

Annual Cumulated Index

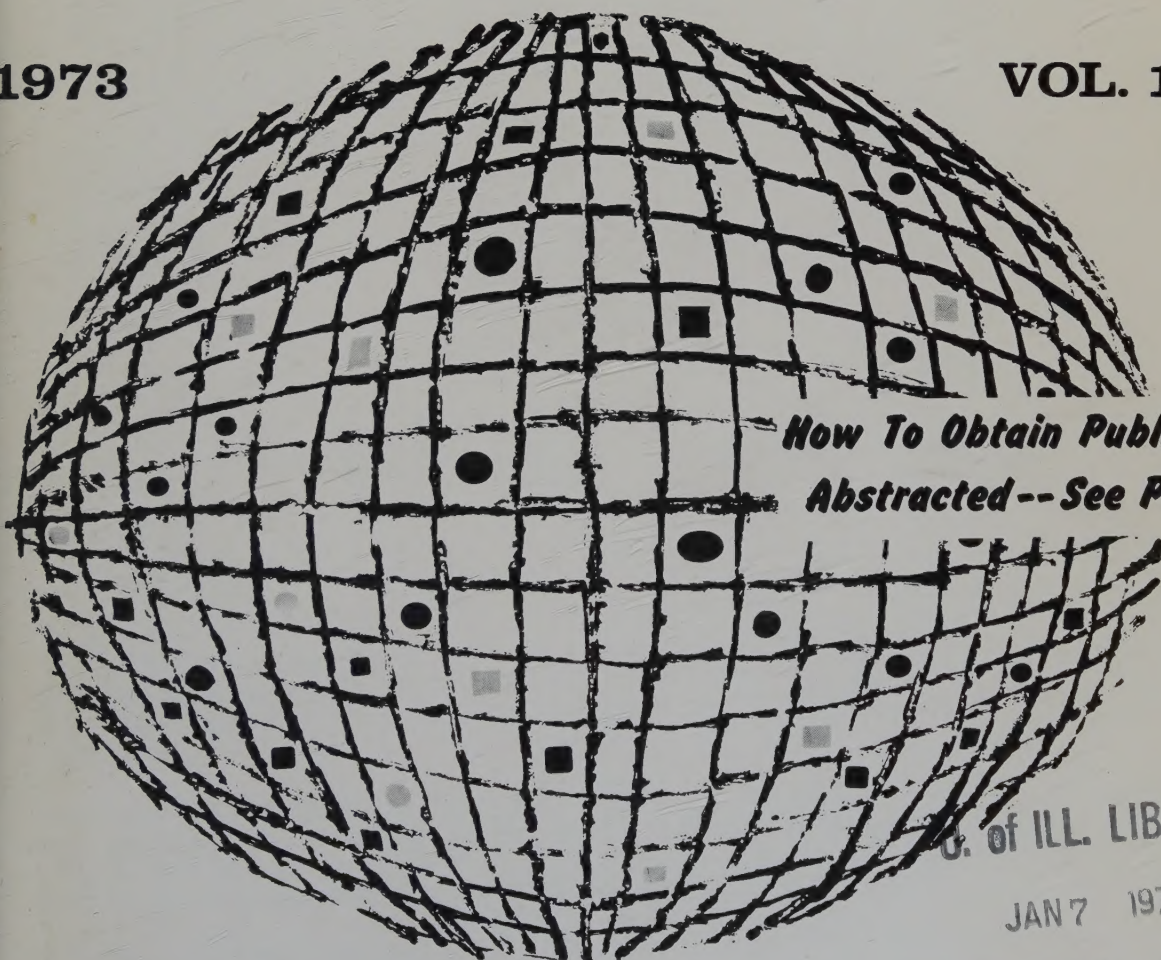
ACCESSION NOS. A73-10001 to A73-45560

INTERNATIONAL AEROSPACE ABSTRACTS

PART 2, SUBJECT INDEX, M - Z

1973

VOL. 13



*How To Obtain Publications
Abstracted-- See Page IV*

U. of ILL. LIBRARY

JAN 7 1974

CHICAGO CIRCLE

PUBLISHED BY THE TECHNICAL INFORMATION SERVICE
AMERICAN INSTITUTE OF AERONAUTICS AND ASTRONAUTICS

INTERNATIONAL AEROSPACE ABSTRACTS

ANNUAL CUMULATED INDEX

PART 2

SUBJECT INDEX, M – Z

VOLUME 13

JANUARY – DECEMBER

1973

ACCESSION NUMBERS A73-10001 to A73-45560

INTERNATIONAL AEROSPACE ABSTRACTS is prepared and published semimonthly (except June and December, which have three issues) by the Technical Information Service, American Institute of Aeronautics and Astronautics, Inc., for the Institute and the National Aeronautics and Space Administration under Contract No. NASW-2532.

SUBSCRIPTION INFORMATION. Semimonthly issues: United States and Possessions, 1 year, \$160 postpaid; all other countries, 1 year, \$175 postpaid. Cumulated index volumes: United States and Possessions, 1 year, \$100 postpaid; all other countries, 1 year, \$115 postpaid. Full service subscription (semimonthly issues and cumulated indexes): United States and Possessions, 1 year, \$240 postpaid; all other countries, 1 year, \$270 postpaid.

EDITORIAL OFFICE: 750 Third Avenue, New York, N.Y. 10017. **SUBSCRIPTION OFFICES:** 750 Third Avenue, New York, N.Y. 10017; Third Avenue and Springtown Road, Alpha, N.J. 08865. Second-class postage paid at New York, N.Y., and at additional mailing offices. Copyright © 1973 by the American Institute of Aeronautics and Astronautics, Inc. (The indexes, however, may be reproduced for any bibliographic purpose.)
TELEPHONE: 212 TN 7-8300

CONTENTS

PART 1

INTRODUCTION	iii
HOW TO OBTAIN PUBLICATIONS ABSTRACTED	iv
CROSS REFERENCES	iv
PERIODICALS SCANNED	v — xxiv
SUBJECT INDEX, A — L	A1 — A988

PART 2

INTRODUCTION	iii
HOW TO OBTAIN PUBLICATIONS ABSTRACTED	iv
CROSS REFERENCES	iv
SUBJECT INDEX, M — Z	A989 — A2008

PART 3

INTRODUCTION	iii
HOW TO OBTAIN PUBLICATIONS ABSTRACTED	iv
PERSONAL AUTHOR INDEX	B1 — B940
CONTRACT NUMBER INDEX	C1 — C35
MEETING PAPER & REPORT NUMBER INDEX	D1 — D13
ACCESSION NUMBER INDEX	E1 — E80

STAFF, TECHNICAL INFORMATION SERVICE

Director, Thomas J. Meskel

Associate Director—Technical, Irene W. Bogolubsky

Abstracts Editor, Nanu Davis

Index Editor, Angelica Mihalakos

Chief Librarian, Patricia M. Marshall

INTRODUCTION

INTERNATIONAL AEROSPACE ABSTRACTS (IAA) is an abstracting and indexing service covering the world's published literature in the field of aeronautics and space science and technology. IAA is issued semimonthly, on the 1st and 15th of each month.

Coverage of Published Literature

The following types of publications are covered in IAA:

- Periodicals (including government-sponsored journals) and books.
- Meeting papers and conference proceedings issued by professional societies and academic organizations.
- Translations of journals and journal articles.

Coverage of Reports ("Unpublished" Literature)

Abstracts and indexes of report literature are issued in SCIENTIFIC AND TECHNICAL AEROSPACE REPORTS (STAR), which is published by the Scientific and Technical Information Office, National Aeronautics and Space Administration.

By special arrangement between NASA and the American Institute of Aeronautics and Astronautics, IAA is issued in coordination with the twice-monthly schedule of STAR, which appears on the 8th and 23rd of each month.

IAA and STAR both utilize identical subject categories and indexes, which are described below.

Thus the two services provide comprehensive access to the national and international unclassified report and published literature of current significance to aerospace science and technology.

Arrangement of the Semimonthly Issues

IAA is arranged in two major sections:

- (1) Abstracts Section. This section contains complete bibliographic citations with informative abstracts as required, arranged by appropriate subject categories to facilitate scanning. The subject categories are numbered from 01 to 34, and the scope of each category is outlined in the Table of Contents and again at the beginning of each category in the Abstracts Section. Each entry is prefixed by the IAA accession number.
- (2) Index Section. Five indexes are contained in this section: Subject, Personal Author, Contract Number, Meeting Paper and Report Number, and Accession Number. Each index is prefaced by explanatory notes.

Cumulated Indexes

The Semiannual Cumulated Index is issued promptly at the end of the first six months and the Annual Cumulated Index is issued promptly at the end of the twelve-month period.

Each cumulated index contains the following sections: A—Subject Index, B—Personal Author Index, C—Contract Number Index, D—Meeting Paper and Report Number Index, and E—Accession Number Index.

Indexing Vocabulary

The Preliminary Edition of the NASA THESAURUS (December 1967) (NASA SP-7030) is the authority for the indexing vocabulary that appears in the subject indexes to STAR and IAA. The NASA Thesaurus should be consulted for a total picture of the current indexing vocabulary and associated cross-reference structure. Copies of the NASA Thesaurus may be obtained from the National Technical Information Service or the U.S. Government Printing Office at a price of \$8.50 for the three-volume set. A one-volume NASA THESAURUS ALPHABETICAL UPDATE (September 1971) of 623 pages is available from the National Technical Information Service (NTIS), Springfield, Va. 22151, for \$6.00.

Information regarding SCIENTIFIC AND TECHNICAL AEROSPACE REPORTS and the availability of INTERNATIONAL AEROSPACE ABSTRACTS to organizations having contractual arrangements with NASA may be obtained from the following address:

National Aeronautics and Space Administration
Scientific and Technical Information Office
Attention: Code KSI
Washington, D. C. 20546

how to obtain publications abstracted

Documents announced are available from the AIAA Technical Information Service as follows:

- Paper copies of accessions announced in IAA and STAR and of other documents in the TIS library are available at \$5.00 per document up to a maximum of 20 pages. The charge for each additional page is \$0.25.
- Microfiche of documents announced in IAA are available at the rate of \$1.00 per microfiche on demand. Documents available in this manner are identified by the symbol # following the accession number in the Abstracts Section and in the Meeting Paper and Report Number and the Accession Number Indexes.
- Minimum air-mail postage to foreign countries is \$1.00.
- A number of publications, because of their special characteristics, are available only for reference in the library.

Address all inquiries and requests to:

Technical Information Service
American Institute of Aeronautics
and Astronautics, Inc.
750 Third Avenue, New York, N. Y. 10017

Telephone: 212 TN 7-8300

**PLEASE REFER TO THE ACCESSION NUMBER
WHEN REQUESTING PUBLICATIONS**

CROSS REFERENCES

The subject index includes two types of cross references to aid the user of the index in locating the material being sought:

1. "USE" references (U) direct the user to alternate headings under which material on the subject will be found, for example

COLUMBIUM
U NIOBIUM

2. "NARROWER TERM" references (NT) refer the user to more specific headings in the same subject area, for example

LUMINESCENCE
NT ELECTROLUMINESCENCE

Either a Notation of Content or the actual title of the publication appears under each subject heading. They are listed under several subject headings which provide multiple access to the subject of each accession. The *IAA* accession number is located under and to the right of the NOC or the title. It is preceded by numbers identifying the issue and page of *International Aerospace Abstracts* where the accession is located.

To illustrate:

Issue Number	Page Number	Accession Number
01	p74	A73-10106

M

M STARS

M giant atmospheric molecular evolution, discussing carbon/oxygen ratios, s-process overabundances and relationships between M, S and C stars

Photospheric and circumstellar H-alpha line profiles in M-supergiant spectra

04 p0496 A73-14971

Hydrostatic, flux constant and LTE stellar atmospheric models at 3800 and 3500 K for Betelgeuse

14 p1801 A73-30737

Bands of the light molecules in Mira variables.

15 p1932 A73-31307

The red dwarf stars of the UV Ceti-type in the neighbourhood of the sun.

15 p1935 A73-31480

Profiles of the photospheric and circumstellar H alpha line in the spectra of type M supergiants.

18 p2354 A73-36731

Cygnids and Taurids - Two classes of infrared objects.

18 p2357 A73-37111

M WINGS

U VARIABLE SWEEP WINGS

MACH CONES

Holographic interferograms for demonstration of acoustic field near supersonic air, nitrogen and helium jets, noting generated Mach wave convection velocity

11 p1346 A73-25382

Acoustic velocity and sound propagation differences in incompressible and compressible fluids related to Mach cone formation and sonic boom effects

24 p3054 A73-45269

MACH INERTIA PRINCIPLE

Some consequences of the Mach-Einstein doctrine for celestial mechanics and geophysics

04 p0498 A73-15280

Experimental test for Mach-Einstein doctrine concerning particle inertial mass variation due to tension or space-time curvature created by interlocking gravitational field

04 p0476 A73-15524

Mach principle incorporation into general relativity, discussing application as selection rule in Einstein field equations solution and other gravitation theories

14 p1798 A73-30238

Matter representation in general theory of relativity in terms of sourceless metric tensor and Einstein matter tensor, examining Mach principle status

22 p2887 A73-42435

MACH NUMBER

Base resistance of axisymmetric bodies with a variable angle of attack - Analysis and interpretation of the physical phenomenon

03 p0242 A73-13375

Method for increasing wind tunnel Mach number for large-scale inlet testing.

[AIAA PAPER 72-1096] 03 p0287 A73-13416

Observations on the macroscopic structure of a near turbulent wake with a Mach number M sub infinity equal 2.3

[ONERA, TP NO. 1176] 03 p0244 A73-13577

Combustion of stabilized ethylene within a supersonic flow by a Mach configuration

03 p0352 A73-13578

Supersonic nozzle design for prescribed flight trajectory and variable gas flow parameters, solving variational problem of optimal contour for given Mach number

03 p0244 A73-13616

Dependence of the base pressure on the ratio of specific heats at supersonic velocities

09 p1027 A73-21917

Isolated reactive and nonreactive Mach stem structure in exothermic systems under conditions encountered behind detonation waves front

10 p1294 A73-23553

Lift and drag at off-design Mach numbers of conically cambered wings with subsonic leading edges and supersonic trailing edge

12 p1458 A73-27927

Control by pressure drop of the radial distribution of the Mach number behind a subsonic annular cascade

[ONERA, TP NO. 1220] 13 p1565 A73-28838

Effect of radial total pressure gradients on the Mach number distribution in turbomachines

13 p1567 A73-29450

Ion Mach number of ion shock embedded in collisional shock wave propagating in electron proton gas plasma

14 p1777 A73-30660

Bottom pressure and specific-heat ratio at supersonic velocities.

15 p1825 A73-32643

Mean flow data analysis of supersonic combustion ramjet turbulent jet mixing at high free stream Mach number

16 p2000 A73-33268

Further data on the pressure recovery performance of straight-channel, plane-divergence diffusers at high subsonic Mach numbers.

[ASME PAPER 73-FE-5] 17 p1552 A73-35005

Mach number and Reynolds number effect on orbiter/tank interference heating.

19 p2491 A73-37403

Investigation of the electron concentration behind strong shock waves

22 p2893 A73-42385

Some effects of pipe flow generated entry conditions on the performance of straight walled conical diffusers with high sub-sonic entry Mach number.

23 p2939 A73-43294

Inlet geometry and axial Mach number effects on fan noise propagation.

24 p3122 A73-44854

Investigation of the diffraction of strong shock waves on convex corners

24 p3081 A73-45536

MACH-ZEHNDER INTERFEROMETERS

Use of a mirror shearing interferometer for gas dynamics research.

01 p0050 A73-10830

Plasma self radiation and absorption, schlieren signals and lasing levels recording methods based on dioxide lasers, using Mach-Zehnder IR interferometer

10 p1253 A73-23517

Alignment technique for the Mach-Zehnder interferometer.

17 p2165 A73-34298

Plasma self radiation and absorption, schlieren signals and lasing levels recording methods based on carbon dioxide lasers, using Mach-Zehnder IR interferometer

17 p2217 A73-35197

Density nonuniformities in a gas dynamic laser cavity.

[AIAA PAPER 73-627] 18 p2321 A73-36174

Quantitative study of an aerodynamic flow by holographic interferometry

18 p2317 A73-37082

High-speed interferometry of expanding and collapsing laser produced plasma.

21 p2744 A73-39964

Electronic fringe-follower for interferometer.

23 p2983 A73-44086

MACHINE LEARNING

U LEARNING MACHINES

MACHINE LIFE

U SERVICE LIFE

MACHINE ORIENTED LANGUAGES

NT LANGUAGE PROGRAMMING

NT SYMBOLIC PROGRAMMING

German monograph - The design of digital filters with minimal storage word length for coefficients and state parameters.

14 p1737 A73-30667

MACHINE RECOGNITION

U ARTIFICIAL INTELLIGENCE

MACHINE STORAGE

U COMPUTER STORAGE DEVICES

U CORE STORAGE

MACHINE TOOLS

NT BORING MACHINES

NT GRINDING MACHINES

NT LATHES

Maximum metal removal rate in ECM.

[SME PAPER MR 72-537] 06 p0697 A73-18092

Investigation of the turning process using diamond cutting tools on M1.-5 magnesium alloy, with the application of mathematical methods in experiment planning

15 p1881 A73-31278

Ionic machine tools for microelectronic manufacture, discussing ion jets properties, optics and construction and implantation, micromachining and deposition technologies

16 p1987 A73-33088

Interactive computer graphic display and interface system effectiveness for programming numerical control operations for tooling and part machining in aircraft production

[AHS PREPRINT 753] 17 p2131 A73-35081

Borazon compact cutting tools.

[SME PAPER MR 73-143] 19 p2436 A73-38500

Turning high-temperature alloys with Borazon tools.

[SME PAPER MR 73-145] 19 p2437 A73-38501

MACHINERY

Machine components dimensioning and testing for fatigue strength, presenting methods for service life determination

03 p0385 A73-13132

Fire suppression for shipboard machinery spaces - Extinguishing and inerting with Halon 1301.

[WSCI PAPER 72-33] 05 p0639 A73-16682

Fundamentals of the theory of combined reliability and service life estimates for machines and instruments

13 p1624 A73-29134

Russian book - Accelerated wear-resistance tests for machine components and machinery.

15 p1881 A73-31582

Solid refractory metal and nonmetal alloys for machine structural components under dynamic and steady cumulative stresses

18 p2326 A73-37000

Isolation of machinery vibration from nonrigid substructures using multiple antivibration mountings.

22 p2927 A73-42923

MACHINING

NT ELECTROCHEMICAL MACHINING

NT HOT MACHINING

NT MILLING [MACHINING]

NT SPARK MACHINING

NT ULTRASONIC MACHINING

Preparation of information for programming machining operations during grinding of a blade profile by the continuous-shaping method

02 p0172 A73-11799

Machining precision in deep-hole boring by a feed-division technique

02 p0174 A73-12578

Applying surface integrity principles in jet engine production.

03 p0312 A73-13272

Beryllium parts machining and surface finishing techniques for maximum fracture strength and fatigue life

05 p0587 A73-16754

Determination of the average duration of a machining process on automatic production lines

05 p0582 A73-16997

Correlation analysis of the accuracy of the machining of micromachine components

09 p1088 A73-22660

Heat resistant Ni alloys residual stresses from machining operations, considering cutting rates, temperature, work piece blanks and cutting tools parameter effects

10 p1226 A73-24798

Automated machining and surface finishing of heat resistant stainless steel nozzles for wind tunnel applications

15 p1855 A73-31200

The laser - A unique tool for /for the time being/ unique applications

15 p1884 A73-31325

Thermal analysis of thin-film micromachining with lasers.

15 p1882 A73-31938

Cold forming stainless steels and other specialty grades.

15 p1883 A73-32168

Surface integrity - A new requirement for improving reliability of aerospace hardware.

16 p2018 A73-33067

Stepped aluminum extrusions - Designing for business aircraft.

[SAE PAPER 730308]

17 p2177 A73-34668

Recognition and control of abusive machining effects on helicopter components.

[AHS PREPRINT 750]

17 p2180 A73-35078

Welded titanium tubes and their applications

19 p2433 A73-37834

Explosive metal forming, considering energy cost, operational speed, achievable tolerances in symmetrical or nonsymmetrical shapes, production quantities and lead time for die preparation

20 p2569 A73-39405

Drop forged Ti alpha-beta alloy textures after heat treatment, quenching, aging and surface machining

22 p2866 A73-42089

Pulsed Nd-YAG laser output spiking for control of materials machining parameters

24 p3098 A73-45552

MACROCLIMATE

U CLIMATE

MACROSCOPIC EQUATIONS

Metal fcc polycrystals macroscopic plasticity theory based on discrete aggregate model, predicting stress-strain curves for partial load cycles

09 p1160 A73-22896

Equivalency and macrophysical validity of Thomson and Clausius theorems for second law of thermodynamics, considering Carathéodory theorem relative to entropy and temperature properties

19 p2504 A73-37654

MACULAR VISION

U VISION

MAFFEI GALAXIES

A radio map of the spiral galaxy Maffei 2 at 1415 MHz.

03 p0370 A73-13210

Optical and near-infrared observations of the nearby spiral galaxy Maffei 2.

10 p1272 A73-23528

MAGELLANIC CLOUDS

Structure and dynamics of barred spiral galaxies, in particular of the Magellanic type.

01 p0096 A73-10298

Remarks on the comparison of the Sanduleak and Fehrenbach-Duflo catalogs of stars belonging to the Large Magellanic Cloud

02 p0223 A73-12718

On the extended van Wijk sequence in the Large Magellanic Cloud.

03 p0371 A73-13217

Measurement of radial velocities with coude spectrograph of the 152-cm telescope of the Haute Provence Observatory

03 p0371 A73-13223

Small Magellanic cloud large depth along line of sight shown from supergiant stars and cepheids observation

03 p0380 A73-14610

Supergiant stars with very strong hydrogen lines in the Great Cloud of Magellan

04 p0502 A73-15998

Structure of the Cepheid instability strip in the small Magellanic Cloud.

04 p0503 A73-16007

Small Magellanic Cloud X-1 X ray source binary nature, occultation, energy spectrum and intensity from Uhuru satellite observation

05 p0626 A73-17345

The radio continuum of the Large Magellanic Cloud. I - The sources at 6 cm wavelength.

06 p0754 A73-18629

The radio continuum of the Large Magellanic Cloud. II - Continuum observations at 11 cm wavelength.

06 p0754 A73-18630

The radio continuum of the Large Magellanic Cloud. III - The sources at 11 cm wavelength.

06 p0754 A73-18631

The radio continuum of the Large Magellanic Cloud. IV - Spectra of sources.

06 p0754 A73-18632

Evidence for ejection of radio sources from supernova remnants.

07 p0873 A73-19056

Light variations of high luminosity O and B stars in

the Large Magellanic Cloud.

07 p0877 A73-19597

Schmidt telescopes in stellar photography of Magellanic clouds, galactic center and Scorpio-Centaurus and globular clusters for southern hemisphere Milky Way structure investigation

08 p1011 A73-21364

A search for neutral hydrogen remnants of strong tidal disruption of the Small Magellanic Cloud.

09 p1141 A73-22012

Chemical composition of classical Cepheids in the Galaxy and Magellanic Clouds

10 p1273 A73-23705

Additional observations of supergiants and foreground stars in the direction of the Large Magellanic Cloud.

10 p1279 A73-24167

Fabry-Perot interferometer with etalon for studying gas movements and planetary nebulae in Large Magellanic Cloud by spectral analysis from pressure scanning

11 p1361 A73-25176

Metagalactic cosmic ray origin models and cosmic ray energy density around Galaxy, considering gamma ray flux, measurement from Magellanic Clouds

12 p1539 A73-27142

A photometric study of the integrated light of clusters in the Magellanic Clouds and the Fornax dwarf galaxy.

14 p1801 A73-30726

Chemical composition of the classical Cepheids in the Galaxy and the Magellanic Clouds.

18 p2354 A73-36730

Polarization of stellar light between the two Magellanic clouds

20 p2606 A73-39063

Model for gas bridge and magnetic field connecting Magellanic Clouds from optical and radio polarization measurements

21 p2779 A73-41535

MAGMA

Genetic significance of chemical, isotopic, and petrographic features of some peralkaline silic rocks from the island of Pantelleria.

05 p0570 A73-16842

Analytical approach to estimating the source rock of basaltic magmas - Major elements.

09 p1076 A73-22147

Europium anomaly in plagioclase feldspar - Experimental results and semiquantitative model.

16 p1976 A73-32902

MAGNESIUM

Practical protective atmospheres for molten magnesium.

03 p0323 A73-13267

The effect of small magnesium additions on microstructure and high-temperature properties of nickel-2-1/2 vol. % alumina.

03 p0326 A73-13966

Cumingtonite temperature dependent Mg and ferric ions order-disorder, estimating crystallization temperatures

03 p0375 A73-14104

Neutral Mg line at 4571 Å in solar atmosphere, computing line profiles from Harvard-Smithsonian Reference Atmosphere and Bilderberg Continuum Atmosphere

03 p0377 A73-14405

Interstellar magnesium abundances and electron density in the direction of Orion and Cassiopeia.

04 p0502 A73-15976

Influence of the degree of purity on the kinetics of the recrystallization of deformed magnesium

05 p0587 A73-17216

Ultraviolet photometry from the Orbiting Astronomical Observatory. VI - Magnesium II 2800 Å emission in cool stars.

05 p0625 A73-17336

Magnesium particle ignition in various media

07 p0923 A73-20419

Magnesium and associated ionospheric processes in Es-layer formation.

08 p0957 A73-20655

Magnesium II doublet profiles of chromospheric inhomogeneities at the center of the solar disk.

08 p1004 A73-20908

Observation of Bardeen-Herring sources in quenched magnesium

08 p0979 A73-21629

Physical characteristics of sponge titanium of a hardness below 100 HB units, obtained by heat treatment with magnesium

09 p1107 A73-23227

Reinforcement of magnesium with boron and tantalum filaments.

10 p1234 A73-24437

Temperature and rate dependence of the critical shearing stress in magnesium single crystals

13 p1636 A73-29056

The photoionization cross section of magnesium near threshold.

14 p1776 A73-29699

Technical note on some mechanical properties of a magnesium-25 vol% boron particulate composite.

14 p1765 A73-30935

The equivalent widths of Mg II lines near 2800 Å in the spectra of 31 stars.

16 p2059 A73-32838

Critical shear stress temperature and rate dependence in magnesium single crystals.

18 p2325 A73-36888

Ignition limit of metallic particles in a mixture of two oxidizers

19 p2503 A73-37517

TD 1 A astronomical satellite detection of UV dayglow emissions above F 2 peak in equatorial zone, considering Mg ions resonance scattering to account for emission features

20 p2551 A73-38940

Influence of magnesium on the structure of heat-resistant nickel-base alloys

21 p2718 A73-40485

High temperature creep in magnesium strengthened by magnesia particles.

21 p2719 A73-40899

The formation of Mg I 4571 Å in the solar atmosphere. III - The Holweger solar model /Research note/.

21 p2777 A73-41480

Temperatures in low-pressure magnesium-vapor diffusion flames.

22 p2899 A73-42820

MAGNESIUM ALLOYS

Temperature dependence of the critical shear stress in single crystals of Al-Mg alloys of various concentration at temperatures between 1.6 and 300 K

01 p0064 A73-10488

Inhomogeneity of the structure and deformability of aluminum and aluminum-magnesium alloys

03 p0324 A73-13506

Influence of deformations on the mechanical properties of magnesium alloys containing yttrium

03 p0324 A73-13509

New magnesium alloys intended for operation at elevated temperatures

03 p0324 A73-13513

Elastic damping properties of binary Mg and Al alloy systems with Cd, Mn, Ni, Si, Zr, Nd and Ca alloying

03 p0324 A73-13515

A study of precipitation at elevated temperatures in a Mg-8.7 pct Y alloy.

04 p0463 A73-15318

Relationship between cavitation and decontamination during ultrasonic processing of aluminum and its magnesium alloys

04 p0454 A73-15663

Double aging time effects on hardness of solution treated, quenched and heat treated two phase Al-Zn-Mg alloy specimens, obtaining transmission electron micrographs

05 p0587 A73-16577

Deep-drawability and some problems after forming by deep-drawing of Al-Mg alloy sheets - Study on Al-Mg alloy sheets for forming use. II.

05 p0581 A73-16580

Composition affects tensile strength of welded aluminum-magnesium alloy.

06 p0709 A73-18385

The formation and structure of precipitates in a dilute magnesium-neodymium alloy.

07 p0838 A73-19121

Filler wire welded joints of Al-Zn-Mg and Al-Mg alloys, testing weldability and mechanical properties susceptibility to hot cracking

07 p0840 A73-20372

The use of macroscopic failure diagrams to determine the quality of materials.

08 p0977 A73-21148

Russian book on extra light engineering alloys covering Mg-Li alloys structure and mechanical properties, aging and strain hardening characteristics, corrosion resistance, etc

08 p0979 A73-21600

Effect of addition of Bi on stress-corrosion cracking of Al-Mg alloy.

09 p1102 A73-22421

Stress corrosion cracking of commercial Al-Mg alloys and its prevention.

09 p1102 A73-22422

Effect of magnesium additions on the ductility of heat-resistant nickel alloys

09 p1108 A73-23230

Effects of beryllium additions on the microstructure and the type of failure in Al-Mg alloys

10 p1233 A73-24423

Ultrasonic treatment of alloy MA2-1 during solidification.

10 p1236 A73-24930

Corrosion fatigue and stress corrosion crack growth in high strength aluminum alloys, magnesium alloys, and titanium alloys exposed to aqueous solutions.

11 p1381 A73-25815

Temperature and concentration dependence of the electrical resistivity of solid alloys in the magnesium-cadmium system

11 p1386 A73-26570

Russian papers on nonferrous metals and alloys metallurgy covering phase equilibria, strengthening, deformation and processing of Al, Mg, Cu and Ti alloys

12 p1510 A73-26902

Temperature dependence of the solubility of scandium in solid magnesium

12 p1510 A73-26908

Improving the properties of the MA5 magnesium alloy by high-temperature thermomechanical treatment

12 p1510 A73-26910

Variation in the kinetics of the natural aging process for Mg-Li-Al alloys as a function of the presence of impurities and small additions of rare-earth elements 12 p1510 A73-26911

Deformation and recrystallization of twin crystals in aluminum and magnesium alloys 12 p1510 A73-26913

Effect of titanium additions on the aging characteristics of an Al-Zn-Mg alloy. 13 p1632 A73-28134

Superconductivity of cadmium-magnesium alloys. 13 p1668 A73-28223

Crystallographic analysis of hexagonal vacancy type Al-Mg alloy cube plane dislocation loops produced by specimen deformation before quenching 13 p1634 A73-28260

Mechanical properties of 6061 Al-Mg-Si alloy after very rapid heating. 13 p1636 A73-28795

Corrosion and corrosion prevention of light metal alloys. [NACE PAPER 114] 13 p1637 A73-29314

Dynamic and static strain aging in Al-Mg solid solution alloys. 13 p1639 A73-29458

Nimonic and Mg alloys creep behavior interpretation by constitutive law, discussing recovery activation and strain hardening from microstructural behavior 13 p1642 A73-29515

Critical shear stress temperature dependence in Al-Mg single crystal alloys of various concentrations in the range 1.6-300 K. 14 p1759 A73-30313

German monograph - Elevation of the yield point and pronounced yield range of multicrystalline aluminum-magnesium alloys. 14 p1762 A73-30673

Catalytic effects in corrosion processes with hydrogen depolarization of multiphase magnesium alloys 14 p1764 A73-30827

Investigation of the turning process using diamond cutting tools on ML-5 magnesium alloy, with the application of mathematical methods in experiment planning 15 p1881 A73-31278

Role of stress in the stress corrosion cracking of a Mg-Al alloy. 17 p2191 A73-35100

Particle combustion mechanism in aluminum-magnesium alloys 19 p2472 A73-37511

Tensile deformation and fracture in high-strength Al-Zn-Mg alloys. 20 p2575 A73-39019

A photographic method for testing the impact strength of metals 21 p2696 A73-39991

Phase diagrams and composition selections for strengthening of multicomponent deformable Mg alloys with rare earth and transition elements 22 p2874 A73-42094

Study of precipitates in an aged Mg-3.6 wt%Zn alloy by an X-ray method. 23 p2993 A73-44124

On the process of precipitation in Mg-Ce alloy. 23 p2994 A73-44155

Discontinuous flow in steady-state creep of Al-Mg alloys at high temperatures. 23 p2995 A73-44162

MAGNESIUM CHLORIDES

Crack corrosion of titanium in a solution of hot concentrated magnesium chloride 07 p0839 A73-20167

Characterization of passivation films formed at the surface of stainless steels in magnesium chloride solutions 08 p0976 A73-20650

Notched austenitic stainless steel stress corrosion cracking tests in boiling magnesium chloride solutions, obtaining relationship between maximum stress and strain rate in graph 15 p1895 A73-32569

MAGNESIUM COMPOUNDS

NT CHLOROPHYLLS

NT ENSTATITE

NT FORSTERITE

NT MAGNESIUM CHLORIDES

NT MAGNESIUM FLUORIDES

NT MAGNESIUM OXIDES

NT MAGNESIUM TITANATES

NT PERCLASE

NT TALC

Struvite precipitation from evaporating sea water with added ammonia, considering importance for prebiotic phosphorylation 07 p0787 A73-19168

The magnesium spinel-bearing rocks from the Fra Mauro formation. 07 p0883 A73-19733

Investigation of the polar and protective properties of magnesium salts of organic acids 10 p1239 A73-24248

Low temperature specific heat of neodymium magnesium nitrate. 18 p2341 A73-36977

Nitride inclusions in titanium ingots - A study of possible sources in the production of magnesium-

reduced sponge. 20 p2576 A73-39026

MAGNESIUM FLUORIDES

Preparation of transmitting coatings for As₂S₃ glass 05 p0605 A73-17293

Use of MgF₂ and LiF photocathodes in the extreme ultraviolet. 08 p0964 A73-21048

MAGNESIUM OXIDES

NT PERCLASE

Thermoluminescence and activation energies in Al₂O₃, MgO and LiF (TLD-100). 12 p1530 A73-27031

On the electrical properties of nonstoichiometric oxides alpha-Nb₂O₅, MnO, and CoO at high temperature 13 p1634 A73-28202

Magnesium oxide crystal dislocation loop shrinkage rate measurement, suggesting oxygen ion diffusion as rate controlling process for dislocation climb 13 p1634 A73-28257

Flow of a dust suspension over an ellipsoid of revolution. 17 p2091 A73-34348

High temperature creep in magnesium strengthened by magnesia particles. 21 p2719 A73-40899

Wettability and interfacial tension of magnesia single crystals by molten magnesium oxide-aluminum trioxide-silicon dioxide glasses, discussing contact angle relationship to temperature 23 p2998 A73-44132

Additive distribution and formation of internal stress in fired magnesia. 23 p2998 A73-44133

MAGNESIUM TITANATES

Influence of grain size on effects of thermal expansion anisotropy in MgTi₂O₅. 21 p2752 A73-40893

MAGNESYN [TRADEMARK]

U SERVOMOTORS

MAGNET COILS

NT FIELD COILS

Magnetic energy storage and transfer from coil into resistive load with superconducting switch, discussing voltage and circuit conditions for full normalization 02 p0200 A73-11830

Model coil test results for a pulsed superconducting magnet energy storage system. 02 p0132 A73-11831

Electromagnetic systems of noise-immunized nuclear-precession sensors 06 p0692 A73-17562

Large-scale applications of superconducting coils. 07 p0863 A73-20107

Performance of a 12-coil superconducting 'bumpy torus' magnet facility. 07 p0809 A73-20460

Operating properties of a helical microwave plasma source in high density high magnetic field regime. 11 p1407 A73-26562

Note on analysis of cryogenic suspensions for space vehicles. 12 p1524 A73-27633

Electromagnetic systems of noiseproof nuclear precession sensors. 16 p2011 A73-32786

MAGNETIC ABSORPTION

U ELECTROMAGNETIC ABSORPTION

MAGNETIC AMPLIFIERS

Application of the superregeneration principle to a ferromagnetic amplifier 13 p1592 A73-28910

MAGNETIC ANNULAR ARC

Magnetic current annular ring near field, noting application to coaxially driven parallel monopole arrays analysis 06 p0666 A73-18198

MAGNETIC ANNULAR SHOCK TUBES

Particular variation of the velocity of the driver gas in a shock tube with electromagnetic blowing with two gases 05 p0601 A73-16429

MAGNETIC ANOMALIES

Non-dipole terms in the magnetic fields of Jupiter and the earth. 02 p0212 A73-11897

Geomagnetic control over evolution of F₂-layer at sunrise. 02 p0159 A73-12183

Magnetically coupled transport of a cold plasma in the outer ionosphere at low latitudes. 05 p0567 A73-16094

Anomaly configuration maps showing westward drift and positions of residual geomagnetic fields and eccentric dipoles during 1885-1965 period 06 p0689 A73-17544

Geographic distribution of anomalies of residual geomagnetic field derived from eccentric dipole and observed field comparing with thermal flux fields and geotectonic features 06 p0689 A73-17546

The electromagnetic perturbation fields of conductivity anomalies within the earth. 06 p0690 A73-17925

Anomalous magnetic and gravitational field models autocorrelation function behavior dependence on circular cylindrical sources depth and spacing 07 p0816 A73-19447

Magnetic irregularities in interplanetary space and

geomagnetic activity. 08 p1007 A73-21004

Penetration of solar protons into the geomagnetic tail 08 p0998 A73-21276

Identification of discontinuities at the magnetosphere boundary 08 p0958 A73-21277

Lower boundary of the occurrence of magnetoacoustic masses 08 p0959 A73-21296

Earth crust inhomogeneities from high altitude aeromagnetic survey, noting informativeness loss increase with height 08 p0960 A73-21308

Nature of the drift of the main eccentric geomagnetic dipole. 10 p1212 A73-24233

Possibility of determining the secular variation of geomagnetic field components from the distribution of variations of the absolute value of the total vector. 10 p1212 A73-24234

A direct method of interpreting gravity and magnetic anomalies - The case of a horizontal cylinder. 11 p1351 A73-25162

The effect of two periodic conductivity anomalies on geomagnetic micropulsation measurements. 13 p1607 A73-28622

Magnetic and gravitational potential anomalies due to uneven nonuniform material layers, using Fourier transforms 13 p1607 A73-28623

Magnetic anomalies in New Guinea-New Zealand region from proton magnetometer measurements, noting effects of andesite-basalt volcanic processes and nuclear precession signal variations 13 p1608 A73-28727

Solar wind proton temperature anomalies relation to interplanetary shock waves, considering solar flare induced material ejection and magnetic bottle formation 14 p1786 A73-29952

The relationship between the structure of the equatorial anomaly and the strength of the equatorial electrojet. 15 p1869 A73-31761

Equatorial electrojet characteristics observation during 1967-1970 with POGO satellite-borne magnetometers, noting anomaly characterized by sharp negative V-signature in width and variable amplitude 15 p1870 A73-31768

Separation of the variable geomagnetic field into normal and anomalous components 15 p1872 A73-31896

Anomaly configuration maps showing westward drift and positions of residual geomagnetic fields and eccentric dipoles during 1885-1965 period 16 p2002 A73-32768

Geographic distribution of anomalies of residual geomagnetic field derived from eccentric dipole and observed field, comparing with thermal flux fields and geotectonic features 16 p2002 A73-32770

Penetration of solar protons into the geomagnetic tail. 19 p2476 A73-37905

Identification of discontinuities at the magnetosphere boundary. 19 p2424 A73-37906

Lower boundary of occurrence of magnetically active masses. 19 p2425 A73-37925

Earth crust inhomogeneities from high altitude aeromagnetic survey, noting information loss increase with height 19 p2425 A73-37937

A geomagnetic variation anomaly across the northern Gulf of California. 21 p2678 A73-39927

Anomalies in geomagnetic variations across the central Gulf of California. 21 p2679 A73-39928

Neutral air wind influences deduced from solar cycle changes in the F₂ region equatorial anomaly. 21 p2679 A73-39932

The detection of 'intermediate' size magnetic anomalies in Cosmos 49 and OGO 2, 4, 6 data. 21 p2691 A73-41374

Ariel 3 evidence of zones of VLF emission at medium invariant latitudes which co-rotate with the earth. 21 p2691 A73-41382

Azimuthal drift and precipitation of electrons into the South Atlantic geomagnetic anomaly during an SC magnetic storm. 22 p2846 A73-41946

Particle precipitation in Brazilian geomagnetic anomaly during magnetic storms. 23 p2971 A73-43687

MAGNETIC CHARGE DENSITY

Search for magnetic monopoles in lunar material using an electromagnetic detector. 19 p2461 A73-38492

MAGNETIC CIRCUITS

Effect of inhomogeneity of normal specimens on measurement error estimation in devices with an incompletely closed magnetic system 01 p0044 A73-10085

Two component magnetic pulsed modulator for electroluminescent and laser diodes, using ac source

- with nonresonance input capacitance charge
01 p0059 A73-10793
- On the phenomenon of parametric resonance of a nonlinear vibrator under the action of electromagnetic force.
04 p0429 A73-15598
- Thermomagnetic shunt for compensation of instrument errors due to temperature effects on magnetoelectric transducers material, calculating magnetic circuit
05 p0577 A73-16988
- Time optimal control for vibrationless starting of electromechanical devices with moving parts, noting linear magnetic circuit
06 p0649 A73-18383
- Analysis of the magnetic systems of calculating transducers
09 p1064 A73-22941
- The application of integrated magnetic devices for circuit checking and error correcting.
10 p1198 A73-24021
- An analog-code follow-up converter based on second-harmonic magnetic modulators
12 p1475 A73-26766
- Wave devices built with ferromagnetic and electrically conducting film strips
12 p1460 A73-26772
- Multiphase even harmonic frequency multipliers using nonlinear magnetic reactors with bridge rectifiers, considering output signal waveforms
12 p1477 A73-26788
- Comparative analysis of the longitudinal and orthogonal magnetic second-harmonic modulators.
12 p1477 A73-26789
- An optimal scheme for excitation of low-threshold magnetically modulated converters and analysis of their operation
13 p1591 A73-28855
- Effects of electron-microscope design features on the accuracy of the microprobe diffraction method
17 p2164 A73-34176
- Analysis of processes occurring during no-load operation of a ferroresonant voltage regulator with an improved shape of the output voltage curve
24 p3057 A73-44608

MAGNETIC COILS

- NT FIELD COILS
- Investigation of cryogenic stability and reliability of operation of Nb₃Sn coils in helium gas environment.
02 p0200 A73-11838
- Crossed-coil nuclear magnetic resonance probe for high sensitivity low temperature measurements.
02 p0168 A73-11962
- Design considerations for high-current-density superconducting saddle magnets for MHD.
07 p0852 A73-20405
- Application of a system of orthogonalized windings with automatically regulated current for plasma stabilization in Tokamak systems
09 p1125 A73-21908
- Equivalent resistance, Q factor and winding capacitance of air-core coils with coplanar spiral winding intended for bandpass filters
09 p1065 A73-23073
- A Lallemand electronic camera focused by a superconducting magnetic coil.
14 p1751 A73-29904
- Experimental study of a conical theta-pinch plasma gun.
14 p1779 A73-29928
- Nuclear spin analogue of a molecular beam maser with cavities in series.
21 p2713 A73-40469
- Structure of currents in a stationary plasma jet in the presence of the Hall effect
23 p3010 A73-43664

MAGNETIC COMPASSES

- Aircraft compass design with magnetic needle free turning capability around two orthogonal axes, noting advantage over conventional devices and suitability for glider navigation
13 p1613 A73-28555
- Simultaneous statistical treatment of the readings of a directional gyroscope and a magnetic compass
24 p3089 A73-44547

MAGNETIC CONTROL

- Magnetic pulse width modulator and power switch subsystem of switching-mode dc regulator, deriving describing function from transfer functions
03 p0282 A73-13928
- Advances in YIG-tuned Gunn effect oscillators.
04 p0426 A73-14734
- Methods of plasma injection into closed magnetic confinement systems
04 p0479 A73-15041
- Engineering problems in the design of controlled thermonuclear reactors.
[AIAA PAPER 73-259]
05 p0596 A73-16980
- Transverse and longitudinal heat flow in a laser-heated magnetically confined plasma.
05 p0603 A73-17162
- Fusion plasma confined by nonpenetrating uniform magnetic field, calculating temperature and density effects on energy balance instabilities from particle conservation equations
05 p0604 A73-17366
- Time optimal control for vibrationless starting of electromechanical devices with moving parts, noting

linear magnetic circuit

- Diademe satellite passive magnetic stabilization system, describing magnet and damper design
06 p0649 A73-18383
- Pioneer Jupiter spacecraft magnetic field control with periodically updated magnetic model for tradeoffs in subsystem moments within allowed magnetic budget
07 p0904 A73-18935
- [IEEE PAPER 41,4]
07 p0905 A73-19364
- Non-local asymptotic treatment of the stability of an inhomogeneous confined plasma.
08 p0991 A73-20819
- Spiral arm structure as standing wave, of magnetically controlled star creation, considering various hydromagnetic models, dust and H I distributions
10 p1002 A73-20879
- Magnetically focused electronographic cameras for far UV imagery and spectrography in astronomical and optical geophysical observations from sounding rockets and space vehicles
08 p0971 A73-21744
- A magnetically controlled tube generator of very-low-frequency sinusoidal oscillations
09 p1063 A73-22337
- Variable-reluctance stepping motor performance capabilities for point-to-point positional control.
10 p1199 A73-24024
- Magnetic intake limitations on interstellar ramjets.
10 p1262 A73-24539
- Magnetic control of near equatorial neutral thermosphere, calculating F region ionization anomaly and molecular nitrogen and atomic oxygen density latitudinal variations
12 p1489 A73-26997
- Small oscillations of gravity gradient satellite in circular near-equatorial orbit, discussing operational efficiency of magnetic damping systems
12 p1549 A73-27648
- Application of methods of mathematical statistics to study the motion of an artificial earth satellite about its center of mass
15 p1931 A73-31234
- Effect of laser pulse rise time on heating of a magnetically confined plasma.
15 p1919 A73-31929
- Magnetic multiple containment of large uniform collisionless quiescent plasmas.
17 p2215 A73-34271
- State-space analysis of a magnetically tuned IMPATT oscillator lumped model.
17 p2136 A73-34973
- Control laws of magnetic attitude stabilization systems of earth satellites
18 p2359 A73-36103
- Magnetic modulation of the optical emission intensity of a plasma from a high-frequency H-discharge
18 p2339 A73-36565
- Computer simulation for time optimal or energy optimal attitude control of spin-stabilized spacecraft.
18 p2360 A73-36837
- Experimental investigations on arc-heated steady plasma flow.
19 p2415 A73-37169
- Investigation of the dynamics of plasma flows in the field of a pulsed magnetic barrier
23 p3010 A73-43658
- Investigation of the efficiency of laser-plasma trapping by a magnetic field
23 p3014 A73-44341

MAGNETIC CORES

- Analysis of limit cycles in a two-transistor saturable-core parallel inverter.
03 p0252 A73-13929
- Ferrite core modular memory characteristics, considering bit capacity and printed circuit technology utilization
05 p0556 A73-16167
- A computer-aided design procedure for flyback step-up dc-to-dc converters.
[IEEE PAPER 4,4]
07 p0779 A73-19361
- Design of a search memory using elements with reluctance modulation
08 p0941 A73-21108
- Megabit capacity ferrite core memories for scientific satellites, using three dimensional organization with pulse program adapted for buffer application
09 p1087 A73-23426
- The application of integrated magnetic devices for circuit checking and error correcting.
10 p1198 A73-24021
- Propagation constant and wave resistance in the case of coaxial and hollow conductors with lossy dielectric and magnetic materials
14 p1730 A73-30920
- A method for thermal stabilization of the parameters of devices with ferrite cores
22 p2833 A73-42371
- Noise and stable operation conditions in associative memory devices
23 p2956 A73-43580

MAGNETIC DIFFUSION

- Hydromagnetic flow about a curved neutral sheet.
01 p0086 A73-11495
- Heat flow and magnetic field diffusion in turbulent fluids.
02 p0199 A73-12841
- Geomagnetic tail and neutral sheet origin based on

geomagnetic flux diffusion through magnetopause, discussing Dungey reconnection mechanism and Kelvin-Helmholtz instability effects
04 p0441 A73-15329

Dayside magnetopause distance calculation at subsolar point for various solar wind parameters, allowing for southward interplanetary field component diffusion
05 p0610 A73-17008

The generation and dissipation of solar and galactic magnetic fields.
22 p2911 A73-42934

MAGNETIC DIPOLES

- Glass reinforced epoxy structure for a lightweight superconducting dipole magnet.
02 p0232 A73-11836
- Asymmetric eigenmodes in a simple model plasmasphere.
03 p0345 A73-12882
- Radiation pattern of longitudinal magnetic dipole ideally conducting infinite circular cylinder parallel to infinite plane screen
04 p0429 A73-15912
- Diffraction of waves generated by a magnetic-dipole current system on a variable-radius sphere
05 p0550 A73-16397
- Anomaly configuration maps showing westward drift and positions of residual geomagnetic fields and eccentric dipoles during 1885-1965 period
06 p0689 A73-17544
- Diffraction of the emission field of a horizontal dipole on a circular hole in a plane screen in the presence of a circular disk coaxial with the hole
06 p0664 A73-17716
- Dipolar coordinate system for geomagnetic field dipole approximation in studies of diffusion and heat conduction in F region and outer ionosphere
07 p0816 A73-19452
- Wave pattern of three dimensional hydromagnetic perturbations produced by harmonic magnetic dipole in anisotropic plasma
07 p0816 A73-19461
- Hydromagnetic waves excited by transverse magnetic dipole in finite-conductivity plasma
07 p0816 A73-19462
- Eccentric geomagnetic dipole drift field as function of time dependent parameters, calculating potential components in spherical coordinates
07 p0817 A73-19467
- Nature of the drift of the main eccentric geomagnetic dipole.
10 p1212 A73-24233
- Geomagnetic field polarity reversal mechanism, interpreting frequency distribution by energy exchange between dynamo models and conversion between kinetic and magnetic energies
11 p1355 A73-25792
- Precise calculation of the magnetosphere surface for a tilted dipole.
11 p1421 A73-25923
- Earth main magnetic field description by cartography and analytic methods based on dipole or spherical harmonic series representations.
13 p1608 A73-28713
- The Ze field, some of its properties, and geophysical information.
13 p1608 A73-28720
- Anomaly configuration maps showing westward drift and positions of residual geomagnetic fields and eccentric dipoles during 1885-1965 period
16 p2002 A73-32768
- Comparison of the two-dipole and empirical magnetospheric models.
18 p2310 A73-36135
- Pulsed magnetic system /terrella/ as earth model with dipole magnetic field for laboratory simulation of geophysical phenomena
19 p2425 A73-37938
- Excitation of the earth-ionosphere waveguide by point dipoles at satellite heights.
20 p2528 A73-38846
- Charged particle acceleration in strong dipole fields.
20 p2595 A73-39077
- Semiconducting ground influence on input impedance and radiation resistance of horizontal magnetic dipoles, covering short wave band for various antenna elevations and conductivity levels
21 p2661 A73-40203
- Jupiter magnetic dipole offset along rotation axis from 11 cm radio centroid measurements with Parkes telescope
24 p3130 A73-44459
- Physical relations of the asymmetric structure of the earth
24 p3088 A73-45448

MAGNETIC DISKS

- An integrated random access memory with full-current recording and readout
14 p1730 A73-30290

MAGNETIC DISTURBANCES

- NT MAGNETIC STORMS
- Ionospheric effects on the transmission of ultralow-frequency plasma waves.
02 p0155 A73-11520
- On the types of current patterns of weak geomagnetic disturbances at the polar caps.
02 p0158 A73-11915
- Drag derived density analysis for geomagnetic

disturbances effect in thermosphere, noting atmospheric reaction time delay and exospheric temperature increment per unit Kp

Geomagnetic indexes Kp, ap, AE and Dst computation, interpretation, reliability and use in statistical studies of solar-terrestrial interactions

Two substorm studies of relations between westward electric fields in the outer plasmasphere, auroral activity, and geomagnetic perturbations.

Study of the effect of the east-west component of the interplanetary magnetic field on the currents equivalent to the magnetic perturbations of high latitude regions

Lower ionosphere at medium latitudes during geomagnetic disturbances.

Solar wind magnetic field and particle concentration disturbances near moon, noting electric field effect on ion motion

Equatorial coronal arches and geomagnetic disturbance.

Solar flare activity during August 1972, discussing sunspots filter- and spectrograms, proton emissions and geomagnetic disturbances

Resonance acceleration of low-energy protons in the earth's radiation belts

Electron acceleration in the outer radiation belt

Molnija 1 satellite slow neutron monitor with photomultiplier scanned scintillator, noting limiting effect of geomagnetic perturbations

Forbush predecrease observation by superneutron monitors, interpreting cosmic ray depletion and rigidity dependence by model of interplanetary magnetic field propagating disturbance from sun

Catalog of geomagnetic activity indices for the years 1841-1864 and 1870

Sector structure of the interplanetary magnetic field, and magnetic disturbances in the circumpolar region

Results of volley flights of radio probes on the Kolsk peninsula during periods of magnetic disturbances in March and April 1971

Time dependent geophysical effects associated with chromospheric and coronal flares, tabulating for 1957-1961

The effects of thermospheric winds on the ionosphere at low and middle latitudes during magnetic disturbances.

Complex studies of the disturbance of March 8, 1970 from observations in the midnight sector

Solar-terrestrial relations in the retrospective world interval from July 26 to August 14, 1972

Geomagnetic disturbance recurrence interval correlation with long term sunspots rotation period

Rocket-borne scientific experiment program Sun-Atmosphere 1971, using meteorological rockets for meteor trail, atmospheric and ionospheric observations during geomagnetic disturbances

Influence of the interplanetary magnetic field on the magnetic perturbations of high latitude regions - Demonstration of an asymmetry in relation to the earth-sun direction

Average high latitude magnetic field: Variation with interplanetary sector and with season. I - Disturbed conditions.

Spatial distribution of H alpha emission in the earth's upper atmosphere, the variations of the emission during a solar cycle, and the dependence of the emission on geomagnetic perturbations

The perturbation of alternating geomagnetic fields by discontinuities with high conductivity contrasts.

Resonance acceleration of low-energy protons in the radiation belts of the earth.

Electron acceleration in the outer radiation belt.

Equatorial spread F layer height nocturnal variations due to magnetic disturbances during solar activity cycles

Solar energy cycle and its relation to geomagnetic activity.

Russian monograph on polar auroras and magnetospheric geomagnetic disturbances from rocket, balloon and ground station soundings covering magnetic storms, solar wind and geoelectric fields

Large-scale auroral-zone electron precipitation event, briefly interrupted during a negative magnetic impulse.

Simulation of driven flare-associated disturbances in the solar wind.

ULF geomagnetic power near L = 4. I - Quiet day power spectra at conjugate points during December solstice.

Sector-patterned structure of interplanetary magnetic field and magnetic disturbances in the circumpolar region.

Ionospheric inhomogeneity parameters and geoelectromagnetic field variations

Method of studying magnetic-ionospheric disturbances and solar flare effects on long-upset periods.

Counter equatorial electrojet currents in the Indian zone.

ULF excitation of plasmopause sinusoidal oscillations by magnetic disturbances exterior to plasmasphere boundary, inferring plasma density from wave frequency and damping rate

Complex studies of corpuscular radiation in the upper atmosphere at midlatitudes during geomagnetic perturbations

Solar-interplanetary disturbances during 5-18 June 1969 /The PPP interval/IASY/.

Geomagnetic disturbance diurnal variation /DS/ component evolution and equatorial electrojet strength changes observation during magnetic storms by globally located stations at various latitudes

Geophysical disturbance environment during the NASA/MPE barium release at 5 earth radii on September 21, 1971.

Short-period interplanetary and polar magnetic field variations.

Dispersion characteristics of whistler atmospherics during higher geomagnetic activity.

MAGNETIC DOMAINS

A new explanation for the creep of domain boundaries with transverse constrictions

Some principles of domain device designing for data processing and means of control.

Features of the domain structure of cobalt-doped lithium ferrite when changing the direction of easy magnetization

A data display device for switching and logic elements constructed from single-crystal ferromagnetic materials

Bubble domain memory materials production, processing and testing, discussing crystal growth, propagation margins, interaction effects and stroboscopic observations

Search for magnetic monopoles in lunar material using an electromagnetic detector.

Optical and polarization study of magnetization processes around individual dislocations in yttrium-iron garnet single crystals

MAGNETIC EFFECTS

NT MAGNETIC RIGIDITY

Geomagnetic activity effects on D layer absorption from vertical soundings during solar flare induced sudden magnetic storms

Variational formulation for hydromagnetic stability

Control of the frequency of Gunn-effect oscillators by a magnetic field

Effect of a magnetic field on emission fluctuations in a ring gas laser

Transfer equations for high-energy electrons and photons in magnetic fields.

Observation of low-charge low-energy geomagnetically forbidden particles.

Effects of the secular magnetic variation on the distribution function of inner-zone protons.

Superconducting-normal phase boundary as func-

MAGNETIC EFFECTS

tion of applied magnetic field and transition temperature in Nb-Ga alloys

Magnetospheric tail plasma sheet near earth structure explained via tangential magnetic field gradient drift velocity coupling to strong pitch-angle diffusion

Stability characteristics of thin elastic plate with time varying temperature under transversal magnetic field, calculating buckling probability

Purification of hydrogen plasmoids by the magnetic field in an injector-diverter.

Horizontal and vertical drift motions in F 2 region caused by electrostatic and geomagnetic fields

Extensive cosmic ray shower production by relativistic dust grain accelerated in interstellar space by galactic radiation pressure and subsequent magnetic processes

Morphic effects. IV - Effects of an applied magnetic field on first-order photon-optical phonon interactions in non-magnetic crystals.

Morphic effects. III - Effects of an external magnetic field on the long wavelength optical phonons.

The equilibrium and stability of uniformly rotating gaseous systems in hydromagnetics. I.

Kinetic theory for calculation of low temperature homogeneous plasma electric conductivity in magnetic field, noting monotonic decrease

Hydrogen atomic structure in magnetic field, using Bohr model, Schrodinger equation and energy eigenvalues

Wave scattering in collisionless magnetoactive plasma, taking into account magnetic field effects, spiral motion of scattering particle and shielding fields

Polytropic subsonic stellar winds with magnetic fields.

Magnetic field effect on friction shear stress in turbulent slipstreams of conducting fluids, calculating mixing zone width

A quick and inexpensive method of monitoring on tape the heart rate during exposure of the human head to pulsed magnetic fields.

Influence of the magnetic field on the heat transfer of a ferromagnetic viscoplastic fluid

Numerical and analytic solutions for dispersion equation for flute-like ion cyclotron instabilities in high beta plasma, noting magnetic field inhomogeneity effect

Investigation of fluctuation and wave phenomena in argon low-current low-pressure discharges, taking place under the influence of a 'brief' axial magnetic field

Stability of nonrotationally symmetric disturbances for inviscid flow between rotating cylinders in the presence of an axial magnetic field.

Magnetospheric trapped particle populations boundaries properties, discussing dynamic boundaries during magnetic disturbances and substorm effect on night magnetosphere configuration

Net-field polarization in a magnetically biased plasma.

Study of the effect of the east-west component of the interplanetary magnetic field on the currents equivalent to the magnetic perturbations of high latitude regions

Influence of a random magnetic field on the properties of stellar absorption lines.

O-type synchronous electron beam waves interaction with electrostatically structured traveling wave, noting linear gain dependence on beam current and magnetic field

Nonspherically symmetric polypole model of azimuthally dependent solar wind in sun equatorial plane, considering coronal temperature, density and radial magnetic component

Steady axisymmetric ring current models computed with energy density distribution parameters variations for effects on magnetic field and particle belt parameters

Magnetic-field-induced one-dimensional behavior in the specific-heat transition in dirty bulk superconductors.

Transverse magnetic field effects on n-type GaAs Gunn diodes microwave power, coherence and

MAGNETIC EFFECTS

dynamic I-V characteristics

05 p0558 A73-16784

ESRO 1A satellite-borne Langmuir probe measurement for anisotropy in ionospheric thermal electron temperature relative to geomagnetic field

05 p0571 A73-17053

Radiation belt buildup from particles moving in magnetic field applied to terrestrial inner belt characteristics, considering extraterrestrial belts

06 p0741 A73-17503

Visible light flash emission due to strong shock wave of laser spark, investigating strong external magnetic field effect and time variation of luminous intensity

06 p0700 A73-17966

The null magnetic field as reference for the study of geomagnetic directional effects in animals and man

06 p0658 A73-18033

Low temperature tests for magnetic field and temperature effects on differential resistance of lead alloy superconductors, calculating viscous friction coefficient

06 p0736 A73-18116

Magnetophotocconductivity of semi-insulating GaAs and its behavior upon electron bombardment

06 p0738 A73-18369

Magnetic transitions observed in sulfide minerals at elevated pressures and their geophysical significance

06 p0691 A73-18576

Microwave properties of n-type InSb in a magnetic field between 4 and 300 K

06 p0739 A73-18792

The application of magnetic after-effects in research on the real structure and migrational properties of metals and alloys

07 p0837 A73-19049

Astrophysical masers. II - Polarization properties

07 p0873 A73-19059

Activities in space research at the Max-Planck-Institut fuer extraterrestrische Physik, Garching bei Muenchen /G.F.R./

07 p0868 A73-19173

Propagation anisotropies of solar flare protons and electrons at low energies in interplanetary space

07 p0869 A73-19227

Pitch angle distribution of solar flare particles in interplanetary space

07 p0869 A73-19228

Turbulence spectra of collisionless magnetized plasma produced in high voltage theta pinch, considering initial magnetic field orientation and instability theories tests

07 p0857 A73-19527

Study of excess Fe metal in the lunar fines by magnetic separation, Moessbauer spectroscopy, and microscopic examination

07 p0788 A73-19745

MHD shock wave decay in oblique magnetic field, considering shock and rarefaction waves interaction

07 p0858 A73-20071

Electromagnetic loss-cone instability of a plasma

07 p0859 A73-20196

Transport equations for dilute plasma in a magnetic field

07 p0860 A73-20479

Magnetic field dependence of the surface resistance of pure and impure superconducting aluminum at photon energies near the energy gap

07 p0864 A73-20573

Stabilization of normal drift modes in an inhomogeneous plasma by a magnetic shear field

07 p0860 A73-20611

Reduction of the thermal flux through a cylindrical pipe containing an ionized gas flow

07 p0860 A73-20617

Microwave filters with single crystal YIG sample as ferrimagnetic resonators, determining magnetic field and temperature effects on resonator cut-off frequency

08 p0942 A73-20705

Magnetic field effects on effective thermal conductivity of partially ionized plasmas, indicating neutral component role in solar magnetoplasma heat transport

08 p1001 A73-20755

Focusing of EM waves in plasmas by inhomogeneous magnetic fields

08 p0993 A73-21205

Cen X-3 and Her X-1 X ray sources emission pulsation explained by model with neutron star accretion of matter from companion via magnetic funnel

09 p1141 A73-22010

Diffusion of charged particles in a random magnetic field

09 p1137 A73-22035

Oppositely directed magnetic fields reconnection rate role in solar flares and small scale turbulent field reduction in photosphere

09 p1142 A73-22037

Plasma diffusion across a magnetic field due to thermal vortices

09 p1126 A73-22217

Equations of motion of ideally conducting medium in MHD approximation, solving under constant magnetic field and magnetic-hydrodynamic pressure equilibrium

09 p1126 A73-22280

Kinetic theory of a two-dimensional magnetized plasma. II - Balescu-Lenard limit

09 p1126 A73-22282

Enhanced energy transfer to a cylindrical plasma by

an Alfvén wave.

09 p1128 A73-22629

A new cosmological model - Formation of organic molecules, planets, and comets.

09 p1151 A73-23147

A study of the stability of slow combustion of gas mixtures subjected to the action of a magnetic field

09 p1167 A73-23351

Magnetic field influence of the Gunn effect threshold.

10 p1258 A73-23568

Characteristics of waveguides filled with homogeneous lossy anisotropic drifting plasma

10 p1192 A73-23574

Synchrotron emission amplification by magnetic field in cosmic sources from analysis of relativistic electron system, noting pulsars and UV Ceti stars

10 p1264 A73-23708

Observation of the entrance of solar protons in the magnetosphere at very high latitudes

10 p1211 A73-23769

Stability of a gravitating fluid layer in the presence of a uniform magnetic field perpendicular to its boundary

10 p1253 A73-23832

Theory of cosmic ray transport with anisotropic particle scattering and convection

10 p1265 A73-23903

Investigation of cosmic-ray propagation in the interplanetary magnetic field on the basis of the kinetic equation

10 p1265 A73-23904

Problems of linear and nonlinear theory of cosmic ray modulation

10 p1266 A73-23913

Putting an electrically conducting fluid in rotation by a rotating magnetic field

10 p1254 A73-24125

Sporadic ionization of the ionospheric E-region at high latitudes as a function of magnetic activity

10 p1212 A73-24221

The effect of an external field on transport phenomena in a Knudsen molecular gas

10 p1252 A73-24453

Uniform variable transverse magnetic field effects on convective instability of plane electrically conducting layer, reducing perturbed equilibrium equations to linear ordinary differential equations

10 p1256 A73-24593

Spontaneous Cerenkov emission of longitudinal waves produced by single particle and cylindrical electron beam moving inside magnetosphere along magnetic field

10 p1269 A73-24722

Disturbance of a magnetized plasma by a fast traveling charge

10 p1257 A73-24758

Characteristics of viscous vortex flows in superconducting alloys near the critical temperature

10 p1261 A73-24765

On the application of Cramer's theorem to axisymmetric, incompressible turbulence

10 p1284 A73-24909

Ambipolar drift, deformation, and diffusion of a plasma in a magnetic field

11 p1402 A73-24989

Parallel magnetic field effect upon plane interface stability between two conducting viscous fluids in uniform relative motion, obtaining neutral shear flow stability curves

11 p1402 A73-25054

Collisional transverse MHD shock wave structure within magnetic field inducing anisotropic plasma transport properties, using singular perturbation approach

11 p1403 A73-25254

Numerical simulation and theory of plasma diffusion across magnetic field at thermal equilibrium, noting collective mode domination at moderate and high fields

11 p1403 A73-25257

Particle kinetic energy vs number density in equilibrium E layer under external and self magnetic fields related to plasma confinement in astron device

11 p1404 A73-25259

Sunspots moving magnetic features analysis from longitudinal magnetograms time series and H alpha filtergrams

11 p1422 A73-25938

Magnetic field effect on plage, prominence and sunspot flares, considering radio, UV and X ray emission

11 p1413 A73-26208

Pair annihilation into neutrinos in strong magnetic fields

11 p1402 A73-26414

Photon neutrino energy losses in strong magnetic fields

11 p1402 A73-26415

Magneto-viscous effects on the ideal and resistive gravitational instabilities in Cartesian geometry

11 p1406 A73-26553

On the evolution of turbulent magnetic fields in a collision dominated plasma

11 p1406 A73-26559

Operating properties of a helical microwave plasma source in high density high magnetic field regime

11 p1407 A73-26562

Investigation of resonance integrals occurring in cosmic-ray diffusion theory

11 p1414 A73-26615

Resistive diffusion of force-free magnetic fields in a passive medium

11 p1428 A73-26620

A note on the heating of magnetoplasma by magnetic perturbations

11 p1407 A73-26659

Solar and geomagnetic modulation of low-energy secondary cosmic ray electrons

12 p1533 A73-26977

Dual magnetometer systems with cross correlation signal enhancement to overcome intrinsic sensor ambient noise and spacecraft magnetic field fluctuation effects on single detection performance

12 p1468 A73-27002

Carnauba wax electrets manufactured under the simultaneous action of magnetic and electric fields

12 p1523 A73-27103

Influence of a transverse electron-temperature gradient on the plasma flow in an axisymmetric magnetic field

12 p1528 A73-27305

Theory of cosmic ray transfer by anisotropically scattered particles

12 p1534 A73-27331

Magnetoelastic vibration of electrically conducting thin shells and plates in steady magnetic field from asymptotic integration of electrodynamics equations

12 p1553 A73-27413

Solar magnetic sector structure - Relation to circulation of the earth's atmosphere

12 p1491 A73-27441

Competition between longitudinal modes in a ring laser with an anisotropic resonator

12 p1507 A73-27508

Effect of a magnetic field on the soft X-ray radiation of a laser plasma

12 p1530 A73-27977

Magneto-oscillatory absorption effect in Sb13

13 p1667 A73-28004

Application of similarity criteria in calculations of a mobile magnetic field to be used for growth stimulation in single crystals of metals

13 p1667 A73-28108

Effect of a high frequency magnetic field on plasma diffusion in a Q-machine

13 p1664 A73-28348

Equatorial electrojet, according to Kosmos-321 measurements

13 p1670 A73-28716

Stability of flute disturbances in a plasma of toroidal geometry

13 p1666 A73-28954

Effect of an external magnetic field on the beat frequency of opposite waves in a ring laser with a noninteracting phase-shifting device

13 p1627 A73-28965

Vanadium galliumide tape preparation and critical temperature and current as function of heat treatment temperature and applied magnetic field, considering pancake current capacity

13 p1669 A73-29069

About the influence of a magnetic field on the model atmosphere of a magnetic star

13 p1687 A73-29657

Parametric instability in the region of low-frequency hybrid resonances

14 p1778 A73-29686

Particle diffusion rate due to poloidal magnetic field component in low beta symmetric toroidal plasma, discussing losses induced by electrostatic field fluctuations

14 p1778 A73-29693

Experiments on CO2-laser heating of magnetically confined underdense plasmas

14 p1780 A73-30123

Determination of magnetic fields in a plasma from the contour of hydrogen spectral lines

14 p1780 A73-30339

Low Hartmann number MHD flow of weakly conducting viscous fluid past nonconducting sphere within aligned uniform magnetic field

14 p1781 A73-30655

Interplanetary scintillations of cosmic rays

14 p1788 A73-30752

Magnetic neutralization and discharge neutralization of an electron beam injected into a magnetoactive plasma

14 p1782 A73-30807

Martensitic transformation in iron-nickel alloys in a pulsed magnetic field

14 p1764 A73-30860

Pi 2 micropulsations occurrence time, morphology change with magnetic activity and source meridian shift from solar wind variations effects

15 p1866 A73-31072

Experimental study of the interaction of a plasma with a magnetic field in the case of a plasma generated by laser irradiation of solids

15 p1917 A73-31249

Predawn enhancement of 6300 A forbidden OI nightglow emission from observations at Abastumani

15 p1867 A73-31263

Influence of a magnetic field on turbulent shear flow

15 p1917 A73-31402

Magnetic field induced energy dissipation in conducting fluid isotropic turbulent flow velocity pulsations, noting Joule dissipation effect on damping

15 p1917 A73-31403

Nonlinear MHD equations solution for conducting

fluid plane index channel flow in traveling magnetic field by net point method

15 p1917 A73-31406

Effect of steady magnetic fields up to 4,500 Oe on the mitotic activity of the corneal epithelium in mice

15 p1838 A73-31510

Redistribution of resonance radiation. II - The effect of magnetic fields.

15 p1913 A73-31559

On the establishment and solution of equations of motion of an electrically conducting fluid set in motion by the slow and uniform rotation of walls of a ring-shaped receiver, in the presence of an axial magnetic field, in the case where the mean value of the intensity of the currents induced in a straight section takes a nonzero value

15 p1918 A73-31569

Solar surface and atmosphere activity due to magnetic field production, transport and dissipation, discussing flares, sunspots, corona, dynamo, plasma turbulence and prominences

15 p1937 A73-31848

Surface oscillations of a weakly ionized plasma in a magnetic field.

15 p1921 A73-32626

Effect of magnetic field curvature on the stability of a plasma confined by a dense neutral gas.

15 p1921 A73-32627

Quasilinear relaxation of a monoenergetic relativistic electron beam in an external magnetic field.

15 p1922 A73-32628

Superconducting magnetic spectrometer technique application to charged primary cosmic rays, discussing calibration, experiments and electron-positron and isotopic separation

16 p2014 A73-33277

Geomagnetic effects on cosmic ray cut-off daily, seasonal and secular variations, considering north-south symmetry and magnetospheric models

16 p2055 A73-33297

Satellite studies of magnetospheric substorms on August 15, 1968. I - State of the magnetosphere.

16 p2004 A73-33449

Luminosity of thermal X-ray sources with a strong magnetic field.

16 p2062 A73-33574

Periodic variations in geomagnetic activity and sector structure of the interplanetary magnetic field.

17 p2157 A73-34075

Anomalous penetration of a magnetic pulse into a plasma.

17 p2214 A73-34098

Generation of intense infrared radiation from an electron beam propagating through a rippled magnetic field.

17 p2214 A73-34204

Calculations on the radio emission resulting from geomagnetic charge separation in an extensive air shower.

17 p2223 A73-34244

Flow of nonisothermal plasma through a magnetic nozzle.

17 p2215 A73-34313

Polarization plane rotation under magnetic field for IR waves in nonmagnetic semiconductors with cubic crystal lattices, explained by magneto-optical Faraday effect

17 p2219 A73-34342

Waves in a plasma amid magnetic and gravitational fields

17 p2226 A73-34373

Interplanetary magnetic field and geomagnetic Dst variations.

17 p2158 A73-34507

Magnetotail response to sudden changes in the interplanetary magnetic field.

17 p2158 A73-34509

Radial variation of magnetic fluctuations and the cosmic-ray diffusion tensor in the solar wind.

17 p2224 A73-34762

Josephson junction interference grating.

17 p2219 A73-34915

Unsteady Couette flow in hydromagnetics.

17 p2154 A73-35121

The effect of a magnetic field on the operation of a dual-base-diode oscillator.

17 p2136 A73-35161

Impulsively started viscous flow past a finite flat plate with and without an applied magnetic field.

17 p2217 A73-35604

Solar energy cycle and its relation to geomagnetic activity.

17 p2236 A73-35777

Influence of transverse magnetic field on Landau damping.

17 p2217 A73-35812

Magneto-fluid-mechanic heat transfer from hot film probes.

17 p2255 A73-35845

Transient flow and expansion of a pinch discharge plasma in self-induced magnetic fields.

[AIAA PAPER 73-689]

18 p2338 A73-36240

Night side electromagnetic response of the moon.

18 p2351 A73-36268

Dependence of the polar cusp on the north-south component of the interplanetary magnetic field.

18 p2351 A73-36273

Synchrotron radiation stimulated amplification by magnetic field in cosmic sources from analysis of

relativistic electron system, noting pulsars and UV Ceti stars

18 p2347 A73-36733

Rarefied collisionless plasma turbulence and dissipation process due to instability, examining magnetic field effects on shock wave front nature

19 p2464 A73-37154

On the energetics and momentum balance of pole-equator temperature differences in the sun.

19 p2485 A73-37620

Influence of an external field on transport effects in a Knudsen molecular gas.

19 p2463 A73-38134

On the effects of uniform high suction on the rotationally symmetric flow of a conducting liquid near a stationary disc in the presence of a transverse magnetic field.

19 p2469 A73-38186

The magnetic channeling of a supersonic axisymmetric plasma jet.

19 p2470 A73-38318

Effect of longitudinal magnetic field on the performance of a channel electron multiplier.

20 p2565 A73-38884

Position of the equatorial boundary of the anomalous ionization occurrence region in relation to the planet's magnetic activity during the solar activity cycle

20 p2554 A73-39175

Geomagnetic field effects in Martin theory of radio wave propagation in ionosphere with oblique and vertical signal incidence

20 p2555 A73-39181

Magnetic field effects on slab surface plasmons in the local limit.

20 p2599 A73-39720

Mesospheric temperature response to variations in geomagnetic activity.

21 p2682 A73-40169

The stability of steady motions of systems with quasi-cyclic coordinates and the stability of mechanical equilibrium under the action of a magnetic field

21 p2736 A73-40177

The effect of toroidal magnets on the sensitivity of photomultipliers.

21 p2699 A73-40410

ULF excitation of plasmapause sinusoidal oscillations by magnetic disturbances exterior to plasmasphere boundary, inferring plasma density from wave frequency and damping rate

21 p2650 A73-40507

Solar proton measurements during August 1972 cosmic ray and magnetic field events caused by chromospheric flares associated with sunspots on east limb

21 p2757 A73-40592

A comparison of the latitudinal variation of auroral absorption at different longitudes.

21 p2684 A73-40785

Book on cosmic ray effective cut-off rigidities calculations in dipole and geomagnetic fields, using trajectory calculations of penumbra function

21 p2760 A73-40805

Wind profiles over Heiss Island.

21 p2685 A73-40812

Influence of a magnetic field on the weld-seam structure during electrosag welding of titanium alloys

21 p2707 A73-40891

Theory of a steady-state nonisothermal positive column in a magnetic field.

21 p2748 A73-40954

Elastoplastic stressed state of a long thick-walled cylinder subjected to the action of a magnetic field

21 p2786 A73-40981

Dense cloud formation and gravitational collapse onset, discussing thermal properties and magnetic field presence

21 p2772 A73-41244

The determination of ionospheric charged particle temperatures from in situ measurements.

21 p2690 A73-41362

Human perception of moderate strength low frequency magnetic fields tested by whole body immersion in large Helmholtz coil field under acoustic isolation

22 p2811 A73-41789

Effects on the geomagnetic tail at 60 earth radii of the geomagnetic storm of April 9, 1971.

22 p2844 A73-41908

Solar magnetic fields and their influence on the earth.

22 p2906 A73-41959

Low temperature thermometry in high magnetic fields.

22 p2856 A73-42017

Apparatus and methods for the precise determination of Boltzmann temperature.

22 p2856 A73-42021

On the stability of a class of plasma flows with helical flow and field lines.

22 p2892 A73-42351

Analysis of force interaction in magnetolectric torque sensors

22 p2860 A73-42364

Longitudinal alignment of working levels in a helium-neon laser

22 p2870 A73-42412

The parallel diffusion of cosmic rays in a random magnetic field.

22 p2904 A73-43011

MAGNETIC EQUATOR

On Kraichnan's direct interaction approximation applied to charged-particle transport in turbulent magnetic fields.

22 p2904 A73-43013

High order nonlinear effects in a gas laser - Saturation anomaly observable on a J equals 1 - J equals 2 transition

22 p2871 A73-43084

Contribution to the theory of cosmic-ray propagation with anisotropic particle scattering.

23 p3020 A73-43229

Improvement of the corrosion-fatigue strength of aluminum alloys by exposure of the medium to a magnetic field

23 p2984 A73-43466

Small amplitude Alfvén waves propagation in solar wind under interplanetary magnetic field, relating wave and wind velocity

23 p3029 A73-43612

Precipitation and magnetic hardening in sintered WC-Co composite materials.

23 p2997 A73-43776

Some electric and spectroscopic properties of the radiofrequency plasma in a steady magnetic field.

23 p3012 A73-43831

Optical orientation in a system of electrons and lattice nuclei within semiconductors - Experiment

23 p3016 A73-44022

Flute stability in a toroidal plasma.

23 p3013 A73-44306

Effect of external magnetic field on the beat frequency in a ring laser with nonreciprocal phase shifter.

23 p2989 A73-44317

Interpretation of distinct type IVmA- and IVmubursts on the basis of micro-instabilities and of resonant nonlinear interaction of waves.

24 p3123 A73-44645

Hydromagnetic gradient waves in the ionosphere

24 p3083 A73-44789

Accretion onto black holes - The emergent radiation spectrum. II Magnetic effects.

24 p3138 A73-45036

Solar wind interaction modes with lunar magnetic fields, discussing moon surface charging, magnetic field compression and wind deflection

24 p3126 A73-45127

Magnetically trapped charged particle pitch angle diffusion and lifetime calculation for radiation belts, taking into account geomagnetic dipole geometry

24 p3127 A73-45138

Triaxial magnetic measurements of field-aligned currents at 800 kilometers in the auroral region - Initial results.

24 p3087 A73-45140

Hot plasma in contact with cold wall, calculating dynamic behavior in magnetic field from numerical solution of one-fluid two-temperature equations

24 p3117 A73-45456

Spectroscopic measurements of plasma temperatures and density at X type magnetic neutral points, suggesting ion acoustic instability role in turbulent conductivity

24 p3118 A73-45461

Unsteady plasma flows behind a moving leading boundary

24 p3119 A73-45539

MAGNETIC EQUATOR

6300 A night airglow emission over the magnetic equator.

01 p0036 A73-10344

E region electromagnetic east-west drift velocity measurement at magnetic equator by incoherent scatter radar

02 p0161 A73-12285

Features of the ionospheric drift over the magnetic equator.

02 p0162 A73-12287

Low energy atmospheric gamma rays near geomagnetic equator.

03 p0360 A73-12890

Drift shell splitting and magnetic equator surface topography model based on charged particle adiabatic motion and trapping in presence of internal geomagnetic multipoles

07 p0813 A73-19236

Equatorial electrojet currents effect on sporadic E layer near magnetic equator, noting cross field irregularities

07 p0819 A73-20066

Some characteristics of the ionospheric irregularities over the magnetic equator derived from spaced fading records.

08 p0957 A73-20656

Metallic ion composition and electron density measurements in equatorial E region, considering three body reaction kinetics with dissociative ion-electron recombination

09 p1074 A73-22064

Ogo 6 measurements of supercooled plasma in the equatorial exosphere.

09 p1074 A73-22066

Charge separation induced vertical electric field calculated for wind motion periodic with height, latitude and longitude at magnetic equator, noting relationship to electrojet

09 p1074 A73-22067

MAGNETIC FIELD COILS

Some effects of the equatorial ionosphere on terrestrial HF radiocommunication.

09 p1051 A73-22500

Ogo 6 retarding potential analyzer observation of vertical and longitudinal gradients in ion concentrations below F region peak near magnetic equator

10 p1214 A73-24738

Equatorial anomaly in the F2 layer during local noon and the IGY and IQSY periods

11 p1350 A73-25089

A theoretical study of the ionospheric F region equatorial anomaly. I - Theory. II - Results in the American and Asian sectors.

11 p1356 A73-25919

Magnetotail model for magnetic field strength and particle drift in magnetic equatorial plane earth, using current sheet from satellite observations

11 p1357 A73-25929

Magnetic control of near equatorial neutral thermosphere, calculating F region ionization anomaly and molecular nitrogen and atomic oxygen density latitudinal variations

12 p1489 A73-26997

Stable auroral red arc equatorial edge observation with photometer during recovery phase of magnetic storm on 18 December 1971 in Southern Africa

12 p1492 A73-27611

Low momentum integral moon spectrum at sea level near the geomagnetic equator.

13 p1670 A73-28211

Determination of the density of protons in the magnetosphere on the basis of observations of Pc-3 type geomagnetic pulsations

13 p1610 A73-29560

Studies of the equatorial anomaly in the F region and outer ionosphere with the aid of spherical ion traps

14 p1746 A73-29860

Total electron content of the equatorial ionosphere.

15 p1865 A73-31063

Formation of blanketing sporadic E-layers at the magnetic equator due to horizontal wind shears.

15 p1866 A73-31070

Magnetic dip equator region ionospheric drifts and electric fields measurements and experimental techniques

15 p1868 A73-31752

Equatorial Esq disappearance relationship to daily magnetic Sr variation inverted latitudinal profiles during magnetical quiet periods, considering counter electrojet current belt hypothesis

15 p1869 A73-31757

Equatorial scintillation variation with magnetic storm from ATS 3 VHF telemetry signal recordings, comparing with spread F observation

15 p1870 A73-31763

Large scale equatorial spread F irregularities motion velocity observation in Africa, interpreting quasi-periodic structures in west-east extension by atmospheric gravity waves

15 p1870 A73-31764

Equatorial ionospheric anomaly related neutral thermospheric composition variation observation from OGO-6 mass spectroscopic data, noting static diffusion model limitations

15 p1870 A73-31767

Equatorial sporadic E layer during geomagnetic storms.

15 p1871 A73-31836

The low-latitude and equatorial outer ionosphere during the magnetic storm of January 2-4, 1964

15 p1871 A73-31881

The effect of polar magnetic sub-storms on the equatorial sporadic E.

15 p1874 A73-32596

Sudden disappearance of Es-q and the reversal of the equatorial electric fields.

16 p2008 A73-33879

Equatorial and auroral zone geomagnetic indices and micropulsations variations relation to 11-18keV protons occurrence in interplanetary space

18 p2345 A73-36120

Satellite observations of strong Balmer alpha atmospheric emissions around the magnetic equator.

18 p2346 A73-36284

Interpretation of the H-alpha atmospheric emissions observed by the D-2A Tournesol satellite around the magnetic equator

19 p2423 A73-37538

Observations of ionospheric storms at low latitudes and their correlation with magnetic field changes near the magnetic equator.

19 p2425 A73-38011

Asymmetrical global O I airglow emission pattern with respect to magnetic equator from Ogo 4 observations, noting poor correlation with ionospheric electron density

20 p2551 A73-38939

Initial observations of geomagnetically trapped alpha particles at the equator.

20 p2552 A73-38950

Magnetic equatorial ionospheric characteristics, discussing F and F regions, diurnal drift variations, field strength, equatorial electrojet, spread F and

sporadic E

20 p2555 A73-39633

D region electron density profiles at geomagnetic equator by rocket sounding, showing ionization production by Lyman alpha radiation and cosmic rays

21 p2690 A73-41361

Balloon and VLF whistler measurements of electric fields, equatorial electron density, and precipitating particles during a barium cloud release in the magnetosphere.

22 p2845 A73-41934

Quiet-time nighttime magnetic field near geomagnetic equator detected by magnetospheric barium cloud injection, revealing taillike structure from atmospheric models

22 p2846 A73-41939

Enhancement of the equatorial anomaly in the topside ionosphere during magnetic storms.

24 p3088 A73-45216

MAGNETIC FIELD COILS

U FIELD COILS

MAGNETIC FIELD CONFIGURATIONS

Theory for the stability of a star with a toroidal magnetic field.

01 p0106 A73-11312

The effect of toroidal magnets on the sensitivity of photomultipliers.

21 p2699 A73-40410

Dispersion relations for parallel-plane waveguide containing transversely magnetized uniaxial and warm plasma in relative motion.

22 p2824 A73-41857

Magnetogasdynamic shock polar - Exact solution in aligned fields.

22 p2893 A73-42393

Equilibrium structure of polytropes with toroidal magnetic fields.

22 p2912 A73-42941

Electric polarization of a plasma beam in an axially symmetrical magnetic field

23 p3009 A73-43655

Shaping of plasma clusters moving in a longitudinal magnetic field

23 p3010 A73-43659

Motion of a plasma in curvilinear magnetic fields of constant and alternating curvature

23 p3010 A73-43661

North-south asymmetry of the interplanetary magnetic field

23 p3025 A73-44250

Relaxation of longitudinal and transverse temperatures in a plasma with directional motion of electrons

23 p3014 A73-44336

A high resolution study in time, position, intensity, and frequency of the radio event of January 14, 1971.

24 p3136 A73-44643

Spherical harmonic analysis of geomagnetic and gravitational field correlation, showing longitudinal shift in magnetic field pattern over six epochs

24 p3084 A73-44812

X-ray observations of characteristic structures and time variations from the solar corona - Preliminary results from Skylab.

24 p3139 A73-45057

MAGNETIC FIELD INTENSITY

U MAGNETIC FLUX

MAGNETIC FIELDS

NT FORCE-FREE MAGNETIC FIELDS

NT GEOMAGNETISM

NT INTERPLANETARY MAGNETIC FIELDS

NT INTERSTELLAR MAGNETIC FIELDS

NT LUNAR MAGNETIC FIELDS

NT MAGNETOSTATIC FIELDS

NT NONUNIFORM MAGNETIC FIELDS

NT PALEOMAGNETISM

NT PLANETARY MAGNETIC FIELDS

NT SOLAR MAGNETIC FIELD

NT STELLAR MAGNETIC FIELDS

NT TRAPPED MAGNETIC FIELDS

Propagation of electromagnetic waves in a plasma with a sheared magnetic field

01 p0081 A73-10206

Excitation of electromagnetic waves in a plasma by a flux of phased oscillators

01 p0082 A73-10207

Nonlinear interaction of two monochromatic Langmuir waves

01 p0016 A73-10209

Slightly oblique shock waves in a collisionless magnetized plasma.

01 p0082 A73-10421

Plasma density measurement by a Langmuir probe in the presence of a magnetic field

01 p0082 A73-10428

Time evolution and functional form of magnetostatic equilibria in axisymmetry.

01 p0082 A73-10452

Use of the virtual-casing principle in calculating the containing magnetic field in toroidal plasma systems.

01 p0084 A73-10464

Arc current, column electric field, mainstream velocity and applied transverse magnetic field relationships in magnetically balanced cross flow plasmas

01 p0084 A73-10738

SUBJECT INDEX

Effect of viscosity on the motion of the inhomogeneities of a nonequilibrium plasma in a magnetic field

01 p0085 A73-10865

Periodic structure of the electric field in a stratified plasma with tensor conductivity

01 p0085 A73-10955

Experimental investigation of millimeter-band electromagnetic wave propagation in a waveguide filled with n-type InSb under a magnetic field

01 p0017 A73-10977

Hydromagnetic flow about a curved neutral sheet.

01 p0086 A73-11495

Calculation of the energy and force process parameters in magnetic-pulse forming of complex shaped elements

02 p0172 A73-11646

Superconducting magnet for a Ku-band maser.

02 p0200 A73-11835

Superconducting Mo-Re alloy thin film prepared by sputtering and deposition onto sapphire substrate, measuring transition temperature, critical current and magnetic field characteristics

02 p0200 A73-11841

Nonlinear waves in a multicomponent plasma with weak dissipation.

02 p0198 A73-12103

Effect of ion viscosity on the stability of a finite-pressure plasma.

02 p0198 A73-12104

Radial and nonradial oscillation modes of gaseous polytrope with toroidal magnetic field, using variational principle

02 p0217 A73-12400

Collisionless plasma compression shock waves thermodynamics, noting entropy variations along shock adiabat under plasma heating in magnetic field

02 p0198 A73-12552

MHD equations for velocity distribution of magnetic field motion in conducting fluid, noting evolution equations of geomagnetic field

02 p0164 A73-12555

Muon track curvatures in Wilson chamber magnetic field for calibrating ionization levels of logarithmic increase

02 p0171 A73-12687

Asymmetric eigenmodes in a simple model plasmasphere.

03 p0345 A73-12882

Three-dimensional MHD duct flows with strong transverse magnetic fields. III - Variable-area rectangular ducts with insulating walls.

03 p0346 A73-13534

Magnetogasdynamic characteristics, transonic and compression regions and pressure losses of conducting gas flow in circular tube within axisymmetric magnetic field

03 p0346 A73-13620

A phenomenological study of the steady-state current sheet speed in a magnetically driven shock tube.

03 p0288 A73-13809

Solar wind interaction with geomagnetic field, discussing magnetosphere polar cusp region and geomagnetic tail neutral sheet structure

03 p0302 A73-13871

Amplatron stability in optimal frequency regime, relating cut-off voltage and plate current as function of magnetic field, input power and geometrical parameters

03 p0284 A73-14068

Injection of an electron beam into a plasma confined by a conducting shell.

03 p0347 A73-14093

Plasma confinement in a racetrack magnetic field with a diverter.

03 p0347 A73-14094

Solution of the Boltzmann equation for a fully ionized plasma in an oscillatory electric field and a steady magnetic field. VI - The first velocity moments of distribution function for a homogeneous plasma in a high-frequency electric field.

03 p0349 A73-14650

Influence of the pinning forces for flux lines on the critical current density in magnetic fields of up to 10 Tesla in superconducting titanium-niobium alloys

03 p0328 A73-14654

Velocity distribution of plasma electrons in the negative H₂- and He-glow with superimposed longitudinal magnetic field.

04 p0477 A73-14897

Leakage field methods of defect detection.

04 p0447 A73-14929

The self-consistent geomagnetic tail under static conditions.

04 p0440 A73-14957

Kinetic and dispersion equations for collisionless plasma interaction with HF magnetic and electric fields, noting conical, drift and cyclotron instabilities prevention

04 p0478 A73-15019

Influence of the degree of uniformity of the magnetic field on the emission of electron cyclotron frequency harmonics from a plasma

04 p0478 A73-15036

Investigation of the stability of plasma-jet motion in the magnetic field of a diverter

04 p0479 A73-15045

Comparison of wave propagation in the stationary and moving plasma - Motion and wave propagation along the magnetic field.

04 p0479 A73-15190

Magnetospheric field distortion relation to ring currents based on satellite-borne magnetometer measurements of magnetic field topology

04 p0442 A73-15338

Characteristics of waveguides containing anisotropic warm plasma in the presence of transverse magnetic field.

04 p0480 A73-15600

Ion distribution function in plasma cylinder flow around thin plate in magnetic field under ionospheric conditions

04 p0481 A73-15617

Measurement of the dc plasma electric resistivity perpendicular to the magnetic surface.

04 p0482 A73-15959

Charged particle beams focusing in combined dual spiral system with uniform magnetic field along axis, applying to imaging of flat object

05 p0556 A73-16067

Concerning the accuracy of conservation of the third adiabatic invariant of the motion of a charged particle in axisymmetric fields. I.

05 p0600 A73-16082

Rotating paraboloid of revolution in viscous conducting fluid, calculating flow velocity and magnetic field from MHD equations

05 p0601 A73-16172

Relaxation of ion beam injected into a plasma transversely to a magnetic field.

05 p0602 A73-16550

Turbulence in the annular flow of a conducting-fluid in a magnetic field

05 p0603 A73-16587

Hydrodynamic instability of the boundary of a viscous plasma in a magnetic field.

05 p0603 A73-16793

Vibrations of circular cylinders of a perfectly conducting elastic material.

05 p0637 A73-17298

Radiative modes of a weakly ionized, collision-dominated, turbulent plasma.

05 p0624 A73-17309

Numerical simulation of high Mach number supercritical magnetosonic collisionless shock wave propagation perpendicular to magnetic field, considering cause of anomalous ion heating

05 p0604 A73-17365

Mechanism of motion of inhomogeneities in a nonequilibrium plasma in a magnetic field.

06 p0726 A73-17401

Propagation of electromagnetic waves in a rarefied plasma which has been placed in an alternating magnetic field.

06 p0726 A73-17402

Motion of plasmoids in a toroidal magnetic multipole.

06 p0727 A73-17421

Motion of a magnetized conducting liquid between two plane electrodes in a transverse magnetic field

06 p0727 A73-17472

Three-dimensional MHD duct flows with strong transverse magnetic fields. IV - Fully insulated, variable-area rectangular ducts with small divergences.

06 p0728 A73-17704

Stream instabilities in a cold plasma in the presence of a magnetic field.

06 p0728 A73-17793

Source excited dielectric wedge surface magnetic field local mode solution compared with plane wave method, noting inaccuracy near surface wave cutoff

06 p0666 A73-18197

Scattering by nonconcentric circular plasma cylinders with axial magnetic fields.

06 p0729 A73-18204

Microwave heating of a plasma and longitudinal electronic thermal conductivity in a magnetic field.

06 p0732 A73-18606

Instability limits of an isothermal weakly ionized plasma in a magnetic field

07 p0855 A73-19282

Method for experimental determination of the magnetic well depth in stellarator-type systems

07 p0855 A73-19285

Investigation of the temperature dependence of the anisotropy parameter K in n-Si and n-Ge by using magneto-plasma waves

07 p0861 A73-19327

Transverse hydromagnetic plane waves in the presence of a temperature gradient.

07 p0856 A73-19339

Transverse particle diffusion across external homogeneous magnetic field under random isotropic large scale hydromagnetic turbulence

07 p0856 A73-19450

Nonlinear thermal convection in electrically conducting Boussinesq fluid subject to temperature

gradient and magnetic field, calculating flow stability limit by energy method

07 p0920 A73-19513

Numerical analysis of magnetohydrodynamic instabilities by the finite element method.

07 p0856 A73-19515

Spatial distributions of plasma density in a high-frequency discharge with a superimposed static magnetic field.

07 p0856 A73-19518

Kelvin-Helmholtz instability in a high-beta collisionless plasma.

07 p0856 A73-19520

Origin of magnetic fields in the early universe.

07 p0877 A73-19607

A semiconductor in a microwave electromagnetic field and in a steady magnetic field

07 p0862 A73-20012

Influence of the thermal effect of the gas on the motion of an electric arc in a transverse magnetic field

07 p0858 A73-20081

Thermomagnetic effect in plasma located in an inhomogeneous magnetic field.

07 p0859 A73-20135

German monograph - Unsteady processes of the interaction between shock-produced plasma flows and magnetic fields - A theoretical investigation.

07 p0859 A73-20384

The a.c. losses of non-ideal type II superconductors under parallel configurations of electric currents and magnetic fields.

07 p0864 A73-20403

Continuum electrostatic probe theory with magnetic field.

07 p0860 A73-20476

Electron bombardment ion rocket engine with large diameter and divergent magnetic field for efficiency improvement, considering application as source in plasma wind tunnel

07 p0868 A73-20486

Hydrodynamic instabilities of current carrying pinch in magnetic field, noting thin walled resistive liner effect on nonlocal modes stabilization

08 p0991 A73-20821

Magnetic surfaces decay for parametric instability in helical magnetic configuration, noting nonlinear equations of magnetic field lines

08 p0991 A73-20822

On the steady flow of a non-equilibrium ionized gas around sharp corners in the presence of a crossed magnetic field.

08 p0992 A73-21009

Influence of radiation damping on the motion of a charge in a uniform magnetic field and in the field of a plane electromagnetic wave

08 p0989 A73-21516

Electric and magnetic field shielding performance of nonmagnetic metallic cylinders, using Sommerfeld approximation

08 p0949 A73-21663

Particle and energy fluxes across magnetic field in axisymmetric toroidal magnetic traps and plasmas with weak collisions, calculating radial electric field

08 p0993 A73-21695

Stability of a ferromagnetic plate within a gas flow in the presence of a magnetic field

08 p0989 A73-21723

Penetration of a solid into a half-space of compressible liquid in the presence of a magnetic field

08 p0994 A73-21724

Electron heat conductivity along a magnetic field in a decaying plasma

09 p1124 A73-21887

Absorption of electromagnetic waves by a magnetoactive plasma at parametric-resonance frequencies

09 p1124 A73-21889

Features of the flow of a nonisothermal plasma, obtained in a beam-plasma discharge, through a magnetic nozzle

09 p1124 A73-21890

Surface oscillations of a weakly ionized plasma in a magnetic field

09 p1124 A73-21901

Influence of magnetic field curvature on the stability of a plasma confined by a dense shell of neutral gas

09 p1124 A73-21902

Quasi-linear relaxation of a monoenergetic relativistic electron beam in an external magnetic field

09 p1124 A73-21903

Cosmic rays in a random magnetic field - Break-down of the quasilinear derivation of the kinetic equation.

09 p1137 A73-22036

Kinetic theory of a two-dimensional magnetized plasma. III - Limit of very large magnetic field.

09 p1127 A73-22283

Convergence of the solution for the far scattered field of a conducting cylinder of arbitrary cross-section.

09 p1050 A73-22397

Influence of the Hall effect on current structure in a plasma flow through a spatially periodic magnetic field

09 p1127 A73-22606

Electromagnetic fields in electrodeless discharges of arbitrary length.

[TTU-SR-Z] 09 p1128 A73-22635

Magnetic field effect on laser radiation intensity and polarization, noting Zeeman component change

09 p1095 A73-22666

Approximate calculation of a thermal boundary layer at a flat plate with allowance for a magnetic field

09 p1167 A73-22859

Drift-like instability in density modulated plasmas in a static magnetic field.

09 p1131 A73-22904

Parametric excitation of circularly polarized and ion waves in a magnetized plasma.

09 p1131 A73-22905

Conductivity tensor and dispersion equation for collisional magnetoactive plasma.

09 p1131 A73-22922

Determination of the electron temperature of a plasma by sounding with an extraordinary wave along a magnetic field

10 p1253 A73-23504

Quantum theory of line formation in a magnetic field.

10 p1249 A73-24134

Collisionless plasma compression shock waves thermodynamics, noting entropy variations along shock adiabat under plasma heating in magnetic field

10 p1254 A73-24179

Ion distribution function in plasma cylinder flow around thin plate in magnetic field under ionospheric conditions

10 p1254 A73-24207

Electromagnetic wave reflection at interface between anisotropic Vlasov plasma and vacuum with external magnetic field, deriving electric and magnetic field characteristics

10 p1255 A73-24260

Straight plasma column confined by static axial and oscillating transverse magnetic fields, deriving stability criteria via viscous fluid model

10 p1255 A73-24264

Numerical simulation of small amplitude whistler waves in thermal plasma, describing particle motion under self consistent and external magnet fields via Lorentz equation

10 p1255 A73-24269

Three phase alternators with two/four poles superconducting inductors and with outer/inner induction winding, determining magnetic field radial distribution

10 p1177 A73-24411

Flow near an accelerated plate in the presence of a magnetic field.

10 p1206 A73-24528

Semiempirical determination of the anisotropy of turbulent MHD flow in a longitudinal field

10 p1256 A73-24592

Alternating spectral oscillations of nonequilibrium photoelectron current in p-InSb in the presence of a quantizing magnetic field

10 p1261 A73-24763

Observation of stationary acceleration of ions to energies of 2 to 20 keV in a nonisothermal plasma

10 p1258 A73-24888

Thermal conductivity of the plasma electron component across the magnetic field

10 p1258 A73-24890

The equilibrium, stability and evolution of a rotating magnetized gaseous disk.

10 p1284 A73-24903

Synthesis of superconducting suspensions with a maximum lifting force

11 p1372 A73-25049

Brownian motion of electrons in time-dependent magnetic fields.

11 p1403 A73-25124

Near field of scattering by a hollow semi-infinite cylinder and its application to sensor booms.

11 p1328 A73-25658

Considerations concerning the solution of Chandrasekhar's system of equations in the case of MHD turbulence

11 p1404 A73-25700

Frequency dependence of circular polarization in three compact radio sources.

11 p1419 A73-25777

Electrodynamics analysis of superconducting vortices interaction with cylindrical cavities (pinning), calculating critical currents in type II superconductors in external magnetic field

11 p1409 A73-26191

Flow of liquid metals with a transversely applied magnetic field. I - Laminar flow in the entrance region.

11 p1406 A73-26341

Current and fields reduced in plasmas by relativistic electron beams with arbitrary radial and axial density profiles.

11 p1407 A73-26560

High field superconductivity in alkali metal intercalates of MoS₂.

11 p1410 A73-26745

Absorption of microwaves by a plasma in a magnetic field in the presence of a large effect due to longitudinal inhomogeneity

12 p1467 A73-26934

MAGNETIC FIELDS

Low energy auroral electron pitch angle diffusion in postbreakup aurora due to injected particle loss in closed magnetic field lines 12 p1488 A73-26987

Magnetic field line velocity associated with Euler potentials set, considering flux preservation properties of particle motion 12 p1489 A73-27000

Two-dimensional steady magneto-fluid-dynamic flows with orthogonal magnetic and velocity field distributions. 12 p1527 A73-27020

The periodic structure of an electric field in stratified plasma with tensor conductivity. 12 p1529 A73-27531

Accuracy of conserving the third adiabatic invariant of the motion of a charged particle in axially symmetrical fields. II. 12 p1535 A73-27634

Influence of viscosity on the motion of nonuniformities of a nonequilibrium plasma in a magnetic field. 12 p1529 A73-27914

Interaction of a high-frequency magnetic field with plasma potential oscillations in a Q machine 12 p1530 A73-27976

Crab Nebula magnetic field origin and internal electron acceleration mechanism nature 13 p1673 A73-28225

Determination of the time interval for orientation of conducting nonmagnetic oblong bodies by a homogeneous alternating magnetic field 13 p1571 A73-28467

Method of experimental study of fields in electromagnetic resonators - Application to helicoidal resonators 13 p1589 A73-28472

Dipole antenna radiation in homogeneous plasma layer magnetized by normal uniform magnetic field, calculating radiation pattern 13 p1583 A73-28661

Stability of a weakly ionized isothermal plasma in a magnetic field. 13 p1665 A73-28682

Experimental determination of magnetic well depth in stellerators. 13 p1665 A73-28685

Investigation of the conversion characteristic of a ferromagnetic rod probe subjected to the simultaneous influence of longitudinal and transverse magnetic fields 13 p1617 A73-28867

Analytical description of the three-dimensional distribution of the scattering of a gyromotor magnetic field 13 p1618 A73-29149

Breakdown of the superheated Meissner state and spontaneous vortex nucleation in type II superconductors. 13 p1669 A73-29183

Alpha-omega dynamo problem of electrically conducting sphere magnetic field, obtaining eigenvalues from variational principle with free decay modes as trial functions 13 p1685 A73-29365

Electrostatic and magnetic fields methods comparison for small angle scanning of electron beam, considering particle trajectories, field energy and circuit electrical parameters 14 p1732 A73-29913

Flow regimes for a magnetic suspension under a rotating magnetic field. 14 p1774 A73-29924

Diffusion of plasma density and temperature perturbations in a magnetic field 14 p1749 A73-30264

Equilibrium equations for vortex lines with allowance for interaction with boundary of ideal superconductor, calculating extremum values of magnetic field 14 p1774 A73-30342

Existence of a new type of rotating equilibrium ellipsoids in the presence of a toroidal magnetic field 14 p1782 A73-30816

Equivalence of geoelectric cross sections in the frequency probing method 14 p1750 A73-30835

On the transport of charged particles in turbulent fields - Comparison of an exact solution with the quasilinear approximation. 15 p1916 A73-31083

Motion of a sphere in a conducting fluid under the action of crossed electric and magnetic fields 15 p1917 A73-31405

Noncirculative MHD inviscid conducting fluid flow past circular cylinder and plane profile in magnetic field, using Fredholm equation 15 p1918 A73-31414

Zone of Poynting vector rotation toward the direction of an applied magnetic field for a wave incident on an inhomogeneous plasma 15 p1919 A73-31707

The field levels near midnight at low and equatorial geomagnetic stations. 15 p1869 A73-31758

Plasma and fields in the vicinity of a rapidly moving body in the presence of an external magnetic field 15 p1919 A73-31880

Existence of stable relative equilibria of an artificial satellite in a model magnetic field 15 p1872 A73-31956

Instabilities in charge sheets and current sheets and their possible occurrence in the aurora. 15 p1873 A73-32235

Nonlinear ion-acoustic and electron-acoustic waves of a plasma in a magnetic field 15 p1921 A73-32324

Equilibrium of a plasma contained between two parallel plates by a magnetic field 15 p1921 A73-32333

German monograph - Investigations regarding the structure of planar boundary layers between magnetic field and plasma. 15 p1921 A73-32584

The dynamical effects of cosmic rays in the Galaxy and the generation of the galactic magnetic field. 16 p2054 A73-33287

Free surface shape of MHD flow due to constant mass source expansion into uniform magnetic field as function of time 16 p2041 A73-33329

Electric coil systems for magnetic field simulation, discussing field size and characteristics and coil configurations 16 p1997 A73-33383

Electromagnetic inductive microsystems with synchronization. I Determination of the characteristic functional magnitudes. II - Determination of the magnetic field in a region with linear and nonlinear media 16 p1992 A73-33664

Anomalous penetration of a magnetic pulse into a plasma. 17 p2214 A73-34098

Investigation of plasma inhomogeneities between coaxial electrodes in a magnetic field 17 p2214 A73-34128

Electron thermal conductivity along the magnetic field in an afterglow. 17 p2215 A73-34310

Absorption of electromagnetic waves at parametric resonances in a magnetoactive plasma. 17 p2215 A73-34312

Memory of early magnetic fields in carbonaceous chondrites. 17 p2228 A73-34421

A self-consistent two-dimensional approach to magnetospheric structures. 17 p2158 A73-34502

Determination of electron temperature of a plasma by probing the extraordinary wave along a magnetic field. 17 p2217 A73-35184

A method for solving the problem of irradiation in anisotropic plasma. 17 p2217 A73-35724

ESRO Geos geostationary satellite for measurement of magnetospheric plasma electric and magnetic fields and drift rate at various frequency regions via electron injection 17 p2176 A73-35816

Re-connexion of magnetic lines of force - Evolution in incompressible MHD fluids. 18 p2338 A73-36181

Current distribution at the zero line of the magnetic field and the turbulent resistance of a plasma 18 p2339 A73-36550

Permittivity of a plasma with transverse nonazimuthal fluxes 18 p2339 A73-36552

Electromagnetic interference caused by a solar array. 18 p2269 A73-36958

Incompressible conducting fluid flows in an arbitrary region in the presence of a strong magnetic field 18 p2340 A73-37015

Cold collisionless plasma flow along magnetic field, deriving quasi-shock wave characteristics from Vlasov-Maxwell equations 19 p2463 A73-37152

Shock waves within the two fluid model in the presence of the magnetic field. 19 p2464 A73-37160

Two field continuum model of magnetic sheath adjacent to absorbing solid surfaces, using Bohm criterion and MHD boundary layer equation approximation 19 p2464 A73-37162

Penetration and crossing of transverse magnetic field barrier by a purely ionic plasma. 19 p2465 A73-37170

Stability of plasma flows in multipolar magnetic fields 19 p2467 A73-37372

Kinematic theory of magnetic field reconnection rate for analysis of turbulent flows in solar photosphere, flare phenomena and galaxy 19 p2467 A73-37439

Russian book on satellite measurement of magnetic fields and plasmas in interplanetary medium, magneto-

sphere, moon and Venus vicinity and geomagnetic field-solar wind interaction region 19 p2486 A73-37772

Series expansion of the magnetic vector-potential computed for a current carrying ring. 19 p2425 A73-37927

Effects of local conductivity anomalies on the magnetic fields of micropulsations. I - Electromagnetic induction in the English Channel. II - Effect of subterranean conductivity anomalies. 19 p2425 A73-38012

Numerical solutions of the kinematic dynamo problem. 19 p2460 A73-38102

Some transient MHD-flows with finite magnetic Reynolds numbers. 19 p2470 A73-38319

The electron kinetics of a weakly ionized Lorentz plasma in arbitrarily oriented external electric and magnetic fields 20 p2596 A73-39192

Study of the stability of a perturbed conducting gas flow in a magnetic field at arbitrary Reynolds magnetic numbers 20 p2597 A73-39276

Low-frequency vibrations of a high-frequency E-discharge plasma in a magnetic field 20 p2598 A73-39398

On an eigenvalue problem in the kinematic approach to dynamo theories of cosmic magnetism. 20 p2609 A73-39571

Generation of magnetic fields in a matter-antimatter universe. 20 p2611 A73-39587

Radiative and convective heat transfer in a magnetic field 20 p2628 A73-39608

High-speed camera study of the shock wave propagation. 21 p2697 A73-39993

Effects of propagation parallel to the magnetic field on the Type I electrojet irregularity instability. 21 p2682 A73-40160

Regular reflection of an oblique shock in a plane flow of ideally dissociating gas in the presence of a transverse magnetic field 21 p2744 A73-40189

Parametric excitation of ion-acoustic oscillations in a plasma situated in an alternating electric field and a constant magnetic field 21 p2746 A73-40519

Study of MHD effects in a viscous conducting fluid flow in a traveling magnetic field 21 p2747 A73-40884

Experimental study of rotational MHD Couette flow in a coplanar field 21 p2747 A73-40886

Magnetohydrodynamic wake behind a body placed in a homogeneous flow in the presence of a longitudinal magnetic field 21 p2747 A73-40890

Conductivity tensor of a collisional plasma in a magnetic field. 21 p2749 A73-41628

Steady-state acceleration of ions to 2-20 keV in a nonisothermal plasma. 21 p2749 A73-41663

Transverse electron thermal conductivity for a plasma in a magnetic field. 21 p2749 A73-41665

Perturbation of the magnetic configuration of a stellarator by a longitudinal current in the plasma. 21 p2750 A73-41678

Numerical methods for solving some problems of the theory of plasma equilibrium in toroidal configurations. 21 p2750 A73-41680

Human perception of moderate strength low frequency magnetic fields tested by whole body immersion in large Helmholtz coil field under acoustic isolation 22 p2811 A73-41789

Barium cloud release near equatorial plane for investigating interaction with ambient medium and electric and magnetic field properties in outer radiation belt 22 p2852 A73-41932

Quiet-time nightside magnetic field near geomagnetic equator detected by magnetospheric barium cloud injection, revealing taillike structure from atmospheric models 22 p2846 A73-41939

High field NMR thermometry below 1 K using HD. 22 p2856 A73-42024

Knudsen free molecular flow explanation of thermomagnetic torque on circular cylinder suspended in axial molecular field, noting apparatus tilt effect 22 p2842 A73-42233

New dispersion relation for a strongly magnetized degenerate electron plasma with anisotropic pressure. 22 p2890 A73-42237

Microwave absorption by a magnetoplasma with a strong longitudinal inhomogeneity. 22 p2891 A73-42268

Investigation of the waveguide properties of a plasma cylinder for axially asymmetric waves 22 p2892 A73-42379

Longitudinal polarization and focusing of plasmoids in a linear multipole magnetic field 22 p2893 A73-42383

Numerical analysis of magnetic field lines of force reconnection along transition layers or at flow stagnation point of incompressible conducting viscous fluid 22 p2894 A73-42396

Study of hydromagnetic stability of a hot rotating layer of fluid by Liapunov method. 22 p2894 A73-42474

Interactions of plasmas with magnetic field boundaries 22 p2851 A73-42977

Induced currents in a stationary plasma flow in an axially-symmetric magnetic field 23 p3010 A73-43663

Structure of currents in a stationary plasma jet in the presence of the Hall effect 23 p3010 A73-43664

Investigation of a turbulent plasma in a reflex discharge with the aid of a double electric probe 23 p3011 A73-43668

Experimental test of the wind-shear theory: A reply - Rocket-borne magnetometers do measure B. 23 p3024 A73-43702

Distribution function of relativistic electrons in a strong magnetic field. 23 p3011 A73-43753

Elastic semispace motion under the action of a shock wave in a magnetic field 23 p3006 A73-43919

Spectroscopic polarization analysis of turbulent plasma noise produced by the annihilation of opposite magnetic fields 23 p3012 A73-44016

Conductivity of Type II superconductors near the transition temperature 23 p3016 A73-44019

Concentration effect in semiconductors with bipolar conductivity in an alternating external magnetic field 23 p3017 A73-44046

Cyclotron oscillations of a plasma in an inhomogeneous magnetic field 23 p3012 A73-44090

Existence of stable relative equilibria for an artificial satellite in a model magnetic field. 24 p3081 A73-44481

Tidal generation of magnetic fields in binary celestial systems, calculating growth times 24 p3134 A73-44578

Phase-sensitive method of electromagnetic flaw detection. 24 p3093 A73-44696

A variation of the Davis-Smith method for in-flight determination of spacecraft magnetic fields. 24 p3139 A73-45107

Electron-molecule collision frequencies in a crossed electric and magnetic field. 24 p3118 A73-45476

MAGNETIC FILMS

High density coupled flat thin film magnetic memories for large capacity storage, using point density/signal amplitude simulation model 05 p0553 A73-16169

Wall contraction in Bloch wall films. 07 p0864 A73-20218

Magnetic reversal mechanisms of obliquely deposited permalloy films possessing perpendicular anisotropy 12 p1530 A73-26833

MAGNETIC FLUX

Generation of the large-scale galactic magnetic field. II. 01 p0107 A73-11329

Magnetic field strength change in equatorial plasmasphere, considering quiet ring current as equatorial sheet current extension of neutral sheet current in magnetospheric tail 02 p0155 A73-11732

Average magnetic field strength relationships with angular velocity and stellar activity cycle period, using Leighton solar cycle model with differential rotation and cyclonic turbulence 02 p0224 A73-12741

Solar active region growth in terms of magnetic flux emergence in shape of new arch filament system 03 p0367 A73-12946

A self-consistent theory of the tail of the magnetosphere. 03 p0302 A73-13872

Geomagnetic tail and neutral sheet origin based on geomagnetic flux diffusion through magnetopause, discussing Dungey reconnection mechanism and Kelvin-Helmholtz instability effects 04 p0441 A73-15329

Line existence in H component magnetic power spectra of geomagnetic field LF components 04 p0445 A73-15552

Density and electric field oscillations of plasma in stellarator, considering magnetic field strength effect,

stabilization by ionic collisions and energy pumping mechanism 06 p0728 A73-17968

Minimum magnetic field energy of two dimensional magnetosphere with neutral sheet for arbitrary dipole inclination to solar wind as function of potential difference on boundary points 07 p0816 A73-19443

Short period geomagnetic pulsations with gradual amplitude increase and abatement, noting latitudinal variation 07 p0816 A73-19465

Design considerations for high-current-density superconducting saddle magnets for MHD. 07 p0852 A73-20405

The energy spectrum of small-scale solar magnetic fields. 08 p1003 A73-20888

The possibility of disappearance of the earth's magnetic field during inversion 08 p0958 A73-21275

'Flux quantization' type of oscillation effects in a normal metal 09 p1130 A73-22709

Hall current effects in the Lewis magnetohydrodynamic generator. 09 p1130 A73-22823

Magnetic field intensity and invariant shell parameters computer programs, assessing error in expansion coefficients 10 p1276 A73-23888

Experience in developing and using laboratory superconducting solenoids with fields up to 119 kOe 10 p1177 A73-23936

On the small-scale structure of solar magnetic fields. 10 p1279 A73-24135

Earth surface magnetic field intensity variations in terms of magnetospheric resonator excitation, assuming three dimensional Alfvén waves 10 p1212 A73-24230

The magnetic field in the immediate vicinity of Mars according to Mars 2 and Mars 3 satellite data 10 p1281 A73-24461

Efficiency of the microwave energy absorption in a plasma at high magnetic fields. 10 p1257 A73-24627

Saturn magnetospheric model for bounds on surface field strength and trapped particle population 10 p1283 A73-24724

Magnetotail model for magnetic field strength and particle drift in magnetic equatorial plane earth, using current sheet from satellite observations 11 p1357 A73-25929

On the random nature of the eruption of magnetic flux at the solar surface. 11 p1422 A73-25939

Solar flares association with emerging flux regions /EFR/ near sunspots, noting correlation between area and brightness changes 11 p1412 A73-25942

Operating properties of a helical microwave plasma source in high density high magnetic field regime. 11 p1407 A73-26562

The growth and decay of the main phase of the September 21-23, 1963 magnetic storm. 12 p1490 A73-27275

Lossless electric energy transmission via superconductivity above 20 K, noting intense magnetic field generation 12 p1531 A73-27689

The normal-tangential form of the equations for the electrodynamics of conducting media 12 p1525 A73-27806

Solar radio burst of 7 August 1972, discussing peak flux density, magnetic field intensity, energy distribution and polarization degree 12 p1536 A73-27850

Identification of interplanetary tangential and rotational discontinuities. 14 p1796 A73-29958

Cosmic ray properties and origin, discussing pulsars and superstrong magnetic fields existence effects 14 p1787 A73-30233

Resistance of superconductors near the critical field Hc2 14 p1784 A73-30813

The problem of choosing a zero approximation of the angular position of an oriented satellite in the case of a nondipolar approximation of the geomagnetic field 15 p1942 A73-31238

The general magnetic field on the sun and its changes with time. 15 p1932 A73-31304

Electrical conductivity and total emission coefficient of air plasma. 15 p1918 A73-31657

Radiation absorption in stellar atmospheres due to photoionization in magnetic field, discussing frequency relation to propagation direction and Larmor frequency 15 p1872 A73-31955

The most important characteristics of magnetizing equipment in the leakage-flux technique - Their measurement and application 15 p1882 A73-32054

NMR spectrometer magnetic field strength-HF field frequency ratio instability spectral density in presence of spin stabilizers 16 p2011 A73-32824

Magnetic field of a horizontal current above a conducting earth. 16 p2004 A73-33448

Quiet time magnetospheric field depression at 2.3-3.6 earth radii. 16 p2005 A73-33464

A self-consistent two-dimensional approach to magnetospheric structures. 17 p2158 A73-34502

Periodic variations of the cosmic radiation. III - The 27-day variation. 18 p2345 A73-36180

Magnetic field in the near vicinity of Mars from data of the Mars-2 and Mars-3 satellites. 19 p2486 A73-38127

Magnetic field intensity and invariant shell parameters computer programs, assessing errors in expansion coefficients 20 p2603 A73-38907

Spectrographic observations of the peculiar Be star with infrared excess HD 45677. 20 p2611 A73-39586

Magnetic equatorial ionospheric characteristics, discussing E and F regions, diurnal drift variations, field strength, equatorial electrojet, spread F and sporadic E 20 p2555 A73-39633

Evaluation of the magnitude of the magnetic field in the solar corona from measurements of the linear polarization of solar radio bursts 21 p2755 A73-40538

The effect of magnetic mass on Alfvén waves. 21 p2701 A73-40624

Simple expressions for the electric and magnetic field strengths between the elements of an infinite array. 22 p2831 A73-41849

Results of the application of the physical modeling method to a study of the tangential component of the magnetic field of a linear inductor on the surface of a massive ferromagnetic body 22 p2800 A73-42214

Anomalous diffusion in a magnetized plasma. 22 p2894 A73-42483

Models of force-free magnetic fields in resistive media. 22 p2911 A73-42938

Resistive diffusion of force-free magnetic fields in a passive medium. II - A nonlinear analysis of the one-dimensional case. 22 p2914 A73-43009

On Kraichnan's direct interaction approximation applied to charged-particle transport in turbulent magnetic fields. 22 p2904 A73-43013

Strong magnetic fields occurrence in sunspot penumbras dark filaments related to hypothesis of penumbral convection rolls existence 23 p3026 A73-43224

Diamagnetism of Penning discharge plasma as function of gas pressure, magnetic field strength and applied voltage, discussing plasma energetic lifetime and current characteristics 23 p3009 A73-43653

Influence of the magnetic field on electrodeless-discharge plasmas 23 p3009 A73-43654

Radiation absorption in stellar atmospheres due to photoionization in magnetic field, discussing frequency relation to propagation direction and Larmor frequency 24 p3081 A73-44480

Observation of plasma flow in the neutral sheet at lunar distance during two magnetic bays. 24 p3139 A73-45137

MAGNETIC FORMING

Calculation of the energy and force process parameters in magnetic-pulse forming of complex shaped elements 02 p0172 A73-11646

An ultrasonic technique for the inspection of magnetic and explosive welds, using a facsimile recording system. 12 p1502 A73-27037

MAGNETIC INDUCTION

Experimental study of the inverse Faraday effect in plasmas 02 p0196 A73-11587

End effects in Faraday type MHD generators with nonequilibrium plasmas. 03 p0254 A73-14185

Inductance and magnetic reversal losses in pulse operated communication, describing bridge circuit for comparing test sample current with capacitor voltage/time characteristics 05 p0559 A73-17241

MAGNETIC INDUCTION PROBES

The induced magnetic field of the moon - Conductivity profiles and inferred temperature.
07 p0892 A73-19835

Influence of annealing under load on the structure and properties of a self-ordering Ni3Mn alloy
09 p1099 A73-21957

Magnetic duct field and induction distributions for liquid metal pump design, using Tozoni integral equations
10 p1177 A73-23475

Induction flowmeter theory in a T-tube of circular section.
10 p1220 A73-24619

EM induction in a semi-infinite solid, impulsively moving in a uniform magnetic field.
11 p1397 A73-25371

Induced lunar magnetosphere and solar wind formed downstream cylindrical cavity for interplanetary magnetic fields arbitrary orientation, assuming lunar core and shell electrical conductivity model
14 p1796 A73-29962

Effect of linear load graduation in the end zones of an inductor on the longitudinal side effect in induction machines
15 p1832 A73-31410

Engineering technique for secondary-medium parameter calculation in the substitution circuits of flat, linear induction MHD machines with side busbars
15 p1832 A73-31411

The perturbation of alternating geomagnetic fields by discontinuities with high conductivity contrasts.
15 p1871 A73-31780

Electromagnetic induction microsystems with synchronization. III - Distribution of magnetic characteristics in complex linear and nonlinear regions. IV - Modeling of nonstationary electromechanical processes
16 p1992 A73-33668

Dynamo theory of earth magnetic field generation, discussing earth core characteristics, electromagnetic induction processes and magnetic field energy sources
17 p2162 A73-35049

Topology of induced lunar magnetic fields.
17 p2235 A73-35736

Effects of local conductivity anomalies on the magnetic fields of micropulsations. I - Electromagnetic induction in the English Channel. II - Effect of subterranean conductivity anomalies.
19 p2425 A73-38012

Magnetically induced collisionless coupling between counterstreaming laser-propagating plasmas.
19 p2469 A73-38290

Study of MHD effects in a viscous conducting fluid flow in a traveling magnetic field
21 p2747 A73-40884

Induced magnetosphere of the moon. II - Experimental results from Apollo 12 and Explorer 35.
22 p2906 A73-41905

Turbulent mean emf in presence of nonvanishing mean conducting fluid flow, modifying Green tensor of induction equation for constant strain rate velocity fields
23 p2969 A73-44050

MAGNETIC INDUCTION PROBES

U MAGNETIC PROBES

MAGNETIC LENSES

Design and modeling of periodic magnetic systems for SHF devices. I, II
01 p0025 A73-10981

An X-ray tube emitting soft and hard radiation with controlled focusing
08 p0969 A73-21721

Properties of magnetic focusing systems for picture tubes
10 p1194 A73-23850

MAGNETIC MATERIALS

NT FERRIMAGNETIC MATERIALS

NT FERROMAGNETIC FILMS

NT FERROMAGNETIC MATERIALS

NT MAGNETITE

NT PERMALLOYS [TRADEMARK]

Experimental investigation of the magnetic properties and magnetization conditions of magnetically solid materials at elevated temperatures
01 p0044 A73-10084

Magnetic semiconductor materials compositions and magneto-electric characteristics, discussing magnetic-electric interactions, fabrication techniques and applications for magnetically controllable diodes, temperature sensors, etc
04 p0483 A73-15323

Improved melting and casting procedures for a cobalt-base magnetic alloy.
04 p0455 A73-15750

Magnetic spheroid mass determination with microbalance and internal cavity observation by X ray photography, noting meteor showers as extraterrestrial source
05 p0621 A73-17055

Investigation of the strength and deformability of thin composite materials used as magnetic recording media. II - Strength and deformability at low temperatures
09 p1110 A73-22156

Influence of magnetic spin resonance in optically transparent magnetic materials on the nature of laser radiation
16 p2024 A73-34001

Magnetic rubber inspection to extend NDT capabilities for locating cracks and defects on or near magnetic material surface
21 p2708 A73-41324

Use of magnetic materials for improvement of screening properties of different types of cables.
22 p2830 A73-41805

The metallurgy of Remendur - Effects of processing variations.
23 p2993 A73-43987

MAGNETIC MEASUREMENT

Effect of inhomogeneity of normal specimens on measurement error estimation in devices with an incompletely closed magnetic system
01 p0044 A73-10085

Continuous Pc micropulsations with discrete latitude dependent frequencies in H components, recording simultaneously at ground based magnetometer stations
02 p0157 A73-11749

Automatic magnetic inspection method using magnetoresistive elements and its application.
02 p0173 A73-11988

Lunar magnetic field measurements, electrical conductivity calculations and thermal profile inferences.
03 p0369 A73-13103

Electromagnetic wave observation in interplanetary medium and in magnetosphere, emphasizing magnetic and electric field measurements
03 p0374 A73-13855

Magnetic fields in solar active regions.
04 p0490 A73-14828

Magnetograph instrumentation and measurements, presenting solar magnetic field fine structure observations
04 p0496 A73-14829

Cosmic ray number density modulation by off-ecliptic phenomena to explain interplanetary magnetic field measurements onboard Heos 1 and 2
05 p0611 A73-17186

Magnetotelluric and geomagnetic depth sounding methods compared.
05 p0572 A73-17189

Marine quantum Cs Z-magnetometer design and compensation for onboard nonmagnetic schooner operation, using vertical gyro mount
06 p0691 A73-17547

Further study of the theta component of the interplanetary magnetic field.
07 p0875 A73-19230

Lunar magnetic field measurements with Apollo 15 subsatellite, discussing surface remanent magnetization, solar wind interactions and limb shocks
07 p0892 A73-19833

Lunar breccia 14321 natural remanent magnetization characteristics from alternating field and thermal demagnetization tests, describing magnetic measurement procedures
07 p0893 A73-19841

Low-frequency applications of superconducting quantum interference devices.
07 p0863 A73-20101

Investigation of the structure of a high-current discharge in a lithium plasma.
08 p0992 A73-20853

Residual geomagnetic field from the satellite Cosmos 49.
09 p1076 A73-22192

Plane film elements demagnetizing factor measurement from material-element hysteresis loop comparison
09 p1084 A73-22655

Use of magnetic probes for diagnostics of pulse plasma.
09 p1086 A73-23149

Measurements of the magnetic field vector of a sunspot.
10 p1275 A73-23827

Preliminary mapping of the lunar magnetic field.
11 p1421 A73-25903

Devices for primary processing of information in controller machines, based on the principles of quantum magnetometry
12 p1495 A73-26778

Cosmos 321 geomagnetic measurement data for construction of satellite geomagnetic survey and geomagnetic field models
12 p1491 A73-27359

GEOS geostationary satellite experiments for dc magnetic fields, dc/ac electric fields and plasma resonances, thermal plasma, electrons and protons
12 p1499 A73-27775

Equatorial electrojet, according to Kosmos-321 measurements.
13 p1670 A73-28716

Magnetic anomalies in New Guinea-New Zealand region from proton magnetometer measurements, noting effects of andesite-basalt volcanic processes and nuclear precession signal variations
13 p1608 A73-28727

Identification of interplanetary tangential and rotational discontinuities.
14 p1796 A73-29958

Marine quantum Cs Z-magnetometer design and compensation for onboard nonmagnetic schooner operation, using vertical gyro mount
16 p2011 A73-32771

Soviet Lunokhod 2 lunar rover design, guidance systems, mineralogical analyses by X ray fluoroscopic spectroscopy, magnetic field measurements and operations site
16 p1996 A73-33225

Satellite studies of magnetospheric substorms on August 15, 1968. IV - Ogo 5 magnetic field observations.
16 p2004 A73-33452

The magnetic field in the vicinity of Venus
16 p2067 A73-33805

Flaw detection and characterization using acoustic emission.
16 p2022 A73-34013

The compensation method for measuring the components of the earth's magnetic field.
17 p2159 A73-34750

Development and qualification of a magnetic technique for the nondestructive measurement of residual stress in CH-47 A rotor blade spars. [AHS PREPRINT 752]
17 p2180 A73-35080

Digital data acquisition and processing from a remote magnetic observatory.
17 p2175 A73-35667

Susceptibility measurements at high frequency - A versatile and sensitive apparatus.
17 p2176 A73-35771

Ground and synchronous orbit magnetic observations of magnetospheric and ionospheric wave propagation to model substorm current system variations
18 p2303 A73-35945

Magnetic measurements in laboratory model tests of solar wind-geomagnetic field interactions
19 p2481 A73-37338

Russian book on satellite measurement of magnetic fields and plasmas in interplanetary medium, magnetosphere, moon and Venus vicinity and geomagnetic field-solar wind interaction region
19 p2486 A73-37772

Magnetic storm inflation analysis from Explorer 45 and ground observation data, noting proton penetration into magnetosphere evening quadrant
20 p2552 A73-38951

Magnetic field in the very close neighborhood of Mars according to data from the Mars 2 and Mars 3 spacecraft.
20 p2604 A73-38959

Solar magnetic field spatial structure in relation to solar activity phenomena, discussing measurements based on Zeeman effect in absorption line spectra formation
20 p2605 A73-39059

Observational comparison with a self-consistent model of the geomagnetic tail.
21 p2691 A73-41377

Surface and orbital magnetic results from Apollo 15.
21 p2691 A73-41398

Cosmos 321 geomagnetic measurement data for construction of satellite geomagnetic survey and geomagnetic field models
23 p2971 A73-43259

Rocket-borne magnetometer measurement of magnetic field changes associated with electron density fluctuations and wind structure, testing wind shear theory of sporadic E formation
23 p3024 A73-43701

A variation of the Davis-Smith method for in-flight determination of spacecraft magnetic fields.
24 p3139 A73-45107

Heos 1 plasma and magnetic field experiments during bow shock crossings for turbulent bow structure, discussing proton velocity distribution
24 p3125 A73-45111

Triaxial magnetic measurements of field-aligned currents at 800 kilometers in the auroral region - Initial results.
24 p3087 A73-45140

MAGNETIC MEMORIES

U MAGNETIC STORAGE

MAGNETIC METALS

U MAGNETIC MATERIALS

U METALS

MAGNETIC MIRRORS

Two-dimensional investigation of absolute instabilities in mirror plasmas.
01 p0083 A73-10458

Theory of electron cyclotron resonance heating. I - Short time and adiabatic effects.
03 p0345 A73-14434

Investigation of a dense plasma produced by an electron beam in a magnetic mirror
04 p0479 A73-15040

Confinement in a magnetic mirror of a plasma generated by laser radiation
04 p0482 A73-15620

Gas-dynamic description of a plasma in a corrugated magnetic field. 05 p0603 A73-17360

Contribution of Coulomb collisions to plasma relaxation in the DECA mirror machine. 05 p0604 A73-17367

Modified negative mass mode stabilization in finite magnetic mirror confined plasmas with highly anisotropic velocity distribution, considering bounce harmonic effects and gyrofrequency 07 p0856 A73-19522

Nonlinear small amplitude behavior of collisionless plasma at mirror flute instability threshold, using modified constant gravity model and magnetic moment variation 07 p0857 A73-19525

Energy distribution functions of kilovolt ions in a modified Penning discharge. 07 p0808 A73-20459

Excitation of low-frequency oscillations by an electron beam in a hot plasma confined in a magnetic mirror 09 p1125 A73-21907

Investigation of the heating mechanism for the electron component of a plasma under beam-instability conditions in a mirror confinement system 09 p1130 A73-22703

Injection of a laser-produced plasma into a magnetic trap. 10 p1254 A73-24210

Numerical studies of charged particle trapping in a time varying magnetic mirror field. 11 p1404 A73-25273

Investigation of the feasibility of the injection of electrons into heliotron-type closed magnetic mirror configurations 13 p1666 A73-28957

Comparison of the hot-electron plasmas produced using two different plasma sources in a magnetic mirror compression experiment. 14 p1781 A73-30657

Coulomb drift of electrons from a mirror confinement system in the case of a positive plasma potential 15 p1920 A73-32306

Electron-beam excitation of low-frequency waves in a hot plasma confined in a mirror machine. 15 p1922 A73-32632

Streaming plasma interaction with variable longitudinal magnetic fields. 19 p2465 A73-37171

Electron injection through the diverter in a heliotron. 23 p3013 A73-44309

Coulomb loss of electrons from a mirror device with a positive plasma potential. 24 p3114 A73-44614

MAGNETIC MOMENTS

Influence of eddy currents on the rotation and orientation of an asymmetric artificial earth's satellite 08 p1014 A73-21547

Critical transition temperatures and magnetic moment measurements of superconducting state of binary Be alloys 11 p1409 A73-25630

Magnetic moment generation in pulsars based on baryon model with superconducting proton fluid and normal electron field 17 p2226 A73-34365

Control laws of magnetic attitude stabilization systems of earth satellites 18 p2359 A73-36103

Magnetic susceptibility of a degenerate electron gas - Interaction of nuclear magnetic moments in normal metals and superconductors 23 p3016 A73-43709

Deflecting moments in magnetic suspensions of gyroscopic devices 24 p3089 A73-44546

MAGNETIC PERMEABILITY

Temperature dependence of magnetic susceptibility in nickel-film-coated iron-silicon alloy specimens 01 p0062 A73-10254

Ti-Al-V alloys ac differential measurement method for metallurgical processing and microstructure effects on superconducting critical temperature and magnetic permeability/susceptibility 02 p0200 A73-11843

AC studies of a superconducting Nb-52 at. % Ti alloy. 02 p0200 A73-11844

Van Vleck paramagnetism and bonding parameters in semiconductors. 02 p0201 A73-11900

Magnetic susceptibility of amorphous semiconductors. 06 p0733 A73-17746

High resolution automatic magnetometer using a superconducting magnet Application to high field susceptibility measurements. 07 p0823 A73-19365 [IEEE PAPER 48,2]

Temperature-dependent magnetic properties of individual glass spherules, Apollo 11, 12, and 14 lunar samples. 07 p0893 A73-19844

Certain physical properties of Nd-Sb system alloys and their correlation with the phase diagram 09 p1134 A73-22679

Magnetic permeability dependence on temperature and composition of hexaferrites with various Sc ion contents 09 p1134 A73-22982

Electromagnetic field of rotating charged oblate ellipsoid of revolution with infinite conductivity and vacuum or infinite magnetic susceptibility 10 p1252 A73-24344

Some physical properties of stephanite in the phase transition region 13 p1667 A73-28002

Performance and possibilities of application of an electromagnetic comparator 15 p1883 A73-32056

Highly permeable nickel-iron-molybdenum alloys containing 33 to 37% nickel 16 p2026 A73-33958

Oscillations of the magnetic susceptibility in n-type semiconductors with a chalcopyrite lattice 16 p2044 A73-34008

Susceptibility measurements at high frequency - A versatile and sensitive apparatus. 17 p2176 A73-35771

Influence of plastic strain on the paramagnetic susceptibility of molybdenum single crystals 18 p2324 A73-36802

Ti-V alloys elastic modulus and paramagnetic susceptibility, considering composition vs property curve salient point indications of changes in interatomic bonding energy and electron structure 21 p2718 A73-40487

Thermometric applications of ferrite permeability dependence on temperature, describing thermometer for magnetically levitated substrate 21 p2702 A73-41108

Magnetic susceptibility of a degenerate electron gas - Interaction of nuclear magnetic moments in normal metals and superconductors 23 p3016 A73-43709

MAGNETIC POLES

Thermal conductivity and hot magnetic poles of pulsars. 03 p0374 A73-13796

Vertical distribution of electron concentration in the Northern Hemisphere at the geomagnetic pole /from top-side and ground-based ionospheric sounding data/ 06 p0689 A73-17554

Mathematical models of the earth's magnetic field. 07 p0818 A73-20030

Vertical electron density distribution at the geomagnetic pole in the Northern Hemisphere /from data of topside and ground-based soundings of the ionosphere/. 16 p2002 A73-32778

Quark search positive results, discussing mathematical models, magnetic monopole searches and existence debate 16 p2054 A73-33289

Magnetic multipole containment of large uniform collisionless quiescent plasmas. 17 p2215 A73-34271

Influence of the polarity of the interplanetary magnetic field on magnetic activity at high latitudes. 21 p2773 A73-41378

MAGNETIC PROBES

Selective differential broadband precision amplifier for weak signals of galvanomagnetic sensor of magnetic induction indicator based on Hall effect 01 p0022 A73-10083

Crossed-coil nuclear magnetic resonance probe for high sensitivity low temperature measurements. 02 p0168 A73-11962

Investigation of the conversion characteristic of a ferromagnetic rod probe subjected to the simultaneous influence of longitudinal and transverse magnetic fields 13 p1617 A73-28867

Some diagnostic methods for dense plasmas from high-pressure pulse discharges 23 p3011 A73-43667

MAGNETIC PROPERTIES

NT ANTIFERROMAGNETISM

NT CURIE TEMPERATURE

NT DIAMAGNETISM

NT FERRIMAGNETISM

NT FERROMAGNETISM

NT GEOMAGNETISM

NT GYROFREQUENCY

NT GYROMAGNETISM

NT MAGNETIC EFFECTS

NT MAGNETIC INDUCTION

NT MAGNETIC MOMENTS

NT MAGNETIC PERMEABILITY

NT MAGNETIC RIGIDITY

NT MAGNETIC SUSPENSION

NT MAGNETOACOUSTICS

NT MAGNETOACTIVITY

NT MAGNETORESISTIVITY

NT MAGNETOSTRICTION

NT PALEOMAGNETISM

NT PARAMAGNETISM

NT POLARIZATION CHARACTERISTICS

NT RELUCTANCE

NT REMANENCE

NT SPIN-LATTICE RELAXATION

NT THERMOMAGNETIC EFFECTS

Experimental investigation of the magnetic properties and magnetization conditions of magnetically solid materials at elevated temperatures 01 p0044 A73-10084

Luna 16 powdery regolith specimens magnetic properties, giving specific susceptibility, remanent magnetization and structure related recession 02 p0213 A73-12236

Comparative analysis of the magnetic properties of lunar rocks and meteorites 02 p0220 A73-12464

Direct observation of the magnetic microstructure in niobium-based superconducting alloys subject to deformation 02 p0201 A73-12554

Superconductivity theory and applications, considering cryogenic problems low-loss and magnetic properties and Josephson junction effect on low power technology 04 p0484 A73-15958

The magnetic properties and morphology of metallic iron produced by subsolidus reduction of synthetic Apollo 11 composition glasses. 05 p0619 A73-16837

Inner planets of the solar system - A comparative study. 06 p0749 A73-18007

INTERMAG Conference, 10th, Kyoto, Japan, April 10-13, 1972, Proceedings. 07 p0861 A73-19360

Magnetic properties of Apollo 14 breccias and their correlation with metamorphism. 07 p0893 A73-19839

Apollo 14 and 15 igneous rock, fines and breccia intrinsic and structure-sensitive magnetic parameters 07 p0893 A73-19842

Lunar surface rock remanent magnetization, considering breccia, igneous samples, thermal demagnetization and Apollo landing sites 07 p0893 A73-19843

Prediction of the low-temperature stability of type 304 stainless steel from a room temperature deformation test. 07 p0840 A73-20414

Influence of nickel on the superconductivity parameters of Nb₃Al + Ni 09 p1098 A73-21845

Uniaxial magnetic anisotropy of single-crystal permalloy films 09 p1132 A73-21958

Calculation of the magnetic properties of a hydrogen molecule with the aid of the method of varying the vector potential and the method of varying the induced current 09 p1122 A73-22017

MOSFET devices with trapezoidal gates - I-V characteristics and magnetic sensitivity. 10 p1194 A73-24157

Direct observation of magnetic microstructure in deformed niobium-based superconducting alloys. 10 p1259 A73-24186

Solar surges magnetic properties analysis from high resolution H alpha filtergrams, matching surge trajectories by computed magnetic lines of force 11 p1422 A73-25941

Mechanical energy storage by flywheel with magnetic fluid hermetic seal and bearing, using anisotropic and whisker materials 11 p1399 A73-25979

Magnetic reversal mechanisms of obliquely deposited permalloy films possessing perpendicular anisotropy 12 p1530 A73-26833

The magnetic characteristics of the alloys of palladium with gadolinium, dysprosium, and holmium 13 p1667 A73-28183

Comparison of the magnetic properties of glass from Luna 20 with similar properties of glass from the Apollo missions. 13 p1677 A73-28332

Austenitic stainless steels at cryogenic temperatures. I - Structural stability and magnetic properties. 13 p1636 A73-29070

Influence of niobium on the magnetic properties of high-titanium Al-Ni-Co alloys - Second communication. 13 p1637 A73-29244

Comparative analysis of the magnetic properties of lunar rocks and meteorites. 15 p1942 A73-32614

High pressure-sintering preparation of barium ferrites, discussing temperature and compression effects on density and magnetic properties 16 p2044 A73-32947

Apollo 17 lunar soil magnetic characteristics, covering ilmenite basalts mineralogy and petrology, electrical properties, orange and green glasses origin, and trace elements 16 p2061 A73-33171

Solar convective motions and associated magnetic fields, discussing photospheric cellular and chromo-

MAGNETIC PUMPING

- spheric vertical motions, fibril structures, sunspot magnetic properties and faculae
16 p2061 A73-33283
- Electromagnetic induction microsystems with synchronization. III - Distribution of magnetic characteristics in complex linear and nonlinear regions. IV - Modeling of nonstationary electromechanical processes
16 p1992 A73-33668
- Annual National Relay Conference, 21st, Oklahoma State University, Stillwater, Okla., May 1, 2, 1973, Proceedings.
17 p2132 A73-34088
- Russian book - Magnetic properties of meteorites: Meteorites in the laboratory.
18 p2348 A73-35871
- Phase characteristics of a rectangular waveguide with symmetrically arranged, transversely magnetized ferrite layers
19 p2407 A73-38342
- Magnetic properties of layered superconductors with a weak layer interaction
21 p2751 A73-40371
- Solar flare forecasting method developed and applied at Crimean observatory, using magnetic instability model for active regions
21 p2762 A73-41391
- MAGNETIC PUMPING**
Neoclassical theory of Landau damping and ion and electron transit-time magnetic pumping (TTPM) in toroidal geometry.
01 p0083 A73-10459
- Inward diffusion of Tokamak-trapped particles by slow magnetic pumping.
01 p0083 A73-10461
- Magnetic pumping of electrons in ohmic dissipation mechanism responsible for neoclassical plasma diffusion rate increase in banana regime
01 p0084 A73-10467
- German monograph on parametric amplification in inverted material covering nonlinear interaction between electromagnetic field and paramagnetic material, dielectric resonator and pumping field strength
03 p0282 A73-13816
- Magnetic duct field and induction distributions for liquid metal pump design, using Tozoni integral equations
10 p1177 A73-23475
- Ejection of supernova shells by magnetic pumping
10 p1273 A73-23701
- Nonthermal radiation from a magnetosheath plasma in the field of a microwave pumping wave.
11 p1405 A73-26182
- Parallel spin-wave pumping in yttrium garnet single crystals.
11 p1409 A73-26188
- Ejection of supernova envelopes by magnetic pumping.
18 p2354 A73-36726
- Direct conversion of thermonuclear plasma energy by high magnetic compression and expansion.
21 p2750 A73-41676

MAGNETIC RECORDING

- A quick and inexpensive method of monitoring on tape the heart rate during exposure of the human head to pulsed magnetic fields.
03 p0270 A73-14289
- High-data-rate, spacecraft tape recorders.
04 p0449 A73-15383
- A brief summary of the meteorological research flight digital magnetic-tape data-recording and data-processing system.
04 p0450 A73-15700
- Reliable, high performance magnetic tape recorder/reproducer for third generation telemetry data computer processing lines, noting human error possibility reduction
07 p0795 A73-18955
- Mechanical and electrical performance of satellite-borne magnetic tape recording system for computer data storage in radio telemetry
07 p0820 A73-18960
- INTERMAG Conference, 10th, Kyoto, Japan, April 10-13, 1972, Proceedings.
07 p0861 A73-19360
- Influence of fluctuations in the tape speed on the accuracy of magnetic recording of measurement signals by the wideband frequency modulation method
07 p0828 A73-20549
- Two dimensional photon counting - A design based on the Aerospace-NASA videomagnetograph.
08 p0972 A73-21756
- Ultrawideband longitudinal magnetic tape recording of 120 MHz biased LF/HF signal frequencies, describing high velocity tape transport and recording heads design
09 p1087 A73-23366
- Effects of tape flutter on notch noise loading test performance of predetection recording of a frequency modulated carrier.
09 p1087 A73-23367

Record/reproduce process induced phase distortion in magnetic tape recorders as function of record head gap length
09 p1087 A73-23368

Magnetic tape recorder parameters effect on PCM telemetry bit error rate, discussing contribution factors and test methods
09 p1087 A73-23370

Portable electro-phonocardiograph using magnetic tape recorder equipped with patient's voice print.
11 p1323 A73-25475

Sunspot observations by means of a vidicon camera.
12 p1545 A73-27833

PCM mobile ground station design covering telemetry receivers, digital data magnetic recording and computer interface circuitry and software
14 p1742 A73-30112

A spectrometric setup for magnetic-tape recording of spectra
15 p1878 A73-32140

Evaluation of phase distortions in the magnetic recording of signals with a high-frequency magnetic bias
20 p2531 A73-39468

Long baseline interferometry with high angular resolution widely separated radio telescopes and video signal magnetic recording tapes, discussing coherence and timing requirements and calibration
23 p2980 A73-43349

MAGNETIC RELAXATION

NT SPIN-LATTICE RELAXATION

MAGNETIC RESONANCE

NT ELECTRON

RESONANCE

NT FERROMAGNETIC RESONANCE

NT NUCLEAR MAGNETIC RESONANCE

NT PARAMAGNETIC RESONANCE

NT PROTON MAGNETIC RESONANCE

NT PROTON RESONANCE

Earth surface magnetic field intensity variations in terms of magnetospheric resonator excitation, assuming three dimensional Alfvén waves
10 p1212 A73-24230

Some results of an analysis of stable geomagnetic Pc4 pulsations at a network of stations.
13 p1608 A73-28719

French monograph - Experimental study of conditions of resonance of tubes of forces of the terrestrial magnetic field.
15 p1874 A73-32594

High-resolution magnetic hyperfine resonance in harmonically bound ground-state Hg-199 ions.
16 p2038 A73-32850

Influence of magnetic spin resonance in optically transparent magnetic materials on the nature of laser radiation
16 p2024 A73-34001

Properties of microwave cavities containing magnetic resonant samples.
17 p2130 A73-35758

Instabilities of drift magnetosonic waves due to the magnetic drift resonance.
22 p2894 A73-42395

Magnetic resonance spectrometer measurements of atomic hydrogen surface recombination.
24 p3113 A73-45425

MAGNETIC RIGIDITY

Rigidity spectrum of helium nuclei above 17 GV and a search for high energy anti-nuclei in primary cosmic rays.
04 p0493 A73-15980

Analysis of the variations of cosmic rays of magnetospheric and interplanetary origins according to spectrographic data
10 p1267 A73-23928

A measurement of cosmic-ray rigidity spectra above 5 GV/c of elements from hydrogen to iron.
11 p1414 A73-26612

Measurement of geomagnetic cutoff rigidities and particle fluxes below geomagnetic cutoff near Palestine, Texas.
12 p1533 A73-26978

Book on cosmic ray effective cut-off rigidities calculations in dipole and geomagnetic fields, using trajectory calculations of penumbra function
21 p2760 A73-40805

MAGNETIC SHIELDING

F-19 chemical shift tensor in group II difluorides.
05 p0546 A73-16046

MAGNETIC SIGNALS

Feasibility of ground-based generation of artificial micropulsations.
04 p0444 A73-15537

MAGNETIC SIGNATURES

Automatic technique for extending magnetograms and for determining variometer sensitivity
05 p0573 A73-16267

Sunspots moving magnetic features analysis from longitudinal magnetograms time series and H alpha filtergrams
11 p1422 A73-25938

Magnetic field signatures of substorms on high-latitude field lines in the nighttime magnetosphere.
12 p1488 A73-26981

Current flow in auroral loops and surges inferred from ground-based magnetic observations.
22 p2902 A73-41917

MAGNETIC SPECTROSCOPY

Line existence in H component magnetic power spectra of geomagnetic field LF components
04 p0445 A73-15532

C-13 nuclear magnetic resonance in organic geochemistry.
11 p1325 A73-25461

Field spinning Zeeman modulation in microwave spectroscopy with cosine distribution magnets.
11 p1366 A73-26302

The magnetic ion-mass spectrometer on Atmosphere Explorer.
13 p1688 A73-28633

Superconducting magnetic spectrometer technique application to charged primary cosmic rays, discussing calibration, experiments and electron-positron and isotopic separation
16 p2014 A73-33277

A magnetic spectrometer for recording particles in a range up to 4 GeV/c
17 p2164 A73-34151

Study of surface by spectrometry of slow electrons
21 p2706 A73-41598

Large wire spark chambers with an information output and storage system
23 p2982 A73-43570

Magnetic resonance spectrometer measurements of atomic hydrogen surface recombination.
24 p3113 A73-45425

MAGNETIC STARS

Periodic components of the density variations of the radio source VRO 42.22.01 /BL Lacertae/
01 p0101 A73-10933

The effect of the Coriolis force on the stability of rotating magnetic stars.
01 p0103 A73-11034

Theory for the stability of a star with a toroidal magnetic field.
01 p0106 A73-11312

He 4, C 12, O 16, Ne 20, Mg 24, Si 28 and Fe 56 abundance computed as function of time for neutron star atmospheres with strong magnetic fields
02 p0223 A73-12728

Polarimeter search for optical circular polarization in eclipsing binaries, magnetic Ap stars, planetary nebulae, Hubble and Orion nebulae, M87 and Sirius
03 p0366 A73-12939

Physical significance of interstellar matter accretion on rotating magnetized star with emphasis on implications for X ray sources
04 p0493 A73-15979

Pulsars as rotating magnetic neutron stars created during catastrophic collapses of old stars, discussing radiation mechanism
06 p0750 A73-18012

HD 215441 and 53 Camelopardalis - Intrinsic polarization of H-beta and the continuum.
07 p0874 A73-19075

Photometric investigations of magnetic stars.
08 p1006 A73-20925

Ultraviolet photometry from the Orbiting Astronomical Observatory. VII alpha squared Canum Venaticorum.
08 p1008 A73-21158

Neutron-star accretion in a stellar wind - Model for a pulsed X-ray source.
08 p0997 A73-21160

Electromagnetic field configuration about aligned rotating magnetic star from relativistic model of rotating magnetosphere
09 p1142 A73-22034

Periodic components in the flux-density variation of the radio source VRO 42.22.01 /BL Lacertae/
09 p1147 A73-22728

Some limits on cosmic-ray heating of H I clouds by magnetic stars.
10 p1263 A73-23487

Spectrophotometric investigation of the star alpha-2 CVn. II
11 p1416 A73-25232

Criticism of Galactic cosmic ray production model with rotating magnetic white dwarfs, noting contrary evidence in magnetic field observations and decay theories
12 p1539 A73-27149

The role of the Coriolis force on the stability of rotating magnetic stars and the origin of convective motions.
12 p1547 A73-27883

About the influence of a magnetic field on the model atmosphere of a magnetic star.
13 p1687 A73-29657

Magnetic stars formation from interstellar matter in presence of interstellar magnetic field, considering critical mass based on Chandrasekhar-Fermi virial theorem
14 p1799 A73-30426

Landstreet null line list revision and null lines tabulation to identify spectra of magnetic Ap star atmospheres
14 p1801 A73-30647

Primordial cosmic ray abundance from rotating magnetic A stars with accelerating ionized interstellar gas particles

15 p1925 A73-31059

The beaming of radiation from an accreting magnetic neutron star and the X-ray pulsars.

17 p2225 A73-35618

Studies of beta Coronae Borealis. I - Identification of the Actinides.

18 p2357 A73-37105

Pulsar model magnetosphere for uniformly rotating infinitely conducting magnetized neutron star with aligned magnetic field

19 p2488 A73-38515

Magnetic stars origin from gravitational collapse of ionized hydrogen clouds, discussing implications of interstellar magnetic fields and critical mass according to Chandrasekhar-Fermi virial theorem

20 p2605 A73-39058

A model for compact X-ray sources - Accretion by rotating magnetic stars.

20 p2602 A73-39443

Spectral variabilities of magnetic peculiar A stars associated with atmospheric chemical composition anomalies, using inclined rotator model

22 p2908 A73-42345

MAGNETIC STORAGE

NT CORE STORAGE

NT MAGNETIC DISKS

Modeling of a bubble-memory organization with self-checking translators to achieve high reliability.

10 p1192 A73-24872

Noise and stable operation conditions in associative memory devices

23 p2956 A73-43580

MAGNETIC STORMS

Response of the ionosphere to the spectrum of acoustic-ionic waves emitted by a localized impulse source in space - Application to suddenly arising geomagnetic storms

01 p0035 A73-10327

Some peculiarities of the development of the magnetic storm on March, 5-10, 1970.

01 p0036 A73-10342

Geomagnetic activity effects on D layer absorption from vertical soundings during solar flare induced sudden magnetic storms

01 p0039 A73-10415

Satellite observations of energetic heavy ions during a geomagnetic storm.

02 p0204 A73-11733

Isis 1 observations of the high-latitude ionosphere during a geomagnetic storm.

[AD-759885]

02 p0155 A73-11735

Inner magnetosphere distortions during magnetic storm development phase from Explorer 26 observations, comparing with Williams-Mead, ring current and compression models

02 p0156 A73-11747

Diurnal latitudinal composition variations in light ion trough fromOGO mass spectrometric observations, noting magnetic storm effects

02 p0157 A73-11904

Spectral analysis of geomagnetic variations to study the tidal and the storm modulation effects.

02 p0158 A73-11906

Spectrographic observation of quasi-periodic pc 1 micropulsation emission after geomagnetic storm associated with geotail plasma bunching in night time magnetosphere

02 p0158 A73-11918

Radiation belt low energy protons intensity and spectrum variations during geomagnetic storms from Molniya 1 satellite measurements, interpreting results in terms of electric field effects

02 p0206 A73-12318

Ionospheric VLF and ELF electric field observation by Alouette 2 satellite, obtaining ion mass distribution from lower hybrid resonance hiss during geomagnetic storm

02 p0164 A73-12623

Ionospheric electron density vertical distribution time dependence for ionospheric storms morphology, noting relationship to geomagnetic storms

03 p0300 A73-13650

Physical mechanisms of magnetospheric processes, discussing matter and energy exchange between solar wind and magnetosphere, substorms, interaction with ionosphere, etc

03 p0302 A73-13853

The pre-midnight asymmetry in the 40 keV electron flux profiles and its relation to magnetospheric substorms.

03 p0363 A73-13866

A theory on the latitude and local time distribution of precipitating electrons during a sudden commencement.

03 p0304 A73-13885

Solar activity effects on geomagnetic variations from spacecraft particle measurements, showing statistical correlations between solar wind, flares and magnetic storms

04 p0491 A73-14838

Solar flare effects in ionosphere, discussing long term variability, sudden ionospheric disturbances, PCA and magnetic storms

04 p0491 A73-14839

Magnetosphere configuration models based on open and closed field line hypotheses, discussing solar wind-magnetosphere interactions, magnetotail, sub-storm growth, flux transport, etc

04 p0441 A73-15327

Magnetotail plasma leakage into magnetosheath during magnetospheric substorms from Vela satellites proton flux measurements

04 p0443 A73-15530

Relation of Pc 1 micropulsations to the ring current and geomagnetic storms.

04 p0444 A73-15536

Geomagnetic storm effects in the nighttime E layer during increasing and maximal solar activities

05 p0568 A73-16215

A satellite study of the mid-latitude trough in electron density and VLF radio emissions during the magnetic storm of 25-27 May 1967.

05 p0571 A73-17060

The ionospheric effects of geomagnetic sudden commencements as measured with an HF Doppler sounder at Hawaii.

05 p0571 A73-17062

Speed of propagation of shock waves responsible for geomagnetic storms and Forbush decreases

06 p0689 A73-17548

Substorm variations of the magnetotail plasma sheet at geocentric distances measured along the solar magnetospheric x-axis from -6 to -60 earth radii.

07 p0813 A73-19235

Global electron concentration disturbances in low and middle latitude F 2 during magnetic storm

07 p0815 A73-19435

Auroral electron spectrum space-time dynamics during magnetospheric substorms, using X ray bremsstrahlung balloon data

07 p0815 A73-19437

Ionospheric anomalies in the night mesosphere after geomagnetic storms.

07 p0817 A73-19543

Coupling between the F-region and protonosphere - Numerical solution of the time-dependent equations.

07 p0818 A73-19665

Magnetic storm of March 8-10, 1970 from Cosmos-321 and ground observations. I - Morphology of the disturbance

08 p0959 A73-21290

Modulation of auroral electron fluxes and the geomagnetic pulsations during the storm of March 8, 1970

08 p0959 A73-21291

Some statistical characteristics of the spectra of polar magnetic substorms

08 p0959 A73-21293

Characteristics of cosmic ray variations near the solar equator plane

08 p0998 A73-21299

Rapid injection of energetic particles into the gap between the inner and outer radiation belts

08 p0998 A73-21300

Geomagnetic storms and wintertime 300-mb trough development in the North Pacific-North America area.

08 p0961 A73-21384

Relationship of magnetospheric substorms on the ground and in the distant magnetotail.

08 p0961 A73-21392

Short-term nonperiodic variations in the intensity of the neutron component of cosmic rays during a period of transition from a quiet to an active sun

09 p1137 A73-22019

Cross-correlation analysis of the AE index and the interplanetary magnetic field Bz component.

09 p1142 A73-22055

Whistler observations of the depletion of the plasmasphere during a magnetospheric substorm.

09 p1074 A73-22060

Evening/forenoon asymmetry in the 27-day oscillation of the low-latitude magnetic field.

09 p1076 A73-22140

Chromospheric flares and shock waves in interplanetary space

09 p1137 A73-22540

Es-q layer at Huanacayo during the March 1970 geomagnetic storm.

09 p1078 A73-22836

Cosmic-ray anisotropy during the disturbed period from Oct. 25 to Nov. 10, 1968

10 p1267 A73-23919

Low energy solar proton events intensity increase near time of magnetic storm sudden commencement and Forbush decrease, using propagation shock wave model

10 p1268 A73-24146

North-south asymmetry in the increase of cosmic-ray intensity before magnetic storms.

10 p1268 A73-24212

Ionospheric magnetic disturbances during March 1970 related to solar flare corpuscular and proton fluxes, generating ring current and PCA absorption

10 p1211 A73-24218

Latitudinal energy distribution of geomagnetic disturbances.

10 p1212 A73-24229

Satellite measurement of variable intensities for geomagnetically trapped protons during magnetic storms, noting ring current source of low-altitude protons

10 p1213 A73-24731

Relationship of southward-drifting auroral arcs to the magnetospheric electric field and substorm activity.

10 p1213 A73-24734

Solar wind flow vector from detection of unshocked wind by plasma detector aboard ATS-5 during 8 March 1970 geomagnetic storm

10 p1270 A73-24741

Magnetospheric substorms correlation with interplanetary magnetic field, discussing balloon and satellite electric field measurements

10 p1215 A73-24784

Latitudinal and longitudinal auroral radio wave absorption in Arctic during IQSY, noting comparison with geomagnetic field disturbances

11 p1350 A73-25086

Results of an investigation of the ionospheric effect of a sudden commencement of a magnetic storm

11 p1351 A73-25097

The causes of storm-time increases of the F-layer at mid-latitudes.

11 p1353 A73-25751

A study of the relationship between geomagnetic storms and ionospheric disturbances at mid-latitudes.

11 p1356 A73-25912

The day-sector polar F-layer during a magnetospheric substorm.

11 p1356 A73-25918

Observations on the time and frequency structure of solar decameter radio bursts.

11 p1413 A73-25951

Inertial magnetic field reconnection and magnetospheric substorms.

11 p1357 A73-26206

Energetic electron precipitation as a source of ionization in the night-time D-region over the mid-latitude rocket range, South Uist.

11 p1358 A73-26701

The nature of seasonal changes in the effects of magnetic storms on mid-latitude F-layer electron concentration.

11 p1358 A73-26708

Enhancements of ionospheric total electron content in the southern auroral zone associated with magnetospheric substorms.

11 p1359 A73-26715

Magnetic field signatures of substorms on high-latitude field lines in the nighttime magnetosphere.

12 p1488 A73-26981

Midlatitude bremsstrahlung X rays, VLF propagation disturbances and electron precipitation during magnetospheric substorm

12 p1468 A73-26983

A study of ionospheric absorption in conjugate regions produced by storm sudden commencements and sudden impulses in the geomagnetic field.

12 p1489 A73-26994

On the relationship between the growth and expansion phases of substorms and magnetospheric convection.

12 p1489 A73-27005

Observations of narrow microburst trains in the geomagnetic storm of August 4-6, 1972.

12 p1490 A73-27007

Solar radiation effects on terrestrial electromagnetic environment, considering interplanetary space, earth internal structure, geomagnetism, upper atmosphere, dynamo action, energetic particles and magnetospheric storms

12 p1538 A73-27053

The growth and decay of the main phase of the September 21-23, 1963 magnetic storm.

12 p1490 A73-27275

Dayside polar aurorae during various substorm phases from IGY data, noting time of glow intensity maximum

12 p1490 A73-27343

Relationship between geomagnetic pulsations of diminishing period and the motion of plasma discontinuities in the magnetosphere

12 p1491 A73-27350

Stable auroral red arc equatorial edge observation with photometer during recovery phase of magnetic storm on 18 December 1971 in Southern Africa

12 p1492 A73-27611

Midday aurora behavior during auroral substorms from all sky photographs at south pole, considering modification of Starkov-Feldstein model

12 p1493 A73-27614

Perpendicular and parallel electric fields in the ionosphere during a magnetospheric substorm

12 p1494 A73-27776

Geomagnetic storm families, direction of the interplanetary magnetic field, and solar activity.

13 p1608 A73-28718

Long term observations of geomagnetic pulsations activity during various phases of magnetic storm at midlatitudes, noting regular and irregular morphological features

13 p1611 A73-29660

Direct measurements of ion drift velocity in the upper ionosphere during a magnetic storm. I - Methodological aspects and some results of measurements in magnetically quiet periods. II - Results of measurements during the magnetic storm of November 3, 1967

14 p1746 A73-29863

Field-aligned currents, plasma waves, and anomalous resistivity in the disturbed polar cusp.

14 p1747 A73-29964

Auroral electrons of energy less than 1 keV observed at rocket altitudes.

14 p1748 A73-29969

Energy and diffusive mass transport relation to thermospheric circulation, composition, temperature and mass density from three dimensional two constituent magnetic storm model

14 p1748 A73-29975

Polar ionospheric electron density distribution near closed field line boundaries for ISIS 1 dayside passes, discussing geomagnetic storm effects

14 p1748 A73-29980

Discontinuous change in earth's spin rate following great solar storm of August 1972.

14 p1800 A73-30602

Isis-2 observations of auroral emissions characteristics in polar region during December 1971 magnetic storm recovery phase

15 p1866 A73-31076

Hydroxyl emission intensity and rotational and vibrational temperatures, discussing statistical properties of geomagnetic storm effects and diurnal, seasonal and latitudinal variations

15 p1867 A73-31260

Distance to the subsolar point of the magnetosphere boundary for various magnetic activity indices

15 p1932 A73-31266

Recurrent magnetic storms in relation to the structure of solar and interplanetary magnetic fields.

15 p1868 A73-31384

On the origin of SC-storms with respect to forecasting geomagnetic activity.

15 p1868 A73-31520

Geomagnetically calm intervals and their forecasts.

15 p1868 A73-31521

Determination of a probable interval for the mean transit time of geomagnetic-storm /SSC/ solar particles

15 p1926 A73-31647

Equatorial scintillation variation with magnetic storm from ATS 3 VHF telemetry signal recordings, comparing with spread F observation

15 p1870 A73-31763

Equatorial sporadic E layer during geomagnetic storms.

15 p1871 A73-31836

The low-latitude and equatorial outer ionosphere during the magnetic storm of January 2-4, 1964

15 p1871 A73-31881

The effect of polar magnetic sub-storms on the equatorial sporadic E.

15 p1874 A73-32596

Propagation velocity of shock waves causing geomagnetic storms and Forbush decreases.

16 p2002 A73-32772

Study of high energy electrons at upper layers of atmosphere during magnetic perturbations.

16 p2054 A73-33282

Electron precipitation patterns and substorm morphology.

16 p2056 A73-33434

Ion cyclotron waves observed in the polar cusp.

16 p2003 A73-33437

Red auroras in the morning sector.

16 p2004 A73-33446

Satellite studies of magnetospheric substorms on August 15, 1968. I - State of the magnetosphere.

16 p2004 A73-33449

Satellite studies of magnetospheric substorms on August 15, 1968. II - Solar wind and outer magnetosphere.

16 p2004 A73-33450

Satellite studies of magnetospheric substorms on August 15, 1968. III - Some features of magnetospheric convection.

16 p2004 A73-33451

Satellite studies of magnetospheric substorms on August 15, 1968. IV - Ogo 5 magnetic field observations.

16 p2004 A73-33452

Satellite studies of magnetospheric substorms on August 15, 1968. V - Energetic electrons, spatial boundaries, and wave-particle interactions at Ogo 5.

16 p2056 A73-33453

Satellite studies of magnetospheric substorms on August 15, 1968. VI - Ogo 5 energetic electron observations - Pitch angle distributions in the nighttime magnetosphere.

16 p2056 A73-33454

Satellite studies of magnetospheric substorms on August 15, 1968. VII - Ogo 5 energetic proton observations - Spatial boundaries.

16 p2056 A73-33455

Satellite studies of magnetospheric substorms on August 15, 1968. VIII - Ogo 5 plasma wave observations.

16 p2004 A73-33456

Satellite studies of magnetospheric substorms on August 15, 1968. IX - Phenomenological model for substorms.

16 p2004 A73-33457

Observation of an unusual multiple mid-latitude 6300-A OI arc from two ground stations.

16 p2009 A73-33895

The behaviour of the topside ionosphere during magnetically disturbed conditions.

16 p2010 A73-33912

Pi 2 and geomagnetic bay maximum occurrence dependence on geomagnetic time, discussing computation methods for geomagnetic time

16 p2010 A73-33922

A search for periodic variations in geomagnetic activity and their solar cycle dependence.

17 p2157 A73-34073

The ionospheric electric field during substorms - An interpretation based on non-uniform reconnection in the geomagnetic tail.

17 p2159 A73-34512

Decay of the magnetic storm ring current by the charge-exchange mechanism.

17 p2159 A73-34782

Particle entry into the equatorial magnetosphere.

18 p2344 A73-35928

Ground and synchronous orbit magnetic observations of magnetospheric and ionospheric wave propagation to model substorm current system variations

18 p2303 A73-35945

Intensity variations of low-energy protons and electrons in the outer magnetosphere at the sudden onset of a magnetic storm

18 p2309 A73-36109

X-ray bremsstrahlung at subauroral latitudes

18 p2345 A73-36111

Atomic hydrogen and water vapour in the lower arctic thermosphere during geomagnetic storm and PCA event.

18 p2310 A73-36141

Neutral wind velocities calculated from temperature measurements during a magnetic storm and the observed ionospheric effects.

18 p2311 A73-36150

Synoptic survey for the neutral line in the magnetotail during the substorm expansion phase.

18 p2352 A73-36275

Interaction between high-frequency turbulence and magnetospheric micropulsations.

18 p2352 A73-36277

Distortions of the nightside ionosphere during magnetospheric substorms.

18 p2312 A73-36279

Occurrence of IPDP events accompanied by cosmic noise absorption in the course of proton aurora substorms.

18 p2312 A73-36298

Semiannual effect in thermosphere due to solar heat input associated with subsolar point migration and auroral heating by magnetic storms

18 p2312 A73-36300

Oscillations of the earth's magnetic tail

19 p2482 A73-37349

Model experiment on solar flares and the neutral sheet. III.

19 p2475 A73-37383

Interplanetary shock waves and cosmic rays.

19 p2476 A73-37759

Magnetic storm of March 8-10, 1970, according to ground-based and Kosmos-321 observations.

19 p2424 A73-37919

Modulation of auroral electron fluxes and geomagnetic pulsations during the storm of March 8, 1970.

19 p2424 A73-37920

Some statistical characteristics of the spectra of polar magnetic substorms.

19 p2425 A73-37922

Characteristics of cosmic-ray variations near the solar equatorial plane.

19 p2476 A73-37928

Fast injection of energetic particles into the gap between the inner and outer radiation belts.

19 p2476 A73-37929

The effect of geomagnetic disturbance on the duct propagation of low-latitude whistlers.

19 p2426 A73-38020

Radio auroral measurements near an auroral electrojet.

20 p2550 A73-38862

Explorer 45 mission objectives discussing magnetospheric ring current, magnetic storm detection, particle energy and interactions, electric and magnetic fields measurements, etc

20 p2614 A73-38949

Magnetic storm inflation analysis from Explorer 45 and ground observation data, noting proton penetration into magnetosphere evening quadrant

20 p2552 A73-38951

Ring current particle distributions during the magnetic storms of December 16-18, 1971.

20 p2552 A73-38952

Energy spectra and pitch angle distributions of storm-time and substorm injected protons.

20 p2552 A73-38953

Plasma wave observations near the plasmapause with the S3-A satellite.

20 p2552 A73-38956

Explorer 45 search coil magnetometer detection of ELF signals during magnetic storms, noting signal variation with storm phases and satellite magnetospheric position

20 p2552 A73-38957

Particle and field observations from Explorer 45 during the December 1971 magnetic storm period.

20 p2552 A73-38958

Relation between coronal 5303-A intensity, recurrent geomagnetic storms, and solar sector structure.

20 p2553 A73-38960

Differences between geomagnetic storms with gradual and sudden commencements

21 p2681 A73-40103

The relation between cosmic ray intensity variations and effects due to the electromagnetic complex

21 p2755 A73-40110

A mechanism for the growth phase of magnetospheric substorms.

21 p2682 A73-40157

The Forbush effect in the nuclear component of primary cosmic rays in August 1972

21 p2757 A73-40588

Heating of the low-latitude upper atmosphere caused by the decaying magnetic storm ring current.

21 p2684 A73-40786

Precipitating protons with E greater than 12.4 keV to 500 keV near the midnight trapping boundary.

21 p2760 A73-40822

Influence of nonadiabatic effects during magnetic storms on the dynamics of proton belts

21 p2760 A73-40907

An analysis of the altitude dependence of the geomagnetic effect by means of 'equivalent durations.'

21 p2689 A73-41353

Tropospheric and stratospheric response to solar influence during geomagnetic disturbances.

21 p2690 A73-41364

Bremsstrahlung X ray measurements over subauroral latitudes during substorms, noting a folding energy correlated with local electrojet and anticorrelated with conjugate electrojet

21 p2760 A73-41366

Effects on the geomagnetic tail at 60 earth radii of the geomagnetic storm of April 9, 1971.

22 p2844 A73-41908

Enhancement of 0.24- to 0.96-MeV trapped protons during the May 25, 1967, magnetic storm.

22 p2901 A73-41909

Periodically structured Pc 1 micropulsations during the recovery phase of intense magnetic storms.

22 p2844 A73-41913

Response of the polar electrojets in the evening sector to polar magnetic substorms.

22 p2902 A73-41916

Geomagnetic disturbance diurnal variation /DS/ component evolution and equatorial electrojet strength changes observation during magnetic storms by globally located stations at various latitudes

22 p2844 A73-41918

Sudden commencement and sudden impulse absorption events at high latitudes.

22 p2845 A73-41928

Azimuthal drift and precipitation of electrons into the South Atlantic geomagnetic anomaly during an SC magnetic storm.

22 p2846 A73-41946

Synoptic survey of geomagnetic field neutral line formation in magnetotail during magnetic substorms noting nightside magnetosphere reconnection and associated plasma sheet behavior

22 p2849 A73-42573

Polar magnetic storm temporal properties and distribution patterns, discussing solar activity, annual and twenty-seven day variations and sudden commencement

22 p2851 A73-42749

Electron precipitation caused auroral zone bremsstrahlung X rays classification with respect to magnetic storm phases

22 p2851 A73-42750

Dayside polar aurorae during various substorm phases from IGY data, noting time of glow intensity maximum

23 p2970 A73-43240

Relationship between geomagnetic PDP pulsations and the motion of plasma inhomogeneities in the magnetosphere.

23 p2970 A73-43247

Particle precipitation in Brazilian geomagnetic anomaly during magnetic storms.

23 p2971 A73-43687

Low latitude whistler activity during geomagnetic storms related to spread F conditions and magnetospheric and ionospheric electron density

23 p2972 A73-43696

On the large scale vertical movements of the F-layer and its effects on the total electron content over low latitude during the magnetic storm of 25 May 1967.

23 p2972 A73-43699

F 2 region critical frequency variations during geomagnetic storms, noting correlation with main phase onset

24 p3082 A73-44728

Drift of radiation-belt particles during substorms

24 p3124 A73-44804

Correlation between the excitation of pi 1 and pc 1 geomagnetic pulsations and magnetospheric substorms

24 p3084 A73-44811

High-latitude proton precipitation and light ion density profiles during the magnetic storm initial phase.

24 p3126 A73-45114

Observation of plasma flow in the neutral sheet at lunar distance during two magnetic bays.

24 p3139 A73-45137

Simultaneous growth of high-latitude positive bay and DR-field in the course of proton aurora substorm.

24 p3127 A73-45215

Enhancement of the equatorial anomaly in the topside ionosphere during magnetic storms.

24 p3088 A73-45216

MAGNETIC SUBSTORMS

U MAGNETIC STORMS

MAGNETIC SURVEYS

Pi 2 type geomagnetic pulsation spectra from simultaneous meridional measurements at equatorial, middle and auroral latitudes, noting secondary amplitude maximum and HF augmentation

01 p0039 A73-10414

German monograph - Short-period transverse variations in the magnetic field data from the Azur research satellite.

01 p0040 A73-10603

Time variation of the geomagnetic main field /on the basis of spherical harmonics analyses of geomagnetic world charts for the period from 1880 to 1960/

04 p0440 A73-15281

Characteristics of spectra of pi2-type geomagnetic pulsations along the meridional profile

06 p0689 A73-17543

Geographic distribution of anomalies of residual geomagnetic field derived from eccentric dipole and observed field comparing with thermal flux fields and geotectonic features

06 p0689 A73-17546

Lower boundary of the occurrence of magnetoactive masses

08 p0959 A73-21296

Earth crust inhomogeneities from high altitude aeromagnetic survey, noting informativeness loss increase with height

08 p0960 A73-21308

Latitudinal rotation direction daytime characteristics of Pc 5 pulsation polarization based on global magnetic observations

10 p1212 A73-24231

Secular geomagnetic field variation of the epoch 1965-1970, according to observatory and satellite observations.

10 p1212 A73-24232

Spherical harmonic analysis of the geomagnetic field during the epoch 1965.0 up to n = 23 from ground data. II - Results

12 p1491 A73-27353

Cosmos 321 geomagnetic measurement data for construction of satellite geomagnetic survey and geomagnetic field models

12 p1491 A73-27359

Earth main magnetic field description by cartography and analytic methods based on dipole or spherical harmonic series representations

13 p1608 A73-28713

Some results of an analysis of stable geomagnetic Pc4 pulsations at a network of stations.

13 p1608 A73-28719

Properties of geomagnetic Pi2 pulsation spectra along a meridional profile.

16 p2001 A73-32767

Geographic distribution of anomalies of residual geomagnetic field derived from eccentric dipole and observed field, comparing with thermal flux fields and geotectonic features

16 p2002 A73-32770

Lower boundary of occurrence of magnetically active masses.

19 p2425 A73-37925

Earth crust inhomogeneities from high altitude aeromagnetic survey, noting information loss increase with height

19 p2425 A73-37937

Spherical harmonic analysis of the geomagnetic field for the 1965 epoch up to n = 23 according to ground-based data. II - Results.

23 p2971 A73-43250

Cosmos 321 geomagnetic measurement data for construction of satellite geomagnetic survey and geomagnetic field models

23 p2971 A73-43259

MAGNETIC SUSCEPTIBILITY

U MAGNETIC PERMEABILITY

MAGNETIC SUSPENSION

Development and application of magnetic bearings.

03 p0313 A73-13924

Maxwell equation for equilibrium force in electromagnetic suspension system of force measuring instrument, noting rigidity dependence on system parameters

05 p0577 A73-16995

Magnetic articulation damping for gravity gradient satellite stabilization, using digital simulation

07 p0904 A73-18937

Note on analysis of cryogenic suspensions for space vehicles.

12 p1524 A73-27633

Flow regimes for a magnetic suspension under a rotating magnetic field.

14 p1774 A73-29924

Theory of cryogenic suspensions for navigational devices

20 p2566 A73-39353

Moments acting on a spherical rotor with magnetically suspended bearings

22 p2860 A73-42360

Deflecting moments in magnetic suspensions of gyroscopic devices

24 p3089 A73-44546

Calculation of the force characteristics of the external spherical suspension of a cryogenic gyroscope

24 p3091 A73-45023

MAGNETIC SWITCHING

Structural complexity and technical realization of formal neurons by means of magnetic current switches

24 p3063 A73-44901

Synthesis of minimized formal neurons by means of magnetic current switches

24 p3063 A73-44902

MAGNETIC TAPE RECORDERS

U MAGNETIC RECORDING

U TAPE RECORDERS

MAGNETIC TAPES

Standard format for reporting electron content data using magnetic tape.

03 p0308 A73-13655

Canadian E.R.T.S. data handling system.

04 p0424 A73-15384

Influence of fluctuations in the tape speed on the accuracy of magnetic recording of measurement signals by the wideband frequency modulation method

07 p0828 A73-20549

Russian book on multichannel magnetic tape recorders in civil aviation ATC for speech communication monitoring and preservation covering design and operation principles

09 p1086 A73-23245

Management of a magnetic tape dubbing and evaluation station.

09 p1087 A73-23408

Magnetic-tape qualification and acceptance testing.

16 p2016 A73-33616

Airborne multimode radar digital data system using high transfer rate magnetic tape recording, discussing 8 track tape storage capacity, coding and logic circuits

19 p2431 A73-38198

MAGNETIC TRANSDUCERS

Thermomagnetic shunt for compensation of instrument errors due to temperature effects on magnetolectric transducers material, calculating magnetic circuit

05 p0577 A73-16988

Characteristics of the OT-series transformer-type transducers of linear displacements

07 p0779 A73-20528

Investigation of the sensitivity of a duct sensor to discontinuities in alternating fields of square-pulse or sinusoidal shape - Detectability of surface defects on nonmagnetic and ferromagnetic specimens. I

08 p0967 A73-21587

Analysis of the magnetic systems of calculating transducers

09 p1064 A73-22941

MAGNETIC TRAPS

U PLASMA CONTROL

MAGNETIC VARIATIONS

NT GEOMAGNETIC MICROPULSATIONS

NT GEOMAGNETIC PULSATIONS

NT NOCTURNAL VARIATIONS

German monograph - Short-period transverse variations in the magnetic field data from the Azur research satellite.

01 p0040 A73-10603

Ion composition and photochemistry of the E-region.

01 p0042 A73-10892

Effects of the secular magnetic variation on the distribution function of inner-zone protons.

02 p0155 A73-11731

Magnetospheric field fluctuations and the penetration of solar protons to low geomagnetic latitude.

03 p0360 A73-12891

Magnetic horizontal component variations on quiet days, suggesting effect of electric field reversal at equatorial electrojet ionospheric region

03 p0299 A73-12949

Inferring the interplanetary magnetic field by observing the polar geomagnetic field.

[AD-755684] 03 p0373 A73-13712

Magnetic field variations at micropulsation frequencies.

03 p0303 A73-13881

Interpretation of magnetic field variations during substorms.

03 p0304 A73-13888

Solar activity and the variations of the geomagnetic K sub p-index. I.

03 p0378 A73-14422

Solar activity effects on geomagnetic variations from spacecraft particle measurements, showing statistical correlations between solar wind, flares and magnetic storms

04 p0491 A73-14838

Time variation of the geomagnetic main field /on the basis of spherical harmonics analyses of geomagnetic world charts for the period from 1880 to 1960/

04 p0440 A73-15281

Magnetospheric plasma instabilities and detectable manifestations in geomagnetic field and particle flux densities variations, considering magnetospheric substorms and auroral breakup

04 p0442 A73-15340

K indices measurements at antipodal earth surface observatories for aa indices, discussing one hundred year series

04 p0444 A73-15547

On the equilibrium configuration of the geomagnetic tail.

05 p0568 A73-16140

ELF signal generation by solar protons observed via tape recording of north-south horizontal geomagnetic field variations in 3-75 Hz resonance range

05 p0571 A73-17064

Book - Geophysics 3, Part 4.

06 p0688 A73-17501

Magnetospheric plasma waves propagation effects on rapid geomagnetic field variations, noting magnetic pulsations and ionospheric propagation

06 p0747 A73-17504

Excitation of natural oscillations in the earth's magnetic tail

06 p0748 A73-17540

Influence of magnetic-field nonuniformity on the fluctuations of the plasma layer in the magnetospheric tail

06 p0690 A73-17559

Seasonal variations in the solar and lunar daily geomagnetic variations.

07 p0813 A73-19024

Geomagnetic activity semiannual and diurnal variations due to interplanetary field southward component interaction with magnetosphere based on model ordered in solar equatorial coordinates

07 p0813 A73-19234

Relationships between the equatorial electrojet and polar magnetic variations.

07 p0818 A73-19662

Geomagnetic variations with the period of a sidereal day.

07 p0818 A73-19672

Lunar and solar geomagnetic tides in declination at Alibag.

07 p0819 A73-20055

Characteristics of hydromagnetic wave propagation in a slowly varying magnetic field /Geometrical optics approximation/

08 p0959 A73-21294

Distribution of electrical conductivity in the earth's mantle from data on the secular variations of the geomagnetic field

08 p0959 A73-21295

Analytical description of the geomagnetic field of past epochs and the determination of the magnetic-wave spectrum in the earth's core

08 p0959 A73-21297

Field-aligned currents between 400 and 3000 km in auroral and polar latitudes.

09 p1078 A73-22834

Possibility of determining the secular variation of geomagnetic field components from the distribution of variations of the absolute value of the total vector.

10 p1212 A73-24234

Spherical analyses of the main geomagnetic field in 1550-1800.

10 p1212 A73-24235

Hourly and daily variations of H values for sunspot minimum, showing uncorrelated night time level departures and range implications for solar flares

11 p1355 A73-25772

A possible current system associated with the Sq variation. 11 p1356 A73-25910

Correspondence of main trough ion temperatures with horizontal drift speed. 12 p1489 A73-27006

Oscillations of the earth's magnetic tail in a quasi-hydrodynamics approximation 12 p1491 A73-27347

Magnetovariational frequency sounding of the earth, using the ratio of magnetic potentials 12 p1491 A73-27352

Day-to-day variability of the quiet-day solar-diurnal variations and the orientation of the interplanetary magnetic field 12 p1540 A73-27358

Liquid core model with precessionally driven magnetoturbulence applied to moon, discussing tidal effects in outer solid and liquid shells 12 p1541 A73-27489

Variations of solar-wind parameters, magnetic activity, and the electron tail of the magnetosphere and of the outer radiation zone. 13 p1608 A73-28714

The Ze field, some of its properties, and geophysical information. 13 p1608 A73-28720

Polar cap magnetic variations and their relationship with the interplanetary magnetic sector structure. 14 p1747 A73-29959

Correspondence of solar field sector direction and polar cap geomagnetic field changes for 1965. 14 p1747 A73-29960

Distance to the subsolar point of the magnetosphere boundary for various magnetic activity indices 15 p1932 A73-31266

Diurnal variations of the vertical component of the magnetic field in high latitude regions as a function of the east-west component of the interplanetary magnetic field 15 p1868 A73-31570

Numerical simulation of equatorial electric fields and magnetic variations based on global ionospheric dynamo and equatorial electrojet models 15 p1869 A73-31753

Equatorial electrojet. I - Development of a model including winds and instabilities. II - Use of the model to study the equatorial ionosphere. 15 p1904 A73-31756

Equatorial Esq disappearance relationship to daily magnetic Sr variation inverted latitudinal profiles during magnetic quiet periods, considering counter electrojet current belt hypothesis 15 p1869 A73-31757

Study of ULF geomagnetic variations in connection with the equatorial electrojet /the Chad-Central African Republic magnetic project/ 15 p1869 A73-31760

POGO satellite observed electrojet signature data comparison with daily geomagnetic variation amplitude measurement at equatorial ground station in India 15 p1870 A73-31769

POGO satellite observation of electrojet profiles compared with H variation around measurements, interpreting data by classical band current model 15 p1871 A73-31773

Geomagnetic variations total field confinement described by Parkinson, discussing primary and secondary fields Maxwell equations linear relationship by induction tensor 15 p1871 A73-31777

Separation of the variable geomagnetic field into normal and anomalous components 15 p1872 A73-31896

Excitation of natural oscillations of the geomagnetic tail. 16 p2058 A73-32764

Effect of magnetic field inhomogeneity on oscillations of the plasma sheet of the magnetospheric tail. 16 p2002 A73-32783

Interplanetary magnetic field and geomagnetic Dst variations. 17 p2158 A73-34507

Equatorial and auroral zone geomagnetic indices and micropulsations variations relation to 11-18keV protons occurrence in interplanetary space 18 p2345 A73-36120

Semi-annual modulation of earth's magnetic field in the equatorial electrojet region. 18 p2311 A73-36187

ULF magnetic fluctuations in the plasma sheet as recorded by the Explorer 34 satellite. 18 p2352 A73-36276

Sector boundary geomagnetic activity average Kp elevation relationship to southward component of interplanetary field, suggesting magnetosphere role 18 p2347 A73-36292

Paleomagnetic excursion recorded in latest Pleistocene deep-sea sediments, Gulf of Mexico. 18 p2313 A73-36513

Ionospheric magnetic field measurements at auroral latitudes. 18 p2313 A73-36647

The sporadic E layer and the variation of the geomagnetic field 18 p2313 A73-36650

Imp-3 satellite measurement-based investigation of variability of interplanetary magnetic field component normal to plane of ecliptic during passage across sector field boundary 19 p2480 A73-37241

Characteristics of hydromagnetic wave propagation in a slowly varying magnetic field /in the approximation of geometric optics/. 19 p2425 A73-37923

Distribution of electric conductivity in the mantle of the earth, according to data on secular geomagnetic field variations. 19 p2425 A73-37924

Analytical description of the geomagnetic field of past epochs and determination of the spectrum of magnetic waves in the core of the earth. 19 p2425 A73-37926

Observations of ionospheric storms at low latitudes and their correlation with magnetic field changes near the magnetic equator. 19 p2425 A73-38011

ULF geomagnetic power near $L = 4$. II - Temporal variation of the radial diffusion coefficient for relativistic electrons. 20 p2551 A73-38936

Particle and field observations from Explorer 45 during the December 1971 magnetic storm period. 20 p2552 A73-38958

Structure of vortical motion systems in the ionosphere that generate Sq variations of the geomagnetic field 20 p2553 A73-39153

Correlation of variations in the horizontal component of the geomagnetic field with drift in the ionosphere 20 p2553 A73-39154

Magnetic fields of the sun and stars 20 p2609 A73-39569

A geomagnetic variation anomaly across the northern Gulf of California. 21 p2678 A73-39927

Anomalies in geomagnetic variations across the central Gulf of California. 21 p2679 A73-39928

Mesospheric temperature response to variations in geomagnetic activity. 21 p2682 A73-40169

Axial symmetry of the magnetosphere and the noon recovery of polar cap absorption 21 p2759 A73-40608

Geomagnetic variation terms neglect in Chapman-Miller method, noting Bartels-Johnston method comparison and possible consequences for lunar tides 21 p2684 A73-40780

Characteristic features of the solar diurnal variation according to data obtained by magnetic observatories in Kazakhstan 21 p2686 A73-40846

Secular geomagnetic variation consequences for steady state inner zone of energetic protons, discussing minimum altitude decrease and mirror point field magnitude increase 21 p2761 A73-41375

Influence of the polarity of the interplanetary magnetic field on magnetic activity at high latitudes. 21 p2773 A73-41378

Magnetic pulsation spectra in a nonisothermal plasma. 22 p2890 A73-41725

Solar cycle control in the 27-day variation of geomagnetic activity. 22 p2846 A73-41945

Oscillations of the earth's magnetic tail in the approximation of quasi-hydrodynamics. 23 p2970 A73-43244

Frequency magnetovariational sounding of the earth, using the ratio of potentials. 23 p2970 A73-43249

Day-to-day variability of quiet-day solar daily variations and the direction of the interplanetary magnetic field. 23 p3027 A73-43258

Short-period interplanetary and polar magnetic field variations. 23 p3029 A73-43691

An analytical expression for the secular variation of the geomagnetic field and a comparison of the activity of secular variations with some astronomical phenomena 23 p2973 A73-43793

Photometric study of a diffuse reinforcement observed in the zodiacal light at a distance of 100 solar radii from the sun 24 p3134 A73-44566

Correlation length for interplanetary magnetic field fluctuations. 24 p3139 A73-45125

E and F layers, discussing formation, collision processes and S and L geomagnetic variations 24 p3087 A73-45204

MAGNETICALLY TRAPPED PARTICLES NT INNER RADIATION BELT

NT OUTER RADIATION BELT

NT PROTON BELTS

NT RADIATION BELTS

Trapping of condensed plasma loops and arcs in cosmic atmospheres. 01 p0103 A73-11020

Conversion of trapped charged particles into untrapped particles in a high-frequency electric field. 06 p0732 A73-18608

Drift shell splitting and magnetic equator surface topography model based on charged particle adiabatic motion and trapping in presence of internal geomagnetic multipoles 07 p0813 A73-19236

Method for experimental determination of the magnetic well depth in stellarator-type systems 07 p0855 A73-19285

Low-energy solar protons in the pseudo-trapping region of the magnetosphere. 09 p1137 A73-22053

Relations between ionospheric electric fields and energetic trapped and precipitating electrons. 09 p1073 A73-22056

Some characteristics of the motion and acceleration of particles in a linearly inhomogeneous magnetic field with a neutral plane 09 p1132 A73-23080

Saturn magnetospheric model for bounds on surface field strength and trapped particle population 10 p1283 A73-24724

Satellite measurement of variable intensities for geomagnetically trapped protons during magnetic storms, noting ring current source of low-altitude protons 10 p1213 A73-24731

Numerical studies of charged particle trapping in a time varying magnetic mirror field. 11 p1404 A73-25273

Jovian decametric emission origin in cyclotron instability of weakly relativistic electrons trapped in magnetic field, considering group velocity in magnetospheric plasma 11 p1424 A73-26129

Pulsar magnetospheres, braking index, polar caps, and period-pulse-width distribution. 11 p1428 A73-26618

Experimental determination of magnetic well depth in stellerators. 13 p1665 A73-28685

Existence of geomagnetically trapped electrons at altitudes below the inner radiation belt. 14 p1749 A73-29985

Influence of transverse magnetic field on Landau damping. 17 p2217 A73-35812

Initial observations of geomagnetically trapped alpha particles at the equator. 20 p2552 A73-38950

Evidence for confinement of low-energy cosmic rays ahead of interplanetary shock waves. 21 p2763 A73-41504

Anomalous transport due to the dissipative trapped-ion instability. 21 p2750 A73-41682

Experimental test to determine the origin of geomagnetically trapped radiation. 22 p2846 A73-41944

Investigation of neoclassical diffusion in toroidal systems with a three-dimensional magnetic axis 23 p3014 A73-44337

Magnetically trapped charged particle pitch angle diffusion and lifetime calculation for radiation belts, taking into account geomagnetic dipole geometry 24 p3127 A73-45138

MAGNETITE

The origin and stability of lunar goethite, hematite and magnetite. 05 p0618 A73-16836

Magnetite absolute zero behavior with restriction to three order parameter theory, showing metallic band resultant from interatomic Coulomb energy ratio to bandwidth 06 p0734 A73-17835

Solubilities of noble gases in magnetite - Implications for planetary gases in meteorites. 13 p1684 A73-29182

Orgueil chondrite magnetite age via $^{129}\text{Xe}/^{129}\text{Xe}$ method compared to Karoonda magnetite age 13 p1684 A73-29250

MAGNETIZATION

Experimental investigation of the magnetic properties and magnetization conditions of magnetically solid materials at elevated temperatures 01 p0044 A73-10084

Amorphous magnetism in F.C.C. Vicalloy II. 01 p0087 A73-10242

Magnetization currents effect on linear hydromagnetic instabilities development in collisionless anisotropic plasmas 02 p0196 A73-11899

Leakage field methods of defect detection. 04 p0447 A73-14929

Iron-titanium-chromite, a possible new carrier of remanent magnetization in lunar rocks. 07 p0892 A73-19836

Features of the domain structure of cobalt-doped lithium ferrite when changing the direction of easy magnetization 10 p1260 A73-24508

Motion of a magnetizable fluid in the lubrication film of a cylindrical bearing 10 p1225 A73-24586

The most important characteristics of magnetizing equipment in the leakage-flux technique - Their measurement and application 15 p1882 A73-32054

Magnetic investigations of lunar soil delivered by AIS Luna 16. 21 p2773 A73-41399

Optical and polarization study of magnetization processes around individual dislocations in yttrium-iron garnet single crystals 23 p3017 A73-44024

MAGNETO-OPTICS

A combined magnetic circular dichroism and electron paramagnetic resonance spectrometer. 02 p0167 A73-11951

Electro-optical, magneto-optical, absorptional and acousto-optical light modulation, noting Kerr effect, Faraday rotation and light absorption 04 p0458 A73-15348

Muller matrix derivation for microwave light modulation studies in quasi-homogeneous magneto-optical and electro-optical media, taking into account finite light speed 04 p0459 A73-15923

Optimum thickness for thermomagnetic laser writing on Fe doped EuO films on quartz substrate 06 p0702 A73-18372

Amorphous thin films of rare earth transition metal alloys for magneto-optic applications, noting SNR in thermomagnetically written film 11 p1409 A73-26325

Book on semiconductor opto-electronics covering solids optical constants, classical and quantum mechanical dispersion theory, absorption processes, magneto-optical and photo-electrical effects, etc 12 p1531 A73-27449

International Conference on the Physics of Semiconductors, 11th, Warsaw, Poland, July 25-29, 1972, Proceedings. Volumes I & 2. 14 p1783 A73-30572

Magneto-optic investigation of MnBi films. 15 p1924 A73-31943

Optical and polarization study of magnetization processes around individual dislocations in yttrium-iron garnet single crystals 23 p3017 A73-44024

MAGNETOACOUSTIC WAVES

Nonlinear magnetic sound in a gravitational field 01 p0016 A73-10202

Linear MHD equations for inviscid medium under external forces, discussing magnetoacoustic wave generation by radially pulsating cylinder and sphere 02 p0196 A73-11605

Diurnal effects in pc 1 hydromagnetic whistlers - An early afternoon source model. 02 p0158 A73-11909

Wave coupling at a collisionless plasma discontinuity. 02 p0198 A73-12408

The propagation of small disturbances in radiative magnetogasdynamics. 03 p0345 A73-12923

LF spectrum of plasma oscillations from amplitude modulation of plasma SHF radiation, noting Langmuir and magnetoacoustic waves interaction 04 p0478 A73-15034

Stability of a plasma with inequilibrium ions with respect to the generation of magneto-sonic waves 04 p0481 A73-15603

Numerical simulation of high Mach number supercritical magnetosonic collisionless shock wave propagation perpendicular to magnetic field, considering cause of anomalous ion heating 05 p0604 A73-17365

High-frequency heating of a plasma under lower hybrid-resonance conditions 07 p0855 A73-19290

An exact helical wave solution to the equations of magnetohydrodynamics. 07 p0859 A73-20233

The diffraction of fast magneto-acoustic waves by a plasma layer of a periodically varying density. 08 p0993 A73-21459

RF plasma heating by the modified two stream instability. 09 p1128 A73-22628

Excitation of magnetosonic waves in a plasma with nonequilibrium ions 09 p1131 A73-23076

Stability of a plasma with nonequilibrium ions with respect to magnetosonic waves. 10 p1254 A73-24193

Strong plasma turbulence at helicon frequencies 10 p1257 A73-24757

A magnetosonic resonator of Pc2,3 pulsations in the earth's magnetosphere 12 p1491 A73-27351

Plasma heating at the lower hybrid resonance. 13 p1665 A73-28690

Theory of turbulent plasma heating by anomalous absorption of magnetosonic waves. 14 p1777 A73-29683

Interaction of fast particles with magneto-hydrodynamical turbulence. 17 p2216 A73-34504

Damping of Alfvén and magnetoacoustic waves at high beta. 17 p2217 A73-35524

Electron-acoustic and drift instabilities in a finite-pressure plasma with a transverse current 21 p2745 A73-40364

Electron-acoustic and ion-cyclotron parametric instabilities of a plasma in an alternating electric field. I, II 21 p2746 A73-40520

Magnetohydrodynamic waves in the solar wind plasma 21 p2763 A73-41506

Parametric instabilities and turbulent heating of a plasma in the field of a fast magneto-acoustic wave. 21 p2750 A73-41677

Mariner 5 observations of solar wind shock-like structures including density, velocity, and proton temperature increases, suggesting nonlinear magnetoacoustic waves under steepening process 22 p2901 A73-41902

Instabilities of drift magnetosonic waves due to the magnetic drift resonance. 22 p2894 A73-42395

Characteristics of the fast and slow magnetosonic waves in layered plasmas. 22 p2894 A73-42397

Vertically nonpropagating magnetoatmospheric waves investigation based on local dispersion relations governing magnetoacoustic and magnetogravitational wave propagation with emphasis on solar atmosphere conditions 22 p2914 A73-43010

Magnetosonic resonator of Pc2,3 pulsations in the earth's magnetosphere. 23 p2970 A73-43248

MAGNETOACOUSTICS

Utilization of hydrostatic compression at high pressures as a means of improving the properties of acoustic nickel ferrite 14 p1765 A73-30890

MAGNETOACTIVITY

NT MAGNETORESISTIVITY

The EM field of a dipole transmitter in the two-layer medium air space-magnetoactive ionosphere 01 p0035 A73-10299

Lower boundary of the occurrence of magnetoactive masses 08 p0959 A73-21296

Nonthermal radiation from a magnetoactive plasma in the field of a microwave pumping wave. 11 p1405 A73-26182

Existence conditions for magnetoactive plasma longitudinal waves with phase velocity near light velocity, investigating increments during synchrotron instability due to relativistic particles 14 p1780 A73-30337

Magnetic neutralization and discharge neutralization of an electron beam injected into a magnetoactive plasma 14 p1782 A73-30807

Lower boundary of occurrence of magnetically active masses. 19 p2425 A73-37925

MAGNETOELASTIC VIBRATIONS

U MAGNETOELASTIC WAVES

NT MAGNETOACOUSTIC WAVES

The thickness of perpendicular collisionless shocks in a hot plasma. 04 p0479 A73-15191

Magnetoelastic vibration of electrically conducting thin shells and plates in steady magnetic field from asymptotic integration of electrodynamics equations 12 p1553 A73-27413

On the propagation of relativistic thermo-magneto-viscoelastic waves in a material of Voigt-type. 19 p2459 A73-37648

Elastic semispace motion under the action of a shock wave in a magnetic field 23 p3006 A73-43919

MAGNETOELASTICITY

U MAGNETOSTRICTION

MAGNETOELECTRIC MEDIA

Magnetic semiconductor materials compositions and magnetoelectric characteristics, discussing magnetic-electric interactions, fabrication techniques and applications for magnetically controllable diodes, temperature sensors, etc 04 p0483 A73-15323

Thermomagnetic shunt for compensation of instrument errors due to temperature effects on magnetoelectric transducers material, calculating magnetic circuit 05 p0577 A73-16988

MAGNETOGASDYNAMICS

U MAGNETOHYDRODYNAMICS

MAGNETOGRAMS

U MAGNETIC SIGNATURES

MAGNETOGRAPHS

U MAGNETOMETERS

U RECORDING INSTRUMENTS

MAGNETOHYDRODYNAMIC ACCELERATION

U PLASMA ACCELERATION

MAGNETOHYDRODYNAMIC FLOW

Streaming two dimensional Oseen MHD flow of conducting fluid past semiinfinite needle within aligned field 01 p0031 A73-10305

One-fluid MHD model for beta and flow effects on stationary axisymmetric self consistent toroidal equilibria, using Bennett relation 01 p0083 A73-10460

Subsonic plasma motion in continuous laser light. 01 p0084 A73-10472

Arc current, column electric field, mainstream velocity and applied transverse magnetic field relationships in magnetically balanced cross flow plasmas 01 p0084 A73-10738

Effect of viscosity on the motion of the inhomogeneities of a nonequilibrium plasma in a magnetic field 01 p0085 A73-10865

Nonlinear boundary-value problem for a conducting source flow in an inhomogeneous magnetic field. 01 p0085 A73-11064

Temperature field and heat transfer equation of unsteady conducting fluid motion on porous plate within magnetic field, allowing for Joule dissipation 01 p0085 A73-11079

Magnetohydrodynamic flow around a hollow sphere 01 p0085 A73-11259

Hydromagnetic flow about a curved neutral sheet. 01 p0086 A73-11495

German book on plasma physics covering MHD equations for incompressible and compressible flow, shock waves, electrical and thermal conductivity, viscosity, flow stability, turbulence, etc 02 p0196 A73-11894

Collisionless plasma flow over a conducting sphere. 02 p0158 A73-11919

Model development of supersonic trough wind with shocks. 03 p0298 A73-12887

The propagation of small disturbances in radiative magnetogasdynamics. 03 p0345 A73-12923

Three-dimensional MHD duct flows with strong transverse magnetic fields. III - Variable-area rectangular ducts with insulating walls. 03 p0346 A73-13534

Magnetic field effect on friction shear stress in turbulent slipstreams of conducting fluids, calculating mixing zone width 03 p0346 A73-13609

Magnetogasdynamic characteristics, transonic and compression regions and pressure losses of conducting gas flow in circular tube within axisymmetric magnetic field 03 p0346 A73-13620

Steady transverse plane magnetogasdynamic flows. 03 p0346 A73-13693

Asymptotic solution for inviscid conducting fluid flow past arbitrary wing profile in magnetic field 03 p0347 A73-14045

The effects of wall conductance on torque of the MHD viscous coupler and hydrostatic thrust bearing. [ASME PAPER 72-LUB-1] 03 p0313 A73-14326

Ionospheric plasma flow past a semi-infinite cylinder. 04 p0440 A73-14967

Ion distribution function in plasma cylinder flow around thin plate in magnetic field under ionospheric conditions 04 p0481 A73-15617

Temperature distribution in non-Newtonian MHD channel flow by shear stress integral evaluation, investigating power law and Prandtl-Eyring fluids 04 p0520 A73-15947

Rotating paraboloid of revolution in viscous conducting fluid, calculating flow velocity and magnetic field from MHD equations 05 p0601 A73-16172

Equations of motion for two dimensional steady conducting gas flow in transverse magnetic field, deriving flow equations for transcritical region via small perturbation theory 05 p0602 A73-16585

Two-dimensional viscid MHD flows in coaxial channels 05 p0603 A73-16588

Effect of the asymmetry of an external magnetic field on a viscous fluid flow in an annular MHD channel 05 p0603 A73-16589

MHD-rotation of a conducting fluid in a rotationally symmetric electromagnet field 05 p0603 A73-16590

Gas-dynamic description of a plasma in a corrugated magnetic field. 05 p0603 A73-17360

Dimension-theory determination of the separation parameter for an incompressible magnetohydrodynamic boundary layer.

06 p0726 A73-17406

Motion of plasmoids in a toroidal magnetic multipole.

06 p0727 A73-17421

Polarization interaction of opposed plasma streams in a linear magnetic octupole.

06 p0727 A73-17422

Hartmann flow stability of conducting incompressible viscous fluid between parallel plates at arbitrary Reynolds numbers under transverse magnetic field

06 p0727 A73-17453

Flow of a two-temperature plasma in the duct of a disk-type magnetohydrodynamic generator with allowance for nonequilibrium ionization and recombination reactions

06 p0727 A73-17464

Motion of a magnetized conducting liquid between two plane electrodes in a transverse magnetic field

06 p0727 A73-17472

Electric probe performance in weakly ionized dense plasma flow for lower ionosphere measurements, considering stagnation point and particle distribution-potential effects

06 p0689 A73-17538

Three-dimensional MHD duct flows with strong transverse magnetic fields. IV - Fully insulated, variable-area rectangular ducts with small divergences.

06 p0728 A73-17704

The development of magnetohydrodynamic flow due to the passage of an electric current past a sphere immersed in a fluid.

06 p0728 A73-17705

Magnetohydrodynamic viscous flow induced by an oscillating disk.

06 p0728 A73-17792

Experiments of magnetohydrodynamic conversion with ionization out of equilibrium

06 p0730 A73-18541

Pressure, temperature, current density and potential difference fluctuations in subsonic flow of combustion products plasma, noting steadiness, ergodicity and distribution functions

06 p0732 A73-18616

Discontinuities propagation in quasi-linear hyperbolic partial differential equation systems, noting MHD flow and crystal optics equations

07 p0850 A73-19016

Magnetohydrodynamic laminar source flow between two parallel disks.

07 p0854 A73-19102

Drift instabilities in nonuniform streaming plasmas.

07 p0855 A73-19337

Unsteady motion of a viscous electrically conducting fluid around a flat plate in the case of orthogonal fields

07 p0858 A73-19999

Flow of a conductive fluid through a cylindrical duct with periodic deformations in the presence of an azimuthal magnetic field

07 p0858 A73-20073

On unsteady magnetohydrodynamic boundary layers in a rotating flow.

07 p0859 A73-20290

German monograph - Unsteady processes of the interaction between shock-produced plasma flows and magnetic fields - A theoretical investigation.

07 p0859 A73-20384

Electrostatic turbulence at colliding plasma streams as the source of ion heating in the solar wind.

08 p0997 A73-20886

Some problems in the theory of an electrochemical velocity sensor for current-conducting fluids

08 p0965 A73-21106

Some extremum principles for pipe flow in magnetohydrodynamics.

08 p0993 A73-21403

Ion saturation currents to planar Langmuir probes in a collision-dominated flowing plasma.

08 p0993 A73-21597

Features of the flow of a nonisothermal plasma, obtained in a beam-plasma discharge, through a magnetic nozzle

09 p1124 A73-21890

Remarks on variational principle for an inviscid, perfect, magnetized plasma.

09 p1126 A73-22122

Equations of motion of ideally conducting medium in MHD approximation, solving under constant magnetic field and magnetic-hydrodynamic pressure equilibrium

09 p1126 A73-22280

Realization of a zero-force magnetic field configuration in the case of axisymmetric magnetohydrodynamic flows

09 p1146 A73-22541

Calculation of the boundary layers of a fully ionized two-temperature plasma for given temperatures of components at the electrodes

09 p1127 A73-22605

Influence of the Hall effect on current structure in a plasma flow through a spatially periodic magnetic field

09 p1127 A73-22606

Structure of a collisionless boundary layer and the turbulent braking of ions

09 p1127 A73-22607

A study of the stability of slow combustion of gas mixtures subjected to the action of a magnetic field

09 p1167 A73-23351

Numerical analysis of the viscous, hypersonic, MHD blunt-body problem.

09 p1132 A73-23455

Ion distribution function in plasma cylinder flow around thin plate in magnetic field under ionospheric conditions

10 p1254 A73-24207

Electromagnetic instability for plasma waves propagating perpendicular to uniform magnetic field in counterstreaming electron-ion plasmas based on linearized Vlasov-Maxwell equations

10 p1255 A73-24262

Unsteady MHD duct flow by the finite element method.

10 p1256 A73-24289

Conducting medium flow in cylinder with nonconducting walls, solving nonlinear elliptic equation /Dirichlet problem/ by projective-iterative method

10 p1256 A73-24509

Flow near an accelerated plate in the presence of a magnetic field.

10 p1206 A73-24528

Motion of a magnetizable fluid in the lubrication film of a cylindrical bearing

10 p1225 A73-24586

Unsteady flow of a conducting viscous fluid between parallel porous walls with heat transfer

10 p1256 A73-24587

Unsteady viscoplastic electrically conducting MHD flow in moving-wall channel, assuming time-variable pressure gradient and uniform transverse magnetic field

10 p1256 A73-24588

Electrically conducting unsteady viscoplastic plane channel Hartmann and Couette MHD flows in presence of uniform transverse magnetic field and time variable electric field

10 p1256 A73-24589

Unsteady motion of a viscoplastic medium in a plane MHD channel at a constant flow rate

10 p1256 A73-24590

Turbulent Hartmann flow based on differential equations for steady isothermic turbulent motion of incompressible electrically conducting fluid in magnetic field

10 p1256 A73-24591

Semiempirical determination of the anisotropy of turbulent MHD flow in a longitudinal field

10 p1256 A73-24592

On unsteady magnetohydrodynamic boundary layers in a rotating flow.

10 p1257 A73-24841

Dynamic viscosity and current distribution model of inhomogeneous Cs plasma flow in coaxial plasma gun with thermionic cathode

10 p1258 A73-24886

Compressible magnetorelativistic flow character in subsonic, supersonic and transonic regions, obtaining pressure coefficient, free stream Mach number and Alfvén speed interrelationships

10 p1210 A73-24921

Nonlinear hydrodynamic and hydromagnetic spin-up driven by Ekman-Hartmann boundary layers.

11 p1403 A73-25156

A note on the unsteady motion of a viscous conducting liquid between two porous concentric circular cylinders acted on by a radial magnetic field.

11 p1404 A73-25368

Second-order solutions for steady magnetohydrodynamic channel flow with anisotropic conductivity.

11 p1404 A73-25746

Nonlinear resistive boundary layer in rotating hydromagnetic flow related to earth dynamo theory, discussing steady solution uniqueness and numerical temporal stability

11 p1355 A73-25794

On MHD flow along an infinite flat wall with constant suction.

11 p1405 A73-25975

Flow of liquid metals with a transversely applied magnetic field. I - Laminar flow in the entrance region.

11 p1406 A73-26341

Laminar free convection flow of an electrically conducting fluid from an inclined isothermal plate.

11 p1452 A73-26369

Equations derived for magnetic field line configuration and plasma flow about rotating object having axisymmetric field with emphasis on pulsar magnetosphere

11 p1427 A73-26614

High speed corotating plasma streams in solar wind from time dependent radial MHD flow model

12 p1533 A73-26979

Solar wind-lunar limb interaction from viscous MHD approach including continuum fluids, kinetic plasma and magnetic boundary layer

12 p1534 A73-27003

Two-dimensional steady magneto-fluid-dynamic flows with orthogonal magnetic and velocity field distributions.

12 p1527 A73-27020

Influence of a transverse electron-temperature gradient on the plasma flow in an axisymmetric magnetic field

12 p1528 A73-27305

Investigation of heat and mass transfer for plasma flows in channels of various shape under conditions of intense condensation

12 p1558 A73-27318

Influence of a variable ionospheric-protonospheric plasma flow on the nighttime F region of the ionosphere

12 p1490 A73-27336

Applied electrical potential effect on heat transfer to tube immersed in highly ionized flow of atmospheric pressure Ar plasma

12 p1529 A73-27696

Influence of viscosity on the motion of nonuniformities of a nonequilibrium plasma in a magnetic field.

12 p1529 A73-27914

Probe device for measuring local parameters of ionized gas flow.

12 p1499 A73-27915

Transonic similarity solution for aligned field MHD nozzle flow.

13 p1599 A73-28089

The channel flow of an electrically conducting Prandtl-Eyring fluid in a magnetic and an electric field

13 p1663 A73-28161

MHD free convective flow in a vertical channel.

13 p1663 A73-28164

Equations for finitely-dimensional probability distributions of pulsating variables in a turbulent flow

13 p1599 A73-28287

Population inversion calculations using near-resonant charge exchange as a pumping mechanism.

13 p1627 A73-28549

A note on the effect of Hall currents on hydromagnetic flow near an accelerated plate.

13 p1664 A73-28617

Variation of parameters in a shock-heated argon plasma flow.

13 p1665 A73-28624

Experiments in magneto-fluid-mechanic natural and forced heat transfer from horizontal hot-film probes.

13 p1620 A73-29254

Solar wind interpenetrating ion streams from Imp 6 electrostatic analyzer measurements, considering origin due to interplanetary high velocity filaments merging into rarefied plasma regions

14 p1786 A73-29954

Low Hartmann number MHD flow of weakly conducting viscous fluid past nonconducting sphere within aligned uniform magnetic field

14 p1781 A73-30655

Chandrasekhar equations for axisymmetric MHD flows generalized for steady and unsteady flows

14 p1781 A73-30701

Transport effects in a turbulent flowing plasma - The moment relations.

15 p1916 A73-31082

A generalized flux-vorticity theorem. I.

15 p1916 A73-31088

Wake past an obstacle in a magnetized plasma flow.

15 p1916 A73-31089

Approximate solution to the problem of a conducting fluid flow in a weakly curved channel

15 p1917 A73-31154

Linearized theory of finite conductivity steady ideal MGD flow past thin wedge in aligned magnetic field using Fourier integral transform

15 p1917 A73-31338

Experimental investigation of the pressure distribution in constrained MHD flows past cylinders

15 p1917 A73-31401

Magnetic field induced energy dissipation in conducting fluid isotropic turbulent flow velocity pulsations, noting Joule dissipation effect on damping

15 p1917 A73-31403

Uses of the equation of pulsation energy balance in the theory of MHD flows in channels and tubes

15 p1917 A73-31404

Nonlinear MHD equations solution for conducting fluid plane periodic channel flow in traveling magnetic field by net point method

15 p1917 A73-31406

Application of the method of characteristics in solving the universal equation of the plane boundary layer of a conducting fluid

15 p1918 A73-31407

Motion of a magnetized fluid between parallel plates

15 p1918 A73-31408

Laminar stratified flow of a conducting medium in ring channels in the event of great MHD-interaction parameters

15 p1918 A73-31409

Velocity structure of a flow in a magnetic field periodically varying along the flow

15 p1918 A73-31413

Noncirculative MHD inviscid conducting fluid flow past circular cylinder and plane profile in magnetic field, using Fredholm equation
15 p1918 A73-31414

On the establishment and solution of equations of motion of an electrically conducting fluid set in motion by the slow and uniform rotation of walls of a ring-shaped receiver, in the presence of an axial magnetic field, in the case where the mean value of the intensity of the currents induced in a straight section takes a nonzero value
15 p1918 A73-31569

Numerical study of the interaction of a shock-wave caused, supersonic, ionized-argon flow with electric and magnetic fields, using the method of characteristics
15 p1918 A73-31571

Plane boundary layer equations of asymmetric MHD incompressible fluid motion for case of high and low electroconductivity
15 p1919 A73-31829

Interaction between an ionized metal vapor flow and a body at Mach numbers equal to or larger than unity
15 p1919 A73-31863

Magnetohydrodynamic boundary layer control with suction or injection.
15 p1864 A73-31931

Magnetogasdynamic compression of a coaxial plasma accelerator flow for micrometeoroid simulation.
15 p1919 A73-31932

Dynamic pressure transducer system for pulsed plasma flow diagnosis.
15 p1876 A73-31977

Solar wind flow in interplanetary space, discussing comets, cometary tail, interplanetary magnetic field and Alfvén waves characteristics
15 p1940 A73-32183

Formation of fast electrons in a plasma under the influence of SHF power near harmonics of the electron cyclotron frequency
15 p1920 A73-32309

Electric probe performance in weakly ionized dense plasma flow for lower ionosphere measurements, considering stagnation point and particle distribution-potential effects
16 p2001 A73-32762

Restrictions on radial magnetic field and flow solutions for the solar wind.
16 p2053 A73-32967

Free surface shape of MHD flow due to constant mass source expansion into uniform magnetic field as function of time
16 p2041 A73-33329

On the solution of magnetohydrodynamic elastico-viscous flow past a plane porous plate.
16 p2042 A73-33370

Ion heating in thermal plasma flows.
16 p2042 A73-33465

Acoustic instability of a bounded weakly ionized plasma
17 p2214 A73-34135

Continuum gas plasma boundary layer flow over flat plate, obtaining ion sheath characteristics and downstream solutions by asymptotic and characteristics methods
17 p2149 A73-34186

Multiring probe in a flowing ionospheric plasma.
17 p2214 A73-34199

Similarity in the flow of a magnetized plasma around a plate and cylinder
17 p2215 A73-34260

Flow of nonisothermal plasma through a magnetic nozzle.
17 p2215 A73-34313

Unsteady Couette flow in hydromagnetics.
17 p2154 A73-35121

Impulsively started viscous flow past a finite flat plate with and without an applied magnetic field.
17 p2217 A73-35604

Sensitivity of the numerical analysis of the three-fluid plasma mixed initial-boundary value problem.
18 p2338 A73-36160

Magnetohydrodynamical steady aligned flow past an oblique flat plate at a high Reynolds number.
18 p2300 A73-36664

Incompressible conducting fluid flows in an arbitrary region in the presence of a strong magnetic field
18 p2340 A73-37015

Cold collisionless plasma flow along magnetic field, deriving quasi-shock wave characteristics from Vlasov-Maxwell equations
19 p2463 A73-37152

Weakly ionized continuum plasma turbulent shear flow and transport properties calculation, noting ratio of Debye shielding length to local integral scale
19 p2463 A73-37153

Interaction of a strong shock wave with electromagnetic field.
19 p2464 A73-37157

Experiments of shock waves in a fully ionized plasma flow.
19 p2464 A73-37159

Plasma channel flow theoretical and experimental review, considering heat transfer studies, turbulent nonequilibrium plasma boundary layers and plasma sheaths
19 p2464 A73-37161

Continuum thick sheath probe studies in hypersonic ionized boundary layers.
19 p2375 A73-37164

A review of electrostatic probe response in a flowing, low density plasma.
19 p2465 A73-37165

Experimental investigations on arc-heated steady plasma flow.
19 p2415 A73-37169

Quasi-steady plasma wind tunnel for Alfvén wave measurements of MHD flow involving shock waves and wakes, using Langmuir probes
19 p2465 A73-37172

Theoretical and experimental research on the electromagnetic acceleration of shock-induced flow in argon.
19 p2419 A73-37174

Linearized MPD jet and channel flows in external magnetic fields with the Hall effect.
19 p2465 A73-37175

Corner expansion flow of ionized argon, calculating electron density, plasma density and recombination rate constant for comparison with measurements
19 p2465 A73-37177

On the flow of a nonequilibrium ionized gas past a wall in the presence of a magnetic field.
19 p2465 A73-37178

System for calibrating on-board instruments and for laboratory simulation of low-density plasma flows past models
19 p2417 A73-37351

Investigation of the high-frequency oscillations in the flow of a pulsed coaxial plasma accelerator - One mechanism of inhomogeneity
19 p2467 A73-37364

Calculation of two-dimensional unsteady plasma flows in channels
19 p2467 A73-37369

Stability of plasma flows in multipolar magnetic fields
19 p2467 A73-37372

Theoretical and experimental study, for different electrical conditions, of the laminar motion of an incompressible and electrically conducting fluid drawn along in a confined medium, and in the presence of an axial magnetic field, by the uniform rotation of a disk
19 p2468 A73-37531

Boundary value problem of steady MHD flow in rotating cylindrical pipe under uniform magnetic field
19 p2468 A73-37647

Numerical simulation of counterstreaming high Mach number plasma laminar interactions, using one dimensional model based on Vlasov equation
19 p2469 A73-37861

Application of cylindrical Langmuir probes to streaming plasma diagnostics.
19 p2469 A73-37862

On the effects of uniform high suction on the rotationally symmetric flow of a conducting liquid near a stationary disc in the presence of a transverse magnetic field.
19 p2469 A73-38186

Development of a turbulent boundary layer in MHD channel.
19 p2470 A73-38316

Some transient MHD-flows with finite magnetic Reynolds numbers.
19 p2470 A73-38319

Potential created by a test particle in one-, two- and three-dimensions in a flowing ion-electron plasma.
20 p2596 A73-38969

Study of the stability of a perturbed conducting gas flow in a magnetic field at arbitrary Reynolds magnetic numbers
20 p2597 A73-39276

The two-dimensional slow flow of a conducting fluid.
20 p2598 A73-39340

Meridional flow and the validity of the two-dimensional approximation in stellar-wind modeling.
20 p2602 A73-39430

Interplanetary gas. XIX - Observational evidence for a meridional solar-wind flow diverging from the plane of the solar equator.
20 p2602 A73-39431

Overheat instability in a flow of electrically conducting incompressible medium under conditions of an internal boundary value problem
20 p2598 A73-39605

Numerical experiment in a study of the separation of a laminar boundary layer in an MHD channel
20 p2598 A73-39611

MPD annular duct flows in crossed external fields for arbitrary values of the Hall parameter
20 p2599 A73-39675

The application of high-speed photography and spectrography for investigations of erosive pulsed plasma streams.
21 p2744 A73-39999

Plasmaspheric quasistatic electric fields and plasma convection, discussing dynamic electric fields and magnetospheric field penetration to low latitudes
21 p2679 A73-40075

Electric field in an MHD channel of rectangular cross section in the presence of the Hall effect
21 p2744 A73-40183

Formation of a plasma focus in erosion-type plasma accelerators. I
21 p2746 A73-40525

Self-similar solutions of the plasma equations
21 p2747 A73-40553

A three-dimensional MHD boundary layer in an incompressible fluid
21 p2747 A73-40882

Study of MHD effects in a viscous conducting fluid flow in a traveling magnetic field
21 p2747 A73-40884

Rotation of an electrically conducting fluid with a free surface in a rotating field
21 p2747 A73-40885

Experimental study of rotational MHD Couette flow in a coplanar field
21 p2747 A73-40886

A numerical study of three-dimensional problems of MHD flow
21 p2747 A73-40887

Conducting fluid jets in a transverse magnetic field
21 p2747 A73-40888

Some integral characteristics of an MHD channel at finite magnetic Reynolds numbers
21 p2747 A73-40889

Magnetohydrodynamic wake behind a body placed in a homogeneous flow in the presence of a longitudinal magnetic field
21 p2747 A73-40890

Measuring the boundary layer temperature distributions using ablating specimens in an air plasma flow.
21 p2791 A73-41052

Solar-wind properties at the earth as predicted by the two-fluid model.
21 p2763 A73-41502

Dynamic viscosity and current distribution model of inhomogeneous Cs plasma flow in coaxial plasma gun with thermionic cathode
21 p2749 A73-41661

Equations for the finite-dimensional probability distributions of pulsating variables in a turbulent flow.
22 p2840 A73-41810

Magnetotail plasma flow observation with Vela 4A oriented perpendicular to ecliptic plane, considering plasma sheet recovery relation to auroral electrojet poleward shift
22 p2844 A73-41907

On the stability of a class of plasma flows with helical flow and field lines.
22 p2892 A73-42351

Longitudinal polarization and focusing of plasmoids in a linear multipole magnetic field
22 p2893 A73-42383

Polarizing interaction between colliding plasma flows in a toroidal magnetic field. II
22 p2893 A73-42384

The numerical prediction of streamer growth in MHD ducts.
22 p2894 A73-42558

Models of force-free magnetic fields in resistive media.
22 p2911 A73-42938

Viscous laminar Hartmann flow of electrically conducting liquid between parallel walls in transverse magnetic field, assessing thermal radiation effects and temperature distribution
23 p3008 A73-43207

Effect of changing ionospheric-protonospheric plasma flow on the nighttime F-region of the ionosphere.
23 p2970 A73-43234

Electric polarization of a plasma beam in an axially symmetrical magnetic field
23 p3009 A73-43655

Experimental investigation of the interaction between plasma fluxes and a spatially-periodic magnetic field
23 p3010 A73-43656

Experimental investigation of a 'poloidal' current in a plasma flow in an inhomogeneous axially-symmetric magnetic field
23 p3010 A73-43657

Investigation of the dynamics of plasma flows in the field of a pulsed magnetic barrier
23 p3010 A73-43658

Induced currents in a stationary plasma flow in an axially-symmetric magnetic field
23 p3010 A73-43663

Weakly-shocked flows of the solar wind plasma through atmospheres of comets and planets.
23 p3024 A73-43682

Free point method finite difference solution for two dimensional nonstationary hydrodynamic problem of continuous media, demonstrating feasibility by plasma pinch effect calculation
23 p2968 A73-43799

- On laminar two-phase flows in magnetohydrodynamics. 23 p3013 A73-44228
- Boundary layer equations of magnetohydrodynamics with moment stresses 23 p3015 A73-44385
- Experimental study of shocked-plasma flows with a double search-coil conductivity probe. 24 p3113 A73-44402
- Inertia effects in MHD lubricated hydrostatic thrust bearing under axial magnetic field investigated by energy integral method, obtaining flow velocity and load carrying capacity 24 p3092 A73-44410
- Production of fast plasma electrons by microwave power at harmonics of the electron cyclotron frequency. 24 p3114 A73-44617
- Equipment for measuring local plasma flow parameters by a thermoanemometer probe 24 p3089 A73-44761
- Interaction between flows with different velocities in the solar wind 24 p3124 A73-44780
- Observation of plasma flow in the neutral sheet at lunar distance during two magnetic bays. 24 p3139 A73-45137
- On the instability of magnetohydrodynamic Couette flow via non-axisymmetric, oscillatory critical modes. 24 p3116 A73-45241
- Effects of thermal conductivity in radiative magnetohydrodynamic channel flow. 24 p3117 A73-45370
- Laser Doppler velocimeter measurement of laminar velocity profiles for developing MHD flow in rectangular duct, noting inlet effects on flow development 24 p3118 A73-45464
- Unsteady plasma flows behind a moving leading boundary 24 p3119 A73-45539
- MAGNETOHYDRODYNAMIC GENERATORS**
- Effect of heterogeneity and Hall current on the MHD power generator. 01 p0005 A73-10434
- Inward diffusion of Tokamak-trapped particles by slow magnetic pumping. 01 p0083 A73-10461
- Glass reinforced epoxy structure for a lightweight superconducting dipole magnet. 02 p0232 A73-11836
- Study of the boundary layers of a completely ionized two-temperature plasma on the nonconducting wall of an MHD channel 03 p0346 A73-13610
- Electric field in a segmented MHD generator for a finite conductivity of the walls at the channel inlet 03 p0346 A73-13621
- End effects in Faraday type MHD generators with nonequilibrium plasmas. 03 p0254 A73-14185
- The influence of spatial temperature distribution and measuring configuration on line-reversal temperature. 05 p0602 A73-16563
- Analysis of optimal conditions for energy conversion in an MHD-generator channel 05 p0602 A73-16586
- Flow of a two-temperature plasma in the duct of a disk-type magnetohydrodynamic generator with allowance for nonequilibrium ionization and recombination reactions 06 p0727 A73-17464
- Large-scale applications of superconducting coils. 07 p0863 A73-20107
- Gas dynamic characteristics of the helium two stage shock tube for MHD power generation experiments. 07 p0808 A73-20117
- Feedback control of ionization instability in MHD generators. 07 p0779 A73-20395
- Electrode and gasdynamic effects in a large nonequilibrium MHD generator. 08 p0928 A73-20713
- Hall current effects in the Lewis magnetohydrodynamic generator. 09 p1130 A73-22823
- Exploratory investigation of an electric power plant utilizing a gaseous core reactor with MHD conversion. 09 p1119 A73-22829
- Influence of ionizational turbulence on the operation of an MHD generator with nonequilibrium plasma 10 p1253 A73-23502
- Optimal, elliptic and circular windings for superconducting nonferrous magnetic MHD generators, comparing cross sections 10 p1178 A73-24594
- Review of liquid-metal magnetohydrodynamic spacecraft energy conversion cycles. 11 p1308 A73-25977
- Investigation of a liquid-metal magnetohydrodynamic power system. 11 p1308 A73-25978
- Certain considerations concerning a magnetoplasma dynamic flux in the one-dimensional hypothesis 12 p1527 A73-27061

- Optimization of the power of a Faraday-type MHD-generator operating with a nonequilibrium plasma 12 p1460 A73-27320
- Qualitative analysis of MHD energy conversion efficiency 12 p1460 A73-27321
- Nonequilibrium ionization in magnetohydrodynamic conversion generators 13 p1571 A73-28071
- Motion of a magnetized fluid between parallel plates 15 p1918 A73-31408
- Engineering technique for secondary-medium parameter calculation in the substitution circuits of flat, linear induction MHD machines with side busbars 15 p1832 A73-31411
- Effects of channel size on the ionization instability in MHD generators. 17 p2108 A73-34185
- Effect of ionization turbulence on the operation of an MHD generator operating with a nonequilibrium plasma. 17 p2217 A73-35182
- Investigation of the discharge structure in a noble gas alkali MHD generator plasma. I. 18 p2338 A73-36303
- Investigation of the discharge structure in a rare gas alkali MHD generator plasma. II. 18 p2339 A73-36304
- Engineering aspects of magnetohydrodynamics; Proceedings of the Thirteenth Symposium, Stanford University, Stanford, Calif., March 26-28, 1973. 19 p2469 A73-38310
- NaK-nitrogen liquid metal MHD converter tests at 30 kW. 19 p2389 A73-38311
- Exploratory study of several advanced nuclear-MHD power plant systems. 19 p2454 A73-38313
- MHD boundary layers on a segmented electrode-wall of a nonequilibrium generator. 19 p2470 A73-38314
- Calculation and measurement of MHD generator boundary layer velocity profiles. 19 p2470 A73-38315
- Exploratory study of several advanced nuclear-MHD power plant systems. 19 p2455 A73-38411
- Microarc current flow and potential drop through cold boundary layer near plasma electrodes in MHD generators 20 p2598 A73-39604
- Experimental investigation of the characteristics of a nonequilibrium MHD generator 20 p2511 A73-39618
- Experimental investigation of the performance of a porous electrode in an MHD converter during the injection of argon with potassium addition 20 p2511 A73-39619
- An MHD generator with a nonequilibrium plasma produced by VHF ionization 23 p3011 A73-43714
- MAGNETOHYDRODYNAMIC STABILITY**
- Book - An introduction to the theory of plasma turbulence. 01 p0081 A73-10124
- Time evolution and functional form of magnetostatic equilibria in axisymmetry. 01 p0082 A73-10452
- Theory of turbulent heating of an isothermal plasma with a transverse current. 01 p0083 A73-10456
- Local hydromagnetic toroidal equilibria without symmetry. 01 p0083 A73-10457
- Two-dimensional investigation of absolute instabilities in mirror plasmas. 01 p0083 A73-10458
- Life-time of ion waves in unstable and turbulent plasmas. 01 p0084 A73-10463
- Use of the virtual-casing principle in calculating the containing magnetic field in toroidal plasma systems. 01 p0084 A73-10464
- Variational formulation for hydromagnetic stability 01 p0084 A73-10550
- The Kelvin-Helmholtz instability in type-I cometary tails 01 p0102 A73-10946
- Onset of turbulence in the interaction between a 'monoenergetic' beam and a plasma 01 p0086 A73-11285
- On the stability of nonlinear cold plasma waves. 01 p0087 A73-11497
- Ring current proton injection instability for ion loss cone and electromagnetic ion cyclotron waves in high beta low density region outside plasmapause 02 p0156 A73-11748
- German book on plasma physics covering MHD equations for incompressible and compressible flow, shock waves, electrical and thermal conductivity, viscosity, flow stability, turbulence, etc. 02 p0196 A73-11894
- Magnetization currents effect on linear hydromagnetic instabilities development in collisionless anisotropic plasmas 02 p0196 A73-11899

- Electromagnetic dispersion relation for two equidense counterstreaming ion beams in warm electron background oscillating plasma, considering ion instability criteria 02 p0197 A73-12066
- Role of trapped particles in plasma waves and instabilities. 02 p0197 A73-12067
- Effect of ion viscosity on the stability of a finite-pressure plasma. 02 p0198 A73-12104
- Stability of a plasma with an axial current surrounded by a cold gas with a pressure gradient. 02 p0198 A73-12108
- Uniform low temperature gas discharge plasma diagnostics in shielded volume, noting application of stable plasma generation effect for isotope analysis 02 p0199 A73-12693
- Parametric instability and anomalous heating due to electromagnetic waves in plasma. 03 p0345 A73-13060
- Effects of Hall currents and collisions with neutrals on the dynamic stability of a composite hydromagnetic plasma. 03 p0346 A73-13292
- Parametric instability of a spatially modulated plasma. 03 p0347 A73-14089
- Surface drift waves in a weakly ionized plasma. 03 p0347 A73-14090
- Instability of a weakly ionized plasma at wavelengths of the order of the Debye radius. 03 p0347 A73-14092
- Plasma confinement in a racetrack magnetic field with a diverter. 03 p0347 A73-14094
- Ion-cyclotron instability of a plasma produced by a fast-ion beam. 03 p0347 A73-14101
- Note on solar plasma irregularities and plasma instabilities. 03 p0378 A73-14420
- Numerical and analytic solutions for dispersion equation for flute-like ion cyclotron instabilities in high beta plasma, noting magnetic field inhomogeneity effect 03 p0348 A73-14436
- Quasi-linear equations for uniform plasma instabilities connected with potential oscillations, noting non-relativistic electron beam relaxation and abnormal plasma resistance 04 p0477 A73-15017
- Hydrodynamic and kinetic instability and oscillations of plasma with non-Maxwellian particle velocity distribution, noting laboratory and cosmic plasmas 04 p0478 A73-15018
- Kinetic and dispersion equations for collisionless plasma interaction with HF magnetic and electric fields, noting conical, drift and cyclotron instabilities prevention 04 p0478 A73-15019
- Hydromagnetic stability of closed plasma configurations 04 p0478 A73-15020
- Cyclotron resonance instability in a rotating plasma 04 p0479 A73-15042
- Multifrequency modulation of electron beam for instability oscillations control and energy transfer to plasma particles 04 p0479 A73-15044
- Investigation of the stability of plasma-jet motion in the magnetic field of a diverter 04 p0479 A73-15045
- Turbulent wave field growth rate and saturation amplitude for nonresonant instability in weak cold beam plasma system, using Dupree plasma turbulence theory 04 p0479 A73-15193
- Instability of a large-amplitude plasma wave due to inverted trapped particle population. 04 p0480 A73-15194
- Magnetospheric plasma instabilities and detectable manifestations in geomagnetic field and particle flux densities variations, considering magnetospheric substorms and auroral breakup 04 p0442 A73-15340
- Stationary turbulence of a parametrically unstable plasma. 04 p0480 A73-15474
- Stable electron density fluctuations in a plasma in the presence of a high-frequency electric field. 04 p0444 A73-15539
- Fluctuations in geomagnetic wake region at 500 earth radii connected with magnetotail Kelvin-Helmholtz instability, using plasma cylinder model 04 p0445 A73-15556
- Stability of a plasma with inequilibrium ions with respect to the generation of magneto-sonic waves 04 p0481 A73-15603
- Electromagnetic-emission energy flux during the development of beam instability in a magnetically confined plasma 04 p0481 A73-15607
- Experimental investigation of the kinetic instabilities in Gabor's alternative magnetron 04 p0481 A73-15610

- The dispersion diagram of the plasma waves on the plasma branch in a beam-created plasma. 04 p0482 A73-15949
- Instability of a relativistically strong electromagnetic wave of circular polarization. [AD-759478] 04 p0482 A73-15960
- Hydromagnetic stability of a laminary boundary layer in a flow past a planar plate 05 p0601 A73-16096
- Stability of a model current sheet with finite transverse field and finite flow velocity. 05 p0568 A73-16141
- Hydrodynamic instability of the boundary of a viscous plasma in a magnetic field. 05 p0603 A73-16793
- Monochromatic plasma wave instability due to induced scattering on thermal plasma electrons and ions with and without magnetic field 05 p0604 A73-17361
- Effect of ion viscosity and thermal conductivity on the drift instability in an inhomogeneous high-pressure collisional plasma. 05 p0604 A73-17362
- Surrounding wall electrical resistivity effects on plasma pinch stabilized by outer region force-free current flow, deriving instability growth rate 05 p0604 A73-17363
- Fusion plasma confined by nonpenetrating uniform magnetic field, calculating temperature and density effects on energy balance instabilities from particle conservation equations 05 p0604 A73-17366
- Electromagnetic radiation caused by the two-stream instability in a bounded plasma. 06 p0726 A73-17416
- Stream instabilities in a cold plasma in the presence of a magnetic field. 06 p0728 A73-17793
- Stationary nonlinear ion acoustic oscillations in dense weakly ionized current carrying plasma, considering wave propagation velocity and instability process 06 p0728 A73-17971
- Excitation of parametric instabilities by microwave pumping in a magnetoactive plasma 06 p0729 A73-18108
- Kinetic theory of longitudinal wave dispersion in nonuniform plasma layer in HF electromagnetic field, noting plasma instability for electron parametric resonance 06 p0729 A73-18109
- Plasma instability in terms of electron oscillations due to parametric interaction with UHF electric field, noting inverse Cerenkov effect for electrons 06 p0729 A73-18111
- Instability of a current-carrying plasma at cyclotron harmonics, and anomalous resistance 06 p0729 A73-18113
- Kadomtsev-Nedospasov helical instability during a strong pinch effect in an electron-hole plasma 06 p0729 A73-18119
- Anomalous ion heating in a laser heated plasma. 06 p0730 A73-18461
- Two dimensional simulation of nonlinear ion-sound instability in current carrying collisionless plasma due to modification of electron distribution function 06 p0730 A73-18464
- Heating of a magnetized plasma under parametrically unstable conditions 06 p0731 A73-18574
- Instability of a magnetoactive plasma with a transverse ion beam. 06 p0731 A73-18602
- High-frequency instabilities in a plasma with a nonlinear ion-acoustic wave. 06 p0731 A73-18603
- Anode sheath plasma current instabilities, examining electron and ion turbulent heating, plasma particle limiting energies and unsteady oscillation spectra 06 p0731 A73-18604
- Necessary and sufficient condition for hydromagnetic stability of the Bennett pinch. 06 p0733 A73-18848
- Macroscopic instability and anomalous diffusion in a glow discharge plasma 07 p0854 A73-19047
- Self trapping modulational instability of electron cyclotron wave whistler in cold and hot dense plasmas, discussing relevance to phenomena in magnetosphere 07 p0814 A73-19239
- Nonphysical noises and instabilities in plasma simulation due to a spatial grid. 07 p0854 A73-19267
- Theory of parametric resonance in an inhomogeneous plasma 07 p0855 A73-19279
- Screw instability of a plasma with a distributed current 07 p0855 A73-19280
- Instability limits of an isothermal weakly ionized plasma in a magnetic field 07 p0855 A73-19282
- Instability of surface ion-acoustic waves of finite amplitude 07 p0855 A73-19291
- Wave pattern of three dimensional hydromagnetic perturbations produced by harmonic magnetic dipole in anisotropic plasma 07 p0816 A73-19461
- Numerical analysis of magnetohydrodynamic instabilities by the finite element method. 07 p0856 A73-19515
- Mode-coupling and wave-particle interactions for unstable ion-acoustic waves. 07 p0856 A73-19521
- Modified negative mass mode stabilization in finite magnetic mirror confined plasmas with highly anisotropic velocity distribution, considering bounce harmonic effects and gyrofrequency 07 p0856 A73-19522
- Computerized simulation for nonlinear evolution of whistler instabilities in anisotropic collisionless plasmas with various Maxwellian electron distributions 07 p0857 A73-19523
- Equilibrium and stability of large-amplitude magnetic Bernstein-Greene-Kruskal waves. 07 p0857 A73-19524
- Nonlinear small amplitude behavior of collisionless plasma at mirror flute instability threshold, using modified constant gravity model and magnetic moment variation 07 p0857 A73-19525
- Theory and simulation of turbulent heating by the modified two-stream instability. 07 p0857 A73-19526
- Turbulence spectra of collisionless magnetized plasma produced in high voltage theta pinch, considering initial magnetic field orientation and instability theories tests 07 p0857 A73-19527
- Alternating current instability produced by the two-stream instability. 07 p0857 A73-19528
- Effects of collisions with neutrals on the dynamic stability of a finitely conducting hydromagnetic composite plasma in the presence of Hall currents. 07 p0858 A73-19600
- The sideband instability of electrostatic waves in an inhomogeneous medium. 07 p0858 A73-19667
- Electron energy loss effect on cross-field electron streaming instability in low density high temperature plasmas, using high voltage theta pinch 07 p0859 A73-20192
- Electromagnetic loss-cone instability of a plasma. 07 p0859 A73-20196
- Parametric excitation of circularly polarized and Langmuir waves in a magnetized plasma. 07 p0859 A73-20197
- Feedback control of ionization instability in MHD generators. 07 p0779 A73-20395
- Privileged equilibria of a collisionless homogeneous or inhomogeneous plasma. 07 p0860 A73-20480
- Large-amplitude stabilization of the drift instability. 07 p0860 A73-20481
- Anomalous plasma ion heating by parametric excitation of lower hybrid instabilities, using long wavelength oscillating electric field [AD-759477] 07 p0860 A73-20482
- Stabilization of normal drift modes in an inhomogeneous plasma by a magnetic shear field 07 p0860 A73-20611
- Non-local asymptotic treatment of the stability of an inhomogeneous confined plasma. 08 p0991 A73-20819
- Hydromagnetic instabilities of current carrying pinch in magnetic field, noting thin walled resistive liner effect on nonlocal modes stabilization 08 p0991 A73-20821
- Magnetic surfaces decay for parametric instability in helical magnetic configuration, noting nonlinear equations of magnetic field lines 08 p0991 A73-20822
- Influence of boundaries of the ionization instability of a plasma in a discharge of coaxial geometry. 08 p0992 A73-20851
- Influence of inelastic energy losses by electrons on the development of ionization instability in a plasma. 08 p0992 A73-20852
- The hydromagnetic oscillations and stability of self-gravitating masses. III - Magnetic polytropes. 08 p1005 A73-20917
- On the instability of longitudinal oscillations in an inhomogeneous isotropic plasma. 08 p0992 A73-20956
- Equatorial sporadic E and cross-field instability. 08 p0958 A73-21150
- Turbulent heating of colliding streams in the solar wind. 08 p0998 A73-21164
- Heat conductivity, plasma instabilities, and radio star scintillations in the solar wind. 08 p0998 A73-21165
- Oblique electromagnetic wave propagation with respect to double stream in plasma, calculating unstable wave oscillation frequency and growth rate dependence on stream direction 08 p0993 A73-21633
- Parametric action of high-power radiation on a plasma near the electron cyclotron frequencies 09 p1123 A73-21876
- Tokamak axisymmetric toroidal plasma filament equilibrium in conducting circular and elliptic cylinder for pressure and current distributions, using numerical MHD equation integration 09 p1123 A73-21877
- Structure of the current front in an unsteady plasma accelerator, and turbulent acceleration of the ions. I 09 p1124 A73-21881
- Structure of the current front in an unsteady plasma accelerator, and turbulent acceleration of the ions. II 09 p1124 A73-21882
- Low threshold unstable nonpotential oscillations of weakly ionized rotating plasma in crossed field centrifuge, noting MHD generator and ionospheric implications 09 p1124 A73-21891
- Parametric excitation of surface waves in a non-homogeneous magnetized plasma 09 p1124 A73-21892
- Surface oscillations of a weakly ionized plasma in a magnetic field 09 p1124 A73-21901
- Influence of magnetic field curvature on the stability of a plasma confined by a dense shell of neutral gas 09 p1124 A73-21902
- Waves in magnetoactive plasma in the presence of a distinct transverse ion velocity 09 p1125 A73-21904
- Application of a system of orthogonalized windings with automatically regulated current for plasma stabilization in Tokamak systems 09 p1125 A73-21908
- Nonlinear frequency correction to plasma instability at half harmonics of electron gyrofrequency as observed by OGO 5 near geomagnetic equator outside plasmopause 09 p1075 A73-22069
- An indirect method for measuring equatorial electrojet currents and its relation to nonlinear saturation of type I instabilities. 09 p1075 A73-22070
- Ion cyclotron instability in current-carrying plasmas with anisotropic temperatures. 09 p1127 A73-22284
- The instability of hydrodynamic longitudinal oscillations in a non-uniform magnetoactive plasma. 09 p1127 A73-22285
- Thermal instability in a viscoelastic fluid layer in hydromagnetics. 09 p1166 A73-22418
- Steady state Lie group solutions to nonlinear partial differential equations of low temperature plasma ionization instability in strong magnetic field 09 p1127 A73-22591
- RF plasma heating by the modified two stream instability. [TTU-SR-2] 09 p1128 A73-22628
- Nonlinear theory of plasma heating by parametric instabilities. [TTU-SR-2] 09 p1128 A73-22633
- Measurement of effective collision frequency in RF heating through parametric instabilities. [TTU-SR-2] 09 p1128 A73-22634
- Analytical and computer simulation of two ion species RF heated magnetoplasmas response to driving electric fields near lower hybrid frequency, observing parametric instabilities [TTU-SR-2] 09 p1129 A73-22640
- Kinetic theory of the spatial instability of a radially bounded plasma-electron beam system with a given radially nonhomogeneous plasma configuration 09 p1129 A73-22688
- Relaxation processes in a parametrically unstable plasma 09 p1130 A73-22707
- Influence of dispersion on the nonlinear evolution of quasi-monochromatic spiral waves in a magnetoactive plasma 09 p1130 A73-22708
- Kelvin-Helmholtz instability in type I comet tails. 09 p1148 A73-22741
- Drift-like instability in density modulated plasmas in a static magnetic field. 09 p1131 A73-22904
- Parametric excitation of circularly polarized and ion waves in a magnetized plasma. 09 p1131 A73-22905
- Propagation of surface waves and instability wave growth in an ion beam-plasma system. 09 p1131 A73-22906
- Excitation of magnetosonic waves in a plasma with nonequilibrium ions 09 p1131 A73-23076
- Anomalous nonlinear dissipation of high-frequency radio waves in a plasma 09 p1053 A73-23330
- Frequency entrainment of a drift instability by nonlinear effects in a plasma. 10 p1253 A73-24114
- Stability of a plasma with nonequilibrium ions with respect to magnetosonic waves. 10 p1254 A73-24193

- Electromagnetic energy in the two-stream instability in a magnetized plasma. 10 p1254 A73-24197
- Experimental investigation of kinetic instabilities in the Gabor magnetron. 10 p1254 A73-24200
- Low-frequency parametric instabilities of magnetized plasmas with two ion species. 10 p1255 A73-24261
- Electromagnetic instability for plasma waves propagating perpendicular to uniform magnetic field in counterstreaming electron-ion plasmas based on linearized Vlasov-Maxwell equations 10 p1255 A73-24262
- Electron-cyclotron drift instability in high-beta plasmas, developing nonlinear theory based on wave kinetic equation for weak turbulence 10 p1255 A73-24263
- Straight plasma column confined by static axial and oscillating transverse magnetic fields, deriving stability criteria via viscous fluid model 10 p1255 A73-24264
- Electromagnetic wave instability characteristics during propagation oblique to electron stream in cold electron-ion plasma 10 p1255 A73-24268
- Internal instabilities derived for electron plasma with electrons rotating about axis of symmetry parallel to confining external magnetic field 10 p1256 A73-24449
- Uniform variable transverse magnetic field effects on convective instability of plane electrically conducting layer, reducing perturbed equilibrium equations to linear ordinary differential equations 10 p1256 A73-24593
- OGO 5 observation of ULF geomagnetic fluctuation at polar cusp boundaries in terms of ionospheric drift wave and Kelvin-Helmholtz instabilities 10 p1214 A73-24744
- Periodic instability induced in semiconductor situated in crossed electric and magnetic fields via electron gas heating, deriving expressions for properties of steady nonlinear waves 10 p1261 A73-24764
- Ambipolar drift, deformation, and diffusion of a plasma in a magnetic field. 11 p1402 A73-24989
- Stability of a plasma rotating in crossed electric and magnetic fields 11 p1403 A73-25240
- Rotational instability of a plasma from a hot-cathode Penning discharge 11 p1403 A73-25243
- Unstable Langmuir or ion acoustic wave saturation in collisionless plasma due to electron trapping, estimating amplitude via adiabatic and sudden approximation 11 p1404 A73-25258
- The ion cyclotron drift loss-cone instability with a coexisting cold plasma. 11 p1404 A73-25271
- On nonlinear transformation and stabilization of beam-plasma instability. 11 p1404 A73-25274
- Rotational discontinuities in an anisotropic plasma. II. 11 p1405 A73-25922
- Refraction by the electromagnetic pump of parametrically generated electrostatic waves. 11 p1405 A73-25973
- Parametric excitation of Langmuir oscillations in the ionosphere in a field of powerful radio waves 11 p1331 A73-26153
- Contribution to the nonlinear theory of kinetic instability of an electron beam in plasma. 11 p1405 A73-26183
- Nonlinear ion sound in a fully ionized current-carrying plasma. 11 p1406 A73-26186
- Inertial magnetic field reconnection and magnetospheric substorms. 11 p1357 A73-26206
- Magneto-viscous effects on the ideal and resistive gravitational instabilities in Cartesian geometry. 11 p1406 A73-26553
- Feedback stabilization of a multimode two-stream instability. 11 p1406 A73-26556
- Long wavelength instability in a perpendicular shock. 11 p1406 A73-26557
- Temperature-waves in connection with drift type instabilities in a Q-plasma. 11 p1406 A73-26558
- Parametric instability in a plasma placed in non-homogeneous magnetic field. 11 p1407 A73-26563
- Parametric instability in an inhomogeneous plasma containing hot ions 12 p1526 A73-26926
- Stability of a magneto-active plasma with a relativistic electron beam, situated in a high-frequency electric field 12 p1527 A73-26927
- Influence of electric drift on the cone instability of a plasma in adiabatic traps 12 p1527 A73-26930
- Electrical explosion of wires at high energy input rates 12 p1523 A73-26936
- Braking of electron beams in a plasma with a high level of Langmuir turbulence 12 p1527 A73-26956
- Hydromagnetic stability of plane heterogeneous shear flow. 12 p1527 A73-27129
- Development of acoustic and overheat instabilities in a plasma with molecular impurities 12 p1528 A73-27303
- Influence of a SHF field on the inhomogeneities of a nonequilibrium plasma from a low-pressure gas discharge 12 p1528 A73-27304
- Czechoslovak Seminar on Plasma Physics, 6th, Liblice, Czechoslovakia, May 10-12, 1972, Research Report. [IPPCZ-167] 12 p1528 A73-27430
- The theoretical situation with the investigations of parametric instabilities in gaseous plasmas. [IPPCZ-167] 12 p1528 A73-27432
- Nonlinear helical waves formation due to Kelvin-Helmholtz instability in type 1 comet tail modeled as plasma cylinder immersed in solar wind 12 p1542 A73-27609
- Nonlinear theory of parametric wave instability in a plasma 12 p1530 A73-27981
- Two-stream instability heating of plasmas by relativistic electron beams. 13 p1663 A73-28186
- Monoenergetic particle beam instabilities in homogeneous plasma due to secondary emission wave interactions 13 p1664 A73-28289
- Effect of a high frequency magnetic field on plasma diffusion in a Q-machine. 13 p1664 A73-28348
- Concerning one exact solution of the theory of quasilinear relaxation of a parametrically unstable plasma in the field of powerful radiation. 13 p1664 A73-28613
- Parametric resonance in an inhomogeneous plasma. 13 p1665 A73-28679
- Screw instability in a plasma with a distributed current. 13 p1665 A73-28680
- Stability of a weakly ionized isothermal plasma in a magnetic field. 13 p1665 A73-28682
- Plasma heating at the lower hybrid resonance. 13 p1665 A73-28690
- Instability of ion-acoustic surface waves of finite amplitude. 13 p1665 A73-28691
- Nature of auroral emission intensity pulsations associated with geomagnetic pulsations of the P2 type. 13 p1607 A73-28706
- Instability of the current in the neutral sheet of the tail of the earth's magnetosphere. 13 p1608 A73-28715
- Instability of hydromagnetic perpendicular shocks in inhomogeneous fluids. 13 p1601 A73-28775
- Stability of a plasma cylinder containing axisymmetric opposite currents 13 p1666 A73-28952
- Suppression of the flute instability of a dense plasma by a magnetic system of feedbacks in an open trap 13 p1666 A73-28953
- Stability of flute disturbances in a plasma of toroidal geometry 13 p1666 A73-28954
- German book on plasma physics covering plasma containment, magnetohydrostatics, gravitational effects, plasma pinch, toroidal plasmas, plasma waves and MHD instabilities 13 p1667 A73-29288
- Theory of turbulent plasma heating by anomalous absorption of magnetosonic waves. 14 p1777 A73-29683
- Parametric instability in the region of low-frequency hybrid resonances. 14 p1778 A73-29686
- Problems associated with the injection of a high-energy neutral beam into a plasma. 14 p1778 A73-29688
- Energy variational principle formulation for stability determination of scalar-pressure toroidal plasma, writing potential energy as one dimensional integral 14 p1778 A73-29689
- 'Drift' instabilities distorting the magnetic surfaces of Tokamak-type toroidal systems. 14 p1778 A73-29690
- High frequency discharges sustained either on a cavity resonance or on a plasma resonance 14 p1779 A73-29923
- Observation of a current-driven plasma instability at the outer zone-plasma sheet boundary. 14 p1747 A73-29966
- Ionospheric plasma waves instabilities induced by energetic electron beam fired perpendicular to magnetic field 14 p1747 A73-29967
- Collisionless magnetized unstable plasma two dimensional adiabatic compression, calculating gamma from temperature distributions 14 p1779 A73-29984
- Symposium on Plasma Heating and Injection, Varenna, Italy, September 21-October 4, 1972, Lectures and Seminars. 14 p1779 A73-30117
- Parametric instabilities and anomalous absorption and heating of plasmas. 14 p1779 A73-30118
- A nonlinear theory for the parametric instability with comparable electron and ion temperatures. 14 p1779 A73-30119
- The use of fast magnetic compression for the production and heating of plasma in Tokamak-like geometries. 14 p1780 A73-30121
- Instabilities in a system of a plasma and an intense relativistic electron beam. 14 p1780 A73-30122
- Existence conditions for magnetoactive plasma longitudinal waves with phase velocity near light velocity, investigating increments during synchrotron instability due to relativistic particles 14 p1780 A73-30337
- Plasma heating by an intense electron beam. 14 p1781 A73-30553
- Correlation between the potential and density fluctuations of a plasma, and the convective transport of particles across the magnetic field in a Penning discharge in the presence of rotational instability 14 p1781 A73-30581
- Stability of solar wind against electromagnetic streaming instability. 14 p1788 A73-30743
- Investigation of low-frequency instabilities in a linear plasma betatron 14 p1782 A73-30805
- Quasi-linear theory of a parametrically unstable magnetoactive plasma 14 p1782 A73-30806
- Electromagnetic instabilities of finite pressure anisotropic plasma with hot electrons. 15 p1916 A73-31084
- The effect of temperature perturbations on ion-acoustic and drift waves in a weakly collisional plasma. 15 p1916 A73-31087
- Linear Z pinch magnetohydrodynamic instability mode and characteristic wavelength determined by discharge tube radius and current buildup rate 15 p1918 A73-31703
- Nonstationary theory of decay instability in a weakly inhomogeneous plasma 15 p1918 A73-31704
- Stochastic heating of a plasma during development of a Langmuir turbulence instability 15 p1918 A73-31705
- Self-induced effects of radio waves in the vicinity of plasma resonance 15 p1918 A73-31706
- Type I and II electron density irregularities due to two-stream and cross field instabilities in E region equatorial electrojet, considering wind shear role 15 p1869 A73-31755
- Electromagnetic instability in a counterstreaming plasma. 15 p1919 A73-31928
- Ionization instability in CO2 laser discharges. 15 p1885 A73-32258
- Dispersion equation for nonpotential oscillations and hydrodynamic instabilities in hot ion plasma with transverse current in magnetic field 15 p1920 A73-32304
- Maximum equilibrium pressure of a plasma in a three-dimensional system with helical geometry 15 p1920 A73-32305
- Intensity of thermal fluctuations of plasma flute instabilities in open confinement systems in the presence of a feedback system 15 p1920 A73-32307
- Limitation of beam instability as a result of the capture of plasma electrons by the wave 15 p1920 A73-32320
- Kinetic instability of a plasma located in an SHF field 15 p1921 A73-32332
- Surface oscillations of a weakly ionized plasma in a magnetic field. 15 p1921 A73-32626
- Effect of magnetic field curvature on the stability of a plasma confined by a dense neutral gas. 15 p1921 A73-32627
- Waves in a magnetoplasma with an isolated transverse ion velocity component. 15 p1922 A73-32629

- Magnetic feedback stabilization in a Tokamak.
15 p1922 A73-32633
- The variational principle and the virial theorem for uniformly rotating magnetohydrodynamic systems.
16 p2040 A73-32926
- Steady state arc discharge physical properties, discussing boundary geometry of plasma column, and stabilities in gas flow and high current and vacuum conditions
16 p2040 A73-32939
- Arc discharge properties in ionized gases, discussing interruption and reignition in terms of instabilities, decay processes, and circuit breaker problem
16 p2040 A73-32940
- Nonlinear evolution of the decay instability in a plasma with comparable electron and ion temperatures.
16 p2041 A73-33324
- Dynamic stabilization of plasmas by means of a high-frequency-modulated electron beam.
16 p2041 A73-33326
- Remote feedback stabilization of ion acoustic type instability in plasma with LF density modulation, noting Van der Pol approach agreement and crossed field diffusion decrease
16 p2041 A73-33327
- Observations of two-stream ion wave instability.
16 p2041 A73-33335
- Ion-ion instability induced by ac electric fields.
16 p2042 A73-33336
- The magnetohydrodynamic stability of white dwarfs and neutron stars.
16 p2062 A73-33573
- Heating of magnetized plasma under conditions of parametric instability.
16 p2042 A73-33599
- Theory of the oscillations and stability of a semiconductor plasma with a small number of carriers in a strong electric field
16 p2042 A73-33734
- Hydromagnetic stability of parallel flow of an ideal heterogeneous fluid.
16 p2043 A73-33872
- Nonlinear radial electron beam focusing in plasma under beam-plasma instability, showing irreversibility conditions dependence on electromagnetic wave propagation mode
16 p2043 A73-34056
- Parametric instabilities in a plasma containing two types of ions
16 p2043 A73-34057
- Nonlinear frequency shift and damping stabilization mechanisms of unstable plasma waves in hot beam-cold plasma system
16 p2043 A73-34058
- Effect of finite resistivity on the dynamic stability of a composite plasma.
17 p2214 A73-34074
- Acoustic instability of a bounded weakly ionized plasma
17 p2214 A73-34135
- Effects of channel size on the ionization instability in MHD generators.
17 p2108 A73-34185
- Edge instability of transverse electromagnetic waves in a weakly ionized plasma
17 p2214 A73-34249
- On the magnetogravitational instability of a plasma which possesses an anisotropic pressure in uniform movement of rotation and under the influence of the Hall current - The equation of dispersion. I
17 p2215 A73-34250
- Instability of plasma waves with nonlinear Landau effect.
17 p2215 A73-34296
- Tokamak axisymmetric toroidal plasma filament equilibrium in conducting circular and elliptic cylinder for pressure and current distributions, using numerical MHD equation integration
17 p2215 A73-34301
- Structure of the current front and turbulent acceleration of ions in a pulsed plasma accelerator. I.
17 p2215 A73-34305
- Structure of current front and turbulent acceleration of ions in a plasma accelerator. II.
17 p2215 A73-34306
- Low threshold unstable nonpotential oscillations of weakly ionized rotating plasma in crossed field centrifuge, noting MHD generator and ionospheric implications
17 p2215 A73-34314
- Parametric excitation of surface waves in an inhomogeneous magnetized plasma.
17 p2215 A73-34315
- Book - Principles of plasma physics.
17 p2216 A73-34467
- A three-dimensional picture of the development of instability during the interaction of a modulated electron beam with a plasma.
17 p2216 A73-35170
- Transformation of high-frequency waves and vanishing of low-frequency instabilities in a radially-inhomogeneous beam-plasma discharge.
17 p2217 A73-35525
- On the explosive instabilities of waves in plasmas with special regard to dissipation and phase effects.
17 p2218 A73-35820
- Five wave interaction - A possibility for enhancement of optical or microwave radiation by nonlinear coupling to explosively unstable plasma waves.
17 p2218 A73-35821
- On the stabilization of explosive instabilities by nonlinear frequency shifts.
17 p2218 A73-35822
- Anomalous heating of dense plasma by laser radiation.
17 p2218 A73-35823
- Statistical theory of weakly interacting perturbations and low amplitude turbulence in fluids, considering diffusion, dispersive and acoustic wave characteristics and plasma instabilities
18 p2299 A73-36504
- Parametric excitation of surface waves in an inhomogeneous magnetized plasma
18 p2339 A73-36556
- Ion cyclotron instability of a rotating plasma
18 p2340 A73-36671
- Rarefied collisionless plasma turbulence and dissipation process due to instability, examining magnetic field effects on shock wave front nature
19 p2464 A73-37154
- Structure of almost collisionless shocks in a magneto-plasma and the ion-acoustic instability.
19 p2464 A73-37158
- Stability of plasma flows in multipolar magnetic fields
19 p2467 A73-37372
- Ionosphere, magnetosphere and interplanetary plasma instabilities effects on magnetosphere dynamics
19 p2476 A73-37758
- Low-frequency flute instabilities of a hollow cathode arc discharge - Theory and experiment.
19 p2468 A73-37858
- Quenching of the beam-plasma instability by mode mixing at a density discontinuity.
19 p2469 A73-37859
- Deceleration of electron beams in a plasma with a high level of Langmuir turbulence.
19 p2469 A73-38133
- Thermal model for streamers in nonequilibrium plasmas.
19 p2470 A73-38317
- Excitation of electromagnetic waves propagating along a magnetic field in a cold plasma by a beam of phased oscillators
19 p2406 A73-38330
- Low-frequency flute instabilities of a bounded plasma column.
20 p2595 A73-38889
- Spread E occurrence relationship to blanketing frequency from cross field plasma instability mechanism
20 p2552 A73-38948
- Magnetospheric implications of the nonlinear whistler instability obtained in a computer experiment.
20 p2553 A73-38961
- The theoretical situation with the investigations of parametric instabilities in gaseous plasmas.
20 p2597 A73-39195
- Potential oscillations with frequencies higher than the gyrofrequency in a plasma containing a cone of losses
20 p2597 A73-39207
- A new type of ionizational instability in a plasma with negative ions
20 p2598 A73-39621
- Current driven ion wave instability in a weakly ionized collisional magnetoplasma.
20 p2599 A73-39725
- Effects of propagation parallel to the magnetic field on the Type I electrojet irregularity instability.
21 p2682 A73-40160
- Plasma stability of electric discharges in molecular gases.
21 p2744 A73-40220
- The decay of perturbations in an electrically conducting and thermally radiating gas.
21 p2789 A73-40246
- Nonlinear ion surface oscillations in a semibounded current-carrying plasma
21 p2745 A73-40361
- Electron-acoustic and drift instabilities in a finite-pressure plasma with a transverse current
21 p2745 A73-40364
- Parametric excitation of ion-acoustic oscillations in a plasma situated in an alternating electric field and a constant magnetic field
21 p2746 A73-40519
- Electron-acoustic and ion-cyclotron parametric instabilities of a plasma in an alternating electric field. I, II
21 p2746 A73-40520
- Linear theory of transverse-current instability in a plasma
21 p2746 A73-40521
- Principal properties of plasma oscillations in an accelerator with closed drift and an extended zone of acceleration /ACDE/
21 p2746 A73-40523
- Inhomogeneous structure of plasma near sun due to drift, slipping and anisotropic temperature distribution instabilities, noting association with radio astronomy observed fine structure
21 p2767 A73-40537
- Rotating cylinder model for plasma gradient-temperature instability in gravitational field, showing heat convection due to Coriolis-caused particle drift
21 p2769 A73-40730
- Nonlinear parametric electron plasma instability due to cyclotron harmonic Bernstein wave interaction in strong electric field
21 p2747 A73-40791
- Growth rates of the ion cyclotron instability in the earth's magnetosphere.
21 p2685 A73-40824
- Plasma instability in a collisional and thermal magnetoplasma.
21 p2748 A73-40928
- MHD frequency wavelength relation to five-minute period oscillation in solar magnetically active regions
21 p2777 A73-41483
- On the possibility of constructing a radiative sunspot model in magnetohydrostatic equilibrium.
21 p2777 A73-41486
- Umbral flashes and running penumbral waves relation to overstable hydromagnetic oscillation in sunspots, noting depth dependence and electrical conductivity variation effects
21 p2777 A73-41487
- Possible mechanism of surge formation in the solar atmosphere.
21 p2777 A73-41493
- A current mechanism for the formation of inhomogeneities resulting in the ionospheric spread F region at high latitudes
21 p2692 A73-41508
- Parametric instabilities and turbulent heating of a plasma in the field of a fast magneto-acoustic wave.
21 p2750 A73-41677
- Parametric instabilities of weakly turbulent plasma, determining collision frequencies characterizing high frequency electric field energy absorption
21 p2750 A73-41681
- Anomalous transport due to the dissipative trapped-ion instability.
21 p2750 A73-41682
- Monoenergetic particle beam bunching instabilities in homogeneous plasma due to secondary emission wave interactions
22 p2890 A73-41813
- Effects of electrostatic instabilities on planetary and interstellar ions in the solar wind.
22 p2902 A73-41940
- Experimental investigation of current-driven ion wave turbulence in plasma.
22 p2890 A73-42224
- Parametric instability in an inhomogeneous plasma with hot ions.
22 p2891 A73-42260
- Stability of a magnetoactive plasma with a relativistic electron beam in an RF electric field.
22 p2891 A73-42261
- Effect of electric drift on the loss-cone plasma instability.
22 p2891 A73-42264
- Exploding wires with high energy input.
22 p2886 A73-42270
- Contribution to the theory of parametric instability of a bounded homogeneous plasma
22 p2892 A73-42380
- Nature of the anomaly of the electrical conductivity of a magnetized plasma
22 p2892 A73-42381
- Nonlinear development and Fourier analysis of the whistler mode instability.
22 p2893 A73-42391
- Instabilities of drift magnetosonic waves due to the magnetic drift resonance.
22 p2894 A73-42395
- Hydromagnetic stability of a composite plasma in the presence of Hall currents.
22 p2894 A73-42439
- Study of hydromagnetic stability of a hot rotating layer of fluid by Liapunov method.
22 p2894 A73-42474
- Flow stability of viscous homogeneous incompressible electrically conducting fluid between nonconducting walls at large magnetic Reynolds numbers
22 p2894 A73-42639
- German monograph - Model of a parallel shock wave with turbulent dissipation in a hot plasma.
22 p2895 A73-42718
- Self-action of electromagnetic wave in plasma under parametric instability.
22 p2895 A73-43022
- Appearance of turbulence during the interaction of a 'monoenergetic' beam with a plasma.
23 p3009 A73-43506

Motion of a plasma in curvilinear magnetic fields of constant and alternating curvature

23 p3010 A73-43661

Theta-pinch instability of plasma beam, relating plasma oscillation frequency to microwave emission and electromagnetic wave scattering

23 p3011 A73-43710

Backward ionization waves linear evolution to nonlinear saturated state from gaseous plasma self oscillation instability viewpoint, noting electron temperature and density increase

23 p3011 A73-43829

Cyclotron oscillations of a plasma in an inhomogeneous magnetic field

23 p3012 A73-44090

Thermonuclear laser synthesis and parametric instabilities

23 p2988 A73-44091

Stability of a plasma cylinder with counterstreaming axisymmetric currents.

23 p3013 A73-44304

Suppression of the flute instability in a dense plasma in an open system by magnetic feedback.

23 p3013 A73-44305

Flute stability in a toroidal plasma.

23 p3013 A73-44306

Theory of parametric resonance in a spatially modulated plasma

23 p3013 A73-44334

Nonpotential gravitationally-dissipative instability of a plasma in toroidal systems

23 p3015 A73-44348

Excitation of parametric instabilities in a magnetoactive plasma by a microwave pumping wave.

24 p3114 A73-44497

Kinetic theory of longitudinal wave dispersion in nonuniform plasma layer in HF electromagnetic field, noting plasma instability for electron parametric resonance

24 p3114 A73-44498

Plasma instability in terms of electron oscillations due to parametric interaction with UHF electric field, noting inverse Cerenkov effect for electrons

24 p3114 A73-44500

Instability of a current-carrying plasma at cyclotron harmonics and the anomalous resistance.

24 p3114 A73-44502

Kadomtsev-Nedospasov helical instability in a strong pinch effect in an electron-hole plasma.

24 p3114 A73-44503

Dispersion equation for nonpotential oscillations and hydrodynamic instabilities in hot ion plasma with transverse current in magnetic field

24 p3114 A73-44612

Maximum equilibrium pressure of a plasma in a spatial system with helical symmetry.

24 p3114 A73-44613

Thermal flute perturbations in an open plasma device with feedback.

24 p3114 A73-44615

Interpretation of distinct type IVmA- and IVmu-bursts on the basis of micro-instabilities and of resonant nonlinear interaction of waves.

24 p3123 A73-44645

Investigation of plasma acceleration in crossed electric and magnetic fields

24 p3115 A73-44751

Plasma instabilities in the region in front of a body moving rapidly in the ionosphere

24 p3115 A73-44790

The ion-sound instability and its associated multimode phenomena.

24 p3115 A73-44874

Heat current and anisotropy-driven instabilities in connection with the solar wind.

24 p3126 A73-45126

Stability of two-dimensional collision-free plasmas.

24 p3116 A73-45237

On the instability of magnetohydrodynamic Couette flow via non-axisymmetric, oscillatory critical modes.

24 p3116 A73-45241

Gaseous plasma thermal conductivity in dynamic equilibrium, relating particle binary correlation to shielding distance under temperature gradients

24 p3116 A73-45243

Magnetically induced electrothermal instability in unseeded partially ionized shock heated argon plasma

24 p3117 A73-45454

Experimental determination of the nonlinear interaction in a one dimensional beam-plasma system.

24 p3117 A73-45458

Parametric instability of strong circularly polarized electromagnetic wave in plasma producing relativistic electrons and backscattered light

24 p3117 A73-45459

Plasma decay instability nonlinear saturation spectrum in small spontaneous emission limit for comparable ion and electron temperatures from kinetic equation numerical solution

24 p3118 A73-45460

Spectroscopic measurements of plasma temperatures and density at X type magnetic neutral points, suggesting ion acoustic instability role in turbulent conductivity

24 p3118 A73-45461

Current driven ion acoustic plasma instability based on ion orbit perturbation by turbulent waves, calculating angular spectrum for comparison with computerized simulation

24 p3118 A73-45463

Nonlinear saturation of the relativistic beam-plasma instability in the presence of ion density fluctuations.

24 p3118 A73-45465

Computerized simulation of electrostatic instabilities development in underdense plasmas during heating by high output lasers with frequencies above electron plasma frequency

24 p3118 A73-45466

MAGNETOHYDRODYNAMIC TURBULENCE

Heat flow and magnetic field diffusion in turbulent fluids.

02 p0199 A73-12841

Turbulence in the annular flow of a conducting-fluid in a magnetic field

05 p0603 A73-16587

Transverse particle diffusion across external homogeneous magnetic field under random isotropic large scale hydromagnetic turbulence

07 p0856 A73-19450

Semiempirical determination of the anisotropy of turbulent MHD flow in a longitudinal field

10 p1256 A73-24592

Considerations concerning the solution of Chandrasekhar's system of equations in the case of MHD turbulence

11 p1404 A73-25700

Influence of a magnetic field on turbulent shear flow

15 p1917 A73-31402

Interaction of fast particles with magnetohydrodynamical turbulence.

17 p2216 A73-34504

Large-scale inhomogeneities in the sector structure of the solar wind

24 p3124 A73-44779

MAGNETOHYDRODYNAMIC WAVES

NT ELECTROSTATIC WAVES

NT PLASMA WAVES

MHD detonation waves properties and propagation velocities within relativistic theory, discussing shock equations nontrivial solution existence and uniqueness

01 p0085 A73-11260

Ergodic behaviour of nonlinear hydromagnetic waves in a cold collisionless plasma.

01 p0087 A73-11496

The propagation of non-uniform slow shock waves.

02 p0198 A73-12092

Alfven waves nonlinear damping mechanism due to magnetosonic wave dissipation, presenting nonlinear coupling rates

02 p0217 A73-12401

Circular polarization of synchrotron radiation in the presence of hydromagnetic waves.

02 p0224 A73-12739

The ducted propagation of PP micropulsations in the magnetosphere and PP dotting.

03 p0298 A73-12877

Asymmetric eigenmodes in a simple model plasmasphere.

03 p0345 A73-12882

Propagation of Pcl micropulsations in a proton-helium magnetosphere.

03 p0298 A73-12883

Magnetospheric field fluctuations and the penetration of solar protons to low geomagnetic latitude.

03 p0360 A73-12891

Alfven wave induced bulk velocity amplitudes in lower solar atmosphere, discussing relationship between energy flux, bulk velocity, wavelengths and scale height

03 p0360 A73-12944

Plasma heating and acceleration due to Landau damping of hydromagnetic waves.

04 p0480 A73-15197

Excitation of a magnetohydrodynamic waveguide by a moving source

05 p0603 A73-16820

Geomagnetic micropulsations within magnetosphere, investigating MHD waves and particle-wave interactions

05 p0570 A73-17051

Nonlinear mode-mode coupling of Alfven waves in the interstellar medium.

06 p0730 A73-18465

Hall current effects on waves in an electrically conducting rotating fluid.

07 p0854 A73-19104

Transverse hydromagnetic plane waves in the presence of a temperature gradient.

07 p0856 A73-19339

Hydromagnetic waves excited by transverse magnetic dipole in finite-conductivity plasma

07 p0816 A73-19462

The behaviour of ULF waves and particles in the magnetosphere.

07 p0792 A73-19666

The laws of reflection and refraction of incompressible magnetohydrodynamic waves at a fluid-solid interface.

07 p0858 A73-20028

On the transmission of the energy in an incompressible magnetohydrodynamic wave into a conducting solid.

07 p0858 A73-20029

MHD shock wave decay in oblique magnetic field, considering shock and rarefaction waves interaction

07 p0858 A73-20071

Collisional absorption of a rapid hydromagnetic wave in a plasma of two kinds of ions - Experiment

07 p0859 A73-20149

Dynamics of the non-linear interaction of magnetohydrodynamic waves.

07 p0859 A73-20236

Classification, orientational characteristics, and some examples of rotational discontinuities in the solar wind

08 p0998 A73-21278

Characteristics of hydromagnetic wave propagation in a slowly varying magnetic field/Geometrical optics approximation/

08 p0959 A73-21294

Analytical description of the geomagnetic field of past epochs and the determination of the magnetic-wave spectrum in the earth's core

08 p0959 A73-21297

Dissipation of hydromagnetic waves with application to the outer solar corona. I - Collisionless protons and collisional electrons. II - Transition from collisional to collisionless electrons.

09 p1142 A73-22038

Characteristics of the electric field far from and close to a radiating antenna around the lower hybrid resonance in the ionospheric plasma.

09 p1049 A73-22277

Enhanced energy transfer to a cylindrical plasma by an Alfven wave.

09 p1128 A73-22629

Theory of fluctuations and particle scattering in ferromagnetic semiconductors and metals

09 p1134 A73-22678

Relativistic MHD formulation in terms of non-holonomic tetrad field for rotating plasma coupled to frozen-in magnetic field, noting Alfven waves propagation velocity

09 p1131 A73-22921

Self-similar cylindrical magnetogasdynamic and ionizing shock waves.

10 p1204 A73-23564

Coefficients of hydromagnetic wave reflection from conjugate ionospheres

10 p1211 A73-23895

On hydromagnetic Rossby waves excited by travelling forcing effects.

11 p1403 A73-25154

Collisional transverse MHD shock wave structure within magnetic field inducing anisotropic plasma transport properties, using singular perturbation approach

11 p1403 A73-25254

Resonance between spin and magnetohydrodynamic waves in antiferromagnetic semiconductors and metals.

11 p1409 A73-26190

Small amplitude hydromagnetic waves for a plasma with a generalized polytrope law.

11 p1406 A73-26555

Dissipation of hydromagnetic waves with application to the outer solar corona. III - Transition from collisional to collisionless protons.

11 p1428 A73-26619

Super-Alfven displacement of hydromagnetic pulses in the earth's radiation belt

12 p1491 A73-27349

Asymmetric eigenmodes in a simple model plasmasphere with non-uniform Alfven speed.

12 p1529 A73-27613

Flare-produced coronal MHD-fast-mode wavefronts and Moreton's wave phenomenon.

12 p1536 A73-27848

'Drift' instabilities distorting the magnetic surfaces of Tokamak-type toroidal systems.

14 p1778 A73-29690

Interplanetary plasma inhomogeneities effect on Alfven wave propagation direction from Pioneer 6 magnetic measurements

14 p1796 A73-29957

Alfven waves in a two-fluid model of the solar wind.

14 p1787 A73-30005

Valve effect of inhomogeneities on anisotropic wave propagation.

14 p1780 A73-30165

Unified geometric and analytical treatment of magnetogasdynamic shocks. I - General solutions and theorems.

15 p1917 A73-31339

Ion-acoustic turbulence as MHD wave damping mechanism in weakly turbulent magnetosphere plasma at high and low frequencies

15 p1919 A73-31893

Absorption of hydromagnetic waves in the plasma layer of the magnetospheric tail

15 p1872 A73-31902

Solar wind flow in interplanetary space, discussing comets, cometary tail, interplanetary magnetic field and Alfvén waves characteristics
15 p1940 A73-32183

French monograph - Experimental study of conditions of resonance of tubes of forces of the terrestrial magnetic field.
15 p1874 A73-32594

Self-consistent calculation of the motion of a sheet of ions in the magnetosphere.
16 p2003 A73-33433

On the existence of critical levels, with applications to hydromagnetic waves.
16 p2043 A73-33869

Book on wave propagation in continuous media covering Hamilton principle, energy theorems, elastic waves, electromagnetic and hydromagnetic waves, Green function and nonlinear effects
17 p2211 A73-34280

The propagation of Alfvén waves and their directional anisotropy in the solar wind.
17 p2223 A73-34501

Interaction of fast particles with magneto-hydrodynamical turbulence.
17 p2216 A73-34504

Damping of Alfvén and magnetoacoustic waves at high beta.
17 p2217 A73-35524

Alfvén waves in the solar wind - Wave pressure, Poynting flux, and angular momentum.
18 p2346 A73-36264

Solar wind interaction with the earth's magnetic field. II - Magnetohydrodynamic bow shock.
18 p2346 A73-36271

Arbitrary propagation of HM waves along the F region.
18 p2312 A73-36285

Hydromagnetic eigenoscillations in the magnetospheric tail.
18 p2352 A73-36295

Radio aurora, storm sudden commencements, and hydromagnetic waves.
18 p2313 A73-36646

High temperature relativistic plasmas, calculating post-shock properties for steady hydromagnetic shock wave production
19 p2464 A73-37156

Two field continuum model of magnetic sheath adjacent to absorbing solid surfaces, using Bohm criterion and MHD boundary layer equation approximation
19 p2464 A73-37162

Quasi-steady plasma wind tunnel for Alfvén wave measurements of MHD flow involving shock waves and wakes, using Langmuir probes
19 p2465 A73-37172

Hydromagnetic waves directed by the geomagnetic field
19 p2481 A73-37337

Weak perturbation propagation in magnetic gasdynamics
19 p2468 A73-37550

Classification, characteristics of orientation, and some examples of rotational discontinuities in the solar wind.
19 p2476 A73-37907

Characteristics of hydromagnetic wave propagation in a slowly varying magnetic field /in the approximation of geometric optics/.
19 p2425 A73-37923

Analytical description of the geomagnetic field of past epochs and determination of the spectrum of magnetic waves in the core of the earth.
19 p2425 A73-37926

Reflection coefficients of hydromagnetic waves from conjugate ionospheres.
20 p2551 A73-38914

Structural determination of electric field conditions in ionizing shock waves.
20 p2596 A73-38964

Structural determination of electric field conditions in ionizing shock waves.
20 p2596 A73-38965

Collisionless damping of hydromagnetic waves in relativistic plasma. I - Weak Landau damping - Heating of the Crab Nebula.
20 p2609 A73-39442

Second-order plasma interaction in the Crab Nebula.
20 p2610 A73-39579

Jupiter magnetospheric interaction with innermost satellite Io, noting magnetic field annihilation enhancement in neutral point by LF MHD waves
21 p2764 A73-40166

The propagation of Alfvén waves along Io's flux tube.
21 p2764 A73-40167

Jupiter satellite Io controlled decametric Alfvén wave emission pattern, considering relationship to coherent cyclotron radiation growth rate
21 p2764 A73-40168

Regular reflection of an oblique shock in a plane flow of ideally dissociating gas in the presence of a transverse magnetic field
21 p2744 A73-40189

The effect of magnetic mass on Alfvén waves.
21 p2701 A73-40624

Magnetohydrodynamic waves in the solar wind plasma
21 p2763 A73-41506

Magnetic pulsation spectra in a nonisothermal plasma.
22 p2890 A73-41725

New dispersion relation for a strongly magnetized degenerate electron plasma with anisotropic pressure.
22 p2890 A73-42237

Magnetogasdynamics shock polar - Exact solution in aligned fields.
22 p2893 A73-42393

Super-Alfvén displacement of hydromagnetic pulses in the radiation belt of the earth.
23 p2970 A73-43246

Small amplitude Alfvén waves propagation in solar wind under interplanetary magnetic field, relating wave and wind velocity
23 p3029 A73-43612

A high resolution study in time, position, intensity, and frequency of the radio event of January 14, 1971.
24 p3136 A73-44643

Hydromagnetic gradient waves in the ionosphere
24 p3083 A73-44789

Plasma conductivity model of current structure of MHD waves propagating from electric dipole source in magnetosphere in relation to geomagnetic pulsations
24 p3084 A73-44805

Role of hydromagnetic waves in cosmic-ray confinement in the disk. I - Theory of behavior in general wave spectra.
24 p3124 A73-45040

MAGNETOHYDRODYNAMICS
An action principle in general relativistic magnetohydrodynamics.
01 p0079 A73-11258

Numerical solutions for MHD equations, considering initial values, time independence and mathematical models including hyperbolic, parabolic and elliptic differential equations
01 p0086 A73-11459

Linear MHD equations for inviscid medium under external forces, discussing magnetoacoustic wave generation by radially pulsating cylinder and sphere
02 p0196 A73-11605

Propagation of surface waves along a plane boundary between two magnetoactive plasmas.
02 p0198 A73-12107

MHD equations for velocity distribution of magnetic field motion in conducting fluid, noting evolution equations of geomagnetic field
02 p0164 A73-12555

The equilibrium and stability of uniformly rotating gaseous systems in hydromagnetics. I.
02 p0225 A73-12806

Low pressure plasma equilibrium in helitron device with stellarator confinement system, calculating plasma pressure from MHD equations
04 p0479 A73-15039

Study of the adiabatic curve of an ionizing shock wave in an inclined magnetic field
06 p0727 A73-17460

Evolutionary aspects of shock waves in the Chew, Goldberg, and Low approximation
06 p0727 A73-17471

An exact helical wave solution to the equations of magnetohydrodynamics.
07 p0859 A73-20233

Design considerations for high-current-density superconducting saddle magnets for MHD.
07 p0852 A73-20405

Special features of the dynamic spectrum of Pi2 type pulsations
08 p0960 A73-21307

Penetration of a solid into a half-space of compressible liquid in the presence of a magnetic field
08 p0994 A73-21724

Approximate calculation of a thermal boundary layer at a flat plate with allowance for a magnetic field
09 p1167 A73-22859

Report on the NATO Advanced Study Institute on magnetohydrodynamic phenomena in rotating fluids.
11 p1404 A73-25851

Steady conditions of a radiating self-constricted high-current discharge in a plasma
11 p1406 A73-26333

Oscillations of the earth's magnetic tail in a quasi-hydrodynamics approximation
12 p1491 A73-27347

Motion of a conducting gas with variable properties between rotating cylinders
12 p1487 A73-27798

Magnetohydrodynamic simulation of toroidal belt-pinch experiments.
14 p1778 A73-29694

Hydrostatic equilibrium conditions for hydromagnetic field, discussing topology of wrapping pattern of lines of force
14 p1782 A73-30741

Radial MHD bearing with a floating bush
15 p1881 A73-31412

Current extension from a quasi-steady MPD arcjet.
15 p1918 A73-31550

Shock waves, jump relations, and structure.
15 p1864 A73-31974

Simultaneous observations of Pcl micropulsation polarization at four low latitude sites.
16 p2008 A73-33877

Magnetohydrodynamics, hydrodynamics and dynamics of solar system model as contracting rotating cloud, discussing effects of turbulence
17 p2226 A73-34403

An approximate method for the solution of a class nonlinear equations in fluid mechanics and magnetohydrodynamics.
17 p2216 A73-35018

Book - Plasma engineering.
17 p2217 A73-35475

Magneto-fluid-mechanic heat transfer from hot film probes.
17 p2255 A73-35845

Re-connexion of magnetic lines of force - Evolution in incompressible MHD fluids.
18 p2338 A73-36181

Magnetopause configuration and dimension calculation methods, noting accurate numerical solutions for magnetohydrodynamic approach to two-dimensional problem
19 p2481 A73-37347

Characteristics of the dynamic spectrum of Pi2 type pulsations.
19 p2425 A73-37936

Solar atmosphere and ionosphere phenomena in terms of conducting gas motion at magnetic field neutral points
21 p2681 A73-40106

Solution of nonlinear problems in magnetofluid-dynamics and non-Newtonian fluid mechanics through parametric differentiation.
22 p2843 A73-42556

Oscillations of the earth's magnetic tail in the approximation of quasi-hydrodynamics.
23 p2970 A73-43244

MHD partial differential equations solution via hyperbolic system indicating shock wave structure existence satisfying Rankine-Hugoniot relation and entropy condition
24 p3116 A73-45221

Classical MHD differential equations solution for uniqueness and existence of shock wave structure based on thermodynamic potential concept
24 p3116 A73-45222

MAGNETOHYDROSTATICS
The effects of wall conductance on torque of the MHD viscous coupler and hydrostatic thrust bearing. [ASME PAPER 72-LUB-1]
03 p0313 A73-14326

German book on plasma physics covering plasma containment, magnetohydrostatics, gravitational effects, plasma pinch, toroidal plasmas, plasma waves and MHD instabilities
13 p1667 A73-29288

MAGNETOIONIC PLASMA
U PLASMAS [PHYSICS]
MAGNETOIONICS
Determination of the apparatus constant during multifrequency measurements of radio-wave absorption by the A1 method
08 p0939 A73-21303

Propagation through a slab of irregularities in a magneto-ionic medium.
09 p1051 A73-22647

Structure of ionospheric inhomogeneities, according to simultaneous observations on two magnetoionic components.
10 p1211 A73-24217

Calculation of the N/h/ profiles in the ionosphere from two magnetoionic components
11 p1351 A73-25096

Group delay times of magnetoionic components for horizontal electron density profiles in magnetic meridian plane, noting comparison with ionospheric sounding data
13 p1608 A73-28708

Frequency analysis of calculated ionospheric reflection coefficients.
16 p1984 A73-33920

Determination of the instrument constant in multifrequency measurements of radio wave absorption by the A1 method.
19 p2404 A73-37932

On the source of the slowly varying component at centimeter and millimeter wavelengths.
21 p2778 A73-41496

MAGNETOMETERS
NT VARIOMETERS
Operating characteristics of cylindrical thin film weak link circuits used as the sensing element in ultra-sensitive magnetometer systems.
02 p0200 A73-11845

Magnetograph instrumentation and measurements, presenting solar magnetic field fine structure observations
04 p0496 A73-14829

Use of magnetometers and asymmetric antenna patterns for attitude determination.
05 p0596 A73-17204

Marine quantum Cs Z-magnetometer design and compensation for onboard nonmagnetic schooner operation, using vertical gyro mount

06 p0691 A73-17547

Electromagnetic systems of noise-immunized nuclear-precession sensors

06 p0692 A73-17562

High resolution automatic magnetometer using a superconducting magnet Application to high field susceptibility measurements.

[IEEE PAPER 48,2] 07 p0823 A73-19365

Surface magnetometer experiments - Internal lunar properties and lunar field interactions with the solar plasma.

07 p0892 A73-19834

The theoretical output of a ring core fluxgate sensor.

07 p0825 A73-20219

Magnetometers using superconducting galvanometers.

07 p0826 A73-20406

Photomultiplier pairs arrays operation as solar magnetograph detector using fiber optics, comparing to photographic methods

08 p0970 A73-21737

Two dimensional photon counting - A design based on the Aerospace-NASA videomagnetograph.

08 p0972 A73-21756

Instrumental polarization concerning magnetographic measurements.

10 p1218 A73-24148

Dual magnetometer systems with cross correlation signal enhancement to overcome intrinsic sensor ambient noise and spacecraft magnetic field fluctuation effects on single detection performance

12 p1468 A73-27002

Bi2Se3 Hall effect magnetometer for reliable low temperature use.

13 p1612 A73-28368

Three axis fluxgate magnetometer/analog to digital converter system onboard Explorer D and E for measuring magnetic fields in auroral zone and equatorial electrojet

13 p1689 A73-28643

Magnetic anomalies in New Guinea-New Zealand region from proton magnetometer measurements, noting effects of andesite-basalt volcanic processes and nuclear precession signal variations

13 p1608 A73-28727

Equipment for recording and computer input of solar magnetograph data

15 p1878 A73-32139

Velocity field in the active regions of the sun

16 p2057 A73-32702

Marine quantum Cs Z-magnetometer design and compensation for onboard nonmagnetic schooner operation, using vertical gyro mount

16 p2011 A73-32771

Electromagnetic systems of noiseproof nuclear precession sensors.

16 p2011 A73-32786

Quiet time magnetospheric field depression at 2.3-3.6 earth radii.

16 p2005 A73-33464

The compensation method for measuring the components of the earth's magnetic field.

17 p2159 A73-34750

Real time digital videomagnetograph at the Aerospace San Fernando Solar Observatory.

17 p2168 A73-34909

Digital data acquisition and processing from a remote magnetic observatory.

17 p2175 A73-35667

An instrument for real-time determination of polar electrojet position and current parameters.

17 p2176 A73-35768

Apollo 15 and 16 subsatellite magnetometer measurements of the lunar magnetic field.

18 p2349 A73-35944

Wind measurement by magnetometers, optical and static pressure sensors.

18 p2310 A73-36136

The effects of the Westinghouse active magnetometer /WD-4/ on implanted cardiac pacemakers.

18 p2286 A73-36936

Angular dependence of optically pumped magnetometer - Effects of collisional mixing in the excited states.

19 p2429 A73-37382

Explorer 45 search coil magnetometer detection of ELF signals during magnetic storms, noting signal variation with storm phases and satellite magnetospheric position

20 p2552 A73-38957

Comments on paper by N. F. Ness, K. W. Behannon, R. P. Lepping, and K. H. Schatten, 'Use of two magnetometers for magnetic field measurements on a spacecraft.'

20 p2615 A73-38963

Specifications of a cryostat for a vibrating sample magnetometer between 1.7 and 300 K

21 p2706 A73-41592

Experimental test of the wind-shear theory: A reply - Rocket-borne magnetometers do measure B.

23 p3024 A73-43702

Triaxial magnetic measurements of field-aligned currents at 800 kilometers in the auroral region - Initial results.

24 p3087 A73-45140

MAGNETOMETRY

U MAGNETIC MEASUREMENT

MAGNETOPOUSE

Magnetopause motions at lunar distance determined from the Explorer 35 plasma experiment.

02 p0155 A73-11730

Shadowing of electron azimuthal-drift motions near the noon magnetopause.

02 p0164 A73-12442

Particle motion and electrostatic instabilities of geomagnetic tail and magnetopause plasma neutral sheets in relation to substorms, using Alfven and Cowley models

03 p0302 A73-13873

An effect of the solar wind on the earth's rotation

04 p0498 A73-15282

Magnetopause physical properties, location and shape from continuum gas dynamics analogies, noting agreement with experimental results

04 p0441 A73-15328

Geomagnetic tail and neutral sheet origin based on geomagnetic flux diffusion through magnetopause, discussing Dungey reconnection mechanism and Kelvin-Helmholtz instability effects

04 p0441 A73-15329

Dayside magnetopause distance calculation at subsolar point for various solar wind parameters, allowing for southward interplanetary field component diffusion

05 p0610 A73-17008

Dependence of the position of the magnetopause on the orientation of the interplanetary magnetic field

06 p0690 A73-17560

Correlation of ground-based measurements of structured Pc 1 micropulsations withOGO-V plasmapause observations.

08 p0937 A73-20652

Heos 2 magnetometer observations of magnetosheath high and low energy electron flux during magnetopause boundary crossings in polar regions

12 p1489 A73-27004

Interaction of the geomagnetic field with the antiparallel solar-wind field

15 p1926 A73-31891

Magnetopause plasma oscillations excitation and transformation into electromagnetic waves, estimating magnetic bremsstrahlung and X ray emission intensities

15 p1926 A73-31892

Dependence of the position of the magnetopause on the orientation of the interplanetary magnetic field.

16 p2002 A73-32784

Model of dayside magnetopause displacement relation to convection currents feeding polar cap ionosphere to estimate electric field and flux return as function of displacement

16 p2003 A73-33432

Magnetopause configuration and dimension calculation methods, noting accurate numerical solutions for magnetohydrodynamic approach to two-dimensional problem

19 p2481 A73-37347

Identification of discontinuities at the magnetosphere boundary.

19 p2424 A73-37906

High energy electrons at the magnetopause above the north pole - Preliminary results from the HEOS 2 satellite.

21 p2761 A73-41376

Satellite measurement of magnetopause location, speed and thickness during satellite immersion within adjacent steep proton flux gradient

24 p3126 A73-45113

MAGNETOPLASMA DYNAMICS

U MAGNETOHYDRODYNAMICS

MAGNETOPLASMAS

U PLASMAS (PHYSICS)

MAGNETORESISTANCE

U MAGNETORESISTIVITY

MAGNETORESISTIVITY

Problem of using the magnetoresistance effect to measure transferred SHF power

01 p0023 A73-10215

Automatic magnetic inspection method using magnetoresistive elements and its application.

02 p0173 A73-11988

Thermal conductivity and hot magnetic poles of pulsars.

03 p0374 A73-13796

Shubnikov-de Haas oscillations in graphite selective scattering by charged impurities.

04 p0468 A73-14871

Influence of the impurity compensation effect on the magnitude of the negative reluctance of alloys of the $\text{In}_2\text{Te}_3/\text{x-Hg}_3\text{Te}_3/1-\text{x}$ system

12 p1532 A73-27940

Thermistors as cryogenic thermometers.

22 p2854 A73-41998

Low temperature thermometry in high magnetic fields.

22 p2856 A73-42017

MAGNETOSONIC RESONANCE

Alfven waves nonlinear damping mechanism due to magnetosonic wave dissipation, presenting nonlinear coupling rates

02 p0217 A73-12401

Nonthermal turbulent heating in the solar envelope.

08 p1003 A73-20887

A magnetosonic resonator of Pc2,3 pulsations in the earth's magnetosphere

12 p1491 A73-27351

Hydromagnetic eigenoscillations in the magnetospheric tail.

18 p2352 A73-36295

Magnetosonic resonator of Pc2,3 pulsations in the earth's magnetosphere.

23 p2970 A73-43248

MAGNETOSPHERE

NT GEOMAGNETIC TAIL

NT MAGNETOPOUSE

Possibilities of measuring the velocity of circulation of the magnetospheric plasma with the help of a quadrupole probe used in the vicinity of the low hybrid frequency

01 p0035 A73-10326

Some peculiarities of the development of the magnetic storm on March, 5-10, 1970.

01 p0036 A73-10342

Ionospheric effects on the transmission of ultralow-frequency plasma waves.

02 p0155 A73-11520

Isis 1 observations of the high-latitude ionosphere during a geomagnetic storm.

[AD-759885] 02 p0155 A73-11735

Quiet time magnetosphere-thermosphere couplings, describing global wind system model and convection and auroral Joule heating

02 p0162 A73-12292

Auroral particle precipitation patterns from satellite observations, discussing electron and proton penetration from magnetosheath plasma and magnetotail

02 p0163 A73-12308

The international magnetospheric study 1975-1977 - Scientific fundamentals and objectives.

02 p0164 A73-12313

Self consistent model of closed field lines of pulsar magnetosphere valid for oblique rotators and unipolar inductors

02 p0216 A73-12382

Quasi-linear interaction of whistler-mode waves and nonthermal electrons.

02 p0141 A73-12390

Effect of the slope of geomagnetic field lines on the field of the magnetosphere-ionosphere current system

02 p0164 A73-12458

The ducted propagation of PP micropulsations in the magnetosphere and PP dotting.

03 p0298 A73-12877

Propagation of Pcl micropulsations in a proton-helium magnetosphere.

03 p0298 A73-12883

Transmission and reflection of magnetospheric whistlers in the ionosphere and lower exosphere at high latitudes.

03 p0298 A73-12884

Geomagnetic field variations caused by changes in the quiet-time solar wind pressure.

03 p0298 A73-12885

Magnetospheric field fluctuations and the penetration of solar protons to low geomagnetic latitude.

03 p0360 A73-12891

Recent satellite measurements of the morphology and dynamics of the plasmasphere.

03 p0301 A73-13709

Results from barium cloud releases in the ionosphere and magnetosphere.

[MPI-PAE-EXTRATERR-67] 03 p0301 A73-13805

Earth's magnetospheric processes; Proceedings of the Symposium, Coriina, Italy, August 30-September 10, 1971.

03 p0302 A73-13851

Magnetospheric structure studies during 1969-1971, discussing bow shock magnetosheath, magnetopause, polar cusps, electric fields and trapped particle composition

03 p0302 A73-13852

Physical mechanisms of magnetospheric processes, discussing matter and energy exchange between solar wind and magnetosphere, substorms, interaction with ionosphere, etc

03 p0302 A73-13853

Ring current effect on plasma convection in magnetosphere, assuming pressure due to proton population

03 p0302 A73-13854

Electromagnetic wave observation in interplanetary medium and in magnetosphere, emphasizing magnetic and electric field measurements

03 p0374 A73-13855

Mechanisms for the injection of protons into the magnetosphere.

03 p0362 A73-13858

Solar wind interaction with geomagnetic field, discussing magnetosphere polar cusp region and geomagnetic tail neutral sheet structure

03 p0302 A73-13871

De electric field measurement with rocket-borne double probes and by satellite and balloon observation, noting ionospheric fields, magnetospheric plasma and auroras

03 p0302 A73-13874

Injun 5 observations of magnetospheric electric fields and plasma convection.

03 p0303 A73-13875

Plasma convection in the vicinity of the geosynchronous orbit.

03 p0303 A73-13878

High energy proton model for the inner radiation belt.

03 p0363 A73-13880

Magnetic field variations at micropulsation frequencies.

03 p0303 A73-13881

Changes in the distribution function of magnetospheric particles associated with gyroresonant interactions.

03 p0303 A73-13882

Magnetospheric observations inOGO-5 plasma wave experiment, emphasizing electrostatic wave particles interaction with plasma

03 p0303 A73-13883

A theory on the latitude and local time distribution of precipitating electrons during a sudden commencement.

03 p0304 A73-13885

Atmospheric model for substorm triggering mechanism, plasma sheath behavior and substorm recovery, noting solar wind interaction with magnetosphere

03 p0304 A73-13886

Interpretation of magnetic field variations during substorms.

03 p0304 A73-13888

Excitation of polar substorms by northward interplanetary magnetic field.

03 p0304 A73-13890

The effect of an electric field induced by a time-dependent ring current on the particle drift motion.

04 p0440 A73-14954

Solar proton intensity structures in the magnetosphere during interplanetary anisotropies.

04 p0492 A73-14962

Analytical study of the evolution of the normal to the wave during the magnetospheric passage of PC 1's

04 p0440 A73-15248

Critical problems of magnetospheric physics; Proceedings of the Symposium, Madrid, Spain, May 11-13, 1972.

04 p0441 A73-15326

Magnetosphere configuration models based on open and closed field line hypotheses, discussing solar wind-magnetosphere interactions, magnetotail, substorm growth, flux transport, etc

04 p0441 A73-15327

Solar wind plasma entry into earth magnetosphere, reviewing major uncertainties in light of current observational knowledge

04 p0442 A73-15330

Auroral and magnetospheric phenomena caused by solar wind particles entry and energization via magnetosheath into magnetosphere and upper atmosphere

04 p0492 A73-15331

Magnetospheric trapped particle populations boundaries properties, discussing dynamic boundaries during magnetic disturbances and substorm effect on night magnetosphere configuration

04 p0442 A73-15332

Magnetospheric electric fields convective motions measurement by Ba ion cloud tracking and symmetric double probe floating potential technique

04 p0442 A73-15333

Electric field and plasma observations in the magnetosphere.

04 p0442 A73-15334

Time dependent and independent electric coupling between magnetosphere and ionosphere, discussing auroral arcs formation and magnetospheric plasma convection

04 p0442 A73-15335

Behavior of thermal plasma in the magnetosphere and topside ionosphere.

04 p0442 A73-15336

Magnetospheric convection, discussing ionospheric twin vortex pattern, reconnection model for solar wind induced generation, plasmasphere response and magnetotail dynamics

04 p0442 A73-15337

Magnetospheric field distortion relation to ring currents based on satellite-borne magnetometer measurements of magnetic field topology

04 p0442 A73-15338

The importance of wave-particle interactions in the magnetosphere.

04 p0492 A73-15339

Magnetospheric plasma instabilities and detectable manifestations in geomagnetic field and particle flux densities variations, considering magnetospheric substorms and auroral breakup

04 p0442 A73-15340

Remarks on the steady and time dependent mathematical convection models.

04 p0443 A73-15341

Physical phenomena of controlled experiments in earth magnetosphere using test particles, radio emission and electron and ion beams

04 p0443 A73-15342

Cosmic-ray scintillations. I - Inside the magnetosphere.

04 p0492 A73-15526

Vela 4 Lyman-alpha observations - Evidence for an aspherical hydrogen geocorona at 18 earth radii.

04 p0492 A73-15528

Two substorm studies of relations between westward electric fields in the outer plasmasphere, auroral activity, and geomagnetic perturbations.

04 p0444 A73-15545

Use of an electron beam for low-temperature plasma measurement in the magnetosphere and interplanetary space.

04 p0450 A73-15553

Demarcation layer between magnetosphere central portion and geomagnetic tail as layer of least resistance to incident solar plasma

05 p0610 A73-17010

Geomagnetic micropulsations within magnetosphere, investigating MHD waves and particle-wave interactions

05 p0570 A73-17051

A theoretical and experimental study of non-ducted VLF waves after propagation through the magnetosphere.

05 p0551 A73-17054

Nonducted whistlers observed in the plasmasphere.

05 p0572 A73-17165

Book - Geophysics 3. Part 4.

06 p0688 A73-17501

Earth magnetosphere essential processes, discussing outermost atmosphere, solar wind theory and sector structure, models, plasmapause, polar cusps, tail theory and ionospheric currents

06 p0688 A73-17502

Magnetospheric plasma waves propagation effects on rapid geomagnetic field variations, noting magnetic pulsations and ionospheric propagation

06 p0747 A73-17504

Activities in space research at the Max-Planck-Institut fuer extraterrestrische Physik, Garching bei Muenchen /G.F.R./.

07 p0868 A73-19173

Strong pitch angle diffusion and magnetospheric solar protons.

07 p0869 A73-19229

Geomagnetic activity semiannual and diurnal variations due to interplanetary field southward component interaction with magnetosphere based on model ordered in solar equatorial coordinates

07 p0813 A73-19234

Observed relationships between electric fields and auroral particle precipitation.

07 p0814 A73-19237

A semiempirical model of large-scale magnetospheric electric fields.

07 p0814 A73-19238

Self trapping modulational instability of electron cyclotron wave whistler in cold and hot dense plasmas, discussing relevance to phenomena in magnetosphere

07 p0814 A73-19239

Incoherent Cerenkov radiation in the magnetosphere and the ground observations of VLF hiss.

07 p0814 A73-19240

Recent studies of magnetospheric electric field emissions above the electron gyrofrequency.

07 p0815 A73-19254

Three layer atmospheric model for neutral gas motion-produced ionosphere and magnetosphere currents, electromagnetic field and charged particle concentration perturbations

07 p0815 A73-19432

Magnetospheric and ionospheric potential electric fields, using variational process based on transverse/longitudinal conductivity ratios in plasma

07 p0815 A73-19433

Minimum magnetic field energy of two dimensional magnetosphere with neutral sheet for arbitrary dipole inclination to solar wind as function of potential difference on boundary points

07 p0816 A73-19443

Characteristic functions of potential distribution on sphere with longitude dependent conductivity for application to ionosphere electrodynamics

07 p0816 A73-19444

Magnetospheric electric fields estimation from electron fluxes intensity on early daylight side

07 p0816 A73-19460

The behaviour of ULF waves and particles in the magnetosphere.

07 p0792 A73-19666

Pulsar magnetosphere evolution, discussing electron and positive ion supply at surface, plasma flow and Crab Nebula characteristics

07 p0900 A73-20276

German monograph - Investigations of the behavior of high energetic protons and electrons in the inner magnetosphere.

07 p0872 A73-20385

Propagation modes of radio whistlers and gyroelectric echoes received in middle latitudes

08 p0937 A73-20651

Identification of discontinuities at the magnetosphere boundary

08 p0958 A73-21277

Acceleration of charged particles in the region of the neutral line of the magnetic field

08 p0959 A73-21292

Formation and decay of a narrow band of energetic electrons in the earth's magnetosphere

08 p0998 A73-21305

Physical conditions in the magnetosphere and interplanetary space during the excitation of pc 1 geomagnetic pulsations

08 p0960 A73-21306

Electromagnetic field configuration about aligned rotating magnetic star from relativistic model of rotating magnetosphere

09 p1142 A73-22034

Nonadiabatic particle motion in the magnetosphere.

09 p1073 A73-22052

Low-energy solar protons in the pseudo-trapping region of the magnetosphere.

09 p1137 A73-22053

Cross-correlation analysis of the AE index and the interplanetary magnetic field Bz component.

09 p1142 A73-22055

Two dimensional model of solar wind passage past magnetosphere, assuming hot plasma current sheath in geomagnetic tail

09 p1077 A73-22485

Interaction of the interplanetary medium with the earth's magnetosphere

09 p1146 A73-22542

Nonducted whistlers observed in the plasmasphere.

09 p1078 A73-22748

Solar particle measurements interpretation for closed vs open magnetospheric model determination, considering electron-proton polar cap differences, magnetotail flux asymmetries, etc

09 p1149 A73-22951

Observation of the entrance of solar protons in the magnetosphere at very high latitudes

10 p1211 A73-23769

Coefficients of hydromagnetic wave reflection from conjugate ionospheres

10 p1211 A73-23895

Polar coupling coefficients and generalization of the spectrographic method for studying cosmic-ray variations of magnetospheric and interplanetary origin

10 p1267 A73-23927

Analysis of the variations of cosmic rays of magnetospheric and interplanetary origins according to spectrographic data

10 p1267 A73-23928

Low latitude equatorial electrojet analysis based on three dimensional electric field equation for ionosphere and magnetosphere

10 p1211 A73-24215

Electron and proton acceleration in the outer regions of the magnetosphere during polar substorms.

10 p1268 A73-24227

Spontaneous Cerenkov emission of longitudinal waves produced by single particle and cylindrical electron beam moving inside magnetosphere along magnetic field

10 p1269 A73-24722

Saturn magnetospheric model for bounds on surface field strength and trapped particle population

10 p1283 A73-24724

Electron pitch angle distributions throughout the magnetosphere as observed on Ogo 5.

10 p1213 A73-24732

Half-harmonic modes for different frequency ranges and wave vectors from infinite homogeneous plasma model for high frequency electrostatic wave propagation in magnetosphere

10 p1213 A73-24733

Relationship of southward-drifting auroral arcs to the magnetospheric electric field and substorm activity.

10 p1213 A73-24734

On what ionospheric workers should know about the plasmapause-plasmasphere.

10 p1215 A73-24781

Magnetospheric substorms correlation with interplanetary magnetic field, discussing balloon and satellite electric field measurements

10 p1215 A73-24784

Analyses of techniques for measuring DC and AC electric fields in the magnetosphere.

11 p1352 A73-25316

The day-sector polar F-layer during a magnetospheric substorm.

11 p1356 A73-25918

Precise calculation of the magnetosphere surface for a tilted dipole.

11 p1421 A73-25923

The effect of the earth's bow shock and magnetosheath on the interaction of a discontinuity in the solar wind with the magnetosphere.

11 p1357 A73-25924

Equations derived for magnetic field line configuration and plasma flow about rotating object having axisymmetric field with emphasis on pulsar magnetosphere

11 p1427 A73-26614

Pulsar magnetospheres, braking index, polar caps, and period-pulse-width distribution.

11 p1428 A73-26618

Some effects of magnetospheric acceleration mechanisms on variations in ultraviolet intensity height profiles, and on consequent rocket spectrograph sensitivities.

11 p1358 A73-26703

Nose extension method based on approximate dispersion function for calculating ducted whistler frequency and associated travel time, discussing ionosphere-magnetosphere interactions

11 p1358 A73-26704

A fast method to determine the nose frequency and minimum group delay of a whistler when the causative spheric is unknown.

11 p1358 A73-26705

Harmonically unrelated spectral components of Pi 2 micropulsations generated by oscillations in magnetospheric tail cavities

11 p1359 A73-26711

Magnetic field signatures of substorms on high-latitude field lines in the nighttime magnetosphere.

12 p1488 A73-26981

Midlatitude bremsstrahlung X rays, VLF propagation disturbances and electron precipitation during magnetospheric substorm

12 p1468 A73-26983

Steady ELF plasmaspheric hiss, studying whistler mode turbulence, band limitation, power spectra and peak intensities

12 p1488 A73-26984

An association of magnetospheric whistler dispersion characteristics with changes in local plasma density.

12 p1488 A73-26985

On the relationship between the growth and expansion phases of substorms and magnetospheric convection.

12 p1489 A73-27005

Solar radiation effects on terrestrial electromagnetic environment, considering interplanetary space, earth internal structure, geomagnetism, upper atmosphere, dynamo action, energetic particles and magnetospheric storms

12 p1538 A73-27053

Anisotropic contact discontinuities at magnetospheric boundary and tail from MHD space plasma data analysis, suggesting sector boundary identification in interplanetary magnetic field

12 p1528 A73-27329

Dynamic model of the interaction between the F region of the ionosphere and the plasmasphere

12 p1490 A73-27335

Magnetosphere boundary location relationship to geomagnetic activity level and solar activity cycle during 1963-68 based on theoretical model

12 p1491 A73-27348

Simultaneous recording of solar cosmic rays near Venus and in the earth magnetosphere

12 p1534 A73-27354

The mean free path in the transition region beyond the boundary of the magnetosphere

12 p1528 A73-27355

Asymmetric eigenmodes in a simple model plasmasphere with non-uniform Alfvén speed.

12 p1529 A73-27613

Nonadiabatic condition effects on ultrarelativistic electron energy losses in geomagnetic trap in remote magnetosphere regions

12 p1535 A73-27649

Longitudinal magnetospheric currents contribution to auroral electrojet from satellite observation data, noting magnetosphere electric field excitation of meridional Pedersen and Hall currents

12 p1493 A73-27650

On the longitudinal extension of electron precipitation during magnetospheric substorms

13 p1606 A73-28152

Method for determining the longitudinal conductivity of the magnetosphere from the pulsations of a Pi-2 type magnetic field

13 p1606 A73-28291

Some results of an analysis of stable geomagnetic Pc4 pulsations at a network of stations.

13 p1608 A73-28719

Scaling laws for outer planet magnetospheres, noting energetic trapped particles radiation belts possibility

14 p1800 A73-30538

Remote sensing of LF nonthermal radio emission for composition and dynamic processes of interplanetary and interstellar media and planetary magnetospheres

14 p1800 A73-30539

Correlation of reported gravitational radiation events with terrestrial phenomena.

14 p1749 A73-30554

Magnetospheric dayside cusp - A topside view of its 6300-angstrom atomic oxygen emission.

14 p1750 A73-30620

Energy and momentum theorems in magnetospheric processes.

15 p1871 A73-31846

Magnetospheric electric field under quiet conditions on the basis of ground-based observations of whistlers

15 p1872 A73-31903

Influence of the inclination of the geomagnetic lines of force on the field of the magnetospheric-ionospheric current system.

15 p1874 A73-32608

Self-consistent calculation of the motion of a sheet of ions in the magnetosphere.

16 p2003 A73-33433

Satellite studies of magnetospheric substorms on August 15, 1968. II - Solar wind and outer magnetosphere.

16 p2004 A73-33450

Satellite studies of magnetospheric substorms on August 15, 1968. IV - Ogo 5 magnetic field observations.

16 p2004 A73-33452

Satellite studies of magnetospheric substorms on August 15, 1968. V - Energetic electrons, spatial boundaries, and wave-particle interactions at Ogo 5.

16 p2056 A73-33453

Satellite studies of magnetospheric substorms on August 15, 1968. VI - Ogo 5 energetic electron observations - Pitch angle distributions in the nighttime magnetosphere.

16 p2056 A73-33454

Satellite studies of magnetospheric substorms on August 15, 1968. IX - Phenomenological model for substorms.

16 p2004 A73-33457

Quiet time magnetospheric field depression at 2.3-3.6 earth radii.

16 p2005 A73-33464

Ion heating in thermal plasma flows.

16 p2042 A73-33465

Three dimensional dynamo theory in the magnetosphere.

17 p2158 A73-34503

Wave propagation in the magnetosphere of Jupiter.

17 p2229 A73-34506

Magnetotail response to sudden changes in the interplanetary magnetic field.

17 p2158 A73-34509

Book - Space physics and space astronomy.

17 p2230 A73-34575

VLF goniometer observations at Halley Bay, Antarctica. I - The equipment and the measurement of signal bearing. II - Magnetospheric structure deduced from whistler observations.

17 p2159 A73-34777

ESRO Geos geostationary satellite for measurement of magnetospheric plasma electric and magnetic fields and drift rate at various frequency regions via electron injection

17 p2176 A73-35816

Russian monograph on polar auroras and magnetospheric geomagnetic disturbances from rocket, balloon and ground station soundings covering magnetic storms, solar wind and geoelectric fields

18 p2302 A73-35873

Particle entry into the equatorial magnetosphere.

18 p2344 A73-35928

Observations of the entry of solar protons into the magnetosphere by use of riometers.

18 p2344 A73-35930

Theory of the excitation of the lower oblique resonance in the magnetospheric plasma.

18 p2302 A73-35939

OGO-5 observations of the physical processes occurring in the disturbed polar cusp and the cusp-magnetosheath interface.

18 p2303 A73-35943

Ground and synchronous orbit magnetic observations of magnetospheric and ionospheric wave propagation to model substorm current system variations

18 p2303 A73-35945

The use of VLF propagation measurements for studies of magnetospheric and meteorological influences on the lower ionosphere.

18 p2303 A73-35953

Ducted propagation of VLF waves through the magnetosphere.

18 p2288 A73-35995

Plasma physics phenomena in the outer planet magnetospheres.

[AIAA PAPER 73-566]

18 p2345 A73-36097

Intensity variations of low-energy protons and electrons in the outer magnetosphere at the sudden onset of a magnetic storm

18 p2309 A73-36109

Comparison of the two-dipole and empirical magnetospheric models.

18 p2310 A73-36135

On solar wind interaction with the earth's magnetosphere.

18 p2346 A73-36184

Solar wind interaction with the earth's magnetic field. I - Magnetosheath.

18 p2346 A73-36270

Dependence of the polar cusp on the north-south component of the interplanetary magnetic field.

18 p2351 A73-36273

Sector boundary geomagnetic activity average Kp elevation relationship to southward component of interplanetary field, suggesting magnetosphere role

18 p2347 A73-36292

Simulation of gyroresonant electron-whistler interactions in the outer radiation belts.

18 p2347 A73-36296

Probe measurement of the electrostatic field in the ionosphere and magnetosphere

18 p2314 A73-37026

Russian book - Interplanetary medium and the physics of the magnetosphere.

19 p2481 A73-37336

Hydromagnetic waves directed by the geomagnetic field

19 p2481 A73-37337

Analysis of methods for measuring electric field intensities in the magnetosphere

19 p2481 A73-37340

Transport of charged particles in the earth's magnetosphere

19 p2474 A73-37348

Use of charged particle beams for low temperature plasma measurement in magnetosphere and interplanetary space.

19 p2429 A73-37381

Generation and decay of a narrow belt of energetic electrons in the earth's magnetosphere.

19 p2476 A73-37934

Physical conditions in the magnetosphere and in interplanetary space during excitation of type Pcl geomagnetic pulsations.

19 p2425 A73-37935

Protonospheric columnar electron content determination. I - Analysis.

19 p2426 A73-38017

Reflection coefficients of hydromagnetic waves from conjugate ionospheres.

20 p2551 A73-38914

Explorer 45 mission objectives discussing magnetospheric ring current, magnetic storm detection, particle energy and interactions, electric and magnetic fields measurements, etc

20 p2614 A73-38949

Explorer 45 search coil magnetometer detection of ELF signals during magnetic storms, noting signal variation with storm phases and satellite magnetospheric position

20 p2552 A73-38957

Auroral arc mechanism of solar wind intrusion and electron and proton energization and precipitation in magnetosphere from Isis photometric and spectrometric observations

20 p2553 A73-39124

Dynamical models of tailed radio sources in clusters of galaxies.

20 p2610 A73-39584

Seasonal and solar cycle dependence of the position of the cusp region of the magnetosphere.

20 p2555 A73-39828

Plasmaspheric quasistatic electric fields and plasma convection, discussing dynamic electric fields and magnetospheric field penetration to low latitudes

21 p2679 A73-40075

Numerical calculation for polar ionospheric current under realistic electric field and conductivity distributions, considering solar wind effect on charged particles in magnetosphere

21 p2681 A73-40155

A mechanism for the growth phase of magnetospheric substorms.

21 p2682 A73-40157

Influence of a sudden compression of the magnetosphere on outer zone electron fluxes measured at arbitrary pitch-angle.

21 p2682 A73-40161

Jovian ionospheric and magnetospheric ionization and temperature distributions from solutions of momentum and chemical equations for electrons, ions and neutrals, and heat transport equation

21 p2764 A73-40165

Jupiter magnetospheric interaction with innermost satellite Io, noting magnetic field annihilation enhancement in neutral point by LF MHD waves

21 p2764 A73-40166

Study of cosmic rays by the Prognostic satellites

21 p2756 A73-40577

Cosmic ray intensity variation observation during August 2-8, 1972, suggesting complex interactions with interplanetary shock waves and magnetic field and magnetosphere

21 p2757 A73-40590

Structural and dynamic features of solar cosmic-ray penetration into polar regions

21 p2758 A73-40606

Limit of the region of low-energy solar proton ir-
ruption into the polar ionosphere 21 p2758 A73-40607

Axial symmetry of the magnetosphere and the noon
recovery of polar cap absorption 21 p2759 A73-40608

Growth rates of the ion cyclotron instability in the
earth's magnetosphere. 21 p2685 A73-40824

Space research XIII; Proceedings of the Fifteenth
Plenary Meeting, Madrid, Spain, May 10-24, 1972.
Volumes 1 & 2. 21 p2687 A73-41325

Thermal positive ions in the dayside polar cusp mea-
sured on the ISIS 1 satellite. 21 p2690 A73-41368

Energetic protons at low L-values of the equatorial
magnetosphere. 21 p2761 A73-41379

Modulation of spectrum and amplitude of VLF
signal in the magnetosphere. 21 p2657 A73-41381

Induced magnetosphere of the moon. II - Experimen-
tal results from Apollo 12 and Explorer 35. 22 p2906 A73-41905

Geophysical disturbance environment during the
NASA/MPE barium release at 5 earth radii on Sep-
tember 21, 1971. 22 p2845 A73-41933

High resolution television imaging of barium cloud
release in magnetosphere, discussing cloud shape
development, striation patterns, core behavior and dif-
fusion characteristics 22 p2845 A73-41936

Computer model of Ba ion cloud expansion in magne-
tosphere, taking into account self-consistent electric
and magnetic field interactions 22 p2846 A73-41938

Quiet-time nightside magnetic field near geomag-
netic equator detected by magnetospheric barium
cloud injection, revealing taillike structure from at-
mospheric models 22 p2846 A73-41939

Electrostatic waves with frequencies exceeding the
gyrofrequency in the magnetosphere. 22 p2851 A73-42933

Vertically nonpropagating magnetoatmospheric
waves investigation based on local dispersion relations
governing magnetoacoustic and magnetogravitational
wave propagation with emphasis on solar atmosphere
conditions 22 p2914 A73-43010

Anisotropic contact discontinuities at magneto-
spheric boundary and tail from MHD space plasma
data analysis, suggesting sector boundary identifica-
tion in interplanetary magnetic field 23 p3008 A73-43227

Dynamic model of interaction of the F-region of the
ionosphere with the plasmasphere. 23 p2970 A73-43233

Magnetosphere boundary location relationship to
geomagnetic activity level and solar activity cycle dur-
ing 1963-68 based on theoretical model 23 p2970 A73-43245

Simultaneous recording of solar cosmic-rays near
Venus and the earth's magnetosphere. 23 p3020 A73-43251

Mean free path in the transition region beyond the
boundary of the magnetosphere. 23 p3008 A73-43253

Densities deduced from perturbations at high al-
titudes. 23 p2972 A73-43688

A magnetospheric field model incorporating the
OGO 3 and 5 magnetic field observations. 23 p2972 A73-43693

VLF input impedance of a loop antenna embedded
in the magnetosphere. 23 p2954 A73-43700

Relationship of the sporadic F2 layer with certain
features of the ionosphere and magnetosphere at sub-
auroral latitudes 24 p3083 A73-44792

Plasma conductivity model of current structure of
MHD waves propagating from electric dipole source
in magnetosphere in relation to geomagnetic pulsa-
tions 24 p3084 A73-44805

Correlation between the excitation of pi 1 and pc 1
geomagnetic pulsations and magnetospheric sub-
storms 24 p3084 A73-44811

Solar wind and magnetosheath electron temperature
measurements by triaxial electron analyzer onboard
Ogo-5, presenting data for bow shock 24 p3125 A73-45112

Diffusion of ring current particles by low-frequency
long-wavelength electrostatic oscillations. 24 p3126 A73-45128

On self-consistent models for the pulsar magneto-
sphere. 24 p3140 A73-45190

ESRO I /Aurora/ satellite observations of aurora,
magnetosphere-ionosphere interaction at high
latitudes and auroral particle flux density 24 p3087 A73-45207

MAGNETOSPHERIC ELECTRON DENSITY

Magnetospheric charged particle populations in
magnetosheath, plasma sheet, extraterrestrial ring cur-
rent, electron trough and trapping regions 03 p0302 A73-13856

Characteristics of magnetosheath plasma observed
at low altitudes in the dayside magnetospheric cusps. 03 p0302 A73-13857

Electron intensity measurements by sounding
rockets over auroral arcs at magnetospheric plasma
boundary 03 p0362 A73-13865

The pre-midnight asymmetry in the 40 keV electron
flux profiles and its relation to magnetospheric sub-
storms. 03 p0363 A73-13866

Some parameters affecting the poleward boundary
of trapped electrons. 03 p0363 A73-13869

Precipitation of low-energy electrons at high
latitudes - Effects of interplanetary magnetic field and
dipole tilt angle. 04 p0493 A73-15531

Annual and semi-annual variations in the electron
density of the inner magnetosphere deduced from
whistler dispersion. 07 p0819 A73-20061

Whistler observations of the depletion of the
plasmasphere during a magnetospheric substorm. 09 p1074 A73-22060

Observations of noise bands associated with the
upper hybrid resonance by the Imp 6 radio astronomy
experiment. 12 p1468 A73-26995

Heos 2 magnetometer observations of magne-
tosheath high and low energy electron flux during
magnetopause boundary crossings in polar regions 12 p1489 A73-27004

Variations of solar-wind parameters, magnetic ac-
tivity, and the electron tail of the magnetosphere and
of the outer radiation zone. 13 p1608 A73-28714

Magnetospheric collisionless drift waves from ATS-
5 electron and proton velocity distribution measure-
ments, comparing with predicted perturbation dis-
tribution function 14 p1750 A73-30659

The plasmasphere during a magnetic recovery
period - A combined study of the OGO 4 and OGO 5
satellite data and of whistlers received at the ground 16 p2008 A73-33876

Convection dominated electrons in auroral zone,
discussing plasma sheet as magnetospheric electron
source, convection electron spatial distribution and
convection-precipitation coupling 17 p2223 A73-34358

Predawn enhancement of 6300-A emission observed
near the plasmapause from the Isis-2 spacecraft. 20 p2551 A73-38945

Balloon and VLF whistler measurements of electric
fields, equatorial electron density, and precipitating
particles during a barium cloud release in the magneto-
sphere. 22 p2845 A73-41934

Low latitude whistler activity during geomagnetic
storms related to spread F conditions and magneto-
spheric and ionospheric electron density 23 p2972 A73-43696

Guided propagation of very low frequency elec-
tromagnetic waves in irregularities of electronic den-
sity in the vicinity of the constant velocity mode 24 p3067 A73-44726

Effect of modified thermal conductivity on the tem-
perature distribution in the protonosphere. 24 p3082 A73-44727

Penetration of thundercloud electric fields into the
ionosphere and magnetosphere. I - Middle and subau-
roral latitudes. 24 p3085 A73-45118

The determination of whistler noise-frequency and
minimum group delay and its implication for the mea-
surement of the east-west electric field and tube con-
tent in the magnetosphere. 24 p3087 A73-45210

MAGNETOSPHERIC INSTABILITY

German monograph - Short-period transverse varia-
tions in the magnetic field data from the Azur research
satellite. 01 p0040 A73-10603

Inner magnetosphere distortions during magnetic
storm development phase from Explorer 26 observa-
tions, comparing with Williams-Mead, ring current
and compression models 02 p0156 A73-11747

A sub-class of pi 1 micropulsations associated with
the diurnal transit of the neutral sheet. 02 p0158 A73-11908

Spectrographic observation of quasi-periodic pc 1
micropulsation emission after geomagnetic storm as-

sociated with geotail plasma bunching in night time
magnetosphere 02 p0158 A73-11918

Particle motion and electrostatic instabilities of
geomagnetic tail and magnetopause plasma neutral
sheets in relation to substorms, using Alfvén and
Cowley models 03 p0302 A73-13873

Ground based goniometric observations of medium
and high latitude VLF emissions due to transverse
resonance instability and auroral oval Cerenkov radia-
tion from magnetosheath 03 p0276 A73-13884

Magnetotail plasma leakage into magnetosheath
during magnetospheric substorms from Vela satellites
proton flux measurements 04 p0443 A73-15530

Morphology and interpretation of magnetospheric
plasma waves at conjugate points during December
solstice. 04 p0443 A73-15535

Theory of diurnal fluctuations of the earth's mag-
netic tail 05 p0620 A73-17011

Auroral electron spectrum space-time dynamics
during magnetospheric substorms, using X ray
bremsstrahlung balloon data 07 p0815 A73-19437

Magnetospheric quasi-stationary pinch effect and
filamentary structure due to electron streams parallel
to geomagnetic field lines 07 p0816 A73-19464

Intrinsic bandwidth of cyclotron resonance in the
geomagnetic field. 07 p0792 A73-19532

Relationship of magnetospheric substorms on the
ground and in the distant magnetotail. 08 p0961 A73-21392

Auroral absorption and magnetospheric plasma
dynamics pattern from arctic stations atmospheric
opacity data 10 p1212 A73-24220

Earth magnetosphere pinch effect related to
geomagnetic field pulsations and polar aurora lu-
minosity fluctuations 10 p1212 A73-24228

Earth surface magnetic field intensity variations in
terms of magnetospheric resonator excitation, assum-
ing three dimensional Alfvén waves 10 p1212 A73-24230

Nonlinear hydrodynamic VLF wave scattering in
the earth's magnetosphere. 11 p1331 A73-25913

Enhancements of ionospheric total electron content
in the southern auroral zone associated with magneto-
spheric substorms. 11 p1359 A73-26715

Observations of narrow microburst trains in the
geomagnetic storm of August 4-6, 1972. 12 p1490 A73-27007

Oscillations of the earth's magnetic tail in a quasi-
hydrodynamics approximation 12 p1491 A73-27347

Relationship between geomagnetic pulsations of
diminishing period and the motion of plasma discon-
tinuities in the magnetosphere 12 p1491 A73-27350

A magnetosonic resonator of Pc2,3 pulsations in the
earth's magnetosphere 12 p1491 A73-27351

Earth outer radiation belt and unstable radiation
zone dynamics during IQSY magnetically quiet and
disturbed period based on Elektron-series satellite
data 12 p1535 A73-27636

Rayed auroral structures and their relation to the
drift current instability in a plasma blob. 13 p1607 A73-28705

Instability of the current in the neutral sheet of the
tail of the earth's magnetosphere. 13 p1608 A73-28715

Threshold of appearance of anomalous resistance
for field-aligned currents in the magnetosphere. 13 p1608 A73-28726

Influence of the interplanetary magnetic field on the
magnetic perturbations of high latitude regions -
Demonstration of an asymmetry in relation to the
earth-sun direction 13 p1611 A73-29563

Observation of a current-driven plasma instability at
the outer zone-plasma sheet boundary. 14 p1747 A73-29966

Distance to the subsolar point of the magnetosphere
boundary for various magnetic activity indices 15 p1932 A73-31266

Interaction of the geomagnetic field with the an-
tiparallel solar-wind field 15 p1926 A73-31891

Ion-acoustic turbulence as MHD wave damping
mechanism in weakly turbulent magnetosphere plasma
at high and low frequencies 15 p1919 A73-31893

Earth magnetosphere ion acoustic turbulence
generation by longitudinal currents and electric fields,

relating turbulence induced current dissipation to plasma heating

15 p1872 A73-31894

Gyrotropic flat ionosphere model with elliptical nonuniform conductivity for electrojet generation by magnetosphere current entering and leaving auroral zone

15 p1872 A73-31895

Anticipated variability of Pulsar NP 0532 emission in the Crab nebula associated with angular velocity jumps

15 p1938 A73-31964

Electron precipitation patterns and substorm morphology.

16 p2056 A73-33434

Theory and computer simulation of whistler turbulence and velocity space diffusion in the magnetospheric plasma.

16 p2003 A73-33439

Satellite studies of magnetospheric substorms on August 15, 1968. I - State of the magnetosphere.

16 p2004 A73-33449

Satellite studies of magnetospheric substorms on August 15, 1968. III - Some features of magnetospheric convection.

16 p2004 A73-33451

Satellite studies of magnetospheric substorms on August 15, 1968. VII - Ogo 5 energetic proton observations - Spatial boundaries.

16 p2056 A73-33455

Satellite studies of magnetospheric substorms on August 15, 1968. VIII - Ogo 5 plasma wave observations.

16 p2004 A73-33456

Hydromagnetic eigenoscillations in the magnetospheric tail.

18 p2352 A73-36295

Oscillations of the earth's magnetic tail

19 p2482 A73-37349

A unified picture of the parallel whistler mode instability.

19 p2403 A73-37440

Ionosphere, magnetosphere and interplanetary plasma instabilities effects on magnetosphere dynamics

19 p2476 A73-37758

Magnetic storm inflation analysis from Explorer 45 and ground observation data, noting proton penetration into magnetosphere evening quadrant

20 p2552 A73-38951

Magnetospheric implications of the nonlinear whistler instability obtained in a computer experiment.

20 p2553 A73-38961

Response of the polar electrojets in the evening sector to polar magnetic substorms.

22 p2902 A73-41916

Sudden commencement and sudden impulse absorption events at high latitudes.

22 p2845 A73-41928

Oscillations of the earth's magnetic tail in the approximation of quasi-hydrodynamics.

23 p2970 A73-43244

Relationship between geomagnetic PDP pulsations and the motion of plasma inhomogeneities in the magnetosphere.

23 p2970 A73-43247

Magnetosonic resonator of Pc2,3 pulsations in the earth's magnetosphere.

23 p2970 A73-43248

Magnetospheric plasma motion during a sudden commencement.

23 p2972 A73-43689

Expected radiative variability of Crab-Nebula pulsar NP 0532, related to abrupt changes in angular velocity.

24 p3132 A73-44489

Guided propagation of very low frequency electromagnetic waves in irregularities of electronic density in the vicinity of the constant velocity mode

24 p3067 A73-44726

Collisionless magnetospheric-solar wind plasmas interactions, noting boundary stability and tail instability

24 p3127 A73-45213

MAGNETOSPHERIC ION DENSITY

NT MAGNETOSPHERIC PROTON DENSITY

Plasmasphere hydrogen, helium, oxygen and nitrogen ions inbound and outbound profiles from OGO 5 mass spectrometric measurements

02 p0164 A73-12320

Magnetospheric thermal plasma and hydrogen cation density profile characteristics in different local time regions explained by time-varying convection model

03 p0303 A73-13879

The light-ion trough, the main trough, and the plasmapause.

04 p0493 A73-15533

French monograph - Experimental study of conditions of resonance of tubes of forces of the terrestrial magnetic field.

15 p1874 A73-32594

The plasmasphere during a magnetic recovery period - A combined study of the OGO 4 and OGO 5 satellite data and of whistlers received at the ground

16 p2008 A73-33876

MAGNETOSPHERIC PROTON DENSITY

Magnetospheric charged particle populations in magnetosheath, plasma sheet, extraterrestrial ring current, electron trough and trapping regions

03 p0302 A73-13856

Characteristics of magnetosheath plasma observed at low altitudes in the dayside magnetospheric cusps.

03 p0302 A73-13857

Turbulent loss mechanism of ring current protons in plasmapause vicinity via electrostatic drift cyclotron loss cone waves

10 p1270 A73-24743

Relationship between geomagnetic pulsations of diminishing period and the motion of plasma discontinuities in the magnetosphere

12 p1491 A73-27350

Determination of the density of protons in the magnetosphere on the basis of observations of Pc-3 type geomagnetic pulsations

13 p1610 A73-29560

Magnetospheric collisionless drift waves from ATS-5 electron and proton velocity distribution measurements, comparing with predicted perturbation distribution function

14 p1750 A73-30659

Energy spectra and pitch angle distributions of storm-time and substorm injected protons.

20 p2552 A73-38953

Relationship between geomagnetic PDP pulsations and the motion of plasma inhomogeneities in the magnetosphere.

23 p2970 A73-43247

MAGNETOSTATIC FIELDS

Radiative losses in a magnetostatic and intense electromagnetic field.

10 p1270 A73-24908

Nonlinear theory of Ubitron microwave oscillator device using fast electromagnetic wave-fast electron beam interaction in spatially periodic magnetostatic field

11 p1332 A73-26164

MAGNETOSTATICS

Magnetodynamic and magnetostatic surface waves in a ferrite layered structure

19 p2470 A73-37724

Amplification of magnetostatic surface waves in the YIG-Ge hybrid system.

24 p3120 A73-45431

MAGNETOSTRICTION

Synthesis of a magnetoelastic control medium for stabilization of hydrodynamic flows

01 p0084 A73-10669

Magnetostriction of stainless steels in relation to heat treatment.

06 p0709 A73-18212

Plane strain dynamics on magneto-thermoviscoelastic materials, noting conductivity, heat sources, potential and rotation

11 p1433 A73-25163

Thermal expansion, Young's modulus, and magnetostriction of a stainless iron-chromium-nickel alloy in the temperature range between 80 and 280 K

14 p1764 A73-30868

Nonlinear magnetoelastic effects in Ni tube torsion spring pendulum due to oscillation damping and stiffness characteristics dependence on amplitude

16 p2025 A73-33214

Thermomechanical theory of ferromagnetic and dielectric materials magnetoelastic and piezoelectric properties, using variational principles

16 p2037 A73-33228

A unified approach to the solution of plane problems of magneto-elasticity with special reference to a hole in a thin infinite conducting plate.

17 p2211 A73-34346

MAGNETOTELLURIC PROFILING

U GEOMAGNETISM

U MAGNETIC SURVEYS

MAGNETOVARIOGRAPHS

U VARIOMETERS

MAGNETRONS

Experimental investigation of the kinetic instabilities in Gabor's alternative magnetron

04 p0481 A73-15610

Critical analysis of Mouthaan-Susskind diffusion theory for magnetron diode electron transport, noting theoretical results discrepancy with experimental data

05 p0556 A73-16064

Experimental investigation of kinetic instabilities in the Gabor magnetron.

10 p1254 A73-24200

Analysis of the static modes of a magnetron with allowance for electron-velocity scatter

11 p1332 A73-26163

Frequency-agile coaxial magnetrons.

12 p1477 A73-26925

Current and energy characteristics of an electron plasma in a magnetron diode

20 p2536 A73-39254

Calculation of the electron trajectories in helical beams produced by axisymmetric magnetron-type injection guns

23 p2961 A73-44346

MAGNETS

NT CRYOGENIC MAGNETS

NT ELECTROMAGNETS

NT SUPERCONDUCTING MAGNETS

MAGNIFICATION

Laser beam steering in confocal unstable resonators, interpreting mirror misalignment effects as far field dependence on magnification and Fresnel number from mode solution

09 p1090 A73-22076

MAGNIFIERS

U MAGNIFICATION

MAGNONS

Raman scattering by phonons and magnons and phonon-magnon interactions in NiO.

02 p0201 A73-12640

Theory of fluctuations and particle scattering in ferromagnetic semiconductors and metals

09 p1134 A73-22678

Parallel spin-wave pumping in yttrium garnet single crystals.

11 p1409 A73-26188

Resonance between spin and magnetohydrodynamic waves in antiferromagnetic semiconductors and metals.

11 p1409 A73-26190

MAGNUS EFFECT

Magnus force and moment coefficients for spinning ogive and cone cylinders and conical bodies in laminar compressible flow, including boundary layer and radial pressure gradient effects

05 p0530 A73-16879

Negative Magnus forces in the critical Reynolds number regime.

05 p0533 A73-17212

Experimental investigation of the Magnus effect at a finned body of revolution of large aspect ratio at a Mach number of 4

08 p0927 A73-21604

Viscous flow over spinning cones at angle of attack.

17 p2096 A73-35132

MAIN SEQUENCE STARS

Mean absolute magnitudes and color indices of the red-giant concentrations in the color-magnitude diagrams of open clusters.

01 p0106 A73-11319

Statistical fractions of variable A and F stars, considering main sequence stars, giants, subgiants and open clusters NGC 2548, Praesepe and Coma

02 p0226 A73-12834

Statistical studies in stellar rotation. II - A method of analyzing rotational coupling in double stars and an introduction to its applications.

03 p0366 A73-12938

Luminosity and mass functions for low main-sequence stars.

03 p0373 A73-13359

Rapid variations of Psi Per shell star H beta line, indicating shell and stellar atmosphere activity

05 p0617 A73-16466

Theoretical evolution of a hydrogen-helium star of 3 solar-mass units from the pre-main sequence to the core helium-exhaustion phase.

05 p0625 A73-17319

Star formation and evolution in spiral galaxies.

07 p0873 A73-19055

Linear series of stellar models. II - Pure carbon stars.

08 p1002 A73-20847

Evolution from the main sequence to the helium flash for population II stars.

08 p1005 A73-20915

Stellar evolution at high mass based on the Ledoux criterion for convection.

08 p1008 A73-21159

A non-LTE study of silicon line formation in early-type main-sequence atmospheres.

10 p1272 A73-23532

Relative proper motions of faint stars in the Pleiades.

10 p1279 A73-24166

Secular stability. V - The perturbation of chemical abundances.

10 p1280 A73-24404

Delta Scuti variables observational and theoretical data, discussing pulsation properties and relationships to other pulsators and nonvariable stars

10 p1281 A73-24405

UBV photometry of 32 Cygni during the 1971 eclipse.

11 p1426 A73-26268

Evolution of stars with suppressed core convection.

11 p1427 A73-26608

Metal-poor stars. IV - The evolution of red giants.

12 p1540 A73-27328

Stellar evolutionary stages of near-main sequence stars and clusters, discussing mass-luminosity and mass-radius relations

13 p1682 A73-28978

Massive main sequence stars structure and evolution within core hydrogen burning models, giving mathematical relation and conditions for convective instability

13 p1682 A73-28979

Perturbation technique investigation of nonlinear pulsations of vibrationally unstable main sequence stars between 70-170 solar masses

17 p2225 A73-34288

Intrinsic ultraviolet colors from OAO-2 Telescope observations for stars on the main sequence.
17 p2225 A73-34290

The ultraviolet flux envelopes of main-sequence B stars.
17 p2234 A73-35613

Zero-age main sequence stellar model calculations compared to observational data derived for nearby low mass stars
20 p2611 A73-39585

Multiple solutions of the equations of stellar structure. II - E model sequences.
24 p3140 A73-45179

MAINTAINABILITY

Book - Applied maintainability engineering.
02 p0238 A73-11883

An exact analysis of the Method-One maintainability demonstration plan in MIL-STD-471.
03 p0336 A73-13731

Maintainability of the Space Shuttle Orbiter main engine.
[SAE PAPER 720808] 05 p0606 A73-16642

Automatic support systems for advanced maintainability; Symposium, Philadelphia, Pa., November 13-15, 1972, Record.
08 p0951 A73-20676

Russian book - Transport aircraft maintainability.
09 p1032 A73-22375

MGC 30 inertial navigation system for civil aviation, emphasizing economics and ease of maintenance
15 p1909 A73-32457

Annual Reliability and Maintainability Symposium, Philadelphia, Pa., January 23-25, 1973, Proceedings.
16 p2020 A73-33601

AEGIS AN/SPY-1 radar system - Design for availability.
16 p1980 A73-33607

Specifying maintainability-demonstration-test parameters.
16 p2020 A73-33635

A synergistic reliability and maintainability prediction package.
16 p1986 A73-33652

Review of engine maintenance concepts applied to wide body jets.
[SAE PAPER 730375] 17 p2178 A73-34714

U.S. instrument landing system performance improvements, considering terrain and weather effects, installation requirements, airport limitations, accuracy, reliability and maintainability
19 p2450 A73-37805

Book - The role of testing in achieving aerospace systems effectiveness.
21 p2675 A73-41201

MAINTENANCE

NT AIRCRAFT MAINTENANCE
NT SPACE MAINTENANCE

Optimal renewal algorithm for control plant with cumulative damage, using failure rate and renewal point spacing model
01 p0058 A73-11421

Ni-Cd battery thermal runaways caused by self sustaining temperature increases, discussing operational and maintenance procedures for avoidance or correction
03 p0251 A73-12906

Optimal planning of technological systems maintenance according to a reliability criterion
07 p0830 A73-19126

Statistical diagnostics and information synthesis relating to the reliability and maintenance of an equipment
07 p0830 A73-19414

Reliability of a self-repairing system with scheduled maintenance.
09 p1088 A73-22443

Maintenance and repair planning and control of complex series-parallel and hierarchical branched systems with discrete sampling of operational status
09 p1064 A73-22553

Prediction of optimal maintenance for devices
13 p1625 A73-29136

Repairable electronic system random failure and repair time related to simulator time available for operation, analyzing MTBF and repair rates
16 p1996 A73-33207

Welding techniques for high strength superalloy turbine blades and vanes repair, discussing controlled preheating and cooling methods for crack prevention
[ASME PAPER 73-GT-44] 16 p2019 A73-33505

A current turbine engine maintenance program and the experience and logic upon which it is based.
[ASME PAPER 73-GT-81] 16 p2049 A73-33526

Nondestructive inspection method for jet engine turbine blades.
[ASME PAPER 73-GT-92] 16 p2019 A73-33530

Fault ambiguity repair optimization (FARO) computer program for electronic circuit card group replacement strategy, using FORTRAN IV for SPEC-TRA 70/55 batch processing
16 p1990 A73-33626

Computerized total On-Line Testing System with diagnostic error visibility and preventive and cor-

rective maintenance functions in multiprogramming mode, discussing design features
16 p1986 A73-33633

Requirements of an economic approach to maintenance.
18 p2373 A73-37142

Book - Hydraulic systems and maintenance.
20 p2510 A73-39142

Safe flying, skilled personnel and aircraft maintenance assurance via safety equipment, initial and recurrent training, protective clothing and shelter from inclement weather, maintenance scheduling, etc
20 p2518 A73-39212

Reliability of some redundant systems with repair.
22 p2867 A73-42968

MAJORITY CARRIERS

Radiation produced trapping effects in devices.
05 p0605 A73-16521

MALFUNCTIONS

Handbook on mechanical face seals covering applications, operational capabilities, design, environmental control, handling, installation, malfunctions, auxiliary equipment, optical flats, etc
03 p0313 A73-13995

Computer-controlled software diagnosis of an airborne computer.
08 p0940 A73-20677

On the improvement in survivability for avionics equipment.
12 p1478 A73-27158

Analyses of flight model spacecraft performance during thermal-vacuum tests.
16 p2072 A73-33149

Failure diagnosis using quadratic programming.
22 p2867 A73-42966

Malfunction diagnostics in digital integrated-circuit devices
23 p2956 A73-43581

MAMMALS

NT BATS
NT CATS
NT CHIMPANZEES
NT MICE

Book - Sensory coding in the mammalian nervous system.
11 p1317 A73-25799

Mammalian tissue response to subcutaneous and intraperitoneal injection of aqueous suspensions of lunar fine material, noting insolubility in tissue and irritant action
11 p1320 A73-26484

The radiobiological effects of heavy ions on mammalian cells and bacteria.
22 p2805 A73-42182

Book on comparative physiology of thermoregulation covering primitive and aquatic mammals, torpidity aspects, evolution and newborns
22 p2809 A73-42859

Primitive mammals phylogeny relationship to homeothermic abilities, discussing body temperature, thermoregulation, basal metabolism rates, hibernation, nycthemeral rhythms and responses to heat and cold
22 p2809 A73-42860

Aquatic and diving mammals in fresh water and marine environments, discussing aquatic thermal conditions, body temperature distribution, thermoregulation, metabolic heat production, etc
22 p2809 A73-42861

Torpor and hibernation physiology in mammals covering evolution, hypothermia, energy conservation, cell and organ adaptations, nervous and cardiovascular system changes. etc
22 p2809 A73-42862

MAN MACHINE SYSTEMS

A method for aiding human operator performance in a noncompensatory tracking task.
01 p0011 A73-10323

Interactive pattern analysis and classification systems - A survey and commentary.
01 p0021 A73-11477

Variations of evoked potentials during various mental stress situations
03 p0268 A73-13825

Computer-mediated human communications in an air traffic control environment A preliminary design.
03 p0340 A73-14658

Apollo program predictive testing for man machine and environmental capabilities in terms of engineering, qualification, manufacturing, maintenance and training aspects
04 p0453 A73-14863

Message switching for multiplexing data of computer users with interactive access onto common facilities, evaluating traffic induced time delay performance
04 p0425 A73-15428

Automated navigation system design for DC 10 long range version, emphasizing control display unit interface functions with pilot
05 p0594 A73-16050

The problem of human efficiency in automated control systems
05 p0542 A73-16410

Technology for man 72; Proceedings of the Sixteenth Annual Meeting, Los Angeles, Calif., October 17-19, 1972.
05 p0542 A73-16701

Performance comparisons for joystick and track ball optimized control configurations operating in rate and position modes
05 p0543 A73-16706

Interactive aspects of man/learning system control teams.
05 p0543 A73-16708

The employment of a spoken language computer applied to an air traffic control task.
05 p0544 A73-16728

Computerized airlines reservations systems with real time conversational interactive characteristics, discussing initial design, simulation, measurement, stability, reliability and data processing techniques
05 p0551 A73-16806

Computer and interactive graphics as applied to mission analysis.
[AIAA PAPER 73-112] 05 p0554 A73-16870

Application of the graphic flight path design program (FPDP) for fast interactive trajectory design.
[AIAA PAPER 73-113] 05 p0619 A73-16871

Preliminary design of the man-powered aircraft, Icarus.
[AIAA PAPER 73-53] 06 p0647 A73-17629

Automation of reliability evaluation procedures through CARE - The computer-aided reliability estimation program.
06 p0670 A73-18058

Studies in interactive communication. I - The effects of four communication modes on the behavior of teams during cooperative problem-solving.
06 p0658 A73-18241

Human factor role in flying personnel errors, noting man machine system performance and medical service engagement
06 p0659 A73-18258

Syntax specification system for computerized hand-drawn pattern grammar generation with user style description for concurrent inputting and analysis at high recognition speed
06 p0671 A73-18535

Use of numerical guidance at the National Weather Service's National Meteorological Center.
06 p0720 A73-18703

German monograph - Work-physiological investigations for the objectivization of the tracking behavior, the mental load, and its psychopharmacological modularity.
07 p0786 A73-20388

Test pilots role in aircraft flying qualities evaluation, discussing spin and longitudinal stability testing
09 p1031 A73-22181

The role of the test pilot in evaluating auto landing systems. I.
09 p1115 A73-22182

Determination of the optimal time of continuous work for operators in man-machine systems
09 p1046 A73-22849

Algorithm for spectrum decomposition during continuous man-computer interaction, noting Gaussian distribution of spectral bands and linear approximation for background
09 p1046 A73-22971

Implications of psychoanalytic factors for Air Force operations.
11 p1323 A73-25340

Automating the design process - Progress, problems, prospects, potential.
[AIAA PAPER 73-410] 11 p1373 A73-25538

RAPID - A system for online radar data reduction and performance analysis.
[AIAA PAPER 73-438] 12 p1476 A73-27825

Response time in the application of interactive graphics in structural analysis.
13 p1693 A73-28244

Computer graphics applied to production structural analysis.
13 p1693 A73-28245

Computer aided design with finite element method for two and three dimensional curved line and surface approximation and representation on interactive graphic console
13 p1587 A73-28850

Ergatic modeling as dynamic goal-oriented physical process based on heuristic autonomous information-structured organization system with regulated model-human operator interaction
13 p1580 A73-29418

Russian book - Engineering psychology in aviation and astronautics.
15 p1838 A73-31375

Anthropotechnical investigation of an above-ground indication and of an artificial horizon with preindication in connection with the manual control of VTOL aircraft
15 p1839 A73-32044

A comparison of visual, auditory, and cutaneous tracking displays when divided attention is required to a cross-adaptive loading task.
15 p1839 A73-32395

Digital computer processing for automatic feature classification of ERTS-borne MSS and RBV imagery data, emphasizing interactive man-machine analysis for image enhancement

16 p1985 A73-33366

System engineering aspects of the man-machine interface.

16 p1975 A73-33645

Man machine systems for flight safety, studying accidents, human factors in system design and implementation of personnel

17 p2113 A73-34078

Air traffic control, discussing man machine systems, multipath with ILS, target indicator radars and flight progress strip preparation

17 p2206 A73-34086

Self destructive behavior of aircraft pilot due to stress accumulation, discussing man machine relationship, coping mechanisms, competence and invulnerability myth

17 p2115 A73-34746

Interactive computer graphic display and interface system effectiveness for programming numerical control operations for tooling and part machining in aircraft production

[AHS PREPRINT 753]

17 p2131 A73-35081

The application of interactive graphics to the numerical methods used in structural analysis.

17 p2250 A73-35314

Teleoperators - Manual/automatic system requirements.

17 p2180 A73-35315

Remote control of planetary surface vehicles.

17 p2148 A73-35316

X-reference frame bilateral control for the Shuttle Attached Manipulator System.

17 p2180 A73-35317

Vehicle management and mission planning in support of shuttle operations.

[AIAA PAPER 73-612]

18 p2358 A73-36090

The multi-moded remote manipulator system.

19 p2416 A73-37314

Some preliminary correlations between control modes of manipulator systems and their performance indices.

19 p2416 A73-37315

Developments in Canada related to remotely manned systems.

19 p2416 A73-37317

Illumination and television considerations in teleoperator systems.

19 p2416 A73-37318

Sorcerer Apprentice head mounted display with wand for interaction with computer generated synthetic objects, describing creation of illusory three dimensional environment

19 p2397 A73-37323

Man-machine interface for controllers and end effectors.

19 p2397 A73-37325

Terminal pointer hand controller and other recent teleoperator controller concepts - Technology summary and application to earth orbital missions.

19 p2397 A73-37326

Evaluation of human operator visual performance capability for teleoperator missions.

19 p2397 A73-37327

Command language for supervisory control of remote manipulation.

19 p2403 A73-37329

Application of self-organizing control to remote piloting of vehicles.

19 p2449 A73-37332

Internal operational environment effects on pilot errors in commercial aircraft flights in terms of man machine interface and flight deck design

19 p2384 A73-37728

The prediction of pilot acceptance for a large aircraft.

19 p2453 A73-38073

Design and evaluation of a backhoe model with a master slave control.

19 p2401 A73-38085

Automatic control of the Skylab Astronaut Maneuvering Research Vehicle.

[AIAA PAPER 73-857]

20 p2586 A73-38795

Experiences with an augmented human intellect system - Computer mediated communication.

21 p2654 A73-40833

Development of pilot-in-the-loop analysis.

[AIAA PAPER 72-898]

22 p2817 A73-43110

Information seeking with multiple sources of conflicting and unreliable information.

24 p3063 A73-44778

MAN OPERATED PROPULSION SYSTEMS

Preliminary design of the man-powered aircraft, Icarus.

[AIAA PAPER 73-53]

06 p0647 A73-17629

MANAGEMENT

NT CONFIGURATION MANAGEMENT

NT CONTRACT MANAGEMENT

NT DATA MANAGEMENT

NT ENGINEERING MANAGEMENT

NT ENVIRONMENT MANAGEMENT

NT FINANCIAL MANAGEMENT

NT INDUSTRIAL MANAGEMENT

NT INFORMATION MANAGEMENT

NT INVENTORY MANAGEMENT

NT LOGISTICS MANAGEMENT

NT PERSONNEL MANAGEMENT

NT PROCUREMENT MANAGEMENT

NT PRODUCTION MANAGEMENT

NT PROJECT MANAGEMENT

NT RESEARCH MANAGEMENT

NT RESOURCES MANAGEMENT

NT SAFETY MANAGEMENT

NT SYSTEMS MANAGEMENT

NT WATER MANAGEMENT

NT WEAPON SYSTEM MANAGEMENT

MANAGEMENT ANALYSIS

Multi-Role Combat Aircraft Program management, discussing international cooperation, industrial arrangements and governmental objectives

13 p1709 A73-29384

Time, space, and energy management in the airways traffic control medium.

22 p2884 A73-42324

Estimation of general aviation air traffic.

[ASCE PREPRINT 2041]

22 p2839 A73-42866

MANAGEMENT INFORMATION SYSTEMS

SAGESS /Analytical System for Managing Space Assemblies and Systems/ - A management system applicable to CNES

01 p0124 A73-11252

Aircraft integrated data systems /AIDS/ utilization for airlines operational flight control and economic exploitation enhancement, discussing aircraft accident investigation, maintenance, navigability, etc

15 p1831 A73-32496

MANAGEMENT METHODS

Book - Management of engineering design.

05 p0642 A73-16351

The role of basic research in the total R&D process.

07 p0923 A73-19185

Apollo project management techniques transfer to socio-economic programs, discussing systems oriented approach to city planning, mass transportation, pollution control, public hygiene, etc

09 p1167 A73-21898

Government request to industry to propose product or service for buyer, discussing procurement role and centralized vs decentralized control

09 p1168 A73-21946

USAF experience in lightweight fighter aircraft acquisition as illustration of requests for industrial proposals simplification and source selection process streamlining

09 p1168 A73-21947

Government request to industry to propose product or service to buyer, discussing communications effectiveness, technical and management requirements and procurement

09 p1168 A73-21948

Charter air fleet maintenance economic management, discussing budget, manpower, time and materials control

09 p1168 A73-23243

Application of Range Commanders Council Document 118-71 test methods to range management - SAMTEC.

09 p1057 A73-23409

The role of the Project Manager in the management of satellite projects.

11 p1454 A73-26262

Mathematical modeling technique for marketing reliability programs in terms of cost/performance assurance for use in management decision making

16 p2089 A73-33638

Stuttgart airport noise abatement supervisor tasks and experience, describing routing specifications, landing and takeoff procedures and traffic flow

[DGLR PAPER 73-022]

17 p2208 A73-34495

Project form of organization adoption for managing innovation, stressing impact of technology on career progression of scientist engineers

17 p2258 A73-35217

Management approach to integration of B-1 avionics, discussing engineering problems, flight tests, electronic equipment and interface requirements

17 p2137 A73-35218

A fundamental methodology for planning and management of research and development programmes.

17 p2258 A73-35836

Management and control of military and commercial flight test programs at Bell Helicopter Company.

23 p3050 A73-44058

Philosophical approaches of technological forecasting and assessment, discussing Dialectical and Singerian inquiring /information/ systems for ill structured problems

23 p3051 A73-44218

MANAGEMENT PLANNING

NT PRODUCTION PLANNING

NT PROJECT PLANNING

GREMEX - A management game for the new public administration.

01 p0124 A73-11007

C-5 program developments and alterations in terms of defense requirements and cost problems, discussing

objectives and management policies in F-15 and B-1 projects

01 p0124 A73-11069

Budgeting role in development and implementation of five year plan of operations at French space research center

01 p0124 A73-11253

Mathematical formulation of linear programming problem, reducing vector valued optimal management plan determination to quadratic programming problem

02 p0144 A73-12126

Organization and management for adhesive bonding aircraft structures.

03 p0333 A73-13048

Aircraft engine development in terms of money, manpower, facilities and knowledge, discussing project organization and scheduling

03 p0251 A73-14469

Air transportation system planning - Progress in noise reduction.

04 p0406 A73-14895

Objective trees as technological forecasting technique in structuring program options for selected strategies, considering R and D, marketing and other functional business programs

08 p1026 A73-21699

Management aspects of the development of the Ariel 4 satellite.

09 p1168 A73-22915

U.S. industry R and D fund cutback caused problems survey by questionnaire, discussing problem minimization with consideration for economic market conditions

10 p1298 A73-24632

Logistics planning with cost reduction for NASA phased programs in conducting R and D and real time inventory control, discussing major activities and objectives

11 p1454 A73-25450

Dynamic prediction model and optimal control of a commercial plant

12 p1561 A73-27081

Industrial material management, considering departments requirements, identification effort, costs and benefit, numbering and standardization systems, and uniform commodity description problem

13 p1624 A73-28788

Engineering management for the Dallas/Fort Worth Airport.

13 p1708 A73-29110

Overview - The role of communication systems in air traffic management.

14 p1725 A73-29876

Formulation of the air traffic system as a management problem.

14 p1772 A73-29878

Book - Interorganizational decision making.

15 p1960 A73-31577

Helicopter design and production cost target and tradeoff considerations based on past programs, supplier quotations, government documents, estimating practices and functional requirements

[AHS PREPRINT 712]

17 p2257 A73-35058

Computer data base use by industrial management for product design, development, manufacturing, testing and documentation coordination to achieve system communication and control improvement

17 p2257 A73-35215

Book - Systems concepts: Lectures on contemporary approaches to systems.

17 p2258 A73-35572

Book - Zero-base budgeting: A practical management tool for evaluating expenses.

17 p2258 A73-35674

Vehicle management and mission planning in support of shuttle operations.

[AIAA PAPER 73-612]

18 p2358 A73-36090

Calculation of the plan for the transportation performance with the aid of electronic data processing

19 p2506 A73-38121

Society of Flight Test Engineers, National Symposium, 3rd, Arlington, Tex., September 11-14, 1972, Proceedings.

23 p3050 A73-44052

Management of Air Force test and evaluation activities.

23 p3050 A73-44055

Management and control of flight test programs of the Naval Air Systems Command.

23 p3050 A73-44056

MANAGEMENT SYSTEMS

NT MANAGEMENT INFORMATION SYSTEMS

Management system for aviation safety.

01 p0005 A73-10825

Management systems for quality cost accounting, time control and productivity analysis based on random time sampling technique

06 p0771 A73-17866

MANDELSTAM REPRESENTATION

Switching of the resonator Q factor by stimulated Mandel'shtam-Brillouin scattering.

20 p2574 A73-39703

The mechanism responsible for shortening of the stimulated Mandelstam-Brillouin scattering light-pulse

duration and for generation of nanosecond-duration pulses

21 p2739 A73-40355

Effect of saturation on light amplification in stimulated Mandelstam-Brillouin scattering

21 p2739 A73-40359

MANDRELS

Part manufacture with plasma arc torch by extending plasma spray coating technology to mandrel design and machining with consideration for base materials

13 p1624 A73-28907

Pressure vessels filament winding with inflatable mandrel in reinforced elastomer, discussing use of balloon as liner

16 p2018 A73-33068

MANEUVERABILITY

Lunokhod 1 vehicle terrestrial mobility tests, simulating lunar gravity, soil and traction on scale and mockup models

02 p0151 A73-12234

Lunokhod 1 vehicle chassis design and mobility characteristics in Mare Imbrium, discussing wheels, suspension, movement control, traction, cohesion and lunar surface maneuverability

02 p0151 A73-12235

Fighter aircraft maneuverability improvement at high subsonic speeds by slotted and unslotted leading- and trailing-edge flaps on delta wing [DGLR PAPER 72-126]

03 p0248 A73-14386

Control configured vehicle (CCV)/ concept application to fighter aircraft design for combat maneuver capabilities and versatility enhancement, using fly by wire technology

05 p0535 A73-16662

Reorganization of airplane manual flight control dynamics.

05 p0595 A73-16707

Control configured vehicle (CCV)/ technology application for fighter aircraft combat control versatility enhancement, presenting F-4 analytical, simulation and wind tunnel test performance results

05 p0535 A73-16907

Birds and aircraft aerodynamics, considering thermal and wind induced updrafts, lift-drag ratio, fuel consumption and maneuverability

06 p0648 A73-18148

'Bank-to-turn steering' for highly maneuverable missiles.

20 p2586 A73-38798

Compensation of the longitudinal-trim and altitude control systems of an aircraft

22 p2800 A73-42949

MANEUVERABLE REENTRY BODIES

Optimization of descent maneuvers for a section of a satellite in a planetary orbit

15 p1931 A73-31227

MANEUVERABLE SATELLITES

U SATELLITES

MANEUVERABLE SPACECRAFT

NT APOLLO SPACECRAFT

NT PERRY SPACECRAFT

NT LIFTING REENTRY VEHICLES

MANEUVERS

NT AIRCRAFT MANEUVERS

NT ORBITAL RENDEZVOUS

NT SIDESLIP

NT SPACECRAFT DOCKING

NT SPACECRAFT MANEUVERS

Manoeuvre in response to collision warning from airborne devices.

01 p0074 A73-10349

Variable mass system dynamic maneuver for maximum payload and given initial weight, noting mathematical model for time optimization

04 p0475 A73-15079

The isolation of critical elements within selected maneuvers during primary flight training.

05 p0544 A73-16727

Long-range energy-state maneuvers for minimum time to specified terminal conditions.

05 p0536 A73-16954

MANGANESE

NT MANGANESE ISOTOPES

Solar Mn abundance derivation based on center-line absorption line profiles, taking into account hyperfine structure broadening

10 p1278 A73-24130

MANGANESE ALLOYS

NT MANGANIN [TRADEMARK]

Strength and ductility of chromium-nickel-manganese steel as a function of the carbon and nitrogen content in the range from 20 to 253 C

01 p0064 A73-10490

Cr and V additions effects on Mn steels mechanical properties and wear resistance, noting strength limit increase

01 p0067 A73-11351

Phase transformations and mechanical properties of highly alloyed Cr-Mn-Ni steels

04 p0466 A73-15664

Structure and composition of certain Laves phases and identification of chi phases in Fe-Mn-Ti alloys

06 p0708 A73-18100

X-ray spectral studies of manganese-aluminum binary alloy systems

06 p0710 A73-18644

The distribution of chromium between ferrite and austenite and the thermodynamics of the alpha/gamma equilibrium in the Fe-Cr and Fe-Mn systems.

06 p0712 A73-18759

Influence of hot rolling on the mechanical properties of unstable austenitic chromium-manganese steels

09 p1098 A73-21848

Influence of annealing under load on the structure and properties of a self-ordering Ni3Mn alloy

09 p1099 A73-21957

Investigation of carbon- and manganese-diffusion processes in the metal-ceramic steel G13M

09 p1103 A73-22466

Crystallochemical analogy between europium, ytterbium, calcium, and barium in their alloys with manganese

09 p1135 A73-23235

Substructure alteration in manganese and nickel austenitic alloys under the action of microimpacts

13 p1630 A73-28013

Strength and ductility of chromium-nickel-manganese steel as a function of carbon and nitrogen contents over the range 20-253 C.

14 p1759 A73-30315

Influence of ordering in a Ni3Mn alloy on the magnitude of the critical shearing stresses

14 p1764 A73-30859

Magneto-optic investigation of MnBi films.

15 p1924 A73-31943

Subscale inclusions formation in solid Fe alloys with small amounts of Mn and other elements, noting inward oxygen thermal diffusion role and metallurgical implications

15 p1891 A73-32171

Temperature dependent crystallization and density of Fe-Mn-C alloys with niobium at 1200-1500 C from gamma ray measurements

16 p2027 A73-34012

Mechanical properties, microstructure and failure characteristics of binary alloys of Al-Mg system determined under different tensile stress rates and temperatures

17 p2187 A73-34339

Variation of the electrical resistance of ordered Ni3Mn alloy during irradiation by fission fragments

20 p2600 A73-39733

Postannealing isothermal decomposition products of Al-Mn alloys studied by transmission electron microscopy, revealing trigonal and hexagonal lattice diffraction patterns

23 p2993 A73-43916

MANGANESE COMPOUNDS

NT PERMANGANATES

Manganese additive effects on emissions from a model gas turbine combustor.

01 p0121 A73-10644

Knudsen measurements of the decomposition and the heat of formation of manganese ditelluride.

09 p1048 A73-22442

X-ray diffraction at high temperatures for a study of thermal expansion of MnSe and MnSe2

15 p1925 A73-32651

MANGANESE IONS

Electron spin resonance of manganoous ions in frozen methanol solution.

04 p0414 A73-15025

MANGANESE ISOTOPES

Study on the cosmic ray produced long-lived Mn-53 in Apollo 14 samples.

07 p0870 A73-19795

Manganese-54 and the lifetime of relativistic cosmic rays.

10 p1264 A73-23541

MANGANESE 53

U MANGANESE ISOTOPES

MANGANESE 54

U MANGANESE ISOTOPES

MANGANESE 56

U MANGANESE ISOTOPES

MANGANIN [TRADEMARK]

Design and development of Manganin and other wire sensors together with a resistance strain gauge transducer for use at pressures up to 200 000 lbf/sq in /1.38 GN/sq m/.

14 p1750 A73-29702

MANIFOLDS

Pressure distributions in manifolds with return ducts.

01 p0032 A73-10699

Prediction of pressure fluctuation in sounding rockets and manifolded recovery systems.

[AIAA PAPER 73-286]

09 p1155 A73-23206

Configuration space and phase space of a system with an infinite number of degrees of freedom

20 p2594 A73-39640

MANIFOLDS [MATHEMATICS]

Existence theorem for integral manifolds of point mappings in resonant and nonresonant cases for differential equations systems with fast rotating phases

05 p0560 A73-16290

MANNED ORBITAL LABORATORIES

Construction of the equations of a programmed motion possessing extremal properties

06 p0722 A73-17715

Evolution equations of motion for program manifold of continuous control system with given transient response

07 p0852 A73-20632

Event manifold curvature tensor as six dimensional bivector space via dyadic projections, applying to gravitational waves description

08 p0989 A73-21521

Control system equations of motion construction based on program manifold, determining multidimensional piecewise continuous controller vectors under assigned inequalities

12 p1484 A73-27455

Integral manifold concept for stability analysis of nonlinear system oscillations, plotting resonance curve for quasi-linear autonomous system

12 p1525 A73-27792

Response functions for mathematical double membrane model of isotropic elastic shell in form of orientable two dimensional differentiable manifold

13 p1694 A73-28284

A survey of recent results in differential equations.

14 p1769 A73-30411

Construction of equations of motion for program manifold of continuous control system with given transient response

15 p1913 A73-31686

A stable manifold theorem for degenerate fixed points with applications to celestial mechanics.

19 p2486 A73-37799

Gravitational waves in a space-time of any dimension.

22 p2885 A73-41773

Pseudo-umbilical manifolds of codimension 2 and of constant mean curvature in an n plus 2 dimensional elliptic space and generalizations

23 p3000 A73-44300

MANIPULATION

U MANIPULATORS

MANIPULATORS

Operation of spacecraft in orbit with the aid of remote-controlled manipulators - A joint project of ERNA, KYBERTRONIC, KLERA

02 p0136 A73-11659

The mathematics of coordinated control of prosthetic arms and manipulators.

[ASME PAPER 72-WA/AUT-4]

04 p0414 A73-15884

X-reference frame bilateral control for the Shuttle Attached Manipulator System.

17 p2180 A73-35317

Shuttle-Attached Manipulator System requirements.

19 p2491 A73-37307

Preliminary design and simulations of a Shuttle-Attached Manipulator System.

19 p2491 A73-37309

Simulation concepts for a full-sized Shuttle manipulator system.

19 p2416 A73-37310

The multi-moded remote manipulator system.

19 p2416 A73-37314

Some preliminary correlations between control modes of manipulator systems and their performance indices.

19 p2416 A73-37315

An anthropomorphic master-slave manipulator system.

19 p2397 A73-37316

Technological survey of machine intelligence for real time autonomous manipulation with computer recognition sensory feedback and programmed task control to eliminate human operator

19 p2417 A73-37330

The control of a manipulator by a computer model of the cerebellum.

19 p2398 A73-37333

Hierarchical hybrid control of manipulators - Artificial intelligence in LSI.

19 p2407 A73-37334

Learning control in remote manipulator and robot systems.

19 p2412 A73-37754

Design and evaluation of a backhoe model with a master slave control.

19 p2401 A73-38085

MANNED ORBITAL LABORATORIES

NT MANNED ORBITAL RESEARCH LABORATORIES

U.S. manned space flight food system development experience assessment, covering Mercury, Gemini, Apollo and manned orbiting laboratory programs

03 p0269 A73-14168

Skylab orbital laboratory design, experiment programs and planned missions schedule, considering rescue measures, life support system and attitude control

03 p0383 A73-14171

Space Treaty legislative provisions for freedom of movement of orbital and lunar laboratories

04 p0521 A73-15127

A 25 kW solar array/battery design for an earth orbiting space station.

11 p1311 A73-26010

An isotope heat source integrated with a 7 kW/e/ to 25 kW/e/ Brayton cycle space power supply.

11 p1312 A73-26019

Sortie module/pallet scientific European space program based on system performing orbital zero-g or earth/celestial bodies observation platforms functions

12 p1549 A73-27381

Sortie lab experiment management, integration and operational techniques, discussing airborne science/shuttle experiment system simulation /AS-SESS/ program

14 p1803 A73-29942

Safety and survival in manned space laboratory, discussing experimental and environment hazard elimination

16 p2071 A73-32673

MANNED ORBITAL RESEARCH LABORATORIES

Modular space station operation as general purpose laboratory with attached or free flying R and D modules for specific projects

09 p1152 A73-22325

Cloud microphysics spaceborne laboratory experimentation under zero-gravity conditions, discussing salt nuclei distribution mechanism due to spray breakup as task for Apollo-Soyuz program [AAS PAPER 73-135]

20 p2583 A73-38590

MANNED ORBITAL SPACE STATIONS

U ORBITAL SPACE STATIONS

MANNED ORBITAL TELESCOPES

NT APOLLO TELESCOPE MOUNT

MANNED REENTRY

Atmospheric braking of a manned spacecraft after interplanetary flight

10 p1286 A73-32879

Atmospheric deceleration of a manned spacecraft returning from an interplanetary flight.

20 p2614 A73-38898

MANNED SPACE FLIGHT

NT APOLLO FLIGHTS

NT APOLLO 11 FLIGHT

NT APOLLO 12 FLIGHT

NT APOLLO 14 FLIGHT

NT APOLLO 15 FLIGHT

NT APOLLO 16 FLIGHT

NT APOLLO 17 FLIGHT

NT MANNED REENTRY

Some of the more important problems of international space rescue.

01 p0110 A73-11106

Interstellar flight and intelligence in the Universe.

03 p0370 A73-13198

U.S. manned space flight food system development experience assessment, covering Mercury, Gemini, Apollo and manned orbiting laboratory programs

03 p0269 A73-14168

Hibernation applications in manned space flight, considering feasibility and advantages

03 p0269 A73-14170

Space shuttle orbiter applications to manned high energy missions from low earth orbit, considering refueling requirements, aerobraking and overall mission capability

05 p0630 A73-16939

Astronauts diurnal life cycle inversion during space flight missions, considering social factors and work-rest cycle effects

12 p1463 A73-27715

Space flight exercise regimen proposals, exploring moving picture/electric muscle stimuli program as earth gravity simulator in weightlessness

15 p1838 A73-31515

Russian book - Optical phenomena in the atmosphere as observed from piloted spacecraft.

18 p2348 A73-35898

Russian book on Soviet news agency space exploration articles for 1971 covering Soyuz, Salyut, Molniya, Luna, Meteor and Lunokhod programs, agricultural satellites and lunar exploration

19 p2486 A73-37771

A digital communications system for manned spaceflight applications.

20 p2527 A73-38763

Proton dosimeter design for distributed body organs.

23 p2949 A73-43389

Long range post-Apollo space exploration goals, considering earth orbital station, moon base, manned Mars landing and interstellar flights

23 p3038 A73-43990

MANNED SPACE FLIGHT NETWORK

Unified S-band ground system design and management for Apollo program, deep space and manned space flight network tracking and communications requirements

01 p0030 A73-11184

MANNED SPACECRAFT

NT APOLLO SPACECRAFT

NT FERRY SPACECRAFT

NT LUNAR MODULE

NT MANNED ORBITAL LABORATORIES

NT MANNED ORBITAL RESEARCH LABORATORIES

NT ORBITAL SPACE STATIONS

NT ORBITAL WORKSHOPS

NT SALLYUT SPACE STATION

NT SOYUZ SPACECRAFT

NT SPACE SHUTTLES

NT SPACE STATIONS

Current status of models for the human operator as a controller and decision maker in manned aerospace systems.

07 p0787 A73-20587

1972 report to the aerospace profession; Proceedings of the Sixteenth Symposium, Beverly Hills, Calif., September 28-30, 1972.

09 p1030 A73-22176

In-core 100 kWe thermionic power system design to meet manned spacecraft shielding requirements, discussing waste heat removal and integration with space base

11 p1395 A73-26026

NASA program manned and unmanned spacecraft system effectiveness survey questionnaire response data concerning various tests

21 p2781 A73-41203

Spectrophotometric investigations of the earth from manned orbital stations

23 p2979 A73-43333

MANOMETERS

Telemetry of venous blood pressure at rest and at muscle activity during running.

03 p0271 A73-14290

Digital readout top-loading balance adaptation as micromanometer, discussing accuracy, sensitivity and repeatability characteristics

03 p0309 A73-14471

Servomanometer designs with two membrane sensing elements for absolute and excess pressure measurements

07 p0827 A73-20542

A noise-immune ionizational manometer for pressures between 1 millitorr and 1 nanotorr

12 p1497 A73-27213

Atmosphere Explorer pressure measurements - Ion gauge and capacitance manometer.

13 p1688 A73-28632

MANTLE [EARTH STRUCTURE]

U EARTH MANTLE

MANUAL CONTROL

NT CONTROL STICKS

NT VISUAL CONTROL

A simple Fourier analysis technique for measuring the dynamic response of manual control systems.

01 p0027 A73-10321

A method for aiding human operator performance in a noncompensatory tracking task.

01 p0011 A73-10323

Automatic frequency control in the case of manually tuned oscillators

04 p0427 A73-14774

Performance comparisons for joystick and track ball optimized control configurations operating in rate and position modes

05 p0543 A73-16706

Reorganization of airplane manual flight control dynamics.

05 p0595 A73-16707

Need for within-trial feedback as a function of task similarity in adaptive training of manual control.

05 p0543 A73-16709

Heuristic response strategies and operator performance errors as function of practice in cross coupled pursuit tracking control tasks

07 p0785 A73-19548

Precision and economy estimates for manual control of spacecraft orientation

10 p1286 A73-23893

Manned vehicle systems analysis techniques application to manual approach-to-landing phase of aircraft flight, developing analytical control model

10 p1247 A73-24011

Analytical design of manual control systems for flight bodies

12 p1549 A73-27896

Manual vs fully automatic landing concepts, discussing pilots abilities and limitations and primary requirements for displays

13 p1656 A73-28905

Electronic control units, discussing automanual transfer, integral desaturation, proportional and compensatory action, position regulation with incorporated memory and computer applications

14 p1737 A73-30923

Anthropotechnical investigation of an above-ground indication and of an artificial horizon with preindication in connection with the manual control of VTOL aircraft

15 p1839 A73-32044

Positioning accuracy with binary selective and fixed gain manual control systems, using finger stick control for operator performance tests

15 p1840 A73-32583

A manual-control approach to development of VTOL automatic landing technology.

[AHS PREPRINT 742]

17 p2209 A73-35075

Teleoperators - Manual/automatic system requirements.

17 p2180 A73-35315

Analytical design of aircraft manual control systems.

18 p2267 A73-36601

A deterministic model of a well trained human operator performing compensatory tracking.

18 p2283 A73-36844

Terminal pointer hand controller and other recent teleoperator controller concepts - Technology summary and application to earth orbital missions.

19 p2397 A73-37326

The development of the F-12 series aircraft manual and automatic flight control system.

[AIAA PAPER 73-822]

Automatic flight control and navigation systems on the L-1011 Capabilities and experiences.

19 p2452 A73-37824

Flight director design for a STOL aircraft.

20 p2508 A73-38649

Evaluation of precision and economy of systems of manual spacecraft orientation.

20 p2614 A73-38912

Time domain analysis of human operator manual control function for second order oscillatory divergent system with error signals for compensatory tracking

21 p2634 A73-40090

Individual and simultaneous tracking of a step input by the horizontal saccadic eye movement and manual control systems.

22 p2811 A73-41735

Systems engineering approach to pneumatic hybrid automatic/manual control system with fluid logical elements and reduced air consumption

23 p2943 A73-43413

MANUALS

Aircraft maintenance manuals optimization for human errors minimization, discussing DC-10 in-flight and ground maintenance fault isolation philosophy and techniques

10 p1226 A73-24716

Safety aspects in documentation system for orientation, training and maintenance of equipment for Poseidon Missile System

16 p2073 A73-33639

MANUFACTURING

NT SPACE MANUFACTURING

Hot extrusion and filled billet techniques to process superalloy powder metallurgy products into complex shapes, bars or wire

01 p0056 A73-10284

State-of-technology for joining TD-NiCr sheet.

02 p0174 A73-12619

Recent advances in automated manufacture of composite structures, e.g., tape laying and pultrusion.

03 p0332 A73-13033

Externally pressurized gas bearings development and applications, considering design, control systems and manufacture

03 p0311 A73-13205

Theoretical foundations of the development of a system of automated information processing for the problems of manufacturing-process design in the metalworking industry

03 p0400 A73-13240

Rocket nozzles fabrication technology, discussing construction materials and manufacturing processes [AIAA PAPER 72-1191]

03 p0358 A73-13481

Thermally stable heterocyclic ladder polymer films preparation techniques in manufacture of solar cells with CdS or CdTe thin films for space applications

07 p0841 A73-18903

Reliability dynamism at the Deutch Company.

07 p0829 A73-19008

Ion implantation method and diffusion process for microelectronics semiconductor components manufacture

13 p1590 A73-28573

Part manufacturing with plasma arc torch by extending plasma spray coating technology to mandrel design and machining with consideration for base materials

13 p1624 A73-28907

Application of human engineering principles and techniques in the design of electronic production equipment.

14 p1722 A73-30497

Russian book - Physics of carbographte materials.

15 p1897 A73-31583

Remanufacture of jet engine compressor components.

[ASME PAPER 73-GT-43]

Developing country industrial product reliability from buying and manufacturing viewpoints, considering local methods, customs, attitudes and working conditions effects on management techniques

16 p2089 A73-33646

Industrial sterilization; Proceedings of the International Symposium, Amsterdam, Netherlands, September 1972.

16 p1975 A73-33691

Aircraft radio equipment manufacture, assembling, mounting, installing and testing, discussing hangar installation, bundle elements, castings, printed circuits and welding techniques

19 p2433 A73-37767

MANY BODY PROBLEM

Renormalized Brueckner-Hartree-Fock theory generalization to calculate intrinsic states of many-body nuclear system with permanent deformation
01 p0079 A73-10243

Earth satellites in resonance with the moon and the sun as objects of laser ranging - Analytical solution for their motion.
01 p0099 A73-10695

Investigation of conditions corresponding to the existence of an energy integral in the generalized n-body problem with variable masses
01 p0077 A73-10918

The n-body problem with variable gravitational constant, and some dynamical consequences for large-scale cosmic systems.
01 p0107 A73-11327

Matrix method for canonical transformations in many body problem of celestial mechanics
03 p0379 A73-14587

Hubble law correspondence in invariant mechanical theory of universe expansion to direct consequence of impulse conservation in inertially moving many body system
03 p0380 A73-14603

Russian monograph on relativistic celestial mechanics covering celestial and solar system bodies motion, Riemann geometry, tensor analysis, N body problem and cosmology
04 p0502 A73-15969

Motion of a body of variable mass in a many-body gravitational field near collision
05 p0615 A73-16326

Stability of clusters of galaxies with mass loss to gravitational radiation.
07 p0873 A73-19053

Investigation of the motion of a body of variable mass within a multibody gravitational field with the aid of a regularizing variable
09 p1121 A73-22852

Singularities and collisions in linear many body problem of Newtonian gravitational systems, noting moment of inertia role
10 p1284 A73-24788

Thermodynamic methods applied to self gravitating n-body systems for different boundary conditions, considering energy transfer
11 p1427 A73-26604

Instability of equilibrium figures consisting of several isolated components rotating jointly
13 p1684 A73-29141

Numerical analysis of the motion of periodic comet Brooks 2.
14 p1791 A73-29800

Homographic motions of Newtonian point mass system interacting through two body forces, considering relativistic interactions
15 p1930 A73-31110

A numerical integration scheme for the N-body gravitational problem.
20 p2604 A73-38973

Relativistic baryon effective masses and thresholds for strongly interacting superdense matter.
21 p2766 A73-40318

An application of integral invariants to the n-body problem
23 p3034 A73-44100

Dynamics of the rotary motions with respect to the center of mass of a system of solids with a variable geometry of the masses
23 p3007 A73-44187

Oscillatory motion existence in expanding n-body gravitational systems with distance bound and particle escape
23 p3034 A73-44208

On global existence and uniqueness theorems for gravitational systems.
24 p3141 A73-45280

Numerical stabilization of all laws of conservation in the many body problem.
24 p3142 A73-45289

MANY PARTICLE THEORY

U MANY BODY PROBLEM

MAP MATCHING GUIDANCE

Radar correlation navigation map matching systems for civilian and military application, noting preprocessing aspects
06 p0721 A73-18280

MAPPING

NT ICE MAPPING

NT PHOTOMAPPING

NT SOIL MAPPING

NT THEMATIC MAPPING

Colour separation and electronic analysis of Gemini V and Apollo spacecraft photography.
01 p0045 A73-10275

Cartesian coordinates for panoramic perspective position of point on conical map, noting relationship to semipolar coordinates of object point
02 p0166 A73-11644

Orbiting altimeter system feasibility for global scale geoidal mapping via satellite altimetry
04 p0439 A73-14803

Double cross-validation of video cartographic symbol location performance.
05 p0543 A73-16719

Mariner 9 Martian surface mapping, describing science instrumentation, orbit characteristics, mapping cycles sequence design and data telecommunications
[AIAA PAPER 73-204]
05 p0630 A73-16938

Radiation balance mapping with multispectral scanner data.
05 p0572 A73-17158

Mapping of atmospheric and sea ice parameters with an imaging microwave radiometer from the Nimbus 5 satellite.
06 p0667 A73-18281

Distortion corrections in geophysically traced gravitational, magnetic and geoelectric field maps, discussing automation
07 p0816 A73-19442

American Society of Photogrammetry and American Congress of Surveying and Mapping, Fall Convention, Columbus, Ohio, October 11-14, 1972, Proceedings.
08 p0968 A73-21701

Computation of the minimum bandwidth for aerotriangulation.
08 p0968 A73-21705

Extremum criteria for Gato differentiable mappings in hypercomplex domains derived for nonlinear Chebyshev problems, extending results to partially ordered sets of operators
09 p1112 A73-22581

D-2A satellite experiments for sky mapping and radiation intensity measurement, discussing attitude correction processing
10 p1285 A73-23623

Contraction-mapping algorithm with guaranteed convergence.
10 p1242 A73-24034

Necessary and sufficient conditions for differentiable nonscalar-valued functions to attain extrema.
10 p1243 A73-24537

Holographic contour mapping using a dye laser.
10 p1221 A73-24874

On the mapping associated with the complex representation of functions and processes.
11 p1333 A73-26645

Instruments and techniques for cartographic processing of space photographs.
12 p1500 A73-27959

Signal color effects on stereoplotters measurements in aerial mapping of built-up areas
12 p1501 A73-27968

Metric calibration of distortion in aerial mapping cameras, using laser, collimator and diffraction grating generated angularly accurate image points matrix
12 p1501 A73-27970

Classification, scale sequence, and nomenclature of lunar maps
13 p1672 A73-28117

Mapping of mangrove and perpendicular-oriented shell reefs in southeastern Panama with side-looking radar.
13 p1606 A73-28170

The hyperelliptical and other new pseudo cylindrical equal area map projections.
13 p1608 A73-28845

Modeling irregular surfaces.
13 p1619 A73-29242

Cost effective land use mapping and resources inventory for Mississippi via high altitude color IR aerial photography and ERTS-1 multispectral imagery
[AIAA PAPER 73-3]
13 p1610 A73-29300

Fixed point theorems and dissipative processes.
14 p1771 A73-30774

The Fredholm alternative in the case of linear approximation-regular operators
15 p1901 A73-32371

Mars topographic and geologic mapping with Mariner 9 TV pictures, ground based radar and IR pressure techniques
16 p2015 A73-33354

Thermal mapping at electrical power generating sites for outfall from fossil or nuclear fuel plants, considering airborne application
16 p2015 A73-33360

Landmark navigational and topographical mapping techniques for planetary surface exploration using unmanned vehicles and earth based computers
17 p2210 A73-35383

New algae mapping technique by the use of an airborne laser fluorosensor.
17 p2163 A73-35412

Nondestructive optical contour mapping for non-contact testing of reflecting surface deformations from interference pattern due to monochromatic illumination of grating
17 p2172 A73-35419

Ground based and airborne microwave radiometer imaging techniques for surface mapping and atmospheric investigations, discussing self calibration, antennas, waveforms and aircraft nose instrumentation
20 p2567 A73-39838

Polarimetric mapping techniques using multichannel digital photometry via remote sensors, discussing terrain types, lunar topographic analysis and soil and vegetation mapping
20 p2568 A73-39860

Remote sensor geological mapping of Rio Grande rift zone /Colorado/ using aerial color infrared photography for compilation of tectonic and geomorphic histories
20 p2560 A73-39893

Strong and weak convergence of the sequence of successive approximations for quasi-nonexpansive mappings.
21 p2724 A73-40297

Integration of remote sensing data into spatial information systems, discussing data specification, acquisition, storage, retrieval, processing, etc
21 p2658 A73-40820

A cartographic projection of photographs of celestial bodies obtained from space
21 p2769 A73-40860

The influence of laser ranging on selenodetic control.
21 p2774 A73-41408

Geophysical field cartographic isoline recording via least generalized course representation of observation points, discussing analytic functions and least squares method
22 p2850 A73-42734

MAPS

NT ASTRONOMICAL MAPS

NT LUNAR MAPS

NT METEOROLOGICAL CHARTS

NT PLANISPHERES

NT RADAR CLUTTER MAPS

NT RADAR MAPS

NT RELIEF MAPS

Ransom /Kansas/ stony meteorites discovery location map, describing megascopic appearance, petrology and chemical group
09 p1139 A73-21859

Mapping of foF2 by means of topside sounder satellites.
19 p2427 A73-38285

MARAGING

Influence of cobalt on the maraging of Fe-Ni-Mo alloys
06 p0705 A73-17876

MARAGING STEELS

Processing of high-performance alloys by powder metallurgy.
01 p0063 A73-10286

Stress corrosion cracking behavior of 18% Ni /300/ maraging steel.
01 p0066 A73-11295

The effect of reverted austenite on the mechanical properties and toughness of 12 Ni and 18 Ni /200/ maraging steels.
02 p0183 A73-12758

Fracture toughness of duplex structures. II - Laminates in the divider orientation.
04 p0460 A73-14701

The properties of 18Ni 350 maraging steel produced from elemental and prealloyed powders.
04 p0466 A73-15800

Maraging steels galvanic corrosion reduction by two layer Fe-Cu protective coatings, presenting salt water stress corrosion/time-to-failure test results
06 p0705 A73-17799

Aging kinetics of maraging nickel and chromium steels
06 p0705 A73-17877

Plastic deformation magnitude and direction /sign/ for maraging steels under heat treatment, noting optimal conditions for maximum hardening
06 p0697 A73-17878

Structure and properties of the weld metal in maraging N18K9M5T steel
06 p0697 A73-17879

Thermal-influence region properties in a maraging steel as a function of welding heat cycles
06 p0697 A73-17880

Resistance to hydroerosion of hard-faced maraging steels
06 p0706 A73-17881

Embrittlement of N18K8M3Ti maraging steel after prolonged cooling from high temperatures
06 p0706 A73-17882

Contribution to the study of the effect of molybdenum on the ageing kinetics of maraging steels.
07 p0838 A73-19499

Forged or homogenized aged maraging steels, discussing microstructure, tensile strength and fracture toughness dependence on precipitates morphology
13 p1637 A73-29243

Influence of alloying on the phase composition and properties of maraging stainless steels
13 p1644 A73-29647

Fatigue crack propagation in martensitic and austenitic steels.
14 p1761 A73-30632

Powder metallurgical preparation /sintering/ of conventional maraging steel and similar alloys with Ni

and/or Mo replacement by Mn and Ti, considering age hardening characteristics

14 p1765 A73-30936

The effect of hydrostatic pressure environment on the low cycle fatigue properties of a maraging steel. [ASME PAPER 73-MAT-K]

18 p2323 A73-36616

The effect of cobalt on the aging mechanism of maraging steels

18 p2324 A73-36771

Maraging steels with strengths from 110 to 130 kgf/sq-mm

21 p2718 A73-40736

Structure and phase composition of a maraging-steel weld

21 p2718 A73-40737

Influence of preloading on the sustained load cracking behavior of maraging steels in hydrogen.

21 p2719 A73-40924

Effect of alloying and phase composition on the properties of maraging stainless steels.

21 p2720 A73-41040

MARIA

NT LUNAR MARIA

Results of contrast measurements of some Martian maria in July-August 1971

08 p1007 A73-21062

Contrast measurement data of Martian maria in July-August, 1971.

18 p2355 A73-36863

MARINE BIOLOGY

Airborne and satellite remote sensing of Anacapa Island for hydrology and aquatic biology.

17 p2161 A73-34944

Remote sensing of chlorophyll and temperature in marine and fresh waters.

17 p2164 A73-35664

Remote sensing of ocean color as an index of biological and sedimentary activity.

18 p2307 A73-36030

MARINE ENVIRONMENTS

Miami offshore airport project rejection reasons, citing commercial and marine ecological considerations

15 p1857 A73-31541

Applications of ERTS data to oceanography and the marine environment.

18 p2302 A73-35935

A review of some possible uses of remote sensing techniques in fishery research and commercial fisheries.

18 p2307 A73-36031

Remote sensing data management from a user's viewpoint.

[AAS PAPER 73-152]

20 p2521 A73-38598

Aquatic and diving mammals in fresh water and marine environments, discussing aquatic thermal conditions, body temperature distribution, thermoregulation, metabolic heat production, etc.

22 p2809 A73-42861

Racemization of amino acids in marine sediments determined by gas chromatography.

23 p2973 A73-43843

MARINE NAVIGATION

U SURFACE NAVIGATION

MARINE PROPULSION

NT UNDERWATER PROPULSION

A testing procedure for flame arrestors for marine spark ignition engines.

[WSCI PAPER 72-34]

05 p0563 A73-16681

French project for high speed hydrofoil marine vehicle with hydrodynamic lifting surfaces, completely submerged wings, gas turbine propulsion and automatic control

09 p1031 A73-22208

Experimental investigation of a gas-augmented water-jet engine model

22 p2841 A73-42126

MARINE TECHNOLOGY

Marine quantum Cs Z-magnetometer design and compensation for onboard nonmagnetic schooner operation, using vertical gyro mount

06 p0691 A73-17547

Naval satellite communications terminal design for shipboard use to meet low cost, small size, light weight and printed circuit module replacement demands

12 p1471 A73-27661

L-band satellite systems for mobile applications.

12 p1472 A73-27664

A shipboard satellite communication experiment.

12 p1473 A73-27675

Maritime Satellite System with broadband and multibeam dish antennas, assessing FDM communication capability as function of channel quality and ship terminal antenna gain

12 p1473 A73-27679

Heavy marine structure engineering in offshore airport planning, discussing construction types and conditions, environmental factors, materials, methods and equipment

15 p1856 A73-31533

A technological development scenario for offshore jetports.

15 p1857 A73-31534

Marine quantum Cs Z-magnetometer design and compensation for onboard nonmagnetic schooner operation, using vertical gyro mount

16 p2011 A73-32771

MARINER PROGRAM

NT MARINER VENUS-MERCURY 1973

Mission building blocks for outer solar system exploration.

14 p1805 A73-30527

Design and construction of a reverberation chamber for high-intensity acoustic testing.

16 p1998 A73-33677

Exploring Jupiter, Saturn and their satellites.

23 p3034 A73-44221

MARINER SPACE PROBES

NT MARINER VENUS-MERCURY 1973

NT MARINER 3 SPACE PROBE

NT MARINER 5 SPACE PROBE

NT MARINER 6 SPACE PROBE

NT MARINER 7 SPACE PROBE

NT MARINER 9 SPACE PROBE

Mariner Jupiter/Saturn 1977 - The mission frame.

02 p0221 A73-12597

The radiation regime of the Martian surface and dusty atmosphere

11 p1418 A73-25628

Influence of horizontal inhomogeneity in the Venusian atmosphere on the accuracy of measurements of its parameters by a radio occultation method

16 p2068 A73-33824

Radiation regime of the surface and dust-filled atmosphere of Mars.

19 p2486 A73-38140

Radio occultation experiments planned for Pioneer and Mariner missions to the outer planets.

22 p2912 A73-42980

MARINER SPACECRAFT

Mariner Mars 1971 orbiter spacecraft with sun-Canopus orientation as references, discussing mission objectives, trajectory characteristics, orbital operations, scientific instruments and system design

10 p1276 A73-24004

Mariner Mars 1971 photogrammetry, discussing spacecraft scan platform mounted TV camera calibration procedure for interior orientation parameters and opto-mechanical orthogonality

12 p1500 A73-27953

Temperature control of the Mariner class spacecraft - A seven mission summary.

[AIAA PAPER 73-769]

18 p2360 A73-36383

A unique method of leak-rate measurements.

18 p2316 A73-36714

Navigation system design for the Mariner Jupiter/Saturn Mission.

[AIAA PAPER 73-838]

21 p2736 A73-40503

MARINER VENUS-MERCURY 1973

Microwave dual frequency propagation experiment using the Mariner Venus Mercury probe.

03 p0275 A73-13628

The Mariner Venus Mercury flight data subsystem.

04 p0425 A73-15423

Application of the graphic flight path design program (FPDP) for fast interactive trajectory design.

[AIAA PAPER 73-113]

05 p0619 A73-16871

Design and fabrication of a flight antenna for a planetary spacecraft.

16 p2018 A73-33057

MARINER 3 SPACE PROBE

Preliminary results of measurements of the infrared temperature of the Mars surface by the Mars 3 interplanetary spacecraft

11 p1418 A73-25629

Preliminary results of infrared temperature measurements of the surface of Mars by the Mars-3 automatic interplanetary station.

19 p2486 A73-38141

MARINER 5 SPACE PROBE

Radio-occultation measurements of the Venusian atmosphere conducted by Mariner 5 in the 10-centimeter band

16 p2067 A73-33802

Plasma near Venus - Comparison of results obtained with the aid of Venus 4 and Mariner 5

16 p2067 A73-33804

Power spectra of solar wind parameters at 20 solar radii derived from Mariner 5 data.

24 p3126 A73-45133

MARINER 6 SPACE PROBE

Error analysis for the Mariner-6 and -7 occultation experiments.

09 p1146 A73-22428

MARINER 7 SPACE PROBE

Error analysis for the Mariner-6 and -7 occultation experiments.

09 p1146 A73-22428

MARINER 9 SPACE PROBE

Michelson interferometer on Mariner 9 space probe for thermal emission spectrum measurement, discussing spectral resolution, external vibration problem and instrument performance

01 p0054 A73-11228

From earth to Mars orbit - Mariner 9 propulsion flight performance with analytical correlations.

[AIAA PAPER 72-1185]

03 p0382 A73-13478

Mariner 9 Martian surface mapping, describing science instrumentation, orbit characteristics, mapping cycles sequence design and data telecommunications

[AIAA PAPER 73-204]

Mariner 9 map analysis of Mars geology, covering cratering, circular basins, volcanism, canyons, chaotic terrain, channels and eolian activity

06 p0745 A73-17476

Mars surface features from Mariner 9 TV photometric observations, discussing albedo variations due to dust storm, topography and craters

06 p0745 A73-17478

Mars atmosphere observation from Mariner 9 TV pictures, discussing global and local dust storms, condensate clouds, albedo and polar cover

06 p0745 A73-17479

Mariner 9 television observations of Phobos and Deimos.

06 p0745 A73-17480

Mariner 9 IR spectral features due to carbon dioxide, water vapor and silicate dust suspended in Mars atmosphere before/after planet-wide dust storm

06 p0746 A73-17482

Mariner 9 ultraviolet spectrometer experiment - Mars airglow spectroscopy and variations in Lyman alpha.

06 p0746 A73-17484

Mariner 9 S-band radio occultation measurements of Mars shape and atmospheric parameters, discussing global dust storm and equatorial surface pressure

06 p0746 A73-17487

Mars shape determination from radio occultation measurements by Mariner 9 probe of signal extinction time and spacecraft ephemeris

06 p0747 A73-17488

Earth-moon mass ratio from Mariner 9 radio tracking data.

07 p0899 A73-20156

Mariner 9 stellar photography and camera parameters for point source photometric calibration and reference for optical navigation

08 p0964 A73-21043

Mariner 9 ultraviolet spectrometer experiment - Seasonal variation of ozone on Mars.

08 p1009 A73-21223

Mariner Mars 1971 project historical background, and Mariner 9 orbiter mission science objects and planning for Mars surface observations and measurements

09 p1144 A73-22265

Real time display, processing and image-data products production system for supporting Mariner 9 TV experiment, discussing computer algorithms

09 p1080 A73-22266

Mariner 9 Ultraviolet Spectrometer experiment - Observations of ozone on Mars.

09 p1144 A73-22267

Gravity field of Mars from Mariner 9 tracking data.

11 p1425 A73-26138

Mars topographic and geologic mapping with Mariner 9 TV pictures, ground based radar and IR pressure techniques

16 p2015 A73-33354

Digital processing of Mariner 9 television data.

17 p2168 A73-34907

Exploration of Mars by Mariner 9 - Television sensors and image processing.

17 p2170 A73-35298

Mars maps based on Mariner 9 pictures and photomosaics, with emphasis on southwest quadrant and south pole topographies

18 p2356 A73-37035

Mariner 9 evidence for wind erosion in the equatorial and mid-latitude regions of Mars.

19 p2477 A73-37209

Variable features on Mars. II - Mariner 9 global results.

19 p2478 A73-37212

Mariner 9 observations of the surface of Mars in the north polar region.

19 p2478 A73-37213

Mars atmosphere during the Mariner 9 Extended Mission - Television results.

19 p2478 A73-37218

Atmospheric and surface properties of Mars obtained by infrared spectroscopy on Mariner 9.

19 p2479 A73-37219

Preliminary report on infrared radiometric measurements from the Mariner 9 spacecraft.

19 p2479 A73-37221

Mariner 9 television observations of Phobos and Deimos. II.

19 p2479 A73-37222

Mariner 9 celestial mechanics experiment - A status report.

19 p2479 A73-37223

Plasma columnar content measurement between earth and Mariner 9 at small solar elongations by phase-group velocity difference technique

19 p2479 A73-37224

Approximations to the mean surface of Mars and Mars atmosphere using Mariner 9 occultations.

19 p2479 A73-37226

Martian surface primary and secondary triangulation networks based on multiphotograph stereophotogrammetry and rectified photographs by Mariner 9, discussing control nets and points
19 p2479 A73-37227

Mars physical ephemeris elements and aerographic coordinate system for Mariner 9 mapping
19 p2479 A73-37228

Photogrammetric evaluation of Mariner 9 photography.
19 p2479 A73-37229

Verification of performance of the Mariner 9 television cameras.
19 p2428 A73-37258

Mariner 9 ultraviolet spectrometer experiment - Mars atomic oxygen 1304-A emission.
20 p2604 A73-38932

MARKET RESEARCH

STOL aircraft technology, operation and markets in view of future European air traffic development, discussing various lift devices, noise aspects and economic factors
[DGLR PAPER 72-054] 02 p0130 A73-11662

A business man views commercial ventures in space.
[AIAA PAPER 73-78] 06 p0771 A73-17640

Boeing 727 design and development in response to airline market requirements, emphasizing profitability
10 p1176 A73-24875

Canadian air transportation survey, outlining history of other modes, transportation investment trends, modal traffic distribution, STOL applications, airline social services and marketing
16 p2087 A73-33177

Short haul aircraft design and marketing, examining competing modes, noise factors, airport traffic density patterns and aircraft types dependence on utilization
16 p2088 A73-33184

Market trends and technical progress in small gas turbine engines for general aviation and executive aircraft and helicopters
17 p2256 A73-34447

Second generation supersonic transport, discussing fuel costs, changing markets, travel patterns, electronic displays and sound suppressor development
[SAE PAPER 730349] 17 p2102 A73-34697

Transport cargo aircraft design requirements and supporting ground system concepts in view of future market demands with emphasis on economic constraints
[SAE PAPER 730352] 17 p2102 A73-34700

Market economic environment change effects on air transport design and use, examining 747 operational requirements in terms of cargo load factor, passenger fares and labor costs
[SAE PAPER 730355] 17 p2103 A73-34703

COS-MOS applications to clock and watch, automotive, aerospace and military, industrial and consumer markets
20 p2533 A73-38654

Future communication satellite technology improvement, market expansion and cost effectiveness, considering foreign domestic, and international light-to-medium and high density systems
20 p2522 A73-38715

Passenger response to airline service and resultant competition dynamics among air carriers in metropolitan area, indicating satellite airports importance
21 p2671 A73-40210

MARKETING

Capital equipment marketing, discussing industry-customer-government interface, marketing and sales techniques and functions, products initiation, etc
10 p1298 A73-24650

MARKING

NT ISOTOPIC LABELING
The problem of the deformation of the photoemulsion layer during artificial marking of points on aerial photos
13 p1621 A73-29417

MARKOV CHAINS

Ergodicity criteria of homogeneous Markov chains in a special phase space. I, II
07 p0844 A73-19326

Uniform estimate of the residual term in the multidimensional limiting theorem for homogeneous Markov chains on the basis of a class of all measured convex sets. II
10 p1242 A73-23814

Simulation of random processes with the aid of piecewise linear transformations of unit interval
11 p1340 A73-25012

Exponential bounds for error and equivocation based on Markov chain observations.
13 p1651 A73-29600

Evaluation of burst error correcting codes using a simple partitioned Markov chain model.
21 p2656 A73-41168

MARKOV PROCESSES

NT MARKOV CHAINS
Displacements of spatially bounded light beams in a turbulent medium using the approximation of a random Markov process
01 p0076 A73-10214

Mathematical model for the buildup of imperfections in plastic isotropic materials
01 p0114 A73-10476

Steady ergodic Markovian random function construction
01 p0071 A73-11271

Reliability and failure sequence characteristics of automatic system, using input rarefaction of Markov renewal process
01 p0058 A73-11423

Parametric vibration of simply supported rectangular plate and cylindrical shell under random excitation, using Markov process theory and Fokker-Planck equation
03 p0388 A73-13318

Application of stochastic stability theory to model-reference systems.
04 p0430 A73-15215

Source encoding with fixed word length and synchronous bit rate.
04 p0425 A73-15420

Dispersion relations for electromagnetic radiation in random media.
05 p0597 A73-16494

Error incidence probability for system control reliability determination, assuming error function as Markov process
06 p0680 A73-17956

Kolmogorov's differential equations for non-stationary, countable state Markov processes with uniformly continuous transition probabilities.
06 p0718 A73-18501

Optimal estimation of operator-valued stochastic processes and applications to distributed parameter systems.
07 p0805 A73-20580

Feedback regulators for jump parameter systems with state and control dependent transition rates.
07 p0806 A73-20597

Techniques for short-term predictions of atmospheric noise levels.
08 p0940 A73-21662

Construction of discrete shaping filters for the digital simulation of linear Markov processes
11 p1340 A73-25011

Viterbi algorithm for recursive optimal estimation of state sequence of discrete time finite state Markov process observed in memoryless noise
11 p1333 A73-26690

Correlated clutter and resultant properties of binary signals.
13 p1585 A73-29208

Optimal damping and stochastic control in certain problems of astrodynamics
15 p1931 A73-31236

Application of the theory of Markov processes in state estimation of dynamic systems and in control of flight-vehicle oscillations
15 p1942 A73-31239

Reliability estimation technique for data transmission processes in remote control systems with redundancy, assuming Markovian randomness of signal input
15 p1854 A73-31806

Optimal Markov sequence signal detection in correlated FM random electronic countermeasure background noise
20 p2529 A73-38929

Optimal detection of binary signals with an arbitrary distribution of state durations at the output of a binary symmetrical Markov channel
20 p2541 A73-38992

A design problem for redundant systems with recovery
20 p2568 A73-38996

Stochastic differential equation solutions for Markov processes with diffuse switching, including limit theorem on convergence
20 p2582 A73-39386

Nonnegative additive functionals of Markov processes and certain limit theorems
20 p2582 A73-39389

Chapman-Enskog-Hilbert expansion for a Markovian model of the Boltzmann equation.
20 p2549 A73-39627

Passive stochastic feedback stability. I - A general theory. II - Applications.
21 p2669 A73-40450

Certain problems in determining the capacity of digital computers
22 p2829 A73-41953

Optimal SAM defense system - An application of optimal control concept to operations research.
23 p2964 A73-43823

Representation of functions of Markov processes as solutions of stochastic equations.
23 p3000 A73-44207

Reliability estimation technique for data transmission processes in remote control systems with redundancy, assuming Markovian randomness of signal input
24 p3075 A73-45350

Random vibrations of elastic nonlinear nonautonomous systems with variable parameters
24 p3112 A73-45502

MARS [PLANET]

MARS [PLANET]
Photographic observations of Mars during the major opposition of 1971
01 p0101 A73-10842

Missions for the systematic unmanned exploration of Mars.
01 p0105 A73-11160

Observation of the region of interaction between the solar-wind plasma and Mars.
05 p0608 A73-16095

Far IR brightness temperature, opacity and emissivity of Jupiter, Venus, Mars and Saturn
05 p0626 A73-17348

Mars shape determination from radio occultation measurements by Mariner 9 probe of signal extinction time and spacecraft ephemeris
06 p0747 A73-17488

Mars diameter optical measurements by earth based refractor telescopes with birefringent double image micrometer
06 p0747 A73-17489

Brightness temperature of Mars thermal emission in two orthogonal polarizations by microwave radiometry from Mars 2 and 3 orbiters
06 p0747 A73-17490

Solar system planets spin rate change and core growth, discussing Mars geology and earth evolution
06 p0749 A73-18006

Properties of solar halos in the Martian limb zone and at the terminator
07 p0902 A73-20322

Structure and evolution of the asteroid ring
07 p0902 A73-20324

Hadamard transform spectrometer designed for airborne IR astronomical observations of Mars, using binary orthogonal pseudonoise codes in multiplexing scheme
08 p0972 A73-21753

New optical measurements of planetary diameters. IV - Size of the North polar cap of Mars.
09 p1145 A73-22273

Martian spin axis wandering resulting from equatorial volcanic convections and gravity field non-hydrostatic low order components
09 p1151 A73-23172

The magnetic field in the immediate vicinity of Mars according to Mars 2 and Mars 3 satellite data
10 p1281 A73-24461

Gravity field of Mars from Mariner 9 tracking data.
11 p1425 A73-26138

Properties of solar halos in the limb zone and at the terminator of Mars.
12 p1540 A73-27294

Photographic observations of Mars during the great opposition of 1971.
15 p1928 A73-30978

Monochromatic and radiometric albedo of Mars and Venus
16 p2067 A73-33811

An experiment in photographic equidensitometry of the moon and planets
16 p2070 A73-33848

Two layer cores in terrestrial planets with emphasis on Mars and Venus, discussing pressure at earth mantle-core boundary, equations of state and composition
17 p2235 A73-35743

Large-scale variations in the obliquity of Mars.
18 p2348 A73-35921

Mariner 9 television observations of Phobos and Deimos. II.
19 p2479 A73-37222

Mariner 9 celestial mechanics experiment - A status report.
19 p2479 A73-37223

Magnetic field in the near vicinity of Mars from data of the Mars-2 and Mars-3 satellites.
19 p2486 A73-38127

Magnetic field in the very close neighborhood of Mars according to data from the Mars 2 and Mars 3 spacecraft.
20 p2604 A73-38959

The figure of Mars and its effect on radar-ranging.
20 p2611 A73-39588

Mars internal structure computed via general relativity application to earth-like model
20 p2612 A73-39711

Mars almanac /ephemerides, rotation data, coordinate data, etc/ for Viking lander position definition and stellar and planetary observations from Mars surface
21 p2733 A73-40031

Climatic change on Mars.
21 p2773 A73-41301

Mars and Jupiter - Radio emission at 1.35 cm.
24 p3128 A73-44399

Mars precession scheme for prolonged equinoctial habitable spring in terms of Sagan model extension
24 p3131 A73-44464

Mars seasonal effects from observations of contrast changes in blue light, discussing diurnal variations and UV contrast reversal
24 p3134 A73-44567

MARS ATMOSPHERE

Transient variation of martian ground-atmosphere thermal boundary layer structure.
01 p0097 A73-10400

Numerical simulation of radiative-conductive heat transfer in the Martian atmosphere-polar cap utilizing Mariner 9 Iris data.
01 p0097 A73-10401

Photographic observations of Mars during the major opposition of 1971
01 p0101 A73-10842

Objectives and first results of the Mars 2, Mars 3 and Mariner 9 planetary probes
01 p0103 A73-10996

Viking Mars program for surface mapping and exploration, atmospheric composition investigation and life evidence search, discussing orbiter and lander phases
01 p0105 A73-11155

Viking lander-borne gas chromatograph mass spectrometer for Martian atmosphere sampling and soil analyses
02 p0168 A73-12000

Diurnal variation of the exospheric temperatures on Venus and Mars.
02 p0214 A73-12253

Restrictions on McElroy theory of Martian chaotic terrain production by permafrost withdrawal, calculating degassed water/carbon dioxide ratios in Mars and earth atmospheres
02 p0218 A73-12418

Mars exploration by spacecraft, discussing erosional processes, atmospheric pressure and composition, heat absorption and radiation and polar caps formation
02 p0221 A73-12575

Mars oxygen photoelectric spectral and aeronomical study, noting water vapor and carbon dioxide photolytic effects
02 p0224 A73-12787

Brief history of the Martian 'violet haze' problem.
03 p0373 A73-13707

Pontryagin maximum principle for optimal terminal velocity control of automatic space probe descent in Mars atmosphere
03 p0383 A73-14556

Martian topography from radar observations and the Mariner 6 and 7 and ground-based CO₂ measurements.
04 p0503 A73-16016

Martian dust storm from photometric observations on board the Automatic Interplanetary Station Mars 3
05 p0620 A73-17018

Mars atmosphere observation from Mariner 9 TV pictures, discussing global and local dust storms, condensate clouds, albedo and polar cover
06 p0745 A73-17479

Mars 3 onboard optical measurements of Mars surface and lower atmosphere, considering temperatures, water vapor content, dust cloud and particle characteristics
06 p0746 A73-17481

Mariner 9 IR spectral features due to carbon dioxide, water vapor and silicate dust suspended in Mars atmosphere before/after planet-wide dust storm
06 p0746 A73-17482

Mars UV reflectance properties from Mariner 9 spectrometer, giving topographic map based on ultraviolet light scattering from atmosphere
06 p0746 A73-17483

Mariner 9 ultraviolet spectrometer experiment - Mars airglow spectroscopy and variations in Lyman alpha.
06 p0746 A73-17484

Carbon monoxide Cameron bands limb intensity profile in Martian airglow from Mariner 9 UV spectrum observations
06 p0746 A73-17485

Preliminary results of measurements of UV emissions scattered in the Martian upper atmosphere.
06 p0746 A73-17486

Mariner 9 S-band radio occultation measurements of Mars shape and atmospheric parameters, discussing global dust storm and equatorial surface pressure
06 p0746 A73-17487

The thermal structure within the stratospheres of Venus and Mars.
06 p0747 A73-17493

Calculation of the transfer coefficients for planetary atmospheres consisting of CO₂-N₂ mixtures
06 p0754 A73-18568

Stability CO₂ in the Martian atmosphere and under radiolysis.
07 p0899 A73-20155

Mariner 9 ultraviolet spectrometer experiment - Seasonal variation of ozone on Mars.
08 p1009 A73-21223

An analytical and numerical study of the Martian planetary boundary layer over slopes.
08 p1011 A73-21381

An alpha particle experiment for chemical analysis of the Martian surface and atmosphere.
09 p1048 A73-22190

Ion velocity temperature observation at Mars surface boundary, suggesting solar plasma interaction with outer atmosphere from ion flux disturbance ahead of shock wave
09 p1126 A73-22264

Mariner 9 Ultraviolet Spectrometer experiment - Observations of ozone on Mars.
09 p1144 A73-22267

Mars dust storm observations at time of great oppositions, suggesting local time and space meteorological conditions and feedback processes favoring global dust spread
09 p1144 A73-22269

Exchange of water vapor between the atmosphere and surface of Mars.
09 p1145 A73-22270

The vertical thermal structure of the Martian atmosphere - Modification by motions.
09 p1145 A73-22271

A new look at the Martian 'violet haze' problem. II - 'Blue clearing' in 1969.
09 p1145 A73-22275

Error analysis for the Mariner-6 and -7 occultation experiments.
09 p1146 A73-22428

Preliminary results of studies of the Martian atmosphere with the aid of the Mars-2 satellite
09 p1146 A73-22486

Some problems of optimal control of space-vehicle trajectories in the Martian atmosphere
10 p1247 A73-23878

Large scale surface structure of Mars.
11 p1417 A73-25268

The radiation regime of the Martian surface and dusty atmosphere
11 p1418 A73-25628

A model of a Martian Great dust storm
11 p1418 A73-25715

Preliminary measurement data on the H₂O content of the Martian atmosphere from the Mars-3 automatic interplanetary station
12 p1540 A73-27451

Mars photographic observations during opposition, analyzing polar caps, surface reliefs, dust storms and atmospheric optical thickness
12 p1542 A73-27498

Investigation of scattered ultraviolet radiation in the upper Martian atmosphere from the Mars-3 automatic interplanetary station
14 p1796 A73-29866

Preliminary results of Martian-atmosphere research with the Mars-2 satellite.
14 p1798 A73-30321

Photographic observations of Mars during the great opposition of 1971.
15 p1928 A73-30978

On the effect of electron-neutral particle collisions upon the refraction of high-frequency radio waves by the lower atmosphere and ionosphere of Mars.
15 p1929 A73-31078

Mars 3 solar wind probe of upper Mars atmosphere, showing plasma interaction with ionosphere measured by energy spectra
15 p1930 A73-31150

Some field characteristics of outgoing thermal radiations in the Venusian and Martian atmospheres
15 p1937 A73-31819

Electrical breakdown caused by dust motion in low-pressure atmospheres - Considerations for Mars.
15 p1941 A73-32267

On the extent of the Martian ionosphere.
16 p2062 A73-33462

Calculation of the transfer coefficients of planetary atmospheres formed by mixtures of CO₂ and N₂.
16 p2039 A73-33593

Spectral studies of the atmospheres of Mars and Venus
16 p2067 A73-33812

Estimates of the intensity of turbulence in the atmospheres of Mars and Venus
16 p2069 A73-33828

Planet Mars atmospheric physics covering optical parameters, brightness distributions, pressure, aerosol, chemical composition, photometric and surface layer properties and topography
16 p2069 A73-33830

Role of water vapor in the meteorology of Mars
16 p2069 A73-33831

Mars blue haze, earth noctilucent clouds and Venus blue clouds, considering mechanism and condensate chemical composition for formation
16 p2069 A73-33833

Criteria for the existence of H₂O crystals on Mars
16 p2069 A73-33836

Photoinduced fixation of CO₂ by amino acids - Implications for nonbiological reactions on the Martian soil.
16 p1977 A73-33874

The atmospheric mixing in the atmospheres of Mars and Venus.
18 p2349 A73-36034

Martian sandstorms and wind erosion, discussing theoretical calculation methods and wind tunnel experiments
19 p2478 A73-37211

Martian polar stacked laminas interpreted in terms of conditions for carbon dioxide liquefaction, considering atmosphere history
19 p2478 A73-37217

Mars atmosphere during the Mariner 9 Extended Mission - Television results.
19 p2478 A73-37218

Atmospheric and surface properties of Mars obtained by infrared spectroscopy on Mariner 9.
19 p2479 A73-37219

Mariner 9 ultraviolet spectrometer experiment - Afternoon terminator observations of Mars.
19 p2479 A73-37220

S band radio occultation measurements of the atmosphere and topography of Mars with Mariner 9 - Extended mission coverage of polar and intermediate latitudes.
19 p2479 A73-37225

Approximations to the mean surface of Mars and Mars atmosphere using Mariner 9 occultations.
19 p2479 A73-37226

Mechanisms for Mars dust storms.
19 p2485 A73-37656

Radiation regime of the surface and dust-filled atmosphere of Mars.
19 p2486 A73-38140

Some problems in the optimal control of spacecraft trajectories in the Martian atmosphere.
20 p2589 A73-38897

Mariner 9 ultraviolet spectrometer experiment - Mars atomic oxygen 1304-A emission.
20 p2604 A73-38932

The photolytic stability of the Martian atmosphere.
21 p2764 A73-40159

Viking Mars 1975 soft landing and search for extraterrestrial life, considering lander transmission of atmospheric and surface data
21 p2766 A73-40414

Climatic change on Mars.
21 p2773 A73-41301

Preliminary results of measurements of the H₂O content of the Martian atmosphere by the unmanned spacecraft Mars 3.
22 p2905 A73-41806

Wave-induced eddy diffusion coefficients in the upper atmosphere of Mars.
22 p2906 A73-41903

Estimate of extreme ultraviolet dayglow of helium in the Martian atmosphere.
22 p2909 A73-42485

The International Planetary Patrol Program - An assessment of the first three years.
22 p2912 A73-42978

Surface wind stress and threshold friction velocity required to raise dust on Mars, discussing mechanisms for production of strong winds in Ekman layer
22 p2912 A73-42981

Ultraviolet observations of Mars made by the Orbiting Astronomical Observatory.
24 p3128 A73-44397

Martian W cloud diurnal brightening observation by Mariners 6 and 7 flyby missions, considering probable water ice formation
24 p3128 A73-44398

Differentiated true abundance Mars air mass calculations for use in spectroscopic observation
24 p3131 A73-44465

Calculation of a model of the neutral atmosphere of Mars above 140 km from ionospheric data
24 p3137 A73-44785

Lyman alpha 1216 A intensity behavior for atomic hydrogen density distribution below 200 km on Mars, calculating radiative transfer
24 p3139 A73-45108

Atmospheric mixing effects for interpretation of oxygen atom concentration in Mars and Venus upper atmospheres obtained by Mariner and Venera space probes
24 p3139 A73-45134

MARS ENVIRONMENT
NT MARS ATMOSPHERE

Solar plasma electron density and temperature measurement by Mars 2 and Mars 3 orbiter-borne retarding potential analyzers, considering solar wind shock front interaction role
09 p1126 A73-22263

Viking type spacecraft rendezvous with the Martian moons.
19 p2482 A73-37401

Soil microbiological tests to evaluate Antarctica as Mars environment model for quarantine standards
22 p2803 A73-42162

On the mechanism of adaptation of micro-organisms to conditions of extreme low humidity.
22 p2803 A73-42164

On the multiplication of xerophilic micro-organisms under simulated Martian conditions.
22 p2803 A73-42165

MARS LANDING

The conjugate gradient method and its application to aerospace vehicle guidance and control. II - Mars entry guidance and control.
08 p0986 A73-21429

Implementation of the 1975 Mars Viking Lander cameras.
08 p0970 A73-21741

- Mars 2 and 3 - Technology and investigation results
11 p1432 A73-26741
Dynamic stress analysis during inflation of disk-gap-band Viking 75 parachute for Mars soft landing
[AIAA PAPER 73-444] 15 p1825 A73-31430
A new approach to performance optimization of the 1975 Mars Viking lander.
[AIAA PAPER 73-889] 20 p2614 A73-38825
Long range post-Apollo space exploration goals, considering earth orbital station, moon base, manned Mars landing and interstellar flights
23 p3038 A73-43990
Investigations of Mars from the Soviet automatic stations Mars 2 and 3.
24 p3128 A73-44431

MARS PROBES

- NT MARINER 3 SPACE PROBE
NT MARINER 6 SPACE PROBE
NT MARINER 7 SPACE PROBE
NT MARS 2 SPACECRAFT
NT MARS 3 SPACECRAFT
NT VIKING LANDER SPACECRAFT
NT VIKING MARS PROGRAM
NT VIKING ORBITER SPACECRAFT
NT VIKING 75 ENTRY VEHICLE
Objectives and first results of the Mars 2, Mars 3 and Mariner 9 planetary probes
01 p0103 A73-10996

- The image-readout system of the combination photographic and television scanners of the Mars-2 and Mars-3 automatic interplanetary space probes.
09 p1086 A73-23050

- Mars 2 and 3 - Technology and investigation results
11 p1432 A73-26741
Magnetic field in the very close neighborhood of Mars according to data from the Mars 2 and Mars 3 spacecraft.
20 p2604 A73-38959

- Ultraminiature X-ray fluorescence spectrometer for in-situ geochemical analysis on Mars.
21 p2765 A73-40241

- Results of solar plasma electron observations on Mars-2 and Mars-3 spacecraft.
22 p2906 A73-41941

MARS SPACECRAFT

- U MARINER SPACECRAFT
MARS SURFACE
Photographic observations of Mars during the major opposition of 1971
01 p0101 A73-10842

- Viking Mars program for surface mapping and exploration, atmospheric composition investigation and life evidence search, discussing orbiter and lander phases
01 p0105 A73-11155

- Mars polar caps formation at aerographic latitudes, assuming water vapor condensation on ground and water presence in carbon dioxide snow
01 p0106 A73-11322

- Restrictions on McElroy theory of Martian chaotic terrain production by permafrost withdrawal, calculating degassed water/carbon dioxide ratios in Mars and earth atmospheres
02 p0218 A73-12418

- Quarantine necessity, protocol and effectiveness for Mars samples, emphasizing risks of foreign replicating agent introduction to earth biosphere
03 p0272 A73-14321

- Martian canals interpretation based on thermodynamic subsurface cells with time-limited cellular convection and densification of dust masses along cell boundaries
04 p0501 A73-15628

- Martian topography from radar observations and the Mariner 6 and 7 and ground-based CO2 measurements.
04 p0503 A73-16016

- Distributions of lunar and Martian craters in relation to their origin
05 p0613 A73-16202

- Mariner 9 Martian surface mapping, describing science instrumentation, orbit characteristics, mapping cycles sequence design and data telecommunications
[AIAA PAPER 73-204] 05 p0630 A73-16938

- Martian dust storm from photometric observations on board the Automatic Interplanetary Station Mars 3
05 p0620 A73-17018

- Mariner 9 map analysis of Mars geology, covering cratering, circular basins, volcanism, canyons, chaotic terrain, channels and eolian activity
06 p0745 A73-17476

- Geological framework of the south polar region of Mars.
06 p0745 A73-17477

- Mars surface features from Mariner 9 TV photometric observations, discussing albedo variations due to dust storm, topography and craters
06 p0745 A73-17478

- Mars 3 onboard optical measurements of Mars surface and lower atmosphere, considering temperatures, water vapor content, dust cloud and particle characteristics
06 p0746 A73-17481

- Mars UV reflectance properties from Mariner 9 spectrometer, giving topographic map based on ultraviolet light scattering from atmosphere
06 p0746 A73-17483

- Interferometric observations of Mars at 21-cm wavelength.
06 p0747 A73-17491

- Mars microwave spectra computation by improved thermal model with seasonal polar cap effects and accurate aspect geometry, noting lunar-like planetary subsurface nature
06 p0747 A73-17492

- Mars surface volcano and canyon features from Mariner 9 photographs and geological map, suggesting internal heating, water erosion, atmospheric evolution and life problem solution
06 p0754 A73-18672

- Mariner spacecraft photographed Mars surface volcanic mountains and water in polar caps, suggesting recurring rainfall and rivers during successive interglacial periods
07 p0875 A73-19166

- Isostasy and relief of the Earth, the Moon and Mars
07 p0878 A73-19661

- The ground surface of planet Mars
07 p0900 A73-20243

- System modeling and optimal design of a Mars-roving vehicle.
07 p0906 A73-20593

- Results of contrast measurements of some Martian maria in July-August 1971
08 p1007 A73-21062

- An alpha particle experiment for chemical analysis of the Martian surface and atmosphere.
09 p1048 A73-22190

- Ground based radar measurement of Martian topography, surface temperature and thermal properties by microwave and IR radiometry and spectral reflectivity observation
09 p1144 A73-22259

- Radar measurement of altitude profiles and reflected power for Martian topography and surface properties, noting heavy cratering
09 p1144 A73-22260

- High resolution radar observation of Martian surface topography and scattering properties, noting dielectric constant and rms surface slope variations
09 p1144 A73-22261

- Ground based spectroscopic observation of carbon dioxide distribution on Mars surface, noting Tharsis region pressure anomaly, ridge slope and dust storm activity
09 p1144 A73-22262

- Mariner Mars 1971 project historical background, and Mariner 9 orbiter mission science objects and planning for Mars surface observations and measurements
09 p1144 A73-22265

- Mars surface ellipticity discrepancy with dynamic value obtained from satellite orbital precession explained by solid state convection in deep interior and Martian evolution
09 p1144 A73-22268

- Exchange of water vapor between the atmosphere and surface of Mars.
09 p1145 A73-22270

- Ground based photometric observations of Mars during 1971 opposition, using conventional photography, multichannel spot photometry and dual channel area scanning
09 p1145 A73-22272

- Permanent frost formation on steep north-facing Mars surface slopes above 25 deg north latitude, considering explanation by insolation and surface albedo
09 p1145 A73-22274

- A new look at the Martian 'violet haze' problem. II - 'Blue clearing' in 1969.
09 p1145 A73-22275

- Retroflecting satellite with laser range finder for Mariner roving vehicle navigation, discussing error analysis and minimization by measurement geometry choice through nonlinear programming
10 p1247 A73-24005

- Terrestrial, Martian and lunar doublet craters origin from simultaneous multiple meteorite impacts, using Lexan plastic projectiles against sand targets in ballistic range tests
10 p1277 A73-24079

- Large scale surface structure of Mars.
11 p1417 A73-25268

- The radiation regime of the Martian surface and dusty atmosphere
11 p1418 A73-25628

- Preliminary results of measurements of the infrared temperature of the Mars surface by the Mars 3 interplanetary spacecraft
11 p1418 A73-25629

- A model of a Martian Great dust storm.
11 p1418 A73-25715

- Fourier analysis of Mars radar topographic data for magnitude and direction of center of mass/center of figure offset, comparing to earth and moon
11 p1419 A73-25862

- Mars photographic observations during opposition, analyzing polar caps, surface reliefs, dust storms and atmospheric optical thickness
12 p1542 A73-27498

- Specific effective scattering area of the surface of the moon, Mars, and Venus in the radio-frequency range.
12 p1543 A73-27639

- Preliminary results of the determination of altitudes on Mars from CO2 2-micron wavelength bands aboard the Mars 3 interplanetary automatic station
13 p1673 A73-28288

- Xenoliths in maars and diatremes with inferences for the moon, Mars, and Venus.
13 p1681 A73-28848

- Mars polar regions layered deposits annual solar insolation variations due to eccentricity
13 p1687 A73-29674

- Chemical evolution before life from carbonaceous meteorites composition, noting porphyryns, optically active substances and isoprenoid hydrocarbons
14 p1715 A73-30130

- Photographic observations of Mars during the great opposition of 1971.
15 p1928 A73-30978

- Mars topographic and geologic mapping with Mariner 9 TV pictures, ground based radar and IR pressure techniques
16 p2015 A73-33354

- Role of water vapor in the meteorology of Mars
16 p2069 A73-33831

- Identification of certain details on photographs of Mars obtained from Mariner 4 and on the ground
16 p2069 A73-33834

- Craters on photographs of the Mars surface taken by the Mariner 4 probe in 1965
16 p2069 A73-33835

- Solar neutrino deficiency related to solar core periodic expansion, considering Martian river-like channel formation and Praesepe cluster distribution through main sequence
17 p2229 A73-34434

- Evidence of active and ancient volcanism on Mars - A review.
17 p2233 A73-35482

- Extraterrestrial life detection from imaging observations on lunar samples and meteorites, discussing application to Mars surface
17 p2113 A73-35804

- Contrast measurement data of Martian maria in July-August, 1971.
18 p2355 A73-36863

- Mars maps based on Mariner 9 pictures and photomosaics, with emphasis on southwest quadrant and south pole topographies
18 p2356 A73-37035

- An overview of geological results from Mariner 9.
19 p2477 A73-37200

- A generalized geologic map of Mars.
19 p2477 A73-37201

- Water and processes of degradation in the Martian landscape.
19 p2477 A73-37202

- Martian volcanic and tectonic features from Mariner 9 photography, comparing evolutionary phases with lunar and terrestrial morphology
19 p2477 A73-37203

- Mars troughs from Mariner 9 pictures, interpreting evolutionary origin in terms of surface and core processes
19 p2477 A73-37204

- Martian lowland terrains fretted and chaotic characteristics, hypothesizing evolutionary processes based on escarpment recession, subsurface ground ice and magma collapse
19 p2477 A73-37205

- Comparison of Martian and lunar multiringed circular basins.
19 p2477 A73-37206

- Martian cratering. IV - Mariner 9 initial analysis of cratering chronology.
19 p2477 A73-37207

- Latitudinal distribution of a debris mantle on the Martian surface.
19 p2477 A73-37208

- Mariner 9 evidence for wind erosion in the equatorial and mid-latitude regions of Mars.
19 p2477 A73-37209

- Mars Hellespontus region identification from Mariner 9 photographs as wind produced dunes, considering albedo features
19 p2477 A73-37210

- Martian sandstorms and wind erosion, discussing theoretical calculation methods and wind tunnel experiments
19 p2478 A73-37211

- Variable features on Mars. II - Mariner 9 global results.
19 p2478 A73-37212

- Mariner 9 observations of the surface of Mars in the north polar region.
19 p2478 A73-37213

- Wind erosion in the Martian polar regions.
19 p2478 A73-37214

MARS 2 SPACECRAFT

Martian south polar region pitted and etched terrain features, interpreting surface layered blanketing material as due to wind action 19 p2478 A73-37215

Nature and origin of layered deposits of the Martian polar regions. 19 p2478 A73-37216

Martian polar stacked laminae interpreted in terms of conditions for carbon dioxide liquefaction, considering atmosphere history 19 p2478 A73-37217

Atmospheric and surface properties of Mars obtained by infrared spectroscopy on Mariner 9. 19 p2479 A73-37219

Preliminary report on infrared radiometric measurements from the Mariner 9 spacecraft. 19 p2479 A73-37221

S band radio occultation measurements of the atmosphere and topography of Mars with Mariner 9 - Extended mission coverage of polar and intermediate latitudes. 19 p2479 A73-37225

Approximations to the mean surface of Mars and Mars atmosphere using Mariner 9 occultations. 19 p2479 A73-37226

Martian surface primary and secondary triangulation networks based on multiphotograph stereophotogrammetry and rectified photographs by Mariner 9, discussing control nets and points 19 p2479 A73-37227

Mars physical ephemeris elements and aerographic coordinate system for Mariner 9 mapping 19 p2479 A73-37228

A study of Martian topography by analytic photogrammetry. 19 p2480 A73-37230

Cartographic products from the Mariner 9 mission. 19 p2480 A73-37231

Martian south polar region albedo map from Mariner 9 photographs, comparing with earth-based telescopic observations 19 p2480 A73-37232

Science aspects of a remotely controlled Mars surface roving vehicle. 19 p2416 A73-37311

Planetary surface rover/remotely manned system concepts and applications from lunar and Mars mission studies 19 p2416 A73-37312

Mars surface exploration by self-guided stereo TV equipped roving vehicle /robot/, describing computerized object and scene ranging and recognition 19 p2429 A73-37321

The dynamical effects of real Mars orography upon the large-scale air flow and some meteorological phenomena of Mars. 19 p2482 A73-37429

Circularity of Martian craters. 19 p2486 A73-37800

Radiation regime of the surface and dust-filled atmosphere of Mars. 19 p2486 A73-38140

Preliminary results of infrared temperature measurements of the surface of Mars by the Mars-3 automatic interplanetary station. 19 p2486 A73-38141

The figure of Mars and its effect on radar-ranging. 20 p2611 A73-39588

Mars equatorial region crustal structure from Bouguer gravity anomalies computed by differencing free air gravity and topographically predicted gravity 20 p2612 A73-39710

Spacecraft television image comparison between earth and Mars surface features and geology, discussing mountain chains, deserts and tectonic mapping techniques 20 p2613 A73-39897

Viking Mars 1975 soft landing and search for extraterrestrial life, considering lander transmission of atmospheric and surface data 21 p2766 A73-40414

Mariner Mars 1969 infrared spectrometer - Gas delivery system and Joule-Thomson cryostat. 21 p2702 A73-41101

Preliminary results of Martian altitude determinations with CO₂ bands /2 micron wavelength/ from the automatic interplanetary space station Mars 3. 22 p2905 A73-41807

Organic geochemical analysis of lunar samples with emphasis on detecting biologically significant organogenic elements, projecting techniques to Mars soil analysis 22 p2803 A73-42163

Absolute measurements and computed values for Martian irradiance between 10.5 and 12.5 microns. 24 p3127 A73-44394

High altitude infrared spectroscopic evidence for bound water on Mars. 24 p3127 A73-44395

Mariner 9 ultraviolet spectrometer experiment - 1971 Mars' dust storm. 24 p3127 A73-44396

Investigations of Mars from the Soviet automatic stations Mars 2 and 3. 24 p3128 A73-44431

Mars surface evolution from analysis of Mariner 6 and 7 equatorial photographs, discussing internal dynamic activity 24 p3128 A73-44432

Mars crustal structure model from analysis of surface markings with Mariner 9 data, showing petrologic distinctions between dark and light regions 24 p3133 A73-44543

Martian surface albedo compared with Mariner-observed topography, noting dark-band correlation with maximum topographic irregularity regions 24 p3133 A73-44551

Seasonal variations of the south polar cap of Mars according to measurements made on photographs taken near the time of the 1971 opposition. 24 p3143 A73-45439

MARS 2 SPACECRAFT

Soviet Mars 1, 2 and 3 lander failure description from western sources, discussing further attempts in July or August 1973 launch windows 17 p2234 A73-35656

Investigations of Mars from the Soviet automatic stations Mars 2 and 3. 24 p3128 A73-44431

MARS 3 SPACECRAFT

Observation of the region of interaction between the solar-wind plasma and Mars. 05 p0608 A73-16095

Martian dust storm from photometric observations on board the Automatic Interplanetary Station Mars 3 05 p0620 A73-17018

Mars 3 onboard optical measurements of Mars surface and lower atmosphere, considering temperatures, water vapor content, dust cloud and particle characteristics 06 p0746 A73-17481

Mars 2 and 3 - Technology and investigation results 11 p1432 A73-26741

Preliminary measurement data on the H₂O content of the Martian atmosphere from the Mars-3 automatic interplanetary station 12 p1540 A73-27451

Mars 3 solar wind probe of upper Mars atmosphere, showing plasma interaction with ionosphere measured by energy spectra 15 p1930 A73-31150

Soviet Mars 1, 2 and 3 lander failure description from western sources, discussing further attempts in July or August 1973 launch windows 17 p2234 A73-35656

Preliminary results of measurements of the H₂O content of the Martian atmosphere by the unmanned spacecraft Mars 3. 22 p2905 A73-41806

Investigations of Mars from the Soviet automatic stations Mars 2 and 3. 24 p3128 A73-44431

MARS '71 PROJECT

Prevention of damage to the science instruments of Mariner-Mars '71 spacecraft due to accidental viewing of the sun during sun-acquisition following exit from earth shadow. 06 p0696 A73-18829

Mariner Mars 1971 orbiter spacecraft with sun-Canopus orientation as references, discussing mission objectives, trajectory characteristics, orbital operations, scientific instruments and system design 10 p1276 A73-24004

Mariner Mars 1971 photogrammetry, discussing spacecraft scan platform mounted TV camera calibration procedure for interior orientation parameters and opto-mechanical orthogonality 12 p1500 A73-27953

Mars topographic and geologic mapping with Mariner 9 TV pictures, ground based radar and IR pressure techniques 16 p2015 A73-33354

MARSHES

U MARSHLANDS

MARSHLANDS

Interpretation of wetlands imagery based on spectral reflectance characteristics of selected plant species. 09 p1077 A73-22388

Mapping of mangrove and perpendicular-oriented shell reefs in southeastern Panama with side-looking radar 13 p1606 A73-28170

Airborne remote sensing of Georgia tidal marshes. 16 p2003 A73-33359

Remote sensing techniques for support of coastal zone resource management. 18 p2306 A73-36020

A comparison of four remote sensing media for assessing salt marsh primary productivity. 20 p2562 A73-39903

MARTENSITE

Low-temperature induced changes in the martensite crystalline structure of iron-aluminum-carbon alloys 01 p0064 A73-10607

Cooling modes effect on heat treated Ti-Nb alloys as function of Nb content, investigating alpha prime and double prime martensites 02 p0181 A73-12500

Martensitic transformation kinetics and martensite morphology in the N25KhT2 alloy after aging 03 p0325 A73-13826

Effect of gamma irradiation on carbon redistribution processes in the martensite lattice 06 p0706 A73-17902

Stacking faults effect on martensitic phase formation during steel hardening based on X ray diffraction analysis and Paterson theory 06 p0735 A73-18034

Martensite transformation in an aged Fe-Ni-Ti alloy 06 p0708 A73-18052

The martensitic transformation during deformation of titanium alloys with metastable beta phase. 06 p0708 A73-18207

Microtwinning factors in plastic deformation, volume changes and carbon solution content of Ni martensite 06 p0710 A73-18645

Investigation of the structural changes in austenite during martensitic transformation in steels with high stacking-fault energy 07 p0841 A73-20521

High strength and plastic properties of two phase austenitic-martensitic Fe alloys after aging in alpha and gamma states 07 p0841 A73-20522

Dependence of martensite morphology on the isothermal transformation temperature of the Fe-24Ni-3Mn alloy 09 p1100 A73-21974

Electron microscopic determination of orientation relationship and habit plane for Ti-Cu martensite. 09 p1101 A73-22406

Correlation of coercive force to microstructure in cyclic martensite/austenite transformations in an Fe-Ni-Co alloy. 10 p1234 A73-24438

Characteristics of martensite decomposition during the tempering of rhenium steels 12 p1509 A73-26894

Plastic deformation, martensite transformation and temperature effects on shape memory of nitinol and other alloys 12 p1509 A73-26896

Hardening by tempering of Fe-Ni-Mo and Fe-Ni-Co-Mo martensites 12 p1514 A73-27987

Strength and ductility of two-phase iron alloy composed of austenite and martensite. 13 p1638 A73-29453

Martensitic transformation in iron-nickel alloys in a pulsed magnetic field 14 p1764 A73-30860

Structural transformations in two-phase titanium alloys 15 p1893 A73-32522

The martensite composition in quenched alloys of the Ti-Mo system 17 p2187 A73-34374

Effect of atom ordering on the martensite decomposition mechanism and kinetics in iron-aluminum-carbon alloys 18 p2324 A73-36769

Twinned plate structure of martensitic transformation dependence on composition in Zr-Ti alloy investigated by transmission electron microscopy 20 p2575 A73-39023

Maraging steels with strengths from 110 to 130 kgf/sq-mm 21 p2718 A73-40736

Decomposition of martensite during tempering of rhenium steels. 21 p2720 A73-41027

Plastic deformation, martensite transformation and temperature effects on shape memory of nitinol and other alloys 21 p2720 A73-41029

Transformation temperatures of martensite in beta-phase nickel aluminide. 23 p2989 A73-43275

On the age-hardening of Fe-Pt-Mn ternary alloys. 23 p2994 A73-44139

Morphology and crystallography of beta prime martensite in TiNi alloys. 23 p2994 A73-44160

Martensitic transformations in Fe-Cr-Ni austenitic stainless steels - Relation between the parameters of the epsilon phase and the transformation mechanisms 24 p3101 A73-45522

MARTENSITIC STAINLESS STEELS

Corrosion behavior of sintered stainless steels. 01 p0065 A73-10815

Premature and delayed fractures of high strength martensitic steels with graduated carbon contents, including brittle and ductile intercrystalline and transcrystalline cleavage fractures 06 p0705 A73-17848

Strength and toughness of Fe-10Ni alloys containing C, Cr, Mo, and Co. 06 p0713 A73-18765

Influence of composition and heat treatments on the structure and mechanical characteristics of marten-

sitic stainless steels derived from the 16 percent chrome and 4 percent nickel type
09 p1098 A73-21924

Plasticity theory, strength-differential /SD/ phenomenon, and volume expansion in metals and plastics.
10 p1234 A73-24428

Study of the mechanical-metallurgical characteristics of martensitic steels in a corrosive medium
12 p1514 A73-27686

The strength of welded joints in high strength stainless steels at cryogenic temperatures.
13 p1625 A73-29615

Redistribution of nickel and chromium during alpha to gamma transformation in stainless nickel-chromium steels
13 p1644 A73-29646

Influence of alloying on the phase composition and properties of maraging stainless steels
13 p1644 A73-29647

Delta ferrite and martensite formation in stainless steels.
14 p1759 A73-30145

Stability of the thermomechanical hardening effect in 60N20 nickel steel
14 p1760 A73-30590

Fatigue crack propagation in martensitic and austenitic steels.
14 p1761 A73-30632

Thermal expansion, Young's modulus, and magnetostriiction of a stainless iron-chromium-nickel alloy in the temperature range between 80 and 280 K
14 p1764 A73-30868

Stacking fault energy in iron-nickel and iron-nickel-chromium alloys
14 p1764 A73-30869

Ferritic martensitic stainless steels stress corrosion cracking, emphasizing heat treatment and environment conditions effects on corrosion resistance
15 p1891 A73-32170

Effect of austenitization temperature on the properties of Kh5Ni2M3Ti steel
21 p2718 A73-40738

Redistribution of nickel and chromium during the alpha to gamma transformation in Cr-Ni stainless steels.
21 p2720 A73-41039

Effect of alloying and phase composition on the properties of maraging stainless steels.
21 p2720 A73-41040

Weldability and weld metal capabilities of a new precipitation-hardenable alloy.
21 p2708 A73-41255

Influence of structural changes arising during the hardening process on element lifetime
23 p2984 A73-43438

Influence of high hydrostatic pressure on the flow stress of 18-8 stainless steel.
23 p2994 A73-44161

MARTIN AIRCRAFT

NT B-57 AIRCRAFT

MARTIN MILITARY AIRCRAFT

U MILITARY AIRCRAFT

MASCONS

Large disks as representations for the lunar mascons with implications regarding theories of formation.
03 p0367 A73-13081

Maria lavas, mascons, layered complexes, achondrites and the lunar mantle.
03 p0368 A73-13088

Lunar gravity model obtained by using spherical harmonics with mascon terms.
04 p0495 A73-14811

Nature of the density reversal beneath the lunar maria.
04 p0496 A73-14821

Lunar Sea of Serenity mascon analysis from Lunar Orbiter and Apollo 15 Doppler gravity data, correlating gravity anomalies with surface mass distribution
05 p0615 A73-16384

Viscosity of the moon. I - After mare formation. II - During mare formation.
10 p1277 A73-24081

Lunar maria basins fast and slow filling implications to moon history, considering meteorite bombardment, maria cooling and mascons
12 p1542 A73-27496

Mare Humorum mascon anomaly characteristics from gravity measurements obtained by Doppler tracking of Apollo 15 subsatellite
23 p3030 A73-43759

MASER OUTPUTS

Space maser with feedback
01 p0060 A73-10934

The superconductor maser - A calculation of the gain from the two-level model and the BCS theory, and some new experimental results.
02 p0175 A73-11848

Simultaneous population inversions observation at Zeeman levels in ruby paramagnetic microwave quantum amplifier, noting pumping efficiency
02 p0177 A73-12499

Rb87 vapor maser with optical pumping, measuring nitrogen or nitrogen argon mixture buffer gas partial pressure effect on power output
04 p0459 A73-15920

Possible cause of the variations of the intensity of an interstellar maser.
04 p0493 A73-16023

Hydrogen maser frequency stability dependence on signal output, magnetic polarization field and relaxation effects, describing automated relaxation rate measurement and atomic line spectrum registration
06 p0699 A73-17588

Plasma heating, emission spectrum distortion and light pressure effects under stimulated Compton scattering, noting upper bound of cosmic maser brightness temperature
06 p0729 A73-18110

Class I OH emission sources structure and variability, considering variable gain maser models
06 p0751 A73-18227

Cosmic maser generator model with resonance scattering feedback for galactic clouds OH molecule radio emission
09 p1147 A73-22729

Galactic nuclei and QSO far IR radiation luminosity explanation by nonthermal maser emission due to gas molecules in dense clouds
09 p1150 A73-23145

Restrictions on the intensity of cosmic masers and the possibility of detecting new OH and H2O sources in a rapid sky survey
10 p1275 A73-23725

Relaxation time measurements by an electronic method.
10 p1217 A73-23998

Extension of the theory of frequency noise of oscillating masers
13 p1630 A73-29558

Quasi-classical calculation of the power output of a cyclotron resonance maser
14 p1758 A73-30944

Stellar maser output observations application to analysis of mass loss rate or physical conditions in circumstellar shell
15 p1934 A73-31477

Constraints on cosmic maser intensity, and the possibility of detecting new OH and H2O radio sources by a rapid sky survey.
18 p2355 A73-36750

Light shift and light broadening in the Rb-87 maser.
20 p2572 A73-38861

Short-term frequency stability of the Rb-87 maser.
21 p2716 A73-41148

Hyperfine structure of furan.
22 p2818 A73-42712

Plasma heating, emission spectrum distortion and light pressure effects under stimulated Compton scattering, noting upper bound of cosmic maser brightness temperature
24 p3114 A73-44499

MASER RESONATORS

U MASERS

MASERS

NT GAS MASERS

NT TRAVELING WAVE MASERS

Signal detection in ruby element quantum paramagnetic amplifier operating at liquid nitrogen temperature
03 p0319 A73-14085

Protoplanet cloud model for cosmic OH and water masers in H II regions to account for anomalous hydrogen deficiency, discussing pumping mechanisms and chemical composition
04 p0497 A73-14974

Observations of maser radio sources with an angular resolution of 0.0002 sec.
04 p0503 A73-16001

Astrophysical masers. II - Polarization properties.
07 p0873 A73-19059

Solid state microwave electronics technology review covering parametric amplifier, maser, tunnel and avalanche diodes, transistors, and transmission, filtering and passive signal processing techniques
08 p0942 A73-20701

Analytic approximation for the saturation behavior of OH emission regions.
10 p1272 A73-23542

Soviet papers on quantum radio physics covering injection lasers, high intensity beams and material interactions, laser dynamics and masers
12 p1505 A73-27135

Infrared emission from the OH/H2O sources in W49.
15 p1940 A73-32196

Compact radio source associated with the OH source ON-1 /OH69.5-1.0/.
16 p2071 A73-34037

Protecting a quantum amplifier from saturation by pulsed modulation of the pumping.
17 p2184 A73-35157

Nuclear spin analogue of a molecular beam maser with cavities in series.
21 p2713 A73-40469

H II region OH maser source pumping by far IR radiation-induced population inversions between Lambda doublet levels
21 p2759 A73-40712

MASKING

Effects of signal duration and masker duration on detectability under diotic and dichotic listening conditions.
01 p0008 A73-10436

Cat optic tract and geniculate unit responses corresponding to human visual masking effects.
02 p0134 A73-12161

Orientation illusion and masking in central and peripheral vision.
03 p0266 A73-12999

Passivation of gallium arsenide with silicon nitride.
07 p0864 A73-20571

Backward masking and enhancement of multisegmented visual targets.
11 p1321 A73-25133

Colour selectivity in orientation masking and aftereffect.
11 p1323 A73-26196

Apparent contraction and disappearance of moving objects in the peripheral visual field.
11 p1318 A73-26198

Interaction between contours in visual masking
19 p2393 A73-37395

Effect of eye movements on backward masking and perceived location.
21 p2639 A73-41184

MASKS

Some new techniques for processing remotely obtained images by self-generated spectral masks.
01 p0078 A73-11219

MASS

NT CRITICAL MASS

NT PARTICLE MASS

NT PLANETARY MASS

NT STELLAR MASS

Experimental test for Mach-Einstein doctrine concerning particle inertial mass variation due to tension or space-time curvature created by interlocking gravitational field
04 p0476 A73-15524

The possibility that nongaseous hydrogen supplies the missing cosmological mass.
05 p0625 A73-17328

Mass formula for Kerr black holes.
06 p0747 A73-17521

Solar mass, earth mass and kilogram re-examined for gravitational constants, discussing geocentric constant
20 p2613 A73-39750

MASS BALANCE

Lateral velocity measurement error analysis in inertial guidance system, noting automatic compensation of mass imbalance effects
05 p0596 A73-16992

The STAN /R/ 'S' Integral Weight and Balance System for the C-130 aircraft.
19 p2385 A73-37889

Early operational experience with the L-1011 On-Board Weight and Balance System.
19 p2386 A73-37890

MASS DISTRIBUTION

Attitude dynamics of a 'nearly-spherical' dual-spin satellite and orbital results for OSO-7.
02 p0227 A73-11600

Dynamic calculation of the stretching of a spring with allowance for redistribution of mass along its length
02 p0230 A73-11720

Approximate conditions to account for spring mass redistribution with kinetic energy conversion into strain energy over small critical time interval
02 p0230 A73-11795

Solar neighborhood dynamically determined mass discrepancy with observed stars and interstellar matter, proposing low mass invisible stars existence
02 p0218 A73-12413

Secondary cosmic ray shower charged particles angular distribution asymmetry in center-of-mass system and azimuthal plane related to single fireball formation
02 p0208 A73-12657

The relative merits of galactic density functions - An orbit computational viewpoint.
03 p0373 A73-13363

Interior point mass earth potential model for satellite geodesy, considering geoid heights, gravity anomalies and spherical harmonics
04 p0438 A73-14791

Elastic force minimization during transient process in mechanical multimass system under time dependent external load
04 p0509 A73-14976

The mass spectrum of interstellar clouds and the assumption of total coalescence.
04 p0500 A73-15489

Lunar Sea of Serenity mascon analysis from Lunar Orbiter and Apollo 15 Doppler gravity data, correlating gravity anomalies with surface mass distribution
05 p0615 A73-16384

Integral equations suitability and solution instability of stellar system models, referring to globular cluster densities and mass distribution equations

05 p0616 A73-16452

Computerized Monte Carlo simulation with program flexibility for mass distribution in particle collision processes, applying to accreting and fragmenting systems including asteroid belt

05 p0624 A73-17316

Associated mass of a simple doubly periodic lattice

06 p0643 A73-17465

Total number and mass of Pultusk meteorite shower fragments, using spatial distribution rule

06 p0748 A73-17838

Mass variation laws in light of Tsiolkovskii hypothesis, considering particle separation rates and thermal energy losses for actual jet engines

08 p1014 A73-21182

Optimized design - Characteristic vibration shapes and resonators.

08 p1017 A73-21191

Investigation of the anisotropy of effective masses in the conduction band of semiconductors under uniaxial compression

09 p1132 A73-21959

Gravitational collapse with a physical singularity on an isotropic hypersurface

10 p1283 A73-24751

Frequencies and virtual masses of a liquid in a cavity formed by eccentric cylinders

11 p1347 A73-25391

Earth-moon system mass and angular momentum distribution anomaly, considering light gases association with Jupiter, Saturn, Uranus and Neptune satellites

11 p1419 A73-25793

Impact interaction of an absolutely hard body and an elastic two-mass system

11 p1400 A73-26455

Effect on shell dynamics of a shell mass distributed within a shell surface area

11 p1446 A73-26461

Principle of virtual work in the dynamics of systems having variable mass solids for constitutive elements

12 p1523 A73-27102

Selection of optimal rigidities for elastic regions of a mechanical system with resonance oscillations

12 p1524 A73-27473

Wave model of Galaxy spiral structure, assuming subsegment mass distribution and old star rotating bar mechanism

12 p1547 A73-27879

Spherical harmonic representation of the gravitational potential of a point mass, a spherical cap, and a spherical rectangle.

13 p1681 A73-28846

Influence of the rotor weight on the changes in the axial rigidity of gyromotors

13 p1572 A73-29146

Influence of the difference in effective masses on the efficiency of heterojunction solar cells.

14 p1713 A73-30000

Aperture synthesis study of neutral hydrogen in NGC 2403 and NGC 4236. II - Discussion.

15 p1929 A73-31057

Apparent added masses of a plate array in an incompressible liquid

15 p1861 A73-31281

Gradient instabilities in a system of gravitating point masses

15 p1938 A73-31954

Density and temperature distributions in hypersonic sphere wakes.

15 p1824 A73-32150

Corresponding function solutions of discrete mechanics problems based on difference polynomials, applying to Lagrange problem of string natural vibrations for distributed point masses

16 p2035 A73-32680

Natural vibrations of variable-thickness shells of revolution with apparent additional masses

16 p2074 A73-32685

Simultaneous flexural and torsional vibrations of multidisk rotors

16 p2075 A73-32691

Time optimal control of satellite pitching motions by variable mass distribution, solving nonlinear optimization problem via maximum principle

16 p2072 A73-33233

Growth features of the embryos of planets

16 p2066 A73-33794

Mass and angular momentum distribution in primitive solar nebula during rotation and contraction hydrodynamics of collapse

17 p2227 A73-34412

Calculation of the natural frequencies and the principal modes of helicopter blades.

18 p2367 A73-37090

Isotopic composition measurements of cosmic-ray nuclei with Z greater than or equal to 10 made using a new technique.

19 p2475 A73-37628

Mass property control of a synchronous meteorological satellite scanning experiment.

[SAWE PAPER 964] 19 p2492 A73-37882

Bounds on the spectral and maximum norms of the finite element stiffness, flexibility and mass matrices.

19 p2500 A73-38110

Observations of neutral hydrogen near the galactic center. II - The nuclear disc.

20 p2610 A73-39578

Comparison of rotation curves of different galaxy types /Research note/.

20 p2611 A73-39592

Natural oscillations of shells of revolution with an open profile and concentrated inclusions

20 p2625 A73-39654

Gravitational analogy of electromagnetic Aharonov-Bohm effect, considering massless Dirac equation for weak gravitational fields arising from mass currents moving between particle beams

22 p2887 A73-42434

Galactic mass distribution models from matter density near sun, discussing halo mass and RR Lyrae effects observation

22 p2912 A73-42940

The angular momentum of spiral galaxies. I - Methods of rotation-curve analysis. II - Detailed models and correlations for 17 galaxies.

22 p2913 A73-43002

Parameter behavior in mass distribution analysis of overdense Geminid trail radio echoes

22 p2915 A73-43041

Gravitational fields calculation in three dimensional mass distribution galaxies, using biorthogonal functions with ultraspherical polynomials

23 p3030 A73-43749

The observational evidence for mass distribution in the meteoritic complex.

23 p3031 A73-43770

Gradient instabilities in a system of gravitating point masses.

24 p3132 A73-44479

The asteroid belt and its evolution.

24 p3134 A73-44565

MASS FILTERS

U FLUID FILTERS

Nonequilibrium thermodynamics description of convective motion, using internal energy and absolute mass flows as generalized convective flow

01 p0123 A73-10867

On the stationary mass outflow from stars. I - The computational method and the results for a 1 solar mass star.

03 p0370 A73-13195

Mass flow and period changes of contact binaries.

03 p0370 A73-13212

Nonequilibrium thermodynamics description of convective motion, using internal energy and absolute mass flows as generalized convective flow

12 p1560 A73-27917

Unstable operation and rotating stall in axial flow compressors.

13 p1566 A73-29024

Contact binary star evolution, discussing adiabatic convection zone entropy, mass flow and relative frequency

15 p1928 A73-31054

Models for compact pulsing X-ray sources.

16 p2050 A73-32738

Theory of mass flow measurement - Its advantages and instrumentation related to same.

17 p2166 A73-34619

MASS FLOW RATE

Peripheral turbocompressors for high pressure rise with small mass flow rate, discussing operational principles, design and performance

02 p0175 A73-12793

Direct measurement of colloid microthruster thrust and propellant mass flow rate, using microbalance

04 p0433 A73-15727

Some extremum principles for pipe flow in magnetohydrodynamics.

08 p0993 A73-21403

Investigation of a single spraying site of a colloid thruster.

08 p0996 A73-21599

Microwave Doppler flowmeter design and performance, discussing free flow monitoring of sand from hopper and pneumatic conveying of alumina through steel pipe

10 p1221 A73-24859

Decomposition of hydrazine on Shell 405 catalyst at high pressure.

15 p1841 A73-32174

Crystal growth by vapor transport of GeSe, GeSe₂, and GeTe and transport mechanism and morphology of GeTe.

15 p1842 A73-32652

Up-rating the fuel system flow capacity with high rotational speed.

16 p2046 A73-32922

Interface effects between a moving supersonic blade cascade and a downstream diffuser cascade.

[ASME PAPER 73-GT-23] 16 p1964 A73-33497

Correlation of the mass flow rate in the laminar boundary layer on a sphere-cone.

17 p2091 A73-34195

Study of incidence loss models in radial and mixed-flow turbomachinery.

17 p2092 A73-34384

Flow studies in radial inflow turbines interspace between nozzles and rotors.

17 p2093 A73-34392

Perfectly stirred reactor - New concept for a CW chemical laser.

17 p2184 A73-34911

Mass flux measurements and correlations in the back flow region of a nozzle plume.

[AIAA PAPER 73-731] 18 p2342 A73-36348

Condition for flameout from a burning droplet

18 p2372 A73-37116

Increasing the transport capacity in a viscous fluid flow by the injection method

19 p2420 A73-37552

High speed cinematographic study of mass flow rate of pressurized subcooled liquid nitrogen inward choked flow through radial gap at various stagnation pressures

21 p2740 A73-40634

Variable mass flow rate air injection from porous flat plate into uniform incompressible air flow, obtaining laminar flow velocity profile and pressure measurements

23 p2940 A73-43932

MASS RATIOS

Deuterium-hydrogen ratio in Jupiter.

05 p0623 A73-17182

The abundance of CH₃D and the D/H ratio in Jupiter.

07 p0874 A73-19066

O-18/O-16, Si-30/Si-28, C-13/C-12, and D/H studies of Apollo 14 and 15 samples.

07 p0887 A73-19771

Sulphur concentrations and isotope ratios in lunar samples.

07 p0887 A73-19775

Earth-moon mass ratio from Mariner 9 radio tracking data.

07 p0899 A73-20156

Oxygen and silicon isotope ratios of the Luna 20 soil.

13 p1677 A73-28337

Comet 1969 g emission spectrum observation with 200-inch telescope, obtaining isotope ratio C-12/C-13

20 p2609 A73-39432

Numerical analysis of families of periodic orbits in restricted three body problem with change in mass ratio mu

21 p2778 A73-41527

Sanduleak 160 variability confirmed, discussing double peaked optical variation, mass ratios and X ray eclipse

22 p2916 A73-43123

Chondrites - Initial strontium-87/strontium-86 ratios and the early history of the solar system.

24 p3137 A73-44688

MASS SPECTRA

Neutral composition measurements of the mesosphere and lower thermosphere.

01 p0040 A73-10879

Equilibrium composite negative ion density profiles in nighttime D region from mass spectrometer measurements

01 p0042 A73-10897

The mass spectrum of interstellar clouds and the assumption of total coalescence.

04 p0500 A73-15489

High energy primary cosmic ray particles total energy and mass spectra measurement

05 p0609 A73-16370

Ion microprobe mass analyzer for solid materials science research, discussing instrument potential and limitations

05 p0576 A73-16675

Complex mixture analysis - Geochemical and environmental applications of a compound classifier based on computer analysis of low resolution mass spectra.

11 p1326 A73-25464

Equation of state of matter at supernuclear densities deduced from particle interactions nature and effective baryon mass spectrum

14 p1777 A73-30739

Direct-sampling studies of combustion processes.

19 p2504 A73-38325

Relaxation time in disk galaxy simulations.

22 p2904 A73-41754

MASS SPECTROMETERS

Atmospheric atomic oxygen density vertical distribution measurement by rocket-borne cryocooled mass spectrometer ion source

02 p0157 A73-11756

Neutral composition measurements in the lower thermosphere by means of a mass spectrometer with helium cooled ion source.

02 p0160 A73-12276

Bending and flexing of the Apollo 15 mass spectrometer boom.

05 p0636 A73-17210

Theoretical analysis of a time-of-flight mass spectrometer with spherical electrodes and radial ion paths.

06 p0693 A73-18270
Lunar orbital mass spectrometer experiment.

07 p0891 A73-19828
Thermal fragmentation of quinoline and isokinoline N-oxides in the ion source of a mass spectrometer.

09 p1048 A73-23470
Digital electrode breakdown potential controller for spark source mass spectrometer automation, using radio frequency pulse amplitude sensing

11 p1367 A73-26315
Atomic oxygen loss in ion source of sounding rocket-borne mass spectrometer for determining lower thermosphere neutral composition

12 p1489 A73-26991
The open-source neutral-mass spectrometer on Atmosphere Explorer-C, -D, and -E.

13 p1616 A73-28628
The magnetic ion-mass spectrometer on Atmosphere Explorer.

13 p1688 A73-28633
Bennett ion-mass spectrometer onboard Explorer C and E, describing operation, data outputs, calibration and data interpretation techniques

13 p1688 A73-28634
Absolute calibration of Apollo lunar orbital mass spectrometer.

13 p1617 A73-28930
A thermosphere composition measurement using a quadrupole mass spectrometer with a side energy focusing quasi-open ion source.

14 p1748 A73-29976
A satellite-borne positive ion mass spectrometer.

14 p1753 A73-30415
Satellite measurements of atmospheric composition in the altitude range 150 to 450 km.

18 p2303 A73-33957
Application of a Thomson mass spectrograph with an electron-optical recorder to the investigation of the mechanism of plasmoid acceleration

19 p2467 A73-37370
Role of gas-surface interactions in the reduction of Ogo 6 neutral particle mass spectrometer data.

20 p2551 A73-38941
Effect of acceleration on distribution of lung perfusion and on respiratory gas exchange.

21 p2643 A73-40274
An appraisal of the mass spectrometer diagnostic technique in the study of afterglow plasmas.

21 p2702 A73-40792
A dynamic mass spectrometer for the study of laser-produced plasmas.

24 p3090 A73-44817

MASS SPECTROMETRY

U MASS SPECTROSCOPY

MASS SPECTROSCOPY

Mass spectrometric measurements of minor constituents in the lower thermosphere.

01 p0041 A73-10880
Recombination of electrons with positive ions of the H₃O⁺/H₂O/n series.

01 p0014 A73-10901
Thermogravimetric-quadrupole mass-spectrometric analysis of geochemical samples.

01 p0015 A73-11251
Viking lander-borne gas chromatograph mass spectrometer for Martian atmosphere sampling and soil analyses

02 p0168 A73-12000
Atomic and molecular interactions investigation by computer aided mass spectrometry, considering applications in bio-organic chemistry, isotope analysis, geochemistry and cosmochemistry

02 p0139 A73-12425
Experimental measurement of the O₂/I- photodetachment cross section.

02 p0195 A73-12433
High vacuum thermal desorption mass spectrometry for electron bombardment activated nitrogen desorption from W surface, discussing lambda state population

04 p0414 A73-14999
Aromatic and heteroatom-containing organic compounds in the lunar samples.

06 p0662 A73-18424
Lunar carbon chemistry - Relations to and implications for terrestrial organic geochemistry.

06 p0662 A73-18429
Pyrolysis system with high sensitivity medium-resolution mass spectroscopy to quantify ions pyrolyzed in lunar fines, confirming presence of indigenous lower hydrocarbons

06 p0662 A73-18431
Ion microprobe analyzers for solid surfaces high resolution mass spectrometric chemical analysis, using focused ion beam sputtering technique

07 p0822 A73-19171
Analysis of single particles of lunar dust for dissolved gases.

07 p0890 A73-19813

Noble gas measurement in powdered aliquots of eleven H-chondrites, using Reynolds type mass spectrometer

07 p0789 A73-20623
Thermal analysis-mass spectrometer computer system and its application to the evolved gas analysis of Green River shale and lunar soil samples.

08 p0936 A73-20824
Mass spectrometric studies of tetrafluorohydrazine and the difluoroamino radical.

08 p0936 A73-21173
UHV outgassing measurements on various carbons.

08 p0937 A73-21621
Mass spectroscopic investigation of dissociation and ionization in a simulated re-entry plasma.

09 p1130 A73-22843
Mass spectrometric determination of the dissociation energies of AlC₂, Al₂C₂, and AlAuC₂.

09 p1048 A73-23247
Mass spectrometry in structural and stereochemical problems. CCXVII - Electron impact promoted fragmentation of O-methyl oximes of some alpha, beta-unsaturated ketones and methyl substituted cyclohexanones.

10 p1186 A73-23550
A mass spectrometric investigation of reactions involving tungsten and molybdenum with potassium-seeded H₂/O₂ flames.

10 p1186 A73-23554
A mass spectrometric investigation of reactions involving vanadium and chromium with potassium-seeded H₂/O₂ flames.

10 p1186 A73-23555
Metal ion density measurement in sporadic E layer during beta Taurids shower by rocket-borne mass spectrometry, noting origin in cosmic debris ablation

13 p1673 A73-28277
Lunar 20 lunar soil samples Pb-207/Pb-206 age determination by ion microprobe mass analysis, determining U, Th and radiogenic Pb concentrations

13 p1674 A73-28304
The gas exchange of hydrogen-adapted algae as followed by mass spectrometry.

17 p2118 A73-34225
Laser probe mass spectrometric in situ measurements of stable and radioactive Ar isotopes in lunar breccia

17 p2232 A73-35263
High temperature thermal cavity system with vitreous carbon tube and end plugs for material and thermochemical environment investigations, discussing mass spectroscopic measurement

17 p2149 A73-35752
Mass spectrometric investigations of the night polar ionospheric structure.

18 p2310 A73-36145
Drift tube and mass spectrometric measurement of molecular positive ion drift velocities in carbon dioxide

21 p2742 A73-40221
Mass-spectrometric investigation of the ion composition of potassium and cesium discharge plasmas

21 p2746 A73-40526
Study of neutral composition of lower thermosphere at Fort Churchill.

21 p2688 A73-41344
Lower thermospheric atomic oxygen profile from 18 May 1971 nitric oxide release and mass spectroscopic observation, noting monotonic density increase to 0.8 trillion/cc

21 p2688 A73-41345
Neutral composition and its variations in the lower thermosphere.

21 p2688 A73-41349
Chemical analysis of surfaces by mass spectrography with secondary ion emission

21 p2648 A73-41595
Interpretation of measurement results with ion traps in a bicomponent medium.

22 p2911 A73-42735
Measurements of recombination of electrons with HCO⁺ ions.

23 p3007 A73-43530
Gas chromatography-mass spectrometry study of sterols from Pinus eliottii tissues.

24 p3065 A73-44698
Atomic oxygen densities in the lower thermosphere as derived from in situ 5577-A night airglow and mass spectrometer measurements.

24 p3086 A73-45122
Oxygen-W/100/ surface interactions investigated simultaneously by secondary ion mass spectrometry /SIMS/ and electron induced desorption /EID/

24 p3066 A73-45330
MASS TRANSFER
Book on momentum, heat and mass transfer at various interfaces based on Prandtl eddy mixing length concept

01 p0030 A73-10049
Electrode phenomena with plasma-MIG welding.

01 p0055 A73-10114
The estimation of ground-level pressure fields from computer analyses and their application to large-scale atmospheric mass transfer.

01 p0072 A73-10144

An autoradiographic investigation of material transfer and wear during high speed/low load sliding.

01 p0056 A73-10438
Heat and mass transfer theory and applications in aerothermoptics, thermoconvective and ferromagnetic fluid studies, chemical engineering, capillary transport and heat pipes

01 p0029 A73-10624
Variational analysis of high mass transfer rates from spherical particles - Boundary-layer injection suction considerations at low particle Reynolds numbers and high Peclet numbers.

01 p0122 A73-10802
Heat transfer from a sphere with injection in a slow moving flow

02 p0152 A73-11611
Theory of the electrodiffusion method for measuring the spectral characteristics of turbulent flows

02 p0165 A73-11614
Effects of vertical mass motions on the composition structure in the thermosphere.

02 p0162 A73-12291
The transmission of mass and angular momentum from a satellite or planetary system to its primary.

02 p0225 A73-12810
Laser induced infrared fluorescence - Thermal heating, mass diffusion, and collisional relaxation in SF₆.

03 p0318 A73-13281
Current distribution prediction in transient response of rotating disk electrode, noting mass transfer for cathodic reduction of ferricyanide

03 p0273 A73-13728
Mass transfer technique for investigation of heat transfer by jet-impingement systems.

03 p0400 A73-14642
Mass transport and energy of impulse compression wave traces in atmosphere due to radiation, inner friction, gravity and rotation effects

04 p0440 A73-15285
Steady two-dimensional heat and mass transfer in the vapor-gas region of a gas-loaded heat pipe.

04 p0518 A73-15821
Enthalpy driving forces for gas cooling data correlation in convective heat transfer in reacting turbulent boundary layers with mass injection

04 p0519 A73-15824
Heat and mass transfer laws for fully turbulent wall flows.

04 p0520 A73-15935
Empirical equations for calculating the heat and mass transfer for the special case of separated flow

04 p0520 A73-15941
Frost and ice column models for analysis of heat and mass transfer and effective thermal conductivity relationship to density in frost layer

05 p0638 A73-16225
Heat pipe operation in a gravity field with liquid pool pumping.

05 p0640 A73-16876
Heat and mass transfer at the surfaces of glass-graphite materials in a high-temperature gas flow

06 p0766 A73-17457
Solid-gas mass transfer in the case of laminar free convection

06 p0768 A73-17919
Condensate droplets heat conductivity as function of drop geometry and vapor mass transport interaction with interior heat conduction, using finite difference method

06 p0768 A73-17920
Calculation of heat and mass transfer in devices employing spray nozzles

06 p0769 A73-18130
Mass transfer during evolution of close binaries within zero velocity surfaces related to nova outbursts and Wolf-Rayet star composition

06 p0753 A73-18246
The mechanism of surface mass transfer in the thin-film Ge-Al system

06 p0738 A73-18651
Mass-transfer effects on higher-order boundary layer solutions - The leading edge of a swept cylinder.

06 p0688 A73-18833
Mass transfer coefficient measurement in turbulent ducted flow, obtaining numerical solution to diffusion equation

06 p0770 A73-18835
Stability of clusters of galaxies with mass loss to gravitational radiation.

07 p0873 A73-19053
Application of the integral balance method to the solution of the problem of interrelated heat and mass transfer in an unbounded plate

07 p0921 A73-20011
Mixing length flow theory for turbulent boundary layer calculation, with allowance for mass transfer

08 p0953 A73-20721
Possible explanation for nonthermal radio noise from binary stars.

08 p1003 A73-20883
A method of calculating heat and mass transfer between liquid droplets and a gaseous phase in an acoustic wave field

08 p1022 A73-21196

MAST SHOCK TUBES

The experimental determination of wall-fluid mass transfer coefficients using plasticized polymer surface coatings.

08 p1023 A73-21261

Mass transfer in close binaries. III - Gaseous rings in algol-like binaries.

08 p1010 A73-21312

Method of determining the mass removal from heat-shield materials on the basis of strain measurements in loaded shells

08 p1023 A73-21369

Study of thermal phenomena in a Hartmann-Sprenger tube

08 p1024 A73-21634

A two-layer model of high speed two- and three dimensional turbulent boundary layers with pressure gradient, surface mass injection and entropy layer swallowing.

[AIAA PAPER 73-135] 08 p0956 A73-21800
Cen X-3 and Her X-1 X ray sources emission pulsation explained by model with neutron star accretion of matter from companion via magnetic funnel

09 p1141 A73-22010

Exchange of water vapor between the atmosphere and surface of Mars.

09 p1145 A73-22270

Elongated shells around novae and concentration near orbital planes resulting from perpetual matter losses, considering close dwarf binaries and recurrent novae

09 p1145 A73-22288

Ejection of matter and gravitational radiation from orbiting bodies.

09 p1149 A73-22961

Dissipation of mechanical energy in a deformable body during thermal diffusion processes

10 p1291 A73-24351

Temperature at the surface of a heat-conducting liquid behind a shock wave in the presence of mass transfer and chemical reactions in the boundary layer

10 p1296 A73-24679

Study of the phase of the wall transfer of heat or mass in incompressible pulsed flow

10 p1297 A73-24850

Principles of evacuated cryogenic insulations.

11 p1450 A73-25581

Analysis of external mass transfer and choice of its parameters for convective removal of reaction-product vapors in a hydrogen-oxygen fuel cell with a capillary membrane

11 p1308 A73-25727

Experimental investigation of heat and mass transfer in the condensation of vapor from gas-vapor mixtures under viscous and viscous-gravitational flow conditions

12 p1558 A73-27315

Investigation of heat and mass transfer for plasma flows in channels of various shape under conditions of intense condensation

12 p1558 A73-27318

Heat and mass transfer during the evaporation of liquids from capillary porous bodies situated in a hot air flow

12 p1559 A73-27474

Compressible boundary layer flow at a three-dimensional stagnation point with intensive suction or injection

12 p1458 A73-27699

Momentum and mass transfer in atmospheric boundary layer from surface drag and evaporation data for weather prediction models

13 p1652 A73-28275

Earth mantle convection theory, calculating polar secular wandering from inertia product change due to mass transfer

13 p1607 A73-28404

High Reynolds number fluid dynamics and heat and mass transfer in real concentrated particulate two-phase systems.

13 p1704 A73-28427

An integral equation approach to heat and mass transfer problem in an infinite cylinder.

13 p1705 A73-28431

Generalization of the integral balance method in problems of correlated heat and mass transfer

13 p1705 A73-28464

Increase of boundary-layer heat transfer by mass injection.

13 p1706 A73-28816

The heat and mass transfer of a binary laminar boundary layer in the presence of simultaneous convection at a vertical permeable flat surface

13 p1708 A73-29350

Heat and mass transfer on the surface of a fiberglass-reinforced plastic in a high-temperature air flow

13 p1708 A73-29403

RY Set detection from search for binary systems with early type star and mass exchange for radio source candidacy

14 p1789 A73-29736

Comet nuclei gas liberation, perihelion mass loss and photometric property dependence on water ice evaporation rate and nongravitational effects

14 p1792 A73-29815

Encke comet icy nucleus core-mantle evolutionary model, investigating mantle sublimation, fading and capture time approximation for nongravitational forces effect in terms of mass output

14 p1793 A73-29822

Ejection of bodies from the solar system in the course of the accumulation of the giant planets and the formation of the cometary cloud.

14 p1793 A73-29825

Energy and diffusive mass transport relation to thermospheric circulation, composition, temperature and mass density from three dimensional two constituent magnetic storm model

14 p1748 A73-29975

Physical conditions of heat transfer and design of heat pipes for the evaporation mode of operation at moderate temperatures

14 p1816 A73-30011

Mass transfer approximation model in unidirectional swirled two phase flow, considering transfer resistance of liquid phase

14 p1816 A73-30016

Boundary layer about a plate assuming an arbitrary gas injection law

14 p1711 A73-30017

Natural convection boundary layer flow over horizontal and slightly inclined surfaces.

14 p1817 A73-30607

Duplicity and its consequences among variable stars in general.

15 p1935 A73-31484

Experimental study of heat exchange in a chemically reacting laminar boundary layer

15 p1958 A73-31874

X ray power derivation from gravitational energy release during matter accretion onto surface of component of mass transfer binary star

16 p2049 A73-32730

Black holes in binary systems - Observational appearances.

16 p2058 A73-32739

HZ Hercules periodically pulsating variable star in binary system detected by Uhuru satellite, detailing X ray emission, rotation pattern and mass exchange mechanism

16 p2059 A73-32948

Electric analogy procedure for simulating heat and mass transfer processes

16 p2085 A73-33380

Mass transport rate in solar nebula model due to turbulence induced by convection

17 p2229 A73-34432

Russian book - Fundamentals of the dynamics and heat and mass transfer of fluids under conditions of weightlessness.

18 p2297 A73-35868

Mass transfer effects on turbulent heating in the vicinity of slots.

[AIAA PAPER 73-766] 18 p2371 A73-36381

Heat and mass transfer processes during thermal decomposition of resin binders in fiberglass reinforced plastics

18 p2328 A73-36814

Certain patterns of heat transfer in a hypersonic shock layer in the presence of mass entrainment

18 p2266 A73-37014

On the mass transfer produced by oscillations in a compressible, dissipative, and inhomogeneous medium

19 p2503 A73-37528

Use of turning ring electrodes for study of the transport of matter in fluid in a laminar or turbulent hydrodynamic regime

19 p2432 A73-38481

The effect of the porous material characteristics on the internal heat and mass transfer.

[ASME PAPER 73-HT-49] 20 p2626 A73-38573

Effects of thermal and mass diffusivities on the burning of fuel droplets.

[AIChE PREPRINT 22] 20 p2626 A73-39249

The eclipsing contact binary VW Cephei.

20 p2610 A73-39577

Burnout of a graphite surface during the blowing of an inert gas through it

21 p2790 A73-40698

Experimental study of heat and mass transfer in chemically reacting laminar boundary layers.

21 p2791 A73-41058

Calculation of the heat resistance of metals at variable temperatures

21 p2721 A73-41230

Influence of nonideal flow conditions in haemodialysers on mass-transfer theories.

22 p2816 A73-42678

Nonstationary mass transfer during the longitudinal flow of a nonlinearly viscous fluid past a flat plate and the forward stagnation point

23 p2967 A73-43440

Cumulus-scale vertical transport of mass, heat and momentum calculated from radar and rain gauge precipitation measurement

23 p3002 A73-43596

Heat and mass transfer in a turbulent layer above permeable plates

24 p3081 A73-45528

MAST SHOCK TUBES

U MAGNETIC ANNULAR SHOCK TUBES

MATCHING

A rapid matching procedure for twin-spool turbopumps.

02 p0202 A73-11593

Microwave bandpass filters formed by shunt and series stubs with quarter wave matching strip lines, noting advantage of equal lengths

09 p1063 A73-22463

MATERIAL ABSORPTION

Mechanisms and kinetics of absorption and desorption reactions in systems of refractory metals with nitrogen, oxygen or carbon.

04 p0462 A73-15302

MATERIAL BALANCE

NT WATER BALANCE

Multi balance measurement of flow systems.

16 p2016 A73-33656

DC-10 Twin design, discussing balance characteristics, loading limits and sample forms [SAWE PAPER 987]

19 p2386 A73-37891

MATERIAL REMOVAL [MACHINING]

U MACHINING

MATERIALS EROSION

U EROSION

MATERIALS HANDLING

NT GROUND HANDLING

NT PROPELLANT TRANSFER

NT REMOTE HANDLING

From theory to practical use of air cushions for transport of heavy loads in the factory

05 p0535 A73-16753

Packaging in aerospace applications

07 p0830 A73-19010

Industrial material management, considering departments requirements, identification effort, costs and benefit, numbering and standardization systems, and uniform commodity description problem

13 p1624 A73-28788

Russian book - Fundamentals of the dynamics and heat and mass transfer of fluids under conditions of weightlessness.

18 p2297 A73-35868

Technical and safety aspects of maintenance work on commercial aircraft wing fuel tanks, considering wing deformation effects and sealant materials and reapplications

18 p2286 A73-36932

Aircraft design for transporting arctic crude oil or liquid natural gas, examining air terminal requirements and handling specifications

21 p2634 A73-41172

Russian book on rocket weapon systems safety handling covering HF electromagnetic, noise and vibration effects, ionizing radiation, fire, etc

22 p2812 A73-41874

MATERIALS RECOVERY

NT WATER RECLAMATION

Influence of recovery and recrystallization on the Young's modulus and its temperature dependence in Invar-type iron-nickel alloys

14 p1760 A73-30586

The availability and cost of curium-244 from power reactor fuel reprocessing wastes.

19 p2457 A73-38430

Recovery of nonferrous metals from scrap automobiles by magnetic fluid levitation.

[AIAA PAPER 73-959] 22 p2878 A73-42531

MATERIALS SCIENCE

Holographic interferometry in materials research and fracture mechanics.

01 p0051 A73-11002

Laser related Bell Laboratories research on light scattering, solid state physics, nonlinear optics, materials science, quantum electronics and ultrashort light pulses

01 p0060 A73-11214

Materials properties data tables on composition, preparation, temperature and field strength parameters of superconducting compounds in Ni alloys

02 p0201 A73-11878

Non-metallic materials selection, processing and environmental behavior; Proceedings of the Fourth National Technical Conference and Exhibition, Palo Alto, Calif., October 17-19, 1972.

03 p0328 A73-13001

General purpose autoclave processable polyimide laminating resin selection, evaluating molding process techniques

03 p0329 A73-13004

Compression and elastic moduli of heterogeneous viscoelastic materials consisting of mechanical mixture of homogeneous phases, using elastic-viscoelastic analogy

03 p0385 A73-13139

Dynamic plastic tensile stress analysis based on equation of motion, kinematic equation and material law with conditions regarding disturbance propagation velocity

03 p0385 A73-13142

Recent studies towards the development of procedures for design of brittle materials.

04 p0508 A73-14725

Opportunities in materials; Proceedings of the Fourth Buhl International Conference, Pittsburgh, Pa., November 16-18, 1971.

Materials processing technology for LSI electronics, considering wafers, doping, diffusion, ion implantation, photomasking and film deposition

A new mathematical theory of simple materials.

Nonstoichiometric yttria crucibles for cold wall Ti melting, noting single batches, cost reduction and alloy homogeneity

Ion microprobe mass analyzer for solid materials science research, discussing instrument potential and limitations

Aircraft brake design and materials, considering thermal, mechanical, friction and wear characteristics of Be, steel, graphite and carbon composites

Material resistance analogies, relating shear, force and strain factors for bar deformation in tension, compression, torsion and bending

Book - Thermal radiative properties: Nonmetallic solids.

Corrosion fatigue considerations in engineering materials selection and design, discussing alleviation and control

Flexural/torsional deformations of material line in continuous body in terms of curvature and bending vectors, using Frenet-Serret equations

On a finite strain theory of elastic-inelastic materials.

Glass fiber for optical communication with existing light source and detector devices, assessing materials and fabrication technology for capacity, attenuation and environmental requirements

Fracture toughness defined as work required for unit area crack extension, discussing toughness as function of material strength and strain characteristics

Book - Fibre-reinforced materials technology.

Book on solids structure effects on materials strength characteristics covering interatomic binding forces, elastic properties, crystal defects, work hardening, heat treatment, temperature effects, etc.

Russian book on aeronautical electric and electronic materials covering physicochemical properties of magnetic, dielectric, conductor, semiconductor, polymer, ferritic, thin film and composite materials

A method for ingredient composition control in binary and quasi-binary systems

Light weight impact protective helmet shell materials and designs, noting E- or S-glass and polyimide resin for oxygen rich space station/shuttle applications

Bubble domain memory materials production, processing and testing, discussing crystal growth, propagation margins, interaction effects and stroboscopic observations

Electric contact materials technology, discussing intermetallics, ordered alloys, metal matrix composites and silver, gold and platinum based dispersion hardened alloys manufacture and properties

New horizons in materials and processing; Proceedings of the Eighteenth National Symposium and Exhibition, Los Angeles, Calif., April 3-5, 1973.

Composite material design criteria, discussing fatigue, stress concentration, safety factors, scaling effects and load characteristics

Reusable space shuttle orbiter design evolution during 1972-1973, discussing payloads, vertical launching capability and advanced materials technology

Society of Plastics Engineers, Annual Technical Conference, 31st, Montreal, Canada, May 7-10, 1973, Proceedings.

Emerging aerospace materials and fabrication techniques.

Fracture mechanics in materials selection and design.

Material damping - An introductory review of mathematical models, measures and experimental techniques.

Material processing with solid-state laser. [SME PAPER EM 73-213]

Papers on materials science covering optical and spectroscopic surface analyses, neutron effects, amorphous semiconductors, high temperature superconductivity, etc

Japan Congress on Materials Research, 16th, Osaka, Japan, August 1972, Proceedings.

Russian book on radiation effects on ferroelectric crystals and ceramic materials covering changes in dielectric, piezoelectric and optical properties, structure and phase transitions

Materials suitable for making far infrared high-pass transmission filters.

Dynamic shaft seal types for high speed continuous shaft rotation, considering service life, failure modes and materials selection

Reference data for thermocouple materials below the ice point.

Nonstandard thermocouple materials, discussing metal and nonmetal thermocouples and ceramic insulating materials

Material resistance analogies, relating shear, force and strain factors for bar deformation in tension, compression, torsion and bending

Russian book - General patterns in the structure of phase diagrams of metal systems.

A survey of compatibility of materials with high pressure oxygen service.

Evolution of the stress state and hardening for certain materials with positive hardening

Deformation history approach compared to internal variables introduced by solution of initial value problem for materials, obtaining constitutive equation

Low-pressure prepress as structural material for light-construction designs

Structural analysis for idealized nonlinear material behavior.

Computational assessment of the numerical influence of the cutting step size and evaluation equation on the precision of experimental and analytical residual-stress determinations

Assembly for studying the characteristics of materials under cyclic loads at elevated temperatures

Investigation of the rheological properties of a model material based on the 'Epidian 2' epoxy resin

Ultrasonic sensing apparatus and eddy current method in NDT, noting radiography, sonics, penetrants and magnetic particles

A method of estimating the probability of faults in material on cyclic loading.

A device for working with extraterrestrial material in an inert-gas medium

Evaluation of materials for underground exposure in extreme environments.

Comparative evaluations of outgassing results between the vacuum thermogravimetric method and the SRI method.

High speed testing of materials mechanical behavior over range of impact loading rates

Testing for prediction of material performance in structures and components, Proceedings of the Symposium, Anaheim, Calif., April 21-23, 1971 and Atlantic City, N.J., June 29-July 1, 1971.

Layout of a thermodynamical theory of the life time scattering in materials testing

Determination of the angle of incidence of angle probes for ultrasonic testing

New method for determining the total radiating power of partially transparent materials at high temperatures.

Flammability comparisons of glass-reinforced unsaturated polyester moldings in various laboratory-scale tests.

Material processing with solid-state laser. [SME PAPER EM 73-213]

Papers on materials science covering optical and spectroscopic surface analyses, neutron effects, amorphous semiconductors, high temperature superconductivity, etc

Japan Congress on Materials Research, 16th, Osaka, Japan, August 1972, Proceedings.

Russian book on radiation effects on ferroelectric crystals and ceramic materials covering changes in dielectric, piezoelectric and optical properties, structure and phase transitions

Materials suitable for making far infrared high-pass transmission filters.

Dynamic shaft seal types for high speed continuous shaft rotation, considering service life, failure modes and materials selection

Reference data for thermocouple materials below the ice point.

Device for investigating the mechanical characteristics of materials in a complex stressed state

Device for endurance testing of materials at low temperatures

New arrangement for testing materials in the volume stressed state and at elevated temperatures /Exchange of experience/.

Low temperature vacuum fatigue testing facility for materials testing under space environment conditions

Concentration of thermal stresses at joints between heterogeneous materials

Laser activated, model surface recession compensator system for testing ablative materials.

Nondestructive flaw detection by holographic interferometry, discussing methods, equipment and applications for materials testing and vibrational analysis

Damping properties of soft viscoelastic materials for certain plane stress combinations

Studies on testing methods and weatherability of plastics.

Viking lander capsule decelerator system candidate materials evaluation, discussing in-situ testing for high density packing and heat sterilization effects on strength

High strength fiber woven cloth materials for inflatable structure, discussing characteristics assembly methods and tests

Performance and possibilities of application of an electromagnetic comparator

An apparatus for work with extraterrestrial water in an inert gas atmosphere.

Spectroscopic measurement of material samples refractive index at submillimeter wavelengths

Book - Advanced experimental techniques in the mechanics of materials.

Development and problems of testing prepress for the purposes of the Czechoslovakian aircraft industry

A survey of nondestructive testing techniques.

A simple method for studying slow crack growth.

Method of studying the resistivity to external effects in fiberglass plastic structural elements with highly dispersed initial-state properties

Viscoelastic panel vibration damping material for ventilation ducts to reduce LF vibrations induced by turbulent air flow

Influence of aluminum on the structure and properties of a Ti + 10% V alloy

Application of the 'differential reflectometer' to materials research in corrosion, ordering and alloying.

Materials testing via ultrasonic spectroscopy developed from pulse-echo technique, discussing application to metal grain size determination and carbon fiber composite quality control

Vacuum effects on materials and environment contamination - Screening method and results obtained at CNES

A device for the investigation of the mechanical characteristics of materials under a complex stress system.

A unit for fatigue testing of materials at low temperatures.

Materials testing by sonic emission analysis /SEA/

MATHEMATICAL ANALYSIS

U APPLICATIONS OF MATHEMATICS

MATHEMATICAL LOGIC

NT ALGORITHMS

NT BOOLEAN ALGEBRA

NT BOOLEAN FUNCTIONS

NT BOREL SETS

NT EQUIVALENCE

NT FORMULAS [MATHEMATICS]

NT LATTICES [MATHEMATICS]

NT SET THEORY

NT THRESHOLD LOGIC

Automatic search system synthesis for linear programming, using gradient method and logic operations for system optimization

MATHEMATICAL MODELS

Algorithm for deriving the equilibrium equations of an electric circuit on the basis of logic rules
21 p2670 A73-41307

Algebraic nature of thought formation structures
24 p3063 A73-44905

MATHEMATICAL MODELS

NT ANALOG SIMULATION
NT DIGITAL SIMULATION
NT THOMAS-FERMI MODEL

Investigation of the macroscopic rheonomic properties of a monodirectional fiberglass-reinforced plastic
01 p0067 A73-10002

Use of a plastic deformation design model of polycrystalline material in the analysis of loading surface transformation
01 p0112 A73-10008

Periodically correlated random processes to model additive and multiplicative rhythmical phenomena, discussing structural properties and theorems
01 p0075 A73-10028

Theoretical and numerical results in the case of the nonlinear Vlasov equation
01 p0069 A73-10073

Book - Lectures in mathematical models of turbulence.
01 p0031 A73-10123

Isovolumic contraction dynamics in man according to two different muscle models.
01 p0007 A73-10158

A continuum analysis of a two-dimensional mechanical model of the lung parenchyma.
01 p0010 A73-10168

Bronchial tree model simulation of pressure-flow-volume relationships during expiration, using gas physics and lung physiology and anatomy data
01 p0011 A73-10169

Analysis of face deformation effects on gas film seal performance.
01 p0055 A73-10246

Mathematical and statistical modeling of wall flow turbulence, considering experimental velocity and temperature measuring techniques
01 p0031 A73-10292

Radiative calculation models for infrared transfer through cloud, aerosol and the continuum.
01 p0073 A73-10358

Low order models representing realizations of turbulence.
01 p0032 A73-10450

Mathematical model for the buildup of imperfections in plastic isotropic materials
01 p0114 A73-10476

Equations of the time-dependent strength of solid bodies
01 p0114 A73-10479

Saturn rings formation explanation by electromagnetic effects, presenting mathematical model
01 p0097 A73-10551

On turbulent flows with fast chemical reactions. II - The distribution of reactants and products near a reacting surface.
01 p0032 A73-10638

Mathematical formulation for classification, realization and evaluation of electronic components and systems reliability tests
01 p0023 A73-10647

Axiomatic formulation of a mathematical model for visual adaptation
01 p0012 A73-10655

Formalization of certain functional aspects of the external respiration system
01 p0012 A73-10657

Mathematical description of certain properties of human sensitivity to vibration
01 p0012 A73-10659

Method of structural synthesis of multivariable systems for automatic control of plants with incomplete information
01 p0028 A73-10672

Lunar motion numerical analysis, discussing flaws due to inadequate solar system model and arithmetic-algebraic procedural deficiencies
01 p0099 A73-10694

Analytical model potential function application to Ar, Kr, Xe, nitrogen, methane and carbon dioxide, applying to different properties
01 p0122 A73-10850

Equations of state and dissociation equilibrium for CsCl plasma, noting thermodynamic model for phase transitions of liquid metal into nonideal ion plasma
01 p0084 A73-10851

Characteristics of the quiet solar wind beyond the earth's orbit.
01 p0092 A73-11042

Reduced dimensionality for minimization of degrees of freedom of skeletal activity models for anthropomorphic locomotion system synthesis
01 p0013 A73-11052

Mathematical models, systems analysis and synthesis in control theory of large scale systems, illustrating on agriculture center planning
01 p0078 A73-11070

Hadron number density model to predict fossil quark abundance in big bang cosmology
01 p0104 A73-11098

Direct Monte Carlo simulation of two-dimensional radiative heat transfer in absorbing-emitting medium bounded by the non-isothermal gray walls.
01 p0123 A73-11139

A derivation of thermal mathematical model with measured nodal temperatures.
01 p0123 A73-11142

Sensitivity analysis method application to spacecraft thermal environment control system design, determining mathematical model input parameters uncertainty effects on temperature determination
01 p0123 A73-11143

Thermal mathematical model development for spacecraft design as exemplified by small scientific satellite, comparing analytical results with test data
01 p0110 A73-11144

A design study of thermal louver system.
01 p0111 A73-11152

Hydrodynamic motions and the vacuum stage in an anisotropic cosmological model
01 p0108 A73-11432

Numerical solutions for MHD equations, considering initial values, time independence and mathematical models including hyperbolic, parabolic and elliptic differential equations
01 p0086 A73-11459

Computation of solutions to the inverse problem of electrocardiography.
01 p0013 A73-11465

Limited space charge accumulation oscillations in gallium arsenide
02 p0199 A73-11530

Bidimensional and surface effects in a coplanar-contact Gunn diode
02 p0144 A73-11533

Some problems in the substantiation and application of discrete large-element design schemes for complex zero-moment shells
02 p0230 A73-11716

Numerical model and computational results for earth bow shock structure, discussing linear dispersion relation for magnetized plasma with counterstreaming ion beams
02 p0155 A73-11728

Mathematical model and error equations of inertial navigation system with two leveled accelerometers, comparing with three component and pendulum gyroscopic systems
02 p0190 A73-11778

Book on functional pavements design covering support condition, quality control and construction tolerance, environmental and landing gear effects, mathematical models, etc
02 p0150 A73-11879

Consistency of fields and particle motion in the 'speiser' model of the current sheet.
02 p0157 A73-11901

A standard format for mathematical models of fluid power systems.
02 p0132 A73-12001

A simple method for determining static parameters of large signal semiconductor diode and transistor models.
02 p0147 A73-12044

Equilibrium model for force-free relativistic electron beam, obtaining solution with maximum beam radius and maximum axial current
02 p0198 A73-12070

Two stage mathematical model of brightness perception operation for stimuli having luminance field with asymmetric discontinuity
02 p0137 A73-12078

The zodiacal light as seen from the Pioneer F/G and Helios probes.
02 p0215 A73-12263

Theoretical model of diurnal variations of the equatorial thermosphere at equinox.
02 p0162 A73-12290

Collisional-radiative coefficients and population coefficients of hydrogen plasma.
02 p0198 A73-12347

Relation of the diffuse reflectance remission function to the fundamental optical parameters.
02 p0193 A73-12350

Biorthogonal function pairs for gravitational field calculations for flat galaxies, deriving algorithms from Hankel-Laguerre functions properties
02 p0216 A73-12380

An asymmetrically rotating fluid disc with applications.
02 p0217 A73-12393

Poisson model of atmospheric noise from lightning discharges as function of thunderstorm distribution and propagation conditions, calculating statistics for narrow band receiver
02 p0142 A73-12528

Gamma time-dependency in Blaxter's compartmental model.
02 p0187 A73-12550

Mathematical model for spectral distribution function of brain waves, noting analysis with RC oscillator
02 p0135 A73-12557

Experimental verification of a digital computer simulation method for predicting gas turbine dynamic behaviour.
02 p0204 A73-12647

Calculations on energy transfer to a diatomic molecule in high-energy head-on collisions.
02 p0195 A73-12723

Two dimensional deep convection rimitive model of pressure perturbation in cumulus cloud with precipitation
02 p0189 A73-12781

A new Monte-Carlo simulation model for the temporal development of cloud droplet spectra.
02 p0144 A73-12782

Terminal velocity equations for ice crystal growth forms and precipitation rates calculation in clouds, using drag coefficients, aspect ratios and densities
02 p0189 A73-12783

Numerical model of energy transfer in carbon monoxide-nitrogen laser, considering electron-molecule excitation and vibration-vibration exchange
02 p0178 A73-12816

Numerical simulation of initial value problem of axisymmetric equatorially trapped oscillation modes of constant density viscous fluid in rotating spherical shell
03 p0384 A73-13064

Nonlinear stress properties in vicinity of crack tip, taking into account finite crack width effect by parabolic model
03 p0385 A73-13131

Mathematical models for elastic solid bodies via similarity theory, noting rheoelectrical simulation for thermal stress analysis
03 p0386 A73-13146

Verification of a comprehensive thrust chamber compatibility model for liquid rocket engines.
03 p0354 A73-13401

Prediction of the critical diameter of composite propellants.
03 p0351 A73-13432

A nonlinear model of combustion instability in liquid propellant rocket engines.
03 p0356 A73-13451

Radiation base heating from solid propellant launch vehicle exhaust plumes.
03 p0397 A73-13466

From earth to Mars orbit - Mariner 9 propulsion flight performance with analytical correlations.
03 p0382 A73-13478

Invariant poles feedback control of flexible highly variable spacecraft.
03 p0285 A73-13522

Computerized radial turbine blades thickness identification, considering temperature distribution and effects and mathematical model parameters for constraints
03 p0312 A73-13565

Long wave disturbance propagation analysis via equations of motion from mathematical model of liquid-gas mixture, determining velocity, pressure and density perturbation propagation
03 p0294 A73-13612

A simple finite element model for elastic-plastic plate bending.
03 p0391 A73-13680

Two stage analytical model for mechanism of heavy nuclei acceleration in solar flares, considering ion Fermi acceleration to higher energies
03 p0362 A73-13720

Reliability optimization of a series-parallel system.
03 p0336 A73-13735

Assessment and operational implications for ATC capital investment decision making by relative capacity estimating process using analytical models
03 p0280 A73-13801

Mathematical treatment of long wave sound propagation in curved ducts and junctions, obtaining principal mode from linearized equation of motion solved for eigenvalues
03 p0343 A73-13832

A self-consistent theory of the tail of the magnetosphere.
03 p0302 A73-13872

Linearized Kalman filtering for turbopump rotating assembly inertial and bearing parameter identification and state estimation, noting state-space model feasibility
03 p0313 A73-13904

Mathematical model, digital filter design and phase error behavior derivation for higher order discrete phase locked loops
03 p0276 A73-13906

Porous cellular structure materials, investigating porosity effects on modulus of elasticity based on central monoporous model
03 p0394 A73-14015

Reversible instantaneous deformations and internal energy in viscoelastic incompressible fluids, using Oldroyd and De Witt hydrodynamic models
03 p0296 A73-14053

Diffusion, recombination and combined models demonstrating shunting and second current conduc-

- tion effects on forward I-V characteristics for dark and illuminated Si solar cells 03 p0254 A73-14211
- Evaluation and reduction on the electromagnetic fields associated with a solar array. 03 p0256 A73-14233
- Calculation of the diffusion current of a finite-base semiconductor diode 03 p0284 A73-14322
- Experimental rotor unbalance response using hydrostatic gas lubrication. [ASME PAPER 72-LUB-31] 03 p0315 A73-14341
- Static and dynamic behavior of spherical hydrostatic bearings - Theory and experiments. [ASME PAPER 72-LUB-35] 03 p0315 A73-14344
- A nondimensional parameter characterizing mixing processes in a model of thermal gas ignition. 03 p0399 A73-14389
- Failure probability distribution models for reliability analysis, considering selection criteria based on application 04 p0507 A73-14708
- Distribution functions with fatigue analysis laws and safety predictions, noting life length and fleet assurance models 04 p0507 A73-14710
- Kinetic model considering cumulative fatigue damage interaction with chance overload on component or structure under probabilistic service load, discussing crack growth in composites 04 p0508 A73-14717
- Analysis of methods for computing an earth gravitational model from a combination of terrestrial and satellite data. 04 p0437 A73-14787
- Theoretical formulation of finite-element methods in linear-elastic analysis of general shells. 04 p0510 A73-15026
- Modeling of the radar scattering characteristics of aircraft. 04 p0416 A73-15057
- Variable mass system dynamic maneuver for maximum payload and given initial weight, noting mathematical model for time optimization 04 p0475 A73-15079
- Human body mathematical model described by kinematic and dynamic equations of joined rigid bodies for investigation of self-controlled movements in specified goal attainment 04 p0411 A73-15207
- Probability model and causal approach to failure mechanisms and reliability of control system elements applied to IC 04 p0424 A73-15208
- Failure diagnostics in mathematical simulators of automatic control systems. 04 p0430 A73-15209
- A new mathematical theory of simple materials. 04 p0511 A73-15221
- Structural reliability under cumulative fatigue damage and chance overload interaction, postulating kinetic fracture model based on probabilistic service load histories 04 p0512 A73-15243
- A method of perturbation for a weakly nonlinear hyperbolic equation with two small parameters - Study of a mathematical model 04 p0471 A73-15246
- Estimation of the statistical parameters of the Kalman-Bucy filter. 04 p0431 A73-15261
- An error sensitivity analysis for nonlinear second order filters. 04 p0431 A73-15269
- Nonlinear estimation theory applied to the interplanetary orbit determination problem. 04 p0498 A73-15271
- Status and prospects of EEG spectral analysis. 04 p0411 A73-15278
- Gold high temperature thermoelectric properties from electron model based on scattering resulting from d band-Fermi level relative position changes 04 p0463 A73-15313
- Remarks on the steady and time dependent mathematical convection models. 04 p0443 A73-15341
- A solar-wind model including proton thermal anisotropy. 04 p0492 A73-15365
- Ground reflection multipath effects on airborne communications. 04 p0422 A73-15439
- A model of signal detection for the instrument landing system. 04 p0474 A73-15441
- System time domain simulation computer aided analysis program for communication systems, presenting mathematical and functional models 04 p0425 A73-15459
- Mathematical model for multipath transmission in aircraft and spacecraft communications, presenting Bayes detector for binary PSK 04 p0422 A73-15462
- Coordinate transformation in arbitrarily dimensional spaces 04 p0443 A73-15509
- Polar ionospheric ion escape /polar wind/ hydrodynamic model equations, discussing singularities and critical points in terms of reduced Mach number 04 p0444 A73-15546
- Electrodynamics models for radio attenuation in ice by electromagnetic absorption and reflection from ice sheet interfaces, noting radar sounding 04 p0445 A73-15572
- Gravitational origin of high energy interactions and general relativity equivalence principle for unitary symmetry, noting quantum geometrodynamics cosmological model 04 p0501 A73-15632
- Equations of motion for mathematical models of turbine rotors with elastic shaft in unsteady operation, calculating resonant angular velocity 04 p0514 A73-15654
- Design and realization of microthruster temperature control subsystems - Optimization through refinement of a mathematical model 04 p0489 A73-15735
- Information theory mathematical models applied to different visual function activity phases, covering Shannon and Fisher probability models, Shreider semantic theory and Kolmogorov algorithm 04 p0412 A73-15784
- Mathematical models for distance perception of earth surface features observed from ascending vehicle, considering convergence, accommodation and monocular parallax mechanisms 04 p0413 A73-15785
- Mathematical description of some visual inertia effects 04 p0413 A73-15786
- Axiomatic mathematical model for human visual edge contrast based on additivity, one-dimensionality and contrast continuity parameters 04 p0413 A73-15788
- Some modeling problems of loudness transformations by the auditory system 04 p0413 A73-15790
- Mathematical and physical models of human long and short term memory, considering information processing and memorization at lower visual perception levels 04 p0413 A73-15793
- Image recognition learning algorithm for expanding neural nets composed of active inputs, receptors, associative elements and recognizers 04 p0426 A73-15794
- Angular velocity magnitude conversion into visually perceived apparent velocity, using psychophysical mathematical model based on axisymmetric annular visual field perception 04 p0413 A73-15796
- Mathematical description of frequency difference hologram obtained by superposition of two holograms of same object produced with light of different frequencies 04 p0451 A73-15924
- Statistical transfer theory in non-homogeneous turbulence. 04 p0520 A73-15937
- Mathematical model for long term creep strength from creep tests, noting crack initiation and microstructural changes 04 p0517 A73-15952
- Frost and ice column models for analysis of heat and mass transfer and effective thermal conductivity relationship to density in frost layer 05 p0638 A73-16225
- A model of VLF band radio wave propagation in the earth-ionosphere waveguide channel 05 p0549 A73-16391
- Adaptation of the P-N junction burnout model to circuit analysis codes. 05 p0557 A73-16506
- Similarity solution for the curved two-dimensional jet. [ASME PAPER 72-APM-JJ] 05 p0564 A73-16527
- Transient dynamic response of viscoelastic structures. [SAE PAPER 720812] 05 p0634 A73-16649
- Steady state spray combustion model, using Nukiyama-Ianasa drop distribution function, Stokes drag and modified Priem-Heidmann or Spalding vaporization rate equations [WSCI PAPER 72-36] 05 p0639 A73-16680
- Visibility of lunar surface features - Apollo 14 orbital observations and lunar landing. 05 p0617 A73-16713
- Modeling of aircraft position errors with independent surveillance. [AIAA PAPER 73-162] 05 p0595 A73-16908
- Analytical and experimental supersonic jet noise research. [AIAA PAPER 73-188] 05 p0531 A73-16926
- A general solution for lift interference in rectangular ventilated wind tunnels. [AIAA PAPER 73-209] 05 p0563 A73-16940
- Decomposition strategies for one on one aerial dog-fight game models with reinforcement learning [AIAA PAPER 73-233] 05 p0536 A73-16958
- Spectral signature variability model based on multispectral band scanner data and clustering experiments, discussing data processing algorithms 05 p0555 A73-17151
- Mathematical model for independent operations complex with rectangular probability distribution of random parameters, noting time optimal control 05 p0562 A73-17282
- Simple mathematical model of shift of threshold voltage induced in an m.o.s. transistor by testing at elevated temperatures. 05 p0560 A73-17324
- Possibility of experimentally dividing a variable magnetic field into poloidal and toroidal components 06 p0690 A73-17561
- Numerical simulation of a plasma. I - General description of the model 06 p0727 A73-17574
- A model for the automatic classification of signals with applications for the automatic language recognition 06 p0663 A73-17591
- An analytical fluid dynamic model of turbulent inlet flow. [AIAA PAPER 73-138] 06 p0644 A73-17647
- Computerized mathematical models of two- and three-dimensional turbulent flow combustion, considering temperature and concentration fluctuations, particle size, NO formation and radiative transfer 06 p0767 A73-17727
- Current kinetic modeling techniques for continuous flow combustors. 06 p0767 A73-17728
- Some observations on flows described by coupled mixing and kinetics. 06 p0767 A73-17729
- Large deflexion elastic-plastic response of certain structures to impulsive load - Numerical solutions and experimental results. 06 p0761 A73-17818
- A stochastic model of creep in the heat-resistant low-alloy CrMoV steel 06 p0705 A73-17846
- Mathematical model for information search and retrieval under Poisson process requests, discussing data processing time minimization sorting algorithms 06 p0670 A73-17856
- Turbulent boundary layers with negligible wall stress - A singular-perturbation theory. 06 p0686 A73-17988
- Mathematical models for yield point dependence on statistical arrangements of ordered precipitated phases, noting crystal dislocations interaction effect 06 p0735 A73-18044
- Automation of reliability evaluation procedures through CARE - The computer-aided reliability estimation program. 06 p0670 A73-18058
- Mathematical model for electric current in granulated media, establishing temperature dependence of tunneling conductivity for tunnel junction with metallic inclusions in oxide layer 06 p0736 A73-18117
- Backscattering of electromagnetic waves from a rough surface model. 06 p0664 A73-18134
- Dynamics of moisture diffusion through a partially liquid filled porous matrix. 06 p0649 A73-18259
- Studies of the potential-curve-crossing problem. II - General theory and a model for close crossings. 06 p0726 A73-18263
- Exhaust plume prediction model for a low-altitude supersonic missile. [AIAA PAPER 72-1170] 06 p0741 A73-18399
- The use of model building in a production environment. 06 p0698 A73-18514
- Mathematical models for critical flow rates of annular two phase mixtures under various discharge conditions 06 p0688 A73-18563
- Mathematical model for plastic deformation of polycrystalline materials with Hookes Law elastic strains 06 p0765 A73-18641
- Discrete maximum principle /local cross sections/ method applications to optimal control and mathematical programming 06 p0718 A73-18676
- Numerical model for three dimensional air parcels trajectories computation from operational wind forecasts, deriving atmospheric moisture, dew and temperature distributions predictions 06 p0720 A73-18705
- A macroscale-mesoscale numerical model of intense baroclinic development. 06 p0720 A73-18708
- Modeling and evaluating the performance of high data rate digital satellite communication systems with limiters. 06 p0669 A73-18830

MATHEMATICAL MODELS

Stochastic ion heating by ion-acoustic turbulence.
06 p0733 A73-18850

Modeling of linear time-varying systems by linear time-invariant systems of lower order.
06 p0682 A73-18867

Noisy data filtering of linear steady state control problems based on nearest neighbor interaction, discussing dimensionality reduction model for saving computer time
06 p0682 A73-18868

Calculus of variations for mathematical model of elastic shell with internal degrees of freedom, noting boundary and discontinuity conditions
06 p0766 A73-18877

A numerical experiment using a general circulation model of the atmosphere.
07 p0846 A73-19037

Optimal planning of technological systems maintenance according to a reliability criterion
07 p0830 A73-19126

The concept of snap-buckling illustrated by a simple model.
07 p0909 A73-19163

Stochastic model application to divergence of horse-pig lineage from common ancestor in terms of hemoglobin and fibrinopeptides alpha and beta chains
07 p0780 A73-19218

Drift shell splitting and magnetic equator surface topography model based on charged particle adiabatic motion and trapping in presence of internal geomagnetic multipoles
07 p0813 A73-19236

A critique of multilayer analyses in application to the propagation of acoustic-gravity waves.
07 p0814 A73-19248

A two-dimensional numerical FET model for dc, ac, and large-signal analysis.
07 p0799 A73-19342

Thermodynamic short range order models for dense substance equilibrium properties calculation, assuming molecular interaction independence and self similar radial function
07 p0851 A73-19397

Mathematical models for failure rates of electronic components, considering tantalum condensers, Zener diodes and n-p-n Si transistors
07 p0830 A73-19413

Anomalous magnetic and gravitational field models autocorrelation function behavior dependence on circular cylindrical sources depth and spacing
07 p0816 A73-19447

Mathematical model of nonstationary linear aeroacousticality
07 p0912 A73-19468

Nonlinear small amplitude behavior of collisionless plasma at mirror flute instability threshold, using modified constant gravity model and magnetic moment variation
07 p0857 A73-19525

The prediction of the optimum performance of ejectors.
07 p0810 A73-19571

Search of optimal biological conservation conditions for a heart, using methods of mathematical experiment planning
07 p0781 A73-19648

Numerical studies of the transport of solar protons in interplanetary space.
07 p0870 A73-19664

Analysis of flow of viscous fluids by the finite-element method.
07 p0811 A73-19953

Numerical calculations for the turbulent arc constrictor.
07 p0858 A73-19960

Application of a variational technique to wedge flow with variable properties.
07 p0775 A73-19963

Prandtl eddy viscosity model for incompressible coaxial jet far field velocity decay prediction with non-dimensional term inclusion
[AD-758488] 07 p0811 A73-19965

Detachment of the outer shock from underexpanded rocket plumes.
07 p0920 A73-19977

Monte Carlo method applications in the solution of gas kinetics problems
07 p0853 A73-19987

Gas-phase ignition model for some solid fuels in a shock tube
07 p0865 A73-19989

Combustion catalysis model of a single-component fuel/as applied to ammonium perchlorate/
07 p0865 A73-19991

Terrestrial thermal history from mathematical model of earth formation with low temperature dust and gas accumulation
07 p0818 A73-19997

Static electric quadrupole interaction of Ta- and Hf-ions in barium and lead titanate.
07 p0862 A73-20018

Mathematical models of the earth's magnetic field.
07 p0818 A73-20030

Experimental determination of the structure of plants with recycling
07 p0805 A73-20045

Response of a general circulation model of the atmosphere to removal of the arctic ice-cap.
07 p0848 A73-20122

Computerized static and dynamic structural analysis, discussing modeling, programs, input preparation, solution algorithms, numerical errors, output interpretation and applications
07 p0914 A73-20209

The photochemical oxidation of iodide to iodine in the presence of oxygen.
07 p0788 A73-20398

Investigation of the burnup process structure under spin conditions
07 p0923 A73-20424

System identification of vibrating structures: Mathematical models from test data; Proceedings of the Winter Annual Meeting, New York, N.Y., November 26-30, 1972.
07 p0915 A73-20426

Engineering systems structure and parameter identification using transfer function, learning model and nonlinear filtering
07 p0796 A73-20427

Methods and application of system identification in shock and vibration.
07 p0916 A73-20429

On the application of parameter identification to high-speed ground transportation systems.
07 p0808 A73-20433

Privileged equilibria of a collisionless homogeneous or inhomogeneous plasma.
07 p0860 A73-20480

A four-level technique for estimation of tactical missile aerodynamic parameters.
07 p0777 A73-20592

Departure from thermodynamic equilibrium of an ionized cesium vapor - Experimental study and comparison with a statistical model
07 p0854 A73-20607

Chaotic photon bunching effect interpretation by theoretical incoherent source model with atomic excitation and emission at stochastically independent times without interaction
07 p0837 A73-20610

A model for the kinetics of oxygen dissociation in a microwave discharge.
07 p0789 A73-20643

IMPATT diode microwave oscillator performance analysis based on model with ac current and voltage superposition on dc, determining avalanche frequency and negative resistance
08 p0942 A73-20706

Finite difference calculation for Gunn effect mathematical model, noting negative slope in electron drift velocity versus electric field characteristics for microwave oscillation
08 p0943 A73-20710

A statistical model for electromigration induced failure in thin film conductors.
08 p0944 A73-20745

Nonlinear Boussinesq convective model for large scale solar circulations.
08 p1001 A73-20751

Mathematical model selection rules for stability studies of linear mechanical or passive electrical network systems with arbitrary degrees of freedom
08 p0987 A73-20787

Electrodynamic mathematical model for electroconductivity of nonuniform plasma with Hall effect, calculating current distribution from Riemann problem solution
08 p0992 A73-20863

Mathematical description of nonlinear systems with distributed parameter
08 p0938 A73-20964

The use of dynamic programming techniques for determining resource allocations among R/D projects - An example.
08 p1025 A73-20970

Benefit-cost analysis of delay reduction with STOL. [ASCE PREPRINT 1507] 08 p1025 A73-21000

Crystal defect model of crack propagation in three dimensional solid, assuming nonlinear dependence of Young modulus on strain with term for time lag
08 p1017 A73-21025

Doppler effect intermodulation distortion derivation by perturbation method for loudspeaker modeled with pulsating sphere, considering boundary condition and nonlinear effect in wave propagation
08 p0987 A73-21123

A mathematical analysis concerning the edge effect of sound absorbing materials.
08 p0987 A73-21124

The structure of a weak shock wave in a gas/liquid medium
08 p0954 A73-21129

The effect of metal gripping during dynamic loading
08 p0973 A73-21132

Conformally invariant cosmological and physical models in terms of Einstein, Maxwell and Dirac equations
08 p1009 A73-21228

Geomagnetic field optimal model with expansion of spherical harmonic series by least squares method
08 p0960 A73-21353

On the lateral boundary conditions for the primitive equations.
08 p0985 A73-21387

Treatment of dynamic snap-through problems by the direct Liapunov method
08 p1018 A73-21410

Theory of a generalized Helmholtz resonator.
08 p0952 A73-21471

A mathematical model to assess changes in the baroreceptor reflex.
08 p0934 A73-21475

A model for the elastic properties of the lung and their effect on expiratory flow.
08 p0934 A73-21502

Constitutive equation for electronic circuits without topologically dependent variables, noting numerical analysis of equations of state for nonlinear circuits
08 p0951 A73-21551

Construction of analytical formulas for functions of linear circuits by means of engineering-application digital computers
08 p0941 A73-21552

Investigation of the applicability of some statistical models to the shock-wave structure problem
08 p0956 A73-21606

Analytical predictions of emissions from and within an Allison J-33 combustor.
08 p1025 A73-21670

A recovery creep model based on dislocation distributions.
08 p0980 A73-21777

A two-layer model of high speed two- and three dimensional turbulent boundary layers with pressure gradient, surface mass injection and entropy layer swallowing.
[AIAA PAPER 73-135] 08 p0956 A73-21800

Monograph - The quasi-biennial oscillation in the stratosphere.
08 p0986 A73-21841

Effects of experimental conditions on parameter estimated when using the Hill model
09 p1044 A73-21872

A numerical model of the structure and evolution of young supernova remnants.
09 p1143 A73-22111

The gradient instability in Gaussian sporadic E-layers.
09 p1075 A73-22133

Performance comparison of suboptimal Kalman filters modeled for a continuous nonlinear system.
09 p1067 A73-22228

Propagation of electronic longitudinal modes in a non-Maxwellian plasma.
09 p1126 A73-22278

A numerical model for predicting mesoscale winds aloft.
09 p1114 A73-22335

Russian book on mathematical models of biological systems covering biogeocenosis, optimal crop, chemostat cultivation, predator-victim society, trophic control, and life support systems
09 p1044 A73-22347

Pure moment loading of axisymmetric finite element models.
09 p1158 A73-22391

One-dimensional numerical experiment on anomalous plasma resistivity
09 p1127 A73-22482

An approximate continuous representation of discrete control systems
09 p1068 A73-22564

Kinetics of the excitation of molecular vibrations by infrared laser radiation
09 p1094 A73-22597

Mathematical model for nonlinear interactions between HF waves and LF acoustic waves applied to electromagnetic wave stability in plasmas and dielectrics
09 p1128 A73-22614

Mathematical model for extinguishing gunpowder combustion via pressure variations, assuming gunpowder surface dependence on combustion rates
09 p1167 A73-22617

Prediction models for surface and air transportation dynamic environments, considering broadband and single frequency continuous and recurrent and intermittent discrete excitation modes
09 p1032 A73-22718

Mathematical model of equilibrium and steady state stability of pulse frequency modulation feedback systems of second kind with time delay filters
09 p1069 A73-22723

One dimensional model for spark ignition Wankel engine combustion, presenting unsteady turbulent flame propagation equations
09 p1136 A73-22824

Molecular model with two interacting terms for time evolution of nonradiative transitions, obtaining expression for energy level populations
09 p1123 A73-22876

Metal fcc polycrystals macroscopic plasticity theory based on discrete aggregate model, predicting stress-strain curves for partial load cycles
09 p1160 A73-22896

Effective use of composite materials directionally reinforced with hollow fibers.

09 p1111 A73-23151

A search for stimulated emission of radiation from superconducting tunnel junctions.

09 p1135 A73-23341

Estimation of possible excitation frequencies for shallow rectangular cavities.

09 p1029 A73-23444

Hybrid stress finite element models for elastic continuum, discussing variational principle and macroscopic equilibrium

09 p1166 A73-23457

Partially ionized nonideal plasma model electron-ion interactions, equilibrium, equations of state and thermodynamic quantities

10 p1252 A73-23501

Mathematical analogy between the bending of a plate and the circulating motion of a liquid in a geometrically similar region

10 p1205 A73-23598

Upper atmosphere analytical density model for satellite motion prediction, allowing for diurnal and semiannual density variations and solar activity and geomagnetic disturbances effects

10 p1211 A73-23883

A mathematical model of the optimization of cosmic ray intensity observation data

10 p1268 A73-23935

Water-salt homeostasis mathematical model, solving equations with analog and digital computers

10 p1184 A73-23941

Earth-atmosphere-ocean energy balance time dependent model equation, using Sellers radiation relationships and turbulent exchange coefficients for numerical solution

10 p1245 A73-23982

Manned vehicle systems analysis techniques application to manual approach-to-landing phase of aircraft flight, developing analytical control model

10 p1247 A73-24011

Dynamics of variable sweep wing aircraft in the course of changing geometry.

10 p1175 A73-24012

Model reduction of multivariable control systems by means of matrix continued fractions.

10 p1200 A73-24046

Order determination and parameter identification of time-invariant state variable models.

10 p1201 A73-24054

Spectral energy transfer models of turbulence decay compared with numerical simulation of three dimensional homogeneous isotropic turbulence, considering eddy viscosity and diffusion models

10 p1246 A73-24252

Turbulent interface structure from eddy viscosity models, discussing equations of motion and Nee-Kovaszny and Prandtl models

10 p1205 A73-24253

Encapsulated common base microwave transistors mathematical models, determining transfer scattering parameters

10 p1195 A73-24420

Application of the fluctuation model of superplasticity to calculate the surface tension of metals during phase transformations

10 p1235 A73-24455

Evaluation of the characteristics of the boundary layer in transitional flow on a flat plate

10 p1296 A73-24497

Radiative heat transport models for evacuated powder to specify IR radiation environment on lunar surface

10 p1282 A73-24645

Boundary conditions model calculations for thermoelastic deformations of continuum body with surface tractions on interface, discussing energy balance laws derivation for loading devices

10 p1292 A73-24659

A self-consistent model of a simple magnetic neutral sheet system surrounded by a cold, collisionless plasma.

10 p1257 A73-24725

Mathematical description by Gaussian error function for metals diffusive saturation and diffusion constants determination

10 p1236 A73-24952

A structural model of random processes and its invariant properties

11 p1340 A73-25007

Experimental models of communication at the molecular and microsystemic levels.

11 p1324 A73-25140

Analysis of swimming motions.

11 p1322 A73-25184

Numerical study of a viscous flow through a pipe orifice.

11 p1346 A73-25213

Numerical modeling of laser produced plasmas - The dynamics and neutron production in dense spherically symmetric plasmas.

11 p1404 A73-25272

Computerized large signal model of IMPATT diode, calculating output power and admittance as function of frequency and amplitude

11 p1336 A73-25320

Structure statistical identification method based on experimental measurements of natural frequencies and mode shapes to modify finite element model structural parameters

[AIAA PAPER 73-339] 11 p1436 A73-25479

Launch vehicle response to inflight winds during ascent, modeling wind velocity as nonstationary random process

[AIAA PAPER 73-398] 11 p1392 A73-25527

Essentially incomplete model construction by non-search method in linear plant parametric control

11 p1341 A73-25620

Kirchhoff and small perturbation methods identity in composite model calculation for rough surface electromagnetic scattering of circularly polarized wave by perfectly conducting body

11 p1329 A73-25678

A simple model of normal shock wave and turbulent boundary-layer interaction.

11 p1347 A73-25710

A model of a Martian Great dust storm.

11 p1418 A73-25715

A model for investigating eddy viscosity effects on mesoscale cellular convection.

11 p1393 A73-25716

Steady state mathematical theory for the insulated gate field effect transistor.

11 p1338 A73-25789

On the superposition model for environmentally-assisted fatigue crack propagation.

11 p1382 A73-25820

Calculations of electrical transport properties of liquid metals at high pressures.

11 p1399 A73-25899

Vibration-to-rotation and vibration-to-vibration energy transfer between diatomic molecules.

11 p1401 A73-25967

Analytical model for radioisotope thermoelectric generator performance prediction in air and vacuum, taking into account modified heat transfer rates

11 p1312 A73-26031

Detailed mathematical models of a radioisotope thermoelectric generator.

11 p1396 A73-26033

Hydrodynamic motions and the vacuum stage in an anisotropic cosmological model.

11 p1423 A73-26052

Experimental method for structure identification in nonlinear objects with recycling processes

11 p1342 A73-26082

Influence of phase fluctuations of the received radiation on the performance of a synthetic antenna

11 p1331 A73-26158

Thermally induced nonlinear propagation of a laser beam in an absorbing fluid medium.

11 p1377 A73-26229

Prediction of heat transfer for turbulent boundary layer with pressure gradient.

11 p1453 A73-26393

Asynchronous linear automatic binary control systems, using interpolation theory of Taylor operators for mathematical modeling

11 p1342 A73-26418

Stagnation conditions in systems with Coulomb friction

11 p1400 A73-26451

Oscillations of a mathematical pendulum of variable length during rectilinear motion of the suspension point

11 p1401 A73-26466

Linear system modeling via optimal finite dimensional approximation based on Sard generalized spline, giving error bounds

11 p1391 A73-26580

Simultaneous radiative and conductive heat transfer in non-gray media.

11 p1453 A73-26583

Radiative transfer in a nongray spherical layer - Simplified rectangular model.

11 p1401 A73-26585

Radar angels cross section statistical distribution model based on radar measurement and direct ornithological data on bird populations density

11 p1332 A73-26630

Measurements of distributed targets with the random signal radar.

11 p1332 A73-26632

Stable-member mounted instrument environment simulation model development.

11 p1395 A73-26638

Economic-mathematics approaches to prognostic air traffic computations

11 p1455 A73-26724

Elasticity theory of three dimensional system of particles in rectangular prismatic or tetrahedral net arrangement as topological model for finite element method

11 p1448 A73-26727

Two component system reliability model, taking into account stress effects under failure normal distribution assumption

11 p1448 A73-26730

Evaluation of the efficiency of automatic control and observation systems on the basis of mathematical models of potential and real automatic systems

12 p1482 A73-26762

Global climatic model based on time and space averaged thermodynamic energy equation for idealized land-water distribution, allowing for continents-oceans seasonal interactions

12 p1519 A73-26801

Radiative transfer theory model of isotropic monochromatic scattering of light in plane layer of finite optical thickness

12 p1538 A73-26862

Differential equations of motion for analog model of M-type TWT performance, proposing block diagram for electron phase and trajectory and field distribution calculations

12 p1478 A73-26950

High speed corotating plasma streams in solar wind from time dependent radial MHD flow model

12 p1533 A73-26979

Lower thermosphere density and composition model from satellite drag and accommodation coefficients

12 p1488 A73-26990

Methodologies for the analysis of transport requirements with particular regard to the aeronautic case

12 p1561 A73-27070

An analytical model for the prediction of liquid rocket plume contamination effects on sensitive surfaces.

12 p1532 A73-27099

A mechanistic model for analysis of pulse-mode engine operation.

12 p1533 A73-27100

On optimal nonlinear estimation. I - Continuous observation.

12 p1517 A73-27147

Calculation of the statistical characteristics of a long waveguide line in a two-wave model

12 p1469 A73-27189

Three-dimensional analytical model of the electron density distribution in a quiet ionosphere

12 p1490 A73-27334

Oscillations of the earth's magnetic tail in a quasi-hydrodynamics approximation

12 p1491 A73-27347

Spherical harmonic analysis of the geomagnetic field during the epoch 1965.0 up to n = 23 from ground data. II - Results

12 p1491 A73-27353

Cosmos 321 geomagnetic measurement data for construction of satellite geomagnetic survey and geomagnetic field models

12 p1491 A73-27359

Book - Reliability concepts in engineering manufacture.

12 p1502 A73-27398

Autonomous second order system model for nonlinear disturbances of multifrequency systems at resonance, using group properties of differential equation

12 p1524 A73-27404

Chetaev concept for experiments with small measurement errors and mathematical model instability and lability properties, applying to biological existence struggle and spacecraft reentry

12 p1524 A73-27405

Mode locking in quantum optics.

12 p1506 A73-27442

Mathematical model of heat conducting medium thermophysical properties based on one dimensional nonlinear thermal conductivity equation solution

12 p1559 A73-27444

A cylindrical shell model of the NASA-MPE barium ion cloud experiment.

12 p1492 A73-27607

Random failure process similarity in redundant schemes for systems with binary elements, noting statistical modeling on specialized Monte Carlo machines

12 p1485 A73-27620

Nonlinear problems in analyzing the observability of the trajectories of spacecraft motion according to measurement data.

12 p1543 A73-27628

Equations of state and dissociation equilibrium for CsCe plasma, noting thermodynamic model for phase transitions of liquid metal into nonideal ion plasma

12 p1529 A73-27901

The pressure and velocity fields of convected vortices.

13 p1599 A73-28067

Probability summation model for heterochromatic luminance additivity failure at absolute visual threshold.

13 p1578 A73-28099

The convergence theorems and their role in the theory of structures.

13 p1692 A73-28227

On further application of the finite element method to three-dimensional elastic analysis.

13 p1693 A73-28241

An evaluation of finite difference and finite element techniques for analysis of general shells.

13 p1694 A73-28256

Mass to wind and wind to mass adjustments in dynamic initialization for primitive equation model of atmospheric motion

13 p1652 A73-28270

Bounds upon the growth rate of errors in quasi-non-divergent prediction models.

13 p1652 A73-28271

Response functions for mathematical double membrane model of isotropic elastic shell in form of orientable two dimensional differentiable manifold

13 p1694 A73-28284

Initial-boundary value problems of nonlinear extensible beam equation as mathematical model for transverse deflections of beam with hinged or clamped ends

13 p1695 A73-28438

Forward and specular scattering from a rough surface - Theory and experiment.

13 p1659 A73-28490

A two-dimensional mathematical model for an acoustically soft parabolic cylinder reflector.

13 p1597 A73-28493

A two-dimensional mathematical model of the insulated-gate field-effect transistor.

13 p1590 A73-28543

Differential equations for digital model of linear quadrupole, discussing digital simulation of analog radio equipment circuits

13 p1591 A73-28659

The numerical models of general circulation and their employment for medium-term and long-term weather prediction

13 p1653 A73-28741

A comparison of time-varying concentrations of air admixtures with those of the corresponding stationary cases

13 p1653 A73-28742

Estimations for queuing and reliability theory

13 p1649 A73-28796

Linear aerodynamic model incorporating torsional oscillations about two dimensional airfoil midchord for stall flutter description

13 p1697 A73-28814

Statistical turbulence model of meteorological and topographical aircraft flight conditions for low altitude critical air turbulence /LO-LOCAT/ environment

13 p1569 A73-28831

Modeling the ignition and cool-flame limits of acetaldehyde oxidation.

13 p1581 A73-28999

A comparison between potential flow studies through blade cascade by theoretical and rheo-electric analogy methods.

13 p1565 A73-29010

A new approach to the problem of predicting the performance of centrifugal compressors.

13 p1565 A73-29012

Accuracy of switching pressure of fluidic OR-NOR device.

13 p1571 A73-29044

Coupled thermoplasticity model of two stress-strain regions characterized by nonevolutionary plastic flow equations and simple wave collapse, with and without thermal conductivity

13 p1698 A73-29087

Linear and nonlinear first order closed loop tracking radar systems, predicting noise performance by Gaussian signal amplitude fluctuation modeling

13 p1585 A73-29206

Least squares and non-linear functions.

13 p1619 A73-29241

Modeling irregular surfaces.

13 p1619 A73-29242

Turbulence in journal bearings, considering Taylor vortices development beyond laminar range and theoretical models based on mixing length flow theory

13 p1625 A73-29261

Some aspects of nonorthogonal data analysis. I - Developing prediction equations.

13 p1650 A73-29298

Statistical model of gust factor relation to lake and terrain surface roughness and height from wind velocity measurement data

13 p1655 A73-29341

Choice of materials on the basis of random vibration and structural fatigue.

13 p1641 A73-29495

Behavior of random micro-structural systems.

13 p1701 A73-29530

Bonding characterization in reinforced composites.

13 p1702 A73-29536

Statistical criteria of ultimate strength and plasticity of materials in the complex stress state.

13 p1703 A73-29620

Self consistent one dimensional plasma layer model with current layer at center described by Vlasov equation and nonexistent normal magnetic field component

14 p1796 A73-29870

Multipath propagation in aircraft digital communication with ground terminal, modeling received signal for detection and estimation theories applications

14 p1726 A73-29902

Optimization of turbulence models by means of a logical search algorithm.

14 p1744 A73-29931

Mass transfer approximation model in unidirectional swirled two phase flow, considering transfer resistance of liquid phase

14 p1816 A73-30016

The employment of an extended theorem of corresponding conditions in the computation of the surface tension of pure substances

14 p1776 A73-30124

Advances in computational methods in structural mechanics and design; Proceedings of the Second U.S.-Japan Seminar, Berkeley, Calif., August 1972.

14 p1806 A73-30176

Finite element models for continuum structural analysis, considering variational principles, element base functions and general purpose computer program

14 p1807 A73-30183

Equivalent finite element model derivation from plate bending triangular element, assumed stress hybrid method and elements with polynomial deflection function

14 p1807 A73-30184

Approximate investigation of the dynamics of a digital phase-lock automatic frequency control system /DPAFC/

14 p1728 A73-30269

Psychoacoustic theory of signal detectability based on mathematical input-output mapping model and memory role in human auditory system

14 p1721 A73-30278

Binaural signal detection - Equalization and cancellation theory.

14 p1716 A73-30284

Group data handling theorems on uniqueness of mathematical model for regression curve reconstruction in polynomial domain with small number of points

14 p1738 A73-30288

A mathematical model of damage accumulation in plastic isotropic materials.

14 p1810 A73-30301

Equations for the time-dependent strength of a solid.

14 p1810 A73-30304

Einstein equations reduction to friction systems in homogeneous cosmological models, investigating Bianchi models solutions isotropization

14 p1798 A73-30327

Model of degenerate semiconductor transition to superconducting state in terms of electron interactions with phonons of low-lying spectral branch

14 p1783 A73-30343

Basic concepts of the mechanics of discretized bodies with an introduction to discrete element calculus.

14 p1775 A73-30548

The calculation of low-Reynolds-number phenomena with a two-equation model of turbulence.

14 p1746 A73-30606

A theoretical model for the elevated temperature deformation of dispersion hardened metals.

14 p1761 A73-30636

Test of statistical models for gases with and without internal energy states.

14 p1818 A73-30653

Modelling and identification theory - A flight control application.

14 p1739 A73-30777

Mathematical models and identification of bilinear systems.

14 p1740 A73-30782

Studies on barotropic and baroclinic energy conversions in wave number regime.

14 p1772 A73-30901

Mathematical model of equilibrium and steady state stability of pulse frequency modulation feedback systems of second kind with time delay filters

14 p1740 A73-30956

A numerical model of the geopotential field with a new profile of the generalized vertical velocity that takes orography into account.

15 p1865 A73-31002

Mathematical model for shimmy auto-oscillations of aircraft landing gear nose wheel with pneumatic tire under velocity changes

15 p1825 A73-31044

Interstellar gas excitation due to supernova explosions using time dependent model based on statistical correlation of gas neutral density, ionization and temperature parameters

15 p1928 A73-31053

Semiinfinite and finite crack motion models comparison without loading restrictions, considering finite length dislocation pile up role and singular integral equation use

15 p1946 A73-31106

Effective-viscosity model for turbulent wall boundary layers.

15 p1860 A73-31119

The problem of choosing a zero approximation of the angular position of an oriented satellite in the case of a nondipolar approximation of the geomagnetic field

15 p1942 A73-31238

Collision induced dissociation - A statistical theory.

15 p1915 A73-31275

A model and calculation procedure for predicting parachute inflation.

[AIAA PAPER 73-453]

15 p1826 A73-31439

Modeling of pulsed propagation problems of radio waves excited by an infinite electric current filament in homogeneous dispersing media

15 p1853 A73-31496

A simple model of uniaxial creep recovery and stress relaxation based on residual-stress redistribution.

15 p1948 A73-31615

Generalized mathematical model for gas turbine dynamic behavior simulation based on one dimensional flow theory with functional integration for rotor speed time derivative

15 p1925 A73-31629

Mixed autoregressive moving average models parameters recursive joint identification and order determination extended for Kalman-Bucy filter transition and covariance parameters estimation

15 p1853 A73-31630

Pulsed laser irradiation effects on solid deuterium slab, deriving two-temperature electron-ion model

15 p1884 A73-31660

Cloud cover probability computation models, showing averaged values for direction of sighting and cumulus cloud cover estimations

15 p1905 A73-31797

Earth shape determination from ellipsoidal model, comparing with spherical functions

15 p1871 A73-31798

Results of the numerical modeling of steady zonal circulation of the atmosphere in the equatorial region

15 p1905 A73-31817

Separation of the variable geomagnetic field into normal and anomalous components

15 p1872 A73-31896

Optimal evasive tactics against a proportional navigation missile with time delay.

15 p1908 A73-31918

Laser mode locking using saturable absorbers.

15 p1885 A73-31941

Existence of stable relative equilibria of an artificial satellite in a model magnetic field

15 p1872 A73-31956

Finite element methods in continuum mechanics.

15 p1950 A73-31973

Shock waves, jump relations, and structure.

15 p1864 A73-31974

Calculation of temperature distribution in the human body.

15 p1839 A73-31999

Mathematical model of elastic flight body behavior in continuous medium based on combination solutions to aerodynamics, automatic control and elasticity theory problems

15 p1952 A73-32063

Structure of a weak shock wave in a gas-liquid medium.

15 p1864 A73-32064

Two component glass fiber reinforced plastic model describing stress-strain state via elastic properties analysis, internal energy production and Hooke's Law application

15 p1952 A73-32085

A consistent finite-difference model for the two-dimensional continuum.

15 p1954 A73-32122

Ray models for sound propagation and attenuation in ducts, in the absence of mean flow.

15 p1865 A73-32153

Simulation of a steady-state integrated human thermal system.

15 p1839 A73-32225

Turbulent scattering phenomenological model for D region partial coherent reflection experiments with measurement noise, presenting amplitude and phase statistics

15 p1845 A73-32230

The mechanism of gyroscopic tracking. I. [ASME PAPER 72-MECH-32]

15 p1883 A73-32284

Calculus of variations for mathematical model of elastic shell with internal degrees of freedom, noting boundary and discontinuity conditions

15 p1956 A73-32402

Simultaneous control of temperature and humidity in a confined space. I - Mathematical modeling of the dynamic behavior of temperature and humidity in a confined space.

15 p1959 A73-32597

Simultaneous control of temperature and humidity in a confined space. II - Feedback control synthesis via classical control theory.

15 p1855 A73-32598

Possibility of experimental separation of the variable geomagnetic field into a poloidal and a toroidal part.

16 p2002 A73-32785

Solar radiation pressure on Mariner 9 Mars orbiter from mathematical model of illuminance and reflectivity characteristics

16 p2052 A73-32906

Distribution of the response of linear systems to Poisson distributed random pulses.

16 p2035 A73-32918

Influence of diffusion on plasma parameters - A qualitative estimate and a physical interpretation.

16 p2040 A73-32941

Mathematical programming methods in structural analysis.

16 p2078 A73-33001

Modified finite difference procedures for structural mechanics, discussing interior and boundary discretization errors and accuracy improvement

16 p2079 A73-33012

Adhesive viscoelasticity effects on sandwich structure performance, presenting mathematical model for adhesive behavior and time dependent loading

16 p2029 A73-33053

Transient oscillator analysis of a high-pressure electrically excited CO laser.

16 p2024 A73-33082

Dynamic analysis procedure to locate vibration sources without simulated service tests, mapping structural surfaces at all frequencies via transfer function or mechanical impedance analysis

16 p2019 A73-33098

A biased model for calculating the evolution in solar absorption.

16 p2060 A73-33128

A doped highly compensated crystal semiconductor as a model of amorphous semiconductors.

16 p2044 A73-33196

Two theoretical models of fatigue crack propagation.

16 p2079 A73-33200

Royal Aircraft Establishment Aerodynamics Flight Division flight simulators for V/STOL and helicopters, emphasizing handling, aircraft mathematical models and cockpit simulation

16 p1996 A73-33211

Discrete /microscopic, atomic/, continuous /macroscopic, phenomenological/ and quasi-continuous models of elastic solids, exemplifying elastic crystals linear model

16 p2037 A73-33230

Quark search positive results, discussing mathematical models, magnetic monopole searches and existence debate

16 p2054 A73-33289

Charge transfer in overlapping gate charge-coupled devices.

16 p1988 A73-33396

Single-fluid model of the distant solar wind.

16 p2056 A73-33459

An analytical model for the response of flueic wall attachment amplifiers.

16 p1970 A73-33474

The use of a hybrid computer in the optimization of gas turbine control parameters.

16 p2047 A73-33491

Newkirk effect - Thermally induced dynamic instability of high-speed rotors.

16 p2047 A73-33499

Simulated weather records experiment for polluted atmosphere effects on climatic change, using numerical circulation model

16 p2007 A73-33568

Mathematical models for critical flow rates of annular two phase mixtures under various discharge conditions

16 p2000 A73-33588

Testing of spacecraft in long-term storage.

16 p2073 A73-33615

Time dependent stress-strength models for non-electrical and electrical systems. I.

16 p2020 A73-33621

Air Force Increase Reliability of Operational Systems computer program and mathematical models for economic logistic resource allocations and cost effective system modification

16 p2088 A73-33627

Statistical and probabilistic MTBF models for parts, sockets and systems reliability

16 p2020 A73-33628

Mathematical modeling technique for marketing reliability programs in terms of cost/performance assurance for use in management decision making

16 p2089 A73-33638

Microorganism heat sterilization process design and control based on logarithmic thermal destruction and Bigelow temperature coefficient models, determining lethality by statistical procedure

16 p1976 A73-33695

Modeling, identification and prediction of a class of nonlinear viscoelastic materials. I.

16 p2082 A73-33904

Spherically symmetric zero energy Einstein-de Sitter cosmological model validity for world geometry from observational data and invalidity of other models

17 p2225 A73-34110

Mathematical formulation of viscous-inviscid interaction problems in supersonic flow.

17 p2091 A73-34178

Approximate method of solution for three-dimensional boundary layers.

17 p2150 A73-34188

An assumed stress hybrid finite element model for linear elastodynamic analysis.

17 p2241 A73-34189

Heat transfer to flowing gas-solid mixtures.

17 p2254 A73-34353

Study of incidence loss models in radial and mixed-flow turbomachinery.

17 p2092 A73-34384

Monte Carlo model of cometary evolution based on hypothetical perturbed orbit calculations, with emphasis on short-period comets

17 p2228 A73-34426

Book - Minicomputers for engineers and scientists.

17 p2130 A73-34455

Finite element analysis of inflatable shells.

17 p2242 A73-34528

Thermodynamic analysis of liquid metal systems by using a cluster model

17 p2188 A73-34555

Book - Nonlinear viscoelastic solids.

17 p2243 A73-34574

Diffraction of a plane electromagnetic wave on arrays of periodically spaced cylinders

17 p2121 A73-34583

The finite element method in fluid mechanics.

17 p2151 A73-34830

Linear structure theory from analysis of structural mechanical models, proposing three dimensional model for behavior of granular materials

17 p2245 A73-34832

Welded steel beam fatigue behavior evaluation via stable crack growth concepts, developing fracture mechanics model for cracks originating from pores

17 p2246 A73-34887

Global circulation numerical modeling problems and aumerical weather forecasting status as basis for GARP programs, considering tropical experiment on deep convective cloud systems

17 p2205 A73-34927

An economical method of analyzing transient motion of gas-lubricated rotor-bearing systems.

[ASLE PREPRINT 73AM-2B-2]

17 p2178 A73-34982

A simple yet theoretically based time domain model for fluid transmission line systems.

[ASME PAPER 73-FE-27]

17 p2153 A73-35021

Investigation of reactionless mode stability characteristics of a stiff inplane hingeless rotor system.

[AHS PREPRINT 734]

17 p2105 A73-35070

A dynamics approach to helicopter transmission noise reduction and improved reliability.

[AHS PREPRINT 772]

17 p2106 A73-35090

A note on compressible flow through a vortex swirl cup.

17 p2154 A73-35120

Partially ionized nonideal plasma model electron-ion interactions, equilibrium equations of state and thermodynamic quantities

17 p2216 A73-35181

Applications of a model of the human visual system to pattern recognition problems.

17 p2116 A73-35242

Computer analysis of the influence of solid state distribution on aircraft power generation.

17 p2109 A73-35250

Intrasystem electromagnetic compatibility analysis program.

17 p2131 A73-35251

Fundamentals of aerodynamic sound theory and flow duct acoustics.

17 p2155 A73-35331

A projection model for Bayesian estimation of distributed functions.

17 p2202 A73-35373

Application of energy model of turbulence to calculation of lubricant flows.

[ASME PAPER 73-LUBS-18]

17 p2181 A73-35397

Mechanical and optical characterization of an anelastic polymer at large strain rates and large strains.

[SESA PAPER 2198A]

17 p2198 A73-35458

Review of some mathematical models of non-linear domain dynamics in bulk-effect semiconductors.

17 p2219 A73-35516

Generalized equation for tensile strength of metal matrix composites from upper bound analysis of simplified model with holes, inclusions and environmental pressure

17 p2251 A73-35528

The engineering of large-scale systems.

17 p2258 A73-35573

A model of psychological annoyance of noise.

17 p2118 A73-35627

The path independence of orbit inclination momentum.

17 p2234 A73-35661

Properties of a superconducting point contact connected to a resonator.

17 p2220 A73-35725

Probabilistic model for radiative transfer problems in cylindrical shell media with complete redistribution in frequency.

17 p2236 A73-35781

Study of the similarity solution in three dimensional compressible laminar boundary layer.

17 p2157 A73-35862

Current status and immediate problems of hydrodynamic short-term weather forecasting

18 p2331 A73-35908

Numerical weather prediction models based on hydrothermodynamic equations and nonadiabatic factors for short term regional, hemispheric and global forecasting

18 p2331 A73-35909

Medium-range forecasting of large-scale atmospheric circulation components on the basis of a nonlinear spectral model

18 p2331 A73-35910

Application of turbulence model equations to axisymmetric wakes.

[AIAA PAPER 73-648]

18 p2260 A73-36203

Aircraft wake vortex transport model.

[AIAA PAPER 73-679]

18 p2267 A73-36230

Multiphase underexpanded plume computational technique including turbulent mixing and nonequilibrium chemistry.

[AIAA PAPER 73-695]

18 p2368 A73-36244

Analysis and interpretation of aspect-dependent ionospheric radar scatter.

18 p2289 A73-36283

Investigation of laminar flow in a porous pipe with variable wall suction.

[AIAA PAPER 73-725]

18 p2299 A73-36342

Thermal modeling of a plate with coupled heat transfer modes.

[AIAA PAPER 73-748]

18 p2370 A73-36364

Three-dimensional nosetip shape changes in hypersonic flow. I - Illustration of a mathematical model characteristic method.

[AIAA PAPER 73-762]

18 p2264 A73-36377

Mathematical modeling for ATTS-F spacecraft louvers and heat pipes thermal control heat rejection capacity, noting correlation with solar environment simulation data

[AIAA PAPER 73-773]

18 p2360 A73-36387

Modeling problems in air traffic control systems.

18 p2335 A73-36427

On Burgers' model equations for turbulence.

18 p2299 A73-36507

Cardiorespiratory transients in exercising man. I - Tests of superposition. II - Linear models.

18 p2278 A73-36656

Mathematical approximation of turbulent cylindrical jets: Initial core - Velocity distribution

18 p2301 A73-36690

Brittle fracture mechanics models of structural materials in terms of elastic continuum with crack

18 p2366 A73-36823

A high-performance, aerodynamically-controlled, tactical missile hybrid 6-DOF simulation.

18 p2296 A73-36835

Airport simulation program describing passenger flow and scheduling considerations, including automobile parking, baggage handling, rapid transit, arrival and departure peaks and passenger decisions

18 p2296 A73-36841

Computer models for air traffic control system simulation.

18 p2335 A73-36843

A deterministic model of a well trained human operator performing compensatory tracking.

18 p2283 A73-36844

Turbine engine control system design based on linearized and nonlinear mathematical models accounting for thermodynamic performance

18 p2343 A73-36995

Possibility of computing the cloud field on the basis of vertical velocities.

18 p2334 A73-37055

Differential games applied to some interception models

18 p2268 A73-37080

Statistical models for rounding-off error studies in linear algebraic problems

18 p2292 A73-37144

Internal structure of the convective shell of the sun

19 p2481 A73-37343

Magnetopause configuration and dimension calculation methods, noting accurate numerical solutions for magnetohydrodynamic approach to two-dimensional problem

19 p2481 A73-37347

An integral transistor model using the quality parameters of a technological process

19 p2409 A73-37400

Study of the behavior of metallic single crystals - Application to the tension of the fcc single crystal

19 p2495 A73-37425

Analysis of some functional parameters of rotary hydrostatic engines under dynamic conditions by modeling on a computer

19 p2388 A73-37557

Implications of the statistical bootstrap model for cosmology and galaxy formation.

19 p2482 A73-37559

Observational nondifferentiability between expanding universe and static world models

19 p2484 A73-37607

Stellar kinetic energy gain in spherical systems by transient external gravitational perturbations, computing dynamic models for compressive shocks
19 p2484 A73-37616

Coupled thermoplasticity model of two stress-strain regions characterized by nonevolutionary plastic flow equations and simple wave collapse, with and without thermal conductivity
19 p2498 A73-37637

Numerical models of the circulation of the atmosphere of Venus.
19 p2485 A73-37657

Numerical modeling of the dynamics and microphysics of warm cumulus convection.
19 p2447 A73-37658

A comparison between axisymmetric and slab-symmetric cumulus cloud models.
19 p2447 A73-37659

ACLS CC-115 model simulation, test analysis and correlation.
19 p2382 A73-37693

A comparison of errors in linear digital models.
19 p2413 A73-38059

Modeling the human in a time-varying anti-aircraft tracking loop.
19 p2401 A73-38071

Material damping - An introductory review of mathematical models, measures and experimental techniques.
19 p2500 A73-38105

Fluctuation model of superplasticity and surface tension of a metal at a phase transition.
19 p2442 A73-38137

Differential equations modelled on nonalgorithmic digital computers.
19 p2408 A73-38144

Quasi-stationary atmospheric waves and mean monthly vorticity production from development term of two level model
19 p2447 A73-38153

Exploratory study of several advanced nuclear-MHD power plant systems.
19 p2454 A73-38313

Limits of applicability of the Delano model for describing the process of wave scattering by a complex-shaped body
19 p2407 A73-38343

Analytical model for long term performance prediction of multihundred watt radioisotope thermoelectric generator with Si-Ge alloy as thermoelectric material, noting degradation mechanisms
19 p2390 A73-38391

Nickel-cadmium battery performance prediction models Apollo Telescope Mount application.
19 p2390 A73-38399

SkyLab ATM solar array performance characteristics prediction via mathematical model, discussing I-V characteristics, test data computer programming and polynomial curves
19 p2391 A73-38407

Comparison of the Beckmann model with bidirectional reflectance measurements.
[ASME PAPER 73-HT-11] 20 p2563 A73-38567

A theoretical model for lunar surface material thermal conductivity.
[ASME PAPER 73-HT-35] 20 p2603 A73-38571

Third- and higher-order intensity correlations in laser light.
20 p2571 A73-38630

Linear acceleration insensitive balanced rotor seismic angular motion sensor with optical pickoff system, discussing mathematical model and performance tests
[AIAA PAPER 73-829] 20 p2564 A73-38774

An approach to the synthesis of separate surface automatic flight control systems.
[AIAA PAPER 73-834] 20 p2508 A73-38777

A 'type one' servo explicit model following adaptive scheme.
[AIAA PAPER 73-862] 20 p2586 A73-38800

Verification of sensitivity enhancement factors for CW ultrasonic resonators.
20 p2565 A73-38887

X-ray emission in laser-produced plasmas.
20 p2595 A73-38890

Upper atmosphere analytical density model for satellite motion prediction, allowing for diurnal and semiannual density variations and solar activity and geomagnetic disturbances effects
20 p2550 A73-38902

Boltzmann equation with Gross-Krook type model for investigation of steady plane shock wave structure in fully ionized gas
20 p2596 A73-38968

Calculation of bending vibrations in beams with the aid of a discrete model
20 p2615 A73-38982

A design problem for redundant systems with recovery
20 p2568 A73-38996

Multivalued models of computer electronic circuits
20 p2532 A73-39001

Probabilistic statistical methods for analysis of impulse flows in nerves
20 p2516 A73-39002

A mathematical model of the peripheral pain signalization mechanism
20 p2516 A73-39003

Mathematical analysis of the operation of regulatory mechanisms of the spinal cord
20 p2517 A73-39005

A programmed control task in a two-level hierarchical system under conditions of uncertainty
20 p2541 A73-39034

Approximate methods for the mathematical description and analysis of processes controlling the spectral characteristics of random vector signals
20 p2542 A73-39047

A study of commensurable motion in the asteroid belt.
20 p2606 A73-39075

Celestial bodies gravitational potential mathematical representation by Lamé functions via series expansion of Laplace differential equation in ellipsoidal coordinates
20 p2606 A73-39080

Stability of periodic oscillations of stars.
20 p2606 A73-39081

Flow theoretical model for nonstationary creep in metals, using Galerkin method for approximate solution of boundary value problem
20 p2616 A73-39099

Numerical model of a two-phase stratiform cloud taking its microstructure into account
20 p2583 A73-39185

Application of information theory to the study of mechanical systems
20 p2592 A73-39260

Nonlinear model for plane unsteady flow resulting from collapse of homogeneous density region in heavy ideal density-stratified fluid
20 p2547 A73-39287

Improved relations in the dynamics of moderately thick shells and plates under the action of massive moving loads
20 p2618 A73-39316

Mathematical theory of nonlinear viscoelasticity
20 p2618 A73-39330

Resource exchange and allocation /a generalized thermodynamic approach/. I
20 p2629 A73-39349

Parametric sensitivity in the problem of control with reference to an incomplete model of the plant
20 p2542 A73-39350

Resource exchange and allocation /a generalized thermodynamic approach/. II
20 p2629 A73-39351

Discrete reproduction of a random parameter change process in standard automation equipment elements
20 p2543 A73-39393

Flutter-divergence transition criteria in certain viscoelastic polygenic systems.
20 p2623 A73-39556

Chapman-Enskog-Hilbert expansion for a Markovian model of the Boltzmann equation.
20 p2549 A73-39627

Natural fluctuations in linear quantum amplifiers.
20 p2574 A73-39699

A study of models of certain digital computer units with the aid of a digital computer
20 p2533 A73-39822

Mathematical equipment of a system of automatic designing of components of logic-type semiconductor integrated circuits
21 p2660 A73-40015

Physical modeling of active microcircuits for the SHF range
21 p2668 A73-40020

Continual mechanochemical model of muscular tissue
21 p2643 A73-40182

Probability distribution of electric fields in thermal and nonthermal plasmas.
21 p2744 A73-40216

Quantum theory of nonlinear optical processes with time-dependent pump amplitude and phase - Frequency conversion.
21 p2711 A73-40222

Maneuvering target motion modeling with binary random variable in state equation, obtaining optimal tracking solution as weighted combination of two Kalman filter estimates
21 p2649 A73-40331

Vibration tests with rotors as a rotor identification problem
21 p2707 A73-40395

Mathematical modeling of spinning elastic bodies for modal analysis.
21 p2784 A73-40421

Evaluation of various analytical models for buckling and vibration of stiffened shells.
21 p2784 A73-40424

Proposal of a new criterion for evaluating the adequacy of models
21 p2669 A73-40499

One dimensional model of electron-phonon system exhibiting Peierls instability for tetrathiofulvalene tetracyanoquinodimethane conductivity, considering

high temperature superconductivity achievement via Peierls instability suppression
21 p2751 A73-40508

Molecular crystals with behavior predictable by discrete quasi-continuous Cosserat model based on system of oriented Newtonian particles with six degrees of freedom
21 p2739 A73-40573

Mathematical model for ISIS satellite attitude and spin rate computerized predictions during electromagnetic torque control operation
21 p2781 A73-40615

The effect of magnetic mass on Alfvén waves.
21 p2701 A73-40624

Concentration and combination limits of heterogeneous ignition
21 p2791 A73-40704

Forced convection of a fluid inside an ellipsoidal cavity
21 p2791 A73-40740

One dimensional computer simulation model of spaced-receiver drift experiment with radio fading produced by reflections from perfectly reflecting ionosphere
21 p2684 A73-40783

The theory of the current-voltage characteristic of diodes fabricated out of compensated semiconductors
21 p2663 A73-40795

Russian monograph on linear signal system models covering steady state, variance and transducers of continuous and discrete signals and random and nonstationary estimates
21 p2669 A73-40798

Two phase alloy internal oxidation kinetics, deriving mathematical model with linear law for penetration velocity fluctuations
21 p2719 A73-40898

Distribution density of small lunar craters - Models and actual distribution
21 p2770 A73-40915

The quantity of initial-parameter information contained in trajectory measurements
21 p2726 A73-40916

Selection of an optimal structure for a tabular model of a control plant
21 p2670 A73-40995

Evaluation of burst error correcting codes using a simple partitioned Markov chain model.
21 p2656 A73-41168

Visually perceived motion in depth resulting from proximal changes. I, II.
21 p2640 A73-41186

Convective heat transfer with allowance for three-dimensional heat sources in the fluid for turbulent flow in a plane slit
21 p2792 A73-41196

Electric connector reliability assessment model based on operating conditions and failure modes analysis without using MTBF
21 p2665 A73-41208

Russian book on statistical properties of ionosphere reflected signals covering statistical modeling, random processes, perturbation method and wave reflection problems
21 p2637 A73-41284

The influence of laser ranging on seismologic control.
21 p2774 A73-41408

Russian book on probabilistic computer simulation and statistical processing techniques covering linear algebra and partial differential equations, Markov chains, random numbers, automata, and analog modeling
21 p2659 A73-41432

Statistical model for phase relations derived from observations of photospheric oscillations, criticizing horizontal propagation theory for phase propagation
21 p2777 A73-41482

Eddies development downstream a pipe orifice.
22 p2840 A73-41738

Mathematics of interaction between blood and electromagnetic fields.
22 p2802 A73-41788

The coupling of high frequency electromagnetic energy into large systems.
22 p2822 A73-41792

Straight wire monopole and dipole antenna near field coupling characteristics prediction, deriving mathematical model by method of moments for computerized analysis
22 p2823 A73-41798

Radio receiver intermodulation characteristics description by generic model, discussing frequency/distance separation criteria to avoid interference, signal measurement procedure and application to equipment standards
22 p2823 A73-41801

Mathematical model of human pitch perception based on acoustic stimulus Fourier transformation by sense organ into peripheral neural activity pattern recognition
22 p2811 A73-41816

Random vibration of distributed systems strongly coupled at discrete points.
22 p2918 A73-41820

- Russian book on scale selection in modeling for analog and digital computers covering similarity theory, error formation, accuracy optimization, etc 22 p2829 A73-41883
- Computer model of Ba ion cloud expansion in magnetosphere, taking into account self-consistent electric and magnetic field interactions 22 p2846 A73-41938
- A new conceptual model for components in measurement/control systems - Practical application to thermocouples. 22 p2859 A73-42050
- Gradient methods for extremum solutions of two-point boundary value problems of dynamics. [ASME PAPER 73-DET-44] 22 p2916 A73-42069
- Transient response simulation model for stability analysis of flexible high speed rotor-bearing system dynamics, examining nonlinear effects [ASME PAPER 73-DET-102] 22 p2865 A73-42079
- Application of strip model to crack tip resistance and crack closure phenomena. 22 p2875 A73-42132
- Safety margins in the implementation of planetary quarantine requirements. 22 p2803 A73-42161
- Compartmental analysis of biological system with a digital computer. 22 p2829 A73-42228
- Thermal conductivity of low density carbon. [ECTP PAPER C-5] 22 p2881 A73-42404
- Gravitational energy quantization model of noncharged particle based on proposed centrosymmetric metric with nonzero Einstein matter tensor and without Schwarzschild singularity 22 p2887 A73-42430
- Nonsingular unified field model for charged particle described by interrelation of gravitational mass, global energy and effective charge, considering comparison with Reissner metric 22 p2887 A73-42432
- Molecular collisions. XIX - The distorted wave approximation to atom-rigid symmetric top rotational excitation. 22 p2889 A73-42445
- Comparison of a suggested polynomial method with the method of F. M. Perelman in the calculation of the solidus surface of the W-Ta-Mo-Nb system 22 p2877 A73-42456
- Rarefied-gas heat transfer in Knudsen layer using ellipsoidal model. 22 p2932 A73-42471
- Rotational relaxation effects in short-pulse CO₂ amplifiers. 22 p2870 A73-42520
- Resonant oscillations of intermediate frequency in a stratified atmosphere. 22 p2848 A73-42539
- Diurnal thermospheric and ionospheric variations from time dependent continuity equations for O⁺, H⁺, O₂⁺, and NO⁺ ions, motion and heat conduction equations 22 p2849 A73-42572
- Application of stochastic programming methods for solving certain optimization problems of multiple-link plants without memory 22 p2836 A73-42612
- Iteration methods for identification of multiple-link controlled plants for self-adaptation purposes 22 p2836 A73-42617
- German monograph - Model of a parallel shock wave with turbulent dissipation in a hot plasma. 22 p2895 A73-42718
- French monograph - On the representation of linear dynamic systems with distributed parameters and its application to the study of intrinsic properties of these systems. 22 p2837 A73-42746
- An analytical and experimental investigation of gravity effects upon laminar gas jet-diffusion flames. 22 p2933 A73-42775
- Stirring factors in combustion chambers - A finite-element model of mixing along an 'information flow path.' 22 p2934 A73-42784
- A computer model for three-dimensional flow in furnaces. 22 p2934 A73-42787
- Mathematical modeling of combustors based on turbulent mixing, droplet evaporation and chemical kinetics, considering stirred reactor heat balance and combustor performance prediction 22 p2935 A73-42789
- Breakup of liquid drops due to convective flow in shocked sprays. 22 p2937 A73-42819
- Recursive methods in photogrammetric data reduction. 22 p2862 A73-42825
- German monograph - Principles concerning proofs regarding optimality conditions in the case of time-dependent processes. 22 p2888 A73-42853
- Runway configuration improvement programming model. [ASCE PREPRINT 2034] 22 p2839 A73-42864
- Use of simulation in airport planning and design. [ASCE PREPRINT 2038] 22 p2839 A73-42865
- GASP simulation of terminal air traffic system. [ASCE PREPRINT 2059] 22 p2839 A73-42868
- Noise reduction by enclosures to block airborne and structure-borne acoustic paths, developing models for insertion loss in different frequency ranges 22 p2888 A73-42924
- Convergent stable three-time level implicit numerical model for phase change problems, evaluating temperature dependent coefficients of parabolic equations at intermediate level 22 p2937 A73-42951
- Reliability of some redundant systems with repair. 22 p2867 A73-42968
- Ultrashort pulses from mode-locked cw dye lasers. 22 p2871 A73-43079
- Mathematical model of collateral blood vessels caliber changes due to hydrodynamic drag /shear stress/ effects on vascular endothelium 22 p2817 A73-43105
- Three-dimensional analytical model of electron density distribution of the quiet ionosphere. 22 p2970 A73-43232
- Oscillations of the earth's magnetic tail in the approximation of quasi-hydrodynamics. 22 p2970 A73-43244
- Spherical harmonic analysis of the geomagnetic field for the 1965 epoch up to n = 23 according to ground-based data. II - Results. 22 p2971 A73-43250
- Cosmos 321 geomagnetic measurement data for construction of satellite geomagnetic survey and geomagnetic field models 22 p2971 A73-43259
- Mathematical model of spacecraft onboard digital guidance computer under data acquisition conditions, using imbedded Markov chains 22 p2955 A73-43261
- Certain algorithmic aspects of flight dynamics simulation on digital computers 22 p3038 A73-43262
- Game theory mathematical model for optimal control of glide modes in conflict situation 22 p2999 A73-43263
- Real-time identification using adaptive discrete model. 22 p2962 A73-43286
- Design of discrete model reference adaptive systems using the positivity concept. 22 p2962 A73-43287
- Design of multivariable adaptive model following control systems. 22 p2962 A73-43288
- The prediction of the performance of variable geometry free gas turbines. 22 p3019 A73-43297
- A model of the dynamic behavior of the coaxial-flow gaseous-core nuclear reactor. 22 p3005 A73-43387
- Oil hydraulic fluidic amplifier mathematical model and computerized design for power consumption optimization at high pressures, testing performance dependence on viscosity 22 p2942 A73-43405
- An approximate model of a separated turbulent flow in an abruptly widening channel 22 p2968 A73-43471
- High energy nucleon inelastic interaction characteristics calculated from artificial event model based on covariant statistical theory of multiple generation of particles 22 p3022 A73-43542
- Multiperipherism and Landau hydrodynamic models of multiple particle collision processes with inhomogeneous and homogeneous energy liberation spaces 22 p3008 A73-43543
- Extensive air showers and nuclear interaction characteristics at superhigh energies 22 p3022 A73-43551
- Calculated characteristics of the electron and muon components of extensive air showers at the 690 g/sq cm level 22 p3022 A73-43553
- Multidimensional scaling methods and data visualization /Review/ 22 p2949 A73-43578
- On the interaction between the zonal mean flow and equatorial waves excited by diabatic heat sources at 20 deg latitude. 22 p3001 A73-43587
- Large amplitude baroclinic waves generation via instabilities of two layer fluid in rapidly rotating cylinder compared with mathematical model based on quasigeostrophic equations 22 p3001 A73-43590
- Mean Reynolds stress tensor model for analytical prediction of turbulence structure of density-stratified atmospheric boundary layer 22 p3002 A73-43592
- Mathematical model for temperature inversion rise velocity under penetrative free surface convection based on unstable atmospheric boundary layer environment 22 p3002 A73-43595
- Role of constraining forces for ultrarelativistic particle motion as a source of gravitational radiation. 22 p3006 A73-43606
- Investigation of the dynamics of plasma flows in the field of a pulsed magnetic barrier 22 p3010 A73-43658
- A computational study of the diffusion of meteor trains using a self-consistent model for the space-charge electric field. 22 p3029 A73-43684
- Classification of methods for solving the direct problem of axisymmetric flow calculation in turboengines 22 p3020 A73-43736
- Gravitational fields calculation in three dimensional mass distribution galaxies, using biorthogonal functions with ultraspherical polynomials 22 p3030 A73-43749
- Use of space techniques for the determination and monitoring of climate parameters and air contaminants 22 p3003 A73-43780
- Comparative studies of model reference adaptive control systems. 22 p2963 A73-43817
- Experimental bases and models for the study of the overall behavior of metals 22 p2993 A73-43964
- Gilbert burst noise model for statistical analysis of nonindependent errors in digital data transmission systems, noting performance and utility in communication theory 22 p2954 A73-43986
- A physical-numerical model for the determination of the meteorological environmental effects produced by cooling towers 22 p3003 A73-43995
- Mixed finite element models for nonlinear thermomechanical responses of continuous dissipative media based on Oden variational principle and theory of thermoplastically simple materials 22 p3044 A73-44049
- Electrical field distribution in the human body. 22 p2950 A73-44216
- A model for estimating joint probabilities of cloud-free lines-of-sight through the atmosphere. 22 p3004 A73-44260
- Existence of stable relative equilibria for an artificial satellite in a model magnetic field. 22 p3081 A73-44481
- Analytical relations of physicochemical, strength and geometrical factors in formation of high strength monolithic glass fiber reinforced structures 22 p3103 A73-44533
- A method for the approximation of processes in homogeneous biological structures 22 p3062 A73-44663
- Optimal macroscopic control and resource exchange model for open market-like systems in economic and thermodynamic terms 22 p3154 A73-44665
- Piecewise-one-dimensional models of supersonic combustion and pseudoshock in a channel 22 p3154 A73-44702
- Equations of linear elastic theory of thin shells based on model of anisotropic Cosserat surface 22 p3147 A73-44744
- Allowance for electron degeneration in a pseudopotential model of a nonideal plasma 22 p3115 A73-44759
- Supersonic jet noise generated by large scale disturbances. [AIAA PAPER 73-992] 22 p3077 A73-44827
- Mathematical model for physical space transformation into subjective field metric for monocular vision 22 p3064 A73-44906
- A mathematical model for controlled image contour sharpness enhancement 22 p3064 A73-44907
- Fundamentals of the theory of plastic flow in discretized bodies 22 p3110 A73-44917
- Line of symmetry for the classical equation of state. 22 p3110 A73-44987
- A mathematical model of real signal spectra 22 p3068 A73-45005
- Numerical experiments on the steady-state meridional structure and ozone distribution in the stratosphere. 22 p3085 A73-45017
- Design criteria for finite-difference models for eddy diffusion with winds that guarantee stability, mass conservation, and nonnegative masses. 22 p3085 A73-45018
- Frequency methods for simulation, analysis and identification of multiply-connected dynamic systems with delay 22 p3074 A73-45097
- On the hybrid stress finite element model for incremental analysis of large deflection problems. 22 p3151 A73-45303

- Development of a mathematical model for vortex configuration in jets and flames. 24 p3157 A73-45376
- Kinetic models and the problem of shock-wave structure 24 p3081 A73-45537
- MATHEMATICAL STATISTICS**
U STATISTICAL ANALYSIS
MATHEMATICAL TABLES
 Improved sixth-order Runge-Kutta formulas and approximate continuous solution of ordinary differential equations. 02 p0188 A73-12822
- Best linear unbiased estimator of the parameter of the Rayleigh distribution. I - Small sample theory for censored order statistics. 09 p1112 A73-22645
- A new method for studying the symmetry reduction of a system by means of a perturbation 11 p1326 A73-25867
- Computer checking of rotational line intensity factors for diatomic transitions. 21 p2744 A73-41212
- Geodetic net optimal design with known configuration matrix, basin, approach on calculus of inverse matrices 22 p2847 A73-42496
- MATHIEU EQUATION**
U MATHIEU FUNCTION
MATHIEU FUNCTION
 Free flexural vibrations of elliptical thin plate with free edge, calculating mode shapes and frequencies by use of Mathieu function 22 p2918 A73-41822
- Mathieu function eigenvalue computation based on Algol program, using Fourier series, Bessel functions, wave equations and elliptic domains 23 p2998 A73-43209
- MATRICES [CIRCUITS]**
 Photodetector array for a holographic optical memory system. 02 p0169 A73-12163
- Description and utilization of the TMS 4062 dynamic memory 05 p0553 A73-16171
- Photodetector matrix circuit for holographic memory converting optical bits into electrical signals 09 p1086 A73-23074
- Cutpoint cellular switching array synthesis by combined cascade simplification rule, noting algorithm efficiency increase 09 p1065 A73-23101
- Satellite-borne programmable communications distribution subsystem, controlling microwave switch matrix by ground command via onboard memory for traffic flow data 09 p1053 A73-23364
- Visible and infrared sensor arrays for imaging systems. 10 p1216 A73-23787
- Standard flexible LSI logic cell arrays with uniform interconnections as fourth generation computer components, discussing microprograms and algorithms for arithmetic operations 10 p1198 A73-24017
- Butler submatrix feed systems for beam forming and scanning networks of linear and circular antenna arrays 11 p1338 A73-25671
- Checkpoint and failure diagnostics of an incompletely homogeneous two-dimensional structure 12 p1482 A73-26754
- Digital computer graphic data feeder with electric pulsed-voltage coordinate matrix and readout probe sensor for input data code coordinate selection 12 p1475 A73-26779
- Acoustical hologram recording by electrostatic transducers using rigid backplate electrode insulated with thin dielectric film transparent to ultrasonic radiation 13 p1614 A73-28584
- Matrix, pyramid and rectangular decoder reliability and operational probability during short circuit/cut-off failures 14 p1736 A73-30566
- Fast random access permanent storage read only optical memory, using light emitting diode matrix addressing, semiconductor laser and holographic lens system 16 p2012 A73-32870
- Broad X band multichannel waveguide matrix for high speed switching from one input to one of four outputs at high power levels 16 p1990 A73-33897
- Experimental use of self-scanned photodiode arrays in astronomy. 17 p2169 A73-35287
- Complementary MOS/silicon on sapphire LSI technology for high speed digital multiplier and correlator logical building blocks design, fabrication and subsystem array implementations 17 p2140 A73-35318

- Design guidelines for 180-degree hybrid type multiple beam phased array forming networks with different element numbers and configurations 21 p2669 A73-40670
- Rapid-switching, broadband 1:4 WG switch matrix. II. 22 p2834 A73-42874
- Cellular dynamic memory array with reduced data-access time. 23 p2956 A73-44116
- MATRICES [MATHEMATICS]**
NT ADJOINTS
NT CANONICAL FORMS
NT EIGENVALUES
NT EIGENVECTORS
NT JORDAN FORM
NT STIFFNESS MATRIX
 Electronic computer design and programming for solving high order linear equations, using matrix determinants and graph trees in letter symbols 01 p0019 A73-10033
- Rational and irrational matrix functions for analysis and synthesis of distributed microwave networks with multiwire lines and lumped nonreactive elements 01 p0027 A73-10578
- Equations for matrix elements in Euclidean quantum electrodynamics 01 p0076 A73-10621
- Doubly relaxed matrix inverse for linear equations system solution with inadequately conditioned coefficient matrices, noting algorithm for improved conditioning 01 p0071 A73-11279
- The range of solutions in the case of optimization problems with parameters in the coefficients of the matrix of the linear restriction conditions 02 p0186 A73-11590
- Nodal admittance matrix method for first and second derivative network sensitivity, noting applicability to network analysis at discrete frequencies 03 p0286 A73-14000
- The solution of linear, constant-coefficient, ordinary differential equations with APL. 04 p0470 A73-15008
- Note on symmetric decomposition of some special symmetric matrices. 04 p0470 A73-15014
- A state covariance matrix computation algorithm for satellite orbit determination sequential filtering. 04 p0431 A73-15267
- Muller matrix derivation for microwave light modulation studies in quasi-homogeneous magneto-optical and electro-optical media, taking into account finite light speed 04 p0459 A73-15923
- Study of modeling of substructure damping matrices. [SAE PAPER 720813] 05 p0634 A73-16645
- Computational variants of the Lanczos method for the eigenproblem. 06 p0716 A73-17984
- Transfer matrices determination for two terminal pair network derived from four terminal pair network, considering bandpass filter circuit design 06 p0677 A73-18397
- Multistep methods with variable matrix coefficients. 06 p0718 A73-18409
- Matrix exponential series approach to distributed parameter systems. 06 p0719 A73-18803
- Matrices, polynomials, and linear time-invariant systems. 06 p0719 A73-18863
- A boundary layer method for the matrix Riccati equation. 06 p0719 A73-18864
- The determination of state-space representations for linear multivariable systems. 07 p0804 A73-19131
- Automated generation and condensation of large mass- and rigidity-matrices 07 p0909 A73-19175
- Stiffness matrix formulation and eigenvalue analysis for high order shallow shell finite element of rectangular plan 07 p0916 A73-20439
- Matrix operator theory of radiative transfer for Rayleigh scattering and radiance calculation of multilayered atmospheres with large optical depths 08 p0958 A73-21040
- Covariance matrices and means of atmospheric Planck function profiles for application to temperature sounding from satellite measurements. 08 p0967 A73-21385
- Use of matrix eigenvalues in the synthesis of symmetrical two terminal pair networks 08 p0947 A73-21397
- Numerical formulation for constant-gain chemical laser calculations. 08 p0975 A73-21411
- Mean vector and covariance matrix estimation for training class sample statistics updating in pattern recognition, applying to crops or any category of objects 08 p0984 A73-21668

- Computerized precession and nutation matrix calculations of rectangular equatorial coordinates with longitude and inclination allowance for radar data processing 09 p1142 A73-22092
- Simple iterative method for determining the eigenvalues of a Hermitian /real-symmetrical/ pair of matrices 09 p1111 A73-22107
- Recursive methods in on-line computer photogrammetric data reduction deriving algorithms for fixed and variable parameter numbers cases with matrix partitioning 09 p1059 A73-22381
- FORTAN IV program and recursive matrix partitioning algorithm for solution of photogrammetric simultaneous equations, noting computation time 09 p1059 A73-22382
- Matrix Riccati differential and quadratic algebraic equations in optimal control and filtering theory, discussing stabilizing solutions, asymptotic properties and computational techniques 09 p1069 A73-23102
- Model reduction of multivariable control systems by means of matrix continued fractions. 10 p1200 A73-24046
- The algorithms of accuracy research of nonstationary linear systems with continuous and discrete elements. 10 p1200 A73-24048
- Feedback control system transfer function matrix synthesis, determining design specifications for required compensation filters from compatibility conditions 10 p1200 A73-24049
- Estimation of noise covariance matrices for a linear time-varying stochastic process. 10 p1201 A73-24053
- Order determination and parameter identification of time-invariant state variable models. 10 p1201 A73-24054
- Matrix eigenvalue search algorithms of Rutishauser-Francis type, showing relationship to linear group decompositions 10 p1243 A73-24124
- Canonical form of hybrid matrix for linear multiple network circuit, discussing synthesis and analysis 10 p1195 A73-24378
- Irreducible canonical realizations from external data sequences. 11 p1390 A73-25191
- Multiinput multioutput linear time invariant discrete system optimal approximation, noting algorithms and weighting matrices computational difficulties 11 p1390 A73-25192
- Application of nonalgebraic digital machines in modeling differential equations 11 p1334 A73-25633
- Calculation of the y-parameters of an integrated-circuit amplifier by reducing the matrix of an n-terminal network to the matrix of a two terminal pair network 11 p1338 A73-26102
- Shear stress and deformation inclusion in elastic plate bending finite element theory, discussing stiffness matrix improvement for thin shells 11 p1447 A73-26651
- Second order approximation to autocorrelation matrix of random variable nonlinear transformation, discussing application to Poisson process and monopulse radar receiver AGC effects 11 p1333 A73-26695
- Calculation of eigenvalues and eigenvectors of normal matrix couples with the aid of Ritz iteration 11 p1392 A73-26726
- Stability of nonlinear systems with a transformed argument 12 p1524 A73-27416
- Formulation of time variant stiffness matrices due to changing joint properties. 12 p1555 A73-27737
- Applications of vector and parallel computers to radar defense systems. [AIAA PAPER 73-428] 12 p1476 A73-27822
- Finite element method for solution of Laplace or wave equation in cylindrical coordinates through base matrices, applying to electromagnetic wave propagation in waveguides 13 p1581 A73-28077
- Effective use of the incremental stiffness matrices in nonlinear geometric analysis. 13 p1694 A73-28252
- Maximal finite groups of $n \times n$ integral matrices and complete groups of integral automorphisms of positive quadratic forms /Bravias types/ 13 p1648 A73-28342
- Spectral analysis of a physical system which can be represented by a stationary linear active electronic network 13 p1589 A73-28474
- Algorithms for finding the coefficients of polynomials of matrix determinants 13 p1587 A73-28864
- Least squares and non-linear functions. 13 p1619 A73-29241

- Kalman filtering of systems with parameter uncertainties - A survey. 13 p1597 A73-29569
- State space approach to mixed boundary value problems. 13 p1651 A73-29571
- Polarization cascade matrix describing arbitrary elliptically polarized microwave transmission through inclined grating of parallel wires 13 p1587 A73-29669
- Matrix analysis of linear antenna arrays of equally spaced elements. 14 p1735 A73-30226
- Zero-solution stability in systems of partial differential equations 14 p1768 A73-30248
- Nonlinear vector matrix differential equations for automatic control systems dynamics, discussing stability, dissipativity and convergence 14 p1768 A73-30344
- Boundary value problem of a system of ordinary differential equations with a complex parameter 14 p1768 A73-30346
- A minimization algorithm for the design of linear multivariable systems. 14 p1769 A73-30504
- Boundary value problem of linear conjugation with a piecewise-continuous matrix coefficient 15 p1900 A73-32104
- Russian book - Design and calculation of microwave stripline elements. 15 p1852 A73-32295
- Implementation of simultaneous iteration for vibration analysis. 16 p2075 A73-32788
- Active networks state equations with singular A matrix, considering algebraic method of reduction to equivalent set of equations with nonsingular A matrix. 16 p1992 A73-32912
- An algebraic method for linear dynamical systems with stationary excitations. 16 p2076 A73-32919
- Computational efficiency comparison for discrete linear filtering Kalman algorithms and information matrix methods, noting Householder square-root implementation identity with Potter technique 16 p2032 A73-33404
- Frequency analysis of calculated ionospheric reflection coefficients. 16 p1984 A73-33920
- On the solution of large systems of linear algebraic equations with sparse, positive definite matrices. 17 p2199 A73-34104
- Isoparametric element forms in finite element analysis. 17 p2245 A73-34834
- Helicopter engineering applications of antiresonance theory, showing eigenvalue nature and matrix iteration determination of antiresonances [AHS PREPRINT 736] 17 p2105 A73-35072
- A generalization of the additive correction methods for the iterative solution of matrix equations. 17 p2203 A73-35729
- Matrix method for the determination of the elastic and mechanical properties of reinforced plastics 18 p2327 A73-36475
- Design of decoupled multivariable control systems. 19 p2412 A73-38032
- Derivation of aggregation matrices for simplified models of linear dynamic systems and their applications for optimal control. 19 p2413 A73-38053
- Output feedback for linear multivariable systems with parameter uncertainty. 19 p2413 A73-38061
- The properties of bond graph junction structure matrices. 19 p2460 A73-38083
- Differential equations modelled on nonalgorithmic digital computers. 19 p2408 A73-38144
- A computational technique for the efficient handling of large matrices. 19 p2445 A73-38191
- Optimum windings for linear induction machines. 19 p2389 A73-38312
- Use of the eigenvalues of a matrix to synthesize symmetrical four-terminal networks. 19 p2415 A73-38355
- Algebraic algorithm for positive realness of real rational functions and matrices relative to unit circle in complex plane, determining real polynomial zeros distribution 19 p2446 A73-38488
- Probabilistic automata minimization for system states reduction by deterministic matrix method 19 p2408 A73-38564
- Study of methods of computing transition matrices [Computer-program description]. 20 p2532 A73-39129
- Construction of a transformation matrix and the differentiability of the formal solution of a system of partial differential equations 20 p2582 A73-39475
- A numerical method in the analytic dynamics of gyrocompasses 20 p2566 A73-39499
- Digital computer simulation program for North Atlantic hybrid navigation systems configurations, using covariance matrix error analysis for planned increase of commercial air traffic capacity 21 p2733 A73-40028
- A practical means of calculating normal forms in problems involving nonlinear oscillations 21 p2738 A73-40178
- Laser transient behavior analysis by quantum theory, obtaining density matrix equation solution in terms of exponentially decaying eigenmodes by truncation method 21 p2711 A73-40214
- A conservative bound on the estimation error covariance matrix in the presence of correlated driving noise and correlated discrete measurement noise. 21 p2724 A73-40295
- A note on pairs of matrices and matrices of monotone kind. 21 p2725 A73-40377
- Linear Kalman filter triangular square root formulation guaranteeing positive covariance matrix, computation and time savings and core storage requirement standardization 21 p2736 A73-40422
- Flexibility matrix coefficients for disk loading under sinusoidal edge loading tabulation and derivation to accommodate boundary conditions 21 p2784 A73-40434
- Polarization phenomena in multiphoton ionization of atoms. 21 p2743 A73-40468
- Conditions of existence of steady representations for discrete linear systems given in terms of unsteady representations 21 p2669 A73-40497
- Linear optimization theory, discussing duality theory, matrix calculations, simplex methods, base points, classical transport problems and industrial production applications 21 p2727 A73-41071
- Speech scrambling by the matrixing of amplitude samples. 21 p2657 A73-41206
- Method of analyzing electronic circuits on the basis of a hybrid-parameter matrix in a canonical system of coordinates 21 p2670 A73-41306
- Algorithm for deriving the equilibrium equations of an electric circuit on the basis of logic rules 21 p2670 A73-41307
- Computer analysis of mixed coordinate base transistor circuits determining matrix numbers without main path or generalized node delineation 21 p2670 A73-41308
- Near fields of wire antennas by matrix methods. 22 p2830 A73-41827
- Analysis and design of circular antenna arrays by matrix methods. 22 p2830 A73-41828
- Inversion techniques for remote sensing of atmospheric temperature profiles. 22 p2883 A73-42056
- Transition probability matrix method for calculating residence times of moving particles in region of space, determining stratosphere residence time against exit to tropopause 22 p2849 A73-42543
- Recursive methods in photogrammetric data reduction. 22 p2862 A73-42825
- Numerical solution of electromagnetic scattering problems. 22 p2827 A73-42841
- German monograph - The computation of periodic motions of multipath nonlinear systems. 22 p2888 A73-42854
- An optimality condition for assessing systematic error 23 p2999 A73-43264
- Standard sensitivity and covariance matrices for statistical estimation of overall performance. 23 p2962 A73-43279
- A simplified minimal-realization algorithm for a symmetric transfer-function matrix. 23 p2999 A73-43382
- Atmospheric oscillations. V - The propagator matrix and the transmission of an electrostatic potential along the geomagnetic field lines. 23 p2971 A73-43686
- Matrix method evaluating an internal radiation field in a plane-parallel atmosphere. 23 p3030 A73-43754
- State-space matrix rank test in locating zeros of linear multivariable systems, noting application to feedforward regulators 23 p2964 A73-43828
- The recursive generation, differentiation, and integration of Hermite interpolation polynomials together with an example concerning the application of the method 23 p3044 A73-44048
- Frequency to time domain sensitivity matrix for equivalent tolerance field and response error evaluation, using Fourier transform 23 p2955 A73-44114
- Unboundedness of solutions and comparison theorems for time-dependent quasilinear differential matrix inequalities. 23 p3000 A73-44202
- Microphone radiated acoustic power directivity measurement enhancement by integral transform, matrix inversion and relaxation techniques, considering application limits, resolution, noise sensitivity and computation [AIAA PAPER 73-1040] 24 p3090 A73-44865
- Vector wave field hologram generation via polarization contrast method, described by correlation matrix formalism 24 p3091 A73-44957
- Effect of unity-rank feedback on the transfer-function matrix of a multivariable system. 24 p3075 A73-45263
- Time-varying network analysis via matrix manipulation and Peano-Baker solution for second and higher order differential equations with periodic coefficients 24 p3075 A73-45477
- ## MATRIX ALGEBRA
- ### U MATRICES [MATHEMATICS]
- ## MATRIX ANALYSIS
- ### U MATRICES [MATHEMATICS]
- ## MATRIX METHODS
- Some problems in the substantiation and application of discrete large-element design schemes for complex zero-moment shells 02 p0230 A73-11716
- Matrix analysis of local instability in plates, stiffened panels and columns. 03 p0390 A73-13339
- Computer method for analysis of multistory structures. 03 p0391 A73-13683
- Computerized multiple level substructuring analysis. 03 p0392 A73-13690
- A strain energy basis for studies of element stiffness matrices. 03 p0395 A73-14184
- Finite elements for axisymmetric solids under arbitrary loadings with nodes on origin. 03 p0395 A73-14192
- Flexibility matrix derived and applied to finite element production for thin walled open tubes under torsion, taking into account warping constraints 03 p0395 A73-14470
- Some crack tip finite elements for plane elasticity. 04 p0506 A73-14683
- Matrix displacement analysis of shells and plates including transverse shear strain effects. 04 p0509 A73-15005
- Hypermatrix solution of large sets of symmetric positive-definite linear equations. 04 p0470 A73-15009
- On the application of the SHEBA shell element. 04 p0510 A73-15016
- Book - Non-linear structures: Matrix methods of analysis and design by computers. 05 p0632 A73-16358
- Use of associated matrices in deriving frequency equations for rods with variable rigidities and masses. 05 p0636 A73-17082
- Constant curvature beam finite elements for in-plane vibration. 05 p0637 A73-17371
- Uniqueness of non-linear elastic equilibrium for prescribed boundary displacements and sufficiently small strains. 06 p0719 A73-18700
- Comparison between sparse stiffness matrix and sub-structure methods. 07 p0907 A73-19031
- FORTAN sequence with economical computer storage requirement for matrix method application to rigid plastic collapse analysis of frame, considering bounded variable problem 07 p0907 A73-19034
- Stiffness matrix for a beam with an axial force. 08 p1015 A73-20725
- Derivatives of eigenvalues and eigenvectors in non-self-adjoint systems. 08 p0983 A73-20728
- Elastoplastic analysis by matrix displacement or finite element method, presenting various direct and iterative solution techniques 08 p1016 A73-20776
- Velocity ratio in the analysis of linear dynamical systems. 08 p0988 A73-21467
- The application of nodal stress concepts to the bending of plates and shells. 08 p1019 A73-21691
- Axisymmetric triangular finite elements for the scalar Helmholtz equation. 09 p1120 A73-22392
- Influence of Poisson's ratio on the condition of the finite element stiffness matrix. 09 p1160 A73-22892

Solution of quadratic matrix equations for free vibration analysis of structures.

10 p1290 A73-24299

Aeroelastic structural weight optimization under strength and flutter constraints, using finite element and displacement methods to describe equations of motion in matrix form.

[AIAA PAPER 73-389]

11 p1439 A73-25518

The free vibrations of a thin circular rotating cylinder.

11 p1443 A73-26088

Dynamic stiffness matrix method for determining natural frequencies of plane frame with axially loaded Timoshenko members of uniform mass distribution

11 p1446 A73-26494

Contribution to the theory of the finite element method applied to the overall stress analysis of a fuselage

12 p1551 A73-27084

Book - Introductory structural analysis with matrix methods.

12 p1554 A73-27548

First-exursion probability in non-stationary random vibration.

13 p1691 A73-28064

Dynamic structural response analysis with eigenvalue problem solution in terms of stiffness and mass matrices, discussing algorithm selection for efficient computation

13 p1691 A73-28081

On further application of the finite element method to three-dimensional elastic analysis.

13 p1693 A73-28241

Finite element matrix formulation of post-buckling stability and imperfection sensitivity.

13 p1694 A73-28253

German book - Elastostatics and elastokinetics in matrix notation: The procedure of transmission matrices.

13 p1695 A73-28300

Effects of polarization on the transmission of coude-spectrometer systems.

13 p1621 A73-29351

Matrix method analysis of stiffened plates free vibrations, deriving governing equation in stiffness matrix form by combining plane stress theory and lateral vibration equation

14 p1807 A73-30186

Automatic nodal point renumbering algorithm for interconnectivity matrix bandwidth reduction in computer aided structural analysis and design

15 p1848 A73-32029

Characteristic matrix method for automatic recognition and extraction of rigid body modes from inconsistent to natural force-deformation relationship of stress and strain elements

16 p2077 A73-32990

The analysis of three dimensional problems of elasticity by integral representation of displacement.

16 p2078 A73-33003

A variational approach to grid optimization in the finite element method.

16 p2079 A73-33010

Matrix theory algorithms for static stresses and elastic deformations in truss structures, deriving equilibrium equations in terms of forces, deformations and node displacements

16 p2080 A73-33258

Matrix analysis of multilayered and sandwich shells by the finite element method

16 p2083 A73-33968

A comparison of structural test results with predictions of finite element analysis.

[SAE PAPER 730340]

17 p2102 A73-34691

Vibration analysis of finite element systems.

17 p2245 A73-34837

Instability analysis using the incremental stiffness matrices.

17 p2245 A73-34838

Micromechanic stresses in photoelastic composite coupons.

[SESA PAPER 2175A]

17 p2251 A73-35456

Book - Computer methods in structural analysis.

17 p2251 A73-35473

A new finite element method for analysing symmetrically loaded thin shells of revolution.

17 p2252 A73-35601

Stiffness matrix displacement analysis via curved elements for plane stress and thin plate bending problems

17 p2252 A73-35606

Program of computation of spectral and modal matrices associated with a linear elastic system

18 p2364 A73-36493

On the flexural vibration frequencies of statically loaded beams.

18 p2367 A73-37091

Matrix formulation of reliability analysis and reliability-based design.

19 p2496 A73-37479

Calculation of the eigenfrequencies for a shaft/bearing system with the aid of transfer matrices

19 p2433 A73-37548

Bounds on the spectral and maximum norms of the finite element stiffness, flexibility and mass matrices.

19 p2500 A73-38110

On a formulation of the bending of elastic plates.

19 p2500 A73-38112

Optimum windings for linear induction machines.

19 p2389 A73-38312

Curved twisted space beam elements, expressing displacement function and inertia property by rotation and mass matrices

20 p2621 A73-39533

Sylvester matrix equation analysis of rigidly connected beam gridworks with weak regularity and translational properties, considering iterative and eigenvalue-eigenvector solutions

20 p2621 A73-39534

Some results of fuselage calculations on a digital computer by the finite-element method

21 p2783 A73-40387

Application of the method of integrating matrices to the calculation of the natural vibrations of a propeller blade with allowance for deflection in two planes and for torsion

21 p2783 A73-40389

Russian book - Matrix methods of calculating the strength of low-aspect-ratio wings.

21 p2785 A73-40799

Application of R-functions to a calculation of the dynamic stability of plates with a complex planform geometry

21 p2786 A73-40984

Specific problems of the dynamics of composite systems

21 p2788 A73-41603

State-change equations relating generalized load increment to response of constraint connected bars, deriving compatibility and equilibrium equations and matrix coefficients

21 p2788 A73-41604

Reduction of the degrees of freedom in solving dynamic problems by the finite element method.

22 p2922 A73-42479

Accelerating the convergence of elastic-plastic stress analysis.

22 p2922 A73-42481

Introduction of shear deformations into a thin plate displacement formulation.

22 p2923 A73-42559

Forced motion of lumped mass systems including the effect of axial force.

22 p2923 A73-42630

Matrix methods application to stress in elastic structures, examining Mohr circles, design implications and orthogonality anisotropy

22 p2929 A73-43173

On the computation of natural modes of an unsupported vibrating structure by simultaneous iteration.

23 p3042 A73-43801

Numerical calculation of simply supported cylindrical shells of arbitrary cross section

23 p3046 A73-44192

Structural analysis for idealized nonlinear material behavior.

24 p3152 A73-45316

MATRIX STRESS CALCULATION

U MATRIX METHODS

MATRIX THEORY

Matrix transformations for spacecraft attitude determination.

02 p0228 A73-11905

Asymptotic estimates for solutions of linear systems of ordinary differential equations having multiple characteristic roots.

02 p0188 A73-12625

Variational aspects of oscillation phenomena for higher order differential equations.

[AD-758575]

02 p0188 A73-12823

Matrix method for direct reduction of astronomical X ray spectral data, taking into account detector resolution and fluorescent escape phenomena effects

03 p0361 A73-13366

A discussion of the Marsh matrix technique applied to fluid flow problems.

03 p0244 A73-13563

Matrix method for canonical transformations in many body problem of celestial mechanics

03 p0379 A73-14587

Modification methods for inverting matrices and solving systems of linear algebraic equations.

05 p0590 A73-16373

Monotonicity and iterative approximations involving rectangular matrices.

05 p0590 A73-16374

Elimination on sparse symmetric systems of a special structure.

05 p0590 A73-16500

Classical minimization procedure without iteration for digital computation of generalized inverse of rectangular matrix with real or complex coefficients

05 p0590 A73-16581

A solution of the bilinear matrix equation $AY + YB = -Q$.

[DFVLR-SONDDR-274]

05 p0591 A73-16607

A matrix Green's formula and optimal control of linear distributed-parameter systems.

06 p0679 A73-17564

Matrix transformation in hyperplanes method for successive solution of boundary value problems of multidimensional differential equations, using space-time functions

06 p0715 A73-17718

Pivoting for size and sparsity in linear programming inversion routes.

06 p0716 A73-17978

Evaluations of matrix functions by real similarity transformation.

06 p0718 A73-18536

Acceleration of the convergence in Nesbet's algorithm for eigenvalues and eigenvectors of large matrices.

07 p0844 A73-19271

Rank-one and rank-two corrections to positive definite matrices expressed in product form.

09 p1113 A73-22956

Application of the finite element method to the study of the stability of plane structures

10 p1287 A73-23618

Unsteady discrete linear systems semisteady realizations existence conditions and matrices elements determination methods

10 p1202 A73-24414

Russian book on rockets as control plants covering dynamics equations of motion for different configurations, linearization and matrix description of rockets

11 p1429 A73-25175

An algorithmic procedure for determining discrete transfer matrices of controlled plants

12 p1485 A73-27624

Nonoscillation and disconjugacy of systems of linear differential equations.

13 p1648 A73-28441

The employment of special methods of the matrix-eigenvalue theory in the calculation of the resistance to buckling according to Vianello

14 p1805 A73-29740

Matrix invariant subspace computation via LU, QR, treppen and bi-iterations, comparing to power method

14 p1768 A73-29940

Haralick-Dinstein iterative clustering procedure limitation and explanation as T transformation linear structure effect in matrix theory

14 p1768 A73-30040

Matrix operator theory of radiative transfer. II - Scattering from maritime haze.

14 p1749 A73-30163

Perturbation method in the analysis of geometrically nonlinear and stability problems.

14 p1808 A73-30196

Standard algorithms application to modified matrix and least squares eigenvalues, determining quadratic forms and Gauss-Radau and Gauss-Lobatto quadrature rules coefficients

14 p1769 A73-30409

Matrix calculus operations and Taylor expansions.

14 p1769 A73-30410

Expansion of nonconjugate differential Dirac operators into a series of eigenvalues over the whole axis, and an analytical expression for a spectral matrix-function

14 p1771 A73-30787

Repetitively switched circuit analysis via matrix formalism and eigenvalue techniques with application to dc-dc converter

16 p1992 A73-33409

An error analysis of a method for solving matrix equations.

17 p2200 A73-34216

Computation of the exponential of a matrix. I - Theoretical considerations.

17 p2203 A73-35521

Convergence of matrix iterations subject to diagonal dominance.

17 p2203 A73-35727

Derivatives of eigensolutions for a general matrix.

18 p2330 A73-36318

Iterative and matrix inversion techniques for antenna electromagnetic radiation and scattering prediction compared for computer storage and execution time

22 p2823 A73-41799

Computerized analysis using sparse matrices/matrices with large number of zero elements/describing sorting, reordering and inverse computing techniques and linear equations solution methods

22 p2922 A73-42480

Geodetic net optimal design with known configuration matrix, basin, approach on calculus of inverse matrices

22 p2847 A73-42496

Decomposition of the solution to optimal synthesis problems of multiple-link control systems

22 p2887 A73-42610

Structural sensitivity transfer matrix for dynamic multiple link control system response minimization with corrections within frequency range

22 p2836 A73-42613

Interior radiances in optically deep absorbing media. I - Exact solutions for one-dimensional model.

24 p3111 A73-45318

Optimal convergence of iterative solution for system of linear equations with real roots based on matrix method
24 p3106 A73-45441

Convergence rate of two-real-parameter iterative solution of linear equations system based on matrix eigenvalues relationship
24 p3106 A73-45442

MATTER (PHYSICS)

The stopping power of atomic matter for relativistic ions, mesons, electrons and positrons.
07 p0852 A73-19036

Thermodynamic short range order models for dense substance equilibrium properties calculation, assuming molecular interaction independence and self similar radial function
07 p0851 A73-19397

Continuous-discrete and probability-deterministic theory of space-time and matter, considering resolution of antagonism between relativity and quantum theories
13 p1658 A73-28373

Rotating neutron star matter and model properties with emphasis on pulsar observations, discussing equations of state, transport processes and relativistic effects
14 p1798 A73-30234

Singularity and matter creation in cosmological models.
14 p1800 A73-30599

Equation of state of matter at supernuclear densities deduced from particle interactions nature and effective baryon mass spectrum
14 p1777 A73-30739

Equations for a plasma consisting of matter and antimatter.
17 p2216 A73-34508

Russian book on radiative and complex heat transfer covering electromagnetic energy-matter interaction, modeling, convective and conductive transfer and thermodynamic equilibrium radiation
17 p2254 A73-34899

Matter representation in general theory of relativity in terms of sourceless metric tensor and Einstein matter tensor, examining Mach principle status
22 p2887 A73-42435

MATURE STREAMS

U STREAMS

MATURE VEGETATION

U VEGETATION

MAXIMA

Rate of convergence of the distribution of the maximum of successive sums of independent random variables
12 p1516 A73-26958

Approximate calculation of the moments of the distribution of the maxima of correlated Gaussian random sequences
12 p1485 A73-27621

MAXIMUM LIKELIHOOD ESTIMATES

RR Lyrae star mean absolute magnitude determination via maximum likelihood method after elimination of stars with high velocity or errors in proper motion
02 p0222 A73-12707

German monograph - Application of estimation procedures for the characteristic parameters of controlled systems on the basis of measurements on the closed control loop.
03 p0285 A73-13811

Equivalence of the likelihood ratio processor, the maximum signal-to-noise ratio filter, and the Wiener filter.
03 p0282 A73-13917

Maximum likelihood estimate of carrier frequency and arrival direction of radio signals in background noise for large aperture antennas
03 p0278 A73-14081

Book - Sequential analysis and optimal design.
05 p0590 A73-16352

Adaptive maximum-likelihood sequence estimation for digital signaling in the presence of intersymbol interference.
06 p0665 A73-18144

Sequentially best estimators for linear systems with non-linear noise-free sensors.
06 p0681 A73-18522

Optimal correlation of sensor data with tracks in surveillance systems.
06 p0682 A73-18822

Dynamic system model identification computational considerations, discussing equation error methods based on regression analysis, maximum likelihood estimates and gradient dependent algorithms for optimization
07 p0845 A73-20428

Optimal estimation of operator-valued stochastic processes and applications to distributed parameter systems.
07 p0805 A73-20580

An analytical method for the filtering error evaluation of sub-optimal filters in a noisy non-linear dynamic system.
08 p0950 A73-21091

Coherent and noncoherent signal burst detection in background noise of unknown intensity, using maximum likelihood estimates
09 p1050 A73-22457

Solar cell fatigue life prediction by statistical analysis and extrapolation for determining failure probability curve as function of stress and time
09 p1036 A73-22808

Exponential bounds for error and equivocation based on Markov chain observations.
13 p1651 A73-29600

Accuracy of target angular coordinate estimates by the maximum likelihood method on a correlated noise background
14 p1729 A73-30557

Maximum likelihood M-ary detection theory application to incoherent optical system model based on photodetectors governed by Laguerre counting statistics, deriving error probability
15 p1875 A73-31734

An empirical Bayes approach for the Poisson life distribution.
15 p1901 A73-32262

Solution of the three-parameter Weibull equations by constrained modified quasilinearization /progressively censored samples/.
15 p1901 A73-32263

Gated phase locked loop tracking device for maximum likelihood estimation of pulsed sinusoid imbedded in noise, predicting phase noise performance
16 p1980 A73-33408

A consistent shape parameter estimator for the Weibull distribution.
16 p2032 A73-33602

Analysis of sudden death tests of bearing endurance.
[ASLE PREPRINT 73AM-3B-2]

Maximum likelihood synchronizer for binary overlapping PCM/NRZ signals.
17 p2179 A73-34984

Bayesian estimation of life parameters in the Weibull distribution.
17 p2127 A73-35641

Identification of YT-2B stability and control derivatives via the maximum likelihood method.
19 p2386 A73-38043

A comparative evaluation of the application of several aircraft parameter identification methods to flight data - with emphasis on the development of rational evaluation criteria.
19 p2386 A73-38044

ML receiver for binary signals with intersymbol interference in Gaussian noise.
20 p2524 A73-38733

Performance evaluation of multispectral scanner classification methods.
20 p2559 A73-39876

Adaptive multispectral scanner recognition via maximum likelihood classifier for agricultural crops, discussing error sources
20 p2559 A73-39877

Monte Carlo technique investigation of subclass number effects in nonoptimum parametric maximum likelihood classification procedure, defining distribution functions of representative subclasses
20 p2559 A73-39878

Unsupervised maximum likelihood classification technique multispectral remote sensing data, using two-part statistical clustering technique of sequential variance analysis
20 p2559 A73-39879

Optimum processing for delay-vector estimation in passive signal arrays.
22 p2825 A73-42198

Increase of closed-loop nominal trajectory likelihood in uncertain systems.
23 p2962 A73-43280

Adaptive maximum-likelihood receiver for synchronous data signals
23 p2957 A73-43320

MAXIMUM PRINCIPLE

A maximum principle for nondiagonal quasi-linear elliptic systems
01 p0071 A73-11267

Optimal horizontal guidance law for aircraft in the terminal area.
03 p0340 A73-13518

Pontryagin maximum principle for optimal terminal velocity control of automatic space probe descent in Mars atmosphere
03 p0383 A73-14556

Laser beams for precision alignment and detection using methods based on maximum and minimum principles
05 p0583 A73-16344

The maximum principle in the identification of distributed-parameter systems
05 p0562 A73-17283

Comparison and maximum theorems for systems of quasilinear elliptic differential equations.
06 p0717 A73-18171

Book on nonlinear optimization covering search, iteration, gradient, algorithmic and computer

techniques, mathematical and dynamic programming, calculus of variations, Pontryagin maximum principle, etc
06 p0717 A73-18401

Discrete maximum principle /local cross sections/ method applications to optimal control and mathematical programming
06 p0718 A73-18676

Pointwise bounds for smooth film profiles Reynolds equation solution based on elliptic equations maximum principle, considering journal bearings
07 p0845 A73-20484

Continuous analog of dynamic-programming allocation process
09 p1112 A73-22889

Iterative optimum control function determination without directly solving the system dynamical equations.
10 p1242 A73-24033

Formulation of Pontryagin's maximality principle in a problem of structural mechanics.
11 p1434 A73-25185

The optimality of variable sampling schemes for a digital encoder.
11 p1374 A73-25194

Maximum principle and uniform convergence for the finite element method.
11 p1390 A73-25435

A proof of the Pontryagin maximum principle for initial-value problems.
12 p1517 A73-27117

Optimal control with probabilistic quadratic performance criterion and constraints, using stochastic principle for reduction to time derivative maximization problem
12 p1485 A73-27897

Application of Pontryagin's maximum principle for minimum weight design of rigid-plastic circular plates.
13 p1696 A73-28754

Optimal control of discrete systems
14 p1738 A73-30348

Optimal control theory for systems with inequality restrictions on control and state variables and time delay, using maximum principle and variational techniques
15 p1855 A73-32580

A geometrical proof of the maximum principle for systems represented by difference-differential equations.
16 p2032 A73-33302

Uniqueness theorems for infinite systems of linear equations
17 p2201 A73-34631

Optimal control with probabilistic quadratic performance criterion and constraints, using stochastic principle for reduction to time derivative maximization problem
18 p2294 A73-36602

Straightforward design of a three-layer cylindrical shell
19 p2494 A73-37183

The maximum principle in problems of optimal control of systems having a nonsmooth right side
20 p2593 A73-39323

Certain problems in the use of the maximum principle to determine optimal controls in the case of special controls and sliding regimes
21 p2670 A73-40858

Convex approximation of the control process and a method for constructing generalized optimum regimes
21 p2727 A73-41064

German monograph - Principles concerning problems regarding optimality conditions in the case of time-dependent processes.
22 p2888 A73-42853

Classical mechanics Noether theorem and variational calculus for optimal control, noting Pontryagin maximum principle equations first integral solution existence condition
22 p2837 A73-43073

A computer program SNR-2 for solving an optimal control problem with state constraints.
23 p2956 A73-44126

A maximum principle and gradient bounds for linear elliptic equations.
24 p3105 A73-44421

Optimality condition based on maximum principle-derived convex reference function for control plants with continuous and discrete times
24 p3105 A73-44601

MAXIMUM USABLE FREQUENCY

Role of the sporadic E layer in short radio wave propagation at frequencies exceeding the maximum usable frequencies of the F2 layer
05 p0548 A73-16264

HF radio signal reception behavior near maximum usable frequency during evening and at midnight, noting SNR
07 p0792 A73-19456

Variations in the M/3000/F2 coefficient as a function of the solar energy entering the earth's atmosphere
20 p2555 A73-39179

MAXWELL BODIES

MAXWELL BODIES

Maxwell kinetic theory of gases with elasticity of shape /modulus of rigidity/ and obeying Hooke's law, deriving expressions for simple shear and relaxation time

14 p1745 A73-30477

MAXWELL EQUATION

Gravitational equations derivation identical to electromagnetic Maxwell equations, noting nonviolation of energy conservation

03 p0373 A73-13358

Book on electromagnetic field theory covering free space Maxwell equations, Lorentz force law, vector analysis, Laplace equation, lossless transmission lines and dipole antennas

03 p0343 A73-13988

Maxwell equations in a spherically symmetric black-hole background and radiation by a radially moving charge.

05 p0597 A73-16470

Green's function of the Maxwell equations in laminar media

05 p0598 A73-16819

Maxwell equation for equilibrium force in electromagnetic suspension system of force measuring instrument, noting rigidity dependence on system parameters

05 p0577 A73-16995

The solution of Maxwell's equation for inhomogeneous dielectric slabs.

06 p0699 A73-17809

Equilibrium and stability of large-amplitude magnetic Bernstein-Greene-Kruskal waves.

07 p0857 A73-19524

Boundary value problems for the Maxwell equations

08 p0988 A73-21130

Electromagnetic propagation in bianisotropic stratified media, obtaining Maxwell and constitutive equations in operator form

09 p1049 A73-22312

Rigorous analogies between elastic and electromagnetic systems.

10 p1250 A73-24873

On Maxwell-type equations in the theory of inertial-gravitational field.

13 p1657 A73-28025

Maxwell equations for lasing modes of bounded region in laser beam with finite spectral width in form of Fourier integrals

14 p1757 A73-30461

Geomagnetic variations total field confinement described by Parkinson, discussing primary and secondary fields Maxwell equations linear relationship by induction tensor

15 p1871 A73-31777

Boundary-value problems for Maxwell's equations.

15 p1900 A73-32065

Electromagnetic emission in the general relativity theory. I

16 p1984 A73-34006

On an initial value problem for a nonlinear system of Vlasov-Maxwell equations.

17 p2200 A73-34320

Einstein-Maxwell fields in conformal space, studying field equations, reducible electromagnetic field in space-time and constraints on metric tensor by Rainich conditions

17 p2212 A73-35560

Relation between the fundamental solutions in cylindrical and spherical coordinates /with identical coordinate origins/ for certain equations of mathematical physics

21 p2753 A73-41025

Maxwell integral equations in problems of wave scattering by moving media

22 p2826 A73-42376

MAXWELL FLUIDS

Thermal instability in a viscoelastic fluid layer in hydromagnetics.

09 p1166 A73-22418

MAXWELL-BOLTZMANN DENSITY FUNCTION

Method for deriving normal solutions to kinetic equations by using boundary conditions

01 p0076 A73-10623

Boltzmann transport equation for plasma probe detector characteristics for Maxwellian and non-Maxwellian distribution functions of electrons in dc and ac electric fields

04 p0480 A73-15602

Boltzmann transport equation for plasma probe detector characteristics for Maxwellian and non-Maxwellian distribution functions of electrons in dc and ac electric fields

10 p1254 A73-24192

Relaxation to Maxwellian distribution of electrons near low voltage Cs arc plasma discharge cathode

13 p1666 A73-28962

Relaxation to Maxwellian distribution of electrons near low voltage Cs arc plasma discharge cathode

23 p3013 A73-44314

MAXWELLIAN DISTRIBUTION [DENSITY]

U MAXWELL-BOLTZMANN DENSITY FUNCTION

MCDONNELL AIRCRAFT

NT DC 10 AIRCRAFT

NT F-4 AIRCRAFT

MCDONNELL DOUGLAS AIRCRAFT

Technical basis for the STOL characteristics of the

McDonnell Douglas/USAF YC-15 prototype airplane.

[SAE PAPER 730366] 17 p2103 A73-34711

Management and control of military flight test programs at McDonnell Douglas St. Louis, Missouri.

23 p3050 A73-44059

MCDONNELL MILITARY AIRCRAFT

U MILITARY AIRCRAFT

MEAN

Conditions for localization of Cesaro's rectangular means and of Abel's method means in the limited summing of a multiple trigonometric Fourier series in the Liouville classes

01 p0071 A73-11439

Convergence of the arithmetic-geometric mean procedure for the complex variables and the calculation of the complete elliptic integrals with complex modulus.

14 p1769 A73-30423

Monte Carlo method for biharmonic boundary value problems solution, using isotropic random walk and mean value relation

20 p2581 A73-39094

MEAN FREE PATH

Laser coupling through nonlinear gas filled absorber cell, discussing molecules mean free path

05 p0585 A73-16783

Mean free path of molecules from a surface in rarefied flow with application to correlating drag data.

05 p0531 A73-16933

Mean path length of high energy galactic cosmic rays in the galactic disk.

07 p0873 A73-20563

Solar protons propagation from instantaneous injection source and inhomogeneities interaction description by mean free path and scattering angle specification

08 p0999 A73-21327

The mean free path in the transition region beyond the boundary of the magnetosphere

12 p1528 A73-27355

Radiative heat transfer through composite materials.

18 p2371 A73-36621

Interplanetary gas. XVIII - Models and the mean free path of protons at 1 astronomical unit.

19 p2489 A73-38523

Mean free path in the transition region beyond the boundary of the magnetosphere.

23 p3008 A73-43253

Role of hydromagnetic waves in cosmic-ray confinement in the disk. I - Theory of behavior in general wave spectra.

24 p3124 A73-45040

New kind of boundary layer over a convex solid boundary in a rarefied gas.

24 p3080 A73-45453

MEAN TIME BETWEEN FAILURES

U MTBF

MEANDERS

Experimental studies on the formation of lunar surface features by fluidization - Discussion.

10 p1280 A73-24349

MEASURANDS

U MEASUREMENT

MEASURE AND INTEGRATION

NT BINARY INTEGRATION

NT BOREL SETS

NT FUNCTIONAL INTEGRATION

NT INTEGRAL CALCULUS

NT LEBESGUE THEOREM

NT NUMERICAL INTEGRATION

NT RUNGE-KUTTA METHOD

NT STIELTJES INTEGRAL

NT WEIGHTING FUNCTIONS

Reynolds equation time dependent numerical integration errors due to phase shifts, indicating correction by extrapolated Crank-Nicolson scheme [ASME PAPER 72-LUB-L] 01 p0055 A73-10223

On the integration of Einstein's equation for energy density inside a perfect fluid sphere.

01 p0076 A73-10250

Solutions and stability of a system of two first-order linear differential equations with variable coefficients

01 p0070 A73-10914

Solution of Troesch's two-point boundary value problem by a combination of techniques.

01 p0035 A73-11470

Stress principle relationship to mechanical power additivity, presenting topological, measure theory and functional analysis theorems

06 p0760 A73-17762

Randomized solutions in stochastic-programming problems

09 p1112 A73-22845

Some oscillatory properties of solutions of fourth-order quasi-linear differential equations

09 p1113 A73-22986

Method of utilizing structural redundancy in a measuring system for processing experimental data with systematic errors

12 p1494 A73-26776

Absolute continuity of estimates corresponding to uniform Gaussian fields

12 p1523 A73-27185

Some general questions in the theory of probability measures in linear spaces

12 p1517 A73-27187

A method of integrating the equations of motion in special coordinates and the elimination of a discontinuity in the theory of the motion of periodic comet Wolf.

14 p1790 A73-29790

A simplified method of calculating thermomodulation curves

15 p1837 A73-31168

Description of the 1/sub o/ class in a special subgroup of probabilistic measures

15 p1899 A73-31243

General linear boundary value problem with measurable coefficients for numerous analytical functions of class E sub p

15 p1900 A73-32092

An integration algorithm for hyperbolic systems having non-zero, non-analytic steady-state solutions.

17 p2203 A73-35610

Riesz representability, sigma-additivity and Daniell-integral properties of measures on uniform spaces

21 p2726 A73-40945

Concentration functions of finite-dimensional and infinite-dimensional random vectors

22 p2882 A73-42649

MEASURE THEORY

U MEASURE AND INTEGRATION

MEASUREMENT

Fundamentals of metrology involving quality and quantity description of reality, emphasizing interrelationship between measurement results in science and technology branches

03 p0305 A73-12895

Iterative method for the statistical processing of measurements with incomplete information on the measurement error characteristics.

15 p1902 A73-32605

MEASURING

U MEASUREMENT

MEASURING APPARATUS

U MEASURING INSTRUMENTS

MEASURING INSTRUMENTS

NT ACCELEROMETERS

NT ACTINOMETERS

NT ALTIMETERS

NT ANALYZERS

NT ANEMOMETERS

NT APPROACH INDICATORS

NT ATOMIC CLOCKS

NT ATTITUDE INDICATORS

NT BATHYMETERS

NT BOLOMETERS

NT CALORIMETERS

NT CERENKOV COUNTERS

NT CHRONOMETERS

NT CINETHEODOLITES

NT CLOCKS

NT CLOUD HEIGHT INDICATORS

NT COMPARATORS

NT COUNTERS

NT DENSITOMETERS

NT DICKE RADIOMETERS

NT DIFFRACTOMETERS

NT DISTANCE MEASURING EQUIPMENT

NT DOSIMETERS

NT DROPSONDES

NT DYNAMOMETERS

NT ELECTROMETERS

NT ELECTRON COUNTERS

NT ELECTRON PROBES

NT ELECTROPHOTOMETERS

NT ELECTROSTATIC PROBES

NT ELLIPSOMETERS

NT ENGINE ANALYZERS

NT ENGINE MONITORING INSTRUMENTS

NT ERGOMETERS

NT FABRY-PEROT INTERFEROMETERS

NT FABRY-PEROT SPECTROMETERS

NT FIELD INTENSITY METERS

NT FLAME CALORIMETERS

NT FLAME PROBES

NT FLIGHT LOAD RECORDERS

NT FLIGHT RECORDERS

NT FLOWMETERS

NT FUEL GAGES

NT GALVANOMETERS

NT GEIGER COUNTERS

NT GONIOMETERS

NT GRAVIMETERS

NT GYROCOMPASSES

NT HELIOMETERS

NT HODOSCOPES

NT HOT-FILM ANEMOMETERS

NT HOT-WIRE ANEMOMETERS

NT HOT-WIRE FLOWMETERS

NT HYGROMETERS

NT IMPEDANCE PROBES
 NT INDICATING INSTRUMENTS
 NT INFRARED DETECTORS
 NT INFRARED INSTRUMENTS
 NT INFRARED INTERFEROMETERS
 NT INFRARED SCANNERS
 NT INFRARED SPECTROMETERS
 NT INFRARED SPECTROPHOTOMETERS
 NT INTERFEROMETERS
 NT ION PROBES
 NT ION TRAPS [INSTRUMENTATION]
 NT IONIZATION GAGES
 NT IONOSONDES
 NT KNUDSEN GAGES
 NT LASER ALTIMETERS
 NT LASER RANGE FINDERS
 NT LUNAR SEISMOGRAPHS
 NT MACH-ZEHNDER INTERFEROMETERS
 NT MAGNETIC PROBES
 NT MAGNETOMETERS
 NT MANOMETERS
 NT MASS SPECTROMETERS
 NT MECHANOGRAMS
 NT METEOROLOGICAL INSTRUMENTS
 NT MICHELSON INTERFEROMETERS
 NT MICROBALANCES
 NT MICRODENSITOMETERS
 NT MICROMETERS
 NT MICROWAVE INTERFEROMETERS
 NT MICROWAVE PLASMA PROBES
 NT MICROWAVE PROBES
 NT MICROWAVE RADIOMETERS
 NT MICROWAVE REFLECTOMETERS
 NT MICROWAVE SENSORS
 NT MOISTURE METERS
 NT MONOCHROMATORS
 NT NEPHELOMETERS
 NT NEUTRON COUNTERS
 NT NOISE METERS
 NT OCULOMETERS
 NT OMEGA NAVIGATION SYSTEM
 NT OPTICAL MEASURING INSTRUMENTS
 NT OPTICAL PYROMETERS
 NT OPTICAL RANGE FINDERS
 NT OPTICAL SCANNERS
 NT OSCILLOGRAPHS
 NT OSMOMETERS
 NT PARTICLE TELESCOPES
 NT PHASE SWITCHING INTERFEROMETERS
 NT PHILIPS IONIZATION GAGES
 NT PHOTOMETERS
 NT PIEZOELECTRIC GAGES
 NT PIEZOMETERS
 NT PLAN POSITION INDICATORS
 NT PLASMA PROBES
 NT PNEUMATIC PROBES
 NT POLARIMETERS
 NT POLARISCOPE
 NT POSITION INDICATORS
 NT POTENTIOMETERS [INSTRUMENTS]
 NT PRESSURE GAGES
 NT PROFILOMETERS
 NT PROPORTIONAL COUNTERS
 NT PYRANOMETERS
 NT PYROHELIOMETERS
 NT PYROMETERS
 NT QUANTUM COUNTERS
 NT RADIATION COUNTERS
 NT RADIATION DETECTORS
 NT RADIATION MEASURING INSTRUMENTS
 NT RADIATION PYROMETERS
 NT RADIO ALTIMETERS
 NT RADIO DIRECTION FINDERS
 NT RADIO FREQUENCY IMPEDANCE PROBES
 NT RADIO INTERFEROMETERS
 NT RADIOGONIOMETERS
 NT RADIOMETERS
 NT RADIOSONDES
 NT RAIN GAGES
 NT RANGE FINDERS
 NT RAWINSONDES
 NT REFLECTOMETERS
 NT REFRACTOMETERS
 NT RESISTANCE THERMOMETERS
 NT RESONANCE PROBES
 NT RESPIROMETERS
 NT RHEOMETERS
 NT RIOMETERS
 NT SATELLITE-BORNE INSTRUMENTS
 NT SCATTEROMETERS
 NT SCINTILLATION COUNTERS
 NT SEISMOGRAPHS
 NT SEXTANTS
 NT SHOCK MEASURING INSTRUMENTS
 NT SIGNAL ANALYZERS
 NT SILICON RADIATION DETECTORS
 NT SOLAR SPECTROMETERS
 NT SONDES
 NT SONIC ANEMOMETERS
 NT SPACECRAFT POSITION INDICATORS
 NT SPARK CHAMBERS
 NT SPECTROHELIOGRAPHS
 NT SPECTROMETERS
 NT SPECTROPHOTOMETERS
 NT SPECTRORADIOMETERS

NT SPEED INDICATORS
 NT STRAIN GAGE ACCELEROMETERS
 NT STRAIN GAGE BALANCES
 NT STRAIN GAGES
 NT TACHOMETERS
 NT TEMPERATURE MEASURING INSTRUMENTS
 NT TEMPERATURE PROBES
 NT TENSOMETERS
 NT THEODOLITES
 NT THERMAL CONDUCTIVITY GAGES
 NT THERMOCOUPLE PYROMETERS
 NT THERMOMETERS
 NT THRESHOLD DETECTORS [DOSIMETERS]
 NT TIME MEASURING INSTRUMENTS
 NT TIMING DEVICES
 NT TORQUEMETERS
 NT TRANSITS
 NT TURBULENCE METERS
 NT ULTRAVIOLET SPECTROMETERS
 NT ULTRAVIOLET SPECTROPHOTOMETERS
 NT VACUUM GAGES
 NT VARIOMETERS
 NT VIBRATION METERS
 NT VISCOMETERS
 NT VOLTMETERS
 NT WATTMETERS
 NT WEATHER DATA RECORDERS
 NT WEIGHT INDICATORS
 Self-compensating digital phase meter with discrete phase shifters 01 p0044 A73-10078
 Design of digital phase meters with intermediate frequency converters 01 p0044 A73-10079
 Investigation of residual resistance in semiconductor switches used to commutate the measuring circuits of alternating-current bridge networks 01 p0022 A73-10080
 Signal amplitude ratios measurement in automatic control applications by digital differential logometer, using time-pulse dividing circuits 01 p0022 A73-10082
 Instrumental considerations in high dispersion requirements of stellar spectroscopy and interstellar absorption and emission line studies, emphasizing spectral resolution and SNR optima determination 01 p0046 A73-10503
 Measuring equipment for multipoint data acquisition and recording, noting modular design of party-line system with programmed data processing 01 p0054 A73-11398
 Thermophysical properties of arc-cast tungsten using the TPRC multi-property apparatus /direct heating method/. 01 p0067 A73-11483
 Component errors of digital frequency meter with nonius estimation of measured quantity smaller digits 02 p0167 A73-11863
 Parameter selection scheme for unit measuring frequency deviation as function of voltage, resistance and circuit sensitivity 02 p0149 A73-11864
 Zener diodes for overvoltage spark protection circuits in automatic control and measuring equipment operating in explosive environment 02 p0147 A73-12175
 Overload tolerance formulas for differential voltage null measuring system with amplifier for trigger circuit drive 02 p0170 A73-12345
 Dynamic errors in force measuring transducers, simulating unsteady processes by analog model with varying step function input signals 02 p0170 A73-12540
 A criterion for establishing the principal dimensions of /metallic/ standard measures of volume 03 p0306 A73-12897
 Cosmic gravitational waves detection and measurement, describing Weber experimental apparatus and theoretical foundations based on Einstein relativity theory 03 p0341 A73-12924
 Diagnostic instrumentation on J-85 engines for gas path and vibration analysis, noting flight test program and installation of remote pressure transducers and signal conditioners 03 p0308 A73-13404
 [AIAA PAPER 72-1081] A very accurate X-band rotary attenuator with an absolute digital angular measuring system. 03 p0310 A73-14498
 Hall effect gimbal angle transducer /HEGAT/ for relative angular orientation measurement between rotor and stator in low cost inertial platform 04 p0447 A73-15066
 Void fraction measurement based on gas-liquid volume ratio by local void velocity measurement with single probe 05 p0638 A73-16224
 Laminar liquid jets thrust measurement apparatus for dilute polymer solutions rheological characteristics determination, using air bearing suspended rotor with discharge capillary 05 p0562 A73-16441

Instrumentation for metallographic structure examination. 05 p0576 A73-16751
 Maxwell equation for equilibrium force in electromagnetic suspension system of force measuring instrument, noting rigidity dependence on system parameters 05 p0577 A73-16995
 Determination of the angle of incidence of angle probes for ultrasonic testing 05 p0582 A73-17068
 Determination of the pass band of a system of measurement of rapidly variable pressures in the air 05 p0579 A73-17228
 Fluidic system for precision positioning of cylindrical machine parts and length and angle measurements, using nozzle jet impingement system for pressure symmetry sensing 05 p0538 A73-17248
 Instrument suspended from tethered balloon for oceanic measurement of average lower atmosphere vertical electric field profile 05 p0579 A73-17251
 An instrument for the simultaneous detection of the OI ground state /2p4 3P/ and first metastable state /2p4 1D/ populations. 05 p0580 A73-17258
 Instrument circuitry, calibration and errors in p-n junction capacitance measurement 06 p0691 A73-17399
 Zero-g propellant gauging 06 p0755 A73-17573
 Time difference measuring instrument for asynchronous and synchronized positive pulses in automatic control system, noting pulse generator and switching, trigger and logic circuits 06 p0677 A73-18384
 A new measurement device for measuring harmonic forces 06 p0695 A73-18434
 Calibration procedure for instruments to measure the delta ferrite content of austenitic stainless steel weld metal. 07 p0832 A73-20272
 Measurement of dynamic mechanical quantities; Scientific-Engineering Conference, 3rd, Warsaw, Poland, October 26-28, 1972, Summaries 07 p0826 A73-20526
 A contactless method of measuring the radial deformations of rotating shafts 07 p0827 A73-20533
 Thermal fluxometry - Heat well influence on detector response 08 p0967 A73-21500
 Measurement of the flexural damping capacity and dynamic Young's modulus of metals and reinforced plastics. 08 p0967 A73-21594
 Measuring apparatus for residual effective stabilizer content in single and double base propellants by passing nitrogen dioxide through ground sample 09 p1135 A73-22300
 Drift phenomena in shaken measurement systems prone to torsional vibrations. III 09 p1086 A73-23116
 Electrical measurement of mechanical forces and displacements, discussing transducers design and measurement standards and units 10 p1215 A73-23633
 Use of lasers for local measurement of velocity components, species densities, and temperatures. 10 p1217 A73-23852
 Prototype skin friction measuring instrument for short period or continuous operation at high temperature, considering alternative feasible systems design and experimental data 10 p1217 A73-24013
 Unified transducers of quantitative and geometrical parameters of different media based on the use of integral properties of electromagnetic fields. 10 p1217 A73-24014
 Semiconductor and semi-insulator resistivity measurements using a direct current four point probe apparatus with non-penetrating tips. 10 p1194 A73-24158
 A measurement stand for reciprocal circuits in a waveguide 10 p1189 A73-24417
 Problem of forming classes of input processes in the study of errors in devices for statistical measurements 11 p1359 A73-25014
 Effect of measuring-device error on the accuracy of the determination of the mathematical expectation and dispersion of a stationary random process 11 p1360 A73-25016
 Statistical synthesis of digital parameter-measuring equipment and analysis of its efficiency 11 p1360 A73-25021
 Level and density sensors using pneumatic repeaters 11 p1364 A73-26099
 Equivalent continuous sound level determination from instantaneous sonic intensity measurement duration. 11 p1364 A73-26099

MECHANICAL DEVICES

ing representative time period, describing electron measuring device and circuitry

11 p1367 A73-26416

Digital measuring devices with a constant range of relative error variations

12 p1495 A73-27777

Aspects of the application of Rogovskii's coil to the measurement of steady currents in a plasma

12 p1528 A73-27306

Complex measuring device for moving object location from multiple autonomous and nonautonomous information sources with different noise spectral compositions

12 p1484 A73-27447

Stochastic-ergodic electronic U-functionmeter for signal electrical characteristics measurement, discussing design, operational features and applications

12 p1499 A73-27874

A high resolution dynamic technique of thermoelectric power measurements.

13 p1612 A73-28370

Testing machine with control panel and vacuum chamber for microhardness measurement at high temperatures with precise test point selection and indentation observation capability

13 p1613 A73-28525

Construction of fuel and oil quantity sensors for high-performance aircraft.

13 p1619 A73-29204

Strain measurements in the solid propellant of a large booster structural test vehicle.

13 p1669 A73-29304

Digital circuits test equipment functional principles, considering time, instantaneous voltage and pulse height measurements

14 p1731 A73-29873

Measurement equipment for the PCM transmission system KPK 30/32

14 p1736 A73-30373

Stress measurement on cloth of inflated solid circular parachute model, noting sensor interference with canopy shape and stress pattern

[AIAA PAPER 73-445] 15 p1825 A73-31431
Akademiia Nauk SSSR, Astronomicheskii Sovet, Meeting of the Commission on Astronomical Instrument Engineering, Sverdlovsk, USSR, July 1-3, 1970, Proceedings

15 p1877 A73-32128

A method of analytical error identification in the inspection of the working profiles of blades

16 p2019 A73-33300

Balloon-borne phosphoric anhydride electrolytic gage measurement of water vapor mixing ratio to 35 km, noting decrease to minimum near tropopause

16 p2008 A73-33884

Circumzenithal instrument for latitude and longitude determination and star transits observation, through almicantar

16 p2017 A73-34048

International Aerospace Instrumentation Symposium, 19th, Las Vegas, Nev., May 21-23, 1973, Proceedings.

17 p2165 A73-34601

The operational performance of reentry vehicle heatshield thermodynamic instrumentation.

17 p2238 A73-34605

On the measuring of soil moisture by microwave radiometric techniques.

17 p2170 A73-35363

Experimental force data reduction equations solved by iterative method for multicomponent force transducers used in load tests, discussing wind tunnel balances

17 p2148 A73-35437

Susceptibility measurements at high frequency - A versatile and sensitive apparatus.

17 p2176 A73-35771

The effect of the rotor pattern on the accuracy of the photoelectric angle-measuring system of a gimbal-less electrostatic gyroscope.

18 p2317 A73-36873

A digital optimization device for directional charged particle measurements in space research.

19 p2428 A73-37148

Early operational experience with the L-1011 On-Board Weight and Balance System.

[SAWE PAPER 986] 19 p2386 A73-37890

An accelerated electron beam position and shape meter

21 p2699 A73-40172

Use of gyro technology to measure small random angular motion.

[AIAA PAPER 73-839] 21 p2700 A73-40504

A non-contacting length comparator with 10 nanometer precision.

21 p2704 A73-41257

Russian book - Aerohydrodynamic methods for measuring input parameters of automatic systems: Fluidic measuring elements.

21 p2704 A73-41288

Optimal dynamic accuracy measurement complexing for combined data processing in multidimensional automatic control systems with various sensors

22 p2836 A73-42618

Pulse generator for testing and measurement, describing pulse frequency, duration and sequence capacity, digital design and normal and alarm sequences

23 p2955 A73-44150

Analyses of some potential problems in cylindrical coordinates in connection with four-point probe technique.

23 p3018 A73-44368

Comparison of results obtained with various sensors used to measure fluctuating quantities in jets.

[AIAA PAPER 73-1043] 24 p3079 A73-44867

Introduction of the viscous force sensing fluctuating probe technique, with measurement in the mixing zone of a circular jet.

[AIAA PAPER 73-1044] 24 p3090 A73-44868

Josephson junction principles for superconducting metals at cryogenic temperatures, considering ultrasensitive electronic measuring instruments and computer components

24 p3073 A73-45224

MECHANICAL DEVICES

The requirements on the parameters of a mechanical modulator for an IR scanning radiometer.

01 p0050 A73-10833

Statistical method of determining the load or stress distribution from the failure characteristics of mechanical systems

01 p0118 A73-11370

Elastic force minimization during transient process in mechanical multimass system under time dependent external load

04 p0509 A73-14976

Statistical linearization of nonlinear single-mass mechanical system for given distribution function of random disturbances, noting amplitude frequency distribution

04 p0475 A73-14977

The properties of a solution of the equations of motion of a mechanical system subject to irregular/singular perturbations.

06 p0722 A73-17755

The influence of nonlinear couplings on the behaviour of the solution of the equations of motion of a mechanical system.

06 p0722 A73-17756

A program for the analysis and design of general dynamic mechanical systems.

[AD-754496] 06 p0671 A73-18063

Resonance characteristics of semiconductor mechanical components.

06 p0676 A73-18344

Stability of incompletely damped mechanical systems

08 p1014 A73-20780

Mathematical model selection rules for stability studies of linear mechanical or passive electrical network systems with arbitrary degrees of freedom

08 p0987 A73-20787

Prediction of optimal maintenance for devices

13 p1625 A73-29136

Partial stability of mechanical systems, analyzing perturbed motion in vector form, using Liapunov functions

15 p1914 A73-32114

Airborne mechanical system for sounding rocket experiments.

16 p2072 A73-33119

Optimization of a vibration generator in the presence of external perturbations

16 p2083 A73-33969

Application of information theory to the study of mechanical systems

20 p2592 A73-39260

High performance vibration isolated tables.

20 p2544 A73-39266

MECHANICAL DRIVES

NT HELICOPTER PROPELLER DRIVE

NT PROPELLER DRIVE

Gear fan engine systems - Their advantages and potential reliability.

[AIAA PAPER 72-1173] 03 p0357 A73-13469

The development of light tracked vehicles for lunar and planetary exploration

08 p0952 A73-20781

Experimental investigation of undulatory multiplication gear systems

10 p1222 A73-23597

Long focal length refractor telescopes for high resolution stellar photography, describing follower drive construction and control

10 p1218 A73-24275

Liquid or solid fueled gas generators applications to driving rocket fuel turbopumps, ejector pumps, gas turbine engine starters, torpedo propulsion, etc

11 p1307 A73-24991

Laser activated, model surface recession compensation system for testing ablative materials.

11 p1343 A73-25510

Twin-engined Anglo-French Lynx helicopter main rotor head, blade and drive train with conformal gearing, discussing design and material features

11 p1374 A73-25790

Reliability analysis of helicopter mechanical transmission components and reduction gearboxes

11 p1306 A73-26596

A high-speed automatic strip-chart recorder

12 p1497 A73-27220

Variable speed single- and multi-quadrant drives using thyristor electronic regulating unit with static converter motor and frequency changers

16 p1971 A73-33961

Helicopter power transfer systems analysis in terms of weight reduction and reliability improvement

[AHS PREPRINT 773] 17 p2106 A73-35091

Helicopter turboshaft engine vibration reduction through engine-airframe interface compatibility design and torsional stability of drive trains with automatic fuel control

[AHS PREPRINT 774] 17 p2106 A73-35092

Basic principles of variable speed drives.

17 p2106 A73-35472

A harmonic drive used as an ultrahigh vacuum rotary feedthrough.

21 p2671 A73-39919

Mechano-optical camera giving ten million images per second

21 p2693 A73-39935

The problem of structural analysis of a wave gear

21 p2708 A73-41198

Helicopter transmission research.

22 p2798 A73-41750

Synchronized operation of a positive-displacement gear pump and a vane pump within the lubricant oil delivery system of a jet engine

23 p3020 A73-43742

MECHANICAL ENGINEERING

Handbook on mechanical face seals covering applications, operational capabilities, design, environmental control, handling, installation, malfunctions, auxiliary equipment, optical flats, etc

03 p0313 A73-13995

Russian book - Nonlinear oscillations and transient processes in machines.

18 p2319 A73-35895

Book on mechanical reliability from engineering standpoint covering statistical probability, performance quality, systems design and manufacturer and user roles

18 p2321 A73-36970

Israel Conference on Mechanical Engineering, 7th, Haifa, Israel, June 27, 28, 1973, Proceedings.

23 p2967 A73-43291

Israel Conference on Theoretical and Applied Mechanics, 20th, Tel Aviv, Israel, April 18, 1973, Proceedings.

23 p3038 A73-43302

MECHANICAL IMPEDANCE

Jet element output impedance for pneumatic circuits transients determination considering load dynamic properties influence

02 p0133 A73-12120

Data analysis criteria and instrumentation requirements for the transient measurement of mechanical impedance.

03 p0343 A73-13837

Experimental determination of three-dimensional liquid rocket nozzle admittances.

09 p1167 A73-23438

Three layered sandwich rings damped vibrations under time-harmonic radial concentrated load, comparing experimental and theoretical mechanical impedance data

09 p1165 A73-23440

Dynamic analysis procedure to locate vibration sources without simulated service tests, mapping structural surfaces at all frequencies via transfer function or mechanical impedance analysis

16 p2019 A73-33098

Operational temperature and frequency effects on radial driving point mechanical impedance of damped thin walled ring with mass segments attached by viscoelastic material

20 p2616 A73-39051

A model to predict the mechanical impedance of the sitting primate during sinusoidal vibration.

[ASME PAPER 73-DET-78] 22 p2813 A73-42073

MECHANICAL MEASUREMENT

NT DISPLACEMENT MEASUREMENT

NT DRAG MEASUREMENT

NT FLOW MEASUREMENT

NT FRICTION MEASUREMENTS

NT PRESSURE MEASUREMENTS

NT STRESS MEASUREMENT

NT THRUST MEASUREMENT

NT VELOCITY MEASUREMENT

NT VIBRATION MEASUREMENT

NT WIND MEASUREMENT

NT WIND VELOCITY MEASUREMENT

NT X RAY STRESS MEASUREMENT

Angular measurements of foot motion for application to the design of foot-pedals.

01 p0013 A73-10773

Luna 16 direct measurements for soil mechanical properties, determining bulk density, failure characteristics, compressibility and shear and bearing strength

02 p0213 A73-12232

Telemetry methods for maximum static muscle strength measurements, considering dynamic force measurement possibilities

03 p0271 A73-14296

Maxwell equation for equilibrium force in electromagnetic suspension system of force measuring instrument, noting rigidity dependence on system parameters
05 p0577 A73-16995

Chemotronic /electrochemical/ transducers of nonelectrical quantities in automatic control
12 p1459 A73-26768

Balancing equipment for jet engine components, compressors, and turbine - Rotating type for measuring unbalance in one or more than one transverse planes.
[SAE ARP 587A] 16 p1993 A73-33013

Fracture toughness and absorbed energy measurements in impact tests on brittle materials.
19 p2500 A73-38094

Surveyor 3 lunar soil shear strength measurements for range of bulk densities obtained by different packing procedures, calculating void ratios
23 p3031 A73-43761

MECHANICAL OSCILLATORS

NT GYROSCOPIC PENDULUMS
NT PENDULUMS

Oscillation damping by pulsed dynamic dampers.
02 p0235 A73-12209

Analysis of the resistance of reed contacts to shock and vibration impacts
05 p0559 A73-17237

Forced vibration of a class of non-linear two-degree-of-freedom oscillators.
07 p0851 A73-19165

German monograph - Harmonically excited forced oscillations of a spring/mass system with controlled Coulomb damping.
07 p0851 A73-19581

Self-synchronization of mechanical vibrators in the event of random disturbances
09 p1120 A73-22356

Generator of rectilinear vibrations for the study of structures at low frequency
[ONERA, TP NO. 1185] 09 p1084 A73-22713

Numerical computation of forced oscillations in coupled Duffing equations.
09 p1113 A73-23022

Signal flow graph methods for four and three degree of freedom linear conservative mechanical vibration systems solution, noting Chan-Mai method superiority
11 p1434 A73-25193

General treatment of the evaluation of tri-diagonal secular determinants.
13 p1700 A73-29379

Kron's method - A consequence of the minimization of the primitive Lagrangian in the presence of displacement constraints.
13 p1700 A73-29381

Qualitative analysis of the behavior of weakly coupled oscillators near the equilibrium position
19 p2458 A73-37191

A quantitative estimate of the effect of the parameters of oscillatory systems on the natural frequencies
19 p2498 A73-37653

Random vibration of distributed systems strongly coupled at discrete points.
22 p2918 A73-41820

Prediction and measurement of the proportionality constant in statistical energy analysis of structures.
22 p2918 A73-41821

Adiabatic variation. I - Exponential property for the simple oscillator.
24 p3112 A73-45543

MECHANICAL PROPERTIES

NT ABRASION RESISTANCE
NT AEROELASTICITY
NT AEROTHERMOELASTICITY
NT ANELASTICITY
NT BRITTLENESS
NT BULK MODULUS
NT COLD STRENGTH
NT COMPRESSIBILITY
NT COMPRESSIVE STRENGTH
NT CREEP PROPERTIES
NT CREEP RUPTURE STRENGTH
NT CREEP STRENGTH
NT DIMENSIONAL STABILITY
NT DUCTILITY
NT DYNAMIC MODULUS OF ELASTICITY
NT ELASTIC PROPERTIES
NT ELASTOPLASTICITY
NT ELECTROSTRICTION
NT FATIGUE LIFE
NT FIBER STRENGTH
NT FLEXIBILITY
NT FRACTURE STRENGTH
NT HARDNESS
NT HIGH STRENGTH
NT HYDROELASTICITY
NT HYPOELASTICITY
NT IMPACT STRENGTH
NT KNOOP HARDNESS
NT MAGNETOSTRICTION
NT MICROHARDNESS
NT MODULUS OF ELASTICITY
NT NOTCH SENSITIVITY
NT NOTCH STRENGTH
NT PHOTOELASTICITY
NT PHOTOPLASTICITY

NT PHOTOVISCOELASTICITY
NT PIEZOELECTRICITY
NT PLASTIC PROPERTIES
NT POISSON RATIO
NT SHEAR PROPERTIES
NT SHEAR STRENGTH
NT SHELL STABILITY
NT STEADY STATE CREEP
NT STIFFNESS
NT STRESS CYCLES
NT STRESS RATIO
NT STRESS RELAXATION
NT STRUCTURAL STABILITY
NT TENSILE CREEP
NT TENSILE PROPERTIES
NT TENSILE STRENGTH
NT THERMAL RESISTANCE
NT THERMOELASTICITY
NT THERMOPLASTICITY
NT THERMOVISCOELASTICITY
NT TOUGHNESS
NT VISCOELASTICITY
NT VISCOPLASTICITY
NT WELD STRENGTH
NT YIELD POINT
NT YIELD STRENGTH

Physical nature of the processes of formation of the set of mechanical properties of quench-hardened alloyed structural steel during tempering
01 p0055 A73-10263

Investigation of the rheological properties of a model material based on the 'Epidian 2' epoxy resin
01 p0068 A73-10571

Sintered chromium-nickel steel of high tungsten content.
01 p0065 A73-10816

Mechanical properties of molybdenum alloys.
01 p0065 A73-10818

Properties and uses of UMoCo-50 and related Co-Cr-Fe alloys.
01 p0066 A73-11051

Prediction of strength of a polymer body with allowance for solar radiation
01 p0068 A73-11078

Investigations of mechanical properties of lunar soil by self-propelled vehicle Lunokhod-1.
01 p0104 A73-11104

Investigations of physical and mechanical properties of lunar soil delivered by Luna-16.
01 p0105 A73-11105

On some relation between the mechanical properties and the bond strength of elastomer to solid inclusion in solid propellant.
01 p0090 A73-11117

The structure of scientific satellites developed by the University of Tokyo.
01 p0110 A73-11119

Balloon polyethylene film materials orthotropic mechanical properties, considering temperature effects on brittle fracture by transverse tension
01 p0005 A73-11206

Discontinuous or short fiber reinforced composites properties, manufacturing procedures and aircraft structural applications
01 p0057 A73-11240

Statistical characteristics for duralumin sheets mechanical properties, fatigue life and crack growth
01 p0117 A73-11298

Effect of various surface-active media on the changes taking place in the strength of U8 steel in the high-strength state.
01 p0066 A73-11337

Mechanical properties anisotropy in heat resistant Ni alloys due to strengthening phase nonmetallic inclusions distribution, suggesting purification by vacuum melting
01 p0066 A73-11346

Nitrided layer effects on austenitic steels mechanical properties at low temperatures, noting improved tensile strength
01 p0067 A73-11347

Ti-V and Ti-Nb alloys mechanical strength and stress concentration resistance at low temperatures
01 p0067 A73-11348

Cr and V additions effects on Mn steels mechanical properties and wear resistance, noting strength limit increase
01 p0067 A73-11351

Mechanical properties of glassy carbon fibres derived from phenolic resin.
01 p0068 A73-11498

PRD 49 high modulus organic fibre as aluminium replacement.
01 p0068 A73-11510

Properties and fabrication of cermet fibers from refractory compounds and of porous materials based on these fibers
02 p0178 A73-11538

Influence of high-temperature annealing on the rupture characteristics of zirconium carbide
02 p0178 A73-11541

Fatigue of duralumin under cyclic loads at ultrasonic frequencies
02 p0179 A73-11566

Correlations between the properties of some heat-resistant alloys
02 p0180 A73-11627

Physicomechanical properties of a structural cold-hardened fiberglass-reinforced plastic
02 p0184 A73-11719

Russian book - Fundamentals of lunar soil science: Physicomechanical properties of lunar soils.
02 p0211 A73-11893

Apparatus for testing reinforced plastics during nonuniform heating, with due allowance for the gas permeability of the material.
02 p0150 A73-12143

Generalized and modified parametric methods for extrapolating results of long term high temperature strength tests for service life determination
02 p0181 A73-12205

The influence of stress concentrators on the properties of steel in cryogenic technology.
02 p0181 A73-12213

Effect of rare-earth metals on mechanical characteristics of chromium.
02 p0181 A73-12214

Luna 16 direct measurements for soil mechanical properties, determining bulk density, failure characteristics, compressibility and shear and bearing strength
02 p0213 A73-12232

Lunar soil bearing strength, shear and cohesion properties in natural state along Lunokhod 1 self propelled vehicle route
02 p0213 A73-12233

Low temperature dynamic mechanical properties of polyurethane-polyether block copolymers.
02 p0185 A73-12426

Glass bead reinforced epoxy and polyester resins mechanical properties as function of volume fraction and interfacial bond strength, discussing beads chemical surface treatment effects
02 p0185 A73-12428

Effects of inhibitors PB-5 and of dialkyl-dimethyl ammonium chloride on the corrosion resistance and mechanical strength of structural materials during the cleaning of heat exchangers from scale by the hydrochloric acid method
02 p0174 A73-12537

Microstructural, mechanical and thermal properties of Nb-W-Ti-Zr alloys, noting cold rolled sheet products
02 p0182 A73-12580

The fracture energy and some mechanical properties of a polyurethane elastomer.
02 p0185 A73-12641

The effect of prior deformation on the strength and annealing of reverted austenite.
02 p0183 A73-12766

Mechanical properties of aluminum matrix composites.
02 p0184 A73-12849

Effects of alloying elements on elevated-temperature mechanical strength of high Cr, Ni-base heat resistant alloy.
03 p0321 A73-12921

Polyimide 2080 molded composites mechanical, thermal and electrical properties, discussing processing techniques
03 p0329 A73-13005

Properties of pultruded composites containing high modulus graphite fibers.
03 p0332 A73-13032

The relationship between dielectric and mechanical properties of polymers.
03 p0332 A73-13036

Effect of heat treatment on filament wound carbon composites.
03 p0332 A73-13043

Vibrational strength of structural members from Woehler lines, calculating service life from S-N diagrams
03 p0385 A73-13138

Mechanical properties of Fe, Al, Ti and heat resistant alloys consolidated powders, establishing coupling between fundamental concepts and engineering application
03 p0322 A73-13261

Mechanical properties of pressed and sintered titanium powder.
03 p0322 A73-13264

Minimum deformation forging of prealloyed steel powder for weapon components, discussing mechanical properties, processing and cost analysis
03 p0322 A73-13265

How deformation affects the mechanical properties of aluminum forgings.
03 p0322 A73-13266

Warm forging of steels for increased precision and mechanical properties.
03 p0323 A73-13269

Covalent bond formation role in Ti strengthening by oxygen from evidence of alpha phase stabilization, ordered structures, abnormal resistivity and high activation energy
03 p0323 A73-13371

Failure criterion for a propellant of a spherical solid rocket motor

[AIAA PAPER 72-1088] 03 p0351 A73-13409

Vacuum arc melting for improved heat resistance and mechanical properties of Ni alloy blanks, comparing with electro-beam and plasma arc melting and powder sintering

03 p0323 A73-13502

Means of improving the quality of heat-resistant metals and their alloys

03 p0324 A73-13504

Influence of deformations on the mechanical properties of magnesium alloys containing yttrium

03 p0324 A73-13509

Strengthening and stabilization effects of alloying elements in metastable Ti beta-alloys as function of atom concentration and position in periodic system

03 p0324 A73-13511

Cast Al-Si alloy strengthening by Mg, Be, Ti, Cu, Cd, Zr and B alloying, refining and modifying techniques

03 p0324 A73-13512

New magnesium alloys intended for operation at elevated temperatures

03 p0324 A73-13513

Ways of enhancing the strength characteristics of heat-resistant and high-strength cast aluminum alloys

03 p0324 A73-13514

Mechanical properties of base and coating metals for explosive plating, noting heat treatment for strain hardening prevention

03 p0312 A73-13584

Preparations and properties of boron and silicon carbide filaments

03 p0334 A73-13588

Prospects offered by high performance composites with a metallic matrix

03 p0325 A73-13589

Influence of aging on the mechanical properties of polyester glass-resin laminated fabrics

03 p0334 A73-13591

Mechanical properties and applications of reinforced plastics for cast alloy elements, machine parts and noncorrosive light structures production, emphasizing glass fiber reinforcement

03 p0334 A73-13593

Some biomechanical properties of the pelvic girdle of man

03 p0267 A73-13743

Effects of process and test variables on the properties of carbon-fibre/epoxide-resin composites.

03 p0335 A73-13800

Ni, Si and Mn alloying effect on structural transformations, phase composition and mechanical properties of cast Cr-Ni steels

03 p0327 A73-14002

Sn alloying effect on heat resistant Ni-Cr alloys plastic strain resistance and strength at room and high temperatures

03 p0327 A73-14003

Hot worked Al alloy machine elements mechanical properties scattering, discussing quality control procedures

03 p0327 A73-14004

Aluminum-stainless steel and Ni-Mo composites prepared by dynamic hot pressing, determining bond strength between fibers and reinforced metal matrix

03 p0328 A73-14013

High speed testing of materials mechanical behavior over range of impact loading rates

03 p0394 A73-14023

Stress analysis and design of silicon solar cell arrays and related material properties.

03 p0255 A73-14224

Consideration of a number of factors involved in determining the long-term strength of dies used for the extrusion of hollow sections of aluminum alloys

03 p0318 A73-14651

The relationship between design allowances and load induced micromechanical damage in composite materials.

04 p0508 A73-14719

Anisotropic material characteristics due to plastic deformation during fabrication processes, presenting tensor analysis

04 p0511 A73-15169

Grain boundary interface and crystal structure effect on elastic and plastic deformation and mechanical properties of metals at low and high temperatures

04 p0462 A73-15301

High temperature tests for chemical vapor deposited W ring and tensile specimens mechanical properties, investigating slip traces and fracture surfaces

04 p0462 A73-15305

Influence of microstructure on the mechanical properties and stress corrosion susceptibility of 7075 aluminum alloy.

04 p0463 A73-15314

Mechanical properties and structure of certain internally oxidized copper alloys

04 p0464 A73-15500

Characteristics of secondary phases in heat-resisting alloys.

04 p0465 A73-15580

Effects of heat treatment on the mechanical properties and microstructure of Inconel Alloy 718.

04 p0465 A73-15582

The problem of strength and aspects of predicting the mechanical properties of metals

04 p0465 A73-15661

Phase transformations and mechanical properties of highly alloyed Cr-Mn-Ni steels

04 p0466 A73-15664

Influence of cold deformation and subsequent heating on the structure and properties of dispersion-strengthened nickel

04 p0466 A73-15666

Alloying effects on Ta binary alloy tensile strength brittleness and yield point at low temperatures

04 p0466 A73-15669

Effective stiffness of randomly oriented fibre composites.

05 p0631 A73-16116

Effect of the cross sectional shape of specimens on their strength under transverse-bending impact loads

05 p0632 A73-16327

The mechanical properties of thermoplastics strengthened by short discontinuous fibres.

05 p0589 A73-16434

Strength and microstructure of nickel-base superalloys after long term heating.

05 p0587 A73-16622

HF dc straight polarity current pulsations effects on quality and mechanical properties of gas tungsten arc welds in Al alloy

05 p0582 A73-16669

Composite materials technology for aircraft and spacecraft structures, discussing various fiber-matrix combinations mechanical properties and production volume/price relations

05 p0589 A73-16759

On the establishment of a diffusion barrier between a boron fiber and its tungsten substrate

05 p0589 A73-17049

Diffusion welding of beryllium. II - The role of the microalloying elements.

06 p0704 A73-17597

Aircraft radome design mechanical, electrical and aerodynamic requirements, taking into account lightning hazards, electrostatic surface charges and plastic components deformations

06 p0648 A73-17997

The mechanical properties of titanium alloys with isomorphous beta-stabilizing elements.

06 p0708 A73-18206

Glass fiber reinforced thermoplastic molding materials mechanical and thermal-dimensional stability properties, considering time dependent behavior under static and dynamic loads

06 p0714 A73-18450

Scale factors of adsorptive reduction in the strength of metals in the presence of melts

06 p0711 A73-18667

Effects of a high-pressure gas medium on the mechanical properties of polymethylmethacrylate

06 p0715 A73-18671

Mechanical behavior of assemblies welded by fusion on steel

06 p0698 A73-18694

Relationship between structure and strength for CVD carbon infiltrated substrates. II - Three dimensional woven, tufted and needled substrates.

06 p0715 A73-18718

Properties of pultruded composites containing high modulus graphite fibers.

06 p0715 A73-18719

High temperature behavior of superalloys exposed to sodium chloride. I - Mechanical properties. II - Corrosion.

06 p0713 A73-18766

Effect of grain refinement on the microstructure and mechanical properties of 4340M.

06 p0713 A73-18773

Beryllium for nonstructural and structural applications in aerospace systems, considering high dimensional stability, mechanical and thermodynamic properties, and metal sintering techniques for production

07 p0828 A73-18904

Superrefractory Ni-based alloys mechanical properties enhancement through unidirectional solidification, considering grain boundary structure

07 p0838 A73-19116

Mechanical properties of interstitial alloys of niobium.

07 p0838 A73-19123

Development and properties of cobalt-base alloys with improved hot-corrosion resistance.

07 p0838 A73-19497

Self lubricating bearing materials strength, friction, wear, thermal and dimensional stability properties, considering plastic, metal matrix and carbon graphite composites

07 p0842 A73-19555

Apollo 12 soil sample strength, compressibility, bulk density, porosity and shear wave velocity

07 p0898 A73-19901

Mechanical properties of lunar soil - Density, porosity, cohesion, and angle of internal friction.

07 p0898 A73-19902

The casting of titanium and its alloys by the lost-mold method

07 p0831 A73-20161

Static and dynamic behavior of welded aluminum beams.

07 p0839 A73-20270

Glass fiber reinforced polyester laminates, testing layer base material and molding condition effects on tensile and bending strengths and other mechanical properties

07 p0843 A73-20326

Hybrid composite of carbon and glass fiber reinforced epoxy resin, testing mechanical properties and optimal fibrous modulus ratios and volume fraction

07 p0844 A73-20327

On the torsional strength of composite materials reinforced with glass fabric laminates and the effect of the voids in matrix.

07 p0915 A73-20332

Filler wire welded joints of Al-Zn-Mg and Al-Mg alloys, testing weldability and mechanical properties susceptibility to hot cracking

07 p0840 A73-20372

Influence of thermal-diffusion coatings on the physicomachanical properties of heat-resistant metals

07 p0840 A73-20512

Possibility of argon-nitrogen gas metal-arc welding of some non-ferrous metals.

08 p0973 A73-21237

Mechanical behaviour of unidirectionally solidified composites.

[ONERA, TP NO. 1147] 08 p0983 A73-21676

Influence of hot rolling on the mechanical properties of unstable austenitic chromium-manganese steels

09 p1098 A73-21848

Influence of composition and heat treatments on the structure and mechanical characteristics of martensitic stainless steels derived from the 16 percent chrome and 4 percent nickel type

09 p1098 A73-21924

Investigation of the strength and deformability of thin composite materials used as magnetic recording media. II - Strength and deformability at low temperatures

09 p1110 A73-22156

Grain size effects on strength and ductility of two phase Ni-Cr and Ni-Mo alloys at high and low deformation temperatures

09 p1101 A73-22164

Static and kinetic strength estimation of ionic and metal single crystals, discussing microcracks in brittle materials and surface quality and pore distribution effects

09 p1160 A73-22900

Analysis of the mechanical and energetic characteristics in pulse-coded regulation of an asynchronous motor

09 p1037 A73-22939

Mechanical behaviour of molybdenum and tantalum under high pressures at elevated temperatures.

09 p1105 A73-23018

Random function theory method for estimation of tensile, compressive and shear strength and elastic constants of monodirectional fiberglass reinforced plastics

09 p1110 A73-23056

Stability of structure and mechanical properties of molybdenum under prolonged influence of temperature and stress.

09 p1106 A73-23160

Investigation of the effect of surface finish and method of surface treatment on the endurance of the steels Kh18N10T and Kh16N6 and of alloy AMG6 at normal and low temperatures.

09 p1106 A73-23163

Effect of heat treatment on the structure and properties of NV10MST3T's alloy

09 p1106 A73-23190

Influence of heat treatment on the mechanical properties of the VT3-1 titanium alloy

09 p1107 A73-23191

Structure and properties of electron-beam-melted 1Kh12N3M3B steel

09 p1107 A73-23194

Effect of hafnium dioxide on grain growth and strength characteristics in niobium

09 p1108 A73-23233

Influence of heat treatment on the high-temperature strength and creep of the NV10MST3T's niobium alloy

10 p1230 A73-23600

Evaluation of static test methods for determining the fundamental mechanical properties of fiberglass-reinforced plastics

10 p1237 A73-23663

Effects of Ni and Fe addition on various properties in heat-resisting aluminum casting alloys.

10 p1231 A73-23675

Mechanical behavior of solid solutions of centered cubic symmetry obtained by limited addition of titanium to the iron

10 p1231 A73-23770

A theoretical study of the effect of the interface on composite toughness.

10 p1288 A73-23955

Effect of fiber-matrix adhesion on the properties of short fiber reinforced ABS.

10 p1237 A73-23956

The effect of long-time thermal exposure on the mechanical properties of graphite/polyimide composites.

10 p1238 A73-23970

Technology, strength, and calculation of bonded circular joints

10 p1224 A73-24090

Adhesive metal/glass laminate bonding, discussing materials, tests and interlaminar strength effects

10 p1224 A73-24092

High strength properties and hardening of epoxy resin bonding materials using dicyanodiamides

10 p1239 A73-24094

Layer strength and vulcanization effects on rubber/metal bonding with MEGUM agent

10 p1239 A73-24095

Carbon-felt, carbon-matrix composites - Dependence of thermal and mechanical properties on fiber volume percent.

10 p1240 A73-24278

Investigation of the sintering process and physicochemical properties of products prepared from spherical bronze pellets

10 p1225 A73-24319

Mechanical properties of recrystallized molybdenum containing vanadium microadditions

10 p1233 A73-24361

Facility for studying the strength and deformability of high-strength brittle materials in biaxial compression

10 p1203 A73-24372

A comparison of the effects of explosive forming and static deformation on the mechanical properties of pressure vessel steels.

10 p1225 A73-24426

Plasticity theory, strength-differential /SD/ phenomenon, and volume expansion in metals and plastics.

10 p1234 A73-24428

Importance of slip mode for dispersion-hardened beta-titanium alloys.

10 p1235 A73-24441

A theory for the mechanical properties of metal-matrix composites at ultimate loading.

10 p1235 A73-24443

Nb refractory alloy sheet mechanical properties for application in space shuttle thermal protection system /TPS/ and space tug aerobraking system

10 p1235 A73-24445

Fabrication procedures, structure, and mechanical properties of BiTeI thin films

10 p1260 A73-24470

Temperature change induced material properties variations effects on impact stresses in graphite and stainless steels, considering impact velocity

10 p1220 A73-24575

Foamed Al production from Al powder mixture with aluminum hydroxide and orthophosphoric acid, discussing mechanical, thermal conductivity and electrical insulating properties

10 p1236 A73-24919

Investigation of the hardening process of alloy D16 in liquid nitrogen.

10 p1226 A73-24929

Structural transitions and mechanical characteristics in the case of multicomponent aluminum bronze

11 p1378 A73-25106

Direct nondestructive prediction of engineering properties.

11 p1372 A73-25129

The state of technology of ceramic radomes, their use and possibilities for the future.

11 p1335 A73-25286

Electrically stabilized alumina as ceramic material for radome applications, tabulating dielectric, thermal and mechanical properties and firing conditions

11 p1408 A73-25287

Fabrication and physical, mechanical and electrical properties of inorganic composite material for aircraft radomes

11 p1387 A73-25288

Mechanical, thermal and electrical properties of machinable glass ceramics, discussing application as electromagnetic window materials

11 p1387 A73-25293

Boron filament reinforced Al and Ti matrices manufactured by pressure-sintering method, investigating filament external silicon carbide effects on mechanical properties

11 p1379 A73-25402

Mechanical properties at high temperature of Ni-based unidirectionally solidified eutectic: Ni-Ni3Ta.

11 p1379 A73-25405

Production and properties of tungsten-wire reinforced NiCr 80 20

11 p1379 A73-25407

Discontinuous fibres alignment in metal composites by plastic deformation.

11 p1372 A73-25409

Ag- or Cu-based fiber reinforced composite materials for springs in electrical contact devices, investigating mechanical strength and contact and wear resistances

11 p1387 A73-25410

Silicon carbide whisker reinforced Al composite production by powder metallurgy, discussing mechanical strength and extrusion process for fiber orientation

11 p1373 A73-25414

A statistical investigation on the mechanical properties of metals impregnated graphites.

11 p1388 A73-25416

Elevated temperature stability of carbon-fibre, nickel-matrix composites Morphological and mechanical property degradation.

11 p1384 A73-26047

Heat treatment effects on the mechanical properties in Ti-6Al-6V-2Sn.

11 p1385 A73-26172

Optical fiber breaking stress distributions obtained by a cantilever method.

11 p1344 A73-26312

Glass fiber reinforced polyester laminates mechanical properties evaluation for structural design, considering failure criteria in terms of fiber bonding and resin and gel coat cracking

12 p1515 A73-26877

Carbon fiber reinforced epoxy resins mechanical properties, correlating test parameters with observed failure mechanism

12 p1515 A73-26878

The nature of the nonuniformity of the structure and properties of semiproducts pressed from titanium and its alpha-alloys

12 p1502 A73-26909

Improving the properties of the MA5 magnesium alloy by high-temperature thermomechanical treatment

12 p1510 A73-26910

Microstructure, microhardness and mechanical strength of ingots and granules of Al alloys with high refractory metal contents

12 p1511 A73-26917

Optimal electrical conductivity and mechanical properties of Cu-Mg-Fe-Si-Zr and Be-B containing heat resistant Al alloys, comparing to Cu at room and elevated temperatures

12 p1511 A73-26918

Realization of the mechanical properties of the fibers in high-modulus polymeric composites

12 p1516 A73-27183

Statistical characteristics of the mechanical constants of glass-fiber-reinforced plastics

12 p1516 A73-27184

Mechanical properties of strip molybdenum with a polygonized single-crystal structure

12 p1513 A73-27265

Thermal and mechanical properties of zirconia cloth, felt and braid for heat shielding of reusable space shuttle

12 p1548 A73-27379

The changes in structural and mechanical properties of construction materials under loads

12 p1513 A73-27500

The pressing of profiles of aluminum casting alloys from granules and the study of their mechanical properties

12 p1503 A73-27560

The strength differential of steel and Ti alloys as influenced by test temperature and microstructure.

12 p1513 A73-27681

Study of the mechanical-metallurgical characteristics of martensitic steels in a corrosive medium

12 p1514 A73-27686

Dynamic strain ageing in some titanium-silicon alloys.

13 p1634 A73-28184

Mechanical behavior of plastically deformed polycrystalline metal subjected to hydrostatic pressure soaking.

13 p1634 A73-28196

The general form of constitutive equations in relativistic physics.

13 p1658 A73-28374

Glass fiber reinforced plastics optimum glass volume fraction for maximum flexural rigidity and strength

13 p1645 A73-28777

The effect of processing on the microstructure of CFRP.

13 p1645 A73-28779

Relationship of mechanical characteristics and microstructural features to the time-dependent edge-notch sensitivity of Inconel 718 sheet.

13 p1637 A73-29200

[ASME PAPER 73-MAT-G] Relationship between structure and strength for CVD carbon infiltrated substrates. III - Fabric lay-up substrates.

13 p1645 A73-29272

German monograph - Effect of creep strains at 700 C on the hardening characteristics of the steel X 8 Cr-NiMoNb 16 16 at room temperature.

13 p1637 A73-29281

Graphite- and boron-epoxy composite curved panels, determining shear buckling stress and post-buckling strength by visual and photographic observations

[SESA PAPER 2030A] 13 p1699 A73-29308

Fiber composite materials properties, technological assessment and future development and application for aerospace flight structures, considering manufacturing cost, tailorability and stiffness requirements

13 p1699 A73-29346

Mechanical behavior of materials: Proceedings of the First International Conference, Kyoto, Japan, August 15-20, 1971. Volume 1 - Deformation and fracture of metals. Volume 2 - Fatigue of metals. Volume 3 - Temperature effects of metals, environmental effects, polymers. Volume 5 - Composites, testing and evaluation.

13 p1638 A73-29451

Theoretical interpretation of residual lattice strains induced in polycrystalline metals by plastic deformation.

13 p1639 A73-29460

The effect of microstructure on fatigue crack propagation in Ti-6Al-6V-2Sn alloy.

13 p1640 A73-29484

Thermal stress analysis of metals with temperature dependent mechanical properties.

13 p1701 A73-29507

Metallurgical and strength studies of heat resisting alloys for gas turbines after long term service.

13 p1625 A73-29519

Nylon copolymers dynamical mechanical properties temperature dependence, discussing alpha peak shifts, polyamides relaxation and ordered structure

13 p1646 A73-29526

A molecular theory of elastomer deformation and rupture.

13 p1646 A73-29528

A variational method for micromechanics of composite materials.

13 p1702 A73-29534

Carbon fibre reinforced ceramics.

13 p1646 A73-29541

Mechanical behavior of WC-Co composite alloys.

13 p1643 A73-29545

Mechanical properties of titanium reinforced with unidirectional molybdenum wires.

13 p1643 A73-29604

Increase in the boundary strength of cast electron-beam-melted molybdenum by microadditions of vanadium.

13 p1643 A73-29634

Book on solids structure effects on materials strength characteristics covering interatomic binding forces, elastic properties, crystal defects, work hardening, heat treatment, temperature effects, etc

14 p1759 A73-29948

Study of the structural and mechanical properties of polyvinyl-chloride pastes used as anticorrosion coatings

14 p1766 A73-30377

German monograph - Effect of the transformation and heat treatment conditions on the mechanical properties and the creep characteristics of the alloy TiAl6V4.

14 p1762 A73-30668

Rotating turbine disks ultimate strength relation to stress-strain state, material mechanical properties and plastic deformation

14 p1814 A73-30684

Bakelite lacquer and epoxy and phenol-formaldehyde solidified resin binders strength at high temperatures

14 p1766 A73-30687

Influence of stress concentrations on the mechanical properties of cast molybdenum with protective coatings

14 p1763 A73-30688

Effect of deep annular grooves on the strength of some metals under static tension and torsion

14 p1763 A73-30693

Steel reinforcement fiber arrangement and volume content influence on aluminum composites strength and fatigue resistance at room and elevated temperatures

14 p1766 A73-30710

Strength and elastic characteristics of ammonium perchlorate whiskers grown with potassium permanganate additions, discussing crystal dislocations and physico-chemical properties

14 p1767 A73-30829

Investigation of the influence of the method of supplying hydrogen to the furnace on the properties of tungsten metal

14 p1765 A73-30885

Dependence of the closeness of two contacting bodies on the load under a high contour-applied pressure with a plastic contact

15 p1880 A73-31143

Investigation of some physicochemical and X-ray structural changes in a superconducting wire prepared from 60T alloy, as a function of the strain level and duration of annealing in vacuum

15 p1887 A73-31187

Effect of lasting high temperatures on the mechanical properties and microstructure of bonded glass mat with an aluminophosphate binder

15 p1896 A73-31213

Viking lander capsule decelerator system candidate materials evaluation, discussing in-situ testing for high density packing and heat sterilization effects on strength

[ALAA PAPER 73-447]

15 p1881 A73-31433

Russian book - Strength of turbine wheels.

15 p1948 A73-31578

Russian book - Physics of carbographite materials.

15 p1897 A73-31583

Characteristics of dynamic hot pressing with high deformation rates

15 p1881 A73-31589

High strength steel developments, discussing chemical compositions, mechanical properties, production technology and applications

15 p1888 A73-31624

Hardening and softening of aluminum alloys under an applied load at 135 to 150 C

15 p1889 A73-31808

Properties of low-alloy steels with small niobium additions

15 p1889 A73-31811

Investigation of titanium alloys containing refractory elements

15 p1889 A73-31813

Work hardened plastic material mechanical properties changes manifested by Bauschinger effect defined as acquired anisotropy, examining plastic deformation conditions

15 p1952 A73-32079

Single crystal mechanical and electrophysical properties in refractory compounds, including temperature effects, microhardness, resistivity, heat transfer, deformation and Hall effect

15 p1898 A73-32241

Mechanical treatment of tungsten powder compacts

15 p1892 A73-32246

A physical basis for solid-solution strengthening and phase stability in alloys of titanium.

15 p1892 A73-32272

Al addition effect on strength of Ti via short range order, considering strengthening by alpha stabilizing solutes

15 p1893 A73-32273

Russian book - Precision alloys with specific thermal-expansion and elastic properties

15 p1893 A73-32293

Phase transformations in alloys of the titanium-molybdenum system

15 p1893 A73-32517

Properties of the 4201 alloy at elevated temperatures

15 p1894 A73-32528

Features of the influence of aluminum on the mechanical properties of titanium

15 p1894 A73-32532

Influence of structure and of stress concentration on the mechanical properties of Ti-Ta-Mo system alloys

15 p1894 A73-32533

Properties of titanium-niobium based stable beta alloys

15 p1894 A73-32534

Investigation of titanium alloys at high temperatures in vacuum

15 p1894 A73-32541

Some mechanical properties of carbon fiber reinforced aluminum.

16 p2025 A73-32849

Heat treatment effects upon the properties of PAN base carbon fibers.

16 p2028 A73-33040

Processing and properties of composites based on NR-150 polyimide binders.

16 p2029 A73-33047

Low void polyimide/glass and graphite reinforced composite properties and fabrication, showing improved interlaminar shear and wet strength

16 p2029 A73-33048

Boron fiber coating by chemical vapor deposition of boron carbide for improved mechanical properties and incorporation in Al alloy matrices

16 p2030 A73-33070

Acoustic fatigue in ceramic materials, analyzing strength degradation as function of microstructure, structural integrity and properties

16 p2030 A73-33194

The consideration of environmental effects in the development of environment-resistant systems

16 p2019 A73-33385

Missile and explosive environmental tests for mechanical properties, outlining test facilities, climatological effects, salt spray, vibration, shock, dropping, vacuum effects and crack propagation

16 p1997 A73-33387

The effects of radiation sterilization on plastics.

16 p2030 A73-33693

High strength low density Hyfil carbon fiber prepreg sheet properties and production for aircraft applications

16 p2021 A73-33986

The effect of cure cycle on the mechanical properties of carbon-fibre/epoxide resin.

16 p2031 A73-33988

The effects of adverse environmental conditions on the resin-glass interface of epoxy composites.

16 p2031 A73-33989

Enhanced ductility in metals /Superplasticity/.

17 p2240 A73-34113

A method of programmed fatigue tests with short-time overloads.

17 p2165 A73-34277

Allowance for the influence of temperature in statistical estimates of the strength of metals in the brittle condition

17 p2186 A73-34328

Effect of additional alloying and heat treatment on the strength of steels

17 p2187 A73-34336

Strength and plasticity of tantalum in rapid tests

17 p2188 A73-34561

Effect of small group-VIII metal additions on the structure and properties of cast molybdenum

17 p2189 A73-34578

Some physicomachanical characteristics of failure in tempered high strength steels

17 p2189 A73-34580

Effect of carbon on the structure and properties of molybdenum

17 p2189 A73-34582

Molybdenum bicrystals mechanical properties dependence on mismatch angle under bending with torsion and brittle cleavage under critical stresses

17 p2189 A73-34636

Polyimide resin dielectric and mechanical properties, discussing syntactic foam composite with aluminum filler for radome construction

17 p2195 A73-34804

The residual strength characteristics of stiffened panels containing fatigue cracks.

17 p2246 A73-34888

Composite materials structure, describing component interactions, major constituents, determinants of mechanical properties, particulate composites, materials applications and fiber types

17 p2195 A73-34974

Moldability, storage stability and thermal, mechanical and electrical properties of epoxy molding compounds for electronic devices

17 p2196 A73-35340

Cold rolling of polymers. III - Properties of rolled crystallized polycarbonates.

17 p2197 A73-35351

Processability/mechanical properties trade-off for reinforced plastics.

17 p2197 A73-35353

Mechanical and optical characterization of an anelastic polymer at large strain rates and large strains. [SESA PAPER 2198A]

17 p2198 A73-35458

Residual stresses and mechanical properties of circumferentially wrapped metal-metal composite cylinders fabricated from plasma sprayed Al reinforced with steel filaments

17 p2251 A73-35534

Emerging aerospace materials and fabrication techniques.

17 p2198 A73-35841

Mechanical properties of weld, base metal and coated columbium FS85.

17 p2182 A73-35842

Study of the hardening and mechanical properties of polyester resins

18 p2327 A73-36468

Matrix method for the determination of the elastic and mechanical properties of reinforced plastics

18 p2327 A73-36475

Mechanical characteristics of thermoplastic materials reinforced with short glass fibers, taking into account various degrees of reinforcement

18 p2327 A73-36479

Interfacial, mechanical and fracture properties of fibre reinforced polycaprolactam.

18 p2328 A73-36480

The effect of a fiberglass reinforcement on the properties of laminates with a polyimide binder

18 p2328 A73-36481

Strength of nonuniformly heated rotating disks

18 p2366 A73-36755

Mo-W alloys mechanical characteristics dependence on temperature and W content

19 p2439 A73-37265

Mechanical, thermal and electrical properties of polymers as functions of temperature, radiation and frequency for cryogenic environment material and design selection

19 p2443 A73-37525

Effect of thermodiffusion coatings on the physicomachanical properties of refractory metals.

19 p2440 A73-37787

Microstructural characteristics of the TA6V alloy as a function of thermomechanical treatments in alpha plus beta - Effects on the mechanical characteristics in tension

19 p2441 A73-37831

Transformations of TA6V6E2Zr alloy in isothermal conditions

19 p2441 A73-37832

Influence of hydrogen and oxygen on the mechanical behavior of unalloyed titanium

19 p2441 A73-37837

The effects of crystallographic texture on the mechanical and fracture properties of Ti-3Al-2.5V hydraulic tubing.

[SAE SP-378]

19 p2434 A73-37871

Mechanical and corrosion resistant properties of titanium castings.

19 p2442 A73-37947

Glass fiber reinforced polypropylene composites fabrication technology and physico-mechanical properties

19 p2444 A73-38162

Effect of autoclave heat treatments on the mechanical properties of the prealloyed-powder cobalt-base alloy HS-31.

19 p2443 A73-38248

French monograph - Mechanical behavior of the titanium alloy TA6V6E2 with reference to hydrogen - Influence of heat treatment and oxygen content.

19 p2443 A73-38362

Mechanical properties of polymeric solids.

19 p2444 A73-38549

Structure and mechanical properties of internally oxidized Ta-8 pct W-2 pct Hf (T-111) alloy.

20 p2576 A73-39025

Mechanical properties of electron-beam-melted molybdenum and dilute Mo-Re alloys.

20 p2576 A73-39032

Aerospace applications of heat resistant alloy diffusion welding techniques, describing mechanical properties, metal bonding, surface cleaning, vacuum levels, temperature effects and microstructure

20 p2569 A73-39246

Study of the photoviscoelasticity method

20 p2619 A73-39331

Changes in the physicomachanical properties of structural polymers after heat treatment

20 p2580 A73-39333

Influence of small oxygen and nitrogen additions on the nature of the temperature dependence of the mechanical properties of niobium

20 p2577 A73-39360

Influence of alloying with elements of group VIII on the mechanical properties of a molybdenum alloy containing carbon in the cast and recrystallized states

20 p2577 A73-39366

Method of studying the resistivity to external effects in fiberglass plastic structural elements with highly dispersed initial-state properties

20 p2580 A73-39380

Anisotropy of the mechanical properties of aluminum hardened by a stainless steel grid

20 p2578 A73-39382

Study of the effect of stress concentration on the variation of stability characteristics in graphites

20 p2580 A73-39383

Effect of the degree of plastic deformation on the structure and mechanical properties of low-alloy molybdenum

20 p2579 A73-39741

The boundary theory of strength and nonlinear programming of boundary value problems of plate bending

20 p2625 A73-39821

Influence of chemical composition on the structure and mechanical properties of polycarbonate films and the possibility of using them as a substrate for moving-picture films

21 p2646 A73-40259

Effect of chemically activated elements on the properties of electron-beam-melted nickel

21 p2718 A73-40482

Influence of hydrogen on the mechanical properties of zirconium and some of its alloys

21 p2718 A73-40483

Preparation and properties of materials containing titanium carbide

21 p2719 A73-40851

Mechanical properties of weldments of AK-3 titanium with an elevated oxygen content.

21 p2720 A73-41036

Mechanical properties of AFC77 stainless steel bolts.

21 p2721 A73-41085

Influence of relief annealing on the mechanical properties of high-strength hydrogenized steel

21 p2721 A73-41228

Grain size effects on strength and ductility of two phase Ni-Cr and Ni-Mo alloys at high and low deformation temperatures

22 p2875 A73-42112

Experimental aspects of the mechanical behavior of fiber composites produced by oriented solidification [ONERA, TP NO. 1205]

22 p2876 A73-42215

Polyquinazolines, thermostable polymers with thermoplastic properties

22 p2881 A73-42218

Book - Ultrasonic investigation of mechanical properties.

22 p2861 A73-42575

Structure and properties of arc-sprayed titanium coatings. 22 p2879 A73-42597

Experimental investigation of the strength and deformability of vacuum-prepared fiberglass-reinforced plastic shells 22 p2881 A73-43062

Linear viscoelasticity theory application to high polymers mechanical properties determination via relaxation spectrum with emphasis on polymethyl methacrylate 22 p2881 A73-43170

Response of glass-fiber-reinforced epoxy specimens to high rates of tensile loading. 23 p2996 A73-43385

Substitution of molybdenum for tungsten in heat resistant cobalt-base alloys 23 p2989 A73-43436

Investigation of the structure and properties of annealed alloys of the Ti-Mo system 23 p2990 A73-43484

Elementary mechanisms and physical models in plasticity and viscoplasticity 23 p3043 A73-43965

Microstructure and its related properties on carbon fiber composites. 23 p2998 A73-44134

Some experiments to crystallize the metal thin films on quartz plates. 23 p3018 A73-44136

Turbine wheel strength, lifetime and safety margin calculations based on classical elasticity and plasticity theories 23 p3020 A73-44225

The relationship of certain mechanical and thermophysical properties of polymer composites with the reduced filler concentration 24 p3102 A73-44512

Process anisotropy of randomly reinforced fiberglass plastics 24 p3102 A73-44515

Mechanical properties of boron fibers 24 p3102 A73-44524

Analytical relations of physicomaterial, strength and geometrical factors in formation of high strength monolithic glass fiber reinforced structures 24 p3103 A73-44533

Influence of small beryllium, titanium, and zirconium additions on the structure and properties of Al9 alloy 24 p3098 A73-44571

Arbeitsgemeinschaft Verstaerkte Kunststoffe, Open Meeting, 10th, Freudenstadt, West Germany, October 3-6, 1972, Reports 24 p3103 A73-44876

The effect of impregnation and wetting characteristics on the mechanical parameters of glass-fiber-reinforced plastics 24 p3103 A73-44877

Glass fiber reinforced casting plastics mechanical properties dependence on processing quality fluctuations, considering laminates with unsaturated polyesters and fiber glass mats 24 p3103 A73-44878

Mechanical properties of unidirectionally reinforced polyester and epoxy resin laminates under combined stresses perpendicular or parallel to glass fiber direction 24 p3104 A73-44886

Mechanical properties of glass fiber reinforced plastic laminate formed by spraying unsaturated polyester resin on fiber rovings 24 p3094 A73-44890

Certain properties of synthetic diamond crystals of various habits 24 p3104 A73-44970

Improved mechanical properties of composites reinforced with neutron-irradiated carbon fibers. 24 p3104 A73-45143

Memory effect on mechanical properties of plastically prestrained Al-Mg alloy sheets 24 p3100 A73-45247

Properties of low-alloy steels with small niobium additions. 24 p3100 A73-45274

Alloys of titanium with refractory elements. 24 p3100 A73-45276

Plastic deformation of Co-Ni-Cr and Co-Ni-Cr-Mo alloys 24 p3101 A73-45525

MEDICAL RESONANCE

U RESONANT VIBRATION

MECHANICAL SHOCK

NT HYDRAULIC SHOCK

Reaction of a damped system to the simultaneous action of an isolated semisinusoidal impact pulse and of vibrational oscillations 01 p0054 A73-11418

Impact of a cylindrical shell against the surface of a compressible fluid 06 p0758 A73-17451

Approximative calculation of flutter regions for collision body systems in phase space, noting fluttering duration as function of post-impact velocity recovery factor 06 p0725 A73-18880

Impact interaction of an absolutely hard body and an elastic two-mass system 11 p1400 A73-26455

Approximative calculation of flutter regions for collision body systems in phase space, noting fluttering duration as function of post-impact velocity recovery factor 15 p1915 A73-32405

Biodynamic applications regarding isolation of humans from shock and vibration. 22 p2816 A73-42926

Generation of electrical current by impact in metallic and semiconductor bodies 23 p3015 A73-43476

MECHANICAL TWINNING

Niobium mechanical twin formation and propagation, discussing continuous nucleation, matrix interface and dislocation core energies 13 p1632 A73-28132

The Bauschinger effect and its role in mechanical anisotropy. 21 p2722 A73-41547

MECHANICS [PHYSICS]

Russian book on tensor calculus fundamentals covering tensor algebra and analysis and applications to mechanics of discrete and continuous systems 02 p0192 A73-11888

Structural design via finite element method, noting object discretization, displacement forms and non-linear problems of deformable body mechanics 02 p0233 A73-11936

Book - Solid-state mechanics 2. 02 p0233 A73-11976

Conference on Mechanics, Berlin, East Germany, October 13-15, 1971, Reports 03 p0386 A73-13151

Southeastern Conference on Theoretical and Applied Mechanics, 6th, University of South Florida, Tampa, Fla., March 23, 24, 1972, Proceedings. 03 p0388 A73-13301

Motion, constitutive and energy balance equations for materials with microstructure, considering elastic bodies 04 p0514 A73-15680

Analytical mechanics algorithms based on characteristic equation and canonical equations of system with integral constraints 10 p1249 A73-24312

Stagnation conditions in systems with Coulomb friction 11 p1400 A73-26451

Method of reducing the order of a differential equation when studying transient processes in mechanical systems 14 p1774 A73-30286

German book - The physics of the scientist: Mechanics, relativity, gravitation. 17 p2229 A73-34465

Book - Advanced experimental techniques in the mechanics of materials. 17 p2176 A73-35834

Interaction of self-excited vibrations in mechanical vibrational systems 19 p2494 A73-37181

MECHANOGRAMS

Muscular activity control mechanism interactions in vertical posture maintenance from stabilogram, mechanogram and electromyogram data 02 p0137 A73-12119

MECHANORECEPTORS

Absence of appreciable cardiovascular and respiratory responses to muscle vibration. 03 p0263 A73-14119

Reflex bradycardia elicited from left ventricular receptors during acute severe hypoxia in cats. 09 p1042 A73-23244

The role of carotid sinuses in the regulation of hemodynamics during motor activity 15 p1833 A73-31161

Circulatory reflexes from mechanoreceptors in the cardio-aortic area. 21 p2638 A73-40637

Measurements of arterial pressure and of pressure-receptor reactions during prolonged pressure shifts in carotid arteries 24 p3062 A73-44720

MEDIA

NT ANISOTROPIC FLUIDS

NT ANISOTROPIC MEDIA

NT ELASTIC MEDIA

NT INTERGALACTIC MEDIA

NT INTERPLANETARY DUST

NT INTERPLANETARY GAS

NT INTERPLANETARY MEDIUM

NT METEOROID DUST CLOUDS

NT ZODIACAL DUST

MEDIAN [STATISTICS]

Application of the algorithm of a median for accuracy and reliability improvement in data processing 01 p0020 A73-10678

The median problem of the theory of elastic mobility with polar effects of spectral type. 18 p2364 A73-36492

MEDICAL ELECTRONICS

Microelectronic technology development and applications in transistor-transistor logic, medical devices, computers and thick film hybrid assemblies 02 p0148 A73-12593

Prolonged control of cardiac bioelectrical activity in man in ground experiments and during spaceflight 06 p0657 A73-17694

Modulated light transmission for electrical isolation in a multichannel physiological monitoring system. 07 p0785 A73-19482

Method for measuring the contractions of small hearts in organ culture. 08 p0933 A73-21218

Rapid eye movement analyzer. 09 p1045 A73-22697

Modification and updating of the bioelectric DS2C amplifier for a FET input. 09 p1046 A73-22936

Miniature single channel narrow-band differential pulse width modulation-FM crystal controlled transmitter for biomedical telemetry system 09 p1047 A73-23381

Electromagnetic 60 Hz interference in ECG recordings, discussing sources, identifying tests, elimination and ECG amplifier design 10 p1183 A73-23648

An IC piezoresistive pressure sensor for biomedical instrumentation. 10 p1183 A73-23649

An electrocardiograph amplifier which satisfies the stringent requirements of long-term monitoring of cardiac activity 10 p1184 A73-23849

Digital temperature-measuring device for medical applications 13 p1578 A73-28338

Multi-information recording and reproduction in the ultrasono-cardio-tomography. 13 p1579 A73-28581

Decatron indicator for a micromanipulator controlled by a stepping motor 14 p1722 A73-30850

Procedure for recording the rate of pressure changes in heart cavities 15 p1837 A73-31167

Technique for measuring the vessel blood pressure in long continued experiments 15 p1838 A73-31394

Russian book - Methods of studying eye movements. 15 p1840 A73-32417

Automatic recognition of electrocardiographic patterns 17 p2116 A73-34964

Book - Biomedical instrumentation and measurements. 17 p2118 A73-35860

Angiotensinotography using an air plethysmograph 18 p2282 A73-36575

The effects of the Westinghouse active magnetometer /WD-4/ on implanted cardiac pacemakers. 18 p2286 A73-36936

A universal preamplifier for bioelectrical signals 21 p2643 A73-40345

Electrofluoroplanigraphy for human body layer single-plane sections synchronization, using X ray tomography and TV imaging followed by roentgenogram electronic summation 21 p2645 A73-41216

Signal/noise ratio in the recording of human nerve-action potentials. 22 p2814 A73-42372

Shaping device for frequency analysis of electrical processes in peripheral neural stems and ganglia 22 p2815 A73-42664

A multiplex cathode-ray-tube display with digital readout for a body plethysmograph. 22 p2815 A73-42666

Circuit diagram of amplifier-filter for analysis of impulse activity of baroreceptor aortic afferent nerves in rabbits 22 p2816 A73-42681

Signal processing in medical technology 23 p2948 A73-43317

Two channel transistor amplifier design with negative capacitance correction for microelectrode applications 24 p3062 A73-44723

MEDICAL EQUIPMENT

NT ARTIFICIAL HEART VALVES

NT MECHANOGRAMS

NT PROSTHETIC DEVICES

NT RESPIRATORS

NT STETHOSCOPES

NT SURGICAL INSTRUMENTS

Influence of the packing and of certain conditions of usage on the medications in portable emergency medicine stores 12 p1465 A73-27720

MEDICAL PERSONNEL

NT FLIGHT SURGEONS

Incidence and severity of altitude decompression sickness in Navy hospital corpsmen. 13 p1576 A73-28511

MEDICAL PHENOMENA
NT PHENOMENOLOGY
MEDICAL SCIENCE

NT DERMATOLOGY
NT EPIDEMIOLOGY
NT HISTOLOGY
NT IMMUNOLOGY
NT NEUROLOGY
NT PHENOMENOLOGY
NT PSYCHIATRY
NT RADIATION MEDICINE
NT RADIOBIOLOGY
NT RADIOLOGY
NT SYMPTOMOLOGY
Book - Ultrasonics: The low- and high-intensity applications.
11 p1366 A73-26273
Predicting coronary heart disease.
14 p1716 A73-30351

MEDICAL SERVICES

Military contributions to aviation medicine.
[AIAA PAPER 73-68] 06 p0656 A73-17636
Human factor role in flying personnel errors, noting man machine system performance and medical service engagement
06 p0659 A73-18258

Physically or mentally disabled passengers handling on scheduled, charter and group flights, discussing rules for attendants, seating and emergency procedures
10 p1176 A73-24709

Medical diagnosis of pilot performance disturbances from viewpoint of flight surgeon responsibilities
15 p1837 A73-31171

MEDITERRANEAN SEA

Critical analysis of the results obtained by SIRS-A in remote sensing of the temperature field over the Mediterranean
17 p2205 A73-34936

The use of satellites for remote sensing of the sea surface
17 p2162 A73-34956

Meteorological satellite TV cloud cover photographs of cyclogenesis over Mediterranean Sea and cyclone arrival to European U.S.S.R. and Scandinavian Peninsula
18 p2334 A73-37074

MEETINGS

U CONFERENCES

MEISSNER EFFECT

U DIAMAGNETISM

U SUPERCONDUCTIVITY

MELANIN

Binding of Melatonin to human and rat plasma proteins.
10 p1182 A73-24657

MELLIN TRANSFORMS

Extended Mellin transforms for boundary value problems, discussing inversion integral, operational properties convolution formulas, and application to circular sector steady state heat problem
13 p1648 A73-28422

MELTING

NT ARC MELTING

NT FUSION (MELTING)

NT VACUUM MELTING

Practical protective atmospheres for molten magnesium.
03 p0323 A73-13267

Dispersive granulation by spinning electrode melting in helium atmosphere for steels and Ti, Ni and Mo alloys powder production
03 p0323 A73-13503

Improved melting and casting procedures for a cobalt-base magnetic alloy.
04 p0455 A73-15750

Initial and boundary value problems for melting propagation from solid cylinder axis and sphere center, assuming pure conductive heat transfer
05 p0638 A73-16595

Linearized hydrodynamic instability initiation in polymer melts extrusion, examining Weissenberg number role in melt fracture onset
10 p1241 A73-24655

Heat resistant and refractory materials contact eutectic melting for surface coating production
10 p1227 A73-24967

Strength of joints produced by melting high-carbon chromium alloys on low-carbon steel
17 p2188 A73-34566

Satellite detection of melting snow and ice by simultaneous visible and near-IR measurements.
20 p2556 A73-39840

MELTING POINTS

Nucleation during solidification and melting of metals and alloys
02 p0181 A73-12363

Determination of degradation of nylon 66 using differential scanning calorimetry.
04 p0468 A73-14857

Influence of annealing at near melting point temperatures on the substructure of aluminum single crystals
06 p0707 A73-18036

Creep in molybdenum single crystals at 0.57 of the melting temperature
06 p0708 A73-18047

A new method for thermographic investigation of high-speed crystallization processes in high-melting-point metals
09 p1103 A73-22483

Electron beam refined niobium melting temperature determination from black body brightness change
10 p1230 A73-23508

Some physicochemical properties of compounds formed by oxides of rare-earth elements and barium
11 p1410 A73-26673

New method of thermographic investigation of rapid processes of crystallization of refractory metals.
15 p1891 A73-32070

Electrical conductivity variations in organic semiconductors in the melting temperature region
16 p2044 A73-34005

Electron beam refined niobium melting temperature determination from black body brightness change
17 p2191 A73-35188

Determination of work functions near melting points of refractory metals by using a direct-current arc.
21 p2722 A73-41563

The melting point of molybdenum as a secondary fixed point on the International Practical Temperature Scale.
[ECTP PAPER G-5] 22 p2877 A73-42407

Some thermophysical properties of titanium in the neighborhood of the melting point.
22 p2878 A73-42508

MEMBRANE ANALOGY

U MEMBRANE STRUCTURES

U STRUCTURAL ANALYSIS

MEMBRANE STRUCTURES

NT SKIN (STRUCTURAL MEMBER)

Stability of a spinning body containing an elastic membrane via Liapunov's direct method.
01 p0077 A73-10728

Progress in the development of the reverse osmosis process for spacecraft wash water recovery.
02 p0137 A73-11993

Finite axisymmetric deformations of elastic membranes.
02 p0234 A73-12089

Finite plastic deformation of pressurized membranes of revolution.
03 p0384 A73-13120

Stress field and deformed shapes of liquid filled axisymmetric sessile neo-Hookean membrane during submergence to various depths
03 p0292 A73-13303

Effect of membrane forces on large deflection of simply supported rectangular plates.
03 p0389 A73-13323

Bending rigidity of an inflated circular cylindrical membrane of rubbery materials.
03 p0395 A73-14183

Axial impact response of semiinfinite cylindrical membrane shell of helically oriented linearly elastic orthotropic fiber reinforced material, solving motion equations
05 p0631 A73-16112

Stress analysis of hyperbolic paraboloid membrane shells for applications in architecture
06 p0757 A73-17395

The concept of snap-buckling illustrated by a simple model.
07 p0909 A73-19163

Beams and membranes nonlinear vibrations via modified perturbation method based on Linstedt-Poincare technique
08 p1018 A73-21406

Anisotropic membrane shells with, if necessary, uniform strength
08 p1018 A73-21407

Stacked membrane elements for plate and shell analysis, noting spurious shear components suppression
09 p1159 A73-22401

Book - Structural analysis of shells.
09 p1164 A73-23273

Investigation of the elastoplastic characteristics of corrugated membranes under cyclic loading conditions
10 p1293 A73-24792

Stability of transverse waves in a spinning membrane disk.
[ASME PAPER 72-APM-MM] 11 p1441 A73-25706

Performance studies on a rechargeable hydrogen-oxygen fuel cell.
11 p1309 A73-25988

Influence of a small bending stiffness on the lateral vibrations of a clamped rectangular membrane
[DFVLR-SONDDR-226] 11 p1445 A73-26425

Hybrid type discrete jet-membrane relay system technology and design for discrete signals transformations
12 p1460 A73-26770

Transverse vibration of membranes of arbitrary shape by the method of constant-deflection contours.
13 p1690 A73-28058

Finite element method analysis of thin shells, discussing reference surface geometry and membrane and bending theory
13 p1693 A73-28234

Response functions for mathematical double membrane model of isotropic elastic shell in form of orientable two dimensional differentiable manifold
13 p1694 A73-28284

The Rayleigh-Faber-Krahn theorem for the characteristic values associated with a class of nonlinear boundary value problems.
13 p1648 A73-28423

Finite deflection of a shallow spherical membrane.
13 p1697 A73-28815

Effect of out-of-planeness of membrane quadrilateral finite elements.
13 p1697 A73-28818

Normal impact of a cone against an elastoplastic membrane
14 p1815 A73-30789

Computerized stress analysis of shock load induced circular elastic membrane interaction with fluid stream via method of characteristics related to aerodynamic decelerator design
15 p1948 A73-31429

The transition from thin plate to membrane in the case of a plate under uniform tension.
15 p1953 A73-32094

Determination of the displacement for a membrane stretched over a constant-curvature surface
16 p2076 A73-32935

Vector field representation of curved elastic membranes oscillatory motions, particularizing equations of motion for small displacements from equilibrium configurations
16 p2076 A73-32937

Non-linear problems of slender webs and of shallow shells.
16 p2078 A73-33006

Variational geometry optimization of thin rotational membrane shells under axisymmetric loading
16 p2079 A73-33011

Circular elastic membrane stability against wrinkling under radial peripheral tension and transverse pressure loading, considering solutions via Foepl-Hencky theory
16 p2080 A73-33246

Strongly curved finite element for shell analysis.
17 p2242 A73-34529

Stability of the general plane membrane adjacent to a supersonic airstream.
[ASME PAPER 72-APM-UUU] 17 p2248 A73-35103

Hydroelastic oscillations in a rigid circular cylinder in the presence of an elastic fluid surface covering
18 p2297 A73-36065

Inextensional approximations in cylindrical shells.
18 p2362 A73-36329

Membrane statics of parachute-like shells.
19 p2496 A73-37480

Acoustic wave fronts in ideal membrane transversely by steady pressure distribution, noting abrupt displacement gradient changes across pressure front
22 p2918 A73-41823

Experimental investigation of hydrodynamic stability for flows past simple membrane surfaces
22 p2840 A73-42117

Effects of axisymmetric loads on inflated non-linear membranes.
23 p3045 A73-44081

MEMBRANE THEORY

U MEMBRANE STRUCTURES

U STRUCTURAL ANALYSIS

MEMBRANES

NT ION EXCHANGE MEMBRANE ELECTROLYTES

NT MEMBRANE STRUCTURES

NT PLEURAE

NT SKIN (STRUCTURAL MEMBER)

A study of basilar membrane vibrations. I - Fuzziness-detection: A new method for the analysis of microvibrations with laser light.
01 p0013 A73-10973

Protein-lipid films as prototypes of biological membranes.
06 p0652 A73-17949

Synthesis of reverse osmosis membranes by plasma polymerization of allylamine.
07 p0780 A73-19169

Spin-labeling studies on the membrane of a facultative thermophilic bacillus.
07 p0782 A73-20027

Servomanometer designs with two membrane sensing elements for absolute and excess pressure measurements
07 p0827 A73-20542

Investigation of the infrastructural organization of interdisk spaces and photoreceptor membranes of the retina in vertebrates during aldehyde fixations, delipidization, and pronase treatment
10 p1181 A73-24458

Measurement of zincate permeation in a polyethylene battery separator with controlled external hydrodynamic conditions.
11 p1307 A73-24974

Cell membrane molecular structure and lipid composition, discussing phospholipid role in membrane potential maintenance in myocardial cells
11 p1315 A73-25591

Cardiac membrane capacitance physiological properties and measurements in Purkinje fibers, ventricular and atrial muscles and heart tissues
11 p1316 A73-25596

The ultrastructural organization of the photoreceptor membranes and the intradiscal spaces of the vertebrate retina as revealed by various experimental treatments.
11 p1321 A73-26717

Influence of ribonuclease on changes in the membrane potential of muscle fibers evoked by stimulation of the sympathetic nerve
11 p1833 A73-31166

Influence of electron transport on the interaction between membrane lipids and Triton X-100 in Halobacterium cutirubrum.
15 p1841 A73-32024

Evaluation of 165 deg F reverse osmosis modules for wastewater purification.
[ASME PAPER 73-ENAS-2] 19 p2399 A73-37964

Development of sulfonated polyphenylene oxide membranes for the reverse osmosis purification of wash water at sterilization temperatures /165 F/.
[ASME PAPER 73-ENAS-16] 19 p2399 A73-37973

NS-1 membranes - Potentially effective new membranes for treatment of wastewater in space cabins.
[ASME PAPER 73-ENAS-19] 19 p2400 A73-37975

Study of the two-frequency natural oscillation regime of a circular membrane on a nonlinearly elastic base
20 p2593 A73-39501

Starch hydrolysis in man - An intraluminal process not requiring membrane digestion.
20 p2519 A73-39789

Ultrafiltration by a compacted clay membrane. I - Oxygen and hydrogen isotopic fractionation. II - Sodium ion exclusion at various ionic strengths.
23 p2973 A73-43845

MEMORY

A model of a memory device based on neuron-like elements which realizes the holographic principles of data recording and readout
04 p0413 A73-15792

Mathematical and physical models of human long and short term memory, considering information processing and memorization at lower visual perception levels
04 p0413 A73-15793

Human memory model with associative linkage between neuronal network information elements
04 p0413 A73-15797

Low body temperature effects on learned behavior retention under hibernation conditions in squirrels
05 p0539 A73-16324

Effect of ethimizol on short term memory and mental working capacity
06 p0653 A73-18160

Rapid eye movement state beneficial effects on memory refuted in favor of delta wave slumber, emphasizing stage 4 sleep
06 p0653 A73-18225

A method for the investigation of interpolated information and time effects in short term retention.
06 p0659 A73-18475

Hippocampus contribution to conditioned reflexes, memory, voluntary motions, orientation and emotional reactions, noting theta rhythm in stimuli response
10 p1180 A73-24326

Memory process in terms of cortex-subcortex interaction, brain lability level and biopotential trace processes
11 p1314 A73-25198

Useful future action models of instrumental reflexes and voluntary actions based on memory role in engram storage of received stimuli
11 p1314 A73-25199

Retention of information in the ionic visual memory during recognition of images of varying complexity
11 p1323 A73-26084

Emotional stimulation traces in the spectra of EEG and cutaneo-galvanic reaction of man under normal conditions and in the case of memory impairment
12 p1461 A73-27106

Visual pattern matching - An investigation of some effects of decision task, auditory codability, and spatial correspondence.
13 p1579 A73-29123

Memory fixation during sleep, discussing EEG, EOG, EMG and ECG recordings for differences between light and paradoxal sleep
15 p1835 A73-31749

Reinforcement of unconscious traces of stimuli in the human being during ontogenesis
19 p2393 A73-37251

Two components and two stages in search performance - A case study in visual search.
24 p3065 A73-45339

MEMORY STORAGE UNITS
U COMPUTER STORAGE DEVICES

U CORE STORAGE

MENISCI
Concerning the stability of the triple-phase boundary in gas-diffusion electrodes of fuel cells.
21 p2636 A73-41320

MENTRUSTATION
Effects of flying and of time changes on menstrual cycle length and on performance in airline stewardesses.
13 p1576 A73-28509

MENTAL HEALTH
Information yield of the Annual Medical Examination for Flying.
20 p2517 A73-39110

MENTAL PERFORMANCE
Intellectual ability and performance on a non-verbal problem-solving task.
03 p0260 A73-13553

An evaluation of sinus arrhythmia as a measure of mental load.
05 p0543 A73-16718

Psychological and physiological components of biorhythm cycles governing periodic variations in physical, emotional and intellectual performance
05 p0544 A73-16720

Statistical correlation between human mental activity and EEG beta rhythm wave energy and frequency characteristics
06 p0653 A73-18159

Effect of ethimizol on short term memory and mental working capacity
06 p0653 A73-18160

German monograph - Work-physiological investigations for the objectivization of the tracking behavior, the mental load, and its psychopharmacological modifiability.
07 p0786 A73-20388

Diurnal psychic working capacity dynamics under conditions of continuous 72-hr wakefulness
08 p0930 A73-20989

Cerebral localization of speech, discussing cortical lesions, aphasia and mental activity correlation theories
08 p0931 A73-21425

Drive and performance modification following multiple/light-light/ shifts in the photoperiod.
09 p1039 A73-22528

Correlation analysis of the bioelectrical activity of the brain during mental work
10 p1178 A73-23678

Experimental study of emotional stress in operators
11 p1321 A73-25038

Ergonomic endurance limits, physiological strains and fatigue assessment in video coding information task performance as function of work shift time length
11 p1323 A73-25649

Forced guidance and distribution of practice in sequential information processing.
11 p1323 A73-26319

Adaptation-level and theory of signal detection - An examination and integration of two judgment models for voluntary stimulus generalization.
12 p1464 A73-26749

Effect of mild acute hypoxia on a decision-making task.
14 p1717 A73-30514

Psychological factors influencing the relationship between cardiac arrhythmia and mental load.
14 p1720 A73-30877

Mental load and the measurement of heart rate variability.
14 p1720 A73-30881

The effects of core temperature elevation and thermal sensation on performance.
15 p1839 A73-32396

Circadian rhythms in human mental performance from waking day, round of clock and simulated shift-work studies
16 p1972 A73-33156

Intellectual performance during prolonged exposure to noise and mild hypoxia.
18 p2283 A73-36783

Aircrew workload during the approach and landing.
19 p2401 A73-38005

Amplitude variations of acoustically evoked potentials as a function of signal information and fatigue due to stress
19 p2396 A73-38161

Continuous radio telemetric recording of pulse rate in radar controllers while on duty
20 p2517 A73-39208

Role of associations in the formation of evoked potentials from the human cerebral cortex
20 p2515 A73-39798

Physiological and operational state of a group of aeroplane pilots under the conditions of stressing tracking tests.
21 p2645 A73-41157

Visual search, complex backgrounds, mental counters, and eye movements.
21 p2639 A73-41185

Keeping track of sequential events - Implications for the design of displays.
23 p2948 A73-43215

The effect of anxiety control on the level of information processing
23 p2946 A73-43848

Effect of prolonged hypokinesia on the higher nervous activity of humans
24 p3058 A73-44668

Algebraic nature of thought formation structures
24 p3063 A73-44905

MENTAL STRESS
U STRESS (PSYCHOLOGY)

MERCURE AIRCRAFT
Test on fuselage models at reduced sizes.
17 p2107 A73-35443

MERCURY (METAL)
NT MERCURY ISOTOPES
NT MERCURY VAPOR
The Os-Pt-Hg abundance peak in Ap stars and the problem of very heavy cosmic rays.
02 p0210 A73-12733

Russian book on spectral composition-dependent photoconductivity in Hg doped amorphous Se films covering effect of quasi-macroscopic centers in semiconductors
02 p0201 A73-12864

High-current gas lasers with a mercury cathode
08 p0976 A73-21717

Icelandic geothermal activity and the mercury of the Greenland icecap.
09 p1079 A73-22949

Certain peculiarities in the distribution of mercury in meteorites.
10 p1278 A73-24106

Nitrogen ionization in an Hg-N2 discharge.
19 p2463 A73-37903

Study of a compact counterflow heat-exchanger with mercury at small Peclet numbers.
20 p2626 A73-38575

MERCURY (PLANET)
Mercury - Surface composition from the reflection spectrum.
02 p0218 A73-12420

Mercury thermal stress and strain fields of elastic deformation from solar heating variations due to resonance rotation
02 p0223 A73-12721

Resonance rotation of celestial bodies and Cassini's laws.
03 p0377 A73-14275

Orbital eccentricity of Mercury and the origin of the moon.
04 p0501 A73-15625

Correction of solar observations for stray light by numerical integration, with application to Mercury's drop.
05 p0621 A73-17032

Symposium on Planetary Atmospheres and Surfaces, Madrid, Spain, May 10-13, 1972, Proceedings.
06 p0743 A73-17427

Review of surface and atmosphere studies of Venus and Mercury.
06 p0743 A73-17428

Cartography of the surface markings of Mercury.
06 p0743 A73-17429

Mercury - Interpretation of optical observations.
06 p0743 A73-17430

General relativity in the equal proper time formalism.
06 p0724 A73-18626

Normal matrix equations for major planet orbital element corrections from optical observations, testing by numerical experiment for Mercury
09 p1143 A73-22096

Mercury, Venus and Pluto satellite system elimination by tidal friction, discussing possible erosion of earth and Mars small satellites
11 p1419 A73-25778

Ultra-violet argon dayglow lines in the atmosphere of Mercury.
11 p1421 A73-25916

Thermal history of the terrestrial planets
16 p2066 A73-33795

Internal structure and chemical composition of Mercury
16 p2066 A73-33796

Photographic measurements of the rotation of Mercury
16 p2066 A73-33797

Radio interferometry of moving sources in the presence of confusion - An application to Mercury at 21-centimeter wavelength.
17 p2231 A73-34763

Technology requirements for ballistic mode Mercury orbiter mission, discussing performance potential with Venus gravity assist and conventional spacecraft propulsion techniques
18 p2350 A73-36073

Solar wind-Mercury atmosphere interaction - Determination of the planet's atmospheric density.
18 p2352 A73-36294

Optical properties of the Mercury surface layer
19 p2480 A73-37233

The effects of scattering and conduction upon radiative transfer in lunar and Mercurian surfaces.
24 p3133 A73-44541

MERCURY ARCS

- Hologram reconstruction by incoherent light. II - Experimental results. 01 p0045 A73-10431
- Vapour density variations in a pulsed mercury discharge. 05 p0601 A73-16432
- Bandpass filter with cooled InSb detector for measurement of far IR radiation and temperature-vs-wavelength characteristics of Hg arc lamp 17 p2176 A73-35774
- Low-frequency vibrations of a high-frequency E-discharge plasma in a magnetic field 20 p2598 A73-39398

MERCURY COMPOUNDS

- NT MERCURY TELLURIDES**
- The effects of mercury compounds on the growth and orientation of cucumber seedlings. 12 p1462 A73-27274
- Gamma detectors using mercuric iodide and other heavy metal compounds as semiconductor with charge carriers for current surge in quantum energy resolution 17 p2134 A73-34247
- Large mercuric iodide single crystals application to high resolution X ray detectors, discussing fabrication by coating platelet face with thin Aquadag film and mounting upon carbon substrate 21 p2699 A73-40465

MERCURY ISOTOPES

- High-resolution magnetic hyperfine resonance in harmonically bound ground-state Hg-199 ions. 16 p2038 A73-32850

MERCURY TELLURIDES

- Electrical properties of evaporated mercury telluride films. 06 p0734 A73-17815
- Influence of the impurity compensation effect on the magnitude of the negative reluctance of alloys of the $\text{In}_2\text{Te}_3/\text{x-Hg}_3\text{Te}_3/1-\text{x}$ system 12 p1532 A73-27940
- Cadmium mercury telluride thin film coatings preparation by HgTe layers deposition onto previously vapor deposited CdTe layers under isothermal conditions 15 p1924 A73-32158
- Principal component determination in mercury and cadmium tellurides and in solid solutions of them 17 p2220 A73-35559

MERCURY VAPOR

- Low current mercury vapor discharge positive column plasma continuous radiation measurements as function of pressure, current density and temperature at 2300-14,000 Å 03 p0348 A73-14624
- Hg vapor laser with He, Ne, Kr, H or N additions, investigating population inversion and lasing properties for optimal performance conditions 12 p1504 A73-26887
- Investigation of the stability of the oscillation frequency of a mercury laser emitting at 1.53 microns. 12 p1507 A73-27511
- Kinetics of physicochemical processes in a shock wave in mercury vapors. II - The relaxation zone: Region of initial ionization 15 p1916 A73-32314
- Thermal conductivity of mercury vapors 20 p2595 A73-39607
- UV radiation measurements of Ar-Hg gas discharge plasma as function of temperature and pressure with emphasis on fluorescent light design 23 p3011 A73-43830

MERIDIANS

- U LATITUDE
U LONGITUDE

MERIDIONAL FLOW

- High-pressure axial fan for air-cushion vehicles 02 p0203 A73-11713
- Incoherent scatter observations of meridional winds in the 150-225 km region. 02 p0161 A73-12283
- On the meridional form of baroclinic waves in a two-layer quasi-geostrophic model. 03 p0304 A73-14312
- On the variance spectra and spatial coherences of equatorial winds. 07 p0846 A73-19038
- Meridional circulation zonal averaging effects on summer hemisphere Hadley cell in tropical regions 07 p0847 A73-19046
- Time dependent hydrodynamics of meridional circulation in rotating star radiative zone, confirming Eddington-Sweet velocity formulation 07 p0877 A73-19599
- Ionospheric plasma interaction with neutral meridional wind, noting effects of east-west gradients in electron concentration 07 p0819 A73-20057
- The mean upper-air flow in Southern Hemisphere temperate latitudes determined from several years of GHOST balloon flights at 200 and 100 mb. 08 p0960 A73-21376
- A climatological analysis of oscillations of Kelvin wave period at 50 mb. 08 p0984 A73-21377

- Experiments on the seasonal variation of the general circulation in a statistical-dynamical model. 08 p0960 A73-21378

- Longitudinal magnetospheric currents contribution to auroral electrojet from satellite observation data, noting magnetosphere electric field excitation of meridional Pedersen and Hall currents 12 p1493 A73-27650

- Stratospheric cooling and perturbation of the meridional flow during the solar eclipse of 7 March 1970. 14 p1771 A73-30765

- Vortex conservation mechanism of earth atmosphere jet stream formation in terms of Hadley cell in meridional divergence/convergence velocity region. 15 p1903 A73-31603
- Relation between the average motion of cyclones and anticyclones and their shape. 15 p1906 A73-32255

- Global meridional cross sections and charts for mesospheric circulation and temperature variability via meteorological rocket network 18 p2302 A73-35925

- Investigations of the 500mb level in relation to the general circulation. I - Transport of relative angular momentum at the 500mb level, by considering daily and monthly eddies that were obtained by applying Fisher's partitioning. 19 p2446 A73-37499

- Evidence for high-frequency synoptic disturbances near the stratopause. 19 p2447 A73-37663

- Meridional flow and the validity of the two-dimensional approximation in stellar-wind modeling. 20 p2602 A73-39430

- Interplanetary gas. XIX - Observational evidence for a meridional solar-wind flow diverging from the plane of the solar equator. 20 p2602 A73-39431

- A method of complex design of the meridional form of the air flow path of a multistage axial-flow compressor 21 p2633 A73-40477

- Book - Atmospheric circulation systems and climates. 21 p2732 A73-41440

- Atmospheric ozone and the movement of the air in the stratosphere. 23 p2977 A73-43903

- Influence of the vertical motion field on ozone concentration in the stratosphere. 23 p2977 A73-43904

- Relation between the intensity of the stratospheric circumpolar vortex and the accumulation of ozone in the winter hemisphere. 23 p2977 A73-43905

- Zonally symmetric global general circulation models with and without the hydrologic cycle. 23 p2978 A73-43981

- The latitudinal motion of sunspots and solar meridional circulations. 24 p3136 A73-44647

- Numerical experiments on the steady-state meridional structure and ozone distribution in the stratosphere. 24 p3085 A73-45017

- Nighttime meridional neutral winds near 350 km at low to mid-latitudes. 24 p3087 A73-45209

MEROMORPHIC FUNCTIONS

- NT ELLIPTIC FUNCTIONS**
NT RATIONAL FUNCTIONS
- Compact integral varieties existence in certain meromorphic Pfaff differential equation systems 21 p2726 A73-40946

MESH

- Metallized fiberglass antenna meshes for spacecraft deployable reflectors, discussing low mass/area, long term stability and performance characteristics and degradation tests 03 p0333 A73-13045
- Automatic mesh generation in two and three dimensional inter-connected domains. 13 p1693 A73-28242
- On the strategy of combining coarse and fine grid meshes in numerical weather prediction. 21 p2728 A73-40055

MESOMETEOROLOGY

- Some specific features of the near-ground temperature field mesostructure and air humidity and their influence on convective processes 13 p1654 A73-28886

- Mesoscale cloud systems analysis from meteorological observations and weather satellite data nephanalysis, applying to weather forecasting 13 p1655 A73-29191

- On the prediction of turbulence in baroclinic zones. 19 p2449 A73-38246

- Certain parameters of cellular convection according to observations by meteorological earth satellites and from a high mast 21 p2731 A73-40492

- Statistical analysis of satellite-observed trade wind cloud clusters in the western North Pacific. 23 p3003 A73-43980

- The mesoscale structure of the atmospheric boundary layer and its interaction with small-scale turbulence 24 p3107 A73-44960

MESONS

NT MUONS

NT PIONS

- Multiple meson production in 250 GeV nucleon-nucleon collisions in LiH targets, noting 40 per cent formation of heavy meson cluster fireballs 02 p0208 A73-12653

- Three meter liquid hydrogen target for K meson production with Serpukhov accelerator, discussing design, operation control and emergency conditions 05 p0538 A73-17289

- The stopping power of atomic matter for relativistic ions, mesons, electrons and positrons. 07 p0852 A73-19036

- Cosmic ray storm effect on midlatitude and polar neutron monitors, noting comparison with underground mu-meson telescopic observations at high rigidities 12 p1534 A73-27001

- Massive singlet f-meson gravitational field effects on gravitational collapse in universe model with ten to eightieth power aligned neutrons 20 p2605 A73-39016

- A meson supertelescope using plastic scintillators and the coupling coefficients for it 21 p2701 A73-40611

- Reactions of pseudoscalar meson production by neutrinos on nucleons near the threshold in the range of high transferred impulses 23 p3008 A73-43544

MESOPAUSE

- An evaluation of the scale of mesospheric wind disturbances. 02 p0160 A73-12272

- The altitude of the scattering layer near the mesopause over the summer poles. 14 p1750 A73-30768

- Midwinter mesospheric cooling during stratospheric warming, discussing circulation, stratosphere-mesosphere interactions and summertime temperature values at midwinter mesopause 18 p2308 A73-36037

MESOSPHERE

- Global mean radiative equilibrium model for Venusian mesosphere, determining horizontal variation of thermal heating and cooling 01 p0097 A73-10361

- Neutral composition measurements of the mesosphere and lower thermosphere. 01 p0040 A73-10879

- Mesospheric nitric oxide concentrations during a PCA. 01 p0041 A73-10881

- A vertical profile of OH in the mesosphere. 01 p0041 A73-10883

- Solar-activity effects and zonal wind in the stratosphere and lower mesosphere 01 p0043 A73-10945

- The diurnal variations of hydrogen and oxygen constituents in the mesosphere and lower thermosphere. 02 p0158 A73-12026

- Mesospheric cosmic dust concentration measurements from particle collection rocket flights, discussing interference from uplifted aerosols of terrestrial or cosmic origin 02 p0215 A73-12259

- An evaluation of the scale of mesospheric wind disturbances. 02 p0160 A73-12272

- Atmospheric stratification stability at heights of 30-90 km from grenade test determined wind and temperature data, presenting Richardson number latitudinal and seasonal distribution 02 p0160 A73-12273

- Rocket sounding and grenade experiments for stratosphere-mesosphere interaction, showing simultaneous winter temperature changes of opposite sign 02 p0165 A73-12789

- Infrared radiative heating and cooling in the Venusian mesosphere. I - Global mean radiative equilibrium. 05 p0613 A73-16197

- Rocket sounding for space charge distribution and electric field strength in stratosphere and mesosphere, noting vertical distribution of atmospheric conductivity 05 p0570 A73-17013

- Atomic hydrogen concentrations in the mesosphere and the hydroxyl emissions. 07 p0815 A73-19257

- Ionospheric anomalies in the night mesosphere after geomagnetic storms. 07 p0817 A73-19543

- Sunrise changes in concentrations of minor neutral constituents in the mesosphere. 07 p0819 A73-20062

- Global time and space changes of satellite radiances received from the stratosphere and lower mesosphere. 09 p1076 A73-22149

- Effects of solar activity on zonal winds in the stratosphere and lower mesosphere. 09 p1078 A73-22740

Observation of mesospheric ozone at low latitudes.
09 p1079 A73-22841

Direct measurements of the electrical conductivity and relaxation time of ionized air in the stratosphere and mesosphere
10 p1211 A73-23890

Infrared radiative heating and cooling in the Venusian mesosphere. II - Day-to-night variation.
11 p1418 A73-25719

Upper stratosphere and lower mesosphere vertical mixing implications of methane observations at 50 km, assuming modelability by eddy transport
15 p1873 A73-32251

Impact of space shuttle orbiter reentry on mesospheric NOx.
[AIAA PAPER 73-525] 16 p2007 A73-33559

A model for studying the effects of injecting contaminants into the stratosphere and mesosphere.
[AIAA PAPER 73-539] 16 p2008 A73-33569

Mesospheric and stratospheric nitrogen oxides behavior from model with nitric oxide photodissociation and nitric acid formation
17 p2119 A73-34779

Mesospheric and lower thermospheric ozone concentration measurement at sunset via occultation technique from rocket payloads
17 p2159 A73-34780

Global meridional cross sections and charts for mesospheric circulation and temperature variability via meteorological rocket network
18 p2302 A73-35925

Mesospheric positive ion observation via measurement of polar electrical conductivities by subsonic parachute-borne blunt probe system launched on meteorological rockets
18 p2305 A73-36006

Midwinter mesospheric cooling during stratospheric warming, discussing circulation, stratosphere-mesosphere interactions and summertime temperature values at midwinter mesopause
18 p2308 A73-36037

The stratospheric-mesospheric circulation over the North Pacific Ocean.
18 p2308 A73-36039

Simultaneous measurements of ion concentration and corpuscular stream intensity at altitudes ranging from 10 to 79 km
18 p2345 A73-36121

Influence of longitudinal variations on the structure of temperature, pressure and wind fields in the stratosphere and mesosphere of the Northern Hemisphere.
18 p2310 A73-36139

Temperature and wind velocity variations in winter mesosphere of polar regions.
18 p2310 A73-36140

A model of formation of the mean diurnal state of the upper atmosphere and its diurnal variations.
18 p2311 A73-36147

The effect of solar activity on temperatures in the equatorial mesosphere.
19 p2426 A73-38015

Wave-mean flow interactions in the upper atmosphere.
19 p2427 A73-38217

Direct measurements of the electrical conductivity and relaxation time of ionized air in the stratosphere and mesosphere.
20 p2551 A73-38909

Mesospheric ozone concentration night and day variations comparison, describing microwave radiometer and remote sensing and photochemical theories
20 p2557 A73-39857

Photochemical model with vertical transport for CO and hydrocarbons profiles in stratosphere and mesosphere, discussing boundary conditions and water vapor
21 p2681 A73-40086

Mesospheric temperature response to variations in geomagnetic activity.
21 p2682 A73-40169

A generalized aeronomical model of the mesosphere and lower thermosphere including ionospheric processes.
21 p2683 A73-40778

The nighttime distribution of ozone in the low-latitude mesosphere.
23 p2975 A73-43881

Ozone and airglow in the mesosphere region.
23 p2976 A73-43886

On the theoretical model for vertical ozone density distributions in the mesosphere and upper stratosphere.
23 p2977 A73-43898

MESSAGES
Optimal fixed message block size for computer communications.
01 p0019 A73-11454

METABOLIC WASTES
NT HUMAN WASTES
NT URINE
Effect of a 30-day stay in a medium with increased oxygen content on the discharge of some gaseous bioactivity products in rats
06 p0650 A73-17676

Gas-chromatography investigation of volatile metabolites in man on reduced food rations and during starvation
06 p0657 A73-17690

Physiological time zone entrainment and stressor effects during prolonged C-141 transmeridian flights, using endocrine-metabolic indices in urine specimens
13 p1574 A73-28283

Influence of hypoxia on the release of certain gaseous wastes in white rats
17 p2111 A73-34228

Zero-gravity and ground testing of a waste collection subsystem for the Space Shuttle.
[ASME PAPER 73-ENAS-42] 19 p2401 A73-37989

METABOLISM
NT ADRENAL METABOLISM
NT ASCORBIC ACID METABOLISM
NT CALCIUM METABOLISM
NT CARBOHYDRATE METABOLISM
NT CATABOLISM
NT ELECTROLYTE METABOLISM
NT ENZYME ACTIVITY
NT HORMONE METABOLISMS
NT HYPOGLYCEMIA
NT LIPID METABOLISM
NT OXYGEN METABOLISM
NT PHOSPHORUS METABOLISM
NT PROTEIN METABOLISM
Current views on the mechanism of the quantum-induced liberation of a mediator from the motor nerve endings of a skeletal muscle
01 p0009 A73-11023

Effects of endotoxin on monoamine metabolism in the rat.
01 p0009 A73-11100

Chemical evolution under the bion hypothesis.
03 p0265 A73-14316

Muscle metabolites with exhaustive static exercise of different duration.
05 p0539 A73-16247

Body thermotopography and some metabolic process characteristics in scuba divers under various underwater exposure conditions
05 p0545 A73-16734

Effect of high-fat diet on thermal acclimation with special reference to thyroid activity.
05 p0541 A73-16800

DNA catabolism in rat tissues in response to transverse accelerations
06 p0650 A73-17679

Modelling of structure and functional unity on coacervate systems.
06 p0652 A73-17950

Hypoxia, an adjunct in helium-cold hypothermia - Sparing effect on hepatic and cardiac metabolites.
07 p0782 A73-20169

Effect of accelerations on the thiamine-S35/ distribution in the organism of white mice
08 p0929 A73-20977

Effect of the administration of free amino acids and metabolic cofactors on the distribution of regional biogenic amine contents in the brain and blood of animals
09 p1040 A73-22864

Predicting heart rate response to work, environment, and clothing.
09 p1046 A73-22931

Intermittent exercise - Metabolites, oxygen pressure, and acid-base equilibrium in the blood.
09 p1041 A73-22933

Frog retinal metabolism in photoreceptors during dark and light adaptation, using ERG, radiopneumetry, oxygen uptake polarography and pyridine spectrophotometric assay
09 p1044 A73-23319

Binding of Melatonin to human and rat plasma proteins.
10 p1182 A73-24657

Vitamin metabolism alteration under increased atmospheric pressure
11 p1321 A73-25036

Chemical volatilization as a technique for the detection of extraterrestrial biopolymers and possible metabolic products.
11 p1319 A73-26479

Nitrogen metabolite dynamics in the brain during repeated hypothermia and subsequent spontaneous warming
12 p1462 A73-27703

Electrical and metabolic manifestations of receptor and higher-order neuron activity in vertebrate retina.
13 p1574 A73-28353

Neurophysiological characteristics of isolated structures of the cerebral cortex
14 p1718 A73-30570

Histochemical investigation of some energy metabolism characteristics in a rat heart after acute fatigue
15 p1834 A73-31393

Effect of prolonged hypokinesia on certain energy transfer characteristics in skeletal muscles and some internal organs
15 p1834 A73-31505

Study of the effect of increased oxygen concentration on the metabolism of Chlorella
15 p1838 A73-31508

Dynamic kalathermometer for measuring the cooling effect of an ambient medium
15 p1838 A73-31512

Validity of Haldane calculation for estimating respiratory gas exchange.
17 p2113 A73-35463

A monkey metabolism pod for space-flight weightlessness studies.
18 p2270 A73-35963

Effect of sympatholytin on metabolism in resting and working muscles in relation to the degree of their adaptation to intensified activity
18 p2276 A73-36571

Activity variations of some renal enzymes during stepwise increased hypoxia
18 p2277 A73-36582

Study of nitrogen balance and creatine and creatinine excretion during recumbency and ambulation of five young adult human males.
18 p2278 A73-36786

Physiologic cost of prolonged double-crew flights in C-5 aircraft.
21 p2644 A73-41152

Solubilization and accumulation of copper from elementary surfaces by *Penicillium notatum*.
21 p2648 A73-41217

Effect of training with eccentric muscle contractions on skeletal muscle metabolites.
21 p2641 A73-41523

Nonthermal metabolic response of rats to He-O₂, N₂-O₂, and Ar-O₂ at 1 atm.
22 p2805 A73-42201

Urea content variations in blood and tissues during muscular activity in relation to the adaptation level of the organism
22 p2807 A73-42660

The energetic metabolism and some reactions of the cardiovascular system during multichannel electrical stimulation and voluntary stressing of muscles
24 p3059 A73-44670

Metabolic and myoelectric reactions under chemical thermoregulation in rats after accelerated cold adaptation
24 p3059 A73-44721

Energy balance and change in body weight and body water in man during a 2-day cold exposure.
24 p3060 A73-45059

Oxygen consumption measurements during continual centrifugation of mice.
24 p3065 A73-45071

METAGALAXY
U UNIVERSE
METAL ALLOYS
U ALLOYS
METAL BONDING
NT METAL-METAL BONDING
Diffusive thermal bonding of cermet elements on steel and iron substrates in vacuum
02 p0172 A73-11537

The chemistry of urethane adhesives incorporating silane coupling agents.
03 p0332 A73-13037

The influence of adhesive components on the corrosion of aluminum honeycomb.
03 p0321 A73-13038

A study of environmental degradation of adhesive bonded titanium structures in Army helicopters.
03 p0332 A73-13039

Selection process for a structural adhesive system for application of the L-1011 aircraft.
03 p0333 A73-13050

Semihydrostatic hot extrusion for Ti plated Cu anode bar, noting metal bonding and current distribution
03 p0312 A73-13583

Assembly by welding and bonding - Introductory report on assemblies
06 p0698 A73-18692

Reflections on the nature of the bond in welding of metals - The particular case of fusion welding
06 p0698 A73-18693

An experimental model of the microelectronic ultrasonic wire bonding mechanism.
08 p0972 A73-20734

The phenomenon of superplasticity of polymorphous metals and alloys and its use for welding - J hardening in the solid state.
08 p0978 A73-21242

Ceramic-to-metal sealing and joining technology assessment, discussing noble filler metal properties, ceramic surface preparation and thermal tests for performance evaluation
09 p1088 A73-22444

Intermetalbond '72; Conference on the Bonding of Metals, 5th, Boboty, Czechoslovakia, November 21-23, 1972, Proceedings
10 p1224 A73-24088

Bonded joints under long-term dynamic load and their resistance to climatic effects
10 p1224 A73-24089

- Technology, strength, and calculation of bonded circular joints 10 p1224 A73-24090
- Calculation of the shear strength of an axisymmetric joint constructed out of Loctite 10 p1224 A73-24091
- Adhesive metal/glass laminate bonding, discussing materials, tests and interlaminar strength effects 10 p1224 A73-24092
- Vinyl plastisols with high adhesion to metals 10 p1239 A73-24093
- Layer strength and vulcanization effects on rubber/metal bonding with MEGUM agent 10 p1239 A73-24095
- Technology of production of bonded sandwich structures 10 p1224 A73-24096
- Fatigue properties of sandwich material with a honeycomb filler 10 p1289 A73-24097
- Transition metal borides ESCA spectra observation for metal-boron bonding energy based on spectral sensitivity to surface oxidation, discussing relevant features 11 p1325 A73-25202
- Linear elastic finite element stress analysis of lap and tapered adhesive joint bonding of composite to metal substrate [AIAA PAPER 73-371] 11 p1438 A73-25505
- German monograph - Investigations regarding the strength characteristics of adhesive bonds involving metals in the case of impact stress. 13 p1625 A73-29277
- Durability of bonded titanium joints increased by new process treatments. 16 p2017 A73-33052
- Factors affecting the survivability of stressed bonds in adverse environments. 16 p2017 A73-33055
- Competitive processes in joining; Proceedings of the Twenty-sixth Autumn Review Course, Eastbourne, England, October 27-29, 1972. 16 p2021 A73-33859
- Joining and assembly by welding. 16 p2021 A73-33860
- Enhancement of polymer adhesion to metals by means of additives with crosslink systems 16 p2030 A73-33941
- Applications in aerospace construction and fallouts of ONERA thermochemical techniques [ONERA, TP NO. 1246] 18 p2320 A73-36688
- Weldbonding/rivetbonding - Application testing of thin gauge aircraft components. [AIAA PAPER 73-805] 19 p2433 A73-37464
- Resistance diffusion bonding boron/aluminum composite to titanium. 19 p2435 A73-38004
- Effect of rivet spacing on crippling loads of joined aluminium angles. 19 p2499 A73-38009
- Electrodeposited Au on TO-5 headers, discussing discoloration measurement and ultrasonic test for bondability from correlation between optical reflectivity and bond pull strength 19 p2435 A73-38441
- Procedure development for brazing Inconel 718 honeycomb sandwich structures. 23 p2985 A73-44001
- Development of corrosion resistant filler metals for brazing molybdenum. 23 p2986 A73-44004
- METAL CARBIDES**
- U CARBIDES**
- METAL COATINGS**
- NT ALUMINUM COATINGS**
- NT GOLD COATINGS**
- NT NICKEL COATINGS**
- Influence of the thickness of a copper coating on the critical current of a superconducting wire made from niobium-based alloys 01 p0089 A73-11435
- Effect of the quality of electrolytic chromium plating on the endurance of steel 02 p0173 A73-11926
- Russian papers on metal corrosion and protection covering additives, annealing, polymer coatings, anodic polarization, electrodeposition, magnetic alloy coatings, etc 02 p0174 A73-12534
- Study of polarization during electrodeposition of tungsten simultaneously with nickel 02 p0174 A73-12539
- Surface properties improvement of Al products by metal coatings, noting corrosion prevention, anodic coatings, enameling and brazing 03 p0312 A73-13580
- Advanced copper and copper alloy conducting wires with metallic coatings 03 p0312 A73-13582
- Mechanical properties of base and coating metals for explosive plating, noting heat treatment for strain hardening prevention 03 p0312 A73-13584
- The deposition of multicomponent phases by ion plating. 04 p0456 A73-15758
- Maraging steels galvanic corrosion reduction by two layer Fe-Cu protective coatings, presenting salt water stress corrosion/time-to-failure test results 06 p0705 A73-17799
- Structure of the borated layer after diffusion saturation with other elements 06 p0707 A73-18040
- Structure and properties of nickel-phosphorus coatings in relation to annealing temperature and time. 06 p0698 A73-18214
- Cermet-oxide plasma jet spray coating of metal surfaces, determining thermal performance characteristics by calorimetric measurements 06 p0714 A73-18448
- Scale factors of adsorptive reduction in the strength of metals in the presence of melts 06 p0711 A73-18667
- Saturation of 1Kh18N9T steel with beryllium and corrosion resistance of the coating in a lithium melt 06 p0711 A73-18669
- Reliability of thin nickel-chromium resistance layers deposited by sublimation under vacuum on a glass substrate 07 p0862 A73-19424
- Metal coating via pastes and organic solvent suspensions application for diffusive metallization of metal surfaces, noting Al coating of heat resistant alloys 07 p0833 A73-20641
- Wear resistant coatings deposition by spark discharge alloying of machine part surfaces, examining surface hardening process and assessing state of art 08 p0946 A73-21083
- Utilization of the detonation phenomenon for the deposition of coatings /Survey/ 09 p1088 A73-22468
- Characteristics of the microstructural wear pattern of carburized chromium coatings 09 p1088 A73-22592
- Protecting metals in corrosive high-temperature environments. 09 p1089 A73-23296
- Thermal conductivity of mixed-composition plasma-sprayed coatings. 09 p1111 A73-23464
- Overview of corrosion cracking of titanium alloys. 10 p1232 A73-23873
- Stress corrosion crack protection from coatings on high strength H-11 steel aerospace bolts. 10 p1232 A73-23874
- Study of the wear resistance of nitrided electrolytic chromium coatings on certain alloy steels 10 p1223 A73-24065
- Metal cladding lubricants tests with powdered lead, copper, zinc, iron, silver and bearing alloys fillers for friction and wear reduction 10 p1239 A73-24249
- Temperature dependence of the adhesive strength and elasticity of some high-melting coatings 10 p1225 A73-24371
- Possibility of reducing the wear of the VD-17 aluminum alloy in a jet of free abrasive particles with the aid of metallic coatings 10 p1226 A73-24796
- Thermodynamic equilibrium calculation and demonstration of Mo siliciding by circulation method in hydrogen-free gaseous medium containing silicon chlorides 10 p1227 A73-24961
- Heat resistant and refractory materials contact eutectic melting for surface coating production 10 p1227 A73-24967
- The spray deposition of oxide-free coatings consisting of special metals with a high affinity to oxygen 11 p1372 A73-25411
- Metallic, nonmetallic, inorganic and organic protective coatings for metals against mechanical and chemical damage, discussing processing methods and applications 11 p1374 A73-25847
- Critical current value for a superconductor niobium-alloy wire as a function of its copper coating thickness. 11 p1409 A73-26062
- Influence of welding parameters on the strength properties of spot welds of MST1X steel with protective coatings 11 p1374 A73-26293
- Hot tinning of aluminum bronze. 11 p1375 A73-26353
- Chromium coated steels corrosion fatigue in normal conditions, aggressive media and high temperature environments 11 p1386 A73-26733
- Influence of gas carburizing on the structure and properties of electrolytically deposited chromium 11 p1375 A73-26734
- Investigation of diffused titanium coatings on refractory metals 13 p1630 A73-28015
- Effect of base material on the formation of thin plasma coatings 15 p1881 A73-31590
- Application of a scanning electron microscope in powder investigations 15 p1892 A73-32239
- Fused salt techniques for metal diffusion coatings with beryllium, boron, silicon, aluminum, titanium and chromium 16 p2017 A73-32697
- Electrolytically deposited noble-metal layers in the electronic industry 16 p1987 A73-32945
- Application of activators in contact diffusion saturation processes in metals and powders 18 p2318 A73-35878
- Plasma sprayed coatings 18 p2318 A73-35882
- Comparative evaluation of the wear resistance of electrolytic and plasma chromium coatings 18 p2318 A73-35883
- Detonation propelled metal particle sprayed coatings adhesion strength relation to particle kinetic energy 18 p2318 A73-35884
- Some physicochemical and technological aspects of obtaining annealed coatings from melts and semimelts 18 p2318 A73-35887
- Synthesis of metal-ceramic and other heat-resistant coatings by the electrochemical method 18 p2319 A73-35890
- Stresses in molybdenum coatings obtained by thermal decomposition of Mo/CO/6 18 p2319 A73-35892
- Flexural vibrations of rods with viscoelastic coating subjected to axial force. 19 p2502 A73-38347
- Schottky barrier diode solar cells using dielectric antireflection coatings, discussing Nb, Mo and Cr diode metal characteristics, photovoltaic characteristics and conducting properties 19 p2391 A73-38406
- Brittleness of coated tungsten wire 20 p2577 A73-39361
- Cadmium embrittlement of high strength, low alloy steels at elevated temperatures. 22 p2873 A73-41968
- On the stability of metal sheathed noble metal thermocouples. 22 p2858 A73-42044
- Alloy or metal coated composite powder thermal spraying applications, discussing bonding properties, wear resistance, low friction applications and abrasibility 22 p2866 A73-42593
- Structure and properties of arc-sprayed titanium coatings. 22 p2879 A73-42597
- Influence of diffusion coating and heat treatment on the wear resistance of VT-8 alloy 23 p2990 A73-43485
- Brazeability of Ni-Cr heat resistant cermets on stainless steel. 23 p2986 A73-44005
- Slot microwave transmission line with thick metal coating on dielectric substrate, calculating phase constant variation with frequency, slot width and coating thickness 23 p2954 A73-44069
- Temperature range for centrifugal thermal diffusion sintering in Cr-Ni powder coatings, relating upper and lower bounds to heating rate 24 p3092 A73-44419
- Pulse method for determining heat-transfer coefficients of coatings 24 p3155 A73-44756
- Structure of lanthanum-hexaboride-coated rhenium filaments. 24 p3105 A73-45401
- METAL COMBUSTION**
- Nitrogen thermochemistry during the combustion of zirconium droplets in N₂/O₂ mixtures. 01 p0123 A73-10922
- Boron combustion, covering thermochemistry application to chemical propulsion systems, temperature effects on oxidation, single particle ignition and powder burning 01 p0089 A73-11112
- Temperatures of aluminum during its combustion in oxygen-argon mixtures, in nitrogen, and in air 01 p0123 A73-11275
- Direct mixing and combustion measurements in ducted, particle-laden jets. 06 p0769 A73-18400
- [AIAA PAPER 72-1177] Propane-oxygen pilot flame ignition of steady flowing Al powder stream in oxygen 07 p0865 A73-20362
- Magnesium particle ignition in various media 07 p0923 A73-20419
- Dispersity of the combustion products of a mechanical mixture of aluminum and cadmium powders 07 p0923 A73-20421
- New phenomena during the burning of condensed systems 12 p1559 A73-27454
- Detonation of explosives containing boron and its organic derivatives 13 p1669 A73-28971

Al filament ignition temperature in carbon dioxide flow at various current values, noting relation to surface oxide film melting temperature
14 p1764 A73-30872

Experimental study of the condensed phase in the combustion products of metallized solid propellants
16 p2086 A73-33965

Application of thermal analysis to the determination of the thermophysical properties and combustion characteristics of metallic particle conglomerates in an oxidizer flow
18 p2342 A73-37119

Effects of additions of metals and metal borides on the burning rates of mixture systems
19 p2503 A73-37509

Mechanism of burning in condensed systems with solid additions in a field of mass forces
19 p2472 A73-37510

Particle combustion mechanism in aluminum-magnesium alloys
19 p2472 A73-37511

Method of selecting particles formed during the burning of metallized compacted systems in a constant-pressure chamber
19 p2503 A73-37518

Russian book - Burning of metal powders in active media.
21 p2753 A73-40418

Spectroscopic studies of supersonic heterogeneous flows with a combustible condensed phase
21 p2754 A73-40702

Determination of the size and the imaginary part of the refractive index of Al₂O₃ drops in a flame
22 p2932 A73-42724

High-temperature fast-flow reactor studies of metal-atom oxidation kinetics.
22 p2898 A73-42761

Temperatures in low-pressure magnesium-vapor diffusion flames.
22 p2899 A73-42820

Combustion of boron particles - Experiment and theory.
22 p2899 A73-42821

Ignition of metal particles in the case of a logarithmic oxidation law
24 p3154 A73-44704

Boron particle ignition limit dependence on particle size and oxygen content, taking into account kinetic and diffusion resistance
24 p3155 A73-44708

METAL COMPOUNDS

Morphology and spontaneous crystallization conditions of silicides of the transition metals from solutions in metallic melts
09 p1104 A73-22976

Russian book - Superconducting alloys and compounds.
15 p1922 A73-31176

Attempted prediction of the superconducting transition temperature for some metallic compounds with the aid of a computer
15 p1922 A73-31177

Physicochemical properties of metal silicides under vacuum at high temperatures, assessing suitability as antiemission materials on Mo grids in high power vacuum electron tubes
15 p1898 A73-31842

METAL CORROSION

U CORROSION

METAL CRYSTALS

Dislocation damping in ultrasound-irradiated molybdenum single crystals
01 p0061 A73-10251

Nickel structure stabilization by multiply alternated thermocyclic treatment and isothermal annealing
01 p0062 A73-10253

Activation energy volume relation to heat of fusion and lattice characteristics for vacancy diffusion along crystal grains in melting metals
01 p0087 A73-10256

Role of the crystalline structure and orientation of single crystals in the formation of the external friction process
01 p0062 A73-10259

Dislocation density in Mo single crystals subject to uniaxial tensile stress or sphere-produced indentation, evaluating plastic strain level
01 p0063 A73-10484

Temperature dependence of the critical shear stress in single crystals of Al-Mg alloys of various concentration at temperatures between 1.6 and 300 K
01 p0064 A73-10488

Low-temperature induced changes in the martensitic crystalline structure of iron-aluminum-carbon alloys
01 p0064 A73-10607

Mosaic-angle and dislocation-density variations in polycrystalline aluminum alloys under tension
01 p0064 A73-10609

Plastic strain anisotropy changes in single crystals of beryllium following programmed load application
01 p0064 A73-10610

Textures of deformation and of primary and secondary recrystallization in high-purity nickel
01 p0064 A73-10614

Microhardness anisotropy of hardened and aged Be single crystal as function of purity
01 p0067 A73-11353

Metal vapor crystallization in rare gas atmosphere for powder production, noting particle size distribution control
02 p0172 A73-11545

Investigation of the interrelation between creep parameters in industrial aluminum during the first and second stages of creep
02 p0179 A73-11567

The thermally activated deformation of niobium-molybdenum and niobium-rhenium alloy single crystals.
02 p0179 A73-11574

Behavior of dislocations in niobium under stress.
02 p0179 A73-11576

Characteristics of the process of plastic deformation of bcc metals in the microyield zone
02 p0179 A73-11622

Statistical evaluation of strength of metals at brittle fracture.
02 p0235 A73-12133

Quadrilateral packet structure and lattice atom positions in single crystal ternary Re-Co-B alloy by X ray analysis
02 p0181 A73-12198

Nucleation during solidification and melting of metals and alloys
02 p0181 A73-12363

Determination of yield locus curves for copper and aluminum crystals with the aid of Knoop hardness measurements
02 p0181 A73-12364

Russian book on ultrasonic processing in metal crystallization covering design of vibrators and transducers and acoustic power measurement
02 p0175 A73-12800

Stress shock waves effect on polycrystalline metals grain structure, discussing strain rate critical value zones
03 p0386 A73-13147

Ultrasonic attenuation measurement of a microplastic memory effect in aluminum single crystals.
03 p0323 A73-13331

Influence of electron concentration on the formation of phases with bcc, fcc, and hexagonal close packed lattices in certain transition-metal alloys
03 p0324 A73-13510

Disordered precipitation effect on steady state creep rate of gamma prime Ni-Al-Ti single crystals
03 p0326 A73-13963

Secondary maximum grain size and even-grained texture in the region of low and moderate deformations during recrystallization of certain nickel- and iron-based alloys
03 p0326 A73-13967

Effects of the state of the surface and of titanium films on the dislocation structure of surface layers in molybdenum single crystals
03 p0326 A73-13969

Stresses governing the high-temperature creep rate in single crystals with a bcc lattice
03 p0326 A73-13971

Substructural changes during high-temperature creep deformation of aluminum single crystals
03 p0327 A73-13978

Internal friction in polycrystalline copper foils after alpha-irradiation at 78 K
03 p0328 A73-14653

Adsorbed barium films on tungsten and molybdenum /011/ face.
04 p0460 A73-14867

Dislocation interstitial impurities interactions in high purity Mo, using dislocation damping techniques
04 p0462 A73-15304

Impurities and cooling rate effects on cast W structure during crystallization from optical metallography
04 p0466 A73-15668

Metallographic orientation determinations on hexagonal polycrystals with the aid of the quantitative polarization equipment of the Neophot.
05 p0577 A73-16752

Calculation of X-ray elastic constants on the basis of single crystal coefficients of metals with a hexagonal structure
05 p0588 A73-17244

A method for performing high precision lattice parameter change measurements on quenched aluminum.
05 p0580 A73-17257

Effect of irradiation on the absolute thermal emf of metals and alloys
06 p0706 A73-17901

Creep characteristics and substructure disorientation in metals with an fcc lattice
06 p0706 A73-17904

Stability of the dislocation structure in cold-deformed Kh18Ni2T and Kh16Ni9M2 steels during high-temperature aging
06 p0707 A73-17905

Metal atom migration acceleration under radioactive radiation, showing diffusion coefficient dependence on free and coupling electron interactions
06 p0735 A73-18038

Creep in molybdenum single crystals at 0.57 of the melting temperature
06 p0708 A73-18047

Structural changes in molybdenum single crystals during high temperature creep
06 p0708 A73-18048

Investigation of dislocation locking by interstitial impurities in bcc-lattice metals
06 p0708 A73-18055

Diffusion in the titanium-aluminum system. I - Interdiffusion between solid Al and Ti or Ti-Al alloys.
06 p0709 A73-18332

Superlattice of voids in neutron-irradiated tungsten.
06 p0709 A73-18353

Energy spectra of Cs⁺ ions scattered from the surface of a tungsten single crystal.
06 p0726 A73-18615

Conduction electrons collective wave properties in metals, discussing energy structure, ground state, Fermi surface and quasi-particle concept for crystal conductivity
06 p0739 A73-18674

The orientation dependence of deformation mode and structure in stoichiometric NiAl single crystals deformed by high temperature steady-state creep.
06 p0712 A73-18758

Creep of precipitation-hardened nickel-base alloy single crystals at high temperatures.
06 p0713 A73-18768

Lattice dynamics, third-order elastic constants, and thermal expansion of titanium.
07 p0839 A73-20173

Dislocation structure of tungsten single crystals grown by electron-beam zone refining
07 p0841 A73-20523

Study of the channeling of light ions of 0.5 to 2 MeV across gold crystals of some hundreds of angstroms thickness
07 p0864 A73-20609

Morphologies of iron crystals from the Haverro meteorite.
09 p1140 A73-21862

Optimal superplasticity model of metallic materials involving interphase surface of new phase fluctuation nuclei in framework of Frenkel theory
09 p1099 A73-21960

Intercrystalline molybdenum fracture
09 p1099 A73-21971

Annealing of discontinuities in deformed aluminum
09 p1100 A73-21973

Critical evaluation of Zhurkov theory of metallic material fracture by successive rupture of atomic bonds due to atom thermal motion
09 p1100 A73-22160

Electron microscopic determination of orientation relationship and habit plane for Ti-Cu martensite.
09 p1101 A73-22406

Symmetry properties of energy zones in rhombohedral-system crystals
09 p1134 A73-22682

Metal fcc polycrystals macroscopic plasticity theory based on discrete aggregate model, predicting stress-strain curves for partial load cycles
09 p1160 A73-22896

Static and kinetic strength estimation of ionic and metal single crystals, discussing microcracks in brittle materials and surface quality and pore distribution effects
09 p1160 A73-22900

Useful penetration in an austenitic stainless steel, of electrons accelerated under a very high voltage /1500 to 2500 kV/
09 p1105 A73-23037

Intergranular precipitation in the oriented bicrystals of aluminum-copper
09 p1105 A73-23039

High temperature mechanical properties measurements verifying metal polycrystal internal friction background origin in diffusion of vacancies formed under grain boundary loading
09 p1105 A73-23060

Determining the technical cohesive strength of polycrystalline metals from the internal energy.
09 p1106 A73-23158

Effect of hafnium dioxide on grain growth and strength characteristics in niobium
09 p1108 A73-23233

Amplitude-dependent anelasticity in aluminum and copper single crystals
10 p1231 A73-23693

Mechanical behavior of solid solutions of centered cubic symmetry obtained by limited addition of titanium to the iron
10 p1231 A73-23770

Contribution to the study of the elasticity of monocrystalline aluminum under very low stresses
10 p1231 A73-23771

Annealing of effects arising during ion-bombardment alloying of metals at energies up to 10 keV
10 p1223 A73-23817

METAL CRYSTALS

- Crystalline structure of the Cr₃AlB₄ compound
10 p1259 A73-24066
- Fine structure of X-ray spectra of nickel and some of its alloys with a nickel arsenide lattice and lattices resembling it
10 p1259 A73-24152
- Mechanical properties of recrystallized molybdenum containing vanadium microadditions
10 p1233 A73-24361
- Application of the fluctuation model of superplasticity to calculate the surface tension of metals during phase transformations
10 p1235 A73-24455
- Thermal oscillations of hexaboride atoms of some metals
10 p1261 A73-24777
- Investigation of the growth of the disperse structure of gold on a germanium surface
11 p1408 A73-25247
- Influence of the intercrystalline structure on the diffusion of zinc in the symmetrical joints of bending of aluminum
11 p1379 A73-25324
- Effects of oxygen environment and surface diffused coatings on fatigue crack development in copper single crystals.
11 p1380 A73-25806
- The soft surface effect in plastic deformation and fatigue of metals and alloys.
11 p1381 A73-25808
- Photoluminescence of ZnTe during laser stimulation
11 p1376 A73-26145
- Resonance between spin and magnetohydrodynamic waves in antiferromagnetic semiconductors and metals.
11 p1409 A73-26190
- On the study of the intergranular corrosion of a stainless steel with the help of twin crystals
11 p1385 A73-26297
- Investigation of radiation defects in silicon and germanium single crystals irradiated by 50-MeV electrons
11 p1410 A73-26449
- Amplitude-dependent anelasticity in aluminum and copper single crystals. II - Studies in amplitude range III during and after plastic deformation
11 p1385 A73-26567
- Change in the dislocation structure during fatigue of nickel prestrained by tension
11 p1386 A73-26732
- X ray and microanalysis of Luna 16 recovered Fe-Ni fragment structure and composition, showing alpha solid solution octahedrite
12 p1538 A73-26893
- Characteristics of martensite decomposition during the tempering of rhenium steels
12 p1509 A73-26894
- Dislocation structure of subgrain boundaries in creep-deformed aluminum.
12 p1511 A73-27028
- Crystalline structure of the TaCoB and NbCoB₂ compounds
12 p1512 A73-27244
- Austenitic steel dislocation density, X ray interference width and hardness changes due to intensified crystal fragmentation from biaxial elongation under tension
12 p1512 A73-27246
- High-cyclic fatigue curves for annealed metals from investigation of defect buildups, lattice distortions, microcrack nucleation and fatigue crack growth
12 p1552 A73-27253
- Influence of plastic deformation on the electrical resistance of molybdenum single crystals
12 p1512 A73-27260
- Mechanical properties of strip molybdenum with a polygonized single-crystal structure
12 p1513 A73-27265
- Possibility of atom displacements in solids under the action of laser light pulses
13 p1626 A73-28003
- Austenite stabilization during inverse transformation in Cr-Co-Mo and Cr-Ni-Co-Mo steels
13 p1630 A73-28012
- Quasi-ternary Mo-TiC-ZrC system
13 p1630 A73-28014
- Metallic crystal growth and defects: All-Union Conference on Metallic Crystal Growth and Imperfections, 2nd, Kiev, Ukrainian SSR, June 15-18, 1970, Proceedings
13 p1631 A73-28101
- Effect of impurities on the substructure and dislocation formation in metal crystals grown from melts
13 p1631 A73-28103
- Effect of the degree of purity on the dislocation structure of tungsten single crystals
13 p1631 A73-28104
- Study of the structure and properties of oriented tungsten single crystals
13 p1631 A73-28105
- Investigation of structure and imperfections in molybdenum single crystals grown by electron-beam zone refining techniques
13 p1631 A73-28106
- Striated, cellular and dendritic substructure formation during growth of Fe-Ni alloy single crystals
13 p1631 A73-28107
- Application of similarity criteria in calculations of a mobile magnetic field to be used for growth stimulation in single crystals of metals
13 p1667 A73-28108
- Temperature conditions of aluminum alloy crystallization at cooling rates of 10,000 to 1,000,000 deg/sec
13 p1632 A73-28111
- Niobium mechanical twin formation and propagation, discussing continuous nucleation, matrix interface and dislocation core energies
13 p1632 A73-28132
- Mechanical behavior of plastically deformed polycrystalline metal subjected to hydrostatic pressure soaking.
13 p1634 A73-28196
- Dislocation structure in molybdenum single crystals after deformation at 293 and 400 deg K.
13 p1634 A73-28221
- Weak-beam high-resolution electron micrographs of plastic deformation-generated extended dislocations in Ge single crystals
13 p1668 A73-28222
- Nickel single crystal target ionization by high voltage electron beam bombardment, using time of flight mass spectroscopic analysis
13 p1663 A73-28666
- Temperature and rate dependence of the critical shearing stress in magnesium single crystals
13 p1636 A73-29056
- Factors controlling the corrosion behavior of titanium and titanium-nickel alloys in saline solutions. [NACE PAPER 64]
13 p1637 A73-29311
- Theoretical interpretation of residual lattice strains induced in polycrystalline metals by plastic deformation.
13 p1639 A73-29460
- Study of plasticity laws of polycrystalline metals at elevated temperatures - Specifically the influence of hydrostatic stress on creep.
13 p1641 A73-29506
- Some observations on grain boundary sliding in aluminum bicrystals deformed at elevated temperatures.
13 p1641 A73-29508
- A static-to-dynamic transition in creep of metallic materials under cyclic stress conditions as caused by an interaction of creep and creep recovery.
13 p1642 A73-29512
- Transgranular stress corrosion cracking of austenitic stainless steels - A single crystal study.
13 p1642 A73-29520
- Increase in the boundary strength of cast electron-beam-melted molybdenum by microadditions of vanadium.
13 p1643 A73-29634
- Corrosion properties and structural transformations of the N70M27 alloy containing vanadium and niobium
13 p1644 A73-29645
- Finite element method application to nonlinear, microscopic and ductile fracture mechanics covering crack tip singularity elastoplastic analysis and elastic constants of metal crystals
14 p1809 A73-30200
- Assessment of the degree of plastic deformation in a crater with ball imprint.
14 p1810 A73-30309
- Critical shear stress temperature dependence in Al-Mg single crystal alloys of various concentrations in the range 1.6-300 K.
14 p1759 A73-30313
- Formation of oriented structures by action of a laser beam on metals.
14 p1760 A73-30325
- Some comments on the importance of third order contributions to the screening of the ionic potential and to the structural energy of metals.
14 p1783 A73-30432
- Crystallostructural investigation of the eutectoid decomposition of copper-beryllium alloys - Ordering accompanied by formation of Cu₂Be metastable solid solution
14 p1760 A73-30587
- Morphology of the structure and the microhardness of Al-Ni, Cu, Be, Fe, Co eutectic compositions
14 p1760 A73-30588
- Dislocation structure of Ni₃Al intermetallic compound during various stages of deformation
14 p1760 A73-30591
- Anomalous creep behavior of crystal bar alpha-Zr during dynamic strain aging at 723-823 K as function of temperature, stress and oxygen content
14 p1760 A73-30626
- German monograph - Elevation of the yield point and pronounced yield range of multicrystalline aluminum-magnesium alloys.
14 p1762 A73-30673
- Some characteristics of the failure by fatigue of mild steel in vacuum
14 p1763 A73-30681
- Mechanical deformation and failure of metals under the action of a 0.01-sec laser light pulse
14 p1758 A73-30714
- Determination of diffusion characteristics in the boundary and volume components of a diffusing hydrogen stream in a polycrystalline metal
14 p1763 A73-30716
- Influence of heating to high temperatures in vacuum on the electrophysical properties of niobium single crystals
14 p1763 A73-30722
- Attenuation of an ultrasonic signal in aluminum deformed according to a harmonic law
14 p1764 A73-30857
- Influence of interstitial impurities on the formation of a cellular structure and on the properties of chromium
14 p1764 A73-30858
- Influence of ordering in a Ni₃Mn alloy on the magnitude of the critical shearing stresses
14 p1764 A73-30859
- Mechanism of plastic deformation and low-temperature brittleness of a Cr alloy containing 45 at.% Fe
14 p1764 A73-30866
- The vanadium-iron-boron, vanadium-cobalt-boron, and vanadium-nickel-boron systems
15 p1887 A73-31202
- Application of a cluster component technique in the interpretation of concentration dependences of the properties of binary metal alloys and anion-substituted spinel solid solutions
15 p1923 A73-31205
- Kinetics of gamma-prime phase precipitation in steel N36T2u2
15 p1887 A73-31322
- Transformations in crystalline boron during mechanical dispersion
15 p1897 A73-31600
- Investigation of defects in GaAs on the basis of the photoluminescence
15 p1923 A73-31717
- Reflection-absorption infrared spectrum of alpha-CO chemisorbed on polycrystalline tungsten.
15 p1841 A73-31971
- Grain boundary dislocations in aluminum bicrystals after high-temperature deformation.
15 p1891 A73-32020
- Effect of specimen thickness on the fracture surface energy of 100 axis tungsten single crystals.
15 p1891 A73-32022
- Russian book on single crystals of high melting and rare metals and alloys covering structure, interatomic bonds, growth, plastic deformation, heat treatment, etc
15 p1893 A73-32297
- German monograph - The spontaneous anisotropy of the resistance in nickel - Measurements involving single crystals of nickel and diluted nickel alloys between 4.2 and 358 K.
15 p1896 A73-32582
- Pre-macro yielding and the orientation dependence of the 'shear' stress in molybdenum single crystals.
16 p2025 A73-33197
- Theory for the inelastic tunneling effect in normal metals
16 p2027 A73-34063
- Mechanism of the micrononhomogeneous deformation of metals throughout a wide interval of temperature
16 p2186 A73-34330
- Special features of high-temperature creep in metals with an fcc lattice
16 p2188 A73-34563
- Temperature dependence of low-temperature strength in aluminum single crystals
16 p2189 A73-34581
- Molybdenum bicrystals mechanical properties dependence on mismatch angle under bending with torsion and brittle cleavage under critical stresses
16 p2189 A73-34636
- An X-ray examination of deformation in beta Ti-V alloys.
16 p2189 A73-34642
- The effect of thermomechanical pretreatment on the allotrop transformation in cobalt.
16 p2190 A73-34645
- Metallurgical investigations of atomic ordering and transformation behavior of close packed ordered nine-layered hexagonal structure /kappa phase/ in V-Co-Ni ternary alloys
16 p2190 A73-34646
- Dislocation-type mechanism of the influence of solid surface films on the deformation and fracture of metals
16 p2319 A73-35891
- Influence of plastic strain on the paramagnetic susceptibility of molybdenum single crystals
16 p2324 A73-36802
- Low temperature tensile tests for strength and plasticity of pure bcc, hcp and fcc polycrystalline metals, indicating stacking fault energy role
16 p2324 A73-36804
- Critical shear stress temperature and rate dependence in magnesium single crystals.
16 p2325 A73-36888

Effect of atom self-diffusion on evaporation processes and porosity development in solid bodies during electron-beam treatment

18 p2320 A73-36900

Molecular beam study of the desorption of cesium ions from tungsten crystals.

18 p2338 A73-36976

X radiation arising during collisions between metal bodies

19 p2458 A73-37249

Study of the behavior of metallic single crystals - Application to the tension of the fcc single crystal

19 p2495 A73-37425

Grain refinement in aluminium-zirconium and aluminium-titanium alloys by metastable phases.

19 p2440 A73-37444

Fluctuation model of superplasticity and surface tension of a metal at a phase transition.

19 p2442 A73-38137

The preparation and anisotropic hardness of tantalum single crystals with principal orientations.

20 p2575 A73-38637

Effects of hydrogen on tantalum by the cathodic charging.

20 p2575 A73-38638

Elastic properties of tantalum over the temperature range 4-300 K.

20 p2575 A73-38886

Propagation of stress wave with plastic deformation in metal obeying the constitutive equation of the Johnston-Gilman type.

20 p2615 A73-38888

Diagrams of cumulative damage during tension of polycrystalline metals

20 p2577 A73-39371

Generation of vacancies in tungsten by rapid-rate deformation at elevated temperature.

20 p2578 A73-39492

Superconductivity and electronic structure of ultrahigh-purity niobium. I - Synthesis of ultrahigh-purity niobium

20 p2600 A73-39732

Structural changes during plastic deformation and annealing of tungsten single crystals

20 p2579 A73-39738

Faulty structure in niobium single crystals deformed by rolling at 77 K

20 p2579 A73-39743

Investigation of the imperfect structure of polycrystalline aluminum after low-temperature rolling and annealing

20 p2579 A73-39747

Reflection of conductivity electrons from an atomically pure $\{110\}$ face of a tungsten crystal

21 p2751 A73-40367

Vapor-liquid-solid type growth in lunar glass covered breccia 15015, noting metallic iron stalks with bulbous tips of iron and sulfur mixture.

21 p2766 A73-40412

X ray and microanalysis of Luna 16 recovered Fe-Ni fragment structure and composition, showing alpha solid solution octahedrite

21 p2771 A73-41026

Decomposition of martensite during tempering of rhodium steels.

21 p2720 A73-41027

Corrosion characteristics and structural transformations in alloy N70M27 with vanadium and niobium.

21 p2720 A73-41038

Effective interchange effects between the ions in metals

21 p2721 A73-41141

Possibility of predicting the residual stress pattern in boronized steels

21 p2721 A73-41229

A detailed investigation of slip line pattern and sub-surface dislocation structure of molybdenum single crystals.

21 p2722 A73-41566

Excitation of surface molecular orbitals on the $\{100\}$ face of molybdenum

21 p2722 A73-41597

Field-ion-microscopic study of interstitial plasticity of tungsten microcrystals.

22 p2872 A73-41726

Ternary systems: Rare earth metal - iron family metal - silicon /Component interaction and crystal structures of compounds/

22 p2873 A73-42084

Calculation of the physicochemical constants of metals associated with the strength of interatomic bonds

22 p2874 A73-42097

Critical evaluation of Zhurkov theory of metallic material fracture by successive rupture of atomic bonds due to atom thermal motion

22 p2874 A73-42108

Russian book - General patterns in the structure of phase diagrams of metal systems.

22 p2877 A73-42451

X-ray investigation of the mechanism of effects of alloying on defect formation in refractory metal alloys

22 p2877 A73-42454

Structure of the phase diagrams of the ternary systems /Mo, W/ - /Ti, Zr, Hf, V, Nb, Ta/ - C

22 p2877 A73-42455

The yield stress of Ni3/Al, W/.

22 p2880 A73-43075

Atomic diffusion mechanisms in multiphase and multicomponent alloys covering relaxation, crystal lattice atom exchange and motion along dislocation lines and to neighboring vacancies

23 p2989 A73-43439

Bcc and fcc metal crystal growth, determining thermodynamic and kinetic conditions, surface texture and favored crystal types

23 p2990 A73-43487

Magnetic susceptibility of a degenerate electron gas - Interaction of nuclear magnetic moments in normal metals and superconductors

23 p3016 A73-43709

Investigation of the substructure in molybdenum single crystals deformed by compression

23 p2991 A73-43712

The plastic deformation of NiAl single crystals between 300 K and 1050 K. I - Experimental evidence on the role of kinking and uniform deformation in crystals compressed along the 001 direction. II - The mechanism of kinking and uniform deformation.

23 p2991 A73-43773

Experimental bases and models for the study of the overall behavior of metals

23 p2993 A73-43964

Elementary mechanisms and physical models in plasticity and viscoplasticity

23 p3043 A73-43965

Electron-electron collisions and the electrical conductivity of metals at low temperatures

23 p3016 A73-44021

Orientation dependent slip in polycrystalline titanium.

23 p2993 A73-44028

Mechanism of ordered dislocation structure formation in metals deformed under high hydrostatic pressure

23 p2993 A73-44043

Morphology and crystallography of beta prime martensite in TiNi alloys.

23 p2994 A73-44160

Creep rate relationship in terms of stress and strain rate for anisotropic metal based on single crystal theory, applying to pressurized thin cylinder

23 p3045 A73-44167

Fracture micromechanism characteristics and crack tip plastic zone formation effects on metal embrittlement, using elastoplasticity theory

23 p3047 A73-44277

The effect of halide impurities on the mass production of metal whiskers by reduction.

24 p3098 A73-44401

Influence of ultrasonic vibrations on the mechanical properties and fine structure of aluminum and an aluminum-magnesium alloy

24 p3098 A73-44570

The Portevin-Le Chatelier effect in compression tests of polycrystalline aluminum

24 p3148 A73-44914

Metal crystal lattice properties and chemical bond nature in terms of valence concept, analyzing p-electron cloud overlapping

24 p3119 A73-45178

Oxygen-W/100/ surface interactions investigated simultaneously by secondary ion mass spectrometry /SIMS/ and electron induced desorption /EID/

24 p3066 A73-45330

Fatigue hardening in niobium single crystals.

24 p3101 A73-45474

METAL CUTTING

Cutting thin metal sheets with the CW CO2 laser.

02 p0175 A73-12819

Russian book on plasma cutting covering electrophysical and thermophysical principles of arc discharges application for metal cutting, arc I-V characteristics, plasmatrons and operation

04 p0457 A73-15962

Cutting and welding using a CO2 laser.

05 p0582 A73-17264

Investigation of adhesion and diffusional interaction of instrumental materials with titanium alloys

12 p1502 A73-27466

Ni-base alloy powder metallurgy from production waste cuttings by oxidation and subsequent oxide reduction with hydrogen and calcium hydride

12 p1503 A73-27553

Investigation of the turning process using diamond cutting tools on ML-5 magnesium alloy, with the application of mathematical methods in experiment planning

15 p1881 A73-31278

Borazon compact cutting tools.

[SME PAPER MR 73-143]

19 p2436 A73-38500

Turning high-temperature alloys with Borazon tools.

[SME PAPER MR 73-145]

19 p2437 A73-38501

Titanium Stressskin panel fabrication and assembly, discussing forming, cutting, thermal processing, welding and applications

19 p2437 A73-38502

Carbon dioxide jet laser cutting technology and rate calculations for metals and dielectrics as function of laser power and material thermal properties

20 p2569 A73-39677

Influence of thermal cutting and its quality on the fatigue strength of steel.

21 p2722 A73-41253

German monograph - Materials removal in the case of the drilling of holes with the aid of solid-state lasers.

22 p2866 A73-42699

METAL DRAWING

Deep-drawability and some problems after forming by deep-drawing of Al-Mg alloy sheets - Study on Al-Mg alloy sheets for forming use. II.

05 p0581 A73-16580

Deep drawability of titanium sheets.

09 p1104 A73-22522

Causes of embrittlement in the 11Kh18M steel

09 p1107 A73-23195

Strain ratio data for commercial Al alloys in various temper conditions as drawability criterion for sheet press performance, discussing single tensile test method

14 p1762 A73-30643

METAL FATIGUE

Facility for investigating low-cycle fatigue of alloys at cryogenic temperatures

01 p0029 A73-10491

Time characteristics of rupture and creep in metals during tension under hydrostatic pressure conditions

01 p0064 A73-10605

Statistical characteristics for duralumin sheets mechanical properties, fatigue life and crack growth

01 p0117 A73-11298

Fatigue of duralumin under cyclic loads at ultrasonic frequencies

02 p0179 A73-11566

Fatigue strength and stress-rupture strength of KhN77Tiur and KhN70VMTiu steels with a protective coating

02 p0180 A73-11628

Simultaneous manifestation of temper brittleness and hydrogen embrittlement during low-cycle fatigue of high-strength structural steel

02 p0180 A73-11927

Structural and energetic analysis of fatigue failure in metals

02 p0232 A73-11929

Influence of cyclic heating on the mechanical fatigue of titanium alloys and their weld joints

02 p0180 A73-11933

Application of the basic concepts of structural-energetic theory to the problem of physical fatigue limit.

02 p0235 A73-12131

The effects of frequency of loading and of nonreactive external media on growth of fatigue cracks.

02 p0235 A73-12132

The influence of preliminary thermocycling on the high-temperature strength of austenitic steel.

02 p0180 A73-12139

Effect of diamond smoothing on the surface finish and fatigue strength of EI961 steel.

02 p0174 A73-12141

A temperature-programmed apparatus for fatigue testing metals.

02 p0150 A73-12218

Corrosion fatigue of type 4140 high strength steel.

02 p0183 A73-12764

Fatigue induced microstructural changes in metals and alloys, considering crystal lattice defects, crack formation and propagation, dislocations and strengthening effects

03 p0321 A73-13133

Studies of fatigue in smooth AlCuMg specimens

03 p0321 A73-13134

Effect of a single plastic deformation on the fatigue behavior of metals

03 p0322 A73-13136

Investigation of fatigue life and residual strength of wing panel for reliability purposes.

03 p0387 A73-13233

Random fatigue of 2024-T3 aluminum under two spectra with identical peak-probability density functions.

03 p0322 A73-13235

Recording of metal hardening during fatigue testing at elevated temperatures.

03 p0307 A73-13287

Cumulative fatigue damage tests of Al alloy, evaluating Miner cycle/stress ratio

03 p0325 A73-13571

Microstructural changes that drilling and reaming can cause in the bore holes in DTD 5014 /RR58 extrusions/.

03 p0325 A73-13573

Resonance test facility using dynamic hysteresis loop method to test metal fatigue and anelasticity in torsion at room and high temperatures

03 p0288 A73-14025

Hold-time effects on the elevated temperature fatigue-crack propagation of type 304 stainless steel.

03 p0328 A73-14448

Size effect in fatigue testing of metals explained, considering implications for bending, torsion and axial loading 03 p0396 A73-14646

Fatigue threshold crack propagation in air and dry argon for a Ti6Al-4V alloy. 04 p0459 A73-14685

Extensive study of low fatigue crack growth rates in A533 and A508 steels. 04 p0459 A73-14686

Fatigue crack propagation growth rates under a wide variation of Delta K for an ASTM A517 Grade F T-1 steel. 04 p0459 A73-14687

Fatigue crack propagation of D6ac steel in air and distilled water. 04 p0459 A73-14688

The effect of frequency upon the fatigue-crack growth of Type 304 stainless steel at 1000 F. 04 p0459 A73-14689

Delay effects in fatigue crack propagation. 04 p0459 A73-14690

Reliability analysis methods for metallic structures. 04 p0452 A73-14714

The additivity of cumulative damage in the test or use environment. 04 p0507 A73-14716

An investigation of fatigue life performance in lap-type solder joints. 04 p0452 A73-14852

Predictive testing in elevated temperature fatigue and creep - Status and problems. 04 p0453 A73-14853

Applications of exoelectron emission to nondestructive evaluation of alloying, crack growth, fatigue, annealing, and grinding processes. 04 p0453 A73-14856

The early detection of fatigue damage by exoelectron emission and acoustic emission. 04 p0453 A73-14858

Verification of structural integrity of pressure vessels by acoustic emission and periodic proof testing. 04 p0453 A73-14859

Techniques for smooth specimen simulation of the fatigue behavior of notched members. 04 p0453 A73-14862

An inelastic stress-strain law for elevated temperature and slowly time varying loads. 04 p0512 A73-15235

Fatigue crack growth measurement on Al alloy wedge-opening-load specimens under constant amplitude sinusoidal loading, comparing data with existing crack propagation results 04 p0462 A73-15241

Fatigue crack propagation in terms of fracture mechanics concepts 04 p0462 A73-15298

The problem of strength and aspects of predicting the mechanical properties of metals 04 p0465 A73-15661

Formation of annular cracks in cylindrical samples intended for estimating resistance to crack propagation. 04 p0514 A73-15673

A plastic-strip specimen for fatigue crack propagation studies in low yield strength alloys. 05 p0581 A73-16127

Porcelain enamels for heat resistant alloys low temperature fatigue strength and high temperature vibration damping increase [SAE PAPER 720809] 05 p0633 A73-16629

Dislocation-point defect interactions in fatigued pure aluminum 05 p0588 A73-17231

Torsional fatigue fixture for high temperature investigation of high strength steels crack growth rate in tensile mode 05 p0563 A73-17254

Determination of constants in the equation for the fatigue-crack propagation rate with allowance for properties of the plastic zone 06 p0761 A73-17847

Thermal fatigue resistance of borided alloy KhN70VMYuT. 06 p0709 A73-18215

Method of analysis and prediction for variable amplitude fatigue crack growth. 06 p0709 A73-18482

Fatigue and fracture basic research at the Langley Research Center. 06 p0764 A73-18486

Tensile and compressive prestressing effects on notched steel cantilever beam specimens low cycle fatigue life 06 p0764 A73-18490

Study of fatigue crack propagation by X-ray diffraction approach. 06 p0698 A73-18496

The influence of stress intensity and microstructure on fatigue crack propagation in ferritic materials. 06 p0710 A73-18498

A note on fatigue crack starter defects produced by a pulsed laser. 06 p0710 A73-18500

Electrostatic field effects on the fatigue of steel in vacuum 06 p0711 A73-18661

Borated steel fracture characteristics in the case of cyclic plane bending 06 p0711 A73-18663

Method for increasing the fatigue strength of hardened steels 06 p0711 A73-18666

Cu-Ni-Zu alloys high ambient temperature tensile and fatigue strengths due to recrystallization and precipitation produced fine grain microstructure, describing annealing and cold working process 06 p0711 A73-18751

Frequency dependent low cycle fatigue crack propagation. 06 p0713 A73-18767

Metal surface active properties effects on fracture characteristics and deformation and failure conditions 07 p0912 A73-19472

The influence of fretting and geometric stress concentrations on the fatigue strength of clamped joints. 07 p0912 A73-19572

Scale effects on the fatigue and corrosion fatigue of steel 07 p0839 A73-19657

The effect of grain size on the fatigue of an Al-Mg alloy. 07 p0839 A73-20114

Effects of surface roughness and form factor on rolling contact fatigue. 07 p0831 A73-20119

Metal tongues in trailing edge of surface pits near fracture path end in rolling contact fatigue of failed ball bearings 07 p0831 A73-20158

Estimation of the fatigue characteristics of D16T and AVT1 aluminum alloys from the breaking stress 07 p0841 A73-20515

Evaluating the variation in fatigue properties of aluminum alloys due to variable loads by using secondary fatigue curves. 08 p0977 A73-21147

High frequency equipment for studying fatigue in sheet materials in conditions of plane stress and elevated temperatures. 08 p0952 A73-21149

Some fatigue properties of welded high temperature alloys. 08 p0978 A73-21241

Measurement of the flexural damping capacity and dynamic Young's modulus of metals and reinforced plastics. 08 p0967 A73-21594

The influence of prior fatigue deformation on creep behaviour. 08 p0979 A73-21672

Book - Fundamentals of cyclic stress and strain. 08 p1020 A73-21836

Parametrization of low-temperature deformation characteristics in single crystals of molybdenum. 09 p1099 A73-21928

Variable-load endurance criteria for steels under conditions of uniaxial and biaxial static tension 09 p1100 A73-22152

Influence of the frequency of the tension-compression cycle on the fatigue life of D16T alloy 09 p1100 A73-22153

Influence of inclusion content on fatigue crack propagation in aluminum alloys. 09 p1101 A73-22409

Ultrafine grained two-phase alloys fatigue properties as function of phase volume fractions and grain size, noting Coffin law type behavior from low cycle fatigue tests 09 p1102 A73-22411

Effect of thermomechanical processing on fatigue crack propagation. 09 p1102 A73-22415

Effects of hold time on low-cycle fatigue behavior of AISI Type 304 stainless steel at 593 C. 09 p1102 A73-22417

Substructure formation around fatigue cracks and its role in the propagation of fatigue cracks in aluminum. 09 p1103 A73-22437

Using fracture mechanics with aluminum alloy structures. 09 p1103 A73-22494

Influence of environment on the appearance of fatigue striations in various alloys 09 p1104 A73-22716

An investigation into the relationships of fatigue fracture and inelastic deformation of metals in torsion. 09 p1161 A73-23052

An apparatus for measuring and recording the electrical resistance of metal specimens during mechanical testing. 09 p1070 A73-23066

Effect of loading frequency on fatigue strength of metals. 09 p1106 A73-23159

Surface work hardening as a means of increasing the resistance of machine parts to low cycle fatigue. 09 p1089 A73-23162

Temperature dependence of conditions for static, quasi-static and fatigue failure of titanium alloys 09 p1107 A73-23193

Fatigue crack growth under C.O.D. cycling. 09 p1163 A73-23252

Fatigue crack initiation and propagation in part through crack metal specimens under cyclic loading, discussing plasticity effects and surface wave interaction 09 p1163 A73-23253

The role of fracture toughness in low-cycle fatigue crack propagation for high-strength alloys. 09 p1108 A73-23254

Effect of mean stress on fatigue crack initiation and propagation from different configurations of notch. 09 p1164 A73-23253

Difference of the plastic deformation of the surface and internal layers of polycrystalline iron under fatigue loading. 10 p1233 A73-24183

Discrete creep of AMg6 aluminum alloy subjected to repeated static loading 10 p1233 A73-24365

Influence of notch and thread rolling on the fatigue strength of samples prepared from VT3-1 and VT16 alloys 10 p1233 A73-24370

Al alloy stress intensity range estimation from surface fatigue striation incidence and modulus of elasticity, noting relationship to crack growth closure in fractography 10 p1235 A73-24447

Increasing the fatigue strength of metals by optimizing the thermal regime during strain hardening 10 p1226 A73-24799

Atmospheric corrosion fatigue tests for environmental conditions and superimposed stress wave effects on Cr-Mo steel fatigue life under rotating bending 10 p1235 A73-24917

Carbon and stainless steels chemical composition effects on diffusion layer structure and fatigue strength after diffusive boriding 10 p1236 A73-24954

Varying-temperature test installation for the interior design of the Concorde 11 p1342 A73-25103

Welded joints fatigue properties, considering porosity, nonmetallic inclusions and cracks effects 11 p1372 A73-25105

Phenomenological approach to low-cycle fatigue fracture of a typical aircraft full scale component static test. 11 p1305 A73-25554

Fatigue crack delay and arrest due to single peak tensile overloads. [AIAA PAPER 73-324] 11 p1441 A73-25555

Metal components wear mechanisms due to adhesion, tribooxidation, abrasion and surface fatigue, discussing prevention by lubrication, suitable mating of materials and surface treatments 11 p1373 A73-25577

Aerospace component failure due to corrosion fatigue in aluminum wing attachment spar, helicopter rotor blade, landing gear cylinder and engine bearings 11 p1380 A73-25803

Metal fatigue crack nucleation behavior and dislocation microstructures, including slip band and extrusion-intrusion pairs 11 p1380 A73-25804

Fatigue damage and dislocation structures in fcc metals surface layers, noting microcrack formation conditions 11 p1380 A73-25805

Effects of oxygen environment and surface diffused coatings on fatigue crack development in copper single crystals. 11 p1380 A73-25806

The soft surface effect in plastic deformation and fatigue of metals and alloys. 11 p1381 A73-25808

The effect of surface films on fatigue crack initiation. 11 p1381 A73-25810

Metal surfaces corrosion fatigue due to environmentally induced localized attack, discussing protective film growth, crack propagation hydrogen interaction and stresses 11 p1381 A73-25811

Shear decohesion mechanism of fatigue crack propagation in ductile metals under cyclic loads, considering secondary microfracture and creep cavitation effects at elevated temperatures 11 p1381 A73-25814

Gaseous environments compatibility with structural alloys under fatigue loading, presenting crack growth rate data 11 p1381 A73-25816

The kinetic and dynamic aspects of corrosion fatigue in a gaseous hydrogen environment. 11 p1382 A73-25817

Oxygen and temperature effects on Ni base superalloys fatigue fracture, discussing trans- and intergranular crack propagation and initiation in single and polycrystals and surface coatings 11 p1382 A73-25818

Environment enhanced corrosion fatigue crack growth and fracture mechanics, discussing inspection intervals to maintain structural integrity

11 p1382 A73-25819

On the superposition model for environmentally-assisted fatigue crack propagation.

11 p1382 A73-25820

Corrosion fatigue crack propagation behavior in steels above/below stress intensity threshold within framework of linear elastic fracture mechanics

11 p1382 A73-25821

Effect of cyclic stress form on corrosion fatigue crack propagation below K_{Isc} in a high yield strength steel.

11 p1382 A73-25822

Effects of stress wave form and cycle frequency on low cycle corrosion fatigue.

11 p1382 A73-25823

Frequency and environmental interactions in the fatigue of aluminum alloys.

11 p1382 A73-25824

The effect of environmental relative humidity upon the ultrasonic fatigue endurance of an age hardening aluminum alloy.

11 p1382 A73-25825

Aircraft structures aluminum alloys fatigue crack growth rate relationship to cracking mode, stress ratio, cyclic frequency and corrosive environment severity

11 p1382 A73-25826

Stress corrosion cracking and corrosion fatigue for hydraulic aluminum pressure cylinders used for landing gear, stabilizers and aircraft systems

11 p1383 A73-25827

The effect of coatings on the fatigue characteristics of notched aluminum alloy sheet specimens.

11 p1383 A73-25829

An ultrasonic device for the study of fatigue crack initiation in anodized aluminum alloys.

11 p1363 A73-25830

Study on the superposition of intergranular corrosion and pitting corrosion by fatigue cracking of stainless steels.

11 p1383 A73-25831

Hot gas environment fatigue analysis from corrosion viewpoint, considering gas-alloy reactions

11 p1383 A73-25833

The effect of vacuum on the high temperature, low cycle fatigue behavior of structural metals.

11 p1383 A73-25834

Fretting fatigue in titanium helicopter components.

11 p1383 A73-25837

Crack toughness evaluation of hot pressed and forged beryllium.

11 p1384 A73-26169

S-200 grade beryllium fracture toughness properties.

11 p1384 A73-26170

Change in the dislocation structure during fatigue of nickel prestrained by tension

11 p1386 A73-26732

Chromium coated steels corrosion fatigue in normal conditions, aggressive media and high temperature environments

11 p1386 A73-26733

Influence of fretting on the endurance of 40KhNMA steel with various thermochemical processing

11 p1386 A73-26735

Coarse grain Al alloys strength characteristics, crack resistance and specific energy of failure due to brittle fracture

11 p1386 A73-26736

Corrosion fatigue due to static and cyclic stress, noting electrochemical adsorption theory

11 p1386 A73-26737

Kinetic strain criteria of cyclic failure at high temperatures

12 p1552 A73-27252

High-cyclic fatigue curves for annealed metals from investigation of defect buildups, lattice distortions, microcrack nucleation and fatigue crack growth

12 p1552 A73-27253

Procedure for studying fatigue failure features in metals under harmonic and complex loading at low temperatures

12 p1486 A73-27254

Thermal stresses arising in high-frequency fatigue tests

12 p1512 A73-27259

Certain fatigue phenomena in aeronautical structures with stiffened shells

12 p1553 A73-27394

Evaluation of torsional fatigue damage from changes in the fatigue properties and microhardness.

13 p1635 A73-28522

A hypothesis of non-propagating fatigue crack.

13 p1635 A73-28644

Rotating bending fatigue tests on Al coated steels, investigating electroplating, hot dip and spraying production methods effects on fatigue strength

13 p1635 A73-28645

Method of studying the fatigue damage of metals with automatic data processing on a computer

13 p1597 A73-29053

Relationship between the strain curves of a material subjected to static and to cyclic loads

13 p1698 A73-29055

Facility for conducting fatigue tests with sheet materials in cyclic tension

13 p1597 A73-29058

Effect of tensile prestrain on fatigue strength of aluminum alloy in high cycle fatigue.

[ASME PAPER 72-MAT-N] 13 p1636 A73-29199

A potential means of using acoustic emission for crack detection under cyclic-load conditions.

13 p1700 A73-29401

Fatigue crack initiation and propagation in low stacking fault energy austenite steel related to plastic deformation induced gamma alpha transformation and martensite failure

13 p1640 A73-29481

X-ray investigation of fatigue-crack growth - On critical strain for fracture at the crack tip.

13 p1625 A73-29482

The effect of microstructure on fatigue crack propagation in Ti-6Al-6V-2Sn alloy.

13 p1640 A73-29484

Residual surface stress changes dependence on fatigue life and steel specimen size during rotating bending fatigue tests from X ray diffraction study

13 p1625 A73-29485

The effect of plastic anisotropy in the low-cycle fatigue behavior of Zircaloy.

13 p1640 A73-29487

A study of fatigue crack propagation in high strength aluminum alloys at high stresses.

13 p1640 A73-29488

Crack initiation and propagation in notched plates subjected to cyclic inelastic strains.

13 p1701 A73-29489

Fatigue crack propagation as successive stochastic processes and fatigue fracture toughness.

13 p1701 A73-29490

Statistical definition of fatigue behavior of strength of low alloy steels.

13 p1641 A73-29492

Correlation between notch sensitivity of a material and its non-propagating crack, under rotating bending stress.

13 p1641 A73-29493

Aspect of cumulative fatigue damage under multiaxial strain cycling.

13 p1701 A73-29497

Fatigue damage by a stress below the endurance limit.

13 p1641 A73-29498

Inelastic strain and hysteresis energy criteria for fatigue fracture of metals.

13 p1641 A73-29499

Evaluation of dissipation and damage in metals submitted to dynamic loading.

13 p1701 A73-29505

Al and Ti alloy corrosion and fretting fatigue in aqueous environment, noting protective oxide surface film effects

13 p1642 A73-29524

The effect of elevated temperature upon the fatigue-crack propagation behavior of two austenitic stainless steels.

13 p1642 A73-29525

Low carbon steel S-N diagram for stresses ranging to fatigue limit, noting cyclic creep, macroplastic cyclic stress and fatigue failure

13 p1703 A73-29603

Effect of loading frequency and directional anisotropy on the fatigue strength of grade AMg6BM aluminum alloy sheet.

13 p1643 A73-29606

Resonant frequency, fatigue and energy dissipation relations for endurance limit determination in Al alloy specimens under vibrational loads

13 p1643 A73-29618

Energy dissipation in metals in high-frequency fatigue tests. I.

13 p1643 A73-29630

Energy dissipation in metals in high-frequency fatigue tests. II.

13 p1643 A73-29631

Machine for investigating the fatigue and inelasticity of metals with programmed load changes both at room and at elevated temperatures.

13 p1599 A73-29636

The effects of out-of-phase biaxial-strain cycling on low-cycle fatigue.

14 p1806 A73-29774

Estimation of fatigue-crack propagation life in butt welds.

14 p1755 A73-30147

Fatigue crack propagation in butt welds containing joint penetration defects.

14 p1755 A73-30148

Effect of loading conditions on the propagation of fatigue cracks in sheet samples of D16T alloy.

14 p1759 A73-30314

A unit for investigating the low-cycle fatigue of alloys at cryogenic temperatures.

14 p1743 A73-30316

Scale effect in fatigue and in corrosion fatigue of steel.

14 p1760 A73-30324

Fatigue crack propagation in martensitic and austenitic steels.

14 p1761 A73-30632

Investigation of fatigue and brittle failure patterns in 15G2AFDps steel at low temperatures

14 p1762 A73-30678

Investigation of crack propagation in small samples under conditions of low-cyclic fatigue

14 p1763 A73-30680

Some characteristics of the failure by fatigue of mild steel in vacuum

14 p1763 A73-30681

Application of fiber optics to the observation of fatigue crack development

14 p1754 A73-30691

Effect of deep annular grooves on the strength of some metals under static tension and torsion

14 p1763 A73-30693

Quantitative classification criterion for corrosion causes in metal under static and cyclic loads, examining failure mechanism

14 p1763 A73-30712

Fatigue failure of a two-phase titanium alloy in vacuum

14 p1763 A73-30713

Some plastic deformation laws for titanium under static and alternating loads

14 p1763 A73-30723

Fracture mechanics approach to fatigue analysis in design.

[ASME PAPER 73-DE-22] 14 p1763 A73-30823

Investigation of fatigue effects in thinnest surface layers of metals with boundary friction

14 p1815 A73-30838

A test machine for fatigue under pulsed moving loads

15 p1855 A73-31144

Localized corrosion - Cause of metal failure; Proceedings of the Symposium, Atlantic City, N.J., June 27-July 2, 1971.

15 p1888 A73-31736

Exfoliation corrosion of aluminum alloys.

15 p1888 A73-31737

Significance of intergranular corrosion in high-strength aluminum alloy products.

15 p1889 A73-31740

Gas saturated surface layer effect on Ti alloy resistance to static cyclic tensile loads, noting increased fatigue strength after etching

15 p1890 A73-31815

Fatigue behaviour of ribbon-reinforced composites.

15 p1898 A73-31840

Failure criterion for metallic materials in the case of multiaxial vibrational stress

15 p1952 A73-32045

Scanning electron microscope analysis of Ti-Al-V specimens under simultaneous fatigue and fretting loads

15 p1883 A73-32148

Corrosion-fatigue crack growth in high-strength aluminum alloys with and without susceptibility to stress-corrosion cracking.

15 p1895 A73-32571

Relation between grain size and the size of fatigue-striated facets in an aluminum alloy

16 p2027 A73-33972

A method of programmed fatigue tests with short-time overloads.

17 p2165 A73-34277

Workhardening, slip band formation and crack initiation during fatigue of titanium.

17 p2190 A73-34882

Welded steel beam fatigue behavior evaluation via stable crack growth concepts, developing fracture mechanics model for cracks originating from pores

17 p2246 A73-34887

The residual strength characteristics of stiffened panels containing fatigue cracks.

17 p2246 A73-34888

On the influence of single and multiple peak overloads on fatigue crack propagation in 7075-T6511 aluminum.

17 p2190 A73-34889

Continuous monitoring of fatigue crack growth by acoustic emission techniques.

[TR-DE-73-2] 17 p2148 A73-35445

Fatigue and creep behavior of aluminum and titanium matrix composites.

17 p2193 A73-35543

The measurement and analysis of fatigue crack growth in cylindrical shapes.

18 p2363 A73-36486

An automatic flash photomicrographic system for fatigue crack initiation studies.

18 p2316 A73-36588

Cyclic inelastic deformation and the fatigue notch factor.

18 p2364 A73-36590

Engineering analysis of the inelastic stress response of a structural metal under variable cyclic strains.

18 p2364 A73-36594

Environment-assisted fracture in engineering alloys. II - Cyclic loading and future work.

[ASME PAPER 73-MAT-S] 18 p2365 A73-36614

- Fatigue and corrosion-fatigue crack propagation in intermediate-strength aluminum alloys.
[ASME PAPER 73-MAT-N] 18 p2323 A73-36615
- The effect of hydrostatic pressure environment on the low cycle fatigue properties of a maraging steel.
[ASME PAPER 73-MAT-K] 18 p2323 A73-36616
- Fatigue strength of materials under a two-frequency load / Review/
18 p2366 A73-36754
- Method of investigating fatigue damage of metals with automatic information processing by computer.
18 p2297 A73-36885
- Relation of strain curves of material in static and cyclical loading.
18 p2366 A73-36887
- Apparatus for fatigue tests on sheet materials subject to cyclical extension.
18 p2297 A73-36890
- Biaxial cyclic high-strain fatigue of aluminium alloy RR58.
19 p2440 A73-37437
- Fracture types in load-controlled low-cycle fatigue.
19 p2498 A73-37666
- Evaluation of the fatigue properties of aluminum alloys D16T and AVT1 on the basis of limit stresses.
19 p2440 A73-37790
- Investigation of fatigue strength of D1T alloy with due regard to dispersion of results.
19 p2440 A73-37791
- The effect of stress amplitude below the fatigue limit on cumulative fatigue lives in perforated round specimens.
19 p2501 A73-38344
- Metal fatigue studies of nucleation and crack propagation through plastic and elastic regimes
19 p2502 A73-38548
- Moisture effect on Ni steel fatigue crack propagation under low stresses
20 p2617 A73-39291
- Investigation of energy criteria for the failure by fatigue of some metals at low and high loading frequencies
20 p2577 A73-39354
- Study of low-cycle fatigue of titanium-base alloys at a temperature of -196 C
20 p2577 A73-39375
- The behavior of materials subjected to multiaxial cyclic stresses. I - Methods of calculation
22 p2917 A73-41781
- Criteria relating to the fatigue life of steels subjected to alternating loads under conditions of uniaxial and biaxial static strain.
22 p2874 A73-42102
- Effect of the frequency of cyclic tension-compression on the fatigue limit of alloy D16T.
22 p2874 A73-42103
- Application of strip model to crack tip resistance and crack closure phenomena.
22 p2875 A73-42132
- Threshold for fatigue crack propagation and the effects of load ratio and frequency.
22 p2875 A73-42137
- Overload effects on subcritical crack growth in austenitic manganese steel.
22 p2875 A73-42138
- Effect of multiple overloads on fatigue crack propagation in 2024-T3 aluminum alloy.
22 p2875 A73-42139
- Fatigue-crack growth under variable-amplitude loading in ASTM A514-B steel.
22 p2875 A73-42140
- Fatigue and corrosion-fatigue crack growth of 4340 steel at various yield strengths.
22 p2875 A73-42142
- Fatigue crack propagation and fracture toughness of 5Ni and 9Ni steels at cryogenic temperatures.
22 p2875 A73-42143
- Influence of stress intensity level during fatigue precracking on results of plane-strain fracture toughness tests.
22 p2876 A73-42149
- Plane-stress fracture toughness and fatigue-crack propagation of aluminum alloy wide panels.
22 p2876 A73-42151
- The fretting fatigue of titanium and some titanium alloys in a corrosive environment.
22 p2876 A73-42356
- Monograph - Fatigue and stochastic loadings.
22 p2923 A73-42673
- German monograph on cyclic stress-strain curves and fracture strength of steels with various compositions covering plastic strain energy, S-N diagrams and test equipment
22 p2879 A73-42739
- Fatigue test apparatus for metals at ultrasonic frequencies consisting of transducers, strain amplitude monitor, cooling circuit and static stress mechanism, discussing S-N response
22 p2867 A73-43169
- Fatigue-crack initiation studied by electrical resistance measurements.
23 p2979 A73-43301
- Influence of structural changes arising during the hardening process on element lifetime
23 p2984 A73-43438

- Improvement of the corrosion-fatigue strength of aluminum alloys by exposure of the medium to a magnetic field
23 p2984 A73-43466
- Fatigue failure analysis of low carbon steel endurance under cyclic loading with time dependent viscoelastic effects, using Hookes-Trouton laws
23 p3040 A73-43469
- Method of determining the susceptibility of metals to brittle fracture under shock loads
23 p2965 A73-43470
- A review of fatigue crack growth in high strength aluminum alloys and the relevant metallurgical factors.
23 p2991 A73-43806
- Fracture analysis of surface- and through-cracked sheets and plates.
23 p3042 A73-43813
- Acoustic emission from low-cycle high-stress-intensity fatigue.
23 p2992 A73-43816
- Metal fatigue phases investigation including strain hardening under cyclic loads and microcrack nucleation due to dislocation formation under hydrostatic pressure
23 p2993 A73-43966
- Investigation on the optimum tightening force of bolted joint in torque control method.
23 p2986 A73-44140
- Kinetics of the development of structural changes in iron in the presence of adsorption fatigue
23 p2995 A73-44224
- Evaluation of the sensitivity of materials to stress concentrations in cyclic loading
23 p3047 A73-44279
- Influence of electrolytic polishing on the stress-concentration sensitivity of some alloys in fatigue
23 p2995 A73-44283
- Influence of heat treatment and surface quality on the endurance of E1961 steel
23 p2995 A73-44288
- Fatigue failure predictions for plates with holes and edge notches.
23 p3047 A73-44350
- The effect of the intermediate principal stress on triaxial fatigue of 7075-T6 aluminum alloy.
23 p3047 A73-44351
- Static and fatigue strength of the KhN40MDTlu /EP 543/ alloy after various hardening treatments
24 p3098 A73-44475
- Gas saturated surface layer effect on Ti alloy resistance to static cyclic tensile loads, noting increased fatigue strength after etching
24 p3100 A73-45278
- Behavior of materials under multiaxial vibrating loads. II - Experimental investigations
24 p3153 A73-45447
- Fatigue hardening in niobium single crystals.
24 p3101 A73-45474
- An inverse torsion pendulum with continuous frequency variation for studies of elastic relaxation and fatigue
24 p3076 A73-45554
- METAL FIBERS**
- The effect of brittle interfacial compounds on deformation and fracture of molybdenum-aluminum fiber composites.
13 p1636 A73-28794
- Three-dimensional scattered-light stress analyses of discontinuous fiber reinforced composites.
[SESA PAPER 2033] 13 p1699 A73-29306
- Metal-filament-reinforced materials and their mechanical behaviour.
13 p1642 A73-29537
- Al filament ignition temperature in carbon dioxide flow at various current values, noting relation to surface oxide film melting temperature
14 p1764 A73-30872
- Stability of metal-based composite materials
15 p1888 A73-31596
- Deformation and fracture behaviours of composites of copper and copper-chromium alloys reinforced with tungsten or molybdenum fibres.
16 p2025 A73-33022
- Failure mode multiplicity in Al-stainless steel and Al-W metal matrix composites under various loading conditions
17 p2191 A73-35527
- The fabrication of fiber-reinforced composites with the aid of high-speed extrusion presses
19 p2435 A73-38272
- Hot-pressed eutectics of oxides and metal fibers.
21 p2723 A73-40895
- High-temperature internal friction in boron fibers
22 p2880 A73-41957
- Influence of alloying additives on the structural changes in a nickel-molybdenum composite
23 p2991 A73-43488
- Fracture behaviour of crystalline Al3Ni intermetallic fibres.
23 p2991 A73-43774
- Antifrictrion materials employing fibers and liquid-metal lubricants
24 p3101 A73-44413

- Shrinkage of reinforced sandwich-type materials during hot pressing
24 p3092 A73-44416
- Mechanical properties of boron fibers
24 p3102 A73-44524
- METAL FILMS**
- Temperature dependence of magnetic susceptibility in nickel-film-coated iron-silicon alloy specimens
01 p0062 A73-10254
- Reflection and transmission coefficients for stratified media, considering total optical reflection attenuator and metal film reflector
01 p0078 A73-11229
- Investigation of the tunnel characteristics of deposited superconducting Nb3Sn films
01 p0089 A73-11290
- Thin film and thick metal film technology comparison and production cost analysis, emphasizing thin film resistors application in hybrid circuits
01 p0026 A73-11399
- Time taken for a laser pulse to make a hole in a metal film.
02 p0176 A73-12114
- Laser-induced stress-wave and impulse augmentation.
02 p0177 A73-12746
- Relative importance of forces of interaction which create, between the grains of a very thin metallic film, the radiation of thermodynamic equilibrium on the one hand, and zero oscillations of the field on the other hand
03 p0349 A73-13605
- Effects of the state of the surface and of titanium films on the dislocation structure of surface layers in molybdenum single crystals
03 p0326 A73-13969
- Adsorbed barium films on tungsten and molybdenum /011/ face.
04 p0460 A73-14867
- Radiation of phonons by metallic films.
04 p0483 A73-15465
- Phase structure of vacuum deposited thin Ta films and molecular beam composition obtained by mass spectroscopy
04 p0484 A73-15667
- Preparation and corrosion properties of a tantalum sputtered thick film.
04 p0456 A73-15759
- The influence of ion bombardment on the microstructure of thick deposits produced by high rate physical vapor deposition processes.
04 p0456 A73-15760
- Stabilization of superconducting beryllium by addition of aluminum.
05 p0605 A73-16794
- Intermetallics formation and diffusion of contacting Al-Au thin films dependence on temperature, thickness ratio and contact time
06 p0706 A73-17903
- Theoretical consideration of soft X-ray absorption by the metallic films of lanthanum and cerium
06 p0737 A73-18220
- Determination of the specific surface resistance of thin metallic layers in the microwave range, based on transmission coefficient measurements
06 p0737 A73-18221
- The mechanism of surface mass transfer in the thin-film Ge-Al system
06 p0738 A73-18651
- Low-temperature epitaxy of Ge films by sputter deposition.
06 p0739 A73-18777
- High reliability technology assessment for metal film resistors production, discussing qualification tests
07 p0829 A73-18921
- Choosing the parameters for plasma anodizing of aluminum
07 p0830 A73-19293
- Solar radiation absorptivity control by metal film coatings, noting thermal control coatings for heat shielding
07 p0778 A73-19300
- Low-frequency creep in CoNiFe films.
[IEEE PAPER 7,1] 07 p0861 A73-19362
- Tantalum thin film capacitors fabrication procedure for hybrid ICs, presenting temperature and frequency responses and I-V characteristics of test samples
07 p0801 A73-19535
- Influence of the substrate and the structure of the metal film on the nature of the annealing treatment of defects formed in the film by proton bombardment
07 p0864 A73-20524
- Study of the channeling of light ions of 0.5 to 2 MeV across gold crystals of some hundreds of angstroms thickness
07 p0864 A73-20609
- Nucleation film/electron beam recorder - Near-real-time display system.
08 p0965 A73-21247
- Ion gun sputter cleaning of thin film metal substrate for in situ corrosion studies by UHV transmission electron microscopy
08 p0990 A73-21616

Uniaxial magnetic anisotropy of single-crystal per-
malloy films 09 p1132 A73-21958

Improved responsivity and sensitivity charac-
teristics of the thin-film bismuth bolometer.
09 p1080 A73-22087

Sensitive platinum film resistance thermometers for
heat transfer measurement. 09 p1083 A73-22509

Electrical and structural properties of low-tempera-
ture bismuth films 09 p1133 A73-22603

Thin In film sealing techniques at temperatures
below 300 C for binding Pyrex to various materials,
using Au layer as alloy flux 09 p1085 A73-22950

Nonequilibrium crystallization of Al-Ru alloys
09 p1108 A73-23228

Diffraction study of fast electrons of the adsorption
layer of oxygen on the surface of a film of epitaxial
copper 10 p1259 A73-23767

Amorphous thin films of rare earth transition metal
alloys for magneto-optic applications, noting SNR in
thermomagnetically written film 11 p1409 A73-26325

Magnetic reversal mechanisms of obliquely
deposited permalloy films possessing perpendicular
anisotropy 12 p1530 A73-26833

Investigation of a pulsed laser utilizing an explod-
ing-film Q switch. 12 p1507 A73-27504

Separation of rotational lines of a CO₂ laser with a
film selector in the resonator. 12 p1508 A73-27527

Copper deposition on ceramic plate, studying inter-
digital slow wave structure and thin film meander-line
coupling impedance and dispersion characteristics
12 p1480 A73-27581

Experimental study of the diffusion of electrons of
conduction by superficial defects of thin gold films
13 p1668 A73-28453

Optical studies of the inhomogeneities of metallic
layers deposited in vacuum 13 p1660 A73-28761

Access to uncombined titanium through an inhibit-
ing film in sublimation pumping of deuterium.
13 p1581 A73-28929

Use of soft X-ray spectroscopy to study corrosion
and oxidation products on metals and alloys.
[NACE PAPER 124] 13 p1638 A73-29319

Quantitative measurement of aluminum film adhe-
sion to polymers, noting influence of substrate nature
on adhesion strength 14 p1755 A73-30724

Response of thermally controlled, vibrating
piezoelectric quartz to the deposition of multiple metal
layers 15 p1924 A73-31843

Cadmium mercury telluride thin film coatings
preparation by HgTe layers deposition onto previously
vapor deposited CdTe layers under isothermal condi-
tions 15 p1924 A73-32158

Heating of an oxidizing metal by CO₂ laser radiation
17 p2184 A73-34634

Effect of adsorption on the electrical conductivity
of thin vanadium films 17 p2220 A73-35557

Dislocation-type mechanism of the influence of
solid surface films on the deformation and fracture of
metals 18 p2319 A73-35891

Evaluation of pinholes in unbacked metal film filters
to be used in rocket- and satellite-borne XUV spec-
troheliographs. 19 p2429 A73-37262

Nd laser radiation thermochemical effects on oxide
formation on thin Cr films, noting resistance and
etching rates 19 p2438 A73-38148

Optimal thick layer nitriding of Ti alloys, discussing
boundary conditions, film, hydrogen effect and
mechanical properties 21 p2707 A73-40739

Characteristics of thin-film metal arrays for laser-
beam information storage. 22 p2869 A73-42254

Exceptional hardness and corrosion resistance of
Mo₅Ru₃ and W₃Ru₂ films. 22 p2866 A73-42581

Investigation of tunnel characteristics of sputtered
superconducting Nb₃Sn films. 23 p3015 A73-43511

Diffusion in thin film couples of platinum-gold.
23 p3015 A73-43528

The rectifying barrier in gallium arsenide Schottky
diodes 23 p2959 A73-43618

The detectability limits of thin coatings measured
with the electron microprobe. 23 p2985 A73-43917

Some experiments to crystallize the metal thin films
on quartz plates. 23 p3018 A73-44136

METAL FINISHING
NT ELECTROPOLISHING
Cleaning and activation of beryllium-copper elec-
tron multiplier dynodes. 02 p0146 A73-11966

METAL FOILS
Fabrication of porous tungsten foils for contact
ionization of cesium [ONERA, TP NO. 1113] 01 p0055 A73-10234

Metal-metal laminar composites for high-tempera-
ture applications. 02 p0182 A73-12620

Internal friction in polycrystalline copper foils after
alpha-irradiation at 78 K 03 p0328 A73-14653

Production of porous tungsten thin walls intended
for cesium ionization by contact 04 p0454 A73-15721

Electron microscopic investigation of cold worked
and annealed thin V and Mo foils recrystallization
characteristics, considering effect of grain boundaries
pinning at surface 05 p0588 A73-17245

Direct observation of tensile and fatigue cracks.
06 p0710 A73-18495

The growth of dielectric aluminum and tantalum
oxide layers 08 p0977 A73-21023

Metal foil panels for radiant heating, describing
historical development, design, fabrication methods
and applications 10 p1177 A73-24175

Fiber reinforced metal production by explosive
welding, discussing fiber winding upon metal foils
11 p1372 A73-25353

Ti-Pd phase diagram eutectoid region configuration
determination through alloy thin foil arc melting
preparation and microstructure examination by elec-
tron microscopy 13 p1633 A73-28146

Aluminum foils crack propagation observation with
electron microscope during tensile tests, noting crystal
dislocation role in ductile fracture process 13 p1639 A73-29467

Twin-jet thinning techniques for transmission elec-
tron microscopy observation of tantalum and niobium.
15 p1891 A73-31995

Electrochemical thinning of a metal disk rotating on
a floating self-moulded cathode. 17 p2182 A73-35766

Radiative property degradation of water impinging
on thermally-controlled surfaces under space condi-
tions. [AIAA PAPER 73-733] 18 p2336 A73-36350

Al foil surface properties from electron spectro-
scopic analysis, determining oxide film thickness, an-
nealing effects and oxidation dependence on surface
hydrocarbon deposits 19 p2442 A73-38171

Anisotropy of low-temperature plasticity and the
tendency of deformed molybdenum toward exfolia-
tion 20 p2578 A73-39377

Investigation of the hypervelocity impact on thin
plastics and metal foils 21 p2696 A73-39990

A titanium-base composite material 21 p2724 A73-41276

METAL FORGING
U FORGING
METAL FORMING
U FORMING TECHNIQUES
U METAL WORKING
METAL GRINDING
Effect of the characteristics of diamond grinding on
the stressed state and strength of hard alloy VK6
24 p3094 A73-44968

METAL HALIDES
NT ALKALI HALIDES
NT ALUMINUM CHLORIDES
NT BARIUM FLUORIDES
NT CADMIUM FLUORIDES
NT CALCIUM CHLORIDES
NT CALCIUM FLUORIDES
NT CESIUM HALIDES
NT CESIUM IODIDES
NT COPPER CHLORIDES
NT LANTHANUM FLUORIDES
NT LITHIUM FLUORIDES
NT MAGNESIUM FLUORIDES
NT POTASSIUM CHLORIDES
NT POTASSIUM IODIDES
NT SILVER BROMIDES
NT SILVER CHLORIDES
NT SILVER HALIDES
NT SILVER IODIDES
NT SODIUM CHLORIDES
NT SODIUM IODIDES
NT STRONTIUM FLUORIDES
METAL HARDENING
U HARDENING [MATERIALS]

METAL HYDRIDES
NT LITHIUM ALUMINUM HYDRIDES
NT LITHIUM HYDRIDES
Dissolution of Ti-6Al-4V at cathodic potentials in
5N HCl. 12 p1512 A73-27249

Titanium hydride and hydronitride thermal stability
analysis from hydrogen vapor pressure and decom-
position measurements in vacuum at 400-1100 C
15 p1888 A73-31601

METAL INSULATOR SEMICONDUCTORS
U MIS [SEMICONDUCTORS]
METAL IONS
NT FERRIC IONS
NT MANGANESE IONS
Oscillator strengths and ground-state photoioniza-
tion cross-sections for Mg⁺ and Ca⁺. 01 p0104 A73-11043

Analyses of light-ion spectra in stellar atmospheres.
I- Magnesium II in B and O stars. 03 p0366 A73-12934

Metal ions implantation to produce alloy or
semiconductor, discussing transmission electron
microscopy use for viewing target material defect
clusters 03 p0350 A73-13794

Ionization balance for ions of Na, Al, P, Cl, A, K,
Ca, Cr, Mn, Fe and Ni. 03 p0345 A73-13949

Magnetospheric electric fields convective motions
measurement by Ba ion cloud tracking and symmetric
double probe floating potential technique 04 p0442 A73-15333

The spectra of highly ionized aluminum [Al VI-X] in
the extreme-ultraviolet and soft X-ray regions.
04 p0492 A73-15369

Non-enzymic beta-decarboxylation of aspartic acid.
04 p0414 A73-16032

Dinuclear anions of molybdenum VI and tungsten
VI with the 'fluoro' and 'oxalato' coordinates
05 p0547 A73-17218

Ultraviolet photometry from the Orbiting As-
tronomical Observatory. VI - Magnesium II 2800 A
emission in cool stars. 05 p0625 A73-17336

Dependence of poly U-directed cell-free system on
ratios of divalent and monovalent cations. 06 p0652 A73-17945

Intensity calculation of X-ray scattering by the atom
and ion of aluminum 06 p0725 A73-18216

Site preferences of Ni²⁺/ and Co²⁺/ in
clinopyroxene and olivine - Limitations of the statisti-
cal approach. 06 p0690 A73-18268

Fe²⁺/-Mg site distribution in Apollo 12021
clinopyroxenes - Evidence for bias in Moessbauer
measurements, and relation of ordering to exsolution.
07 p0881 A73-19706

Static electric quadrupole interaction of Ta- and Hf-
ions in barium and lead titanate. 07 p0862 A73-20018

Spectroscopy of optical centers of Nd³⁺/ in CaF₂
and SrF₂ crystals 07 p0836 A73-20203

Optical properties of Nd³⁺/ in lanthanum oxy-
fluoride single crystals 07 p0837 A73-20205

Electron-hole processes in CaF₂ crystals doped
with rare-earth ions 07 p0837 A73-20208

Magnesium and associated ionospheric processes in
Es-layer formation. 08 p0957 A73-20655

Solar two-component atmospheric model for predic-
tion of Ca II emission arches in spectrogram of strong
lines near limb from kinetic equilibrium calculation
08 p1001 A73-20753

The metallic-line star 15 UMa and the F 5 V star 5
And. 09 p1141 A73-22013

The extreme-ultraviolet spectrum of Fe XV in a
solar flare. 09 p1137 A73-22039

Metallic ion composition and electron density mea-
surements in equatorial E region, considering three
body reaction kinetics with dissociative ion-electron
recombination 09 p1074 A73-22064

Effect of copper ions on the functional state of the
neuromuscular apparatus 09 p1039 A73-22369

Magnetic permeability dependence on temperature
and composition of hexaferrites with various Sc ion
contents 09 p1134 A73-22982

Galvanic interaction between active and passive
titanium. 09 p1106 A73-23167

Obtaining beams of singly charged metal ions with
the aid of giant ruby laser pulses 10 p1227 A73-23815

Optical resolution of DL-aspartic acid in the presence of optically active amino acid and copper (II) ion.

11 p1324 A73-25146

Metal ion density measurement in sporadic A layer during beta Taurids shower by rocket-borne mass spectrometry, noting origin in cosmic debris ablation

13 p1673 A73-28277

Metal ions role in sporadic E layer formation in terms of magnesium ions profile redistribution by vertical gradient in neutral particle wind

13 p1608 A73-28723

Excitation of the Fe XIII spectrum in the solar corona.

13 p1684 A73-29353

Fe XVII emission from the solar corona.

13 p1685 A73-29356

New observations of Fe XVII in the solar X-ray spectrum.

13 p1685 A73-29357

Photometric analysis of monochromatic photographs of the solar corona taken in the green line (5303 Å) and the red line (6374 Å).

13 p1685 A73-29363

Cavity-like instability observed in quiescent prominence from H alpha slit-yaw pictures shown with Ca ion 8542 Å spectra

13 p1670 A73-29371

Optical absorption spectrum of excited Cr³⁺/ions in yttrium aluminum garnet.

13 p1629 A73-29432

Equatorial spread F formation convective electric fields generation by neutral winds and conductivity caused by metallic ion concentrations

14 p1749 A73-29988

Valency transfers of vanadium ions in ruby

14 p1783 A73-30582

Application of an extended method of calculation to rare-earth atoms and ions in the 4fN configuration

14 p1784 A73-30852

Mossbauer and X-ray spectral studies of a nickel-cobalt ferrite subjected to thermomagnetic treatment

15 p1886 A73-31034

Visible luminescence of Yb³⁺ and Er³⁺ during IR excitation

15 p1884 A73-31712

Cooperative mechanisms during laser excitation of luminescence in Yb-Tb and Yb-Eu ion activated glass

15 p1884 A73-31713

Effects of electron-phonon interaction in the luminescence spectra of transition and rare-earth impurity ions in crystals

15 p1885 A73-31715

Quantum losses during excitation of ruby luminescence

15 p1924 A73-31721

Metallic lines in the solar flare of July 12, 1961 and properties of the corresponding emission regions

15 p1938 A73-31957

The equivalent widths of Mg II lines near 2800 Å in the spectra of 31 stars.

16 p2059 A73-32838

Stark broadening and shift of singly ionized aluminum lines.

16 p2040 A73-32845

High-resolution magnetic hyperfine resonance in harmonically bound ground-state Hg-199 ions.

16 p2038 A73-32850

Selection and preliminary evaluation of three structures as potential solid conductors of alkali ions - Two hollandites, a titanate, and a tungstate.

17 p2219 A73-35325

Anisotropy of absorption bands in some lunar, meteoritic, and terrestrial pyroxenes.

17 p2235 A73-35738

Positive ion composition in the lower ionosphere during the Geminid meteorshower and the occurrence of a winter anomaly.

18 p2305 A73-36005

Meteoritic ions in the D and E-regions.

18 p2310 A73-36132

Meteor ions in the polar ionosphere according to the rocket mass-spectrometric measurements and theoretical calculations.

18 p2311 A73-36146

TD 1 A astronomical satellite detection of UV dayglow emissions above F 2 peak in equatorial zone, considering Mg ions resonance scattering to account for emission features

20 p2551 A73-38940

A semiempirical description of the structure of metals

20 p2577 A73-39295

High-resolution photodetachment study of Se⁻ ions.

21 p2710 A73-40213

Violet and UV laser transitions in Ca II and Sr II resulting from impact radiation recombination of doubly charged metal ions

21 p2712 A73-40358

Ruby coloring centers and orange coloration dependence in corundum crystals on additive Mg, Cr, V and Ti ions

21 p2752 A73-40560

Computer model of Ba ion cloud expansion in magnetosphere, taking into account self-consistent electric and magnetic field interactions

22 p2846 A73-41938

Stimulation of two-valent rare earth ion luminescence in CaF₂ crystals by ruby and neodymium lasers

22 p2870 A73-42725

Energy level transitions in Ca XVII and Ti XIX UV spectra, basing identifications on extrapolation method

22 p2914 A73-43016

EPR-line splitting in irradiated ruby containing impurities

23 p3017 A73-44039

Metal lines in the solar flare of July 12, 1961, and the properties of the emission region.

24 p3132 A73-44482

Proton collisional excitation in the ground configuration of Fe⁺/12/.

24 p3123 A73-44634

Layering of the neutral metals of meteoric origin in the lower ionosphere.

24 p3066 A73-44733

Probe electric field measurements near a midlatitude ionospheric barium release.

24 p3085 A73-45119

METAL JOINTS

NT SOLDERED JOINTS

NT SPOT WELDS

NT WELDED JOINTS

Russian book on ultrasonic welding of metals and plastics covering equipment, transducers, welded joints stabilization, quality control and efficiency

04 p0457 A73-15970

Glued metal joints polished samples interface corrosion under alternate immersions and withdrawals in baths of different compositions

04 p0468 A73-15991

Filler wire welded joints of Al-Zn-Mg and Al-Mg alloys, testing weldability and mechanical properties susceptibility to hot cracking

07 p0840 A73-20372

Technology, strength, and calculation of bonded circular joints

10 p1224 A73-24090

Calculation of the shear strength of an axisymmetric joint constructed out of Loctite

10 p1224 A73-24091

Linear elastic finite element stress analysis of lap and tapered adhesive joint bonding of composite to metal substrate

11 p1438 A73-25505

[AIAA PAPER 73-371]

Book - Welding and welding technology.

17 p2177 A73-34454

Strength of joints produced by melting high-carbon chromium alloys on low-carbon steel

17 p2188 A73-34566

Prediction of weld metal hydrogen levels obtained under test conditions.

21 p2708 A73-41252

Investigation on the optimum tightening force of bolted joint in torque control method.

23 p2986 A73-44140

METAL MATRIX COMPOSITES

Processing of high-performance alloys by powder metallurgy.

01 p0063 A73-10286

Experimental investigation of the thermal expansion of filamentary composite materials

01 p0068 A73-10859

Influence of fiber/matrix interfaces on the plasticity and strength of fiber-reinforced composites

02 p0184 A73-11623

Material and structural studies of metal and polymer matrix composites.

02 p0182 A73-12621

Mechanical properties of aluminum matrix composites.

02 p0184 A73-12849

Failure mechanisms in transversely loaded boron-aluminum.

02 p0184 A73-12861

Preparation and high-temperature properties of carbon fiber-Ni composites.

03 p0321 A73-12919

Reinforcement of aluminum alloys by high strength steel ribbons

03 p0312 A73-13581

Prospects offered by high performance composites with a metallic matrix

03 p0325 A73-13589

Effects of alloying on structural stability and cohesion between phases in oxide/metal composites.

03 p0326 A73-13964

Aluminum-stainless steel and Ni-Mo composites prepared by dynamic hot pressing, determining bond strength between fibers and reinforced metal matrix

03 p0328 A73-14013

Fracture toughness of duplex structures. I - Tough fibers in a brittle matrix.

04 p0460 A73-14700

Metallic materials developments in aircraft construction and gas turbine engine applications,

discussing superalloys, refractory metals, composites and directionally solidified alloys

04 p0460 A73-14741

B-Al matrix composites environmental properties, costs and development for aerospace systems, considering corrosion, erosion and thermal cycling effects on tensile strength

04 p0467 A73-15934

Boron fiber-aluminum alloy matrix composite structure Charpy impact energy absorbing capacity explained via energy dissipation of matrix by plastic deformation

05 p0588 A73-16111

Deformation by Paoletti-Lueders bands observed on composites of oriented solidification

[ONERA, TP NO. 1192]

Composite Al- and Ni-base alloys strengthened by B and W/Mo fibers respectively for reduced weight wing spars and high temperature applications

06 p0708 A73-18099

Self lubricating bearing materials strength, friction, wear, thermal and dimensional stability properties, considering plastic, metal matrix and carbon graphite composites

06 p0710 A73-18638

The yield point phenomenon in a Be-Al composite.

07 p0832 A73-20449

Structural fabrication of advanced metal-matrix composites.

[SME PAPER EM 72-108]

The influence of a thoria dispersion on preferred orientation in nickel alloys.

07 p0832 A73-20449

Effects of thermal loading on foil and sheet composites with constituents of differing thermal expansivities.

08 p0977 A73-21012

[ASME PAPER 72-MAT-E]

Effects of thermal loading on fiber-reinforced composites with constituents of differing thermal expansivities.

08 p0979 A73-21572

[ASME PAPER 72-MAT-F]

Unidirectional filament reinforced metal matrix composites compositional changes due to temperature induced interatomic diffusion, using diffusion equation finite difference solutions superposition technique

08 p0979 A73-21573

Investigation of the compatibility of boron fibers with tungsten substrates and titanium matrices

09 p1101 A73-22404

Microstructural observations of arc welded boron-aluminum composites.

09 p1103 A73-22469

Fiber reinforced metal matrix composites mixing rule, determining tensile strength, deformation energy and flow curve

10 p1223 A73-23630

Phase equilibria in three-component alloys containing an interstitial element, and the stability of composite materials

10 p1231 A73-23694

Creep and creep-rupture-strength of titanium strengthened by molybdenum fibers

10 p1233 A73-24317

Failure analysis and heat resistance optimization factors of reinforced metal sheet under thermal cycling

10 p1233 A73-24356

Reinforcement of magnesium with boron and tantalum filaments.

10 p1233 A73-24369

Experimental observations of tensile fracture in unidirectional boron filament reinforced aluminum sheet.

10 p1234 A73-24437

A theory for the mechanical properties of metal-matrix composites at ultimate loading.

10 p1235 A73-24439

Fiber reinforced metal production by explosive welding, discussing fiber winding upon metal foils

10 p1235 A73-24443

Composite materials; Meeting, 2nd, Konstanz, West Germany, March 15, 16, 1972, Technical Reports

11 p1372 A73-25353

Boron filament reinforced Al and Ti matrices manufactured by pressure-sintering method, investigating filament external silicon carbide effects on mechanical properties

11 p1372 A73-25401

Directionally solidified eutectic high temperature alloys.

11 p1379 A73-25402

Mechanical properties at high temperature of Ni-based unidirectionally solidified eutectic: Ni-Ni₃Ta.

11 p1379 A73-25403

Production and properties of tungsten-wire reinforced NiCr 80 20

11 p1379 A73-25407

Networks of polycrystalline metal whiskers for composite materials

11 p1379 A73-25408

Discontinuous fibres alignment in metal composites by plastic deformation.

11 p1372 A73-25409

Ag- or Cu-based fiber reinforced composite materials for springs in electrical contact devices, investigating mechanical strength and contact and wear resistances

11 p1387 A73-25410

Compatibility between material components in metal-ceramics composites

11 p1387 A73-25412

Plasma sprayed boron fiber reinforced titanium oxide and Al matrix composites, discussing temperature control for particle size and SiC coating effects on strength

11 p1388 A73-25413

Silicon carbide whisker reinforced Al composite production by powder metallurgy, discussing mechanical strength and extrusion process for fiber orientation

11 p1373 A73-25414

Steel wire, boron or carbon filament reinforced Al alloys shaped parts fabrication, discussing sintering, pressure impregnation and filament winding processes

11 p1373 A73-25415

Design and manufacture of structure components made of fiber-reinforced materials

11 p1373 A73-25417

Effect of water vapor on fatigue behavior of an aluminum-boron composite.

11 p1383 A73-25828

Stability of micromorphology of carbon fibres and their interstitial compounds.

11 p1389 A73-25858

Reactivity and interface characteristics of titanium-alumina composites.

11 p1384 A73-26043

Elevated temperature stability of carbon-fibre, nickel-matrix composites Morphological and mechanical property degradation.

11 p1384 A73-26047

Microscopic, kinetic and microhardness observations of Ti-W metal matrix composite solid state interface reactions, showing enhanced shear resistance

11 p1384 A73-26049

Theoretical and experimental investigation of the nonlinear behavior of angleplid boron/aluminum composites.

11 p1385 A73-26524

Bivariant eutectic alloys located on liquidus surface within Ni-Nb-Cr-Al quaternary, permitting production of aligned delta Ni-Nb lamellae within nichrome matrix containing Ni-Al fcc precipitate

12 p1509 A73-26845

Analysis of the energy losses during dynamic hot pressing of reinforced metals

12 p1503 A73-27557

Metal matrix composites microstructural alignment by solid state transformation process involving eutectoid decomposition and cellular precipitation

12 p1513 A73-27682

Experimental investigation of thermal expansion in composite fibrous materials.

12 p1516 A73-27908

Use of high cooling rates to obtain aluminum alloys with special properties

13 p1623 A73-28110

Transverse creep and stress-rupture of Borsic-aluminum composites and Borsic-aluminum composites containing stainless steel and titanium.

13 p1633 A73-28143

Directionally solidified eutectic alloy composites for high temperature turbine blade and vane applications, considering morphology, crystallography and thermal stability properties

13 p1635 A73-28778

The effect of brittle interfacial compounds on deformation and fracture of molybdenum-aluminum fiber composites.

13 p1636 A73-28794

A study of the effects of prestrain on the tensile properties of filamentary composites.

[ASME PAPER 72-MAT-K]

13 p1699 A73-29198

Mechanical behavior of WC-Co composite alloys.

13 p1643 A73-29545

Mechanical properties of titanium reinforced with unidirectional molybdenum wires.

13 p1643 A73-29604

Book - Fibre-reinforced materials technology.

13 p1644 A73-29675

Precipitation and dispersion hardened alloys, fiber reinforced metal matrix composites, carbon-carbon composites, and dispersed system, eutectics application in aerospace industry

14 p1759 A73-30067

Compatibility of components in metal-ceramics composites

14 p1766 A73-30442

Layered and aggregate product displacement reaction kinetics in solid state /metal-metal oxide/ couples for metal matrix composites at 1000 C from thermodynamic and diffusion data

14 p1783 A73-30634

A theoretical model for the elevated temperature deformation of dispersion hardened metals.

14 p1761 A73-30636

Steel reinforcement fiber arrangement and volume content influence on aluminum composites strength and fatigue resistance at room and elevated temperatures

14 p1766 A73-30710

Technical note on some mechanical properties of a magnesium-25 vol% boron particulate composite.

14 p1765 A73-30935

Compatibility of silicon carbide fiber with a tungsten base and a titanium matrix

15 p1888 A73-31595

Stability of metal-based composite materials

15 p1888 A73-31596

Theoretical post-yielding behavior of composite laminates. I - Inelastic micromechanics.

15 p1897 A73-31678

Yielding in unidirectional composites under external loads and temperature changes.

15 p1949 A73-31679

Fatigue behaviour of ribbon-reinforced composites.

15 p1898 A73-31840

Effect of treatment factors on the properties of friction materials. II - Effect of sintering conditions on the structure and friction and wear properties of friction materials

15 p1892 A73-32244

Techniques for fabrication of composite materials.

16 p2017 A73-32699

Some mechanical properties of carbon fiber reinforced aluminum.

16 p2025 A73-32849

Electric contact materials technology, discussing intermetallics, ordered alloys, metal matrix composites and silver, gold and platinum based hardened alloys manufacture and properties

16 p2027 A73-32946

Deformation and fracture behaviours of composites of copper and copper-chromium alloys reinforced with tungsten or molybdenum fibres.

16 p2025 A73-33022

Thermal cycling effects on void formation in boron-aluminum matrix composites at 70-670 F, considering jet turbine compressor blade applications

16 p2084 A73-33037

Boron fiber coating by chemical vapor deposition of boron carbide for improved mechanical properties and incorporation in Al alloy matrices

16 p2030 A73-33070

Monograph - Fibre reinforcement.

17 p2240 A73-34125

Room temperature creep of Borsic-aluminum composites.

17 p2189 A73-34644

A study on some metal-base self-lubricating composites containing tungsten disulfide. [ASLE PREPRINT 73AM-3C-1]

17 p2196 A73-34986

A nondestructive measurement of the elastic constants of unidirectional borsic fiber reinforced aluminum composites.

17 p2182 A73-35439

Failure mode multiplicity in Al-stainless steel and Al-W metal matrix composites under various loading conditions

17 p2191 A73-35527

Generalized equation for tensile strength of metal matrix composites from upper bound analysis of simplified model with holes, inclusions and environmental pressure

17 p2251 A73-35528

Direct observation of the failure of a fibre reinforced composite.

17 p2192 A73-35529

Brass matrix composites tensile strain characteristics and fracture mode dependence on fiber volume fraction and properties

17 p2192 A73-35531

Borsic/Ti-Al-V composite properties, fracture modes and fabrication, discussing tensile strength and temperature dependence of longitudinal strength

17 p2192 A73-35532

Filament orientation effect on Al and Ti matrix composite tensile properties, using boron, borsic and silicon carbide fibers

17 p2192 A73-35533

Residual stresses and mechanical properties of circumferentially wrapped metal-metal composite cylinders fabricated from plasma sprayed Al reinforced with steel filaments

17 p2251 A73-35534

High modulus fiber reinforced metal and plastic matrix composites fracture within linear elastic fracture mechanics framework, reviewing standard notch toughness test

17 p2192 A73-35536

Borsic-aluminum composites fracture and flexural behavior from Charpy impact and slow bend tests

17 p2192 A73-35537

Deformation and fracture mechanisms in aluminium reinforced by high strength steel ribbons.

17 p2192 A73-35539

Borsic-Al composites fiber-matrix debonding for toughening mechanism of crack blunting, noting notch insensitivity and delamination

17 p2193 A73-35540

Noncumulative fracture mode of unidirectional boron filament-aluminum matrix composite under axial tension, measuring critical filament stress

17 p2193 A73-35542

Fatigue and creep behavior of aluminum and titanium matrix composites.

17 p2193 A73-35543

Tension-tension low cycle fatigue failure mechanism in uniaxially and biaxially reinforced boron fiber-aluminum alloy composites, considering matrix plasticity role

17 p2193 A73-35544

High temperature tensile and stress rupture tests of tungsten /Nichrome laminar composites and tungsten alloy/ Inconel sheet and foil specimens

17 p2193 A73-35545

Selection of the composition for the matrix of a composite material, which will not dissolve the reinforcing fibers

18 p2328 A73-36860

Resistance diffusion bonding boron/aluminum composite to titanium.

19 p2435 A73-38004

The influence of primary precipitates on the tensile strength of unidirectionally solidified /Fe, Cr/-/Cr, Fe/7C3 in-situ grown composites containing 30 wt % Cr.

19 p2442 A73-38088

The effect of elevated temperatures on the mechanical properties of B-Al composites.

19 p2442 A73-38095

Observations on the directional solidification of cobalt-base alloys strengthened by carbide fibers.

19 p2443 A73-38249

The fabrication of fiber-reinforced composites with the aid of high-speed extrusion presses

19 p2435 A73-38272

Structures and properties of cobalt base-TaC eutectic alloys.

20 p2575 A73-39020

Partitioning of stress between fiber and matrix during tensile deformation of the Al-Al3Ni eutectic composite.

20 p2576 A73-39024

Carbide reinforcement in two directionally solidified alloyed nickel eutectic alloys.

20 p2576 A73-39028

Properties of boron fibers and of boron-aluminum composites in uniaxial compression

20 p2580 A73-39358

Investigation of the transition zone structure in composite materials under cyclic loads

20 p2580 A73-39379

Anisotropy of the mechanical properties of aluminum hardened by a stainless steel grid

20 p2578 A73-39382

Ultrahigh speed cinematography with rotating Ti drums bound by monocrystalline boron fibers, noting prototype performance

21 p2693 A73-39937

A titanium-base composite material

21 p2724 A73-41276

Possible reinforcement of the tungsten-nickel-iron composite with tungsten fibers.

21 p2722 A73-41586

Deformation and microfracture characteristics of two-phase tungsten-composite materials sintered with the liquid phase

22 p2872 A73-41948

Experimental aspects of the mechanical behavior of fiber composites produced by oriented solidification [ONERA, TP NO. 1205]

22 p2876 A73-42215

Grain boundary cavitation and sliding in copper/tungsten composites due to thermal stresses.

22 p2876 A73-42339

Fibre-reinforced metallic and ceramic composites produced by thermal spraying.

22 p2866 A73-42592

Generalized initial yield surfaces for unidirectional composites.

[ASME PAPER 73-APMW-24]

22 p2925 A73-42886

Al-aluminum nickelide eutectic fiber composite impact strength dependence on crystallization rate, examining crack propagation rate relation to fiber spacing

23 p2996 A73-43437

Influence of the method of preparing a Ni + ThO₂ composite and of its strengthening-oxide content on heat resistance

23 p2990 A73-43486

Influence of alloying additives on the structural changes in a nickel-molybdenum composite

23 p2991 A73-43488

Precipitation and magnetic hardening in sintered WC-Co composite materials.

23 p2997 A73-43776

Soldering and brazing of advanced metal-matrix structures.

23 p2986 A73-44003

The stability of sapphire whiskers in nickel at elevated temperatures. I - General morphological and chemical stability. II - The kinetics of morphological changes over the temperature range 1100 to 1400 C.

23 p2986 A73-44032

METAL OXIDE SEMICONDUCTORS

The copper-boron eutectic - Unidirectionally solidified. 23 p2993 A73-44035

Deformation behaviour and deviation from the simple rule of mixture for the ultimate tensile strength in the cold rolled fibre-reinforced composites. 23 p2998 A73-44151

Testing of composite materials with the aid of annular samples 23 p2998 A73-44295

Kinetics of shrinkage during the sintering of porous glass/metal composites 24 p3092 A73-44415

Shrinkage of reinforced sandwich-type materials during hot pressing 24 p3092 A73-44416

METAL OXIDE SEMICONDUCTORS

Influence of strong external factors on the characteristics of semiconductor devices sensitive to the state of the surface /Review/ 01 p0022 A73-10036

The degradation of MOS transistors resulting from junction avalanche breakdown. 01 p0023 A73-10648

M.O.S.F.E.T. temperature-drift performance limitations. 04 p0427 A73-14983

Threshold voltage shift for low voltage operation of transistor circuits with boron ion implanted MOS 04 p0427 A73-15322

Exact frequency dependent complex admittance of the MOS diode including surface states, Shockley-Read-Hall /SRH/ impurity effects, and low temperature dopant impurity response. 04 p0427 A73-15347

Method of calculating high-frequency parameters of m.o.s. transistors in the nonpinch-off region 05 p0556 A73-16163

N-type Si MNOS random access memory devices for data storage without applied voltage, noting threshold shifts vs writing pulse width for various oxide thicknesses 05 p0553 A73-16166

Description and utilization of the TMS 4062 dynamic memory 05 p0553 A73-16171

Performance of hardened P-MOS devices in severe neutron environments. 05 p0557 A73-16517

Current saturation mechanisms in junction field-effect transistors. 05 p0558 A73-16605

Buried channel MOS, double junction and Schottky barrier charge coupled devices, noting higher speeds, charge transfer efficiencies and radiation resistance 05 p0559 A73-16810

Investigation of surface states in the MOS system by gate controlled diode structure. 05 p0559 A73-17170

Simple mathematical model of shift of threshold voltage induced in an m.o.s. transistor by testing at elevated temperatures. 05 p0560 A73-17324

Certain electrophysical properties of zinc oxide base semiconductor ceramics with admixtures of transition-metal oxides 06 p0735 A73-18079

Influence of low-temperature heat treatment on the electrical and recombination properties of silicon-silicon dioxide systems 06 p0736 A73-18085

Charged coupled IC image sensors based on MOS capacitors for low light level TV, considering operation, performance and production technologies 06 p0676 A73-18301

Effects of ionizing radiations on MOS components 07 p0860 A73-18914

MOS field effect components integration on Si operation, performance and application to logic circuits 07 p0797 A73-18916

MOS production line with individual manufacturing operation reliability assurance based on failure analysis, process perfection, material control and experimental verification 07 p0829 A73-18917

Improving the performance of M.I.S. circuits under radiation. 07 p0797 A73-18918

Co-60 source gamma irradiation of Mo-Au doped p-type Si MOS transistors, noting threshold voltage increase and current carrier mobility decrease 07 p0862 A73-19541

Electron tunnelling into amorphous germanium and silicon. 07 p0864 A73-20454

A procedure for the evaluation and failure analysis of M.O.S. memory circuits using the scanning electron microscope in potential contrast mode. 08 p0943 A73-20730

Design and fabrication of MOS/LSI circuits for reliability, discussing layout rules and protective circuitry 08 p0943 A73-20733

Degradation of MNOS memory transistor characteristics and failure mechanism model. 08 p0944 A73-20741

Low-dissipation memories by p-channel MOS technology with special processes and by complementary-channel MOS technology 08 p0945 A73-21073

The breakdown mechanism and methods for measuring breakdown voltages in insulated-gate MOS field-effect transistors 08 p0946 A73-21081

Low-field tunnelling current in thin-oxide M.N.O.S. memory transistors. 08 p0946 A73-21115

Statistical approach to the prediction of M.O.S.-device performance. 08 p0946 A73-21116

Numerical calculation of low-frequency capacitance/voltage curves of M.O.S. capacitors with nonconstant doping profiles. 08 p0947 A73-21122

The low temperature strain sensitivity of MOS transistors. 08 p0948 A73-21476

Resistive MOS-gated diode light sensor. 08 p0948 A73-21477

Book - MOS/LSI design and application. 08 p0950 A73-21840

Bulk lifetime determination from current and capacitance transient response of MOS capacitors. 09 p1062 A73-22307

Electrical properties of MOS capacitors with oxide grown in the presence of HCl. 09 p1062 A73-22308

The effect of an interfacial layer on minority carrier injection in forward-biased silicon Schottky diodes. 09 p1135 A73-23044

Threshold voltage of nonuniformly doped MOS structures. 09 p1064 A73-23046

A linear voltage-tunable distributed null device. 09 p1066 A73-23246

Complementary MOS/silicon-on-sapphire LSI technology developments, assessing impact of incorporated Al and Si gates applications on high speed and low power capabilities 10 p1259 A73-23791

Complementary MOS LSI microprogrammed digital computer design, for Space Ultrareliable Modular Computer Demonstration Vehicle, discussing instruction operation codes, I/O peripherals and software support 10 p1191 A73-23795

MOSFET devices with trapezoidal gates - I-V characteristics and magnetic sensitivity. 10 p1194 A73-24157

A nanovolt-level MOSFET reversing switch for low temperature applications. 11 p1367 A73-26310

Precision low frequency adaptive MOSFET IC electronic oscillators with loose tolerance component timers for cost reduction 12 p1478 A73-27167

Influence of gate metal on gamma-ray induced defects in MOS structures. 13 p1589 A73-28421

The extension of self-registered gate and doped-oxide diffusion technology to the fabrication of complementary MOS transistors. 13 p1595 A73-29576

Anomalous low-frequency noise in MOS transistors at low temperatures. 14 p1731 A73-29749

Two-phase charge-coupled devices with overlapping polysilicon and aluminum gates. 15 p1850 A73-31373

Equivalent circuit HF model of MOS transistor active region based on transient response equation, voltage and structural parameters 15 p1850 A73-31492

Influence of the substrate on the transfer admittance of a saturated MOS transistor 15 p1850 A73-31495

Book - The physics and circuit properties of transistors. 15 p1850 A73-31574

Avalanche injection effects in MIS structures and realization of n-channel enhancement type MOS FETS. 15 p1851 A73-32017

Book - MOS integrated circuits: Theory, fabrication, design and systems applications of MOS LSI. 15 p1852 A73-32579

Transient analysis of complementary MOS IC inverter. 16 p1990 A73-33688

Integrated semiconductor storage devices, discussing bipolar transistor, Schottky diode and MOS memories and RAM, ROM and PROM types with circuit compatibility considerations 16 p1991 A73-33960

Binary capacitors made with p-channel MOS Si gate technology, discussing threshold voltage effects,

structural characteristics, bootstrapping and artificial voltage enhancement 16 p1991 A73-33962

Light sensitive MNOS /metal-nitride-oxide-silicon/ memory transistor space charge layers current-field relationships and steady state I-V measurements 17 p2134 A73-34221

Custom LSI technology utilization in low volume avionic systems, discussing handcrafted chip design, full wafer, array logic and MOS cell approaches and costs 17 p2138 A73-35227

Modular MOS LSI digital data bus system design for integrated avionics and remote sensors interconnection in aerospace vehicles 17 p2139 A73-35232

Complementary MOS/silicon on sapphire LSI technology for high speed digital multiplier and correlator logical building blocks design, fabrication and subsystem array implementations 17 p2140 A73-35318

Book - MOS integrated circuit design. 18 p2294 A73-36966

Low-frequency 1/f noise in MOSFET's. 19 p2409 A73-37581

Semiconductor failures due to oxide defects and diffusion faults, describing nematic liquid crystals application to pinholes detection in oxide layers 19 p2410 A73-38447

Metal oxide semiconductor/large scale integration circuit failure analysis and diagnosis, discussing short circuits, cholesteric liquid crystal coloring and aluminum anodization 19 p2411 A73-38448

Process control stress test of MOS IC circuit susceptibility to charge spreading with channel formation 19 p2436 A73-38452

Book - RCA COS/MOS technology. 20 p2533 A73-38653

COS/MOS applications to clock and watch, automotive, aerospace and military, industrial and consumer markets 20 p2533 A73-38654

Fundamentals of COS/MOS integrated circuits. 20 p2534 A73-38655

High reliability manufacturing technology for COS/MOS IC devices, discussing failure mechanisms and MIL-STD-883 and MIL-M-38510 tests for quality control 20 p2534 A73-38656

COS/MOS phase-locked-loop - A versatile building block for micro-power digital and analog applications. 20 p2534 A73-38657

Analysis and design of single-cycle stages in MOS transistors with allowance for nonlinear distortions 20 p2535 A73-38857

Unpaired electrons and charge carriers in oxide semiconductor glasses based on the oxides of titanium, vanadium, and phosphorus 20 p2599 A73-39394

Design of MOS-transistor integrated-circuit amplifiers 21 p2660 A73-40021

Acoustic surface wave energy detection via combination of MOSFET array and ZnO overlay piezoelectric transducer, deriving signal processing technique 21 p2660 A73-40100

CODYMOS frequency dividers achieve low power consumption and high frequency. 21 p2670 A73-41111

An automated system for designing integrated circuits 21 p2666 A73-41305

Diffusion profile measurements in the base of a microwave transistor. 21 p2668 A73-41560

A new type of charge trapping in MOS systems. 22 p2896 A73-42275

Three layer semiconductor dielectric interface model of structural and electrical properties of silicon-silicon dioxide system involving amorphous regions 23 p3015 A73-43614

Interface properties of oxidized germanium-doped silicon. 23 p3016 A73-43778

Complementary MOS transistor inverter application to quartz oscillator in terms of frequency, temperature and supply voltage 23 p2960 A73-44112

V groove MOS transistor fabrication by preferential silicon etching and masking process with noncritical alignment tolerances 23 p2960 A73-44115

Investigation of low-frequency noise in MOS transistors 24 p3071 A73-44593

Calculation of the nonstationary electric field, carrier concentration, and current distribution in semiconductor integrated circuits 24 p3119 A73-45177

Effects of stress on metal-oxide-semiconductor structures. 24 p3120 A73-45415

Trap-assisted charge injection in MNOS structures.
24 p3120 A73-45419

METAL OXIDES

NT ALKALINE EARTH OXIDES
NT ALUMINUM OXIDES
NT BARIUM OXIDES
NT BERYLLIUM OXIDES
NT BISMUTH OXIDES
NT CALCIUM OXIDES
NT CESIUM OXIDES
NT CHROMITES
NT CHROMIUM OXIDES
NT COBALT OXIDES
NT HAFNIUM OXIDES
NT HEMATITE
NT ILMENITE
NT IRON OXIDES
NT KAOLINITE
NT LANTHANUM OXIDES
NT LEAD OXIDES
NT LITHIUM OXIDES
NT MAGNESIUM OXIDES
NT MAGNETITE
NT MOLYBDENUM OXIDES
NT NICKEL OXIDES
NT NIOBIUM OXIDES
NT PERICLASE
NT PLUTONIUM OXIDES
NT POTASSIUM OXIDES
NT PYROPHYLLITE
NT RUTILE
NT SAPPHIRE
NT SCANDIUM OXIDES
NT TANTALUM OXIDES
NT THORIUM OXIDES
NT TITANIUM OXIDES
NT TUNGSTEN OXIDES
NT VANADIUM OXIDES
NT YTTRIUM OXIDES
NT ZINC OXIDES
NT ZIRCONIUM OXIDES

The effect of oxide thickness on the hot salt stress corrosion susceptibility of Ti-6Al-4V.

01 p0061 A73-10137

Electron-microscopic investigations of metal oxide powders

02 p0178 A73-11543

Operation, fabrication, characterization, I-V performance and application of transient voltage suppressor using metal oxide varistor

03 p0283 A73-13941

Mechanical properties and structure of certain internally oxidized copper alloys

04 p0464 A73-15500

Investigation of the structure of sodium silicate glass containing oxides of multivalent metals by nuclear spectroscopy methods

09 p1110 A73-22980

Interpretation of K X-ray emission spectra and chemical bonding in oxides of Mg, Al and Si using quantitative molecular orbital theory.

10 p1211 A73-24107

Some physicochemical properties of compounds formed by oxides of rare-earth elements and barium

11 p1410 A73-26673

The chemical stage in the mechanism of metal oxide reduction

13 p1581 A73-28937

Samarium oxide neodymium oxide activated glass fiber output power under lasing conditions

14 p1766 A73-30468

Layered and aggregate product displacement reaction kinetics in solid state /metal-metal oxide/ couples for metal matrix composites at 1000 C from thermodynamic and diffusion data

14 p1783 A73-30634

Microstructure and phase composition of oxide scale formation on Ti-Al alloys, noting dependence on Al concentration

17 p2188 A73-34557

Application of refractory oxide coatings in extensometry

18 p2314 A73-35886

Effect of oxides on certain properties of glass-ceramic coatings for titanium

18 p2319 A73-35889

Method of selecting particles formed during the burning of metallized compacted systems in a constant-pressure chamber

19 p2503 A73-37518

The relationship between relative oxide ion content of Na₂SO₄, the presence of liquid metal oxides and sulfidation attack.

20 p2575 A73-39022

Structure and mechanical properties of internally oxidized Ta-8 pct W-2 pct Hf /T-111/ alloy.

20 p2576 A73-39025

Hot-pressed eutectics of oxides and metal fibers.

21 p2723 A73-40895

Metal oxide absorption coefficients for use in intense laser interaction with solids.

21 p2715 A73-40961

Russian book - High-temperature strain gauges based on heat-resistant oxides.

21 p2704 A73-41286

High reliability protective coatings for high temperature technology.

22 p2879 A73-42596

Investigation of the possibility of obtaining andesite-based alkali-resistant glass compositions for a continuous glass fiber

23 p2998 A73-44298

METAL PARTICLES

NT METAL POWDER
NT POWDERED ALUMINUM

Phase diagrams, microstructure and interface composition of two phase metallic particles from lunar soils and rocks, determining equilibrium temperature and equilibration time

03 p0376 A73-14110

Metallic mounds produced by reduction of material of simulated lunar composition and implications on the origin of metallic mounds on lunar glasses.

07 p0884 A73-19738

Metallic particles in the Apollo 14 lunar soil.

07 p0884 A73-19744

On lunar metallic particles and their contribution to the trace element content of Apollo 14 and 15 soils.

07 p0884 A73-19746

Experimental investigation of the electrical conductivity of a coaxial high-temperature jet with dispersed particles of Ti

07 p0858 A73-20010

Investigation of the Canyon Diablo metallic spheroids and their relationship to the breakup of the Canyon Diablo meteorite.

09 p1144 A73-22145

Emission spectrographic analysis of used aero engine oil - A tool of maintenance.

09 p1136 A73-23242

Metallic dust particles in quasi circular solar orbit, discussing evolution, thermal evaporation, atomization and size

10 p1274 A73-23720

Investigation of iron content of lubricating oil using a ferrograph and an emission spectrometer.

10 p1218 A73-24165

Apollo 15 soil samples structure and phase equilibrium data noting metal particles of high cobalt content

12 p1466 A73-27544

Meteoritic vs lunar origin of Luna 20 lunar soil samples metal particles and metallic inclusions discussing meteoritic microstructural obliteration due to shock reheating of crust

13 p1675 A73-28315

Apollo lunar fines ferromagnetic resonance spectral line shape anomaly and anisotropy energy attributed to Fe particles with body centered cubic structure

13 p1684 A73-29177

Composition of metal in type III carbonaceous chondrites and its relevance to the source-assignment of lunar metal.

13 p1686 A73-29564

Metallic dust particles in quasi-circular solar orbit, discussing evolution, thermal evaporation, atomization and size

18 p2355 A73-36745

Application of thermal analysis to the determination of the thermophysical properties and combustion characteristics of metallic particle conglomerates in an oxidizer flow

18 p2342 A73-37119

Ignition limit of metallic particles in a mixture of two oxidizers

19 p2503 A73-37517

High temperature creep in magnesium strengthened by magnesia particles.

21 p2719 A73-40899

Influence of cooling on surface dispersion during the friction process

24 p3092 A73-44417

Ignition of metal particles in the case of a logarithmic oxidation law

24 p3154 A73-44704

Boron particle ignition limit dependence on particle size and oxygen content, taking into account kinetic and diffusion resistance

24 p3155 A73-44708

Specific surface changes in tungsten and molybdenum oxides during reduction processes

24 p3099 A73-44738

METAL PLATES

Large elasto-plastic deflection of a circular plate of mild steel under cyclic loading.

03 p0396 A73-14626

Sharp-notch tension testing of thick aluminum alloy plate with cylindrical specimens.

04 p0460 A73-14698

Fracture toughness of duplex structures. II - Laminates in the divider orientation.

04 p0460 A73-14701

Study of the diffusion of carbon in structural steel plates clad with stainless steels

04 p0467 A73-15951

Crack growth and failure of aluminum plate under in-plane shear.

[AIAA PAPER 73-253]

05 p0635 A73-16975

METAL POWDER

Heat exchange between gas and air cooled porous metal plate prepared from stainless steel powder under induction and resistance heating

06 p0768 A73-18129

Stress analysis of sharply notched plates and measurement of notch tip blunting.

06 p0764 A73-18487

Lamellar tearing and the slice bend test.

07 p0832 A73-20275

An examination of the perforation of a mild steel plate by a flat-ended cylindrical projectile.

08 p1016 A73-20828

Neutron bombardment radiative effects on thin metal plate stability, considering compressive force, lattice defects and critical flux relations

08 p1020 A73-21771

Simple test apparatus for a 100% defect-detection probability in ultrasonic surface scanning of plates and strips

09 p1070 A73-22219

Incident radio wave resonance effect on stationary electric and magnetic fields and standing magnetoplasma wave excitation in Bi plates

09 p1127 A73-22604

Plastic strain rates within discrete crack tip zones at running brittle cracks in mild steel plates, identifying twinning as main deformation mode

09 p1163 A73-23258

Small-scale explosion seam welding.

10 p1223 A73-23626

Stress redistribution and rupture due to creep in a uniformly stretched thin plate containing a circular hole.

[ASME PAPER 72-APM-KKK] Stud welding on 5083 aluminum and 9% Ni steel for cryogenic use.

11 p1442 A73-25709

Metal barrier maximum puncturable thickness dependence on high velocity meteorite particle impact parameters

12 p1375 A73-26352

Finite element method application to elastoplastic analysis of cracked metal plates, discussing plate thickness effects on plastic zone growth and stress distributions along crack tip

12 p1554 A73-27642

The drilling of a metal plate by a laser beam.

[ASME PAPER 73-PROD-6] The residual strength characteristics of stiffened panels containing fatigue cracks.

13 p1701 A73-29476

Transient temperatures in a plate from a Gaussian distribution of normal heat flux and current flow with application to the free arc discharge.

16 p2019 A73-33535

Mechanical and corrosion resistant properties of titanium castings.

17 p2255 A73-35843

Instability of the interface between colliding metal surfaces

19 p2442 A73-37947

Contactless on-line NDT of metal plates for concealed defects by Lamb wave excitation through wave generation from air

21 p2707 A73-40706

Pulse method for determining heat-transfer coefficients of coatings

21 p2708 A73-41138

Laser-induced deformation modes in thin metal targets.

24 p3155 A73-44756

24 p3097 A73-45417

METAL POLISHING

NT ELECTROPOLISHING

Influence of heat treatment and surface quality on the endurance of EI961 steel

23 p2995 A73-44288

METAL POWDER

NT POWDERED ALUMINUM

The early stages of the mechanism of sintering.

01 p0062 A73-10277

Fundamental principles of powder preform forging.

01 p0056 A73-10278

Processing and properties of powder forgings.

01 p0056 A73-10279

Book - Research in powder metallurgy.

01 p0065 A73-10812

Sinterability of stainless steel powders.

01 p0065 A73-10813

Effect of various methods of oxide introduction on the properties of dispersion-hardened nickel.

01 p0065 A73-10814

Mechanical properties of molybdenum alloys.

01 p0065 A73-10818

Effect of high isostatic pressures on the compressibility and sinterability of tungsten powders.

01 p0065 A73-10819

Preparation and sintering of tungsten-rhenium alloy powders.

01 p0065 A73-10820

Hydrogenation as a means of utilization of industrial titanium scrap.

01 p0065 A73-10821

General analysis and synthesis of alloys and materials with inhomogeneous physical properties, noting

METAL SHEETS

thermal physicochemical methods for laminates and metal powders

01 p0066 A73-11340

Porosity measurement of porous bronze, nichrome and steel sintered specimens by fluid displacement technique

02 p0178 A73-11540

Sintering of nonstoichiometric nickel monoxide

02 p0179 A73-11546

Yield and plastic flow theory for porous metal powder compacts and preforms, discussing stress-strain and deformation-densification relations

03 p0388 A73-13260

Consolidation of tungsten and molybdenum powders.

03 p0322 A73-13262

Titanium powder properties, production, alloying, costs and hardware fabrication by pressing, casting, molding, coining and forging

03 p0322 A73-13263

Mechanical properties of pressed and sintered titanium powder.

03 p0322 A73-13264

Minimum deformation forging of prealloyed steel powder for weapon components, discussing mechanical properties, processing and cost analysis

03 p0322 A73-13265

Dispersive granulation by spinning electrode melting in helium atmosphere for steels and Ti, Ni and Mo alloys powder production

03 p0323 A73-13503

Tensile strength dependence on temperature and interstitial oxygen and nitrogen concentration in powdered Nb, noting microhardness and yield point

03 p0326 A73-13968

Heat resistant Ni and Cr alloys powder metallurgy, discussing inert and solute gas atomization, rotating electrode and gatorizing processes for powder fabrication

04 p0461 A73-15023

Studies of the elastic properties of molybdenum

04 p0464 A73-15372

The role of pore size in the ultimate densification achievable during P/M forging.

04 p0456 A73-15799

The properties of 18Ni 350 maraging steel produced from elemental and prealloyed powders.

04 p0466 A73-15800

Compression tests for plastic deformation and fracturing of Al alloy powder at hot working temperatures, noting limiting deformations in forging

[ASME PAPER 72-WA/MAT-5] 04 p0456 A73-15808

Electron density reduction in high temperature air via boron powder aerosol, presenting shock tube data for temperature range 2800-4200 K and pressure range 1-2 atm

[AIAA PAPER 73-261] 05 p0603 A73-16982

Ignition of systems having refractory reaction products

07 p0920 A73-19988

Magnesium particle ignition in various media

07 p0923 A73-20419

Chemical stability of tantalum germanide powders in air and aggressive media, including acids, fluorine ions and perhydrol

09 p1133 A73-22465

Influence of rare-earth metal dust containing radioactive components on the development of reticulosarcoma of the lungs

10 p1183 A73-23680

Crystalline structure of the Cr3AlB4 compound

10 p1259 A73-24066

Metal cladding lubricants tests with powdered lead, copper, zinc, iron, silver and bearing alloys fillers for friction and wear reduction

10 p1239 A73-24249

Investigation of the crystallization of metallic powders obtained by liquid-phase atomization

10 p1224 A73-24313

Compressibility of heterogeneous powder mixtures during rolling

10 p1224 A73-24314

Hot deformation of metal ceramic titanium preforms

10 p1225 A73-24321

Investigation of metal droplet shaping during atomization

10 p1225 A73-24688

The role of plastic deformation in metal powder compaction.

11 p1374 A73-26270

Highly disperse Fe powder electrodeposition on cathode, examining electrolyte concentration, acidity, current density and bath temperature effects on current efficiency for optimal deposition conditions

12 p1503 A73-27552

Conditions for powder compaction over the deformation zone width during rolling

12 p1503 A73-27554

Investigation of the influence of the method of supplying hydrogen to the furnace on the properties of tungsten metal

14 p1765 A73-30885

The vanadium-iron-boron, vanadium-cobalt-boron, and vanadium-nickel-boron systems

15 p1887 A73-31202

Characteristics of dynamic hot pressing with high deformation rates

15 p1881 A73-31589

Preparation of porous electrodes from titanium nitrides

15 p1881 A73-31592

Oxidation of powdered germanium, tin and lead tellurides under atmospheric conditions

15 p1887 A73-31594

Effect of dispersity on spectral analysis data for alloyed powders

15 p1888 A73-31597

Structure of powdered solders with a Ni-Cr-Si-Fe-B-C-Mo/base

15 p1892 A73-32245

Mechanical treatment of tungsten powder compacts

15 p1892 A73-32246

Effect of some activators on the molybdenum and niobium siliciding process

15 p1892 A73-32247

Application of activators in contact diffusion saturation processes in metals and powders

18 p2318 A73-35878

The combustibility of aluminum-nickel powders

18 p2325 A73-36862

Russian book - Burning of metal powders in active media.

21 p2753 A73-40418

Powder geometry and structural design of the high volumetric efficiency tantalum electrolytic capacitor.

21 p2663 A73-40770

Alloy or metal coated composite powder thermal spraying applications, discussing bonding properties, wear resistance, low friction applications and abrasibility

22 p2866 A73-42593

Reactive kinetic observations for spraying with Ni-Al powder.

22 p2879 A73-42594

Investigations into the mechanism of exothermically reacting nickel-aluminum spraying materials.

22 p2879 A73-42595

Compacting of metallic powders by plane high-explosive charges. I

24 p3092 A73-44414

Temperature range for centrifugal thermal diffusion sintering in Cr-Ni powder coatings, relating upper and lower bounds to heating rate

24 p3092 A73-44419

Hot closed-die forging of powder titanium

24 p3093 A73-44739

Creep during the hot compression of titanium diboride powder

24 p3093 A73-44740

A gasdynamic test stand and its use in studying sprayer nozzles for spraying metallic solutions. I

24 p3075 A73-44742

METAL SHEETS

Cold rolling of dispersion-strengthened nickel.

01 p0063 A73-10282

Re-interpretation of some simple tension and bulge test data for anisotropic metals.

01 p0065 A73-10764

Fracture characteristics of some aluminum alloy sheets in Charpy impact test at super-low temperatures.

02 p0179 A73-11595

Investigation of the first forming phase of transverse corrugations

02 p0172 A73-11722

Conductivity of 2024-T42 aluminum sheet solution heat treated at various temperatures.

02 p0168 A73-11986

State-of-technology for joining TD-NiCr sheet.

02 p0174 A73-12619

Dependence of the deformability of the Kh17 high-chromium steel on texture

03 p0326 A73-13827

Flat Ti alloy sheet creep under variable loads at 300-400 C comparing prediction with test data

03 p0328 A73-14016

Deep-drawability and some problems after forming by deep-drawing of Al-Mg alloy sheets - Study on Al-Mg alloy sheets for forming use. II.

05 p0581 A73-16580

Influence of condensation temperature on microstructure and tensile properties of titanium sheet produced by high-rate physical vapor deposition process.

06 p0711 A73-18752

Effects of the initial structures of pressed semi-finished products made of AK-8 alloy on their weldability.

07 p0832 A73-20370

The use of macroscopic failure diagrams to determine the quality of materials.

08 p0977 A73-21148

High frequency equipment for studying fatigue in sheet materials in conditions of plane stress and elevated temperatures.

08 p0952 A73-21149

Characteristics of elastic anisotropy and the textural development of sheet titanium

09 p1099 A73-21968

Texture and anisotropy of the thermal emf of sheet titanium

09 p1099 A73-21969

Experiment on the mechanical anisotropy of titanium, zirconium, and Zircaloy-2 rolled sheets.

09 p1104 A73-22521

Deep drawability of titanium sheets.

09 p1104 A73-22522

Effects of circular holes on the fatigue resistance of AMg6BM aluminum-alloy sheet in symmetrical bending.

09 p1105 A73-23053

Structural features of surface layers in molybdenum alloy sheets

09 p1106 A73-23188

Determination of tensile stresses in wide flat samples

09 p1165 A73-23359

Calculation of the elastic anisotropy of Ti-6Al-4V alloy sheet from pole figure data.

10 p1234 A73-24431

Experimental observations of tensile fracture in unidirectional boron filament reinforced aluminum sheet.

10 p1235 A73-24439

Nb refractory alloy sheet mechanical properties for application in space shuttle thermal protection system (TPS) and space tug aerobraking system

10 p1235 A73-24445

Zr additions effect on quenched and aged Al-Mg-Li alloy having phases in equilibrium with solid solution

10 p1236 A73-24928

The effect of coatings on the fatigue characteristics of notched aluminum alloy sheet specimens.

11 p1383 A73-25829

The fracture toughness of beryllium.

11 p1384 A73-26168

High speed welding of sheet steel with a CO2 laser.

11 p1375 A73-26351

A modernized device for testing metal sheet and welded joints under conditions of planar tension

12 p1486 A73-27464

Stability of sheet metal drawn by a rigid stamp to cylindrical and conical shapes

12 p1503 A73-27476

Conditions for powder compaction over the deformation zone width during rolling

12 p1503 A73-27554

Strain hardening and instability in biaxially stretched sheets.

13 p1623 A73-28139

Facility for conducting fatigue tests with sheet materials in cyclic tension

13 p1597 A73-29058

Thin Al alloy sheet fracture toughness from crack growth resistance curves, discussing failure modes and critical stress intensities

13 p1640 A73-29480

Effect of loading frequency and directional anisotropy on the fatigue strength of grade AMg6BM aluminum alloy sheet.

13 p1643 A73-29606

Experimental and theoretical investigation of the fracture of sheet materials in the presence of cracks.

13 p1703 A73-29625

Precipitation in EB welded beryllium ingot sheet.

14 p1759 A73-30146

Strain ratio data for commercial Al alloys in various temper conditions as drawability criterion for sheet press performance, discussing single tensile test method

14 p1762 A73-30643

Influence of stress concentrations on the mechanical properties of cast molybdenum with protective coatings

14 p1763 A73-30688

Testing assembly for sheet metals and welded joints under static and low-cycle biaxial tension under low temperature conditions

15 p1855 A73-31147

Thin Al alloy sheet plane stress testing with zero K gradient specimen based on tapered double cantilever beam modification, considering fracture toughness and crack propagation

15 p1950 A73-31985

Effect of load sequences on crack propagation under random and program loading.

17 p2190 A73-34879

A microscopic study of crack initiation mechanisms in 7075 aluminum alloy sheets.

17 p2190 A73-34885

Mechanical properties of weld, base metal and coated columbium FS85.

17 p2182 A73-35842

Apparatus for fatigue tests on sheet materials subject to cyclical extension.

18 p2297 A73-36890

Fine structure of rolled annealed tungsten sheet, discussing subsurface layer recrystallization and deformation effects based on radiographic examination

19 p2440 A73-37443

The effect of stiffeners on the sound radiation and the transmission loss of metal walls 19 p2460 A73-38181

Titanium Stressskin panel fabrication and assembly, discussing forming, cutting, thermal processing, welding and applications 19 p2437 A73-38502 [SME PAPER MF 73-158]

Vibration and noise damping of steel structures by prebonded laminates or viscoelastic layer additions, discussing steel sheets 21 p2717 A73-40236

Texture and anisotropy of the properties of titanium sheet 21 p2719 A73-40852

Influence of sheet thickness upon the fracture resistance of structural aluminum alloys. 22 p2876 A73-42150

Plane-stress fracture toughness and fatigue-crack propagation of aluminum alloy wide panels. 22 p2876 A73-42151

Memory effect on mechanical properties of plastically prestrained Al-Mg alloy sheets 24 p3100 A73-45247

METAL SHELLS

Spot welded stainless steel cylindrical strip shells supercritical behavior, analyzing equilibrium states dependence on axial loads and buckling forces 01 p0119 A73-11441

Experimental investigation of the behavior of cylindrical shells under dynamic loads 02 p0229 A73-11626

Characteristics of inversion tubes under axial loading. 03 p0396 A73-14640

Experimental investigation of the stability of shells with holes 11 p1434 A73-25390

Spot welded stainless steel cylindrical shells post-critical loading behavior, analyzing equilibrium states dependence on axial loads and buckling forces 11 p1443 A73-26058

The influence of back pressure on the point of instability of axisymmetric shells deformed by fluid pressure. 14 p1813 A73-30662

Influence of preliminary dynamic loading on the load-bearing capacity of cylindrical shells 16 p2075 A73-32693

Experimental investigation of the stability of oblique conical panels under the action of uniform external pressure 20 p2617 A73-39308

Effect of the yield point of the material on the stability of cylindrical shells under axial compression 20 p2625 A73-39658

Elastoplastic strains and carrying capacity of shallow shells /Review/ 21 p2786 A73-40976

Stability of cylindrical shells beyond the elastic limit 21 p2786 A73-40979

Influence of the geometrical configuration of a structure on its carrying capacity 21 p2786 A73-40982

Thin Ni shell electroforming for applications in structural tests, discussing plating bath composition, Al and wax mandrels preparation 22 p2867 A73-42999

METAL SPINNING

Dispersive granulation by spinning electrode melting in helium atmosphere for steels and Ti, Ni and Mo alloys powder production 03 p0323 A73-13503

METAL SPRAYING

International Metal Spraying Conference, 7th, London, England, September 10-14, 1973, Proceedings. 22 p2879 A73-42591

Investigations into the mechanism of exothermically reacting nickel-aluminum spraying materials. 22 p2879 A73-42595

METAL STRIPS

Spot welded stainless steel cylindrical strip shells supercritical behavior, analyzing equilibrium states dependence on axial loads and buckling forces 01 p0119 A73-11441

Metal stripline connector technology to fabricate flexible silicon solar cell arrays, noting cost reduction 03 p0256 A73-14232

Coupled thermoelastic stability effect on critical thermal buckling of strip under compression in temperature field 06 p0765 A73-18686

Simple test apparatus for a 100% defect-detection probability in ultrasonic surface scanning of plates and strips 09 p1070 A73-22219

Flow stress dependence on grain size in microstrain region of Ni strip machined to produce different grain sizes 10 p1235 A73-24444

Solution of a boundary value problem for the oblique incidence of a plane E-polarized wave on a metallic strip array with an optically active medium 13 p1623 A73-29682

Deflection of a thin, nonlinearly heated, rectangular strip 15 p1946 A73-31142

Critical load analysis of strip /beam/ with arched crack under compressive stress and bending moments 21 p2786 A73-40985

Thermal stress calculation for elastic half strip in nonuniform temperature field by functions in terms of Castigliano variational principle 21 p2786 A73-40986

Analysis of stress intensity factors for the tension of a centrally cracked strip with stiffened edges. 23 p2992 A73-43812

METAL SURFACES

Contribution to the theory of the current-voltage characteristic of a contact between a metal and a thin-film semiconductor 01 p0087 A73-10042

Pressure distribution vs porosity and load variation with permeability for squeeze fluid films in porous metal journal bearings [ASME PAPER 72-LUB-P] 01 p0055 A73-10219

Certain characteristics of the initial phase of the nitriding process 01 p0055 A73-10255

New morphological element of the microsurface of ductile fracture of hypoeutectoid steel. 01 p0066 A73-11336

Effect of various surface-active media on the changes taking place in the strength of U8 steel in the high-strength state. 01 p0066 A73-11337

Nonstationary interaction of thermal radiation with surfaces of pure metals 01 p0124 A73-11434

Effect of laser working on the wear of machine parts in an abrasive-lubricant medium 02 p0173 A73-11935

Application of the basic concepts of structural-energetic theory to the problem of physical fatigue limit. 02 p0235 A73-12131

Spectral characteristics in visible and UV regions of laser plasma-air interaction, using focused beams on metal targets at atmospheric pressure and vacuum 02 p0176 A73-12351

Complex phenomena in metal surface layers after high velocity impact loading in Ar atmosphere 02 p0182 A73-12698

Book - Corrosion and corrosion control: An introduction to corrosion science and engineering /2nd edition/. 03 p0321 A73-13125

Investigation of hole scattering in surface inversion channels arising on a cleaved germanium surface 03 p0349 A73-13659

Surface preparation and pit propagation in stainless steels. 03 p0325 A73-13726

Effects of the state of the surface and of titanium films on the dislocation structure of surface layers in molybdenum single crystals 03 p0326 A73-13969

Investigation of anti wear additives under various loads and at different sliding speeds. [ASLE PREPRINT 72LC-3C-4] 03 p0316 A73-14359

Microcorrosion studies with functional fluids. [ASLE PREPRINT 72LC-4C-1] 03 p0335 A73-14360

Metallic contact resistance and friction behavior under microdisplacement for lead/gold surfaces with lubricant or oxide film, noting consistency with Greenwood theory [ASLE PREPRINT 72LC-6B-1] 03 p0316 A73-14364

The relative validity of the concepts of coefficient of friction and interface friction shear factor for use in metal deformation studies. [ASLE PREPRINT 72LC-7A-3] 03 p0316 A73-14368

Antifriction bearing with lubricated rubber and metal laminations for wear elimination in limited rotation applications, discussing design guidelines and advantages 03 p0317 A73-14424

Surface effects during fretting fatigue of Ti-6Al-4V. 04 p0461 A73-14998

High vacuum thermal desorption mass spectrometry for electron bombardment activated nitrogen desorption from W surface, discussing lambda state population 04 p0414 A73-14999

Ni-Cr-thoria alloy surface oxidation induced by sprayed coating of sodium sulfate for gas turbine blade hot corrosion investigation 04 p0468 A73-15316

Metal-dielectric-semiconductor junction transistor HF response analysis by digital computer, deriving switching time as function of impurity concentration and electrode voltage 05 p0556 A73-16069

Boundary lubrication and wear of slow moving sliding concentrated hardened steel contacts as function of geometry, load, speed, lubricant and oxygen content 05 p0580 A73-16104

Solid-state sliding friction and wear in the case of iron, cobalt, copper, silver, magnesium, and alu-

minum, kept in an oxygen-nitrogen mixture at pressures from 760 torr to 0.2 micrororr 05 p0581 A73-16107

Total electron backscatter and backemission yields from metals bombarded at several angles by 0.4 to 1.4 MeV electrons. 05 p0604 A73-16514

Absolute yields of X-ray induced photoemission from metals. 05 p0604 A73-16515

Surface roughness effects on bidirectional reflectance. [AIAA PAPER 73-152] 05 p0598 A73-16900

Laser-induced fast thermal desorption from solid surfaces 06 p0699 A73-17914

Emission of metals under the action of non-relativistic electrons 06 p0725 A73-18102

Backscattering of electromagnetic waves from a rough surface model. 06 p0664 A73-18134

Determination of the specific surface resistance of thin metallic layers in the microwave range, based on transmission coefficient measurements 06 p0737 A73-18221

Thermal processes in metals exposed to high power laser pulses 06 p0702 A73-18571

Transition of oxide film on a molybdenum surface from a two-dimensional structure to a three-dimensional structure. 06 p0738 A73-18617

Manifestation of the adsorption-induced loss of strength in metals under conditions of selective transfer in boundary friction. 06 p0698 A73-18637

Investigation of high-temperature evaporation of heat-resistant ceramic coatings on metals 06 p0714 A73-18656

The role of electrochemical processes in the fretting corrosion of metals 06 p0710 A73-18660

Boundary conditions for diffusion in the pack-aluminizing of nickel. 06 p0713 A73-18774

A gas cell method for the measurement of secondary electron ejection coefficients for metastable atoms on metal surfaces. 06 p0726 A73-18846

Metal surface active properties effects on fracture characteristics and deformation and failure conditions 07 p0912 A73-19472

Tunneling observation of bound states in a normal metal-superconductor sandwich. 07 p0862 A73-19606

Occurrence of oriented structures under the action of a laser beam in metals 07 p0839 A73-19658

The use of the thermal accommodation coefficients of a rare gas for studying the adsorption of an active gas on a metal, such as in the case of nitrogen and oxygen on tungsten 07 p0839 A73-20150

Crack corrosion of titanium in a solution of hot concentrated magnesium chloride 07 p0839 A73-20167

Interaction of TEA-CO₂-laser pulses with metals enhanced by liquid layers. 07 p0836 A73-20195

Metal coating via pastes and organic solvent suspensions application for diffusive metallization of metal surfaces, noting Al coating of heat resistant alloys 07 p0833 A73-20641

Apparatus for measuring spectral emissivity of metals. 08 p0962 A73-20868

The effect of metal gripping during dynamic loading 08 p0973 A73-21132

The effect of stress on metal semiconductor junctions. 08 p0995 A73-21482

Distinguishing characteristics of pitting and crevice corrosion. 08 p0980 A73-21775

Processes determining the composition of a two-dimensional oxide film on a molybdenum surface 09 p1098 A73-21886

Electric charges on stainless steel surfaces - The effects of hydrogen, charged particles, illumination, and electric fields on the work function. 09 p1133 A73-22195

Spectroscopic investigation of the interaction of oxides with a metallic surface. III - Systems Al₂O₃-Me/Al, Cu, Ti, Kh18N9T steel, Ni, Co, Mo, W, Si/ 09 p1103 A73-22470

'Flux quantization' type of oscillation effects in a normal metal 09 p1130 A73-22709

Features of the influence of the ambient medium on the friction of plastics against metal during intermittent travel 09 p1089 A73-22855

METAL VAPORS

Thermionic constants and electron reflection for Ta/100/ by the Shelton retarding field method.
10 p1259 A73-23695

Variation of the work function of W/100/ by adsorption of oxygen, cesium, and coadsorption of oxygen and cesium
10 p1186 A73-23696

Annealing of effects arising during ion-bombardment alloying of metals at energies up to 10 keV
10 p1223 A73-23817

Effects of metal grain size on friction and wear characteristics
10 p1223 A73-24067

The mechanism responsible for luminescence of polymer films during their formation by ion-beam bombardment of solids
10 p1252 A73-24762

Photoconductor-metal contact at higher densities.
11 p1407 A73-24985

Metallic and nonmetallic surface investigation by scanning electron microscopy, discussing operational features and applications to wear, fracture and corrosion studies
11 p1361 A73-25107

The solid-vacuum interface; Proceedings of the Second International Symposium on Surface Physics, Technische Hogeschool Twente, Enschede, Netherlands, June 21-23, 1972.
11 p1325 A73-25201

Decomposition of carbon monoxide on a /110/ nickel surface.
11 p1325 A73-25203

Nd laser radiation thermochemical effects on oxide formation on thin Cr films, Fe-Ni-Co and Cr-SiO alloys and MgO-MnO ferrites, noting resistance and etching rates
11 p1376 A73-25636

Investigation of the heat conductivity of aluminum oxide deposited by plasma spraying
11 p1373 A73-25731

Fatigue damage and dislocation structures in fcc metals surface layers, noting microcrack formation conditions
11 p1380 A73-25805

The soft surface effect in plastic deformation and fatigue of metals and alloys.
11 p1381 A73-25808

Metal surfaces structure, chemical segregation, electronic properties, space charge and electrode behavior
11 p1381 A73-25809

The effect of surface films on fatigue crack initiation.
11 p1381 A73-25810

Metal surfaces corrosion fatigue due to environmentally induced localized attack, discussing protective film growth, crack propagation hydrogen interaction and stresses
11 p1381 A73-25811

Nonstationary interaction of thermal radiation with surfaces of pure metals.
11 p1452 A73-26061

Investigation of adhesional and diffusional interaction of instrumental materials with titanium alloys
12 p1502 A73-27466

Influence of the physical properties of metal melts on the spheroidization of droplets in the process of their crystallization
12 p1503 A73-27551

The influence of the thermal properties of the heating-surface on the heat-transfer of bubble boiling
12 p1559 A73-27698

Experimental evaluation of the role of surface reactions in studies of hydrogen penetration through titanium, nickel and copper
13 p1630 A73-28009

The interaction between two hydrogen atoms adsorbed on /100/ tungsten.
13 p1580 A73-28215

Access to uncombined titanium through an inhibiting film in sublimation pumping of deuterium.
13 p1581 A73-28929

Surface solid solutions and chemical compounds formation due to gas sorption by titanium and barium
13 p1663 A73-28968

French monograph on metal-semiconductor junction electron tunneling effect covering phonon interaction mechanisms, control and characterization problems
13 p1669 A73-29290

Use of soft X-ray spectroscopy to study corrosion and oxidation products on metals and alloys.
[NACE PAPER 124]
13 p1638 A73-29319

Formation of oriented structures by action of a laser beam on metals.
14 p1760 A73-30325

Behavior of the electrode potential of a metal under conditions of fretting corrosion
14 p1763 A73-30711

Mechanical deformation and failure of metals under the action of a 0.01-sec laser light pulse
14 p1758 A73-30714

Radio-frequency size effect in a normal metal layer adjacent to a superconducting phase
14 p1784 A73-30810

Investigation of fatigue effects in thinnest surface layers of metals with boundary friction
14 p1815 A73-30838

Nitrides and oxides formed on a niobium surface at high temperatures in vacuum
15 p1887 A73-31203

Strongly active surfactant effects on metal surface fracture characteristics under various loading conditions
15 p1952 A73-32071

Investigation of friction behavior in titanium alloy with 3.8% Al
15 p1894 A73-32535

Oxidation of OT4 and OT4-1 alloys in the process of prolonged heating in air at temperatures from 200 to 400 deg
15 p1894 A73-32539

Study of multiple surface compound precipitation during passivation of D6AC-steel.
15 p1895 A73-32566

Surface morphology after pretreatment in relation with bondability of aluminum alloys.
16 p2018 A73-33056

Thermal processes in metals irradiated by powerful laser pulses.
16 p2086 A73-33596

Current-voltage characteristic of a metal-dielectric contact with allowance for thermionic and field emission of electrons
16 p1972 A73-34010

Composition of a two-dimensional oxide film on a molybdenum surface.
17 p2186 A73-34309

Heating of an oxidizing metal by CO2 laser radiation
17 p2184 A73-34634

Static-kinetic dichotomy in friction theory, examining atmospheric contaminants effects on surfaces, theoretical basis of static friction postulation and sliding velocity effect on theory
[ASLE PREPRINT 73AM-8A-2]
17 p2179 A73-34992

The application of strip strain gages for measuring residual surface stresses in beryllium.
17 p2191 A73-35438

Detection of optical and infrared radiation with dc-biased electron-tunneling metal-barrier-metal diodes.
17 p2143 A73-35792

Phase formation investigation in the Mo-Al and W-Al systems when the Mo and W surfaces are saturated with aluminum by diffusion from a vapor phase in a vacuum
18 p2318 A73-35879

Protective coating-metal adhesion dependence on chemical bonds, double electric layers at interface and thermoelastic stresses
18 p2319 A73-35893

Angular dependence of the impulse of recoil in the case of high-speed impact
18 p2362 A73-36123

The role of surface states in the formation of a Schottky barrier at a metal/gallium arsenide contact
18 p2341 A73-36717

The role of physicochemical processes in surface wear under rolling friction in low-molecular hydrocarbon media
18 p2343 A73-36821

A theory of adhesion at a bimetallic interface - Overlap effects.
18 p2287 A73-37032

Detonation shock wave against metal surface with hemispherical notch, investigating expelled metal jet dimensions relation to notch radius and Reynolds number
19 p2433 A73-37515

Surface treatments of titanium and its alloys
19 p2441 A73-37828

Spatial distributions of H2 desorbed from Fe, Pt, Cu, Nb, and stainless steel surfaces.
19 p2402 A73-37951

Investigation of the plasticity of coatings on heat-resistant alloys
20 p2566 A73-39367

Effect of supersonic gas flows on the structure and heat resistance of metal alloys
21 p2717 A73-40481

Instability of the interface between colliding metal surfaces
21 p2707 A73-40706

Theory of successive electron transfer steps in cyclic voltammetry Application to oxygen pseudocapacitance on platinum.
21 p2636 A73-40843

Influence of hydrogen, alcohols, and moisture on the ultimate strength and electrical resistance of tungsten and steel wire samples
21 p2721 A73-41227

Residual-stress measurement using surface displacements around an indentation.
21 p2704 A73-41265

Chemical analysis of surfaces by mass spectrography with secondary ion emission
21 p2648 A73-41595

Measurement of temperature distribution over metal objects using single-wire thermocouples.
22 p2858 A73-42048

An application of topographical analysis to the wear of polymers.
22 p2881 A73-42352

Determination of thermal contact resistance using a pulse technique.
22 p2878 A73-42511

The wall condition of the specific density of a radiation field
22 p2888 A73-43040

The nature of the high microhardness of surface strain-hardened by friction
23 p2984 A73-43462

Generation of electrical current by impact in metallic and semiconductor bodies
23 p3015 A73-43469

Diffusionless theory of the current-voltage characteristics of a metal/monopolar semiconductor contact in the case of current limiting by an arbitrary space charge
23 p3015 A73-43621

Changes in surface structure during high-temperature creep flow.
23 p2994 A73-44159

Kinetics of the development of structural changes in iron in the presence of adsorption fatigue
23 p2995 A73-44224

Surface solid solutions and chemical compounds formation due to gas sorption by titanium and barium
23 p3008 A73-44320

The possibility of field emission from metal surface with a Q-switched laser pulse.
24 p3095 A73-44404

Influence of cooling on surface dispersion during the friction process
24 p3092 A73-44417

Free surface profile of wedge-shaped cavity in metal during collapse due to incident shock wave with decreasing pressure behind shock front
24 p3093 A73-44711

Structure of lanthanum-hexaboride-coated rhenium filaments.
24 p3105 A73-45401

Stationary charge transport in metal-semiconductor-metal /MSM/ structures.
24 p3120 A73-45421

METAL VAPORS

NT MERCURY VAPOR

NT SODIUM VAPOR

Characteristics of a thermionic converter with a cesium-barium filling at a high anodic temperature
01 p0006 A73-10855

Metal vapor crystallization in rare gas atmosphere for powder production, noting particle size distribution control
02 p0172 A73-11545

Supersonic electrical-discharge copper vapor laser.
04 p0457 A73-14746

Q switched ruby laser emission absorption by diatomic Rb vapor, noting molecular fluorescence intensity changes
04 p0458 A73-15560

Vacuum deposition of alloys - Theoretical and practical considerations.
04 p0456 A73-15756

The formation of primary gas discharge zones in electrical wire explosions
06 p0723 A73-17911

Gasdynamic structure of a plasma flame arising during vaporization of metals by strong optical radiation
06 p0729 A73-18107

Plasma parameters in gas discharges for positive-column He-Sc+/ lasers.
06 p0701 A73-18360

The equation of state of a dense metal vapor plasma and electron mobility
06 p0730 A73-18552

Molecular beam study on BaO and SrO formation for clarifying interaction of metal-vapors with upper atmosphere oxygen.
07 p0818 A73-19668

CW He-Cd and He-Se metal vapor lasers, discussing atomic energy states, energy emission and absorption by electrons He storage levels and Penning ionization
07 p0836 A73-19933

Photography of a lithium vapor trail during the daytime.
07 p0820 A73-20068

Thermal behavior of a plasma-heated tungsten probe in the presence of tungsten vapor.
[ECS PAPER 88]
07 p0788 A73-20447

Solid material ion source discharge chamber with cathode sputtering-introduced metal vapor, based on conventional ion source with electrons oscillating in magnetic field
08 p0993 A73-21515

Deformation of laser pulses in resonant media.
09 p1096 A73-22902

A hollow cathode device for CW helium-metal vapor laser systems.
10 p1229 A73-24617

Heat pipe oven as instrument for laser absorption and fluorescence spectroscopy of metal vapors,

vapor-gas, vapor-vapor mixtures and metal vapor plasmas

11 p1361 A73-25148

Experimental determination of the integral radiative capacity of nickel

11 p1398 A73-25739

Thermodynamics of heterogeneous gas equilibria. VII - Gas phase composition and chemical transport reactions in the tungsten-oxygen-hydrogen system

11 p1386 A73-26568

Pulsed gas laser employing substances of low volatility

12 p1506 A73-27218

Possible utilization of a vapor, formed by the action of a high-power electron beam on a target, as an active medium for stimulated emission of light.

12 p1507 A73-27517

Characteristics of thermionic converter with cesium-barium filling at high anode temperature.

12 p1461 A73-27905

Experimental investigation of the pressure of the saturated vapor of rubidium and cesium.

12 p1526 A73-27907

Observations of stimulated anti-Stokes radiation in barium vapour.

14 p1776 A73-29697

Absorption spectrum analysis of free Cu, Ca, Na, Zn, Ni and Cr atom concentration in acetylene air flame zones

14 p1817 A73-30458

Spectral diagnostics of a plasma flare during well-developed vaporization of metals by laser radiation

14 p1782 A73-30804

Interaction between an ionized metal vapor flow and a body at Mach numbers equal to or larger than unity

15 p1919 A73-31863

CW metal vapor lasers, discussing discharge conditions, excitation processes, cathoporetic effect and He-Se and He-Cd lasers output characteristics

16 p2023 A73-32858

Equation of state of a plasma of a dense metal vapor and the electron mobility.

16 p2042 A73-33577

Coherent light propagation and scattering in vaporized alkali metal atmosphere as function of refractive index and coherent to incoherent transformation

16 p2086 A73-34002

The gas carrier problem during the crystallization of metals from a gas phase

18 p2323 A73-35880

Effect of particle collisions in a resonance gas medium on the deformation of laser pulses

18 p2322 A73-36677

Adiabatic following and the self-defocusing of light in rubidium vapor.

20 p2571 A73-38632

Pulsed lead vapor laser with high peak and average output powers.

20 p2574 A73-39693

Combined LEED, Auger electron and flash desorption spectroscopy of metals on single crystal surfaces.

21 p2706 A73-41596

Evaporation of metallic targets caused by intense optical radiation.

22 p2868 A73-41727

High-temperature fast-flow reactor studies of metal-atom oxidation kinetics.

p2898 A73-42761

Temperatures in low-pressure magnesium-vapor diffusion flames.

22 p2899 A73-42820

Fluxless brazing of aluminum using protective gas.

23 p2985 A73-43997

Study of induced four-photon parametric scattering of laser light in alkali metal vapor

23 p2988 A73-44009

Gas-dynamic structures of a plasma flare produced during the evaporation of metals by high-intensity optical radiation.

24 p3114 A73-44496

METAL WHISKER REINFORCEMENT

U WHISKER COMPOSITES

METAL WORKING

NT AUSFORMING

NT BULGING

NT CLADDING

NT EXPLOSIVE FORMING

NT FORGING

NT MAGNETIC FORMING

NT METAL DRAWING

NT METAL SPINNING

Powder metallurgy for high-performance applications; Proceedings of the Eighteenth Sagamore Army Materials Research Conference, Raquette Lake, N.Y., August 31-September 3, 1971.

01 p0062 A73-10276

Fabrication of high-strength aluminum products from powder.

01 p0063 A73-10281

Upper bounds to the load for the plane strain working of anisotropic metals.

01 p0057 A73-10696

Calculation of the energy and force process parameters in magnetic-pulse forming of complex shaped elements

02 p0172 A73-11646

Investigation of the first forming phase of transverse corrugations

02 p0172 A73-11722

Problem of the influence of an instantaneous change in normal pressure on the magnitude of contact friction force

02 p0172 A73-11796

Book - Forging design handbook.

02 p0173 A73-11884

Russian book on physics of explosive hardening and welding covering high velocity inelastic collisions, shock wave generation, strengthening mechanisms of metals, etc

02 p0173 A73-11892

Theoretical foundations of the development of a system of automated information processing for the problems of manufacturing-process design in the metalworking industry

03 p0400 A73-13240

Metal deformation processes, discussing hot working, fracture, hydrostatic extrusion, superplastic forming, diffusion bonding and powder fabrication

04 p0452 A73-14742

Development of a process utilizing heated rolls for hot rolling metals.

04 p0454 A73-15001

Powder metallurgy production of structural shapes.

04 p0461 A73-15022

Maximum metal removal rate in ECM.

[SME PAPER MR 72-537] 06 p0697 A73-18092

Problems in electron-beam welding of non-ferrous metals.

08 p0973 A73-21243

Effect of thermomechanical processing on fatigue crack propagation.

09 p1102 A73-22415

Compressibility of heterogeneous powder mixtures during rolling

10 p1224 A73-24314

Steel wire, boron or carbon filament reinforced Al alloys shaped parts fabrication, discussing sintering, pressure impregnation and filament winding processes

11 p1373 A73-25415

Influence of fretting on the endurance of 40KhNMA steel with various thermochemical processing

11 p1386 A73-26735

Conditions for powder compaction over the deformation zone width during rolling

12 p1503 A73-27554

Analysis of the energy losses during dynamic hot pressing of reinforced metals

12 p1503 A73-27557

Tensile properties of high strength Al-Zn-Mg and Al-Zn-Mg-Cu alloy products processed by T-AHA type final thermomechanical treatments

13 p1633 A73-28141

German monograph - Effect of the transformation and heat treatment conditions on the mechanical properties and the creep characteristics of the alloy TiAl6V4.

14 p1762 A73-30668

German monograph - Investigations concerning the hot working of heterogeneous iron-molybdenum alloys with differing precipitation distribution.

14 p1762 A73-30670

Application of inverse boundary value problems in the theory of dimensional electrochemical working

15 p1881 A73-31153

High feed rate electrochemical machining Fe in aqueous NaCl, using high supply voltage, electrolyte pressures and flow velocities

[ASME PAPER 73-PROD-3] 16 p1971 A73-33533

Flow stress of metals and its application in metal forming analyses.

[ASME PAPER 73-PROD-4] 16 p2019 A73-33534

The influence of fabrication and structure processes on the result of control by ultrasonics of semifinished products of titanium alloys

19 p2441 A73-37830

Hot fluomachining of Ti alloy tubes and turbine casings, noting dimensional accuracy dependence on temperature

19 p2441 A73-37835

Explosive metal forming, considering energy cost, operational speed, achievable tolerances in symmetrical or nonsymmetrical shapes, production quantities and lead time for die preparation

20 p2569 A73-39405

Tungsten inert gas arc welding for refractory or active metals working in gas-tight chamber, noting effects of reduced pressure on cathode zone energy density

20 p2569 A73-39666

Effect of mechanothermal treatment on the heat-resistant properties of 1Kh14N18V2B steel with boron additives

21 p2718 A73-40735

Aluminum and aluminum alloys extrusion processes, discussing form shape, weldability, hardening and metal transformations

21 p2707 A73-41067

How composition affects properties of a ferritic stainless steel.

21 p2721 A73-41084

Explosive and electrohydraulic forming techniques cost effectiveness in metal technology, considering welding methods and metal powder compaction

22 p2865 A73-41779

METAL-GAS SYSTEMS

The influence of oxygen concentration on the internal stress and dislocation arrangements in alpha titanium.

02 p0184 A73-12768

Effects of alloying elements on the solubility of hydrogen in beta titanium.

03 p0321 A73-12920

Hydrogen distribution between the phases in metals

03 p0324 A73-13507

Mechanisms and kinetics of absorption and desorption reactions in systems of refractory metals with nitrogen, oxygen or carbon.

04 p0462 A73-15302

Influence of hydrogen on the technological plasticity of the alloy Ti + 9% Al

04 p0464 A73-15499

Possibility of argon-nitrogen gas metal-arc welding of some non-ferrous metals.

08 p0973 A73-21237

The solubility of hydrogen in rhodium, ruthenium, iridium and nickel.

09 p1047 A73-21981

The spray deposition of oxide-free coatings consisting of special metals with a high affinity to oxygen

11 p1372 A73-25411

Effect of high dislocation density on stress corrosion cracking and hydrogen embrittlement of type 304L stainless steel.

11 p1385 A73-26174

Influence of gas carburizing on the structure and properties of electrolytically deposited chromium

11 p1375 A73-26734

The low-temperature embrittlement of niobium and vanadium by both dissolved and precipitated hydrogen.

14 p1761 A73-30630

Oxygen in titanium alloyed with aluminum and zirconium

15 p1889 A73-31812

Gas saturated surface layer effect on Ti alloy resistance to static cyclic tensile loads, noting increased fatigue strength after etching

15 p1890 A73-31815

Critical survey of studies of phase diagrams in the titanium-oxygen system in connection with the formation of suboxides

15 p1893 A73-32515

Phase equilibria in the metal-rich side of the Ta-N system.

16 p2025 A73-33110

A study of the process of oxidation of zirconium-oxygen alloys

17 p2188 A73-34558

Anelastic studies of hydrogen diffusion in niobium.

17 p2193 A73-35622

Internal friction in niobium quenched from premelting temperatures

18 p2324 A73-36772

Book - Elevated temperature properties as influenced by nitrogen additions to types 304 and 316 austenitic stainless steels.

18 p2325 A73-36971

Diffusion of hydrogen and deuterium in Ta, Nb, and V.

20 p2576 A73-39134

Influence of small oxygen and nitrogen additions on the nature of the temperature dependence of the mechanical properties of niobium

20 p2577 A73-39360

Thermodynamics of the Al-O and Al-O-C systems

21 p2718 A73-40847

Influence of relief annealing on the mechanical properties of high-strength hydrogenized steel

21 p2721 A73-41228

Omega-phase stability in the Ti-Zr-O system

22 p2873 A73-42085

Diffusion parameters of oxygen in alpha and beta titanium modifications

22 p2874 A73-42098

Thermodynamics of transition metal-hydrogen solid solutions.

22 p2880 A73-43076

Porous and dense layers in Nb-Ti-O system analyzed by X-ray spectroscopy, finding element content influence

23 p2990 A73-43481

Phase equilibrium technique to measure oxygen solubility in liquid Co at 1510 to 1700 C, determining thermodynamic characteristics and deoxidation curves

23 p2990 A73-43482

Phase composition of Cu-Ni-O alloys with Ir additions, examining oxygen content influence on Ir distribution and solid solution formation

23 p2990 A73-43483

METAL-METAL BONDING

Chemical stability and features of the formation of complex nitrides of III-B subgroup elements /Al-B-N system/ 24 p3119 A73-44952

Oxygen in alloys of titanium with aluminum and zirconium. 24 p3100 A73-45275

Gas saturated surface layer effect on Ti alloy resistance to static cyclic tensile loads, noting increased fatigue strength after etching 24 p3100 A73-45278

METAL-METAL BONDING

The mechanism of the metallic adhesion bond. 01 p0087 A73-10473

High temperature adhesive shear tests at ambient temperature as function of loading rate and bond overlap length 03 p0332 A73-13040

Evaluating adhesives for joining aluminum. 03 p0334 A73-13271

Aluminum-stainless steel and Ni-Mo composites prepared by dynamic hot pressing, determining bond strength between fibers and reinforced metal matrix 03 p0328 A73-14013

Weld quality of explosive welded industrial metals, noting role of thermal processes and materials thermophysical properties 07 p0831 A73-19995

Sliding friction welding of nonferrous Cu, wrought Al alloy and Ti, resting rubbing speed and axial pressure effects on equilibrium condition transition 08 p0973 A73-21238

Environmental stress cracking of epoxy adhesives. 11 p1388 A73-25840

Epoxy adhesive bonding of Concorde light alloy sandwich structure elevons, discussing surface treatment, polymerization and ultrasonic testing 13 p1623 A73-28468

Epoxy resin adhesive for metal-to-metal and honeycomb sandwich bonding, featuring high flow during cure for high structural strength 16 p2029 A73-33054

Joining of plastics to plastics and to metals. 16 p2021 A73-33861

Use of honeycomb and bonded structures in light aircraft. [SAE PAPER 730307] 17 p2101 A73-34667

A theory of adhesion at a bimetallic interface - Overlap effects. 18 p2287 A73-37032

Bonding degradation in the tantalum nitride-chromium-gold metallization system. 19 p2435 A73-38440

Failure analysis of wire bonds. 19 p2436 A73-38446

Technique for resistance brazing of thin copper conductors. 23 p2985 A73-43998

Soldering technique using reaction flux for metal deposition, obtaining strong joints of Al with other metals 23 p2985 A73-43999

Soldering and brazing of advanced metal-matrix structures. 23 p2986 A73-44003

Spot weld adhesive bonding procedures, examining process and quality control, tooling, curing, surface preparation, adhesive types and corrugated panel application 24 p3093 A73-44766

METAL-NITRIDE-OXIDE-SILICON

Polarization charge capture dependence of two layer dielectric metal-silicon nitride-silica-silicon semiconductor structures on pulse duration and temperature 16 p1991 A73-34003

Light sensitive MNOS /metal-nitride-oxide-silicon/ memory transistor space charge layers current-field relationships and steady state I-V measurements 17 p2134 A73-34221

Properties of anodic oxide films formed in the anodization of silicon nitride. [ECS PAPER 81] 21 p2702 A73-40844

Trap-assisted charge injection in MNOS structures. 24 p3120 A73-45419

METAL-WATER REACTIONS

Composition and structure of rust layers and corrosion rate of chromium steels exposed to a marine atmosphere. 05 p0586 A73-16137

Some results in the erosion of prestressed materials due to water-jet impact. 19 p2443 A73-38299

Pitting of titanium. I - Titanium-foil experiments. II - One-dimensional pit experiments. 23 p2991 A73-43521

METALLIC HYDROGEN

Thermodynamic parameters for metallic hydrogen-helium alloy of Saturn and Jupiter interiors, using Monte Carlo chains and dielectric function theory 11 p1420 A73-25888

Transport properties of liquid metal hydrogen under high pressures. 11 p1401 A73-25907

On convection and gravitational layering in Jupiter and in stars of low mass. 14 p1797 A73-30009

Metallic hydrogen concept and experimental investigations, considering high temperature superconductivity and role in outer planets structure 24 p3110 A73-45225

METALLIC PLASMAS
NT CESIUM PLASMA
NT URANIUM PLASMAS

Investigation of the temporal-spatial distribution of optical density in a plasma of high-current Li and In discharges 01 p0085 A73-10853

Fluctuation characteristics of dense plasmas from high-current discharges produced by electric explosion of metallic wires in vacuum 01 p0086 A73-11283

Momentum transfer interaction of a laser-produced plasma with a low-pressure background. [AD-755558] 02 p0197 A73-12062

Possibilities of using organic compound lasers in spectral analysis 02 p0176 A73-12095

Ion density and electron temperature calculations for metallic plasma population inversion possibility by near resonant charge exchange with inert gas ions 02 p0194 A73-12847

Gasdynamic structure of a plasma flame arising during vaporization of metals by strong optical radiation 06 p0729 A73-18107

The equation of state of a dense metal vapor plasma and electron mobility 06 p0730 A73-18552

Investigation of the structure of a high-current discharge in a lithium plasma. 08 p0992 A73-20853

Heat pipe oven as instrument for laser absorption and fluorescence spectroscopy of metal vapors, vapor-gas, vapor-vapor mixtures and metal vapor plasmas 11 p1361 A73-25148

Investigation of heat and mass transfer for plasma flows in channels of various shape under conditions of intense condensation 12 p1558 A73-27318

Investigation of the space-time distribution of the optical density of the plasma in high-current Li-In discharges. 12 p1529 A73-27903

Interaction between an ionized metal vapor flow and a body at Mach numbers equal to or larger than unity 15 p1919 A73-31863

Equation of state of a plasma of a dense metal vapor and the electron mobility. 16 p2042 A73-33577

Characteristics of the electrode-adjointing potential layer in an alkali metal plasma in the presence of adsorption 17 p2214 A73-34131

Nitrogen ionization in an Hg-N₂ discharge. 19 p2463 A73-37903

Tungsten target surface contaminants produced fast ion current peak measured by ion collector in expanding laser produced plasma 21 p2716 A73-40972

Raman scattering of SHF radiation in a bounded plasma of a solid 21 p2657 A73-41509

Fluctuation characteristics of a dense plasma of high current discharges produced by electric explosion of metallic wires. 23 p3009 A73-43504

Temperature and ion energy spectra of laser plasma produced by giant-pulse ruby laser heating metallic targets 23 p3012 A73-43849

Gas-dynamic structures of a plasma flare produced during the evaporation of metals by high-intensity optical radiation. 24 p3114 A73-44496

Turbulent motions in an artificial plasma inhomogeneity released in the ionosphere. 24 p3088 A73-45238

METALLIZING

Metallized fiberglass antenna meshes for spacecraft deployable reflectors, discussing low mass/area, long term stability and performance characteristics and degradation tests 03 p0333 A73-13045

A novel high area ratio T-burner for characterizing metallized propellants. [AIAA PAPER 73-219] 05 p0563 A73-16949

Solid-phase epitaxial growth of Si mesas from Al metallization. 06 p0738 A73-18650

Metal coating via pastes and organic solvent suspensions application for diffusive metallization of metal surfaces, noting Al coating of heat resistant alloys 07 p0833 A73-20641

Metallization failures caused by organic adhesives used in hybrid microelectronic devices. 08 p0944 A73-20747

Vacuum contactless metallization of carbon steels, stainless steels and nickel alloys, considering Si, Cr and Al coatings 10 p1227 A73-24964

Gas turbine engine turbine blades service life increase by Cr and Al vacuum diffusion metallization, presenting full scale endurance test results 10 p1227 A73-24965

Bonding degradation in the tantalum nitride-chromium-gold metallization system. 19 p2435 A73-38440

Screening of metallization step coverage on integrated circuits. 19 p2411 A73-38456

Influence of diffusion coating and heat treatment on the wear resistance of VT-8 alloy 23 p2990 A73-43485

METALLOGRAPHY

Metallographic investigation of electrodeposited iron-nickel-chromium alloys 02 p0174 A73-12535

An observation of the effect of grain structure on the appearance of Kirkendall porosity. 02 p0184 A73-12772

Instrumentation for metallographic structure examination. 05 p0576 A73-16751

Metallographic orientation determinations on hexagonal polycrystals with the aid of the quantitative polarization equipment of the Neophot. 05 p0577 A73-16752

High temperature and metallographic investigation of Nd-Y alloys, measuring heat and electrical conductivity, thermal expansion and emf, magnetic susceptibility and Hall coefficient 06 p0735 A73-18050

Electrical measurements, metallographic microscopy and chemical analysis for failure analysis 07 p0800 A73-19409

Metallic particles in the Apollo 14 lunar soil. 07 p0884 A73-19744

Metallographic investigation and notch, tensile and hardness tests for electrosag welding of austenitic stainless steels 07 p0831 A73-19949

Investigation of the morphology and decomposition kinetics of Co-Ni-Ti alloys 10 p1232 A73-24153

Cast and annealed chromium-yttrium and chromium-lanthanum alloys peak solubility from metallographic, durometric and differential thermal analyses 12 p1512 A73-27245

Phenomena of precipitation observed in carburized tantalum in the vapor phase 15 p1896 A73-32645

Field electron emission microscopic study of titanium 24 p3098 A73-44474

METALLOIDS

NT ARSENIC
NT BORON
NT GERMANIUM
NT SILICON
NT SILICON ISOTOPES
NT TELLURIUM
NT TELLURIUM ISOTOPES

Superconductor/exiton-dielectric phase transition in a semimetal 01 p0089 A73-11292

The superconductor-excitonic dielectric phase transition in a semimetal. 23 p3015 A73-43513

METALLORGANIC COMPOUNDS
U ORGANOMETALLIC COMPOUNDS

METALLURGY

Influence of metallurgical factors on the corrosion cracking under tension of TA6V titanium alloy in an aqueous medium at ambient temperature [ONERA, TP NO. 1100] 01 p0061 A73-10231

Russian papers on nonferrous metal alloys covering physical and mechanical properties, crystallization, casting, solid solutions and heat treatment 03 p0323 A73-13501

Japan-U.S. Seminar on the Physical Metallurgy of Heat Resisting Alloys, Diamond Point, N.Y., September 13-15, 1972, Proceedings. 04 p0464 A73-15576

Metallurgical, chemical and electrochemical production and refining of refractory metals, including titanium, fluorotitanates and artificial rutile 04 p0465 A73-15660

Application possibilities of atomic resonance absorption spectroscopy in vacuum metallurgy. 04 p0455 A73-15754

Some aspects of the metallurgy and wear resistance of surface coatings. 05 p0580 A73-16102

Product quality concept definition in terms of use requirements, characteristic properties reproducibility /quality control/ and cost, discussing steel metallurgy and fabrication methods 05 p0582 A73-16999

Book - The superalloys. 06 p0708 A73-18073

Metallurgical principle guidance of alloy design, discussing gas turbine alloys, dispersion hardened and composite alloys, high damping alloys and superalloys
08 p0979 A73-21657

Russian papers on nonferrous metals and alloys metallurgy covering phase equilibria, strengthening, deformation and processing of Al, Mg, Cu and Ti alloys
12 p1510 A73-26902

Study of the mechanical-metallurgical characteristics of martensitic steels in a corrosive medium
12 p1514 A73-27686

High strength steel developments, discussing chemical compositions, mechanical properties, production technology and applications
15 p1888 A73-31624

Interdisciplinary communications problems of metal physicists, fracture mechanists, structural designers and reliability analysts for fatigue crack generation and growth
17 p2246 A73-34886

Russian papers on metal alloys chemistry covering atomic structure, physicochemical properties, phase diagrams, X ray analysis, laser microanalysis, etc
22 p2873 A73-42083

Influence of the offset on the experimental yield surfaces of metals - A theoretical evaluation.
24 p3147 A73-44747

METALS

NT ACTINIDE SERIES
NT ACTINIUM
NT ALKALI METALS
NT ALKALINE EARTH METALS
NT ALUMINUM
NT ALUMINUM COATINGS
NT ALUMINUM 26
NT BARIUM
NT BERYLLIUM
NT BISMUTH
NT CADMIUM
NT CALCIUM
NT CERIUM
NT CESIUM
NT CESIUM VAPOR
NT CHROMIUM
NT COBALT
NT COBALT ISOTOPES
NT COBALT 60
NT CURIUM ISOTOPES
NT CURIUM 244
NT DYSPROSIUM
NT ERBIUM
NT EUROPIUM
NT FERROUS METALS
NT GADOLINIUM
NT GALLIUM
NT GOLD
NT GOLD COATINGS
NT HAFNIUM
NT HOLMIUM
NT INDIUM
NT IRIIDIUM
NT IRON
NT IRON 57
NT LANTHANUM
NT LEAD (METAL)
NT LEAD ISOTOPES
NT LIQUID METALS
NT LIQUID POTASSIUM
NT LIQUID SODIUM
NT LITHIUM
NT LITHIUM ISOTOPES
NT MAGNESIUM
NT MANGANESE
NT MANGANESE ISOTOPES
NT MERCURY (METAL)
NT MERCURY ISOTOPES
NT MERCURY VAPOR
NT METAL COATINGS
NT METAL CRYSTALS
NT METAL FILMS
NT METAL FOILS
NT METAL MATRIX COMPOSITES
NT METAL POWDER
NT METAL VAPORS
NT MOLYBDENUM
NT NEODYMIUM
NT NEPTUNIUM ISOTOPES
NT NICKEL
NT NICKEL COATINGS
NT NIOBIUM
NT NOBLE METALS
NT NONFERROUS METALS
NT OSMIUM
NT PALLADIUM
NT PLATINUM
NT PLUTONIUM ISOTOPES
NT PLUTONIUM 238
NT POLONIUM 210
NT POTASSIUM
NT POTASSIUM ISOTOPES
NT POWDERED ALUMINUM
NT PROMETHIUM
NT RARE EARTH ELEMENTS
NT REFRACTORY METALS

NT RHENIUM
NT RHENIUM ISOTOPES
NT RUBIDIUM
NT RUBIDIUM ISOTOPES
NT SAMARIUM
NT SCANDIUM
NT SILVER
NT SINTERED ALUMINUM POWDER
NT SODIUM
NT SODIUM ISOTOPES
NT SODIUM VAPOR
NT SODIUM 22
NT SODIUM 24
NT STRONTIUM
NT STRONTIUM ISOTOPES
NT STRONTIUM 90
NT TANTALUM
NT THALLIUM
NT THALLIUM ISOTOPES
NT THORIUM
NT THORIUM ISOTOPES
NT TIN
NT TITANIUM
NT TRANSITION METALS
NT TUNGSTEN
NT ULTRAPURE METALS
NT URANIUM
NT URANIUM ISOTOPES
NT URANIUM 238
NT VANADIUM
NT YTTERBIUM
NT YTTRIUM
NT ZIRCONIUM

Differing roles of electron scattering processes in the thermodynamics of metals in the normal and superconducting states
01 p0088 A73-10613

Surface gravities, Doppler broadening velocities, effective temperatures and metal abundances of K giants from narrow band photometry
03 p0371 A73-13224

Analyzing failures of metal components.
03 p0323 A73-13270

Frequency dependence of the damping of mechanical vibrations in some commercially pure metals
03 p0327 A73-13976

Development and use of relaxation tests for study of the long-term creep of metals
[ONERA, TP NO. 1146]
04 p0511 A73-15095

Frequency spectra of acoustic emissions generated by deforming metals and ceramics.
04 p0448 A73-15122

Bending and rolling methods for tensile testing of metals without local necking, considering fracture under reduced axial stress
05 p0581 A73-16130

Evaluation of multiaxial theories for room-temperature plasticity and elevated-temperature creep and relaxation of several metals.
06 p0759 A73-17599

Correlation between the diffusion activation energy, the heat of fusion, and the bond energy in metals
06 p0708 A73-18046

Time variation of metal abundance in galaxies - Super-metal-rich stage.
07 p0902 A73-20446

On the metal abundance of RR Lyrae stars in the globular cluster M22.
08 p1009 A73-21169

On dynamic plasticity. I
08 p1020 A73-21823

Design stability of composite samples with a soft interlayer in static tension
10 p1291 A73-24352

Investigation of the durability of metals under conditions of transition from brittle to plastic failure
10 p1235 A73-24456

High temperature superconductivity in three dimensional systems of metals and nonmetals, discussing electron collectivization in metals, dielectrics, organic compounds, semiconductors and molecular crystals
10 p1261 A73-24692

Diffusion processes electron mechanism in metal-metal and metal-nonmetal systems, using configurational model for valence electrons localization
10 p1236 A73-24951

Mathematical description by Gaussian error function for metals diffusive saturation and diffusion constants determination
10 p1236 A73-24952

A statistical investigation on the mechanical properties of metals impregnated graphites.
11 p1388 A73-25416

Measurement of a set of thermal properties of metals at high temperatures by the periodic-heating method
11 p1379 A73-25426

Deformation bounds for a creeping structure approaching rupture.
11 p1447 A73-26654

An examination of dynamic fracture under biaxial-strain conditions.
12 p1550 A73-27022

Mechanical behavior of materials: Proceedings of the First International Conference, Kyoto, Japan, August 15-20, 1971. Volume 1 - Deformation and fracture of metals. Volume 2 - Fatigue of metals. Volume 3 - Temperature effects of metals, environmental effects, polymers. Volume 5 - Composites, testing and evaluation.
13 p1638 A73-29451

Deformation mechanism and strength of metals under impulsive loading.
13 p1639 A73-29463

Minimum creep lives of structural metallic materials at elevated temperatures.
13 p1701 A73-29514

Ultrasonic attenuation measurements in metals at low temperatures.
13 p1662 A73-29639

International Congress on Metallic Corrosion, 5th, Tokyo, Japan, May 21-27, 1972, Proceedings.
15 p1895 A73-32564

Book - Techniques involving extreme environment, nondestructive techniques, computer methods in metals research, and data analysis. Part 1.
16 p2017 A73-32696

Experimental methods regarding the thermodynamics of metals and alloys. I
16 p2026 A73-33953

Allowance for the influence of temperature in statistical estimates of the strength of metals in the brittle condition
17 p2186 A73-34328

Influence of the reflection forces and the tunnel effect on the current-voltage characteristic of a metal-semiconductor contact with a Schottky barrier
18 p2340 A73-36668

Investigation of the durability of metals under conditions of a transition from brittle fracture to plastic flow.
19 p2442 A73-38138

A solar engine using the thermal expansion of metals.
19 p2392 A73-38473

Japan Congress on Materials Research, 16th, Osaka, Japan, August 1972, Proceedings.
20 p2575 A73-38636

Acoustic emission measurements during plastic deformation of metals.
22 p2919 A73-41975

Experiment involving the application of the LMA-1 laser microanalyzer to the investigation of metallic materials
22 p2868 A73-42100

Russian book - General patterns in the structure of phase diagrams of metal systems.
22 p2877 A73-42451

Response function class for constitutive equations in nonlinear isothermal theory of elastic-plastic metals, discussing free energy and stress response as measure of deformation
[ASME PAPER 73-APMW-30]
22 p2925 A73-42890

Procedure and device for the study of the behavior of metals subjected to dynamic torsional stresses
22 p2868 A73-43171

High rotational velocity correlation with metal abundance interpreted by coronal mass loss rate in metal-poor stars
24 p3140 A73-45184

METAMORPHISM [GEOLOGY]

Lunar breccias lithification and metamorphism model construction from experimental and analytical data, discussing scale of lunar metamorphic temperatures
02 p0220 A73-12476

Metamorphism of Apollo 14 breccias.
07 p0882 A73-19717

Magnetic properties of Apollo 14 breccias and their correlation with metamorphism.
07 p0893 A73-19839

Radiation and shock effects on Apollo 14 and 15 breccias substructure history, reporting optical microscope observations of solar flares and cosmic ray tracks
07 p0896 A73-19872

Temperature scaling of heat metamorphism evolved during lunar and meteoritic brecciation, evaluating dust sintering degree
07 p0896 A73-19874

The age and petrography of two Luna 20 fragments and inferences for widespread lunar metamorphism.
13 p1675 A73-28319

Deformation and transformation of rock-forming minerals by natural and experimental shock processes. I - Behavior of minerals under shock compression.
14 p1750 A73-30958

METASTABILITY

U METASTABLE STATE
METASTABLE ATOMS

SST related ozone photochemical reactions and metastable oxygen system below 100 km, discussing oxygen dissociation and recombination, photolysis, UV absorption, etc
01 p0042 A73-10898

Processes leading to 6300 A radiation during determinations of O(1D) quenching by nitrogen and oxygen molecules in F region, using model of neutral atmosphere composition
[AD-754996]
02 p0156 A73-11742

A possible method for estimating any indirect process in the production of the O/I/S atoms in aurora
02 p0157 A73-11902

Pumping rate in He-Cd laser from metastable atoms concentration measurement and plasma diagnostics, noting upper level population dependence on Penning effect
03 p0319 A73-13753

A gas cell method for the measurement of secondary electron ejection coefficients for metastable atoms on metal surfaces.
06 p0726 A73-18846

Optical orientation of metastable He-3 atoms and its influence on the electron density and on the emission of helium atoms in a plasma
10 p1257 A73-24755

Relaxation processes in metastable beta titanium alloys.
11 p1385 A73-26498

Metastable oxygen atoms radiative lifetime quenching rate as function of altitude in lower ionosphere based on auroral observations and atmospheric model
23 p2972 A73-43692

METASTABLE STATE

Energetic metastable molecular oxygen as a source of ionization in the D region.
02 p0157 A73-11757

Pulsar glitches and the metastability of the superfluid core.
02 p0211 A73-11895

Strengthening and stabilization effects of alloying elements in metastable Ti beta-alloys as function of atom concentration and position in periodic system
03 p0324 A73-13511

An instrument for the simultaneous detection of the OI ground state /2p4 3P/ and first metastable state /2p4 1D/ populations.
05 p0580 A73-17258

Effect of overheating on creep resistance in metastable alloys.
06 p0710 A73-18639

Spatial and temporal ionization growth characteristics in nitrogen at moderate electric field strength, noting dominant secondary emission effect due to cathode bombardment by metastable molecules
09 p1122 A73-22120

Helium superleak metastable persistent current quantum states use to provide nondecaying angular momentum for gyroscopic element
15 p1876 A73-31942

Diffusional and nondiffusional metastable-phase transformations in titanium alpha + beta alloys
15 p1893 A73-32520

Influence of plastic deformation and of alloying with small additions of oxygen on the decomposition of the metastable beta phase in the TS6 alloy
15 p1894 A73-32526

Effect of thermomechanical treatment on the stress corrosion cracking of metastable beta III titanium.
15 p1896 A73-32574

Phase composition and properties of metastable alloys of titanium with nickel
16 p2027 A73-34072

Microstructure and hardness investigations of alpha prime, alpha double prime and omega metastable phases formed during quenching of Ti-Ru alloys
17 p2188 A73-34567

Experimental investigation of collisions of He atoms in the ground state and the 2/S/ metastable state
19 p2462 A73-37248

Grain refinement in aluminum-zirconium and aluminum-titanium alloys by metastable phases.
19 p2440 A73-37444

Electron diffraction study of a noncrystalline Zr-Ni phase.
20 p2575 A73-39021

Measurement of superheating and supercooling fields of superconducting thin films.
20 p2599 A73-39724

Metastable phase diagrams of eutectic and peritectic alloys crystallization during rapid cooling from liquid state
22 p2877 A73-42458

Metastable phases produced by laser melt quenching.
22 p2878 A73-42576

Quantum yield of metastable oxygen atoms and molecules via ozone photolysis by UV absorption, noting uncertainties in secondary reaction kinetics
23 p2951 A73-43899

Ionospheric metastable particle production and annihilation during photochemical reactions, determining neutral and ionized particle abundance profiles
23 p2978 A73-43979

Time of flight spectral measurements of metastable lifetimes in molecular beams with different excited states
24 p3089 A73-44814

METAZOA

U ANIMALS

METEOR BURSTS

U METEOROID SHOWERS

METEOR TRAILS

Investigation of fading radio echoes from meteor trails. I
01 p0016 A73-10201

Meteorite ablation coefficient and brightness dependence on velocity and atmospheric density, considering molecular screen effect
01 p0101 A73-10847

Upper-atmosphere motion, as determined by observations of radio echoes from meteor trails.
02 p0159 A73-12145

Analysis of the meteor wind data.
05 p0622 A73-17167

Shock waves and flares by meteors.
08 p0101 A73-21317

On the source of the 3840 A persistent emission by meteors.
08 p0101 A73-21318

Galactic cosmic ray modulation region evaluation from meteoroid orbit, velocity and radioactive dating data
08 p1000 A73-21342

Determination of upper atmosphere parameters from measurements of the ambipolar diffusion coefficient by radar observations of meteor trails.
10 p1212 A73-24223

The telescopic radiant areas of the Perseids and the Orionids.
11 p1426 A73-26572

Meteorite ablation coefficient and brightness dependence on velocity and atmospheric density, considering molecular screen effect
15 p1928 A73-30983

Meteor trail drift observations in equatorial region /Somalia/ for lower thermosphere wind velocity and direction calculation via harmonic analysis
15 p1902 A73-31223

Russian monograph on meteor observation covering telescopic and photographic methods, meteor trail plotting, radiant determination, stream counts and bolide data
15 p1941 A73-32416

The Budrio station of the meteoric radar system of the CNR for the systematic study of the upper atmosphere
17 p2147 A73-34959

Results of simultaneous wind velocity profile measurements in the lower thermosphere by the meteor radar and rocket methods.
18 p2310 A73-36130

Upper atmospheric turbulence kinetic energy spectrum from radio meteor trails observations, noting relationship to structure function for isotropic turbulence
18 p2312 A73-36288

Unusual LF radio absorption events during a major meteor shower.
18 p2289 A73-36302

Method of detecting meteor streams and associations
19 p2480 A73-37236

Meteor lifetime and the position of the maximum brightness point
19 p2480 A73-37238

Structure of the Perseids radiants in 1971
19 p2481 A73-37243

Evolution of the orbits and radiants of meteor swarms of the Jupiter family
21 p2768 A73-40724

Parameter behavior in mass distribution analysis of overdense Geminid trail radio echoes
22 p2915 A73-43041

Variation of the colour index along the meteor trail.
22 p2915 A73-43042

Fireball spectral data reduction for self absorption, Fe abundance, excitation temperatures, relaxation time and optical thickness effects
22 p2915 A73-43043

A computational study of the diffusion of meteor trains using a self-consistent model for the space-charge electric field.
23 p3029 A73-43684

METEORITE COLLISIONS

Model for meteorite impact generated gas flow on moon as function of mass, velocity and composition, noting wind effects on lunar erosion
02 p0223 A73-12719

Iron and stony-iron meteorites kamacite hardness and shock histories, hypothesizing preterrestrial collisions between asteroid sized objects
05 p0615 A73-16377

Biogenic elemental distribution and isotopic abundance in lunar samples, discussing heavy isotopes enrichment by solar wind irradiation, meteorite impacts and hydrogen stripping
06 p0654 A73-18417

Lunar maria basins fast and slow filling implications to moon history, considering meteorite bombardment, maria cooling and mascons
12 p1542 A73-27496

Laboratory modeling of 'vaporization-condensation and spilling' type processes taking place on the lunar surface
13 p1672 A73-28118

Zinc, lead, chlorine and FeOOH-bearing assemblages in the Apollo 16 sample 66095 - Origin by impact of a comet or a carbonaceous chondrite.
13 p1686 A73-29565

Development of soil on the lunar surface.
15 p1941 A73-32226

Moon surface physical properties from earth based observations and lunar soil samples, noting effects of cosmic dust and meteorite impacts
16 p2063 A73-33752

The origin of large lunar craters and circular seas
16 p2065 A73-33786

Urey meteoritic chondrule impact theory confirmation from Apollo sites and Lomar Crater /India/ impact generated silicate spherules
17 p2236 A73-35748

Lunar and terrestrial impact crater spherules.
17 p2236 A73-35749

Apollo 17 'orange soil' and meteorite impact on liquid lava.
19 p2482 A73-37390

Forces acting upon an asteroid moving through a meteoroid stream.
23 p3029 A73-43745

Production of lunar fragmental material by meteoroid impact.
24 p3129 A73-44447

Meteoroids impact rate on lunar and earth surfaces for given geocentric and selenocentric velocity distributions, taking into account gravitational effects
24 p3131 A73-44461

METEORITE COMPRESSION TESTS

U COMPRESSION TESTS

U MECHANICAL PROPERTIES

U METEORITES

METEORITE CRATERS

Petrographic and electron microprobe study of the Monturaqui impactite.
01 p0040 A73-10575

Major, minor and trace elements, specific gravities and refraction indices of Ivory Coast tektites, comparing composition to Bosumtwi crater glasses and Apollo lunar materials
01 p0109 A73-11475

Micrometeoroid particle flux impacting on lunar surface measured by observation of Surveyor 3 glass surfaces craters
02 p0214 A73-12256

Meteoroid activity on the lunar surface from the Surveyor 3 sample examination.
02 p0214 A73-12257

Petrographic and electron microprobe study of the Monturaqui impactite.
02 p0165 A73-12626

Distributions of lunar and Martian craters in relation to their origin
05 p0613 A73-16202

Extralunar materials in Apollo 16 soils and the decay rate of the extralunar flux 4.0 Gy ago.
05 p0618 A73-16835

Neutron activation analysis for geochemical origin and trace element compositions of moldavites and source rocks from Ries impact crater
07 p0877 A73-19652

Spall/pit diameter ratio decrease in lunar microcraters with decreasing size, considering origin from interplanetary dust particles impact
07 p0896 A73-19866

Crater frequency age determinations for the proposed Apollo 17 site at Taurus-Littrow.
09 p1148 A73-22873

Displaced mass, depth, diameter, and effects of oblique trajectories for impact craters formed in dense crystalline rocks.
10 p1276 A73-24077

Terrestrial, Martian and lunar doublet craters origin from simultaneous multiple meteorite impacts, using Lexan plastic projectiles against sand targets in ballistic range tests
10 p1277 A73-24079

Spatial distribution of elements in tektites and comparable materials by charged particle activation analysis.
11 p1418 A73-25584

The tsunami model of the origin of ring structures concentric with large lunar craters.
11 p1419 A73-25791

French monograph - Study of craters formed on glass surfaces by the impact of artificial micrometeoroids.
15 p1898 A73-32591

Circularity of Martian craters.
19 p2486 A73-37800

Two probable astroblemes in Brazil, considering meteorite impact origin by discovery of diagnostic shock-metamorphic effects in rocks from ERTS-1 satellite and aerial photographs
21 p2771 A73-41078

Lunar surface meteoritic material composition, distribution and amounts from trace element studies, discussing micrometeorites, ancient planetesimal debris and recent crater-forming projectiles
23 p3030 A73-43758

The Canyon Diablo meteorite.
24 p3137 A73-44949

- METEORITES**
- NT ACHONDrites 02 p0220 A73-12464
- NT BRÜDERHEIM METEORITE 02 p0221 A73-12690
- NT CARBONACEOUS METEORITES 06 p0749 A73-17839
- NT CHONDRITES 09 p1148 A73-22875
- NT IRON METEORITES 15 p1942 A73-32614
- NT MICROMETEORITES 17 p2229 A73-34470
- NT ORGUEIL METEORITE 20 p2348 A73-35871
- NT SIKHOTE-LIN METEORITE 20 p2486 A73-37775
- NT STONY METEORITES 24 p3076 A73-44656
- NT TEKTITES 01 p0108 A73-11474
- NT TUNGUSK METEORITE 01 p0109 A73-11475
- Comparative analysis of the magnetic properties of lunar rocks and meteorites 02 p0220 A73-12464
- Meteorite apheia calculation from activity levels of accumulated cosmogenic radioisotope due to cosmic ray irradiation 02 p0221 A73-12690
- Thermal effects experienced by meteoritic particles during atmospheric flight and upon earth surface impact 06 p0749 A73-17839
- Saint Severin meteorite irradiation age from thermoluminescence measurements, considering saturation of natural thermoluminescence from calibration curves 09 p1148 A73-22875
- Comparative analysis of the magnetic properties of lunar rocks and meteorites. 15 p1942 A73-32614
- Book - Meteorites and their origins. 17 p2229 A73-34470
- Russian book - Magnetic properties of meteorites: Meteorites in the laboratory. 18 p2348 A73-35871
- Russian book on cosmogenic nuclear reactions in meteorites and asteroid and lunar surface layers covering vertical /depth/ distributions of isotopes and nuclear-active particles 19 p2486 A73-37775
- Investigation of some theoretical point-explosion problems by the difference method 24 p3076 A73-44656
- METEORITIC COMPOSITION**
- Petrographic and electron microprobe study of the Monturaqui impactite. 01 p0040 A73-10575
- Chemical fractionation in iron meteorites and its interpretation. 01 p0108 A73-11474
- Major, minor and trace elements, specific gravities and refraction indices of Ivory Coast tektites, comparing composition to Bosumtwi crater glasses and Apollo lunar materials 01 p0109 A73-11475
- Relation between solar and planetary neon in carbonaceous chondrites. 02 p0211 A73-11744
- Chlorine, bromine, iodine, and uranium in tektites, obsidians, and impact glasses. 02 p0223 A73-12720
- The Angra dos Reis /stone/ mineral assemblage and the Genesis of stony meteorites. 03 p0374 A73-13797
- Xenon in carbonaceous chondrites. 04 p0501 A73-15631
- Double spiral DNA-like nucleotide analog in carbonaceous chondrite, indicating organic compound synthesis at low temperature 05 p0619 A73-16843
- Organic compounds in the Murchison meteorite. 06 p0752 A73-18234
- Siberian iron meteorites and chondrites characteristics and histories during 1965-1971 06 p0753 A73-18247
- Resolution by gas-liquid chromatography of diastereomers of five nonprotein amino acids known to occur in the Murchison meteorite. 06 p0662 A73-18468
- Abundance patterns of thirteen trace elements in primitive carbonaceous and unequilibrated ordinary chondrites. 07 p0877 A73-19651
- Lunar crater Copernicus - Search for debris of impacting body at Apollo 12 site. 07 p0877 A73-19653
- Elements abundances in Apollo 14 and 15 soils and breccias in eucrite Juvinas and howardite Kapocsa, suggesting initial chemical layering of moon 07 p0886 A73-19758
- Major impacts on the moon - Characterization from trace elements in Apollo 12 and 14 samples. 07 p0887 A73-19768
- A comparison of noble gases released from lunar fines /no. 15601.64/ with noble gases in meteorites and in the earth. 07 p0889 A73-19806
- Allende meteorite carbonaceous phase - Intractable nature and scanning electron morphology. 07 p0900 A73-20283
- Inter-element relationships between trace elements in primitive carbonaceous and unequilibrated ordinary chondrites. 07 p0903 A73-20619
- Fine structures of mutually normalized rare-earth patterns of chondrites. 07 p0789 A73-20620
- Gallium and germanium in the metal and silicates of L- and LL-chondrites. 07 p0789 A73-20621
- Chemical fractionations in meteorites. VI - Accretion temperatures of H-, LL-, and E-chondrites, from abundance of volatile trace elements. 07 p0789 A73-20622
- Noble gas measurement in powdered aliquots of eleven H-chondrites, using Reynolds type mass spectrometer 07 p0789 A73-20623
- Solar nebula Lu 176-Hf 176 pair and Zr abundance determinations, using chondrite fraction and s-process model 08 p1006 A73-20937
- Stony meteorite discovery at Ness County, Kansas, noting three separate falls and composition and mineralogical differences from Kansada, Franklinville and Wellmanville meteorites 09 p1138 A73-21851
- Mineralogy and petrology of the Yilmia enstatite chondrite. 09 p1139 A73-21852
- Petrography, mineralogy and composition of plagioclase and pyroxenes of Washougal howardite by density and refraction measurements 09 p1139 A73-21853
- Seminole meteorite external form chondrite composition and structure, noting brecciation and chondrules 09 p1139 A73-21854
- The Gosnells iron - A fragment of the Mount Dooling octahedrite. 09 p1139 A73-21855
- The Oro Grande, New Mexico, chondrite and its lithic inclusion. 09 p1139 A73-21858
- Havero stony ureilite origin modes, composition, textural features, mineralogy and petrology 09 p1139 A73-21860
- Forms of carbon in the new Havero ureilite of Finland. 09 p1140 A73-21863
- The chemical composition of the Havero meteorite and the genesis of the ureilites. 09 p1140 A73-21864
- The highly reflecting and opaque components in the mineral content of the Havero meteorite. 09 p1140 A73-21866
- Neutron activation and irradiation analyses of Havero ureilite elemental abundances 09 p1140 A73-21867
- Elemental abundances and chemistry of Havero carbonaceous ureilite, noting similarity to Allende inclusions pattern 09 p1047 A73-21868
- Havero ureilite - Evidence for recrystallization and partial reduction. 09 p1140 A73-21869
- Mineralogy and texture of Havero ureilite, noting preterrestrial shock evidence, recrystallized olivine and metal grain, and graphite conversion into diamonds from petrographic observation 09 p1140 A73-21870
- Investigation of the Canyon Diablo metallic spheroids and their relationship to the breakup of the Canyon Diablo meteorite. 09 p1144 A73-22145
- Historical treatment and inconclusiveness of evidence of extraterrestrial life traces and organic matter in carbonaceous and other meteorites 09 p1146 A73-22545
- Tillaberi /Niger/ stony meteorite elements abundance and radioactivity determination by gamma ray spectrometry 09 p1149 A73-23032
- Isotopic and crystalline structure changes in lunar rock and meteorite constituents for cosmic ray nuclei intensity and energy spectrum 09 p1138 A73-23169
- Spatial variations of cosmic rays on the basis of data for the radioactivity of meteorites with known orbits 10 p1266 A73-23910
- Heterocyclic compounds extraction and identification from carbonaceous meteorites by gas chromatography and mass spectrometry, noting pyrimidine distribution and absence of biological heterocycles 10 p1277 A73-24101
- Volatile organic compounds from Murchison, carbonaceous chondrite by vaporization-pyrolysis at different temperatures, comparing with Allende meteorite and terrestrial rocks 10 p1277 A73-24102
- Spallation production of He-3, Ne-21, and Ar-38 from target elements in the Bruderheim chondrite. 10 p1277 A73-24103
- Noble gas and carbon abundances of the Havero, Dingo Pup Donga, and North Haig ureilites. 10 p1277 A73-24104
- Certain peculiarities in the distribution of mercury in meteorites. 10 p1278 A73-24106
- High-temperature condensates in chondrites and the environment in which they formed. 10 p1278 A73-24109
- Argon 40-argon 39 chronology of four calcium-rich achondrites. 10 p1278 A73-24110
- New data on the cosmic history of the Sikhote-Alin meteorite 10 p1281 A73-24462
- Depth variation of cosmogenic noble gases in the approximately 120-kg Keyes chondrite. 11 p1418 A73-25587
- Applications of activation analysis to geochemical, meteoritic and lunar studies. 11 p1326 A73-25800
- Double spiral DNA-like polynucleotide analog in carbonaceous chondrite, indicating organic compound synthesis at low temperature 11 p1423 A73-26053
- Indium abundances in cosmos, meteorites, tektites, rock-forming and ore minerals and igneous rocks, considering behavior in magmatogenic processes and rock weathering and alteration 12 p1490 A73-27125
- Mineralogical density of sporadic meteoric bodies 13 p1673 A73-28298
- Meteoritic vs lunar origin of Luna 20 lunar soil samples metal particles and metallic inclusions discussing meteoritic microstructural obliteration due to shock reheating of crust 13 p1675 A73-28315
- Mineralogical characteristics of the Rechki meteorite 13 p1677 A73-28349
- Hammond Downs, a new chondrite from the Tenham area, Queensland, Australia. 13 p1680 A73-28618
- Allende carbonaceous chondrite Ca-Al rich inclusion refractory trace metals condensation temperature calculation, indicating high temperature primitive solar nebula condensates 13 p1684 A73-29176
- Cu content comparison of Eaton meteorite to true extraterrestrial meteorites, determining dendritic structure and terrestrial origin from similarity to brass 13 p1684 A73-29179
- The isotopic composition of 'graphitic' carbon from iron meteorites and some remarks on the troilite sulfur of iron meteorites. 13 p1684 A73-29180
- Carbonaceous chondrite neutron activation analysis for trace elements, revealing compositional homogeneity 13 p1684 A73-29181
- Solubilities of noble gases in magnetite - Implications for planetary gases in meteorites. 13 p1684 A73-29182
- Orgueil chondrite magnetite age via I 129/Xe 129 method compared to Karoonda magnetite age 13 p1684 A73-29250
- Composition of metal in type III carbonaceous chondrites and its relevance to the source-assignment of lunar metal. 13 p1686 A73-29564
- Chemical evolution before life from carbonaceous meteorites composition, noting porphyrins, optically active substances and isoprenoid hydrocarbons 14 p1715 A73-30130
- Minor and trace elements in some meteoritic minerals. 15 p1941 A73-32387
- Chemical fractionations in meteorites. VII - Cosmochemistry and cosmochemistry. 15 p1841 A73-32390
- Time differences in the formation of meteorites as determined from the ratio of lead-207 to lead-206. 17 p2225 A73-34096
- Accretion processes to account for chemical differences among chondrites formed in cooling solar nebula 17 p2227 A73-34414
- The A, B, C's of trapped helium, neon, and argon in meteorites and lunar samples. 17 p2228 A73-34417
- Cosmic radiation intensity constancy from observations of cosmic ray induced transmutations in meteorites 17 p2223 A73-34419
- Chondrule chemical variations in chondrite compared to predictions for different chondrule formation mechanisms 17 p2119 A73-34425
- Book - Meteorites and their origins. 17 p2229 A73-34470
- Pb isotopic composition measurement in chondrites and achondrite for model ages, noting 50 My variations 17 p2233 A73-35265
- Isotopic composition of solar wind xenon in carbonaceous chondrites, discussing evolution of meteoritic matter 17 p2233 A73-35266
- Radioactivities and He, Ne and Ar stable isotopes measured in meteorites for cosmic ray exposure ages 17 p2233 A73-35267

Anisotropy of absorption bands in some lunar, meteoritic, and terrestrial pyroxenes.

17 p2235 A73-35738

He, Ne and Ar in chondritic Ni-Fe as irradiation hardness sensors.

17 p2120 A73-35801

Radiochemical neutron activation analysis for U and Th abundance measurement in achondrites and pallasite olivines

17 p2120 A73-35802

Aluminum-26 in meteorites. VII - Ureilites, their unique radiation history.

17 p2237 A73-35803

Extraterrestrial life detection from imaging observations on lunar samples and meteorites, discussing application to Mars surface

17 p2113 A73-35804

Russian book - Magnetic properties of meteorites: Meteorites in the laboratory.

18 p2348 A73-35871

Elemental abundance determinations for meteors by spectroscopy.

18 p2352 A73-36287

Thermal models of inhomogeneously accreted meteorite parent bodies.

18 p2356 A73-37048

New data on the cosmic history of the Sikhote-Alin meteorite.

19 p2486 A73-38128

Evidence for solar flare rare gases in the Khor Temiki aubrite.

21 p2764 A73-40231

Lead isotopic composition ages of carbonaceous chondritic meteorites with correction for terrestrial lead contamination

21 p2765 A73-40239

Characteristics of tracks of ions of 14 less than or equal to Z less than or equal to 36 in common rock silicates.

21 p2682 A73-40242

Sequential nondestructive neutron activation analysis for bulk abundance of Fe, Al, Na, Mn, Cr, Sc, Co and Ir in chondrules from chondrites

21 p2647 A73-40563

The chemical classification of iron meteorites. VII - A reinvestigation of irons with Ge concentrations between 25 and 80 ppm.

21 p2647 A73-40564

Chromium and phosphorous enrichment in the metal of type II/C2 carbonaceous chondrites.

21 p2771 A73-41007

Variability of the He-3 and Ne-21 production rates in ordinary chondrites.

21 p2771 A73-41008

Distribution of Ni, Ga, Ge and Ir between metal and silicate portions of H-group chondrites.

21 p2771 A73-41009

Amino acids in the Murchison meteorite.

21 p2771 A73-41010

Ablation debris and primary micrometeoroids in the stratosphere.

21 p2775 A73-41419

Mineralogical density of sporadic meteoric bodies.

21 p2779 A73-41542

Primordial abundance values for heavy nuclei related to content of type 1 and 2 carbonaceous chondrites

23 p2950 A73-43752

Lunar surface meteoritic material composition, distribution and amounts from trace element studies, discussing micrometeorites, ancient planetesimal debris and recent crater-forming projectiles

23 p3030 A73-43758

X ray and electron diffraction studies of Ni-containing etched brown rims in meteoritic taenite (Ni-Fe alloy) associated with kamacite, noting Widmanstätten pattern

23 p2951 A73-43844

Comparisons of meteorite and asteroid spectral reflectivities.

24 p3132 A73-44538

Rare-earth elements in matrix, inclusions, and chondrules of the Allende meteorite.

24 p3133 A73-44539

Photometric and polarimetric properties of the Bruderheim chondritic meteorite.

24 p3133 A73-44557

The Canyon Diablo meteorite.

24 p3137 A73-44949

The Mighei meteorite.

24 p3137 A73-44950

METEORITIC DAMAGE

Meteoroid activity on the lunar surface from the Surveyor 3 sample examination.

02 p0214 A73-12257

Petrographic and electron microprobe study of the Monturaqui impactite.

02 p0165 A73-12626

Spall/pit diameter ratio decrease in lunar microcraters with decreasing size, considering origin from interplanetary dust particles impact

07 p0896 A73-19866

Reflection from the earth's surface of shock waves generated by falling meteorites

08 p0958 A73-21065

Metal barrier maximum puncturable thickness dependence on high velocity meteorite particle impact parameters

12 p1554 A73-27642

Impact tests for aid in data interpretation of measured meteor particles impact on spacecraft structures, noting transducer response dependence on impact angle

12 p1554 A73-27643

Reflection of meteorite generated shock waves from the earth's surface.

18 p2313 A73-36866

Lunar cross hatching lineament patterns at Silver Spur on Apollo 15 landing site, relating to geological, lighting or meteorite impact gas flow effects

23 p3034 A73-43962

METEORITIC DIAMONDS

Forms of carbon in the new Haverro ureilite of Finland.

09 p1140 A73-21863

The highly reflecting and opaque components in the mineral content of the Haverro meteorite.

09 p1140 A73-21866

Transformation of meteorite material in experiments on explosively produced shock compression at pressures of 500 and 1000 kbar

24 p3137 A73-44710

METEORITIC DUST

U MICROMETEORITIDS

METEORITIC IONIZATION

U ATMOSPHERIC IONIZATION

U METEOR TRAILS

METEORITIC MICROSTRUCTURES

Seminole meteorite external form chondrite composition and structure, noting brecciation and chondrules

09 p1139 A73-21854

The structure of a meteorite, its formation and transformation during heating

17 p2230 A73-34565

Cosmic ray bombardment of meteorites allowing solar system age estimation from spallation product concentration and subatomic particle track distribution

17 p2232 A73-34975

X ray and electron diffraction studies of Ni-containing etched brown rims in meteoritic taenite (Ni-Fe alloy) associated with kamacite, noting Widmanstätten pattern

23 p2951 A73-43844

METEOROID CONCENTRATION

Spacecraft-borne IR optical remote sensor for detection, identification and distribution measurement of asteroid and meteoroid particles

01 p0105 A73-11205

Meteoroid activity on the lunar surface from the Surveyor 3 sample examination.

02 p0214 A73-12257

Conditions of Leonid meteor shower encounters with the earth in occurrences of the years 1898-2000

09 p1146 A73-22546

Micrometeoroid mass, velocity and composition from Heos 2 and Helios satellite experiments, using hypervelocity dust particle impacting plasma emission

10 p1218 A73-24119

Correction for angle of incidence of meteoric particle with penetration and piezoelectric sensors in estimates of spatial density of meteoric matter.

12 p1554 A73-27644

Meteoroid ions in the D and E-regions.

18 p2310 A73-36132

Meteoroid ions in the polar ionosphere according to the rocket mass-spectrometric measurements and theoretical calculations.

18 p2311 A73-36146

Lunar asymmetries in crustal thickness, maria distribution and gamma radioactivity due to intense early bombardment by interplanetary meteoroid flux

23 p3031 A73-43762

The observational evidence for mass distribution in the meteoritic complex.

23 p3031 A73-43770

METEOROID CRATERS

U METEORITE CRATERS

METEOROID DUST CLOUDS

NT ZODIACAL DUST

The meteoroid influx and the maintenance of the solar system dust cloud.

03 p0365 A73-12889

METEOROID PROTECTION

Computerized design of an outer planets spacecraft structure to survive the meteoroid environment.

11 p1430 A73-25487

METEOROID SHOWERS

NT AQUARIID METEORITIDS

NT DRACONID METEORITIDS

NT GEMINID METEORITIDS

NT LEONID METEORITIDS

NT ORIONID METEORITIDS

NT PERSEID METEORITIDS

NT QUADRANTID METEORITIDS

NT TAURID METEORITIDS

Meteor shower and cosmic dust effects on twilight sky brightness from mountain top and balloon observations

02 p0215 A73-12261

Cometary structure from ground based observations of meteor showers, noting fireball characteristics difference

04 p0495 A73-14763

Tunable dye laser radar observation for Na layer nocturnal vertical distribution, suggesting meteor shower effect on layer content increase

04 p0444 A73-15543

Magnetic spheroid mass determination with microbalance and internal cavity observation by X ray photography, noting meteor showers as extraterrestrial source

05 p0621 A73-17051

Total number and mass of Pultusk meteorite shower fragments, using spatial distribution rule

06 p0748 A73-17831

The Iarkovskii-Radzievskii effect and the evolution of condensations in a meteor stream

08 p1007 A73-21066

The epsilon-Lyrid, alpha-Coronid, and phi-Draconid meteor streams in 1969

08 p1007 A73-21069

Cometary parent bodies transfer to short period orbits by Jupiter caused gravitational disturbances, noting qualitative analysis of orbits evolution

08 p1012 A73-21576

Statistical model of meteor streams. III - Stream search among 19303 radio meteors.

11 p1425 A73-26135

Hammond Downs, a new chondrite from the Tenham area, Queensland, Australia.

13 p1680 A73-28618

Deformation of a meteor stream caused by an approach to Jupiter.

14 p1795 A73-29843

Orbital evolution of the alpha Virginid and alpha Capricornid meteor streams.

14 p1795 A73-29844

Theoretical cometary radiants and the structure of meteor streams.

14 p1795 A73-29845

Focusing effect of planetary perturbations on meteor stream particles for comet formation

14 p1795 A73-29846

Meteor streams and comet orbital statistics from radar observations during 1967-1968

14 p1795 A73-29847

Monte Carlo technique application to meteor stream formation process modeling, discussing mass ejection from cometary nuclei

14 p1795 A73-29848

Genetic relationship between short period comets and meteor streams, considering radial and longitudinal focusing mechanism for particles in meteor streams

15 p1939 A73-32009

Russian monograph on meteor observation covering telescopic and photographic methods, meteor trail plotting, radiant determination, stream counts and bolide data

15 p1941 A73-32416

Unusual LF radio absorption events during a major meteor shower.

18 p2289 A73-36302

Yarkovskii-Radzievskii effect and the evolution of meteor swarms.

18 p2355 A73-36867

The meteor showers epsilon-Lyrids, alpha-Coronids, and phi-Draconids in 1969.

18 p2355 A73-36870

Some characteristics of the surface scattering of the Sikhote-Alin meteorite shower

19 p2480 A73-37240

Interaction of the lower thermosphere with the solid component of the interplanetary medium.

21 p2682 A73-40151

Evolution of the orbits and radiants of meteor swarms of the Jupiter family

21 p2768 A73-40724

Mie scattering computation of cosmic dust flux in upper atmosphere from twilight luminance increase during meteor showers

21 p2775 A73-41418

Airborne photographic and visual observation of material from Comet Giacobini-Zinner produced meteor showers due to orbit perturbation and perihelion changes by Jupiter

22 p2909 A73-42588

Forces acting upon an asteroid moving through a meteoroid stream.

23 p3029 A73-43745

METEORITIDS

NT AQUARIID METEORITIDS

NT BOLIDES

NT DRACONID METEORITIDS

NT GEMINID METEORITIDS

NT LEONID METEORITIDS

NT METEOROID DUST CLOUDS

NT MICROMETEORITIDS

NT ORIONID METEORITIDS

NT PERSEID METEORITIDS

NT QUADRANTID METEORITIDS

NT RADIO METEORS

NT SPORADIC METEORITIDS

NT TAURID METEORITIDS

NT ZODIACAL DUST

Meteor dust motion in the upper atmosphere and in the vicinity of the earth's orbit.

Statistical analysis of atmospheric sudden changes in VLF bands, suggesting lower ionosphere ionization increase due to meteors incidence

Low energy solar nuclear particle irradiation of lunar and meteoritic breccias.

Light distribution in photographic meteors by means of multicolour photometry.

On the source of the 3840 A persistent emission by meteors.

Galactic cosmic ray modulation region evaluation from meteoroid orbit, velocity and radioactive dating data

Ablation of large meteor particles

Photometric error of the NA-MK-25 camera field

Impact gages for detecting meteoroid and other orbital debris impacts on space vehicles.

Elemental abundance determinations for meteors by spectroscopy.

Meteor lifetime and the position of the maximum brightness point

Recording of the angular velocity of meteors by sequential photography

Meteorite production mechanism from asteroid belt via asteroidal collision fragments perihelion changes and orbit perturbation by Jupiter into earth-crossing orbital elements

METEOROLOGICAL BALLOONS

The balloon launch stations of the EOLE program.

Eole meteorological balloon scientific instruments, describing pressure sensor and electronic circuit design for signal transmission via satellite

Battery charge regulator for Eole meteorological balloons power supply, describing printed circuit design and construction

Isentropic/isopycnic mountain waves tracing from superpressure balloon flights synchronous radar, temperature and pressure data

EOLE balloon clusters horizontal trajectories as indicators of southern hemisphere atmospheric circulation, estimating rms divergence as function of scale

METEOROLOGICAL CHARTS

Typification of circulation processes in the atmosphere over the Northern Hemisphere and the possibility for its objectivization with the aid of numerical characteristics

Utilization of meteorological data from earth satellites in the analysis of global weather maps and in studies of planetary atmospheric circulation

Use of numerical guidance at the National Weather Service's National Meteorological Center.

Present state and further developments in short-range hydrodynamic weather forecasting

Forecasting with a global, three-layer, primitive-equation model.

Forecast maps for seasonal variations in the geometrical parameters of the F2 layer

Weather forecasts in tabulated and worded form by computer interpretation of forecast charts.

Russian thunderstorms mean annual duration chart and calculation nomograms

Diurnal tropopause maps divergence from average tropopause altitude profile, commenting on Eole experiment

Ground wind component calculations from synoptic parameters

Statistical properties of precipitation patterns.

The global distribution of the maximum 24-hour totals of precipitation

Compression of weather charts by the segmented Lynch-Davison code.

Global meridional cross sections and charts for mesospheric circulation and temperature variability via meteorological rocket network

The stratospheric-mesospheric circulation over the North Pacific Ocean.

Aerological soundings of the atmosphere from NOAA-2 data for operational systems.

Features of the evolution of depressions and their cloud systems over the Pacific Ocean.

Investigations of the 500mb level in relation to the general circulation. I - Transport of relative angular momentum at the 500mb level, by considering daily and monthly eddies that were obtained by applying Fisher's partitioning.

Selection of analogs to composite kinematic charts of natural synoptic periods

Use of meteorological rocketsonde and satellite radiation data for constant-pressure analyses at levels between 5 and 0.4 mb.

Relationship between midstratospheric temperatures and tropospheric synoptic features.

METEOROLOGICAL FLIGHT

An airborne instrument system for atmospheric boundary-layer research.

Microwave radiometric measurements of atmospheric temperature and water from an aircraft.

CAT association with Kelvin-Helmholtz wave structures in baroclinic zone, correlating meteorological radar and aircraft observations [AD-751724]

A brief summary of the meteorological research flight digital magnetic-tape data-recording and data-processing system.

Gun launched sounding rockets and sabot projectiles for low cost meteorological and geophysical data acquisition, considering cost advantages

Meteorological rocket observations of amplitudes and phases of zonal wind quasi-biennial oscillations at 25-60 km during 1962-1969

Turbulence variations during the high altitude clear air turbulence (HICAT) program.

Intensive probing of a clear air convective field by radar and instrumental drone aircraft.

Scheme for evaluating the influence of convective-cloud modifications aimed at controlling precipitations artificially, and the results of cumulus cloud structure investigations from aircraft

Some scale estimates of the three-dimensional structure of cloud fields from aircraft-based aerial photographs

METEOROLOGICAL INSTRUMENTS

NT CLOUD HEIGHT INDICATORS

NT DROPSONDES

NT IONOSONDES

NT RADIOSONDES

NT RAIN GAGES

NT RAWINSONDES

NT WEATHER DATA RECORDERS

An airborne instrument system for atmospheric boundary-layer research.

Observations of precipitation zones from satellites using microwave radiometers.

Eole meteorological balloon scientific instruments, describing pressure sensor and electronic circuit design for signal transmission via satellite

Rocket motor, Dart vehicle, booster and launcher design and instruments and payload description for Super Loki meteorological rocket systems [AIAA PAPER 73-303]

Utilization of vacuum ultraviolet radiation for measurement of humidity pulsations

Digital readout wind measurement and indicator system for data acquisition, processing and display in airports for aircraft wind information service

Current trends in the refinement of scientific equipment for meteorological satellites

Worldwide variations in atmospheric transmission. I - Baseline results from Smithsonian observations.

METEOROLOGICAL PARAMETERS

Cup anemometer input/output frequency characteristics, determining nonlinear behavior via inertia considerations

Airports automated meteorological instrumentation, describing cloud base height telemeter and transmissometer for runway visibility measurement

Low-inertia ultraviolet hygrometer

Lidar measurements for the exploration of the atmosphere

METEOROLOGICAL PARAMETERS

Meteorological effects on SST operations during various flight phases, considering ATC and communications aspects

Meteorological parameters conducive to ice formation on aircraft, analyzing data statistics on atmospheric moisture content, temperature and drop size [DGLR PAPER 72-109]

Use of space techniques in the detection and monitoring of climate parameters and air pollutants [DGLR PAPER 72-081]

Missile range dispersions produced by meteorological factors, drag differences and mass changes during passive ballistic flight

Meteorological and atmospheric physics observations by Soyuz manned spacecraft, analyzing spectrophotometry, photography and visual observation data of twilight, night and day horizons

Approach for obtaining prognostic relations on the basis of meteorological data

Investigation of the electrical parameters and meteorological elements of the atmosphere close to the ground during thunderstorm and thunderstorm-free periods

Upper bounds for long range numerical weather forecasts errors due to inadequate knowledge of frictional constants, heating and initial conditions

Status of remote sensing of the troposphere.

Thermospheric parameters seasonal and latitudinal variations calculation based on atmospheric model with components ionization and molecular oxygen dissociation as main heat sources

Information transfer satellite system (ITSS) design for earth resource and meteorological data collection and relay from remote sensing platforms

'Barycentric' averaging of the hydro-dynamical equations with respect to coordinate systems with arbitrary vertical coordinate

Russian book on atmospheric circulation covering temperature distribution, tropospheric and stratospheric winds, jet streams and Southern Hemisphere meteorological features

Russian book - Meteorological effects on cosmic rays.

Utilization of the convergence of atmospheric processes during construction of long-range weather forecasts

Application of structural-temporal functions for analysis of periodicities in atmospheric motions

Utilization of meteorological data from earth satellites in the analysis of global weather maps and in studies of planetary atmospheric circulation

Vertical scintillation propagation from ground characterized by log normal probability distribution, universal spectral function and variance behavior dependent on near ground meteorological conditions

Atmospheric attenuation of noise measured in a range of climatic conditions.

Atmospheric conditions effects on line-of-sight microwave PCM data transmission system performance, comparing predicted error probability vs predetection SNR with measurement

Mapping of atmospheric and sea ice parameters with an imaging microwave radiometer from the Nimbus 5 satellite.

A radiative-convective model for the prediction of radiation fog.

Experiments on objectively predicting some atmospheric and oceanic variables for the winter of 1971-72.

The use of model output statistics (MOS) in objective weather forecasting. 06 p0720 A73-18706

Parameter value selection in Saraki's meteorological field coordination method 06 p0721 A73-18731

Vertical profiles of liquid water content and other cloud parameters for cumulus and cumulus congestus clouds from aircraft measurements over Ukraine 06 p0985 A73-21454

Study on the solar activity dependence of the E region peak electron density and some atmospheric parameters. 08 p0961 A73-21652

Ion angular distribution around Explorer 31, discussing observed ion flux relation to ionospheric parameters derived from ambient ion and electron measurements 09 p1075 A73-22136

Analog, digital and hybrid simulation of a planetary boundary layer meteorological forecast model. 09 p1114 A73-22333

Equivalent number method of optimal interval selection for meteorological observations with independent statistical samplings 09 p1114 A73-22853

Possible correlation between the concentration and density of alpha-radioactive fallouts and types of meteorological processes 09 p1115 A73-22995

Application of some numerical techniques in combining satellite and conventional data in the tropics. 09 p1115 A73-23175

An operational upper air analysis using the variational method. 10 p1244 A73-23645

One method of computing the meteorological variables for mesoscale processes. 11 p1394 A73-26192

F 2 layer characteristics forecasts by extrapolation of critical F 2 frequency data from Moscow, Sverdlovsk, Irkutsk, Alma-Ata and Salehard 12 p1490 A73-27338

Spatial-temporal analysis of asynchronous meteorological data 12 p1521 A73-27743

Method for calculating turbulent flows from network data 12 p1521 A73-27744

Weather condition caused aircraft accident avoidance, considering meteorological factors of air temperature, humidity, cloud formation, fog, haze, precipitation and visibility deterioration 13 p1568 A73-28554

A comparison of time-varying concentrations of air admixtures with those of the corresponding stationary cases 13 p1653 A73-28742

Project VEMNO - North Sea-Baltic measuring network. 13 p1608 A73-28787

Statistical turbulence model of meteorological and topographical aircraft flight conditions for low altitude critical air turbulence (LO-LOCAT) environment 13 p1569 A73-28831

Spectra of star and planet scintillation and dependence of their characteristics on meteorological conditions 13 p1683 A73-29097

A discretization method for atmosphere dynamics equations and for the construction of numerical weather forecast schemes 13 p1654 A73-29151

Structure of the lower 300-meter atmospheric layer during the passage of a cold front 13 p1655 A73-29194

Precipitation forecasting by numerical scheme using dew point depression as moisture parameter and gradual onset techniques 13 p1655 A73-29336

Determination of coefficients of vertical diffusion between 0 and 100 m with the help of radon and of ThB 13 p1655 A73-29342

Influence of atmospheric parameters on the wavelength of single-frequency laser radiation 14 p1756 A73-30023

German book - Long-term weather forecaster: Fundamentals of a new experiment with monthly predictions. 15 p1903 A73-31473

A basis for four-dimensional /continuous/ processing of meteorological observation data, using a dynamic statistical approach 15 p1904 A73-31608

Estimation of errors arising in calculations of the fluxes and influxes of thermal radiation due to errors in the initial meteorological parameters 15 p1905 A73-31786

Meteorological time series persistence tendency representation by autocorrelation coefficients, summation, determining independent values effective number by white noise bandpass filtering 15 p1906 A73-32344

The regression relations for turbulence parameters in the air layer near the ground in the case of an inhomogeneous base 15 p1907 A73-32359

Coordinated measurements of atmospheric parameters at stratospheric levels. 16 p2007 A73-33560

The characteristics of millimeter wavelength satellite-to-ground space diversity links. 16 p1981 A73-33707

Atmospheric attenuation interrelations at 12 and 35 GHz with meteorological parameters derivation for homogeneous atmosphere, testing dynamic atmospheric model 16 p1981 A73-33709

Atmospheric temperature measurement with X and K band radiometers, discussing meteorological conditions variation effects on microwave propagation and comparison with spacecraft tracking data 16 p1983 A73-33730

Atmosphere and ionosphere of Venus on the basis of data obtained by Mariner 5 in the S band during radio occultation 16 p2067 A73-33801

Influence of horizontal inhomogeneity in the Venusian atmosphere on the accuracy of measurements of its parameters by a radio occultation method 16 p2068 A73-33824

Satellite monitoring of climate parameters, discussing energy transfer in atmosphere, energy distribution, radiation balance, climatic models 17 p2205 A73-34928

Low altitude satellite networks for recording programmable earth atmosphere parameters related to terrestrial environment control 17 p2205 A73-34929

Three to five day numerical forecasting making use of the complete hydrodynamics equations, and problems of correlating the original fields of meteorological elements 18 p2331 A73-35911

Development of methods of forecasting meteorological conditions for aviation 18 p2331 A73-35912

The use of VLF propagation measurements for studies of magnetospheric and meteorological influences on the lower ionosphere. 18 p2303 A73-35953

Differences in circulation of the upper atmosphere in low latitudes of the southern and northern hemispheres. 18 p2310 A73-36138

A model of formation of the mean diurnal state of the upper atmosphere and its diurnal variations. 18 p2311 A73-36147

The sensitivity of optimal flight paths to variations in aircraft and atmospheric parameters. 19 p2386 A73-38051

Turbulence spectra, length scales and structure parameters in the stable surface layer. 19 p2448 A73-38216

Capabilities of radar, sodar and lidar for measuring the structure and motion of the stably stratified atmosphere. 19 p2405 A73-38239

Scintillation measurements for large integrated-path turbulence. 19 p2461 A73-38486

Clear air turbulence mesoscale history from sequential analysis of rawinsonde stations network observed data 21 p2728 A73-40057

Certain parameters of cellular convection according to observations by meteorological earth satellites and from a high mast 21 p2731 A73-40492

Atmospheric models for 110-2000 km region, considering composition, temperature profiles, thermosphere and exosphere variations, density and boundary condition computation, etc 21 p2683 A73-40629

Thermospheric structural parameter diurnal variations from satellite orbit decay, rocket measurements of vertical temperature distribution and atmospheric component concentrations and incoherent scatter observations 21 p2688 A73-41348

Variations in density and chemical composition at 120 km from chemical and dynamical processes. 21 p2689 A73-41355

Observations of electron fluxes and related variations of ionospheric plasma parameters in the south polar cusp. 21 p2690 A73-41369

Allowance for the effects of the relief and of the Coriolis force in forecasting meteorological elements. 22 p2883 A73-41954

The effect of atmospheric and physiological conditions on the homogeneity of observations of noctilucent clouds 22 p2847 A73-42448

A meteorological and a geophysical example of the use of the scale autocorrelation coefficient to deter-

mine ratios of frequencies present in periodic phenomena. 22 p2883 A73-42542

Diurnal cycles of the refractive index structure function coefficient. 22 p2849 A73-42545

F 2 layer characteristics forecasts by extrapolation of critical F 2 frequency data from Moscow, Sverdlovsk, Irkutsk, Alma-Ata and Salehard 23 p2970 A73-43236

Nonlinear methods for evaluating the informative value of meteorological parameters and for classifying meteorological phenomena /Functional methods and algorithms/ 23 p3001 A73-43464

Intensity variations of electron-photon shower particles in the atmosphere 23 p3023 A73-43557

Optical radar measurements of meteorological parameters and air pollution related to environment protection, using Raman effect and resonance and Mie scattering 24 p3096 A73-44896

National Center for Atmospheric Research collected synoptic meteorological data from earth surface, upper air and satellite observations for handling on computers 24 p3075 A73-45087

METEOROLOGICAL PROBES

U SONDES

METEOROLOGICAL RADAR

Airborne radar set for weather surveillance, independent landing monitoring, ground visualization and collision avoidance 02 p0190 A73-11854

Radar Meteorology Conference, 15th, Urbana, Ill., October 10-12, 1972, Preprints. 03 p0337 A73-14504

Evaluation of a dual-wavelength radar hail detector. 03 p0337 A73-14505

Pulse Doppler radar observations of hailstone maximum diameters as function of time 03 p0337 A73-14506

Doppler radar evidence of severe storm high-reflexivity cores acting as obstacles to airflow. 03 p0337 A73-14507

Results of precipitation backscatter measurements at 1.8 cm with a polarization diversity radar. 03 p0338 A73-14509

Storm cell models from digital radar data. 03 p0338 A73-14510

Radar and Nimbus 4 infrared measurements of the Oklahoma City tornados, 30 April 1970. 03 p0338 A73-14512

Meteorological radar site selection factors, discussing antenna towers installation 03 p0288 A73-14514

Digitized radar experiments project for data acquisition and processing and weather forecasting techniques development, describing test bed configuration, equipment and operation 03 p0288 A73-14515

Radar measurement errors due to rain attenuation compensation and improper system calibration, discussing error reduction procedures 03 p0279 A73-14518

Multiple contrail streamers observed by radar. 03 p0279 A73-14519

Type and time of integration in precision digital video integrator for meteorological radar, describing equipment and operation [AD-751726] 03 p0281 A73-14521

Automated procedures for mapping and display of digitized radar data. 03 p0281 A73-14522

Project Cloud Catcher weather radar data system revisions in radar set, echo pulse integrator, data logging and analysis and graphic displays 03 p0289 A73-14523

Uncertainties in coherent measurement of the mean frequency and variance of the Doppler spectrum from meteorological echoes. 03 p0279 A73-14525

A modified coefficient for the weather radar equation. 03 p0279 A73-14526

Pulse pair estimation of Doppler spectrum parameters. 03 p0279 A73-14527

Coherent signal from incoherent meteorological radar echoes for atmospheric turbulence intensity measurement, noting autocorrelation function for average frequency 03 p0338 A73-14531

Life cycle of brief CAT episodes determined by mesoscale analysis. 03 p0338 A73-14533

CAT association with Kelvin-Helmholtz wave structures in baroclinic zone, correlating meteorological radar and aircraft observations [AD-751724] 03 p0339 A73-14534

Inverse problem in the theory of turbulence filtering by the radar pulse volume. 03 p0279 A73-14538

Radar observations of intense undulance in an evaporating cloud layer.

Simultaneous FM-CW radar and lidar observations of climatological regions, convective activity, cloud echoes, layered structures, insects and breaking Kelvin-Helmholtz waves

A study of tropospheric radar propagation characteristics during an unusual spell of persistent haze followed by thunderstorm over Delhi during May 1966.

Computerized weather radar data central processor design, implementation and programs for data reduction and calibration

Meteorological echoes movement and evolution measurement potential of conventional radars connected to programmable real time processor

The University of Oklahoma acoustic radar.

Meteorological lidar use to obtain backscatter curve produced by aerosols suspended in atmosphere [ONERA, TP NO. 1130]

A note on the use of airborne 30-millimetre radar at long ranges.

Form of the spectrum of radar signals due to precipitation

Microwave remote sensor technology review, discussing target-sensor interaction, spatial resolution concepts and meteorological applications of radiometric and radar systems

Updating of numerical precipitation guidance.

Acoustic sounding of meteorological phenomena in the planetary boundary layer.

Intensive probing of a clear air convective field by radar and instrumental drone aircraft.

Weather radar surveillance data short term distribution to airline users through weather message switching center, describing data coding, teletype network and data plotting operations

Doppler radar characteristics of precipitation at vertical incidence.

Precipitation patterns effective fall velocity determination from three dimensional radar scan data, discussing interpolation/extrapolation technique to improve coarse sampling time effects

Meteorological radar and the WILM landing aid

Meteorological lidar for determining aerological data above launching base prior to rocket firing

The shape of the spectrum of radar echoes from precipitation.

Observations of aerosol layers in the upper atmosphere by laser radar.

Light aircraft-borne low cost phased array X band radar and display design requirements for weather detection and ground mapping

Digitized weather radar data models of intense storm cells with 1-2 km resolution and 10 dBZ reflectivity

Turbo and jet powered general aviation aircraft-borne weathervision memory radar system with digital processing technique to eliminate direct view storage tube

Doppler radar with polarization diversity.

The Budrio station of the meteoric radar system of the CNR for the systematic study of the upper atmosphere

Doppler radar measurements and observations of precipitation velocity fields.

Real-time estimates of mean velocity by averaging quantized phase displacements of Doppler radar echoes.

Meteor radar observations of long period waves in the 80-100 km altitudes range.

A new lidar for meteorological application.

New developments in FM-CW radar sounding.

A note on the FM-CW radar as a remote probe of the Pacific Trade-Wind Inversion.

Russian book on UHF meteorological radar techniques and applications covering precipitation and cloud monitoring radiolocation stations, lidar, sonar, echo signals and meteorological satellites

Doppler spectrum turbulence spreading updraft velocity estimation from observation by pulsed radar, noting average value and standard deviation in small thunderstorm

Dual wavelength synchronized and slaved radars for hail shaft boundaries detection based on average echo power ratio logarithm range derivative computation

Experimental investigation of the velocities of vertical motions in convective clouds

Certain results of radar studies of the evolution of convective clouds

Autocorrelation functions for meteorological scatterer velocity measurements in Doppler spectrum from linear, quadratic and logarithmic radar signal detectors

A comparison of radar-determined cloud height and reflected solar radiance measured from the geosynchronous satellite ATS-3.

Meteorological Doppler radar for measurements of particle velocity and horizontal winds inside convective storms, discussing signal processing and multiple radar method

METEOROLOGICAL ROCKETS

U SOUNDING ROCKETS

METEOROLOGICAL SATELLITES

NT AEROS SATELLITE

NT ELEKTRON SATELLITES

NT EOLE SATELLITES

NT METEOSAT SATELLITE

NT NIMBUS SATELLITES

NT NIMBUS 3 SATELLITE

NT NIMBUS 4 SATELLITE

NT NIMBUS 5 SATELLITE

NT SAN MARCO SATELLITE

NT SYNCHRONOUS SATELLITE

NT TIROS SATELLITES

Weather satellite Meteosat operational features and objectives, describing instrumentation, communication, data acquisition and processing facilities [DGLR PAPER 72-082]

Vertical resolution of temperature profiles obtained from remote radiation measurements.

The Meteosat system - Europe space contribution to global atmosphere observation.

A method for reproducing pictures transmitted by meteorological satellites.

Prospects for the utilization of satellite information in studies of the general atmospheric circulation

Utilization of meteorological data from satellites in studies of the general atmospheric circulation

Interpretation of numerical observations of meteorological satellites with infrared and monochromatic vision by means of high resolution satellites - The case of storm cloud systems

Meteorological satellites data acquisition, storage, reproduction, recall, use and costs

Antenna design for meteorological Meteosat satellite, transmitting and receiving radiation patterns

A synoptic climatology of satellite observed cloud vortices over the Southern Hemisphere.

Weather forecasting with the aid of satellite data. [AIAA PAPER 73-21]

Weather forecasting with the aid of satellite data. GARP Global Experiment design with satellite and balloon borne systems for meteorological observation and atmospheric research, discussing sounding data numerical simulation

Measurements of solar energy reflected by the earth and atmosphere from meteorological satellites.

Weather satellite capabilities - Present and future.

Aeros meteorological research satellite for F region aeronomic parameters and solar UV radiation measurements, discussing performance since launch

Mesoscale cloud systems analysis from meteorological observations and weather satellite data nephanalysis, applying to weather forecasting

Technological weather forecasting advances, including use of satellites, global meteorological network, computer techniques and mechanical recorders

The estimation of extratropical cyclone parameters from satellite radiation measurements.

A system of four geosynchronous satellites for global observations

Current trends in the refinement of scientific equipment for meteorological satellites

Book on earth satellites covering transmission technology, cost effectiveness and materials development for communication, meteorological, earth resources, navigational, research and military applications

Meteorological satellites in the service of aeronautics

Role of the meteorological satellites of the earth atmosphere observation system for the first global experiment of the 'Global Atmospheric Research Programme'

Providing satellite systems for the national weather satellite services.

International cooperation in the field of spatial meteorology

Book - Advances in satellite meteorology.

Meteorological satellite TV cloud cover photographs of cyclogenesis over Mediterranean Sea and cyclone arrival to European U.S.S.R. and Scandinavian Peninsula

Very short range local area weather forecasting using measurements from geosynchronous meteorological satellites.

Russian book on UHF meteorological radar techniques and applications covering precipitation and cloud monitoring radiolocation stations, lidar, sonar, echo signals and meteorological satellites

Use of meteorological rocketsonde and satellite radiation data for constant-pressure analyses at levels between 5 and 0.4 mb.

Geostationary meteorological satellite network development for static and cinematographic image transmission based on international cooperation

Stratospheric temperature measuring instrument development for Tiros N satellites and ESRO geostationary meteorological satellite development for cloud photography

Commencement of routine meteorological rocket observation at Ryori, Japan.

Communication satellite application to shipping company operations for cost benefits and alleviation of distress alerting, search and rescue, and heavy weather damage problems

Lidar anemometry and atmospheric sounding [ONERA, TP NO. 1151]

Prospects of developing an automated hydrometeorological system

Weather radar surveillance data short term distribution to airline users through weather message switching center, describing data coding, teletype network and data plotting operations

Weather satellite capabilities - Present and future.

Role of commercial aircraft in global monitoring systems.

Weather forecasting in the recent past, at the present time, and in the near future

Ground communications networks for aeronautical operations.

Technological weather forecasting advances, including use of satellites, global meteorological network, computer techniques and mechanical recorders

Digital readout wind measurement and indicator system for data acquisition, processing and display in airports for aircraft wind information service

Rational distribution of meteorological stations as a problem of operation studies

- VOLMET transmission automation with the aid of the 'DECLAM' system using a speech synthesizer 15 p1846 A73-32429
- Meteorological satellites in the service of aeronautics 15 p1907 A73-32562
- Participation of the Air Force Weather Service in the Eole experiment 17 p2206 A73-34940
- An automatic system for broadcasting weather data to international civil aviation 17 p2122 A73-34962
- Hydrometeorological data processing and dissemination techniques and equipment, with emphasis on computerized regional centers and space-based systems 18 p2295 A73-35907
- Providing satellite systems for the national weather satellite services. [AIAA PAPER 73-586] 18 p2373 A73-36077
- Survey of clear air turbulence detection methods. 19 p2430 A73-37822
- Weather modification activities, discussing state and local funding, research, federal programs, precipitation, hail and warm fog 21 p2729 A73-40092
- The Marsta micro-meteorological field project - Profile measurement system and some preliminary data. 21 p2732 A73-41567
- The role of computers in the development of numerical weather prediction. 24 p3108 A73-45085
- National Center for Atmospheric Research collected synoptic meteorological data from earth surface, upper air and satellite observations for handling on computers 24 p3075 A73-45087

METEOROLOGICAL STATIONS

U WEATHER STATIONS

METEOROLOGY

- NT AEROLOGY
- NT HYDROMETEOROLOGY
- NT LONG RANGE WEATHER FORECASTING
- NT MESOMETEOROLOGY
- NT MICROMETEOROLOGY
- NT NUCLEAR METEOROLOGY
- NT NUMERICAL WEATHER FORECASTING
- NT POLAR METEOROLOGY
- NT RADIO METEOROLOGY
- NT STATISTICAL WEATHER FORECASTING
- NT SYNOPTIC METEOROLOGY
- NT TROPICAL METEOROLOGY
- NT WEATHER FORECASTING
- Highlights of the COSPAR Symposium on the solar eclipse of 7 March 1970. 01 p0101 A73-10911

Principal trends of investigations in the field of theoretical meteorology performed in Hungary. 04 p0473 A73-15284

Russian book - Problems of the general circulation of the atmosphere. 05 p0392 A73-16226

Group classification of the hydrodynamics equations of an ideal fluid 12 p1487 A73-27409

Operations research methods application to meteorological forecasting, discussing optimization algorithm and feedback systems 15 p1907 A73-32354

Russian book - Analysis of meteorological conditions for aviation. 17 p2204 A73-34539

All-Union Meteorological Conference, 5th, Leningrad, USSR, June 21-25, 1971, Transactions. Volume 1 - General information, resolutions and plenary reports. Volume 2 - Weather prediction section. Volume 3 - Climate section. Volume 4 - Section on seeding effects on atmospheric processes 18 p2331 A73-35905

Evolution of the hydrodynamic methods for weather forecasting 18 p2331 A73-35906

Solar magnetic fields and their influence on the earth. 22 p2906 A73-41959

METEOR

U METEOROLIDS

METEOSAT SATELLITE

Optics, image scanning mechanism and response characteristics of visible/IR radiometer onboard stationary satellite for earth imagery 07 p0822 A73-18988

Dual channel high resolution radiometer of French synchronous meteorological satellite Meteosat for full time cloud coverage of earth in visible and IR ranges 11 p1368 A73-26508

Meteosat geosynchronous satellite for European meteorological space program, discussing picture taking, data broadcasting and rebroadcasting, central control station and peripheral terminals 12 p1549 A73-27380

Meteosat - Project of a European geostationary meteorological satellite - Status: 9/15/1972 13 p1689 A73-28743

METEERS

U MEASURING INSTRUMENTS

METHACRYLATE RESINS

U ACRYLIC RESINS

METHANE

Analytical model potential function application to Ar, Kr, Xe, nitrogen, methane and carbon dioxide, applying to different properties 01 p0122 A73-10850

Densities of compressed liquid methane, and the equation of state. 02 p0238 A73-12630

Methane pyrolysis in a low current DC discharge. 03 p0399 A73-13798

Methane-air mixtures burning velocity as function of equivalence ratio at atmospheric pressure, using bomb/hot-wire and corrected density ratio techniques 03 p0399 A73-14398

Titan atmosphere composition of methane hydrate with ammonia impurity, discussing hydrogen and hydrocarbon production, liquid water existence and greenhouse effects 04 p0497 A73-14973

Thermophysical properties of methane. 04 p0517 A73-15050

Pollutants from methane fueled gas turbine combustion. [ASME PAPER 72-WA/GT-3] 04 p0485 A73-15867

Deuterium-hydrogen ratio in Jupiter. 05 p0623 A73-17182

Investigation of NO formation kinetics in combustion processes - The methane-oxygen-nitrogen reaction. 06 p0767 A73-17731

The abundance of CH3D and the D/H ratio in Jupiter. 07 p0874 A73-19066

Distribution of methane and carbide in Apollo 11 fines. 07 p0900 A73-20188

Comparison of four simple models of steady flow combustion of pyrolyzed methane and air. 07 p0865 A73-20360

Intensity variation across Uranus disk during limb darkening-brightening cycles observations to test cloud absence theory, predicting limb brightening in methane bands 08 p1003 A73-20889

Measurements on the infrared lines of planetary gases at low temperatures. I - Nu-3 fundamental of methane. 08 p1003 A73-20891

Jupiter upper atmosphere temperature inversion to explain brightness temperature variation in 7.9 micron methane band, observing limb brightening 08 p1004 A73-20900

Some results of spectrophotometry of the methane absorption band (7250 A) on the Jovian disk 08 p1007 A73-21063

Investigation of molecular absorption in the atmospheres of the giant planets 08 p1007 A73-21064

Spectroscopy of Jupiter - 3200 to 11,200 A. 11 p1418 A73-25720

Phase equilibria in fluid mixtures at high pressures - The He-CH4 system. 11 p1399 A73-25889

Reactions of O/ID/ with methane and ethane. 12 p1466 A73-27126

Titan model arising from observations and methane-rich atmosphere thermodynamics, photochemistry and optical properties, considering origins and volatile content of outer planets satellites 12 p1539 A73-27140

Interpretation of hydrogen quadrupole and methane observations of Jupiter and the radiative properties of the visible clouds. 13 p1673 A73-28280

Use of narrow resonances in methane for frequency stabilization of a 3.39-micron He-Ne laser 13 p1627 A73-28763

The chemical stage in the mechanism of metal oxide reduction 13 p1581 A73-28937

Reduction of oxygen compounds of cobalt by methane 14 p1724 A73-30828

Upper stratosphere and lower mesosphere vertical mixing implications of methane observations at 50 km, assuming modelability by eddy transport 15 p1873 A73-32251

Vertical profiles of molecular H2 and CH4 in the stratosphere. [AIAA PAPER 73-518] 16 p2006 A73-33555

Investigation of molecular absorption features in the spectrum of Jupiter 16 p2070 A73-33839

Results of observations of methane /6190 A/ and ammonia /6441 and 6478 A/ absorption bands on the Jovian disk over a period of three years 16 p2070 A73-33840

Saturn - A study of the 3 nu sub 3 methane band. 17 p2231 A73-34765

New infrared spectra of the Jovian planets from 12,000 to 4000/cm by Fourier transform spectroscopy. I - Study of Jupiter in the 3 nu-sub 3 CH4 band. 17 p2234 A73-35617

Spectrophotometry of the 7250-A methane absorption band over the disk of Jupiter. 18 p2355 A73-36864

Molecular absorption in the atmospheres of the giant planets. 18 p2355 A73-36865

Balloon-borne measurement of stratospheric methane as function of altitude absorption spectroscopy, obtaining mixing ratios 21 p2680 A73-40076

Tropospheric and stratospheric vertical profiles of methane concentration via air sampling and gas chromatography, noting temporal and spatial variations 21 p2680 A73-40077

Theoretical model of vertical distributions of CO and CH4 in the mesosphere and upper stratosphere. 21 p2680 A73-40085

Vacuum IR spectrometer measurement of C 12 methane absorption band at 1.1 microns, describing technique for extending standards to photomultiplier region of spectra 21 p2743 A73-40936

Experimental study of heat and mass transfer in chemically reacting laminar boundary layers. 21 p2791 A73-41058

Formation of lunar carbide from lunar iron silicates. 21 p2780 A73-41643

Mode competition in the 3s sub 2-3p sub 4 transition in a neon laser with a methane absorbing cell. 22 p2869 A73-42256

Reaction of H atoms with CH2Cl2 - Application to the inhibition of flames. 22 p2819 A73-42779

Turbulent flow reactor for oxidation of moist CO and postoxidation phase oxidation of methane, using chemical sampling and gas chromatographic analysis 22 p2820 A73-42804

The temperature dependence of the half widths of some self- and foreign-gas-broadened lines of methane. 22 p2821 A73-42989

Stratospheric methane and nitrogen dioxide from infrared spectra. 23 p2976 A73-43887

The concentration of molecular H2 and CH4 in the stratosphere. 23 p2976 A73-43891

On the vertical distribution of carbon monoxide and methane in the stratosphere. 23 p2976 A73-43894

OH radical concentration in the stratosphere. 23 p2976 A73-43895

Multicolor astronomical photography of Jupiter using wideband filters, emphasizing Red Spot, atmospheric bright belts and methane absorption variations above clouds 23 p3032 A73-43941

Minimum detectable frequency deviations in output of He-Ne laser stabilized by external methane absorption cell 23 p2989 A73-44366

Methane absorption in the atmosphere of Saturn - Rotational temperature and abundance from the 3 nu sub 3 band. 24 p3129 A73-44445

Formation of spectral lines in planetary atmosphere. IV - Theoretical evidence for structure of the Jovian clouds from spectroscopic observations of methane and hydrogen quadrupole lines. 24 p3129 A73-44449

Methane absorption in the Jovian atmosphere. I - The Lorentz half-width in the 3nu/sub 3/ band at 1.1 microns. 24 p3132 A73-44537

Methane absorption in the Jovian atmosphere. II - Absorption line formation. 24 p3133 A73-44559

Line strength measurements of the 2 nu sub 3 band of methane. 24 p3066 A73-45320

METHIONINE

Effect of the administration of free amino acids and metabolic cofactors on the distribution of regional biogenic amine contents in the brain and blood of animals 09 p1040 A73-22864

METHOD OF CHARACTERISTICS

Possibility of using the method of time characteristics for solving applied problems concerning the bending of sandwich plates with allowance for creep of the materials 02 p0230 A73-11641

Evaluation of the method of characteristics applied to a pressure transient analysis of the B.A.C./S.N.I.A.S. Concorde refueling system. 02 p0133 A73-12645

Possibilities of rationalizing the design of flow-through turbomachine components 03 p0353 A73-13239

A new algorithm for three-dimensional method of characteristics. 03 p0337 A73-14201

Numerical solution to kinetic equations of rarefied supersonic steady gas flow normal to plate by method of characteristics 06 p0643 A73-17461

Intrinsic coordinate method of characteristics application to supersonic steady two dimensional nonisotropic inviscid flow, noting shock wave interaction [ONERA, TP NO. 1186] 09 p1072 A73-22714

Accuracy studies of the numerical method of characteristics for axisymmetric, steady supersonic flows. 10 p1171 A73-23602

Periodic method of characteristics for solution of hyperbolic partial differential equations of physical system specified by two boundary conditions at single spatial location 10 p1241 A73-23604

The shape of a supersonic three-dimensional nozzle with a maximum thrust 11 p1302 A73-26334

Minimum-energy terminal state control of first order linear hyperbolic systems in one spatial variable using the method of characteristics. 14 p1769 A73-30453

An explicit second order method of characteristics for the initial value problem in the case of quasi-linear hyperbolic differential-equations systems of the first order with two independent variables 15 p1899 A73-31361

Application of the method of characteristics in solving the universal equation of the plane boundary layer of a conducting fluid 15 p1918 A73-31407

Numerical study of the interaction of a shock-wave caused, supersonic, ionized-argon flow with electric and magnetic fields, using the method of characteristics 15 p1918 A73-31571

A contribution to the theoretical and experimental examination of the flow through plane supersonic deceleration cascades and supersonic compressor rotors. [ASME PAPER 73-GT-17] 16 p2047 A73-33494

The analysis of nonequilibrium, chemically reacting, supersonic flow in three dimensions using a bicharacteristics method. 17 p2151 A73-34891

An investigation of velocity flowfields in chemical laser nozzles. [AIAA PAPER 73-641] 18 p2322 A73-36199

Three-dimensional nosetip shape changes in hypersonic flow. I - Illustration of a mathematical model-characteristic method. [AIAA PAPER 73-762] 18 p2264 A73-36377

Linearized characteristics method for supersonic flow past vibrating shells. 21 p2632 A73-40426

German monograph - A method for the calculation of mixing and combustion processes in a rocket propulsion system with air-augmentation. 22 p2900 A73-42851

The calculation of flow in nozzles using a time-marching technique based on the method of characteristics. 24 p3079 A73-44894

METHODOLOGY

Algorithmic design methodology, describing functional representation of suitable effect chains 11 p1371 A73-24994

Advances in computational methods in structural mechanics and design; Proceedings of the Second U.S.-Japan Seminar, Berkeley, Calif., August 1972. 14 p1806 A73-30176

METHODS

U METHODOLOGY

METHYL ALCOHOLS

Electron spin resonance of manganous ions in frozen methanol solution. 04 p0414 A73-15025

Electrode kinetic studies on the anodic oxidation of methanol. 04 p0406 A73-15102

Hydrogen-air electrolytic fuel cell stack and auxiliary systems for use with methanol feedstock hydrogen generator 04 p0408 A73-15117

Cracking of Ti-6Al-4V in methanol solutions containing sulfates. 11 p1385 A73-26175

On the E sub 1-E sub 2 labeling of energy levels and the anomalous excitation of interstellar methanol. 22 p2914 A73-43005

METHYL COMPOUNDS

NT METHYL POLYSILOXANE

Methyl nitrite photolysis reaction products under various ambient gas mixture environments, noting irradiation time and gas pressure effects 10 p1186 A73-24656

The diagenesis and maturation of phytol - The stereochemistry of 2,6,10,14-tetramethylpentadecane from an ancient sediment. 11 p1326 A73-25466

Vibrational spectra of substituted hydrazines. IV - Raman and far-infrared spectra and structure of tetramethylhydrazine. 15 p1841 A73-32220

Vibrational spectrum of bis(trifluoromethyl) trioxide. 15 p1841 A73-32221

Microwave spectrum, structure, dipole moment and low frequency vibrations of dimethyl cyanamide. 24 p3066 A73-44771

METHYL POLYSILOXANE

IR spectroscopic study of polydimethylsiloxane thin film structure and polymerization under glow discharge 11 p1400 A73-26144

METRIC PHOTOGRAPHY

Testing of the Apollo 15 Metric Camera System. 08 p0968 A73-21703

METRIC SPACE

NT HILBERT SPACE

Integral bounds of generalized derivative solutions of second-order equations of elliptic type in the Lp metric and certain related embedding theorems 02 p0187 A73-12181

Estimation of the state vector of a plant by minimization of a distance in metric space when using discrete sampling 05 p0561 A73-17281

A class of almost periodic motions in systems with impulses 06 p0724 A73-18681

A non-parametric method with applications to pattern recognition and mode estimation. 06 p0672 A73-18805

Randomized solutions in stochastic-programming problems 09 p1112 A73-22845

Anisotropic and isotropic descriptions of physical process speeds in special relativity theory space-time metric 10 p1250 A73-24944

Model universe generalization to minisuperspace with Einstein equation solution and nondiagonal metric replacing wave equation, considering commutation relations for quantization in curved space 11 p1397 A73-25309

Integral estimates of the derivatives of solutions of elliptic homogeneous linear equations of arbitrary order with variable coefficients in the metric Lp, p ranging between 1 and infinity, and some of their applications 12 p1519 A73-27819

Estimation of the state vector of a linear plant by the method of distance minimization in metric space on the basis of continuous measurement of plant inputs and outputs 12 p1485 A73-27894

Method of trigonometric sums in the metric theory of Diophantine approximations of dependent variables 13 p1648 A73-28343

Metric tensor properties of physical space with deformable continuum in terms of kinetic stress function, approximating Einstein constant 15 p1945 A73-31041

Approximation of differentiable functions of numerous variables by Fourier sums in an L sub p metric 15 p1899 A73-31218

Kinematic invariants and their relation to chronometric invariants in Einstein's theory of gravitation 15 p1913 A73-31246

Probability series weak uniform convergence based on Billingsley-Topsoe uniformity theorem, using Borel set theory for separable metric space 16 p2031 A73-33107

A new theory of gravity. 16 p2036 A73-33123

Type-III Einsteinian void spaces with a G/2/Abelian group of motions and solvable G/3/ groups 17 p2212 A73-35565

Nonconformally plane relativistic recurrent-curvature spaces 17 p2212 A73-35567

Configuration space and phase space of a system with an infinite number of degrees of freedom 20 p2594 A73-39640

On the uniqueness of search directions in variable-metric algorithms. 21 p2726 A73-40837

Riesz representability, sigma-additivity and Daniell-integral properties of measures on uniform spaces 21 p2726 A73-40945

Nonsingular unified field model for charged particle described by interrelation of gravitational mass, global energy and effective charge, considering comparison with Reissner metric 22 p2887 A73-42432

Mathematical model for physical space transformation into subjective field metric for monocular vision 24 p3064 A73-44906

METRIC SYSTEM

U INTERNATIONAL SYSTEM OF UNITS

METROLOGY

UV light intensities calibration in astrophysics and high temperature metrology with thermal arc plasma

as radiation sources, discussing intensity standard establishment 02 p0199 A73-12715

International Symposium on Metrology, Bratislava, Czechoslovakia, September 5-8, 1972, Proceedings 03 p0305 A73-12893

General optimization criteria with allowance for economic factors and their use in measurement technology 03 p0305 A73-12894

Fundamentals of metrology involving quality and quantity description of reality, emphasizing interrelationship between measurement results in science and technology branches 03 p0305 A73-12895

Problem of forming classes of input processes in the study of errors in devices for statistical measurements 11 p1359 A73-25014

The problem of temperature in vacuum metrology. II 11 p1371 A73-26552

An analog-code follow-up converter based on second-harmonic magnetic modulators 12 p1475 A73-26766

Method of utilizing structural redundancy in a measuring system for processing experimental data with systematic errors 12 p1494 A73-26776

An optimal scheme for excitation of low-threshold magnetically modulated converters and analysis of their operation 13 p1591 A73-28855

Why exact metrology in an ultrahigh-speed cinematographic system - An application example: Calibration of image converters with a view to photometric measurements 21 p2694 A73-39951

Tape recording, off-line digitalization and time series analysis of dynamic field measurement analog data for computerized power spectral density calculation 22 p2859 A73-42197

MICE

Effects of a synchronizer phase-shift on circadian rhythms in response of mice to ethanol or ouabain. 20 p2513 A73-39481

MICHELL THEOREM

On the uniqueness of solutions of stress equations of motion of the Beltrami-Michell type. 14 p1809 A73-30254

Monograph on optimal structure design by linear programming and calculus of variations covering pin jointed frameworks, beams, circular sandwich plates, Michell continua, etc 19 p2502 A73-38364

MICHELSON INTERFEROMETERS

The quasi-linear intensity interferometer. 01 p0045 A73-10184

Design features and observational feasibility of high resolution Michelson interferometer for use in visible spectral range at coude focus of astronomical telescope 01 p0049 A73-10533

Minicomputer based CAMAC modular system for astronomical telescope instrumentation, discussing hardware and software interfaces, squad scaler, photoelectric photometer, Michelson interferometer and multichannel spectrometers 01 p0019 A73-10547

Michelson interferometer on Mariner 9 space probe for thermal emission spectrum measurement, discussing spectral resolution, external vibration problem and instrument performance 01 p0054 A73-11228

Optical sweep generator using single frequency He-Ne lasers with Michelson interferometer for mode selection to provide smooth tuning throughout Doppler width 03 p0319 A73-14065

Q switched carbon dioxide laser based on PM by rotating mirror in one arm of Michelson interferometer, establishing phase relationships 05 p0583 A73-16062

An application of the Michelson interferometer to nonthermalized spectral features in the night airglow. 08 p0963 A73-20870

Laser interferometric alignment sensor for the large space telescope /LST/. 08 p0970 A73-21732

Interferometric spectrometry for infrared astronomy. 11 p1369 A73-26517

A SISAM interferometer and a simple Michelson-interferometer with spherical mirrors for space application. 11 p1369 A73-26519

Michelson shearing interferometer with piezoelectric scanner for atmospheric optical mean transfer function measurements from airborne platform, using laser or white light sources 13 p1621 A73-29332

A modified interferometer for vibration amplitude measurement. 16 p2013 A73-32878

Interference phenomena obtained by replacing the mirrors of a Michelson interferometer by Fabry-Perot couples 19 p2429 A73-37540

Temperature measurement, monitoring, and control on a Michelson interferometer for ambient-temperature emission spectroscopy. 22 p2856 A73-42025

Measurement of the atmospheric brightness temperature at submillimeter wavelengths 22 p2847 A73-42330

Laser interferometer for displaying small rapid motions 24 p3092 A73-45468

MICROANALYSIS

Activated oxygen ashing of biological specimens for the microdetermination of Na, K, Mg, and Ca by atomic absorption spectrophotometry. 02 p0139 A73-12546

Study of the composition of inclusions in synthetic diamond crystals by microanalysis. 02 p0185 A73-12691

Trace phase analysis as an aid in the study of heterogeneous raw material impurities in powder metallurgy 04 p0464 A73-15370

Ion microprobe analyzers for solid surfaces high resolution mass spectrometric chemical analysis, using focused ion beam sputtering technique 07 p0822 A73-19171

Electron microprobe investigations of the oxidation states of Fe and Ti in ilmenite in Apollo 11, Apollo 12, and Apollo 14 crystalline rocks. 07 p0880 A73-19696

Mineralogy, petrology, and surface features of some fragmental material from the Fra Mauro site. 07 p0885 A73-19748

Microphysical, microchemical, and adhesive properties of lunar material. III - Gas interaction with lunar material. 07 p0892 A73-19832

Laser microspectral analyzer operation in Q switched mode, discussing microplasma generation under inert gas at variable pressure 07 p0836 A73-20162

Concentration profiles through thin oxide scales by ion-probe microanalysis. 09 p1101 A73-22402

Microchemical urinalysis. VIII - Determination of urinary 17-hydroxycorticosteroids. 11 p1324 A73-25138

X ray and microanalysis of Luna 16 recovered Fe-Ni fragment structure and composition, showing alpha solid solution octahedrite 12 p1538 A73-26893

A microspectrophotometer that records the first derivative of the absorption spectrum 12 p1496 A73-26957

Stereometric microanalysis of conglomerate, colony and dispersed structures of binary eutectic Fe, Al, Cu and low melting alloys 13 p1631 A73-28109

Luna 20 soil - Abundance and composition of phases in the 45-125 micron fraction. 13 p1677 A73-28330

Petrology of some lithic fragments from Luna 20. 13 p1677 A73-28331

Characterization of boron carbide with an electronic microprobe 13 p1645 A73-28346

Lunar core sample structure morphology and composition examined by microanalysis, revealing tenite to martensite transformation 15 p1930 A73-31220

Application of a microanalyzer to the investigation of the interaction between titanium and coatings 18 p2323 A73-35894

Spectral discharge plasma emission analysis with controlled electrical synchronization of laser vaporized microsamples of steel and wolframite 21 p2711 A73-40302

X ray and microanalysis of Luna 16 recovered Fe-Ni fragment structure and composition, showing alpha solid solution octahedrite 21 p2771 A73-41026

Microchemical urinalysis. IX - Determination of hydroxyproline in urine. 21 p2648 A73-41213

Lunar core sample structure morphology and composition examined by microanalysis, revealing tenite to martensite transformation 22 p2905 A73-41808

Experiment involving the application of the LMA-1 laser microanalyzer to the investigation of metallic materials 22 p2868 A73-42100

MICROBALANCES

Ultrahigh vacuum quartz spring microbalance for determination of evaporation rate and vapor pressure. 02 p0168 A73-11965

Evaporation rate and vapor pressure of selected polymeric lubricating oils. [ASLE PREPRINT 73AM-1A-3] 17 p2195 A73-34978

MICROBE U MICROORGANISMS

Investigation of stress state at fatigue crack tip by means of X-ray microbeam. 10 p1293 A73-24918

Ionic machine tools for microelectronic manufacture, discussing ion jets properties, optics and construction and implantation, micromachining and deposition technologies 16 p1987 A73-33088

MICROBIOLOGY NT BACTERIOLOGY

Cinematographic study of the development of subsurface colonies of *Staphylococcus aureus* in soft agar. 08 p0933 A73-21828

Electric discharge and microbiological experiments in simulated Jovian atmosphere for investigation of Jupiter life prospects 11 p1319 A73-26478

Results and prospects of microbiological studies in outer space. 11 p1320 A73-26487

Microbiological testing of Skylab foods. 12 p1464 A73-27075

International literature survey of microbiological space research for 1930-1970, discussing high altitude balloon, rocket and satellite experiments, weightlessness effects, mutagenesis, etc 15 p1838 A73-31501

Monitoring for microbial flora contamination on spacecraft surface, discussing cultural techniques and sampling methods for microorganisms detection and sterilization 16 p1976 A73-33698

Spacecraft microbial burden reduction due to atmospheric entry heating - Jupiter. 18 p2281 A73-36100

Microbial contamination of water - Traditional and space-age problems and approaches. [ASME PAPER 73-ENAS-33] 19 p2395 A73-37988

Protection of mineral oils from microbiological damage by compounds of the quinone group 21 p2723 A73-41069

MICROCALORIMETERS

U CALORIMETERS

Microchannel image intensifiers - Applications to ultrahigh-speed photography 06 p0697 A73-18860

MICROCIRCUITS

U MICROELECTRONICS

Thermal protective garment using independent regional control of coolant temperature. 07 p0785 A73-19481

MICROCRACKS

Cracking of Zircaloy as a result of unusual localized texturing. 02 p0183 A73-12756

Accommodation of the stress field at a grain boundary under heterogeneous shear by initiation of microcracks. 02 p0237 A73-12812

Fatigue scoring - A new form of lubricant failure. [ASLE PREPRINT 72LC-3B-1] 03 p0316 A73-14356

Microfracture effects on seismic wave propagation velocity and Q factor in lunar rocks by Rayleigh ultrasonic surface wave technique 04 p0497 A73-15125

Fretting-fatigue mechanisms and the effect of direction of fretting motion on fatigue strength. 05 p0581 A73-16128

Annealing of discontinuities in deformed aluminum 09 p1100 A73-21973

Transmission electron microscope study on initiation of fatigue crack in 18-8 austenitic steel. 09 p1104 A73-22523

Static and kinetic strength estimation of ionic and metal single crystals, discussing microcracks in brittle materials and surface quality and pore distribution effects 09 p1160 A73-22900

Ductile fracture strain criteria from known stress-strain relationships, predicting microscopic crack and void nucleation strain 09 p1164 A73-23322

Fatigue damage and dislocation structures in fcc metals surface layers, noting microcrack formation conditions 11 p1380 A73-25805

Shear decohesion mechanism of fatigue crack propagation in ductile metals under cyclic loads, considering secondary microfracture and creep cavitation effects at elevated temperatures 11 p1381 A73-25814

High-cyclic fatigue curves for annealed metals from investigation of defect buildups, lattice distortions, microcrack nucleation and fatigue crack growth 12 p1552 A73-27253

Machine parts fatigue life and linear cumulative damage at stresses below endurance limit, including plastic strain, microcracking and S-N curves 13 p1641 A73-29496

Nonlinear thermodynamics of irreversible processes for polymer microfracture process under mechanical, thermal, diffusion and chemical actions 14 p1766 A73-30479

German monograph on frictional fatigue failure covering microcrack initiation due to shear induced vibrational stresses 15 p1956 A73-32587

Some specific features of crack initiation and development in heat-resistant alloys under various loading conditions 20 p2578 A73-39376

Influence of grain size on effects of thermal expansion anisotropy in MgTi2O5. 21 p2752 A73-40893

Influence of hydrogen on the fracture micromechanism of OT4 and OT4-1 titanium alloys 21 p2721 A73-41231

Heat resistant materials cracking and fracturing caused by ductility loss at high temperatures, discussing cavitation mechanisms, microcracks, creep tests and time dependence 21 p2722 A73-41576

Deformation and microfracture characteristics of two-phase tungsten-composite materials sintered with the liquid phase 22 p2872 A73-41948

Metal fatigue phases investigation including strain hardening under cyclic loads and microcrack nucleation due to dislocation formation under hydrostatic pressure 23 p2993 A73-43966

The creep of sapphire filament with orientations close to the c-axis. 23 p2997 A73-44029

Mechanism of surface microcracking of matrix in glass-reinforced polyester by artificial weathering. 23 p2997 A73-44034

The influence of flaw density and flaw size distribution on the static and dynamic fatigue behaviour of graphite. 23 p2998 A73-44037

Fracture micromechanism characteristics and crack tip plastic zone formation effects on metal embrittlement, using elastoplasticity theory 23 p3047 A73-44277

MICRODENSITOMETERS

Sensitometric instruments for black and white and color photographic material and image measurements, including recording microdensitometer, reflection goniodensitometer, automatic granulometer and projection resolvometer 01 p0051 A73-10837

The suitability of the microdensitometer PDS 1000 for the measurement of radial velocities 20 p2565 A73-39065

MICROELECTRONICS

NT LARGE SCALE INTEGRATION

Flying-spot scanned or computer controlled electron beam fabrication system for generating high packing density pattern of LSI microelectronic circuit components 01 p0023 A73-10548

Low pass Butterworth and Chebyshev filters designed with Sallen-Key network for fabrication of microelectronic circuits 01 p0024 A73-10682

New design concepts for microwaves power transistor. 01 p0024 A73-10721

Microelectronic technology development and applications in transistor-transistor logic, medical devices, computers and thick film hybrid assemblies 02 p0148 A73-12593

Microelectronic technologies for SAM-D system, discussing thick film hybrid circuits and microstrip applications 02 p0148 A73-12594

Microelectronic metal-dielectric-semiconductor devices for physical properties of multilayer multiphase systems, noting field effect transistors, integrated circuits and electro-optical elements 03 p0349 A73-13656

Multilayer thin film microcircuit and printed circuit conductors partial capacitance and potential coefficients, using matrix method for approximate calculation 03 p0284 A73-14070

Terminal modeling and photocompensation of complex microcircuits. 05 p0557 A73-16508

The design of electronic equipment for biotelemetry using microcircuit techniques. 06 p0673 A73-17674

Reliability tests on miniature ceramic capacitors encapsulated by epoxy-novolac block polymer compounds 06 p0677 A73-18398

One degree of freedom fluid suspension gyros, direct drive gimbal motors and microelectronic control

assemblies review, noting miniature inertial platforms availability

07 p0820 A73-18941

Accelerated life tests of microelectronic components by operational power dissipation, noting efficiency and profitability

07 p0799 A73-19404

Failure modes of hybrid microcircuits in thick films

07 p0800 A73-19410

An experimental model of the microelectronic ultrasonic wire bonding mechanism.

08 p0972 A73-20734

Operational amplifier microcircuits intermittent failure due to input offset voltage drift, describing testing and analysis methods

08 p0944 A73-20740

Metallization failures caused by organic adhesives used in hybrid microelectronic devices.

08 p0944 A73-20747

Effect of engineering-design factors on the parameters of microstrip transmission lines

08 p0951 A73-21109

Transmission zeros in microstrip discontinuities, considering structure effective width for TEM and higher modes

09 p1049 A73-22315

Book - Heat transfer in microelectronic equipment: A practical guide.

10 p1194 A73-23900

Determination of the proper integration level of the unified functional units of a complex of statistical-measurement methods

11 p1340 A73-25002

Book - Engineering means in automatic control.

12 p1481 A73-26751

Diagnostic tests and failure checkout for interconnected combinational micrologic circuit components in manufacturing process, tabulating individual failure functions

12 p1474 A73-26755

Methods of constructing control and diagnosis tests for homogeneous microelectronic circuits

12 p1476 A73-26757

Automation considerations in technological methods for microcircuit fabrication, emphasizing electron-ion technology

12 p1477 A73-26783

Microelectronics developments and limitations, considering bipolar IC, metal-dielectric-semiconductor structures and optoelectronic communication links

12 p1480 A73-27267

Determination of parameter tolerances for microstrip transmission lines

12 p1470 A73-27580

Coupled asymmetrical microstrip transmission lines odd and even mode wave impedances as functions of conductor strip width and spacing

12 p1481 A73-27582

Design of temperature-controlled substrates for hybrid microcircuits.

13 p1588 A73-28044

Reliability considerations in hybrid microcircuits.

13 p1588 A73-28045

Thermal/electrical design of spaceborne microelectronic components.

13 p1588 A73-28046

Pulse rebalance gyro electronic system with hybrid microcircuitry for digitizing sensor inputs to computer

13 p1589 A73-28047

Ion implantation method and diffusion process for microelectronics semiconductor components manufacture

13 p1590 A73-28573

Air traffic control technology progress review and future forecast, noting microelectronics and automation need in civil avionics

15 p1960 A73-32479

Ionic machine tools for microelectronic manufacture, discussing ion jets properties, optics and construction and implantation, micromachining and deposition technologies

16 p1987 A73-33088

International Microelectronic Symposium, Washington, D.C., October 30-November 1, 1972, Proceedings.

16 p1989 A73-33466

Investigation of mounting discrete chip components for hybrid microelectronic applications.

16 p1989 A73-33467

Epoxy adhesive materials evaluation for microelectronic assemblies of hermetically sealed hybrid circuits with semiconductor chips and thin film substrates

16 p1989 A73-33468

Mathematical functional modular building block implementation in LSI microelectronics for signal and data processing, discussing primitive functions and 8-bit family design example

17 p2138 A73-35229

Analysis and temperature control of hybrid microcircuits.

[ASME PAPER 73-ENAS-6]

19 p2412 A73-37968

An elusive open-circuit failure mode in thin-film chip resistors.

19 p2410 A73-38444

Failure analysis of wire bonds.

19 p2436 A73-38446

Microwave integrated circuit technology.

19 p2411 A73-38535

A method of computer design of microelectronic equipment

20 p2534 A73-38852

Morphological indices of digital microelectronic structures

21 p2660 A73-40016

Physical modeling of active microcircuits for the SHF range

21 p2668 A73-40020

Viscous dielectric materials for application in microwave microcircuits.

21 p2668 A73-41589

Microelectronic circuitry for monitoring stray electromagnetic energy coupled into electroexplosive device, using fiber optic transmission with photovoltaic energy conversion to eliminate wiring caused interference

22 p2822 A73-41794

Low pass filter design for FDM and PCM systems, discussing active RC realization techniques and microelectronics model tests

22 p2832 A73-42293

Development of a hybrid microelectronics solid state relay for 2500 volts isolation and -120 C to 80 C thermal cycling range.

22 p2835 A73-42914

A square-law voltmeter based on elements with a thermal coupling

24 p3071 A73-44544

MICROFILMS

Computer output microfilm system technology assessment, discussing two dimensional acousto-optic laser scanner to write on dry process film

06 p0700 A73-18294

MICROGRAPHY

U PHOTOMICROGRAPHY

MICROHARDNESS

Microhardness anisotropy of hardened and aged Be single crystal as function of purity

01 p0067 A73-11353

Changes in microhardness as a basis of service life estimates for smooth AlCuMg specimens

03 p0321 A73-13135

Borating kinetics and coating phase composition and thickness on cobalt and cobalt base alloys by metallographic, microhardness and X ray analyses

09 p1103 A73-22467

Influence of the combined effect of plastic deformation and high temperatures on the diffusion mobility of carbon

09 p1108 A73-23241

Carbon content relationship to rhodium microhardness, determining cast specimens phase composition by X ray analysis and microstructure observations

10 p1234 A73-24424

Relaxation of diagonal length and indentation depth of Vickers microhardness measurements on plastics

11 p1388 A73-25449

Influence of gas carburizing on the structure and properties of electrolytically deposited chromium

11 p1375 A73-26734

Study of the variations of the microhardness of the surface layer hardened by ball rolling in relation to the heating temperature

12 p1502 A73-26799

Some physical properties of stephanite in the phase transition region

13 p1667 A73-28002

Evaluation of torsional fatigue damage from changes in the fatigue properties and microhardness.

13 p1635 A73-28522

Machine for measuring hardness and microhardness at high temperatures.

13 p1613 A73-28524

Testing machine with control panel and vacuum chamber for microhardness measurement at high temperatures with precise test point selection and indentation observation capability

13 p1613 A73-28525

Thin ferrosilicon intermediate cylindrical layer tensile strength, microhardness and yield point determination at 20-1000 C

13 p1624 A73-29064

Morphology of the structure and the microhardness of Al-Ni, Cu, Be, Fe, Co eutectic compositions

14 p1760 A73-30588

Influence of heating to high temperatures in vacuum on the electrophysical properties of niobium single crystals

14 p1763 A73-30722

Hard WC-Co alloys as dispersion strengthened materials

15 p1887 A73-31591

Niobium-gold alloys crystal structure, phase diagrams, peritectic crystallization and microhardness, noting intermetallics formation by solid state reactions

16 p2026 A73-33957

Influence of interstitials on the behavior in tension of niobium between 20 and 1000 C

17 p2193 A73-35624

Characteristics of the temperature dependence of the microhardness of a highly heat resistant dispersion-hardened nickel alloy

18 p2324 A73-36765

Influence of prolonged aging on the behavior of the microhardness and substructure of E1257 austenitic steel

18 p2324 A73-36806

Thin ferrosilicon intermediate cylindrical layer tensile strength, microhardness and yield point determination at 20-1000 C

18 p2320 A73-36896

Changes in the microhardness of lithium fluoride crystals subjected to cyclic elastic compression

19 p2470 A73-37954

The preparation and anisotropic hardness of tantalum single crystals with principal orientations.

20 p2575 A73-38637

Investigations regarding structure, preparation, and hardness properties in the system Ta-Hf-C-N

22 p2873 A73-41949

The nature of the high microhardness of surfaces strain-hardened by friction

23 p2984 A73-43467

Influence of diffusion coating and heat treatment on the wear resistance of VT-8 alloy

23 p2990 A73-43485

MICROINDENTATION

U MICROHARDNESS

MICROINSTRUMENTATION

Micromensor measurement of spatial correlation between pressure fluctuations of turbulent boundary layer

08 p0965 A73-21188

The electroretinogram, as analyzed by microelectrode studies.

09 p1047 A73-23318

Decatron indicator for a micromanipulator controlled by a stepping motor

14 p1722 A73-30850

Theory and performance of a tritium battery for the microwatt range.

21 p2737 A73-39922

Ultraminiature X-ray fluorescence spectrometer for in-situ geochemical analysis on Mars.

21 p2765 A73-40241

Two channel transistor amplifier design with negative capacitance correction for microelectrode applications

24 p3062 A73-44723

Intracellular measurements in a closed hyperbaric chamber.

24 p3065 A73-45072

MICROMANOMETERS

U MANOMETERS

MICROMETEORITES

Lunar surface meteoritic material composition, distribution and amounts from trace element studies, discussing micrometeorites, ancient planetesimal debris and recent crater-forming projectiles

23 p3030 A73-43758

MICROMETEORITIDS

NT METEOROID DUST CLOUDS

NT ZODIACAL DUST

Micrometeoroid particle flux impacting on lunar surface measured by observation of Surveyor 3 glass surface craters

02 p0214 A73-12256

Nighttime atmosphere emission of atomic oxygen /5577 A/ and its connection with penetrating micrometeorites

07 p0818 A73-19592

Lunar micrometeoroid flux, calculating rocks survival time before impact damage and mass wasting rate by single particle abrasion

07 p0895 A73-19865

Scanning electron microscope and energy dispersive X-ray analysis of the surface features of Surveyor III television mirror.

07 p0872 A73-19899

Micrometeoroid mass, velocity and composition from Heos 2 and Helios satellite experiments, using hypervelocity dust particle impacting plasma emission

10 p1218 A73-24119

Meteoritic particles orbits secular evolution under planetary perturbation and Poynting-Robertson effects, considering oscillating orbital elements long term variations via simplified model

14 p1795 A73-29842

Magnetogasdynamic compression of a coaxial plasma accelerator flow for micrometeoroid simulation.

15 p1919 A73-31932

French monograph - Study of craters formed on glass surfaces by the impact of artificial micrometeoroids.

15 p1898 A73-32591

A linear accelerator for simulated micrometeoroids.

17 p2145 A73-34274

Meteoritic ions in the D and E-regions.

18 p2310 A73-36132

Meteor ions in the polar ionosphere according to the rocket mass-spectrometric measurements and theoretical calculations.

18 p2311 A73-36146

Differential equations for ballistic motion of meteoric particles in earth atmosphere, noting orbit stability

19 p2480 A73-37237

Interaction of the lower thermosphere with the solid component of the interplanetary medium.

21 p2682 A73-40158

Investigations of meteoritic matter in the vicinity of the earth and the moon from the orbiting station Salyut and the moon satellite Luna 19.

21 p2775 A73-41409

Preliminary measurements of spherules of the Pontina Plain and of micrometeorites of Apollo 12 and related impact studies.

21 p2775 A73-41412

Near-earth micrometeorite flux measurement by rocket-borne acoustic detectors, noting consistency with previous observations

21 p2775 A73-41415

Ablation debris and primary micrometeoroids in the stratosphere.

21 p2775 A73-41419

Micrometeorite and cosmic dust studied for solar system and universe origin and evolution and for medium range weather forecasting, discussing cosmic matter infall to earth

22 p2913 A73-42988

Micrometeoroid flux measurement during the 1970 Geminid meteor shower.

22 p2915 A73-43035

A magnetogasdynamic accelerometer for the simulation of micrometeoroids

23 p2966 A73-43781

Urey hypothesis for tektites origin via earth-comet collisions dependence on cometary structure, considering solid nucleus vs meteoric particle swarms

23 p3033 A73-43953

MICROMETEOROLOGY

Fine structure of the temperature stratification in the troposphere and stratosphere.

07 p0848 A73-20348

Correlation of microthermal turbulence data with meteorological soundings in the troposphere.

08 p0985 A73-21382

Temperature and humidity spectra in the atmospheric surface layer.

11 p1393 A73-25693

Logarithmic wind profile in neutral barotropic planetary boundary layers, discussing von Karman constant

11 p1394 A73-25717

Study of droplet size distribution in a two-phase stratiform cloud - A numerical experiment

13 p1653 A73-28877

Numerical model of a two-phase stratiform cloud taking its microstructure into account

20 p2583 A73-39185

A physical-numerical model for the determination of the meteorological environmental effects produced by cooling towers

23 p3003 A73-43995

MICROMETEORS

U MICROMETEORIODS

MICROMETERS

Combined determination of the turn value and screw errors of the position micrometer of an astronomical universal instrument

19 p2432 A73-38553

MICROMINIATURIZATION

NT LARGE SCALE INTEGRATION

Fast response coaxial miniature thermoelements for rapid temperature change measurements in droplets, turbulence and bubbles

12 p1499 A73-27875

Detection of random chip defects in monolithic microcircuits.

17 p2135 A73-34732

Technological forecasting for microcomputer architecture and fabrication on LSI chip, considering cost effectiveness, pins number, packing density, power and speed factors

17 p2131 A73-35226

MICROMINIATURIZED ELECTRONIC DEVICES

NT MICROMODULES

Surgically implanted single and multichannel telemetry systems for monitoring single and multiple physiological parameters, discussing size and power requirements

03 p0271 A73-14302

Miniature pressure transducers with a silicon diaphragm.

09 p1084 A73-22692

Field of view and target uncertainty in visual search and inspection.

11 p1322 A73-25181

Feedback in microminiaturized transistor amplifiers

21 p2659 A73-40010

MICROMODULES

Switching stepdown dc-to-dc converter with analog signal to discrete interval converter, hybrid micromodule and two-loop control subsystem, discussing circuitry and performance

03 p0283 A73-13935

A method of computer design of microelectronic equipment

20 p2534 A73-38852

MICROMOTORS

Telecontrol system for particle accelerator target displacement via micromotor electronic control with emphasis on adaptation to ultrahigh vacuum chamber simulating ionospheric plasma

22 p2838 A73-41868

MICROORGANISMS

NT ANAEROBES

NT AZOTOBACTER

NT BACILLUS

NT BACTERIA

NT NITROBACTER

NT PROTOZOA

NT STAPHYLOCOCCUS

Resistance of soil microorganisms to starvation.

02 p0136 A73-12627

Biological, chemical and cytological methods of microorganism detection integrated into single instrument

03 p0272 A73-14320

Russian book on radiation genetics of microorganisms covering lethal and mutagenic action of radiation on fungi, microscopical algae, bacteria and viruses

04 p0410 A73-15701

Microorganisms induced biological corrosion, considering oxidizing agents, inhibitors, protective coatings and cathodic protection

06 p0704 A73-17507

Microflora of a sealed cabin with human subjects in a 3-day experiment with reduced temperature and high relative humidity

06 p0657 A73-17697

Survival of micro-organisms on the moon.

07 p0780 A73-19111

A method for studying the action of high-intensity electric fields on microorganisms

10 p1184 A73-24419

A technique for extracting Radiolaria from radiolarian cherts.

11 p1324 A73-25141

Results and prospects of microbiological studies in outer space.

11 p1320 A73-26487

Estimating the number of terrestrial organisms on the moon.

11 p1320 A73-26488

Upper Cretaceous Spumellariina from the Great Valley Sequence, California coast ranges.

13 p1605 A73-28023

Late Precambrian microfossils - A new stromatolitic biota from Boorthanna, South Australia.

14 p1713 A73-29723

Responses of indigenous microorganisms to soil incubation as viewed by transmission electron microscopy of cell thin sections.

14 p1714 A73-29724

Biological indicators and the effectiveness of sterilization procedures.

16 p1976 A73-33692

Formaldehyde gas as a sterilant.

16 p1976 A73-33694

Microorganism heat sterilization process design and control based on logarithmic thermal destruction and Bigelow temperature coefficient models, determining lethality by statistical procedure

16 p1976 A73-33695

The synergistic inactivation of biological systems by thermoradiation.

16 p1976 A73-33696

Ten years of development of the Planetary Quarantine Program of the United States.

16 p2281 A73-35966

The significance of outer planet satellite quarantine constraints on aim-point selection.

18 p2359 A73-36096

Developments in the analysis of planetary quarantine requirements.

22 p2803 A73-42159

Safety margins in the implementation of planetary quarantine requirements.

22 p2803 A73-42161

Soil microbiological tests to evaluate Antarctica as Mars environment model for quarantine standards

22 p2803 A73-42162

Estimation of the biological danger of the very high energy component of space radiation.

22 p2805 A73-42180

Directed Panspermia theory of terrestrial bioevolution, suggesting microorganism transmission to earth by intelligent technologically advanced civilization via spacecraft

24 p3058 A73-44553

MICROPARTICLES

Studies of plasma production at hypervelocity microparticle impact.

13 p1667 A73-29424

Method for the determination of impurity particle dispersion in fuels and lubricants

15 p1876 A73-31834

Holographic investigations and measurements in a cloud of moving microparticles

21 p2696 A73-39979

MICROPHONES

Contribution to the study of noise measured by a microphone placed in a gaseous flow

03 p0290 A73-12973

Microphone radiated acoustic power directivity measurement enhancement by integral transform, matrix inversion and relaxation techniques, considering application limits, resolution, noise sensitivity and computation

[AIAA PAPER 73-1040] 24 p3090 A73-44865

A new device for measuring local acoustic power output of subsonic jets.

[AIAA PAPER 73-1042] 24 p3090 A73-44866

MICROPHOTOGRAPHS

Methods of birefringence-parameter determination in tension studies by photoelasticity techniques

05 p0635 A73-17077

MICROPHOTOMETERS

U PHOTOMETERS

MICROPLASMAS

Ionization energy of adhesion levels and heat-generation centers in the microplasma volume in germanium p-n junctions

08 p0995 A73-21274

MICROPOLAR FLUIDS

Boundary layer growth of a micropolar fluid.

02 p0154 A73-12093

Micropolar model of blood steady flow through rigid circular tubes, presenting equations solutions and velocity profiles

03 p0266 A73-13302

Numerical solutions to flow and heat transfer characteristics of free convection micropolar flow with Newtonian solvent substructure

08 p1023 A73-21260

Decay of the kinetic energy of compressible micropolar fluids.

20 p2547 A73-39341

Statistical continuum mechanics and constitutive theories governing microfluid behavior, noting relations with aid of tables

20 p2547 A73-39343

Solution of nonlinear problems in magnetofluid-dynamics and non-Newtonian fluid mechanics through parametric differentiation.

22 p2843 A73-42556

Lubricating properties of micropolar fluids in composite and step slider bearings, obtaining analytic expressions for load carrying capacity and skin friction

24 p3092 A73-44409

MICROPOROSITY

The role of pore size in the ultimate densification achievable during P/M forging.

04 p0456 A73-15799

Correlation between pore formation at grain boundaries and internal friction during creep of nickel

09 p1099 A73-21970

The role of micropores in the fracture of forged sintered steel.

13 p1639 A73-29468

Some consequences of introducing the geometrical-dynamic characteristic ratio in studies of the heat transfer to surfaces with artificial roughnesses or to microwaving surfaces

19 p2504 A73-37655

MICROPROGRAMMING

Microprogrammable processors applied to telemetry processing systems.

09 p1057 A73-23411

Microprogrammed digital filters for strapdown guidance application.

12 p1483 A73-27168

CPU design for command and control system with programmable read-only control memory, discussing self microdiagnostics for control store error detection

17 p2144 A73-35258

Designing with microprocessors instead of wired logic asks more of designers.

23 p2956 A73-44122

MICROPULSATIONS

NT GEOMAGNETIC MICROPULSATIONS

Short period pulsating radio auroras properties, determining apparent Doppler characteristics of long period echo sequences

01 p0017 A73-10340

Asymmetric eigenmodes in a simple model plasmasphere.

03 p0345 A73-12882

MICROROCKET ENGINES

Continuing development of the short-pulsed ablative space propulsion system.

03 p0356 A73-13457

The RIT engine family. - From microthruster to main propulsion units.

04 p0488 A73-15716

Emitter efficiency increase in annular colloid microthrusters with single sharp tips for high specific charge of conducting liquid droplets under low potential

04 p0488 A73-15723

Direct measurement of colloid microthruster thrust and propellant mass flow rate, using microbalance

04 p0433 A73-15727

Description of power conditioning systems intended for satellite stabilization thrusters

04 p0489 A73-15732

Design and realization of microthruster temperature control subsystems - Optimization through refinement of a mathematical model

04 p0489 A73-15735

Geostationary satellites stabilization by microthrusters based on solid sublimation or hydrazine monopropellant, describing propulsion system development 07 p0866 A73-18926

Subliming solid propellant microthruster for satellite stabilization, discussing operational principles and design features 07 p0866 A73-18927

Heat exchanging and catalytic dissociation of ammonia flowing through tubes - Application to micropropulsion. 07 p0867 A73-18931

Visual display of the spatial distribution of colloidal particle beams. 09 p1136 A73-23448

Scattering of light by the medium generated by a space vehicle. I - Emission of vapor jets by spacecraft microthrusters. 12 p1549 A73-27641

MICROSCALES

U MICROBALANCES

MICROSCOPES

NT ELECTRON MICROSCOPES

NT ION MICROSCOPES

NT OPTICAL MICROSCOPES

Electrical measurements, metallographic microscopy and chemical analysis for failure analysis 07 p0800 A73-19409

Automatic microscopy for mitotic cell location. 12 p1464 A73-27144

Laser beam scanned 1.1 GHz acoustic microscope based on photoconductive CdS piezoelectric transducer 13 p1614 A73-28580

Image contrast in a microscope with synchronous scanning of the object by point or raster field diaphragms 13 p1616 A73-28771

MICROSCOPY

NT ULTRAVIOLET MICROSCOPY

Application of optical methods to the verification of microscopic data on polymer materials 04 p0468 A73-15693

Real time high resolution 100 MHz acoustic image or holograph microscope using optical measurement of boundary displacement by incident angular sound wave 13 p1614 A73-28579

Reflected light holographic microscopy of moving objects. 16 p2014 A73-33174

Phase measurement microscopy consisting of phase modulation optical system using interferometry and optical heterodyning, and phase detection system using digital processing 21 p2698 A73-40144

MICROSEISMS

The elastic energy and character of quakes in solid stars and planets. 11 p1420 A73-25894

MICROSONICS

Book - RCA advanced technology. 10 p1216 A73-23781

Microsonics /acoustic surface waves/ technology developments covering materials, heteroepitaxial systems, propagation, electron phonon interaction, acoustic amplifiers and waveguides, electromechanical transducers and signal processing 10 p1223 A73-23782

MICROSTRUCTURE

NT METEORITIC MICROSTRUCTURES

NT WIDMANSTATTEN STRUCTURE

Structural changes during the deformation of molybdenum alloys 01 p0061 A73-10252

Structural changes following annealing in a dispersion-strengthened tungsten alloy 01 p0062 A73-10261

Grain growth in alloyed molybdenum under conditions of creep 01 p0063 A73-10486

Intergrain boundary shape effects on the impact strength and character of brittle fracture 01 p0064 A73-10606

Investigation of structural changes during the heat treatment of carbonized fibers with the aid of a scanning electron microscope 01 p0068 A73-11246

New morphological element of the microsurface of ductile fracture of hypoeutectoid steel. 01 p0066 A73-11336

Structured changes and phase transformations of welded joints of Al alloy with Cu addition during welding thermal cycles 01 p0067 A73-11352

Microstructure, hardness, electrical resistivity and thermal properties of Ni alloys with Al and Ta, noting composition of heat resistant alloys 01 p0067 A73-11436

Sintering of nonstoichiometric nickel monoxide 02 p0179 A73-11546

Metallographic macro- and microstructural study of semiconductor compounds, discussing single crystal imperfections, polycrystals and semiconductor films 02 p0199 A73-11582

Refinement of primary silicon crystals in a hypereutectic Al-20% Si alloy by sulphur addition. 02 p0179 A73-11597

Ti-Al-V alloys ac differential measurement method for metallurgical processing and microstructure effects on superconducting critical temperature and magnetic permeability/susceptibility 02 p0200 A73-11843

Vibratory loads effect on metal microstructure under sliding friction, noting rheological criteria for fretting corrosion wear resistance 02 p0180 A73-11934

Direct observation of the magnetic microstructure in niobium-based superconducting alloys subject to deformation 02 p0201 A73-12554

Microstructural, mechanical and thermal properties of Nb-W-Ti-Zr alloys, noting cold rolled sheet products 02 p0182 A73-12580

Microstructure and phase relations for Ti-Mo-Al alloys. 02 p0182 A73-12751

Structural studies of Laves intermetallic phase precipitation in Fe-Ta alloys by microscopic, X ray diffraction and electron probe techniques 02 p0182 A73-12754

Microstructure and microsegregation effects in the intergranular corrosion of austenitic stainless steel. 02 p0183 A73-12765

Interdendritic structures of a directionally solidified cobalt-base alloy. 02 p0184 A73-12770

High resolution marker transport sintering study. 02 p0175 A73-12771

Use of LEED, Auger emission spectroscopy and field ion microscopy in microstructural studies. 02 p0171 A73-12843

Fatigue induced microstructural changes in metals and alloys, considering crystal lattice defects, crack formation and propagation, dislocations and strengthening effects 03 p0321 A73-13133

Boundary-layer methods in microstructure theories of elasticity. 03 p0390 A73-13330

Changes in the fine structure of heat-resistant nickel-chromium alloys during the creep process 03 p0324 A73-13505

New magnesium alloys intended for operation at elevated temperatures 03 p0324 A73-13513

Influence of microstructure on the corrosion behavior of Ti-2% Ni in hot acidic chloride solutions with particular reference to weld regions. 03 p0325 A73-13730

Microstructure and plastic deformation of the Ni4Mo alloy. 03 p0325 A73-13804

Liquation-induced microinhomogeneity of heat resistant submerged-arc-smelted steel 4Kh12N8G8MFB /EI481/ 03 p0326 A73-13829

Secondary maximum grain size and even-grained texture in the region of low and moderate deformations during recrystallization of certain nickel- and iron-based alloys 03 p0326 A73-13967

Substructural changes during high-temperature creep deformation of aluminum single crystals 03 p0327 A73-13978

Ni, Si and Mn alloying effect on structural transformations, phase composition and mechanical properties of cast Cr-Ni steels 03 p0327 A73-14002

Phase diagrams, microstructure and interface composition of two phase metallic particles from lunar soils and rocks, determining equilibrium temperature and equilibration time 03 p0376 A73-14110

Microstructures and transformation kinetics of continuously cooled carbon free Fe-Mo-Ni alloys. 04 p0463 A73-15311

Microstructure alignment in Ni-In system eutectic alloys due to directional solidification 04 p0463 A73-15312

Influence of microstructure on the mechanical properties and stress corrosion susceptibility of 7075 aluminum alloy. 04 p0463 A73-15314

Acoustic model of HF damping and microstructure of dispersed aluminum oxide ceramics systems, using Hugoniot elastic limits for Young modulus and fracture determination 04 p0468 A73-15373

Mechanical properties and structure of certain internally oxidized copper alloys 04 p0464 A73-15500

The effect of alloying elements on creep rupture strength and microstructure of 12 percent chromium heat resisting steel. 04 p0465 A73-15581

Effects of heat treatment on the mechanical properties and microstructure of Inconel Alloy 718. 04 p0465 A73-15582

High temperature strength and microstructure of nickel-base heat resisting No. 64BC alloy. 04 p0465 A73-15583

Influence of cold deformation and subsequent heating on the structure and properties of dispersion-strengthened nickel 04 p0466 A73-15666

Method for fractographic investigation of high-tensile aluminum alloys. 04 p0466 A73-15674

Motion, constitutive and energy balance equations for materials with microstructure, considering elastic bodies 04 p0514 A73-15680

The effect of substrate temperature on the structure of titanium carbide deposited by activated reactive evaporation. 04 p0456 A73-15757

The influence of ion bombardment on the microstructure of thick deposits produced by high rate physical vapor deposition processes. 04 p0456 A73-15760

Strength and microstructure of nickel-base superalloys after long term heating. 05 p0587 A73-16622

Instrumentation for metallographic structure examination. 05 p0576 A73-16751

Structure and properties of the weld metal in maraging N18K9M5T steel 06 p0697 A73-17879

Weldability, corrosion resistance and heat resistance increase in Nb alloyed steels, noting aging temperature effects and microstructure 06 p0706 A73-17886

The 'second' plane distortion problem of the theory of micropolar elasticity. 06 p0761 A73-17891

Structural and phase transformations in silicon steels during heat treatment 06 p0707 A73-18035

Structure of the borated layer after diffusion saturation with other elements 06 p0707 A73-18040

Structural changes arising in nickel under the action of ultrasound and subsequent thermal annealings 06 p0708 A73-18053

Field-ion microscopic investigation of the microstructure of deformable superconducting niobium-based alloys 06 p0736 A73-18115

Possibilities of changing the microstructure of turbulent flow in investigations of convective heat transfer 06 p0686 A73-18133

X ray analysis of high coercivity Ticonal alloy single crystal microstructure after isothermal thermomagnetic treatment 06 p0709 A73-18210

Study of fatigue crack propagation by X-ray diffraction approach. 06 p0698 A73-18496

The influence of stress intensity and microstructure on fatigue crack propagation in ferritic materials. 06 p0710 A73-18498

Cu-Ni-Zn alloys high ambient temperature tensile and fatigue strengths due to recrystallization and precipitation produced fine grain microstructure, describing annealing and cold working process 06 p0711 A73-18751

Influence of condensation temperature on microstructure and tensile properties of titanium sheet produced by high-rate physical vapor deposition process. 06 p0711 A73-18752

Directionally solidified NiAl-Cr and NiAl-Mo eutectic composites microstructural stability as function of time and temperature 06 p0711 A73-18753

Substructure and dispersion hardening in aged, cold worked, and annealed Al-4 wt pct Cu alloy. 06 p0711 A73-18754

Dendritic solidification of Cu-Ni alloys. II - The influence of initial dendrite growth temperature on microsegregation. 06 p0712 A73-18757

Morphological factors influencing the initial stages of coarsening in the Al-Al3Ni eutectic composite. 06 p0712 A73-18761

Effect of grain refinement on the microstructure and mechanical properties of 4340M. 06 p0713 A73-18773

Occurrence of oriented structures under the action of a laser beam in metals 07 p0839 A73-19658

Microstructure and mineral compositions of impact produced lunar chondrules from Apollo 14 breccia by electron microprobe X ray analyzer 07 p0882 A73-19722

Deformation of silicates in some Fra Mauro breccias. 07 p0883 A73-19734

Structure of lunar glasses by Raman and soft X-ray spectroscopy. 07 p0788 A73-19737

MICROSTRUCTURE

Fine grained weld structures.

- 07 p0832 A73-20273
Structural service life from carrying capacity during rupturing stage, noting microstructural properties effect
- 07 p0917 A73-20504
Investigation of the structural changes in austenite during martensitic transformation in steels with high stacking-fault energy
- 07 p0841 A73-20521
Application of the method of polarizational ultraviolet fluorescence microscopy to study giant muscle fibers *Balanus rostratus* Hook
- 08 p0930 A73-21135
The influence of microstructure on creep properties of low alloy ferritic chromium-molybdenum-vanadium steel.
- 08 p0980 A73-21675
Influence of the surface microstructure on the evolution of the combustion velocity of ammonium perchlorate composite solid propellants as a function of pressure
- 08 p0995 A73-21678
[ONERA, TP NO. 1167]
The effect of a dispersed phase on the creep properties of a Cr-Ni steel.
- 08 p0980 A73-21779
The influence of structure upon the notched creep strength of a nickel-base alloy.
- 08 p0982 A73-21795
Effects of composition and structure on the creep strength of molybdenum bearing ferritic steels.
- 08 p0982 A73-21796
Effect of microstructure on measurements of fracture energy of Al₂O₃.
- 08 p0983 A73-21842
[ACS PAPER 44-BN-71P]
Influence of composition and heat treatments on the structure and mechanical characteristics of martensitic stainless steels derived from the 16 percent chrome and 4 percent nickel type
- 09 p1098 A73-21924
Thermal stability of the microstructure in the eutectic composition Al-Al₃Ni
- 09 p1099 A73-21966
Microstructural control of Ti-6Al-4V forgings.
- 09 p1088 A73-22495
Characteristics of the microstructural wear pattern of carbided chromium coatings
- 09 p1088 A73-22592
The effect of the structure of the titanium alloys VT3-1 and VT-18 on their fatigue resistance under asymmetrical cyclic loading.
- 09 p1106 A73-23164
Structural features of surface layers in molybdenum alloy sheets
- 09 p1106 A73-23188
Effect of heat treatment on the structure and properties of NV10M5T3Ts alloy
- 09 p1106 A73-23190
Structure and properties of electron-beam-melted 1Kb12N3M3B steel
- 09 p1107 A73-23194
Physical characteristics of sponge titanium of a hardness below 100 HB units, obtained by heat treatment with magnesium
- 09 p1107 A73-23227
Ductility of recrystallized molybdenum as a function of oxygen concentration and grain size
- 09 p1108 A73-23231
Influence of material properties on dynamic fracture toughness of steels.
- 09 p1109 A73-23259
Enhancement of fracture toughness in high strength steel by microstructural control.
- 09 p1109 A73-23262
Effects of composition on embrittlement of austenitic stainless steels.
- 10 p1230 A73-23628
Microstructural observations of arc welded boron-aluminum composites.
- 10 p1223 A73-23630
Short time aging characteristics of Inconel X-750.
- 10 p1230 A73-23631
Effects of Ni and Fe addition on various properties in heat-resisting aluminum casting alloys.
- 10 p1231 A73-23675
Grain growth inhibition by carbide additives in hard metal alloys of the ISO-K 10 type
- 10 p1231 A73-23688
High modulus graphite fiber-epoxy composite shear strength and structural observation by X ray and electron diffraction and surface dark field electron microscopy
- 10 p1239 A73-23977
Direct observation of magnetic microstructure in deformed niobium-based superconducting alloys.
- 10 p1259 A73-24186
Carbon-felt, carbon-matrix composites - Dependence of thermal and mechanical properties on fiber volume percent.
- 10 p1240 A73-24278
Damping properties of VT3-1, VT-9, and VT-18 titanium alloys of various microstructure
- 10 p1233 A73-24359
Effects of beryllium additions on the microstructure and the type of failure in Al-Mg alloys
- 10 p1233 A73-24423

An electron microscopy study of precipitation in Cu-Ti sideband alloys.

- 10 p1234 A73-24434
Quantitative characterization of the substructure of AISI 316 stainless steel resulting from creep.
- 10 p1234 A73-24436
Correlation of coercive force to microstructure in cyclic martensite/austenite transformations in an Fe-Ni-Co alloy.
- 10 p1234 A73-24438
The effect of carbon and titanium on the hot workability of 25Cr-6Ni stainless steels.
- 10 p1235 A73-24440
Importance of slip mode for dispersion-hardened beta-titanium alloys.
- 10 p1235 A73-24441
Flow stress dependence on grain size in microstrain region of Ni strip machined to produce different grain sizes
- 10 p1235 A73-24444
Investigation of the infrastructural organization of interdisk spaces and photoreceptor membranes of the retina in vertebrates during aldehyde fixations, delipidization, and pronase treatment
- 10 p1181 A73-24458
Zr additions effect on quenched and aged Al-Mg-Li alloy having phases in equilibrium with solid solution
- 10 p1236 A73-24928
Tests concerning the production of gas turbine blades with directionally solidified structure
- 11 p1372 A73-25104
Corrosion fatigue: Chemistry, mechanics and microstructure; Proceedings of the International Conference, University of Connecticut, Storrs, Conn., June 14-18, 1971.
- 11 p1380 A73-25801
Metal fatigue crack nucleation behavior and dislocation microstructures, including slip band and extrusion-intrusion pairs
- 11 p1380 A73-25804
Preferred a axis orientation parallel to fiber axis in commercial carbon fibers due to lower surface energy of basal plane configuration
- 11 p1389 A73-25857
Stability of micromorphology of carbon fibres and their interstitial compounds.
- 11 p1389 A73-25858
Microstructure, hardness, electrical resistivity and thermal properties of Ni alloys with Al and Ta, noting composition of heat resistant alloys
- 11 p1384 A73-26063
Determination of alpha plus gamma/gamma phase boundaries in Fe-Cr-Ni, Fe-Cr-Co, and Fe-Cr-Mn systems
- 11 p1384 A73-26108
Phase diagrams, microstructure and superconducting properties of thermally diffused Nb-Sn system
- 12 p1508 A73-26835
Investigation with an electron microscope of the structure of wires prepared from the 60T superconducting alloy
- 12 p1509 A73-26841
X ray and microanalysis of Luna 16 recovered Fe-Ni fragment structure and composition, showing alpha solid solution octahedrite
- 12 p1538 A73-26893
The nature of the nonuniformity of the structure and properties of semiproducts pressed from titanium and its alpha-alloys
- 12 p1502 A73-26909
The nature of slated cleavage planes in pressed VAD 23 alloy
- 12 p1511 A73-26915
Microstructure, microhardness and mechanical strength of ingots and granules of Al alloys with high refractory metal contents
- 12 p1511 A73-26917
Effect of neutron irradiation on the structure and properties of zirconium carbide
- 12 p1512 A73-27200
The changes in structural and mechanical properties of construction materials under loads
- 12 p1513 A73-27500
Determination of the boundaries of single-phase edge regions in the Mo-Cu-Ni system in solid state
- 12 p1513 A73-27559
The strength differential of steel and Ti alloys as influenced by test temperature and microstructure.
- 12 p1513 A73-27681
Metal matrix composites microstructural alignment by solid state transformation process involving eutectoid decomposition and cellular precipitation
- 12 p1513 A73-27682
Structural evolution of an austenitic-ferritic stainless steel by keeping it between 600 and 1150 C
- 12 p1514 A73-27986
Deformable body with reticular structure, studying microstructural transitions using physical model with isolated-valence bond coupling
- 13 p1690 A73-27992
Substructure alteration in manganese and nickel austenitic alloys under the action of microimpacts
- 13 p1630 A73-28013
Investigation of diffused titanium coatings on refractory metals
- 13 p1630 A73-28015

Free vibrations of a laminated beam by a microstructure theory.

- 13 p1691 A73-28063
Ti-Al-Sn alloy microstructure effects on low temperature creep, discussing creep stresses, activation energy and yield stress
- 13 p1632 A73-28127
Effect of titanium additions on the aging characteristics of an Al-Zn-Mg alloy.
- 13 p1632 A73-28134
Cast microstructure and fatigue behavior of a high strength aluminum alloy /KO-1/.
- 13 p1633 A73-28137
Ti-Pd phase diagram eutectoid region configuration determination through alloy thin foil arc melting preparation and microstructure examination by electron microscopy
- 13 p1633 A73-28146
The effect of processing on the microstructure of CFRP.
- 13 p1645 A73-28779
Grain growth of chemical vapour deposited tungsten-22 wt % rhenium alloy.
- 13 p1636 A73-28927
Relationship of mechanical characteristics and microstructural features to the time-dependent edge-notch sensitivity of Inconel 718 sheet.
- 13 p1637 A73-29200
[ASME PAPER 73-MAT-G]
Forged or homogenized aged maraging steels, discussing microstructure, tensile strength and fracture toughness dependence on precipitates morphology
- 13 p1637 A73-29243
Relationship between structure and strength for CVD carbon infiltrated substrates. III - Fabric lay-up substrates.
- 13 p1645 A73-29272
Effect of microstructure and environment on stress corrosion of 7075 aluminum alloy.
- 13 p1637 A73-29312
[NACE PAPER 97]
Mechanical behavior of high-strength beta-titanium alloys.
- 13 p1638 A73-29456
Interpretation of mechanical behavior of pure aluminum in terms of microstructure.
- 13 p1639 A73-29459
The interaction of material and geometric aspects in the fracture of aluminum alloys.
- 13 p1640 A73-29475
The effect of microstructure on fatigue crack propagation in Ti-6Al-6V-2Sn alloy.
- 13 p1640 A73-29484
Creep properties of low alloy steel in relation to microstructure.
- 13 p1641 A73-29509
Nimonic and Mg alloys creep behavior interpretation by constitutive law, discussing recovery activation and strain hardening from microstructural behavior
- 13 p1642 A73-29515
The micro-structural approach toward a kinetic theory of polymer fracture.
- 13 p1646 A73-29529
Behavior of random micro-structural systems.
- 13 p1701 A73-29530
Increase in the boundary strength of cast electron-beam-melted molybdenum by microadditions of vanadium.
- 13 p1643 A73-29634
Properties and structure of Ti-Nb-base superconducting alloys
- 13 p1643 A73-29644
Corrosion properties and structural transformations of the N70M27 alloy containing vanadium and niobium
- 13 p1644 A73-29645
Book on solids structure effects on materials strength characteristics covering interatomic binding forces, elastic properties, crystal defects, work hardening, heat treatment, temperature effects, etc
- 14 p1759 A73-29948
Delta ferrite and martensite formation in stainless steels.
- 14 p1759 A73-30145
Solidification structure and tensile properties of 2014 aluminum alloy welds.
- 14 p1755 A73-30149
Grain growth during creep of alloyed molybdenum.
- 14 p1759 A73-30311
Formation of oriented structures by action of a laser beam on metals.
- 14 p1760 A73-30325
Structure stability of austenitic chromium-nickel steels at the temperature of liquid helium
- 14 p1760 A73-30420
Precipitation of iron in rapidly solidified aluminum-iron alloys
- 14 p1760 A73-30439
Morphology of the structure and the microhardness of Al-/Ni, Cu, Be, Fe, Co/ eutectic compositions
- 14 p1760 A73-30588
Effects of some carbide stabilizing elements on creep-rupture strength and microstructural changes of 18-10 austenitic steel.
- 14 p1761 A73-30627

Martensitic transformation in iron-nickel alloys in a pulsed magnetic field

14 p1764 A73-30860

Aluminum structure effects on thermal activation parameters of plastic deformation, proposing strain rate control mechanism

14 p1764 A73-30867

Structure and superconducting properties of alloys of the vanadium-tantalum system

15 p1923 A73-31183

Properties of the superconducting alloy 35BT

15 p1887 A73-31188

Molybdenum-rhenium alloy microstructure changes due to nitriding in ammonia vapors from metallographic and X ray structural analysis

15 p1887 A73-31206

Effect of oxygen on the structure and properties of Bi₂Te₃-based alloys

15 p1923 A73-31209

Effect of lasting high temperatures on the mechanical properties and microstructure of bonded glass mat with an aluminophosphate binder

15 p1896 A73-31213

Lunar core sample structure morphology and composition examined by microanalysis, revealing tenite to martensite transformation

15 p1930 A73-31220

Grain-boundary sliding and recrystallization of Nimonic 108 during creep.

15 p1887 A73-31352

Mo-W-C phase equilibria study at 1000 C, obtaining isothermal cross sections for various carbon contents from X ray and microstructural analysis

15 p1888 A73-31598

Saturation of Kh18N10T steel by molybdenum from the vapor phase

15 p1889 A73-31807

Investigation of titanium alloys containing refractory elements

15 p1889 A73-31813

Superplasticity of the Kh18N10T steel

15 p1890 A73-31816

Experimental observations of dendritic duplex crystals grown in complex Ni base alloys.

15 p1890 A73-31841

Twin-jet thinning techniques for transmission electron microscopy observation of tantalum and niobium.

15 p1891 A73-31995

A scanning electron microscope study of the surface morphology of TD-NiCr oxidized at 800 C to 1200 C.

15 p1892 A73-32270

Critical survey of studies of the equilibrium phase diagram of the Ti-W system

15 p1893 A73-32513

Investigation of the phase equilibrium of ternary Ti-Al-Nb system alloys

15 p1893 A73-32514

Effect of ordering on the properties of oxygen solid solutions in titanium

15 p1893 A73-32516

Phase transformations in alloys of the titanium-molybdenum system

15 p1893 A73-32517

Structural transformations in two-phase titanium alloys

15 p1893 A73-32522

Phase and structural changes in titanium under impulsive loads

15 p1894 A73-32523

Phase transformations during heat treatment of the VT18 alloy

15 p1894 A73-32524

Failure retardation mechanism in plastic titanium alloys

15 p1894 A73-32529

Influence of structure and of stress concentration on the mechanical properties of Ti-Ta-Mo system alloys

15 p1894 A73-32533

Properties of titanium-niobium based stable beta alloys

15 p1894 A73-32534

Investigation of the structure and corrosion behavior of alloys of the Ti-Ta-Cr system

15 p1895 A73-32542

Investigation of corrosion stability in alloys of the Ti-Ta-Nb system

15 p1895 A73-32543

Scanning electron microscopic observation of fracture surfaces of austenitic stainless steels in stress corrosion cracking.

16 p2025 A73-33021

Three dimensional microstructure of carbonized polyacrylonitrile (PAN) fibers dependence on basal plane alignment and process cycle treatment

16 p2028 A73-33039

Diffusional creep and creep-degradation in dispersion-strengthened Ni-Cr base alloys.

16 p2025 A73-33111

Structure, strength, and fracture of electrodeposited nickel and Ni-Co alloys.

16 p2025 A73-33113

Acoustic fatigue in ceramic materials, analyzing strength degradation as function of microstructure, structural integrity and properties

16 p2030 A73-33194

The influence of prior thermal treatment of cast blocks on the coarse grain characteristics in extruded bars and profiles of alloys of the type AlCuSiMn

16 p2021 A73-33952

The precipitation behavior of a commercial aluminum-copper-lithium alloy. I - The microstructure after isothermal heat treatment

16 p2026 A73-33954

Relation between grain size and the size of fatigue-striated facets in an aluminum alloy

16 p2027 A73-33972

Phase composition and properties of metastable alloys of titanium with nickel

16 p2027 A73-34072

Enhanced ductility in metals /Superplasticity/.

17 p2240 A73-34113

Mechanism of the micrononhomogeneous deformation of metals throughout a wide interval of temperature

17 p2186 A73-34330

Microstructure and phase composition of oxide scale formation on Ti-Al alloys, noting dependence on Al concentration

17 p2188 A73-34557

Microstructure and hardness investigations of alpha prime, alpha double prime and omega metastable phases formed during quenching of Ti-Ru alloys

17 p2188 A73-34567

Effect of small group-VIII metal additions on the structure and properties of cast molybdenum

17 p2189 A73-34578

Relation between the brittle-viscous transition temperature and structural characteristics in certain low-alloyed chromium alloys

17 p2189 A73-34579

Some physicochemical characteristics of failure in tempered high strength steels

17 p2189 A73-34580

Effect of carbon on the structure and properties of molybdenum

17 p2189 A73-34582

Physical and chemical analysis of germanium tunnel diodes.

17 p2219 A73-34865

Thermal cyclization of 1,2-polybutadiene and 3,4-polyisoprene.

17 p2119 A73-34925

Composite materials structure, describing component interactions, major constituents, determinants of mechanical properties, particulate composites, materials applications and fiber types

17 p2195 A73-34974

Structure of sputtered molybdenum disulfide films at various substrate temperatures. [ASLE PREPRINT 73AM-3C-3]

17 p2196 A73-34988

Dynamic yield strength determination at elevated temperatures after nanosecond pulse heating. [SESA PAPER 2141A]

17 p2148 A73-35450

Influence of cold work on the stress corrosion susceptibility of Ti-13V-11Cr-3Al.

17 p2194 A73-35675

Axial alignment of basal planes in polyacrylonitrile base carbon fibers, increasing axial and radial microstructural textures via heat treatment temperature

17 p2198 A73-35837

Some physicochemical and technological aspects of obtaining annealed coatings from melts and semimelts

18 p2318 A73-35887

Certain law controlling the temperature dependence of the microdeformation of Fe-Cu-Ti, W, and W-Re bcc alloys

18 p2324 A73-36803

Some characteristics of the microplastic deformation of the surface layers of semiconductor crystals at temperatures below and above the thermal brittleness threshold

18 p2341 A73-36805

Influence of prolonged aging on the behavior of the microhardness and substructure of EI257 austenitic steel

18 p2324 A73-36806

Austenitic grain structure and strength changes associated with aging in 14Cr-14Ni type steels

18 p2325 A73-36810

Influence of stresses on the nature of the distribution of dislocations in Kh18N10T steel at a temperature of 650 C

18 p2325 A73-36820

Apollo program contributions to lunar cosmology and composition, discussing core-mantle structure, earth-moon gravitational system, mineral types and cosmological hypotheses

18 p2356 A73-37044

Structure and phase composition of welded joints of zirconium alloy with 2.5% Nb

19 p2439 A73-37266

Fine structure of rolled annealed tungsten sheet, discussing subsurface layer recrystallization and

deformation effects based on radiographic examinations

19 p2440 A73-37443

Grain refinement in aluminum-zirconium and aluminum-titanium alloys by metastable phases.

19 p2440 A73-37444

Structural service life from carrying capacity during rupturing stage, noting microstructural properties effect

19 p2499 A73-37779

The influence of fabrication and structure processes on the result of control by ultrasonics of semifinished products of titanium alloys

19 p2441 A73-37830

Microstructural characteristics of the TA6V alloy as a function of thermomechanical treatments in alpha plus beta - Effects on the mechanical characteristics in tension

19 p2441 A73-37831

Transformations of TA6V6E2Zr alloy in isothermal conditions

19 p2441 A73-37832

Grain refinement by titanium in the unidirectionally solidified aluminum alloys.

19 p2442 A73-37949

Resistance diffusion bonding boron/aluminum composite to titanium.

19 p2435 A73-38004

A comparison of the capabilities of continuous drive friction and inertia welding. [SME PAPER AD 73-221]

19 p2436 A73-38493

Structure and mechanical properties of internally oxidized Ta-8 pct W-2 pct Hf /T-11/ alloy.

20 p2576 A73-39025

Aerospace applications of heat resistant alloy diffusion welding techniques, describing mechanical properties, metal bonding, surface cleaning, vacuum levels, temperature effects and microstructure.

20 p2569 A73-39246

Investigation of the transition zone structure in composite materials under cyclic loads

20 p2580 A73-39379

Substructure of type 316 stainless steel deformed in slow tension at temperatures between 21 and 816 C.

20 p2578 A73-39491

Effect of the degree of plastic deformation on the structure and mechanical properties of low-alloy molybdenum

20 p2579 A73-39741

Investigation of the imperfect structure of polycrystalline aluminum after low-temperature rolling and annealing

20 p2579 A73-39747

Changes in the disorientation of the substructure of a nickel-aluminum alloy under ultrasonic treatment and creep

20 p2579 A73-39748

Effect of supersonic gas flows on the structure and heat resistance of metal alloys

21 p2717 A73-40481

Fine structure of an explosion-hardened chromium-nickel-manganese austenitic steel

21 p2718 A73-40484

Influence of magnesium on the structure of heat-resistant nickel-base alloys

21 p2718 A73-40485

The nature of the interaction between scandium and aluminum in the aluminum-rich part of the Al-Sc system

21 p2718 A73-40486

Structure and phase composition of a maraging-steel weld

21 p2718 A73-40737

Effect of austenitization temperature on the properties of Kh5N12M3TiU steel

21 p2718 A73-40738

Influence of aluminum on the structure and properties of a Ti + 10% V alloy

21 p2719 A73-40850

X ray and microanalysis of Luna 16 recovered Fe-Ni fragment structure and composition, showing alpha solid solution octahedrite

21 p2771 A73-41026

Properties and structure of superconducting Ti-Nb alloys.

21 p2720 A73-41037

Corrosion characteristics and structural transformations in alloy N70M27 with vanadium and niobium.

21 p2720 A73-41038

Microstructure of recrystallized alloy Kh20N80.

21 p2721 A73-41042

Investigation of the effective heat conductivity of plasma-sprayed alumina coatings subject to radiative heating in the temperature range from 100 to 900 C

21 p2792 A73-41220

Influence of thermal cutting and its quality on the fatigue strength of steel.

21 p2722 A73-41253

Lunar core sample structure morphology and composition examined by microanalysis, revealing tenite to martensite transformation

22 p2905 A73-41808

MICROTHRUST

Study of the structure and properties of alloys of the V-Al, Cr-Al and V-Cr-Al systems in the region of solid solution bcc ordering

22 p2873 A73-42088

Experimental aspects of the mechanical behavior of fiber composites produced by oriented solidification [ONERA, TP NO. 1205]

22 p2876 A73-42215

Structure and properties of arc-sprayed titanium coatings.

22 p2879 A73-42597

The effect of change of polarisation of the illuminating beam on the microstructure of speckles produced by a random diffuser.

22 p2871 A73-43095

Influence of structural changes arising during the hardening process on element lifetime

23 p2984 A73-43438

Investigation of the structure and properties of annealed alloys of the Ti-Mo system

23 p2990 A73-43484

Influence of alloying additives on the structural changes in a nickel-molybdenum composite

23 p2991 A73-43488

Microstructural characteristics of the plastic deformation and recrystallization of an aluminum alloy of various heterophase structure

23 p2991 A73-43489

Investigation of the substructure in molybdenum single crystals deformed by compression

23 p2991 A73-43712

The effect of cold and hot rolling on the microstructure and fracture characteristics of titanium-to-steel explosion welds.

23 p2985 A73-43912

Phase transformations in beta-Cu-Al during extremely rapid cooling from the melt

23 p2992 A73-43914

The metallurgy of Remendur - Effects of processing variations.

23 p2993 A73-43987

Structural changes caused in glassy arsenic trisulfide and triselenide by penetrating radiation

23 p3017 A73-44042

Additive distribution and formation of internal stress in fired magnesia.

23 p2998 A73-44133

Microstructure and its related properties on carbon fiber composites.

23 p2998 A73-44134

Changes in surface structure during high-temperature creep flow.

23 p2994 A73-44159

Diagram of continuous cooling transformation of a titanium alloy with 6 per cent Al, 6 per cent V, and 2 per cent Sn /TA 6-V 6-E 2/ homogenized in the beta /sub 0/ phase

23 p2995 A73-44177

Kinetics of the development of structural changes in iron in the presence of adsorption fatigue

23 p2995 A73-44224

Investigation of the softening processes in molybdenum and its alloys under conditions of creep

23 p2995 A73-44281

Field electron emission microscopic study of titanium

24 p3098 A73-44474

Influence of ultrasonic vibrations on the mechanical properties and fine structure of aluminum and an aluminum-magnesium alloy

24 p3098 A73-44570

Influence of small beryllium, titanium, and zirconium additions on the structure and properties of Al9 alloy

24 p3098 A73-44571

Deformation characteristics and ductility of two-phase titanium alloys of laminated structure

24 p3099 A73-44573

Influence of the microstructure of water aerosol on the phase function, its asymmetry, and polarization of scattered light

24 p3084 A73-44963

Displacements and rotations in micropolar elastic body with external loading and permanent distortions

24 p3149 A73-45004

Spatial orientation of phases in the Al-Al3Ni eutectic system

24 p3099 A73-45169

Microstructural features of Cr12NiWMoV/Ti /T60/ steel after electrosalt remelting

24 p3100 A73-45170

Saturation of steel Kh18NiOT with molybdenum from the vapor phase.

24 p3100 A73-45270

Alloys of titanium with refractory elements.

24 p3100 A73-45276

Superplasticity of steel Kh18NiOT.

24 p3100 A73-45279

Determination of the parameters of particle density and size distribution functions from measurements of attenuation and backscattering coefficients

24 p3112 A73-45519

MICROTHRUST

Direct measurement of colloid microthruster thrust and propellant mass flow rate, using microbalance

04 p0433 A73-15727

Space charge neutralized Hall ion microthrusters, discussing ion exhaust velocity, thrust and efficiency relationships

04 p0489 A73-15729

MICROTOPOGRAPHY U TERRAIN

MICROWAVE AMPLIFIERS

M/W power transistors and MIC amplifiers - State-of-the-art.

01 p0024 A73-10719

A wideband transistor amplifier at the 4 GHz band for communication satellite use.

01 p0026 A73-11176

Gunn diodes - Physical principles and simulation calculations

02 p0144 A73-11529

Microwave amplifier design based on negative differential mobility in Gunn diodes

02 p0144 A73-11531

Simultaneous population inversions observation at Zeeman levels in ruby paramagnetic microwave quantum amplifier, noting pumping efficiency

02 p0177 A73-12499

Material concerns, fabrication procedure, cooling techniques, performance and stability characteristics of transferred electron microwave amplifiers and oscillators

03 p0282 A73-13893

High-power avalanche IMPATT reflection amplifier using the Rucker combining circuit.

03 p0282 A73-13894

A review of microwave parametric amplifiers with particular reference to satellite communications and radio astronomy.

03 p0284 A73-13999

Arsenic emitter silicon bipolar transistor and gallium arsenide FET transistor devices for low noise microwave amplification to 10 GHz

04 p0426 A73-14731

Computer-aided design of high-frequency transistor amplifiers.

04 p0427 A73-15053

High power SHF transmitter experiment using TWT depressed collector beam microwave amplifier for flight testing on communications technology satellite /CTS/

04 p0428 A73-15447

Stabilization bandwidth reduction in microwave parallel tuned tunnel diode amplifier circuits synthesis

04 p0429 A73-15919

Minimum noise coefficients of M-type microwave beam amplifiers with crossed fields taking into account distributed losses in slow wave structure

04 p0429 A73-15922

Parametric regeneration in Josephson superconducting point contacts for combination frequency signal amplification and conversion in microwave application

05 p0556 A73-16073

Effect of ionizing radiation on Gunn diode amplifiers.

05 p0557 A73-16502

Neutron irradiation effects on microwave transistor amplifiers.

05 p0558 A73-16520

Nonreciprocal circulator coupled reflection type microwave amplifier gain and stability characteristics, presenting scattering matrix and signal flow diagram

06 p0673 A73-17590

The GaAs traveling-wave amplifier as a new kind of microwave transistor.

06 p0673 A73-17788

Platinotron crossed field microwave amplifier tube phase response characteristics, considering anode current fluctuations and statistical phase variations at constant operating conditions

06 p0674 A73-17823

Microwave amplifier with internal negative feedback, using IF output for frequency modulation of mixer oscillator signal

06 p0677 A73-18394

Circuit model for characterizing the nearly linear behavior of avalanche diodes in amplifier circuits. [AD-757849]

06 p0677 A73-18738

On the theory of the avalanche transit-time diode reflection amplifier.

06 p0678 A73-18838

Optimum R.F.-power transport in Nd-limited gallium-arsenide travelling-wave amplifiers.

07 p0798 A73-19159

High-Q toroidal cavities for high frequency klystrons.

07 p0803 A73-20550

Integrated electrically tuned X-band power amplifier utilizing Gunn and IMPATT diodes.

07 p0803 A73-20551

Waveguide cavity multistage Gunn reflection amplifiers for FM-CW systems, discussing stabilization techniques, bandwidth, noise, power variation with temperature and group delay distortion

07 p0803 A73-20552

Design and performance of transferred electron amplifiers using distributed equalizer networks.

07 p0803 A73-20553

X- and Ku-band amplifiers with GaAs Schottky-barriers field-effect transistors.

07 p0803 A73-20555

Microwave lumped passive and active circuit components properties assessment, considering inductor, capacitor, resistor, gyrator, tunnel diode amplifier, varactor Gunn oscillator, and parametric amplifier

08 p0942 A73-20703

Hydrogen maser amplifier performance characteristics, discussing relaxation time measurements, frequency stability and performance enhancement via resonator cavity magnetic shielding improvement

08 p0974 A73-20774

Characteristics of a gallium-arsenide travelling-wave amplifier with Schottky-barrier contacts.

08 p0946 A73-21118

Wideband class-C Trapatt amplifiers.

08 p0947 A73-21145

1-2 GHz high-power linear transistor amplifier.

08 p0947 A73-21146

On the mechanism for microwave amplification in 'supercritically' doped n-GaAs.

08 p0947 A73-21212

Two stage microwave monolithic integrated circuit power amplifier design with matched transistors, calculating distributed matching network

08 p0950 A73-21826

Design a 4 to 8 GHz FET amplifier with a 7 dB NF.

08 p0950 A73-21827

Design criteria for high gain, wide band, microwave amplifiers.

09 p1062 A73-22304

TRAPATT amplifiers for phased-array radar systems.

09 p1051 A73-22497

Noise in single-frequency oscillators and amplifiers.

10 p1196 A73-24864

Microwave transistor power amplifier.

11 p1338 A73-26149

Optimal passband of a double-tuned selective amplifier during the simultaneous passage of rectangular radio pulses and white noise

12 p1477 A73-26874

Considerations about jump effect in microwave power amplifier.

12 p1478 A73-27073

Combination and crosstalk distortions in microwave parametric systems.

13 p1583 A73-28665

Gain-bandwidth limitations of microwave transistor amplifiers.

14 p1735 A73-30247

Wideband monopulse radio direction finding measurement improvement, using receiver with log video IF amplifier, multiplexing filters and detectors to provide signal normalization

16 p1990 A73-33850

Linear theory of an IMPATT diode distributed microwave amplifier.

16 p1991 A73-33983

C band low noise IC microwave amplifier for phased array module in multiple access communication links, discussing photofabrication for low cost batch processing

17 p2135 A73-34727

Time-domain analysis of intermodulation effects caused by nonlinear amplifiers.

17 p2136 A73-34868

Experimental gain and noise parameters of microwave GaAs FET's in the L and S bands.

17 p2136 A73-34972

Broadband TWT microwave amplifier failure modes in airborne systems related to physical mechanism, fabrication processes and field operator handling

17 p2140 A73-35259

Two terminal large signal circular coupled wideband TRAPATT diode microwave amplifiers, noting negative resistance characteristics and dc-to-rf conversion efficiency

17 p2140 A73-35321

Performance and advantages of FET's as microwave solid state amplifiers.

17 p2141 A73-35322

Microwave amplifier design with discrete variable components, testing power output and efficiency, bandwidth, and temperature, vacuum and vibration effects on performance

17 p2141 A73-35324

Baseplate heat pipe system for waste heat dispersion and temperature control of TWT microwaves amplifier in space shuttle communication equipment, discussing design and performance

18 p2370 A73-36371

Design of the 14/11 GHz repeater for the European Orbital Test Satellite.

20 p2525 A73-38745

Design and application of low noise GaAs FET amplifiers.

20 p2534 A73-38749

Active electronic devices - Microwave diodes

20 p2535 A73-39054

Book - Gallium arsenide microwave bulk and transit-time devices.

20 p2536 A73-39137

High power GaAs double-drift IMPATT devices.
22 p2834 A73-42693
Microwave cross field and traveling wave tube amplifier characteristics for ECM systems, discussing bandwidth, dual mode, modulation and size and weight tradeoffs
22 p2834 A73-42872
Experimental study of the dynamic parameters of varactor diodes
24 p3072 A73-44929

MICROWAVE ANTENNAS

NT HORN ANTENNAS
NT LENS ANTENNAS
NT SLOT ANTENNAS
Low-side-lobe paraboloidal antenna with microwave absorber.

01 p0018 A73-11054
X band microstripline slot antenna measurement for input impedance and radiation pattern dependence on slot-to-reflector spacing, applying to array design
02 p0141 A73-12100
Comparing ECM antennas - Horns vs spirals.
02 p0147 A73-12568

Class of stepped-reflector antennas with improved frequency response.
05 p0547 A73-16159
Dielectric layers in the radiation field of microwave antennas

05 p0550 A73-16475
The 'Paradise' antenna - A novel technique to improve the axial ratio of a circularly polarized high gain antenna system.

06 p0676 A73-18195
Diffraction by double circular irises and scattering by two elliptical reflectors.

06 p0666 A73-18196
Height-gain experimental data for groundwave propagation. II - Heterogeneous paths.
07 p0791 A73-19378

Antennas have it tough - when forced to ride on spacecraft.
07 p0803 A73-20491

A new earth-station antenna for domestic satellite communications.
08 p0947 A73-21144

Wideband squintless linear arrays.
10 p1192 A73-23605
Computer design of antenna reflectors.
[ALAA PAPER 73-351]
11 p1437 A73-25489

Design of multiple-edge bladders for large horn reflector antennas.
11 p1337 A73-25653

Radiation properties of a composite-dielectric-rod aerial.
11 p1332 A73-26286

The disc antenna - A possible L-band aircraft antenna.
12 p1471 A73-27655

Frequency-selective surfaces for multiple-frequency antennas Design data plus experimental results.
14 p1737 A73-30625

Radiating slot antenna immittance reactive term due to energy storage in feeding waveguide, discussing resonance characteristics
15 p1849 A73-31097

Size-reduced log-periodic dipole array antenna.
16 p1988 A73-33299

Antenna admittance determination of electron density.
17 p2121 A73-34187

Design techniques for multiple beam reflector antennas.
17 p2142 A73-35636

Radiation efficiency of an X-band waveguide antenna.
17 p2127 A73-35637

Remote sensing using microwave radiometry.
17 p2174 A73-35639

Accurate measurement of antenna gain and polarization at reduced distances by an extrapolation technique.
17 p2127 A73-35676

A practical method for measuring the complex polarization ratio of arbitrary antennas.
17 p2127 A73-35677

Probe compensated near-field measurements on a cylinder.
17 p2127 A73-35678

Corrugated horn antenna with high efficiency and monotonic amplitude in microwave pattern ranges applicable as calibrating standard
17 p2143 A73-35693

Large parabolic reflector microwave antenna antismattem effects on radiation pattern, discussing focusing procedure for phase error reduction
17 p2143 A73-35695

Microwave radiation hazards around large microwave antenna.
19 p2397 A73-37274

Microwave Landing System with air-derived sample data and scanning narrow beam antennas for signal-in-space generation, discussing design requirements and performance test
21 p2735 A73-40046

Phased array antenna feed systems developments, discussing relative merits, problems and design choices for air surveillance radar applications in microwave region
21 p2672 A73-40664

Bias controlled step recovery diode as combined frequency multiplier and analog phase shifter for applications in microwave phased array antenna systems
21 p2663 A73-40668

Antenna radiation pattern measurement using time-to-frequency transformation /TFT/ techniques.
22 p2831 A73-41842

Short axial length broad-band horns.
22 p2831 A73-41846

Experimental determination of the field parameters in a sectorial horn aperture with the aid of a passive probe
22 p2826 A73-42337

Low-noise microwave receiving systems in a worldwide network of large antennas.
23 p2958 A73-43376

Some data for the design of low-crosspolarisation feeds.
24 p3069 A73-45255

Comparative focusing properties of spherical and plane microwave zone plate antennas.
24 p3069 A73-45480

MICROWAVE ATTENUATION

Dual frequency antenna design using hollow fin as TE mode waveguide with sidewall radiating elements, calculating attenuation for comparison with experiment
01 p0023 A73-10189

Microwave-power attenuation in Gunn diodes
01 p0025 A73-10979

A very accurate X-band rotary attenuator with an absolute digital angular measuring system.
03 p0310 A73-14498

Millimeter wave propagation measurement for attenuation probability statistics by ATS-5 satellite, considering impact on space communication system design
04 p0418 A73-15387

Absorption in the 220 GHz atmospheric window.
04 p0418 A73-15394

Rain attenuation of vertically and horizontally polarized signals of 18 GHz communication system
04 p0419 A73-15395

A note on the use of airborne 30-millimetre radar at long ranges.
04 p0423 A73-15699

Dimensional and material effects on microwave waveguide damping and bandwidth characteristics in long distance communications
06 p0663 A73-17583

Argon plasma density and energy distribution development during microwave radiation absorption at upper hybrid resonance
06 p0732 A73-18605

Microwave power absorption by a plasma outside the electron cyclotron resonance region.
06 p0733 A73-18795

Path diversity for mm-wave earth-to-satellite links.
[AD-757967]
07 p0791 A73-19376

Atomic oxygen formation times obtained from measurements of electron density profiles behind shock waves in air.
07 p0853 A73-19510

Unusually high earth-space path attenuations measured using a 6.4-GHz radiometer.
07 p0793 A73-20111

Submillimeter radio telescope employing an n-InSb detector
07 p0825 A73-20311

Absorption of microwaves by a plasma in a magnetic field in the presence of a large effect due to longitudinal inhomogeneity
12 p1467 A73-26934

Submillimeter radio telescope with an n-InSb detector.
12 p1497 A73-27283

Absorption of the microwave energy in a magnetoactive plasma.
[IPPCZ-167]
12 p1529 A73-27433

Modified X band microwave calorimeter design for precision power and attenuation measurements in GHz and MHz ranges
12 p1498 A73-27752

Absorption of waves by a two-dimensionally inhomogeneous plasma in the vicinity of singularity points
13 p1666 A73-28960

On the absorption of microwave through laboratory plasma.
14 p1782 A73-30800

Atmospheric lens effect - Another loss for the radar range equation.
16 p1980 A73-33407

Atmospheric attenuation interrelations at 12 and 35 GHz with meteorological parameters derivation for homogeneous atmosphere, testing dynamic atmospheric model
16 p1981 A73-33709

The respective influences of multi-path configurations and precipitation rates for frequencies lying between 10 GHz and 30 GHz.
16 p1981 A73-33710

Atmospheric attenuation measurement for nine millimeter wavelength signal from radio source, discussing solar power, radiosonde, emission temperature and nodding solar methods
16 p1982 A73-33719

Earth-space slant path radio attenuation measurements above 10 GHz over four year period, noting caution in use of long term statistics
16 p1982 A73-33721

Linear cross-polarisation and attenuation measurements at 11 and 36 GHz.
16 p1982 A73-33723

Radio-occultation measurements of the Venusian atmosphere conducted by Mariner 5 in the 10-centimeter band
16 p2067 A73-33802

Absorption of centimeter radio waves in the Venusian atmosphere
16 p2068 A73-33821

Atmospheric attenuation anomalies at 2.7 mm from sky noise temperature measurements compared with water vapor and oxygen line strength calculations
17 p2159 A73-34571

Microwave energy absorbing elements based on Pd/Ag
17 p2141 A73-35549

Electromagnetic wave absorbers and anechoic chambers through the years.
17 p2128 A73-35683

Raindrops in satellite communications.
18 p2289 A73-36515

Effect of scattering on radiometer measurements of attenuation in rain.
19 p2403 A73-37426

An approximation method for calculating the attenuation characteristic of dielectric-lined circular waveguides.
19 p2404 A73-37723

A method of providing rain margins for 18/30 GHz communications satellites without increasing the solar power requirement.
20 p2524 A73-38731

Corrugated circular waveguide boundary value problem solution to predict lower attenuation for HE sub 11 mode
20 p2538 A73-39598

Elaborated attenuation computation for elliptic waveguide with corrected expressions for axial and transverse surface impedances and TE and TM modes
21 p2656 A73-41112

Laser-induced gas breakdown in superhigh pressure region.
22 p2869 A73-42227

Microwave absorption by a magnetoplasma with a strong longitudinal inhomogeneity.
22 p2891 A73-42268

Damping in a strip waveguide with a central conductor composed of two equipotential strips
23 p2959 A73-43517

Modified H guide for millimeter and submillimeter wavelengths.
23 p2960 A73-44072

Wave absorption near singular points in a two-dimensional inhomogeneous plasma.
23 p3013 A73-44312

The damping of electromagnetic waves in smooth, superconductive waveguides.
24 p3068 A73-44945

MICROWAVE CIRCUITS

Rational and irrational matrix functions for analysis and synthesis of distributed microwave networks with multiwire lines and lumped nonreactive elements
01 p0027 A73-10578

New design concepts for microwaves power transistor.
01 p0024 A73-10721

Statistical method of calculating scattering matrix elements and parameter deviations of SHF octupole networks /square bridge, hybrid ring or directional junction/
02 p0146 A73-12025

Uniform junction microwave transistor fabrication by automatically controlled diffusion technique, using low temperature phosphosilicate glass films on silicon wafers
02 p0147 A73-12164

Designing limiter/detectors for ECM receivers.
02 p0143 A73-12569

Phase and amplitude balance - Key to image rejection mixers.
02 p0148 A73-12571

Microwave harmonic generator using the nonlinearity of negative resistance in n-type GaAs.
03 p0281 A73-12997

An accurate bridge method for impedance measurements of impatt diodes.
03 p0281 A73-13175

Voltage-controlled variable power divider.
04 p0428 A73-15454

MICROWAVE COUPLING

Wideband microwave device with diode and single component correction circuits Q factors measurement from frequency dependence of input traveling wave coefficients

04 p0429 A73-15927

Radiation damage effects in microwave dielectric substrate materials.

05 p0557 A73-16507

Gunn diodes oscillating circuit with waveguide cavity in push-pull mode at 42 GHz for high power parametric amplifier pump applications

05 p0558 A73-16807

The noise of microwave Schottky diodes at 70 MHz

06 p0673 A73-17579

Computer analysis of latching phase shifters in rectangular waveguide.

06 p0678 A73-18743

Microwave properties of n-type InSb in a magnetic field between 4 and 300 K.

06 p0739 A73-18792

Russian book on pulse radar circuits covering signal and device characteristics, shaping circuits, amplifiers, limiters, frequency dividers and generators

07 p0794 A73-20231

High efficiency microwave avalanche diode capability for digital applications, describing GHz rate 100 V pulse generator circuit

07 p0804 A73-20556

Microstrip transmission line microwave IC, discussing electrical characteristics, dielectric and conductor materials, photo-etching processes, connection fabrication and circuit encapsulation

08 p0942 A73-20702

Microwave lumped passive and active circuit components properties assessment, considering inductor, capacitor, resistor, gyrator, tunnel diode amplifier, varactor Gunn oscillator, and parametric amplifier

08 p0942 A73-20703

Microwave integrated circuits on a ferrite substrate.

08 p0942 A73-20704

Gunn diode characteristics under large and small signal conditions, noting applications for FM oscillators and voltage tuned and magnetically tuned oscillators

08 p0943 A73-20711

Millimeter-wave frequency response of hot electrons in n-type GaAs.

08 p0994 A73-20845

Microwave baritt /barrier-injection-transit-time/ diodes large signal performance, noting phase delay between injected and total current densities

08 p0945 A73-21074

Effect of engineering-design factors on the parameters of microstrip transmission lines

08 p0951 A73-21109

Measurement of admittance of Gunn diodes in passive and active regions of bias voltage.

08 p0947 A73-21432

Electrically controlled microwave polarization transformer

09 p1064 A73-22675

Microwave characteristics of ion-implanted bipolar transistors.

10 p1194 A73-24156

A quick accurate method to measure the dielectric constant of microwave integrated-circuit substrates.

10 p1197 A73-24866

An analytical expression for the limits of error in the measurement of reflection-coefficient phase.

10 p1190 A73-24867

Microwave electronic packaging with integrated multifunction assemblies, considering stripline choice for transmission line

11 p1338 A73-26113

Review of microwave-integrated-circuit technology.

13 p1588 A73-28043

Small-signal analysis of punch-through injection microwave devices.

13 p1590 A73-28541

Microwave signal source amplitude stabilization, analyzing circuit with doubly balanced electronically regulated attenuator with p-i-n diodes

14 p1733 A73-30055

Description of the measurement design and the measurement principle in the measurement of the chip impedance of coaxially mounted semiconductor diodes in the microwave range

14 p1733 A73-30058

Ge-doped p-type epitaxial GaAs for microwave device application.

15 p1923 A73-31399

Microwave integrated circuit applications at special microwave devices operation.

15 p1851 A73-32274

Microwave power transistors - The present and the future.

15 p1852 A73-32275

Mechanical design of microwave integrated circuit enclosures.

16 p1989 A73-33469

Ceramic waveguide microwave

16 p1989 A73-33470

Small-signal modelling and characterization of microwave transistors.

16 p1990 A73-33687

Microwave-package measurements at the Q band.

16 p1991 A73-34019

Design of second-order phase circuits constructed with TEM-line segments

17 p2144 A73-34592

Thin film hybrid microwave integrated circuit.

17 p2141 A73-35323

Josephson junction mixing of monochromatic sources at two microwave frequencies, noting output power dependence on dc bias

18 p2340 A73-36624

Enhancement of the sensitivity of microwave admittance measurements through the use of 'matching' two-ports

19 p2409 A73-37717

Preparation and RF properties of MIS mesa varactors.

19 p2409 A73-37720

Microwave integrated circuit technology.

19 p2411 A73-38535

A calculation of the equilibrium temperature distributions in multiple-emitter microwave transistors.

20 p2535 A73-38926

Book - Design performance and applications of microwave semiconductor control components.

20 p2535 A73-39136

Microwave IC devices covering circulators, directional couplers, frequency multipliers, phase shifters, power amplifiers and reference oscillators, discussing technological development and applications

21 p2668 A73-40019

Physical modeling of active microcircuits for the SHF range

21 p2668 A73-40020

Thermal response of microwave transistors under pulsed power operation.

21 p2663 A73-40774

Continuum centimeter wave radiometers circuits, parameters, sensitivity and atmospheric radio emission fluctuations

21 p2705 A73-41460

Viscous dielectric materials for application in microwave microcircuits.

21 p2668 A73-41589

Prediction methods for the susceptibility of solid state devices to interference and degradation from microwave energy.

22 p2823 A73-41796

Pulse burnout of microwave mixer diodes.

22 p2835 A73-42965

Analysis of microwave circuit for characterization of negative-conductance devices by transients.

23 p2964 A73-44076

MICROWAVE COUPLING

NT COUPLING CIRCUITS

Modulation type microwave receiver with selective filter and ferrite resonator in waveguide coupling

08 p0949 A73-21561

Computational estimate of applicability of infinite-array theory.

09 p1065 A73-23099

Panoramic measurement of the coupling impedance of delay systems by the heterodyne method

12 p1479 A73-27210

Surface acoustic wave multistrip components and their applications.

12 p1484 A73-27567

Several parallel-plate guides with screen as phased array - Effect of the coupling on the directive gain

16 p1979 A73-33374

Five wave interaction - A possibility for enhancement of optical or microwave radiation by nonlinear coupling to explosively unstable plasma waves.

17 p2218 A73-35821

Generalized representation of electric fields in interaction gaps of klystrons and traveling-wave tubes.

18 p2292 A73-36595

A circular waveguide 'hybrid-T' and its applications.

18 p2292 A73-36606

Off-resonance microwave-created plasmas.

20 p2597 A73-39196

Use of cancellation techniques in the measurement of atmospheric crosspolarisation.

23 p2955 A73-44111

MICROWAVE EMISSION

Infrared stars with strong 1665/1667-MHz OH microwave emission.

01 p0104 A73-11040

A noncoherent model for microwave emissions and backscattering from the sea surface.

02 p0164 A73-12362

Aircraft measurements of microwave emission from Arctic Sea ice.

02 p0171 A73-12773

Hydrogen recombination line and continuum observations at 5000 MHz of 13 southern HII regions.

03 p0372 A73-13347

The design of broad-band resistive radiation probes.

03 p0310 A73-14492

Free-free absorption of gyrosynchrotron radiation in solar microwave bursts.

04 p0492 A73-15366

Measurements of flux fluctuation in solar radio emission at a wavelength of 3 cm

05 p0573 A73-16270

Some studies on the solar microwave bursts in relation to the slowly varying component.

05 p0621 A73-17038

X-radiation /E greater than 10 keV/, H-alpha and microwave emission during the impulsive phase of solar flares.

05 p0610 A73-17041

Centimeter radiation associated with the solar limb prominence of 8 February 1972.

08 p0996 A73-20762

Observation of beam-plasma interaction in a toroidal plasma in a large electric field.

08 p0993 A73-21631

Infrared and microwave emission from nebulae in the galaxy.

09 p1150 A73-23133

Galactic nuclei and QSO far IR radiation luminosity explanation by nonthermal maser emission due to gas molecules in dense clouds

09 p1150 A73-23145

Some studies on the association of solar optical flares and microwave bursts with sudden ionospheric disturbances.

11 p1354 A73-25769

Thermal radio emission from Jupiter and Saturn.

11 p1420 A73-25883

Study of the effect of a plasma on the microwave radiation of a helical beam in a waveguide

12 p1527 A73-26935

Microwave oscillations and the visible radiation spectrum of a cesium plasma diode

12 p1527 A73-26938

Quiet sun millimeter wave emission and brightness temperature, discussing observational difficulties arising from fog, cloud and rain attenuation

12 p1543 A73-27725

Further evidence for a complex limb structure in the solar radial brightness distribution at mm wavelengths.

12 p1545 A73-27841

Solar microwave emission height determination from latitude shift, noting precision comparable with observation based on rate of motion in longitude

12 p1536 A73-27842

Low-temperature negative differential microwave conductivity in semiconductors following elastic scattering of electrons.

13 p1669 A73-28614

The Perseus spiral arm at 21-cm.

13 p1685 A73-29354

On the generation of high-energy particles in solar flares.

15 p1925 A73-31068

Stellar maser output observations application to analysis of mass loss rate or physical conditions in circumstellar shell

15 p1934 A73-31477

The correlation between 10.7-cm /2800 MHz/ solar radio emission and chromospheric flares

15 p1926 A73-31646

Solar limb brightening at the 8-mm wavelength

16 p2057 A73-32705

Interstellar microwave radiation measured by spectroscopic analysis of chemical composition, distribution, excitation and emission data

16 p2058 A73-32722

Studies of the solar chromosphere from millimeter and sub-millimeter observations. I - Isophotometric mapping.

16 p2060 A73-32953

Absolute calibration of solar radio flux density in the microwave region.

16 p1993 A73-32968

Development of moving type IV solar radio bursts and relation to expanding magnetic bottles from flare regions.

16 p2054 A73-33096

Lunar radio emission in the 1.25- to 2.5-cm band

16 p2064 A73-33767

Radio emission from the moon and sun at the 2.25-mm wavelength and from Jupiter at the 2.1-mm wavelength

16 p2064 A73-33768

Radio emission from Venus and Jupiter at 2 and 8 mm wavelengths

16 p2068 A73-33817

Results of Jupiter observations in the centimeter wavelength range

16 p2070 A73-33844

Generation-recombination noise and the microwave emission from InSb.

17 p2219 A73-34912

Microwave signatures of first-year and multiyear sea ice.

17 p2163 A73-35466

19-20 May 1969, an example of type III emission during the impulsive phase of flares.

18 p2344 A73-36013

OH observations of sixteen interstellar dust clouds.

20 p2607 A73-39118

Surface microwave emissivities dependence on humidity, vegetable cover and surface structure, considering water influence on sand emissivity

20 p2556 A73-39839

A new estimate of the fluctuation of relict radiation in the universe

21 p2759 A73-40708

Remote sounding of water surface conditions from aboard artificial satellites.

21 p2657 A73-41333

Effect of a plasma on the microwave radiation from a helical beam in a waveguide.

22 p2892 A73-42269

Microwave oscillations and visible emission in a cesium diode.

22 p2892 A73-42272

Remote measurement of salinity in an estuarine environment.

22 p2850 A73-42730

On the spectrum of the S- and B-components of solar radio emission at dm-wavelengths.

22 p2915 A73-43038

Theta-pinch instability of plasma beam, relating plasma oscillation frequency to microwave emission and electromagnetic wave scattering

23 p3011 A73-43710

Microwave emission mechanism of frequency dependent pulse profile changes in pulsar, using cooled parametric amplifier observations

23 p3034 A73-43963

A search for narrow band 21-cm wavelength signals from ten nearby stars.

24 p3133 A73-44552

A study of solar radio emission in the light of Sengupta's model of coronal active regions.

24 p3123 A73-44637

On the observation of linear polarization of solar microwave bursts.

24 p3136 A73-44644

Interpretation of atmospheric radio emission in the 5-mm spectral region

24 p3068 A73-44961

MICROWAVE EQUIPMENT

NT BACKWARD WAVE TUBES

NT CATHODE RAY TUBES

NT CELESTROSCOPES

NT GYRATORS

NT HELITRONS

NT HORN ANTENNAS

NT IMAGE ORTHOCOSINS

NT IMAGE TUBES

NT KLYSTRONS

NT LENS ANTENNAS

NT MAGNETRONS

NT MICROWAVE AMPLIFIERS

NT MICROWAVE ANTENNAS

NT MICROWAVE FILTERS

NT MICROWAVE INTERFEROMETERS

NT MICROWAVE OSCILLATORS

NT MICROWAVE PLASMA PROBES

NT MICROWAVE PROBES

NT MICROWAVE RADIOMETERS

NT MICROWAVE TUBES

NT PHOTOMULTIPLIER TUBES

NT PICTURE TUBES

NT PLANOTRONS

NT SLOT ANTENNAS

NT THERMIONIC DIODES

NT THYRATRONS

NT TRAVELING WAVE TUBES

NT VIDICONS

Book - Handbook of microwave techniques and equipment.

01 p0021 A73-10025

Pulse communication at microwave bit rates using Gunn domains.

02 p0145 A73-11534

Radar engineering developments, discussing microwave and optical systems, plan position indicators, antennas, displays, receivers, transmitters, solid state IC devices and signal processing

06 p0668 A73-18440

Operation, fabrication and structural features of pulsed/CW microwave p-n diodes, presenting diode impedance and resistance as function of conduction current

07 p0797 A73-18898

Solid state microwave electronics technology review covering parametric amplifier, maser, tunnel and avalanche diodes, transistors, and transmission, filtering and passive signal processing techniques

08 p0942 A73-20701

Point contact and Schottky barrier microwave mixer diodes reliability under X band RF pulse operating conditions, considering burnout alleviating fabrication techniques

08 p0943 A73-20735

Conversion losses of a point contact presenting the Josephson effect used in a microwave mixer

08 p0938 A73-20968

Narrow band and broad band step-recovery diode frequency multipliers for microwave power generation.

08 p0947 A73-21138

Microwave and millimeter wave receiver noise performance state of art and acoustic measurement methods, discussing traveling wave maser, parametric and transistor amplifiers and tunnel diodes

08 p0940 A73-21625

Semiconductors for microwave frequencies.

08 p0949 A73-21649

Nonlinear properties of microwave avalanche diodes operated in IMPATT mode, discussing current density effect and power efficiency

09 p1063 A73-22489

Propagation in periodically loaded waveguides with higher symmetries.

09 p1063 A73-22490

Solid-state devices and components for mm-wave receiver-transmitter systems.

09 p1064 A73-22498

Microwave small signal bipolar transistor evolution, design and applications, noting cost effectiveness and surface geometry control

09 p1064 A73-22499

Microwave system with direct, AM, FM and pulse propagation techniques for swept-frequency group delay measurement, discussing error sources and various distortions

10 p1193 A73-23610

Caloric vestibular stimulation via UHF-microwave irradiation.

10 p1178 A73-23650

Microwave landing system /MLS/ with Doppler scanning technique for aircraft guidance precision improvement over standard VHF/UHF ILS, detailing five-year development plan

10 p1246 A73-23652

Digital microwave receiver with passive discriminator for precise and instantaneous pulsed RF signal frequency measurement

10 p1188 A73-24168

Encapsulated common base microwave transistors mathematical models, determining transfer scattering parameters

10 p1195 A73-24420

Microwave Doppler flowmeter design and performance, discussing free flow monitoring of sand from hopper and pneumatic conveying of alumina through steel pipe

10 p1221 A73-24859

High power linear beam microwave klystrons, coupled cavity TWTs and hybrid tubes design and operation, considering electron gun and focusing system

11 p1339 A73-26693

Quantitative analysis of specific gases by means of a microwave cavity spectrometer.

13 p1612 A73-28224

High power microwave nanosecond pulse generator with waveguide standing wave resonator, noting power gain and pulse shape

13 p1583 A73-28672

Microwave Landing System under U.S. national development plan for replacing ILS, discussing system requirements and design, precision DME and flare-out guidance

14 p1773 A73-29884

Printed circuit meander line polarizer for converting microwaves in 1-20 GHz range from linear to circular polarization, describing construction and performance

14 p1735 A73-30221

Miniature phase/amplitude tracking RF receiver front ends.

14 p1737 A73-30623

Cd doped CdTe microwave film detectors sensitivity, frequency response, thermal characteristics and stability

14 p1737 A73-30855

Mathematical description and calculation of the static mode of operation of a microwave power regulator with a semiconductor attenuator.

15 p1849 A73-30993

Ferrite component for waveguide commutator used as microwave switching element and modulator, noting application in navigation instruments and avionics

15 p1849 A73-30995

Allowance for the influence of the space charge in the kinematic theory of microwave devices

15 p1850 A73-31491

Microwave integrated circuit applications at special microwave devices operation.

15 p1851 A73-32274

French civil aviation inexpensive C band landing system with ILS angular coding and simplified on-board equipment for STOL and Alpine airports

15 p1910 A73-32467

Microwave guidance system for aircraft landing, discussing civil and military requirements, position measurement capability, shadowing in propagation, and ground reflection induced signal fading

15 p1910 A73-32468

Pulse coded scanning beam microwave landing system technology assessment for civil aviation application, describing ground equipment and procedures

15 p1910 A73-32469

Multiple path induced position errors in microwave landing systems, considering beating beam and Doppler systems based on time and frequency division multiplexing respectively

15 p1910 A73-32471

Frequency hopping principle for precision L band DME as complementary aid to microwave landing system

15 p1911 A73-32490

The multipath challenge for the microwave landing system.

15 p1912 A73-32503

M.A.D.G.E. - Microwave Aircraft Digital Guidance Equipment: Description of the system

15 p1912 A73-32504

Propagation studies and the development of terrestrial microwave radio relay systems above 10 GHz in the UK.

16 p1980 A73-33702

ECM systems with TWT dual moding to provide distinct CW and pulsed microwave power levels, evaluating performance beyond octave in bandwidth

16 p1990 A73-33849

Oscillographic equipment for research in the field of semiconductor microwave electronics

17 p2218 A73-34160

Mixed CTOL-QTOL traffic effects on air traffic controller tasks, microwave landing and radio navigation systems, airport operation and ground equipment [MBB-UH-05-73]

17 p2207 A73-34487

Flight-path control device for generating curvilinear flight path profiles using microwave landing systems [DGLR PAPER 73-016]

17 p2208 A73-34492

Aircraft microwave landing system development, including conventional system history and shortcomings, program objectives and implementation schedule for ATC

17 p2208 A73-34611

Computerized automatic microwave testing with pulse measurements of phase and power from Reliable Advanced Solid State Radar phased array modules, discussing system design

17 p2135 A73-34724

Techniques for digital-microwave hybrid real-time radar simulation.

17 p2131 A73-35303

Microwave equipment reliability design for aerospace environment applications, considering vibration, shock, humidity and temperature effects and frequency stability

18 p2293 A73-36778

C band microwave landing system for increased guidance signal accuracy and reliability in azimuth, elevation and range relative to touchdown point

19 p2450 A73-37494

Modular building block microwave landing system for automatic flight in CAT, discussing ICAO and NIAG missions

19 p2450 A73-37495

United States Microwave Landing System development program.

19 p2451 A73-37815

Millimeter wave solid state technology for 60 GHz communication systems, discussing silicon Schottky diode and varactor mixer/receiver, parametric amplifiers and upconverters

20 p2534 A73-38748

Nonlinear trajectory following in the terminal area - Guidance, control and flight mechanics concepts using the microwave landing system.

[AIAA PAPER 73-903]

20 p2589 A73-38837

Evaluation of effects of the microwave oven /915 and 2450 MHz/ and radar /2810 and 3050 MHz/ electromagnetic radiation on noncompetitive cardiac pacemakers.

20 p2520 A73-39824

Microwave Landing System with air-derived sample data and scanning narrow beam antennas for signal-in-space generation, discussing design requirements and performance test

21 p2735 A73-40046

Ground based microwave landing system for aircraft navigation, guidance and control in terminal area, discussing system requirements for flight safety

21 p2735 A73-40047

Microwave landing system elevation data or altimeter information for flare-out guidance, considering airport, aircraft autopilot and ground equipment and cost factors

21 p2736 A73-40050

Microwave acoustic surface wave devices design tradeoffs, considering propagation losses, air loading, beam steering and diffraction, and transducer effects in curves and data

22 p2833 A73-42399

New device techniques for microwave bipolar power transistors.

22 p2833 A73-42692

Evolution of blind landing systems

22 p2885 A73-43032

MICROWAVE FILTERS

An initialization technique for improved MTI performance in phased array radars.

06 p0664 A73-17790

Compact YIG bandpass filter with finite-pole frequencies for applications in microwave integrated circuits.

06 p0678 A73-18742

Precision design of millimeter-wave band-pass filter.

07 p0799 A73-19371

Microwave filters with single crystal YIG sample as ferrimagnetic resonators, determining magnetic field

MICROWAVE FREQUENCIES

and temperature effects on resonator cut-off frequency 08 p0942 A73-20705

Band-splitting filters in oversized rectangular waveguide. 08 p0946 A73-21119

Microwave bandpass filters formed by shunt and series stubs with quarter wave matching strip lines, noting advantage of equal lengths 09 p1063 A73-22463

Microstrip bandpass filters with reduced radiation effects. 09 p1065 A73-23098

General cavity analysis for corrugation in rectangular waveguide microwave filters, using admittance method with consideration for propagation modes 10 p1192 A73-23606

Design and manufacture of delay equalized comb-line filters. 10 p1193 A73-23608

The optimization of delay equalized comb-line filters. 10 p1193 A73-23609

Narrow band microwave active bandpass filter with inverted-common-collector transistor circuit, discussing design algorithm, insertion loss, stability, sensitivity and frequency selectivity 10 p1201 A73-24169

VHF and microwave surface acoustic wave bandpass filter design with impulse model for frequency response and interdigital transducer input admittance calculation 12 p1484 A73-27563

The use of surface-elastic-wave reflection gratings in large time-bandwidth pulse-compression filters. 12 p1480 A73-27566

Ranging and data transmission using digital encoded FM-'chirp' surface acoustic wave filters. 12 p1470 A73-27571

Potential applications of acoustic matched filters to air-traffic control systems. 12 p1522 A73-27572

Surface elastic wave microwave bandpass filter for miniaturized frequency synthesizer in satellite communications systems, noting insertion loss and sidelobe reduction 12 p1484 A73-27573

A programmable surface acoustic wave matched filter for phase-coded spread spectrum waveforms. 12 p1484 A73-27574

Microwave filters physical volume relation to losses, discussing intrinsic and loaded Q factors from frequency attenuation curves and graphical design procedures 15 p1850 A73-31252

Three layer concentric sphere microwave filter resonators, considering eigenvalue equation for arbitrary conductivity and complex permittivity and permeability effects on resonant frequencies and Q factors 16 p1987 A73-33092

Determination of the geometrical dimensions of a bandpass filter for a microwave hybrid integrated circuit 17 p2134 A73-34584

High performance surface wave bandpass filters for signal processing applications. 17 p2140 A73-35320

The present state of the microwave filter art. 19 p2415 A73-38533

Experimental characteristics of certain types of semi-open, multi-circuit microwave ferrite filters. 20 p2535 A73-38920

The theory of half-open ferrite microwave filters. 20 p2535 A73-38925

Linear signal processing by acoustic surface-wave transversal filters. 21 p2705 A73-41426

Tapered corrugated waveguide low-pass filters. 21 p2666 A73-41427

Two dimensional microstrip transmission line with step discontinuities, predicting microwave filtering behavior by broadband equivalent circuit for comparison with experiment 22 p2835 A73-42465

German monograph on microwave filters for communication channels separation at millimeter wavelengths covering coupling circuits design and resonant frequencies of coaxial resonator 22 p2827 A73-42701

Implementation problems of a multichannel digital filter in the case of beat frequencies in the MHz range 23 p2957 A73-43316

Coupling coefficient/frequency characteristics of rectangular dielectric waveguide channel dropping coupled line filter for millimeter wave 23 p2961 A73-44118

Electronically tunable microwave bandpass filters 24 p3071 A73-44606

MICROWAVE FREQUENCIES
 NT C BAND
 NT EXTREMELY HIGH FREQUENCIES
 NT SUPERHIGH FREQUENCIES

Radio wave propagation effects in a three-dimensionally inhomogeneous magnetoactive ionosphere 01 p0016 A73-10204

Practical and precise means of microwave power meter calibration transfer. 03 p0310 A73-14499

Equivalent circuits for microwave frequency converter design, noting small and large signal operation and power efficiency of variable capacity diode circuit 06 p0673 A73-17578

Physiological effects of microwave electromagnetic fields on human and animal organisms, considering etiology, diagnostics and prophylaxis 06 p0659 A73-18256

Velocity measurements of microwave ultrasonic waves in quartz. 06 p0724 A73-18776

A semiconductor in a microwave electromagnetic field and in a steady magnetic field 07 p0862 A73-20012

Analog-computer studies on microwave mixing in superconducting weak links. 07 p0863 A73-20103

Frequency multipliers for the millimeter wave band employing gallium arsenide diodes. 07 p0802 A73-20146

The influence of substrate properties on microwave losses in thin films of semiconductors. 09 p1064 A73-23041

Spatial distributions of intensity and polarization over the source of microwave impulsive bursts. 10 p1275 A73-23828

Ionization front propagation velocity as function of microwave power density, showing dependence on precursor electron density profiles 10 p1251 A73-24257

Venus - Microwave opacity of the minor atmospheric constituents. 11 p1417 A73-25267

Book - Microwave power measurement. 12 p1480 A73-27425

Millimeter wave burst mean duration relation to PCA event intensity derived from relationship between impulsive single frequency microwave bursts and solar proton events 12 p1543 A73-27616

A survey of elliptical galaxies at 6 cm. 13 p1685 A73-29361

High-resolution microwave holographic technique - Application to the imaging of objects obscured by dielectric media. 13 p1622 A73-29668

Rainfall crosspolarization at microwave frequencies with differential phase shift and attenuation, considering rain models 13 p1587 A73-29670

On Compton models of the isotropic X-ray background. 14 p1796 A73-30001

Ultrahigh energy photons, electrons, and neutrinos, the microwave background, and the universal cosmic-ray hypothesis. 15 p1927 A73-32004

A high-temperature plasma state in a high-power microwave discharge 17 p2214 A73-34136

MICROWAVE HOLOGRAPHY
 Real time microwave hologram data acquisition by double circular scanning of single sensor over recording aperture, presenting optical bench simulation 13 p1618 A73-29122

Image quality of binary and multigradation microwave holograms, noting HF components and background noise 17 p2168 A73-35164

On numerical reconstruction of the image from a microwave hologram. 21 p2655 A73-41045

MICROWAVE IMAGERY
 Aircraft measurements of microwave emission from Arctic Sea ice. 02 p0171 A73-12773

An airborne Ka-band microwave radiometric measurement mapping system. 04 p0451 A73-15783

Low energetic efficiency of semiconductor microwave scanning converters for radio images of fog obscured objects 05 p0556 A73-16072

Coherent optical processing and display techniques for microwave imagery generation from synthetic aperture radar system data, discussing hologram and side-looking radar 06 p0667 A73-18279

Mapping of atmospheric and sea ice parameters with an imaging microwave radiometer from the Nimbus 5 satellite. 06 p0667 A73-18281

On the numerical reconstruction of images from a microwave hologram. 06 p0669 A73-18737

Study of antenna cross-polarization characteristics by using microwave holography 09 p1065 A73-23087

Recent progress in infrared and microwave techniques of astronomical interest. 09 p1086 A73-23128

Millimeter wave imagery of complex three dimensional target by diffuse reflection with spatial filtering, discussing range, resolution and view field capabilities 10 p1188 A73-23798

A two-satellite microwave occultation system for determining pressure altitude references. 12 p1521 A73-26813

Diffraction theory treatment of long wave holography to demonstrate spiral scan and other circular sampling formats in microwave or acoustic hologram recording 13 p1615 A73-28585

Experimental investigation of the direct quasi-optical radio-wave imaging of small objects. 13 p1583 A73-28673

Double balanced microwave mixer circuit with local oscillator input and IF outputs for achieving low noise and image rejection 14 p1737 A73-30622

Microwave holography application to landing without visibility 15 p1911 A73-32497

Remote sensing and photointerpretation, discussing black and white, color and IR photography, microwave imagery, atmospheric attenuation, reflectance and potential application for ERTS satellites 16 p2014 A73-33100

Dark field method for phase diffraction grating visualization by microwave holography, using radio lens for object microwave spectrum formation 17 p2168 A73-35165

Hologram matrix and its application to a novel radar. 19 p2428 A73-37145

Airborne and spaceborne microwave imaging techniques for earth surface surveys, discussing resolution capabilities and applications for side-looking radar, microwave radiometers and scatterometers [AAS PAPER 73-111] 20 p2533 A73-38577

Polar region soil moisture content remote sensing based on electromagnetic backscattering and depolarization by ice and terrain, considering radar, microwave and IR sensors 21 p2654 A73-40814

MICROWAVE INTERFEROMETERS
 Ionospheric vertical electron density profiles from geophysical rocket-borne microwave dispersing interferometer 11 p1350 A73-25079

A balloon-borne helium-cooled interferometer for investigation of the isotropic submillimetre background. 11 p1368 A73-26506

The 73.5-cm wavelength radio interferometer of the Biurakan Observatory 12 p1479 A73-27226

High resolution radio observation of sun at 3.71 and 11.1 cm with three-element interferometer, noting flare near east limb 16 p2060 A73-33097

High-resolution interferometric observations of Venus at the 3.1-cm wavelength 16 p2068 A73-33818

Some characteristics of an operational system for measuring UT 1 using very long baseline interferometry. 21 p2705 A73-41330

Fixed baseline millimeter wave interferometer with aperture synthesis telescope of antenna array for interstellar and planetary water vapor and radio sources mapping 23 p2980 A73-43364

An 8-mm interferometer for solar radio astronomy at Bordeaux, France. 23 p2980 A73-43365

An aperture-synthesis interferometer at Ooty for operation at 327 MHz. 23 p2980 A73-43366

Radio astronomy interferometer receiver IF control for centimeter wave polarized signal processing and parabolic antenna instrumentation 23 p2980 A73-43377

Local measurements of plasma parameters by a microwave interferometer with a moving emitter 23 p3011 A73-43666

High-angular-resolution observations of Saturn at 21.1-centimeter wavelength. 24 p3138 A73-45051

MICROWAVE OSCILLATORS
 NT BACKWARD WAVE TUBES
 Resonant feedback loops and impedance matching network analysis of pulsed and CW transistor microwave power oscillators 01 p0024 A73-10722

Linear rapid frequency settling time solid state voltage controlled oscillators (VCO) for electronic countermeasure and B-scan tracking radar applications 01 p0024 A73-10723

Control of the frequency of Gunn-effect oscillators by a magnetic field 01 p0024 A73-10978

Nonlinear computation of a resonant O-type oscillator featuring constant wave amplitude in the presence of losses

01 p0025 A73-10984

Large-signal calculations on IMPATT oscillators with voltage waveforms giving close-to-optimum efficiency.

01 p0026 A73-11297

50 GHz gallium-arsenide IMPATT oscillator.

02 p0144 A73-11519

Gunn diodes - Physical principles and simulation calculations

02 p0144 A73-11529

Limited space charge accumulation oscillations in gallium arsenide

02 p0199 A73-11530

Microwave Gunn diode oscillators applications, noting use as Doppler radar and synchronized oscillators

02 p0144 A73-11532

LF noise in n-type GaAs and its correlation with HF noise of Gunn-diode oscillators

02 p0145 A73-11535

Indium phosphide as a new material for microwave/transferred electron effect/oscillators.

02 p0199 A73-11536

Standing wave approximation of distributed dual frequency parametric oscillators consisting of semiconductor diodes and transmission line in steady state

02 p0147 A73-12490

Material concerns, fabrication procedure, cooling techniques, performance and stability characteristics of transferred electron microwave amplifiers and oscillators

03 p0282 A73-13893

Transit effects in grid plate gap of triode for generating microwave oscillations in regime similar to IMPATT diode

03 p0284 A73-14069

Optimal output power of tunnel drift diode oscillator in millimeter band as function of electric field and diode geometry

03 p0284 A73-14086

Measurement of admittances of microwave oscillators with injection locking.

03 p0310 A73-14497

Wideband varactor-tuned Gunn effect oscillators.

04 p0426 A73-14732

Some theoretical and practical considerations in the design of wideband varactor tuned Gunn oscillators.

04 p0426 A73-14733

Advances in YIG-tuned Gunn effect oscillators.

04 p0426 A73-14734

Subharmonic generation and its implications in Gunn effect devices.

04 p0427 A73-15055

CW microwave oscillations of reach-through p-n-p barrier injection transit time /BARITT/ diodes, calculating small signal impedance and noise measure for comparison with experiment

04 p0427 A73-15346

Permanent and transient radiation effects in BARITT microwave oscillators.

05 p0558 A73-16518

Transient ionizing radiation effects on IMPATT diode oscillators.

05 p0558 A73-16519

Gunn diodes oscillating circuit with waveguide cavity in push-pull mode at 42 GHz for high power parametric amplifier pump applications

05 p0558 A73-16807

Silicon X band oscillation TRAPATT diodes with high power efficiency, presenting electric field variation with distance

05 p0559 A73-16809

GaAs transferred electron /Gunn/ device microwave oscillator with harmonic tuning, noting reactive termination and bias voltage effects on efficiency optimization

05 p0559 A73-16813

On some noise properties of high frequency solid-state oscillators.

06 p0673 A73-17714

Large-signal noise, frequency conversion, and parametric instabilities in IMPATT diode networks.

06 p0679 A73-17789

Optimize Gunn circuits for wideband varactor tuning.

06 p0675 A73-17841

Varactor or YIG tuned Gunn effect microwave oscillators for ECM applications, noting low noise octave tuning and high sweep rates

06 p0675 A73-17842

CW Q band Gunn diode microwave oscillator fabricated by integral heat sink technique for high power output and efficiency

06 p0677 A73-18345

Display of microwave pulse response via the real-time Fourier transform of the transfer function.

06 p0677 A73-18346

Microwave oscillator subharmonic phase locking, discussing nonlinear capacitance and linear frequency-dependent parameter and broadband tuning characteristics comparison with fundamental injection locking

06 p0677 A73-18739

Nonlinear analysis for local microwave oscillator voltage waveform across nonlinear junction of Schottky barrier mixer diode, comparing results with analog simulation

06 p0677 A73-18740

Theoretical and experimental study of GaAs IMPATT oscillator efficiency.

06 p0678 A73-18789

Noise of local oscillators of high capacity radio links

07 p0798 A73-19179

Intrinsic FM noise of Gunn oscillators.

07 p0798 A73-19341

Attainment of a low-noise high-power and highly stable Gunn oscillator by coupling to a superconducting cavity.

07 p0801 A73-20109

Direct frequency demodulation with CW Gunn and IMPATT oscillators.

07 p0795 A73-20554

Microwave lumped passive and active circuit components properties assessment, considering inductor, capacitor, resistor, gyrator, tunnel diode amplifier, varactor Gunn oscillator, and parametric amplifier

08 p0942 A73-20703

IMPATT diode microwave oscillator performance analysis based on model with ac current and voltage superposition on dc, determining avalanche frequency and negative resistance

08 p0942 A73-20706

IMPATT diode microwave oscillator performance analysis for I-V characteristics, output power, efficiency and starting current from equivalent circuit

08 p0943 A73-20707

IMPATT diode anomalous microwave oscillation mode performance analysis, calculating I-V variation, power and efficiency from equivalent circuit

08 p0943 A73-20708

Finite difference calculation for Gunn effect mathematical model, noting negative slope in electron drift velocity versus electric field characteristics for microwave oscillation

08 p0943 A73-20710

Microwave oscillation in germanium avalanche diodes. I, II.

08 p0947 A73-21461

Doppler signal detection with negative-resistance diode oscillators.

09 p1062 A73-22321

X band Gunn oscillator FM noise spectrum dependence on quality factor of resonant circuit

09 p1062 A73-22322

Transistor harmonic oscillator design.

10 p1192 A73-23573

Tuning nonlinearity of oscillatory systems made of long-line segments containing a varicap

10 p1193 A73-23728

Tunnel and Gunn diode oscillators coupled to superconducting cavity as S and X band frequency standards

10 p1195 A73-24397

The elimination of tuning-induced burnout and bias-circuit oscillations in IMPATT oscillators.

10 p1196 A73-24622

J-band transferred-electron oscillators.

10 p1196 A73-24863

Noise in single-frequency oscillators and amplifiers.

10 p1196 A73-24864

Wide-band varactor-tuned X-band Gunn oscillators in full-height waveguide cavity.

10 p1197 A73-24865

Overlength modes of transferred-electron oscillators.

11 p1337 A73-25359

Development of cavities for microwave solid state oscillator

11 p1338 A73-26150

Nonlinear theory of Ubitron microwave oscillator device using fast electromagnetic wave-fast electron beam interaction in spatially periodic magnetostatic field

11 p1332 A73-26164

Injection-locked IMPATT oscillations applied to F.D.M. microwave transmission.

11 p1338 A73-26285

On combined frequency oscillations of the forced Van der Pol oscillator.

11 p1339 A73-26696

Pulse avalanche diode oscillators with an injected CW signal.

11 p1339 A73-26698

Analysis of an oscillator using a sequence of negative resistance devices

12 p1477 A73-26871

Laddertron oscillator /klystron/ cavity dispersion characteristics via electrodynamic analysis of dispersion equation for surface wave operation and coupled modes

12 p1477 A73-26948

Gunn microwave oscillators electron temperature dependent noise in absence of 1/f type, considering thermal or Johnson noise augmented by carriers hopping

12 p1478 A73-27111

Investigation of the synchronization of Gunn diode oscillators having a stripline resonance system

12 p1480 A73-27448

Use of an yttrium-iron garnet sphere as the tuning element in Gunn oscillators

12 p1481 A73-27592

Certain problems in controlling phase of microwave electromagnetic oscillations using an inductive transistor.

13 p1591 A73-28670

A tunnel diode regenerative frequency multiplier with a high multiplication factor.

13 p1591 A73-28734

Injection phase locked microwave oscillator for FM amplifier, calculating frequency drift caused gain limitation in terms of diode and circuit properties temperature effects

13 p1593 A73-29116

Computer simulations of large-signal oscillation behavior of avalanche diodes.

13 p1594 A73-29235

Injection frequency locking of the avalanche transit-time oscillator.

13 p1594 A73-29292

Noise in cavity-stabilized microwave oscillators.

13 p1595 A73-29294

Extension of the theory of frequency noise of oscillating masers

13 p1630 A73-29558

Noise at large RF amplitudes in IMPATT oscillators.

14 p1731 A73-29713

Circuits for power density reduction in TRAPATT diodes.

14 p1732 A73-29927

Narrowband time domain reflectometer uses pulse modulated Gunn-oscillator to measure small reflections in 6 and 7.5 GHz band waveguides.

14 p1733 A73-30057

High-power high-efficiency operation of Read-type IMPATT-diode oscillators.

14 p1736 A73-30447

A theory of oscillator noise and its application to IMPATT diodes.

15 p1851 A73-31939

X band oscillators for microwave generation based on silicon avalanche diodes, presenting power and efficiency dependence on frequency and bias current

15 p1851 A73-32160

Aftereffects in IMPATT oscillators with transient ionizing radiation.

15 p1851 A73-32187

Measurement of external Q factor of microwave oscillators using frequency pulling or frequency locking.

15 p1852 A73-32646

Microwave capabilities of transferred-electron devices.

16 p1986 A73-32720

Wideband varactor-tuned solid-state sources to 20 GHz.

16 p1991 A73-33898

Q band /38 GHz/ varactor-tuned Gunn oscillators.

16 p1991 A73-34018

A study of millimeter-wave GaAs IMPATT oscillator and amplifier noise.

17 p2133 A73-34217

Design considerations of high-efficiency GaAs IMPATT diodes.

17 p2134 A73-34219

An electronically tuned Gunn oscillator circuit.

17 p2134 A73-34222

Compatible ILS involving pilot signal from microwave oscillator and precision ILS involving linear antenna array of emitter elements

17 p2207 A73-34484

Quenched-domain mode oscillation in waveguide circuits.

17 p2136 A73-34969

State-space analysis of a magnetically tuned IMPATT oscillator lumped model.

17 p2136 A73-34973

Temperature effects on modulation sensitivity and vibrational spectra in Gunn diode oscillators, suggesting frequency stability improvement method

17 p2136 A73-35162

An X-band Gunn-diode generator with varactor tuning

17 p2126 A73-35550

Electronically-regulated power supplies for microwave backward-wave oscillators.

17 p2142 A73-35643

The effects of the microwave structure parameters on the behavior of X-band Gunn oscillator.

17 p2142 A73-35650

Gunn diode parameters from a small signal analysis.

17 p2142 A73-35651

Frequency distortions of signals in frequency-modulated oscillators with a delayed feedback.

17 p2130 A73-35714

Mutual synchronization of oscillators which are coupled by a segment of a long line.

17 p2143 A73-35715

Highly stabilized IMPATT oscillators at millimeter wavelengths.

18 p2293 A73-36607

A technique for gating short microwave pulses.

19 p2410 A73-38000

MICROWAVE PHOTOGRAPHY

- Electron beams as carriers of optical coherence. 20 p2570 A73-38621
- Active electronic devices - Microwave diodes 20 p2535 A73-39054
- Book - Gallium arsenide microwave bulk and transit-time devices. 20 p2536 A73-39137
- Intrinsic AM noise in singly tuned IMPATT diode oscillators. 20 p2537 A73-39417
- Analytic theory for silicon double-sided n/+/-n-p-p/+/-TRAPATT-diode structures. 20 p2538 A73-39594
- Design of Gunn-diode oscillators on the basis of normalized characteristics 21 p2659 A73-40007
- Summation of the output power from two Gunn diodes 21 p2659 A73-40008
- Thermally induced FM noise in Gunn oscillators and jitter in Gunn-effect digital devices. 21 p2660 A73-40096
- Graphical analysis of traveling-wave-tube oscillator with external feedback loop. 21 p2663 A73-41046
- Frequency-following injection microwave oscillator with bias voltage control for tracking speed to provide amplifier or noise improvement circuit 21 p2664 A73-41091
- Self excited mixer/detector of Gunn diode oscillator, calculating detection characteristics from combined equivalent circuit and computer simulated analysis 21 p2664 A73-41092
- Low noise Si multijunction IMPATT diode measurements for large signal FM X band oscillator performance 21 p2668 A73-41588
- Russian book on wideband microwave oscillatory systems covering stepwise and smoothly irregular stripline and coaxial line resonators for radio receivers, multipliers, etc 22 p2832 A73-41881
- Approximate nonlinear theory of orotron as SHF hybrid-type monotron oscillator, calculating output power and efficiency as function of tube electrical parameters and geometry 22 p2826 A73-42338
- Boost klystron efficiency with three-cavity design. 22 p2833 A73-42400
- Book - Avalanche-diode microwave oscillators. 22 p2833 A73-42490
- Construction techniques for an S-band high-power fluid-cooled TWT helix. 22 p2834 A73-42697
- Some general observations on the tuning characteristics of 'electromechanically' tuned Gunn oscillators. 23 p2960 A73-44070
- Increasing the locking bandwidth of a waveguide-cavity oscillator through the use of a double-tuned circuit. 23 p2965 A73-44109
- Short-term frequency stability of an L band oscillator with a superconducting cavity. 23 p2961 A73-44117
- Microwave transistor oscillators design based on Si overlay transistors and microstrip transmission lines as passive elements, obtaining negative resistance between collector-base terminals 23 p2961 A73-44144
- Calculation of the energetic characteristics of Gunn diode oscillators in retarded- and quenched-domain modes 24 p3072 A73-44928
- Parametric oscillations in an oscillating circuit utilizing negative resistance. 24 p3075 A73-45479
- Gunn diode negative resistance microwave oscillators with simultaneous lower frequency mode and individual tunings of two frequencies 24 p3073 A73-45483

MICROWAVE PHOTOGRAPHY

- Microwave or acoustic holographic synthetic aperture interferometry with pulsed techniques, noting single scan, resolution and fringe number advantages 07 p0824 A73-20110

MICROWAVE PLASMA PROBES

- Measurement of plasma density in a torsatron by a multimode resonator technique 07 p0855 A73-19283
- Measurement of spatial plasma-density distributions with the aid of an open barrel-shaped resonant cavity 09 p1124 A73-21879
- Determination of the electron temperature of a plasma by sounding with an extraordinary wave along a magnetic field 10 p1253 A73-23504
- Microwave cavity measurements of electron densities in a shock tube. 10 p1220 A73-24620
- Application of the collisionless absorption of an extraordinary wave to the determination of plasma electron temperatures 12 p1528 A73-27302

- Multimode cavity measurements of plasma density in a torsatron. 13 p1665 A73-28683

- Measurement of plasma density distribution using an open barrel-shaped cavity. 17 p2215 A73-34303

- Determination of electron temperature of a plasma by probing the extraordinary wave along a magnetic field. 17 p2217 A73-35184

MICROWAVE PROBES

- NT MICROWAVE PLASMA PROBES
- Determination of solid-propellant transient regression rates using a microwave Doppler shift technique. [ALAA PAPER 72-1118] 03 p0351 A73-13433

MICROWAVE RADIATION

U MICROWAVES

MICROWAVE RADIOMETERS

- Observations of precipitation zones from satellites using microwave radiometers. 02 p0160 A73-12267
- Precipitation detection over the ocean using microwave satellite radiometry. 02 p0188 A73-12268
- Microwave radiometric measurements of atmospheric temperature and water from an aircraft. 02 p0164 A73-12361
- Spectral characteristics and black body radiation sensitivity of submillimeter band radiometer based on n-type epitaxial GaAs films 02 p0147 A73-12496
- An airborne Ka-band microwave radiometric measurement mapping system. 04 p0451 A73-15783
- The abundance of NH₃ on Jupiter inferred from UHF radiometry data. [ALAA PAPER 73-128] 05 p0619 A73-16881
- Brightness temperature of Mars thermal emission in two orthogonal polarizations by microwave radiometry from Mars 2 and 3 orbiters 06 p0747 A73-17490
- Microwave remote sensor technology review, discussing target-sensor interaction, spatial resolution concepts and meteorological applications of radiometric and radar systems 06 p0667 A73-18278
- Mapping of atmospheric and sea ice parameters with an imaging microwave radiometer from the Nimbus 5 satellite. 06 p0667 A73-18281
- The earth resources experiment package on Skylab and proposed resource investigations. 09 p1082 A73-22389
- Radiometer measurements of atmospheric attenuation at 19 and 37 GHz along sun-earth paths. 09 p1052 A73-22957
- Microwave noise measurement with Dicke type radiometers, discussing measurement error reduction 09 p1052 A73-23109
- Formamide rotational transition microwave emission detection in interstellar medium in Sgr B2 and Sgr A direction 09 p1150 A73-23140
- Microwave radiometric observations of simulated sea surface conditions. 11 p1355 A73-25774
- The moon as a proposed radiometric standard for microwave and infrared observations of extended sources. 11 p1426 A73-26545
- Parabolic 10 m antenna-8.4 mm wavelength radiometer system for radio astronomy 12 p1498 A73-27724
- An electronically switched microwave radiometer. 13 p1622 A73-29423
- A wideband radiometer for the four-millimeter band built with semiconductor devices 14 p1735 A73-30272
- Atmospheric attenuation measurements via solar microwave radiometer yielding excess attenuation statistics for communications systems planners 16 p1982 A73-33722
- Correction of electrical path length by passive microwave radiometry. 16 p1983 A73-33729
- Passive microwave radiometry and its potential applications to earth resources surveys. 17 p2162 A73-34958
- On the measuring of soil moisture by microwave radiometric techniques. 17 p2170 A73-35363
- Remote sensing using microwave radiometry. 17 p2174 A73-35639
- Oil spills - Measurements of their distributions and volumes by multifrequency microwave radiometry. 17 p2164 A73-35806
- Ground based and airborne microwave radiometer imaging techniques for surface mapping and atmospheric investigations, discussing self calibration, antennas, waveforms and aircraft nose instrumentation 20 p2567 A73-39838
- Mesospheric ozone concentration night and day variations - comparison, describing microwave

- radiometer and remote sensing and photochemical theories 20 p2557 A73-39857

- Salinity surveys using an airborne microwave radiometer. 20 p2558 A73-39865

- Radiometric terrain mapping at 3 mm wavelength. 20 p2568 A73-39870

- Continuum centimeter wave radiometers circuits, parameters, sensitivity and atmospheric radio emission fluctuations 21 p2705 A73-41460

- Microwave radiometric systems. 22 p2859 A73-42059

- Estimation of atmospheric moisture profiles from satellite measurements by a combination of linear and non-linear methods. 23 p3001 A73-43526

MICROWAVE REFLECTOMETERS

- Electron density measurements in time varying plasmas with a microwave reflectometer system. 01 p0044 A73-10120
- Optical wavelengths and microwaves operated holographic refractometers and reflectometers based on dielectric microwaveguides 09 p1085 A73-23013
- Precise measurement of reflection coefficients by means of tuned microwave reflectometers. 12 p1478 A73-27047
- IMEKO Symposium on Microwave Measurement, Budapest, Hungary, May 10-13, 1972, Proceedings. 14 p1733 A73-30054
- Reflectometric bridge in Q band /8 mm/ - Power detected in an unbalanced bridge 19 p2403 A73-37532

MICROWAVE RESONANCE

- Transverse resonance solutions for a long slot leaky wave antenna. 01 p0023 A73-10187
- Series-connected operation of Gunn diodes in a coaxial resonator 01 p0025 A73-10980
- Domain-wall related, natural, submillimeter-wave resonance in orthoferrites 06 p0736 A73-18114
- Satellite dimensional resonances in microwave helicon transmission through semiconductors. 06 p0739 A73-18788
- Microwave filters with single crystal YIG sample as ferrimagnetic resonators, determining magnetic field and temperature effects on resonator cut-off frequency 08 p0942 A73-20705
- Plasma diagnostics with open microwave cavities 08 p0963 A73-21014
- Study of the geometrical resonances of superconducting tunnel junctions. 08 p0994 A73-21207
- The design, analysis, and performance of resonant and nonresonant microwave transmission devices with theoretically infinite rejection. 09 p1080 A73-22103
- Incident radio wave resonance effect on stationary electric and magnetic fields and standing magnetoplasma wave excitation in Bi plates 09 p1127 A73-22604
- Resonant RLC tank circuit design with coupled stripline segments, using lumped and distributed parameter system synthesis theory 13 p1592 A73-28895
- Three layer concentric sphere microwave filter resonators, considering eigenvalue equation for arbitrary conductivity and complex permittivity and permeability effects on resonant frequencies and Q factors 16 p1987 A73-33092
- Dielectric properties of ferrites in the microwave band 17 p2141 A73-35548
- Estimate of error in the solution of interior problems of microwave electrodynamics. 17 p2143 A73-35706
- Properties of microwave cavities containing magnetic resonant samples. 17 p2130 A73-35758
- The theory of half-open ferrite microwave filters. 20 p2535 A73-38925

MICROWAVE SCATTERING

- HF microwave scattering by perfectly conducting four-sided involuted pyramid, deriving principally polarized radar cross section at small aspect angles [AD-753370] 01 p0016 A73-10193
- Stimulated Raman scattering of microwaves in a layer of collisionless plasma. 01 p0082 A73-10423
- Antennas for measurement of microwave electromagnetic field by a light-modulated scattering technique. 01 p0025 A73-11055
- Backscattering of electromagnetic waves from a rough surface model. 06 p0664 A73-18134
- Diffraction by double circular irises and scattering by two elliptical reflectors. 06 p0666 A73-18196

Scattering of microwaves by a stratified overdense plasma at high collision frequencies.
[AD-756733] 06 p0732 A73-18780

Height-gain experimental data for groundwave propagation. II - Heterogeneous paths.
07 p0791 A73-19378

Microwave reflection from detonation waves in equimolar C₂H₂-O₂ at low pressures.
10 p1294 A73-23557

Reduction of ILS errors caused by building reflections.
11 p1330 A73-25784

Two-position scattering of radio waves by the sea surface at small slip angles
11 p1331 A73-26154

Certain methods of numerical calculation in problems of microwave scattering from cylindrical obstacles
13 p1581 A73-28125

Microwave-propagation studies regarding the isotropy characteristics of the turbulent fine structure of the refractive index in the troposphere
15 p1874 A73-32361

Investigation of scattering of microwaves in a plasma-beam discharge.
17 p2217 A73-35716

Scattering properties of oblate raindrops and cross polarization of radio waves due to rain - Calculations at 19.3 and 34.8 GHz.
18 p2290 A73-36880

Electromagnetic interactions with turbulent plasmas.
19 p2465 A73-37167

Effect of scattering on radiometer measurements of attenuation in rain.
19 p2403 A73-37426

Quenching of the beam-plasma instability by mode mixing at a density discontinuity.
19 p2469 A73-37859

Tall buildings induced microwave scattering coefficient measurement with helicopter-borne bistatic pulse radar, explaining coefficient dependence on azimuth, elevation and range
20 p2530 A73-39127

MICROWAVE SENSORS

Problem of using the magnetoresistance effect to measure transferred SHF power
01 p0023 A73-10215

Sensitivity of Josephson junctions in video detection of microwave and millimeter-wave radiation.
06 p0677 A73-18371

Remote sensing of atmospheric and surface temperatures with microwaves.
22 p2825 A73-42060

Book - The surveillance science: Remote sensing of the environment.
23 p2971 A73-43605

MICROWAVE SPECTRA

The short-wavelength spectrum of the microwave background.
01 p0015 A73-10062

Observations at 750, 1400, and 2700 MHz of radio sources in the Vermilion River Observatory survey.
01 p0096 A73-10312

A survey of linear polarization at 1415 MHz. III - Method of reduction and results for the galactic spurs.
01 p0096 A73-10319

Time dependence of Cygnus X-3 8 GHz flux density and spectral index during outburst decay, describing source model
02 p0204 A73-11553

Spectrum and polarization of the Cygnus X-3 outburst.
02 p0210 A73-11556

Thermal radio source DR 21 centimeter flux density measurements for antenna aperture calibration, comparing with standard sources
03 p0366 A73-12932

Very long baseline interferometer observations of Taurus A and other sources at 121.6 MHz.
03 p0366 A73-12933

Glyoxal cis form as source of microwave spectra from rotational spectrum investigations of B-type transitions
03 p0273 A73-13286

Pulsars spectrum measurements with 100 m radio telescope, using 2.8 cm receiver in prime focus and cryogenically cooled parametric amplifier
04 p0502 A73-15977

Interferometric observations of Mars at 21-cm wavelength.
06 p0747 A73-17491

Mars microwave spectra computation by improved thermal model with seasonal polar cap effects and accurate aspect geometry, noting lunar-like planetary subsurface nature
06 p0747 A73-17492

Microwave method of investigating the quality of ruby boules.
06 p0734 A73-17813

Intensity variations in a complete sample of radio sources at 2,300 MHz.
07 p0902 A73-20558

Cyg X-3 flux density measurements at 365 MHz with broadband synthesis interferometer, comparing radio flares with Laan model
07 p0902 A73-20559

Evidence for a common origin of the electrons responsible for the impulsive X-ray and type III radio bursts.
08 p0996 A73-20766

Polarization structure of a solar flare region at 9.5 mm wavelength.
08 p0997 A73-20767

On the long-term behaviour of the circular polarization from coronal condensation radio emission at 4.3 cm wavelength.
08 p0997 A73-20769

The infrared and microwave spectra of stars; International Colloquium on Astrophysics, 17th, Universite de Liege, Liege, Belgium, June 28-30, 1971, Proceedings
09 p1149 A73-23126

Recent experimental and theoretical investigations of infrared and microwave molecular spectra of astronomical interest [Introductory report].
09 p1123 A73-23127

Observational, theoretical, and predicted data on the infrared and microwave spectra of interstellar matter [Introductory report].
09 p1150 A73-23135

Observational data and interpretation of infrared spectra and microwaves of galaxies and the intergalactic matter
09 p1150 A73-23143

The Parkes 2700 MHz survey. IV - Catalogue for the south polar cap zone, declinations -75 deg to -90 deg.
10 p1275 A73-23751

Microwave rotational spectroscopy - A technique for specific pollutant monitoring.
10 p1221 A73-24891

Microwave range-difference measurements on 65-km slanted overwater path, interpreting tropospheric noise power spectra and rms values as function of baseline length
11 p1330 A73-25685

Solar microwave burst radiation spectrum, explaining burst intensity decreasing phase by gyromagnetic absorption model
11 p1413 A73-25946

Field spinning Zeeman modulation in microwave spectroscopy with cosine distribution magnets.
11 p1366 A73-26302

Microwave spectrometer with internal dc glow discharge for transient paramagnetic molecules observation, discussing design features and operating parameters effects on spectrum
11 p1366 A73-26303

Application of acoustic surface-wave technology to spread spectrum communications.
12 p1470 A73-27570

Radiation temperatures of the earth's blankets in the microwave and infrared ranges according to experiment data on the Cosmos-384 artificial earth satellite
13 p1609 A73-29154

Investigation of cloud cover parameters from measurements on the Cosmos 384 satellite
13 p1654 A73-29155

High temperature-microwave spectrometer for Zeeman-effect measurements involving diamagnetic molecules
14 p1753 A73-30235

Long wave measurements of brightness temperature for thermal structure of major planet atmospheres at great depths, discussing Jupiter and Saturn microwave spectra
14 p1800 A73-30537

Interstellar microwave radiation measured by spectroscopic analysis of chemical composition, distribution, excitation and emission data
16 p2058 A73-32722

Experimental study of a new geometry for a microwave molecular-beam spectrometer
16 p2038 A73-33173

Laboratory measurements of electromagnetic properties of atmospheric gases at millimeter wavelengths.
16 p1983 A73-33731

Interpretation of radar measurements of Venus in the microwave range
16 p2068 A73-33820

Dark field method for phase diffraction grating visualization by microwave holography, using radio lens for object microwave spectrum formation
17 p2168 A73-35165

Crop identification by microwave remote sensing obtained spectral response data from fields with corn, sorghum, soybeans and alfalfa
20 p2562 A73-39902

Temperature gradient in gaseous nebulae
21 p2768 A73-40716

Measurement of antenna parameters and calibration of the sensitivity of the RATAN-600 radio telescope in the radar mode of operation at the 8-mm wavelength
21 p2667 A73-41467

FORTH computer program for National Radio Astronomy Observatory telescope observed millimeter

wave spectral line data reduction, summarizing language capabilities
23 p2956 A73-43380

Sensitive search for microwave pulses from the galactic centre.
23 p3033 A73-43961

Statistical properties of radio sources at centimeter wavelengths in a range of terminally weak flux densities
23 p3034 A73-44229

Planetary brightness temperature measurements at 8.6 mm and 3.1 mm wavelengths.
24 p1310 A73-44458

Microwave spectrum, structure, dipole moment and low frequency vibrations of dimethyl cyanamide.
24 p3066 A73-44771

Microwave optical double resonance spectra of CW dye laser pumped transitions in BaO
24 p3096 A73-44976

Octave bandwidth microwave spectral response.
24 p3068 A73-44996

MICROWAVE SWITCHING

Series diode SP4T switch for satellite applications.
04 p0428 A73-15455

P-I-N switching diodes in phase-shifters for electronically scanned aerial arrays.
08 p0943 A73-20712

Dynamic behavior of Josephson tunnel junctions in the subnanosecond range.
09 p1132 A73-21941

Satellite-borne programmable communications distribution subsystem, controlling microwave switch matrix by ground command via onboard memory for traffic flow data
09 p1053 A73-23364

Semiconductor diodes for controlling microwave power.
12 p1480 A73-27266

Microwave tunnel diode ring counter with displaced nonlinear load line in multistage transistor driver and current switching configuration
13 p1593 A73-29120

Broad X band multichannel waveguide matrix for high speed switching from one input to one of four outputs at high power levels
16 p1990 A73-33897

A satellite-switched SDMA/TDMA system for a wideband multibeam satellite.
20 p2524 A73-38730

Observation of turn-on action in a gate-triggered thyristor using a new microwave technique.
20 p2543 A73-39414

Rapid-switching, broadband 1:4 WG switch matrix. II.
22 p2834 A73-42874

MICROWAVE TRANSMISSION

NT MANDELSTAM REPRESENTATION

Book - Handbook of microwave techniques and equipment.
01 p0021 A73-10025

Microwave varactor upconverter in radio repeater for domestic wideband communication satellite, emphasizing transmission characteristics design
01 p0006 A73-11177

Field distribution formulas for fast wave attenuation in thin walled tubular dielectric waveguide within external absorbing diaphragms
02 p0142 A73-12495

Microwave dual frequency propagation experiment using the Mariner Venus Mercury probe.
03 p0275 A73-13628

Electromagnetic measurement at submillimeter wavelengths for solids and liquids absorption and refraction and atmospheric gases and plasmas emission based on Fourier transform spectrometry
03 p0310 A73-14496

ATS-F COMSAT millimeter wave propagation experiment.
04 p0418 A73-15386

Millimeter wave propagation measurement for attenuation probability statistics by ATS-5 satellite, considering impact on space communication system design
04 p0418 A73-15387

Rain attenuation of vertically and horizontally polarized signals of 18 GHz communication system
04 p0419 A73-15395

Diurnal variation of the effective earth's radius factor /k/ over India and its influence on microwave propagation.
04 p0423 A73-15599

Synchronous satellite solar power station for solar energy conversion to microwaves for transmission to earth discussing technical, economic and social aspects [ASME PAPER 72-WA/SOL-6]
04 p0408 A73-15801

Diurnal variation of the effective earth's radius factor /k/ over India and its influence on microwave propagation.
04 p0423 A73-15928

Higher-order evanescent modes on slow-wave structures.
05 p0547 A73-16160

MICROWAVE TRANSMISSION

Mirror corner for use with overmoded circular waveguide. 05 p0548 A73-16165

Dimensional and material effects on microwave waveguide damping and bandwidth characteristics in long distance communications 06 p0663 A73-17583

Design of modern semiconductor senders for frequency-modulated directional radio systems. I 06 p0663 A73-17585

Book - Microwave transmission. 06 p0663 A73-17670

Satellite solar power station for solar energy conversion and transmission to earth via microwave beam, discussing technology status and weight and cost projections 06 p0750 A73-18027

Atmospheric conditions effects on line-of-sight microwave PCM data transmission system performance, comparing predicted error probability vs predetection SNR with measurement 06 p0665 A73-18187

Triangular obstacle caused microwave shadow zone diffraction pattern calculation by ray optics theory, comparing with scale model test results 06 p0666 A73-18201

Determination of the specific surface resistance of thin metallic layers in the microwave range, based on transmission coefficient measurements 06 p0737 A73-18221

Transmission of microwave through perforated flat plates of finite thickness. 06 p0669 A73-18735

Cut-off frequency calculation for TE and TM modes in doubly ridged circular and elliptical microwave waveguides, using Mathieu function and eigenfunctions 06 p0669 A73-18736

Experimental investigation of the transient formation of a microwave-generated ionized sheath in air. 06 p0732 A73-18781

Satellite dimensional resonances in microwave helicon transmission through semiconductors. 06 p0739 A73-18788

Height-gain experimental data for groundwave propagation. I - Homogeneous paths. 07 p0791 A73-19377

Experimental investigation of the parameters of a statistical Gaussian model of the field below the radio horizon at centimeter wavelengths. 07 p0794 A73-20131

Buildup of a narrow plasma channel by microwaves. 08 p0992 A73-20954

On the procedures of measuring microwave Faraday rotation in semiconductors. 08 p0994 A73-21016

Selectively faded nondiversity and space diversity narrowband microwave radio channels. 08 p0939 A73-21086

Reflection of a microwave signal from a semiconductor plate of finite thickness 08 p0995 A73-21517

The design, analysis, and performance of resonant and nonresonant microwave transmission devices with theoretically infinite rejection. 09 p1080 A73-22103

Satellite solar power station for solar energy conversion into electricity and transmission to ground receiving stations via microwave beams 09 p1035 A73-22791

Satellite solar power station systems engineering study, examining basic concept technical and economic feasibility 09 p1154 A73-22814

Radiometer measurements of atmospheric attenuation at 19 and 37 GHz along sun-earth paths. 09 p1052 A73-22957

Fundamental and parasitic modes of a shielded microstrip transmission line 09 p1052 A73-23085

Canadian domestic ANIK communication satellite with all-microwave 12-channel repeater, discussing system components, antenna design and performance parameters 09 p1059 A73-23437

Near-equatorial synchronous orbit Satellite Solar Power Station system with photovoltaic cell arrays energy conversion into microwave power for transmission to earth 10 p1285 A73-23601

Experimental investigation of the effective permittivity and of the resonator Q of slot lines on ceramic substrates in the frequency range from 1 to 18 GHz 10 p1194 A73-23994

Frequency entrainment of a drift instability by nonlinear effects in a plasma. 10 p1253 A73-24114

Satellite electric power station for conversion of solar energy to microwaves beamed to earth, discussing structural design, flight control, transportation and technology assessment 10 p1178 A73-24554

Efficiency of the microwave energy absorption in a plasma at high magnetic fields. 10 p1257 A73-24627

Spectra of short-term fluctuations of line-of-sight signals - Electromagnetic and acoustic. 10 p1190 A73-24893

Comparison of observed and predicted phase-front distortion in line-of-sight microwave signals. 11 p1330 A73-25687

L-band satellite systems for mobile applications. 12 p1472 A73-27664

The Canadian/U.S. High-Power Communications Technology Satellite. 12 p1472 A73-27669

Centimeter wave propagation beyond horizon, considering terrestrial surface curvature and mountain effects on deflection and atmospheric refractivity inhomogeneity caused scattering 12 p1473 A73-27754

Applications of methods of geometric optics in the case of tropospheric propagation 12 p1473 A73-27755

Determination of the parameters of a fluctuating plasma from the modulation of microwave signals 13 p1666 A73-28961

Polarization cascade matrix describing arbitrary elliptically polarized microwave transmission through inclined grating of parallel wires 13 p1587 A73-29669

A study of frequency sharing between satellite and terrestrial broadcasting systems. 14 p1725 A73-29748

Nonlinear mechanisms for self-focusing of microwaves in semiconductors. 14 p1732 A73-29920

Russian book - Design and calculation of microwave stripline elements. 15 p1852 A73-32295

Microwave guidance system for aircraft landing, discussing civil and military requirements, position measurement capability, shadowing in propagation, and ground reflection induced signal fading 15 p1910 A73-32468

Experimental investigation of microwave signal fluctuations for propagation above the sea at low slip angles 16 p1978 A73-32889

Single and dual path propagation at 18 GHz with application to the design of digital radio relay systems. 16 p1981 A73-33703

Atmospheric refractivity effects on maximum antenna gain and correlation coefficient in design of microwave line of sight links for high reliability 16 p1981 A73-33704

Rain attenuation and fade duration statistics for design of satellite-based communication system, predicting outage for 16 GHz path diversity system 16 p1981 A73-33706

Multipath propagation effects on 11, 20 and 37 GHz FM-FDM systems at different path lengths 16 p1981 A73-33711

Microwave transhorizon propagation in atmospheric evaporative duct layer by superdiffraction, using Monin-Obukhov similarity theory for computerized prediction 16 p1981 A73-33712

The influence of the sea evaporation duct on the phase of the received field on a line-of-sight path. 16 p1981 A73-33713

Atmospheric refractivity fluctuation caused transit time variation effects on propagation noise and frequency stability in microwave radio link signal reception at 36 GHz 16 p1982 A73-33714

Millimeter wave propagation measurements from an orbiting earth satellite. 16 p1982 A73-33716

The R.S.R.S. ground stations for receiving 11.6 GHz transmission from the SIRIO satellite. 16 p1982 A73-33717

Microwave radiometer measurement at 17 GHz to investigate atmospheric attenuation and radio noise and interference sources for optimal satellite communication systems design 16 p1982 A73-33718

Zenith atmospheric emission noise temperature and attenuation measurements including multiple and single frequency statistical observations at 85-118 GHz during 1970-1971 16 p1982 A73-33720

Microwave propagation in atmosphere with oblate spheroidal raindrops, discussing linear and circular cross-polarization effectiveness statistical analysis with allowance for raindrop orientation 16 p1983 A73-33724

Atmospheric temperature measurement with X and K band radiometers, discussing meteorological conditions variation effects on microwave propagation and comparison with spacecraft tracking data. 16 p1983 A73-33730

Fading correlation on terminal point and spaced microwave paths, discussing switched path diversity to overcome rain attenuation effects 16 p1983 A73-33732

Atmospheric refractivity variation, precipitation and wind effects on two orthogonal linearly polarized microwave signals transmission over radio link at 22 and 37 GHz 16 p1983 A73-33733

Absorption of centimeter radio waves in the Venusian atmosphere 16 p2068 A73-33821

Reflection coefficient of an electromagnetic wave by a plasma column of variable electron density in a waveguide. 16 p1984 A73-33994

Ionospheric scintillation at 4 and 6 GHz. 17 p2122 A73-34869

Two-way wideband microwave communication system oriented toward PCM-TDM digital technique for covering telephone, videophone and radio broadcasting services 17 p2123 A73-34968

On the optimum design of tapered waveguide transitions. 17 p2136 A73-34970

Scattering of waves at a step in a circular multiwaveguide. 17 p2123 A73-35152

An experimental investigation of the propagation of electromagnetic waves in a rectangular waveguide, partially filled with n-InSb in a transverse magnetic field. 17 p2123 A73-35166

Electric power generation on earth via satellite solar power station, assessing technologies of energy collection and conversion, microwave transmission and rectification 17 p2110 A73-35313

The generalized multiprobe reflectometer and its application to automated transmission line measurements. 17 p2143 A73-35691

A 180-deg phase-shift keying modulator for microwave broadband application 18 p2292 A73-36398

Analysis of thick rectangular waveguide windows with finite conductivity. 18 p2292 A73-36605

On rainfall and space diversity for millimeter-wave earth-satellite communications systems. 18 p2289 A73-36709

Domestic communication satellite systems with microwave transmission links and coast-to-coast earth stations and receivers, detailing design and interference problems 18 p2289 A73-36776

Wave propagation between two plane, parallel reactive walls. 19 p2404 A73-37721

Waveguide transitions especially for excitation of the H sub 11 mode in a circular waveguide 19 p2404 A73-37722

Optical and millimeter line-of-sight propagation effects in the turbulent atmosphere. 19 p2405 A73-38220

Some developments in semi-direct broadcast satellites and community receiving systems. [AAS PAPER 73-155] 20 p2521 A73-38599

Design features of an unattended earth terminal for satellite communications. 20 p2522 A73-38716

Orbital design strategy for domestic communication satellite systems. 20 p2527 A73-38761

Optimization in the design of a 12 GHz low cost ground receiving system for broadcast satellites. 20 p2527 A73-38762

Surface strip coplanar waveguide characteristic impedance measurement as function of aspect ratio and substrate thickness 20 p2538 A73-39595

Analysis of ground tests of a microwave, earth-occultation, pressure-reference-level system. 21 p2729 A73-40065

Statistical analysis of microwave transmission line coefficients, discussing line losses, inhomogeneity distribution, input voltage standing wave ratios and rms deviations 21 p2648 A73-40204

Maritime communications via satellites employing phased arrays. 21 p2649 A73-40330

Performance degradation plots for comparison of signal fading and intersymbol interference effects in two-component specular multipath digital microwave communication channel 21 p2649 A73-40336

Propagation of microwaves in a solid-state plasma 21 p2753 A73-41292

Low-noise microwave down-converter with optimum matching at idle frequencies. 21 p2666 A73-41428

On inhomogeneously filled rectangular waveguides. 21 p2657 A73-41430

Angle and Doppler measurements of the quasi-coherent and incoherent components of microwave transhorizon signals. 22 p2824 A73-41859

Theory of power rectification and harmonic generation processes at super-high frequencies 22 p2800 A73-42213

Octave-bandwidth, acoustic M/W frequency-memory loop. 22 p2834 A73-42873

Slot microwave transmission line with thick metal coating on dielectric substrate, calculating phase constant variation with frequency, slot width and coating thickness 23 p2954 A73-44069

The eigenvalue solution of asymmetric-ridge waveguides using the mode-matching method. 23 p2955 A73-44146

Determination of the parameters of a fluctuating plasma from modulation of a microwave signal. 23 p3013 A73-44313

Optical modulation of X band microwave transmission by acoustoelectric domains in semiconducting CdS single crystal, noting domain conductivity and permittivity changes 23 p3018 A73-44365

Parameter evaluation method for lossy strip transmission lines, assuming microwave propagation in waveguide system with dielectric between two conducting plates 24 p3074 A73-45007

MICROWAVE TUBES

NT BACKWARD WAVE TUBES

NT CATHODE RAY TUBES

NT CELESTROSCOPES

NT HELITRONS

NT IMAGE ORTHOCONS

NT IMAGE TUBES

NT KLYSTRONS

NT MAGNETRONS

NT MICROWAVE OSCILLATORS

NT PHOTOMULTIPLIER TUBES

NT PICTURE TUBES

NT PLANOTRONS

NT THERMIONIC DIODES

NT THYRATRONS

NT TRAVELING WAVE TUBES

Reliability-performance comparisons between tube and transistor power modules for ground-based and airborne radar applications 01 p0024 A73-10718

50 GHz helix type travelling wave tube 'W-5028'. 07 p0799 A73-19372

High power microwave tubes design trends, considering output capacity and quality, bandwidth, gain, linearity, low noise and intermodulation performance factors 11 p1339 A73-26691

The continuous-cathode /emitting-sole/ crossed-field amplifier. 11 p1339 A73-26694

Temperature field calculation for certain elements located in microwave channels 12 p1558 A73-27247

Microwave transmitter tubes for surface-based and airborne radar applications, considering ATC, output power, stability, spectrum, size, weight, reliability, maintainability and cost requirements 13 p1590 A73-28532

Dual mode microwave tube parameters for ECM power amplifiers based on systems rationale analysis, considering TWT and injected-beam crossed field amplifier 14 p1736 A73-30621

Designing high efficiency TWT's. 18 p2293 A73-36777

Helix support, focusing, fabrication and performance tests of miniature traveling wave tubes (TWT), using rare earth-cobalt (RAECO) magnets 22 p2834 A73-42696

High power airborne radar CW tube-transmitter interface failures due to design, maintenance, handling and environment effects 22 p2834 A73-42875

MICROWAVES

NT DECIMETER WAVES

NT MICROWAVE EMISSION

NT MILLIMETER WAVES

Third harmonic generation in Ge induced by conduction nonlinearity during bulk heating of charge carriers by microwave fields 03 p0350 A73-14077

Application of the Stark effect to the determination of the fields in the region of microwave/plasma interaction 04 p0423 A73-15611

Nonprimordial hypothesis for cosmic microwave background radiation generation by ordinary astronomical processes and subsequent thermalization by interaction with dust grains 08 p1008 A73-21152

Microwave background radiation in terms of isotropy, universe mass density, sky brightness temperature spectra investigations and H distribution in intergalactic space 08 p1010 A73-21229

Microwave heating and resonant diffusion of electron plasmas, considering relativistic theory and Fokker-Planck equation 09 p1129 A73-22641

Computer simulation of ion heating by pulsed microwaves. 09 p1129 A73-22642

Determination of field strength in a microwave-plasma interaction by means of the Stark effect. 10 p1254 A73-24201

Nonthermal radiation from a magnetoactive plasma in the field of a microwave pumping wave. 11 p1405 A73-26182

Microwave heating of electrons of a dense plasma column at frequencies higher than electron cyclotron frequency. 14 p1782 A73-30771

Changes in the quantity of overall sulfhydryl groups in the blood of persons coming in contact with microwave radiation sources 15 p1837 A73-31169

The combined influence of microwave radiation and an adverse climate on the organism 15 p1837 A73-31170

Biophysical hazards of microwave radiation. 16 p1974 A73-32723

Search for small-scale anisotropy in the 2.7 K cosmic background radiation at a wavelength of 3.56 centimeters. 17 p2231 A73-34768

Absorber theory of radiation and the future of the universe. 19 p2460 A73-38172

Occurrence and features of ducted modes of internal gravity waves over Western Europe and their influence on microwave propagation. 19 p2405 A73-38225

Hot-electron production and anomalous microwave absorption near the plasma frequency. 19 p2469 A73-38289

Changes in the peripheral blood of the rat exposed to microwave radiation /2400 MHz/ in conditions of chronic exposure. 21 p2645 A73-41159

MICROWEIGHING

U WEIGHT MEASUREMENT

MIDAIR COLLISIONS

Manoeuvre in response to collision warning from airborne devices. 01 p0074 A73-10349

Rocket sled facility for impact tests with friable balloon platforms, describing braking and accelerating jet configurations, vibration damping measures and telemetry system 07 p0808 A73-19004

Aircraft in-flight visibility /conspicuity/ during daytime, discussing exterior paints, tapes and high intensity lighting effectiveness for midair collision avoidance 16 p1965 A73-32661

Digital synchronization of synchronous collision prevention systems in aviation 17 p2207 A73-34480

Optimal aircraft collision avoidance. 19 p2452 A73-38050

Systems for collision avoidance - An overview. 19 p2453 A73-38467

SECANT - A solution to the problem of midair collisions. 19 p2454 A73-38469

Midair collision avoidance strategies for ATC improvement, discussing relative effectiveness of structural airspace, airborne and ground-based systems based on US statistics 21 p2733 A73-40030

USA government and industry efforts on aircraft midair collision avoidance systems technology advancement, comparing cost effectiveness between airborne and ground based options [ASME PAPER 73-ICT-49] 23 p3005 A73-43495

MIDCOURSE GUIDANCE

Propellant requirements for midcourse velocity corrections. [AIAA PAPER 73-172] 05 p0630 A73-16916

MIDDLE EAR

Spontaneous middle ear muscle activity in man - A rapid eye movement sleep phenomenon. 02 p0134 A73-12423

The dynamic properties of the acoustic middle ear reflex in nonanesthetized rabbits - Quantitative aspects of a polysynaptic reflex system. 05 p0539 A73-16249

Dynamic properties of human and animal middle ear in terms of acoustic impedance, transfer function, impulse response, sound diffraction and reflex sensitivity 14 p1715 A73-30279

Evaluation of auditory disorders in pilots by examining intratympanic muscles reflexes. 18 p2279 A73-36934

Loudness changes resulting from an electrically induced middle-ear reflex. 22 p2811 A73-41815

MIDLATITUDE ATMOSPHERE

Refraction of whistler-mode waves by large-scale gradients in the middle-latitude ionosphere. 01 p0017 A73-10328

Rocket measurements of electron fluxes in the upper atmosphere at midlatitudes. 01 p0041 A73-10887

Electron-density and energetic-electron measurements of the midlatitude lower ionosphere during winter. 01 p0041 A73-10888

The standard profile of the mid-latitude F region of the ionosphere as deduced from bottomside and topside ionograms. 02 p0163 A73-12301

Simultaneous measurements of height wind profiles and electron concentration for verifying theory of sporadic E layer formation in midlatitudes under wind shear action 02 p0163 A73-12306

Midlatitude excess radiation energy density relation to primary cosmic ray background from spectrum measurement data 02 p0208 A73-12460

Ground based geomagnetic observations of medium and high latitude VLF emissions due to transverse resonance instability and auroral oval Cerenkov radiation from magnetosheath 03 p0276 A73-13884

Long term German observations of auroral activity compared to other midlatitude observations 04 p0445 A73-15551

Lower ionosphere at medium latitudes during geomagnetic disturbances. 05 p0568 A73-16214

Altitude variations of the sporadic E layer at geographical mid-latitudes 05 p0568 A73-16217

Passage of medium-frequency radio waves through the ionosphere 05 p0550 A73-16395

A satellite study of the mid-latitude trough in electron density and VLF radio emissions during the magnetic storm of 25-27 May 1967. 05 p0571 A73-17060

Midlatitude sporadic E layer vertical electron and ion distributions from rocket experimental wind velocity profile, assuming molecular and metallic ions in ionosphere 06 p0742 A73-17535

Composition of radiation excess over primary cosmic ray background recorded by Cosmos satellites below midlatitude belt region 07 p0870 A73-19426

Coupling between the F-region and protonosphere - Numerical solution of the time-dependent equations. 07 p0818 A73-19665

Global electron density distributions from the Ariel 3 satellite at mid-latitudes during quiet magnetic periods. 07 p0819 A73-20054

Mid-latitude winter anomalies in radio absorption and stratospheric temperature distribution - Observations concerning the influence of auroral and magnetic activity. 07 p0819 A73-20058

Propagation modes of radio whistlers and gyroelectric echoes received in middle latitudes 08 p0937 A73-20651

Midlatitude signal fading during sunrise and sunset transitions, noting amplitude ratio independence of propagation direction in earth-ionosphere waveguide 09 p1049 A73-22131

Mode coupling importance in midlatitude nonblanketing sporadic E layers from observations of ordinary and extraordinary blanketing frequencies 09 p1076 A73-22142

Simultaneous occurrences of hydrogen arcs and mid-latitude stable auroral red arcs. 10 p1214 A73-24740

Spatial correlation of the critical frequencies of the F2 layer on the basis of data from stationary mid-latitude stations 11 p1351 A73-25091

The causes of storm-time increases of the F-layer at mid-latitudes. 11 p1353 A73-25751

The effects of thermospheric winds on the ionosphere at low and middle latitudes during magnetic disturbances. 11 p1353 A73-25752

Structure at the poleward edge of a mid-latitude F-region trough. 11 p1353 A73-25756

The topside ionosphere at mid-latitudes during local sunrise. 11 p1353 A73-25757

A study of the relationship between geomagnetic storms and ionospheric disturbances at mid-latitudes. 11 p1356 A73-25912

Energetic electron precipitation as a source of ionization in the night-time D-region over the mid-latitude rocket range, South Uist. 11 p1358 A73-25701

The nature of seasonal changes in the effects of magnetic storms on mid-latitude F-layer electron concentration. 11 p1358 A73-26708

Diurnal, seasonal and solar cycle changes in southern midlatitude ionosphere electron content from June 1965-August 1971 11 p1359 A73-26712

Analytical model of the unsteady nighttime F2 region of the ionosphere at mid-latitudes 12 p1490 A73-27337

- Midlatitude standard ionospheric profile to construct F2 region noon electron density profiles and thermal response to solar activity changes
12 p1493 A73-27761
- An analysis of seasonal changes in electron densities at middle latitudes in the lower D-region.
13 p1606 A73-28207
- Long term observations of geomagnetic pulsations activity during various phases of magnetic storm at midlatitudes, noting regular and irregular morphological features
13 p1611 A73-29660
- Comment on the effect of a vorticity centre on a frontal boundary.
13 p1656 A73-29663
- Anomalous winter time absorption of radio waves in the middle latitude ionosphere
15 p1844 A73-31900
- Midlatitude excess radiation energy density relation to primary cosmic ray background from spectrum measurement data
15 p1927 A73-32610
- Midlatitude sporadic E layer vertical electron and ion distributions from rocket experimental wind velocity profile, assuming molecular and metallic ions in ionosphere
16 p2052 A73-32759
- Monthly mean values of eddy diffusion coefficients in the lower stratosphere.
[AIAA PAPER 73-498] 16 p2005 A73-33540
- Observation of an unusual multiple mid-latitude 6300-A OI arc from two ground stations.
16 p2009 A73-33895
- Atmospheric composition changes and the F2-layer seasonal anomaly.
16 p2010 A73-33915
- Observation of quasitrapped and precipitating electrons at midlatitude.
18 p2344 A73-35927
- Ionospheric electron content and its horizontal gradients at high and middle latitudes from radiowave propagation from satellites.
18 p2304 A73-35972
- Comparison of electron density profiles in the lower ionosphere at Equator and midlatitudes.
18 p2305 A73-36007
- Electron temperature profile and its solar activity dependence in the middle latitude region.
18 p2308 A73-36047
- A rocket observation of the disturbed mid-latitude nighttime ionosphere.
18 p2308 A73-36048
- Distortions of the nighttime ionosphere during magnetospheric substorms.
18 p2312 A73-36279
- Spectrum analysis of tropical cloudiness. II.
19 p2446 A73-37430
- Fine-scale inhomogeneities of the mid-latitude sporadic E layer
19 p2427 A73-38332
- Midlatitude ionospheric disturbances
20 p2554 A73-39172
- Midlatitude F 2 layer critical frequency fluctuations as ionosphere disturbance criteria during magnetically quiet days
21 p2681 A73-40104
- Midlatitude spread F relationship to F region trough formation, considering multiple reflections emanating from steep ionization contours
21 p2684 A73-40784
- Complex studies of corpuscular radiation in the upper atmosphere at midlatitudes during geomagnetic perturbations
21 p2760 A73-40918
- The establishment of the winter polar vortex in middle latitudes in 1971.
21 p2687 A73-41338
- Investigation of mid-latitude ionospheric currents by combined rocket techniques.
21 p2689 A73-41359
- Ariel 3 evidence of zones of VLF emission at medium invariant latitudes which co-rotate with the earth.
21 p2691 A73-41382
- Characteristics of the redistribution of charged particles in the nighttime E region at mid-latitudes
22 p2847 A73-42331
- Analytical model of the nocturnal nonstationary F2-region of the ionosphere at middle latitudes.
23 p2970 A73-43235
- Radiation production and energy deposition by ring current protons precipitated into the mid-latitude upper atmosphere.
23 p3024 A73-43685
- The slab thickness of the mid-latitude ionosphere.
23 p2972 A73-43694
- Statistical characteristics of the vertical ozone distribution in mid-latitudes.
23 p2975 A73-43874
- Spectral analysis of traveling planetary scale waves - Vertical structure in middle latitudes of Northern Hemisphere.
23 p2978 A73-43982

- Diurnal and semidiurnal variations in amplitude and phase of midlatitude ionosphere tidal motions, using sodium cloud drift rate
24 p3082 A73-44732
- Formation of the sporadic E layer and the nighttime E region of the ionosphere at midlatitudes
24 p3083 A73-44794
- Positive nitrogen ions in midlatitude atmosphere, discussing concentration dependence on height, solar zenith angle and activity level
24 p3084 A73-44801
- Penetration of thundercloud electric fields into the ionosphere and magnetosphere. I - Middle and subauroral latitudes.
24 p3085 A73-45118
- Probe electric field measurements near a midlatitude ionospheric barium release.
24 p3085 A73-45119

MIDLATITUDES

U TEMPERATE REGIONS

MIE SCATTERING

NT RAYLEIGH SCATTERING

An inversion technique developed to determine characteristics of mie scatterers differing in index of refraction interspersed in the stratosphere.

Condensation trail effects on atmospheric radiation budget from model calculation for ice particle layer near tropopause, using Mie scattering and radiative transfer approximation
01 p0037 A73-10353

Atmospheric aerosol Mie scattering calculation as function of polarization parameters based on models for three laser wavelengths and two materials
01 p0038 A73-10389

A direct solution of the radiative transfer equation - Application to Rayleigh and Mie atmospheres.
03 p0341 A73-12900

Size determination of a perfectly conducting sphere from the extrema of Mie scattering intensities.
07 p0852 A73-20220

An explicit form of the Mie phase matrix for multiple scattering calculations in the I, Q, U and V representation.
11 p1329 A73-25679

Optical properties of single-component zodiacal light models.
11 p1390 A73-25718

Twilight circular polarization due to Mie scattering, analyzing polarimeter measurements in IR and UV spectral bands
11 p1357 A73-25926

Calculation of the radiative characteristics of polydisperse concentric spheres
12 p1490 A73-27150

Mie scattering computation of cosmic dust flux in upper atmosphere from twilight luminance increase during meteor showers
20 p2531 A73-39728

Electromagnetic resonances and Q-factors of lossy dielectric spheres.
21 p2775 A73-41418

23 p2960 A73-44067

MIE THEORY

U MIE SCATTERING

MIGRATION

The service life of rocket motors filled with double base propellants.

[AIAA PAPER 72-1109] 03 p0351 A73-13424

MILITARY AIRCRAFT

Airframe structural testing and safety design for military aircraft, discussing static, dynamic and fatigue tests and environmental effects
04 p0454 A73-14865

Forward scatter chaff system for air-ground long haul communications.
04 p0418 A73-15393

TF34 and F101 turbofan engines for Navy S-3A ASW aircraft and USAF B-1 strategic bomber, respectively, discussing design features, manufacturing techniques and testing procedures
[SAE PAPER 720841] 05 p0607 A73-16655

Prototype development for Army personnel and equipment airborne mobility, considering various aircraft conceptual designs feasibility relative to logistics requirements
[SAE PAPER 720846] 05 p0534 A73-16658

Digital Avionics Information System (DAIS)/development for military supersonic all-weather precision weapon delivery system, emphasizing modular design for different aircraft types
05 p0534 A73-16658

The USAF aircraft structural integrity program /ASIP/.
[AIAA PAPER 73-18] 06 p0759 A73-17611

1972 report to the aerospace profession; Proceedings of the Sixteenth Symposium, Beverly Hills, Calif., September 28-30, 1972.
09 p1030 A73-22176

Aerial targets for weapon systems performance testing, discussing converted aircraft, pilotless drones and towed targets
09 p1168 A73-23120

Neurological fatigue-indices of flight crews of long-range and military transport aviation
11 p1321 A73-25040

Augmentor wing design and performance tests for multimission XFV-12 V/STOL prototype aircraft
12 p1459 A73-27733

Two approaches to aircraft development - The U.S.A. and Europe.
13 p1568 A73-28177

Hydrolytic reversion of elastomeric potting compounds.
13 p1646 A73-29247

New inhibited elastomeric finish system designed by corrosion engineers to solve acute corrosion problems on military aircraft.
[NACE PAPER 118] 13 p1638 A73-29316

Multi-Role Combat Aircraft Program management, discussing international cooperation, industrial arrangements and governmental objectives
13 p1709 A73-29368

Naval air weaponry logistics support, discussing criteria for management effectiveness evaluation
13 p1709 A73-29573

ESCAPAC IE stabilized ejection seat for Navy S-3A and Air Force A-9A aircraft, describing propulsion, stabilization, separation and lateral divergence subsystems
16 p1966 A73-32669

The simulator industry and its contribution to military training requirements.
16 p1996 A73-33208

TACAN based SETAC and L band DME based DLS approach and landing systems for military aircraft, discussing time division multiplexing and antenna array
[DGLR PAPER 73-019] 17 p2208 A73-34493

The Air Force/Boeing advanced medium STOL transport prototype.
[SAE PAPER 730365] 17 p2103 A73-34710

Technical basis for the STOL characteristics of the McDonnell Douglas/USAF YC-15 prototype airplane.
[SAE PAPER 730366] 17 p2103 A73-34711

Applications and concepts for the incorporation of composites in large military transport aircraft.
17 p2104 A73-34816

Military aircraft onboard Digital Avionics Information System for computerized integration of navigation, guidance, weapon delivery, cockpit display, communication, flight control and energy management
17 p2136 A73-35202

The C-401, a STOL transport for many applications
17 p2107 A73-35666

USAF aircraft structural integrity requirements, discussing safety and durability concepts for designing, evaluating and substantiating flight systems
18 p2267 A73-36169

Civil and military aircraft
18 p2268 A73-36689

Psychophysiological characteristic of the activity of military-transport-aviation flight crews during low-altitude flights
19 p2397 A73-37196

Military aircraft structure computerized design optimization procedures based on local optimum and stiffness requirements
19 p2495 A73-37407

Air cushion landing systems application to tactical airlift aircraft for personnel, and equipment delivery to dispersed sites under diverse climatic, terrain and combat conditions
19 p2380 A73-37678

The Navy SETOLS program and its potential applications to Navy aircraft.
19 p2381 A73-37680

Drone launch and recovery reliability requirements for target, reconnaissance, air-to-air combat, high altitude endurance and defense suppression missions
19 p2381 A73-37681

ACLS trade study for application to STOL tactical aircraft.
19 p2381 A73-37683

Air cushion landing system applications and operational considerations.
19 p2381 A73-37684

The aircraft modification phase of the joint U.S./Canadian ACLS program.
19 p2382 A73-37689

Air cushion landing system /ACLS/ design and drone flight tests for low cost unmanned military aircraft recovery, comparing with mid air retrieval system /MARS/
19 p2383 A73-37699

The potential influence of the ACLS on the development of logistical cargo aircraft.
19 p2383 A73-37701

The utility of data link to military aircraft communication - An operational view.
20 p2527 A73-38760

US Department of Defense aircraft system effectiveness tests survey questionnaire response data from component, subsystem and system suppliers
21 p2635 A73-41204

Electromagnetic interference in military transport aircraft, discussing RF terminal voltage and current, radiated field, fuselage attenuation and power supply impedance measurements
22 p2821 A73-41693

The capabilities of army test facilities.
23 p2966 A73-44064

MILITARY AVIATION

- Realistic pilot training and aircraft handling qualities in pilot error risk minimization for military, commercial and general aviation 05 p0545 A73-16733
- Military contributions to aviation medicine. [ALAA PAPER 73-68] 06 p0656 A73-17636
- Case histories of valvular cardiopathies in military pilots, determining tolerance to flight 07 p0784 A73-19209
- Proteinuria and military aircrew 08 p0931 A73-21539
- Productivity estimates of the strategic airlift system by the use of simulation. 10 p1297 A73-23774
- Military ATC systems and equipment in U.S. National Aviation System, discussing operations, organizational and facility interfaces, communications, navigation, and surveillance radar requirements 14 p1773 A73-29889
- Automated system of mixed /civil and military/ control 15 p1847 A73-32444
- New constraints of military aviation 18 p2267 A73-36684
- Discourse on comparisons between commercial and military aircraft logistics. 20 p2629 A73-39274

MILITARY HELICOPTERS

- NT CH-46 HELICOPTER
- NT CH-47 HELICOPTER
- NT H-53 HELICOPTER
- NT H-56 HELICOPTER
- NT HH-43 HELICOPTER
- NT S-61 HELICOPTER
- NT UH-1 HELICOPTER
- Fiberglass reinforced composite material application to light weight ballistic damage tolerant military helicopter flight control components previously vulnerable to small arms fire 04 p0452 A73-14722
- Military helicopter avionics for communication, surveillance, navigation, landing approach, flight control, power management, ASW and weapons aiming 06 p0648 A73-18509
- A flight research program to define VTOL visual simulator requirements. 16 p1996 A73-33210
- Experimental autostabilized tethered rotor platform for reconnaissance, communications and ECM, discussing control system effectiveness from flight test results 16 p1969 A73-33736
- Future technology and economy of the VTOL aircraft; International Helicopter Forum, 10th, Buebeckburg, West Germany, June 5-7, 1973, Proceedings 17 p2098 A73-34251
- Progress in the development of a practically applicable VTOL aircraft with low disk loading 17 p2098 A73-34254
- Military VTOL combat and commercial efficiency considerations, including convertiplane substitution, Mach number effects and reverse flow on blades, rotor design and speed limitations 17 p2098 A73-34256
- The application of system analysis techniques for the solution of complex helicopter crew station design problems. [AHS PREPRINT 723] 17 p2105 A73-35064
- U.S. Army helicopter vibration data for OH-6A, OH-58A, UH-1H and CH-54B models obtained from triaxial accelerometer locations, presenting spectral and statistical analyses 17 p2106 A73-35086
- [AHS PREPRINT 763] Community noise impact study from military helicopter operations. 22 p2800 A73-42947

MILITARY PSYCHIATRY

U MILITARY PSYCHOLOGY

- MILITARY PSYCHOLOGY**
- Implications of psychoanalytic factors for Air Force operations. 11 p1323 A73-25340
- Naval aviator training program dropouts identification in terms of physiological, safety, security, social, self-esteem and self-actualization needs 14 p1722 A73-30513
- Clinical psychology diagnostic methods in military aviation medicine, considering neurotic symptoms and psychosomatic disorders in flight fitness examinations 22 p2817 A73-43129

MILITARY SPACECRAFT

- NT VELA SATELLITES
- Space shuttle cost effectiveness studies from viewpoint of combined civil and military payloads and simplified systems design 05 p0613 A73-16182
- The impact of satellites on military communications. 14 p1729 A73-30874

MILITARY TECHNOLOGY

- Army studies cost effectiveness of communications satellites. 03 p0274 A73-13075

Financial problems related to aircraft and ships development and production for Defense Department, stressing C-5A, Cheyenne helicopter and DD-963 class of automated destroyers

- Air Force weapon system procurement needs, considering industry technological capabilities, nonlinear estimation in cruise navigation and nonlinear systems design, test and implementation 03 p0401 A73-13897
- The 600 knot Yankee escape system. 04 p0430 A73-15252
- Army 1500 shp advanced technology engine development program, discussing in components design and fabrication, air leakage losses, environmental testing and maintainability oriented design [SAE PAPER 720828] 05 p0606 A73-16627
- F100/F401 augmented turbopfan engines - High thrust-to-weight jet propulsion systems. [SAE PAPER 720842] 05 p0607 A73-16657
- Suitability of the CL-84 tiltwing aircraft for the sea control ship system. [SAE PAPER 720852] 05 p0534 A73-16660
- Harrier trial operations onboard Sea Control Ship /SCS/ U.S.S. Guam as model for future V/STOL aircraft-carrier systems [SAE PAPER 720833] 05 p0534 A73-16661
- Military contributions to civil aviation. [ALAA PAPER 73-67] 06 p0647 A73-17635
- Military helicopter avionics for communication, surveillance, navigation, landing approach, flight control, power management, ASW and weapons aiming 06 p0648 A73-18509
- Optimisation in construction of the Jaguar and other military aircraft. 08 p0928 A73-20947
- Electronic display devices for command, monitoring, surveillance, simulation and training in military applications, considering reliability, cost and performance specifications in procurement decision making 08 p0965 A73-21245
- Distance measurement by laser based on reflected pulse time measurement, discussing operating principle and military applications 10 p1228 A73-24174
- Book - Introduction to defense radar systems engineering. 13 p1587 A73-29677
- The MADGE system - Operational results and stretch potential. 15 p1912 A73-32505
- Realism in environmental design criteria - MIL-STD-210B. 16 p2034 A73-33139
- Design and service environment standardization /Military electronic equipment/. 16 p2087 A73-33143
- MIL-STD-810 uniform test methods for determining military equipment environmental resistance, discussing inadequacies, misapplications and planned revision for improvement 16 p2087 A73-33144
- Evaluation of remote sensor imagery for military geographic information. 16 p2016 A73-33365
- The simulation of environmental effects in military technology 16 p1997 A73-33386
- System engineering aspects of the man-machine interface. 16 p1975 A73-33645
- Air Force propulsion maintenance concepts. [SAE PAPER 730373] 17 p2177 A73-34712
- NAECON 73; Proceedings of the National Aerospace Electronics Conference, Dayton, Ohio, May 14-16, 1973. 17 p2136 A73-35201
- Environment effects on tape recorder design for in-flight data collection in military aircraft 19 p2431 A73-38197
- Navy Transit navigation satellite system, discussing flight test for feasibility of military application to YP-3C Antisubmarine Warfare Weapons System aircraft. 21 p2735 A73-40040
- International cooperation in weapons systems development, discussing military R and D technology interdependence within NATO, duplication and security 21 p2793 A73-41173
- Overview of Department of Defense Electromagnetic Radiation Hazards Standardization Program. 22 p2822 A73-41790
- Prediction of RS01 design requirements for MIL-STD-461A. 22 p2823 A73-41803
- Technical and economic problems in use of military passive night vision systems including image intensifiers, IR detectors and thermographic imaging devices 23 p2979 A73-43219
- The role of a military flight test engineer in test management. 23 p3051 A73-44062

The capabilities of government test facilities at the Air Force Systems Command. 23 p2966 A73-44065

Naval test and evaluation capabilities for aircraft, emphasizing organizational relationships 23 p3051 A73-44066

MILKY WAY GALAXY

- Velocity structures in hydrogen profiles. 01 p0096 A73-10315
- An approximate form of the third integral in the Galaxy. 01 p1013 A73-11017
- Cosmic-ray production of deuterium, He/3, lithium, beryllium, and boron in the galaxy. 02 p0208 A73-12412
- Adiabatic propagation of cosmic rays in the Galaxy. 03 p0360 A73-12929
- Russian book - Problems of galactic and extragalactic astronomy. 05 p0616 A73-16451
- Stochastic wave model of spiral galaxy rotation based on weak interaction, obtaining frequency spectrum integrals for Milky Way Galaxy 05 p0616 A73-16454
- Neutral hydrogen cloud rotation and recurrent eflux from central region of Galaxy, considering material and energy resources limitation 05 p0616 A73-16457
- Solution on a BESM-3M electronic computer of the equation for transfer of diffuse radiation in two-layer plane-parallel models of galaxies 05 p0617 A73-16461
- Gas shell surrounding Galaxy with temperatures intermediate between corona and disk due to hot gas accretion from intergalactic space of Local Group 05 p0622 A73-17179
- VV 281-427, variable stars in a Cepheus-Lacerta field of the Milky Way. 07 p0874 A73-19117
- Stokes polarization parameters of optical emission scattered in absorbing medium calculated for Galaxy and M 82 galaxy, assuming thermal IR radiation from nucleus 07 p0901 A73-20312
- Stellar distances, magnitude and mass measurements methods, noting distance to globular clusters and center of Galaxy 07 p0903 A73-20638
- Galactic differential rotation derived from the radial velocities of some population I objects. 08 p1005 A73-20912
- Equatorial coordinates and photographic magnitudes for new carbon stars in Northern Milky Way, noting classification by spectral discontinuity 08 p1005 A73-20916
- High velocity clouds as part of Galactic spiral arms, obtaining spiral structure maps from observations of Galactic plane 08 p1005 A73-20918
- Three-colour photometry of a field in the galactic anticentre section near NGC 1664. 08 p1005 A73-20922
- Three-colour photometry in a field in the direction of the galactic anticentre near M 35. 08 p1005 A73-20923
- A soft X-ray survey from the galactic center to Cassiopeia. 08 p1008 A73-21163
- A model for peaking of galactic gravitational radiation. 08 p1009 A73-21201
- Schmidt telescopes in stellar photography of Magellanic clouds, galactic center and Scorpio-Centaurus and globular clusters for southern hemisphere Milky Way structure investigation 08 p1011 A73-21364
- Galactic structure at high galactic latitudes. 08 p1011 A73-21365
- 327-MHz observations of the galactic center - Possible detection of a deuterium absorption line. 08 p1013 A73-21808
- H beta emitting diffuse nebulae as reflection nebulae illuminated by galactic light, based on photometric observation of H alpha emitting external spiral galaxies 08 p1013 A73-21809
- Galactic interstellar molecules, discussing physical, chemical and spectral characteristics, hydroxyl emission, occurrence regions, hydrogen clouds, isotope ratios, interstellar masers and probes 09 p1146 A73-22446
- Observations of the outer spiral structure of the Milky Way and its relation to the high velocity clouds. 09 p1151 A73-23292
- An estimate of the energy spectrum of gamma rays from the central region of the Galaxy and some implications. 10 p1263 A73-23486
- Statistical significance of some optical evidence for the bending of the galactic plane. 10 p1271 A73-23492
- Chemical composition of classical Cepheids in the Galaxy and Magellanic Clouds 10 p1273 A73-23705

MILLIMETER WAVES

- Particle motion diffusion model for cosmic ray propagation in Galaxy, investigating electron component energy spectra and background radio emission 10 p1265 A73-23908
- Energy spectrum of galactic cosmic rays beyond the region of modulation and the anisotropy of cosmic rays in the Galaxy 10 p1267 A73-23925
- The distribution of X-ray sources in our galaxy. 11 p1415 A73-25178
- Russian book - Physics of stars and nebulae. 11 p1416 A73-25226
- Luminescence of isolated dark clouds caused by the integral field of stellar galactic radiation 11 p1416 A73-25234
- Investigation of star orbits in stellar clusters with allowance for the disturbing force of the galaxy 12 p1538 A73-26863
- Metagalactic cosmic ray origin models and cosmic ray energy density around Galaxy, considering gamma ray flux, measurement from Magellanic Clouds 12 p1539 A73-27142
- Stokes polarization parameters of optical emission scattered in absorbing medium calculated for Galaxy and M 82 galaxy, assuming thermal IR radiation from nucleus 12 p1539 A73-27284
- Wave model of Galaxy spiral structure, assuming subsystem mass distribution and old star rotating bar mechanism 12 p1547 A73-27879
- The Perseus spiral arm at 21-cm. 13 p1685 A73-29354
- Young open star clusters. II - Their nature and their significance for galaxy research 14 p1798 A73-30274
- On the kinematical and spatial coincidence of optical and radio spiral arms in our galaxy. 15 p1929 A73-31055
- Gamma-ray observations of the galactic centre. 15 p1933 A73-31354
- Southern Milky Way early type star interstellar extinction curves, considering position with regard to galactic plane and local dust cloud conditions 15 p1939 A73-32046
- Chemical composition of the classical Cepheids in the Galaxy and the Magellanic Clouds. 18 p2354 A73-36730
- A stochastic model of the galactic magnetic field. 18 p2356 A73-36974
- Universe evolutionary model construction based on observations of high flux gravitational radiation generated within Milky Way Galaxy 20 p2609 A73-39434
- Observations of neutral hydrogen near the galactic center. II - The nuclear disc. 20 p2610 A73-39578
- Residual velocities of clusters and indications of the existence of a local cluster 21 p2768 A73-40713
- Galactic spiral arm structure mapping by 21 cm data taken at different latitudes, discussing high velocity hydrogen clouds distribution 21 p2778 A73-41533
- Infrared maps of the galactic nucleus. 22 p2904 A73-41757
- Pulsar search in Galactic nucleus region at 430 MHz with 140 foot telescope, discussing data reduction and results 22 p2909 A73-42484
- Galactic nucleosynthesis time interval from birth to solar system formation /Galactic age/ from radioactive decay nuclear yield ratios 22 p2916 A73-43049
- Neutral hydrogen spectral line observation for Milky Way Galaxy mapping, discussing role of spiral structure density wave theory in interpretation 23 p3028 A73-43348
- Spectral line radio astronomy observations of interstellar molecular clouds in Galaxy, relating to stellar and life evolution 23 p3028 A73-43350
- Neutral hydrogen rotational motions near galactic center and 3-kpc arm, using dispersion ring model 24 p3140 A73-45180
- Bending of the galactic plane and the nature of the high velocity clouds. 24 p3140 A73-45189
- ## MILLIMETER WAVES
- Unit for wideband measurements of dielectric parameters at millimeter wavelengths 01 p0050 A73-10794
- Experimental investigation of millimeter-band electromagnetic wave propagation in a waveguide filled with n-type InSb under a magnetic field 01 p0017 A73-10977
- 50 GHz gallium-arsenide IMPATT oscillator. 02 p0144 A73-11519
- Optimal output power of tunnel drift diode oscillator in millimeter band as function of electric field and diode geometry 03 p0284 A73-14086
- Newly developed bolometer mounts for the short millimeter wave region. 03 p0310 A73-14500

- Molecular clouds in the galactic center region - Carbon monoxide observations at 2.6 millimeters. 04 p0499 A73-15357
- ATS-F COMSAT millimeter wave propagation experiment. 04 p0418 A73-15386
- Millimeter wave propagation measurement for attenuation probability statistics by ATS-5 satellite, considering impact on space communication system design 04 p0418 A73-15387
- Absorption in the 220 GHz atmospheric window. 04 p0418 A73-15394
- Experimental study of millimeter-wave characteristics of hot electrons in n-type GaAs by electrodeless method. 05 p0558 A73-16525
- Millimeter-wave investigation of electronic conduction in semiconducting III-V compounds. 06 p0737 A73-18366
- Sensitivity of Josephson junctions in video detection of microwave and millimeter-wave radiation. 06 p0677 A73-18371
- On the reduction of rainfall outages by space diversity for millimeter-wave earth-satellite communications systems. 06 p0668 A73-18712
- Precision design of millimeter-wave band-pass filter. 07 p0799 A73-19371
- 50 GHz helix type travelling wave tube 'W-5028.' 07 p0799 A73-19372
- Path diversity for mm-wave earth-to-satellite links. [AD-757967] 07 p0791 A73-19376
- Brightness distribution of the sun at 8.6 mm wavelength. 07 p0877 A73-19596
- Millimeter and submillimeter wave detection and mixing with superconducting weak links. 07 p0863 A73-20102
- Josephson junction millimeter microwave source and homodyne detector. 07 p0863 A73-20104
- Unusually high earth-space path attenuations measured using a 6.4-GHz radiometer. 07 p0793 A73-20111
- Results of radio source observations at short millimeter wavelengths 07 p0901 A73-20310
- Waveguide millimeter wave diode, ECL-2173. 07 p0804 A73-20568
- GaAs diffused diode, ECL-1350. 07 p0804 A73-20570
- A three-cavity ring type filter. 07 p0804 A73-20572
- Polarization structure of a solar flare region at 9.5 mm wavelength. 08 p0997 A73-20767
- Semicircular waveguide-type, band-splitting filter for millimeter waves. 08 p0945 A73-20807
- Millimeter-wave frequency response of hot electrons in n-type GaAs. 08 p0994 A73-20845
- Microwave and millimeter wave receiver noise performance state of art and acoustic measurement methods, discussing traveling wave maser, parametric and transistor amplifiers and tunnel diodes 08 p0940 A73-21625
- Solid-state devices and components for mm-wave receiver-transmitter systems. 09 p1064 A73-22498
- Solar oscillatory phenomenon at 9.6 mm with atmospheric absorption effects minimized, discussing power spectra 09 p1149 A73-22962
- Interstellar organic molecules millimeter wave line spectra and transition rotational quantum numbers 09 p1150 A73-23141
- Semiconductor diode mixer for millimeter-wave frequencies. 10 p1193 A73-23665
- Equivalent circuits of diodes in millimeter and submillimeter wave frequencies. 10 p1193 A73-23667
- Millimeter wave imagery of complex three dimensional target by diffuse reflection with spatial filtering, discussing range, resolution and view field capabilities 10 p1188 A73-23798
- The radio diameter of the sun from interferometer measurements at 9 mm wavelength. 10 p1284 A73-24773
- Equivalent noise temperature equation relating HF noise in mm wave Schottky barrier diodes to barrier transport mechanism 11 p1339 A73-26697
- Observations of radio sources at short millimeter wavelengths. 12 p1539 A73-27282
- Millimeter wave burst mean duration relation to PCA event intensity derived from relationship between impulsive single frequency microwave bursts and solar proton events 12 p1543 A73-27616

- Parabolic 10 m antenna-8.4 mm wavelength radiometer system for radio astronomy 12 p1498 A73-27724
- Quiet sun millimeter wave emission and brightness temperature, discussing observational difficulties arising from fog, cloud and rain attenuation 12 p1543 A73-27725
- A recalibration of the quiet sun millimeter spectrum based on the moon as an absolute radiometric standard. 12 p1545 A73-27840
- Further evidence for a complex limb structure in the solar radial brightness distribution at mm wavelengths. 12 p1545 A73-27841
- Frequency stability of millimetre-band reflex klystrons with various cooling techniques. 13 p1589 A73-28049
- Ground-based measurement of millimetre-wavelength emission by upper stratospheric O2. 14 p1751 A73-29718
- A null-reading method of measuring the complex reflection coefficient in the short-wave end of the millimeter band 14 p1728 A73-30271
- A wideband radiometer for the four-millimeter band built with semiconductor devices 14 p1735 A73-30272
- Rain-attenuation measurements of millimetre waves over short paths. 15 p1848 A73-32647
- Solar limb brightening at the 8-mm wavelength 16 p2057 A73-32705
- EHF radio wave limitations and potentialities for high speed data communications systems, considering applications in urban short range relays 16 p1981 A73-33705
- The characteristics of millimeter wavelength satellite-to-ground space diversity links. 16 p1981 A73-33707
- Millimeter wave propagation measurements from an orbiting earth satellite. 16 p1982 A73-33716
- Atmospheric attenuation measurement for nine millimeter wavelength signal from radio source, discussing solar power, radiosonde, emission temperature and nodding solar methods 16 p1982 A73-33719
- Zenith atmospheric emission noise temperature and attenuation measurements including multiple and single frequency statistical observations at 85-118 GHz during 1970-1971 16 p1982 A73-33720
- Millimeter wave backscatter measurements for snow, ice and sea ice, discussing penetration into snow and ice 16 p1983 A73-33728
- Laboratory measurements of electromagnetic properties of atmospheric gases at millimeter wavelengths. 16 p1983 A73-33731
- Radio emission from the moon and sun at the 2.25-mm wavelength and from Jupiter at the 2.1-mm wavelength 16 p2064 A73-33768
- Radio emission of the moon at millimeter and submillimeter wavelengths 16 p2064 A73-33769
- Distribution of radio brightness across the disk of Venus at the 8-mm wavelength 16 p2068 A73-33816
- Radio emission from Venus and Jupiter at 2 and 8 mm wavelengths 16 p2068 A73-33817
- Radiation patterns and structural design of two mirror millimeter wave Cassegrain antennas with horn radiator 16 p1991 A73-33985
- Determination of changes in the reflection coefficient of absorbing coatings in the millimeter wavelength band 17 p2120 A73-34156
- Visualization of the amplitude-phase structure of electromagnetic fields in the millimeter and submillimeter ranges 17 p2121 A73-34158
- A study of millimeter-wave GaAs IMPATT oscillator and amplifier noise. 17 p2133 A73-34217
- Atmospheric attenuation anomalies at 2.7 mm from sky noise temperature measurements compared with water vapor and oxygen line strength calculations 17 p2159 A73-34571
- Experimental investigation of a millimeter band frequency converter on n-InSb at 4.2 K. 17 p2136 A73-35158
- Highly stabilized IMPATT oscillators at millimeter wavelengths. 18 p2293 A73-36607
- On rainfall and space diversity for millimeter-wave earth-satellite communications systems. 18 p2289 A73-36709
- Reflectometric bridge in Q band /8 mm/ - Power detected in an unbalanced bridge 19 p2403 A73-37532

Search for solar recombination lines in the frequency range 110-115 GHz. 19 p2488 A73-38521

Millimeter wave solid state technology for 60 GHz communication systems, discussing silicon Schottky diode and varactor mixer/receiver, parametric amplifiers and upconverters 20 p2534 A73-38748

A low temperature bolometer heterodyne receiver for millimeter wave astronomy. 20 p2564 A73-38878

Circular polarized emission from solar active regions at millimeter wavelengths. 20 p2601 A73-39070

Radiometric terrain mapping at 3 mm wavelength. 20 p2568 A73-39870

Radio astronomy millimeter wave receiver techniques and atmospheric restrictions for coherent radio/detection 21 p2771 A73-41237

German monograph on microwave filters for communication channels separation at millimeter wavelengths covering coupling circuits design and resonant frequencies of coaxial resonator 22 p2827 A73-42701

Properties of a light-modified-breakdown detector in GaAs. 22 p2864 A73-43164

Fixed baseline millimeter wave interferometer with aperture synthesis telescope of antenna array for interstellar and planetary water vapor and radio sources mapping 23 p2980 A73-43364

An 8-mm interferometer for solar radio astronomy at Bordeaux, France. 23 p2980 A73-43365

Millimeter wave radio telescope with high resolution for obtaining heliograph, discussing fast rotational synthesis and array redundancy design features 23 p2958 A73-43373

Modified H guide for millimeter and submillimeter wavelengths. 23 p2960 A73-44072

Reactions of living organisms to the action of electromagnetic waves in the millimeter range 23 p2949 A73-44094

Effects of electromagnetic waves of the millimeter range on a cell and on some structural elements of a cell 23 p2949 A73-44095

Prospects for studying mechanisms responsible for the nonthermal effects of millimeter- and submillimeter-band electromagnetic radiation on biologically active compounds 23 p2949 A73-44096

Coupling coefficient/frequency characteristics of rectangular dielectric waveguide channel dropping coupled line filter for millimeter wave 23 p2961 A73-44118

Planetary brightness temperature measurements at 8.6 mm and 3.1 mm wavelengths. 24 p3130 A73-44458

Interpretation of atmospheric radio emission in the 5-mm spectral region 24 p3068 A73-44961

MILLING [MACHINING]

Surface roughness of turbine blades machined by circular milling 02 p0174 A73-12579

MILLING [MIXING]

U COMPOUNDING

MINERAL EXPLORATION

Natural resources research and development in Lesotho using ERTS imagery. 18 p2308 A73-36045

MINERAL OILS

Oxystearate-based multipurpose lithium lubricants 07 p0843 A73-20013

Experimental determination of the temperature and pressure dependence of the absolute viscosity of mineral oils 10 p1237 A73-23661

Frictional traction in elastohydrodynamic lubrication. 13 p1623 A73-28198

A comparison of hydraulic fluid characterizations in two evaluation systems. [ASLE PREPRINT 73AM-9A-2] 17 p2196 A73-34997

Protection of mineral oils from microbiological damage by compounds of the quinone group 21 p2723 A73-41069

Gas solubility in hydraulic liquids from measurements of air in mineral oils, noting oil molecular weight effect 21 p2724 A73-41579

MINERALOGY

The composition and crystalline structure of the minerals of regolith from the Sea of Fertility. 02 p0214 A73-12243

Stability relations of ilmenite and ulvöspinel in the Fe-Ti-O system and application of these data to lunar mineral assemblages. 02 p0220 A73-12482

Hornblendes from calc-alkaline volcanic rocks of island arcs and continental margins. 02 p0165 A73-12635

The Angra dos Reis /stone/ mineral assemblage and the Genesis of stony meteorites. 03 p0374 A73-13797

Comparison of the analytical results from the Surveyor, Apollo, and Luna missions. 04 p0498 A73-15185

The mineralogy, petrology and geochemistry of lunar samples - A review. 04 p0498 A73-15186

Magnetic transitions observed in sulfide minerals at elevated pressures and their geophysical significance. 06 p0691 A73-18576

Lunar Science Conference, 3rd, Houston, Tex., January 10-13, 1972, Proceedings. Volume 1 - Mineralogy and petrology. Volume 2 - Chemical and isotope analyses, organic chemistry. Volume 3 - Physical properties. 07 p0878 A73-19676

Mineralogical evidence for subsolidus vapor-phase transport of alkalis in lunar basalts. 07 p0880 A73-19693

Fra Mauro crystalline rocks - Mineralogy, geochemistry and subsolidus reduction of the opaque minerals. 07 p0880 A73-19698

Mineralogical and petrographic features of two Apollo 14 rocks. 07 p0880 A73-19699

Lunar plagioclase - A mineralogical study. 07 p0881 A73-19712

Apollo 14 breccia 14313 - A mineralogical and petrologic report. 07 p0882 A73-19719

Mineralogy and origin of Fra Mauro fines and breccias. 07 p0883 A73-19726

Mineralogy, petrology, and chemical composition of lunar samples 15085, 15256, 15271, 15471, 15475, 15476, 15535, 15555, and 15556. 07 p0883 A73-19727

Experimental petrology and origin of Fra Mauro rocks and soil. 07 p0883 A73-19728

Compositions and mineralogy of lithic fragments in 1-2 mm soil samples 14002, 7 and 14258, 33. 07 p0884 A73-19739

Chromatographic and mineralogical study of Apollo 14 fines. 07 p0884 A73-19743

Mineralogy, petrology, and surface features of some fragmental material from the Fra Mauro site. 07 p0885 A73-19748

A new titanium and zirconium oxide from the Apollo 14 samples. 07 p0885 A73-19749

Electron microscopy of some experimentally shocked counterparts of lunar minerals. 07 p0885 A73-19750

Apollo 14 mineral ages and the thermal history of the Fra Mauro formation. 07 p0887 A73-19776

Apollo 14 samples with Fe-bearing minerals examined by Mossbauer spectroscopy, noting parallelism with Apollo 11 and 12 samples 07 p0893 A73-19845

Stony meteorite discovery at Ness County, Kansas, noting three separate falls and composition and mineralogical differences from Karsada, Franklinville and Wellmanville meteorites 09 p1138 A73-21851

Mineralogy and petrology of the Yilmia enstatite chondrite. 09 p1139 A73-21852

Petrography, mineralogy and composition of plagioclase and pyroxenes of Washougal howardite by density and refraction measurements 09 p1139 A73-21853

The Oro Grande, New Mexico, chondrite and its lithic inclusion. 09 p1139 A73-21858

Havero stony ureilite origin modes, composition, textural features, mineralogy and petrology 09 p1139 A73-21860

The highly reflecting and opaque components in the mineral content of the Havero meteorite. 09 p1140 A73-21866

Havero ureilite - Evidence for recrystallization and partial reduction. 09 p1140 A73-21869

Mineralogy and texture of Havero ureilite, noting preterrestrial shock evidence, recrystallized olivine and metal grain, and graphite conversion into diamonds from petrographic observation 09 p1140 A73-21870

Apollo 15 soil and rock particle tracks density and stability and uranium content 12 p1542 A73-27547

Preliminary data on lunar soil recovered by the Luna 16 automatic station 13 p1672 A73-28114

Mineralogical density of sporadic meteorite bodies 13 p1673 A73-28298

An unusual basalt fragment in Luna 20 sample L2010. 13 p1675 A73-28309

Luna 20 - Mineral chemistry of spinel, pleonaste, chromite, ulvöspinel, ilmenite and rutile. 13 p1675 A73-28316

Luna 20 highland soil samples mineralogical and petrological analysis, comparing chemical composition with Apollo 16 soil samples 13 p1676 A73-28322

Luna 20 - Mineralogy and petrology of fragments less than 125-micron size. 13 p1676 A73-28324

Mineralogy, petrology and chemistry of lithic fragments from Luna 20 fines - Origin of the cumulate ANT suite and its relationship to high-alumina and mare basalts. 13 p1676 A73-28328

Mineralogical characteristics of the Rechki meteorite 13 p1677 A73-28349

Apollo 17 basalt ortho- and para-armalcolite, noting differences in optical properties, crystal habit and distribution between coarse and fine grained rocks 14 p1789 A73-29739

Soviet Lunokhod 2 lunar rover design, guidance systems, mineralogical analyses by X ray fluoroscopic spectroscopy, magnetic field measurements and operations site 16 p1996 A73-33225

Changes in the optical properties of minerals and their atomization caused by ion bombardment 16 p1977 A73-33756

Mineralogical density of sporadic meteoric bodies. 21 p2779 A73-41542

Major and trace elements in igneous rocks from Apollo 15. 23 p2950 A73-43765

The Canyon Diablo meteorite. 24 p3137 A73-44949

MINERALS

NT ARAGONITE

NT ASBESTOS

NT CALCITE

NT CHROMITES

NT ENSTATITE

NT FELDSPARS

NT FLUORITE

NT FORSTERITE

NT GARNETS

NT GRAPHITE

NT HEMATITE

NT ILMENITE

NT KAMACITE

NT KAOLINITE

NT MAGNETITE

NT OLIVINE

NT PEROVSKITES

NT PROUSTITE

NT PYRITES

NT PYROPHYLLITE

NT PYROXENES

NT QUARTZ

NT SIDERITES

NT SPINEL

NT STISHOVITE

NT TALC

NT TROILITE

NT WURTZITE

NT ZINCBLENDE

The kinetics of ulvöspinel reduction - Synthetic study and applications to lunar rocks. 08 p0936 A73-20840

Some physical properties of stephanite in the phase transition region 13 p1667 A73-28002

Deformation and transformation of rock-forming minerals by natural and experimental shock processes. I - Behavior of minerals under shock compression. 14 p1750 A73-30958

Minor and trace elements in some meteoritic minerals. 15 p1941 A73-32387

MINES [EXCAVATIONS]

Satellite imagery in national resource surveys and vegetation growth monitoring on mine dumps from ERTS-1 data 18 p2311 A73-36151

MINIATURE ELECTRONIC EQUIPMENT

Development and adjustment of a multi-channel miniaturized FM/AM telemetering system adapted to the primates. 03 p0270 A73-14284

An implantable blood pressure and flow transmitter. 04 p0447 A73-14845

Attempt at estimating the parameters of soldering processes 04 p0454 A73-15349

Miniature biotelemeter giving 10 channels of wide-band biomedical data. 04 p0412 A73-15388

Miniature four-channel radiotelemetry system for the transmission of cerebral biopotentials 06 p0658 A73-18167

MINIATURIZATION

Miniature single channel narrow-band differential pulse width modulation-FM crystal controlled transmitter for biomedical telemetry system
09 p1047 A73-23381

Technique for measuring the vessel blood pressure in long continued experiments
15 p1838 A73-31394

Helix support, focusing, fabrication and performance tests of miniature traveling wave tubes (TWT), using rare earth-cobalt /RAECO/ magnets
22 p2834 A73-42696

MINIATURIZATION

NT MICROMINIATURIZATION

Recent research results in the field of hermetically sealed miniature silver-zinc storage batteries.
02 p0133 A73-12513

Some effects of temperature on material properties and device reliability.
07 p0797 A73-19134

Multiparametric optimization of a thermionic electric power generating element
07 p0778 A73-19286

Six-channel strain-gauge system for dynamic measurements
07 p0827 A73-20539

Miniaturized unstable and bistable fluidic switching elements performance characteristics, considering vibration, velocity, pressure and laminar/turbulent flow effects on switching time and stability
13 p1571 A73-28482

Multiparameter optimization of a thermionic fuel cell.
13 p1571 A73-28686

Miniature phase/amplitude tracking RF receiver front ends.
14 p1737 A73-30623

Low cost strapdown inertial navigator with miniature electrostatically suspended gyros, discussing system performance goal in terms of position, velocity and attitude errors
21 p2734 A73-40037

Miniaturized Nd-YAG laser end pumped by single incoherent gallium-arsenide-phosphide light emitting diode to achieve threshold at room temperature
21 p2713 A73-40457

MINICOMPUTERS

Real time programmable data compression system with minicomputers for operation between TV data acquisition ground stations and ATS satellites
04 p0425 A73-15442

Automated vibration shaker calibration data acquisition and analysis system with minicomputer for working transfer standard voltage monitoring and acceleration level determination
09 p1070 A73-22508

Small digital computer program packet organization for central processor productivity and use coefficient improvement, discussing graph-algorithm language for program splicing
15 p1848 A73-31694

New structure of on-board microcomputers using large-scale integrated logic circuits
15 p1852 A73-32478

French monograph on numerical data processing organs for real time process control, describing modular computer design project
15 p1849 A73-32590

Microcomputer programs for data reduction and quality control chart work, using Olivetti P-101, HP 9100-B and Wang 700-A calculators
16 p1986 A73-33642

Book - Minicomputers for engineers and scientists.
17 p2130 A73-34455

Digital pulse counting astronomical spectrograph system with TV camera tube, image intensifier and minicomputer for camera scan control and video data processing
17 p2169 A73-35282

Airborne flight-test strain gage instrumentation from installation, calibration and data recording and reduction standpoint, discussing ground and airborne minicomputer use
17 p2148 A73-35442

A precision control system for a large astronomical telescope.
19 p2430 A73-38079

Designing with microprocessors instead of wired logic asks more of designers.
23 p2956 A73-44122

MINIMAX TECHNIQUE

Dynamic programming and a max-min problem in the theory of structures.
01 p0019 A73-10199

A Chebyshev minimax technique oriented to aerospace trajectory optimization problems.
01 p0100 A73-10729

Estimation of the state vector of a plant by minimization of a distance in metric space when using discrete sampling
05 p0561 A73-17281

One- and multistage multivariable function max-min problem solution by random search type method through regression curve construction based on statistical test and root determination
06 p0715 A73-17563

Sufficiently informative functions and the minimax feedback control of uncertain dynamic systems.
10 p1202 A73-24535

A method of feasible directions using function approximations, with applications to min max problems.
11 p1390 A73-25474

Determining the trend of a random sequence
12 p1518 A73-27224

Best rational approximation and strict quasi-convexity.
13 p1649 A73-28602

Game problem of the rigid collision of two points with impulsive thrust in a linear central field
13 p1660 A73-29080

A minimax filter for systems with large plant uncertainties using measurements corrupted by colored noise.
13 p1593 A73-29205

Degeneracy phenomenon in minimax rational approximation behavior in neighborhood of approximating function pole
13 p1650 A73-29396

Output feedback for linear multivariable systems with parameter uncertainty.
19 p2413 A73-38061

Necessary conditions for Chebyshev-Bolza optimal control problems.
19 p2415 A73-38489

Optimality and lower and upper bound conditions for multistep games with saddle point and minimax/maximin strategies, extending to differential games
20 p2539 A73-38678

Chebyshev minimax functional solution for optimal control system design, noting flexible rocket and nuclear reactor control applications
20 p2592 A73-38683

Optimum minimax strategy in pursuit game with observation of evading player phase vector at fixed times
21 p2724 A73-40180

German monograph on regularization and penalty function methods of numerical analysis in Hilbert or Banach space covering minimax technique and optimal control theory application
22 p2882 A73-42847

MINIMUM DRAG

Calculus of variations for functional conditional extremum, determining minimum drag shape for body of revolution in hypersonic flow
04 p0403 A73-14886

Optimization of drag minimums including effects of flow separation.
[ASME PAPER 72-WA/AERO-1]

The development of reciprocating engine installation data for general aviation aircraft.
[SAE PAPER 730325]

Construction of a minimum-wave-drag profile in inhomogeneous supersonic flow
21 p2631 A73-40184

The wave drag of circular nose cones at zero angle of attack at Mach numbers from 1.5 to 4 and thickness ratios from 0.05 to 0.5
23 p2940 A73-43782

MINITRACK OPTICAL TRACKING SYSTEM

U MINITRACK SYSTEM
MINITRACK SYSTEM
Geos 1 and 2 long periodic and secular orbit perturbations, discussing oscillating elements transformation with maximum accuracy via minitrack system
11 p1423 A73-26070

MINKOWSKI SPACE

Stress equations solutions existence near Minkowskian solution for asymptotic behavior, demonstrating flat space-time stability
[AD-756017]

The interaction of weak gravitational waves with a gas.
11 p1400 A73-26177

Unaccelerated-returning-twin paradox in flat space-time.
23 p3006 A73-43608

The Minkowski problem generalized for ovaloids
23 p2999 A73-43613

MINOR CIRCLE TURNING FLIGHT

Performance and stability of hypervelocity aircraft flying on a minor circle.
05 p0534 A73-16179

MINORITY CARRIERS

Effects of transverse diffusion and transverse stored charge in alloy transistor base.
01 p0023 A73-10681

On the measurement of the specific 'emitter efficiency factor in bipolar transistors.'
02 p0147 A73-12043

Vertical multijunction solar cells light generated current spectral response and I-V characteristics derivation from minority carrier diffusion equations
03 p0254 A73-14208

Minority carrier lifetime and diffusion constant as function of impurity concentration in double junction vertical solar cell, determining power efficiency
03 p0254 A73-14213

Electron irradiated float-zone Si solar cell I-V performance degradation due to photon irradiation, noting base region minority carrier lifetime role
03 p0257 A73-14244

Beta irradiation of silicon junction devices - Effects on diffusion length.
05 p0537 A73-16522

Bulk lifetime determination from current and capacitance transient response of MOS capacitors.
09 p1062 A73-22301

Two dimensional analysis of minority carriers on drift p-n-p junction transistor base for low level injection and constant mobility and diffusivity
09 p1062 A73-22301

The effect of an interfacial layer on minority carrier injection in forward-biased silicon Schottky diodes.
09 p1135 A73-23044

Cooling associated with minority carriers exclusion effect in semiconductors, discussing influence of electroconductivity and forbidden bandwidth
17 p2219 A73-35165

MINUTEMAN ICBM

ARIES, the Minuteman I second stage as a controlled sound rocket.
[AIAA PAPER 73-287]

Circumvention design of active circuitry and passive shielding for electromagnetic pulse environments with application to Minuteman ICBM system
22 p2822 A73-41786

MINUTEMAN MISSILES

U MINUTEMAN ICBM
MIRRORS
NT CELESTROSCOPES
NT FRESNEL REFLECTORS
NT MAGNETIC MIRRORS
NT PARABOLOID MIRRORS
NT ROTATING MIRRORS

Auxiliary instruments for 4-m reflectors related to astronomical telescope focal positions, discussing correlators, cameras, sensitometers, film, rotator-adaptor, guider, echelle spectrograph and photometers
01 p0046 A73-10504

Instrumentation and some principal programs of the McDonald Observatory 2.75-meter /107-inch/ reflector.
01 p0046 A73-10505

Schmidt and Maksutov spectrographic cameras, discussing correcting devices for mirror aberrations
01 p0047 A73-10512

The coude of the 1.2 meter telescope at Victoria.
01 p0048 A73-10527

Use of a mirror shearing interferometer for gas dynamics research.
01 p0050 A73-10830

Variable reflectivity unstable laser resonator mode selectivity solution by perturbation analysis for mirror misalignment effects, obtaining Fresnel number and output coupling conditions
01 p0060 A73-11223

Interferometric testing of large optical components with circular computer holograms.
01 p0053 A73-11225

Lunar laser observatory equipment modifications, noting change of Cassegrain primary mirror from spherical metal alloy to hyperboloid glass construction
02 p0176 A73-12244

Elastic deformation of lightweight mirrors.
02 p0236 A73-12375

Coupling losses in hollow waveguide laser resonators.
02 p0177 A73-12573

Spectrum of stimulated radiation in a flat-mirror resonator.
02 p0177 A73-12695

Mutual compensation of the unloading-force errors in the axial- and lateral-unloading systems of an astronomical mirror
05 p0575 A73-16317

Image quality and energy distribution for mirror cone and toroidal annular mirror optical coordinators in wide angle measuring instruments
05 p0575 A73-16318

Four-field parametric frequency selection in stimulated emission lines from nonlinear mirror, noting reflection coefficient
05 p0584 A73-16554

Analysis of sublimation-cooled coated mirrors in convective and radiative environments.
05 p0641 A73-17108

Stress distribution on astronomical telescope mirror outer surface, calculating deflection and relief load
06 p0693 A73-18157

Scanning electron microscope and energy dispersive X-ray analysis of the surface features of Surveyor III television mirror.
07 p0872 A73-19899

Wave transformation by a phase corrector
07 p0793 A73-19923

Analysis of He-Ne laser surface reflections from an off-axis parabolic mirror.
08 p0974 A73-21032

Modal control applied to the real-time figure control of a spaceborne telescope mirror.
08 p0969 A73-21729

- Multiple mirror telescope consisting of six Cassegrainian telescopes combined for common focal surface, noting light gathering power equivalent to 180 inch standard telescope
08 p0970 A73-21738
- Some design aspects of a multiple-mirror telescope.
08 p0970 A73-21739
- Laser beam steering in confocal unstable resonators, interpreting mirror misalignment effects as far field dependence on magnification and Fresnel number from mode solution
09 p1090 A73-22076
- Semiconductor electron-beam-pumped lasers of the radiating mirror type.
09 p1092 A73-22248
- Laser system output mirrors alignment for beam quality and power performance optimization and external optical component premature degradation prevention, using autocollimator
09 p1094 A73-22445
- Optimization studies in the support design for the Large Space Telescope.
[AIAA PAPER 73-350]
11 p1437 A73-25488
- Problem of the reflection of pulse signals from a moving mirror
11 p1332 A73-26167
- A SISAM interferometer and a simple Michelson-interferometer with spherical mirrors for space application.
11 p1369 A73-26519
- Emission of a ruby laser with a moving mirror in the presence of a selector in the resonator
12 p1505 A73-26955
- Graphs for the design of laser mirrors at normal incidence.
13 p1627 A73-28598
- Parametric studies on CO₂ TEA lasers with extracavity and intracavity electrodes.
13 p1628 A73-29187
- Effects of polarization on the transmission of coude-spectrometer systems.
13 p1621 A73-29351
- The polished surface of a telescope mirror as seen in an electron microscope
14 p1752 A73-30060
- Field properties and losses in a three-mirror optical ring resonator with a Gaussian diaphragm
15 p1886 A73-32341
- Computerized Ritchey-Chretien computation method for telescopic optical system, controlling mirror shape via transparent screen
16 p2011 A73-32715
- Effects of mirror reflectivity in a distributed-feedback laser.
16 p2024 A73-33081
- Feasibility experiments for high capacity Hertzian cables to distribute and collect data within urban areas, using cylindrical mirrors
16 p1982 A73-33715
- Improvement of absolute accuracy for a multiple bounce reflectometer through a detailed effort to reduce systematic errors.
17 p2172 A73-35420
- Optical effects of cryodeposits on low scatter mirrors.
[AIAA PAPER 73-732]
18 p2336 A73-36349
- Mass property control of a synchronous meteorological satellite scanning experiment.
[SAWE PAPER 964]
19 p2492 A73-37882
- Generation in a ruby laser with moving mirror and a selector in the resonator.
19 p2438 A73-38132
- Design study of a glass meridian circle.
20 p2565 A73-39064
- Determination of the centering conditions of two-mirror systems with the aid of Hartmann photographs
20 p2565 A73-39067
- Czerny-Turner monochromator design using small spherical mirror off-axis angles to eliminate multiply dispersed light, discussing mirror types and focal length
21 p2697 A73-40129
- Characteristics of a laser using a grid as the resonator output mirror
21 p2713 A73-40528
- Interference patterns and operation of four unit interferometer consisting of beam splitter, mirrors and analyzer
21 p2704 A73-41261
- Main-mirror aberrations in a variable-profile antenna and beam scanning by displacement of the primary radiating element
21 p2667 A73-41446
- Design of the reflecting elements and secondary mirror of the RATAN-600 radio telescope
21 p2675 A73-41449
- Indicator and setting devices for circular-mirror sections of the RATAN-600 radio telescope
21 p2675 A73-41451
- Reference indication and setting devices for circular mirror sections of the RATAN-600 radio telescope
21 p2675 A73-41452
- Divergence of the output radiation of electron-beam-pumped 'radiating mirror' lasers.
22 p2869 A73-42258
- Properties of laser mirrors at non-normal incidence.
22 p2872 A73-43186
- Real laser cavity with nonideal reflecting mirrors, showing Q factor increase relation to mode order for plane monochromatic linearly polarized waves
23 p2987 A73-43650
- Elastomechanical model measurements conducted with the aid of holographic approaches in the case of a mirror cell
24 p3090 A73-44897
- MIS [SEMICONDUCTORS]**
- Negative resistance in metal-semiconductor-metal (MSM) diodes.
01 p0023 A73-10579
- Circuit variants of dynamically operated MIS /metal-insulator-semiconductor/ structures
03 p0281 A73-13241
- Theory of dynamic charge and capacitance characteristics in MIS systems containing discrete surface traps.
04 p0427 A73-15344
- Theory of dynamic charge current and capacitance characteristics in MIS systems containing distributed surface traps.
04 p0427 A73-15345
- N-type Si MNOS random access memory devices for data storage without applied voltage, noting threshold shifts vs writing pulse width for various oxide thicknesses
05 p0553 A73-16166
- MIS and Schottky barrier microstrip devices consisting of microstrip transmission line fabricated on semiconductor substrate, causing capacitance dependence on electric field
05 p0559 A73-16818
- Improving the performance of M.I.S. circuits under radiation.
07 p0797 A73-18918
- Surface oxide transistor with MIS and base contacts, investigating I-V characteristics as function of oxide thickness and contact separation distance
08 p0948 A73-21480
- Feasibility analysis of MIS sandwich structure for pulsed laser based on calculation for field distribution and TE and TM modes in optical cavity
09 p1093 A73-22254
- Microelectronics developments and limitations, considering bipolar IC, metal-dielectric-semiconductor structures and optoelectronic communication links
12 p1480 A73-27267
- Avalanche injection effects in MIS structures and realization of n-channel enhancement type MOS FETS.
15 p1851 A73-32017
- Photoeffect applications in MDS systems with a nonstationary depletion layer in ionizing radiation detectors
18 p2316 A73-36716
- Preparation and RF properties of MIS mesa varactors.
19 p2409 A73-37720
- MIS structures with reversible charge capture capability, discussing I-V characteristics and applications similar to FET, image storage and charge coupled devices
20 p2534 A73-38853
- Metal-insulator-semiconductor-insulator-metal information storage system with optical write and read operations.
20 p2533 A73-39683
- Present state and future prospects of the design of large-scale integrated circuits using MIS transistors
21 p2660 A73-40018
- Measurement of the doping level distribution in the surface region of a semiconductor
21 p2753 A73-41097
- German monograph - Investigation of time-variable currents in Al-Al₂O₃-Al thin-film structures.
22 p2897 A73-42855
- Photoelectric methods of determining the electrical characteristics of MDS systems
23 p3006 A73-43616
- Hartree-Fock model for metal to insulator transition in vanadium oxide based on electronic band structure at zero and finite temperatures
23 p2961 A73-44163
- MISALIGNMENT**
- Variable reflectivity unstable laser resonator mode selectivity solution by perturbation analysis for mirror misalignment effects, obtaining Fresnel number and output coupling conditions
01 p0060 A73-11223
- PM signal cross-correlated receiver output SNR in presence of random misalignments with respect to carrier frequency and signal arrival time
05 p0547 A73-16058
- Instrument axes trihedron orientation relative to reference, deriving expressions for angular misalignment statistical estimation
09 p1115 A73-22353
- Estimation and correction of electric thruster misalignment effects on a geostationary satellite.
17 p2238 A73-34866
- Effects of misalignment on the pre-macroyield region of the uniaxial stress-strain curve.
20 p2576 A73-39030
- MISCIBILITY**
- U SOLUBILITY**
- MISFIRE**
- U FIRING [IGNITING]**
- MISMATCH**
- U IMPEDANCE MATCHING**
- MISORIENTATION**
- U MISALIGNMENT**
- MISS DISTANCE**
- Noise processes in a homing radar seeker.
18 p2290 A73-37088
- Optimal aircraft collision avoidance.
19 p2452 A73-38050
- New missile guidance concepts as applied to command guidance control system.
20 p2584 A73-38778
- Horizontal aircraft maneuver strategy for maximum miss distance and minimum course deviation, examining filtering techniques, collision avoidance system and signal error analysis
21 p2734 A73-40032
- MISSILE ANTENNAS**
- Development of loaded resin one-piece radomes
11 p1387 A73-25294
- MISSILE BODIES**
- Optimum shapes of slender axisymmetric missile bodies with minimum ballistic factor, using calculus of variations
16 p2071 A73-32904
- MISSILE CASES**
- U MISSILE BODIES**
- MISSILE COMPONENTS**
- NT MISSILE ANTENNAS**
- NT MISSILE BODIES**
- Microelectronic technologies for SAM-D system, discussing thick film hybrid circuits and microstrip applications
02 p0148 A73-12594
- Electronic equipment computerized radiation hardness assurance program for retaliatory or deterrent missile system, discussing supplier data monitoring, verification test and radiation shield assurance
11 p1342 A73-26637
- Turbine powerplants for missiles - Cost improvement requirements.
17 p2222 A73-34709
- Load currents in missile circuits excited by a plane polarized field.
19 p2409 A73-37272
- MISSILE CONFIGURATIONS**
- An empirical flowfield analysis technique for preliminary evaluation of inlet systems operating in a vehicle generated flowfield.
01 p0003 A73-11132
- Exhaust plume prediction model for a low-altitude supersonic missile.
[AIAA PAPER 72-1170]
06 p0741 A73-18399
- Russian book on rockets as control plants covering dynamics equations of motion for different configurations, linearization and matrix description of rockets.
11 p1429 A73-25175
- Asymmetric missile subharmonic response to nonlinear aerodynamic moments, considering spin and aerodynamic damping effects
15 p1943 A73-31667
- Aircraft-store separation design for angular momentum increase of external weapon with internally mounted spinning flywheel
20 p2508 A73-38652
- The panel method for the calculation of the pressure distribution on missiles in the subsonic range
22 p2797 A73-43028
- MISSILE CONSTRUCTION**
- U MISSILE STRUCTURES**
- MISSILE CONTROL**
- Phase space trajectory analysis of pulsed laser spot pursuit tracking problem for autonomous line-of-sight interceptor missile with flip-flop controls
03 p0287 A73-14483
- Missile guidance and control systems optical linking, using fiber optics and light emitting diodes and photodetectors as optical/electrical transducers
06 p0757 A73-18324
- Suboptimal guidance for attitude angle constrained flight trajectories.
06 p0721 A73-18825
- Titan III-C guidance with the Carousel VB inertial guidance system.
06 p0721 A73-18826
- Launching base telelimiter apparatus with image superposition on TV screen for controlling missile or rocket from going beyond security limits during initial flight
07 p0789 A73-18950
- A four-level technique for estimation of tactical missile aerodynamic parameters.
07 p0777 A73-20592
- A discrete separation principle with a stochastic terminal constraint.
07 p0806 A73-20599
- A semiinertial homing guidance system
10 p1247 A73-24498
- A four-level technique for estimation of tactical missile aerodynamic parameters.
10 p1172 A73-24538

Russian book on rockets as control plants covering dynamics equations of motion for different configurations, linearization and matrix description of rockets 11 p1429 A73-25175

Radome precision testing for fire control, missile aiming, Doppler navigation and bombing 11 p1335 A73-25277

Optimal stochastic guidance laws for tactical missiles. 15 p1908 A73-31917

Optimal evasive tactics against a proportional navigation missile with time delay. 15 p1908 A73-31918

Russian book - Radio devices for flight vehicle control systems. 15 p1908 A73-32421

Real-time hybrid hardware-in-the-loop simulation of a terminal homing missile. 18 p2291 A73-36834

A high-performance, aerodynamically-controlled, tactical missile hybrid 6-DOF simulation. 18 p2296 A73-36835

Differential games applied to some interception models 18 p2268 A73-37080

Noise processes in a homing radar seeker. 18 p2290 A73-37088

Airborne IRP alignment using acceleration and angular rate matching. 19 p2386 A73-38048

New missile guidance concepts as applied to command guidance control system. [ALAA PAPER 73-835] 20 p2584 A73-38778

Direct statistical evaluation of nonlinear guidance systems. [ALAA PAPER 73-836] 20 p2584 A73-38779

The P-star technique and its application to inertial guidance. [ALAA PAPER 73-837] 20 p2584 A73-38780

The application of digital filters using observers to the design of an ICBM flight control system. [ALAA PAPER 73-845] 20 p2541 A73-38784

"Bank-to-turn steering" for highly maneuverable missiles. [ALAA PAPER 73-860] 20 p2586 A73-38798

Information content subsetting of highly correlated error sources. [ALAA PAPER 73-867] 20 p2586 A73-38805

A real-time six-degree-of-freedom hybrid simulation facility for guidance system testing. [ALAA PAPER 73-876] 20 p2543 A73-38813

SAM-D guidance system simulator for design verification, preflight checkout and performance demonstration based on real time digital communication between missile computer and simulator hybrid computer [ALAA PAPER 73-877] 20 p2587 A73-38814

System performance prediction by modeling test data in digital simulations. [ALAA PAPER 73-880] 20 p2543 A73-38816

Russian book on rocketry principles covering jet propulsion, jet engine combustion chambers, rocket propellants, design, aerodynamics, flight control and aircraft rockets 23 p3038 A73-43334

A hot gas actuator for missile control. 23 p2942 A73-43398

Recent advances in thrust vector control for tactical missiles. 24 p3144 A73-44693

MISSILE DEFENSE

BMD requirements for phased array radars. 21 p2651 A73-40644

MISSILE DEFENSE SYSTEMS

U MISSILE SYSTEMS

MISSILE DESIGN

Development of aft inlets for a ramjet powered missile. 03 p0246 A73-14133

Hypervelocity tactical missile radome materials with noncharring ablator and fiberglass substructure for thermal protection against aerodynamic heating with negligible effects on radio transmission 11 p1336 A73-25307

Approach to reliability for the SM-2 missile. 16 p2073 A73-33610

Exploratory development of composite missile fuselages. 17 p2181 A73-35354

MISSILE DETECTION

NT RADAR DETECTION

MISSILE ENGINE CASES

U ROCKET ENGINE CASES

MISSILE GUIDANCE

U MISSILE CONTROL

MISSILE LAUNCHERS

NT MOBILE MISSILE LAUNCHERS

Predicting the service life of neoprene launch tube liner pads for the Poseidon missile. 04 p0468 A73-14861

MISSILE RANGES

Application of Range Commanders Council Document 118-71 test methods to range management - SAMTEC. 09 p1057 A73-23409

Space missile test center development for checkout, launch and data processing for space boosters, intermediate and intercontinental range ballistic missiles and supersonic aircraft 16 p1993 A73-33087

MISSILE ROLL CONTROL

U LATERAL CONTROL

U MISSILE CONTROL

MISSILE SIMULATION [MATH MODELS]

U MATHEMATICAL MODELS

U MISSILES

MISSILE SIMULATORS [TRAINING]

U MISSILES

U TRAINING SIMULATORS

MISSILE STABILIZATION

U MISSILE CONTROL

U STABILIZATION

MISSILE STAGING

U MISSILES

U STAGE SEPARATION

MISSILE STRUCTURES

Graphite-epoxy composite missile adapter design, fabrication, tooling, bonded assembly and costs, comparing with boron-aluminum material 03 p0331 A73-13022

Reinforced all-plastic quadrat molded missile airframes design, fabrication and flight testing 03 p0333 A73-13052

Test rails possibilities for rain erosion phenomena study on aircraft or missile structures 11 p1335 A73-25296

Exploratory development of composite missile fuselages. 17 p2181 A73-35354

MISSILE SYSTEMS

Selected analytic procedures for range safety analysis. 01 p0117 A73-11200

AEGIS Demineralizer/Water Cooler - Design for availability. 16 p1989 A73-33608

B-52 aircraft-borne short range attack missile weapon system air conditioner thermal performance fulfillment with Freon refrigerant and air distribution in heat exchangers [ALAA PAPER 73-723] 18 p2269 A73-36340

MISSILE TEST LABORATORIES

U MISSILE TESTS

MISSILE TEST RANGES

U MISSILE RANGES

MISSILE TESTS

Measured thermal response to the MIL-STD 210B cold atmosphere. 16 p2034 A73-33140

MISSILE TRACKING

French Guiana space center facilities for missile tracking, telemetry, data processing and transmission of command instructions, discussing PCM, PAM and PDM links equipment 07 p0807 A73-18942

High speed cinetheodolite for missile tracking incorporating LED /light emitting diode/ system for metric data recording 10 p1222 A73-24950

MISSILE TRAJECTORIES

Short term bounds for the effect of oblateness on ballistic trajectories. 03 p0373 A73-13495

Systems analysis applied to a hybrid computer simulation of a missile reentering the atmosphere. 08 p0941 A73-20825

Rocket rectilinear motion, comparing Meshcherskii and Gantmacher-Levin equations in light of contact interaction hypothesis 08 p1014 A73-21181

Free flight and re-entry of a missile with a high ballistic coefficient. 09 p1147 A73-22625

Russian book - Solid-fuel ballistic rockets. 14 p1804 A73-30356

Asymmetric missile subharmonic response to nonlinear aerodynamic moments, considering spin and aerodynamic damping effects 15 p1943 A73-31667

The rocket motion in resisting medium on a given trajectory. 18 p2353 A73-36490

The P-star technique and its application to inertial guidance. [ALAA PAPER 73-837] 20 p2584 A73-38780

MISSILE WINGS

U LOW ASPECT RATIO WINGS

MISSILES

NT AIR TO AIR MISSILES

NT AIR TO SURFACE MISSILES

NT ANTIAIRCRAFT MISSILES

NT ANTIMISSILE MISSILES

NT BALLISTIC MISSILES

NT CHAPARRAL MISSILE

NT INTERCONTINENTAL BALLISTIC MISSILES

NT MINUTEMAN ICBM

NT POLARIS MISSILES

NT POSEIDON MISSILES

NT RAMJET MISSILES

NT SURFACE TO AIR MISSILES

NT TALOS MISSILE

Missile and explosive environmental tests for mechanical properties, outlining test facilities, climatological effects, salt spray, vibration, shock, dropping, vacuum effects and crack propagation 16 p1997 A73-33387

MISSILE U MISSILES

MISSION PLANNING

German-NASA joint Aeros aeronomy satellite project, discussing mission objectives and related instrumentation 01 p0109 A73-10470

Missions for the systematic unmanned exploration of Mars. 01 p0105 A73-11160

Experience obtained so far in connection with the German scientific spacecraft program [DGLR PAPER 72-052] 02 p0227 A73-11654

Helios A and B interplanetary exploration objectives, considering solar plasma, high energy particles and interplanetary dust characteristics [DGLR PAPER 72-068] 02 p0227 A73-11688

German-American cooperative solar probe project Helios, discussing design features, mission objectives and project development status [DGLR PAPER 72-104] 02 p0228 A73-11706

Space shuttle abort - Downrange basing and cross-range capability requirements. 02 p0228 A73-12371

Plans and objectives of the remaining Apollo missions. 03 p0368 A73-13086

Engineering potential for lunar missions after Apollo. 03 p0380 A73-13087

Computerized operational simulation for space shuttle program in terms of flight units, launch rate, success probabilities and costs 03 p0381 A73-13298

Mission performance of a 360 mw nuclear rocket engine. [ALAA PAPER 72-1064] 03 p0381 A73-13393

Dual mode applications of nuclear rocket engine for spacecraft propulsion and electrical power generation, considering payloads and missions competitiveness with nondual system [ALAA PAPER 72-1092] 03 p0341 A73-13413

The use of orbital photography for earth-resources satellite mission planning. 03 p0301 A73-13843

Skylab experiments in life sciences, solar physics, earth observations, astrophysics, engineering and technology 03 p0376 A73-14172

Comets Tago-Sato-Kosaka and Bennett spectra twilight observation by 200 inch reflector, considering Comet d'Arrest for in situ study by instrumented space probe 04 p0495 A73-14761

Space shuttle missions and configurations, discussing payload, external tank, solid rocket engines, orbiter vehicle and alternate delivery system costs 05 p0627 A73-16183

Computer and interactive graphics as applied to mission analysis. [ALAA PAPER 73-112] 05 p0554 A73-16870

A computerized technique for mission profile design analysis. [ALAA PAPER 73-114] 05 p0629 A73-16872

Venus atmosphere engineering models for use in spacecraft design and mission planning for Mariner 5 and Venera spacecraft and earth based measurements [ALAA PAPER 73-130] 05 p0619 A73-16883

Research and applications modules /RAM/ program for manned space research satellites transportation and support, discussing mission requirements and design concepts [ALAA PAPER 73-72] 06 p0755 A73-17637

Conference on Planetology and Space Mission Planning, 3rd, New York, N.Y., October 28-30, 1970, Proceedings. 06 p0749 A73-18001

Space shuttle cost effectiveness from earth orbital mission analysis, discussing potential performance and shuttle derived high energy transportation system 06 p0756 A73-18017

Grand Tour missions to the outer solar system with Saturn /Intermediate 20/. 06 p0750 A73-18024

The experimental telecommunication satellite Project Symphonic. 07 p0905 A73-19140

The ground operations system for the AEROS research satellite. 08 p0953 A73-21661

Mariner Mars 1971 project historical background, and Mariner 9 orbiter mission science objects and planning for Mars surface observations and measurements 09 p1144 A73-22265

Development of a global cloud model for simulating earth-viewing space missions. 10 p1244 A73-23979

Mariner Mars 1971 orbiter spacecraft with sun-Canopus orientation as references, discussing mission objectives, trajectory characteristics, orbital operations, scientific instruments and system design
10 p1276 A73-24004

Orbit selection for satellite missions, determining elements of sun-synchronous, recurrent, near-recurrent, polar, synchronous and stationary orbits
13 p1684 A73-29246

Mission building blocks for outer solar system exploration.
14 p1805 A73-30527

Cometary Science Working Group, Meeting, Williams Bay, Wis., June 9-11, 1971, Proceedings.
15 p1941 A73-32413

Digitally integrated cockpit simulation facility for display systems and avionics to plan mission/human program and airborne equipment requirements
17 p2139 A73-35236

Mission planning for remote exploration of the surface of Venus.
[AIAA PAPER 73-580] 18 p2350 A73-36072

Technology requirements for ballistic mode Mercury orbiter mission, discussing performance potential with Venus gravity assist and conventional spacecraft propulsion techniques
[AIAA PAPER 73-581] 18 p2350 A73-36073

Solar electric propulsion comet and asteroid rendezvous missions, examining asteroid perihelion data base, optimum mission length, flight time and exploration vehicle power levels
[AIAA PAPER 73-597] 18 p2350 A73-36081

Space shuttle solid rocket boosters mission and systems requirements, considering thrust vector control and staging/separation, electrical and recovery systems
[AIAA PAPER 73-606] 18 p2358 A73-36086

Representative Space Shuttle missions and their impact on shuttle design.
[AIAA PAPER 73-608] 18 p2358 A73-36087

Reusable space tug system and missions for space shuttle operations with 1980s planned payloads, discussing interfaces and configuration alternatives
[AIAA PAPER 73-609] 18 p2358 A73-36088

Vehicle management and mission planning in support of shuttle operations.
[AIAA PAPER 73-612] 18 p2358 A73-36090

Temperature control of the Mariner class spacecraft - A seven mission summary.
[AIAA PAPER 73-769] 18 p2360 A73-36383

The application of simulation to mission planning for communications and data relay satellites.
18 p2291 A73-36424

Comet exploration - Scientific objectives and mission strategy for a rendezvous with comet Encke.
[AIAA PAPER 73-550] 18 p2353 A73-36496

Pioneer Venus mission plan for atmospheric probes and an orbiter.
[AIAA PAPER 73-579] 18 p2353 A73-36499

Pioneer spacecraft for atmospheric entry missions to the outer planets.
[AIAA PAPER 73-595] 18 p2360 A73-36500

Cometary exploration - A case for Encke.
[AIAA PAPER 73-596] 18 p2353 A73-36501

Impact of the space tug concept on space program economics.
19 p2490 A73-37192

Space shuttle program, discussing master planning schedule, vehicle design, payloads and initial flight tests
19 p2491 A73-37592

Space shuttle payload definition, design and planning, using computers for scheduling and costing
19 p2491 A73-37593

Vehicle and ground support in space shuttle sortie and delivery-retrieval mission profiles
19 p2491 A73-37594

Space Shuttle solid rocket stage recovery, retrieval, and refurbishment.
19 p2492 A73-37599

Design considerations for space mission wash water processing by reverse osmosis.
[ASME PAPER 73-ENAS-3] 19 p2493 A73-37965

Communication satellites future use in Europe, considering mission requirements, data transmission, specialized TV distribution, cost effectiveness and shuttle/tug launch system
[AAS PAPER 73-148] 20 p2521 A73-38596

Asteroid belt observation, spatial distribution and mission planning, considering IR, spectrophotometric, interferometric, polarization and Doppler measurement techniques
23 p3034 A73-43991

MISSISSIPPI
Cost effective land use mapping and resources inventory for Mississippi via high altitude color IR aerial photography and ERTS-1 multispectral imagery
[AIAA PAPER 73-3] 13 p1610 A73-29300

MIST
A study of mist cooling /1st Report - Investigation of mist cooling/.
05 p0638 A73-16222

MITOCHONDRIA
Effects of exercise on activity of heart and muscle mitochondria.
01 p0006 A73-10135

High energy phosphate deficit-produced myocardial cell genetic apparatus activation as cardiac hypertrophy mechanism, discussing mitochondrial biogenesis and cardiac hyperfunction roles
02 p0134 A73-12511

Methodical studies concerning the polarographic measurement of respiration and 'critical oxygen pressure' in mitochondria and isolated cells with the aid of the membrane-covered platinum electrode
03 p0272 A73-14647

Myeloperoxidase, the peroxidase of a primitive cell - Its reaction with Fe and H2O2.
06 p0652 A73-17944

Influence of ultrasound and of a superhigh-frequency electromagnetic field in the three-centimeter band on the oxidative phosphorylation of liver and kidney mitochondria
09 p1044 A73-22368

Effects of altitude stress on mitochondrial function.
14 p1717 A73-30430

MITOSIS
The effect of temperature on the mitotic activity of human peripheral blood lymphocytes in a culture
07 p0781 A73-19649

Mitotic activity in dorsal epidermis of Rana pipiens.
07 p0784 A73-20456

Automatic microscopy for mitotic cell location.
12 p1464 A73-27144

Proliferative activity of bone marrow cells in dogs exposed to chronic and repeated acute gamma irradiation
12 p1463 A73-27708

Effect of steady magnetic fields up to 4,500 Oe on the mitotic activity of the corneal epithelium in mice
15 p1838 A73-31510

MIXED CRYSTALS
Characteristics of the reflection spectra of CdS/xSe/1-x/ mixed crystals in their exciton absorption region
14 p1783 A73-30578

Investigation of some electrooptical properties of liquid crystals
14 p1784 A73-30854

Angular dependence of optical scattering in mixed nematic-cholesteric liquid crystals.
21 p2751 A73-40453

MIXED FLOW
U MULTIPHASE FLOW

MIXERS
Conversion losses of a point contact presenting the Josephson effect used in a microwave mixer
08 p0938 A73-20968

MIXING
NT COMPOUNDING
NT DISSOLVING
NT HOMOGENIZING
NT LAMINAR MIXING
NT SIGNAL MIXING
NT SUSPENDING (MIXING)
NT TURBULENT MIXING

Solutions of the chemical kinetic equations for initially inhomogeneous mixtures.
[AIAA PAPER 73-101] 05 p0546 A73-16861

The atmospheric mixing in the atmospheres of Mars and Venus.
18 p2349 A73-36034

MIXING CIRCUITS
Phase and amplitude balance - Key to image rejection mixers.
02 p0148 A73-12571

Conversion coefficients of optical heterodyne receiver mixer for various amplitude-phase distributions of interfering signal
03 p0319 A73-14067

Electron beam fabrication of submillimeter diameter mixer diodes for millimeter and submillimeter wavelengths.
05 p0559 A73-16811

Nonlinear analysis for local microwave oscillator voltage waveform across nonlinear junction of Schottky barrier mixer diode, comparing results with analog simulation
06 p0677 A73-18740

Point contact and Schottky barrier microwave mixer diodes reliability under X band RF pulse operating conditions, considering burnout alleviating fabrication techniques
08 p0943 A73-20735

Semiconductor diode mixer for millimeter-wave frequencies.
10 p1193 A73-23665

Digital single sideband mixing circuit for sum or difference frequency conversion in phase quadrature, using exclusive-or logic gates
13 p1593 A73-29117

Double balanced microwave mixer circuit with local oscillator input and IF outputs for achieving low noise and image rejection
14 p1737 A73-30622

Self excited mixer/detector of Gunn diode oscillator, calculating detection characteristics from combined equivalent circuit and computer simulated analysis
21 p2664 A73-41092

Pulse burnout of microwave mixer diodes.
22 p2835 A73-42965

MIXING LENGTH FLOW THEORY
Book on momentum, heat and mass transfer at various interfaces based on Prandtl eddy mixing length concept
01 p0030 A73-10049

A relation between the energy distribution of the main flow and the corresponding fluctuating quantities in boundary layers
03 p0292 A73-13171

Calculation methods of three-dimensional boundary layers with and without rotation of the walls.
[ONERA, TP NO. 1135] 04 p0403 A73-15093

The stability of lifted turbulent diffusion and premixed flames.
[WSCIPAPER 72-39] 05 p0638 A73-16678

Possible construction of semiempirical turbulent flow theories
07 p0812 A73-20092

Mixing length flow theory for turbulent boundary layer calculation, with allowance for mass transfer
08 p0953 A73-20721

A unified view of the law of the wall using mixing-length theory.
[AD-759043] 08 p0926 A73-21441

The mixing length derived from Karman's similarity hypothesis.
08 p0955 A73-21442

Solution of the direct problem of mixed subsonic and supersonic gas flow in a nozzle of finite length
09 p1072 A73-22480

Euler, Lagrange and time turbulence scales for Prandtl mixing length, relating with velocity and pressure pulsations in steady turbulent gas flow
10 p1204 A73-23474

Turbulence in journal bearings, considering Taylor vortices development beyond laminar range and theoretical models based on mixing length flow theory
13 p1625 A73-29261

Supersonic mixing nozzle for gas-dynamic lasers.
17 p1783 A73-34205

Turbulent mixing of cylindrical jet with parallel stream in terms of mixing length concepts and velocity profiles
17 p2157 A73-35515

Calculation of free turbulent mixing by interaction approach.
[AIAA PAPER 73-649] 18 p2297 A73-36204

On the convective diffusion in tubes of circular section
18 p2299 A73-36489

Euler, Lagrange and time turbulence scales for Prandtl mixing length, relating with velocity and pressure pulsations in steady turbulent gas flow
21 p2678 A73-41321

On the possibility of constructing a radiative sun-spot model in magnetohydrostatic equilibrium.
21 p2777 A73-41486

Linear convective modes and the energy transport in stellar convection zones.
22 p2905 A73-41761

Experiments on the propagation of mixing and combustion injecting hydrogen transversely into hot supersonic streams.
22 p2934 A73-42785

MIXTURES
NT ADMIXTURES
NT AEROSOLS
NT AQUEOUS SOLUTIONS
NT BINARY FLUIDS
NT BINARY MIXTURES
NT COLLOIDAL PROPELLANTS
NT COLLOIDS
NT DETONABLE GAS MIXTURES
NT DISPERSIONS
NT EMULSIONS
NT EUTECTIC ALLOYS
NT EUTECTICS
NT FOG
NT GAS MIXTURES
NT LIQUID-GAS MIXTURES
NT METAL MATRIX COMPOSITES
NT NUCLEAR EMULSIONS
NT PHOTOGRAPHIC EMULSIONS
NT SMOKE
NT SOLID SOLUTIONS
NT SOLID SUSPENSIONS
NT SOLUTIONS

Continuum thermodynamics-based formulation of mixture theory using Boolean algebra with emphasis on partial stress tensors, considering force, moment and energy balance equations
22 p2885 A73-41771

Acceleration waves in ideal fluid mixtures with several temperatures.
22 p2929 A73-41772

MNOS
U METAL-NITRIDE-OXIDE-SILICON

- Application of the method of slipping modulating functions for identification of plants with time lag 21 p2670 A73-40993
- Continuous information theory and modulation methods. 22 p2826 A73-42463
- Optical modulation of X band microwave transmission by acoustoelectric domains in semiconducting CdS single crystal, noting domain conductivity and permittivity changes 23 p3018 A73-44365

MODULATORS

- Two component magnetic pulsed modulator for electroluminescent and laser diodes, using ac source with nonresonance input capacitance charge 01 p0059 A73-10793
- Stable optico-mechanical Q-factor modulator for a laser resonator 01 p0059 A73-10797
- The requirements on the parameters of a mechanical modulator for an IR scanning radiometer. 01 p0050 A73-10833
- Push-pull ac modulator design allowing balanced thermal load on plasma electrodes in pulsed high power short arc Xe flash lamps 03 p0282 A73-13933
- Real time coherent electro-optic two dimensional on-line spatial light modulator role in optical data processing system 06 p0693 A73-18286
- Acousto-optical modulator for carbon dioxide lasers based on Bragg scattering concept, discussing design parameters and application to lidar system 06 p0700 A73-18295
- Experimental verification and assessment of an infra-red radiation modulator based on a Fabry-Perot etalon. 07 p0825 A73-20373
- Russian book on onboard distance measuring systems for flight vehicles covering design of cw and pulsed devices, modulators, error analysis, noise, logic elements, etc 07 p0825 A73-20378
- Optical modulator based on coupled waveguides for integrated optical circuits, presenting design and dynamic characteristics 08 p0974 A73-20810
- Modulation type microwave receiver with selective filter and ferrite resonator in waveguide coupling 08 p0949 A73-21561
- Weaver modulator with digital filter for single side-band transmission in radio communication and telemetry, discussing FORTRAN simulation for cost, computation time and accuracy 10 p1186 A73-23499
- Analysis of the nonlinearity of the modulation characteristic of a single-circuit phase modulator employing a varactor 10 p1195 A73-24382
- An analog-code follow-up converter based on second-harmonic magnetic modulators 12 p1475 A73-26766
- Comparative analysis of the longitudinal and orthogonal magnetic second-harmonic modulators. 12 p1477 A73-26789
- A modulator with inherent bandwidth limiting for use with a bi-phase PSK data transmission system. 12 p1472 A73-27663
- An optimal scheme for excitation of low-threshold magnetically modulated converters and analysis of their operation 13 p1591 A73-28855
- Influence of the parasitic capacitance of a field effect transistor and of the input capacitance of the amplifier on the null shift of a modulator 13 p1591 A73-28856
- Null level of a field-effect-transistor modulator of small constant-voltage signals 13 p1592 A73-28873
- Effect of the input capacitance of an ac amplifier on the performance of key modulators 13 p1592 A73-28874
- Ferrite component for waveguide commutator used as microwave switching element and modulator, noting application in navigation instruments and avionics 15 p1849 A73-30995
- A pulse-width modulator operating on dc integral amplifiers 18 p2293 A73-36855
- A symmetry correcting pulse-width modulator for power conditioning applications. 22 p2802 A73-42919
- MODULATORS-DEMODULATORS**
- MODULES**
- NT AIRLOCK MODULES
- NT APOLLO LUNAR EXPERIMENT MODULE
- NT COMMAND MODULES
- NT COMMAND SERVICE MODULES
- NT ELECTRONIC MODULES
- NT LUNAR MODULE
- NT MICROMODULES
- NT SERVICE MODULES
- NT SPACECRAFT MODULES

- Measuring equipment for multipoint data acquisition and recording, noting modular design of party-line system with programmed data processing 01 p0054 A73-11398
- Fluidic system design based on miniaturized modular high power fluidic logic elements, discussing applications in production process control 10 p1177 A73-23761
- A unified method for analyzing mission reliability for fault tolerant computer systems. 15 p1901 A73-32261
- Some practical methods for development of modular fluidic devices. 23 p2943 A73-43415

MODULUS OF ELASTICITY

- NT DYNAMIC MODULUS OF ELASTICITY**
- Compression and elastic moduli of heterogeneous viscoelastic materials consisting of mechanical mixture of homogeneous phases, using elastic-viscoelastic analogy 03 p0385 A73-13139
- High modulus Be-Al alloy strengthening and aging as function of Cu, Mg and Zn additions 03 p0325 A73-13517
- Strength limits correlation to modulus of elasticity for compact bone material from compression tests, noting anisotropy tensor analysis 03 p0267 A73-13744
- Porous cellular structure materials, investigating porosity effects on modulus of elasticity based on central monoporous model 03 p0394 A73-14015
- A fourth-order nonlinear equation of state - Application to the determination of the elastic moduli of single-crystal and polycrystalline solids 03 p0350 A73-14601
- Determination of Young's modulus and of the Poisson coefficient by a method of resonant bars 04 p0462 A73-15247
- Studies of the elastic properties of molybdenum 04 p0464 A73-15372
- On the effective moduli of composite materials - Slender rigid inclusions at dilute concentrations. 05 p0630 A73-16099
- A new method for simultaneous measurement of total respiratory resistance and compliance. 05 p0545 A73-16799
- Structural design with allowance for shakedown in the case of temperature-dependent elastic constants 06 p0760 A73-17780
- Partial yielding of cylindrical pressure vessel with elastic modulus and yield function as arbitrary functions of radial coordinate, assuming elastoplastic strain hardening material 06 p0761 A73-17895
- The compressional modulus of a material permeated by a random distribution of circular cracks. 07 p0915 A73-20335
- Variational bounds of unidirectional fiber-reinforced composites. 09 p1157 A73-21931
- Young modulus anomaly in precipitation-hardening subjected Invars 09 p1099 A73-21962
- Influence of the nonlinear compliance of rolling contact bearings on the vibrations of a balanced shaft 09 p1088 A73-22479
- Determination of the modulus of elasticity of metallic and nonmetallic fibers based on bending oscillations 10 p1231 A73-23691
- A theoretical study of the effect of the interface on composite toughness. 10 p1288 A73-23955
- Solid composite material thermostatics and overall thermoelastic modulus determination, considering arbitrarily anisotropic phases, binary composite and self consistent theory 10 p1295 A73-24099
- Al alloy stress intensity range estimation from surface fatigue striation incidence and modulus of elasticity, noting relationship to crack growth closure in fractography 10 p1235 A73-24447
- Direct nondestructive prediction of engineering properties. 11 p1372 A73-25129
- Possibilities regarding the development and the employment of fiber-reinforced composites in comparison with conventional materials 11 p1454 A73-25419
- Ultrasonic measurement of elastic moduli in slender specimens using extensional and torsional wave pulses. 11 p1365 A73-26171
- Composite solid with two contacting or bonded half planes of different elastic moduli, considering interplane force transmission from stress distribution calculation 11 p1443 A73-26277
- 'Invar' and 'Elinvar' - Alloys with controllable thermal expansion and elastic properties 11 p1385 A73-26564

- Transversely isotropic /anisotropic/ elastic beam bending and torsion, determining frequency dependent compliances by approximate analytic solution via variational method 11 p1447 A73-26655
- Anisotropy of gallium elasticity and thermal expansion 12 p1531 A73-27936
- Probability characteristics of the shear modulus of fiberglass-strengthened plastics 13 p1644 A73-27997
- Determining elasticity constants of disc-shaped specimens of material. 13 p1613 A73-28521
- Interpretation of mechanical behavior of pure aluminum in terms of microstructure. 13 p1639 A73-29459
- Application of fracture mechanics to the analysis of statically indeterminate structure. 13 p1700 A73-29466
- Influence of recovery and recrystallization on the Young's modulus and its temperature dependence in Invar-type iron-nickel alloys 14 p1760 A73-30586
- Thermal expansion, Young's modulus, and magnetostriction of a stainless iron-chromium-nickel alloy in the temperature range between 80 and 280 K 14 p1764 A73-30868
- Technical note on some mechanical properties of a magnesium-25 vol% boron particulate composite. 14 p1765 A73-30935
- Solution uniqueness for elasticity problem with modulus diversity based on deformation potential energy as convex function 15 p1950 A73-31826
- Temperature dependence of the single-crystal elastic constants of Co-rich Co-Fe alloys. 15 p1890 A73-31926
- Effect of nonlinear compliance in rolling motion bearings on the vibrations of a balanced shaft. 15 p1883 A73-32066
- High modulus graphite fiber preparation from polyacrylonitrile yarn, discussing graphitization, properties and stabilization oxidation treatment 16 p2028 A73-33042
- Thermal expansion compatibility of ceramic chip capacitors mounted on alumina substrates. 16 p1989 A73-33472
- The role of a porous filler structure in strengthening polymers 16 p2030 A73-33929
- Method for determining Young's dynamic modulus for curvilinear specimens 16 p2030 A73-33938
- Phase composition and properties of metastable alloys of titanium with nickel 16 p2027 A73-34072
- Young modulus of elasticity measurement in alloys of Fe with Cr, W and Mo, examining concentration dependence at 20 to 500 C 17 p2187 A73-34334
- Young elastic modulus determination in steel and alloy disks by contact method 17 p2177 A73-34338
- An appreciation of the design of carbon fibre rigid solar panels for spacecraft. 17 p2238 A73-34812
- Processability/mechanical properties trade-off for reinforced plastics. 17 p2197 A73-35353
- The use of a high modulus inclusion gauge in non-linear viscoelastic materials. [SESA PAPER 2187A] 17 p2173 A73-35457
- High modulus fiber reinforced metal and plastic matrix composites fracture within linear elastic fracture mechanics framework, reviewing standard notch toughness test 17 p2192 A73-35536
- Book - Experimental techniques in fracture mechanics. 17 p2252 A73-35668
- Compliance measurement for determination of crack extension force, specimen dimensions and elastic constants in linear fracture mechanics, discussing instrumentation, precautions and data reduction 17 p2252 A73-35671
- Causes of changes in the properties of resite in aqueous and alkaline media 18 p2328 A73-36822
- Modulus reinforcement in elastomer composites. I - Inorganic fillers. 18 p2328 A73-36980
- Modulus reinforcement in elastomer composites. II - Polymeric fillers. 18 p2328 A73-36981
- Fracture mechanics of carbon fibers at high temperatures due to fine structure, discussing effects of ribbon unbending during extension 19 p2444 A73-38089
- Influence of cycle ratio on the elastic modulus of glassfiber reinforced plastics subjected to repeated tensile load. 20 p2580 A73-38644

MOHR CIRCLES

Differential equations of the asymmetrical mathematical theory of elasticity and their solution when Young's modulus varies according to an exponential law

20 p2620 A73-39505

Problem of an elastic semiinfinite cover plate fastened to a linearly deformable base

20 p2624 A73-39646

Ti-V alloys elastic modulus and paramagnetic susceptibility, considering composition vs property curve salient point indications of changes in interatomic bonding energy and electron structure

21 p2718 A73-40487

Texture and anisotropy of the properties of titanium sheet

21 p2719 A73-40852

Fiber glass reinforced plastics measurement for ratio of elastic modulus to mean thermal conduction for use in cryostat to resist large forces

21 p2723 A73-41106

Torsional elasticity of human skin in vivo.

21 p2642 A73-41625

Applications of the compliance concept in fracture mechanics.

22 p2920 A73-42154

Nature and significance of alterations in myocardial compliance.

22 p2808 A73-42689

Load capacity of rings formed by winding of composites reinforced with high-modulus anisotropic fibers

24 p3093 A73-44528

Manufacture and properties of compressor blades made of plastics reinforced with carbon filaments

24 p3122 A73-44880

MOHR CIRCLES

U FRACTURE MECHANICS

MOIRE EFFECTS

Application of the moire effect for studying flows of a continuous medium

02 p0230 A73-11721

An experimental investigation of a rigid-plastic state of deformation with the aid of the Moire method

03 p0306 A73-13148

Interference grating production for viscoelasticity investigation by moire method, noting tensile tests of viscoelastic plates

03 p0306 A73-13159

Wavelength dependence of moire patterns

05 p0577 A73-16822

Moire phenomena theory and applications extension by diffraction and Fourier optics

06 p0696 A73-18696

Diffraction moire technique illustrated by determination of beam deflections.

08 p1016 A73-20797

Some investigations on the methods of measuring 3-dimensional plastic deformations by laser.

09 p1086 A73-23321

Moire fringe method for stationary and running cracks length and crack opening displacement measurements in composite materials

10 p1240 A73-24287

A modification of the moire fringes technique for the analysis of moments and deflections in a laterally loaded plate.

10 p1220 A73-24573

Moire topography for full size living human body contour stereophotographic pictures with high contrast, discussing instrument construction, performance and accuracy

11 p1365 A73-26239

Improvement on moire technique for in-plane deformation measurements.

11 p1365 A73-26241

Circular carrier-frequency photography for observing phase objects.

12 p1495 A73-26832

Dynamic moire methods for the bending of plates.

12 p1550 A73-27023

Moire techniques of incoherent and coherent light filtering, line multiplication and contrast amelioration in framework of physical optics and diffraction theory for stress analysis

13 p1612 A73-28470

Moire gauging by projected interference fringes.

13 p1616 A73-28600

Developments in the optical spatial filtering of superposed, crossed gratings.

13 p1620 A73-29302

Strain analysis of composites by moire methods.

15 p1956 A73-32269

Determination of slope and strain contours by double-exposure shearing interferometry.

17 p2174 A73-35459

MOISTURE

NT SOIL MOISTURE

MOISTURE CONTENT

NT ATMOSPHERIC MOISTURE

The determination of moisture in propellant charge powders and solid propellants

02 p0202 A73-11565

Water frost absorptions in IR reflectivities of Jupiter Galilean satellites, discussing surface cover distributions and underlying material reflectivity

04 p0497 A73-15070

Remote sensing of the near-surface moisture profile of specular soils with multi-frequency microwave radiometry.

04 p0446 A73-15782

Venus atmosphere water vapor content from IR spectra observed by airborne Fourier interferometric spectrometer, discussing different models for abundance

06 p0744 A73-17434

Mars 3 onboard optical measurements of Mars surface and lower atmosphere, considering temperatures, water vapor content, dust cloud and particle characteristics

06 p0746 A73-17481

Dynamics of moisture diffusion through a partially liquid filled porous matrix.

06 p0649 A73-18259

Vertical profiles of liquid water content and other cloud parameters for cumulus and cumulus congestus clouds from aircraft measurements over Ukraine

08 p0985 A73-21454

Moisture absorption characteristics of solid lubricant coatings

10 p1239 A73-24247

Calculation of the moisture content correction in measuring the quantity of gas flowing through an orifice

12 p1498 A73-27595

Water sources in lunar atmosphere, calculating minimum depth for existence from water density values

13 p1681 A73-28844

A rapidly convergent procedure for computing large-scale condensation in a dynamical weather model.

13 p1655 A73-29338

Estimates of water content in the atmosphere of Venus on the basis of radio-astronomical measurements and space probe data

16 p2068 A73-33823

A model of a long-term process of heat and moisture transfer in the atmosphere over the ocean

17 p2158 A73-34344

Elasticity of water-saturated rocks as a function of temperature and pressure.

17 p2163 A73-35271

A flowmeter to measure cloud liquid content.

17 p2174 A73-35578

Light beam dispersal of fog with various drop sizes based on energy equation, considering cloud water content, cross wind effects and front velocity

18 p2337 A73-36561

Cumuli structure at various stages of development.

18 p2333 A73-36705

Integral moisture content determination in rain clouds by simultaneous thermal radiation and radar measurements

20 p2584 A73-39190

Progress report on aircraft gamma-ray surveys for soil-moisture detection at a NOAA test site near Phoenix, Arizona.

20 p2558 A73-39871

Long wave radiation flux, water content and temperature measurements in stratus and cumulostratus clouds by aircraft radiometry

21 p2731 A73-40496

On the mechanism of adaptation of micro-organisms to conditions of extreme low humidity.

22 p2803 A73-42164

On the multiplication of xerophilic micro-organisms under simulated Martian conditions.

22 p2803 A73-42165

High altitude infrared spectroscopic evidence for bound water on Mars.

24 p3127 A73-44395

Air-hydrogen-carbon fuel mixtures chemical composition determination by measuring carbon dioxide and moisture content of combustion products, presenting nomogram

24 p3157 A73-45378

MOISTURE DETECTORS

U MOISTURE METERS

MOISTURE METERS

NT HYGROMETERS

Use of cellulose crystallite structures with solid state strain gages for humidity and moisture measurement.

17 p2166 A73-34621

MOL [ORBITAL LABORATORIES]

U MANNED ORBITAL LABORATORIES

MOLDAVITE

Neutron activation analysis for geochemical origin and trace element compositions of moldavites and source rocks from Ries impact crater

07 p0877 A73-19652

MOLDING MATERIALS

General purpose autoclave processable polyimide laminating resin selection, evaluating molding process techniques

03 p0329 A73-13004

Polyimide 2080 molded composites mechanical, thermal and electrical properties, discussing processing techniques

03 p0329 A73-13004

Non polar thermosetting resins for high temperature electrical/electronic components.

03 p0332 A73-13003

Glass fiber reinforced polyester laminates, testing layer base material and molding condition effects on tensile and bending strengths and other mechanical properties

07 p0843 A73-20326

Flammability comparisons of glass-reinforced unsaturated polyester moldings in various laboratory scale tests.

08 p0983 A73-21822

Preparation and thermomechanical properties of pyrrone moldings.

10 p1237 A73-23961

Moldability, storage stability and thermal, mechanical and electrical properties of epoxy molding compounds for electronic devices

17 p2196 A73-35340

Ultimate tensile properties and composite structures of flow-molded short fiber composites.

17 p2197 A73-35352

Electrochemical thinning of a metal disk rotating on a floating self-moulded cathode.

17 p2182 A73-35766

Hardening with UV radiation in the manufacture of glass-fiber-reinforced unsaturated polyester resin molding materials

24 p3093 A73-44889

MOLECULAR ABSORPTION

Book - Emission, absorption, and transfer of radiation in heated atmospheres.

01 p0119 A73-10125

4830 MHz observations of the formaldehyde molecule in the direction of discrete radio sources.

03 p0371 A73-13214

Pressure of radiation due to the absorption of resonant light

03 p0318 A73-13604

Q switched ruby laser emission absorption by diatomic Rb vapor, noting molecular fluorescence intensity changes

04 p0458 A73-15560

On calculating the radiation from two plane isothermal layers of carbon dioxide and/or water vapor.

08 p1021 A73-20859

Investigation of molecular absorption in the atmospheres of the giant planets

08 p1007 A73-21064

On ultraviolet absorption by molecular hydrogen in stellar atmospheres.

09 p1148 A73-22867

Molecular absorption spectra of S-type stars in the one-micron region.

09 p1123 A73-23130

Interferometric observations of formaldehyde absorption in front of strong galactic sources.

09 p1150 A73-23139

Optical absorption cell with water vapor cross flow instrument designed for wall decontamination and open air meteorological simulation, examining thermodynamic parameters effects

11 p1367 A73-26318

Interpretation of hydrogen quadrupole and methane observations of Jupiter and the radiative properties of the visible clouds.

13 p1673 A73-28280

High resolution spectroscopy with lasers.

14 p1756 A73-29925

Interferometric observations of formaldehyde absorption in front of strong galactic sources.

14 p1801 A73-30735

Investigation of molecular absorption features in the spectrum of Jupiter

16 p2070 A73-33839

Molecular absorption in the atmospheres of the giant planets.

18 p2355 A73-36865

Absorption saturation effects on high-power CO₂ laser beam transmission.

21 p2710 A73-40152

MOLECULAR BEAMS

Determination of the molecular velocity distribution function in a molecular beam by the method of mechanical selection

02 p0194 A73-11606

Molecular beam simulation of planetary atmospheric entry - Some recent results.

03 p0287 A73-13564

Phase structure of vacuum deposited thin Ta films and molecular beam composition obtained by mass spectroscopy

04 p0484 A73-15667

Molecular beam study of the K+CH₃I reaction - Energy dependence of the detailed differential reactive cross section.

05 p0546 A73-16047

Speed distribution measurements of N₂ and Ar molecular beams produced by a multichannel source.

06 p0726 A73-18261

Electromagnetic wave reflection by two level medium analog of moving molecular beam, considering fields penetration and surface impedance effects
06 p0668 A73-18647

Molecular beam study on BaO and SrO formation for clarifying interaction of metal-vapors with upper atmosphere oxygen.
07 p0818 A73-19668

RF field space-time modulation devices to obtain molecular beam velocity distribution and Zeeman pattern components shift
13 p1662 A73-28345

Absorption of He-Ne laser radiation by an iodine molecule beam
13 p1627 A73-28773

Gas molecule-solid surface interactions, considering rainbow scattering, roughness at molecular scale, potential well and statistical analysis procedures
13 p1663 A73-28912

Absolute calibration of Apollo lunar orbital mass spectrometer.
13 p1617 A73-28930

Diffusion processes in the mixing zone of a low-density supersonic jet
13 p1567 A73-29170

Study of gas-solid chemical interactions by the molecular beam technique. V - Reactions of oxygen and carbon monoxide with polycrystalline tantalum strips
15 p1841 A73-31970

Experimental study of a new geometry for a microwave molecular-beam spectrometer
16 p2038 A73-33173

Molecular beam study of the desorption of cesium ions from tungsten crystals.
18 p2338 A73-36976

Direct-sampling studies of combustion processes.
19 p2504 A73-38325

An aerodynamic test facility with free molecular flow and high stagnation temperature
20 p2545 A73-39615

Investigation of the intensity distribution in a molecular beam expelled from a conical ring source
22 p2889 A73-42387

MOLECULAR BIOLOGY

Triparanol inhibition of sterol biosynthesis in *Chlorella emersonii*.
02 p0139 A73-12547

Chemical evolution under the bion hypothesis.
03 p0265 A73-14316

Concepts related to the origin of the genetic apparatus.
03 p0265 A73-14317

Symposium on Capillary Exchange and the Interstitial Space, Bad Duerkheim, West Germany, May 3-6, 1972, Proceedings.
03 p0265 A73-14649

Russian book - Information macromolecules during radiation injury to cells.
04 p0410 A73-15707

A note on the hypothesis - Protein polymorphism as a phase of molecular evolution.
04 p0410 A73-16033

Book - Molecular evolution: Prebiological and biological.
06 p0651 A73-17926

Life origin on earth, considering hydrocarbon molecules and macromolecular synthesis under earth atmospheric evolutionary conditions
06 p0651 A73-17928

Atomic, molecular, cellular, genetic, multicellular, neural, mental, social and suprasocial levels of evolution, discussing systems constituents, interactions and selective focus
06 p0651 A73-17929

Proteins and nucleic acids in prebiotic evolution.
06 p0652 A73-17937

Model experiments on the prebiological formation of protein.
06 p0652 A73-17938

Informational biopolymer structure in early living forms.
06 p0652 A73-17946

Trypsinogen activation peptides - An example of molecular epigenesis.
06 p0652 A73-17947

Modelling of structure and functional unity on coacervate systems.
06 p0652 A73-17950

Coacervate systems and evolution of matter on the earth.
06 p0652 A73-17951

Ribosomal RNA base composition and molecular evolution in plants and animals of various taxonomic groups
07 p0780 A73-19220

Photochemical reactions in condensed phase relevant to biology, discussing molecular energy states, isomerization reactions and bond making/breaking processes
09 p1121 A73-23305

Investigation of the infrastructural organization of interdisk spaces and photoreceptor membranes of the

retina in vertebrates during aldehyde fixations, delipidization, and pronase treatment
10 p1181 A73-24458

Experimental models of communication at the molecular and microsystemic levels.
11 p1324 A73-25140

A study of the secondary structure of ilamycin B1 by 300 MHz proton magnetic resonance.
11 p1326 A73-25572

Cell membrane molecular structure and lipid composition, discussing phospholipid role in membrane potential maintenance in myocardial cells
11 p1315 A73-25591

Quaternary structure /subunit composition/ of human ceruloplasmin
11 p1316 A73-25638

Book - Molecular evolution and the origin of life.
12 p1461 A73-27049

Relationship of theoretical physics to molecular biology, considering synthesis, ontogenesis, phylogenesis, evolution models, thermodynamic applications and Eugen prebiological evolution theory
15 p1835 A73-31823

Self organized biological systems analysis, including deterministic and phenomenological selection theories, molecular level cell instructive properties and self reproducing hypercycles
15 p1835 A73-31825

Abnormal biochemistry in myocardial failure.
22 p2808 A73-42686

Theoretical study of primary photosynthesis processes in higher plants and algae
23 p2946 A73-43707

Hemoglobin molecule oxygenation mechanism in various animals, discussing erythrocytes as hemoglobin carriers, ecological factors and physicochemical conditions
23 p2947 A73-43929

MOLECULAR BONDS

U CHEMICAL BONDS

MOLECULAR CHAINS

Evolution from amino acids - Lunar occurrence of their precursors.
01 p0008 A73-10249

Drag reduction in non-Newtonian turbulent flow, considering viscosity change with strain in long-chain molecules /polymers/ fluid solutions
01 p0034 A73-11134

Extended chain crystals of linear high polymers.
02 p0139 A73-12650

Theory of one-dimensional Mott semiconductors and electronic structure of long molecules with conjugate bonds
06 p0734 A73-17923

Syntheses and conformational studies of polyacidic amino acids containing optical active side chains.
06 p0661 A73-17942

Polymer chain model with internal rotations for elastic body stress-strain state, internal work, elastic energy and equations of motion
10 p1240 A73-24307

Theory of cooperative defect formation in a biopolymer molecule under the action of radiation
11 p1323 A73-25637

Branched-chain carbohydrate structures resulting from formaldehyde condensation.
15 p1842 A73-32550

Branched-chain mechanism of propane-oxygen-fluorine explosions.
22 p2819 A73-42778

On the dimensions of intramolecularly crosslinked polymer molecules. I - The synthesis and chemical characterization of intramolecularly crosslinked polystyrene molecules having a narrow distribution of molecular weight. II - The theoretical prediction of the dimensions in solution of intramolecularly crosslinked polystyrene molecules. III - The measurement of the dimensions of intramolecularly crosslinked polystyrene.
23 p3008 A73-43795

Theory of one-dimensional Mott semiconductors and the electronic structure of long molecules having conjugated bonds.
23 p3018 A73-44323

MOLECULAR COLLISIONS

Semiclassical theory for low-energy molecular collisions - H₂/+/-H₂ vibrational excitation.
01 p0080 A73-10564

Vibrational relaxation in CO₂ with selected collision partners. I - H₂O and D₂O.
01 p0080 A73-10775

A computer program for molecular dynamics of dilute gases.
01 p0081 A73-11472

Calculations on energy transfer to a diatomic molecule in high-energy head-on collisions.
02 p0195 A73-12723

Foreign gas collision broadening effects on 15 micron carbon dioxide bands radiation absorption lines
03 p0345 A73-13697

Molecular gas presence effect on electron energy balance in atomic gases, noting inelastic collisions loss

factor in heated Ar plasma containing nitrogen molecules
03 p0347 A73-14098

Rayleigh and Brillouin scattering from fluids in thermal equilibrium and light scattering from macromolecules in solution, discussing light and medium properties interrelationship
05 p0583 A73-16345

Dissociative excitation of molecular hydrogen by electron impact.
05 p0600 A73-16596

Mean free path of molecules from a surface in rarefied flow with application to correlating drag data. [ALAA PAPER 73-198]
05 p0531 A73-16933

Thermal conductivity and resonant multipole interactions.
06 p0725 A73-18121

Studies of the potential-curve-crossing problem. II - General theory and a model for close crossings.
06 p0726 A73-18263

Studies in molecular dynamics by collision-induced infrared absorption in H₂-rare gas mixtures. I - Profile analysis and the autocorrelation interference effect.
08 p0990 A73-21630

Prohibited autodetachment in OD- formed by collisions of O- with D₂.
09 p1048 A73-22075

Spatial and temporal ionization growth characteristics in nitrogen at moderate electric field strength, noting dominant secondary emission effect due to cathode bombardment by metastable molecules
09 p1122 A73-22120

Deformation of laser pulses in resonant media.
09 p1096 A73-22902

Recent experimental and theoretical investigations of infrared and microwave molecular spectra of astronomical interest /Introductory report/.
09 p1123 A73-23127

Formation of spectral lines in planetary atmospheres. V - Collision narrowed profiles of quadrupole lines in hydrogen atmospheres.
13 p1680 A73-28456

Theory of an infrared high-pressure chemical laser
13 p1627 A73-28762

Processes altering charge state in collisions of hydrogen atoms with H₂ molecules.
14 p1777 A73-30330

Application of the Poisson stochastic process for collision relaxation calculations in a nonequilibrium gas
15 p1915 A73-30968

Collision induced dissociation - A statistical theory.
15 p1915 A73-31275

Evolution of the CO vibrational energy distribution in a transverse flow laser.
15 p1884 A73-31313

Photographic studies of the transition between continuum and free molecular flow.
15 p1864 A73-31935

Momentum transfer and total scattering cross sections for ions with polar molecules.
17 p2213 A73-35178

Condensation in CO₂ free jet expansions. II - Growth of small clusters.
21 p2743 A73-40938

Change in the hyperfine state of the hydrogen atom during its collisions with unsaturated hydrocarbon molecules in the gaseous state.
22 p2889 A73-41719

Dissociation of diatomic molecules. I.
22 p2889 A73-42443

Molecular collisions. XIX - The distorted wave approximation to atom-rigid symmetric top rotational excitation.
22 p2889 A73-42445

Collisional radiative processes and molecular lasers
23 p2988 A73-44013

Stripping cross sections for production of forward scattered molecular ions in hydrogen and deuterium molecular collisions at kinetic energies below 500 eV, noting isotope effect
23 p3007 A73-44119

Reorientation /collision/ cross sections for hydrogen intermolecular potentials, taking into account quadrupole-quadrupole interaction effects
24 p3113 A73-44980

MOLECULAR DIFFUSION

Flame-sheet analysis of C.W. diffusion-type chemical lasers. II - Coupled radiation.
01 p0059 A73-10727

Effect of molecular shape and flexibility on gamma-ray directional correlations.
06 p0725 A73-18122

Diffusion processes in the mixing zone of a low-density supersonic jet
13 p1567 A73-29170

The photochemistry of hydrocarbons in the Jovian atmosphere.
14 p1802 A73-30766

Microscopic aspects of turbulent and laminar mixing in terms of molecular, eddy and bulk diffusional operations
17 p2156 A73-35502

MOLECULAR DISSOCIATION

Combined temperature, diffusion coefficient and density measurements of photoluminescent A10 releases.

18 p2303 A73-35949

Molecular diffusion model of cardiogenic gas mixing during inspiration at alveolar boundary in dogs

18 p2277 A73-36652

Theoretical studies and experimental verifications of thermal and electrical conductivity, molecular diffusivity and viscosity of a partially ionized suspension in an electric field.

22 p2894 A73-42512

MOLECULAR DISSOCIATION

U DISSOCIATION

MOLECULAR ELECTRONICS

NT LARGE SCALE INTEGRATION

MOLECULAR ENERGY LEVELS

NT INTERMOLECULAR FORCES

Energy distribution among reaction products. VII - H + F2.

04 p0414 A73-14820

Organic dye lasers use as continuously tunable sources of coherent light, discussing molecular energy level systems and transitions

05 p0583 A73-16337

Oxygen anions excited electronic states, analyzing energy curves and wave functions via configuration-interaction results obtained by multiconfiguration self consistent field techniques

07 p0853 A73-19333

Problem of the nuclear pumping of molecular gas lasers

09 p1096 A73-22702

Molecular model with two interacting terms for time evolution of nonradiative transitions, obtaining expression for energy level populations

09 p1123 A73-22876

Photochemical reactions in condensed phase relevant to biology, discussing molecular energy states, isomerization reactions and bond making/breaking processes

09 p1121 A73-23305

A quantum model for bending vibrations and thermodynamic properties of C3.

12 p1526 A73-27019

Structure of beryllium boron hydrides BeBH5 and BeB2H8.

12 p1466 A73-27045

Electron impact excitation of H2O.

12 p1526 A73-27687

Group theory generalization of Dicke quantum theory for spontaneous coherent radiation of multilevel molecules, noting angular distribution of photon echo effects

14 p1757 A73-30332

Chemical laser and molecular amplifiers characteristics covering population inversion and vibrational energy generation, storage, distribution and transfer

18 p2321 A73-35902

New thermodynamic functions for the C3 molecule.

18 p2287 A73-36326

Triply ionized Pm in lithium yttrium fluoride laser, calculating crystal field split energy levels and radiative transition probabilities

21 p2715 A73-40764

Vibrational relaxation of oxygen in an unsteady expansion wave.

22 p2889 A73-42441

E and F regions nitrogen vibration energy content by numerical integration of time dependent species continuity equation and species equation of motion

22 p2848 A73-42537

On the E sub 1-E sub 2 labeling of energy levels and the anomalous excitation of interstellar methanol.

22 p2914 A73-43005

Airglow hydroxyl emission IR spectral bands intensity measurements with allowance for atmospheric extinction, deriving vibrational level excitation rates from spontaneous emission transition probabilities

23 p2972 A73-43690

Determination of dissociation energies for some alkaline earth/hydro- / oxides in CO/N2O flames.

24 p3156 A73-44985

MOLECULAR EXCITATION

Energy transfer between impurity molecules in the presence of relaxation

01 p0080 A73-11243

Russian papers on nonlinear optics and hyperacoustics covering laser use in ultrasound propagation study and thermal and stimulated molecular light scattering effects

02 p0194 A73-11944

Stimulated molecular light scattering in gases

02 p0195 A73-11946

Quenching of vibrationally excited N2 by atomic oxygen.

02 p0139 A73-12085

Gain distribution in a CO2 TEA laser.

02 p0177 A73-12434

Dynamics of the CO2 atmospheric pressure laser with transverse pulse excitation.

[AD-760231] 02 p0177 A73-12435

Numerical model of energy transfer in carbon monoxide-nitrogen laser, considering electron-molecule excitation and vibration-vibration exchange

02 p0178 A73-12816

Electron scattering by molecules with and without vibrational excitation. VI - Elastic scattering by CO at 6-80 eV.

03 p0344 A73-13284

Chemical lasers population inversion mechanism and excitation energy comparison with other molecular gas lasers including carbon dioxide systems, considering efficiency

04 p0458 A73-14749

Vibrational excitation in CO by electron impact in the energy range 10-90 eV.

04 p0477 A73-14770

Photoionization of vibrationally excited N2. II - Quenching by CO2 and N2O.

04 p0414 A73-14817

Measurements of temperatures of vibrationally excited N2.

04 p0477 A73-14819

Thermal conductivity in vibrationally excited gases.

05 p0600 A73-16048

Dissociative excitation of molecular hydrogen by electron impact.

05 p0600 A73-16596

Calculation of shock wave relaxation zones including dissipative transport phenomena.

05 p0567 A73-17114

Excited molecules in a medium with a negative dielectric constant

06 p0725 A73-18105

Direct overtone excitation of hydrogen fluoride second vibrational level, measuring global deactivation rate by temperature tuned Nd-YAG laser excited fluorescence technique

06 p0703 A73-18750

Nitrous oxide laser optical pumping at high pressures with TEA hydrogen bromide laser, considering application to other linear triatomic molecules

06 p0704 A73-18796

Oxygen anions excited electronic states, analyzing energy curves and wave functions via configuration-interaction results obtained by multiconfiguration self consistent field techniques

07 p0853 A73-19333

Intracavity breakdown in CO and CO2 lasers.

07 p0835 A73-19638

Parametric studies of pulsed HF lasers using transverse excitation.

07 p0835 A73-19641

[AD-760268] Collision cross sections for electrons with atmospheric species.

08 p0957 A73-20659

Multiphoton excitations in vibrational-rotational states of diatomic molecules in an intense electromagnetic field.

08 p0990 A73-21003

Generation of vibrationally excited O2 and nonthermal infrared emission in the upper atmosphere

08 p0959 A73-21289

HF chemical lasers kinetics, radiative interactions and gas dynamics, deriving closed form solutions for excited states populations

08 p0976 A73-21671

Excitation mechanism of the far-infrared sulfur dioxide molecular laser.

09 p1090 A73-21938

[AD-760378] Kinetics of the excitation of molecular vibrations by infrared laser radiation

09 p1094 A73-22597

Protein molecules peptide groups excitation interpretation by quantum theory, noting application to muscle contraction

09 p1046 A73-23297

Prolonged luminescence of complex molecules in the gas phase

09 p1123 A73-23334

Energy transfer between impurity molecules during relaxation.

10 p1251 A73-24180

Vibrationally-excited nitrogen in the upper atmosphere.

10 p1212 A73-24226

Doppler broadening of OI 1304 A multiplet in dissociative excitation of CO2 and O2.

10 p1251 A73-24243

A plasma laser operating on molecular electronic transitions

10 p1228 A73-24454

Spectroscopic study of the vibrational-energy dissipation of the I2 molecule excited by a He-Ne laser

10 p1228 A73-24577

Effect of atomic oxygen on the N2 vibrational temperature in the lower thermosphere.

10 p1214 A73-24748

Carbon dioxide laser active medium excitation by ionizing radiation from external source during electric current passage, discussing gain dependence on pressure and mixture

10 p1229 A73-24756

Influence of excitation power on the energetic characteristics of phthalimide solutions

11 p1376 A73-26143

Feasibility of high-pressure noble-gas lasers.

11 p1378 A73-26360

Bounds on mean excitation energies-Lamb shift, stopping power, straggling, and grazing collision of high-energy charged particle.

12 p1526 A73-27128

Electron impact excitation of H2O.

12 p1526 A73-27687

Chemical reaction stimulation by laser radiation

12 p1467 A73-27979

The heating of interstellar clouds by vibrationally excited molecular hydrogen.

13 p1673 A73-28279

Investigation of the inversion medium of a quasi-stationary CO2 laser with 'pulsed' excitation

13 p1628 A73-29162

Heterodyne detection of frequency sweeping in the output of transverse-excitation CO2 lasers.

13 p1628 A73-29186

Autoionizing transitions in N2 and H2 produced by electron impact.

14 p1776 A73-29695

Observation of the effects of rotational transitions in the resonant scattering of electrons from N2.

14 p1776 A73-29696

Influence of CO on the population inversion in CO2 lasers.

14 p1756 A73-29921

Investigation of the excitation of vibrational levels of the N-14/H3 molecule by carbon dioxide laser radiation

14 p1758 A73-30801

Narrow nonlinear resonances of excited molecule densities in a standing wave of light

14 p1775 A73-30802

Vibrational excitation of H2 by proton impact.

14 p1777 A73-30957

Quantum oscillators employing the luminescence of self-localized excitons in condensed inert gases

15 p1885 A73-31714

Stimulation of nonradiating transitions during intense excitation by light

15 p1885 A73-31720

Transient oscillator analysis of a high-pressure electrically excited CO laser.

16 p2024 A73-33082

Electron impact excitation of N2. I, II.

16 p2039 A73-33866

CW IR laser action in slowly flowing premixed He-air-CO mixture with simultaneous molecular excitation and carbon dioxide generation by discharge-initiated CO oxidation

17 p2186 A73-35799

Production of vibrationally excited O2 and nonthermal infrared emission in the upper atmosphere.

19 p2424 A73-37918

Electron transitions of molecules in a plasma laser.

19 p2438 A73-38135

Emission of infrared molecular hydrogen lines from a cooled-gas laser.

20 p2574 A73-39694

Study of excitation transfer in dye mixtures by measurements of gain spectra.

21 p2716 A73-40968

Parametric study of a helical TEA CO2 laser.

21 p2716 A73-41050

Molecular collisions. XIX - The distorted wave approximation to atom-rigid symmetric top rotational excitation.

22 p2889 A73-42445

Postsunset oxygen emission observation by radiometer on rocket launched at Natal, Brazil, observing 10-km thick emission layer

22 p2848 A73-42536

On the E sub 1-E sub 2 labeling of energy levels and the anomalous excitation of interstellar methanol.

22 p2914 A73-43005

Behavior of excited atoms and molecules in the upper atmosphere at heights from 40 to 300 km

24 p3084 A73-44803

Time of flight spectral measurements of metastable lifetimes in molecular beams with different excited states

24 p3089 A73-44814

Chemiluminescence spectra from cool and blue flames - Electronically excited formaldehyde.

24 p3066 A73-45163

Theoretical study of a photodissociation model in polyatomic molecules

24 p3113 A73-45326

MOLECULAR FLOW

NT SLIP FLOW

NT TRANSITION FLOW

Molecular transmission probability through duct connecting two large vessels calculated from data on cylindrical tubes, comparing with Monte Carlo data for error correction

03 p0341 A73-12905

Some problems of gas-solid surface interaction.

05 p0638 A73-16177

Knudsen flow in a rectangular duct of finite length.

06 p0684 A73-17426

Circular cones and cylinder drag in molecular flow, using Schamberg model of molecules/solid surface interaction

09 p1030 A73-23461

Molecular gas dynamics, considering molecules internal degrees of freedom, Navier-Stokes and Knudsen layer boundary conditions, heterogeneous reactions, evaporation, condensation and surface shocks

A distribution of molecular flow in the interior of a cylindrical space-simulation chamber with spherical gas source

Fluid turbulence equations for large molecular drift velocity gradients in rarefied gas, near surface and stellar system motions, using Predvoditelev hydrodynamic equations

The flow of highly rarefied gases.

Method for the interpretation of surface pressure measurements under rarefied hypersonic conditions.

Two-variable asymptotic solution to unsteady three dimensional turbulent flow equations describing small scale deformation, determining hot spot or macromolecular size statistical behavior

MOLECULAR GASES

NT DIATOMIC GASES

NT POLAR GASES

NT POLYATOMIC GASES

A computer program for molecular dynamics of dilute gases.

Breakdown thresholds in rare and molecular gases using pulsed 10.6-micron radiation.

Energy flux intensity in IR bands of selectively radiating molecular gas nonisothermal layer from radiative transfer equation and mathematical model

Quantum kinetic equation for monatomic and molecular gases optical characteristics calculation, considering spontaneous emission spectrum of atoms

Time history of laser power pulses from molecular gas lasers.

The Navier-Stokes equations and the bulk viscosity of simple gases.

Laser coupling through nonlinear gas filled absorber cell, discussing molecules mean free path

Statistical mechanics and virial functions for equation of state of dense gas with spherical nonpolar molecules, calculating compressibility factor for methane and Ar

Combustion molecular gases radiative heat transfer, emissivity and absorptivity calculation, presenting high speed computer routine

Molecular nitrogen ionization growth characteristics as function of electric field strength and gas pressure, using thin gold film electrodes

Luminescence of a molecular gas under the action of a carbon dioxide laser pulse

The effect of an external field on transport phenomena in a Knudsen molecular gas

Photoabsorption cross sections of H₂, D₂, N₂, O₂, Ar, Kr, and Xe at the 584-A line of neutral helium.

Nongray radiative transfer and simultaneous turbulent diffusion in layer of molecular gas enclosed by parallel black walls, presenting temperature profiles

Statistical mechanics and virial functions for equation of state of dense gas with spherical nonpolar molecules, calculating compressibility factor for methane and Ar

Self-focusing of CO₂ laser radiation in resonantly absorbing gases.

Investigation of the molecular composition of the vapors and the structure of the condensate during the evaporation of arsenic chalcogenides by laser radiation

Influence of an external field on transport effects in a Knudsen molecular gas.

Treatment of molecular reaction equilibria and opacity calculations for cool circumstellar envelopes

Plasma stability of electric discharges in molecular gases.

Dissociation and bleaching of a multilevel molecular gas under the influence of radiation from a powerful CO₂ laser

Far infrared and Raman spectra of gaseous carbon suboxide and the potential function for the low frequency bending mode.

Change in the hyperfine state of the hydrogen atom during its collisions with unsaturated hydrocarbon molecules in the gaseous state.

The absorption cross sections of N₂, O₂, CO, NO, CO₂, N₂O, CH₄, C₂H₄, C₂H₆, and C₄H₁₀ from 180 to 700 Å.

Theory of nonequilibrium phenomena in chemically reacting gas mixtures

MOLECULAR INTERACTIONS

NT MOLECULAR COLLISIONS

Review of laboratory measurements of aeronomic ion-neutral reactions.

Influence of roughness on the process of interaction between a rarefied gas and the surface of a solid

Experimental investigation of thermal and induced molecular scattering of light in solutions within a wide spectral range

Atomic and molecular interactions investigation by computer aided mass spectrometry, considering applications in bio-organic chemistry, isotope analysis, geochemistry and cosmochemistry

Gas-phase acidities of binary hydrides.

Galerkin stress functions for non-local theories of elasticity.

Cosmic-ray heating and molecular cooling of dense clouds.

Investigation of long-chain molecule dynamics in condensed state by the IR-spectroscopy and Rayleigh-scattering methods

Valence-bond study of the H₂, D₂/ exchange reaction mechanism.

Laser spectroscopy of stimulated Raman scattering of weakly interacting molecules, and its applications

Theory of cooperative defect formation in a biopolymer molecule under the action of radiation

Correlation of theory and experiment for high-pressure hydrogen.

Vibration-to-rotation and vibration-to-vibration energy transfer between diatomic molecules.

On the product rotational state distribution in exoergic atom-diatom molecule reactions.

Book - Statistical mechanics, kinetic theory, and stochastic processes

The employment of an extended theorem of corresponding conditions in the computation of the surface tension of pure substances

Evaluation of the intermolecular energy between two hydrogen molecules near the van der Waals minimum, from a perturbative procedure.

Short-acting repulsive forces between atoms and molecules of atmospheric gases

Treatment of molecular reaction equilibria and opacity calculations for cool circumstellar envelopes

Boundaries effect on dispersion interaction between molecules in bounded region, applying method to two oscillators between conducting plates

Self consistent microscopic theory of Rayleigh light scattering by molecular aggregates based on random phase modulation and stochastic theories

Life origin hypothesis based on interstellar molecular concentration in gas clouds, examining radical types and molecular Doppler spectra

State variables and transport coefficients of binary gaseous mixtures. II - The binary interaction between identical and nonidentical molecules [DFVLR-SONDDR-279]

Elementary reactions in the combustion of small inorganic molecules.

Estimation of rate constants of elementary processes - A review of the state of the art.

Estimate of the effect of photoionization and ion-molecule reactions on the diffusion coefficient in the ionosphere.

Moment equation solutions for plane nonisothermal Poiseuille gas flow slip rate and temperature and pressure gradients in terms of molecular models

MOLECULAR IONS

Multiquantum ionization of a molecule represented by a nonorthogonal wave function system

Positive ion composition measurements in disturbed D region, noting positive molecular oxygen ions as major source of water cluster ions

The charge transfer spectrum of LiNa⁺.

Dissociative recombination at elevated temperatures. III - O₂⁺/ dominated afterglows.

Proton-impact dissociation and ionization of H₂⁺ molecular ions.

Interaction of haemoglobin with ions - Binding of inorganic phosphate to human oxyhaemoglobin.

Search for interstellar absorption in 4250 Å line of singly ionized CO in direction of different stars

Negative oxygen molecular ion formation in low energy electron collision and attachment obtaining capture cross section and resonance width

Fluorescent cross sections and yields of CO₂⁺/ from threshold to 185 Å.

Self consistent field calculations of CO positive ion dipole moment in ground state

Cavity perturbation technique for determining the presence of molecular ions of helium in a dc discharge plasma.

Oscillator strength calculations for vibrational transitions of X-A electronic system of interstellar CH positive ion, noting agreement with astrophysical observations of line spectra

Dissociative recombination rate for CH positive ions in interstellar clouds

Drift tube and mass spectrometric measurement of molecular positive ion drift velocities in carbon dioxide

Excitation of the CO fourth positive system by the dissociative recombination of CO₂⁺/ ions.

Ionised molecules in BCA photospheric model.

N₂⁺/ Meinel and O₂⁺/ second negative bands laser theory.

Measurements of recombination of electrons with HCO⁺ ions.

Stripping cross sections for production of forward scattered molecular ions in hydrogen and deuterium molecular collisions at kinetic energies below 500 eV, noting isotope effect

MOLECULAR ORBITALS

An 'ab initio' Gaussian orbital calculation of the /100/ surface of crystalline lithium hydride.

Projected states of open shell molecules - The pi-electron states of the cyclopentadienyl cation.

Interpretation of K X-ray emission spectra and chemical bonding in oxides of Mg, Al and Si using quantitative molecular orbital theory.

Superexchange potential and kinetic energy theory in molecular orbital and configurational interaction approximation for three center four electron model of ferrimagnetic materials

Excitation of surface molecular orbitals on the /100/ face of molybdenum

MOLECULAR OSCILLATIONS

Vibrational relaxation in CO₂ with selected collision partners. I - H₂O and D₂O.

Navier-Stokes approximation for gas dynamics equations of molecular oscillations in diatomic gas, noting relaxation pressure proportionality to energy density equilibrium deviation

Frequency distribution function for free rotation and uniform angular distribution of molecules, detecting conformations from vibrational spectrum characteristics

Molecular nitrogen vibrational temperature in E and F regions, using positive ion data and model for ionic reaction rate and continuity equation numerical solution

Electron scattering by molecules with and without vibrational excitation. VI - Elastic scattering by CO at 6-80 eV.

03 p0344 A73-13284

Shock-tube study of vibrational energy transfers in the CO₂-N₂ and the CO₂-CO systems.

03 p0345 A73-14442

Energy distribution among reaction products. VII - H + F₂.

04 p0414 A73-14820

Thermal conductivity in vibrationally excited gases.

05 p0600 A73-16048

Carbon dioxide-nitrogen gasdynamic lasers, predicting population inversion from numerical model of vibrational relaxation of anharmonic diatomic oscillators in supersonic expansions

07 p0834 A73-19511

Laser-excited vibrational energy transfer studies of HF, CO, and NO.

07 p0834 A73-19627

Experimental determination of the vibrational temperature of a supersonic gas flow.

08 p1021 A73-20854

Kinetics of the excitation of molecular vibrations by infrared laser radiation

09 p1094 A73-22597

Vibration-to-rotation and vibration-to-vibration energy transfer between diatomic molecules.

11 p1401 A73-25967

Role of exchange in shifted scattering of light for a double hole

13 p1660 A73-28760

Vibrational relaxation measurements in CO₂ employing an incremental TEA laser gain technique.

16 p2024 A73-33083

Chemical lasers and chemical reactions induced by lasers.

17 p2182 A73-34112

Vibrational relaxation in the HF-HCl, HF-HBr, HF-HI, and HF-DF systems.

17 p2119 A73-35176

Chemical laser and molecular amplifiers characteristics covering population inversion and vibrational energy generation, storage, distribution and transfer

18 p2321 A73-35902

High power carbon dioxide-nitrogen gasdynamic laser vibration kinetics model, suggesting closed cycle photon generator engine for energy conversion to work

21 p2710 A73-40094

HF and DF molecules vibrational relaxation investigation by recording IR radiation behind incident shock wave at 1500-5000 K

21 p2743 A73-40360

Nuclear spin analogue of a molecular beam maser with cavities in series.

21 p2713 A73-40469

Dissociation of diatomic molecules. I.

22 p2889 A73-42443

E and F regions nitrogen vibration energy content by numerical integration of time dependent species continuity equation and species equation of motion

22 p2848 A73-42537

Determination of vibrational and translational temperatures in gas-dynamic lasers.

24 p3095 A73-44588

Bending potential of an H₂O molecule.

24 p3113 A73-44977

MOLECULAR OSCILLATORS

Kinetics of the deactivation of the vibrations of highly excited oscillators in an inert gas medium with allowance for spontaneous emission

02 p0194 A73-11607

Frequency generators performance with stability associated with atomic/molecular transition, considering rubidium and hydrogen clocks and He-Ne lasers

10 p1219 A73-42496

Classical calculation of intensity distribution in the oscillatory-rotational spectra of diatomic molecules

15 p1916 A73-32338

Ultrastable atomic and molecular oscillators and their applications to navigation

19 p2429 A73-37384

Oscillator strength calculations for vibrational transitions of X-A electronic system of interstellar CH positive ion, noting agreement with astrophysical observations of line spectra

19 p2488 A73-38512

MOLECULAR PHYSICS

Thermodynamic functions and molecular parameters of rhombic dimeric molecules of alkali metal halides

01 p0080 A73-10857

Radio spectroscopy superiority for interstellar cloud chemical composition studies, detecting formaldehyde, X-ogen, HNC and other exotic molecular species

05 p0546 A73-16305

Organogenic elements in stars, interstellar matter, comets, meteorites and planets, discussing molecular distribution and formation, prebiological chemical evolution, and terrestrial and extraterrestrial biology

06 p0754 A73-18430

On the presence of H₂ molecules inside neutral globules imbedded in H II regions.

09 p1140 A73-22005

Molecular abundances in stellar atmospheres. II.

11 p1417 A73-25265

Oxidation of organic molecules by photoproduct holes of ZnO.

15 p1841 A73-31969

Boundaries effect on dispersion interaction between molecules in bounded region, applying method to two oscillators between conducting plates

20 p2538 A73-39705

The influence of electron plasma formation on superbroadening in light filaments.

22 p2871 A73-43077

Molecular rupture mechanism, self reinforcement and failure modes of elastomeric materials dependence on strain, temperature, filler and crosslink density

23 p2997 A73-43808

MOLECULAR PUMPS

Calculation of the pumping characteristic of a turbomolecular vacuum pump

12 p1461 A73-27475

The axial flow molecular pump. IV - Performance of a rotor with a single blade row in the transition flow regime.

19 p2433 A73-37673

The performance characteristics of modern vacuum pumps.

21 p2707 A73-39915

MOLECULAR RELAXATION

Vibrational relaxation in CO₂ with selected collision partners. I - H₂O and D₂O.

01 p0080 A73-10775

Energy transfer between impurity molecules in the presence of relaxation

01 p0080 A73-11243

Navier-Stokes approximation for gas dynamics equations of molecular oscillations in diatomic gas, noting relaxation pressure proportionality to energy density equilibrium deviation

02 p0152 A73-11602

Kinetics of the deactivation of the vibrations of highly excited oscillators in an inert gas medium with allowance for spontaneous emission

02 p0194 A73-11607

Quenching of vibrationally excited N₂ by atomic oxygen.

02 p0139 A73-12085

Acoustical studies of rotational relaxation in gases.

03 p0342 A73-12986

Relaxation of excess populations in the lower laser level CO₂/100/.

03 p0318 A73-13278

Monte Carlo classical trajectory calculation of the rates of F-atom vibrational relaxation of HF and DF.

03 p0318 A73-13279

Monte Carlo classical trajectory calculation of the rates of H and D-atom vibrational relaxation of HF and DF.

03 p0318 A73-13280

Laser induced infrared fluorescence - Thermal heating, mass diffusion, and collisional relaxation in SF₆.

03 p0318 A73-13281

Study of excitation transfer in a flowing helium afterglow pumped with a tuneable dye laser. II - Measurement of the rate coefficient for the rotational relaxation of He₂/3p 3Pi-g/.

05 p0600 A73-16045

The Navier-Stokes equations and the bulk viscosity of simple gases.

05 p0597 A73-16591

Calculation of shock wave relaxation zones including dissipative transport phenomena.

05 p0567 A73-17114

The application of magnetic after-effects in research on the real structure and migrational properties of metals and alloys

07 p0837 A73-19049

A new integral-variational method for calculation of relaxation regions behind shock and detonation waves.

07 p0809 A73-19050

Carbon dioxide-nitrogen gasdynamic lasers, predicting population inversion from numerical model of vibrational relaxation of anharmonic diatomic oscillators in supersonic expansions

07 p0834 A73-19511

Laser-excited vibrational energy transfer studies of HF, CO, and NO.

07 p0834 A73-19627

Measurement of the temperature dependence of the vibrational relaxation rate of HF and the effect of SF₆, N₂, and F₂ as diluents.

07 p0853 A73-19628

Chemical laser studies of vibrational energy distributions - The equal-gain and zero-gain temperature techniques.

07 p0834 A73-19629

Far IR molecular lasers evaluation, discussing excitation, line assignment, relaxation, frequency measurement and development predictions

07 p0835 A73-19636

Vibrational relaxation times of oxygen in the pressure range 10-110 atm.

07 p0853 A73-19927

Calculation of probabilities of energy transfer - Application to the vibrational relaxation of the CS radicals in the presence of argon

07 p0854 A73-20608

Relaxation and pumping processes in thermally excited carbon dioxide lasers.

08 p0975 A73-21194

Vibrational relaxation theory of diatomic and molecular single component and gas mixture systems for molecular laser mechanisms, using oscillator simulation

09 p1097 A73-23331

Flux magnitude and single transition probabilities as a function of electron density and temperature in relaxation model ionization and recombination channels

10 p1253 A73-23503

Kinetic equations for vibrational energy relaxation in a polyatomic gas mixture

10 p1250 A73-23579

The Knudsen layer in a flow with two-temperature relaxation

10 p1250 A73-23580

Energy transfer between impurity molecules during relaxation.

10 p1251 A73-24180

Vibrational relaxation in hydrogen-rare-gases mixtures.

11 p1402 A73-25969

Concerning one exact solution of the theory of quasilinear relaxation of a parametrically unstable plasma in the field of powerful radiation.

13 p1664 A73-28613

Relaxation processes in electrically excited discharge pumped gasdynamic lasers with supersonic gas mixture flow

13 p1627 A73-28967

Low-temperature relaxations in amorphous polymers.

14 p1765 A73-30134

Vibrational relaxation effects in weak shock waves in air and the structure of sonic bangs.

14 p1711 A73-30174

Application of the Poisson stochastic process for collision relaxation calculations in a nonequilibrium gas

15 p1915 A73-30968

Relaxation of a partially ionized gas in a nozzle

15 p1824 A73-32327

Vibrational relaxation measurements in CO₂ employing an incremental TEA laser gain technique.

16 p2024 A73-33083

Vibrational relaxation of CO by O atoms.

17 p2119 A73-35174

Quantum scattering theory of rotational relaxation and spectral line shapes in H₂-He gas mixtures.

17 p2119 A73-35175

Vibrational relaxation in the HF-HCl, HF-HBr, HF-HI, and HF-DF systems.

17 p2119 A73-35176

Flux magnitude and single transition probabilities as a function of electron density and temperature in relaxation model ionization and recombination channels

17 p2217 A73-35183

Laser absorption study of carbon monoxide vibrational relaxation behind incident shock waves, discussing vibration-rotation levels, shock tubes, oscilloscope traces and Boltzmann distributions

19 p2437 A73-37900

Direct-sampling studies of combustion processes.

19 p2504 A73-38325

Influence of vibrational, rotational, and reorientational relaxation on pulse amplification in molecular amplifiers.

21 p2742 A73-40217

HF and DF molecules vibrational relaxation investigation by recording IR radiation behind incident shock wave at 1500-5000 K

21 p2743 A73-40360

The carbon monoxide laser - Mechanism of formation of population inversion

21 p2712 A73-40444

Vibrational relaxation of oxygen in an unsteady expansion wave.

22 p2889 A73-42441

Rotational relaxation effects in short-pulse CO₂ amplifiers.

22 p2870 A73-42520

Studies of the relaxation of internal energy of molecular hydrogen.

22 p2898 A73-42762

Catalytic efficiencies of atoms in the vibrational relaxation of HF and DF.

22 p2818 A73-42763

Relaxation processes in electrically excited discharge pumped gasdynamic lasers with supersonic gas mixture flow

23 p2989 A73-44319

Vibrational relaxation of CO₂ /nu sub 3/ by ozone.

24 p3066 A73-44988

MOLECULAR ROTATION

Vibration-rotation bands of NH in the spectrum of alpha Orionis.

01 p0104 A73-11041

Laser power density calculation with complete rotational analysis for molecular hydrogen Lyman and Werner bands vibrational-rotational transitions

01 p0061 A73-11224

Frequency distribution function for free rotation and uniform angular distribution of molecules, detecting conformations from vibrational spectrum characteristics

02 p0195 A73-12099

Acoustical studies of rotational relaxation in gases.

03 p0342 A73-12986

Glyoxal cis form as source of microwave spectra from rotational spectrum investigations of B-type transitions

03 p0273 A73-13286

Measurements of temperatures of vibrationally excited N₂.

04 p0477 A73-14819

Energy distribution among reaction products. VII - H + F₂.

04 p0414 A73-14820

Effect of molecular shape and flexibility on gamma-ray directional correlations.

06 p0725 A73-18122

Chemical laser studies of vibrational energy distributions - The equal-gain and zero-gain temperature techniques.

07 p0834 A73-19629

Vibration-rotation state populations and laser output spectra of CW chemical hydrogen halide lasers under subsonic transverse flow

07 p0835 A73-19640

Rotational temperature measurements in nitrogen at hypersonic flow using an electron beam technique [ONERA, TP NO. 1206]

07 p0853 A73-20605

Multiphoton excitations in vibrational-rotational states of diatomic molecules in an intense electromagnetic field.

08 p0990 A73-21003

Carbon monoxide rotational transitions as dark cloud cooling mechanism during protostar formation

08 p0103 A73-21814

Polymer chain model with internal rotations for elastic body stress-strain state, internal work, elastic energy and equations of motion

10 p1240 A73-24307

Microwave rotational spectroscopy - A technique for specific pollutant monitoring.

10 p1221 A73-24891

Rotational and vibrational hydroxyl excitation in the laboratory and in the night airglow.

11 p1354 A73-25761

Vibration-to-rotation and vibration-to-vibration energy transfer between diatomic molecules.

11 p1401 A73-25967

On the product rotational state distribution in exoergic atom-diatom molecule reactions.

11 p1402 A73-25968

An evaluation of molecular constants and transition probabilities for the NH free radical.

11 p1402 A73-26582

Separation of rotational lines of a CO₂ laser with a film selector in the resonator.

12 p1508 A73-27527

Rotational spectral lines of water vapor dimers in the upper troposphere

13 p1609 A73-29152

Observation of the effects of rotational transitions in the resonant scattering of electrons from N₂.

14 p1776 A73-29696

High temperature-microwave spectrometer for Zeeman-effect measurements involving diamagnetic molecules

14 p1753 A73-30235

Viscosity coefficients and heat conductivity of dense gases with rotational degrees of freedom

15 p1915 A73-31022

Plastic crystals structural, thermodynamic and mechanical properties, noting high deformability due to molecular rotational freedom

15 p1923 A73-31415

Classical calculation of intensity distribution in the oscillatory-rotational spectra of diatomic molecules

15 p1916 A73-32338

Rotational temperature measurement of gases using laser Raman scattering techniques.

17 p2166 A73-34623

Lamb-dip-stabilized carbon dioxide laser line frequency separations, discussing beat frequencies, C 12 and O 16 molecular rotation constants and vibration level reduction

21 p2712 A73-40324

Computer checking of rotational line intensity factors for diatomic transitions.

21 p2744 A73-41212

A device for the on-line measurement of nitrogen rotational temperature in low density flows.

22 p2854 A73-41995

Dissociation of diatomic molecules. I.

22 p2889 A73-42443

Molecular collisions. XIX - The distorted wave approximation to atom-rigid symmetric top rotational excitation.

22 p2889 A73-42445

Hyperfine structure of furan.

22 p2818 A73-42712

Methane absorption in the atmosphere of Saturn - Rotational temperature and abundance from the 3 nu sub 3 band.

24 p3129 A73-44445

Dipole moment of water from Stark measurements of H₂O, HDO, and D₂O.

24 p3113 A73-44978

MOLECULAR SIEVES

U ABSORBENTS

MOLECULAR SPECTRA

NT ELECTRONIC SPECTRA

NT RAMAN SPECTRA

NT VIBRATIONAL SPECTRA

The short-wavelength spectrum of the microwave background.

01 p0015 A73-10062

Eta Aquilae star molecular abundances of CO, CN, carbon, OH, NH and CH with respect to dissociation equilibrium and light curve correspondence

01 p0103 A73-11022

Laser power density calculation with complete rotational analysis for molecular hydrogen Lyman and Werner bands vibrational-rotational transitions

01 p0061 A73-11224

Long wavelength spectrometry and photometry of M, S and C-stars.

02 p0222 A73-12708

Glyoxal cis form as source of microwave spectra from rotational spectrum investigations of B-type transitions

03 p0273 A73-13286

Foreign gas collision broadening effects on 15 micron carbon dioxide bands radiation absorption lines

03 p0345 A73-13697

The spectrum of FeH - Laboratory and solar identification.

03 p0374 A73-13718

Molecular clouds and stellar origin in interstellar space

03 p0376 A73-14175

Comet spectra and excitation mechanism for spectrum production, discussing structural subdivision into nucleus, coma and tail

04 p0494 A73-14760

Cometary heads observations indicating precursor decay lengths from 100-10,000 km, considering visible and UV molecular and atomic emissions

04 p0495 A73-14764

Calculation of pressure-broadened linewidths of SO₂ and NO₂.

04 p0414 A73-14815

Interstellar molecules detection, sources and destruction observed via visible, UV and radio wave spectra

04 p0501 A73-15627

The mechanism of vacuum ultraviolet emission from the Lewis-Rayleigh nitrogen afterglow.

05 p0600 A73-16560

New laser technique for the identification of molecular transitions.

05 p0585 A73-16597

Interstellar molecular hydrogen observed in the ultraviolet spectrum of delta Scorpii.

07 p0874 A73-19071

On the differing molecular line widths in dense interstellar clouds.

07 p0874 A73-19072

Galactic interstellar molecules, discussing physical, chemical and spectral characteristics, hydroxyl emission, occurrence regions, hydrogen clouds, isotope ratios, interstellar masers and probes

09 p1146 A73-22446

On the detection of H₂ from interstellar clouds in the wavelength range 4.4 to 28.2 microns.

09 p1148 A73-22870

Recent experimental and theoretical investigations of infrared and microwave molecular spectra of astronomical interest [Introductory report].

09 p1123 A73-23127

Observational, theoretical, and predicted data on the infrared and microwave spectra of interstellar matter [Introductory report].

09 p1150 A73-23135

Interstellar organic molecules millimeter wave line spectra and transition rotational quantum numbers

09 p1150 A73-23141

Prolonged luminescence of complex molecules in the gas phase

09 p1123 A73-23334

Interstellar Na I, K I, Ca II, and CH₃/+ line profiles toward zeta Ophiuchi.

10 p1273 A73-23549

Probabilities of infrared and RF transitions in OH and CH molecules

10 p1250 A73-23710

Isotopic combination identification in interstellar clouds through radio spectral line observations, discussing millimeter wave astronomy, molecular clouds, excitation mechanisms, galactic structure, etc

10 p1280 A73-24323

Transition metal borides ESCA spectra observation for metal-boron bonding energy based on spectral sensitivity to surface oxidation, discussing relevant features

11 p1325 A73-25202

Asymmetric intensities of Zeeman components of electronic transitions of diatomic molecular spectra in sunspots, considering CN red lines

11 p1422 A73-25936

Determination of the temperature of a methane-fluorine diffusion flame by means of the vibration-rotation spectrum of the HF molecule

11 p1453 A73-26586

Interferometric studies of interstellar CH₃/+ molecules.

11 p1427 A73-26617

Atoms and molecules in astrophysics; Proceedings of the Twelfth Session of the Scottish Universities Summer School in Physics, University of Stirling, Stirling, Scotland, August 1971.

12 p1538 A73-26920

Solar rotational and vibrational temperature based on turbulent velocity determined from CN molecular line profiles half widths

12 p1547 A73-27870

The Perseus spiral arm at 21-cm.

13 p1685 A73-29354

Ground-based measurement of millimetre-wavelength emission by upper stratospheric O₂.

14 p1751 A73-29718

High temperature-microwave spectrometer for Zeeman-effect measurements involving diamagnetic molecules

14 p1753 A73-30235

Bands of the light molecules in Mira variables.

15 p1932 A73-31307

The absence of formaldehyde radiation toward cold regions of the galactic plane - Further investigation.

15 p1936 A73-31554

The variation of the electronic transition moment, Re, in the intensity theory of diatomic molecules.

15 p1916 A73-32392

Long-path infrared spectra of CO, NO₂, NO, SO₂ and N₂O observed in a simulated atmosphere in trace amounts.

16 p1976 A73-32700

IR and molecular radio emissions from interstellar clouds representing formation stage of normal stars, discussing dust screening effects

17 p2229 A73-34433

Infrared and radio transition probabilities of OH and CH.

18 p2338 A73-36735

Observations of carbon monoxide at 4.7 microns in IRC + 10216, VY Canis Majoris, and NML Cygni.

19 p2484 A73-37612

A new method for determining the degree of oxygenation of hemoglobin spectra in the case of inhomogeneous light paths, explained in an analysis of spectra of the human skin

20 p2517 A73-39145

Solar rotational and vibrational temperature based on turbulent velocity determined from CN molecular line profiles half widths

20 p2608 A73-39244

The cosmological significance of molecular band strengths in the infrared spectra of elliptical galaxies.

20 p2609 A73-39447

Vacuum IR spectrometer measurement of C 12 methane absorption band at 1.1 microns, describing technique for extending standards to photomultiplier region of spectra

21 p2743 A73-40936

Synthesis and characterization of isomeric cis- and trans-pyrone model compounds.

21 p2648 A73-41215

Carbon, CN, CH, MgH, NH and OH line behavior in solar photospheric spectra

21 p2778 A73-41528

Spectroscopic studies of low-pressure hydrogen-fluorine flames.

22 p2898 A73-42760

Spectral line radio astronomy observations of interstellar molecular clouds in Galaxy, relating to stellar and life evolution

23 p3028 A73-43350

Background concentrations of photochemically active trace constituents in the stratosphere and upper troposphere.

23 p2976 A73-43889

Development of an H₂O atmosphere around Comet Kohoutek /1973/ and its possible detection.

23 p3033 A73-43955

Methane absorption in the Jovian atmosphere. I - The Lorentz half-width in the 3 nu/sub 3/ band at 1.1 micron.

24 p3132 A73-44537

Methane absorption in the Jovian atmosphere. II - Absorption line formation.

24 p3133 A73-44559

Absorption at about 4.3 microns by /N₂-N₂/ and /N₂-O₂/ complexes in the terrestrial atmosphere

24 p3084 A73-44964

Spectral data for the nu sub 2 bands of ammonia with applications to radiative transfer in the atmosphere of Jupiter.

24 p3142 A73-45324

MOLECULAR SPECTROSCOPY NT RAMAN SPECTROSCOPY

Nitric oxide detection by use of Zeeman-effect and CO laser.

03 p0318 A73-12871

Molecular branching-ratio method for intensity calibration of optical systems in the vacuum ultraviolet.

05 p0597 A73-16495

Double charge transfer spectroscopy of diatomic molecules.

09 p1122 A73-22118

Spectroscopy of tetrabenzoporphin molecules and possible astrophysical implications.

09 p1048 A73-23136

Microwave spectrometer with internal dc glow discharge for transient paramagnetic molecules observation, discussing design features and operating parameters effects on spectrum

11 p1366 A73-26303

Interstellar molecules and radio spectroscopy in the cm- and mm-wave range

12 p1544 A73-27779

Investigation by the laser photolysis method of the spectral and time characteristics of tetrapyrrole molecules in a triplet state

13 p1628 A73-29050

High resolution spectroscopy with lasers.

14 p1756 A73-29925

Spectroscopy of the vapors of weakly volatile compounds, supercooled in a supersonic flow

16 p2038 A73-34054

Interference filter laser Raman spectrometry of gases and volatile liquids, discussing instrument sensitivity and response linearity, signal to noise ratios, and bandwidths

21 p2698 A73-40140

Computer checking of rotational line intensity factors for diatomic transitions.

21 p2744 A73-41212

Hyperfine structure of furan.

22 p2818 A73-42712

Microwave optical double resonance spectra of CW dye laser pumped transitions in BaO

24 p3096 A73-44976

Bending potential of an H2O molecule.

24 p3113 A73-44977

MOLECULAR STRUCTURE

Thermodynamic functions and molecular parameters of rhombic dimeric molecules of alkali metal halides

01 p0080 A73-10857

Spectroscopic study and molecular structure of 1,1-dimethylhydrazine-mono-borane.

02 p0139 A73-12628

Neodymium energy level shifts in three oxygen-compensated sites of neodymium oxide-doped calcium fluoride crystals

03 p0349 A73-13288

Vibrational spectra and structure of tetrakis(trifluoromethyl)hydrazine in the crystalline and fluid states.

04 p0414 A73-16036

On supposedly five-co-ordinate titanium (IV) complexes - The crystal and molecular structure of C13Ti/C5H7O2/.

06 p0661 A73-18266

Infrared and Raman spectroscopic studies of structural variations in minerals from Apollo 11, 12, 14, and 15 samples.

07 p0897 A73-19887

Calculation of the magnetic properties of a hydrogen molecule with the aid of the method of varying the vector potential and the method of varying the induced current

09 p1122 A73-22017

Molecular model with two interacting terms for time evolution of nonradiative transitions, obtaining expression for energy level populations

09 p1123 A73-22876

Low frequency vibrations and molecular structure of /CH3/2NPF2.

11 p1326 A73-25567

A study of the secondary structure of ilamycin B1 by 300 MHz proton magnetic resonance.

11 p1326 A73-25572

Quaternary structure /subunit composition/ of human ceruloplasmin

11 p1316 A73-25638

Criteria for distinguishing biogenic and abiogenic amino acids - Preliminary considerations.

11 p1319 A73-26480

The ultrastructural organization of the photoreceptor membranes and the intradiscal spaces of the vertebrate retina as revealed by various experimental treatments.

11 p1321 A73-26717

Cometary nuclei chemical composition and molecular structure, suggesting radial-forming organic

molecules synthesis by solar and galactic cosmic radiation

14 p1723 A73-29816

Investigation of some electrooptical properties of liquid crystals

14 p1784 A73-30854

Vibrational spectra of substituted hydrazines. IV - Raman and far-infrared spectra and structure of tetramethylhydrazine.

15 p1841 A73-32220

Structure of the lipid phase in cell envelope vesicles from Halobacterium cutirubrum.

17 p2112 A73-34599

Study of the dependence of the properties of radicals on the characteristics of the initial hydrazine structure

17 p2220 A73-34638

X ray data refinement on proteins, discussing backbone and side chain dihedral angles adjustment by least squares fitting to relieve atomic overlaps

17 p2112 A73-34893

The anisotropy of creep behaviour in oriented thermoplastics.

17 p2196 A73-35342

Cold rolling of polymers. III - Properties of rolled crystallized polycarbonates.

17 p2197 A73-35351

Superconducting fluctuations in complexes of tetracyanoquinodimethane and structural imperfections.

19 p2482 A73-37387

Physical nature of gelatin as polymer material, emphasizing low temperature restoration of collagen structure, supermolecular structure formation capability and glassy-elastic state transition temperature

21 p2647 A73-40265

Molecular crystals with behavior predictable by discrete quasi-continuous Cosserat model based on system of oriented Newtonian particles with six degrees of freedom

21 p2739 A73-40573

Hyperfine structure of furan.

22 p2818 A73-42712

Mathematical model for fracture strength of material undergoing molecular orientation during tensile strain, accounting for anomalous polymer characteristics

24 p3144 A73-44508

Microwave spectrum, structure, dipole moment and low frequency vibrations of dimethyl cyanamide.

24 p3066 A73-44771

MOLECULAR THEORY

Investigation of long-chain molecule dynamics in condensed state by the IR-spectroscopy and Rayleigh-scattering methods

09 p1122 A73-21956

Kinetic equations solved for population of different molecular quantum states via quasi-steady state approximation

12 p1526 A73-27307

A molecular theory of elastomer deformation and rupture.

13 p1646 A73-29528

Terrestrial and extraterrestrial stable organic molecules.

14 p1724 A73-30131

MOLECULAR WEIGHT

NT LOW MOLECULAR WEIGHTS

Structure of helium burning regions in stars - Dependence on molecular weight and burning rates.

19 p2483 A73-37560

Russian book - High-molecular-weight compounds in photographic processes.

21 p2646 A73-40252

Physicochemical principles of the photographic process on vesicular films and the high-molecular-weight compounds used for these films

21 p2646 A73-40254

Gas solubility in hydraulic liquids from measurements of air in mineral oils, noting oil molecular weight effect

21 p2724 A73-41579

Analysis of spikes in occultation curves - A critique of Brinkmann's method.

24 p3129 A73-44444

MOLECULES

NT DIATOMIC MOLECULES

NT POLYATOMIC MOLECULES

NT TRIATOMIC MOLECULES

MOLIERE FORMULA

U COSMIC RAY SHOWERS

U SECONDARY COSMIC RAYS

U SPATIAL DISTRIBUTION

MOLNIYA SATELLITES

Resonance acceleration of low-energy protons in the earth's radiation belts

06 p0742 A73-17526

Resonance acceleration of low-energy protons in the radiation belts of the earth.

16 p2051 A73-32751

MOLTEN SALT ELECTROLYTES

Cell assemblies for a molten carbonate fuel battery. I - The construction of cell assemblies. II - Electrolyte paste discs for molten carbonate fuel cells.

04 p0406 A73-14985

MOLYBDATES

Some optical properties of CaMoO4 single crystals

01 p0088 A73-10626

A mass spectrometric investigation of reactions involving tungsten and molybdenum with potassium-seeded H2/O2 flames.

10 p1186 A73-23554

Molybdenum metal by the aluminothermic reduction of calcium molybdate.

10 p1234 A73-24430

Investigation of cobalt molybdate polymorphism

15 p1887 A73-31207

MOLYBDENUM

Dislocation damping in ultrasound-irradiated molybdenum single crystals

01 p0061 A73-10251

Dislocation density in Mo single crystals subject to uniaxial tensile stress or sphere-produced indentation, evaluating plastic strain level

01 p0063 A73-10484

Hot extrusion and properties of rods from sintered molybdenum and tungsten blanks.

01 p0065 A73-10817

Impurities effect on Mo plastic properties and toughness, suggesting lower vacuum arc welding rates and increased electron beam zone refining runs

01 p0066 A73-11343

Diffusive boronizing of molybdenum and niobium in boron carbide powder

02 p0178 A73-11544

Consolidation of tungsten and molybdenum powders.

03 p0322 A73-13262

Effects of the state of the surface and of titanium films on the dislocation structure of surface layers in molybdenum single crystals

03 p0326 A73-13969

Effect of hydrogen on internal friction in molybdenum

03 p0327 A73-13975

Adsorbed barium films on tungsten and molybdenum /011/ face.

04 p0460 A73-14867

The mechanism of stage III recovery of electron irradiated molybdenum.

04 p0461 A73-14870

Dislocation interstitial impurities interactions in high purity Mo, using dislocation damping techniques

04 p0462 A73-15304

Studies of the elastic properties of molybdenum

04 p0464 A73-15372

On the point defect production in electron-irradiated molybdenum.

06 p0705 A73-17832

Investigation of molybdenum after exposure to single-charge helium atom radiation

06 p0707 A73-17909

Creep in molybdenum single crystals at 0.57 of the melting temperature

06 p0708 A73-18047

Structural changes in molybdenum single crystals during high temperature creep

06 p0708 A73-18048

Contribution to the study of the effect of molybdenum on the ageing kinetics of maraging steels.

07 p0838 A73-19499

Temperature dependent pitting corrosion tests of Mo containing austenitic stainless steels

07 p0840 A73-20354

Parametrization of low-temperature deformation characteristics in single crystals of molybdenum.

09 p1099 A73-21928

Intercrystalline molybdenum fracture

09 p1099 A73-21971

Deformation and rupture of molybdenum under conditions of creep

09 p1100 A73-22161

Mechanical behaviour of molybdenum and tantalum under high pressures at elevated temperatures.

09 p1105 A73-23018

Ductility of recrystallized molybdenum as a function of oxygen concentration and grain size

09 p1108 A73-23231

Creep and creep-rupture-strength of titanium strengthened by molybdenum fibers

10 p1233 A73-24356

Molybdenum metal by the aluminothermic reduction of calcium molybdate.

10 p1234 A73-24430

Thermodynamic equilibrium calculation and demonstration of Mo siliciding by circulation method in hydrogen-free gaseous medium containing silicon chlorides

10 p1227 A73-24961

The effect of an addition of molybdenum on the quenched and aged structure of a Ti-1 wt % Si alloy.

11 p1384 A73-26048

Effect of prestraining on the brittleness of molybdenum.

12 p1511 A73-27058

Creep and long-term strength of molybdenum with a boron silicide coating in vacuum at temperatures from 1000 to 1400 C

12 p1512 A73-27257

Influence of plastic deformation on the electrical resistance of molybdenum single crystals
12 p1512 A73-27260

Mechanical properties of strip molybdenum with a polygonized single-crystal structure
12 p1513 A73-27265

Investigation of structure and imperfections in molybdenum single crystals grown by electron-beam zone refining techniques
13 p1631 A73-28106

Dislocation structure in molybdenum single crystals after deformation at 293 and 400 deg K.
13 p1634 A73-28221

Assessment of the degree of plastic deformation in a crater with ball imprint.
14 p1810 A73-30309

Influence of stress concentrations on the mechanical properties of cast molybdenum with protective coatings
14 p1763 A73-30688

The interaction of tungsten and molybdenum melts with gaseous oxygen
15 p1890 A73-31924

Pre-macro yielding and the orientation dependence of the 'shear' stress in molybdenum single crystals.
16 p2025 A73-33197

Molybdenum evaporation rates in oxygen, air, and water vapor at high temperatures and low pressures
16 p2026 A73-33956

Molybdenum bicrystals mechanical properties dependence on mismatch angle under bending with torsion and brittle cleavage under critical stresses
17 p2189 A73-34636

Phase formation investigation in the Mo-Al and W-Al systems when the Mo and W surfaces are saturated with aluminum by diffusion from a vapor phase in a vacuum
18 p2318 A73-35879

Stresses in molybdenum coatings obtained by thermal decomposition of Mo/CO/6
18 p2319 A73-35892

Influence of temperature and strain rate on the load-elongation curve and plastic properties of molybdenum
18 p2324 A73-36801

Influence of plastic strain on the paramagnetic susceptibility of molybdenum single crystals
18 p2324 A73-36802

Molybdenum-oxygen-sulfur fuel cell anode catalysts capable of oxidizing low cost fuels in acid electrolytes
19 p2390 A73-38401

Anisotropy of low-temperature plasticity and the tendency of deformed molybdenum toward exfoliation
20 p2578 A73-39377

Effect of ultrasound on the dislocation structure and mechanical properties of molybdenum
20 p2579 A73-39745

A detailed investigation of slip line pattern and sub-surface dislocation structure of molybdenum single crystals.
21 p2722 A73-41566

Molybdenum sintering and the molybdenum-oxygen-carbon system.
21 p2722 A73-41585

Excitation of surface molecular orbitals on the /100/ face of molybdenum
21 p2722 A73-41597

The deformation and fracture of molybdenum under creep conditions.
22 p2874 A73-42109

Anomalous behaviour during interdiffusion in the system Nb-Mo.
22 p2876 A73-42340

Investigation of the thermal expansion of molybdenum and tungsten at high temperatures.
[ECTP PAPER E-5] 22 p2876 A73-42406

The melting point of molybdenum as a secondary fixed point on the International Practical Temperature Scale.
[ECTP PAPER G-5] 22 p2877 A73-42407

Investigation of the substructure in molybdenum single crystals deformed by compression
23 p2991 A73-43712

Impurity diffusion of iron in molybdenum.
23 p2994 A73-44157

MOLYBDENUM ALLOYS

NT RENE 41

Structural changes during the deformation of molybdenum alloys
01 p0061 A73-10252

Grain growth in alloyed molybdenum under conditions of creep
01 p0063 A73-10486

Mechanical properties of molybdenum alloys.
01 p0065 A73-10818

C and Re effects on brittleness threshold temperature and plasticity of Mo-Re alloy
01 p0066 A73-11342

Superconducting Mo-Re alloy thin film prepared by sputtering and deposition onto sapphire substrate, measuring transition temperature, critical current and magnetic field characteristics
02 p0200 A73-11841

Microstructure and phase relations for Ti-Mo-Al alloys.
02 p0182 A73-12751

Alloy hardening and softening in binary molybdenum alloys as related to electron concentration.
03 p0323 A73-13300

Microstructure and plastic deformation of the Ni4Mo alloy.
03 p0325 A73-13804

Ni-Mo-W alloys hardness rating and corrosion resistance to sulfuric and hydrochloric acids, discussing dispersion hardening, quenching and aging treatments
03 p0327 A73-14001

Carbide hardening of chromium-molybdenum-vanadium steel.
03 p0327 A73-14005

Mo addition effect on high temperature creep resistance and diffusion activation energy of Nb alloys tested in torsion and tension at 1100-1500 C in vacuum
03 p0328 A73-14018

Microstructures and transformation kinetics of continuously cooled carbon free Fe-Mo-Ni alloys.
04 p0463 A73-15311

Molybdenum corner in Mo-Ti-B and Mo-Zr-B ternary systems
04 p0464 A73-15494

A stochastic model of creep in the heat-resistant low-alloy CrMoV steel
06 p0705 A73-17846

Influence of cobalt on the maraging of Fe-Ni-Mo alloys
06 p0705 A73-17876

Temperature and concentration effects on heterodiffusion coefficient of diffusion welded Mo-W alloy rods
06 p0707 A73-17907

Effects of heat treatment on the properties of a molybdenum-carbon-nickel alloy and joints in it.
07 p0840 A73-20371

Effects of composition and structure on the creep strength of molybdenum bearing ferritic steels.
08 p0982 A73-21796

Investigation of partially dissolved secondary-phase precipitates in a molybdenum-based alloy
09 p1098 A73-21849

Observations on the interaction of twins with grain boundaries in Mo-35 at.% Re alloy.
09 p1100 A73-21982

Recrystallization in Ti-15 Mo base beta titanium alloys.
09 p1103 A73-22423

Interaction between zirconium diboride and molybdenum
09 p1105 A73-22981

Stability of structure and mechanical properties of molybdenum under prolonged influence of temperature and stress.
09 p1106 A73-23160

Temperature range of maximum aging of Mo-Re-C alloys after quenching and tempering, noting carbon solubility effects due to Re content
09 p1106 A73-23187

Structural features of surface layers in molybdenum alloy sheets
09 p1106 A73-23188

Electrothermal annealing via electrical heating in vacuum for improved plasticity of thin walled molybdenum alloy elements after cold working
09 p1107 A73-23196

Molybdenum and nickel alloying effect on time and temperature range of reversible temper brittleness of chromium steels
09 p1107 A73-23200

Effect of carbon on the fine structure of cast molybdenum
09 p1108 A73-23232

Determination of the composition of Ni-NiMo eutectic by the zone recrystallization method
09 p1108 A73-23239

Work function of the principal faces of single crystals of rhenium solutions in molybdenum
10 p1231 A73-23818

Mechanical properties of recrystallized molybdenum containing vanadium microadditions
10 p1233 A73-24361

Interaction of molybdenum with elements of the iron group and carbon
12 p1510 A73-26903

Mo-W-B alloy phase equilibria, isothermal cross sections, liquidus, solubility and mechanical properties by thermal, X ray and microstructural analyses
12 p1510 A73-26904

Mo-Nb-Ta alloys phase and composition-hardness diagrams for 20-1100 C, establishing mutual solubility of system components
12 p1510 A73-26905

Fracture characteristics of thermally strengthened titanium beta-alloys
12 p1510 A73-26914

Determination of the boundaries of single-phase edge regions in the Mo-Cu-Ni system in solid state
12 p1513 A73-27559

Quasi-ternary Mo-TiC-ZrC system
13 p1630 A73-28014

Experimental and thermodynamic study of the equilibria between ferrite, austenite and intermediate phases in the Fe-Mo, Fe-W, and Fe-Mo-W systems.
13 p1633 A73-28136

A high-temperature thermodynamic investigation of the Nb-Mo system.
13 p1633 A73-28140

High temperature tests of microalloying effect on creep and stress rupture characteristics of hot rolled and annealed Mo alloys
13 p1643 A73-29605

Increase in the boundary strength of cast electron-beam-melted molybdenum by microadditions of vanadium.
13 p1643 A73-29634

Grain growth during creep of alloyed molybdenum.
14 p1759 A73-30311

Characteristics of the decomposition of an interstitial-impurities solid solution in molybdenum during recrystallization
14 p1760 A73-30589

German monograph - Investigations concerning the hot working of heterogeneous iron-molybdenum alloys with differing precipitation distribution.
14 p1762 A73-30670

Influence of annealing temperature on the changes in the chemical and phase compositions of the intercrystalline boundaries of weakly-alloyed molybdenum
14 p1764 A73-30865

Molybdenum-rhenium alloy microstructure changes due to nitriding in ammonia vapors from metallographic and X ray structural analysis
15 p1887 A73-31206

Mo-W-C phase equilibria study at 1000 C, obtaining isothermal cross sections for various carbon contents from X ray and microstructural analysis
15 p1888 A73-31598

Saturation of Kh18N10T steel by molybdenum from the vapor phase
15 p1889 A73-31807

Properties of HSLA steels, with and without molybdenum.
15 p1891 A73-32169

Phase transformations in alloys of the titanium-molybdenum system
15 p1893 A73-32517

Transformations during heat treatment of Ti-Mo system alloys with additions of aluminum, zirconium, and tin
15 p1893 A73-32518

Properties of the 4201 alloy at elevated temperatures
15 p1894 A73-32528

Influence of structure and of stress concentration on the mechanical properties of Ti-Ta-Mo system alloys
15 p1894 A73-32533

Highly permeable nickel-iron-molybdenum alloys containing 33 to 37% nickel
16 p2026 A73-33958

Certain physical properties of a new alloy of the nickel-rhenium-molybdenum system
17 p2186 A73-34137

AC polarographic determination of sulfur in molybdenum-rhenium alloy.
17 p2118 A73-34276

The martensite composition in quenched alloys of the Ti-Mo system
17 p2187 A73-34374

Investigation of molybdenum-rich Mo-Ni-C, Mo-Ni-Zr, and Mo-Zr-Ni-C alloys
17 p2188 A73-34569

Ti-Ta-V-Mo system phase diagram in Ti corner region for 600-900 C, investigating solubility, electrical resistivity and hardness
17 p2189 A73-34570

Effect of group VIII elements on the temperature of plastic-to-brittle transition of states in molybdenum-carbon alloys
17 p2189 A73-34576

Inter crystalline failure in recrystallized low-alloyed molybdenum alloys
17 p2189 A73-34577

Effect of small group-VIII metal additions on the structure and properties of cast molybdenum
17 p2189 A73-34578

Effect of carbon on the structure and properties of molybdenum
17 p2189 A73-34582

X ray diffraction analysis of Mo-Ta and Mo-C solid solutions, relating transition and nontransition metal electronic structures and stacking fault energy
18 p2325 A73-36808

Limit of the two-phase region of Mo/Ni, Cu/ and Cu/Ni, Mo/ solid solutions in the Mo-Cu-Ni system
18 p2325 A73-36859

Mo-W alloys mechanical characteristics dependence on temperature and W content
19 p2439 A73-37265

The effect of molybdenum on gamma prime coarsening and on elevated-temperature hardness in some experimental nickel-base superalloys.
20 p2576 A73-39029

Mechanical properties of electron-beam-melted molybdenum and dilute Mo-Re alloys.
20 p2576 A73-39032

Influence of alloying with elements of group VIII on the mechanical properties of a molybdenum alloy containing carbon in the cast and recrystallized states.
20 p2577 A73-39366

Experimental investigation of the integral hemispherical emissivity of refractory metals and alloys.
20 p2593 A73-39426

Effect of the degree of plastic deformation on the structure and mechanical properties of low-alloy molybdenum.
20 p2579 A73-39741

The homogeneity regions of superconducting phases in the molybdenum-platinum system.
21 p2717 A73-40320

A study of the extraction of oxygen from molybdenum by dissolving it in metallic carbon-containing melts in a vacuum.
21 p2717 A73-40479

A study of the heat resistance of Nb-Mo alloys containing titanium and zirconium.
21 p2718 A73-40489

Phase diagram thermal sections and concentration corner of Mo-Zr-B system by microstructure, X ray and electron microscope analysis.
21 p2718 A73-40490

Heat resistance of chromium-nickel and chromium-nickel-molybdenum steels with additions of boron.
21 p2718 A73-40734

Preparation and properties of materials containing titanium carbide.
21 p2719 A73-40851

Interaction of interstitial impurities with iron-subgroup metals in as-cast molybdenum-based dilute solid solutions.
22 p2873 A73-42090

Structural transformations in molybdenum-carbon alloys during quenching and aging.
22 p2874 A73-42091

Elastic properties of alloys of the Ti-Al-Mo system as a function of the composition and heat treatment.
22 p2874 A73-42095

Electrical resistivity and thermal conductivity of alloys of the tungsten-molybdenum system.
[ECTP PAPER B1-6] 22 p2876 A73-42402

Isothermal cross sections of the phase diagram of the nickel-molybdenum-tungsten system at 1200 and 700 C.
22 p2877 A73-42459

Interaction of molybdenum with cobalt and carbon.
22 p2877 A73-42460

The influence of carbon on the interdiffusion of Mo and Ni.
22 p2878 A73-42579

Mo content influence on heat resistant Ni base alloys corrosion and oxidation resistance and gamma-prime phase solution temperature and amount.
23 p2989 A73-43435

Substitution of molybdenum for tungsten in heat resistant cobalt-base alloys.
23 p2989 A73-43436

Investigation of the structure and properties of annealed alloys of the Ti-Mo system.
23 p2990 A73-43484

Influence of alloying additives on the structural changes in a nickel-molybdenum composite.
23 p2991 A73-43488

Development of corrosion resistant filler metals for brazing molybdenum.
23 p2986 A73-44004

Steady-state creep characteristics of an Fe alloy containing 3.5 at.% Mo.
23 p2994 A73-44153

Investigation of the softening processes in molybdenum and its alloys under conditions of creep.
23 p2995 A73-44281

Saturation of steel Kh18N10T with molybdenum from the vapor phase.
24 p3100 A73-45270

MOLYBDENUM CARBIDES

Activity of carbon and solubility of carbides in the fcc Fe-Mo-C, Fe-Cr-C, and Fe-V-C alloys.
02 p0183 A73-12755

The effect of carbon and oxygen on the brittleness characteristics of molybdenum.
08 p0978 A73-21417

Structural transformations in molybdenum-carbon alloys during quenching and aging.
22 p2874 A73-42091

MOLYBDENUM COMPOUNDS

NT MOLYBDATES

NT MOLYBDENUM DISULFIDES

NT MOLYBDENUM OXIDES

Optical band gap energies and stacking sequences of molybdenum tellurides and tungsten selenides derived from dielectric constant measurements.
04 p0482 A73-14868

Mo disilicide-Ti disilicide system phase diagram based on metallographic, X ray structural and high temperature differential thermal analyses.
05 p0587 A73-16846

Dinuclear anions of molybdenum VI and tungsten VI with the 'fluoro' and 'oxalato' coordinates.
05 p0547 A73-17218

Thermodynamic characteristics of molybdenum silicides in the temperature interval between 400 and 1200 K.
06 p0710 A73-18560

Thermodynamic properties of molybdenum silicides in the temperature range 400-1200 K.
16 p2026 A73-33585

Effect of interphase boundaries on the kinetics of molybdenum silicizing.
18 p2318 A73-35881

Molybdenum sintering and the molybdenum-oxygen-carbon system.
21 p2722 A73-41585

MOLYBDENUM DISULFIDES

Molybdenum disulfide in oils and greases under boundary conditions.
[ASME PAPER 72-LUB-37] 03 p0335 A73-14345

Electron microscopic investigation of lubricating mechanism of dry and oil-suspended molybdenum disulfide powder, discussing physical and chemical properties effects.
05 p0589 A73-17067

Evaluation of the lubricating properties of chemically upgraded MoS₂.
07 p0842 A73-19553

Alkali metal intercalates of molybdenum disulfide.
08 p0937 A73-21174

High field superconductivity in alkali metal intercalates of MoS₂.
11 p1410 A73-26745

Structure of sputtered molybdenum disulfide films at various substrate temperatures.
[ASLE PREPRINT 73AM-3C-3] 17 p2196 A73-34988

MOLYBDENUM OXIDES

Transition of oxide film on a molybdenum surface from a two-dimensional structure to a three-dimensional structure.
06 p0738 A73-18617

Processes determining the composition of a two-dimensional oxide film on a molybdenum surface.
09 p1098 A73-21886

Comparative estimation of thermodynamic characteristics for reduction of tungsten and molybdenum oxides.
09 p1107 A73-23226

Reduction kinetics and phase transformations of tungsten and molybdenum oxides.
13 p1636 A73-28938

Composition of a two-dimensional oxide film on a molybdenum surface.
17 p2186 A73-34309

Specific surface changes in tungsten and molybdenum oxides during reduction processes.
24 p3099 A73-44738

MOLYBDENUM SULFIDES

NT MOLYBDENUM DISULFIDES

Frictional behaviour of molybdenum disulfide in high vacuum.
04 p0454 A73-14997

MOMENT DISTRIBUTION

A finite element, linear programming method for the limit analysis of thin plates.
07 p0906 A73-19026

Pure moment loading of axisymmetric finite element models.
09 p1158 A73-22391

Approximate calculation of the moments of the distribution of the maxima of correlated Gaussian random sequences.
12 p1485 A73-27621

A variant of the moment theory of elasticity for a one-dimensional continuous medium with a non-homogeneous periodic structure.
13 p1698 A73-29085

On kinematics and statics of finite-strain force and moment stress elasticity.
17 p2252 A73-35829

Dirac's distribution in the study of statically indeterminate beams.
18 p2364 A73-36491

Post-buckling behavior of cold-formed thin-walled stainless steel beams.
19 p2496 A73-37481

Neighboring body effects on bluff body tipping moment.
20 p2507 A73-39520

Stability of the state of moment stress of a toroidal shell.
20 p2624 A73-39650

Bounds estimation for normalized second spectral moment of random radar signal process in terms of measured quantities statistics without weighting.
21 p2650 A73-40343

Closed-form lift and moment for Osborne's unsteady thin-airfoil theory.
21 p2632 A73-40442

Moments acting on a spherical rotor with magnetically suspended bearings.
22 p2860 A73-42360

Plane boundary layer equations for viscous incompressible fluid with asymmetric stress tensor produced by moment stresses and mass moments.
23 p2968 A73-43922

Boundary layer equations of magnetohydrodynamics with moment stresses.
23 p3015 A73-44385

MOMENTS

NT BENDING MOMENTS

NT DIPOLE MOMENTS

NT DISTRIBUTION MOMENTS

NT ELECTRIC MOMENTS

NT LOADING MOMENTS

NT MAGNETIC MOMENTS

NT MEAN

NT MOMENTS OF INERTIA

NT PITCHING MOMENTS

NT ROLLING MOMENTS

NT STABILITY DERIVATIVES

NT STANDARD DEVIATION

NT TORQUE

NT VARIANCE (STATISTICS)

NT YAWING MOMENTS

Zero and first velocity moments of Boltzmann equation with complications placed on Ohm Law in plasmas, considering momentum exchange.
06 p0730 A73-18462

Fluctuating lift and moment coefficients for cascaded airfoils in a nonuniform compressible flow.
09 p1028 A73-22432

Calculation of structures by superrelaxation iterations over moments.
19 p2497 A73-37549

Flight vehicle extensive attitude control theory, deriving kinematic relations for optimal control moment selection to ensure required rotation.
21 p2780 A73-40385

Aggregation scheme solution for uniform asymptotic stability of large dimensionality system, using L-problem moment theory.
24 p3112 A73-45505

MOMENTS OF INERTIA

Moments of inertia for fluid-filled rotating bodies, solving Laplace and Navier-Stokes equations for cylinder and sphere.
01 p0030 A73-10089

Instability of rotation about a centroidal axis of maximum moment of inertia.
01 p0077 A73-10743

Certain problems of dynamics and accuracy of gyroscopes in gimbals.
01 p0053 A73-11197

Intersection line of axes cone with sphere and locus of angular velocity vectors for uniform gyroscope rotation with different moments of inertia.
02 p0191 A73-11764

Equations of motion for Kovalevskaja gyroscope uniform rotation about axes differing from inertia ellipsoid principal axes, noting sufficient stability conditions.
02 p0167 A73-11765

Newtonian force field effect on gyroscope motion for coordinate axes coincident with inertia tensor axes, solving equations of motion by energy integral.
02 p0192 A73-11769

Lunar interior density constraints from moon moment of inertia and mean density calculations and seismometer data on lunar crust mass and density.
02 p0220 A73-12484

Rotatory inertia and hub radius effects on transverse vibrational characteristics of clamped Rayleigh beam, using Galerkin method.
03 p0388 A73-13316

Optimal efficiency of satellite passive nutation damper, noting system moment of inertia and flywheel axis relationship and viscous friction coefficient.
03 p0383 A73-14558

Buckling of columns with variable moment of inertia.
05 p0633 A73-16538

Gyroscopic device for compensating external moments of sextants or binoculars optical axis due to spontaneous hand movements.
09 p1084 A73-22673

Computation of the deflections of straight beams with any variation of the moment of inertia by the method of the three unknowns.
10 p1287 A73-23617

Incomplete/complete feedback and off-on control moments for prescribed orientation of solid body in rotational motion.
10 p1248 A73-23744

Periodic small parameter solutions of rotary gyroscope motions about axis of ellipsoid of inertia, using Euler-Poisson equations.
10 p1220 A73-24678

Singularities and collisions in linear many body problem of Newtonian gravitational systems, noting moment of inertia role.
10 p1284 A73-24788

Nonsingular control, determining optimum shape of straight bar under stress and inertial moment restrictions.
12 p1482 A73-26793

- Dynamic figure of the moon and the density distribution in the lunar interior 12 p1546 A73-27866
- Gyroscopic moment effect on rotating shafts lowest critical velocity, plotting convergence characteristics 15 p1949 A73-31668
- Steady motions of three nonpoint bodies moving freely in space with centers of inertia describing uniform circle 16 p2059 A73-32908
- Torsional vibrations of a bar of variable cross-section. 16 p2079 A73-33075
- Motion of a free solid body about its center of mass when the body is stabilized by rotation about a non-principal axis of inertia 18 p2336 A73-36163
- Earth-moon system angular momentum loss from paleontological data and earth rotational moment of inertia effect 18 p2354 A73-36509
- Mass property control of a synchronous meteorological satellite scanning experiment. [SAWE PAPER 964] 19 p2492 A73-37882
- Inertial symmetrization of large spin-stabilized spacecraft. [SAWE PAPER 965] 19 p2493 A73-37883
- Dynamical figure of the moon and the density distribution of the lunar interior. 20 p2608 A73-39240
- Dynamics of the rotary motions with respect to the center of mass of a system of solids with a variable geometry of the masses 23 p3007 A73-44187
- Inertia effects in MHD lubricated hydrostatic thrust bearing under axial magnetic field investigated by energy integral method, obtaining flow velocity and load carrying capacity 24 p3092 A73-44410

MOMENTUM

NT ANGULAR MOMENTUM

MOMENTUM ENERGY

U KINETIC ENERGY

MOMENTUM PRECESSION

U PRECESSION

MOMENTUM THEORY

- Optimal stabilization of nonlinear control systems for given region of initial perturbations, reducing optimal synthesis to moments problem 01 p0077 A73-10671
- Momentum formulae derived for quasi-monochromatic wave packets of transverse and longitudinal waves in plasma without magnetic field 02 p0195 A73-11522
- Linearly elastic materials theory covering kinematics, momentum balance, constitutive relation, boundary value problems and field equations 02 p0233 A73-11977
- Binary stars tidal evolution theory, deriving energy and momentum equations for arbitrary internal structures 02 p0218 A73-12411
- Axial flow turbomachines annulus wall boundary layer growth calculation methods, deriving momentum integral equations from passage averaged equations of motion through cascaded blades 03 p0249 A73-14645
- An explicit numerical method for the solution of jet flows. [ASME PAPER 72-WA/FE-20] 04 p0435 A73-15846
- Relative importance of terms in the turbulent-energy and momentum equations as applied to the problem of a surface roughness change. 05 p0591 A73-16191
- Protoplanet formation models with floccule accumulation, discussing momentum considerations and supersonically turbulent collapsing gas cloud 05 p0625 A73-17318
- Multiplicity link to transverse momenta in ultrahigh energy nucleon-nucleon interaction processes, considering resonance formation and expected average elasticity 06 p0743 A73-17830
- Semiclassical theory of inelastic collisions. II - Momentum-space formulation. 06 p0726 A73-18262
- Electromagnetic interactions of cosmic ray muons in iron. II - Momentum dependence of the interaction probabilities. 06 p0743 A73-18387
- A simple integration method for the momentum and energy theorem of boundary layer theory 14 p1745 A73-30300
- Energy and momentum theorems in magnetospheric processes. 15 p1871 A73-31846
- Momentum and moment of momentum differential equations of turbulent flow, reviewing and extending Mattioli theory to three dimensional flow 15 p1865 A73-32119
- An upper bound on the stress in plane Couette flow. [ASME PAPER 73-FE-8] 17 p2152 A73-35007
- The momentum-energy tensor of an electromagnetic field 21 p2739 A73-40446

The laws of conservation of energy and momentum during emission of electromagnetic waves /photons/ in a medium and the energy-momentum tensor in macroscopic electrodynamics 21 p2739 A73-40447

The momentum potential field description of fluctuating fluid motion as a basis for a unified theory of internally generated sound. [AIAA PAPER 73-1000] 24 p3077 A73-44835

MOMENTUM TRANSFER

- Book on momentum, heat and mass transfer at various interfaces based on Prandtl eddy mixing length concept 01 p0030 A73-10049
- Stellar structure and angular momentum evolution of rotating stars, describing interaction in terms of redistribution processes of momentum 01 p0094 A73-10054
- An experimental and analytical investigation of angular momentum exchange in a rotating fluid. 01 p0073 A73-10444
- Cryoprobe with truncated circular cross sectioned Cu cone with copper slug heat sink for momentum flow rate measurement in hypersonic low density flow 01 p0003 A73-10755
- Multiple scattering of cosmic ray muons in the range 10-70 GeV/c. 01 p0091 A73-10787
- Momentum transfer interaction of a laser-produced plasma with a low-pressure background. [AD-755558] 02 p0197 A73-12062
- Momentum deposition by atmospheric waves, and its effects on thermospheric circulation. 02 p0162 A73-12297
- A numerical hydrodynamic study of coalescence in head-on collisions of identical stars. 02 p0223 A73-12727
- The transmission of mass and angular momentum from a satellite or planetary system to its primary. 02 p0225 A73-12810
- The relation between momentum transfer and capture and total scattering cross sections for ion-dipole collisions. 02 p0195 A73-12842
- Convective storm updraft shape calculation based on horizontal momentum changes in rising air, noting effects of mixing and aerodynamic drag 05 p0592 A73-16195
- A mechanism for the exploding granule phenomenon. [AD-759887] 05 p0621 A73-17029
- Transfer and moment equations obtained for radiation transfer in spherically moving medium with relativistic corrections, discussing matter-radiation coupling and energy conservation 05 p0612 A73-17382
- Optically thin stellar winds in early-type stars. 07 p0873 A73-19061
- Analysis of internally generated sound in continuous materials. III - The momentum potential field description of fluctuating fluid motion as a basis for a unified theory of internally generated sound. 07 p0909 A73-19097
- High-energy electron-beam deposition onto a hot graphite surface. 08 p0990 A73-21210
- Ultrarelativistic plasma momentum loss perpendicular to pulsar magnetic field, considering synchrotron compression of electrons leading to emission mechanisms 09 p1144 A73-22172
- Primordial random motions and angular momenta of galaxies and galaxy clusters. 11 p1427 A73-26601
- Momentum and mass transfer in atmospheric boundary layer from surface drag and evaporation data for weather prediction models 13 p1652 A73-28275
- Lunar rotation secular acceleration and tidal friction related to earth rotational velocity and creep properties 13 p1677 A73-28378
- On the torques due to tidal friction of the oceans and adjacent seas. 13 p1607 A73-28409
- Integral properties of viscous channel or pipe flow satisfying mixed no-slip and no-shear conditions from total momentum flux considerations 13 p1599 A73-28417
- Solar rotation angular velocity variation with heliographic latitude, depth and time, considering superficial circulation as cause of angular momentum transport 14 p1797 A73-30139
- Application of the momentum translation method to multiphoton ionization of hydrogen by intense electromagnetic fields. 16 p2039 A73-33864
- Momentum transfer to laser-irradiated targets, indicating the nonlinear interaction force. 17 p2184 A73-34897
- State space attitude control synthesis for a satellite with flexible appendages. 17 p2239 A73-34951

Momentum transfer and total scattering cross sections for ions with polar molecules. 17 p2213 A73-35178

Earth-moon system angular momentum loss from paleontological data and earth rotational moment of inertia effect 18 p2354 A73-36509

Angular momentum decrease of slowly rotating Kerr black holes due to stationary distribution of outside matter 21 p2766 A73-40314

Ceramic component strength degradation by projectile impacts in terms of momentum and elasticity relation 21 p2723 A73-40892

Impulse reaction resulting from the in-air irradiation of aluminum by a pulsed CO2 laser. 21 p2715 A73-40960

Solar wind interaction with Comet Bennett near earth, examining photographs for momentum flux change-ion tail kink correlations 21 p2763 A73-41501

Dense argon plasma expansion into vacuum or low density partially ionized hydrogen plasma, examining momentum transfer, electron density and electric field effects 22 p2891 A73-42239

Large transverse momenta and the structure of extensive air shower cores 23 p3022 A73-43548

Cumulus-scale vertical transport of mass, heat and momentum calculated from radar and rain gage precipitation measurement 23 p3002 A73-43596

Laser supported gaseous detonation wave propagation above solid surface, calculating momentum transfer as functions of laser energy, pulse duration, and beam and target areas 24 p3097 A73-45455

Determination of the impulses and moments imparted by shock waves to bodies of revolution 24 p3055 A73-45542

MONATOMIC GASES

- Circular orifice flow of monatomic rarefied gas between two reservoirs, observing pressure ratio effect 03 p0295 A73-13773
- Book - Kinetic theory. Volume 3 - The Chapman-Enskog solution of the transport equation for moderately dense gases. 03 p0345 A73-13991
- Quantum kinetic equation for monatomic and molecular gases optical characteristics calculation, considering spontaneous emission spectrum of atoms 04 p0459 A73-15565
- Some problems of gas-solid surface interaction. 05 p0638 A73-16177
- Electron energy distribution in a low-temperature plasma. 06 p0727 A73-17419
- Monatomic gas flow around uniformly heated sphere for small Reynolds numbers, noting drag decrease due to thermal stresses 06 p0646 A73-18884
- Viscosity of atomic hydrogen. 11 p1397 A73-25075
- A simple theory of breakdown for nightlight gases in fields of any frequencies ranging from low to optical 13 p1663 A73-29165
- Test of statistical models for gases with and without internal energy states. 14 p1818 A73-30653
- Monatomic gas flow around uniformly heated sphere for small Reynolds numbers, noting drag decrease due to thermal stresses 15 p1824 A73-32409
- Effects of translational disequilibrium on the structure of a shock wave in an ionized monatomic gas 22 p2895 A73-43045
- Gasdynamic equations for low temperature monatomic gas, showing Wigner distribution function independence of density gradient in agreement with nonequilibrium statistical thermodynamics concepts 23 p2939 A73-43704

MONAURAL SIGNALS

Loudness enhancement following contralateral stimulation. 01 p0013 A73-10827

MONEL [TRADEMARK]

Study of fretting wear in titanium, Monel-400, and cobalt-25 percent molybdenum using scanning electron microscopy. [ASLE PREPRINT 73AM-8A-3] 17 p2190 A73-34993

MONITORS

- Analysis of a nonisothermal, spherical detector for monitoring the earth's radiative energy budget. 01 p0045 A73-10382
- Molecular fluorine concentration and pressure change monitor based on UV absorption spectrum during chemical reactants mixing, noting measurement accuracy 02 p0168 A73-11967

MONOCHROMATIC RADIATION

Gas path analysis applied to turbine engine condition monitoring.
[AIAA PAPER 72-1082] 03 p0354 A73-13405

Design and function of sweat sensor to monitor motion sickness sweat response
03 p0269 A73-14160

Broad-band isotropic electromagnetic radiation monitor.
03 p0310 A73-14493

Monitoring and modeling of airport air pollution.
04 p0432 A73-14891

The prediction of team monitoring performance under conditions of varied team size and decision rules.
05 p0543 A73-16710

Satellite frequency division multiple access communication net, examining channel monitoring and self regulating downlink power output for performance improvement
09 p1053 A73-23363

Microwave rotational spectroscopy - A technique for specific pollutant monitoring.
10 p1221 A73-24891

Computer executive system for design automation file network creation and monitoring to permit input/output operations, storage information updating and display
[AIAA PAPER 73-355] 11 p1334 A73-25492

Automatic checkout and monitoring in the AN TPQ-27 radar system.
13 p1585 A73-29210

Independent Landing Monitor for economic Category 3 operation with fail-operational autoland, fog dissipation or fail-passive autoland plus visibility augmentation
15 p1911 A73-32499

Air quality monitoring instruments involving atmospheric pollution chemiluminescent reactions and CO IR, optical absorption and laser detectors
16 p2016 A73-33402

Monitoring for microbial flora contamination on spacecraft surface, discussing cultural techniques and sampling methods for microorganisms detection and sterilization
16 p1976 A73-33698

Monitoring interruptions at the satellite earth station.
17 p2122 A73-34870

New methods for studying gas solid reaction kinetics using automated resistance monitoring.
17 p2175 A73-35756

Nuclear submarine atmospheric constituent monitoring, covering mass spectrometers, IR carbon monoxide sensors, system development, requirements testing and spacecraft applications
[ASME PAPER 73-ENAS-9] 19 p2399 A73-37970

Gas management system for control, bleeding, evacuating and radiological and pressure monitoring of He atmosphere in multihundred watt heat source
19 p2457 A73-38428

Development of a practical remote sensing water quality monitoring system.
20 p2567 A73-39830

ILS capability improvements on localizer and glide-slope antenna arrays and monitors, considering effects of reflecting objects on or near aerodrome and terrain
21 p2736 A73-40049

ERTS-1 satellite-borne multispectral scanner remote sensor for global pollution monitoring, geological and heat balance surveys, and storm and earthquake caused damage
21 p2692 A73-41520

Microelectronic circuitry for monitoring stray electromagnetic energy coupled into electroexplosive device, using fiber optic transmission with photovoltaic energy conversion to eliminate wiring caused interference
22 p2822 A73-41794

The solar radio patrol network of the USAF and its application.
23 p2958 A73-43371

MONOCHROMATIC RADIATION

Interaction of opposed beams of electromagnetic waves in a transparent nonlinear medium
01 p0016 A73-10208

Nonlinear interaction of two monochromatic Langmuir waves
01 p0016 A73-10209

Talbot shearing interferometer based on Fourier imaging behind grating illuminated by plane monochromatic wave with spatial filtering, obtaining radial and lateral derivatives
01 p0053 A73-11227

Planetary nebulae NGC 7635, 7008, 1514, 650-1, 7139, 3587, 6781 and 6543 monochromatic images, centering filters on H alpha, N II and O III forbidden lines
02 p0221 A73-12703

Landau attenuation in a plasma excited by a monochromatic electron beam
05 p0601 A73-16394

Monochromatic plasma wave instability due to induced scattering on thermal plasma electrons and ions with and without magnetic field
05 p0604 A73-17361

Nonlinear damping of potential monochromatic waves in inhomogeneous plasma, obtaining resonance particle distribution function
06 p0728 A73-17967

Wave spectrum transformation in an active nonlinear medium
07 p0792 A73-19907

On the near- and far-field radiation patterns generated by the non-linear interaction of two separate and non-planar monochromatic sources.
08 p0988 A73-21469

Visual sensitivity in the presence of alternating monochromatic fields of light.
08 p0932 A73-21567

Quasi-monochromatic radiation pulse reflection from rough surfaces, analyzing echoes statistical properties
09 p1120 A73-22575

Solution of equations for one-dimensional propagation of a monochromatic light pulse in absorbing media
09 p1095 A73-22623

Effect of a laser field on the gain line profile of an adjacent transition in an argon laser
09 p1096 A73-22968

A tunable laser based on an organic dye solution and providing highly monochromatic, stable single-frequency emission
09 p1097 A73-23010

Propagation of monochromatic waves in an initially stressed infinite micropolar elastic plate.
09 p1160 A73-23024

The energy-momentum tensor for an electromagnetic wave in plasma.
10 p1254 A73-24115

Stability of the monochromatic mode of emission in a multimode solid-state laser
11 p1376 A73-25631

Stationary emission of monochromatic spatially banded laser beams from active medium with thin lens type inhomogeneity due to flat wave converter /resonator/ structure
11 p1376 A73-26142

Photoemission diode standards with high sensitivity, time stability and response uniformity for accurate measurement of monochromatic UV light, discussing design and construction
11 p1365 A73-26234

The wave length dependence of the transfer properties of photographic materials for holography.
11 p1370 A73-26536

Radiative transfer theory model of isotropic monochromatic scattering of light in plane layer of finite optical thickness
12 p1538 A73-26862

Single-frequency ruby laser with electrooptical Q switching and smooth frequency tuning
12 p1504 A73-26886

On the momentum of quasi-monochromatic waves in a plasma.
[IPPCZ-167] 12 p1529 A73-27435

Reflection of plane heterogeneous and uniform electromagnetic waves and the reflected wave displacement
13 p1658 A73-28072

Attenuation of monochromatic light in bottom layer of atmosphere and some properties of aerosols.
13 p1653 A73-28518

Quasi-monochromatic measurements of homogeneous arc plasmas.
15 p1841 A73-32393

Monochromatic field frequency misalignment effect on polarization and population ratio instabilities of single frequency traveling wave laser with broadened active medium
16 p2024 A73-32894

Monochromatic and radiometric albedo of Mars and Venus
16 p2067 A73-33811

Thermal structure and evolution of interstellar gas exposed to a soft X-ray burst.
17 p2231 A73-34757

Method to apply homogeneous-path transmittance models to inhomogeneous atmospheres.
17 p2205 A73-34856

Radiating power of a system consisting of a semitransparent isothermal coating and a flat non-transparent substrate.
17 p2212 A73-35194

The optical design of the 40-in. telescope and of the Irene Dupont telescope at Las Campanas Observatory, Chile.
17 p2171 A73-35408

Nondestructive optical contour mapping for non-contact testing of reflecting surface deformations from interference pattern due to monochromatic illumination of grating
17 p2172 A73-35419

Plane monochromatic electromagnetic waves in general relativity theory
17 p2212 A73-35562

Calculation of the radiation field in a semiinfinite medium in the presence of isotropic scattering
19 p2460 A73-37850

Stability of the monochromatic generation mode in multimode solid-state lasers.
19 p2438 A73-38147

Distribution of a monochromatic electromagnetic field and of temperature in a plane conductor with temperature dependent conductivity
19 p2471 A73-38340

An investigation of the combined amplification of monochromatic and noise signals in a TWT.
20 p2529 A73-38930

Nonlinear theory of a quasi-monochromatic electrostatic wave packet in an inhomogeneous plasma
21 p2745 A73-40364

Real laser cavity with nonideal reflecting mirrors showing Q factor increase relation to mode order for plane monochromatic linearly polarized waves
23 p2987 A73-43650

A self-similar regime of powder combustion with variable optical constants
24 p3154 A73-44708

Clearing of a cloudy atmosphere containing water drops by intense monochromatic radiation
24 p3108 A73-45520

MONOCHROMATORS

Application of the method of least squares to the determination of optical constants of uniaxial isotropic and anisotropic substances, and of the rate of polarization of monochromators in the far UV
05 p0597 A73-16148

Comparison between a double and triple monochromator in Raman laser spectrometry
07 p0836 A73-20166

Nebular Fabry-Perot, Pepsios, and Sisam monochromators.
08 p0964 A73-21039

Single beam spectrophotometer for transmittance measurement constructed from off-axis parabolic mirrors and plane grating monochromator, considering systematic errors
17 p2172 A73-35426

Czerny-Turner monochromator design using small spherical mirror off-axis angles to eliminate multiply dispersed light, discussing mirror types and focal length
21 p2697 A73-40129

MONOCLINAL VALLEYS

U VALLEYS

MONOCOQUE CYLINDERS

U CYLINDRICAL SHELLS

U MONOCOQUE STRUCTURES

MONOCOQUE STRUCTURES

Nondestructive shell-stability estimation by a combined-loading technique.
21 p2708 A73-41266

MONOCRYSTALS

U SINGLE CRYSTALS

MONOCULAR VISION

Cortical area of neural loci involved in monoptic and dichoptic metacortical occurring for target and masking stimuli imaged on different retinal regions
03 p0261 A73-13764

Monocular and binocular clues interaction in depth perception and spatial orientation, discussing stereopsis testing
05 p0542 A73-16483

Threshold variance analysis of monocular vs binocular visual stimulation in apparent movement perception
07 p0783 A73-20262

Eye dominance measurement relationship to image sharpness or visual acuity from binocular and monocular tests, obtaining dominance normal distribution
09 p1039 A73-21893

Corpus callosum role in monocular system transcommisural interactions from binocular interaction studies of stimulus-evoked potentials in rat visual cortex
10 p1180 A73-24332

Monocular fixation tests and prediction model for time course of aftereffect of eye turn on autokinetic illusion direction
13 p1578 A73-28098

Monocular contribution to binocular vision in normals and amblyopes.
13 p1575 A73-28359

Extended border enhancement during intermittent illumination - Binocular effects.
17 p2112 A73-34842

Monocular pilot ability in securing and retaining license as compared to controls
21 p2639 A73-41163

Mathematical model for physical space transformation into subjective field metric for monocular vision
24 p3064 A73-44906

MONOLITHIC CIRCUITS

U INTEGRATED CIRCUITS

MONOMOLECULAR FILMS

Reflection of conductivity electrons from an atomically pure 110° face of a tungsten crystal
21 p2751 A73-40367

MONOPLANES

NT A-4 AIRCRAFT

NT A-7 AIRCRAFT

NT AN-24 AIRCRAFT

NT B-52 AIRCRAFT

NT B-57 AIRCRAFT

NT B-70 AIRCRAFT

NT BOEING 737 AIRCRAFT

NT C-130 AIRCRAFT
 NT C-141 AIRCRAFT
 NT CESSNA 172 AIRCRAFT
 NT DHC 5 AIRCRAFT
 NT DO-31 AIRCRAFT
 NT F-8 AIRCRAFT
 NT HFB-320 AIRCRAFT
 NT IL-62 AIRCRAFT
 NT JINDIVIK TARGET AIRCRAFT
 NT P-3 AIRCRAFT
 NT T-33 AIRCRAFT
 NT T-39 AIRCRAFT
 NT TU-134 AIRCRAFT
 SOKO Galeb 3 cantilever low wing trainer-fighter monoplane with Bristol-Siddeley Viper 20 turbojet engine, describing flight control, loading gear, fuel system and avionics
 14 p1712 A73-30240

MONOPOLE ANTENNAS

NT WHIP ANTENNAS
 Towards faithful radio transmission of very wide bandwidth signals.
 01 p0015 A73-10176

The extended boundary condition solution of the dipole antenna of revolution.
 01 p0016 A73-10186

Electromagnetic near field energy flow characteristics of dipole/monopole receiving rod antenna, investigating frequency dependence of antenna effective area shape
 02 p0145 A73-11824

Impedance and radiation pattern of antennas above flat discs.
 06 p0676 A73-18191

Efficiency transition point for inductively loaded monopole.
 11 p1337 A73-25364

Geometrical diffraction theory for radiation pattern of extended vertical monopole antenna over infinitely conducting ground plane, noting back radiation level
 11 p1329 A73-25662

First order effects of terrain on the radiation pattern of a non-directional LF beacon.
 11 p1332 A73-26204

Flush mountable elliptically polarized low silhouette blade antenna for aircraft, describing polarization and radiation characteristics
 12 p1478 A73-27043

The performance of transistor fed monopoles in active antennas.
 14 p1735 A73-30219

Computer evaluation of large low-frequency antennas.
 14 p1735 A73-30227

Radiation pattern of a low-frequency beacon antenna located on a semi-elliptic terrain irregularity.
 19 p2409 A73-37716

A projection method in the problem of the excitation of a dielectric antenna
 21 p2667 A73-41512

Straight wire monopole and dipole antenna near field coupling characteristics prediction, deriving mathematical model by method of moments for computerized analysis
 22 p2823 A73-41798

MONOPOLES

Monopole aspects of solar magnetic field at sunspot cycle maximum and minimum, considering different explanations
 04 p0496 A73-14972

Quark search positive results, discussing mathematical models, magnetic monopole searches and existence debate
 16 p2054 A73-33289

Formulation of the basic approximations of the field theory of static current-voltage characteristics of quasi-monopolar semiconductors
 18 p2341 A73-36724

Search for magnetic monopoles in lunar material using an electromagnetic detector.
 19 p2461 A73-38492

MONOPROPELLANTS

Long-life firings of a catalytic reactor for monopropellant hydrazine.
 03 p0350 A73-13378

[AIAA PAPER 72-1045]
 Mono- and multipropellant, storable and cryogenic, liquid rocket propulsion engines developments including gas generators and engines
 03 p0355 A73-13422

[AIAA PAPER 72-1104]
 Asymptotic analysis of premixed burning with large activation energy.
 03 p0397 A73-13531

Decomposition and hybrid combustion of hydrazine, MMH and UDMH as droplets in a combustion gas environment.
 03 p0352 A73-14392

Design and analysis of an APU monopropellant gas generator.
 05 p0537 A73-16635

[SAE PAPER 720834]
 Auxiliary power units and their application to the space shuttle.
 09 p1153 A73-22778

Monopropellant hydrazine system for satellite attitude control, reporting catalysts properties, decomposition mechanisms and activities
 12 p1532 A73-27064

MONOPULSE ANTENNAS

Precision of amplitude-comparison direction finding by phased array antennas
 12 p1470 A73-27579

Corrugated circular waveguide horn as monopulse antenna feed for optimal tracking performance, using difference-sum patterns with hybrid modes
 14 p1731 A73-29705

Wideband monopulse radio direction finding measurement improvement, using receiver with log video IF amplifier, multiplexing filters and detectors to provide signal normalization
 16 p1990 A73-33850

MONOPULSE RADAR

Digital modeling of multipath induced monopulse angle tracking errors.
 04 p0416 A73-15056

A brief survey of monopulse techniques.
 11 p1331 A73-26148

Dynamic AGC correction for angle signal variations in monopulse radar receivers with reference signal, analyzing signal statistics
 12 p1469 A73-27163

Signal processing in the Air Traffic Control Radar Beacon System.
 12 p1469 A73-27165

The Corail radar - Automatic equipment for runway surveillance
 15 p1846 A73-32431

Russian book on design and operational principles of monopulse and moving target radar, atomic time and frequency measuring devices, radio navigation and optical processing
 21 p2650 A73-40510

Monopulse radar equipment
 21 p2651 A73-40511

MONOTONE FUNCTIONS

Difference procedures of monotonic type for non-linear parabolic boundary value problems
 01 p0069 A73-10072

Iteration approach for elliptic /nonlinear/ difference operators in divergence form
 01 p0069 A73-10075

Monotonicity and iterative approximations involving rectangular matrices.
 05 p0590 A73-16374

Sturm-Liouville problem monotone proper function zeros lower and upper bounds evaluation using Barta inequality and Schwartz iteration
 09 p1113 A73-23026

A note on pairs of matrices and matrices of monotone kind.
 21 p2725 A73-40377

Necessary and sufficient conditions for solvability of certain boundary value problems for a second-order ordinary differential equation
 21 p2727 A73-41272

MONSOONS

Southeast Asia weather during southwest monsoon in summer, discussing relation to westward moving equatorial waves from wind, pressure and cloudiness synoptic pattern analysis
 12 p1520 A73-26805

On the interaction between the zonal mean flow and equatorial waves excited by diabatic heat sources at 20 deg latitude.
 23 p3001 A73-43587

Mediterranean, south Sahara and northwest India rainfall records analysis, correlating general circulation changes with winter-spring and monsoon rainfall fluctuations
 23 p3003 A73-43954

MONTE CARLO METHOD

Direct Monte Carlo simulation of two-dimensional radiative heat transfer in absorbing-emitting medium bounded by the non-isothermal gray walls.
 01 p0123 A73-11139

Backward Monte Carlo calculations of the polarization characteristics of the radiation emerging from spherical-shell atmospheres.
 01 p0078 A73-11233

Rocket payload designs simulated by Monte Carlo method for aerodynamic properties during D region composition measurements
 02 p0156 A73-11740

Nuclear-electron cascades longitudinal evolution calculation in ionization calorimeter for primary nucleons and pions, using Monte Carlo method
 02 p0171 A73-12654

A new Monte-Carlo simulation model for the temporal development of cloud droplet spectra.
 02 p0144 A73-12782

Molecular transmission probability through duct connecting two large vessels calculated from data on cylindrical tubes, comparing with Monte Carlo data for error correction
 03 p0341 A73-12905

Application of the Monte Carlo technique to fatigue-failure analysis under random loading.
 03 p0388 A73-13236

Monte Carlo classical trajectory calculation of the rates of F-atom vibrational relaxation of HF and DF.
 03 p0318 A73-13279

Monte Carlo classical trajectory calculation of the rates of Hand D-atom vibrational relaxation of HF and DF.
 03 p0318 A73-13280

Monte Carlo solution of structural dynamics.
 03 p0391 A73-13681

Cell averaging constant-false-alarm-rate radar receiver with noise estimated from logarithmic detector output, determining performance in Gaussian noise by Monte Carlo simulation
 03 p0277 A73-13910

Degree and direction of polarization of multiple scattered light. I - Homogeneous cloud layers.
 03 p0344 A73-14427

Impact loading on structures with random properties.
 04 p0510 A73-15028

Implications of a quadratic stream definition in radiative transfer theory.
 05 p0592 A73-16196

Isotropic and incoherent light scattering by atomic slab, calculating Doppler effect induced diffuse radiation energy partial redistribution by Monte Carlo method
 05 p0597 A73-16562

Computerized Monte Carlo simulation with program flexibility for mass distribution in particle collision processes, applying to accreting and fragmenting systems including asteroid belt
 05 p0624 A73-17316

Monte Carlo computer technique for one-dimensional random media.
 06 p0665 A73-18188

Contrast transmittance Monte Carlo computation for atmospheric haze models based on aircraft measurement data from various geographical areas
 06 p0694 A73-18302

Monte Carlo simulation for electron diffusion in Cd Te, noting effects of applied electric field near threshold value for negative differential mobility
 06 p0739 A73-18799

A modified Monte Carlo model for the ionospheric heating rates.
 07 p0815 A73-19380

Monte Carlo method applications in the solution of gas kinetics problems
 07 p0853 A73-19987

Gamma-ray lines from an expanding supernova shell.
 08 p1008 A73-21162

Monte Carlo simulation of a model ionosphere. II - Energy flow and energy dissipation.
 09 p1075 A73-22129

Sufficient conditions for the applicability of the Monte-Carlo method to the solution of systems of nonlinear equations
 09 p1112 A73-22888

A probabilistic approach to a differential-difference equation arising in analytic number theory.
 10 p1241 A73-23643

Analytical and Monte Carlo analysis of rms beam pointing errors of planar phased arrays with isotropic elements
 11 p1328 A73-25660

Characterization of boron carbide with an electronic microprobe
 13 p1645 A73-28346

Lyman alpha radiation transfer in spherically symmetric hydrogen nebula from Monte Carlo techniques, computing for different optical depths
 13 p1685 A73-29358

Monte Carlo technique application to meteor stream formation process modeling, discussing mass ejection from cometary nuclei
 14 p1795 A73-29848

Numerical experiments by Monte Carlo method to examine comet orbits evolution within solar system, noting Trojan, horseshoe and Jupiter-Saturn midrange orbits
 15 p1938 A73-31949

Single point solutions of Dirichlet boundary value problems by Monte Carlo and successive over-relaxation.
 15 p1899 A73-32037

Radiation configuration factors for annular rings and hemispherical sectors.
 15 p1959 A73-32281

Probabilistic Monte Carlo computerized simulation of surface to air missile systems reaction time from aircraft attack in non-jamming environment and over flat terrain
 16 p1985 A73-33418

Time dependent worldwide distribution of atmospheric neutrons and of their products. I, II, III.
 16 p2055 A73-33427

A consistent shape parameter estimator for the Weibull distribution.
 16 p2032 A73-33602

Thermal dissociation and recombination of hydrogen according to the reversible reactions H₂ + H to H + H + H.
 16 p1977 A73-33674

MOON

- Monte Carlo model of cometary evolution based on hypothetical perturbed orbit calculations, with emphasis on short-period comets 17 p2228 A73-34426
- Monte Carlo simulation on CRT display for training and learning system reliability and early decision effects on life cycle cost effectiveness 17 p2140 A73-35261
- Numerical techniques in two- and three-dimensional radiation hydrodynamics. 17 p2255 A73-35596
- Monte Carlo calculations of reaction rates and energy distributions among reaction products. IV - F + HF/nu/ yields HF/nu-prime/ + F and F + DF/nu/ yields DF/nu-prime/ + F. 19 p2463 A73-37898
- Monte Carlo method for biharmonic boundary value problems solution, using isotropic random walk and mean value relation 20 p2581 A73-39094
- Monte Carlo technique investigation of subclass number effects in nonoptimum parametric maximum likelihood classification procedure, defining distribution functions of representative subclasses 20 p2559 A73-39878
- Plant canopy models for simulating composite scene spectroradiance in the 0.4 to 1.05 micrometer region. 20 p2562 A73-39906
- Monte-Carlo-method based calculation of the linearity and resolving power of a Cerenkov spectrometer for purposes of gamma astronomy 21 p2701 A73-40613
- Reflection of a shock wave from a thermally accommodating wall - Molecular simulation. 22 p2842 A73-42234
- Comparison of calculated characteristics of extensive atmospheric showers with experimental results at various altitudes 22 p2903 A73-42733
- Monte Carlo computer simulation of lunar regolith evolution, considering buffering regolith effect via computation for debris produced by crater 24 p3130 A73-44460
- A variant of the Monte-Carlo method for solving the linear dynamics problems of a rarefied gas 24 p3076 A73-44660
- Numerical solution of linearized kinetic equations for coagulation of cloud particles by the Monte-Carlo method 24 p3107 A73-44965
- MOON**
- Ultraviolet photometry of the moon with the telescope experiment on the OAO-II. 01 p0096 A73-10317
- Literal expressions for the co-ordinates of the moon. I - The first degree terms. 01 p0099 A73-10687
- The moon; Proceedings of the Second Symposium, University of Newcastle-upon-Tyne, Newcastle-upon-Tyne, England, March 22-26, 1971. 03 p0367 A73-13076
- Lunar axis inclination to ecliptic axis as function of time, tabulating variations during 1971 03 p0367 A73-13078
- Lunar thermal convection via solid state creep processes, discussing departure from hydrostatic equilibrium figure 03 p0369 A73-13105
- The role of occultations in the improvement of the lunar ephemeris. 03 p0369 A73-13107
- Soviet Union-proposed draft International Treaty governing lunar exploration and use 04 p0522 A73-15135
- UN space treaty proposals relating to moon and other celestial bodies natural resources utilization 04 p0524 A73-15158
- The secular accelerations of the moon's orbital motion and the earth's rotation. 04 p0497 A73-15176
- On surface photometry of the moon. 04 p0448 A73-15188
- Orbital eccentricity of Mercury and the origin of the moon. 04 p0501 A73-15625
- Solar wind magnetic field and particle concentration disturbances near moon, noting electric field effect on ion motion 05 p0620 A73-17009
- Search for biogenic structures and viable organisms in lunar samples - A review. 06 p0654 A73-18416
- Analytical solution of lunar ephemerides, considering sun-earth-moon problem and required corrections and perturbation methods 09 p1147 A73-22710
- Statistical distribution of albedo over the lunar disk 12 p1546 A73-27863
- A method for determining the position of the moon's center of mass from earth-based observations. 15 p1927 A73-30976
- Russian book - Physics of the moon and planets. 16 p2063 A73-33751

- Long term heliometric Moesting crater distance measurements applied to moon libration relationship to lunar radius 16 p2064 A73-33775
- An experiment in photographic equidensitometry of the moon and planets 16 p2070 A73-33848
- Solid state convection role in moon from analysis of models with homogeneous initial distribution of radioactive heat sources 17 p2232 A73-35262
- Statistical distribution of the albedo over the lunar disk. 20 p2608 A73-39237
- MOON ILLUSION**
- An explanation of transient lunar phenomena from studies of static and fluidized lunar dust layers. 07 p0895 A73-19863
- MOON-EARTH TRAJECTORIES**
- Sighting methods during flights from the moon to the earth 18 p2351 A73-36107
- MOONMOBILES**
- U LUNAR SURFACE VEHICLES
- MOONQUAKES**
- Moonquakes and lunar tectonism results from the Apollo passive seismic experiment. 07 p0894 A73-19848
- New seismic data on the state of the deep lunar interior. 17 p2237 A73-35805
- MOPS (PROPULSION SYSTEMS)**
- U MAN OPERATED PROPULSION SYSTEMS
- MORAINAL LAKES**
- U LAKES
- MORAINES**
- U GLACIAL DRIFT
- MORL**
- U MANNED ORBITAL RESEARCH LABORATORIES
- MORNING**
- Proton energy spectra from recent rocket measurements in the night and morning time auroral zone. 02 p2006 A73-12315
- Energy transport by photoelectrons in the early morning ionosphere. 18 p2348 A73-37027
- MORPHOLOGY**
- NT GEOMORPHOLOGY
- NT ISOMORPHISM
- NT LUNG MORPHOLOGY
- NT POLYMORPHISM
- Morphological, physiological and pharmacological investigations of rat cerebellar cortex synaptic structure and function maturation and neurotransmitter receptivity development 03 p0264 A73-14256
- Morphological, structural and electrical nonuniformities correlation in epitaxial GaAs films on planes, noting Miller indices effects on morphological and electrical properties 05 p0605 A73-17290
- Dependence of martensite morphology on the isothermal transformation temperature of the Fe-24Ni-3Mn alloy 09 p1100 A73-21974
- Morphology and spontaneous crystallization conditions of silicides of the transition metals from solutions in metallic melts 09 p1104 A73-22976
- The morphological organization of the vertebrate retina. 09 p1042 A73-23304
- Morphological changes in the liver of dogs induced by chronic gamma irradiation 12 p1463 A73-27707
- Morphology of the structure and the microhardness of Al-Ni, Cu, Be, Fe, Co/ eutectic compositions 14 p1760 A73-30588
- Morphological changes in kidneys during exposure to variously oriented accelerations at a level of 4 g for many hours 17 p2111 A73-34226
- Morphological and electron-microscopic alterations of the myocardium in dogs subjected to lasting chronic gamma irradiation 17 p2111 A73-34230
- Book - Pathological effects of radio waves. 19 p2395 A73-37774
- MORPHOTROPISM**
- U ISOMORPHISM
- MORTALITY**
- Relationship between ventricular premature contractions on routine electrocardiography and subsequent sudden death from coronary heart disease. 14 p1715 A73-30051
- Risk factors for developing myocardial infarction and other diseases - The 'Men born in 1913' study. 14 p1716 A73-30352
- MOS (SEMICONDUCTORS)**
- U METAL OXIDE SEMICONDUCTORS

MOSAICS

- E resonance line broadening due to superhyperfine interactions in ruby, noting angular dependence of mosaic structure mechanism 09 p1132 A73-21954
- Photomosaic construction high altitude photographs, approximating surface curved areas by planes 13 p1621 A73-29323
- Organization of a reliability study on an electromechanical product 16 p1970 A73-33271
- Optical mosaics for large field visual simulation display systems. [AIAA PAPER 73-926] 21 p2673 A73-40873
- MOSFET**
- U FIELD EFFECT TRANSISTORS
- MOSS (SPACE STATIONS)**
- U ORBITAL SPACE STATIONS
- MOSSBAUER EFFECT**
- Amorphous magnetism in F.C.C. Vicalloy II. 01 p0087 A73-10242
- Mossbauer spectroscopic analysis of Sea of Fertility regolith core samples, noting olivine content increase with depth 02 p0214 A73-12242
- X-ray study and Moessbauer spectroscopy on lunar ilmenites (Apollo 11). 02 p0220 A73-12480
- A versatile Moessbauer spectrometer and its applications in structural mechanics. 03 p0305 A73-12875
- Temperature-dependent hyperfine interactions in Fe2B. 06 p0734 A73-17833
- High resolution Mossbauer spectrometer design and applications, describing electromechanical Doppler shifter, control electronics and data storage 07 p0822 A73-19170
- Moessbauer spectroscopy of lunar regolith returned by the automatic station Luna 16. 07 p0879 A73-19683
- Fe/2+/-Mg site distribution in Apollo 12021 clinopyroxenes - Evidence for bias in Moessbauer measurements, and relation of ordering to exsolution. 07 p0881 A73-19706
- On the amount of ferric iron in plagioclases from lunar igneous rocks. 07 p0882 A73-19716
- Study of excess Fe metal in the lunar fines by magnetic separation, Moessbauer spectroscopy, and microscopic examination. 07 p0788 A73-19745
- Apollo 14 samples with Fe-bearing minerals examined by Mossbauer spectroscopy, noting parallelism with Apollo 11 and 12 samples 07 p0893 A73-19845
- Electrical conductivity and Moessbauer study of Apollo lunar samples. 07 p0898 A73-19896
- Investigation of the structure of sodium silicate glass containing oxides of multivalent metals by nuclear spectroscopy methods 09 p1110 A73-22980
- Application of the Moessbauer effect to the study of the mechanism of iron diffusion in beta-titanium 09 p1108 A73-23240
- Moessbauer spectroscopic studies of iron-doped rutile. 10 p1258 A73-23567
- Mixed valencies and site occupancies of iron in silicate minerals from Moessbauer spectroscopy. 11 p1324 A73-25142
- Temperature dependence of the Moessbauer spectra of iron-cobalt-vanadium alloys 12 p1509 A73-26839
- Properties of iron impurity in aluminium matrix studied by Mossbauer spectroscopy. 13 p1634 A73-28220
- The vibrational frequency of Fe-57 atoms in Pt-Fe solid solution from measurements of the second-order Moessbauer Doppler shift. 13 p1634 A73-28258
- 'Anomalous' alteration of the Moessbauer isomer shift of Te125 in defect diamond-like semiconductors 14 p1784 A73-30809
- Mossbauer and X-ray spectral studies of a nickel-cobalt ferrite subjected to thermomagnetic treatment 15 p1886 A73-31034
- Moessbauer effect in Nb3Sn as a function of heat treatment 15 p1922 A73-31180
- Theoretical possibilities for the creation of a gamma laser /gazer/ using nuclear transitions 23 p2988 A73-44092
- Stimulated gamma emission in long-lived nuclear isomers, proposing gamma lasers based on Mossbauer line broadening effect 23 p2988 A73-44093
- MOTILITY**
- U LOCOMOTION
- MOTION AFTEREFFECTS**
- Tilt discrimination and motion aftereffect independence of flicker rate of stroboscopically illuminated contours visual stimuli 06 p0660 A73-18624

Disparity detectors in human depth perception - Evidence for directional selectivity. 21 p2637 A73-40413

MOTION EQUATIONS
U EQUATIONS OF MOTION
MOTION PERCEPTION
U SPACE PERCEPTION
MOTION PICTURES
Moving radiography for photographic recording and display of transient or cyclic motion, emphasizing application to aircraft gas turbines under dynamic conditions 07 p0832 A73-20451
Storage and transmission of sequences of moving images 08 p0941 A73-21559
Ultrasonic holography by one-dimensional moving of the source or the object. 10 p1216 A73-23664
Phase characteristic function of holographic images of objects in parabolic motion. 11 p1366 A73-26248
Holographic motion picture camera allows front surface detail to be recorded in real time using a continuous wave laser. 11 p1366 A73-26249
Flight simulation visual image innovations, including closed circuit television, motion pictures and computer generated imagery with wide angle presentation and day/night realizations 16 p1995 A73-33205
The use of holographic techniques for recording high-speed events. 21 p2695 A73-39962
A streak technique for measuring the initial movement of a rocket with four unknown and two known degrees of motion. 21 p2696 A73-39986
National Center for Atmospheric Research utility plotting programs for computer graphics, two and three dimensional fields display and movie generation 24 p3070 A73-45089

MOTION SICKNESS
Semicircular canals as a primary etiological factor in motion sickness. 02 p0135 A73-12560
Direction-specific adaptation effects acquired in a slow rotation room. 03 p0268 A73-14154
Design and function of sweat sensor to monitor motion sickness sweat response 03 p0269 A73-14160
Motion sickness symptomatology and performance decrements occasioned by hurricane penetrations in C-121, C-130 and P-3 Navy aircraft. 03 p0269 A73-14161
Findings on American astronauts bearing on the issue of artificial gravity for future manned space vehicles. 09 p1045 A73-22531
Effectiveness of some hemodynamic indices in the detection of vestibulo-vegetative disorders under ordinary conditions and those of hypoxia 17 p2110 A73-34121
The role of the sympathetic section of the vegetative nervous system in the training of the organism for the influence of statokinetic irritants. 18 p2279 A73-36903
Human statokinetic stability as component of non-specific resistance, discussing revolving, altitude, hypoxic and orthostatic stress dependence tests 18 p2279 A73-36904
Altered susceptibility to motion sickness as a function of subgravity level. 20 p2518 A73-39486

MOTION SICKNESS DRUGS
Use of sodium hydrocarbonate for medication and prophylaxis of motion sickness 08 p0933 A73-20990
Effects of some antimotion sickness drugs and secobarbital on postural equilibrium functions at sea level and at 12,000 feet/simulated/. 09 p1045 A73-22529
Prophylaxis and treatment of the motion sickness syndrome 13 p1580 A73-29410

MOTION STABILITY
NT AERODYNAMIC STABILITY
NT AIRCRAFT STABILITY
NT ATTITUDE STABILITY
NT BOUNDARY LAYER STABILITY
NT DIRECTIONAL STABILITY
NT FLAME STABILITY
NT FLOW STABILITY
NT GYROSCOPIC STABILITY
NT HOVERING STABILITY
NT LONGITUDINAL STABILITY
NT MAGNETOHYDRODYNAMIC STABILITY
NT ROTARY STABILITY
NT SPACECRAFT STABILITY
R-function numerical analysis method for motion stability criteria, developing algorithms for Liapunov function construction and controller design for conservative control system stability 01 p0076 A73-10096

Liapunov function for complex system motion stability analysis, noting stability criteria for subsystems satisfying Routh-Hurwitz conditions 01 p0076 A73-10668
Theory of the motion of a rigid model of an aircraft with a vertical landing-gear strut on a runway 01 p0005 A73-10917
Multiple correction procedure for motion control ensuring arrival at final state without complete initial state information 01 p0079 A73-11419
Equations of motion for Kovalevskaya gyroscope uniform rotation about axes differing from inertia ellipsoid principal axes, noting sufficient stability conditions 02 p0167 A73-11765
Similar normal mode vibrations in certain conservative systems with two degrees-of-freedom. 02 p0193 A73-12515
Liapunov function for Hamilton-Jacobi equation for motion stability of linear and nonlinear mechanical systems, calculating vibration damping factor 03 p0342 A73-13157
Liapunov function application to stability of unperturbed motion of system of differential equations with respect to part of variables 03 p0344 A73-14056
Motion stability of librational points in gravitational field of rotating triaxial ellipsoid, applying to planets of solar system 03 p0376 A73-14266
About the motion of a heavy flexible string attached to the satellite in the central field of attraction. 03 p0376 A73-14267
Equilibrium motions of rigid spinning satellite in circular orbit around central body subject to gravitational torque 03 p0376 A73-14268
On the stability of triangular points of equilibrium in the restricted elliptic problem 03 p0376 A73-14270
Newtonian differential equations of Kepler motion, analyzing stability by numerical integration based on Floquet theorem and Runge-Kutta method 04 p0497 A73-15013
Investigation of the stability of plasma-jet motion in the magnetic field of a diverter 04 p0479 A73-15045
Numerical integration of equations of Ba cloud motion in ionosphere with end shorting, noting critical electric field for motion stability 04 p0445 A73-15649
Dynamics of three-axis spacecraft orientation 05 p0628 A73-16405
The motion and stability of a dual-spin satellite during the momentum wheel spin-up maneuver. [AIAA PAPER 73-142] 05 p0629 A73-16891
Equations for the compass motion of a triaxial gyro-stabilizer in gyrocompass operation 05 p0577 A73-16993
Couplings effect on Liapunov stability estimation of higher order linear nonstationary systems, using aggregation method 05 p0599 A73-17084
Three dimensional self oscillating motion study of roll and pitch stabilized vehicle with thrust vector control under resonance, using averaging method 05 p0599 A73-17086
The influence of viscosity on the stability of a relative motion of two media. 06 p0685 A73-17761
Frequency stability criterion for a variable-structure automatic control system. 06 p0680 A73-17958
Asymptotic motion stability analysis with respect to part of variables, using Liapunov functions for solution boundedness conditions 07 p0850 A73-19012
Stability of the libration points of a triaxial ellipsoid under constantly acting disturbances in the first approximation 09 p1143 A73-22093
Spinning Skylab space station dynamics, investigating motion stability from simplified models with flexible appendages by digital simulation 10 p1286 A73-24003
Resonance phenomena associated with nonlinear vibrations of solid bodies 10 p1249 A73-24303
Unsteady three-dimensional motion of a flight vehicle during hypersonic reentry in the atmosphere 10 p1286 A73-24304
Stability of planar oscillations of a satellite in an elliptic orbit. 10 p1287 A73-24663
Nelson Tyler helicopter camera mount for aerial reconnaissance photography providing camera balance and motion stability under combat flight conditions 10 p1222 A73-24949
Linear system unperturbed motion stability in finite time interval, formulating first approximation vector matrix equation 11 p1397 A73-25045

Conformal mapping method application to unsteady motion of arbitrary deformable contour in potential flow of ideal incompressible fluid 11 p1348 A73-26426
Controlling the angular motions of a flight vehicle with the aid of flywheels 12 p1522 A73-27083
Integral manifold concept for stability analysis of nonlinear system oscillations, plotting resonance curve for quasi-linear autonomous system 12 p1525 A73-27792
Analytical design of manual control systems for flight bodies 12 p1549 A73-27896
Aerosol particle downward motion in vertical electric field, discussing stability of major axis orientation of ellipsoid of revolution 13 p1654 A73-28881
Whirling shafts motion stability necessary and sufficient conditions analysis based on Liapunov method, taking into account internal and external damping effects 15 p1955 A73-32166
Contribution to the theory of electron-beam stability in an inhomogeneous dielectric medium 15 p1920 A73-32302
Stable tumbling motions of a dual-spin satellite subject to gravitational torques. 17 p2237 A73-34177
Stability of motion in a controlled system consisting of two elastically butted bodies one of which has cavities partially filled with a liquid 17 p2243 A73-34733
Analytical design of aircraft manual control systems. 18 p2267 A73-36601
Adaptive control of forced motions in discrete extremal systems with independent search 20 p2542 A73-39346
Bifurcation and stability of steady motions of complex mechanical systems 21 p2738 A73-40176
The stability of steady motions of systems with quasi-cyclic coordinates and the stability of mechanical equilibrium under the action of a magnetic field 21 p2738 A73-40177
Containment stability of charged particles captured by a plane electromagnetic wave propagating at a slowly varying velocity 22 p2826 A73-42377
Solar pressure induced librations of spinning axisymmetric satellites. 22 p2910 A73-42633
Numerical exploration of commensurable periodic solutions of the restricted problem of three bodies and their stability. 23 p3029 A73-43746
About the stability of the libration points of a rotating triaxial ellipsoid in a degenerate case. 23 p3032 A73-43838
Analysis of the perturbed motion of a solid with cavities partially filled with liquid 23 p2969 A73-44198
Oscillatory motion existence in expanding n-body gravitational systems with distance bound and particle escape 23 p3034 A73-44208
Stability of an electron beam in an inhomogeneous dielectric medium. 24 p3114 A73-44610
Application of the sensitivity theory to an analysis of the high-frequency components of motion 24 p3074 A73-45096
Vertical perturbation stability of three dimensional periodic orbits in restricted three body problem 24 p3142 A73-45295
Three dimensional computer plots of zero velocity contours for restricted three and four body problems, discussing motion stability near equilibrium points 24 p3142 A73-45297
Stability of Lagrange solutions to the three-dimensional elliptic problem of three bodies 24 p3111 A73-45299

MOTIVATION
Motivation in vigilance - A test of the goal-setting hypothesis of the effectiveness of knowledge of results. 17 p2113 A73-34149

MOTOR SYSTEMS [BIOLOGY]
U EFFERENT NERVOUS SYSTEMS
MOTORS
NT ELECTRIC MOTORS
NT MICROMOTORS
NT SERVOMOTORS
NT SYNCHRONOUS MOTORS
NT TORQUE MOTORS
Speed control for an air motor using fluidic techniques. [ASME PAPER 73-DE-35] 14 p1713 A73-30824

MOTS [TRACKING SYSTEM]
U MINITRACK SYSTEM

MOUNTAIN INHABITANTS

MOUNTAIN INHABITANTS

- High altitude adaptation in mountain inhabitants of Tian Shan and Pamir, discussing effects on hemodynamic and pulmonary functions 02 p0133 A73-11922
- Hemocoagulation system function in mountain inhabitants and during altitude acclimatization, noting parasympathetic nervous system tonus 02 p0133 A73-11923
- Comparative evaluation of the general and specific efficiencies of athletes under normal barometric pressure and in the process of training and acclimatization under highland conditions of Pamir 02 p0136 A73-11925
- Mountain inhabitants physiological characteristics due to altitude effects, investigating human tolerance and adaptation to ambient environment 07 p0784 A73-19212
- Influence of developmental adaptation on aerobic capacity at high altitude. 09 p1041 A73-22928
- Physiological studies of human organism adaptation to high altitudes in temporary and permanent mountain inhabitants, discussing oxygen uptake, lung ventilation and cardiac ventricle hypertrophy 10 p1181 A73-24514
- Mechanics of breathing in high altitude and sea level subjects. 11 p1318 A73-26217

MOUNTAINS

NT ALPS MOUNTAINS [EUROPE]

- Preliminary observations of stratified rocks of the Hadley Appennines photographed by the Apollo 15 astronauts 01 p0095 A73-10268
- Mountain waves and CAT encountered by the XB-70 in the stratosphere. 11 p1394 A73-25785
- Theory of mountain lee waves for an arbitrary-profile elevation 15 p1905 A73-31818
- Mountain range effects on tropopausal turbulence with mountain waves, examining tropopause layer inversions, vertical wind vectors, temperature distribution and buffeting intensity 17 p2204 A73-34542
- Linearized models of two dimensional steady air flow around mountain obstacle for constant temperature gradients and invariant velocity 21 p2731 A73-40741

MOUNTING

- Improved mount and alignment procedures for a rapid-scan Fabry-Perot interferometer. 06 p0691 A73-17498
- The dependence of piezo-electric accelerometer response on method of attachments. 12 p1496 A73-26974
- A kinematically designed mount for the precise location of specimens for holographic interferometry. 14 p1753 A73-30414
- Investigation of mounting discrete chip components for hybrid microelectronic applications. 16 p1989 A73-33467
- Resiliently mounted objects holographic system sensitivity threshold control by proper selection of support stiffness and vibration damping 21 p2698 A73-40132
- The drifts of a gyroscope mounted on the oscillating housing. 23 p2983 A73-44271

MOUNTS

U SUPPORTS

MOVING TARGET INDICATORS

- Low cost monolithic range gated radar moving target indicator using bucket brigade delay line circuits 02 p0141 A73-12360
- Recursive MTI radar filter design for sharp spectrum rolloff and flat pass band, investigating clutter rejection performance vs spectral spread 05 p0558 A73-16808
- An initialization technique for improved MTI performance in phased array radars. 06 p0664 A73-17790
- Ground and angel clutter in radar systems - The two-beam antenna solution. 07 p0794 A73-20250
- Moving-target-indicator recursive radar filter using bucket-brigade circuits. 09 p1065 A73-23096
- Open-loop tracking of moving targets with an Aerobee sounding rocket. 09 p1117 A73-23221
- Range-gated moving target indicator with digital filters. 12 p1469 A73-27161
- Quantization and roundoff errors in a digital MTI filter. 13 p1590 A73-28478
- MTI radar filter with adaptively controlled double canceller for frequency shifted clutter spectra effects minimization 13 p1594 A73-29222

- Phase coded moving target indicators, describing phase measurement technique to discriminate between moving and fixed targets 15 p1846 A73-32433
- Clutter spectra of low PRF AMTI pulse-Doppler radar. 16 p1980 A73-33413
- The staggering of pulse sequences in the case of a pulsed radar providing moving target indication 18 p2289 A73-36399
- Operational principles and testing of a digital radar target extractor 19 p2404 A73-37584
- The effect of staggered PRF's on MTI signal detection. 21 p2650 A73-40344
- Russian book on design and operational principles of monopulse and moving target radar, atomic time and frequency measuring devices, radio navigation and optical processing 21 p2650 A73-40510
- Electronic moving-target selection systems 21 p2651 A73-40512
- Limitation of m.t.i. improvement factor due to oscillator instability. 24 p3069 A73-45259

MTBF

- Estimating the mean time until follow-up cutoff in a nonlinear sampled-data servosystem for irregular arrival of the signal. 04 p0430 A73-15205
- Reliability of systems with shifting redundancy in servicing a random demand flow 05 p0560 A73-16274
- Reliability tests on fire control airborne radars prototypes, measuring MTBF 07 p0800 A73-19416
- Electronic equipment burn-in for repairable equipment. 08 p0945 A73-20949
- Reliability of a self-repairing system with scheduled maintenance. 09 p1088 A73-22443
- The concept of coverage and its effect on the reliability model of a repairable system. 10 p1226 A73-24871
- Mean time of the failure-free operation of a redundant system with allowance for monitoring of operational efficiency 12 p1504 A73-27619
- Heat resistant nickel alloys creep rupture strength diagram, determining time to failure as function of loads 13 p1636 A73-29062
- Reliability analysis of time to failure distribution of redundant system with failing elements number as periodic function of time 15 p1880 A73-30998
- Repairable electronic system random failure and repair time related to simulator time available for operation, analyzing MTBF and repair rates 16 p1996 A73-33207
- Universal operating characteristic curves for sequential probability ratio tests. 16 p2020 A73-33611
- Reliability of GaAs/I-xP/x/light emitting diodes. 16 p1990 A73-33623
- Statistical and probabilistic MTBF models for parts, sockets and systems reliability 16 p2020 A73-33628
- Specifying maintainability-demonstration-test parameters. 16 p2020 A73-33635
- Probabilistic analysis of sequential test plans. 16 p1986 A73-33636
- Probabilistic analysis of a two-unit system with a warm standby and a single repair facility. 17 p2149 A73-35809
- Heat resistant nickel alloys creep rupture strength diagram, determining time to failure as function of loads 18 p2325 A73-36894
- Failure detection and isolation techniques for gimbaled and strapdown inertial systems examining redundant system reliability relationship to MTBF [ALAA PAPER 73-852] 22 p2884 A73-41969
- Reliability of some redundant systems with repair. 22 p2867 A73-42968
- Product reliability management, providing MTBF charts for relationships between part count, laboratory test results and operational performance 22 p2867 A73-42969
- Equivalence of redundant systems with respect to time to failure. 22 p2867 A73-42970

MTI RADAR

U MOVING TARGET INDICATORS

MUD

- Biogeochemistry of aragonite mud and oolites. 03 p0266 A73-14662

MULLITES

- Possibility of obtaining mullite at high dynamic pressures 02 p0178 A73-11542

- Thermal characterization of reusable external insulation for the space shuttle. 22 p2931 A73-42403 [ECTP PAPER B2-8]
- MULTICHANNEL COMMUNICATION**
- Conditions for the absence of periodic conditions in multivariable pulse-coded systems 01 p0027 A73-10592
- Constant-envelope spread spectrum random access satellite communication system, discussing message and multiple access modem, signal acquisition, tracking, ranging, etc 01 p0018 A73-11178
- Optimization of input-signal levels during amplification in a TWT 01 p0026 A73-11266
- Comparison of digital-signal multiplexing methods by means of sequencing 01 p0021 A73-11485
- Multichannel communication system in adaptive system with automatic channel selection based on random parameter extremum criterion for maximum usage time of extremal channel 03 p0278 A73-14063
- A three channel telemetry system, compatible with the British medical and biological telemetry regulations. 03 p0269 A73-14277
- Multichannel PDM-FM biomedical radio telemetry system for ECG, respiratory rate and oxygen consumption during exercise, considering transmitter and receiver design 03 p0269 A73-14278
- A time-division multiplexed telemetry system using delta-modulation. 03 p0270 A73-14279
- A programmable four channel system for long-time radio telemetry of biomedical parameters. 03 p0270 A73-14280
- Development and adjustment of a multi-channel miniaturized FM/AM telemetering system adapted to the primates. 03 p0270 A73-14284
- Three channel FM telemetry system for long term EEG monitoring, discussing routine clinical operation results 03 p0271 A73-14298
- Surgically implanted single and multichannel telemetry systems for monitoring single and multiple physiological parameters, discussing size and power requirements 03 p0271 A73-14302
- Multichannel telemetry of physiological parameters/body temperature ecg, eeg/ in the rat. I - Design and methods. 03 p0272 A73-14305
- Differentially encoded multiple phase shift keyed signals transmission and detection, analyzing digital communication system performance 04 p0415 A73-14991
- Channel filters with longitudinally coupled flexural mode resonators. 04 p0427 A73-15320
- Miniature biotelemetry giving 10 channels of wide-band biomedical data. 04 p0412 A73-15388
- Detection of multichannel FSK signals using chirp dispersion method. 04 p0419 A73-15407
- Single channel per carrier FCM FDMA demand assignment satellite communications system /SPADE/ for INTELSAT, discussing hardware and software introduction at first terminal 04 p0420 A73-15414
- Two channel multimode feed for circular horn tracking antenna applications, discussing channel patterns, coupling, isolation and frequency response 04 p0428 A73-15417
- Time division multiple access for tactical trunking via satellite. 04 p0420 A73-15424
- Earth resources sensing technology - 24-channel multispectral sensor system development. 04 p0449 A73-15463
- Communication satellite technology development, discussing INTELSAT and Russian Orbita systems, spectrum and orbit utilization, modulation, multiplexing, electron devices, radiation environment and power generation 05 p0550 A73-16604
- Intermodulation noise and system analysis in SSB-PM multiple access system. 05 p0552 A73-17169
- Transmission quality in noiseless multiple-access systems with feedback 06 p0679 A73-17855
- Multiple access analog and digital satellite telecommunication systems, discussing Intelsat /FM/ and Spade /frequency division/ systems 07 p0790 A73-19181
- Multichannel television coupling modulation experiments using a CO2 laser. 07 p0833 A73-19195

Common-bandwidth transmission of data signals and wide-band pseudonoise synchronization waveforms. 07 p0790 A73-19200

The resistance of discrete phase modulation to random interference 07 p0793 A73-20023

Optical birefringent multichannel splitting and combining wideband FDM communications filters, considering crosstalk, pulse response, extinction ratio and detuning 08 p0939 A73-21046

Preemphasis for an S-band constant bandwidth FM/FM system. 08 p0939 A73-21085

Synthesis of functions for polynomial linear-phase amplifiers with feedback 08 p0947 A73-21396

TDMA system and full scale test programs for Symphonic satellite telecommunication with ground 09 p1049 A73-22316

Study of a phase displacement modulation mode for a time division multiple access system 09 p1050 A73-22318

High capacity digital concentrator of telephone circuits for a TDMA station/CELTIC/ 09 p1050 A73-22319

TDMA satellite telephonic communication network with preassigned channeled radio carrier, describing four phase demodulator and channel units regrouping 09 p1050 A73-22320

The accuracy of an approximate representation of the correlation functions of complex signals distorted in the linear stages of a radio channel 09 p1051 A73-22461

Intelsat 4 communications system, discussing radio transponders, earth stations, and multiple access, modulation and multiplexing methods 09 p1051 A73-22700

Satellite frequency division multiple access communication net, examining channel monitoring and self regulating downlink power output for performance improvement 09 p1053 A73-23363

Acquisition detectability parameter/output SNR/ for unrestricted random access through ideal hard-limiter in multiple access communication systems 09 p1053 A73-23365

Convolutional coding for multiple-access satellite communication. 09 p1056 A73-23399

Canadian domestic ANIK communication satellite with all-microwave 12-channel repeater, discussing system components, antenna design and performance parameters 09 p1059 A73-23437

A combined coding and modulation approach for communication over dispersive channels. 10 p1186 A73-23496

Multichannel wideband FM communication systems, discussing method for channel density increase with reduced linearity requirement and enhanced noise immunity 10 p1187 A73-23732

Modulation distortions during fading in frequency-modulated multichannel radio communication 10 p1187 A73-23740

Internally modulating and multiplexing mode locked Nd-YAG laser techniques for one gigabit optical communication, noting system efficiency improvement over conventional approaches 10 p1227 A73-23783

Commercial communications satellite technology trends, stressing wideband capabilities, flexibility, multiple access and channel capacity increase 10 p1189 A73-24561

Error probability in an atmospheric twin-channel optical link. 10 p1190 A73-24628

A method for smoothing level fluctuations caused by echoes in the case of FM directional radio links 11 p1328 A73-25344

Second-order phase-lock-loop acquisition time in the presence of narrow-band Gaussian noise. 12 p1468 A73-27010

Calculation of the average usage time of a channel in an adaptive multichannel communications system 12 p1471 A73-27585

Maritime Satellite System with broadband and multibeam dish antennas, assessing FDM communication capability as function of channel quality and ship terminal antenna gain 12 p1473 A73-27679

Parallel optical channel communications system with separate laser sources for suppressing mode competition noise due to beam intensity fluctuations/beats/ 13 p1584 A73-28898

Multiple access system by time division with synchronization in the S2 TDMA satellite 13 p1584 A73-28908

Study of carrier and bit-timing recovery of ultrahigh speed PSK-TDMA systems 13 p1584 A73-28909

Multiple access technique for future communication, surveillance and navigation subsystems to meet ATC demands, considering satellite surveillance radar system 14 p1725 A73-29893

Multibeam satellite Effective Isotropic Radiative Power /EIRP/ for aeronautical communications, discussing carrier-to-noise density increase and communication load per channel decrease 14 p1726 A73-29900

Remote feed, control, and signalization in transmission lines of multichannel systems with pulse code modulation 14 p1728 A73-30374

Output signal-to-noise ratio for a random-access repeater link with an ideal hard limiter. 15 p1844 A73-31733

Interference into angle-modulated systems carrying multichannel telephony signals. 16 p1983 A73-33742

Broad X band multichannel waveguide matrix for high speed switching from one input to one of four outputs at high power levels 16 p1990 A73-33897

Optimization of input signal levels in TWT amplifiers. 17 p2134 A73-34319

Demand-assignment multiple-access control techniques. 17 p2144 A73-35304

Multiple access techniques for the Canadian domestic satellite communications systems. 17 p2124 A73-35305

Time division multiple access in the INTELSAT system. 17 p2124 A73-35306

Wideband multidrop asynchronous TDM/FDM multichannel data distribution system for space station application, discussing analog and digital buses design 17 p2124 A73-35308

Asymptotic methods for the effectiveness computation of a sampling scheme of active sub-channels in an adaptive, multi-channel communication system. 17 p2129 A73-35712

Optimal processing of signals in systems with multiple elements/channels/ of reception. 17 p2130 A73-35723

Synthesis of the functions of polynomial linear-phase feedback amplifiers. 19 p2410 A73-38354

Multiple-beam satellite repeater tradeoffs applied to a multifunctional system. 20 p2524 A73-38732

Communication system with self limiting multiple access repeaters, calculating critical intermodulation power levels resulting from N equal amplitude carriers for comparison with measurements 20 p2526 A73-38750

An investigation of the combined amplification of monochromatic and noise signals in a TWT. 20 p2529 A73-38930

Probability of error in a bandlimited quadriphase communication system. 21 p2649 A73-40334

Combined effects of intersymbol, interchannel, and co-channel interferences in M-ary CPSK systems. 21 p2656 A73-41167

ATS-1 borne Random Access Discrete Address System for Multiple access satellite communication, discussing repeater performance concerning CW signal transmission efficiency, intermodulation and SNR 22 p2825 A73-42187

High altitude remotely piloted vehicle /RPV/ platforms for tactical pseudo-satellite multichannel relay transponder systems 22 p2826 A73-42423

Implementation problems of a multichannel digital filter in the case of beat frequencies in the MHz range 23 p2957 A73-43316

Coupling coefficient/frequency characteristics of rectangular dielectric waveguide channel dropping coupled line filter for millimeter wave 23 p2961 A73-44118

MULTICHANNEL RECEIVERS

U MULTICHANNEL COMMUNICATION RECEIVERS

MULTICHANNEL TRANSMITTERS

U MULTICHANNEL COMMUNICATION TRANSMITTERS

MULTILAYER INSULATION

High performance cryogenic multilayer thermal insulation with plastic films coated by vapor deposited metal, discussing heat transfer mechanism for comparison with microsphere insulation 05 p0642 A73-17285

Conical liquid hydrogen target with large exit aperture and multilayer insulation between inner vessel and vacuum jacket for experiments on leptonic decays 05 p0538 A73-17288

Analysis of gas flow through a multilayer insulation system. 17 p2149 A73-34184

Radiation heat transfer in multilayer insulation having perforated shields. 18 p2369 A73-36337

[AIAA PAPER 73-718] Multilayer foil insulated Si-Ge thermoelectric converters with multihundred watt power capacity, presenting thermal performance stability under vacuum operating conditions 19 p2392 A73-38423

Multilayer foil insulated Si-Ge thermopile design for multihundred watt radioisotope thermoelectric generator to withstand launch environments, evaluating performance under shock and vibration loads 19 p2392 A73-38424

The design and construction of an anechoic chamber lined with panels and intended for investigation of aerodynamic noise 21 p2674 A73-40942

Properties of laser mirrors at non-normal incidence. 22 p2872 A73-43186

MULTILAYER STRUCTURES

U LAMINATES

MULTILOOP SYSTEMS

U CASCADE CONTROL

MULTIMODE RESONATORS

Application of longitudinal multimode laser coherence properties to increase the holographic depth of field. 12 p1504 A73-26830

Electrooptical and piezoelectric alignment of a composite resonator in a semiconductor laser 13 p1627 A73-28764

Iterative diffraction calculations of transverse mode distributions in confocal unstable laser resonators. 14 p1756 A73-30156

Unsteady processes in multimode lasers with a nonuniformly widening line of lasing 15 p1886 A73-32329

MULTIPATH TRANSMISSION

The influence of chordal paths on signals propagating to the near antipode of an HF radio transmitter. 01 p0015 A73-10182

Digital modeling of multipath induced monopulse angle tracking errors. 04 p0416 A73-15056

Ground reflection multipath effects on airborne communications. 04 p0422 A73-15439

Multipath fading and ionospheric scintillation modes of propagation anomalies measurement to formulate models of propagation media 04 p0422 A73-15440

Mathematical model for multipath transmission in aircraft and spacecraft communications, presenting Bayes detector for binary PSK 04 p0422 A73-15462

Selectively faded nondiversity and space diversity narrowband microwave radio channels. 08 p0939 A73-21086

Effects of multipath fading on low data-rate space communications. 09 p1058 A73-23422

Modulation distortions during fading in frequency-modulated multichannel radio communication 10 p1187 A73-23740

First order effects of terrain on the radiation pattern of a non-directional LF beacon. 11 p1332 A73-26204

Multipaths by diffusion on the ground and application to the transmission of digital messages affected by jumps of the carrier frequency 14 p1725 A73-29732

Aircraft-satellite multipath communication characteristics, considering surface scatter, ionospheric scintillation and refraction and tropospheric refraction and scatter 14 p1725 A73-29891

Effect of multipath on ranging error for an airplane-satellite link. 14 p1725 A73-29892

Satellite-aircraft multipath and ranging experiment results at L band. 14 p1726 A73-29898

Multipath propagation in aircraft digital communication with ground terminal, modeling received signal for detection and estimation theories applications 14 p1726 A73-29902

Multiple path induced position errors in microwave landing systems, considering beating beam and Doppler systems based on time and frequency division multiplexing respectively 15 p1910 A73-32471

The multipath challenge for the microwave landing system. 15 p1912 A73-32503

The MADGE system - Operational results and stretch potential. 15 p1912 A73-32505

Propagation of radio waves at frequencies above 10 GHz; Proceedings of the Conference, London, England, April 10-13, 1973. 16 p1980 A73-33701

Single and dual path propagation at 18 GHz with application to the design of digital radio relay systems. 16 p1981 A73-33703

MULTIPHASE FLOW

- Methods for investigating the effects of multipath fading on 2-phase digital radio systems.
16 p1981 A73-33708
- The respective influences of multipath configurations and precipitation rates for frequencies lying between 10 GHz and 30 GHz.
16 p1981 A73-33710
- Multipath propagation effects on 11, 20 and 37 GHz FM-FDM systems at different path lengths
16 p1981 A73-33711
- Possibilities for improving conventional ILS systems
17 p2207 A73-34479
- Pseudo random modulation - An effective means of enhancing PSK signal transmission in a diffuse multipath environment.
17 p2125 A73-35376
- Simulation results for a radar multipath angle error reduction method.
17 p2127 A73-35633
- Decomposition of pulse-type data by cepstrum techniques.
17 p2127 A73-35635
- Recursive ideal observer detection of known M-ary signals in multiplicative and additive Gaussian noise.
19 p2407 A73-38385
- The effects of multipath on the design of ship board satellite communications antennas.
20 p2523 A73-38726
- Multipath channel characterization for Aerosat.
20 p2526 A73-38755
- Performance degradation plots for comparison of signal fading and intersymbol interference effects in two-component specular multipath digital microwave communication channel
21 p2649 A73-40336
- ILS technology assessment, considering landing glide path determination, interference due to multipath propagation and ground effects, and operating frequency range problem
21 p2737 A73-41075
- Cepstrum signal processing with complex algorithm involving Fourier transforms and logarithm for multipath interference distortion reduction in single sideband or multiplexed transmission channels
23 p2953 A73-43321
- ## MULTIPHASE FLOW
- ### NT TWO PHASE FLOW
- Boundary value problem for flow equation of multiphase viscous fluid with given velocity distribution, noting equations of motion for incompressible micropolar fluid flow
03 p0291 A73-13164
- Equations of motion in electrohydrodynamics of multiphase one dimensional flow, noting shock wave propagation and attenuation
03 p0346 A73-13611
- Population inversion by mixing in a shock tube flow.
05 p0600 A73-16556
- Flow equations of a multiphase mixture with one coherent liquid or gaseous phase.
06 p0685 A73-17758
- Multiphase flow past thin symmetrical airfoil, applying three velocity model with incident two phase and reflected particle flow components
09 p1027 A73-21993
- Shock wave pattern visualization and static pressure distribution in supersonic diffusers for mixed flow supersonic compressors, using closed Freon loop test rig [ASME PAPER 73-FE-35]
17 p2095 A73-35026
- Multiphase underexpanded plume computational technique including turbulent mixing and nonequilibrium chemistry.
18 p2368 A73-36244
- ### MULTIPLE DEGREES OF FREEDOM
- #### U DEGREES OF FREEDOM
- #### MULTIPLETS
- #### U FINE STRUCTURE
- #### MULTIPLY TRANSMISSION
- #### U MULTIPLEXING
- #### MULTIPLIERS
- #### U MULTIPLEXING
- #### MULTIPLYING
- #### NT FREQUENCY DIVISION MULTIPLEXING
- #### NT TIME DIVISION MULTIPLEXING
- Double exposure holographic interferometry for comparison of object of two points in time evolution, discussing space division multiplexing of exposures onto photographic plate
01 p0054 A73-11234
- Comparison of digital-signal multiplexing methods by means of sequencing
01 p0021 A73-11485
- Message switching for multiplexing data of computer users with interactive access onto common facilities, evaluating traffic induced time delay performance
04 p0425 A73-15428
- High-frequency electro-optic prism deflector with application to optical demultiplexing and multiplexing.
06 p0701 A73-18363
- Bragg diffraction by standing ultrasonic waves with application to optical demultiplexing.
06 p0701 A73-18364

- Energy spectra of mixed discrete random processes in statistical multiplexing systems with pulse position, delta and pulse code modulation
06 p0668 A73-18390
- Telemetry data acquisition, transmission lines and delayed time processes onboard spacecraft and at ground receiving stations and center, discussing multiplexing and computer control
07 p0795 A73-18953
- Recording and reconstruction method for image plane hologram multiplexed tenfold in small area, using He-Cd laser
08 p0964 A73-21052
- Three-dimensional holograms by rotational multiplexing of two-dimensional films.
08 p0964 A73-21055
- A broadband antenna and multiplexer system in the decimeter-wave range for solar radio astronomy
12 p1481 A73-27782
- An efficient multiplexing approach for adaptive aircraft communications via a relay satellite.
14 p1726 A73-29899
- PCM multiplexing system for incorporation into telemetry systems of large ballistic missiles or spacecraft launch vehicles
14 p1727 A73-30110
- Code division multiplexing system for multiple signal binary transmission in branched glass fiber optical communication network
14 p1729 A73-30696
- High speed serial multiplexed holographic recording for large capacity random access memories, using piezoelectric deflector and ferroelectric ceramic array modulators
16 p2013 A73-32872
- Flight test and demonstration of digital multiplexing in a fly-by-wire flight control system.
17 p2107 A73-35225
- Multiplex data bus techniques for digital avionics, discussing transmission media, modulation methods, remote control and reliability
17 p2138 A73-35231
- Application of multiplexing to the B-1 aircraft.
17 p2107 A73-35247
- B-1 aircraft electrical multiplex system.
17 p2110 A73-35309
- Control of multiplexed communications channels.
17 p2144 A73-35310
- Design and structure of a flexible recursive digital filter
23 p2957 A73-43315
- ## MULTIPLICATION
- Additions and multiplications number required for fast evaluation of polynomials, investigating savings through preconditioning
01 p0068 A73-10043
- Convergence to logarithmic distribution laws
09 p1112 A73-22884
- Rank-one and rank-two corrections to positive definite matrices expressed in product form.
09 p1113 A73-22956
- Comparative analysis of algorithms for measurement of correlation functions by the multiplication method /Review/
11 p1360 A73-25018
- ## MULTIPLIER PHOTOTUBES
- ### U PHOTOMULTIPLIER TUBES
- ### MULTIPLIERS
- #### NT CHANNEL MULTIPLIERS
- New transistor squaring stage with a 'smooth' parabolic characteristic for realizing a simple high-precision parabolic multiplier
01 p0024 A73-10924
- Improvement of the product accuracy in analog multipliers with the aid of the negative-feedback principle
06 p0672 A73-17400
- Optical device for three dimensional multiplication of input signal recorded on photographic film, noting pattern recognition and optical communication applications
07 p0823 A73-19909
- Inertial smoothing of multiplier signals in automatic control system under sinusoidal signal, noting analog simulation of inertialess synchronous detector for self adaptive control
09 p1069 A73-22654
- Bipolar LSI building blocks for digital filtering applications.
17 p2138 A73-35228
- High speed parallel multiplier design based on threshold logic adder using integrated logic circuits
17 p2139 A73-35238
- A new technique for designing high-speed frequency counters.
21 p2658 A73-41146
- Use of switching circuits as redundant multiplier elements in canonic digital networks.
21 p2658 A73-41209
- Four-quadrant analog multiplier synthesis for IC implementation based on logarithmic addition in all n-p-n bipolar transistor configuration for algebraic product derivation
24 p3074 A73-45260

MULTIPOLAR FIELDS

- Motion of plasmoids in a toroidal magnetic multipole.
06 p0727 A73-17421
- Polarization interaction of opposed plasma streams in a linear magnetic octupole.
06 p0727 A73-17422
- Thermal conductivity and resonant multipole interactions.
06 p0725 A73-18121
- Drift shell splitting and magnetic equator surface topography model based on charged particle adiabatic motion and trapping in presence of internal geomagnetic multipoles
07 p0813 A73-19236
- Radiation fields in the Schwarzschild background.
08 p0988 A73-21202
- Magnetic multipole containment of large uniform collisionless quiescent plasmas.
17 p2215 A73-34271
- Stability of plasma flows in multipolar magnetic fields
19 p2467 A73-37372
- Multipoint distribution calculation of the isotropic turbulent energy spectrum.
19 p2421 A73-37854
- Debye representation and multipole expansion of the quantized free electromagnetic field.
20 p2591 A73-38609
- Longitudinal polarization and focusing of plasmoids in a linear multipole magnetic field
22 p2893 A73-42383
- ## MULTIPOLES
- Statistical method of calculating scattering matrix elements and parameter deviations of SHF octupole networks /square bridge, hybrid ring or directional junction/
02 p0146 A73-12025
- Multipole sine-cosine azimuth patterns for wide aperture Adcock direction finders, determining spacing and reradiation errors and array pickup factor
02 p0142 A73-12529
- Discretized elastic multipolar bodies equations of motion and conservation laws from variational formulation, considering virtual work, Betti principle and Somigliana formulae
06 p0761 A73-17892
- Modulation functions and transmission coefficients for static frequency converter representation in form of equivalent multipole networks for reactive loads
13 p1592 A73-28939
- ## MULTIPROCESSING [COMPUTERS]
- A simulation model for a memory organization for a multiprocessor.
12 p1475 A73-27155
- Aerospace multiprocessor for A-7D aircraft digital fly by wire flight control, discussing design requirements, software development and reliability
17 p2107 A73-35223
- Station Data Acquisition and Control System.
17 p2147 A73-35301
- ## MULTIPROGRAMMING
- Teleprocessing systems communication software functions and construction, considering network control, message preprocessing, queueing and error recovery in multiprogramming and multiprocessing environment
05 p0551 A73-16803
- Scheduling algorithms for multiprogramming in a hard-real-time environment.
08 p0941 A73-20961
- Design philosophy and operation of hardware and data flow of TELFILE real time multiprogrammed telemetry system, discussing support of Minuteman III Weapons Systems
09 p1057 A73-23415
- Computerized total On-Line Testing System with diagnostic error visibility and preventive and corrective maintenance functions in multiprogramming mode, discussing design features
16 p1986 A73-33633
- ## MULTIPROPELLANTS
- ### U ROCKET PROPELLANTS
- ## MULTISPECTRAL BAND SCANNERS
- Multispectral cloud type identification based on Nimbus 3 medium resolution IR radiometer measurements, using radiative transfer theory
01 p0073 A73-10381
- Radiometric techniques for observing the atmosphere from aircraft.
01 p0073 A73-10404
- The ERTS wideband image communication system.
04 p0418 A73-15382
- Earth resources sensing technology - 24-channel multispectral sensor system development.
04 p0449 A73-15463
- A digital processing and analysis system for multispectral scanner and similar data.
05 p0554 A73-17147
- Variance reduction in remotely sensed multispectral data caused by random noises and systematic variations in system angular response and in apparent scene radiance
05 p0554 A73-17148

Rapid processing of multispectral scanner data using linear techniques. 05 p0554 A73-17150

Spectral signature variability model based on multispectral band scanner data and clustering experiments, discussing data processing algorithms 05 p0555 A73-17151

Texture dependent features recognition in terms of spatial frequencies of remotely sensed multispectral data small sections 05 p0555 A73-17152

Radiation balance mapping with multispectral scanner data. 05 p0572 A73-17158

A dual polarization laser backscatter system for water quality studies. 06 p0700 A73-18306

ERTS-1 satellite-borne high resolution multispectral radiometer scanner, discussing optical surface performance during exposure to direct and reflected sunlight 13 p1621 A73-29331

Optimum astronomical photoelectric photometry - Terrestrial operations in the UV-IR band up to 1 micron wavelength. 16 p2011 A73-32829

Airborne photography with multispectral scanners for remote sensing of large area features, discussing cost and feasibility of computerized pattern recognition and automatic identification 16 p2015 A73-33361

Monitoring earth's resources from space. 17 p2157 A73-34279

The use of remote sensing for the detection of natural resources - Definition of the platforms, technical-organizational considerations 17 p2160 A73-34930

Satellite remote monitoring of earth environment and natural resources by high resolution multispectral scanners for European requirements 17 p2160 A73-34931

Key technological challenges of the Earth Resources Technology Satellite program. 17 p2161 A73-34943

ERTS-1 satellite-borne multispectral scanner photographic mapping of Israel vegetation, hydrology, geological structure, atmospheric phenomena and oceanography 17 p2162 A73-34947

Remote sensing technology - The 24-channel multispectral scanner. 17 p2171 A73-35365

A low-cost system for reproducing ERTS imagery. 18 p2315 A73-36018

ERTS-1 MSS imagery - A tool for identifying soil associations. 18 p2306 A73-36023

Hydrological phenomena teledetection based on multispectral band scanners for IR and visible frequency ranges 18 p2307 A73-36027

Remote sensing - The application of space technology to the survey of the earth and its environment. 19 p2423 A73-37497

Equipment for checking of terrestrial resources 19 p2431 A73-38177

Computer processing of earth resources data from mono- and multispectral band scanners and IR photography 19 p2431 A73-38178

Enhancement of Earth Resources Technology Satellite /ERTS/ and aircraft imagery using atmospheric corrections. 20 p2567 A73-39835

Corn blight epiphytotic remote sensing, data acquisition and crop identification by photointerpretation and computer aided multispectral band scanner data analysis 20 p2556 A73-39836

Land use classification in the southeastern forest region by multispectral scanning and computerized mapping. 20 p2557 A73-39849

Multispectral survey of power plant thermal effluents in Lake Michigan. 20 p2558 A73-39862

The interpretation of multispectral imagery - An analysis of automated versus human interpretation techniques. 20 p2558 A73-39875

Performance evaluation of multispectral scanner classification methods. 20 p2559 A73-39876

Adaptive multispectral scanner recognition via maximum likelihood classifier for agricultural crops, discussing error sources 20 p2559 A73-39877

Multispectral scanner data analysis by application of spectral radiance signature extension techniques based on preprocessing to reduce atmospheric and scanner look angle effects 20 p2559 A73-39880

Remotely sensed multispectral scanner data collection over agricultural area, discussing spatial resolution modification for crops and unresolved objects classification 20 p2559 A73-39882

Experimental design to produce visible-reflective IR ratio image from ERTS data for geological mapping of iron compounds 20 p2561 A73-39899

Multispectral reflectance scanning of crop image signatures during April-July growing season, examining time dependent image changes, discrimination tests and crop types 20 p2561 A73-39900

Multispectral scanner imagery in aerial photography of plant communities, discussing reflectance effects, digital processing, vegetation types, classification errors and spectrum analysis 20 p2561 A73-39901

ERTS-1 satellite return beam vidicon and multispectral scanner comparative evaluation for image quality, considering response functions, resolution, measurability, detectability and image motion effects 20 p2563 A73-39912

ERTS-1 satellite-borne multispectral scanner remote sensor for global pollution monitoring, geological and heat balance surveys, and storm and earthquake caused damage 21 p2692 A73-41520

ERTS-1 satellite-borne TV cameras and multispectral band scanners for remote sensing and data collection with applications in agriculture, forestry, and water resources survey 21 p2692 A73-41521

An analysis of the earth's resources satellite /ERTS-1/ data. 22 p2850 A73-42732

MULTISPECTRAL PHOTOGRAPHY

NT INFRARED PHOTOGRAPHY

NT RADAR PHOTOGRAPHY

Geology, hydrology, land use and transportation net of Dallas-Fort Worth area from Apollo 6 photographs, comparing with ground based data 01 p0035 A73-10139

Multiband and multiemulsion digitized aerial photographs automatic processing by digital computer techniques and statistical pattern recognition algorithms 01 p0044 A73-10140

Digital image registration by correlation techniques. 04 p0449 A73-15413

Electro-optical multiband cameras for spaceborne remote sensing, discussing optical multiplexing, return beam vidicon, intensifier vidicon storage tube, image spectrophotometer and dissector 04 p0450 A73-15770

An electronic multiband camera film viewer. 04 p0450 A73-15771

Satellite-borne solid state multispectral image remote sensors with photodiode linear arrays for data acquisition, noting system performance and reliability advantages 04 p0451 A73-15781

The cost-effectiveness of high altitude systems for regional resource assessment. 05 p0642 A73-17139

Supervised and unsupervised category identification and classification systems consistency with ERTS satellites high rate multispectral data requirements 05 p0572 A73-17142

ERTS two-inch RBV cameras performance characteristics. 05 p0579 A73-17144

Multispectral additive color viewer for ERTS satellite photography, discussing colorimetric measurement usefulness and photo processing and image density control effects on color characteristics 05 p0579 A73-17145

An integrated feature selection and supervised learning scheme for fast computer classification of multi-spectral data. 05 p0555 A73-17153

Automatic classification by sequential statistical variance and K-means clustering techniques for remote multispectral earth resource observation data. 05 p0555 A73-17154

Remote sensing of lunar color differences using isoluminous enhancement techniques. 09 p1082 A73-22384

A 35mm aerial photographic system. 09 p1082 A73-22387

The earth resources experiment package on Skylab and proposed resource investigations. 09 p1082 A73-22389

Multispectral imagery data compression for earth resources satellites, comparing performance of spectral-spatial-delta-interleave and Rice coding algorithms 09 p1055 A73-23391

Color encoded multispectral image recording on black-and-white photographic film with synthetically generated diffraction gratings, noting color recognition, resolution and contrast ratio 10 p1216 A73-23786

The application of color and multispectral techniques to the collection of military geographic information. 12 p1500 A73-27952

Block adjustment for color and multispectral high altitude frame photography in photogrammetry, considering terrain caused sun angle effect as discriminant for automatic photointerpretation 12 p1500 A73-27955

Skylab A solar and terrestrial observation and photography hardware, including solar observatory, microwave scanner, IR spectrometer and multispectral photographic facility 13 p1612 A73-28276

Atmospheric effects in multispectral photographs. 13 p1619 A73-29239

Sensor development - An overview of recent Canadian experience. 20 p2533 A73-38578

The use of small-scale multi-band photography for detecting land-use change. 20 p2557 A73-39847

Multispectral remote sensing of elements of water and radiation balances. 20 p2558 A73-39864

Unsupervised maximum likelihood classification technique multispectral remote sensing data, using two-part statistical clustering technique of sequential variance analysis 20 p2559 A73-39879

Environment models and algorithm for obtaining statistically optimal proportions estimates for category mixtures in multispectral sensor data processing 20 p2559 A73-39883

Southern California coastal processes as analyzed from multi-sensor data. 20 p2560 A73-39886

A statistical-temporal image merging technique for automatic bathymetry applied to southern California coastal waters. 20 p2560 A73-39887

Radiometric calibration of a multi-spectral aerial camera. 22 p2862 A73-42824

MULTISTAGE COMPRESSORS

U TURBOCOMPRESSORS

MULTISTAGE ROCKET VEHICLES

NT ASTROBEE ROCKET VEHICLES

NT ATLAS CENTAUR LAUNCH VEHICLE

NT BLACK KNIGHT ROCKET VEHICLE

NT DIAMANT LAUNCH VEHICLE

NT ELDO LAUNCH VEHICLE

NT LAMBDA ROCKET VEHICLES

NT SATURN LAUNCH VEHICLES

NT SKYLARK ROCKET VEHICLE

NT TITAN 3 LAUNCH VEHICLE

Lambda-4S solid propellant four-stage sounding rocket and scientific satellite launcher, describing design, operational and performance features 01 p0091 A73-11157

Rocket stages separation distance measurement by monitoring gamma ray flux variation, noting separation mechanisms and retromotor performances 01 p0052 A73-11166

Structural weight analysis of single stage and multistage spacecraft for given payload and initial vehicle weight, considering optimization problem 02 p0229 A73-12469

Structural weight optimization of single stage and multistage spacecraft for given payload and initial vehicle weight 15 p1944 A73-32619

Possibility of utilizing the ERIDAN rocket probe as an experimental vehicle 16 p2071 A73-32817

MULTIVARIATE STATISTICAL ANALYSIS

NT BIVARIATE ANALYSIS

NT COVARIANCE

NT DISCRETE FUNCTIONS

NT ORTHOGONALITY

NT REGRESSION ANALYSIS

Non-interacting control of non-linear multivariable systems. 01 p0028 A73-11517

Multivariate analysis applied to aircraft optimisation - Some effects of research advances on the design of future subsonic transport aircraft. 02 p0130 A73-11661

MULTIVIBRATORS

P wave analysis in 2464 orthogonal electrocardiograms from normal subjects and patients with atrial overload.

22 p2806 A73-42341

High energy nucleon inelastic interaction characteristics calculated from artificial event model based on covariant statistical theory of multiple generation of particles

23 p3022 A73-43542

Multidimensional scaling methods and data visualization /Review/

23 p2949 A73-43578

MULTIVIBRATORS

NT FLIP-FLOPS

Russian book on nanosecond multiphase multivibrators covering transistorized single- and dual-stage amplifiers and wave shaping circuits for digital control and computer logic applications

02 p0146 A73-11887

Multivibrator with p-n-p and n-p-n transistors, noting circuit diagram, operation and power dissipation

10 p1197 A73-24940

Linearization of the relaxation time control of a transistor multivibrator.

15 p1849 A73-30992

Optimum nonlinear characteristic of the supply element in the astable multivibrator with a tunnel diode.

19 p2410 A73-38309

The optimal nonlinear characteristic of the drive element in an astable multivibrator with a tunnel diode

20 p2536 A73-39201

Information dependent frequency control of an automatic typewriter.

23 p2944 A73-43423

Cascade n-phase transistorized astable multivibrator circuit design for digital and tool control clock applications

23 p2983 A73-44142

MUONS

Multiple scattering of cosmic ray muons in the range 10-70 GeV/c.

01 p0091 A73-10787

High energy muons /not less than 150 GeV/ in extensive air showers.

01 p0092 A73-10788

The possibility of a consistent explanation of various phenomena involving cosmic ray muons.

01 p0092 A73-10789

Measurement of the local production of muons underground.

01 p0080 A73-11009

Cosmic ray muon component integral multiplicity calculations with allowance for angular distribution of secondary particles in elementary collision event on atmospheric boundary, using computer

02 p0205 A73-12172

Primary proton-air atom nuclei interaction study of negative and positive cosmic ray muon coupling coefficients with angular distribution allowance

02 p0205 A73-12173

Electron and muon density fluctuations, trajectory distribution and azimuthal symmetry in cosmic ray air showers

02 p0209 A73-12673

Extensive air shower spectra based on electron and muon number for given shower development mechanism and primary cosmic ray chemical composition

02 p0209 A73-12677

Extensive air shower characteristics and muon counts at different level observations relative to particle number and primary energy spectra

02 p0209 A73-12678

High energy cosmic ray interactions at one TeV, including X process, horizontal showers and muon poor showers

02 p0209 A73-12679

High energy muon energy and angular distributions from electron-photon cascades, using emulsion chamber with X ray films

02 p0209 A73-12680

Energy spectrum of muon formed electromagnetic cascades in vertical cosmic radiation flux

02 p0209 A73-12681

Spectral calculations of electromagnetic and nuclear showers, studying cosmic ray muons interactions with matter

02 p0210 A73-12682

Muon densities in penetrating high energy particles, comparing with extensive air showers

02 p0210 A73-12683

Muon generated cascade showers in iron, using ionization calorimeter and hodoscopic detectors

02 p0210 A73-12684

Muon track curvatures in Wilson chamber magnetic field for calibrating ionization levels of logarithmic increase

02 p0171 A73-12687

Nonconventional processes in anomalous cosmic-ray experiments.

06 p0743 A73-17865

Electromagnetic interactions of cosmic ray muons in iron. I - Search for a charge asymmetry.

06 p0743 A73-18386

Electromagnetic interactions of cosmic ray muons in iron. II - Momentum dependence of the interaction probabilities.

06 p0743 A73-18387

Coupling function for the vertical muon telescope at 60-meters-water-equivalent depth.

07 p0869 A73-19251

Energy spectra of cosmic pions and nucleons at the top of the atmosphere.

07 p0872 A73-20015

Predicting light flashes due to alpha-particle flux on SST planes.

07 p0777 A73-20157

Low momentum integral muon spectrum at sea level near the geomagnetic equator.

13 p1670 A73-28211

Abundance and lateral distribution of muons in inclined showers.

13 p1670 A73-28371

Neutron emission after muon capture in Ce, Ba and Sn, analyzing delayed gamma ray energies and branching ratios to excited nuclear states

13 p1662 A73-28650

Measurement of cosmic-ray muon charge ratio at sea level between energies of 10 and 1500 GeV.

14 p1787 A73-30455

Muon observations, discussing high energy cosmic ray neutrino experiments and production via pion and kaon decay, neutrino interactions and nuclear collisions

16 p2055 A73-33291

Interpretation of the charge ratio of cosmic ray muons.

17 p2223 A73-34242

The lateral distribution of muons in near vertical EAS.

17 p2223 A73-34243

Large underground showers and multiple muons in association with E.A.S.

19 p2475 A73-37574

Muon production in large air showers, determining mean origin height via magnetic spectrography, distance from shower core, geomagnetic deflection and trajectory angles

20 p2603 A73-39707

Cosmic ray muon zenith angle distribution during horizontal air showers, discussing kaon and pion decay, spectrum characteristics, bremsstrahlung effects and flux upper limits

20 p2603 A73-39708

A survey on the recent measurements of the absolute vertical cosmic-ray muon flux at sea level.

20 p2603 A73-39825

Low energy gamma ray spectrum following muon capture by oxygen 16 leading to bound states of nitrogen 16

21 p2743 A73-40475

The multiplicity distribution of shower particles underground and the cosmic-ray primary spectrum.

21 p2764 A73-41633

Measurements of absolute intensities of cosmic-ray muons in the vertical and greatly inclined directions at geomagnetic latitudes 16 N.

22 p2903 A73-42437

Measurement of the absolute vertical integral and differential cosmic-ray single-muon flux at 3.6 GeV and a measurement of the showerless penetrating particle-pair flux above 3.6 GeV.

22 p2903 A73-42440

Comparison of calculated characteristics of extensive atmospheric showers with experimental results at various altitudes

22 p2903 A73-42733

Intense air showers with an electron-photon core of complex structure

23 p3022 A73-43545

Large transverse momenta and the structure of extensive air shower cores

23 p3022 A73-43548

An arrangement for studying horizontal air showers - Initial results

23 p2966 A73-43549

Calculated characteristics of the electron and muon components of extensive air showers at the 690 g/sq cm level

23 p3022 A73-43553

The energy spectrum of cosmic ray muons at sea level

23 p3023 A73-43559

Generation of high-energy muons in cosmic rays

23 p3023 A73-43560

Experimental characteristics of a muon stream with energies above 10 GeV, contained in an extensive air shower

23 p3023 A73-43561

Some characteristics of the muon component of extensive air showers at mountain level

23 p3023 A73-43562

Muon decay/transmission ratios at 60 and 850 mwe measured by scintillation counter

23 p3023 A73-43563

Energy spectrum and angular distribution of outer space muons and the processes of their production in the 1 TeV energy range

23 p3024 A73-43564

Spark calorimetry investigation of trident and extensive air showers muon component generated highly energy penetrating particles at large zenith angles

23 p3024 A73-43565

Large wire spark chambers with an information output and storage system

23 p2982 A73-43570

MUSCLES

Effect of increased atmospheric pressure on the dynamics of free oxygen content in animal muscle tissues

01 p0007 A73-10156

Diet, exercise, and glycogen changes in human muscle fibers.

01 p0007 A73-10160

Absence of appreciable cardiovascular and respiratory responses to muscle vibration.

03 p0263 A73-14119

Oxidation effects on rate of C 14-labeled leucine incorporation into rat skeletal muscle protein

05 p0538 A73-16152

Myosin ATPase and fiber composition from trained and untrained rat skeletal muscle.

05 p0538 A73-16155

Some physiological reactions to acceleration in albino rats in a state of hypothermia

05 p0541 A73-16737

Application of the method of polarizational ultraviolet fluorescence microscopy to study giant muscle fibers Balanus rostratus Hock

08 p0930 A73-21135

Effect of training on enzyme activity and fiber composition of human skeletal muscle.

08 p0935 A73-21508

Possibility of modeling the relationship between the intracellular potential of individual muscle fibers and the overall electromyogram for tonic muscles

10 p1179 A73-23810

Periodic conditions in artificial muscle: autopsaltors

14 p1721 A73-30289

Influence of ribonuclease on changes in the membrane potential of muscle fibers evoked by stimulation of the sympathetic nerve

15 p1833 A73-31166

Space flight exercise regimen proposals, exploring moving picture/electric muscle stimuli program as earth gravity simulator in weightlessness

15 p1838 A73-31515

Technique for recording muscle biopotentials by means of implanted electrodes

15 p1839 A73-31799

Continual mechanochemical model of muscular tissue

21 p2643 A73-40182

MUSCULAR FATIGUE

Energy cost of muscle work in a state of fatigue

05 p0541 A73-16697

Functional condition changes of biceps brachii in man under the effect of fatiguing physical stress

07 p0780 A73-19643

Oxygen consumption alteration effects on human endurance capacity as function of relative work, muscle blood flow and anaerobic metabolism

14 p1714 A73-29753

Erythrocyte volume in acidified venous blood from exercising limbs.

24 p3062 A73-45557

MUSCULAR FUNCTION

Effects of exercise on activity of heart and muscle mitochondria.

01 p0006 A73-10135

Activity relation between internal organ receptors and skeletal muscles in terms of laws controlling process coordination

01 p0007 A73-10154

Interrelation between hardness, viscosity, strength, and bioelectric activity of human muscles

01 p0007 A73-10155

Role of the sympathetic-adrenal system during a period of rest and in adaptation to muscular activity

01 p0007 A73-10157

Isovolumic contraction dynamics in man according to two different muscle models.

01 p0007 A73-10158

Polysynaptic pathways role in tonic vibration and monosynaptic reflexes due to muscle vibratory or nerve electric stimulation, respectively, discussing tetanization effects

01 p0008 A73-10409

Peripheral electromyography spike and ventral root unit discharge intervals during tonic vibration reflex of cat soleus motoneuron

01 p0008 A73-10410

Investigation of the recovery dynamics of the mimic muscle function and choice of an optimal bioelectric stimulation program with the aid of an electronic digital computer

01 p0012 A73-10656

Effect of eccentric and concentric muscle conditioning on tension and electrical activity of human muscle.

01 p0013 A73-10774

Microvascular responses to alterations in oxygen tension.

01 p0009 A73-11010

Electromyographic study on human standing posture in experimental hypogravic state.

01 p0013 A73-11211

Muscular activity control mechanism interactions in vertical posture maintenance from stabilogram, mechanogram and electromyogram data

02 p0137 A73-12119

Importance of the Lohmann reaction in the response of the heart to anoxic aggression

02 p0133 A73-12152

The role of muscle stiffness in meeting the changing postural and locomotor requirements for force development by the ankle extensors.

02 p0138 A73-12166

Spontaneous middle ear muscle activity in man - A rapid eye movement sleep phenomenon.

02 p0134 A73-12423

Myocardial function and ultrastructure in chronically hypoxic rats.

03 p0259 A73-13369

EMG measurement on male adults for muscular relaxation reaction time interval from light stimulus onset to elbow flexor response

03 p0267 A73-13699

The role of extrinsic vagal innervation in the motility of the smooth-muscle portion of the esophagus - Electromyographic study in the cat and the baboon

03 p0262 A73-13785

Correlation between the voltage-time curves of H- and M-responses of a human muscle during various functional states of the spinal center

03 p0262 A73-13819

Telemetry methods for maximum static muscle strength measurements, considering dynamic force measurement possibilities

03 p0271 A73-14296

EMG from smooth musculature [uterus, ureter, gut] in unrestrained animals monitored by telemetry.

03 p0271 A73-14297

Reliability of electromyographic measurements by means of surface electrodes

04 p0412 A73-15520

Effects of physical training on cardiac actomyosin adenosine triphosphatase activity.

05 p0539 A73-16157

Muscle metabolites with exhaustive static exercise of different duration.

05 p0539 A73-16247

Muscle control models of joint angle spatial motions, including circle, ellipse and straight line trajectories and orientations in space

06 p0680 A73-17960

Mechanical modeling of eye muscle dynamics.

06 p0660 A73-18816

Adenonucleotides, NAD⁺, and NADN in skeletal muscles during intensive work and at rest

07 p0780 A73-19475

Functional condition changes of biceps brachii in man under the effect of fatiguing physical stress

07 p0780 A73-19643

A method for chronocyclographical motion analysis with the aid of an on-line computer

07 p0785 A73-20036

The interaction between muscle groups in a complex motor act in humans

08 p0930 A73-21320

Contributions of quick and slow muscle fibers to changes in the electrical activity of skeletal muscles in rats under acute and chronic effects of cold

08 p0931 A73-21323

Blood vessels simulation by muscle pump represented by elastically deformable pipe with valves, solving Navier-Stokes equation for viscous fluid flow

08 p0934 A73-21375

Effects of anesthesia and muscle paralysis on respiratory mechanics in normal man.

08 p0934 A73-21505

An implantable glass electrode used for pH measurement in working skeletal muscle.

08 p0935 A73-21510

Effect of copper ions on the functional state of the neuromuscular apparatus

09 p0139 A73-22369

Organization of spontaneous muscular activity in man

09 p0140 A73-22863

A frequency response analysis of fusimotor-driven muscle spindles.

09 p0141 A73-22934

Protein molecules peptide groups excitation interpretation by quantum theory, noting application to muscle contraction

09 p0146 A73-23297

Changes in gaseous metabolism and cardiac output per minute during local muscle work in man

10 p1179 A73-23809

Electromyographic alterations in articular muscles during emotional shifts

10 p1180 A73-24328

Rise time of the spike potential in fast and slowly contracting muscle of man.

10 p1181 A73-24500

Voluntary activation of individual motor units in man

10 p1181 A73-24519

Human forearm-muscle blood supply regimes after 'static' exercise with increasing stress

10 p1181 A73-24522

Reflex reaction of antagonist muscles during an evoked tendon reflex

10 p1182 A73-24598

Organization of the activity of a group of motor neurons in man during voluntary contraction of a muscle

10 p1182 A73-24599

The nature of the optimum muscular performance achieved in the execution of fast eye rotations.

10 p1185 A73-24772

Calcium movements and excitation-contraction coupling in cardiac cells.

11 p1316 A73-25601

Posture responses of upper limb muscles during electric stimulation of the vestibular apparatus

11 p1317 A73-26087

A new phenomenon of an active intraorgan pumping function of skeletal muscles

12 p1462 A73-27446

Heart function mechanism explanation by activation potential stimulation of muscular contraction via calcium ions

12 p1462 A73-27690

Effect of adaptation to cold on the energy characteristics of muscular activity

13 p1574 A73-28295

Exogenous free fatty acid effects on hypoxic myocardial function in isolated isometric rat papillary muscles

13 p1577 A73-29572

Electrical activity of the external ear muscles in man /at rest and during identification of acoustic signals/

14 p1719 A73-30843

Motor, thermal and sensory factors in heart rate variation A methodology for indirect estimation of intermittent muscular work and environmental heat loads.

14 p1720 A73-30880

Functional condition of skeletal muscles in rats under lasting movement constraints /up to 120 days/

15 p1834 A73-31504

Effect of prolonged hypokinesia on certain energy transfer characteristics in skeletal muscles and some internal organs

15 p1834 A73-31505

Mechanism of working hyperemia condition alteration in the forearm muscles of man under increased loads

18 p2276 A73-36570

Effect of sympatholytin on metabolism in resting and working muscles in relation to the degree of their adaptation to intensified activity

18 p2276 A73-36571

Changes in respiration effectiveness during muscular activity

18 p2277 A73-36580

Ribes Nigrum anthocyanosides in ophthalmology

18 p2280 A73-36935

The capacity for muscular work in acute hypoxia

18 p2286 A73-36946

Electromyographic study of repetitive fasciculation potentials in triceps and adductor pollicis in normal subjects and patients with motor neuron diseases, noting postcontraction pause

20 p2514 A73-39761

Variations in the motor potential with force exerted during voluntary arm movements in man.

21 p2638 A73-41013

Relationship between cyclic AMP, phosphodiesterase activity, calcium and contraction in intestinal smooth muscle.

21 p2638 A73-41130

Oxygen uptake, muscle high-energy phosphates, and lactate in exercise under acute hypoxic conditions in man.

21 p2638 A73-41131

Effect of training with eccentric muscle contractions on skeletal muscle metabolites.

21 p2641 A73-41523

Effect of hind-limb immobilization on contractile and histochemical properties of skeletal muscle.

21 p2642 A73-41624

Investigation of the nature of biological rhythm sensors by means of automatic networks

22 p2812 A73-41865

Effect of chronic pyramid insufficiency on the function of spinal centers of shin and foot muscles in man

22 p2807 A73-42658

Reflex arch lability in rabbits at synchronous maximum frequency of electromyographic and muscle stretching vibration measurement

22 p2807 A73-42659

Urea content variations in blood and tissues during muscular activity in relation to the adaptation level of the organism

22 p2807 A73-42660

Human phasic reflex response to parameters of a mechanical stimulus as an index of muscle-spindle sensitivity.

22 p2816 A73-42679

Myocardial oxygen consumption in experimental hypertrophy and congestive heart failure due to pressure overload.

22 p2808 A73-42688

Study of the nature of the active tonus with the aid of a discrete Wiener-medium analog

22 p2816 A73-42973

The energetic metabolism and some reactions of the cardiovascular system during multichannel electrical stimulation and voluntary stressing of muscles

24 p3059 A73-44670

Use of the conditioned reflex method to study the motor analyzer during hygienic evaluation of working conditions in the presence of vibrations

24 p3062 A73-44673

MUSCULAR STRENGTH

Interrelation between hardness, viscosity, strength, and bioelectric activity of human muscles

01 p0007 A73-10155

Utilization extent of the muscle apparatus capabilities during maximum voluntary force exertion

05 p0541 A73-16696

MUSCULAR TONUS

Cerebral circulation alteration during hypothermia

05 p0541 A73-16698

Action of a serum protein on muscular contraction.

08 p0930 A73-21200

Possibility of modeling the relationship between the intracellular potential of individual muscle fibers and the overall electromyogram for tonic muscles

10 p1179 A73-23810

Contraction kinetics of ventricular muscle from hibernating and nonhibernating mammals.

20 p2514 A73-39603

Human sensorimotor coordination following space flights.

22 p2814 A73-42170

Action of stable and pulsed noise on the processes of skeletal muscle excitation

22 p2815 A73-42662

Study of the nature of the active tonus with the aid of a discrete Wiener-medium analog

22 p2816 A73-42973

A method for the approximation of processes in homogeneous biological structures

24 p3062 A73-44663

MUSCULOSKELETAL SYSTEM

NT BONES

NT CEREBRUM

NT COLLAGENS

NT CONNECTIVE TISSUE

NT CONSTRICTORS

NT CRANIUM

NT ELBOW [ANATOMY]

NT FLEXORS

NT INTRACRANIAL CAVITY

NT JOINTS [ANATOMY]

NT KNEE [ANATOMY]

NT PELVIS

NT SKULL

NT ULNA

NT VERTEBRAE

NT VERTEBRAL COLUMN

Current views on the mechanism of the quantum-induced liberation of a mediator from the motor nerve endings of a skeletal muscle

01 p0009 A73-11023

Reduced dimensionality for minimization of degrees of freedom of skeletal activity models for anthropomorphic locomotion system synthesis

01 p0013 A73-11052

An implantable glass electrode used for pH measurement in working skeletal muscle.

08 p0935 A73-21510

A new phenomenon of an active intraorgan pumping function of skeletal muscles

12 p1462 A73-27446

Functional condition of skeletal muscles in rats under lasting movement constraints /up to 120 days/

15 p1834 A73-31504

Dynamic analyses of hybrid bio/mechanical networks with feedback characterization.

16 p1975 A73-33161

Prolonged space flight and hypokinesia.

18 p2278 A73-36789

Motor unit reactions of man to spinal and supraspinal inhibitory stimuli

19 p2395 A73-37943

Volume-pressure characteristics of rib cage-diaphragm interaction in standing subjects during voluntary relaxation

20 p2518 A73-39778

Action of stable and pulsed noise on the processes of skeletal muscle excitation

22 p2815 A73-42662

Age-dependent characteristics of myoglobin content and distribution in the heart and skeletal muscles

24 p3059 A73-44669

MUTATIONS

A note on the hypothesis - Protein polymorphism as a phase of molecular evolution.

04 p0410 A73-16033

Stochastic model application to divergence of horse-pig lineage from common ancestor in terms of hemoglobin and fibrinopeptides alpha and beta chains

07 p0780 A73-19218

International literature survey of microbiological space research for 1930-1970, discussing high altitude

MYOCARDIAL INFARCTION

- balloon, rocket and satellite experiments, weightlessness effects, mutagenesis, etc 15 p1838 A73-31501
- Influence of simulated weightlessness on the mutational rate of *Tribolium confusum*. 18 p2270 A73-35984
- Survival and mutability of *Chlorella* under various orientation in the earth's gravitational field. 18 p2270 A73-35997
- Chemical protection from genetic damages induced by radiation in the period of aftereffect of acceleration. 21 p2643 A73-40815
- Results of cytogenetic studies of seeds after their extended orbital flight aboard the Salyut orbital scientific station. 22 p2804 A73-42169
- Heavy ion irradiation effects on bacteria mutations in balloon flight and accelerator experiments, comparing with cosmic rays 22 p2805 A73-42184
- MYOCARDIAL INFARCTION**
- Echocardiographic findings in experimental myocardial infarction of the posterior left ventricular wall. 02 p0138 A73-12446
- Left ventricular performance after myocardial infarction assessed by radioisotope angiocardiography. 08 p0932 A73-21801
- Intravascular platelet aggregation in the heart induced by stress. 08 p0933 A73-21805
- Electrocardiographic evidence of left atrial hypertension in acute myocardial infarction. 11 p1319 A73-26287
- Angina pectoris in men - Prognostic significance of selected medical factors. 11 p1319 A73-26288
- Unreliability of conventional electrocardiographic monitoring for arrhythmia detection in coronary care units. 12 p1465 A73-27891
- Immediate and remote prognostic significance of fascicular block during acute myocardial infarction. 14 p1715 A73-30052
- Risk factors for developing myocardial infarction and other diseases - The 'Men born in 1913' study. 14 p1716 A73-30352
- Echocardiographic detection of regional myocardial infarction - An experimental study. 15 p1839 A73-31997
- A new method for diagnosing myocardial damage in patients with normal electrocardiograms and vector cardiograms. 16 p1973 A73-33375
- Book on vectorcardiography covering equipment, techniques, lead systems and abnormalities associated with atrial and ventricular hypertrophy, bundle branch blocks, myocardial infarction and arrhythmia 17 p2114 A73-34452
- Diagnostic power of the Q wave - Critical assay of its significance in both detection and localization of myocardial deficit. 18 p2274 A73-36527
- Coronary atherosclerosis and ischemic myocardial damage. 18 p2275 A73-36538
- Experimental myocardial infarction - Hemodynamic evaluation. 18 p2275 A73-36540
- Clinical manifestations of acute myocardial infarction. 18 p2275 A73-36543
- Electrocardiographic diagnosis of myocardial infarction - Pitfalls of a graphic technique. 18 p2282 A73-36544
- Cell viability in acute myocardial infarction, discussing pathogenesis, histological, histochemical and biochemical responses to ischemia, homeostasis maintenance and treatment methods 18 p2276 A73-36545
- Drug therapy for treatment of cardiogenic shock syndrome following myocardial infarction, discussing sympathomimetics, alpha-adrenergic blocks and combinations 18 p2276 A73-36546
- Power failure of the heart in acute myocardial infarction. 18 p2276 A73-36547
- Evaluation, diagnosis and treatment of common structural complications of acute myocardial infarction. 18 p2276 A73-36548
- The prognosis of myocardial infarction. 18 p2276 A73-36549
- Responsibility for ischemic cardiopathies in civil aviation flight personnel 18 p2284 A73-36902
- A diagnostic program - Problems of predicting myocardial infarction on a digital computer 20 p2516 A73-38998
- Prediction of the outcomes of myocardial infarction from formulas derived by the dynamic programming method 20 p2516 A73-39000

- The complications of coronary arteriography. 22 p2806 A73-42343
- Significance of arterial obstructive lesions in early diagnosis of coronary heart disease. 22 p2808 A73-42829
- Myocardial infarction susceptibility correlated with psychosocial factors in life change measurement studies 22 p2809 A73-42833
- MYOCARDIUM**
- Isovolumic contraction dynamics in man according to two different muscle models. 01 p0007 A73-10158
- Computation of solutions to the inverse problem of electrocardiography. 01 p0013 A73-11465
- Q waves and coronary arteriography in cardiomyopathy. 01 p0010 A73-11507
- Importance of the Lohmann reaction in the response of the heart to anoxic aggression 02 p0133 A73-12152
- High energy phosphate deficit-produced myocardial cell genetic apparatus activation as cardiac hypertrophy mechanism, discussing mitochondrial biogenesis and cardiac hyperfunction roles 02 p0134 A73-12511
- Relationship of anginal symptoms to lung mechanics during myocardial ischemia. 02 p0136 A73-12820
- Myocardial function and ultrastructure in chronically hypoxic rats. 03 p0259 A73-13369
- Evaluation of cardiac performance in exercise. 03 p0259 A73-13359
- Diagnostic value of vectorcardiogram in strictly posterior infarction. 03 p0268 A73-13891
- Effects of hypoxemia and acute coronary occlusion on myocardial metabolism in dogs. 05 p0538 A73-16154
- Effects of physical training on cardiac actomyosin adenosine triphosphatase activity. 05 p0539 A73-16157
- Systolic time intervals in constrictive pericarditis and severe primary myocardial disease. 06 p0649 A73-17596
- Geometry of left ventricular contraction in the systolic click syndrome - Characterization of a segmental myocardial abnormality. 06 p0655 A73-18870
- Adaptation to high altitude hypoxia as a factor preventing development of myocardial ischemic necrosis. 07 p0780 A73-19151
- Assessment of hypoxia in the human heart. 07 p0781 A73-19928
- The use of glycolytic metabolism in the assessment of hypoxia in human hearts. 07 p0781 A73-19929
- The contractile function of the myocardium in two types of cardiac adaptation to a chronic load. 07 p0781 A73-19931
- Transglucosidase activity of heart-muscle per-glucosylase 08 p0930 A73-21136
- Morphometric and histochemical investigation on human right atrial and mitral papillary muscle. 08 p0930 A73-21215
- Ventriculographic patterns and hemodynamics in primary myocardial disease. 08 p0933 A73-21804
- Order and disorder in the rhythm of the heart /Fifth Annual George C. Griffith Lecture/. 08 p0933 A73-21806
- Myocardial metabolism during exposure to carbon monoxide in the conscious dog. 09 p1042 A73-22935
- Regional myocardial dynamics from single-plane coronary cineangiograms. 10 p1185 A73-24771
- Embryonic chick heart cell age dependent electrophysiological studies, discussing structure, metabolism, ATPase activity, membrane potential and cell interactions 11 p1315 A73-25589
- Morphological and experimental excitation models of cardiac muscle ultrastructure, transmission activity and intercellular contact relationships 11 p1315 A73-25590
- Cell membrane molecular structure and lipid composition, discussing phospholipid role in membrane potential maintenance in myocardial cells 11 p1315 A73-25591
- Ionic current mechanisms for cardiac muscle repolarization time course of Purkinje fibers and other heart cells, relating charge transfer data to earlier studies 11 p1316 A73-25593
- Electrogenic potassium inward transport involvement in mechanism of enhanced repolarization, correlating cardiac excitation with Na, K and Ca ions transfer and active ion transport 11 p1316 A73-25594

- Cardiac membrane capacitance physiological properties and measurements in Purkinje fibers, ventricular and atrial muscles and heart tissues 11 p1316 A73-25596
- Vertebrate cardiac innervation via parasympathetic and sympathetic nervous system, considering synaptic transmission, nerve endings, stimulation and electrical effects 11 p1316 A73-25597
- Cardiac activity potentials, P-R interval and impulse propagation across atrioventricular node, ventricular conduction and Purkinje fiber-muscle junctions 11 p1316 A73-25598
- Neurogenic and myogenic mechanisms of myocardium cell electrical activity and excitation in vertebrate and invertebrate neural and muscle tissues 11 p1316 A73-25599
- Physical/electrical sealing mechanisms of myocardial and muscle fiber healing after surface injury, considering ionic factors, sodium and calcium rates and contraction relation 11 p1316 A73-25600
- Calcium movements and excitation-contraction coupling in cardiac cells. 11 p1316 A73-25601
- Myocardial contraction velocity and acceleration in man measured by ultrasound echocardiography differentiation. 12 p1461 A73-27026
- Heart function mechanism explanation by activation potential stimulation of muscular contraction via calcium ions 12 p1462 A73-27690
- High-fidelity left ventricular pressure measurements for the assessment of cardiac contractility in man. 12 p1464 A73-27888
- Exogenous free fatty acid effects on hypoxic myocardial function in isolated isometric rat papillary muscles 13 p1577 A73-29572
- German monograph - Comparative investigations regarding the phenomenon of force potentiation in the case of the heart muscle of cold-blooded and warm-blooded animals. 14 p1719 A73-30669
- Myoglobin distribution in the heart of growing rats exposed to a simulated altitude of 3500 m in their youth or born in the low pressure chamber. 14 p1720 A73-30910
- Study of myocardial antigen localization using the immunofluorescence method 15 p1834 A73-31392
- Effect of prolonged hypokinesia on certain energy transfer characteristics in skeletal muscles and some internal organs 15 p1834 A73-31505
- Assessment of left ventricular performance in man - Instantaneous tension-velocity-length relations obtained with the aid of an electromagnetic velocity catheter in the ascending aorta. 15 p1836 A73-31996
- Nutritional circulation in the heart. IV - Effect of calcium chloride and potassium chloride on myocardial hemodynamics and clearance of rubidium-86. 16 p1973 A73-33990
- Effect of maximal work load on cardiac function. 16 p1973 A73-33991
- Heart muscle viability following hypoxia - Protective effect of acidosis. 17 p2110 A73-34097
- Morphological and electron-microscopic alterations of the myocardium in dogs subjected to lasting chronic gamma irradiation 17 p2111 A73-34230
- Factors influencing coronary blood flow in the presence of coronary obstructive disease. 18 p2275 A73-36539
- Some metric characteristics of myocardial cells under various conditions of cardiac and cardiovascular pathology 18 p2280 A73-36962
- The effect of exercise on intrinsic myocardial performance. 19 p2396 A73-38258
- Contraction kinetics of ventricular muscle from hibernating and nonhibernating mammals. 20 p2514 A73-39603
- Influence of preliminary adaptation to the main environmental factors on the ATP level and phosphorylation potential in the myocardium during severe heart strain 21 p2640 A73-41278
- A simple cardiac contractility computer. 22 p2815 A73-42677
- Structural conditions in the hypertrophied and failing heart. 22 p2807 A73-42685
- Abnormal biochemistry in myocardial failure. 22 p2808 A73-42686
- Ribonucleic acid (RNA) polymerase and adenylylase in cardiac hypertrophy and cardiomyopathy. 22 p2808 A73-42687

- Myocardial oxygen consumption in experimental hypertrophy and congestive heart failure due to pressure overload. 22 p2808 A73-42688
- Nature and significance of alterations in myocardial compliance. 22 p2808 A73-42689
- Alterations of cardiac sympathetic neurotransmitter activity in congestive heart failure. 22 p2808 A73-42690
- Polyparametric information of the electrocardiogram in injured tissue. 22 p2809 A73-42834
- Age-dependent characteristics of myoglobin content and distribution in the heart and skeletal muscles. 24 p3059 A73-44669
- Hemoglobin-oxygen equilibrium and coronary blood flow - An analog model. 24 p3064 A73-45060
- Comparison of ultrasound and cineangiographic measurements of left ventricular performance in patients with and without wall motion abnormalities. 24 p3062 A73-45400
- MYOELECTRIC POTENTIALS**
- Possibility of modeling the relationship between the intracellular potential of individual muscle fibers and the overall electromyogram for tonic muscles. 10 p1179 A73-23810
- Rise time of the spike potential in fast and slowly contracting muscle of man. 10 p1181 A73-24500
- Voluntary activation of individual motor units in man. 10 p1181 A73-24519
- Organization of the activity of a group of motor neurons in man during voluntary contraction of a muscle. 10 p1182 A73-24599
- Embryonic chick heart cell age dependent electrophysiological studies, discussing structure, metabolism, ATPase activity, membrane potential and cell interactions. 11 p1315 A73-25589
- Morphological and experimental excitation models of cardiac muscle ultrastructure, transmission activity and intercellular contact relationships. 11 p1315 A73-25590
- Cardiac action potential rising phase and generation mechanism, discussing pacemaker potential and slow depolarization initiating upstroke in spontaneously active cardiac cells. 11 p1316 A73-25592
- Ionic current mechanisms for cardiac muscle repolarization time course of Purkinje fibers and other heart cells, relating charge transfer data to earlier studies. 11 p1316 A73-25593
- Electrogenic potassium inward transport involvement in mechanism of enhanced repolarization, correlating cardiac excitation with Na, K and Ca ions transfer and active ion transport. 11 p1316 A73-25594
- Sinoatrial node pacemaker cell functions, discussing ionic and metabolic principles, electrical activity, membranar effects of neurohormonal control factors and cardioactive drug effects. 11 p1316 A73-25595
- Cardiac activity potentials, P-R interval and impulse propagation across atrioventricular node, ventricular conduction and Purkinje fiber-muscle junctions. 11 p1316 A73-25598
- Neurogenic and myogenic mechanisms of myocardial cell electrical activity and excitation in vertebrate and invertebrate neural and muscle tissues. 11 p1316 A73-25599
- Influence of ribonuclease on changes in the membrane potential of muscle fibers evoked by stimulation of the sympathetic nerve. 15 p1833 A73-31166
- Technique for recording muscle biopotentials by means of implanted electrodes. 15 p1839 A73-31799
- Electromyographic study of repetitive fasciculation potentials in triceps and adductor pollicis in normal subjects and patients with motor neuron diseases, noting postcontraction pause. 20 p2514 A73-39761
- Conditional computer analysis of the onset-to-onset duration of spikes from the electromyographic interference pattern of extraocular muscles. 22 p2802 A73-41731
- Human phasic reflex response to parameters of a mechanical stimulus as an index of muscle-spindle sensitivity. 22 p2816 A73-42679
- MYOELECTRICITY**
- NT MYOELECTRIC POTENTIALS**
- Interrelation between hardness, viscosity, strength, and bioelectric activity of human muscles. 01 p0007 A73-10155
- Polysynaptic pathways role in tonic vibration and monosynaptic reflexes due to muscle vibratory or nerve electric stimulation, respectively, discussing tetanization effects. 01 p0008 A73-10409

- Peripheral electromyography spike and ventral root unit discharge intervals during tonic vibration reflex of cat soleus motoneuron. 01 p0008 A73-10410
- Effect of eccentric and concentric muscle conditioning on tension and electrical activity of human muscle. 01 p0013 A73-10774
- The role of muscle stiffness in meeting the changing postural and locomotor requirements for force development by the ankle extensors. 02 p0138 A73-12166
- Some physiological reactions to acceleration in albino rats in a state of hypothermia. 05 p0541 A73-16737
- Contributions of quick and slow muscle fibers to changes in the electrical activity of skeletal muscles in rats under acute and chronic effects of cold. 08 p0931 A73-21323
- Cardiac membrane capacitance physiological properties and measurements in Purkinje fibers, ventricular and atrial muscles and heart tissues. 11 p1316 A73-25596
- Electrical activity of the external ear muscles in man /at rest and during identification of acoustic signals/. 14 p1719 A73-30843
- A method for the approximation of processes in homogeneous biological structures. 24 p3062 A73-44663
- Metabolic and myoelectric reactions under chemical thermoregulation in rats after accelerated cold adaptation. 24 p3059 A73-44721

MYOGLOBIN

- Myoglobin distribution in the heart of growing rats exposed to a simulated altitude of 3500 m in their youth or born in the low pressure chamber. 14 p1720 A73-30910
- Age-dependent characteristics of myoglobin content and distribution in the heart and skeletal muscles. 24 p3059 A73-44669

N

N-N JUNCTIONS

- Observation of doping profiles in Gunn diodes with a scanning electron microscope using the beta-conductivity. 23 p2960 A73-43777

N-P JUNCTIONS

U P-N JUNCTIONS

N-P-N JUNCTIONS

- New transistor squaring stage with a 'smooth' parabolic characteristic for realizing a simple high-precision parabolic multiplier. 01 p0024 A73-10924
- GaAs-GaAlAs heterojunction transistor for high frequency operation. 02 p0147 A73-12046
- The effect of surface recombination velocity on the performance of vertical multi-junction solar cell. 03 p0255 A73-14214
- Mathematical models for failure rates of electronic components, considering tantalum condensers, Zener diodes and n-p-n Si transistors. 07 p0830 A73-19413
- Ion-implanted bipolar transistor carrier concentration profiles. 10 p1194 A73-24155
- Microwave characteristics of ion-implanted bipolar transistors. 10 p1194 A73-24156
- Multivibrator with p-n-p and n-p-n transistors, noting circuit diagram, operation and power dissipation. 10 p1197 A73-24940
- Selection of conditions for the fabrication of planar n-p-n silicon transistors with the application of the ion-beam alloying method. 20 p2535 A73-38858
- A calculation of the equilibrium temperature distributions in multiple-emitter microwave transistors. 20 p2535 A73-38926
- A two-dimensional numerical analysis of a silicon n-p-n transistor. 20 p2536 A73-39413
- Evolution of the shape of the current-voltage characteristics of n-p-n and p-n-p three-layer degenerate semiconductor structures. 24 p3119 A73-44607
- Influence of emitter current concentration effects on the temperature distribution in power transistors. 24 p3072 A73-44930
- Four-quadrant analog multiplier synthesis for IC implementation based on logarithmic addition in all n-p-n bipolar transistor configuration for algebraic product derivation. 24 p3074 A73-45260

N-TYPE SEMICONDUCTORS

- LF noise in n-type GaAs and its correlation with HF noise of Gunn-diode oscillators. 02 p0145 A73-11535

- Comparison of data on irradiation of germanium by 1- and 28-MeV electrons. 02 p0201 A73-12592

- Microwave harmonic generator using the nonlinearity of negative resistance in n-type GaAs. 03 p0281 A73-12997
- Investigation of the phonon drag effect in n-GaAs. 04 p0482 A73-14866
- Electron impulse interactions of heat in semiconductors. 04 p0483 A73-15470
- Quasi-discrete acceptor states in zero forbidden gap n-type semiconductors, showing noncompensation at low temperatures. 04 p0484 A73-15567

- N-type Si MNOS random access memory devices for data storage without applied voltage, noting threshold shifts vs writing pulse width for various oxide thicknesses. 05 p0553 A73-16166

- Purity evaluation of n type GaAs LSA diodes from low-field temperature-dependent mobility. 05 p0556 A73-16435

- Experimental study of millimeter-wave characteristics of hot electrons in n-type GaAs by electrodeless method. 05 p0558 A73-16525

- Transverse magnetic field effects on n-type GaAs Gunn diodes microwave power, coherence and dynamic I-V characteristics. 05 p0558 A73-16784

- Electrical properties of nickel-low-doped n-type gallium arsenide Schottky-barrier diodes. 05 p0559 A73-17072

- Shot noise in a Schottky barrier diode in the presence of surface electronic states at the contact. 06 p0675 A73-18077

- Dependence of the current-voltage characteristic of a p-n-p drift triode on the donor concentration in the n-type base. 06 p0675 A73-18081

- Characteristics of recombination centers defining the high sensitivity of n-CdSb photoresistors. 06 p0675 A73-18082

- Influence of low-temperature heat treatment on the electrical and recombinational properties of silicon-silicon dioxide systems. 06 p0736 A73-18085

- Millimeter-wave investigation of electronic conduction in semiconducting III-V compounds. 06 p0737 A73-18366

- Thermal emf of indium antimonide of a p- and n-type of conductivity at room temperature. 06 p0738 A73-18652

- Microwave properties of n-type InSb in a magnetic field between 4 and 300 K. 06 p0739 A73-18792

- Doping dependence of photon yield as a function of excitation energy in optically-excited n-type GaAs at 300 K. 06 p0704 A73-18844

- Electrical contacts to ion cleaned n-type gallium arsenide. 07 p0797 A73-19136

- Diffusion of hot electrons in n indium phosphide. 07 p0861 A73-19157

- Investigation of the temperature dependence of the anisotropy parameter K in n-Si and n-Ge by using magneto-plasma waves. 07 p0861 A73-19327

- Faraday effect in n-GaAs in the intermediate doping region. 07 p0862 A73-20009

- Gunn diode effect in n-type GaAs, discussing electron drift velocity relationship to electric field, I-V characteristics and fabrication. 08 p0943 A73-20709

- Millimeter-wave frequency response of hot electrons in n-type GaAs. 08 p0994 A73-20845

- On the procedures of measuring microwave Faraday rotation in semiconductors. 08 p0994 A73-21016

- On the mechanism for microwave amplification in 'supercritically' doped n-GaAs. 08 p0947 A73-21212

- Electrical properties of InAs to very high pressures. 08 p0995 A73-21535

- Semiconductor strain transducer. 08 p0950 A73-21720

- Gain-current relation for GaAs lasers with n-type and undoped active layers. 09 p1091 A73-22239

- Resonant enhancement of photoexcited nitrogen trap n-type GaAs laser electron-hole recombination probability by crystal composition variation and gamma conduction band degeneration. 09 p1093 A73-22255

- Photovoltaic and photoconductivity measurements on p- and n-type GaSe, determining light polarization direction effect, photovoltage relaxation times and minority carriers diffusion lengths. 10 p1259 A73-23569

NACELLES

- On a 'memory' effect in N-type silicon Schottky diodes in the presence of metallic impurities
11 p1338 A73-25872
- Boltzmann transport equation solution for electron mobility in ellipsoidal valleys of n-type GaAs and GaP, taking into account arbitrary magnetic fields and scattering mechanisms
13 p1668 A73-28217
- Bi₂Se₃ Hall effect magnetometer for reliable low temperature use.
13 p1612 A73-28368
- Determination of the diffusion length of excess carriers in semiconductors under a polyethylene film
13 p1668 A73-28462
- Determination of the diffusivity-mobility ratio in highly degenerate semiconductors at low temperatures from linewidth measurements in junction lasers.
16 p1990 A73-33689
- Oscillations of the magnetic susceptibility in n-type semiconductors with a chalcopyrite lattice
16 p2044 A73-34068
- Experimental investigation of a millimeter band frequency converter on n-InSb at 4.2 K.
17 p2136 A73-35158
- An experimental investigation of the propagation of electromagnetic waves in a rectangular waveguide, partially filled with n-InSb in a transverse magnetic field.
17 p2123 A73-35166
- Parameters of fast recombination centers in CdS single crystals and the effect of the parameters on photosensitivity
18 p2340 A73-36669
- The role of surface states in the formation of a Schottky barrier at a metal/gallium arsenide contact
18 p2341 A73-36717
- Refractive index of n-type gallium arsenide.
20 p2599 A73-38892
- The theory of the current-voltage characteristic of diodes fabricated out of compensated semiconductors
21 p2663 A73-40795
- Planar conductance transistor based on charge carrier accumulation due to n-n junction, featuring steep negative resistance characteristics and low sustaining voltage
21 p2655 A73-41048
- Ion-implanted varicaps with a steep capacitance-voltage characteristic
21 p2664 A73-41096
- Effective recombination levels in N- and P-type silicon irradiated by 4.5 MeV electrons.
21 p2753 A73-41558
- The rectifying barrier in gallium arsenide Schottky diodes
23 p2959 A73-43618
- Interface properties of oxidized germanium-doped silicon.
23 p3016 A73-43778

NACELLES

- Powered model wind tunnel investigation to determine performance trends with nacelle location.
[AIAA PAPER 72-1114] 03 p0243 A73-13429
- Subsonic commercial transport aircraft reduced noise and increased cruise Mach number effects on nacelle design in terms of inlet, fan, cowl and nozzle
[AIAA PAPER 72-1204] 03 p0358 A73-13488
- Flight and wind tunnel investigation of the effects of Reynolds number on installed boattail drag at subsonic speeds.
[AIAA PAPER 73-139] 05 p0530 A73-16888

NAPHTHALENE

- Mass transfer technique for investigation of heat transfer by jet-impingement systems.
03 p0400 A73-14642
- Drift mobilities of holes and electrons in naphthalene single crystals.
11 p1407 A73-24988

NARCOSIS

- Effects of vagotomy on the impulse activity of respiratory neurons
15 p1833 A73-31160

NARCOTICS

- Characteristics of the narcotic action of hexenal in combination with aminothyl-series radioprotective drugs in irradiated animals
15 p1838 A73-31391

NASA PROGRAMS

- NT APOLLO APPLICATIONS PROGRAM
NT APOLLO PROJECT
NT EARTH RESOURCES PROGRAM
NT EARTH RESOURCES SURVEY PROGRAM
NT GLOBAL ATMOSPHERIC RESEARCH PROGRAM
NT HELIOS PROJECT
NT JUPITER PROJECT
NT MARINER PROGRAM
NT MARS 71 PROJECT
NT QUIET ENGINE PROGRAM
NT ROVER PROJECT
NT SATURN PROJECT
NT SKYLAB PROGRAM
NT VIKING MARS PROGRAM

German-NASA joint Aeros aeronomy satellite project, discussing mission objectives and related instrumentation
01 p0109 A73-10470

Objectives and first results of the Mars 2, Mars 3 and Mariner 9 planetary probes
01 p0103 A73-10996

Scientific mission and German and U.S. plans/design for Helios cooperative solar probe, stressing advanced technology requirements
01 p0110 A73-11103

Missions for the systematic unmanned exploration of Mars.
01 p0105 A73-11160

Some experiences in the scaling of the NASA 8-stage transonic axial flow compressor.
[SAE PAPER 720711] 02 p0203 A73-12008

Mariner Jupiter/Saturn 1977 - The mission frame.
02 p0221 A73-12597

NASA Quiet Engine Program review and test results, discussing noise reduction technology application to transport aircraft
02 p0204 A73-12845

NASA technology program for auxiliary and primary electric propulsion systems, noting flight tests and solar arrays
[AIAA PAPER 72-1127] 03 p0355 A73-13437

The National Aeronautics and Space Administration-U.S. Public Health Service Health Evaluation and Enhancement Program - Summary of results.
03 p0260 A73-13545

U.S. manned space flight food system development experience assessment, covering Mercury, Gemini, Apollo and manned orbiting laboratory programs
03 p0269 A73-14168

NASA's Technology Utilization Program.
04 p0521 A73-14730

NASA's space station and the need for quantifiable components of a responsive legal regime.
04 p0522 A73-15134

NASA space research costs balanced with scientific and technological achievements in relation to space law
04 p0524 A73-15156

Synchronous meteorological satellite (SMS) system responsibilities of NASA and Commerce Department, discussing program objectives, payload, spacecraft subsystems and ground systems
04 p0504 A73-15451

NASA space program value to humanity, discussing Skylab solar and earth observations and communications satellites
05 p0613 A73-16181

NASA lift fan V/STOL transport technology status.
[SAE PAPER 720856] 05 p0535 A73-16663

NASA airframes structures program, discussing automated design, composites, supersonic and hypersonic technologies, control systems, load and aerodynamic prediction and integrity concepts
[AIAA PAPER 73-17] 06 p0759 A73-17610

Research on future short-haul aircraft at the NASA Langley Research Center.
[AIAA PAPER 73-27] 06 p0647 A73-17616

Research and applications modules (RAM) program for manned space research satellites transportation and support, discussing mission requirements and design concepts
[AIAA PAPER 73-72] 06 p0755 A73-17637

Space technology transfer to community and industry; Proceedings of the Eighteenth Annual Meeting and Tenth Goddard Memorial Symposium, Washington, D.C., March 13, 14, 1972.
06 p0771 A73-17673

Space transportation systems and payload concepts for proposed space missions, discussing available and projected technology and environmental, economic and political aspects
06 p0757 A73-18096

U.S. and U.S.S.R. Venus probes data on Venus atmosphere, discussing atmospheric heat transfer mechanism and cloud structure
07 p0874 A73-19110

ERTS program, describing satellite design and imaging and data collection systems for real time or delayed taped transmission to ground stations
07 p0905 A73-19112

Apollo-Soyuz docking project for flight testing systems compatibility for safe and reliable crew transfer, discussing program objectives, technical requirements and solutions
09 p1152 A73-22187

Space shuttle phase B program, discussing orbiter and booster configurational studies, ground simulation, propulsion systems, structure, avionics, environment control and life support systems, etc
09 p1152 A73-22189

AEC/NASA thermionic reactor program with emphasis on technology utilization, comparing with French, German and Soviet programs
09 p1036 A73-22815

Radio telemetering trends in post-Apollo space programs, emphasizing service lifetimes and orbiting space station data bit generation rate
09 p1053 A73-23362

The DOT/NASA Civil Aviation Research and Development Policy Study.
10 p1298 A73-24552

Logistics planning with cost reduction for NASA phased programs in conducting R and D and real time inventory control, discussing major activities and objectives
11 p1454 A73-25450

The American space program for the future.
12 p1560 A73-27062

Space shuttle missions relationship to post-Apollo European and joint European-U.S. space exploration programs
13 p1690 A73-29387

Organization and operations at National Aeronautics and Space Administration Wallops Station.
14 p1741 A73-30078

Measurement of high-altitude air quality using aircraft.
[AIAA PAPER 73-517] 16 p2006 A73-33554

Sterilization technology in the United States space program.
16 p1976 A73-33697

NASA in general aviation research: Past - present - future.
[SAE PAPER 730317] 17 p2257 A73-34675

The evolution of location and data collection systems in the United States.
[AIAA PAPER 73-584] 18 p2372 A73-36076

Representative Space Shuttle missions and their impact on shuttle design.
[AIAA PAPER 73-608] 18 p2358 A73-36087

NASA airframe structures program, discussing automated analysis and design, advanced composites, supersonic and hypersonic vehicles technology, active controls, aircraft loads and aeroelasticity prediction methods
18 p2362 A73-36168

Space Shuttle Program; Proceedings of the Short Course, Boulder, Colo., October 6, 7, 1972.
19 p2491 A73-37591

Space shuttle program budget difficulties, discussing consequences of cost increase or program suspension
21 p2793 A73-40234

NASA program manned and unmanned spacecraft system effectiveness survey questionnaire response data concerning various tests
21 p2781 A73-41203

Technology transfer in New York City - The NASA/NYC Applications Project.
[AIAA PAPER 73-978] 22 p2938 A73-42532

NATIONAL AIRSPACE UTILIZATION SYSTEM
ATC concepts and air/ground data link requirements for U.S. airspace structure in 1980s to support anticipated Los Angeles basin traffic densities in 1995
14 p1772 A73-29879

Ground communications networks for aeronautical operations.
14 p1740 A73-29885

NATIONAL AVIATION SYSTEM
Status of funded improvements to the National Aviation System and planned improvements not yet funded.
12 p1561 A73-27363

Improvements in the use of FAA resources for system performance assurance.
12 p1561 A73-27364

National aviation system improvement via cost effectiveness, considering FAA facilities and equipment program, ATC automation and terminal aids
12 p1522 A73-27365

Military ATC systems and equipment in U.S. National Aviation System, discussing operations, organizational and facility interfaces, communications, navigation, and surveillance radar requirements
14 p1773 A73-29889

NATURAL FREQUENCIES

U RESONANT FREQUENCIES

NATURAL GAS

Aircraft design for transporting arctic crude oil or liquid natural gas, examining air terminal requirements and handling specifications
21 p2634 A73-41172

NATURAL SATELLITES

NT DEIMOS

NT EUROPA

NT IAPETUS

NT IO

NT MOON

NT PHOBOS

NT TITAN

The mass and figure of Saturn by photographic astrometry of its satellites.
01 p0096 A73-10316

Normality condition derivation for algorithm of first order solution to ideal resonance problem, applying to critical inclination of oblate planet satellite
01 p0077 A73-10686

Brightness temperature measurement of Callisto satellite thermal radio emission, using ice layer model
01 p0101 A73-10845

Evidence for objects of lunar mass in the early solar system and for capture as a general process for the origin of satellites.

02 p0217 A73-12394

Theoretical model for tidal evolution induced capture of natural satellite pairs into orbit-orbit resonance, discussing Titan and Hyperion relationship with Saturn

02 p0219 A73-12421

The transmission of mass and angular momentum from a satellite or planetary system to its primary.

02 p0225 A73-12810

Gravitational constant variations from natural satellites and lunar observation, discussing tidal problems solution from lunar orbit tracking

03 p0377 A73-14310

Water frost absorptions in IR reflectivities of Jupiter Galilean satellites, discussing surface cover distributions and underlying material reflectivity

04 p0497 A73-15070

On the origin of the commensurabilities amongst the satellites of Saturn.

06 p0752 A73-18238

Potential atmospheric composition of smaller bodies in the solar system and some aspects of planetary evolution.

07 p0875 A73-19249

Mutual phenomena of Jupiter's satellites in 1973-74.

07 p0875 A73-19260

Analytical theory of the motion of the fifth Jupiter satellite

07 p0876 A73-19395

Infrared spectra of the Galilean satellites of Jupiter.

08 p1004 A73-20901

On the analytical study of Saturn's satellites, Enceladus-Dione

08 p1005 A73-20921

The role of the satellite swarm in the origin of the earth's rotation.

08 p1012 A73-21579

Satellite-caused energy dissipation via tides in spinning planet leading to orbital decay induced destruction or escape or to stable synchronism

09 p1142 A73-22041

Survey of the outer planets Jupiter, Saturn, Uranus, Neptune, Pluto, and their satellites.

11 p1417 A73-25315

Mercury, Venus and Pluto satellite system elimination by tidal friction, discussing possible erosion of earth and Mars small satellites

11 p1419 A73-25778

Earth-moon system mass and angular momentum distribution anomaly, considering light gases association with Jupiter, Saturn, Uranus and Neptune satellites

11 p1419 A73-25793

Solar system planets and satellites fundamental properties, considering observational uncertainty in masses and dimensions

11 p1419 A73-25878

A survey of dynamical data for the major planets and satellites.

11 p1420 A73-25880

Galilean satellites surface thermal properties from radiometry of 20-micron band during eclipses of Jupiter

11 p1424 A73-26132

Ten-micron eclipse observations of Io, Europa, and Ganymede.

Position and velocity components for Jupiter VIII-XII.

11 p1429 A73-26684

Observations of the satellites Jupiter VI and VII.

12 p1540 A73-27429

Outer planet satellites and atmospheres composition and structure from low temperature condensation accretion models

14 p1724 A73-30530

Outer solar system, including planetary atmospheres, natural satellites, solar wind, interstellar cosmic rays and spacecraft missions

14 p1800 A73-30616

Brightness temperature measurement of Callisto thermal radio emission, using ice layer model

15 p1928 A73-30981

Evolution of satellite resonances by tidal dissipation.

15 p1938 A73-31950

New techniques for determining sizes of satellites and asteroids.

15 p1940 A73-32075

Contribution to the dynamic study of the Galilean system of Jupiter. I - The intermediate solution in the nonresonant case

16 p2059 A73-32839

Jupiter's radiation belts and the sweeping effect of its satellites.

16 p2062 A73-33429

New determinations of the diameters of planets and satellites

16 p2066 A73-33792

Saturn ring thickness according to 1966 observation data of the Pic-du-Midi Observatory

16 p2070 A73-33845

Night sky photographic evidence for natural retrograde earth satellites explanation for Vulcan type observations, considering group C orbit anomaly and terrestrial day length errors

16 p2071 A73-34000

Evidence for objects of lunar mass in the early solar system and for capture as a general process for the origin of satellites.

Bode's law and the preference for near-commensurability among pairs of orbital periods in the solar system.

17 p2228 A73-34415

Distribution of satellite bodies according to their mean distances in the systems of the sun, Jupiter, Saturn and Uranus

17 p2229 A73-34429

Planetary quarantine constraints for outer planet satellite encounter missions, determining spacecraft impact probability in terms of trajectory analysis and navigation error numerical integration

18 p2349 A73-35976

The significance of outer planet satellite quarantine constraints on aim-point selection.

[AIAA PAPER 73-553]

18 p2359 A73-36096

Canonical elements of the translational-rotational motion of a planet satellite

19 p2476 A73-37199

Viking type spacecraft rendezvous with the Martian moon.

19 p2482 A73-37401

Narrow-band photometry of the Galilean satellites.

19 p2483 A73-37577

Spectral albedos of the Galilean satellites.

19 p2483 A73-37578

Effect of noble gases on an atmospheric greenhouse /Titan/.

19 p2487 A73-38173

The occultations and the mutual eclipses of the Galilean satellites of Jupiter

20 p2604 A73-39009

On the 3-7 commensurability between Jupiter's outer two Galilean satellites.

21 p2778 A73-41531

An atmosphere on Ganymede from its occultation of SAO 186800 on 7 June 1972.

23 p3027 A73-43337

Orbit improvement from satellite imaging data obtainable from outer planet missions.

23 p3032 A73-43840

Exploring Jupiter, Saturn and their satellites.

23 p3034 A73-44221

Topography on satellite surfaces and the shape of asteroids.

24 p3129 A73-44446

Titan satellite optical polarization observation in three spectral regions, noting inconsistency with scattering from planetary surface or pure molecular atmosphere

24 p3130 A73-44452

Determination of radii of satellites and asteroids from radiometry and photometry.

24 p3130 A73-44453

Mutual Jupiter satellite-satellite eclipses and occultation observations for improved ephemerides, albedo maps, radii and limb darkening estimation

24 p3130 A73-44454

Area-scanning photometric observations of Galilean satellite surface color variations due to orbital phase and Jupiter environment

24 p3130 A73-44455

Refutation of Bagby moonlet theory via analysis of supporting evidence

24 p3133 A73-44542

NAVIER-STOKES EQUATION

Moments of inertia for fluid-filled rotating bodies, solving Laplace and Navier-Stokes equations for cylinder and sphere

01 p0030 A73-10089

Existence and stability of the secondary periodic solution figuring in Navier-Stokes type evolution problems

[ONERA, TP NO. 1172]

01 p0033 A73-10780

Navier-Stokes equations numerical solution for steady state axisymmetric flow of incompressible Newtonian fluid between two parallel infinite rotating disks

01 p0122 A73-10805

Exact vorticity solutions of the incompressible Navier-Stokes equations.

01 p0034 A73-11358

Navier-Stokes approximation for gas dynamics equations of molecular oscillations in diatomic gas, noting relaxation pressure proportionality to energy density equilibrium deviation

02 p0152 A73-11602

On certain parabolic differential equations and an equivalent variational problem.

02 p0186 A73-11972

A relation between the energy distribution of the main flow and the corresponding fluctuating quantities in boundary layers

03 p0292 A73-13171

Computer methods for simulation of multidimensional, nonlinear, subsonic, incompressible flow.

[ASME PAPER 72-HT-61]

03 p0294 A73-13546

NAVIER-STOKES EQUATION

Existence theorems for Navier-Stokes equations periodic solution bifurcation in convection between two horizontal plates at different time periodical temperature

[ONERA, TP NO. 1179]

03 p0343 A73-13602

A note on a minimum principle in Benard convection.

04 p0520 A73-15940

Navier-Stokes equation solutions for steady laminar viscous flow of incompressible fluid with mixed no-slip and no-shear conditions

05 p0563 A73-16097

Stability investigation in the case of an oscillating Couette flow. I Nonlinear theory. II - Linear theory [DFVLR-SONDDR-257]

05 p0563 A73-16098

Numerical solution of a boundary value problem for the Navier-Stokes equations

05 p0564 A73-16449

Numerical solutions of the Navier-Stokes equations in inlet regions.

[ASME PAPER 72-APM-DD]

05 p0564 A73-16526

On the numerical solution of two-dimensional, laminar compressible flows with imbedded shock waves.

[ASME PAPER 72-FE-7]

05 p0564 A73-16545

The Navier-Stokes equations and the bulk viscosity of simple gases.

05 p0597 A73-16591

Transformation of the hypersonic compressible Navier-Stokes equations.

05 p0567 A73-17120

On the solution of the Navier-Stokes equations for a spherically symmetric expanding flow.

06 p0684 A73-17707

Steady rectilinear universal motions of a Navier-Stokes fluid.

06 p0685 A73-17861

Boundary value problems of viscous fluid dynamic system generated by Navier-Stokes equations, using Hopf theory

06 p0724 A73-18634

Mass-transfer effects on higher-order boundary layer solutions - The leading edge of a swept cylinder.

06 p0688 A73-18833

On generalized hydrodynamic equations used in heat transfer theory.

06 p0688 A73-18834

Energy conserving finite difference approximation for solution of unaveraged Navier-Stokes equations of three dimensional incompressible turbulent flow in square duct

07 p0810 A73-19263

Numerical solution of the Navier-Stokes equations by the finite element method.

07 p0810 A73-19501

Decaying unsteady viscous vortex flow under conditions of streamlines and vortex lines coincidence, deriving Navier-Stokes equations solution

07 p0812 A73-20340

Supersonic flow of a viscous gas about a spherically blunt cooled object

09 p1028 A73-22620

Free boundary flow invariant solutions of Navier-Stokes equations for optimal S/H subgroup systems, using continuous transformation group operators

10 p1204 A73-23583

Three dimensional boundary layer theory, applying Navier-Stokes equations to Newtonian fluids continuous flow over solid bodies or through finite ducts

10 p1171 A73-23863

Molecular gas dynamics, considering molecules internal degrees of freedom, Navier-Stokes and Knudsen layer boundary conditions, heterogeneous reactions, evaporation, condensation and surface shocks

10 p1251 A73-23865

Prandtl's boundary-layer theory from the viewpoint of a mathematician.

10 p1172 A73-23866

A numerical solution of the Navier-Stokes equations using the finite element technique.

11 p1345 A73-25116

Numerical study of a viscous flow through a pipe orifice.

11 p1346 A73-25213

Navier-Stokes equation solution for steady state, tandem and Rankine capillary viscometer precision measurements, including compressibility correction

11 p1361 A73-25367

On the numerical treatment of the Navier-Stokes equations for an incompressible fluid.

13 p1599 A73-28090

Steady universal motions of a Navier-Stokes fluid - The case when the velocity magnitude is constant on a Lamb surface.

13 p1599 A73-28285

Rain fall deceleration effect on flow velocity of infinitely deep water mass, solving Navier-Stokes equations via Laplace transforms

13 p1600 A73-28419

Capacity theory and removable sets for finite energy harmonic functions extended to nonlinear Navier-Stokes equations, using multiple trigonometric series

13 p1648 A73-28539

Study of a new family of solutions of Navier-Stokes equations

14 p1744 A73-29758

NAVIGATION

On the connection between the elliptic equations of the Navier-Stokes type and the theory of harmonic functionals.

14 p1769 A73-30521

The theory of fluctuating flow fields near walls.

14 p1746 A73-30704

Numerical solution of the viscous flow in the entrance region of parallel plates.

14 p1746 A73-30907

Multistep computer algorithm for Navier-Stokes equations of two dimensional viscous incompressible flow in channel with complex geometry

15 p1860 A73-30965

Intermittency in fully developed turbulence as a consequence of the Navier-Stokes equations.

15 p1860 A73-31092

Numerical solution for the flow of a fluid in a heated closed cavity.

16 p2084 A73-32929

Steady solutions of a nonlinear problem for the Navier-Stokes equations

16 p2031 A73-32933

Time dependent one dimensional Navier-Stokes differential equations solved via difference scheme, determining reflected shock wave structure and end wall pressure

16 p1999 A73-33251

The numerical integration of the Navier-Stokes equations for the two-dimensional incompressible flow along a planar plate

16 p2000 A73-33261

Finite-difference approximations of the Navier-Stokes equations applied to a geophysical flow. I. II - Three-dimensional approximations on a region homeomorphic to a plane region. III - Three-dimensional approximations over the totality of a spherical region represented by means of a regular polyhedron

16 p2009 A73-33886

Analyticity of the plane steady state solutions of the Navier-Stokes equation.

17 p2150 A73-34324

Book - Lectures on fluid mechanics.

17 p2150 A73-34457

Numerical solution method for Navier-Stokes equations of a compressible gas over a wide range of Reynolds numbers

17 p2151 A73-34632

Computational considerations in application of the finite element method for analysis of unsteady flow around airfoils.

17 p2096 A73-35138

Numerical solution of the three-dimensional Navier-Stokes equations in integro-differential form - Flow about a finite body.

17 p2155 A73-35139

Alternating direction implicit finite difference computational method for solving two dimensional Navier-Stokes equations for high and low speed flows

17 p2202 A73-35140

On the solution of the unsteady Navier-Stokes equations including multicomponent finite rate chemistry.

18 p2259 A73-36157

Numerical solutions of time-dependent incompressible Navier-Stokes equations using an integro-differential formulation.

18 p2297 A73-36159

Calculation of viscous gas flows in flat channels

18 p2265 A73-36990

Mises variables in problems with a free boundary for the Navier-Stokes equations

19 p2419 A73-37245

Turbulent Couette flow statistical theory, applying stochastic analysis to Navier-Stokes equation

19 p2421 A73-37855

Numerical study of viscous flow in a cavity.

20 p2545 A73-38971

Steady separated flow over finite flat plate in linearly decelerated free stream, using numerical solution of two dimensional Navier-Stokes equation

20 p2546 A73-39089

Vortex interaction with plane in viscous fluid, discussing free parameter related to insufficient boundary conditions for solving Navier-Stokes equations

20 p2547 A73-39289

Second-approximation boundary layer equations in Prandtl-Mises variables

20 p2549 A73-39610

The equations of fast-process hydrodynamics

21 p2676 A73-40205

Numerical integration method for Navier-Stokes equation of time dependent flow past impulsively started circular cylinder, calculating length of separated wake and pressure distribution

21 p2631 A73-40248

Asymptotic behavior of the solutions to the Navier-Stokes equations near ribs

21 p2678 A73-41275

Global atmospheric wind distribution computed by solving Navier-Stokes equations with models at upper atmospheric densities and ion distribution

21 p2689 A73-41354

Inertial range differences between Kolmogoroff energy spectrum formula for turbulence and modified Navier-Stokes equation, considering mu value deductibility

22 p2840 A73-41733

The integrals of the system of Navier-Stokes equations for axisymmetric motion of an incompressible fluid

22 p2841 A73-42123

French monograph - Study of the behavior of the laminar boundary layer in the presence of a positive or negative pressure gradient in hypersonic flow around obstacles.

22 p2797 A73-42744

Navier-Stokes equation formulation in parabolic coordinates for flow in trailing vortex, obtaining asymptotic expansions for stream function and angular momentum

23 p2939 A73-43205

Applicability of difference methods for solving Navier-Stokes equations at large Reynolds numbers

24 p3076 A73-44426

Calculation of supersonic flow around blunt bodies using complete and simplified Navier-Stokes equations

24 p3053 A73-44657

NAVIGATION

NT AIR NAVIGATION

NT ALL-WEATHER AIR NAVIGATION

NT ASTRONAVIGATION

NT CELESTIAL NAVIGATION

NT DECCA NAVIGATION

NT DIGITAL NAVIGATION

NT DOPPLER NAVIGATION

NT HYBRID NAVIGATION SYSTEMS

NT HYPERBOLIC NAVIGATION

NT INERTIAL NAVIGATION

NT INTERPLANETARY NAVIGATION

NT LORAN

NT LORAN C

NT OMEGA NAVIGATION SYSTEM

NT RADAR NAVIGATION

NT RADIO NAVIGATION

NT SPACE NAVIGATION

NT SURFACE NAVIGATION

NT TACAN

NT VHF OMNIRANGE NAVIGATION

Radio noise contaminated area avoidance by vehicles dependent on navigation or communication radio receivers, giving equations and curves for navigational problem

12 p1523 A73-27887

NAVIGATION AIDS

NT GYROCOMPASSES

NT LASER ALTIMETERS

NT MAGNETIC COMPASSES

NT NAVIGATION INSTRUMENTS

NT RADAR BEACONS

NT RADIO BEACONS

NT RADIO DIRECTION FINDERS

Solution of navigation problems with a hybrid analog computer

01 p0075 A73-11400

Summary of navigation aids to civil aviation - Current state and prospects

02 p0190 A73-11851

S-61N helicopter all-weather IFR operation for North Sea oil rigs supply and harbor pilots transportation, describing onboard instrumentation, navigation and communication systems

05 p0535 A73-16847

Financing of route installations and services to aircraft in flight, suggesting international rules for rental collection

06 p0771 A73-17862

Flight planning and navigation for thermal-IR surveys.

07 p0849 A73-20019

Image formation radiometers for blind landing, aerial reconnaissance over land and sea, horizon detection and detection of obstacles at sea

08 p0986 A73-21087

Doppler TACAN navigation system for helicopters obtaining data through computer display method

10 p1247 A73-24475

Operation of current navigation aids and future prospects.

14 p1773 A73-29883

Military ATC systems and equipment in U.S. National Aviation System, discussing operations, organizational and facility interfaces, communications, navigation, and surveillance radar requirements

14 p1773 A73-29889

Ship positioning by sonar group and ultrasonic transponder beacons with tracking station axis direction definition capability

14 p1741 A73-30083

Diver lockout submarine Shelf Diver evaluation for missile recovery use, noting design and navigation systems

14 p1742 A73-30089

Russian book - Air navigation: Application of radio navigational aids and automated navigation complexes.

15 p1908 A73-31471

Roskilde airport for Copenhagen metropolitan area general aviation and domestic air traffic, describing runways, taxiways, drainage, terminal facilities, lighting and navigation aids

15 p1858 A73-32364

Area navigation computer TCE-71 A system, discussing central control display and data entry units, inputs/outputs and operating modes

15 p1909 A73-32455

Doppler VOR area navigation operational principles, emphasizing bearing accuracy improvements compared to conventional VOR systems

15 p1909 A73-32455

The lowering of minima of third-level and business aircraft

15 p1831 A73-32474

Helicopter night and bad weather navigation aids, examining ground-independent navigation, low flight, obstacle warning, terrain detectors, blind landing and optoelectric sensing

17 p2206 A73-34258

Flight control problems during STOL landing approaches, considering navigation aids, pilot work load and flight safety

17 p2207 A73-34483

Airtransit - The Canadian demonstration interurban STOL service.

[SAE PAPER 730356] 17 p2103 A73-34706

Scaled illustration of unit sphere geometry with navigation applications.

17 p2209 A73-34874

A manual-control approach to development of VTOL automatic landing technology.

[AHS PREPRINT 742] 17 p2209 A73-35075

Ultrastable atomic and molecular oscillators and their applications to navigation

19 p2429 A73-37384

Navigation and landing aid systems in-flight and ground performance monitoring, discussing safety, legal, operational and economic aspects

19 p2450 A73-37802

Area navigation as means for airspace optimal utilization, considering navigation equipment and methods and ATC procedures reorganization

19 p2452 A73-37817

Simplification of navigation and flight control systems without compromising integrity.

19 p2452 A73-37826

Digital information management system of navigational and flight data for post-1975 fighter aircraft.

[AIAA PAPER 73-897] 20 p2589 A73-38832

Russian book on design and operational principles of monopulse and moving target radar, atomic time and frequency measuring devices, radio navigation and optical processing

21 p2650 A73-40510

Aircraft and spacecraft radio navigation systems, discussing Doppler, inertial and VHF omnirange techniques, Apollo spacecraft guidance systems, TACAN, Harrier and Swedish SAAB37 aircraft navigation

21 p2736 A73-40514

NAVIGATION INSTRUMENTS

NT ATTITUDE INDICATORS

NT GYROCOMPASSES

NT MAGNETIC COMPASSES

NT RADIO ALTIMETERS

NT RADIO DIRECTION FINDERS

Air and naval gyroscopic instruments development in Germany during 1927-1945, discussing inertial platforms, antiaircraft fire control, gas bearings and accelerometers

05 p0577 A73-16766

Book - Aircraft Instruments: Principles and applications.

06 p0693 A73-18075

Digital simulation of the Lunar Roving Vehicle navigation system.

06 p0722 A73-18828

Aircraft compass design with magnetic needle free turning capability around two orthogonal axes, noting advantage over conventional devices and suitability for glider navigation

13 p1613 A73-28555

Vertical aircraft flight control and navigation instrumentation avionics developments, emphasizing Inertial-lead Vertical Speed Indicator design and command and advisory information displays

13 p1621 A73-29345

Russian book on civil aviation aircraft and helicopter equipment covering navigation, automatic control, electrical and oxygen systems and aircraft instruments

15 p1829 A73-31548

Aircraft VLF radio navigation, discussing propagation characteristics, Omega and Global Navigation systems and historical development

[SAE PAPER 730313] 17 p2209 A73-34673

Strapdown air navigation with dry inertial instruments and high speed general purpose digital computer predicting system performance by position error analysis

17 p2210 A73-35211

LN-33 airborne inertial navigation system with low cost precision instruments and miniaturized digital computer, noting built-in calibration and test capability for minimizing maintenance

17 p2210 A73-35212

On-board navigation and landing systems for local airlines in the USSR 19 p2452 A73-37819

Navigation of the Titan IIIC space launch vehicle using the Carousel VB IMU. [ALAA PAPER 73-905] 20 p2589 A73-38839

The impact of space navigation on the spherical gas bearing gyro. 21 p2697 A73-40025

Redundant independent guidance, navigation and control system application to space shuttle, estimating channel output divergence due to sensor bias and scale factor errors 21 p2735 A73-40043

Russian book - The laser gyroscope. 21 p2704 A73-41295

Analysis of force interaction in magnetoelectric torque sensors 22 p2860 A73-42364

NAVIGATION SATELLITES

NT TRANSIT SATELLITES

Application of electron content observations in navigational ranging. 03 p0275 A73-13654

Oceanic ATC by application of aeronautical satellite technology, discussing system design requirements, performance evaluation and international program 14 p1773 A73-29888

Multiple access technique for future communication, surveillance and navigation subsystems to meet ATC demands, considering satellite surveillance radar system 14 p1725 A73-29893

Geodetic control point accurate position determination by Navy navigation Doppler satellite observations with geoeceiver and teletype tape 15 p1873 A73-32268

Book on earth satellites covering transmission technology, cost effectiveness and materials development for communication, meteorological, earth resources, navigational, research and military applications 15 p1944 A73-32292

Optimal digital modulation techniques for aeronautical communications via satellite, considering air navigational systems for transoceanic flight 15 p1847 A73-32480

Prospects of automation of air traffic control systems using satellites for radio navigation 17 p2209 A73-34961

Aeronautical and maritime traffic control by stationary orbit navigation satellites, discussing frequency ranges, aircraft distance control, antenna arrays and multiple data access 17 p2125 A73-35477

Synchronous satellite systems for civilian air, ship and land vehicle traffic control, communication, navigation and surveillance, discussing technology requirements for continental and oceanic systems [ALAA PAPER 73-583] 18 p2288 A73-36075

National Aerospace Meeting, Washington, D.C., March 13, 14, 1973, Proceedings. 21 p2734 A73-40035

NAVY

Large floating ocean platforms for US Navy bases, discussing concrete construction techniques and costs for different configurations 19 p2418 A73-37749

Naval test and evaluation capabilities for aircraft, emphasizing organizational relationships 23 p3051 A73-44066

NC-130 AIRCRAFT

U C-130 AIRCRAFT

NEAR INFRARED RADIATION

Polarization of near-infrared sunlight reflected by terrestrial clouds. 01 p0073 A73-10363

Energy distribution in the near infrared from nuclei of galaxies. I - M31, M32, NGC 3115, NGC 4151, NGC 4406. 01 p0098 A73-10552

Heterojunction photocell, sensitive in the near infrared. 01 p0051 A73-10834

A near-infrared view of the Uranus system. 01 p0109 A73-11491

Continuous near-infrared spectrum of two Be stars - HD 50138 and HD 51585 02 p0224 A73-12735

The generation of tunable near IR radiation using a nitrogen laser pumped dye laser. 03 p0318 A73-12869

Solar spectra line intensities in band 201 of visible and near IR regions, noting water vapor bands presence in sunspot spectra 03 p0377 A73-14412

Gravity-darkening of the secondary component of RW monocerotis. 05 p0624 A73-17315

Response characteristics of photodiodes, phototransistors and photoresistors in near IR range, showing output signal levels as function of wavelength and illumination intensity 06 p0692 A73-17837

Study and development of a dye laser with coupled modes excited by a flash tube and emitting in the near infrared 08 p0976 A73-21493

Spectrophotometric measurements of noctilucent clouds. 09 p1079 A73-23339

Near infra-red magnitudes of 248 early-type emission-line stars and related objects. 11 p1415 A73-25172

Polarization of the cloudless daytime sky in the 1.25- to 2.42-micron range 11 p1353 A73-25645

Visible and near-infra-red transmission and reflectance measurements of the Luna 20 soil. 13 p1674 A73-28303

A review of near-infra-red optically pumped solid-state lasers. 16 p2023 A73-32856

The impact of silicon technology on near-infra-red and low-light-level imaging. 16 p2012 A73-32867

Optical and near IR absorption line spectra of quasar 1331+170, discussing red shift and line locking process 19 p2487 A73-38508

Minor planets and related objects. X - Spectrophotometric study of the composition of /1685/ Toro. 20 p2607 A73-39120

Statistical spectral attenuation characteristics of transmittance windows for visible and near IR under various optical weather conditions 21 p2731 A73-40746

Possibilities of calculating the spectral albedo of Venus in the near infrared 21 p2770 A73-40914

Vacuum IR spectrometer measurement of C 12 methane absorption band at 1.1 microns, describing technique for extending standards to photomultiplier region of spectra 21 p2743 A73-40936

Near-infrared radiation intensity from restrikes of exploding wires. 21 p2740 A73-40955

Lower atmospheric intensity-calibrated thermal emission spectra with digital recording near IR spectrometer, discussing applications to pollutant detection 21 p2692 A73-41574

NEAR ULTRAVIOLET RADIATION

Optical properties and structure of the atmosphere of Saturn. II - Latitudinal variations of absorption in the CH4 0.62-micron line and the characteristic features of the planet in the near ultraviolet 12 p1546 A73-27862

Space observations of the variability of solar irradiance in the near and far ultraviolet. 16 p2062 A73-33428

The extinction coefficients of NO2 between 195 nm and 410 nm. 16 p2005 A73-33544

[ALAA PAPER 73-503] Experimental results on combined ultraviolet-proton excitation of moon rock luminescence. 17 p2233 A73-35273

Optical properties and structure of Saturn's atmosphere. II - Latitudinal variations of absorption in the 0.62-micron CH4 band and characteristics of the planet in the near ultraviolet. 20 p2608 A73-39236

The near ultraviolet spectrum of early type stars obtained with S 59. 21 p2769 A73-40825

Line identifications in the near ultraviolet spectrum of the peculiar A star epsilon Ursae Majoris. 21 p2769 A73-40829

NEAR WAKES

An investigation of the near wake properties which lead to the generation of vortex shedding sound from airfoils. 03 p0242 A73-12976

Observations on the macroscopic structure of a near turbulent wake with a Mach number M sub infinity equal 2.3 [ONERA, TPNO. 1176] 03 p0244 A73-13577

Comparison of theory with experiment for electron density distribution in the near wake of an ionospheric satellite. 04 p0444 A73-15541

Experiments on flow about a yawed circular cylinder. 05 p0527 A73-16546

[ASME PAPER 72-FE-2] Wind tunnel study of flow structure and turbulent wakes on base surfaces of sharp or blunt edged flat bodies at various Mach and Reynolds numbers 06 p0643 A73-17456

Variational determination of electric field induced by charge separation in near wake of negatively charged body moving at mesothermal speeds in collisionless plasma 10 p1254 A73-24116

Two dimensional inviscid flow model of shear layer motion and vortex shedding in near wake of bluff-based body, using Schwarz-Christoffel transformation 11 p1300 A73-25155

Electron depletion in the wake of ionospheric spacecraft - A comparison between results from Langmuir probes and antennas. 17 p2159 A73-34783

NEARSHORE WATER

NT COASTAL WATER

NEBULAE

NT CASSIOPEIA A

NT CRAB NEBULA

NT GUM NEBULA

NT PLANETARY NEBULAE

The image tube nebular spectrograph of the Asiago Observatory. 01 p0050 A73-10543

Rocket infrared observations of H II regions. 01 p0103 A73-11026

Investigation of the faint nebula identified with radio source HB-21. 01 p0106 A73-11304

Two quantum induced photon-plasma transition probability for hydrogen atom in processes of nebulae and stellar chromospheres 01 p0080 A73-11308

Observations of planets, nebulae, and galaxies at 350 microns. 03 p0374 A73-13716

Molecular clouds and stellar origin in interstellar space 03 p0376 A73-14175

Spectroscopic study of the nebula NGC 7635 and the star BD +60.2522 deg. 04 p0503 A73-16005

Possibility of emission-line polarization in diffuse nebulae with a C + E spectrum 05 p0617 A73-16462

Spectrophotometric survey of diffuse galactic nebulae 05 p0617 A73-16463

Absolute intensity of the H-alpha line in the nebulae NGC 2068 and S-57 05 p0617 A73-16464

The kinematical distribution of dark clouds surveyed in the 4830 MHz H2CO line. 08 p1004 A73-20904

Measurements of the electron temperatures in M42 from the profiles of H-alpha, forbidden N II, H-beta, and forbidden O III. 08 p1004 A73-20906

Spectra of the Becklin-Neugebauer point source and the Kleinmann-Low nebula from 2.8 to 13.5 microns. 08 p1008 A73-21157

H beta emitting diffuse nebulae as reflection nebulae illuminated by galactic light, based on photometric observation of H alpha emitting external spiral galaxies 08 p1013 A73-21809

The X-ray surface brightness of the Cygnus Loop. 08 p1013 A73-21811

Carbon monoxide rotational transitions as dark cloud cooling mechanism during protostar formation 08 p1013 A73-21814

Infrared and microwave emission from nebulae in the galaxy. 09 p1150 A73-23133

Interferometric investigations of the A21 nebula /Y/M29, Medusa/ 10 p1273 A73-23704

Russian book - Physics of stars and nebulae. 11 p1416 A73-25226

Polarization of continuous-spectrum emission in the Larger Orion Nebula 11 p1416 A73-25227

Photometric characteristics and structure of nebulae NGC 6914a, IC 5076, and Ced 201 11 p1416 A73-25228

Optical system and performance potential of telescopic high-aperture-ratio Schmidt camera designed for photographic studies of faint extended objects 11 p1361 A73-25230

Optical and radio observations of the Orion Nebula. 11 p1425 A73-26265

Kinematics of the Huygenian region of the Orion Nebula. 11 p1427 A73-26605

Path length distribution of cosmic rays from pulsar nebula complexes. 12 p1536 A73-27880

Nebular stage of Nova Delphini 1967. I 13 p1672 A73-28039

High radio frequency observations of the Omega nebula. 15 p1932 A73-31268

IR objects in Orion Nebula, discussing temperature range and pre T Tauri evolutionary stage 15 p1934 A73-31419

O-B stars in young star clusters associated with nebulae 15 p1934 A73-31420

Photoelectric photometric investigation of brightness behavior of Orion nebula variable stars 15 p1934 A73-31422

The absence of formaldehyde radiation toward cold regions of the galactic plane - Further investigation. 15 p1936 A73-31554

Motion of fourteen stars in the Orion nebula cluster. 15 p1936 A73-31555

Some remarks on solar nebula type theories of the origin of the solar system.

17 p2227 A73-34406

Interferometry of the Medusa nebula A21 /YM 29/.

18 p2354 A73-36729

On the nature of the infrared point source in the Orion Nebula.

18 p2356 A73-36975

Radial velocity measurements of the Cetus Arc nebulosity around Loop II.

19 p2483 A73-37571

Infrared spectrum of the Orion Nebula between 55 and 200 microns.

19 p2484 A73-37614

2.2- and 3.5-micron polarization measurements of the Becklin-Neugebauer object in the Orion Nebula.

19 p2489 A73-38528

Ground based photometry of planets, stars and galactic nebulae at 34 microns

19 p2489 A73-38529

A catalog of data on optically visible H II regions.

20 p2607 A73-39084

Shell nebulae and Wolf-Rayet stars - Observations of NGC 2359

21 p2768 A73-40714

Temperature gradient in gaseous nebulae

21 p2768 A73-40716

Linear polarization in the Orion Nebula.

22 p2908 A73-42313

Wolf-Rayet stars effective temperature estimation from UVB photometry of surrounding ring nebulae with optically thick H II region excited by stellar Lyman radiation

23 p3025 A73-43195

The H II region G333.6-0.2, a very powerful 1-20 micron source.

23 p3028 A73-43527

Density and velocity fluctuations in young nebulae of Orion type

23 p3035 A73-44232

Simeiz 59 /Sharpless 104/ nebula radial and expansion velocity indicating type I supernova origin, discussing spectral and interferometric measurements and relativistic electron energy and density

23 p3035 A73-44233

Electronographic observations of the forbidden O II ratio in the core of the Orion Nebula.

24 p3140 A73-45183

The shapes of neutral globules associated with diffuse nebulae.

24 p3141 A73-45194

NECK [ANATOMY]

Some effects of cooling and heating areas of the head and neck on body temperature measurement at the ear.

13 p1575 A73-28504

Vestibular and spinal control of eye movements.

18 p2272 A73-36440

NEEDLES

Streaming two dimensional Oseen MHD flow of conducting fluid past semiinfinite needle within aligned field

01 p0031 A73-10305

Combined forced and free-convection heat transfer from vertical thin needles in a uniform stream.

02 p0238 A73-12052

Combined forced and free-convection over thin needles.

18 p2371 A73-36697

NEGATIVE CONDUCTANCE

Instability nature in Gunn diode type system with negative differential conductivity, presenting expressions for oscillation threshold and gain

01 p0088 A73-10629

Oscillations of injected carriers in p-type indium antimonide.

04 p0482 A73-14869

Infrared detection by reconfiguration of high field domains in CdS:Ag, Al.

06 p0733 A73-17500

Energy absorption inelastic surface mechanisms effect on I-V characteristics profile for bounded semiconductor with negative differential conductivity

06 p0735 A73-17974

Analysis of an inhomogeneous bulk 'S-shaped' negative differential conductivity element in a circuit containing reactive elements.

09 p1061 A73-21989

Computer simulations of the large signal characteristics of supercritical GaAs transferred electron amplifiers.

09 p1063 A73-22492

Book - Transferred electron devices.

09 p1066 A73-23299

Low-temperature negative differential microwave conductivity in semiconductors following elastic scattering of electrons.

13 p1669 A73-28614

Effect of donor density and temperature on the performance of stabilized transferred-electron devices.

17 p2134 A73-34220

Self-resonant LSA oscillator diode of rectangular cross-section.

22 p2832 A73-41895

NEGATIVE FEEDBACK

NT SENSORY FEEDBACK

Improvement of the product accuracy in analog multipliers with the aid of the negative-feedback principle

06 p0672 A73-17400

Microwave amplifier with internal negative feedback, using IF output for frequency modulation of mixer oscillator signal

06 p0677 A73-18394

Certain feedbacks generated during turbulent cellular convection in the atmosphere

08 p0986 A73-21456

Mechanism of passive negative feedback in the cavity of a solid-state laser

12 p1504 A73-26884

Pulse amplifier with active gain adjustment for constant bandwidth

13 p1590 A73-28571

A simple method for obtaining a constant input resistance in broadband amplifiers

13 p1590 A73-28572

SNR improvement by negative feedback and deterioration by positive feedback in amplifiers, discussing input circuit thermal noise

13 p1591 A73-28735

Reduction of nonlinear distortions in a two-port network exhibiting a small nonlinearity

13 p1592 A73-28894

Selectivity enhancement of certain low-sensitivity RC active networks.

14 p1738 A73-29711

Self-stabilizing power amplifiers with combination-type negative feedback

14 p1736 A73-30564

Nonlinear distortions of series-connected two-port networks

15 p1850 A73-31253

Mutual synchronization of oscillators which are coupled by a segment of a long line.

17 p2143 A73-35715

Frequency-time domain stability criterion for nonlinear negative feedback system with linear transfer function, using Zame positive operator theory

17 p2203 A73-35731

Feedback in microminiaturized transistor amplifiers

21 p2659 A73-40010

Generation of microsecond pulses with controllable pulse width in a ruby laser

21 p2713 A73-40527

NEGATIVE RESISTANCE CIRCUITS

Combined operations with negative resistance and nonlinear characteristics in an avalanche diode.

07 p0804 A73-20569

Stabilization of relaxation oscillators based on devices with an S-type current-voltage characteristic.

10 p1197 A73-24933

A modified GaAs IMPATT structure for high-efficiency operation.

13 p1595 A73-29577

Wideband negative resistance by synthesizing parallel tank converter circuit, discussing input and load admittance

15 p1853 A73-31258

System oscillations from negative input resistance at power input port of switching-mode regulator, amplifier, dc/dc converter, or dc/ac inverter.

22 p2802 A73-42911

Microwave transistor oscillators design based on Si overlay transistors and microstrip transmission lines as passive elements, obtaining negative resistance between collector-base terminals

23 p2961 A73-44144

Two-terminal current-fed negative admittance incorporating field effect transistors.

23 p2961 A73-44145

NEGATIVE RESISTANCE DEVICES

Negative resistance in metal-semiconductor-metal /MSM/ diodes.

01 p0023 A73-10579

Microwave amplifier design based on negative differential mobility in Gunn diodes

02 p0144 A73-11531

Microwave harmonic generator using the nonlinearity of negative resistance in n-type GaAs.

03 p0281 A73-12997

Analysis of limit cycles in a two-transistor saturable-core parallel inverter.

03 p0252 A73-13929

Impurity centers effect on I-V characteristics of double injection level semiconductors, noting negative resistance region

04 p0482 A73-14877

GaAs Gunn diode LSA operation mode in multiloop circuit to extend high frequency limit

05 p0558 A73-16788

Large-signal noise, frequency conversion, and parametric instabilities in IMPATT diode networks.

06 p0679 A73-17789

Semiconductor-insulator-semiconductor /SIS/ tunneling current characteristics, noting negative resistance feature for degenerate p-n diode

06 p0677 A73-18359

Regenerative amplifier based on multiple IMPATT diodes

07 p0802 A73-20295

Design and performance of transferred electron amplifiers using distributed equalizer networks.

07 p0803 A73-20553

IMPATT diode microwave oscillator performance analysis based on model with ac current and voltage superposition on dc, determining avalanche frequency and negative resistance

08 p0942 A73-20706

Finite difference calculation for Gunn effect mathematical model, noting negative slope in electron drift velocity versus electric field characteristics for microwave oscillation

08 p0943 A73-20710

Diffusion effects in the double injection negative-resistance problem.

08 p0948 A73-21487

Doppler signal detection with negative-resistance diode oscillators.

09 p1062 A73-22321

Double-injection negative differential resistance in compensated gold-doped germanium.

10 p1259 A73-23752

The elimination of tuning-induced burnout and bias-circuit oscillations in IMPATT oscillators.

10 p1196 A73-24622

Analysis of an oscillator using a sequence of negative resistance devices

12 p1477 A73-26871

Small-signal analysis of punch-through injection microwave devices.

13 p1590 A73-28541

Noise in cavity-stabilized microwave oscillators.

13 p1595 A73-29294

Phenomenon of negative differential resistance in silicon carbide crystals

14 p1783 A73-30384

Two terminal large signal circular coupled wideband TRAPATT diode microwave amplifiers, noting negative resistance characteristics and dc-to-rf conversion efficiency

17 p2140 A73-35321

Review of some mathematical models of non-linear domain dynamics in bulk-effect semiconductor.

17 p2219 A73-35516

An X-band Gunn-diode generator with varactor tuning

17 p2126 A73-35550

Gunn diode parameters from a small signal analysis.

17 p2142 A73-35651

Regenerative multidiode IMPATT amplifier.

18 p2294 A73-37132

Negative resistance oscillators, predicting fundamental, harmonic and subharmonic locking characteristics by nonlinear models and equivalent circuit

19 p2410 A73-38307

Optimum nonlinear characteristic of the supply element in the astable multivibrator with a tunnel diode.

19 p2410 A73-38309

Parallel resonator with a resistance and a frequency dependent negative resistance realized with a single operational amplifier.

19 p2411 A73-38536

Realization of canonical bandpass filters with frequency-dependent and frequency-independent negative resistances.

19 p2412 A73-38537

Temperature dependence of the parameters of an n-p-i structure with negative resistance

20 p2535 A73-38860

Analysis of limit cycles in a two-transistor saturable-core parallel inverter.

21 p2662 A73-40339

Planar conductance transistor based on charge carrier accumulation due to n-n junction, featuring steep negative resistance characteristics and low sustaining voltage

21 p2655 A73-41048

IMPATT diode frequency-independent small-signal equivalent circuit incorporated with negative resistance element and white noise source for terminal behavior prediction

23 p2964 A73-44074

Analysis of microwave circuit for characterization of negative-conductance devices by transients.

23 p2964 A73-44076

Oscillation amplitude curve determination of negative resistance oscillator connected to LC circuit, obtaining device I-V characteristics

23 p2961 A73-44147

Parametric oscillations in an oscillating circuit utilizing negative resistance.

24 p3075 A73-45479

Gunn diode negative resistance microwave oscillators with simultaneous lower frequency mode and individual tunings of two frequencies

24 p3073 A73-45483

NEODYMIUM

Polycrystalline organic compounds effect on second harmonic generation of neodymium laser, noting relation between nonlinear susceptibility and intramolecular charge transport

02 p0176 A73-12097

Neodymium energy level shifts in three oxygen-compensated sites of neodymium oxide-doped calcium fluoride crystals
03 p0349 A73-13288

Phononless lines shift and broadening during electron phonon interaction in lanthanum trifluoride-Nd crystal, obtaining temperature dependence of non-radiative transition probability
04 p0484 A73-15566

Mode locking picosecond pulse Nd glass laser design for reliable and reproducible operation as function of pump power, mirror alignment and saturable absorber
06 p0700 A73-18293

Large-aperture Nd-glass laser amplifier for high-peak-power application.
06 p0704 A73-18791

Optical properties of Nd³⁺ in lanthanum oxyfluoride single crystals
07 p0837 A73-20205

Quasi-stationary emission from ruby and neodymium-glass lasers
08 p0976 A73-21718

Spectroscopic and lasing studies of a new laser crystal, KY(WO₄/2-Nd³⁺)
09 p1134 A73-22984

Lasing characteristics of neodymium glasses at the 0.92-micron wavelength
10 p1260 A73-24581

Neodymium-glass laser with tunable pulse width
11 p1376 A73-25433

Improving the angular divergence of the emission from a neodymium-glass laser with a high pulse energy level
12 p1505 A73-26963

Observation of dislocations and inclusions in neodymium-doped yttrium aluminium garnet by transmission electron microscopy.
14 p1782 A73-29744

A controlled single-pulse neodymium-glass laser
14 p1757 A73-30369

Improving the angular divergence of a neodymium-glass laser beam having a high radiation energy per pulse.
19 p2438 A73-38146

A neodymium-doped yttrium-aluminum-garnet laser amplifier with an integrated design
20 p2572 A73-38669

NEODYMIUM ALLOYS
Phase diagram of the neodymium-yttrium system
01 p0088 A73-10919

Phase diagram and certain properties of alloys of the neodymium-antimony system
06 p0707 A73-18041

High temperature and metallographic investigation of Nd-Y alloys, measuring heat and electrical conductivity, thermal expansion and emf, magnetic susceptibility and Hall coefficient
06 p0735 A73-18050

The formation and structure of precipitates in a dilute magnesium-neodymium alloy.
07 p0838 A73-19121

Moessbauer effect in Nb₃Sn as a function of heat treatment
15 p1922 A73-31180

NEODYMIUM COMPOUNDS
Enthalpy and specific heat of the orthophosphates of lanthanum, neodymium, and yttrium at high temperatures
06 p0738 A73-18654

Certain physical properties of Nd-Sb system alloys and their correlation with the phase diagram
09 p1134 A73-22679

Samarium oxide neodymium oxide activated glass fiber output power under lasing conditions
14 p1766 A73-30468

Low temperature specific heat of neodymium magnesium nitrate.
18 p2341 A73-36977

NEON
NT NEON ISOTOPES
Gas discharge efficiency from populations comparison of Ne absorbing levels in hollow cathode and positive column discharges, measuring laser output power peak
02 p0176 A73-12096

Mapping the solar corona in X-ray lines of O VII and Ne IX.
03 p0375 A73-13956

Projectile structure effects on neon K X-ray production by fast, highly ionized argon beams.
04 p0476 A73-14769

Local transient phenomena induced in an inert gas plasma by a short pulse.
10 p1257 A73-24626

Measurement by double resonance of Lande factors of the 3 s/2 and 2 p/4 of neon pumped optically by a laser beam
13 p1627 A73-28568

The kinetic characteristics of the electrons of the anisothermal homogeneous steady neon plasma in the ionization level range from 10 to the minus 9th power to 0.01
16 p2043 A73-34022

Data acquisition technique for Fabry-Perot spectroscopy, noting application to Brillouin spectra recording of solid Ne
17 p2171 A73-35403

Exponential projectile charge dependence of Ar K and Ne K X-ray production by fast, highly ionized argon beams in thin neon targets.
22 p2890 A73-42710

NEON ISOTOPES
Relation between solar and planetary neon in carbonaceous chondrites.
02 p0211 A73-11744

Spallation production of He-3, Ne-21, and Ar-38 from target elements in the Bruderheim chondrite.
10 p1277 A73-24103

The A, B, C's of trapped helium, neon, and argon in meteorites and lunar samples.
17 p2228 A73-34417

He, Ne and Ar in chondritic Ni-Fe as irradiation hardness sensors.
17 p2120 A73-35801

Variability of the He-3 and Ne-21 production rates in ordinary chondrites.
21 p2771 A73-41008

NEON 19
U NEON ISOTOPES
NEOFLASMS
NT CANCER
NEOPRENES
U CHLOROPRENE RESINS
NEPHANALYSIS
Mesoscale cloud systems analysis from meteorological observations and weather satellite data nephanalysis, applying to weather forecasting
13 p1655 A73-29191

NEPHELOMETERS
A nephelometric method for transparency determination in scattering media
14 p1771 A73-30463

NEPTUNE (PLANET)
Neptune model calculation from mass, radius and rotation period, comparing with gravitational moment
01 p0101 A73-10844

Limits of possible position of tenth planet at 50-100 AU from analysis of Neptune orbit
05 p0622 A73-17180

Temperatures of Uranus and Neptune at 24 microns.
07 p0874 A73-19067

Survey of the outer planets Jupiter, Saturn, Uranus, Neptune, Pluto, and their satellites.
11 p1417 A73-25315

Multicolor photoelectric photometry of Neptune.
11 p1429 A73-26682

Neptune model calculation from mass, radius and rotation period, comparing computed gravitational moments with observation
15 p1928 A73-30980

Atmospheric Uranus and Neptune models with massive atmospheres above solid cores, discussing Uranus solid methane cloud layer
22 p2913 A73-42987

The wavelength dependence of the albedos of Uranus and Neptune from 0.3 to 1.1 micron.
22 p2914 A73-43014

H2 pressure-induced lines in the spectra of the major planets.
24 p3138 A73-45050

NEPTUNIUM
NT NEPTUNIUM ISOTOPES
NEPTUNIUM ISOTOPES
Np-237, U-236, and other actinides on the moon.
07 p0888 A73-19785

NERNST HEAT THEOREM
U NERNST-ETTINGSHAUSEN EFFECT
NERNST-ETTINGSHAUSEN EFFECT
Theory of quantum oscillations of the Nernst-Ettingshausen thermomagnetic coefficient in semiconductors
20 p2599 A73-39397

NERVA (ENGINE)
U NUCLEAR ENGINE FOR ROCKET VEHICLES
NERVES
On the causes of the changes of the second heart sound in left bundle branch block.
01 p0009 A73-11008

The role of the vagus nerves in the respiratory response to CO2 under hyperoxic conditions.
01 p0010 A73-11501

The role of the carotid chemoreceptors in the CO2-hyperpnea under hyperoxia.
01 p0010 A73-11502

Derivation of a function of nerve-fiber distribution according to fiber diameters on the basis of electrophysiological measurements
04 p0413 A73-15787

Study of intraventricular conduction times in patients with left bundle-branch block and left axis deviation and in patients with left bundle-branch block and normal QRS axis using His bundle electrograms.
05 p0540 A73-16582

Device for analyzing the electrical activity of nerve fibers in intact nerves
10 p1183 A73-23812

Corpus callosum role in monocular system transcommisural interactions from binocular interaction studies of stimulus-evoked potentials in rat visual cortex
10 p1180 A73-24332

Electrophysiological study of the topographic organization of Deiters' lateral vestibular nucleus
10 p1181 A73-24515

Results of electron microscopic studies in the rat brain under oxygen at high pressure.
11 p1314 A73-25330

Anatomical and neurophysiological investigations of centrifugal control of retinal activity via efferent optic nerve fibers
14 p1714 A73-29875

Neuroanatomy of the auditory system.
14 p1715 A73-30280

Impact acceleration effects on rabbit central nervous system, noting changes in nerve tissue elements and cerebral vessels
17 p2111 A73-34227

Evoked potentials in the hypothalamus in response to stimulation of the vagus and sciatic nerves
19 p2395 A73-37941

Force output of the diaphragm as a function of phrenic nerve firing rate and lung volume.
20 p2515 A73-39780

Signal/noise ratio in the recording of human nerve-action potentials.
22 p2814 A73-42372

Computer acquisition of multiunit nerve-spike signals.
22 p2815 A73-42671

NERVOUS SYSTEM
NT AFFERENT NERVOUS SYSTEMS
NT AUTONOMIC NERVOUS SYSTEM
NT AXONS
NT BRAIN
NT BRAIN STEM
NT CENTRAL NERVOUS SYSTEM
NT CEREBELLUM
NT CEREBRAL CORTEX
NT CEREBRUM
NT DIENCEPHALON
NT EFFERENT NERVOUS SYSTEMS
NT GANGLIA
NT HIPPOCAMPUS
NT NERVES
NT NEUROGLIA
NT NEURONS
NT PERIPHERAL NERVOUS SYSTEM
NT SPINAL CORD
NT SPINE
NT SYMPATHETIC NERVOUS SYSTEM
NT SYNAPSES
NT THALAMUS
Sleep and the maturing nervous system; Proceedings of the Symposium on the Maturation of Brain Mechanisms Related to Sleep Behavior, Boiling Springs, Pa., June 21-24, 1970.
03 p0263 A73-14255

Nervous system transmitter biochemistry in terms of excitation and inhibition coordination with emphasis on gamma-aminobutyric acid (GABA) function in cerebellum
03 p0264 A73-14258

Comparative anatomy of the vestibular nuclear complex in submammalian vertebrates.
06 p0655 A73-18575

Structural models of simple sensory motor co-ordination.
06 p0660 A73-18890

Investigation of certain indices of higher nervous activity in man during prolonged stay in a water environment
09 p1039 A73-22364

Book - Sensory coding in the mammalian nervous system.
11 p1317 A73-25799

Vector correlation theory and neural mechanisms of binaural signal detection in human auditory system
14 p1716 A73-30283

Hypothalamo-adenohypophysis-adrenal neurosecretory system under hyperthermia
14 p1719 A73-30847

Correlational inter-relationships between the neuroendocrinal system and the genotype in the formation of protective reactions of the organism
15 p1835 A73-31875

Determination of the type of higher nervous activity from the aftereffect characteristics of multidimensional stimuli
18 p2277 A73-36577

Biological effects due to single accelerated heavy particles and the problems of nervous system exposure in space.
22 p2814 A73-42181

Visual perception dominance over touch related to threshold changes, analyzing nervous system reliance on sense with lower threshold
23 p2946 A73-43847

Influence of physical stress on the state of human higher nervous activity under conditions of underwater labor
24 p3059 A73-44672

NETS

NT NEURAL NETS

Elasticity theory of three dimensional system of particles in rectangular prismatic or tetrahedral net arrangement as topological model for finite element method

11 p1448 A73-26727

NETWORK ANALYSIS

NT CRITICAL PATH METHOD

Application of the asymptotic method to third-order oscillatory systems

01 p0021 A73-10030

Rational and irrational matrix functions for analysis and synthesis of distributed microwave networks with multiwave lines and lumped nonreactive elements

01 p0027 A73-10578

New transistor squaring stage with a 'smooth' parabolic characteristic for realizing a simple high-precision parabolic multiplier

01 p0024 A73-10924

Signal search networks for enlargement of locking bandwidth of tracking filters in automatic control systems, examining transistorized signal search and acquisition circuits

02 p0145 A73-11793

Parameter selection scheme for unit measuring frequency deviation as function of voltage, resistance and circuit sensitivity

02 p0149 A73-11864

Statistical method of calculating scattering matrix elements and parameter deviations of SHF octupole networks /square bridge, hybrid ring or directional junction/

02 p0146 A73-12025

Photomultiplier operation pulse control in semiconductor circuit for background cosmic radiation noise error minimization in air shower station

02 p0171 A73-12688

Nodal admittance matrix method for first and second derivative network sensitivity, noting applicability to network analysis at discrete frequencies

03 p0286 A73-14000

Nonlinear harmonic analysis of reflex klystrons with high electron conductance, using average method in second approximation

05 p0556 A73-16065

Linear time-invariant feedback systems with multiple inputs and outputs, deriving necessary and sufficient conditions for stable closed loop impulse response

05 p0561 A73-16493

Large-signal behaviour of R.F. power transistors. I - Analysis of the equivalent circuit

05 p0559 A73-17125

Large-signal noise, frequency conversion, and parametric instabilities in IMPATT diode networks

06 p0679 A73-17789

Globally equivalent representations for reciprocal stationary nonlinear systems in equilibrium or steady state conditions, considering electric circuits and thermodynamic system examples

06 p0716 A73-17993

Digital-computer analysis of linear electronic circuits by the method of structural numbers

07 p0804 A73-18894

Design of active filter sections performing biquadratic transfer functions on the basis of a branched operational-amplifier configuration

07 p0796 A73-18895

Design of selective third-order active RC filters exhibiting high Q values at low Q sensitivities

07 p0796 A73-18896

A low-sensitivity third-order active filter constructed with DVCCS/DVCCS universal sources

07 p0796 A73-18897

A two-dimensional numerical FET model for dc, ac, and large-signal analysis

07 p0799 A73-19342

Lumped parameter network modeling for spacecraft surface thermal environment analysis, discussing computer program and application to Skylab ATM

07 p0919 A73-19496

Analysis of active RC circuits with nonhomogeneously distributed parameters in the time domain

07 p0805 A73-20024

A laser scanner for integrated circuit testing

08 p0974 A73-20731

An algebraic algorithm for the design and analysis of linear dynamical systems

08 p0984 A73-21468

Integral methods of calculating unsteady processes in nonlinear electric systems

08 p0951 A73-21556

Analysis of an inhomogeneous bulk 'S-shaped' negative differential conductivity element in a circuit containing reactive elements

09 p1061 A73-21989

The design, analysis, and performance of resonant and nonresonant microwave transmission devices with theoretically infinite rejection

09 p1080 A73-22103

A new analysis of the digital data transition tracking loop

09 p1062 A73-22302

Feedback control theory as general network analysis tool based on circuit decomposition

09 p1067 A73-22303

RC planar distributed networks one and two dimensional analysis techniques and frequency response characterization, noting FORTRAN program use

09 p1067 A73-22309

Cyclic binary coding and decoding circuits for high reliability data and command transmission, discussing analytical relations and design aspects

09 p1060 A73-22923

Allowable set construction of noncrossing branched paths over prescribed length in unidirectional finite multinetworks

10 p1201 A73-24062

Canonical form of hybrid matrix for linear multipole network circuit, discussing synthesis and analysis

10 p1195 A73-24378

An analytical expression for the limits of error in the measurement of reflection-coefficient phase

10 p1190 A73-24867

Equivalent circuit analysis of noise in bulk semiconductor devices

10 p1197 A73-24869

A representation of uncorrelated random processes by stochastic integrals

11 p1340 A73-25010

Analysis of an oscillator using a sequence of negative resistance devices

12 p1477 A73-26871

A current-excited large-signal analysis of IMPATT devices and its circuit implications

12 p1478 A73-27112

Asilomar Conference on Circuits and Systems, 6th, Pacific Grove, Calif., November 15-17, 1972, Conference Record

12 p1483 A73-27151

Output characteristics of high frequency transistor power amplifiers

12 p1479 A73-27169

Errors of the formal theory of amplifiers with a feedback

12 p1481 A73-27594

Formation and solution of the equations of state of electronic circuits

12 p1485 A73-27623

Resonant bipolar linear networks representation by matched equivalent circuits

13 p1589 A73-28121

Stationary multiport networks frequency response and representation by equivalent circuits

13 p1589 A73-28122

Automatic measurement of the Q factor of stationary bipolar networks and multiports

13 p1589 A73-28123

Spectral analysis of a physical system which can be represented by a stationary linear active electronic network

13 p1589 A73-28474

Shaping circuit for complex RF pulse consisting of simultaneous equilength square pulses with different frequencies, discussing carrier frequencies selection

13 p1583 A73-28730

Modulation functions and transmission coefficients for static frequency converter representation in form of equivalent multipole networks for reactive loads

13 p1592 A73-28939

Transient analysis of multiple-input integrated digital structures

13 p1595 A73-29580

Optimal feedback characteristics of transistor amplifiers

14 p1736 A73-30372

The features of disk shape piezoelectric ceramic transducer equivalent circuit

14 p1754 A73-30892

Operational modes of the feedback circuit of an asynchronous logical network

14 p1731 A73-30939

Methods of calculating high-power rectifier and inverter circuits

15 p1832 A73-31696

Kirchhoff mode theory application to electrical network analysis with arbitrary branch couplings including ideal transformers and controlled sources

16 p1992 A73-32909

Active networks state equations with singular A matrix, considering algebraic method of reduction to equivalent set of equations with nonsingular A matrix

16 p1992 A73-32912

Repetitively switched circuit analysis via matrix formalism and eigenvalue techniques with application to dc-dc converter

16 p1992 A73-33409

Transient analysis of complementary MOS IC inverter

16 p1990 A73-33688

An electronically tuned Gunn oscillator circuit

17 p2134 A73-34222

Time-domain analysis of intermodulation effects caused by nonlinear amplifiers

17 p2136 A73-34868

Effect of upper sideband impedance on a lower sideband up-converter

17 p2123 A73-34971

Book - Introduction to servomechanism system design

17 p2110 A73-35275

Modes of operation of the feedback loop in an asynchronous logical network

19 p2414 A73-38193

International Symposium on Circuit Theory, Toronto, Canada, April 9-11, 1973, Proceedings

19 p2411 A73-38532

A comparison of the times of computation required by two approaches for determining a shortest route in a network - A contribution to the economy of programming

20 p2533 A73-39631

Determination of optimal regimes of a common-emitter transistor cascade which ensure minimal distortions

21 p2659 A73-40012

Phased array analysis by circuit and field theory approaches, discussing boundary value problems formulation and solutions for systems with current carrying and aperture elements

21 p2651 A73-40650

Network analysis of infinite regular antenna arrays, discussing unified approach based on electromagnetic interaction among subarrays as distinguished from boundary value problem solution

21 p2651 A73-40651

Analysis of infinite planar array of rectangular waveguides by generalized scattering matrix approach

21 p2651 A73-40652

Graphical analysis of traveling-wave-tube oscillator with external feedback loop

21 p2663 A73-41046

Electrical network analysis and synthesis problems concerning sensitivity characteristics relationship to circuit parameters and structure determination to satisfy behavioral requirements respectively

21 p2670 A73-41074

Self excited mixer/detector of Gunn diode oscillator, calculating detection characteristics from combined equivalent circuit and computer simulated analysis

21 p2664 A73-41092

Method of analyzing electronic circuits on the basis of a hybrid-parameter matrix in a canonical system of coordinates

21 p2670 A73-41306

Computer analysis of mixed coordinate base transistor circuits determining matrix numbers without main path or generalized node delineation

21 p2670 A73-41308

Polynomial approximations of the characteristics of low-sensitivity filters

21 p2666 A73-41315

Russian book on operation and design of bipolar transistor circuits for video amplifiers covering TV, radar, oscilloscope, automatic control and computer applications

22 p2832 A73-41878

Impulse analysis of subharmonic oscillations in control systems with thyristor converters

22 p2835 A73-42299

Two dimensional microstrip transmission line with step discontinuities, predicting microwave filtering behavior by broadband equivalent circuit for comparison with experiment

22 p2835 A73-42465

Multicircuit structural analysis of linear multiple link control systems with dynamic interchannel cross couplings

22 p2836 A73-42608

Power Electronics Specialists Conference, California Institute of Technology, Pasadena, Calif., June 11-13, 1973, Record

22 p2801 A73-42901

Analysis of starting circuits for a class of hard oscillators - Two-transistor saturable-core parallel inverters

22 p2834 A73-42909

Semiconductor rectifiers analysis, considering triac and thyristor tetrode circuits, trigger devices and circuit diagrams

22 p2835 A73-43128

Investigations on fluidic jet deflection amplifiers in dc- and ac networks

23 p2942 A73-43400

Digital-computer aided analysis and synthesis of specialized functional diode converter circuits

23 p2959 A73-43579

Small signal duality theory of linear optoelectronic circuits with optical coupling for equivalent circuit computerized design and analysis

23 p2963 A73-43615

Analysis of microwave circuit for characterization of negative-conductance devices by transients

23 p2964 A73-44076

Frequency to time domain sensitivity matrix for equivalent tolerance field and response error evaluation, using Fourier transform

23 p2955 A73-44114

Linear system resonance effects in single loop controlled frequency tank circuit with variable capacitor under variable or constant emf

24 p3074 A73-44591

- Analysis of the detection characteristics of frequency discriminators with nonminimum-phase loops
24 p3071 A73-44597
- Analysis of processes occurring during no-load operation of a ferroresonant voltage regulator with an improved shape of the output voltage curve
24 p3057 A73-44608
- An analytical solution of the problem of a frequency tripler employing a varactor diode with an arbitrary voltage-charge characteristic
24 p3072 A73-44927
- Analysis of a frequency-modulated tunnel-diode oscillator.
24 p3072 A73-44941
- Efficient numerical solution of the transmission-line equivalent-circuit model of a semiconductor.
24 p3119 A73-45261
- Time-varying network analysis via matrix manipulation and Peano-Baker solution for second and higher order differential equations with periodic coefficients.
24 p3075 A73-45477
- Tunnel diode equivalent circuit analysis based on empirical expressions for composite T-V characteristics, predicting series resistance effect on switching time
24 p3073 A73-45485
- ## NETWORK SYNTHESIS
- Rational and irrational matrix functions for analysis and synthesis of distributed microwave networks with multiwire lines and lumped nonreactive elements
01 p0207 A73-10578
- Synthesis of active controllers for vibratory systems.
01 p0057 A73-10697
- Synthesis of active RC circuits by means of equivalent circuits of impedance converters
02 p0148 A73-11549
- A decoupling supply network for small antenna arrays
02 p0145 A73-11825
- Systematic method of designing fluidic-pneumatic control circuits.
02 p0133 A73-12646
- Time-averaged power stage models transient and frequency responses characterization and circuit component values derivation for switched dc-dc converters design
03 p0282 A73-13927
- Circuit design of triode thyristors and companion rectifiers for high frequency power conditioning, discussing emitter selection, lifetime control, encapsulation and interdigitation optimization
03 p0283 A73-13943
- Loss compensation in the case of filters with additional resistors
03 p0284 A73-14124
- Noise characteristics, channel capacities, power requirements and transmission efficiencies of various semiconductor transmitter designs for FM directional radio systems
03 p0284 A73-14125
- Logic network design for digital waveform shaping of polyphase voltage generator, noting application for airborne and marine gyroscope power supply
03 p0258 A73-14618
- A digital echo suppressor for satellite circuits.
04 p0416 A73-14995
- Low-sensitivity, frequency-selective amplifier circuits for hybrid and bipolar fabrication.
04 p0427 A73-15054
- Equivalent, filter realization and threshold CNR determination for optimum design of extended range phase locked loop
04 p0421 A73-15436
- Stabilization bandwidth reduction in microwave parallel tuned tunnel diode amplifier circuits synthesis
04 p0429 A73-15919
- Computerized synthesis of wideband series stabilized tunnel diode amplifier based on distributed constant elements
05 p0555 A73-16061
- Logidyn analog components regulator systems for industrial current and speed control, amplifier output voltage control, digital-analog converters, analog storage devices, etc
05 p0556 A73-16075
- Digital and hybrid computational aspects of the discrete representation theorem of nonlinear estimation.
06 p0670 A73-17803
- Optimize Gunn circuits for wideband varactor tuning.
06 p0675 A73-17841
- Transfer matrices determination for two terminal pair network derived from four terminal pair network, considering bandpass filter circuit design.
06 p0677 A73-18397
- Frequency domain synthesis algorithm for linear multivariable system via state variable feedback combined with input dynamics compensation, applying to decoupling and model matching
06 p0682 A73-18866
- Design of active filter sections performing biquadratic transfer functions on the basis of a branched operational-amplifier configuration
07 p0796 A73-18895
- Design of selective third-order active RC filters exhibiting high Q values at low Q sensitivities
07 p0796 A73-18896
- A low-sensitivity third-order active filter constructed with DVCCS/DVCCVS universal sources
07 p0796 A73-18897
- Fluidic circuits fabrication and design technology for rocket guidance and attitude control
07 p0778 A73-18939
- High-frequency converter for power supply applications.
[IEEE PAPER 17.3]
07 p0779 A73-19363
- A relationship between the antenna synthesis for a given radiation pattern and the statistical synthesis of systems for spatial signal processing.
07 p0801 A73-20129
- Radio pulse shaping network synthesis composed of lumped elements, noting pulse duration limitation by network efficiency
07 p0805 A73-20134
- Synthesis of a system with a Pi-shaped amplitude-frequency characteristic and a 'zero' equivalent phase-frequency characteristic
07 p0794 A73-20293
- A wide-band low-shape-factor amplifier module using an acoustic surface-wave bandpass filter.
07 p0804 A73-20557
- A three-cavity ring type filter.
07 p0804 A73-20572
- Design and fabrication of MOS/LSI circuits for reliability, discussing layout rules and protective circuitry
08 p0943 A73-20733
- Improvement of frequency characteristics of digital filters.
08 p0945 A73-20801
- Semicircular waveguide-type, band-splitting filter for millimeter waves.
08 p0945 A73-20807
- Narrow band and broad band step-recovery diode frequency multipliers for microwave power generation.
08 p0947 A73-21138
- Synthesis of functions for polynomial linear-phase amplifiers with feedback
08 p0947 A73-21396
- Use of matrix eigenvalues in the synthesis of symmetrical two terminal pair networks
08 p0947 A73-21397
- An algebraic algorithm for the design and analysis of linear dynamical systems.
08 p0984 A73-21468
- Construction of analytical formulas for functions of linear circuits by means of engineering-application digital computers
08 p0941 A73-21552
- Realization of two-dimensional state space digital filters.
09 p1068 A73-22398
- Theoretical fundamentals of constructing parametric filters equivalent to linear filters
09 p1063 A73-22451
- Dynamic operating regime of multistage diode-capacitor storage networks
09 p1063 A73-22459
- Cutpoint cellular switching array synthesis by combined cascade simplification rule, noting algorithm efficiency increase
09 p1065 A73-23101
- Matched filters for extracting synchronization in signaling, nonreturn-to-zero and split phase PCM systems, using finite-time-duration trigonometric pulse synthesis
09 p1056 A73-23402
- The complex digital filter and its applications in digital signal processing.
09 p1058 A73-23425
- Transistor harmonic oscillator design.
10 p1192 A73-23573
- Design and manufacture of delay equalized comb-line filters.
10 p1193 A73-23608
- Synthesis of gyrator RC filters from the cascaded model
10 p1193 A73-23729
- Active RC filter synthesis with decoupling stage and third order element for minimizing impedance mismatching and overall capacitance
10 p1193 A73-23734
- Speed active multipole filter design with a flexible computer program that calculates the component values for optimum performance.
10 p1191 A73-23755
- Narrow band microwave active bandpass filter with inverted-common-collector transistor circuit, discussing design algorithm, insertion loss, stability, sensitivity and frequency selectivity
10 p1201 A73-24169
- Bending waves dispersion properties in rod applied to acoustic LF dispersion delay line design, analyzing signal distortion and attenuation during propagation
10 p1291 A73-24366
- Synthesis of nonrecurrent digital filters utilizing the knowledge of the spectral characteristics of the input signal
10 p1195 A73-24421
- Active RC filter circuit design based on Pukhov generalized two subcircuit model, determining complex transfer function
10 p1195 A73-24511
- Electrical interference /noise/ effects on measurements of high accuracy low-level differential data signals, discussing noise reduction, capacitive coupling problem and design principles
10 p1189 A73-24570
- A numerical algorithm to design multivariable low-pass equiripple filters.
10 p1202 A73-24600
- Real time digital computer algorithm for linear and nonlinear electronic circuit modeling in state variable form for static and dynamic regimes
10 p1196 A73-24607
- Synthesis of RC gyrator circuits with a constant characteristic resistance
10 p1196 A73-24608
- Method of designing digital devices for bandpass filtration of signals
11 p1333 A73-25023
- Design procedures for matched and broadbanding filters for scanning tests.
11 p1341 A73-25074
- Iterative computer-aided design of optimum cascaded digital recursive filter, using unconstrained Fletcher-Powell algorithm for frequency domain synthesis
11 p1327 A73-25189
- Calculation of the y-parameters of an integrated-circuit amplifier by reducing the matrix of an n-terminal network to the matrix of a two terminal pair network
11 p1338 A73-25102
- Active electromagnetic horn antenna with tunnel diode.
11 p1331 A73-26124
- Cyclic binary codes circuit technology, discussing error types and decoding circuits for error detection and correction
11 p1332 A73-26254
- High Q bandpass low sensitivity RC amplifier-filter networks, discussing two-step decomposition of denominator polynomial of second order filter transfer function
11 p1338 A73-26417
- Optimal control theory for constant gain radar filter design with weighted variance average minimization comparable with Kalman filter performance
11 p1339 A73-26643
- Questionnaire approach for technical diagnostics problem formulation covering hardware failure analysis coding, combinational switching device synthesis and optimal program construction
12 p1482 A73-26752
- Construction of verification tests for digital devices with delay elements
12 p1482 A73-26753
- Multiple input system with feedback loops and majority decision for performance optimization, discussing design principles and applications for structural synthesis and circuit design
12 p1482 A73-26759
- Wave devices built with ferromagnetic and electrically conducting film strips
12 p1460 A73-26772
- Frequency characteristics of directional loop-type bandpass filters
12 p1477 A73-26870
- Nonrecursive digital filter hardware design based on analysis of bit level counting operations in convolution, using fixed and floating point representations
12 p1483 A73-27115
- Counting operation based recursive digital filter hardware design in canonic and direct forms, emphasizing low cost, low speed and high flexibility
12 p1483 A73-27116
- Data aided phase locked loops for phase estimation improvement in coherent demodulator to obtain loop acquisition characteristics design flexibility
12 p1483 A73-27157
- VHF and microwave surface acoustic wave bandpass filter design with impulse model for frequency response and interdigital transducer input admittance calculation
12 p1484 A73-27563
- The design and applications of highly dispersive acoustic surface-wave filters.
12 p1484 A73-27564
- Analog voltage squaring circuits with series-connected resistors shunted by semiconductor diodes or ladder network, discussing design, construction and operation principles
12 p1481 A73-27591
- Formation and solution of the equations of state of electronic circuits
12 p1485 A73-27623
- Method for synthesizing built-in control circuits of automatic systems with memory
12 p1476 A73-27899

Inductive flow meter sensor design for optimal electrode diameter to ensure signal quality and impedance matching, proposing circuit diagram

Review of microwave-integrated-circuit technology.

A computer program for filter design having arbitrary magnitude specifications in the frequency domain.

Wave resistance determination in synthesis of oscillatory circuits with homogeneous line segments for given resonant frequencies spectrum

Analysis of the operation of a diode phase detector with allowance for the diode recovery time

Active analog bandpass RC and LC filters design calculation by wave parameters

Resonant RLC tank circuit design with coupled stripline segments, using lumped and distributed parameter system synthesis theory

Synthesis of regenerative amplifiers with isoeutremal approximation of the amplitude-frequency characteristics

High-speed frequency count-down circuit using a tunnel diode and a delay line.

Selectivity enhancement of certain low-sensitivity RC active networks.

Active LC, RC and C/gyrator/ filters design, operation, tolerance, cost and noise characteristics

Control systems synthesis via digital computer techniques, describing numerical optimization procedure and analog simulation method

Multidigit switching circuit synthesis for functionally complete redundant systems with incomplete splicing correlation

Nonlinear distortions of series-connected two-port networks

Wideband negative resistance by synthesizing parallel tank converter circuit, discussing input and load admittance

Russian book - Design and calculation of microwave stripline elements.

Papers on digital signal processing covering digital filters, fast Fourier transform, finite word length effects, algorithms, and design and programming considerations

Approximate procedure for synthesis of interdigital bandpass filters with lumped capacitance loaded band ends, deriving transmission response from Kirchhoff nodal law

Analysis of the dynamic operation of a four-terminal network with slight nonlinearity.

A user-oriented guide to the design and application of solid state relays.

Load transfer between AC sources within relay ratings through circuit design.

Inductive relaxation oscillator design using common emitter avalanche transistors with N-shaped I-V characteristics at base input

Theory of optimal AGC system synthesis.

Book - Design of modern transistor circuits.

Determination of the geometrical dimensions of a bandpass filter for a microwave hybrid integrated circuit

Design of second-order phase circuits constructed with TEM-line segments

On the optimum design of tapered waveguide transitions.

Thin film hybrid microwave integrated circuit.

Design of nonlinear resistive networks with prescribed input-output behavior.

Book - Low-noise electronic design.

A new technique for synthesis of broad-band parametric amplifiers.

Method of synthesizing built-in monitoring arrangements for automata with memory.

Book - MOS integrated circuit design.

Design principles for phase-measuring attachments with automatic error corrections

Synthesis of a system of pi-shaped amplitude-frequency and 'zero' equivalent phase-frequency characteristics.

Suboptimal filter design for dynamic measurement systems, deriving bias and Kalman covariance formulae for error analysis and model sensitivity

Synthesis of the functions of polynomial linear-phase feedback amplifiers.

Use of the eigenvalues of a matrix to synthesize symmetrical four-terminal networks.

International Symposium on Circuit Theory, Toronto, Canada, April 9-11, 1973, Proceedings.

The present state of the microwave filter art.

Realization of canonical bandpass filters with frequency-dependent and frequency-independent negative resistances.

Near-harmonic integrated oscillators in the 10 MHz to 40 MHz range.

Multivalued models of computer electronic circuits

Optimal matching by using band filters

Approaches to the design of low-voltage pulse generators using avalanche semiconductor devices

Optimization and design of varicap-diode tuned transistor oscillators

Synthesis of combination circuits in a universal basis and its use in estimating the complexity of digital structures containing integrated circuits

Present state and future prospects of the design of large-scale integrated circuits using MIS transistors

Synthesis of digital filters for the control of short periodic angular oscillations of aerospace vehicles.

Synthesis of reactive ladder filters with uniform losses, discussing iterative solution for nonlinear equations and low, high and band pass filters loss compensation

Monopulse radar equipment

Design guidelines for 180-degree hybrid type multiple beam phased array forming networks with different element numbers and configurations

Computerized synthesis of optimal fault-diagnosable logical circuits capable of detecting and repairing faulty modules for circuit reliability and availability improvements

Electrical design requirements for electrolytic capacitors used in regulated low voltage DC power supplies.

A design approach for LSI using chip selection and circuit modification techniques.

Electrical network analysis and synthesis problems concerning sensitivity characteristics relationship to circuit parameters and structure determination to satisfy behavioral requirements respectively

AM radio receiver diode resonance circuit design for large signal processing, considering FET pinch-off voltage effects and correct circuit parameter selection

Operation, design and applications of inductorless digital IC selective N-path filters

The approximation problem in the synthesis of circuits with distributed RC parameters

Analog to digital converters with logarithmic input-output law, comparing performance and complexity of various realizations

A new technique for designing high-speed frequency counters.

Use of switching circuits as redundant multiplier elements in canonic digital networks.

The use of logic simulation in the design of a large computer system.

Automated systems for designing electronic circuits

An automated system for designing integrated circuits

Algorithm for deriving the equilibrium equations of an electric circuit on the basis of logic rules

Computer simulation of complex electronic circuit equations derived from subcircuit equations combined with coupling equations, noting topological modification ease and run time savings

Means of improving the effectiveness of designing nonlinear electronic circuits on a digital computer by the method of nodular potentials

Optimization of electronic circuits with characteristics depending on a continuously varying parameter

An effective algorithm for optimizing electronic circuits

Electronic circuit optimization via Powell iterative method, describing search techniques, matrix methods and transistor hybrid equivalent circuit application

Circumvention design of active circuitry and passive shielding for electromagnetic pulse environment with application to Minuteman ICBM system

On the design of wave digital filters with low sensitivity properties.

Low pass filter design for FDM and PCM systems, discussing active RC realization techniques and microelectronics model tests

A computer for modeling and calculating technological dimensional circuits

Boost klystron efficiency with three-cavity design.

Octave-bandwidth, acoustic M/W frequency-memory loop.

High voltage waveform generation at low power levels by circuit techniques and system configurations involving parallel series chains of light triggered bilateral switches

Linearized stability analysis and design of a flyback dc-dc boost regulator.

Logic-controlled solid-state switchgear for 270 volt dc.

Design and structure of a flexible recursive digital filter

Digital-computer aided analysis and synthesis of specialized functional diode converter circuits

Approximation of transfer functions for filters with equalized group-delay characteristics.

Microwave transistor oscillators design based on Si overlay transistors and microstrip transmission lines as passive elements, obtaining negative resistance between collector-base terminals

Interconnecting computer network theory and system types, discussing data coordination and transformation, host computer links with system participants and network applications

Synthesis of a transverse digital filter defined in the complex plane

Nonminimum-phase difficulties in multivariable-control-system design.

Four-quadrant analog multiplier synthesis for IC implementation based on logarithmic addition in all n-p-n bipolar transistor configuration for algebraic product derivation

NEUMANN PROBLEM

Application of the Meler-Fok complex conversion formulas in the solution of certain problems of heat conductivity

Finite element model for discontinuous potential flow field analysis leading to Dirichlet, Neumann and mixed boundary value problems solution

Higher order numerical solution of the integral equation for the two-dimensional Neumann problem.

Point matching /collocation/ computation of transverse resonances by complex valued solutions of Helmholtz equation with Neumann or Dirichlet problems, applying to electromagnetic waveguides

Nonlinear acoustics of inviscid fluid in duct with varying cross section, obtaining propagation velocity potential as power series for reduction to Neumann problem 15 p1865 A73-32154

Inconsistencies and S.O.R. convergence for the discrete Neumann problem. 17 p2202 A73-35519

A priori L sub 2 error estimates for Galerkin approximations to parabolic partial differential equations. 21 p2725 A73-40383

The exterior Neumann problem for the Helmholtz equation. 24 p3112 A73-45470

The Dirichlet and Neumann problems for parabolic equations with a Bessel operator in Dini spaces 24 p3106 A73-45510

NEURAL NETS

Visual field image analysis via investigation of receptor-furnished signal analysis by network of neuron-like structures 04 p0413 A73-15789

A model of a memory device based on neuron-like elements which realizes the holographic principles of data recording and readout 04 p0413 A73-15792

Image recognition learning algorithm for expanding neural nets composed of active inputs, receptors, associative elements and recognizers 04 p0426 A73-15794

Human memory model with associative linkage between neuronal network information elements 04 p0413 A73-15797

Space-time dynamics of the impulse activity in human-brain neuron populations 05 p0540 A73-16692

A model of image-shape analysis based on fiber-optics elements and on the principle of photoelectric conversion 06 p0671 A73-18084

Information processing in the visual system. 07 p0786 A73-20374

Dynamics of changes in neuron activity regimes of the ascending auditory pathways 11 p1317 A73-26079

Step-wise changes in thermoregulatory responses to slowly changing thermal stimuli. 13 p1576 A73-28535

Neuroanatomy of the auditory system. 14 p1715 A73-30280

Conditioned reflex switching effects in higher nervous system reactions as function of experimental stimuli background conditions /arousal, diurnal rhythms, test conditions, physiological condition/ 14 p1718 A73-30567

Forward and backward conditional link formation as physiological mechanism for reinforcement conditioning connection 14 p1718 A73-30568

Circulation of nervous impulses in the cerebral cortex 14 p1718 A73-30569

Loss of information during central summation of local postsynaptic potentials 14 p1719 A73-30825

Electrophysiological evidence that abnormal early visual experience can modify the human brain. 15 p1838 A73-31371

Correlative function formalism for neuron networks with limited communication channels and active-refractive-storing signal action 21 p2645 A73-41277

On the electronic simulation of acceleratory system. 22 p2816 A73-42683

Structural complexity and technical realization of formal neurons by means of magnetic current switches 24 p3063 A73-44901

Synthesis of minimized formal neurons by means of magnetic current switches 24 p3063 A73-44902

Probability estimate models for reliable function of redundant systems with adaptable and inadaptably neuron-like restoration organs 24 p3063 A73-44904

Optical electronic model of local detectors of the visual analyzer 24 p3064 A73-44912

NEURISTORS

Integrated neuristor lines based on p-n-p-n structures with diffused resistors 10 p1193 A73-23727

NEUROGLIA

Analysis of the changes in glial cell numbers in the auditory cortex during the application of acoustic stimuli of various intensities 22 p2807 A73-42653

Influence of histotoxic hypoxia on the activity of lactic dehydrogenase isoenzymes in neurons and neuroglia of various sections of the central nervous system 24 p3058 A73-44429

NEUROLOGY

Neurological fatigue-indices of flight crews of long-range and military transport aviation 11 p1321 A73-25040

Development of neurosurgical instrumentation and procedures for emergency use in null and low-gravity environments - A speculative approach. 11 p1323 A73-25342

Human visual system model based on neurological connectivity data from anatomical dissection, in vivo physiological measurements and psychological experimentation 17 p2116 A73-35239

Central nervous system influence upon electrocardiographic waveforms. 18 p2275 A73-36530

NEUROMUSCULAR TRANSMISSION

Polysynaptic pathways role in tonic vibration and monosynaptic reflexes due to muscle vibratory or nerve electric stimulation, respectively, discussing tetanization effects 01 p0008 A73-10409

Current views on the mechanism of the quantum-induced liberation of a mediator from the motor nerve endings of a skeletal muscle 01 p0009 A73-11023

Atrioventricular block response to exercise and intraventricular conduction at rest. 01 p0010 A73-11506

Usefulness of vectorcardiography combined with His bundle recordings and cardiac pacing in evaluation of the preexcitation /Wolff-Parkinson-White/ syndrome. 02 p0138 A73-12445

Phasic discharge activity and localization of sheep medullary neurons in relation to swallowing reflex after superior laryngeal nerve stimulation 03 p0262 A73-13786

Extent of engagement of various cardiovascular effectors to alterations of carotid sinus pressure. 05 p0539 A73-16250

Effect of hypercapnia on the electrical discharges of the bulbar respiratory neurons and motor neuron ganglia of respiratory muscles 05 p0541 A73-16735

Correlation between the impulse activity of bulbar respiratory neurons, the electrical activity of respiratory muscles, and pulmonary respiration volume during obstructed respiration 06 p0650 A73-17683

Research on the displacement of blood-plasma proteins and on the nerve conduction velocity in rats subjected to accelerations and hypokinesia 06 p0650 A73-17769

Pathological cardiac conduction system lesions anatomy associated with arrhythmia, discussing atrioventricular, His bundle and bundle branch blocks 06 p0655 A73-18872

Cardiac arrhythmias generation by impulse initiation and conduction abnormalities, considering depressed excitability, reentrant excitation, summation, inhibition and parasytote 06 p0656 A73-18874

Cortico- and rubrofugal activation of interneurons forming proprioceptive paths in the dorsolateral funiculi of the cat spinal cord 07 p0781 A73-20002

Changes in the amplitudinal and temporal characteristics of sensorimotor-cortex evoked potentials after deactivation of spinocervical tracts in cats 07 p0781 A73-20004

Ontogenic cerebrospinal reflex activity studies, covering spinal cord morphology, reflex arches, inhibition, intracortical responses and post-tetanic potentiation 07 p0784 A73-20366

Contributions of quick and slow muscle fibers to changes in the electrical activity of skeletal muscles in rats under acute and chronic effects of cold 08 p0931 A73-21323

Order and disorder in the rhythm of the heart /Fifth Annual George C. Griffith Lecture/. 08 p0933 A73-21806

Effect of copper ions on the functional state of the neuromuscular apparatus 09 p1039 A73-22369

Synaptic activation of thoracic spinal cord interneurons through reticulo-spinal pathways 09 p1039 A73-22576

Cortico-pyramidal and cortico-extrapyramidal synaptic effects on lumbar motor neurons in monkeys 09 p1040 A73-22578

Investigation of evoked activity in the ventral horn of lumbar segments during the interaction of efferent extrapyramidal and cortical stimuli 09 p1040 A73-22579

Organization of spontaneous muscular activity in man 09 p1040 A73-22863

A frequency response analysis of fusimotor-driven muscle spindles. 09 p1041 A73-22934

Features of supraspinal control of the reflex paths of the spinal cord during walking 10 p1178 A73-23677

NEUROMUSCULAR TRANSMISSION

Alternative mechanisms of apparent supernormal atrioventricular conduction. 10 p1184 A73-23843

Rise time of the spike potential in fast and slowly contracting muscle of man. 10 p1181 A73-24500

Features of the spontaneous and evoked neuronal activity of deep brain structures in man during voluntary movements 10 p1181 A73-24517

Voluntary activation of individual motor units in man 10 p1181 A73-24519

Reflex reaction of antagonist muscles during an evoked tendon reflex 10 p1182 A73-24598

Organization of the activity of a group of motor neurons in man during voluntary contraction of a muscle 10 p1182 A73-24599

Functional and morphological structures of motor activity events, noting central integration ensemble of cerebrum transmitter sequences 11 p1314 A73-25200

Effect of whole-body vibration on peripheral nerve conduction time in the Rhesus monkey. 11 p1315 A73-25335

Morphological and experimental excitation models of cardiac muscle ultrastructure, transmission activity and intercellular contact relationships 11 p1315 A73-25590

Vertebrate cardiac innervation via parasympathetic and sympathetic nervous system, considering synaptic transmission, nerve endings, stimulation and electrical effects 11 p1316 A73-25597

Cardiac activity potentials, P-R interval and impulse propagation across atrioventricular node, ventricular conduction and Purkinje fiber-muscle junctions 11 p1316 A73-25598

Neurogenic and myogenic mechanisms of myocardium cell electrical activity and excitation in vertebrate and invertebrate neural and muscle tissues 11 p1316 A73-25599

Motor functions and control of sensorial messages of somatic origin 13 p1576 A73-29174

Immediate and remote prognostic significance of fascicular block during acute myocardial infarction. 14 p1715 A73-30052

Influence of increased air atmosphere pressure on the excitability of the neuro-motor apparatus in man 14 p1719 A73-30845

Anatomo-functional bases of cerebello-cerebral interrelations 15 p1836 A73-32287

The behavior of eye movement motoneurons in the alert monkey. 18 p2271 A73-36433

Unit activity in the brainstem related to eye movement - Possible inputs to the motor nuclei. 18 p2271 A73-36434

The neuronal mechanism of nystagmus. 18 p2271 A73-36437

Supranuclear structures regulating binocular eye and head movements. 18 p2272 A73-36451

QRS abnormalities in AV block - Variations and their significance. 18 p2274 A73-36521

The clinical causes and mechanisms of intraventricular conduction disturbances. 18 p2274 A73-36524

Investigation of the distribution of synaptic inputs on an analog model of the motoneurons 19 p2399 A73-37942

Force output of the diaphragm as a function of phrenic nerve firing rate and lung volume. 20 p2515 A73-39780

Russian book - Electrical activity of the human brain in the process of motor action. 21 p2640 A73-41289

Effects of beta-blocking agents on atrio-ventricular and intraventricular conduction in man. 21 p2641 A73-41564

Effect of the electrical stimulation of the sensorimotor cortex on the potentials of dorsal roots and on the depolarization of primary spinal afferents 22 p2807 A73-42652

Effect of chronic pyramid insufficiency on the function of spinal centers of shin and foot muscles in man 22 p2807 A73-42658

Alterations of cardiac sympathetic neurotransmitter activity in congestive heart failure. 22 p2808 A73-42690

Signal and noise in the human oculomotor system. 22 p2810 A73-42964

Structurally functional properties of the dendrites of central neurons 23 p2947 A73-43926

A method for the approximation of processes in homogeneous biological structures 24 p3062 A73-44663

The presence in the heart of compounds which participate in the neurohumoral regulation of coronary circulation 24 p3059 A73-44769

NEURON TRANSMISSION

Intracellular measurements in a closed hyperbaric chamber. 24 p3065 A73-45072

Spinal and spino-bulbo-spinal neuron mechanisms of somatic and visceromotor reflex transfer in the thoracic spinal cord 24 p3061 A73-45249

NEURON TRANSMISSION U BIOELECTRICITY NEURONS

Neuron networks modeling from viewpoint of intracellular and cell-medium interaction, discussing coding properties and nonsingular self adjusting system response 01 p0012 A73-10652

Computerized correlation analysis of single and multiple neuron pulse activity, considering temporal, sequential and entropy characteristics 01 p0012 A73-10653

Complex processing of discrete biological information 01 p0012 A73-10662

Y-chromosome localization in the interphase nuclei of cerebral neurons in man 01 p0010 A73-11444

Stable frequency and synchronicity alterations in the discharges of cortical neuron populations in feedback experiments 01 p0010 A73-11445

Cat optic tract and geniculate unit responses corresponding to human visual masking effects. 02 p0134 A73-12161

Analysis of the response characteristics of optic tract and geniculate units and their mutual relationship. 02 p0134 A73-12162

Topochemical differences in RNA content in spinal cord motoneurons during hypoxia and hypokinesia 02 p0135 A73-12558

Phasic discharge activity and localization of sheep medullary neurons in relation to swallowing reflex after superior laryngeal nerve stimulation 03 p0262 A73-13786

Response of motoneurons of the spinal cord to gamma radiation - A cytochemical study. 03 p0262 A73-13808

Recording and discrimination of pulsed neuron activity responses to stimulus application and removal 03 p0268 A73-13823

Response of single units of the posterior hypothalamus to thermal stimulation. 03 p0262 A73-14111

Maturing neuronal subsystems - The dendrites of spinal motoneurons. 03 p0264 A73-14257

Telemetered EEG and neuronal spike activity in olfactory bulb and amygdala in free moving rabbits. 03 p0271 A73-14299

Visual receptive fields sensitive to absolute and relative motion during tracking. 04 p0409 A73-15072

Responses of bulbar respiratory neurons to apparatus-aided artificial respiration 05 p0541 A73-16699

Correlation between the impulse activity of bulbar respiratory neurons, the electrical activity of respiratory muscles, and pulmonary respiration volume during obstructed respiration 06 p0650 A73-17683

Neural channel mechanism for real light and equivalent background coding, using test flashes under bleaching and field adaptation 07 p0783 A73-20258

Structural characteristics of connections between medial efferent systems and spinal cord neurons 09 p1040 A73-22577

Electrophysiological investigation of noise rejection in an auditory system receiving sound from a localized source 09 p1040 A73-22580

Statistical investigation of the impulse activity of neurons in various hypothalamic regions 10 p1179 A73-23802

Role of the medial area of the medulla oblongata in the rhythmic activity of respiratory-center neurons 10 p1179 A73-23804

Neuron analyzer technique for poststimulus histogram plotting of neuron excitation as function of stimulus onset time 10 p1183 A73-23811

Amplitude discriminator with variable effective range design for use with/without digital computer in neuron pulsed activity analysis 10 p1184 A73-24516

Voluntary activation of individual motor units in man 10 p1181 A73-24519

Reflex excitability of spinal motor neurons in man under high atmospheric pressure 10 p1182 A73-24525

Short-term latent reactions of the lateral geniculate body neurons in the rat to electrical stimulation of the optical tract 10 p1182 A73-24595

Characteristics of the electrical activity of the superior olivary bodies of Vespertilionidae and Rhinolophidae bats in response to ultrasonic stimuli of different frequencies 10 p1182 A73-24596

Hypothalamus, septum and ventrobasal thalamus nuclei single neuron responses to skin thermal stimulation, indicating afferent connections between cerebrium thermoregulation center and peripheral thermoreceptors 11 p1317 A73-26086

On neural inhibition, contrast effects and visual sensitivity. 11 p1318 A73-26197

Influence of synchronized sleep upon spontaneous and induced discharges of single units in visual system. 11 p1319 A73-26223

Single unit reactions in the visual cortex of the unanesthetized rabbit to the light flashes of different intensities. 11 p1321 A73-26719

Autoradiographic study of protein synthesis in perikaryons and of nitrogen migration into the axons of hypertrophic sympathetic neurons 13 p1574 A73-28296

Electrical and metabolic manifestations of receptor and higher-order neuron activity in vertebrate retina. 13 p1574 A73-28353

Intranuclear organization of the center median nucleus of the thalamus. 13 p1576 A73-29175

Processing of auditory information by medial superior-olivary neurons. 14 p1715 A73-30281

Loss of information during central summation of local postsynaptic potentials 14 p1719 A73-30825

Effects of vagotomy on the impulse activity of respiratory neurons 15 p1833 A73-31160

Mechanisms of secretion of neurohypophyseal hormones - Cellular and subcellular aspects 15 p1836 A73-32286

Transmission of nerve pulses at the switching locations of the brain 16 p1973 A73-33424

The visual cortex as a spatial frequency analyzer. 17 p2112 A73-34840

The behavior of eye movement motoneurons in the alert monkey. 18 p2271 A73-36433

Unit activity in the brainstem related to eye movement - Possible inputs to the motor nuclei. 18 p2271 A73-36434

Cholinergic activation of vestibular neurones leading to rapid eye movements in the mesencephalic cat. 18 p2272 A73-36439

Some functional characteristics of the superior colliculus of the Rhesus monkey. 18 p2272 A73-36442

Neuronal elements of the orienting response - Microrecordings and stimulation experiments in rabbits. 18 p2272 A73-36444

The role of the superior colliculus in visually-evoked eye movements. 18 p2272 A73-36445

Comparative physiology of movement-detecting neuronal systems in lower vertebrates (anura and urodela). 18 p2273 A73-36454

Orientation specificity and response variability of cells in the striate cortex. 19 p2394 A73-37421

Functional characteristics of different neurons in the auditory cortex 19 p2395 A73-37940

Effects of round window stimulation on unit discharges in the visual cortex and superior colliculus. 20 p2513 A73-39146

Determinants of hypothalamic neuronal thermosensitivity in ground squirrels and rats. 20 p2513 A73-39600

Changes in thermosensitive characteristics of hypothalamic units over time. 20 p2514 A73-39601

Computer controlled automatic TV-microscope system for tracking and measuring nerve cell processes in designated axons and dendrites 20 p2518 A73-39763

Reaction of neurocytes of the paraventricular hypothalamic nucleus to unilateral thyroidectomy 21 p2637 A73-40283

Correlative function formalism for neuron networks with limited communication channels and active-refractive-storing signal action 21 p2645 A73-41277

Objective method for classification of multicellular activity patterns of neuron population in the cerebrium of man 22 p2807 A73-42656

An assembly for electrophysiological and thermometric studies 22 p2815 A73-42663

Rectifier-like color dependent phase shifts in electrophysiological responses to different colored stimuli at evoked potential and single neuron levels 22 p2810 A73-42961

Gamma-aminobutyric acid antagonism in visual cortex - Different effects on simple, complex, and hypercomplex neurons. 23 p2946 A73-43338

Structurally functional properties of the dendrites of central neurons 23 p2947 A73-43926

Influence of histotoxic hypoxia on the activity of lactic dehydrogenase isoenzymes in neurons and neuroglia of various sections of the central nervous system 24 p3058 A73-44425

Inferior colliculus neuron responses to an amplitude-modulated signal with varying intensity levels. 24 p3061 A73-45248

Spinal and spino-bulbo-spinal neuron mechanisms of somatic and visceromotor reflex transfer in the thoracic spinal cord 24 p3061 A73-45249

NEUROPHYSIOLOGY

Changes in ventilatory patterns after ablation of various respiratory feedback mechanisms. 01 p0007 A73-10162

Investigation of the recovery dynamics of the mimic muscle function and choice of an optimal bioelectric stimulation program with the aid of an electronic digital computer 01 p0012 A73-10656

Structural organization and electrophysiological properties of the intercentral functional systems of the hypothalamic region of the brain 01 p0009 A73-11024

Inhibitive mechanisms activity in behavior control by neostriatum, discussing suppressive reactions, evoked sleep, conditioned and instrumental reflexes and neurophysiological aspects 01 p0009 A73-11025

Structural change in the paradoxical phase of sleep due to the stimulation of the reticular formation and hypothalamus on a background of deep slow sleep 01 p0009 A73-11081

A relationship between the detection of size, rate, orientation and direction in the human visual system. 03 p0261 A73-13758

Recording and discrimination of pulsed neuron activity responses to stimulus application and removal 03 p0268 A73-13823

Morphological, physiological and pharmacological investigations of rat cerebellar cortex synaptic structure and function maturation and neurotransmitter receptivity development 03 p0264 A73-14256

Maturing neuronal subsystems - The dendrites of spinal motoneurons. 03 p0264 A73-14257

Nervous system transmitter biochemistry in terms of excitation and inhibition coordination with emphasis on gamma-aminobutyric acid (GABA) function in cerebellum 03 p0264 A73-14258

Developmental changes in neurochemistry during the maturation of sleep behavior. 03 p0264 A73-14261

Maturation of neurobiochemical systems related to the ontogeny of sleep behavior. 03 p0264 A73-14262

Multichannel telemetry of physiological parameters/body temperature, EKG, EEG/ in the rat. II - Applications in neuropharmacology. 03 p0272 A73-14306

Derivation of a function of nerve-fiber distribution according to fiber diameters on the basis of electrophysiological measurements 04 p0413 A73-15787

Characteristic of collicular responses to stimulation of various sections of the visual afferent pathway in cats 05 p0539 A73-16332

Space-time dynamics of the impulse activity in human-brain neuron populations 05 p0540 A73-16692

Intercortical functional connections in lower monkeys, Macacus rhesus, exhibited by evoked responses 05 p0540 A73-16693

The control of sensitivity in the retina. 06 p0655 A73-18673

Electrophysiological investigation of supraspinal motor control systems evolution through Cyclostoma-Primate series, noting preservation of reticulomotor neuron projection characteristics 07 p0781 A73-20001

Cortico- and rubrofugal activation of interneurons forming propriospinal paths in the dorsolateral funiculi of the cat spinal cord 07 p0781 A73-20002

Rabbit hippocampal neuron activity relation to theta-wave phases from cell potential and extracellular recording analyses 07 p0782 A73-20005

Statistical investigation of the impulse activity of neurons in various hypothalamic regions 10 p1179 A73-23802

Neurochemical aspects of the formation of electrographical and behavioral reactions

Brain tissue functional organization based on models for cell pseudorandom behavior, information processing, learning and memory, considering spontaneous wave and unit firing

Functional and morphological structures of motor activity events, noting central integration ensemble of cerebrum transmitter sequences

Neurogenic and myogenic mechanisms of myocardium cell electrical activity and excitation in vertebrate and invertebrate neural and muscle tissues

The visual system: Neurophysiology, biophysics, and their clinical applications; Proceedings of the Ninth Symposium, Brighton, England, July 1971.

Theoretical models of the generation of steady-state evoked potentials, their relation to neuroanatomy and their relevance to certain clinical problems.

Posthyperventilation breathing - Different effects of active and passive hyperventilation.

Anatomical and neurophysiological investigations of centrifugal control of retinal activity via efferent optic nerve fibers

On the functional significance of subcortical single unit activity during sleep.

Forward and backward conditional link formation as physiological mechanism for reinforcement conditioning connection

Neurophysiological characteristics of isolated structures of the cerebral cortex

Supranuclear connections to oculomotor nuclei in terms of stimulus relation to eye movements

The neuronal mechanism of nystagmus.

Vestibular and cerebellar control of oculomotor functions.

Optomotor integration in the colliculus superior of the cat.

Brain stem reticular formation influence on lateral geniculate body neurons during eye movements, suggesting cortical oculomotor impulse influence mediation by perigeniculate nucleus

Neurophysiological correlates of eye movements in the visual cortex.

Comparative physiology of movement-detecting neuronal systems in lower vertebrates /anura and urodelae/.

Monkey rod receptor potential suppression at photopic stimulus intensities by neurophysiological inhibitory mechanism for clearing cone initiated visual pathway

The effect of social-emotional environmental stress on the functional state of the neocortical structures of rhesus monkeys

Quantitative evoked-potential analyses for the neurophysiological characterization of faulty learning processes in the experimental arterial hypertension-pathogenesis

Role of specific and nonspecific thalamic nuclei in the genesis of certain slow rhythms on the human electrocorticogram

Investigation of the geometry of the dendritic tree of retinal ganglion cells

Probabilistic statistical methods for analysis of impulse flows in nerves

Structural changes in the adrenal nerve apparatus during experimental subtotal pancreatectomy

Electromyographic study of repetitive fasciculation potentials in triceps and adductor pollicis in normal subjects and patients with motor neuron diseases, noting postcontraction pause

Functional properties of auditory cortex neurons in a controlled experiment

Diminution of uncertainty in the firing of hippocampal units in response to a stimulus

Successive differentiation of visual stimuli in monkeys under various conditions of presentation

Symmetry of the visual evoked potential in normal subjects.

The psychophysical inquiry into binocular summation.

Russian book on structural and functional plasticity of interneuron synapses during readjustment to chemical and physical damage covering degenerative and regenerative changes

Visual field defects after missile injuries to the geniculo-striate pathway in man.

Spatial integration in the crustacean visual system - Peripheral and central sources of non-linear summation.

Investigation of complex and hypercomplex receptive fields of visual cortex of the cat as spatial frequency filters.

Stimulus specificity in the human visual system.

The effect of low X-ray doses on the central nervous system

Neuronal activity of the sensorimotor and visual cortex in rabbits during development of a summation focus in the reticular formation

Anatomic and functional organization of the ventral anterior and reticular nuclei of the thalamus

Some physiological mechanisms of alpha-rhythm frequency fluctuations in man under conditions of relative rest

Electronic simulation and analog computer studies of the influence of temperature on the process of nerve impulse shaping

Ventilation at transition from rest to exercise.

NEUROSCIENCE

U NEUROLOGY

NEUROSES

Functional alterations in the auditory and visual analyzer systems of monkeys during experimental neurosis

Characteristics of the higher nervous activity of monkeys during a postneurotic period

Clinical psychology diagnostic methods in military aviation medicine, considering neurotic symptoms and psychosomatic disorders in flight fitness examinations

NEUTRAL BEAMS

NT MOLECULAR BEAMS

NT NEUTRON BEAMS

A neutral-potassium-beam measurement of plasma density.

Problems associated with the injection of a high-energy neutral beam into a plasma.

Investigation of the possibility of developing a wide-aperture injector of fast neutral atoms

Influence of Langmuir electron oscillations on the degree of neutralization of an ion beam

NEUTRAL PARTICLES

NT FAST NEUTRONS

NT NEUTRONS

NT THERMAL NEUTRONS

Measurement of the macroscopic velocity of the neutral component of weakly ionized gas in the crossed fields.

Energy and mass analysis of neutral particles emitted from a toroidal theta-pinch plasma.

Neutral composition measurements of the mesosphere and lower thermosphere.

D and E ionospheric regions behavior, emphasizing water cluster ions formation, minor neutral constituents measurement and daytime ionization sources

Neutral composition measurements in the lower thermosphere by means of a mass spectrometer with helium cooled ion source.

Turbopause effect on latitudinal diurnal variation of upper atmosphere neutral species, using turbulent diffusion coefficients and photochemical transport theory

A short description of the ESRO-IV satellite.

Steady-state charged and neutral particle densities in a bounded turbulent high-temperature plasma.

Sunrise changes in concentrations of minor neutral constituents in the mesosphere.

Magnetic field effects on effective thermal conductivity of partially ionized plasmas, indicating neutral component role in solar magnetoplasma heat transport

On the presence of H₂ molecules inside neutral globules imbedded in H II regions.

Auroral heating and the composition of the neutral atmosphere.

Near-satellite neutral gas temperature determination from measurement of molecular nitrogen velocity distribution

Explorer satellite triaxial accelerometer system to determine neutral atmosphere density, monitoring orbit adjust propulsion thrust and measuring spacecraft roll, describing instrument calibration

Metal ions role in sporadic E layer formation in terms of magnesium ions profile redistribution by vertical gradient in neutral particle wind

Edge instability of transverse electromagnetic waves in a weakly ionized plasma

ALADDIN II ionospheric composition measurements, obtaining ion and neutral vertical density profiles and dynamic parameters for E region nighttime ion layering prediction model

Interaction of plasma streams with a neutral gas cloud.

Neutral composition and its variations in the lower thermosphere.

Aperture synthesis of interstellar neutral hydrogen in absorption. I - The Perseus arm feature of Casiopeia A.

Gravitational energy quantization model of noncharged particle based on proposed centrosymmetric metric with nonzero Einstein matter tensor and without Schwarzschild singularity

Layering of the neutral metals of meteoric origin in the lower ionosphere.

The shapes of neutral globules associated with diffuse nebulae.

NEUTRAL SHEETS

Particle motion and electrostatic instabilities of geomagnetic tail and magnetopause plasma neutral sheets in relation to substorms, using Alfven and Cowley models

Minimum magnetic field energy of two dimensional magnetosphere with neutral sheet for arbitrary dipole inclination to solar wind as function of potential difference on boundary points

A self-consistent model of a simple magnetic neutral sheet system surrounded by a cold, collisionless plasma.

Thermal instability of coronal neutral sheets and the formation of quiescent prominences.

Inertial magnetic field reconnection and magnetospheric substorms.

Instability of the current in the neutral sheet of the tail of the earth's magnetosphere.

Electron current estimation along auroral zone-plasma neutral sheet field line from steady state one dimensional model

Model experiment on solar flares and the neutral sheet. III.

Acceleration of charged particles in the region of the neutral line of the magnetic field.

A magnetospheric field model incorporating the OGO 3 and 5 magnetic field observations.

Observation of a possible neutral sheet in the corona.

Role of the neutral sheet in the illumination of polar caps by solar protons.

Observation of plasma flow in the neutral sheet at lunar distance during two magnetic bays.

NEUTRALIZERS

Some results of flight tests of an ion-engine model using surface ionization of cesium on tungsten.

NEUTRINOS

- Transient ion neutralization by electrons.
24 p3111 A73-45411
- NEUTRINOS**
Solar neutrino detection methods, capture cross sections, model construction and results
01 p0091 A73-10053
Dynamics of gravitating systems against the neutrino background of the universe
01 p0100 A73-10712
Effect of a neutrino-photon interaction on the solar-neutrino flux.
02 p0205 A73-12165
Neutrino contribution to relativistic interacting matter-radiation cosmological models, presenting cosmological interpretation of quasars
02 p0218 A73-12410
Neutrino archaeology - The simulation of double beta-decay by solar neutrinos.
03 p0344 A73-13293
Effects of sudden mixing in the solar core on solar neutrinos and ice ages.
05 p0623 A73-17188
Neutrino energy loss in neutron star matter.
07 p0902 A73-20444
Solar neutrino problem - No low energy He-3 + He-3 resonance.
08 p1000 A73-21530
Criticism of solar core mixing hypothesis of solar neutrino problem, discussing implications for semiconvection theory
08 p1012 A73-21532
Solar neutrino flux prediction discrepancies with observation, considering cosmic ray background and flaws in calculation of capture rate
09 p1136 A73-21995
Neutrino hindrance of density irregularities growth in expanding radiation dominated cosmological model from numerical integration of perturbation equations
09 p1141 A73-22026
Nonzero neutrino rest mass to account for virial mass discrepancy in Coma cluster and missing cosmological mass needed to close universe
09 p1141 A73-22027
Thermal conductivity approximation for gasdynamic equations describing stellar gravitational collapse, calculating neutrino and antineutrino energy and momentum transport processes
09 p1147 A73-22701
A four-component hypermass equation possibly applying to unstable neutrinos.
10 p1251 A73-23754
Solar He abundance from neutrino flux, He lines intensity in prominences and chromosphere spectra, solar cosmic rays and solar wind He/H ratio
10 p1284 A73-24780
Gamma-gamma total hadronic cross section and absorption of extragalactic gamma-rays.
11 p1413 A73-26107
Pair annihilation into neutrinos in strong magnetic fields.
11 p1402 A73-26414
Photon-neutrino energy losses in strong magnetic fields.
11 p1402 A73-26415
Metal-poor stars. IV - The evolution of red giants.
12 p1540 A73-27328
URCA process and the evolution of carbon stellar core.
13 p1673 A73-28173
Solar neutrino flux, discussing effects of temperature oscillations on neutrino and photon luminosities
15 p1926 A73-31358
Solar neutrino flux deficiency explanation based on solar core nuclear reactions theory with consequences for luminosity and earth climate
15 p1937 A73-31849
Ultrahigh energy photons, electrons, and neutrinos, the microwave background, and the universal cosmic-ray hypothesis.
15 p1927 A73-32004
Solar neutrino deficiency related to solar core periodic expansion, considering Martian river-like channel formation and Praesepe cluster distribution through main sequence
17 p2229 A73-34434
Low solar neutrino flux explained by evolution model emphasizing internal rotation effects on solar structure
19 p2488 A73-38519
Solar neutrinos. IV - Effect of radiative opacities on calculated neutrino fluxes.
20 p2602 A73-39427
Nonspherically symmetric thermal instabilities implied by discrepancy between theory and observation for solar neutrino problem, noting absence in solar numerical model
20 p2608 A73-39429
Solar neutrino fluxes on earth from solar model and analytical approach, discussing neutrino capture rate contributions
21 p2764 A73-41539
Solar structure and evolution, calculating neutrino emission for Pleistocene glacial age caused by solar luminosity reduction
21 p2764 A73-41613

- Neutrino losses effects on 4-8 solar mass stars leading to collapse of degenerate carbon-oxygen cores, discussing type II supernovae and pulsar formation
22 p2914 A73-43008
Reactions of pseudoscalar meson production by neutrinos on nucleons near the threshold in the range of high transferred impulses
23 p3008 A73-43544
- NEUTRON ACTIVATION ANALYSIS**
Neutron activation analysis of lunar soil brought by 'Luna-16' from Mare Poecunditatis
05 p0620 A73-17021
Distribution of elements between different phases of Apollo 14 rocks and soils.
07 p0885 A73-19751
Isotopic anomalies in lunar rhodium.
07 p0889 A73-19805
Total nitrogen contents of some Apollo 14 lunar samples by neutron activation analysis.
07 p0890 A73-19815
Neutron activation and irradiation analyses of Haverlo ureilite elemental abundances
09 p1140 A73-21867
Applications of activation analysis to geochemical, meteoritic and lunar studies.
11 p1326 A73-25800
Luna 20 and Apollo 16 lunar soil samples rare earth, iron and other trace elements contents from neutron activation analysis, noting Eu anomaly
13 p1675 A73-28317
Luna 20 soil and rock fragments chemical composition from neutron activation analysis, noting low rare earth content and contamination with W and Mo
13 p1676 A73-28321
Luna 20 metaigneous rocks, breccia and soil and Apollo 16 soils chemical composition by neutron activation analysis, tabulating major, minor and trace elements
13 p1676 A73-28323
Carbonaceous chondrite neutron activation analysis for trace elements, revealing compositional homogeneity
13 p1684 A73-29181
Radiochemical neutron activation analysis for U and Th abundance measurement in achondrites and pallasite olivines
17 p2120 A73-35802
Sequential nondestructive neutron activation analysis for bulk abundance of Fe, Al, Na, Mn, Cr, Sc, Co and Ir in chondrules from chondrites
21 p2647 A73-40563
Sample preparation, irradiation, and counting and data reduction scheme for trace element analysis of coal using neutron activation
21 p2737 A73-40632
Radiochemical neutron activation analysis for extralunar trace elements in Apollo 14 lunar soil 14141, comparing with mature samples and Fra Mauro subregolith materials
23 p2951 A73-43846
- NEUTRON BEAMS**
Nuclear laser realizability for gamma quanta production from population inversion during radiative capture of neutrons, considering constraints imposed on heating of active medium
10 p1229 A73-24754
The analytically determined response of silicon detectors to a polyenergetic neutron beam.
11 p1365 A73-26210
- NEUTRON COUNTERS**
Molnira 1 satellite slow neutron monitor with photomultiplier scanned scintillator, noting limiting effect of geomagnetic perturbations
07 p0823 A73-19428
The Elbrus cosmic ray spectrograph
10 p1203 A73-23926
Analysis of the quality of the cosmic ray data recorded by the neutron supermonitor at Krasnaia Pakhra
10 p1217 A73-23934
Nuclear track etching in radiation and fast neutron dosimetry and health physics, discussing counter materials and fission and alpha particles and recoil nucleus recordings
11 p1362 A73-25421
Dose equivalent determinations in neutron fields by means of moderator techniques.
11 p1362 A73-25424
The analytically determined response of silicon detectors to a polyenergetic neutron beam.
11 p1365 A73-26210
Cosmic ray storm effect on midlatitude and polar neutron monitors, noting comparison with underground mu-meson telescopic observations at high rigidities
12 p1534 A73-27001
The BD-9 integral discriminator in the circuit of a scintillation-type fast neutron detector
12 p1497 A73-27207
Electronic safety test replaces radioactive test source.
14 p1712 A73-30928
Contribution of atmospheric multiple neutron production to the multiplicity distribution observed in cosmic ray neutron monitor.
15 p1926 A73-31385

- Calculated cosmic ray neutron monitor response to solar modulation of galactic cosmic rays.
16 p2056 A73-33444
Gamma ray and neutron measurements and their relation to the solar flare problem.
18 p2345 A73-36126
A photoneutron antimony-124-beryllium system for fissile materials assay.
21 p2738 A73-40769
- NEUTRON DECAY**
Cosmic ray albedo neutron decay injection theory for proton belt, considering radial diffusion, atmospheric losses, geomagnetic models, atmospheric density, etc
21 p2755 A73-40071
- NEUTRON DETECTORS**
U NEUTRON COUNTERS
NEUTRON DISTRIBUTION
Neutron diffusion from a distributed source in a homogeneous atmosphere
06 p0742 A73-17549
Boltzmann equation integral form derived tensorial formulation of monoenergetic neutron diffusion theory, evaluating components of diffusion coefficient tensor
11 p1401 A73-25211
Neutron diffusion from a distributed source in an inhomogeneous atmosphere.
16 p2052 A73-32773
Singular eigenfunction solution of the monoenergetic neutron transport equation for finite radially reflected critical cylinders.
24 p3109 A73-44700
- NEUTRON EMISSION**
Solar white light flares induced neutron and gamma ray emission, discussing acceleration mechanism through high energy proton bombardment induced photospheric heating
02 p0206 A73-12322
Estimation of an upper limit for the solar neutron emission during large flares.
11 p1413 A73-25953
Neutron emission after muon capture in Ce, Ba and Sn, analyzing delayed gamma gamma rays and branching ratios to excited nuclear states
13 p1662 A73-28650
Energetic neutrons leaking from the top of the atmosphere.
19 p2474 A73-37299
Dynamics of plasma column constriction and electromagnetic acceleration of ions
21 p2745 A73-40362
Neutron emission from laser produced plasmas and collisionless electrostatic shock waves.
24 p3116 A73-45242
- NEUTRON FLUX**
U FLUX [RATE]
NEUTRON FLUX DENSITY
A measurement of the atmospheric neutron flux in the energy range 50 less than E less than 350 MeV.
03 p0298 A73-12886
Cosmic ray produced neutron flux equilibrium for lunar surface compositions, calculating isotopic production rates as function of depth
03 p0364 A73-14105
Neutron flux anisotropy from plasma focus measured by gamma spectroscopy of activated Ag target, discussing axial concentration
07 p0857 A73-19529
Rare-gas analyses on neutron irradiated Apollo 12 samples.
07 p0889 A73-19798
Diurnal, sporadic and yearly variations in cosmic ray flux based on neutron component data, noting relation to solar activity cycles
08 p1000 A73-21345
Epithermal neutron differential flux spectrum in equilibrium layers of atmosphere at 57 degrees north
08 p1000 A73-21350
On the self-shielding coefficient of plates against neutron fluxes.
09 p1117 A73-22018
Short-term nonperiodic variations in the intensity of the neutron component of cosmic rays during a period of transition from a quiet to an active sun
09 p1137 A73-22019
Statistical analysis of continuous neutron component intensity measurements in cosmic rays
09 p1137 A73-22020
Solar cosmic ray anisotropy 27-day variations during IGY from global network stations neutron component data
10 p1268 A73-24237
Calculations of neutron flux spectra induced in the earth's atmosphere by galactic cosmic rays.
16 p2055 A73-33426
Time dependent worldwide distribution of atmospheric neutrons and of their products. I, II, III.
16 p2055 A73-33427
Apollo 16 neutron stratigraphy.
18 p2354 A73-36514
Neutron flux and energy spectra measurements in space related to theoretical predictions, discussing neutron leakage flux, solar neutron observations and radiation detector configurations
18 p2347 A73-36645

Inner belt equilibrium equatorial proton flux computation from albedo neutron measurements, including effects of atmospheric collisions, radial diffusion and geomagnetic secular decrease

20 p2601 A73-38943

The question of the method of studying cosmic ray anisotropy

21 p2755 A73-40111

Seasonal variations of the barometric effect of the cosmic ray neutron component intensity

21 p2755 A73-40114

Co-60 concentration measurement for lunar soil and rock samples, determining lunar neutron production rate

21 p2765 A73-40238

Flux measurements of galactic cosmic-ray albedo neutrons by the Molnia 1 satellite in 1972

21 p2758 A73-40605

Energy spectra and angular distribution measurement for 10-100 MeV earth albedo neutrons by balloon sounding at 116,000 ft

21 p2761 A73-41380

Quiet-time solar neutron flux upper limit from OGO-6 neutron detector, evaluating solar cosmic ray acceleration, nuclear reaction and energy region

21 p2763 A73-41498

NEUTRON IRRADIATION

The Bauschinger effect in annealed and irradiated titanium

01 p0064 A73-10495

Effects of chemical impurities, oxygen and dopant, on the gamma and neutron damage of silicon solar cells.

01 p0006 A73-11163

Change in critical current of superconducting NbTi by neutron irradiation.

02 p0200 A73-11842

Imaging techniques for low-flux neutron radiography.

05 p0573 A73-16279

Performance of hardened P-MOS devices in severe neutron environments.

05 p0557 A73-16517

Permanent and transient radiation effects in BARITT microwave oscillators.

05 p0558 A73-16518

Neutron irradiation effects on microwave transistor amplifiers.

05 p0558 A73-16520

Radiation produced trapping effects in devices.

05 p0605 A73-16521

Neutron damage in GaAs laser diodes - At and above laser threshold.

05 p0584 A73-16523

Third side of the Lambert triangle - Evidence of traps-filled-limit single-carrier injection.

05 p0605 A73-17349

Effect of irradiation on the absolute thermal emf of metals and alloys

06 p0706 A73-17901

Superlattice of voids in neutron-irradiated tungsten.

06 p0709 A73-18353

Influence of the dose of neutron irradiation on the anelastic behavior of an aluminum deformed at 80 K

06 p0710 A73-18542

Postirradiation mechanical properties of Types 304 and 304 + 0.15% titanium stainless steel.

06 p0710 A73-18545

Antiradiation properties of DNA and of its denaturation products

06 p0656 A73-18875

Rare-gas analyses on neutron irradiated Apollo 12 samples.

07 p0889 A73-19798

Apollo 14 and 15 lunar rocks and soils rare gas content via fast neutron irradiation, noting radioactive age determination

07 p0889 A73-19802

Neutron bombardment radiative effects on thin metal plate stability, considering compressive force, lattice defects and critical flux relations

08 p1020 A73-21771

Neutron activation and irradiation analyses of Haverro uricite elemental abundances

09 p1140 A73-21867

Neutron radiography as a diagnostic tool in the study of corrosion in lithium-filled heat pipes.

09 p1079 A73-21991

Device for investigating the mechanical characteristics of materials in a complex stressed state

09 p1070 A73-22167

Dielectric dispersion of irradiated BaTiO₃ in the phase transition region

09 p1134 A73-22983

Attenuation of 15 MeV neutrons in multilayer shields composed of steel, polyethylene and borated materials.

10 p1248 A73-23571

Solid state neutron radiation dosimeter for hands of medical and industrial personnel working with spontaneously fissionable fuels, describing Th foil detector and automatic spark counter

11 p1361 A73-25312

LiF albedo dosimeter for fast neutron and gamma irradiation measurement on personnel, using Cf-252 source for calibration

11 p1361 A73-25313

Neutron irradiation effects on room and high temperature fatigue behavior of stainless steel, noting fatigue life enhancement at low temperature and strains

11 p1383 A73-25832

Application of an electronic image analyzer to dimensional measurements from neutron radiographs.

11 p1371 A73-26743

Effect of neutron irradiation on the structure and properties of zirconium carbide

12 p1512 A73-27200

The effect of neutron irradiation damage on the low temperature deformation characteristics of b.c.c. metals and their alloys.

13 p1638 A73-29454

Bauschinger effect in annealed and irradiated titanium.

14 p1759 A73-30320

Radiation-induced strengthening and embrittlement in aluminum.

14 p1761 A73-30628

Preparation of high-level alpha-particle sources for the Surveyor Alpha Scattering Experiment.

16 p2035 A73-32975

Papers on materials science covering optical and spectroscopic surface analyses, neutron effects, amorphous semiconductors, high temperature superconductivity, etc

19 p2502 A73-38547

Measured drift of irradiated and unirradiated W3%Re/W25%Re thermocouples at a nominal 2000 K.

22 p2858 A73-42046

A device for the investigation of the mechanical characteristics of materials under a complex stress system.

22 p2838 A73-42115

Influence of neutron bombardment on the mechanical properties of titanium and the magnitude of the programmed-hardening effect

23 p2995 A73-44284

Determination of the temperature fields of turbine disks and blades, using irradiated diamond indicators

23 p2987 A73-44294

Influence of radiation on the current-voltage characteristic of tunnel diodes /Survey/

24 p3072 A73-44926

Improved mechanical properties of composites reinforced with neutron-irradiated carbon fibers.

24 p3104 A73-45143

NEUTRON SCATTERING

On the self-shielding coefficient of plates against neutron fluxes.

09 p1117 A73-22018

Coupled waves and particle scattering processes in ferromagnetic semiconductors and metals

09 p1133 A73-22677

Theory of fluctuations and particle scattering in ferromagnetic semiconductors and metals

09 p1134 A73-22678

Proton beam measurement of absolute cross section for neutron knockout reaction on C 12 at pion-nucleon resonance, correcting for muon and electron contamination

21 p2743 A73-40686

NEUTRON SOURCES

Neutron diffusion from a distributed source in a homogeneous atmosphere

06 p0742 A73-17549

Numerical modeling of laser produced plasmas - The dynamics and neutron production in dense spherically symmetric plasmas.

11 p1404 A73-25272

Contribution of atmospheric multiple neutron production to the multiplicity distribution observed in cosmic ray neutron monitor.

15 p1926 A73-31385

Neutron diffusion from a distributed source in an inhomogeneous atmosphere.

16 p2052 A73-32773

Technical and experimental investigations of a plasma focus neutron source

21 p2744 A73-39976

NEUTRON SPECTRA

K-neutal pion inelasticity factor measurement for nucleon interactions in carbon corresponding to primary neutron energy transferred to pions

02 p0209 A73-12663

Cosmic ray exposure ages from Apollo 14 lunar rocks isotopic anomalies due to neutron capture effect in Gd, Br and Ba

07 p0871 A73-19803

Epithermal neutron differential flux spectrum in equilibrium layers of atmosphere at 57 degrees north

08 p1000 A73-21350

Neutron flux and energy spectra measurements in space related to theoretical predictions, discussing neutron leakage flux, solar neutron observations and radiation detector configurations

18 p2347 A73-36645

Investigation of isotropic and anisotropic effects of cosmic rays during October through November 1968

21 p2758 A73-40600

NEUTRON STARS

NT PULSARS

Pulsar structure theory with respect to rotating neutron star hypothesis, discussing evolutionary elements

01 p0095 A73-10065

Single gaseous object and stellar cluster models of quasars and galactic nuclei stability, noting neutron and collapsing star lifetimes

01 p0106 A73-11302

Unsteady accretion of optically thick gas cloud on neutron star as hydrodynamic phenomenon due to supernova explosions or collision with ordinary star

01 p0106 A73-11303

Pulsar glitches and the metastability of the superfluid core.

02 p0211 A73-11895

Observational evidence relating to a recent theory on the origin of the universal X-ray background /Research note/.

02 p0207 A73-12395

The nature of radio emission from pulsars.

02 p0218 A73-12407

Neutron star vibration damping from semirelativistic neutron star models with magnetic field, superfluid component, outer crust, normal neutron composition and quantum crystals

02 p0222 A73-12714

He 4, C 12, O 16, Ne 20, Mg 24, Si 28 and Fe 56 abundance computed as function of time for neutron star atmospheres with strong magnetic fields

02 p0223 A73-12728

Equations of motion for steady state spherically symmetric flow of polytropic gases into or out of neutron stars, black holes or Schwarzschild singularities

02 p0223 A73-12729

Gaseous star as first limit to nebular matter gravitational collapse, considering equilibrium, neutron stars, black holes, forbidden lines and ionized hydrogen clouds

03 p0365 A73-12913

Numerical model of transient behavior of radiation dominated shock calculated for neutron star core of imploding supernovae

03 p0372 A73-13354

Subnuclear density state equation for minimum mass and binding energy of neutron star converting into white dwarf

04 p0502 A73-15978

Self similar procedure derived for gas infall to solid surface in constant gravitational field, applying to initial phase of neutron star matter accretion

04 p0503 A73-16003

Crab Nebula evolution from 1054 supernova to neutron star and nebula expansion, discussing pulsar properties

05 p0614 A73-16304

Pulsars as rotating magnetic neutron stars created during catastrophic collapses of old stars, discussing radiation mechanism

06 p0750 A73-18012

Determination of properties of cold stars in general relativity by a variational method

07 p0874 A73-19065

Soft X-ray pulsations from PSR 0833-45.

07 p0872 A73-20153

Neutrino energy loss in neutron star matter.

07 p0902 A73-20444

Neutron-star accretion in a stellar wind - Model for a pulsed X-ray source.

08 p0997 A73-21160

Mass differentiation of X ray sources based on Roche model, identifying pulsating sources with neutron stars and black holes as nonpulsating sources

08 p1013 A73-21810

Cen X-3 and Her X-1 X ray sources emission pulsation explained by model with neutron star accretion of matter from companion via magnetic funnel

09 p1141 A73-22010

Rotating neutron star gas cocoon heating by LF radiation absorption, noting X ray emission

10 p1263 A73-23481

Ejection of supernova shells by magnetic pumping

10 p1273 A73-23701

Quasi-radial pulsations of rotating white dwarfs and neutron stars in the relativistic theory of gravitation

10 p1274 A73-23711

Formation of neutron star spots and its connection with pulsars. II - Close similarities between radiation from the sun and pulsars.

10 p1275 A73-23829

Influence of interaction on the stability and pulsations of rotating neutron stars

10 p1283 A73-24704

Remarks on the soft X-ray emission from the galactic radio spurs.

10 p1270 A73-24904

Pair annihilation into neutrinos in strong magnetic fields.

11 p1402 A73-26414

- Massive X ray binaries consisting of early type star with neutron stars or black holes as companions 12 p1535 A73-27597
- Integral parameters and pulsation frequencies for equilibrium configurations of rotating neutron stars, expanding energy characteristics into series of relativistic members 12 p1546 A73-27854
- Radio emission from pulsars and surface temperature of neutron stars. 13 p1681 A73-28925
- Neutron stars physical model, deriving mass-density-energy relationships for degenerate electron gas 13 p1682 A73-28985
- Stellar structure deviation from neutron star models, deriving equations for relativistic models with deviation from Einstein principle of equivalence 13 p1686 A73-29655
- The effect of interstellar medium parameters on the accretion by neutron stars. 13 p1687 A73-29658
- White dwarfs, neutron stars and black hole identification by satellite X ray astronomy, discussing gas temperature and mass relation to cluster parameters 14 p1797 A73-30075
- Rotating neutron star matter and model properties with emphasis on pulsar observations, discussing equations of state, transport processes and relativistic effects 14 p1798 A73-30234
- Iron energy spectra due to acceleration at neutron star surface vs primary cosmic rays 14 p1787 A73-30618
- Positron-annihilation radiation from neutron stars. 14 p1788 A73-30738
- Differentially rotating neutron star models calculation for given state equation, examining mass increase relationship to rotational rigidity relaxation via Ostriker-Tassoul instability criterion 15 p1929 A73-31093
- Models for compact pulsing X-ray sources. 16 p2050 A73-32738
- Neutron matter solidification in neutron star cores, discussing energy minimization through strongly interacting baryon system via arrangement into lattice structure 16 p2061 A73-33220
- The magnetohydrodynamic stability of white dwarfs and neutron stars. 16 p2062 A73-33573
- The beaming of radiation from an accreting magnetic neutron star and the X-ray pulsars. 17 p2225 A73-35618
- Ejection of supernova envelopes by magnetic pumping. 18 p2354 A73-36726
- Quasiradial pulsation of rotating white dwarfs and neutron stars in general relativity. 18 p2354 A73-36736
- Light curves of the gravitational lens-like action for binaries with degenerate stars. 19 p2483 A73-37563
- Pulsar model magnetosphere for uniformly rotating infinitely conducting magnetized neutron star with aligned magnetic field 19 p2488 A73-38515
- Integral parameters and pulsation frequencies for equilibrium configurations of rotating neutron stars, expanding energy characteristics into series of relativistic members 20 p2608 A73-39228
- A model for compact X-ray sources - Accretion by rotating magnetic stars. 20 p2602 A73-39443
- Stimulated linear acceleration radiation - A pulsar radio emission mechanism. 20 p2602 A73-39444
- Temperature aspects of Landau orbital ferromagnetism in white dwarfs and neutron stars. 20 p2610 A73-39573
- Electrically neutral condensate of pions arises in nuclear matter at neutron star densities, discussing phase transitions 21 p2771 A73-41022
- Magnetized and nonmagnetized rotating neutron star reactions to applied torques for pulsar slowdown, discussing magnetosphere and wind zone 21 p2778 A73-41529
- Neutrino losses effects on 4-8 solar mass stars leading to collapse of degenerate carbon-oxygen cores, discussing type II supernovae and pulsar formation 22 p2914 A73-43008
- On self-consistent models for the pulsar magnetosphere. 24 p3140 A73-45190
- NEUTRON THERMALIZATION**
- Small nuclear light bulb engines with cold beryllium reflectors. [AIAA PAPER 72-1093] 04 p0475 A73-14907
- NEUTRON TRANSMUTATION**
- U NUCLEAR REACTIONS**
- NEUTRONS**
- NT FAST NEUTRONS
- NT THERMAL NEUTRONS

A shielding application of perturbation theory to determine changes in neutron and gamma doses due to changes in shield layers. 01 p0075 A73-10244

Cold matter consisting of atomic nuclei submerged in electron-neutron gas, relating subnuclear density relation to existence and binding energy of neutron-rich nuclei 01 p0081 A73-11310

Probabilistic integral multiplicity of generation of primary cosmic ray particles from count rate and primary spectrum relationship, using definition for neutron component calculations 08 p1000 A73-21352

Calculations of the transport of neutrons and secondary gamma rays through concrete for incident neutrons in the energy range 15 to 75 MeV. 08 p0987 A73-21528

Altitude and latitude dependences of the partial coefficients and integral multiplicity of the cosmic-ray neutron component 10 p1268 A73-23933

Advanced radiographic imaging techniques. 18 p2316 A73-36680

Massive singlet f-meson gravitational field effects on gravitational collapse in universe model with ten to eightieth power aligned neutrinos 20 p2605 A73-39016

NEUTRON PRESSURE LAW

Newtonian aerodynamic forces from Poisson's equation. 11 p1303 A73-26382

NEUTRON THEORY

Newtonian analysis of cosmological model for galactic accretion from small initial perturbation of central black hole 01 p0104 A73-11048

Newtonian dynamics canonical formulation in Galilean relativity framework, representing motions of bodies as integral manifolds of 2-form characteristic distribution 01 p0079 A73-11256

Newtonian and relativistic gravitational theories, discussing gravitational waves generating mechanism and black holes formation 06 p0753 A73-18274

A classification of particle motions in the equatorial plane of a gravitational monopole-quadrupole field in Newtonian mechanics and general relativity. 09 p1148 A73-22910

A method for the calculation of the aerodynamic coefficients of a body of any form. 12 p1457 A73-27067

Nongravitational forces and periodic comet Giacobini-Zinner. 14 p1791 A73-29803

Homographic motions of Newtonian point mass system interacting through two body forces, considering relativistic interactions 15 p1930 A73-31110

Overall existence of a solution of the Cauchy problem for the system of equations with Liouville-Newton partial derivatives 17 p2201 A73-35045

A deduction of the inverse square law from Newtonian cosmology. 19 p2486 A73-38169

Structural characteristics of galaxies caused by screening of the Newtonian gravitational potential 23 p3029 A73-43646

On a criterion for the occurrence of a Dedekind-like point of bifurcation along a sequence of axisymmetric systems. II - Newtonian theory for differentially rotating configurations. 24 p3110 A73-45033

NEUTON-RAPHSON METHOD

A modified conjugate gradient method for optimization problems. 04 p0471 A73-15216

The use of interval arithmetic to bound the zeros of real polynomials. 04 p0471 A73-15232

The application of Newton's method to the problem of elastic stability. [ASME PAPER 72-APM-P] 05 p0632 A73-16531

A numerical method for solving optimal control problems with unspecified terminal time. 06 p0681 A73-18520

Application of the extended Newton method to the creep analysis of shells of revolution. 11 p1432 A73-24998

Newton method for calculation of viscous flow around circular cylinder with Fourier series truncation for stream function and vorticity, evaluating numerical error 11 p1345 A73-25115

Superlinear convergent multistep procedure of the regula falsi and the Newton type 11 p1392 A73-26728

Solution of systems of nonlinear differential equations by the Newton-Raphson method 12 p1518 A73-27396

Geometrically nonlinear static and dynamic analysis of shells of revolution. 13 p1693 A73-28239

A rapidly convergent procedure for computing large-scale condensation in a dynamical weather model. 13 p1655 A73-29338

Some efficient algorithms for solving systems of nonlinear equations. 14 p1768 A73-29939

An historical survey of computational methods in optimal control. 14 p1738 A73-30413

Extensions of Newton's method and Simplex methods for solving quadratic programs. 16 p2033 A73-33856

Some computational techniques for the nonlinear least squares problem. 17 p2199 A73-34105

Kantorovich functional analysis algorithms providing rigorous theory for convergence of iterative methods to nonlinear functional equations on Banach spaces, emphasizing Newton method 17 p2163 A73-35268

Quasi-Newton methods for discretized non-linear boundary problems. 17 p2202 A73-35520

Newton method relationship to Floquet theory for nonlinear vibration problems, considering Van der Pol equation periodic solutions for breathing and bending modes [ASME PAPER 73-APMW-20] 22 p2924 A73-42883

NEWTONIAN FLUIDS

Navier-Stokes equations numerical solution for steady state axisymmetric flow of incompressible Newtonian fluid between two parallel infinite rotating disks 01 p0122 A73-10805

Relativistic gas dynamics problems reduction to equivalent Newtonian flow via transformation of governing equations 01 p0034 A73-11138

Some refinements of the theory of the viscous screw pump. [ASME PAPER 72-LUB-24] 03 p0314 A73-14337

Convective transport terms effect on laminar flow-field of Newtonian fluid between rotating cylinders, using adapted finite difference solution technique 03 p0298 A73-14643

Study of plane flows of viscous fluid around a body 04 p0404 A73-15652

Flow in the entrance region at low Reynolds numbers. [ASME PAPER 72-WA/FE-21] 04 p0435 A73-15847

Order c-square bulk stress derivation for force-free spherical particles suspension in Newtonian ambient fluid with uniform viscosity, noting error bounds 06 p0722 A73-17701

Numerical solutions to flow and heat transfer characteristics of free convection micropolar flow with Newtonian solvent substructure 08 p1023 A73-21260

Three dimensional boundary layer theory, applying Navier-Stokes equations to Newtonian fluids continuous flow over solid bodies or through finite ducts 10 p1171 A73-23863

The free surface on a liquid between cylinders rotating at different speeds. I. 10 p1207 A73-24789

Newtonian and non-Newtonian liquids rotating adjacent to a stationary surface. 11 p1346 A73-25369

Pulsatile Newtonian frictional losses in a rigid tube. 17 p2151 A73-34532

Solution for the pressure and temperature in thrust bearings operating in the thermohydrodynamic turbulent regime. [ASME PAPER 73-LUBS-14] 17 p2181 A73-35394

Creeping flow of Newtonian fluids in curved rectangular channels. 22 p2840 A73-41745

Capillary breakup length and stability of Newtonian and viscoelastic cylindrical liquid jets in terms of dimensionless viscosity and relaxation time 23 p2967 A73-43307

NICHROME [TRADEMARK]

Metal-metal laminar composites for high-temperature applications. 02 p0182 A73-12620

NICKEL

Nickel structure stabilization by multiply alternated thermocyclic treatment and isothermal annealing 01 p0062 A73-10253

Dry oxidation of nickel by anhydrous carbon dioxide under pressure 01 p0062 A73-10271

Cold rolling of dispersion-strengthened nickel. 01 p0063 A73-10282

Textures of deformation and of primary and secondary recrystallization in high-purity nickel 01 p0064 A73-10614

Study of polarization during electrodeposition of tungsten simultaneously with nickel 02 p0174 A73-12539

Preparation and high-temperature properties of carbon fiber-Ni composites. 03 p0321 A73-12919

Cs vapors thermal conductivity at various temperatures and pressures, using low emissivity Ni cylinders 03 p0396 A73-13181

Two phase recrystallization temperatures and structural inhomogeneity of dispersion hardened Ni after cold working and annealing at 1300-1400 C 03 p0324 A73-13508

Raney-Ni catalysts preparation for carbon-PTFE fuel cell electrodes from Ni-Al alloy, discussing rolling technique suitability and electrode characteristics 04 p0407 A73-15115

Influence of cold deformation and subsequent heating on the structure and properties of dispersion-strengthened nickel 04 p0466 A73-15666

Cyclic endurance and alteration nature of the dislocation structure in nickel before and after programmed strengthening 06 p0707 A73-17906

Structural changes arising in nickel under the action of ultrasound and subsequent thermal annealings 06 p0708 A73-18053

Investigation of static and transient current-voltage characteristics of diodes made of nickel-modified silicon 06 p0676 A73-18248

Chemisorption and catalysis of hydrogen on polycrystalline wires of tungsten and nickel. 06 p0661 A73-18253

Site preferences of Ni²⁺ and Co²⁺ in clinopyroxene and olivine - Limitations of the statistical approach. 06 p0690 A73-18268

Boundary conditions for diffusion in the pack-aluminizing of nickel. 06 p0713 A73-18774

Influence of nickel on the superconductivity parameters of Nb₃Al + Ni 09 p1098 A73-21845

Correlation between pore formation at grain boundaries and internal friction during creep of nickel 09 p1099 A73-21970

Ni diffusion in Nb at 988 to 1246 C, using residual activity technique with Ni-63 as tracer 09 p1103 A73-22436

Influence of the degree of deformation and annealing temperature on the recovery of 99.999% pure nickel after plastic deformation at -196 C and 25 C, respectively 10 p1231 A73-23690

Flow stress dependence on grain size in microstrain region of Ni strip machined to produce different grain sizes 10 p1235 A73-24444

Decomposition of carbon monoxide on a 1110/nickel surface. 11 p1325 A73-25203

Experimental determination of the integral radiative capacity of nickel 11 p1398 A73-25739

Temperature dependence of the activity and solubility of carbon in pure nickel 11 p1384 A73-26110

Change in the dislocation structure during fatigue of nickel prestrained by tension 11 p1386 A73-26732

The role of annealing twins in the primary recrystallization of nickel 270 work hardened in tension 12 p1514 A73-27988

Composition of metal in type III carbonaceous chondrites and its relevance to the source-assignment of lunar metal. 13 p1686 A73-29564

Some effects of prestraining nickel at various rates on its subsequent tensile properties. 14 p1761 A73-30637

Effect of rare earth metal additions on the recrystallization of nickel 14 p1765 A73-30887

A study of the adsorption of oxygen on Ni(111) using Auger electron spectroscopy - Chemical shifts and valence spectra. 15 p1840 A73-31968

Nonlinear magnetoelastic effects in Ni tube torsion spring pendulum due to oscillation damping and stiffness characteristics dependence on amplitude 16 p2025 A73-33214

Grain boundary destruction mechanisms in pure nickel polycrystals following plastic deformation, discussing annealing, fault concentration, microscopic techniques and critical loads 20 p2578 A73-39735

Work hardening of copper, nickel, and alloy H31 by compression and explosion 21 p2707 A73-40705

Thin Ni shell electroforming for applications in structural tests, discussing plating bath composition, Al and wax mandrels preparation 22 p2867 A73-42999

Influence of the method of preparing a Ni + ThO₂ composite and of its strengthening-oxide content on heat resistance 23 p2990 A73-43486

The stability of sapphire whiskers in nickel at elevated temperatures. I - General morphological and chemical stability. II - The kinetics of morphological changes over the temperature range 1100 to 1400 C. 23 p2986 A73-44032

NICKEL ALLOYS

NT INCONEL [TRADEMARK]

NT KAMACITE

NT MONEL [TRADEMARK]

NT NICHROME [TRADEMARK]

NT NITINOL ALLOYS

NT RENE 41

NT UDIMET ALLOYS

NT WASPALOY

Some aspects of the instability of superrefractory alloys rich in nickel 01 p0062 A73-10270

Development of IN-100 powder-metallurgy disks for advanced jet engine application. 01 p0063 A73-10283

Processing of high-performance alloys by powder metallurgy. 01 p0063 A73-10286

Damping in copper-aluminum-nickel alloys and its causes 01 p0064 A73-10611

Effect of various methods of oxide introduction on the properties of dispersion-hardened nickel. 01 p0065 A73-10814

Mechanical properties anisotropy in heat resistant Ni alloys due to strengthening phase nonmetallic inclusions distribution, suggesting purification by vacuum melting 01 p0066 A73-11346

Microstructure, hardness, electrical resistivity and thermal properties of Ni alloys with Al and Ta, noting composition of heat resistant alloys 01 p0067 A73-11436

Interaction of chromium carbide with copper-nickel melts 02 p0178 A73-11539

Influence of repeated loads on the resistance to relaxation of a heat-resistant nickel-chromium alloy 02 p0180 A73-11624

Correlations between the properties of some heat-resistant alloys 02 p0180 A73-11627

Hall mobility measurements on iron rich nickel ferrites from room temperature to 600 C. 02 p0199 A73-11725

Ultrasonic inspection of nickel-base alloy products. 02 p0174 A73-12150

The influence of test temperature on the fatigue strength of Zr56K alloy. 02 p0181 A73-12204

Metallographic investigation of electrodeposited iron-nickel-chromium alloys 02 p0174 A73-12535

State-of-technology for joining TD-NiCr sheet. 02 p0174 A73-12619

The high temperature thermodynamic properties of Ni-Ti alloys. 02 p0182 A73-12753

Electron-vacancy prediction methods for sigma phase precipitation in residual matrix compositions of austenitic Niand Co-base superalloys 02 p0183 A73-12757

High resolution marker transport sintering study. 02 p0175 A73-12771

An observation of the effect of grain structure on the appearance of Kirkendall porosity. 02 p0184 A73-12772

The growth process of oxide layers during the initial oxidation of a 80Ni-20Cr alloy. 03 p0321 A73-12917

Effects of alloying elements on elevated-temperature mechanical strength of high Cr, Ni-base heat resistant alloy. 03 p0321 A73-12921

Vacuum arc melting for improved heat resistance and mechanical properties of Ni alloy blanks, comparing with electro-beam and plasma arc melting and powder sintering 03 p0323 A73-13502

Changes in the fine structure of heat-resistant nickel-chromium alloys during the creep process 03 p0324 A73-13505

Phase diagrams of ternary Ni-Re alloys with La, Y, Sc, Hf, Si and Mo for cathode applications in electronic vacuum devices 03 p0325 A73-13516

Microstructure and plastic deformation of the Ni4Mo alloy. 03 p0325 A73-13804

Martensitic transformation kinetics and martensite morphology in the N25KhT2 alloy after aging 03 p0325 A73-13826

Disordered precipitation effect on steady state creep rate of gamma prime Ni-Al-Ti single crystals 03 p0326 A73-13963

Effects of alloying on structural stability and cohesion between phases in oxide/metal composites. 03 p0326 A73-13964

The effect of small magnesium additions on microstructure and high-temperature properties of nickel-2 1/2 vol. % alumina. 03 p0326 A73-13966

Secondary maximum grain size and even-grained texture in the region of low and moderate deformations during recrystallization of certain nickel- and iron-based alloys 03 p0326 A73-13967

Ni-Mo-W alloys hardness rating and corrosion resistance to sulfuric and hydrochloric acids, discussing dispersion hardening, quenching and aging treatments 03 p0327 A73-14001

Sn alloying effect on heat resistant Ni-Cr alloys plastic strain resistance and strength at room and high temperatures 03 p0327 A73-14003

The high-temperature oxidation of nickel-20 wt. % chromium alloys containing dispersed oxide phases. 04 p0461 A73-14923

Heat resistant Ni and Cr alloys powder metallurgy, discussing inert and solute gas atomization, rotating electrode and gatorizing processes for powder fabrication 04 p0461 A73-15023

Microstructures and transformation kinetics of continuously cooled carbon free Fe-Mo-Ni alloys. 04 p0463 A73-15311

Microstructure alignment in Ni-In system eutectic alloys due to directional solidification 04 p0463 A73-15312

Ni-Cr-thoria alloy surface oxidation induced by sprayed coating of sodium sulfate for gas turbine blade hot corrosion investigation 04 p0468 A73-15316

Chromium diffusion in Ni-20 wt pct Cr-3 vol pct Y2O3 and Co-21 wt pct Cr-3 vol pct Y2O3. 04 p0463 A73-15317

The effect of a hydrogen preheat-treatment on the oxidation behavior of Ni-Cr-Al-ThO₂ alloys. 04 p0463 A73-15319

High temperature strength and microstructure of nickel-base heat resisting No. 648C alloy. 04 p0465 A73-15583

Effects of rare earth elements on the oxidation resistance of iron and nickel base alloys. 04 p0465 A73-15584

Precipitation hardening effect on Co-Ni-Ti-Al alloys stress-strain, grain size and strain resistance behavior in micro- and macrodeformation yield point region 04 p0465 A73-15639

Temperature dependence of the elastic micro- and macro-stiffness of dispersion hardenable Co-Ni-Ti and Co-Ni-Ti-Al alloys. II 04 p0465 A73-15640

Preparation of alloy deposits by continuous electron beam evaporation from a single rod-fed source. 04 p0456 A73-15761

X ray diffraction measurement of ordering kinetics in Ni-Pt alloy at annealing temperatures, showing disorder-order transitions relation to nucleation and growth 04 p0467 A73-15982

Strength and microstructure of nickel-base superalloys after long term heating. 05 p0587 A73-16622

Material variability as measured by low temperature electrical resistivity. 05 p0588 A73-17287

Influence of cobalt on the maraging of Fe-Ni-Mo alloys 06 p0705 A73-17876

Cyclic loads for decrease in relaxation softening of heat resistant Ni-Cr alloys, noting working temperature effects 06 p0706 A73-17885

Martensite transformation in an aged Fe-Ni-Ti alloy 06 p0708 A73-18052

X ray analysis of high coercivity Ticonal alloy single crystal microstructure after isothermal thermomagnetic treatment 06 p0709 A73-18210

Mechanical properties of heat and corrosion resistant nonmagnetic Ni-Cr-Nr spring alloys with W addition tested in aggressive and nitric acid media. 06 p0709 A73-18211

Composite Al- and Ni-base alloys strengthened by B and W/Mo fibers respectively for reduced weight wing spars and high temperature applications 06 p0710 A73-18638

Microtwinning factors in plastic deformation, volume changes and carbon solution content of Ni martensite 06 p0710 A73-18645

Directionally solidified NiAl-Cr and NiAl-Mo eutectic composites microstructural stability as function of time and temperature 06 p0711 A73-18753

Dendritic solidification of Cu-Ni alloys. I - Initial growth of dendrite structure. 06 p0712 A73-18756

Dendritic solidification of Cu-Ni alloys. II - The influence of initial dendrite growth temperature on microsegregation. 06 p0712 A73-18757

The orientation dependence of deformation mode and structure in stoichiometric NiAl single crystals deformed by high temperature steady-state creep.

06 p0712 A73-18758

Nickel-base alloys hot corrosion mechanism due to sodium sulfate induced accelerated or catastrophic oxidation as result of protective oxide scale dissolution

06 p0712 A73-18763

Creep of precipitation-hardened nickel-base alloy single crystals at high temperatures.

06 p0713 A73-18768

Thoria stability in TD-NiCr at high temperatures in the presence of chromium in solution.

06 p0713 A73-18771

The application of magnetic after-effects in research on the real structure and migrational properties of metals and alloys

07 p0837 A73-19049

Superrefractory Ni-based alloys mechanical properties enhancement through unidirectional solidification, considering grain boundary structure

07 p0838 A73-19116

A specific type of carbide phase precipitation during the aging of KhN77TiRu alloy

07 p0841 A73-20640

The influence of a thoria dispersion on preferred orientation in nickel alloys.

08 p0977 A73-21012

Stress rupture behavior of a dispersion strengthened superalloy.

[ASME PAPER 72-MAT-G] 08 p0978 A73-21570

Shock deformation of K-state in Ni-Cr alloys.

08 p0979 A73-21626

Steel and Ni-based alloys structural stability during long term high temperature creep, noting matrix structure dependence on initial dislocation and interparticle spacing

08 p0980 A73-21780

The influence of some structural factors on the creep strength of wrought precipitation-hardened Ni-Cr alloys.

08 p0982 A73-21793

The influence of structure upon the notched creep strength of a nickel-base alloy.

08 p0982 A73-21795

Influence of annealing under load on the structure and properties of a self-ordering Ni3Mn alloy

09 p1099 A73-21957

Young modulus anomaly in precipitation-hardening subjected Invars

09 p1099 A73-21962

Grain-boundary internal friction of copper-nickel alloys

09 p1099 A73-21965

Electrical conductivity of a directionally crystallized Al-Al3Ni composition

09 p1099 A73-21972

Dependence of martensite morphology on the isothermal transformation temperature of the Fe-24Ni-3Mn alloy

09 p1100 A73-21974

Grain size effects on strength and ductility of two phase Ni-Cr and Ni-Mo alloys at high and low deformation temperatures

09 p1101 A73-22164

Concentration profiles through thin oxide scales by ion-probe microanalysis.

09 p1101 A73-22402

Ni-Ti alloy aging effects on yield strength explained by internal strain due to lattice modulation and Ti rich region volume fraction

09 p1103 A73-22520

High temperature creep in nickel and its alloys

09 p1108 A73-23229

Effect of magnesium additions on the ductility of heat-resistant nickel alloys

09 p1108 A73-23230

Determination of the composition of Ni-NiMo eutectic by the zone recrystallization method

09 p1108 A73-23239

Advances in directional solidification spur usage in turbine airfoil shapes.

09 p1089 A73-23293

Protecting metals in corrosive high-temperature environments.

09 p1089 A73-23296

Thermodynamic properties of the nickel-tungsten system as determined from its hydrogen solubility

10 p1231 A73-23689

Stress corrosion cracking behavior of nickel and nickel alloys.

10 p1232 A73-23870

Fine structure of X-ray spectra of nickel and some of its alloys with a nickel arsenide lattice and lattices resembling it

10 p1259 A73-24152

Investigation of the morphology and decomposition kinetics of Co-Ni-Ti alloys

10 p1232 A73-24153

Development and investigation of fine-grain metal ceramic contacts of silver/graphite and silver/nickel/graphite composition for low-voltage device applications

10 p1225 A73-24320

An observation of vacancy sources during substitutional diffusion in thoriated nickel alloys.

10 p1234 A73-24433

Fine precipitate within coarse gamma-prime particles in cast Ni-base superalloy during elevated temperature exposure

10 p1235 A73-24446

Heat resistant Ni alloys residual stresses from machining operations, considering cutting rates, temperature, work piece blanks and cutting tools parameter effects

10 p1226 A73-24798

Diffusion aluminizing of Ni and Ni-base alloys by gas circulation method, investigating gas flow velocity effect relationship to specimen weight gain

10 p1226 A73-24957

Cr diffusion into Ni-Cr alloys in presence of aluminized layer, noting increased diffusive mobility

10 p1226 A73-24959

Si addition effect on Ni-Cr alloy calorized layer depth, microhardness, phase structure, chemical composition and scaling resistance

10 p1227 A73-24960

Vacuum contactless metallization of carbon steels, stainless steels and nickel alloys, considering Si, Cr and Al coatings

10 p1227 A73-24964

Stabilization of the austenitic phase of iron-nickel base alloys by cumulative thermal cycling

11 p1379 A73-25323

Directionally solidified eutectic high temperature alloys.

11 p1379 A73-25404

Mechanical properties at high temperature of Ni-based unidirectionally solidified eutectic: Ni-Ni3Ta.

11 p1379 A73-25405

Composite material production by grinding Ni-Al-Ti alloy powder with other mixed powders, noting alloying elements effects on corrosion resistance and ductility

11 p1372 A73-25406

Production and properties of tungsten-wire reinforced NiCr80 20

11 p1379 A73-25407

Oxygen and temperature effects on Ni base superalloys fatigue fracture, discussing trans- and intergranular crack propagation and initiation in single and polycrystals and surface coatings

11 p1382 A73-25818

Determination of the resistivity of nickel and of some of its alloys as a function of pressure up to 60 kbar

11 p1384 A73-25873

Microstructure, hardness, electrical resistivity and thermal properties of Ni alloys with Al and Ta, noting composition of heat resistant alloys

11 p1384 A73-26063

'Invar' and 'Elinvar' - Alloys with controllable thermal expansion and elastic properties

11 p1385 A73-26564

Bivariant eutectic alloys located on liquidus surface within Ni-Nb-Cr-Al quaternary, permitting production of aligned delta Ni-Nb lamellae within nichrome matrix containing Ni-Al fcc precipitate

12 p1509 A73-26845

Phase structure and composition during the crystallization of eutectic-type alloys of the Ni-Cr system

12 p1509 A73-26897

Relaxation stability of iron and nickel alloys at high temperatures

12 p1509 A73-26898

Precipitation and its hardening effect in Ni-rich NiTi.

12 p1511 A73-27057

Nickel base alloys high temperature steady creep rate and stress relations

12 p1512 A73-27256

Ni-base alloy powder metallurgy from production waste cuttings by oxidation and subsequent oxide reduction with hydrogen and calcium hydride

12 p1503 A73-27553

'Glazes' produced on nickel-base alloys during high temperature wear.

12 p1513 A73-27598

X-ray spectral study of the K state in a nickel-chromium alloy

12 p1514 A73-27943

Dendritic liquation of hypoeutectic binary, ternary and complex Fe- and Ni-base alloys dependence on phase diagram

13 p1631 A73-28102

Striated, cellular and dendritic substructure formation during growth of Fe-Ni alloy single crystals

13 p1631 A73-28107

Crystallization of nickel-based alloys and indium-lithium system alloys at ultrahigh cooling rates

13 p1632 A73-28112

Unidirectional solidification formed interdendritic eutectic composition related to solidification variables, discussing Al-Cu and Al-Cu-Ni systems

13 p1632 A73-28131

The partitioning of refractory metal elements in hafnium-modified cast nickel-base superalloys.

13 p1633 A73-28138

The effect of lattice disorder on the thermodynamic properties of the f.c. tetragonal beta-one NiZn alloys.

13 p1635 A73-28262

Heat resistant nickel alloys creep rupture strength diagram, determining time to failure as function of loads

13 p1636 A73-29062

Changes in the electrical resistance of heat-resistant EI 826 alloy in the presence of creep

13 p1636 A73-29065

Factors controlling the corrosion behavior of titanium and titanium-nickel alloys in saline solutions.

[NACE PAPER 64] 13 p1637 A73-29311

Strength and ductility of two-phase iron alloy composed of austenite and martensite.

13 p1638 A73-29453

Energy dissipation in metals in high-frequency fatigue tests. II.

13 p1643 A73-29631

Investigation of the structure of turbine disc materials after use.

13 p1643 A73-29632

Corrosion properties and structural transformations of the N70M27 alloy containing vanadium and niobium

13 p1644 A73-29645

Study of precipitates formed by internal oxidation in cobalt-nickel-chromium alloys with a cobalt base. I. - Precipitates formed by oxidation in air

14 p1759 A73-29750

Effects of deformation on diffusion in iron-nickel and iron-chrome systems

14 p1760 A73-30379

Calculation of the binary phase diagrams of iron, chromium, nickel and cobalt.

14 p1760 A73-30440

Influence of recovery and recrystallization on the Young's modulus and its temperature dependence in Invar-type iron-nickel alloys

14 p1760 A73-30586

Dislocation structure of Ni3Al intermetallic compound during various stages of deformation

14 p1760 A73-30591

Thoria particle dispersion TD-nickel creep and tensile deformation at elevated temperature dependence on grain size and L/D ratio

14 p1761 A73-30635

Nickel niobide tested along crystal growth direction for twinning mode of intermetallic phase in tensile deformation, projecting crystallographic structure upon crystal plane

14 p1762 A73-30640

Influence of ordering in a Ni3Mn alloy on the magnitude of the critical shearing stresses

14 p1764 A73-30859

Martensitic transformation in iron-nickel alloys in a pulsed magnetic field

14 p1764 A73-30860

Kinetics of changes in deformability of a heat-resistant nickel-base alloy

14 p1764 A73-30861

Electron-microscopic investigation of the spatial distribution parameters of second-phase precipitation in aging nickel-base alloys

14 p1764 A73-30862

Investigation of interdiffusion in the nickel-tungsten and palladium-tungsten systems

14 p1764 A73-30864

Liquid Ni-Si alloy short range order structure analyzed by X ray scattering, revealing Ni atoms position relation to Si atoms

14 p1764 A73-30870

Utilization of hydrostatic compression at high pressures as a means of improving the properties of acoustic nickel ferrite

14 p1765 A73-30890

Powder metallurgical preparation/sintering/ of conventional maraging steel and similar alloys with Ni and/or Mo replacement by Mn and Ti, considering age hardening characteristics

14 p1765 A73-30936

The effect of stacking-fault energy on the stress-strain curve of dispersion-hardened Ni-Co alloys.

15 p1887 A73-31351

Interpretation of tensile and compressive creep behaviour of two nickel alloys.

15 p1888 A73-31618

Intergranular corrosion in iron and nickel base alloys.

15 p1888 A73-31739

Experimental observations of dendritic duplex crystals grown in complex Ni base alloys.

15 p1890 A73-31841

Electronic specific heat of nickel-base alloys containing small amounts of transition metals

[ONERA, TP NO. 1250] 15 p1924 A73-32210

Structure of powdered solders with a Ni-Cr-Si-Fe-B-C/Mo/ base

15 p1892 A73-32245

A scanning electron microscope study of the surface morphology of TD-NiCr oxidized at 800 C to 1200 C.

15 p1892 A73-32270

Mach 1 oxidation of thoriated nickel chromium at 1204 C /2200 F/.

15 p1892 A73-32271

Russian book - Precision alloys with specific thermal-expansion and elastic properties 15 p1893 A73-32293

Effect of chloride ions on the dissolution behavior of Fe-Ni alloys. 15 p1895 A73-32565

Na₂SO₄-induced attack of Ni-20Cr-2ThO₂. 15 p1896 A73-32575

German monograph - The spontaneous anisotropy of the resistance in nickel - Measurements involving single crystals of nickel and diluted nickel alloys between 4.2 and 358 K. 15 p1896 A73-32582

The role of yttrium in high-temperature oxidation behavior of Ni-Cr-Al alloys. 16 p2025 A73-33077

Diffusional creep and creep-degradation in dispersion-strengthened Ni-Cr base alloys. 16 p2025 A73-33111

Phase constitution of the Ni-Cr-S alloy system between 600 and 850 C. 16 p2025 A73-33112

Structure, strength, and fracture of electrodeposited nickel and Ni-Co alloys. 16 p2025 A73-33113

Eutectic superalloys strengthened by aligned delta, Ni₃Co lamellae, gamma-prime, Ni₃Al precipitates and reduced interlamellar spacing. 16 p2026 A73-33425

Highly permeable nickel-iron-molybdenum alloys containing 33 to 37% nickel 16 p2026 A73-33958

Hot fatigue strength during fluctuating axial tension of PER 7 and IN 100 superalloys 16 p2026 A73-33971

Hall effect and electrical resistance in Ni, Co and Ni-Co alloys 16 p2027 A73-34009

Phase composition and properties of metastable alloys of titanium with nickel 16 p2027 A73-34072

Certain physical properties of a new alloy of the nickel-rhenium-molybdenum system 17 p2186 A73-34137

Composition and temperature effects on hydrogen solubility in Ni-Al liquid alloys 17 p2187 A73-34553

Behavior of hafnium dioxide particles in dispersively hardened nickel during isothermal annealing 17 p2188 A73-34560

Investigation of molybdenum-rich Mo-Ni-C, Mo-Ni-Zr, and Mo-Zr-Ni-C alloys 17 p2188 A73-34569

Nickel-titanium memory material stress measurement methods, energy absorption capacity and cyclic response, discussing nickel foil surface temperature sensing devices 17 p2166 A73-34616

Tracer diffusion of Ni-63 in Fe-17 wt pct Cr-12 wt pct Ni. 17 p2189 A73-34641

Stress relaxation measurements for strain rate sensitivity of dispersion hardened thoriated Ni alloys as function of applied stress concentration 17 p2190 A73-34647

Direct observation of the failure of a fibre reinforced composite. 17 p2192 A73-35529

Ni-Fe-Cr alloy and austenitic stainless steel cyclic stress-strain behavior at 70-1400 F 18 p2323 A73-36586

Characteristics of the temperature dependence of the microhardness of a highly heat resistant dispersion-hardened nickel alloy 18 p2324 A73-36765

Effect of temperature on true energy dissipation in heat resistant E1893 nickel alloy 18 p2324 A73-36766

Limit of the two-phase region of Mo/Ni, Cu/ and Cu/Ni, Mo/ solid solutions in the Mo-Cu-Ni system 18 p2325 A73-36859

Heat resistant nickel alloys creep rupture strength diagram, determining time to failure as function of loads 18 p2325 A73-36894

The change in the electrical resistance of E1826 refractory alloy with creep. 18 p2325 A73-36897

Effect of temperature on the effectiveness of hardening components made of heat-resistant alloys 19 p2439 A73-37268

High temperature cyclic oxidation resistance tests on Ni-, Co- and Fe-base alloys for aircraft gas turbine engines 19 p2440 A73-37496

Brazing of nickel base alloys. [SME PAPER AD 73-222] 19 p2436 A73-38494

Electron diffraction study of a noncrystalline Zr-Ni phase. 20 p2575 A73-39021

The relationship between relative oxide ion content of Na₂SO₄, the presence of liquid metal oxides and sulfidation attack. 20 p2575 A73-39022

Carbon deposition and the role of reducing agents in hot-corrosion processes. 20 p2576 A73-39027

Carbide reinforcement in two directionally solidified alloyed nickel eutectic alloys. 20 p2576 A73-39028

The effect of molybdenum on gamma prime coarsening and on elevated-temperature hardness in some experimental nickel-base superalloys. 20 p2576 A73-39029

Investigation of energy criteria for the failure by fatigue of some metals at low and high loading frequencies 20 p2577 A73-39354

Some specific features of crack initiation and development in heat-resistant alloys under various loading conditions 20 p2578 A73-39376

The effect of vanadium, niobium, and tantalum on the electrical resistance of nickel 20 p2578 A73-39396

Variation of the electrical resistance of ordered Ni₃Mn alloy during irradiation by fission fragments 20 p2600 A73-39733

Continuous decomposition of gamma solid solution in iron-nickel-titanium alloys 20 p2579 A73-39736

Study of the mechanism of plastic deformation of aging nickel-aluminum alloys with a large volume fraction of gamma prime phase 20 p2579 A73-39740

Dislocation structure of Ni₃Fe and Ni₃FeCr alloys in various stages of strain hardening 20 p2579 A73-39742

Changes in the disorientation of the substructure of a nickel-aluminum alloy under ultrasonic treatment and creep 20 p2579 A73-39748

Effect of chemically activated elements on the properties of electron-beam-melted nickel 21 p2718 A73-40482

Influence of magnesium on the structure of heat-resistant nickel-base alloys 21 p2718 A73-40485

Phase composition of Ni-Al and Ni-Ga alloys hardened from the liquid state 21 p2719 A73-40849

Preparation and properties of materials containing titanium carbide 21 p2719 A73-40851

Structure and composition of phases during solidification of Ni-Cr alloys of the eutectic type. 21 p2720 A73-41030

Relaxation resistance of alloys based on iron and nickel at high temperatures. 21 p2720 A73-41031

Ti, Al, W and Mo concentrations effect on heat resistance of precipitation hardened Ni-based alloys 21 p2720 A73-41035

Corrosion characteristics and structural transformations in alloy N70M27 with vanadium and niobium. 21 p2720 A73-41038

Microstructure of recrystallized alloy Kh20N80. 21 p2721 A73-41042

Possible reinforcement of the tungsten-nickel-iron composite with tungsten fibers. 21 p2722 A73-41586

Deformation and microfracture characteristics of two-phase tungsten-composite materials sintered with the liquid phase 22 p2872 A73-41948

Grain size effects on strength and ductility of two phase Ni-Cr and Ni-Mo alloys at high and low deformation temperatures 22 p2875 A73-42112

Isothermal cross sections of the phase diagram of the nickel-molybdenum-tungsten system at 1200 and 700 C 22 p2877 A73-42459

Thermodynamic properties and Cr activity measurements in solid Cr-Ni-Fe alloys by solid oxide electrolyte technique 22 p2878 A73-42577

The influence of carbon on the interdiffusion of Mo and Ni. 22 p2878 A73-42579

Superplasticity and residual tensile properties of a microduplex copper-nickel-zinc alloy. 22 p2879 A73-42582

Reactive kinetic observations for spraying with Ni-Al powder. 22 p2879 A73-42594

Investigations into the mechanism of exothermically reacting nickel-aluminum spraying materials. 22 p2879 A73-42595

The effect of stacking fault energy on the plastic deformation of polycrystalline Ni-Co alloys. 22 p2879 A73-43074

The yield stress of Ni₃Al, W/. 22 p2880 A73-43075

Transformation temperatures of martensite in beta-phase nickel aluminide. 23 p2989 A73-43275

Mo content influence on heat resistant Ni base alloys corrosion and oxidation resistance and gamma-prime phase solution temperature and amount 23 p2989 A73-43435

Al-aluminum nickelide eutectic fiber composite impact strength dependence on crystallization rate, examining crack propagation rate relation to fiber spacing 23 p2996 A73-43437

Book - Advances in corrosion science and technology. Volume 3. 23 p2990 A73-43455

Corrosion and deposition of steels and nickel-base alloys in liquid sodium. 23 p2990 A73-43456

Intergranular corrosion of iron-nickel-chromium alloys. 23 p2990 A73-43458

Phase composition of Cu-Ni-O alloys with Ir additions, examining oxygen content influence on Ir distribution and solid solution formation 23 p2990 A73-43483

Influence of alloying additives on the structural changes in a nickel-molybdenum composite 23 p2991 A73-43488

Thermodynamic properties and phase composition of the In-Ni system 23 p2991 A73-43706

The plastic deformation of NiAl single crystals between 300 K and 1050 K. I - Experimental evidence on the role of kinking and uniform deformation in crystals compressed along the 001 direction. II - The mechanism of kinking and uniform deformation. 23 p2991 A73-43773

X ray and electron diffraction studies of Ni-containing etched brown rims in meteoritic taenite [Ni-Fe alloy] associated with kamacite, noting Widmanstätten pattern 23 p2951 A73-43844

Ni-based ternary alloy element segregation after addition of third element during crystallization, showing Si addition influence on segregation direction of Co, Cr and Mo 23 p2992 A73-43915

Brazeability of Ni-Cr heat resistant cermets on stainless steel. 23 p2986 A73-44005

Morphology and crystallography of beta prime martensite in TiNi alloys. 23 p2994 A73-44160

Static and fatigue strength of the KhN40MDTi/EP 543/ alloy after various hardening treatments 24 p3098 A73-44475

Spatial orientation of phases in the Al-Al₃Ni eutectic system 24 p3099 A73-45169

Dynamic strain ageing in creep of beta-NiAl. 24 p3100 A73-45331

The precipitation of titanium in copper and copper-nickel base alloys. 24 p3100 A73-45473

Plastic deformation of Co-Ni-Cr and Co-Ni-Cr-Mo alloys 24 p3101 A73-45525

NICKEL CADMIUM BATTERIES

Ni-Cd battery thermal runaways caused by self sustaining temperature increases, discussing operational and maintenance procedures for avoidance or correction 03 p0251 A73-12906

The reflex principle of charging nickel-cadmium and other batteries. 03 p0253 A73-13938

Sealed cylindrical high energy density Ni-Cd batteries, discussing electrode design and performance characteristics 09 p1034 A73-22754

Spacecraft Ni-Cd battery cycle life performance tests, noting cycle life-cycle duration relationship 09 p1034 A73-22755

High energy density long life Ni-Cd battery systems for synchronous satellites, discussing radiation protection, charge and discharge control electronics and temperature control 09 p1034 A73-22756

Intelsat 4 power subsystem with solar panels, Ni-Cd batteries, controller and relays for bus paralleling, discussing spacecraft and system configurations and performance 09 p1154 A73-22788

Heat pipe thermal control of spacecraft batteries. 11 p1309 A73-25992

Design and performance of the TACSAT power subsystem. 11 p1312 A73-26020

Unmanned interplanetary spacecraft power systems with nickel-cadmium batteries, solar panels or radioisotope thermoelectric generators 11 p1312 A73-26022

Power supply requirements during the AEROS acquisition phase. 13 p1689 A73-28784

Evaluation of Intelsat IV nickel-cadmium cells. 13 p1572 A73-29582

NICKEL COATINGS

- OA0 2 satellite nickel-cadmium batteries with auxiliary electrodes for overcharge control, discussing operation and degradation mechanism
13 p1572 A73-29583
- Nickel-cadmium cells for low earth orbit applications.
13 p1572 A73-29584
- Long-life, high energy Ni-Cd aerospace cells.
13 p1572 A73-29585
- Primary cells hybridization with sealed nickel cadmium batteries for power supply operation over wide temperature ranges and discharge rates
13 p1573 A73-29588
- Sealed aircraft battery with integral power conditioner.
13 p1573 A73-29589
- Nickel-cadmium battery performance prediction models Apollo Telescope Mount application.
19 p2390 A73-38399

NICKEL COATINGS

- Temperature dependence of magnetic susceptibility in nickel-film-coated iron-silicon alloy specimens
01 p0062 A73-10254
- Structure and properties of nickel-phosphorus coatings in relation to annealing temperature and time.
06 p0698 A73-18214
- Method of plasticity enhancement in aluminum and nickel-aluminum diffusion coatings on medium-carbon steel
06 p0711 A73-18665
- Stability of nickel coated sapphire whiskers.
11 p1389 A73-26044
- Improved corrosion protection for solid rocket propulsion systems.
13 p1645 A73-29273
- Influence of a solid-phase nickel coating on the sintering kinetics of tungsten wire
18 p2320 A73-36858

NICKEL COMPOUNDS

- NT NICKEL OXIDES
Kinetics of the formation of passivating nickel hydroxide layers on nickel carbonyl
07 p0788 A73-20397
- Certain resonance properties of nickel-cadmium ferrites
08 p0995 A73-21513
- Ternary nickel-vanadium-oxygen compound and solid solutions formation by vacuum calcination of vanadium and nickel oxides mixtures
13 p1634 A73-28203
- Carbonyl nickel recrystallization characteristics from hardness-temperature graphs and X ray analyses
14 p1765 A73-30891
- Study of the electronic structure of iron, cobalt, and nickel monosilicides by X-ray photoelectron spectroscopy and X-ray spectroscopy
20 p2578 A73-39734

NICKEL OXIDES

- Activated sintering of ThO₂ and ThO₂-Y₂O₃ with NiO.
01 p0066 A73-11014
- Thermogravimetry system designed for use in dispersion strengthening studies.
01 p0015 A73-11449
- Sintering of nonstoichiometric nickel monoxide
02 p0179 A73-11546
- Raman scattering by phonons and magnons and phonon-magnon interactions in NiO.
02 p0201 A73-12640
- The concentration-dependent diffusion of chromium in nickel oxide.
06 p0712 A73-18760
- NiO and CoO single crystal thermal conductivities, reporting specific heat and electrical resistivity near magnetic transition
20 p2600 A73-39826

NICKEL STEELS

- Strength and ductility of chromium-nickel-manganese steel as a function of the carbon and nitrogen content in the range from 20 to 253 C
01 p0064 A73-10490
- Sinterability of stainless steel powders.
01 p0065 A73-10813
- Corrosion behavior of sintered stainless steels.
01 p0065 A73-10815
- Sintered chromium-nickel steel of high tungsten content.
01 p0065 A73-10816
- Stress corrosion cracking behavior of 18% Ni/300/maraging steel.
01 p0066 A73-11295
- Austenite deformation effect on thermal stability and hardness of Ni steels at various C and Ni concentrations
01 p0067 A73-11349
- Certain regularities in the influence of preliminary loading by alternating tensile stress on the long-term strength of Kh18N10T steel
02 p0180 A73-11928
- Influence of cerium and boron additions on the corrosion properties of Kh18N9TL steel
02 p0181 A73-12538

The effect of reverted austenite on the mechanical properties and toughness of 12 Ni and 18 Ni/200/maraging steels.

- Temper embrittlement response and toughness of a rare earth treated Ni-Cr-Mo steel.
02 p0183 A73-12758
- Delta-ferrite alteration in steel 1Kh16N4B during homogenization
02 p0183 A73-12762
- Liquation-induced microinhomogeneity of heat resistant submerged-arc-smelted steel 4Kh12N8G8MFB/EI481/
03 p0326 A73-13828
- Ni, Si and Mn alloying effect on structural transformations, phase composition and mechanical properties of cast Cr-Ni steels
03 p0327 A73-14002
- The influence of certain experimental factors on the fracture toughness of a high-strength steel
04 p0462 A73-15299
- Low-cycle fatigue behavior of quenched and tempered UNI 38NiCrMo4 steel
04 p0462 A73-15300
- Phase transformations and mechanical properties of highly alloyed Cr-Mn-Ni steels
04 p0466 A73-15664
- The properties of 18Ni 350 maraging steel produced from elemental and prealloyed powders.
04 p0466 A73-15800
- Aging kinetics of maraging nickel and chromium steels
06 p0705 A73-17877
- Magnetostriiction of stainless steels in relation to heat treatment.
06 p0709 A73-18212
- Strength and toughness of Fe-10Ni alloys containing C, Cr, Mo, and Co.
06 p0713 A73-18765
- Alloy composition and temperature effects on nitrogen solubility in austenitic Cr-Ni steels, noting nitride precipitation effect on impact strength reduction
07 p0839 A73-19950
- Investigation of the structural changes in austenite during martensitic transformation in steels with high stacking-fault energy
07 p0841 A73-20521
- Cr-Ni carbon steel testing for stress and temperature dependencies of secondary creep rate, noting grain boundary diffusion controlled mechanism
08 p0980 A73-21674
- A recovery creep model based on dislocation distributions.
08 p0980 A73-21777
- The effect of a dispersed phase on the creep properties of a Cr-Ni steel.
08 p0980 A73-21779
- Dislocation distributions during creep and recovery of a 20% Cr-35% Ni steel at 700 deg C.
08 p0981 A73-21784
- Irradiation creep in some austenitic stainless steels, nimonic PE16 alloy and nickel.
08 p0982 A73-21794
- The influence of nickel content on the structure and high temperature properties of a 12% Cr Mo V Nb steel.
08 p0982 A73-21799
- Molybdenum and nickel alloying effect on time and temperature range of reversible temper brittleness of chromium steels
09 p1107 A73-23200
- Corrosion and electrochemical characteristics of oxidized steels Kh15N5D2T and Kh15N4AM3.
10 p1236 A73-24926
- Effect of chemical composition on the heat resistance of steel Kh25Ni16G7AR.
10 p1236 A73-24932
- Dynamic potential method of estimating the susceptibility of corrosion-resistant steels to intercrystalline corrosion
11 p1364 A73-26112
- Stud welding on 5083 aluminum and 9% Ni steel for cryogenic use.
11 p1375 A73-26352
- Substructure alteration in manganese and nickel austenitic alloys under the action of microimpacts
13 p1630 A73-28013
- Some observations of crack initiation and propagation of notched specimens under creep conditions.
13 p1641 A73-29510
- Investigation of the thermal fatigue of type Kh18N10T steel under complex stress distributions.
13 p1643 A73-29623
- Redistribution of nickel and chromium during alpha to gamma transformation in stainless nickel-chromium steels
13 p1644 A73-29646
- Mo and W alloying effects on low carbon chromium nickel steels intergranular corrosion resistance
13 p1644 A73-29648
- Delta ferrite and martensite formation in stainless steels.
14 p1759 A73-30145

Strength and ductility of chromium-nickel-manganese steel as a function of carbon and nitrogen contents over the range 20-253 C.

- Structure stability of austenitic chromium-nickel steels at the temperature of liquid helium
14 p1759 A73-30315
- Stability of the thermomechanical hardening effect in 60N20 nickel steel
14 p1760 A73-30420
- Thermal expansion, Young's modulus, and magnetostriiction of a stainless iron-chromium-nickel alloy in the temperature range between 80 and 280 K
14 p1764 A73-30868
- Stacking fault energy in iron-nickel and iron-nickel-chromium alloys
14 p1764 A73-30869
- Strengthening of chromium-nickel steels with unstable austenite
15 p1889 A73-31809
- Nonisothermal creep of chrome-nickel steel
15 p1890 A73-31830
- High strength Ni-Cr-Mo steel plane-strain fracture toughness measured with circumferentially cracked-notched round bars, discussing heat treatment and test temperature effects
17 p2190 A73-34890
- Austenitic grain structure and strength changes associated with aging in 14Cr-14Ni type steels
18 p2325 A73-36810
- Influence of coherency strains on precipitate shape in a Fe-Ni-Ta alloy.
20 p2577 A73-39223
- Moisture effect on Ni steel fatigue crack propagation under low stresses
20 p2617 A73-39291
- Heat resistance of chromium-nickel and chromium-nickel-molybdenum steels with additions of boron
21 p2718 A73-40734
- Redistribution of nickel and chromium during the alpha to gamma transformation in Cr-Ni stainless steels.
21 p2720 A73-41039
- Mo and W alloying effects on low carbon chromium nickel steels intergranular corrosion resistance
21 p2721 A73-41041
- Fatigue crack propagation and fracture toughness of 5Ni and 9Ni steels at cryogenic temperatures.
22 p2875 A73-42143
- Gas metal arc welding of 9% Ni steel using ferritic filler metal.
22 p2866 A73-42226
- Microstructural features of Cr12NiWMoVTi/T600 steel after electroslag remelting
24 p3100 A73-45170
- Strengthening of Cr-Ni steels with unstable austenite.
24 p3100 A73-45272
- Investigation of the kinetics of the redistribution of alloying elements between the alpha solid solution and cementite in cobalt and nickel steels
24 p3100 A73-45362

NICKEL ZINC BATTERIES

- Sealed nickel zinc cells with nonsintered and supplementary oxygen recombination electrodes and layer structure inorganic separators
13 p1572 A73-29587

NIGHT

- Night search and rescue techniques over sea in poor visibility by helicopter, discussing automatic flight control systems, radar, plotting facility and pilot training
15 p1825 A73-31094
- An aid for the prediction of the nighttime minimum temperature
15 p1906 A73-32352
- Determination of the density of the surface covering of the moon from given surface temperatures during eclipse and lunar-night periods
16 p2063 A73-33754
- Helicopter night and bad weather navigation aids, examining ground-independent navigation, low flight, obstacle warning, terrain detectors, blind landing and optoelectric sensing
17 p2206 A73-34258
- Response of the polar electrojets in the evening sector to polar magnetic substorms.
22 p2902 A73-41916
- Absorption of whistler waves during night.
22 p2850 A73-42623
- Nighttime meridional neutral winds near 350 km at low to mid-latitudes.
24 p3087 A73-45209

NIGHT AIRGLOW

- U AIRGLOW
U NIGHT SKY
NIGHT E LAYER
U E REGION
U NIGHT SKY
NIGHT F LAYER
U F REGION
U NIGHT SKY

NIGHT SKY

- The IR emission spectrum of N₂ excited under auroral conditions. 01 p0036 A73-10337
- A nighttime ionospheric E-region model. 01 p0042 A73-10893
- Proton energy spectra from recent rocket measurements in the night and morning time auroral zone. 02 p0206 A73-12315
- A dual wavelength ground-based auroral scanner. 03 p0299 A73-12888
- Hawaii's Mauna Kea Observatory today. 03 p0287 A73-13549
- Instabilities resulting from gravity wave perturbation of ionization via neutral-charged particle collisions in nighttime E region 03 p0305 A73-14595
- Constant height sporadic E velocities and heights at night explained via instabilities generated from recombination and photoionization rate variations induced by gravity wave perturbations 03 p0305 A73-14596
- Tunable dye laser radar observation for Na layer nocturnal vertical distribution, suggesting meteor shower effect on layer content increase 04 p0444 A73-15543
- Geomagnetic storm effects in the nighttime E layer during increasing and maximal solar activities 05 p0568 A73-16215
- Observations of the He II 304-A radiation in the night sky. 07 p0869 A73-19232
- HF radio signal reception behavior near maximum usable frequency during evening and at midnight, noting SNR 07 p0792 A73-19456
- Ionospheric anomalies in the night mesosphere after geomagnetic storms. 07 p0817 A73-19543
- Night sky background radiation measurement by far IR radiometer carried on rocket launched from Hawaii 07 p0825 A73-20187
- Clusters of galaxies and the cosmic light. 08 p1002 A73-20876
- Nighttime ionospheric wave propagation curves in the broadcast band 08 p0939 A73-21286
- Nighttime midionosphere dynamical perturbations on ionizations from solutions of time dependent continuity equation with charge transport effects, considering semidiurnal atmospheric tide propagation mode 09 p1075 A73-22130
- Nighttime electron density in the E region at auroral latitudes in sunspot maximum. 09 p1078 A73-22747
- Measurement of the integral parameters of the nighttime ionosphere from observations of Intercompos-2 signals. 10 p1212 A73-24238
- Physics and chemistry of upper atmospheres. 11 p1425 A73-26209
- An infrared photometer for the balloon-borne telescope Thibse. 11 p1368 A73-26505
- High angular resolution photography of complex OH airglow structures in IR night sky 11 p1358 A73-26666
- Energetic electron precipitation as a source of ionization in the night-time D-region over the mid-latitude rocket range, South Uist. 11 p1358 A73-26701
- Total electron content measurements during visible auroras. 11 p1359 A73-26714
- Magnetic field signatures of substorms on high-latitude field lines in the nighttime magnetosphere. 12 p1488 A73-26981
- Influence of a variable ionospheric-protonospheric plasma flow on the nighttime F region of the ionosphere 12 p1490 A73-27336
- Analytical model of the unsteady nighttime F2 region of the ionosphere at mid-latitudes 12 p1490 A73-27337
- Averaged nighttime altitude profile of atmospheric emission at 6300 Å 12 p1491 A73-27345
- B system calculation of night airglow stellar component from cataloged photometric scales, obtaining night sky brightness 12 p1546 A73-27857
- Formation of optical discontinuities in the atmospheric inversion layer 15 p1903 A73-31424
- High speed photoelectric photometer for night sky scanning 15 p1878 A73-32137
- Extra-atmospheric observations of the luminosity of the sky from the Cosmos 51 and Cosmos 213 satellites. I - Method and calibration of the measurements 16 p2011 A73-32706

- Extra-atmospheric observations of the luminosity of the sky from the Cosmos 51 and Cosmos 213 satellites. II - Measurement data and their interpretation 16 p2001 A73-32707
- Satellite studies of magnetospheric substorms on August 15, 1968. VI - Ogo 5 energetic electron observations - Pitch angle distributions in the nighttime magnetosphere. 16 p2056 A73-33454
- Vertical distribution and temperature profile of the night time atmospheric sodium layer obtained by laser backscatter. 16 p2009 A73-33890
- Penetration and reflection of VLF waves through the ionosphere - Full wave calculations with ground effect. 16 p1984 A73-33921
- Night sky photographic evidence for natural retrograde earth satellites explanation for Vulcan type observations, considering group C orbit anomaly and terrestrial day length errors 16 p2071 A73-34000
- A rocket-borne instrument for the measurement of nighttime atmospheric densities. 17 p2164 A73-34270
- Magnetotail response to sudden changes in the interplanetary magnetic field. 17 p2158 A73-34509
- Propagation of VLF waves in the earth-ionosphere waveguide under nighttime ionospheres. 17 p2126 A73-35629
- Downward transport of nighttime Es layers into the lower E-region at Arecibo. 18 p2302 A73-35941
- Preliminary results obtained with astrophotometer installed on Lunokhod II. 18 p2315 A73-35992
- A rocket observation of the disturbed mid-latitude nighttime ionosphere. 18 p2308 A73-36048
- Mass spectrometric investigations of the night polar ionospheric structure. 18 p2310 A73-36145
- Distortions of the nightside ionosphere during magnetospheric substorms. 18 p2312 A73-36279
- Photographic parallax heights of infrared airglow structures. 18 p2313 A73-36510
- Propagation curves of an ionospheric wave at night for the broadcasting range. 19 p2404 A73-37915
- Photometric measurements of zenith night sky over Fritz Peak /CO/ for diurnal and seasonal variation of nightglow continuum 19 p2425 A73-38013
- Whistlers association with sudden changes in amplitude of long distance nighttime subionospheric VLF transmission 20 p2530 A73-38944
- B system calculation of night airglow stellar component from cataloged photometric scales, obtaining night sky brightness 20 p2608 A73-39231
- Maintenance of the F-region at night - Incoherent scatter measurements at a mid-latitude station. 21 p2683 A73-40776
- On the detection of X-rays from celestial sources through their ionization of the terrestrial atmosphere. 21 p2762 A73-41394
- Effects of interhemisphere transport on plasma temperatures at low latitudes. 22 p2844 A73-41919
- Characteristics of the redistribution of charged particles in the nighttime E region at mid-latitudes 22 p2847 A73-42331
- Postsunset oxygen emission observation by radiometer on rocket launched at Natal, Brazil, observing 10-km thick emission layer 22 p2848 A73-42536
- French monograph - Contribution to the ultraviolet spectrophotometry of the night sky /1900 to 3400 Å/. 22 p2850 A73-42742
- Effect of changing ionospheric-protonospheric plasma flow on the nighttime F-region of the ionosphere. 23 p2970 A73-43234
- Analytical model of the nocturnal nonstationary F2-region of the ionosphere at middle latitudes. 23 p2970 A73-43235
- Average nighttime vertical profile of the 6300 Å atmospheric emission. 23 p2970 A73-43242
- The nighttime distribution of ozone in the low-latitude mesosphere. 23 p2975 A73-43881
- Nighttime sporadic E layer measurements and integrated content measurements at Arecibo Observatory, using Barker coded incoherent scatter radar pulses 24 p3087 A73-45142

NIGHT VISION

- Psychophysical effects of night vision perceptual contrast in terms of central visual receptive field organization 03 p0261 A73-13759

- Reduced illumination effects on visual acuity, color vision, dark adaptation, accommodation, visual fields and glare 05 p0540 A73-16480
- Perceptual considerations for a wide field of view, helicopter night landing system /HENILAS/. 05 p0543 A73-16705
- Miniaturized second generation night vision image intensifier system operation and performance based on secondary photoelectron emission 06 p0694 A73-18300
- Pulsed GaAs illuminators for night-vision systems. 10 p1216 A73-23785
- Design considerations for night-vision system optics. 16 p2012 A73-32865
- Touchdown performance with a computer graphics night visual attachment. 21 p2673 A73-40874
- Technical and economic problems in use of military passive night vision systems including image intensifiers, IR detectors and thermographic imaging devices 23 p2979 A73-43219
- Design and performance of light-intensification night vision telescopes 23 p2979 A73-43220
- Performances and physical limitations of image intensifiers 23 p2979 A73-43221
- Microchannel image intensifiers for detection at low light levels 23 p2979 A73-43222

NIGHTGLOW

- 6300 Å night airglow emission over the magnetic equator. 01 p0036 A73-10344
- Research of the emission at 5577 Å in the period of 1958-1967 in Ashkhabad. 01 p0036 A73-10345
- Excitation of the Herzberg bands of O₂ in laboratory afterglow and night airglow. 02 p0156 A73-11743
- Correcting the OH contribution in emission line measurements in the night airglow filter photometry. 04 p0440 A73-14969
- Nighttime atmosphere emission of atomic oxygen /5577 Å/ and its connection with penetrating micrometeorites 07 p0818 A73-19592
- 6300 Å night airglow enhancements in low latitudes. 07 p0818 A73-20051
- An application of the Michelson interferometer to nonthermalized spectral features in the night airglow. 08 p0963 A73-20870
- Excitation of oxygen permitted line emissions in the tropical nightglow. 10 p1214 A73-24739
- Rotational and vibrational hydroxyl excitation in the laboratory and in the night airglow. 11 p1354 A73-25761
- Seasonal and diurnal variations of forbidden oxygen and sodium lines emission, stressing nightglow zenith intensity fluctuations connection to F layer electric fields 12 p1489 A73-26992
- Diurnal variation of nightglow Na emission, noting linear intensity variation with time, oscillatory and anticovariation characteristics 13 p1610 A73-29337
- Diurnal variations of H-alpha nightglow emission intensity 15 p1867 A73-31261
- Predawn enhancement of 6300 Å forbidden OI nightglow emission from observations at Abastumani 15 p1867 A73-31263
- Investigation of the hydrogen in the upper atmosphere and geocorona from observations of the H-alpha emission line in the nightglow spectrum /Survey/ 15 p1867 A73-31267
- Diurnal, annual and solar cycle variations of hydroxyl and sodium nightglow intensities in the Europe-Africa sector. 17 p2160 A73-34785
- Photometric measurements of zenith night sky over Fritz Peak /CO/ for diurnal and seasonal variation of nightglow continuum 19 p2425 A73-38013
- Geocorona originated low intensity nighttime H alpha and H beta emission components from high resolution observation, considering Balmer line producing mechanism 20 p2555 A73-39433
- An atlas of low-latitude 6300-Å forbidden O I night airglow from Ogo 4 observations. 22 p2845 A73-41924
- Ozone and airglow in the mesosphere region. 23 p2976 A73-43886
- Extinction coefficient /point source light loss due to atmospheric scattering/ significance in reduction of night airglow data 24 p3082 A73-44734
- Atomic oxygen densities in the lower thermosphere as derived from in situ 5577-Å night airglow and mass spectrometer measurements. 24 p3086 A73-45122

NIMBUS SATELLITES

NIMBUS SATELLITES

NT NIMBUS 3 SATELLITE
NT NIMBUS 4 SATELLITE
NT NIMBUS 5 SATELLITE
Environmental data transmission from arctic data buoys via polar orbiting satellite.

04 p0421 A73-15431
The growth of remote sensing through the Nimbus and ERTS spacecraft.

19 p2430 A73-37712
Low cost modular power systems for multi mission earth observations.

19 p2494 A73-38435

NIMBUS 3 SATELLITE

The SNAP-19 radioisotopic thermoelectric generator experiment - Flight performance on the Nimbus III observatory.

11 p1396 A73-26037

Application of temperature soundings by the Nimbus 3 satellite to the analysis of the hemispheric-scale stratospheric environment

17 p2206 A73-34937

Satellite radiances and clear air turbulence probabilities.

19 p2448 A73-38218

NIMBUS 4 SATELLITE

Four dimensional forecast assimilation of temperature data from Nimbus 4 SIRS radiance measurements, using two level model with geostrophic wind adjustment

15 p1902 A73-31314

Satellite radiances and clear air turbulence probabilities.

19 p2448 A73-38218

The Nimbus-4 backscatter ultraviolet (BUV) atmospheric ozone experiment 2 years' operation.

23 p2975 A73-43877

Variations in the stratospheric ozone field inferred from Nimbus satellite observations.

23 p2975 A73-43878

NIMBUS 5 SATELLITE

ATS-F and Nimbus-E satellites use for range and range rate determination, earth gravity anomaly detection and orbital position determination

13 p1656 A73-28391

The design, construction and calibration of an infrared temperature profile radiometer (ITPR) for Nimbus E.

17 p2238 A73-34602

Vertical temperature profiles from satellites - Results from second generation instruments aboard Nimbus-5.

18 p2307 A73-36029

Remote sounding of atmospheric temperature from satellites. IV - The selective chopper radiometer for Nimbus 5.

21 p2706 A73-41601

NIMONIC ALLOYS

Creep life and strain estimation for Nimonic alloy by monitoring cavity density under optical microscope

03 p0326 A73-13965

High temperature strength and microstructure of nickel-base heat resisting No. 64BC alloy.

04 p0465 A73-15583

Investigation of the temperature dependence of hardening characteristics in an aging nimonic alloy

06 p0707 A73-17908

The influence of scatter on some simple variable-stress creep predictions.

08 p1016 A73-20798

Some fatigue properties of welded high temperature alloys.

08 p0978 A73-21241

Irradiation creep in some austenitic stainless steels, nimonic PE16 alloy and nickel.

08 p0982 A73-21794

Nimonic and Mg alloys creep behavior interpretation by constitutive law, discussing recovery activation and strain hardening from microstructural behavior

13 p1642 A73-29515

Grain-boundary sliding and recrystallization of Nimonic 108 during creep.

15 p1887 A73-31352

Interpretation of tensile and compressive creep behaviour of two nickel alloys.

15 p1888 A73-31618

NIMPE (ENGINE)

U HYDRAZINE ENGINES

NIOBATES

NT LITHIUM NIOBATES

Fracture of nonlinear crystals /KDP and LiNbO3/ by radiation from a ruby laser.

02 p0176 A73-12112

Effect of surface states on surface-wave amplification in a composite structure of CdSe film on LiNbO3.

05 p0559 A73-17073

Phenomenological theory of antiferroelectricity and ferroelectricity applied to NaNbO3 and the system KNbO3-NaNbO3.

06 p0737 A73-18354

Conductivity and solubility measurements and potentiometry for composition of yttrium nitrate-potassium metaniobate/potassium niobate-water system

09 p1134 A73-22979

An X-ray diffraction and DTA study of the ferroelectric transition in barium sodium niobate.

15 p1924 A73-31839

Single crystals for optical applications - Problem of index homogeneity of double niobates Ba_x/Sr_{1-x}/Nb₂O₆ and Ba₂Nb₅O₁₅.

16 p2043 A73-32862

Resistance anomaly in semiconductor barium and strontium niobates

17 p2219 A73-35554

Biaxial potassium niobate single crystal nonlinear optical coefficients determination by Marker fringe pattern method, using CW Nd doped yttrium-aluminum garnet laser

23 p3018 A73-44369

NIOBIUM

Diffusive boronizing of molybdenum and niobium in boron carbide powder

02 p0178 A73-11544

Behavior of dislocations in niobium under stress.

02 p0179 A73-11576

Tensile strength dependence on temperature and interstitial oxygen and nitrogen concentration in powdered Nb, noting microhardness and yield point

03 p0326 A73-13968

Dislocation dynamics in niobium-oxygen solid solutions.

04 p0462 A73-15303

Plastic anisotropy of low-carbon, low-manganese steels containing niobium.

04 p0463 A73-15309

Electron beam float zone melting and vacuum degassing of niobium single crystals

04 p0456 A73-15762

Anomalous slip in high-purity niobium single crystals deformed at 77 K in tension.

04 p0467 A73-15931

Wave attenuation in superconducting elliptical waveguides

07 p0793 A73-19924

Body centered cubic transition metal stage 3 electrical resistivity recovery mechanism from experiment on recrystallized and stress-relieved plastically deformed Nb wire

07 p0839 A73-20112

Some further comments on Stage III recovery in Group VA body-centered cubic transition metals.

07 p0839 A73-20113

The oxidation of tantalum and niobium in the temperature range 400-600 C.

08 p0978 A73-21416

The temperature dependence of steady state creep in 20% Cr, 25% Ni, Nb stabilized stainless steel.

08 p0981 A73-21785

The effect of niobium content on the steady-state creep of stabilized 20/25 austenitic stainless steels.

08 p0981 A73-21786

The effect of creep strain on stacking-fault precipitation in Nb-stabilized 20/25 austenitic stainless steels.

08 p0981 A73-21787

Ni diffusion in Nb at 988 to 1246 C, using residual activity technique with Ni-63 as tracer

09 p1103 A73-22436

Niobium and tungsten cementation in a glow-discharge plasma

09 p1089 A73-23197

Effect of hafnium dioxide on grain growth and strength characteristics in niobium

09 p1108 A73-23233

Electron beam refined niobium melting temperature determination from black body brightness change

10 p1230 A73-23508

Nb nitriding kinetics and external effects observations, noting nitrogen diffusion through crystal lattices

10 p1236 A73-24955

Compatibility between material components in metal-ceramics composites

11 p1387 A73-25412

Kinetics of the degassing of oxygen-containing niobium in flowing acetylene to form carbon monoxide

11 p1375 A73-26565

Niobium mechanical twin formation and propagation, discussing continuous nucleation, matrix interface and dislocation core energies

13 p1632 A73-28132

Influence of niobium on the magnetic properties of high-titanium Al-Ni-Co alloys - Second communication.

13 p1637 A73-29244

Relaxation spectra of niobium irradiated at low temperature.

13 p1638 A73-29455

Production of a niobium-stainless steel bimetal by explosion welding

14 p1755 A73-30386

The low-temperature embrittlement of niobium and vanadium by both dissolved and precipitated hydrogen.

14 p1761 A73-30630

Influence of heating to high temperatures in vacuum on the electrophysical properties of niobium single crystals

14 p1763 A73-30722

Properties of low-alloy steels with small niobium additions

15 p1889 A73-31811

Enhanced strain aging of niobium by cyclic deformation.

15 p1890 A73-31990

Twin-jet thinning techniques for transmission electron microscopy observation of tantalum and niobium.

15 p1891 A73-31995

The kinetics of the dissolution of oxygen in niobium at low oxygen pressures and high temperatures

16 p2026 A73-33955

Thermal conductivity and temperature dependence of energy gaps in niobium samples containing large amounts of impurity atoms

16 p2027 A73-34061

Electron beam refined niobium melting temperature determination from black body brightness change

17 p1291 A73-35188

Anelastic studies of hydrogen diffusion in niobium.

17 p1293 A73-35622

Thermodynamics of b.c.c. solid solutions of hydrogen in niobium, vanadium and tantalum.

17 p1293 A73-35623

Influence of interstitials on the behavior in tension of niobium between 20 and 1000 C

17 p1293 A73-35624

Mechanical properties of weld, base metal and coated columbium FS85.

17 p1282 A73-35842

Internal low-frequency friction in niobium in a normal and superconducting state

18 p2323 A73-36676

Internal friction in niobium quenched from premelting temperatures

18 p2324 A73-36772

Ultrahigh-speed quenching of niobium and vanadium

19 p2439 A73-37250

Influence of small oxygen and nitrogen additions on the nature of the temperature dependence of the mechanical properties of niobium

20 p2577 A73-39360

Superconductivity and electronic structure of ultrahigh-purity niobium. I - Synthesis of ultrahigh-purity niobium

20 p2600 A73-39732

Faulty structure in niobium single crystals deformed by rolling at 77 K

20 p2579 A73-39743

Superconductivity of films made from aluminum oxide and niobium mixtures

20 p2579 A73-39744

Chromatographic separation of niobium from titanium, tungsten, molybdenum, and vanadium on the fluoroform of the AV-16 anion exchanger

20 p2520 A73-39820

Nb electrical resistance change under elastic distortion due to lattice distortions and dimensional change

21 p2717 A73-40323

Russian book - Spectrophotometry of niobium and tantalum.

21 p2648 A73-40803

Oxygen interaction with tantalum and niobium at high temperatures

21 p2722 A73-41594

Anomalous behaviour during interdiffusion in the system Nb-Mo.

22 p2876 A73-42340

The activation energy for creep of columbium/niobium.

22 p2879 A73-42580

Dislocation locking by interstitial oxygen atoms and the temperature dependence of the yield point in niobium

24 p3099 A73-44574

Properties of low-alloy steels with small niobium additions.

24 p3100 A73-45274

Fatigue hardening in niobium single crystals.

24 p3101 A73-45474

Recrystallization and precipitation induced by high temperature deformation - Case of a weldable construction steel containing niobium

24 p3101 A73-45524

NIOBIUM ALLOYS

A sintered Nb-Ti-Zr alloy.

01 p0065 A73-10822

Investigation of the tunnel characteristics of deposited superconducting Nb₃Sn films

01 p0089 A73-11290

Singularities of the temperature dependences of the heat conduction coefficients of solid solutions of the niobium-zirconium system.

01 p0066 A73-11338

Cast Nb alloys ductility enhancement by heat treatment, discussing solid solution decay kinetics and carbides composition of Nb-Mo-Zr-C system

01 p0066 A73-11344

Ti-V and Ti-Nb alloys mechanical strength and stress concentration resistance at low temperatures

01 p0067 A73-11348

Influence of the thickness of a copper coating on the critical current of a superconducting wire made from niobium-based alloys

01 p0089 A73-11435

The thermally activated deformation of niobium-molybdenum and niobium-rhenium alloy single crystals.

02 p0179 A73-11574

Superconducting-normal phase boundary as function of applied magnetic field and transition temperature in Nb-Ga alloys

02 p0200 A73-11840

Change in critical current of superconducting NbTi by neutron irradiation.

02 p0200 A73-11842

AC studies of a superconducting Nb-52 at. % Ti alloy.

02 p0200 A73-11844

Materials properties data tables on composition, preparation, temperature and field strength parameters of superconducting compounds in Ni alloys

02 p0201 A73-11878

Cooling modes effect on heat treated Ti-Nb alloys as function of Nb content, investigating alpha prime and double prime martensites

02 p0181 A73-12500

Direct observation of the magnetic microstructure in niobium-based superconducting alloys subject to deformation

02 p0201 A73-12554

Microstructural, mechanical and thermal properties of Nb-W-Ti-Zr alloys, noting cold rolled sheet products

02 p0182 A73-12580

Hydrogen self-diffusion in the niobium-zirconium-hydrogen system

03 p0327 A73-13973

Mo addition effect on high temperature creep resistance and diffusion activation energy of Nb alloys tested in torsion and tension at 1100-1500 C in vacuum

03 p0328 A73-14018

Influence of the pinning forces for flux lines on the critical current density in magnetic fields of up to 10 Tesla in superconducting titanium-niobium alloys

03 p0328 A73-14654

Solubility of zirconium and niobium in solid-state copper

04 p0464 A73-15495

Characteristics of the ingot crystallization process under conditions of melting in vacuum furnaces with a consumable electrode, and the stability of the cast structure in alloys of the Nb-Ti system

04 p0464 A73-15496

Weldability, corrosion resistance and heat resistance increase in Nb alloyed steels, noting aging temperature effects and microstructure

06 p0706 A73-17886

Heat resistance of alloys of the compound TiAl with niobium at 800 and 1000 C

06 p0708 A73-18049

Field-ion microscopic investigation of the microstructure of deformable superconducting niobium-based alloys

06 p0736 A73-18115

Mechanical properties of heat and corrosion resistant nonmagnetic Ni-Cr-Nr spring alloys with W addition tested in aggressive and nitric acid base media

06 p0709 A73-18211

Investigation of the corrosion-erosion resistance of niobium alloys

06 p0711 A73-18668

Mechanical properties of interstitial alloys of niobium.

07 p0838 A73-19123

Influence of nickel on the superconductivity parameters of Nb3Al + Ni

09 p1098 A73-21845

Effect of heat treatment on the structure and properties of NV10M5T3Ts alloy

09 p1106 A73-23190

Phase composition of Nb-1% Zr-C and Nb-2% Hf-C alloys

09 p1108 A73-23237

Influence of heat treatment on the high-temperature strength and creep of the NV10M5T3Ts niobium alloy

10 p1230 A73-23600

Metallurgical investigations of phase equilibria in the titanium-niobium-germanium ternary system

10 p1231 A73-23692

Direct observation of magnetic microstructure in deformed niobium-based superconducting alloys.

10 p1259 A73-24186

Nb refractory alloy sheet mechanical properties for application in space shuttle thermal protection system /TPS/ and space tug aerobraking system

10 p1235 A73-24445

Evaluation of columbium alloy thermal protection systems for space shuttle.

[AIAA PAPER 73-378]

11 p1380 A73-25508

Critical current value for a superconducting niobium-alloy wire as a function of its copper coating thickness.

11 p1409 A73-26062

Mechanical properties of weld, base metal and coated columbium alloy Cb 752.

11 p1375 A73-26356

Phase diagrams, microstructure and superconducting properties of thermally diffused Nb-Sn system

12 p1508 A73-26835

Investigation with an electron microscope of the structure of wires prepared from the 60T superconducting alloy

12 p1509 A73-26841

Mo-Nb-Ta alloys phase and composition-hardness diagrams for 20-1100 C, establishing mutual solubility of system components

12 p1510 A73-26905

Precipitation processes in Nb microalloyed converter steel

12 p1514 A73-27685

Investigation of the ferroniobium oxidation process

13 p1630 A73-28010

A high-temperature thermodynamic investigation of the Nb-Mo system.

13 p1633 A73-28140

Properties and structure of Ti-Nb-base superconducting alloys

13 p1643 A73-29644

Nb-Al alloys sigma phase superconductivity characteristics, investigating critical temperature, composition and heat treatment relations

14 p1759 A73-30236

Solid solution strengthening of high purity niobium alloys.

14 p1761 A73-30631

German monograph - The effect of germanium additions on the superconductor characteristics and the transition processes in technical titanium-niobium alloys.

14 p1762 A73-30666

Superconductivity and electron structures of a solid solution of titanium in niobium

14 p1784 A73-30811

Phase diagram of the niobium-gallium system

15 p1922 A73-31182

Specific heat of alloys of the niobium-titanium system near the superconducting transition temperature

15 p1886 A73-31184

Influence of heat treatment on the critical currents in binary alloys of niobium with zirconium and titanium

15 p1887 A73-31185

Investigation of some physicomachanical and X-ray structural changes in a superconducting wire prepared from 60T alloy, as a function of the strain level and duration of annealing in vacuum

15 p1887 A73-31187

Properties of the superconducting alloy 35BT

15 p1887 A73-31188

Changes in the superconducting transition temperature of alloys of variable composition, as exemplified by the niobium-tantalum system

15 p1887 A73-31189

Temperature effects in quadrupole interaction in NbHf alloys

15 p1923 A73-31710

Study of a niobium-aluminum-silicon system. I - Partial isothermal sections at 1500 and 1300 deg C, and the behavior of the Nb/Si, Al/2 phase

15 p1890 A73-31991

Study of a niobium-aluminum-silicon system. II - Analysis of ternary niobium-aluminum-silicon alloys by atom absorption spectrophotometry

15 p1890 A73-31992

Investigation of the phase equilibrium of ternary Ti-Al-Nb system alloys

15 p1893 A73-32514

Properties of titanium-niobium based stable beta alloys

15 p1894 A73-32534

Eutectic superalloys strengthened by aligned delta, Ni3Cb lamellae, gamma-prime, Ni3Al precipitates and reduced interlamellar spacing.

16 p2026 A73-33425

Niobium-gold alloys crystal structure, phase diagrams, peritectic crystallization and microhardness, noting intermetallics formation by solid state reactions

16 p2026 A73-33957

Temperature dependent crystallization and density of Fe-Mn-C alloys with niobium at 1200-1500 C from gamma ray measurements

16 p2027 A73-34012

Simultaneous measurement of specific heat, electrical resistivity, and hemispherical total emittance of niobium-1 wt. % zirconium alloy in the range 1500 to 2700 K by a transient /subsecond/ technique.

17 p2187 A73-34499

Effects of cold deformation and heat treatment on the elastic properties of niobium

17 p2188 A73-34562

Prediction of the heat-resistance characteristics of high melting materials

18 p2323 A73-36757

Superconducting properties of alloys of the vanadium-niobium-chromium system

18 p2325 A73-36898

An arrangement for carrying out metal creep and stress-rupture strength tests under high vacuum conditions

20 p2545 A73-39384

The effect of vanadium, niobium, and tantalum on the electrical resistance of nickel

20 p2578 A73-39396

Effect of zirconium concentration on creep of niobium-zirconium alloys

20 p2579 A73-39739

Preparation of zirconium-niobium alloy by carbide-oxide reaction.

21 p2717 A73-40321

A study of the heat resistance of Nb-Mo alloys containing titanium and zirconium

21 p2718 A73-40489

Properties and structure of superconducting Ti-Nb alloys.

21 p2720 A73-41037

Electrical conductivity and superconductivity of vanadium, niobium, and chromium solid solutions

22 p2873 A73-41963

Anomalous concentration dependence of thermal expansion coefficients of tungsten-rhenium and tungsten-niobium alloys.

22 p2878 A73-42509

Porous and dense layers in Nb-Ti-O system analyzed by X-ray spectroscopy, finding element content influence

23 p2990 A73-43481

Investigation of tunnel characteristics of sputtered superconducting Nb3Sn films.

23 p3015 A73-43511

Concentration curves and phase diagram plotted for Nb-Zr system diffusion layers during annealing at 700 to 1700 C

23 p2991 A73-43649

Superconductivity of copper containing small amounts of niobium.

23 p3017 A73-44033

Investigation of the elastic stiffness of niobium low-alloys subjected to small plastic strains

24 p3099 A73-44572

NIOBIUM CARBIDES

L-beta /2/ and K-alpha X ray spectra of niobium and carbon in NbC compound, assuming collectivized valence electrons

02 p0180 A73-12174

Flat dendritic carbide effects on crack formation in Ti and Nb stabilized austenitic Cr-Ni corrosion resistant steels after heating to 1250 C

06 p0705 A73-17850

The temperature dependence of steady state creep in 20% Cr, 25% Ni, Nb stabilized stainless steel.

08 p0981 A73-21785

Low stress creep tests of niobium stabilized austenitic steels.

08 p0981 A73-21789

The effect of niobium carbide on the creep rupture properties of austenitic stainless steels.

08 p0981 A73-21790

Thermal diffusivity and thermal conductivity of pyrolytic titanium and niobium carbides and of titanium nitride at high temperatures

11 p1380 A73-25740

Investigation of the enthalpy and heat capacity of niobium carbide based materials at high temperatures

12 p1513 A73-27310

Effects of small amounts of carbide-forming elements on the elevated temperature strength of austenitic stainless steel.

13 p1642 A73-29517

Titanium carbide nitride and zirconium niobium carbide solid solutions electromotive forces, examining temperature-concentration dependencies, carbide and carbonitride conductivity mechanisms, resistivity and Hall effect

18 p2325 A73-36964

Effect of porosity on creep in niobium carbide and other powder materials under uniaxial loads

20 p2578 A73-39381

NIOBIUM COMPOUNDS

NT NIOBATES

NT NIOBIUM CARBIDES

NT NIOBIUM OXIDES

NT NIOBIUM STANNIDES

Materials properties data tables on composition, preparation, temperature and field strength parameters of superconducting compounds in Ni alloys

02 p0201 A73-11878

Electron microprobe chemical analysis and structural formula of niobium rutile in Apollo 14 microbreccia sample KREEP fragment

09 p1139 A73-21856

Crystalline structure of the TaCoB and NbCoB2 compounds

12 p1512 A73-27244

Investigation of the oxygen content in superconducting vanadium- and niobium-base compounds

15 p1922 A73-31181

NIOBIUM OXIDES

On the electrical properties of nonstoichiometric oxides alpha-Nb2O5, MnO, and CoO at high temperature

13 p1634 A73-28202

NiO-CoO solid solutions defect structure from high temperature measurements of integrated Bragg peak intensities

13 p1645 A73-28934

NIOBIUM STANNIDES

The use of nitride intermediates in the preparation of metals - A study of the reduction of Nb₂O₅ with NH₃.

14 p1761 A73-30629

Nitrides and oxides formed on a niobium surface at high temperatures in vacuum

15 p1887 A73-31203

NIOBIUM STANNIDES

Twisted, multifilament Nb₃Sn superconductive ribbon.

01 p0087 A73-10245

Effect of hydrostatic extrusion on the composition and properties of Nb₃Sn compounds.

06 p0736 A73-18213

Electron microscopy study of Nb₃Sn strips

10 p1259 A73-23674

NITINOL ALLOYS

Plastic deformation, martensite transformation and temperature effects on shape memory of nitinol and other alloys

12 p1509 A73-26896

Plastic deformation, martensite transformation and temperature effects on shape memory of nitinol and other alloys

21 p2720 A73-41029

NITRATES

NT AMMONIUM NITRATES

NT CELLULOSE NITRATE

NT NITROGLYCERIN

NT POTASSIUM NITRATES

The occurrence of nitrate on the early earth and its role in the evolution of the prokaryotes.

11 p1320 A73-26490

Effect of nitrite and nitrate on chlorophyll fluorescence in green algae.

16 p1973 A73-33226

Low temperature specific heat of neodymium magnesium nitrate.

18 p2341 A73-36977

NITRATION

An anomalous reaction of aceto-4-/or 6-/ nitro-2,5-ylidides with hydrochloric acid.

03 p0273 A73-13900

NITRIC ACID

Ignition of nonhypergolic rocket fuels with fuming nitric acid under suitable conditions.

01 p0089 A73-10736

Distribution of nitric acid vapor in the stratosphere as determined from infrared atmospheric emission data.

02 p0189 A73-12786

Corrosion tests for rocket propulsion system components materials for use with nitric acid-nitrogen tetroxide blend oxidizer

03 p0329 A73-13007

Red fuming nitric acid suitability for nonhypergolic rocket fuel ignition in presence of chromate and dichromate catalysts

07 p0865 A73-19986

Ignition of nonhypergolic bipropellants in presence of suitable catalysts.

14 p1784 A73-30044

NITRIC OXIDE

The production of nitric oxide in ammonia oxidation flames.

01 p0121 A73-10640

Analysis of NO formation in single droplet combustion.

01 p0014 A73-10645

Global nitric oxide and gamma emission measurements with Ebert-Fastie scanning spectrometer on-board polar orbiting OGO 4 satellite

01 p0040 A73-10878

Mesospheric nitric oxide concentrations during a PCA.

01 p0041 A73-10881

Estimation of nitric oxide concentration in the lower E region from rocket and satellite measurements of electron densities and X-ray fluxes.

01 p0041 A73-10882

Nuclear explosions released nitric oxide effect on atmospheric ozone concentration compared with potential effect from SST flights

01 p0043 A73-11068

E and F regions ion composition measurement with rockets, noting nitric oxide variation with molecular/atomic oxygen cations ratios at different solar activity phases

02 p0206 A73-12305

Nitric oxide detection by use of Zeeman-effect and CO laser.

03 p0318 A73-12871

Radial concentration profiles of NO and combustion products formation in laminar diffusion flames, using vertical coaxial burner and quartz microprobe

06 p0740 A73-17730

Investigation of NO formation kinetics in combustion processes - The methane-oxygen-nitrogen reaction.

06 p0767 A73-17731

Measurement of nitric oxide formation within a multifueled turbine combustor.

06 p0740 A73-17734

Pressure broadening of magnetically-tuned infrared absorption spectrum of NO using a CO laser.

07 p0833 A73-19145

Reaction kinetics of nitric oxide positive ion with ozone yielding nitrogen dioxide positive ion and oxygen, noting impact on ionospheric chemistry

07 p0787 A73-19258

The role of mixing in burner-generated carbon monoxide and nitric oxide.

07 p0919 A73-19392

Laser-excited vibrational energy transfer studies of HF, CO, and NO.

07 p0834 A73-19627

Nitric oxide densities during sunrise derived from overhead emission measurement as function of altitude

09 p1074 A73-22065

Nitric oxide formation and radical overshoot in premixed hydrogen flames.

10 p1294 A73-23558

Amplified laser absorption - Detection of nitric oxide.

12 p1505 A73-27121

Atmosphere Explorer satellite-borne two channel fixed grating Ebert spectrometer for measurement of airglow at 21.50 Å, yielding altitude profiles of nitric oxide density

13 p1689 A73-28640

Nitric oxide formation in gas turbine combustors.

13 p1670 A73-28805

Reactions of HO₂ with carbon monoxide and nitric oxide and of O(1D) with water.

14 p1723 A73-30069

Amplified laser absorption - Detection of nitric oxide.

15 p1885 A73-31844

Sampling nitric oxide from combustion gases.

16 p2085 A73-33348

Concentration of OH and NO in YJ93-GE-3 engine exhausts measured in situ by narrow-line UV absorption.

16 p2045 A73-33546

Subsonic jet aircraft contribution to NO_x in the stratospheric ozone layer - 1968 to 1990.

16 p2046 A73-33566

The production of nitric oxide in the stratosphere by oxidation of nitrous oxide.

16 p2008 A73-33885

Parameters controlling nitric oxide emissions from gas turbine combustors.

17 p2221 A73-34474

Nitric oxide detection in stratosphere from characteristic absorption line spectrum via airborne IR spectrometer, obtaining molecular concentration [ONERA, TP NO. 1256]

17 p2159 A73-34552

Atmospheric attenuation effects on nitric oxide dissociation in mesosphere and stratosphere, noting dissociation profile dependence on absorption of discrete oxygen Schumann-Runge bands

17 p2119 A73-34778

Nitric oxide emissions from tube combustor burning premixed gaseous propane-air mixture, considering inlet conditions for equivalence ratios

17 p2222 A73-35468

Observation of stratospheric nitric oxide by infrared absorption spectrometry from a balloon

19 p2423 A73-37533

Real time nitrogen dioxide and nitric oxide pollution measurement by molecular fluorescence induced by argon laser beam

21 p2671 A73-40135

Lower thermospheric atomic oxygen profile from 18 May 1971 nitric oxide release and mass spectroscopic observation, noting monotonic density increase to 0.8 trillion/cc

21 p2688 A73-41345

Satellite ultraviolet measurements of nitric oxide fluorescence with a diffusive transport model.

22 p2845 A73-41925

Ozone composition and nitric oxide injection upper and lower limits for stratosphere by nuclear bomb tests, comparing to estimated SST contribution

22 p2848 A73-42534

Shock tube kinetics of NO decomposition in mixtures with Ar, measuring ground state atomic oxygen formation rate by resonance absorption spectrophotometry

22 p2818 A73-42766

Air afterglow radiative recombination reaction of NO with O yielding nitrogen dioxide, considering pressure dependence in chemiluminescence spectral region

22 p2819 A73-42772

Nitric oxide formation kinetics in combustion processes, discussing formation from nitrogen-containing compounds

22 p2819 A73-42791

Kinetics of nitric oxide formation in premixed laminar flames.

22 p2820 A73-42792

Formation of nitric oxide in fuel-lean and fuel-rich flames.

22 p2820 A73-42794

The effects of imperfect fuel-air mixing in a burner on NO formation from nitrogen in the air and the fuel.

22 p2820 A73-42795

Effects of turbulent mixing and chemical kinetics on nitric oxide production in a jet-stirred reactor.

22 p2820 A73-42796

Nitric oxide formation weightless in diffusion flame ethanol drop combustion as function of air temperature and diffusion and spray characteristics

22 p2935 A73-42797

Nitric oxide generation in turbulent diffusion flames, discussing limits for constant pressure turbulent reacting mixing zone between parallel flowing streams of fuel and oxidizer

22 p2935 A73-42798

On the behavior of nitrogen oxides in the stratosphere.

23 p2976 A73-43896

IR absorption spectrometry to determine vertical distribution of nitric oxide abundance in stratosphere

23 p2978 A73-43959

NITRIDES

NT ALUMINUM NITRIDES

NT BORON NITRIDES

NT SILICON NITRIDES

NT TANTALUM NITRIDES

NT TITANIUM NITRIDES

NT ZIRCONIUM NITRIDES

Synthesis and fabrication of high purity hafnium nitride and hafnium carbide.

04 p0455 A73-15752

Alloy composition and temperature effects on nitrogen solubility in austenitic Cr-Ni steels, noting nitride precipitation effect on impact strength reduction

07 p0839 A73-19950

Low-field tunnelling current in thin-oxide M.N.O.S. memory transistors.

08 p0946 A73-21115

Phase equilibria in V-N-Sc/Y, Ce, Pr alloys

09 p1108 A73-23238

Obtaining of carbide and nitride dispersions in iron

13 p1633 A73-28182

Nitrides and oxides formed on a niobium surface at high temperatures in vacuum

15 p1887 A73-31203

Titanium hydride and hydronitride thermal stability analysis from hydrogen vapor pressure and decomposition measurements in vacuum at 400-1100 C

15 p1888 A73-31601

Investigations regarding structure, preparation, and hardness properties in the system Ta-Hf-C-N

22 p2873 A73-41949

Influence of Co, Ni, Mo, and W on the solubility of Fe₁₆N₂ in alpha-iron.

23 p2994 A73-44156

NITRIDING

Certain characteristics of the initial phase of the nitriding process

01 p0055 A73-10255

Nitrided layer effects on austenitic steels mechanical properties at low temperatures, noting improved tensile strength

01 p0067 A73-11347

Oxidation and nitriding of Cr-W alloy.

03 p0325 A73-13803

Nitriding by ion bombardment of 18-10 stainless steels

04 p0457 A73-15954

Study of nitriding by ion bombardment of titanium and titanium alloys

04 p0457 A73-15955

Cr effect on N solubility increase during Fe alloy nitriding, noting temperature effect on nitrides precipitation

06 p0697 A73-18054

Kinetics of transformation of carbon- and nitrogen-enriched austenite by carbonitriding in the gas phase

09 p1105 A73-23038

Study of the wear resistance of nitrided electrolytic chromium coatings on certain alloy steels

10 p1223 A73-24065

Nb nitriding kinetics and external effects observations, noting nitrogen diffusion through crystal lattices

10 p1236 A73-24955

Alloy steels supercooled austenite nitriding in ammonia flow, examining diffusion layers by X ray analysis and hardness tests

10 p1236 A73-24956

The use of nitride intermediates in the preparation of metals - A study of the reduction of Nb₂O₅ with NH₃.

14 p1761 A73-30629

Molybdenum-rhenium alloy microstructure changes due to nitriding in ammonia vapors from metallographic and X ray structural analysis

15 p1887 A73-31206

Optimal thick layer nitriding of Ti alloys, discussing boundary conditions, film, hydrogen effect and mechanical properties

21 p2707 A73-40739

NITRILES

NT ACRYLONITRILES

- Protobiochemical developments in terms of extraterrestrial life search and roles of nitriles and urea in prebiological chemical evolution
03 p0265 A73-14319
- NITRITES**
Methyl nitrite photolysis reaction products under various ambient gas mixture environments, noting irradiation time and gas pressure effects
10 p1186 A73-24656
Effect of nitrite and nitrate on chlorophyll fluorescence in green algae.
16 p1973 A73-33226
- NITRO COMPOUNDS**
NT NITROGLYCERIN
NT TRINITROTOLUENE
An anomalous reaction of aceto-4/-or 6/-nitro-2,5-xylidides with hydrochloric acid.
03 p0273 A73-13900
- NITROAMINES**
An intumescent coating for improved fuel fire protection of heat sensitive articles.
02 p0185 A73-12642
Study of the dependence of the properties of radicals on the characteristics of the initial hydrazine structure
17 p2220 A73-34638
Comparative study of the combustion of 6-, 5-, 4-, and 3-amines of nitrate of cobalt/III/
21 p2647 A73-40703
- NITROBACTER**
The occurrence of nitrate on the early earth and its role in the evolution of the prokaryotes.
11 p1320 A73-26490
- NITROBENZENES**
NT TRINITROTOLUENE
NITROCELLULOSE
U CELLULOSE NITRATE
NITROGEN
NT LIQUID NITROGEN
NT NITROGEN ATOMS
NT NITROGEN IONS
NT NITROGEN ISOTOPES
NT SOLID NITROGEN
The IR emission spectrum of N₂ excited under auroral conditions.
01 p0036 A73-10337
The infrared spectrum of nitrogen excited by fast electrons.
01 p0036 A73-10338
Ionization cross sections for H₂, N₂, and CO₂ clusters by electron impact.
01 p0080 A73-10563
New mechanism for generating coherent emission from ionized oxygen and nitrogen in the visible region of the spectrum
01 p0059 A73-10630
Nitrogen thermochemistry during the combustion of zirconium droplets in N₂/O₂ mixtures.
01 p0123 A73-10922
Temperatures of aluminum during its combustion in oxygen-argon mixtures, in nitrogen, and in air
01 p0123 A73-11275
Quenching of vibrationally excited N₂ by atomic oxygen.
02 p0139 A73-12085
Molecular nitrogen vibrational temperature in E and F regions, using positive ion data and model for ionic reaction rate and continuity equation numerical solution
02 p0161 A73-12279
Effects of immersion with the head above water on tissue nitrogen elimination in man.
02 p0135 A73-12563
Enhanced N₂ vibrational temperatures in the thermosphere.
03 p0298 A73-12881
Tensile strength dependence on temperature and interstitial oxygen and nitrogen concentration in powdered Nb, noting microhardness and yield point
03 p0326 A73-13968
Molecular gas presence effect on electron energy balance in atomic gases, noting inelastic collisions loss factor in heated Ar plasma containing nitrogen molecules
03 p0347 A73-14098
Production of gaseous nitrogen during human steady state exercise.
03 p0269 A73-14163
Shock-tube study of vibrational energy transfers in the CO₂-N₂ and the CO₂-CO systems.
03 p0345 A73-14442
Photoionization of vibrationally excited N₂. II - Quenching by CO₂ and N₂O.
04 p0414 A73-14817
Measurements of temperatures of vibrationally excited N₂.
04 p0477 A73-14819
High vacuum thermal desorption mass spectrometry for electron bombardment activated nitrogen desorption from W surface, discussing lambda state population
04 p0414 A73-14999
Dislocation interstitial impurities interactions in high purity Mo, using dislocation damping techniques
04 p0462 A73-15304
- The mechanism of vacuum ultraviolet emission from the Lewis-Rayleigh nitrogen afterglow.
05 p0600 A73-16560
Speed distribution measurements of N₂ and Ar molecular beams produced by a multichannel source.
06 p0726 A73-18261
Mixed-venous oxygen tension by nitrogen rebreathing - A critical, theoretical analysis.
06 p0654 A73-18336
Pulsed nitrogen laser emitting at 3371 Å.
06 p0702 A73-18587
Photoelectron precipitation induced dissociation of atmospheric nitrogen molecules during moderate solar activity
07 p0816 A73-19459
Analysis of single particles of lunar dust for dissolved gases.
07 p0890 A73-19813
Total nitrogen contents of some Apollo 14 lunar samples by neutron activation analysis.
07 p0890 A73-19815
Chemically bound nitrogen abundances in lunar samples, and active gases released by heating at lower temperatures /250 to 500 C/.
07 p0890 A73-19817
Alloy composition and temperature effects on nitrogen solubility in austenitic Cr-Ni steels, noting nitride precipitation effect on impact strength reduction
07 p0839 A73-19950
Rotational temperature measurements in nitrogen at hypersonic flow using an electron beam technique [ONERA, TP NO. 1206]
07 p0853 A73-20605
Thermoregulatory reactions of rats in a nitrogen and helium-diluted hypoxic atmosphere
08 p0929 A73-20979
Low cost nitrogen laser design for dye laser pumping.
08 p0974 A73-21027
Comparative investigations regarding the determination of nitrogen in tantalum
08 p0978 A73-21418
Effects of lung volume and disease on the lung nitrogen decay curve.
08 p0934 A73-21501
Features of the structure and of plastic deformation in zirconium saturated with nitrogen and oxygen
09 p1099 A73-21967
Flow of a supersonic nitrogen jet and of a low-density nitrogen-hydrogen mixture around a blunt body
10 p1171 A73-23582
Vibrationally-excited nitrogen in the upper atmosphere.
10 p1212 A73-24226
Measurement of vibrational temperature of CO and N₂ using the He/2 3S/ Penning ionization technique.
10 p1218 A73-24246
Effect of atomic oxygen on the N₂ vibrational temperature in the lower thermosphere.
10 p1214 A73-24748
Nb nitriding kinetics and external effects observations during nitrogen diffusion through crystal lattices
10 p1236 A73-24955
Single breath nitrogen washout method for measurement of functional residual capacity.
11 p1315 A73-25332
Nitrogen and oxygen molecules, photodissociation continua from absorption and ionization cross sections, calculating upper atmosphere emission rates
12 p1489 A73-26993
Nitrogen laser with a longitudinal discharge and high power density
12 p1506 A73-27214
Nitrogen laser with a transverse discharge
12 p1506 A73-27215
Nitrogen metabolite dynamics in the brain during repeated hypothermia and subsequent spontaneous warming
12 p1462 A73-27703
Near-satellite neutral gas temperature determination from measurement of molecular nitrogen velocity distribution
13 p1687 A73-28630
Second positive system of nitrogen bands in dayglow, according to Kosmos-224 data.
13 p1607 A73-28703
Laminar flame propagation in hydrogen, oxygen, nitrogen mixtures.
13 p1707 A73-29001
Solubility of nitrogen and hydrogen in cobalt and cobalt alloys - A review.
13 p1637 A73-29245
Procedure for preparing an oxygen-nitrogen gas mixture for respiration in a pressure chamber
13 p1580 A73-29409
Development of austenitic heat-resistant steel containing a high concentration of nitrogen.
13 p1642 A73-29516
Autoionizing transitions in N₂ and H₂ produced by electron impact.
14 p1776 A73-29695
Observation of the effects of rotational transitions in the resonant scattering of electrons from N₂.
14 p1776 A73-29696
- Ionospheric nitrogen ion density from rocket-borne dayglow spectrometry, considering charge exchange with metastable oxygen ions and solar EUV photoionization as ionizing mechanisms
14 p1723 A73-29953
Spatial separation of 3914- and 3160-Å emissions of nitrogen in an aurora.
14 p1749 A73-29987
Calculation of the composition of 79% N₂ + 21% O₂ and 50% N₂ + 50% O₂ mixtures containing carbon at high temperatures
15 p1840 A73-31853
The interaction of gases and carbon with refractory metals
15 p1890 A73-31925
Nitrogen pulsed ultraviolet laser.
16 p2023 A73-32861
Phase equilibria in the metal-rich side of the Ta-N system.
16 p2025 A73-33110
Electron impact excitation of N₂. I, II.
16 p2039 A73-33866
Experimental determination of thermal conductivity of nitrogen in the temperature range 100-2200 C.
17 p2254 A73-34372
Validation of open-circuit method for the determination of oxygen consumption.
17 p2117 A73-35462
Validity of Haldane calculation for estimating respiratory gas exchange.
17 p2113 A73-35463
Repetitively pulsed high power nitrogen laser for UV radiation at room temperature, discussing electrical design and construction
17 p2185 A73-35767
Steady-state equality of respiratory gaseous N₂ in resting man.
18 p2278 A73-36660
Study of nitrogen balance and creatine and creatinine excretion during recumbency and ambulation of five young adult human males.
18 p2278 A73-36786
Hematological, biochemical, and immunological studies during a 14-day continuous exposure to 5.2% O₂ in N₂ at pressure equivalent to 100 FSW /4 ata/.
18 p2278 A73-36794
Book - Elevated temperature properties as influenced by nitrogen additions to types 304 and 316 austenitic stainless steels.
18 p2325 A73-36971
Experimental study of the heat transfer in the vicinity of the critical point during nonequilibrium physicochemical transformations and determination of the nitrogen recombination rate constant
18 p2287 A73-37013
New vapour pressure measurements for argon and nitrogen and a new method for establishing rational vapour pressure equations.
19 p2461 A73-38200
Gallium phosphide with nitrogen doping from the gas phase
20 p2599 A73-38666
Respiratory nitrogen elimination - A potential source of error in closed-circuit spirometry.
20 p2512 A73-39113
Influence of small oxygen and nitrogen additions on the nature of the temperature dependence of the mechanical properties of niobium
20 p2577 A73-39360
Fluorescence efficiencies of electrons in second positive bands of N₂ and first negative bands of N₂⁺.
21 p2682 A73-40164
Oxygen and nitrogen thermodynamic state equation determination by least squares fitting to experimental PVT, isochoric heat capacity and saturation density data
21 p2740 A73-41104
Diurnal and semidiurnal nitrogen density and temperature variations from thermosphere probe measurements.
22 p2845 A73-41926
A device for the on-line measurement of nitrogen rotational temperature in low density flows.
22 p2854 A73-41995
Absorption of gas bubbles in flowing blood.
22 p2806 A73-42414
New measurements of the thermal conductivity of argon and nitrogen to 200 C and 1600 atmospheres.
22 p2932 A73-42502
E and F regions nitrogen vibration energy content by numerical integration of time dependent species continuity equation and species equation of motion
22 p2848 A73-42537
Kinetics of gas absorption by refractory metals in dissociated environments - The nitrogen/tantalum system.
22 p2879 A73-42583
Curve crossing theory for N molecule-O atom reactions in terms of spin-orbit coupling, considering nitrous oxide unimolecular decomposition and molecular N vibrational relaxation
24 p3113 A73-44979

NITROGEN ATOMS

- Differences between inspired and expired minute volumes of nitrogen in man. 24 p3060 A73-45069
- Energy deposition of protons in molecular nitrogen and applications to proton auroral phenomena. 24 p3126 A73-45116
- Electron-molecule collision frequencies in a crossed electric and magnetic field. 24 p3118 A73-45476

NITROGEN ATOMS

- Photoionization of atomic nitrogen and atomic oxygen. 13 p1662 A73-28190
- Excitation of atomic nitrogen by electron impact. 16 p2038 A73-33099
- Atomic nitrogen and nitrogen oxide in the perturbed ionosphere at heights ranging from 100 to 200 km. 24 p3066 A73-44802

NITROGEN COMPOUNDS

- NT ACETANILIDE
- NT ALUMINUM NITRIDES
- NT AMIDES
- NT AMMONIA
- NT AMMONIUM NITRATES
- NT AZIDES [ORGANIC]
- NT AZO COMPOUNDS
- NT BORON NITRIDES
- NT CELLULOSE NITRATE
- NT CYANAMIDES
- NT CYANO COMPOUNDS
- NT HYDROCYANIC ACID
- NT HYOSCINE
- NT IMIDES
- NT IMINES
- NT ISOCYANATES
- NT LIQUID AMMONIA
- NT NITRATES
- NT NITRIC ACID
- NT NITRIC OXIDE
- NT NITRIDES
- NT NITRITES
- NT NITRO COMPOUNDS
- NT NITROAMINES
- NT NITROGEN DIOXIDE
- NT NITROGEN FLUORIDES
- NT NITROGEN HYDRIDES
- NT NITROGEN OXIDES
- NT NITROGEN POLYMERS
- NT NITROGEN TETROXIDE
- NT NITROGLYCERIN
- NT NITROUS OXIDES
- NT POLYIMIDES
- NT POTASSIUM NITRATES
- NT QUINOLINE
- NT SILICON NITRIDES
- NT TANTALUM NITRIDES
- NT THIURONIUM
- NT TITANIUM NITRIDES
- NT TRINITROTOLUENE
- NT TRYPTOPHAN
- NT UREAS
- NT ZIRCONIUM NITRIDES

- Combustion products of polymeric materials containing nitrogen in their chemical structure. 08 p0983 A73-21821

- Measurements of some hydrogen-oxygen-nitrogen compounds in the stratosphere from Concorde 002. 09 p1079 A73-22947

- Influence of thermally stabilizing alloying additions on the antifriction properties of lamellar graphites with a organic silicon binders. 09 p1110 A73-22978

NITROGEN DIOXIDE

- Calculation of pressure-broadened linewidths of SO₂ and NO₂. 04 p0414 A73-14815
- Stratospheric nitrogen dioxide from infrared absorption spectra. 04 p0445 A73-15626
- Measuring apparatus for residual effective stabilizer content in single and double base propellants by passing nitrogen dioxide through ground sample. 09 p1135 A73-22300
- Photoionization and charge exchange reaction kinetics inadequacy for explanation of observed positive nitrogen dioxide ion concentration in lower ionosphere, considering alternative mechanism. 10 p1214 A73-24749
- Real time nitrogen dioxide and nitric oxide pollution measurement by molecular fluorescence induced by argon laser beam. 21 p2671 A73-40135
- Nitrogen dioxide and ozone photolysis as oxygen atom sources for high pressure addition reaction rate studies, discussing quantum yields and photolysis dependence on pressure. 22 p2819 A73-42769
- Stratospheric methane and nitrogen dioxide from infrared spectra. 23 p2976 A73-43887
- On the behavior of nitrogen oxides in the stratosphere. 23 p2976 A73-43896

NITROGEN FLUORIDES

- Investigation of heat transfer in a rarefied molecular gas with the aid of the Senfleben effect. 11 p1453 A73-26445
- Spectrophotometric determination of the rate of dissociation of nitrogen trifluoride behind shock waves. 16 p1977 A73-34017

NITROGEN HYDRIDES

- Nitrogen hydride as a possible stratospheric constituent. 02 p0159 A73-12225

NITROGEN IONS

- Ionic reaction mechanism for F region nitrogen vibrational temperature, using positive ion composition. 01 p0042 A73-10894
- Nitriding by ion bombardment of 18-10 stainless steels. 04 p0457 A73-15954
- Study of nitriding by ion bombardment of titanium and titanium alloys. 04 p0457 A73-15955
- Absolute cross section for producing C-11 from carbon by 270-MeV/nucleon N-14 ions. 06 p0725 A73-17519
- Dissociative recombination at elevated temperatures. IV - N₂⁺/+ dominated afterglows. 07 p0853 A73-19149
- Measurements of the electron temperatures in M42 from the profiles of H-alpha, forbidden N II, H-beta, and forbidden O III. 08 p1004 A73-20906
- Molecular nitrogen ionization growth characteristics as function of electric field strength and gas pressure, using thin gold film electrodes. 09 p1122 A73-22119
- Spatial and temporal ionization growth characteristics in nitrogen at moderate electric field strength, noting dominant secondary emission effect due to cathode bombardment by metastable molecules. 09 p1122 A73-22120
- Dayglow nitrogen ion 3914 A emission profiles for average solar activity at 110-240 km heights from Cosmos 224 observations. 13 p1607 A73-28704

- Atomic nitrogen ion density measurements for loss rate coefficient of N⁺ reaction with oxygen at 150-220 km. 16 p2009 A73-33892

- Positive nitrogen ions in midlatitude atmosphere, discussing concentration dependence on height, solar zenith angle and activity level. 24 p3084 A73-44801

- Ion-implanted nitrogen in gallium arsenide. 24 p3120 A73-45402

NITROGEN ISOTOPES

- Theory of interstellar abundances of the isotopes of carbon, nitrogen and oxygen. 22 p2914 A73-43006
- Nitrogen quadrupole coupling constants in cis-propyleneimine. 23 p2950 A73-43272

NITROGEN OXIDES

- NT NITRIC OXIDE
- NT NITROGEN DIOXIDE
- NT NITROGEN TETROXIDE
- NT NITROUS OXIDES
- Gas turbine combustion rig simulation of pollutant carbon and nitrogen oxide emissions as function of air-fuel mixing, metallic additions and chamber design. 06 p0767 A73-17732
- Reduction of nitrogen oxide emissions from a gas turbine by fuel modifications. 16 p2045 A73-33483
- [ASME PAPER 73-GT-5] The extinction coefficients of NO₂ between 195 nm and 410 nm. 16 p2005 A73-33544
- [AIAA PAPER 73-503] Impact of space shuttle orbiter reentry on mesospheric NO_x. 16 p2007 A73-33559
- [AIAA PAPER 73-525] On the possible effect of NO_x injection in the stratosphere due to past atmospheric nuclear weapons tests. 16 p2011 A73-34047
- [AIAA PAPER 73-538] Mesospheric and stratospheric nitrogen oxides behavior from model with nitric oxide photodissociation and nitric acid formation. 17 p2119 A73-34779
- The effects of water vapor and oxides of nitrogen on the ozone and temperature structure of the stratosphere. 17 p2160 A73-34857
- Photochemistry of the ozone in the stratosphere. 18 p2287 A73-36938
- Nitrogen oxide turbojet emissions minimization with hydrogen compared to kerosene (JP) fuels due to flammability limits, burning velocity and introduction in combustor as gas. 19 p2473 A73-37498
- Nitrogen oxides, nuclear weapon testing, Concorde and stratospheric ozone. 21 p2686 A73-41076
- Experimental and theoretical studies of NO_x formation in a jet-stirred combustor. 22 p2820 A73-42793

- Recent developments in photochemistry of atmospheric ozone. 23 p2951 A73-43892

- The production and distribution of nitrogen oxides in the lower stratosphere. 23 p2977 A73-43897

- Nitrogen oxides role in global stratospheric ozone balance demonstrated by observed instantaneous photochemical rates comparison with Chapman ozone formation theory. 23 p2952 A73-43900

- The effects of water vapour and oxides of nitrogen on ozone and temperature structure of the stratosphere. 23 p2977 A73-43902

- Atomic nitrogen and nitrogen oxide in the perturbed ionosphere at heights ranging from 100 to 200 km. 24 p3066 A73-44802

NITROGEN PLASMA

- The transport coefficients and material functions of a plasma with different electron and gas temperatures. 11 p1404 A73-25343
- Recombination rate measurements in nitrogen. 16 p2039 A73-33673
- Cylindrical probe in a glowing-discharge nitrogen plasma at medium pressures. 17 p2215 A73-34261
- Calculation of components, electrical conductivity, and total radiative source strength of nitrogen plasma in local thermodynamic equilibrium. 18 p2339 A73-36360
- [AIAA PAPER 73-744] Continuum emission from recombining oxygen and nitrogen plasmas. 18 p2338 A73-36799
- Nitrogen ionization in an Hg-N₂ discharge. 19 p2463 A73-37903

NITROGEN POLYMERS

- New fire resistant polymers - Poly(phosphazenes). 17 p2197 A73-35356
- Physical nature of gelatin as polymer material, emphasizing low temperature restoration of collagen structure, supermolecular structure formation capability and glassy-elastic state transition temperature. 21 p2647 A73-40265

NITROGEN TETROXIDE

- Corrosion tests for rocket propulsion system components materials for use with nitric acid-nitrogen tetroxide blend oxidizer. 03 p0329 A73-13007
- Experimental study of heat transfer in the boiling of nitrogen tetroxide. 03 p0397 A73-13188

NITROGLYCERIN

- The thermal decomposition of nitroglycerin and its relation to the stability of CMDB propellants. 05 p0605 A73-16685
- [WSCI PAPER 72-30] Experimental study of the critical conditions of powder ignition and combustion. 24 p3155 A73-44707

NITROUS OXIDES

- Fuel-rich and stoichiometric carbon monoxide-nitrous oxide premixed laminar flames with varying water contents, determining flame temperature by line reversal method. 03 p0399 A73-14396
- Nitrous oxide laser optical pumping at high pressures with TEA hydrogen bromide laser, considering application to other linear triatomic molecules. 06 p0704 A73-18796
- Frequency stabilization of a CO₂ or N₂O power laser by a fast sampling method. 08 p0976 A73-21444
- High-temperature oxidation of hydrogen by nitrous oxide in shock waves. 22 p2933 A73-42756
- A single-pulse shock-tube study of the reaction between nitrous oxide and carbon monoxide. 22 p2933 A73-42757
- Curve crossing theory for N molecule-O atom reactions in terms of spin-orbit coupling, considering nitrous oxide unimolecular decomposition and molecular N vibrational relaxation. 24 p3113 A73-44979

NOBLE GASES

- U RARE GASES
- NOBLE METALS
- NT GOLD
- NT SILVER
- Ceramic-to-metal sealing and joining technology assessment, discussing noble filler metal properties, ceramic surface preparation and thermal tests for performance evaluation. 09 p1088 A73-22444
- Electrolytically deposited noble-metal layers in the electronic industry. 16 p1987 A73-32945
- Electric contact materials technology, discussing intermetallics, ordered alloys, metal matrix composites and silver, gold and platinum based dispersion hardened alloys manufacture and properties. 16 p2027 A73-32946
- Long-term drift of some noble and refractory-metal thermocouples at 1600 K in air, argon, and vacuum. 22 p2857 A73-42033

The effects of catalysis in measuring the temperature of incompletely-burned gases with noble-metal thermocouples.

22 p2857 A73-42035

On the stability of metal sheathed noble metal thermocouples.

22 p2858 A73-42044

NOCTILUCENCE

U LUMINESCENCE

NOCTILUCENT CLOUDS

The contrast and the visibility of noctilucent clouds in the twilight sky

04 p0441 A73-15293

Spectrophotometric measurements of noctilucent clouds.

09 p1079 A73-23339

Noctilucent clouds seasonal distribution, altitude and displacement velocity from German observations during 1885-1941

15 p1873 A73-32347

Mars blue haze, earth noctilucent clouds and Venus blue clouds, considering mechanism and condensate chemical composition for formation

16 p2069 A73-33833

Interpretation of the results of photometric observations of noctilucent clouds

21 p2732 A73-40859

Preliminary results from the noctilucent sampling from Kiruna in 1970.

21 p2775 A73-41413

Noctilucent cloud sampling by a multi-experiment payload.

21 p2775 A73-41414

Solar atmosphere origin for submicrometer cosmic dust in ionosphere and noctilucent clouds, noting anomalously high atomic weight

21 p2775 A73-41416

Dust measurements in the upper atmosphere during and in the absence of noctilucent cloud display.

21 p2691 A73-41417

The effect of atmospheric and physiological conditions on the homogeneity of observations of noctilucent clouds

22 p2847 A73-42448

NOCTURNAL VARIATIONS

6300 A night airglow enhancements in low latitudes.

07 p0818 A73-20051

Equatorial spread F layer height nocturnal variations due to magnetic disturbances during solar activity cycles

16 p2008 A73-33878

Bandpass filter IR observations of hydroxyl airglow, mapping mean nightly level spatial and temporal fluctuations in brightness

24 p3087 A73-45208

NODES [STANDING WAVES]

Steady state vibrational frequencies of grid stiffened rectangular plates with monolithic connection at node points for simply supported case

07 p0909 A73-19095

Space-time cross spectral method to resolve transient disturbances into quasi-standing wave oscillations, giving formulas for node and antinode location

12 p1521 A73-26814

NOISE [SOUND]

NT AERODYNAMIC NOISE

NT AIRCRAFT NOISE

NT ENGINE NOISE

NT JET AIRCRAFT NOISE

NT ROCKET ENGINE NOISE

NT SONIC BOOMS

NT THERMAL NOISE

The interaction of auditory noise and subjective noise annoyance sensitivity with peripheral visual sensitivity.

05 p0543 A73-16703

Acoustic radiation from plates excited by flow noise.

08 p0988 A73-21470

Impairment to hearing from exposure to noise.

16 p1973 A73-33676

A model of psychological annoyance of noise.

17 p2118 A73-35627

Rotor noise due to inflow turbulence.

[AIAA PAPER 73-632] 18 p2259 A73-36191

NOISE ATTENUATION

U NOISE REDUCTION

NOISE ELIMINATION

U NOISE REDUCTION

NOISE GENERATORS

Attenuation of airplane /747/ air-conditioning noise in lined and unlined ducts.

03 p0289 A73-12959

Performance and noise generation studies of supersonic air ejectors.

03 p0290 A73-12972

An investigation of the near wake properties which lead to the generation of vortex shedding sound from airfoils.

03 p0242 A73-12976

Analysis of internally generated sound in continuous materials. II - A critical review of the conceptual adequacy and physical scope of existing theories of

aerodynamic noise, with special reference to supersonic jet noise.

03 p0246 A73-13840

Noise sources analysis for high and low bypass ratio turbofan engines, considering jet, compressor, fan and turbine sound generation mechanisms

03 p0359 A73-14138

Pseudorandom noise for telemetry error rate measurement applications and limitations.

04 p0449 A73-15457

Disturbance of the environment by jet aircraft noise

05 p0535 A73-16760

Current Pratt & Whitney engine noise reduction programs.

06 p0740 A73-17603

Internal additive noise generated by a random pulse process

08 p0939 A73-21395

Low vs high speed propeller fan noise, discussing pseudosound generation by rotating aerodynamic pressure fields

13 p1603 A73-29030

Turbulent jet noise generation theory relationship between flow and acoustic characteristics, obtaining intensity expression with velocity space-time derivatives for moving and stationary coordinates

13 p1603 A73-29138

Helicopter rotor blade passing close to tip vortex, calculating fluctuating lift induced harmonic blade loads and generated cyclic banging noise

13 p1570 A73-29382

Noise at large RF amplitudes in IMPATT oscillators.

14 p1731 A73-29713

Some noise generation mechanisms in transonic gas jets

14 p1712 A73-30947

Monograph - Two causality correlation techniques applied to jet noise.

17 p2155 A73-35150

Fundamentals of aerodynamic sound theory and flow duct acoustics.

17 p2155 A73-35331

Rotating blades and aerodynamic sound.

17 p2096 A73-35333

Application of the coherence function to acoustic noise measurements.

19 p2458 A73-37284

Effect of spanwise circulation on compressor noise generation.

19 p2473 A73-37292

Internal additive interference produced by a pulsed random process.

19 p2407 A73-38353

Subsonic and supersonic turbulent shear layer aerodynamic noise emission derivation from differential wave equations via Fourier transformation and WKBJ method

20 p2507 A73-39087

Sound generation by open supersonic rotors.

22 p2795 A73-41712

Refraction, convection, and diffusion flame effects in combustion-generated noise.

22 p2934 A73-42780

Signal transmission in analog fluidic systems mainly with respect to noise influence.

23 p2944 A73-43421

Noise and stable operation conditions in associative memory devices

23 p2956 A73-43580

Studies on a band limited white noise with a uniform bispectrum.

23 p2965 A73-44135

Supersonic jet noise generated by large scale disturbances.

[AIAA PAPER 73-992] 24 p3077 A73-44827

Broadband noise generation by aerofoils and axial flow fans.

[AIAA PAPER 73-1018] 24 p3054 A73-44850

Multiple pure tone noise generation and control.

[AIAA PAPER 73-1021] 24 p3122 A73-44853

Noise generation by turbulent combustion, discussing sound power, spectral content, enclosure effect, and importance in turbopropulsion system core engine noise

[AIAA PAPER 73-1023] 24 p3155 A73-44855

Spectral trends in rotor noise generation.

[AIAA PAPER 73-1033] 24 p3056 A73-44862

NOISE HAZARDS

U HAZARDS

U NOISE [SOUND]

NOISE INJURIES

Electron-microscopy investigation of Corti's organ after noise trauma

05 p0539 A73-16333

Damage-risk criteria - The trading relation between intensity and the number of nonreverberant impulses.

16 p1973 A73-33678

Hearing conservation studies covering impulse noise produced threshold shift, damage risk criteria, ultrasound hazards and hearing protection

17 p2117 A73-35326

Impulse noise damage risk criteria.

17 p2117 A73-35327

Evaluation of auditory disorders in pilots by examining intratympanic muscles reflexes.

18 p2279 A73-36934

Survey of the civil responsibility for damages caused by aircraft noise in American and French law

19 p2506 A73-37998

Corti organ lesion effects on signal perception in patients with noise induced hearing loss, correlating speech discrimination with age and sound level

19 p2396 A73-38182

Conventional and high frequency hearing of naval airmen as a function of noise exposure.

23 p2949 A73-43500

NOISE INTENSITY

Statistical analysis of the sound-level distribution of aircraft noise as a function of time. II

02 p0131 A73-12449

Inlet sound power of axial compressors.

03 p0241 A73-12956

On evaluation of aircraft noise around air-bases by factor analysis.

03 p0249 A73-12957

Osaka airport effective continuous perceived noise level measurements, area contour map and noise duration allowance vs aircraft distance diagram

03 p0249 A73-12977

Techniques for determining the noise zones in the vicinity of the central Berlin-Schoenefeld airport, and related problems

03 p0249 A73-12978

The second noise and social survey around Heathrow, London airport.

03 p0266 A73-12980

An acceptable exposure level for aircraft noise in residential communities.

03 p0250 A73-13838

Low noise regenerative amplifier with direct coupling to load, noting optimal use at moderately high frequencies

03 p0284 A73-14033

Neumann-Pearson-optimal signal detection procedure invariant with respect to amplitude and random noise intensity

03 p0278 A73-14073

Study of the influence of the volumetric mass of a jet on acoustic sound emission

03 p0359 A73-14143

Minimum noise coefficients of M-type microwave beam amplifiers with crossed fields taking into account distributed losses in slow wave structure

04 p0429 A73-15922

Noise magnitude calculation for intensity quantized hologram based on Laplace transform for nonlinear device analysis and Gaussian random process

05 p0579 A73-17220

Noise performance of gallium-arsenide and indium-phosphide injection-limited diodes.

07 p0798 A73-19158

Pulse interference suppression during noise signal intensity measurements with a modulation radiometer

07 p0792 A73-19111

Comparative studies of noise limitations in superconducting thin-film radiation detectors.

07 p0863 A73-20105

Sound pressure level spectra measurements for four- and three-engine jet transport during concrete and grassy surface runup and flyover

08 p0927 A73-20693

Some perspectives on receiver noise performance and its measurement.

08 p0940 A73-21624

Microwave and millimeter wave receiver noise performance state of art and acoustic measurement methods, discussing traveling wave maser, parametric and transistor amplifiers and tunnel diodes

08 p0940 A73-21625

Techniques for short-term predictions of atmospheric noise levels.

08 p0940 A73-21662

A new analysis of the digital data transition tracking loop.

09 p1062 A73-22302

Variation of atmospheric radio noise level with sunspot number.

09 p1051 A73-22493

Aircraft turboengine noise, discussing noise level/power output relations

10 p1262 A73-23861

Acoustic dipole source strength on flat plate and simple airfoil surfaces from local surface and far field acoustic pressure cross correlation

11 p1345 A73-24982

Noise intensity in the field of subsonic turbulent jets

11 p1347 A73-25738

Target-detection performance as a function of noise intensity and task difficulty.

11 p1323 A73-26320

Huygens principle, power spectrum and photon and photographic noise intensities effects in holography, discussing optical information transmission by eigen-solutions

11 p1369 A73-26529

Variations in the sound field of a STOL aircraft as a function of wing-flap deflection

11 p1306 A73-26592

NOISE MEASUREMENT

- Investigation of the permissible power level of FM radio interference at the input of the frequency converter in an FM-signal receiver 12 p1477 A73-26873
- Book - Human factor aspects of aircraft noise. 12 p1465 A73-27450
- Short term frequency stability and single sideband phase noise measurements on signal generators, considering frequency deviation and amplitude modulation produced by noise 13 p1582 A73-28570
- Low noise temperature measurement converter with electrical oscillation frequency output, presenting computer calculations of sensor components 13 p1617 A73-28860
- Correlation of random noise levels in short-wave radio channels 13 p1584 A73-28888
- Evaluation of the noise immunity of pulsed systems for transmission of continuous messages with allowance for quantization and interpolation errors. I 13 p1584 A73-28891
- Turbulent jet noise generation theory relationship between flow and acoustic characteristics, obtaining intensity expression with velocity space-time derivatives for moving and stationary coordinates 13 p1603 A73-29138
- Acoustic radiation intensity of a turbulent boundary layer on a plate 14 p1746 A73-30952
- Low-frequency noise characteristics of commercial silicon and gallium arsenide IMPATT diodes. 15 p1851 A73-32188
- Prediction and measurement of aircraft noise. 16 p2014 A73-33133
- Determination of maximum ground noise during a rocket launch - Discussion and simple prediction method. 16 p2072 A73-33142
- Experimental educational noise surveys of rural, suburban, urban and industrial areas at various times of day, using computerized data processing 16 p2036 A73-33216
- Social acceptability of heliports particularly from the standpoint of noise. 17 p2146 A73-34441
- Human response to transportation noise and vibration. 17 p2117 A73-35328
- Maximum air transportation service with minimum community noise. 19 p2388 A73-38369
- [AIAA PAPER 73-796] A status report on jet noise suppression as seen by an aircraft manufacturer. 19 p2388 A73-38374
- [AIAA PAPER 73-816] Overall sound pressure levels of STOL thrust reverse noise as function of jet velocity at touchdown 20 p2600 A73-38650
- Two-stage detection of signals in normal noise of unknown intensity. 20 p2529 A73-38922
- Determination of the root-mean-square and mean intensity of the atmospheric radio noise field 21 p2648 A73-40208
- Amplifier with distributed gain for use in radiometry 21 p2700 A73-40540
- Interactive effects of intense noise and low-level vibration on tracking performance and response time. 21 p2644 A73-41153
- Perceived noise level ratings for helicopter noise, discussing blade slap, tail rotor whine, broadband noise and PNL rating shortcomings 22 p2798 A73-41708
- Aircraft flyover noise - Spectral analysis of sounds and sound intensity fluctuations. 22 p2800 A73-42946
- Cognitions and 'placebos' in behavioral research on ambient noise. 22 p2816 A73-42950
- Intensity of sound radiation from a turbulent boundary layer on a plate. 23 p2969 A73-44328
- ## NOISE MEASUREMENT
- ### U ACOUSTIC MEASUREMENTS
- #### NOISE METERS
- Direct-reading measurement of receiver-noise parameters. 13 p1590 A73-28531
- A new device for measuring local acoustic power output of subsonic jets. [AIAA PAPER 73-1042] 24 p3090 A73-44866
- #### NOISE POLLUTION
- The influence of background noise on disturbance due aircraft. 03 p0249 A73-12979
- The aeroplane as a threat to the environment. 03 p0251 A73-14468
- Disturbance of the environment by jet aircraft noise 05 p0535 A73-16760
- Technology and operation of Olympus engine cycle on Concorde aircraft, discussing chemical and noise pollution and economic factors 05 p0536 A73-17190

- Technology and operation of Olympus engine cycle on Concorde aircraft, discussing chemical and noise pollution and economic factors 08 p0996 A73-21687
- Determinants for aircraft noise annoyance - A comparison between French and Scandinavian data. 16 p1967 A73-32915
- Realism in environmental testing and control: Proceedings of the Nineteenth Annual Technical Meeting, Anaheim, Calif., April 2-5, 1973. 16 p1993 A73-33126
- Aircraft produced environmental noise and air pollution, discussing related aircraft power plant technology evolution 16 p2047 A73-33191
- A model of psychological annoyance of noise. 17 p2118 A73-35627
- Turbine engine research activity evolution, considering entry temperature increase, pollution sources nonstationary aerodynamics and aeroelasticity in compressors, and noise problem 18 p2343 A73-36991
- Possibilities and problems of achieving community noise acceptance of VTOL. 19 p2386 A73-38010
- Contributions of the DFVLR to environmental research and environment protection. II - Noise control, water environment protection, nature and landscape, environmental protection techniques 19 p2506 A73-38266
- Interactive effects of intense noise and low-level vibration on tracking performance and response time. 21 p2644 A73-41153
- Methods for quantifying the effect of noise on people. 22 p2811 A73-41707
- Runway sideline aircraft noise measurements on takeoff and approach for enforcing community noise levels based on FAA aircraft type certification, noting associated problems 22 p2800 A73-42945
- Community noise impact study from military helicopter operations. 22 p2800 A73-42947
- Human noise sensitivity, discussing personality effects, Maplin airport planning and population separation into sensitive and imperturbable groups 24 p3062 A73-44770
- ## NOISE PROPAGATION
- Helicopter internal and external noise level measurements under various flight conditions, obtaining noise radiation directivity patterns via time measuring tractography equipment [ONERA, TP NO. 1136] 01 p0004 A73-10241
- Model study of aircraft noise reverberation in a city street. 02 p0130 A73-12199
- Effect of wake-wake interactions on the generation of noise in axial-flow turbomachinery. 03 p0246 A73-14129
- Passage of useful and noise signals through a nonlinear circuit containing a p-n junction capacitance 08 p0946 A73-21111
- Enhanced energetic electron intensities at 100 km altitude and a whistler propagating through the plasma-sphere. 09 p1079 A73-22839
- Determination of maximum ground noise during a rocket launch - Discussion and simple prediction method. 16 p2072 A73-33142
- Aircraft engine fan noise radiation from inlet and discharge ducts, describing wind tunnel tests and noise spectra at various blade tip speeds 19 p2472 A73-37288
- Helicentric Pioneers 8 and 9 hyperbolic cosmic dust data suggesting cosmic dust origin of previously solar effect generated noise 21 p2775 A73-41410
- Atmospheric absorption considerations in airplane flyover noise at altitudes above sea level. 22 p2799 A73-42943
- A difference theory for noise propagation in an acoustically lined duct with mean flow. [AIAA PAPER 73-1007] 24 p3078 A73-44840
- Inlet geometry and axial Mach number effects on fan noise propagation. [AIAA PAPER 73-1022] 24 p3122 A73-44854
- Combustion noise radiation by open turbulent flames. [AIAA PAPER 73-1025] 24 p3156 A73-44856
- ## NOISE REDUCTION
- High efficiency dc-to-dc converter with second non-saturable transformer for eliminating collector current spike to reduce electromagnetic interference and transistor damage 01 p0005 A73-10247
- Optimum configurations for bangless sonic booms. 01 p0031 A73-10302
- On-line digital recording of stellar spectrum with photoelectron-counting spectrophotometer, noting discrimination against spurious signals from noise and pulse height distribution measurements 01 p0048 A73-10531

- Sonic boom avoidance by flight path maneuvers, investigating shock front development in curved flight 02 p0130 A73-11856
- Further studies of the aeroacoustics of jets perturbed by screens. 02 p0154 A73-12200
- Phase and amplitude balance - Key to image rejection mixers. 02 p0148 A73-12571
- NASA Quiet Engine Program review and test results, discussing noise reduction technology application to transport aircraft 02 p0204 A73-12845
- Aerodynamic noise characteristics, discussing turbulent fluid acoustic propagation equation modification and antinoise legislation 03 p0241 A73-12952
- Attenuation of airplane /747/ air-conditioning noise in lined and unlined ducts. 03 p0289 A73-12959
- An experimental study on noise reduction of axial flow fans. 03 p0241 A73-12961
- Sound field for noise extinction via controlled interference, stressing sonic generators installation near noise sources 03 p0341 A73-12962
- Supersonic jet noise suppression using coaxial flow interaction. 03 p0241 A73-12964
- Subsonic aircraft noise - A solution by the wider application of today's new engines. 03 p0249 A73-13062
- Solid propellant combustion instability suppression devices. [AIAA PAPER 72-1051] 03 p0353 A73-13382
- Geared fan engine systems - Their advantages and potential reliability. [AIAA PAPER 72-1173] 03 p0357 A73-13469
- Subsonic commercial transport aircraft reduced noise and increased cruise Mach number effects on nacelle design in terms of inlet, fan, cowl and nozzle [AIAA PAPER 72-1204] 03 p0358 A73-13488
- Real time linear and nonlinear motion desmearing of imagery telemeasured from airborne platform, discussing inverse filter error analysis and analog simulation 03 p0276 A73-13907
- Jet noise suppression for commercial CTOL, STOL and SST aircraft, discussing various devices effectiveness 03 p0251 A73-14130
- Directional devices for noise reduction of high speed jets 03 p0359 A73-14142
- Variable pitch fan experimental design for quiet STOL propulsion, testing blade designs for aerodynamic and acoustic performance 03 p0359 A73-14147
- Some experiments on the noise emission of coaxial jets. 03 p0360 A73-14148
- SST aircraft wing design for sonic boom avoidance and noise reduction in airport vicinity, describing aerodynamic characteristics from wind tunnel and flying model tests 04 p0405 A73-14673
- Airlines responsibility and measures for aircraft noise abatement, considering economic and safety aspects 04 p0406 A73-14893
- Aircraft noise as a continuing national problem. 04 p0521 A73-14894
- Air transportation system planning - Progress in noise reduction. 04 p0406 A73-14895
- A DPCM codec using edge coding and line replacement. 04 p0422 A73-15443
- Attenuation of spiral modes in a circular and annular lined duct. 04 p0487 A73-15591
- Thermodynamic considerations for the design of a sonic-boom reducing powerplant. [ASME PAPER 72-WA/AERO-3] 04 p0404 A73-15907
- Application of external aerodynamic diffusion to reduce shrouded propeller noise. 05 p0528 A73-16623
- Disturbance of the environment by jet aircraft noise 05 p0535 A73-16760
- Recursive MTI radar filter design for sharp spectrum rolloff and flat pass band, investigating clutter rejection performance vs spectral spread 05 p0558 A73-16808
- The effects of leading-edge serrations on reducing flow unsteadiness about airfoils. [AIAA PAPER 73-89] 05 p0529 A73-16853
- Effect of bulk-reacting liners on wave propagation in ducts. [AIAA PAPER 73-227] 05 p0566 A73-16952
- Atmospheric attenuation of noise measured in a range of climatic conditions. [AIAA PAPER 73-242] 05 p0570 A73-16966

Externally blown flap trailing edge noise reduction by slot blowing - A preliminary study.
[AIAA PAPER 73-245] 05 p0532 A73-16969

Recent progress in the field of aircraft noise technology
05 p0537 A73-17272

Engine noise reduction by fan blade tip speed reduction and high lift coefficient operation, presenting full scale test results
06 p0740 A73-17571

Aircraft noise reduction problems, noting trained personnel and research laboratories shortage and full scale tests requirements
[AIAA PAPER 73-5] 06 p0646 A73-17601

Current Pratt & Whitney engine noise reduction programs.
[AIAA PAPER 73-8] 06 p0740 A73-17603

Sonic boom reduction through aircraft design and operation.
[AIAA PAPER 73-241] 06 p0647 A73-17666

Digital transmission performance on fading dispersive diversity channels.
06 p0664 A73-17711

On some noise properties of high frequency solid-state oscillators.
06 p0673 A73-17714

A sampling FM wide-band demodulator useful for laser Doppler velocimeters.
06 p0673 A73-17786

Security system signal detector with time delay and prediction filters and optimal noise suppression, noting detection time dependence on cost effectiveness
06 p0679 A73-17806

Noisy data filtering of linear steady state control problems based on nearest neighbor interaction, discussing dimensionality reduction model for saving computer time
06 p0682 A73-18868

Precision design of millimeter-wave band-pass filter.
07 p0799 A73-19371

Ducts, nacelles, power source components and cabin noise sources identified for aircraft noise control research, considering prerequisites for quiet operations
[SAE AIR 1079] 08 p0928 A73-20698

Coherent optical processing with spatial frequency diversity speckle and reflection noise reduction, discussing coding by illuminating input transparency through square screen mesh
08 p0964 A73-21045

Noise reduction in acousto-optic /Bragg/ imaging systems by holographic recording.
08 p0965 A73-21209

A new type of PSK anti-ambiguity system for satellite applications.
09 p1156 A73-23431

Multichannel wideband FM communication systems, discussing method for channel density increase with reduced linearity requirement and enhanced noise immunity
10 p1187 A73-23732

Tunnel diodes in receivers to reduce noise level and improve selectivity, discussing distortions, crosstalk and passband dependence on signal amplitude
10 p1195 A73-24385

EASCON '72; Electronics and Aerospace Systems Convention, Washington, D.C., October 16-18, 1972, Record.
10 p1298 A73-24551

Aircraft noise reduction technology and certification standards, reviewing federal laws and regulations
10 p1175 A73-24553

Jet aircraft engine noise reduction.
10 p1263 A73-24555

Electrical interference /noise/ effects on measurements of high accuracy low-level differential data signals, discussing noise reduction, capacitive coupling problem and design principles
10 p1189 A73-24570

Method of increasing the noise immunity of optical communications lines
10 p1190 A73-24615

Noise abatement two-segment, precision and category I, II and III approaches considerations covering altimetry, cost and safety problems in ATC
10 p1247 A73-24768

Synthesis of helicopter rotor tips for less noise.
11 p1299 A73-24981

A single number rating for effective noise reduction.
11 p1397 A73-25000

The optimality of variable sampling schemes for a digital encoder.
11 p1327 A73-25194

Noise control modification to HH-43B helicopter for 50 percent reduction in forward flight octave band sound pressure level signature
11 p1304 A73-25383

Noise reduction for subsonic fluid flow over flat plate via interposition of secondary fluid layer at trailing edge
11 p1300 A73-25386

Active electromagnetic horn antenna with tunnel diode.
11 p1331 A73-26124

Zero-steering antenna system for receiving a signal close to the direction of strong interference.
11 p1332 A73-26284

Airport noise control and minimization for community and airline industry interests by technology application and legal-political approaches
11 p1455 A73-26350

Theory of sound scattering by turbulence applied to scattering cross section calculation for turbulent jet flow and wind, discussing jet noise reduction
11 p1349 A73-26496

Evaluation of the efficiency of the polarization selection method in suppressing fluctuating polarization noise
12 p1468 A73-26946

Dual magnetometer systems with cross correlation signal enhancement to overcome intrinsic sensor ambient noise and spacecraft magnetic field fluctuation effects on single detection performance
12 p1468 A73-27002

Acoustic and fluid dynamic tests of multilobed discharge silencers scale models, noting optimum jet noise attenuation configuration
12 p1486 A73-27390

Cryogenically cooled parametric amplifiers for 100 meter radio telescope low noise operation, describing system design and performance
12 p1481 A73-27780

The first two receivers for the radio astronomy programme on the 100 meter radiotelescope - An assessment of performance.
13 p1581 A73-28000

Coaxial anode for background suppression in X-ray proportional counters.
13 p1612 A73-28367

Parallel optical channel communications system with separate laser sources for suppressing mode competition noise due to beam intensity fluctuations /beats/
13 p1584 A73-28898

Airports: Challenges of the future; Proceedings of the Airports Specialty Conference, Dallas, Tex., March 7-9, 1973.
13 p1598 A73-29101

Recent advances in aircraft noise reduction.
13 p1570 A73-29104

Application of adaptive arrays to suppress strong jammers in the presence of weak signals.
13 p1593 A73-29215

Suppressing spurious signals in saturated switching systems.
13 p1595 A73-29394

Reduction of aircraft noise during stationary runs
13 p1570 A73-29651

Variable-pitch fans - Progress in Britain.
14 p1785 A73-29770

Variable-pitch fans - Hamilton Standard and the Q-fan.
14 p1785 A73-29771

Double balanced microwave mixer circuit with local oscillator input and IF outputs for achieving low noise and image rejection
14 p1737 A73-30622

Insulating houses against aircraft noise.
14 p1743 A73-30913

Reduction of noise generated by flow of fluid over plate.
14 p1746 A73-30915

Concorde engine noise reduction at takeoff, initial climb and landing, discussing noise sources research and exhaust system nozzle modifications
14 p1785 A73-30930

Theory of shot noise depression in a modified diode
14 p1737 A73-30943

Fundamental statistical characteristics of a modified phase AFC /PAFC/ system.
15 p1842 A73-30989

Noise rejection estimation for sinusoidal signal detectors which use information on zero-crossing moments
15 p1842 A73-31251

A method of assigning noise-resistant analog-to-digital converters
15 p1848 A73-31915

Jet noise suppression technology progress review, discussing Lighthill theory of aerodynamic noise, machinery noise and quiet aircraft future
15 p1830 A73-32186

VFW 614 twin-jet short haul aircraft, discussing layout, auxiliary power supply system for ground handling independence, surface movements maneuverability and low noise characteristics
15 p1830 A73-32365

Aircraft noise abatement technological and social aspects, considering aircraft design, airport noise pattern minimization and population removal
15 p1831 A73-32560

Determinants for aircraft noise annoyance - A comparison between French and Scandinavian data.
16 p1967 A73-32915

Aircraft engine noise reduction state of art, discussing FAA requirements, Concorde, DC-9 and Bertin Aladin II aircraft
16 p1967 A73-32970

STOL jet aircraft with variable pitch fan, discussing engine handling, noise reduction and efficiency
16 p2046 A73-33189

High bypass fan engines for quiet propulsion and optimal aircraft performance in military and commercial applications
16 p2046 A73-33190

Single-loop delay line integrator SNR enhancement properties in additive zero mean correlated noise channels for finite signal observation times
16 p1979 A73-33406

Noise immunity of optical communications links with radio and optical AGC systems.
16 p1984 A73-33977

Hydraulic system noise measurements and control, discussing source, vibrating parts isolation, transmission path and acoustic barriers and enclosures
16 p1971 A73-33993

High bypass ratio quiet turbofan engine for STOL aircraft, emphasizing noise reducing design based on low-speed variable pitch fan concept
16 p2049 A73-34040

Pilot operation practices for helicopter noise level reduction, with emphasis on flight altitude increase and routing over noise insensitive areas
17 p2099 A73-34442

Mixed CTOL-QTOL traffic effects on air traffic controller tasks, microwave landing and radio navigation systems, airport operation and ground equipment [MBB-UH-05-73] 17 p2207 A73-34487

Noise reduction of STOL aircraft during landing approach and takeoff via thrust reduction and steepest descent flight paths
[MBB-UH-06-73] 17 p2100 A73-34488

Stuttgart airport noise abatement supervisor tasks and experience, describing routing specifications, landing and takeoff procedures and traffic flow [DGLR PAPER 73-022] 17 p2208 A73-34495

Status of international noise certification standards for business aircraft.
[SAE PAPER 730286] 17 p2101 A73-34651

Progress in the development of optimally quiet turboprop engines and installations.
[SAE PAPER 730287] 17 p2221 A73-34652

Quiet aspects of the Pratt & Whitney Aircraft JT15D turbofan.
[SAE PAPER 730289] 17 p2101 A73-34654

Aircraft cabin noise reduction through composite material insulation, discussing engine noise sources, aircraft fuselage transmission loss characteristics, vibration damping and sandwich structures
[SAE PAPER 730339] 17 p2102 A73-34690

Engine cycle considerations for future transport aircraft.
[SAE PAPER 730345] 17 p2222 A73-34693

Noise reduction modifications in JT3D and JT8D gas turbine engine by single stage fan replacements
[SAE PAPER 730346] 17 p2222 A73-34694

Profitable transport engines for the environment of the eighties.
[SAE PAPER 730347] 17 p2257 A73-34695

Second generation supersonic transport, discussing fuel costs, changing markets, travel patterns, electronic displays and sound suppressor development
[SAF PAPER 730349] 17 p2102 A73-34697

Fundamental aspects of noise reduction from powered-lift devices.
[SAE PAPER 730376] 17 p2103 A73-34715

Status of current development activity related to STOL propulsion noise reduction.
[SAE PAPER 730377] 17 p2222 A73-34716

Design studies of low-noise propulsive-lift airplanes.
[SAE PAPER 730378] 17 p2103 A73-34717

An investigation of the vibratory and acoustic benefits obtainable by the elimination of the blade tip vortex.
[AHS PREPRINT 735] 17 p2105 A73-35071

A dynamics approach to helicopter transmission noise reduction and improved reliability.
[AHS PREPRINT 772] 17 p2106 A73-35090

Speckle reduction in holography by means of random spatial sampling.
17 p2172 A73-35429

Engine-over-the-wing noise research.
[AIAA PAPER 73-631] 18 p2267 A73-36190

Inter-noise 72; International Conference on Noise Control Engineering, Washington, D.C., October 4-6, 1972, Proceedings and Tutorial Papers.
19 p2472 A73-37276

On the role of the radiation directivity in noise reduction for STOL aircraft.
19 p2378 A73-37277

The ultimate noise barrier - Far field radiated aerodynamic noise.
19 p2375 A73-37278

Noise certification of a transport airplane.
19 p2378 A73-37279

A proposed littoral airport.
19 p2415 A73-37280

Predicting the reduction in noise exposure around airports.
19 p2378 A73-37281

Inglewood /California/ airport noise abatement monitoring program, discussing landing approach slopes, monitoring equipment and techniques and noise effects on property value

19 p2505 A73-37283

Jet engine noise reduction technology and design, discussing sonic pressure probes, high bypass turbofan engines, noise source fluctuations and far field measurements

19 p2472 A73-37287

Recent studies of fan noise generation and reduction.

19 p2473 A73-37293

Extraneous modes in sound absorbent ducts.

19 p2459 A73-37294

Noise reducing choked /sonic/ inlet design for V/STOL jet aircraft, discussing aerodynamic theoretical and experimental studies

19 p2375 A73-37295

Engineering design considerations in the noise control of commercial jet aircraft's vent and drain systems.

19 p2378 A73-37297

Vibration isolation and the use of controlled flexibility for noise reduction.

19 p2495 A73-37298

Effects of noise curfews on airline operations.

19 p2379 A73-37461

Noise from turbomachinery.

[AIAA PAPER 73-798]

Noise from turbomachinery.

[AIAA PAPER 73-815]

The design or operation of aircraft to minimize their sonic boom.

[AIAA PAPER 73-817]

Consequences of aircraft noise reduction alternatives on communities around airports.

[AIAA PAPER 73-818]

Noise and pollution - The Federal Aviation Administration's views.

19 p2384 A73-37812

Transport aircraft noise reduction in airport areas through low noise engine design, traffic control, flight maneuvers and architectural planning

19 p2384 A73-37818

Jet aircraft noise abatement near airports during takeoff, approach and landing, discussing noise measurement standards and regulatory and noise reduction design efforts

19 p2385 A73-37825

Possibilities and problems of achieving community noise acceptance of VTOL.

19 p2386 A73-38010

Testing noise-reducing approach techniques with the HFB 320 research aircraft of the DFVLR

19 p2387 A73-38265

Contributions of the DFVLR to environmental research and environment protection. II - Noise control, water environment protection, nature and landscape, environmental protection techniques

19 p2506 A73-38266

A status report on jet noise suppression as seen by an aircraft manufacturer.

[AIAA PAPER 73-816]

Optimum propulsion system design for advanced technology commercial transport, emphasizing low noise and emission, performance, reliability, maintainability and economics

[AIAA PAPER 72-760]

An adaptive scheme for PCM transmission.

20 p2523 A73-38728

ML receiver for binary signals with intersymbol interference in Gaussian noise.

20 p2524 A73-38733

Crosstalk compensation in optical beam transmission.

20 p2528 A73-38769

Damping of glass-like materials at high temperatures.

20 p2580 A73-39272

Application of the method of equivalent nonlinear systems to noise rejection analysis in FM tracking receivers

20 p2537 A73-39451

Wave dispersion equation for large eccentric elliptic jet stability calculations for noise suppression, using approximate Mathieu functions

20 p2549 A73-39807

Coherent imaging system suppression of noise /extraneous non-image light/ through multiple-wave illumination, periodic phase modulation and diffuse wave illumination

21 p2698 A73-40148

Vibration and noise damping of steel structures by prebonded laminates or viscoelastic layer additions, discussing steel sheets

21 p2717 A73-40236

A rational approach to the synthesis of one-dimensional acoustic filters.

21 p2739 A73-40285

Small-scale suppressor of the aerodynamic noise of a subsonic gas jet

21 p2754 A73-40404

Signal extraction from channel with noise- and signal-like interferences, analyzing clipping effect on SNR in time averaging processor

21 p2650 A73-40452

Peak subsonic noise level reduction by jet refraction, showing directivity patterns as function of jet velocities and temperature ratios

21 p2754 A73-40753

Frequency-following injection microwave oscillator with bias voltage control for tracking speed to provide amplifier or noise improvement circuit

21 p2664 A73-41091

Symbol set for multiregenerated digital transmission featuring highly redundant timing for low frequency phase noise suppression

21 p2656 A73-41110

Reduction of noise in high-power crossed-field amplifiers.

21 p2665 A73-41114

A method of reducing the influence of interference on the operation of a correlation interferometer

21 p2667 A73-41511

Boundary layer induced cockpit noise.

22 p2795 A73-41706

Reduction of fan noise by annulus boundary layer removal.

22 p2795 A73-41713

Rolls-Royce RB-211 jet engine noise reduction program, considering fan, compressor, turbine and tail-pipe noise and acoustic linings and powerplant configurations

22 p2900 A73-41717

Low-noise instrumentation for Raman and luminescence spectrometry with ruby and argon laser excitation.

22 p2868 A73-41783

Europlane QSTOL economical solution to noise and congestion problem in short and medium haul transport

22 p2798 A73-41862

Isolation of mechanical vibration, impact, and noise; Proceedings of the Colloquium, Cincinnati, Ohio, September 9-12, 1973.

22 p2926 A73-42920

Noise reduction by enclosures to block airborne and structure-borne acoustic paths, developing models for insertion loss in different frequency ranges

22 p2888 A73-42924

Redundant speckle free hologram production without spurious background patterns, blocking intensity by cutting of lower order frequencies

22 p2862 A73-43089

Speckle noise reduction by the composition of diffused Fraunhofer holograms.

22 p2863 A73-43093

Cepstrum signal processing with complex algorithm involving Fourier transforms and logarithm for multipath interference distortion reduction in single band or multiplexed transmission channels

23 p2953 A73-43321

Suppression of equichannel interference in the case of binary phase shift keying employing a limiter

23 p2953 A73-43324

Noise factor of a multiple-circuit input device

23 p2953 A73-43518

Turbulent boundary layer noise minimization by acoustic oscillation control, discussing suction and gas injection techniques

23 p2969 A73-43976

A model for the pressure excitation spectrum and acoustic impedance of sound absorbers in the presence of grazing flow.

[AIAA PAPER 73-995]

Subsonic and supersonic jets and supersonic suppressor characteristics.

[AIAA PAPER 73-999]

Swirling flow effect on jet noise suppression based on acoustic field and engine thrust measurements with and without stationary swirl vanes in exhaust nozzle

[AIAA PAPER 73-1003]

The influence of aerodynamic flow noise in turbofan engines.

[AIAA PAPER 73-1016]

Multiple pure tone noise generation and control.

[AIAA PAPER 73-1021]

Progress in source noise suppression of subsonic tip speed fans.

[AIAA PAPER 73-1032]

A study to determine the feasibility of a low sonic boom supersonic transport.

[AIAA PAPER 73-1035]

Maplin airport planning history, noise reduction features and government surveys, noting future air traffic trends and planning alternatives

24 p3077 A73-44830

Swirling flow effect on jet noise suppression based on acoustic field and engine thrust measurements with and without stationary swirl vanes in exhaust nozzle

[AIAA PAPER 73-1003]

The influence of aerodynamic flow noise in turbofan engines.

[AIAA PAPER 73-1016]

Multiple pure tone noise generation and control.

[AIAA PAPER 73-1021]

Progress in source noise suppression of subsonic tip speed fans.

[AIAA PAPER 73-1032]

A study to determine the feasibility of a low sonic boom supersonic transport.

[AIAA PAPER 73-1035]

Maplin airport planning history, noise reduction features and government surveys, noting future air traffic trends and planning alternatives

24 p3076 A73-45373

Aircraft noise reduction alternatives for operational aircraft, noting noise generation upstream of final nozzle, reengining, refanning and suppressor techniques

24 p3123 A73-45374

NOISE SPECTRA

LF noise in n-type GaAs and its correlation with HF noise of Gunn-diode oscillators

02 p0145 A73-11535

Some results on zero crossing distribution of non-stationary random noise.

02 p0143 A73-12857

Aerodynamic noise and alternating loads in an idealized turbine stage.

03 p0242 A73-12981

Acoustic power spectrum of a subsonic jet.

03 p0295 A73-14040

CW microwave oscillations of reach-through p-n-p barrier injection transit time /BARITT/ diodes, calculating small signal impedance and noise measure for comparison with experiment

04 p0427 A73-15346

A revised low-frequency cosmic noise spectrum.

04 p0500 A73-15516

Pyrotechnic shock synthesis using nonstationary broad band noise.

[ASME PAPER 72-WA/APM-19]

04 p0516 A73-15897

FM noise spectrum measurement in feedback harmonic oscillators with crystal or transmission cavity resonators as discriminator for frequency stability

05 p0556 A73-16164

Equations of motion for precession theory of two rotor gyroscopes on earth satellites for orbit plane determination, noting noise spectrum transformation

05 p0628 A73-16407

Evaluation of the noise autocorrelation function of stationary and moving noise sources by a cross correlation method.

[AIAA PAPER 73-186]

Intrinsic FM noise of Gunn oscillators.

07 p0798 A73-19341

Sound pressure level spectra measurements for four- and three-engine jet transport during concrete and grassy surface runup and flyover

[SAE AIR 1216]

08 p0927 A73-20693

X band Gunn oscillator FM noise spectrum dependence on quality factor of resonant circuit

09 p1062 A73-22322

Phase locked loop and coherent detection performance prediction, considering desirable phase detector characteristics in terms of SNR and noise spectral density

09 p1058 A73-23433

Characteristics of the VLF-noise spectrum during excitation of the earth-ionosphere resonator by cosmic sources.

10 p1188 A73-24222

Noise in single-frequency oscillators and amplifiers.

10 p1196 A73-24864

Equivalent circuit analysis of noise in bulk semiconductor devices.

10 p1197 A73-24869

Microwave range-difference measurements on 65-km slanted overwater path, interpreting tropospheric noise power spectra and rms values as function of baseline length

11 p1330 A73-25685

Digitally scanned spectral convolution by computerized filtering for noise spectra quality improvement with instrument signature removal

11 p1334 A73-26679

Observations of noise bands associated with the upper hybrid resonance by the Imp 6 radio astronomy experiment.

12 p1468 A73-26995

Complex measuring device for moving object location from multiple autonomous and nonautonomous information sources with different noise spectral compositions

12 p1484 A73-27447

Flat circular acoustic transducer for pressure spectrum analysis, deriving flow noise response correction factor in terms of polynomial coefficients and frequency-dependent constants

13 p1613 A73-28492

A unified analysis of fan stator noise.

13 p1563 A73-28500

Thermal noise measurements on space-charge-limited hole current in silicon.

13 p1668 A73-28542

On the existence in Schottky diodes of correlation laws between the parameters of the direct characteristic and the amplitude of low frequency background noise

13 p1590 A73-28565

Linear and nonlinear first order closed loop tracking radar systems, predicting noise performance by Gaussian signal amplitude fluctuation modeling

13 p1585 A73-29206

Noise in cavity-stabilized microwave oscillators.

13 p1595 A73-29294

Two-bladed large rotor mounted on tower in inverted mode to overcome recirculation effects, analyzing broadband noise spectra and directivity pattern

13 p1570 A73-29380

Noise at large RF amplitudes in IMPATT oscillators.

14 p1731 A73-29713

Anomalous low-frequency noise in MOS transistors at low temperatures.

14 p1731 A73-29749

A theory of oscillator noise and its application to IMPATT diodes.

15 p1851 A73-31939

French monograph - Contribution to the study of background noise in Gunn effect diodes.

15 p1852 A73-32589

A contribution to the proof of the formula for resistance noise
16 p1978 A73-32910

Spectral moving frame representation of jet noise by far field acoustic pressure autocorrelation and density function
16 p2000 A73-33681

Experimental gain and noise parameters of microwave GaAs FET's in the L and S bands.
17 p2136 A73-34972

Laboratory for the automatic treatment of analog signals
18 p2297 A73-37086

Spatial coherence characteristics of noise emission in active waveguide channel, considering Raman scattering of focused beam
19 p2437 A73-37247

Distribution of peaks in atmospheric radio noise.
19 p2403 A73-37269

Application of the coherence function to acoustic noise measurements.
19 p2458 A73-37284

Aircraft engine fan noise radiation from inlet and discharge ducts, describing wind tunnel tests and noise spectra at various blade tip speeds
19 p2472 A73-37288

Fan acoustic measurements by hot-wire anemometers in anechoic chamber, discussing turbulent flow characteristics, noise spectra, wire velocity spectra and blade tip shape
19 p2472 A73-37289

Low-frequency 1/f noise in MOSFET's.
19 p2409 A73-37581

Turbofan suction noise level measurements, discussing octave noise analysis, angular velocity distributions, discharge coefficient, takeoff and landing operations
19 p2473 A73-37816

Short term gyro drift measurements.
19 p2430 A73-38081

Quasi-periodic noises in a He-Ne laser.
19 p2438 A73-38166

An investigation of the combined amplification of monochromatic and noise signals in a TWT.
20 p2529 A73-38930

Intrinsic AM noise in singly tuned IMPATT diode oscillators.
20 p2537 A73-39417

Bipolar transistor base region noise current correlation with effective voltage, proposing equivalent circuit
20 p2538 A73-39597

Natural fluctuations in linear quantum amplifiers.
20 p2574 A73-39699

Noise loading analysis of a memoryless nonlinearity characterized by a Taylor series of finite order.
21 p2656 A73-41147

Noise caused by supersonic jet shock waves as function of jet pressure ratio, determining spectral characteristics
22 p2795 A73-41702

Noise from an isolated rotor due to inflow turbulence.
22 p2795 A73-41711

Aircraft flyover noise - Spectral analysis of sounds and sound intensity fluctuations.
22 p2800 A73-42946

Signal and noise in the human oculomotor system.
22 p2810 A73-42964

Dynamic range and frequency response of the vortex rate sensor.
23 p2942 A73-43406

An innovations approach to least-squares estimation. V - Innovations representations and recursive estimation in colored noise.
23 p2954 A73-43819

Spectroscopic polarization analysis of turbulent plasma noise produced by the annihilation of opposite magnetic fields
23 p3012 A73-44016

Studies on a band limited white noise with a uniform bispectrum.
23 p2965 A73-44135

The frequency stability and noise of passive Rb standard.
23 p2965 A73-44137

Some results in predicting the states of semiconductor triodes from noise factors on the basis of the statistical theory of pattern recognition
23 p2961 A73-44297

Noise comparisons from full-scale fan tests at NASA Lewis Research Center.
24 p3121 A73-44849

[AIAA PAPER 73-1017] Low frequency noise generation within aircraft gas turbine engine core portion, discussing sources prediction, model and full scale engine tests, and future technology
24 p3122 A73-44858

[AIAA PAPER 73-1027] Mechanisms of externally blown flap noise.
24 p3056 A73-44859

[AIAA PAPER 73-1029] Progress in source noise suppression of subsonic tip speed fans.
24 p3122 A73-44861

[AIAA PAPER 73-1032] Spectral trends in rotor noise generation.
24 p3056 A73-44862

[AIAA PAPER 73-1033]

Comparison of aircraft noise measured in flight test and in the NASA Ames 40- by 80-foot wind tunnel.
24 p3056 A73-44871

Spectral analysis of frequency noise of oscillators by the Hadamard variance
24 p3073 A73-44974

A comparison of the overall and broadband noise characteristics of full-scale and model helicopter rotors.
24 p3057 A73-45264

NOISE STORMS
Correlation analysis of the continuum radio emission of noise storms.
04 p0504 A73-16028

Structure of a noise-storm source according to observations of the eclipse of September 22, 1968 at the 1.37-m wavelength
16 p2057 A73-32704

Dependence of some noise-storm characteristics on the solar activity cycle
23 p3036 A73-44249

NOISE SUPPRESSORS
U NOISE REDUCTION
NOISE TEMPERATURE
Noise factor and power formula for cooled SHF broadband frequency converters with semiconductor mixer diode
01 p0026 A73-11265

Noise temperature and signal characteristics of parametric microwave superheterodyne receiver with downconverter for satellite communication, radio and TV transmission
03 p0277 A73-13986

The 15 m Cracow radiotelescope. I - Technical description and observational possibilities.
08 p0952 A73-20850

Measurement of amplifier noise.
08 p0949 A73-21623

Some perspectives on receiver noise performance and its measurement.
08 p0940 A73-21624

Semiconductor diode mixer for millimeter-wave frequencies.
10 p1193 A73-23665

Performance of multifrequency parametric converter with resonant circuits as function of input and parametric diode characteristics, using gain and noise temperature coefficients
10 p1196 A73-24605

Equivalent noise temperature equation relating HF noise in mm wave Schottky barrier diodes to barrier transport mechanism
11 p1339 A73-26697

The first two receivers for the radio astronomy programme on the 100 meter radiotelescope - An assessment of performance.
13 p1581 A73-28000

Direct-reading measurement of receiver-noise parameters.
13 p1590 A73-28531

NASA computer generated 136/400-MHz radio sky maps covering whole celestial sphere for earth-based receiver noise temperature determination in satellite communication
13 p1585 A73-29115

Zenith atmospheric emission noise temperature and attenuation measurements including multiple and single frequency statistical observations at 85-118 GHz during 1970-1971
16 p1982 A73-33720

Noise factor and power formula for cooled SHF broadband frequency converters with semiconductor mixer diode
17 p2134 A73-34317

Atmospheric attenuation anomalies at 2.7 mm from sky noise temperature measurements compared with water vapor and oxygen line strength calculations
17 p2159 A73-34571

Calculation of the antenna noise temperature in the RATAN-600 radio telescope
21 p2667 A73-41448

Radio astronomical traveling wave maser with ruby or doped rutile single crystals, superconducting magnet, cryogenic equipment and low noise temperature
23 p2953 A73-43375

Low-noise microwave receiving systems in a world-wide network of large antennas.
23 p2958 A73-43376

Noise factor of a multiple-circuit input device
23 p2953 A73-43518

Experimental investigation of the frequency dependence of the steady-state noise temperature of reverse-biased tunnel diodes between 0.001 and 30 MHz
24 p3072 A73-44931

NOISE THRESHOLD
Temporary threshold shift caused by combined steady-state and impulse noises.
01 p0077 A73-10785

Conditions for termination of tracking in electronic servo systems
10 p1202 A73-24610

NOISE TOLERANCE
Noise effects on the critical tracking performance of the human operator.
01 p0010 A73-10107

Annoyance reactions from aircraft noise exposure.
01 p0005 A73-10781

Temporary threshold shift caused by combined steady-state and impulse noises.
01 p0077 A73-10785

Model study of aircraft noise reverberation in a city street.
02 p0130 A73-12199

The second noise and social survey around Heathrow, London airport.
03 p0266 A73-12980

Effects of intermittent and continuous noise on serial search performance.
03 p0267 A73-13560

The interaction of auditory noise and subjective noise annoyance sensitivity with peripheral visual sensitivity.
05 p0543 A73-16703

Effects of noise and response complexity upon vigilance performance.
06 p0656 A73-17523

Effects of aircraft noise on human sleep.
06 p0659 A73-18546

Electrophysiological investigation of noise rejection in an auditory system receiving sound from a localized source
09 p1040 A73-22580

Combined effects of noise and vibration on human tracking performance and response time.
11 p1323 A73-25334

Definitions and procedures for computing the effective perceived noise level for flyover aircraft noise.
16 p1967 A73-33015

Intellectual performance during prolonged exposure to noise and mild hypoxia.
18 p2283 A73-36783

Noise immunity of autocorrelation reception of single PSK signals.
18 p2291 A73-37135

Aircraft noise disruption in public schools - A definition of an impasse.
19 p2505 A73-37282

Action of stable and pulsed noise on the processes of skeletal muscle excitation
22 p2815 A73-42662

Human noise sensitivity, discussing personality effects, Maplin airport planning and population separation into sensitive and imperturbable groups
24 p3062 A73-44770

NOMENCLATURES
Origin, classification, nomenclature and incidence of the atrial arteries in normal human hearts, with special reference to their clinical importance.
04 p0409 A73-15522

Extending lunar nonmenclature to the far side of the moon.
05 p0612 A73-16089

Classification, scale sequence, and nomenclature of lunar maps
13 p1672 A73-28117

NOMINAL VALUES
U APPROXIMATION
NOMOGRAPHS
Ionospheric electron density profiles calculation from ionograms via nomograph relating gradients of possible and actual height in given frequency interval of integration
02 p0159 A73-12184

Method of solving the interplanetary orbit optimization problem with an invariant nomographic scale.
05 p0613 A73-16093

Book - Calculation of wave propagation by nomograms - Frequencies above 30 MHz.
05 p0548 A73-16325

Approximate nomograms for the characteristics of chemical-fuel combustion products
12 p1532 A73-27087

A nomographic comparison of coherent and non-coherent detection statistics.
16 p1980 A73-33415

Nomograms for determining horizontal coordinates of artificial earth satellites
16 p2063 A73-33662

Total ozone increase over North America during the 1960's.
23 p2973 A73-43857

Reliability estimation for repairable and nonrepairable flight vehicles, considering nomographs for failure rate and probability of defined requirements satisfaction
24 p3057 A73-45197

NONADIABATIC CONDITIONS
U ADIABATIC CONDITIONS
NONADIABATIC THEORY
Nonadiabatic temperature change in rapidly expanded or compressed gas, discussing shearing and volume viscosity effects
05 p0597 A73-16350

Nonadiabatic condition effects on ultrarelativistic electron energy losses in geomagnetic trap in remote magnetosphere regions
12 p1535 A73-27649

Numerical weather prediction models based on hydrothermodynamic equations and nonadiabatic fac-

tors for short term regional, hemispheric and global forecasting
18 p2331 A73-35909

Influence of nonadiabatic effects during magnetic storms on the dynamics of proton belts
21 p2760 A73-40907

NONAXISYMMETRY

U ASYMMETRY

NONCONDENSABLE GASES

Effects of forced flow, noncondensables, and variable properties on film condensation of pure and binary vapors at the forward stagnation point of a horizontal cylinder.
01 p0122 A73-10806

Steady two-dimensional heat and mass transfer in the vapor-gas region of a gas-loaded heat pipe.
[ASME PAPER 72-WA/HT-34] 04 p0518 A73-15821

The effect of noncondensable gas on laminar film condensation of liquid metals.
[ASME PAPER 72-WA/HT-9] 04 p0520 A73-15836

Apollo 17 mass spectrometer indication of rare gases and molecular hydrogen in lunar atmosphere, confirming noncondensable gas model
18 p2349 A73-35973

NONCONDUCTORS

U ELECTRICAL INSULATION

NONCONSERVATIVE FORCES

Beams subjected to follower force within the span.
04 p0508 A73-14938

Effect of external-load nonconservativeness on the stability of an idealized elastoplastic rod
05 p0635 A73-17076

Book - On elastic stability under nonconservative loads.
06 p0762 A73-18275

Damping configurations that have a stabilizing influence on nonconservative systems.
07 p0908 A73-19088

Application of the complementary energy method to two non-conservative problems of elastic stability.
10 p1291 A73-24393

Canonical perturbation theory solution for nonconservative dynamic systems equations of motion, considering Duffing and van der Pol equations
10 p1283 A73-24665

On the role of the adjoint problem in dissipative, nonconservative problems of elastic stability.
11 p1434 A73-25214

Application of a variational method to dissipative, non-conservative problems of elastic stability.
13 p1700 A73-29376

Rayleigh-Ritz coefficient application in variational principle calculations of instability and flutter load of nonconservative systems
16 p2031 A73-32980

Variational methods applied to nonconservative stability problems of elastic continua.
16 p2078 A73-32995

Column instability under nonconservative forces, with internal and external damping - Finite element using adjoint variational principles.
20 p2621 A73-39540

An approximate analysis of non-linear, non-conservative systems using orthogonal polynomials.
21 p2740 A73-40755

Vibration and stability of nondivergent elastic systems.
22 p2922 A73-42551

NONDESTRUCTIVE TESTS

NT PRELAUNCH TESTS

NT STATIC FIRING

Development and present state of the non-destructive testing of semi-finished products
01 p0056 A73-10587

An electromagnetic comparator system with improved possibilities in regard of sorting and recording of absolute test parameters
01 p0056 A73-10588

The resolution of flaw depth of angle probes for ultrasonic testing
01 p0056 A73-10589

Measurement of surface temperatures by means of an infrared camera - Application in non-destructive testing
01 p0050 A73-10590

Ultrasonic sensing apparatus and eddy current method in NDT, noting radiography, sonics, penetrants and magnetic particles
01 p0057 A73-11001

Computer based data processing system with display for improving ultrasonic pulse echo NDT test equipment resolution and SNR
02 p0173 A73-11983

Dual sensitivity liquid penetrants for improving NDT inspection of minute defects in military aircraft structures during rework and repair, noting comparative advantages
02 p0173 A73-11984

The influence of X-ray parameters on crack detection capability.
[NA-72-779] 02 p0173 A73-11985

Ultrasonic measurements of cold-work percentages in Type 316 stainless steel.
02 p0173 A73-11987

Automatic magnetic inspection method using magnetoresistive elements and its application.
02 p0173 A73-11988

The acoustic emission response of mechanically stressed ceramics.
02 p0173 A73-11989

Optimum operation conditions of thyatron generator circuit in electroacoustic system for excitation of quartz piezoelectric vibrators in ultrasonic NDT
02 p0168 A73-12147

Use of ultrasonic emission in nondestructive inspection.
02 p0169 A73-12148

Determining the size of defects in standardizing sensitivity using a spherical reflector.
02 p0169 A73-12149

Ultrasonic inspection of nickel-base alloy products.
02 p0174 A73-12150

Applications of dynamic photoelasticity in flaw detection analysis. I.
02 p0175 A73-12868

Computer technique for automated acoustical inspection of rotating machines
03 p0311 A73-12958

The relationship between dielectric and mechanical properties of polymers.
03 p0332 A73-13036

Liquid crystals for nondestructive testing of composite structures.
03 p0349 A73-13041

Ultrasonic holography application to NDT, discussing small angle approximation to spherical beam, hologram formation, image reproduction and wavelength change effect
04 p0446 A73-14674

Holographic correlation offers new possibilities for acoustical NDT.
04 p0446 A73-14675

Applications of exoelectron emission to nondestructive evaluation of alloying, crack growth, fatigue, annealing, and grinding processes.
04 p0453 A73-14856

The early detection of fatigue damage by exoelectron emission and acoustic emission.
04 p0453 A73-14858

Verification of structural integrity of pressure vessels by acoustic emission and periodic proof testing.
04 p0453 A73-14859

NDT applications of acoustic or stress wave, ultrasonic spectroscopy, imaging, critical angle reflectivity and holography
04 p0447 A73-14927

Pattern classification in scan-type nondestructive tests.
04 p0447 A73-14928

Leakage field methods of defect detection.
04 p0447 A73-14929

Some results using the ultrasonic goniometer - The corner reflector method.
04 p0447 A73-14930

Nondestructive detection of hydrides and alpha-case in titanium alloys.
04 p0461 A73-15217

Laser irradiation testing - A new method for the nondestructive study of plastic material
04 p0458 A73-15324

Nondestructive eddy current tests of Al bronze alloy fillet size and flatwise distribution in Ti honeycomb sandwich panels
05 p0581 A73-16131

Imaging techniques for testing and inspection; Proceedings of the Seminar-in-Depth, Los Angeles, Calif., February 14, 15, 1972.
05 p0573 A73-16276

An overview - Advantages of imaging techniques for nondestructive testing.
05 p0573 A73-16277

Imaging techniques for low-flux neutron radiography.
05 p0573 A73-16279

Bragg-diffraction imaging and its application for non destructive testing.
05 p0574 A73-16281

Application of graphic display to ultrasonic testing.
05 p0574 A73-16282

Ultrasonic isometric imaging.
05 p0574 A73-16283

Acoustic holographic scanning techniques for imaging flaws in thick metal sections.
05 p0574 A73-16284

Holographic interferometry techniques and applications, discussing gas and ruby lasers in imaging, measurements and NDT of materials and mechanical components
05 p0574 A73-16286

Nondestructive screening and pulse damage mechanism for thermal second breakdown of semiconductor junction diodes
05 p0557 A73-16504

Nondestructive and impulsive testing of electroexplosive devices.
05 p0606 A73-17207

Cholesteric liquid crystals thermophysical properties application in aerospace sciences and engineering,
05 p0606 A73-17207

noting temperature measurement and nondestructive tests
06 p0733 A73-17767

Determination of the extent of ultrasonically detected defects - Application to welded butt joint quality control
07 p0831 A73-19904

Some new developments in nondestructive testing.
08 p0963 A73-20869

Radiography and ultrasonic tests for weldment and flaw inspection, discussing choice based on economic, technical and application considerations
08 p0952 A73-21076

Non-destructive testing in industry - Non-ferrous metals.
08 p0973 A73-21077

Visualization of pulsed ultrasound using stroboscopic photoelasticity.
08 p0973 A73-21078

Investigation of the sensitivity of a duct sensor to discontinuities in alternating fields of square-pulse or sinusoidal shape - Detectability of surface defects on nonmagnetic and ferromagnetic specimens. I
08 p0967 A73-21587

Possibilities of determining the permissible reverse-bias current and voltage in semiconductor devices by a nondestructive method
09 p1061 A73-21979

Neutron radiography as a diagnostic tool in the study of corrosion in lithium-filled heat pipes.
09 p1079 A73-21991

Unconventional methods of generating, detecting and coupling of ultrasound in non-destructive testing
09 p1088 A73-22218

Simple test apparatus for a 100% defect-detection probability in ultrasonic surface scanning of plates and strips
09 p1070 A73-22219

Multielement scanning system for acoustic holography application in nondestructive testing, combining multiple mechanical sensors with simultaneous electronic commutation
09 p1080 A73-22297

Ultrasonic structure analyzer for nondestructive inspection of fine grained metallic materials
09 p1080 A73-22298

Investigation of the detectability of defects in the ultrasonic testing of joints obtained by friction welding.
09 p1088 A73-22299

Instrument Society of America, Annual Conference, 27th, New York, N.Y., October 9-12, 1972, Proceedings. Part 2.
09 p1082 A73-22501

Holographic laboratory practice for NDT, discussing data reduction, display and pulse laser development
09 p1083 A73-22513

Acoustical holography applications in nondestructive testing.
09 p1083 A73-22514

Defect detection in solid materials with the aid of holographic vibration analysis
09 p1089 A73-23115

Holographic interferometry as nondestructive testing method, discussing applications to defects detection in tires, metal-rubber vibration isolators and glass fiber reinforced plastic tubing
10 p1218 A73-24173

Elastic wave analysis in nondestructive testing.
10 p1292 A73-24630

A mechanized eddy current scanning system for aircraft struts.
10 p1225 A73-24631

Design procedures for matched and broadbanding filters for scanning tests.
11 p1341 A73-25074

Direct nondestructive prediction of engineering properties.
11 p1372 A73-25129

Holographic nondestructive evaluation of interference fit fasteners.
11 p1366 A73-26247

Non-destructive testing of adhesive bonding.
11 p1374 A73-26299

Eddy current testing - The present situation, results, new developments.
11 p1374 A73-26300

Use of reflection-coefficient amplitude-phase diagrams for choosing and analyzing the operating modes of a radio defectoscope.
11 p1375 A73-26363

Comparative investigation of sensitivities of the xeroradiographic and the roentgenographic methods of flaw detection.
11 p1375 A73-26364

Fringe control in real time and double exposure holography for nondestructive testing of multilaminated and thin laminated structures and vibration analysis
11 p1370 A73-26541

Nondestructive flaw detection by holographic interferometry, discussing methods, equipment and applications for materials testing and vibrational analysis
11 p1371 A73-26551

Temperature sensitivity of cfrp honey-comb structures under holographic ndt. 12 p1496 A73-27036

An ultrasonic technique for the inspection of magnetic and explosive welds, using a facsimile recording system. 12 p1502 A73-27037

Measuring projection weld strength by acoustic emission. 12 p1502 A73-27038

Use of Sirtl etch for silicon-slice evaluation. 12 p1530 A73-27044

Bragg-diffraction imaging - A potential technique for medical diagnosis and material inspection. 13 p1614 A73-28582

Graphic display for ultrasonic nondestructive testing. 13 p1615 A73-28586

Russian book on ultrasonic methods for weld testing covering flaw detection, emitters/receivers, acoustic channels, echo and mirror shadow methods, automatic testing, etc 13 p1624 A73-28949

Multiple-fault detection in large logical networks. 13 p1588 A73-29296

Laser illumination for infrared nondestructive testing. 15 p1874 A73-31050

Russian book on ionizing radiation introscopic methods for nondestructive flaw detection in non-transparent objects covering imaging techniques and quality control equipment 15 p1875 A73-31580

Integral equations for nondestructive determination of buckling loads for elastic plates and bars. 15 p1948 A73-31634

The ultrasonic pulse-echo technique as applied to adhesion testing. 15 p1882 A73-31673

Techniques and equipment for thermal nondestructive quality control of products and materials. 15 p1882 A73-31692

Setting of sensitivity of ultrasonic equipment for weld inspection. 15 p1882 A73-32025

The use of the terms nearfield and farfield in ultrasonic non-destructive testing 15 p1882 A73-32052

The attenuation of ultrasonic waves in cylindrical work pieces with central bore-hole 15 p1882 A73-32053

The most important characteristics of magnetizing equipment in the leakage-flux technique - Their measurement and application 15 p1882 A73-32054

Performance and possibilities of application of an electromagnetic comparator 15 p1883 A73-32056

Book - Techniques involving extreme environment, nondestructive techniques, computer methods in metals research, and data analysis. Part 1. 16 p2017 A73-32696

Nondestructive inspection method for jet engine turbine blades. [ASME PAPER 73-GT-92] 16 p2019 A73-33530

Forecasting failures with acoustic emission. 16 p2022 A73-33992

Flaw detection and characterization using acoustic emission. 16 p2022 A73-34013

Application of frequency analysis to ultrasonic non-destructive testing 16 p2016 A73-34014

Device for nondestructive measurement of secondary-breakdown parameters in transistors 17 p2133 A73-34161

Acoustic emission coincidence detector for monitoring high residual stress areas in symmetrical pressure vessels. 17 p2166 A73-34620

Development and qualification of a magnetic technique for the nondestructive measurement of residual stress in CH-47 A rotor blade spars. [AHS PREPRINT 752] 17 p2180 A73-35080

Non-destructive testing of plastics by means of holographic interferometry. 17 p2181 A73-35355

Nondestructive optical contour mapping for non-contact testing of reflecting surface deformations from interference pattern due to monochromatic illumination of grating 17 p2172 A73-35419

A nondestructive measurement of the elastic constants of unidirectional borsic fiber reinforced aluminum composites. [SC-DC-72-1644] 17 p2182 A73-35439

A new non-destructive method for three-dimensional photoelasticity. [SESA PAPER 2143A] 17 p2182 A73-35451

Acoustic emission instrumentation and application for plastic deformation, flaw detection monitoring of fatigue crack growth, stress corrosion and hydrogen embrittlement 17 p2175 A73-35670

Nondestructive testing of fiberglass reinforced plastic plates by means of holographic interferometry 18 p2316 A73-36477

Fracture and flaws; Proceedings of the Thirteenth Annual Symposium, Albuquerque, N. Mex., March 1, 2, 1973. 18 p2363 A73-36482

Fracture mechanics in materials selection and design. 18 p2363 A73-36483

A survey of nondestructive testing techniques. 18 p2320 A73-36484

Some applications of spectral analysis in ultrasonic testing. 18 p2316 A73-36485

A real-time software operating system for a computer-controlled acoustic emission flow monitor. 18 p2316 A73-36679

Visualization of surface elastic waves on structural materials. 19 p2432 A73-37449

Method of measuring the size of defects without using calibrating standards and adjusting the sensitivity of ultrasonic defectoscopes. 19 p2432 A73-38358

Method of holography in nondestructive testing. 19 p2432 A73-38359

On the ultrasonic inspection of separation in solid propellant rocket motors. 20 p2568 A73-38646

Inspecting thin tubes by ultrasounds - Choice of examination frequency 21 p2707 A73-41068

Contactless on-line NDT of metal plates for concealed defects by Lamb wave excitation through wave generation from air 21 p2708 A73-41138

Commercial aircraft system effectiveness survey questionnaire response data concerning various tests in manufacturing and operational environments 21 p2635 A73-41205

Scribe line technique detects incomplete fusion in EB welds. 21 p2708 A73-41251

Nondestructive shell-stability estimation by a combined-loading technique. 21 p2708 A73-41266

Magnetic rubber inspection to extend NDT capabilities for locating cracks and defects on or near magnetic material surface 21 p2708 A73-41324

Electroexplosive device pin-pin firing frequency mathematical modeling and prediction based on RF impedance data obtained nondestructively by automatic network analyzer 22 p2822 A73-41793

The nondestructive tests in the maintenance of commercial aircraft 22 p2799 A73-42186

Applications of liquid crystals to information display, fault detection, and medical thermography. 22 p2897 A73-42524

Ultrasonic spectroscopy for NDT of composite material tube, noting role of frequency signature and pulse spreading in flaw detection 23 p2984 A73-43641

Acoustic emission from low-cycle high-stress-intensity fatigue. 23 p2992 A73-43816

Expanding the capability of a laboratory ultrasonic testing facility. 23 p2966 A73-44168

A technique for placing known defects in weldments. 23 p2986 A73-44170

Some results of the application of the nondestructive ultrasonic method to the measurement of residual stresses 23 p2996 A73-44289

Phase-sensitive method of electromagnetic flaw detection. 24 p3093 A73-44696

Determination of the point at which damage occurs in glass-reinforced laminates - New nondestructive methods and their suitability as production control procedures 24 p3103 A73-44879

Materials testing by sonic emission analysis/SEA/ 24 p3094 A73-45445

NONEQUILIBRIUM CONDITIONS

Hypersonic, viscous shock layer with chemical nonequilibrium for spherically blunted cones. 01 p0002 A73-10746

Nonequilibrium thermodynamics description of convective motion, using internal energy and absolute mass flows as generalized convective flow 01 p0123 A73-10867

Condensation of excitons in momentum space under the influence of optical pumping. 02 p0177 A73-12696

Calculation of shock wave relaxation zones including dissipative transport phenomena. 05 p0567 A73-17114

NONEQUILIBRIUM IONIZATION

A non-equilibrium thermodynamical analysis of the origin of life. 06 p0651 A73-17931

A new integral-variational method for calculation of relaxation regions behind shock and detonation waves. 07 p0809 A73-19030

Kinetics of the excitation of molecular vibrations by infrared laser radiation 09 p1094 A73-22597

Nonequilibrium radiative and inelastic collisional transitions structuring of ionizing shock waves in He and Ar 11 p1449 A73-25253

Nonequilibrium thermodynamics description of convective motion, using internal energy and absolute mass flows as generalized convective flow 12 p1560 A73-27917

Multiphase underexpanded plume computational technique including turbulent mixing and nonequilibrium chemistry. 18 p2368 A73-36244

Experimental study of the heat transfer in the vicinity of the critical point during nonequilibrium physicochemical transformations and determination of the nitrogen recombination rate constant 18 p2287 A73-37013

Nonequilibrium velocity distributions and reaction rates in fast highly exothermic reactions. 19 p2402 A73-37897

Effects of translational disequilibrium on the structure of a shock wave in an ionized monatomic gas 22 p2895 A73-43045

NONEQUILIBRIUM DRAG

U FRICTION DRAG

NONEQUILIBRIUM FLOW

Aerodynamics of blunted bodies in hypersonic stream at the angle of attack. 01 p0003 A73-11133

On the multi-parameter characteristic perturbation method - Application to nonlinear supersonic nonequilibrium flow over a wedge. 01 p0004 A73-11425

A numerical analysis for chemical non-equilibrium boundary layer of dissociated gases over a flat plate with arbitrary catalyticity. 03 p0291 A73-13068

Vibrational and chemical nonequilibrium in a stoichiometric turbojet engine using kerosene-type fuel. [AIAA PAPER 72-1208] 03 p0273 A73-13491

Calculation of the supersonic region of three-dimensional nonequilibrium air flow past bodies 03 p0245 A73-13618

Effects of a fully catalytic wall on a non-equilibrium boundary layer including ablation products. [ASME PAPER 72-WA/HT-28] 04 p0519 A73-15826

Method of approximate calculation of the laminar boundary layer outside of vibrational equilibrium 08 p1023 A73-21259

Russian book - Nonequilibrium physicochemical processes in aerodynamics. 09 p1029 A73-23225

Three-dimensional motion of a reacting gas mixture around a blunt body 15 p1822 A73-31290

The analysis of nonequilibrium, chemically reacting, supersonic flow in three dimensions using a bicharacteristics method. 17 p2151 A73-34891

On the solution of the unsteady Navier-Stokes equations including multicomponent finite rate chemistry. 18 p2259 A73-36157

Engineering approximations for radiating nonequilibrium shock layers. 18 p2297 A73-36224

Analysis of nonequilibrium particulate flow. [AIAA PAPER 73-687] 18 p2298 A73-36238

Linear theory for chemically reacting flows. [AIAA PAPER 73-688] 18 p2298 A73-36239

An integral procedure for estimating boundary layer parameters and heat transfer in arbitrary pressure gradients. 18 p2298 A73-36249

Calculation of hypersonic nonequilibrium nozzle flows with excited vibrational degrees of freedom. 18 p2266 A73-37018

On an equilibrium-frozen flow approximation in the analysis of nonequilibrium nozzle flows. 19 p2422 A73-38282

Interaction of parametrically coupled waves in nonequilibrium media /Survey/ 19 p2406 A73-38326

A method of calculating a chemically nonequilibrium flow of gas in a heated tube under conditions close to the equilibrium or frozen state 24 p3081 A73-45527

NONEQUILIBRIUM IONIZATION

Stationary state of the radially symmetrical motion of vapors heated by laser radiation with allowance for thermal and ionizational nonequilibrium 02 p0175 A73-11601

Flow of a two-temperature plasma in the duct of a disk-type magnetohydrodynamic generator with al-

NONEQUILIBRIUM PLASMAS

lowance for nonequilibrium ionization and recombination reactions

06 p0727 A73-17464

Experiments of magnetohydrodynamic conversion with ionization out of equilibrium

06 p0730 A73-18541

Effect of ionization nonequilibrium on the shock wave in the stagnation region

07 p0776 A73-20616

Influence of boundaries of the ionization instability of a plasma in a discharge of coaxial geometry.

08 p0992 A73-20851

Influence of inelastic energy losses by electrons on the development of ionization instability in a plasma.

08 p0992 A73-20852

On the steady flow of a non-equilibrium ionized gas around sharp corners in the presence of a crossed magnetic field.

08 p0992 A73-21009

Nonequilibrium transport process calculation by theoretical microscopic model for interaction between ionized gas and solid particles in suspension, noting free electron concentration change

09 p1130 A73-22826

Excitation of magnetosonic waves in a plasma with nonequilibrium ions

09 p1131 A73-23076

Influence of ionizational turbulence on the operation of an MHD generator with nonequilibrium plasma

10 p1253 A73-23502

Nonequilibrium ionization in magnetohydrodynamic conversion generators

13 p1571 A73-28071

Discharge characteristics in cesium-seeded argon.

13 p1665 A73-28807

Small perturbation method study of nonlinear weak D-type unsteady ionization front geometry with radiation source in interstellar incompressible gas medium

15 p1932 A73-31295

Effect of ionization turbulence on the operation of an MHD generator operating with a nonequilibrium plasma.

17 p2217 A73-35182

On the flow of a nonequilibrium ionized gas past a wall in the presence of a magnetic field.

19 p2465 A73-37178

A new type of ionizational instability in a plasma with negative ions

20 p2598 A73-39621

Structure of ionizing shock waves with radiative energy loss.

22 p2841 A73-42200

Kinetics of impact-radiation ionization and recombination.

22 p2892 A73-42344

NONEQUILIBRIUM PLASMAS

Effect of viscosity on the motion of the inhomogeneities of a nonequilibrium plasma in a magnetic field

01 p0085 A73-10865

Computation of the axisymmetrical free expansion of a nonequilibrium hydrogen plasma

02 p0196 A73-11604

End effects in Faraday type MHD generators with nonequilibrium plasmas.

03 p0254 A73-14185

Stability of a plasma with inequilibrium ions with respect to the generation of magneto-sonic waves

04 p0481 A73-15603

Mechanism of motion of inhomogeneities in a nonequilibrium plasma in a magnetic field.

06 p0726 A73-17401

Nonequilibrium plasma wave scattering cross section dependence on energy bands shape and field orientation in semiconductors

06 p0735 A73-17975

Feedback control of ionization instability in MHD generators.

07 p0779 A73-20395

Electrode and gasdynamic effects in a large nonequilibrium MHD generator.

08 p0928 A73-20713

High-frequency instability of an electromagnetic wave in a nonequilibrium magnetized plasma

09 p1130 A73-22705

Influence of ionizational turbulence on the operation of an MHD generator with nonequilibrium plasma

10 p1253 A73-23502

Stability of a plasma with nonequilibrium ions with respect to magnetosonic waves.

10 p1254 A73-24193

Absorption and amplification of electromagnetic waves in a nonstationary magnetoactive plasma with allowance for spatial dispersion

11 p1405 A73-26151

Influence of a SHF field on the inhomogeneities of a nonequilibrium plasma from a low-pressure gas discharge

12 p1528 A73-27304

Optimization of the power of a Faraday-type MHD-generator operating with a nonequilibrium plasma

12 p1460 A73-27320

ARC discharge plasma diagnostics for nonuniform nonequilibrium turbulent sources, including automatic methods for control applications

12 p1528 A73-27322

Influence of viscosity on the motion of nonuniformities of a nonequilibrium plasma in a magnetic field.

12 p1529 A73-27914

Effects of channel size on the ionization instability in MHD generators.

17 p2108 A73-34185

Electron energy distribution function validity for nonequilibrium plasma in presence of electric field verified for ionized cesium vapor positive column

17 p2216 A73-34551

Effect of ionization turbulence on the operation of an MHD generator operating with a nonequilibrium plasma.

17 p2217 A73-35182

Nonlinear wave interaction and fluctuations in plasma.

17 p2217 A73-35818

Entry of a high-frequency longitudinal field into a nonequilibrium plasma

18 p2339 A73-36554

Plasma channel flow theoretical and experimental review, considering heat transfer studies, turbulent nonequilibrium plasma boundary layers and plasma sheaths

19 p2464 A73-37161

MHD boundary layers on a segmented electrode-wall of a nonequilibrium generator.

19 p2470 A73-38314

Thermal model for streamers in nonequilibrium plasmas.

19 p2470 A73-38317

Effect of an isotropic nonequilibrium plasma on electron temperature measurements.

20 p2552 A73-38947

Experimental investigation of the characteristics of a nonequilibrium MHD generator

20 p2511 A73-39618

A numerical investigation of the current and density distributions for a non-equilibrium plasma in a segmented electrode duct.

21 p2748 A73-40926

Magnetic pulsation spectra in a nonisothermal plasma.

22 p2890 A73-41725

The numerical prediction of streamer growth in MHD ducts.

22 p2894 A73-42558

On the determination of electron temperature in diffusion-dominated non-L.T.E. plasmas.

22 p2896 A73-43167

An MHD generator with a nonequilibrium plasma produced by VHF ionization

23 p3011 A73-43714

Wave-wave contribution to the high-frequency resistivity of nonequilibrium plasma.

24 p3117 A73-45457

NONEQUILIBRIUM RADIATION

Nonequilibrium effects on shock-layer radiometry during earth entry.

18 p2338 A73-36798

NONEQUILIBRIUM THERMODYNAMICS

Nonequilibrium statistical operators and quasi-means in the theory of irreversible processes

21 p2741 A73-41298

Gasdynamic equations for low temperature monatomic gas, showing Wigner distribution function independence of density gradient in agreement with nonequilibrium statistical thermodynamics concepts

23 p2939 A73-43704

NONEUCLIDIAN GEOMETRY

U DIFFERENTIAL GEOMETRY

NONFERROUS METALS

Russian papers on nonferrous metal alloys covering physical and mechanical properties, crystallization, casting, solid solutions and heat treatment

03 p0323 A73-13501

Ferrous and nonferrous metal alloys melting and remelting in plasma induction and beam furnaces, noting cost reduction and ingots homogeneity

04 p0455 A73-15748

Non-destructive testing in industry - Non-ferrous metals.

08 p0973 A73-21077

Welding and fabrication of non-ferrous metals; Proceedings of the International Conference, Eastbourne, Sussex, England, May 2, 3, 1972. Volume 1.

08 p0973 A73-21235

Possibility of argon-nitrogen gas metal-arc welding of some non-ferrous metals.

08 p0973 A73-21237

Sliding friction welding of nonferrous Cu, wrought Al alloy and Ti, resting rubbing speed and axial pressure effects on equilibrium condition transition

08 p0973 A73-21238

Problems in electron-beam welding of non-ferrous metals.

08 p0973 A73-21243

Investigation of the detectability of defects in the ultrasonic testing of joints obtained by friction welding.

09 p1088 A73-22299

An investigation into the electron beam welding of five non-ferrous alloys.

11 p1372 A73-25125

Russian papers on nonferrous metals and alloys, metallurgy covering phase equilibria, strengthening, deformation and processing of Al, Mg, Cu and Ti alloys

12 p1510 A73-26902

Recovery of nonferrous metals from scrap automobiles by magnetic fluid levitation.

22 p2878 A73-42531

NONFLAMMABLE MATERIALS

Weibull distribution government of dispersion of destructive temperature gradients characteristic of fireproof ceramic materials heat resistance

09 p1110 A73-23061

Recent developments in commercial fire resistant fibrous materials.

11 p1389 A73-26414

New fire resistant polymers - Poly(phosphazenes).

17 p2197 A73-35356

Flame resistant and nonflammable textile fibers.

17 p2198 A73-35836

NONGRAY ATMOSPHERES

Nongray atmospheric model to assess radiative effects of water vapor and carbon dioxide layer injected into lower stratosphere by SST and HST exhaust gases

01 p0038 A73-10388

Opacity probability distribution functions for application to non-gray late-type stars model atmospheres.

09 p1149 A73-23131

Effect of line or band shape on the radiative flux of an isothermal spherical layer.

22 p2938 A73-42990

Titan molecular hydrogen greenhouse effect responsibility for IR temperature disagreement with atmosphereless equilibrium temperature from analysis of nongray radiative and gray convective equilibrium

24 p3129 A73-44450

NONGRAY GAS

A simple method for calculating nongray radiation.

01 p0119 A73-10109

Nongray theory for temperature wave propagation without turbulent or convective motions, discussing diurnal waves simulation for planetary atmospheres

01 p0039 A73-10396

An approximation to radiative transfer in a nongray gas.

01 p0121 A73-10733

Non-gray radiative heat transfer in the picket-fence approximation.

08 p1020 A73-20790

Simultaneous radiative and conductive heat transfer in non-gray media.

11 p1453 A73-26583

Radiative transfer in a nongray spherical layer - Simplified rectangular model.

11 p1401 A73-26585

Nongray radiative transfer and simultaneous turbulent diffusion in layer of molecular gas enclosed by parallel black walls, presenting temperature profiles

13 p1705 A73-28433

Approximation nature and error magnitude in radial radiative heat flux within optically thin nongray isothermal gas cylinder

15 p1959 A73-32282

Thermal stability of radiating fluids - The Benard problem.

16 p2085 A73-33313

Thermal stability of radiating fluids - Asymmetric slot problem.

16 p2085 A73-33314

Fully coupled nongray radiating gas flows with ablation product effects about planetary entry bodies.

18 p2368 A73-36223

Planetary atmospheric entry vehicles shock layer energy transport with nongray radiation, using optical thick-thin approximation for radiative transfer in temperature distribution calculation

18 p2369 A73-36334

Radiative transfer in homogeneous, nongray gases with non-isotropic particle scattering.

20 p2625 A73-38566

NONHOLONOMIC EQUATIONS

Relations between the first integrals of a non-holonomic mechanical system and of the corresponding system freed of constraints.

07 p0850 A73-19013

Relativistic MHD formulation in terms of non-holonomic tetrad field for rotating plasma coupled to frozen-in magnetic field, noting Alfvén waves propagation velocity

09 p1131 A73-22921

Basic trends in the development of modern analytic mechanics

15 p1913 A73-31622

Equations of motion for systems with nonlinear, second-order, nonholonomic connections

17 p2211 A73-34147

Nonholonomic generalization of the Stokes theorem

19 p2462 A73-38542

Motion of a solid with a nonholonomic constraint at a fixed point

23 p3007 A73-44200

NONHOMOGENEITY
U INHOMOGENEITY
NONISENTROPICITY

A theoretical analysis of non-isentropic flow of a compressible, viscous gas in narrow passages.
 [ASLE PREPRINT 72LC-3A-1]

03 p0297 A73-14355

NONISOTHERMAL PROCESSES

U ISOTHERMAL PROCESSES

NONISOTROPIC PLATES

U ANISOTROPIC PLATES

NONISOTROPY

U ANISOTROPY

NONLINEAR EQUATIONS

NT DUFFING DIFFERENTIAL EQUATION

NT QUADRATIC EQUATIONS

Numerical solution of nonlinear partial differential and integrodifferential equations; Meeting, Oberwolfach, West Germany, November 28-December 4, 1971, Reports

01 p0069 A73-10066

Application of the boundary-value method to the solution of weakly nonlinear parabolic differential equations

01 p0069 A73-10070

Some numerical experiments with Dafermos's method for nonlinear hyperbolic equations.

01 p0069 A73-10071

Theoretical and numerical results in the case of the nonlinear Vlasov equation

01 p0069 A73-10073

A method for nonlinear plasma wave kinetics.

01 p0082 A73-10419

Study of a mixed problem for a third-order nonlinear differential equation with degeneration or singularity

01 p0070 A73-10920

Nonlinear differential equations with logarithmically small perturbations.

01 p0071 A73-11268

Existence theorem for nonlinear parabolic equations of evolution in real Banach space

01 p0071 A73-11270

Operators tolerated by the dynamics equations in the three-dimensional problem of elasticity theory

02 p0230 A73-11781

Nonlinear initial and boundary value problems of thermoviscoplasticity, discussing uses of Vainberg theorem and functional convolution in variational principle formulation
 [AD-758580]

02 p0236 A73-12516

Non-linear oscillations of a nonuniform fixed circular plate.

02 p0236 A73-12519

A note on modified optimal linear multistep methods.

02 p0188 A73-12614

Numerical integration of nonlinear integrodifferential equations of thin viscoelastic beams deflection, considering cantilever beam under uniformly distributed loads

03 p0390 A73-13343

A fourth-order nonlinear equation of state - Application to the determination of the elastic moduli of single-crystal and polycrystalline solids

03 p0350 A73-14601

Oscillatory and asymptotic behavior of functional differential equations.

04 p0469 A73-14663

Theorems on periodic noncritical approximate solutions of nonlinear oscillations differential equations

04 p0469 A73-14667

Stressed state of a planar elliptical, hyperbolic shell

04 p0511 A73-15088

A method of perturbation for a weakly nonlinear hyperbolic equation with two small parameters - Study of a mathematical model

04 p0471 A73-15246

Russian book - Variational method and the method of monotonic operators in the theory of nonlinear equations.

04 p0472 A73-15963

Phase space structure of neutral-type quasi-linear differential equations

05 p0589 A73-16294

Variational solution to the radiative equation by the use of a step function. II - Extension to nonlinear case by iteration method.

05 p0641 A73-17102

Computer-aided solution of nonlinear differential equations in electrical engineering, using an extension of Wolinkin's procedure

06 p0669 A73-17595

The problem of the excitation of subharmonics and higher harmonics in circuits, determined by a nonlinear differential equation of second order

06 p0715 A73-17698

Solvability in the large of the first boundary value problem for a certain class of quasi-linear one-dimensional parabolic equations

06 p0716 A73-17719

Applications of Jacobi polynomials to non-linear differential equation associated with generalized hypergeometric function.

06 p0716 A73-17791

Comparison and maximum theorems for systems of quasilinear elliptic differential equations.

06 p0717 A73-18171

Convergent finite difference schemes for nonlinear parabolic equations.

06 p0717 A73-18405

Nonlinear natural vibrations of rectangular plates and cylindrical panels.

06 p0765 A73-18640

Multipoint boundary problem for differential equations with a deviating argument

06 p0718 A73-18685

Approximate method for the synthesis of the optimal control of a dynamic system subjected to random disturbances

06 p0725 A73-18879

Method of solution of certain boundary value problems for nonlinear hyperbolic equations and propagation of weak shock waves.

07 p0809 A73-19015

Estimate of the time of occurrence of discontinuities in the solution of a boundary value problem for a second order quasilinear hyperbolic system.

07 p0844 A73-19023

Construction of exact solutions to certain systems of linear and nonlinear Volterra integral equations by using a power series

07 p0844 A73-19129

Some results of finite element applications in finite elasticity.

07 p0914 A73-20213

The existence and the numerical evaluation of generalized solutions of semilinear initial value problems

07 p0845 A73-20288

Magnetic surfaces decay for parametric instability in helical magnetic configuration, noting nonlinear equations of magnetic field lines

08 p0991 A73-20822

Crystal defect model of crack propagation in three dimensional solid, assuming nonlinear dependence of Young modulus on strain with term for time lag

08 p1017 A73-21025

Contact problem with one governing parameter in elasticity theory

08 p1017 A73-21099

Axisymmetric Stefan problem with boundary conditions of the third kind

08 p1022 A73-21100

Numerical formulation for constant-gain chemical laser calculations.

08 p0975 A73-21411

An instability theorem for certain nonlinear hyperbolic equations

08 p0984 A73-21488

On the solution of the nonlinear heat conduction equations by numerical methods.

08 p1024 A73-21636

Convergence of difference methods for certain degenerating quasi-linear parabolic equations

09 p1111 A73-21919

Investigation of the motion of the medium near the point of contact of shock waves in linear and nonlinear formulations

09 p1070 A73-21921

An iteration procedure for the solution of special nonlinear boundary-value problems

09 p1112 A73-22448

Initial circuit equation transformation into equation of variable states, noting linear and nonlinear circuits in static and dynamic regimes

09 p1068 A73-22452

Sufficient conditions for the applicability of the Monte-Carlo method to the solution of systems of nonlinear equations

09 p1112 A73-22888

Periodic solution of a second-order non-linear differential equation.

09 p1113 A73-22985

Some oscillatory properties of solutions of fourth-order quasi-linear differential equations

09 p1113 A73-22986

Remarks on a system of nonlinear equations

09 p1113 A73-22987

Solution of the Cauchy problem for a nonlinear equation describing a gas flow in the presence of strong blowing

09 p1029 A73-23352

Nonstationary equations of the nonlinear theory of elasticity in Euler coordinates

10 p1287 A73-23590

On the instability of leap-frog and Crank-Nicolson approximations of a nonlinear partial differential equation.

10 p1241 A73-23640

Boundary value problems for a nonlinear differential equation with a deviating argument of neutral type

10 p1241 A73-23742

Nonlinear problem for a plane continuous medium in Euler coordinates

10 p1292 A73-24489

Application of the averaging method to the solution of the mixed boundary value problem for a class of nonlinear partial differential equations

10 p1243 A73-24504

Construction of the solution to a nonlinear boundary value problem for a heat-radiating body of complex shape

10 p1296 A73-24510

Initial conditioned solutions of a second-order nonlinear conservative differential equation with a periodically varying coefficient.

10 p1244 A73-24706

The analytical treatment of the nonlinear aeroelastic galloping problem
 [DFVLR-SONDRER-289]

11 p1432 A73-24997

An approximate solution to a strongly non-linear, second-order, differential equation.

11 p1390 A73-25195

A case of application of the variational method in the theory of the eigenfunctions of nonlinear equations

11 p1391 A73-26076

Comparison and oscillation theory for Lienard's equation with positive damping.

11 p1391 A73-26367

Parametron circuit current fluctuations analysis via successive approximation solution of nonlinear differential equation, investigating operational mode stability

11 p1400 A73-26452

Bending problem for shell of revolution with finite displacements, axisymmetric loading and nonlinear strain functions

11 p1445 A73-26460

Application of the Chaplygin method to the solution of Volterra-type nonlinear integro-differential equations

11 p1391 A73-26521

An iterative method for generalized nonlinear complementarity problems.

11 p1391 A73-26577

Solvability of the mixed boundary value problem for higher-order parabolic quasi-linear equations with discontinuous and rapidly growing coefficients in the Orlicz classes

11 p1392 A73-26599

Second order closed form asymptotic solution to Donnell type nonlinear equations of elastic homogeneous conical shells for displacement and stress resultants

11 p1447 A73-26650

Superlinear convergent multistep procedure of the regula falsi and the Newton type

11 p1392 A73-26728

Existence and stability of the solution of the Volterra nonlinear integral equation

12 p1517 A73-27101

Construction of asymptotic solutions to the Cauchy problem with an initial jump for nonlinear systems of integrodifferential equations containing a small parameter at the higher derivative

12 p1518 A73-27298

Temperature calculation for heat emitting surface in transparent gas flow, using linearizing function method for heat transfer problems with nonlinear boundary conditions

12 p1558 A73-27316

Solution of systems of nonlinear differential equations by the Newton-Raphson method

12 p1518 A73-27396

Mathematical model of heat conducting medium thermophysical properties based on one dimensional nonlinear thermal conductivity equation solution

12 p1559 A73-27444

Nonlinear integral equations for the electrodynamic of conducting media

12 p1525 A73-27805

Some error estimates for approximate solutions of nonlinear integral Hammerstein-type equations

12 p1519 A73-27818

Symposium on Ordinary Differential Equations, University of Minnesota, Minneapolis, Minn., May 29, 30, 1972, Proceedings.

12 p1519 A73-27919

Global solutions to a class of nonlinear hyperbolic systems of equations.

13 p1647 A73-28024

Implicit separation of variables [via superposition principle/ and explicit and implicit traveling wave methods of solving nonlinear partial differential equations

13 p1648 A73-28437

Initial-boundary value problems of nonlinear extensible beam equation as mathematical model for transverse deflections of beam with hinged or clamped ends

13 p1695 A73-28438

Singular perturbations for a nonlinear differential equation with a small parameter.

13 p1648 A73-28537

Capacity theory and removable sets for finite energy harmonic functions extended to nonlinear Navier-Stokes equations, using multiple trigonometric series

13 p1648 A73-28539

Numerical stability criteria for fourth order nonlinear difference equations, using discrete form of Liapunov direct method

13 p1649 A73-28699

Conditions for evading a point in a second-order differential game

13 p1660 A73-29078

NONLINEAR FEEDBACK

Rayleigh-Ritz method for approximate solutions to nonlinear ordinary differential equations with nonlinear boundary conditions

13 p1650 A73-29399

A quadrature-iterative method of solving linear and nonlinear integral equations

13 p1651 A73-29679

Nonlinear heat flow in anisotropic media with property variations and nonlinear heat generation.

14 p1816 A73-29915

Some efficient algorithms for solving systems of nonlinear equations.

14 p1768 A73-29939

Convergence of the net-point method for multidimensional quasi-linear heat-conduction problems

14 p1816 A73-30020

Nonlinear vector matrix differential equations for automatic control systems dynamics, discussing stability, dissipativity and convergence

14 p1768 A73-30344

Some aspects of the asymptotic behavior of solutions of nonlinear differential equations with delayed argument

14 p1768 A73-30345

The Cauchy problem in classes of increasing functions for some second-order quasi-linear degenerate parabolic equations

14 p1769 A73-30347

Solution of certain nonlinear boundary value problems for regions of complex shape by a structural method

14 p1769 A73-30349

Stability considerations for a Volterra integral equation with discontinuous nonlinearity.

14 p1769 A73-30403

Determining unknown coefficients in a nonlinear heat conduction problem.

14 p1817 A73-30406

Some computation-steeples in fluid mechanics.

14 p1745 A73-30412

Numerical solutions by the continuation method.

14 p1769 A73-30454

On asymptotic solutions of nonlinear differential equations with time lag.

14 p1770 A73-30759

Oscillations of nonlinear functional differential equations generated by retarded actions.

14 p1770 A73-30761

Investigation of a weakly generalized solution to the mixed self-conjugate problem of a class of quasi-linear second-order hyperbolic systems with a nonlinear right-hand operator member

14 p1771 A73-30791

Convergence of the Bubnov-Galerkin method for a type of nonlinear operator equation

15 p1898 A73-30966

Effect of nonlinearity in a coherent pulse integrator on signal-to-noise gain.

15 p1842 A73-30988

A modified quasilinearization technique for optimal control problems with unspecified final time.

15 p1853 A73-31627

Convergence, accuracy and stability of finite element approximations of a class of non-linear hyperbolic equations.

15 p1899 A73-32030

The non-linear theory of thin elastic sheets.

15 p1954 A73-32118

Existence and uniqueness of positive eigenfunctions for a class of quasilinear elliptic boundary value problems of sublinear type.

15 p1900 A73-32181

Book - Two-point boundary value problems: Shooting methods.

15 p1901 A73-32299

Approximate synthesis method for optimal control of a system subjected to random perturbations.

15 p1915 A73-32404

Nonlinear shell theory, obtaining differential equilibrium equations and boundary conditions from three dimensional variational energy expression by kinematic hypothesis and Ritz method

16 p2078 A73-32996

New problems pertaining to nonlinear integro-differential equations with several independent variables. I - Search for solutions in the case of initial integral boundary conditions

16 p2032 A73-33172

Forming energy in rigid-plastic materials unsteady molding processes, obtaining nonlinear equations system solution by iterative procedure

16 p2037 A73-33237

Modeling, identification and prediction of a class of nonlinear viscoelastic materials. I.

16 p2082 A73-33904

Numerical solution of systems of nonlinear algebraic equations; Proceedings of the Regional Conference, University of Pittsburgh, Pittsburgh, Pa., July 10-14, 1972.

17 p2199 A73-34101

Nonlinear algebraic equations in continuum mechanics.

17 p2199 A73-34102

Some computational techniques for the nonlinear least squares problem.

17 p2199 A73-34105

Computer oriented algorithms for solving systems of simultaneous nonlinear algebraic equations.

17 p2199 A73-34107

On the choice of relaxation parameters for nonlinear problems.

17 p2199 A73-34108

Equations of motion for systems with nonlinear, second-order, nonholonomic connections

17 p2211 A73-34147

Liapunov direct method extended to stability of nonlinear parabolic systems, noting application to Burgers equation

17 p2200 A73-34398

Multivalued solutions and the classification principle for nonlinear differential equations

17 p2200 A73-34628

Russian book - Linear and nonlinear boundary value problems.

17 p2201 A73-34640

An approximate method for the solution of a class nonlinear equations in fluid mechanics and magnetohydrodynamics.

[ASME PAPER 73-FE-22]

17 p2216 A73-35018

Linearized implicit schemes for the computation of viscous incompressible flow - with applications.

17 p2155 A73-35141

Quasi-Newton methods for discretized non-linear boundary problems.

17 p2202 A73-35520

Examination of the parameters in solutions to systems of two-dimensional nonlinear Volterra-type integral equations

17 p2203 A73-35590

Nonlinear boundary value problems and several Lyapunov functions.

17 p2203 A73-35730

Approximate method for determining the natural frequencies of flexible rectangular plates

18 p2363 A73-36408

Oscillation theorems for a second order damped nonlinear differential equation.

18 p2330 A73-36694

On the iterative solution of Dirichlet problem for some mildly non-linear elliptic equations.

19 p2445 A73-38027

Stability criteria for explicit finite difference solutions of the parabolic diffusion equation with non-linear boundary conditions.

19 p2445 A73-38189

Accurate approximate solutions to oscillatory problems with perturbing singular damping.

19 p2461 A73-38490

An indirect trajectory optimization algorithm based on the continuation method for solution of nonlinear equations.

[AIAA PAPER 73-890]

20 p2588 A73-38826

Some nonoscillation theorems for a second order nonlinear differential equation.

20 p2581 A73-38976

Series representation of the solution of nonlinear partial differential equations and its use in determining the dynamic characteristics of nonlinear plants with distributed parameters

20 p2581 A73-38986

Nonlinear boundary value problem with permissible zeros on the contour

20 p2582 A73-39206

Normal third-order shapes of nonlinear oscillations

20 p2593 A73-39320

Mathematical theory of nonlinear viscoelasticity

20 p2618 A73-39330

Special periodic solutions and asymptotic properties of a class of quasi-linear differential equations with delayed argument

20 p2583 A73-39509

Mixed finite-difference scheme for a class of linear and nonlinear structural mechanics problems.

20 p2621 A73-39544

Deviation of the solution of a quasi-linear wave equation from the solution of the linear equation in the region of continuous first derivatives

21 p2724 A73-40181

Finite difference approximation of the weak solution of a mildly nonlinear Dirichlet problem.

21 p2725 A73-40379

Sound propagation in gases, liquids and solids, discussing effects of nonlinear terms in wave and state equations and boundary conditions on solution

21 p2739 A73-40621

Pairs of positive solutions of nonlinear elliptic partial differential equations.

21 p2726 A73-40695

Integration of a nonlinear partial differential mixed boundary value problem

21 p2792 A73-41065

Russian book - Qualitative theory of boundary value problems for quasi-linear second-order parabolic equations.

22 p2881 A73-41701

Local and global theorems of existence and uniqueness for solutions to nonlinear singular integral equations on a denumerable set of contours

22 p2882 A73-42472

Liapunov-like behavior and separation of solutions to nonlinear and linear differential equations

23 p3000 A73-42404

Group properties and invariant solutions in the problem of the analytic design of controllers for a process with distributed parameters

24 p3074 A73-44661

Quasi-steady Stefan problem solutions for nonlinear heat conduction in two phase /liquid-solid/ state crystallizer

24 p3158 A73-45501

The problem of an iteration method for solving a nonlinear system of partial differential equations given in implicit form with time lag

24 p3106 A73-45507

NONLINEAR FEEDBACK

Effect of nonlinearity in the feedback loop of a recirculation comb filter.

10 p1203 A73-24935

Nonlinear feedback systems and weakly stationary stochastic processes.

14 p1739 A73-30503

Limit cycle stability determination for nonlinear system with single loop feedback, using describing function method and z transform

17 p2202 A73-35517

Oscillations in nonlinear feedback systems.

19 p2414 A73-38069

Instability of feedback systems containing several time-varying nonlinear amplifiers.

19 p2414 A73-38078

Stability circle criteria extended to signal power gain mean-square criteria for nonlinear feedback distributed parameter system defined by transfer function

22 p2837 A73-43066

NONLINEAR FILTERS

Application of the asymptotic method to third-order oscillatory systems

01 p0021 A73-10030

Low pass Butterworth and Chebyshev filters design with Sallen-Key network for fabrication of microelectronic circuits

01 p0024 A73-10682

Symposium on Nonlinear Estimation Theory and its Applications, 3rd, San Diego, Calif., September 11-13, 1972, Proceedings.

04 p0430 A73-15251

An application of Bayes-law estimation to nonlinear phase demodulation.

04 p0471 A73-15253

System identification using approximate nonlinear filters.

04 p0430 A73-15257

Evaluation of the performance of a variance estimation algorithm using order statistics.

04 p0471 A73-15259

A higher measurement space filter for passive tracking.

04 p0431 A73-15262

Functional analysis approach of the partial differential equation arising from non-linear filtering theory.

04 p0472 A73-15263

Solution structure duality between nonlinear filtering with finite dimensional sensor orbit and nonlinear control with involuntary actuator orbit

04 p0431 A73-15264

A state covariance matrix computation algorithm for satellite orbit determination sequential filtering.

04 p0431 A73-15267

An error sensitivity analysis for nonlinear second order filters.

04 p0431 A73-15269

Nonlinear estimation theory applied to the interplanetary orbit determination problem.

04 p0498 A73-15271

Optimum quantization and parallel algorithms for nonlinear state estimation.

04 p0472 A73-15276

Pseudo state measurements applied to recursive nonlinear filtering.

04 p0431 A73-15277

Digital and hybrid computational aspects of the discrete representation theorem of nonlinear estimation.

06 p0670 A73-17803

On parameter identification for distributed systems using Galerkin's criterion.

07 p0804 A73-19130

Engineering systems structure and parameter identification using transfer function, learning model and nonlinear filtering

07 p0796 A73-20427

Nonlinear estimation theory applied to the interplanetary orbit determination problem.

07 p0805 A73-20582

Adaptive nonlinear filtering for tracking with measurements of uncertain origin.

07 p0805 A73-20584

An analytical method for the filtering error evaluation of sub-optimal filters in a noisy non-linear dynamic system.

08 p0950 A73-21091

Nonlinear filter with a Pi-shaped amplitude-frequency characteristic

08 p0946 A73-21110

- Estimation theory and system state and parameter identification, developing algorithms for optimum linear sequential and nonlinear filters
10 p1200 A73-24051
- Effect of nonlinearity in the feedback loop of a recirculation comb filter.
10 p1203 A73-24935
- On optimal nonlinear estimation. I - Continuous observation.
12 p1517 A73-27147
- Stochastic equations of nonlinear filtering of random processes
12 p1518 A73-27222
- Time characteristics of a ring laser with a bleachable filter.
12 p1507 A73-27509
- Harmonic balance method for spectral investigation of periodic and disturbing functions of nonlinear systems in radio engineering, using autofiltration hypothesis
14 p1739 A73-30555
- Nonlinear filter evaluation for estimating vehicle position and velocity using satellites.
16 p1988 A73-33410
- Linear and nonlinear filtering techniques for estimating the state of reentry vehicles from optical tracking data.
17 p2125 A73-35371
- Detection of weak signals in narrowband noises.
20 p2529 A73-38921
- Motion cue method featuring coordinated adaptive washout circuitry in flight simulator using nonlinear filter, discussing heave, yaw and six degrees of freedom application
[AIAA PAPER 73-930] 21 p2674 A73-40877
- NONLINEAR OPTICS**
Phase matching in second-harmonic generation using artificial periodic structures.
07 p0834 A73-19538
- Nonlinear optical susceptibility measurements for zinc silver indium sulfide quaternary compounds, noting agreement with bond charge theory
09 p1120 A73-22090
- Generation of the second harmonic of laser emission in organic crystals
10 p1228 A73-24583
- Theory of image conversion in nonlinear optical systems
13 p1660 A73-28772
- Generalized theory of nonlinear susceptibilities and linear electrooptic coefficients based on a three-dimensional anharmonic oscillator model.
14 p1756 A73-29926
- Calculation of the nonlinear polarizability of a gas at a lasing transition with allowance for capture of resonance emission
14 p1757 A73-30367
- Narrow nonlinear resonances of excited molecule densities in a standing wave of light
14 p1775 A73-30802
- Theory of the nonlinear power resonances in gas lasers
14 p1758 A73-30803
- An optical parametric generator with a large length of nonlinear interaction and weak feedback
14 p1754 A73-30853
- Quantum theory of frequency conversion in nonlinear optics
15 p1886 A73-32330
- Vacuum evaporation method for manufacturing neutral density filters with nonlinear density profiles.
15 p1914 A73-32380
- Trends in physics; General Conference, 2nd, Wiesbaden, West Germany, October 3-6, 1972, Lectures.
17 p2256 A73-34109
- Book - Applied nonlinear optics.
17 p2212 A73-35274
- On the stabilization of explosive instabilities by nonlinear frequency shifts.
17 p2218 A73-35822
- Nonlinear light scattering in crystals
19 p2462 A73-38539
- Nonlinear radiation reaction field effects on operator self-field and oscillating dipole, taking into account one-atom spontaneous emission and superradiance theories
20 p2590 A73-38607
- Amplitude stabilization of pulses from a Q-switched ruby laser by means of interaction with a non-linear medium.
20 p2570 A73-38614
- Unified thermodynamics of dissipative structures and coherence in nonlinear optics.
20 p2571 A73-38633
- Linearization of Cauchy's problem for quadratic semilinear partial differential equations.
20 p2581 A73-38865
- Intensity limitation and energy spreading in an optical field under transient thermal defocusing conditions.
20 p2574 A73-39689
- Amplification of stimulated Raman scattering of light in various nonlinear amplifier pumping circuits
21 p2711 A73-40306
- Nonlinear effects in the emission and absorption spectra of gases in resonant optical fields
21 p2712 A73-40443
- Influence of inhomogeneities in a nonlinear crystal on the conversion of an image by sum-frequency generation.
22 p2869 A73-42245
- Phase fluctuations in a parametric light source operating inside a laser resonator.
22 p2869 A73-42246
- Some features of second-harmonic generation in a lithium metaniobate crystal.
22 p2896 A73-42247
- Generation of high-power light pulses at wavelengths 1.06 and 0.53 microns and their application in plasma heating. II - Neodymium-glass laser with a second-harmonic converter.
22 p2869 A73-42248
- Self-focusing and self-trapping of light beams in a non-linear medium.
22 p2888 A73-43050
- Bulk and surface damage mechanisms of laser crystalline and nonlinear optical materials and thin films, noting plasma thresholds and surface polishing
23 p2989 A73-44210
- Biaxial potassium niobate single crystal nonlinear optical coefficients determination by Marker fringe pattern method, using CW Nd doped yttrium-aluminum garnet laser
23 p3018 A73-44369
- NONLINEAR PROGRAMMING**
Absolute minima determination for homogeneous polynomial real valued goal function under equality constraints, solving nonlinear programming problem by penalty function method
06 p0716 A73-17851
- Simplex gradientless algorithm for unconstrained static optimization, noting effectiveness for arbitrary goal functions in nonlinear programming
06 p0670 A73-17858
- Method of branches and bounds as a regular method for the solution of irregular mathematical programming problems. I.
06 p0716 A73-17961
- Nonlinear programming in design of control systems with specified handling qualities.
07 p0777 A73-20588
- System modeling and optimal design of a Mars-roving vehicle.
07 p0906 A73-20593
- Optimization of system reliability using a parametric approach.
09 p1112 A73-22646
- A mathematical programming approach to identification and optimization of a class of unknown systems.
10 p1242 A73-23773
- Book - Iterative methods for nonlinear optimization problems.
10 p1242 A73-23947
- Optimization methods in control systems design, discussing nonlinear and linear programming, variational and maximum principles, dynamic programming and game and graph theories
10 p1242 A73-24032
- Study of recurrence relationships and their applications by the Laboratoire d'Automatique et de ses Applications Spatiales.
10 p1200 A73-24042
- A method of feasible directions using function approximations, with applications to min max problems.
11 p1390 A73-25474
- Mathematical programming optimization procedure applicable to minimum weight structural design, considering static stress and displacement constraints under alternative loading conditions
[AIAA PAPER 73-341] 11 p1436 A73-25480
- Cutting planes for programs with disjunctive constraints.
11 p1391 A73-26578
- Methods of quadratic Liapunov vector-function construction for linear systems
12 p1525 A73-27895
- A convergence theory for a class of nonlinear programming problems.
13 p1649 A73-28610
- Extremal controls in a nonlinear differential game
13 p1660 A73-29077
- Mathematical programming methods in structural analysis.
16 p2078 A73-33001
- An approach to nonlinear programming.
16 p2032 A73-33301
- Numerical methods for non-linear optimization; Proceedings of the Conference, University of Dundee, Dundee, Scotland, June 28-July 1, 1971.
16 p2033 A73-33851
- The choice of step length, a crucial factor in the performance of variable metric algorithms.
16 p2033 A73-33853
- Nonlinear least squares calculations by Gauss-Newton and Levenberg, Marquardt and Morrison methods, discussing algorithm convergence rate and numerical computational scheme
16 p2033 A73-33854
- A combinatorial method to compute a global solution of certain non-convex optimization problems.
16 p2033 A73-33855
- A survey of methods for solving constrained minimization problems via unconstrained minimization.
16 p2033 A73-33857
- Generalization of an exact method for solving equality constrained problems to deal with inequality constraints.
16 p2033 A73-33858
- Nonlinear functional minimization under auxiliary constraints, discussing convergence conditions and iterative solution algorithm performance for least squares weighted sum problem
17 p2199 A73-34106
- A comparison of the complex method of optimization with the penalty function approach using Zangwill's method for constrained optimization problems.
17 p2202 A73-35385
- Methods of constructing quadratic Lyapunov vector functions for linear systems.
18 p2330 A73-36600
- Duality relationships for a nonlinear version of the generalized Neyman-Pearson problem.
18 p2330 A73-36636
- Control configuration optimization of linear engineering systems.
19 p2414 A73-38082
- Synthesis of a class of optimal discrete systems for correcting the trajectories of dynamic systems
20 p2592 A73-38697
- A nonlinear programming algorithm for the automated design and optimization of flexible space vehicle autopilots.
20 p2588 A73-38828
- The boundary theory of strength and nonlinear programming of boundary value problems of plate bending
20 p2625 A73-39821
- Some method of nonlinear programming suitable for solving the task of optimization of a small transport aircraft
21 p2634 A73-40478
- Optimization of electronic circuits with characteristics depending on a continuously varying parameter
21 p2666 A73-41311
- Journal bearings computerized design optimization by geometric programming with volume, dimensions, torque and horsepower absorption, shaft strength, speed, load, pressure and Sommerfeld number as constraints
21 p2708 A73-41668
- Comparison of some penalty function based optimization procedures for the synthesis of a planar truss.
22 p2922 A73-42478
- Application of stochastic programming methods for solving certain optimization problems of multiple-link plants without memory
22 p2836 A73-42612
- Algorithmic and computational aspects of the use of optimization methods in engineering design.
24 p3070 A73-45235
- NONLINEAR SYSTEMS**
Equations of motion integral properties-based construction of Liapunov functions used to derive sufficient conditions for perturbed nonlinear system solution stability
01 p0075 A73-10090
- Linearization method for analytic solution optimization of oscillatory motion differential equations of elastic nonlinear system, studying combinations of free and forced vibrations
01 p0075 A73-10093
- A method of construction and the structure of asymptotic approximations of the solutions of nonlinear mixed boundary value problems in studies of multifrequency oscillation modes
01 p0076 A73-10097
- Validity of averaging methods for certain systems with periodic solutions.
01 p0070 A73-10273
- Generation and stability of subharmonic and modulated subharmonic oscillations in nonlinear systems.
01 p0076 A73-10303
- Stability of large-scale systems under structural perturbations.
01 p0070 A73-10322
- White noise signal correction for nonlinear nonstationary systems, using orthonormalized functionals
01 p0027 A73-10593
- Investigation of the dissipativity of a pulse-frequency modulated system of stabilizing an unsteady plant
01 p0027 A73-10596
- Abstract theory of systems - Current state and development trends
01 p0027 A73-10664
- Optimal stabilization of nonlinear control systems for given region of initial perturbations, reducing optimal synthesis to moments problem
01 p0077 A73-10671

Equipment for determining the amplitude-frequency characteristics of nonlinear elements in the range of low and extra-low frequencies

01 p0023 A73-10679

Liapunov vector functions in stability analysis of nonlinear dynamic distributed parameter, interconnected and multivariable systems

01 p0078 A73-11073

Analysis of an altitude control system of a low flying vehicle.

01 p0075 A73-11195

Analysis of non-linear systems defined by their response to arbitrary disturbances.

01 p0028 A73-11456

Non-interacting control of non-linear multivariable systems.

01 p0028 A73-11517

Variational method in the invariance problem for controlled systems.

02 p0149 A73-12117

Evaluation of the coefficients of the effect of errors in the original information and in the model of optimization results.

02 p0149 A73-12122

Transient curve construction for analysis and synthesis of automatic control systems with asymmetrical nonlinearities, comparing with harmonic linearization

02 p0149 A73-12342

A new circle criterion for the stability of nonlinear control system.

02 p0149 A73-12346

Amplitude-frequency and stability characteristics of parametric amplification by triple-frequency interaction in nonlinear nonautonomous system

02 p0147 A73-12491

Similar normal mode vibrations in certain conservative systems with two degrees-of-freedom.

02 p0193 A73-12515

Response of a system of cascaded nonlinear springs

02 p0193 A73-12521

Worst inputs and a bound on the highest peak statistics of a class of non-linear systems.

02 p0188 A73-12602

Liapunov function for Hamilton-Jacobi equation for motion stability of linear and nonlinear mechanical systems, calculating vibration damping factor

03 p0342 A73-13157

Variable stability simulation techniques for non-linear rate-dependent systems.

03 p0285 A73-13521

On the stability of steady-state response of certain nonlinear dynamic systems subjected to harmonic excitations.

03 p0393 A73-13792

Optimal control of nonlinear time-lag systems.

03 p0285 A73-13899

Damping perturbation of high order nonlinear autonomous Liapunov system, reducing system equations integration to quadratures via transformation to lower order quasi-linear nonautonomous system

03 p0344 A73-14054

Computerized design and algorithm for linear and nonlinear regulators by mathematical programming approach involving vector determination for objective function minimization

03 p0286 A73-14480

Large scale systems with linear and nonlinear subsystems and coupling connections, investigating connective stability under perturbations due to subsystem on-off participation

03 p0337 A73-14484

Modeling of nonlinear systems for the example of a single-shaft jet turbine engine

03 p0360 A73-14615

Linear and nonlinear systems dynamic stability conditions for incomplete coefficients data, determining worst disturbance from Pontryagin principle

04 p0475 A73-14887

Dynamic response of nonlinear media at large strains.

04 p0509 A73-14947

Statistical linearization of nonlinear single-mass mechanical system for given distribution function of random disturbances, noting amplitude frequency distribution

04 p0475 A73-14977

Nonlinear analysis of double feedback loop tracking system with coupling, obtaining steady state phase error probability density functions with application to satellite transponder

04 p0429 A73-14994

Absolute instability of nonlinear pulse-amplitude control systems - Frequency criteria.

04 p0430 A73-15204

Estimating the mean time until follow-up cutoff in a nonlinear sampled-data servosystem for irregular arrival of the signal.

04 p0430 A73-15205

Air Force weapon system procurement needs, considering industry technological capabilities, nonlinear estimation in cruise navigation and nonlinear systems design, test and implementation

04 p0430 A73-15252

Solution structure duality between nonlinear filtering with finite dimensional sensor orbit and nonlinear control with involutory actuator orbit

04 p0431 A73-15264

Relaxation algorithms for nonlinear system modal trajectory estimation by approximate step with lower triangular matrix inversions sequence, comparing convergence with Gauss-Newton method

04 p0472 A73-15265

On-line parameter estimation of nonlinear dynamic system with unknown impulsive inputs by Kalman filter with application to maneuvering spacecraft tracking

04 p0431 A73-15270

Nonlinear heat transfer systems design optimization based on physical properties cost functionals, presenting geometric programming method

[ASME PAPER 72-WA/HT-15] 04 p0519 A73-15833

Determination of root locus for nonlinear multi-variable system.

[ASME PAPER 72-WA/AUT-21]

04 p0472 A73-15879

Nonlinear modeling and dynamic simulation of vehicle air cushion suspensions.

[ASME PAPER 72-WA/AUT-5] 04 p0406 A73-15883

Investigation of the dynamics of nonlinear sampled-data automatic control systems

05 p0560 A73-16296

Control of electro-hydraulic shaker by digital iteration techniques.

[SAE PAPER 720823] 05 p0562 A73-16636

Critical lag of the driving element in a parametric system

05 p0561 A73-16990

Free vibrations in nonlinear systems with two degrees of freedom

05 p0599 A73-17087

Combinational servosystem with a self-adjusting loop

05 p0561 A73-17250

Computer adaptive optimization system for problems with nonlinear criteria function and constraints, noting algorithms of deterministic and stochastic categories

05 p0555 A73-17284

On the dynamics of randomly excited nonlinear systems.

06 p0715 A73-17393

Parameter identification using the Galerkin procedure in nonlinear boundary-value problems.

[ASME PAPER 73-AUT-C] 06 p0716 A73-17724

Decoupling in a class of nonlinear systems by state variable feedback.

[ASME PAPER 72-AUT-V] 06 p0679 A73-17725

Nonlinear dynamic systems controllability theorem formulation and proof using matrix theory

06 p0716 A73-17853

Synthesis of statistically optimal multiloop control systems containing essentially nonlinear elements.

06 p0679 A73-17955

Globally equivalent representations for reciprocal stationary nonlinear systems in equilibrium or steady state conditions, considering electric circuits and thermodynamic system examples

06 p0716 A73-17993

A program for the analysis and design of general dynamic mechanical systems.

[AD-754496] 06 p0671 A73-18063

An iterative approach to nonlinear dynamic stability problems.

06 p0717 A73-18145

Nonsearch algorithms for parametric synthesis of stochastic automatic control systems

06 p0680 A73-18381

Describing functions, circle criteria and multiloop feedback systems.

06 p0680 A73-18444

Periodic oscillations in feedback systems with combined pulse modulation.

06 p0680 A73-18518

A numerical method for solving optimal control problems with unspecified terminal time.

06 p0681 A73-18520

Complete identification of some non-linear closed-loop systems.

06 p0681 A73-18525

Invariance conditions and controllability relation of linear and nonlinear dynamic systems, including composite systems and systems with deviating argument

06 p0724 A73-18678

Nonlinear time-varying control systems transformation, deriving conditions for existence of observable system representation and corresponding scalar differential equation

06 p0719 A73-18802

Identification of multivalued nonlinearities in a class of noisy time invariant dynamic systems.

06 p0681 A73-18811

State estimation of nonlinear system by applying stochastic approximation method.

06 p0681 A73-18813

Absolute stability of nonlinear systems with a constraint on the derivative - Some extensions.

06 p0682 A73-18820

Free vibration of multi-degree-of-freedom nonlinear systems.

07 p0909 A73-19168

Forced vibration of a class of non-linear two-degree-of-freedom oscillators.

07 p0851 A73-19165

Experimental determination of the structure of plants with recycling

07 p0805 A73-20043

Absolute stability of nonlinear control systems with nonstationary nonlinearities and tachometric feedback

07 p0805 A73-20044

An analytical method for certain weakly nonlinear periodic differential systems.

07 p0845 A73-20228

Dynamics of the non-linear interaction of magneto-hydrodynamic waves.

07 p0859 A73-20228

Analysis of the stability and periodic motions of nonlinear automatic pulsed systems by the root-locus curve method

07 p0806 A73-20636

Mathematical description of nonlinear systems with distributed parameter

08 p0938 A73-20964

Comparative study of methods of analysis of nonlinear systems subjected to random input

08 p0938 A73-20969

Integral methods of calculating unsteady processes in nonlinear electric systems

08 p0951 A73-21556

Nonlinear system analysis based on Fokker-Planck equation, simplifying solution sequence for steady state or variance of states combination

09 p1111 A73-22114

Performance comparison of suboptimal Kalman filters modeled for a continuous nonlinear system.

09 p1067 A73-22228

Approach and evasion games in conflict controlled system with nonlinear control, deriving necessary condition for winning

09 p1068 A73-22355

Construction of quality diagrams for transient processes in nonlinear systems

09 p1068 A73-22558

Determination of limits bounding the bifurcational relationship between parameters of two-stage nonlinear servo mechanisms

09 p1033 A73-22653

Liapunov vector functions in stability analysis of nonlinear dynamic distributed parameter, interconnected and multivariable systems

09 p1121 A73-22998

Numerical computation of forced oscillations in coupled Duffing equations.

09 p1113 A73-23022

A first-approximation theory of discrete nonautonomous stabilization systems

10 p1248 A73-23745

Book - Digital simulation of physical systems.

10 p1191 A73-23946

On the application of the method of decoupling of motions to the analysis and synthesis of nonlinear systems.

10 p1199 A73-24031

The evaluation of the domain of attraction of nonlinear control systems with hybrid computing systems.

10 p1192 A73-24040

New criteria for bounded-input-bounded-output and asymptotic stability of nonlinear systems.

10 p1199 A73-24041

The use of operators with degenerated kernel for nonlinear system investigation.

10 p1242 A73-24043

Trajectory optimization for the nonlinear combined estimation and control problem.

10 p1200 A73-24044

Wide-sense adaptive dual control for nonlinear stochastic systems.

10 p1202 A73-24533

A survey of data smoothing for linear and nonlinear dynamic systems.

10 p1243 A73-24546

Calculation of the characteristics of nonlinear elements in first-order circuits for given signal conversion conditions

10 p1196 A73-24603

Russian book on military application oriented automatic control systems design covering amplifiers, servo elements, stability, performance, optimization, and nonlinear and sampled data systems

10 p1203 A73-24972

Linear or nonlinear dynamic systems response to arbitrary input functions, describing numerical computation method with provision for discontinuities

11 p1389 A73-25110

Field of attraction of a singularity of a nonlinear recurrence of the second order - Method of determination of the boundary

11 p1389 A73-25137

Converse theorems for Liapunov stability and boundedness of nonlinear discrete-time systems described by difference equations

11 p1389 A73-25186

- Nonlinear dynamic feedback control system state variable observers reconstruction error convergence and digital simulation for performance 11 p1390 A73-25187
- Nonlinear delay-differential control systems described by periodic functional differential equations with small real parameter, investigating asymptotic stability in Liapunov sense 11 p1390 A73-25190
- Parametric synchronization of self-oscillators with feedback delay and nonlinear circuit 11 p1337 A73-25429
- Method of Liapunov vector functions in the analysis of complex systems with distributed parameters /Survey/ 11 p1398 A73-25617
- Experimental method for structure identification in nonlinear objects with recycling processes 11 p1342 A73-26082
- Efficiency estimates of methods for analyzing the precision of nonlinear control systems 11 p1342 A73-26094
- Dynamics of a two-frequency self-oscillator with 'hard' excitation 11 p1331 A73-26157
- Time-related behavior of causal, anticausal, memoryless and crosscausal nonlinear control systems modeled as operator on group-valued function space 11 p1391 A73-26366
- Application of the harmonic balance method for studying oscillations of nonlinear systems with distributed parameters 11 p1400 A73-26464
- Optimal inputs and sensitivities for parameter estimation. 11 p1391 A73-26579
- Resonant oscillations of conservative system with nonlinear component, obtaining differential equations of motion solution 11 p1448 A73-26731
- The quorum element and its application in the design of adaptive automatic control systems 12 p1482 A73-26758
- Group properties and invariant solutions of the Bellman equation in the problem of optimal control synthesis for second-order systems 12 p1483 A73-27079
- Some methods of assuring the stability of certain classes of nonlinear systems by the intentional use of an additional nonlinearity. 12 p1517 A73-27156
- Autonomous second order system model for nonlinear disturbances of multifrequency systems at resonance, using group properties of differential equations 12 p1524 A73-27404
- Stability of nonlinear systems with a transformed argument 12 p1524 A73-27416
- Solid body on elastic supports as model for helicopter stability and nonlinear oscillations analysis 12 p1459 A73-27791
- Integral manifold concept for stability analysis of nonlinear system oscillations, plotting resonance curve for quasi-linear autonomous system 12 p1525 A73-27792
- Stability of coupled systems of nonlinear differential delayed-argument equations 12 p1525 A73-27947
- Vibrations of a system with memory, non-linear elasticity, friction and relaxation. 13 p1690 A73-28055
- Methods for the approximate computation of the periodic solutions of systems of nonlinear periodic differential equations 13 p1647 A73-28193
- Analytical approximation of high order Galerkin solutions to ordinary differential equations describing forced oscillations of systems with polynomial nonlinearities, considering first-order harmonic effects 13 p1648 A73-28440
- Auto-oscillations, stability at the origin, overall stability of nonlinear systems with distributed parameter 13 p1596 A73-28473
- Two coupled nonlinear oscillators driven by sinusoidal input, calculating fractional harmonic frequency pairs relationship to driving and resonance frequencies 13 p1659 A73-28487
- Normal coordinates in the analysis of the principal resonances of nonlinear vibrating systems with multiple degrees of freedom 13 p1695 A73-28557
- Other stability criteria for distributed and Gaussian stochastic systems with diagonal nonlinearity 13 p1596 A73-28564
- Nonlinear elements piecewise and continuous approximations for constructing current-voltage characteristic functions 13 p1596 A73-28871
- Reduction of nonlinear distortions in a two-port network exhibiting a small nonlinearity 13 p1592 A73-28894
- Influence of the nonlinearity of the phase characteristic of the RF signal path in an FM receiver on the signal distortions 13 p1584 A73-28897
- Small perturbation evolutionary motion equations for forced vibrations of quasi-linear two frequency autonomous systems at resonance 13 p1661 A73-29082
- Periodic rectilinear solutions close to normal mode shapes of vibration of nonlinear conservative system described by differential equations generated by homogeneous potential systems 13 p1661 A73-29083
- Arrangement of integral surfaces in weakly-nonlinear systems of differential equations 13 p1650 A73-29137
- Determination of the absolute-stability domain of nonlinear time-lag systems 13 p1596 A73-29143
- Transmission characteristics of PSK wave in nonlinear system - Application to INTELSAT IV satellite systems. 13 p1586 A73-29234
- German monograph - Rapid excitation of quasi-harmonic oscillations in a class of nonlinear oscillators. 13 p1594 A73-29285
- Book - Theory of vibration with applications. 13 p1703 A73-29676
- Construction of upper and lower functions during approximate integration of a nonlinear system containing a biharmonic operator 13 p1651 A73-29678
- A first-harmonic method for nonlinear distributed-parameter systems subjected to deterministic or stochastic loads 14 p1738 A73-29707
- Perturbed bifurcations problems due to initial imperfections caused by small deviations from ideal configuration in nonlinear theory 14 p1767 A73-29764
- Approximate investigation of the dynamics of a digital phase-lock automatic frequency control system /DPAFC/ 14 p1728 A73-30269
- Synthesis of a control coupling in a nonlinear servosystem 14 p1738 A73-30287
- A criterion for the bounded-input, bounded-output stability of time-varying nonlinear systems. 14 p1738 A73-30404
- Cone-bounded nonlinearities and mean-square bounds - Estimation upper bound. 14 p1769 A73-30505
- Frequency-domain criteria for stability of a class of nonlinear stochastic systems. 14 p1739 A73-30506
- Suboptimal terminal feedback control of nonstationary, nonlinear systems. 14 p1739 A73-30507
- Harmonic balance method for spectral investigation of periodic and disturbing functions of nonlinear systems in radio engineering, using autofiltration hypothesis 14 p1739 A73-30555
- Relationship between the control range and the variation in passband width in a controlled-gain amplifier with nonlinear shunting of the load 14 p1736 A73-30563
- Quantum theory of nonlinear oscillators interacting with a medium 14 p1775 A73-30812
- Use of computers for calculation of the capture band of nonlinear phase-automatic-frequency-control systems. 15 p1842 A73-30990
- Varactor frequency multipliers of the parallel type. I - Spectrum analysis of the voltage on a partially open-circuited varactor. 15 p1849 A73-30991
- Book on perturbation methods for nonlinear differential equations covering canonical transformation theory, Hamiltonian and integrable systems, area preserve mapping and resonance problem 15 p1899 A73-31472
- Suboptimal adaptive control of a class of non-linear systems. 15 p1853 A73-31628
- Stability of a stochastically excited nonlinear cylindrical shell. 13 p1949 A73-31654
- Analysis of stability and periodic motions in nonlinear sampled-data systems by the root locus method. 15 p1854 A73-31690
- Cup anemometer input/output frequency characteristics, determining nonlinear behavior via inertia considerations 15 p1879 A73-32345
- Extension of the Caratheodory theory to multivalued differential systems with nonlinear boundary conditions 16 p2031 A73-32932
- Determining the stability of nonlinear systems. 16 p2033 A73-33699
- Optimal parallel-type varactor frequency multiplier calculation for reverse-biased conditions in terms of nonlinear conductance loss and diffusion capacitance Q factor 16 p1991 A73-33981
- Minimization of quadratic functionals in the presence of quadratic constraints and the necessity of a frequency condition in the quadratic criterion of absolute stability for nonlinear control systems 16 p2034 A73-34071
- Numerical solution of systems of nonlinear algebraic equations; Proceedings of the Regional Conference, University of Pittsburgh, Pittsburgh, Pa., July 10-14, 1972. 17 p2199 A73-34101
- Russian book - Lectures on the theory of stability of the solutions of systems with an aftereffect. 17 p2211 A73-34224
- On an initial value problem for a nonlinear system of Vlasov-Maxwell equations. 17 p2200 A73-34320
- Book - Methods of nonlinear analysis. Volume 2. 17 p2200 A73-34453
- Remarks on the optimum rate of convergence of the on-line identification of non-stationary systems. 17 p2144 A73-34600
- Russian book - Asymptotic and qualitative methods in the theory of nonlinear oscillations. 17 p2211 A73-34850
- Design of nonlinear resistive networks with prescribed input-output behavior. 17 p2145 A73-35378
- Limit cycle stability determination for nonlinear system with single loop feedback, using describing function method and z transform 17 p2202 A73-35517
- Nonlinear optimal control synthesis for oscillating second-order systems with a convex control region 17 p2213 A73-35589
- Oscillations of a system with two degrees of freedom during resonance 17 p2213 A73-35591
- Limit cycles resulting from quantization in digital control systems. 17 p2145 A73-35642
- Frequency-time domain stability criterion for nonlinear negative feedback system with linear transfer function, using Zame positive operator theory 17 p2203 A73-35731
- Russian book - Nonlinear oscillations and transient processes in machines. 18 p2319 A73-35895
- A nonlinear oscillator analog of rigid body dynamics. 18 p2337 A73-36416
- The transformational behaviour of perturbation theories. 18 p2352 A73-36421
- Nonlinear gas oscillations in pipes. I - Theory. 18 p2299 A73-36505
- A perturbation treatment for optimal slightly nonlinear systems with linear control and quadratic criteria. 18 p2294 A73-36637
- Solving M. A. Aizerman's first problem of absolute stability of nonlinear systems on the basis of the general theory of root trajectories 18 p2337 A73-37025
- Computation of the nonlinear dynamic stability functions of a reentry body in hypersonic flight 18 p2361 A73-37081
- Interaction of self-excited vibrations in mechanical vibrational systems 19 p2494 A73-37181
- Small perturbation evolutionary motion equations for forced vibrations of quasi-linear two frequency autonomous systems at resonance 19 p2445 A73-37633
- Periodic solutions close to rectilinear normal mode shapes of vibration of nonlinear conservative system described by differential equations generated by homogeneous potential systems 19 p2459 A73-37634
- Approximate solution of second-order nonlinear systems with heredity of a single independent variable 19 p2445 A73-37642
- Stability of nonlinear oscillations with unsteady impulsive excitation 19 p2459 A73-37650
- Discrete stochastic linear servomechanism with observation costs, deriving optimal control solution with extension to nonlinear systems suggested by dynamic population models 19 p2412 A73-38029
- Parallel algorithms for optimum nonlinear state estimation. 19 p2413 A73-38041
- Polynomial estimators for systems with polynomial nonlinearities. 19 p2445 A73-38042
- Suboptimal design of a class of nonlinear controllers. 19 p2414 A73-38068

A note on the period of oscillation of non-linear systems. 19 p2460 A73-38108

The transient response of certain third-order non-linear systems. 19 p2460 A73-38109

Nonlinear time-varying differential system stability and asymptotic stability study using equivalent inner product method, discussing global and regional stability 19 p2445 A73-38255

Spontaneous emission and self-excitation of a small volume in a classical, nonlinear active medium 19 p2463 A73-38540

Controllability and synthesis of optimal dynamic systems 20 p2591 A73-38672

Optimal invariant solution for compensating circuit of nonlinear control system under disturbances, using unperturbed motion prediction 20 p2538 A73-38676

Construction of improving variations during the optimization of determinate and stochastic systems 20 p2539 A73-38677

Computerized analytical methods for optimal control synthesis of linear and nonlinear systems with constraints, using integral quadratic weighting function estimates 20 p2539 A73-38679

Nonlinear control systems analysis, discussing phase space method, Taylor-Cauchy transform, Volterra functions, Liapunov stability, Popov-Kalman-Yakubovich theorems and limit cycle oscillations 20 p2592 A73-38691

Approximate methods for analysis and synthesis of nonlinear systems 20 p2592 A73-38692

Conditions, based on the estimation of the sensitivity of a periodic solution, for the application of the harmonic linearization method to higher harmonics and small parameters 20 p2592 A73-38693

Influence of low-frequency periodic interference on the operation of a complex system with variable structure 20 p2539 A73-38694

Fundamentals of the theory of nonlinear control systems with pulsed frequency and width modulation 20 p2539 A73-38696

Determination of the structural features of nonlinear dynamic systems 20 p2540 A73-38709

Direct statistical evaluation of nonlinear guidance systems. [AIAA PAPER 73-836] 20 p2584 A73-38779

Bifurcations and certain qualitative characteristics of a phase-locked automatic frequency control system with a second-order filter 20 p2535 A73-38979

Certain results of the application of the method of sections to typical classes of nonlinear automatic systems 20 p2541 A73-38985

A general quadratic criterion for absolute stability of nonlinear automatic control systems and its application to sampled-data systems with pulse-width modulation 20 p2541 A73-38988

Russian book - Complex control systems. 20 p2541 A73-39033

Synthesis of multidimensional automatic optimization systems with allowance for constraints 20 p2542 A73-39040

Stability and dissipativity of control systems containing unsteady nonlinearities 20 p2542 A73-39041

Successive approximation technique for dynamic-load problems of nonlinear viscoelastic systems 20 p2593 A73-39322

Application of the method of equivalent nonlinear systems to noise rejection analysis in FM tracking receivers 20 p2537 A73-39451

Calculation of the current of a nonlinear element with inertia in the presence of a biharmonic input 20 p2537 A73-39454

Approximation of the characteristics of two-port networks with a complex nonlinearity 20 p2537 A73-39464

Conditionally periodic oscillations in nonlinear systems 20 p2593 A73-39500

Multiwave interactions in nonlinear distributed systems 20 p2593 A73-39511

Zeroth-order approximation by multiple scaling method to analyze nonlinear oscillations with small speed-dependent damping, applying to pendulum problem 20 p2593 A73-39536

A practical means of calculating normal forms in problems involving nonlinear oscillations 21 p2738 A73-40178

Effects of non-linearity due to large deflections in the derivation of frequency response data from the impulse response of structures. 21 p2783 A73-40287

Suboptimal algorithms for nonlinear smoothing. 21 p2669 A73-40333

Use of piecewise linearization for suboptimal control of nonlinear systems. 21 p2669 A73-40451

An approximate analysis of non-linear, non-conservative systems using orthogonal polynomials. 21 p2740 A73-40755

Certain problems in the use of the maximum principle to determine optimal controls in the case of special controls and sliding regimes 21 p2670 A73-40858

Russian book on nonlinear waves in dispersive media covering unsteady waves, gravity waves in deep water, electromagnetic waves in nonlinear dielectric, etc 21 p2741 A73-41285

Means of improving the effectiveness of designing nonlinear electronic circuits on a digital computer by the method of nodular potentials 21 p2666 A73-41310

Method of calculating the amplitude and phase-amplitude characteristics of high-frequency amplifiers 21 p2666 A73-41314

A method for selecting a nonlinear clutch in a system undergoing vibration forced by polyharmonic excitation 21 p2708 A73-41583

Parametric amplification and generation of pulses in nonlinear distributed systems 22 p2826 A73-42333

Approximate nonlinear theory of orotron as SHF hybrid-type monotron oscillator, calculating output power and efficiency as function of tube electrical parameters and geometry 22 p2826 A73-42338

Linearization technique for synthesis of nonlinear two dimensional automatic control systems with cross disturbances, imposing constraints on motion coordinate deviations 22 p2836 A73-42615

Quasi-autonomous dynamic control subsystem interrelation and location for nonlinear multiple link automatic control synthesis with iterative integration of motion equations 22 p2836 A73-42616

Analysis of a damped, non-linear, non-autonomous system. 22 p2887 A73-42621

Root locus analysis of stability of a class of nonlinear systems. 22 p2837 A73-42624

German monograph - The computation of periodic motions of multipath nonlinear systems. 22 p2888 A73-42854

Analysis of transient oscillations in nonlinear control systems. 22 p2837 A73-43019

On the Volterra series functional evaluation of the response of non-linear discrete-time systems. 22 p2837 A73-43069

Synthesis of parameter and state insensitive feedback systems with constraints based on piecewise constant linear control laws. 23 p2962 A73-43283

Nonlinear regulator theory and an inverse optimal control problem. 23 p2963 A73-43820

Monofrequent oscillations in mechanical systems governed by second order hyperbolic differential equations with small non-linearities. 23 p3044 A73-44077

A new method of analysing the stability of nonlinear dynamic systems. 23 p3006 A73-44084

System stability analysis technique for nonlinear oscillation via Van der Pol and Duffing equations, noting ease of approximating higher harmonics 23 p3007 A73-44085

An existence and uniqueness theorem for the solution of a stochastic integrodifferential equation 23 p2999 A73-44101

Unboundedness of solutions and comparison theorems for time-dependent quasilinear differential matrix inequalities. 23 p3000 A73-44202

Discrete time invariant bilinear systems analysis for controllability, using decomposition by multiplicative feedback and linear compensation loops 24 p3073 A73-44585

Weak invariance conditions and synthesis algorithms for control systems with discontinuities on hypersurfaces in phase space 24 p3074 A73-44666

On the stability limit of nonlinear resonances in multiple-degree-of-freedom vibrating systems. 24 p3146 A73-44681

Eigenfunction expansions for randomly excited non-linear systems. 24 p3151 A73-45265

Random vibrations of elastic nonlinear nonautonomous systems with variable parameters 24 p3112 A73-45502

Reduction of systems of nonlinear differential equations to normal form 24 p3107 A73-45511

Compensation method for non-linear systems having jump and hysteresis properties. 24 p3075 A73-45553

On the limit-cycle characteristics of a bang-bang servo. 24 p3075 A73-45556

NONLINEARITY

Ultrasonic studies of the nonlinear properties of solids. 01 p0057 A73-11003

Photomultiplier tubes nonlinear response in radiation measurements, suggesting fatigue avoidance through pulsed operation 01 p0053 A73-11222

Alfven waves nonlinear damping mechanism due to magnetosonic wave dissipation, presenting nonlinear coupling rates 02 p0217 A73-12401

Russian papers on phosphor crystal luminescence and nonlinear optics covering spectral line decomposition, GaAs laser and electromagnetic wave interaction 05 p0584 A73-16551

Four-field parametric frequency selection in stimulated emission lines from nonlinear mirror, noting reflection coefficient 05 p0584 A73-16554

Accurate measurements of and corrections for nonlinearities in radiometers. 06 p0693 A73-17898

Book on nonlinear optimization covering search, iteration, gradient, algorithmic and computer techniques, mathematical and dynamic programming, calculus of variations, Pontryagin maximum principle, etc 06 p0717 A73-18401

Galerkin methods for parabolic equations with nonlinear boundary conditions. 07 p0844 A73-19138

The effect of a nonlinearity upon signals in the presence of noise. 07 p0795 A73-20499

Combined operations with negative resistance and nonlinear characteristics in an avalanche diode. 07 p0804 A73-20569

Nonlinear acoustics of a radiating gas. I - General analysis of the equations 09 p1119 A73-21920

Nonlinear properties of microwave avalanche diodes operated in IMPATT mode, discussing current density effect and power efficiency 09 p1063 A73-22489

Analysis of the nonlinearity of the modulation characteristic of a single-circuit phase modulator employing a varactor 10 p1195 A73-24382

Effect of the nonlinearity of the junction capacitance on the spectral characteristics of the current of a tunnel diode. 10 p1197 A73-24939

On the origin of oscillations appearing in shock profiles calculated by difference methods. 11 p1390 A73-25868

Bending of a circular nonlinearly-elastic plate by a concentrated force 12 p1555 A73-27794

Large amplitude vibrations of certain deformable bodies. I - Discs, membranes and rings. 12 p1556 A73-27929

Finite element static structural analysis for small elastoplastic strains and geometric nonlinearities, considering total Lagrangian and incremental moving coordinate formulations 14 p1807 A73-30189

Incremental formulation for problems with geometric and material nonlinearities. 14 p1808 A73-30190

Progress in nonlinear finite element analysis using asymptotic solution techniques. 14 p1808 A73-30191

Nonlinear thermal elastoplastic structural analysis, using principle of virtual work in finite element method 14 p1808 A73-30192

Incremental solution procedures for finite element nonlinear structural analysis, considering combined material and geometric nonlinearities 14 p1808 A73-30193

Variational principles in nonlinear continuum mechanics. 16 p2036 A73-32979

Analysis of the dynamic operation of a four-terminal network with slight nonlinearity. 16 p1993 A73-33979

Book - Nonlinear viscoelastic solids. 17 p2243 A73-34574

Nonlinear wave interaction and fluctuations in plasma. 17 p2217 A73-35818

Axisymmetrical bending of circular plates and shallow spherical cupolas with allowance for physical and geometrical nonlinearities

20 p2618 A73-39310

Certain approximations in the solution of shell and plate bending problems with allowance for physical and geometrical nonlinearity

20 p2618 A73-39311

Study of the two-frequency natural oscillation regime of a circular membrane on a nonlinearly elastic base

20 p2593 A73-39501

Effects of modulation nonlinearity on the range response of FM radars.

21 p2650 A73-40341

Nonlinear elasticity of random inhomogeneous materials reinforced by grains or oriented fibers, using Kauderer stress relation

21 p2787 A73-40987

Noise loading analysis of a memoryless nonlinearity characterized by a Taylor series of finite order.

21 p2656 A73-41147

Gravity wave nonlinear interactions producing secondary waves of opposite polarization, discussing tide polarization

21 p2688 A73-41343

A study of the physics and non-linear effects in photomultipliers.

22 p2860 A73-42302

Bezold-Bruecke effect and visual nonlinearity.

23 p2946 A73-43342

NONNEWTONIAN FLOW

A non-similar solution of heat transfer in external non-Newtonian flow with thermal radiation.

[AIAA PAPER 73-116] 05 p0640 A73-16873

A non-Newtonian model for fluid flow in the semicircular canals.

18 p2281 A73-36431

Solution of nonlinear problems in magnetofluid-dynamics and non-Newtonian fluid mechanics through parametric differentiation.

22 p2843 A73-42556

NONNEWTONIAN FLUIDS

Drag reduction in non-Newtonian turbulent flow, considering viscosity change with strain in long-chain molecules /polymers/ fluid solutions

01 p0034 A73-11134

Turbulent non-Newtonian liquid power dissipation steadiness during motion as function of viscous forces balanced variation

02 p0152 A73-11571

The statistical evaluation of the measurement of viscosity of a non-Newtonian liquid.

03 p0306 A73-12899

A variational solution of the Rayleigh problem for a power law non-Newtonian conducting fluid.

03 p0347 A73-13790

Temperature distribution in non-Newtonian MHD channel flow by shear stress integral evaluation, investigating power law and Prandtl-Eyring fluids

04 p0520 A73-15947

Fluid film lubrication fluid mechanical theory, considering non-Newtonian fluids, turbulence, inertia and elastohydrodynamic effects in various bearing types

10 p1223 A73-23858

Inertia effects in laminar radial flow of power law fluids.

10 p1206 A73-24660

The free surface on a liquid between cylinders rotating at different speeds. II.

10 p1207 A73-24790

Newtonian and non-Newtonian liquids rotating adjacent to a stationary surface.

11 p1346 A73-25369

Asymptotic Nusselt numbers for dissipative non-Newtonian flow through ducts.

11 p1346 A73-25370

The channel flow of an electrically conducting Prandtl-Eyring fluid in a magnetic and an electric field

13 p1663 A73-28161

Development of convection in horizontal layers of a non-Newtonian fluid

16 p2084 A73-32679

NONOHMIC EFFECT

Non-ohmic transport and phonon amplification in polar semiconductors.

04 p0484 A73-16035

NONOSCILLATORY ACTION

Nonoscillation and oscillation of a linear differential equation of the n-th order

20 p2582 A73-39318

NONPARAMETRIC STATISTICS

Nonparametric signal detectors in the case of dependent sampled magnitudes

12 p1467 A73-26868

NONPOLAR CASES

Thermodynamic properties of gases dissolved in electrolyte solutions.

07 p0789 A73-20642

NONREFLECTION

U ENERGY ABSORPTION

NONRELATIVISTIC MECHANICS

Solar soft X-ray bursts data recorded by satellite telemetry, considering production by thermal plasma

and nonrelativistic electrons with power law energy distribution

08 p0996 A73-20765

NONRESONANCE

A method of studying oscillatory systems subject to the action of external periodic forces in the nonresonant case

12 p1525 A73-27812

Helicopter engineering applications of antiresonance theory, showing eigenvalue nature and matrix iteration determination of antiresonances [AHS PREPRINT 736]

17 p2105 A73-35072

NONRIGIDITY

U FLEXIBILITY

NONSTABILIZED OSCILLATION

Analysis of the vibrational characteristics of a liquid contained in a tank [ONERA, TP NO. 1197]

07 p0812 A73-20074

Wave periodic structure solution instability and unstable oscillation growth rates for nonlinear drift waves and solitons in collisionless plasma

14 p1778 A73-29692

Orthotropic viscoelastic shells and plates dynamic behavior reduced to eigenvalue and quasi-static solutions for nonstabilized oscillation

17 p2241 A73-34326

Time domain analysis of human operator manual control function for second order oscillatory divergent system with error signals for compensatory tracking

21 p2634 A73-40090

NONUNIFORM FLOW

Calculation of the mean parameters of an inhomogeneous flow by the method of sections

06 p0645 A73-17720

An evaluation of the heat pulse anemometer for velocity measurement in inhomogeneous turbulent flow. [AD-758460]

09 p1071 A73-22102

Hydromagnetic stability of plane heterogeneous shear flow.

12 p1527 A73-27129

Flow through non-uniform gauze screens.

20 p2508 A73-39811

Construction of a minimum-wave-drag profile in inhomogeneous supersonic flow

21 p2631 A73-40184

The Lagrange function for a gas bubble in an inhomogeneous flow

21 p2676 A73-40206

Flow field over pointed wedges in isoenergetic flow of thermally and calorically perfect gases with nonuniform incident supersonic flow, noting attached shock formation

24 p3056 A73-45547

NONUNIFORM MAGNETIC FIELDS

Nonlinear boundary-value problem for a conducting source flow in an inhomogeneous magnetic field.

01 p0085 A73-11064

Effect of the asymmetry of an external magnetic field on a viscous fluid flow in an annular MHD channel

05 p0603 A73-16589

Gas-dynamic description of a plasma in a corrugated magnetic field.

05 p0603 A73-17360

Influence of magnetic-field nonuniformity on the fluctuations of the plasma layer in the magnetospheric tail

06 p0690 A73-17559

Possibility of experimentally dividing a variable magnetic field into poloidal and toroidal components

06 p0690 A73-17561

Thermomagnetic effect in plasma located in an inhomogeneous magnetic field.

07 p0859 A73-20135

Characteristics of hydromagnetic wave propagation in a slowly varying magnetic field /Geometrical optics approximation/

08 p0959 A73-21294

Investigation of the heating mechanism for the electron component of a plasma under beam-instability conditions in a mirror confinement system

09 p1130 A73-22703

Synchrotron emission, adiabatic invariant, and gradient drift of particles in a linearly inhomogeneous magnetic field

09 p1132 A73-23079

Some characteristics of the motion and acceleration of particles in a linearly inhomogeneous magnetic field with a neutral plane

09 p1132 A73-23080

Measurement of plasmoid energy in a time-variable magnetic field

10 p1258 A73-24881

Parametric instability in a plasma placed in nonhomogeneous magnetic field.

11 p1407 A73-26563

Experiments on the containment of an alkali plasma in a corrugated magnetic field.

13 p1664 A73-28612

Valve effect of inhomogeneities on anisotropic wave propagation.

14 p1780 A73-30165

Analysis of EH inhomogeneities and singular H inhomogeneities in a rectangular-section waveguide

14 p1729 A73-30560

Velocity structure of a flow in a magnetic field periodically varying along the flow

15 p1918 A73-31413

Separation of the variable geomagnetic field into normal and anomalous components

15 p1872 A73-31896

Effect of magnetic field inhomogeneity on oscillations of the plasma sheet of the magnetospheric tail.

16 p2002 A73-32783

Possibility of experimental separation of the variable geomagnetic field into a poloidal and a toroidal part.

16 p2002 A73-32785

Generation of energetic ion fluxes from a high temperature electron discharge in an inhomogeneous magnetic field

19 p2466 A73-37358

Characteristics of hydromagnetic wave propagation in a slowly varying magnetic field /is the approximation of geometric optics/.

19 p2425 A73-37923

The rate of separation of magnetic lines of force in a random magnetic field.

19 p2489 A73-38522

Measurement of plasmoid energy in a time-varying magnetic field.

21 p2749 A73-41656

Experimental investigation of the interaction between plasma fluxes and a spatially-periodic magnetic field

23 p3010 A73-43656

Experimental investigation of a 'poloidal' current in a plasma flow in an inhomogeneous axially-symmetric magnetic field

23 p3010 A73-43657

Plasma cluster movements in guides using straight stellarator magnetic fields and axisymmetric-straight rod produced field combination

23 p3010 A73-43660

Single particle approximation analysis of particle velocity changes influence on plasma motion across nonhomogeneous magnetic field, examining energy exchange between particles

23 p3010 A73-43662

Unsteady plasma flows behind a moving leading boundary

24 p3119 A73-45539

NONUNIFORM PLASMAS

Kinetic theory of electromagnetic fluctuations in an anisotropic plasma half-space

01 p0082 A73-10210

Anomalous absorption of electromagnetic radiation at double the plasma frequency.

01 p0082 A73-10425

Thermal instability of nonuniform plasma in steady state D-T fusion reactor operated by charged particle heating with spatially uniform fuel injection

01 p0084 A73-10463

Periodic structure of the electric field in a stratified plasma with tensor conductivity

01 p0085 A73-10955

Second harmonic generation in an inhomogeneous laser plasma

01 p0086 A73-11288

Magnetization currents effect on linear hydromagnetic instabilities development in collisionless anisotropic plasmas

02 p0196 A73-11899

Sawtooth, solitary, and turbulent waves in a weakly ionized plasma.

02 p0196 A73-12058

Coupled wave equations for propagation in generally inhomogeneous compressible magnetoplasma.

03 p0345 A73-13069

Plasma inhomogeneity in crossed electromagnetic fields, comparing motion velocity to ion component transverse drift rate in polarized electric field

03 p0347 A73-14090

Study of the boundary layers of a completely ionized two-temperature plasma on the nonconducting wall of an MHD channel

03 p0346 A73-13610

Surface drift waves in a weakly ionized plasma.

03 p0347 A73-14090

Interaction of an intense electron beam with a homogeneous and a nonhomogeneous plasma

04 p0478 A73-15031

Nonlinear radio-frequency response of a nonuniform plasma slab-condenser system with realistic density and velocity profiles.

04 p0479 A73-15189

Diagnostic procedures for nonhomogeneous plasma based on geometrical optics approximation, irradiating plasma by plane wave at oblique incidence

05 p0601 A73-16070

Electrostatic ion cyclotron waves in an anisotropic plasma.

05 p0611 A73-17305

Effect of ion viscosity and thermal conductivity on the drift instability in an inhomogeneous high-pressure collisional plasma. 05 p0604 A73-17362

Mechanism of motion of inhomogeneities in a nonequilibrium plasma in a magnetic field. 06 p0726 A73-17401

Diffusion of weak inhomogeneities in a magnetoactive two-ion plasma 06 p0727 A73-17536

New procedure for measuring the radial temperature distribution in inhomogeneous and unsteady plasma columns with considerable self-absorption 06 p0728 A73-17913

Nonlinear damping of potential monochromatic waves in inhomogeneous plasma, obtaining resonance particle distribution function 06 p0728 A73-17967

Quasi-hydrodynamic equations for transverse quanta in inhomogeneous plasma, using geometric optics approximation 06 p0728 A73-17969

Kinetic theory of longitudinal wave dispersion in nonuniform plasma layer in HF electromagnetic field, noting plasma instability for electron parametric resonance 06 p0729 A73-18109

Diffraction of electromagnetic plane wave by an infinite slit embedded in an anisotropic plasma. 06 p0668 A73-18356

A specific feature of surface waves at the boundary of inhomogeneous plasma. 06 p0730 A73-18466

Anode sheath plasma current instabilities, examining electron and ion turbulent heating, plasma particle limiting energies and unsteady oscillation spectra 06 p0731 A73-18604

Absorption of light at oblique incidence on a plasma layer. 07 p0854 A73-19262

Use of Olver's algorithm to evaluate certain definite integrals of plasma physics involving Chebyshev polynomials. 07 p0854 A73-19270

Theory of parametric resonance in an inhomogeneous plasma 07 p0855 A73-19279

Drift instabilities in nonuniform streaming plasmas. 07 p0855 A73-19337

Wave pattern of three dimensional hydromagnetic perturbations produced by harmonic magnetic dipole in anisotropic plasma 07 p0816 A73-19461

Magnetospheric quasi-stationary pinch effect and filamentary structure due to electron streams parallel to geomagnetic field lines 07 p0816 A73-19464

Kelvin-Helmholtz instability in a high-beta collisionless plasma. 07 p0856 A73-19520

Effect of collision frequency on the characteristics of waveguide filled with homogeneous anisotropic plasma. 07 p0857 A73-19533

The complete iso-thermalization by collective electromagnetic interactions of strongly anisotropic magnetized collisionless plasmas. 07 p0859 A73-20235

Privileged equilibria of a collisionless homogeneous or inhomogeneous plasma. 07 p0860 A73-20480

Departure from thermodynamic equilibrium of an ionized cesium vapor - Experimental study and comparison with a statistical model 07 p0854 A73-20607

Stabilization of normal drift modes in an inhomogeneous plasma by a magnetic shear field 07 p0860 A73-20611

Lower-hybrid-resonance heating of a plasma in a parallel-plate waveguide. 08 p0991 A73-20816

Ion cyclotron wave generation in a two-ion plasma. 08 p0991 A73-20817

Non-local asymptotic treatment of the stability of an inhomogeneous confined plasma. 08 p0991 A73-20819

Electrodynamic mathematical model for electroconductivity of nonuniform plasma with Hall effect, calculating current distribution from Riemann problem solution 08 p0992 A73-20863

On the instability of longitudinal oscillations in an inhomogeneous isotropic plasma. 08 p0992 A73-20956

The rate of motion of weak inhomogeneities in the ionospheric plasma 08 p0959 A73-21302

Parametric excitation of surface waves in a nonhomogeneous magnetized plasma 09 p1124 A73-21892

Momentum method extension to thermal conduction laser heating of nonhomogeneous plasma, obtaining closed form solutions for plane waves 09 p1126 A73-22171

Energy absorption in cold inhomogeneous plasmas - The Herlofson paradox. 09 p1126 A73-22276

Effect of the plasma inhomogeneity on the nonlinear damping of monochromatic waves. 09 p1126 A73-22281

The instability of hydrodynamic longitudinal oscillations in a non-uniform magnetoactive plasma. 09 p1127 A73-22285

Wave number space analysis of propagation in nonuniform media. 09 p1120 A73-22474

Effect of plasma inhomogeneity on the spectral-line profile and the reversal temperature 09 p1129 A73-22662

Kinetic theory of the spatial instability of a radially bounded plasma-electron beam system with a given radially nonhomogeneous plasma configuration 09 p1129 A73-22688

Obliquely incident electromagnetic wave propagation through plane-stratified weakly ionized plasma with electron density inhomogeneity scale length comparable with mean free path 09 p1052 A73-23077

Nonlinear interactions between Langmuir waves in a weakly inhomogeneous plasma 10 p1253 A73-23576

Efficiency of the microwave energy absorption in a plasma at high magnetic fields. 10 p1257 A73-24627

Dynamic viscosity and current distribution model of inhomogeneous Cs plasma flow in coaxial plasma gun with thermionic cathode 10 p1258 A73-24886

Enhanced laser-light absorption by optical resonance in inhomogeneous plasma. 11 p1405 A73-25970

Light scattering from weakly ionized nonhomogeneous plasmas. 11 p1405 A73-25971

Electromagnetic wave scattering by an inhomogeneous magnetoplasma column moving in the axial direction. 11 p1407 A73-26700

Parametric instability in an inhomogeneous plasma containing hot ions 12 p1526 A73-26926

Inhomogeneous plasma density distribution relation to ambipolar diffusion and ionization balance processes of electron cooling, particle recombination and ground state, step wise and Penning ionization 12 p1527 A73-26932

Absorption of microwaves by a plasma in a magnetic field in the presence of a large effect due to longitudinal inhomogeneity 12 p1467 A73-26934

ARC discharge plasma diagnostics for nonuniform nonequilibrium turbulent sources, including automatic methods for control applications 12 p1528 A73-27322

Reflection of electromagnetic waves from nonhomogeneous anisotropic plasma layers /normal incidence/ 12 p1470 A73-27356

On the momentum of quasi-monochromatic waves in a plasma. 12 p1529 A73-27435

[IPPCZ-167] The periodic structure of an electric field in stratified plasma with tensor conductivity. 12 p1529 A73-27531

Nonlinear ion sound waves in a plasma with three-dimensional random inhomogeneities 12 p1530 A73-27980

Nonlinear behavior of stimulated Brillouin and Raman scattering in laser-irradiated plasmas. 13 p1664 A73-28187

Parametric resonance in an inhomogeneous plasma. 13 p1665 A73-28679

Diffusion spreading of weak plasma inhomogeneities in the presence of two kinds of positive ions. 13 p1608 A73-28710

Investigation of the absorption and emission of electron-beam-induced waves in an inhomogeneous magnetoactive plasma 13 p1666 A73-28958

Absorption of waves by a two-dimensionally inhomogeneous plasma in the vicinity of singularity points 13 p1666 A73-28960

Effect of plasma inhomogeneity on the relaxation of the electron distribution function in the electrode area of a low voltage arc 13 p1667 A73-28963

Theory of surface wave dispersion in an inhomogeneous plasma situated in a strong HF field 13 p1667 A73-29161

Diffusion of plasma density and temperature perturbations in a magnetic field 14 p1749 A73-30264

Electromagnetic instabilities of finite pressure anisotropic plasma with hot electrons. 15 p1916 A73-31084

Nonstationary theory of decay instability in a weakly inhomogeneous plasma 15 p1918 A73-31704

Zone of Poynting vector rotation toward the direction of an applied magnetic field for a wave incident on an inhomogeneous plasma 15 p1919 A73-31707

Diffusion of weak inhomogeneities in a magnetically active plasma consisting of two ions. 16 p2039 A73-32760

Propagation of frequency-modulated pulses in a randomly stratified plasma. 17 p2214 A73-34095

Investigation of plasma inhomogeneities between coaxial electrodes in a magnetic field 17 p2214 A73-34128

Parametric excitation of surface waves in an inhomogeneous magnetized plasma. 17 p2215 A73-34315

Surface oscillations of a magneto-active plasma. 17 p2217 A73-35522

Damping of Alfvén and magnetoacoustic waves at high beta. 17 p2217 A73-35524

Transformation of high-frequency waves and vanishing of low-frequency instabilities in a radially inhomogeneous beam-plasma discharge. 17 p2217 A73-35525

A method for solving the problem of irradiation in anisotropic plasma. 17 p2217 A73-35724

One-dimensional model for nonlinear reflection of laser radiation by an inhomogeneous plasma layer. 17 p2218 A73-35824

Resonant absorption of an electromagnetic wave by an inhomogeneous magnetoactive plasma at electron cyclotron frequency harmonics 18 p2289 A73-36563

Wavenumber space analysis of oscillations in weakly non-uniform magnetoplasmas. 19 p2468 A73-37442

Electromagnetic load propagation for an oblique incidence in a nonhomogeneous magnetized plasma 19 p2468 A73-37447

Traveling longitudinal electrostatic waves excitation in warm nonuniform plasma by external HF electric fields, using kinetic theory 19 p2468 A73-37857

Velocity of weak inhomogeneities in the ionospheric plasma. 19 p2425 A73-37931

Theory of electromagnetic wave in a nonuniformly moving magnetoactive plasma 19 p2406 A73-38328

Passage of pulses through an inhomogeneous plasma medium 19 p2406 A73-38329

Excitation of transverse extraordinary mode in an inhomogeneous magnetoplasma. 20 p2598 A73-39300

Nonlinear theory of a quasi-monochromatic electrostatic wave packet in an inhomogeneous plasma 21 p2745 A73-40363

Wave absorption by a plasma with a nonmonotonic longitudinal distribution of the concentration 21 p2746 A73-40524

Quasar scintillations at an inhomogeneous interstellar plasma 21 p2767 A73-40535

Variations of pulsar intensity as a result of scintillations at an inhomogeneous plasma 21 p2767 A73-40536

Inhomogeneous structure of plasma near sun due to drift, slipping and anisotropic temperature distribution instabilities, noting association with radio astronomy observed fine structure 21 p2767 A73-40537

Dynamic viscosity and current distribution model of inhomogeneous Cs plasma flow in coaxial plasma gun with thermionic cathode 21 p2749 A73-41661

Nonlinear interacting longitudinal and transverse electron oscillations due to plasma density inhomogeneity in HF hybrid resonance region 21 p2750 A73-41683

Parametric instability in an inhomogeneous plasma with hot ions. 22 p2891 A73-42260

Inhomogeneous plasma density distribution relation to ambipolar diffusion and ionization balance processes of electron cooling, particle recombination and ground state, step wise and Penning ionization 22 p2891 A73-42266

Microwave absorption by a magnetoplasma with a strong longitudinal inhomogeneity. 22 p2891 A73-42268

Incident electromagnetic wave reflection in inhomogeneous plasma with local nonlinearity, discussing reflection point shift and dielectric permittivity effect 22 p2892 A73-42328

Nonlinear propagation of electromagnetic waves in a plasma containing random irregularities. 22 p2894 A73-42398

Small angle multiple backscattering from randomly spaced cylindrical plasma cloud striations, obtaining ray density via Fokker-Planck transport equation 22 p2896 A73-43182

Reflection of electromagnetic waves from inhomogeneous anisotropic plasma sheets /normal incidence/.
23 p2952 A73-43255

Second-harmonic generation in an inhomogeneous laser plasma.
23 p3009 A73-43509

Local measurements of plasma parameters by a microwave interferometer with a moving emitter
23 p3011 A73-43666

Absorption and emission of waves generated by an electron beam in an inhomogeneous magnetoplasma.
23 p3013 A73-44310

Wave absorption near singular points in a two-dimensional inhomogeneous plasma.
23 p3013 A73-44312

Effect of plasma inhomogeneity on the relaxation of the electron distribution near the electrodes in a low-voltage arc.
23 p3013 A73-44315

Langmuir wave attenuation in collisionless plasma of variable density due to field generated by resonant particle currents moving toward lower density region
23 p3015 A73-44349

Kinetic theory of longitudinal wave dispersion in nonuniform plasma layer in HF electromagnetic field, noting plasma instability for electron parametric resonance
24 p3114 A73-44498

On coupled fields in stratified plasmas with tensor pressure perturbations.
24 p3115 A73-44625

Large-scale inhomogeneities in the sector structure of the solar wind
24 p3124 A73-44779

NONUNIFORMITY
A non-uniform relativistic cosmological model.
01 p0098 A73-10581

NONVISCOUS FLOW
U TURBULENT FLOW

NOON
The standard electron density profile of the F2-layer at noon.
09 p1078 A73-22746

Equatorial anomaly in the F2 layer during local noon and the IGY and IQSY periods
11 p1350 A73-25089

NOREPINEPHRINE
Hypothalamic norepinephrine - Circadian rhythms and the control of feeding behavior.
02 p0134 A73-12417

Energy requirements of ouabain-sensitive Na-K positive ion membrane pump during norepinephrine induced thermogenesis of brown adipose tissue in cold-exposed hamsters
09 p1040 A73-22649

Circadian rhythms in catecholamines in organs of the golden hamster.
11 p1318 A73-26120

Alterations of cardiac sympathetic neurotransmitter activity in congestive heart failure.
22 p22808 A73-42690

NORMAL DENSITY FUNCTIONS
A systematic approach to the problem of crossings by a random process.
01 p0070 A73-10577

Experimental investigation of the parameters of a statistical Gaussian model of the field below the radio horizon at centimeter wavelengths.
07 p0794 A73-20131

Algorithm for spectrum decomposition during continuous man-computer interaction, noting Gaussian distribution of spectral bands and linear approximation for background
09 p1046 A73-22971

Normalization of stochastic system analog of linear determinate system with combined normal distribution of input/output signal, noting theorems for random variable distributions
11 p1341 A73-25632

Approximate log normal distribution of normalized power antenna patterns, relating first sidelobe level and antenna size to 0.5 probability level
11 p1337 A73-25668

Absolute continuity of estimates corresponding to uniform Gaussian fields
12 p1523 A73-27185

Approximate calculation of the moments of the distribution of the maxima of correlated Gaussian random sequences
12 p1485 A73-27621

On the robustness of properties characterizing the normal distribution.
13 p1650 A73-28797

Distribution law of light-ray direction fluctuations in telescopes
13 p1618 A73-29098

Ionospheric and pulse compression induced distortions in chirped Gaussian electromagnetic pulses
14 p1728 A73-30232

Transient temperatures in a plate from a Gaussian distribution of normal heat flux and current flow with application to the free arc discharge.
17 p2255 A73-35843

Normalization of stochastic system analog of linear determinate system with combined normal distribution of input/output signal, noting theorems for random variable distributions
19 p2414 A73-38143

Two-stage detection of signals in normal noise of unknown intensity.
20 p2529 A73-38922

Statistical representation of the strength of fiberglass-reinforced plastic samples
22 p2880 A73-41956

NORMAL DISTRIBUTIONS
U NORMAL DENSITY FUNCTIONS
NORMAL FORCE DISTRIBUTION
U FORCE DISTRIBUTION
NORMAL SHOCK WAVES
Combustion of stabilized ethylene within a supersonic flow by a Mach configuration
03 p0352 A73-13578

Weak normal shock wave interactions with materials, investigating incident pressure ratio, thickness, perforation diameter, close area and flow resistance effects on acoustic reflectance
[AIAA PAPER 73-244]
05 p0598 A73-16968

Radiating-conducting thick-transparent normal shock solution.
07 p0919 A73-19507

A simple model of normal shock wave and turbulent boundary-layer interaction.
11 p1347 A73-25710

Long wavelength instability in a perpendicular shock.
11 p1406 A73-26557

Generation of acoustic waves during the passage of a shock wave through a heated gaseous element.
13 p1705 A73-28494

Instability of hydromagnetic perpendicular shocks in inhomogeneous fluids.
13 p1601 A73-28775

Engineering approximations for radiating nonequilibrium shock layers.
[AIAA PAPER 73-673]
18 p2297 A73-36224

NORMALITY
Normality condition derivation for algorithm of first order solution to ideal resonance problem, applying to critical inclination of oblate planet satellite
01 p0077 A73-10686

NORMALIZING
Normal third-order shapes of nonlinear oscillations
20 p2593 A73-39320

A practical means of calculating normal forms in problems involving nonlinear oscillations
21 p2738 A73-40178

Reference image /brightness distribution functions/ existence and normalization under additive and multiplicative groups of transformations in visual field
24 p3064 A73-44908

NORMALIZING [STATISTICS]
Normalization of stochastic system analog of linear determinate system with combined normal distribution of input/output signal, noting theorems for random variable distributions
11 p1341 A73-25632

Normalization properties of resonance wave functions of quantum systems associated with poles of Green function in terms of Siegert and Kapur-Peierls energy definitions
14 p1776 A73-30244

Analysis of the operation of devices for normalizing random signals
18 p2293 A73-36851

Normalization of stochastic system analog of linear determinate system with combined normal distribution of input/output signal, noting theorems for random variable distributions
19 p2414 A73-38143

Design of Gunn-diode oscillators on the basis of normalized characteristics
21 p2659 A73-40007

NORTH AMERICA
Geomagnetic storms and wintertime 300-mb trough development in the North Pacific-North America area.
08 p0961 A73-21384

Whistler observations of the depletion of the plasmasphere during a magnetospheric substorm.
09 p1074 A73-22060

Possible stratotype sequences for the basal Paleozoic in North America.
15 p1865 A73-31025

NORTH AMERICAN AIRCRAFT
NT B-1 AIRCRAFT
NT B-70 AIRCRAFT
NT T-39 AIRCRAFT
NORTH AMERICAN MILITARY AIRCRAFT
U MILITARY AIRCRAFT
NORTH SEA
Project VEMNO - North Sea-Baltic measuring network.
13 p1608 A73-28787

NORTHERN HEMISPHERE
NT ARCTIC REGIONS
D region HF radio wave noontime absorption correlation to winds and temperature in Northern Hemisphere during IQSY
03 p0304 A73-14593

Typification of circulation processes in the atmosphere over the Northern Hemisphere and the possibility for its objectivization with the aid of numerical characteristics
05 p0593 A73-16238

Vertical distribution of electron concentration in the Northern Hemisphere at the geomagnetic pole /from top-side and ground-based ionospheric sounding data/
06 p0689 A73-17554

Long term atmospheric pressure fluctuations in relationship to solar activity over Northern Hemisphere, confirming 22 year cycle
07 p0816 A73-19448

Differences in auroral intensity at conjugate points.
09 p1074 A73-22059

Northern Hemisphere climatic trend from monthly atmospheric temperature and water vapor content calculations over five year period, noting humidity decrease and cooling
11 p1358 A73-26663

New estimate of annual poleward energy transport by Northern Hemisphere oceans.
13 p1610 A73-29225

Study of the effect of heat influxes on the formation of lower and higher baric fields in the Northern Hemisphere
15 p1903 A73-31602

Kinetic energy conversions by horizontal and vertical eddy processes from 5 years of hemispheric data.
15 p1873 A73-32253

Map series for description of annual temperature wave in lower stratosphere in Northern Hemisphere, establishing easterly circulation on south side of Aleutian high
15 p1873 A73-32254

Relation between the average motion of cyclones and anticyclones and their shape.
15 p1906 A73-32255

Vertical electron density distribution at the geomagnetic pole in the Northern Hemisphere /from data of topside and ground-based soundings of the ionosphere/.
16 p2002 A73-32778

Speed variation in the earth's rotation and the baric field of the earth's Northern Hemisphere
17 p2159 A73-34637

Application of temperature soundings by the Nimbus 3 satellite to the analysis of the hemispheric-scale stratospheric environment
17 p2206 A73-34937

Analysis of atmosphere circulation and climate fluctuations in different portions of the Northern Hemisphere of the earth
18 p2331 A73-35913

Differences in circulation of the upper atmosphere in low latitudes of the southern and northern hemispheres.
18 p2310 A73-36138

Influence of longitudinal variations on the structure of temperature, pressure and wind fields in the stratosphere and mesosphere of the Northern Hemisphere.
18 p2310 A73-36139

Experiments on incorporating radiative heat influx in numerical forecasting.
18 p2334 A73-37077

Oceanic contribution to atmospheric CO budget estimation from Northern Hemisphere water carbon monoxide content, comparing to anthropogenic production
21 p2680 A73-40083

NORTHROP AIRCRAFT
Cobra P-530 air superiority fighter adaption to ground attack for international requirements for multipurpose aircraft, discussing avionics for multimission version
21 p2634 A73-40301

NORTHROP MILITARY AIRCRAFT
U MILITARY AIRCRAFT
U NORTHROP AIRCRAFT
NOSE [ANATOMY]
Aspects of air flow to the olfactory region of the human nose
15 p1833 A73-31163

NOSE CAPS
U NOSE CONES
NOSE CONES
NT ROCKET NOSE CONES
Thin shell theory for thermal stresses in ogival shell used in nose cone design
01 p0113 A73-10016

Hyperonic, viscous shock layer with chemical nonequilibrium for spherically blunted cones.
01 p0002 A73-10746

Thermal stress analysis of reentry vehicle nosetips at angle of attack.
03 p0392 A73-13688

Tibere rocket launched Electre nose cones reentry impact safety optimization policy based on probabilistic viewpoint
[ONERA, TP NO. 1152]
08 p1014 A73-21679

A method for calculating aerodynamic heating on sounding rocket tangent ogive noses.
[AIAA PAPER 73-281]
09 p1167 A73-23202

NOSE WHEELS

Numerical computation for entropy layer on blunt nosed cone in terms of shock layer fraction for given free stream and Mach number

11 p1299 A73-25113

Structural testing of ceramic nose cap and leading edge components for a reusable entry vehicle.

11 p1388 A73-25507

Experimental study of wakes produced by hyper-sonic cones in free flight.

15 p1823 A73-31312

Airborne mechanical system for sounding rocket experiments.

16 p2072 A73-33119

Investigation of multiple slot film cooling to a blunt nose cone.

[AIAA PAPER 73-698]

18 p2368 A73-36247

Transpiration nosetip coolant flow control.

[AIAA PAPER 73-767]

18 p2371 A73-36382

Functional tests with hypersonic flight vehicles, using an infrared heating system to simulate the temperature loads in flight

19 p2419 A73-38269

Geometrical characteristics of flat-faced bodies of revolution.

22 p2842 A73-42425

The wave drag of circular nose cones at zero angle of attack at Mach numbers from 1.5 to 4 and thickness ratios from 0.05 to 0.5

23 p2940 A73-43782

NOSE WHEELS

Hydraulic system on de Havilland Twin Otter STOL aircraft for flaps, wheel brakes and nose wheel steering, noting power supply mounting

03 p0252 A73-13350

Mathematical model for shimmy auto-oscillations of aircraft landing gear nose wheel with pneumatic tire under velocity changes

15 p1825 A73-31044

NOSES (FOREBODIES)

NT NOSE CONES

NT ROCKET NOSE CONES

An investigation into the flow around a family of elliptically nosed cylinders at zero incidence at free-stream Mach numbers of 2.5 and 4.

02 p0129 A73-12507

Buffalo aircraft fiberglass laminated polyester nose boom for mounting horizontal and vertical wind sensing probes, describing instruments and measurement procedures

17 p2174 A73-35576

Effect of nose geometry on the aerothermodynamic environment of shuttle entry configurations.

[AIAA PAPER 73-638]

18 p2260 A73-36196

Three-dimensional nosetip shape changes in hypersonic flow. I - Illustration of a mathematical model-characteristic method.

[AIAA PAPER 73-762]

18 p2264 A73-36377

A method for computing roughwall heat transfer rates on reentry nosetips.

[AIAA PAPER 73-763]

18 p2264 A73-36378

Analytic solutions for potential flow over a class of semi-infinite two-dimensional bodies having circular-arc noses.

23 p2940 A73-43931

NOTATION

U CODING

NOTCH SENSITIVITY

The effect of tin on the strength and plasticity of titanium at low temperatures.

02 p0181 A73-12212

Notch induced stress concentrations at elastic rectangular core /inclusion/ in extended rectangular plate with rigidly supported edges, using finite element method

07 p0910 A73-19196

The dependence of the notch sensitivity of Waspaloy at 1000-1400 deg F on the gamma prime phase.

[ASME PAPER 72-MAT-J]

08 p0979 A73-21571

TRIP steel embrittlement and notch sensitivity in high pressure hydrogen environment resulting from interaction between hydrogen and stress-assisted martensite during deformation

13 p1633 A73-28144

Relationship of mechanical characteristics and microstructural features to the time-dependent edge-notch sensitivity of Inconel 718 sheet.

[ASME PAPER 73-MAT-G]

13 p1637 A73-29200

Correlation between notch sensitivity of a material and its non-propagating crack, under rotating bending stress.

13 p1641 A73-29493

Evaluation of the sensitivity of materials to stress concentrations in cyclic loading

23 p3047 A73-44279

Influence of electrolytic polishing on the stress-concentration sensitivity of some alloys in fatigue

23 p2995 A73-44283

NOTCH STRENGTH

Low-temperature mechanical properties of the alloys AT3 and AT6.

02 p0180 A73-12136

Study of the effect of small elastoplastic deformations on the load-bearing capacity of specimens with

stress concentrators under repeated variable loading.

02 p0181 A73-12203

The influence of structure upon the notched creep strength of a nickel-base alloy.

08 p0982 A73-21795

Embrittlement of 2-1/4Cr-1Mo steel weld metal by postweld heat treatment.

11 p1375 A73-26354

Influence of temperature on the initial yield of notch strength.

13 p1641 A73-29511

High modulus fiber reinforced metal and plastic matrix composites fracture within linear elastic fracture mechanics framework, reviewing standard notch toughness test

17 p2192 A73-35536

NOTCH TESTS

NT CHARPY IMPACT TEST

The influence of stress concentrators on the properties of steel in cryogenic technology.

02 p0181 A73-12213

Brittle crack initiation at the elastic-plastic interface.

02 p0182 A73-12752

Significance of the sequence of treatment for the notch impact strength of cold-worked steel samples

02 p0175 A73-12850

Low-cycle fatigue of titanium alloys.

03 p0327 A73-14007

Sharp-notch tension testing of thick aluminum alloy plate with cylindrical specimens.

04 p0460 A73-14698

Techniques for smooth specimen simulation of the fatigue behavior of notched members

04 p0453 A73-14862

Local stress-strain response of notched members to predict fatigue life of stress relieved and as-received weldments with internal cavities

04 p0453 A73-14864

Method of determining the energy of fracture of aluminum alloys during impact-bend tests with sharp notches.

04 p0466 A73-15675

Elastic-plastic deformation in edge-notched tension specimens under plane stress conditions.

[ASME PAPER 72-WA/MAT-3]

04 p0514 A73-15809

Experimental analysis of the low-temperature strength of notched bars

06 p0705 A73-17779

Stress analysis of sharply notched plates and measurement of notch tip blunting.

06 p0764 A73-18487

Tensile and compressive prestressing effects on notched steel cantilever beam specimens low cycle fatigue life

06 p0764 A73-18490

Fracture mechanics application to initial notch extension under tension in quasi-isotropic fiberglass reinforced laminates, noting transplanar buckling effects on fracture toughness

07 p0841 A73-19186

Temperature and loading rate effects on yield stress and specific fracture work in tempered carbon steel from notch tests, correlating with linear fracture mechanics

07 p0838 A73-19215

Metallographic investigation and notch, tensile and hardness tests for electrosag welding of austenitic stainless steels

07 p0831 A73-19949

The dependence of the notch sensitivity of Waspaloy at 1000-1400 deg F on the gamma prime phase.

[ASME PAPER 72-MAT-J]

08 p0979 A73-21571

Effect of mean stress on fatigue crack initiation and propagation /from different configurations of notch/.

09 p1164 A73-23323

Izod impact tests of carbon fiber composites strength, measuring residual compressive strength

10 p1238 A73-23973

Stresses in a partly yielded notched bar - An assessment of three alternative programs.

10 p1290 A73-24294

Influence of notch and thread rolling on the fatigue strength of samples prepared from VT3-1 and VT16 alloys

10 p1233 A73-24370

Measurement of the critical crack displacement with the help of double-notched specimens

11 p1434 A73-25325

The effect of coatings on the fatigue characteristics of notched aluminum alloy sheet specimens.

11 p1383 A73-25829

Brittle fracture initiation characteristics of twin notches.

13 p1700 A73-29469

Plane strain elastic-plastic state and fracture in cracked blunt notched steel plates under tensile loads

13 p1701 A73-29477

Crack initiation and propagation in notched plates subjected to cyclic inelastic strains.

13 p1701 A73-29489

Random and program fatigue tests of Cr-Mo steel specimen with V-grooved notch.

13 p1641 A73-29494

A method for the calculation of the fatigue life of unnotched and notched specimens loaded with alternating stresses.

13 p1641 A73-29500

Some observations of crack initiation and propagation of notched specimens under creep conditions.

13 p1641 A73-29511

Application of cylindrical specimens with a ring crack for determining the brittle strength in materials

14 p1814 A73-30719

Macromechanic model of notch size effects on tensile fracture strength in angle ply laminated composites

15 p1897 A73-31688

Notched austenitic stainless steel stress corrosion cracking tests in boiling magnesium chloride solutions, obtaining relationship between maximum stress and strain rate in graph

15 p1895 A73-32569

A microscopic study of crack initiation mechanisms in 7075 aluminum alloy sheets.

17 p2190 A73-34885

High strength Ni-Cr-Mo steel plane-strain fracture toughness measured with circumferentially cracked-notched round bars, discussing heat treatment and temperature effects

17 p2190 A73-34890

The effect of load interaction and sequence on the fatigue behavior of notched coupons.

18 p2364 A73-36589

Cyclic inelastic deformation and the fatigue notch factor.

18 p2364 A73-36590

Applications of finite element stress analysis and stress-strain properties in determining notch fatigue specimen deformation and life.

18 p2364 A73-36591

Quantitative estimation of the fatigue crack propagation under varying load conditions.

19 p2501 A73-38346

Experimental investigation of changes in the fracture toughness of aluminum alloys

20 p2577 A73-39359

High-frequency fatigue tests at low temperatures

20 p2619 A73-39363

Study of the effect of stress concentration on the variation of stability characteristics in graphites

20 p2580 A73-39383

Some further results of J-integral analysis and estimates.

22 p2920 A73-42144

Gamma to alpha transformation and notch depth effects on metastable austenitic steel impact strength at cryogenic temperatures

23 p2995 A73-44282

Fatigue failure predictions for plates with holes and edge notches.

23 p3047 A73-44350

NOTCHED METALS

U NOTCH TESTS

NOTCHED STEEL

U NOTCH TESTS

U STEELS

NOTCHES

Determination of elastic stresses at notches and corners by integral equations.

02 p0234 A73-12075

Infinite triangular wedge, with a notch at its bisectrix, under the action of concentrated forces applied to the edges of the notch

07 p0911 A73-19312

A problem for a half-plane with a finite vertical cut

08 p1019 A73-21727

Antiplane deformation near a cut in a hardening elastoplastic material

11 p1445 A73-26458

Elliptic notch interaction with nearby crack in elastic solid under longitudinal shear, obtaining stress intensity factor

13 p1697 A73-28914

Detonation shock wave against metal surface with hemispherical notch, investigating expelled metal jet dimensions relation to notch radius and Reynolds number

19 p2433 A73-37515

J-integral and equivalent energy method parameter relationship from elastic and inelastic stress concentration factors for notches and cracks

22 p2920 A73-42146

NOVAE

NT HERCULES NOVA

Preliminary report on the infrared spectrum of Nova Serpentis 1970.

01 p0095 A73-10269

The state of ionization in nova shells.

02 p0222 A73-12706

Polarization of light by circumstellar material.

02 p0226 A73-12828

Mass transfer during evolution of close binaries within zero velocity surfaces related to nova outbursts and Wolf-Rayet star composition

06 p0753 A73-18246

- Hydrodynamic calculations for novae origin and mass ejection from luminous red giants, considering planetary nebulae and plausible models
07 p0903 A73-20628
- Luminous blue variables in M 31 and 33, discussing light curves, color index and luminosity
09 p1141 A73-22014
- Elongated shells around novae and concentration near orbital planes resulting from perpetual matter losses, considering close dwarf binaries and recurrent novae
09 p1145 A73-22288
- Thermal wave generation and transformation into shock waves due to energy release in stellar interior, considering nova outburst
09 p1146 A73-22547
- Nebular stage of Nova Delphini 1967, I
13 p1672 A73-28039
- Novae physical processes during subdwarf-explosive variable-subdwarf evolution, describing spectroscopic indications for various luminous stages vs time
13 p1682 A73-28984
- Eruptive binary stars evolutionary origin, outburst mechanisms and effects on Galactic evolution
15 p1935 A73-31487
- Nova and supernova stars as sources of relativistic particles
21 p2756 A73-40580
- NOXIOUS MATERIALS**
U CONTAMINANTS
NOZZLE COEFFICIENT
U NOZZLE FLOW
NOZZLE DESIGN
- Criteria concerning the adaptation of the rear components of a propulsion system to the subsonic and transonic altitude flight
[DGLR PAPER 72-065] 02 p0128 A73-11690
- Implementing the design of airplane engine exhaust systems.
[AIAA PAPER 72-1112] 03 p0355 A73-13427
- Axisymmetric gas-particle flows maximum thrust nozzle design, investigating particle size, nozzle geometry and heat transfer coefficient effects
[AIAA PAPER 72-1189] 03 p0357 A73-13479
- Rocket nozzle design and analysis techniques, considering requirements for high energy propellants, multiple pulse operation and long duration high temperature exposure
[AIAA PAPER 72-1190] 03 p0358 A73-13480
- Supersonic nozzle design for prescribed flight trajectory and variable gas flow parameters, solving variational problem of optimal contour for given Mach number
03 p0244 A73-13616
- Inverse problem approach to the design of short two-dimensional diffusers.
[ASME PAPER 72-WA/GT-6] 04 p0404 A73-15870
- An engineering approach to the design of laminarizing nozzle flows.
[ASME PAPER 72-FE-19] 05 p0565 A73-16549
- Solid propellant rocket engines - Design and development of components in refractory and stratified materials.
07 p0867 A73-18992
- Improved flexible supersonic wind-tunnel nozzle operated by a single jack.
07 p0808 A73-19972
- Investigation of the heat transfer between the gas and casing in the area of the apertures between the nozzle diaphragm blades and guide vanes of turbines
07 p0868 A73-20086
- Relationship among various parameters used in ejector-nozzle performance estimates
07 p0776 A73-20097
- Design analysis of plane asymmetric nozzles with a supersonic velocity at the inlet
08 p0927 A73-21608
- Concorde engine noise reduction at takeoff, initial climb and landing, discussing noise sources research and exhaust system nozzle modifications
14 p1785 A73-30930
- Determination of the shape of a plane supersonic nozzle
15 p1822 A73-31196
- A feed nozzle for hydraulic amplifiers
16 p1971 A73-33671
- Theoretical and experimental analysis of the design and off-design performance of supersonic turbine nozzles.
17 p2093 A73-34387
- Aerodynamic parameters affecting practical gas dynamic laser design.
[AIAA PAPER 73-626] 18 p2321 A73-36173
- Specie number density, pitot pressure, and flow visualization in the near field of two supersonic nozzle banks used for chemical laser systems.
[AIAA PAPER 73-642] 18 p2322 A73-36200
- Noise reducing choked /sonic/ inlet design for V/STOL jet aircraft, discussing aerodynamic theoretical and experimental studies
19 p2375 A73-37295
- Space science terrestrial applications in biomedical data exchange and telediagnosis, propellant technology, life support atmospheres without fire hazard, industrial mixers and nozzle materials
[AAS PAPER 73-133] 20 p2629 A73-38589
- Russian book - Solid-propellant rocket engines.
22 p2900 A73-41880
- Nozzle design for subsonic flow in axisymmetric contractions based on potential flow theory and visual observation, obtaining velocity distribution along wall
22 p2798 A73-43029
- Experimental study on optimization parameters of a supersonic jet ejector thrust augmentor.
22 p2798 A73-43113
- Acoustic investigation of the engine-over-the-wing concept using a D-shaped nozzle.
[AIAA PAPER 73-1030] 24 p3122 A73-44860
- Experimental and theoretical determination of the admittances of a family of nozzles subjected to axial instabilities.
24 p3122 A73-45267
- Solution of the variational problem of designing the contour of a two-mode nozzle
24 p3055 A73-45533
- NOZZLE EFFICIENCY**
Thrust nozzle optimization including boundary-layer effects.
02 p0129 A73-12508
- Axisymmetric gas-particle flows maximum thrust nozzle design, investigating particle size, nozzle geometry and heat transfer coefficient effects
[AIAA PAPER 72-1189] 03 p0357 A73-13479
- Circular conical diffuser inlet velocity profile effect on efficiency, presenting experimental results for different cone angles and expansion ratios
07 p0774 A73-19616
- Lift engine bleed flow management for a V/STOL fighter reaction control system.
[ASME PAPER 73-GT-70] 16 p2048 A73-33521
- Performance of jet V/STOL tactical aircraft nozzles.
[ASME PAPER 73-GT-77] 16 p1969 A73-33523
- NOZZLE EXPANSION**
U GAS EXPANSION
U NOZZLE FLOW
NOZZLE FLOW
- Density and temperature measurement in laminar boundary layer and free jet of hypersonic nozzles by electron beam probe.
[ONERA, TP NO. 1131] 01 p0045 A73-10239
- Flow and heat transfer on a flat plate normal to a two-dimensional laminar jet issuing from a nozzle of finite height.
01 p0033 A73-10804
- Pressure drop, gas content, liquid drop size and nozzle length effects on flow velocity and heat transfer in two phase nozzle flow
01 p0033 A73-10863
- Theoretical consideration on the supersonic axisymmetrical nozzle.
01 p0003 A73-11131
- Approximate method based on quasi-one dimensional theory for calculation of transonic wave propagation in slender nozzles
01 p0034 A73-11368
- Computation of the axisymmetrical free expansion of a nonequilibrium hydrogen plasma
02 p0196 A73-11604
- Numerical calculations of the flow field of low Reynolds number viscous flow with or without real-gas-effects in slender-channel-nozzles.
[DGLR PAPER 72-110] 02 p0152 A73-11674
- Alternating-pressure measurements involving mushroom-nozzle flows with regard to dynamic stresses in the case of the skin structures of reusable carrier rockets
[DGLR PAPER 72-076] 02 p0128 A73-11686
- Ethanol condensation by homogeneous nucleation and growth of liquid droplets in steady state supersonic nozzle flow of ethanol-air and ethanol-nitrogen mixtures
02 p0153 A73-12051
- Some details of the pressure and velocity fields near the nozzle of a round turbulent jet.
03 p0293 A73-13311
- Review of nozzle damping in solid rocket instabilities.
[AIAA PAPER 72-1050] 03 p0353 A73-13381
- Inverse Laval problem of three dimensional subsonic and supersonic flows in nozzles and ducts of variable cross section in terms of asymptotic series
03 p0246 A73-14046
- Effect of nozzle boundary layers on rocket exhaust plumes.
03 p0247 A73-14193
- CW dye laser with dye solution pumped through simple nozzles to provide unconfined flowing thin streams with optical quality and long term stability
03 p0320 A73-14460
- Development of a submerged round laminar jet from an initially parabolic profile.
[ASME PAPER 72-WA/FLCS-3] 04 p0408 A73-15861
- Calculation of transonic flow in three-dimensional nozzles
05 p0527 A73-16447
- An engineering approach to the design of laminarizing nozzle flows.
[ASME PAPER 72-FE-19] 05 p0565 A73-16549
- Theoretical study of a by-pass convergent-divergent nozzle
05 p0533 A73-17191
- Variational mixed boundary value problems of subsonic gas flows for plane parallel symmetric Laval nozzle and transonic wedge, using singular integral equation
06 p0646 A73-18888
- Hypersonic flows in large-scale inlet models.
07 p0773 A73-19189
- Transonic nozzle flow with a parabolic temperature distribution.
07 p0811 A73-19985
- Motion of a fluid outside a turbulent jet system
07 p0812 A73-20091
- The effect of nozzle inlet shape, lip thickness, and exit shape and size on subsonic jet noise.
[AIAA PAPER 73-187] 07 p0776 A73-20465
- Transonic nozzle flow with nonuniform gas properties.
08 p0925 A73-20719
- Effects of contraction geometry on non-isotropic free-stream turbulence.
08 p0955 A73-21438
- Design analysis of plane asymmetric nozzles with a supersonic velocity at the inlet
08 p0927 A73-21608
- Periodic nozzle flow with heat addition.
[AD-758555] 08 p1025 A73-21669
- Features of the flow of a nonisothermal plasma, obtained in a beam-plasma discharge, through a magnetic nozzle
09 p1124 A73-21890
- Solution of the direct problem of mixed subsonic and supersonic gas flow in a nozzle of finite length
09 p1072 A73-22480
- A one-dimensional problem concerning the discharge of a two-phase fluid from a nozzle
09 p1073 A73-23353
- The behavior of vapors of soluble binary systems during expansion in supersonic nozzles - Droplet coalescence in a potential vortex flow
10 p1205 A73-24162
- Cavitation erosion in geometrically similar nozzles with lead and plastic liners, presenting expressions for erosion rates dependence on scale
10 p1206 A73-24669
- On the Kutta-condition at the trailing edge of a nozzle in a weakly nonstationary jet flow.
10 p1209 A73-24827
- Calculation of the relaxed one-dimensional flow of a gas in a convergent-divergent sonic nozzle
11 p1348 A73-25869
- Calculation of nozzle flows using Pade fractions.
11 p1303 A73-26386
- Nonlinear behavior of capillary liquid jets ejected from nonsymmetric nozzles, showing effect on flow stability
11 p1349 A73-26432
- Study of disturbance reflection from the subsonic section of a Laval nozzle
11 p1411 A73-26437
- Application of the principle of corresponding states to two-phase choked flow.
11 p1349 A73-26744
- Pressure drop, gas content, liquid drop size and nozzle length effects on flow velocity and heat transfer in two phase nozzle flow
12 p1560 A73-27912
- Transonic similarity solution for aligned field MHD nozzle flow.
13 p1599 A73-28089
- Two-dimensional calculation of revolution of the relaxed flow of a gas in a convergent-divergent sonic nozzle
13 p1563 A73-28563
- German monograph on compressible turbulent boundary layer equations solution for heat transfer in divergent nozzle flow based on modified Patankar-Spalding difference method
13 p1605 A73-29276
- German monograph on laser and schlieren photographic investigation of supersonic free jet flow from nozzle at supercritical pressure ratio into free atmosphere
13 p1567 A73-29286
- Liquid propellant rockets, discussing effective exhaust velocity, nozzle expansion, chamber pressure effects on equilibrium performance and kinetic recombinations
14 p1784 A73-30136
- Book on aerospace propulsion covering nozzle, combustors and diffusers flow, space power generation, electrothermal engines, chemical rockets and central force fields
14 p1785 A73-30361
- An accurate method for solving some theoretical problems of spatial supersonic gas flows
14 p1712 A73-30826
- Behavior of a weak turbulent jet in a cross flow
15 p1822 A73-31199
- Calculation of the flow of a two-phase mixture in a Laval nozzle with allowance for turbulent diffusion of particles
15 p1822 A73-31300

NOZZLE GEOMETRY

Solution of the direct problem on mixed subsonic and supersonic flow of a gas in a nozzle of finite length.

15 p1824 A73-32067

Relaxation of a partially ionized gas in a nozzle

15 p1824 A73-32327

Variational mixed boundary value problems of subsonic gas flows for plane parallel symmetric Laval nozzle and transonic wedge, using singular integral equation

15 p1824 A73-32412

Hypersonic nozzle flow of air with high initial dissociation levels.

16 p2001 A73-33870

Flow of nonisothermal plasma through a magnetic nozzle.

17 p2215 A73-34313

Theoretical and experimental analysis of the design and off-design performance of supersonic turbine nozzles.

17 p2093 A73-34387

Flow studies in radial inflow turbines interspace between nozzles and rotors.

17 p2093 A73-34392

Total pressure tube measurements in turbomachine-simulating pulsating nozzle flow generator supplemented by pneumatic tube probes for averaging error comparison

17 p2166 A73-34608

An evaluation of hypermixing for VSTOL aircraft augmentors.

[AIAA PAPER 73-654]

18 p2267 A73-36208

Recombination effects in chemical laser nozzles.

[AIAA PAPER 73-643]

18 p2287 A73-36258

Mass flux measurements and correlations in the back flow region of a nozzle plume.

[AIAA PAPER 73-731]

18 p2342 A73-36348

Investigation of the flow in regions of turbulent boundary layer separation in front of a subsonic jet blown from a circular nozzle

18 p2265 A73-37003

Some characteristics of two-phase nozzle flows

18 p2265 A73-37005

Gas expelled from a strongly underexpanded nozzle upstream into a hypersonic flow

18 p2265 A73-37010

Calculation of hypersonic nonequilibrium nozzle flows with excited vibrational degrees of freedom

18 p2266 A73-37018

Flow properties fluctuations in a convergent-divergent nozzle.

19 p2375 A73-37402

Comparison of electron and electronic temperatures in recombining nozzle flow of ionized nitrogen-hydrogen mixture. I, II.

19 p2462 A73-37441

Non-reacting and equilibrium chemically reacting turbulent boundary-layer flows.

19 p2421 A73-38187

On an equilibrium-frozen flow approximation in the analysis of nonequilibrium nozzle flows.

19 p2421 A73-38282

Approximate determination of the inverted population and amplification factor of a gas expanding adiabatically in a nozzle

20 p2572 A73-39280

Incompressible flow planar-nozzle discharge coefficient computations for one dimensional inviscid flow, considering nozzle geometry, flow cross sections and turbulence

20 p2548 A73-39526

Visualization of gas flows by means of high-speed holography

21 p2696 A73-39978

Structure of the base flow in a four-nozzle cluster rocket engine

21 p2696 A73-40392

Analysis of gas flow in multinozzle jets

21 p2631 A73-40393

Contribution to the study of the development of a jet issuing from a nozzle of small elongation and confined between two lateral walls

21 p2677 A73-40620

Investigation of nozzles with cryogenic suction of the boundary layer

21 p2678 A73-41221

Dependence of the output power of CO₂ gas-dynamic laser on the distance from nozzle throat.

22 p2869 A73-42225

Thermodynamic expansion processes for argon plasma in a convergent-divergent nozzle.

22 p2894 A73-42632

Turbulence generation by supersonic nozzle gas flow interaction with plasmas, discussing high current electric arc in axis

22 p2895 A73-43166

Axial vortex and Coanda vortex flow controllers.

23 p2941 A73-43392

An analog investigation of the gas jet resonance tube.

23 p2967 A73-43401

Output pressure-displacement and flow pattern characteristics of digital limit Schrenk, wall attachment and nozzle receiver fluidic switches

23 p2945 A73-43426

Fluidic linear nozzle-flapper valve accelerometer for ship motion sensing, describing circuit configuration and performance tests

23 p2981 A73-43428

Precise method for solving certain problems of the theory of three-dimensional supersonic gas flows.

23 p2939 A73-43582

Total shock-tube working time in the investigation of the discharge through holes in the end face

24 p3076 A73-44755

Use of a relaxation technique in nozzle wave propagation problems.

[AIAA PAPER 73-1011]

24 p3078 A73-44843

The calculation of flow in nozzles using a time-marching technique based on the method of characteristics.

24 p3079 A73-44894

NOZZLE GEOMETRY

Pressure drop, gas content, liquid drop size and nozzle length effects on flow velocity and heat transfer in two phase nozzle flow

01 p0033 A73-10863

Thrust nozzle optimization including boundary-layer effects.

02 p0129 A73-12508

Investigation of the effect of the nozzle cone angle on the parameters of a rarefied gas flow

03 p0245 A73-13624

Calculation of transonic flow in three-dimensional nozzles

05 p0527 A73-16447

Optimal profiles of a nozzle for axisymmetric supersonic discharge of a Lighthill dissociating gas

05 p0534 A73-17270

Stress intensity factors for nozzle corner cracks.

07 p0912 A73-19564

Effects of contraction geometry on non-isotropic free-stream turbulence.

08 p0955 A73-21438

Nozzle-target system geometry and gas dynamics parameters effect on supersonic underexpanded jets interaction with walls, noting frequency response and pressure oscillations

08 p0927 A73-21610

Experimental determination of three-dimensional liquid rocket nozzle admittances.

09 p1167 A73-23438

The shape of a supersonic three-dimensional nozzle with a maximum thrust

11 p1302 A73-26334

Pressure drop, gas content, liquid drop size and nozzle length effects on flow velocity and heat transfer in two phase nozzle flow

12 p1560 A73-27912

Determination of the shape of a plane supersonic nozzle

15 p1822 A73-31196

Automated machining and surface finishing of heat resistant stainless steel nozzles for wind tunnel applications

15 p1855 A73-31200

Two dimensional Mach 5 supersonic nozzle configurations with hot nitrogen expansion for mixing carbon dioxide gasdynamic laser, calculating and measuring gain distribution

18 p2321 A73-36170

Velocity decay and acoustic characteristics of various nozzle geometries with forward velocity.

18 p2263 A73-36256

A note on residual drop and single drop formation.

22 p2840 A73-41748

Analysis of the effects of a probe in the transonic region of a nozzle.

22 p2796 A73-42568

The prediction of the performance of variable geometry free gas turbines.

23 p3019 A73-43297

Optimal parameters on fluidic noncontact sensors for drives of exact positioning.

23 p2945 A73-43427

Fluidic vortex-type proximity sensor with analog to digital converter, investigating output nozzle diameter and pressure by steepest ascent method

23 p2981 A73-43431

Solution of the variational problem of designing the contour of a two-mode nozzle

24 p3055 A73-45533

NOZZLE INSERTS

An approximate rigid-plastic analysis of shell intersections loaded dynamically.

[ASME PAPER 72-WA/DE-1]

09 p1164 A73-23272

Axisymmetric gas-particle flows maximum thrust nozzle design, investigating particle size, nozzle geometry and heat transfer coefficient effects

[AIAA PAPER 72-1189]

03 p0357 A73-13479

Experimental tests on scale models of conical variable geometry propulsion nozzle with short petals for fighter aircraft, discussing aerodynamic and thrust coefficients

12 p1533 A73-27388

NOZZLES

The possibility of crystallization of condensed combustion products in nozzles

21 p2753 A73-40697

NRX-A REACTOR
U NUCLEAR ENGINE FOR ROCKET VEHICLES

NUCLEAR AUXILIARY POWER UNITS

NT SNAP

NT SNAP 19

NT SNAP 27

NT SNAP 29

NT SPACE POWER REACTORS

NT SPACE POWER UNIT REACTORS

Russian book - Power systems of spacecraft.

04 p0408 A73-15704

The optimization of nuclear reactor energy supply installations with turbogenerators

11 p1395 A73-25352

Development of a plutonium-fueled miniature power supply based on thermionic conversion.

11 p1396 A73-26028

NUCLEAR BINDING ENERGY

Cold matter consisting of atomic nuclei submerged in electron-neutron gas, relating subnuclear density relation to existence and binding energy of neutron-rich nuclei

01 p0081 A73-11310

Subnuclear density state equation for minimum mass and binding energy of neutron star converting into white dwarf

04 p0502 A73-15978

Temperature dependent nuclear mass and its application to astrophysical problems.

15 p1939 A73-32013

Electrostatic Hellmann-Feynman theorem applied to long-range interatomic forces - The hydrogen molecule.

24 p3113 A73-44981

NUCLEAR CAPTURE

NT ELECTRON CAPTURE

Capture of primary cosmic rays in the upper atmosphere as a source of excess radiation

10 p1268 A73-23931

Nuclear laser realizability for gamma quanta production from population inversion during radiative capture of neutrons, considering constraints imposed on heating of active medium

10 p1229 A73-24754

NUCLEAR ELECTRIC POWER GENERATION

NT NUCLEAR AUXILIARY POWER UNITS

NT NUCLEAR POWER PLANTS

NT NUCLEAR POWER REACTORS

NT SNAP

NT SNAP 19

NT SNAP 27

NT SNAP 29

NT SPACE POWER REACTORS

NT SPACE POWER UNIT REACTORS

NT THERMONUCLEAR POWER GENERATION

Spacecraft nuclear power source optimization, considering radioisotope and reactor heat sources, cryogenic cooler cycle types and spacecraft design

09 p1118 A73-22799

A review of radioisotope power source development at Atomic Energy of Canada Limited.

09 p1038 A73-23286

Operational safety experience and advances of space nuclear power systems fueled with Pu-238, discussing modular heat sources

09 p1119 A73-23287

Standardized space shuttle launched multipurpose spacecraft design using nuclear electric power systems with radioisotope thermoelectric generators or Brayton cycle alternators

19 p2455 A73-38393

Nuclear safety considerations for the design of a shuttle launched 500 to 2000 watt isotope Brayton power system.

19 p2457 A73-38432

NUCLEAR ELECTRIC PROPULSION

Thermionic reactor ion propulsion system /TRIPS/- Its multi-mission capability.

[AIAA PAPER 72-1060]

03 p0381 A73-13389

Investigation of a liquid-metal magnetohydrodynamic power system.

11 p1308 A73-25978

Multi-mission nuclear electric propulsion stage design.

19 p2457 A73-38433

Development costs for a nuclear electric propulsion stage.

19 p2458 A73-38434

NUCLEAR EMULSIONS

Nuclear photoemulsions under bombardment by pion beam of 60 GeV/c momentum, investigating pion-nucleon interactions involving recoil protons

02 p0195 A73-12667

Semiautomatic photometer for determining the charge of heavy cosmic-ray nuclei in photonuclear emulsions

09 p1085 A73-23001

Upper limit of the antineutrino abundance in primary cosmic rays

10 p1265 A73-23899

Methods for determining the charges of heavy primary nuclei /Z greater than 26/ in photonuclear emulsions of different sensitivities

10 p1267 A73-23922

Experimental methods of correlation between the trajectories of cosmic heavy ions and biological objects: Dosimetric results - Experiment Biostack on Apollo XVI and XVII. 18 p2270 A73-35946

AgCl detectors in the Biostack II experiment aboard Apollo 17. 18 p2314 A73-35986

Upper limit of antinuclei content in primary cosmic rays. 20 p2601 A73-38918

Photographic nuclear emulsions with total replacement of gelatin by synthetic polymers 21 p2647 A73-40269

Preliminary results of the Pamir-20-71 experiment on interactions at energies of about 1000 Tev 23 p3021 A73-43534

Events in a photoemulsion indicating the formation of superheavy fireballs 23 p3021 A73-43535

Interkosmos 6 cosmic ray shower experiment using emulsion stack, spark chamber and scintillation counter to measure particle energy, angular distribution and production multiplicity 23 p2981 A73-43540

Inelastic interaction between pions and emulsion nuclei at an energy of 60 GeV 23 p3021 A73-43541

Study of low-energy heavy-nucleus track regression in plastic detectors /cellulose triacetate and polyethylene terephthalate/ and in low-sensitivity nuclear photoemulsion 23 p2981 A73-43567

Charged particle track detector design with electric field control of nuclear photoemulsion sensitivity, discussing microcrystals, trajectory recording and proton irradiation 23 p2982 A73-43569

Observation of cosmic-ray particles with Z greater than 35. 23 p3024 A73-43609

NUCLEAR ENERGY

Nuclear energy sources in superdense celestial bodies. 01 p0106 A73-11311

Star magnetic field origin in dynamo action associated with nuclear energy generation in stellar evolution, discussing effects on flares, chromosphere and coronal activities 10 p1271 A73-23489

Nuclear Science Symposium, 19th, and Nuclear Power Systems Symposium, 4th, Miami, Fla., December 6-8, 1972, Proceedings. 11 p1363 A73-25955

Stellar evolution lifetime shortening due to thermal instability of nuclear energy generation shell, discussing relaxation oscillations and S-process nucleosynthesis 13 p1683 A73-28990

Intersociety Energy Conversion Engineering Conference, 8th, University of Pennsylvania, Philadelphia, Pa., August 13-16, 1973, Proceedings and Addendum. 19 p2390 A73-38386

Configurations of hot white dwarfs with nuclear energy sources 23 p3025 A73-44360

NUCLEAR ENERGY LABORATORIES

U NUCLEAR RESEARCH

NUCLEAR ENGINE FOR ROCKET VEHICLES

Space propulsion future assessment, discussing space shuttle and tug, NERVA project and electric and photon propulsion 10 p1262 A73-23611

Economic tradeoff study of design criteria cost effectiveness, applying to reusable nuclear shuttle /RNS/ engine concepts 16 p2035 A73-33650

Fluidic programmer for nuclear engine application. 19 p2454 A73-38054

NUCLEAR EXPLOSION EFFECT

Selection and application of the protective coating system for the AWACS radome. 03 p0329 A73-13008

Ionization of the atmosphere and attenuation of radar waves after a nuclear explosion. 15 p1844 A73-32198

On the possible effect of NOx injection in the stratosphere due to past atmospheric nuclear weapons tests. 16 p2011 A73-34047

[AIAA PAPER 73-538] Nuclear meteorology as branch of atmospheric physics, examining natural and artificial fission products, nuclear explosion effects, atmospheric purification and radioactive tracers for meteorological process investigation 21 p2730 A73-40115

Ozone composition and nitric oxide injection upper and lower limits for stratosphere by nuclear bomb tests, comparing to estimated SST contribution 22 p2848 A73-42534

NUCLEAR EXPLOSIONS

NT THERMONUCLEAR EXPLOSIONS

Nuclear explosions released nitric oxide effect on atmospheric ozone concentration compared with potential effect from SST flights 01 p0043 A73-11068

Nitrogen oxides, nuclear weapon testing, Concorde and stratospheric ozone. 21 p2686 A73-41076

NUCLEAR FISSION

Superheavy element fissionability on r-process path, considering experimental search methods and doubly magic nucleus concept 10 p1272 A73-23536

The possibility of microfission explosions by laser or relativistic electron-beam high-density compression. 11 p1378 A73-26657

On Pu-244 in lunar rocks from Fra Mauro and implications regarding their origin. 23 p2951 A73-43771

Curium-248 in the early solar system. 24 p3143 A73-45348

NUCLEAR FORCES

U NUCLEAR BINDING ENERGY

NUCLEAR FUEL ELEMENTS

Development of a radioisotope-fueled thruster for satellite propulsion. 03 p0354 A73-13395

[AIAA PAPER 72-1066] Thermionic fuel elements for in-core reactor power plant space applications, summarizing operating and environmental requirements and technology development 09 p1036 A73-22819

ZrH space power reactors design, discussing long life fuel elements, high temperature hard vacuum irradiation environment control drive components and shield fabrication 11 p1395 A73-26011

Development of a plutonium-fueled miniature power supply based on thermionic conversion. 11 p1396 A73-26028

Thermoelectric nuclear batteries fabrication in milliwatt power range combining bismuth telluride thermopiles with plutonia fuel capsules 19 p2455 A73-38410

NUCLEAR FUELS

An analysis of the operating characteristics of the Colloid Core Reactor. 03 p0341 A73-13414

[AIAA PAPER 72-1094] Co-60 fueled tubular radioisotope thermoelectric generator, correlating long term test data with performance prediction model results 09 p1117 A73-22764

Application of an electronic image analyzer to dimensional measurements from neutron radiographs. 11 p1371 A73-26743

Developments in Canada related to remotely manned systems. 19 p2416 A73-37317

The availability and cost of curium-244 from power reactor fuel reprocessing wastes. 19 p2457 A73-38430

Real-time X-ray inspection system for fast flux test facility fuel. 23 p2966 A73-44169

NUCLEAR FUSION

NT CONTROLLED FUSION

Thermal instability of nonuniform plasma in steady state D-T fusion reactor operated by charged particle heating with spatially uniform fuel injection 01 p0084 A73-10465

Evolutionary sequences for massive stars with various initial chemical compositions, studying convection effects on core helium burning star distribution in H-R diagram 01 p0104 A73-11037

Thermal instability of the hydrogen-burning shell in nondegenerate stars. 03 p0366 A73-12937

Prospects for rocket propulsion with laser-induced fusion microexplosions. 03 p0353 A73-13392

[AIAA PAPER 72-1063] Averaged equations of cumulative-laser heating of plasma in Z-pinch with consideration of the recovery of the energy of nuclear fusion. 03 p0347 A73-13782

Averaged equations of cumulative-laser heating of two-temperature plasma in Z-pinch taking into account the nuclear fusion energy. 03 p0347 A73-13783

Thermal pulses in helium shell-burning stars. 04 p0499 A73-15364

Equations of laser heating of plasma in a system of the 'focus' type, the recovered energy of nuclear fusion being taken into consideration. 04 p0480 A73-15593

Averaged equations of laser heating of two-temperature plasma in Z-pinch, the thermonuclear fusion energy being taken into consideration. 04 p0480 A73-15594

Cumulation-laser heating of two-temperature plasma, the recovered energy of nuclear fusion being taken into consideration. 04 p0480 A73-15596

NUCLEAR FUSION

Solar luminance via light nuclei fusion into heavier nuclei with temperature gradient maintenance by gravity, relating to H-R diagram of different star clusters 05 p0614 A73-16302

He 3 burning burst complication of mixing in solar core for solar luminosity variations resulting from central temperature decrease 05 p0611 A73-17187

Theoretical evolution of a hydrogen-helium star of 3 solar-mass units from the pre-main sequence to the core helium-exhaustion phase. 05 p0625 A73-17319

Interaction contributions to the solar proton-proton reaction. 05 p0612 A73-17339

Fusion plasma confined by nonpenetrating uniform magnetic field, calculating temperature and density effects on energy balance instabilities from particle conservation equations 05 p0604 A73-17366

Laser-initiated fusion - Key experiments looming. 06 p0727 A73-17570

Gravitational contraction and energy dissipation and compensation in stellar nuclear reactions, noting He thermonuclear reactions and nucleosynthesis 06 p0751 A73-18158

Advanced evolution of massive stars. III - Hydrostatic carbon-burning nucleosynthesis and energy generation. 07 p0874 A73-19062

Neutron flux anisotropy from plasma focus measured by gamma spectroscopy of activated Ag target, discussing axial concentration 07 p0857 A73-19529

Large-scale applications of superconducting coils. 07 p0863 A73-20107

He core burning and shell hydrogen burning in horizontal and posthorizontal branch stars 07 p0903 A73-20627

Light elements D 2, He 3-4, Li 6-7, Be 9 and B 10-11 origin and history in universe, considering nucleosynthesis sites 08 p0997 A73-20885

Elemental synthesis during high temperature phase of expansion of big bang universes, obtaining universal baryon density relationship to primordial deuterium abundance 08 p1008 A73-21151

Papers on cosmology and nuclear fusion covering big bang and expanding universe models, conformal invariance, microwave astronomy, neutrino physics, gravitational constant, cosmic rays, etc 08 p1009 A73-21226

Gamow contributions to cosmology and primeval nucleosynthesis theories, discussing big bang model, residual cosmic black body radiation, stellar energy sources and cosmonumerology 08 p1009 A73-21227

Nucleocosmochronology and stellar nucleosynthesis models for Galaxy origin and solar system formation 08 p1010 A73-21231

Charged particle thermonuclear reactions in nucleosynthesis. 10 p1271 A73-23479

Thermal cumulation equations for concentric conductive laser heating of two temperature D-T plasma with nuclear fusion energy recovery 11 p1406 A73-26411

Hydrogen ignition in flat rotating disk shape of stellar formation, determining central conditions from total mass and adiabatic constant 12 p1542 A73-27575

Nuclear reactions in carbon stars. 13 p1672 A73-28038

URCA process and the evolution of carbon stellar core. 13 p1673 A73-28173

Pb 205 as chronometer for s-process nucleosynthesis mechanism, discussing cosmochemistry implications and abundance at solidification 13 p1657 A73-28923

Thermonuclear reactions and nucleosynthesis in stellar interiors, initial big bang, supermassive objects and supernovae explosions 13 p1663 A73-28989

Stellar evolution lifetime shortening due to thermal instability of nuclear energy generation shell, discussing relaxation oscillations and S-process nucleosynthesis 13 p1683 A73-28990

Secular stability of an 8 solar mass star during central helium burning. 13 p1685 A73-29355

Pulsational instability of a star of 0.5 solar mass during core hydrogen burning. 13 p1685 A73-29362

Averaged equations of cumulative laser heating of a plasma focus with consideration of the heat of nuclear fusion. 13 p1667 A73-29389

Concentric laser cumulation of plasma with consideration of the heat of nuclear fusion. 13 p1667 A73-29393

- Stellar nuclear hydrogen burning shell thermal stability to radial perturbations, discussing growth rate, energy generation and temperature increases
15 p1929 A73-31058
- Thermal instability of the helium-burning shell in massive stars.
15 p1936 A73-31557
- Planetary cosmogony theory review emphasizing cold evolution through dust-gas protoplanetary cloud nucleosynthesis, discussing iron fractionation, organic compounds and planetary thermal history
16 p2066 A73-33793
- Trends in physics; General Conference, 2nd, Wiesbaden, West Germany, October 3-6, 1972, Lectures.
17 p2256 A73-34109
- Numerical analysis of the averaged equations of concentric laser cumulation of plasma with consideration of nuclear fusion energy.
17 p2216 A73-34323
- Nearly spherical constant-power detonation waves as driven by focused radiation.
[AIAA PAPER 73-674]
18 p2322 A73-36225
- Structure of helium burning regions in stars - Dependence on molecular weight and burning rates.
19 p2483 A73-37560
- Dynamics of step heat waves in gases and plasmas.
20 p2592 A73-38863
- Book - Introduction to the physics of stellar interiors.
20 p2607 A73-39144
- Stability of the sun against spherical thermal perturbations.
20 p2608 A73-39428
- Effects of nuclear reactions with fast protons in a supernova shell and the origin of cosmic rays
21 p2756 A73-40581
- Stellar explosive nucleosynthesis foundations in nuclear experiments and numerical schemes for solutions in limits of strong and weak coupling of abundances by nuclear reactions
21 p2771 A73-41238
- Origin of cosmic rays, atomic nuclei, and pulsars in explosions of massive stars.
22 p2905 A73-41765
- Theory of interstellar abundances of the isotopes of carbon, nitrogen and oxygen.
22 p2914 A73-43006
- Galactic nucleosynthesis time interval from birth to solar system formation /Galactic age/ from radioactive decay nuclear yield ratios
22 p2916 A73-43049
- Thermonuclear laser synthesis and parametric instabilities
23 p2988 A73-44091
- NUCLEAR HEAT**
Concentric laser cumulation of plasma with consideration of the heat of nuclear fusion.
13 p1667 A73-29393
- NUCLEAR INTERACTIONS**
NT ELECTRON CAPTURE
NT NUCLEAR CAPTURE
NT SPIN-ORBIT INTERACTIONS
Primary proton-air atom nuclei interaction study of negative and positive cosmic ray muon coupling coefficients with angular distribution allowance
02 p0205 A73-12173
- Inelastic nuclear interactions between 200-GeV cosmic ray particles and polyethylene targets, correlating similarity property, momentum spectra and secondary particle pairs
02 p0208 A73-12652
- Particle multiplicity and momentum spectra for high energy inelastic nuclear interactions in Wilson chamber with polyethylene target
02 p0208 A73-12655
- Ionization calorimeter measurement of energy transfer to electron photon cascade secondary particles during hadron interaction with lead nuclei
02 p0209 A73-12662
- Spectral calculations of electromagnetic and nuclear showers, studying cosmic ray muons interactions with matter
02 p0210 A73-12682
- Study of strong interactions between cosmic-ray hadrons and nuclei at 200 to 2000 GeV energies
10 p1264 A73-23816
- Influence of interaction on the stability and pulsations of rotating neutron stars
10 p1283 A73-24704
- Alpha particles in solar cosmic rays over the last 80,000 years.
11 p1412 A73-25375
- Hydrogen and helium isotopes differential energy spectra during solar flare particle acceleration related to nuclear interaction processes
11 p1414 A73-26610
- Charged stopping pions from nuclear-electromagnetic cascades in rock, calculating number and energy spectra by Monte Carlo method
13 p1671 A73-29667
- Re-187, recycling r-process elements through stars, and the age of the Galaxy.
15 p1939 A73-32014
- Null correlation method for estimation of the primary energies of cosmic ray jets.
15 p1927 A73-32149
- Asymptotic electron terms of colliding identical heavy nuclei
21 p2742 A73-40353
- Low-energy cosmic ray protons from nuclear interactions of cosmic rays with the interstellar medium.
22 p2902 A73-41927
- Study of nucleon interactions with carbon, iron and lead nuclei in the energy range 600 to 10,000 GeV
23 p3008 A73-43532
- Events in a photoemulsion indicating the formation of superheavy fireballs
23 p3021 A73-43535
- Extensive air showers and nuclear interaction characteristics at superhigh energies
23 p3022 A73-43551
- NUCLEAR LIGHTBULB ENGINES**
Small nuclear light bulb engines with cold beryllium reflectors.
[AIAA PAPER 72-1093]
04 p0475 A73-14907
- On the emission coefficient of uranium plasmas.
23 p3005 A73-43388
- NUCLEAR MAGNETIC RESONANCE**
NT PROTON MAGNETIC RESONANCE
NT PROTON RESONANCE
Crossed-coil nuclear magnetic resonance probe for high sensitivity low temperature measurements.
02 p0168 A73-11962
- Study of the effect of cobalt on redistribution of atoms of alloying elements in iron-base alloys by the nuclear gamma resonance method.
02 p0182 A73-12697
- Hydrogen self-diffusion in the niobium-zirconium-hydrogen system
03 p0327 A73-13973
- Carbon-13 nuclear magnetic resonance in biosynthetic studies of lipids.
03 p0274 A73-14550
- F-19 chemical shift tensor in group II difluorides.
05 p0546 A73-16046
- Solar Rb isotopic ratio from Rb I resonance lines at 7800 and 7947 Å in photospheric spectrum
05 p0620 A73-17026
- Programmable digital pulse generator for NMR applications based on master clock, several counters and inexpensive ICs
05 p0559 A73-17256
- Atomic nuclei physical properties for space navigation system gyroscopes, noting nuclear magnetic resonance and nuclei polarization
06 p0692 A73-17774
- Effect of molecular shape and flexibility on gamma-ray directional correlations.
06 p0725 A73-18122
- The synthesis and characterization of tin complexes using inert atmosphere techniques - An advanced laboratory experiment.
06 p0661 A73-18272
- Nuclear magnetic resonance properties of lunar samples.
07 p0893 A73-19846
- The nuclear resonance in liquid helium three at very low temperatures
08 p0987 A73-20647
- The nuclear resonance in a hypothetical superfluid phase of helium three
08 p0989 A73-21491
- Calculation of the coverage factor of a NMR sensor for an externally located sample
09 p1080 A73-22339
- Modern developments in flow measurement; Proceedings of the International Conference, Harwell, Berks., England, September 21-23, 1971.
10 p1220 A73-24852
- Recent measurements of flow using nuclear magnetic resonance techniques.
10 p1185 A73-24855
- C-13 nuclear magnetic resonance in organic geochemistry.
11 p1325 A73-25461
- Influence of deformation and heat treatment on the structural changes of the OKh12N13M alloy
12 p1508 A73-26836
- CW NMR millidegree thermometer using oscillator to detect resonance, noting Curie law, magnetogyric ratio, spin-lattice relaxation time and low electrical conductivity
13 p1618 A73-29072
- NMR measurements of the speed of vortices in flux flow in a type II superconductor.
14 p1783 A73-30433
- Temperature effects in quadrupole interaction in NbHf alloys
15 p1923 A73-31710
- NMR spectrometer magnetic field strength-HF field frequency ratio instability spectral density in presence of spin stabilizers
16 p2011 A73-32824
- The compensation method for measuring the components of the earth's magnetic field.
17 p2159 A73-34750
- Resonant nuclear measurement of hydrogen concentration vs depth in Apollo 11, 15 and 16 lunar soil fragments and platinum foil exposed to solar event
21 p2765 A73-40237
- Nuclear spin analogue of a molecular beam maser with cavities in series.
21 p2713 A73-40469
- Nuclear magnetic resonance thermometry.
22 p2856 A73-42022
- Instrumentation errors in nuclear resonance thermometry.
22 p2856 A73-42023
- High field NMR thermometry below 1 K using HD.
22 p2856 A73-42024
- Optical orientation in a system of electrons and lattice nuclei within semiconductors - Theory
23 p3017 A73-44023
- Theoretical possibilities for the creation of a gamma laser /gazer/ using nuclear transitions
23 p2988 A73-44092
- NUCLEAR METEOROLOGY**
Russian book - Certain problems concerning solar-terrestrial links and physics of the atmosphere.
21 p2730 A73-40102
- Nuclear meteorology as branch of atmospheric physics, examining natural and artificial fission products, nuclear explosion effects, atmospheric purification and radioactive tracers for meteorological process investigation
21 p2730 A73-40115
- NUCLEAR PARTICLES**
NT ALPHA PARTICLES
NT ANTINEUTRINOS
NT ANTIPARTICLES
NT ANTIPROTONS
NT BETA PARTICLES
NT MESONS
NT NUCLEONS
NT PHOTOELECTRONS
NT PHOTONS
NT PIONS
NT POSITRONS
Solar corpuscular irradiation induced latent and etched nuclear particle tracks in lunar dust grains, presenting electron microscopic studies of Apollo 11/12 lunar soil samples
03 p0361 A73-13099
- Nuclear particle fluxes and radioactive isotopes production rate distribution from cosmic rays data along orbits, calculating iron meteorite dimensions prior to atmosphere entry
08 p1012 A73-21582
- Nuclear track etching in radiation and fast neutron dosimetry and health physics, discussing counter materials and fission and alpha particles and recoil nucleus recordings
11 p1362 A73-25421
- A low noise, very low power charge sensitive amplifier for space applications.
17 p2134 A73-34272
- Study by the method of nuclear tracking of the soil of Mare Fecunditatis /Luna 16/
21 p2770 A73-41002
- Solid state AgCl detectors for nuclear tracks with on- and off-response at choice - Applications to life sciences.
22 p2814 A73-42179
- NUCLEAR PHYSICS**
NT FIELD THEORY [PHYSICS]
NT PLASMA PHYSICS
NT QUANTUM THEORY
NUCLEAR POWER
U NUCLEAR ENERGY
NUCLEAR POWER GENERATION
U NUCLEAR ELECTRIC POWER GENERATION
NUCLEAR POWER PLANTS
Concepts for application of 500- to 2500-We Brayton power systems for shuttle-launched missions.
09 p1154 A73-22794
- Solar/battery space station power plants combined with nuclear configurations, discussing rectified alternator current, direct energy transfer, and high voltage dc sources
11 p1311 A73-26008
- Power plants, cost estimates, freighter missions, commercial feasibility and technology for nuclear air cushion vehicles
15 p1912 A73-32194
- Thermal mapping at electrical power generating sites for outfall from fossil or nuclear fuel plants, considering airborne application
16 p2015 A73-33360
- Exploratory study of several advanced nuclear-MHD power plant systems.
19 p2454 A73-38313
- Exploratory study of several advanced nuclear-MHD power plant systems.
19 p2455 A73-38411
- The Satellite Nuclear Power Station - An option for future power generation.
19 p2455 A73-38412
- NUCLEAR POWER REACTORS**
NT SPACE POWER REACTORS
NT SPACE POWER UNIT REACTORS

Technical and economic analysis of nuclear power reactors application for international cargo ship and air transportation, noting feasibility study of airborne power plants
[AIAA PAPER 72-1061] 03 p0340 A73-13390

ZrH space power reactors design, discussing long life fuel elements, high temperature hard vacuum irradiation environment control drive components and shield fabrication
11 p1395 A73-26011

Performance of the thermoelectric converter for the zirconium hydride reactor thermoelectric space power supply.
11 p1396 A73-26036

Atmospheric entry and impact behavior of modular disk shaped radioactive isotope heat source for space nuclear power
19 p2454 A73-38387

The availability and cost of curium-244 from power reactor fuel reprocessing wastes.
19 p2457 A73-38430

NUCLEAR POWERED SHIPS

Technical and economic analysis of nuclear power reactors application for international cargo ship and air transportation, noting feasibility study of airborne power plants
[AIAA PAPER 72-1061] 03 p0340 A73-13390

NUCLEAR PROPELLED AIRCRAFT
Engine technology for large subsonic nuclear powered aircraft.
[AIAA PAPER 72-1062] 03 p0353 A73-13391

NUCLEAR PROPULSION
NT NUCLEAR ELECTRIC PROPULSION
Technology assessment of nuclear rocket engines based on solid core reactors for space propulsion
02 p0191 A73-11995

Chemical and nuclear space tugs in the earth orbital shuttle mission.
02 p0216 A73-12372

Engine technology for large subsonic nuclear powered aircraft.
[AIAA PAPER 72-1062] 03 p0353 A73-13391

Prospects for rocket propulsion with laser-induced fusion microexplosions.
[AIAA PAPER 72-1063] 03 p0353 A73-13392

High performance reactorless nuclear propulsion of reusable orbital space tug by laser rocket engine
[AIAA PAPER 72-1095] 03 p0341 A73-13415

German book - Flight propulsion systems: Principles, systematics, and technology of aeronautical and astronautical propulsion systems.
05 p0606 A73-16355

Nuclear pulse propulsion system for interplanetary space flight, describing operational principles and design concepts
06 p0722 A73-18022

Reaction equilibrium and energy balance in thermonuclear fusion propulsion for interstellar space flight, discussing nuclear fuel and ion temperature effects
10 p1262 A73-24544

NUCLEAR QUADRUPOLE RESONANCE

Temperature dependence of the Na-23 quadrupole coupling constants in Rochelle salt.
11 p1409 A73-25875

Nuclear gamma resonance spectra of Sn119 and Te125 and the electron structure of ternary diamond-like semiconductors Cu2SnS3, Cu2SnSe3 and Cu2SnTe3
14 p1784 A73-30851

Elastic properties of tantalum over the temperature range 4-300 K.
20 p2575 A73-38886

Nitrogen quadrupole coupling constants in cis-propyleneimine.
23 p2950 A73-43272

NUCLEAR RADIATION

NT BETA PARTICLES
NT FAST NEUTRONS
NT GAMMA RAYS
NT NEUTRON BEAMS
NT SPALLATION
NT THERMAL NEUTRONS
Book - Fundamentals of nuclear hardening of electronic equipment.
03 p0283 A73-13990

Annual Conference on Nuclear and Space Radiation Effects, 9th, University of Washington, Seattle, Wash., July 24-27, 1972, Proceedings.
05 p0557 A73-16501

The propagation of the energetic very heavy nuclei in the cosmic radiation.
07 p0870 A73-19340

A digital measurement converter of pulsed flows
13 p1591 A73-28872

Nuclear hardness assurance and radiation specifications for overall system assurance, listing electronic component failure modes
16 p2035 A73-33651

NUCLEAR RADIATION SPECTROSCOPY

Application of gamma-resonance emission spectroscopy to the study of the structure of laminar compounds of graphite with Co-57-labeled cobalt and cobalt chloride
10 p1186 A73-24466

NUCLEAR REACTIONS

NT ALPHA DECAY
NT ANNIHILATION REACTIONS
NT CONTROLLED FUSION
NT ELECTRON CAPTURE
NT ELECTRON SCATTERING
NT HIGH ENERGY INTERACTIONS
NT NEUTRON EMISSION
NT NEUTRON SCATTERING
NT NUCLEAR CAPTURE
NT NUCLEAR FISSION
NT NUCLEAR FUSION
NT NUCLEAR INTERACTIONS
NT NUCLEAR SCATTERING
NT PHOTONUCLEAR REACTIONS
NT PHOTOPRODUCTION
NT POSITRON ANNIHILATION
NT PROTON SCATTERING
NT PROTON-PROTON REACTIONS
NT RADIOACTIVE DECAY
NT RESONANCE SCATTERING
NT SPALLATION
NT SPIN-ORBIT INTERACTIONS
NT THERMONUCLEAR REACTIONS

Lunar rock C 14 production rate as function of depth, discussing solar and galactic cosmic radiation induced nuclear reactions
02 p0220 A73-12479

Solar corona properties and nuclear reactions in flares from August 1972 OSO 7 observation, noting hard X ray bursts from electron streams
04 p0502 A73-15971

Problem of the nuclear pumping of molecular gas lasers
09 p1096 A73-22702

Relativistic cosmology of interacting hadronic matter-radiation models, discussing compatibility with Hagedorn equation of state based on statistical mechanics
15 p1939 A73-32002

Russian book on cosmogenic nuclear reactions in meteorites and asteroid and lunar surface layers covering vertical /depth/ distributions of isotopes and nuclear-active particles
19 p2486 A73-37775

Reactions of pseudoscalar meson production by neutrinos on nucleons near the threshold in the range of high transferred impulses
23 p3008 A73-43544

NUCLEAR REACTOR CONTROL

Optimal control problems of spacecraft mass minimization and nuclear power engine operation under uncontrollable perturbations due to errors and external field interactions
05 p0596 A73-16414

Nuclear Science Symposium, 19th, and Nuclear Power Systems Symposium, 4th, Miami, Fla., December 6-8, 1972, Proceedings.
11 p1363 A73-25955

NUCLEAR REACTOR MATERIALS

U REACTOR MATERIALS

NUCLEAR REACTORS

NT ASTRON THERMONUCLEAR REACTOR
NT FAST TEST REACTORS
NT GASEOUS FISSION REACTORS
NT HIGH TEMPERATURE NUCLEAR REACTORS

NT LIQUID METAL COOLED REACTORS
NT NUCLEAR POWER REACTORS
NT ORGANIC COOLED REACTORS
NT SPACE POWER REACTORS
NT SPACE POWER UNIT REACTORS
NT THERMAL REACTORS
NT TOKAMAK FUSION REACTORS

Thermal instability of nonuniform plasma in steady state D-T fusion reactor operated by charged particle heating with spatially uniform fuel injection
01 p0084 A73-10465

Technology assessment of nuclear rocket engines based on solid core reactors for space propulsion
02 p0191 A73-11995

Performance potential of the colloid core reactor concept in near-earth applications.
[AIAA PAPER 72-1065] 03 p0340 A73-13394

Nuclear rocket engine reactor utilization as energy center for propulsion, attitude control, refrigeration and scientific experiments, emphasizing dual mode electrical power generation
[AIAA PAPER 72-1091] 03 p0340 A73-13412

Post impact behavior of mobile reactor core containment systems.
07 p0850 A73-20468

Thermonuclear reactor model with core surrounded by dense cold plasma, noting temperature profile effects on fusion and energy release locations
08 p0991 A73-20818

Thermoelectric radioisotope generators and nuclear thermoelectronic reactors, noting anaerobic self contained reliable operation and suitability for underwater energy sources
09 p1032 A73-22203

Calculation of the steady thermal and stress boundary conditions in the Phoebus 2 reactor
10 p1248 A73-24495

NUCLEAR-ELECTRIC MOMENTS

66 kWe ZrH reactor-organic Rankine power systems for large manned orbiting space systems.
11 p1311 A73-26014

Nuclear thermionic power plants in the 50-300 kWe range.
11 p1396 A73-26027

An evolutionary approach for a compact-split-core reactor.
17 p2211 A73-35470

Exploratory study of several advanced nuclear-MHD power plant systems.
19 p2455 A73-38411

Amorphous alloy resistance thermometer development.
22 p2856 A73-42015

NUCLEAR RESEARCH

Versatile logic system for use in nuclear experiments on scientific satellites.
19 p2412 A73-37147

NUCLEAR RESEARCH AND TEST REACTORS
NT HIGH TEMPERATURE NUCLEAR REACTORS

NUCLEAR ROCKET ENGINES

NT NUCLEAR LIGHTBULB ENGINES

Technology assessment of nuclear rocket engines based on solid core reactors for space propulsion
02 p0191 A73-11995

Thermionic reactor ion propulsion system /TRIPS/ - Its multi-mission capability.
[AIAA PAPER 72-1060] 03 p0381 A73-13389

Mission performance of a 360 mw nuclear rocket engine.
[AIAA PAPER 72-1064] 03 p0381 A73-13393

Performance potential of the colloid core reactor concept in near-earth applications.
[AIAA PAPER 72-1065] 03 p0340 A73-13394

Unmanned outer planets and round trip mission nuclear rocket engine design for carrying payload into orbit by single earth orbital shuttle
[AIAA PAPER 72-1090] 03 p0340 A73-13411

Nuclear rocket engine reactor utilization as energy center for propulsion, attitude control, refrigeration and scientific experiments, emphasizing dual mode electrical power generation
[AIAA PAPER 72-1091] 03 p0340 A73-13412

Dual mode applications of nuclear rocket engine for spacecraft propulsion and electrical power generation, considering payloads and missions competitiveness with nonnuclear system
[AIAA PAPER 72-1092] 03 p0341 A73-13413

Comparison of advanced propulsion concepts for deep space exploration.
05 p0608 A73-17201

Planetary exploration with electrically propelled vehicles.
06 p0750 A73-18021

Thermionic reactor power systems design for spacecraft auxiliary power supply and electrical propulsion, discussing performance and design guidelines for various applications
09 p1118 A73-22798

High temperature core thermocouple development for the Nuclear Rocket Engine Program /Rover/.
22 p2885 A73-42047

NUCLEAR SCATTERING

NT NEUTRON SCATTERING

NT RESONANCE SCATTERING

Recoilless nuclear transition based gamma laser, using resonant gamma rays or thermal neutron beam irradiation and selective photoionization
16 p2024 A73-34055

NUCLEAR SHIELDING

U RADIATION SHIELDING

NUCLEAR SPIN

Indirect interaction of nuclear spins through valence band electrons in semiconductors
03 p0350 A73-13754

Electromagnetic systems of noise-immunized nuclear-precession sensors
06 p0692 A73-17562

Electromagnetic systems of noiseproof nuclear precession sensors.
16 p2011 A73-32786

Magnetic susceptibility of a degenerate electron gas - Interaction of nuclear magnetic moments in normal metals and superconductors
23 p3016 A73-43709

NUCLEAR STRUCTURE

Renormalized Brueckner-Hartree-Fock theory generalization to calculate intrinsic states of many-body nuclear system with permanent deformation
01 p0079 A73-10243

NUCLEAR SUBMARINES

U NUCLEAR POWERED SHIPS

U SUBMARINES

NUCLEAR WEAPONS

On the possible effect of NOx injection in the stratosphere due to past atmospheric nuclear weapons tests.
[AIAA PAPER 73-538] 16 p2011 A73-34047

NUCLEAR-ELECTRIC MOMENTS

U ELECTRIC MOMENTS

NUCLEASE

Activity of acid nucleases in eye tissues under the action of corticosteroid hormones 24 p3058 A73-44430

NUCLEATE BOILING

NT LEIDENFROST PHENOMENON

Equation of motion and bubble size distribution function for nucleate boiling, noting balance equation for two phase fluid 08 p1022 A73-21096

Influence of heating-surface orientation in a gravitational field on the nucleate boiling crisis of liquid 11 p1450 A73-25729

The influence of the thermal properties of the heating-surface on the heat-transfer of bubble boiling 12 p1559 A73-27698

Optical method for studying the heat transfer mechanism in bubble boiling 13 p1708 A73-29173

Heat transfer during helium boiling in narrow channels of different orientations 13 p1661 A73-29405

High-speed cine-photography and oscillography in a boiling simulation. 21 p2697 A73-39994

Law of micro-liquid-layer formation between a growing bubble and a solid surface with a special reference to nucleate boiling. 21 p2792 A73-41144

Comparison of experimental microlayer thickness results. 21 p2793 A73-41690

NUCLEATION

NT CLOUD SEEDING

Ethanol condensation by homogeneous nucleation and growth of liquid droplets in steady state supersonic nozzle flow of ethanol-air and ethanol-nitrogen mixtures 02 p0153 A73-12051

Nucleation during solidification and melting of metals and alloys 02 p0181 A73-12363

Experimental approaches to well controlled studies of thin-film nucleation and growth. 02 p0201 A73-12633

X ray diffraction measurement of ordering kinetics in Ni-Pt alloy at annealing temperatures, showing disorder-order transitions relation to nucleation and growth 04 p0467 A73-15982

Conjugation of proteinoid microspheres - A model of primordial recombination. 06 p0652 A73-17952

A note on fatigue crack starter defects produced by a pulsed laser. 06 p0710 A73-18500

Nucleation film/electron beam recorder - Near-real-time display system. 08 p0965 A73-21247

Alloying elements effects on voids nucleation in irradiated Al alloys, tabulating defect concentration 09 p1101 A73-22175

Continuously recording cloud nuclei counter, describing diffusion chamber with separate functions of sample supersaturation and photoelectric droplets recording 10 p1217 A73-23990

A technique for measuring relative threshold nucleation temperatures for active nucleation catalysts. 12 p1521 A73-26816

Niobium mechanical twin formation and propagation, discussing continuous nucleation, matrix interface and dislocation core energies 13 p1632 A73-28132

Growth rate calculation for hygroscopic condensation nuclei in the presence and absence of a monolayer of a surface-active substance 13 p1654 A73-28880

Breakdown of the superheated Meissner state and spontaneous vortex nucleation in type II superconductors. 13 p1669 A73-29183

Capillarity induced stresses effects on dislocations generation during early stage sintering, predicting plastic flow via modified Hirth method of surface nucleation 20 p2576 A73-39221

Condensation in CO₂ free jet expansions. II - Growth of small clusters. 21 p2743 A73-40938

NUCLEI

Comet nucleus existence in terms of optical effect and particle swarm model of coma 04 p0494 A73-14753

The compact central region of the galaxy NGC 1614. 04 p0499 A73-15356

Continuous flow condensation nucleus counter 04 p0451 A73-15999

Vertical plate steady flow thermal diffusion chamber for cloud condensation nucleus counter, featuring long available growth time for operation below 0.2 percent supersaturation 21 p2697 A73-40059

NUCLEI [NUCLEAR PHYSICS]

NT ALPHA PARTICLES

NT DEUTERONS

NT HEAVY NUCLEI

Cold matter consisting of atomic nuclei submerged in electron-neutron gas, relating subnuclear density relation to existence and binding energy of neutron-rich nuclei 01 p0081 A73-11310

Composition of relativistic cosmic rays near the earth and at the sources. 02 p0207 A73-12327

High energy cosmic ray pions and nucleons interactions with atomic nuclei, using ionization calorimeter and spark chambers system 02 p0209 A73-12661

The Fermi mechanism and the source spectrum of cosmic ray nuclei. 03 p0361 A73-13365

The abundances of solar accelerated nuclei from carbon to iron. 03 p0362 A73-13719

Upper limit of the antinucleus abundance in primary cosmic rays 10 p1265 A73-23899

A phenomenological study of cosmic ray propagation. I - The nuclei component. 11 p1412 A73-25263

Retinal change induced in the primate *Macaca mulatta* by oxygen nuclei radiation. 18 p2271 A73-36125

On the abundance of secondary nuclei in cosmic rays. 19 p2475 A73-37572

Isotopic composition measurements of cosmic-ray nuclei with Z greater than or equal to 10 made using a new technique. 19 p2475 A73-37628

Upper limit of antinuclei content in primary cosmic rays. 20 p2601 A73-38918

The Forbush effect in the nuclear component of primary cosmic rays in August 1972 21 p2757 A73-40588

Study of nucleon interactions with carbon, iron and lead nuclei in the energy range 600 to 10,000 GeV 23 p3008 A73-43532

Measurement of the effective cross section of inelastic interaction between protons and carbon nuclei in the energy range 0.1 TeV to 1.0 TeV, on the Proton-4 space station 23 p3021 A73-43539

NUCLEIC ACIDS

NT RIBONUCLEIC ACIDS

Concepts related to the origin of the genetic apparatus. 03 p0265 A73-14317

Proteins and nucleic acids in prebiotic evolution. 06 p0652 A73-17937

NUCLOGENESIS

Russian book - Information macromolecules during radiation injury to cells. 04 p0410 A73-15707

Ribosomal RNA base composition and molecular evolution in plants and animals of various taxonomic groups 07 p0780 A73-19220

NUCLEON-NUCLEON INTERACTIONS

Multiple meson production in 250 GeV nucleon-nucleon collisions in LiH targets, noting 40 per cent formation of heavy meson cluster fireballs 02 p0208 A73-12653

K-neutral pion inelasticity factor measurement for nucleon interactions in carbon corresponding to primary neutron energy transferred to pions 02 p0209 A73-12663

Inelastic scattering calculations with projected Hartree-Fock wave functions. II - Coupled-channel treatment. 03 p0345 A73-13806

Multiplicity link to transverse momenta in ultrahigh energy nucleon-nucleon interaction processes, considering resonance formation and expected average elasticity 06 p0743 A73-17830

High energy nucleon inelastic interaction characteristics calculated from artificial event model based on covariant statistical theory of multiple generation of particles 23 p3022 A73-43542

NUCLEONS

Nuclear-electron cascades longitudinal evolution calculation in ionization calorimeter for primary nucleons and pions, using Monte Carlo method 02 p0171 A73-12654

Inelasticity factor dependence on particle energy spectra to explain nucleon flux calculations and Proton satellite data, considering scattering cross sections 02 p0208 A73-12658

High energy cosmic ray pions and nucleons interactions with atomic nuclei, using ionization calorimeter and spark chambers system 02 p0209 A73-12661

Secondary particles in pion-nucleon and coherent interactions, measuring momentum from multiple Coulomb scattering 02 p0209 A73-12666

Nuclear photoemulsions under bombardment by pion beam of 60 GeV/c momentum, investigating pion-nucleon interactions involving recoil protons 02 p0195 A73-12667

Pion-nucleon high energy interactions, determining inelasticity coefficient distribution 02 p0195 A73-12668

Description of a device for studying inelastic nuclear processes with nucleons at energies from .1 to 10 TeV and analysis of its operation at an altitude of 3250 m above sea level 05 p0577 A73-16823

Barometric coefficients of the nucleon components of cosmic rays of various energies 06 p0742 A73-17550

Three dimensional cosmic ray anisotropy and density distribution at earth orbit and in interplanetary space with allowance for primary particle and nucleon energy spectrum 08 p1000 A73-21343

Nucleon and electromagnetic component generation, energy spectrum and diffusion during solar flares 08 p1000 A73-21349

Intermediate energy nucleon-deuteron scattering theory. 14 p1776 A73-29766

Composition of galactic cosmic rays with energy ranging between 10 and 30 MeV/nucleon. 15 p1926 A73-31355

Barometric coefficients of the nucleon component of cosmic rays of different energies. 16 p2052 A73-32774

Study of nucleon interactions with carbon, iron and lead nuclei in the energy range 600 to 10,000 GeV 23 p3008 A73-43532

Pion-nucleon interaction structure based on negative pion beam data from Serpukhov accelerator, showing secondary particle energy distribution asymmetry 23 p3021 A73-43537

Reactions of pseudoscalar meson production by neutrinos on nucleons near the threshold in the range of high transferred impulses 23 p3008 A73-43544

NUCLEOSIDES

NT ADENOSINE DIPHOSPHATE [ADP]

NT ADENOSINE TRIPHOSPHATE [ATP]

NT ADENOSINES

Gamma irradiation induced abiogenic radiochemical synthesis of deoxynucleosides from dry mixtures of purine bases with deoxyribose and ribose 22 p2803 A73-42166

NUCLEOSYNTHESIS

U NUCLEAR FUSION

NUCLEOTIDES

NT ADENOSINE DIPHOSPHATE [ADP]

NT ADENOSINE TRIPHOSPHATE [ATP]

NT ADENOSINES

NT PYRIDINE NUCLEOTIDES

Double spiral DNA-like nucleotide analog in carbonaceous chondrite, indicating organic compound synthesis at low temperature 05 p0619 A73-16843

Genetic code evolution in terms of abiotic polynucleotide synthesis, suggesting alternating sequences of purines and pyrimidines as polypeptide codes 09 p1044 A73-23469

Double spiral DNA-like polynucleotide analog in carbonaceous chondrite, indicating organic compound synthesis at low temperature 11 p1423 A73-26053

Prebiotic reactions combining amino acids and ribonucleotides into polypeptides and polynucleotides in presence of urea, imidazole and Mg positive ion, suggesting contemporary biosynthesis parallels 21 p2637 A73-40372

NUCLIDES

NT ALUMINUM 26

NT ARGON ISOTOPES

NT CARBON ISOTOPES

NT CARBON 12

NT CARBON 13

NT CARBON 14

NT CESIUM VAPOR

NT COBALT ISOTOPES

NT COBALT 60

NT CURIUM ISOTOPES

NT CURIUM 244

NT DEUTERIUM

NT EUROPIUM ISOTOPES

NT HELIUM ISOTOPES

NT HYDROGEN ISOTOPES

NT IODINE ISOTOPES

NT IRON 57

NT ISOTOPES

NT KRYPTON ISOTOPES

NT LEAD ISOTOPES

NT LITHIUM ISOTOPES

NT MANGANESE ISOTOPES

NT MERCURY ISOTOPES

NT NEON ISOTOPES
 NT NITROGEN ISOTOPES
 NT OXYGEN ISOTOPES
 NT OXYGEN 18
 NT PLUTONIUM ISOTOPES
 NT PLUTONIUM 238
 NT POLONIUM 210
 NT POTASSIUM ISOTOPES
 NT RADIOACTIVE ISOTOPES
 NT RADON ISOTOPES
 NT RUBIDIUM ISOTOPES
 NT SODIUM ISOTOPES
 NT SODIUM 22
 NT SODIUM 24
 NT STRONTIUM ISOTOPES
 NT STRONTIUM 90
 NT TELLURIUM
 NT TELLURIUM ISOTOPES
 NT THORIUM ISOTOPES
 NT TRITIUM
 NT URANIUM ISOTOPES
 NT URANIUM 238
 NT XENON ISOTOPES
 NT XENON 129
 Depth variation of cosmogenic noble gases in the approximately 120-kg Keyes chondrite. 11 p1418 A73-25587

NULL HYPOTHESIS
 Evidence for the existence of galactic superclusters near the galactic North Pole 16 p2063 A73-33661

NULL REFERENCE GLIDE PATH
 U GLIDE PATHS

NUMBER THEORY
 NT ARITHMETIC
 NT DIOPHANTINE EQUATION
 NT DIVIDING [MATHEMATICS]
 NT MULTIPLICATION
 A probabilistic approach to a differential-difference equation arising in analytic number theory. 10 p1241 A73-23643

NUMERICAL ANALYSIS
 NT APPROXIMATION
 NT BORN APPROXIMATION
 NT BORN-OPPENHEIMER APPROXIMATION
 NT CHEBYSHEV APPROXIMATION
 NT DIFFERENCE EQUATIONS
 NT EDDINGTON APPROXIMATION
 NT ERROR ANALYSIS
 NT FINITE DIFFERENCE THEORY
 NT HARTREE APPROXIMATION
 NT INTERPOLATION
 NT ITERATION
 NT ITERATIVE SOLUTION
 NT LEAST SQUARES METHOD
 NT MONTE CARLO METHOD
 NT NEWTON-RAPHSON METHOD
 NT NOMOGRAMS
 NT NUMERICAL INTEGRATION
 NT OSEEN APPROXIMATION
 NT PADE APPROXIMATION
 NT PARTICLE IN CELL TECHNIQUE
 NT RAYLEIGH-RITZ METHOD
 NT RELAXATION METHOD [MATHEMATICS]
 NT RITZ AVERAGING METHOD
 NT RUNGE-KUTTA METHOD
 NT SCHWARTZ METHOD
 NT SOMMERFELD APPROXIMATION
 NT TRUNCATION ERRORS
 R-function numerical analysis method for motion stability criteria, developing algorithms for Liapunov function construction and controller design for conservative control system stability 01 p0076 A73-10096
 Transverse resonance solutions for a long slot leaky wave antenna. 01 p0023 A73-10187
 A new program for the dc one-dimensional analysis of semiconductor devices. 01 p0023 A73-10576
 Lunar motion numerical analysis, discussing flaws due to inadequate solar system model and arithmetic-algebraic procedural deficiencies 01 p0099 A73-10694
 Analysis of non-linear systems defined by their response to arbitrary disturbances. 01 p0028 A73-11456
 Numerical solutions for MHD equations, considering initial values, time independence and mathematical models including hyperbolic, parabolic and elliptic differential equations 01 p0086 A73-11459
 A discrete numerical approach to fluid dynamics. 01 p0071 A73-11461
 Numerical method for describing turbulent, compressible, subsonic separated jet flows. 01 p0035 A73-11467
 Three dimensional potential flow past arbitrarily shaped aerodynamic configurations, using Hess-Smith numerical method [DGLR PAPER 72-105] 02 p0127 A73-11657
 Numerical calculations of the flow field of low Reynolds number viscous flow with or without real-gas-effects in slender-channel-nozzles. [DGLR PAPER 72-110] 02 p0152 A73-11674

Numerical analysis of spontaneous electric activity of the brain - Study of the statistical properties of the power density spectra 02 p0138 A73-12160
 A numerical method considering the Bauschinger effect for large deflection analysis of elastic-plastic circular plates. 02 p0236 A73-12522
 The dynamical evolution of triple star systems - A numerical study. 02 p0221 A73-12702
 A numerical analysis for chemical non-equilibrium boundary layer of dissociated gases over a flat plate with arbitrary catalytic. 03 p0291 A73-13068
 Linear integral equation, wave function and parameter optimization for numerical analysis of remote sensing problem 03 p0337 A73-14488
 Numerical predictions of some three-dimensional boundary layers in ducts. 04 p0433 A73-15006
 A transformation for the numerical solution of two-dimensional free mixing flow problems. [ASME PAPER 72-WA/FE-3] 04 p0434 A73-15841
 An explicit numerical method for the solution of jet flows. [ASME PAPER 72-WA/FE-20] 04 p0435 A73-15846
 Calculation of transonic flow in three-dimensional nozzles 05 p0527 A73-16447
 Numerical analysis of eddy viscosity models in supersonic turbulent boundary layers. [AIAA PAPER 73-164] 05 p0566 A73-16910
 Numerical computation of the hypersonic rarefied flow near the sharp leading edge of a flat plate. [AIAA PAPER 73-200] 05 p0531 A73-16934
 Numerical solution of viscous reacting blunt body flows of a multicomponent mixture. [AIAA PAPER 73-202] 05 p0532 A73-16936
 Finite element analysis of the post-buckling behavior of structures. [AIAA PAPER 73-255] 05 p0635 A73-16977
 Nonlinear stability analysis of nonhomogeneous self-gravitating unstable equilibrium stellar systems, using numerical techniques and water bag configurations 05 p0624 A73-17317
 Numerical analysis of far turbulent wakes in ideal gas, determining hydrodynamic field moments, turbulence levels and mean square enthalpy fluctuations 06 p0643 A73-17454
 Analysis of active RC circuits with nonhomogeneously distributed parameters in the time domain 07 p0805 A73-20024
 Computerized static and dynamic structural analysis, discussing modeling, programs, input preparation, solution algorithms, numerical errors, output interpretation and applications 07 p0914 A73-20209
 An efficient parallel algorithm for the solution of a tridiagonal linear system of equations. 08 p0983 A73-20960
 Constitutive equation for electronic circuits without topologically dependent variables, noting numerical analysis of equations of state for nonlinear circuits 08 p0951 A73-21551
 Construction of analytical formulas for functions of linear circuits by means of engineering-application digital computers 08 p0941 A73-21552
 Orthotropic material plane crack problem numerical solutions by polynomial approximation and modified mapping-collocation technique involving conformal mapping 09 p1161 A73-23178
 Alternating method with combined analytical and numerical calculations for two dimensional edge and three dimensional surface crack problems 09 p1162 A73-23181
 Mixed boundary value problems in solid contact and crack mechanics, discussing numerical solution of singular integral equations with simple and generalized Cauchy kernels 09 p1162 A73-23184
 Numerical analysis of the viscous, hypersonic, MHD blunt-body problem. 09 p1132 A73-23455
 Partial differential post-Newtonian equations numerically solved for stellar models with polytropic pressure-density relation for uniform rotation 10 p1271 A73-23490
 A numerical-analytical method of calculating stream flow of a heavy liquid around curvilinear obstacles 10 p1205 A73-23585
 Accuracy studies of the numerical method of characteristics for axisymmetric, steady supersonic flows. 10 p1171 A73-23602
 Numerical solution of the optimal control problem by the direct method 10 p1197 A73-23999
 A numerical method for the analysis of longitudinal elastic-plastic stress wave propagation. 10 p1290 A73-24297

Vertical two axis gyrostabilizer equations of motion analysis by averaging method 11 p1360 A73-25048
 Linear or nonlinear dynamic systems response to arbitrary input functions, describing numerical computation method with provision for discontinuities 11 p1389 A73-25110
 Numerical computation for entropy layer on blunt nosed cone in terms of shock layer fraction for given free stream and Mach number 11 p1299 A73-25113
 Unsteady viscous jet flow into stationary surroundings. 11 p1345 A73-25117
 Numerical analysis of the properties of an avalanche diode in the avalanche multiplication range 11 p1337 A73-25321
 Clamped orthotropic skew plates under uniformly distributed transverse load, considering nonlinear analysis based on numerical technique of dynamic relaxation involving critically damped vibration 11 p1444 A73-26381
 Book - Numerical methods for unconstrained optimization. 12 p1518 A73-27549
 Flexural response of tapered beam on elastic-plastic foundation, solving in closed form to evaluate efficiency of numerical methods 12 p1557 A73-27932
 Numerical Master Geometry computer programs for smooth surface shape mathematical representation, manipulation, definition and interrogation in design and production 13 p1623 A73-28053
 Certain methods of numerical calculation in problems of microwave scattering from cylindrical obstacles 13 p1581 A73-28125
 High speed computing of elastic structures; Proceedings of the Symposium, Universite de Liege, Liege, Belgium, August 23-28, 1970. Volumes 1 & 2. 13 p1692 A73-28226
 The mechanical interpretation of high accuracy multipoint difference methods for plates and shells. 13 p1694 A73-28255
 The numerical treatment of natural eigenvalue problems of the 4th order according to the collocation method with a Lagrange polynomial approach 13 p1695 A73-28411
 Numerical study of the stochasticity of dynamical systems with more than two degrees of freedom. 13 p1648 A73-28425
 Analysis of self-excited and forced vibrations of a rectangular plate on many supports in supersonic flow. 13 p1700 A73-29392
 A library of standard programmes for constructing numerical theories for studying the motion and evolution of the orbits of the minor bodies of the solar system. 14 p1790 A73-29789
 On the determination of nongravitational forces acting on comets. 14 p1791 A73-29798
 Russian book - Methods for calculating electromagnetic fields by electronic digital computers. 14 p1774 A73-30026
 On numerical convergence of moment solutions of moderately thick wire antennas using sinusoidal basis functions. 14 p1734 A73-30216
 Some computation-steeples in fluid mechanics. 14 p1745 A73-30412
 Numerical solutions by the continuation method. 14 p1769 A73-30454
 Numerical methods for functional differential equations. 14 p1770 A73-30755
 Numerical experiments for the determination of characteristic dimensions and intensities of convection cells 15 p1902 A73-31138
 A numerical solution for the transonic flow around blunt wedges 15 p1823 A73-31330
 Nonplanar wings in nonplanar ground effect. 15 p1824 A73-31744
 The solution of heat conduction problems with the aid of the Laplace transformation. II - Numerical evaluation and graphical representation of two specific boundary value problems 15 p1958 A73-31907
 A numerical technique for determining the effect of singularities in finite difference solutions illustrated by application to plane elastic problems. 15 p1951 A73-32031
 Book - Mathematical programming and the numerical solution of linear equations. 15 p1901 A73-32300
 German monograph - The flow around wings of arbitrary planform in the case of supersonic flow - A computational method. 15 p1824 A73-32581
 Solution on a digital computer of boundary value problems for three-dimensional rod systems with branchings 16 p2075 A73-32692

Numerical method for mixed elliptical-hyperbolic nonlinear Cauchy problem with boundary conditions, applying to sonic flow around wing sections

16 p1961 A73-32807

Hypoelastic approximation for plastic media axisymmetric deformation, determining grid for numerical analysis from orthogonality relations

16 p2079 A73-33239

Numerical methods for non-linear optimization; Proceedings of the Conference, University of Dundee, Dundee, Scotland, June 28-July 1, 1971.

16 p2033 A73-33851

Numerical experience with algorithms for unconstrained minimization.

16 p2033 A73-33852

The choice of step length, a crucial factor in the performance of variable metric algorithms.

16 p2033 A73-33853

Nonlinear least squares calculations by Gauss-Newton and Levenberg, Marquardt and Morrison methods, discussing algorithm convergence rate and numerical computational scheme

16 p2033 A73-33854

Numerical solution of systems of nonlinear algebraic equations; Proceedings of the Regional Conference, University of Pittsburgh, Pittsburgh, Pa., July 10-14, 1972.

17 p2199 A73-34101

Numerical analysis of the averaged equations of concentric laser cumulation of plasma with consideration of nuclear fusion energy.

17 p2216 A73-34323

Numerical solution method for Navier-Stokes equations of a compressible gas over a wide range of Reynolds numbers

17 p2151 A73-34632

The analysis of nonequilibrium, chemically reacting, supersonic flow in three dimensions using a bicharacteristics method.

17 p2151 A73-34891

Cylindrical shell postbuckling behavior under axial compression using multiple scale averaging technique, concluding predominance of diamond shaped postbuckling pattern

[ASME PAPER 73-APM-7]

17 p2247 A73-35032

Computational Fluid Dynamics Conference, Palm Springs, Calif., July 19, 20, 1973, Proceedings.

17 p2095 A73-35126

Numerical solution of the three-dimensional Navier-Stokes equations in integro-differential form - Flow about a finite body.

17 p2155 A73-35139

A new numerical technique for solving the time-dependent radiation transport equation.

17 p2255 A73-35595

Chemically reacting gas flow numerical calculations from stiff nonlinear ordinary differential equations solution in finite difference form

17 p2119 A73-35609

Results of numerical solution of the complex dispersion equation for the HE₁₁ wave in a two-layer circular waveguide.

17 p2143 A73-35718

Book - Analysis of discretization methods for ordinary differential equations.

18 p2329 A73-35904

The effect of nonlinear transformations on the computation of weak solutions.

18 p2330 A73-36610

Calculations of real gas properties from tables of thermodynamic functions

18 p2372 A73-36817

Effectiveness of utilizing cloudiness data obtained from satellites in objective analysis of the wind field.

18 p2334 A73-37071

A procedure for solving problems of elasto-plastic flow.

19 p2496 A73-37484

Numerical solution of ordinary and retarded differential equations with discontinuous derivatives.

19 p2444 A73-37523

Numerical models of the circulation of the atmosphere of Venus.

19 p2485 A73-37657

Numerical modeling of the dynamics and microphysics of warm cumulus convection.

19 p2447 A73-37658

Numerical simulation of counterstreaming high Mach number plasma laminar interactions, using one dimensional model based on Vlasov equation

19 p2469 A73-37861

The transient response of certain third-order nonlinear systems.

19 p2460 A73-38109

Numerical investigation of internal waves in jet streams including nonlinear effects.

19 p2449 A73-38233

Numerical and analytical prediction methods for time dependent reactions in homogeneous gas mixtures, considering accuracy and computing times

20 p2626 A73-39095

A two-dimensional numerical analysis of a silicon n-p-n transistor.

20 p2536 A73-39413

Stability and postbuckling behavior of hyperelastic bodies at finite strain by the finite element method.

20 p2620 A73-39529

A numerical analysis of some practical aspects of airborne urea seeding for warm fog dispersal at airports.

21 p2728 A73-40056

Numerical solution of nonlinear resonant wave equation of radiating gas between parallel walls by parametric differentiation

21 p2790 A73-40250

Computer program for determining system resonance frequencies and damping via numerical analysis of vector modal response loci plots

21 p2783 A73-40290

A note on pairs of matrices and matrices of monotone kind.

21 p2725 A73-40377

Nonlinear eigenvalue problem of square matrix of analytic functions of complex number lambda, comparing algorithms convergence by numerical tests

21 p2725 A73-40380

A finite step algorithm for determining the "strict" Chebyshev solution to $Ax = b$.

21 p2725 A73-40381

A numerical study of three-dimensional problems of MHD flow

21 p2747 A73-40887

A numerical investigation of the current and density distributions for a non-equilibrium plasma in a segmented electrode duct.

21 p2748 A73-40926

Numerical analysis of families of periodic orbits in restricted three body problem with change in mass ratio μ

21 p2778 A73-41527

A numerical study of damping in viscoelastic sandwich beams.

[ASME PAPER 73-DET-73]

22 p2919 A73-42071

Electromagnetic flowmeters with point electrodes and finite length insulating liners, discussing performance numerical analysis accuracy by comparison with exact analytic solutions

22 p2860 A73-42300

Computerized analysis using sparse matrices/matrices with large number of zero elements/describing sorting, reordering and inverse computing techniques and linear equations solution methods

22 p2922 A73-42480

The calculation of open circular cylindrical shells with the aid of partial discretization

22 p2922 A73-42528

Numerical solution of wire antenna boundary value problems based on integral equations formulation, considering Yagi-Uda array, antenna design and radiation patterns

22 p2827 A73-42840

Numerical solution of electromagnetic scattering problems.

22 p2827 A73-42841

Hybrid numerical solution to electromagnetic wave scattering and diffraction with application to microstrip transmission lines, echelette gratings and dielectric step discontinuities in waveguides

22 p2828 A73-42844

German monograph on regularization and penalty function methods of numerical analysis in Hilbert or Banach space covering minimax technique and optimal control theory application

22 p2882 A73-42847

German monograph - The computation of periodic motions of multipath nonlinear systems.

22 p2888 A73-42854

Amplification of short pulses in CO₂ laser amplifiers.

22 p2871 A73-43025

Analytic solutions for potential flow over a class of semi-infinite two-dimensional bodies having circular-arc noses.

23 p2940 A73-43931

Efficient numerical solution of the transmission-line equivalent-circuit model of a semiconductor.

24 p3119 A73-45261

Numerical methods of boundary layer type for stiff systems of differential equations.

24 p3106 A73-45333

Computational assessment of the numerical influence of the cutting step size and evaluation equation on the precision of experimental and analytical residual-stress determinations

24 p3153 A73-45446

NUMERICAL CONTROL

A high-precision computer-controlled dual-channel polarizing radiometer.

01 p0045 A73-10383

A digital system for shaping, analysis and control of a random vibration spectrum

01 p0027 A73-10598

Coding technique to record computer generated binary hologram on numerically controlled CRT with resolution cell of two beam spots

01 p0019 A73-11235

A fast computational algorithm for optimum digital control systems.

01 p0021 A73-11463

Contributions to the standardization of control systems for satellites and peak payloads

02 p0228 A73-11705

Preparation of information for programming machining operations during grinding of a blade profile by the continuous-shaping method

02 p0172 A73-11799

Radio telescope for high resolution radio source mapping, discussing system design, computerized control and calibration

02 p0150 A73-11869

Portable self contained computerized in-aircraft engine analyzer with cassette tape resident program control and digital display and punched card indicators

[AIAA PAPER 72-1080]

03 p0307 A73-13403

An automated jet-engine-blade inspection system.

03 p0312 A73-13524

An advanced concept in electrical power distribution control and management.

03 p0253 A73-13945

A digitally controlled scanning device for a high resolution spectrograph.

05 p0576 A73-16439

Field experience with digital control systems for vibration and acoustic testing.

[SAE PAPER 720821]

05 p0554 A73-16637

Computer-controlled environmental test systems - Criteria for selection, installation, and maintenance.

[SAE PAPER 720819]

05 p0562 A73-16638

Computer-controlled differential review-time payoff as a training aid.

05 p0544 A73-16725

Digital control mounts on jet engine.

05 p0608 A73-17249

Computer control algorithms for transient response optimization in on/off motor control system synthesis

06 p0741 A73-17963

Design of dynamic programming feedback controllers for multivariable time-invariant linear systems.

06 p0680 A73-18517

Numerically controlled plotters THD 605.

07 p0795 A73-18944

AUTOMATE - A self-contained automatic test system.

08 p0951 A73-20680

Computer controlled automatic test system for circuits, assemblies and systems performance and test programs on-line generation, editing and validation

08 p0940 A73-20682

Scheduling algorithms for multiprogramming in a hard-real-time environment.

08 p0941 A73-20961

Contributions to the design of future on-board data processing systems for scientific spacecraft experiments.

09 p1061 A73-23379

Data quality assurance in a shipboard computer-controlled telemetry system.

09 p1057 A73-23410

Micromovement servocontrollers in closed loop system, using piezoelectric device, ceramic element actuators and rotary switch derived logic control signal

10 p1199 A73-24027

Airport computerized departure control for check-in, load control, cargo and catering operations, discussing load optimization and passenger acceptance control /LOPAC/ system

11 p1343 A73-25210

Book - Engineering means in automatic control.

12 p1481 A73-26751

Dynamic characteristics, stability and steady state accuracy for orbital gyroscope with digital control, noting bit density requirements of onboard computer

12 p1523 A73-27632

Blocking oscillator multipulse mode operation digital control by supply voltage regulation

13 p1593 A73-29119

Algorithm for statistical error detection in digital control computers

14 p1730 A73-30038

The universal automatic reflector AZT-12

15 p1877 A73-32129

The automatic telescope AZT-11

15 p1877 A73-32130

Electrophotometer control system for the AZT-24 telescope

15 p1877 A73-32131

French monograph on numerical data processing organs for real time process control, describing modular computer design project

15 p1849 A73-32590

Performance and methodology of a digital random vibration control system.

16 p1993 A73-33134

Surveillance and correction of gas analysis devices and the analysis evaluation with the aid of a process computer

16 p2014 A73-33223

An integrated, modular approach to automatic testing and data monitoring.

16 p1986 A73-33632

Multi balance measurement of flow systems.

16 p2016 A73-33656

Interactive computer graphic display and interface system effectiveness for programming numerical control operations for tooling and part machining in aircraft production [AHS PREPRINT 753] 17 p2131 A73-35081

Aerospace multiprocessor for A-7D aircraft digital fly by wire flight control, discussing design requirements, software development and reliability 17 p2107 A73-35223

Algorithm construction for the stabilization of a deformable spacecraft using an onboard digital computer 18 p2359 A73-36105

A real-time software operating system for a computer-controlled acoustic emission flaw monitor. 18 p2316 A73-36679

Fluidic programmer for nuclear engine application. 19 p2454 A73-38054

Performance of LQG control systems using optimal k-step-ahead control laws. 19 p2413 A73-38062

Metering and spacing with computerized ARTS III ATC system, discussing display for heading, speed and altitude commands 19 p2453 A73-38462

Computer controlled automatic TV-microscope system for tracking and measuring nerve cell processes in designated axons and dendrites 20 p2518 A73-39763

SAFE - Six axis frequency evaluation of a motion simulator. [AIAA PAPER 73-932] 21 p2674 A73-40879

Computerized control system for fuel flow into and out of fuel cells and aircraft gravity center optimization during supersonic cruise and takeoff 21 p2634 A73-40939

Some problems associated with the construction of scanner employing a cathode-ray tube and programmed control 21 p2665 A73-41270

Russian book on accuracy of automatic systems using digital computers as control devices covering analysis and synthesis, stochastic inputs, system errors and operator methods 21 p2658 A73-41282

Computer processing of RF neutral-hydrogen line observations carried out with a fixed antenna 21 p2659 A73-41468

Sampling phase rotator for removal of Doppler shift in a lunar radar. 21 p2658 A73-41590

Certain problems in determining the capacity of digital computers 22 p2829 A73-41953

A laser raster setup with programmed control for image lithoplate synthesis 22 p2869 A73-42362

Adaptive measurement of vigilance decrement. 23 p2947 A73-43211

Use of a digital computer for studying velocity judgements of radar targets. 23 p2948 A73-43213

Computer controlled steerable radio telescope construction and performance for decimeter and centimeter wavelength observations 23 p2958 A73-43367

Fluidic logic circuits applications under adverse environmental conditions, considering sequential control devices and rocket engine roll axis numerical control 23 p2941 A73-43394

Optimal parameters on fluidic noncontact sensors for drives of exact positioning. 23 p2945 A73-43427

Cascade n-phase transistorized astable multivibrator circuit design for digital and tool control clock applications 23 p2983 A73-44142

NUMERICAL FLOW VISUALIZATION

Eddies development downstream a pipe orifice. 22 p2840 A73-41738

NUMERICAL INTEGRATION

NT RUNGE-KUTTA METHOD

Numerical solution of nonlinear partial differential and integrodifferential equations; Meeting, Oberwolfach, West Germany, November 28-December 4, 1971, Reports 01 p0069 A73-10066

Numerical integration of a problem of a second-order equation with discontinuous coefficients 01 p0070 A73-10088

An approximate form of the third integral in the Galaxy. 01 p0103 A73-11017

A method for incorporating nested finite grids in the solution of systems of geophysical equations. 02 p0165 A73-12776

Numerical integration of nonlinear integrodifferential equations of thin viscoelastic beams deflection, considering cantilever beam under uniformly distributed loads 03 p0390 A73-13343

A brief comparison of the accuracy of time-dependent integration schemes for the Reynolds equation. [ASME PAPER 72-LUB-L] 03 p0297 A73-14352

Error sources in numerical integration of spacecraft equations of motion in solar and planetary gravitational fields, suggesting methods for improving accuracy 03 p0379 A73-14553

Stabilization of constraints and integrals of motion in dynamical systems. 04 p0470 A73-15002

Newtonian differential equations of Kepler motion, analyzing stability by numerical integration based on Floquet theorem and Runge-Kutta method 04 p0497 A73-15013

Extended validity of single segment stepwise integration schemes for solution of two-point boundary value problems. 04 p0510 A73-15015

A numerical computer method for computing the electrostatic field and electron paths of focusing optoelectronic systems 04 p0448 A73-15078

Stability of Richtmyer type difference schemes in any finite number of space variables and their comparison with multistep Strang schemes. 04 p0471 A73-15233

Numerical integration of equations of Ba cloud motion in ionosphere with end shorting, noting critical electric field for motion stability 04 p0445 A73-15649

A multi-step method for the numerical integration of ordinary differential equations. 05 p0589 A73-16100

Application of certain stable methods for numerical solution of forecasting equations 05 p0592 A73-16228

Numerical integration of rotating body dynamic and kinematic equations, noting orthogonalization, normalization and error minimization methods 05 p0595 A73-16423

Numerical solution of integral equations of the first kind using a priori information on the function to be determined. 05 p0591 A73-16789

Accelerated numerical integration of the equations of motion of celestial mechanics 05 p0619 A73-17002

Correction of solar observations for stray light by numerical integration, with application to Mercury's drop. 05 p0621 A73-17032

Variational solution to the radiative equation by the use of a step function. II - Extension to nonlinear case by iteration method. 05 p0641 A73-17102

Inverse method of designing two-dimensional transonic airfoil sections. 05 p0533 A73-17104

Numerical solution of elastoplastic problems by the method of local variations 06 p0760 A73-17777

An efficient numerical technique for evaluating large quantities of highly oscillatory integrals. 06 p0716 A73-17982

Comparing numerical methods for ordinary differential equations. 06 p0717 A73-18406

A simple interpolation algorithm for improvement of the numerical solution of a differential equation. 06 p0717 A73-18407

Multistep methods with variable matrix coefficients. 06 p0718 A73-18409

Numerical solution of the integral equations for optimal sequential filtering. 06 p0719 A73-18814

Numerical integration over Brillouin zone for solids spectral properties calculation, considering crystal optical spectra, phonon effects, IR absorption, electron emission and magnetic susceptibilities 07 p0861 A73-19266

Numerical analysis of anisotropic rotational shells subjected to nonsymmetric loads. 07 p0914 A73-20210

The existence and the numerical evaluation of generalized solutions of semilinear initial value problems 07 p0845 A73-20288

Numerical formulation for constant-gain chemical laser calculations. 08 p0975 A73-21411

Integration of the equations of meteorology. III - Integration in time 08 p0986 A73-21485

Integral methods of calculating unsteady processes in nonlinear electric systems 08 p0951 A73-21556

Neutrino hindrance of density irregularities growth in expanding radiation dominated cosmological model from numerical integration of perturbation equations 09 p1141 A73-22026

Numerical solution of mixed boundary value problems using numerical Green's functions. 09 p1112 A73-22394

Studies in the application of recurrence relations to special perturbation methods. 09 p1149 A73-22914

Numerical solution of Volterra integral equations. 09 p1113 A73-23020

Studies in the application of recurrence relations to special perturbation methods. II - Comparison of the Encke and Cowell methods of integration in the restricted three-body problem. 10 p1283 A73-24668

Direct time numerical integration of spatially discretized linear elastodynamics integral equations, comparing one-step algorithms for stability and accuracy in terms of frequency spectrum 11 p1435 A73-25439

Errors associated with Rodrigues-Hamilton parameters /vector space basis quaternions/ calculation by numerical integration of kinematic equations of moving body orientation 11 p1400 A73-26454

Satellite ascent transfer trajectories equations of motion numerical integration, replacing time parameter by regularizing independent variable for gravitational singularity elimination [DFVLR-SONDDR-283] 12 p1537 A73-26822

Method for successively increasing the step of numerical integration for systems of ordinary differential equations 12 p1516 A73-26952

A self starting predictor corrector algorithm of arbitrary order having exact stability. 12 p1517 A73-27170

Integrated force method for discrete structural analysis, discussing analogy with continuous problem Beltrami-Michell formulation and applications to pin and rigid connected frames 13 p1691 A73-28082

Finite element incremental solutions for geometrically nonlinear problems based on second variations of variational functionals, discussing numerical integration and variational principles 13 p1692 A73-28228

Computer programs for analysis of shells of revolution based on numerical integration and finite difference procedures 13 p1693 A73-28236

Numerical integration of orbits for evolution of different configurations, discussing Titius-Bode law and stability limits of planetoid and hypothetical planet orbits 13 p1686 A73-29366

On the stability of numerical integration routines for ordinary differential equations. 13 p1650 A73-29397

The numerical solution of parabolic partial differential equations using the method of Lanczos. 13 p1650 A73-29398

Construction of upper and lower functions during approximate integration of a nonlinear system containing a biharmonic operator 13 p1651 A73-29678

Systematic analysis of perturbations of orbits - The case of drag. 14 p1788 A73-29717

A numerical method of integration by means of Taylor-Steffensen series and its possible use in the study of the motions of comets and minor planets. 14 p1790 A73-29788

An algorithm for numerical integration in triangular domains. 14 p1806 A73-30047

Numerical time integration methods in shell transient response finite element analysis, considering conditionally stable explicit and unconditionally or conditionally stable implicit schemes 14 p1807 A73-30187

Integral equation formulation for electromagnetic scattering by conducting cylinders, investigating coupling between complementary boundary value problem and nonuniqueness consequences on numerical resolution 14 p1727 A73-30215

Convergence of the arithmetic-geometric mean procedure for the complex variables and the calculation of the complete elliptic integrals with complex modulus. 14 p1769 A73-30423

An adaptive precision gradient method for optimal control. 14 p1738 A73-30452

The particle resonance in spiral galaxies - Nonlinear effects. 14 p1801 A73-30727

Nonstationarity effects on planetary boundary layer by numerical integration of time dependent boundary layer model 14 p1772 A73-30903

A new method for the Lebedev-Ufliand integral equation for contact problems of elasticity. 15 p1946 A73-31103

Riccati transformation for optimal control linear two-point boundary value problems formulated from first order numerical integration methods 15 p1908 A73-31666

Optimal algorithms for numerical solutions of singular integral equations 15 p1900 A73-32096

A numerical integration method for the determination of flutter speeds. 15 p1955 A73-32163

A numerical method for integrating the unsteady boundary-layer equations when there are regions of backflow. 16 p1998 A73-32799

Numerical integration errors due to differential equations instability for Kepler orbits, discussing error reduction procedure by substituting for time as independent variable 16 p2061 A73-33231

The numerical integration of the Navier-Stokes equations for the two-dimensional incompressible flow along a planar plate 16 p2000 A73-33261

A modified Butcher formula for integration of stiff systems of ordinary differential equations. 17 p2199 A73-34212

Asymptotic expansions for product integration. 17 p2200 A73-34213

Note on error bounds for numerical integration. 17 p2200 A73-34214

Solution of incorrect problems by methods of successive approximations 17 p2201 A73-34630

Unconditional stability in numerical time integration methods. 17 p2201 A73-35027

[ASME PAPER 73-APM-1] Some aspects of numerical integration. 17 p2202 A73-35372

Numerical investigation of unsteady boundary-layer separation. 19 p2420 A73-37852

Ion trajectories in plasma focusing devices based on numerical integration of three dimensional equations of motion 19 p2468 A73-37856

Matching the geopotential and wind fields with the aim of improving the accuracy of objective analysis 19 p2449 A73-38544

Attitude determination for a strapdown inertial system using the Euler axis/angle and quaternion parameters. 20 p2589 A73-38834

A numerical integration scheme for the N-body gravitational problem. 20 p2604 A73-38973

A study of systems with time-variable coefficients by the definite-integral method 20 p2542 A73-39037

Study of methods of computing transition matrices /Computer-program description/. 20 p2532 A73-39129

A method for calculating three-dimensional turbulent boundary layer by using streamline co-ordinates. 20 p2546 A73-39225

Numerical integration method for Navier-Stokes equation of time dependent flow past impulsively started circular cylinder, calculating length of separated wake and pressure distribution 21 p2631 A73-40248

Numerical evaluation of integrals around simple closed curves. 21 p2725 A73-40378

Application of the method of integrating matrices to the calculation of the natural vibrations of a propeller blade with allowance for deflection in two planes and for torsion 21 p2783 A73-40389

Integration of certain ordinary differential equations based on the approximation of continuous functions by linear functions 21 p2727 A73-41063

Computerized simultaneous numerical integration of motion equations for solar system, star cluster and galaxies, considering radar observations of moon, Mercury, Venus, Mars and Icarus 21 p2772 A73-41241

On the evaluation of the principal value integral in the scattering problems. 21 p2728 A73-41475

Shock wave structure analysis via averaging over nonsinusoidal functions, discussing shock front length in cubic nonlinear medium, adiabatic invariants and harmonic functions 21 p2749 A73-41518

Use of the numerical method of Estoque and Bhumerikar for the planetary boundary layer. 21 p2732 A73-41572

E and F regions nitrogen vibration energy content by numerical integration of time dependent species continuity equation and species equation of motion 22 p2848 A73-42537

Stability of the De Vogelaere method for time-wise numerical integration. 22 p2882 A73-42557

Quasi-autonomous dynamic control subsystem interrelation and location for nonlinear multiple link automatic control synthesis with iterative integration of motion equations 22 p2836 A73-42616

Numerical integration of shell equations using the field method. [ASME PAPER 73-APMW-27] 22 p2925 A73-42888

Computer analysis of clamped-clamped and clamped-supported cylindrical shells. 22 p2927 A73-42995

Prediction of satellite motion by a combined method of recurrent relations 23 p3027 A73-43267

Numerical solution of Fredholm integral equation describing incompressible inviscid potential flow past three dimensional bodies 23 p2939 A73-43474

Technically oriented algorithms for unsteady pipe flow. 23 p2968 A73-43800

A method for solving ill-posed integral equations of the first kind. 23 p2999 A73-43803

A note on relative motion in the general three-body problem. 23 p3031 A73-43834

Thickness of liquid film on a rotating disk. 23 p2969 A73-44128

Automatic integration algorithm for computer calculation of definite integral within specified tolerance, discussing computation failures and algorithm reliability 23 p2957 A73-44390

Numerical integration of the equations of chemical kinetics 24 p3065 A73-44703

Superposition technique in numerical integration of generalized Ekman equation for wind profile determination, taking into account eddy diffusivity variation 24 p3108 A73-45019

Three body problem triple close approaches within escape mechanism, discussing method to control numerical integrations accuracy 24 p3141 A73-45281

Multistep-multistage-multiderivative methods for ordinary differential equations. 24 p3106 A73-45334

The problem of an iteration method for solving a nonlinear system of partial differential equations given in implicit form with time lag 24 p3106 A73-45507

NUMERICAL STABILITY

Stability theory of difference approximations for mixed initial boundary value problems. II. 02 p0188 A73-12616

Rayleigh scattering influence on stimulated Raman effect, determining occurrence conditions for absolute instability due to feedback 06 p0702 A73-18593

Solution stability of autonomous differential equations with holomorphic members under perturbation by time dependent auxiliary functions 06 p0724 A73-18683

Stability of difference approximations to differential equations. 07 p0845 A73-20494

Conditional stability and separation of solutions to differential equations. 07 p0845 A73-20496

Stability of certain finite-difference schemes for solving heat conduction equations with a nonself-conjugate elliptic operator 09 p1167 A73-22582

Semivariational approximation for solution of parabolic differential equation with inhomogeneous mixed boundary conditions and abstract equation with operators, noting convergence and stability 09 p1113 A73-23025

Matrix Riccati differential and quadratic algebraic equations in optimal control and filtering theory, discussing stabilizing solutions, asymptotic properties and computational techniques 09 p1069 A73-23102

A note on the stability of an iterative finite-difference method for hyperbolic systems. 10 p1241 A73-23639

On the instability of leap-frog and Crank-Nicolson approximations of a nonlinear partial differential equation. 10 p1241 A73-23640

Local extrapolation in the solution of ordinary differential equations. 10 p1241 A73-23641

Heat conductivity equation solution stabilization for Cauchy problem with oblique derivative and arbitrary number of geometrical variables 10 p1295 A73-24061

Discrete-time fixed-lag smoothing algorithms. 10 p1243 A73-24547

Explicit and implicit difference schemes for solving complex equations of motion, deriving approximation stability conditions 11 p1397 A73-25033

On the stability of finite difference schemes in transient semiconductor problems. 11 p1408 A73-25438

Direct time numerical integration of spatially discretized linear elastodynamics integral equations, comparing one-step algorithms for stability and accuracy in terms of frequency spectrum 11 p1435 A73-25439

Nonlinear resistive boundary layer in rotating hydromagnetic flow related to earth dynamo theory, discussing steady solution uniqueness and numerical temporal stability 11 p1355 A73-25794

Accuracy and convergence of absolutely stable finite difference procedures for solution of multidimensional heat conductivity equation with discontinuous coefficients 11 p1452 A73-26327

Stability of the solutions of differential equations with a nonlinear potential operator in a Hilbert space 12 p1516 A73-26959

Necessary and sufficient condition for stability of a class of difference-type boundary value problems 12 p1517 A73-26962

Existence and stability of the solution of the Volterra nonlinear integral equation 12 p1517 A73-27101

A self starting predictor corrector algorithm of arbitrary order having exact stability. 12 p1517 A73-27170

Inequalities for the large deviation probabilities of sums of independent random quantities in the case of a limiting stable law 12 p1518 A73-27221

Stability of heat transfer during boiling at a nonisothermal surface 12 p1558 A73-27314

Chetaev concept for experiments with small measurement errors and mathematical model instability and liability properties, applying to biological existence struggle and spacecraft reentry 12 p1524 A73-27405

Stability of nonlinear systems with a transformed argument 12 p1524 A73-27416

Book - Numerical methods for unconstrained optimization. 12 p1518 A73-27549

Cauchy problem solution stability for non-homogeneous heat conduction equation with two space variables, allowing specular reflection on rectangular boundary 12 p1560 A73-27809

Numerical stability criteria for fourth order nonlinear difference equations, using discrete form of Liapunov direct method 13 p1649 A73-28699

On the robustness of properties characterizing the normal distribution. 13 p1650 A73-28797

Periodic solutions of piecewise-continuous systems with a small parameter 13 p1661 A73-29084

On the stability of numerical integration routines for ordinary differential equations. 13 p1650 A73-29397

Routh-Hurwitz method for optimal algebraic stability of ordinary differential equations of fourth order systems with linear control law 13 p1597 A73-29419

Wave periodic structure solution instability and unstable oscillation growth rates for nonlinear drift waves and solitons in collisionless plasma 14 p1778 A73-29692

Stability of difference equations and convergence of iterative processes. 14 p1767 A73-29937

Quadrature errors effect on finite element method solutions accuracy, considering stiffness matrix numerical stability 14 p1806 A73-30179

Stability and convergence of finite element methods for elastic structures vibration analysis, stressing application to mixed boundary value problems 14 p1807 A73-30185

Perturbation method in the analysis of geometrically nonlinear and stability problems. 14 p1808 A73-30196

Fourier decomposition for antenna near field reconstruction from far field pattern data, investigating numerical stability and convergence bounds 14 p1727 A73-30213

Zero-solution stability in systems of partial differential equations 14 p1768 A73-30248

Nonlinear vector matrix differential equations for automatic control systems dynamics, discussing stability, dissipativity and convergence 14 p1768 A73-30344

Some aspects of the asymptotic behavior of solutions of nonlinear differential equations with delayed argument 14 p1768 A73-30345

An upper bound for the singular parameter in a stable, singularly perturbed system. 14 p1770 A73-30592

Oscillations of higher-order retarded differential equations generated by the retarded argument. 14 p1770 A73-30756

Asymptotic stability and perturbations for linear Volterra integrodifferential systems. 14 p1770 A73-30757

- Oscillations of nonlinear functional differential equations generated by retarded actions. 14 p1770 A73-30761
- Stability in the critical case of purely imaginary roots for neutral functional differential equations. 14 p1771 A73-30773
- Analysis of a system of differential equations with a small parameter at the higher derivatives. 14 p1771 A73-30832
- Regulators providing control system autonomy. 14 p1740 A73-30938
- Nonlocal continuance of solutions to vibration-stable differential equations. 15 p1899 A73-31219
- Stability, solvability and adjoint conditions for time periodic perturbation solutions to subcritical bifurcating plane Poiseuille flow. 15 p1863 A73-31340
- Analysis of stability and periodic motions in nonlinear sampled-data systems by the root locus method. 15 p1834 A73-31690
- Convergence, accuracy and stability of finite element approximations of a class of non-linear hyperbolic equations. 15 p1899 A73-32030
- Numerical integration errors due to differential equations instability for Kepler orbits, discussing error reduction procedure by substituting for time as independent variable. 16 p2061 A73-33231
- Comparison of the solutions obtained by Tikhonov's and Sparrow's methods for the inverse unsteady-heat-conductivity problem. 17 p2253 A73-34134
- Analysis of gas flow through a multilayer insulation system. 17 p2149 A73-34184
- A modified Butcher formula for integration of stiff systems of ordinary differential equations. 17 p2199 A73-34212
- An error analysis of a method for solving matrix equations. 17 p2200 A73-34216
- Russian book - Lectures on the theory of stability of the solutions of systems with an aftereffect. 17 p2211 A73-34224
- Formulation of stable difference schemes for systems of initial-value partial differential equations. 17 p2200 A73-34284
- Liapunov direct method extended to stability of nonlinear parabolic systems, noting application to Burgers equation. 17 p2200 A73-34398
- Implicit finite difference scheme for Eulerian fluid dynamics of time dependent one dimensional polytropic gas flow, noting numerical stability. 17 p2151 A73-34894
- Unconditional stability in numerical time integration methods. [ASME PAPER 73-APM-1] 17 p2201 A73-35027
- Hopscotch method for one-space dimensional bending beam elliptic differential equation solution, noting mesh ratio stability range. 17 p2251 A73-35518
- Frequency-time domain stability criterion for nonlinear negative feedback system with linear transfer function, using Zame positive operator theory. 17 p2203 A73-35731
- Russian book on linear differential delay equations covering solvability theorems, solution properties, stable and unstable equations, first and second order equations, periodic equations, etc. 18 p2329 A73-35897
- Sensitivity of the numerical analysis of the three-fluid plasma mixed initial-boundary value problem. 18 p2338 A73-36160
- Numerical stability of boundary layers with massive blowing. 18 p2298 A73-36321
- Global stability and the restricted 3-body problem. 18 p2352 A73-36417
- A serial CSDT predictor-corrector technique for the hybrid computer solution of partial differential equations. 18 p2291 A73-36425
- Eigenproblem solution by a combined Sturm sequence and inverse iteration technique. 19 p2408 A73-38188
- Stability criteria for explicit finite difference solutions of the parabolic diffusion equation with nonlinear boundary conditions. 19 p2445 A73-38189
- Stability and convergence of streamline curvature flow analysis procedures. 19 p2421 A73-38190
- Regulators guaranteeing the autonomy of a controlled system. 19 p2414 A73-38192
- Dynamics and stability of the algorithm of a digital adaptive system using a prediction technique. 20 p2532 A73-38688
- An initial value method for the eigenvalue problem for systems of ordinary differential equations. 20 p2581 A73-38970
- Lyapunov theory and perturbations of differential equations. 20 p2581 A73-38974
- Investigation of the stability of solutions to a quasi-stationary system of linear differential equations with quasi-periodic coefficients. 20 p2581 A73-38987
- Stability of periodic oscillations of stars. 20 p2606 A73-39081
- Stability of an almost periodic solution to a generalized Duffing equation. 20 p2593 A73-39493
- Excitation of parametric vibrations in stochastic systems with two degrees of freedom. 20 p2594 A73-39641
- The solution and stability of a system of two first-order linear ordinary differential equations with variable coefficients. 21 p2727 A73-41066
- Russian book - Qualitative theory of boundary value problems for quasi-linear second-order parabolic equations. 22 p2881 A73-41701
- Higher order accuracy finite difference algorithms for quasi-linear, conservation law hyperbolic systems. 22 p2882 A73-42518
- Semiempirical time dependent climate models formulated for stability of asymptotic steady state equilibrium solutions to perturbations. 22 p2883 A73-42540
- Stability of the De Vogelaere method for timewise numerical integration. 22 p2882 A73-42557
- On the behavior of a numerical approximation to the rotatory inertia and transverse shear plate. [ASME PAPER 73-APMW-7] 22 p2924 A73-42880
- On the construction of accurate difference schemes for hyperbolic partial differential equations. 23 p3000 A73-43208
- Numerical exploration of commensurable periodic solutions of the restricted problem of three bodies and their stability. 23 p3029 A73-43746
- A method for solving ill-posed integral equations of the first kind. 23 p2999 A73-43803
- Numerical stability of various summation schemes in a floating-type R subset. 23 p2999 A73-44098
- An application of integral invariants to the n-body problem. 23 p3034 A73-44100
- Exponential stability theorems of multivalued difference equations for discrete dynamical systems. 23 p3000 A73-44206
- Design criteria for finite-difference models for eddy diffusion with winds that guarantee stability, mass conservation, and nonnegative masses. 24 p3085 A73-45018
- Numerical stabilization of all laws of conservation in the many body problem. 24 p3142 A73-45289
- Stability of Lagrange solutions to the three-dimensional elliptic problem of three bodies. 24 p3111 A73-45299
- Nonlinear difference schemes for linear partial differential equations. 24 p3106 A73-45332
- Stability and small parameter perturbations of a critical neutral functional differential equation. 24 p3106 A73-45336
- NUMERICAL WEATHER FORECASTING**
- An efficient, one-level, primitive-equation spectral model. 01 p0072 A73-10248
- The Air Force Global Weather Central operational boundary-layer model. 01 p0074 A73-10499
- A method for incorporating nested finite grids in the solution of systems of geophysical equations. 02 p0165 A73-12776
- Upper bounds for long range numerical weather forecasts errors due to inadequate knowledge of frictional constants, heating and initial conditions. 02 p0189 A73-12777
- Application of certain stable methods for numerical solution of forecasting equations. 05 p0592 A73-16228
- Interrelation between processes occurring along a vertical, and the forecasting of stratospheric wind. 05 p0592 A73-16232
- Random forcing effects on numerical weather predictability, assessing atmospheric variables computational space truncation impact. 06 p0720 A73-18701
- Use of numerical guidance at the National Weather Service's National Meteorological Center. 06 p0720 A73-18703
- Numerical model for three dimensional air parcels trajectories computation from operational wind forecasts, deriving atmospheric moisture, dew and temperature distributions predictions. 06 p0720 A73-18705
- Climatic presentations for short-range forecasting based on event occurrence and reoccurrence profiles. 06 p0720 A73-18707
- A macroscale-mesoscale numerical model of intense baroclinic development. 06 p0720 A73-18708
- Updating of numerical precipitation guidance. 06 p0720 A73-18709
- Parameter value selection in Sasaki's meteorological field coordination method. 06 p0721 A73-18731
- A numerical experiment using a general circulation model of the atmosphere. 07 p0846 A73-19037
- Present state and further developments in short-range hydrodynamic weather forecasting. 07 p0848 A73-20624
- Rossby wave barotropic instability effects on errors leading to large scale atmosphere predictability experiments by numerical simulation of two dimensional turbulence. 08 p0985 A73-21386
- On the lateral boundary conditions for the primitive equations. 08 p0985 A73-21387
- Barotropic model of local forecasts of katabatic winds. 08 p0985 A73-21451
- Integration of the equations of meteorology. III - Integration in time. 08 p0986 A73-21485
- Forecasting with a global, three-layer, primitive-equation model. 09 p1114 A73-22124
- Use of model output statistics for predicting ceiling height. 09 p1114 A73-22125
- Analog, digital and hybrid simulation of a planetary boundary layer meteorological forecast model. 09 p1114 A73-22333
- A numerical model for predicting mesoscale winds aloft. 09 p1114 A73-22335
- Application of some numerical techniques in combining satellite and conventional data in the tropics. 09 p1115 A73-23175
- Explicit and implicit weather forecast expressions based on differential hydrodynamics equation relating horizontal and vertical wind velocity, geopotential and temperature gradients. 10 p1244 A73-23813
- Global numerical atmospheric circulation model predictive sensitivity to equator-to-pole temperature gradient changes, applying variance analysis technique to Mintz-Arakawa model. 10 p1245 A73-23983
- Boundary conditions in the problem of short-range weather forecasting on the basis of a baroclinic model of the atmosphere. 11 p1393 A73-25639
- Comparison of grids and difference approximations for numerical weather prediction over a sphere. 12 p1519 A73-26803
- Weather forecasts in tabulated and worded form by computer interpretation of forecast charts. 12 p1520 A73-26806
- Spatial-temporal analysis of asynchronous meteorological data. 12 p1521 A73-27743
- Blocking anticyclones over Siberia in the cold half-year period and the possibility of forecasting them. 12 p1521 A73-27745
- The numerical models of general circulation and their employment for medium-term and long-term weather prediction. 13 p1653 A73-28741
- A discretization method for atmosphere dynamics equations and for the construction of numerical weather forecast schemes. 13 p1654 A73-29151
- A first experiment in constructing a weather forecast for a month by the synoptic method on a computer. 13 p1655 A73-29193
- Precipitation forecasting by numerical scheme using dew point depression as moisture parameter and gradual onset techniques. 13 p1655 A73-29336
- A rapidly convergent procedure for computing large-scale condensation in a dynamical weather model. 13 p1655 A73-29338
- Boundary conditions in primitive equation weather prediction models with special emphasis on the control of gravity wave propagation. 14 p1772 A73-30902
- Four dimensional forecast assimilation of temperature data from Nimbus 4 SIRS radiance measurements, using two level model with geostrophic wind adjustment. 15 p1902 A73-31314
- Results of the numerical modeling of steady zonal circulation of the atmosphere in the equatorial region. 15 p1905 A73-31817

Considerations concerning the quasi-geostrophic model equations for an energetically open system
15 p1907 A73-32360

The analytical aspects of the reduction of boundary errors in the case of numerical weather predictions
16 p2034 A73-33074

The effect of forecast error accumulation on four-dimensional data assimilation.
17 p2205 A73-34853

Global circulation numerical modeling problems and numerical weather forecasting status as basis for GARP programs, considering tropical experiment on deep convective cloud systems
17 p2205 A73-34927

Numerical weather prediction models based on hydrothermodynamic equations and nonadiabatic factors for short term regional, hemispheric and global forecasting
18 p2331 A73-35909

Three to five day numerical forecasting making use of the complete hydrodynamics equations, and problems of correlating the original fields of meteorological elements
18 p2331 A73-35911

Computation of heat flux in numerical weather forecasting.
18 p2334 A73-37059

Experiments on incorporating radiative heat influx in numerical forecasting.
18 p2334 A73-37077

Numerical study on the effects controlling the low-level jet.
18 p2335 A73-37100

Numerical forecasting experiments based on the conservation of potential vorticity on isentropic surfaces.
21 p2728 A73-40053

On the strategy of combining coarse and fine grid meshes in numerical weather prediction.
21 p2728 A73-40055

Numerical one dimensional cumulus model of stratification and cloud depth-radius relations for convective layer prediction
21 p2729 A73-40068

Allowance for the effects of the relief and of the Coriolis force in forecasting meteorological elements
22 p2883 A73-41954

Numerical simulation of maritime warm cumulus by one dimensional cylindrical cloud model incorporating nucleation and raindrop breakup processes
22 p2883 A73-42546

An exact solution to the system of prognostic equations of a barotropically divergent model of the atmosphere
23 p3001 A73-43461

The role of computers in the development of numerical weather prediction.
24 p3108 A73-45085

Numerical weather prediction and analysis in isentropic coordinates.
24 p3108 A73-45091

Northern summer tropical upper tropospheric large scale flow dynamics, energy exchange diagram and limited area numerical weather prediction problems
24 p3108 A73-45094

Parametrizing turbulent-friction effects in a planetary boundary layer
24 p3108 A73-45450

NUSSELT NUMBER

Convection heat transfer in a contained fluid subjected to vibration.
03 p0398 A73-13547

Free convective heat transfer between vertical parallel plates One plate isothermally heated and the other thermally insulated.
05 p0638 A73-16221

Comparison of exact and mean beam length results for a radiating hydrogen plasma.
07 p0859 A73-20221

Experimental investigation of heat transfer using facilities for testing heatproof materials
08 p1022 A73-21094

Entrance region heat transfer between parallel plates with uniform wall temperature.
09 p1167 A73-23460

Influence of the Reynolds number on nonstationary convective heat transfer in a pipe during a change in the thermal load
10 p1204 A73-23511

An experimental study of combined forced- and free-convective heat transfer from flat plates to air at low Reynolds numbers.
10 p1295 A73-23777

Closed form solution for heat transfer through Rankine vortex, noting square root dependence of Nusselt number on Peclet number
10 p1295 A73-23780

Asymptotic Nusselt numbers for dissipative non-Newtonian fluid through ducts.
11 p1346 A73-25370

Natural convective heat transfer between vertical parallel plates - One plate with a uniform heat flux and the other thermally insulated.
15 p1958 A73-32057

Effect of Reynolds number on nonstationary convective heat exchange in a tube with variable heat load.
17 p2255 A73-35191

Heat transfer through free convection of air between vertical plates, obtaining Nusselt and Grashof numbers, and temperature and pressure effects
20 p2628 A73-39407

Heat transfer from an enclosed rotating disk with uniform suction and injection.
22 p2938 A73-42998

Forced convective heat transfer from isothermal sphere in steady incompressible flow at low Reynolds and various Prandtl numbers, obtaining mean Nusselt number
23 p3049 A73-43934

NUTATION

A theory of perturbations in angle-action variables: Application to the motion of a solid about a fixed point - Precession-nutation
01 p0107 A73-11362

The effects of viscous friction on the precession and nutation of celestial bodies.
02 p0217 A73-12396

Communications satellite Symphonic stability during perigee-apogee transfer in terms of liquid filled spinning top nutation
03 p0381 A73-13295

Computerized precession and nutation matrix calculations of rectangular equatorial coordinates with longitude and inclination allowance for radar data processing
09 p1142 A73-22092

Ponderous nutational motion of gyroscope in gimbal suspension, calculating precession rate from reduced equations of motion
09 p1081 A73-22351

Spectrum of the earth's pole coordinates over the period from 1846 to 1971
10 p1274 A73-23723

Investigation of the influence of precession, nutation, and yearly aberration on the average equatorial coordinates, azimuth, and elevation of the North Star
10 p1281 A73-24476

Dynamical latitude correction requiring changes in ephemeris and time determination, discussing applicability to nutation of pole of earth figure
11 p1429 A73-26689

General considerations about the revision of all the calculations of the International Latitude Service.
13 p1678 A73-28379

Chandler polar motion due to elastic earth free nutation using models based on historical data
13 p1678 A73-28380

Earth axis 14 month variation with latitude /Eulerian nutation/ as free vibration subject to damping, obtaining nonuniform drift rate from seven year interval observations
13 p1678 A73-28382

On the regularity of fluctuations in annual and secular polar motions.
13 p1678 A73-28385

Comparison of the coordinates of the pole as obtained by classical astrometry /IPMS, BIH/ and as obtained by Doppler measurements on artificial satellites /Dahlgren polar monitoring service/.
13 p1679 A73-28390

Earth liquid core effect on axis annual nutation, deriving Z term for correction of International Latitude Service latitude variation data
13 p1606 A73-28400

On the comparison of diurnal nutation derived from separate series of latitude and time observations.
13 p1679 A73-28402

On the correlation between earthquake occurrence and disturbances in the path of the rotation pole.
13 p1607 A73-28405

Excitation of the Chandler wobble by large earthquakes.
13 p1607 A73-28407

Time and fuel consumption optimal nutation damping and attitude-angular velocity control of spin-stabilized flight vehicles
16 p2072 A73-33234

Spectrum of the coordinates of the earth's pole during the period 1846-1971.
18 p2355 A73-36748

Dual spin spacecraft minimum energy and nutational dynamic trap states due to asymmetric or unbalanced rotors, analyzing single degree of freedom dynamic model
20 p2614 A73-38842

Energy-sink analysis for asymmetric dual-spin spacecraft.
20 p2614 A73-38843

Simultaneous determination of pole coordinates and the nonuniformity of the earth's rotation
21 p2768 A73-40727

Effect of the elastic deformation of a gimbal suspension on the nutation oscillation frequency of a gyroscope
22 p2860 A73-42359

NUTATION DAMPERS

Experimental satellite for attitude control. IV - Nutational damping of a spinning satellite.
01 p0112 A73-11191

Attitude dynamics of a 'nearly-spherical' dual-spin satellite and orbital results for OSO-7.
02 p0227 A73-11600

Optimal efficiency of satellite passive nutation damper, noting system moment of inertia and flywheel axis relationship and viscous friction coefficient
03 p0383 A73-14558

The motion and stability of a dual-spin satellite during the momentum wheel spin-up maneuver.
05 p0629 A73-16891

Spinning satellite with partially filled viscous ring damper, solving equations of motion for nutation-synchronous and spin-synchronous modes
05 p0629 A73-16892

[AIAA PAPER 73-143] Analytical design of optimal nutation dampers.
05 p0630 A73-17206

French Monograph - Contribution to the study of the stabilization of gyroscopic satellites - Conception and development of an active nutation damper.
06 p0757 A73-18097

Nutation dampers vs precession dampers for asymmetric spinning spacecraft.
11 p1432 A73-26670

The use of a spinning dissipator for attitude stabilization of earth-orbiting satellites.
13 p1690 A73-29216

Inertial force field patterns due to nutational motion of spinning satellites.
19 p2492 A73-37709

An attitude control system for earth observation spacecraft.
20 p2585 A73-38792

[AIAA PAPER 73-854] Techniques for flat-spin recovery of spinning satellites.
20 p2614 A73-38797

[AIAA PAPER 73-859] On the use of a dual spin vehicle for scanning a celestial body.
20 p2614 A73-38844

NUTATIONAL OSCILLATION

U NUTATION

NUTRIENTS

Reactivity and certain metabolic indices during prolonged sustenance of animals in artificial nutrient conditions
15 p1833 A73-31162

Effect of protein quality in the diet of rats on their tolerance to severe hypoxia
15 p1835 A73-31511

NUTRITION

Nutritional circulation in the heart. IV - Effect of calcium chloride and potassium chloride on myocardial hemodynamics and clearance of rubidium-86.
16 p1973 A73-33990

NUTRITIONAL REQUIREMENTS

Nutrition systems for pressure suits.
20 p2517 A73-39105

NYLON [TRADEMARK]

Determination of degradation of nylon 66 using differential scanning calorimetry.
04 p0468 A73-14857

Use of the linear heat flow for poor conductors and its application to the thermal conductivity of nylon.
09 p1166 A73-22200

[AD-758307] Nylon copolymers dynamical mechanical properties temperature dependence, discussing alpha peak shifts, polyamides relaxation and ordered structure
13 p1646 A73-29526

The relation between tensile bond strength and crystalline properties of the adhesive on the steel-nylon 12-steel system.
13 p1642 A73-29531

NYLON RESINS

U POLYAMIDE RESINS

NYQUIST FREQUENCIES

Linear multivariable control systems - A survey.
10 p1201 A73-24058

A contribution to the proof of the formula for resistance noise
16 p1978 A73-32910

Digital communication system with known channel characteristics, discussing intersymbol interference dependence on signalling rate based on Nyquist criteria consideration
24 p3070 A73-45482

NYSTAGMUS

Vestibular reactions to Coriolis accelerations under hypoxia conditions
06 p0650 A73-17691

Role of the visual cortex in the organization of nystagmic reactions evoked by optokinetic stimulation
06 p0653 A73-18165

Effect of some pharmacological preparations on the fall-out nystagmus and Bechterew nystagmus
08 p0929 A73-20982

Clinical applications of averaging techniques in studies of vestibulo-oculomotor function. I - Basic techniques and illustrative cases.
11 p1315 A73-25339

[AD-758545] Differential effects of central versus peripheral vision on egocentric and exocentric motion perception.
11 p1318 A73-26221

Harmonic spectral analysis of nystagmus waveform frequency content for clinical vestibular examination via digital computer
13 p1579 A73-28502

Nystagmic response persistence to Fitzgerald-Hallpike caloric tests as function of directional cupular deflections due to head movement
13 p1576 A73-28510

Experimental-mathematical analysis of the effects of rotational accelerations on the vestibular apparatus
17 p2110 A73-34120

Pontine reticular formation as origin of neural mechanism generating saccades and nystagmus quick phases in horizontal plane, investigating effects of various brain lesions
18 p2271 A73-36436

The neuronal mechanism of nystagmus.
18 p2271 A73-36437

Cross coupling between effects of linear and angular acceleration on vestibular nystagmus.
18 p2272 A73-36441

Cerebellar ablations and spontaneous eye movements in monkey.
18 p2272 A73-36447

Optokinetic stimulation of an immobilized eye in the monkey.
18 p2273 A73-36457

Ambivalent optokinetic stimulation and motion detection.
18 p2273 A73-36458

Quantitative studies on optokinetic nystagmus in the monkey.
18 p2273 A73-36459

The significance of pendulum nystagmography in aviation medicine
18 p2286 A73-36941

On the electronic simulation of acceleratory nystagmus.
22 p2816 A73-42683

O

O RING SEALS

The effect of environmental factors on seal performance of VITON E-60C fluoroc elastomer.
03 p0331 A73-13027

Feasibility study of a slanted 'O-ring' as a high pressure rotary seal.
[ASME PAPER 72-WA/DE-14] 04 p0457 A73-15873

Elastomer compatibility considerations relative to O-ring and sealant selection.
[SAE AIR 786 A] 08 p0982 A73-20691

Determination of displacements during compression of an oval seal ring
16 p2021 A73-33942

The effects of environment on performance of fluoroc elastomers in seal applications.
[ASLE PREPRINT 73AM-8B-2] 17 p2179 A73-34994

Expanding split ring seal types for pistons, discussing straight cut, step, two piece and three piece rings and pressure and friction effects
22 p2865 A73-41777

O STARS

Element abundances in O- and early B-stars.
01 p0096 A73-10296

Possibility of accelerating the matter of hot stars by absorption in spectral lines
01 p0100 A73-10706

New ultraviolet line identifications for early-type stars.
02 p0226 A73-12831

The spiral arm structure on the southwestern border of M31
02 p0227 A73-12840

Analyses of light-ion spectra in stellar atmospheres. I - Magnesium II in B and O stars.
03 p0366 A73-12934

O stars line spectra from high dispersion photographic spectrograms at 3059-6683 Å, tabulating absorption and emission lines identifications, equivalent widths and profiles
05 p0618 A73-16742

Spectroscopic studies of O-type stars. III - The effective-temperature scale.
07 p0873 A73-19060

Luminosity classification of stars earlier than O9.
07 p0875 A73-19120

Light variations of high luminosity O and B stars in the Large Magellanic Cloud.
07 p0877 A73-19597

Spectrophotometric observation of He-rich subliminous subdwarf peculiar O-type star CPD-31 1701, noting spectrum dominance by extremely stark-broadened He lines
08 p1003 A73-20894

Problem of the selective mechanism for the excitation of the C III 5696-Å line in the spectra of certain stars. I
08 p1012 A73-21549

Dust emission nebulae around Orion O and B stars.
11 p1427 A73-26606

Blue OB stars detection by flicker comparison, astronomical photography and two color diagrams, discussing classification as quasars and white dwarfs
13 p1673 A73-28148

A problem in distance-determination for Mira variables with an appendix on OB-star distances.
15 p1932 A73-31306

O-B stars in young star clusters associated with nebulae
15 p1934 A73-31420

Mariner 9 ultraviolet spectrometer experiment - Interstellar absorption at Lyman alpha in OB stars.
15 p1936 A73-31556

Early type stellar line spectra, discussing LTE, hydrogen and helium lines, stellar element abundance and O and B stars
18 p2356 A73-36875

The He I lambda 5876 line in O-star spectra.
18 p2356 A73-36973

O, Of, Oe and Wolf-Rayet star comparison in terms of emission and absorption line spectra, noting relationship to evolutionary status on H-R diagram
23 p3026 A73-43197

Study of the kinematics of O and B spectral type stars
23 p3036 A73-44241

OA O

NT OAO 2
NT OAO 3

Space astronomy-developments in the sixties to scientific achievements in the seventies.
01 p0112 A73-11203

Cygnus X-3 intensity drop and principal period observation by X ray instrument onboard OAO Copernicus
02 p0204 A73-11563

Ultraviolet photometry from the Orbiting Astronomical Observatory. VII alpha squared Canum Venaticorum.
08 p1008 A73-21158

Instrumentation in astronomy; Proceedings of the Seminar-in-Depth, Tucson, Ariz., March 13-15, 1972.
08 p0969 A73-21726

Observing from space with the Orbiting Astronomical Observatory.
08 p1015 A73-21727

Spectrophotometric results from the Copernicus satellite. I - Instrumentation and performance.
14 p1754 A73-30744

Orbiting Astronomical Observatory heat pipe flight performance data.
[AIAA PAPER 73-758] 18 p2370 A73-36373

An insight into the features of the OAO-C thermal design.
[ASME PAPER 73-ENAS-4] 19 p2493 A73-37966

OA O 2

Ultraviolet photometry of the moon with the celestec experiment on the OAO-II.
01 p0096 A73-10317

Ultraviolet photometry from the orbiting astronomical observatory. IV - Photometry of late-type stars.
05 p0626 A73-17381

OAO 2 satellite nickel-cadmium batteries with auxiliary electrodes for overcharge control, discussing operation and degradation mechanism
13 p1572 A73-29583

OAO-2 observations of HD 153919 = 2U 1700-37.
14 p1797 A73-30007

OAO-2 observations of Beta Lyrae and a provisional interpretation.
15 p1935 A73-31489

Report on the telescope ultraviolet observations from the OAO-2 satellite and associated research at the Smithsonian Astrophysical Observatory.
18 p2349 A73-35996

OA O 3

Fine pointing performance characteristics of the Orbiting Astronomical Observatory /OAO-3/.
[AIAA PAPER 73-869] 20 p2587 A73-38807

OA O-A2

U OAO 2

OA O-C

U OAO 3

OBESITY

Special physical training of pilots as a prophylactic measure against obesity
15 p1837 A73-31172

OBLATE SPHEROIDS

Expansion of the force function of two homogeneous spheroids with noncoincident symmetry planes.
04 p0503 A73-16021

Stress-strain state of a spheroidal inclusion/measuring device/ embedded in a thermoelastic medium
05 p0633 A73-16616

Closed form analytical solution for secondary flow in viscoelastic liquids axisymmetric flow past oblate and prolate ellipsoids
06 p0687 A73-18507

Black hole polar flattening and equatorial circumference lengthening as function of angular momentum, considering effects of highly curved space-time
07 p0899 A73-20176

Electromagnetic field of rotating charged oblate ellipsoid of revolution with infinite conductivity and vacuum or infinite magnetic susceptibility
10 p1252 A73-24344

Stress-strain state of a thermoelastic spheroidal insert in a thermal viscoelastic medium
11 p1434 A73-25388

Equations of planet figures solved for third order accuracy, covering flattening, density distribution, Jupiter and Saturn models and gravitational moments corrections for radii
12 p1546 A73-27860

On the motion of short-period comets in the neighbourhood of Jupiter.
14 p1790 A73-29786

Motion of a satellite in the equatorial plane of a spheroid.
15 p1929 A73-31107

Free vibration of an inflated oblate spheroidal shell.
15 p1955 A73-32155

Scattering properties of oblate raindrops and cross polarization of radio waves due to rain - Calculations at 19.3 and 34.8 GHz.
18 p2290 A73-36880

Equations of planet figures solved for third order accuracy, covering flattening, density distribution, Jupiter and Saturn models and gravitational moments corrections for radii
20 p2608 A73-39234

OBLIQUE SHOCK WAVES

Reflexion and diffraction of shocks interacted by yawed wedges.
01 p0002 A73-10272

Slightly oblique shock waves in a collisionless magnetized plasma.
01 p0082 A73-10421

Oblique shock waves heating of high beta plasma ions, suggesting Landau damping of wave energy
02 p0197 A73-12059

Oblique shock wave interaction with approach boundary layer at combustor entrance in supersonic scramjet engines, observing wall pressure distribution [AIAA PAPER 72-1181] 03 p0357 A73-13476

Unsteady flow generated by shock-turbulent boundary layer interactions.
[AIAA PAPER 73-168] 05 p0566 A73-16913

Use of oblique shock waves in high-temperature shock-tube studies.
06 p0683 A73-18793

Oblique shock-sound interaction at a freestream Mach number of about 20 in helium.
07 p0775 A73-19984

MHD shock wave decay in oblique magnetic field, considering shock and rarefaction waves interaction
07 p0858 A73-20071

Oblique shock wave generation and quenching in curved supersonic diffusers at Mach 1.6, noting dependence on boundary layer properties
13 p1566 A73-29021

Some relations for high pressure flows with and without heat transfer.
14 p1817 A73-30604

Study of the similarity solution in three dimensional compressible laminar boundary layer.
17 p2157 A73-35862

High-speed photographic observation of the propagation of a shockwave in a branched-tunnel system
21 p2676 A73-39983

Regular reflection of an oblique shock in a plane flow of ideally dissociating gas in the presence of a transverse magnetic field
21 p2744 A73-40189

Pioneer 10 flyby trajectory relationship to analogy between earth and Jupiter bow shocks with emphasis on oblique shock structure
22 p2906 A73-41942

Influence of aerodynamic field on shock-induced combustion of hydrogen and ethylene in supersonic flow.
22 p2934 A73-42786

OBSCURATION

U OCCULTATION

OBSERVATION

NT SATELLITE OBSERVATION

NT VISUAL OBSERVATION

Optimal control of observation processes, formulating solvability conditions in terms of ordinary differential equations
03 p0286 A73-14043

Stochastic linear system observer eigenvalue optimal placement with respect to quadratic error criterion for adaptation to digital computation and applicability to higher order system
07 p0849 A73-19966

Optimal observation laws for certain controlled motions
09 p1069 A73-22565

Evaluation of the efficiency of automatic control and observation systems on the basis of mathematical models of potential and real automatic systems
12 p1482 A73-26762

Phase coordinates estimation optimization, deriving observable vector relations from sampling laws
12 p1524 A73-27417

Optimal observer techniques for linear discrete time systems. 17 p2144 A73-34361

OBSERVATION AIRCRAFT

NT CL-84 AIRCRAFT

OBSERVATORIES

NT ASTRONOMICAL OBSERVATORIES

NT GEOPHYSICAL OBSERVATORIES

NT HEAO

NT LUNAR OBSERVATORIES

NT OAO

NT OSO

NT OSO-7

NT POGO

NT SOLAR OBSERVATORIES

OBSIDIAN

NT MOLDAVITE

Chlorine, bromine, iodine, and uranium in tektites, obsidians, and impact glasses. 02 p0223 A73-12720

OBSTACLES

U BARRIERS

OBSTRUCTING

U BLOCKING

OCCLUDED FRONTS

U FRONTS [METEOROLOGY]

OCCLUSION

Left ventricular receptors activated by severe asphyxia and by coronary artery occlusion. 01 p0008 A73-10549

Gas occlusions in arterial heat pipes. 18 p2369 A73-36341

[AIAA PAPER 73-724] Comparison of plethysmographic and electromagnetic flow measurements. 23 p2950 A73-44215

OCCULTATION

NT LUNAR OCCULTATION

NT RADIO OCCULTATION

NT SOLAR ECLIPSES

NT STELLAR OCCULTATION

A technique for recovering the vertical number density profile of atmospheric gases from planetary occultation data. 02 p0158 A73-11913

Small Magellanic Cloud X-1 X ray source binary nature, occultation, energy spectrum and intensity from Uhuru satellite observation 05 p0626 A73-17345

Mars shape determination from radio occultation measurements by Mariner 9 probe of signal extinction time and spacecraft ephemeris 06 p0747 A73-17488

Mutual phenomena of Jupiter's satellites in 1973-74. 07 p0875 A73-19260

Error analysis for the Mariner-6 and -7 occultation experiments. 09 p1146 A73-22428

A two-satellite microwave occultation system for determining pressure altitude references. 12 p1521 A73-26813

Mesospheric and lower thermospheric ozone concentration measurement at sunset via occultation technique from rocket payloads 17 p2159 A73-34780

The occultations and the mutual eclipses of the Galilean satellites of Jupiter 20 p2604 A73-39009

Analysis of ground tests of a microwave, earth-occultation, pressure-reference-level system. 21 p2729 A73-40065

Jupiter satellite Europa polar cap from photoelectric observation of occultations by satellite Io 21 p2687 A73-41077

Mutual Jupiter satellite-satellite eclipses and occultation observations for improved ephemerides, albedo maps, radii and limb darkening estimation 24 p3130 A73-44454

OCEAN BOTTOM

Bottle green microtektites from Australasian and Ivory Coast deep sea sediments, discussing physical and chemical properties, age and origin 05 p0615 A73-16383

Geochemical significance of perylene occurrence in marine sediments, discussing land organism biogenic pigment precursors and polycyclic aromatic hydrocarbon conversion 10 p1211 A73-24105

Deep sea drilling core sample analysis methods and results relation to sediment age and fossil fauna and flora 11 p1325 A73-25462

On the torques due to tidal friction of the oceans and adjacent seas. 13 p1607 A73-28409

Worldwide sea level pulsations and interpolations relation to elevation and subsidence of oceanic ridge systems, discussing sea floor spreading hypotheses 17 p2164 A73-35858

North American microtektites from the Caribbean Sea and their fission track age. 18 p2354 A73-36511

Paleomagnetic excursion recorded in latest Pleistocene deep-sea sediments, Gulf of Mexico. 18 p2313 A73-36513

Distribution and diagenesis of organic compounds in JOIDES sediment from Gulf of Mexico and western Atlantic. 21 p2683 A73-40562

OCEAN CURRENTS

NT COASTAL CURRENTS

Upwelling of a stratified fluid in a rotating annulus - Steady state. I - Linear theory. 06 p0684 A73-17702

Instability of a two-layer geostrophic flow with an antisymmetric velocity profile in the upper layer 06 p0691 A73-18728

New estimate of annual poleward energy transport by Northern Hemisphere oceans. 13 p1610 A73-29225

Remote sensing in a circulatory survey of Boston Harbor. 16 p2003 A73-33356

Horizontal electric fields and currents caused by depths-to-surface oceanic water exchange in geomagnetic field, discussing electric field distribution and magnetic field distortion 19 p2426 A73-38175

On the prediction of turbulence in baroclinic zones. 19 p2449 A73-38246

Ocean currents observation by ship and satellite tracking of free-drifting Lagrangian platforms [AAS PAPER 73-144] 20 p2550 A73-38593

Wind modification of structure of thermally driven tropical undercurrent, considering stratified and constant density models, surface winds, monsoons, thermocline jets and meridional circulation 21 p2679 A73-40069

Suspended sediment observations from ERTS-1. 22 p2850 A73-42726

OCEAN MODELS

Wind modification of structure of thermally driven tropical undercurrent, considering stratified and constant density models, surface winds, monsoons, thermocline jets and meridional circulation 21 p2679 A73-40069

OCEAN SURFACE

Precipitation detection over the ocean using microwave satellite radiometry. 02 p0188 A73-12268

A noncoherent model for microwave emissions and backscattering from the sea surface. 02 p0164 A73-12362

Average return pulse form and bias for the S193 radar altimeter on Skylab as a function of wave conditions. 04 p0446 A73-14804

Surface winds from sun-glitter measurements from a spacecraft. 04 p0474 A73-15777

Ocean color measurements utilizing a noon orbit for earth resources satellite applications. 04 p0445 A73-15778

High altitude remote spectroscopy of the ocean. 04 p0451 A73-15779

Doppler spectral width of radar signal reflected from sea surface as function of illuminated region dimensions, waviness scale and emission factors 04 p0423 A73-15913

The specific ozone destruction at the ocean surface and its dependence on horizontal wind velocity from profile measurements. 05 p0594 A73-16348

Resonant coupling of ocean Rayleigh waves to atmospheric shock waves from Apollo rockets. [AD-755609] 05 p0569 A73-16380

Space wave field produced by a vertical electric dipole above a perfectly conducting sinusoidal ocean surface. 06 p0665 A73-18181

Experiments on objectively predicting some atmospheric and oceanic variables for the winter of 1971-72. [AD-758469] 06 p0720 A73-18702

High-altitude photographs of the Oregon coast. 09 p1078 A73-22719

Macroscale interaction between the atmosphere and oceans and the role of the latter in the formation of anomalous circulation in the stratosphere 10 p1246 A73-24374

Microwave range-difference measurements on 65-km slanted overwater path, interpreting tropospheric noise power spectra and rms values as function of baseline length 11 p1330 A73-25685

Microwave radiometric observations of simulated sea surface conditions. 11 p1355 A73-25774

Two-position scattering of radio waves by the sea surface at small slip angles 11 p1331 A73-26154

On the estimation of the directional spectrum of surface gravity waves from a programmed aircraft altimeter. 11 p1358 A73-26347

Optimum processor accuracy for radar altimetry for geodesy over sea, considering surface reflectivity, height variation additive noise and pointing errors 11 p1371 A73-26631

Computerized maritime sea level atmospheric pressure field analysis, using pressure and wind velocity data 12 p1519 A73-26802

Ground-wave perturbation over a transition zone between two different sections. 13 p1583 A73-28798

Experiments in the determination of turbulent layer thickness in monochromatic-type waves 13 p1655 A73-29160

Atmospheric effects on ocean surface temperature sensing from the NOAA satellite scanning radiometer. 13 p1610 A73-29195

Comments on the determination of the total heat flux from the sea with a two-wavelength radiometer system as developed by McAlister. 13 p1610 A73-29197

Fog frequency and characteristics at the site of the proposed New York offshore airport, as compared with those at J. F. Kennedy International Airport - A preliminary report. 15 p1903 A73-31546

Remote sensing of atmosphere and ocean by lidar, radar, bistatic radio, IR optics, microwave radiometry, crossed-beam correlation, etc 16 p2003 A73-33368

The influence of the sea evaporation duct on the phase of the received field on a line-of-sight path. 16 p1981 A73-33713

A model of a long-term process of heat and moisture transfer in the atmosphere over the ocean 17 p2158 A73-34344

Radiometric measurements of temperature of the ocean surface - Improvement brought by use of a polarizing radiometer 17 p2161 A73-34946

The use of satellites for remote sensing of the sea surface 17 p2162 A73-34956

On radar mapping of sea surface. 17 p2123 A73-35153

The composite scattering model for radar sea return. 17 p2163 A73-35364

Prospects for physical oceanography from space. 18 p2306 A73-36024

Remote sensing of ocean color as an index of biological and sedimentary activity. 18 p2307 A73-36030

Gulf Stream eddies - Recent observations in the western Sargasso Sea. 18 p2313 A73-36642

Some problems associated with wind drag and infrared images of the sea surface. 18 p2313 A73-36643

Optical wave measurement technique and experimental comparison with conventional wave height probes. 19 p2458 A73-37263

Some effects of surface anomalies in a global general circulation model. 19 p2446 A73-37539

Remote sensing of the ocean. 19 p2405 A73-38240

Oceanographic satellite capabilities, considering sea-air interactions, currents, upwellings, deep sea tides, sea-earth interactions and water mass identification [AAS PAPER 73-145] 20 p2550 A73-38594

IR quasi-synoptic global sensing of ocean surface temperature, covering IR theory, airborne radiation thermometry and single band satellite data analysis techniques [AAS PAPER 73-146] 20 p2550 A73-38595

Multipath channel characterization for Aerosat. 20 p2526 A73-38755

Relationship between sea wave parameters and the spectra of aerial photography and radar imagery of sea surface. 20 p2531 A73-39891

Oil spill radar scatterometer detection at 13.3 GHz through backscattering cross sections, discussing ground truth, data correlation and wind velocity 20 p2560 A73-39892

Improvements brought to the measurement of the ocean surface temperature by utilization of a polarizing infrared radiometer 21 p2698 A73-40142

Remote sounding of water surface conditions from aboard artificial satellites. 21 p2657 A73-41333

Two frequency radar interferometry applied to the measurement of ocean wave height. 22 p2843 A73-41832

Mapping of North Atlantic winds by HF radar sea backscatter interpretation. 22 p2882 A73-41836

The determination of surface temperature from satellite 'window' radiation measurements. 22 p2846 A73-42057

A direct comparison of satellite and aircraft infrared /10 to 12 microns/ remote measurements of surface temperature. 22 p2850 A73-42729

The specific ozone destruction rate of the ocean surface and its dependence on horizontal wind velocity. 23 p2974 A73-43867

An investigation of the numerical properties of the surface heat-balance equation. 23 p3004 A73-44265

OCEANOGRAPHY

Satellite oceanographic measurements and observations and required sensors assessment, noting benefits to marine and coastal interests and to weather forecasting [AIAA PAPER 73-11] 06 p0690 A73-17605

Orbit analysis for coastal zone oceanography observations. [AIAA PAPER 73-207] 06 p0748 A73-17659

Experiments on objectively predicting some atmospheric and oceanic variables for the winter of 1971-72. [AD-758469] 06 p0720 A73-18702

Geopause satellite orbit, tracking, environment, gravity and station position properties and applications to earth and oceanographic dynamics studies 11 p1430 A73-25317

Project VEMNO - North Sea-Baltic measuring network. 13 p1608 A73-28787

New estimate of annual poleward energy transport by Northern Hemisphere oceans. 13 p1610 A73-29225

Applications of ERTS data to oceanography and the marine environment. 18 p2302 A73-35935

Prospects for physical oceanography from space. 18 p2306 A73-36024

The role of applications satellites in the management of the human environment. 19 p2424 A73-37713

Radio techniques applied to oceanography and earth science - Oceanic wind measurement and overland imaging as examples. 21 p2654 A73-40817

Oceanographic analysis of orbital photographs of the upper Gulf of California. 21 p2692 A73-41634

OCEANS

NT ARCTIC OCEAN

NT ATLANTIC OCEAN

NT INDIAN OCEAN

NT PACIFIC OCEAN

OCTAHEDRAL RESEARCH SATELLITES

U ENVIRONMENTAL RESEARCH SATELLITES

OCTAHEDRITE

U MINERALS

OCTAVES

Harmonic enhancement for airborne low voltage lightweight TWT amplifier band edge performance improvement to provide bandwidth in excess of two octaves 16 p1988 A73-33298

OCULAR CIRCULATION

Investigation of the exchange between the blood and the intraocular fluid with the aid of radioactive phosphorus 10 p1185 A73-24520

Possibilities of barotherapy in ophthalmology 21 p2637 A73-40349

Glycogen content in the rabbit retina in relation to blood circulation. 22 p2802 A73-41732

Fluorescent angiographic technique for fundus oculi 23 p2946 A73-43788

OCULOGRAPHIC ILLUSIONS

Moving visual scenes influence the apparent direction of gravity. 04 p0411 A73-15250

Disorienting effects of aircraft catapult launchings. 07 p0785 A73-19480

Inversion illusion in the so-called zero-gravity conditions of parabolic flight. 14 p1722 A73-30511

Visual-vestibular interaction and motion perception. 18 p2273 A73-36460

OCULOMETERS

A combined photoelectric method for detecting eye movements. 02 p0137 A73-12079

Linearity of the horizontal component of the electro-oculogram. 07 p0784 A73-19125

Two dimensional eye movement recording using a photo-electric matrix method. 07 p0786 A73-20259

Rapid eye movement analyzer. 09 p1045 A73-22697

A vecto-oculographic approach to fast sleep eye movements in man. 14 p1715 A73-29994

Russian book - Methods of studying eye movements. 15 p1840 A73-32417

Involuntary eye movements in the presence and absence of points 18 p2276 A73-36568

The oculometer in remote viewing systems. 19 p2397 A73-37320

The oculometer - A new approach to flight management research. [AIAA PAPER 73-914] 21 p2702 A73-40862

OCULOMOTOR NERVES

Mechanical modeling of eye muscle dynamics. 06 p0660 A73-18816

Clinical applications of averaging techniques in studies of vestibulo-oculomotor function. I - Basic techniques and illustrative cases. [AD-758545] 11 p1315 A73-25339

Adjustment of saccade characteristics during head movements. 11 p1319 A73-26222

Accuracy of saccadic eye movements and maintenance of eccentric eye positions in the dark. 14 p1716 A73-30390

Accommodation of the eye during sleep and anesthesia. 14 p1716 A73-30391

The behavior of eye movement motoneurons in the alert monkey. 18 p2271 A73-36433

Supranuclear connections to oculomotor nuclei in terms of stimulus relation to eye movements 18 p2271 A73-36435

Pontine reticular formation as origin of neural mechanism generating saccades and nystagmus quick phases in horizontal plane, investigating effects of various brain lesions 18 p2271 A73-36436

The neuronal mechanism of nystagmus. 18 p2271 A73-36437

Vestibular and cerebellar control of oculomotor functions. 18 p2271 A73-36438

Cholinergic activation of vestibular neurones leading to rapid eye movements in the mesencephalic cat. 18 p2272 A73-36439

Some functional characteristics of the superior colliculus of the Rhesus monkey. 18 p2272 A73-36442

Optomotor integration in the colliculus superior of the cat. 18 p2272 A73-36443

Neuronal elements of the orienting response - Microrecordings and stimulation experiments in rabbits. 18 p2272 A73-36444

Cerebellar ablations and spontaneous eye movements in monkey. 18 p2272 A73-36447

Brain stem reticular formation influence on lateral geniculate body neurons during eye movements, suggesting cortical oculomotor impulse influence mediation by perigeniculate nucleus 18 p2272 A73-36448

Saccade correlated events in the lateral geniculate body. 18 p2272 A73-36449

Conditional computer analysis of the onset-to-onset duration of spikes from the electromyographic interference pattern of extraocular muscles. 22 p2802 A73-41731

Signal and noise in the human oculomotor system. 22 p2810 A73-42964

OFF-ON CONTROL

Dynamic response of an on-off type secondary injection thrust vector control. 01 p0091 A73-11196

Phase space trajectory analysis of pulsed laser spot pursuit tracking problem for autonomous line-of-sight interceptor missile with flip-flop controls 03 p0287 A73-14483

Large scale systems with linear and nonlinear subsystems and coupling connections, investigating connective stability under perturbations due to subsystem on-off participation 03 p0337 A73-14484

Necessary conditions for optimal controls of elliptic or parabolic problems. 05 p0590 A73-16487

Computer control algorithms for transient response optimization in on/off motor control system synthesis 06 p0741 A73-17963

Disturbance accommodation in linear systems with chattering controllers. 06 p0681 A73-18818

Incomplete/complete feedback and off-on control moments for prescribed orientation of solid body in rotational motion 10 p1248 A73-23744

Linearization limits for optimal pulse controller adjustments, using comparison with continuous controller and extrapolation 10 p1198 A73-24000

Start/stop motor incremental motion system design for optimal control with minimized energy dissipation and operating temperature under inertial and constant torque load 10 p1198 A73-24023

A time-optimal response inverter. 11 p1308 A73-25981

A power and load priority control concept as applied to a Brayton cycle turbo-electric generator. 11 p1309 A73-25984

Quasi time-optimal spacecraft reorientation maneuvers using single gimbal control moment gyros /SG CMG's/. 12 p1548 A73-27153

Reduction of the switching time of a liquid-crystal optical transparency. 12 p1498 A73-27514

Digital control of a pneumatic isolation system for inertial instrument testing. [AIAA PAPER 73-830] 20 p2543 A73-38775

On-off control of an unstable plant with time lag 20 p2542 A73-39345

Sensitivity of optimal control systems with bang-bang control. 22 p2837 A73-43068

On the limit-cycle characteristics of a bang-bang servo. 24 p3075 A73-45556

OFFSHORE PLATFORMS

Offshore airport design, construction and operation on basis of cost/benefit considerations, emphasizing ATC problems generated by ILS localizer and glide path signal reflection 18 p2296 A73-36682

A proposed littoral airport. 19 p2415 A73-37280

International Conference on Offshore Airport Technology, 1st, Bethesda, Md., April 29-May 2, 1973, Proceedings. Volume 2. 19 p2417 A73-37741

Environmental considerations for offshore airports. 19 p2417 A73-37742

Urban and regional planning aspects of offshore airport technology. 19 p2417 A73-37743

An offshore airport in Sydney region - Review of a 1972 feasibility study. 19 p2418 A73-37744

Machinery to be developed for an offshore airport constructed by reclamation. 19 p2418 A73-37746

Floating offshore airport in Osaka Bay, Japan - Digest of preliminary engineering study. 19 p2418 A73-37747

Floating superport. 19 p2418 A73-37748

Large floating ocean platforms for US Navy bases, discussing concrete construction techniques and costs for different configurations 19 p2418 A73-37749

New York offshore airport feasibility study. [FAA-RD-73-45] 19 p2418 A73-37750

OGEE WINGS

U VARIABLE SWEEP WINGS

OGIVES

Thin shell theory for thermal stresses in ogival shell used in nose cone design 01 p0113 A73-10016

A method for calculating aerodynamic heating on sounding rocket tangent ogive noses. [AIAA PAPER 73-281] 09 p1167 A73-23202

Calculation of the temperature distribution within an ogival radome in supersonic flight 11 p1336 A73-25302

The wave drag of circular nose cones at zero angle of attack at Mach numbers from 1.5 to 4 and thickness ratios from 0.05 to 0.5 23 p2940 A73-43782

OGO

NT POGO

OGO-E

Satellite studies of magnetospheric substorms on August 15, 1968. IV - Ogo 5 magnetic field observations. 16 p2004 A73-33452

Satellite studies of magnetospheric substorms on August 15, 1968. V - Energetic electrons, spatial boundaries, and wave-particle interactions at Ogo 5. 16 p2056 A73-33453

Satellite studies of magnetospheric substorms on August 15, 1968. IX - Phenomenological model for substorms. 16 p2004 A73-33457

OGO-5 observations of the physical processes occurring in the disturbed polar cusp and the cusp-magnetosheath interface. 18 p2303 A73-35943

OGO-F

Comparison of Te and Ti from Ogo 6 and from various incoherent scatter radars. 07 p0790 A73-19241

Additional results from an Ogo 6 experiment concerning ionospheric electric and electromagnetic fields in the range 20 Hz to 540 kHz. 16 p2003 A73-33438

Global temperature distributions from OGO VI 6300 A airglow measurements. 18 p2309 A73-36058

OHMIC DISSIPATION

Magnetic pumping of electrons in ohmic dissipation mechanism responsible for neoclassical plasma diffusion rate increase in banana regime

01 p0084 A73-10467

Temperature field and heat transfer equation of unsteady conducting fluid motion on porous plate within magnetic field, allowing for Joule dissipation

01 p0085 A73-11079

Current sheet model for sunspot structure, considering ohmic dissipation as decay mechanism

03 p0377 A73-14408

Character of acoustic dispersion in plasma

06 p0726 A73-17403

Auroral atmosphere temperature variations relation to nightly auroral streamer length variations, assuming ionospheric current dissipation as heat source

12 p1491 A73-27344

Influence of longitudinal thermal conductivity on the ohmic heating of plasma in the Tuman-1 facility

13 p1666 A73-28959

Time behavior of hydrogen discharge in ST-Tokamak based on measured radial electron temperature and density profiles and ohmic-heating current and voltage

14 p1778 A73-29691

Proximity effects for parallel rectangular conductors in nontransmission-line mode

17 p2129 A73-35703

Auroral atmosphere temperature variations relation to nightly auroral streamer length variations, assuming ionospheric current dissipation as heat source

23 p2970 A73-43241

Investigation of temperature pulsations accompanying the heating of a laminar sample by alternating and pulsating currents

23 p3048 A73-43446

Global distribution of thermospheric heat sources - EUV absorption and Joule dissipation

23 p2971 A73-43681

Determination of the temperature fields and thermal stresses in a bimetallic layer subjected to induction heating

23 p3046 A73-44194

Effect of longitudinal thermal conductivity on ohmic heating in Tuman-1

23 p3013 A73-44311

OHMS LAW

Zero and first velocity moments of Boltzmann equation with complications placed on Ohm Law in plasmas, considering momentum exchange

06 p0730 A73-18462

OIL ADDITIVES

Protection of mineral oils from microbiological damage by compounds of the quinone group

21 p2723 A73-41069

OIL EXPLORATION

17alpha/H/ hopane identified in oil shale of the Green River formation /Eocene/ by carbon-13 NMR

14 p1746 A73-29734

Rotary wing aircraft ecological advantages in logging, off shore oil exploration and short haul passenger transport for airport size reduction

16 p2088 A73-33185

OIL SLICKS

Detection of oil spills using a 13.3-GHz radar scatterometer

13 p1610 A73-29196

Oil spills - Measurements of their distributions and volumes by multifrequency microwave radiometry

17 p2164 A73-35806

Oil spread over Arctic ice, considering spread rate and oil slick size attainment for pollution potential during spills on tundra or pack ice [AIAA PAPER 73-701]

18 p2312 A73-36250

Oil spill radar scatterometer detection at 13.3 GHz through backscattering cross sections, discussing ground truth, data correlation and wind velocity

20 p2560 A73-39892

Polarization - A key to an airborne optical system for the detection of oil on water

23 p2979 A73-43225

OILS

NT CRUDE OIL
NT FUEL OILS
NT LUBRICATING OILS
NT MINERAL OILS

Construction of fuel and oil quantity sensors for high-performance aircraft

13 p1619 A73-29204

Photoluminescence and optical transmission of diffusion-pump oils

21 p2698 A73-40139

OKLAHOMA

The diurnal wind variation in the lowest 1500 ft in central Oklahoma - June 1966-May 1967

10 p1245 A73-23987

OLEFINS

U ALKENES

OLEIC ACID

Perchlorate degradation of ethyl oleate in solid propellants

10 p1262 A73-23758

OLFACTORY PERCEPTION

Comparative physiological characteristics of functional relations among the hypothalamus and the olfactory and limbic systems of the brain

01 p0006 A73-10151

Aerodynamic and temporal parameters of olfactory stimulation - Discussion concerning the lowering of the threshold by prenasal injection in man

03 p0262 A73-13787

Telemetered EEG and neuronal spike activity in olfactory bulb and amygdala in free moving rabbits

03 p0271 A73-14299

Aspects of air flow to the olfactory region of the human nose

15 p1833 A73-31163

High-frequency synchronized activity of the amygdaloid complex as an EEG indicator of certain psychophysiological states

21 p2636 A73-40277

OLIVINE

Mossbauer spectroscopic analysis of Sea of Fertility regolith core samples, noting olivine content increase with depth

02 p0214 A73-12242

Apollo 14 lunar rock ultrabasic fragments chemical analysis, noting pyroxene and olivine compositions

02 p0219 A73-12441

Cation determinative curves for Mg-Fe-Mn olivines from vibrational spectra

02 p0139 A73-12636

The valence states of 3d - Transition elements in Apollo 11 and 12 rocks

03 p0369 A73-13097

A point of phase equilibria interpretation in connection with lavas from the Apollo 12 site

03 p0375 A73-14106

Earth crust materials high temperature lattice and radiative thermal conductivity from laser IR measurements, discussing single crystal and polycrystal fosterite-rich olivines and enstatite

05 p0569 A73-16378

Site preferences of Ni²⁺ and Co²⁺ in clinopyroxene and olivine - Limitations of the statistical approach

06 p0690 A73-18268

Rock 14068 - An unusual lunar breccia

07 p0883 A73-19732

Electron microscopy of some experimentally shocked counterparts of lunar minerals

07 p0885 A73-19750

Electrical conductivity, internal temperatures and thermal evolution of the moon

17 p2235 A73-35741

Radiochemical neutron activation analysis for U and Th abundance measurement in achondrites and pallasite olivines

17 p2120 A73-35802

Study of a chondrule extracted from Lot 118-111 of the lunar soil of Mare Fecunditatis

21 p2770 A73-41006

OMEGA NAVIGATION SYSTEM

Comparison of medium-distance navigation systems. II

02 p0191 A73-12014

Clock comparisons by short wave, ULF and VLF signals, Loran C and Omega methods, onboard aircraft atomic clocks and TV synchronizing pulses

03 p0307 A73-13246

Omega navigation system

04 p0474 A73-15061

Nonsolar related D region semilunar variation effects on Omega navigation systems signal phase shift from harmonic analysis of VLF propagation data periodicities

04 p0416 A73-15062

Omega v.l.f. wave propagation and the 1922-23 Marconi expedition

06 p0668 A73-18442

VLF/Omega digital airborne area navigation system evaluation tests, discussing transmitting stations and system performance

13 p1656 A73-28904

VLF and Omega signal air navigation at 3 to 30 kHz supplementing VOR-DME and Loran-A navigation frequencies, considering transmission techniques

17 p2209 A73-34614

VLF navigation development at NAE

17 p2209 A73-34849

A modified composite wave technique for OMEGA

22 p2884 A73-42325

OMNIDIRECTIONAL ANTENNAS

NT MONOPOLE ANTENNAS
NT TURNSTILE ANTENNAS

Omnidirectional satellite antennas with radiation pattern distortion minimization by adjustment of antenna inclination, height above spacecraft structure and angle with metallic objects

01 p0111 A73-11173

Multipaths by diffusion on the ground and application to the transmission of digital messages affected by jumps of the carrier frequency

14 p1725 A73-29732

OMNIRANGE NAVIGATION

U VHF OMNIRANGE NAVIGATION

ON-LINE PROGRAMMING

Use of an on-line computer in a study of cardiac arrhythmia

04 p0412 A73-15644

Computer controlled automatic test system for circuits, assemblies and systems performance and test programs on-line generation, editing and validation

08 p0940 A73-20682

A five-channel time-scale converter

09 p1064 A73-23007

Computerized total On-Line Testing System with diagnostic error visibility and preventive and corrective maintenance functions in multiprogramming mode, discussing design features

16 p1986 A73-33633

Contactless on-line NDT of metal plates for concealed defects by Lamb wave excitation through wave generation from air

21 p2708 A73-41138

Certain problems in determining the capacity of digital computers

22 p2829 A73-41953

ONBOARD COMPUTERS

U AIRBORNE/SPACEBORNE COMPUTERS

ONBOARD EQUIPMENT

NT AIRBORNE EQUIPMENT
NT AIRBORNE/SPACEBORNE COMPUTERS
NT AIRCRAFT EQUIPMENT
NT SPACECRAFT ELECTRONIC EQUIPMENT

Test chamber for on board moving parts in ultrahigh vacuum

01 p0030 A73-11148

Physical and thermal constraints on batteries of electrochemical power supply systems onboard satellites, sounding and booster rockets and balloons

07 p0778 A73-18977

Spacecraft-borne optical components and systems design and operational requirements, considering thin film filters and mirrors, detectors, diffraction gratings and materials

07 p0821 A73-18978

Operational reliability of onboard equipment subjected to very long idling periods

07 p0831 A73-19418

Russian book on onboard data measuring systems for flight vehicles covering design of cw and pulsed devices, modulators, error analysis, noise, logic elements, etc

07 p0825 A73-20378

Crew station lighting - Commercial aircraft

[SAE ARP 1161]

08 p0925 A73-20692

Contributions to the design of future on-board data processing systems for scientific space-craft experiments

09 p1061 A73-23379

Megabit capacity ferrite core memories for scientific satellites, using three dimensional organization with pulse program adapted for buffer application

09 p1087 A73-23426

Naval satellite communications terminal design for shipboard use to meet low cost, small size, light weight and printed circuit module replacement demands

12 p1471 A73-27661

Aircraft onboard data link and Aerosat equipment integration, considering antenna, duplexer, amplifier and receiver systems

15 p1846 A73-32428

Onboard electronic equipment optimization and redundancy

15 p1852 A73-32460

New structure of on-board microcomputers using large-scale integrated logic circuits

15 p1852 A73-32478

System of recording based on partial on-board processing

15 p1880 A73-32494

Early operational experience with the L-1011 On-Board Weight and Balance System

[SAWE PAPER 986]

19 p2386 A73-37890

Aircraft and spacecraft radio navigation systems, discussing Doppler, inertial and VHF omnirange techniques, Apollo spacecraft guidance systems, TACAN, Harrier and Swedish SAAB37 aircraft navigation

21 p2736 A73-40514

Study of cosmic rays by the Prognostic satellites

21 p2756 A73-40577

Russian book on aircraft onboard instruments and equipment arrangement and housing for weight reduction covering electric, radar, navigation, control, display and auxiliary devices

21 p2635 A73-41425

ONBOARD NAVIGATION

U NAVIGATION

ONE DIMENSIONAL FLOW

An investigation of particle trajectories in two-phase flow systems

01 p0002 A73-10439

Numerical solution of one-dimensional non-steady flow with supersonic and subsonic flows and heat transfer

01 p0003 A73-10765

- One-dimensional electrohydrodynamic flows with a variable mobility coefficient - Evaporation and condensation discontinuities
01 p0077 A73-10954
- Equations of motion in electrohydrodynamics of multiphase one dimensional flow, noting shock wave propagation and attenuation
03 p0346 A73-13611
- Unsteady one-dimensional compressible frictional flow with heat transfer.
03 p0298 A73-14639
- One-dimensional shock waves in heat conducting materials with memory. II.
04 p0511 A73-15225
- MHD-rotation of a conducting fluid in a rotationally symmetric electromagnetic field
05 p0603 A73-16590
- A one-dimensional flow model for an air-augmented rocket.
05 p0607 A73-16848
- One dimensional steady electrohydrodynamic duct flow with shock waves for continuous and discontinuous electric fields
06 p0733 A73-18882
- One-dimensional electrogasdynamic flow with shock waves in the case of a small parameter of the electrohydraulic interaction
06 p0733 A73-18883
- Perturbation about one dimensional parabolic flow field in three dimensional boundary layer separation, obtaining skin friction from linear equation eigensolutions
[AD-755557] 07 p0774 A73-19502
- Calculation of one-dimensional hydrodynamic in Eulerian coordinates
09 p1070 A73-21922
- Two phase channel flow behavior from three dimensional phase diagram for one dimensional steady flow of ideal gas carrying solid particles
09 p1072 A73-22621
- A one-dimensional problem concerning the discharge of a two-phase fluid from a nozzle
09 p1073 A73-23353
- One dimensional supersonic shock front location by sonic circle involute point by point plotting, using geometric considerations
09 p1030 A73-23467
- An evaluation of cell type finite difference methods for solving viscous flow problems.
[AD-757443] 11 p1345 A73-25112
- Calculation of the relaxed one-dimensional flow of a gas in a convergent-divergent sonic nozzle
11 p1348 A73-25869
- Simplification of one-dimensional heat-conduction problems in the case of impulsive radiative heating of flat bodies
12 p1558 A73-27317
- Possibility of gasdynamic effects at the critical point of the phase equilibrium
12 p1487 A73-27418
- One-dimensional electrohydrodynamic flows with variable mobility coefficient, evaporation and condensation jumps.
12 p1524 A73-27530
- Numerical solution to transient heat flow problems.
13 p1704 A73-28172
- Variational formalism of a quasi-linear compressible fluid flow with heat exchange.
13 p1602 A73-29022
- Cauchy problem solution for motion of piston generating shock wave after fast impact under influence of one dimensional gas flow
15 p1822 A73-31289
- The local role of the limit line in the well-posing of steady state problems in gas dynamics. I - Problems involving one space dimension.
15 p1862 A73-31328
- Generalized mathematical model for gas turbine dynamic behavior simulation based on one dimensional flow theory with functional integration for rotor speed time derivative
15 p1925 A73-31629
- One dimensional steady electrohydrodynamic duct flow with shock waves for continuous and discontinuous electric fields
15 p1921 A73-32407
- One-dimensional electro-gasdynamic flow with shock waves and a small electrohydraulic interaction parameter.
15 p1921 A73-32408
- Electric analogy procedure for simulating heat and mass transfer processes
16 p2085 A73-33380
- Implicit finite difference scheme for Eulerian fluid dynamics of time dependent one dimensional polytropic gas flow, noting numerical stability
17 p2151 A73-34894
- Numerical solution procedure for calculating the unsteady, one-dimensional flow of compressible fluid /with allowance for the effects of heat transfer and friction/.
[ASME PAPER 73-FE-30] 17 p2153 A73-35022
- Solution by characteristics at fixed time interval of the equations of one dimensional unsteady flow.
18 p2300 A73-36608
- Unsteady combustion of a confined spray.
[AICHE PREPRINT 23] 20 p2626 A73-39250
- Exact solutions of some problems of the Stefan type
20 p2627 A73-39335
- A new method of solving one-dimensional unsteady flow equations and its application to shock wave stability in sonic inlets.
20 p2548 A73-39522
- Incompressible flow planar-nozzle discharge coefficient computations for one dimensional inviscid flow, considering nozzle geometry, flow cross sections and turbulence
20 p2548 A73-39526
- Piecewise-one-dimensional models of supersonic combustion and pseudoshock in a channel
24 p3154 A73-44702
- The calculation of flow in nozzles using a time-marching technique based on the method of characteristics.
24 p3079 A73-44894
- ONISOTROPY**
U ANISOTROPY
ONSAGER RELATIONSHIP
Collisionless magnetoactive plasma nonlinear responses tensors symmetry properties, stressing Onsager relations generalization
01 p0083 A73-10454
- Equilibrium point asymptotic stability for nonlinear generalization of Onsager theory for entropy functions construction with applications to chemical reaction kinetics
20 p2627 A73-39338
- ONTOGENESIS**
U ONTOGENY
ONTOGENY
Maturation of neurobiochemical systems related to the ontogeny of sleep behavior.
03 p0264 A73-14262
- Patterns of reflex excitability during the ontogenesis of sleep and wakefulness.
03 p0264 A73-14264
- Ontogenic cerebrospinal reflex activity studies, covering spinal cord morphology, reflex arches, inhibition, intracranial responses and post-tetanic potentiation
07 p0784 A73-20366
- Relation between the frequency-amplitude characteristics of cerebral electrical activity and gonadotropic hormone excretion levels at various stages of ontogenesis
08 p0930 A73-21319
- Histological studies on the vestibular organ of frog embryos and larvae after the influence of simulated weightlessness.
18 p2270 A73-35979
- Reinforcement of unconscious traces of stimuli in the human being during ontogenesis
19 p2393 A73-37251
- Gravitational effects on animal ontogeny from centrifugation studies of acceleration tolerance, considering egg and embryo development, body composition, etc
22 p2804 A73-42174
- OPACITIES**
U GEMETOCYTES
OPACITY
Fra Mauro crystalline rocks - Mineralogy, geochemistry and subsolidus reduction of the opaque minerals.
07 p0880 A73-19698
- On the He-H2 thermal opacity in planetary atmospheres.
08 p1003 A73-20890
- Particle seeded RF hydrogen plasma opacity, emission spectra, heat transfer and temperature profile at high temperatures
09 p1128 A73-22636
- Opacity probability distribution functions for application to non-grey late-type stars model atmospheres.
09 p1149 A73-23131
- Venus - Microwave opacity of the minor atmospheric constituents.
11 p1417 A73-25267
- Simplified Hartree-Fock approximation for complex atom opacity efficient calculation based on homogeneous one-electron orbital equation solution with effective potential optimization
13 p1662 A73-28455
- Stellar opacity and energy transport based on radiation-matter interactions, discussing radiative transfer, absorption and scattering cross sections, quantum mechanical methods, etc
13 p1682 A73-28987
- CN red system line opacity codes for late star model atmosphere calculation
19 p2488 A73-38513
- Solar neutrinos. IV - Effect of radiative opacities on calculated neutrino fluxes.
20 p2602 A73-39427
- Portable pulse X-ray micro and nanosecond range apparatus for studying fast-going processes in opaque media.
21 p2696 A73-39977
- OPEN PIT MINES**
U MINES [EXCAVATIONS]
- OPENINGS**
NT APERTURES
NT IRISES [MECHANICAL APERTURES]
NT PORTS [OPENINGS]
NT SLITS
Effect of openings on stresses in rigid pavements.
15 p1856 A73-31387
- Torsion and extension of a cylinder with an outer annular cut
17 p2240 A73-34143
- Torsion of a cylindrical shaft having an annular semicircular cutout
17 p2244 A73-34791
- OPERATING SYSTEMS [COMPUTERS]**
Problems of the synthesis of spacecraft onboard data computation units
05 p0553 A73-16417
- Computer protection mechanisms design principles for operating system and hardware architecture implementation, considering access matrix storage, efficiency and subject and object selection
09 p1059 A73-22223
- Computer executive system for design automation file network creation and monitoring to permit input/output operations, storage information updating and display
[AIAA PAPER 73-355] 11 p1334 A73-25492
- Centralized coalition control in data processing systems
15 p1848 A73-31804
- Certain problems in determining the capacity of digital computers
22 p2829 A73-41953
- Large-scale systems and operations management decentralized coalitional control in data processing systems.
23 p2956 A73-44333
- OPERATING TEMPERATURE**
Linear solar collector conversion efficiency over wide operating temperature range via model consisting of long pipe with energy injection at points along length
[ASME PAPER 72-WA/SOL-7] 04 p0408 A73-15802
- Non-steady-state thermal analysis of a rolling aircraft tire.
[SAE PAPER 720871] 05 p0535 A73-16667
- Low peak temperatures and hydrodynamic bearings - Key to long life organic Rankine cycle systems.
09 p1034 A73-22770
- Heat resistant alloys stress-rupture strength tests for operating temperatures based on equivalent high temperatures damageability
09 p1106 A73-23156
- Start/stop motor incremental motion system design for optimal control with minimized energy dissipation and operating temperature under inertial and constant torque load
10 p1198 A73-24023
- Experimental operation of constant temperature heat pipes.
11 p1451 A73-25989
- Low temperature-reactor Brayton cycle for Space Station/Base application.
11 p1311 A73-26013
- Selection of brazing solders according to technical requirements and economy
16 p2026 A73-33350
- Damping properties of turbine blade materials at operational temperatures
17 p2221 A73-34327
- Operational temperature and frequency effects on radial driving point mechanical impedance of damped thin walled ring with mass segments attached by viscoelastic material
20 p2616 A73-39051
- A study of startup regimes of high-temperature heat pipes.
21 p2792 A73-41060
- Development of methods for long-term prediction of heat-resistance characteristics
24 p3099 A73-44768
- OPERATIONAL CALCULUS**
Operational methods for analysis of discontinuous systems with multiple lumped parameter attachments and concentrated forces, obtaining steady state closed form solutions
09 p1159 A73-22648
- OPERATIONAL HAZARDS**
Safety management of air to surface nuclear short range attack missile /SRAM/ at fabrication, testing and operation levels
16 p2073 A73-33640
- OPERATIONAL PROBLEMS**
A mechanistic model for analysis of pulse-mode engine operation.
[AIAA PAPER 72-1184] 12 p1533 A73-27100
- Mobile satellite communication systems constraints imposed by international institution disagreements on management, procurement and operation, considering US and European conflicts on Aerosat project
12 p1471 A73-27653
- Mean risk determination in radio-electronic device control
14 p1735 A73-30291

OPERATIONS RESEARCH

Some remarks on operational problems associated with the introduction of automatic data processing into air traffic control.

15 p1909 A73-32447

Corporate aircraft design and operational problems, including supercritical wing and wasp-waist body design, airport private/airline interfaces, noise criteria, flight simulation and ATC

20 p2509 A73-39218

Skylab flight schedule emphasizing Command Service, Module, discussing meteoroid shield deployment difficulties and rescue team development of solar heat shield

21 p2767 A73-40415

OPERATIONS RESEARCH

Book - Civil aviation development - A policy and operations analysis.

08 p1026 A73-21837

Rational distribution of meteorological stations as a problem of operation studies

15 p1903 A73-31604

Operations research methods application to meteorological forecasting, discussing optimization algorithm and feedback systems

15 p1907 A73-32354

Book - Systems concepts: Lectures on contemporary approaches to systems.

17 p2258 A73-35572

Numerical methods for solving some problems in studies of operations

18 p2331 A73-36985

Linear optimization theory, discussing duality theory, matrix calculations, simplex methods, base points, classical transport problems and industrial production applications

21 p2727 A73-41071

OPERATOR PERFORMANCE

Noise effects on the critical tracking performance of the human operator.

01 p0010 A73-10107

Operator remnant power spectral density measurement during compensatory tracking task by serial segments method, noting Fourier coefficient processing

01 p0011 A73-10324

Variations of evoked potentials during various mental stress situations

03 p0268 A73-13825

Telemetric transmission of ergonomic and time study data to describe work load of radar controllers.

03 p0272 A73-14308

The problem of human efficiency in automated control systems

05 p0542 A73-16410

High resolution radar target recognition, discussing effects of transfer curves of radar signal strength vs display luminance on operator performance

05 p0550 A73-16716

Computer programs for operator performance time prediction and workspace design

05 p0544 A73-16721

Work requirements test program for operator proficiency in tasks analogous to aircraft piloting under difficulty variation, deriving workload capability limits

05 p0544 A73-16722

The employment of a spoken language computer applied to an air traffic control task.

05 p0544 A73-16728

Quality /probability/ evaluation of human operator ergatic processes controlling spacecraft during rendezvous and docking with orbital station

06 p0657 A73-17686

Heuristic response strategies and operator performance errors as function of practice in cross coupled pursuit tracking control tasks

07 p0785 A73-19548

Human operators and automatic adaptive controllers - A comparative study on a particular control task.

07 p0786 A73-20399

Current status of models for the human operator as a controller and decision maker in manned aerospace systems.

07 p0787 A73-20587

Comparison of human operator critical tracking task performance with aural and visual displays.

08 p0936 A73-21667

Determination of the optimal time of continuous work for operators in man-machine systems

09 p1046 A73-22849

Heart activity characteristics in a human operator during a control process

10 p1183 A73-23806

Experimental study of emotional stress in operators

11 p1321 A73-25038

Russian book - Engineering psychology in aviation and astronautics.

15 p1838 A73-31375

Self-estimates of distractibility as related to performance decrement on a task requiring sustained attention.

15 p1839 A73-32394

A comparison of visual, auditory, and cutaneous tracking displays when divided attention is required to a cross-adaptive loading task.

15 p1839 A73-32395

Positioning accuracy with binary selective and fixed gain manual control systems, using finger stick control for operator performance tests

15 p1840 A73-32583

Informative parameters of the psychophysiological state of flight personnel when working with indicators

17 p2114 A73-34237

Nonadjectival rating scales in human response experiments.

17 p2117 A73-35400

A deterministic model of a well trained human operator performing compensatory tracking.

18 p2283 A73-36844

Evaluation of human operator visual performance capability for teleoperator missions.

19 p2397 A73-37327

The air traffic controller and control capacity.

19 p2451 A73-37811

Modeling the human in a time-varying anti-aircraft tracking loop.

19 p2401 A73-38071

Time domain analysis of human operator manual control function for second order oscillatory divergent system with error signals for compensatory tracking

21 p2634 A73-40090

Operator response to sinusoidally varying normal and emergency cycles in dynamic control task, testing anticipatory aversion response ability and error response

22 p2812 A73-41885

Dynamic operative image formation and function features during extrapolation tracking of visibly moving target, noting image reaction to operator performance

22 p2812 A73-41886

Effect of the information panel structure on operator activity

22 p2812 A73-41889

Operator reaction functional readiness manifestation in evoked potential characteristics of stimulus-response situations, obtaining response amplitude distribution

22 p2812 A73-41891

Effect of a subjective ambiguity estimate concerning the duration of work on activity regulation

22 p2812 A73-41892

Ability of a human operator to estimate the probability characteristics of alternative stimuli

22 p2813 A73-41893

Adaptive measurement of vigilance decrement.

23 p2947 A73-43211

Use of a digital computer for studying velocity judgements of radar targets.

23 p2948 A73-43213

Use of a response surface to optimize digital telecommunication systems.

23 p2948 A73-43214

Keeping track of sequential events - Implications for the design of displays.

23 p2948 A73-43215

Optimal work-rest schedules under prolonged vibration.

23 p2948 A73-43217

Performance prediction in a single-operator simulated surveillance system.

24 p3063 A73-44775

Prediction equation validity for response surface methodology analysis of surveillance tracking by human operators, comparing variance and regression procedures

24 p3063 A73-44776

OPERATORS [MATHEMATICS]

NT BERGMAN OPERATOR

Conformal transformation of semiordered linear space via inclusion statement, considering second order differential operators

01 p0069 A73-10068

Iteration approach for elliptic /nonlinear/ difference operators in divergence form

01 p0069 A73-10075

Variational methods for linear numerical filtering with operator and transfer function spreads compromise, presenting graphical data [ONERA, TP NO. 1127]

01 p0070 A73-10236

Reduction of integral equations in elasticity theory to infinite systems

01 p0116 A73-10960

Finite difference solution to Vekua thin shell equations, using differential and equivalent energetic operators

01 p0116 A73-11076

Uniqueness of a solution to an inverse problem in the case of a second order equation with continuous boundary conditions: Regularized sums of a portion of eigenvalues - Factorization of the characteristic determinant

01 p0071 A73-11440

Singular elliptic perturbations of vanishing first-order differential operators.

02 p0186 A73-11970

The deficiency indices and spectrum associated with self-adjoint differential expressions having complex coefficients.

02 p0186 A73-11971

A selfadjoint formulation of overdamped systems.

02 p0193 A73-12093

The representation of functions determined by a class of hypoelliptic operators

02 p0187 A73-12180

Grid model to derive biharmonic difference operators with computer programming application, assessing errors in boundary conditions

02 p0236 A73-12512

Spectrum of the self-adjoint extensions of a minimal operator generated by the Sturm-Liouville equation with an operator potential

04 p0470 A73-14931

Approximate solution of the Cauchy problem by the method of polynomial operators

04 p0470 A73-14936

Stability of the Bubnov-Galerkin method for unstable operator equations with variable coefficients

04 p0470 A73-15068

Hyperbolic equations and systems with multiple characteristics.

04 p0471 A73-15224

On the prediction of the expansion coefficients in a variational calculation.

04 p0471 A73-15228

Proof of the eigenvalues 0 and -1 in the spectra of integral operators of two-dimensional elasticity theory

04 p0514 A73-15677

Russian book - Variational method and the method of monotonic operators in the theory of nonlinear equations.

04 p0472 A73-15963

Fredholm operator theory application to linear feedback system input-output stability in terms of origin encirclement counting in complex plane

05 p0561 A73-16488

Localization principle for a polyharmonic operator expanded in a Fourier series of a fundamental system of functions

05 p0591 A73-16614

Eigenfunction expansions and scattering theory for perturbed elliptic partial differential equations.

06 p0719 A73-18698

Boundary value problems for non-elliptic first-order systems of pseudo-differential operators.

06 p0719 A73-18699

Differential operators transformation into integral functions by Green function and distributions theory methods in structural analysis

06 p0719 A73-18727

The determination of state-space representations for linear multivariable systems.

07 p0804 A73-19131

A proposal for the calculation of characteristic functions for certain differential and integral operators via initial-value methods.

07 p0845 A73-20490

The asymptotic behavior of solutions of second order systems of partial differential equations.

07 p0845 A73-20495

Study of the dynamic theory of BaTiO3 in the cubic phase

07 p0864 A73-20612

Matrix operator theory of radiative transfer for Rayleigh scattering and radiance calculation of multilayered atmospheres with large optical depths

08 p0958 A73-21040

Probability estimates of the accuracy of a solution to the problem of antenna synthesis in the case of an experimental determination of the direct operator of the problem

08 p0946 A73-21104

Solvability of mixed boundary value problems for second-order parabolic equations with degeneration

08 p0983 A73-21126

Fractional exponents of an elliptic operator and parabolic differential equations in spaces of Hoelder-continuous functions

08 p0983 A73-21250

On degenerate elliptic-parabolic operators of second order and their associated diffusions.

09 p1111 A73-21996

Green operator evaluation by Fourier transform method for wave propagation in bianisotropic media, obtaining constitutive equations

09 p1049 A73-22311

Extremum criteria for Gato differentiable mappings in hypercomplex domains derived for nonlinear Chebyshev problems, extending results to partially ordered sets of operators

09 p1112 A73-22581

Stability of certain finite-difference schemes for solving heat conduction equations with a nonself-conjugate elliptic operator

09 p1167 A73-22582

Lie operators admitted by Lamé equations in three dimensional dynamic elasticity theory for arbitrary particle velocity and displacement and linear stress-strain tensor relation

09 p1159 A73-22585

Quantum mechanical operator for photon flux density passing through spatial point over infinite time, interpreting photon wave functions

09 p1094 A73-22598

Equivalent initial conditions for automatic control systems with variable parameters
09 p1069 A73-22943

Dielectric modulation of single mode CW gas laser by acoustic wave, solving equations for creation and annihilation operators to obtain quantum number
09 p1096 A73-22973

The use of operators with degenerated kernel for nonlinear system investigation.
10 p1242 A73-24043

Statistical characteristics of phase variable states and phase operators in optical quantum fields by intrinsic state factorization method
10 p1228 A73-24151

Nonlinear singular multipoint boundary value problems.
10 p1243 A73-24161

Potential operator theory in Hilbert spaces applied to rigorous definition of conservative loading, examining pressure loading case
11 p1434 A73-25212

Statistically orthogonal functions for finite intervals of a random process
11 p1390 A73-25642

A case of application of the variational method in the theory of the eigenfunctions of nonlinear equations
11 p1391 A73-26076

Time-related behavior of causal, anticausal, memoryless and crosscausal nonlinear control systems modeled as operator on group-valued function space
11 p1391 A73-26366

Asymptotic behavior of the eigenvalues of self-conjugate expansions of the Schroedinger operator in a multidimensional bounded domain
11 p1391 A73-26463

Nonlinear plane cavity flow past flexible barrier, deriving uniqueness theorem by variational operator formulation in terms of potentialness conditions
11 p1391 A73-26547

An iterative method for generalized nonlinear complementarity problems.
11 p1391 A73-26577

Stability of the solutions of differential equations with a nonlinear potential operator in a Hilbert space
12 p1516 A73-26959

Boundary value problems in elastoplastic plate theory, obtaining solution through reduction to operator equations
12 p1552 A73-27370

On the reduction of integral equations of the theory of elasticity to infinite systems.
12 p1554 A73-27536

Conditions for convergence of spectral decompositions corresponding to self-adjoint expansions of elliptic operators. IV - Negative-type theorems for arbitrary expansion of a general self-adjoint second-order elliptic operator
12 p1518 A73-27726

Construction of doubly branched fundamental solutions of the Cauchy problem for homogeneous rotationally invariant hyperbolic operators with constant coefficients
12 p1518 A73-27817

Direct numerical solution of three-dimensional equations containing elliptic operators.
13 p1647 A73-28080

Gaussian quadrature formula derivation by integration of linear interpolation operator replacing Hermite polynomial with vanishing derivative for error minimization
13 p1647 A73-28194

Solutions of some Fredholm integral equations using fractional integration, with an application to a forced convection problem.
13 p1704 A73-28413

Conjugating a Chaplygin operator with a differential operator in gasdynamics
13 p1563 A73-28443

Rigorous resolution of the hierarchy of grand-canonical-ensemble Green functions.
13 p1662 A73-28552

Generalized smoothing spline functions for operators.
13 p1649 A73-28604

Mean frequency response characteristics of graphical smoothing operator for latitude observations analysis
13 p1683 A73-29099

Construction of upper and lower functions during approximate integration of a nonlinear system containing a biharmonic operator
13 p1651 A73-29678

The asymptotic behavior of the first real eigenvalue of a second order elliptic operator with a small parameter in the highest derivatives.
14 p1769 A73-30457

Expansion of nonconjugate differential Dirac operators into a series of eigenvalues over the whole axis, and an analytical expression for a spectral matrix-function
14 p1771 A73-30787

Investigation of a weakly generalized solution to the mixed self-conjugate problem of a class of quasi-linear second-order hyperbolic systems with a nonlinear right-hand operator member
14 p1771 A73-30791

Fundamental solution to a single-parameter family of Laplace-parameter difference approximations on a plane
15 p1898 A73-30961

Convergence of the Bubnov-Galerkin method for a type of nonlinear operator equation
15 p1898 A73-30966

Boundary value problems for a first-order differential equation with operator coefficients and for the expansion of this equation in a series of its eigenvalues
15 p1899 A73-31216

Differential operators of constant force and a comparison of differential operators
15 p1899 A73-31217

A solution operator for ordinary differential equations and its application in fluid dynamics
15 p1862 A73-31329

Differential and pseudodifferential operators with an infinite number of independent variables, and their applications
15 p1900 A73-32081

Multivariable linear passive systems
15 p1900 A73-32087

A priori estimates for solution operators of diffusion equations.
15 p1901 A73-32368

The Fredholm alternative in the case of linear approximation-regular operators
15 p1901 A73-32371

Spectral resolution of differential operators associated with symmetric hyperbolic systems.
15 p1901 A73-32373

Integral operators and the first initial boundary value problem for pseudoparabolic equations with analytic coefficients.
15 p1902 A73-32399

Variational principles in nonlinear continuum mechanics.
16 p2036 A73-32979

Book - Non-homogeneous boundary value problems and applications. Volume 3.
17 p2200 A73-34464

Finite element formulation of nonlinear boundary-value problems.
17 p2201 A73-34831

A perturbation method for obtaining approximate solutions of an equation with two small parameters
17 p2201 A73-35046

Numerical techniques in two- and three-dimensional radiation hydrodynamics.
17 p2255 A73-35596

Umbra/finite operator/ calculus in combinatorial theory of special polynomial sequences as technique for expressing one polynomial set in terms of another
17 p2204 A73-35732

Effects of the boundary conditions and of the deformation of a region on the spectrum of operators which are generated by boundary value problems with a spectral parameter contained in the boundary conditions on a boundary section
18 p2329 A73-36161

Formal treatment and optimization of Boolean expressions.
18 p2292 A73-36956

A projection operator algorithm for optimal control problems with unspecified initial state values.
19 p2414 A73-38064

A generalization of the concept of equivalent linearization.
19 p2445 A73-38257

Nonlinear radiation reaction field effects on operator self-field and oscillating dipole, taking into account one-atom spontaneous emission and superradiance theories
20 p2590 A73-38607

Debye representation and multipole expansion of the quantized free electromagnetic field.
20 p2591 A73-38609

Solution of a multipoint problem about the eigenvalues and eigenfunctions of an ordinary linear differential operator using a decomposition technique
20 p2582 A73-39251

Gevrey hypoelliptic differential operators for subelliptic boundary value problems, considering relationship to size of derivative fractional loss in subelliptic estimate
20 p2583 A73-39626

Scalar waves in the mixmaster universe. I - The Helmholtz equation in a fixed background.
21 p2766 A73-40317

Proposal of a new criterion for evaluating the adequacy of models
21 p2669 A73-40499

Initial-value problems for pseudo-parabolic partial differential equations.
21 p2726 A73-40694

Russian book on topological spaces and groups with continuous operations covering rings, Lie group, compact groups, homomorphism, automorphism, isomorphism, etc
21 p2726 A73-40801

Nonequilibrium statistical operators and quasimeans in the theory of irreversible processes
21 p2741 A73-41298

The integrals of the system of Navier-Stokes equations for axisymmetric motion of an incompressible fluid
22 p2841 A73-42123

Electromagnetic field equations in operator form for anisotropic conducting media
22 p2886 A73-42212

Stability of the De Vogelaere method for timewise numerical integration.
22 p2882 A73-42557

Monograph - Singular perturbation problems for partial differential equations.
22 p2882 A73-42715

Singlet s-wave electron-hydrogen scatter below first excitation threshold, computing phase shift in Feshback operator and static exchange approximation
22 p2890 A73-43127

Boundary value problems for elliptic equations in domains with an unlimited boundary
23 p2999 A73-43622

Practical implementation of the perturbation method in an inhomogeneous boundary value problem of thermoviscoelasticity
23 p3046 A73-44189

Perturbation method applications to elasticity theory three-dimensional problems, discussing differential operator construction via recursion relations
23 p3046 A73-44190

Differential operator hypoellipticity, taking into account necessary and sufficient conditions for existence based on Ehrenpreis-Palamodov theorem
23 p3000 A73-44205

Representation of functions of Markov processes as solutions of stochastic equations.
23 p3000 A73-44207

Singular integral equations with a Carleman shift in the case of discrete coefficients and investigation of the Noetherian character of a class of linear operators with involution
24 p3105 A73-44425

Convergence of the Bazley-Fox method in the problem of eigenvalues of a bilinear form relative to another bilinear form
24 p3109 A73-44649

Topology of linear operators in Banach space generalized to invariant polynomials for minimum Schatten ideals in Hilbert space
24 p3105 A73-45008

Topological analysis of integral operators with Agmon kernel in Sobolev spaces within Hilbert space framework
24 p3105 A73-45009

The formation of resonance lines in multidimensional media. II - Radiation operators and their numerical representation.
24 p3113 A73-45041

Interior radiances in optically deep absorbing media. I - Exact solutions for one-dimensional model.
24 p3111 A73-45318

Operator of thin plate reinforced with thin-walled ribs.
24 p3152 A73-45440

Constitutive equations, creep laws, stress functions, variational principles and differential operators in dynamic and static linear viscoelasticity theory
24 p3153 A73-45496

OPERATORS [PERSONNEL]
NT AIRCRAFT PILOTS
NT TEST PILOTS
Solid state neutron radiation dosimeter for hands of medical and industrial personnel working with spontaneously fissionable fuels, describing Th foil detector and automatic spark counter
11 p1361 A73-25312

Continuous radio telemetric recording of pulse rate in radar controllers while on duty
20 p2517 A73-39208

OPHTHALMODYNAMOMETRY
Ophthalmodynamography in pilots to test internal carotid insufficiency - Comparison of blood-pressure responses.
21 p2639 A73-41162

OPHTHALMOLOGY
NT EYE EXAMINATIONS
Ophthalmological assessment of visual functional impairment due to glare, stimulus motion and aging changes
05 p0540 A73-16485

Binocular color resolution capability of the eyes as a function of the characteristics of vision during anisometropia
15 p1832 A73-30999

Vein wall changes as the main cause of acute disturbance of blood circulation in the Vena centralis retinae system
15 p1833 A73-31173

Glaucoma development in aging flight personnel.
18 p2285 A73-36926

OPTICAL ABSORPTION

- Ribes Nigrum anthocyanosides in ophthalmology 18 p2280 A73-36935
- Ocular tension in flying personnel 21 p2637 A73-40347
- Possibilities of barotherapy in ophthalmology 21 p2637 A73-40349
- Fluorescent angiographic technique for fundus oculi 23 p2946 A73-43788

OPTICAL ABSORPTION

U ELECTROMAGNETIC ABSORPTION

U LIGHT TRANSMISSION

OPTICAL ACTIVITY

- Optically active materials light reflection polarization characteristics, comparing theories based on wave vector and permittivity tensor and on polarization/magnetization current constitutive equations 10 p1261 A73-24693
- Solution of a boundary value problem for the oblique incidence of a plane E-polarized wave on a metallic strip array with an optically active medium 13 p1623 A73-29682
- Racemization of amino acids in marine sediments determined by gas chromatography. 23 p2973 A73-43843

OPTICAL AMPLIFIERS

U LIGHT AMPLIFIERS

OPTICAL COMMUNICATION

- Future optical communication systems problems, potentialities and development prospects, considering bandwidth, laser modulation, directionality, fiber transmission, reception, detection, power and efficiency 01 p0018 A73-11066
- Bell Laboratories optical communications research and development on lasers, transmission media, principles, methods and components for systems 01 p0060 A73-11212
- Double-reverse-scatter interference in optical fiber communication systems. 01 p0018 A73-11217
- Optical communication systems with glass fiber waveguide, using semiconductor lasers and photodiodes as transmitters and receivers respectively 01 p0019 A73-11486
- Airborne laser-beam scintillation measurements at high altitudes. 03 p0305 A73-14657
- Phase and frequency tracking accuracy in direct-detection optical-communication systems. 04 p0416 A73-14993
- Active terminal devices for wide band time multiplexed laser PCM communication systems. 04 p0417 A73-15069
- Laser communication lines in atmospheric ground layer, comparing SNR for direct-reception and super-heterodyne video systems 05 p0585 A73-16787
- Electro-optical multiplexers and demultiplexers for time-multiplexed PCM laser communication systems. 06 p0700 A73-18297
- High-frequency electro-optic prism deflector with application to optical demultiplexing and multiplexing. 06 p0701 A73-18363
- Bragg diffraction by standing ultrasonic waves with application to optical demultiplexing. 06 p0701 A73-18364
- Applications for quantum amplifiers in simple digital optical communication systems. 06 p0668 A73-18404
- Multichannel television coupling modulation experiments using a CO2 laser. 07 p0833 A73-19195
- Optical device for three dimensional multiplication of input signal recorded on photographic film, noting pattern recognition and optical communication applications 07 p0823 A73-19909
- Laser beam spreading, deflection and collimation under atmospheric effects on long high path 08 p0938 A73-21028
- Optical birefringent multichannel splitting and combining wideband FDM communications filters, considering crosstalk, pulse response, extinction ratio and detuning 08 p0939 A73-21046
- Optimization of detection systems for quasi-classical optical signals 08 p0940 A73-21558
- Optical communications links with EDM digital data channels, examining signal optimal reception and noise stability 09 p1048 A73-22043
- Atmospheric turbulence effects on laser beam transmitted signals, considering filtering and detection based on doubly stochastic Poisson process 09 p1067 A73-22229
- Double heterojunction [GaAl]As laser pulse modulation at 200 Mbits/sec continuous operation at room temperature, considering lasing delay time and damped oscillations problems 09 p1093 A73-22257
- International Telemetry Conference, Los Angeles, Calif., October 10-12, 1972, Proceedings. 09 p1053 A73-23361

- Decimicrometer band laser operated communication system to link earth observation satellites with geosynchronous satellites, discussing key technologies 09 p1055 A73-23393
- IR laser terrestrial communication system with 5 Mbit/sec digital data capacity, using intracavity optical frequency modulation or frequency shift keying modulation 09 p1055 A73-23394
- Airborne visible laser optical communication experiment between high altitude aircraft and ground station, discussing tracker-transmitter equipment and atmospheric effects on performance 09 p1055 A73-23395
- Optical communication theory application to free space, turbulent and scatter channels, discussing background noise, detector statistical model and quantum receivers 10 p1188 A73-23757
- Internally modulating and multiplexing mode locked Nd-YAG laser techniques for one gigabit optical communication, noting system efficiency improvement over conventional approaches 10 p1227 A73-23783
- Information in the time of arrival of a photon packet - Capacity of PPM channels. 10 p1188 A73-23836
- Depolarization of laser radiation in an optical channel 10 p1229 A73-24612
- Method of increasing the noise immunity of optical communications lines 10 p1190 A73-24615
- Error probability in an atmospheric twin-channel optical link. 10 p1190 A73-24628
- Two dimensional signals Fourier transformations, discussing digital techniques application to linear and optical systems 11 p1397 A73-24993
- Low loss fiber optics communication technology with almost infinite bandwidth potential, discussing transmission lines, light sources, detectors, integrated circuits, systems and applications 11 p1399 A73-26118
- Glass fiber optical waveguides for laser communications systems. 11 p1376 A73-26119
- High data rate YAG laser communication experimental systems with partial cavity dumping, orthogonal setup or harmonic mode locking, investigating internal modulation feasibility 11 p1378 A73-26246
- Stabilized two-pulse operation of the phase-modulated, frequency-doubled laser. 12 p1504 A73-26831
- Use of semiconductor lasers in compact communication systems. 12 p1470 A73-27521
- CO2 laser communication through an urban atmosphere. 13 p1582 A73-28481
- Coherent optical signal superregenerative amplification in Q switched gas laser, calculating sensitivity of He-Ne laser light amplifier 13 p1627 A73-28663
- Calculation of the amplitude of pulse signals at the output of linear filters in optical communications systems. 13 p1583 A73-28671
- Parallel optical channel communications system with separate laser sources for suppressing mode competition noise due to beam intensity fluctuations /beats/ 13 p1584 A73-28898
- Glass fiber for optical communication with existing light source and detector devices, assessing materials and fabrication technology for capacity, attenuation and environmental requirements 13 p1585 A73-29114
- Optical fibre guide measurements with short coherent light pulses. 14 p1756 A73-30056
- Utilization of optical-frequency carriers for low- and moderate-bandwidth channels. 14 p1728 A73-30418
- Spectral analysis of optical pulse signals in application to the problem of synchronizing PCM laser communications lines 14 p1729 A73-30556
- Code division multiplexing system for multiple signal binary transmission in branched glass fiber optical communication network 14 p1729 A73-30696
- Photoelectron statistics and calculation of the characteristics of optical communications lines 15 p1842 A73-31257
- German monograph on data transmission by laser covering analysis of electromagnetic wave diffraction by narrow slits via Mathieu function solution of boundary value problem 15 p1847 A73-32585

- Recent progress in fibres for optical communications. 16 p2023 A73-32862
- GaAs and GaAlAs semiconductor injection lasers: discussing system design and applications for ranging, illumination and communication with peak power and repetition rate requirements 16 p2023 A73-32866
- Fiber laser amplifier properties and light dispersion due to fiber structure and materials in optical communication 16 p2024 A73-32888
- Optical transceiver system requirements for local communications, discussing GaAs light emitting diode lasing modes, transmission links, installation, maintenance and environmental error factors 16 p1978 A73-32888
- Noise immunity of optical communications links with radio and optical AGC systems. 16 p1984 A73-33977
- Error probability of binary optical communications in turbulent atmosphere - Experimental results. 16 p1984 A73-33995
- Optical communication channel optimization with binary signals preamplified in optical parametric amplifier, noting amplifier gain and SNR 17 p2123 A73-35155
- High speed bit synchronizer for mode-locked laser communications. 17 p2138 A73-35220
- The transversely adjusted gap laser for optical communication systems. 17 p2186 A73-35795
- Equivalent circuit and transfer function of the multimode glass fiber with random mode conversions. 20 p2521 A73-38658
- Multimode glass fiber as transmission medium for digital signals. 20 p2521 A73-38659
- Glass fiber transmission characteristics as optical waveguides for communication systems, considering transit time and attenuation 20 p2522 A73-38660
- Double heterostructure lasers for optical communications systems 20 p2572 A73-38664
- Use of laser amplifiers in a glass-fiber communications system. 20 p2522 A73-38667
- A pulse-regenerating optical transmission line. 20 p2522 A73-38668
- Crosstalk compensation in optical beam transmission. 20 p2528 A73-38769
- A semiconductor-laser communication system using differential pulse position modulation. 21 p2656 A73-41094
- Optical communication system performance with tracking error induced signal fading. 21 p2657 A73-41171
- Matched-filter detection of mode-locked laser signals. 22 p2872 A73-43152
- Computer simulation of light pulse propagation for communication through thick clouds. 22 p2828 A73-43156
- Experiments on light pulse communication and propagation through atmospheric clouds. 22 p2828 A73-43157
- A model for estimating joint probabilities of cloud-free lines-of-sight through the atmosphere. 23 p3004 A73-44260
- Optical information transmission over rectangular waveguide communication channels in terms of geometry-wavelength ratio, transparency and repeater functions 23 p2955 A73-44296

OPTICAL CORRECTION PROCEDURE

- Limiting resolution of reconstructed image of focused hologram in electron microscopes as function of aberration and spatial coherence 03 p0309 A73-14088
- Calculation of a photoelectric system for stabilizing the optical axis of an instrument 05 p0575 A73-16316
- Drobyshev stereograph corrector operation for aerial photographs processing with transformed beam of stereoprojector 07 p0824 A73-20043
- Analysis of He-Ne laser surface reflections from an off-axis parabolic mirror. 08 p0974 A73-21032
- Speckle reduction by simulation of partially coherent object illumination in holography. 08 p0964 A73-21037
- Block defocused spherical Fabry-Perot interferometer. 08 p0964 A73-21038
- Schmidt telescopes for northern and southern hemispheres, discussing optical design with achromatic corrector to achieve high angular resolution and conversion to Cassegrain configuration 08 p0966 A73-21366

- Load and support configurations associated with aspherical diopter of revolution with variable thickness profile generating diopters deformed by elasticity
08 p0967 A73-21492
- Modal control applied to the real-time figure control of a spaceborne telescope mirror.
08 p0969 A73-21729
- Aberrations, astigmatism and coma control for far UV stellar spectrograph design by grating shape and ruling space modification
08 p0972 A73-21752
- Laser speckle for determining ametropia and accommodation response of the eye.
11 p1377 A73-26232
- Mathematical principles of optical image deblurring by holography for photographic and electron micrographic applications
11 p1371 A73-26543
- Approximate calculation of the small-reflector surface from the deformations of the large reflector of a Cassegrainian antenna
12 p1480 A73-27235
- Ray optics model analysis for spherical aberration effects on acoustic hologram resolution in image reconstruction, discussing computer generated correction for quality improvement
13 p1615 A73-28591
- Longitudinal and lateral magnification distortion correction in three dimensional long wavelength holography from standpoint of observer visual perception
13 p1616 A73-28596
- Correction formulas for aerial photograph distortions due to internal refraction of light rays in separation of gas media by lateral surface of circular cylinder
16 p2038 A73-34050
- Astronomical optics, including two mirror systems, aspherical plates, lens type field correctors, spectrograph cameras, focal reducers and optical adjustments
17 p2171 A73-35407
- Atmospheric radiative transfer model for correction of Apollo photographic remote imagery data degradation due to radiation scattering
20 p2559 A73-39881
- Television guidance for astronomical telescopes
23 p2984 A73-44362
- ## OPTICAL COUPLING
- Flame-sheet analysis of C.W. diffusion-type chemical lasers. II - Coupled radiation.
01 p0059 A73-10727
- Variable reflectivity unstable laser resonator mode selectivity solution by perturbation analysis for mirror misalignment effects, obtaining Fresnel number and output coupling conditions
01 p0060 A73-11223
- Coupling losses in hollow waveguide laser resonators.
02 p0177 A73-12573
- An experimental study of unstable confocal CO2 resonators.
03 p0320 A73-14456
- Coupling losses between cylindrical multimode fibers and laser diodes
04 p0458 A73-15321
- Laser coupling through nonlinear gas filled absorber cell, discussing molecules mean free path
05 p0585 A73-16783
- Missile guidance and control systems optical linking, using fiber optics and light emitting diodes and photodetectors as optical/electrical transducers
06 p0757 A73-18324
- Normal-mode analysis of anisotropic and gyrotropic thin-film waveguides for integrated optics.
06 p0702 A73-18365
- An antiresonant ring interferometer for coupled laser cavities, laser output coupling, mode locking, and cavity dumping.
09 p1091 A73-22085
- Book - Optical waveguides.
09 p1066 A73-23274
- Frequency selective coupler with thin film waveguides in periodic medium, discussing bandwidth and coupling factor from Brillouin diagram
12 p1504 A73-26827
- Optoelectronic step-up voltage transformer with optical coupling electrical isolation, using light emitting diode and semiconductor film with high photovoltage levels
12 p1496 A73-26964
- An analysis of pulsation in coupled-cavity structure semiconductor lasers.
12 p1505 A73-27014
- A tunnel diode trigger with an optical output
14 p1737 A73-30797
- Effects of mirror reflectivity in a distributed-feedback laser.
16 p2024 A73-33081
- Effect of rotational level coupling on pulse sharpening in CO2 amplifiers.
17 p2143 A73-35791
- Five wave interaction - A possibility for enhancement of optical or microwave radiation by nonlinear coupling to explosively unstable plasma waves.
17 p2218 A73-35821
- Unstable cavities with a central coupling hole in lasers and amplifiers
18 p2322 A73-36559
- Optical coupling system for photon-photon coincidence experiments.
19 p2462 A73-37255
- Perturbation analysis of holographic grating couplers in thin film waveguides, discussing coupling efficiency dependence on evanescent tail length, refractive index and gelatin film thickness
21 p2699 A73-40149
- Theoretical and experimental investigations of the coupling of two glass-fiber light waveguides
22 p2861 A73-42424
- Small signal duality theory of linear optoelectronic circuits with optical coupling for equivalent circuit computerized design and analysis
23 p2963 A73-43615
- Optical directional coupler tolerance improvement by tapered propagation coefficients based on numerical model
23 p2955 A73-44113
- Generation of complex phase-shift-keyed signals by the optical correlation method
24 p3067 A73-44595
- ## OPTICAL DATA PROCESSING
- Image photon counting technique nature, performance, merits, implementation and applications, noting photoelectronic components and image information treatment at quantum level
01 p0048 A73-10529
- Some new techniques for processing remotely obtained images by self-generated spectral masks.
01 p0078 A73-11219
- Digital image processing for the earth resources technology satellite data.
01 p0020 A73-11457
- Digital image-processing activities in remote sensing for earth resources.
01 p0021 A73-11476
- Incoherent optical correlation with a hologram - An example of identifying fingerprints
01 p0054 A73-11489
- Lunar laser ranging system for experimental data acquisition, discussing preliminary design, SNR, photodetection method and data processing
02 p0141 A73-12245
- The data-handling problem with television recording of spectra.
02 p0170 A73-12340
- Computerized analyses of radar photographs.
03 p0281 A73-14524
- Optical Characters Reading and facsimile terminals reduction of message preparation time for electrical transmission in Defense Communications System, considering cost effectiveness and maximum benefit
04 p0418 A73-15380
- Canadian E.R.T.S. data handling system.
04 p0424 A73-15384
- High resolution image data sensors and recorders characteristics and performance limits, describing transmission system
04 p0449 A73-15385
- Real time digital spacecraft TV with data compression/error correction test system, evaluating source encoding algorithm performance from processed picture quality
04 p0449 A73-15409
- Color image quantization error assessment from noninferior bit assignment determination for several coordinate systems by color shift comparison, using computer simulation
04 p0449 A73-15444
- Computerized terrain classification system software features for automatic interpretation of aerial photographic imagery by laser scanning system
04 p0445 A73-15772
- Theoretical and experimental automatic exposure control study.
04 p0451 A73-15775
- Prototype data processing system design for automatic correlation of earth resources image data collected from remote sensors and gyrating vehicle platforms
04 p0426 A73-15776
- Computer development of holographic mass memory plans
05 p0553 A73-16168
- Semiconductor photodetection matrices for holographic memory reading
05 p0553 A73-16170
- Quantitative materials evaluation and inspection with the image analyzing computer.
05 p0575 A73-16288
- Investigation of color detail, color analysis and false-color representation in satellite photographs.
05 p0578 A73-17136
- Automatic analysis and classification methods based on statistical characteristics of aerial photometric and TV photographs, noting contour related interval distribution
05 p0579 A73-17143
- Two dimensional digital Fourier transform applications to picture processing, noting economy in computer storage
05 p0554 A73-17146
- A digital processing and analysis system for multispectral scanner and similar data.
05 p0554 A73-17147
- Rapid processing of multispectral scanner data using linear techniques.
05 p0554 A73-17150
- An integrated feature selection and supervised learning scheme for fast computer classification of multi-spectral data.
05 p0555 A73-17153
- Automatic classification by sequential statistical variance and K-means clustering techniques for remote multispectral earth resource observation data
05 p0555 A73-17154
- Universal data system for image processing of earth resources observations, discussing input/output film, tape and multispectral data, interactive control and video color displays
05 p0555 A73-17155
- Carrier-frequency photography - Principle and application of lattice-coded image tracing
06 p0692 A73-17754
- The reconstruction of three-dimensional objects from two orthogonal projections and its application to cardiac cineangiography.
06 p0657 A73-17801
- The representation and matching of pictorial structures.
06 p0692 A73-17804
- Picture information acquisition, storage and transmission characteristics of film and vidicon systems for photographic reconnaissance of planets
06 p0750 A73-18010
- Ancillary information effects on photointerpretation performance under four imagery system operation modes, noting identification accuracy independence on information variables
06 p0658 A73-18245
- Coherent optical processing and display techniques for microwave imagery generation from synthetic aperture radar system data, discussing hologram and side-looking radar
06 p0667 A73-18279
- Real time coherent electro-optic two dimensional on-line spatial light modulator role in optical data processing system
06 p0693 A73-18286
- Coherent and non-coherent optical processing of analog signals.
06 p0667 A73-18313
- Viking lander vehicles ground reconstruction equipment for Martian surface digital magnetic tape video data conversion into high quality hard copy
06 p0683 A73-18321
- Aerial imagery data statistical processing, discussing probability density and autocorrelation functions and power spectra for automatic pattern recognition
06 p0695 A73-18322
- Electron-beam tube with semiconducting laser screen.
06 p0677 A73-18636
- Quantitative temperature data from Direct-Readout Infrared (DRIR) pictures.
06 p0696 A73-18711
- A non-parametric method with applications to pattern recognition and mode estimation.
06 p0672 A73-18805
- Quantitative size and shape analyses of Apollo 14 and 15 fines by computer evaluation of scanning electron microscope images
07 p0898 A73-19898
- Computer aided recognition of objects shapes on aerial photographs, discussing image derivatives and histograms use and flying spot scanner principle
07 p0825 A73-20165
- Endogenic craters count and measurement by Hyginus Rille floor, establishing size distributions by Lunar Orbiter 5 photographs processing
07 p0900 A73-20278
- German monograph - Properties and dimensions of storage image intensifiers with lens raster storage, magnetic guiding field and micro lens cathode.
07 p0803 A73-20392
- Auto- and cross-correlations of diffuse objects for coherent optical data processing, using single lensless Fresnel hologram
08 p0963 A73-21036
- Relation between object position and autocorrelation spots in the Vander Lugt filtering process. II - Influence of the volume nature of the photographic emulsion.
08 p0964 A73-21044
- Lunar control densification with panoramic space photography.
08 p0968 A73-21702
- An automated two-channel scanning spectrophotometer system.
08 p0970 A73-21740
- Real time display, processing and image-data products production system for supporting Mariner 9 TV experiment, discussing computer algorithms
09 p1080 A73-22266
- Reduction of lunar panoramic photography on the analytical stereoplotter.
09 p1081 A73-22379

Holographic laboratory practice for NDT, discussing data reduction, display and pulse laser development

09 p1083 A73-22513

TV vidicon image converter with arbitrary scanning format and computer-compatible output signals, using power spectrum redistribution functions

09 p1060 A73-22945

Communication system for digital image processing services over Advanced Research Project Agency computer network, describing hardware facilities and software capacity

09 p1061 A73-23390

Adaptive algorithm with error control for line by line encoder for image transmission, noting reconstructed image quality improvement

09 p1055 A73-23392

Block quantizers for encoding pictures at low bit rates, noting maximum nonstationary error signal incurred at block edges

10 p1186 A73-23497

Range-azimuth-coupling aberrations in pulse-scanned imaging systems.

10 p1188 A73-23833

A finite element method for block adjustment problems of photogrammetry.

10 p1218 A73-24291

Adaptation algorithms in multilayer pattern-recognition systems

10 p1192 A73-24502

A probabilistic model of an optical-field and the statistical properties of a videosegment from a vidicon target

11 p1360 A73-25025

Image processing using acoustic surface waves.

11 p1334 A73-25358

Coherent light optical filtering, holographically produced complex filters, imaging systems and pattern recognition multiplex arrangement for optical data processing, discussing image reconstruction

11 p1370 A73-26533

Computer generated binary synthetic holograms, discussing information coding and processing, detour phase effect and kinoforms

11 p1370 A73-26534

Holographic approach to real time correction of optical instruments images, discussing restoration by spatial frequency filtering

11 p1370 A73-26535

A numerical algorithm for identifying spread functions of shift-invariant imaging systems.

12 p1475 A73-27114

Automatic microscopy for mitotic cell location.

12 p1464 A73-27144

Image analysis techniques associated with automatic data base generation.

[AIAA PAPER 73-430]

12 p1499 A73-27823

Instruments and techniques for cartographic processing of space photographs.

12 p1500 A73-27959

Electronic image enhancement in remote sensing by information content reduction before computer read-in, discussing electronic image transformations

12 p1501 A73-27961

Photogrammetric solution for precision processing of E.R.T.S. images.

12 p1501 A73-27964

Graphic display for ultrasonic nondestructive testing.

13 p1615 A73-28586

Reference fringes in holographic interferometry.

13 p1616 A73-28599

Experimental investigation of the direct quasi-optical radio-wave imaging of small objects.

13 p1583 A73-28673

Diffuse auroral belt observation by Isis-2 scanning auroral photometer verified by analysis of ground based all sky photographs

15 p1866 A73-31074

Artificial satellites photographic observations reduction by Turner and colineation methods, considering IBM 360 FORTRAN program application

15 p1843 A73-31648

Satellite rotation period determination from visual photometric observations reduction, noting solar and geomagnetic activity effects

15 p1843 A73-31649

Digital image processing for information extraction.

15 p1875 A73-31800

Computerized stellar spectrogram processing using semiautomatic diagram-code converters, least squares method and reference spectral lines

15 p1878 A73-32141

Implementation of a frog's eye type discriminator, responsive only to pattern changes, as a pre-processor for visual data.

16 p2014 A73-33127

Operational remote sensing; Proceedings of the Seminar, Houston, Tex., February 1-4, 1972.

16 p2002 A73-33351

Controlled-quality images from synthetic-aperture radar data.

16 p2015 A73-33358

Airborne photography with multispectral scanners for remote sensing of large area features, discussing

cost and feasibility of computerized pattern recognition and automatic identification

16 p2015 A73-33361

Digital computer processing for automatic feature classification of ERTS-borne MSS and RBV imagery data, emphasizing interactive man-machine analysis for image enhancement

16 p1985 A73-33366

Hybrid techniques for automatic imagery interpretation.

16 p2016 A73-33367

Compression of weather charts by the segmented Lynch-Davison code.

16 p1983 A73-33744

Certain conclusions concerning the morphometry of sections of the moon photographed by the Luna 12 probe

16 p2065 A73-33779

A real-time simulator for image data systems.

17 p1417 A73-34903

Digital processing of Mariner 9 television data.

17 p1268 A73-34907

The University College London image photon counting system - Performance and observing configuration.

17 p2169 A73-35279

Digital pulse counting astronomical spectrograph system with TV camera tube, image intensifier and minicomputer for camera scan control and video data processing

17 p2169 A73-35282

Imaging techniques in spaceborne X ray astronomy, discussing ray focusing, data processing and observational requirements of single photon detection and high time resolution

17 p2170 A73-35294

Exploration of Mars by Mariner 9 - Television sensors and image processing.

17 p2170 A73-35298

Restoration of degraded images by composite gratings in a coherent optical processor.

17 p2173 A73-35435

Single step detection of blurred images in a coherent optical processor.

17 p2173 A73-35436

Computer processing and analysis of TV cloud photographs.

18 p2334 A73-37058

Recent developments in digital image processing at the Image Processing Laboratory of JPL.

19 p2429 A73-37324

Computer processing of earth resources data from mono- and multispectral band scanners and IR photography

19 p2431 A73-38178

Digital processing of stereoscopic image pairs.

19 p2432 A73-38534

The application of constrained least squares estimation to image restoration by digital computer.

20 p2533 A73-39401

Thermal IR image recording, processing and enhancement, discussing prevention of defects or irregularities caused by aircraft motion, weather and electronic noise

20 p2566 A73-39670

Two-dimensional statistic analysis of radar imagery of sea ice.

20 p2556 A73-39843

Unsupervised maximum likelihood classification technique multispectral remote sensing data, using two-part statistical clustering technique of sequential variance analysis

20 p2559 A73-39879

Multispectral scanner data analysis by application of spectral radiance signature extension techniques based on preprocessing to reduce atmospheric and scanner look angle effects

20 p2559 A73-39880

Environment models and algorithm for obtaining statistically optimal proportions estimates for category mixtures in multispectral sensor data processing

20 p2559 A73-39883

A new method for evaluating and mapping colours in aerial photographs.

20 p2568 A73-39884

Time sensing and analysis of coastal water dynamic features obtained from aircraft and satellite provided sequential photographic data

20 p2560 A73-39885

Southern California coastal processes as analyzed from multi-sensor data.

20 p2560 A73-39886

A statistical-temporal image merging technique for automatic bathymetry applied to southern California coastal waters.

20 p2560 A73-39887

Holographic method of recording temporal characteristics of optical signals.

21 p2695 A73-39958

Automatic surface mapping via holographic system, describing Q switched ruby laser holograms, image disector, computer video signal analysis and scan signals

21 p2699 A73-40150

High-molecular compounds and recording of information on thermoplastic films

21 p2646 A73-40252

A fast IR spectral transform imager.

21 p2699 A73-40272

Russian book on design and operational principles of monopulse and moving target radar, atomic time and frequency measuring devices, radio navigation and optical processing

21 p2650 A73-40342

Optical processing of radar signals

21 p2651 A73-40343

Venus upper atmosphere four-day retrograde rotation derived from statistical analysis of telephoto graphic observation of Y-shaped feature

21 p2767 A73-40366

A wave propagation method for conversion of g pictures into line figures.

21 p2654 A73-40646

On numerical reconstruction of the image from microwave hologram.

21 p2655 A73-41044

Solar photospheric granulation plate statistical properties, establishing two dimensional autocorrelation function and power spectrum as function of wave number

21 p2776 A73-41477

Space-variant system analysis of image motion.

21 p2706 A73-41609

Oceanographic analysis of orbital photographs of the upper Gulf of California.

21 p2692 A73-41634

Preliminary analysis of NASA optical data obtained in barium ion cloud experiment of September 21, 1971

22 p2846 A73-41933

High resolution image formation through the turbulent atmosphere.

22 p2863 A73-43099

Automated data reduction of holographic interferometry translational measurement of diffusely reflecting rigid body by reconstructed virtual image processing on CDC 6600 computer

22 p2863 A73-43147

Numerical method for computer generated kinoform image reconstruction error minimization comparing with random phase method

22 p2863 A73-43148

Multidimensional Fourier transforms and image processing with finite scanning apertures.

22 p2864 A73-43156

Electrooptical radio spectroscopy design for high resolution in time and frequency based on photographic film recording density and coherent optical processing data rate

23 p2980 A73-43374

The use of Skylab and ERTS data in an integrated natural resources development programme.

23 p2973 A73-43782

OPTICAL DENSITY

Investigation of the temporal-spatial distribution of optical density in a plasma of high-current Li and Li discharges

01 p0085 A73-10853

Computerized flying spot scanner/analyzer for automatic mensuration analysis of droplets, particles and cell preparations from 35 mm film density distributions

03 p0309 A73-14445

Random optical density fields pertaining to analysis of aerial photo imaging of aerial topographic objects

06 p0693 A73-18153

Measurement of the transparency of the atmospheric ground layer at different wavelengths

11 p1363 A73-25611

Investigation of the space-time distribution of the optical density of the plasma in high-current Li-Li discharges.

12 p1529 A73-27900

Human cone optical density estimation implication of conflicting results for luminosity at bleaching intensities in dichromats related to use of psychophysical data

14 p1717 A73-30400

Determination of the transmittance of an optically not dense plasma by an intracavity method

24 p3115 A73-44763

OPTICAL DEPOLARIZATION

Depolarization of laser radiation in an optical channel

10 p1229 A73-24611

Relative Raman cross section of O3 for four Ar+ laser frequencies.

20 p2595 A73-38899

OPTICAL EMISSION

U LIGHT EMISSION

OPTICAL EMISSION SPECTROSCOPY

Astronomical telescope research programs emphasizing spectrographic instrumentation to detect and record extragalactic light sources spectra

01 p0046 A73-10500

Laser applications to spectroscopic analysis of Raman, maximum resolution and excited state spectroscopies, and spectral instruments manufacture

02 p0177 A73-12722

Spectroscopic remote sensing of lunar surface composition.
 [AD-756154] 04 p0448 A73-15181
 Apparatus for measuring spectral emissivity of metals.
 08 p0962 A73-20868
 High resolution spectra of the stratosphere between 30 and 200/cm.
 08 p0961 A73-21533
 Spectral shift between components of homogeneous /radiation or shock/ line, using ring laser spatial and frequency burnout effects
 10 p1228 A73-24464
 An interference filter radiometer with cooled optics and a cooled PbS detector for rocket application.
 11 p1368 A73-26507
 Spectral shift between components of homogeneous /radiation or shock/ line, using ring laser spatial and frequency burnout effects
 19 p2438 A73-38136
 Ultrahigh resolution holographic spectroscopy by double exposure of light scattering medium interferogram recording and reconstruction, noting equivalence to use of narrower laser line width
 22 p2861 A73-42413

OPTICAL EQUIPMENT

NT ASTRONOMICAL TELESCOPES
 NT BINOCULARS
 NT CAMERAS
 NT CELESTIALS
 NT CINETHODOLITES
 NT COLLIMATORS
 NT DIFFRACTION LIMITED CAMERAS
 NT DIFFRACTOMETERS
 NT ELECTROPHOTOMETERS
 NT ELLIPSOMETERS
 NT EYEPIECES
 NT FRAMING CAMERAS
 NT HELIOMETERS
 NT HIGH SPEED CAMERAS
 NT IMAGE CONVERTERS
 NT IMAGE TUBES
 NT INFRARED SPECTROMETERS
 NT INFRARED SPECTROPHOTOMETERS
 NT LALLEMAND CAMERAS
 NT MICRODENSITOMETERS
 NT MICROWAVE REFLECTOMETERS
 NT MULTISPECTRAL BAND SCANNERS
 NT NEPHELOMETERS
 NT OPTICAL GYROSCOPES
 NT OPTICAL MEASURING INSTRUMENTS
 NT OPTICAL MICROSCOPES
 NT OPTICAL PYROMETERS
 NT OPTICAL RADAR
 NT OPTICAL RANGE FINDERS
 NT OPTICAL SCANNERS
 NT PANORAMIC CAMERAS
 NT PHOTOMETERS
 NT POLARIMETERS
 NT POLARISCOPE
 NT PRISMATIC BARS
 NT PRISMS
 NT PYROHELIOMETERS
 NT REFLECTOMETERS
 NT REFRACTOMETERS
 NT SCHMIDT CAMERAS
 NT SEXTANTS
 NT SPECTROHELIOGRAPHS
 NT SPECTROPHOTOMETERS
 NT SPECTROSCOPIC TELESCOPES
 NT STRATOSCOPE TELESCOPES
 NT STROBOSCOPES
 NT TELEVISION CAMERAS
 NT THEODOLITES
 NT TRANSITS
 NT ULTRAVIOLET SPECTROMETERS
 NT ULTRAVIOLET SPECTROPHOTOMETERS
 NT WIDE ANGLE LENSES
 NT X RAY TELESCOPES
 Fourier spectrometer design for high resolution solar optical spectra, emphasizing short scan time
 01 p0049 A73-10534
 Bell Laboratories laser optics development and technology applications, discussing CW lasers, light deflectors, holography, optical memories, pattern generator, remote blackboard and micrographs
 01 p0060 A73-11213
 Holo-diagram coherent optics device for studying interference patterns of object near focal points representing illumination and/or observation points
 01 p0053 A73-11220
 Spaceborne high resolution solar telescopes optical systems, discussing construction, alignment and thermal control problems
 02 p0169 A73-12338
 Laser anemometry developments review covering reference-beam, fringe and single-beam modes optical arrangements, signal processing systems and light scattering particles
 03 p0308 A73-13535
 An optical model of a detector of oriented segments of the visual analyzer in animals
 04 p0413 A73-15795

Optical computer technology based on Fourier transform optics and holography, discussing speed and parallel processing capabilities, image deblurring, and applications
 04 p0426 A73-15957
 Calculation of a photoelectric system for stabilizing the optical axis of an instrument
 05 p0575 A73-16316
 Molecular branching-ratio method for intensity calibration of optical systems in the vacuum ultraviolet.
 05 p0597 A73-16495
 Spacecraft-borne optical components and systems design and operational requirements, considering thin film filters and mirrors, detectors, diffraction gratings and materials
 07 p0821 A73-18978
 Optical instrumentation for satellite attitude control, solar direction and earth magnetic field sensors, thermal detection, star tracking and Lunokhod 1 laser reflector
 07 p0821 A73-18979
 The Toulouse centre's space environment simulator - 'The sun.'
 07 p0807 A73-19002
 Optical device for three dimensional multiplication of input signal recorded on photographic film, noting pattern recognition and optical communication applications
 07 p0823 A73-19909
 IR radiometers for free jets sound emission mechanism probing, describing optical and electronic equipment
 [ONERA, TP NO. 1212] 07 p0825 A73-20164
 Russian book - Optoelectronic devices in spacecraft.
 07 p0825 A73-20379
 Holographic optical element for visual display applications.
 08 p0963 A73-21034
 Removal of hydrocarbon contaminant film from spacecraft optical surfaces using a radiofrequency-excited oxygen plasma.
 [AIAA PAPER 72-263] 08 p0989 A73-21835
 Images of truncated triangular-wave periodic targets in optical systems in the presence of linear image-motion.
 10 p1248 A73-23614
 The detection and resolution of incoherent objects by an aberrated optical system in the presence of background noise.
 10 p1229 A73-24618
 Integrated microoptical circuit technology with lenses, prisms, reflectors, mixers, detectors, gratings, filters, lasers, amplifiers and modulators fabricated around waveguides, assessing advantages and potentials
 11 p1399 A73-26117
 Holographic approach to real time correction of optical instruments images, discussing restoration by spatial frequency filtering
 11 p1370 A73-26535
 Optical space astronomy and goals of the large space telescope.
 12 p1497 A73-27436
 A high performance large aperture window for photography from a space platform.
 13 p1621 A73-29326
 The 2.2-m telescope of the Max-Planck Institute for Astronomy
 14 p1743 A73-30273
 Polarization-dependent intensity transmittance of optical systems.
 15 p1913 A73-31125
 Television in the control system of an optical telescope
 15 p1877 A73-32135
 Broadband ultraviolet reflectance filters for space applications.
 15 p1914 A73-32381
 Computerized Ritchey-Chretien computation method for telescopic optical system, controlling mirror shape via transparent screen
 16 p2011 A73-32715
 Design considerations for night-vision system optics.
 16 p2012 A73-32865
 Noise immunity of optical communications links with radio and optical AGC systems.
 16 p1984 A73-33977
 Choice of optimal light characteristics for marks in optical sighting devices
 17 p2114 A73-34241
 Laser guided weapon system optical countermeasures /OCM/ vulnerability evaluation, discussing use of LED laser in computerized simulation at low cost
 17 p2147 A73-35208
 Spacecraft environmental optical contamination problems associated with thermal control surface outgassing.
 [ASME PAPER 73-ENAS-32] 19 p2395 A73-37987
 Experimental test of optical antenna-gain reciprocity.
 19 p2439 A73-38487

Optical system imaging in partially coherent light, noting Rayleigh criterion insensitivity to aberration as characteristic of two-point resolution criteria
 22 p2889 A73-43187

OPTICAL FILTERS

NT INFRARED FILTERS

NT ULTRAVIOLET FILTERS

Long slit spectrographs /Focal reducers - Fabry-Perot spectrographs - Array spectrographs/
 01 p0049 A73-10535
 Ultrashort light pulse generation in lasers with bleachable filters, covering mode formation, secondary effects and two photon recording of emission time structures
 01 p0061 A73-11354
 Filters for solar corona polarization observations, deriving equations for arbitrary settings to obtain data reduction with simplified polarization direction calculation
 02 p0170 A73-12370
 Automatic control for aircraft photographic camera pitch compensation via optical space filters and frequency methods, noting flight velocity to altitude relation
 06 p0693 A73-18154
 Coherent intensity spatial filtering applied to inspection of photolithography masks for LSI.
 06 p0694 A73-18288
 Report on results of research conducted by the Thin Film Department of SEAVOM, under CNES contract.
 07 p0821 A73-18980
 Visualization of thermal fields in saturated porous media by the Christiansen effect.
 08 p0963 A73-21030
 Nebular Fabry-Perot, Pepsios, and Sisam monochromators.
 08 p0964 A73-21039
 Relation between object position and autocorrelation spots in the Vander Lugt filtering process. II - Influence of the volume nature of the photographic emulsion.
 08 p0964 A73-21044
 Coherent optical processing with spatial frequency diversity speckle and reflection noise reduction, discussing coding by illuminating input transparency through square screen mesh
 08 p0964 A73-21045
 Optical birefringent multichannel splitting and combining wideband FDM communications filters, considering crosstalk, pulse response, extinction ratio and detuning
 08 p0939 A73-21046
 Schmidt telescopes for quasars and blue stars radio astronomy in southern sky survey, considering UV filtering-out for image quality improvement
 08 p1011 A73-21362
 The use of solid etalon devices as narrow band interference filters.
 08 p0970 A73-21736
 Method of increasing the noise immunity of optical communications lines
 10 p1190 A73-24615
 An interference filter radiometer with cooled optics and a cooled PbS detector for rocket application.
 11 p1368 A73-26507
 Coherent light optical filtering, holographically produced complex filters, imaging systems and pattern recognition multiplex arrangement for optical data processing, discussing image reconstruction
 11 p1370 A73-26533
 Influence of the spectral characteristics of liquid filters on the thermal regime and efficiency of a neodymium-glass laser
 12 p1505 A73-26891
 Analysis of the information capacity of optical matched filters.
 12 p1498 A73-27516
 Calculation of the amplitude of pulse signals at the output of linear filters in optical communications systems.
 13 p1583 A73-28671
 Rhodamine laser frequency locking using Faraday filter for tuning to sodium D lines
 13 p1628 A73-29249
 Developments in the optical spatial filtering of superposed, crossed gratings.
 13 p1620 A73-29302
 Vacuum evaporation method for manufacturing neutral density filters with nonlinear density profiles.
 15 p1914 A73-32380
 Solutions of certain difference equations describing transformation of the temporal characteristics of radiation in a laser
 16 p2024 A73-32891
 Use of interferential filters for optical control during deposition of reflecting coatings
 17 p2183 A73-34171
 Dichromatic convergence points obtained by subtractive colour matching.
 19 p2398 A73-37420
 An adaptation of the Stromgren four-color system to photographic photometry.
 19 p2430 A73-37568
 Signal/noise ratio in optical radar systems.
 20 p2528 A73-38849

OPTICAL GENERATORS

- Emission spectrum of a Q-switched ruby laser and its dependence on the density of the bleachable filter
21 p2711 A73-40304
- Extraction of Tacheysheff design data for the low-pass dielectric multilayer.
21 p2665 A73-41135
- Lytot birefringent filter contrast element thickness effects on SNR performance and transmission loss
21 p2706 A73-41505
- Matched-filter detection of mode-locked laser signals.
22 p2872 A73-43152

OPTICAL GENERATORS

U LASERS

OPTICAL GYROSCOPES

Russian book - The laser gyroscope.

21 p2704 A73-41295

OPTICAL HETERODYNYING

Earth based and spaceborne stellar interferometer with optical balanced mixer system for coherent detection, discussing principles, construction, SNR and sensitivity

02 p0170 A73-12341

Optical sweep generator using single frequency He-Ne lasers with Michelson interferometer for mode selection to provide smooth tuning throughout Doppler width

03 p0319 A73-14065

Conversion coefficients of optical heterodyne receiver mixer for various amplitude-phase distributions of interfering signal

03 p0319 A73-14067

Sensitivity of optical autodyne quantum receiver in presence of output noise, using photomultiplier signal model

03 p0319 A73-14076

Single band optical mixer heterodyne spectrum analyzer for laser radiation image spectrum suppression

03 p0319 A73-14083

Reciprocity theorem for antenna directivity pattern measurement of optical superheterodyne receiver for carbon dioxide laser radiation

03 p0284 A73-14084

Investigation of the time characteristics of the phase fluctuations of optical waves propagating through the earth atmosphere boundary layer

07 p0792 A73-19914

IR interferometry with heterodyne detection and tuned laser focusing for stellar envelopes, interstellar dust, planetary surfaces and low temperature sources observation

07 p0825 A73-20242

Production of a coherent submillimetric radiation by a heterodyne method

09 p1097 A73-23030

Carbon dioxide laser technological advances and applications including frequency stability systems, remote sensing, air pollution detection, optical heterodyning and pumping

16 p2023 A73-32860

Problems connected with an employment of carbon dioxide lasers in space communications systems

18 p2290 A73-37087

Difference frequency generation by optical mixing of two dye lasers in proustite.

19 p2438 A73-38165

Dispersion characteristic of a three-mode gas laser during modulation of relative excitation

19 p2406 A73-38335

Optical heterodyne radiometry of the solar surface.

20 p2611 A73-39591

General method for the calculation of the frequency of beats in a single-mode ring laser.

20 p2573 A73-39678

Phase measurement microscopy consisting of phase modulation optical system using interferometry and optical heterodyning, and phase detection system using digital processing

21 p2698 A73-40144

Laser mode locking effect on conversion efficiency of beat frequency excitation in multimode emission, using two photon fluorescence method

21 p2712 A73-40308

Maximum SNR performance calculation for heterodyne laser detection system with parameters optimization under assumed total cost

24 p3096 A73-44875

Photomixing of the fundamental and reference laser beams during analysis of the frequency spectrum of laser radiation by the method of optical heterodyning

24 p3096 A73-44955

OPTICAL ILLUSION

Influence of border and background on perception of straightness.

02 p0137 A73-12081

Orientation illusion and masking in central and peripheral vision.

03 p0266 A73-12999

Influence of a visual frame and vertical-horizontal illusion of shape and size perception.

04 p0411 A73-15219

A new illusion - The underestimation of distance during pursuit eye movements.

06 p0656 A73-17575

Sensory, learned, and cognitive mechanisms of size perception.

06 p0657 A73-18031

Apennine Front lineaments origin at Apollo 15 landing site, interpreting topographic irregularities in terms of obliquely incident sunlight illusions

07 p0878 A73-19678

Attention field and perception probability distribution mechanisms of Muller-Lyer illusion due to angle contour

07 p0783 A73-20255

Apparent contraction and disappearance of moving objects in the peripheral visual field.

11 p1318 A73-26198

After-effects of movement contingent on direction of gaze.

11 p1324 A73-26721

Constancy and illusion of apparent direction of rotary motion in depth - Tests of a theory.

13 p1577 A73-28094

Monocular fixation tests and prediction model for time course of aftereffect of eye turn on autokinetic illusion direction

13 p1578 A73-28098

Space-time adaptation of visual position constancy.

17 p2114 A73-34223

The superiority of the pair-comparisons method for scaling visual illusions.

17 p2118 A73-35497

Spatial determinants of the aftereffect of scan motion.

19 p2394 A73-37415

A comparison of the Ponzo illusion with a textural analogue.

21 p2639 A73-41180

Spatial frequency selectivity of a visual tilt illusion.

21 p2642 A73-41642

OPTICAL MASER MODULATION

U LIGHT MODULATION

OPTICAL MASERS

U LASERS

OPTICAL MEASUREMENT

NT ASTRONOMICAL PHOTOMETRY

NT COLORIMETRY

NT ELECTROPHOTOMETRY

NT OPTOMETRY

NT PHOTOMETRY

NT POLARIMETRY

NT SPECTROPHOTOMETRY

NT STELLAR SPECTROPHOTOMETRY

NT ULTRAVIOLET PHOTOMETRY

NT VISUAL PHOTOMETRY

Measurement of the complex index of refraction of atmospheric aerosols using optical spectral analysis techniques.

01 p0045 A73-10375

Theoretical calculation of light scattering and measurements with grating UV double monochromator for anomalous atmospheric transparency

01 p0039 A73-10402

Light polarization measurement with multichannel polarimeters, considering achromatic modulators to convert polarization information into intensity modulation before light beam split into constituent wavelengths

01 p0050 A73-10542

Holographic inspection of shapes of unpolished surfaces.

01 p0051 A73-10835

Measuring the spread function of infrared spectrometers by means of gas lasers.

01 p0060 A73-10838

Spacecraft-borne IR optical remote sensor for detection, identification and distribution measurement of asteroid and meteoroid particles

01 p0105 A73-11205

Measurement of the angular distribution of light scattered from a glass fiber optical waveguide.

01 p0078 A73-11215

Russian papers on nonlinear optics and hyperacoustics covering laser use in ultrasound propagation study and thermal and stimulated molecular light scattering effects

02 p0194 A73-11944

Optical measurements of lunar albedo, angular illumination, diffuse and specular reflectance and scattering coefficients on Mare Fecunditatis regolith powder of various sizes

02 p0213 A73-12238

Fiber-dispersion measurements using a mode-locked krypton laser.

02 p0177 A73-12574

Laser interferometer for measuring high velocities of any reflecting surface.

02 p0171 A73-12818

Line and continuous excitation sources for measuring wavelength dependence, angular distribution and polarization of scattered light intensity in turbulent and laminar flames

03 p0396 A73-12925

German monograph - Effect of spatial partial coherence on the measurement of optical transfer functions.

03 p0343 A73-13813

Calorimetric measurement of optical power from pulsed lasers.

03 p0310 A73-14499

A calorimeter for high-power CW lasers.

03 p0310 A73-14499

Airborne laser-beam scintillation measurements at high altitudes.

03 p0305 A73-14655

Design and field tests of astronomical optical theodolite, noting latitude, longitude and azimuth determination and objective aberration

04 p0447 A73-14844

Application of optical methods to the verification of microscopic data on polymer materials

04 p0468 A73-15699

Optimal optical measurement for two dimensional object position on plane in Gaussian background noise, calculating mean square error for false identification probability determination

05 p0547 A73-16085

Optical transfer function (OTF)/ measurement standards and specification for high quality aerial photographic mapping lens, discussing error sources

05 p0573 A73-16147

Course on Physical and Technical Measurements with Lasers, Erice, Italy, May 8-21, 1971. Proceedings.

05 p0583 A73-16336

Mode locked laser system generated picosecond pulses envelope and phase structure measurement methods

05 p0583 A73-16339

Direct measurement of pulse broadening in the second harmonic of mode-locked Nd:glass laser.

05 p0585 A73-17221

Mars diameter optical measurements by earth based refractor telescopes with birefringent double image micrometer

06 p0747 A73-17489

Ellipsometric polarized light methods application to corrosion technology, discussing surface film optical properties and measurement techniques

06 p0704 A73-17508

He-Ne laser beam intrinsic third order intensity statistical correlation function measurement by digital technique for comparison with calculations

06 p0699 A73-17520

Comparative study of reflectivity measurements performed in the visible and infrared wavelengths.

07 p0824 A73-19945

Optical constants measurement for far IR materials: of crystalline quartz, sapphire, Ge and Si at room temperature and 1.5 K

08 p0994 A73-21045

Spectroelectrophotometer for atmospheric optical measurements in the near infrared region of the spectrum

11 p1362 A73-25610

Measurement of the transparency of the atmospheric ground layer at different wavelengths

11 p1363 A73-25612

Optical properties of single-component zodiacal light models.

11 p1357 A73-25926

Direct measurement of the fluorescence energy yield of a rhodamine 6G solution with the aid of an Ar+ laser

11 p1377 A73-26146

Method of measuring the parameters of axisymmetric mirror antennas on the basis of the emission of a 'black' disk positioned in the Fresnel region

11 p1332 A73-26162

Interference fringes and surface displacement interrelationship in holographic interferometry, discussing fringe localization, visibility and interpretation after postrecording techniques

11 p1369 A73-26534

Comparison of methods of photomultiplier photocurrent recording in measurements of weak luminous fluxes

12 p1495 A73-26866

Visible and near-infrared transmission and reflectance measurements of the Luna 20 soil.

13 p1674 A73-28303

An absolute method of measuring energy outputs from CO2 lasers.

13 p1626 A73-28365

Moire techniques of incoherent and coherent light filtering, line multiplication and contrast amelioration in framework of physical optics and diffraction theory for stress analysis

13 p1612 A73-28476

Adjustment of thick-film resistors by laser and new pastes for the thick-film technology

13 p1627 A73-28574

Michelson shearing interferometer with piezoelectric scanner for atmospheric optical mean transfer function measurements from airborne platform, using laser or white light sources

13 p1621 A73-29333

On the results of observations of occultations of stars by the moon according to the double image principle

13 p1686 A73-29555

A null-reading method of measuring the complex reflection coefficient in the short-wave end of the millimeter band

14 p1728 A73-30271

Measurement of the temperature coefficient of the refractive index of infrared materials with the aid of a carbon dioxide laser

14 p1757 A73-30371

Q switched ruby laser optical diagnostic system for plasma shock waves and plasmoid observation, noting schlieren photographs of exploding wire experiments

14 p1782 A73-30925

The determination of plasma electron density from refraction measurements.

15 p1916 A73-31085

Temperature and velocity profiles measurement in hybrid rocket engine combustion, using optical method based on Na line reversal technique

15 p1957 A73-31636

Holographic method for measuring spatial coherence functions

15 p1879 A73-32339

Two-component dual-scatter laser Doppler velocimeter with frequency burst signal readout.

15 p1880 A73-32383

Remote measurement of the thickness, distance and velocity of objects by means of a piezoelectric laser beam deflector.

16 p2023 A73-32877

Recent measurements of stratospheric reactions by flash photolysis resonance fluorescence.

[AIAA PAPER 73-502]

16 p2005 A73-33543

Comparison of determinations of the rotational velocity of Venus by radar, optical Doppler effect, and spot measurement methods

16 p2067 A73-33809

High-pressure chamber for optical studies at low temperatures

17 p2164 A73-34174

Assembly for optical studies of semiconductors under pressures up to 10 kbar at 77 K

17 p2145 A73-34175

A rocket-borne instrument for the measurement of nighttime atmospheric densities.

17 p2164 A73-34270

Spectral line absorption measurement using optical cavities.

17 p2184 A73-34913

Single beam spectrophotometer for transmittance measurement constructed from off-axis parabolic mirrors and plane grating monochromator, considering systematic errors

17 p2172 A73-35426

Progress in remote optical analysis of lunar surface composition.

17 p2119 A73-35747

A reflectance analog computer for the determination of thin film optical properties.

17 p2132 A73-35773

Laser measurement of high-altitude aircraft emissions.

[AIAA PAPER 73-704]

18 p2315 A73-36253

Peak height measurement system for pulsed laser experiments.

20 p2572 A73-38876

Application of G. V. Rozenberg's asymptotic formulas in the interpretation of cloud brightness measurements

20 p2584 A73-39189

Method of observing processes in the interior of explosives

21 p2695 A73-39966

Optimum detection of an optical image on a photoelectric surface.

21 p2650 A73-40338

A photometric system for automatic recording of optical absorption spectra

21 p2700 A73-40561

Rocket measurements of electric field and optical aurora during weak PCA event, noting rocket passage through discrete auroral forms

21 p2684 A73-40781

A linear method of autonomous space navigation and guidance

21 p2737 A73-40906

Interference patterns and operation of four unit interferometer consisting of beam splitter, mirrors and analyzer

21 p2704 A73-41261

Residual-stress measurement using surface displacements around an indentation.

21 p2704 A73-41265

Interaction of vision with optical aids.

21 p2645 A73-41608

Speckle effect use in laser photography for vibration and displacement measurement of mechanical systems, discussing diffraction patterns and measurement methods

23 p2982 A73-43675

Holographic shearing interferometer using two linearly polarized reference light beams with application to refractivity and density gradient measurements in aqueous solutions

24 p3088 A73-44406

Optical identifications of radio sources using accurate radio and optical positions.

24 p3135 A73-44579

HF and molecular fluorine refractive indices in visible spectral region computed from interferometer fringe shift vs pressure measurements

24 p3113 A73-44983

Laser Doppler velocimeter measurement of laminar velocity profiles for developing MHD flow in rectangular duct, noting inlet effects on flow development

24 p3118 A73-45464

Laser interferometer for displaying small rapid motions

24 p3092 A73-45468

OPTICAL MEASURING INSTRUMENTS

NT CINETHEODOLITES

NT DIFFRACTOMETERS

NT ELECTROPHOTOMETERS

NT ELLIPSOMETERS

NT INFRARED SPECTROMETERS

NT INFRARED SPECTROPHOTOMETERS

NT MICRODENSITOMETERS

NT MICROWAVE REFLECTOMETERS

NT NEPHELOMETERS

NT OCULOMETERS

NT OPTICAL PYROMETERS

NT OPTICAL RANGE FINDERS

NT OPTICAL SCANNERS

NT PHOTOMETERS

NT POLARIMETERS

NT REFLECTOMETERS

NT REFRACTOMETERS

NT SEXTANTS

NT SPECTROPHOTOMETERS

NT THEODOLITES

NT TRANSITS

NT ULTRAVIOLET SPECTROMETERS

NT ULTRAVIOLET SPECTROPHOTOMETERS

An optical bridge for the assessment of mode-locked CO2 lasers.

01 p0058 A73-10471

Two-stream heterogeneous mixing measurements using laser Doppler velocimeter.

01 p0050 A73-10741

Gas density measurements in a jet using Raman scattering.

01 p0050 A73-10763

Use of a mirror shearing interferometer for gas dynamics research.

01 p0050 A73-10830

Utilization of electro-optical methods in designing angular- and linear-displacement sensors

01 p0052 A73-11074

Observation of upper atmospheric constituents by laser radar systems.

01 p0018 A73-11202

Measurement of particle size, number density, and velocity using a laser interferometer.

01 p0053 A73-11226

Remotely sensing strain-rate meter based on the Doppler shift of laser light.

02 p0168 A73-11961

Molecular fluorine concentration and pressure change monitor based on UV absorption spectrum during chemical reactants mixing, noting measurement accuracy

02 p0168 A73-11967

Optical modeling of antenna radiation patterns by radio holograms of aperture fields

02 p0146 A73-12020

Laser Doppler anemometer theory and application to radial flow velocity measurement in oscillating boundary layer in front of blunt body

02 p0171 A73-12559

Laser applications to spectroscopic analysis, Raman, maximum resolution and excited state spectroscopies, and spectral instruments manufacture

02 p0177 A73-12725

Laser anemometry in an unseeded supersonic wind tunnel by means of photon correlation spectroscopy of backscattered light.

02 p0172 A73-12860

Correlation analysis as applied to the observation of fluctuations of laser light diffracted on an ultrasonic wave in an inhomogeneous medium.

03 p0318 A73-12994

A small model of the Nusselt-Fric diaphanous and position determination

03 p0307 A73-13245

Accuracy requirements for an objectivized astrolabe

03 p0307 A73-13250

Two beam optical recording instrument for atmospheric IR transmissivity, discussing spectrophotometers with changeable NaCl, KBr and LiF prisms

04 p0450 A73-15575

High altitude remote spectroscopy of the ocean.

04 p0451 A73-15779

Holographic interferometry techniques and applications, discussing gas and ruby lasers in imaging, measurements and NDT of materials and mechanical components

05 p0574 A73-16286

OPTICAL MEASURING INSTRUMENTS

A graph-analytical method for precalculation of the moments of solar transition through the field of view of electrooptical systems

05 p0575 A73-16313

Image quality and energy distribution for mirror cone and toroidal annular mirror optical coordinators in wide angle measuring instruments

05 p0575 A73-16318

Laser Doppler velocity measurements in a supersonic flow without artificial seeding.

05 p0576 A73-16361

An optical system for measurement of mean and fluctuating concentrations in a turbulent air stream.

05 p0576 A73-16437

Optical anemometers applicability to steady atomized fuel sprays, obtaining particle velocity profiles and probability density distributions

05 p0565 A73-16761

Measurements of turbulence-transport properties with a laser Doppler velocimeter.

[AIAA PAPER 73-169]

05 p0566 A73-16914

Electro-optical fiducial system for shock wave interferometry relating impact time to free surface motion

05 p0580 A73-17261

Laser velocity meters - A comparative study.

05 p0580 A73-17265

Acousto-optical profilometer system with two diffracted laser beams for surface topography holographic measurements

06 p0694 A73-18290

A dynamic polariscope for stress wave analysis.

08 p0962 A73-20668

A laser optical lever system for measuring the pitch and yaw of a ground-launched rocket.

08 p0974 A73-20669

Optical pyrometers with dual spectral ratios to eliminate instrument error due to selective radiation

08 p0962 A73-20862

Effect of Doppler ambiguity on the measurement of turbulence spectra by laser Doppler velocimeter.

[AD-756047]

08 p0965 A73-21211

Broadening of the measured frequency spectrum in a differential laser anemometer due to interference plane gradients.

08 p0967 A73-21596

New optical measurements of planetary diameters.

IV - Size of the North polar cap of Mars.

09 p1145 A73-22273

Length measurement interferometry principles and limitations imposed by available coherent sources, discussing laser source techniques and fringe counting method

09 p1093 A73-22313

Photo-optic instrumentation of magnetic flyer plate facility for pressure-time response measurement of impact loaded test specimens, using streak and high speed framing cameras

09 p1083 A73-22512

Accuracy of interferometric plasma investigations involving heating of the optical elements

09 p1131 A73-22883

An optical Doppler meter of the velocity of a moving surface

09 p1096 A73-22970

Statistical analysis and computer simulation of laser Doppler velocimeter systems.

10 p1217 A73-23997

Modern developments in flow measurement; Proceedings of the International Conference, Harwell, Berks., England, September 21-23, 1971.

10 p1220 A73-24852

An evaluation of optical anemometers for volumetric flow measurement of liquids and gases.

10 p1221 A73-24858

Laser application for remote analysis of gaseous air pollutants emission based on Raman scattering, resonance fluorescence or absorption measurements

11 p1375 A73-25399

Displacement comparator based on laser interferometer with photoelectric counter for monitoring inside and outside dimensions of cylinder bores, shafts, spheres, etc

11 p1364 A73-26103

Laser speckle for determining ametropia and accommodation response of the eye.

11 p1377 A73-26232

Limitations of the use of vacuum photodiodes in instruments for the measurement of laser power and energy.

11 p1377 A73-26233

Improvement on moire technique for in-plane deformation measurements.

11 p1365 A73-26241

Automatic sensor with parabola null test and ray intercept error measurement for optical system wave front error determination, noting interferometric sensitivity

11 p1365 A73-26242

High temperature density measuring apparatus using the photon attenuation technique.

11 p1367 A73-26309

Hologram interferometry adaptation to industrial conditions for dimensions, deformation, vibration and

refractivity measurements, noting advantages over ordinary interferometry

11 p1370 A73-26540

A system for instantaneous measurement of flame temperature

12 p1557 A73-27071

Optical interferometry for ultrasonic surface wave detection, using two coherent light beams focusing for recording standing wave ratio, attenuation, transmission and harmonic content

13 p1613 A73-28497

Problems of theory and practical application of Doppler-laser rate measuring devices in turbulent flow studies

13 p1628 A73-29169

The comparison of a new constant temperature anemometer with several laser anemometer configurations.

13 p1620 A73-29268

The application of photon correlation spectroscopy to the measurement of turbulent flows.

13 p1622 A73-29421

Experimental measurement of ambiguity noise in a laser anemometer.

13 p1622 A73-29641

Some limiting parameters of an optoelectronic device for determining the orientation of a spacecraft with respect to the sun

14 p1803 A73-29872

Measurement using the Doppler effect of small velocities in flows occurring in the free convection of fluids.

15 p1864 A73-32069

Air quality monitoring instruments involving atmospheric pollution chemiluminescent reactions and CO IR, optical absorption and laser detectors

16 p2016 A73-33402

Optical method for submillimeter band phase measurements by probing spatially separated compared fields and summing two signals at detector

17 p2120 A73-34155

Book - Flow visualization: Optical methods of analyzing fluid flows.

17 p2165 A73-34459

Interferometric surface strain measurement with optical strain gage using laser-generated interference pattern with linear fringe motion-intensity relation [SESA PAPER 2158A]

17 p2173 A73-35453

A flowmeter to measure cloud liquid content.

17 p2174 A73-35578

Large antennas and radomes boresight measurement with angular accuracy by laser mirror system incorporated into pattern range for antenna tower alignment

17 p2143 A73-35696

Wind measurement by magnetometers, optical and static pressure sensors.

18 p2310 A73-36136

The application of a scanning laser Doppler velocimeter to trailing vortex definition and alleviation.

[ALAA PAPER 73-680]

18 p2315 A73-36231

Measurements of aerosol size distributions with a laser Doppler velocimeter (LDV).

[ALAA PAPER 73-705]

18 p2315 A73-36254

Optical wave measurement technique and experimental comparison with conventional wave height probes.

19 p2458 A73-37263

Strain analysis of a disk subjected to diametral compression by means of holographic interferometry.

19 p2429 A73-37264

Compact carbon monoxide sensor utilizing a confocal optical cavity.

[ASME PAPER 73-ENAS-20]

19 p2400 A73-37976

Linear acceleration insensitive balanced rotor seismic angular motion sensor with optical pickoff system, discussing mathematical model and performance tests

[ALAA PAPER 73-829]

20 p2564 A73-38774

Comparison of Langmuir double probe and laser scattering measurements of plasma parameters.

20 p2595 A73-38880

Design study of a glass meridian circle.

20 p2565 A73-39064

Analysis of the control circuit of a seeing measurement device

20 p2565 A73-39069

Frequency-domain analysis of laser Doppler signals for estimation of turbulence parameters.

20 p2572 A73-39130

Argon laser application in a study of velocity in flames

20 p2573 A73-39620

Portable respirable dust monitor for continuous concentration measurement by light scattering of gas laser cavity beam

21 p2708 A73-39923

A high vacuum, low temperature specimen transfer device for use in measuring optical properties of thin films.

21 p2693 A73-39925

Space-variant system analysis of image motion.

21 p2706 A73-41609

Lidar measurements for the exploration of the atmosphere

22 p2823 A73-41825

Measuring transient high temperatures by optical pyrometry.

22 p2853 A73-41989

Laser Doppler instrument for measurement of vibration of moving turbine blades.

22 p2869 A73-42297

Confocal backscatter laser velocimeter with on-axis sensitivity.

22 p2864 A73-43162

The laser-Doppler velocimeter and its application to the measurement of turbulence.

23 p2982 A73-43937

Spectroscopic polarization analysis of turbulent plasma noise produced by the annihilation of opposite magnetic fields

23 p3012 A73-44016

Holographic technique for coherent optical imaging system superresolution via storage of image amplitude

23 p2983 A73-44088

A laser Doppler velocimeter for studying fast gas-dynamic flows

24 p3089 A73-44714

Signal conditioning electronics for a laser vector velocimeter.

24 p3090 A73-44819

Measurement of turbulence transport properties in a supersonic boundary-layer flow using laser velocimeter and hot-wire anemometer techniques.

[ALAA PAPER 73-1045]

24 p3090 A73-44869

Hypersonic flow velocity measurements using laser velocimeter.

[ALAA PAPER 73-1046]

24 p3090 A73-44870

Reducing the level of additive noise in the output signal of a laser velocimeter

24 p3096 A73-44958

OPTICAL MEMORY [DATA STORAGE]

Photodetector array for a holographic optical memory system.

02 p0169 A73-12163

INTERMAG Conference, 10th, Kyoto, Japan, April 10-13, 1972, Proceedings.

07 p0861 A73-19360

German monograph - Properties and dimensions of storage image intensifiers with lens raster storage, magnetic guiding field and microlens cathode.

07 p0803 A73-20392

Application of lens-raster optics for recording holograms with discrete information

09 p1079 A73-21916

Self-enhancement of LiNbO₃ holograms.

09 p1079 A73-21943

Recording of paraseph-coded binary information on phase holograms

09 p1085 A73-22881

Photodetector matrix circuit for holographic memory converting optical bits into electrical signals

09 p1086 A73-23074

Holographic read-only memory with high speed and density optical storage on low-cost changeable media, discussing feasibility model design, construction and test

10 p1216 A73-23796

Photochromic glass as reversible optical recording storage medium, discussing image resolution, configuration improvements, merits and applications in holography, random access memory and displays

11 p1370 A73-26537

Holographic optical memory superiority over conventional localized computer storage devices, considering capacity, access time, immunity to local imperfections, and crosstalk problem

11 p1370 A73-26538

Establishment of hologram memory system with capacity as high as 10,000,000 bits.

13 p1588 A73-29236

Some problems in the optimization of holographic memories.

13 p1622 A73-29435

Study of a read-only optical memory addressed by an array of electroluminescent diodes

14 p1755 A73-29726

High-density image-storage holograms by sampling and random phase shifter method.

15 p1876 A73-31946

Lens raster optics for holograms with digital information.

15 p1880 A73-32642

A fast access holographic memory.

16 p2012 A73-32868

Block organized holographic read only optical memory /ROOM/ model for random access large storage capacities with electro-optical or acousto-optical light deflection system

16 p2012 A73-32869

Fast random access permanent storage read only optical memory, using light emitting diode matrix addressing, semiconductor laser and holographic lens system

16 p2012 A73-32870

Holographic read-write memory, optical organization and capacity enhancement by three-dimensional storage.

16 p2013 A73-32877

High speed serial multiplexed holographic recording for large capacity random access memories, using piezoelectric deflector and ferroelectric ceramic array modulators

16 p2013 A73-32878

Holographic document data recording and storage for single- and multiterminal information processing system, emphasizing Fourier and carrier frequency photography techniques

16 p2013 A73-32879

Optical data storage and data processing, and holography in aerospace and electronic instrumentation.

17 p2131 A73-35135

Holographic coding plate - A new application of holographic memory.

17 p2173 A73-35433

Block oriented random access and read-only archival holographic memories design, considering relationships between lens geometric parameters, laser power and packing density requirements

17 p2173 A73-35433

Increasing the storage density of holographic recording by spatial frequency multiplexing.

20 p2563 A73-38676

Metal-insulator-semiconductor-insulator-metal information storage system with optical write and read operations.

20 p2533 A73-39683

Storage tube with silicon target captures very fast transients.

21 p2661 A73-40222

Characteristics of thin-film metal arrays for laser beam information storage.

22 p2869 A73-42255

Probabilistic analysis of random and deterministic phase coding for lowering Fourier transform spectrum dynamic range in digitally generated hologram and kinoform memories

22 p2864 A73-43141

The behavior of nematic liquid crystals in the electric field

23 p3019 A73-44387

OPTICAL METHODS

U OPTICS

OPTICAL MICROSCOPES

Differential interference contrast microscope with continuously variable wavefront shear and pupil compensation.

05 p0573 A73-16150

Instrumentation for metallographic structure examination.

05 p0576 A73-16755

Incident-light double-refracting interference microscope with variable wavefront shear.

21 p2703 A73-41134

OPTICAL MODULATION

U LIGHT MODULATION

OPTICAL PATHS

Line-by-line computations of transmittance for non-homogeneous paths in designing application-oriented representations for water vapor and carbon dioxide channels IR spectral responses

01 p0037 A73-10366

Heat and mass transfer theory and applications in aerothermoptics, thermoconvective and ferromagnetic fluid studies, chemical engineering, capillary transport and heat pipes

01 p0029 A73-10622

Laser beam spreading, deflection and collimation under atmospheric effects on long high path

08 p0938 A73-21020

Analysis of electromagnetic-wave modes in lens-like media.

10 p1248 A73-23833

Projective properties of an anamorphic bundle of projecting beams

10 p1219 A73-24488

Theory of light deviation by sheets of circular conic geometry

11 p1397 A73-25566

Optical beam hybrid lens waveguide with central aperture and surrounding lens, comparing transmission loss and bending effects with iris guides

11 p1365 A73-26233

Applications of methods of geometric optics in the case of tropospheric propagation

12 p1473 A73-27755

Sensitivity and resolution in holographic interferometry of focused images

13 p1616 A73-28766

Eikonal properties for real rays chromatic aberration formulas in terms of path length, image space and lens parameters

13 p1660 A73-28766

Calculation of the constants of an infinitely narrow beam in spectral devices

13 p1660 A73-28766

The illumination distribution in the image plane from the radiation of a plane-parallel plate with the actual ray paths taken into consideration.

13 p1621 A73-29322

- Calculation of phase difference power spectrum for slant-path propagation. 13 p1661 A73-29327
- A new method for determining the degree of oxygenation of hemoglobin spectra in the case of inhomogeneous light paths, explained in an analysis of spectra of the human skin 20 p2517 A73-39145
- Aircraft measurements of effective photon paths in cloud-reflected and transmitted light in the 0.76-micron oxygen band 20 p2583 A73-39184
- Use of gyro technology to measure small random angular motion. [AIAA PAPER 73-839] 21 p2700 A73-40504
- Electronic fringe-follower for interferometer. 23 p2983 A73-44086
- ### OPTICAL POLARIZATION
- Stress concentration at circular holes in a cylindrical shell of moderate thickness 01 p0114 A73-10480
- Light polarization measurement with multichannel polarimeters, considering achromatic modulators to convert polarization information into intensity modulation before light beam split into constituent wavelengths 01 p0050 A73-10542
- Filters for solar corona polarization observations, deriving equations for arbitrary settings to obtain data reduction with simplified polarization direction calculation 02 p0170 A73-12370
- Viscoelastic properties of amorphous polymers employed in stress investigations by the optical polarization method 03 p0335 A73-13737
- Degree and direction of polarization of multiple scattered light. I - Homogeneous cloud layers. 03 p0344 A73-14427
- Degree and direction of polarization of multiple scattered light. II - Earth's atmosphere with aerosols. 03 p0344 A73-14428
- Discovery of circular polarization in the red degenerate star G99-47. 04 p0502 A73-15687
- Isochromatic curves modeling for stress-strain state of doubly connected regions by optical polarization and photoelastic analysis, using isopach field method. 05 p0578 A73-17092
- Polarization properties of a traveling-wave laser. 06 p0703 A73-18611
- Polarimetric properties of the lunar surface and its interpretation. V - Apollo 14 and Luna 16 lunar samples. 07 p0897 A73-19891
- Stokes polarization parameters of optical emission scattered in absorbing medium calculated for Galaxy and M 82 galaxy, assuming thermal IR radiation from nucleus 07 p0901 A73-20312
- Behavior of threshold current and polarization of stimulated emission of GaAs injection lasers under uniaxial stress. 09 p1092 A73-22247
- Faraday pulsations and circular polarization of optical radiation from cosmic sources in terms of angle between interstellar dust orientation vector and galactic plane 10 p1273 A73-23709
- Optical resolution of DL-aspartic acid in the presence of optically active amino acid and copper (II) ion. 11 p1324 A73-25146
- Polarization of continuous-spectrum emission in the Larger Orion Nebula 11 p1416 A73-25227
- Investigation of thermoelastic stresses by means of 'freezing' involving the realization of a prescribed temperature gradient 11 p1435 A73-25454
- Brightness and polarization of the sky in the solar almucantar in the near infrared region of the spectrum 11 p1353 A73-25604
- Optical characteristics of bright day sky in the visual region of the spectrum and the atmospheric aerosol 11 p1353 A73-25606
- Polarization of the cloudless daytime sky in the 1.25- to 2.42-micron range 11 p1353 A73-25645
- Influence of laser field polarization on nonlinear interference effects. 11 p1377 A73-26180
- Polarization of the emission from the solar corona in the 5303 Å line 12 p1538 A73-26859
- Stokes polarization parameters of optical emission scattered in absorbing medium calculated for Galaxy and M 82 galaxy, assuming thermal IR radiation from nucleus 12 p1539 A73-27284
- Altitudinal variations of the brightness indicatrices and angular characteristics of polarization levels in daytime skies in the 1.27-micron oxygen emission band 13 p1609 A73-29157
- Influence of magnetic spin resonance in optically transparent magnetic materials on the nature of laser radiation 16 p2024 A73-34001
- Theory of optical polarization measurements of the turbulence spectrum in a plasma 17 p2216 A73-34627
- A new non-destructive method for three-dimensional photoelasticity. [SESA PAPER 2143A] 17 p2182 A73-35451
- Faraday pulsations and circular polarization of optical radiation from cosmic sources in terms of angle between interstellar dust orientation vector and galactic plane 18 p2354 A73-36734
- The optical polarization of the Crab Nebula pulsar. I - A relativistic vector model. 19 p2488 A73-38517
- Optical polarization of the Crab Nebula pulsar. II - Observational results and fits by the relativistic vector model. 19 p2488 A73-38518
- Nonlinear light scattering in crystals 19 p2462 A73-38539
- Gas discharge plasma diagnostics based on polarization plane rotation of submillimeter laser radiation 20 p2598 A73-39622
- Interferograms of high optical quality by double exposure. 21 p2695 A73-39963
- Optical mosaics for large field visual simulation display systems. [ALAA PAPER 73-926] 21 p2673 A73-40873
- Polarization characteristics of a regenerative laser with a Faraday cell and a partial polarizer 22 p2870 A73-42721
- Optical orientation in a system of electrons and lattice nuclei within semiconductors - Experiment 23 p3016 A73-44022
- Titan satellite optical polarization observation in three spectral regions, noting inconsistency with scattering from planetary surface or pure molecular atmosphere 24 p3130 A73-44452
- Generation of nonunidirectionally polarized modes by a gas laser oscillator with a mode selector. 24 p3096 A73-45031
- A double image chopping polarimeter. 24 p3091 A73-45185
- ### OPTICAL PROPERTIES
- NT ABSORPTANCE
- NT ABSORPTIVITY
- NT BIREFRINGENCE
- NT BRIGHTNESS
- NT COLOR
- NT DICHROISM
- NT GYROTROPISM
- NT LUMINOSITY
- NT OPACITY
- NT OPTICAL REFLECTION
- NT PHOTOCONDUCTIVITY
- NT PHOTOELECTRIC EFFECT
- NT PHOTOELECTRIC EMISSION
- NT PHOTOIONIZATION
- NT PHOTOVISCOELASTICITY
- NT PHOTOVOLTAIC EFFECT
- NT RADIANCE
- NT REFLECTANCE
- NT REFRACTIVITY
- NT SKY BRIGHTNESS
- NT SPECTRAL REFLECTANCE
- NT STELLAR LUMINOSITY
- NT TRANSMISSIVITY
- NT TRANSMITTANCE
- NT TRANSPARENCE
- NT TURBIDITY
- Investigation of the rheological properties of a model material based on the 'Epidian 2' epoxy resin 01 p0068 A73-10571
- Light waves interaction in nonlinear medium, noting operational principles and optical properties of parametric optical generators with semiconductors 01 p0059 A73-10717
- Transmittance of the atmosphere and the relationship among optical parameters in the ultraviolet spectral region 01 p0040 A73-10873
- Liquid crystal optical and physical characteristics and applications to display design, emphasizing field effect and twisted nematic devices 02 p0201 A73-12083
- The infrared reflection, emission and absorption spectra of regolith from the Sea of Fertility and its scattering coefficient. 02 p0213 A73-12237
- Solar cell optical properties effects on electrical and thermal performance and cost savings in panel design optimization 03 p0255 A73-14226
- Linear and nonlinear optical properties of some ternary selenides. 03 p0350 A73-14458
- Measured physical and optical properties of the passive geodetic satellite /Pages/ and Echo 1. 04 p0446 A73-14809
- Optical band gap energies and stacking sequences of molybdenum tellurides and tungsten selenides derived from dielectric constant measurements 04 p0482 A73-14868
- Quantum kinetic equation for monatomic and molecular gases optical characteristics calculation, considering spontaneous emission spectrum of atoms 04 p0459 A73-15565
- Conformal mapping for Cs ion engine beam optical system with laminar flux, calculating design parameters for current limitation by Cs flow 04 p0488 A73-15722
- Application of the method of least squares to the determination of optical constants of uniaxial isotropic and anisotropic substances, and of the rate of polarization of monochromators in the far UV 05 p0597 A73-16148
- Energy structure, I-V characteristics and optical and photoelectrical properties of heterojunctions between different semiconductor materials, noting interface state effects 06 p0736 A73-18091
- Optical constitutive equation derivation for Tresca type plastic dielectrics, calculating birefringence and extinction angle in simple shear 06 p0723 A73-18458
- Change in sign of thermal lens of glass laser rods with change in thermo-optical constant of glass. 06 p0703 A73-18635
- Optical and thermal properties of hydrated yttrium vanadates in aqueous solutions, showing decomposition during thermal dehydration 06 p0739 A73-18655
- Numerical integration over Brillouin zone for solids spectral properties calculation, considering crystal optical spectra, phonon effects, IR absorption, electron emission and magnetic susceptibilities 07 p0861 A73-19266
- Optical properties of lunar glass spherules from Apollo 14 fines. 07 p0898 A73-19893
- Grain size analysis, optical reflectivity measurements, and determination of high-frequency electrical properties for Apollo 14 lunar samples. 07 p0898 A73-19897
- Energy loss measurements with 60 keV electrons in the case of amorphous and polycrystalline selenium and tellurium and the determination of optical constants 07 p0862 A73-20017
- Optical properties of Nd³⁺/ in lanthanum oxyfluoride single crystals 07 p0837 A73-20205
- Optical resolution of aspartic acid by using copper complexes of optically active amino acids. 07 p0789 A73-20457
- Optical characteristics and structure of the Jovian atmosphere. V - Probable structure of the ammonia aerosol layer. 08 p1012 A73-21577
- The highly reflecting and opaque components in the mineral content of the Haverro meteorite. 09 p1140 A73-21866
- Nonlinear optical susceptibility measurements for zinc silver indium sulfide quaternary compounds, noting agreement with bond charge theory 09 p1120 A73-22090
- Optical properties of Apollo 12 moon samples. 09 p1144 A73-22191
- Thermodynamic and optical properties of elements vaporized by monochromatic laser light, considering carbon and aluminum vapor stream characteristics 09 p1095 A73-22612
- Influence of absorption on the optical properties of solids - Propagation of uniform, plane, heterogeneous electromagnetic waves in isotropic and homogeneous mediums 09 p1121 A73-22963
- Ultraviolet effects on the chemical composition and optical properties of interstellar grains. 09 p1150 A73-23138
- Dioptric apparatus of arthropod compound eyes, describing optical characteristics of apposition eye 09 p1043 A73-23310
- Optical properties of vertebrate eyes. 09 p1043 A73-23312
- Structure diagram, crystal growth, band structure, physical, optical and photoelectric properties of A/II/B/V/ compounds, emphasizing CdSb-ZnSb solid solutions 10 p1258 A73-23566
- Statistical characteristics of phase variable states and phase operators in optical quantum fields by intrinsic state factorization method 10 p1228 A73-24151
- Optical orientation of metastable He-3 atoms and its influence on the electron density and on the emission of helium atoms in a plasma 10 p1257 A73-24755
- CsI optical and photoemission spectra computed from first order allowed transitions between Bloch-wave states, using energy band data 11 p1407 A73-24987
- Optical constants of water in the 200-nm to 200-micron wavelength region. 11 p1350 A73-25060

Optical properties of polydisperse media with different size distributions of particles

11 p1398 A73-25611

Output power saturation with a discharge current in powerful continuous argon lasers.

11 p1377 A73-26179

Optical properties and structure of the atmosphere of Saturn. II - Latitudinal variations of absorption in the CH₄ 0.62-micron line and the characteristic features of the planet in the near ultraviolet

12 p1546 A73-27862

Luna 20: A study of samples from the lunar highlands returned by the unmanned Luna 20 spacecraft.

13 p1674 A73-28301

Atmospheric transparency and the relationships between optical variables in the ultraviolet.

13 p1607 A73-28697

Optical studies of the inhomogeneities of metallic layers deposited in vacuum

13 p1660 A73-28761

Apollo 17 basalt ortho- and para-armalcolite, noting differences in optical properties, crystal habit and distribution between coarse and fine grained rocks

14 p1789 A73-29739

Dispersion relation derivation and approximation applications for generalized optical potential use in analysis of energy dependence of empirical potential strength

14 p1774 A73-30237

International Conference on the Physics of Semiconductors, 11th, Warsaw, Poland, July 25-29, 1972, Proceedings. Volumes 1 & 2.

14 p1783 A73-30572

Aperture synthesis study of neutral hydrogen in NGC 2403 and NGC 4236. II - Discussion.

15 p1929 A73-31057

Propagation laws of a spatially bounded radiation flow in a scattering medium

15 p1903 A73-31324

Study of a narrow-band interference filter at various angles of incidence

16 p2012 A73-32844

Physiological factors and optical parameters as bases of vegetation discrimination and stress analysis.

16 p2003 A73-33355

Changes in the optical properties of minerals and their atomization caused by ion bombardment

16 p1977 A73-33756

Jupiter and Saturn optical observations, discussing atmospheric composition, cloud layers and temperature distribution

16 p2069 A73-33837

Preliminary data on the optical properties of solid ammonia and scattering parameters for ammonia cloud particles.

17 p2211 A73-34858

Aqueous ammonium sulfate aerosol optical properties via attenuated total reflectance /ATR/ spectroscopy

17 p2171 A73-35402

Analysis of multiwavelength observations of optical scintillation.

17 p2212 A73-35418

Mechanical and optical characterization of an anelastic polymer at large strain rates and large strains. [SESA PAPER 2198A]

17 p2198 A73-35458

Optical and luminescent properties of CdBr₂-Sn and CdCl₂-Sn single crystals

17 p2219 A73-35553

Mathematical method for calculating the optical characteristics of cone-shaped cockpit windscreens.

18 p2266 A73-36069

Nature of some optical effects observed on spacecraft at sunrise

18 p2309 A73-36122

Optical stability of coatings exposed to four years space environment on OSO-III.

18 p2336 A73-36351

Operative determination of the characteristics of polydisperse systems

18 p2338 A73-37114

Optical properties of the Mercury surface layer

19 p2480 A73-37233

Coherence and quantum optics; Proceedings of the Third Rochester Conference, University of Rochester, Rochester, N.Y., June 21-23, 1972.

20 p2569 A73-38601

Optical properties and structure of Saturn's atmosphere. II - Latitudinal variations of absorption in the 0.62-micron CH₄ band and characteristics of the planet in the near ultraviolet.

20 p2608 A73-39236

Study of the photoviscoelasticity method

20 p2619 A73-39331

Photoluminescence and optical transmission of diffusion-pump oils.

21 p2698 A73-40139

Materials suitable for making far infrared high-pass transmission filters.

21 p2701 A73-40692

Optical properties of the lower atmosphere of Venus /for interpreting measurements of the Venera 8 planetary probe/

21 p2686 A73-40913

Measurement of the thermo-optical characteristics of satellite thermal control coatings

22 p2929 A73-41872

Optical and electrical properties of doped semiconductors in a strong electromagnetic field.

22 p2896 A73-42252

Design and performance of light-intensification night vision telescopes

23 p2979 A73-43220

Glass and plastic optical fiber properties, performance, limitations and applications

23 p3007 A73-44211

The optical properties of Venus and the Jovian planets. I - The atmosphere of Jupiter according to polarimetric observations.

24 p3129 A73-44442

Terrestrial rock optical constants, finding refractive index and reflectivity for andesite, basalt, basaltic glass, obsidian and obsidian glass through spectrophotometric analysis

24 p3081 A73-44558

OPTICAL PUMPING

Simultaneous two-wavelength selection in the N₂ laser-pumped dye laser.

01 p0058 A73-10126

Use of light pressure for selective evacuation of gases

01 p0059 A73-10627

Parameter calculation and design of synchronization circuit for firing pumping lamp of laser with modulator employing total internal reflection prism for Q switching

01 p0059 A73-10831

An 11 megawatt 6.8 joule flashlamp pumped coaxial liquid dye laser.

02 p0175 A73-11956

Space discharge instability in carbon dioxide laser pumping by ionization source and electric field for time difference in heat removal and gas heating

02 p0177 A73-12553

Condensation of excitons in momentum space under the influence of optical pumping.

02 p0177 A73-12696

Laser oscillation and anisotropic gain in the 1 to 0 vibrational band of optically pumped HF gas.

02 p0177 A73-12747

The generation of tunable near IR radiation using a nitrogen laser pumped dye laser.

03 p0318 A73-12869

Pumping rate in He-Cd laser from metastable atoms concentration measurement and plasma diagnostics, noting upper level population dependence on Penning effect

03 p0319 A73-13753

Spin saturation and pump depletion in continuous spin-flip Raman oscillation.

03 p0319 A73-14452

Internal upconversion and doubling of an optical parametric oscillator to extend the tuning range.

03 p0320 A73-14463

Tunable polarized violet light pulse emission from anthracene doped organic molecular fluorene crystal laser pumped with nitrogen laser, noting pulse amplitude and duration

04 p0458 A73-14873

Molecular iodine photolysis in photodissociative laser due to selective pumping, noting recombination-like storage mechanism

04 p0458 A73-15561

Rb87 vapor maser with optical pumping, measuring nitrogen or nitrogen argon mixture buffer gas partial pressure effect on power output

04 p0459 A73-15920

Study of excitation transfer in a flowing helium afterglow pumped with a tuneable dye laser. I - Measurement of the rate coefficient for selected quenching reactions involving He(5-3P).

05 p0600 A73-16044

Study of excitation transfer in a flowing helium afterglow pumped with a tuneable dye laser. II - Measurement of the rate coefficient for the rotational relaxation of He2(3p 3Pi-g).

05 p0600 A73-16045

New laser technique for the identification of molecular transitions.

05 p0585 A73-16597

Cavity detuning and multimode operation of an optically pumped gas laser.

[AD-758495]

05 p0585 A73-16598

Frequency shift in a mode-selected dye laser.

05 p0586 A73-17225

Short pulse laser based on versatile 60 kV fast switching circuit, noting application as pump source for organic dye molecule solutions

05 p0586 A73-17252

Waveguide properties, modes and optical pumping effects on thin film organic dye lasers, noting temperature effects on refractivity and laser modes

06 p0699 A73-17808

Threshold pump energy value of liquid lasers in quasi-steady-state operation

06 p0699 A73-17915

Five temperature model of pumping and output power pulse shape predictions for carbon dioxide-nitrogen-helium TEA lasers

06 p0701 A73-18362

Emission spectrum of a polyhedral-resonator laser pumped by long pulses.

06 p0702 A73-18390

Nonlinear polarization coefficients of proustite and tellurium.

06 p0738 A73-18590

Time dependence of the gain of an optically pumped solution of rhodamine 6G.

06 p0703 A73-18598

Efficient pumping of a CW garnet laser by water-cooled metal-halide lamps.

06 p0703 A73-18600

110-J pulsed laser using a solution of rhodamine 6G in ethyl alcohol.

06 p0703 A73-18612

Direct overtone excitation of hydrogen fluoride-second vibrational level, measuring global deactivation rate by temperature tuned Nd-YAG laser excited fluorescence technique

06 p0703 A73-18750

Light emitting diode pumped Nd-YAG laser analysis for pumping rate and output dependence on temperature, using circular and transverse intensity distribution

06 p0704 A73-18787

Nitrous oxide laser optical pumping at high pressures with TEA hydrogen bromide laser, considering application to other linear triatomic molecules

06 p0704 A73-18796

Doping dependence of photon yield as a function of excitation energy in optically-excited n-type GaAs at 300 K.

06 p0704 A73-18844

Two-pass-internal second-harmonic generation using a prism coupler.

07 p0834 A73-19539

The effect of an electric field on the active medium in a dye laser.

07 p0834 A73-19540

Saturation resonances by magnetic mode crossing in optical pumping with a multimode gas laser.

07 p0837 A73-20606

Low cost nitrogen laser design for dye laser pumping.

08 p0974 A73-21027

Thin film YAG-Nd laser light sources, discussing material selection, incoherent pumping sources, geometrical configuration, heat dissipation, gain saturation and feedback methods

08 p0975 A73-21143

Relaxation and pumping processes in thermally excited carbon dioxide lasers.

08 p0975 A73-21194

Submillimeter-band gas laser pumped by a CO₂ laser.

08 p0976 A73-21654

High-resolution study of anomalous dispersion in the ruby R lines.

09 p1090 A73-21940

Loss analysis and design improvement for a continuous dye laser.

09 p1090 A73-22080

A tunable flashlamp-pumped dye ring laser of extremely narrow bandwidth.

09 p1091 A73-22083

Room temperature pulsed n-type GaAs cleaved platelet lasers bulk optically pumped near band gap by tunable parametric oscillator, noting emission peak at threshold

[AD-758950]

09 p1092 A73-22240

Broad-band laser emission from optically pumped PbS/1-x/Se/x.

[AD-759091]

09 p1092 A73-22249

A photochemical method of determining the optical pumping energy absorbed by rhodamine dyes under conditions corresponding to stimulated emission of radiation

09 p1095 A73-22668

Influence of thermo-optical distortions on the emission spectrum of a rhodamine 6G laser with incoherent pumping

09 p1096 A73-22972

Optically pumped gas laser steady state solution for population inversion, gain coefficient, radiative intensity and power output, noting Doppler broadening role

09 p1097 A73-23070

Space discharge instability in carbon dioxide laser pumping by ionization source and electric field for time difference in heat removal and gas heating

10 p1228 A73-24182

Effect of concentration on laser threshold of organic dye laser.

10 p1229 A73-24695

Broadly tunable, narrow linewidth dye laser emission in the near infrared.

11 p1375 A73-25366

Influence of excitation power on the energetic characteristics of phthalimide solutions

11 p1376 A73-26143

A plasma-beam discharge laser.

11 p1377 A73-26181

- Superradiant waveguide dye laser pumped by flash lamps, noting power output and stable mode pattern insensitivity to disturbance and thermal effects
11 p1378 A73-26324
- Influence of saturable-absorber transmission and optical pumping on the reproducibility of passive mode locking.
12 p1505 A73-27013
- Continuous-wave laser with a vortex-stabilized lamp.
12 p1506 A73-27503
- Operation of a laser with a planar resonator at high pumping levels.
12 p1507 A73-27507
- Quantum oscillations and pump depletion effects in an efficient high-power tunable spin-flip laser.
13 p1626 A73-28216
- Measurement by double resonance of Lande factors of the 3 s/2l and 2 p/4l of neon pumped optically by a laser beam
13 p1627 A73-28568
- Investigation of the delay of stimulated emission from a CaF₂:Dy²⁺/laser relative to pumping pulses.
13 p1629 A73-29431
- Thermal deformation of an injection laser crystal during the passage of pumping current pulses.
13 p1630 A73-29443
- Damping time of a ruby laser with flat mirrors
13 p1630 A73-29556
- Temperature stability of the disperse phase component of the output emission of an optical quantum amplifier
14 p1758 A73-30576
- Investigation of the excitation of vibrational levels of the /N-14/H3 molecule by carbon dioxide laser radiation
14 p1758 A73-30801
- Injection of a short light pulse into a laser with extensive length of the resonator
15 p1884 A73-31247
- Quantum theory of frequency conversion in nonlinear optics
15 p1886 A73-32330
- High-resolution magnetic hyperfine resonance in harmonically bound ground-state Hg-199 ions.
16 p2038 A73-32850
- Current status of Nd:YAG lasers.
16 p2022 A73-32855
- A review of near-infra-red optically pumped solid-state lasers.
16 p2023 A73-32856
- Lamp pumping system for lasers based on organic compound solutions
17 p2183 A73-34170
- Single mode operation of flashlamp pumped dye laser achieved after emission spectrum line narrowing by interference filter and successive quartz Fabry-Perot etalons
17 p2185 A73-35769
- Stability of the output oscillation amplitude in a linear laser amplifier
18 p2322 A73-36665
- Angular dependence of optically pumped magnetometer - Effects of collisional mixing in the excited states.
19 p2429 A73-37382
- Optimal pumping focusing in parametric single-resonator lasers
19 p2439 A73-38336
- Laser-pumped tunable spin-flip InSb Raman lasers in terms of low field operation, linewidth measurement technique, power output and applications
20 p2571 A73-38623
- Tuning and bandwidth control of laser pumped continuous dye lasers for obtaining stable single axial mode operation
20 p2571 A73-38624
- Stimulated Raman scattering in sulfur hexafluoride.
20 p2574 A73-39688
- Asymptotic nature of threshold conditions and multimode laser emission.
20 p2574 A73-39691
- Quantum theory of nonlinear optical processes with time-dependent pump amplitude and phase - Frequency conversion.
21 p2711 A73-40222
- Amplification of stimulated Raman scattering of light in various nonlinear amplifier pumping circuits
21 p2711 A73-40306
- Lasing mode generation during normal competition in channels with common upper level, assuming line broadening and atomic diffusion
21 p2712 A73-40307
- Laser action from optically pumped epitaxial GaAs crystal waveguides with feedback provided by surface corrugation
21 p2713 A73-40455
- Stimulated emission in multiple-photon-pumped xenon and argon excimers.
21 p2713 A73-40456
- Miniaturized Nd-YAG laser end pumped by single incoherent gallium-arsenide-phosphide light emitting diode to achieve threshold at room temperature
21 p2713 A73-40457
- Carbon dioxide laser pumped dielectric and metallic far IR waveguide, discussing size, mirror coupling and gas medium
21 p2713 A73-40461
- High quantum efficiency IR up-conversion into visible photons through three wave interactions in nonlinear medium, using laser pump light feedback technique
21 p2699 A73-40464
- Excited state absorption spectroscopy of alkaline earths selectively pumped by tunable dye lasers. I - Barium arc spectra.
21 p2713 A73-40472
- Saturation effect in RF spectroscopy for transverse optical pumping.
21 p2713 A73-40473
- H II region OH maser source pumping by far IR radiation-induced population inversions between Lambda doublet levels
21 p2759 A73-40712
- Far IR laser lines measurements in carbon dioxide laser pumped ethylene glycol, dimethyl ether, formic acid, and monomethyl amine, using grating spectrometer and Golay-cell detector
21 p2715 A73-40765
- Generation of reproducible giant pulses with an optically regenerative Q switch.
21 p2715 A73-40959
- Study of excitation transfer in dye mixtures by measurements of gain spectra.
21 p2716 A73-40968
- Self-termination of free oscillations in ruby at low temperatures.
22 p2896 A73-42251
- Nonstationarity of the three-mode regime in a gas laser in the case of mode-frequency symmetry
22 p2870 A73-42388
- Radiation pulse development time instability in electrooptically Q switched lasers due to flash lamp output fluctuations
22 p2870 A73-42722
- Self diffraction of coherent wave radiation by absorption from excited levels of Nd laser light induced phase diffraction gratings in thin layer rhodamine
22 p2870 A73-42723
- Quenching effects in flashlamp-excited polymethine dye lasers.
22 p2871 A73-43083
- High order nonlinear effects in a gas laser - Saturation anomaly observable on a J equals 1 - J equals 2 transition
22 p2871 A73-43084
- Q switched Nd-YAG laser third harmonic for pumping dye laser, extending tunable output range to blue region
23 p2989 A73-44373
- Optically pumped 33-atm CO₂ laser.
24 p3095 A73-44587
- Rapidly fading absorption induced in polymethine dyes by nanosecond pulses of ruby laser radiation
24 p3096 A73-44959
- Microwave optical double resonance spectra of CW dye laser pumped transitions in BaO
24 p3096 A73-44976
- Influence of photodecomposition on the emission of a lamp-pumped dye laser
24 p3098 A73-45518
- OPTICAL PYROMETERS**
High-temperature thermal analysis of high boron alloys using automatic optical pyrometry.
01 p0015 A73-11450
- Opto-thermal gas concentration detector operation by measuring temperature variations caused by chopped laser beam in sample cell, using pyroelectric material as temperature sensor
21 p2701 A73-40691
- Measurement of the heat capacity of graphite in the range 1500 to 3000 K by a pulse heating method.
22 p2881 A73-42510
- OPTICAL RADAR**
Laser radar measurements of atmospheric backscattering turbidity.
01 p0073 A73-10403
- Compact laser radar for remote atmospheric probing.
01 p0060 A73-11059
- Observation of upper atmospheric constituents by laser radar systems.
01 p0018 A73-11202
- Daytime laser radar measurements of the atmospheric sodium layer.
02 p0157 A73-11875
- Detection probability in the case of laser distance measurements involving moving targets
03 p0274 A73-13256
- Simultaneous FM-CW radar and lidar observations of climatological regions, convective activity, cloud echoes, layered structures, insects and breaking Kelvin-Helmholtz waves
03 p0280 A73-14545
- Meteorological lidar use to obtain backscatter curve produced by aerosols suspended in atmosphere
04 p0432 A73-15091
- Large ruby laser radar for remote detection and recording of atmospheric scattering data, describing tracking mount, optics, electronic signal processing and display features
04 p0433 A73-15768
- Tunable dye lidar techniques for measurement of atmospheric constituents.
04 p0423 A73-15769
- Acousto-optical modulator for carbon dioxide lasers based on Bragg scattering concept, discussing design parameters and application to lidar system
06 p0700 A73-18295
- Lidar illuminator/sensor system for range and/or angle spatial resolution enhancement, discussing pulse shape, optical characteristics and atmospheric effects on performance
06 p0667 A73-18303
- A dual polarization laser backscatter system for water quality studies.
06 p0700 A73-18306
- Optimal and suboptimal systems for detecting fluctuating optical radar pulses.
06 p0668 A73-18393
- Radar engineering developments, discussing microwave and optical systems, plan position indicators, antennas, displays, receivers, transmitters, solid state IC devices and signal processing
06 p0668 A73-18440
- Compact laser radar probes the upper atmosphere.
07 p0834 A73-19573
- Remote probing by laser radar.
07 p0793 A73-19947
- Influence of the geometrical parameters of a lidar on the applicability of single-scattering approximation
08 p0986 A73-21457
- Lidar anemometry and atmospheric sounding
08 p0986 A73-21680
- Sierra Nevada mountain lee waves atmospheric structure from lidar, rawinsonde and aircraft observations, delineating atmospheric flow patterns from particulate matter concentrations induced echoes
10 p1245 A73-23988
- Operational features of an FM rangefinder employing a gas laser
10 p1229 A73-24602
- Remote measurement of wind speed by laser Doppler systems.
11 p1375 A73-25062
- FM laser noise effects on optical Doppler radar systems.
11 p1333 A73-26639
- Observation of Raman scattering by SO₂ in a generating plant stack plume.
13 p1607 A73-28547
- Meteorological lidar for determining aerological data above launching base prior to rocket firing
14 p1771 A73-30115
- Observations of aerosol layers in the upper atmosphere by laser radar.
15 p1868 A73-31383
- Lidar measurements of the variability of stratospheric particulates.
16 p2007 A73-33556
- Polarization properties of lidar backscattering from clouds.
17 p2125 A73-35416
- Reflection coefficients for wires, cables, ropes and chains from scanning laser radar, discussing wire avoidance system for airplanes and helicopters
17 p2210 A73-35421
- Remote measurement of atmospheric temperatures by Raman lidar.
17 p2163 A73-35467
- A new lidar for meteorological application.
18 p2353 A73-36708
- Detection probability of laser radars for satellite ranging.
18 p2290 A73-36882
- New developments in FM-CW radar sounding.
19 p2405 A73-38210
- Capabilities of radar, sodar and lidar for measuring the structure and motion of the stably stratified atmosphere.
19 p2405 A73-38239
- Sensor development - An overview of recent Canadian experience.
20 p2533 A73-38578
- Study of laser remote sensing techniques from space platforms.
20 p2521 A73-38591
- Signal/noise ratio in optical radar systems.
20 p2528 A73-38849
- Daytime applications of Raman technique of laser backscatter to measure atmospheric composition profiles
21 p2729 A73-40067
- Lidar measurements for the exploration of the atmosphere
22 p2823 A73-41825
- Optical radar measurements of meteorological parameters and air pollution related to environment protection, using Raman effect and resonance and Mie scattering
24 p3096 A73-44896

- Numerical experiments in laser sounding of aerosol stratification in the atmosphere 24 p3085 A73-44966
- Measurement of short distances with optical pulse radars 24 p3069 A73-45467
- OPTICAL RANGE FINDERS**
- NT LASER RANGE FINDERS**
- Detection probability in the case of laser distance measurements involving moving targets 03 p0274 A73-13256
- Prototype distance measuring instrument for modulated light beam transit time determination 11 p1367 A73-26308
- Detection probability of laser radars for satellite ranging. 18 p2290 A73-36882
- OPTICAL REFLECTION**
- General solution for polarized radiation in a homogeneous-slab atmosphere. 01 p0078 A73-11033
- Reflection and transmission coefficients for stratified media, considering total optical reflection at attenuator and metal film reflector 01 p0078 A73-11229
- Relation of the diffuse reflectance remission function to the fundamental optical parameters. 02 p0193 A73-12350
- Small view field high resolution all-reflective optical image scanner capable of straight line production for space applications 02 p0170 A73-12374
- Surface winds from sun-glitter measurements from a spacecraft. 04 p0474 A73-15777
- Four-field parametric frequency selection in stimulated emission lines from nonlinear mirror, noting reflection coefficient 05 p0584 A73-16554
- Preparation of transmitting coatings for As2S3 glass 05 p0605 A73-17293
- Source limited gray scale and color selection capabilities for direct and reflected light scanners. 06 p0701 A73-18308
- An explanation of transient lunar phenomena from studies of static and fluidized lunar dust layers. 07 p0895 A73-19863
- Equivalence relationships between diffuse radiation fields for finite slabs bounded by a perfect specular reflector and a perfect absorber. 09 p1121 A73-23072
- The emissivity of a system consisting of a semitransparent isothermal coating and a flat opaque substrate 10 p1294 A73-23514
- Analysis of the first laser echoes obtained on the reflector of Luna 21 13 p1686 A73-29561
- Influence of saturation effects on stimulating scattering in laser heating of a plasma. 16 p2041 A73-33079
- Reflected light holographic microscopy of moving objects. 16 p2014 A73-33174
- Lunar surface light reflection phase function, discussing topsoil atomization and brightness distribution over lunar disk 16 p2063 A73-33755
- Calculation of the diffuse reflection and transmission of light by a semiinfinite atmosphere 16 p2066 A73-33791
- Radiating power of a system consisting of a semitransparent isothermal coating and a flat non-transparent substrate. 17 p2212 A73-35194
- Optical effects of cryodeposits on low scatter mirrors. [AIAA PAPER 73-732] 18 p2336 A73-36349
- Aircraft measurements of effective photon paths in cloud-reflected and transmitted light in the 0.76-micron oxygen band 20 p2583 A73-39184
- Diffraction of optical radiation by a reflecting disk in a turbulent atmosphere. 20 p2531 A73-39680
- Generation of high-power light pulses at wavelengths 1.06 and 0.53 micron and their application in plasma heating. I - Experimental investigations of reflection of light of two wavelengths in laser heating of plasma. 20 p2573 A73-39684
- Methods for alignment of lasers with unstable resonators. 20 p2573 A73-39686
- Reflection of a laser beam from an interface between isotropic dielectrics 21 p2714 A73-40569
- Diffraction grating model in terms of amplitude and phase modulation to explain angular spectrum of light reflection from corrugated surface for various incidence angles 21 p2740 A73-40790
- Evaluation of a high accuracy reflectometer for specular materials. 22 p2864 A73-43160

- Leaky rays cause failure of geometric optics on optical fibres. 23 p2955 A73-44105
- OPTICAL RESONANCE**
- Diffraction losses and corrections for lower order transverse modes and resonance conditions in optical resonators with cylindrical mirrors 03 p0319 A73-14079
- Laser optical double resonance and efficient infrared quantum counter upconversion in LaCl3:Pr3+/ and LaF3:Pr3+/+. 09 p1090 A73-21936
- Deformation of laser pulses in resonant media. 09 p1096 A73-22902
- A laser amplifier with resonator natural frequencies misaligned with respect to the gain profile of the active medium 09 p1096 A73-22969
- Enhanced laser-light absorption by optical resonance in inhomogeneous plasma. 11 p1405 A73-25970
- Single-frequency neodymium-glass lasers under nonspiking free-oscillation and Q-switched conditions. 12 p1506 A73-27502
- Propagation of ultrashort light pulses in a semiconductor under two-photon resonance conditions. 13 p1630 A73-29445
- Amplitude characteristics of a helium-neon laser at the 0.63-micron wavelength in the region of strong interaction between two modes. 13 p1630 A73-29446
- Narrow nonlinear resonances of excited molecule densities in a standing wave of light 14 p1775 A73-30802
- Theory of the nonlinear power resonances in gas lasers 14 p1758 A73-30803
- Self-focusing of CO2 laser radiation in resonantly absorbing gases. 17 p2186 A73-35811
- Effect of double optical resonance on frequency interaction and selection in a gas laser 21 p2711 A73-40303
- Nonlinear effects in the emission and absorption spectra of gases in resonant optical fields 21 p2712 A73-40443
- Saturation effect in RF spectroscopy for transverse optical pumping. 21 p2713 A73-40473
- Mode competition in the 3s sub 2-3p sub 4 transition in a neon laser with a methane absorbing cell. 22 p2869 A73-42256
- Distribution of hot phonons generated by laser radiation 23 p2988 A73-44020
- Optical orientation in a system of electrons and lattice nuclei within semiconductors - Theory 23 p3017 A73-44023
- Microwave optical double resonance spectra of CW dye laser pumped transitions in BaO 24 p3096 A73-44976
- OPTICAL RESONATORS**
- Emission spectrum of a polyhedral-resonator laser pumped by long pulses. 06 p0702 A73-18580
- Waveguide resonator structure of an electron-beam-pumped semiconductor laser. 06 p0702 A73-18584
- Possibilities of control of radiation emitted by lasers with telescopic resonators. 06 p0702 A73-18588
- Optimization of the parameters of a quasi-CW YAG:Nd3+/ laser with a nonlinear element in the resonator. 06 p0703 A73-18599
- Resonator polarization parameters effect on backward wave attenuation in three and four mirror TW ring laser, noting colliding waves intensity dependence on polarization angle 06 p0703 A73-18619
- Cylindrical laser resonators with partial radial radiation and strong axial energy focusing, relating low-loss cavity modes to Gaussian beam modes 07 p0833 A73-19273
- Laser beam steering in confocal unstable resonators, interpreting mirror misalignment effects as far field dependence on magnification and Fresnel number from mode solution 09 p1090 A73-22076
- /GaAl/As lasers with a heterostructure for optical confinement and additional heterojunctions for extreme carrier confinement. 09 p1092 A73-22243
- Lasing characteristics of flat resonator carbon dioxide-nitrogen-helium gasdynamic laser in terms of mirror reflection index, resonator length and gas pressure and composition 09 p1095 A73-22609
- Outlet of second harmonic emission for the laser resonant cavity 09 p1097 A73-23011
- Frequency selection schemes based on combined use of dispersive prism and interferometer in laser resonator 09 p1097 A73-23012

- Open resonator operating at 337-micron wavelength 09 p1097 A73-23094
- Density homogeneity in a laser cavity due to energy release. 09 p1098 A73-23450
- Resonator parameters effect on stability characteristics of ultrashort pulse produced by ruby laser using mirror and thin reflector 10 p1227 A73-24076
- Stationary emission of monochromatic spatially-bounded laser beams from active medium with thin lens type inhomogeneity due to flat wave converter/resonator/ structure 11 p1376 A73-26140
- Lowest-order mode selection in a laser interferometer. 12 p1504 A73-26842
- Luminescence line width in ruby crystals of a laser resonator 12 p1505 A73-26892
- Emission of a ruby laser with a moving mirror in the presence of a selector in the resonator 12 p1505 A73-26953
- Properties of unstable resonators with large equivalent Fresnel numbers. 12 p1507 A73-27505
- Influence of a nonlinear lens on the stability of steady-state laser emission. 12 p1507 A73-27506
- Operation of a laser with a planar resonator at high pumping levels. 12 p1507 A73-27507
- Competition between longitudinal modes in a ring laser with an anisotropic resonator. 12 p1507 A73-27508
- Electron-beam tube with a semiconductor target - An electron-beam-pumped scanning laser. 12 p1508 A73-27526
- Separation of rotational lines of a CO2 laser with a film selector in the resonator. 12 p1508 A73-27527
- Theory of the shape of pulses produced by transient parametric generation of light. 13 p1629 A73-29438
- Influence of self-focusing on the stability of steady-state laser emission. 13 p1629 A73-29441
- Generation of opposed waves polarized in different planes in a ring laser 14 p1757 A73-30368
- Measurement of the temperature coefficient of the refractive index of infrared materials with the aid of a carbon dioxide laser 14 p1757 A73-30371
- An optical parametric generator with a large length of nonlinear interaction and weak feedback 14 p1754 A73-30853
- Injection of a short light pulse into a laser with extensive length of the resonator 15 p1884 A73-31247
- Application of the perturbation method in a polarization analysis of anisotropic laser resonators 15 p1886 A73-32334
- Field properties and losses in a three-mirror optical ring resonator with a Gaussian diaphragm 15 p1886 A73-32341
- Geometric magnification and collimation of traveling wave unidirectional unstable ring lasers, comparing with standing wave resonators 15 p1886 A73-32382
- Papers on laser theory covering historical evolution, optical resonators, oscillators, amplifiers, pulse propagation, gain saturation effects, internal modulation, mode locking and noise problems 15 p1886 A73-32424
- Influence of a reflected signal on the operation of a laser 16 p1978 A73-32892
- Detection and measurement of low-level backscattering of laser radiation 16 p1978 A73-32893
- Spectral line absorption measurement using optical cavities. 17 p2184 A73-34913
- Electrooptical Q-switching /EQQS/ in solid-state laser resonators 17 p2184 A73-34917
- Investigation of the characteristics of organic compound lasers with dispersive resonators 17 p2184 A73-34920
- Density nonuniformities in a gas dynamic laser cavity. [AIAA PAPER 73-627] 18 p2321 A73-36174
- An electrooptical modulator based on a coaxial step-shaped resonator 18 p2322 A73-36856
- Generation in a ruby laser with moving mirror and a selector in the resonator. 19 p2438 A73-38137
- Optimal pumping focusing in parametric single-resonator lasers 19 p2439 A73-38336

Single-line operation of a 2-W longitudinal cw CO chemical laser with no frequency-selective element in the optical cavity.

19 p2439 A73-38475

Spatially locked laser mode formation of coherent wave fields with improved angular divergence by degenerate oscillation superposition in laser resonator

20 p2573 A73-39681

Methods for alignment of lasers with unstable resonators.

20 p2573 A73-39686

Coherent oscillation modes of optical waveguide resonators, noting selectivity and thermo-optic insensitivity to pumping and active medium deformation

20 p2574 A73-39692

Calculation of the power of polarized emission from a laser with an anisotropic resonator

21 p2712 A73-40312

Dependence of the induced phase-locking of modes in relationships among laser parameters

21 p2714 A73-40557

Hole-type confocal active optical cavity resonator loss distribution, discussing Fresnel zone oscillation type intensity within resonator and diffraction at cavity

21 p2714 A73-40559

Finite aperture waveguide laser resonators with external reflectors by matrices coupling linearly polarized modes, calculating power efficiency, resonant frequencies and radiation patterns

21 p2714 A73-40760

Laser resonator mode structure during interaction with active medium, considering combined effects of gain and refractivity variations for arbitrary mirror configurations

21 p2714 A73-40761

Influence of mechanical treatment of the resonator on the parameters of an electron-beam-pumped cadmium sulfide laser.

22 p2869 A73-42259

Three-dimensional diffraction calculations of laser resonator modes.

22 p2872 A73-43151

Sealed carbon dioxide laser design for transverse mode output power in terms of beam, transmission loss, Fresnel number and cavity parameters

22 p2872 A73-43155

Collective spontaneous emission of polyatomic systems

23 p2988 A73-44010

A possible Q-factor modulation mechanism in a ruby laser with a misaligned resonator

23 p2988 A73-44047

OPTICAL SCANNERS

NT FLYING SPOT SCANNERS

NT MULTISPECTRAL BAND SCANNERS

A computer-controlled digital spectrum scanner for La Silla.

01 p0047 A73-10515

The coude spectrograph and echelle scanner of the 2.7 m telescope at McDonald Observatory.

01 p0048 A73-10525

Fourier spectrometer design for high resolution solar optical spectra, emphasizing short scan time

01 p0049 A73-10534

Real-time computer for monitoring a rapid-scanning Fourier spectrometer.

01 p0020 A73-11231

Linear photoelectric scanning techniques for achieving high resolution, comparing with two dimensional scanning at telescope or of electronographic images

02 p0169 A73-12332

Small view field high resolution all-reflective optical image scanner capable of straight line production for space applications

02 p0170 A73-12374

Computerized analyses of radar photographs.

03 p0281 A73-14524

Computerized terrain classification system software features for automatic interpretation of aerial photographic imagery by laser scanning system

04 p0445 A73-15772

Optical design of an imaging spectral radiometer for earth resources applications.

04 p0451 A73-15780

A digitally controlled scanning device for a high resolution spectrograph.

05 p0576 A73-16439

Improved mount and alignment procedures for a rapid-scan Fabry-Perot interferometer.

06 p0691 A73-17498

Computer output microfilm system technology assessment, discussing two dimensional acousto-optic laser scanner to write on dry process film

06 p0700 A73-18294

High speed wideband laser scanning technology for extremely small focal points

06 p0701 A73-18307

Source limited gray scale and color selection capabilities for direct and reflected light scanners.

06 p0701 A73-18308

High bandwidth and resolution laser scanners and recorders for imagery transmission, discussing com-

ponent constraints and integrated optics utilization in modulator and scanner development

06 p0701 A73-18310

A four-channel scanning photometer for remote sensing.

07 p0824 A73-19944

A laser scanner for integrated circuit testing.

08 p0974 A73-20731

Television rate laser raster scanner, discussing deflectors, beam-shaping and image-forming optics, electronic system and scanning beam frequency response

08 p0975 A73-21141

Television rate laser scanner with anisotropic Bragg device of paratellurite as acousto-optic horizontal deflector, noting operation efficiency and limiting resolution

08 p0975 A73-21142

Astrometry with Schmidt telescopes, discussing automated computerized plate scanner and measuring machine for star position and relative motion determination

08 p0966 A73-21356

An automated two-channel scanning spectrophotometer system.

08 p0970 A73-21740

The image-readout system of the combination photographic and television scanners of the Mars-2 and Mars-3 automatic interplanetary space probe.

09 p1086 A73-23050

Visible and infrared sensor arrays for imaging systems.

10 p1216 A73-23787

The Coude spectrum scanner at the Lowell Observatory.

11 p1360 A73-25069

Thermal reference system with linear temperature profile down fin axis for thermography, using scanning IR camera as image detector

11 p1366 A73-26305

Real time quantitative display for visible and IR scanning radiometer in ITOS-D satellite-borne automatic picture transmission system with stations access to computers

12 p1520 A73-26811

A progress report on the laser scanned acoustic

13 p1614 A73-28577

Laser beam scanned 1.1 GHz acoustic microscope based on photoconductive CdS piezoelectric transducer

13 p1614 A73-28580

Image contrast in a microscope with synchronous scanning of the object by point or raster field diaphragms

13 p1616 A73-28771

ERTS-1 satellite-borne high resolution multispectral radiometer scanner, discussing optical surface performance during exposure to direct and reflected sunlight

13 p1621 A73-29331

Michelson shearing interferometer with piezoelectric scanner for atmospheric optical mean transfer function measurements from airborne platform, using laser or white light sources

13 p1621 A73-29332

Pick-up storage tube having an electronic shutter, automatic exposure control, wobbling correction, and slow scanning.

14 p1751 A73-29911

Photosensor aperture shaping to reduce aliasing in optical-mechanical line-scan imaging systems.

14 p1753 A73-30161

High speed photoelectric photometer for night sky scanning

15 p1878 A73-32137

The effect of system blocking in an intensifier detector scanner.

17 p2169 A73-35284

A rapid-scanning image intensifier spectrometer for astronomy.

17 p2169 A73-35286

Use of a stable polarization modulator in a scanning spectrophotometer and ellipsometer.

17 p2175 A73-35751

ISIS-II scanning auroral photometer.

19 p2428 A73-37256

Application of a photoelectric area scanner to various astronomical problems

19 p2430 A73-37605

The sensitivity of optoelectronic scanning systems with out-of-phase connection of the radiation detector elements.

20 p2564 A73-38850

Storage tube with silicon target captures very fast transients.

21 p2661 A73-40228

Some problems associated with the construction of scanner employing a cathode-ray tube and programmed control

21 p2665 A73-41270

Multidimensional Fourier transforms and image processing with finite scanning apertures.

22 p2864 A73-43150

First-order probability densities of laser speckle patterns observed through finite-size scanning apertures.

22 p2872 A73-43188

OPTICAL SENSORS

U OPTICAL MEASURING INSTRUMENTS

OPTICAL SIGNALS

U OPTICAL COMMUNICATION

OPTICAL SPECTRUM

U LIGHT [VISIBLE RADIATION]

OPTICAL THICKNESS

Concentration distribution and effective lifetimes of excited atoms at small optical thicknesses of the plasma

01 p0085 A73-11083

Absorption line profile and equivalent line width derivation for planetary atmosphere with low and high optical thicknesses, assuming arbitrary scattering coefficients

01 p1016 A73-11321

On the formation of Saturn's rings.

02 p0225 A73-12805

Measurement of temperature by recording the absolute line intensity with apparent increase of plasma optical thickness.

03 p0348 A73-14439

Small Magellanic cloud large depth along line of sight shown from supergiant stars and cepheids observations

03 p0380 A73-14610

On the radio optical depth of the layer where the temperature equals the brightness temperature.

08 p1002 A73-20761

Radiative and collisional effects in a cylindrically confined plasma. I - Optically thin considerations. II - Absorption effects.

08 p1021 A73-20793

Measurement of the temperature of an optically thick luminous gas layer in the upper atmosphere by the homodyne detection method

08 p0960 A73-21304

Effects of multiple scattering on laser pulses transmitted through clouds.

08 p0976 A73-21423

The relation of brightness phase functions to the optical thickness of the atmosphere.

08 p0986 A73-21585

On the relation between optical scale height and density scale height in a stellar atmosphere.

10 p1281 A73-24406

Correlation between the absolute brightness characteristic of day sky and the optical thickness of the atmosphere

11 p1353 A73-25605

Investigations of atmospheric extinction using direct solar radiation measurements made with a multiple wavelength radiometer.

12 p1520 A73-26810

Radiative transfer theory model of isotropic monochromatic scattering of light in plane layer of finite optical thickness

12 p1538 A73-26862

Mars photographic observations during opposition, analyzing polar caps, surface reliefs, dust storms and atmospheric optical thickness

12 p1542 A73-27498

Luminosity levels in deep planetary atmosphere layers

12 p1536 A73-27858

Solar photosphere turbulent velocity relation to optical depth and deviation from LTE based on Goldberg-Unno method

13 p1683 A73-29093

Reflection and transmission of a narrow beam of light in a thick turbid medium layer with isotropic scattering and absorption

13 p1609 A73-29158

Lyman alpha radiation transfer in spherically symmetric hydrogen nebula from Monte Carlo techniques, computing for different optical depths

13 p1685 A73-29358

Fluctuations of light fluxes propagating in a scattering medium

15 p1903 A73-31323

Transmission of solar radiation by stratified cloudiness as a function of the statistical characteristics of its structure

15 p1905 A73-31796

Atmosphere optical thickness determination from satellite and ground measurements of scattered light in solar vertical

15 p1905 A73-31820

Optical thickness of Saturn rings along cross section from intensity of radiation transmitted through rings, considering dark side illumination sources

15 p1939 A73-32008

Approximation nature and error magnitude in radial radiative heat flux within optically thin nongray isothermal gas cylinder

15 p1959 A73-32282

Thermal stability of radiating fluids - Asymmetric slot problem.

16 p2085 A73-33314

Luminosity of thermal X-ray sources with a strong magnetic field.

16 p2062 A73-33574

- Time dependent radiative transfer. III - Development of the formalism. 19 p2503 A73-37565
- Measurement of the temperature of an optically dense layer of luminous gas in the upper atmosphere by the homodyne detection method. 19 p2425 A73-37933
- Radiation field in the deep layers of planetary atmospheres. 20 p2602 A73-39232
- Numerical solution of the radiative transfer equation in spherical shells. 21 p2727 A73-41000
- Static stellar envelopes at radiative equilibrium for power law dependence of opacity on temperature and density 22 p2911 A73-42935
- Saha's equation under deviation from thermodynamic equilibrium. 22 p2915 A73-43040
- Fireball spectral data reduction for self absorption, Fe abundance, excitation temperatures, relaxation time and optical thickness effects 22 p2915 A73-43043
- Properties of laser mirrors at non-normal incidence. 22 p2872 A73-43186
- Combined lidar and radiometric measurements of cirrus clouds for IR emissivity, optical thickness and albedo 23 p3003 A73-43600
- Planetary spectrum formation in atmospheric model with lower and upper layers of infinite and small optical thickness respectively 23 p3029 A73-43623
- Mariner 9 ultraviolet spectrometer experiment - 1971 Mars' dust storm. 24 p3127 A73-44396
- Disk integrated polarization observation for Titan at small phase angles, noting optically thin Rayleigh atmosphere on opaque cloud deck 24 p3130 A73-44451
- Interior radiances in optically deep absorbing media. I - Exact solutions for one-dimensional model. 24 p3111 A73-45318
- Interior radiances in optically deep absorbing media. II - Rayleigh scattering. 24 p3111 A73-45319
- OPTICAL TRACKING**
- Noise effects on the critical tracking performance of the human operator. 01 p0010 A73-10107
- Astronomical observatory lunar ranging system with high radiance neodymium-glass laser and transmitting telescope, noting tracking accuracy 02 p0151 A73-12246
- Center of mass coordinates of Baker-Nunn camera tracking stations from Geos 1 and Geos 2 optical flash data 04 p0437 A73-14785
- Earth gravitational field representation via potential of simple layer in satellite geodesy applied to satellite optical observations and Doppler data 04 p0438 A73-14789
- Visual receptive fields sensitive to absolute and relative motion during tracking. 04 p0409 A73-15072
- A new illusion - The underestimation of distance during pursuit eye movements. 06 p0656 A73-17575
- A method for the analysis of optical tracking systems. 07 p0822 A73-19194
- Autokinetic movement as a function of the implied movement of target shape. 07 p0785 A73-19549
- Influence of high ambient temperatures on the performance and some physiological parameters in a tracking problem and an optical vigilance problem 08 p0935 A73-21575
- Choosing the optimal distribution of radar and optical observations of Venus 09 p1142 A73-22091
- Normal matrix equations for major planet orbital element corrections from optical observations, testing by numerical experiment for Mercury 09 p1143 A73-22096
- Wide view field laser target designation seeker system with photodetector for multiple returns discrimination, discussing sensor broadband model, signal processing and design feasibility 10 p1216 A73-23788
- Combined effects of noise and vibration on human tracking performance and response time. [AD-759329] 11 p1323 A73-25334
- Photographic satellite observations with the Automatic Camera for Astrogeodesy. 13 p1611 A73-28150
- Pole position studied with artificial earth satellites. 13 p1656 A73-28393
- Limiting magnitude techniques with the Corralitas 24 inch Cassegrain image orthicon system. 17 p2169 A73-35290
- Linear and nonlinear filtering techniques for estimating the state of reentry vehicles from optical tracking data. 17 p2125 A73-35371

- Investigations of the eye tracking system through stabilized retinal images. 18 p2273 A73-36456
- A deterministic model of a well trained human operator performing compensatory tracking. 18 p2283 A73-36844
- The interaction between horizontal and vertical eye-rotations in tracking tasks. 19 p2394 A73-37417
- Modeling the human in a time-varying anti-aircraft tracking loop. 19 p2401 A73-38071
- A precision control system for a large astronomical telescope. 19 p2430 A73-38079
- Interference of 'attend to and learn' tasks with tracking. 19 p2401 A73-38377
- Beacon Explorer C satellite laser tracking for effects of lunar and solar tides on orbit, noting geogravitational field distortion 21 p2765 A73-40275
- Sleep deprivation effects on accuracy and speed of response selection and execution. 21 p2644 A73-40853
- Phase-tracking performance of direct-detection optical receivers. 21 p2656 A73-41169
- Optical communication system performance with tracking error induced signal fading. 21 p2657 A73-41171
- Individual and simultaneous tracking of a step input by the horizontal saccadic eye movement and manual control systems. 22 p2811 A73-41735
- Dynamic operative image formation and function features during extrapolation tracking of visibly moving target, noting image reaction to operator performance 22 p2812 A73-41886
- Recognition of component differences in two-dimensional oculomotor tracking tasks. 22 p2810 A73-42959

OPTICAL TRANSITION

- Fe ions optical transition lines in solar flares soft X ray spectra, noting continuum emission near 8 Å 03 p0367 A73-12945
- CW neutral Ar laser line competition effect observation, establishing correct transition assignment 03 p0320 A73-14461
- Possibility of generating ultrashort laser pulses on combination vibrational-rotational transitions of molecular hydrogen. 04 p0458 A73-15472
- New laser technique for the identification of molecular transitions. 05 p0585 A73-16597
- Chemical lasers with molecular gas excitation and population inversion by chemical reactions, discussing lasing conditions, vibrational transition and pumping mechanism 05 p0585 A73-16602
- Absorption coefficient due to band-band optical transitions in heavily doped semiconductor, obtaining electron and hole quasi-Fermi levels 06 p0738 A73-18586
- Multiphoton transitions. III - Rates of multiphotodetachment of negative ions. 07 p0852 A73-19147
- Energy and threshold characteristics of chemical lasers. 08 p0975 A73-21213
- Numerical formulation for constant-gain chemical laser calculations. 08 p0975 A73-21411
- Dependence of He-Ne laser output power on discharge current, gas pressure and tube radius. 08 p0976 A73-21462
- Lamb dip measurements on low pressure CO laser vibrational-rotational lines, determining line widths, velocity-changing collision rate and saturation intensities with curve fitting 09 p1090 A73-22078
- Efficient parametric conversion in cesium vapor irradiated by 3470-Å mode-locked pulses. 09 p1090 A73-22079
- Deformation of laser pulses in resonant media. 09 p1096 A73-22902
- Effect of a laser field on the gain line profile of an adjacent transition in an argon laser 09 p1096 A73-22968
- Some characteristics of transition processes in He-Ne lasers operating at the 0.63-micron wavelength 10 p1227 A73-24073
- A plasma laser operating on molecular electronic transitions 10 p1228 A73-24454
- Lasing characteristics of neodymium glasses at the 0.92-micron wavelength 10 p1260 A73-24581
- He-Ne laser low order transverse modes self mode locking at six transition wavelengths, attributing effect to oscillating modes reduction due to hole burning and cross relaxation 10 p1229 A73-24616

- Semiconductor injection lasers, discussing optical transitions threshold effects, radiative recombination coherent emission, etc 12 p1506 A73-27113
- Mode locking in quantum optics. 12 p1506 A73-27444
- Theory of an infrared high-pressure chemical laser 13 p1627 A73-28767
- Studies of noble-gas lasers for continuous operation 13 p1627 A73-28797
- Ar laser output characteristics variation due to mutual influence of 4880 and 5145 Å transitions, solving ion density formation rate equations 13 p1628 A73-29118
- Optical absorption spectrum of excited Cr³⁺/ion in yttrium aluminum garnet. 13 p1629 A73-29118
- Calculation of the nonlinear polarizability of a gas at a lasing transition with allowance for capture of resonance emission 14 p1757 A73-30366
- Laser power and vibrational energy transfer in CO lasers. 17 p2185 A73-35177
- Electron transitions of molecules in a plasma laser. 19 p2438 A73-38133
- Amplified spontaneous emission comparison with laser stimulated emission during He-Ne transitions noting threshold condition relation to population inversion density 20 p2570 A73-38619
- Nd doped YAG laser crystal relaxation time describing population inversion, beam gain time dependence and phonon spectra 20 p2574 A73-39699
- Violet and UV laser transitions in Ca II and Sr I resulting from impact radiation recombination of doubly charged metal ions 21 p2712 A73-40350
- Polarization phenomena in multiphoton ionization of atoms. 21 p2743 A73-40466
- Triply ionized Pm in lithium yttrium fluoride laser calculating crystal field split energy levels and radiative transition probabilities 21 p2715 A73-40766
- Far IR laser lines measurements in carbon dioxide laser pumped ethylene glycol, dimethyl ether, formic acid, and monomethyl amine, using grating spectrometer and Golay-cell detector 21 p2715 A73-40766
- Mode competition in the 3s sub 2-3p sub 4 transition in a neon laser with a methane absorbing cell. 22 p2869 A73-42255
- Longitudinal alignment of working levels in a helium-neon laser 22 p2870 A73-42411
- Determination of valence electron plasma frequencies and optical permittivity in single crystals of trisulfide of antimony 22 p2897 A73-42644
- Quantum-beat g-value measurements on transitions from levels of aligned fast ions. 22 p2890 A73-42977
- Measurements of the upper and lower level lifetimes in He-Ne lasers. 22 p2871 A73-43088
- Optical characteristics of phononless lines 24 p3109 A73-44427
- Rotational line overlap in CO₂ laser transitions. 24 p3096 A73-44877
- Multiphotonic absorption spectroscopy without Doppler effect 24 p3096 A73-45322
- OPTICAL WAVEGUIDES**
- Measurement of the angular distribution of light scattered from a glass fiber optical waveguide. 01 p0078 A73-11211
- Double-reverse-scatter interference in optical fiber communication systems. 01 p0018 A73-11211
- Helical gas lenses for guiding optical beam over long distances, calculating irradiance patterns for various propagation mode numbers and temperatures 01 p0053 A73-11211
- Optical communication systems with glass fiber waveguide, using semiconductor lasers and photodiodes as transmitters and receivers respectively 01 p0019 A73-11488
- Book - Light transmission optics. 02 p0192 A73-11888
- Coupling losses in hollow waveguide laser resonators. 02 p0177 A73-12577
- Mode-locked high-pressure waveguide CO₂ laser. 02 p0178 A73-12747
- Mode losses in hollow-waveguide lasers. 04 p0457 A73-14747
- The refractive index profile in a glass-fiber light waveguide 05 p0584 A73-16447
- Beam trajectory distortions due to turbulent refractive index fluctuations in optical waveguides 05 p0551 A73-16788

- Quartz light pipe for scanning electron microscope, noting photomultiplier voltage reduction and indefinite service life 05 p0580 A73-17259
- Waveguide properties, modes and optical pumping effects on thin film organic dye lasers, noting temperature effects on refractivity and laser modes 06 p0699 A73-17808
- Normal-mode analysis of anisotropic and gyrotropic thin-film waveguides for integrated optics. 06 p0702 A73-18365
- Quartz optical waveguide by ion implantation. 06 p0703 A73-18745
- Intensity fluctuations of a light beam propagating through a wave guide channel with random refraction-index inhomogeneities 07 p0792 A73-19915
- Wave propagation along radially inhomogeneous glass fibres. 08 p0937 A73-20832
- Laser oscillation modes in corrugated optical waveguides with passive core, calculating wavelengths for hybrid modes 08 p0975 A73-21060
- Laser oscillation in leaky corrugated optical waveguides. 08 p0975 A73-21206
- Proposal of periodic layered waveguide structures for distributed lasers. 09 p1090 A73-21935
- Investigation of the dielectric waveguide modes in homostructure GaAs laser. 09 p1091 A73-22238
- Energy resolution of scintillation counters employing a light guide 09 p1085 A73-23004
- Photoresist technology for passive ICs production with optical waveguides, describing vaporization deposition and processing for glass films 09 p1086 A73-23075
- Book - Optical waveguides. 09 p1066 A73-23274
- Pulse amplitude modulation of a CO₂ laser in an electro-optic thin-film waveguide. 09 p1098 A73-23337
- Optical fiber waveguide operational principles, discussing information transfer rate capability, channel characteristics and input and output devices 09 p1055 A73-23396
- Optical fiber element image microcontrast dependence on fiber lightguide output and light-tight shell illuminance difference 10 p1228 A73-24584
- Tube waveguide for optical transmission. 10 p1196 A73-24624
- Optical waveguide structures for CO₂ lasers. 11 p1375 A73-25058
- Integrated microoptical circuit technology with lenses, prisms, reflectors, mixers, detectors, gratings, filters, lasers, amplifiers and modulators fabricated around waveguides, assessing advantages and potentialities 11 p1399 A73-26117
- Glass fiber optical waveguides for laser communication systems. 11 p1376 A73-26119
- Influence of external self-focusing on the performance of laser amplifiers 11 p1364 A73-26156
- Optical beam hybrid lens waveguide with central aperture and surrounding lens, comparing transmission loss and bending effects with iris guides 11 p1365 A73-26230
- Superradiant waveguide dye laser pumped by flash lamps, noting power output and stable mode pattern insensitivity to disturbance and thermal effects 11 p1378 A73-26324
- Gain and saturation intensity measurements in a waveguide CO₂ laser. 12 p1505 A73-27017
- German monograph on signal transmission and radiation distribution in optical waveguide consisting of glass fibers with refractive index gradient and optically dense envelope 13 p1628 A73-29282
- Measurement of the radius of curvature of a laser beam by an interferometric method. 13 p1629 A73-29442
- Waveguide laser mode patterns in the near and far field. 14 p1756 A73-30157
- Monomode optical fiber waveguide propagation attenuation due to random curvature, analyzing radiation losses for clad cores with uniform and gradient refractive index profiles 14 p1729 A73-30695
- Direct modulation of a double heterostructure laser at a rate of 2.3 Gbit/s 14 p1758 A73-30700
- Recent progress in fibres for optical communications. 16 p2023 A73-32863
- A self-stabilized 3.5-micron waveguide He-Xe laser. 17 p2183 A73-34206
- Low loss light guiding polymer thin film with continuously adjustable refractivity, discussing fabrication and refractivity and scattering loss measurements 17 p2172 A73-35423
- Papers on integrated optics covering waveguides, mode launching, radiation losses, lasers, parametric devices, light deflectors and thin film deposition 17 p2185 A73-35599
- Glass fiber transmission characteristics as optical waveguides for communication systems, considering transit time and attenuation 20 p2522 A73-38660
- Detachable liquid filled capillary waveguide connector for glass fiber multimode optical transmission lines, discussing propagation efficiency as function of dimensional tolerances 20 p2522 A73-38662
- Determining the absorption coefficients of low-loss bulk glass materials. 20 p2563 A73-38663
- Crosstalk compensation in optical beam transmission. 20 p2528 A73-38769
- Cross focusing possibility between two coaxial laser beams in dielectrics with optical inhomogeneities and oscillatory waveguide characteristics, noting critical power role 20 p2572 A73-38848
- Coherent oscillation modes of optical waveguide resonators, noting selectivity and thermooptic insensitivity to pumping and active medium deformation 20 p2574 A73-39692
- Perturbation analysis of holographic grating couplers in thin film waveguides, discussing coupling efficiency dependence on evanescent tail length, refractive index and gelatin film thickness 21 p2699 A73-40149
- Laser action from optically pumped epitaxial GaAs crystal waveguides with feedback provided by surface corrugation 21 p2713 A73-40455
- Carbon dioxide laser pumped dielectric and metallic far IR waveguide, discussing size, mirror coupling and gas medium 21 p2713 A73-40461
- Finite aperture waveguide laser resonators with external reflectors by matrices coupling linearly polarized modes, calculating power efficiency, resonant frequencies and radiation patterns 21 p2714 A73-40760
- Sealed-off waveguide carbon dioxide laser, investigating gas mixture and pressure effects on power gain and output and optical properties effects on losses 21 p2715 A73-40763
- Optical waveguides in GaAs-AlGaAs epitaxial layers. 21 p2752 A73-40969
- New developments regarding wide-band communication with waveguide, glass fiber, and superconductivity 21 p2655 A73-41072
- Optical waveguide refractive index control process for glass film during deposition by sputtering power density variance 21 p2665 A73-41116
- Theoretical and experimental investigations of the coupling of two glass-fiber light waveguides 22 p2861 A73-42424
- Propagation of optical pulses through clad fibers - Modified theory. 22 p2828 A73-43163
- Leaky rays cause failure of geometric optics on optical fibres. 23 p2955 A73-44105
- Optical directional coupler tolerance improvement by tapered propagation coefficients based on numerical model 23 p2955 A73-44113
- Optical information transmission over rectangular waveguide communication channels in terms of geometry-wavelength ratio, transparency and repeater functions 23 p2955 A73-44296
- Some experiments on a voltage-induced optical waveguide in LiNbO₃. 23 p3019 A73-44374
- Mode guidance parallel to the junction plane of double-heterostructure GaAs lasers. 24 p3097 A73-45423
- OPTICS**
- NT NONLINEAR OPTICS**
- Book - Light transmission optics. 02 p0192 A73-11881
- Geometrical optics calculation of radar cross sections. 04 p0416 A73-15058
- Diagnostic procedures for nonhomogeneous plasma based on geometrical optics approximation, irradiating plasma by plane wave at oblique incidence 05 p0601 A73-16070
- Edge diffraction cone detection by illuminating razor blade edge with laser beam, noting agreement with geometrical theory prediction 05 p0585 A73-16812
- Interference patterns of a horizontal electric dipole over layered dielectric media. 17 p2123 A73-35270
- Wave amplitude calculation for propagation in inhomogeneous isotropic media by optical ray tracing consisting of integration of first and second order differential equations 22 p2885 A73-41817
- OPTIMAL CONTROL**
- NT TIME OPTIMAL CONTROL**
- Atmospheric reentry optimal lateral guidance for low lift/drag ratio space shuttle vehicle, presenting formulation as optimal stochastic control problem [AIAA PAPER 71-914] 01 p0074 A73-10106
- A method for aiding human operator performance in a noncompensatory tracking task. 01 p0011 A73-10323
- Iteration accuracy effect on optimal discrete control system synthesis and stability, applying to Zubov damping problem 01 p0027 A73-10591
- Investigation of a class of nonsearching extremal-control systems with pulse frequency modulation 01 p0027 A73-10594
- Wiener-Kolmogoroff optimal filtration theory for synthesis of linear stabilization systems under steady random external perturbations, noting control optimality conditions 01 p0028 A73-10670
- Optimal stabilization of nonlinear control systems for given region of initial perturbations, reducing optimal synthesis to moments problem 01 p0077 A73-10671
- Synthesis of a multidimensional automatic optimization system with constraints 01 p0028 A73-10674
- Automatic search system synthesis for linear programming, using gradient method and logic operations for system optimization 01 p0028 A73-10675
- Optimal control problems in differential games of pursuit and evasion involving deterministic, random and controlled motion 01 p0028 A73-11071
- Optimal processes theory, discussing Pontryagin principle, special controls, dynamic programming, discrete systems, algorithms, identification and controllability 01 p0028 A73-11072
- Discrete control algorithms for spaceborne terminal systems. 01 p0075 A73-11194
- Sufficient conditions for the optimal control problem 01 p0071 A73-11269
- Optimal renewal algorithm for control plant with cumulative damage, using failure rate and renewal point spacing model 01 p0058 A73-11421
- A fast computational algorithm for optimum digital control systems. 01 p0021 A73-11463
- Space booster control system computerized design algorithm for forward loop compensation filter selection based on minimization of penalty function of stability margin violations 01 p0021 A73-11516
- Effects of controller dynamics on the stability of a class of optimal control systems. 01 p0028 A73-11518
- Homogeneous linear partial differential equation for optimal control with boundary condition formed by terminal component, noting weighting functions for linear plant 02 p0149 A73-12116
- Optimization of control and observation processes in dynamic systems under random perturbations. 02 p0149 A73-12118
- Evaluation of the coefficients of the effect of errors in the original information and in the model of optimization results. 02 p0149 A73-12122
- Linear dynamic control system synthesis methods based on aggregation and suboptimal control by decomposition, minimizing quadratic performance criterion 02 p0149 A73-12124
- Mathematical formulation of linear programming problem, reducing vector valued optimal management plan determination to quadratic programming problem 02 p0144 A73-12126
- Application of the conditional-gradient method to the solution of an optimum control problem in a Hilbert space 02 p0187 A73-12188
- Synthesis of optimal control over the motion of a material point in a thin spherical layer of a central gravitational field with noncollinear vectors of the final gross error in the radius vector and velocity vector 02 p0193 A73-12452
- Optimal energetic characteristics of the parallel guidance method in satellite rendezvous 02 p0219 A73-12456

OPTIMAL CONTROL

Minimization of spacecraft maximum acceleration in atmosphere after reentry, applying results to reentry trajectory optimization and associated optimal control problems

02 p0219 A73-12457

Algorithm for automatic optimal control of radio telescope parabolic antenna with extremal characteristic in radiation pattern, noting quasi-steady and steady operation

02 p0147 A73-12497

Application of relaxed solutions to minimum sensitivity optimal control

02 p0149 A73-12509

Russian book - The designing of quasi-optimal combined-control servosystems

02 p0149 A73-12867

Optimal lift control by Miele's method for the atmospheric entry of a hypersonic glider. I - Simple type problems

03 p0245 A73-13766

German monograph - Application of estimation procedures for the characteristic parameters of controlled systems on the basis of measurements on the closed control loop

03 p0285 A73-13811

Optimal control of nonlinear time-lag systems

03 p0285 A73-13899

Book on control engineering covering dynamic system state representation, finite and infinite dimensional optimization, dynamic programming, stochastic estimation, applications, etc

03 p0285 A73-13987

Book on linear optimal control theory covering systems analysis, state reconstruction, stochastic nature and feedback control

03 p0286 A73-13992

Optimal control of observation processes, formulating solvability conditions in terms of ordinary differential equations

03 p0286 A73-14043

Pontryagin maximum principle application to optimal linear filtration for multivariable systems with signal processing

03 p0286 A73-14082

Optimal control approximations for time delay systems

03 p0286 A73-14195

A new filter for optimal tracking in dense multitarget environments

03 p0286 A73-14477

Nonlinear stochastic optimal control theory application to guidance policies determination of nonmaneuvering target interception or rendezvous and goal-tending game

03 p0286 A73-14478

The optimal control of merging aircraft-derivation of the hybrid air traffic controller

03 p0340 A73-14489

Pontryagin maximum principle for optimal terminal velocity control of automatic space probe descent in Mars atmosphere

03 p0383 A73-14556

Spacecraft optimal control after transfer from hyperbolic trajectory to planetary orbit by atmospheric drag, minimizing engine thrust

03 p0340 A73-14570

Pulsed motion of gravity gradient vehicle in central gravity field, presenting expressions of optimized attitude control

03 p0383 A73-14573

Calculus of variations for maximum payload of partitioned variable mass system, considering optimal weight control effect on motion

04 p0475 A73-15084

Optimal lift control by Miele's method for the atmospheric entry of a hypersonic glider. II - Isoperimetric type problems

04 p0404 A73-15168

Optimal trajectory control system synthesis via Pontryagin maximum principle, taking into account system dynamics, control constraints and boundary conditions

04 p0429 A73-15201

Choice of a rational control law for control systems for delayed objects subjected to random load disturbances

04 p0429 A73-15202

Optimal risk equation and solution existence and uniqueness of dual control problems with unknown parameter and additive noise

04 p0429 A73-15203

Adaptive feedback control without complete plant identification, deriving vector cost function and algorithm for performance optimization

04 p0430 A73-15214

A modified conjugate gradient method for optimization problems

04 p0471 A73-15216

Position and rate aided tracking for conventional pointing systems

04 p0430 A73-15256

Optimal nonlinear estimator algorithms for tracking in face of incorrect sensor returns in multitarget environments

vironments, using posteriori probability selective measurements

04 p0431 A73-15260

Optimum quantization and parallel algorithms for nonlinear state estimation

04 p0472 A73-15276

Theoretical and experimental automatic exposure control study

04 p0451 A73-15775

The selection of performance indices for optimal control problems

[ASME PAPER 72-WA/AUT-15]

04 p0432 A73-15880

Search stability and steady motion region characteristics of self oscillatory extremal automatic control system under additive disturbances on controlled object input

05 p0560 A73-16293

Synthesis of an optimal discrete control system in the presence of control delay

05 p0560 A73-16295

Extremal control system efficiency enhancement by information storage, noting algorithms for sequential data storage

05 p0560 A73-16298

Russian book - Control of moving objects

05 p0528 A73-16401

Pontryagin principle for variational problem of controllability region in three dimensional pursuit tracking, noting rendezvous optimal control system

05 p0560 A73-16403

Methods of optimization of a spacecraft angular position control program

05 p0594 A73-16412

Optimal control problems of spacecraft mass minimization and nuclear power engine operation under uncontrollable perturbations due to errors and external field interactions

05 p0596 A73-16414

Flight vehicle /FV/ control optimization taking into account control-function and phase-coordinate constraints

05 p0594 A73-16415

Synthesis of optimal control problems with allowance for a prescribed reliability

05 p0561 A73-16416

Statistical synthesis of optimal pulsed control systems for spacecraft while taking into account system structural constraints

05 p0595 A73-16419

Automatic control system synthesis for optimal correction, maximum accuracy and stability of linear unsteady final action systems under deterministic and random actions

05 p0561 A73-16420

Optimal control of extratmospheric spacecraft motion stability by variable structure system with logic circuits

05 p0528 A73-16421

An optimal orbit control system for a stationary artificial earth satellite

05 p0616 A73-16427

Control of functional differential equations of retarded and neutral type to target sets in function space. [AD-758569]

05 p0561 A73-16486

Necessary conditions for optimal controls of elliptic or parabolic problems

05 p0590 A73-16487

Existence theorems for multidimensional control systems with lower-dimensional controls

05 p0561 A73-16489

Finite-dimensional approximations of state-constrained continuous optimal control problems

05 p0561 A73-16490

Performance comparisons for joystick and track ball optimized control configurations operating in rate and position modes

05 p0543 A73-16706

Optimal flight control system design for aircraft with large flight envelopes, using optimal control theory with limited measurement feedback

[AIAA PAPER 73-159]

05 p0535 A73-16906

Energy management in aerial combat weapon systems maneuvering and delivery tactics, computing optimal feedback control laws for supersonic aircraft minimum time turning trajectories

[AIAA PAPER 73-231]

05 p0536 A73-16956

Optimal control of a combined propulsion system of a rotating spacecraft

05 p0630 A73-17003

Mathematical model for independent operations complex with rectangular probability distribution of random parameters, noting time optimal control

05 p0562 A73-17282

Computer adaptive optimization system for problems with nonlinear criteria function and constraints, noting algorithms of deterministic and stochastic categories

05 p0555 A73-17284

A matrix Green's formula and optimal control of linear distributed-parameter systems

06 p0679 A73-17564

An optimization technique for the transient response of passively stable satellites

06 p0755 A73-17566

Summary and comparison of gradient-restoration algorithms for optimal control problems

06 p0715 A73-17567

Suboptimal feedback control of linear gyroscopic systems

06 p0679 A73-17568

High-order necessary conditions of optimality for singular controls of discrete systems

06 p0679 A73-17717

The method of Lyapunov functions in control problems for distributed-parameter systems [A survey]

06 p0723 A73-17933

On an application of Lie group theory to the optimal control problem for linear dynamic systems with time-varying parameters

06 p0679 A73-17954

Synthesis of statistically optimal multiloop control systems containing essentially nonlinear elements

06 p0679 A73-17955

Computer control algorithms for transient response optimization in on/off motor control system synthesis

06 p0741 A73-17963

An analysis of optimal control system algorithms

06 p0670 A73-18059

A new method of calculating controller constants according to an optimal modulus criterion

06 p0680 A73-18160

An optimum settling problem for time lag systems

06 p0717 A73-18172

Relationship between conventional-control-theory figures of merit and quadratic performance index in optimal control theory for a single-input/single-output system

06 p0680 A73-18445

Time-invariant single input/output controllable and observable tracking servosystem, discussing dynamic trajectory controller and cost functional selection for zero steady state error

06 p0680 A73-18516

Design of dynamic programming feedback controllers for multivariable time-invariant linear systems

06 p0680 A73-18517

Dynamic system optimal control problems with higher order state variable inequality constraints, obtaining solutions with boundary arcs and isolated points

06 p0680 A73-18519

Optimal control of a class of linear multivariable systems with integral quadratic energy constraint

06 p0681 A73-18521

Sequentially best estimators for linear systems with non-linear noise-free sensors

06 p0681 A73-18522

Fuzzy multi-stage decision-making, fuzzy state and terminal regulators and their relationship to non-fuzzy quadratic state and terminal regulators

06 p0681 A73-18523

Discrete maximum principle /local cross sections/ method applications to optimal control and mathematical programming

06 p0718 A73-18676

Computerized optimal control problem formulation in calculus of variations, discussing flexible user-oriented algorithm for terminal point transversality boundary conditions numerical implementation

06 p0672 A73-18806

Some preliminary notions towards improved stochastic controller synthesis via transformed indices of performance

06 p0681 A73-18817

Adaptive real time control for defense systems - A minimum risk algorithm

06 p0682 A73-18823

Suboptimal guidance for attitude angle constrained flight trajectories

06 p0721 A73-18822

Approximate method for the synthesis of the optimal control of a dynamic system subjected to random disturbances

06 p0725 A73-18879

Adaptive control of linear stochastic systems

07 p0804 A73-19132

Type I linear multivariable systems with state integral feedback control, deriving optimal conditions for zero steady state error compensatory tracking by frequency domain techniques

07 p0805 A73-19133

Necessary condition of optimality for some problems of optimal control theory

07 p0844 A73-19296

Stochastic linear system observer eigenvalue optimal placement with respect to quadratic error criterion for adaptation to digital computation and applicability to higher order system

07 p0849 A73-19966

Stochastically optimal terminal control system synthesis for loss function dependence on finite phase coordinates of dynamic system, considering soft landing of flight vehicle

07 p0805 A73-20037

Optimal control of stochastic systems with continuous and discontinuous random disturbances, obtaining problem solution conditions for linear system via dynamic programming

07 p0805 A73-20038

- Bayes criteria and previous test data for industrial equipment test optimization, using linear and quadratic programming 07 p0831 A73-20076
- An attainable sets approach to optimal control of functional differential equations with function space terminal conditions. 07 p0846 A73-20497
- Optimal estimation of operator-valued stochastic processes and applications to distributed parameter systems. 07 p0805 A73-20580
- Recent advances and applications in the prediction of pilot acceptance of aircraft flying qualities. 07 p0777 A73-20586
- Minimum fuel control solution for linear discrete systems, discussing finite iterative algorithm based on dual problem of functional analysis 07 p0806 A73-20595
- An approximate method for the synthesis of optimal control of distributed systems. 07 p0806 A73-20596
- Feedback regulators for jump parameter systems with state and control dependent transition rates. 07 p0806 A73-20597
- Dual characterizations of optimal control systems governed by linear and nonlinear differential equations with dynamic constraints, using complementary variational principle in Hilbert space 07 p0846 A73-20598
- A discrete separation principle with a stochastic terminal constraint. 07 p0806 A73-20599
- An actively adaptive control for linear systems with random parameters via the dual control approach. [AD-751587] 07 p0806 A73-20601
- On the adaptive control of linear systems using the open-loop-feedback-optimal approach. 07 p0806 A73-20602
- Comparison of theoretical and simulated performance of optimal and suboptimal filters in a dense multitarget environment. 07 p0806 A73-20604
- Minimum fuel rocket maneuvers in horizontal flight. 08 p1014 A73-20714
- Near-optimal control of high-order systems using low-order models. 08 p0950 A73-21090
- An analytical method for the filtering error evaluation of sub-optimal filters in a noisy non-linear dynamic system. 08 p0950 A73-21091
- Distributed parameter system a priori stochastic optimal control, deriving canonical differential equations from dynamic programming formulation for insight into feedback control problem 08 p0950 A73-21093
- The conjugate gradient method and its application to aerospace vehicle guidance and control. I - Basic results in the conjugate gradient method. 08 p0951 A73-21428
- Optimal stabilization of the Rayleigh-Taylor instability in the multiarm fluid pendulum. 09 p1119 A73-21942
- Application of four methods for approximating optimal feedback gains. 09 p1067 A73-22234
- Extremal targeting in a nonlinear rendezvous game 09 p1112 A73-22476
- Vector-valued optimization of linear systems 09 p1112 A73-22478
- Optimal sequence for introducing elements of large system into operation, using resource allocation cost criterion 09 p1068 A73-22551
- Optimal control system design with respect to vector quality criterion, noting linear system described by differential equations 09 p1068 A73-22560
- Approximate solution of certain optimal-control and discrete-programming problems 09 p1068 A73-22561
- Algorithmic construction of optimal controllers on the basis of incomplete information about the state of the plan 09 p1068 A73-22562
- Solution of the Fokker-Planck-Kolmogorov equation for a dynamic system with analytical characteristics 09 p1068 A73-22563
- Optimal observation laws for certain controlled motions 09 p1069 A73-22565
- Optimal control problems under conditions of a priori indeterminateness 09 p1069 A73-22566
- Application of the principle of invariant imbedding in the solution of optimal control problems 09 p1069 A73-22722
- Continuous analog of dynamic-programming allocation process 09 p1112 A73-22889
- Optimal self learning classification of point in set for image recognition systems, using proximity functions 09 p1060 A73-22944
- Optimal control of n-order system with transport delay by variational calculation, comparing with proportional integrator /PI/ controller 09 p1069 A73-22974
- Optimal control problems in differential games of pursuit and evasion involving deterministic, random and controlled motion 09 p1113 A73-22996
- Optimal processes theory, discussing Pontryagin principle, special controls, dynamic programming, discrete systems, algorithms, identification and controllability 09 p1069 A73-22997
- Optimal lift control by Miele's method for the atmospheric entry of a hypersonic glider. III. 10 p1285 A73-23616
- Some problems of optimal control of space-vehicle trajectories in the Martian atmosphere 10 p1247 A73-23878
- Numerical solution of the optimal control problem by the direct method 10 p1197 A73-23999
- Linearization limits for optimal pulse controller adjustments, using comparison with continuous controller and extrapolation 10 p1198 A73-24000
- All-weather aircraft landing automation, discussing efficient optimal feedback control law selection based on trajectory termination or terminal control requirements 10 p1247 A73-24010
- Optimum operational flow characteristics derivation for control valves based on frequency distribution of relative pressure drop occurring in practical applications 10 p1223 A73-24015
- Start/stop motor incremental motion system design for optimal control with minimized energy dissipation and operating temperature under inertial and constant torque load 10 p1198 A73-24023
- The design of optimally parameter insensitive control systems. 10 p1199 A73-24030
- Optimization methods in control systems design, discussing nonlinear and linear programming, variational and maximum principles, dynamic programming and game and graph theories 10 p1242 A73-24032
- Iterative optimum control function determination without directly solving the system dynamical equations. 10 p1242 A73-24033
- Contraction-mapping algorithm with guaranteed convergence. 10 p1242 A73-24034
- Discrete dynamic adaptive control algorithms for estimation of minimum loss function point trajectory characterizing system quality in nonstationary conditions 10 p1242 A73-24035
- An adaptive convex feedback method for linear control systems with quadratic performance index. 10 p1199 A73-24038
- Linear stochastic, multivariable, optimal control, realization and time-varying systems theory developments covering external and internal representations and variance computation problems 10 p1200 A73-24045
- Optimal filtering for systems described by linear partial differential equations. 10 p1200 A73-24050
- A comparison of the effectiveness of some adaptive optimal filtering techniques applied to the gyrocompassing problem. 10 p1201 A73-24052
- On optimization of control systems according to vector-valued performance criteria. 10 p1201 A73-24056
- Linear multivariable control systems - A survey. 10 p1201 A73-24058
- Wide-sense adaptive dual control for nonlinear stochastic systems. 10 p1202 A73-24533
- Sufficiently informative functions and the minimax feedback control of uncertain dynamic systems. 10 p1202 A73-24535
- Optimal stochastic linear systems with exponential performance criteria and their relation to deterministic differential games. 10 p1202 A73-24536
- Discrete-time fixed-lag smoothing algorithms. 10 p1243 A73-24547
- An optimal control problem for a class of distributed parameter systems. 10 p1202 A73-24549
- Solution of the stochastic control problem in unbounded domains. 10 p1203 A73-24705
- Russian book on military application oriented automatic control systems design covering amplifiers, servo elements, stability, performance, optimization, and nonlinear and sampled data systems 10 p1203 A73-24972
- Optimal control methods for combined signal processing, using complex filtration-compensation system principles and mean square measurement error criteria 11 p1340 A73-25003
- Random analog signal quantization and reconstruction from discrete sample values by optimal filtration according to statistical criteria 11 p1341 A73-25013
- Functional analysis and optimal control of linear discrete systems, deriving algorithms for minimum fuel, energy or amplitude from linear equations solution 11 p1390 A73-25188
- The optimality of variable sampling schemes for a digital encoder. 11 p1327 A73-25194
- Two quadratic cost functionals equivalence conditions derivation in terms of system parameters and weighting matrices for optimal control law generation 11 p1341 A73-25196
- Suboptimal input signal synthesis for linear control system identification based on output SNR maximization, bandwidth matching and pseudorandom binary noise nature 11 p1327 A73-25197
- Extension of the principle of variable structure systems to the case where the slip hypersurface is nonlinear - Application to suboptimal control 11 p1341 A73-25574
- Synthesis, with the aid of Liapunov functions, of optimal and suboptimal discrete systems for controlling determinate and stochastic plants 11 p1341 A73-25619
- The principle of complexity and the method of regularization in stochastic problems of optimal automatic control system synthesis 11 p1341 A73-25634
- An optimal control approach to terminal area air traffic control. 11 p1394 A73-25786
- On a solution of an optimization problem in linear control systems with quadratic performance index. 11 p1342 A73-26224
- Optimal inputs and sensitivities for parameter estimation. 11 p1391 A73-26579
- Optimal control for functional differential systems through Krasovskii generalization for time delay systems and resulting Riccati equations numerical solution 11 p1392 A73-26581
- Optimal control theory for constant gain radar filter design with weighted variance average minimization comparable with Kalman filter performance 11 p1339 A73-26643
- Multiple input system with feedback loops and majority decision for performance optimization, discussing design principles and applications for structural synthesis and circuit design 12 p1482 A73-26759
- Choosing the transmission ratio of position servomechanism reduction gears 12 p1460 A73-26792
- Nonsingular control, determining optimum shape of straight bar under stress and inertial moment restrictions 12 p1482 A73-26793
- Group properties and invariant solutions of the Bellman equation in the problem of optimal control synthesis for second-order systems 12 p1483 A73-27079
- Dynamic prediction model and optimal control of a commercial plant 12 p1561 A73-27081
- A proof of the Pontryagin maximum principle for initial-value problems. 12 p1517 A73-27117
- General theory of optimal trajectory for rocket flight in a resisting medium. 12 p1538 A73-27119
- On optimal nonlinear estimation. I - Continuous observation. 12 p1517 A73-27147
- Asilomar Conference on Circuits and Systems, 6th, Pacific Grove, Calif., November 15-17, 1972, Conference Record. 12 p1483 A73-27151
- Minimum fuel problem link to Kalman controllability theorem, deriving solution based on state transition and controllability matrices 12 p1517 A73-27152
- Practical quadratic optimal control for systems with large parameter variations. 12 p1483 A73-27166
- Phase coordinates estimation optimization, deriving observable vector relations from sampling laws 12 p1524 A73-27417
- Optimization of the parameters of heterogeneous multipurpose controlled systems using standard elements 12 p1484 A73-27456
- Synthesis of an approximately optimal control for one class of controlled systems. 12 p1484 A73-27457

Response-optimum control of the angular and torsional oscillations of an elastic flying wing.

12 p1459 A73-27459

Analytical design of manual control systems for flight bodies

12 p1549 A73-27896

Optimal control with probabilistic quadratic performance criterion and constraints, using stochastic principle for reduction to time derivative maximization problem

12 p1485 A73-27897

Optimal estimation of the phase coordinates for a linear dynamic system

12 p1485 A73-27898

Linear systems with aftereffects of delayed feedback described by differential equations, obtaining optimal control solution in terms of parameters and boundary value problem

12 p1486 A73-27950

Optimal search scanning for electronic surveillance radar based on antenna beam position with highest echo signal for maximum likelihood target acquisition

13 p1581 A73-27999

Application of mathematical programming methods to determine the optimal control for systems described by heat conduction equations

13 p1704 A73-28016

The Ritz-Galerkin procedure for nonlinear control problems.

13 p1649 A73-28607

Computerized adaptive flight control for helicopter dynamic systems based on identification and optimization methods

13 p1569 A73-28829

Optimal data sampling in communication channels system, discussing algorithms for data transmission and control

13 p1587 A73-28870

Thermodynamic optimization of current leads into low temperature regions.

13 p1707 A73-29067

Extremal controls in a nonlinear differential game

13 p1660 A73-29077

A minimax filter for systems with large plant uncertainties using measurements corrupted by colored noise.

13 p1593 A73-29205

Optimal aircraft go-around and flare maneuvers.

13 p1657 A73-29217

MTI radar filter with adaptively controlled double canceller for frequency shifted clutter spectra effects minimization

13 p1594 A73-29222

Routh-Hurwitz method for optimal algebraic stability of ordinary differential equations of fourth order systems with linear control law

13 p1597 A73-29419

Book - Optimal control of differential and functional equations.

13 p1651 A73-29550

Zeros determination in large-scale multivariable systems.

13 p1651 A73-29568

Application of a modified quasilinearization technique to totally singular optimal control problems.

13 p1597 A73-29570

Algorithms of formal selection for optimal control systems of digital computers

14 p1730 A73-30034

Mean risk determination in radio-electronic device control

14 p1735 A73-30291

Optimal control of discrete systems

14 p1738 A73-30348

Optimal feedback characteristics of transistor amplifiers

14 p1736 A73-30372

Solution of a dual problem in optimal control theory.

14 p1738 A73-30405

An historical survey of computational methods in optimal control.

14 p1738 A73-30413

Inverse problem of linear optimal control.

14 p1738 A73-30451

An adaptive precision gradient method for optimal control.

14 p1738 A73-30452

Minimum-energy terminal state control of first order linear hyperbolic systems in one spatial variable using the method of characteristics.

14 p1769 A73-30453

A minimization algorithm for the design of linear multivariable systems.

14 p1769 A73-30504

Suboptimal terminal feedback control of nonstationary, nonlinear systems.

14 p1739 A73-30507

Book - Optimal control theory for the damping of vibrations of simple elastic systems.

14 p1813 A73-30674

Control of functional differential equations with function space boundary conditions.

14 p1770 A73-30754

The infinite time quadratic cost problem for certain classes of infinite dimensional control systems.

14 p1770 A73-30758

Some results on the abstract realization theory of multilinear systems.

14 p1740 A73-30781

Optimal control synthesis in the observation problem. I, II

14 p1802 A73-30788

Control systems synthesis via digital computer techniques, describing numerical optimization procedure and analog simulation method

14 p1730 A73-30921

Regulators providing control system autonomy

14 p1740 A73-30938

Use of the principle of invariant imbedding in solving an optimal control problem.

14 p1740 A73-30955

Optimal transfer between coplanar elliptic orbits with the aid of tangential impulses applied at the apsidal points

15 p1931 A73-31232

Optimal damping and stochastic control in certain problems of astrodynamics

15 p1931 A73-31236

Russian book on remote guidance control systems covering theory, optimization and constraints for steady, unsteady, linear and nonlinear automatic control systems

15 p1853 A73-31374

Analysis of various automatic homing techniques for gliding airdrop systems with comparative performance in adverse winds.

[AIAA PAPER 73-462]

15 p1827 A73-31448

A computational scheme used with the epsilon-technique in synthesizing optimal controls.

15 p1853 A73-31625

Optimal and linear sub-optimal control of second-order saturating control systems.

15 p1853 A73-31626

A modified quasilinearization technique for optimal control problems with unspecified final time.

15 p1853 A73-31627

Suboptimal adaptive control of a class of non-linear systems.

15 p1853 A73-31628

Integral action in the optimal control of linear systems with some inaccessible state variables.

15 p1854 A73-31631

Riccati transformation for optimal control linear two-point boundary value problems formulated from first order numerical integration methods

15 p1908 A73-31666

Optimal control in a finite time interval for discrete systems in the minimization problem of an inhomogeneous quadratic functional / a case of fixed terminals/

15 p1854 A73-31802

Synthesis of optimal discrete control systems with persisting perturbations

15 p1854 A73-31803

Optimal stochastic guidance laws for tactical missiles.

15 p1908 A73-31917

Optimal evasive tactics against a proportional navigation missile with time delay.

15 p1908 A73-31918

The method of penalty functions and necessary conditions of optimality for generalized solutions of the optimal control problem

15 p1901 A73-32367

Approximate synthesis method for optimal control of a system subjected to random perturbations.

15 p1915 A73-32404

Simultaneous control of temperature and humidity in a confined space. III Feedback control synthesis via optimal control theory.

15 p1855 A73-32549

Optimal control theory for systems with inequality restrictions on control and state variables and time delay, using maximum principle and variational techniques

15 p1855 A73-32580

Contribution to the synthesis of optimum control of motion of a point mass in a spherical lamella of a central gravitational field with finite miss vectors noncollinear with respect to radius vector and velocity vector.

15 p1915 A73-32602

Optimum energetic characteristics of the parallel-guidance method of bringing satellites into proximity.

15 p1941 A73-32606

Minimization of spacecraft maximum acceleration in atmosphere after reentry, applying results to reentry trajectory optimization and associated optimal control problems

15 p1941 A73-32607

Minimum-norm control of linear systems with partially known initial conditions.

16 p1992 A73-33163

A geometrical proof of the maximum principle for systems represented by difference-differential equations.

16 p2032 A73-33302

Optimal control solution existence for relaxed linear systems with strictly convex Hamiltonian

16 p1992 A73-33303

Intermediate-thrust arcs and their optimality in a central, time-invariant force field.

16 p2062 A73-33305

The use of a hybrid computer in the optimization of gas turbine control parameters.

[ASME PAPER 73-GT-13]

16 p2047 A73-33491

An approach to the analysis of performance of quasi-optimum digital phase-locked loops.

16 p1992 A73-33743

Gradient methods with penalty functions for solution of optimal control with terminal constraints, noting convergence superiority of conjugate gradient algorithm

16 p2034 A73-33998

Papers on optimal control and dynamic system theory covering linear discrete systems observers, quasi-linearization, national economic policy, decision theory and closed loop formulation

17 p2143 A73-34360

Optimal observer techniques for linear discrete time systems.

17 p2144 A73-34361

Modified quasilinearization method for mathematical programming problems and optimal control problems.

17 p2200 A73-34362

Closed loop formulations of optimal control problems for minimum sensitivity.

17 p2144 A73-34363

Solution of coupled and singular perturbation methods using duality theory.

17 p2202 A73-35358

Unsupervised learning of the optimal linear signal estimator in the presence of unknown multiplicative, additive, and message generating noise.

17 p2144 A73-35374

Nonlinear optimal control synthesis for oscillating second-order systems with a convex control region

17 p2213 A73-35589

Application of the dynamic filtration method to spacecraft orientation control problems

18 p2359 A73-36104

Neighboring extremals for optimal control problems.

18 p2294 A73-36308

Optimal control of linear systems in the case of continuous and discrete controls

18 p2337 A73-36410

Hybrid computer technique for desensitized optimal design of system with uncertain plant parameters, with application to Saturn 5 Apollo attitude control system design

18 p2291 A73-36426

Analytical design of aircraft manual control systems.

18 p2267 A73-36601

Optimal control with probabilistic quadratic performance criterion and constraints, using stochastic principle for reduction to time derivative maximization problem

18 p2294 A73-36602

Optimal estimation of the phase coordinates of a linear dynamic system.

18 p2294 A73-36603

A perturbation treatment for optimal slightly nonlinear systems with linear control and quadratic criteria.

18 p2294 A73-36637

Chattering arcs and chattering controls.

18 p2294 A73-36639

On the existence of an optimal solution of the epsilon variational problem.

18 p2330 A73-36641

Optimal feedback control and Kalman filter design via an interactive computing and visual display system.

18 p2295 A73-36839

Spinning HEOS-A2 satellite active deconing with pulse sequence from attitude reorientation system, discussing optimal control pulse number and timing.

18 p2361 A73-36957

Existence of optimal controls for processes described by a system of hyperbolic equations

18 p2331 A73-36986

Use of weighting functions in conjugate gradient methods

18 p2295 A73-37079

The scope for electron-optical devices for the optimal processing of composite signals in communication systems.

18 p2290 A73-37127

Synthesis of the optimal characteristics of the engines of multiengine systems

19 p2388 A73-37187

A parameter optimisation technique applied to the design of flight control systems.

19 p2378 A73-37409

Non-singular control problems. II - Integral equation function-space method applied to the solution of optimization problems in the mechanics of deformable bodies.

19 p2498 A73-37649

Joint Automatic Control Conference, 14th, Ohio State University, Columbus, Ohio, June 20-22, 1973, Preprints of Technical Papers.

Discrete stochastic linear servomechanism with observation costs, deriving optimal control solution with extension to nonlinear systems suggested by dynamic population models

Suboptimal filter design for dynamic measurement systems, deriving bias and Kalman covariance formulae for error analysis and model sensitivity

Design of decoupled multivariable control systems.

A sensitivity approach to the decoupling of linear systems with parameter disturbances.

A constraining hyperplane technique for state variable constrained optimal control techniques.

A comparative study of two basic approaches to extremum control.

On the use of singular perturbation methods in the solution of variational problems.

Second-order optimality conditions for the Bolza problem with variable endpoints and separated end conditions.

An application of truncated power series controllers for optimization of dynamic systems.

Parallel algorithms for optimum nonlinear state estimation.

Polynomial estimators for systems with polynomial nonlinearities.

Identification of YT-2B stability and control derivatives via the maximum likelihood method.

A practical filter for noisy dynamic systems with unknown time-varying parameters.

Optimal aircraft collision avoidance.

Feedback controller design for multivariable systems by linear programming.

Derivation of aggregation matrices for simplified models of linear dynamic systems and their applications for optimal control.

A hybrid fluidic directional gyro.

An optimal feedback control law for regulator problems with linear state inequality constraints.

Output feedback for linear multivariable systems with parameter uncertainty.

Performance of LQG control systems using optimal k-step-ahead control laws.

A new approach to the 'inverse problem of optimal control theory' by use of a generalized performance index /GPI/.

A projection operator algorithm for optimal control problems with unspecified initial state values.

A computational algorithm for design of regulators for linear jump parameter systems.

Controllability of discrete bilinear systems with bounded control.

Suboptimal design of a class of nonlinear controllers.

Modeling the human in a time-varying anti-aircraft tracking loop.

Control configuration optimization of linear engineering systems.

Comparison of optimized active and passive vibration absorbers.

Synthesis of optimal automatic control systems by use of the complexity principle and of the regularization method.

Regulators guaranteeing the autonomy of a controlled system.

The Ritz-Galerkin procedure for parabolic control problems.

Modern control techniques applied to energy conservation flight control systems.

Necessary conditions for Chebyshev-Bolza optimal control problems.

Russian book - Optimal and adaptive systems.

Controllability and synthesis of optimal dynamic systems

Controllability conditions and optimization solution to finite control problem during prescribed time for lumped parameter system

Approximate synthesis theory in problems of optimization of automatic control systems

Discontinuous solutions of hyperbolic optimum problems

Optimal invariant solution for compensating circuit of nonlinear control system under disturbances, using unperturbed motion prediction

Construction of improving variations during the optimization of determinate and stochastic systems

Computerized analytical methods for optimal control synthesis of linear and nonlinear systems with constraints, using integral quadratic weighting function estimates

Determination of an optimal dynamic system according to complex statistical criteria in the presence of constraints

Some problems in the analysis and synthesis of statistically optimal constrained control

Chebyshev minimax functional solution for optimal control system design, noting flexible rocket and nuclear reactor control applications

Synthesis problems of adaptive systems for processing information and accepting solutions

Multidimensional linear extrapolation in problems of optimal design and control

Synthesis of a class of optimal discrete systems for correcting the trajectories of dynamic systems

Correctness, regularization, and the maximum complexity principle in the statistical dynamics of automatic control systems

Stochastic process control with a regulated control interval duration

Methods for calculating and enhancing the efficiency of automatic systems

Certain methods of determining the dynamic characteristics of stochastic objects

An adaptive scheme for PCM transmission.

Direct statistical evaluation of nonlinear guidance systems.

[ALAA PAPER 73-836]

Digital flight control design using implicit model following.

[ALAA PAPER 73-844]

Optimum inertial sensor orientation for earth inertial navigation systems allowing for azimuth error and g-sensitive instrument error effects

[ALAA PAPER 73-850]

Automatic control of adverse yaw in the landing environment using optimal control theory.

[ALAA PAPER 73-861]

A practical load relief control system designed with modern control techniques.

[ALAA PAPER 73-863]

Large orbiting telescopes fine guidance system for ultrahigh pointing stability based on disturbance accommodation standard deviation optimal controller design

[ALAA PAPER 73-882]

An indirect trajectory optimization algorithm based on the continuation method for solution of nonlinear equations.

[ALAA PAPER 73-890]

A nonlinear programming algorithm for the automated design and optimization of flexible space vehicle autopilots.

[ALAA PAPER 73-892]

Some problems in the optimal control of spacecraft trajectories in the Martian atmosphere.

Multiple queueing system of control plants, determining optimal order and initiation moments for minimized total time for all requests

Choice of optimal parameters for flight-vehicle control systems in the presence of random disturbances

19 p2415 A73-38489

20 p2538 A73-38671

20 p2591 A73-38672

20 p2591 A73-38673

20 p2591 A73-38674

20 p2581 A73-38675

20 p2538 A73-38676

20 p2539 A73-38677

20 p2539 A73-38679

20 p2539 A73-38680

20 p2539 A73-38681

20 p2592 A73-38683

20 p2531 A73-38684

20 p2539 A73-38687

20 p2592 A73-38697

20 p2540 A73-38699

20 p2540 A73-38701

20 p2540 A73-38705

20 p2540 A73-38710

20 p2523 A73-38728

20 p2584 A73-38779

20 p2508 A73-38783

20 p2585 A73-38789

20 p2586 A73-38799

20 p2508 A73-38801

20 p2588 A73-38818

20 p2588 A73-38826

20 p2588 A73-38828

20 p2589 A73-38897

20 p2530 A73-38989

20 p2590 A73-38991

Optimal statistical solution methods in recognition, data processing, and control problems

A programmed control task in a two-level hierarchical system under conditions of uncertainty

Optimal stabilization of moving control plants during multichannel measurement of their coordinates

Synthesis of multidimensional automatic optimization systems with allowance for constraints

The maximum principle in problems of optimal control of systems having a nonsmooth right side

Statistically optimal sampled data terminal guidance algorithm for complex probabilistic multipurpose control system, using linearized equations

Adaptive control of forced motions in discrete extremal systems with independent search

Parametric sensitivity in the problem of control with reference to an incomplete model of the plant

Optimal control of stochastic systems with random shocks and discontinuous trajectories, using functional minimization

Reproduction of a useful signal by linear feedback systems

Optimal active damping of vibrations

Dynamic systems stability under influence of white noise-Gaussian random processes, discussing optical control, Markov processes, linear equations and vector fields

Optimization and design of varicap-diode tuned transistor oscillators

Space shuttle ascent guidance, using quadratic performance index and reference trajectory kinematics to obtain optimal time-varying feedback control gain

Approximate solution of Bellman's equation for a class of problems involving optimal terminal control

Optimum minimax strategy in pursuit game with observation of evading player phase vector at fixed times

Optimum cross-coupled tracker for pulse-Doppler radar.

Maneuvering target motion modeling with binary random variable in state equation, obtaining optimal tracking solution as weighted combination of two Kalman filter estimates

Suboptimal algorithms for nonlinear smoothing.

A finite algorithm for the minimum l-infinity solution to a system of consistent linear equations.

Flight vehicle extensive attitude control theory, deriving kinematic relations for optimal control moment selection to ensure required rotation

Use of piecewise linearization for suboptimal control of nonlinear systems.

Computerized simulation of radio telescope control for minimum rms error and system parameter optimization

Russian book on mathematical theory of optimal control of discrete time systems covering multidimensional geometry, convex sets, Pontryagin maximum principle and dynamic programming

On the uniqueness of search directions in variable-metric algorithms.

Lower bounds on the cost functional for systems governed by partial differential equations.

Certain problems in the use of the maximum principle to determine optimal controls in the case of special controls and sliding regimes

Optimal motions of a spacecraft relative to its center of mass

Selection of an optimal structure for a tabular model of a control plant

Convex approximation of the control process and a method for constructing generalized optimum regimes

A method of optimization of algorithms for secondary processing of radio signals

Possibilities of suboptimal control in a linear-quadratic problem 21 p2671 A73-41606

Optimum processing for delay-vector estimation in passive signal arrays. 22 p2825 A73-42198

Synthesis of optimal control with allowance for the real characteristics of the executive mechanism 22 p2835 A73-42363

German monograph - Passive and active satellite attitude control with the aid of rod-like torsion pendula. 22 p2917 A73-42599

Russian book - Theory and methods for constructing multiple-link control systems. 22 p2835 A73-42601

Sufficient optimality conditions for control system described by ordinary differential equations in Banach space with Lebesgue measure of material quantity set 22 p2882 A73-42604

Gradient control laws in stabilization problems of multidimensional control systems 22 p2887 A73-42605

Optimal control of multiple-link plants with bounded phase coordinates 22 p2887 A73-42607

Decomposition of the solution to optimal synthesis problems of multiple-link control systems 22 p2887 A73-42610

Application of stochastic programming methods for solving certain optimization problems of multiple-link plants without memory 22 p2836 A73-42612

Structural sensitivity transfer matrix for dynamic multiple link control system response minimization with corrections within frequency range 22 p2836 A73-42613

Optimal dynamic accuracy measurement complexing for combined data processing in multidimensional automatic control systems with various sensors 22 p2836 A73-42618

German monograph on regularization and penalty function methods of numerical analysis in Hilbert or Banach space covering minimax technique and optimal control theory application 22 p2882 A73-42847

German monograph - Principles concerning proofs regarding optimality conditions in the case of time-dependent processes. 22 p2888 A73-42853

Analysis of transient oscillations in nonlinear control systems. 22 p2837 A73-43019

Dynamic programming application to extremal fields topological singularity in optimal control theory for flight vehicle with state variables satisfying initial conditions and ordinary differential equations 22 p2917 A73-43030

Synthesis of optimal control of the longitudinal motion of an elastic tank containing liquid 22 p2843 A73-43059

Sensitivity of optimal control systems with bang-bang control. 22 p2837 A73-43068

Optimal feedback control solution existence and uniqueness conditions for asymptotic stability, discussing relationships with Pontryagin equations and linear regulator problem with quadratic cost functions 22 p2837 A73-43070

Optimal discrete-time feedback control of mixed distributed and lumped parameter systems. 22 p2837 A73-43072

Classical mechanics Noether theorem and variational calculus for optimal control, noting Pontryagin maximum principle equations first integral solution existence condition 22 p2837 A73-43073

Game theory mathematical model for optimal control of glide modes in conflict situation 23 p2999 A73-43263

Sensitivity, adaptivity and optimality; Proceedings of the Third Symposium, Ischia, Italy, June 18-23, 1973. 23 p2961 A73-43277

Synthesis of parameter and state insensitive feedback systems with constraints based on piecewise constant linear control laws. 23 p2962 A73-43283

Optimal landing flare control of aircrafts with sensitivity consideration. 23 p2940 A73-43284

Reduction of the sensitivity of optimal control systems by using two degrees of freedom. 23 p2962 A73-43285

Oil hydraulic button vortex valve optimization experiment for power consumption reduction, noting Reynolds number effects on turn down and pressure ratios 23 p2942 A73-43404

Servomechanism design techniques and applications - Aerospace problems. 23 p2945 A73-43450

Application of finite integral transformations to optimal control problems 23 p2963 A73-43576

Problem of synthesizing a control system in the case of a plant involving random jerky forces 23 p2963 A73-43577

Optimal SAM defense system - An application of optimal control concept to operations research. 23 p2964 A73-43823

Optimum mean-square decision feedback equalization. 23 p2964 A73-43988

A computer program SNR-2 for solving an optimal control problem with state constraints. 23 p2956 A73-44126

Synthesis of optimal sampled-data control systems in the presence of continuous disturbances. 23 p2965 A73-44332

Synthesis of cascaded multiple-loop feedback systems with large plant parameter ignorance. 24 p3073 A73-44584

Optimality condition based on maximum principle-derived convex reference function for control plants with continuous and discrete times 24 p3105 A73-44601

Certain problems of the correctness of the minimum-impulse linear optimal control problem. I - Dependence of the optimal control on the initial state and parameters 24 p3105 A73-44602

Group properties and invariant solutions in the problem of the analytic design of controllers for a process with distributed parameters 24 p3074 A73-44661

Optimal macroscopic control and resource exchange model for open market-like systems in economic and thermodynamic terms 24 p3154 A73-44665

On the limit-cycle characteristics of a bang-bang servo. 24 p3075 A73-45556

OPTIMIZATION

NT FLIGHT OPTIMIZATION

NT OPTIMAL CONTROL

NT TIME OPTIMAL CONTROL

NT TRAJECTORY OPTIMIZATION

Dynamic programming and a max-min problem in the theory of structures. 01 p0019 A73-10199

Optimum configurations for bangless sonic booms. 01 p0031 A73-10302

Structural members optimal shaping in terms of stress concentration, analyzing plane elasticity boundary value problem 01 p0114 A73-10600

Optimization of hybrid gas lubricated conical bearings. 01 p0057 A73-10698

A note on optimality conditions for trusses with a zero minimum cross-section. 01 p0115 A73-10766

Grillages of maximum strength and maximum stiffness. 01 p0115 A73-10767

Variational optimization problems for hyperbolic-type equations 01 p0077 A73-10952

Optimal thickness of a cylindrical shell under external pressure 01 p0116 A73-10964

Optimization study of the satellite broadcasting system for television. 01 p0018 A73-11180

The optimum allocation of redundancy - An application of mathematical programming to system design. 01 p0071 A73-11199

Investigation of the effectiveness of the variable-step simplex optimization method in a noise environment 01 p0028 A73-11420

Optimal fixed message block size for computer communications. 01 p0019 A73-11454

The range of solutions in the case of optimization problems with parameters in the coefficients of the matrix of the linear restriction conditions 02 p0186 A73-11590

A rapid matching procedure for twin-spool turbobfans. 02 p0202 A73-11593

Multivariate analysis applied to aircraft optimization - Some effects of research advances on the design of future subsonic transport aircraft. [DGLR PAPER 72-093] 02 p0130 A73-11661

Optimization of the apogee impulse during the positioning of a geostationary satellite. [ONERA, TP NO. 1218] 02 p0228 A73-11992

Application of the device of linear programming to solve certain optimal problems of reliability theory. 02 p0187 A73-12121

Method of minimization of description of classes in pattern recognition. 02 p0143 A73-12125

Analytical expressions for postmaneuver velocity and transfer impulse optimizing elliptic-to-hyperbolic orbital transfer 02 p0219 A73-12453

Thrust nozzle optimization including boundary-layer effects. 02 p0129 A73-12508

Steady state conditions for maximal and minimal energy transfer between any load form and any system displacement shape, examining coincidence and resonance 02 p0194 A73-12604

Optimization of spectral intervals for remote sensing of atmospheric temperature profiles. 02 p0171 A73-12774

Design study for long-lived compact 750 kW industrial gas turbine, discussing optimal aerodynamic proportioning and size determination [ONERA, TP NO. 1174] 02 p0204 A73-12791

General optimization criteria with allowance for economic factors and their use in measurement technology 03 p0305 A73-12894

The optimisation of sound attenuation in lined ducts containing uniform, axial, subsonic, mean flow. 03 p0291 A73-12987

On optimal design of prestressed elastic structures. 03 p0384 A73-13119

Hydrostatic journal bearings design review covering pad coefficients, flow control, optimization, dynamic behavior, thermal effects, turbulence and tolerances 03 p0311 A73-13207

Axisymmetric gas-particle flows maximum thrust nozzle design, investigating particle size, nozzle geometry and heat transfer coefficient effects [AIAA PAPER 72-1189] 03 p0357 A73-13479

Optimality criteria for structural design of statically determinate or indeterminate truss with prescribed compliance and cross sectional area 03 p0391 A73-13679

Reliability optimization of a series-parallel system. 03 p0336 A73-13735

FM threshold performance of the frequency demodulator with feedback. 03 p0276 A73-13903

Partially coherent detection of binary FSK system with adaptive receiver, determining optimum and sub-optimum estimators of channel parameters for phase and bit synchronization 03 p0277 A73-13909

Equivalence of the likelihood ratio processor, the maximum signal-to-noise ratio filter, and the Wiener filter. 03 p0282 A73-13917

Far-field simulation of circular antenna arrays on the analog/hybrid computer 03 p0277 A73-13988

Optimal matched Wiener discrete filters investigated with operator-matrix concepts, considering signal decorrelation 03 p0278 A73-14030

Neumann-Pearson-optimal signal detection procedure invariant with respect to amplitude and random noise intensity 03 p0278 A73-14073

Performance optimization for supersonic ramjet - Theoretical and experimental studies [ONERA, TP NO. 1106] 03 p0359 A73-14144

Computerized design and algorithm for linear and nonlinear regulators by mathematical programming approach involving vector determination for objective function minimization 03 p0286 A73-14480

Gravitational stabilization systems parameters determination for minimum amplitude of satellite eccentric vibrations 03 p0383 A73-14557

Minimum weight rectangular beam grillages and reinforced plates of given strength or stiffness presenting solutions for various boundary conditions 04 p0508 A73-14937

Elastic force minimization during transient process in mechanical multimass system under time dependent external load 04 p0509 A73-14976

Optimum detection and signal design for channels with non-but near-Gaussian additive noise. 04 p0415 A73-14988

Minimum weight design of plastic and elastic grillages and fiber reinforced plates of given strength or stiffness, presenting optimal solutions for various boundary conditions 04 p0509 A73-15011

Constrained optimal design of columns against buckling. 04 p0510 A73-15029

Minimum-weight plastic design of continuous beams subjected to one single moveable load. 04 p0510 A73-15030

On the weight optimization problem for supersonic rectangular flat panels with specified flutter speed. 04 p0511 A73-15170

Boundary techniques for the multistep formulation of the optimized Lax-Wendroff method for non-linear hyperbolic systems in two space dimensions. 04 p0471 A73-15227

Optimum Runge-Kutta-Fehlberg methods for second-order differential equations. 04 p0471 A73-15231

Optimal equalization of discrete signals passed through a random channel.

04 p0420 A73-15418

Data return maximization for unpredictable channel capacity, considering planetary entry probe to Venus or Jupiter with unknown atmospheric transmission characteristics

04 p0420 A73-15425

Equivalent, filter realization and threshold CNR determination for optimum design of extended range phase locked loop

04 p0421 A73-15436

Parameter optimization technique for remote radio probing and diagnostics of inhomogeneous media with properties variation along single dimension

04 p0422 A73-15478

Design and realization of microthruster temperature control subsystems - Optimization through refinement of a mathematical model

04 p0489 A73-15735

Error minimization methods for Planck law remote measurements of single and two color temperature, considering multiple wavelengths

04 p0445 A73-15773

Nonlinear heat transfer systems design optimization based on physical properties cost functionals, presenting geometric programming method

[ASME PAPER 72-WA/HT-15] 04 p0519 A73-15833

Linear analytical procedure for adhesively bonded flat joints design with minimized shear stress concentration, presenting finite element and automated iterative procedure

[ASME PAPER 72-WA/DE-13] 04 p0514 A73-15874

Modulating /multiplicative/ noise effects on output signal characteristics of receiver designed for optimal reception against background of Gaussian noise

04 p0423 A73-15915

Optimal distribution of resources in automatic detector-meters determining number of random concentrated radio noises in assigned frequency range

04 p0423 A73-15926

A note on a minimum principle in Benard convection.

04 p0520 A73-15940

Allowance for the correlation of factors in the method of priorities for electrical system optimization

05 p0560 A73-16272

Book - Sequential analysis and optimal design.

05 p0590 A73-16352

Classical minimization procedure without iteration for digital computation of generalized inverse of rectangular matrix with real or complex coefficients

05 p0590 A73-16581

A class of airfoils designed for high lift in incompressible flow.

[AIAA PAPER 73-86] 05 p0528 A73-16851

Optimal and stiffened simply supported circular plates comparison under uniform pressure and uniform compression loads

[AIAA PAPER 73-254] 05 p0635 A73-16976

Analytical design of optimal nutation dampers.

05 p0630 A73-17206

Probabilistic minimum weight limit design of one dimensional pin jointed structures with random continuous variables, using stochastic programming

06 p0757 A73-17397

The effects of various parameters on an aeroelastic optimization problem.

06 p0758 A73-17565

Digital and hybrid computational aspects of the discrete representation theorem of nonlinear estimation.

06 p0670 A73-17803

Optimize Gunn circuits for wideband varactor tuning.

06 p0675 A73-17841

Optimal sampling and quantization rates for analog signal by mean-square-error estimates and information content quantitative measure, describing probabilistic properties estimation

06 p0664 A73-17854

Simplex gradientless algorithm for unconstrained static optimization, noting effectiveness for arbitrary goal functions in nonlinear programming

06 p0670 A73-17858

Comparison of the Powell 1, Powell 2, and Zangwill static optimization methods

06 p0670 A73-17859

Quadratic termination properties of minimization algorithms. I - Statement and discussion of results. II - Proofs of theorems.

06 p0716 A73-17983

Explosive forming for axisymmetric dish shells without clamped blank around edge, discussing design parameters, formability limits and optimization techniques

[SME PAPER MF 72-237] 06 p0698 A73-18095

Mean square error automatic equalizer for synchronous data transmission by gradient projection method for parameter optimization in discrete frequency domain, noting algorithm convergence

06 p0665 A73-18141

Constrained optimal design of circular plates against buckling.

06 p0762 A73-18338

Limit design in the absence of a given layout - A finite element, zero-one programming approach.

06 p0762 A73-18340

A unified formulation of the theory of optimal plastic design with convex cost function.

06 p0763 A73-18343

Optimal and suboptimal systems for detecting fluctuating optical radar pulses.

06 p0668 A73-18393

Book on nonlinear optimization covering search, iteration, gradient, algorithmic and computer techniques, mathematical and dynamic programming, calculus of variations, Pontryagin maximum principle, etc

06 p0717 A73-18401

Least square approach for system reliability optimization.

06 p0681 A73-18524

Numerical solution of the integral equations for optimal sequential filtering.

06 p0719 A73-18814

Weight minimization of axisymmetric clamped plates subject to constraints.

07 p0908 A73-19092

Optimum R.F.-power transport in Nd-limited gallium-arsenide travelling-wave amplifiers.

07 p0798 A73-19159

Automatic optimization of Symbolic Algol programs. I - General principles.

07 p0796 A73-19269

Multiparametric optimization of a thermionic electric power generating element

07 p0778 A73-19286

Multiparameter optimal design of plates and shells.

07 p0912 A73-19367

The prediction of the optimum performance of ejectors.

07 p0810 A73-19571

Thin walled beam composed indeterminate elastic framed structures minimum weight design, obtaining solutions by nonlinear programming algorithm

07 p0912 A73-19951

Second derivatives of the flutter velocity and the optimization of aircraft structures.

07 p0912 A73-19952

Multiple element airfoils optimized for maximum lift coefficient.

07 p0775 A73-19956

Optimization of antenna parameters in the presence of random errors.

07 p0801 A73-20128

One dimensional elastoplastic system optimal design by stochastic programming, determining limiting stresses and random load distribution

07 p0914 A73-20151

Approximate solutions to some static and dynamic optimal structural design problems.

07 p0915 A73-20341

Dynamic system model identification computational considerations, discussing equation error methods based on regression analysis, maximum likelihood estimates and gradient dependent algorithms for optimization

07 p0845 A73-20428

System modeling and optimal design of a Mars-roving vehicle.

07 p0906 A73-20593

The minimum weight structural configuration of pin-jointed truss cantilevers of given external shape.

08 p1015 A73-20671

On optimizing thermal stresses in cylindrical shells.

08 p1015 A73-20674

A nonlinear, nonconvex optimization problem

08 p0983 A73-20778

On the theory of optimal, constant thickness fibre-reinforced plates. II.

08 p1016 A73-20830

Optimisation in construction of the Jaguar and other military aircraft.

08 p0928 A73-20947

Optimized design - Characteristic vibration shapes and resonators.

08 p1017 A73-21191

Computer optimisation of double-dielectric-region IMPATT diodes.

08 p0947 A73-21433

Tibere rocket launched Electre nose cones reentry impact safety optimization policy based on probabilistic viewpoint

08 p1014 A73-21679

Weight optimization for multilayered plates and shells with given load, end conditions and middle surface shape and dimension

08 p1019 A73-21762

An algorithmically and physically oriented design approach. I - Problems analysis

09 p1087 A73-21900

Algorithms for calculating disjunctive normal form with minimum number of variables of completely/incompletely determined Boolean functions

09 p1111 A73-22108

Gas turbine combustor optimization dependence on combustion length and efficiency, cutoff pressure fall, wall cooling and pollution

09 p1135 A73-22213

Laser system output mirrors alignment for beam quality and power performance optimization and external optical component premature degradation prevention, using autocollimator

09 p1094 A73-22445

An optimal algorithm for measuring the dispersion of a random process in the case of separate allowance for the influence of external and internal additive noise

09 p1051 A73-22462

Mathematical properties of and optimization methods for bandlimited function systems, discussing applications to engineering problems

09 p1051 A73-22491

Determination of the optimal physical load in the local heating of a cylindrical shell

09 p1159 A73-22589

Optimization of system reliability using a parametric approach.

09 p1112 A73-22646

Determination of the optimal time of continuous work for operators in man-machine systems

09 p1046 A73-22849

Equivalent number method of optimal interval selection for meteorological observations with independent statistical samplings

09 p1114 A73-22853

Optimum holographic recording of complex light fields generated by diffusive objects in presence of point sources, maximizing SNR or distortion-free diffraction level

09 p1084 A73-22880

Rank-one and rank-two corrections to positive definite matrices expressed in product form.

09 p1113 A73-22956

Optimization of finite element grids based on minimum potential energy.

[ASME PAPER 72-PVP-3] 09 p1163 A73-23268

Weight minimization constrained design of rotational shallow spherical shells, comparing simplex and variable metric methods

09 p1165 A73-23446

The optimization of delay equalized comb-line filters.

10 p1193 A73-23609

Aircraft operations computerized simulation for commercial flight schedules evaluation and optimization, describing operational modeling and programming

10 p1203 A73-23685

Best approximation in digital filtering

10 p1242 A73-23764

A mathematical programming approach to identification and optimization of a class of unknown systems.

10 p1242 A73-23773

Investigation of the dynamics of a rotation scheme of a spacecraft composed of two units

10 p1286 A73-23877

A mathematical model of the optimization of cosmic ray intensity observation data

10 p1268 A73-23935

Book - Iterative methods for nonlinear optimization problems.

10 p1242 A73-23947

Optimal conductive heating of hollow cylinder inner surface with temperature dependent thermal stress limits for internal/external surfaces

10 p1289 A73-24063

Positive solutions of infinite equation and inequality systems and Lagrange multipliers for infinite differentiable optimization problems

10 p1243 A73-24163

Chebyshev projections properties, determining method for minimum linear distortion in class of conformal mappings of given region

10 p1212 A73-24300

Complex target resolution with the random signal radar.

10 p1189 A73-24560

Optimal, elliptic and circular windings for superconducting nonferrous magnetic MHD generators, comparing cross sections

10 p1178 A73-24594

Optimal reconstruction of a stationary random process from discrete readings

10 p1202 A73-24611

Comparative analysis of optimal failure search procedures, considering criteria, failure extent, initial data, reliability and compatibility

10 p1226 A73-24696

Structural design for weight or volume minimization in deformable body under combined loads, comparing structures with different boundary configurations

10 p1226 A73-24791

Russian book on analytical theory of optimization in gravitational fields covering orbital transfer trajectories, variational optimization problems, Lagrange multiplier properties, etc

10 p1284 A73-24800

Symmetrical airfoils optimized for small flap deflection.

10 p1174 A73-24915

Design of lowest-cost prestressed combined metallic systems

11 p1371 A73-25035

Computerized optimal tube heat exchanger design, discussing programming for heat transfer surface area and operating point determination 11 p1448 A73-25102

Iterative computer-aided design of optimum cascaded digital recursive filter, using unconstrained Fletcher-Powell algorithm for frequency domain synthesis 11 p1327 A73-25189

Multiinput multioutput linear time invariant discrete system optimal approximation, noting algorithms and weighting matrices computational difficulties 11 p1390 A73-25192

Strength and weight optimization of strengthened spherical shells under external pressure 11 p1434 A73-25389

Automated structural synthesis using a reduced number of design coordinates. [AIAA PAPER 73-336] 11 p1436 A73-25476

A unified approach to the problem of optimization in the design of structures. [AIAA PAPER 73-337] 11 p1436 A73-25477

Mathematical programming optimization procedure applicable to minimum weight structural design, considering static stress and displacement constraints under alternative loading conditions [AIAA PAPER 73-341] 11 p1436 A73-25480

Optimum design of stressed skin structures using a sequence of linear programs method. [AIAA PAPER 73-342] 11 p1436 A73-25481

Mathematical programming techniques of dimensionless index solutions for optimal structural design by iterative search on computer, applying to beam column steel structures [AIAA PAPER 73-344] 11 p1436 A73-25483

Computer programs for structural design optimization, discussing automated structural optimization program /ASOP/, component display analysis and stiffened panel programs [AIAA PAPER 73-345] 11 p1436 A73-25484

Optimization studies in the support design for the Large Space Telescope. [AIAA PAPER 73-350] 11 p1437 A73-25488

Application of computer-aided aircraft design in a multidisciplinary environment. [AIAA PAPER 73-353] 11 p1304 A73-25490

Rayleigh quotient minimization and eigenvalue/eigenvector errors of mode convergence in dynamic structural analysis, using gradient algorithm and scaling transformation [AIAA PAPER 73-361] 11 p1438 A73-25497

Isogrid as integral stiffened waffle with triangular pattern to allow simple graphical solution for optimizing spherical caps or cylinders under various buckling loads [AIAA PAPER 73-365] 11 p1438 A73-25500

Aeroelastic structural weight optimization under strength and flutter constraints, using finite element and displacement methods to describe equations of motion in matrix form [AIAA PAPER 73-389] 11 p1439 A73-25518

Gradient optimization of structural weight for specified flutter speed. [AIAA PAPER 73-390] 11 p1439 A73-25519

Numerical procedure for determining optimal member sizes of aircraft structural components with weight minimization and flutter speed lower bound [AIAA PAPER 73-391] 11 p1439 A73-25520

Eigenvalue problem and stiffness optimization procedure for incremental flutter analysis, describing method use in computer graphics mode [AIAA PAPER 73-392] 11 p1439 A73-25521

Optimization of the loop-coupled log-periodic antenna. 11 p1337 A73-25652

Synthesis of broad-band arrays with arbitrary frequency-independent elements. 11 p1329 A73-25664

Optimum bandlimited signal synthesis with pulse compression for transionospheric propagation along vertical path, considering statistical effects of total ionospheric electron content variations 11 p1330 A73-25689

Statistical method for fiber-reinforced plate design optimization for important boundary conditions, noting topographies associated with piecewise linear specific cost functions 11 p1443 A73-26092

Optimization of aircraft structures with multiple stiffness requirements. 11 p1444 A73-26298

Optimization problems with large parameters. 11 p1391 A73-26365

Minimum-mass design of multielement structures under a frequency constraint. 11 p1444 A73-26380

Geometric programming with signomial transformation into equivalent posynomials minimized under inequality constraints and generalization by equilibrium solutions to reverse programs in larger class 11 p1391 A73-26576

An iterative method for generalized nonlinear complementarity problems. 11 p1391 A73-26577

Cutting planes for programs with disjunctive constraints. 11 p1391 A73-26578

Linear system modeling via optimal finite dimensional approximation based on Sard generalized spline, giving error bounds 11 p1391 A73-26580

Viterbi algorithm for recursive optimal estimation of state sequence of discrete time finite state Markov process observed in memoryless noise 11 p1333 A73-26690

Questionnaire approach for technical diagnostics problem formulation covering hardware failure analysis coding, combinational switching device synthesis and optimal program construction 12 p1482 A73-26752

Automatic control system components optimization for minimal cost, demonstrating algorithm efficiency for servosystem 12 p1482 A73-26775

Inertial air navigation system error minimization, using discrete-sampled position fixing and star sighting data in computerized calculations 12 p1522 A73-26821

Choice of the quantization step and sampling interval for analog measurement signals 12 p1482 A73-26848

Amplitude-modulated pulse code sequence demodulation using physically realizable linear filter for reconstruction of discrete sample message at optimum mean-square error level 12 p1467 A73-26943

Analysis of the operational parameters of a bypass turbojet 12 p1532 A73-27069

Temperature field in front of or behind gas turbine with additive white noise, deriving optimal filter for dynamic programming technique in random fields analysis 12 p1483 A73-27080

Aircraft design parameters optimization based on criterion function representing overall deviation for specifications with application to subsonic passenger aircraft 12 p1458 A73-27095

Quadratically convergent algorithms and one-dimensional search schemes. 12 p1517 A73-27118

The evolution of a computer program for obtaining optimum computer simulation solutions. 12 p1475 A73-27133

Aerospace systems evaluation and optimization via systems analysis, discussing capability, dependability and availability and cost 12 p1561 A73-27384

Unit batch size optimization in mass production, discussing labor efficiency, operational cycle length, unfinished volume and total cost 12 p1562 A73-27477

Variational optimization problems for equations of hyperbolic type. 12 p1518 A73-27528

On optimal thickness of a cylindrical shell loaded by external pressure. 12 p1554 A73-27540

Book - Numerical methods for unconstrained optimization. 12 p1518 A73-27549

Highly dispersive Fe powder electrodeposition on cathode, examining electrolyte concentration, acidity, current density and bath temperature effects on current efficiency for optimal deposition conditions 12 p1503 A73-27552

Multistep conjugate gradient search methods with memory, describing convergence of iterative procedure for functional minimization 12 p1485 A73-27617

Optimum design of composite shells subject to natural frequency constraints. 12 p1554 A73-27734

Design optimization of prestressed concrete spans for high speed ground transportation. 12 p1554 A73-27735

Selection of optimal parameters for unidirectionally compressed three-layer plates 12 p1555 A73-27795

Optimizing sensitometric data for color and black and white aerial film. 12 p1501 A73-27966

Continuous analog signals optimal discretization involving selected quantization steps and sampling rates 13 p1595 A73-28017

Application of Liapunov functions for studying the convergence of unconstrained minimization methods 13 p1657 A73-28018

Multiparameter optimization of a thermionic fuel cell. 13 p1571 A73-28686

Glass fiber reinforced plastics optimum glass volume fraction for maximum flexural rigidity and strength 13 p1645 A73-28777

Triggering apparatus for optimal recording of slowly evolving phenomena using electrical impulse or mechanical contact signal 13 p1617 A73-28840

Prediction of optimal maintenance for devices 13 p1625 A73-29136

Optimizing power efficiency of hydrazine-oxygen fuel cells. 13 p1574 A73-29596

Radiating waveguide antenna elliptical beam off-axis gain maximization, applying to geostationary satellite 13 p1587 A73-29671

The optimization of the supporting structures of parabolic antennas 14 p1740 A73-29744

On the optimal design of statically indeterminate elastic structures subjected to multiple loading systems and multiple constraints. 14 p1805 A73-29760

Solution of linear equations in remote sensing and picture reconstruction. 14 p1767 A73-29767

Optimization of turbulence models by means of a logical search algorithm. 14 p1744 A73-29931

Launching operations organization and optimization and information supply, discussing vehicle reliability impact 14 p1741 A73-30086

Optimal antenna array signal to noise ratio gain comparison with conventional array for narrow band signal environment 14 p1735 A73-30222

Minimum potential and complementary energy rate principle formulation for finite plastic deformation, applying to cylindrical shell under uniformly distributed internal load 14 p1809 A73-30258

Optimal shapes of simply supported vibrating elastic beams for maximum fundamental frequency under axial compressive load 14 p1812 A73-30494

Optimisation theory of elastic-rigid bodies under repeated variable deformation. 14 p1812 A73-30495

Optimal lighting for visual tasks, discussing color, type, transillumination, crossed polarization, brightness patterns, diffuse reflection and surface shadowgraphing 14 p1722 A73-30498

Application of the optimal linearization method to the heat transfer problem. 14 p1817 A73-30605

Rotors and turbine disks fracture resistance optimization at high temperatures from plane strain toughness criteria 14 p1813 A73-30679

On the weight minimization of supersonic, axisymmetric circular cylindrical shells of finite length. 14 p1814 A73-30709

A procedure for the minimization of the costs of a project in the case of a given project duration 15 p1959 A73-31224

Optimal forms of the thin-walled closed cross-section of a beam subjected to bending 15 p1947 A73-31365

Parameters of rational airfield pavement design system. [ASCE PREPRINT 1700] 15 p1855 A73-31386

An asymptotically optimal rank detection algorithm for a signal in noise of unknown distribution 15 p1842 A73-31490

Optimal reception of digital signals on an additive noise background 15 p1843 A73-31493

Optimal algorithms for numerical solutions of singular integral equations 15 p1900 A73-32096

Structural components shape optimization for stress concentration reduction, solving complex boundary value problem via conformal transformation to curvilinear coordinates 15 p1954 A73-32108

The optimization of modal sound attenuation in ducts, in the absence of mean flow. 15 p1865 A73-32152

Propulsion system optimization for interstellar probes. 15 p1943 A73-32217

Operations research methods application to meteorological forecasting, discussing optimization algorithm and feedback systems 15 p1907 A73-32354

Onboard electronic equipment optimization and redundancy 15 p1852 A73-32460

Analytical expressions for postmaneuver velocity and transfer impulse optimizing elliptic-to-hyperbolic orbital transfer 15 p1941 A73-32603

Optimal design of layered structures under dynamic loading. 16 p2075 A73-32790

- Optimum shapes of slender axisymmetric missile bodies with minimum ballistic factor, using calculus of variations 16 p2071 A73-32904
- Optimal structural design of elastic rotating disks by dynamic programming 16 p2079 A73-33009
- A variational approach to grid optimization in the finite element method. 16 p2079 A73-33010
- Variational geometry optimization of thin rotational membrane shells under axisymmetric loading 16 p2079 A73-33011
- Mutual coupling in the signal-to-noise ratio optimization of antenna arrays. 16 p1979 A73-33168
- The optimization of the cross-sectional profile of rods and plates subjected to dynamic stress 16 p2080 A73-33241
- Utilization of realization to optimize the choices of reliability from the economic point of view 16 p2088 A73-33270
- Dual extremum principles relating to optimum beam design. 16 p2081 A73-33748
- Numerical methods for non-linear optimization; Proceedings of the Conference, University of Dundee, Dundee, Scotland, June 28-July 1, 1971. 16 p2033 A73-33851
- Numerical experience with algorithms for unconstrained minimization. 16 p2033 A73-33852
- The choice of step length, a crucial factor in the performance of variable metric algorithms. 16 p2033 A73-33853
- A combinatorial method to compute a global solution of certain non-convex optimization problems. 16 p2033 A73-33855
- A survey of methods for solving constrained minimization problems via unconstrained minimization. 16 p2033 A73-33857
- Generalization of an exact method for solving equality constrained problems to deal with inequality constraints. 16 p2033 A73-33858
- Optimum finite element idealization characterization based on displacement formulation, system potential energy true minimum, stiffness matrix gradients and geometry considerations 16 p2082 A73-33909
- Book - Optimum structural design: Theory and applications. 17 p2242 A73-34350
- Remarks on the optimum rate of convergence of the on-line identification of non-stationary systems. 17 p2144 A73-34600
- Optimal modular redundancy over a set of configurations for attaining specified system availability and reliability requirements. 17 p2139 A73-35257
- A comparison of the complex method of optimization with the penalty function approach using Zangwill's method for constrained optimization problems. 17 p2202 A73-35385
- An optimization technique utilizing the deflected gradient algorithm for dynamic testing of electromechanical equipment. 17 p2202 A73-35386
- Systems engineering at the Jet Propulsion Laboratory. 17 p2258 A73-35574
- Book - Graph theory in modern engineering: Computer aided design, control, optimization, reliability analysis. 17 p2132 A73-35600
- Fuel-optimal angular momentum vector control for spinning and dual-spin spacecraft. 17 p2240 A73-35663
- Estimates of unknown parameter from quantized observations given as sequence of evenly distributed random values, noting optimal grouping equations for general distribution function 17 p2130 A73-35722
- Optimal processing of signals in systems with multiple elements/channels/of reception. 17 p2130 A73-35723
- Graphite fiber optimization and evaluation efforts for utilization as fiber-epoxy composites reinforcement in tensile-critical applications 17 p2198 A73-35838
- Optimal plastic design for partially preassigned strength distribution. 18 p2365 A73-36638
- Fractured solutions in the calculus of variations. 18 p2330 A73-36640
- Formal treatment and optimization of Boolean expressions. 18 p2292 A73-36956
- Numerical methods for solving some problems in studies of operations 18 p2331 A73-36985
- Propulsion system optimisation for a single-stage constant-thrust relativistic rocket. 18 p2361 A73-37037
- Problems of minimum-weight turbomachine rotor designs 18 p2367 A73-37140
- A digital optimization device for directional charged particle measurements in space research. 19 p2428 A73-37148
- Symposium on Optimisation in Aircraft Design, London, England, November 15, 1972, Proceedings. 19 p2378 A73-37405
- Simplex method for linear programming for computerized design global optimization problems involving large numbers of equations and variables 19 p2407 A73-37406
- Military aircraft structure computerized design optimization procedures based on local optimum and stiffness requirements 19 p2495 A73-37407
- The optimisation of wing design. 19 p2495 A73-37408
- Algorithm for optimal material selection by seeking tradeoff between conflicting multifunctional structural design objectives 19 p2496 A73-37477
- Structural optimization by methods of feasible directions. 19 p2496 A73-37478
- Optimum windings for linear induction machines. 19 p2389 A73-38312
- Monograph on optimal structure design by linear programming and calculus of variations covering pin jointed frameworks, beams, circular sandwich plates, Michell continua, etc 19 p2502 A73-38364
- Computerized optimization of interrelated airframe/engine design parameters against variable criteria to satisfy performance constraints in air superiority fighter design [AIAA PAPER 73-800] 19 p2388 A73-38370
- Probabilistic automata minimization for system states reduction by deterministic matrix method 19 p2408 A73-38564
- Optimality and lower and upper bound conditions for multistep games with saddle point and minimax/maximin strategies, extending to differential games 20 p2539 A73-38678
- Gradient method of nonsmooth function minimization on an analog computer 20 p2531 A73-38682
- Dynamics of a twisting mode for a two-section space vehicle. 20 p2614 A73-38896
- Nonparametric properties of detectors optimized for Gaussian interference of unknown intensity. 20 p2529 A73-38923
- The fastest transfer from one circular orbit to another under the action of a small thrust 20 p2604 A73-38990
- Optimal detection of binary signals with an arbitrary distribution of state durations at the output of a binary symmetrical Markov channel 20 p2541 A73-38992
- Transmission strategy and optimal block size in high-speed data communication. 20 p2530 A73-39128
- The optimal nonlinear characteristic of the drive element in an astable multivibrator with a tunnel diode 20 p2536 A73-39201
- Optimal matching by using band filters 20 p2537 A73-39452
- Engineering design and optimization of the parameters of frequency doublers for the visible range. 20 p2573 A73-39685
- Determination of optimal regimes of a common-emitter transistor cascade which ensure minimal distortions 21 p2659 A73-40012
- Image restoration filter with preprocessing to minimize distortion due to truncation errors and edge effects 21 p2697 A73-40131
- Constrained optimization using a nondifferentiable penalty function. 21 p2725 A73-40384
- Russian book on radar signal synthesis optimization problems covering proximity criterion, ambiguity and autocorrelation functions and FM and PSK signals 21 p2650 A73-40419
- Some method of nonlinear programming suitable for solving the task of optimization of a small transport aircraft 21 p2634 A73-40478
- Linear programming for optimization, discussing definitions, practical examples, simplex algorithm, duality theory, heuristic interpretations and integer solutions 21 p2726 A73-40836
- Optimum tapering design of vibrating cantilever beams, considering geometrically similar and rectangular cross sections and degenerated end mass case 21 p2785 A73-40839
- Optimal design of linearly elastic vibrating structural members for minimized total mass and maximized fundamental frequency respectively, noting solution existence dependence on boundary conditions 21 p2785 A73-40840
- The filtering of random sequences with gaps by optimal discrete filters with a constant memory volume 21 p2658 A73-40857
- An optimized video output from a wide angle optical probe. [AIAA PAPER 73-918] 21 p2673 A73-40866
- Multicriterial optimization problems solution by method of effective sets defined in criterion or variable vector spaces, noting advantages over global criteria and additive value methods 21 p2670 A73-40992
- Linear optimization theory, discussing duality theory, matrix calculations, simplex methods, base points, classical transport problems and industrial production applications 21 p2727 A73-41071
- Unsupervised learning of the Kalman filter. 21 p2664 A73-41109
- Optimization of electronic circuits with characteristics depending on a continuously varying parameter 21 p2666 A73-41311
- An effective algorithm for optimizing electronic circuits 21 p2671 A73-41312
- Electronic circuit optimization via Powell iterative method, describing search techniques, matrix methods and transistor hybrid equivalent circuit application 21 p2671 A73-41313
- Journal bearings computerized design optimization by geometric programming with volume, dimensions, torque and horsepower absorption, shaft strength, speed, load, pressure and Sommerfeld number as constraints 21 p2708 A73-41668
- Nonlinear optimization reduces the sidelobes of Yagi antenna. 22 p2831 A73-41847
- An analytical method of designing long turbine blades 22 p2918 A73-41960
- Optimal utilization of redundant information in thermal radiation in thermophysical measurements. [ECTP PAPER II-2] 22 p2931 A73-42408
- Prestressing force and tendon configuration optimization for indeterminate structure with prescribed cross sectional dimensions, using linear programming and design variable transformation 22 p2922 A73-42476
- Comparison of some penalty function based optimization procedures for the synthesis of a planar truss. 22 p2922 A73-42478
- Geodetic net optimal design with known configuration matrix, basin, approach on calculus of inverse matrices 22 p2847 A73-42496
- Experimental substantiation of the optimal method for scaling the duration of acoustic stimuli 22 p2814 A73-42654
- Computer-aided design of airport system plans. [ASCE PREPRINT 2058] 22 p2839 A73-42867
- Evaluation of error bounds in an optimization problem using the finite-element method. [ASME PAPER 73-APMW-15] 22 p2924 A73-42882
- Identification of damping coefficients in multidimensional linear systems. [ASME PAPER 73-APMW-43] 22 p2926 A73-42899
- Optimization of exposure time in linear hologram recording by pre-exposure or post-exposure. 22 p2862 A73-43090
- Use of a response surface to optimize digital telecommunication systems. 23 p2948 A73-43214
- Optimal work-rest schedules under prolonged vibration. 23 p2948 A73-43217
- An optimality condition for assessing systematic errors 23 p2999 A73-43264
- Optimal navigation function for spacecraft orbit defined by initial conditions and acting force constants, determining matrix minimizing variance estimate 23 p3005 A73-43270
- Finite journal bearings with stepwise discontinuity in hydrodynamic film shape, predicting optimal performance as function of step height, eccentricity and L/D ratios 23 p2984 A73-43293
- Fluidic vortex-type proximity sensor with analog to digital converter, optimizing output nozzle diameter and pressure by steepest ascent method 23 p2981 A73-43431
- Synthesis and analysis of optimal dual-mirror antennas 23 p2959 A73-43516
- Digital-computer aided analysis and synthesis of specialized functional diode converter circuits 23 p2959 A73-43579

Performance criteria selection for complex system parameter optimization based on minimum deviation from extremal values

23 p2963 A73-43737

A new approach to optimal design of elastic structures.

23 p3042 A73-43798

Analysis of hurricane data using the variational optimization approach with a dynamic constraint.

23 p3004 A73-44258

Choice of the duration of an elementary signal in the presence of fluctuations in the synchronization channel

24 p3067 A73-44605

State minimization of incompletely defined deterministic automaton by imbedding one-to-one mapping into homomorphism

24 p3074 A73-44664

Maximum SNR performance calculation for heterodyne laser detection system with parameters optimization under assumed total cost

24 p3096 A73-44875

Receiving antenna optimum polarization determination by mapping on Poincare sphere for maximum ratio of signal to summed external interference and internal noise

24 p3068 A73-44943

Optimum design of lattice structures in creep conditions with consideration of the Kempner-Hoff theory of buckling.

24 p3148 A73-45002

Bellman dynamic programming principle for elastically-plastic beam structure design optimization with respect to cross-sections, span lengths and weight

24 p3148 A73-45003

Respiratory work minimization during exercise, using respiratory frequency, functional residual capacity and air flow pattern effects as controlled variables

24 p3060 A73-45066

Algorithmic and computational aspects of the use of optimization methods in engineering design.

24 p3070 A73-45235

Structural design optimization by iterative analysis using proper stiffness matrix with applications to sandwich plate and frame problems

24 p3150 A73-45236

Optimization of fiber reinforced composite structures.

24 p3151 A73-45304

Optimal force transmission by flexure-clamped boundaries.

24 p3152 A73-45317

Optimization of compression constants for cumulated plane shock waves in a closed tube.

24 p3117 A73-45428

Optimal convergence of iterative solution for system of linear equations with real roots based on matrix method

24 p3106 A73-45441

Solution of the variational problem of designing the contour of a two-mode nozzle

24 p3055 A73-45533

OPTIMUM CONTROL

U OPTIMAL CONTROL

OPTIMUM THRUST PROGRAMMING

U THRUST PROGRAMMING

OPTIONS

Objective trees as technological forecasting technique in structuring program options for selected strategies, considering R and D, marketing and other functional business programs

08 p1026 A73-21699

OPTOMETRY

Two dimensional eye movement recording using a photo-electric matrix method.

07 p0786 A73-20259

Apparatus for measurement of vision acuity restoration time after brief macula lutea exposures to light

23 p2949 A73-43791

OR-GATES

U GATES (CIRCUITS)

ORBIT CALCULATION

Gravity thrust Jupiter orbiter trajectories generated by encountering the Galilean satellites.

01 p0095 A73-10103

An approximate form of the third integral in the Galaxy.

01 p1013 A73-11017

Comparison of Kalman filter and stepwise methods for real time orbit determination.

01 p1015 A73-11187

Elliptical orbits of mass point under Newtonian gravitational forces of two fixed centers with different mass in Cartesian coordinates as function of time

02 p0211 A73-11776

Processing of results of observations of the satellite 65-011-04 carried out within the framework of INTEROBS program 1966.

02 p0159 A73-12170

Meteorite aphelia calculation from activity levels of accumulated cosmogenic radioisotope due to cosmic ray irradiation

02 p0221 A73-12690

Eclipsing binary system orbital eccentricity deduction from observed epochs of light minima

02 p0223 A73-12734

Analysis of the orbit of Cosmos 316/1969-108 A/.

02 p0225 A73-12824

Computation of Schwarzschild's periodic solutions in the restricted three-body problem.

02 p0226 A73-12838

A numerical investigation of secular terms of the planetary disturbing function.

03 p0372 A73-13351

Geostationary artificial satellite orbital parameters calculation, taking into account lunar, solar and light pressure perturbations

03 p0378 A73-14551

Optimum elliptic orbit characteristics of planetary artificial satellite based on earth-planet-earth flight

03 p0379 A73-14572

A new method for calculating the preliminary orbit of an artificial satellite with the aid of simultaneous observations

03 p0379 A73-14579

On the Napier method for the photometric reflection effect in close binary stars.

03 p0379 A73-14583

Comet orbit calculation in terms of nongravitational force effects, emphasizing periodic comet return predictions

04 p0495 A73-14762

Propagation of errors in orbits computed from density layer models.

04 p0438 A73-14790

A state covariance matrix computation algorithm for satellite orbit determination sequential filtering.

04 p0431 A73-15267

Nonlinear estimation theory applied to the interplanetary orbit determination problem.

04 p0498 A73-15271

Subsatellite point coordinates calculation for artificial earth satellites with nearly circular orbits, noting ephemeris application

05 p0613 A73-16203

Analytical approach to orbit determination in the presence of model errors.

[ALAA PAPER 73-170] 05 p0619 A73-16915

Accelerated numerical integration of the equations of motion of celestial mechanics

05 p0619 A73-17002

Alteration of the Laplace spheres of planetary influence during the application of a new intermediate orbit

05 p0620 A73-17022

Limits of possible position of tenth planet at 50-100 AU from analysis of Neptune orbit

05 p0622 A73-17180

French computation center equipment for satellite orbit calculations and attitude corrections, describing links between teleprocessing and data transmission

05 p0555 A73-17300

Orbit determination capability analysis for the Mariner-Jupiter-Saturn 1977 mission.

[ALAA PAPER 73-171] 06 p0748 A73-17650

Earth-based orbit determination for solar electric spacecraft with application to a Comet Encke rendezvous.

06 p0748 A73-17651

Spinning test bodies motion in metric fields, applying to spinning stars in orbit around black holes

06 p0749 A73-17869

Solution of the low-altitude satellite equations.

06 p0757 A73-18072

Book - The Titius-Bode Law of planetary distances: Its history and theory.

06 p0753 A73-18403

Nonlinear estimation theory applied to the interplanetary orbit determination problem.

07 p0805 A73-20582

Computational aspects of multilevel trajectory optimization.

07 p0903 A73-20589

Determination of the elements of an orbit from known values of the velocity vector at three different moments of time

08 p1012 A73-21550

Definitive orbit of the comet 1937 V Finsler.

08 p1012 A73-21580

Orbit determination by range-only data.

08 p1013 A73-21816

Normal matrix equations for major planet orbital element corrections from optical observations, testing by numerical experiment for Mercury

09 p1143 A73-22096

Literary theory of the motion of a satellite in the terrestrial-harmonic field of the earth's gravitational potential at small eccentricities

09 p1143 A73-22097

Geometrical dynamics method for orbit geometry in configuration space of dynamical system, using polar coordinates as generalized coordinates for circular restricted three body problem

09 p1148 A73-22911

Predicting network for artificial satellite tracking data acquisition and preprocessing and orbit parameters computation

10 p1187 A73-23622

Note on Brady's hypothetical trans-Plutonian planet.

10 p1275 A73-23847

Mathematical processing of measurement data in the orbital method of space geodesy

10 p1281 A73-24480

Determination of the coordinates of points in a cosmic geodetic grid by the orbital method

10 p1281 A73-24481

Calculation of higher-order perturbations in the motion of celestial bodies

10 p1282 A73-24482

Relative motion of near orbiting satellites.

10 p1283 A73-24662

Lunar gravity derived from long-period satellite motion - A proposed method.

10 p1283 A73-24664

Periodic solutions of the third sort for restricted problem of three bodies and their stability.

11 p1423 A73-26068

Exact analytical solutions basic to a class of two-body orbits.

11 p1423 A73-26072

An analytical iterative algorithm for the prediction of special satellite orbit points with the Brouwer orbit theory.

11 p1423 A73-26075

Preliminary orbit determination for lunar satellites.

11 p1426 A73-26396

Investigation of star orbits in stellar clusters with allowance for the disturbing force of the galaxy

12 p1538 A73-26863

Trigonometric series for earth rotation velocity around solar system center of mass

12 p1540 A73-27297

Least squares method for satellite motion parameters determination in orbital plane, using altimeter distance to planet surface measurements

12 p1543 A73-27627

Transcendental equations solution for satellite Kepler orbit determination from coordinates, velocity and time components, using Lambert-Euler relation

12 p1543 A73-27629

Artificial satellite orbit determination from range measurements, applying to orbits around earth and other planets

12 p1543 A73-27722

Determination of the circular orbit of an artificial earth satellite from optical observations at undetermined moments of time

12 p1547 A73-27867

Polydynamic equilibrium equation for steady particle motion along stationary orbits in central body attraction field, comparing with Schroedinger wave equation

13 p1657 A73-28001

The origin of Jupiter's family of comets.

13 p1672 A73-28037

Earth rotation axis motion determination through satellite tracking via laser range observation, estimating orbit computation error sources

13 p1656 A73-28392

Pole position studied with artificial earth satellites.

13 p1656 A73-28393

Orbit selection for satellite missions, determining elements of sun-synchronous, recurrent, near-recurrent, polar, synchronous and stationary orbits

13 p1684 A73-29246

Numerical integration of orbits for evolution of different configurations, discussing Titius-Bode law and stability limits of planetoid and hypothetical planet orbits

13 p1686 A73-29366

Comet orbit and ephemeris calculations with reference to position and magnitude to facilitate reobservation with long focus telescopes

14 p1789 A73-29782

Chebyshev polynomial series solution method for highly eccentric perturbed orbits of comets, using modified Hansen method of partial anomalies

14 p1790 A73-29783

On the application of Hansen's method of partial anomalies to the calculation of perturbations in cometary motions.

14 p1790 A73-29784

Disturbing functions application to secular perturbation calculation for periodic comets with validity for any eccentricity and inclination

14 p1790 A73-29787

A method of integrating the equations of motion in special coordinates and the elimination of a discontinuity in the theory of the motion of periodic comet Wolf.

14 p1790 A73-29790

A numerical interpretation of the homogenization of observational material for one-apparition comets.

14 p1790 A73-29792

The influence of properties of a set of observations on the weights of determination of the orbital elements of a one-apparition comet.

14 p1790 A73-29794

Standardization of the calculation of nearly parabolic cometary orbits.

14 p1790 A73-29795

Determination of parabolic orbits on the basis of N observations, by means of an electronic computer
14 p1790 A73-29796

A search for Encke's comet in ancient Chinese records - A progress report.
14 p1791 A73-29799

Numerical analysis of the motion of periodic comet Brooks 2.
14 p1791 A73-29800

Linkage of seven apparitions of periodic comet Faye 1925-1970 and investigation of the orbital evolution during 1660-2060.
14 p1791 A73-29801

Pons-Brooks comet orbit calculation based on observations in 1812, 1883-1884 and 1953-1954, noting impossibility of single orbit fitting
14 p1791 A73-29806

Periodic comet Tempel-Tuttle orbital elements relation to Leonid meteor shower, using computer program for numerical integration
14 p1791 A73-29807

Periodic comet Stephan-Oterma orbit, taking into account perturbations by major planets
14 p1792 A73-29808

Determination of planetary masses from the motions of comets.
14 p1792 A73-29809

Saturn mass determination from Hidalgo orbit trajectory and variational equation, obtaining probable error from fitted parabola
14 p1792 A73-29813

Evolution of short-period cometary orbits due to close approaches to Jupiter.
14 p1794 A73-29832

Evolution of the orbits of selected minor planets during an interval of 1000 years.
14 p1794 A73-29840

Theoretical cometary radiants and the structure of meteor streams.
14 p1795 A73-29845

The particle resonance in spiral galaxies - Nonlinear effects.
14 p1801 A73-30727

Basic theory for PROD, a program for computing the development of satellite orbits.
15 p1930 A73-31108

First order perturbation theory for geostationary satellites orbit calculation, taking into account earth oblateness, equator ellipticity and solar and lunar gravitational effects
15 p1930 A73-31114

Optimal orbital transfer in the equatorial plane of an axisymmetric planet with a supplementary accuracy requirement
15 p1931 A73-31228

Optimal transfer between weakly elliptic orbits with a supplementary accuracy requirement and with allowance for nonsphericity
15 p1931 A73-31229

Intermediate orbit of an artificial earth satellite obtained by the averaging method - First order perturbations
15 p1936 A73-31644

Numerical experiments by Monte Carlo method to examine comet orbits evolution within solar system, noting Trojan, horseshoe and Jupiter-Saturn midrange orbits
15 p1938 A73-31949

Contribution to the dynamic study of the Galilean system of Jupiter. I - The intermediate solution in the nonresonant case
16 p2059 A73-32839

Nomograms for determining horizontal coordinates of artificial earth satellites
16 p2063 A73-33662

Differential transformation for satellite injection.
16 p2070 A73-33999

Monte Carlo model of cometary evolution based on hypothetical perturbed orbit calculations, with emphasis on short-period comets
17 p2228 A73-34426

Differential equations for ballistic motion of meteoric particles in earth atmosphere, noting orbit stability
19 p2480 A73-37237

Third integral of motion and the velocity field for a quasi-Newtonian potential. I
19 p2486 A73-37848

Minor planets and related objects. XIII - Long-term orbital evolution of /1685/ Toro.
20 p2607 A73-39123

Determination of a circular orbit for an earth satellite from optical observations at unknown times.
20 p2608 A73-39241

Experiments to determine satellite orbit geometry in spherically symmetric gravitational field, discussing aging asymmetry in clock paradox
21 p2739 A73-40623

Numerical analysis of families of periodic orbits in restricted three body problem with change in mass ratio μ
21 p2778 A73-41527

Realisation of rendezvous by the transfer orbit which is tangential to the original and terminal orbits.
21 p2779 A73-41550

The cause of the residuals in the motion of Halley's comet.
22 p2907 A73-42210

Russian book - Accuracy of comet and satellite orbits.
22 p2910 A73-42640

Determination of the orbital period of a satellite moving in the earth's gravitational field
23 p3027 A73-43268

Optimal navigation function for spacecraft orbit defined by initial conditions and acting force constants, determining matrix minimizing variance estimate
23 p3005 A73-43270

Orbit osculation control algorithm guaranteeing satellite repeated passage over given point of earth surface, deriving functional for satellite thrust control
23 p3027 A73-43271

Evolution of a 'class two' family of periodic orbits in the general planar problem of three bodies.
23 p3031 A73-43835

The global solution of the problem of the critical inclination.
23 p3031 A73-43836

Some useful results on initial node locations for near-equatorial circular satellite orbits.
23 p3031 A73-43837

Orbit improvement from satellite imaging data obtainable from outer planet missions.
23 p3032 A73-43840

Satellite intermediate orbit and secular perturbations due to second zonal harmonics of planetary potential and outer body attraction
23 p3037 A73-44254

The next return of the comet of the Perseid meteors.
24 p3135 A73-44583

A global solution in the resonance problem of Poincare.
24 p3141 A73-45288

Fast computation of high eccentricity orbits by the stroboscopic method.
24 p3142 A73-45292

The evolution of periodic orbits close to homoclinic points.
24 p3142 A73-45296

ORBIT DECAY
Satellite-caused energy dissipation via tides in spinning planet leading to orbital decay induced destruction or escape or to stable synchronism
09 p1142 A73-22041

Atmospheric density values from radar-determined low altitude satellite orbit decay and accelerometer data
18 p2302 A73-35942

Air density at heights near 200 km from the orbit of 1970-65D.
18 p2309 A73-36052

ORBIT EQUATIONS
U ORBITAL MECHANICS
ORBIT PERTURBATION
NT SATELLITE PERTURBATION
Algorithms for spacecraft trajectory optimization programs for orbit perturbations caused by random measurement errors and minimum mathematical expectancy of energy dissipation
02 p0220 A73-12468

Circular orbit stability in restricted two body problem with secular variations, giving disturbing function secular terms to eighth order
02 p0222 A73-12710

Computation of Schwarzschild's periodic solutions in the restricted three-body problem.
02 p0226 A73-12838

Trans-Plutonian planet calculations by Brady, discussing Halley, Olbert and Pons-Brook comet trajectories and perturbations and planet parameters
03 p0370 A73-13199

Expansions of the derivatives of the disturbing function in planetary problems.
03 p0377 A73-14272

Orbital period variations of eclipsing binary TW Draconis caused by third body effect, apsidal motion and matter exchange
03 p0379 A73-14582

Gravity anomalies determination from satellite orbit perturbations, using least squares method
04 p0439 A73-14799

Observed effects of earth-reflected radiation and hydrogen drag on the orbital accelerations of balloon satellites.
04 p0439 A73-14802

Resonances and encounters in the inner solar system.
04 p0500 A73-15519

A variation-of-parameters perturbation theory for the restricted three-body problem.
05 p0619 A73-16893

[AIAA PAPER 73-144]
Effects of the sun and the moon on a near-equatorial synchronous satellite.
08 p1011 A73-21430

Cometary parent bodies transfer to short period orbits by Jupiter caused gravitational disturbances, noting qualitative analysis of orbits evolution
08 p1012 A73-21576

Ejection of matter and gravitational radiation from orbiting bodies.
09 p1149 A73-22961

Differential equations in terms of the osculatory elements of a solid for the motion of the solid about its center of mass
09 p1121 A73-23355

Calculation of higher-order perturbations in the motion of celestial bodies
10 p1282 A73-24482

Lunar gravity derived from long-period satellite motion - A proposed method.
10 p1283 A73-24664

Studies in the application of recurrence relations to special perturbation methods. II - Comparison of the Encke and Cowell methods of integration in the restricted three-body problem.
10 p1283 A73-24668

Planetary masses, dynamic flattening and orbital elements determination by perturbation analysis for disturbed planet, space probe and satellite
11 p1420 A73-25882

Geos 1 and 2 long periodic and secular orbit perturbations, discussing osculating elements transformation with maximum accuracy via minitrack system
11 p1423 A73-26070

Nonsingular differential equations derivation for parabolic, hyperbolic, elliptic and rectilinear orbit perturbations via simple osculating element coordinate transformations and Lagrange planetary equations
11 p1423 A73-26073

Resonances and librations of some Apollo and Amor asteroids with the Earth.
11 p1429 A73-26688

Nongravitational force variation with heliocentric distances computed for long and short period comets, deriving force law from water snow vaporization rate
12 p1540 A73-27428

Systematic analysis of perturbations of orbits - The case of drag.
14 p1788 A73-29717

Chebyshev polynomial series solution method for highly eccentric perturbed orbits of comets, using modified Hansen method of partial anomalies
14 p1790 A73-29783

On the application of Hansen's method of partial anomalies to the calculation of perturbations in cometary motions.
14 p1790 A73-29784

Orbital characteristics of comets passing through the 1:1 commensurability with Jupiter.
14 p1790 A73-29785

On the motion of short-period comets in the neighbourhood of Jupiter.
14 p1790 A73-29786

Disturbing functions application to secular perturbation calculation for periodic comets with validity for any eccentricity and inclination
14 p1790 A73-29787

Nongravitational effects on comets - The current status.
14 p1791 A73-29797

On the determination of nongravitational forces acting on comets.
14 p1791 A73-29798

Numerical analysis of the motion of periodic comet Brooks 2.
14 p1791 A73-29800

Linkage of seven apparitions of periodic comet Faye 1925-1970 and investigation of the orbital evolution during 1660-2060.
14 p1791 A73-29801

Investigation of the motion of periodic comet Giacobini-Zinner and the origin of the Draconid meteor showers of 1926, 1933 and 1946.
14 p1791 A73-29802

Nongravitational forces and periodic comet Giacobini-Zinner.
14 p1791 A73-29803

Osculating orbital elements and nongravitational parameters for non-Newtonian orbit of periodic comet Borrelly
14 p1791 A73-29804

Borrelly periodic comet motion, including secular acceleration due to nongravitational forces and orbital elements perturbations by planets from Venus to Pluto
14 p1791 A73-29805

Periodic comet Stephan-Oterma orbit, taking into account perturbations by major planets
14 p1792 A73-29808

The determination of Jupiter's mass from large perturbations on cometary orbits in Jupiter's sphere of action.
14 p1792 A73-29810

Determination of the mass of Jupiter from observations of 10 Hygiea during 1932-1969.
14 p1792 A73-29811

Hidalgo orbit near Saturn, discussing resemblance to extinct comet nucleus, nongravitational force effects and planetary mass determination
14 p1792 A73-29812

On nongravitational effects in two classes of models for cometary nuclei.
14 p1793 A73-29820

ORBITAL ASSEMBLY

Rotation effects in the nongravitational parameters of comets.

14 p1793 A73-29821

A nongravitational effect in the simulation of cometary phenomena.

14 p1793 A73-29824

Determination of the form of the Oort cometary cloud as the Hill surface in the galactic field.

14 p1793 A73-29827

Diffusion of comets from parabolic into nearly parabolic orbits.

14 p1793 A73-29828

Comet motion and hyperbolic orbital statistics, discussing secular accelerations, decelerations and nongravitational effects

14 p1794 A73-29830

The effect of the ellipticity of Jupiter's orbit on the capture of comets to short-period orbits.

14 p1794 A73-29831

Evolution of short-period cometary orbits due to close approaches to Jupiter.

14 p1794 A73-29832

The major planets as powerful transformers of cometary orbits.

14 p1794 A73-29834

Investigation of the orbital stability of minor planets with cometary eccentricities.

14 p1794 A73-29839

Meteoritic particles orbits secular evolution under planetary perturbation and Poynting-Robertson effects, considering osculating orbital elements long term variations via simplified model

14 p1795 A73-29842

Deformation of a meteor stream caused by an approach to Jupiter.

14 p1795 A73-29843

Orbital evolution of the alpha Virginid and alpha Capricornid meteor streams.

14 p1795 A73-29844

Theoretical cometary radiants and the structure of meteor streams.

14 p1795 A73-29845

Optimal control synthesis in the observation problem. I, II

14 p1802 A73-30788

On approximate calculation of the principal part of disturbances in an interior bounded three-body problem.

14 p1802 A73-30953

First order perturbation theory for geostationary satellites orbit calculation, taking into account earth oblateness, equator ellipticity and solar and lunar gravitational effects

15 p1930 A73-31114

Application of the theory of Markov processes in state estimation of dynamic systems and in control of flight-vehicle oscillations

15 p1942 A73-31239

Evolution of satellite resonances by tidal dissipation.

15 p1938 A73-31950

Algorithms for spacecraft trajectory optimization programs for orbit perturbations caused by random measurement errors and minimum mathematical expectancy of energy dissipation

15 p1942 A73-32618

Vaporization theory of cometary nucleus prediction of law of dependence of nongravitational force on heliocentric distance

17 p2228 A73-34427

Barnard star multiplanet system, discussing inclinations of planetary orbits and cosmogonic implications.

17 p2229 A73-34430

Characteristics of the future orbital evolution of the comet Churumov-Gerasimenko, 1969h

17 p2230 A73-34597

Large-scale variations in the obliquity of Mars.

18 p2348 A73-35921

Density scale height and geopotential coefficients evaluations from analysis of Cosmos 54 rocket orbit perturbations due to drag and odd-zonal harmonics

18 p2351 A73-36176

Gyroscopic orbit errors caused by random perturbations

18 p2317 A73-36853

A study of commensurable motion in the asteroid belt.

20 p2606 A73-39075

Modification of weak turbulence theory due to perturbed orbit effects. II - Nonlinear Landau damping of electron plasma waves.

20 p2598 A73-39302

Evolution of the orbits and radiants of meteor swarms of the Jupiter family

21 p2768 A73-40724

On the 3-7 commensurability between Jupiter's outer two Galilean satellites.

21 p2778 A73-41531

The cause of the residuals in the motion of Halley's comet.

22 p2907 A73-42210

Airborne photographic and visual observation of material from Comet Giacobini-Zinner produced

meteor showers due to orbit perturbation and perihelion changes by Jupiter

22 p2909 A73-42588

Meteorite production mechanism from asteroid belt via asteroidal collision fragments perihelion changes and orbit perturbation by Jupiter into earth-crossing orbital elements

23 p3027 A73-43336

Densities deduced from perturbations at high altitudes.

23 p2972 A73-43688

Forces acting upon an asteroid moving through a meteoroid stream.

23 p3029 A73-43745

Numerical exploration of commensurable periodic solutions of the restricted problem of three bodies and their stability.

23 p3029 A73-43746

Gravitational perturbations of equatorial orbits.

23 p3032 A73-43839

Orientation-dependent effects in Oort's theory of comet origin. II - Anisotropies in the distribution of long-period comet orbits.

24 p3131 A73-44467

Nonlinear saturation of the gradient drift instability in the equatorial electrojet.

24 p3087 A73-45141

Vertical perturbation stability of three dimensional periodic orbits in restricted three body problem

24 p3142 A73-45295

A tenth order solution in explicit form to the 'restricted' three-body problem.

24 p3143 A73-45434

Current driven ion acoustic plasma instability based on ion orbit perturbation by turbulent waves, calculating angular spectrum for comparison with computerized simulation

24 p3118 A73-45463

ORBITAL ASSEMBLY

On-orbit checkout and repair as a factor in economical spacecraft design and operation.

12 p1549 A73-27439

ORBITAL ELEMENTS

Satellite orbit inclination function computation as representative problem in symbolic programming applied to celestial mechanics

01 p0099 A73-10688

Influence of selectivity on the observed orbital-parameter distribution of radio meteors

01 p0101 A73-10846

Lunar occultation of stars to determine moon diameter and orbital elements, noting time measurement difficulties due to scintillation effects

01 p0102 A73-10994

Processing of results of observations of the satellite 65-011-04 carried out within the framework of INTEROBS program 1966.

02 p0159 A73-12170

Very long baseline interferometry observations of radio emissions from geostationary satellites.

02 p0215 A73-12270

Theoretical model for tidal evolution induced capture of natural satellite pairs into orbit-orbit resonance, discussing Titan and Hyperion relationship with Saturn

02 p0219 A73-12421

Eclipsing binary system orbital eccentricity deduction from observed epochs of light minima

02 p0223 A73-12734

Improved orbit and ephemeris of the periodic Comet Reinmuth 1 for its apparition in 1972-73.

03 p0370 A73-13197

Determination of lunar orbital elements by the method of equal altitudes.

03 p0372 A73-13247

Stability criteria for equal mass triple star systems, considering direct or retrograde revolution and outer periastron distance to inner semimajor axis ratio

03 p0376 A73-14271

Statistical data processing method for accuracy evaluation of satellite orbit parameters obtained from onboard measurements of two stars angular positions

03 p0379 A73-14554

Data processing method for optimal prediction of spacecraft orbital elements, using dynamic and quadratic programming

03 p0379 A73-14555

Orbital period variations of eclipsing binary TW Draconis caused by third body effect, apsidal motion and matter exchange

03 p0379 A73-14582

Orbital elements and geopotential coefficients estimation with increased accuracy by satellite-satellite tracking

04 p0438 A73-14794

Improvement of zonal harmonics by the use of observations of low-inclination satellites Dial, SAS, and Peole.

04 p0438 A73-14795

Analysis of the orbit of Cosmos 268 rocket /1969-208/.

04 p0496 A73-14964

Secular inequalities in the motion of earth satellites.

04 p0503 A73-16020

Analysis of the effect of errors in determining the orbit parameters of a satellite on the accuracy of prediction of its motion

05 p0614 A73-16312

Computer and interactive graphics as applied to mission analysis.

[AIAA PAPER 73-112]

05 p0554 A73-16870

Orbital parameters optimization of circular orbit earth satellites network for continuous earth observation, using group theory

05 p0620 A73-17004

Correction of solar observations for stray light by numerical integration, with application to Mercury's drop.

05 p0621 A73-17032

Effects of resonant tesseral gravity coefficients on Viking-type orbits.

[AIAA PAPER 73-146]

06 p0748 A73-17648

Orbit analysis for coastal zone oceanography observations.

[AIAA PAPER 73-207]

06 p0748 A73-17659

Total solar eclipses of great duration.

07 p0876 A73-19400

Violet shift of the H alpha absorption line of the hydrogen-depleted star HD 30353

07 p0877 A73-19598

Determination of the elements of an orbit from known values of the velocity vector at three different moments of time

08 p1012 A73-21550

Normal matrix equations for major planet orbital element corrections from optical observations, testing by numerical experiment for Mercury

09 p1143 A73-22096

Close binary systems orbital elements perturbations due to stellar material viscosity effects on dynamical tide lag

10 p1271 A73-23478

Perturbed satellite motion differential equations, on basis of fixed center problem and perturbing forces with no force function

10 p1274 A73-23721

Note on Brady's hypothetical trans-Plutonian planet.

10 p1275 A73-23847

Determination of the coordinates of points in a cosmic geodetic grid by the orbital method

10 p1281 A73-24481

Perturbation function expansion in series of orbital elements for satellite motion in rotating oblate planet gravitational field with two fixed centers

10 p1282 A73-24493

Lunar gravity derived from long-period satellite motion - A proposed method.

10 p1283 A73-24664

Investigation of long-term periodic changes of the orbital elements of artificial earth satellites

10 p1283 A73-24699

Planetary masses, dynamic flattening and orbital elements determination by perturbation analysis for disturbed planet, space probe and satellite

11 p1420 A73-25882

Precession, nutation and the choice of reference system for close earth satellite orbits.

11 p1423 A73-26067

Geos 1 and 2 long periodic and secular orbit perturbations, discussing osculating elements transformation with maximum accuracy via minitrack system

11 p1423 A73-26070

Nonsingular differential equations derivation for parabolic, hyperbolic, elliptic and rectilinear orbit perturbations via simple osculating element coordinate transformations and Lagrange planetary equations

11 p1423 A73-26073

On the determination of the long period tidal perturbations in the elements of artificial earth satellites.

11 p1423 A73-26074

Preliminary orbit determination for lunar satellites.

11 p1426 A73-26396

The light variation and orbital elements of VW Bootis.

11 p1429 A73-26680

The eclipsing binary system RU Ursae Minoris.

11 p1429 A73-26681

Differential coefficient computation for spacecraft orbital velocity component variations in case of universal elements utilization for orbit improvement problems

12 p1538 A73-26864

Structure and evolution of the asteroid belt.

12 p1540 A73-27296

Trigonometric series for earth rotation velocity around solar system center of mass

12 p1540 A73-27297

Orbit selection for satellite missions, determining elements of sun-synchronous, recurrent, near-recurrent, polar, synchronous and stationary orbits

13 p1684 A73-29246

The influence of properties of a set of observations on the weights of determination of the orbital elements of a one-apparition comet.

14 p1790 A73-29794

Investigation of the motion of periodic comet Giacobini-Zinner and the origin of the Draconid meteor showers of 1926, 1933 and 1946.

14 p1791 A73-29802

Osculating orbital elements and nongravitational parameters for non-Newtonian orbit of periodic comet Borrelly

14 p1791 A73-29804

Borrelly periodic comet motion, including secular acceleration due to nongravitational forces and orbital elements perturbations by planets from Venus to Pluto

14 p1791 A73-29805

Periodic comet Tempel-Tuttle orbital elements relation to Leonid meteor shower, using computer program for numerical integration

14 p1791 A73-29807

Comet motion and hyperbolic orbital statistics, discussing secular accelerations, decelerations and nongravitational effects

14 p1794 A73-29830

Orbital classification for short period comets based on minimum approach distances to respective planets

14 p1794 A73-29833

Meteoritic particles orbits secular evolution under planetary perturbation and Poynting-Robertson effects, considering osculating orbital elements long term variations via simplified model

14 p1795 A73-29842

Meteor streams and comet orbital statistics from radar observations during 1967-1968

14 p1795 A73-29847

Determination of the motion and rotation parameters of an asteroid by the measurement of distances to a space station situated on the asteroid surface

14 p1796 A73-29858

Effect of selectivity on the observed distribution of orbital parameters for radio meteors.

15 p1928 A73-30982

Effects of motion of the equatorial plane on the orbital elements of an earth satellite.

15 p1930 A73-31112

Gaussian variational equations for osculating elements of an arbitrary separable reference orbit.

15 p1930 A73-31113

The effect of multiple encounters on short-period comet orbits.

17 p2226 A73-34291

Systematic elevation errors in maps of the lunar edge zone

17 p2230 A73-34594

Characteristics of the future orbital evolution of the comet Churiumov-Gerasimenko, 1969h

17 p2230 A73-34597

Zonal gravity harmonics from long satellite arcs by a seminumeric method.

17 p2233 A73-35269

The path independence of orbit inclination momentum.

17 p2234 A73-35661

Approximate description of the evolution of a synchronous-satellite orbit

18 p2350 A73-36101

Planetary elements for 10 000 000 years.

18 p2352 A73-36418

Perturbed satellite motion differential equations derivation on basis of fixed center problem and perturbing forces with no force function, obtaining intermediate orbital elements

18 p2355 A73-36746

Inclination of the moon's orbit - The early history.

20 p2605 A73-39055

Determination of equations of conditions between harmonics of resonance of the order of 14 starting with observations from the Eole satellite

21 p2781 A73-41327

On the 3-7 commensurability between Jupiter's outer two Galilean satellites.

21 p2778 A73-41531

Transformation between orbital parameters in different coordinate systems of the general relativistic Schwarzschild problem.

22 p2886 A73-41967

Accuracy of photographic artificial earth satellite observations at the observational station in Riga

22 p2910 A73-42644

Prediction of satellite motion by a combined method of recurrent relations

23 p3027 A73-43267

Impulse application for optimal correction of angular position of orbital plane line of apsides, expressing axis angle of rotation as linear function

23 p3027 A73-43269

Optimal navigation function for spacecraft orbit defined by initial conditions and acting force constants, determining matrix minimizing variance estimate

23 p3005 A73-43270

Meteorite production mechanism from asteroid belt via asteroidal collision fragments perihelion changes and orbit perturbation by Jupiter into earth-crossing orbital elements

23 p3027 A73-43336

Densities deduced from perturbations at high altitudes.

23 p2972 A73-43688

The global solution of the problem of the critical inclination.

23 p3031 A73-43836

Effects of physical librations of the moon on the orbital elements of a lunar satellite.

23 p3032 A73-43841

Comet Kohoutek development predictions for various orbital locations, discussing brightness changes, tail production, nucleus ice melting by solar heating at perihelion, etc

23 p3033 A73-43956

Orientation-dependent effects in Oort's theory of comet origin. II - Anisotropies in the distribution of long-period comet orbits.

24 p3131 A73-44467

ORBITAL LAUNCHING

Satellite orbits allocation by international conventions to prevent interference with existing vehicles, noting international cooperation in communication frequencies allocation

04 p0524 A73-15157

A possible application of large orbiting space laboratories - An artificial moon

05 p0613 A73-16201

ORBITAL MECHANICS

NT KEPLER LAWS

Approximate method to determine collision probabilities, hyperbolas, and direct and retrograde ellipses during single close encounters in three body planetary problem

01 p0099 A73-10693

Lunar motion numerical analysis, discussing flaws due to inadequate solar system model and arithmetic-algebraic procedural deficiencies

01 p0099 A73-10694

Physical processes responsible for Bode law, noting sufficiency of point mass perturbations for existing distributions of satellite and planetary orbits

02 p0211 A73-11874

The secular accelerations of the moon's orbital motion and the earth's rotation.

04 p0497 A73-15176

Optimal correction of a planetary-approach trajectory for transfer to an artificial-satellite orbit

05 p0616 A73-16428

Russian book on celestial and space flight mechanics covering trajectory and orbit evolution problems, resonance effects, relative motion dynamics and mathematical treatment

09 p1146 A73-22350

Stability of planar oscillations of a satellite in an elliptic orbit.

10 p1287 A73-24663

Three body system successive states classified as triple approach, simple interplay, ejection without escape and escape /final state/ during course of motion

13 p1683 A73-29140

All order stability of Hamiltonian systems with two degrees of freedom.

14 p1773 A73-29756

The motion, evolution of orbits, and origin of comets; Proceedings of the Symposium, Leningrad, USSR, August 4-11, 1970.

14 p1789 A73-29776

Orbital characteristics of comets passing through the 1:1 commensurability with Jupiter.

14 p1790 A73-29785

Cometary and asteroidal orbits discrimination using Jacobi integral in three body system with sun and Jupiter

14 p1795 A73-29849

Optimal transfer between coplanar elliptic orbits with the aid of tangential impulses applied at the apsidal points

15 p1931 A73-31232

Two dimensional nonlinear oscillations around center of mass of vehicle moving along circular orbit with magnetic damping under gravitational field and external perturbation

15 p1942 A73-31233

Book on Cartesian vortex theory of planetary motions covering celestial mechanics theories of Galileo, Kepler, Descartes, Leibniz and Newton

15 p1960 A73-32422

Numerical integration errors due to differential equations instability for Kepler orbits, discussing error reduction procedure by substituting for time as independent variable

16 p2061 A73-33231

Pallas evolution on basis of orbital eccentricity and inclination, discussing accumulation in asteroid belt in quiescent solar nebula, collisions and planetary gravitational encounters

17 p2229 A73-34428

Bode's law and the preference for near-commensurability among pairs of orbital periods in the solar system.

17 p2229 A73-34429

Distribution of satellite bodies according to their mean distances in the systems of the sun, Jupiter, Saturn and Uranus

17 p2231 A73-34598

Global stability and the restricted 3-body problem.

18 p2352 A73-36417

Planetary elements for 10 000 000 years.

18 p2352 A73-36418

ORBITAL POSITION ESTIMATION

Stromgen doubly asymptotic orbits analyzed by Hamiltonian functions with two degrees of freedom, investigating homoclinic and heteroclinic orbits in restricted three body problem

18 p2352 A73-36419

Elastic and inelastic scattering in orbital clustering.

18 p2357 A73-37109

Statistical dynamics formulation of motion equations for particle system in gravitational interaction with neither gas law nor hydromagnetic effects, applying to solar system evolution

21 p2766 A73-40313

Evolution of the orbits and radiants of meteor swarms of the Jupiter family

21 p2768 A73-40724

Properties of galactic orbits and motion integrals of high-velocity stars. II - Periodic and nonperiodic orbits in the 2nd Schmidt potential

22 p2907 A73-42303

German book on rocket propulsion theory covering orbital mechanics, equations of motion, performance parameters and nuclear, electric and chemical propulsion types

22 p2909 A73-42493

Determination of nongravitational forces in the motion of comets. I - Analysis of observation errors

22 p2910 A73-42643

An application of integral invariants to the n-body problem

23 p3034 A73-44100

Motion of a solid with a nonholonomic constraint at a fixed point

23 p3007 A73-44200

Barnard star proper motion and planetary system orbital analysis, indicating massive planet companions in inclined orbits

24 p3133 A73-44556

Quadrature solution for the general relativistic motion of a satellite or a planet.

24 p3142 A73-45291

Kustaanheimo-Stiefel transformation in Kepler motion perturbation theory derived from general solution of two body problem, noting application to collision orbits and Lagrange solutions

24 p3142 A73-45298

ORBITAL POSITION ESTIMATION

Orbit determination for the scientific satellite in Japan.

01 p0105 A73-11186

Comet orbit calculation in terms of nongravitational force effects, emphasizing periodic comet return predictions

04 p0495 A73-14762

Geos-C mini arc orbit determination from radar altimeter observations under perturbations from gravitational anomalies

04 p0437 A73-14784

Subsatellite point coordinates calculation for artificial earth satellites with nearly circular orbits, noting ephemeris application

05 p0613 A73-16203

Analysis of the effect of errors in determining the orbit parameters of a satellite on the accuracy of prediction of its motion

05 p0614 A73-16312

Methods of optimization of a spacecraft angular position control program

05 p0594 A73-16412

Selection of the measurement frequency in the determination of satellite orientation

05 p0630 A73-17007

A simple method for precise attitude determination of a spinning spacecraft.

06 p0722 A73-18827

Nonlinear estimation theory applied to the interplanetary orbit determination problem.

07 p0805 A73-20582

Recurrent orbit estimation biases by filtering, using method representing motion by finite difference equations

09 p1143 A73-22098

Upper atmosphere analytical density model for satellite motion prediction, allowing for diurnal and semiannual density variations and solar activity and geomagnetic disturbances effects

10 p1211 A73-23883

Least squares method for satellite motion parameters determination in orbital plane, using altimeter distance to planet surface measurements

12 p1543 A73-27627

ATS-F and Nimbus-E satellites use for range and range rate determination, earth gravity anomaly detection and orbital position determination

13 p1656 A73-28391

On the results of observations of occultations of stars by the moon according to the double image principle

13 p1686 A73-29559

Zero order approximation for attitude angle of stabilized satellite at high orbits under solar pressure perturbation, using trigonometric polynomials based on magnetometer data

15 p1943 A73-31241

ORBITAL RENDEZVOUS

Satellite operation mode coordination with space program mission, considering orbital position and velocity and time at ground station horizon

17 p2160 A73-34932

Upper atmosphere analytical density model for satellite motion prediction, allowing for diurnal and semiannual density variations and solar activity and geomagnetic disturbances effects

20 p2550 A73-38902

Mathematical model for ISIS satellite attitude and spin rate computerized predictions during electromagnetic torque control operation

21 p2781 A73-40615

Accuracy of the determination of satellite orbits

22 p2910 A73-42641

Sky region mobile barrier concept to predict satellite appearance for telescopic visual observation

22 p2910 A73-42642

Determination of nongravitational forces in the motion of comets. I - Analysis of observation errors

22 p2910 A73-42643

Evaluation of the accuracy of predicting the motion parameters of low-orbit artificial earth satellites

23 p3027 A73-43266

Prediction of satellite motion by a combined method of recurrent relations

23 p3027 A73-43267

ORBITAL RENDEZVOUS

Optimal energetic characteristics of the parallel guidance method in satellite rendezvous

02 p0219 A73-12456

Propulsion systems for orbital maneuvering stages. [SAE PAPER 720843]

05 p0607 A73-16656

Quality [probability]/ evaluation of human operator ergatic processes controlling spacecraft during rendezvous and docking with orbital station

06 p0657 A73-17686

Optimum strategy for the correction of orbit-injection errors of arbitrary orientation.

09 p1151 A73-23451

Optimum energetic characteristics of the parallel-guidance method of bringing satellites into proximity.

15 p1941 A73-32606

ORBITAL SHOTS

AEROS research satellite acquisition phase performance, considering injection, attitude determination and control, trajectory measurement and correction, nutation reduction, solar alignment, etc

13 p1689 A73-28782

ORBITAL SIMULATORS

U SPACE SIMULATORS

ORBITAL SPACE STATIONS

NT ORBITAL WORKSHOPS

NT ORBITING LUNAR STATIONS

NT SALLYUT SPACE STATION

Space stations and shuttle vehicles design and placement in earth orbit, reviewing life support, energy production and data transmission systems

01 p0096 A73-10300

NASA's space station and the need for quantifiable components of a responsive legal regime.

04 p0522 A73-15134

A possible application of large orbiting space laboratories - An artificial moon

05 p0613 A73-16201

Electrical and isotope power from space for terrestrial use.

06 p0750 A73-18028

The legal position of earth orbiting stations

07 p0923 A73-19201

Modular space station operation as general purpose laboratory with attached or free flying R and D modules for specific projects

09 p1152 A73-22325

Large solar array photovoltaic power systems for manned orbital space stations, discussing technology evaluation and design feasibility studies

09 p1153 A73-22780

A solar array and battery electrical power subsystem for the shuttle-launched modular space station.

09 p1153 A73-22783

Space station solar array-energy storage-power control and distribution system based on regenerative fuel cell integrated with life support system

09 p1153 A73-22784

An integrated system for space station power, life support, and propulsion.

11 p1311 A73-26009

A 25 kW solar array/battery design for an earth orbiting space station.

11 p1311 A73-26010

Reactor-thermoelectric power systems for NASA Space Station/Space Base.

11 p1395 A73-26012

66 kWe ZrH reactor-organic Rankine power systems for large manned orbiting space systems.

11 p1311 A73-26014

Preliminary design of reactor power systems for the manned space base.

11 p1395 A73-26018

Space shuttle implementation prognosis, discussing spacecraft configurations, international cooperation,

research possibilities in TR telescopic, space physics laboratories and exobiology

18 p2348 A73-35937

Precession rate matching for a space station in orbit about an oblate planet.

18 p2351 A73-36153

Russian book - Studies of the natural environment from manned orbital stations.

23 p2971 A73-43330

Visual observations of the earth and of the circumterrestrial space environment from manned orbital stations

23 p2971 A73-43331

Spectrophotometric investigations of the earth from manned orbital stations

23 p2979 A73-43333

Two stage recoverable space shuttle structural design, discussing configurations, costs and orbiter and booster materials and thermal protection systems

23 p3038 A73-43786

Long range post-Apollo space exploration goals, considering earth orbital station, moon base, manned Mars landing and interstellar flights

23 p3038 A73-43990

Skylab 26 day rescue mission diary, describing docking, communications, extravehicular activity, repair work, medical checkouts, physical exercises, solar array problems, etc

23 p3038 A73-43992

ORBITAL TRANSFER

U TRANSFER ORBITS

ORBITAL VELOCITY

The structure of the close vicinity of the sun - Investigations concerning star troops, star families, and star streams

02 p0212 A73-12017

Analytical expressions for postmaneuver velocity and transfer impulse optimizing elliptic-to-hyperbolic orbital transfer

02 p0219 A73-12453

Optimum strategy for the correction of orbit-injection errors of arbitrary orientation.

09 p1151 A73-23451

Position and velocity components for Jupiter VIII-XII.

11 p1429 A73-26684

Differential coefficient computation for spacecraft orbital velocity component variations in case of universal elements utilization for orbit improvement problems

12 p1538 A73-26864

Splitting and sudden outbursts of comets as indicators of nongravitational effects.

14 p1793 A73-29819

Analytical expressions for postmaneuver velocity and transfer impulse optimizing elliptic-to-hyperbolic orbital transfer

15 p1941 A73-32603

Satellite operation mode coordination with space program mission, considering orbital position and velocity and time at ground station horizon

17 p2160 A73-34932

ORBITAL WORKSHOPS

Solar Array System for the Skylab Orbital Workshop.

03 p0257 A73-14238

Space shuttle orbiter system planning and operational modes, considering propulsion into orbit, automated observatories, sortie workshop and European cooperation

14 p1803 A73-29943

Skylab program mission profile, vehicle components, ground station data links, Apollo telescope mount, Saturn V rocket, solar cells and Salyut spacecraft comparison

20 p2615 A73-39150

ORBITALS

NT ELECTRON ORBITALS

NT MOLECULAR ORBITALS

ORBITER PROJECT

Space Shuttle Orbiter aerodynamics, discussing wing/body matching, lateral/directional stability, control and reaction systems

19 p2491 A73-37595

Space Shuttle Orbiter radiative, ablative and insulative thermal protection system design, performance and reliability

19 p2492 A73-37596

Space shuttle external tank, discussing Orbiter engine, propellant conditioning, solid rocket boosters structural support, environment effects and safe disposals

19 p2492 A73-37598

Space Shuttle development, qualification, acceptance and horizontal/vertical flight tests for Orbiter, solid rocket motor and drop tank element subsystems

19 p2492 A73-37602

Space Shuttle Orbiter Environmental Control and Life Support System for atmosphere revitalization, crew life support, thermal conditioning and airlock support

19 p2400 A73-37979

ORBITING ASTRONOMICAL OBSERVATORY

U OAO

ORBITING LUNAR STATIONS

Terrestrial law adaption to lunar surface or orbital space laboratories requirements

04 p0521 A73-15130

ORBITING SATELLITES

U ARTIFICIAL SATELLITES

ORBITING SOLAR OBSERVATORY

U OSO

ORBITS

NT APHELIONS

NT APOGEES

NT CIRCULAR ORBITS

NT EARTH ORBITS

NT ECCENTRIC ORBITS

NT ELLIPTICAL ORBITS

NT EQUATORIAL ORBITS

NT INTERPLANETARY TRANSFER ORBITS

NT LUNAR ORBITS

NT PERIGEEES

NT PERIHELIONS

NT PLANETARY ORBITS

NT POLAR ORBITS

NT SATELLITE ORBITS

NT SOLAR ORBITS

NT SPACECRAFT ORBITS

NT STATIONARY ORBITS

NT TRANSFER ORBITS

NT TROJAN ORBITS

NT TWENTY-FOUR HOUR ORBITS

ORDER-DISORDER TRANSFORMATIONS

High temperature effects on near order transformations in TiC-WC solid solutions during heat treatment and cooling, using X ray diffusion scattering measurements

01 p0064 A73-10615

Microstructure and plastic deformation of the Ni4Mo alloy.

03 p0325 A73-13804

Disordered precipitation effect on steady state creep rate of gamma prime Ni-Al-Ti single crystals

03 p0326 A73-13963

Cumingtonite temperature dependent Mg and ferric ions order-disorder, estimating crystallization temperatures

03 p0375 A73-14104

X ray diffraction measurement of ordering kinetics in Ni-Pt alloy at annealing temperatures, showing disorder-order transitions relation to nucleation and growth

04 p0467 A73-15982

Magnetite absolute zero behavior with restriction to three order parameter theory, showing metallic band resultant from interatomic Coulomb energy ratio to bandwidth

06 p0734 A73-17835

Thermodynamic stability of ordered phase atomic structure state for antiphase domain formation, noting superstructures in face centered and body centered cubic solutions

06 p0736 A73-18118

Shock deformation of K-state in Ni-Cr alloys.

08 p0979 A73-21626

Confirmation of electronic paramagnetic resonance of the existence of an ordered phase in the zirconium-calcium system

09 p1135 A73-23031

Order-disorder alpha and gamma phase transformations as function of temperature in Co-Fe-V alloy by dilatometric, magnetostructural, neutron diffraction and X ray analyses

12 p1508 A73-26834

Study of crystalline transformations at high temperature above 2000 K; International Colloquium, Odeillo, Pyrenees-Orientales, France, September 27-30, 1971, Proceedings

12 p1514 A73-27918

Corrosion properties and structural transformations of the N70M27 alloy containing vanadium and niobium

13 p1644 A73-29645

The Portevin-Le Chatelier effect in the case of alloys of copper with aluminum, gallium, germanium, arsenic, and indium

14 p1760 A73-30443

Effect of ordering on the properties of oxygen solid solutions in titanium

15 p1893 A73-32516

Papers on earth and planetary sciences, volume I covering earth planetary structure, red beds, planetary interiors, mineral deposits and order-disorder relationship in silicates

17 p2158 A73-34356

Metallurgical investigations of atomic ordering and transformation behavior of close packed ordered nine-layered hexagonal structure /kappa phase/ in V-Co-Ni ternary alloys

17 p2190 A73-34646

Effect of atom ordering on the martensite decomposition mechanism and kinetics in iron-aluminum-carbon alloys

18 p2324 A73-36769

Laser threshold behavior analogy with thermodynamic ferromagnetic order-disorder phase transition, using self consistent field theory

20 p2571 A73-38628

Application of the 'differential reflectometer' to materials research in corrosion, ordering and alloying. 21 p2719 A73-40897

Corrosion characteristics and structural transformations in alloy N70M27 with vanadium and niobium. 21 p2720 A73-41038

Study of the structure and properties of alloys of the V-Al, Cr-Al and V-Cr-Al systems in the region of solid solution bcc ordering. 22 p2873 A73-42088

Electron paramagnetic resonance studies of a viscous nematic liquid crystal. II - Evidence counter to a second-order phase change. 22 p2897 A73-42711

Influence of ion ordering on the induced anisotropy in Li-Fe ferrites. 23 p3018 A73-44175

Mathematical model for fracture strength of material undergoing molecular orientation during tensile strain, accounting for anomalous polymer characteristics. 24 p3144 A73-44508

ORDINATES
U COORDINATES
OREGON

High-altitude photographs of the Oregon coast. 09 p1078 A73-22719

ORGAN WEIGHT

Organ and body mass changes in restrained and fasted domestic fowl. 04 p0409 A73-14975

Structural conditions in the hypertrophied and failing heart. 22 p2807 A73-42685

Regression of altitude-produced cardiac hypertrophy. 24 p3060 A73-45065

ORGANIC CHEMISTRY

The organic analysis and carbon chemistry of lunar samples: Their significance for exobiology; Proceedings of the Conference, University of Maryland, College Park, Md., October 26-28, 1971. 06 p0753 A73-18410

Review of methods used in lunar organic analysis - Extraction and hydrolysis techniques. 06 p0661 A73-18412

Search for biogenic structures and viable organisms in lunar samples - A review. 06 p0654 A73-18416

Organogenic elements in stars, interstellar matter, comets, meteorites and planets, discussing molecular distribution and formation, prebiological chemical evolution, and terrestrial and extraterrestrial biology. 06 p0754 A73-18430

Advances in organic geochemistry 1971; Proceedings of the Fifth International Meeting, Hanover, West Germany, September 7-10, 1971. 11 p1325 A73-25459

Complex mixture analysis - Geochemical and environmental applications of a compound classifier based on computer analysis of low resolution mass spectra. 11 p1326 A73-25464

Terrestrial and extraterrestrial stable organic molecules. 14 p1724 A73-30131

Organic geochemical analysis of lunar samples with emphasis on detecting biologically significant organogenic elements, projecting techniques to Mars soil analysis. 22 p2803 A73-42163

ORGANIC COMPOUNDS

NT ADENOSINE DIPHOSPHATE [ADP]
NT ADENOSINE TRIPHOSPHATE [ATP]
NT ADENOSINES
NT AMINO ACIDS
NT ASPARTIC ACID
NT CARBON TETRAFLUORIDE
NT CHOLINE
NT FATTY ACIDS
NT FLUORINE ORGANIC COMPOUNDS
NT FLUOROCARBONS
NT FLUOROXYDROCARBONS
NT GLUTAMIC ACID
NT LEUCINE
NT LYSINE
NT METHIONINE
NT NUCLEASE
NT NUCLEOTIDES
NT OLEIC ACID
NT ORGANIC LIQUIDS
NT OXIDASE
NT PEPTIDES
NT PHENYLALANINE
NT PYRIDINE NUCLEOTIDES
NT QUINOLINE
NT SEROTONIN
NT THYROXINE
NT TRYPTOPHAN

Polycrystalline organic compounds effect on second harmonic generation of neodymium laser, noting relation between nonlinear susceptibility and intramolecular charge transport. 02 p0176 A73-12097

Vapor deposition of thin films of DPPH and BDPA. 02 p0201 A73-12639

Organic compounds catalytic activity comparison for use in fuel cell, noting superiority of dihydrodibenzo-tetraazannulene cobalt complex. 04 p0407 A73-15109

On the origin of strongly conducting states in thin insulator films. 06 p0734 A73-17812

The origin of life problem - A brief critique. 06 p0651 A73-17927

Organic compounds in the Murchison meteorite. 06 p0752 A73-18234

Cosmochemical evolution of large organic molecules - Illustrative laboratory simulations for porphyrins. 06 p0752 A73-18235

Nanogram level lunar organic compound separation and detection by gas-liquid chromatography. 06 p0661 A73-18413

Low molecular weight compounds of organogenic elements on Apollo 11 and 12 fines and breccias obtained by vacuum pyrolysis, acid hydrolysis and crushing. 06 p0654 A73-18418

Aromatic and heteroatom-containing organic compounds in the lunar samples. 06 p0662 A73-18424

Lunar samples organic analysis avoiding organic molecules synthesis from indigenous constituents, considering pyrosynthetic and ionic reactions in solution. 06 p0662 A73-18426

Indigenous lunar organic compound search, considering prebiological chemistry and composition possibility in deeper region under surface. 06 p0655 A73-18428

Sterically controlled syntheses of optically active organic compounds. XV - Syntheses of optically active aspartic acid through beta-lactam. 07 p0787 A73-19204

Analysis of organogenic compounds in Apollo 11, 12, and 14 lunar samples. 07 p0890 A73-19819

Directly excited subsonically flowing CW gas laser with carbon monoxide and dioxide generation as reaction products formed by organic molecule electrochemical oxidation. 09 p1091 A73-22084

Interstellar organic molecules millimeter wave line spectra and transition rotational quantum numbers. 09 p1150 A73-23141

Volatile organic compounds from Murchison, carbonaceous chondrite by vaporization-pyrolysis at different temperatures, comparing with Allende meteorite and terrestrial rocks. 10 p1277 A73-24102

Investigation of the polar and protective properties of magnesium salts of organic acids. 10 p1239 A73-24248

High temperature superconductivity in three dimensional systems of metals and nonmetals, discussing electron collectivization in metals, dielectrics, organic compounds, semiconductors and molecular crystals. 10 p1261 A73-24692

Organic coating technology review, discussing binders, pigments and various processing techniques. 11 p1388 A73-25848

Sterically controlled syntheses of optically active organic compounds. XVI - Temperature dependence of hydrogenolytic asymmetric transamination. 12 p1467 A73-27974

The addition of tert-butyl hypochlorite to isocyanates. 13 p1580 A73-28022

Cometary nuclei chemical composition and molecular structure, suggesting radial-forming organic molecules synthesis by solar and galactic cosmic radiation. 14 p1723 A73-29816

Prebiological synthesis of organic compounds. 14 p1724 A73-30129

High strength organic fiber PRD-49 reinforced plastics compared to materials reinforced with glass, graphite and boron, discussing weight required to achieve Al faced sandwich performance. 17 p2194 A73-34802

Organic compounds chemical analysis with cold trap to allow materials evaporation according to vapor pressure characteristics for replacing gas chromatography. 17 p2175 A73-35760

Superconducting fluctuations in complexes of tetracyanoquinodimethane and structural imperfections. 19 p2482 A73-37387

Distribution and diagenesis of organic compounds in JOIDES sediment from Gulf of Mexico and western Atlantic. 21 p2683 A73-40562

Organic compounds oxidation and combustion reactions, discussing hydrogen dioxide radical role and reaction rate. 22 p2933 A73-42753

ORGANIC COOLED REACTORS

66 kWc ZrH reactor-organic Rankine power systems for large manned orbiting space systems. 11 p1311 A73-26014

ORGANIC FLUORINE COMPOUNDS
U FLUORINE ORGANIC COMPOUNDS

ORGANIC LASERS
NT DYE LASERS

Simultaneous two-wavelength selection in the N2 laser-pumped dye laser. 01 p0058 A73-10126

Passive mode locking of the cw dye laser. 01 p0058 A73-10129

Organic dye lasers tuning by diffraction gratings and prisms, noting CW, pulsed and mode locking operations. 01 p0059 A73-10716

An 11 megawatt 6.8 joule flashlamp pumped coaxial liquid dye laser. 02 p0175 A73-11956

Possibilities of using organic compound lasers in spectral analysis. 02 p0176 A73-12095

The generation of tunable near IR radiation using a nitrogen laser pumped dye laser. 03 p0318 A73-12869

Combined nonlinear amplification and absorption role in ultrashort pulse generation of mode locked quasi-continuous dye laser in absence of short relaxation time. 03 p0318 A73-12870

Transient analysis of an electronically tunable dye laser. I - Simulation study. 03 p0320 A73-14457

CW dye laser with dye solution pumped through simple nozzles to provide unconfined flowing thin streams with optical quality and long term stability. 03 p0320 A73-14460

The effect of pH on photobleaching of organic laser dyes. 03 p0320 A73-14462

Tunable polarized violet light pulse emission from anthracene doped organic molecular fluorene crystal laser pumped with nitrogen laser, noting pulse amplitude and duration. 04 p0458 A73-14873

Tunable dye laser radar observation for Na layer nocturnal vertical distribution, suggesting meteor shower effect on layer content increase. 04 p0444 A73-15543

Tunable dye lidar techniques for measurement of atmospheric constituents. 04 p0423 A73-15769

Study of excitation transfer in a flowing helium afterglow pumped with a tuneable dye laser. I - Measurement of the rate coefficient for selected quenching reactions involving He/5-3P/. 05 p0600 A73-16044

Study of excitation transfer in a flowing helium afterglow pumped with a tuneable dye laser. II - Measurement of the rate coefficient for the rotational relaxation of He/2/3p 3Pi-g/. 05 p0600 A73-16045

Organic dye lasers use as continuously tuneable sources of coherent light, discussing molecular energy level systems and transitions. 05 p0583 A73-16337

Electromechanical techniques for rapid frequency tuning of lasers. 05 p0584 A73-16443

Picosecond pulses from a passively mode-locked cw dye laser. 05 p0585 A73-17222

Frequency shift in a mode-selected dye laser. 05 p0586 A73-17225

Short pulse laser based on versatile 60 kV fast switching circuit, noting application as pump source for organic dye molecule solutions. 05 p0586 A73-17252

Waveguide properties, modes and optical pumping effects on thin film organic dye lasers, noting temperature effects on refractivity and laser modes. 06 p0699 A73-17808

Threshold pump energy value of liquid lasers in quasi-steady-state operation. 06 p0699 A73-17915

Time dependence of the gain of an optically pumped solution of rhodamine 6G. 06 p0703 A73-18598

110-I pulsed laser using a solution of rhodamine 6G in ethyl alcohol. 06 p0703 A73-18612

The effect of an electric field on the active medium in a dye laser. 07 p0834 A73-19540

Compact laser radar probes the upper atmosphere. 07 p0834 A73-19573

Angular dispersion of an acoustooptic Bragg cell used in the wavelength tuning of an organic dye laser. 08 p0975 A73-21056

Angular dispersion of diffraction gratings used for tuning organic dye lasers. 08 p0975 A73-21057

Study and development of a dye laser with coupled modes excited by a flash tube and emitting in the near infrared 08 p0976 A73-21493

Loss analysis and design improvement for a continuous dye laser. 09 p1090 A73-22080

A tunable flashlamp-pumped dye ring laser of extremely narrow bandwidth. 09 p1091 A73-22083

A photochemical method of determining the optical pumping energy absorbed by rhodamine dyes under conditions corresponding to stimulated emission of radiation 09 p1095 A73-22668

Influence of thermo-optical distortions on the emission spectrum of a rhodamine 6G laser with incoherent pumping 09 p1096 A73-22972

A tunable laser based on an organic dye solution and providing highly monochromatic, stable single-frequency emission 09 p1097 A73-23010

Two-photon excitation of luminescence in $\text{CaF}_2:\text{Er}^{3+}$ crystals by a frequency-scanning laser employing organic dye solutions 10 p1227 A73-24075

Possibility of smoothly tuning the emission frequency of a mixed-dye laser 10 p1228 A73-24582

Generation of the second harmonic of laser emission in organic crystals 10 p1228 A73-24583

Effect of concentration on laser threshold of organic dye laser. 10 p1229 A73-24695

Holographic contour mapping using a dye laser. 10 p1221 A73-24874

Influence of excitation power on the energetic characteristics of phthalimide solutions 11 p1376 A73-26143

Superradiant waveguide dye laser pumped by flash lamps, noting power output and stable mode pattern insensitivity to disturbance and thermal effects 11 p1378 A73-26324

Lamp pumping system for lasers based on organic compound solutions 17 p2183 A73-34170

Experimental studies of pulse lasers using organic-dye solutions covering the spectral range from 7,100 to 11,000 Å - Analysis of optimal generation conditions 17 p2184 A73-34918

Investigation of the characteristics of organic compound lasers with dispersive resonators 17 p2184 A73-34920

Far IR laser lines measurements in carbon dioxide laser pumped ethylene glycol, dimethyl ether, formic acid, and monomethyl amine, using grating spectrometer and Golay-cell detector 21 p2715 A73-40765

ORGANIC LIQUIDS

Heat transfer as function of temperature on small horizontal wires in water and organic liquids noting application for heater low gravity behavior prediction 01 p0122 A73-10801

3000 hour endurance test of a 6 kWe organic Rankine cycle power system. 09 p1034 A73-22769

Low peak temperatures and hydrodynamic bearings - Key to long life organic Rankine cycle systems. 09 p1034 A73-22770

New formaldehyde base disinfectants. 23 p2948 A73-43276

Influence of nonexplosive liquids on the detonation rate of solid explosives 24 p3157 A73-45380

ORGANIC MATERIALS

Oxygen plasma for cleaning polymerized organic material contaminated oil-pumped channel electron multiplier arrays used as vacuum UV to visible radiation converters 01 p0054 A73-11237

PRD 49 high modulus organic fibre as aluminium replacement. 01 p0068 A73-11510

Spectrophotofluorometers for returned lunar samples and geological materials organic analyses, discussing optical component performance and calibration to avoid instrumental artifacts effect on spectra 06 p0662 A73-18415

Quantitative evaluation of superficial organic contaminants, soluble in halogenated solvents, discussing sampled surface solvent extraction method and subsequent IR absorption spectrographic analysis 06 p0660 A73-18547

High modulus organic fibre composites in aircraft applications. 09 p1110 A73-22519

Historical treatment and inconclusiveness of evidence of extraterrestrial life traces and organic matter in carbonaceous and other meteorites 09 p1146 A73-22545

The origin and incorporation of organic molecules in sediments as elucidated by studies of the sedimentary sequence from a residual Pleistocene lake. 11 p1326 A73-25468

Metallic, nonmetallic, inorganic and organic protective coatings for metals against mechanical and chemical damage, discussing processing methods and applications 11 p1374 A73-25847

Sensitometric tests on plane-parallel organic photochromic bulk material film samples of styrene, methylmethacrylate and inoline spiropyran, evaluating photosensitivity suitability for holography 13 p1622 A73-29436

Mechanism of failure in transparent organic-glass-type dielectrics under the action of laser radiation 16 p2030 A73-33927

The yielding of a two-dimensional void assembly in an organic glass. 19 p2444 A73-38090

Stable high energy nonaqueous lithium-organic electrolyte batteries, discussing discharge rates, temperature effects, energy density and voltage regulation 19 p2390 A73-38396

ORGANIC NITRATES

NT CELLULOSE NITRATE

NT NITROGLYCERIN

ORGANIC PHOSPHORUS COMPOUNDS

Investigation of anti wear additives under various loads and at different sliding speeds. [ASLE PREPRINT 72LC-3C-4]

Lactate, alpha-GP, and Krebs cycle in sea-level and high-altitude native guinea pigs. 11 p1318 A73-26122

Analysis of the mechanism of the therapeutic action of pressurized oxygen in organic phosphorus poisoning 14 p1722 A73-30848

Responses to graded hypoxia at high and low 2,3-diphosphoglycerate concentrations. 17 p2112 A73-35460

ORGANIC SEMICONDUCTORS

Electric properties of 5,12-6,11-tetraoxotetrasene crystals 07 p0862 A73-20007

Photocurrent pulse shape in thin organic semiconductor films 07 p0862 A73-20008

Oxidation of organic molecules by photoproduct holes of ZnO . 15 p1841 A73-31969

Electrical conductivity variations in organic semiconductors in the melting temperature region 16 p2044 A73-34005

ORGANIC SILICON COMPOUNDS

Heat conductivity of system composed of a silicon-glass elastomer and a powdered mineral filler 05 p0589 A73-16771

Influence of thermally stabilizing alloying additions on the antifraction properties of lamellar graphites with a organic silicon binders 09 p1110 A73-22978

ORGANIC TIN COMPOUNDS

Some anionic tetrahalo/2,4-pentanedionato/stannate/IV complexes. 06 p0661 A73-18271

The synthesis and characterization of tin complexes using inert atmosphere techniques - An advanced laboratory experiment. 06 p0661 A73-18272

ORGANISMS

Multidimensional judgments in design of ideal organisms with integral number of resource units allocated among characteristics such as memory, vision, resourcefulness, etc 03 p0261 A73-13559

Body temperature effect on protein conformation stability in healthy and diseased organisms, noting blood plasma albumin fractions 04 p0409 A73-14822

Ergatic organism defined as multipurpose nonautonomous control system with homeostasis with respect to functional operations conservation 07 p0786 A73-20048

Gravity, weightlessness and organismic genetic structures. 18 p2269 A73-35923

ORGANIZATIONS

Book - Interorganizational decision making. 15 p1960 A73-31577

History, evolution, and role of the Civil Aviation Secretariat General 15 p1960 A73-32554

New initiatives in engineering computer software sharing. 20 p2533 A73-39515

ORGANIZING

The role of basic research in the total R&D process. 07 p0923 A73-19185

ORGANOMETALLIC COMPOUNDS

NT CARBOXYHEMOGLOBIN

NT CHLOROPHYLLS

NT HEMOGLOBIN

NT ORGANIC TIN COMPOUNDS

NT OXYHEMOGLOBIN

NT PORPHINES

Russian book on titanium chemistry covering physicochemical and electrochemical properties, hydrolysis and production of metal-organic and complex titanium compounds 02 p0139 A73-11890

The evolution of ferredoxins from primitive life to higher organisms. 03 p0265 A73-14318

Organic compounds catalytic activity comparison for use in fuel cell, noting superiority of dihydro-dibenzo-tetraazaannulene cobalt complex 04 p0407 A73-15109

On supposedly five-co-ordinate titanium (IV) complexes - The crystal and molecular structure of C13Ti/C5H7O2 . 06 p0661 A73-18266

Electron absorption spectra of benzochromium-dicarbonyltriphenylphosphine and benzochromium-tricarbonyl and their application to studies of the decomposition kinetics of these compounds 10 p1186 A73-24457

The oxidation of metal alkyls in the presence of isobutane. 13 p1581 A73-29002

ORGANS

NT ESOPHAGUS

NT KIDNEYS

NT LIVER

NT LUNGS

NT PITUITARY GLAND

NT TESTES

Activity relation between internal organ receptors and skeletal muscles in terms of laws controlling process coordination 01 p0007 A73-10154

A new phenomenon of an active intraorgan pumping function of skeletal muscles 12 p1462 A73-27446

RNA and DNA of internal organs during a remote postreanimation period in animals with complete and incomplete functional recovery of the central nervous system 14 p1719 A73-30842

Histopathological and histochemical studies of one year isolation and six months immobilization effects on rhesus monkeys internal organs and tissues 18 p2270 A73-35983

Properties of biological fluids and solids: Mechanics of tissues and organs; Proceedings of the Biomechanics Symposium, Georgia Institute of Technology, Atlanta, Ga., June 20-22, 1973. 18 p2281 A73-36428

Relationship between organ weight and blood flow in rats adapted to simulated high altitude. 21 p2639 A73-41156

Ocular antigens. IV - A comparative study of the localization of immunogenic determinants of ocular structural glycoproteins in connective tissues of various organs. 22 p2802 A73-41729

Proton dosimeter design for distributed body organs. 23 p2949 A73-43389

ORGEL REACTOR

U ORGANIC COOLED REACTORS

ORGUEIL METEORITE

Orgueil chondrite magnetite age via I 129/Xe 129 method compared to Karoonda magnetite age 13 p1684 A73-29250

ORIENTATION

Effect of forward head inclination on visual orientation during lateral body tilt. 03 p0266 A73-13000

Reorientation of a spacecraft 04 p0504 A73-14885

Biological clocks in animal orientation and in other functions. 06 p0651 A73-17825

The null magnetic field as reference for the study of geomagnetic directional effects in animals and man. 06 p0658 A73-18033

Kinematic problem of orientation in a rotating coordinate system 09 p1116 A73-22354

Interstellar and interplanetary dust grains orientation distribution function in anisotropic corpuscular or radiation fluxes 10 p1271 A73-23482

Incomplete/complete feedback and off-on control moments for prescribed orientation of solid body in rotational motion 10 p1248 A73-23744

Preferred a axis orientation parallel to fiber axis in commercial carbon fibers due to lower surface energy of basal plane configuration 11 p1389 A73-25857

Spacecraft reorientation by successive rotations about nonorthogonal axes, deriving classical Euler angles as special case of general solution 15 p1908 A73-31662

ORIFICE FLOW

Equivalent solid obstacle for gas injection into a supersonic stream. 01 p0002 A73-10734

Circular orifice flow of monatomic rarefied gas between two reservoirs, observing pressure ratio effect

03 p0295 A73-13773

Theoretical and experimental pressure distribution in supersonic domain for an inherently compensated circular thrust bearing.

[ASME PAPER 72-LUB-43] 03 p0315 A73-14349
Discharge coefficients for air outflow through a single orifice in the wall of a tube.

03 p0297 A73-14597

The measurement of a pulsating air flow using a sharp-edged orifice meter.

[ASME PAPER 72-WA/FE-36] 04 p0451 A73-15853
Theory of a generalized Helmholtz resonator.

08 p0952 A73-21471

Viscous energy transfer from elliptical orifice originated laminar three dimensional jet, using boundary layer assumptions in jet mixing region

09 p1072 A73-22827

Turbulent wake development in oscillating flow, deriving flow equations for sinusoidally time dependent orifice flow

10 p1208 A73-24814

Long bore thick plate orifices performance in flow velocity measurement at low Reynolds numbers, calculating uncalibrated uncertainty in discharge coefficient

10 p1221 A73-24860

Numerical study of a viscous flow through a pipe orifice.

11 p1346 A73-25213

Calculation of the moisture content correction in measuring the quantity of gas flowing through an orifice

12 p1498 A73-27595

Photographic studies of the transition between continuum and free molecular flow.

15 p1864 A73-31935

Numerical studies of viscous, incompressible flow through an orifice for arbitrary Reynolds number.

17 p2157 A73-35602

Utilization of miniature diaphragm-leakport devices in fluidic applications.

20 p2511 A73-39752

The effect of valve area gain on the performance of the hydraulic servomechanism.

20 p2511 A73-39755

Eddies development downstream a pipe orifice.

22 p2840 A73-41738

Rarefied gas flow through an orifice at low pressure gradients

23 p2969 A73-44347

ORIFICES

Evaluation of an orifice probe for plasma diagnostics.

05 p0601 A73-16431

ORION AIRCRAFT

U P-3 AIRCRAFT

ORION CONSTELLATION

Kinematics of the Huyghenian region of the Orion Nebula.

11 p1427 A73-26605

Interstellar light absorption in the Orion constellation area

12 p1537 A73-26856

Spatial distribution of stars in the Orion constellation region

14 p1799 A73-30385

Electronographic observations of the forbidden O II ratio in the core of the Orion Nebula.

24 p3140 A73-45183

ORIONID METEOROIDS

Optical manifestations of meteoric aerosols. I - The 1970 Orinoids

01 p0096 A73-10332

The telescopic radiant areas of the Perseids and the Orionids.

11 p1426 A73-26572

ORNITHOPTER AIRCRAFT

U RESEARCH AIRCRAFT

ORNSTEIN-UHLENBECK PROCESS

Application of the Ornstein-Uhlenbeck stochastic process to the study of dynamic systems in an environment of stochastic disturbances.

18 p2330 A73-36829

OROGRAPHY

Numerical model for calculation of the geopotential field with a new generalized vertical velocity profile incorporating the influence of orography

05 p0572 A73-17352

A numerical model of the geopotential field with a new profile of the generalized vertical velocity that takes orography into account.

15 p1865 A73-31002

A three-level model for calculating vertical motions generated by planetary orography.

18 p2314 A73-37073

The dynamical effects of real Mars orography upon the large-scale air flow and some meteorological phenomena of Mars.

19 p2482 A73-37429

Parametrization of orographical effects in the planetary boundary layer.

21 p2732 A73-41570

ORR-SOMMERFELD EQUATIONS

Integration of an extended Orr-Sommerfeld equation in connection with a stability investigation of laminar boundary-layer flows

16 p1963 A73-33252

Stability of a plane boundary layer with allowance for nonparallelism

23 p2968 A73-43472

ORRERIES

U ASTRONOMICAL MODELS

ORTHICONS

NT IMAGE ORTHICONS

ORTHO HYDROGEN

The non-equilibrium ortho/para spin state ratio for molecular H₂ formed in the hydrolysis of lithium aluminum hydride.

07 p0787 A73-19144

ORTHO PARA CONVERSION

The non-equilibrium ortho/para spin state ratio for molecular H₂ formed in the hydrolysis of lithium aluminum hydride.

07 p0787 A73-19144

ORTHOGONAL FUNCTIONS

NT WALSH FUNCTION

Orthogonal function approximation of uniform thickness plate temperature distribution, using reduced two dimensional unsteady heat conduction equations

01 p0119 A73-10010

Stress analysis for two stamps impression into linearly deformable base, solving integral stress equation by orthogonal polynomials method

01 p0118 A73-11411

Biorthogonal function pairs for gravitational field calculations for flat galaxies, deriving algorithms from Hankel-Laguerre functions properties

02 p0216 A73-12380

A new numerical method for the inversion of the Laplace transform.

04 p0471 A73-15229

An application of Bayes-law estimation to nonlinear phase demodulation.

04 p0471 A73-15253

Orthogonalization method application to problems of wave diffraction from several bodies through reduction to integral equations

05 p0547 A73-16053

An economical approximation for the coefficients in the development of a function with respect to an orthogonal system.

08 p0984 A73-21413

An 'orthogonalization' method for determining the dynamic characteristics of an elastic body from static vibration tests

09 p1161 A73-23090

Orthogonal polynomials for computerized construction of equations of state for substances under thermodynamic restrictions

10 p1293 A73-23505

Statistically orthogonal functions for finite intervals of a random process

11 p1390 A73-25642

Nonoscillation and disconjugacy of systems of linear differential equations.

13 p1648 A73-28441

Orthogonal polynomials for computerized construction of equations of state for substances under thermodynamic restrictions

17 p2255 A73-35185

Orthogonal operators and phase space distributions in quantum optics.

20 p2591 A73-38629

Signal theory problems of discrete signal representation decomposition and characterization by Walsh and orthogonal functions, noting voiced speech analysis

23 p2952 A73-43309

Gravitational fields calculation in three dimensional mass distribution galaxies, using biorthogonal functions with ultraspherical polynomials

23 p3030 A73-43749

Orthogonal MULTIPLEXING THEORY

Synchronous multiplexing of digital signals using a combination of time- and code-division multiplexing /t.d.m. and c.d.m./.

02 p0140 A73-11588

Error probabilities estimates for digital communication systems using orthogonal multiposition signals in data transmission

03 p0278 A73-14029

L. orthogonal signaling scheme transmission bandwidth tradeoff with error probability performance of associated receiver used for data detection

09 p1054 A73-23383

ORTHOGONALITY

Computational variants of the Lanczos method for the eigenproblem.

06 p0716 A73-17984

On forced vibrations in the linear theory of micropolar elasticity.

06 p0762 A73-17987

Orthogonal versus planar vector-electrocardiography.

07 p0785 A73-19930

ORTHOTROPIC CYLINDERS

Systems with internal parameters obeying the orthogonality condition.

08 p0987 A73-20777

Restoring the orthogonality of two polarizations in radio communication systems. II.

10 p1190 A73-24623

Bragg diffraction of light by two orthogonal ultrasonic waves in water.

15 p1914 A73-32256

Hypoelastic approximation for plastic media axisymmetric deformation, determining grid for numerical analysis from orthogonality relations

16 p2079 A73-33239

Fibrous composite materials orthogonal shear properties related to laminate construction, discussing shear load tests, fiber orientation, boron, graphite, aluminum and titanium properties

19 p2443 A73-37893

[SAWE PAPER 993] An approximate analysis of non-linear, non-conservative systems using orthogonal polynomials.

21 p2740 A73-40755

Matrix methods application to stress in elastic structures, examining Mohr circles, design implications and orthogonality anisotropy

22 p2929 A73-43173

ORTHONORMAL FUNCTIONS

Numerical solution of integral equations of the first kind using a priori information on the function to be determined.

05 p0591 A73-16789

Optimal control of a class of linear multivariable systems with integral quadratic energy constraint.

06 p0681 A73-18521

Geometrical properties of normed spaces, associated with the convexity and smoothness moduli of a unit sphere

24 p3106 A73-45353

ORTHOGRAPHY

Cartographic applications of high-altitude aircraft photographs.

16 p2016 A73-33362

IR scanner for aerial stereoscopic photography, discussing use of computer controlled orthophoto printer for image distortion reduction by rectification

20 p2566 A73-39671

ORTHOSTATIC TOLERANCE

Airline flight and ground personnel fatigue and orthostatic hypotension syndrome manifested by variations in retinal arterial pressure and brain circulation

02 p0134 A73-12156

Vertical posture control after Soiz 6, 7 and 8 flights and 120-day hypokinesia

08 p0933 A73-20985

Influence of an oxygen and carbon dioxide rich gas mixture on the human orthostatic stability

08 p0933 A73-20988

Proteinuria and civil aviation aircrew

08 p0931 A73-21538

Effect of passive 70-deg head-up tilt on peripheral visual response time.

10 p1185 A73-24566

Certain features of hemodynamics during orthostatic tests with persons of different vestibulo-vegetative tolerance levels

17 p2111 A73-34236

Human statokinetic stability as component of non-specific resistance, discussing revolving, altitude, hypoxic and orthostatic stress dependence tests

18 p2279 A73-36904

Intracranial hemodynamic changes in pilots to tilting.

18 p2279 A73-36916

Ophthalmodynamography in pilots to test internal carotid insufficiency - Comparison of blood-pressure responses.

21 p2639 A73-41162

ORTHOTROPIC CYLINDERS

Propagation of harmonic waves in orthotropic circular cylindrical shells.

04 p0515 A73-15893

[ASME PAPER 72-WA/APM-23] Axial impact response of semifinite cylindrical membrane shell of helically oriented linearly elastic orthotropic fiber reinforced material, solving motion equations

05 p0631 A73-16112

Approximate method of studying the symmetrical deformation of orthotropic bodies

07 p0911 A73-19311

Orthotropic almost cylindrical beams - Bending by a transverse load.

09 p1160 A73-23023

Multilocal difference method for free vibration analysis of closed and open orthotropic noncircular cylindrical shells with supported curved edges

12 p1511 A73-27035

Stress concentration near a cutout on the surface of an orthotropic cylindrical shell

16 p2075 A73-32694

Large deflections and stability of a long shallow orthotropic cylindrical panel under the action of a local load

20 p2618 A73-39312

ORTHOTROPIC PLATES

- Investigation of the stress-strain state at a strengthened hole in an orthotropic cylindrical shell 23 p3046 A73-44193
- Critical stresses of compressed cylindrical shells consisting of orthotropic layers with various orientations 24 p3145 A73-44529
- The use of glass-fiber-reinforced plastics for containers which are subjected to external pressure 24 p3147 A73-44881

ORTHOTROPIC PLATES

- Some exact solutions in the design of technically orthotropic axisymmetric plates. 01 p0118 A73-11365
- Modified shear-flexible orthotropic plate theory application to simply supported rectangular sandwich plates buckling problem, comparing results with Reissner theory and experimental data. 04 p0509 A73-14946
- Analysis of transverse cracks in an orthotropic strip with edge stiffeners. [ASME PAPER 72-WA/APM-4] 04 p0516 A73-15904
- Lateral rigidity of longitudinally stiffened plates. 05 p0633 A73-16543
- Orthotropic panel flutter at arbitrary yaw angles - Experiment and correlation with theory. [AIAA PAPER 73-192] 05 p0634 A73-16924
- Monograph - Grid analysis of orthotropic plates. 06 p0761 A73-17873
- Vibration of cylindrically orthotropic circular plates. 07 p0913 A73-19968
- Postbuckling analysis of rectangular orthotropic plates. 08 p1015 A73-20673
- Stress concentration in rotating orthotropic elliptic disks solution via Chen-Hsu modification of stress function for bounded plates 08 p1017 A73-20943
- Large deflections and stability of a long cylindrical panel prepared from an orthotropic fiberglass plastic under the action of piecewise-uniform loading 08 p1017 A73-21370
- The influence of orthotropy on the stability of some multi-plate structures in compression. 08 p1018 A73-21435
- Stresses and displacements in reinforced orthotropic panels under static loads, obtaining differential equations solution as numerically derived transfer matrices 09 p1161 A73-23091
- Post-buckling behaviour of rectangular orthotropic plates. 10 p1288 A73-23699
- Vibration analysis of clamped, rectangular plates of generalized orthotropy. 10 p1291 A73-24387
- Elastic deformation of an orthotropic semi-infinite plate with straight boundary asymmetric with respect to the elastic axes of the material under uniform partial loading. 10 p1293 A73-24922
- Incremental deformations in orthotropic laminated plates under initial stress. [ASME PAPER 72-APM-VV] 11 p1441 A73-25707
- Shear correction factors for orthotropic laminates under static load. 11 p1442 A73-25713
- Clamped orthotropic skew plates under uniformly distributed transverse load, considering nonlinear analysis based on numerical technique of dynamic relaxation involving critically damped vibration 11 p1444 A73-26381
- Rayleigh-Ritz method for natural frequencies of transversely vibrating polar orthotropic annular perforated plates, proposing coordinate transformations for asymmetric mode solutions 11 p1446 A73-26495
- Eigenfunction analysis for bending of clamped rectangular, orthotropic plates. 11 p1447 A73-26653
- Static, vibration and buckling analysis of axisymmetric circular plates using finite elements. 12 p1555 A73-27738
- Vibration of simply supported-clamped skew plates at large amplitudes. 13 p1690 A73-28057
- Clamped orthotropic triangular plates free nonlinear vibrations, solving equations of motion in first order approximation by von Karman plate theory 13 p1697 A73-28808
- Postbuckling behavior of orthotropic skew plates. 13 p1697 A73-28813
- Planar shear wave motions polarized in plane of bonded elastic orthotropic layered plates with each layer having distinct mechanical and inertial properties and thickness 13 p1697 A73-28820
- Internal stress-strain boundary layer theory of shells and orthotropic plates with zero stress conditions at upper and lower planes and edge distance dependent attenuation 14 p1815 A73-30815

- The large deflection and post-buckling behaviour of some laminated plates. 15 p1946 A73-31117
- Orthotropic characteristics of glass-fibre-epoxy laminates under plane stress. 15 p1897 A73-31698
- Estimates of the eigenvalues of a difference problem for a plate 16 p2074 A73-32690
- Flexural vibrations of clamped orthotropic plates. 16 p2081 A73-33680
- Free vibrations of multilayered composite plates. 17 p2241 A73-34192
- Orthotropic viscoelastic shells and plates dynamic behavior reduced to eigenvalue and quasi-static solutions for nonstabilized oscillation 17 p2241 A73-34326
- Thin elastic orthotropic annular plate postbuckling behavior under planar edge compression loads, analyzing axisymmetric deformations via nondimensional equations and Keller-Reiss numerical method [ASME PAPER 73-APM-5] 17 p2247 A73-35030
- Nonlinear vibration of a rectangular plate arbitrarily laminated of anisotropic material. 17 p2249 A73-35105
- [ASME PAPER 73-APM-F] 17 p2249 A73-35105
- Nondestructive testing of fiberglass reinforced plastic plates by means of holographic interferometry 18 p2316 A73-36477
- Elastic stresses in rotating orthotropic discs of variable thickness. 19 p2496 A73-37436
- Boundary layer concept /attenuating stress-strain state with homogeneous boundary conditions/ incorporation into internal stress-strain state theory for orthotropic rectangular elastic plates 19 p2499 A73-37763
- Nonlinear bending of rectangular orthotropic plates. 19 p2500 A73-38116
- A unified method for determination of fundamental natural frequency of orthotropic plate with arbitrary boundary. 20 p2622 A73-39546
- On stress-concentration analysis of laminated composite plates. 20 p2622 A73-39551
- Free and forced nonlinear oscillations of anisotropic orthotropic annular plate with free inner boundary and fixed immovable outer boundary 20 p2623 A73-39561
- Antisymmetrical bending of a circular orthotropic plate of variable thickness 20 p2625 A73-39656
- Buckling of continuous circular plates. 21 p2782 A73-40004
- Large amplitude flexural vibration of simply supported skew plates. 21 p2784 A73-40423
- Temperature stresses in a partly reinforced orthotropic plate 21 p2787 A73-40991
- Thermoelastic dilatational deformation in two perfectly bonded orthotropic half-planes, showing linear relations between elastic and homogeneous field 21 p2789 A73-41674
- Dynamic behaviour of orthotropic plates using finite difference technique. 22 p2917 A73-41716
- High frequency vibrations and waves in laminated orthotropic plates. 22 p2928 A73-43135
- Thermal stresses in heated orthotropic plates with variable heat-transfer coefficients 23 p3046 A73-44195
- Mixed finite-difference scheme for analysis of simply supported thick plates. 24 p3150 A73-45226

ORTHOTROPIC SHELLS

- Basic behavioral characteristics of viscoelastic orthotropic shell prepared from a generalized thermorheologically simple material 01 p0112 A73-10001
- Free vibration of prestressed cylindrical shells having arbitrary homogeneous boundary conditions. 01 p0114 A73-10730
- Existence of solutions in nonlinear shallow shell theory 01 p0116 A73-10962
- Helios solar probe structural adapter design for linking to booster rocket end stage, investigating orthotropic cylindrical shell carrying capacity [DGLR PAPER 72-101] 02 p0227 A73-11685
- On higher-order theory for thermoelastic analysis of heterogeneous orthotropic cylindrical shells. 03 p0389 A73-13327
- A finite element analysis of an axisymmetrically loaded orthotropic shell of revolution. 03 p0391 A73-13677
- Influence areas for some cross sectional parameters of shallow double-curvature shells 04 p0513 A73-15507
- Russian book on orthotropic laminated cylindrical shells strength and optimal design covering glass ribbon reinforced zero moment shells and interlayer shear theory 04 p0514 A73-15702

- Variable thickness orthotropic shell of revolution with bending suppressed. 05 p0633 A73-16537
- Axisymmetric deformation of a laminar, orthotropic, cylindrical shell 08 p1017 A73-21368
- Deformation of a frame coupled to a fiberglass-plastic shell under the action of local loads 08 p1017 A73-21372
- Stability of the state of moment stress of a three-layer orthotropic cylindrical shell under uniform and nonuniform external pressure 08 p1018 A73-21374
- Iterative method for solving some boundary value problems for the equations of an orthotropic shell of revolution 10 p1292 A73-24501
- Stability of a cylindrical anisotropic shell under the action of a ring load with allowance for subcritical deflection 12 p1553 A73-27373
- Supersonic flutter of truncated multilayered orthotropic conical thin shells. 14 p1814 A73-30702
- Natural vibrations of variable-thickness shells of revolution with apparent additional masses 16 p2074 A73-32685
- Effect of transverse shear on the stability of an orthotropic cylindrical shell with an elastic filler under axial compression 16 p2082 A73-33931
- Dynamic stability of an orthotropic cylindrical shell allowing for transversal shear 16 p2083 A73-33937
- Orthotropic viscoelastic shells and plates dynamic behavior reduced to eigenvalue and quasi-static solutions for nonstabilized oscillation 17 p2241 A73-34326
- Meridional geometries for orthotropic shells with bending suppressed for different loading conditions, deriving shell configurations for combined loading via equilibrium equations 17 p2243 A73-34530
- Vibration of layered shells. 18 p2367 A73-37029
- Inverse bending problems for two-layer orthotropic shallow shells 20 p2618 A73-39313
- Symmetrical three-layer shells with a light-weight elastic filler 20 p2618 A73-39328
- Natural oscillations of shells of revolution with an open profile and concentrated inclusions 20 p2625 A73-39654
- Calculation of shear-sensitive orthotropic shells with residual stresses 21 p2786 A73-40977
- Function space approach to prestressed nonlinear orthotropic shallow shell theory boundary value problems 24 p3149 A73-45006

ORTHOTROPISM

- Nonlinear effect of initial stress on crack propagation between similar and dissimilar orthotropic media. 07 p0915 A73-20334
- Bending of an orthotropic prismatic beam by a transverse force in a geometrically nonlinear formulation 08 p1020 A73-21769
- Natural vibrations of laminated orthotropic spheres. 09 p1160 A73-22890
- Orthotropic material plane crack problem numerical solutions by polynomial approximation and modified mapping-collocation technique involving conformal mapping 09 p1161 A73-23175
- On the elastic properties of fiber composite laminates with statistically dispersed fiber and ply orientations. 10 p1288 A73-23959
- Method of initial functions for the plane problem of a linearly orthotropic body in the theory of elasticity 11 p1445 A73-26457
- Elastostatic invariance in the composite plane. 13 p1696 A73-28747
- Oblique bending of a homogeneous orthotropic prismatic beam by a force couple in the quadratic theory of elasticity 14 p1815 A73-30785
- Photoelastic analysis of an orthotropic ring under diametral compression. 15 p1949 A73-31653
- Effect of orthotropy on singular stresses for a finite crack. [ASME PAPER 72-APM-VVV] 17 p2249 A73-35109
- On stress concentration factors in orthotropic glass-fiber reinforced plastics. 18 p2327 A73-36474
- Torsional and anti-plane strain delamination of an orthotropic layered composite. 20 p2622 A73-39549
- Effect of orthotropy on singular stresses produced near a crack tip by incident SH-waves. 21 p2786 A73-40933

The effect of plasticity and crack blunting on the stress distribution in orthotropic composite materials. [ASME PAPER 73-APMW-2] 22 p2924 A73-42876
 Static theory of plane micropolar strain for homogeneous orthotropic elastic solids, deriving existence and uniqueness theorems and reducing boundary value problems to Fredholm equations 24 p3147 A73-44684

OSCILLATING CYLINDERS

An experimental study of the dynamic lift on a cylinder subjected to a high Reynolds number flow perpendicular to its axis. [ONERA, TP NO. 1073] 01 p0001 A73-10226
 Dynamic stability of the state of moment stress in a cylindrical shell with allowance for inertia of the sub-critical state 01 p0117 A73-11093
 Oscillations of nonshallow cylindrical shells loaded by distributed and concentrated masses 01 p0118 A73-11407
 Oscillations of open cylindrical shells of variable curvature 02 p0233 A73-11941
 Application of the method of summary representations to problems of cylindrical shell oscillations 04 p0511 A73-15086
 Law governing the oscillations of a circular cylindrical shell of finite length containing a liquid with a variable level 04 p0434 A73-15505
 Vortex induced vibration of circular cylindrical structures. [ASME PAPER 72-WA/FE-39] 04 p0404 A73-15856
 Finite element analysis of unsteady incompressible flow around an oscillating obstacle of arbitrary shape. [AIAA PAPER 73-91] 05 p0529 A73-16855
 Approximate determination of the hydrodynamic coefficients for the sloshing of a liquid in moving cylindrical cavities 10 p1206 A73-24309
 Lift forces on an oscillating cylinder at low Reynolds number. 10 p1173 A73-24822
 Effect on shell dynamics of a shell mass distributed within a shell surface area 11 p1446 A73-26461
 Vertical free vibrations of rectangular vessel partially filled with perfect incompressible liquid analyzed by power series 15 p1860 A73-31045
 Stability of elliptical cylinder consisting of perfect incompressible gravitating fluid subject to arbitrary perturbations 15 p1860 A73-31048
 Reaction of a cylindrical shell to periodic shock waves propagating in its interior 17 p2243 A73-34735
 Nonlinear parametric vibrations of closed cylindrical shells 19 p2499 A73-37764
 Heat transfer from a vibrating circular cylinder. 19 p2505 A73-38478
 Application of the method of normal waves to the study of the oscillations of a cylindrical shell in contact with an elastic medium 20 p2615 A73-38984
 Nonlinear streaming effects associated with viscous incompressible fluid near oscillating cylinder, considering theory based on outer-inner expansion technique with Stokes drift correction 20 p2546 A73-39088
 Vibration analysis of circular cylinders by holographic interferometry. 21 p2701 A73-40756
 On the radiation from an aerodynamic acoustic dipole source 21 p2633 A73-40943
 Vibrations of a rotating solid body with a cavity partly filled with an arbitrary viscous fluid 21 p2677 A73-40988
 Eigenmodes in vibrations of circular cylindrical shells with free boundaries, calculating frequencies from theory of inextensional vibrations 21 p2788 A73-41614
 Gradient instabilities in a system of gravitating point masses. 24 p3132 A73-44479
 Nonlinear parametric vibrations of cylindrical shells prepared from composite materials 24 p3145 A73-44517

OSCILLATING FLOW

A variant of the solution of problems of fluid oscillations in cylindrical cavities by the Bubnov-Galerkin method 01 p0031 A73-10101
 Two-dimensional boundary layers in a free stream which oscillates without reversing. 01 p0032 A73-10446
 The oscillations of supersonic gas flows 03 p0289 A73-12953
 Numerical simulation of initial value problem of axisymmetric equatorially trapped oscillation modes of constant density viscous fluid in rotating spherical shell 03 p0384 A73-13064

The stability of oscillatory Stokes layers.

03 p0291 A73-13065
 Time-periodic fluid surface wave radiation and scattering by partially immersed objects in short wave asymptotic limit of nondimensional wavelength approaching zero 03 p0397 A73-13533
 Hydrodynamics in weak gravitational fields - Plane oscillations of an ideal fluid in a rectangular channel 03 p0294 A73-13606
 Calculation of the natural oscillations of an ideal liquid in an axisymmetrical container with allowance for surface forces 03 p0294 A73-13607
 Analysis of unsteady laminar boundary layer flow by an integral method. [ASME PAPER 72-WA/FE-2] 04 p0434 A73-15839
 The oscillatory boundary layer growth over the top and bottom plates of a rotating channel. [ASME PAPER 72-WA/FE-5] 04 p0434 A73-15842
 Effect of an oscillating free stream on the unsteady pressure on a circular cylinder. [ASME PAPER 72-WA/FE-12] 04 p0434 A73-15843
 Experimental analysis of lift on a fixed cylinder subjected to a flow perpendicular to its axis at high Reynolds numbers 04 p0405 A73-15990
 Stability investigation in the case of an oscillating Couette flow. I. Nonlinear theory. II - Linear theory [DFVLR-SONDDR-257] 05 p0563 A73-16098
 Nonlinear longitudinal combustion instability in rocket motors. 05 p0641 A73-16947
 Finite-amplitude convection occurring in a modulated gravitational field 06 p0767 A73-17463
 Containers with isochronous fluid oscillations. 06 p0686 A73-18147
 Critical conditions for steady/unsteady laminar shear flow breakdown into HF oscillations, using kinematic wave theory [AD-758579] 06 p0687 A73-18533
 The use of aerosols for the visualization of flow phenomena. 06 p0683 A73-18837
 Investigation of auto-oscillations of a continuous medium, occurring at loss of stability of a stationary mode. 07 p0809 A73-19018
 Time-periodic solution of the system of boundary layer equations. 07 p0809 A73-19019
 An iterative procedure for the oscillatory laminar boundary layer. 07 p0809 A73-19035
 Unsteady thin-airfoil theory for subsonic flow. 08 p0925 A73-20718
 Planetary boundary layer flow of a stable atmosphere over the globe. 08 p0960 A73-21380
 Some diagnostic applications of wind speed and component spectra for mesoscale through synoptic scale frequencies. 09 p1114 A73-22336
 Characteristics of the motion of a system composed of a shell and fluid within the limits of hydraulic approximation 09 p1072 A73-22587
 Oscillation of axisymmetric bodies in a stratified fluid. 10 p1205 A73-23625
 Unsteady boundary layer flow, considering Stokes, Rayleigh and Heisenberg-Tollmien theories application to oscillatory, fluctuating, impulsive and rotational effects 10 p1207 A73-24802
 On the response of laminar boundary layers to periodic changes in free-stream speed. 10 p1207 A73-24803
 Turbulent wake development in oscillating flow, deriving flow equations for sinusoidally time dependent orifice flow 10 p1208 A73-24814
 Development of unsteady boundary layers under variable suction. 10 p1209 A73-24831
 Acoustic streaming and forces generated on circular cylinder in radially oscillatory incompressible fluid, considering steady and unsteady flow 10 p1174 A73-24847
 Oscillations arising when parallel flows of a viscous liquid lose stability relative to periodic long-wave disturbances 11 p1349 A73-26430
 Influence of the flexibility of the walls on the oscillations of the liquid masses of storage tanks 12 p1487 A73-27395
 On oscillatory instability of plane-parallel convective motion in a vertical channel. 12 p1559 A73-27542
 Axisymmetric inertial oscillations of a fluid in a rotating spherical shell. 13 p1601 A73-28916
 A study of frequency selection and jumping peculiar to some fluidic oscillations. 13 p1603 A73-29034

The unpolarized electrode in a pulsating Poiseuille pipe flow. 13 p1620 A73-29258

Heat transfer by fluctuating flow of an elastico-viscous liquid past an infinite plate with time varying suction. 14 p1816 A73-29999
 Free convection effects on the oscillatory flow past an infinite, vertical, porous plate with constant suction. I, II. 14 p1816 A73-30049
 The theory of fluctuating flow fields near walls. 14 p1746 A73-30704
 Experimental study of cavitation oscillations in a centrifugal screw pump 15 p1832 A73-31499
 Oscillatory flow phenomena in diffusers at low Reynolds numbers. [ASME PAPER 73-FE-14] 17 p2152 A73-35011
 Concentrated vortex nonlinear oscillations, discussing vortex ring and helical vortex filament stability, mode shape and frequency changes and standing and traveling wave solutions 18 p2301 A73-37004
 Calculation of hypersonic nonequilibrium nozzle flows with excited vibrational degrees of freedom 18 p2266 A73-37018
 Investigation of the high-frequency oscillations in the flow of a pulsed coaxial plasma accelerator - One mechanism of inhomogeneity 19 p2467 A73-37364
 A study of a feedback fluidic jet oscillator. I, II. 19 p2389 A73-38077
 Nonlinear streaming effects associated with viscous incompressible fluid near oscillating cylinder, considering theory based on outer-inner expansion technique with Stokes drift correction 20 p2546 A73-39088
 Shock oscillation associated with Hartmann resonance tubes excited by underexpanded sonic jets, using schlieren streak photography 21 p2677 A73-40616
 The dynamic stability of a pipe conveying a pulsatile flow. 21 p2678 A73-41671
 Finite amplitude dynamic motion of viscoelastic materials. 23 p3038 A73-43273
 Experimental investigation of turbulent flow characteristics in a rotating channel 23 p2968 A73-43443
 Flare triggering by coherent oscillations. 24 p3124 A73-45048

OSCILLATION DAMPERS

Oscillation damping by pulsed dynamic dampers. 02 p0235 A73-12209
 Investigation of damping methods for low frequency augmentor combustion instability. [AIAA PAPER 72-1207] 03 p0358 A73-13490
 Screen and porous absorbing liner design for damping pressure oscillations in ramjet combustors based on acoustic absorption efficiency and combustion instability calculation 06 p0767 A73-17665
 Experimental verification of the energy dissipation mechanism in acoustic dampers. 08 p1024 A73-21472
 Nutation dampers vs precession dampers for asymmetric spinning spacecraft. 11 p1432 A73-26670
 Frequency method of synthesis for an active dynamic vibration damper 12 p1525 A73-27948
 Errors of the gravitational stabilization system of a satellite with gyro damping 14 p1803 A73-29869
 Tuned dampers for randomly excited dynamic systems. [ASME PAPER 73-DET-70] 22 p2919 A73-42070
 Experimental investigation of a simple squeeze film damper. [ASME PAPER 73-DET-101] 22 p2865 A73-42078

OSCILLATIONS

NT ELECTRON OSCILLATIONS
 NT H WAVES
 NT HARMONIC OSCILLATION
 NT MOLECULAR OSCILLATIONS
 NT NONOSCILLATORY ACTION
 NT NONSTABILIZED OSCILLATION
 NT PLASMA OSCILLATIONS
 NT PRESSURE OSCILLATIONS
 NT SELF OSCILLATION
 NT STABLE OSCILLATIONS
 NT TRANSIENT OSCILLATIONS
 NT TRANSVERSE OSCILLATION
 NT UNDAMPED OSCILLATIONS
 NT WING OSCILLATIONS
 Variational aspects of oscillation phenomena for higher order differential equations. [AD-758575] 02 p0188 A73-12823
 Theorems on periodic noncritical approximate solutions of nonlinear oscillations differential equations 04 p0469 A73-14667

OSCILLATORS

Solution of an inhomogeneous boundary value problem with continuous discrete parameters in the presence of discrete disturbances

04 p0470 A73-14934

Spacecraft oscillatory motion as function of attitude control impulse magnitude

05 p0627 A73-16080

A quasi-inertial attitude mode for orbiting spacecraft.

05 p0630 A73-17203

Representation of oscillations in piecewise-linear systems by the phase-shift-averaging method.

06 p0717 A73-18146

Periodic oscillations in feedback systems with combined pulse modulation.

06 p0680 A73-18518

Flow in the wake of a cascade of oscillating airfoils.

07 p0774 A73-19954

Vertical velocity field oscillations in photospheric sunspot umbrae interpretation in terms of gravity or acoustic waves traveling along magnetic field lines

08 p1001 A73-20756

H alpha observations of vertical velocity distribution periodic oscillations in sunspot, noting transverse waves formation and propagation to penumbral boundary

08 p1001 A73-20757

Nonoscillation of second-order, linear differential equations with retarded argument.

09 p1112 A73-22420

Second order differential equations with complex-valued coefficients.

09 p1112 A73-22425

Variational aspect of the integration of partial differential equations for the oscillations of elastic bodies

12 p1517 A73-27097

Integral manifold concept for stability analysis of nonlinear system oscillations, plotting resonance curve for quasi-linear autonomous system

12 p1525 A73-27792

A method of studying oscillatory systems subject to the action of external periodic forces in the nonresonant case

12 p1525 A73-27812

Nonoscillation and disconjugacy of systems of linear differential equations.

13 p1648 A73-28441

Oscillatory waves in intracranially recorded electroretinograms in primates, considering electrode depth, stimulus duration and intensity and background illumination, anesthesia and tetrodotoxin effects

14 p1717 A73-30393

Oscillations of higher-order retarded differential equations generated by the retarded argument.

14 p1770 A73-30756

Oscillations of nonlinear functional differential equations generated by retarded actions.

14 p1770 A73-30761

The period of nonlinear vibrations of autonomous dynamical systems of the order n

15 p1947 A73-31366

Vector field representation of curved elastic membranes oscillatory motions, particularizing equations of motion for small displacements from equilibrium configurations

16 p2076 A73-32937

Russian book - Asymptotic and qualitative methods in the theory of nonlinear oscillations.

17 p2211 A73-34850

Russian book - Nonlinear oscillations and transient processes in machines.

18 p2319 A73-35895

On the mass transfer produced by oscillations in a compressible, dissipative, and inhomogeneous medium

19 p2503 A73-37528

A note on the period of oscillation of non-linear systems.

19 p2460 A73-38108

Application of the averaging method to the study of oscillatory systems with distributed parameters and time lag

20 p2592 A73-38978

Book on oscillation theory covering classical, abstract and complex theories, nonselfadjoint differential equations, hyperbolic and elliptic equations, Sturm-Picone theorem, etc

20 p2582 A73-39141

Nonoscillation and oscillation of a linear differential equation of the n-th order

20 p2582 A73-39318

Normal third-order shapes of nonlinear oscillations

20 p2593 A73-39320

Combined density of the probability distribution of instantaneous values for the phase difference of two oscillations and for the phase difference derivatives

20 p2593 A73-39390

Oscillatory motions of an axisymmetric spin-stabilized solid body

20 p2593 A73-39495

Conditionally periodic oscillations in nonlinear systems

20 p2593 A73-39500

Multiwave interactions in nonlinear distributed systems

20 p2593 A73-39511

The description of vortex-excited oscillations of prismatic bodies by means of a sequence of pulses having random time differences

20 p2594 A73-39770

A practical means of calculating normal forms in problems involving nonlinear oscillations

21 p2738 A73-40178

Small oscillations of a heavy solid body about a stationary point and certain cases of the existence of 'linear integrals'

21 p2738 A73-40188

Comments on the mathematical theory of small oscillations of an inviscid gas

21 p2738 A73-40191

Oscillation amplitude curve determination of negative resistance oscillator connected to LC circuit, obtaining device I-V characteristics

23 p2961 A73-44147

A new weighting function for solving nonlinear oscillation problems.

24 p3148 A73-44893

OSCILLATORS

NT AUTODYNES

NT CRYSTAL OSCILLATORS

NT GYROSCOPIC PENDULUMS

NT HARMONIC OSCILLATORS

NT HELITRONS

NT MAGNETRONS

NT MECHANICAL OSCILLATORS

NT MICROWAVE OSCILLATORS

NT MICROWAVE TUBES

NT MOLECULAR OSCILLATORS

NT PENDULUMS

NT PLANOTRONS

NT RELAXATION OSCILLATORS

NT SYNCHRONIZED OSCILLATORS

NT VACUUM TUBE OSCILLATORS

High voltage square pulse oscillator and recording circuit for negative and positive autoelectron emission properties

01 p0024 A73-10795

Investigation of the dynamics of a pulsed phase-lock automatic frequency control system

02 p0142 A73-12493

German monograph - Contributions to the calculation of natural frequencies of undamped oscillator chains by the transfer method.

03 p0343 A73-13815

Parasitic oscillations in external excitation oscillators due to internal feedback in transistor, investigating frequency dependence of stability coefficient in common emitter stage

03 p0284 A73-14032

Voltage controlled subcarrier oscillator design and performance for FM/FM multiplex telemetry system for ECG recording during exercise

03 p0271 A73-14293

Automatic frequency control in the case of manually tuned oscillators

04 p0427 A73-14774

Almost-coherent detection of phase-shift-keyed signals using an injection-locked oscillator.

05 p0549 A73-16368

Continuous measurement of internal friction and modulus with a regenerative feedback loop and composite oscillator.

05 p0559 A73-17255

Feedback networks for RC oscillators with maximum frequency stability

06 p0673 A73-17581

Radio oscillators short term frequency instability, examining relations between time domain and frequency domain sample variance definitions

07 p0798 A73-19176

Properties and applications of the iterative synthesizer with a search oscillator

07 p0798 A73-19178

Application of ultrastable oscillators to the aerospace field

07 p0798 A73-19180

Gunn diode characteristics under large and small signal conditions, noting applications for FM oscillators and voltage tuned and magnetically tuned oscillators

08 p0943 A73-20711

High gain gas laser oscillators saturation, verifying with 3.51 micron Xe oscillator having unsaturated single pass intensity gain of ten million

09 p1091 A73-22086

Self excited LC and RC oscillator networks based on FETs, discussing frequency tuning and FM methods

10 p1197 A73-24941

A high performance 4500 volt electron multiplier bias supply for satellite use.

11 p1363 A73-25959

Dynamics of a two-frequency self-oscillator with 'hard' excitation

11 p1331 A73-26157

Parametron circuit current fluctuations analysis via successive approximation solution of nonlinear differential equation, investigating operational mode stability

11 p1400 A73-26452

Precision low frequency adaptive MOSFET IC electronic oscillators with loose tolerance component timers for cost reduction

12 p1478 A73-27167

Wave resistance determination in synthesis of oscillator circuits with homogeneous line segments for given resonant frequencies spectrum

13 p1591 A73-28660

Blocking oscillator multipulse mode operation digital control by supply voltage regulation

13 p1593 A73-29119

High-speed frequency count-down circuit using a tunnel diode and a delay line.

13 p1594 A73-29222

German monograph - Rapid excitation of quasi-harmonic oscillations in a class of nonlinear oscillators.

13 p1594 A73-29285

Quadratically coupled oscillators interaction at semiresonant frequencies, considering time dependent Duffing equation and frequency divider application

13 p1661 A73-29375

Truncated general equations and a characteristic equation of a self-excited transistor oscillator

14 p1736 A73-30562

Quantum theory of nonlinear oscillators interacting with a medium

14 p1775 A73-30812

Two-phase radio-frequency generators employing phase-lock AFC

17 p2135 A73-34590

Pulse modulation of Gunn-effect oscillator.

17 p2142 A73-35652

A nonlinear oscillator analog of rigid body dynamics.

18 p2337 A73-36416

Spontaneous emission and self-excitation of a small volume in a classical, nonlinear active medium

19 p2463 A73-38540

Boundaries effect on dispersion interaction between molecules in bounded region, applying method to two oscillators between conducting plates

20 p2538 A73-39705

Optimization and design of varicap-diode tuned transistor oscillators

21 p2659 A73-40009

On the radiation from an aerodynamic acoustic dipole source

21 p2633 A73-40943

Analysis of starting circuits for a class of hard oscillators - Two-transistor saturable-core parallel inverters.

22 p2834 A73-42909

Spectral analysis of frequency noise of oscillators by the Hadamard variance

24 p3073 A73-44974

Limitation of m.t.i. improvement factor due to oscillator instability.

24 p3069 A73-45259

On the gyroscopic coupling of a Van der Pol oscillator in the forced regime and of a free linear oscillator

24 p3111 A73-45396

OSCILLOGRAMS

U OSCILLOGRAMS

OSCILLOGRAMS

Two coordinate oscillograph recording device with automatic reversing for stress-strain tests under static and cyclic loads

02 p0168 A73-12144

Operational tests of the K-115 loop oscillograph

07 p0828 A73-20548

Investigation of the operation of a polarographic sensor under the action of surge-type polarizing voltage, using an electric analog

08 p0965 A73-21107

High-speed stereoscopic investigation of paths of luminous objects

08 p0969 A73-21719

Modification of a ballisto-oscillograph for extremities

09 p1046 A73-22865

Procedure for recording stresses by dielectric sensors in the case of impulsive loads

10 p1219 A73-24367

Oscillographic equipment for research in the field of semiconductor microwave electronics

17 p2218 A73-34160

Laser pulse shape measurement by successive oscillographing of pulse front areas and concurrent signal amplitude variation

17 p2183 A73-34168

Oscillographic registration of the occurrence of off-axis modes in a gas laser

17 p2183 A73-34169

High-speed cine-photography and oscillography in a boiling simulation

21 p2697 A73-39994

OSCILLOSCOPES

A moderately-priced modern cathode-ray tube without intensifier electrode

16 p1987 A73-33166

CRT designs for high-sensitivity high speed broadband oscilloscopes, discussing brightness characteristics enhancement
16 p1987 A73-33167

An automatic sweep generator for a strobed oscilloscope
21 p2664 A73-41098

An improved method of triggering oscilloscopes for dynamic-strain measurements.
21 p2704 A73-41267

OSCILLATIONS
U DOUBLE CUSPS
OSCILLATORY INTERPOLATION
U ORBIT CALCULATION
U ORBIT PERTURBATION
OSEEN APPROXIMATION
Streaming two dimensional Oseen MHD flow of conducting fluid past semiinfinite needle within aligned field
01 p0031 A73-10305

An extension of the modified Oseen solution for laminar viscous flow past a semi-infinite flat plate.
06 p0688 A73-18849

On the Oseen limiting movements around a rectilinear profile placed under a free line
19 p2459 A73-37526

OSMIUM
The Os-Pt-Hg abundance peak in Ap stars and the problem of very heavy cosmic rays.
02 p0210 A73-12733

Reflectance and optical constants of evaporated osmium in the vacuum ultraviolet from 300 to 2000 Å.
13 p1660 A73-28936

OSMOMETERS
Apparatus for measuring the colloid osmotic pressure in blood serum
23 p2949 A73-43792

OSMOSIS
Progress in the development of the reverse osmosis process for spacecraft wash water recovery.
02 p0137 A73-11993

Symposium on Capillary Exchange and the Interstitial Space, Bad Duerkheim, West Germany, May 3-6, 1972, Proceedings.
03 p0265 A73-14649

Synthesis of reverse osmosis membranes by plasma polymerization of allylamine.
07 p0780 A73-19169

Effect of ultrafiltration and plasma osmolality upon the flow properties of blood - A possible mechanism for control of blood flow in the renal medullary Vasa recta.
08 p0930 A73-21199

Evaluation of 165 deg F reverse osmosis modules for washwater purification.
[ASME PAPER 73-ENAS-2] 19 p2399 A73-37964

Design considerations for space mission wash water processing by reverse osmosis.
[ASME PAPER 73-ENAS-3] 19 p2493 A73-37965

Reverse osmosis for wash water recovery in space vehicles.
[ASME PAPER 73-ENAS-12] 19 p2399 A73-37971

Development of sulfonated polyphenylene oxide membranes for the reverse osmosis purification of wash water at sterilization temperatures /165 F/.
[ASME PAPER 73-ENAS-16] 19 p2399 A73-37973

NS-1 membranes - Potentially effective new membranes for treatment of washwater in space cabins.
[ASME PAPER 73-ENAS-19] 19 p2400 A73-37975

Reverse osmosis for recovering and recycling water in Space Station Prototype Environmental Thermal Control/Life Support System Integrated Water and Waste Management
[ASME PAPER 73-ENAS-22] 19 p2400 A73-37978

Effect of prior adaptation to cold on the development of experimental hypertonia
21 p2636 A73-40209

Apparatus for measuring the colloid osmotic pressure in blood serum
23 p2949 A73-43792

OSMOTIC PRESSURE
U OSMOSIS
OSO
NT OSO-7
Attitude dynamics of a 'nearly-spherical' dual-spin satellite and orbital results for OSO-7.
02 p0227 A73-11600

The Harvard experiment on OSO-6 - Instrumentation, calibration, operation, and description of observations.
18 p2357 A73-37108

OSO-7
Solar corona properties and nuclear reactions in flares from August 1972 OSO 7 observation, noting hard X ray bursts from electron streams
04 p0502 A73-15971

Maneuvering a tumbling dual-spin spacecraft - The recovery of OSO-7.
[AIAA PAPER 73-248] 05 p0630 A73-16971

Space application of SEC vidicons - The OSO 7 coronagraph.
17 p2170 A73-35293

OTOLITH ORGANS

Vestibular influences on orientation in zero gravity, produced by parabolic flight.
06 p0653 A73-18032

Findings on American astronauts bearing on the issue of artificial gravity for future manned space vehicles.
09 p1045 A73-22531

Inversion illusion in the so-called zero-gravity conditions of parabolic flight.
14 p1722 A73-30511

Asymmetry of otolith responses in fish
15 p1834 A73-31507

Analysis of vestibular effects in experiments on swings
17 p2111 A73-34235

Vestibular and spinal control of eye movements.
18 p2272 A73-36440

OUTER PLANET MISSIONS

U GRAND TOURS
OUTER PLANET SPACECRAFT
U OUTER PLANETS EXPLORERS
OUTER PLANETS EXPLORERS

Unmanned outer planets and round trip mission nuclear rocket engine design for carrying payload into orbit by single earth orbital shuttle
[AIAA PAPER 72-1090] 03 p0340 A73-13411

Solar escape achievement by solid propulsion augmentation system and design independent of multiplanetary swingby, analyzing cost effectiveness of different programs
[AIAA PAPER 72-1163] 03 p0382 A73-13464

The radiation environments of outer-planet missions.
05 p0617 A73-16511

Estimating trajectory correction requirements for multiple outer planet missions.
05 p0623 A73-17205

Computerized design of an outer planets spacecraft structure to survive the meteoroid environment.
[AIAA PAPER 73-349] 11 p1430 A73-25487

Planetary quarantine constraints for outer planet satellite encounter missions, determining spacecraft impact probability in terms of trajectory analysis and navigation error numerical integration
18 p2349 A73-35976

The significance of outer planet satellite quarantine constraints on aim-point selection.
[AIAA PAPER 73-553] 18 p2359 A73-36096

Thermal control subsystem design of a Saturn/Uranus atmospheric entry probe for descent missions to 20 bars.
[AIAA PAPER 73-770] 18 p2360 A73-36384

Thermal control and structures approach for fluorinated propulsion.
[AIAA PAPER 73-772] 18 p2360 A73-36386

Pioneer spacecraft for atmospheric entry missions to the outer planets.
[AIAA PAPER 73-595] 18 p2360 A73-36500

A failure tolerant power subsystem for outer planet spacecraft.
22 p2801 A73-42902

Orbit improvement from satellite imaging data obtainable from outer planet missions.
23 p3032 A73-43840

Exploring Jupiter, Saturn and their satellites.
23 p3034 A73-44221

OUTER RADIATION BELT
Observations suggesting weak pitch angle diffusion of protons.
04 p0493 A73-15532

Electron acceleration in the outer radiation belt
06 p0742 A73-17527

Earth outer radiation belt and unstable radiation zone dynamics during IQSY magnetically quiet and disturbed period based on Elektron-series satellite data
12 p1535 A73-27636

Variations of solar-wind parameters, magnetic activity, and the electron tail of the magnetosphere and of the outer radiation zone.
13 p1608 A73-28714

Exponential distributions of protons according to adiabatic invariants in the outer radiation belt
15 p1926 A73-31898

Electron acceleration in the outer radiation belt.
16 p2051 A73-32752

Simulation of gyroresonant electron-whistler interactions in the outer radiation belts.
18 p2347 A73-36296

Influence of a sudden compression of the magnetosphere on outer zone electron fluxes measured at arbitrary pitch-angle.
21 p2682 A73-40161

Barium cloud release near equatorial plane for investigating interaction with ambient medium and electric and magnetic field properties in outer radiation belt
22 p2852 A73-41932

Steady state exponential distribution function of outer radiation belt low energy protons in terms of adiabatic invariants
24 p3124 A73-44807

OUTGASSING

Response of lunar atmosphere to volcanic gas releases.
03 p0365 A73-12880

Vacuum thermogravimetric analysis system for determination of continuous weight change and total condensable materials.
03 p0330 A73-13018

Comparative evaluations of outgassing results between the vacuum thermogravimetric method and the SRI method.
03 p0330 A73-13019

Outgassing and contamination properties of prospective Apollo Telescope Mount materials.
03 p0330 A73-13020

UHV outgassing measurements on various carbons.
08 p0937 A73-21621

Experimental studies on the formation of lunar surface features by fluidization - Discussion.
10 p1280 A73-24349

The evacuating and outgassing of a vacuum UV spectrophotometer for rockets
10 p1220 A73-24683

Leakable gases and water vapor loss rates and service life predictions for sealed alkaline cells in vacuum or aerospace environments, using mass transfer equations [ECS PAPER 32] 11 p1307 A73-24973

High and ultra-high vacuum by pumping with cryocooled surfaces.
11 p1398 A73-25579

Role of pressure transients in the detection and identification of lunar surface gas sources.
14 p1752 A73-29963

Volatile elements in Apollo 16 samples - Possible evidence for outgassing of the moon.
15 p1933 A73-31370

Spacecraft environmental optical contamination problems associated with thermal control surface outgassing.
[ASME PAPER 73-ENAS-32] 19 p2395 A73-37987

OUTLETS
Theoretical and experimental work on losses in 2-D turbine cascades with supersonic outlet flow.
17 p2092 A73-34377

OUTLETS [GEOLOGY]

U ESTUARIES

OUTPUT

NT LASER OUTPUTS

NT MASER OUTPUTS

OUTWASH PLAINS

U GLACIAL DRIFT

OVERCAST

U CLOUD COVER

OVERESTIMATION

U ESTIMATING

OVEREXPOSURE

U RADIATION DOSAGE

OVERPRESSURE

Prediction of inlet duct overpressures resulting from engine surge.
[AIAA PAPER 72-1142] 03 p0243 A73-13448

Characteristic overpressure of a supersonic transport of given length in a homogeneous atmosphere.
19 p2377 A73-38006

Effects of repeated simulated sonic booms of 1.0 PSF on the sleep behavior of young and old subjects.
21 p2644 A73-41151

A study to determine the feasibility of a low sonic boom supersonic transport.
[AIAA PAPER 73-1035] 24 p3056 A73-44863

OVERTONES

U HARMONICS

OVERVOLTAGE

Overload tolerance formulas for differential voltage null measuring system with amplifier for trigger circuit drive
02 p0170 A73-12345

OXIDASE

Biochemical processes during the maturation of erythrocytes - Further results with regard to the action site of the respiratory inhibitor F from reticulocytes in the respiratory chain
02 p0134 A73-12510

OXIDATION

NT ELECTROCHEMICAL OXIDATION

NT PHOTOOXIDATION

NT RUSTING

Dry oxidation of nickel by anhydrous carbon dioxide under pressure
01 p0062 A73-10271

Boron combustion, covering thermochemistry application to chemical propulsion systems, temperature effects on oxidation, single particle ignition and powder burning
01 p0089 A73-11112

The growth process of oxide layers during the initial oxidation of a 80Ni-20Cr alloy.
03 p0321 A73-12917

High-temperature oxidation of a Ti-15Mo-5Zr alloy at low pressure of oxygen /40 microtorr to roughly 0.2 millitorr/.
03 p0321 A73-12918

Soot particles oxidation by oxygen diffusion in laminar hydrocarbon flames, deriving kinetic expression from observed time dependent particle concentration variations

03 p0399 A73-14395

Ni-Cr-thoria alloy surface oxidation induced by sprayed coating of sodium sulfate for gas turbine blade hot corrosion investigation

04 p0468 A73-15316

Chromium diffusion in Ni-20 wt pct Cr-3 vol pct Y2O3 and Co-21 wt pct Cr-3 vol pct Y2O3.

04 p0463 A73-15317

The effect of a hydrogen preheat-treatment on the oxidation behavior of Ni-Cr-Al-ThO2 alloys.

04 p0463 A73-15319

Mechanical properties and structure of certain internally oxidized copper alloys

04 p0464 A73-15500

Oxidation effects on rate of C 14-labeled leucine incorporation into rat skeletal muscle protein

05 p0538 A73-16152

Oxidation of amino acids by diaphragms from fed and fasted rats.

05 p0538 A73-16153

Cool flame oxidation studies of acyclic and cyclic hydrocarbons.

05 p0606 A73-16691

Myeloperoxidase, the peroxidase of a primitive cell - Its reaction with Fe and H2O2.

06 p0652 A73-17944

Nickel-base alloys hot corrosion mechanism due to sodium sulfate induced accelerated or catastrophic oxidation as result of protective oxide scale dissolution

06 p0712 A73-18763

Passivation of chrome steels under isothermal oxidation at 1020 deg C

07 p0839 A73-19660

Evidence of lunar surface oxidation processes - Electron spin resonance spectra of lunar materials and simulated lunar materials.

07 p0893 A73-19840

Kinetics of the formation of passivating nickel hydroxide layers on nickel carbonyl

07 p0788 A73-20397

Radiation-induced oxidation of impurities in the water obtained from human moisture-containing bioactivity products

08 p0933 A73-20984

Internal oxidation of silver-beryllium and silver-lithium alloys.

08 p0977 A73-21022

A review of the diffusion path concept and its application to the high-temperature oxidation of binary alloys.

08 p0978 A73-21414

Superalloys oxidation behavior under long term exposure to high temperatures for suitability as Co-60 heat sources encapsulation materials

08 p0978 A73-21415

The oxidation of tantalum and niobium in the temperature range 400-600 C.

08 p0978 A73-21416

UV-induced lipid peroxidation in human epidermis, dermis, and hypodermis in vitro

09 p1038 A73-21873

Investigation of the failure characteristics of electrically heated samples of heat-resistant steels and alloys in a high-pressure oxidizing flow

09 p1069 A73-21980

Concentration profiles through thin oxide scales by ion-probe microanalysis.

09 p1101 A73-22402

Improvement of the friction and wear behavior of T-A6V alloy by a new anodic oxidation treatment

09 p1104 A73-22966

Organic and species-related differences in the action of certain hydrazine derivatives and of aminoperoxidase on the oxidative deamination of serotonin

10 p1183 A73-23679

Acids obtained by oxidation of kerogens of ancient sediments of different geographic origin.

11 p1326 A73-25467

Metal components wear mechanisms due to adhesion, tribooxidation, abrasion and surface fatigue, discussing prevention by lubrication, suitable mating of materials and surface treatments

11 p1373 A73-25577

Oxygen and temperature effects on Ni base superalloys fatigue fracture, discussing trans- and intergranular crack propagation and initiation in single and polycrystals and surface coatings

11 p1382 A73-25818

Soot oxidation kinetics at combustion temperatures.

12 p1557 A73-26844

Planetary and lunar surface color as geochemical history indicator in terms of oxidation state, solar wind access to atmosphere and planetary moisture content

12 p1541 A73-27484

Surface temperature measurement of regressing polymethyl methacrylate slabs burning in oxygen-nitrogen mixtures, discussing chemical mechanism for condensed phase depolymerization

13 p1707 A73-28994

Modeling the ignition and cool-flame limits of acetaldehyde oxidation.

13 p1581 A73-28999

The oxidation of metal alkyls in the presence of isobutane.

13 p1581 A73-29002

Study of precipitates formed by internal oxidation in cobalt-nickel-chromium alloys with a cobalt base. I - Precipitates formed by oxidation in air

14 p1759 A73-29750

Oxidation of powdered germanium, tin and lead tellurides under atmospheric conditions

15 p1887 A73-31594

Oxidation of acrylic fibres for carbon fibre formation.

15 p1898 A73-32049

A scanning electron microscope study of the surface morphology of TD-NiCr oxidized at 800 C to 1200 C.

15 p1895 A73-32270

Mach 1 oxidation of thoriated nickel chromium at 1204 C /2200 F/.

15 p1892 A73-32271

Oxidation of OT4 and OT4-1 alloys in the process of prolonged heating in air at temperatures from 200 to 400 deg

15 p1894 A73-32539

High-temperature oxidation of tungsten boride in oxygen and the effect of scale evaporation.

16 p1976 A73-33076

Shock-tube measurements of soot oxidation rates.

16 p2085 A73-33344

A study of the process of oxidation of zirconium-oxygen alloys

17 p2188 A73-34558

Heating of an oxidizing metal by CO2 laser radiation

17 p2184 A73-34634

Graphite oxidation at low temperature in subsonic air

[AIAA PAPER 73-735]

18 p2326 A73-36352

Oxidation of titanium between 25 C and 400 C

19 p2442 A73-37950

CW laser action from acetylene oxidation, noting sensitivity to total pressure and helium, oxygen and acetylene partial pressure changes

20 p2573 A73-39676

Two phase alloy internal oxidation kinetics, deriving mathematical model with linear law for penetration velocity fluctuations

21 p2719 A73-40898

Calculation of the heat resistance of metals at variable temperatures

21 p2721 A73-41230

Spectrophotometric study of products formed in the course of superficial oxidation of titanium and TA6V alloy

21 p2722 A73-41587

Organic compounds oxidation and combustion reactions, discussing hydrogen dioxide radical role and reaction rate

22 p2933 A73-42753

High-temperature oxidation of hydrogen by nitrous oxide in shock waves.

22 p2933 A73-42756

Sulfur hexafluoride pyrolysis and subsequent oxidation in mixtures with oxygen atoms and molecules, measuring decomposition rate at high temperature in shock tube experiment

22 p2818 A73-42767

Kinetics of carbon monoxide oxidation in postflame gases.

22 p2820 A73-42803

Turbulent flow reactor for oxidation of moist CO and postoxidation phase oxidation of methane, using chemical sampling and gas chromatographic analysis

22 p2820 A73-42804

Pyrolysis and oxidation of polymers at high heating rates.

22 p2936 A73-42806

Study of the spatial development of oxidation and combustion reactions by means of image photoelectric receivers, and of a thermometric method

24 p3091 A73-45398

OXIDATION RESISTANCE

Practical protective atmospheres for molten magnesium

03 p0323 A73-13267

Oxidation and nitridation of Cr-W alloy.

03 p0325 A73-13803

The high-temperature oxidation of nickel-20 wt. % chromium alloys containing dispersed oxide phases.

04 p0461 A73-14923

The functional form of rate curves for the high-temperature oxidation of dispersion-containing alloys forming Cr2O3 scales.

04 p0461 A73-14924

The high-temperature oxidation of cobalt-21 wt % chromium-3 vol. % Y2O3 alloys.

04 p0461 A73-14925

Effects of rare earth elements on the oxidation resistance of iron and nickel base alloys.

04 p0465 A73-15584

Heat resistance of alloys of the compound TiAl with niobium at 800 and 1000 C

06 p0708 A73-18049

Effect of oxygen on the scale resistance of titanium-tin alloys.

06 p0709 A73-18208

W-Ta alloys prepared by electron beam melting, testing Ta content effects on oxidation resistance and hardness at high temperatures

09 p1103 A73-22424

Perchlorate degradation of ethyl oleate in solid propellants.

10 p1262 A73-23758

Corrosion and electrochemical characteristics of oxidized steels Kh15N5D2T and Kh15N4AM3.

10 p1236 A73-24926

Transition metal borides ESCA spectra observation for metal-boron bonding energy based on spectral sensitivity to surface oxidation, discussing relevant features

11 p1325 A73-25202

Investigation of the ferriobionium oxidation process

13 p1630 A73-28016

Variation of chemical composition on the surface of cobalt-base alloys by oxidation in air.

15 p1891 A73-32016

Oxidizability of the IVT1 beta titanium alloy and its protection from gaseous corrosion

15 p1894 A73-32537

Oxidizability of AN-type beta titanium alloys and their protection from gaseous corrosion

15 p1894 A73-32538

Oxidation resistant carbon-carbon composite for Space Shuttle application.

16 p2028 A73-33043

The role of yttrium in high-temperature oxidation behavior of Ni-Cr-Al alloys.

16 p2025 A73-33077

Protection of certain borides from oxidation in air at 1200 C

18 p2318 A73-35888

High temperature cyclic oxidation resistance tests on Ni-, Co- and Fe-base alloys for aircraft gas turbine engines

19 p2440 A73-37496

The oxidation of binary alloys of chromium with metals of the first long period.

19 p2442 A73-38098

High reliability protective coatings for high temperature technology.

22 p2879 A73-42596

Mo content influence on heat resistant Ni base alloys corrosion and oxidation resistance and gamma-prime phase solution temperature and amount

23 p2989 A73-43435

Microstructure and its related properties on carbon fiber composites.

23 p2998 A73-44134

Ten years' experience of UMCo-type alloys in a special steel foundry.

24 p3099 A73-45074

OXIDES

NT ALKALINE EARTH OXIDES
NT ALUMINUM OXIDES
NT ANHYDRIDES
NT BARIUM OXIDES
NT BERYLLIUM OXIDES
NT BISMUTH OXIDES
NT BORON OXIDES
NT CALCIUM OXIDES
NT CARBON DIOXIDE
NT CARBON MONOXIDE
NT CESIUM OXIDES
NT CHROMITES
NT CHROMIUM OXIDES
NT COBALT OXIDES
NT ENSTATITE
NT GERMANIUM OXIDES
NT HAFNIUM OXIDES
NT HEAVY WATER
NT HEMATITE
NT ILMENITE
NT INORGANIC PEROXIDES
NT IRON OXIDES
NT LANTHANUM OXIDES
NT LEAD OXIDES
NT LITHIUM OXIDES
NT MAGNESIUM OXIDES
NT MAGNETITE
NT METAL OXIDES
NT MOLYBDENUM OXIDES
NT NICKEL OXIDES
NT NIOBATES
NT NIOBIUM OXIDES
NT NITRIC OXIDE
NT NITROGEN DIOXIDE
NT NITROGEN OXIDES
NT NITROGEN TETROXIDE
NT NITROUS OXIDES
NT PERICLASE
NT PEROXIDES
NT PLUTONIUM OXIDES
NT POTASSIUM OXIDES
NT PYROXENES
NT QUARTZ
NT RUTILE
NT SCAPHIRE
NT SCANDIUM OXIDES

NT SILICON DIOXIDE
NT SILICON OXIDES
NT SULFUR OXIDES
NT TANTALUM OXIDES
NT THORIUM OXIDES
NT TITANIUM OXIDES
NT TUNGSTEN OXIDES
NT VANADIUM OXIDES
NT YTTRIUM OXIDES
NT ZINC OXIDES
NT ZIRCONIUM OXIDES

An assessment of some mixed-oxide systems as low-cost electrocatalysts for oxygen electrodes.

04 p0407 A73-15110

Electronically conducting oxides as cathodes or interconnection materials in high-temperature fuel cell batteries.

04 p0407 A73-15111

Theory of scattering of electrons in a non-degenerate-semiconductor-surface inversion layer by surface-oxide charges.

06 p0733 A73-17747

Investigation of the preparation of high-temperature strain gauges based on heat-resistant oxides

11 p1362 A73-25455

Oxide minerals in lithic fragments from Luna 20 fines.

13 p1674 A73-28306

The extension of self-registered gate and doped-oxide diffusion technology to the fabrication of complementary MOS transistors.

13 p1595 A73-29576

Far infrared and Raman spectra of gaseous carbon suboxide and the potential function for the low frequency bending mode.

21 p2740 A73-40935

Effects of additions of Al and Ti on electrical resistivities of oxide films of Fe-18 Cr sealing alloy.

23 p2986 A73-44152

OXIDIZERS

NT FLOX
NT LIQUID OXYGEN
NT ROCKET OXIDIZERS

Scanning electron microscope investigation of interaction between pyrolytic carbon fibers and oxidizer, noting periodic variations of carbon chemical activity in radial direction

02 p0185 A73-12556

Microorganisms induced biological corrosion, considering oxidizing agents, inhibitors, protective coatings and cathodic protection

06 p0704 A73-17507

Ignition of systems having refractory reaction products

07 p0920 A73-19988

Influence of oxidizer dispersity on the efficiency of combustion catalyzers

13 p1669 A73-28973

Application of thermal analysis to the determination of the thermophysical properties and combustion characteristics of metallic particle conglomerates in an oxidizer flow

18 p2342 A73-37119

Ignition limit of metallic particles in a mixture of two oxidizers

19 p2503 A73-37517

Combustion of a solid fuel in a gaseous oxidizer flow

21 p2754 A73-40701

A method for calculating the burning rates of solid fuels in a turbulent gaseous oxidizer flow at Le unequal to unity

23 p3049 A73-43729

Ignition of metal particles in the case of a logarithmic oxidation law

24 p3154 A73-44704

Burn-up of the high temperature products of incomplete combustion in a supersonic flow by a second injection of oxidizer

24 p3156 A73-45076

OXIMETRY

A new method for determining the degree of oxygenation of hemoglobin spectra in the case of inhomogeneous light paths, explained in an analysis of spectra of the human skin

20 p2517 A73-39145

OXYACETYLENE

Microwave reflection from detonation waves in equimolar C2H2-O2 at low pressures.

10 p1294 A73-23557

OXYGEN

NT HIGH PRESSURE OXYGEN
NT LIQUID OXYGEN
NT OXYGEN ATOMS
NT OXYGEN ISOTOPES
NT OXYGEN PLASMA
NT OXYGEN 18
NT OZONE

6300 A night airglow emission over the magnetic equator.

01 p0036 A73-10344

New mechanism for generating coherent emission from ionized oxygen and nitrogen in the visible region of the spectrum

01 p0059 A73-10630

Temperature changes in hydrogen-oxygen explosions.

01 p0121 A73-10646

Positive ion composition measurements in disturbed D region, noting positive molecular oxygen ions as major source of water cluster ions

01 p0041 A73-10890

SST related ozone photochemical reactions and metastable oxygen system below 100 km, discussing oxygen dissociation and recombination, photolysis, UV absorption, etc

01 p0042 A73-10898

Rates of clustering of oxygen negative ions with water vapor.

01 p0014 A73-10902

Energetic metastable molecular oxygen as a source of ionization in the D region.

02 p0157 A73-11757

Calcium stabilized zirconia electrolyte with appreciable oxygen ionic diffusivity used as permeation membrane for oxygen leak source

02 p0167 A73-11955

The diurnal variations of hydrogen and oxygen constituents in the mesosphere and lower thermosphere.

02 p0158 A73-12026

Molecular oxygen densities in atmosphere near 100 km from solar hydrogen Lyman alpha absorption measurements by Intercoms 4 satellite and Vertical 1 rocket

02 p0160 A73-12275

E and F regions ion composition measurement with rockets, noting nitric oxide variation with molecular/atomic oxygen cations ratios at different solar activity phases

02 p0206 A73-12305

Experimental measurement of the O2-/photodetachment cross section.

02 p0195 A73-12433

The influence of oxygen concentration on the internal stress and dislocation arrangements in alpha titanium.

02 p0184 A73-12768

Thermal and near-thermal electron transport coefficients in O2 determined with a time-of-flight swarm experiment using a drift-dwell-drift technique.

03 p0344 A73-13276

Neodymium energy level shifts in three oxygen-compensated sites of neodymium oxide-doped calcium fluoride crystals

03 p0349 A73-13288

Covalent bond formation role in Ti strengthening by oxygen from evidence of alpha phase stabilization, ordered structures, abnormal resistivity and high activation energy

03 p0323 A73-13371

Tensile strength dependence on temperature and interstitial oxygen and nitrogen concentration in powdered Nb, noting microhardness and yield point

03 p0326 A73-13968

Dislocation dynamics in niobium-oxygen solid solutions.

04 p0462 A73-15303

The diffusivity and solubility of oxygen in liquid tin and solid silver and the diffusivity of oxygen in solid nickel.

04 p0463 A73-15315

Oxygen and nonmetallic inclusions in chromium and aluminothermic ferrochrome

04 p0465 A73-15662

The influence of atmospheric oxygen on velocity of flame spread along a solid.

[ASME PAPER 72-WA/HT-23]

04 p0519 A73-15831

Analysis of oxygen in aluminum by activation by means of charged particles and gamma photons

05 p0547 A73-17217

Reaction mechanisms of the CS2-O2 chemical laser.

06 p0702 A73-18370

Solubility of oxygen in ZrC.

07 p0838 A73-19199

Oxygen anions excited electronic states, analyzing energy curves and wave functions via configuration-interaction results obtained by multiconfiguration self consistent field techniques

07 p0853 A73-19333

Gain measurements on CO P-branch transitions in a C2H2-O2 flame.

07 p0788 A73-19634

Oxygen and bulk element composition studies of Apollo 14 and other lunar rocks and soils.

07 p0885 A73-19752

Vibrational relaxation times of oxygen in the pressure range 10-110 atm.

07 p0853 A73-19927

Study of the ignition reaction in an oxygen-hydrogen mixture at relatively high pressures and low temperatures in the shock tube

07 p0920 A73-19993

Upper self-ignition limit of hydrogen in oxygen

07 p0921 A73-19994

Sunrise changes in concentrations of minor neutral constituents in the mesosphere.

07 p0819 A73-20062

Features of the structure and of plastic deformation in zirconium saturated with nitrogen and oxygen

09 p1099 A73-21967

Prohibited autodetachment in OD- formed by collisions of O- with D2.

09 p1048 A73-22075

Performance improvement of cesium thermionic converters by addition of oxygen.

09 p1036 A73-22818

Effect of excited states of atomic oxygen ions on the reaction rates and thermal balance in the F-region.

09 p1078 A73-22832

Ductility of recrystallized molybdenum as a function of oxygen concentration and grain size

09 p1108 A73-23231

Variation of the work function of W(100) by adsorption of oxygen, cesium, and coadsorption of oxygen and cesium

10 p1186 A73-23696

Diffraction study of fast electrons of the adsorption layer of oxygen on the surface of a film of epitaxial copper

10 p1259 A73-23767

Coadsorption of oxygen and carbon monoxide on tungsten - Desorption spectra, electron stimulated desorption and field emission microscopy.

11 p1325 A73-25204

Hydrogen promoted corrosion of tungsten by oxygen in an electric field A field ion microscopy study.

11 p1325 A73-25205

Effects of oxygen environment and surface diffused coatings on fatigue crack development in copper single crystals.

11 p1380 A73-25806

Surface effects on trapping and recombination processes in Bi13 single crystals

12 p1531 A73-27938

Contribution to the study of the behavior of liquid cobaltous oxide in an oxidizing atmosphere

13 p1634 A73-28204

Oxygen and bulk element abundances in Luna 20 fines from instrumental neutron activation analysis, noting comparison with Apollo lunar soil samples

13 p1676 A73-28320

States of absorption, velocities of absorption, of desorption of oxygen on rhodium, and mechanisms of atomization and oxidation at high temperature and low pressure

13 p1580 A73-28451

Temperature dependence of the cross section of O+ ion desorption by electrons from an oxygen layer adsorbed on a tungsten surface

13 p1663 A73-28969

Laminar flame propagation in hydrogen, oxygen, nitrogen mixtures.

13 p1707 A73-29001

Negative oxygen molecular ion formation in low energy electron collision and attachment obtaining capture cross section and resonance width

14 p1777 A73-30775

Investigation of the oxygen content in superconducting vanadium- and niobium-base compounds

15 p1922 A73-31181

Effect of oxygen on the structure and properties of Bi2Te3-based alloys

15 p1923 A73-31209

Oxygen in titanium alloyed with aluminum and zirconium

15 p1889 A73-31812

Influence of air oxygen concentration on the thermochemical stability of jet fuels

15 p1925 A73-31833

Calculation of the composition of 79% N2 + 21% O2 and 50% N2 + 50% O2 mixtures containing carbon at high temperatures

15 p1840 A73-31853

The interaction of tungsten and molybdenum melts with gaseous oxygen

15 p1890 A73-31924

The interaction of gases and carbon with refractory metals

15 p1890 A73-31925

A study of the adsorption of oxygen on Ni(111)/using Auger electron spectroscopy - Chemical shifts and valence spectra.

15 p1840 A73-31968

Study of gas-solid chemical interactions by the molecular beam technique. V - Reactions of oxygen and carbon monoxide with polycrystalline tantalum strips

15 p1841 A73-31970

Critical survey of studies of phase diagrams in the titanium-oxygen system in connection with the formation of suboxides

15 p1893 A73-32515

Effect of ordering on the properties of oxygen solid solutions in titanium

15 p1893 A73-32516

Influence of plastic deformation and of alloying with small additions of oxygen on the decomposition of the metastable beta phase in the Ti6 alloy

15 p1894 A73-32526

Certain systematic errors in determining parameters of oxygen diffusion in alpha titanium

15 p1894 A73-32540

A proposed correction to the solar abundances of carbon and oxygen utilizing new and accurate theoretical forbidden transition probabilities.

16 p2060 A73-32952

- The kinetics of the dissolution of oxygen in niobium at low oxygen pressures and high temperatures 16 p2026 A73-33955
- A study of the process of oxidation of zirconium-oxygen alloys 17 p2188 A73-34558
- A comment on the measurement of atmospheric density by absorption of Lyman-alpha. 18 p2309 A73-36054
- Investigation of the kinetics of high-temperature aluminum/oxygen interaction by the ignition method 19 p2503 A73-37504
- Ignition limit of metallic particles in a mixture of two oxidizers 19 p2503 A73-37517
- Influence of hydrogen and oxygen on the mechanical behavior of unalloyed titanium 19 p2441 A73-37837
- Height distribution of O+ and H+ ions in the ionosphere F2 region. I 19 p2427 A73-38333
- French monograph - Mechanical behavior of the titanium alloy TA6V6E2 with reference to hydrogen - Influence of heat treatment and oxygen content. 19 p2443 A73-38362
- Molybdenum-oxygen-sulfur fuel cell anode catalysts capable of oxidizing low cost fuels in acid electrolytes 19 p2390 A73-38401
- Influence of small oxygen and nitrogen additions on the nature of the temperature dependence of the mechanical properties of niobium 20 p2577 A73-39360
- Thermodynamics of the Al-O and Al-O-C systems 21 p2718 A73-40847
- The partial molar thermodynamic magnitudes of oxygen and the nonstoichiometry of oxides - Model with interactions 21 p2791 A73-40950
- Mechanical properties of weldments of AK-3 titanium with an elevated oxygen content. 21 p2720 A73-41036
- Oxygen and nitrogen thermodynamic state equation determination by least squares fitting to experimental PVT, isochoric heat capacity and saturation density data 21 p2740 A73-41104
- Elements of a model of oxygen interactions under low pressure with transition metals at high temperature 21 p2648 A73-41562
- Oxygen interaction with tantalum and niobium at high temperatures 21 p2722 A73-41594
- Omega-phase stability in the Ti-Zr-O system 22 p2873 A73-42085
- Diffusion parameters of oxygen in alpha and beta titanium modifications 22 p2874 A73-42098
- Inhibition of the first limit of the hydrogen-oxygen reaction by ethyl bromide. 22 p2898 A73-42777
- Branched-chain mechanism of propane-oxygen-fluorine explosions. 22 p2819 A73-42778
- Porous and dense layers in Nb-Ti-O system analyzed by X-ray spectroscopy, finding element content influence 23 p2990 A73-43481
- Study of aluminum-oxygen equilibrium in liquid iron at 1600 deg C with the aid of a solid ThO2-Y2O3 electrolyte cell 23 p2995 A73-44178
- Temperature dependence of the cross section for electron-induced O+ desorption from tungsten. 23 p3008 A73-44321
- Rocket-borne spectrometer measurement of solar UV flux for thermospheric vertical distribution of molecular oxygen 24 p3135 A73-44632
- Electron cooling rates calculation based on measured impact cross sections of molecular oxygen for vibrational and low lying electronic excitation 24 p3086 A73-45123
- Oxygen in alloys of titanium with aluminum and zirconium. 24 p3100 A73-45275
- Oxygen-W(100) surface interactions investigated simultaneously by secondary ion mass spectrometry (SIMS) and electron induced desorption (EID) 24 p3066 A73-45330
- OXYGEN AFTERGLOW**
- Excitation of the Herzberg bands of O2 in laboratory afterglow and night airglow. 02 p0156 A73-11743
- Dissociative recombination at elevated temperatures. III - O2+/+ dominated afterglows. 07 p0852 A73-19148
- OXYGEN ATOMS**
- Atomic oxygen profiles in the lower thermosphere. 01 p0041 A73-10884
- Dependence of the D-region positive-ion composition on the atomic oxygen and atomic hydrogen concentrations. 01 p0041 A73-10891

- Atmospheric atomic oxygen density vertical distribution measurement by rocket-borne cryocooled mass spectrometer ion source 02 p0157 A73-11756
- A possible method for estimating any indirect process in the production of the O(1S) atoms in aurora. 02 p0157 A73-11902
- Quenching of vibrationally excited N2 by atomic oxygen. 02 p0139 A73-12085
- Relative rate measurements for oxygen atom addition to simple olefins in liquid Ar at 87.5 K, noting activation energies during reactions 02 p0139 A73-12086
- Molecular beam simulation of planetary atmospheric entry - Some recent results. 03 p0287 A73-13564
- Absorption measurements at Calcutta compared with current D region models for atomic oxygen production and loss processes 03 p0305 A73-14594
- An instrument for the simultaneous detection of the OI ground state /Zp4 3P/ and first metastable state /Zp4 1D/ populations. 05 p0580 A73-17258
- Selective reabsorption leading to multiple oscillations in the 8446-A atomic-oxygen laser. 07 p0834 A73-19335
- Interactions among multiple lines in the 8446-A atomic-oxygen laser. 07 p0834 A73-19336
- Ionospheric electrons and neutral particles temperature and concentration profiles explanation by electron gas cooling due to atomic oxygen excitation, calculating heat flow 07 p0815 A73-19441
- Atomic oxygen formation times obtained from measurements of electron density profiles behind shock waves in air. 07 p0853 A73-19510
- A model for the kinetics of oxygen dissociation in a microwave discharge. 07 p0789 A73-20643
- Effect of atomic oxygen on the N2 vibrational temperature in the lower thermosphere. 10 p1214 A73-24748
- Reactions of O(1D) with methane and ethane. 12 p1466 A73-27126
- Photoionization of atomic nitrogen and atomic oxygen. 13 p1662 A73-28190
- O I 4368 airglow tropical emission excitation due to conjugate photoelectron escape flux, discussing radiative recombination contribution to intensity 14 p1749 A73-29981
- Planetary atmospheres chemistry, discussing physical factors, atomic oxygen reactions, ozone, airglow and mathematical models 14 p1723 A73-30128
- Magnetospheric dayside cusp - A topside view of its 6300-angstrom atomic oxygen emission. 14 p1750 A73-30620
- The excitation of atomic oxygen to the O(1 S) level by energy transfer from N2/A 3 Sigma u+/ molecules in aurora. 15 p1866 A73-31075
- Predawn enhancement of 6300 A forbidden OI nightglow emission from observations at Abastumani 15 p1867 A73-31263
- New rate measurements on the reaction of O(3P), O3, and OH. [ALAA PAPER 73-501] 16 p1977 A73-34045
- Lower thermospheric oxygen photodissociation evaluation for global average and hemispheric imbalance, discussing wind system to compensate for solar thermal input imbalance 17 p2159 A73-34784
- Vibrational relaxation of CO by O atoms. 17 p2119 A73-35174
- Atomic oxygen profiles determined by EUV absorption analysis. 18 p2308 A73-36049
- Reactions of singlet oxygen with pine pollen. 19 p2402 A73-38295
- Lower thermospheric atomic oxygen profile from 18 May 1971 nitric oxide release and mass spectroscopic observation, noting monotonic density increase to 0.8 trillion/cc 21 p2688 A73-41345
- Shock tube kinetics of NO decomposition in mixtures with Ar, measuring ground state atomic oxygen formation rate by resonance absorption spectrophotometry 22 p2818 A73-42766
- Sulfur hexafluoride pyrolysis and subsequent oxidation in mixtures with oxygen atoms and molecules, measuring decomposition rate at high temperature in shock tube experiment 22 p2818 A73-42767
- Atomic oxygen reaction with acetylene in low pressure fast flow system, measuring free radical formation rate by photoionization mass spectrometer 22 p2818 A73-42768

- Nitrogen dioxide and ozone photolysis as oxygen atom sources for high pressure addition reaction rate studies, discussing quantum yields and photolysis dependence on pressure 22 p2819 A73-42769
- Formation of nitric oxide in fuel-lean and fuel-rich flames. 22 p2820 A73-42794
- Metastable oxygen atoms radiative lifetime quenching rate as function of altitude in lower ionosphere based on auroral observations and atmospheric model 23 p2972 A73-43692
- Dislocation locking by interstitial oxygen atoms and the temperature dependence of the yield point in niobium 24 p3099 A73-44574
- Curve crossing theory for N molecule-O atom reactions in terms of spin-orbit coupling, considering nitrous oxide unimolecular decomposition and molecular N vibrational relaxation 24 p3113 A73-44979
- Distribution of atomic oxygen in the upper atmosphere deduced from Ogo 6 airglow observations. 24 p3086 A73-45121
- Atomic oxygen densities in the lower thermosphere as derived from in situ 5577-A night airglow and mass spectrometer measurements. 24 p3086 A73-45122
- Energetic dissociative recombination oxygen atom production and exospheric redistribution for high/low solar conditions in terms of ballistic trajectories and neutral density models 24 p3086 A73-45131
- Atmospheric mixing effects for interpretation of oxygen atom concentration in Mars and Venus upper atmospheres obtained by Mariner and Venera space probes 24 p3139 A73-45134
- OXYGEN BREATHING**
- The effect of O2 breathing on maximal aerobic power. 01 p0010 A73-11504
- Effects of immersion with the head above water on tissue nitrogen elimination in man. 02 p0135 A73-12563
- EEG activity of rats compressed by inert gases to 700 feet and oxygen-helium to 4000 feet. 11 p1314 A73-25327
- Results of electron microscopic studies in the rat brain under oxygen at high pressure. 11 p1314 A73-25330
- Physiological criteria of early toxic normobaric hyperoxia manifestations 17 p2110 A73-34123
- Development of effective means for desaturation of the human organism as a prophylactic measure against altitude decompression disturbances 17 p2111 A73-34231
- Hematological, biochemical, and immunological studies during a 14-day continuous exposure to 5.2% O2 in N2 at pressure equivalent to 100 FSW /4 ata/. 18 p2278 A73-36794
- Endocrine studies during a 14-day continuous exposure to 5.2% O2 in N2 at pressure equivalent to 100 FSW /4 ata/. 18 p2279 A73-36795
- Body fluid volume changes during a 14-day continuous exposure to 5.2% O2 in N2 at pressure equivalent to 100 FSW /4 ata/. 18 p2279 A73-36796
- Aerobic capacity of relatively sedentary males. 19 p2396 A73-38360
- Respiratory nitrogen elimination - A potential source of error in closed-circuit spirometry. 20 p2512 A73-39113
- OXYGEN COMPOUNDS**
- On some oxygenated compounds of titanium and alkalis /Li, Na/ - Study of the binaries M2O-TiO2 in the zones rich in alkaline oxide 05 p0547 A73-17219
- Measurements of some hydrogen-oxygen-nitrogen compounds in the stratosphere from Concorde 002. 09 p1079 A73-22947
- Ternary nickel-vanadium-oxygen compound and solid solutions formation by vacuum calcination of vanadium and nickel oxides mixtures 13 p1634 A73-28203
- Concentration dependence of the degree of occupancy of a lattice element in cubic titanium oxycarbide 15 p1896 A73-31210
- Charge transport bands in the electronic spectra of Fe(III) complexes with certain oxygen-containing ligands 21 p2751 A73-40310
- OXYGEN CONSUMPTION**
- Effects of exercise on activity of heart and muscle mitochondria. 01 p0006 A73-10135
- Arterial oxygen increase by high-carbohydrate diet at altitude. 01 p0007 A73-10164

Oxygen uptake, heart rate and pulmonary ventilation during swimming for different speeds and styles, comparing to running and cycling data
 01 p0008 A73-10171
 The effect of O₂ breathing on maximal aerobic power.
 01 p0010 A73-11504
 Evaluation of cardiac performance in exercise.
 03 p0259 A73-13539
 Perceived exertion, heart rate, oxygen uptake and blood lactate in different work operations.
 03 p0267 A73-13698
 Interdependence of oxygen uptake, heart rate and ventilation during treadmill exercise from regression slope analysis of lag logarithms
 03 p0263 A73-14118
 Production of gaseous nitrogen during human steady state exercise.
 03 p0269 A73-14163
 Multichannel PDM-FM biomedical radio telemetry system for ECG, respiratory rate and oxygen consumption during exercise, considering transmitter and receiver design
 03 p0269 A73-14278
 Telemetry and ergometry associated to the measure of oxygen consumption during sports events.
 03 p0270 A73-14285
 Radio telemetric measurements of oxygen consumption during exercise via respiratory air flow and oxygen partial pressure monitors, considering water vapor and temperature
 03 p0270 A73-14288
 Energy cost of muscle work in a state of fatigue
 05 p0541 A73-16697
 Cerebral circulation alteration during hypothermia
 05 p0541 A73-16698
 Some physiological reactions to acceleration in albino rats in a state of hypothermia
 05 p0541 A73-16737
 Competitive oxidation and pyrolysis of ethane in the presence of low concentrations of oxygen
 05 p0641 A73-17050
 Thermoregulatory reactions of animals in a helium-oxygen medium
 06 p0650 A73-17695
 Statistical correlations of maximum oxygen consumption, body weight and endurance /work/ performance in exercise-oxygen studies
 06 p0659 A73-18472
 Central, femoral, and brachial circulation during exercise in hypoxia.
 08 p0934 A73-21506
 Influence of developmental adaptation on aerobic capacity at high altitude.
 09 p1041 A73-22928
 Oxygen consumption and its "critical" tension for the cerebral cortex in situ
 10 p1179 A73-23801
 Maximal oxygen intake and nomographic assessment of functional aerobic impairment in cardiovascular disease.
 11 p1319 A73-26362
 Oxygen consumption alteration effects on human endurance capacity as function of relative work, muscle blood flow and anaerobic metabolism
 14 p1714 A73-29753
 Oscillations in oxygen consumption of man at rest.
 14 p1714 A73-29755
 Breath to breath cyclical variations in functional residual capacity, oxygen uptake, carbon dioxide release, tidal volume, respiratory period, alveolar gas tension and heart rate
 15 p1834 A73-31346
 Optimal duration of endurance performance on the cycle ergometer in relation to maximal oxygen intake.
 15 p1836 A73-32397
 Effects of oxygen-augmented atmosphere on the immune response.
 17 p2115 A73-34743
 Validation of open-circuit method for the determination of oxygen consumption.
 17 p2117 A73-35462
 Specific features in the activity of the oxygen transport system of the organism during hand-performed working cycles of submaximum intensity
 18 p2277 A73-36579
 The effects of training on some parameters of hemodynamics and of the oxygen transportation function of the blood during static strains
 18 p2277 A73-36581
 Adequacy of the Haldane transformation in the computation of exercise oxygen consumption in man.
 18 p2278 A73-36658
 Oxygen delivery and oxygen return to the lungs at onset of exercise in man.
 20 p2519 A73-39788
 Human intrapair twin differences, examining age, height, weight, heart volume, metabolism, respiratory rate and monozygous/dizygous differences
 20 p2519 A73-39792
 Oxygen uptake, muscle high-energy phosphates, and lactate in exercise under acute hypoxic conditions in man.
 21 p2638 A73-41131

Oxygen uptake during maximal work at lowered and raised ambient air pressures.
 21 p2638 A73-41132
 Effect of training with eccentric muscle contractions on skeletal muscle metabolites.
 21 p2641 A73-41523
 Advantage or disadvantage of a decrease of blood oxygen affinity for tissue oxygen supply at hypoxia - A theoretical study comparing man and rat.
 21 p2641 A73-41620
 Effect of hypothermia on renal sodium reabsorption.
 21 p2641 A73-41623
 Rebreathing and steady state pulmonary diffusing capacity for O₂ in the dog and in inhomogeneous lung models.
 21 p2645 A73-41639
 Nonthermal metabolic response of rats to He-O₂, N₂-O₂, and Ar-O₂ at 1 atm.
 22 p2805 A73-42201
 Myocardial oxygen consumption in experimental hypertrophy and congestive heart failure due to pressure overload.
 22 p2808 A73-42688
 Changes in indices of the carbohydrate and fat metabolism, the state of the sympathoadrenal system, and oxidative processes under varying-intensity cold effects
 24 p3059 A73-44671
 Hemoglobin-oxygen equilibrium and coronary blood flow - An analog model.
 24 p3064 A73-45060
 Oxygen kinetics for constant work loads at various altitudes.
 24 p3060 A73-45062
 Oxygen consumption measurements during continual centrifugation of mice.
 24 p3065 A73-45071

OXYGEN DEFICIENCY

U HYPOXIA

OXYGEN ISOTOPES

NT OXYGEN 18

Possibility of using a laser flame as a source of light in the isotope spectral method
 02 p0176 A73-12094

Astrophysical CO isotopic constituents from H II regions line emissions, determining relative abundances
 04 p0502 A73-15688

Elastic scattering of negative pions from O-16 in the region of the $\{3, 3\}$ resonance.
 04 p0477 A73-16037

Oxygen isotopic compositions and oxygen concentrations of Apollo 14 and Apollo 15 rocks and soils.
 07 p0887 A73-19772

Luna 20 lunar soil elemental and oxygen isotopic composition compared to Apollo 11, 12, 14 and 15 abundances
 13 p1675 A73-28310

Isotope separation factor of carbon dioxide-water system and isotopic composition of atmospheric oxygen.
 15 p1873 A73-32252

Low energy gamma ray spectrum following muon capture by oxygen 16 leading to bound states of nitrogen 16
 21 p2743 A73-40475

O-18/O-16 ratios in Luna 16 fines.
 21 p2770 A73-41003

Theory of interstellar abundances of the isotopes of carbon, nitrogen and oxygen.
 22 p2914 A73-43006

Ultrafiltration by a compacted clay membrane. I - Oxygen and hydrogen isotopic fractionation. II - Sodium ion exclusion at various ionic strengths.
 23 p2973 A73-43845

OXYGEN METABOLISM

Effect of increased atmospheric pressure on the dynamics of free oxygen content in animal muscle tissues
 01 p0007 A73-10156

Determination of the value of blood oxygen capacity and of the oxyhemoglobin dissociation curves by polarographic coulombometry
 03 p0267 A73-13750

A criterion for oxygen supply optimality in tissues and the capillary circulation rate
 03 p0268 A73-13821

Cardiac output and oxygen transport in early ontogenesis
 05 p0541 A73-16738

Biological role of atmospheric oxygen in the mechanism of blood coagulation
 06 p0650 A73-17678

Assessment of hypoxia in the human heart.
 07 p0781 A73-19928

Myocardial metabolism during exposure to carbon monoxide in the conscious dog.
 09 p1042 A73-22935

Changes in gaseous metabolism and cardiac output per minute during local muscle work in man
 10 p1179 A73-23809

Effect of excessive glucose administration on the lipid level, glycolysis rates, and oxygen uptake in the tissues of the liver, heart, cerebrum and aorta
 11 p1314 A73-25042
 Kinetics of oxygen uptake and recovery for supramaximal work of short duration.
 11 p1323 A73-25648
 Effect of antioxidants on the blood deoxygenation rate in animals exposed to altered atmospheres
 12 p1465 A73-27702
 Effect of adaptation to cold on the energy characteristics of muscular activity
 13 p1574 A73-28295
 Relative rates of arterial lactate and oxygen-deficit accumulation in hypoxic dogs.
 15 p1836 A73-31922
 Responses to graded hypoxia at high and low 2,3-diphosphoglycerate concentrations.
 17 p2112 A73-35460
 Changes in respiration effectiveness during muscular activity
 18 p2277 A73-36580
 Aerobic capacity of relatively sedentary males.
 19 p2396 A73-38360
 Anaerobic threshold and respiratory gas exchange during exercise.
 20 p2519 A73-39785
 Hemoglobin molecule oxygenation mechanism in various animals, discussing erythrocytes as hemoglobin carriers, ecological factors and physicochemical conditions
 23 p2947 A73-43929
 Hemoglobin species diffusion effect on oxygen transport in moving and stationary flat films of hemoglobin solution
 23 p2949 A73-43993

OXYGEN PLASMA

Oxygen plasma for cleaning polymerized organic material contaminated oil-pumped channel electron multiplier arrays used as vacuum UV to visible radiation converters
 01 p0054 A73-11237

Removal of hydrocarbon contaminant film from spacecraft optical surfaces using a radiofrequency-excited oxygen plasma.
 08 p0989 A73-21835

Study by electronic paramagnetic resonance of the molecular dissociation in an oxygen plasma
 13 p1664 A73-28566

Continuum emission from recombining oxygen and nitrogen plasmas.
 18 p2338 A73-36799

Estimates of thermospheric neutral constituents from ion composition measurements.
 21 p2688 A73-41350

OXYGEN PRODUCTION

Oxygen from electrolyzed lunar rocks - A discussion of the energetics.
 03 p0253 A73-14169

Atmospheric regeneration in closed chambers by potassium superoxide
 18 p2287 A73-36951

A study of the extraction of oxygen from molybdenum by dissolving it in metallic carbon-containing melts in a vacuum
 21 p2717 A73-40479

OXYGEN RECOMBINATION

Three component static thermosphere model for oxygen radiative recombination and thermal diffusion dependence on underlying layers and solar UV radiation
 06 p0689 A73-17539

Lower thermosphere thermal energy and oxygen transport due to photochemical reactions, noting Schumann-Runge band absorption, atomic recombination and collisional deactivation
 11 p1358 A73-26706

Atomic oxygen loss in ion source of sounding rocket-borne mass spectrometer for determining lower thermosphere neutral composition
 12 p1489 A73-26991

Sealed nickel zinc cells with nonsintered and supplementary oxygen recombination electrodes and layer structure inorganic separators
 13 p1572 A73-29587

Three component static thermosphere model for oxygen radiative recombination and thermal diffusion dependence on underlying layers and solar UV radiation
 16 p2001 A73-32763

Location in magnetic latitude and local time of the tropical ultraviolet bands seen from Apollo 16.
 21 p2684 A73-40788

Air afterglow radiative recombination reaction of NO with O yielding nitrogen dioxide, considering pressure dependence in chemiluminescence spectral region
 22 p2819 A73-42772

Average nighttime vertical profile of the 6300 Å atmospheric emission.
 23 p2970 A73-43242

Energetic dissociative recombination oxygen atom production and exospheric redistribution for high/low

solar conditions in terms of ballistic trajectories and neutral density models 24 p3086 A73-45131

OXYGEN REGULATORS

The diluter-demand oxygen system used during the international Himalayan expedition to Mount Everest. 11 p1322 A73-25145

OXYGEN SPECTRA

Oxygen emission volume rate in auroras due to direct electron impact excitation, obtaining integral cross sections and quenching rate. 01 p0036 A73-10336

Research of the emission at 5577 Å in the period of 1958-1967 in Ashkhabad. 01 p0036 A73-10345

Airglow 6300 Å emission predawn enhancement amplitude variation with geomagnetic and solar activity 01 p0037 A73-10347

Processes leading to 6300 Å radiation during determinations of O(1D) quenching by nitrogen and oxygen molecules in F region, using model of neutral atmosphere composition [AD-754996] 02 p0156 A73-11742

Excitation of the Herzberg bands of O₂ in laboratory afterglow and night airglow. 02 p0156 A73-11743

Possibility of O III 304-Å emissions in the extreme ultraviolet airglow. 02 p0157 A73-11755

A possible method for estimating any indirect process in the production of the O(1S) atoms in aurora. 02 p0157 A73-11902

A technique for recovering the vertical number density profile of atmospheric gases from planetary occultation data. 02 p0158 A73-11913

Atomic oxygen concentration from the forbidden O I 5577 Å line emission at the auroral zone latitude. 02 p0158 A73-11916

Rocket photometric observations of dayglow sky radiation in O green line, noting aerosol scattering coefficient and particle concentration 02 p0161 A73-12277

Mars oxygen photoelectric spectral and aeronomical study, noting water vapor and carbon dioxide photolytic effects 02 p0224 A73-12787

Mapping the solar corona in X-ray lines of O VII and Ne IX. 03 p0375 A73-13956

Changes in thermospheric molecular oxygen abundance inferred from twilight 6300 Å airglow. 04 p0440 A73-14963

Airglow height profiles of forbidden O I 6300 and 5577 Å line emissions in morning ionosphere from rocket photometric measurement 04 p0444 A73-15542

Atmospheric transmittance calculation from 0.76-micron oxygen band fine structure parameters 04 p0473 A73-15571

Oxygen 1S production efficiency of photons at 812-1216 Å measured by O I 5577 Å green line detection during carbon dioxide photodissociation 05 p0546 A73-16049

Human endocrine-metabolic responses to graded oxygen pressures. 07 p0785 A73-19479

Nighttime atmosphere emission of atomic oxygen (5577 Å) and its connection with penetrating micrometeorites 07 p0818 A73-19592

Oxygen D line collisional quenching by atmospheric oxygen, nitrogen, carbon monoxide and dioxide, water vapor and ozone, determining absolute rate constants 07 p0788 A73-20239

Measurements of the electron temperatures in M42 from the profiles of H-alpha, forbidden N II, H-beta, and forbidden O III. 08 p1004 A73-20906

Generation of vibrationally excited O₂ and nonthermal infrared emission in the upper atmosphere 08 p0959 A73-21289

Simultaneous observations of low energy electron fluxes and the polar red emission at 6300 Å. 09 p1075 A73-22137

Intensities and half-widths of lines in the A and B bands of the red atmospheric system of O₂ bands 09 p1077 A73-22664

On the nature of X Persei - Evidence from the 1957 outburst. 10 p1275 A73-23845

Doppler broadening of O I 1304 Å multiplet in dissociative excitation of CO₂ and O₂. 10 p1251 A73-24243

Twilight airglow. I - Photoelectrons and forbidden O I 5577-angstrom radiation. 10 p1214 A73-24737

Excitation of oxygen permitted line emissions in the tropical nightglow. 10 p1214 A73-24739

Seasonal variations in the telluric lines of oxygen and water vapor 11 p1392 A73-25614

Stellar occultation measurements of molecular oxygen in the lower thermosphere. 11 p1356 A73-25911

Nitrogen and oxygen molecules, photodissociation continuums from absorption and ionization cross sections, calculating upper atmosphere emission rates 12 p1489 A73-26993

Upper atmospheric temperatures from Doppler line widths. V - Auroral electron energy spectra and fluxes deduced from the 5577 and 6300 Å atomic oxygen emissions. 12 p1492 A73-27605

Altitudinal variations of the brightness indicatrices and angular characteristics of polarization levels in daytime skies in the 1.27-micron oxygen emission band 13 p1609 A73-29157

Ground-based measurement of millimetre-wavelength emission by upper stratospheric O₂. 14 p1751 A73-29718

O I 4368 airglow tropical emission excitation due to conjugate photoelectron escape flux, discussing radiative recombination contribution to intensity 14 p1749 A73-29981

Magnetospheric dayside cusp - A topside view of its 6300-angstrom atomic oxygen emission. 14 p1750 A73-30620

Predawn enhancement of 6300 Å forbidden O I nightglow emission from observations at Abastumani 15 p1867 A73-31263

Spectral investigations of 6300 Å forbidden O I twilight emission at Abastumani 15 p1867 A73-31264

Twilight enhancement of forbidden-O I 6300 Å airglow. 15 p1868 A73-31382

The O I 1304- and 1356-Å emissions from the atmosphere of Venus. 16 p2062 A73-33431

Laboratory measurements of electromagnetic properties of atmospheric gases at millimeter wavelengths. 16 p1983 A73-33731

Equivalent widths of the oxygen A-band absorption lines at different pressures 16 p2039 A73-33815

Observation of an unusual multiple mid-latitude 6300-Å O I arc from two ground stations. 16 p2009 A73-33895

Photometric investigation of the 4278 Å and 5577 Å emissions in aurora. 16 p2010 A73-33918

Atmospheric attenuation effects on nitric oxide dissociation in mesosphere and stratosphere, noting dissociation profile dependence on absorption of discrete oxygen Schumann-Runge bands 17 p2119 A73-34778

ISIS-2 red line photometer for global distribution mapping of atomic oxygen 6300 Å emission in airglow and auroras, discussing atomic excitation processes in upper atmosphere 19 p2428 A73-37257

Production of vibrationally excited O₂ and nonthermal infrared emission in the upper atmosphere. 19 p2424 A73-37918

Mariner 9 ultraviolet spectrometer experiment - Mars atomic oxygen 1304-Å emission. 20 p2604 A73-38932

Asymmetrical global O I airglow emission pattern with respect to magnetic equator from Ogo 4 observations, noting poor correlation with ionospheric electron density 20 p2551 A73-38939

Predawn enhancement of 6300-Å emission observed near the plasmopause from the Isis-2 spacecraft. 20 p2551 A73-38945

Aircraft measurements of effective photon paths in cloud-reflected and transmitted light in the 0.76-micron oxygen band 20 p2583 A73-39184

An atlas of low-latitude 6300-Å forbidden O I night airglow from Ogo 4 observations. 22 p2845 A73-41924

Aeronomic consequences of solar flux variations between 2000 and 1325 angstroms. 22 p2902 A73-41931

Vibrational relaxation of oxygen in an unsteady expansion wave. 22 p2889 A73-42441

Ozone transition detection in earth atmospheric absorption and emission, comparing measured ozone absorption profiles with theoretical computations 22 p2848 A73-42535

Postsunset oxygen emission observation by radiometer on rocket launched at Natal, Brazil, observing 10-km thick emission layer 22 p2848 A73-42536

Quantum-beat g-value measurements on transitions from levels of aligned fast ions. 22 p2890 A73-42974

Variations in the distribution and physical properties of Perseid meteors. 22 p2914 A73-43015

Temperature and oxygen abundance determination in the sun from the oxygen lines 23 p3037 A73-44257

Interpretation of atmospheric radio emission in the 5-mm spectral region 24 p3068 A73-44961

Electronographic observations of the forbidden O II ratio in the core of the Orion Nebula. 24 p3140 A73-45182

ISIS 2 scanning photometric analysis of E and F region airglow at O I 5577 Å, noting height difference of airglow components at midlatitudes and near equator. 24 p3088 A73-45214

OXYGEN SUPPLY EQUIPMENT

Research on ignition and combustion in oxygen systems. 13 p1708 A73-29446

Russian book on passenger aircraft high altitude equipment covering cabin pressurization, air conditioning and temperature and pressure control, human tolerances, reliability factors, etc 14 p1712 A73-30355

Concorde emergency power supply, oxygen and escape systems design and operational features 14 p1713 A73-30929

Russian book on civil aviation aircraft and helicopter equipment covering navigation, automatic control, electrical and oxygen systems and aircraft instruments 15 p1829 A73-31548

Fire hazard reduction in corporate aircraft oxygen system, covering hoses, regulators, manifolds, cylinders, leakage, combustion conditions and servicing procedures 20 p2518 A73-39215

OXYGEN SYSTEMS

U OXYGEN SUPPLY EQUIPMENT

OXYGEN TENSION

NT HYPOXEMIA

Microvascular responses to alterations in oxygen tension. 01 p0009 A73-11010

Studies of blood gas analysis at abnormal environment. 01 p0013 A73-11210

Methodical studies concerning the polarographic measurement of respiration and 'critical oxygen pressure' in mitochondria and isolated cells with the aid of the membrane-covered platinum electrode 03 p0272 A73-14647

Effects of cardiac output on O₂/18/2 lung diffusion in normal resting man. 06 p0654 A73-18335

Mixed-venous oxygen tension by nitrogen rebreathing - A critical, theoretical analysis. 06 p0654 A73-18336

Russian book - Tissue, oxygen in the presence of extremal flight factors. 07 p0780 A73-19425

Human endocrine-metabolic responses to graded oxygen pressures. 07 p0785 A73-19479

Intermittent exercise - Metabolites, oxygen pressure, and acid-base equilibrium in the blood. 09 p1041 A73-22933

Influence of histamine on cutaneous capillary circulation and on the oxygen tension of subcutaneous cellular tissue in various age periods 10 p1178 A73-23676

Gas dynamic theory of gas exchange in organisms based on oxygen and carbon dioxide permanent partial pressure gradients in tissues, blood and lungs 10 p1181 A73-24523

Procedures for polarocochleography and for pressure measurement in the inner ear perilymph in acute experiments on animals 11 p1314 A73-25043

Changes in microvascular diameter and oxygen tension induced by carbon dioxide. 11 p1317 A73-26116

Studies of alveolar-mixed venous CO₂ and O₂ gradients in the rebreathing dog lung. 11 p1318 A73-26219

Changes in the gas content of blood in man during exposure to high ambient temperatures 12 p1463 A73-27711

Characteristics of spontaneous oxygen tension variations in human brain structures 14 p1719 A73-30844

Analysis of the mechanism of the therapeutic action of pressurized oxygen in organic phosphorus poisoning 14 p1722 A73-30848

Determination of diffusive capacity components in lungs and of alveolararterial oxygen gradients for the estimation of oxygen transport conditions in lungs 14 p1719 A73-30849

Hypoxic pulmonary steady-state diffusing capacity for CO and cardiac output in rats born at a simulated altitude of 3500 m. 14 p1720 A73-30911

Study of the effect of increased oxygen concentration on the metabolism of Chlorella 15 p1838 A73-31508

Oxygen affinity and electrolyte distribution of human blood - Changes induced by propranolol. 24 p3062 A73-44689

Response of coronary blood flow to pH-induced changes in hemoglobin-O₂ affinity. 24 p3060 A73-45061

An equation for the oxygen hemoglobin dissociation curve. 24 p3064 A73-45070

OXYGEN TOXICITY

U HYPEROXIA

OXYGEN II

Oxygen and silicon isotope ratios of the Luna 20 soil. 13 p1677 A73-28337

OXYGENATION

Exercise during hyperoxia and hyperbaric oxygenation. 19 p2396 A73-38160

The ignition of solid materials in oxygen by electrical sparks. 19 p2504 A73-38275

Oxygen transport augmentation mechanism for human hemoglobin, considering hemoglobin translational mobility absence effects 20 p2515 A73-39795

OXYHEMOGLOBIN

Determination of the value of blood oxygen capacity and of the oxyhemoglobin dissociation curves by polarographic coulombometry 03 p0267 A73-13750

Significance of the Bohr and Haldane effects in the pulmonary capillary. 08 p0935 A73-21614

Effect of antioxidants on the blood deoxygenation rate in animals exposed to altered atmospheres 12 p1465 A73-27702

Interaction of haemoglobin with ions - Binding of inorganic phosphate to human oxyhaemoglobin. 14 p1714 A73-29850

Responses to graded hypoxia at high and low 2,3-diphosphoglycerate concentrations. 17 p2112 A73-35460

Oxygen transport augmentation mechanism for human hemoglobin, considering hemoglobin translational mobility absence effects 20 p2515 A73-39795

Hemoglobin molecule oxygenation mechanism in various animals, discussing erythrocytes as hemoglobin carriers, ecological factors and physicochemical conditions 23 p2947 A73-43929

Hemoglobin-oxygen equilibrium and coronary blood flow - An analog model. 24 p3064 A73-45060

An equation for the oxygen hemoglobin dissociation curve. 24 p3064 A73-45070

OZONE

Rates of clustering of oxygen negative ions with water vapor. 01 p0014 A73-10902

Nuclear explosions released nitric oxide effect on atmospheric ozone concentration compared with potential effect from SST flights 01 p0043 A73-11068

Aeronomic chemistry of the stratosphere. 02 p0158 A73-11910

The specific ozone destruction at the ocean surface and its dependence on horizontal wind velocity from profile measurements. 05 p0594 A73-16348

Reaction kinetics of nitric oxide positive ion with ozone yielding nitrogen dioxide positive ion and oxygen, noting impact on ionospheric chemistry 07 p0787 A73-19258

Measurement of the cross section for photodetachment of O₃-. 08 p0957 A73-20658

Photochemical ozone formation in the atmosphere over southern England. 08 p0957 A73-20667

Observation of mesospheric ozone at low latitudes. 09 p1079 A73-22841

Rotational and vibrational hydroxyl excitation in the laboratory and in the night airglow. 11 p1354 A73-25761

Detection of a temporary ozone content decrease in the upper atmosphere at the moment of sunrise 13 p1605 A73-28074

Rate constants for the reactions of hydroxyl and hydroperoxyl radicals with ozone. 14 p1724 A73-30619

An analytic formula for heating due to ozone absorption. 14 p1750 A73-30767

Some results of ozone observations by satellite on June 17 and 18, 1966 15 p1868 A73-31607

Some statistical characteristics of atmospheric ozone measurements 15 p1868 A73-31612

Trace gases, aerosols, and solar radiation in the stratosphere - Explored and unexplored problem areas. 16 p2006 A73-33547

[AIAA PAPER 73-509] The characteristics of the solar ultraviolet radiation at Arosa. 16 p2056 A73-33558

[AIAA PAPER 73-523] Numerical atmospheric circulation model of SST effects on stratospheric ozone distribution 16 p2007 A73-33563

[AIAA PAPER 73-529] Subsonic jet aircraft contribution to NO_x in the stratospheric ozone layer - 1968 to 1990. 16 p2046 A73-33566

[AIAA PAPER 73-534] New rate measurements on the reaction of O(3P), O₃, and OH. 16 p1977 A73-34045

[AIAA PAPER 73-501] Mesospheric and lower thermospheric ozone concentration measurement at sunset via occultation technique from rocket payloads 17 p2159 A73-34780

The effects of water vapor and oxides of nitrogen on the ozone and temperature structure of the stratosphere. 17 p2160 A73-34857

Vertical ozone profiles from observations of eclipsing satellites. 18 p2304 A73-35971

Photochemistry of the ozone in the stratosphere 18 p2287 A73-36938

Reaction of HO₂ with O₃. 19 p2402 A73-37674

Infrared spectrum and geometry of ozone isolated in inert gas matrices at 20.4 K. 19 p2463 A73-37904

Relative Raman cross section of O₃ for four Ar+ laser frequencies. 20 p2595 A73-38893

Pulmonary function in man after short-term exposure to ozone. 21 p2642 A73-40001

Nitrogen oxides, nuclear weapon testing, Concorde and stratospheric ozone. 21 p2686 A73-41076

Russian book - Physics of atmospheric ozone. 21 p2691 A73-41435

Ozone composition and nitric oxide injection upper and lower limits for stratosphere by nuclear bomb tests, comparing to estimated SST contribution 22 p2848 A73-42534

Ozone transition detection in earth atmospheric absorption and emission, comparing measured ozone absorption profiles with theoretical computations 22 p2848 A73-42535

Nitrogen dioxide and ozone photolysis as oxygen atom sources for high pressure addition reaction rate studies, discussing quantum yields and photolysis dependence on pressure 22 p2819 A73-42769

Symposium on Atmospheric Ozone, Arosa, Switzerland, August 21-25, 1972, Proceedings. 23 p2973 A73-43851

Total ozone measurements in cloudy weather. 23 p2973 A73-43853

Principles and possibilities of a new method of ozone measurements within the Huggins bands. 23 p2982 A73-43854

Total ozone increase over North America during the 1960's. 23 p2973 A73-43857

Global climatological ozone changes in terms of secular, annual and sunspot cycle-related variability 23 p2974 A73-43858

Meridional distribution of tropospheric ozone from measurements aboard commercial airliners. 23 p2974 A73-43859

Meridional tropospheric ozone distribution north of 50 deg from airplane measurements. 23 p2974 A73-43860

A theoretical investigation of tropospheric ozone and stratospheric-tropospheric exchange processes. 23 p2974 A73-43861

The average tropospheric ozone content and its variation with season and latitude as a result of the global ozone circulation. 23 p2974 A73-43862

Problems experienced in continuous recording of surface ozone by the electrochemical method at Poona. 23 p2982 A73-43864

Short-term ground ozone fluctuations at Poona. 23 p2974 A73-43865

The specific ozone destruction rate of the ocean surface and its dependence on horizontal wind velocity. 23 p2974 A73-43867

Ozone concentration studies and ozone flux measurements near the ground at Poona. 23 p2974 A73-43868

Studies of variations in the vertical ozone profiles over India. 23 p2975 A73-43871

Studies of the vertical distribution of atmospheric ozone in association with western disturbances over India. 23 p2975 A73-43872

Statistical characteristics of the vertical ozone distribution in mid-latitudes. 23 p2975 A73-43874

Description of a photometer suitable for measuring twilight ozone content variations from a stratospheric balloon gondola 23 p2982 A73-43875

The Nimbus-4 backscatter ultraviolet (BUV) atmospheric ozone experiment Two years' operation. 23 p2975 A73-43877

Aerosols - A limitation on the determination of ozone from BUV observations. 23 p2975 A73-43879

The nighttime distribution of ozone in the low-latitude mesosphere. 23 p2975 A73-43881

Statistical analysis for autocorrelation and cross correlation coefficients of mean annual total atmospheric ozone and relative sunspot number as solar activity indicator 23 p2976 A73-43883

Recent developments in photochemistry of atmospheric ozone. 23 p2951 A73-43892

On the theoretical model for vertical ozone density distributions in the mesosphere and upper stratosphere. 23 p2977 A73-43898

Quantum yield of metastable oxygen atoms and molecules via ozone photolysis by UV absorption, noting uncertainties in secondary reaction kinetics 23 p2951 A73-43899

Nitrogen oxides role in global stratospheric ozone balance demonstrated by observed instantaneous photochemical rates comparison with Chapman ozone formation theory 23 p2952 A73-43900

Ozone and temperature change in the winter stratosphere. 23 p2977 A73-43901

The effects of water vapour and oxides of nitrogen on ozone and temperature structure of the stratosphere. 23 p2977 A73-43902

Atmospheric ozone and the movement of the air in the stratosphere. 23 p2977 A73-43903

Influence of the vertical motion field on ozone concentration in the stratosphere. 23 p2977 A73-43904

Relation between the intensity of the stratospheric circumpolar vortex and the accumulation of ozone in the winter hemisphere. 23 p2977 A73-43905

On the vertical ozone and wind profiles near the tropopause. 23 p2977 A73-43907

Ozone variation in the lower stratosphere and its mechanism. 23 p2977 A73-43908

Application of general circulation models to the study of stratospheric ozone. 23 p2978 A73-43909

Vibrational relaxation of CO₂/nu sub 3/ by ozone. 24 p3066 A73-44988

Numerical experiments on the steady-state meridional structure and ozone distribution in the stratosphere. 24 p3085 A73-45017

OZONOMETRY

Atmospheric ozone distribution from remote sensing with spaceborne IR interferometer spectrometer, estimating error due to cloud cover 01 p0038 A73-10384

Distribution of the total ozone content in the atmosphere according to satellite observations. 07 p0820 A73-20346

Mariner 9 ultraviolet spectrometer experiment - Seasonal variation of ozone on Mars. 08 p1009 A73-21223

Mariner 9 Ultraviolet Spectrometer experiment - Observations of ozone on Mars. 09 p1144 A73-22267

A simple technique to estimate large-scale eddy coefficients in the stratosphere. 16 p2005 A73-33541

[AIAA PAPER 73-499] A two-dimensional theoretical model for stratospheric ozone density distributions in the meridional plane. 16 p2008 A73-33571

[AIAA PAPER 73-541] Experimental determination of small scale transport mechanisms in the stratosphere. 16 p2010 A73-34044

[AIAA PAPER 73-496] Remote sensing of atmospheric O₃ and H₂O to 70 km by aircraft measurements of radiation at 1.64 mm wavelength. 20 p2557 A73-39855

Mesospheric ozone concentration night and day variations comparison, describing microwave radiometer and remote sensing and photochemical theories 20 p2557 A73-39857

Russian book - Physics of atmospheric ozone. 21 p2691 A73-41435

P

Symposium on Atmospheric Ozone, Arosa, Switzerland, August 21-25, 1972, Proceedings.

23 p2973 A73-43851

Spectrophotometer design for total ozone measurement for Dobson instrument replacement, describing spectrograph, reeds, electronic control, photon counter, readout system and accuracy

23 p2982 A73-43852

Principles and possibilities of a new method of ozone measurements within the Huggins bands.

23 p2982 A73-43854

An automated Dobson spectrophotometer.

23 p2982 A73-43855

Inference of total ozone from photometric measurements of sky radiation.

23 p2973 A73-43856

Total ozone increase over North America during the 1960's.

23 p2973 A73-43857

Meridional tropospheric ozone distribution north of 50 deg from airplane measurements.

23 p2974 A73-43860

The average tropospheric ozone content and its variation with season and latitude as a result of the global ozone circulation.

23 p2974 A73-43862

A new automatic ozone recorder for near-surface measurements working at 19 stations on a meridional chain between Norway and South Africa.

23 p2982 A73-43863

Problems experienced in continuous recording of surface ozone by the electrochemical method at Poona.

23 p2982 A73-43864

Surface ozone in the arctic atmosphere.

23 p2974 A73-43866

Ozone concentration studies and ozone flux measurements near the ground at Poona.

23 p2974 A73-43868

Fourteen-year series of vertical ozone distribution over Arosa, Switzerland, from Umkehr measurements.

23 p2974 A73-43869

Six years of regular ozone soundings over Switzerland.

23 p2974 A73-43870

Radiosonde ground station ozone concentration measurements as stratospheric motions Lagrangian tracer, noting sonde data inadequacy and alternative measurement possibilities

23 p2975 A73-43873

Remote sensing of the global distribution of total ozone and the inferred upper-tropospheric circulation from Nimbus IRIS experiments.

23 p2975 A73-43876

Variations in the stratospheric ozone field inferred from Nimbus satellite observations.

23 p2975 A73-43878

The mean ozone distribution from several series of rocket soundings to 52 km at latitudes from 58 deg S to 64 deg N.

23 p2975 A73-43880

Ozone related spectral measurements of total solar radiation.

23 p2975 A73-43882

Variations of the total amount of ozone and the behaviour of some ionospheric parameters in the winter time upper atmosphere.

23 p2976 A73-43885

Ozone and airglow in the mesosphere region.

23 p2976 A73-43886

OZONOSPHERE

SST related ozone photochemical reactions and metastable oxygen system below 100 km, discussing oxygen dissociation and recombination, photolysis, UV absorption, etc

01 p0042 A73-10898

Secular variation of the stratospheric ozone layer over middle Europe during the solar cycles from 1951 to 1972.

04 p0445 A73-15635

Stellar survey at 2000-4100 Å via balloon-borne observations, discussing intensity distributions and earth atmospheric ozone layer density

09 p1140 A73-22006

Ozone variation in the lower stratosphere and its mechanism.

13 p1611 A73-29664

The 27-day variations of the hard cosmic ray component and the atmospheric ozone X-layer according to IGY data

21 p2755 A73-40109

Russian book - Physics of atmospheric ozone.

21 p2691 A73-41435

The influence of solar activity on the stratospheric ozone layer.

23 p2976 A73-43884

P WAVES

P and S waves propagation velocity distribution for lunar mantle and crust composition, noting petrological models with differentiated mantle

07 p0894 A73-19849

Apollo 17 seismic profiling - Probing the lunar crust.

16 p2059 A73-32903

Effect of orthotropy on singular stresses for a finite crack.

[ASME PAPER 72-APM-VVV] 17 p2249 A73-35109

P-I-N DIODES

U DIODES

U P-I-N JUNCTIONS

P-I-N JUNCTIONS

Recent advances in diode and ferrite phaser technology for phased-array radars. II.

01 p0024 A73-10720

Study of the ac small-signal dynamic characteristic of p-i-n silicon diodes

01 p0024 A73-10921

Instabilities and small-signal response of double injection structures with deep traps.

02 p0146 A73-12042

Series diode SP4T switch for satellite applications.

04 p0428 A73-15455

Features of voltage-capacitance relationships in Si/Li p-i-n detectors

06 p0675 A73-18080

Semiconductor-insulator-semiconductor (SIS) tunneling current characteristics, noting negative resistance feature for degenerate p-i-n diode

06 p0677 A73-18359

Operation, fabrication and structural features of pulsed/CW microwave p-i-n diodes, presenting diode impedance and resistance as function of conduction current

07 p0797 A73-18898

Quality control of semiconductor elements manufactured in low-run series production - Ultrahigh frequency components

07 p0801 A73-19422

Low-frequency current oscillations in high-resistivity, Au-doped silicon junctions with two Schottky contacts.

07 p0864 A73-20190

P-I-N switching diodes in phase-shifters for electronically scanned aerial arrays.

08 p0943 A73-20712

Investigation of a high-level power switch based on p-i-n diodes

08 p0948 A73-21560

Design curves for PIN diode transmitter receiver switch based on lumped circuit filter suited to high frequency bands

09 p1063 A73-22496

Semiconductor diodes for controlling microwave power.

12 p1480 A73-27266

An electronically switched microwave radiometer.

13 p1622 A73-29423

Microwave signal source amplitude stabilization, analyzing circuit with doubly balanced electronically regulated attenuator with p-i-n diodes

14 p1733 A73-30055

A computer study of the design and operating performance of a photovoltaic cell for thermophotovoltaic energy conversion applications.

19 p2391 A73-38405

Application of distributed p-n and p-i-n structures in the development of integrated circuits for electrically controlled SHF devices

20 p2535 A73-38856

Some photoelectrical characteristics of photoelectric converters with a p-i-n structure

20 p2510 A73-39448

P-N JUNCTIONS

Heterojunction photocell, sensitive in the near infrared.

01 p0051 A73-10834

Structure and electrical characteristics of epitaxial palladium silicide contacts on single crystal silicon and diffused P-N diodes.

02 p0147 A73-12045

Noise measurement in p-n junction surface of Si semiconductor wafer under transverse electric field, noting reverse current contribution

03 p0350 A73-13665

An electronic method of temperature compensation in hydrostatic pressure transducers with semiconductor p-n junctions.

03 p0308 A73-13784

Solar cell graded band gap materials, determining I-V characteristics, junction capacitance and photovoltaic spectral response

03 p0254 A73-14207

New results on the development of a thin-film p-CdTe-n-CdS heterojunction solar cell.

03 p0255 A73-14220

Summary of results of JPL lithium-doped solar cell development program.

03 p0257 A73-14240

Li and Si p-n solar cells performance comparison for simulated earth orbit environment by real time irradiation with Sr 90 beta particles

03 p0257 A73-14243

Calculation of the diffusion current of a finite-base semiconductor diode

03 p0284 A73-14322

On the potential difference between two immiscible media.

04 p0483 A73-15106

Naturally alloyed n-p structures in cadmium telluride

04 p0484 A73-15642

P-n-p-n junction thyristor turnoff process under reverse anode voltage at high injection level, examining current voltage curve and switching time constant

05 p0556 A73-16068

Adaptation of the P-N junction burnout model to circuit analysis codes.

05 p0557 A73-16506

Instrument circuitry, calibration and errors in p-n junction capacitance measurement

06 p0691 A73-17399

P-n junction size effect on thermal resistance of reverse biased Si mesa-type diode, considering junction area, mesa height and power dissipation

06 p0674 A73-17795

Measurements of the photomultiplication factor of silicon avalanche photodiodes.

06 p0674 A73-17796

Influence of recombinations in the base contact and on the base surface upon static and dynamic characteristics of the p-n junction.

06 p0674 A73-17816

Features of voltage-capacitance relationships in Si/Li p-i-n detectors

06 p0675 A73-18080

Forward biased P-N junction photoelectric current shown resulting from photovoltaic, photoresistive and electric injection currents superposition

06 p0738 A73-18544

Melchly thermodynamics hypotheses based on average electron energy for examination of equilibrium and steady state conditions in semiconductor p-n junctions

06 p0770 A73-18840

Semiconductor radiation detectors fabrication methods, discussing p-n junctions diffusion and ion implantation techniques and surface barrier, dE/dx, chessboard and rod type counters

07 p0822 A73-19172

Diffusion equation for current carriers in solar cell with inhomogeneous internal electric field, determining photoelectric current in p-n junction

07 p0778 A73-19299

Fine structure in the optical-absorption edge of silicon.

07 p0863 A73-20175

GaAs diffused diode, ECL-1350.

07 p0804 A73-20570

Passage of useful and noise signals through a nonlinear circuit containing a p-n junction capacitance

08 p0946 A73-21111

Effects of boron density on radiation resistance of copper-contaminated n/p type silicon solar cells.

08 p0928 A73-21114

Ionization energy of adhesion levels and heat-generation centers in the microplasma volume in germanium p-n junctions

08 p0995 A73-21274

Characterization of p-n junctions under the influence of a time varying mechanical strain.

08 p0951 A73-21481

Investigation of the dielectric waveguide modes in homostructure GaAs laser.

09 p1091 A73-22238

Calculation of series and shunt resistances on the basis of the current-voltage characteristics of a solar cell

09 p1033 A73-22720

Integrated neuristor lines based on p-n-p-n structures with diffused resistors

10 p1193 A73-23727

Improved analysis of the steady-state operation of a resistive parametron

10 p1189 A73-24381

Effect of the nonlinearity of the junction capacitance on the spectral characteristics of the current of a tunnel diode.

10 p1197 A73-24939

Numerical analysis of the properties of an avalanche diode in the avalanche multiplication region

11 p1337 A73-25321

Pressure effects on contact potential in diode p-n junction, discussing potential barrier height variation, minority carrier concentration changes and relative position of energy bands

11 p1338 A73-26520

Te-doped GaAs injection laser with nonplanar p-n junction for enhanced power output, discussing diode construction and fabrication by Zn diffusion

12 p1505 A73-26890

Electrical fluctuations in ideal forward-biased non-degenerate diodes.

12 p1480 A73-27272

Influence of heat treatment on characteristics of injection lasers. 12 p1507 A73-27522

Output radiation influence on catastrophic and slow degradation process in heterojunction injection lasers, noting service life dependence on current density 12 p1508 A73-27525

A transport equation treatment of tunnelling in semiconductors. 13 p1668 A73-28218

A modified GaAs IMPATT structure for high-efficiency operation. 13 p1595 A73-29577

Linear theory of an IMPATT diode distributed microwave amplifier. 16 p1991 A73-33983

A study of millimeter-wave GaAs IMPATT oscillator and amplifier noise. 17 p2133 A73-34217

Design considerations of high-efficiency GaAs IMPATT diodes. 17 p2134 A73-34219

Theory of the threshold of an injection laser operating at the experimental band tails 17 p2184 A73-34922

Method for plotting frequency cutoff measurements for GaAs varactor diodes. 18 p2292 A73-36596

Main trends of development of avalanche photodiodes as high-speed photodetectors /Review/ 18 p2293 A73-36715

Application of the semiconductor p-n junction to measurements of rapidly varying pressures. 19 p2432 A73-38308

Degradation studies of diffused GaAs electroluminescent diodes subjected to mechanical stress. 19 p2439 A73-38458

Application of distributed p-n and p-i-n structures in the development of integrated circuits for electrically controlled SHF devices 20 p2535 A73-38856

Calculation of the base layer conductivity of a transistor structure 20 p2535 A73-38859

A technique for the investigation of deep-level states in diffused p-n junction devices - Application to GaAs electroluminescent diodes. 20 p2536 A73-39412

Determination of the parameters A and j /sub 0/ in the loaded portion of the current-voltage characteristic of a photoelectric converter 20 p2510 A73-39450

Analytic theory for silicon double-sided n/+/-n-p-p/+/-TRAPATT-diode structures. 20 p2538 A73-39594

Determination of the bulk carrier lifetime in the low-doped region of a silicon power diode, by the method of open circuit voltage decay. 21 p2665 A73-41123

Heterojunction injection lasers /Review/. 22 p2869 A73-42244

Book - Avalanche-diode microwave oscillators. 22 p2833 A73-42490

Determination of hole and electron traps from capacitance measurements. 24 p3119 A73-44405

Two-loop frequency multipliers employing the barrier capacitance of a p-n junction and exhibiting maximum energetic indices 24 p3071 A73-44592

Measurement of the p-n junction depth in photocells with epitaxial layers 24 p3058 A73-45254

P-N-P N JUNCTIONS

CW microwave oscillations of reach-through p-n-p barrier injection transit time /BARITT/ diodes, calculating small signal impedance and noise measure for comparison with experiment 04 p0427 A73-15346

Dependence of the current-voltage characteristic of a p-n-p drift triode on the donor concentration in the n-type base 06 p0675 A73-18081

Effect of carrier multiplication in the collector junction of an alloyed transistor on the behavior of the transistor at high current densities 07 p0798 A73-19292

Two dimensional analysis of minority carriers in drift p-n-p junction transistor base for low level injection and constant mobility and diffusivity 09 p1062 A73-22310

Inductance and Q factor measurements of inductive p-n-p transistor element in IC circuit as function of frequency, temperature and junction capacitance 10 p1196 A73-24613

Multivibrator with p-n-p and n-p-n transistors, noting circuit diagram, operation and power dissipation 10 p1197 A73-24940

Small-signal analysis of punch-through injection microwave devices. 13 p1590 A73-28541

Evolution of the shape of the current-voltage characteristics of n-p-n and p-n-p three-layer degenerate semiconductor structures 24 p3119 A73-44607

P-N-P-N JUNCTIONS

Semiconductor rectifiers and thyristor devices, discussing transistor switching, Zener diode, controlled and light activated p-n-p-n diodes 21 p2668 A73-41619

Switching transients in conducting channel-broadened p-n-p-n structure thyristors, predicting voltage change during current growth avalanche phase and settling at saturation point 24 p3072 A73-44932

P-TYPE SEMICONDUCTORS

The growth and electrical characteristics of epitaxial layers of zinc sulphide and of zinc selenide on p-type gallium phosphide. 01 p0088 A73-10683

Oscillations of injected carriers in p-type indium antimonide. 04 p0482 A73-14869

Performance of hardened P-MOS devices in severe neutron environments. 05 p0557 A73-16517

Galvanomagnetic effects measured in p-type bismuth selenide single crystal within magnetic field for Hall and conductivity mobilities, determining temperature dependences 06 p0733 A73-17741

Thermal emf of indium antimonide of a p- and-n type of conductivity at room temperature 06 p0738 A73-18652

Optical and electrical properties of proton-bombarded p-type GaAs. 06 p0739 A73-18786

Co-60 source gamma irradiation of Mo-Au doped p-type Si MOS transistors, noting threshold voltage increase and current carrier mobility decrease 07 p0862 A73-19541

Equivalent circuit of unbent p-PbS point diodes 09 p1061 A73-22022

Photovoltaic and photoconductivity measurements on p- and n-type GaSe, determining light polarization direction effect, photovoltaic relaxation times and minority carriers diffusion lengths 10 p1259 A73-23569

Alternating spectral oscillations of nonequilibrium photoelectron current in p-InSb in the presence of a quantizing magnetic field 10 p1261 A73-24763

Determination of the parameters of r-type recombination centers in germanium-doped GaTe single crystals 11 p1410 A73-26587

Ge-doped p-type epitaxial GaAs for microwave device application. 15 p1923 A73-31399

Electromagnetic wave propagation in p-type Ge and Si semiconductor plasmas, studying dispersion, cyclotron resonance, and kinetic equations 15 p1925 A73-32214

Effect of an electric field on the negative photoconductivity of high-resistance ZnTe-CdTe crystals 17 p2219 A73-35552

Electrical properties of single-crystal films of p-type PbTe 17 p2219 A73-35556

Bi implant CdS studies, discussing sputtering, surface concentration, p-type behavior and light emission characteristics 21 p2752 A73-40951

Effective recombination levels in N- and P-type silicon irradiated by 4.5 MeV electrons. 21 p2753 A73-41558

A new type of charge trapping in MOS systems. 22 p2896 A73-42275

The rectifying barrier in gallium arsenide Schottky diodes 23 p2959 A73-43618

Interface properties of oxidized germanium-doped silicon. 23 p3016 A73-43778

P-3 AIRCRAFT

Navy Transit navigation satellite system, discussing flight test for feasibility of military application to YP-3C Antisubmarine Warfare Weapons System aircraft 21 p2735 A73-40040

P-531 HELICOPTER

The application of system analysis techniques for the solution of complex helicopter crew station design problems. [AHS PREPRINT 723] 17 p2105 A73-35064

PACIFIC OCEAN

Secor range observations on Geos 1 satellite in Pacific tracking network, determining station coordinates, relative positions and geodetic heights 04 p0437 A73-14783

Geomagnetic storms and wintertime 300-mb trough development in the North Pacific-North America area. 08 p0961 A73-21384

Intratropical convergence zone in the eastern portion of the Pacific Ocean 09 p1115 A73-22990

Rapid intensification and low-latitude weakening of tropical cyclones of the western North Pacific Ocean. 10 p1245 A73-23986

Statistical aspects of lower atmospheric disturbances delineated from conventional and satellite data over the tropical Pacific. 11 p1394 A73-25724

Investigation of cloud cover parameters from measurements on the Cosmos 384 satellite 13 p1654 A73-29155

Ionospherically propagated backscatter from Pacific Ocean via swept frequency continuous wave recordings, noting sky wave polarization rotation modulation of received signal 15 p1845 A73-32228

The stratospheric-mesospheric circulation over the North Pacific Ocean. 18 p2308 A73-36039

Features of the evolution of depressions and their cloud systems over the Pacific Ocean. 18 p2334 A73-37061

A note on the FM-CW radar as a remote probe of the Pacific Trade-Wind Inversion. 19 p2448 A73-38211

PACKAGES

NT APOLLO LUNAR SURFACE EXPERIMENTS PACKAGE

NT INSTRUMENT PACKAGES

PACKAGING

NT ELECTRONIC PACKAGING

Packaging in aerospace applications 07 p0830 A73-19010

Influence of the packing and of certain conditions of usage on the medications in portable emergency medicine stores 12 p1465 A73-27720

A solid state bonding and packaging technique for integrated sensor transducers. 17 p2166 A73-34618

PACKING DENSITY

Flying-spot scanned or computer controlled electron beam fabrication system for generating high packing density pattern of LSI microelectronic circuit components 01 p0023 A73-10548

Sphere packings constructed from BCH and Justesen codes. 13 p1584 A73-28919

Suppressing spurious signals in saturated switching systems. 13 p1595 A73-29394

Viking lander capsule decelerator system candidate materials evaluation, discussing in-situ testing for high density packing and heat sterilization effects on strength [AIAA PAPER 73-447] 15 p1881 A73-31433

Technological forecasting for microcomputer architecture and fabrication on LSI chip, considering cost effectiveness, pins number, packing density, power and speed factors 17 p2131 A73-35226

Block oriented random access and read-only archival holographic memories design, considering relationships between lens geometric parameters, laser power and packing density requirements 17 p2173 A73-35432

Model for lunar near surface thermal conductivity in terms of contact conductivity, pressure and packing density 20 p2613 A73-39719

Surveyor 3 lunar soil shear strength measurements for range of bulk densities obtained by different packing procedures, calculating void ratios 23 p3031 A73-43761

PADE APPROXIMATION

Calculation of nozzle flows using Pade fractions. 11 p1303 A73-26386

PAGEOS SATELLITE

Observed effects of earth-reflected radiation and hydrogen drag on the orbital accelerations of balloon satellites. 04 p0439 A73-14802

Measured physical and optical properties of the passive geodetic satellite /Pageos/ and Echo 1. 04 p0446 A73-14809

Vertical ozone profiles from observations of eclipsing satellites. 18 p2304 A73-35971

PAIN SENSITIVITY

A mathematical model of the peripheral pain signalization mechanism 20 p2516 A73-39003

PAINTS

White and black paints for satellite thermal control coatings, discussing space environment radiation effects on emissivity and solar absorptance 07 p0841 A73-18909

A new approach to aircraft exterior lighting. 17 p2108 A73-35808

Radiative property degradation of water impinging on thermally-controlled surfaces under space conditions. [AIAA PAPER 73-733] 18 p2336 A73-36350

The testing of varnishing products used in aeronautics 21 p2724 A73-41557

PAIR PRODUCTION

Heavy elements in surface materials - Determination by alpha particle scattering.

23 p2981 A73-43529

PAIR PRODUCTION

Quantum electrodynamical models of coherent plasma electron-positron pair production and pulsed radiation in electric field, relating to pulsars

05 p0626 A73-17383

The influence of negative-ion changes in the D-region during sudden ionospheric disturbances.

09 p1075 A73-22126

Vacuum state of a relativistic system interacting with an external field

11 p1397 A73-25245

Coherent production of electron-positron pairs and bremsstrahlung on a corundum crystal

11 p1410 A73-26447

Secondary electrons and energy per ion-pair in a thermal gas for electron, proton and X-ray ionization.

16 p2052 A73-32826

Dipole-quadrupole dispersion coefficient calculation for interactions of atomic pairs formed from hydrogen, alkali and rare gas atoms, using perturbation and variation methods

23 p3007 A73-43522

Pair production near energy threshold by electron oscillation and acceleration to relativistic velocities at laser beam focus with plasma wave excitation

23 p2989 A73-44121

PALEOMAGNETISM

Natural remanent magnetizations of carbonaceous chondrites and the magnetic field in the early solar system.

05 p0619 A73-16839

Natural remanent magnetization and thermomagnetic properties of the Allende meteorite.

05 p0619 A73-16840

Lunar breccia 14321 natural remanent magnetization characteristics from alternating field and thermal demagnetization tests, describing magnetic measurement procedures

07 p0893 A73-19841

Mathematical models of the earth's magnetic field.

07 p0818 A73-20030

Analytical description of the geomagnetic field of past epochs and the determination of the magnetic-wave spectrum in the earth's core

08 p0959 A73-21297

Lunar magnetic field model with primeval liquid shell dynamo driven by thermal convection or earth tidal motions

14 p1789 A73-29722

Memory of early magnetic fields in carbonaceous chondrites.

17 p2228 A73-34421

Paleomagnetic excursion recorded in latest Pleistocene deep-sea sediments, Gulf of Mexico.

18 p2313 A73-36513

Analytical description of the geomagnetic field of past epochs and determination of the spectrum of magnetic waves in the core of the earth.

19 p2425 A73-37926

Geomagnetic field, cosmic rays, and radiocarbon content in the earth's atmosphere

21 p2756 A73-40585

PALEONTOLOGY

Paleontological evidence on the earth's rotational history since early Precambrian.

02 p0217 A73-12387

Carboxylic acids derived from Tasmanian tasmanite by extractions and kerogen oxidations.

10 p1211 A73-24108

Organic inclusions within hydrothermal minerals from S.W. Africa and elsewhere.

11 p1352 A73-25472

Trace fossils from the Nama Group, south-west Africa.

12 p1490 A73-27250

Possible stratotype sequences for the basal Paleozoic in North America.

15 p1865 A73-31025

Earth-moon system angular momentum loss from paleontological data and earth rotational moment of inertia effect

18 p2354 A73-36509

PALLADIUM

Laser-induced fast thermal desorption from solid surfaces

06 p0699 A73-17914

PALLADIUM ALLOYS

Ti-Pd phase diagram eutectoid region configuration determination through alloy thin foil arc melting preparation and microstructure examination by electron microscopy

13 p1633 A73-28146

The magnetic characteristics of the alloys of palladium with gadolinium, dysprosium, and holmium

13 p1667 A73-28183

Investigation of interdiffusion in the nickel-tungsten and palladium-tungsten systems

14 p1764 A73-30864

Amorphous alloy resistance thermometer development.

22 p2856 A73-42015

PALLADIUM COMPOUNDS

Structure and electrical characteristics of epitaxial palladium silicide contacts on single crystal silicon and diffused P-N diodes.

02 p0147 A73-12045

PAM (MODULATION)

U PULSE AMPLITUDE MODULATION

PANCREAS

Mechanisms of certain functional shifts during change in the blood of the content level of external pancreatic-gland secretion components

05 p0541 A73-16700

Structural changes in the adrenal nerve apparatus during experimental subtotal pancreatectomy

20 p2513 A73-39400

Starch hydrolysis in man - An intraluminal process not requiring membrane digestion.

20 p2519 A73-39789

PANEL FLUTTER

Dynamics of a rotating free system of bodies with an oriented axis of rotation

02 p0192 A73-11774

Acoustic resonance during the vibrations of a plate cascade in subsonic gas flow

03 p0294 A73-13619

Flutter of flat rectangular sandwich type panels in a supersonic, coplanar gas flow, with arbitrary direction.

03 p0392 A73-13768

Perturbation and harmonic balance methods for nonlinear panel flutter.

03 p0395 A73-14182

On the weight optimization problem for supersonic rectangular flat panels with specified flutter speed.

04 p0511 A73-15170

Orthotropic panel flutter at arbitrary yaw angles - Experiment and correlation with theory.

[AIAA PAPER 73-192] 05 p0634 A73-16924

The effects of various parameters on an aeroelastic optimization problem.

06 p0758 A73-17565

Nonlinear natural vibrations of rectangular plates and cylindrical panels.

06 p0765 A73-18640

Investigation of the flutter of cylindrical panels in a supersonic gas flow

12 p1550 A73-26954

Cylindrically curved panels flutter characteristics in supersonic flow parallel to generators, investigating in-plane boundary conditions and panel geometry effects

15 p1949 A73-31652

Natural frequencies and normal modes of a four plate structure.

16 p2083 A73-33948

First-order frequency effects in supersonic panel flutter of finite cylindrical shells.

[ASME PAPER 73-APM-K] 17 p2249 A73-35106

Investigation of the flutter of cylindrical panels in a supersonic gas flow.

19 p2500 A73-38139

A direct method of stability analysis for elastic circulatory systems.

20 p2621 A73-39535

Viscoelastic panel vibration damping material for ventilation ducts to reduce LF vibrations induced by turbulent air flow

21 p2723 A73-40235

Linearized characteristics method for supersonic flow past vibrating shells.

21 p2632 A73-40426

Vibration and stability of nondivergent elastic systems.

22 p2922 A73-42551

PANELS

NT CURVED PANELS

NT RECTANGULAR PANELS

NT WING PANELS

Large deflections and stability of a long cylindrical panel prepared from an orthotropic fiberglass plastic under the action of piecewise-uniform loading

08 p1017 A73-21370

Thin panels stresses diffusion analysis, comparing Bleich, variational, Conway finite difference and finite element methods

09 p1159 A73-22717

Synthesis of compression panels having non-uniform stiffener sections.

[AIAA PAPER 73-347] 11 p1437 A73-25485

Stresses in bonded joints of circular cylindrical shells and panels

12 p1551 A73-27182

Light-weight Al isogrid panel design with triangular reinforcement elements for aerospace structural applications, discussing load response characteristics, fabrication and cost reduction

13 p1624 A73-28906

Calculation of three-layer minimum-weight panels as a problem of mathematical programming

20 p2625 A73-39651

PANIC

Aircraft evacuation and safety procedures during emergencies, discussing negative panic, flight crew training and impact injury minimization

18 p2268 A73-36849

PANORAMIC CAMERAS

Apollo 15 panoramic camera with 24 inch focal length for stereophotography of lunar surface, presenting pictures of lunar craters and landing sites

07 p0824 A73-20021

Stereophotogrammetric compilation of large scale topographic chart using convergent panoramic photos obtained with Apollo 15 spacecraft

07 p0824 A73-20022

Lunar control densification with panoramic space photography.

08 p0968 A73-21702

Apollo 15 optical bar panoramic lunar surface photography, considering luminance, exposure time, resolution and camera performance

08 p0970 A73-21731

Reduction of lunar panoramic photography on the analytical stereoplotter.

09 p1081 A73-22379

Panoramic and frame cameras for aerial phototopographic survey, noting photo quality and high resolution advantages

12 p1497 A73-27423

UV photography of star field by Eridan rocket-borne wide angle camera, noting inertial guidance system pointing errors data reduction problems

18 p2315 A73-35994

PANORAMIC SCANNING

Sensitivity and resolution of panoramic analyzers

20 p2537 A73-39455

PAPILLAE

Visual work duration and intensity effects on optic papillae expansions and shape alterations, noting differences between trained and untrained subjects

05 p0540 A73-16694

PARA HYDROGEN

The non-equilibrium ortho/para spin state ratio for molecular H₂ formed in the hydrolysis of lithium aluminum hydride.

07 p0787 A73-19144

PARABOLAS

On the equivalent parabola technique to predict the performance characteristics of a Cassegrainian system with an offset feed.

14 p1734 A73-30211

PARABOLIC ANTENNAS

Off-axis polarization characteristics of Cassegrainian and front-fed paraboloidal antennas.

01 p0022 A73-10177

Low-sidelobe paraboloidal antenna with microwave absorber.

01 p0018 A73-11054

Results of an experimental investigation of a two-mirror antenna with a modified counter reflector

02 p0146 A73-12019

Algorithm for automatic optimal control of radio telescope parabolic antenna with external characteristic in radiation pattern, noting quasi-steady and steady operation

02 p0147 A73-12497

Remote sensor for atmospheric physical properties with FM-CW scanning radar, parabolic antennas and waveguide feeds for linear and circular polarization

03 p0339 A73-14544

Parabolic, Cassegrain, spherical and horn-parabolic axisymmetric mirror antennas, calculating primary radiating element orientation effects on radiation polarization characteristics

05 p0547 A73-16052

Calculation of the satellite tracking accuracy for ground stations with medium-diameter parabolic antennas

07 p0791 A73-19373

Study of the Rayleigh zone of circular radiating apertures

11 p1328 A73-25283

Computer design of antenna reflectors.

[AIAA PAPER 73-351] 11 p1437 A73-25489

Determination of the maximum scan-gain contours of a beam-scanning paraboloid and their relation to the Petzval surface.

11 p1328 A73-25651

Project management and installation of the Arvi satellite communication earth station.

11 p1344 A73-26147

Method of measuring the parameters of axisymmetrical mirror antennas on the basis of the emission of a 'black' disk positioned in the Fresnel region

11 p1332 A73-26162

Skyнет satellite communication service for small dish antenna equipped mobile ground stations, emphasizing necessity of rapid central control response to configuration and propagation condition changes

12 p1471 A73-27660

Parabolic 10 m antenna-8.4 mm wavelength radiometer system for radio astronomy

12 p1498 A73-27724

The optimization of the supporting structures of parabolic antennas

14 p1740 A73-29742

Design and fabrication of a flight antenna for a planetary spacecraft.

16 p2018 A73-33057

Directional properties of horn-parabolic antennas

21 p2661 A73-40193

Transverse displacements of the radiating element of the parabolic antenna of a mobile radio telescope
21 p2672 A73-40548

Longitudinal displacements of the secondary mirror of a parabolic antenna
21 p2672 A73-40550

Phase errors at the aperture of a curvilinear antenna during displacement of the primary radiating element from the focal point
21 p2667 A73-41447

Stanford radio telescope array with five paraboloid antennas for fast image forming interferometry, using earth rotation synthesis to produce sky continuous radiation brightness map
23 p2957 A73-43359

Southern Hemisphere earth rotational synthesis radio telescope array with paraboloids arranged as compound grating interferometer for astronomical radio sources mapping
23 p2958 A73-43361

Radio astronomy interferometer receiver IF control for centimeter wave polarized signal processing and parabolic antenna instrumentation
23 p2980 A73-43377

A fan-beam dual reflector antenna.
24 p3069 A73-45030

PARABOLIC BODIES

Calculation of the flow of a viscous compressible fluid past a parabolic obstacle
[ONERA, TP NO. 1129]
01 p0002 A73-10238

Rotating paraboloid of revolution in viscous conducting fluid, calculating flow velocity and magnetic field from MHD equations
05 p0601 A73-16172

Stability of a shell in the form of a hyperbolic paraboloid subjected to compression along straight generating lines
11 p1435 A73-25397

A contribution to Hertz's theory of elastic impact.
13 p1696 A73-28748

Equilibrium of an elastic paraboloid of revolution under a concentrated load applied to its apex
22 p2927 A73-43052

Experiments on free vibration of shells of revolution.
23 p3039 A73-43384

PARABOLIC DIFFERENTIAL EQUATIONS

Application of the boundary-value method to the solution of weakly nonlinear parabolic differential equations
01 p0069 A73-10070

Difference procedures of monotonic type for nonlinear parabolic boundary value problems
01 p0069 A73-10072

Existence theorem for nonlinear parabolic equations of evolution in real Banach space
01 p0071 A73-11270

A priori estimate of the solution to a Cauchy problem with data prescribed on a time-like surface for a 2-nd order parabolic equation and the uniqueness theorems associated with it
01 p0071 A73-11426

On a semi-variational method for parabolic equations. I.
02 p0186 A73-11589

On certain parabolic differential equations and an equivalent variational problem.
02 p0186 A73-11972

The representation of functions determined by a class of hypoelliptic operators
02 p0187 A73-12180

Semidiscrete-least squares methods for a parabolic boundary value problem.
02 p0188 A73-12615

The convergence of separation /Galerkin/ formulations in the case of time-dependent equations
03 p0336 A73-13165

Boundary value problems with variable boundaries for a special differential equation
03 p0337 A73-14630

Integral representation of positive solutions of linear elliptic and parabolic differential equations with constant coefficients
04 p0470 A73-14898

Cauchy problem and mixed boundary value problems for parabolic and hyperbolic wave equations of heat conductivity for boundary operators given on hyperplane
04 p0517 A73-14935

Practical techniques for estimating the accuracy of finite-difference solutions to parabolic equations.
[ASME PAPER 72-WA/APM-12]
04 p0472 A73-15900

Necessary conditions for optimal controls of elliptic or parabolic problems.
05 p0590 A73-16487

Solvability in the large of the first boundary value problem for a certain class of quasi-linear one-dimensional parabolic equations
06 p0716 A73-17719

Convergent finite difference schemes for nonlinear parabolic equations.
06 p0717 A73-18405

Galerkin methods for vibration problems in two space variables.
06 p0717 A73-18408

Approximate method for the synthesis of the optimal control of a dynamic system subjected to random disturbances
06 p0725 A73-18879

Galerkin methods for parabolic equations with nonlinear boundary conditions.
07 p0844 A73-19138

Lower bound estimates of solutions to a second boundary-value problem for a second-order parabolic equation in regions with unrestricted spatial variables
07 p0845 A73-19655

A unified boundary controllability theory for hyperbolic and parabolic distributed parameter systems.
07 p0846 A73-20591

Solvability of mixed boundary value problems for second-order parabolic equations with degeneration
08 p0983 A73-21126

Fractional exponents of an elliptic operator and parabolic differential equations in spaces of Hoelder-continuous functions
08 p0983 A73-21250

Convergence of difference methods for certain degenerating quasi-linear parabolic equations
09 p1111 A73-21919

On degenerate elliptic-parabolic operators of second order and their associated diffusions.
09 p1111 A73-21996

Semivariational approximation for solution of parabolic differential equation with inhomogeneous mixed boundary conditions and abstract equation with operators, noting convergence and stability
09 p1113 A73-23025

A finite element collocation method for quasilinear parabolic equations.
10 p1241 A73-23638

Solution of the stochastic control problem in unbounded domains.
10 p1203 A73-24705

Solvability of the mixed boundary value problem for higher-order parabolic quasi-linear equations with discontinuous and rapidly growing coefficients in the Orlicz classes
11 p1392 A73-26599

Power series solution of quasi-linear parabolic heat conduction equation for temperature wave propagation in soil
12 p1560 A73-27807

The numerical solution of parabolic partial differential equations using the method of Lanczos.
13 p1650 A73-29398

Asymptotic behavior of solutions of the Cauchy problem and the first boundary value problem on a half-axis for a linear second-order parabolic equation with the absolute value of x approaching infinity and at large values of the parameter
13 p1651 A73-29680

Uniqueness theorems for the Dirichlet boundary value problem in the case of elliptic-parabolic differential equations and lower bounds for the smallest eigenvalue
14 p1767 A73-29765

The Cauchy problem in classes of increasing functions for some second-order quasi-linear degenerate parabolic equations
14 p1769 A73-30347

Convergence of a difference procedure for quasi-linear parabolic initial boundary-value problems in cylinder symmetry
14 p1769 A73-30422

Estimated solutions for the second and third boundary value problems of a second-order parabolic equation in regions with unbounded spatial variables
14 p1771 A73-30836

Convergence, accuracy and stability of finite element approximations of a class of non-linear hyperbolic equations.
15 p1899 A73-32030

Integral operators and the first initial boundary value problem for pseudoparabolic equations with analytic coefficients.
15 p1902 A73-32399

Approximate synthesis method for optimal control of a system subjected to random perturbations.
15 p1915 A73-32404

A difference method of solving boundary value problem for a parabolic-type quasi-linear integro-differential equation
16 p2034 A73-34070

On the numerical computation of parabolic problems for preceding times.
17 p2199 A73-34211

Liapunov direct method extended to stability of nonlinear parabolic systems, noting application to Burgers equation
17 p2200 A73-34398

Book - Non-homogeneous boundary value problems and applications. Volume 3.
17 p2200 A73-34464

Russian book - Linear and nonlinear boundary value problems.
17 p2201 A73-34640

A generalization of the additive correction methods for the iterative solution of matrix equations.
17 p2203 A73-35729

The Ritz-Galerkin procedure for parabolic control problems.
19 p2446 A73-38375

The Cauchy problem and some basic problems of mathematical physics about parabolic systems with discontinuous coefficients
20 p2582 A73-39252

The numerical solution of nonlinear parabolic problems by variational methods.
21 p2725 A73-40382

A priori L sub 2 error estimates for Galerkin approximations to parabolic partial differential equations.
21 p2725 A73-40383

Initial-value problems for pseudo-parabolic partial differential equations.
21 p2726 A73-40694

A method of treating boundary singularities in time-dependent problems.
21 p2726 A73-40997

Convergence of perturbation-theory series in the problem of short-wave propagation through a randomly nonhomogeneous medium
21 p2657 A73-41514

Russian book - Qualitative theory of boundary value problems for quasi-linear second-order parabolic equations.
22 p2881 A73-41701

Shear layer effect on acoustic duct wall impedance for sound propagation in uniform flow in terms of parabolic cylinder functions
22 p2900 A73-43138

Quasi-periodic solutions existence, uniqueness and asymptotic behavior to quasi-linear parabolic equations, demonstrating vanishing conditions at boundary
23 p3049 A73-43611

The 'multiplexing' CTDS method of solving certain second-order partial differential equations on a hybrid computer system
23 p2956 A73-43951

Efficient subroutines for the solution of general elliptic and parabolic partial differential equations.
24 p3106 A73-45093

Integral representations of solutions for general parabolic boundary value problems and the correct solution in spaces of increasing functions
24 p3106 A73-45352

The Dirichlet and Neumann problems for parabolic equations with a Bessel operator in Dini spaces
24 p3106 A73-45510

PARABOLIC FLIGHT

Vestibular influences on orientation in zero gravity, produced by parabolic flight.
06 p0653 A73-18032

Hohmann trajectories efficiency for interplanetary transfers of spacecraft between circular coplanar orbits, considering earth-Mars-earth flight and transition to parabolic trajectory
12 p1538 A73-27065

Standardization of the calculation of nearly parabolic cometary orbits.
14 p1790 A73-29795

Diffusion of comets from parabolic into nearly parabolic orbits.
14 p1793 A73-29828

Inversion illusion in the so-called zero-gravity conditions of parabolic flight.
14 p1722 A73-30511

PARABOLIC REFLECTORS

NT PARABOLOID MIRRORS

A fixed reflector, steerable beam, earth station antenna.
04 p0428 A73-15415

Class of stepped-reflector antennas with improved frequency response.
05 p0547 A73-16159

Reflector antenna radiation pattern analysis by equivalent edge currents.
06 p0665 A73-18179

The 15 m Cracow radiotelescope. I - Technical description and observational possibilities.
08 p0952 A73-20850

Analysis of He-Ne laser surface reflections from an off-axis parabolic mirror.
08 p0974 A73-21032

Analysis of generalized dual-mirror antennas
08 p0947 A73-21399

Feed arrangement for axis definition of paraboloid reflector.
08 p0947 A73-21434

Computer design of antenna reflectors.
[AIAA PAPER 73-51]
11 p1437 A73-25489

Design of multiple-edge blinders for large horn reflector antennas.
11 p1337 A73-25653

Coaxial feeds for high aperture efficiency and low spillover of paraboloidal reflector antennas.
11 p1337 A73-25655

A two-dimensional mathematical model for an acoustically soft parabolic cylinder reflector.
13 p1597 A73-28493

Shaping of subreflectors in Cassegrainian antennas for maximum aperture efficiency.
14 p1734 A73-30207

Offset parabolic reflector antennas linearly and circularly polarized excitations, discussing dependence on angle between dual mode feed and axis

14 p1734 A73-30212

Large parabolic reflector microwave antenna astigmatism effects on radiation pattern, discussing focusing procedure for phase error reduction

17 p2143 A73-35695

Analysis of two-mirror antennas of a general type.

19 p2410 A73-38357

Large scanning and multibeam reflector antennas for space communications.

20 p2524 A73-38738

New multiple-support radially-symmetric design of the parabolic-reflector suspension for a radio telescope

21 p2672 A73-40547

Advances in the theory and technology of horn antennas and reflector antennas

21 p2664 A73-41073

Design of the reflecting elements and secondary mirror of the RATAN-600 radio telescope

21 p2675 A73-41449

Experimental verification of the analysis of umbrella parabolic reflectors.

22 p2831 A73-41844

On separating aberrant effects from random scattering effects in radio telescopes.

23 p2958 A73-43379

Some data for the design of low-crosspolarisation feeds.

24 p3069 A73-45255

PARABOLIC VELOCITY

U ESCAPE VELOCITY

PARABOLOID MIRRORS

Method of measuring the parameters of axisymmetrical mirror antennas on the basis of the emission of a 'black' disk positioned in the Fresnel region

11 p1332 A73-26162

Approximate calculation of the small-reflector surface from the deformations of the large reflector of a Cassegrainian antenna

12 p1480 A73-27235

Single beam spectrophotometer for transmittance measurement constructed from off-axis parabolic mirrors and plane grating monochromator, considering systematic errors

17 p2172 A73-35426

Changes in the geometrical parameters of a radio-telescope parabolic mirror experiencing radially symmetric deformations

21 p2672 A73-40549

Interferometric test of an f/8, 24-inch /60.96 cm/ diameter paraboloidal mirror in the atmosphere.

21 p2704 A73-41260

PARABOLOIDS

U PARABOLIC BODIES

PARACHUTE DESCENT

Evaluation of the state of the cardiovascular system from polycardiographic test data

06 p0650 A73-17749

Visual-motor coordination characteristics of parachute jumpers

06 p0657 A73-17750

Effect of suspension-line viscous damping on parachute opening load amplification.

07 p0777 A73-19495

A linearised theory of parachute opening dynamics.

08 p0928 A73-21692

Recovery of sounding rocket payloads by center-of-gravity position control.

09 p1155 A73-23213

Parachute opening dynamic analysis, taking into account risers, shrouds and canopy cloth elastic properties on opening history and loads

10 p1176 A73-24647

Aerodynamic decelerator dynamics modeling for Viking lander parachute deployment, analyzing unfurling process with attention to longitudinal and rotational dynamics

12 p1549 A73-27440

Viking aerodynamic decelerator for Mars lander mission in 1976, discussing mortared disk-gap-band parachute, qualification flight tests and atmospheric environment effects

15 p1825 A73-31428

Dynamic stress analysis during inflation of disk-gap-band Viking 75 parachute for Mars soft landing

15 p1825 A73-31430

Dynamic parachute inflation model for dimensionless time and maximum force predictions at high altitudes

15 p1826 A73-31436

Parachute axisymmetric self excited breathing oscillations dependence on descent velocity, Froude number, canopy/line length ratio, drag and line stiffness

15 p1826 A73-31438

Development of the Viking parachute configuration by wind tunnel investigation.

15 p1826 A73-31440

Low altitude flight test phase of Viking decelerator system development, considering low density environment loading condition simulation method

15 p1826 A73-31441

Viking 75 Mars lander parachute high altitude qualification flight tests for camera, telemetry and radar performance, using ground based computer-radar monitoring system

[AIAA PAPER 73-456] 15 p1826 A73-31442

Viking 75 Mars lander spacecraft mortar system design and environmental requirements, stressing manufacturing and qualification tests and parachute ejection

[AIAA PAPER 73-458] 15 p1827 A73-31444

Mortar design for parachute ejection and deployment into airstream to decelerate spacecraft and aircraft pilot escape modules, estimating hardware weight and reaction load

[AIAA PAPER 73-459] 15 p1827 A73-31445

Computerized six degree of freedom parachute deployment model for predicting entry vehicle-decelerator dynamic response to aerodynamic forces and physical property changes

[AIAA PAPER 73-460] 15 p1827 A73-31446

Performance/stability of midair recovery system with tandem parachute configuration, discussing gliding and nongliding systems

[AIAA PAPER 73-461] 15 p1827 A73-31447

A parachute snatch force theory incorporating line disengagement impulses.

[AIAA PAPER 73-464] 15 p1827 A73-31450

Development of a high-performance ringsail parachute cluster.

[AIAA PAPER 73-468] 15 p1828 A73-31452

Development of an improved midair-retrieval parachute system for drone/RPV aircraft.

[AIAA PAPER 73-469] 15 p1828 A73-31453

A technique for the calculation of the opening-shock forces for several types of solid cloth parachutes.

[AIAA PAPER 73-477] 15 p1829 A73-31461

Predicting descent rate for aircraft parachute flares.

[AIAA PAPER 73-482] 15 p1829 A73-31464

Parachute-payload system performance prediction for cause and effect relationships by parametric sensitivity and regression analysis for optimal design with computer simulation

[AIAA PAPER 73-487] 15 p1829 A73-31469

Several computerized techniques to aid in the design and optimization of parachute deceleration and aerial-delivery systems.

[AIAA PAPER 73-488] 15 p1829 A73-31470

Sea survival after ejection and parachute descent, describing hand operated canopy connector release to free pilot from entanglement or dragging

16 p1974 A73-32665

Mesospheric positive ion observation via measurement of polar electrical conductivities by subsonic parachute-borne blunt probe system launched on meteorological rockets

18 p2305 A73-36006

Thermal control subsystem design of a Saturn/Uranus atmospheric entry probe for descent missions to 20 bars.

[AIAA PAPER 73-770] 18 p2360 A73-36384

Initial results of a psychophysiological study of certified parachutists

18 p2284 A73-36917

A new approach to performance optimization of the 1975 Mars Viking lander.

[AIAA PAPER 73-889] 20 p2614 A73-38825

Helium bubble survey of an opening parachute flowfield.

22 p2798 A73-43112

PARACHUTE FABRICS

Stress measurement on cloth of inflated solid circular parachute model, noting sensor interference with canopy shape and stress pattern

[AIAA PAPER 73-445] 15 p1825 A73-31431

Force-strain characteristics of dacron parachute suspension-line cord under dynamic loading conditions.

[AIAA PAPER 73-446] 15 p1825 A73-31432

Parachute webbing designs for opening shock energy absorption and force limitation, discussing drop tower and ballistic piston test results for various designs

16 p2018 A73-33066

PARACHUTES

NT DRAG CHUTES

NT RECOVERY PARACHUTES

NT RIBBON PARACHUTES

A model and calculation procedure for predicting parachute inflation.

[AIAA PAPER 73-453] 15 p1826 A73-31439

Parachute gore shape and flow visualization during transient and steady-state conditions.

[AIAA PAPER 73-474] 15 p1828 A73-31458

Relative merit of the disc-gap-band parachute applied to individual aircrew member escape.

[AIAA PAPER 73-483] 15 p1829 A73-31465

Parachutes computer aided design and performance analysis system development and operation, presenting information storage and retrieval tasks mechanics

[AIAA PAPER 73-484] 15 p1829 A73-31466

Single point emergency equipment divestment system for instantaneous parachute harness, lap belt and leg restraint release, describing pyrotechnic actuation system

16 p1966 A73-32666

PARACHUTING

U PARACHUTE DESCENT

PARAGLIDERS

NT FLEXIBLE WINGS

NT PARAWINGS

PARALLAX

Hyades stellar flux parallaxes for cosmic scale photometric distance determinations and calibration

03 p0372 A73-1324

Catalog of angular diameters, absolute magnitudes, spectroscopic parallaxes and linear diameters for 230 stars, discussing accuracy and frequency distribution of log functions

03 p0375 A73-1394

Secular parallaxes of stars and the speed of the sun according to absolute intrinsic motions of 14,600 stars with respect to galaxies

15 p1938 A73-3196

Photographic parallax heights of infrared airflow structures.

18 p2313 A73-3651

Data reduction for annual, diurnal and satellite observation aberrations via rectangular coordinate method, discussing parallax, refraction, instrument eccentricity and computer applications

22 p2915 A73-4303

Secular parallaxes and space velocity of the sun from absolute proper motions of 14,600 stars relative to galaxies.

24 p3132 A73-4448

Calibration of luminosity criteria for G and K giants by means of trigonometric parallaxes.

24 p3140 A73-4518

PARALLEL COMPUTERS

High speed parallel multiplier design based on threshold logic adder using integrated logic circuits

17 p2139 A73-35238

PARALLEL DRAINAGE

U DRAINAGE PATTERNS

PARALLEL FLOW

NT GAS FLOW

NT LAMINAR FLOW

NT PIPE FLOW

NT STEADY FLOW

NT THREE DIMENSIONAL FLOW

Pressure surfaces and flow lines geometry of three dimensional parallel steady flow, noting geodesics for motion on surfaces of constant pressure

06 p0686 A73-18174

Linear viscoelastic fluid parallel flow in straight duct of uniform cross section under axial pressure gradient

13 p1602 A73-28914

Free parallel shear flow approximation by velocity discontinuity involving Kelvin-Helmholtz waves longer than shear layer thickness

13 p1605 A73-29448

Linear stability of nearly parallel flows. II - The Blasius boundary layer

14 p1744 A73-29759

Nonlinear development of disturbances in a plane-parallel Poiseuille flow

15 p1861 A73-31283

A numerical solution for the transonic flow around blunt wedges

15 p1823 A73-31336

Thin rectangular lifting wing investigation at small angle of attack in parallel flow based on Prandtl acceleration potential theory

15 p1955 A73-32128

Experimental investigation of secondary instabilities in the unstable laminar boundary layer of a concave wall in parallel flow

16 p1999 A73-33203

Spatially growing wave trails of an inviscid fluid discontinuity.

16 p2001 A73-33868

Hydromagnetic stability of parallel flow of an ideal heterogeneous fluid.

16 p2043 A73-33872

Turbulent mixing of cylindrical jet with parallel stream in terms of mixing length concepts and velocity profiles

17 p2157 A73-35515

Numerical solutions of time-dependent incompressible Navier-Stokes equations using an integral differential formulation.

18 p2297 A73-36159

Boundary conditions and stability of inviscid plane parallel flows.

19 p2420 A73-37751

Non-parallel flow corrections for the stability of shear flows.

20 p2546 A73-39097

Stability of parallel flow of a dusty gas in an annulus.

20 p2548 A73-39522

Two types of instability of steady convective motion caused by internal heat sources

21 p2789 A73-40197

Stability of a plane boundary layer with allowance for nonparallelism

23 p2968 A73-43477

PARALLEL PLATES

Effect of gas-surface interaction on the transmission of sound through a collisionless gas. 01 p0077 A73-10972

Study of the natural convection between two plane, vertical plates parallel and isothermal 02 p0238 A73-12795

Applying quasilinearization to the steady laminar flow between two parallel porous plates. 03 p0292 A73-13307

Inertia and energy effects in the developing gas film between two parallel flat plates. [ASME PAPER 72-1-UB-33] 03 p0297 A73-14343

Transient free-convection horizontal laminar flow between two parallel plates. 04 p0517 A73-15681

Free convective heat transfer between vertical parallel plates One plate isothermally heated and the other thermally insulated. 05 p0638 A73-16221

Aperture fields and gain of open-ended parallel-plate waveguides. 06 p0676 A73-18178

A comparison of mode match, geometrical theory of diffraction, and Kirchhoff radiation. 06 p0666 A73-18192

Numerical prediction of the phenomenon of transition for a flow between two parallel planes 06 p0687 A73-18537

Non-grey radiative heat transfer in the picket-fence approximation. 08 p1020 A73-20790

Parallel plate electromagnetic shock tube, investigating drive current, gas pressure and electrode material effects on electrode ablation and current sheet velocity 08 p0953 A73-21632

Variable properties laminar gas flow heat transfer in the entry region of parallel porous plates. [AD-759455] 08 p1024 A73-21640

Electromagnetic pulse penetration through small apertures. 08 p0940 A73-21664

Entrance region heat transfer between parallel plates with uniform wall temperature. 09 p1167 A73-23460

Inertia effects in laminar radial flow of power law fluids. 10 p1206 A73-24660

Scattering from a periodic corrugated surface - Semi-infinite alternately filled plates. 13 p1659 A73-28484

The illumination distribution in the image plane from the radiation of a plane-parallel plate with the actual ray paths taken into consideration. 13 p1621 A73-29325

A position sensitive proportional counter with high spatial resolution. 13 p1622 A73-29643

Numerical solution of the viscous flow in the entrance region of parallel plates. 14 p1746 A73-30907

Motion of a magnetized fluid between parallel plates 15 p1918 A73-31408

Heat transfer in the case of free convection of air between vertical surfaces 15 p1958 A73-31908

Natural convective heat transfer between vertical parallel plates - One plate with a uniform heat flux and the other thermally insulated. 15 p1958 A73-32057

Equilibrium of a plasma contained between two parallel plates by a magnetic field 15 p1921 A73-32333

Poiseuille flow and thermal creep of a rarefied gas between parallel plates. 16 p2085 A73-33315

Several parallel-plate guides with screen as phased array - Effect of the coupling on the directive gain 16 p1979 A73-33374

Effect of a connecting plane link on the excitation and propagation of flexural oscillations in parallel plates 17 p2244 A73-34737

Wave propagation between two plane, parallel reactive walls. 19 p2404 A73-37721

Turbulent flow development characteristics in channel inlets. 19 p2421 A73-38184

Heat transfer in an absorbing, emitting and scattering slug flow between parallel plates. [ASME PAPER 73-HT-13] 20 p2625 A73-38568

Combined forced convection and radiation heat transfer in the thermal entrance region of a non-isothermal parallel plate channel - Optical thin gases. [ASME PAPER 73-HT-14] 20 p2625 A73-38569

Electromagnetic scattering by discontinuities in weakly inhomogeneous parallel plane waveguides or ducts, noting edge diffraction singularities role from ray optical calculation 20 p2528 A73-38847

Variational analysis of the flow development in the entrance region of circular tubes and parallel-plate channels. 20 p2548 A73-39527

Contribution to the study of the development of a jet issuing from a nozzle of small elongation and confined between two lateral walls 21 p2677 A73-40620

Unsteady, combined radiation and conduction in an absorbing, scattering, and emitting medium. [ASME PAPER 73-HT-1] 22 p2930 A73-42288

Evaluation of error bounds in an optimization problem using the finite-element method. [ASME PAPER 73-APMW-15] 22 p2924 A73-42882

Heat transfer in plane Couette flow of rarefied gas between parallel plates, determining temperature jumps at plates from transfer equations 23 p3048 A73-43206

Fluid pad resistor for linear laminar flow resistance between parallel plates with emphasis on fluidic circuits application 23 p2945 A73-43425

On laminar two-phase flows in magnetohydrodynamics. 23 p3013 A73-44228

PARALLEL PROCESSING [COMPUTERS]

Airborne associative parallel array digital computer built with MOS LSI technology for size and weight reduction, discussing design and applications 04 p0424 A73-15065

Optimum quantization and parallel algorithms for nonlinear state estimation. 04 p0472 A73-15276

Optical computer technology based on Fourier transform optics and holography, discussing speed and parallel processing capabilities, image deblurring, and applications 04 p0426 A73-15957

On the number of operations simultaneously executable in Fortran-like programs and their resulting speedup. 05 p0553 A73-16450

Teleprocessing systems communication software functions and construction, considering network control, message preprocessing, queuing and error recovery in multiprogramming and multiprocessing environment 05 p0551 A73-16803

A cellular processor for task assignments in polymorphic, multiprocessor computers. 06 p0671 A73-18061

An efficient parallel algorithm for the solution of a tridiagonal linear system of equations. 08 p0983 A73-20960

Applications of vector and parallel computers to radar defense systems. [AIAA PAPER 73-428] 12 p1476 A73-27822

Parallel algorithms for optimum nonlinear state estimation. 19 p2413 A73-38041

A parallel algorithm for high subsonic compressible flow over a circular cylinder. 21 p2727 A73-41474

Noise and stable operation conditions in associative memory devices 23 p2956 A73-43580

Parallel and string array processor hardware design and computer programs for computing speed increase over conventional series computers 24 p3070 A73-45086

PARALLEL PROGRAMMING

The 'multiplexing' CTDS method of solving certain second-order partial differential equations on a hybrid computer system 23 p2956 A73-43951

PARALLELEPIPEDS

Solid deformable body mean stress determination by statistical summation of stress squares on faces of parallelepiped rotated within Euler angle limits 02 p0235 A73-12207

A chart for the computation of the gravitational attraction of a right rectangular prism. 11 p1351 A73-25160

Construction of a stress tensor according to Papkovitch-Filonenko-Borodich method 20 p2618 A73-39324

PARALYSIS

Effects of anesthesia and muscle paralysis on respiratory mechanics in normal man. 08 p0934 A73-21505

Effect of chronic pyramid insufficiency on the function of spinal centers of shin and foot muscles in man 22 p2807 A73-42658

PARAMAGNETIC AMPLIFIERS

U MASERS

PARAMAGNETIC RESONANCE

NT ELECTRON

RESONANCE

German monograph on parametric amplification in inverted material covering nonlinear interaction between electromagnetic field and paramagnetic material, dielectric resonator and pumping field strength 03 p0282 A73-13816

PARAMETRIC AMPLIFIERS

E resonance line broadening due to superhyperfine interactions in ruby, noting angular dependence of mosaic structure mechanism 09 p1132 A73-21954

Paramagnetic resonance line broadening in ferrite garnets with small additions of rare-earth elements 10 p1261 A73-24703

PARAMAGNETISM

Amorphous magnetism in F.C.C. Vicalloy II. 01 p0087 A73-10242

Van Vleck paramagnetism and bonding parameters in semiconductors. 02 p0201 A73-11900

Morphic effects. V - Time reversal symmetry and the mode properties of long wavelength optical phonons. 03 p0349 A73-12901

Magnetic susceptibility of amorphous semiconductors. 06 p0733 A73-17746

Nature of localized states in amorphous semiconductors - A study by electron spin resonance. 07 p0863 A73-20174

Effect of paramagnetic impurities on Josephson currents through junctions with normal-metal barriers. 07 p0864 A73-20574

Microwave spectrometer with internal dc glow discharge for transient paramagnetic molecules observation, discussing design features and operating parameters effects on spectrum 11 p1366 A73-26303

Influence of plastic strain on the paramagnetic susceptibility of molybdenum single crystals 18 p2324 A73-36802

PARAMETERIZATION

The range of solutions in the case of optimization problems with parameters in the coefficients of the matrix of the linear restriction conditions 02 p0186 A73-11590

Parameter optimization technique for remote radio probing and diagnostics of inhomogeneous media with properties variation along single dimension 04 p0422 A73-15478

Parameter identification using the Galerkin procedure in nonlinear boundary-value problems. [ASME PAPER 73-AUT-C] 06 p0716 A73-17724

Comparative considerations concerning parametric stress concentration studies involving finite elements and complex stress functions 07 p0910 A73-19208

Systems with internal parameters obeying the orthogonality condition. 08 p0987 A73-20777

A nonlinear, nonconvex optimization problem 08 p0983 A73-20778

Signal processing device with parametric interaction between opposite acoustic waves passing through delay line considering real time convolution and time inversion capabilities 12 p1470 A73-27569

Computer aided parametric analysis for general aviation aircraft. [SAE PAPER 730332] 17 p2130 A73-34685

A perturbation method for obtaining approximate solutions of an equation with two small parameters 17 p2201 A73-35046

Antenna radiation pattern recording as functions of two simultaneous parameters, considering measurement time savings 17 p2129 A73-35699

Parametrization of orographical effects in the planetary boundary layer. 21 p2732 A73-41570

Solution of nonlinear problems in magnetofluid-dynamics and non-Newtonian fluid mechanics through parametric differentiation. 22 p2843 A73-42556

Parameterization of baroclinicity effects in the planetary boundary layer. 24 p3088 A73-45366

Parametrizing turbulent-friction effects in a planetary boundary layer 24 p3108 A73-45450

PARAMETERS

U INDEPENDENT VARIABLES

PARAMETRIC AMPLIFIERS

Standing wave approximation of distributed dual frequency parametric oscillators consisting of semiconductor diodes and transmission line in steady state 02 p0147 A73-12490

Amplitude-frequency and stability characteristics of parametric amplification by triple-frequency interaction in nonlinear nonautonomous system 02 p0147 A73-12491

German monograph on parametric amplification in inverted material covering nonlinear interaction between electromagnetic field and paramagnetic material, dielectric resonator and pumping field strength 03 p0282 A73-13816

Noise temperature and signal characteristics of parametric microwave superheterodyne receiver with

PARAMETRIC DIODES

downconverter for satellite communication, radio and TV transmission

03 p0277 A73-13986

A review of microwave parametric amplifiers with particular reference to satellite communications and radio astronomy.

03 p0284 A73-13999

Internal upconversion and doubling of an optical parametric oscillator to extend the tuning range.

03 p0320 A73-14463

Parametric subharmonic oscillators - Static behaviour.

04 p0429 A73-15929

Parametric amplification of a UHF signal by plasma-beam interaction in the presence of a magnetic field of finite amplitude

04 p0424 A73-15996

Parametric regeneration in Josephson superconducting point contacts for combination frequency signal amplification and conversion in microwave application

05 p0556 A73-16073

Gunn diodes oscillating circuit with waveguide cavity in push-pull mode at 42 GHz for high power parametric amplifier pump applications

05 p0558 A73-16807

Noise considerations in space communication antennas.

07 p0794 A73-20228

Combined operations with negative resistance and nonlinear characteristics in an avalanche diode.

07 p0804 A73-20569

Solid state microwave electronics technology review covering parametric amplifier, maser, tunnel and avalanche diodes, transistors, and transmission, filtering and passive signal processing techniques

08 p0942 A73-20701

Microwave lumped passive and active circuit components properties assessment, considering inductor, capacitor, resistor, gyrator, tunnel diode amplifier, varactor Gunn oscillator, and parametric amplifier

08 p0942 A73-20703

Phase-amplitude and amplitude characteristics of a regenerative parametric amplifier

08 p0948 A73-21555

Interference protection of regenerative parametric amplifiers.

09 p1061 A73-22042

Room temperature pulsed n-type GaAs cleaved platelet lasers bulk optically pumped near band gap by tunable parametric oscillator, noting emission peak at threshold

[AD-758950]

09 p1092 A73-22240

Analysis of parametron oscillation characteristics based on the collector-junction capacitance of the transistor.

10 p1193 A73-23666

Cryogenically cooled parametric amplifiers for 100 meter radio telescope low noise operation, describing system design and performance

12 p1481 A73-27780

Radio astronomy telescope all sky survey procedure and data acquisition systems development for use with parametric amplifiers

12 p1544 A73-27781

Combination and crosstalk distortions in microwave parametric systems.

13 p1583 A73-28665

Application of the superregeneration principle to a ferromagnetic amplifier

13 p1592 A73-28910

Pulsar positions and periods with He cooled parametric receiver at 11 cm, confirming PSR 0355 position at 218 cm

13 p1681 A73-28920

An optical parametric generator with a large length of nonlinear interaction and weak feedback

14 p1754 A73-30853

French monograph - Contribution to the study of systems with periodically variable parameters in time, intended for the continuous amplification of signals of weak amplitude.

15 p1847 A73-32588

Optical parametric oscillators.

16 p2023 A73-32857

Optical communication channel optimization with binary signals preamplified in optical parametric amplifier, noting amplifier gain and SNR

17 p2123 A73-35155

A new technique for synthesis of broad-band parametric amplifiers.

18 p2292 A73-36604

Phase fluctuations in a parametric light source operating inside a laser resonator.

22 p2869 A73-42246

Microwave emission mechanism of frequency dependent pulse profile changes in pulsar, using cooled parametric amplifier observations

23 p3034 A73-43963

Complete photon conversion in backward-travelling-wave parametric amplification and oscillation.

23 p2955 A73-44108

Parametric oscillations in an oscillating circuit utilizing negative resistance.

24 p3075 A73-45479

PARAMETRIC DIODES

Performance of multifrequency parametric converter with resonant circuits as function of input and parametric diode characteristics, using gain and noise temperature coefficients

10 p1196 A73-24605

PARAMETRIC FREQUENCY CONVERTERS

Synchronously pulsed high repetition rate IR up converter based on Nd-YAG pump laser and proustite nonlinear crystal, describing experimental arrangement and operation

01 p0044 A73-10133

Microwave varactor upconverter in radio repeater for domestic wideband communication satellite, emphasizing transmission characteristics design

01 p0006 A73-11177

Internal upconversion and doubling of an optical parametric oscillator to extend the tuning range.

03 p0320 A73-14463

Parametric regeneration in Josephson superconducting point contacts for combination frequency signal amplification and conversion in microwave application

05 p0556 A73-16073

Controllable matched filter model for single circuit and twin circuit parametric converters

05 p0558 A73-16786

Laser optical double resonance and efficient infrared quantum counter upconversion in LaCl₃:Pr³⁺ and LaF₃:Pr³⁺/+

09 p1090 A73-21936

Efficient parametric conversion in cesium vapor irradiated by 3470-A mode-locked pulses.

09 p1090 A73-22079

Performance of multifrequency parametric converter with resonant circuits as function of input and parametric diode characteristics, using gain and noise temperature coefficients

10 p1196 A73-24605

Quantum theory of frequency conversion in nonlinear optics

15 p1886 A73-32330

Effect of upper sideband impedance on a lower sideband up-converter.

17 p2123 A73-34971

Quantum theory of nonlinear optical processes with time-dependent pump amplitude and phase - Frequency conversion.

21 p2711 A73-40222

High quantum efficiency IR up-conversion into visible photons through three wave interactions in nonlinear medium, using laser pump light feedback technique

21 p2699 A73-40464

PARAMETRIC OSCILLATORS

U PARAMETRIC AMPLIFIERS

PARAMETRONS

Analysis of parametron oscillation characteristics based on the collector-junction capacitance of the transistor.

10 p1193 A73-23666

Improved analysis of the steady-state operation of a resistive parametron

10 p1189 A73-24381

Parametron circuit current fluctuations analysis via successive approximation solution of nonlinear differential equation, investigating operational mode stability

11 p1400 A73-26452

PARANASAL SINUSES

The frequency of barotraumas as determined by nasal findings and X-rays of the paranasal sinuses

22 p2817 A73-43132

PARAPSYCHOLOGY

U EXTRASENSORY PERCEPTION

PARAWINGS

Parawing-drag chute system operation on wind shear energy to maintain payload flight altitude

11 p1305 A73-25787

PARITY

He odd parity states computed via Hylleraas trial wave function with nonlinear parameters, considering mass-polarization correction and electron transitions

05 p0600 A73-16599

PARKINSON DISEASE

Characteristics of spontaneous oxygen tension variations in human brain structures

14 p1719 A73-30844

PARTIAL DIFFERENTIAL EQUATIONS

NT BIHARMONIC EQUATIONS

NT BURGER EQUATION

NT ELLIPTIC DIFFERENTIAL EQUATIONS

NT FOKKER-PLANCK EQUATION

NT GAUSS EQUATION

NT HELMHOLTZ VORTICITY EQUATION

NT LIOUVILLE EQUATIONS

NT PARABOLIC DIFFERENTIAL EQUATIONS

NT VLASOV EQUATIONS

Numerical solution of nonlinear partial differential and integrodifferential equations; Meeting, Oberwolfach, West Germany, November 28-December 4, 1971, Reports

01 p0069 A73-10066

Automation of solutions to mathematical physics problems described by partial differential equations

01 p0019 A73-10100

The role of interpolation and approximation theory in variational and projectional methods for solving partial differential equations.

01 p0071 A73-11458

Numerical solutions for MHD equations, considering initial values, time independence and mathematical models including hyperbolic, parabolic and elliptic differential equations

01 p0086 A73-11459

Continuous methods based on particular solutions for free boundary problems in partial differential equations, considering heat equation Stefan problem and Laplace equation interface

01 p0071 A73-11462

Conference on the Theory of Ordinary and Partial Differential Equations, Dundee, Scotland, March 28-31, 1972, Proceedings.

02 p0186 A73-11968

Approximation by functions of fewer variables.

02 p0186 A73-11969

On certain parabolic differential equations and an equivalent variational problem.

02 p0186 A73-11972

Elliptic partial differential equations may be related by a change of independent variables

02 p0186 A73-11975

Homogeneous linear partial differential equation for optimal control with boundary condition formed by terminal component, noting weighting functions for linear plant

02 p0149 A73-12116

Solution of an inhomogeneous boundary value problem with continuous discrete parameters in the presence of discrete disturbances

04 p0470 A73-14934

A second-order accurate difference method for systems of hyperbolic partial differential equations.

04 p0470 A73-15007

Partial differential equations with random coefficients and boundary conditions for stochastic processes in plasma, using parabolic equations for distribution function

04 p0479 A73-15037

Stressed state of a planar elliptical, hyperbolic shell

04 p0511 A73-15088

Boundary techniques for the multistep formulation of the optimized Lax-Wendroff method for non-linear hyperbolic systems in two space dimensions.

04 p0471 A73-15227

Optimum Runge-Kutta-Fehlberg methods for second-order differential equations.

04 p0471 A73-15231

Asymptotic waves and Cauchy problem with singular data for a system of linear equations with a double characteristic

04 p0471 A73-15245

Functional analysis approach of the partial differential equation arising from non-linear filtering theory.

04 p0472 A73-15263

Practical techniques for estimating the accuracy of finite-difference solutions to parabolic equations. [ASME PAPER 72-WA/APM-12]

04 p0472 A73-15900

Existence theorems for multidimensional control systems with lower-dimensional controls.

05 p0561 A73-16489

Existence of analytic solutions of partial differential equations with constant coefficients in an arbitrary number of variables

05 p0591 A73-17246

The maximum principle in the identification of distributed-parameter systems

05 p0562 A73-17283

Approximate perturbation solution in Chebyshev polynomials for partial differential equation of heat conduction with cylindrical, spherical or hyperspheric symmetry

06 p0769 A73-18503

The direct and inverse boundary value problems for the heat-conduction equation

06 p0770 A73-18682

Classical solvability of a problem of conjugation of two equations with the third boundary condition

06 p0718 A73-18684

Matrix exponential series approach to distributed parameter systems.

06 p0719 A73-18803

Method of solution of certain boundary value problems for nonlinear hyperbolic equations and propagation of weak shock waves.

07 p0809 A73-19015

Discontinuities propagation in quasi-linear hyperbolic partial differential equation systems, noting MHD flow and crystal optics equations

07 p0850 A73-19016

On parameter identification for distributed systems using Galerkin's criterion. 07 p0804 A73-19130

Automatic optimization of Symbolic Algol programs. I - General principles. 07 p0796 A73-19269

Boundary value problem solution method for hyperbolic partial differential equations based on theory of retarded potentials 07 p0845 A73-20440

The asymptotic behavior of solutions of second order systems of partial differential equations. 07 p0845 A73-20495

An economical approximation for the coefficients in the development of a function with respect to an orthogonal system. 08 p0984 A73-21413

An instability theorem for certain nonlinear hyperbolic equations 08 p0984 A73-21488

Asymptotic scheme for a class of partial differential equations 09 p1112 A73-22477

Steady state Lie group solutions to nonlinear partial differential equations of low temperature plasma ionization instability in strong magnetic field 09 p1127 A73-22591

Remarks on a system of nonlinear equations 09 p1113 A73-22987

Partial differential post-Newtonian equations numerically solved for stellar models with polytropic pressure-density relation for uniform rotation 10 p1271 A73-23490

Periodic method of characteristics for solution of hyperbolic partial differential equations of physical system specified by two boundary conditions at single spatial location 10 p1241 A73-23604

A note on the stability of an iterative finite-difference method for hyperbolic systems. 10 p1241 A73-23639

On the instability of leap-frog and Crank-Nicolson approximations of a nonlinear partial differential equation. 10 p1241 A73-23640

'Farfield' behavior of solutions to partial differential equations asymptotic expansions and maximal rates of decay along a ray. 10 p1241 A73-23700

Optimal filtering for systems described by linear partial differential equations. 10 p1200 A73-24050

Application of the averaging method to the solution of the mixed boundary value problem for a class of nonlinear partial differential equations 10 p1243 A73-24504

Method of Liapunov vector functions in the analysis of complex systems with distributed parameters /Surya/. 11 p1398 A73-25617

Quasi-linear partial differential equations of nonlinear pulse shock wave propagation in two- and three-dimensional steady transonic gas flow near critical point 11 p1302 A73-25854

Variational aspect of the integration of partial differential equations for the oscillations of elastic bodies 12 p1517 A73-27097

Solution in Dirichlet series to a system of linear partial differential equations 12 p1518 A73-27223

The mathematical foundations of the finite element method with applications to partial differential equations; Proceedings of the Symposium, University of Maryland, Baltimore, Md., June 26-30, 1972. 12 p1519 A73-27921

Direct numerical solution of three-dimensional equations containing elliptic operators. 13 p1647 A73-28080

Numerical solution to transient heat flow problems. 13 p1704 A73-28172

Implicit separation of variables /via superposition principle/ and explicit and implicit traveling wave methods of solving nonlinear partial differential equations 13 p1648 A73-28437

Symmetries of differential equations - The hypergeometric and Euler-Darboux equations. 13 p1648 A73-28538

General treatment of the evaluation of tri-diagonal secular determinants. 13 p1700 A73-29379

The numerical solution of parabolic partial differential equations using the method of Lanczos. 13 p1650 A73-29398

Numerical implementation of the Schwarz alternating procedure for elliptic partial differential equations. 14 p1768 A73-29938

Convergence of the net-point method for multidimensional quasi-linear heat-conduction problems 14 p1816 A73-30020

Zero-solution stability in systems of partial differential equations 14 p1768 A73-30248

The global aspect of the complex analysis in the theory of the morphic functions 15 p1900 A73-32106

The non-linear theory of thin elastic sheets. 15 p1954 A73-32118

Singularities of solutions to linear, second order, analytic elliptic equations in two independent variables. II - The piecewise regular boundary. 15 p1901 A73-32374

Initial-value problems in potential theory. 16 p2032 A73-33304

Formulation of stable difference schemes for systems of initial-value partial differential equations. 17 p2200 A73-34284

Overall existence of a solution of the Cauchy problem for the system of equations with Liouville-Newton partial derivatives 17 p2201 A73-35045

An integration algorithm for hyperbolic systems having non-zero, non-analytic steady-state solutions. 17 p2203 A73-35610

On the convergence of two-stage iterative processes for solving linear equations. 17 p2203 A73-35726

A serial CSDT predictor-corrector technique for the hybrid computer solution of partial differential equations. 18 p2291 A73-36425

The effect of nonlinear transformations on the computation of weak solutions. 18 p2330 A73-36610

Finite element and finite difference energy techniques for the numerical solution of partial differential equations. 18 p2330 A73-36827

Numerical methods based on very accurate approximation of partial derivatives. 18 p2330 A73-36828

Membrane statics of parachute-like shells. 19 p2496 A73-37480

The Ritz-Galerkin procedure for parabolic control problems. 19 p2446 A73-38375

Linearization of Cauchy's problem for quadratic semilinear partial differential equations. 20 p2581 A73-38865

Improvable estimates in some non-well-posed problems for a system of elliptic equations. 20 p2581 A73-38975

Series representation of the solution of nonlinear partial differential equations and its use in determining the dynamic characteristics of nonlinear plants with distributed parameters 20 p2581 A73-38986

Application of a truncation method in the derivation of a multiperiodic solution of a denumerable system of partial differential equations 20 p2582 A73-39473

Asymptotic representation of the fundamental solution of an elliptic equation with a small parameter in the presence of a higher derivative 20 p2582 A73-39474

Construction of a transformation matrix and the differentiability of the formal solution of a system of partial differential equations 20 p2582 A73-39475

Initial-value problems for pseudo-parabolic partial differential equations. 21 p2726 A73-40694

Pairs of positive solutions of nonlinear elliptic partial differential equations. 21 p2726 A73-40695

Lower bounds on the cost functional for systems governed by partial differential equations. 21 p2726 A73-40838

A method of treating boundary singularities in time-dependent problems. 21 p2726 A73-40997

Free boundary problem involving elliptic differential equation, discussing iterative method instabilities inhibition of convergence 21 p2727 A73-40998

Integration of a nonlinear partial differential mixed boundary value problem 21 p2792 A73-41065

A method of solving a slightly disturbed mixed problem for a hyperbolic equation with a small delay of the argument 22 p2881 A73-42277

The use of singularity programming in finite-difference and finite-element computations of temperature. [ASME PAPER 73-HT-K] 22 p2930 A73-42287

Higher order accuracy finite difference algorithms for quasi-linear, conservation law hyperbolic systems. 22 p2882 A73-42518

Monograph - Singular perturbation problems for partial differential equations. 22 p2882 A73-42715

Computer analysis of clamped-clamped and clamped-supported cylindrical shells. 22 p2927 A73-42995

Numerical convective schemes based on accurate computation of space derivatives. 24 p3105 A73-45026

MHD partial differential equations solution via hyperbolic system indicating shock wave structure existence satisfying Rankine-Hugoniot relation and entropy condition 24 p3116 A73-45221

Nonlinear difference schemes for linear partial differential equations. 24 p3106 A73-45332

The problem of an iteration method for solving a nonlinear system of partial differential equations given in implicit form with time lag 24 p3106 A73-45507

PARTIAL PRESSURE
 NT HYPOKEMIA
 NT OXYGEN TENSION
 Oxygen partial pressure measurement in respiratory air via radio telemetry system with polarographic catheter electrode pressure sensor 03 p0270 A73-14287

Radio telemetric measurements of oxygen consumption during exercise via respiratory air flow and oxygen partial pressure monitors, considering water vapor and temperature 03 p0270 A73-14288

Inert-gas transport in liquid metals during boiling experiments. 08 p1023 A73-21263

Chlorine trifluoride chemical laser emission, discussing output power dependence on partial pressures and chemical reaction kinetics 13 p1630 A73-29444

PARTICLE ACCELERATION
 Energy balance in the current sheath of a solar flare and the acceleration of cosmic rays by plasma waves 01 p0092 A73-10936

Extensive cosmic ray shower production by relativistic dust grain accelerated in interstellar space by galactic radiation pressure and subsequent magnetic processes 02 p0207 A73-12388

The Fermi mechanism and the source spectrum of cosmic ray nuclei. 03 p0361 A73-13365

The abundances of solar accelerated nuclei from carbon to iron. 03 p0362 A73-13719

Two stage analytical model for mechanism of heavy nuclei acceleration in solar flares, considering ion Fermi acceleration to higher energies 03 p0362 A73-13720

Ion acceleration in a plasma boundary layer formed by two electron groups 03 p0347 A73-13755

Acceleration of auroral particles by electric double layers. 03 p0303 A73-13877

Geomagnetic tail plasma sheet thinning and auroral zone negative bays development during magnetospheric substorms, suggesting auroral particles acceleration along magnetic field lines 03 p0304 A73-13887

The transient highly excited solar flare plasma. 03 p0364 A73-13960

Solar flare development particle acceleration phase model, noting association with white light emission, hard X-rays and PCA 04 p0490 A73-14833

Pulsars and the evolution of supernova remnants. 04 p0501 A73-15686

Electron acceleration in the outer radiation belt 06 p0742 A73-17527

Influence of ionization losses on the conditions of cosmic ray generation on the sun 06 p0742 A73-17530

The generation of the highest cosmic ray energies. 07 p0872 A73-20193

Ion acceleration in the current sheath of a solar flare 07 p0872 A73-20320

Acceleration of charged particles in the region of the neutral line of the magnetic field 08 p0959 A73-21292

Solar cosmic ray heavy nuclei acceleration independence from solar activity phenomena, based on Elektron 4 satellite observation 08 p0999 A73-21332

Emission from a bunch of charged particles in multiple transit through a cylindrical resonant cavity 09 p1061 A73-21885

Plasma effects and the acceleration of charged particles in pulsar fields. 09 p1141 A73-22016

Energy balance in the current sheet of a solar flare, and the acceleration of cosmic rays by plasma waves. 09 p1138 A73-22831

Radio halos around old pulsars - Ghost supernova remnants. 09 p1148 A73-22871

Some characteristics of the motion and acceleration of particles in a linearly inhomogeneous magnetic field with a neutral plane 09 p1132 A73-23080

Electron and proton acceleration in the outer regions of the magnetosphere during polar substorms. 10 p1268 A73-24227

PARTICLE ACCELERATOR TARGETS

Hydrogen and helium isotopes differential energy spectra during solar flare particle acceleration related to nuclear interaction processes

11 p1414 A73-26610

Some effects of magnetospheric acceleration mechanisms on variations in ultraviolet intensity height profiles, and on consequent rocket spectrograph sensitivities.

11 p1358 A73-26703

Observations of narrow microburst trains in the geomagnetic storm of August 4-6, 1972.

12 p1490 A73-27007

Ion acceleration in the current layer of a solar flare.

12 p1534 A73-27292

Studies of plasma production at hypervelocity microparticle impact.

13 p1667 A73-29424

Particle acceleration by a moving laser focus, focusing front or ultrashort laser pulse front.

14 p1757 A73-30338

Ion energy spectra due to acceleration at neutron star surface vs primary cosmic rays

14 p1787 A73-30618

Theory of shot noise depression in a modified diode

14 p1737 A73-30943

Formation of fast electrons in a plasma under the influence of SHF power near harmonics of the electron cyclotron frequency

15 p1920 A73-32309

Electron acceleration in the outer radiation belt.

16 p2051 A73-32752

Effect of ionization losses on cosmic-ray generation conditions on the sun.

16 p2052 A73-32754

A linear accelerator for simulated micrometers.

17 p2145 A73-34274

Interaction of fast particles with magneto-hydrodynamical turbulence.

17 p2216 A73-34504

Influence of transverse magnetic field on Landau damping.

17 p2217 A73-35812

Statistical acceleration of ultrarelativistic electrons by random electromagnetic waves.

19 p2462 A73-37558

Acceleration of charged particles in the region of the neutral line of the magnetic field.

19 p2425 A73-37921

Periodic analysis of arrival times in delayed cosmic-ray coincidences.

19 p2476 A73-38086

Deceleration of electron beams in a plasma with a high level of Langmuir turbulence.

19 p2469 A73-38133

Lunar thermal ionosphere acceleration and detection within lunar electric field for electric potential of moon in solar wind or magnetosheath

20 p2604 A73-38933

Charged particle acceleration in strong dipole fields.

20 p2595 A73-39077

Helios probe design for solar wind acceleration mechanism, magnetic and electric fields, interplanetary dust and cosmic radiation

21 p2780 A73-40449

Possibility of radiative acceleration of the gas in stellar atmospheres

21 p2767 A73-40554

Preferential acceleration of heavy nuclei on the sun

21 p2756 A73-40582

Nonthermal electromagnetic and thermal X ray sources of accelerated electrons during solar flares

21 p2761 A73-41384

Quiet-time solar neutron flux upper limit from OGO-6 neutron detector, evaluating solar cosmic ray acceleration, nuclear reaction and energy region

21 p2763 A73-41498

Ion acceleration upon expansion of a rarefied plasma.

22 p2890 A73-41724

Acceleration of heavy ions by radiation pressure.

22 p2900 A73-41759

Analysis and synthesis of coronal and interplanetary energetic particle, plasma, and magnetic field observations over three solar rotations.

22 p2901 A73-41901

Biological effects due to single accelerated heavy particles and the problems of nervous system exposure in space.

22 p2814 A73-42181

Computer simulation of the acceleration of charged particles captured by plane electromagnetic waves

22 p2826 A73-42378

Auroral electron and proton flux density, energy spectra, acceleration and precipitation mechanisms and turbulent diffusion from rocket and satellite measurements

22 p2850 A73-42748

Solar activity forecasting, considering flare site identification from active center microscopic magnetic components, and particle acceleration observations

23 p3021 A73-43370

A magnetogasdynamic accelerometer for the simulation of micrometeoroids

23 p2966 A73-43781

Ion acceleration by relativistic electron beam extracted from discharge plasma, discussing proton acceleration and beam composition and energy distribution

23 p3014 A73-44339

Production of fast plasma electrons by microwave power at harmonics of the electron cyclotron frequency.

24 p3114 A73-44617

Drift of radiation-belt particles during substorms

24 p3124 A73-44804

Transient ion neutralization by electrons.

24 p3111 A73-45411

Spectrometer design with particle preacceleration for measuring energy spectra of secondary electrons and photoelectrons with high resolution

24 p3092 A73-45553

PARTICLE ACCELERATOR TARGETS

Multiple meson production in 250 GeV nucleon-nucleon collisions in LiH targets, noting 40 per cent formation of heavy meson cluster fireballs

02 p0208 A73-12653

Conical liquid hydrogen target with large exit aperture and multilayer insulation between inner vessel and vacuum jacket for experiments on leptonic decays

05 p0538 A73-17288

Three meter liquid hydrogen target for K meson production with Serpukhov accelerator, discussing design, operation control and emergency conditions

05 p0538 A73-17289

A target design for irradiation of NaI at high beam current.

07 p0853 A73-20469

Reaction Li-6/p, p/t at 590 MeV.

21 p2743 A73-41018

Telecontrol system for particle accelerator target displacement via micromotor electronic control with emphasis on adaptation to ultrahigh vacuum chamber simulating ionospheric plasma

22 p2838 A73-41868

PARTICLE ACCELERATORS

NT BETATRONS

NT ELECTRON ACCELERATORS

NT ION ACCELERATORS

NT LINEAR ACCELERATORS

NT STORAGE RINGS [PARTICLE ACCELERATORS]

Spark calorimeter calibration by particle accelerator induced high energy pions, noting neutral and charged particles track detectors high geometric resolution

02 p0171 A73-12686

A magnetic spectrometer for recording particles in a range up to 4 GeV/c

17 p2164 A73-34151

Low cost beam current integrator for use with dc accelerators in ion implantation experiments

17 p2175 A73-35759

Pion-nucleon interaction structure based on negative pion beam data from Serpukhov accelerator, showing secondary particle energy distribution asymmetry

23 p3021 A73-43537

PARTICLE BEAMS

NT ATOMIC BEAMS

NT ELECTRON BEAMS

NT ION BEAMS

NT MOLECULAR BEAMS

NT NEUTRAL BEAMS

NT NEUTRON BEAMS

NT PION BEAMS

NT PROTON BEAMS

One dimensional periodic slow wave structure interaction with charged particles beam, considering system operation as TWT and backward wave tube

05 p0556 A73-16063

Charged particle beams focusing in combined dual spiral system with uniform magnetic field along axis, applying to imaging of flat object

05 p0556 A73-16067

Nonlinear theory of interaction between restricted relativistic particle beam and plasma, determining field amplitudes and beam radii

06 p0728 A73-17972

Visual display of the spatial distribution of colloidal particle beams.

09 p1136 A73-23448

Free particle gravitating cylindrical model for gravitational kinetic instabilities, calculating natural vibration spectrum and parameters for beam instability development

10 p1253 A73-23714

Relativistic particle beam stability and electromagnetic oscillations in plasma rectangular waveguide under longitudinal magnetic field

10 p1258 A73-24887

On nonlinear transformation and stabilization of beam-plasma instability.

11 p1404 A73-25274

Monoenergetic particle beam instabilities in homogeneous plasma due to secondary emission wave interactions

13 p1664 A73-28289

Effect of radial profile of a charged particle pulse on the electromagnetic wake in a plasma.

14 p1779 A73-29710

Reliability testing of high-perveance three-electrode guns

15 p1851 A73-32215

Free particle gravitating cylindrical model for gravitational kinetic instabilities, calculating natural vibration spectrum and parameters for beam instability development

18 p2340 A73-36739

Methods of corpuscular plasma diagnostics in a pulsed coaxial accelerator

19 p2467 A73-37371

Use of charged particle beams for low temperature plasma measurement in magnetosphere and interplanetary space.

19 p2429 A73-37381

Excitation of electromagnetic waves propagating along a magnetic field in a cold plasma by a beam of phased oscillators

19 p2406 A73-38330

Relativistic particle beam stability and electromagnetic oscillations in plasma rectangular waveguide under longitudinal magnetic field

21 p2749 A73-41662

Monoenergetic particle beam bunching instabilities in homogeneous plasma due to secondary emission wave interactions

22 p2890 A73-41813

Gravitational analogy of electromagnetic Aharonov-Bohm effect, considering massless Dirac equation for weak gravitational fields arising from mass currents moving between particle beams

22 p2887 A73-42434

Theory of parametric resonance in a spatially modulated plasma

23 p3013 A73-44334

PARTICLE CLOUDS

U CLOUDS

PARTICLE COLLISIONS

Integral of collisions for a rarefied plasma /Quantum theory/

01 p0086 A73-11287

Cosmic ray muon component integral multiplicity calculations with allowance for angular distribution of secondary particles in elementary collision event on atmospheric boundary, using computer

02 p0205 A73-12172

Three dimensional jet stream dynamics based on particle population evolution numerical simulation, interpreting solar system evolution

02 p0218 A73-12415

Multiple production processes hydrodynamic-type models validated by high energy particle collision collective interactions

02 p0208 A73-12659

Investigation of the process of the explosive disintegration and simultaneous collision of a gravitating material points

05 p0619 A73-16844

Computerized Monte Carlo simulation with program flexibility for mass distribution in particle collision processes, applying to accreting and fragmenting systems including asteroid belt

05 p0624 A73-17316

Vertical profiles of the effective collision number in the E and F regions of the ionosphere

06 p0689 A73-17552

A general study of the effect of collision parameters on the cosmic-ray fluxes in the atmosphere.

06 p0743 A73-17831

Simulated collisions in collision processes with transitions between atomic levels and free and bound states, noting population density stabilization

06 p0725 A73-17910

Disturbed ionospheric electron and ion kinetics, detailing dissociative recombination as regulating process for temporal evolution

07 p0816 A73-19454

Effects of collisions with neutrals on the dynamic stability of a finitely conducting hydromagnetic composite plasma in the presence of Hall currents.

07 p0858 A73-19600

On the collisional absorption of radio waves in cosmology.

07 p0877 A73-19602

Collision effects on electromagnetic wave propagation in a plasma generated by a moving ionization source

07 p0858 A73-19906

Surface oscillations of a weakly ionized plasma in a magnetic field

09 p1124 A73-21901

Collisional effect on the saturation amplitude of nonlinearly excited plasma waves.

09 p1125 A73-22023

Effects of collisions and gyroviscosity on gravitational instability in a two-component plasma.

09 p1127 A73-22286

Kinetic theory of the spatial instability of a radially bounded plasma-electron beam system with a given radially nonhomogeneous plasma configuration

09 p1129 A73-22688

Symmetry properties of the collision integral and nonisotropic steady-state solutions in the theory of weak turbulence

10 p1207 A73-24759

Singularities and collisions in linear many body problem of Newtonian gravitational systems, noting moment of inertia role
10 p1284 A73-24788

Explosive disintegration and simultaneous collision of a material gravitating points.
11 p1423 A73-26054

Bounds on mean excitation energies-Lamb shift, stopping power, straggling, and grazing collision of high-energy charged particle.
12 p1526 A73-27128

Particle trapping effect on conductivity of toroidal plasma with like-particle collisions taken into account, obtaining results applicable to all aspect ratios
14 p1778 A73-29687

On the absorption of microwave through laboratory plasma.
14 p1782 A73-30800

Theory of the nonlinear power resonances in gas lasers
14 p1758 A73-30803

Surface oscillations of a weakly ionized plasma in a magnetic field.
15 p1921 A73-32626

Vertical profiles of the effective collision frequency in the E- and F-regions of the ionosphere.
16 p2002 A73-32776

Probabilistic radiative transfer - Mean number of scatterings.
16 p2038 A73-33739

Scattering of a nonlocalized exciton on phonons in thin quantized semiconductor films
17 p2218 A73-34118

Effect of particle collisions in a resonance gas medium on the deformation of laser pulses
18 p2322 A73-36677

High-transverse-momentum secondaries and rising total cross sections in cosmic-ray interactions.
19 p2476 A73-38292

Effects of collisions on whistler-mode ray tracing.
20 p2531 A73-39404

Laboratory studies of collisions of energetic H⁺/+ and hydrogen with atmospheric constituents.
21 p2679 A73-40072

Asymptotic electron terms of colliding identical heavy nuclei
21 p2742 A73-40353

Collision integral for a low-density plasma/quantum theory/.
23 p3009 A73-43508

Multiperipherism and Landau hydrodynamic models of multiple particle collision processes with inhomogeneous and homogeneous energy liberation spaces
23 p3008 A73-43543

Thunderstorm electrification by the inductive charging mechanism. I - Particle charges and electric fields. II - Possible effects of updraft on the charge separation process.
23 p3002 A73-43599

Computerized simulation of plasma particle collisions, using electric dipole expansion method for grid charge density and electrostatic force determination with Fourier transformation
24 p3116 A73-45027

Electron-molecule collision frequencies in a crossed electric and magnetic field.
24 p3118 A73-45476

PARTICLE COUNTERS

U RADIATION COUNTERS

PARTICLE DECAY

U RADIOACTIVE DECAY

PARTICLE DENSITY [CONCENTRATION]

NT ELECTRON DENSITY [CONCENTRATION]
NT ELECTRON DENSITY PROFILES
NT ELECTRON DISTRIBUTION
NT ION DENSITY [CONCENTRATION]
NT IONOSPHERIC ELECTRON DENSITY
NT IONOSPHERIC ION DENSITY
NT MAGNETOSPHERIC ELECTRON DENSITY
NT MAGNETOSPHERIC ION DENSITY
NT MAGNETOSPHERIC PROTON DENSITY
NT PLASMA DENSITY
NT PROTON DENSITY [CONCENTRATION]

Hadron number density model to predict fossil quark abundance in big bang cosmology
01 p0104 A73-11098

Measurement of particle size, number density, and velocity using a laser interferometer.
01 p0053 A73-11226

Electric potential and particle concentration of a plasma in the proximity of a projectile moving rapidly toward the plasma
01 p0086 A73-11289

Lunar surface observation with cold cathode ionization gage left by Apollo 14, noting low concentration atmospheric particles and gas clouds
02 p0213 A73-12239

Interplanetary dust particle flux curves, number densities and size distributions from zodiacal light investigations
02 p0215 A73-12262

Rocket photometric observations of dayglow sky radiation in O green line, noting aerosol scattering coefficient and particle concentration.
02 p0161 A73-12277

Extensive air showers vertical distribution at aircraft heights, constructing integral spectrum based on particle number
02 p0209 A73-12674

A short description of the ESRO-IV satellite.
03 p0381 A73-13274

Influence of distributed grit-type roughness on the spectrum of wall pressure fluctuations of turbulent flow in a tube.
03 p0295 A73-14038

An optical system for measurement of mean and fluctuating concentrations in a turbulent air stream.
05 p0576 A73-16437

Solar wind magnetic field and particle concentration disturbances near moon, noting electric field effect on ion motion
05 p0620 A73-17009

Cosmic-ray particle density
06 p0742 A73-17771

Steady-state charged and neutral particle densities in a bounded turbulent high-temperature plasma.
06 p0732 A73-18607

Investigation of the scattered-light-flux magnitude dependence on the drop size in the aerosol photoelectric counter
06 p0691 A73-18734

Three layer atmospheric model for neutral gas motion-produced ionosphere and magnetosphere currents, electromagnetic field and charged particle concentration perturbations
07 p0815 A73-19432

Eruptive, loop shaped prominences and rapid irreversible bursts relation to high energy particle concentrations
10 p1265 A73-23905

Particle kinetic energy vs number density in equilibrium E layer under external and self magnetic fields related to plasma confinement in astron device
11 p1404 A73-25259

Optical properties of single-component zodiacal light models.
11 p1357 A73-25926

A method for calculating the sedimentation characteristics of particles in linear dextrane-density gradients and its application to the separation of red blood cells according to the sedimentation rate
13 p1578 A73-28476

Concentration dependence of the degree of occupancy of a lattice element in cubic titanium oxycarbide
15 p1896 A73-31210

Plasma and fields in the vicinity of a rapidly moving body in the presence of an external magnetic field
15 p1919 A73-31880

Experimental investigation of the plasma focus in erosion-source plasma accelerators. I
15 p1921 A73-32325

Relative efficiencies of filters and impactors for collecting stratospheric particulate matter.
17 p2167 A73-34863

Small hypervelocity particle in-flight detection against background noise using forward scattering from laser illuminated particle distribution
17 p2172 A73-35415

Second phase particle redistribution in dispersion-hardened alloys by directed particle diffusion via chemical potential control
18 p2325 A73-36807

Some characteristics of two-phase nozzle flows
18 p2265 A73-37005

Operative determination of the characteristics of polydisperse systems
18 p2338 A73-37114

Dynamic electron bunching theory applied to moving solid particles and liquid droplets, describing synchronization mechanism for mechanical particles in oscillating gas
20 p2598 A73-39494

Cyclotron resonance in a weakly ionized hydrogen plasma with nitrogen, oxygen and air impurities
22 p2890 A73-41864

Electric potential and particle concentration of a plasma in the vicinity of a rapidly moving charge.
23 p3009 A73-43510

Behavior of excited atoms and molecules in the upper atmosphere at heights from 40 to 300 km
24 p3084 A73-44803

Determination of the parameters of particle density and size distribution functions from measurements of attenuation and backscattering coefficients
24 p3112 A73-45519

Determination of the size distribution function of erythrocytes by the spectral transparency method
24 p3065 A73-45521

PARTICLE DETECTORS

U RADIATION COUNTERS

PARTICLE DIFFUSION

NT ELECTRON DIFFUSION

NT IONIC DIFFUSION

Characteristics of quiet as well as enhanced diurnal anisotropy of cosmic radiation.
03 p0360 A73-12876

Adiabatic propagation of cosmic rays in the Galaxy.
03 p0360 A73-12929

Minority carrier lifetime and diffusion constant as function of impurity concentration in double junction vertical solar cell, determining power efficiency
03 p0254 A73-14213

On the potential difference between two immiscible media.
04 p0483 A73-15106

Diffusion time of charged particles in a plasma with volume ionization.
06 p0726 A73-17417

Neutron diffusion from a distributed source in a homogeneous atmosphere
06 p0742 A73-17549

Physical principles in incompressible fluid and plasma turbulence comparison, noting quasi-linear approximation for nonlinear particle diffusion in turbulent oscillations
06 p0728 A73-17924

Steady-state charged and neutral particle densities in a bounded turbulent high-temperature plasma.
06 p0732 A73-18607

Strong pitch angle diffusion and magnetospheric solar protons.
07 p0869 A73-19229

Transverse particle diffusion across external homogeneous magnetic field under random isotropic large scale hydromagnetic turbulence
07 p0856 A73-19450

Mass variation laws in light of Tsolkovskii hypothesis, considering particle separation rates and thermal energy losses for actual jet engines
08 p1014 A73-21182

Cosmic ray source composition calculated from diffusion-produced path length spreads
08 p0998 A73-21232

Simultaneous diffusion of photons and particles in a semiinfinite space. I - Distribution of excited atoms in a semiinfinite space
09 p1123 A73-23068

Simultaneous diffusion of photons and particles in a semiinfinite space. II - Concentration of excited atoms before a shock wavefront
09 p1123 A73-23069

Boltzmann equation integral form derived tensorial formulation of monoenergetic neutron diffusion theory, evaluating components of diffusion coefficient tensor
11 p1401 A73-25211

A phenomenological study of cosmic ray propagation. I - The nuclei component.
11 p1412 A73-25263

A diffusion model for the electron density distribution along the earth's magnetic field in an F-region plasma cloud.
11 p1354 A73-25768

Investigation of resonance integrals occurring in cosmic-ray diffusion theory.
11 p1414 A73-26615

Theory of cosmic ray transfer by anisotropically scattered particles
12 p1534 A73-27331

Selection of a propagation model for computing the solar-proton injection spectrum
12 p1534 A73-27333

Similarity theory of diffusion and the observed vertical spread in the diabatic surface layer.
13 p1655 A73-29339

Particle diffusion rate due to poloidal magnetic field component in low beta symmetric toroidal plasma, discussing losses induced by electrostatic field fluctuations
14 p1778 A73-29693

Calculation of the flow of a two-phase mixture in a Laval nozzle with allowance for turbulent diffusion of particles
15 p1822 A73-31300

Neutron diffusion from a distributed source in an inhomogeneous atmosphere.
16 p2052 A73-32773

Second phase particle redistribution in dispersion-hardened alloys by directed particle diffusion via chemical potential control
18 p2325 A73-36807

Kinetic equation for one particle cosmic ray distribution function in static random magnetic field on basis of diffusion theory
19 p2476 A73-38291

Bilinear hydrodynamics and the Stokes-Einstein law.
21 p2676 A73-40218

Trapped-particle scattering by electrostatic turbulence in toroidal plasmas.
21 p2749 A73-41675

A nonstationary model of charged-particle diffusion in a gravitational field
22 p2902 A73-41955

The parallel diffusion of cosmic rays in a random magnetic field.
22 p2904 A73-43011

On Kraichnan's direct interaction approximation applied to charged-particle transport in turbulent magnetic fields.
22 p2904 A73-43013

PARTICLE EMISSION

- Contribution to the theory of cosmic-ray propagation with anisotropic particle scattering.
23 p3020 A73-43229
- Selection of a propagation model for calculating the injection spectrum of solar protons.
23 p3020 A73-43231
- Atomic diffusion mechanisms in multiphase and multicomponent alloys covering relaxation, crystal lattice atom exchange and motion along dislocation lines and to neighboring vacancies
23 p2989 A73-43439
- A computational study of the diffusion of meteor trains using a self-consistent model for the space-charge electric field.
23 p3029 A73-43684
- Physical principles in incompressible fluid and plasma turbulence comparison, noting quasi-linear approximation for nonlinear particle diffusion in turbulent oscillations
23 p3013 A73-44326
- Investigation of neoclassical diffusion in toroidal systems with a three-dimensional magnetic axis
23 p3014 A73-44337
- Diffusion of ring current particles by low-frequency long-wavelength electrostatic oscillations.
24 p3126 A73-45128
- Magnetically trapped charged particle pitch angle diffusion and lifetime calculation for radiation belts, taking into account geomagnetic dipole geometry
24 p3127 A73-45138

PARTICLE EMISSION

- NT ELECTRON EMISSION
NT FIELD EMISSION
NT ION EMISSION
NT NEUTRON EMISSION
NT PHOTOELECTRIC EMISSION
NT SECONDARY EMISSION
NT THERMIONIC EMISSION
- Energy and mass analysis of neutral particles emitted from a toroidal theta-pinch plasma.
01 p0084 A73-10466
- On the mechanism of particle emission from graphite during pulsed laser heating.
01 p0068 A73-10923
- Book - Engine emissions: Pollutant formation and measurement.
19 p2474 A73-38321
- Solar structure and evolution, calculating neutrino emission for Pleistocene glacial age caused by solar luminosity reduction
21 p2764 A73-41613

PARTICLE ENERGY

- NT ELECTRON ENERGY
NT ELECTRON STATES
NT PROTON ENERGY
- A search for the quark in extensive air showers, using a counter-controlled cloud chamber.
01 p0093 A73-11249
- Corpuscular radiation as an upper atmospheric energy source.
02 p0205 A73-12289
- High-latitude precipitation of low-energy particles as observed by ESRO I A.
02 p0206 A73-12312
- Study of energy spectra of primary cosmic rays at very high energies on the proton series of satellites.
02 p0207 A73-12328
- Inelasticity factor dependence on particle energy spectra to explain nucleon flux calculations and Proton satellite data, considering scattering cross sections
02 p0208 A73-12658
- A measurement of the atmospheric neutron flux in the energy range 50 less than E less than 350 MeV.
03 p0298 A73-12886
- Auroral and magnetospheric phenomena caused by solar wind particles entry and energization via magnetosheath into magnetosphere and upper atmosphere
04 p0492 A73-15331
- Investigations of high-energy charged particles and VLF radiation with the Interkosmos 3 satellite.
05 p0608 A73-16085
- High energy primary cosmic ray particles total energy and mass spectra measurement
05 p0609 A73-16370
- Influence of ionization losses on the conditions of cosmic ray generation on the sun
06 p0742 A73-17530
- Barometric coefficients of the nucleon components of cosmic rays of various energies
06 p0742 A73-17550
- Activities in space research at the Max-Planck-Institut fuer extraterrestrische Physik, Garching bei Muenchen (G.F.R.).
07 p0868 A73-19173
- Evidence for differences in the energy spectra of cosmic ray nuclei.
07 p0873 A73-20562
- Energy dependence of primary cosmic ray nuclei abundance ratios.
07 p0873 A73-20564
- Heating of the upper atmosphere during aurorae and auroral rays length.
08 p0957 A73-20663

- Ionization loss effects on cosmic ray lifetime in galactic interstellar medium, noting dependence on particle energy
08 p0999 A73-21335
- A possible cosmic ray primary particle energy spectrum above 10 TeV and its astrophysical implications.
08 p1000 A73-21824
- Data processing technique and calculation procedure for cosmic rays hard particle and neutron components coupling coefficients
10 p1268 A73-23932
- Auroral oval spectral features as basis for particle precipitation and energy deposition determination
10 p1215 A73-24782
- Particle kinetic energy vs number density in equilibrium E layer under external and self magnetic fields related to plasma confinement in astron device
11 p1404 A73-25259
- Additional evidence for the existence of a very high energy solar particle component.
11 p1413 A73-26473
- Intermediate energy nucleon-deuteron scattering theory.
14 p1776 A73-29766
- Ultrahigh energy photons, electrons, and neutrinos, the microwave background, and the universal cosmic-ray hypothesis.
15 p1927 A73-32004
- Effect of ionization losses on cosmic-ray generation conditions on the sun.
16 p2052 A73-32754
- Barometric coefficients of the nucleon component of cosmic rays of different energies.
16 p2052 A73-32774
- The theory of charged particle temperatures in the upper atmosphere.
17 p2224 A73-35593
- Normal Doppler shifted cyclotron radiation from a cold plasma.
18 p2338 A73-36189
- Thermodynamic heat concept, discussing kinetic and potential particle energy, internal energy, heat absorption and release and thermal energy
20 p2627 A73-39293
- Interaction of fast particles with waves in cosmic magnetoactive plasma.
21 p2748 A73-41248
- High energy cosmic rays and elementary particles, discussing detection, sources, nature and properties
21 p2764 A73-41611
- The spectral comparison method for temperature measurement in two-phase flames.
22 p2853 A73-41987
- German monograph - The back-scattering method as a procedure for the determination of the radiation damage profile in silicon doped by ion implantation.
22 p2897 A73-42852
- Interkosmos 6 cosmic ray shower experiment using emulsion stack, spark chamber and scintillation counter to measure particle energy, angular distribution and production multiplicity
23 p2981 A73-43540
- Multiperipherism and Landau hydrodynamic models of multiple particle collision processes with inhomogeneous and homogeneous energy liberation spaces
23 p3008 A73-43543
- Large transverse momenta and the structure of extensive air shower cores
23 p3022 A73-43548
- Fluctuations of the total path of charged particles in electron-photon showers caused by gamma-quanta with energies of 40, 60 and 200 m/c-squared/
23 p3023 A73-43555
- Experimental characteristics of a muon stream with energies above 10 GeV, contained in an extensive air shower
23 p3023 A73-43561
- Spark calorimetry investigation of trident and extensive air showers muon component generated high energy penetrating particles at large zenith angles
23 p3024 A73-43565
- A new method of analysing the stability of nonlinear dynamic systems.
23 p3006 A73-44084

PARTICLE FLUX

- U FLUX [RATE]
PARTICLE FLUX DENSITY
- NT ELECTRON FLUX DENSITY
NT NEUTRON FLUX DENSITY
NT PROTON FLUX DENSITY
- Effect of a neutrino-photon interaction on the solar-neutrino flux.
02 p0205 A73-12165
- Micrometeoroid particle flux impacting on lunar surface measured by observation of Surveyor 3 glass surfaces craters
02 p0214 A73-12256
- Measurements of the isotopic composition of particle fluxes carried out on spacecrafts Soyuz, Zond 8 and Luna 16.
02 p0206 A73-12317
- Inelasticity factor dependence on particle energy spectra to explain nucleon flux calculations and

Proton satellite data, considering scattering cross sections
02 p0208 A73-12658

- Electron and muon density fluctuations, trajectory distribution and azimuthal symmetry in cosmic ray air showers
02 p0209 A73-12673
- Muon densities in penetrating high energy particles, comparing with extensive air showers
02 p0210 A73-12683
- Electron photon shower particle flux transition effect on ionization chamber and scintillation counter readings
02 p0210 A73-12685
- Studies of the chemical composition of cosmic rays with Z = 3-30 at high and low energies.
02 p0210 A73-12737
- Auroral flux enhancements due to solar proton injection at medium energies during flares from ESRO 2 satellite measurements
03 p0362 A73-13859
- Preferential particle arrival at polar caps during solar events, noting north pole flux increase from ESRO 1 measurements
03 p0362 A73-13861
- Observation of solar particle fluxes over extended solar longitudes.
03 p0365 A73-14421
- Magnetospheric plasma instabilities and detectable manifestations in geomagnetic field and particle flux densities variations, considering magnetospheric substorms and auroral breakup
04 p0442 A73-15340
- Analysis of the isotopic composition of low-energy cosmic ray particles in plastic detectors, taking into account the elements boron, carbon, nitrogen, and oxygen
05 p0611 A73-17275
- Pulsed galactic nuclei and the origin of cosmic rays.
05 p0611 A73-17308
- The heliocentric radial gradient in cosmic ray density and the 'Swinson' sidereal time variation.
07 p0870 A73-19671
- Auroral particle influx behavior and electric field aligned electron precipitation observation by Ba release and electrostatic probe in rocket and satellite experiments
08 p0957 A73-20662
- Primary cosmic rays alpha particles and protons energy spectra similarity and intensity difference at .05 to 1.6 TeV, using Proton satellites data
08 p0999 A73-21331
- Probabilistic integral multiplicity of generation of primary cosmic ray particles from count rate and primary spectrum relationship, using definition for neutron component calculations
08 p1000 A73-21352
- Particle and energy fluxes across magnetic field in axisymmetric toroidal magnetic traps and plasmas with weak collisions, calculating radial electric field
08 p0993 A73-21695
- Electrometric amplifiers for inductive measurement of charges
08 p0949 A73-21713
- Solar neutrino flux prediction discrepancies with observation, considering cosmic ray background and flaws in calculation of capture rate
09 p1136 A73-21995
- Ionospheric and plasma sheet particle densities, fluxes and bulk velocities along auroral magnetic field line for collisionless ion-exosphere model
09 p1079 A73-22842
- Isotopic and crystalline structure changes in lunar rock and meteorite constituents for cosmic ray nuclei intensity and energy spectrum
09 p1138 A73-23169
- On-board registration and redundancy reduction method for quasi-stationary Poisson processes.
09 p1058 A73-23420
- Direct measurements of solar-wind fluctuations between 0.0048 and 13.3 Hz.
10 p1264 A73-23539
- Esro 4 performance of abandoned TD-2 experiments for particle measurements over polar regions, describing satellite construction, thermal control, power supply, attitude control and measurement
10 p1285 A73-23748
- Certain data concerning heavy primary nuclei /Z above 33/ obtained outside the earth's magnetosphere
10 p1266 A73-23915
- Investigation of charged-particle fluxes at altitudes of 200 to 300 km with the aid of the Saliut orbital station
10 p1267 A73-23930
- Possibility of estimating the flux of energetic particles in the ionospheric D-region at sunrise and during the daytime.
10 p1212 A73-24219
- Auroral oval spectral features as basis for particle precipitation and energy deposition determination
10 p1215 A73-24782
- Auroral He precipitation flux and charge state measurements for auroral ions source location by com-

parison with ionospheric and solar wind ion abundances

10 p1215 A73-24783

Alpha particles in solar cosmic rays over the last 80,000 years.

11 p1412 A73-25375

Particle injection in the Cygnus X-3 radio outburst.

11 p1419 A73-25859

Charge states and energy-dependent composition of solar-flare particles.

11 p1413 A73-26207

The structure of the Eta Aquarid meteor stream.

11 p1426 A73-26573

A rigorous cosmic-ray transport equation with no restrictions on particle energy.

11 p1414 A73-26609

Measurement of geomagnetic cutoff rigidities and particle fluxes below geomagnetic cutoff near Palestine, Texas.

12 p1533 A73-26978

Distributions and characteristics of high-latitude field-aligned electron precipitation.

12 p1534 A73-26988

Amplitude analysis of extensive air shower particle fluxes

12 p1496 A73-27202

Electrostatic toroidal analyzer for studying charged particle fluxes in outer space

12 p1496 A73-27203

Rocket measurements of particle flux during the April 1969 solar cosmic ray event.

12 p1535 A73-27651

Low momentum integral muon spectrum at sea level near the geomagnetic equator.

13 p1670 A73-28211

Distribution of flux of charge-exchange atoms from a plasma over the cross section of the plasma filament in the Tokamak-4 apparatus.

13 p1664 A73-28611

Intercomos 5 investigation of VLF electromagnetic signals and emissions, discussing onboard instruments to measure particle fluxes

13 p1622 A73-29662

Solar cosmic-ray burst of July 7, 1966 and its measurement by Proton-3 satellite.

15 p1927 A73-32611

Continuum analysis of the photoionization chamber in the transition from low to high rates of ionization.

16 p2015 A73-33321

Solar flare cosmic rays at and beyond the modulation boundary.

16 p2056 A73-33458

Cosmic antiproton production in interstellar pp collisions.

17 p2223 A73-34099

Some characteristics of charged particle flux studies using traps and analyzers. II - Modulation trap utilization for investigating the solar wind

18 p2345 A73-36113

Solar cosmic ray alpha particles and protons flux measurement after events in 1967-1969 for 1-10 MeV particles

18 p2347 A73-36289

Initial observations of geomagnetically trapped alpha particles at the equator.

20 p2552 A73-38950

Solar neutrines. IV - Effect of radiative opacities on calculated neutrino fluxes.

20 p2602 A73-39427

A survey on the recent measurements of the absolute vertical cosmic-ray muon flux at sea level.

20 p2603 A73-39825

Observational comparison with a self-consistent model of the geomagnetic tail.

21 p2691 A73-41377

Investigations of meteoritic matter in the vicinity of the earth and the moon from the orbiting station Salyut and the moon satellite Luna 19.

21 p2775 A73-41409

Near-earth micrometeorite flux measurement by rocket-borne acoustic detectors, noting consistency with previous observations

21 p2775 A73-41415

Solar neutrino fluxes on earth from solar model and analytical approach, discussing neutrino capture rate contributions

21 p2764 A73-41539

Investigation of the intensity distribution in a molecular beam expelled from a conical ring source

22 p2889 A73-42387

Auroral electron and proton flux density, energy spectra, acceleration and precipitation mechanisms and turbulent diffusion from rocket and satellite measurements

22 p2850 A73-42748

Micrometeoroid flux measurement during the 1970 Geminid meteor shower.

22 p2915 A73-43035

Particle number fluctuations and transient effects in electron-photon showers in lead at energies above 20 GeV

23 p3021 A73-43531

Intense air showers with an electron-photon core of complex structure

23 p3022 A73-43545

The assembly edge effect and the spatial distribution of extensive air shower particles in an assembly with widely spaced detectors

23 p3022 A73-43547

Extensive air showers and nuclear interaction characteristics at superhigh energies

23 p3022 A73-43551

Fluctuations of the total path of charged particles in electron-photon showers caused by gamma-quanta with energies of 40, 60 and 200 m/c-squared/

23 p3023 A73-43555

Intensity variations of electron-photon shower particles in the atmosphere

23 p3023 A73-43557

Experimental characteristics of a muon stream with energies above 10 GeV, contained in an extensive air shower

23 p3023 A73-43561

Some characteristics of the muon component of extensive air showers at mountain level

23 p3023 A73-43562

Muon decay/transmission ratios at 60 and 850 mwc measured by scintillation counter

23 p3023 A73-43563

Energy spectrum and angular distribution of outer space muons and the processes of their production in the 1 TeV energy range

23 p3024 A73-43564

Observation of cosmic-ray particles with Z of 50 or greater and interpretation of the charge spectrum.

23 p3024 A73-43610

Higher order Compton-Getting anisotropies in particle population distribution function of low energy solar protons in interplanetary space

23 p3024 A73-43698

Observations of water vapor ions at the lunar surface.

23 p3031 A73-43764

Meteoroids impact rate on lunar and earth surfaces for given geocentric and selenocentric velocity distributions, taking into account gravitational effects

24 p3131 A73-44461

Physical characteristics of the set of scientific devices used to record the cosmic-ray ionizing component on "Prognoz" satellites

24 p3089 A73-44784

ESRO I/Aurora/satellite observations of aurora, magnetosphere-ionosphere interaction at high latitudes and auroral particle flux density

24 p3087 A73-45207

PARTICLE IN CELL TECHNIQUE

Large particle method for calculation of transonic supercritical vortex flow fields around flat and axisymmetric bodies

11 p1302 A73-26330

Nonlinear development and Fourier analysis of the whistler mode instability.

22 p2893 A73-42391

PARTICLE INTENSITY

Galactic cosmic ray particle intensity decrease relationship to low energy proton flux increase based on interplanetary Zond 3 and Venera probes measurements

08 p0999 A73-21326

PARTICLE INTERACTIONS

NT ELECTRON CAPTURE
NT ELEMENTARY PARTICLE INTERACTIONS

NT ION ATOM INTERACTIONS
NT MOLECULAR COLLISIONS
NT MOLECULAR INTERACTIONS
NT NUCLEAR CAPTURE
NT NUCLEAR INTERACTIONS
NT SPIN-ORBIT INTERACTIONS

Cool giant star-ejected high velocity dust grains interaction with interstellar clouds, discussing solid state defect accumulation, sputtering and grain and cloud heating

01 p0098 A73-10582

Effect of a neutrino-photon interaction on the solar-neutrino flux.

02 p0205 A73-12165

Raman scattering by phonons and magnons and phonon-magnon interactions in NiO.

02 p0201 A73-12640

Cosmic ray particle high energy inelastic interactions, discussing pion and nucleon interaction angular and energy characteristics and muon production mechanism

02 p0209 A73-12664

Nuclear photoemulsions under bombardment by pion beam of 60 GeV/c momentum, investigating pion-nucleon interactions involving recoil protons

02 p0195 A73-12667

Pion-nucleon high energy interactions, determining inelasticity coefficient distribution

02 p0195 A73-12668

Amplification of signal by Cerenkov resonance interaction.

04 p0415 A73-14958

International conference of the CNRS on the physics of very high frequency phonons, Sainte-Maxime, Var, France, June 27-30, 1972, Proceedings

04 p0483 A73-15464

Interaction of stars with local dust formations.

04 p0503 A73-16008

Chemical kinetics equations of lower ionosphere and D region particle interactions for aeronomic problems

05 p0569 A73-16396

Geomagnetic micropulsations within magnetosphere, investigating MHD waves and particle-wave interactions

05 p0570 A73-17051

Cosmic-ray evolution due to interactions with self-excited plasma waves.

05 p0612 A73-17385

Exciton-phonon interaction in recrystallized CdTe layers

06 p0737 A73-18219

Relative motion integrals of interacting identical mass particles in terms of Hamiltonian function and momentum relation

06 p0725 A73-18887

Rocket rectilinear motion, comparing Meshcherskii and Gantmacher-Levin equations in light of contact interaction hypothesis

08 p1014 A73-21181

Description of hydrodynamics in the theory of gravitation on the basis of covariant statistical equations

08 p0989 A73-21522

Solution to a time-dependent Schroedinger equation in the case of a specific potential

09 p1122 A73-22021

Inelastic collision of fast charged particles with arbitrary levelled hydrogen-like atoms.

10 p1250 A73-23575

Intermolecular potential energy curve crossing probabilities and associated phases determination for low energy elastic scattering cross section of He cations by Ne, noting rainbow effect

10 p1250 A73-23670

Determination of the characteristics of light-scattering particles in the atmosphere of Venus from photometric measurements.

12 p1543 A73-27640

Emulsion and suspension effective viscosity dependence on dispersed phase volume concentration and particle interactions in two phase flows

13 p1580 A73-28465

A Hamiltonian theory for weakly interacting vortices.

13 p1609 A73-28917

Equation of state of matter at supernuclear densities deduced from particle interactions nature and effective baryon mass spectrum

14 p1777 A73-30739

Third-order treatment of combined effects of space charge and external fields on cylindrical ion and electron beams.

15 p1915 A73-31933

Klein-Gordon equation for a charged particle interacting with an electromagnetic wave.

16 p1979 A73-33164

Superfluidity of the Fermi component in a Fermi-Bose gas and in He3-He4 solutions

16 p2038 A73-34067

Equilibrium properties of a one-dimensional kinetic system.

19 p2463 A73-37899

Charged particle acceleration in strong dipole fields.

20 p2595 A73-39077

Fredholm-uniformization computation of elastic scattering amplitudes in the presence of arbitrarily many open channels.

21 p2738 A73-40212

Book on cosmic ray effective cut-off rigidities calculations in dipole and geomagnetic fields, using trajectory calculations of penumbra function

21 p2760 A73-40805

Interaction of fast particles with waves in cosmic magnetoactive plasma.

21 p2748 A73-41248

Solar wind interaction with Comet Bennett near earth, examining photographs for momentum flux change-ion tail kink correlations

21 p2763 A73-41501

Carbon particles size distribution and charged fraction in acetylene-oxygen flame using molecular beam system and electron microscopy, noting particle interaction formation mechanism

22 p2936 A73-42801

Dipole-quadrupole dispersion coefficient calculation for interactions of atomic pairs formed from hydrogen, alkali and rare gas atoms, using perturbation and variation methods

23 p3007 A73-43522

Forces acting upon an asteroid moving through a meteoroid stream.

23 p3029 A73-43745

Accretion and electrostatic interaction of interstellar dust grains - Interstellar grit.

23 p3030 A73-43757

One-component two dimensional plasma, calculating equilibrium pair correlation function by Debye approximation for particle interaction via Coulomb potential

23 p3013 A73-44172

Production of gamma radiation in dense interstellar clouds by cosmic-ray interactions.

24 p3125 A73-45054

PARTICLE MASS

PARTICLE MASS

He odd parity states computed via Hylleraas trial wave function with nonlinear parameters, considering mass-polarization correction and electron transitions
05 p0600 A73-16599

Magnetic spheroid mass determination with microbalance and internal cavity observation by X ray photography, noting meteor showers as extraterrestrial source
05 p0621 A73-17055

Modified negative mass mode stabilization in finite magnetic mirror confined plasmas with highly anisotropic velocity distribution, considering bounce harmonic effects and gyrofrequency
07 p0856 A73-19522

Nonzero neutrino rest mass to account for virial mass discrepancy in Coma cluster and missing cosmological mass needed to close universe
09 p1141 A73-22027

A four-component hypermass equation possibly applying to unstable neutrinos.
10 p1251 A73-23754

Photon rest mass limit determination from Galactic magnetic field measurements, utilizing maximum current density capability of plasmas
11 p1415 A73-25121

A photon rest mass and the propagation of longitudinal electric waves in interstellar and intergalactic space.
11 p1417 A73-25562

Quasar red shift mechanism based on atomic energy levels and particle rest masses variations in scalar gravitational field
15 p1929 A73-31062

Evidence for the possible existence of a charged particle with large mass.
16 p2016 A73-33700

Relativistic baryon effective masses and thresholds for strongly interacting superdense matter.
21 p2766 A73-40318

Solar atmosphere origin for submicrometer cosmic dust in ionosphere and noctilucent clouds, noting anomalously high atomic weight
21 p2775 A73-41416

General relativistic time analysis leading to scalar Hamiltonian formalism for particle mass based on Riemannian metric, considering Hamilton-Jacobi equation in particle dynamics
22 p2888 A73-43048

PARTICLE MOTION

Dispersion relation for Cerenkov radiation of moving test particles in a magnetoplasma.
01 p0083 A73-10453

Universal dimensionless formulas for physical property and trajectory computation in cosmic spherical media, applying to Kepler orbits, particle motions and radio wave paths
01 p0103 A73-11019

Transition radiation from a plasma boundary.
01 p0085 A73-11063

Electric potential and particle concentration of a plasma in the proximity of a projectile moving rapidly toward the plasma
01 p0086 A73-11289

Particle motions in coronal streamers and type III radio bursts.
01 p0093 A73-11393

Calculation of the energy and force process parameters in magnetic-pulse forming of complex shaped elements
02 p0172 A73-11646

Consistency of fields and particle motion in the 'speiser' model of the current sheet.
02 p0157 A73-11901

Cherenkov and transient radiation of uniformly moving charge in random inhomogeneous medium.
02 p0193 A73-12381

Radar measurement of ionosphere motion in the presence of current-induced spectral asymmetries.
02 p0143 A73-12532

Field dynamics equilibrium equation for particle rotational motion in gravitational field of central body, noting energy spectra of stationary orbits
03 p0374 A73-13751

Particle motion and electrostatic instabilities of geomagnetic tail and magnetopause plasma neutral sheets in relation to substorms, using Alfvén and Cowley models
03 p0302 A73-13873

The effect of an electric field induced by a time-dependent ring current on the particle drift motion.
04 p0440 A73-14954

Concerning the accuracy of conservation of the third adiabatic invariant of the motion of a charged particle in axisymmetric fields. I.
05 p0600 A73-16082

Drag coefficient for particles in rarefied, low Mach-number flows.
05 p0564 A73-16354

Gravitational field effects on processes near stars and galaxies in late evolution phases, describing particle motion and light propagation near rotating sources
05 p0623 A73-17197

Radiation belt buildup from particles moving in magnetic field applied to terrestrial inner belt characteristics, considering extraterrestrial belts
06 p0741 A73-17503

Order c-square bulk stress derivation for force-free spherical particles suspension in Newtonian ambient fluid with uniform viscosity, noting error bounds
06 p0722 A73-17701

Time /T-field/ solutions to Einstein equations of test particles and light rays in nonstatic spherically symmetric gravitational field
06 p0724 A73-18646

Relative motion integrals of interacting identical mass particles in terms of Hamiltonian function and momentum relation
06 p0725 A73-18887

Auroral electron spectrum space-time dynamics during magnetospheric substorms, using X ray bremsstrahlung balloon data
07 p0815 A73-19437

The behaviour of ULF waves and particles in the magnetosphere.
07 p0792 A73-19666

The Iarkovskii-Radzievskii effect and the evolution of condensations in a meteor stream
08 p1007 A73-21066

Influence of radiation damping on the motion of a charge in a uniform magnetic field and in the field of a plane electromagnetic wave
08 p0989 A73-21516

Multiphase flow past thin symmetrical airfoil, applying three velocity model with incident two phase and reflected particle flow components
09 p1027 A73-21993

Diffusion of charged particles in a random magnetic field.
09 p1137 A73-22035

Nonadiabatic particle motion in the magnetosphere.
09 p1073 A73-22052

Effect of the plasma inhomogeneity on the nonlinear damping of monochromatic waves.
09 p1126 A73-22281

A classification of particle motions in the equatorial plane of a gravitational monopole-quadrupole field in Newtonian mechanics and general relativity.
09 p1148 A73-22910

Application of lateral illumination in holography of small objects
09 p1085 A73-23015

Synchrotron emission, adiabatic invariant, and gradient drift of particles in a linearly inhomogeneous magnetic field
09 p1132 A73-23079

Some characteristics of the motion and acceleration of particles in a linearly inhomogeneous magnetic field with a neutral plane
09 p1132 A73-23080

Nonlinear theory of a relativistic monotron
09 p1065 A73-23086

The motion of dust and gas in the heads of comets with type II tails.
10 p1271 A73-23494

Particle scattering in interplanetary space and the properties of solar corpuscular streams
10 p1265 A73-23902

Theory of cosmic ray transport with anisotropic particle scattering and convection
10 p1265 A73-23903

Particle motion diffusion model for cosmic ray propagation in Galaxy, investigating electron component energy spectra and background radio emission
10 p1265 A73-23908

Numerical simulation of small amplitude whistler waves in thermal plasma, describing particle motion under self consistent and external magnet fields via Lorentz equation
10 p1255 A73-24269

Relative motion of near orbiting satellites.
10 p1283 A73-24662

Initial conditioned solutions of a second-order nonlinear conservative differential equation with a periodically varying coefficient.
10 p1244 A73-24706

Radiative losses in a magnetostatic and intense electromagnetic field.
10 p1270 A73-24908

Sidereal periods in a gravitational field characterized by Schwarzschild's internal solution
11 p1416 A73-25237

Motion of fast particles in a spherically-symmetric gravitational field
11 p1416 A73-25239

Changes in the mean energy of an electron in the field of a plane wave with allowance for radiation damping
12 p1526 A73-26969

Magnetic field line velocity associated with Euler potentials set, considering flux preservation properties of particle motion
12 p1489 A73-27000

The frequency dispersion of the transverse electrical conductivity of ionospheric plasma
12 p1491 A73-27357

Accuracy of conserving the third adiabatic invariant of the motion of a charged particle in axially symmetrical fields. II.
12 p1535 A73-27634

Polydynamic equilibrium equation for steady particle motion along stationary orbits in central body attraction field, comparing with Schroedinger wave equation
13 p1657 A73-28001

Fundamental equations of a mixture of gas and small spherical solid particles from simple kinetic theory.
13 p1600 A73-28616

Holographic recording of three-dimensional ensembles of rapidly moving particles
13 p1616 A73-28767

Aerosol particle downward motion in vertical electric field, discussing stability of major axis orientation of ellipsoid of revolution
13 p1654 A73-28881

The stochastic and deterministic aspects of the 'classical' approach to problems of quantum mechanics.
13 p1661 A73-29388

Correlation between the potential and density fluctuations of a plasma, and the convective transport of particles across the magnetic field in a Penning discharge in the presence of rotational instability
14 p1781 A73-30581

German book on physical foundations of electronics covering charged particle motions in electric and magnetic fields, relativistic effects, electron and ion optics, etc
14 p1736 A73-30597

On the transport of charged particles in turbulent fields - Comparison of an exact solution with the quasilinear approximation.
15 p1916 A73-31083

Homographic motions of Newtonian point mass system interacting through two body forces, considering relativistic interactions
15 p1930 A73-31110

Insensitivity of single particle time domain measurements to laser velocimeter 'Doppler ambiguity.'
15 p1875 A73-31671

Theory of transient radiation in a waveguide with a piecewise-homogeneous dielectric filler
16 p1978 A73-32898

Reflected light holographic microscopy of moving objects.
16 p2014 A73-33174

Analysis of nonequilibrium particulate flow.
[AIAA PAPER 73-687] 18 p2298 A73-36238

Permittivity of a plasma with transverse nonazimuthal fluxes
18 p2339 A73-36552

Yarkovskii-Radzievskii effect and the evolution of meteor swarms.
18 p2355 A73-36867

Medium-velocity and electric-current concepts in restricted relativity
19 p2459 A73-37535

Smoothed distribution function of equilibrium states and probability of particle occurrence in thermodynamic systems, using Liouville equation
20 p2627 A73-39294

Dynamic electron bunching theory applied to moving solid particles and liquid droplets, describing synchronization mechanism for mechanical particles in oscillating gas
20 p2598 A73-39494

Measurement of change in a cross section and position of small particles by diffraction techniques.
21 p2695 A73-39959

Holographic investigations and measurements in a cloud of moving microparticles
21 p2696 A73-39979

The slow unsteady settling of two fluid spheres along their line of centres.
22 p2840 A73-41742

Application of transverse reference beams in holographic investigations of small particles.
22 p2860 A73-42253

Particle streams along the force lines of a magnetic field in a multicomponent ionospheric plasma in the presence of longitudinal currents
22 p2892 A73-42329

Containment stability of charged particles captured by a plane electromagnetic wave propagating at a slowly varying velocity
22 p2826 A73-42377

Shielding of moving test particles in warm, isotropic plasma.
22 p2893 A73-42392

Transition probability matrix method for calculating residence times of moving particles in region of space, determining stratosphere residence time against exit to tropopause
22 p2849 A73-42543

On the theoretical possibility of the libration cloud.
22 p2911 A73-42936

Polarizable particle entrainment in electromagnetic field consisting of wave packets propagating in opposite directions
22 p2889 A73-43099

Frequency dispersion of transverse electrical conductivity of ionospheric plasma.

23 p2971 A73-43256

Electric potential and particle concentration of a plasma in the vicinity of a rapidly moving charge.

23 p3009 A73-43510

Role of constraining forces for ultrarelativistic particle motion as a source of gravitational radiation.

23 p3006 A73-43606

Single particle approximation analysis of particle velocity changes influence on plasma motion across nonhomogeneous magnetic field, examining energy exchange between particles

23 p3010 A73-43662

Relaxation of longitudinal and transverse temperatures in a plasma with directional motion of electrons

23 p3014 A73-44336

Physical particle description of moderately dense gases. II - Equilibrium properties.

24 p3111 A73-45397

Strong plasma turbulence theory, discussing convergence of perturbation series formed with renormalized particle propagator

24 p3118 A73-45462

PARTICLE PRODUCTION

NT PAIR PRODUCTION

Measurement of the local production of muons underground.

01 p0080 A73-11009

Multiple meson production in 250 GeV nucleon-nucleon collisions in LiH targets, noting 40 per cent formation of heavy meson cluster fireballs

02 p0208 A73-12653

Particle multiplicity and momentum spectra for high energy inelastic nuclear interactions in Wilson chamber with polyethylene target

02 p0208 A73-12655

Multiple production processes hydrodynamic-type models validated by high energy particle collision collective interactions

02 p0208 A73-12659

Production of different non-thermal electron groups in small solar flares.

03 p0364 A73-13959

Three meter liquid hydrogen target for K meson production with Serpukhov accelerator, discussing design, operation control and emergency conditions

05 p0538 A73-17289

Interaction contributions to the solar proton-proton reaction.

05 p0612 A73-17339

Multiple production of hadrons at cosmic ray energies - Experimental results and theoretical concepts.

07 p0870 A73-19374

Energy spectra of cosmic pions and nucleons at the top of the atmosphere.

07 p0872 A73-20015

Solar protons propagation from instantaneous injection source and inhomogeneities interaction description by mean free path and scattering angle specification

08 p0999 A73-21327

Nucleon and electromagnetic component generation, energy spectrum and diffusion during solar flares

08 p1000 A73-21349

Probabilistic integral multiplicity of generation of primary cosmic ray particles from count rate and primary spectrum relationship, using definition for neutron component calculations

08 p1000 A73-21352

Nuclear particle fluxes and radioactive isotopes production rate distribution from cosmic rays data along orbits, calculating iron meteorite dimensions prior to atmosphere entry

08 p1012 A73-21582

Secondary particles multiplicity law validity in cosmic ray showers highest energy interactions

09 p1138 A73-23035

Solar proton energy spectra recorded in stratosphere during two solar cycles, approximating generation spectra by power law

10 p1266 A73-23917

Contribution of pion production by primary cosmic-ray nucleons to the interstellar electron-positron flux.

10 p1269 A73-24348

Charged particle production and plasma electron/ion current discharges from W targets under laser beam, noting dependence on electric field strength, pressure and operation mode

11 p1378 A73-26522

Contribution of atmospheric multiple neutron production to the multiplicity distribution observed in cosmic ray neutron monitor.

15 p1926 A73-31385

Muon observations, discussing high energy cosmic ray neutrino experiments and production via pion and kaon decay, neutrino interactions and nuclear collisions

16 p2055 A73-33291

Cosmic antiproton production in interstellar pp collisions.

17 p2223 A73-34099

Muon production in large air showers, determining mean origin height via magnetic spectrography,

distance from shower core, geomagnetic deflection and trajectory angles

20 p2603 A73-39707

Complete hydrogen and helium particle spectra from 30- to 60-MeV proton bombardment of nuclei with $A = 12$ to 209 and comparison with the intranuclear cascade model.

21 p2744 A73-41019

Low-energy cosmic ray protons from nuclear interactions of cosmic rays with the interstellar medium.

22 p2902 A73-41927

High energy gamma quanta families and multiple generation processes in electron photon cascades detected by nuclear emulsion X ray chamber

23 p3021 A73-43536

Intercomets 6 cosmic ray shower experiment using emulsion stack, spark chamber and scintillation counter to measure particle energy, angular distribution and production multiplicity

23 p2981 A73-43540

Inelastic interaction between pions and emulsion nuclei at an energy of 60 GeV

23 p3021 A73-43541

High energy nucleon inelastic interaction characteristics calculated from artificial event model based on covariant statistical theory of multiple generation of particles

23 p3022 A73-43542

Reactions of pseudoscalar meson production by neutrinos on nucleons near the threshold in the range of high transferred impulses

23 p3008 A73-43544

Generation of high-energy muons in cosmic rays

23 p3023 A73-43560

Energy spectrum and angular distribution of outer space muons and the processes of their production in the 1 TeV energy range

23 p3024 A73-43564

Spark calorimetry investigation of trident and extensive air showers muon component generated high energy penetrating particles at large zenith angles

23 p3024 A73-43565

Ionospheric metastable particle production and annihilation during photochemical reactions, determining neutral and ionized particle abundance profiles

23 p2978 A73-43979

PARTICLE SIZE DISTRIBUTION

An inversion technique developed to determine characteristics of mie scatterers differing in index of refraction interspersed in the stratosphere.

01 p0037 A73-10353

An electrostatic cloud droplet probe.

01 p0052 A73-11058

Metal vapor crystallization in rare gas atmosphere for powder production, noting particle size distribution control

02 p0172 A73-11545

The analysis of particulate contaminants in hydraulic fluids.

02 p0132 A73-12004

Optical measurements of lunar albedo, angular illumination, diffuse and specular reflectance and scattering coefficients on Mare Foecunditatis regolith powder of various sizes

02 p0213 A73-12238

The morphology, types and distribution of sizes of regolith particles in the Sea of Fertility.

02 p0214 A73-12241

Interplanetary dust particle flux curves, number densities and size distributions from zodiacal light investigations

02 p0215 A73-12262

Particle size spectra measurement in cirrus generating cells, deriving particle concentration, crystal length, ice water content, reflectivity and precipitation rate

02 p0189 A73-12784

Contrail ice budget measurements with optical array particle size spectrometer onboard Sabreliner, noting water abundance reduction at subropopause jet traffic levels

02 p0189 A73-12785

Size effect in fatigue testing of metals explained, considering implications for bending, torsion and axial loading

03 p0396 A73-14646

Type II comet model for head and tail regions release of dust particles having wide size distribution

04 p0494 A73-14759

The mechanisms of growth of gamma prime particles and tensile yield in Udimet 520.

04 p0464 A73-15578

Freeze drying - A unique approach to the synthesis of ultrafine powders.

04 p0455 A73-15753

Droplets size and velocity distribution in air-kerosene atomized spray flame as function of fuel-air ratio from double image high speed photographic measurements

[ASME PAPER 72-WA/HT-25] 04 p0519 A73-15829

The use of a gas laser for sizing single particles of airborne dust.

05 p0584 A73-16444

Apollo 14 soils - Size distribution and particle types.

07 p0884 A73-19740

PARTICLE SIZE DISTRIBUTION

Grain size analysis, optical reflectivity measurements, and determination of high-frequency electrical properties for Apollo 14 lunar samples.

07 p0898 A73-19897

Quantitative size and shape analyses of Apollo 14 and 15 fines by computer evaluation of scanning electron microscope images

07 p0898 A73-19898

On-surface and laboratory size measurements of fine lunar particles.

07 p0900 A73-20184

Magnesium particle ignition in various media

07 p0923 A73-20419

Finson-Probststein model for dust comets applied to calibrated photographic plates of Comet Bennett, giving dust size distribution, emission rate and initial velocities

07 p0902 A73-20443

Tests of coherence for the empirical laws of distribution of raindrops

08 p0938 A73-20966

Equation of motion and bubble size distribution function for nucleate boiling, noting balance equation for two phase fluid

08 p1022 A73-21096

Solute rejection by porous glass membranes. II - Pore size distributions and membrane permeabilities.

09 p1048 A73-22525

Metallic dust particles in quasi circular solar orbit, discussing evolution, thermal evaporation, atomization and size

10 p1274 A73-23720

Optical properties of polydisperse media with different size distributions of particles

11 p1398 A73-25611

Approximation of empirical size distributions of cloud droplets and other aerosol particles

11 p1393 A73-25644

Estimate of the mean size of cloud layer particles in the Jovian atmosphere

11 p1423 A73-26080

The energetic degree of shielding provided by hail-protection screens in the case of certain distribution spectra of hailstone diameters

11 p1394 A73-26373

The structure of the Eta Aquarid meteor stream.

11 p1426 A73-26573

Study of droplet size distribution in a two-phase stratiform cloud - A numerical experiment

13 p1653 A73-28877

Calculation of the growth and melting of ice particles and the radar signal reflection profiles in cumulonimbus clouds

13 p1653 A73-28878

Cometary nucleus evolution dependence on secular brightness decrease relationship to dust particle size distribution, nuclear radius and screened surface area

14 p1792 A73-29817

Ostwald ripening of transition-metal carbides in liquid nickel and cobalt

14 p1760 A73-30441

A nephelometric method for transparency determination in scattering media

14 p1771 A73-30463

The effect of the size distribution of the rain drops on the standard visibility

15 p1902 A73-31139

Droplet size distribution resulting from liquid jet injection across a supersonic stream.

15 p1863 A73-31659

Behavior of hafnium dioxide particles in dispersively hardened nickel during isothermal annealing

17 p2188 A73-34560

Forward scattering method for determination of atmospheric aerosols particle size distribution, considering angle-dependent scattering at fixed wave number

17 p2161 A73-34938

Measurements of aerosol size distributions with a laser Doppler velocimeter (LDV).

[ASME PAPER 73-705] 18 p2315 A73-36254

Cumuli structure at various stages of development.

18 p2333 A73-36705

Metallic dust particles in quasi-circular solar orbit, discussing evolution, thermal evaporation, atomization and size

18 p2355 A73-36745

The combustibility of aluminum-nickel powders

18 p2325 A73-36862

Some characteristics of two-phase nozzle flows

18 p2265 A73-37005

Method of selecting particles formed during the burning of metallized compacted systems in a constant-pressure chamber

19 p2503 A73-37518

A study of droplet spectra in fogs.

19 p2447 A73-37660

Radiative transfer in homogeneous, nongray gases with non-isotropic particle scattering.

[ASME PAPER 73-HT-9] 20 p2625 A73-38566

Airborne remote sensing of cloud particle size and shapes via IR polarimeter, obtaining polarization vs phase angle curve for thick tropical cirrus clouds

20 p2567 A73-39859

Effect of coagulation and spatial redistribution of cloud particles on the precipitation spectrum

21 p2730 A73-40120

Optical and mechanical models of interplanetary dust.

21 p2776 A73-41420

The multiplicity distribution of shower particles underground and the cosmic-ray primary spectrum.

21 p2764 A73-41633

Mixed particle sizes in fast carbon thermometry.

22 p2854 A73-41997

Determination of the size and the imaginary part of the refractive index of Al₂O₃ drops in a flame.

22 p2932 A73-42724

Electrical control of particulate pollutants from flames.

22 p2935 A73-42799

Carbon particles size distribution and charged fraction in acetylene-oxygen flame using molecular beam system and electron microscopy, noting particle interaction formation mechanism

22 p2936 A73-42801

The observational evidence for mass distribution in the meteoritic complex.

23 p3031 A73-43770

Production of lunar fragmental material by meteoroid impact.

24 p3129 A73-44447

Determination of the parameters of particle density and size distribution functions from measurements of attenuation and backscattering coefficients

24 p3112 A73-45519

Determination of the size distribution function of erythrocytes by the spectral transparency method

24 p3065 A73-45521

PARTICLE SPIN

NT ELECTRON SPIN

NT NUCLEAR SPIN

Fermions spin polarization reversal for HF high intensity gravitational waves generation and detection, suggesting superconducting metals for waves receiver

04 p0476 A73-15633

PARTICLE TELESCOPES

Coupling function for the vertical muon telescope at 60-meters-water-equivalent depth.

07 p0869 A73-19251

Investigation of rigid gamma rays in the atmosphere with the aid of a telescope with an acoustic spark chamber

10 p1267 A73-23923

Preliminary Pioneer-10 intensity gradients of galactic cosmic rays.

11 p1414 A73-26622

Cosmic ray storm effect on midlatitude and polar neutron monitors, noting comparison with underground mu-meson telescopic observations at high rigidities

12 p1534 A73-27001

Geometric factor optimization for a telescope performing charged-particle recording in space

18 p2315 A73-36115

Isotopic composition measurements of cosmic-ray nuclei with Z greater than or equal to 10 made using a new technique.

19 p2475 A73-37628

A low-background counter telescope for recording alpha particles in \ln , alpha-reactions

21 p2699 A73-40173

A meson supertelescope using plastic scintillators and the coupling coefficients for it

21 p2701 A73-40611

PARTICLE THEORY

CP-noninvariance model of baryon asymmetry of universe, postulating kappa particle /neutral massive fermion/

02 p0221 A73-12669

Conduction electrons collective wave properties in metals, discussing energy structure, ground state, Fermi surface and quasi-particle concept for crystal conductivity

06 p0739 A73-18674

PARTICLE TRACKS

U PARTICLE TRAJECTORIES

PARTICLE TRAJECTORIES

NT ELECTRON TRAJECTORIES

An investigation of particle trajectories in two-phase flow systems.

01 p0002 A73-10439

Experimental study of the turbulent flow of a suspension: Trajectories and velocities of particles - Heat transfers between the two phases

01 p0122 A73-10810

Distortion of particle trajectories by dynamic effects in the problem of two bodies with corpuscular emission

01 p0102 A73-10947

A search for the quark in extensive air showers, using a counter-controlled cloud chamber.

01 p0093 A73-11249

Corpuscular radiation as an upper atmospheric energy source.

02 p0205 A73-12289

Muon track curvatures in Wilson chamber magnetic field for calibrating ionization levels of logarithmic in-crease

02 p0171 A73-12687

Solar corpuscular irradiation induced latent and etched nuclear particle tracks in lunar dust grains,

presenting electron microscopic studies of Apollo 11/12 lunar soil samples

03 p0361 A73-13099

Fossil particle tracks in lunar materials, discussing track densities implications, production rates via cosmic ray spallation and interpretation for rock ages and erosion rates

03 p0361 A73-13102

The location and size of the hot spot in catalytic variable stars.

04 p0499 A73-15486

Semiclassical theory of inelastic collisions. I - Classical picture and semiclassical formulation.

06 p0726 A73-18264

The propagation of the energetic very heavy nuclei in the cosmic radiation.

07 p0870 A73-19340

DR ring current belt formation due to electron and proton gradient drift in inhomogeneous geomagnetic field, calculating charged particles trajectories

07 p0816 A73-19446

Initial free-surface motion of an impulsively loaded half-space.

07 p0810 A73-19509

Chemistry and particle track studies of Apollo 14 glasses.

07 p0884 A73-19736

Lunar craters and exposure ages derived from crater statistics and solar flare tracks.

07 p0896 A73-19869

Cosmic ray track densities of Apollo 14 breccias, igneous rock and soils from Fra Mauro, indicating surface residence times

07 p0871 A73-19871

Radiation effects in soils from five lunar missions.

07 p0896 A73-19875

Charge assignment to cosmic ray heavy ion tracks in lunar pyroxenes.

07 p0872 A73-19877

Interlaboratory comparison for solar flare track density data on feldspars in individual sections of lunar rock 14310, noting depth dependence and irradiation history

07 p0896 A73-19878

Monte Carlo method applications in the solution of gas kinetics problems

07 p0853 A73-19987

Large-amplitude stabilization of the drift instability.

07 p0860 A73-20481

The anisotropic Kepler problem in two dimensions.

08 p0988 A73-21204

Solar protons propagation from instantaneous injection source and inhomogeneities interaction description by mean free path and scattering angle specification

08 p0999 A73-21327

Error analysis of approximate formula for transform of rarefied gas particle reflection from homogeneous anisotropic random surface

09 p1123 A73-22615

Dynamical effects of the curvature of particle trajectories in the two-body problem with corpuscular radiation.

09 p1148 A73-22742

Upper limit of the antineutrino abundance in primary cosmic rays

10 p1265 A73-23899

Tracks from extinct radioactivity, ancient cosmic rays, and calibration ions.

10 p1269 A73-24271

Nuclear track etching in radiation and fast neutron dosimetry and health physics, discussing counter materials and fission and alpha particles and recoil nucleus recordings

11 p1362 A73-25421

Delta ray particle track structure theory for radiation dosimetry and biological cell response to heavy ions, fast neutrons, stopped pions and mixed radiation fields

11 p1323 A73-25423

Magnetotail model for magnetic field strength and particle drift in magnetic equatorial plane earth, using current sheet from satellite observations

11 p1357 A73-25929

Particle track densities in 100-200 micron crystalline grains from soil column returned from lunar highlands by Luna 20 and 16

12 p1541 A73-27487

Apollo 15 soil and rock particle tracks density and stability and uranium content

12 p1542 A73-27547

Path length distribution of cosmic rays from pulsar nebula complexes.

12 p1536 A73-27880

Search for quarks using a flash-tube chamber.

13 p1670 A73-28210

Fossil track and thermoluminescence studies of Luna 20 material.

13 p1675 A73-28312

East-west asymmetry of cosmic rays at sea level at geomagnetic latitudes from 50 N to 20 S.

13 p1670 A73-28702

Particle track record in Apollo 15 deep core from 54 to 80 cm depths.

13 p1686 A73-29566

Electrostatic and magnetic fields methods comparison for small angle scanning of electron beam, considering particle trajectories, field energy and circuit electrical parameters

14 p1732 A73-29913

Structure of the wall zone of a longitudinal disperse flow over a plane plate

14 p1711 A73-30014

Study on the charge and isotope composition of medium cosmic ray particles.

16 p2054 A73-33278

Aluminum-26 in meteorites. VII - Ureilites, their unique radiation history.

17 p2237 A73-35803

Experimental methods of correlation between the trajectories of cosmic heavy ions and biological objects: Dosimetric results - Experiment Biostack on Apollo XVI and XVII.

18 p2270 A73-35946

A search for laser-amplified cosmic ray tracks.

19 p2437 A73-37254

Ion trajectories in plasma focusing devices based on numerical integration of three dimensional equations of motion

19 p2468 A73-37856

The geometrical factor of large aperture hemispherical electrostatic analyzers.

20 p2564 A73-38877

Upper limit of antinuclei content in primary cosmic rays.

20 p2601 A73-38918

Mechanical erasure of particle tracks - A tool for lunar microstratigraphic chronology.

20 p2612 A73-39713

Characteristics of tracks of ions of 14 less than or equal to Z less than or equal to 36 in common rock silicates.

21 p2682 A73-40242

Study by the method of nuclear tracking of the soil of Mare Fecunditatis /Luna 16/

21 p2770 A73-41002

Uneven illumination of the polar caps by solar protons - Comparison of different particle entry models.

22 p2901 A73-41906

Solid state AgCl detectors for nuclear tracks with on- and off-response at choice - Applications to life sciences.

22 p2814 A73-42179

Perturbation of ion density by a body moving through the ionosphere.

23 p3008 A73-43254

Study of low-energy heavy-nucleus track regression in plastic detectors /cellulose triacetate and polyethylene terephthalate/ and in low-sensitivity nuclear photoemulsion

23 p2981 A73-43567

Charged particle track detector design with electric field control of nuclear photoemulsion sensitivity, discussing microcrystals, trajectory recording and proton irradiation

23 p2982 A73-43569

Observation of cosmic-ray particles with Z greater than 35.

23 p3024 A73-43609

Track density gradient and light noble gas isotope analysis of lunar breccia, postulating higher solar flux densities during early brecciation history

23 p2950 A73-43766

Investigation of neoclassical diffusion in toroidal systems with a three-dimensional magnetic axis

23 p3014 A73-44337

Drift of radiation-belt particles during substorms

24 p3124 A73-44804

PARTICLES

NT AEROSOLS

NT ALPHA PARTICLES

NT ANIONS

NT ANTINEUTRINOS

NT ANTIPARTICLES

NT ANTIPROTONS

NT ARGON PLASMA

NT BETA PARTICLES

NT CATIONS

NT CESIUM PLASMA

NT CHARGED PARTICLES

NT COLD PLASMAS

NT COLLISIONLESS PLASMAS

NT CONDUCTION ELECTRONS

NT CORPUSCULAR RADIATION

NT COSMIC PLASMA

NT CYCLOTRON RADIATION

NT DEUTERIUM PLASMA

NT DEUTERONS

NT DROPS [LIQUIDS]

NT ELECTRON BEAMS

NT ELECTRON PLASMA

NT ELECTRON PRECIPITATION

NT ELECTRON RADIATION

NT ELECTRONS

NT ELEMENTARY PARTICLES

NT FAST NEUTRONS

NT FERMIONS

NT FERRIC IONS

NT FINES

NT FOG

NT FREE ELECTRONS
 NT HADRONS
 NT HELIUM PLASMA
 NT HIGH ENERGY ELECTRONS
 NT HOT ELECTRONS
 NT HYDROGEN PLASMA
 NT INNER RADIATION BELT
 NT ION CYCLOTRON RADIATION
 NT LEPTONS
 NT LIGHT BEAMS
 NT MAGNETICALLY TRAPPED PARTICLES
 NT MANGANESE IONS
 NT MESONS
 NT METAL IONS
 NT METAL PARTICLES
 NT METALLIC PLASMAS
 NT MICROPARTICLES
 NT MIST
 NT NEUTRAL PARTICLES
 NT NEUTRINOS
 NT NEUTRONS
 NT NONEQUILIBRIUM PLASMAS
 NT NONUNIFORM PLASMAS
 NT NUCLEAR PARTICLES
 NT NUCLEONS
 NT OUTER RADIATION BELT
 NT OXYGEN PLASMA
 NT PHOTOELECTRONS
 NT PHOTONS
 NT PI-ELECTRONS
 NT PIONS
 NT PLASMA CLOUDS
 NT PLASMA JETS
 NT PLASMA LAYERS
 NT PLASMA SHEATHS
 NT PLASMA SLABS
 NT PLASMAS [PHYSICS]
 NT POLARONS
 NT POLLEN
 NT POSITRONS
 NT POWDER [PARTICLES]
 NT POWDERED ALUMINUM
 NT PRIMARY COSMIC RAYS
 NT PROTON BELTS
 NT PROTONS
 NT QUARKS
 NT RADIATION BELTS
 NT RAINDROPS
 NT RAREFIED PLASMAS
 NT RECOIL PROTONS
 NT RELATIVISTIC PARTICLES
 NT RELATIVISTIC PLASMAS
 NT ROTATING PLASMAS
 NT SOLAR CORPUSCULAR RADIATION
 NT SOLAR COSMIC RAYS
 NT SOLAR ELECTRONS
 NT SOLAR PROTONS
 NT SOLAR WIND
 NT SOOT
 NT STELLAR WINDS
 NT THERMAL NEUTRONS
 NT THERMAL PLASMAS
 NT TOROIDAL PLASMAS
 NT TRAPPED PARTICLES

PARTICULATE FILTERS
 U FLUID FILTERS

PARTICULATE SAMPLING
 Pioneer 10 space probe measurement of interplanetary particulates and aggregates via reflected and scattered sunlight, with emphasis on distribution in asteroid belt
 [AIAA PAPER 73-546] 18 p2350 A73-36095
 Thermal conductivity measurement for particulate materials in vacuum, comparing line and differential-line source methods in terms of test and data reduction times
 20 p2565 A73-38882
 Portable respirable dust monitor for continuous concentration measurement by light scattering of gas laser cavity beam
 21 p2708 A73-39923

PARTITIONS [MATHEMATICS]
 Solution of Troesch's two-point boundary value problem by a combination of techniques.
 01 p0035 A73-11470
 Scalar and vector partitions of the probability score.
 II - N-state situation.
 06 p0720 A73-18704
 A non-parametric method with applications to pattern recognition and mode estimation.
 06 p0672 A73-18805
 FORTRAN IV program and recursive matrix partitioning algorithm for solution of photogrammetric simultaneous equations, noting computation time
 09 p1059 A73-22382
 Partitioning techniques for solving large systems of equations in structural analysis.
 11 p1442 A73-25844
 Partition function derived for liquid Fe from Eyring method of significant structures, describing solid at high temperature via Einstein approximation
 11 p1355 A73-25904
 Vector partition of probability /Brier/ score providing reliability and resolution measures of weather forecasts
 18 p2332 A73-36703

Design of discrete model reference adaptive systems using the positivity concept.
 23 p2962 A73-43287

Solution of plane problems of elasticity utilizing partitioning concepts.
 [ASME PAPER 73-APM-C] 23 p3047 A73-44378

PARTS
 U COMPONENTS

PASCHEN SERIES
 Work function and surface ionization currents in stearite ceramics from nickel electrode and thermocouple measurements, plotting temperature dependent Paschen curves
 16 p2031 A73-34011

PASSEBANDS
 U BANDPASS FILTERS
 U BANDWIDTH

PASSENGER AIRCRAFT
 NT A-300 AIRCRAFT
 NT BOEING 727 AIRCRAFT
 NT BOEING 737 AIRCRAFT
 NT BOEING 747 AIRCRAFT
 NT CESSNA 172 AIRCRAFT
 NT CH-46 HELICOPTER
 NT CH-47 HELICOPTER
 NT DC 10 AIRCRAFT
 NT EUROPEAN AIRBUS
 NT H-53 HELICOPTER
 NT H-56 HELICOPTER
 NT HFB-320 AIRCRAFT
 NT IL-62 AIRCRAFT
 NT L-1011 AIRCRAFT
 NT T-39 AIRCRAFT
 NT TU-134 AIRCRAFT
 Management system for aviation safety.
 01 p0005 A73-10825
 Optimum position of the center of gravity of a passenger plane in cruising flight
 02 p0129 A73-11649
 Short haul twin jet passenger aircraft Iak-40 for small airfields, noting flight characteristics and cost analysis
 03 p0249 A73-13070
 Russian book on passenger aircraft and air transport design covering technical and economic efficiency, airbus concept, weight and size problems and aft-mounted engine design
 07 p0777 A73-20377
 Arava STOL turboprop passenger aircraft flutter flight test program, describing measurement instrumentation and data recording system
 09 p1031 A73-22185
 Commercial aircraft passenger cabins interior design, considering seating arrangements, cabin architecture and fittings, materials and color schemes and maintainability
 10 p1183 A73-23687
 Aeritalia-Boeing passenger aircraft design features in short, medium and long haul versions
 10 p1175 A73-24474
 Airliner radomes erosion by atmospheric precipitation, water penetration, icing, bird and stone impact and lightning
 11 p1335 A73-25297
 Aircraft design parameters optimization based on criterion function representing overall deviation for specifications with application to subsonic passenger aircraft
 12 p1458 A73-27095
 Air transport and commercial aviation developments, including revenues, passenger traffic statistics, charter flights and fare levels
 13 p1709 A73-29383
 Russian book on passenger aircraft high altitude equipment covering cabin pressurization, air conditioning and temperature and pressure control, human tolerances, reliability factors, etc
 14 p1712 A73-30355
 Skyjacking - Its domestic civil and criminal ramifications.
 16 p2087 A73-33102
 Independently targeted short haul individual rotorcraft for air taxi service, considering traffic control system, market possibilities, environmental impact and projected utilization
 16 p2088 A73-33186
 Helicopters for business executive transport between cities or to isolated locations, police use, ambulance service, etc
 17 p2256 A73-34445
 Aircraft accident statistics for passenger fatalities, worldwide jet hull losses and estimated costs to suggest proposals for approach, landing and takeoff accident reduction
 18 p2268 A73-36846
 STOL passenger aircraft ride smoothing control system based on vertical and lateral acceleration limits for design flight condition of 7 fps rms gust velocity
 [AIAA PAPER 73-885] 20 p2509 A73-38821

PASSENGERS
 Airport internal transportation systems for passengers and baggage, considering time scheduled, continuously moving and individually controlled systems
 01 p0029 A73-10306
 Medical considerations for aircraft passengers.
 03 p0267 A73-13802

Advanced transport systems for airports.
 05 p0562 A73-16566

Physically or mentally disabled passengers handling on scheduled, charter and group flights, discussing rules for attendants, seating and emergency procedures
 10 p1176 A73-24709

Post-crash survival planning and procedures, discussing passenger instructions and control, crew training and rescue signalling devices
 10 p1176 A73-24711

Dusseldorf airport passenger terminal facilities project, considering handling capacity, building and wide bodied jet traffic requirements
 11 p1343 A73-25206

Air-ground transportation interface at airports, examining baggage handling, ticketing, security procedures, rapid transit access, in-airport time and walking distances
 16 p1995 A73-33178

Concorde aircraft introduction into airline network, discussing time gain over various routes, operating costs, passenger service, departure and arrival problems, maintenance, etc
 [SAE PAPER 730351] 17 p2102 A73-34699

Airport simulation program describing passenger flow and scheduling considerations, including automobile parking, baggage handling, rapid transit, arrival and departure peaks and passenger decisions
 18 p2296 A73-36841

Automation of airline passenger processing.
 19 p2506 A73-37804

Seattle-Tacoma's unconventional concept.
 22 p2839 A73-42315

PASSIVATION
 U PASSIVITY

PASSIVE SATELLITES
 NT BEACON SATELLITES
 NT ECHO 1 SATELLITE
 NT ECHO 2 SATELLITE
 NT PAGESO SATELLITE

PASSIVITY
 Passivation of chrome steels under isothermal oxidation at 1020 deg C
 07 p0839 A73-19660
 Passivation of gallium arsenide with silicon nitride.
 07 p0864 A73-20571
 Characterization of passivation films formed at the surface of stainless steels in magnesium chloride solutions
 08 p0976 A73-20650
 Study of the conditions defining the passivating action of surface-active substances on hygroscopic condensation nuclei
 18 p2332 A73-35918

PASTES
 Metal coating via pastes and organic solvent suspensions application for diffusive metallization of metal surfaces, noting Al coating of heat resistant alloys
 07 p0833 A73-20641

FASTURES
 U GRASSLANDS

PATCH TESTS
 Introduction of shear deformations into a thin plate displacement formulation.
 22 p2923 A73-42559

PATCHING
 U MAINTENANCE

PATENTS
 Book - Holography: State of the art review 1971-72.
 03 p0309 A73-14440

PATHOGENESIS
 Pathogenesis of some respiration and circulation reactions to barometric pressure gradients
 08 p0929 A73-20980
 The pathogenesis and clinical significance of primary T-wave abnormalities.
 18 p2274 A73-36529

PATHOLOGICAL EFFECTS
 Russian monograph on radioactive isotopes effects on organisms covering metabolism, elimination acceleration methods, pathogenesis and treatment of damage, toxicity, biological action, etc
 02 p0138 A73-12865
 Pathomorphological and histochemical analysis of Luna 16 fine lunar soil fraction biological effect on mice
 03 p0272 A73-14569
 Clinical diagnosis of angina pectoris, implicating obstructive disease of coronary arteries and effects of paroxysmal events on heart rate and blood pressure
 05 p0542 A73-17277
 Biophysical properties of vibration energy transfer to human body structure, noting harmful effects dependence on frequency range
 06 p0657 A73-17748
 Physiological effect of air nitrogen replacement by inert gases under high and low temperature conditions
 12 p1465 A73-27701
 RNA and DNA of internal organs during a remote postreanimation period in animals with complete and incomplete functional recovery of the central nervous system
 14 p1719 A73-30842

Physiological criteria of early toxic normobaric hyperoxia manifestations 17 p2110 A73-34123

Histopathological and histochemical studies of one year isolation and six months immobilization effects on rhesus monkeys internal organs and tissues 18 p2270 A73-35983

Retinal change induced in the primate /Macaca mulatta/ by oxygen nuclei radiation. 18 p2271 A73-36125

Circadian rhythms of free radical state concentrations in the organs of mice. 20 p2512 A73-39104

Sudden incapacitation in flight - 1 Jan. 1966-30 Nov. 1971. 20 p2512 A73-39112

Structural changes in the adrenal nerve apparatus during experimental subtotal pancreatectomy 20 p2513 A73-39400

Effects of a synchronizer phase-shift on circadian rhythms in response of mice to ethanol or ouabain. 20 p2513 A73-39481

Russian book on structural and functional plasticity of interneuron synapses during readjustment to chemical and physical damage covering degenerative and regenerative changes 21 p2640 A73-41280

The effect of low X-ray doses on the central nervous system 23 p2947 A73-44179

PATHOLOGY

NT HUMAN PATHOLOGY

PATTERN RECOGNITION

NT CHARACTER RECOGNITION

Book - Introduction to mathematical techniques in pattern recognition. 01 p0019 A73-10050

Multiband and multiemulsion digitized aerial photographs automatic processing by digital computer techniques and statistical pattern recognition algorithms 01 p0044 A73-10140

Digital filters applicable to electroencephalographic pattern recognition. 01 p0013 A73-11464

Digital image-processing activities in remote sensing for earth resources. 01 p0021 A73-11476

Interactive pattern analysis and classification systems - A survey and commentary. 01 p0021 A73-11477

A comparison of analog and digital techniques for pattern recognition. 01 p0021 A73-11478

Features selection by heuristic method with figure of merit in pattern recognition 01 p0021 A73-11488

Incoherent optical correlation with a hologram - An example of identifying fingerprints 01 p0054 A73-11489

Target detection during picture transmission through a TV system [DGLR PAPER 72-099] 02 p0166 A73-11682

Method of minimization of description of classes in pattern recognition. 02 p0143 A73-12125

A minor perturbing effect of retinal locus on dot pattern recognition - Rejection of a possible artifact. 02 p0135 A73-12524

Psychological test for relative contributions of specific and nonspecific components to intersensory transfer between vision and touch 03 p0266 A73-13525

Computerized radial turbine blades thickness identification, considering temperature distribution and effects and mathematical model parameters for constraints 03 p0312 A73-13565

Parametric and nonparametric classification techniques for pattern recognition in remote sensed data processing, noting crop identification 03 p0281 A73-14485

Application of pattern recognition techniques to digitized radar data. 03 p0279 A73-14517

Pattern classification in scan-type nondestructive tests. 04 p0447 A73-14928

Numerical classification and coding of electrocardiograms. 04 p0412 A73-15647

Psychophysical studies of visual image normalization mechanisms in man 04 p0413 A73-15791

Image recognition learning algorithm for expanding neural nets composed of active inputs, receptors, associative elements and recognizers 04 p0426 A73-15794

Theoretical foundations for synthesis of learning-type recognition algorithms by the method of R-functions in the complex-plant control problem 05 p0560 A73-16275

Quantitative materials evaluation and inspection with the image analysing computer. 05 p0575 A73-16288

Applications of the discriminant function in automatic pattern recognition of side-looking radar imagery. 05 p0553 A73-16289

On the probability of error and the expected Bhattacharyya distance in multiclass pattern recognition. 05 p0554 A73-16814

Automatic analysis and classification methods based on statistical characteristics of aerial photometric and TV photographs, noting contour related interval distribution 05 p0579 A73-17143

Texture dependent features recognition in terms of spatial frequencies of remotely sensed multispectral data small sections 05 p0555 A73-17152

An integrated feature selection and supervised learning scheme for fast computer classification of multi-spectral data. 05 p0555 A73-17153

Automatic classification by sequential statistical variance and K-means clustering techniques for remote multispectral earth resource observation data 05 p0555 A73-17154

The representation and matching of pictorial structures. 06 p0692 A73-17804

A partitioning algorithm with application in pattern classification and the optimization of decision trees. 06 p0670 A73-17805

Clustering phenomena in side-looking radar /SLR/ microtexture. 06 p0667 A73-18285

Aerial imagery data statistical processing, discussing probability density and autocorrelation functions and power spectra for automatic pattern recognition 06 p0695 A73-18322

Syntax specification system for computerized hand-drawn pattern grammar generation with user style description for concurrent inputting and analysis at high recognition speed 06 p0671 A73-18535

A non-parametric method with applications to pattern recognition and mode estimation. 06 p0672 A73-18805

Optical device for three dimensional multiplication of input signal recorded on photographic film, noting pattern recognition and optical communication applications 07 p0823 A73-19909

Inter-hemispheric transfer of meaningful visual information in normal human subjects. 07 p0782 A73-20123

Three dimensional models images information content increase in coherent light by interference shadow marking, noting automatic systems for distant objects recognition 07 p0824 A73-20140

Computer aided recognition of objects shapes on aerial photographs, discussing image derivatives and histograms use and flying spot scanner principle 07 p0825 A73-20165

Electrical stimulation effects of human eye on photic threshold for square wave vision as function of wavelength, orientation and spatial frequency 07 p0783 A73-20260

The role of colour perception and 'pattern' recognition in stereopsis. 07 p0783 A73-20266

Dynamic programming as applied to feature subset selection in a pattern recognition system. 08 p0941 A73-21666

Mean vector and covariance matrix estimation for training class sample statistics updating in pattern recognition, applying to crops or any category of objects 08 p0984 A73-21668

Linear decision rule for probabilistic signal estimation in image recognition problems with sampling 09 p1060 A73-22556

Optimal self learning classification of point in set for image recognition systems, using proximity functions 09 p1060 A73-22944

On the solution of linear inequalities with applications to threshold logic. 10 p1191 A73-23746

Adaptation algorithms in multilayer pattern-recognition systems 10 p1192 A73-24502

Pattern recognition based on visual perception relation to transformations and identification by coded sentences 11 p1334 A73-25621

Retention of information in the iconic visual memory during recognition of images of varying complexity 11 p1323 A73-26084

Coherent light optical filtering, holographically produced complex filters, imaging systems and pattern recognition multiplex arrangement for optical data processing, discussing image reconstruction 11 p1370 A73-26533

Automatic classification of G5-K5 stars by means of 166 A/mm objective prism spectra /4000-4550 A/. 12 p1538 A73-26858

Implications of measurement of eye fixations for a psychophysics of form perception. 13 p1577 A73-28092

Monocular contribution to binocular vision in normals and amblyopes. 13 p1575 A73-28359

Visual pattern matching - An investigation of some effects of decision task, auditory codability, and spatial correspondence. 13 p1579 A73-29123

Properties of human visual orientation detectors - A new approach using patterned afterimages. 13 p1579 A73-29124

Dynamic scheduling of large digital computer systems using adaptive control and clustering techniques. 14 p1730 A73-30039

Digital correlator-computer-pattern recognition system for VLF phenomena investigation, discussing electromagnetic waves structure and spectrum analysis 15 p1845 A73-32234

Implementation of a frog's eye type discriminator, responsive only to pattern changes, as a pre-processor for visual data. 16 p2014 A73-33127

Airborne photography with multispectral scanners for remote sensing of large area features, discussing cost and feasibility of computerized pattern recognition and automatic identification 16 p2015 A73-33361

Digital computer processing for automatic feature classification of ERTS-borne MSS and RBV imagery data, emphasizing interactive man-machine analysis for image enhancement 16 p1985 A73-33366

Automatic recognition of electrocardiographic patterns 17 p2116 A73-34964

Automatic cataloging of electrocardiographic patterns 17 p2116 A73-34965

Automatic analysis and classification of electroencephalograms 17 p2116 A73-34966

Pattern recognition techniques suggested from psychological correlates of a model of the human visual system. 17 p2116 A73-35241

Applications of a model of the human visual system to pattern recognition problems. 17 p2116 A73-35242

Interaction between contours in visual masking 19 p2393 A73-37395

Uses of image recognition methods without teaching, in product quality control and lost observation estimations 20 p2568 A73-38712

Optimal statistical solution methods in recognition, data processing, and control problems 20 p2532 A73-38997

Automatic terrain mapping by texture recognition. 20 p2568 A73-39873

Multispectral reflectance scanning of crop image signatures during April-July growing season, examining time dependent image changes, discrimination tests and crop types 20 p2561 A73-39900

A probabilistic algorithm for grouped handling of arguments with sequential discrimination of input features 21 p2638 A73-40994

Sufficient conditions for the discrimination of motion. 21 p2639 A73-41181

Pattern recognition learning machine design heuristics, discussing analysis, synthesis and convergence of algorithms 21 p2639 A73-41290

A recognition learning program based on selecting statistically useful attributes 21 p2639 A73-41291

Mathematical model of human pitch perception based on acoustic stimulus Fourier transformation by sense organ into peripheral neural activity pattern recognition 22 p2811 A73-41816

Human recognition of dynamic pattern changes in numerical series displayed on spatiotemporal panels, discussing learning times and reactions to pattern disruptions 22 p2812 A73-41887

On an asymptotic property of the least-mean-square-error design criterion in pattern recognition. 22 p2835 A73-42274

Application of a computer image recognition technique to the determination of phase diagram types for binary metal systems 22 p2877 A73-42457

Recognition of component differences in two-dimensional oculomotor tracking tasks. 22 p2810 A73-42959

Failure diagnosis using quadratic programming. 22 p2867 A73-42966

Noise blurred image recognition probability characteristics from experimental investigation, showing difference from statistical decision theory data
24 p3062 A73-44667

PATTERN REGISTRATION
Digital image registration by correlation techniques.
04 p0449 A73-15413
Two direct methods for reconstructing pictures from their projections - A comparative study.
09 p1080 A73-22224
Colored aftereffects after prolonged inspection of convex lines of one color and concave lines of another color
21 p2640 A73-41303

PAVEMENTS
Airfield pavement full scale performance tests under simulated C-5A load conditions, evaluating construction joint systems
01 p0029 A73-10823
Book on functional pavements design covering support condition, quality control and construction tolerance, environmental and landing gear effects, mathematical models, etc
02 p0150 A73-11879
German book - Soil mechanics of retaining structures, roads, and runways.
11 p1344 A73-26255
Aircraft-airport system R and D program in terms of efficient planning, lighting and marking, geometric design, safety and pavements
13 p1598 A73-29103
Analytical elasticity methods for airfield pavement structural stress-strain, failure and reliability performance evaluation
13 p1598 A73-29106
Airport planning trends and engineering, discussing systems analysis, pavement design, modular terminal facilities, costs and economic efficiency
13 p1598 A73-29111
Parameters of rational airfield pavement design system.
[ASCE PREPRINT 1700] 15 p1855 A73-31386
Effect of openings on stresses in rigid pavements.
15 p1856 A73-31387
Subgrade strengthening of existing airfield runways.
15 p1856 A73-31388
Technical studies and research on airport infrastructure
15 p1859 A73-32561
Book - Prestressed pavements of airports and roads.
21 p2675 A73-41287

PAYLOADS
Prediction of the landing point of a balloon payload.
01 p0005 A73-11208
Scientific payload of Aeros German aeronomy satellite for atmospheric upper layers investigation, discussing instruments operation and location and measurement technique
[DGLR PAPER 72-069] 02 p0190 A73-11656
Rocket payload designs simulated by Monte Carlo method for aerodynamic properties during D region composition measurements
02 p0156 A73-11740
Structural weight analysis of single stage and multistage spacecraft for given payload and initial vehicle weight, considering optimization problem
02 p0229 A73-12469
Apollo 14 mission, discussing extravehicular activities time and payload increase via enlarged propellant tanks
03 p0368 A73-13085
Dual mode applications of nuclear rocket engine for spacecraft propulsion and electrical power generation, considering payloads and missions competitiveness with nondual system
[AIAA PAPER 72-1092] 03 p0341 A73-13413
Thrust reversal systems for solid propellant rocket motors last stage separation from payloads, examining pressure decay under isothermal and adiabatic assumptions
[AIAA PAPER 72-1110] 03 p0355 A73-13425
Spacecraft low thrust propulsion systems applications to earth orbital and planetary missions, discussing payload capabilities vs flight time
[AIAA PAPER 72-1125] 04 p0486 A73-14911
Solar electric propulsion for payloads earth orbit injection, discussing communication satellites and space shuttle/tug system applications
[AIAA PAPER 72-1126] 04 p0486 A73-14912
Variable mass system dynamic maneuver for maximum payload and given initial weight, noting mathematical model for time optimization
04 p0475 A73-15079
Calculus of variations for maximum payload of partitioned variable mass system, considering optimal weight control effect on motion
04 p0475 A73-15084
Revolutionary implications of the space shuttle.
06 p0756 A73-18018
Sounding rocket payload recovery systems
[ONERA, TP NO. 1153] 08 p1014 A73-21681
Balloon-borne UV stellar spectrometer telescope pointing and stabilization, discussing in-house feasibility studies by small scale test payload experiments
08 p0971 A73-21750

ARIES, the Minuteman I second stage as a controlled sound rocket.
[AIAA PAPER 73-287] 09 p1155 A73-23207
Two concepts for the reduction of payload attitude slewing times.
[AIAA PAPER 73-290] 09 p1155 A73-23209
A digital attitude control system for orientation of rocket launched scientific payloads.
[AIAA PAPER 73-292] 09 p1116 A73-23211
Dispersion of the direction of the angular momentum vector of sounding rocket payloads due to atmosphere exit and certain vehicle activities.
[AIAA PAPER 73-293] 09 p1116 A73-23212
Recovery of sounding rocket payloads by center-of-gravity position control.
[AIAA PAPER 73-294] 09 p1155 A73-23213
Real-time analysis and ground command control to achieve accurate vehicle and payload event functions.
[AIAA PAPER 73-298] 09 p1117 A73-23217
Recoverable sounding rocket payload field refurbishment for data acquisition with time and monetary savings, noting micrometeorite collection experiments
[AIAA PAPER 73-301] 09 p1156 A73-23220
Rocket motor, Dart vehicle, booster and launcher design and instruments and payload description for Super Loki meteorological rocket systems
[AIAA PAPER 73-303] 09 p1156 A73-23222
A probabilistic evaluation of helicopter lift capability.
10 p1175 A73-23775
An apparatus for the orientation of stratospheric-balloon payloads
11 p1304 A73-25355
Parawing-drag chute system operation on wind shear energy to maintain payload flight altitude
11 p1305 A73-25787
Refurbishable spacecraft - Modules and components for the Shuttle era.
12 p1549 A73-27437
Shuttle payloads - Saving dollars by offsetting risks.
12 p1549 A73-27438
Lower payload costs through refurbishment and module replacement.
14 p1803 A73-29944
Recovery objectives - Review of the most interesting aspects of problems related to this technique
14 p1804 A73-30087
Sounding rocket payload recovery systems
14 p1804 A73-30088
Satellite payloads preparation and launching methods in European space programs, evaluating firing range apparatus and firing range/satellite interfaces
14 p1804 A73-30106
Payload/launcher radio compatibility, discussing RF link parameters choice, terminal devices quality and test schedule
14 p1742 A73-30113
Parachute-payload system performance prediction for cause and effect relationships by parametric sensitivity and regression analysis for optimal design with computer simulation
15 p1829 A73-31469
Structural weight optimization of single stage and multistage spacecraft for given payload and initial vehicle weight
15 p1944 A73-32619
Reusable space shuttle orbiter design evolution during 1972-1973, discussing payloads, vertical launching capability and advanced materials technology
16 p2072 A73-33063
A sequential programmer for rocket payloads.
16 p1992 A73-33105
Airborne mechanical system for sounding rocket experiments.
16 p2072 A73-33119
Large payload aircraft for Alaskan and Canadian gas-oil transportation, examining alternative pipeline economic factors and possible new North Canadian island fuel fields
16 p2088 A73-33183
WB-57F aircraft with instrument package for nuclear test detection and upper atmosphere research, discussing range, altitude, speed, payload capacity and onboard equipment
[AIAA PAPER 73-510] 16 p1969 A73-33548
The Space Shuttle and its utilization.
18 p2357 A73-35936
The impact of launch vehicle reliability on the financial risks associated with multiple payload space functions.
[AIAA PAPER 73-591] 18 p2358 A73-36079
A concept for Space Shuttle payload ground operations.
[AIAA PAPER 73-615] 18 p2359 A73-36093
Electric propulsion interactive effects with spacecraft science payloads.
[AIAA PAPER 73-559] 18 p2353 A73-36497
Space shuttle payload definition, design and planning, using computers for scheduling and costing
19 p2491 A73-37593
The telecommunication payload of the satellite Symphonie
21 p2655 A73-41081

PCM [MODULATION]
U PULSE CODE MODULATION

PCM TELEMETRY
TDM link with digitized voice channel and PCM telemetry sequence coding for error correction, comparing tested performance with prediction and computer simulation
04 p0419 A73-15401
Third generation satellite PCM telemetry data processing with computer control for optimization and supervision, discussing system reliability, automatic control and diagnostic routine
07 p0795 A73-18954
Circuit diagrams, electronic modules and design of PCM telemetry encoder for Eole satellite, noting data multiplexing and processing
07 p0789 A73-18957
Sounding balloon system SITTEL for upper atmosphere physical parameters measurement, noting PCM telemetry, remote control and vehicle localization
07 p0790 A73-18971
European space operations control center subsystems for PCM telemetry data acquisition and processing
07 p0790 A73-18973
Data collecting and sequencing equipment for Prospero satellite PCM telemetry system, describing encoders, programming unit and tape recorder for orbital data storage
09 p1051 A73-22918
Magnetic tape recorder parameters effect on PCM telemetry bit error rate, discussing contribution factors and test methods
09 p1087 A73-23370
Utilization of PCM telemetry for the control of the Europa III launcher
14 p1804 A73-30111
PCM mobile ground station design covering telemetry receivers, digital data magnetic recording and computer interface circuitry and software
14 p1742 A73-30112
Crosstalk interference and regenerative amplifier noise effects on PCM signal transmission over twin- and four-conductor lines
23 p2954 A73-43784

PDM [MODULATION]
U PULSE DURATION MODULATION

PEARLITE
Influence of vanadium, niobium, carbon, and silicon on the properties of low-pearlite steel
15 p1889 A73-31810
Effect of vanadium, niobium, and silicon on the properties of low-pearlite steel.
24 p3100 A73-45273

PECLET NUMBER
Closed form solution for heat transfer through Rankine vortex, noting square root dependence of Nusselt number on Peclet number
10 p1295 A73-23780
Determination of the turbulent exchange coefficients in the case of tube bundles in crossflow
11 p1448 A73-25109
Study of a compact counterflow heat-exchanger with mercury at small Peclet numbers.
[ASME PAPER 73-HT-54] 20 p2626 A73-38575

PEDALS
Angular measurements of foot motion for application to the design of foot-pedals.
01 p0013 A73-10773

PEDOLOGY
U SOIL SCIENCE

PEGASUS ENGINE
U BRISTOL-SIDDELEY BS 53 ENGINE

PELLETS
Development of a small end-burning type motor by using pellet impregnated propellant.
01 p0090 A73-11108
Investigation of the sintering process and physicochemical properties of products prepared from spherical bronze pellets
10 p1225 A73-24319

PELLICLE
Dye laser tuning with pellicles.
22 p2870 A73-42707

FELTIER EFFECTS
Experimental investigation of unsteady-state thermoelectric cooling. III - Combined regime
05 p0639 A73-16772

FELVES
Some biomechanical properties of the pelvic girdle of man
03 p0267 A73-13743

PENALTIES
Variational principle with penalty for finite element solution of model Poisson equation with homogeneous Dirichlet boundary conditions, noting convergence
17 p2199 A73-34209
Constrained optimization using a nondifferentiable penalty function.
21 p2725 A73-40384
Comparison of some penalty function based optimization procedures for the synthesis of a planar truss.
22 p2922 A73-42478

PENDULOUS GYROSCOPES
U GYROSCOPIC PENDULUMS

PENDULUMS

PENDULUMS

NT GYROSCOPIC PENDULUMS

A simple illustration of the principle of correspondence in quantum mechanics

02 p0193 A73-12542

Optimal stabilization of the Rayleigh-Taylor instability in the multiarm fluid pendulum.

09 p1119 A73-21942

Dynamic error of solid body-elastic rod pendulum system hinged on vibrating suspension point in terms of tensile rigidity finiteness

11 p1399 A73-26096

Oscillations of a mathematical pendulum of variable length during rectilinear motion of the suspension point

11 p1401 A73-26466

Some aspects of the inverted pendulum problem for modelling of locomotion systems.

19 p2460 A73-38035

Zeroth-order approximation by multiple scaling method to analyze nonlinear oscillations with small speed-dependent damping, applying to pendulum problem

20 p2593 A73-39536

The characteristics of hydraulic tensile-test machines of the pendulum type and their effect on the tensile test

20 p2545 A73-39629

Periodic solutions of a spring-pendulum system.

24 p3111 A73-45294

Adiabatic variation. I - Exponential property for the simple oscillator.

24 p3112 A73-45543

An inverse torsion pendulum with continuous frequency variation for studies of elastic relaxation and fatigue

24 p3076 A73-45554

PENETRANTS

Dual sensitivity liquid penetrants for improving NDT inspection of minute defects in military aircraft structures during rework and repair, noting comparative advantages

02 p0173 A73-11984

PENETRATING PARTICLES

U CORPUSCULAR RADIATION

PENETRATION

An examination of the perforation of a mild steel plate by a flat-ended cylindrical projectile.

08 p1016 A73-20828

Anomalous penetration of a magnetic pulse into a plasma.

17 p2214 A73-34098

PENCILLIN

Solubilization and accumulation of copper from elementary surfaces by Pencillium notatum.

21 p2648 A73-41217

PENNING DISCHARGE

CW He-Cd and He-Se metal vapor lasers, discussing atomic energy states, energy emission and absorption by electrons He storage levels and Penning ionization

07 p0836 A73-19933

Energy distribution functions of kilovolt ions in a modified Penning discharge.

07 p0808 A73-20459

Rotation of the ion component of a plasma from a hot-cathode Penning discharge

09 p1125 A73-21955

Measurement of vibrational temperature of CO and N₂ using the He/2 3S/ Penning ionization technique.

10 p1218 A73-24246

Electrostatic turbulence and ion thermalization in modified Penning discharge, investigating ion heating processes

10 p1251 A73-24259

Rotational instability of a plasma from a hot-cathode Penning discharge

11 p1403 A73-25243

Correlation between the potential and density fluctuations of a plasma, and the convective transport of particles across the magnetic field in a Penning discharge in the presence of rotational instability

14 p1781 A73-30581

Energy distribution functions of kilovolt ions in a modified Penning discharge.

20 p2597 A73-39197

Diamagnetism of Penning discharge plasma as function of gas pressure, magnetic field strength and applied voltage, discussing plasma energetic lifetime and current characteristics

23 p3009 A73-43653

Self-sustaining Penning avalanche discharge in crossed electric and magnetic fields, discussing anode surface boundary effects and maximum discharge intensity conditions

23 p3015 A73-44345

PENNING EFFECT

Pumping rate in He-Cd laser from metastable atoms concentration measurement and plasma diagnostics, noting upper level population dependence on Penning effect

03 p0319 A73-13753

Inhomogeneous plasma density distribution relation to ambipolar diffusion and ionization balance

processes of electron cooling, particle recombination and ground state, step wise and Penning ionization

12 p1527 A73-26932

Electron temperature and density in the He-Cd12 positive column used for an I/+ laser.

17 p2186 A73-35798

Inhomogeneous plasma density distribution relation to ambipolar diffusion and ionization balance processes of electron cooling, particle recombination and ground state, step wise and Penning ionization

22 p2891 A73-42266

PENTACHLORIDES

U CHLORIDES

PENTANES

Laser Raman spectrum of crystalline cyclopentane-d/sub 0/ and -d/sub 10/.

03 p0318 A73-13282

Slow combustion of n-pentane in single pulse chemical shock tube, discussing yields of oxygenated products

07 p0788 A73-20356

Experimental studies on the flame structure in the wake of a burning droplet.

22 p2937 A73-42816

PENUMBRAE

Observations of the intensity of the penumbra of sunspots.

03 p0377 A73-14409

Running waves in quiet sunspots with well developed penumbras, noting intensity fluctuation in H alpha centerline or wing

05 p0626 A73-17347

Morphological and kinematic study of the fine structures of a sunspot

16 p2052 A73-32956

Book on cosmic ray effective cut-off rigidities calculations in dipole and geomagnetic fields, using trajectory calculations of penumbra function

21 p2760 A73-40805

Umbral flashes and running penumbral waves relation to overstable hydromagnetic oscillation in sunspots, noting depth dependence and electrical conductivity variation effects

21 p2777 A73-41487

Strong magnetic fields occurrence in sunspot penumbras dark filaments related to hypothesis of penumbral convection rolls existence

23 p3026 A73-43224

On the generation of umbral flashes and running penumbral waves.

24 p3136 A73-44638

PEPTIDES

Evolution of ribonuclease in relation to polypeptide folding mechanisms.

04 p0409 A73-15047

A mechanism for polypeptide synthesis on a protein template.

06 p0652 A73-17943

Trypsinogen activation peptides - An example of molecular epigenesis.

06 p0652 A73-17947

Polymerization of amino acids under primitive earth conditions.

07 p0787 A73-19217

Stochastic model application to divergence of horse-pig lineage from common ancestor in terms of hemoglobin and fibrinopeptides alpha and beta chains

07 p0780 A73-19218

Protein molecules peptide groups excitation interpretation by quantum theory, noting application to muscle contraction

09 p1046 A73-23297

Genetic code evolution in terms of abiotic polynucleotide synthesis, suggesting alternating sequences of purines and pyrimidines as polypeptide codes

09 p1044 A73-23469

IR-spectroscopic investigation of the thermal stability of albumin at different levels of its ionization

10 p1182 A73-24685

A study of the secondary structure of ilamycin B1 by 300 MHz proton magnetic resonance.

11 p1326 A73-25572

Origin of terrestrial polypeptides - A theory based on data from discharge-tube experiments.

20 p2513 A73-39484

Prebiotic reactions combining amino acids and ribonucleotides into polypeptides and polynucleotides in presence of urea, imidazole and Mg positive ion, suggesting contemporary biosynthesis parallels

21 p2637 A73-40372

PERCENTAGE

U RATIOS

PERCEPTION

NT AUDITORY PERCEPTION

NT AUTOKINESIS

NT BINAURAL HEARING

NT CONSCIOUSNESS

NT CRITICAL FLICKER FUSION

NT EXTRASENSORY PERCEPTION

NT OLFACTORY PERCEPTION

NT PAIN SENSITIVITY

NT PROPRIOCEPTION

NT SENSORY PERCEPTION

NT SOUND LOCALIZATION

NT SPACE PERCEPTION

NT TACTILE DISCRIMINATION

NT VERTICAL PERCEPTION

NT VIBRATION PERCEPTION

NT VISUAL DISCRIMINATION

NT VISUAL PERCEPTION

Reflex act structural components interaction in terms of reflection, creativity and organism-environment relations, noting subjective and objective perception and attitude formation

04 p0410 A73-15796

PERCEPTORS

U SELF ORGANIZING SYSTEMS

PERCEPTUAL SPEED

U PERCEPTUAL TIME CONSTANT

PERCEPTUAL TIME CONSTANT

Visual temporal integration for threshold, signal detectability, and reaction time measures.

13 p1578 A73-28097

PERCHLORATES

NT AMMONIUM PERCHLORATES

PERCHLORIC ACID

The gas-phase reaction of perchloric acid with hydrogen.

07 p0787 A73-19387

The gas-phase reaction of perchloric acid with ethylene.

10 p1186 A73-23556

Kinetics of the catalytic reactions of the thermal decomposition of perchloric acid and ammonium perchlorate

19 p2402 A73-37505

Effect of composite propellant catalysts on the stabilities of HClO₄ and the HClO₄-NH₃ system.

22 p2899 A73-42814

PERFLUORO COMPOUNDS

The evaporation of various lubricant fluids in vacuum.

[ASLE PREPRINT 72LC-6C-2]

03 p0335 A73-14366

PERFORATED PLATES

Plane stress analysis of an annular disk with distorted inner hole.

01 p0115 A73-10754

Stress concentration in disk with radial slot and with outer boundary subject to arbitrary continuous load, using plane elasticity theory

01 p0117 A73-11095

Stressed state of an anisotropic plate with a finite number of curvilinear holes

02 p0230 A73-11783

Generalized dynamic problem of thermoelasticity for an infinite plate with a circular hole

02 p0232 A73-11931

Curvilinear holes bi-periodic array in isotropic plane, determining hole shape for constant shear stress around contours

02 p0235 A73-12193

Stress concentration near a circular hole reinforced with a wide ring in the case of a nonlinear law of elasticity

02 p0236 A73-12584

Stress concentration in a plane weakened by two different circular holes in the presence of small elastoplastic strains

02 p0237 A73-12585

Temperature distribution at a thermally insulated crack in a plate for various boundary conditions

05 p0640 A73-16774

Elastic-plastic analysis of stresses near fastener holes.

[AIAA PAPER 73-252]

05 p0635 A73-16974

Nonlinearity of Helmholtz resonators

05 p0599 A73-17269

Surface tractions, heat fluxes and body forces required for deformation of flat perforated thermoelastic circular plate into pierced spherical cap

06 p0759 A73-17757

A time hardening transient creep solution for steadily loaded uniaxial tension panels containing circular and elliptical holes under conditions of plane stress.

06 p0761 A73-17820

Effectiveness of the thermal protection of a plane wall during injection of air through two rows of rectangular holes arranged in a checkered order

06 p0768 A73-18127

A couple-stresses elastic solution of an infinite tension plate bounded by an elliptical hole.

06 p0717 A73-18173

On the buckling of thin tensioned sheets with cracks and slots.

06 p0764 A73-18497

Transmission of microwave through perforated flat plates of finite thickness.

06 p0669 A73-18735

Microinhomogeneous plane with a circular hole in tension

07 p0911 A73-19320

Transmission of the load from an annular cover piece to a plane with a circular hole

07 p0911 A73-19321

Nonlinear vibrations of rectangular plates with cutouts.

07 p0913 A73-19978

Thermal stresses in an anisotropic plate with a circular hole. 07 p0914 A73-20199

Equilibrium method for stress concentration around hole in plate under tension, comparing with Kolosov-Muskhelishvili potential method 08 p1015 A73-20699

Free vibrations of square plates with stiffened square openings. 08 p1016 A73-20826

An examination of the perforation of a mild steel plate by a flat-ended cylindrical projectile. 08 p1016 A73-20828

Cyclically symmetrical heat conduction problems for perforated plates and shells in the presence of heat transfer 08 p1021 A73-20997

Optical stress rosette based on caustics for stress distribution and differences measurement in perforated plate, using gas laser light for interferometry 08 p0964 A73-21047

Stressed state of an isotropic elliptical plate weakened by elliptical holes 08 p1020 A73-21767

Propagation of a transverse harmonic wave in a plate with a statistically rough circular hole 08 p1020 A73-21770

Difference iterative solution for two dimensional boundary value problem for rectangular elastic plate with rectangular cutout 09 p1159 A73-22584

Effects of circular holes on the fatigue resistance of AMg6BM aluminum-alloy sheet in symmetrical bending. 09 p1105 A73-23053

Elastoplastic deformation and hardening function of perforated plates under in-plane tensile loads 09 p1164 A73-23346

Small perturbation approximations of plane biaxial tensile deformation of semilinear elastic medium with cavity, using Piola-Kirchhoff stress functions 09 p1164 A73-23347

Action of a concentrated force on an elastic ring pressed into a circular hole in an isotropic plate 09 p1165 A73-23357

Nonlinear problem for a plane continuous medium in Euler coordinates 10 p1292 A73-24489

Stress distribution in a half-plane with a hole strengthened by an elastic insert 11 p1432 A73-25026

Stress concentration in an anisotropic plate with an insert in pure bending 11 p1433 A73-25031

Stress redistribution and rupture due to creep in a uniformly stretched thin plate containing a circular hole. [ASME PAPER 72-APM-KKK] 11 p1442 A73-25709

Rayleigh-Ritz method for natural frequencies of transversely vibrating polar orthotropic annular perforated plates, proposing coordinate transformations for asymmetric mode solutions 11 p1446 A73-26495

Brittle failure of infinite plate with circular hole and radial cracks under two perpendicular uniformly distributed tensile loads 12 p1556 A73-27802

Equilibrium of an anisotropic plane reinforced by an isotropic circular ring 13 p1698 A73-29131

Stress-strain state of thin circular perforated Cu plate under uniform tensile load, showing applicability of small elastoplastic finite deformation theory 13 p1703 A73-29601

Couple-stress effects near an interior hole of an infinite elastic plate subjected to a concentrated force. 14 p1813 A73-30593

Stress concentration determination near a small hole on a plate in three-dimensional representation 14 p1813 A73-30682

Influence on the stress-strain state of the way a concentrated force is applied to the tip of a crack in a plate 14 p1814 A73-30718

Study of the elastoplastic stressed state and plastic zones of a plate with a circular hole under tension 14 p1815 A73-30794

Effect of a crack in an infinite plate containing a circular hole under uniform normal pressure. 15 p1947 A73-31333

Strains and stress-concentration factors in plates under out-of-phase biaxial cyclic loads. 15 p1948 A73-31614

Testing machine to determine perforated plate biaxial tension creep rupture strength and fatigue life at high temperature 15 p1858 A73-31617

Stresses in a fiber-reinforced elastic sheet containing a circular hole. 15 p1949 A73-31655

Accuracy of the finite element analysis for the elastic plate with a circular hole. 15 p1951 A73-32036

Stress distribution near holes 15 p1953 A73-32097

First fundamental problem of the theory of elasticity for a bi-periodic system of cuts 15 p1953 A73-32100

Stress concentration in plates with holes for large curvatures at the points of inflection 16 p2074 A73-32688

Effectiveness and heat transfer with full-coverage film cooling. [ASME PAPER 73-GT-18] 16 p2086 A73-33495

Stresses in a symmetrically-laminar plate weakened by a central crack 17 p2240 A73-34145

A unified approach to the solution of plane problems of magneto-elasticity with special reference to a hole in a thin infinite conducting plate. 17 p2211 A73-34346

Stress distribution near a circular hole on a plane consisting of a stochastically inhomogeneous material 17 p2244 A73-34798

Alleviation of stress concentration with analogue reinforcement. [SESA PAPER 2102] 17 p2250 A73-35446

Effects of material and stacking sequence on behavior of composite plates with holes. [SESA PAPER 2157A] 17 p2198 A73-35452

Thermoelastic state of an anisotropic plate with an elliptic hole and mixed boundary conditions 18 p2363 A73-36406

Stress concentration determination under biaxial tension in a plate weakened by a randomly-shaped hole 18 p2363 A73-36414

Contact problem for infinite elastic isotropic plate weakened by rectilinear cut with free, slipping and adhesive segments and uniformly distributed load at infinity 18 p2363 A73-36415

The acoustic impedance of perforates at medium and high sound pressure levels. 18 p2337 A73-37030

Temperature field calculation for a plate of a complex shape with systems of double-periodic holes, inclusions, and energy sources 20 p2627 A73-39255

Determination of the critical load for a compressed plate weakened by a circular hole and by cracks propagating toward the hole contour 20 p2617 A73-39263

Stress-concentration at a hole with periodic irregularities 20 p2619 A73-39334

Effectiveness of film cooling of an adiabatic wall downstream of the perforated section. 20 p2628 A73-39424

On stress-concentration analysis of laminated composite plates. 20 p2622 A73-39551

The elastic layer with a cylindrical hole subjected to a nonuniform axisymmetric radial displacement. 20 p2624 A73-39566

Flexural wave propagation in a thin plate with circular holes. 21 p2787 A73-41142

Stress distribution around an elliptic hole in an infinite micropolar elastic plate. 22 p2924 A73-42684

Normalized stresses around an elliptic hole in a finite plate of linear material subjected to large uniform in-plane loading. 23 p3039 A73-43386

Deformation and failure of boron-epoxy plate with circular hole. 23 p3040 A73-43631

Determination of the strained state of a thick elastoplastic plate with an elliptical hole 23 p3046 A73-44201

Fatigue failure predictions for plates with holes and edge notches. 23 p3047 A73-44350

Strip weakened by array of holes, investigating plastic zone initiation and propagation under uniaxial tension for load bearing capacity estimation 24 p3147 A73-44685

Determination of the temperature field in a perforated plate with convective heat transfer 24 p3157 A73-45171

Stress concentration in infinite strip with periodically spaced circular holes under uniformly distributed bending loads 24 p3149 A73-45176

Free vibration of square plates under different boundary conditions, determining opening geometry effects on fundamental frequencies by grid framework model with finite difference operators 24 p3151 A73-45266

Determination of shape for apertures of equal strength in thin isotropic plates 24 p3152 A73-45356

PERFORATED SHELLS

Stress concentration at circular holes in a cylindrical shell of moderate thickness 01 p0114 A73-10480

Design of a shallow shell with a large rectangular hole 02 p0231 A73-11803

Elastoplastic stressed state of cylindrical shells weakened by a circular hole 02 p0237 A73-12590

Shear strains and elastic anisotropy of transversely isotropic cylindrical shell with circular hole under uniform internal pressure, using shallow shell equations 03 p0394 A73-14020

Effect of a circular hole on the buckling of cylindrical shells loaded by axial compression. 03 p0395 A73-14181

Cyclically symmetrical heat conduction problems for perforated plates and shells in the presence of heat transfer 08 p1021 A73-20997

Calculation of the stress concentration produced by an internal pressure in the region where a cylindrical shell is connected to a branch pipe. 09 p1161 A73-23058

The effect of a transverse shear acting on the edge of a circular cutout in a simply supported circular cylindrical shell. 09 p1161 A73-23092

Stress state around an elliptic hole in a conical shell under tension. [ASME PAPER 72-PVP-11] 09 p1163 A73-23269

Torsion of a circular-section bar weakened by two longitudinal circular-cylindrical cavities 10 p1293 A73-24702

Experimental investigation of the stability of shells with holes 11 p1434 A73-25390

Experimental investigation of oscillation damping in shells with holes 11 p1435 A73-25398

Investigation of the stress-strain state of spherical shells with an eccentric hole on the basis of the three-dimensional theory of elasticity by the finite element method 12 p1552 A73-27262

Calculation of the stress-strain state of a toroidal shell with holes 12 p1555 A73-27787

Perforated water tunnel to decrease wall effect on deflected cavitation flow, studying suction coefficient, pressure losses and blowing parameters 13 p1597 A73-28450

Investigation of the elastoplastic state of a spherical shell with a unreinforced circular hole 13 p1698 A73-29061

Conformal mapping technique for stress concentration around elliptical hole in shallow spherical shell under internal pressure 14 p1806 A73-30045

Stress concentrations close to circular holes in a cylindrical shell of medium thickness. 14 p1810 A73-30305

Zero moment equilibrium stress state for multiply connected convex shells with curvilinear holes 15 p1945 A73-31031

Stresses in a pressurized ribbed cylindrical shell with a reinforced hole. 15 p1948 A73-31621

Axissymmetrical and antisymmetrical stresses and deformations in shells of revolution with a meridional cutout 16 p2074 A73-32683

Stress concentration near a cutout on the surface of an orthotropic cylindrical shell 16 p2075 A73-32694

Shell stability effects of holes from review of published studies, emphasizing cylindrical shells under uniformly distributed compression loads 17 p2244 A73-34789

Study of elastoplastic state of a spherical shell with round unsupported apertures. 18 p2366 A73-36893

Stress concentration in tubes with a hole of star-shaped profile 19 p2494 A73-37185

Limit pressures for cylindrical shells with two adjacent circular cut outs. 22 p2929 A73-43175

Determination of the stressed state near a curvilinear hole in a transversely isotropic spherical shell 23 p3043 A73-43924

Investigation of the stress-strain state at a strengthened hole in an orthotropic cylindrical shell 23 p3046 A73-44193

Thermoelasticity problem of a spherical shell with multiply connected regions 24 p3149 A73-45175

PERFORATION

Example of utilization of a wind tunnel with perforated variable-geometry walls 16 p1993 A73-32818

Radiation heat transfer in multilayer insulation having perforated shields. [AIAA PAPER 73-718] 18 p2369 A73-36337

PERFORMANCE

Hydrogen maser amplifier performance characteristics, discussing relaxation time measurements, frequency stability and performance enhancement via resonator cavity magnetic shielding improvement 08 p0974 A73-20774

Microwave oscillation in germanium avalanche diodes. I, II. 08 p0947 A73-21461

On optimization of control systems according to vector-valued performance criteria. 10 p1201 A73-24056

PERFORMANCE CHARACTERISTICS

U PERFORMANCE

PERFORMANCE DECREMENT

U PERFORMANCE

PERFORMANCE PREDICTION

NT PREDICTION ANALYSIS TECHNIQUES

Observers detecting a signal in two multiple observation tasks. 01 p0011 A73-10350

Holographic gratings application to astronomical spectrograph design for IR to extreme UV and X rays, considering characteristics advantage 01 p0447 A73-10519

Simulation program for satellite operation status prediction in space environment. 01 p0110 A73-11146

The accurate prediction of radiation environment and solar cell degradation. 01 p0006 A73-11164

The prediction of resolving power of air and space photographic systems. 02 p0171 A73-12567

Computer programs for air cooled gas turbine engine design and performance prediction, noting aerodynamic effect of turbine coolant 02 p0129 A73-12848

The steady state performance of an externally pressurized gas lubricated porous thrust bearing with a uniform film. 03 p0311 A73-13203

Evaluation of a two-pocket hydrostatic journal bearing suitable for use over a wide range of temperature. 03 p0311 A73-13204

The performance of a four-pocket conical hydrostatic bearing. 03 p0311 A73-13206

Optimum performance of static propellers and rotors. 03 p0242 A73-13308

Research on combustion instability and application to solid propellant rocket motors. II. [AIAA PAPER 72-1049] 03 p0353 A73-13380

Mission performance of a 360 mw nuclear rocket engine. [AIAA PAPER 72-1064] 03 p0381 A73-13393

Performance potential of the colloid core reactor concept in near-earth applications. [AIAA PAPER 72-1065] 03 p0340 A73-13394

Verification of a comprehensive thrust chamber compatibility model for liquid rocket engines. [AIAA PAPER 72-1078] 03 p0354 A73-13401

Solid propellant rocket service life prediction based on propellant grain structural failure analysis, discussing surveillance program rationale for various conditions [AIAA PAPER 72-1085] 03 p0354 A73-13407

Aft-end design criteria and performance prediction methods applicable to air superiority fighters having twin buried engines and dual nozzles. [AIAA PAPER 72-1111] 03 p0250 A73-13426

From earth to Mars orbit - Mariner 9 propulsion flight performance with analytical correlations. [AIAA PAPER 72-1185] 03 p0382 A73-13478

Analog simulation for transient and steady state performance of group-triggered cycloconverter supplying controlled slip induction motor, discussing commutation failures 03 p0253 A73-13932

Psychiatric and psychometric predictability of test pilot school performance. [AD-754148] 03 p0269 A73-14165

Analysis of an arched outer-race ball bearing considering centrifugal forces. [ASME PAPER 72-LUB-28] 03 p0314 A73-14339

Optimal speed sharing characteristics of a series-hybrid bearing. [ASME PAPER 72-LUB-39] 03 p0315 A73-14346

Testing for prediction of material performance in structures and components, Proceedings of the Symposium, Anaheim, Calif., April 21-23, 1971 and Atlantic City, N.J., June 29-July 1, 1971. 04 p0452 A73-14851

Analytical correlation technique for air breathing and rocket engines combustor design and performance prediction based on hydrogen oxygen engines test data [AIAA PAPER 72-1074] 04 p0486 A73-14904

Experimental evaluation of a 600 lbf spacecraft rocket engine. [AIAA PAPER 72-1129] 04 p0486 A73-14914

Phase and frequency tracking accuracy in direct-detection optical-communication systems. 04 p0416 A73-14993

Speed-torque characteristics of a solar cell motor. 04 p0406 A73-15068

Prediction of failure for a multiple load-path system under random loading. 04 p0510 A73-15075

Evaluation of the performance of a variance estimation algorithm using order statistics. 04 p0471 A73-15259

Performance versus complexity of Viterbi and sequential decoding. 04 p0424 A73-15397

Performance of correlation receivers in the presence of impulse noise. 04 p0419 A73-15406

Comparison of coherent and noncoherent detection of phase continuous binary FM signals. 04 p0420 A73-15410

Optimal equalization of discrete signals passed through a random channel. 04 p0420 A73-15418

Source encoding with fixed word length and synchronous bit rate. 04 p0425 A73-15420

Digital phase locked loops for incoming signal phase tracking, predicting performance from nonlinear difference equation model for comparison with digital simulation 04 p0421 A73-15435

The problem of strength and aspects of predicting the mechanical properties of metals 04 p0465 A73-15661

Upper bound predictions of composite tensile strength as function of transitions from homogeneous to nonhomogeneous deformation [ASME PAPER 72-WA/PROD-8] 04 p0469 A73-15806

Predicting performance of heat pipes with partially saturated wicks. [ASME PAPER 72-WA/HT-38] 04 p0518 A73-15817

A combined theoretical and empirical method of axial compressor cascade prediction. 04 p0404 A73-15869

The selection of performance indices for optimal control problems. [ASME PAPER 72-WA/AUT-15] 04 p0432 A73-15880

The prediction of team monitoring performance under conditions of varied team size and decision rules. 05 p0543 A73-16710

Computer programs for operator performance time prediction and workspace design 05 p0544 A73-16721

Critical skills and procedures isolation within replacement air group /RAG/ training for F-4 pilot performance prediction 05 p0544 A73-16723

Analysis of high aspect ratio jet flap wings of arbitrary geometry. [AIAA PAPER 73-125] 05 p0530 A73-16880

Evaluation of turbulent heating predictions with flight data. [AIAA PAPER 73-213] 05 p0532 A73-16943

Air combat roles identification by reachable sets technique, evaluating aircraft/weapon systems potential performance vs given threat [AIAA PAPER 73-232] 05 p0536 A73-16957

Comparison of advanced propulsion concepts for deep space exploration. 05 p0608 A73-17201

Digital transmission performance on fading dispersive diversity channels. 06 p0664 A73-17711

Performance of M-ary PSK systems in Gaussian noise and intersymbol interference. 06 p0665 A73-18140

Adaptive maximum-likelihood sequence estimation for digital signaling in the presence of intersymbol interference. 06 p0665 A73-18144

Atmospheric conditions effects on line-of-sight microwave PCM data transmission system performance, comparing predicted error probability vs predetection SNR with measurement 06 p0665 A73-18187

Source limited gray scale and color selection capabilities for direct and reflected light scanners. 06 p0701 A73-18308

Probability of stress-corrosion fracture under random loading. 06 p0763 A73-18483

Fracture due to damage from projectile impact. 06 p0763 A73-18484

Circuit model for characterizing the nearly linear behavior of avalanche diodes in amplifier circuits. [AD-757849] 06 p0677 A73-18738

Adaptive trackers based on continuous learning theory. 06 p0682 A73-18821

Modeling and evaluating the performance of high data rate digital satellite communication systems with limiters. 06 p0669 A73-18830

Predicting method of the change in stage performance of axial flow machinery for the variation of cascade geometry. 07 p0867 A73-19225

The prediction of the optimum performance of ejectors. 07 p0810 A73-19571

Relationship among various parameters used in ejector-nozzle performance estimates 07 p0776 A73-20097

Recent advances and applications in the prediction of pilot acceptance of aircraft flying qualities. 07 p0777 A73-20586

Current status of models for the human operator as a controller and decision maker in manned aerospace systems. 07 p0787 A73-20587

Wiener and Kalman-Bucy filters design with error covariance bound for performance divergence prevention under stochastic processes with unknown signal and noise densities 07 p0806 A73-20603

Comparison of theoretical and simulated performance of optimal and suboptimal filters in a dense multitarget environment. 07 p0806 A73-20604

IMPATT diode microwave oscillator performance analysis based on model with ac current and voltage superposition on dc, determining avalanche frequency and negative resistance 08 p0942 A73-20706

IMPATT diode microwave oscillator performance analysis for I-V characteristics, output power, efficiency and starting current from equivalent circuit 08 p0943 A73-20707

Prediction of IC and LSI performance by specialized vibration/detection test for presence of conductive particles. 08 p0943 A73-20732

IC plastic package performance prediction, discussing procedure to estimate degradation rate due to moisture effects 08 p0944 A73-20738

Carre method for optimum overrelaxation factor determination in electron gun performance analysis by digital simulation, discussing choice of parameters for rapid iterative convergence 08 p0990 A73-20836

The design, analysis, and performance of resonant and nonresonant microwave transmission devices with theoretically infinite rejection. 09 p1080 A73-22103

Global asymptotic stability estimation for large scale systems of interconnected exponentially stable subsystems, using aggregated comparison and Liapunov function description 09 p1120 A73-22227

Performance comparison of suboptimal Kalman filters modeled for a continuous nonlinear system. 09 p1067 A73-22228

Co-60 fueled tubular radioisotope thermoelectric generator, correlating long term test data with performance prediction model results 09 p1117 A73-22764

Computer program for the transient analysis of radioisotope thermoelectric generators. 09 p1060 A73-22768

An approach to performance assessment and management of a large solar array/battery power system. 09 p1035 A73-22775

SNAP 19/Pioneer radioisotope thermoelectric generator program status report, stressing Jupiter first mission converters performance prediction 09 p1118 A73-22800

Viking Orbiter power subsystem performance prediction computer program simulating solar array, battery charge controls, zener diodes and power conditioning equipment characteristics and interactions 09 p1060 A73-22802

Solar cell fatigue life prediction by statistical analysis and extrapolation for determining failure probability curve as function of stress and time 09 p1036 A73-22808

The determination and treatment of temperature coefficients of silicon solar cells for interplanetary spacecraft application. 09 p1036 A73-22810

Delta modulation and differential PCM systems performance comparison at high sampling rates for color video signal coding 09 p1055 A73-23389

Digitally implemented clock acquisition loops for low SNR data signals. 09 p1056 A73-23405

Concatenated coding for deep space interplanetary communication with low data rate and SNR, comparing performance of three binary codes 09 p1058 A73-23424

A new FM system with a novel modulator design yielding high linearity and thermal stability. 09 p1058 A73-23430

Tracking performance of a phase locked loop with a linear phase detector. 09 p1058 A73-23432

Phase locked loop and coherent detection performance prediction, considering desirable phase detector characteristics in terms of SNR and noise spectral density 09 p1058 A73-23433

PCM and DPCM digital modulators design and performance comparison for sampling rate effects on 09 p1058 A73-23433

quantizing noise, noting tradeoffs between cost and system efficiency

09 p1059 A73-23435

Weaver modulator with digital filter for single sideband transmission in radio communication and telemetry, discussing FORTRAN simulation for cost, computation time and accuracy

10 p1186 A73-23499

Air cushion landing gears for transport aircraft, discussing peripheral jet stream performance prediction and system installation on Buffalo STOL

10 p1174 A73-23659

Radar filter asymptotic efficiency analysis for pass-band and impulse response duration increase, considering realization of approximate Urkowitz filter with controlled memory

10 p1194 A73-23737

Variable-reluctance stepping motor performance capabilities for point-to-point positional control.

10 p1199 A73-24024

The design of optimally parameter insensitive control systems.

10 p1199 A73-24030

Accelerated testing of solid film lubricants.

10 p1225 A73-24635

Flow twisting in front of rotor for centrifugal blower operation control, predicting efficiency criteria

10 p1173 A73-24671

Direct nondestructive prediction of engineering properties.

11 p1372 A73-25129

Effect of edge reflections on the performance of antenna ground screens.

11 p1329 A73-25673

The design of components for an advanced Rankine cycle test facility.

11 p1344 A73-25995

Analytical model for radioisotope thermoelectric generator performance prediction in air and vacuum, taking into account modified heat transfer rates

11 p1312 A73-26031

Detailed mathematical models of a radioisotope thermoelectric generator.

11 p1396 A73-26033

Temperature reducing solar cell arrangements for spin stabilized planetary and solar probes, analyzing thermal performance

11 p1313 A73-26668

Evaluation of the efficiency of automatic control and observation systems on the basis of mathematical models of potential and real automatic systems

12 p1482 A73-26762

Comparative analysis of the longitudinal and orthogonal magnetic second-harmonic modulators.

12 p1477 A73-26789

Pseudoelastic design method for bottle-plate stack instability performance prediction through failure by creep buckling, assessing effectiveness by comparison with measurements

12 p1514 A73-26876

Qualitative analysis of MHD energy conversion efficiency

12 p1460 A73-27321

IMCON reflection mode dispersive delay line in large time-bandwidth product pulse compression systems, deriving operational characteristics from transfer function

12 p1480 A73-27565

Quantizer functions and their use in the analyses of digital beamformer performance.

13 p1582 A73-28496

Ultrasonic acoustic holography for wave source and object in relative motion, predicting reconstructed image aberration elimination performance in point-by-point mapping technique

13 p1616 A73-28597

Two dimensional steady subsonic flow through airfoil cascades, predicting turbomachine performance from boundary layer calculation for comparison with experiments

13 p1565 A73-29005

Influence of the variation of cascade geometry on the performance in axial flow machinery.

13 p1565 A73-29007

A new approach to the problem of predicting the performance of centrifugal compressors.

13 p1565 A73-29012

The switching of wall-reattachment fluidic devices.

13 p1571 A73-29041

Fundamentals of the theory of combined reliability and service life estimates for machines and instruments

13 p1624 A73-29134

High gain hydromechanical servomechanism with multiplating, mass damping and feedback control, deriving transfer function response, with application to aircraft control surface actuator design

13 p1596 A73-29150

Linear and nonlinear first order closed loop tracking radar systems, predicting noise performance by Gaussian signal amplitude fluctuation modeling

13 p1585 A73-29206

Application of holographic interferometry to predict long time torsional relaxation.

13 p1620 A73-29301

Life prediction of metals subjected to high temperature fatigue.

13 p1708 A73-29503

Hydrodynamic tilting pad thrust bearings performance estimation in turbulent region based on laminar flow operation data

14 p1755 A73-30062

Spiral top-loaded antenna (STLA) characteristics and design procedure derivation via self consistent field method, noting VLF applications

14 p1734 A73-30204

On the equivalent parabola technique to predict the performance characteristics of a Cassegrainian system with an offset feed.

14 p1734 A73-30211

Relativistic electron beam focusing by neutral gas filled conical guide tube, comparing efficiency, fluence gain, energy loss and pressure variation predictions with experiments

14 p1777 A73-30658

Predicting descent rate for aircraft parachute flares. [AIAA PAPER 73-482]

15 p1829 A73-31464

Parachute-payload system performance prediction for cause and effect relationships by parametric sensitivity and regression analysis for optimal design with computer simulation

[AIAA PAPER 73-487]

15 p1829 A73-31469

Proportional counter energy deposition spectral quality prediction from experimental data, using folding procedure to produce composite energy absorption distributions for biological materials

15 p1839 A73-31549

Optimal and linear sub-optimal control of second-order saturating control systems.

15 p1853 A73-31626

A note on the use of a simple technique for failure prediction using resistance curves.

15 p1951 A73-31989

Three bladed model rotor gust induced impulsive discrete noise characteristics prediction by point dipole and rotational noise theories for comparison with measurement

16 p1967 A73-32917

Adhesive viscoelasticity effects on sandwich structure performance, presenting mathematical model for adhesive behavior and time dependent loading

16 p2029 A73-33053

Transient oscillator analysis of a high-pressure electrically excited CO laser.

16 p2024 A73-33082

Signal bandwidth consideration for electromagnetic compatibility specifications, comparing broad and narrow band measurements performance by computerized simulation

16 p1979 A73-33169

Gated phase locked loop tracking device for maximum likelihood estimation of pulsed sinusoid imbedded in noise, predicting phase noise performance

16 p1980 A73-33408

The effectiveness of flow control devices and circuits.

16 p1970 A73-33473

Comparative analysis of turbine loss parameters. [ASME PAPER 73-GT-91]

16 p1964 A73-33529

An approach to the analysis of performance of quasi-optimum digital phase-locked loops.

16 p1992 A73-33743

Modeling, identification and prediction of a class of nonlinear viscoelastic materials. I.

16 p2082 A73-33904

Study of incidence loss models in radial and mixed-flow turbomachinery.

17 p2092 A73-34384

Theoretical and experimental analysis of the design and off-design performance of supersonic turbine nozzles.

17 p2093 A73-34387

Book - Gas turbine theory /2nd edition/.

17 p2221 A73-34471

Performance of low-aspect-ratio diffusers with fully developed turbulent inlet flows. II - Development and application of a performance prediction method.

[ASME PAPER 73-FE-13]

17 p2152 A73-35010

Aerodynamic design parameters effects on static performance of short ducted fans for helicopter tail rotor applications, comparing theoretical analysis and experimental results

[AHS PREPRINT 701]

17 p2104 A73-35052

Strapdown air navigation with dry inertial instruments and high speed general purpose digital computer predicting system performance by position error analysis

17 p2210 A73-35211

Gunn-effect digital functional devices and their performance evaluation.

17 p2143 A73-35814

Solid propellant rocket burning rate optimization at constant thrust by imbedded inert heat conducting fibers, analyzing flight performance

18 p2342 A73-36064

Reflecting heat-shield entry analysis computer program for planetary probes.

[AIAA PAPER 73-714]

18 p2368 A73-36333

A probabilistic approach to the design of heat pipes. [AIAA PAPER 73-754]

18 p2370 A73-36370

Computer models for air traffic control system simulation.

18 p2335 A73-36843

Stationary high-current plasma accelerators

19 p2466 A73-37359

Whole aircraft and component design optimization, discussing criteria, constraints and performance prediction accuracy during feasibility analysis and project design

19 p2378 A73-37410

FET for AM large signal processing and regulation without distortion in resonant circuits, discussing characteristics and harmonic analysis

19 p2409 A73-37433

Design method of the axial-flow blade row on modified isolated aerofoil theory with interference coefficient. II - The influence of the aerodynamic parameter on the fan performance at low flow rate.

19 p2377 A73-37671

The prediction of pilot acceptance for a large aircraft.

19 p2453 A73-38073

Negative resistance oscillators, predicting fundamental, harmonic and subharmonic locking characteristics by nonlinear models and equivalent circuit

19 p2410 A73-38307

Analytical model for long term performance prediction of multihundred watt radioisotope thermoelectric generator with Si-Ge alloy as thermoelectric material, noting degradation mechanisms

19 p2390 A73-38391

Nickel-cadmium battery performance prediction models Apollo Telescope Mount application.

19 p2390 A73-38399

GOES system data collection performance estimates.

20 p2525 A73-38743

Communication system with self limiting multiple access repeaters, calculating critical intermodulation power levels resulting from N equal amplitude carriers for comparison with measurements

20 p2526 A73-38750

Performance estimate for coherent QPSK with random intersymbol interference due to time-varying scatter.

20 p2527 A73-38765

System performance prediction by modeling test data in digital simulations.

[AIAA PAPER 73-880]

20 p2543 A73-38816

Fluidic strain gages based on detection of flow resistance or pressure drop changes due to elongation, comparing various type gage factors

20 p2564 A73-38873

Effect of longitudinal magnetic field on the performance of a channel electron multiplier.

20 p2565 A73-38884

Analytic theory for silicon double-sided n+/n-p-p+/n TRAPATT-diode structures.

20 p2538 A73-39594

Prediction of the dynamic and quasi-static performance characteristics of fluoric wall-attachment amplifiers.

20 p2511 A73-39756

Linear fire control predictor with non-Gaussian inputs, calculating on-target probability lower bounds for verification by digital simulation

21 p2649 A73-40332

Performance degradation plots for comparison of signal fading and intersymbol interference effects in two-component specular multipath digital microwave communication channel

21 p2649 A73-40336

Prediction of long-term heat-pipe performance from accelerated life tests.

21 p2643 A73-40438

Considerations concerning the evaluation of the detection probability in radar systems

21 p2650 A73-40500

Design of a phased array radiating face for prevention of performance degradation in the presence of rain.

21 p2663 A73-40663

Analog to digital converters with logarithmic input-output law, comparing performance and complexity of various realizations

21 p2658 A73-41145

Evaluation of burst error correcting codes using a simple partitioned Markov chain model.

21 p2656 A73-41168

Phase-tracking performance of direct-detection optical receivers.

21 p2656 A73-41169

Prediction methods for the susceptibility of solid state devices to interference and degradation from microwave energy.

22 p2823 A73-41796

Theory and performance of plated thermocouples.

22 p2859 A73-42051

Laser Doppler velocity measuring system parameters and SNR analysis, comparing photomultiplier, p-i-n and avalanche photodiode detectors for performance

22 p2825 A73-42298

PERFORMANCE TESTS

Electromagnetic flowmeters with point electrodes and finite length insulating liners, discussing performance numerical analysis accuracy by comparison with exact analytic solutions

22 p2860 A73-42300

Mathematical modeling of combustors based on turbulent mixing, droplet evaporation and chemical kinetics, considering stirred reactor heat balance and combustor performance prediction

22 p2935 A73-42789

Standard sensitivity and covariance matrices for statistical estimation of overall performance.

23 p2962 A73-43279

Finite journal bearings with stepwise discontinuity in hydrodynamic film shape, predicting optimal performance as function of step height, eccentricity and L/D ratios

23 p2984 A73-43293

The prediction of the performance of variable geometry free gas turbines.

23 p3019 A73-43297

Evaluating the performance of shell-and-tube heat-exchangers.

23 p3048 A73-43299

Of fluid mechanics and fluidics and of analysis and physical insight.

23 p2945 A73-43432

Bipolar transistor emitter efficiency calculation, considering heavy doping induced impurity profiles effects on current gain

23 p2958 A73-43451

Fiber reinforced composite crack model performance prediction and tests, noting fiber volume fraction for maximum fracture toughness

23 p3040 A73-43629

IMPATT diode frequency-independent small-signal equivalent circuit incorporated with negative resistance element and white noise source for terminal behavior prediction

23 p2964 A73-44074

Fall-off of base component of f_T/f at low currents in a bipolar transistor.

23 p2961 A73-44148

Three-component sonic anemometer for wind speed measurement, calculating transfer functions for effect of line averaging and path separation on spectral response

23 p2983 A73-44266

Some results in predicting the states of semiconductor triodes from noise factors on the basis of the statistical theory of pattern recognition

23 p2961 A73-44297

Development of methods for long-term prediction of heat-resistance characteristics

24 p3099 A73-44768

Performance prediction in a single-operator simulated surveillance system.

24 p3063 A73-44775

Prediction equation validity for response surface methodology analysis of surveillance tracking by human operators, comparing variance and regression procedures

24 p3063 A73-44776

Hirs turbulent lubrication theory, discussing plane inclined slider thrust bearing applications and performance predictions

24 p3094 A73-44891

Some comments to mathematical interpretation of performance characteristics of jet engine combustion chambers.

24 p3123 A73-45381

The effect of amplifier gain-bandwidth product on the performance of active filters.

24 p3073 A73-45393

Predicted electron transport coefficients and operating characteristics of CO₂-N₂-He laser mixtures.

24 p3097 A73-45420

Darlington composite transistor frequency properties concerning alpha and beta cut-off points and high frequency power gain in common-emitter configuration

24 p3073 A73-45481

PERFORMANCE TESTS

Mathematical formulation for classification, realization and evaluation of electronic components and systems reliability tests

01 p0023 A73-10647

Thermal analysis and its verification test of a small probe for space use.

01 p0052 A73-11147

M-4 S four-stage solid propellant rocket launch vehicle for scientific satellites, detailing design and performance characteristics

01 p0111 A73-11158

Laboratory experience with long-term bearing lubrication.

01 p0057 A73-11278

Model coil test results for a pulsed superconducting magnet energy storage system.

02 p0132 A73-11831

Design and model tests for a 5 Tesla superconducting saddle magnet.

02 p0132 A73-11837

Channel electron multiplier prepared from shaped glass tubing with inner conductive coating, discussing electron and photon detection characteristics

02 p0146 A73-11954

System design, breadboard construction and tests of slope reversal video processor based on tapped delay line estimation with timing discriminator

02 p0167 A73-11957

A fundamental method for evaluating the contaminant tolerance of fluid power control valves.

02 p0132 A73-12003

Design and test of a small, high-pressure ratio, axial compressor with tandem and swept stators.

[SAE PAPER 720713] 02 p0203 A73-12010

Designing limiter/detectors for ECM receivers.

02 p0143 A73-12569

A versatile silver oxide-zinc battery for synchronous orbit and planetary missions.

02 p0133 A73-12622

Experimental approaches to well controlled studies of thin-film nucleation and growth.

02 p0201 A73-12633

Performance characteristics of a helical TEA CO₂ laser.

02 p0177 A73-12745

The effect of environmental factors on seal performance of VITON E-60C fluoroelastomer.

03 p0331 A73-13027

United States SST electrical power system evaluation.

[AIAA PAPER 72-1055] 03 p0252 A73-13386

Effects of transverse ribs on pressure recovery in two-dimensional subsonic diffusers.

[AIAA PAPER 72-1141] 03 p0243 A73-13447

Ammonium perchlorate/aluminum powder propellant rocket engine feasibility evaluation, considering test firing results on performance and stability characteristics for various injector configurations

[AIAA PAPER 72-1162] 03 p0357 A73-13463

Installation effects on performance of multiple model V-STOL lift fans.

[AIAA PAPER 72-1175] 03 p0250 A73-13471

Gas generator system with continuously burning driver propellant and demand propellant combustion during exposure to driver gas flow, testing performance

[AIAA PAPER 72-1193] 03 p0358 A73-13483

ATS-F satellite borne radio beacon transmitter experiment for obtaining ionospheric electron content, discussing design, in-orbit performance, calibration information dissemination and propagation measurement

03 p0275 A73-13639

Supersonic compressor performance for gas turbine engines, discussing cascade, single stage compressor rigs and experimental engine test results

03 p0360 A73-14152

Solar cell optical properties effects on electrical and thermal performance and cost savings in panel design optimization

03 p0255 A73-14226

Performance test of flexible rolled-up solar array /FRUSA/ via telemetered data from accelerometers, strain gages and temperature sensors, noting feasibility for spacecraft power supply

03 p0256 A73-14236

Solar array and supporting technologies development, discussing manufacturing, handling, design qualification tests in space environment and comparison between fold-up and roll-up types

03 p0257 A73-14237

Li and Si p-n solar cells performance comparison for simulated earth orbit environment by real time irradiation with Sr 90 beta particles

03 p0257 A73-14243

ATS-5 solar cell experiment after 699 days in synchronous orbit.

03 p0257 A73-14244

Performance of liquid jet pumps at elevated temperatures.

03 p0317 A73-14502

Experimental investigations concerning pneumatic ejectors, with special reference to the effect of dimensional parameters on performance characteristics.

03 p0297 A73-14503

An investigation of fatigue life performance in lap-type solder joints.

04 p0452 A73-14852

Fuel cell air cathode for high current densities at low polarization and ambient temperature, noting performance improvement with pure oxygen supply

04 p0407 A73-15112

Manned spacecraft digital TV system channel error correcting encoder and decoder performance test data including bit error rate versus SNR and decoding depth

04 p0419 A73-15400

TDM link with digitized voice channel and PCM telemetry sequence coding for error correction, comparing tested performance with prediction and computer simulation

04 p0419 A73-15401

Real time digital spacecraft TV with data compression/error correction test system, evaluating source

encoding algorithm performance from processed picture quality

04 p0449 A73-15409

Pressure vessel proof test variables and flaw growth.

05 p0581 A73-16129

Performance of hardened P-MOS devices in severe neutron environments.

05 p0557 A73-16517

Neutron irradiation effects on microwave transistor amplifiers.

05 p0558 A73-16520

Performance comparisons for joystick and track ball optimized control configurations operating in rate and position modes

05 p0543 A73-16706

Results of an experimental program for the development of sonic inlets for turbofan engines.

[AIAA PAPER 73-222] 06 p0645 A73-17664

Intrinsic models for computer storage allocation program locality concept, comparing performance in terms of working set size and missing page probability by experiments

06 p0670 A73-18060

Ancillary information effects on photointerpretation performance under four imagery system operation modes, noting identification accuracy independence on information variables

06 p0658 A73-18245

Electro-optical laser beam deflector with lithium niobate for low resolution and high speed operation, discussing system design, construction and tests

06 p0700 A73-18296

Low power thermoelectric cascade for cooling substrates to 145 K, discussing materials electrical and thermal properties, design optimization, computerized performance simulation, fabrication and testing

06 p0683 A73-18316

Design, production, reliability analysis and testing of Eole satellite decoder for balloon sounding data, noting performance tests

07 p0790 A73-18966

Ion thruster thermal characteristics and performance.

07 p0867 A73-19488

Minimum performance standards - Airborne distance measuring equipment /DME/ operating within the radio-frequency range of 960-1215 megahertz.

07 p0849 A73-19575

Cone shaped arc discharge driver chamber for high energy shock tube, presenting performance characteristics test data

07 p0808 A73-19969

Bayes criteria and previous test data for industrial equipment test optimization, using linear and quadratic programming

07 p0831 A73-20076

Pressure gage performance tests for air turbine through flow static pressure measurement

07 p0824 A73-20100

The space environment simulation chamber of the Toulouse space center

07 p0808 A73-20245

Operational tests of the K-115 loop oscillograph

07 p0828 A73-20548

A modular approach to an automated digital test system.

08 p0940 A73-20678

Computer controlled automatic test system for circuits, assemblies and systems performance and test programs on-line generation, editing and validation

08 p0940 A73-20682

Fluidics test methods and instrumentation.

[SAE ARP 1254] 08 p0928 A73-20695

Central nervous system stresses effects estimation, discussing ocular positioning movements functional significance and psychological processes

08 p0935 A73-21542

Electrostatic getter-ion pump performance.

08 p0989 A73-21618

A summary of wind tunnel research on tilt-rotors from hover to cruise flight.

[ONERA, TP NO. 1133] 08 p0928 A73-21683

Use of open-structure channel electron multipliers in sounding rocket experiments.

09 p1080 A73-22105

Gradual degradation of GaAs double-heterostructure lasers.

09 p1092 A73-22241

Sealed cylindrical high energy density Ni-Cd batteries, discussing electrode design and performance characteristics

09 p1034 A73-22754

Spacecraft Ni-Cd battery cycle life performance tests, noting cycle life-cycle duration relationship

09 p1034 A73-22755

Nonleaking battery terminals design for polyphenylene oxide plastic cased Ag-Zn battery for synchronous satellite applications, describing life tests under thermal and electrical cycling

09 p1034 A73-22757

Thermoelectric generators long term tests, discussing SNAP 11, 19 and 27, TEM-10 and

SiGe/PbTe cascaded generator performance characteristics 09 p1136 A73-22760

Co-60 fueled tubular radioisotope thermoelectric generator, correlating long term test data with performance prediction model results 09 p1117 A73-22764

SNAP 19 thermoelectric generator long term performance tests, attributing output degradation to sublimation and hot junction bond loss due to internal gas cover depletion 09 p1118 A73-22765

Thermoelectric panel array of hybrid thermocouples with p-type Si-Ge encapsulated PbTe/Si-Ge n-legs, presenting performance test results as function of test time 09 p1134 A73-22766

Radioisotope thermoelectric converter for Navy TRANSIT navigational satellite 5 year power supply, describing design and performance test data 09 p1034 A73-22767

3000 hour endurance test of a 6 kWe organic Rankine cycle power system. 09 p1034 A73-22769

Thermionic fuel unit cell major component materials selection for life and performance improvements, giving out-of-pile and in-pile results 09 p1036 A73-22816

Testing of the improved SNAP 19-primary power for advanced space missions. 09 p1038 A73-23285

Subjective comparisons of analog and digital TV transmission system, considering spectral occupancy and picture quality 09 p1055 A73-23387

Impact of solar calibration on telemetry system testing and checkout. 09 p1057 A73-23407

Filling tests in single and double arm plenum configuration models used in gasdynamic laser systems, noting wave controlled unsteady flow processes 09 p1030 A73-23447

Criteria for self loosening of fasteners under vibration. III. 10 p1222 A73-23524

Theoretical and experimental study of the performance of quasi-steady MPD thrusters 10 p1262 A73-24499

Joint operation of the last gas-turbine stage and a diagonal diffuser 11 p1299 A73-25050

Radome precision testing for fire control, missile aiming, Doppler navigation and bombing 11 p1335 A73-25277

Development of loaded resin one-piece radomes 11 p1387 A73-25294

Terrain-vehicle dynamic interaction studies of a mobility concept (ELMS) for planetary surface exploration. [AIAA PAPER 73-407] 11 p1343 A73-25536

Ti alloy coating and surface treatment to prolong fatigue life by eliminating fretting damage, discussing design parameters selection, screening and strength tests and performance evaluation 11 p1383 A73-25838

Performance of an auxiliary power unit on anhydrous hydrazine. 11 p1308 A73-25980

Performance studies on a rechargeable hydrogen-oxygen fuel cell. 11 p1309 A73-25988

Solar cell dark I-V characteristics and their applications. 11 p1310 A73-26003

TRANSIT radioisotope thermoelectric generator technology, discussing structural design, thermal efficiency, performance prediction, panel configurations and life test data 11 p1312 A73-26034

The SNAP-19 radioisotopic thermoelectric generator experiment - Flight performance on the Nimbus III observatory. 11 p1396 A73-26037

Preliminary testing of a SNAP-19 TAGS RTG in support of the Pioneer F and G missions. 11 p1396 A73-26039

Measurement of hydrazine gas generator performance by gas chromatography. 11 p1326 A73-26398

InSb and Ga-doped Ge bolometers performance tests, discussing detector circuitry and dc, noise and responsivity measurements 11 p1368 A73-26512

Diagnostic tests and failure checkout for interconnected combinational micrologic circuit components in manufacturing process, tabulating individual failure functions 12 p1474 A73-26755

Hg vapor laser with He, Ne, Kr, H or N additions, investigating population inversion and lasing properties for optimal performance conditions 12 p1504 A73-26887

Empirical estimation of the service life of injection lasers from short-term tests. 12 p1507 A73-27523

Aerial cameras functional testing and calibration, discussing film plane flatness measurement methods and camera applications to ice surface photography 12 p1502 A73-27971

Studies of noble-gas lasers for continuous operation 13 p1627 A73-28790

Design and evaluation of combustors for reducing aircraft engine pollution. 13 p1670 A73-28932

Effect of solidity on rocket pump inducer performance. 13 p1624 A73-29011

Low speed of sound modeling of a high pressure ratio centrifugal compressor. 13 p1566 A73-29020

Oblique shock wave generation and quenching in curved supersonic diffusers at Mach 1.6, noting dependence on boundary layer properties 13 p1566 A73-29021

Constant current and temperature hot-wire anemometer systems evaluation via ratio of changes in bridge balance to heat transfer changes between sensor and environment 13 p1620 A73-29257

Study on material for investment cast turbine wheel. 13 p1642 A73-29518

Influence of transient conditions on the overall service life of turbine blades 14 p1785 A73-30676

Evaluation of the performance of a signal detection system by counting the overshoots of an internal threshold 15 p1842 A73-31359

Drag effectiveness of aerodynamic brakes in series on high speed train-like vehicle, considering fixed and moving model testing techniques [AIAA PAPER 73-476] 15 p1828 A73-31460

Reliability testing of high-perveance three-electrode guns 15 p1851 A73-32215

Aircraft flight control head-up display system design, equipment installation particulars, performance tests and merits evaluation 15 p1831 A73-32508

Positioning accuracy with binary selective and fixed gain manual control systems, using finger stick control for operator performance tests 15 p1840 A73-32583

Protective helmets performance evaluation for design optimization, considering failure analysis from aircraft accident reports 16 p1973 A73-32655

Ultrafast spark gaps for electro-optical device control, discussing trigger system design and performance in terms of delay, jitter and internal voltage time response 16 p2013 A73-32874

Phenomena associated with bench and thermal-vacuum testing of super conductors - Heat pipes. 16 p2084 A73-33131

Investigation of the aerodynamic performance of small axial turbines. 16 p1963 A73-33481

Experimental evaluation of the effects of a blunt leading edge on the performance of a transonic rotor. [ASME PAPER 73-GT-60] 16 p1964 A73-33515

The role of testing in achieving aerospace systems effectiveness. 16 p2020 A73-33605

Universal operating characteristic curves for sequential probability ratio tests. 16 p2020 A73-33611

Magnetic-tape qualification and acceptance testing. 16 p2016 A73-33616

DC9-30 refrigeration system diagnosis by computer. 16 p1969 A73-33654

Low-speed performance of a compressor cascade designed for prescribed velocity distribution and tested with variable axial velocity ratio. 17 p2093 A73-34393

Performance measurements of aircraft electrical systems having highly distorted voltage and current waveforms. 17 p2135 A73-34604

Performance and economic advantages offered by a diffused semiconductor strain gage pressure transducer. 17 p2167 A73-34626

High strength continuous filament wound carbon fiber reinforced plastic performance evaluation for use in light weight rocket motors 17 p2195 A73-34810

The effects of environment on performance of fluoroclastomers in seal applications. [ASLE PREPRINT 73AM-8B-2] 17 p2179 A73-34994

Performance of low-aspect-ratio diffusers with fully developed turbulent inlet flows. I - Some experimental results. [ASME PAPER 73-FE-12] 17 p2152 A73-35009

Flight-critical fail-operative and endurance tests for SST electrical power system 17 p2109 A73-35252

Book - Handbook of adhesive bonding. 17 p2180 A73-35337

The orbital test satellite for the European Communication Satellites Programme - Performance and growth capability. [DGLR PAPER 73-044] 17 p2126 A73-35481

Shop level maintenance of inertial platforms without a surveyed site. 17 p2148 A73-35644

Certification program for the DC-10 slide/raft. 17 p2108 A73-35807

Construction and testing of a gas-loaded, passive-control, variable-conductance heat pipe. [AIAA PAPER 73-727] 18 p2369 A73-36344

Wind tunnel and flight tests for Saturn S-2 stage polyurethane spray foam insulation erosion under aerodynamic heating, shear stress and static pressure [AIAA PAPER 73-740] 18 p2326 A73-36357

Orbiting Astronomical Observatory heat pipe flight performance data. [AIAA PAPER 73-758] 18 p2370 A73-36373

Thermal design and testing of the Apollo 17 lunar traverse gravimeter. [AIAA PAPER 73-771] 18 p2316 A73-36385

Verification of performance of the Mariner 9 television cameras. 19 p2428 A73-37258

Comparative study of patches for liquid cooled garments. 19 p2398 A73-37404

Compatibility and satisfactory performance of individual Space Shuttle elements, discussing development/flight cost tradeoff, booster thrust vector and optimal control 19 p2492 A73-37600

Space Shuttle development, qualification, acceptance and horizontal/vertical flight tests for Orbiter, solid rocket motor and drop tank element subsystems 19 p2492 A73-37602

ACLS CC-115 model simulation, test analysis and correlation. 19 p2382 A73-37693

Navigation and landing aid systems in-flight and ground performance monitoring, discussing safety, legal, operational and economic aspects 19 p2450 A73-37802

NaK-nitrogen liquid metal MHD converter tests at 30 kW. 19 p2389 A73-38311

Thrust stand performance measurements of a lithium fueled applied field MPD arcjet. 19 p2473 A73-38320

Performance test equipment of Transit generator with lightweight Isotec thermoelectric panels 19 p2455 A73-38395

Design and testing of a 150 watt SNAP 19 high performance generator. [IEECR PAPER 739090] 19 p2458 A73-38437

Study of a compact counterflow heat-exchanger with mercury at small Peclet numbers. [ASME PAPER 73-HT-54] 20 p2626 A73-38575

Concepts of high-capacity communications satellites. 20 p2613 A73-38714

Linear acceleration insensitive balanced rotor seismic angular motion sensor with optical pickoff system, discussing mathematical model and performance tests [AIAA PAPER 73-829] 20 p2564 A73-38774

The selection of test frequencies for system fault diagnosis. [AIAA PAPER 73-864] 20 p2586 A73-38802

A study of the characteristics of surface charge transfer devices 20 p2534 A73-38854

Questionnaire survey covering development, qualification, acceptance and flight test roles in achieving aerospace vehicles systems effectiveness/reliability, maintainability and safety/ 20 p2544 A73-39248

Microwave Landing System with air-derived sample data and scanning narrow beam antennas for signal-in-space generation, discussing design requirements and performance test 21 p2735 A73-40046

Large phased array antenna pattern measurements for performance, monitoring and maintenance checks 21 p2653 A73-40679

Relative performance of a variety of NF3/+/- hydrogen-donor transverse-discharge HF chemical-laser systems. 21 p2714 A73-40757

FFTF probe-type eddy-current flowmeter - Wet versus dry performance evaluation in sodium. 21 p2738 A73-40768

Book - The role of testing in achieving aerospace systems effectiveness. 21 p2675 A73-41201

Manned and unmanned aerospace launch vehicle liquid and solid rocket propulsion system effectiveness survey questionnaire response data concerning various tests 21 p2781 A73-41202

US Department of Defense aircraft system effectiveness tests survey questionnaire response data from component, subsystem and system suppliers

21 p2635 A73-41204

Commercial aircraft system effectiveness survey questionnaire response data concerning various tests in manufacturing and operational environments

21 p2635 A73-41205

Simulator performance validation and improvement through recorded data.

[AIAA PAPER 73-938] 22 p2838 A73-41972

Studies of the performance of W-Re type thermocouples.

22 p2858 A73-42039

Monograph - Development and performance of a solar hard X-ray spectrometer.

22 p2861 A73-42674

Helix support, focusing, fabrication and performance tests of miniature traveling wave tubes /TWT/, using rare earth-cobalt /RAECO/ magnets

22 p2834 A73-42696

Product reliability management, providing MTBF charts for relationships between part count, laboratory test results and operational performance

22 p2867 A73-42969

Design and performance of light-intensification night vision telescopes

23 p2979 A73-43220

Performances and physical limitations of image intensifiers

23 p2979 A73-43221

Oil hydraulic fluidic amplifier mathematical model and computerized design for power consumption optimization at high pressures, testing performance dependence on viscosity

23 p2942 A73-43405

Fluidic linear nozzle-flapper valve accelerometer for ship motion sensing, describing circuit configuration and performance tests

23 p2981 A73-43428

Fiber reinforced composite crack model performance prediction and tests, noting fiber volume fraction for maximum fracture toughness

23 p3040 A73-43629

Oversize waveguide polarization diplexers based on metal grating or dielectric plate at Brewster angle, measuring performances in microwave circuit and with HCN IR laser

23 p2960 A73-44071

The scale effect and design method of the regenerative pump with non-radial vanes.

23 p2986 A73-44274

The effects of modulated blade spacing on static rotor acoustics and performance.

[AIAA PAPER 73-1020] 24 p3121 A73-44852

A new device for measuring local acoustic power output of subsonic jets.

[AIAA PAPER 73-1042] 24 p3090 A73-44866

Pseudorandom Poisson process binary pulse generator, discussing digital hardware implementation and test results

24 p3069 A73-45256

Performance of a large-bore high-power argon ion laser.

24 p3097 A73-45422

PERICLASE

Investigation of the effect of pressed-powder grain composition on the physico-mechanical properties of magnesia refractory materials

17 p2187 A73-34337

Effect of aluminum-containing components on phase alloying in periclas ceramic materials

24 p3104 A73-44953

PERIODOTTE

Analytical approach to estimating the source rock of basaltic magmas - Major elements.

09 p1076 A73-22147

PERIGEE

Analysis of the orbit of Cosmos 316 /1969-108 A/.

02 p0225 A73-12824

PERIHELIONS

Calculation of the perihelion advance of planets in a field approach to gravitation.

02 p0225 A73-12802

General relativity in the equal proper time formalism.

06 p0724 A73-18626

Comets origin in interstellar space or solar system evaluated with reference to comet streaming from perihelions statistical analysis, assuming Oort cloud accretion

14 p1794 A73-29838

New statistical laws governing the system of long-period comets

19 p2480 A73-37235

The cause of the residuals in the motion of Halley's comet.

22 p2907 A73-42210

Airborne photographic and visual observation of material from Comet Giacobini-Zinner produced meteor showers due to orbit perturbation and perihelion changes by Jupiter

22 p2909 A73-42588

Meteorite production mechanism from asteroid belt via asteroidal collision fragments perihelion changes and orbit perturbation by Jupiter into earth-crossing orbital elements

23 p3027 A73-43336

Orientation-dependent effects in Oort's theory of comet origin. II - Anisotropies in the distribution of long-period comet orbits.

24 p3131 A73-44467

The next return of the comet of the Perseid meteors.

24 p3135 A73-44583

PERIOD EQUATIONS

U PERIODIC FUNCTIONS

PERIODIC FUNCTIONS

NT TRIGONOMETRIC FUNCTIONS

Validity of averaging methods for certain systems with periodic solutions.

01 p0070 A73-10273

Doubly-periodic problem in elasticity theory for an isotropic medium weakened by congruent groups of arbitrary holes

01 p0116 A73-10961

Uniqueness and stability of positive periodic solutions of differential equations with a delayed argument

02 p0187 A73-12357

Behavior of the periodic surface for a periodically perturbed autonomous system and periodic solutions.

04 p0469 A73-14665

Existence theorem for nonlinear oscillatory equations of motion transformation into normal form, noting quasi-periodic functions with arbitrary frequencies

04 p0475 A73-14888

Convergence of the small parameter method in deriving periodic solutions to ordinary neutral-type differential equations with small delay

06 p0718 A73-18680

A class of almost periodic motions in systems with impulses

06 p0724 A73-18681

Time-periodic solution of the system of boundary layer equations.

07 p0809 A73-19019

An analytical method for certain weakly nonlinear periodic differential systems.

07 p0845 A73-20226

Fourier transformation of two-dimensional signals. I

09 p1119 A73-21899

Periodic solution of a second-order non-linear differential equation.

09 p1113 A73-22985

Periodic method of characteristics for solution of hyperbolic partial differential equations of physical system specified by two boundary conditions at single spatial location

10 p1241 A73-23604

The use of operators with degenerated kernel for nonlinear system investigation.

10 p1242 A73-24043

Stability of planar oscillations of a satellite in an elliptic orbit.

10 p1287 A73-24663

Initial conditioned solutions of a second-order nonlinear conservative differential equation with a periodically varying coefficient.

10 p1244 A73-24706

Periodic solutions of the third sort for restricted problem of three bodies and their stability.

11 p1423 A73-26068

Doubly-periodic problem of the theory of elasticity for an isotropic medium weakened by congruent groups of arbitrary holes.

12 p1554 A73-27537

A method of studying oscillatory systems subject to the action of external periodic forces in the nonresonant case

12 p1525 A73-27812

Methods for the approximate computation of the periodic solutions of systems of nonlinear periodic differential equations

13 p1647 A73-28193

Periodic solutions of piecewise-continuous systems with a small parameter

13 p1661 A73-29084

Extension of the Favard theory to the case of a system of linear differential equations with unbounded coefficients which are nearly periodic according to Levin

14 p1771 A73-30837

Approximation of differentiable functions of numerous variables by Fourier sums in an L sub p metric

15 p1899 A73-31218

Periodic solutions of the restricted three-body problem encompassing a large number of revolutions about the smaller body

15 p1931 A73-31240

The period of nonlinear vibrations of autonomous dynamical systems of the order n

15 p1947 A73-31366

Algebraic criteria for positive realness relative to the unit circle.

16 p2032 A73-33162

Periodic solutions of singularly perturbed equations arising from gyroscopic systems.

16 p2032 A73-33310

Convergence of periodic solutions of differential equations for resonance circuits with nonlinear semiconductor capacitance

17 p2144 A73-34585

Oscillations of a system with two degrees of freedom during resonance

17 p2213 A73-35591

The numerical derivation of a periodic solution of a second order differential difference equation.

17 p2203 A73-35728

Russian book - Linear differential equations with periodic coefficients and their applications.

18 p2329 A73-35903

Finite amplitude Kelvin-Helmholtz billows, describing periodic solutions of nonlinear Boussinesq equation

19 p2448 A73-38230

Application of the averaging method to the study of oscillatory systems with distributed parameters and time lag

20 p2592 A73-38978

Stress-concentration at a hole with periodic irregularities

20 p2619 A73-39334

Application of a truncation method in the derivation of a multiperiodic solution of a denumerable system of partial differential equations

20 p2582 A73-39473

Stability of an almost periodic solution to a generalized Duffing equation

20 p2593 A73-39493

Special periodic solutions and asymptotic properties of a class of quasi-linear differential equations with delayed argument

20 p2583 A73-39509

Quasi-periodic solutions existence, uniqueness and asymptotic behavior to quasi-linear parabolic equations, demonstrating vanishing conditions at boundary

23 p3049 A73-43611

Numerical exploration of commensurable periodic solutions of the restricted problem of three bodies and their stability.

23 p3029 A73-43746

On the Stepanov-almost periodic solution of an abstract differential equation.

24 p3105 A73-44420

Time-varying network analysis via matrix manipulation and Peano-Baker solution for second and higher order differential equations with periodic coefficients.

24 p3075 A73-45477

PERIODIC OSCILLATIONS

U OSCILLATIONS

PERIODIC VARIATIONS

NT ANNUAL VARIATIONS

NT DIURNAL VARIATIONS

NT NOCTURNAL VARIATIONS

NT SECULAR VARIATIONS

Periodically correlated random processes to model additive and multiplicative rhythmic phenomena, discussing structural properties and theorems

01 p0075 A73-10028

Short-term pulsar intensity variation in the frequency range 70-115 MHz. I - Correlation measurements.

01 p1006 A73-11306

Scanning electron microscope investigation of interaction between pyrolytic carbon fibers and oxidizer, noting periodic variations of carbon chemical activity in radial direction

02 p0185 A73-12556

Periodicities in seismic response caused by pulsar CPI133.

03 p0367 A73-13056

Possible sidereal period for the seismic lunar activity.

03 p0367 A73-13057

Existence theorems for Navier-Stokes equations periodic solution bifurcation in convection between two horizontal plates at different time periodical temperature

[ONERA, TP NO. 1179] 03 p0343 A73-13602

Nonsolar related D region semilunar variation effects on Omega navigation systems signal phase shift from harmonic analysis of VLF propagation data periodicities

04 p0416 A73-15062

Stability of the solar system - Evidence from the asteroids.

04 p0497 A73-15179

12.5-minute periodicity in solar proton fluxes at balloon altitude and in magnetic micropulsations.

04 p0492 A73-15527

Application of structural-temporal functions for analysis of periodicities in atmospheric motions

05 p0593 A73-16240

Electromagnetic wave propagation in a medium with two-dimensionally periodic variations of the refractive index

05 p0548 A73-16268

Comments on a PLC relationship for Cepheids and on the comparison between pulsation and evolution masses for Cepheids.

05 p0625 A73-17334

7.8-GHz flux density measurements of variable radio sources.

07 p0876 A73-19355

Long term atmospheric pressure fluctuations in relationship to solar activity over Northern Hemisphere, confirming 22 year cycle 07 p0816 A73-19448

The heliocentric radial gradient in cosmic ray density and the 'Swinson' sidereal time variation. 07 p0870 A73-19671

Observations of periodic variations in the X-ray intensity of Cygnus X-3. 07 p0872 A73-20240

Cyclic variations of the Be star beta-one Monocerotis. 08 p1006 A73-20924

Stratospheric cosmic ray short period variations at 30 km by spectral density method 08 p1000 A73-21351

Blocking situations lasting less than five days over the Euro-Atlantic region in the 20-year period from 1951 through 1970 08 p0986 A73-21486

Monograph - The quasi-biennial oscillation in the stratosphere. 08 p0986 A73-21841

Quasi-periodic variations in X ray emission from black holes for accretion-formed disk with surface bright spots 10 p1273 A73-23703

Frequency spectrum of cosmic ray intensity and solar activity variations 10 p1267 A73-23924

Delta Scuti variables observational and theoretical data, discussing pulsation properties and relationships to other pulsators and nonvariable stars 10 p1281 A73-24405

Spatial and temporal variations of the Lyman-alpha airglow and related atomic hydrogen distributions. 11 p1356 A73-25909

Long-periodicity fading of short-wave signals 12 p1473 A73-27759

Solar surface photospheric oscillation spatiotemporal power spectrum observation, considering long-period oscillation correlation with chromospheric flare 12 p1544 A73-28288

The effect of two periodic conductivity anomalies on geomagnetic micropulsation measurements. 13 p1607 A73-28622

Determination of the information-forecasting indices of biometeorological phenomena 13 p1579 A73-28861

Cepheid variables model characteristics, determining luminosity, radial velocity and radius time dependent variations 13 p1682 A73-28981

Investigation of the motion of periodic comet Giacobini-Zinner and the origin of the Draconid meteor showers of 1926, 1933 and 1946. 14 p1791 A73-29802

Experimental investigations regarding the behavior of turbulent boundary layers in the case of small periodic pressure changes 14 p1745 A73-30299

Breath to breath cyclical variations in functional residual capacity, oxygen uptake, carbon dioxide release, tidal volume, respiratory period, alveolar gas tension and heart rate 15 p1834 A73-31346

Period determination method for variable stars using interpolation in light curves, noting applicability to light curves with few branches 15 p1936 A73-31645

High pass filter and power spectral analysis of periodicity in solar activity time series, applying statistical tests to sunspot and flare indices 16 p2060 A73-32955

Dynamic gas temperature measurements in a gas turbine transition duct exit. 16 p2047 A73-33485

[ASME PAPER 73-GT-7] Continuing activity of Jupiter and comparison of the 1871-1880 and 1961-1965 flare-ups 16 p2057 A73-33842

A search for periodic variations in geomagnetic activity and their solar cycle dependence. 17 p2157 A73-34073

Periodic variations in geomagnetic activity and sector structure of the interplanetary magnetic field. 17 p2157 A73-34073

Limit cycles resulting from quantization in digital control systems. 17 p2145 A73-35642

Meteor radar observations of long period waves in the 80-100 km altitudes range. 18 p2304 A73-35968

Periodic variations of the cosmic radiation. III - The 27-day variation. 18 p2345 A73-36180

Measurements of ionospheric reflectivity from 6 to 35 kHz. 18 p2289 A73-36286

Quasi-periodic variations in X ray emission from black holes for accretion-formed disk with surface bright spots 18 p2354 A73-36728

Generation of time-periodic secondary convective flows 18 p2301 A73-37006

Comparison and synthesis of the characteristics of long- and short-duration blocking systems over the Euroatlantic region 19 p2447 A73-38124

Conditionally periodic oscillations in nonlinear systems 20 p2593 A73-39500

Research of short-period variations in cosmic rays at Moscow's latitude 21 p2759 A73-40610

Operator response to sinusoidally varying normal and emergency cycles in dynamic control task, testing anticipatory aversion response ability and error response 22 p2812 A73-41885

The investigation of the periodicity of hydrometeorological phenomena according to the autocorrelation method of Fuhrich 22 p2883 A73-42449

Vertical phase variation and mechanical flux in the solar 5-minute oscillation. 22 p2916 A73-43124

Pulsar properties covering galactic distribution, pulse periodicity computed from arrival time measurements, models, emission mechanisms, total intensity pulse shapes, etc 23 p3028 A73-43351

Structure of global geopotential fields in view of the quasi-two-year cyclicity in the equatorial stratosphere 23 p3001 A73-43463

The slab thickness of the mid-latitude ionosphere. 23 p2972 A73-43694

Use of a relaxation technique in nozzle wave propagation problems. [AIAA PAPER 73-1011] 24 p3078 A73-44843

Far field effects of weak spatially periodic inhomogeneities. [AIAA PAPER 73-1036] 24 p3109 A73-44864

PERIODICITY
U PERIODIC VARIATIONS
PERIODICITY (BIOLOGY)
U RHYTHM (BIOLOGY)

PERIPHERAL CIRCULATION
Microvascular responses to alterations in oxygen tension. 01 p0009 A73-11010

Studies of blood gas analysis at abnormal environment. 01 p0013 A73-11210

Ultrasonic Doppler locators for peripheral vessel blood circulation and myocardium and valvular motor activity measurements 06 p0656 A73-17682

Book - Peripheral vascular diseases: Diagnosis and management. 06 p0651 A73-17871

Influence of histamine on cutaneous capillary circulation and on the oxygen tension of subcutaneous cellular tissue in various age periods 10 p1178 A73-23676

Peripheral blood composition changes in cosmonauts during 18- and 24-day space flights 12 p1463 A73-27710

Sustained human skin and muscle vasoconstriction with reduced baroreceptor activity. 15 p1833 A73-31344

Study of lymphocyte chromosome aberrations in human peripheral blood under in vitro exposures to 645-MeV protons and X-rays 15 p1835 A73-31517

Control of forearm skin blood flow during periods of steadily increasing skin temperature. 18 p2278 A73-36657

Changes in the peripheral blood of the rat exposed to microwave radiation /2400 MHz/ in conditions of chronic exposure. 21 p2645 A73-41159

Comparison of plethysmographic and electromagnetic flow measurements. 23 p2950 A73-44215

Cardiovascular adjustments to progressive dehydration. 24 p3060 A73-45063

PERIPHERAL JET FLOW
Air cushion landing gears for transport aircraft, discussing peripheral jet stream performance prediction and system installation on Buffalo STOL 10 p1174 A73-23659

Static performance of plenum and peripheral jet air cushions. 19 p2377 A73-37703

Theory and experiments for air cushion landing system - A ground jet concept. 19 p2383 A73-37704

PERIPHERAL NERVOUS SYSTEM
Study of the peripheral auditory adaptation in a psycho-acoustic experiment 10 p1179 A73-23807

Functional model of the frequency channel of the peripheral auditory analyzer 10 p1183 A73-23808

Role of nerve structures in the action of low-frequency sinusoidally modulated currents on synovial membrane permeability in the knee joint 10 p1180 A73-23943

Effect of whole-body vibration on peripheral nerve conduction time in the Rhesus monkey. 11 p1315 A73-25335

A mathematical model of the peripheral pain signalization mechanism 20 p2516 A73-39003

Mathematical model of human pitch perception based on acoustic stimulus Fourier transformation by sense organ into peripheral neural activity pattern recognition 22 p2811 A73-41816

Shaping device for frequency analysis of electrical processes in peripheral neural stems and ganglia 22 p2815 A73-42664

PERIPHERAL VISION
Peripheral threshold of perceived contrast of the human eye. 09 p1046 A73-22964

Effect of passive 70-deg head-up tilt on peripheral visual response time. 10 p1185 A73-24566

Apparent contraction and disappearance of moving objects in the peripheral visual field. 11 p1318 A73-26198

Differential effects of central versus peripheral vision on egocentric and exocentric motion perception. 11 p1318 A73-26221

Information processing in the visual periphery. 17 p2113 A73-34150

Reaction times for focal and nonfocal peripheral/processing of simultaneously presented color and form stimuli 21 p2639 A73-41182

Visual field defects after missile injuries to the geniculo-striate pathway in man. 21 p2641 A73-41600

Increment thresholds for multiple identical flashes in the peripheral retina. 23 p2946 A73-43343

PERIPHERIES
U BOUNDARIES

PERMAFROST
Restrictions on McElroy theory of Martian chaotic terrain production by permafrost withdrawal, calculating degassed water/carbon dioxide ratios in Mars and earth atmospheres 02 p0218 A73-12418

Lunar permafrost - Dielectric identification. 10 p1282 A73-24629

Lunar sinuous rilles as inverted eskers formed by volatiles /water and carbon dioxide/ moving in channel between basement surface and permafrost layer 17 p2237 A73-35859

PERMALLOYS (TRADEMARK)
Uniaxial magnetic anisotropy of single-crystal permalloy films 09 p1132 A73-21958

Some principles of domain device designing for data processing and means of control. 10 p1198 A73-24022

Magnetic reversal mechanisms of obliquely deposited permalloy films possessing perpendicular anisotropy 12 p1530 A73-26833

PERMANGANATES
Ignition of nonhypergolic rocket fuels with fuming nitric acid under suitable conditions. 01 p0089 A73-10736

PERMEABILITY
NT DIELECTRIC PERMEABILITY
Pressure distribution vs porosity and load variation with permeability for squeeze fluid films in porous metal journal bearings [ASME PAPER 72-LUB-P] 01 p0055 A73-10219

Heat transfer and friction in the turbulent boundary layer of a compressible gas on a permeable surface 08 p0926 A73-20992

Solute rejection by porous glass membranes. II - Pore size distributions and membrane permeabilities. 09 p1048 A73-22525

Measurement of zincate permeation in a polyethylene battery separator with controlled external hydrodynamic conditions. 11 p1307 A73-24974

Investigation of the influence of biologically active substances on the permeability of the skin 15 p1838 A73-31174

Supersonic-hypersonic motion past a permeable cone at zero angle of attack 19 p2376 A73-37544

PERMEATING
Calcia stabilized zirconia electrolyte with appreciable oxygen ionic diffusivity used as permeation membrane for oxygen leak source 02 p0167 A73-11955

Determination of hydrogen permeation parameters in alpha titanium using the mass spectrometer. 09 p1102 A73-22412

PERMITTIVITY
Electromagnetic wave diffraction by ideally conducting homogeneous bodies of revolution with arbitrary complex permittivity and permeability, using separation of variables method 05 p0547 A73-16054

Propagation of radio waves in a triple-layer medium with spheroidal boundary surfaces

05 p0549 A73-16388

Measurement of dielectric constant of nonmagnetic materials in a waveguide system with an unknown movable reflecting load.

06 p0696 A73-18618

Calculation of the asymptotic behaviour of the TDR step response related to the asymptotic behaviour of dielectrics in the frequency domain.

07 p0797 A73-19107

Experimental investigation of the effective permittivity and of the resonator Q of slot lines on ceramic substrates in the frequency range from 1 to 18 GHz

10 p1194 A73-23994

Loaded and artificial dielectric materials with variable permittivity for sandwich radomes, discussing weight saving, multiband coverage and cross polarization reduction

11 p1335 A73-25281

Influence of the illumination law on the radioelectric performance of radomes - Contribution to the determination of apparent illumination of the antenna

11 p1328 A73-25284

Influence of fabrication inaccuracies on the axis deviation of an airborne radome

11 p1328 A73-25295

Radome material technology in UK, summarizing permittivity, loss tangent, internal phase difference, attenuation, aberration, cross polarization and pattern distortion measurements and environmental tests

11 p1336 A73-25308

Reflection and transmission of radio waves at a dielectric slab with variable permittivity.

11 p1329 A73-25675

Intensity and displacement fields of microinhomogeneous medium with random permittivity tensor field described by step functions, using renormalization method

12 p1530 A73-26929

Determination of parameter tolerances for microstrip transmission lines

12 p1470 A73-27580

Nonstationary emission from dipole sources in a plasma with a diagonal permittivity tensor

14 p1780 A73-30263

Mono- and polycrystalline barium titanate structural and physical properties, discussing thermally induced structural changes effects on polarization, permittivity and loss tangent

15 p1924 A73-31775

Remote sensing of complex permittivity by multiple resonances in RCS.

17 p2128 A73-35692

Properties of microwave cavities containing magnetic resonant samples.

17 p2130 A73-35758

Permittivity of a plasma with transverse nonazimuthal fluxes

18 p2339 A73-36552

Semiconductor laser beam self focusing action due to combined effects of linear and nonlinear dielectric constant and absorption coefficients, considering n-InSb sample

21 p2711 A73-40226

Viscous dielectric materials for application in microwave microcircuits.

21 p2668 A73-41589

Bounds on effective dielectric constant of inhomogeneous material.

22 p2896 A73-42263

Short-wave propagation in a randomly inhomogeneous medium with an arbitrary law of permittivity fluctuations

22 p2826 A73-42335

Determination of valence electron plasma frequencies and optical permittivity in single crystals of trisulfide of antimony

22 p2897 A73-42648

Finite-boundary corrections to the coplanar waveguide analysis.

23 p2954 A73-44075

PEROVSKITES

Raman spectrum of PbZrO₃.

21 p2752 A73-40894

High temperature electron transfer and Bi and Sb ion valency pair predictions in ordered perovskite-type oxides, using lattice constants

23 p3017 A73-44129

PEROXIDES

NT INORGANIC PEROXIDES

UV-induced lipid peroxidation in human epidermis, dermis, and hypodermis in vitro

09 p1038 A73-21873

PERSEID METEORIDS

Complex parameter B of Perseids meteors from photographic observations at Dushanbe, giving logarithms

02 p0216 A73-12358

Radio-echo measurements of the flux of the Quadrantid, Perseid and Geminid meteor streams.

11 p1415 A73-25169

The telescopic radiant areas of the Perseids and the Orionids.

11 p1426 A73-26572

Structure of the Perseids radiants in 1971

19 p2481 A73-37243

Variations in the distribution and physical properties of Perseid meteors.

22 p2914 A73-43015

The next return of the comet of the Perseid meteors.

24 p3135 A73-44583

PERSONALITY

Daytime human performance and temperament rhythms as function of individual introversion-extroversion rating

16 p1972 A73-33157

Individual personality variability difficulties in measurement of human psychophysiological reactions to flight stress, emphasizing psychological interview and evaluation methods

22 p2817 A73-43130

PERSONNEL

NT AIRCRAFT PILOTS

NT COSMONAUTS

NT CREWS

NT FLIGHT CREWS

NT FLIGHT SURGEONS

NT FLYING PERSONNEL

NT GROUND CREWS

NT INSTRUCTORS

NT MEDICAL PERSONNEL

NT OPERATORS [PERSONNEL]

NT SCIENTISTS

NT TEST PILOTS

PERSONNEL DEVELOPMENT

Computer assisted instruction for commercial programmer and systems analyst education and training, discussing government use, pretest importance and future developments

09 p1168 A73-22222

Engineering personnel, technical and flight instructors training for introduction to and effective utilization of new civil and military aircraft and weapon systems

13 p1624 A73-28789

Project form of organization adoption for managing innovation, stressing impact of technology on career progression of scientist engineers

17 p2258 A73-35217

Air traffic controller responsibilities and performance evaluation criteria development, discussing manager/monitor functions, field evaluation tests and training criteria

19 p2402 A73-38472

Comparison of the job attitudes of personnel in three air traffic control specialties.

20 p2517 A73-39108

Safe flying, skilled personnel and aircraft maintenance assurance via safety equipment, initial and recurrent training, protective clothing and shelter from inclement weather, maintenance scheduling, etc

20 p2518 A73-39212

PERSONNEL MANAGEMENT

Maintaining vitality and productivity in R & D - Steps to maintain high level staff performance.

10 p1298 A73-24633

Airline pilots problems in terms of job security, working conditions, management relations, public relations, flight safety due to noise abatement rules, etc

12 p1562 A73-27599

Man machine systems for flight safety, studying accidents, human factors in system design and implementation of personnel

17 p2113 A73-34078

Aerospace industry project managers and support personnel authority perceptions based on assessment of situational factors surrounding decision making, tabulating empirical investigation statistics

17 p2257 A73-35214

A survey of behavioral science contributions to laboratory management.

17 p2257 A73-35216

Crew discipline factors in aircraft accident statistics, linking pilot-related accidents to crew carelessness, flight regulation infractions and unfamiliarity with flight conditions

20 p2509 A73-39216

Airline flight crew management and coordination procedures, outlining self-discipline philosophies and criteria, flight training and simulation, and performance records

20 p2509 A73-39217

Flight test programs management and control, considering weapon systems performance tests relative to contractual requirements, personnel allocation and supporting facilities

23 p3051 A73-44060

The capabilities of army test facilities.

23 p2966 A73-44064

PERSONNEL SELECTION

NT PILOT SELECTION

Flight personnel training meetings, covering decision making, cockpit personnel selection and instructor role analysis

03 p0266 A73-13073

Proposed new test for aptitude screening of air traffic controller applicants.

09 p1045 A73-22535

Initial results of a psychophysiological study of certified parachutists

18 p2284 A73-36917

Psychotechnical selection of flight crews in South Vietnam

18 p2284 A73-36918

Hybrid computer laboratory construction, organization and operation principles, including computer selection and personnel requirements

23 p2956 A73-43956

PERSEX [TRADEMARK]

Limit of linear viscoelastic behavior - An energy criterion.

13 p1700 A73-29461

PERSPIRATION

Perspiration secretion distribution over human body based on extended Kerslake cylinder model, comparing with predicted 4 hr sweat rate

03 p0259 A73-13122

Design and function of sweat sensor to monitor motion sickness sweat response

03 p0269 A73-14160

Differential thermal sensitivity in the human skin.

14 p1720 A73-30912

Blood electrolytes and exercise in relation to temperature regulation in man.

18 p2280 A73-36983

Sodium Na-24 and potassium K-42 availability for sweat production after intravenous injection and their handling by sweat glands.

19 p2395 A73-37757

Desoxyribonucleases in sweat gland secretion of man

24 p3059 A73-44674

PERTURBATION

NT ORBIT PERTURBATION

NT SATELLITE PERTURBATION

Optimal stabilization of nonlinear control systems for given region of initial perturbations, reducing optimal synthesis to moments problem

01 p0077 A73-10671

Oscillations of spacecraft with on-off attitude control under constant perturbation moment, calculating energy expenditures for desired orientation maintenance

03 p0383 A73-14559

Application of the ray method to a study of the propagation of large-scale perturbations in a barotropic atmosphere with a mean wind

17 p2204 A73-34345

PERTURBATION THEORY

Equations of motion integral properties-based construction of Liapunov functions used to derive sufficient conditions for perturbed nonlinear system solution stability

01 p0075 A73-10090

A shielding application of perturbation theory to determine changes in neutron and gamma doses due to changes in shield layers.

01 p0075 A73-10244

Stability of large-scale systems under structural perturbations.

01 p0070 A73-10322

Reductive perturbation theory application to nonlinear Schroedinger equation for plasma of cold ions and isothermal electrons, investigating ion oscillation mode automodulation

01 p0082 A73-10420

Effects of gravity-gradient torque on the rotational motion of a triaxial satellite in a precessing elliptic orbit.

01 p0099 A73-10685

Plane stress analysis of an annular disk with distorted inner hole.

01 p0115 A73-10735

Series expansion of the perturbation function

01 p0102 A73-10948

Newtonian analysis of cosmological model for galactic accretion from small initial perturbation of central black hole

01 p0104 A73-11048

Dynamical interaction in biaxial control systems.

01 p0075 A73-11198

Variable reflectivity unstable laser resonator mode selectivity solution by perturbation analysis for mirror misalignment effects, obtaining Fresnel number and output coupling conditions

01 p0060 A73-11223

Nonlinear differential equations with logarithmically small perturbations.

01 p0071 A73-11268

Rotational perturbations in anisotropic cosmology.

01 p0107 A73-11328

Shear waves and perturbations in linearized steady plane flows of a thermally nonconducting compressible ideal fluid

01 p0034 A73-11359

A theory of perturbations in angle-action variables: Application to the motion of a solid about a fixed point - Precession-nutation

01 p0107 A73-11362

On the multi-parameter characteristic perturbation method - Application to nonlinear supersonic nonequilibrium flow over a wedge.

01 p0004 A73-11425

Solution of Troesch's two-point boundary value problem by a combination of techniques.

01 p0035 A73-11470

Dynamics of a rotating free system of bodies with an oriented axis of rotation

02 p0192 A73-11774

Analysis of the longitudinal perturbed motion of a ground-effect flight vehicle

02 p0128 A73-11785

The superconductor maser - A calculation of the gain from the two-level model and the BCS theory, and some new experimental results.

02 p0175 A73-11848

Physical processes responsible for Bode law, noting sufficiency of point mass perturbations for existing distributions of satellite and planetary orbits

02 p0211 A73-11874

Resonance, particle trapping, and Landau damping in finite amplitude obliquely propagating waves.

02 p0197 A73-12068

The propagation of non-uniform slow shock waves.

02 p0198 A73-12092

Low-frequency oscillations in a bounded low-density plasma.

02 p0198 A73-12105

Optimization of control and observation processes in dynamic systems under random perturbations.

02 p0149 A73-12118

An asymmetrically rotating fluid disc with applications.

[AD-751727]

02 p0217 A73-12393

Perturbation technique for approximation of sound radiation from controlled boundary layer on thin plate, deriving random stationary functions in terms of Fourier integral

03 p0291 A73-12992

Lunar librations results of Koziel reevaluated, noting elasticity effects and elastic strain perturbation on satellite

03 p0367 A73-13077

Square well fluid liquid-vapor interface density profiles from perturbation expansion in chemical potential, comparing to BGVB and excess free energy minimization approaches

03 p0342 A73-13277

Boundary-layer methods in microstructure theories of elasticity.

03 p0390 A73-13330

A numerical investigation of secular terms of the planetary disturbing function.

03 p0372 A73-13351

Study of the asymptotic behavior of axial perturbation velocities in the vicinity of singularities

03 p0245 A73-13770

Damping perturbation of high order nonlinear autonomous Liapunov system, reducing system equations integration to quadratures via transformation to lower order quasi-linear nonautonomous system

03 p0344 A73-14054

Perturbation and harmonic balance methods for nonlinear panel flutter.

03 p0395 A73-14182

Behavior of the periodic surface for a periodically perturbed autonomous system and periodic solutions.

04 p0469 A73-14665

A method of perturbation for a weakly nonlinear hyperbolic equation with two small parameters - Study of a mathematical model

04 p0471 A73-15246

Complete spectrum of pulsation frequencies for a polytropic atmosphere.

04 p0504 A73-16029

Error analysis of ionospheric parameter measurement by satellite transmitted or reflected multiple frequency pulsed radiation signal, using perturbation method

05 p0547 A73-16051

Sinusoidal thermal wave propagation in horizontal fluid layer with small Prandtl number, deriving induced mean flow from nonlinear equation solution by perturbation approach

05 p0591 A73-16188

Spacecraft motion control as stochastic dynamic problem formulated according to single criterion for deterministic programmed and stochastic perturbed motions

05 p0629 A73-16425

Stability conditions for strongly flattened galaxy model with respect to axisymmetric disturbances of gaseous subsystem in finite isothermal layer

05 p0616 A73-16456

A stability theory for perturbed difference equations.

05 p0590 A73-16491

A variation-of-parameters perturbation theory for the restricted three-body problem.

05 p0619 A73-16893

Four body problem reduction to three body problem via perturbation region, noting Moon-Earth-Sun system

05 p0623 A73-17198

Effects of resonant tesseral gravity coefficients on Viking-type orbits.

[AIAA PAPER 73-146]

06 p0748 A73-17648

Piston motion in semiclosed tube under high initial pressure, using gas-to-piston mass ratio as perturbation parameter in analysis based on Lagrange solution [DFVLR-SONDDR-255]

06 p0685 A73-17739

The properties of a solution of the equations of motion of a mechanical system subject to irregular /singular/ perturbations.

06 p0722 A73-17755

The electromagnetic perturbation fields of conductivity anomalies within the earth.

06 p0690 A73-17925

Turbulent boundary layers with negligible wall stress - A singular-perturbation theory.

06 p0686 A73-17988

Solution of the low-altitude satellite equations.

06 p0757 A73-18072

Conservation of quasiparticles in weakly turbulent plasmas.

06 p0730 A73-18273

Singular perturbation and turbulent shear flow near walls.

06 p0686 A73-18378

Approximate perturbation solution in Chebyshev polynomials for partial differential equation of heat conduction with cylindrical, spherical or hyperspheric symmetry

06 p0769 A73-18503

A class of almost periodic motions in systems with impulses

06 p0724 A73-18681

Solution stability of autonomous differential equations with holomorphic members under perturbation by time dependent auxiliary functions

06 p0724 A73-18683

Eigenfunction expansions and scattering theory for perturbed elliptic partial differential equations.

06 p0719 A73-18698

A boundary layer method for the matrix Riccati equation.

06 p0719 A73-18864

Perturbation about one dimensional parabolic flow field in three dimensional boundary layer separation, obtaining skin friction from linear equation eigensolutions

[AD-755557]

07 p0774 A73-19502

Equilibrium and stability of large-amplitude magnetic Bernstein-Greene-Kruskal waves.

07 p0857 A73-19524

First-order perturbations of the two finite body problem.

07 p0877 A73-19594

Asymptotic solution to the problem of optimal low-thrust energy increase.

07 p0899 A73-19962

Steady almost parallel flows linear stability, using multiple scales method for perturbation waves analysis

[ONERA, TP NO. 1235]

07 p0811 A73-20072

Small perturbations solution for spatially homogeneous expanding gravitating medium, using Vlasov kinetic equation with self consistent Newtonian field

07 p0901 A73-20315

Nonlinear multiple-scale solution of a cylindrical shell.

07 p0915 A73-20337

Thermodynamic properties of gases dissolved in electrolyte solutions.

07 p0789 A73-20642

On the simplest example of the barotropic instability of Rossby wave motion.

08 p0985 A73-21388

Beams and membranes nonlinear vibrations via modified perturbation method based on Linstedt-Poincare technique

08 p1018 A73-21406

Neutrino hindrance of density irregularities growth in expanding radiation dominated cosmological model from numerical integration of perturbation equations

09 p1141 A73-22026

Stability of the libration points of a triaxial ellipsoid under constantly acting disturbances in the first approximation

09 p1143 A73-22093

Nighttime midionosphere dynamical perturbations on ionizations from solutions of time dependent continuity equation with charge transport effects, considering semidiurnal atmospheric tide propagation mode

09 p1075 A73-22130

Application of a singular perturbation method to the study of beginning cavitation

09 p1071 A73-22215

Analytical solution of lunar ephemerides, considering sun-earth-moon problem and required corrections and perturbation methods

09 p1147 A73-22710

Studies in the application of recurrence relations to special perturbation methods.

09 p1149 A73-22914

Conversion of the wave spectrum in a medium with smooth spatial-temporal fluctuations

09 p1052 A73-23082

Tensor theory of perturbations in atmospheric dynamics

09 p1115 A73-23150

Stress state around an elliptic hole in a conical shell under tension.

[ASME PAPER 72-PVP-11]

09 p1163 A73-23269

Perturbation method for linearizing equations of supersonic flow over conical bodies, obtaining potential velocity and entropy solutions

10 p1171 A73-23615

Perturbation function expansion in series of orbital elements for satellite motion in rotating oblate planet gravitational field with two fixed centers

10 p1282 A73-24493

Canonical perturbation theory solution for nonconservative dynamic systems equations of motion, considering Duffing and van der Pol equations

10 p1283 A73-24665

Parallel perturbation solution for ideal resonance problem characterized by one degree of freedom Hamiltonian system, considering singularities at separatrix

10 p1283 A73-24666

The free surface on a liquid between cylinders rotating at different speeds. I.

10 p1207 A73-24789

Kaplan perturbation method for incipient flow separation, considering three dimensional, compressible and unsteady boundary layers

10 p1208 A73-24815

Small perturbations in flat galaxies. I - Equilibrium models and adiabatic perturbations.

10 p1284 A73-24913

Effect of electron-electron collisions on the thermal conductivity of a dense plasma.

11 p1402 A73-25120

On Howard's technique for perturbing neutral solutions of the Taylor-Goldstein equation.

11 p1345 A73-25157

Perturbation theory for multistrip acoustoelectric surface-wave amplifier.

11 p1337 A73-25362

Perturbation theory for the surface-wave multistrip coupler.

11 p1337 A73-25363

On the stability of finite difference schemes in transient semiconductor problems.

11 p1408 A73-25438

Kirchhoff and small perturbation methods identity in composite model calculation for rough surface electromagnetic scattering of circularly polarized wave by perfectly conducting body

11 p1329 A73-25678

A new method for studying the symmetry reduction of a system by means of a perturbation

11 p1326 A73-25867

Planetary masses, dynamic flattening and orbital elements determination by perturbation analysis for disturbed planet, space probe and satellite

11 p1420 A73-25882

Thin uniform circular rings axial and radial bending vibrations under perturbing effect of circumferentially attached small cylinder, comparing theoretical with experimental results

11 p1444 A73-26290

Laminar symmetry-plane boundary layer on a sharp spinning body at incidence.

11 p1303 A73-26397

Sonic line for a coaxial axisymmetric nozzle.

11 p1303 A73-26403

Elastic domain similar to half plane with perturbed boundaries, comparing small parameter method accuracy with exact solutions

11 p1446 A73-26467

A note on the heating of magnetoplasma by magnetic perturbations.

11 p1407 A73-26659

Galaxies as local perturbations in homogeneous universe, considering galactic manufacture within Einstein theory context

12 p1539 A73-27141

Small perturbations solution for spatially homogeneous expanding gravitating medium, using Vlasov kinetic equation with self consistent Newtonian field

12 p1539 A73-27287

Behavior of eigenfunctions and values in elliptical boundary value problems in a variable region

12 p1518 A73-27728

Solid profile wing motion in ideal incompressible fluid at variable distance from screen in terms of small perturbation theory

12 p1488 A73-27815

Perturbation techniques in the analysis of geometrically nonlinear shells.

13 p1694 A73-28251

Singular perturbation analysis of a certain Volterra integral equation.

13 p1648 A73-28412

The stability of Poiseuille flow - An analysis of two- and three-dimensional disturbances.

13 p1600 A73-28418

Application of small perturbation method in calculations of turbulent boundary layers on a curvilinear surface with suction 13 p1600 A73-28447

Method of experimental study of fields in electromagnetic resonators - Application to helicoidal resonators 13 p1589 A73-28472

Nonlinear transverse vibrations of beams with properties that vary along the length. 13 p1695 A73-28488

Singular perturbations for a nonlinear differential equation with a small parameter. 13 p1648 A73-28537

Ground-wave perturbation over a transition zone between two different sections. 13 p1583 A73-28798

Advanced elastic postbuckling analysis by a perturbation procedure. 13 p1697 A73-28826

Representative shear wave passage through plane flame front, determining wave refraction and modification, flame generated turbulence and noise and perturbation of front 13 p1707 A73-28993

Small perturbation evolutionary motion equations for forced vibrations of quasi-linear two frequency autonomous systems at resonance 13 p1661 A73-29082

Computational algorithm for three dimensional mixed boundary value problem for perturbing potential in earth figure theory 13 p1609 A73-29130

'Drift' instabilities distorting the magnetic surfaces of Tokamak-type toroidal systems. 14 p1778 A73-29690

All order stability of Hamiltonian systems with two degrees of freedom. 14 p1773 A73-29756

Perturbed bifurcations problems due to initial imperfections caused by small deviations from ideal configuration in nonlinear theory 14 p1767 A73-29764

The determination of Jupiter's mass from large perturbations on cometary orbits in Jupiter's sphere of action. 14 p1792 A73-29810

Focusing effect of planetary perturbations on meteor stream particles for comet formation 14 p1795 A73-29846

Perturbation method in the analysis of geometrically nonlinear and stability problems. 14 p1808 A73-30196

Electromagnetic wave radiation and reflection at guiding structure discontinuity, calculating TE mode surface wave by boundary perturbation technique 14 p1727 A73-30214

Some comments on the importance of third order contributions to the screening of the ionic potential and to the structural energy of metals. 14 p1783 A73-30432

Asymptotic stability and perturbations for linear Volterra integrodifferential systems. 14 p1770 A73-30757

Stability of elliptical cylinder consisting of perfect incompressible gravitating fluid subject to arbitrary perturbations 15 p1860 A73-31048

First order perturbation theory for geostationary satellites orbit calculation, taking into account earth oblateness, equator ellipticity and solar and lunar gravitational effects 15 p1930 A73-31114

Stability, solvability and adjoint conditions for time periodic perturbation solutions to subcritical bifurcating plane Poiseuille flow 15 p1863 A73-31340

Book on perturbation methods for nonlinear differential equations covering canonical transformation theory, Hamiltonian and integrable systems, area preserve mapping and resonance problem 15 p1899 A73-31472

Basic trends in the development of modern analytic mechanics 15 p1913 A73-31622

Perturbation solution for shock waves in a dissipative lattice. 15 p1913 A73-31937

A theory of oscillator noise and its application to IMPATT diodes. 15 p1851 A73-31939

Estimate of the influence of the seasonal redistribution of air masses on the motion of the earth's poles 15 p1939 A73-31967

Partial stability of mechanical systems, analyzing perturbed motion in vector form, using Liapunov functions 15 p1914 A73-32114

Analysis of externally pressurized gas bearings with journal rotation. 15 p1883 A73-32147

Application of the perturbation method in a polarization analysis of anisotropic laser resonators 15 p1886 A73-32334

Book - Applications of the electromagnetic reciprocity principle. 15 p1915 A73-32577

Book on perturbation methods covering parameter variation, strained coordinates, averaging, multiple scale and matched and composite asymptotic expansions 15 p1902 A73-32578

Hagen-Poiseuille flow stability with superimposed rigid rotation, deriving perturbed differential flow equations from Navier-Stokes and continuity equations 16 p1999 A73-33253

Periodic solutions of singularly perturbed equations arising from gyroscopic systems. 16 p2032 A73-33310

Correlation measurements on the complex amplitude of stellar plane waves perturbed by atmospheric turbulence. 16 p2037 A73-33684

Angular quadrature perturbations in radiative transfer theory. 16 p2037 A73-33738

Bifurcated small parameter perturbation solutions in boundary layer theory, applying to Falkner-Skan equation and instability in stratified shear flow 16 p2001 A73-33871

Damped lateral vibration in an axially creeping beam with random material parameters. 16 p2082 A73-33902

Perturbation technique investigation of nonlinear pulsations of vibrationally unstable main sequence stars between 70-170 solar masses 17 p2225 A73-34288

Small perturbations analysis of hydrodynamic relations of shock front propagation in inhomogeneous medium 17 p2150 A73-34311

Interaction of fast particles with magneto-hydrodynamical turbulence. 17 p2216 A73-34504

Vibration of plates subject to arbitrary in-plane loads - A perturbation approach. 17 p2248 A73-35042

A perturbation method for obtaining approximate solutions of an equation with two small parameters 17 p2201 A73-35046

A perturbation method for low-frequency fluid-structure interaction problems. 17 p2248 A73-35102

Perturbation theory for field moments in an inhomogeneous medium. 17 p2123 A73-35151

Solution of coupled and singular perturbation methods using duality theory. 17 p2202 A73-35358

Book - Acoustic fields and waves in solids. Volumes 1 & 2. 17 p2213 A73-35597

Small perturbations in flat galaxies. II - Time-dependent azimuthal perturbations. 17 p2236 A73-35782

On stability of large-scale systems under structural perturbations. 17 p2213 A73-35827

Motion of a free solid body about its center of mass when the body is stabilized by rotation about a non-principal axis of inertia 18 p2336 A73-36163

Oriental dependence of certain RF impedance probes in the ionosphere. 18 p2288 A73-36188

The transformational behaviour of perturbation theories. 18 p2352 A73-36421

Satellite vibration-rotation motions studied via canonical transformations. 18 p2352 A73-36422

Statistical theory of weakly interacting perturbations and low amplitude turbulence in fluids, considering diffusion, dispersive and acoustic wave characteristics and plasma instabilities 18 p2299 A73-36504

A perturbation treatment for optimal slightly nonlinear systems with linear control and quadratic criteria. 18 p2294 A73-36637

Weak perturbation propagation in magnetic gasdynamics 19 p2468 A73-37550

On the equivalence between Hori and Lacina perturbations theories. 19 p2483 A73-37564

Small perturbation evolutionary motion equations for forced vibrations of quasi-linear two frequency autonomous systems at resonance 19 p2445 A73-37633

Boundary conditions and stability of inviscid plane-parallel flows. 19 p2420 A73-37751

Poincare-Lighthill and linear-time-scales methods for linear perturbation problems. 19 p2445 A73-37752

On the use of singular perturbation methods in the solution of variational problems. 19 p2386 A73-38038

Accurate approximate solutions to oscillatory problems with perturbing singular damping. 19 p2461 A73-38490

Coupled superradiance master equations - Application to fluctuations in coherent pulse propagation in resonant media. 20 p2571 A73-38627

Self organizing behavior of multivariable stochastic extremal control systems with environmental or intrinsic positive feedback under perturbation 20 p2539 A73-38689

Lyapunov theory and perturbations of differential equations. 20 p2581 A73-38974

Perturbation analysis of holographic grating couplers in thin film waveguides, discussing coupling efficiency dependence on evanescent tail length, refractive index and gelatin film thickness 21 p2699 A73-40149

Quantum theory of nonlinear optical processes with time-dependent pump amplitude and phase - Frequency conversion. 21 p2711 A73-40222

The decay of perturbations in an electrically conducting and thermally radiating gas. 21 p2789 A73-40246

Effects of non-linearity due to large deflections in the derivation of frequency response data from the impulse response of structures. 21 p2783 A73-40287

Effect of small perturbations on the behavior of thermodynamic variables near the point of a phase transition of the second kind 21 p2790 A73-40445

Digitally scanned planar phased arrays, deriving optimum phase perturbation function for quantization and reflection lobe dispersion in terms of aperture distribution amplitude 21 p2652 A73-40667

Interference parameters in the problem of estimating the accuracy of prediction of spacecraft motion 21 p2781 A73-40904

Propagation of acoustic waves in a fluid flowing through a cylindrical duct 21 p2677 A73-40944

Convergence of perturbation-theory series in the problem of short-wave propagation through a randomly nonhomogeneous medium 21 p2657 A73-41514

A method of solving a slightly disturbed mixed problem for a hyperbolic equation with a small delay of the argument 22 p2881 A73-42277

Coupling between thermal conduction and radiative transfer in a moving atmosphere. 22 p2907 A73-42305

Short-wave propagation in a randomly inhomogeneous medium with an arbitrary law of permittivity fluctuations 22 p2826 A73-42335

Asymptotic properties of solutions to single-point and two-point problems with singular perturbations for systems of ordinary linear differential equations 22 p2882 A73-42473

Semiempirical time dependent climate models formulated for stability of asymptotic steady state equilibrium solutions to perturbations 22 p2883 A73-42540

Analysis of a damped, non-linear, non-autonomous system. 22 p2887 A73-42621

Monograph - Singular perturbation problems for partial differential equations. 22 p2882 A73-42715

Electromagnetic theory of Fresnel holograms in the first perturbation theory approximation 22 p2862 A73-42927

Increase of closed-loop nominal trajectory likelihood in uncertain systems. 23 p2962 A73-43280

On stability of large-scale systems under structural perturbations. 23 p2963 A73-43290

Collective spontaneous emission of polyatomic systems 23 p2988 A73-44010

Practical implementation of the perturbation method in an inhomogeneous boundary value problem of the thermoviscoelasticity 23 p3046 A73-44189

Perturbation method applications to elasticity theory three-dimensional problems, discussing differential operator construction via recursion relations 23 p3046 A73-44190

Estimated seasonal redistribution of air masses affecting motion of earth's poles. 24 p3081 A73-44492

Stability of two-dimensional collision-free plasmas. 24 p3116 A73-45237

Kustaanheimo-Stiefel transformation in Kepler motion perturbation theory derived from general solution

of two body problem, noting application to collision orbits and Lagrange solutions

24 p3142 A73-45298

Stability and small parameter perturbations of a critical neutral functional differential equation.

24 p3106 A73-45336

On the gyroscopic coupling of a Van der Pol oscillator in the forced regime and of a free linear oscillator

24 p3111 A73-45396

A tenth order solution in explicit form to the 'restricted' three-body problem.

24 p3143 A73-45434

Nonlinear stability of cylindrical vortex enclosing a central jet of light or dense fluid.

24 p3080 A73-45452

Strong plasma turbulence theory, discussing convergence of perturbation series formed with renormalized particle propagator

24 p3118 A73-45462

PERVEANCE

Investigation of the structure of an electron beam formed by a high-perveance triode gun under controlled-current conditions

01 p0025 A73-10989

PETREL SOUNDING ROCKET

An IRIG FM-FM telemetry system for the Petrel sounding rocket.

05 p0551 A73-16850

PETROGRAPHY

Petrographic and electron microprobe study of the Monturaqui impactite.

01 p0040 A73-10575

Sedimentology of clastic rocks returned from the moon by Apollo 15.

01 p0103 A73-11016

Petrographic and electron microprobe study of the Monturaqui impactite.

02 p0165 A73-12626

Comparative petrology of Apollo 16 sample 68415 and Apollo 14 samples 14276 and 14310.

03 p0375 A73-14103

The Apollo 16 lunar samples - Petrographic and chemical description.

05 p0614 A73-16319

Volatile-rich lunar soil - Evidence of possible cometary impact.

05 p0615 A73-16321

Breccias from the lunar highlands - Preliminary petrographic report on Apollo 16 samples 60017 and 63335.

05 p0615 A73-16322

A crustal-upper-mantle model for the Colorado plateau based on observations of crystalline rock fragments in the Moses Rock dike.

05 p0569 A73-16381

Genetic significance of chemical, isotopic, and petrographic features of some peralkaline salic rocks from the island of Pantelleria.

05 p0570 A73-16842

Petrography and crystallization history of basalts 14310 and 14072.

07 p0879 A73-19685

Electron petrography of Apollo sample 14310.

07 p0880 A73-19692

Mineralogical and petrographic features of two Apollo 14 rocks.

07 p0880 A73-19699

Analysis of Fra Mauro samples and the origin of the Imbrium Basin.

07 p0880 A73-19701

Electron petrography of Apollo 14 and 15 rocks.

07 p0881 A73-19702

Lunar plagioclase - A mineralogical study.

07 p0881 A73-19712

Petrology and chemistry of some Apollo 14 lunar samples.

07 p0882 A73-19721

Rock 14068 - An unusual lunar breccia.

07 p0883 A73-19732

Chemical and petrographic characterization of Fra Mauro soils.

07 p0884 A73-19742

Havero ureilite - Evidence for recrystallization and partial reduction.

09 p1140 A73-21869

Mineralogy and texture of Havero ureilite, noting preterrestrial shock evidence, recrystallized olivine and metal grain, and graphite conversion into diamonds from petrographic observation

09 p1140 A73-21870

Volatilization studies on a terrestrial basalt and their applicability to volatilization from the lunar surface.

10 p1275 A73-23738

Apollo 15 mare olivine and quartz basalts major and trace element composition and petrogenesis, deriving model of magma genesis

12 p1466 A73-27545

The age and petrography of two Luna 20 fragments and inferences for widespread lunar metamorphism.

13 p1675 A73-28319

PETROLEUM

U CRUDE OIL

PETROLOGY

NT PETROGRAPHY

Lunar breccias lithification and metamorphism model construction from experimental and analytical data, discussing scale of lunar metamorphic temperatures

02 p0220 A73-12476

The Rb-Sr age of a crystalline rock from Apollo 16.

02 p0220 A73-12483

Petrochemistry and chemical features of lunar glass spherules.

03 p0273 A73-13089

Lunar gabbroic rock internal origin hypothesis support by petrologic data, giving temperature interval of crystallization from dry silicate melt

03 p0369 A73-13095

The mineralogy, petrology and geochemistry of lunar samples - A review.

04 p0498 A73-15186

Spinel troctolite and anorthosite in Apollo 16 samples.

05 p0615 A73-16323

Lunar Science Conference, 3rd, Houston, Tex., January 10-13, 1972, Proceedings. Volume 1 - Mineralogy and petrology. Volume 2 - Chemical and isotope analyses, organic chemistry. Volume 3 - Physical properties.

07 p0878 A73-19676

Petrology of Apollo 14 high-alumina basalt.

07 p0879 A73-19684

Petrology of Fra Mauro basalt 14310.

07 p0879 A73-19687

Some textures in Apollo 12 lunar igneous rocks and in terrestrial analogs.

07 p0879 A73-19688

Lunar rocks petrogenesis, determining liquidus and solidus temperatures and crystalline phases sequence in lunar samples and synthesized oxides and silicates.

07 p0879 A73-19689

Experimental petrology and petrogenesis of Apollo 14 basalts.

07 p0880 A73-19690

Petrographic features and petrologic significance of melt inclusions in Apollo 14 and 15 rocks.

07 p0880 A73-19694

Pyroxenes as recorders of lunar basalt petrogenesis - Chemical trends due to crystal-liquid interaction.

07 p0881 A73-19704

Plagioclase and Ba-K phases from Apollo samples 12063 and 14310.

07 p0881 A73-19714

Apollo 14 breccia 14313 - A mineralogic and petrologic report.

07 p0882 A73-19719

Mineralogy, petrology, and chemical composition of lunar samples 15085, 15256, 15271, 15471, 15475, 15476, 15535, 15555, and 15556.

07 p0883 A73-19727

Experimental petrology and origin of Fra Mauro rocks and soil.

07 p0883 A73-19728

Petrology and origin of lithic fragments in the Apollo 14 regolith.

07 p0883 A73-19730

Mineralogy, petrology, and surface features of some fragmental material from the Fra Mauro site.

07 p0885 A73-19748

P and S waves propagation velocity distribution for lunar mantle and crust composition, noting petrological models with differentiated mantle

07 p0894 A73-19849

Constrained least-squares analysis of petrologic problems with an application to lunar sample 12040.

08 p0936 A73-20842

Mineralogy and petrology of the Yilmia enstatite chondrite.

09 p1139 A73-21852

Ransom /Kansas/ stony meteorites discovery location map, describing megascopic appearance, petrology and chemical group

09 p1139 A73-21859

Havero stony ureilite origin modes, composition, textural features, mineralogy and petrology

09 p1139 A73-21860

Carboxylic acids derived from Tasmanian tasmanite by extractions and kerogen oxidations.

10 p1211 A73-24108

Photomicrographic investigation of plutonic and metamorphic equilibration in polished thin sections of Apollo 16 feldspathic microbreccia samples from North Ray crater rim

11 p1326 A73-25863

Indium abundances in cosmos, meteorites, tektites, rock-forming and ore minerals and igneous rocks, considering behavior in magmatogenic processes and rock weathering and alteration

12 p1490 A73-27125

Petrology of fine-grained rock fragments and petrologic implications of single crystal from the Luna 20 soil.

13 p1674 A73-28307

Petrology of Luna 20 regolith from the lunar highlands.

13 p1675 A73-28311

Luna 20 pyroxenes - Exsolution and phase transformation as indicators of petrologic history.

13 p1675 A73-28313

Luna 20 highland soil samples mineralogical and petrological analysis, comparing chemical composition with Apollo 16 soil samples

13 p1676 A73-28322

Luna 20 - Mineralogy and petrology of fragments less than 125-micron size.

13 p1676 A73-28324

Mineralogy, petrology and chemistry of lithic fragments from Luna 20 fines - Origin of the cumulate ANT suite and its relationship to high-alumina and mare basalts.

13 p1676 A73-28328

Petrology of some lithic fragments from Luna 20.

13 p1677 A73-28331

The Luna 20 lithic fragments, and the composition and origin of the lunar highlands.

13 p1677 A73-28336

Apollo 16 rocks - Petrology and classification.

15 p1937 A73-31850

Petrology of the 2-4 mm soil fraction from the Hadley-Apennine region of the moon.

17 p2230 A73-34517

Ventifact evolution in Wright Valley, Antarctica.

21 p2687 A73-41211

Ancient lunar mega-regolith and subsurface structure.

24 p3129 A73-44448

Mars crustal structure model from analysis of surface markings with Mariner 9 data, showing petrologic distinctions between dark and light regions

24 p3133 A73-44543

PPFAFF EQUATION

Topological equivalence of linear systems of Pfaff equations in the neighborhoods of their one-dimensional closed characteristics

06 p0718 A73-18677

Compact integral varieties existence in certain meromorphic Pfaff differential equation systems

21 p2726 A73-40946

PFM [MODULATION]

U PULSE FREQUENCY MODULATION

PH

Hydrogen ion concentration in the blood of man under high mountain conditions with physical loads

02 p0133 A73-11924

Properties of phosphoribulokinase from Thiobacillus neapolitanus.

03 p0261 A73-13597

The effect of pH on photobleaching of organic laser dyes.

03 p0320 A73-14462

Carbon dioxide concentration, pH and nutrient concentration effects on blue-green algae relative abundance to green algae in lakes

06 p0655 A73-18577

Plasma electrolytes, pH, and ECG during and after exhaustive exercise.

15 p1834 A73-31347

Effect of stimulation of the hypothalamus on the pH of arterial and venous blood

21 p2637 A73-40281

Response of coronary blood flow to pH-induced changes in hemoglobin-O₂ affinity.

24 p3060 A73-45061

PH FACTOR

An implantable glass electrode used for pH measurement in working skeletal muscle.

08 p0935 A73-21510

Zirconium sorption by and release from carboxyl cationates in nitric and sulfuric acids, discussing pH dependence

14 p1765 A73-30884

PHANTOM AIRCRAFT

NT F-4 AIRCRAFT

PHARMACOLOGY

Hemodynamic effects of physical maneuvers /Val-salva, effort, respiration/ and of pharmacodynamic tests - Their clinical application

02 p0138 A73-12159

The role of biogenic amines in sleep.

03 p0264 A73-14260

Multichannel telemetry of physiological parameters /body temperature, EKG, EEG/ in the rat. II - Applications in neuropharmacology.

03 p0272 A73-14306

A hybrid broad-band EEG frequency analyzer for use in long-term experiments.

04 p0411 A73-14847

Influence of different motor regimes on the convulsive reactivity of the central nervous system.

05 p0542 A73-17178

Effect of some pharmacological preparations on the fall-out nystagmus and Bechterew nystagmus

08 p0929 A73-20982

The effects of Dalmene /flurazepam hydrochloride/ on human EEG characteristics.

08 p0931 A73-21464

Adaptive hormone action and nonspecific adaptive function of steroid hormones, discussing stress resistance mechanisms of steroids pharmacologically classified as syntoxic and catatonic

09 p1045 A73-22536

Psychopharmacology in treating psychiatric diseases, negative emotions, and nerve stimulation, discussing tranquilizers synthesis and effects

12 p1465 A73-27497

PHASE ANGLE

Characteristics of the narcotic action of hexenal in combination with aminothiol-series radioprotective drugs in irradiated animals

15 p1838 A73-31391

Techniques for microinjection of biologically active substances into subcortical structures of the brain

18 p2282 A73-36574

The inhibiting action of 5-oxytryptophan on thermal regulation during the awakening from hibernation

19 p2393 A73-37252

Coronary heart disease; Proceedings of the Second International Symposium, Frankfurt am Main, West Germany, June 1972.

22 p2809 A73-42856

Gamma-aminobutyric acid antagonism in visual cortex - Different effects on simple, complex, and hypercomplex neurons.

23 p2946 A73-43338

PHASE ANGLE

U PHASE SHIFT

PHASE CHANGES

U PHASE TRANSFORMATIONS

PHASE COHERENCE

Statistical characteristics of phase variable states and phase operators in optical quantum fields by intrinsic state factorization method

10 p1228 A73-24151

Phase correlations of longitudinal modes in a laser under free emission conditions

15 p1886 A73-32336

Lunar surface light reflection phase function, discussing topsoil atomization and brightness distribution over lunar disk

16 p2063 A73-33755

Image reconstruction from the modulus of the correlation function - A practical approach to the phase problem of coherence theory.

20 p2570 A73-38616

Performance estimate for coherent QPSK with random intersymbol interference due to time-varying scatter.

20 p2527 A73-38765

PHASE CONTRAST

Phase contrast transfer damping functions for various beam apertures in high resolution electron microscopy

21 p2702 A73-40949

PHASE CONTROL

Electronically controlled phased arrays for radar tracking systems, considering military, earth resources and planetary topography applications

06 p0677 A73-18447

Phase matching in second-harmonic generation using artificial periodic structures.

07 p0834 A73-19538

Wave transformation by a phase corrector

07 p0793 A73-19923

German monograph - Synchronization of digital telephone networks by means of phase averaging with parameter transfer.

07 p0794 A73-20386

A positional, asynchronous, thyristor-based, electrical servo actuating element with directional shaping of the phase trajectories

12 p1460 A73-26787

Synthesis of a linear antenna in a class of piecewise-constant current-distribution functions

12 p1479 A73-27228

Certain problems in controlling phase of microwave electromagnetic oscillations using an inductive transistor.

13 p1591 A73-28670

Influence of the nonlinearity of the phase characteristic of the RF signal path in an FM receiver on the signal distortions

13 p1584 A73-28897

Fundamental statistical characteristics of a modified phase AFC /PAFC/ system.

15 p1842 A73-30989

On-axis computer generated hologram with multimulsion color film for retaining kinoform advantages and effective control over amplitude and phase transmittance

17 p2171 A73-35401

Time scanned array radar with time delay or phase gradient for electronic beam steering control by signal

21 p2652 A73-40669

Synchronization range of phase control systems

21 p2665 A73-41271

PHASE DEMODULATORS

An application of Bayes-law estimation to nonlinear phase demodulation.

04 p0471 A73-15253

Majority logic detection scheme of differentially phase-modulated waves.

08 p0937 A73-20802

Data aided phase locked loops for phase estimation improvement in coherent demodulator to obtain loop acquisition characteristics design flexibility

12 p1483 A73-27157

The effect of carrier recovery and bit timing errors in the coherent reception of 2 and 4 phase PSK signals.

20 p2527 A73-38766

PHASE DETECTORS

Measurement of phase fluctuation dispersion for narrow-band signals

01 p0015 A73-10077

Digital phase locked loops for incoming signal phase tracking, predicting performance from nonlinear difference equation model for comparison with digital simulation

04 p0421 A73-15435

Second order phase lock AFC system transient response duration calculation for rectangular and sawtooth characteristics of phase detector, using averaging method

05 p0547 A73-16059

Analysis of a dual mode digital synchronization system employing digital rate-locked loops.

05 p0549 A73-16369

Tracking performance of a phase locked loop with a linear phase detector.

09 p1058 A73-23432

Phase locked loop and coherent detection performance prediction, considering desirable phase detector characteristics in terms of SNR and noise spectral density

09 p1058 A73-23433

High voltage phase meter with electrostatic logometer for loss angle measurements in capacitors and power cables during operation

12 p1495 A73-26790

Phase discriminator of a nonregular signal.

12 p1480 A73-27270

Analysis of the operation of a diode phase detector with allowance for the diode recovery time

13 p1591 A73-28866

Phase coded moving target indicators, describing phase measurement technique to discriminate between moving and fixed targets

15 p1846 A73-32433

Phase measurement microscopy consisting of phase modulation optical system using interferometry and optical heterodyning, and phase detection system using digital processing

21 p2698 A73-40144

A computing digital phase meter

21 p2664 A73-41083

Synchronization range of phase control systems

21 p2665 A73-41271

Ideal laser amplifier as a phase measuring system of a microscopic radiation field.

22 p2870 A73-42516

A phase discriminator with feedbacks

24 p3071 A73-44545

PHASE DEVIATION

Measurement of phase fluctuation dispersion for narrow-band signals

01 p0015 A73-10077

Platinotron crossed field microwave amplifier tube phase response characteristics, considering anode current fluctuations and statistical phase variations at constant operating conditions

06 p0674 A73-17823

Some problems in methods for determining the parameters of scattering inhomogeneities

08 p0959 A73-21284

Study of ionospheric phase distortion at Ahmedabad.

10 p1188 A73-24170

Investigation of the phase variation of a NWC signal /22.3 kHz/ along a transequatorial path

12 p1469 A73-27339

Calculation of phase difference power spectrum for slant-path propagation.

13 p1661 A73-29327

Waveguide channel point source electric field level and phase derived by Rytov smooth perturbation technique, obtaining correlation functions, energy spectra and phase fluctuations

19 p2406 A73-38338

Measurement methods for sudden ionospheric disturbances caused by solar flares, discussing short wave fading, sudden phase anomaly and sudden enhancement of atmospheric techniques

22 p2904 A73-43036

Vertical phase variation and mechanical flux in the solar 5-minute oscillation.

22 p2916 A73-43124

Study of phase changes of the NWC signal /22.3 kHz/ on a transequatorial path.

23 p2952 A73-43237

PHASE DIAGRAMS

Phase diagram of the neodymium-yttrium system

01 p0088 A73-10919

On the ternary compound G in the Al-Mn-Cr system.

02 p0179 A73-11598

Microstructure and phase relations for Ti-Mo-Al alloys.

02 p0182 A73-12751

Influence of electron concentration on the formation of phases with bcc, fcc, and hexagonal close packed lattices in certain transition-metal alloys

03 p0324 A73-13510

Phase diagrams of ternary Ni-Re alloys with La, Y, Sc, Hf, Si and Mo for cathode applications in electronic vacuum devices

03 p0325 A73-13516

A point of phase equilibria interpretation in connection with lavas from the Apollo 12 site.

03 p0375 A73-14106

Phase diagrams, microstructure and interface composition of two phase metallic particles from lunar soils and rocks, determining equilibrium temperature and equilibration time

03 p0376 A73-14110

Phase diagrams and properties of binary alloys of refractory metals, taking into account the electronic structure of the atoms of the components

03 p0328 A73-14652

Metal-semiconductor system phase diagram for temperature dependence of substrate surface epitaxial film thickness during single crystal growth, determining equilibrium saturation time

04 p0483 A73-14880

Growth of ternary composites from the melt. II.

04 p0463 A73-15310

Molybdenum corner in Mo-Ti-B and Mo-Zr-B ternary systems

04 p0464 A73-15494

Phase structure of vacuum deposited thin Ti films and molecular beam composition obtained by mass spectroscopy

04 p0484 A73-15667

Phase equilibrium diagram of the lanthanum-germanium system

04 p0484 A73-15692

Mo disilicide-Ti disilicide system phase diagram based on metallographic, X ray structural and high temperature differential thermal analyses

05 p0587 A73-16846

Phase equilibrium in the TeO₂-V₂O₅ system

05 p0589 A73-17173

Stable or metastable phase crystallization rate of Cd-Sb liquid alloys as function of time, composition and temperature above liquidus line

05 p0605 A73-17294

Phase diagram and certain properties of alloys of the neodymium-antimony system

06 p0707 A73-18041

Interaction between the ZrCr₂ intermetallic compound and some zirconium compounds with iron, cobalt, and nickel

06 p0708 A73-18056

Effect of hydrostatic extrusion on the composition and properties of Nb₃Sn compounds.

06 p0736 A73-18213

Diffusion in the titanium-aluminum system. II - Interdiffusion in the composition range between 25 and 100 at.% Ti.

06 p0709 A73-18333

Phase separation analysis of ternary Co-W-Ti alloy during high temperature aging by X ray and electron microscopy method

09 p1099 A73-21963

Two phase channel flow behavior from three dimensional phase diagram for one dimensional steady flow of ideal gas carrying solid particles

09 p1072 A73-22621

Certain physical properties of Nd-Sb system alloys and their correlation with the phase diagram

09 p1134 A73-22679

Interaction between zirconium diboride and molybdenum

09 p1105 A73-22981

Laves phases in hafnium alloys containing period-IV transition metals

09 p1108 A73-23234

Study of the W-Ta-Re phase diagram by the diffusion layer method

09 p1108 A73-23236

Phase equilibria in V-N-Sc/Y, Ce, Pr/ alloys

09 p1108 A73-23238

Metallurgical investigations of phase equilibria in the titanium-niobium-germanium ternary system

10 p1231 A73-23692

Phase equilibria in three-component alloys containing an interstitial element, and the stability of composite materials

10 p1233 A73-24317

Phase equilibria and crystal structure of intermediate phases in Er-Rh binary alloys

10 p1260 A73-24435

Cerium-germanium system state diagram based on microstructural, differential thermal, dilatometric and X ray phase analyses, emphasizing intermetallics observation

10 p1260 A73-24684

Phase equilibria in fluid mixtures at high pressures - The He-CH₄ system.

11 p1399 A73-25889

Equation of state and phase diagram of dense hydrogen.

11 p1399 A73-25890

Constitution and phase relationships in copper-silver-aluminum ternary system.

11 p1385 A73-26566

- Rare earth-rhodium systems intermediate phase equilibria and crystal structures, using powder X ray diffraction technique 11 p1410 A73-26569
- Phase diagrams, microstructure and superconducting properties of thermally diffused Nb-Sn system 12 p1508 A73-26835
- Carbide separation and carbide equilibrium in the Co-Cr-C system 12 p1509 A73-26895
- Phase structure and composition during the crystallization of eutectic-type alloys of the Ni-Cr system 12 p1509 A73-26897
- Interaction of molybdenum with elements of the iron group and carbon 12 p1510 A73-26903
- Mo-W-B alloy phase equilibria, isothermal cross sections, liquidus, solubility and mechanical properties by thermal, X ray and microstructural analyses 12 p1510 A73-26904
- Mo-Nb-Ta alloys phase and composition-hardness diagrams for 20-1100 C, establishing mutual solubility of system components 12 p1510 A73-26905
- Phase equilibria in the aluminum-chromium-zirconium system 12 p1510 A73-26906
- Apollo 15 soil samples structure and phase equilibrium data noting metal particles of high cobalt content 12 p1466 A73-27544
- Investigation of the sintering of binary alloys with limited solubility in the solid state. I - Concentration dependence of shrinkage during sintering of two-component systems with a eutectic type of phase diagram 12 p1503 A73-27558
- Equilibrium of vanadium carbide with an alpha or gamma solid solution in the iron-rich Fe-Cr-V-C system at temperatures from 700 to 1150 C and at a carbon concentration of 0.30% 12 p1513 A73-27684
- Quasi-ternary Mo-TiC-ZrC system 13 p1630 A73-28014
- Dendritic liquation of hypoeutectic binary, ternary and complex Fe- and Ni-base alloys dependence on phase diagram 13 p1631 A73-28102
- Experimental and thermodynamic study of the equilibria between ferrite, austenite and intermediate phases in the Fe-Mo, Fe-W, and Fe-Mo-W systems. 13 p1633 A73-28136
- Ti-Pd phase diagram eutectoid region configuration determination through alloy thin foil arc melting preparation and microstructure examination by electron microscopy 13 p1633 A73-28146
- Determination of the boundaries of fluorite-type Y2O3 solid solutions in HfO2 13 p1645 A73-28292
- Delta ferrite and martensite formation in stainless steels. 14 p1759 A73-30145
- Calculation of the binary phase diagrams of iron, chromium, nickel and cobalt. 14 p1760 A73-30440
- Influence of annealing temperature on the changes in the chemical and phase compositions of the intercrystalline boundaries of weakly-alloyed molybdenum 14 p1764 A73-30865
- Phase diagram of the niobium-gallium system 15 p1922 A73-31182
- Structure and properties of alloys of the V3Si-V3Ga-V3Ge system 15 p1923 A73-31190
- The vanadium-iron-boron, vanadium-cobalt-boron, and vanadium-nickel-boron systems 15 p1887 A73-31202
- Mo-W-C phase equilibria study at 1000 C, obtaining isothermal cross sections for various carbon contents from X ray and microstructural analysis 15 p1888 A73-31598
- A combinational method of calculating the average velocity and the mean-mass temperature of a gas flow from the phase diagram of the substance 15 p1957 A73-31865
- Critical survey of studies of the equilibrium phase diagram of the Ti-W system 15 p1893 A73-32513
- Investigation of the phase equilibrium of ternary Ti-Al-Nb system alloys 15 p1893 A73-32514
- Critical survey of studies of phase diagrams in the titanium-oxygen system in connection with the formation of suboxides 15 p1893 A73-32515
- Influence of heating rate on the phase composition of the VT3-1 alloy 15 p1894 A73-32525
- Investigation of the structure and corrosion behavior of alloys of the Ti-Ta-Cr system 15 p1895 A73-32542
- Investigation of corrosion stability in alloys of the Ti-Ta-Nb system 15 p1895 A73-32543
- Phenomena of precipitation observed in carburized tantalum in the vapor phase 15 p1896 A73-32645
- Phase equilibria in the metal-rich side of the Ta-N system. 16 p2025 A73-33110
- Phase constitution of the Ni-Cr-S alloy system between 600 and 850 C. 16 p2025 A73-33112
- Niobium-gold alloys crystal structure, phase diagrams, peritectic crystallization and microhardness, noting intermetallics formation by solid state reactions 16 p2026 A73-33957
- Microstructure and phase composition of oxide scale formation on Ti-Al alloys, noting dependence on Al concentration 17 p2188 A73-34557
- Polythermal and isothermal sections of Ti-Al-W phase diagram for Ti corner investigation, determining phase region boundary locations by X ray analysis 17 p2188 A73-34568
- Investigation of molybdenum-rich Mo-Ni-C, Mo-Ni-Zr, and Mo-Zr-Ni-C alloys 17 p2188 A73-34569
- Ti-Ta-V-Mo system phase diagram in Ti corner region for 600-900 C, investigating solubility, electrical resistivity and hardness 17 p2189 A73-34570
- Limit of the two-phase region of Mo/Ni, Cu/ and Cu/Ni, Mo/ solid solutions in the Mo-Cu-Ni system 18 p2325 A73-36859
- Selection of the composition for the matrix of a composite material, which will not dissolve the reinforcing fibers 18 p2328 A73-36860
- Superconducting properties of alloys of the vanadium-niobium-chromium system 18 p2325 A73-36898
- Ti rich corner of Ti-Al alloys phase diagrams investigated by differential thermal analysis and radiography for thermal resistance and intermetallic compounds existence 19 p2441 A73-37838
- The nature of the interaction between scandium and aluminum in the aluminum-rich part of the Al-Sc system 21 p2718 A73-40486
- Ta-Nb-Re system phase diagram plotted by physicochemical analysis methods, establishing region of existence of ternary solid solutions and temperature dependence 21 p2718 A73-40488
- Phase diagram thermal sections and concentration corner of Mo-Zr-B system by microstructure, X ray and electron microscope analysis 21 p2718 A73-40490
- Binary and ternary Laves phases in systems composed of zirconium and transition metals of the V through VII groups of the periodic system 21 p2718 A73-40848
- Phase composition of Ni-Al and Ni-Ga alloys hardened from the liquid state 21 p2719 A73-40849
- Carbide precipitation and carbide equilibrium in the Co-Cr-C system. 21 p2720 A73-41028
- Structure and composition of phases during solidification of Ni-Cr alloys of the eutectic type. 21 p2720 A73-41030
- Phase method of investigation of short time scale disturbances and motions in space plasma. 21 p2748 A73-41373
- Molybdenum sintering and the molybdenum-oxygen-carbon system. 21 p2722 A73-41585
- Russian book - The structure of zirconium alloys. 22 p2873 A73-41973
- Russian papers on metal alloys chemistry covering atomic structure, physicochemical properties, phase diagrams, X ray analysis, laser microanalysis, etc 22 p2873 A73-42083
- Ternary systems: Rare earth metal - iron family metal - silicon /Component interaction and crystal structures of compounds/ 22 p2873 A73-42084
- Omega-phase stability in the Ti-Zr-O system 22 p2873 A73-42085
- Investigation of the phase composition of alloys in the Ti-Al-Fe ternary system 22 p2873 A73-42086
- Specific structural features of the phase diagrams of the Ti-Cr-V, Ti-Cr-Nb and Ti-Cr-Ta ternary systems 22 p2873 A73-42087
- Phase diagrams and composition selections for strengthening of multicomponent deformable Mg alloys with rare earth and transition elements 22 p2874 A73-42094
- Russian book - General patterns in the structure of phase diagrams of metal systems. 22 p2877 A73-42451
- Patterns of the structure of transition metal/interstitial element diagrams /Me - B, C, N, O, H/ 22 p2877 A73-42452
- Specific structural features of the binary phase diagrams of some transition metals in a region containing Laves phases 22 p2877 A73-42453
- X-ray investigation of the mechanism of effects of alloying on defect formation in refractory metal alloys 22 p2877 A73-42454
- Structure of the phase diagrams of the ternary systems /Mo, W/ - /Ti, Zr, Hf, V, Nb, Ta/ - C 22 p2877 A73-42455
- Comparison of a suggested polynomial method with the method of F. M. Perelman in the calculation of the solidus surface of the W-Ta-Mo-Nb system 22 p2877 A73-42456
- Application of a computer image recognition technique to the determination of phase diagram types for binary metal systems 22 p2877 A73-42457
- Metastable phase diagrams of eutectic and peritectic alloys crystallization during rapid cooling from liquid state 22 p2877 A73-42458
- Isothermal cross sections of the phase diagram of the nickel-molybdenum-tungsten system at 1200 and 700 C 22 p2877 A73-42459
- Interaction of molybdenum with cobalt and carbon. 22 p2877 A73-42460
- Phase diagrams of ruthenium and rhodium systems with carbon 22 p2878 A73-42461
- Phase equilibrium technique to measure oxygen solubility in liquid Co at 1510 to 1700 C, determining thermodynamic characteristics and deoxidation curves 23 p2990 A73-43482
- Phase composition of Cu-Ni-O alloys with Ir additions, examining oxygen content influence on Ir distribution and solid solution formation 23 p2990 A73-43483
- Concentration curves and phase diagram plotted for Nb-Zr system diffusion layers during annealing at 700 to 1700 C 23 p2991 A73-43649
- Thermodynamic properties and phase composition of the In-Ni system 23 p2991 A73-43706
- A thermodynamic calculation of the iron-chromium-vanadium equilibrium diagram. 23 p2993 A73-43918
- Phase relations and diagram investigation for zirconium silicate-titanium dioxide system by quenching method, obtaining solid solution formation conditions and lattice constants 23 p2998 A73-44131
- Diagram of continuous cooling transformation of a titanium alloy with 6 per cent Al, 6 per cent V, and 2 per cent Sn /TA 6-V 6-E 2/ homogenized in the beta /sub 0/ phase 23 p2995 A73-44177

PHASE ERROR

- Mathematical model, digital filter design and phase error behavior derivation for higher order discrete phase locked loops 03 p0276 A73-13906
- Application of the spatial spectral power density to the calculation of resolution limits. 03 p0277 A73-13916
- Nonlinear analysis of double feedback loop tracking system with coupling, obtaining steady state phase error probability density functions with application to satellite transponder 04 p0429 A73-14994
- The nonlinear analysis and design constraints of a multi-filter phase-lock loop. 04 p0421 A73-15434
- Digital simulation of imperfect second-order hybrid phase locked loop operating in RF interference background, determining phase error variance and probability density function 04 p0422 A73-15438
- Sinusoidal signal and stationary quasi-white Gaussian noise mixture effects on stochastic phase locked AFC system operation, noting phase error probability density function 05 p0547 A73-16060
- The effect of a bandpass nonlinearity on signal detectability. 06 p0664 A73-17713
- On the unequal accuracy of radio range finder measurements in the reflection of radio waves from an underlying surface. 07 p0793 A73-20041
- Synthesis of a system with a Pi-shaped amplitude-frequency characteristic and a 'zero' equivalent phase-frequency characteristic 07 p0794 A73-20293
- The effect of carrier phase and timing on a single-sideband data signal. 10 p1187 A73-23500
- An analytical expression for the limits of error in the measurement of reflection-coefficient phase. 10 p1190 A73-24867

- Radome insertion phase delay errors due to element impedance, frequency uncertainty, power instability and heat effects
11 p1327 A73-25278
- Adaptive control for correction of flexible linear array phase error with resistance strain gages and ferrite phase shifter, noting radiation pattern performance
11 p1332 A73-26283
- Radio direction finder of increased accuracy with a moving antenna.
16 p1991 A73-33976
- The effects of cycle slips and phase jitter on the probability of bit error in suppressed carrier phase-shift keyed communications.
17 p2126 A73-35628
- Spatial statistics of instrument-limited angular measurement errors in phased array radars.
17 p2128 A73-35687
- Large parabolic reflector microwave antenna astigmatism effects on radiation pattern, discussing focusing procedure for phase error reduction
17 p2128 A73-35687
- Dependence of sidelobe level on random phase error in a linear array antenna.
17 p2129 A73-35697
- Synthesis of a system of pi-shaped amplitude-frequency and 'zero' equivalent phase-frequency characteristics.
18 p2291 A73-37130
- The effect of carrier recovery and bit timing errors in the coherent reception of 2 and 4 phase PSK signals.
20 p2527 A73-38766
- On the effects of eliminating the passive elements from a thinned array.
21 p2652 A73-40655
- Digitally scanned planar phased arrays, deriving optimum phase perturbation function for quantization and reflection lobe dispersion in terms of aperture distribution amplitude
21 p2652 A73-40667
- Phase-locked loop operation in the presence of impulsive and Gaussian noise.
21 p2656 A73-41166
- Phase-tracking performance of direct-detection optical receivers.
21 p2656 A73-41169
- Phase errors at the aperture of a curvilinear antenna during displacement of the primary radiating element from the focal point
21 p2667 A73-41447
- On separating aberrant effects from random scattering effects in radio telescopes.
23 p2958 A73-43379
- The accuracy of phase-comparison angle tracking by phased-array antennas
24 p3071 A73-44594

PHASE LOCK DEMODULATORS

- Simulation of sequential decoding with phase-locked demodulation.
07 p0794 A73-20498
- Nonlinear system analysis based on Fokker-Planck equation, simplifying solution sequence for steady state or variance of states combination
09 p1111 A73-22114
- Carrier-phase tracking-loop computer simulation and performance evaluation in high-speed SSB data transmission.
23 p2953 A73-43322

PHASE LOCKED SYSTEMS

- Signal search networks for enlargement of locking bandwidth of tracking filters in automatic control systems, examining transistorized signal search and acquisition circuits
02 p0145 A73-11793
- Investigation of the dynamics of a pulsed phase-lock automatic frequency control system
02 p0142 A73-12493
- Mathematical model, digital filter design and phase error behavior derivation for higher order discrete phase locked loops
03 p0276 A73-13906
- Design of communication systems using short-constraint-length convolutional codes.
04 p0419 A73-15396
- Cascade phase-lock loops for the generation of harmonic and subharmonic components.
04 p0421 A73-15433
- The nonlinear analysis and design constraints of a multi-filter phase-lock loop.
04 p0421 A73-15434
- Digital phase locked loops for incoming signal phase tracking, predicting performance from nonlinear difference equation model for comparison with digital simulation
04 p0421 A73-15435
- Equivalent, filter realization and threshold CNR determination for optimum design of extended range phase locked loop
04 p0421 A73-15436
- Transient phenomena in a phase-locked loop with a noisy reference.
04 p0421 A73-15437

Digital simulation of imperfect second-order hybrid phase locked loop operating in RF interference background, determining phase error variance and probability density function
04 p0422 A73-15438

Second order phase lock AFC system transient response duration calculation for rectangular and sawtooth characteristics of phase detector, using averaging method
05 p0547 A73-16059

Sinusoidal signal and stationary quasi-white Gaussian noise mixture effects on stochastic phase locked AFC system operation, noting phase error probability density function
05 p0547 A73-16060

Short term instability of frequency standard using AFC of quartz crystal oscillator by phase locking to optically pumped Rb 87 vapor clock
05 p0583 A73-16071

Operating modes of a phase-loop AFC system with a low control circuit time lag under the action of additive harmonic noise
05 p0560 A73-16292

Fast accurate phase lock loop with self calibrating frequency discriminator, showing dynamic response of frequency lock-up
06 p0675 A73-17843

Microwave oscillator subharmonic phase locking, discussing nonlinear capacitance and linear frequency-dependent parameter and broadband tuning characteristics comparison with fundamental injection locking
06 p0677 A73-18739

Demodulation of pulse modulated signals using Kalman filtering techniques.
06 p0669 A73-18809

Transient analysis of phase-locked tracking systems in the presence of noise.
09 p1066 A73-22113

Second order digital phase locked loop for Viking Orbiter 1975 command system, using filtered sequence of phase error polarity to correct system clocks
09 p1053 A73-23372

Digital phase locked loop for FM demodulation in real time, computing SNR for frequency offsets and sinusoidal modulation
09 p1054 A73-23373

Digital phase locked loops with sequential loop filters - A case for coarse quantization.
09 p1054 A73-23374

Phase locked bit synchronization design tradeoffs between acquisition and noise performance, considering frequency tolerance of decision-directed loop with nonreturn-to-zero input
09 p1056 A73-23403

First order phase locked loop statistical transient behavior in presence of noise from differential equation numerical solution, noting correlation with computer simulation
09 p1056 A73-23404

Improvements in deep-space tracking by use of third-order loops.
09 p1056 A73-23406

Recent development results on the HELIOS S-band command receiver.
09 p1057 A73-23416

Tracking performance of a phase locked loop with a linear phase detector.
09 p1058 A73-23432

Phase locked loop and coherent detection performance prediction, considering desirable phase detector characteristics in terms of SNR and noise spectral density
09 p1058 A73-23433

Noise in single-frequency oscillators and amplifiers.
10 p1196 A73-24864

Pulse avalanche diode oscillators with an injected CW signal.
11 p1339 A73-26698

Second-order phase-lock-loop acquisition time in the presence of narrow-band Gaussian noise.
12 p1468 A73-27010

Data aided phase locked loops for phase estimation improvement in coherent demodulator to obtain loop acquisition characteristics design flexibility
12 p1483 A73-27157

Probability density characteristics of elapsed time interval to synchronization disruption in phase locked AFC systems
13 p1584 A73-28890

Special features of the suppression of low-frequency modulation in a direct-coupled frequency converter
13 p1593 A73-28943

Injection phase locked microwave oscillator for FM amplifier, calculating frequency drift caused gain limitation in terms of diode and circuit properties temperature effects
13 p1593 A73-29116

Measurement of semiconductor junction parameters using lock-in amplifiers.
13 p1595 A73-29578

Frequency synthesizer technology review, discussing direct frequency synthesis and frequency analysis /phase lock/ techniques
14 p1732 A73-29874

Approximate investigation of the dynamics of a digital phase-lock automatic frequency control system /DPAFC/
14 p1728 A73-30269

Use of computers for calculation of the capture band of nonlinear phase-automatic-frequency-control systems.
15 p1842 A73-30990

Synthesis and analysis of tracking systems with optimal acquisition.
15 p1854 A73-31727

HYPHA analog-to-digital converters with phase-locked loops.
16 p1991 A73-33979

Gated phase locked loop tracking device for maximum likelihood estimation of pulsed sinusoid imbedded in noise, predicting phase noise performance
16 p1980 A73-33406

An approach to the analysis of performance of quasi-optimum digital phase-locked loops.
16 p1992 A73-33743

Two-phase radio-frequency generators employing phase-lock AFC
17 p2135 A73-34590

On the explosive instabilities of waves in plasmas with special regard to dissipation and phase effects.
17 p2188 A73-35820

COS/MOS phase-locked-loop - A versatile building block for micro-power digital and analog applications.
20 p2534 A73-38657

Bifurcations and certain qualitative characteristics of a phase-locked automatic frequency control system with a second-order filter
20 p2535 A73-38979

Book - Frequency synthesis: Theory, design and applications.
20 p2542 A73-39143

Superconducting Josephson junction power flow relations dependence on harmonically or subharmonically phase locked autonomous frequency
20 p2536 A73-39411

A square-wave generator with digital frequency setting
21 p2662 A73-40346

Dependence of the induced phase-locking of modes in relationships among laser parameters
21 p2714 A73-40557

Frequency-following injection microwave oscillator with bias voltage control for tracking speed to provide amplifier or noise improvement circuit
21 p2664 A73-41091

Phase-locked loop operation in the presence of impulsive and Gaussian noise.
21 p2656 A73-41166

PHASE MODULATION

NT PHASE SHIFT KEYING

- Measurement of phase fluctuation dispersion for narrow-band signals
01 p0015 A73-10077
- Theory of multistep coding and its application to multiphase-modulation communication systems.
01 p0018 A73-11053
- Mathematical expectation of angularly modulated signal in unsteady linear random noise, using Marchenko formula
03 p0278 A73-14074
- Variance estimate of random process second order moment by nonlinear correlator in presence of additive amplitude and phase modulated and normal noise processes
03 p0278 A73-14075
- Phase and frequency tracking accuracy in direct-detection optical-communication systems.
04 p0416 A73-14993
- Pulsed random process energy spectra methods for spectral distribution of signal power in multichannel AM, FM and PM PCM systems with time division multiplexing
04 p0423 A73-15918
- Indeterminacy functions aside maxima for phase manipulated signals with low sidelobe levels in autocorrelation functions, noting Doppler frequency shift effect
04 p0423 A73-15925
- PM signal cross-correlated receiver output SNR in presence of random misalignments with respect to carrier frequency and signal arrival time
05 p0547 A73-16058
- Q switched carbon dioxide laser based on PM by rotating mirror in one arm of Michelson interferometer, establishing phase relationships
05 p0583 A73-16062
- Velocity measurements made holographically of diffusely reflecting objects.
05 p0574 A73-16287
- Frequency and time description of mode locked laser system, discussing active and passive phase locking of longitudinal standing wave modes in laser cavity
05 p0583 A73-16338
- Intermodulation noise and system analysis in SSB-PM multiple access system.
05 p0552 A73-17169
- Two-dimensional optical phased-array beam steering.
06 p0694 A73-18287

Investigation of the time characteristics of the phase fluctuations of optical waves propagating through the earth atmosphere boundary layer
07 p0792 A73-19914

The resistance of discrete phase modulation to random interference
07 p0793 A73-20023

Detection of signals using receivers with processing of moduli.
07 p0794 A73-20133

Electromagnetic measurement of frequency and amplitude of mechanical vibration, based on echo signal phase modulation, explaining heterodyne detection system
07 p0827 A73-20532

Intelligible crosstalk and AM-PM transfer in commercial communication satellites. II
08 p0937 A73-20773

Reduction of phase non linearities in Traveling Wave Tubes /TWT/.
09 p1062 A73-22305

State of the art in the techniques of digital phase modulation
09 p1050 A73-22317

Study of a phase displacement modulation modem for a time division multiple access system
09 p1050 A73-22318

Bandwidth efficiency for digital communication via a hard limiting channel.
09 p1054 A73-23382

Investigation of the mutual ambiguity function of a wideband signal with complex angle modulation
10 p1187 A73-23731

Influence of signal amplitude changes in systems with phase and frequency modulation
10 p1189 A73-24377

Analysis of the nonlinearity of the modulation characteristic of a single-circuit phase modulator employing a varactor
10 p1195 A73-24382

Stabilized two-pulse operation of the phase-modulated, frequency-doubled laser.
12 p1504 A73-26831

Holographic visualization of large amplitude vibration using reference beam phase modulation.
13 p1622 A73-29642

Possibility of independent control of frequency characteristic and coverage band in a PAFS system.
15 p1842 A73-30987

Signal interference and improvement of signal-to-noise ratios in a half-wave linear detector.
15 p1843 A73-31729

Phase modulated data transmission with partial pilot signals, interpolating reference demodulation signals at receiving end by maximum cross correlation
16 p1884 A73-33978

First order theory of steady state single optical pulses /solitons/ phase modulation during propagation in nonlinear absorbers, predicting nonchirped and chirped pulse trains
20 p2591 A73-38626

Correlation of random phases spaced over oscillation frequencies
20 p2531 A73-39457

Spectra of signals with functional phase modulation in digital frequency synthesizers
20 p2537 A73-39461

Derivative light scattering photometer, using angular modulation with photomultiplier entrance slit vibration to obtain gain improvement over conventional technique
21 p2697 A73-40130

Self consistent microscopic theory of Rayleigh light scattering by molecular aggregates based on random phase modulation and stochastic theories
21 p2739 A73-40219

Diffraction grating model in terms of amplitude and phase modulation to explain angular spectrum of light reflection from corrugated surface for various incidence angles
21 p2740 A73-40790

Probabilistic analysis of random and deterministic phase coding for lowering Fourier transform spectrum dynamic range in digitally generated hologram and kinoform memories
22 p2864 A73-43149

A digital system for receiving binary phase-coded signals
23 p2952 A73-43319

Propagation velocity of picosecond pulse from mode locked Nd-glass laser investigated by optically induced birefringence, self phase modulation and self focused light
23 p2988 A73-44120

Josephson junction I-V characteristics and measurements of phase modulated quasi-particle current in superconducting weak links, taking into account thermal noise
23 p3018 A73-44174

Calculation of the spectrum of a sinusoidal signal modulated by phase displacement with one, two, or three states for any values of phase jumps
24 p3068 A73-44972

PHASE SHIFT

Hilbert transform for single and narrow band signal analysis with 90 deg spectral component phase shift in frequency region
01 p0015 A73-10076

Phase switched FM-CW radio altimeter, noting error reduction by controlled switching of phase difference between emitted and echo signals
02 p0165 A73-11526

Antenna radiation pattern synthesis, discussing current phase and amplitude distribution determination by iterative and quadratures solutions respectively
03 p0284 A73-14059

Nonsolar related D region semilunar variation effects on Omega navigation systems signal phase shift from harmonic analysis of VLF propagation data periodicities
04 p0416 A73-15062

Q switched carbon dioxide laser based on PM by rotating mirror in one arm of Michelson interferometer, establishing phase relationships
05 p0583 A73-16062

Outer-scale effects in turbulence-degraded light-beam spectra.
05 p0597 A73-16498

Representation of oscillations in piecewise-linear systems by the phase-shift-averaging method.
06 p0717 A73-18146

Fluctuations in the level and phase of a field in a waveguide with a random boundary
07 p0793 A73-19916

Differential phase experiment on signal reflections from D region, noting systematic error in phase jitter calculation with pulse nonoverlap explanation
07 p0820 A73-20067

Wavefront tilter for double-exposure holographic interferometry.
08 p0963 A73-20874

Microwave barrier /barrier-injection-transit-time/ diodes large signal performance, noting phase delay between injected and total current densities
08 p0945 A73-21074

Oscillator synchronization by FM signal for constant central frequency-sideband phase difference operation
08 p0946 A73-21112

Rytov method to predict random vibration amplitude and phase fluctuations range and frequency dependence in Mintzer region, noting applicability domain
08 p0988 A73-21193

Block diagram of transistorized phase instability meter for statistical analysis of one dimensional density distributions, noting two series connected identical delay lines
09 p1064 A73-23008

Selective amplifier with zero group delay in pass-band phase characteristics for sinusoidal frequency signal measurement
09 p1066 A73-23118

Record/reproduce process induced phase distortion in magnetic tape recorders as function of record head gap length
09 p1087 A73-23368

Spectra of short-term fluctuations of line-of-sight signals - Electromagnetic and acoustic.
10 p1190 A73-24893

Interference measurement techniques for small phase difference changes, noting diffraction and noise effects as limiting factors
10 p1222 A73-24945

Influence of phase fluctuations of the received radiation on the performance of a synthetic antenna
11 p1331 A73-26158

Gaussian light beam transmitted intensity derivation for thermal lensing in solids by vector Kirchhoff approach, obtaining time dependent shift in diffraction focus
11 p1377 A73-26228

Lowest-order mode selection in a laser interferometer.
12 p1504 A73-26842

Investigation of series pattern-forming circuits for multiple-beam antennas
12 p1479 A73-27231

Horn-element antenna phase center position calculation for directivity characteristics by power series of radiation patterns
12 p1480 A73-27236

Mode locking in quantum optics.
12 p1506 A73-27442

A simple method for converting a pulse code into a phase code by using parametrons
12 p1481 A73-27590

Solar prominences during period between sunspot minimum and maximum, investigating secondary polar zone coronal activity phase shift relationship to main zone anomaly
12 p1545 A73-27837

Analysis of primary currents in a three-phase/single-phase frequency converter with direct coupling and artificial commutation
13 p1592 A73-28940

PHASE SHIFT CIRCUITS

Turbine vane vibration simulation tests with phase shift generation, using tube type phase inverters
13 p1599 A73-29638

The effects of out-of-phase biaxial-strain cycling on low-cycle fatigue.
14 p1806 A73-29774

Phase effect in RC transistor oscillator with single transistor or tube as amplifying element, determining vibration frequency, reverse communication amplification and frequency dependence
14 p1737 A73-30793

Phase-difference distributions in a D-region partial-reflection experiment.
15 p1845 A73-32231

Phase coded moving target indicators, describing phase measurement technique to discriminate between moving and fixed targets
15 p1846 A73-32433

Phase progression of the QRS complexes in electrocardiograms versus the inscribing directions of the QRS loops in vectorcardiograms.
16 p1975 A73-33116

Optical method for submillimeter band phase measurements by probing spatially separated compared fields and summing two signals at detector
17 p2120 A73-34155

A practical method for measuring the complex polarization ratio of arbitrary antennas.
17 p2127 A73-35677

Phase characteristics of a rectangular waveguide with symmetrically arranged, transversely magnetized ferrite layers
19 p2407 A73-38342

The sensitivity of optoelectronic scanning systems with out-of-phase connection of the radiation detector elements.
20 p2564 A73-38850

Some results and accuracy of satellite measurements of the electron content in the ionosphere
20 p2554 A73-39166

Combined density of the probability distribution of instantaneous values for the phase difference of two oscillations and for the phase difference derivatives
20 p2593 A73-39390

Evaluation of phase distortions in the magnetic recording of signals with a high-frequency magnetic bias
20 p2531 A73-39468

Effects of a synchronizer phase-shift on circadian rhythms in response of mice to ethanol or ouabain.
20 p2513 A73-39481

Method of calculating the amplitude and phase-amplitude characteristics of high-frequency amplifiers
21 p2666 A73-41314

Sampling phase rotator for removal of Doppler shift in a lunar radar.
21 p2658 A73-41590

Influence of inhomogeneities in a nonlinear crystal on the conversion of an image by sum-frequency generation.
22 p2869 A73-42245

Phase fluctuations in a parametric light source operating inside a laser resonator.
22 p2869 A73-42246

Some features of second-harmonic generation in a lithium metaniobate crystal.
22 p2896 A73-42247

Singlet s-wave electron-hydrogen scatter below first excitation threshold, computing phase shift in Feshbach operator and static exchange approximation
22 p2890 A73-43127

Uses of tunnel diodes for zero-transition discrimination in phasometric devices
23 p2959 A73-43477

Zero-transition discrimination in phase-measuring devices with amplifier-limiters and tunnel diodes
23 p2959 A73-43478

Slot microwave transmission line with thick metal coating on dielectric substrate, calculating phase constant variation with frequency, slot width and coating thickness
23 p2954 A73-44069

Electronic fringe-follower for interferometer.
23 p2983 A73-44086

Ultrasonic holography free from phase turbulence - Construction of the device and experimental results.
23 p2983 A73-44087

Phase-sensitive method of electromagnetic flaw detection.
24 p3093 A73-44696

Short-time fluctuations of the VLF field along polar paths
24 p3067 A73-44809

PHASE SHIFT CIRCUITS
NT CIRCULATORS [PHASE SHIFT CIRCUITS]
Transistorized varicap diode frequency modulator circuit with restricted parasitic AM, using phase shift control and frequency multiplication
01 p0022 A73-10031

Self-compensating digital phase meter with discrete phase shifters
01 p0044 A73-10078

Design of digital phase meters with intermediate frequency converters
01 p0044 A73-10079

PHASE SHIFT KEYING

Quadrature phase splitter with indications of the quadrature and equality of output voltage amplitudes
01 p0022 A73-10081

Recent advances in diode and ferrite phase technology for phased-array radars. II.
01 p0024 A73-10720

An application of pneumatic phase shifting to stabilization of externally pressurized journal gas bearings.
[ASME PAPER 72-LUB-4] 03 p0313 A73-14327

Computer analysis of latching phase shifters in rectangular waveguide.
06 p0678 A73-18743

P-I-N switching diodes in phase-shifters for electronically scanned aerial arrays.
08 p0943 A73-20712

Electronic six-channel phase shifter
08 p0950 A73-21715

Design and performance of electrically regulated phase shifter comprising rectangular waveguide section containing two ferrite resonators magnetized at ferromagnetic-resonance frequency
12 p1477 A73-26945

High power latching ferrite phase shifters for AEGIS.
13 p1591 A73-28620

Effect of an external magnetic field on the beat frequency of opposite waves in a ring laser with a noninteracting phase-shifting device
13 p1627 A73-28965

A new statistical design method for thinned solid-state phased arrays.
13 p1594 A73-29231

High-density image-storage holograms by sampling and random phase shifter method.
15 p1876 A73-31946

Two-phase radio-frequency generators employing phase-lock AFC
17 p2135 A73-34590

Design of second-order phase circuits constructed with TEM-line segments
17 p2144 A73-34592

Design principles for phase-measuring attachments with automatic error corrections
18 p2294 A73-36999

Book - Design performance and applications of microwave semiconductor control components.
20 p2535 A73-39136

Baseband modeling and distortion equalization of the DeLange FM oscillator by functional methods.
21 p2662 A73-40337

Digitally switched phase shifter operating at metric wavelengths
21 p2662 A73-40544

Diode and ferrite phase configurations for phased array antenna system, discussing digital and analog versions, driver requirements and design trends
21 p2663 A73-40665

Planar phased array beam steering methods, emphasizing electronic driver and logic circuit sharing between phase shifters for cost reduction
21 p2652 A73-40666

Bias controlled step recovery diode as combined frequency multiplier and analog phase shifter for applications in microwave phased array antenna systems
21 p2663 A73-40668

Mechanically and electronically switched circular symmetric phased arrays with hybrid matrix phase shifter and lens switch combinations, assessing design and performance characteristics
21 p2672 A73-40675

Rapid-switching, broadband 1:4 WG switch matrix. II.
22 p2834 A73-42874

Effect of external magnetic field on the beat frequency in a ring laser with nonreciprocal phase shifter.
23 p2989 A73-44317

Analysis of the detection characteristics of frequency discriminators with nonminimum-phase loops
24 p3071 A73-44597

PHASE SHIFT KEYING

Effects of a finite-width decision threshold on binary CPSK and PSK communication systems.
03 p0277 A73-13911

Differentially encoded multiple phase shift keyed signals transmission and detection, analyzing digital communication system performance
04 p0415 A73-14991

Quadrature amplitude-shift key satellite communication feasibility based on SNR and transmitter power efficiency comparison with multiphase-shift key system
04 p0420 A73-15411

Effects of hardlimiting on bandlimited transmissions with conventional and offset QPSK modulation.
04 p0420 A73-15412

Mathematical model for multipath transmission in aircraft and spacecraft communications, presenting Bayes detector for binary PSK
04 p0422 A73-15462

Almost-coherent detection of phase-shift-keyed signals using an injection-locked oscillator.
05 p0549 A73-16368

The effect of a bandpass nonlinearity on signal detectability.
06 p0664 A73-17713

Performance of M-ary PSK systems in Gaussian noise and intersymbol interference.
06 p0665 A73-18140

8-phase and 16-phase high speed PSK modems for PCM-TDMA satellite communication.
07 p0791 A73-19370

Noise immunity of autocorrelated reception of singly phase-shift-keyed signals
07 p0794 A73-20298

State of the art in the techniques of digital phase modulation
09 p1050 A73-22317

Noise immunity in detection of pseudorandom PSK signals with allowance for synchronization errors, noting reception fidelity dependence on signal to noise ratio
09 p1050 A73-22455

Digital coherent demodulator techniques for moderate data rate PSK signal reception in real time, describing synchronous bandpass sampling receiver with IF signal A/D conversion
09 p1053 A73-23371

Bandwidth efficiency for digital communication via a hard limiting channel.
09 p1054 A73-23382

Amplitude-phase-keying with M-ary alphabets - A technique for bandwidth reduction.
09 p1054 A73-23385

Convolutional coding for multiple-access satellite communication.
09 p1056 A73-23399

A single channel command detector for deep space missions.
09 p1057 A73-23417

A new type of PSK anti-ambiguity system for satellite applications.
09 p1156 A73-23431

A combined coding and modulation approach for communication over dispersive channels.
10 p1186 A73-23496

High volume wideband PSK system design for minimal sidelobe, calculating signal number relationship to maximum sidelobe level of cross correlation and autocorrelation
10 p1187 A73-23733

Noise immunity of quasi-coherent reception of phase-shift keyed signals with respect to additive fluctuation noise.
10 p1191 A73-24938

A modulator with inherent bandwidth limiting for use with a bi-phase PSK data transmission system.
12 p1472 A73-27663

A shipboard satellite communication experiment.
12 p1473 A73-27675

Noise immunity evaluation for noncoherent demodulators or FSK and PSK signals in short wave channels, using minimum a priori information on additive noise properties
13 p1592 A73-28899

Study of carrier and bit-timing recovery of ultrahigh speed PSK-TDMA systems
13 p1584 A73-28909

Transmission characteristics of PSK wave in nonlinear system - Application to INTELSAT IV satellite systems.
13 p1586 A73-29234

Application of acoustic surface-wave technology to spread spectrum communications.
14 p1733 A73-29934

Spectral-energy dispersal in digital communication-satellite systems.
15 p1842 A73-31096

Methods for investigating the effects of multipath fading on 2-phase digital radio systems.
16 p1981 A73-33708

Analysis of the correlation properties of certain PSK signal systems
17 p2121 A73-34586

Effects of cochannel interference and Gaussian noise in M-ary PSK systems.
17 p2122 A73-34871

Pseudo random modulation - An effective means of enhancing PSK signal transmission in a diffuse multipath environment.
17 p2125 A73-35376

The effects of cycle slips and phase jitter on the probability of bit error in suppressed carrier phase-shift keyed communications.
17 p2126 A73-35628

A 180-deg phase-shift keying modulator for microwave broadband application
18 p2292 A73-36398

Noise immunity of autocorrelation reception of single PSK signals.
18 p2291 A73-37135

Signal set design for bandwidth constrained multiple phase amplitude shift keyed /MPASK/ communication system, considering minimum error probability for given energy/noise ratio
20 p2522 A73-38717

Nonlinear transformation by a travelling wave tube and power spectral density of a PSK-signal.
20 p2522 A73-38718

A proposed time division multiple access /TDMA/ satellite system for Anik I.
20 p2523 A73-38719

Error rate of a 4-phase coherent PSK satellite channel with non-Gaussian interference.
20 p2523 A73-38721

The domain analysis of intersymbol interference effects on phase shift keyed /PSK/ and quadrature phase shift keyed /QPSK/ communication systems.
20 p2524 A73-38734

Effect of nonlinear channel characteristics on QPSK system performance.
20 p2526 A73-38752

High-bit-rate transmissions through a channelized repeater.
20 p2526 A73-38753

Adjacent-channel interference between unfiltered and filtered QPSK signals.
20 p2526 A73-38754

Variable data rate multimode quadriphase modem for PSK or QPSK operation in digital communication links, noting optimum overall system performance
20 p2527 A73-38764

Performance estimate for coherent QPSK with random intersymbol interference due to time-varying scatter.
20 p2527 A73-38765

The effect of carrier recovery and bit timing errors in the coherent reception of 2 and 4 phase PSK signals.
20 p2527 A73-38766

Calculation of structurally compressed satellite radio lines
20 p2531 A73-39469

Combined effects of intersymbol, interchannel, and co-channel interferences in M-ary CPSK systems.
21 p2656 A73-41167

Suppression of equichannel interference in the case of binary phase shift keying employing a limiter
23 p2953 A73-43324

Generation of complex phase-shift-keyed signals by the optical correlation method
24 p3067 A73-44595

PHASE SWITCHING INTERFEROMETERS

Multiple-beam lateral-shear interferometer.
22 p2863 A73-43146

PHASE TRANSFORMATIONS

NT ARC MELTING
NT BOILING
NT EVAPORATION
NT FILM BOILING
NT FREEZING
NT FUSION [MELTING]
NT LEIDENFROST PHENOMENON
NT MELTING
NT NUCLEATE BOILING
NT PROPELLANT EVAPORATION
NT SUBLIMATION
NT TRANSPIRATION
NT VACUUM MELTING
NT VAPORIZING
NT VIBRATIONAL FREEZING
NT ZONE MELTING

Structural changes during the deformation of molybdenum alloys
01 p0061 A73-10252

Characteristics of the formation of austenite during rapid heating of cold-worked KVK-42 /42Kh2NGSM/ steel
01 p0062 A73-10260

Phase diagram of the neodymium-yttrium system
01 p0088 A73-10919

Comment on the nature of the disaccommodation in HCP Co-C alloys.
01 p0066 A73-10999

Solid-solid phase transitions determined by differential scanning calorimetry.
01 p0014 A73-11062

Thermochromic cuprous mercuric iodide for IR recording applications, observing phase transition hysteresis from reflectance-vs-temperature, specific heat and sensitivity measurements
01 p0054 A73-11230

Superconductor/exiton-dielectric phase transition in a semimetal
01 p0089 A73-11292

Structured changes and phase transformations of welded joints of Al alloy with Cu addition during welding thermal cycles
01 p0067 A73-11352

High-temperature thermal analysis of high boron alloys using automatic optical pyrometry.
01 p0015 A73-11450

Mechanism of transformation of a low-carbon 18-10 stainless steel by reaction in liquid tin
02 p0178 A73-11525

Automatic two-coordinate compensator for resistance-measurement studies of steels and special alloys
02 p0167 A73-11867

- Hydrogen reactions and detection by line broadening in beta transformed Ti-Al-V alloy, using X ray diffraction analysis 02 p0183 A73-12759
- The tempering of low carbon steels containing tungsten. 02 p0183 A73-12760
- The effect of prior deformation on the strength and annealing of reverted austenite. 02 p0183 A73-12766
- The solidification sequence in an 18-8 stainless steel, investigated by directional solidification. 02 p0184 A73-12769
- Shock wave and isentropic compression/expansion in plasma with anomalous thermodynamic properties due to strong particle interactions, discussing phase transitions types 03 p0346 A73-13190
- Two phase recrystallization temperatures and structural inhomogeneity of dispersion hardened Ni after cold working and annealing at 1300-1400 C 03 p0324 A73-13508
- Martensitic transformation kinetics and martensite morphology in the N25Kh2 alloy after aging 03 p0325 A73-13826
- Delta-ferrite alteration in steel 1Kh16N4B during homogenization 03 p0326 A73-13828
- Phase transformations in the VT9 quenched titanium alloy during heating 03 p0327 A73-13974
- Ni, Si and Mn alloying effect on structural transformations, phase composition and mechanical properties of cast Cr-Ni steels 03 p0327 A73-14002
- Nature of the density reversal beneath the lunar maria. 04 p0496 A73-14821
- Plastic anisotropy of low-carbon, low-manganese steels containing niobium. 04 p0463 A73-15309
- Microstructures and transformation kinetics of continuously cooled carbon free Fe-Mo-Ni alloys. 04 p0463 A73-15311
- Characteristics of secondary phases in heat-resisting alloys. 04 p0465 A73-15580
- Phase transformations and mechanical properties of highly alloyed Cr-Mn-Ni steels 04 p0466 A73-15664
- Study of transformations of TA6V6E2 titanium alloy with 6.4 per cent zirconium, in isothermal conditions after putting in solution in the beta domain 04 p0466 A73-15691
- Phase transformations in Al-rich Al-W alloys rapidly quenched from the melt. 04 p0468 A73-15983
- Stacking faults effect on martensitic phase formation during steel hardening based on X ray diffraction analysis and Paterson theory 06 p0735 A73-18034
- Structural and phase transformations in silicon steels during heat treatment 06 p0707 A73-18035
- Polymorphous transformation mechanism in thallium 06 p0735 A73-18045
- Martensite transformation in an aged Fe-Ni-Ti alloy 06 p0708 A73-18052
- The mechanical properties of titanium alloys with isomorphous beta-stabilizing elements. 06 p0708 A73-18206
- The martensitic transformation during deformation of titanium alloys with metastable beta phase. 06 p0708 A73-18207
- Transition of oxide film on a molybdenum surface from a two-dimensional structure to a three-dimensional structure. 06 p0738 A73-18617
- The formation and structure of precipitates in a dilute magnesium-neodymium alloy. 07 p0838 A73-19121
- Lunar rocks petrogenesis, determining liquidus and solidus temperatures and crystalline phases sequence in lunar samples and synthesized oxides and silicates 07 p0879 A73-19689
- Lunar plagioclase and pyroxene observation for lamella thicknesses by X ray diffraction, noting twinning, exsolution and crystal disorder effects 07 p0788 A73-19711
- Investigation of the structural changes in austenite during martensitic transformation in steels with high stacking-fault energy 07 p0841 A73-20521
- Axisymmetric Stefan problem with boundary conditions of the third kind 08 p1022 A73-21100
- Dynamic yield, compressional, and elastic parameters for several lightweight intermetallic compounds. 09 p1099 A73-21926
- Optimal superplasticity model of metallic materials involving interphase surface of new phase fluctuation nuclei in framework of Frenkel theory 09 p1099 A73-21960
- Dependence of martensite morphology on the isothermal transformation temperature of the Fe-24Ni-3Mn alloy 09 p1100 A73-21974
- Analytical approach to estimating the source rock of basaltic magmas - Major elements. 09 p1076 A73-22147
- Phase transformational kinetics and hardenability of low-carbon, boron-treated steels. 09 p1102 A73-22416
- Ni-Ti alloy aging effects on yield strength explained by internal strain due to lattice modulation and Ti rich region volume fraction 09 p1103 A73-22520
- Dielectric dispersion of irradiated BaTiO3 in the phase transition region 09 p1134 A73-22983
- Kinetics of transformation of carbon- and nitrogen-enriched austenite by carbonitriding in the gas phase 09 p1105 A73-23038
- Austenite stabilization in Kh17N6M3 transition-type steel 09 p1107 A73-23201
- Cast, annealed and hardened zirconium binary alloys cubic to hexagonal phase transitions from X ray and differential thermal analysis 10 p1233 A73-24318
- Correlation of coercive force to microstructure in cyclic martensite/austenite transformations in an Fe-Ni-Co alloy. 10 p1234 A73-24438
- Application of the fluctuation model of superplasticity to calculate the surface tension of metals during phase transformations 10 p1235 A73-24455
- Peritectic solid phase transformations in cast homogenized Al-Cu-Li-Mn-Cd alloy, noting Li strengthening effect 10 p1236 A73-24927
- Structural transitions and mechanical characteristics in the case of multicomponent aluminum bronze 11 p1378 A73-25106
- Additives alloying with cobalt, discussing allotropic transformation dependence, recrystallization, mobile dislocations, and iron deformation by twinning 11 p1408 A73-25322
- Shock induced phase change in single crystal orthoclase at 115 kb, noting high pressure phase with hollandite-structure properties 11 p1352 A73-25586
- Analytical investigation of heat transfer in bodies with moving boundaries 11 p1450 A73-25622
- Ultrasonic investigation of the nematic-isotropic phase transition in MBBA. 11 p1409 A73-26213
- Order-disorder alpha and gamma phase transformations as function of temperature in Co-Fe-V alloy by dilatometric, magnetostuctural, neutron diffraction and X ray analyses 12 p1508 A73-26834
- Influence of deformation and heat treatment on the structural changes of the OKh12N13M alloy 12 p1508 A73-26836
- Plastic deformation, martensite transformation and temperature effects on shape memory of nitinol and other alloys 12 p1509 A73-26896
- Phase transformations in the bismuth ferrites BiFeO3 and Bi2Fe4O9 12 p1531 A73-27199
- Possibility of silicon carbide recrystallization in the process of reactive sintering 12 p1503 A73-27555
- Metal matrix composites microstructural alignment by solid state transformation process involving eutectoid decomposition and cellular precipitation 12 p1513 A73-27682
- Study of crystalline transformations at high temperature above 2000 K; International Colloquium, Odeillo, Pyrenées-Orientales, France, September 27-30, 1971, Proceedings 12 p1514 A73-27918
- Influence of the chrome content and the interstitial impurities content /carbon and nitrogen/ on the volumetric and intergranular diffusion of iron 59' in iron-chrome alloys with from 0 to 15 per cent chrome - Relations with alpha to alpha plus gamma reversible transformations 12 p1514 A73-27985
- Some physical properties of stephanite in the phase transition region 13 p1667 A73-28002
- Austenite stabilization during inverse transformation in Cr-Co-Mo and Cr-Ni-Co-Mo steels 13 p1630 A73-28012
- Luna 2 pyroxenes - Exsolution and phase transformation as indicators of petrologic history. 13 p1675 A73-28313
- Reduction kinetics and phase transformations of tungsten and molybdenum oxides 13 p1636 A73-28938
- German monograph on calculation of thermal and transformation stresses in long circular cylinders covering austenite-martensite transformation, thermal expansion and viscous bodies 13 p1699 A73-29284
- Fatigue crack initiation and propagation in low stacking fault energy austenite steel related to plastic deformation induced gamma alpha transformation and martensite failure 13 p1640 A73-29481
- An X-ray study of hydrogen induced phenomena affecting mechanical behaviours of austenitic stainless steels. 13 p1625 A73-29522
- Redistribution of nickel and chromium during alpha to gamma transformation in stainless nickel-chromium steels 13 p1644 A73-29646
- Book on statistical mechanics, covering thermodynamics, canonical ensembles, quantum statistics, simple gases, ensemble theory, phase transitions, cluster expansions and interacting systems 14 p1775 A73-30360
- Alpha phase decomposition and precipitation measurement in titanium rich Ti-Al alloys by electrical resistivity and microscopic methods 14 p1761 A73-30638
- Effect of tensile deformation in the austenite range on transformation kinetics of a high-strength low-alloy /HSLA/ steel. 14 p1762 A73-30641
- German monograph - Effect of the transformation and heat treatment conditions on the mechanical properties and the creep characteristics of the alloy TiAl6V4. 14 p1762 A73-30668
- Martensitic transformation in iron-nickel alloys in a pulsed magnetic field 14 p1764 A73-30860
- Titanium and zirconium alpha-omega transformation hysteresis at room temperature from dilatometry, X ray phase analysis and electrical resistance and shear measurements 14 p1764 A73-30863
- Some characteristics of the influence of alloying elements on the polymorphous transformation temperature of zirconium 14 p1765 A73-30886
- Investigation of phase transitions in BaTiO3 15 p1923 A73-31204
- Lunar core sample structure morphology and composition examined by microanalysis, revealing tenite to martensite transformation 15 p1930 A73-31220
- Transformations in crystalline boron during mechanical dispersion 15 p1897 A73-31600
- Method for boundary condition selection in the heat transfer problem with phase transition 15 p1958 A73-31872
- Study of a niobium-aluminum-silicon system. I - Partial isothermal sections at 1500 and 1300 deg C, and the behavior of the Nb/Si, Al/2 phase 15 p1890 A73-31991
- Study of the isothermal transformations of the titanium alloy beta sub III 15 p1892 A73-32212
- Phase transformations in alloys of the titanium-molybdenum system 15 p1893 A73-32517
- Transformations during heat treatment of Ti-Mo system alloys with additions of aluminum, zirconium, and tin 15 p1893 A73-32518
- Structure and decay characteristics of unstable beta-solid solutions of the Ti-V system 15 p1893 A73-32519
- Diffusional and nondiffusional metastable-phase transformations in titanium alpha + beta alloys 15 p1893 A73-32520
- Structural transformations in two-phase titanium alloys 15 p1893 A73-32522
- Phase and structural changes in titanium under impulsive loads 15 p1894 A73-32523
- Phase transformations during heat treatment of the VT18 alloy 15 p1894 A73-32524
- Influence of plastic deformation and of phase transformations at negative temperatures on the properties of titanium alloys 15 p1894 A73-32531
- Phase composition and properties of metastable alloys of titanium with nickel 16 p2027 A73-34072
- The structure of a meteorite, its formation and transformation during heating 17 p2230 A73-34565
- Microstructure and hardness investigations of alpha prime, alpha double prime and omega metastable phases formed during quenching of Ti-Ru alloys 17 p2188 A73-34567

PHASE VELOCITY

The effect of thermomechanical pretreatment on the allotropic transformation in cobalt.

17 p2190 A73-34645

Heat pipe and phase changing material (PCM)/sounding rocket experiment.

18 p2371 A73-36374

[AIAA PAPER 73-759]

Investigation of the impact toughness of construction materials at temperatures of 20 and 4.2 K

18 p2324 A73-36767

Transformations of TA6V6E2Zr alloy in isothermal conditions

19 p2441 A73-37832

Principal aspects of thermal treatments of the alloy Ti-11, 5 Mo-6, Zr-4, 5 Sn /Beta III/

19 p2441 A73-37833

Equilibrium properties of a one-dimensional kinetic system.

19 p2463 A73-37899

Fluctuation model of superplasticity and surface tension of a metal at a phase transition.

19 p2442 A73-38137

Laser threshold behavior analogy with thermodynamic ferromagnetic order-disorder phase transition, using self consistent field theory

20 p2571 A73-38628

Electron diffraction study of a noncrystalline Zr-Ni phase.

20 p2575 A73-39021

Twinned plate structure of martensitic transformation dependence on composition in Zr-Ti alloy investigated by transmission electron microscopy

20 p2575 A73-39023

Stabilized gamma phase U-Nb-Zr alloy observation by electron microscopy, noting displacement reaction role in transition phase formation

20 p2578 A73-39489

Theory of the phase transition in group IV-VI compound semiconductors

21 p2751 A73-40369

Vapor-liquid-solid type growth in lunar glass covered breccia 15015, noting metallic iron stalks with bulbous tips of iron and sulfur mixture.

21 p2766 A73-40412

Effect of small perturbations on the behavior of thermodynamic variables near the point of a phase transition of the second kind

21 p2790 A73-40445

Structure and phase composition of a maraging-steel weld

21 p2718 A73-40737

Influence of aluminum on the structure and properties of a Ti + 10% V alloy

21 p2719 A73-40850

Electrically neutral condensate of pions arises in nuclear matter at neutron star densities, discussing phase transitions

21 p2771 A73-41022

Plastic deformation, martensite transformation and temperature effects on shape memory of nitinol and other alloys

21 p2720 A73-41029

Redistribution of nickel and chromium during the alpha to gamma transformation in Cr-Ni stainless steels.

21 p2720 A73-41039

Ehrenfest equations for thermodynamic equilibrium in classical body second order phase changes using calorific equations of state, relating specific heat discontinuities and equilibrium manifold

22 p2885 A73-41737

Lunar core sample structure morphology and composition examined by microanalysis, revealing tenite to martensite transformation

22 p2905 A73-41808

Vapour pressures of liquid oxygen and nitrogen.

22 p2930 A73-41979

Omega-phase stability in the Ti-Zr-O system

22 p2873 A73-42085

Structural transformations in molybdenum-carbon alloys during quenching and aging

22 p2874 A73-42091

Metastable phases produced by laser melt quenching.

22 p2878 A73-42576

Venus atmosphere water vapor phase transformation possibilities, discussing ice crystal and supercooled water drop formation

22 p2911 A73-42736

Convergent stable three-time level implicit numerical model for phase change problems, evaluating temperature dependent coefficients of parabolic equations at intermediate level

22 p2937 A73-42951

Transformation temperatures of martensite in beta-phase nickel aluminide.

23 p2989 A73-43275

The superconductor-excitonic dielectric phase transition in a semimetal.

23 p3015 A73-43513

Phase transformations in beta-Cu-Al during extremely rapid cooling from the melt

23 p2992 A73-43914

Hydrogen-induced transformation and embrittlement in 18-8 stainless steel.

23 p2994 A73-44158

Diagram of continuous cooling transformation of a titanium alloy with 6 per cent Al, 6 per cent V, and 2 per cent Sn /TA 6-V 6-E 2/ homogenized in the beta /sub 0/ phase

23 p2995 A73-44177

Gamma to alpha transformation and notch depth effects on metastable austenitic steel impact strength at cryogenic temperatures

23 p2995 A73-44282

Field electron emission microscopic study of titanium

24 p3098 A73-44474

Transformation of meteorite material in experiments on explosively produced shock compression at pressures of 500 and 1000 kbar

24 p3137 A73-44710

Least squares methods for thermal equations of state parameters of substances and solutions, taking into account phase equilibrium lines

24 p3155 A73-44753

Chemical stability and features of the formation of complex nitrides of III-B subgroup elements /Al-B-N system/

24 p3119 A73-44952

Stability of the gamma-prime Co3Ti compound in simple and complex cobalt alloys.

24 p3099 A73-45075

Stability criteria for two phase transpiration, cooling system with equilibrium phase transition inside porous wall

24 p3156 A73-45079

Contribution to the phase stabilization of ammonium nitrate

24 p3066 A73-45201

Martensitic transformations in Fe-Cr-Ni austenitic stainless steels - Relation between the parameters of the epsilon phase and the transformation mechanisms

24 p3101 A73-45522

PHASE VELOCITY

Numerical solution for propagation of longitudinal waves along the geomagnetic field using a three-fluid ionosphere model.

01 p0016 A73-10197

Influence of an important region of the ionospheric layer on ELF propagation characteristics

01 p0016 A73-10203

Nonlinear interaction of two monochromatic Langmuir waves

01 p0016 A73-10209

Reduction of antenna length via wave channel type antenna design with modulated phase velocity and multiple use of antenna array

03 p0284 A73-14031

A mechanism of steady-turbulence development in a plasma

04 p0477 A73-14876

Elastic wave propagation in a circular cylinder subjected to finite deformation Compressible material

04 p0513 A73-15503

The dispersion diagram of the plasma waves on the plasma branch in a beam-created plasma.

04 p0482 A73-15949

Lower F region ionospheric wave dispersion observation for horizontal phase and group velocities relationship to period, considering interpretation by internal gravity wave hypothesis

05 p0552 A73-17056

Character of acoustic dispersion in plasma.

06 p0726 A73-17403

Calculation of the field amplitude and phase velocity of low-frequency waves in the earth's spherical waveguide

08 p0939 A73-21285

On the simplest example of the barotropic instability of Rossby wave motion.

08 p0985 A73-21388

Upper sporadic E layer downward velocity, considering corkscow mechanism, ionization following gravity wave particular phase and velocity decrease

10 p2125 A73-24750

Small amplitude surface and plate waves propagation in incompressible biaxially stressed elastic media, obtaining dispersion equation for various phase velocities

11 p1434 A73-25166

Ionosphere spatial resonance as result of internal gravity wave phase velocity equal to ionization irregularity drift rate

11 p1356 A73-25908

Small amplitude hydromagnetic waves for a plasma with a generalized polytrope law.

11 p1406 A73-26555

Dynamics of strongly nonlinear beam-plasma interaction.

12 p1529 A73-27434

[IPPCZ-167]

Theory for errors, resolution, and separation of unknown variables in inverse problems, with application to the mantle and the crust in Southern Africa and Scandinavia.

13 p1607 A73-28621

Phase velocities and angle of inclination for frequency components in fully developed turbulent flow through pipes.

13 p1604 A73-29266

Electron density phase velocity, drift rate and ion temperatures from radar echoes power spectrum near equatorial electrojet

14 p1748 A73-29972

On linear parasitic array of dipoles with reactive loading.

14 p1734 A73-30203

Quasi-monochromatic viscoelastic waves energy velocity equivalence to phase velocity for medium represented by standard linear solid or Maxwell model

15 p1955 A73-32176

Observations of two-stream ion wave instability.

16 p2041 A73-33335

Eddy power flow of electromagnetic waves.

16 p1980 A73-33690

Wave propagation in uniform laminar cylindrical shells, discussing group and phase velocities on wave numbers in sandwich walls

17 p2243 A73-34734

Arbitrary propagation of HM waves along the F region.

18 p2312 A73-36285

Radar aurora type III spectra with phase velocities exceeding ion acoustic velocity, discussing relation to current-excited ionospheric electrostatic ion cyclotron oscillations

18 p2312 A73-36299

Optokinetic stimulation of an immobilized eye in the monkey.

18 p2273 A73-36457

Experimental investigation of a fast ion-acoustic wave in a multicomponent plasma

18 p2339 A73-36564

Phase velocity dispersion for transverse normal elastic wave propagation through sandwiched CdS and molten quartz or germanium layers

18 p2340 A73-36672

Computations of the field amplitude and phase velocity of low-frequency waves in a spherical surface waveguide.

19 p2404 A73-37914

Containment stability of charged particles captured by a plane electromagnetic wave propagating at a slowly varying velocity

22 p2826 A73-42377

Dynamic stability of transverse axisymmetric waves in circular/cylindrical shells.

22 p2925 A73-42887

[ASME PAPER 73-APMW-26]

Stability of a potential vortex with a non-rotating and rigid-body rotating top-hat jet core.

24 p3055 A73-45309

PHASE-SPACE INTEGRAL

Characteristic phase mixing time for spherical systems with different stellar mean velocity at each individual integral phase space surface

01 p0100 A73-10710

A nonlinear, nonconvex optimization problem

08 p0983 A73-20778

Optimal estimation of the phase coordinates for a linear dynamic system

12 p1485 A73-27898

Optimal estimation of the phase coordinates of a linear dynamic system.

18 p2294 A73-36603

Orthogonal operators and phase space distributions in quantum optics.

20 p2591 A73-38629

Configuration space and phase space of a system with an infinite number of degrees of freedom

20 p2594 A73-39640

Phase integral corrections to radio wave absorption and virtual height for model ionospheric layers.

21 p2654 A73-40777

PHASED ARRAYS

Aperture matching of wideband phased array radar antennas, using digital ferrite phase shifters and dielectric transformer with magnetic resonance limiting

01 p0022 A73-10178

Performance of a protruding-dielectric waveguide element in a phased array.

01 p0022 A73-10180

Recent advances in diode and ferrite phaser technology for phased-array radars. II.

01 p0024 A73-10720

VLF-ELF radiation characteristics of a 90 degree-phased crossed-dipole array in a cold multicomponent magnetoplasma.

02 p0140 A73-11739

A decoupling supply network for small antenna arrays

02 p0145 A73-11825

Effects of cross-coupling and of the edge effect on the characteristics of linear phased antenna arrays

02 p0146 A73-12021

Computation of element patterns of an E plane sectoral-horn planar phased array.

04 p0415 A73-14987

Antenna beam focusing and deflection with the aid of a digital phase computer, in a radiation-fed electronically controlled antenna

06 p0673 A73-17580

An initialization technique for improved MTI performance in phased array radars.

06 p0664 A73-17790

Electronically controlled phased arrays for radar tracking systems, considering military, earth resources and planetary topography applications
06 p0677 A73-18447

A statistical estimate of the achievable sidelobe level in phased array antennas with nonlinear initial phase distribution.
07 p0801 A73-20130

P-I-N switching diodes in phase-shifters for electronically scanned aerial arrays.
08 p0943 A73-20712

TRAPATT amplifiers for phased-array radar systems.
09 p1051 A73-22497

Computational estimate of applicability of infinite-array theory.
09 p1065 A73-23099

Analytical and Monte Carlo analysis of rms beam pointing errors of planar phased arrays with isotropic elements
11 p1328 A73-25660

Precision of amplitude-comparison direction finding by phased array antennas
12 p1470 A73-27579

A maritime communications concept using spaceborne phased arrays.
12 p1472 A73-27665

A new statistical design method for thinned solid-state phased arrays.
13 p1594 A73-29231

Mutual coupling effects in semi-infinite arrays.
14 p1734 A73-30202

Broad-band impedance matching of rectangular waveguide phased arrays.
14 p1734 A73-30205

A wide-band square-waveguide array polarizer.
14 p1735 A73-30228

Experimental investigations of coupling phenomena in a periodic linear antenna array
14 p1729 A73-30697

Concept of phase centre of an array applied to elevation-angle measurements.
15 p1842 A73-31098

Self complementary wire element phased array antennas, discussing matching, operating bandwidth, structural design and isolation
15 p1850 A73-31255

Light aircraft-borne low cost phased array X band radar and display design requirements for weather detection and ground mapping
15 p1909 A73-32451

Several parallel-plate guides with screen as phased array - Effect of the coupling on the directive gain
16 p1979 A73-33374

Computerized automatic microwave testing with pulse measurements of phase and power from Reliable Advanced Solid State Radar phased array modules, discussing system design
17 p2135 A73-34724

Coherent optical processing of linear phased array radar signals.
17 p2132 A73-35649

Spatial statistics of instrument-limited angular measurement errors in phased array radars.
17 p2128 A73-35687

Linear phased array antenna focused in Fresnel region, noting radiation pattern indoor measurement simplicity advantage over far field observation in performance monitoring
17 p2128 A73-35694

Effect of modulating /multiplicative/ interference on signal processing in a system consisting of a phased array antenna and a receiver.
17 p2129 A73-35710

Adaptive ground implemented phased arrays.
20 p2523 A73-38729

Effect of a statistically uneven underlying surface on the radiation characteristics of a phased antenna array
20 p2537 A73-39453

Frequency dependence of radiation-pattern orientation in phased-array antennas
21 p2661 A73-40196

Maritime communications via satellites employing phased arrays.
21 p2649 A73-40330

Phased array antennas; Proceedings of the Symposium, Polytechnic Institute of Brooklyn, Farmingdale, N.Y., June 2-5, 1970.
21 p2651 A73-40643

BMD requirements for phased array radars.
21 p2651 A73-40644

Phased array antennas in ground based remote sensor system, assessing technologies of AN/FPS-85, HAPDAR and AP/TPN-19 radar systems
21 p2672 A73-40645

Development programs status report on airborne planar, conformal and distributed aperture phased array antennas for use in radar and communication systems
21 p2662 A73-40646

Phased array antennas for applications on spacecraft.
21 p2662 A73-40647

Design, performance, and cost considerations for solid-state arrays.
21 p2662 A73-40648

Phased array element types comparison, discussing dipole and open-ended waveguide radiator designs with emphasis on driving point impedance accuracy and active element pattern
21 p2663 A73-40649

Phased array analysis by circuit and field theory approaches, discussing boundary value problems formulation and solutions for systems with current carrying and aperture elements
21 p2651 A73-40650

Surface-wave effects and blindness in phased-array antennas.
21 p2651 A73-40653

Numerical solution of edge effects of external coupling between elements in linear phased array of slots covered by dielectric slab, using scattering matrix
21 p2651 A73-40654

On the effects of eliminating the passive elements from a thinned array.
21 p2652 A73-40655

Small arrays - Their analysis and their use for the design of array elements.
21 p2652 A73-40656

A survey of the simulator technique for designing a radiating element in a phased-array antenna.
21 p2652 A73-40657

A new procedure for the design of a waveguide element for a phased-array antenna.
21 p2652 A73-40658

Wide-angle impedance matching of phased-array antennas - A survey of theory and practice.
21 p2652 A73-40659

The design of a wide band wide scan-angle waveguide radiating element.
21 p2652 A73-40660

Multimode phased array element for wide scan angle impedance matching.
21 p2652 A73-40661

A new flush mounted antenna element for phased array application.
21 p2663 A73-40662

Design of a phased array radiating face for prevention of performance degradation in the presence of rain.
21 p2663 A73-40663

Phased array antenna feed systems developments, discussing relative merits, problems and design choices for air surveillance radar applications in microwave region
21 p2672 A73-40664

Diode and ferrite phaser configurations for phased array antenna system, discussing digital and analog versions, driver requirements and design trends
21 p2663 A73-40665

Planar phased array beam steering methods, emphasizing electronic driver and logic circuit sharing between phase shifters for cost reduction
21 p2652 A73-40666

Digitally scanned planar phased arrays, deriving optimum phase perturbation function for quantization and reflection lobe dispersion in terms of aperture distribution amplitude
21 p2652 A73-40667

Bias controlled step recovery diode as combined frequency multiplier and analog phase shifter for applications in microwave phased array antenna systems
21 p2663 A73-40668

Design guidelines for 180-degree hybrid type multiple beam phased array forming networks with different element numbers and configurations
21 p2669 A73-40670

Bandwidth criteria for phased array antennas.
21 p2652 A73-40671

High resolution beam steering phased array radar antenna design by subarray techniques, using time delay circuit for cost effective driver control simplification
21 p2653 A73-40672

Transient frequency response analysis and far field measurement of linear phased array with tandem series feed network, noting instantaneous bandwidth
21 p2653 A73-40673

Mutual coupling effects in circular arrays on cylindrical surfaces Aperture design implications and analysis.
21 p2653 A73-40674

Mechanically and electronically switched circular symmetric phased arrays with hybrid matrix phase shifter and lens switch combinations, assessing design and performance characteristics
21 p2672 A73-40675

Conformal arrays on surfaces with rotational symmetry.
21 p2653 A73-40676

Basic theoretical aspects of spherical phased arrays.
21 p2653 A73-40678

Large phased array antenna pattern measurements for performance, monitoring and maintenance checks
21 p2653 A73-40679

Limited scan phased array antenna design, featuring electronic beam deflection from few beamwidths to twenty degrees with cost reduction
21 p2653 A73-40680

Pattern measurements of phased-arrayed antennas by focusing into the near zone.
21 p2653 A73-40681

A method of locating defective elements in large phased arrays.
21 p2653 A73-40682

Dual beam antenna - A unique waveguide phased array with independently steered beams.
21 p2653 A73-40683

A single-plane electronically scanned antenna for airborne radar applications.
21 p2653 A73-40684

Physical design considerations for airborne electronic-scanning antennas.
21 p2654 A73-40685

Polarization characteristics of phased arrays of elliptically polarized elementary radiators
21 p2664 A73-41082

An array technique with grating-lobe suppression for limited-scan applications.
22 p2830 A73-41826

Narrow beam phased array of identical isotropic elements, estimating far field beam width with consideration for element position error effects
22 p2831 A73-41839

The accuracy of phase-comparison angle tracking by phased-array antennas
24 p3071 A73-44594

The effect of interaction of array elements with arbitrary amplitude distribution on the radiation pattern.
24 p3068 A73-44942

PHENACETIN

U ACETANILIDE

PHENOL FORMALDEHYDE

Bakelite lacquer and epoxy and phenol-formaldehyde solidified resin binders strength at high temperatures
14 p1766 A73-30687

PHENOLIC RESINS

Phenolic resin char-formation during hyperthermal ablation.
01 p0124 A73-11448

Mechanical properties of glassy carbon fibres derived from phenolic resin.
01 p0068 A73-11498

Effect of additives on ablation of phenolic-silica composites.
07 p0842 A73-19486

Vinyl plastisols with high adhesion to metals
10 p1239 A73-24093

Missile ablation shields erosion by high velocity dust, considering wind tunnel test data on phenolic cork for various dust materials, particle sizes and velocities
11 p1388 A73-25509

Phenolic binder decomposition in silica-phenolic ablator, determining reaction mechanism from Arrhenius rate equations for various temperatures
11 p1452 A73-26376

A comparison of quasi-static uniaxial-strain and Hugoniot tests for quartz-phenolic composite.
12 p1550 A73-27024

Surface ablation of silica-reinforced composites.
18 p2368 A73-36316

Investigation of failure of a fiberglass plastic due to differential carbon burnup
18 p2328 A73-36813

Causes of changes in the properties of resite in aqueous and alkaline media
18 p2328 A73-36822

PHENOMENOLOGY

A method for phenomenological analysis of ecological data.
02 p0188 A73-12629

PHENYLALANINE

An automated gas chromatographic analysis of phenylalanine in serum.
11 p1326 A73-25571

On the asymmetric adsorption of phenylalanine enantiomers by kaolin.
24 p3066 A73-44772

PHENYLS

NT POLYPHENYLS

Photoisomerization of 2-isocyanato- and 2,x'-diisocyanobiphenyls in cyclohexane.
12 p1466 A73-27600

PHILIPS IONIZATION GAGES

Photoabsorption cross sections of H2, D2, N2, O2, Ar, Kr, and Xe at the 584-A line of neutral helium.
12 p1465 A73-26989

PHOBOS

Mariner 9 television observations of Phobos and Deimos.
06 p0745 A73-17480

Mariner 9 television observations of Phobos and Deimos. II.
19 p2479 A73-37222

PHONEMES

Time and frequency functional analysis of speech for quantitative information parameters determination

PHONOARTERIOGRAPHY

and signal recognition, considering German phoneme system twoformant signal structure
06 p0663 A73-17592

PHONOARTERIOGRAPHY

Transcutaneous measurement of blood velocity profiles and flow.
22 p2817 A73-43108

PHONOCARDIOGRAMS

U PHONOCARDIOGRAPHY

PHONOCARDIOGRAPHY

NT ECHOCARDIOGRAPHY

On the causes of the changes of the second heart sound in left bundle branch block.
01 p0009 A73-11008

The value of the ultrasonic Doppler method and apexcardiography as reference tracings in phonocardiography.
01 p0014 A73-11509

Unusual diastolic heart beat in pericardial effusion.
03 p0259 A73-13059

Geometry of left ventricular contraction in the systolic click syndrome - Characterization of a segmental myocardial abnormality.
06 p0655 A73-18870

Portable electro-phonocardiograph using magnetic tape recorder equipped with patient's voice print.
11 p1323 A73-25475

Stethoscope- or phonocardiograph-detectable systole-associated left atrial sound in terms of activity recording, sound genesis, hemodynamic correlations and clinical applications
11 p1317 A73-25696

Familial syndrome of midsystolic click and late systolic murmur.
11 p1317 A73-25697

Phonocardiogram and apex cardiogram in systolic click-late systolic murmur syndrome.
11 p1317 A73-25698

Intracardiac heart murmurs and sounds influenced by respiration.
15 p1836 A73-32546

Assessing the severity of aortic stenosis by phonocardiography and external carotid pulse recordings.
20 p2516 A73-38867

PHONON BEAMS

The solid-solid interface in thermal phonon radiation.
04 p0483 A73-15468

PHONONS

NT PHONON BEAMS

Influence of the polarization of phonons on the thermal conductivity of single crystals of indium phosphide between 300 and 800 K
01 p0087 A73-10430

Investigation of the emission of donor-acceptor pairs and of their phonon echoes in CdS single crystals
01 p0088 A73-10634

Morphic effects. IV - Effects of an applied magnetic field on first-order photon-optical phonon interactions in non-magnetic crystals.
02 p0201 A73-12637

Morphic effects. III - Effects of an external magnetic field on the long wavelength optical phonons.
02 p0201 A73-12638

Raman scattering by phonons and magnons and phonon-magnon interactions in NiO.
02 p0201 A73-12640

Morphic effects. V - Time reversal symmetry and the mode properties of long wavelength optical phonons.
03 p0349 A73-12901

International conference of the CNRS on the physics of very high frequency phonons, Sainte-Maxime, Var, France, June 27-30, 1972, Proceedings
04 p0483 A73-15464

Radiation of phonons by metallic films.
04 p0483 A73-15465

Superconducting tunnel junctions as phonon sources and detectors.
04 p0428 A73-15466

Experimental results on absolute phonon detection sensitivity of superconducting tunnelling junctions.
04 p0483 A73-15467

Bottleneck of 29/cm phonons in ruby.
04 p0484 A73-15471

Strong electromagnetic waves in semiconductors under conditions of inelastic scattering of current carriers by optical phonons.
04 p0484 A73-15568

Exciton-phonon interaction in recrystallized CdTe layers
06 p0737 A73-18219

Single-phonon contribution to the hopping conductivity of amorphous solids.
08 p0994 A73-20955

Raman scattering from phonon bath using quantum mechanical model with random and stochastic Stokes and anti-Stokes coupled modes in light fields
13 p1658 A73-28209

Luminescence quenching and zero-phonon line broadening associated with defect interactions in diamond.
13 p1667 A73-28212

Detection of gravitational waves by the method of light scattering by elastic oscillations
15 p1913 A73-31321

Multiplicity of dielectric local modes - Bound states of phonons with impurity centers
15 p1885 A73-31719

Scattering of a nonlocalized exciton on phonons in thin quantized semiconductor films
17 p2218 A73-34118

Two-phonon absorption in SbSI single crystals
23 p3016 A73-43713

Distribution of hot phonons generated by laser radiation
23 p2988 A73-44020

PHOSPHATES

NT ADENOSINE DIPHOSPHATE [ADP]

NT ADENOSINE TRIPHOSPHATE [ATP]

NT ADENOSINES

NT AMMONIUM PHOSPHATES

NT CALCIUM PHOSPHATES

NT DIPHOSPHATES

NT NUCLEOTIDES

NT POTASSIUM PHOSPHATES

NT PYRIDINE NUCLEOTIDES

Preferential adsorption in the lubrication process of zinc dialkylidithiophosphate.
[ASLE PREPRINT 72LC-3C-3]

Enthalpy and specific heat of the orthophosphates of lanthanum, neodymium, and yttrium at high temperatures
03 p0274 A73-14358

Interaction of haemoglobin with ions - Binding of inorganic phosphate to human oxyhaemoglobin.
06 p0738 A73-18654

Amine phosphates as antiwear additives in neopentyl polyol esters.
14 p1714 A73-29850

Selection of phosphate impregnants for graphite oxidation inhibition
17 p2196 A73-34996

PHOSPHIDES

NT GALLIUM PHOSPHIDES

NT INDIUM PHOSPHIDES

Cobalt phosphide CoP₃ as a catalyst for electrochemical H₂ oxidation in acid fuel cells.
04 p0407 A73-15108

Structure and properties of nickel-phosphorus coatings in relation to annealing temperature and time.
06 p0698 A73-18214

PHOSPHENES

Low frequency vibrations and molecular structure of /CH₃2NPF₂.
11 p1326 A73-25567

PHOSPHORIC ACID

The phosphoric acid fuel cell, a long life power source for the low to medium wattage range.
09 p1037 A73-22821

PHOSPHORS

NT RADIOPHOSPHORS

Russian papers on phosphor crystal luminescence and nonlinear optics covering spectral line decomposition, GaAs laser and electromagnetic wave interaction
05 p0584 A73-16551

Phosphor crystals for electromagnetic emission recording based on optical and thermal effects on luminescent screens, considering optimal extinguishing and color alteration conditions
05 p0584 A73-16552

Influence of thionyl chloride on the lasing characteristics of the liquid phosphor POC13-SnCH₃Nd³⁺/
12 p1506 A73-27197

Comparison of an aluminum-coated phosphor layer and a Channeltron Electron Multiplier Array as extreme ultraviolet-to-visible image converters for use in space applications.
14 p1752 A73-30155

PHOSPHORUS

Internal friction study of intercrystalline phosphorus adsorption during temper brittleness development in iron alloys
01 p0064 A73-10608

P II Zeeman effect spectral line observation for J-value assignments with check on wave functions obtained from energy level least squares fitting
05 p0600 A73-16497

The sources of phosphorus on the primitive earth - An inquiry.
06 p0651 A73-17933

The electrical properties of phosphorus doped silicon layers obtained by ion implantation through a passivating oxide.
17 p2220 A73-35654

Chromium and phosphorus enrichment in the metal of type II /C2/ carbonaceous chondrites.
21 p2771 A73-41007

Detection of phosphorus in heavily diffused silicon by He⁺/ backscattering.
24 p3120 A73-45262

PHOSPHORUS COMPOUNDS

NT ADENOSINE DIPHOSPHATE [ADP]

NT ADENOSINE TRIPHOSPHATE [ATP]

NT ADENOSINES

NT AMMONIUM PHOSPHATES

NT CALCIUM PHOSPHATES

NT DIPHOSPHATES

NT GALLIUM PHOSPHIDES

NT INDIUM PHOSPHIDES

NT NUCLEOTIDES

NT ORGANIC PHOSPHORUS COMPOUNDS

NT PHOSPHATES

NT PHOSPHIDES

NT PHOSPHINES

NT PHOSPHORIC ACID

NT PHOSPHORUS POLYMERS

NT POTASSIUM PHOSPHATES

NT PYRIDINE NUCLEOTIDES

Muscle metabolites with exhaustive static exercise of different duration.
05 p0539 A73-16247

Development and properties of CdP₂S₄
24 p3119 A73-44951

PHOSPHORUS METABOLISM

Role of nerve structures in the action of low-frequency sinusoidally modulated currents on synovial membrane permeability in the knee joint
10 p1180 A73-23943

Investigation of the exchange between the blood and the intraocular fluid with the aid of radioactive phosphorus
10 p1185 A73-24520

Cell membrane molecular structure and lipid composition, discussing phospholipid role in membrane potential maintenance in myocardial cells
11 p1315 A73-25591

Interaction of haemoglobin with ions - Binding of inorganic phosphate to human oxyhaemoglobin.
14 p1714 A73-29850

Analysis of the mechanism of the therapeutic action of pressurized oxygen in organic phosphorus poisoning
14 p1722 A73-30848

Glycolytic intermediates and adenosine phosphates in rat liver at high altitude /3,800 m/.
20 p2514 A73-39602

Oxygen uptake, muscle high-energy phosphates, and lactate in exercise under acute hypoxic conditions in man.
21 p2638 A73-41131

Studies on the metabolism of glucose-1,6-diphosphate in human erythrocytes.
21 p2639 A73-41139

PHOSPHORUS POLYMERS

Polyphosphazene fluoroclastomers preparation, properties and potential applications.
03 p0331 A73-13029

New fire resistant polymers - Polyphosphazenes/.
17 p2197 A73-35356

PHOSPHORYLATION

Struvite precipitation from evaporating sea water with added ammonia, considering importance for prebiotic phosphorylation
07 p0787 A73-19168

Influence of ultrasound and of a superhigh-frequency electromagnetic field in the three-centimeter band on the oxidative phosphorylation of liver and kidney mitochondria
09 p1044 A73-22368

Influence of preliminary adaptation to the main environmental factors on the ATP level and phosphorylation potential in the myocardium during severe heart strain
21 p2640 A73-41278

PHOTOABSORPTION

Light enhanced decarboxylations by proteinoids.
06 p0661 A73-17941

Photoabsorption cross section of argon in the 180-700-A wavelength region.
08 p0990 A73-21050

Oscillator strength and photoionization cross section computation for Cs ground state during photoabsorption, using semiempirical model potential with adjustable parameters
10 p1250 A73-23672

Photoabsorption cross sections of H₂, D₂, N₂, O₂, Ar, Kr, and Xe at the 584-A line of neutral helium.
12 p1465 A73-26989

Laser photons multiple absorption by atoms, determining transition probabilities from Schrodinger equation solution via space translation operation
14 p1776 A73-29698

PHOTOCATHODES

Design and operation of high power pulsed X ray tube with photocathode and nitrogen laser illumination for electron beam generation
02 p0175 A73-11960

Use of MgF₂ and LiF photocathodes in the extreme ultraviolet.
08 p0964 A73-21048

Spectracon camera for astronomical telescope prime focus operation, discussing image tube extended area photocathode and mica window
14 p1751 A73-29906

Electronographic image tube development at the Royal Greenwich Observatory.
14 p1732 A73-29908

Electron-optical image transfer using opaque photocathodes with electromagnetic lens in image tubes
17 p2136 A73-34905

- Television sensors for ultraviolet space astronomy.
17 p2170 A73-35292
- The effect of toroidal magnets on the sensitivity of photomultipliers.
21 p2699 A73-40410
- Microchannel image intensifiers for detection at low light levels
23 p2979 A73-43222
- Investigation of some characteristics of UM-92 image converters with oxygen-cesium photocathodes
23 p2983 A73-44361

PHOTOCELLS

U PHOTOELECTRIC CELLS

PHOTOCHEMICAL REACTIONS

- NT PHOTOCROMISM
NT PHOTODECOMPOSITION
NT PHOTOLYSIS
NT PHOTOSYNTHESIS
NT RADIOLYSIS

Extraterrestrial solar flux attenuation and photodissociation cross sections effects on errors in photochemical kinetic model calculations
01 p0014 A73-10369

Ion composition and photochemistry of the E-region.
01 p0042 A73-10892

SST related ozone photochemical reactions and metastable oxygen system below 100 km, discussing oxygen dissociation and recombination, photolysis, UV absorption, etc
01 p0042 A73-10898

The effect of pH on photobleaching of organic laser dyes.
03 p0320 A73-14462

Photochemical ignition and combustion enhancement in high speed flows of fuel-air mixtures.
[ALAA PAPER 73-216] 05 p0641 A73-16946

Sterically controlled syntheses of optically active organic compounds. XV - Syntheses of optically active aspartic acid through beta-lactam.
07 p0787 A73-19204

The photochemical oxidation of iodide to iodine in the presence of oxygen.
07 p0788 A73-20398

Photochemical ozone formation in the atmosphere over southern England.
08 p0957 A73-20667

Ion composition and photochemistry of the E region
08 p0958 A73-21282

Generation of vibrationally excited O₂ and nonthermal infrared emission in the upper atmosphere
08 p0959 A73-21289

A photochemical method of determining the optical pumping energy absorbed by rhodamine dyes under conditions corresponding to stimulated emission of radiation
09 p1095 A73-22668

Photochemical reactions in condensed phase relevant to biology, discussing molecular energy states, isomerization reactions and bond making/breaking processes
09 p1121 A73-23305

Lower thermosphere thermal energy and oxygen transport due to photochemical reactions, noting Schumann-Runge band absorption, atomic recombination and collisional deactivation
11 p1358 A73-26706

Photo-decarbonylation of beta-styryl isocyanates.
12 p1466 A73-27225

Photoisomerization of 2-isocyanato- and 2,x'-diisocyanobiphenyls in cyclohexane.
12 p1466 A73-27600

Photochemistry of minor constituents in the troposphere.
12 p1466 A73-27603

Photo-induced isomerization of aryl isocyanides into cyanides.
13 p1580 A73-28200

The photochemistry of hydrocarbons in the Jovian atmosphere.
14 p1802 A73-30766

Photochemical, radiative and dynamic modeling of the stratosphere.
[ALAA PAPER 73-527] 16 p2007 A73-33561

A two-dimensional theoretical model for stratospheric ozone density distributions in the meridional plane.
[ALAA PAPER 73-541] 16 p2008 A73-33571

Photoinduced fixation of CO₂ by amino acids - Implications for nonbiological reactions on the Martian soil.
16 p1977 A73-33874

New improved laser dye for the blue-green spectral region.
17 p2186 A73-35800

Photochemical reactions in the Jovian atmosphere.
17 p2237 A73-35835

Photochemistry of the ozone in the stratosphere
18 p2287 A73-36938

Ion composition and photochemistry of the E-region.
19 p2424 A73-37911

Production of vibrationally excited O₂ and nonthermal infrared emission in the upper atmosphere.
19 p2424 A73-37918

Mesospheric ozone concentration night and day variations comparison, describing microwave radiometer and remote sensing and photochemical theories
20 p2557 A73-39857

Photochemical model for homogeneous gas phase radical chain mechanism to remove tropospheric methane, carbon monoxide, molecular hydrogen and formaldehyde
21 p2646 A73-40082

Photochemical model with vertical transport for CO and hydrocarbons profiles in stratosphere and mesosphere, discussing boundary conditions and water vapor
21 p2681 A73-40086

Dissociation and bleaching of a multilevel molecular gas under the influence of radiation from a powerful CO₂ laser
21 p2712 A73-40357

A generalized aeronomic model of the mesosphere and lower thermosphere including ionospheric processes.
21 p2683 A73-40778

Evidence of features in atmospheric spectra at around 8 per cm of probable solar origin.
21 p2687 A73-41079

Ammonia density profiles and photochemical destruction above Jovian tropopause as function of eddy diffusion coefficient, considering background atmosphere scale height
23 p3028 A73-43601

Background concentrations of photochemically active trace constituents in the stratosphere and upper troposphere.
23 p2976 A73-43889

Recent developments in photochemistry of atmospheric ozone.
23 p2951 A73-43892

Nitrogen oxides role in global stratospheric ozone balance demonstrated by observed instantaneous photochemical rates comparison with Chapman ozone formation theory
23 p2952 A73-43900

Ozone variation in the lower stratosphere and its mechanism.
23 p2977 A73-43908

Application of general circulation models to the study of stratospheric ozone.
23 p2978 A73-43909

Ionospheric aeronomy problems with emphasis on photochemical processes of neutral and ionized components, discussing nighttime ionizing agents, ion recombination, water vapor and nitrogen oxide behavior, etc
23 p2978 A73-43977

Ionospheric metastable particle production and annihilation during photochemical reactions, determining neutral and ionized particle abundance profiles
23 p2978 A73-43979

Determination of the rate coefficients of ionospheric reactions from experimental data for electron concentration
24 p3083 A73-44787

PHOTOCHEMISTRY

U PHOTOCHEMICAL REACTIONS

PHOTOCROMISM

Photochemical receptor mechanism of chromatic vision and scotopic contrast hue sensation due to cone and rod activity interaction
07 p0783 A73-20261

Photochromic glass as reversible optical recording storage medium, discussing image resolution, configuration improvements, merits and applications in holography, random access memory and displays
11 p1370 A73-26537

The recording of three-dimensional holograms on photochromic glass with the use of an optical bleaching process. I
13 p1616 A73-28765

Sensitometric tests on plane-parallel organic photochromic bulk material film samples of styrene, methylmethacrylate and inoline spiropyran, evaluating photosensitivity suitability for holography
13 p1622 A73-29436

Indoline series spirochromene polymer matrices for holographic recordings with argon and helium-neon lasers in green and UV spectral regions
14 p1753 A73-30365

Three-dimensional hologram recordings on photochromic glass with the application of an optical discoloration process. II
15 p1879 A73-32340

Kinetic equations for time behavior of solid photochromic film in photocoloration, photobleaching and thermal bleaching, evaluating absorption cross sections and quantum yields
17 p2172 A73-35422

Chromatic photosensitization of a variable-index material for the recording of high-efficiency phase holograms
24 p3091 A73-45011

PHOTOCONDUCTIVITY

Russian book on spectral composition-dependent photoconductivity in Hg doped amorphous Se films

covering effect of quasi-macroscopic centers in semiconductors
02 p0201 A73-12864

Magnetophotocurrent of semi-insulating GaAs and its behavior upon electron bombardment.
06 p0738 A73-18369

Forward biased P-N junction photoelectric current shown resulting from photovoltaic, photoresistive and electric injection currents superposition
06 p0738 A73-18544

IR and thermal extinction spectra of luminescence and photoconductivity of zinc cadmium sulfide solid solution films doped with Cu and Cl
06 p0738 A73-18643

Influence of an electric field on the laser-induced impurity photoconductivity of gallium selenide
07 p0861 A73-19398

Photoresist technology for passive ICs production with optical waveguides, describing vaporization deposition and processing for glass films
09 p1085 A73-23075

Photovoltaic and photoconductivity measurements on p- and n-type GaSe, determining light polarization direction effect, photovoltage relaxation times and minority carriers diffusion lengths
10 p1259 A73-23569

Temperature dependence of kinetic properties of photoconductivity produced by carrier redistribution across attachment centers, discussing results with Ag and Al doped ZnS single crystals
10 p1260 A73-24468

Electrophysical parameters of TiSbSe₂ thin films
10 p1260 A73-24471

Determination of the parameters of r-type recombination centers in germanium-doped GaTe single crystals
11 p1410 A73-26587

International Conference on Luminescence, Leningrad, USSR, August 17-22, 1972, Proceedings
15 p1884 A73-31711

Electrical properties and photoconductivity of CdS thin films obtained in a hydrogen atmosphere
17 p2219 A73-34281

Effect of an electric field on the negative photoconductivity of high-resistance ZnTe-CdTe crystals
17 p2219 A73-35552

Photoelectric methods of determining the electrical characteristics of MDS systems
23 p3006 A73-43616

PHOTOCONDUCTORS

Response characteristics of photodiodes, phototransistors and photoresistors in near IR range, showing output signal levels as function of wavelength and illumination intensity
06 p0692 A73-17837

Characteristics of recombination centers defining the high sensitivity of n-CdSb photoresistors
06 p0675 A73-18082

Saturation and acoustoelectric oscillations of a photocurrent in CdS and CdSe
06 p0737 A73-18218

Sensitivity limits for extrinsic and intrinsic infrared detectors.
08 p0967 A73-21422

CdS-metal contact at higher current densities.
11 p1407 A73-24984

Photoconductor-metal contact at higher densities.
11 p1407 A73-24985

Infrared detectors - Survey of the present state of the art.
11 p1368 A73-26509

Photoresistor synchronous detector circuits with rectangular light pulse switching elements for capacitive and resistive loads
13 p1592 A73-28900

Theory for the steady-state operation of a thin-film regenerative optron
23 p2959 A73-43617

PHOTOCURRENTS

U ELECTRIC CURRENT

U PHOTOELECTRIC EMISSION

PHOTODECOMPOSITION

Influence of photodecomposition on the emission of a lamp-pumped dye laser
24 p3098 A73-45518

PHOTODETACHMENT

Experimental measurement of the O₂-I photodetachment cross section.
02 p0195 A73-12433

Multiphoton transitions. III - Rates of multiphoton detachment of negative ions.
07 p0852 A73-19147

Measurement of the cross section for photodetachment of O₃-I.
08 p0957 A73-20658

The negative-ion composition of the daytime D-region.
09 p1048 A73-22127

High-resolution photodetachment study of Se-I ions.
21 p2710 A73-40213

PHOTODIODES

PHOTODIODES

- Optical communication systems with glass fiber waveguide, using semiconductor lasers and photodiodes as transmitters and receivers respectively 01 p0019 A73-11486
- Superconducting time variant filter tracking test for RF signal amplitude modulation, using photodiodelectric perturbation in semiconductor cavity resonant frequency 02 p0146 A73-11847
- Satellite-borne solid state multispectral image remote sensors with photodiode linear arrays for data acquisition, noting system performance and reliability advantages 04 p0451 A73-15781
- Single photon detection and timing - Experiments and techniques. 05 p0576 A73-16603
- Measurements of the photomultiplication factor of silicon avalanche photodiodes. 06 p0674 A73-17796
- Response characteristics of photodiodes, phototransistors and photoresistors in near IR range, showing output signal levels as function of wavelength and illumination intensity 06 p0692 A73-17837
- Photodiode structure performance dependence on surface properties in static and kinetic operations, noting surface recombination and photoeffect relaxation 06 p0676 A73-18086
- High speed, high performance [Hg,Cd/Te photodiode detectors. 06 p0667 A73-18314
- Ultrafast photodiode for mode locked laser pulses detection, estimating rise time 06 p0678 A73-18851
- Fast solid state IR detection photodiodes design, properties and utilization, investigating high speed response conditions and quantum efficiency 06 p0678 A73-18853
- Resistive MOS-gated diode light sensor. 08 p0948 A73-21477
- Limitations of the use of vacuum photodiodes in instruments for the measurement of laser power and energy. 11 p1377 A73-26233
- Photoemission diode standards with high sensitivity, time stability and response uniformity for accurate measurement of monochromatic UV light, discussing design and construction 11 p1365 A73-26234
- Optoelectronic semiconductor components under the influence of ionizing radiation 14 p1733 A73-30070
- The effect of unmodulated sunlight on the integral voltage sensitivity of some radiation detectors. 14 p1754 A73-30954
- The fine solar sensor of the Astronomical Netherlands Satellite. 16 p2012 A73-32852
- A monolithic pair of dielectrically isolated high-sensitivity photodiodes operating in the visible spectrum. 16 p2012 A73-32854
- Implementation of a frog's eye type discriminator, responsive only to pattern changes, as a pre-processor for visual data. 16 p2014 A73-33127
- Photon counting with a self-scanned diode array. 17 p2169 A73-35283
- Experimental use of self-scanned photodiode arrays in astronomy. 17 p2169 A73-35287
- A flowmeter to measure cloud liquid content. 17 p2174 A73-35578
- Main trends of development of avalanche photodiodes as high-speed photodetectors [Review/ 18 p2293 A73-36715
- Generation of reproducible giant pulses with an optically regenerative Q switch. 21 p2715 A73-40959
- Image tube systems for ground based and spaceborne astronomical observations, considering self scanning diode array, phosphor screen output devices, electronography, etc 21 p2703 A73-41239
- The design, fabrication, and evaluation of a silicon junction field-effect photodetector. 23 p2981 A73-43453
- Uniaxial pressure effects on diode structures volt-ampere characteristics, examining potential barrier height and photo emf changes 23 p2960 A73-43787
- PHOTODISSOCIATION**
- Extraterrestrial solar flux attenuation and photodissociation cross sections effects on errors in photochemical kinetic model calculations 01 p0014 A73-10369
- Aeronomical chemistry of the stratosphere. 02 p0158 A73-11910
- Molecular iodine photolysis in photodissociative laser due to selective pumping, noting recombination-like storage mechanism 04 p0458 A73-15561

Photochemistry chemical kinetics in the interstellar medium. 06 p0752 A73-18236

Nitrogen and oxygen molecules, photodissociation continuums from absorption and ionization cross sections, calculating upper atmosphere emission rates 12 p1489 A73-26993

Diurnal thermospheric heat budget in terms of electron-ion recombination, photodissociation and neutral wind energy transfer and conductive and radiative cooling 12 p1492 A73-27604

Lower thermospheric oxygen photodissociation evaluation for global average and hemispheric imbalance, discussing wind system to compensate for solar thermal input imbalance 17 p2159 A73-34784

Kinetics of the generation spectrum of a photodissociation iodine laser. 22 p2868 A73-41722

The production and distribution of nitrogen oxides in the lower stratosphere. 23 p2977 A73-43897

Theoretical study of a photodissociation model in polyatomic molecules 24 p3113 A73-45326

PHOTOELASTIC ANALYSIS

- Photoelastic model analysis of sandwich beams. 01 p0050 A73-10737
- Stress separation in the photoelastic study of centrifugal stresses. 01 p0116 A73-11013
- Photoelastic stress analysis of solid propellant grains. 01 p0090 A73-11118
- Axial compression buckling of single metal fiber embedded in plastic matrix, using photoelastic stress analysis and finite element method 02 p0236 A73-12432
- Applications of dynamic photoelasticity in flaw detection analysis. I. 02 p0175 A73-12868
- Viscoelastic properties of amorphous polymers employed in stress investigations by the optical polarization method 03 p0335 A73-13737
- Shear stresses below asperities in Hertzian contact as measured by photoelasticity. 03 p0314 A73-14330
- A study of local stresses near surface flaws in bending fields. 04 p0505 A73-14678
- Crack tip stress field variation via elastic pulses for crack path alteration and subsequent fracturing process termination, using photoelastic analysis 05 p0634 A73-16795
- Methods of birefringence-parameter determination in tension studies by photoelasticity techniques 05 p0635 A73-17077
- Isochromatic curves modeling for stress-strain state of doubly connected regions by optical polarization and photoelastic analysis, using isopach field method 05 p0578 A73-17092
- Application of elastooptical modeling studies in determining optimal shapes for plane structures 06 p0760 A73-17782
- An assessment of factors influencing data obtained by the photoelastic stress freezing technique for stress fields near crack tips. 06 p0764 A73-18488
- Stress intensity factors for nozzle corner cracks. 07 p0912 A73-19564
- Photoelastic investigation of serrated plastic flow in 6061 Al alloy, considering Luders bands effects relative to type A and B serrations 09 p1101 A73-22408
- Some results of a study of the interaction between Rayleigh pulses and edge cracks 10 p1287 A73-23591
- Investigation of the load-carrying capacity of rotating disks by the method of optically sensitive coatings 10 p1291 A73-24364
- Strain gages and photoelastic coating methods of thermal stress determination for model and full scale tests 11 p1435 A73-25452
- Mechanical simulation of thermoelastic stresses on the basis of a given temperature field 11 p1435 A73-25453
- Dual-beam polariscope and framing camera for dynamic photoelasticity. 12 p1496 A73-27025
- Moire techniques of incoherent and coherent light filtering, line multiplication and contrast amelioration in framework of physical optics and diffraction theory for stress analysis 13 p1612 A73-28470
- Symmetrical crack branching in polymethyl methacrylate plates, using method of caustics for stress intensity factor evaluation 13 p1645 A73-28842
- Three-dimensional scattered-light stress analyses of discontinuous fiber reinforced composites. [SESA PAPER 2033] 13 p1699 A73-29306

Three-dimensional photoelastic tests of thin shell pressure vessels. 13 p1699 A73-29307

Stress differentiation procedure for screen technique studies in dynamic photoelasticity, giving expressions for elastic modulus and Poisson ratio 13 p1703 A73-29613

Photoelasticity - An improvement in the sandwich technique. 14 p1765 A73-29703

Photoelastic analysis of an orthotropic ring under diametral compression. 15 p1949 A73-31653

Determination of displacements during compression of an oval seal ring 16 p2021 A73-33942

High precision photoelastic and ultrasonic techniques for determining absolute and differential thermal expansion of titania-silica glasses. 17 p2107 A73-35443

Test on fuselage models at reduced sizes. 17 p2171 A73-35410

Micromechanic stresses in photoelastic composite coupons. [SESA PAPER 2175A] 17 p2251 A73-35456

The use of a high modulus inclusion gauge in non-linear viscoelastic materials. [SESA PAPER 2187A] 17 p2173 A73-35457

Book - Experimental techniques in fracture mechanics. 17 p2252 A73-35668

Two dimensional static, dynamic and three dimensional photoelasticity measurement techniques for stress intensity, factors determination in boundary value problems of fracture mechanics 17 p2252 A73-35673

Stress concentration in tubes with a hole of star-shaped profile 19 p2494 A73-37185

Photoelastic study of rectangular plates under bending. 19 p2498 A73-37667

Study of the photoviscoelasticity method 20 p2619 A73-39331

Photoelastic investigation of dynamic stress conditions involving rapidly varying principal stress directions 21 p2695 A73-39965

Repetitive recording of stress waves in a photoelastic material using a multi-pulsed laser and an inexpensive streak camera. 21 p2695 A73-39970

Local stresses near deep surface flaws under cylindrical bending fields. 22 p2880 A73-42135

Holographic photo-elasticity - Independent observation of the isochromatic and isopachic fringes for a single model subjected to only one process. 24 p3091 A73-45335

PHOTOELASTIC MATERIALS

- Liquid rubber formulation for cold and hot urethane casting of photoelastic models, including membranes and thin walled structures 07 p0843 A73-19566
- Photoelasticity - An improvement in the sandwich technique. 14 p1765 A73-29703
- On the limitations of interferometric methods in three-dimensional photoelasticity. [SESA PAPER 2165] 17 p2251 A73-35455
- Repetitive recording of stress waves in a photoelastic material using a multi-pulsed laser and an inexpensive streak camera. 21 p2695 A73-39970

PHOTOELASTIC STRESS MEASUREMENT

- U PHOTOELASTIC ANALYSIS**
- PHOTOVISCOELASTICITY**
- NT PHOTOVISCOELASTICITY
- A certain case of stress-concentration analysis by an elastooptical method 01 p0114 A73-10574
- Photoelastic methods of studying dynamic stress problems 03 p0306 A73-13163
- Similarity condition for the lateral contraction coefficient in photoelasticity 06 p0761 A73-17785
- Dioptric powers of transparent plates in a plane state of tension 06 p0765 A73-18697
- Optical stress rosette based on caustics for stress distribution and differences measurement in perforated plate, using gas laser light for interferometry 08 p0964 A73-21047
- Visualization of pulsed ultrasound using stroboscopic photoelasticity. 08 p0973 A73-21078
- On the uniqueness of solutions of stress equations of motion of the Beltrami-Michell type. 14 p1809 A73-30254
- A new non-destructive method for three-dimensional photoelasticity. [SESA PAPER 2143A] 17 p2182 A73-35451

German book - Practical photoelasticity /3rd revised and enlarged edition/ 20 p2566 A73-39273

Absolute instability of the interaction between optical and acoustic waves. 20 p2594 A73-39679

PHOTOELECTRIC CELLS
NT PHOTOVOLTAIC CELLS
 A combined photoelectric method for detecting eye movements. 02 p0137 A73-12079

Diffusion and conduction processes in CdS-Cu_xS thin film photocells. 03 p0350 A73-14217

Calculation of a photoelectric system for stabilizing the optical axis of an instrument 05 p0575 A73-16316

Accurate measurements of and corrections for nonlinearities in radiometers. 06 p0693 A73-17898

Choice of thermal parameters for a photoelectric switch operating with a capacitive load 06 p0676 A73-18087

The pulse-controlled photoelectric switch as an element in automatic control circuits and in computer equipment 06 p0676 A73-18088

Investigation of the scattered-light-flux magnitude dependence on the drop size in the aerosol photoelectric counter 06 p0691 A73-18734

Comparison of the efficiency of photocells with stepwise and exponential distributions of the impurities in the doped layer 09 p1033 A73-22721

Investigation of high-voltage photoelectric converters at low radiation intensities 14 p1713 A73-30948

Possibility of using semiconductor photocells as receivers of ultraviolet radiation 14 p1713 A73-30949

Photoelectron statistics and calculation of the characteristics of optical communications lines 15 p1842 A73-31257

A light amplifier display device. 16 p2013 A73-32882

Synthesis of a universal cell with increased reliability for the realization of an iterative automatic system 16 p1986 A73-33667

Application of silicon photoelectric converters in solar orientation sensors 20 p2510 A73-39449

CIE interlaboratory comparison of measurements of photocell spectral sensitivity. 21 p2698 A73-40141

Series resistance of rectangular and cylindrical semiconductor photocells with linear and circular contacts and thin base, noting dependence on contact strip width 24 p3058 A73-45251

Measurement of the p-n junction depth in photocells with epitaxial layers 24 p3058 A73-45254

PHOTOELECTRIC EFFECT
NT PHOTOIONIZATION
 Passage of electric current through an illuminated semiconductor under conditions where the anisotropy parameters, the electrical conductivity, and the relaxation time are nonuniform. I 04 p0484 A73-15641

Some characteristics of isopotential curves of photoelectret state formation in compressed polycrystalline anthracene 05 p0605 A73-17176

Photodiode structure performance dependence on surface properties in static and kinetic operations, noting surface recombination and photoeffect relaxation 06 p0676 A73-18086

Angle to digital photoelectric converter for azimuthal telescope, discussing accuracy and temperature effects 15 p1877 A73-32132

Study of the influence of various parameters on the method used for determining the attenuation lengths through photoelectric yield measurements in the far ultraviolet 15 p1878 A73-32211

Photoeffect applications in MDS systems with a nonstationary depletion layer in ionizing radiation detectors 18 p2316 A73-36716

The wall condition of the specific density of a radiation field 22 p2888 A73-43046

Photoelectric methods of determining the electrical characteristics of MDS systems 23 p3006 A73-43616

PHOTOELECTRIC EMISSION
 Design and operation of high power pulsed X ray tube with photocathode and nitrogen laser illumination for electron beam generation 02 p0175 A73-11960

Vertical multijunction solar cells light generated current spectral response and I-V characteristics derivation from minority carrier diffusion equations 03 p0254 A73-14208

Terminal modeling and photocompensation of complex microcircuits. 05 p0557 A73-16508

Absolute yields of X-ray induced photoemission from metals. 05 p0604 A73-16515

Effects of ionizing radiation on dielectrically isolated junction field effect transistors. [AD-757969] 05 p0558 A73-16524

Diffusion equation for current carriers in solar cell with inhomogeneous internal electric field, determining photoelectric current in p-n junction 07 p0778 A73-19299

Polarization dependence of a photoelectric current during the modulated illumination of a system composed of an electrolyte, a porous pigment film, and a metal 07 p0851 A73-19473

Photoemission from lunar surface fines and the lunar photoelectron sheath. 07 p0895 A73-19860

Photocurrent pulse shape in thin organic semiconductor films 07 p0862 A73-20008

Fine structure in the optical-absorption edge of silicon. 07 p0863 A73-20175

Use of MgF₂ and LiF photocathodes in the extreme ultraviolet. 08 p0964 A73-21048

A relationship between photoemission-determined valence band gaps in semiconductors and insulators and ionicity parameters. 09 p1134 A73-22903

Improvement of photomultiplier performance in astronomical applications. 10 p1215 A73-23483

Photoemission from cesium-oxide-activated In-GaAsP. 10 p1259 A73-23839

CsI thin film photoemission spectra resolution maximization, rejecting localized ionic state transitions model 11 p1407 A73-24986

CsI optical and photoemission spectra computed from first order allowed transitions between Bloch-wave states, using energy band data 11 p1407 A73-24987

Determination of attachment center parameters in semiconductors from the temperature dependence of the photocurrent 11 p1408 A73-25248

Photoemission diode standards with high sensitivity, time stability and response uniformity for accurate measurement of monochromatic UV light, discussing design and construction 11 p1365 A73-26234

Comparison of methods of photomultiplier photocurrent recording in measurements of weak luminous fluxes 12 p1495 A73-26866

O I 4368 airglow tropical emission excitation due to conjugate photoelectron escape flux, discussing radiative recombination contribution to intensity 14 p1749 A73-29981

Influence of the difference in effective masses on the efficiency of heterojunction solar cells. 14 p1713 A73-30000

Photoelectric statistics and calculation of the characteristics of optical communications lines 15 p1842 A73-31257

Properties of the satellite photoelectron sheath derived from photoemission laboratory measurements. 16 p2062 A73-33435

Time delay statistics of photoelectric emissions - An experimental test of classical radiation theory. 20 p2570 A73-38606

Optimum detection of an optical image on a photoelectric surface. 21 p2650 A73-40338

PHOTOELECTRIC GENERATORS
 Determination of the parameters A and j/sub 0/ in the loaded portion of the current-voltage characteristic of a photoelectric converter 20 p2510 A73-39450

PHOTOELECTRIC MATERIALS
 Some photoelectrical characteristics of photoelectric converters with a p-i-n structure 20 p2510 A73-39448

PHOTOELECTRIC PHOTOMETRY
U ELECTROPHOTOMETERS
PHOTOELECTRICITY
 Photoelectric measurement of satellite camera shutter opening time delay and photographic plate motion synchronization, calculating root-mean-square error in observation time 03 p0307 A73-13253

Method for calculating the delay in a time-service photoelectric phase apparatus. 04 p0451 A73-16019

Semiconductor photodetection matrices for holographic memory reading 05 p0553 A73-16170

Energy structure, I-V characteristics and optical and photoelectrical properties of heterojunctions between different semiconductor materials, noting interface state effects 06 p0736 A73-18091

Kinetics of electrostatic image formation during exposure of electrophotographic layers 07 p0823 A73-19331

Structure diagram, crystal growth, band structure, physical, optical and photoelectric properties of A/II(B)/V compounds, emphasizing CdSb-ZnSb solid solutions 10 p1258 A73-23566

Photosensor aperture shaping to reduce aliasing in optical-mechanical line-scan imaging systems. 14 p1753 A73-30161

Structure, composition and photoelectrical properties of cadmium sulfide and selenide epitaxial films subjected to heat treatment 14 p1784 A73-30856

A rotation angle-to-digital code photoelectric converter 15 p1877 A73-32133

Astronomic follow-up systems with mismatch signal buildup 15 p1877 A73-32134

Russian book - Methods of studying eye movements. 15 p1840 A73-32417

Digital photoelectric tracking systems with accumulation of the mismatch signal 16 p1977 A73-32716

Multichannel quick-response photoelectric micropyrometer 17 p2164 A73-34173

Photoelectric phenomena in amorphous chalcogenide semiconductors. 20 p2599 A73-39133

High precision photoelectric azimuthal polarimeter design, construction and operation for determining angular rotation of polarized light beam 21 p2704 A73-41258

PHOTOELECTROMAGNETIC DETECTORS
U RADIATION MEASURING INSTRUMENTS
PHOTOELECTRONICS
U ELECTRONICS
U PHOTOELECTRICITY
PHOTOELECTRONS
 On-line digital recording of stellar spectrum with photoelectron-counting spectrophotometer, noting discrimination against spurious signals from noise and pulse height distribution measurements 01 p0048 A73-10531

Revised calculations of F region ambient electron heating by photoelectrons. 02 p0157 A73-11751

Solar UV Lyman alpha radiation intensity measurements, using Vertikal-1 rocket-borne photometer and photoelectron analyzer 03 p0379 A73-14565

Characteristics of the lunar photoelectron layer in the geomagnetic tail. 04 p0492 A73-15529

Single photon detection and timing - Experiments and techniques. 05 p0576 A73-16603

The effect of photoelectrons on kinetic polar wind models. 05 p0572 A73-17159

Miniaturized second generation night vision image intensifier system operation and performance based on secondary photoelectron emission 06 p0694 A73-18300

The process of reinforcement of lead shields in electroradiography 07 p0822 A73-19330

A modified Monte Carlo model for the ionospheric heating rates. 07 p0815 A73-19380

Photoelectron precipitation induced dissociation of atmospheric nitrogen molecules during moderate solar activity 07 p0816 A73-19459

Photoelectron layer detection above sunlit lunar surface with ion-electron spectrometer in Apollo 14 charged particle lunar environment experiment, noting energy spectra 07 p0895 A73-19859

Photoemission from lunar surface fines and the lunar photoelectron sheath. 07 p0895 A73-19860

Photoelectron detection ability increase of image dissector by buffer intensifier tube, noting application for photon counting spectroscopy 08 p0971 A73-21745

Digicon multichannel image tube photoelectron counter for astronomical spectroscopy, discussing design information density and accuracy, noise and quantum efficiency 08 p0971 A73-21747

Study of the time correlation of multifrequency-laser emission by the photon coincidence method 09 p1096 A73-22877

PHOTOEMISSION

Investigation of geoeactive corpuscular particles and photoelectrons on board the Cosmos 261 satellite. V - Spectra of ionospheric photoelectrons and migration of the latter from the conjugate ionosphere
10 p1211 A73-23887

Twilight airglow. I - Photoelectrons and forbidden O I 5577-angstrom radiation.
10 p1214 A73-24737

Alternating spectral oscillations of nonequilibrium photoelectron current in p-InSb in the presence of a quantizing magnetic field
10 p1261 A73-24763

Measurement of the absorption of solar ultraviolet radiation with the aid of a photoelectron analyzer
11 p1350 A73-25080

Description of the photoelectron interaction with ambient electrons in the ionosphere.
11 p1357 A73-25927

Photoelectrons and solar wind/lunar limb interaction.
12 p1534 A73-27495

The photoelectron-spectrometer experiment on Atmosphere Explorer.
13 p1689 A73-28641

ESCA study of fractional monolayer quantities of chemisorbed gases on tungsten.
14 p1724 A73-30421

Anisotropy and energy spectra of newly-generated photoelectrons
15 p1867 A73-31265

Photoelectron excitation of the Jupiter dayglow.
16 p2062 A73-33430

Properties of the satellite photoelectron sheath derived from photoemission laboratory measurements.
16 p2062 A73-33435

Cylindrical X ray source with Al K-alpha radiation production for spherical photoelectron spectrometer, discussing radiation intensity with minimum bremsstrahlung
17 p2176 A73-35765

Fluorescence excitation and photoelectron spectra of CO₂ induced by vacuum ultraviolet radiation between 185 and 716 angstroms.
18 p2346 A73-36266

Photoelectron layer above sunlit lunar surface due to solar photon flux, using models neglecting solar wind electron flux
18 p2351 A73-36267

Energy transport by photoelectrons in the early morning ionosphere.
18 p2348 A73-37027

Rocket measurement of photoelectrons in the ionosphere by K-9 M-40.
19 p2474 A73-37379

Investigation of geoeactive corpuscles and photoelectrons with the Cosmos 261 satellite. V - Spectra of ionospheric photoelectrons and their transfer from the conjugate ionosphere.
20 p2550 A73-38906

Photoelectron energy spectra for atomic and molecular binding energies, examining spectrum signatures, angular distribution, autoionization, rare gases, carbon monoxide and cyanocobalamin
20 p2520 A73-39634

A study of geoeactive corpuscles and photoelectrons on the Cosmos 261 satellite. VI - Epithermal electrons in the energy range from 30 to 150 eV in the region of the dayside and nightside polar cusps
21 p2686 A73-40909

Electroradiography technique involving photoproduction of free electrons via Townsend avalanche amplification in diode/triode/gap, noting increased quantum efficiency
23 p2950 A73-44214

Thermalization and transport of photoelectrons - A comparison of theoretical approaches.
24 p3086 A73-45124

PHOTOEMISSION

U PHOTOELECTRIC EMISSION

PHOTOEMISSION

U EMISSION

U PHOTOELECTRIC EMISSION

PHOTOEMITTERS

U PHOTOELECTRIC MATERIALS

PHOTOLOGY

Radar imagery and aerial photography for geological remote sensing applications in coastal mapping, land-form analysis, engineering and reconnaissance
06 p0667 A73-18282

Mars surface volcano and canyon features from Mariner 9 photographs and geological map, suggesting internal heating, water erosion, atmospheric evolution and life problem solution
06 p0754 A73-18672

Photogeologic interpretations of Apollo 14 orbital photographs of far side craters and lunar surface formations
07 p0879 A73-19681

Astronaut observations from lunar orbit and their geologic significance.
07 p0879 A73-19682

A generalized geologic map of Mars.
19 p2477 A73-37201

PHOTOGRAMMETRY

On a method of determining the interaction coefficient in convective clouds
01 p0074 A73-11273

Daytime and nighttime stereophotogrammetric photography of moving object using stroboscopic effect, noting pulsed light sources for fast moving near objects
05 p0575 A73-16314

Affine and nonlinear transformations for aerial photography film deformation effects on photogrammetry accuracy
05 p0575 A73-16315

Central projection parameter determination of photographed objects
06 p0693 A73-18153

Time lapse stereo photogrammetry of ring vortex type circulation in cumulonimbus cloud tops of hail bearing storms
07 p0847 A73-19042

Stereophotogrammetric compilation of large scale topographic chart using convergent panoramic photos obtained with Apollo 15 spacecraft
07 p0824 A73-20022

American Society of Photogrammetry and American Congress of Surveying and Mapping, Fall Convention, Columbus, Ohio, October 11-14, 1972, Proceedings.
08 p0968 A73-21701

Camera orientation with peripheral image coordinates of oblique circles.
08 p0968 A73-21704

Computation of the minimum bandwidth for aerotriangulation.
08 p0968 A73-21705

Calibration of the aerial photographic system by the method of mixed ranges.
08 p0969 A73-21706

Fine verticality readout accuracy test on film format of each photograph obtained by prime camera, describing aerial photogrammetric data reduction methods
08 p0969 A73-21708

Coordinates correction for atmospheric refraction in aerial photography, noting effects of ground elevation, atmospheric pressure and temperature
08 p0969 A73-21709

Apollo 15 optical bar panoramic lunar surface photography, considering luminance, exposure time, resolution and camera performance
08 p0970 A73-21735

American Society of Photogrammetry, Annual Meeting, 38th, Washington, D.C., March 12-17, 1972, Proceedings.
09 p1081 A73-22376

Close range photogrammetry of objects moving at high speed.
09 p1081 A73-22377

Graphical method of profiling and contouring microcraters on lunar rocks from stereomicrograph pair obtained by scanning electron microscope
09 p1081 A73-22378

Reduction of lunar panoramic photography on the analytical stereoplotter.
09 p1081 A73-22379

Airborne photogrammetric system with mapping and geodetic surveying data acquisition capability, discussing inertial navigation subsystem, terrain profile recorder and electronic distance measuring equipment
09 p1081 A73-22380

Recursive methods in on-line computer photogrammetric data reduction deriving algorithms for fixed and variable parameter numbers cases with matrix partitioning
09 p1059 A73-22381

FORTAN IV program and recursive matrix partitioning algorithm for solution of photogrammetric simultaneous equations, noting computation time
09 p1059 A73-22382

Collinear theory of photogrammetry developed from projective equations in three dimensional space through singular transformation with 11 independent parameters
09 p1082 A73-22383

ERTs return beam vidicon TV cameras and ground based electron beam recording system resolution and distortion characteristics from preflight and in-flight simulation and calibration studies
09 p1082 A73-22385

A finite element method for block adjustment problems of photogrammetry.
10 p1218 A73-24291

An analytic expression for the radial photogrammetric distortion of aerial photo cameras
10 p1219 A73-24479

Projective properties of an anamorphic bundle of projecting beams
10 p1219 A73-24484

Mariner Mars 1971 photogrammetry, discussing spacecraft scan platform mounted TV camera calibration procedure for interior orientation parameters and opto-mechanical orthogonality
12 p1500 A73-27953

Block adjustment for color and multispectral high altitude frame photography in photogrammetry, considering terrain caused sun angle effect as discriminant for automatic photointerpretation
12 p1500 A73-27955

Photogrammetric solution for precision processing of E.R.T.S. images.
12 p1501 A73-27964

Apollo 15 photogrammetric measurements of lunar figure, describing system characteristics and analytical triangulation techniques
12 p1501 A73-27967

Aerial radar photograph restitution for photogrammetric application, discussing geometric qualities and methods and instruments for partial removal of distortion
12 p1502 A73-27972

Photomosaic construction high altitude photographs, approximating surface curved areas by planes
13 p1621 A73-29323

Experiment in stereophotogrammetric processing of aerial photographs with decentrations on an STD-2 stereometer
14 p1753 A73-30417

Martian surface primary and secondary triangulation networks based on multiphotograph stereophotogrammetry and rectified photographs by Mariner 9, discussing control nets and points
19 p2479 A73-37227

Photogrammetric evaluation of Mariner 9 photography.
19 p2479 A73-37229

A study of Martian topography by analytic photogrammetry.
19 p2480 A73-37230

Photogrammetry in Apollo lunar roving vehicle conducted geometry and geology exploration, using horizontal stereophotography with special gnomon for sun-line and vertical control
20 p2611 A73-39669

Statistical comparison of airborne laser and stereophotogrammetric sea ice profiles.
22 p2850 A73-42731

Recursive methods in photogrammetric data reduction.
22 p2862 A73-42825

Satellite-borne photography of earth surface covering environment and flight dynamics effects, space photogrammetry principles, natural environment imagery interpretation and natural resource photography
23 p2971 A73-43332

The precision of contour lines and contour intervals of large- and medium-scale maps.
23 p2979 A73-44123

PHOTOGRAPH INTERPRETATION

U PHOTOINTERPRETATION

PHOTOGRAPH DEVELOPERS

Photographic processing of aerial imagery for earth resources, discussing photographic developers, film and materials
19 p2431 A73-38179

PHOTOGRAPHIC EMULSIONS

NT NUCLEAR EMULSIONS

High resolution apparatus at the focus of large telescopes
01 p0049 A73-10532

Comparison of high-resolution photographic emulsions for recording three-dimensional holograms.
01 p0051 A73-10839

Radiative transfer theory application to stellar images in photographic emulsions, deriving theoretical relation between star brightness and photographic effective radius
08 p1006 A73-20926

Relation between object position and autocorrelation spots in the Vander Lugt filtering process. II - Influence of the volume nature of the photographic emulsion.
08 p0964 A73-21044

Some questions on the evidence of laser X-ray emission from CuSO₄ doped gelatin.
08 p0975 A73-21061

Photographic process based on ultrathin photosensitive molecular dispersion layer of benzenediazophenyl and autocatalytic Ag deposition during development process
09 p1084 A73-22691

The wave length dependence of the transfer properties of photographic materials for holography.
11 p1370 A73-26536

The problem of the deformation of the photoemulsion layer during artificial marking of points on aerial photos
13 p1621 A73-29417

Camera design with deep-cooled photographic emulsion for low intensity light photography, discussing gas filling and vacuum techniques for water condensation avoidance
14 p1753 A73-30275

Investigation of the dependence of the quality of a reconstructed holographic image on the parameters of the photoemulsion layer. I - Diffractive efficiency of the hologram
14 p1753 A73-30370

On-axis computer generated hologram with multi-emulsion color film for retaining kinoform advantages and effective control over amplitude and phase transmittance

17 p2171 A73-35401

Russian book - High-molecular-weight compounds in photographic processes.

21 p2646 A73-40252

Stability of silver bromide dispersions in the presence of gelatin and other surface-active substances

21 p2647 A73-40267

Physicochemistry of the deposition of gelatinous photographic emulsion layers on a substrate

21 p2647 A73-40268

Photographic nuclear emulsions with total replacement of gelatin by synthetic polymers

21 p2647 A73-40269

Influence of certain wetting agents on the optical sensitization and retention of the photographic properties of a finished layer

21 p2647 A73-40271

Semiautomatic recorder for photometry of black spots produced by electron-photon cascades on RT-6 type X-ray films

23 p2982 A73-43568

PHOTOGRAPHIC EQUIPMENT

NT CAMERAS

NT DIFFRACTION LIMITED CAMERAS

NT FRAMING CAMERAS

NT HIGH SPEED CAMERAS

NT LALLEMAND CAMERAS

NT PANORAMIC CAMERAS

NT PHOTOGRAPHIC PROCESSING EQUIPMENT

NT SCHMIDT CAMERAS

NT TELEVISION CAMERAS

Photographic equipment for astronomical telescopes, considering mechanical devices for plate translation and rotation, guiding microscope and digitally controlled servomotors with incremental feedback

01 p0049 A73-10541

Nelson Tyler helicopter camera mount for aerial reconnaissance photography providing camera balance and motion stability under combat flight conditions

10 p1222 A73-24949

A high performance large aperture window for photography from a space platform.

13 p1621 A73-29326

Radiometric calibration of a multi-spectral aerial camera.

22 p2862 A73-42824

PHOTOGRAPHIC FILM

NT MICROFILMS

Computerized flying spot scanner/analyzer for automatic mensuration analysis of droplets, particles and cell preparations from 35 mm film density distributions

03 p0309 A73-14449

Comparative data of investigations of aerial films on lavsan and triacetate bases

04 p0447 A73-14850

Affine and nonlinear transformations for aerial photography film deformation effects on photogrammetry accuracy

05 p0575 A73-16315

Optical device for three dimensional multiplication of input signal recorded on photographic film, noting pattern recognition and optical communication applications

07 p0823 A73-19909

Real time 3-D holographic display, discussing reusable thermoplastic photoconducting recording film and frequency compensation with short laser pulses and acousto-optic modulator

08 p0965 A73-21246

Simple method of obtaining high-sensitivity interferograms

09 p1085 A73-22882

Color encoded multispectral image recording on black-and-white photographic film with synthetically generated diffraction gratings, noting color recognition, resolution and contrast ratio

10 p1216 A73-23786

Circular carrier-frequency photography for observing phase objects.

12 p1495 A73-26832

Long duration radio signals reception on noise background, recording signal/noise mixture on photographic film

12 p1470 A73-27578

Examination of film deformation for aerial photography

12 p1500 A73-27960

Optimizing sensitometric data for color and black and white aerial film.

12 p1501 A73-27966

Video-to-film color-image recorder.

13 p1619 A73-29240

Sensitometric tests on plane-parallel organic photochromic bulk material film samples of styrene, methylmethacrylate and inoline spiropyran, evaluating photosensitivity suitability for holography

13 p1622 A73-29436

Kinetic equations for time behavior of solid photochromic film in photocoloration, photobleaching and thermal bleaching, evaluating absorption cross sections and quantum yields

17 p2172 A73-35422

Photographic processing of aerial imagery for earth resources, discussing photographic developers, film and materials

19 p2431 A73-38179

Image converter intensification for ultrahigh speed photography, discussing photographic film sensitivity, optical fiber output, slit analysis and camera types

21 p2694 A73-39941

Russian book - High-molecular-weight compounds in photographic processes.

21 p2646 A73-40252

High-molecular compounds and recording of information on thermoplastic films

21 p2646 A73-40253

Physicochemical principles of the photographic process on vesicular films and the high-molecular-weight compounds used for these films

21 p2646 A73-40254

Certain features of sensitive layers containing bifunctional polymers /fixatives/ on a blank film

21 p2646 A73-40257

Influence of chemical composition on the structure and mechanical properties of polycarbonate films and the possibility of using them as a substrate for moving-picture films

21 p2646 A73-40259

Investigation of the possibility of using acetylated oxyethylcellulose as a film forming substance for a moving-picture film base

21 p2647 A73-40262

Physico-mechanical properties and damage mechanism of moving-picture photographic materials as film systems

21 p2699 A73-40270

An electronically synchronized drum-type film camera

21 p2706 A73-41580

Properties of thin-film holograms on chalcogenide glasses

22 p2860 A73-42409

Holographic image nonlinear distortion analysis based on photographic film material characteristic curve representation by Taylor series

22 p2861 A73-42410

Semiautomatic recorder for photometry of black spots produced by electron-photon cascades on RT-6 type X-ray films

23 p2982 A73-43568

PHOTOGRAPHIC MEASUREMENT

NT PHOTOGRAMMETRY

Sensitometric instruments for black and white and color photographic material and image measurements, including recording microdensitometer, reflection goniodensitometer, automatic granulometer and projection resoluometer

01 p0051 A73-10837

A new dimension in front-light laser photography.

03 p0309 A73-14199

Geometrical adjustment with simultaneous laser and photographic observations on the European datum.

04 p0437 A73-14781

Criterion for the choice of exposure time in atmospheric turbulence investigation with an optical wave.

06 p0691 A73-17497

Interstellar extinction curve structure via photographic techniques, considering optical observation extension into UV with OAO-C telescope

06 p0751 A73-18228

Redintegrated somatotyping technique for physique measurement and classification based on limb and torso photographic diameter integration with height, using photoelectric cell and electronics

06 p0659 A73-18474

Computational solution for positions on whole Schmidt-plates - Report on reduction of coordinates measured on 22 plates of the Bergedorf Schmidt telescope.

08 p0966 A73-21357

Photo-optic instrumentation of magnetic flyer plate facility for pressure-time response measurement of impact loaded test specimens, using streak and high speed framing cameras

09 p1083 A73-22512

Photometric analysis of earth photographs from Zond space station, determining earth sidereal magnitude

10 p1281 A73-24477

Hologram interferometry adaptation to industrial conditions for dimensions, deformation, vibration and refractivity measurements, noting advantages over ordinary interferometry

11 p1370 A73-26540

New phenomena during the burning of condensed systems

12 p1559 A73-27454

Error estimates for turbulent flow characteristics by visualization and solid particle photography

13 p1601 A73-28738

PHOTOGRAPHIC PROCESSING

Optical method for studying the heat transfer mechanism in bubble boiling

13 p1708 A73-29173

Automatic coordinate-measuring machine for astrophotography purposes

15 p1878 A73-32144

Measurement of small movements and vibrations by laser photography.

16 p2013 A73-32879

Slope angle determination with respect to photograph surface from visible horizon line configuration

16 p2017 A73-34049

Solar eclipse of July 10, 1972 - Comparison of photographic-photometry and K-coronometer measurement data

20 p2611 A73-39589

Flashlamp pumped CW mode-locked dye laser picosecond light pulse duration measurement by electro-optical streak camera

21 p2694 A73-39946

Hypervelocity projectile holography for application to bullets and shells, calculating rotational velocity and flight direction from fringe on wave front reconstruction

21 p2694 A73-39957

Measurement of change in a cross section and position of small particles by diffraction techniques.

21 p2695 A73-39959

Holographic investigations and measurements in a cloud of moving microparticles

21 p2696 A73-39979

Spallation and fracture resulting from reflected and intersecting stress waves.

21 p2782 A73-39989

High-speed camera study of the shock wave propagation.

21 p2697 A73-39993

High-speed cine-photography and oscillography in a boiling simulation.

21 p2697 A73-39994

Measurement accuracy achievable in photographed isochromatic pictures

21 p2706 A73-41605

On the possibility of determining stellar radial velocities to 0.01 km per sec.

22 p2907 A73-42207

Photographic instrumentation in Hyperballistic Range /G/ of the von Karman Gas Dynamics Facility.

22 p2864 A73-43189

The Saturn rings in 1969: Morphological and photometric study. I - Photograph acquisition and evaluation

24 p3128 A73-44434

PHOTOGRAPHIC PLATES

A program for plate reduction in the case of satellite observations with a satellite observation camera

03 p0274 A73-13254

Cartography of the surface markings of Mercury.

06 p0743 A73-17429

Finson-Probst model for dust comets applied to calibrated photographic plates of Comet Bennett, giving dust size distribution, emission rate and initial velocities

07 p0902 A73-20443

Astrometry with Schmidt telescopes, discussing automated computerized plate scanner and measuring machine for star position and relative motion determination

08 p0966 A73-21356

Astronomical spectroscopy with prism in front of Schmidt correcting plate, considering spectral resolution and light loss characteristics in plate field

08 p0966 A73-21359

Vibration measurement by vibrating-plate holograms.

09 p1079 A73-21997

Reflection plate interferometer with thin glass shearing plate replacing knife edge in Schlieren system, noting optimum operating range and fringe spacing

11 p1365 A73-26238

Holographic coding plate - A new application of holographic memory.

17 p2173 A73-35431

Properties and fabrication of micro Fresnel zone plates.

17 p2173 A73-35434

Solar photospheric granulation plate statistical properties, establishing two dimensional autocorrelation function and power spectrum as function of wave number

21 p2776 A73-41477

A laser raster setup with programmed control for image lithoplate synthesis

22 p2869 A73-42362

Shakhbazian I compact galactic cluster, discussing red shift, angular size, galactic type, velocity dispersion, mass/light ratio and photographic plates

22 p2909 A73-42586

PHOTOGRAPHIC PROCESSING

An electronic multiband camera film viewer.

04 p0450 A73-15771

Multispectral additive color viewer for ERTS satellite photography, discussing colorimetric measure-

ment usefulness and photo processing and image density control effects on color characteristics
05 p0579 A73-17145

Drobyshev stereograph corrector operation for aerial photographs processing with transformed beam of stereoprojector
07 p0824 A73-20043

Photographic process based on ultrathin photosensitive molecular dispersion layer of benzenediazosulphide and autocatalytic Ag deposition during development process
09 p1084 A73-22691

The problem of the deformation of the photoemulsion layer during artificial marking of points on aerial photos
13 p1621 A73-29417

Photographic processing of aerial imagery for earth resources, discussing photographic developers, film and materials
19 p2431 A73-38179

Statistical analysis of the influence of various factors on the quality of photolithographic operations in the production of integrated circuits
20 p2534 A73-38851

Physicochemical principles of the photographic process on vesicular films and the high-molecular-weight compounds used for these films
21 p2646 A73-40254

Certain features of sensitive layers containing bifunctional polymers/fixatives/ on a blank film
21 p2646 A73-40257

Advantages of using polymer bases as fixing agents in hydrotype printing
21 p2646 A73-40258

Silver halogenide bichromatic gelatin chemical and photographic properties, noting decelerating development effect
21 p2647 A73-40266

Influence of certain wetting agents on the optical sensitization and retention of the photographic properties of a finished layer
21 p2647 A73-40271

PHOTOGRAPHIC PROCESSING EQUIPMENT
Rapid in situ processing for real-time holographic interferometry.
21 p2692 A73-39918

PHOTOGRAPHIC RECORDING
Holographic image polarization recording and sum wave simulation on photoanisotropic materials, using Weigert effect
01 p0052 A73-11086

Double exposure holographic interferometry for comparison of object of two points in time evolution, discussing space division multiplexing of exposures onto photographic plate
01 p0054 A73-11234

Coding technique to record computer generated binary hologram on numerically controlled CRT with resolution cell of two beam spots
01 p0019 A73-11235

Solar flares recognition from H-alpha centered birefringent filtered photographs, determining statistical pattern of filament movements
04 p0491 A73-14842

Wavefront sampling in holographic interferometry.
05 p0579 A73-17223

Modulated laser beam photographic recorder/reproducer system bandwidth and SNR tradeoff alternatives consideration for high dynamic range performance, suggesting FM recording technique superiority
06 p0701 A73-18309

High data rate holographic recorder with six-channel acousto-optical modulator array as input composer and mode locked Ar laser as light source
06 p0694 A73-18311

Moving radiography for photographic recording and display of transient or cyclic motion, emphasizing application to aircraft gas turbines under dynamic conditions
07 p0832 A73-20451

Holographic optical element for visual display applications.
08 p0963 A73-21034

Relation between object position and autocorrelation spots in the Vander Lugt filtering process. II - Influence of the volume nature of the photographic emulsion.
08 p0964 A73-21044

Amplitudes of mth order holographic images recorded on film with power law characteristics.
08 p0964 A73-21054

Noise reduction in acousto-optic /Bragg/ imaging systems by holographic recording.
08 p0965 A73-21209

Image intensifier systems and their applications to astronomy.
08 p0971 A73-21743

Application of lens-raster optics for recording holograms with discrete information
09 p1079 A73-21916

Two direct methods for reconstructing pictures from their projections - A comparative study.
09 p1080 A73-22224

A 35mm aerial photographic system.
09 p1082 A73-22387

Holographic recording of focused images in multimode laser radiation
09 p1084 A73-22879

Optimum holographic recording of complex light fields generated by diffusive objects in presence of point sources, maximizing SNR or distortion-free diffraction level
09 p1084 A73-22880

Recording of paraphase-coded binary information on phase holograms
09 p1085 A73-22881

Holographic recording and reproduction of wave polarization information by correlation matrix and Stokes parameter method
09 p1087 A73-23333

Holographic recording of moving objects.
10 p1215 A73-23613

Color encoded multispectral image recording on black-and-white photographic film with synthetically generated diffraction gratings, noting color recognition, resolution and contrast ratio
10 p1216 A73-23786

Advances in high-speed photography 1957-1972.
11 p1359 A73-24995

A light and compact X-ray image read-out system for space applications.
11 p1364 A73-26050

Phase characteristic function of holographic images of objects in parabolic motion.
11 p1366 A73-26248

Mathematical principles of optical image deblurring by holography for photographic and electron micrographic applications
11 p1371 A73-26543

Reversible recording of holograms on chalcogenide glass films
12 p1495 A73-26940

Holographic focused image recording and reconstruction in white light, considering source size, shape and spectral composition effects and interferometry
12 p1497 A73-27424

Controllable liquid-crystal transparency for recording of holograms.
12 p1498 A73-27513

Large sunspot high dispersion line spectrum at 6610-6770 A, noting umbral/photospheric contrast and drift curves across limb from photographic recording
12 p1547 A73-27925

Remote sensor dynamic imageries produced by stereo systems, discussing line-by-line and section-by-section orientation methods and triple channel recording scheme
12 p1500 A73-27956

Multistage image converter tubes for studying high-speed phenomena.
13 p1611 A73-28175

Effect of some external factors on accuracy of observations of active satellites.
13 p1680 A73-28516

The recording of three-dimensional holograms on photochromic glass with the use of an optical bleaching process. I
13 p1616 A73-28765

Holographic recording of three-dimensional ensembles of rapidly moving particles
13 p1616 A73-28767

Establishment of hologram memory system with capacity as high as 10,000,000 bits.
13 p1588 A73-29236

Indoline series spirochromene polymer matrices for holographic recordings with argon and helium-neon lasers in green and UV spectral regions
14 p1753 A73-30365

Thermal expansion coefficient measurement of diffusely reflecting samples by holographic interferometry.
15 p1877 A73-31980

Thermal expansion coefficient measurements of specularly reflecting samples.
15 p1877 A73-31981

Three-dimensional hologram recordings on photochrome glass with the application of an optical discoloration process. II
15 p1879 A73-32340

Burst-mode frequency-doubled YAG:Nd3+/ laser for time-sequenced high-speed photography and holography.
15 p1886 A73-32384

Lens raster optics for holograms with digital information.
15 p1880 A73-32642

Holographic document data recording and storage for single- and multiterminal information processing system, emphasizing Fourier and carrier frequency photography techniques
16 p2013 A73-32873

Oscillographic equipment for research in the field of semiconductor microwave electronics
17 p2218 A73-34160

Investigation of thermal deformations by methods of holographic interferometry
17 p2164 A73-34172

The optical design of the 40-in. telescope and of the Irene Dupont telescope at Las Campanas Observatory, Chile.
17 p2171 A73-35408

Distortionless recording in double-exposure holographic interferometry.
17 p2173 A73-35430

Applications of the speckle pattern techniques to the visualization of modulation transfer functions and quantitative study of vibrations of mechanical structures.
17 p2173 A73-35433

Recording of the angular velocity of meteors by sequential photography
19 p2480 A73-37239

A direct approach to reduce recording time in stroboscopic holographic interferometry.
19 p2429 A73-37541

Remote sensing experiments with balloons
19 p2431 A73-38180

Thermal IR image recording, processing and enhancement, discussing prevention of defects or irregularities caused by aircraft motion, weather and electronic noise
20 p2566 A73-39670

Literature survey on high speed photography and cinematography, discussing gas discharge tube and open spark equipment, Kerr cells, image dissection and holographic interferometry
21 p2693 A73-39934

Mechano-optical camera giving ten million images per second
21 p2693 A73-39935

Resetting in time of recordings in ultrahigh-speed cinematography
21 p2694 A73-39952

Utilization for high speed cinematography of phased-locked CW lasers
21 p2709 A73-39954

A method for the calibration of a quantitative high-speed schlieren procedure involving photographic recording
21 p2694 A73-39955

Holographic method of recording temporal characteristics of optical signals.
21 p2695 A73-39958

The use of holographic techniques for recording high-speed events.
21 p2695 A73-39962

Method of observing processes in the interior of explosives
21 p2695 A73-39966

Recording of diffraction patterns by X-ray pulses of materials subjected to a shock wave compression
21 p2695 A73-39967

Repetitive recording of stress waves in a photoelastic material using a multi-pulsed laser and an inexpensive streak camera.
21 p2695 A73-39970

Utilization of the laser as a source in ultrahigh-speed cinematography
21 p2709 A73-39972

Practical lasers for photographic and holographic recording.
21 p2709 A73-39973

A multiflash high-speed camera developed to register phase objects with good spatial resolution without parallax.
21 p2696 A73-39980

Holographic interferometry applied to aerodynamics
21 p2696 A73-39984

A streak technique for measuring the initial movement of a rocket with four unknown and two known degrees of motion.
21 p2696 A73-39986

High-speed photographic study of failure processes in composite materials.
21 p2723 A73-39988

A photographic method for testing the impact strength of metals
21 p2696 A73-39991

Kerr-cell studies of exploding wires in vacuum.
21 p2738 A73-39996

Degree of coherence mapping of single ruby laser pulses using holographic interferometry, discussing self-coherence, length and photographic recording
21 p2710 A73-40146

A system for the photographic recording of pulsar pulses
21 p2700 A73-40552

Solar eclipse of 10 July 1972 observed by visual and photographic method from aircraft, taking into account coronal structure
21 p2767 A73-40565

Elimination of a fundamental defect of two-dimensional holograms
21 p2700 A73-40570

Study of the properties of thick-film chalcogenide glass holograms
21 p2701 A73-40571

Image contrast and efficiency of nonlinearly recorded holograms of diffusely reflecting objects.
21 p2703 A73-41133

Some problems associated with the construction of scanner employing a cathode-ray tube and programmed control

21 p2665 A73-41270

Properties of thin-film holograms on chalcogenide glasses

22 p2860 A73-42409

Ultrahigh resolution holographic spectroscopy by double exposure of light scattering medium interferogram recording and reconstruction, noting equivalence to use of narrower laser line width

22 p2861 A73-42413

Speckle effect use in laser photography for vibration and displacement measurement of mechanical systems, discussing diffraction patterns and measurement methods

23 p2982 A73-43675

Holographic photo-elasticity - Independent observation of the isochromatic and isopachic fringes for a single model subjected to only one process.

24 p3091 A73-45335

PHOTOGRAPHIC RECORDING INSTRUMENTS

U OPTICAL MEASURING INSTRUMENTS

U PHOTOGRAPHIC RECORDING

U RECORDING INSTRUMENTS

PHOTOGRAPHIC TRACKING

Photographic satellite tracking instrument technology and data reduction methods, describing various camera types and for photogrammetric and astrometric position determination

03 p0274 A73-13252

Artificial earth satellites photographic position determination, discussing instrumental and procedural technologies

03 p0274 A73-13255

Photographic satellite observations with the Automatic Camera for Astrogeodesy.

13 p1611 A73-28150

Artificial satellites photographic observations reduction by Turner and collineation methods, considering IBM 360 FORTRAN program application

15 p1843 A73-31648

Russian monograph on meteor observation covering telescopic and photographic methods, meteor trail plotting, radiant determination, stream counts and bo-
lide data

15 p1941 A73-32416

Accuracy of photographic artificial earth satellite observations at the observational station in Riga

22 p2910 A73-42644

PHOTOGRAPHS

NT CLOUD PHOTOGRAPHS

NT LUNAR PHOTOGRAPHS

NT MICROPHOTOGRAPHS

NT MOTION PICTURES

PHOTOGRAPHY

NT AERIAL PHOTOGRAPHY

NT ALL SKY PHOTOGRAPHY

NT ASTRONOMICAL PHOTOGRAPHY

NT AUTORADIOGRAPHY

NT BLACK AND WHITE PHOTOGRAPHY

NT CHRONOPHOTOGRAPHY

NT CINEMATOPHOTOGRAPHY

NT CLOUD PHOTOGRAPHY

NT COLOR PHOTOGRAPHY

NT ELECTRO-OPTICAL PHOTOGRAPHY

NT ELECTRON PHOTOGRAPHY

NT FRACTOGRAPHY

NT FRAME PHOTOGRAPHY

NT HOLOGRAPHY

NT INFRARED IMAGERY

NT INFRARED PHOTOGRAPHY

NT LUNAR PHOTOGRAPHY

NT METRIC PHOTOGRAPHY

NT MICROWAVE PHOTOGRAPHY

NT MULTISPECTRAL PHOTOGRAPHY

NT ORTHOPHOTOGRAPHY

NT PHOTOMICROGRAPHY

NT RADAR PHOTOGRAPHY

NT ROCKET-BORNE PHOTOGRAPHY

NT SATELLITE-BORNE PHOTOGRAPHY

NT SCHLIEREN PHOTOGRAPHY

NT SHADOWGRAPH PHOTOGRAPHY

NT SPACEBORNE PHOTOGRAPHY

NT SPECTROPHOTOGRAPHY

NT STEREOGRAPHY

NT ULTRAVIOLET PHOTOGRAPHY

NT ULTRAVIOLET PHOTOMETRY

Thoracic X-ray photography technique for tubercular lesion detection in flight personnel, comparing to standard radiography and radioscopy

02 p0137 A73-12155

Pulsed X-ray photography of a shock wave in cesium vapor using two X-ray tubes

06 p0731 A73-18554

Camera design with deep-cooled photographic emulsion for low intensity light photography, discussing gas filling and vacuum techniques for water condensation avoidance

14 p1753 A73-30275

Pulse X-ray photography of a shock wave in cesium vapor using two X-ray tubes.

16 p2042 A73-33579

PHOTOINTERPRETATION

Colour separation and electronic analysis of Gemini V and Apollo spacecraft photography.

01 p0045 A73-10275

Computerized terrain classification system software features for automatic interpretation of aerial photographic imagery by laser scanning system

04 p0445 A73-15772

Applications of the discriminant function in automatic pattern recognition of side-looking radar imagery.

05 p0553 A73-16289

The representation and matching of pictorial structures.

06 p0692 A73-17804

Central projection parameter determination of photographed objects

06 p0693 A73-18153

Random optical density fields pertaining to analyses of aerial photo imaging of aerial topographic objects

06 p0693 A73-18155

Ancillary information effects on photointerpretation performance under four imagery system operation modes, noting identification accuracy independence on information variables

06 p0658 A73-18245

Similarities and differences in the interpretation of air photos and SLAR imagery.

06 p0693 A73-18284

Perception of tone differences from film transparencies.

06 p0695 A73-18388

Measurements regarding the color of aerial photographs in studies of the vegetation

06 p0695 A73-18437

Computer aided recognition of objects shapes on aerial photographs, discussing image derivatives and histograms use and flying spot scanner principle

07 p0825 A73-20165

The utility of a low flying aircraft or helicopter when collecting ground data for regional resource surveys.

08 p0961 A73-21710

Apollo 15 optical bar panoramic lunar surface photography, considering luminance, exposure time, resolution and camera performance

08 p0970 A73-21735

Analysis and interpretation of air-borne multifrequency side-looking radar sea ice imagery.

09 p1080 A73-22150

Interpretation of wetlands imagery based on spectral reflectance characteristics of selected plant species.

09 p1077 A73-22388

A new interpretation of interferometric fringe patterns.

10 p1220 A73-24661

A BESM-3M computer program for processing photographic observations of extended objects

11 p1333 A73-25231

Panoramic and frame cameras for aerial phototopographic survey, noting photo quality and high resolution advantages

12 p1497 A73-27423

Block adjustment for color and multispectral high altitude frame photography in photogrammetry, considering terrain caused sun angle effect as discriminant for automatic photointerpretation

12 p1500 A73-27955

Skylab earth terrain camera for high resolution photography of areas covered by other Earth Resources Experiment Package sensors to aid in data interpretation

12 p1500 A73-27958

Digital image processing for information extraction.

15 p1875 A73-31800

Remote sensing and photointerpretation, discussing black and white, color and IR photography, microwave imagery, atmospheric attenuation, reflectance and potential application for ERTS satellites

16 p2014 A73-33100

Operational remote sensing; Proceedings of the Seminar, Houston, Tex., February 1-4, 1972.

16 p2002 A73-33351

Hybrid techniques for automatic imagery interpretation.

16 p2016 A73-33367

Certain conclusions concerning the morphometry of sections of the moon photographed by the Luna 12 probe

16 p2065 A73-33779

Identification of certain details on photographs of Mars obtained from Mariner 4 and on the ground

16 p2069 A73-33834

Holography, radar data and interpreter performance.

17 p2165 A73-34286

Mars troughs from Mariner 9 pictures, interpreting evolutionary origin in terms of surface and core processes

19 p2477 A73-37204

Corn blight epiphytotic remote sensing, data acquisition and crop identification by photointerpre-

tion and computer aided multispectral band scanner data analysis

20 p2556 A73-39836

The interpretation of multispectral imagery - An analysis of automated versus human interpretation techniques.

20 p2558 A73-39875

Small scale Gemini photographs of Indian regions for interpretation of tonal variations, geomorphologic, geologic and structural features and drainage patterns

20 p2561 A73-39898

A study of lineaments from a Zond 5 photograph of northern Africa.

21 p2687 A73-41332

Multi-stage acquisition of forest information from space and aircraft imagery and ground sampling.

21 p2687 A73-41334

Oceanographic analysis of orbital photographs of the upper Gulf of California.

21 p2692 A73-41634

The use of near-infrared photography in the analysis of surface morphology of an Argentine alluvial floodplain.

22 p2850 A73-42728

Satellite-borne photography of earth surface covering environment and flight dynamics effects, space photogrammetry principles, natural environment imagery interpretation and natural resource photography

23 p2971 A73-43332

Book - The surveillant science: Remote sensing of the environment.

23 p2971 A73-43605

Mars surface evolution from analysis of Mariner 6 and 7 equatorial photographs, discussing internal dynamic activity

24 p3128 A73-44432

The Saturn rings in 1969: Morphological and photometric study. II - Deconvolution of the raw photometric curves

24 p3128 A73-44435

Short-term Jovian rotation profiles, 1970-1972.

24 p3134 A73-44562

Some scale estimates of the three-dimensional structure of cloud fields from aircraft-based aerial photographs

24 p3107 A73-44962

Picture of the month - NOAA 2 scanning radiometer visual and infrared imagery received real-time over a 50,000-mile transmission link.

24 p3085 A73-45020

PHOTOIONIZATION

Oscillator strengths and ground-state photoionization cross-sections for Mg+ and Ca+.

01 p0104 A73-11043

Cross sections for the production of excited products in the photoionization of N2, O2, CO, and N2O by 58.4-nm radiation.

02 p0157 A73-11752

Ionizing potential wave analysis for gas breakdown, noting photoionization role in avalanche propagation and velocity, electron densities and temperature as function of electric field

02 p0197 A73-12063

The feasibility of producing laser plasmas via photoionization.

02 p0177 A73-12572

Breakdown thresholds in rare and molecular gases using pulsed 10.6-micron radiation.

02 p0195 A73-12859

Theoretical models of photoionized intergalactic hydrogen.

03 p0365 A73-12926

Photoionization of vibrationally excited N2. II - Quenching by CO2 and N2O.

04 p0414 A73-14817

Laser plasma generation with high electron densities by photoionization from flashlamp or coherent UV source from harmonic generation or gas lasers

05 p0601 A73-16362

Observation of laser oscillation in a 1-atm CO2-N2-He laser pumped by an electrically heated plasma generated via photoionization.

06 p0703 A73-18649

Laser-induced gas breakdown initiated by ultraviolet photoionization.

06 p0703 A73-18749

An efficient electrical CO2 laser using preionization by ultraviolet radiation.

06 p0704 A73-18797

Impact and bremsstrahlung photoionization due to precipitating electrons in the lower ionosphere.

08 p0957 A73-20657

Photoinitiated transversely sustained CO2 laser.

08 p0975 A73-21208

Resonant multiphoton ionization of a cesium atomic beam by a tunable-wavelength Q-switched neodymium-glass laser.

09 p1098 A73-23472

Oscillator strength and photoionization cross section computation for Cs ground state during photoabsorption, using semiempirical model potential with adjustable parameters

10 p1250 A73-23672

Threshold energies of K-shell photoionization cross sections for various cosmic ionic species

10 p1251 A73-23756

Photoionization and charge exchange reaction kinetics inadequacy for explanation of observed positive nitrogen dioxide ion concentration in lower ionosphere, considering alternative mechanism

10 p1214 A73-24749

Simplified photoionization analysis of quasar emission spectra.

11 p1427 A73-26616

Photoionization of atomic nitrogen and atomic oxygen.

13 p1662 A73-28190

The photoionization cross section of magnesium near threshold.

14 p1776 A73-29699

Focused high power CW carbon dioxide laser sustained Xe, Kr and Ar continuous plasmas, investigating plasma radiative properties by calorimetric techniques

14 p1779 A73-29922

Radiation absorption in stellar atmospheres due to photoionization in magnetic field, discussing frequency relation to propagation direction and Larmor frequency

15 p1872 A73-31955

Pulsed interferometric holography of laser-produced air breakdown.

16 p2014 A73-33175

Continuum analysis of the photoionization chamber in the transition from low to high rates of ionization.

16 p2015 A73-33321

Recoilless nuclear transition based gamma laser, using resonant gamma rays or thermal neutron beam irradiation and selective photoionization

16 p2024 A73-34055

Continuous uniform excitation of medium-pressure CO₂ laser plasmas by means of controlled avalanche ionization.

17 p2183 A73-34207

Continuum emission from recombining oxygen and nitrogen plasmas.

18 p2338 A73-36799

Large aperture atmospheric pressure excited carbon dioxide laser discharges, using weak volumetric gas preionization to obtain high power for plasma production

21 p2714 A73-40762

Incompatibility of solar EUV fluxes and incoherent scatter measurements at Arecibo.

22 p2902 A73-41923

French monograph - Preparation of a space experiment intended for high resolution study of the far ultraviolet spectrum of the star gamma Geminii.

22 p2910 A73-42714

Estimate of the effect of photoionization and ion-molecule reactions on the diffusion coefficient in the ionosphere.

23 p2971 A73-43257

An electrostatic suspension method for determining photoionization energies of solids.

23 p3015 A73-43447

Radiation absorption in stellar atmospheres due to photoionization in magnetic field, discussing frequency relation to propagation direction and Larmor frequency

24 p3081 A73-44480

PHOTOLUMINESCENCE

NT X RAY FLUORESCENCE

Phosphor crystals for electromagnetic emission recording based on optical and thermal effects on luminescent screens, considering optimal extinguishing and color alteration conditions

05 p0584 A73-16552

Extinction of photoluminescence by electron irradiation and energy transfer in molecular crystals

05 p0660 A73-16555

Resonant enhancement of photoexcited nitrogen trap n-type GaAs laser electron-hole recombination probability by crystal composition variation and gamma conduction band degeneration

09 p1093 A73-22255

Radiophotoluminescence dosimetry for personnel monitoring, discussing thermoluminescence of phosphate and silver activated glasses, energy compensation filters and measurement techniques

11 p1362 A73-25425

Photoluminescence of ZnTe during laser stimulation

11 p1376 A73-26145

Luminescence quenching and zero-phonon line broadening associated with defect interactions in diamond.

13 p1667 A73-28212

Investigation of defects in GaAs on the basis of the photoluminescence

15 p1923 A73-31717

Luminescence of CdS single crystals doped with various donors and acceptors

19 p2471 A73-37955

Kinetics of recovery of luminescence properties of gallium arsenide single crystals irradiated with high-energy electrons.

20 p2574 A73-39697

Photoluminescence and optical transmission of diffusion-pump oils.

21 p2698 A73-40139

Emission spectra of ZnS:Cu single crystals

21 p2751 A73-40311

Stimulation of two-valent rare earth ion luminescence in CaF₂ crystals by ruby and neodymium lasers

22 p2870 A73-42725

Si and Ge doping characteristics and energy levels in vapor phase epitaxially grown GaAs from sample photoluminescence spectra

23 p3018 A73-44370

PHOTOLYSIS

NT RADIOLYSIS

Molecular iodine photolysis in photodissociative laser due to selective pumping, noting recombination-like storage mechanism

04 p0458 A73-15561

Methyl nitrite photolysis reaction products under various ambient gas mixture environments, noting irradiation time and gas pressure effects

10 p1186 A73-24656

Reactions of O(1D) with methane and ethane.

12 p1466 A73-27126

Investigation by the laser photolysis method of the spectral and time characteristics of tetrapyrrole molecules in a triplet state

13 p1628 A73-29050

Recent measurements of stratospheric reactions by flash photolysis resonance fluorescence.

[ALAA PAPER 73-502] 16 p2005 A73-33543

New rate measurements on the reaction of O(3P), O₃, and OH.

[ALAA PAPER 73-501] 16 p1977 A73-34045

Reaction of HO₂ with O₃.

19 p2402 A73-37674

The photolytic stability of the Martian atmosphere.

21 p2764 A73-40159

Nitrogen dioxide and ozone photolysis as oxygen atom sources for high pressure addition reaction rate studies, discussing quantum yields and photolysis dependence on pressure

22 p2819 A73-42769

Quantum yield of metastable oxygen atoms and molecules via ozone photolysis by UV absorption, noting uncertainties in secondary reaction kinetics

23 p2951 A73-43899

Jovian ammonia photolysis to nitrogen, explaining ammonia observations by deep and hot atmosphere and/or electrical discharge phenomena

24 p3065 A73-44536

Thermokinetics and combustion phenomena in non-flowing gaseous systems - An invited review.

24 p3157 A73-45165

PHOTOMAGNETIC EFFECTS

Magnetophotconductivity of semi-insulating GaAs and its behavior upon electron bombardment.

06 p0738 A73-18369

PHOTOMAPPING

Results of contrast measurements of some Martian maria in July-August 1971

08 p1007 A73-21062

Jupiter surface maps from synoptic observations with refracting telescope, considering white cloud formations and atmosphere motions

08 p1012 A73-21584

Photographic experiments during a spacecraft flight lasting a number of days

13 p1611 A73-28008

Wetlands mapping in New Jersey.

13 p1619 A73-29237

Photomosaic construction high altitude photographs, approximating surface curved areas by planes

13 p1621 A73-29232

Computer program analysis of errors in mutual orientation elements on aerial photographs with different lengthwise overlaps, discussing error minimization

13 p1621 A73-29324

Experience in constructing analytical planar phototriangulation grids from 1:40,000 and 1:75,000 scale aerial photographs for the preparation of 1:10,000 scale photographic maps

14 p1753 A73-30416

Pioneer 10 spacecraft spin-scan imaging photopolarimetric optical system for Jupiter mapping

15 p1880 A73-32385

ERTS-1 satellite-borne multispectral scanner photographic mapping of Israel vegetation, hydrology, geological structure, atmospheric phenomena and oceanography

17 p2162 A73-34947

The cartographic and scientific application of ERTS-1 imagery in polar regions.

18 p2306 A73-36019

EROS Program and ERTS-1 satellite applications to geophysical problems.

18 p2307 A73-36032

Contrast measurement data of Martian maria in July-August, 1971.

18 p2355 A73-36863

Mars maps based on Mariner 9 pictures and photomosaics, with emphasis on southwest quadrant and south pole topographies

18 p2356 A73-37035

An overview of geological results from Mariner 9.

19 p2477 A73-37200

A generalized geologic map of Mars.

19 p2477 A73-37201

Photogrammetric evaluation of Mariner 9 photography.

19 p2479 A73-37229

Cartographic products from the Mariner 9 mission.

19 p2480 A73-37231

Remote sensing to detect regional change in land use characteristics, using aerial photo mosaics and high altitude photography

20 p2557 A73-39846

Radiometric terrain mapping at 3 mm wavelength.

20 p2568 A73-39870

A new method for evaluating and mapping colours in aerial photographs.

20 p2568 A73-39884

Hailswaths mapping with airborne fixed beam and scanning IR radiometers, noting dimensions, orientation and fine structure

21 p2729 A73-40062

Earth surveys by remote sensing in Israel.

21 p2685 A73-40816

The use of Skylab and ERTS data in an integrated natural resources development programme.

23 p2973 A73-43785

PHOTOMECHANICS

U PHOTOGRAPHY

U PRINTING

PHOTOMETERS

NT ELECTROPHOTOMETERS

NT ULTRAVIOLET SPECTROMETERS

NT ULTRAVIOLET SPECTROPHOTOMETERS

Design of an extremely sensitive flame-photometer for analyses in the picogram range using a lock-in amplifier

01 p0051 A73-10925

Photodetector array for a holographic optical memory system.

02 p0169 A73-12163

Experience with the cross-beam photometer system.

05 p0579 A73-17156

High speed, high performance /Hg,Cd/Te photodiode detectors.

06 p0667 A73-18314

The microchannel Picoscope - A tube with high-temporal-resolution scanning for studying luminous phenomena in the subnanosecond range

06 p0679 A73-18862

A four-channel scanning photometer for remote sensing.

07 p0824 A73-19944

Polarimeter-photometer to study solar corona or disk over wide photon arrival rate range, measuring magnitude of polarization effects

08 p0971 A73-21746

Semiautomatic photometer for determining the charge of heavy cosmic-ray nuclei in photonuclear emulsions

09 p1085 A73-23001

Photodetector matrix circuit for holographic memory converting optical bits into electrical signals

09 p1086 A73-23074

Solar 1.9 A X ray spectral line effects on SOLRAD satellite-borne photometer sensitivity and lower ionospheric ion production rate

11 p1354 A73-25771

Calibrations of the airglow photometers and spectrometers.

11 p1365 A73-26237

Iris photometer electronic control system, presenting NGC 1778 cluster stars photoelectric UVB magnitudes

12 p1498 A73-27723

Conventional filter photometer onboard Explorer satellite for 3000-7500 A airglow and auroral thermospheric emission features monitoring

13 p1688 A73-28639

Some problems in the optimization of holographic memories.

13 p1622 A73-29435

Statistics of photoelectric sensor readings during propagation of light in a turbulent medium

14 p1753 A73-30270

Maximum likelihood M-ary detection theory application to incoherent optical system model based on photodetectors governed by Laguerre counting statistics, deriving error probability

15 p1875 A73-31734

Photometric device for an ISP-28 spectrograph in optical atmospheric studies

15 p1875 A73-31822

Low cost two-beam multimode nebular/stellar photometer design, construction and use on extended and discrete objects emitting 3700-9000 A radiation

15 p1877 A73-32007

Device for spectral line interspace measurements

15 p1878 A73-32145

Two descriptions for the photocounting detection of radiation passed through a random medium - A comparison for the turbulent atmosphere.
15 p1914 A73-32291

Pioneer 10 spacecraft spin-scan imaging photopolarimetric optical system for Jupiter mapping
15 p1880 A73-32385

The Schottky-barrier silicon photodetector in perspective with other detection devices in the 200 nm to 1100 nm range.
16 p2013 A73-32885

Hybrid optoelectronics - High frequency modulation and detection of light by semiconductor sources and sensors.
16 p1978 A73-32886

Astronomical educational aids design and application, including photometers for star cluster detection, ocular comparators and projection devices for photograph examination
16 p2014 A73-32950

Main trends of development of avalanche photodiodes as high-speed photodetectors [Review/
18 p2293 A73-36715

On the Zeeman photometer observing upper atmospheric winds in the daytime.
19 p2429 A73-37377

Photodetection volume of coherence for thermal optical source with given intensity and spectral density, defining photon phase space cell concept
20 p2570 A73-38610

Derivative light scattering photometer, using angular modulation with photomultiplier entrance slit vibration to obtain gain improvement over conventional technique
21 p2697 A73-40130

Design and test of a photometer with nine wavelength bands for the measurement of astronomical objects
22 p2852 A73-41784

PHOTOMETRY
NT ASTRONOMICAL PHOTOMETRY
NT ELECTROPHOTOMETRY
NT SPECTROPHOTOMETRY
NT STELLAR SPECTROPHOTOMETRY
NT ULTRAVIOLET PHOTOMETRY
NT VISUAL PHOTOMETRY
A computer-controlled digital spectrum scanner for La Silla.
01 p0047 A73-10515

Photometric measurements with the aid of image converter tubes
06 p0696 A73-18859

A photometric investigation of the packing state of Apollo 11 lunar regolith samples.
07 p0878 A73-19669

Optical emission of a ball-lightning
09 p1113 A73-21913

Photometric and polarimetric analysis of the coronal streamers observed at the March 7, 1970 Mexican eclipse.
11 p1425 A73-26263

Optical emission from ball lightning.
15 p1915 A73-32639

Artificial earth satellite brightness attenuation and rotation periods from spectral analyses of photometric curves by mathematical simulation
18 p2315 A73-36142

Interpretation of the results of photometric observations of noctilucent clouds
21 p2732 A73-40859

Semiautomatic recorder for photometry of black spots produced by electron-photon cascades on RT-6 type X-ray films
23 p2982 A73-43568

Photometric strip blurring and brightness contrast measurements of visual perception in turbulent atmosphere as function of distance, turbulence and exposure
23 p3001 A73-43573

PHOTOMICROGRAPHY
Advances in high-speed photography 1957-1972.
11 p1359 A73-24995

An automatic flash photomicrographic system for fatigue crack initiation studies.
18 p2316 A73-36588

Phase contrast transfer damping functions for various beam apertures in high resolution electron microscopy
21 p2702 A73-40949

PHOTOMULTIPLIER TUBES
Design of an extremely sensitive flame-photometer for analyses in the picogram range using a lock-in amplifier
01 p0051 A73-10925

Photomultiplier tubes nonlinear response in radiation measurements, suggesting fatigue avoidance through pulsed operation
01 p0053 A73-11222

Oxygen plasma for cleaning polymerized organic material contaminated oil-pumped channel electron multiplier arrays used as vacuum UV to visible radiation converters
01 p0054 A73-11237

Channel electron multiplier prepared from shaped glass tubing with inner conductive coating, discussing electron and photon detection characteristics
02 p0146 A73-11954

Cleaning and activation of beryllium-copper electron multiplier dynodes.
02 p0146 A73-11966

Photomultiplier operation pulse control in semiconductor circuit for background cosmic radiation noise error minimization in air shower station
02 p0171 A73-12688

Sensitivity of optical autodyne quantum receiver in presence of output noise, using photomultiplier signal model
03 p0319 A73-14076

Book - Advances in electronics and electron physics. Volume 31.
05 p0558 A73-16601

Single photon detection and timing - Experiments and techniques.
05 p0576 A73-16603

Quartz light pipe for scanning electron microscope, noting photomultiplier voltage reduction and indefinite service life
05 p0580 A73-17259

Measurements of the photomultiplication factor of silicon avalanche photodiodes.
06 p0674 A73-17796

The HR 300 ultrafast photomultiplier with a microchannel plate
06 p0678 A73-18852

Microchannel electron multipliers application to X ray cinematography of laser generated plasma
06 p0697 A73-18861

The microchannel Picoscope - A tube with high-temporal-resolution scanning for studying luminous phenomena in the subnanosecond range
06 p0679 A73-18862

Photomultipliers for UV radiation detection, discussing high sensitivity and speed features, components, photon detection, tube types and applications
07 p0821 A73-18981

Molnaya 1 satellite slow neutron monitor with photomultiplier scanned scintillator, noting limiting effect of geomagnetic perturbations
07 p0823 A73-19428

A dynamic polariscope for stress wave analysis.
08 p0962 A73-20668

Photomultiplier pairs arrays operation as solar magnetograph detector using fiber optics, comparing to photographic methods
08 p0970 A73-21737

The calibration of electrostatic analyzers and channel electron multipliers using laboratory simulated omnidirectional electron beams.
09 p1080 A73-22104

Use of open-structure channel electron multipliers in sounding rocket experiments.
09 p1080 A73-22105

Improvement of photomultiplier performance in astronomical applications.
10 p1215 A73-23483

A high performance 4500 volt electron multiplier bias supply for satellite use.
11 p1363 A73-25959

Radiation effects on multiplier phototubes.
11 p1363 A73-25960

Comparison of methods of photomultiplier photocurrent recording in measurements of weak luminous fluxes
12 p1495 A73-26866

Experimental studies of a method of detecting microwave-modulated laser radiation in a photosensitive detector
13 p1628 A73-29415

The effect of unmodulated sunlight on the integral voltage sensitivity of some radiation detectors.
14 p1754 A73-30954

Influence of illumination on the temporal resolution of photomultipliers
16 p1988 A73-33273

Laser spectrometer for combination scattering, recording polarized spectra with thermoelectrically cooled photomultiplier by photon count
17 p2164 A73-34164

Spectrophotometric setup with a detector for individual photon count
17 p2164 A73-34165

The equipment for photoelectric photometry in the Graz observatory
20 p2565 A73-39068

Characteristics and limitation of microchannel plates used in shutters for ultrahigh-speed photography
21 p2694 A73-39943

The microchannel picoscope - A high temporal resolution scanning tube for study of luminous phenomena in the subnanosecond range
21 p2694 A73-39949

Technique of an ultrahigh-speed sampling camera based on the use of a unique photomultiplier
21 p2697 A73-39995

Derivative light scattering photometer, using angular modulation with photomultiplier entrance slit

vibration to obtain gain improvement over conventional technique
21 p2697 A73-40130

The effect of toroidal magnets on the sensitivity of photomultipliers.
21 p2699 A73-40410

A study of the physics and non-linear effects in photomultipliers.
22 p2860 A73-42302

PHOTON ABSORPTION
U ELECTROMAGNETIC ABSORPTION
PHOTON BEAMS
NT LIGHT BEAMS
Chaotic photon bunching effect interpretation by theoretical incoherent source model with atomic excitation and emission at stochastically independent times without interaction
07 p0837 A73-20610

Information in the time of arrival of a photon packet - Capacity of PPM channels.
10 p1188 A73-23836

Laser photons multiple absorption by atoms, determining transition probabilities from Schroedinger equation solution via space translation operation
14 p1776 A73-29698

Path-length distributions of photons diffusely reflected from a semi-infinite atmosphere.
18 p2314 A73-37110

Optical coupling system for photon-photon coincidence experiments.
19 p2462 A73-37255

Aircraft measurements of effective photon paths in cloud-reflected and transmitted light in the 0.76-micron oxygen band
20 p2583 A73-39184

PHOTON DENSITY
Effect of a magnetic field on emission fluctuations in a ring gas laser
01 p0060 A73-11089

Polarimeter-photometer to study solar corona or disk over wide photon arrival rate range, measuring magnitude of polarization effects
08 p0971 A73-21746

Two dimensional photon counting - A design based on the Aerospace-NASA videomagnetograph.
08 p0972 A73-21756

Quantum mechanical operator for photon flux density passing through spatial point over infinite time, interpreting photon wave functions
09 p1094 A73-22598

Kinetics of high-pressure chemical lasers
14 p1758 A73-30577

Redistribution of resonance radiation. II - The effect of magnetic fields.
15 p1913 A73-31559

Spectrophotometric setup with a detector for individual photon count
17 p2164 A73-34165

Capabilities and limitations of infrared imaging systems.
17 p2167 A73-34902

An investigation of the statistical properties of the radiation of a laser, operating in several axial modes, by the photon counting method.
17 p2184 A73-35156

Photon counting with a self-scanned diode array.
17 p2169 A73-35283

The effect of system blocking in an intensifier disector scanner.
17 p2169 A73-35284

Statistical effects in the transient response of a He-Ne laser with a given initial photon distribution
21 p2714 A73-40568

Dynamics of a laser with regulated cavity Q
21 p2716 A73-41510

Calculation of the fluctuations of the Cerenkov radiation of an electron-photon shower in the atmosphere
23 p3022 A73-43554

PHOTON-ELECTRON INTERACTION
Interaction between intense optical radiation and free electrons [Nonrelativistic case/
01 p0061 A73-11248

Transfer equations for high-energy electrons and photons in magnetic fields.
01 p0080 A73-11309

Multiphoton transitions. III - Rates of multiphotodetachment of negative ions.
07 p0852 A73-19147

Differential light scattering cross section derivation for photon interaction with relativistic electrons, comparing with quantum electrodynamics calculation and Thomson scattering experiment
07 p0851 A73-19516

The possibility of storing laser radiation scattered by an electron beam.
13 p1627 A73-28662

Propagation of ultrashort light pulses in a semiconductor under two-photon resonance conditions.
13 p1630 A73-29445

Interaction of intense optical radiation with free electrons /nonrelativistic case/.
22 p2892 A73-42346

Photon retinue and infra-red divergence problem in quantum electrodynamics. 22 p2889 A73-42426

PHOTONIC PROPULSION

Propulsion by impinging laser beams. 05 p0585 A73-17211
Space propulsion future assessment, discussing space shuttle and tug, NERVA project and electric and photon propulsion 10 p1262 A73-23611

PHOTONS

NT LIGHT BEAMS
Image photon counting technique nature, performance, merits, implementation and applications, noting photoelectronic components and image information treatment at quantum level 01 p0048 A73-10529

Two quantum induced photon-plasma transition probability for hydrogen atom in processes of nebulas and stellar chromospheres 01 p0080 A73-11308

Transfer of resonance radiation and photon random walks. 02 p0207 A73-12403

Morphic effects. IV - Effects of an applied magnetic field on first-order photon-optical phonon interactions in non-magnetic crystals. 02 p0201 A73-12637

Propagation of Pcl micropulsations in a proton-helium magnetosphere. 03 p0298 A73-12883

Ion beam lifetimes measurement by temporal correlation of photons emitted in cascades 03 p0341 A73-12912

Properties of photons determined by interferometric spectroscopy. 04 p0475 A73-15046

Oxygen $1S$ production efficiency of photons at 812-1216 Å measured by O I 5577 Å green line detection during carbon dioxide photodissociation 05 p0546 A73-16049

Analysis of oxygen in aluminum by activation by means of charged particles and gamma photons 05 p0547 A73-17217

Quasi-hydrodynamic equations for transverse quanta in inhomogeneous plasma, using geometric optics approximation 06 p0728 A73-17969

Photon counting statistics of the superposition of coherent and chaotic light of arbitrary spectrum passed through the turbulent atmosphere or a Gaussian medium. 08 p0987 A73-20952

Multiphoton excitations in vibrational-rotational states of diatomic molecules in an intense electromagnetic field. 08 p0990 A73-21003

Photoelectron detection ability increase of image dissector by buffer intensifier tube, noting application for photon counting spectroscopy 08 p0971 A73-21745

Limulus photoreceptor response to single photon stimulation, discussing flash intensity, dim lights, discrete waves and subliminal responses 09 p1042 A73-23308

Results of volley flights of radio probes on the Kola peninsula during periods of magnetic disturbances in March and April 1971 10 p1267 A73-23929

Two-photon excitation of luminescence in $\text{CaF}_2:\text{Er}^{3+}$ crystals by a frequency-scanning laser employing organic dye solutions 10 p1227 A73-24075

Photon rest mass limit determination from Galactic magnetic field measurements, utilizing maximum current density capability of plasmas 11 p1415 A73-25121

A photon rest mass and the propagation of longitudinal electric waves in interstellar and intergalactic space. 11 p1417 A73-25562

Antenna effective area lower limit based on photon limited localizability and Heisenberg uncertainty principle, deriving directivity dependence on area 11 p1338 A73-25672

A high resolution position sensitive detector for ultraviolet and X-ray photons. 11 p1363 A73-25958

Changes in the mean energy of an electron in the field of a plane wave with allowance for radiation damping 12 p1526 A73-26969

Certain quantum-gravitational effects in central classical fields 12 p1538 A73-26970

Emission of 'soft' photons in the field of a strong electromagnetic wave 12 p1468 A73-26972

Russian book on quantum radio physics, Volume I covering photons and nonlinear media, matter-radiation interaction, electromagnetic fields, relaxation, emission, solid state physics, etc 12 p1508 A73-27924

Quantum theory of a high energy gas laser 14 p1757 A73-30363

Ultrahigh energy photons, electrons, and neutrinos, the microwave background, and the universal cosmic-ray hypothesis. 15 p1927 A73-32004

Probabilistic radiative transfer - Mean number of scatterings. 16 p2038 A73-33739

Application of the momentum translation method to multiphoton ionization of hydrogen by intense electromagnetic fields. 16 p2039 A73-33864

Bose-Einstein condensation of dipole-active excitons and photons 16 p2039 A73-34064

Absorption of ultrahigh energy photons in the universe 17 p2223 A73-34368

Experimental verification of the effective photon theory of laser induced gas ionization. 17 p2186 A73-35832

Photodetection volume of coherence for thermal optical source with given intensity and spectral density, defining photon phase space cell concept 20 p2570 A73-38610

Two-photon time distributions in mixed light beams. 20 p2570 A73-38615

Radiative corrections and soft-photon emission in magnetic bremsstrahlung. 20 p2602 A73-39445

Photon lateral distribution sensitivity to longitudinal development of electron cascade via computer simulations of optical Cerenkov emission from cosmic ray showers 20 p2603 A73-39704

Rotational line structure in three-photon scattering by symmetric top molecules. 20 p2574 A73-39723

The laws of conservation of energy and momentum during emission of electromagnetic waves /photons/ in a medium and the energy-momentum tensor in macroscopic electrodynamics 21 p2739 A73-40447

Polarization phenomena in multiphoton ionization of atoms. 21 p2743 A73-40468

Study of induced four-photon parametric scattering of laser light in alkali metal vapor 23 p2988 A73-44009

Complete photon conversion in backward-travelling-wave parametric amplification and oscillation. 23 p2955 A73-44108

PHOTONUCLEAR REACTIONS

Methods for determining the charges of heavy primary nuclei Z greater than 26 in photonuclear emulsions of different sensitivities 10 p1267 A73-23922

Abundance and lateral distribution of muons in inclined showers. 13 p1670 A73-28371

Charged stopping pions from nuclear-electromagnetic cascades in rock, calculating number and energy spectra by Monte Carlo method 13 p1671 A73-29667

PHOTOOXIDATION

Kinetics of a pulsed chemical CO laser with photostimulation based on the carbon disulfide oxidation reaction 06 p0700 A73-18103

The photochemical oxidation of iodide to iodine in the presence of oxygen. 07 p0788 A73-20398

Nd laser radiation thermochemical effects on oxide formation on thin Cr films, Fe-Ni-Co and Cr-SiO alloys and MgO-MnO ferrites, noting resistance and etching rates 11 p1376 A73-25636

Determination of the temperature of a sample undergoing pulsed irradiation by sunlight 15 p1896 A73-30997

Oxidation of organic molecules by photoproducts of holes of ZnO. 15 p1841 A73-31969

Nd laser radiation thermochemical effects on oxide formation on thin Cr films, noting resistance and etching rates 19 p2438 A73-38148

PHOTOPEAK

Characteristics of infrared photodetectors produced by radiation doping. 09 p1079 A73-21934

PHOTOPHILIC PLANTS

Quantitative estimation of the gas metabolism of continuous higher plant cultures as a life support system component 06 p0656 A73-17680

PHOTOPIEZOELECTRICITY**U PHOTOELECTRICITY****U PIEZOELECTRICITY****PHOTOPLASTICITY**

On the similarity conditions in the phototheological method of stress analysis. 05 p0632 A73-16430

Use of chromoplastic models for the study of the behaviour of rectangular plates after buckling. 08 p1017 A73-20946

Polycarbonate as a model material for three-dimensional photoplasticity. 17 p2247 A73-35029

[ASME PAPER 73-APM-4] Experimental determination of the transient uniaxial stress in a bar by dynamic photoplasticity. 22 p2926 A73-42894

PHOTOPRODUCTION

Gravitational Compton effect and graviton photoproduction by electrons 21 p2742 A73-40351

PHOTORECEPTORS

ERG late photoreceptor potential components time course in macaque monkey cones and rods, noting pure cone foveal response 03 p0261 A73-13761

Visual field image analysis via investigation of receptor-field signal analysis by network of neuron-like structures 04 p0413 A73-15789

Rod vision chemistry in terms of rhodopsin, visual cycle and pigment-vision relations, considering dark and light adaptation 05 p0540 A73-16479

Photochemical receptor mechanism of chromatic vision and scotopic contrast hue sensation due to cone and rod activity interaction 07 p0783 A73-20261

Modified rhodopsin in the pigment epithelium. 07 p0783 A73-20263

Book - Physiology of photoreceptor organs. 09 p1042 A73-23301

The structural organization of the compound eye in insects. 09 p1042 A73-23302

Vertebrate photoreceptor cell /rods and cones/ development and structure, discussing light pathway, ciliary connective and microtubules, outer and inner segments, etc. 09 p1042 A73-23303

The structure and reactions of visual pigments. 09 p1042 A73-23306

Light evoked responses in invertebrate photoreceptor cells, considering cell organization, microvilli, lateral eye of Limulus, generator potentials, visual responses, etc 09 p1042 A73-23307

Limulus photoreceptor response to single photon stimulation, discussing flash intensity, dim lights, discrete waves and subliminal responses 09 p1042 A73-23308

Inhibitory interaction in the retina of Limulus. 09 p1043 A73-23311

Light-induced potential and resistance changes in vertebrate photoreceptors. 09 p1043 A73-23313

Retinal S-potential receptive field relationship to light energy and wavelength, considering cone and rod potentials, ganglion cells and vision 09 p1043 A73-23314

Receptive fields of retinal ganglion cells. 09 p1043 A73-23315

Retinal mechanisms of colour vision. 09 p1043 A73-23316

Duplex vision theory of photoreceptor /rods and cones/ light and dark adaptation, discussing rhodopsin regeneration, bleaching and desensitization mechanisms 09 p1043 A73-23317

The electroretinogram, as analyzed by microelectrode studies. 09 p1047 A73-23318

Frog retinal metabolism in photoreceptors during dark and light adaptation, using ERG, radiopirrometry, oxygen uptake polarography and pyridine spectrophotometric assay 09 p1044 A73-23319

Investigation of the infrastructural organization of interdisk spaces and photoreceptor membranes of the retina in vertebrates during aldehyde fixations, delipidation, and pronase treatment 10 p1181 A73-24458

The ultrastructural organization of the photoreceptor membranes and the intradisk spaces of the vertebrate retina as revealed by various experimental treatments. 11 p1321 A73-26717

Probability summation model for heterochromatic luminance additivity failure at absolute visual threshold. 13 p1578 A73-28099

Changes caused by illumination in the Na^+ , K^+ adenosine-triphosphatase and n -nitrophenylphosphatase activities of the external segments of the retina 13 p1574 A73-28294

Light adaptation of the late receptor potential in the cat retina. 13 p1574 A73-28352

New method of stimulation for the study of photoreceptors. 13 p1578 A73-28362

The Stiles-Crawford effect - Explanation and consequences. 14 p1717 A73-30396

Retinal receptive fields - Correlations between psychophysics and electrophysiology.
14 p1717 A73-30397

Human cone optical density estimation implications of conflicting results for luminosity at bleaching intensities in dichromats related to use of psychophysical data
14 p1717 A73-30402

Monkey rod receptor potential suppression at photopic stimulus intensities by neurophysiological inhibitory mechanism for clearing cone initiated visual pathway
19 p2393 A73-37412

Slowed decay of the monkey's cone receptor potential by intense stimuli, and protection from this effect by light adaptation.
19 p2394 A73-37413

Contrast sensitivity, Westheimer function and Stiles-Crawford effect in a blue cone monochromat.
19 p2394 A73-37414

Spatial integration in the crustacean visual system - Peripheral and central sources of non-linear summation.
22 p2810 A73-42956

Recovery of cone receptor activity in the frog's isolated retina.
22 p2810 A73-42962

Frog red rod dark adaptation from recorded receptor potentials of isolated retina, examining permanent sensitivity loss due to pigment bleaching
22 p2810 A73-42963

Bee image detection by ommatidium based on physical model using electromagnetic analysis of light absorption in photoreceptor
23 p2946 A73-43344

PHOTORECONNAISSANCE
Binary coded aircraft flight data block inclusion in aerial reconnaissance photographs for automated data processing
10 p1222 A73-24948

The application of color and multispectral techniques to the collection of military geographic information.
12 p1500 A73-27952

Natural resources research and development in Lesotho using ERTS imagery.
18 p2308 A73-36045

Aerial-survey aircraft of the new generation
22 p2799 A73-42590

PHOTOREDUCTION
U PHOTOCHEMICAL REACTIONS
U REDUCTION [CHEMISTRY]

PHOTOSENSITIVITY
U PHOTOCONDUCTIVITY
U PHOTOSENSITORS
U PHOTOCONDUCTORS

PHOTOSENSITIVITY
NT LIGHT ADAPTATION
Regulation of testis function in golden hamsters - A circadian clock measures photoperiodic time.
02 p0134 A73-12422

Russian book on color recognition methods and devices covering algorithms for radiation color identification and optimal spectra of photosensitive radiation detector
02 p0144 A73-12862

The control of sensitivity in the retina.
06 p0655 A73-18673

Photomultipliers for UV radiation detection, discussing high sensitivity and speed features, components, photon detection, tube types and applications
07 p0821 A73-18981

Satellite-borne TV vidicon design requirements and operational specifications, considering storage, relaxation, resolution, sensitivity, electrostatic focusing and deflection, image magnification and enhancement
07 p0821 A73-18982

Reversible high speed high resolution imaging in amorphous semiconductors.
07 p0862 A73-19609

Photosensitized inhibitor formation in isolated, aging chloroplasts.
07 p0784 A73-20453

Improved responsivity and sensitivity characteristics of the thin-film bismuth bolometer.
09 p1080 A73-22087

Influence of changes in the contact region on the basic characteristics of a semiconductor in the illuminated mode
09 p1134 A73-22685

Simple method of obtaining high-sensitivity interferograms
09 p1085 A73-22882

Methods for determining the charges of heavy primary nuclei /Z greater than 26/ in photonuclear emulsions of different sensitivities
10 p1267 A73-23922

Effect of passive 70-deg head-up tilt on peripheral visual response time.
10 p1185 A73-24566

Solar 1.9 A X ray spectral line effects on SOLRAD satellite-borne photometer sensitivity and lower ionospheric ion production rate
11 p1354 A73-25771

Limitations of the use of vacuum photodiodes in instruments for the measurement of laser power and energy.
11 p1377 A73-26233

Spectral sensitivities of colour mechanisms isolated by the human visual evoked response.
12 p1461 A73-26919

Photostimulation significance in electroencephalographic examinations of pilots and aviation school applicants
12 p1465 A73-27717

Multistage image converter tubes for studying high-speed phenomena.
13 p1611 A73-28175

Cone spectral sensitivity studied with an ERG method.
13 p1575 A73-28358

Sensitometric tests on plane-parallel organic photochromic bulk material film samples of styrene, methylmethacrylate and inoline spiropyrans, evaluating photosensitivity suitability for holography
13 p1622 A73-29436

The signal-to-noise ratio of a photodetector with a virtual cathode.
17 p2168 A73-35172

Parameters of fast recombination centers in CdS single crystals and the effect of the parameters on photosensitivity
18 p2340 A73-36669

Contrast sensitivity, Westheimer function and Stiles-Crawford effect in a blue cone monochromat.
19 p2394 A73-37414

The sensitivity of optoelectronic scanning systems with out-of-phase connection of the radiation detector elements.
20 p2564 A73-38850

Investigation of the photosensitivity of polyvinylcinnamate
21 p2646 A73-40255

Investigation of the spectral properties of sensitized polyvinylcinnamate
21 p2646 A73-40256

Certain features of sensitive layers containing bifunctional polymers /fixatives/ on a blank film
21 p2646 A73-40257

Influence of certain wetting agents on the optical sensitization and retention of the photographic properties of a finished layer
21 p2647 A73-40271

Spatial integration in the crustacean visual system - Peripheral and central sources of non-linear summation.
22 p2810 A73-42956

Recovery of cone receptor activity in the frog's isolated retina.
22 p2810 A73-42962

Frog red rod dark adaptation from recorded receptor potentials of isolated retina, examining permanent sensitivity loss due to pigment bleaching
22 p2810 A73-42963

Increment thresholds for multiple identical flashes in the peripheral retina.
23 p2946 A73-43343

Inhibition by selenium of the free-radical states of the retina of the eye
24 p3059 A73-44724

Chromatic photosensitization of a variable-index material for the recording of high-efficiency phase holograms
24 p3091 A73-45011

PHOTOSENSORS
U PHOTOELECTRICITY
U RADIATION MEASURING INSTRUMENTS

PHOTOSPHERE
Relative polarization of type III solar radio bursts at 23.5 and 30 MHz.
01 p0093 A73-11315

Photospheric height gradient and solar rotation measurements for Fraunhofer lines by magnetograph, considering telluric lines effect
01 p0107 A73-11376

The empirical determination of line source functions, beta-L-values, and the microturbulent and convective velocity components as functions of depth in the photosphere-chromosphere transition region.
01 p0107 A73-11378

Solar outer layer models of convective zone, photosphere, chromosphere, corona and solar wind, using electron density dependence
01 p0107 A73-11379

Tunnel-effect and propagation of 5-min oscillations in the solar atmosphere.
01 p0107 A73-11381

Photospheric network properties and transition to sunspot of solar bright points in 3840 A and H alpha, comparing with Ellerman bomb
01 p0108 A73-11384

Solar white light flares induced neutron and gamma ray emission, discussing acceleration mechanism through high energy proton bombardment induced photospheric heating
02 p0206 A73-12322

Moustaches in solar H alpha filtergrams and spectra, studying relations to photospheric and chromospheric phenomena
03 p0378 A73-14413

Solar activity and the variations of the geomagnetic K sub p-index. I.
03 p0378 A73-14422

Heliographic and spectroscopic observations of solar southern hemisphere active region during August 1971 cycle, noting photospheric changes, sunspots and flares
03 p0379 A73-14581

Behavior of carbon monoxide in the upper photosphere.
04 p0504 A73-16027

Large-scale photospheric magnetic field - The diffusion of active region fields.
05 p0620 A73-17028

Methods of studying solar granulation fields in the presence of atmospheric disturbances
07 p0876 A73-19396

Magnetic fields and the vibrational motions of the solar photosphere
07 p0901 A73-20319

Vertical velocity field oscillations in photospheric sunspot umbras interpretation in terms of gravity or acoustic waves traveling along magnetic field lines
08 p1001 A73-20756

Observations of the variation of temperature with latitude in the upper solar photosphere. II - Magnetic-field comparison, implications for solar-oblateness measurements, and harmonic analysis.
08 p1009 A73-21166

Oppositely directed magnetic fields reconnection rate role in solar flares and small scale turbulent field reduction in photosphere
09 p1142 A73-22037

Photospheric and circumstellar H-alpha line profiles in M-supergiant spectra
10 p1273 A73-23706

Quasi-periodic /wave/ motions in the solar photosphere. I - Preliminary results
10 p1274 A73-23718

Solar cosmic ray heavy nucleus abundances relation to oxygen nuclei in solar corona and photosphere
10 p1265 A73-23898

High resolution spectroscopic analysis for photospheric Eu II lines with spectrum synthesis techniques, determining solar isotopic composition and abundance
10 p1278 A73-24129

Line source functions with variable Doppler width and noncoherent scattering.
11 p1415 A73-25135

Photospheric convective network as a determining factor in sunspot and group development and stabilization.
11 p1426 A73-26574

Magnetic fields and oscillatory motion in the solar photosphere.
12 p1540 A73-27291

Solar surface photospheric oscillation spatiotemporal power spectrum observation, considering long-period oscillation correlation with chromospheric flare
12 p1544 A73-27828

Equator-pole temperature difference and the solar oblateness /Research note/.
12 p1544 A73-27831

Solar pole-equator temperature distribution in high photosphere layers from Mg spectral line observations
12 p1544 A73-27832

Determination of damping constants and turbulent speed in the solar photosphere by the Voigt method
15 p1938 A73-31958

Solar convective motions and associated magnetic fields, discussing photospheric cellular and chromospheric vertical motions, fibril structures, sunspot magnetic properties and faculae
16 p2061 A73-33283

Profiles of the photospheric and circumstellar H alpha line in the spectra of type M supergiants.
18 p2354 A73-36731

Quasiperiodic /wavelike/ motions in the solar photosphere. I - Preliminary results.
18 p2355 A73-36743

Kinematic theory of magnetic field reconnection rate for analysis of turbulent flows in solar photosphere, flare phenomena and galaxy
19 p2467 A73-37439

Photospheric faculae and the solar oblateness - A reply to 'Faculae and the solar oblateness' by R. H. Dicke.
19 p2488 A73-38520

Solar cosmic ray heavy nucleus abundances relation to oxygen nuclei in solar corona and photosphere
20 p2601 A73-38917

On the nature and origin of the solar five-minute oscillations.
20 p2606 A73-39071

Determination of the temperature behavior in a photospheric facula through the solution of an integral equation by the gradient-random search method
21 p2759 A73-40721

Microturbulence and the effect of departures from LTE on photospheric iron lines.
21 p2777 A73-41481

- Statistical model for phase relations derived from observations of photospheric oscillations, criticizing horizontal propagation theory for phase propagation
21 p2777 A73-41482
- Carbon, CN, CH, MgH, NH and OH line behavior in solar photospheric spectra
21 p2778 A73-41528
- Structure of the solar chromosphere. I - Basic computations and summary of the results.
22 p2905 A73-41762
- Absolute oscillator strengths in neutral chromium and the solar chromium abundance.
22 p2905 A73-41764
- Ionised molecules in BCA photospheric model.
22 p2915 A73-43039
- Vertical phase variation and mechanical flux in the solar 5-minute oscillation.
22 p2916 A73-43124
- Damping constants and turbulence velocities in the solar photosphere determined by the Voigt method.
24 p3132 A73-44483
- Solar abundance of Th and Pb based on photospheric line spectrum analysis for comparison with chondritic composition data
24 p3135 A73-44627
- PHOTOSYNTHESIS**
Quantitative estimation of the gas metabolism of continuous higher plant cultures as a life support system component
06 p0656 A73-17680
- Circadian rhythms - Subcellular and biochemical aspects.
06 p0651 A73-17824
- Photosensitized inhibitor formation in isolated, aging chloroplasts.
07 p0784 A73-20453
- Variable photosynthetic units, energy transfer and light-induced evolution of hydrogen in algae and bacteria.
08 p0932 A73-21685
- Study of the effect of increased oxygen concentration on the metabolism of *Chlorella*
15 p1838 A73-31508
- Photoinduced fixation of CO₂ by amino acids - Implications for nonbiological reactions on the Martian soil.
16 p1977 A73-33874
- Theoretical study of primary photosynthesis processes in higher plants and algae
23 p2946 A73-43707
- PHOTOTHERMOTROPISM**
U ANISOTROPY
U TEMPERATURE EFFECTS
- PHOTOTRANSISTORS**
Response characteristics of photodiodes, phototransistors and photoresistors in near IR range, showing output signal levels as function of wavelength and illumination intensity
06 p0692 A73-17837
- Light sensitive MNOS /metal-nitride-oxide-silicon/ memory transistor space charge layers current-field relationships and steady state I-V measurements
17 p2134 A73-34221
- PHOTOTUBES**
NT PHOTOMULTIPLIER TUBES
- PHOTOVISCOELASTICITY**
Study of the photoviscoelasticity method
20 p2619 A73-39331
- PHOTOVOLTAGES**
Some characteristics of isopotential curves of photoelectret state formation in compressed polycrystalline anthracene
05 p0605 A73-17176
- Uniaxial pressure effects on diode structures volt-ampere characteristics, examining potential barrier height and photo emf changes
23 p2960 A73-43787
- PHOTOVOLTAIC CELLS**
Heterojunction photocell, sensitive in the near infrared.
01 p0051 A73-10834
- Photovoltaic Specialists Conference, 9th, Silver Spring, Md., May 2-4, 1972, Record.
03 p0254 A73-14203
- Laser energy conversion into electrical energy with photovoltaic cells, noting Si and GaAs cells power efficiencies improvement compared to operation in sunlight
03 p0254 A73-14210
- Photovoltaic and I-V characteristics of integral diode solar cells as function of temperature and radiation exposure
03 p0256 A73-14231
- Calculation of series and shunt resistances on the basis of the current-voltage characteristics of a solar cell
09 p1033 A73-22720
- A model of a thermophotovoltaic radionuclide battery.
09 p1037 A73-23279
- Near-equatorial synchronous orbit Satellite Solar Power Station system with photovoltaic cell arrays energy conversion into microwave power for transmission to earth
10 p1285 A73-23601

- Application of heat pipes to unmanned space power systems.
11 p1452 A73-25994
- Principles of photovoltaic solar energy conversion.
13 p1573 A73-29591
- A computer study of the design and operating performance of a photovoltaic cell for thermophotovoltaic energy conversion applications.
19 p2391 A73-38405
- PHOTOVOLTAIC CONVERSION**
Large solar array photovoltaic power systems for manned orbital space stations, discussing technology evaluation and design feasibility studies
09 p1153 A73-22780
- Radiophotovoltaic devices power and energy conversion efficiency limits, investigating phosphors deterioration and nuclide layer optimal thickness
09 p1037 A73-23280
- PHOTOVOLTAIC EFFECT**
Solar cell graded band gap materials, determining I-V characteristics, junction capacitance and photovoltaic spectral response
03 p0254 A73-14207
- Optical degradation and thermal restoration - New inputs to the mechanism of the photovoltaic effects in Cu₂S-CdS heterojunctions.
03 p0350 A73-14218
- Investigations of the inhomogeneity of polycrystalline Cu_x/S-CdS solar cells.
03 p0255 A73-14222
- Voltage and power relationships in lithium-containing solar cells.
03 p0257 A73-14241
- Low-resistance CdTe films exhibiting a constant emf under the action of an ac field
06 p0737 A73-18222
- Forward biased P-N junction photoelectric current shown resulting from photovoltaic, photoresistive and electric injection currents superposition
06 p0738 A73-18544
- Surface photovoltage spectroscopy - A new approach to the study of high-gap semiconductor surfaces.
08 p0968 A73-21620
- Radioisotopic energy conversion by radiovoltaic effect, describing titanium-tritium sources and semiconductor converter
09 p1037 A73-23278
- Photovoltaic and photoconductivity measurements on p- and n-type GaSe, determining light polarization direction effect, photovoltage relaxation times and minority carriers diffusion lengths
10 p1259 A73-23569
- Book on semiconductor opto-electronics covering solids optical constants, classical and quantum mechanical dispersion theory, absorption processes, magneto-optical and photo-electrical effects, etc
12 p1531 A73-27449
- PHUGOID OSCILLATIONS**
U OSCILLATIONS
U OSCILLATORS
U PITCH [INCLINATION]
- PHYSICAL CHEMISTRY**
General analysis and synthesis of alloys and materials with inhomogeneous physical properties, noting thermal physicochemical methods for laminates and metal powders
01 p0066 A73-11340
- Physicochemical distinction between separating similar and different materials in terms of cohesive or adhesive fracture energy in continuum mechanics
03 p0312 A73-13334
- Friction in ultrahigh vacuum, discussing physicochemical problems, self lubricating material advantages and drawbacks, and solid lubricant choice for space applications
07 p0828 A73-18906
- Physicochemical principles of the photographic process on vesicular films and the high-molecular-weight compounds used for these films
21 p2646 A73-40254
- Physicochemistry of the deposition of gelatinous photographic emulsion layers on a substrate
21 p2647 A73-40268
- Russian book - Burning of metal powders in active media.
21 p2753 A73-40418
- Hemoglobin molecule oxygenation mechanism in various animals, discussing erythrocytes as hemoglobin carriers, ecological factors and physicochemical conditions
23 p2947 A73-43929
- PHYSICAL ENDURANCE**
U PHYSICAL FITNESS
- PHYSICAL EXAMINATIONS**
Photostimulation significance in electroencephalographic examinations of pilots and aviation school applicants
12 p1465 A73-27717
- Detection of atherosclerosis in examinations of flight personnel
18 p2284 A73-36913
- Surveillance of the vertebral column in pilots who have undergone an ejection
18 p2284 A73-36914

- Binocular vision variation with age in flight crews
18 p2285 A73-36928
- Information yield of the Annual Medical Examination for Flying.
20 p2517 A73-39110
- Evaluation of the physical conditions of individual airmen
23 p2949 A73-43790
- PHYSICAL EXERCISE**
Effects of exercise on activity of heart and muscle mitochondria.
01 p0006 A73-10135
- Diet, exercise, and glycogen changes in human muscle fibers.
01 p0007 A73-10160
- Cardiorespiratory responses to exercise in air and underwater.
01 p0007 A73-10161
- Oxygen uptake, heart rate and pulmonary ventilation during swimming for different speeds and styles, comparing to running and cycling data
01 p0008 A73-10171
- Effect of eccentric and concentric muscle conditioning on tension and electrical activity of human muscle.
01 p0013 A73-10774
- The effect of O₂ breathing on maximal aerobic power.
01 p0010 A73-11504
- Atrioventricular block response to exercise and intraventricular conduction at rest.
01 p0010 A73-11506
- Hydrogen ion concentration in the blood of man under high mountain conditions with physical loads
02 p0133 A73-11924
- Maximal treadmill exercise electrocardiography - Correlations with coronary arteriography and cardiac hemodynamics.
02 p0136 A73-12821
- Passive and active warm-up effects on track athletes heart and respiration rates
03 p0266 A73-13123
- Normal pulmonary pressure-flow relationship during exercise in the sitting position.
03 p0266 A73-13124
- Intensity of exercise and heart tissue catecholamine content.
03 p0259 A73-13498
- Control of exercise hyperpnea under varying durations of exposure to moderate hypoxia.
03 p0259 A73-13499
- Exercise testing for evaluation of cardiac performance.
03 p0259 A73-13538
- Evaluation of cardiac performance in exercise.
03 p0259 A73-13539
- Exercise electrocardiography and vasoregulatory abnormalities.
03 p0260 A73-13541
- Exercise testing for detecting changes in cardiac rhythm and conduction.
03 p0260 A73-13542
- Correlation of computer-quantitated treadmill exercise electrocardiogram with arteriographic location of coronary artery disease.
03 p0260 A73-13543
- Cardiac dysrhythmias associated with exercise stress testing.
03 p0260 A73-13544
- The National Aeronautics and Space Administration-U.S. Public Health Service Health Evaluation and Enhancement Program - Summary of results.
03 p0260 A73-13545
- Multiple hormonal responses to graded exercise in relation to physical training.
03 p0263 A73-14116
- Multiple hormonal responses to prolonged exercise in relation to physical training.
03 p0263 A73-14117
- Interdependence of oxygen uptake, heart rate and ventilation during treadmill exercise from regression slope analysis of lag logarithms
03 p0263 A73-14118
- Production of gaseous nitrogen during human steady state exercise.
03 p0269 A73-14163
- Respiratory air flow telemetry during exercise, discussing flowmeter working conditions and equipment testing
03 p0270 A73-14286
- Voltage controlled subcarrier oscillator design and performance for FM/FM multiplex telemetry system for ECG recording during exercise
03 p0271 A73-14293
- Telemetrical measurements during sport performance on sportsmen with cardiac arrhythmias.
03 p0271 A73-14294
- Elevated ST segments with exercise in ventricular aneurysm.
04 p0410 A73-15643
- Myosin ATPase and fiber composition from trained and untrained rat skeletal muscle.
05 p0538 A73-16155
- Energy balance and lactic acid production in the exercising rabbit.
05 p0538 A73-16156

Effects of physical training on cardiac actomyosin adenosine triphosphatase activity. 05 p0539 A73-16157

Muscle metabolites with exhaustive static exercise of different duration. 05 p0539 A73-16247

Effect of hypoxia on free fatty acid metabolism during exercise. 05 p0540 A73-16609

Augmentation of chemosensitivity during mild exercise in normal man. 05 p0540 A73-16610

Influence of different motor regimes on the convulsive reactivity of the central nervous system. 05 p0542 A73-17178

Visual after-images in athletes and coaches as a prestart condition index 06 p0658 A73-18161

The effects of hypoxia, hypercapnia, and asphyxia on the baroreceptor-cardiac reflex at rest and during exercise in man. 06 p0654 A73-18348

Statistical correlations of maximum oxygen consumption, body weight and endurance /work/ performance in exercise-oxygen studies 06 p0659 A73-18472

Investigations concerning the coordination of heart rate and respiration rate /pulse-respiration quotient/ during exercise 07 p0782 A73-20034

A comparison between the effects of dynamic and isometric exercise as evaluated by the systolic time intervals in normal man. 07 p0784 A73-20369

Cardiovascular changes in middle-aged men during two years of training. 08 p0934 A73-21504

Central, femoral, and brachial circulation during exercise in hypoxia. 08 p0934 A73-21506

Changes in total plasma content of electrolytes and proteins with maximal exercise. 08 p0934 A73-21507

Effect of training on enzyme activity and fiber composition of human skeletal muscle. 08 p0935 A73-21508

On-line computer analysis and breath-by-breath graphical display of exercise function tests. 08 p0935 A73-21511

Inability of the submaximal treadmill stress test to predict the location of coronary disease. 08 p0932 A73-21802

Thirty-month follow-up of maximal treadmill stress test and double Master's test in normal subjects. 08 p0932 A73-21803

Isometric effects on treadmill exercise response in healthy young men. 10 p1179 A73-23842

Controlled tachycardia through voluntary change in exercise regime, investigating relation between heart rate and blood circulation 10 p1185 A73-24521

Human forearm-muscle blood supply regimes after 'static' exercise with increasing stress 10 p1181 A73-24522

Effect of physical exercises on the lung rheogram 10 p1182 A73-24524

Physiological response to exercise after space flight - Apollo 7 to Apollo 11. 11 p1314 A73-25326

Cardiac arrhythmias during exercise testing in healthy men. 11 p1315 A73-25336

Portable electro-phonocardiograph using magnetic tape recorder equipped with patient's voice print. 11 p1323 A73-25475

Adrenal influence on the supercompensation of cardiac glycogen following exercise. 11 p1318 A73-26121

Maximal oxygen intake and nomographic assessment of functional aerobic impairment in cardiovascular disease. 11 p1319 A73-26362

Comparison of isometric exercise and angiotensin infusion as stress test for evaluation of left ventricular function. 12 p1464 A73-27889

Exercise-induced ventricular arrhythmias in patients with coronary artery disease - Their relation to angiographic findings. 12 p1464 A73-27890

Diurnal rhythm of a corticosteroid reaction to ACTH and physical load 14 p1719 A73-30841

Effect of body temperature on ventilatory transients at start and end of exercise in man. 15 p1832 A73-31127

The role of carotid sinuses in the regulation of hemodynamics during motor activity 15 p1833 A73-31161

Special physical training of pilots as a prophylactic measure against obesity 15 p1837 A73-31172

Energy balance during moderate exercise at altitude. 15 p1833 A73-31343

Assessment of left heart function by noninvasive exercise test in normal subjects. 15 p1834 A73-31345

Plasma electrolytes, pH, and ECG during and after exhaustive exercise. 15 p1834 A73-31347

Space flight exercise regimen proposals, exploring moving picture/electric muscle stimuli program as earth gravity simulator in weightlessness 15 p1838 A73-31515

Optimal duration of endurance performance on the cycle ergometer in relation to maximal oxygen intake. 15 p1836 A73-32397

Polarcardiographic responses to maximal exercise and to changes in posture in healthy middle-aged men. 16 p1972 A73-33114

Cardiovascular responses to sudden strenuous exercise - Heart rate, blood pressure, and ECG. 17 p2112 A73-35461

Gravitational stress and exercise. 18 p2270 A73-35980

Postural effects on respiration, pulmonary ventilation, oxygen uptake and inhalation and exhalation volumes during asana /yoga gymnastics/ exercises executed by athletes 18 p2276 A73-36573

The effects of training on some parameters of hemodynamics and of the oxygen transportation function of the blood during static strains 18 p2277 A73-36581

Red cell volume with changes in plasma osmolality during maximal exercise. 18 p2277 A73-36654

Cardiorespiratory transients in exercising man. I - Tests of superposition. II - Linear models. 18 p2278 A73-36656

Adequacy of the Haldane transformation in the computation of exercise oxygen consumption in man. 18 p2278 A73-36658

Blood electrolytes and exercise in relation to temperature regulation in man. 18 p2280 A73-36983

Exercise during hyperoxia and hyperbaric oxygenation. 19 p2396 A73-38160

The effect of exercise on intrinsic myocardial performance. 19 p2396 A73-38258

Effects of posture on exercise performance - Measurement by systolic time intervals. 19 p2396 A73-38260

Circadian variations in presumably healthy men under conditions of peace-time army reserve unit training. 20 p2513 A73-39482

Anaerobic threshold and respiratory gas exchange during exercise. 20 p2519 A73-39785

Oxygen delivery and oxygen return to the lungs at onset of exercise in man. 20 p2519 A73-39788

Oxygen uptake during maximal work at lowered and raised ambient air pressures. 21 p2638 A73-41132

Effect of training with eccentric muscle contractions on skeletal muscle metabolites. 21 p2641 A73-41523

The significance of an increased RQ after sucrose ingestion during prolonged aerobic exercise. 21 p2641 A73-41621

Plasma insulin and carbohydrate metabolism after sucrose ingestion during rest and prolonged aerobic exercise. 21 p2641 A73-41622

The correlation of coronary angiography and the electrocardiographic response to maximal treadmill testing in 76 asymptomatic men. 22 p2806 A73-42342

Work-heat tolerance derived from interval training. 22 p2806 A73-42416

External airway resistance effects on ventilation and carbon dioxide response during human steady state exercise 22 p2806 A73-42417

Climbing and cycling with additional weights on the extremities. 22 p2806 A73-42418

Submaximal exercise with increased inspiratory resistance to breathing. 22 p2806 A73-42419

Ischemic heart disease prediction via exercise ECG tests, discussing work load standardization 22 p2809 A73-42835

Ischemic polarcardiographic changes induced by exercise - A new criterion. 24 p3060 A73-44946

Respiratory work minimization during exercise, using respiratory frequency, functional residual capacity and air flow pattern effects as controlled variables 24 p3060 A73-45066

Rebreathing equilibration of CO2 during exercise. 24 p3060 A73-45068

Ventilation at transition from rest to exercise. 24 p3061 A73-45375

PHYSICAL FITNESS

Practical exercise test for physical fitness and cardiac performance. 03 p0259 A73-13540

Aerobic capacity of relatively sedentary males. 19 p2396 A73-38360

PHYSICAL OPTICS

Bell Laboratories laser optics development and technology applications, discussing CW lasers, light deflectors, holography, optical memories, pattern generator, remote blackboard and micrographics 01 p0060 A73-11213

Laser related Bell Laboratories research on light scattering, solid state physics, nonlinear optics, materials science, quantum electronics and ultrashort light pulses 01 p0060 A73-11214

Kirchhoff and small perturbation methods identify in composite model calculation for rough surface electromagnetic scattering of circularly polarized wave by perfectly conducting body 11 p1329 A73-25678

Possibility of correlating the field of a wide wave beam in a smoothly nonhomogeneous medium with the field of a beam in vacuum 11 p1331 A73-26161

Optical and acoustical holography; Proceedings of the Advanced Study Institute, Milan, Italy, May 24-June 4, 1971. 11 p1369 A73-26526

Moire techniques of incoherent and coherent light filtering, line multiplication and contrast amelioration in framework of physical optics and diffraction theory for stress analysis 13 p1612 A73-28470

Calculation of the constants of an infinitely narrow beam in spectral devices 13 p1660 A73-28769

Mode locking in quantum optics. 13 p1627 A73-28928

Optical model of a holographic television system 15 p1879 A73-32331

Three-dimensional diffraction calculations of laser resonator modes. 22 p2872 A73-43151

PHYSICAL PROPERTIES

Investigations of physical and mechanical properties of lunar soil delivered by Luna-16. 01 p0105 A73-11105

General analysis and synthesis of alloys and materials with inhomogeneous physical properties, noting thermal physicochemical methods for laminates and metal powders 01 p0066 A73-11340

Physicomechanical properties of a structural cold-hardened fiberglass-reinforced plastic 02 p0184 A73-11719

Russian book on titanium chemistry covering physicochemical and electrochemical properties, hydrolysis and production of metal-organic and complex titanium compounds 02 p0139 A73-11890

Russian book - Fundamentals of lunar soil science: Physicomechanical properties of lunar soils. 02 p0211 A73-11893

Liquid crystal optical and physical characteristics and applications to display design, emphasizing field effect and twisted nematic devices 02 p0201 A73-12083

Cosmic black glassy spherules composition, mineralogy and physical properties compared to lunar fines, considering possible common origin 02 p0214 A73-12254

Physical and chemical properties of solid propellant igniter materials, determining averaged heat of reaction and burning rate values [AIAA PAPER 72-1195] 03 p0352 A73-13485

Prospects offered by high performance composites with a metallic matrix 03 p0325 A73-13589

Microelectronic metal-dielectric-semiconductor devices for physical properties of multilayer multiphase systems, noting field effect transistors, integrated circuits and electro-optical elements 03 p0349 A73-13656

Measured physical and optical properties of the passive geodetic satellite /Pagesos/ and Echo 1. 04 p0446 A73-14809

H I clouds with spin temperatures less than 25 K. II - Physical properties of two neutral hydrogen clouds. 04 p0500 A73-15517

Bottle green microtektites from Australasian and Ivory Coast deep sea sediments, discussing physical and chemical properties, age and origin 05 p0615 A73-16383

Physicochemical parameters associated with surfactants, investigating effects on hydrocarbon fuels coalescence [SAE PAPER 720863] 05 p0582 A73-16674

Atomic nuclei physical properties for space navigation system gyroscopes, noting nuclear magnetic resonance and nuclei polarization 06 p0692 A73-17774

Sounding balloon system SITTEL for upper atmosphere physical parameters measurement, noting PCM telemetry, remote control and vehicle localization
07 p0790 A73-18971

Influence of thermal-diffusion coatings on the physicochemical properties of heat-resistant metals
07 p0840 A73-20512

Alkali metal intercalates of molybdenum disulfide
08 p0937 A73-21174

Cosmic dilute collisionless plasma physical properties, discussing plasma wave turbulence characteristics, particle acceleration, relativistic plasmas, synchrotron emission, pulsars and galactic nuclei
12 p1537 A73-26850

The physics and chemistry of high pressures.
12 p1523 A73-26923

Influence of the physical properties of metal melts on the spheroidization of droplets in the process of their crystallization
12 p1503 A73-27551

X ray sources in Centaurus X-3 and Hercules X-1 eclipsing binaries, determining upper and lower limits on physical parameters from assumption involving mass function
12 p1536 A73-27878

Planetary atmospheres chemistry, discussing physical factors, atomic oxygen reactions, ozone, airglow and mathematical models
14 p1723 A73-30128

Investigation of some physicochemical and X-ray structural changes in a superconducting wire prepared from 60T alloy, as a function of the strain level and duration of annealing in vacuum
15 p1887 A73-31187

Mono- and polycrystalline barium titanate structural and physical properties, discussing thermally induced structural changes effects on polarization, permittivity and loss tangent
15 p1924 A73-31775

Physicochemical properties of metal silicides under vacuum at high temperatures, assessing suitability as antineutron materials on Mo grids in high power vacuum electron tubes
15 p1898 A73-31842

Extragalactic X ray source physical properties, discussing thermal bremsstrahlung X ray generation by synchrotron mechanism or by Compton scattering
16 p2051 A73-32743

Russian book - Physics of the moon and planets.
16 p2063 A73-33751

Moon surface physical properties from earth based observations and lunar soil samples, noting effects of cosmic dust and meteorite impacts
16 p2063 A73-33752

Electric relay contacts physical characteristics and state changes during dry circuit, low level, intermediate and power switchings
17 p2132 A73-34090

Plastic bonded, thermally stable explosive for an Apollo experiment.
18 p2341 A73-36152

Effect of thermomodification coatings on the physicochemical properties of refractory metals.
19 p2440 A73-37787

Glass fiber reinforced polypropylene composites fabrication technology and physico-mechanical properties
19 p2444 A73-38162

Changes in the physicochemical properties of structural polymers after heat treatment
20 p2580 A73-39333

Physico-mechanical properties and damage mechanism of moving-picture photographic materials as film systems
21 p2699 A73-40270

Cometary atmospheric dust chemical composition and physical properties estimated from colorimetric, polarimetric and IR data, using models of optically thin polydisperse media
21 p2776 A73-41421

Russian papers on metal alloys chemistry covering atomic structure, physicochemical properties, phase diagrams, X ray analysis, laser microanalysis, etc
22 p2873 A73-42083

Variations in the distribution and physical properties of Perseid meteors.
22 p2914 A73-43015

Certain properties of synthetic diamond crystals of various habits
24 p3104 A73-44970

PHYSICAL WORK

Hemodynamic effects of physical maneuvers /Valsalva, effort, respiration/ and of pharmacodynamic tests - Their clinical application
02 p0138 A73-12159

Effect of a 5-day space flight on cardiodynamics during physical work of moderate intensity
02 p0138 A73-12467

Perceived exertion, heart rate, oxygen uptake and blood lactate in different work operations.
03 p0267 A73-13698

Muscle, skin and esophageal temperature measurement during transient and steady state phases of negative work exercise on bicycle ergometer
03 p0262 A73-14112

Utilization extent of the muscle apparatus capabilities during maximum voluntary force exertion
05 p0541 A73-16696

Energy cost of muscle work in a state of fatigue
05 p0541 A73-16697

Physical work induced hyperthermia effects on detection rate in visual vigilance task performance in hot and humid environment
06 p0659 A73-18469

Adenonucleotides, NAD+, and NADN in skeletal muscles during intensive work and at rest
07 p0780 A73-19475

Functional condition changes of biceps brachii in man under the effect of fatiguing physical stress
07 p0780 A73-19643

Predicting heart rate response to work, environment, and clothing.
09 p1046 A73-22931

Work-heat test comparisons of dry and wet heat and exercise programs for heat acclimatization
09 p1041 A73-22932

Changes in gaseous metabolism and cardiac output per minute during local muscle work in man
10 p1179 A73-23809

Laddermil and ergometry - A comparative summary.
11 p1322 A73-25183

Kinetics of oxygen uptake and recovery for supramaximal work of short duration.
11 p1323 A73-25648

Interrelations among the supranal glucocorticoid activity, the cardiovascular systems, and the electrolyte metabolism during prolonged work
11 p1317 A73-26085

Carbon monoxide content in the exhaled air and carboxyhemoglobin in the blood of subjects equipped with an isolating protective garment
12 p1463 A73-27712

Motor, thermal and sensory factors in heart rate variation A methodology for indirect estimation of intermittent muscular work and environmental heat loads.
14 p1720 A73-30880

Effect of a 5-day space flight on the cardiac dynamics during moderately severe physical work.
15 p1840 A73-32617

Effect of maximal work load on cardiac function.
16 p1973 A73-33991

Development of effective means for desaturation of the human organism as a prophylactic measure against altitude decompression disturbances
17 p2111 A73-34231

Effect of stepwise adaptation to high-mountain areas on the respiratory function and the acid-alkali equilibrium of blood in subjects with different motor activity stresses
17 p2111 A73-34232

Effect of sympatholytin on metabolism in resting and working muscles in relation to the degree of their adaptation to intensified activity
18 p2276 A73-36571

Specific features in the activity of the oxygen transport system of the organism during hand-performed working cycles of submaximum intensity
18 p2277 A73-36579

Physical energy expenditure in long-haul cabin crew.
18 p2283 A73-36793

The capacity for muscular work in acute hypoxia
18 p2286 A73-36946

Influence of physical stress on the state of human higher nervous activity under conditions of underwater labor
24 p3059 A73-44672

Oxygen kinetics for constant work loads at various altitudes.
24 p3060 A73-45062

PHYSICS

Trends in physics; General Conference, 2nd, Wiesbaden, West Germany, October 3-6, 1972, Lectures.
17 p2256 A73-34109

PHYSIOGRAPHY

U GEOMORPHOLOGY

PHYSIOLOGICAL ACCELERATION

Vestibular adaptation in man - Effects of increased acceleration during different phases of adaptation.
04 p0411 A73-15218

Adequate vestibular stimulants on earth and in space
17 p2110 A73-34122

Analysis of vestibular effects in experiments on swings
17 p2111 A73-34235

PHYSIOLOGICAL DEFENSES

The effects of bilateral destruction of certain medial-hypothalamus structures on the formation of complement-binding antibodies
07 p0781 A73-19647

PHYSIOLOGICAL EFFECTS

NT HEMODYNAMIC RESPONSES

NT PHYSIOLOGICAL RESPONSES

Insensitivity of the alveolar septum to local hypoxia.
01 p0006 A73-10134

Mathematical description of certain properties of human sensitivity to vibration
01 p0012 A73-10639

Changes in the vibratory sensation threshold after exposure to powerful vibration.
01 p0013 A73-10772

Effect of eccentric and concentric muscle conditioning on tension and electrical activity of human muscle.
01 p0013 A73-10774

The effect of O2 breathing on maximal aerobic power.
01 p0010 A73-11504

Fatigue in flight personnel during long flights
02 p0137 A73-12153

Effect of a 5-day space flight on cardiodynamics during physical work of moderate intensity
02 p0138 A73-12467

Effect of sleep-wake reversal and sleep deprivation on the circadian rhythm of oxygen toxicity seizure susceptibility.
02 p0135 A73-12561

Effect of altitude acclimatization and simultaneous acclimatization to altitude and cold on critical flicker frequency at 11,000 ft. altitude in man.
02 p0135 A73-12562

Effects of the space flight environment on man's immune system. II - Lymphocyte counts and reactivity.
02 p0135 A73-12565

Passive and active warm-up effects on track athletes heart and respiration rates
03 p0266 A73-31233

Effect of chronic centrifugation on body composition in the rat.
03 p0259 A73-13370

Intensity of exercise and heart tissue catecholamine content.
03 p0259 A73-13498

Medical considerations for aircraft passengers.
03 p0267 A73-13802

Changes in cardiac rhythm during sustained high levels of positive +Gz acceleration.
03 p0269 A73-14157

Effect of hydrochlorothiazide on +Gz tolerance in normotensives.
03 p0269 A73-14159

Wakefulness and sleep states in developing organism, discussing REM sleep deprivation effects on behavior, brain excitability, pharmacology and biochemistry
03 p0265 A73-14265

The use of telemetry to study the physiological and clinical variations of intracranial pressure in man.
03 p0271 A73-14300

Hypobaric hypoxia - Within-subject transition effects in albino rats.
06 p0649 A73-17525

Developments in space medicine.
06 p0649 A73-17569

Physiological effects of microwave electromagnetic fields on human and animal organisms, considering etiology, diagnostics and prophylaxis
06 p0659 A73-18256

Mountain inhabitants physiological characteristics due to altitude effects, investigating human tolerance and adaptation to ambient environment
07 p0784 A73-19212

Influence of high ambient temperatures on the performance and some physiological parameters in a tracking problem and an optical vigilance problem
08 p0935 A73-21575

Investigation of certain indices of higher nervous activity in man during prolonged stay in a water environment
09 p1039 A73-22364

Study of the influence of weak electromagnetic field gradients on man
09 p1046 A73-22850

Vitamin metabolism alteration under increased atmospheric pressure
11 p1321 A73-25036

The effect of prolonged immobilization on diuresis and water intake in rats.
11 p1320 A73-26489

Human respiration under increased pressures.
12 p1461 A73-26924

Effects of chronic irradiation of dogs with Co-60 gamma rays on the level of auto-antibodies
12 p1462 A73-27706

Effects of ethyl alcohol on pilot performance.
13 p1579 A73-28501

Sensory versus perceptual isolation - A comparison of their electrophysiological effects.
14 p1722 A73-30517

Aircraft cabin altitude hypoxia effects on mother, embryo and fetus during first trimester of pregnancy in air hostesses and women passengers
14 p1718 A73-30519

Physical and psychological effects of electromagnetic fields on human and animal central nervous system
14 p1718 A73-30571

- Heart rate variability analysis for ergonomics purposes, discussing interpolations, algorithms and physiological effects and spectral analysis methods
14 p1720 A73-30882
- The combined influence of microwave radiation and an adverse climate on the organism
15 p1837 A73-31170
- Effect of steady magnetic fields up to 4,500 Oe on the mitotic activity of the corneal epithelium in mice
15 p1838 A73-31510
- Changes in cardiac activity and in the latter's phase structure during decompression of the lower half of the body
15 p1835 A73-31513
- Work-rest cycle effects on airline pilots performance, considering central nervous system changes measurement techniques
15 p1839 A73-32059
- Intracardiac heart murmurs and sounds influenced by respiration.
15 p1836 A73-32546
- Effect of a 5-day space flight on the cardiac dynamics during moderately severe physical work.
15 p1840 A73-32617
- Physiological criteria of early toxic normobaric hyperoxia manifestations
17 p2110 A73-34123
- Influence of hypoxia on the release of certain gaseous wastes in white rats
17 p2111 A73-34228
- Effect of stepwise adaptation to high-mountain areas on the respiratory function and the acid-alkali equilibrium of blood in subjects with different motor activity stresses
17 p2111 A73-34232
- Physiological effects of acceleration and weightlessness during space flight, discussing cardiovascular system, renal function, respiration, blood volume, metabolism, work capacity, etc
17 p2113 A73-35856
- Changes in functional construction of bone in rats under conditions of simulated increased gravity.
17 p2113 A73-35863
- Determination of the type of higher nervous activity from the aftereffect characteristics of multidimensional stimuli
18 p2277 A73-36577
- Cardiovascular reactions of a healthy man exposed to sonic booms
18 p2284 A73-36909
- Effect of sonic boom on hearing and vestibular equilibrium
18 p2284 A73-36910
- Physiological shifts in the human organism under increased neuropsychic stresses
19 p2393 A73-37392
- Changes in some behavioral reactions and in the bioelectric activity of the brain in cats during the development of sleep under polarization of individual brain structures
19 p2393 A73-37393
- Structural changes in the adrenal nerve apparatus during experimental subtotal pancreatectomy
20 p2513 A73-39400
- Effect of convulsions on certain aspects of the biosynthesis of proteins in the brain cortex
21 p2638 A73-40750
- Biodegradation from evolution viewpoint as physiological function and fundamental cellular process regulating biological equilibrium, explained by intracellular digestion and phagocytic cells association
21 p2638 A73-41024
- Apollo 16 flight program for investigating physiological effects of prolonged weightlessness on central nervous system, vestibular, neuromuscular and cardiovascular functions, metabolism, radiation sensitivity and body weight
22 p2814 A73-42176
- Chronic acceleration effects on homeotherm physiological adaptation in terms of body weight, tolerable field intensity, growth and fat deposition inhibition, etc
22 p2804 A73-42177
- Spinal cord heating effects on frog thermoregulatory behavior in aqueous thermal gradient, noting preference for colder ambient temperature
23 p2947 A73-43994
- Effect of prolonged hypokinesia on the higher nervous activity of humans
24 p3058 A73-44668
- Inhibition by selenium of the free-radical states of the retina of the eye
24 p3059 A73-44724
- PHYSIOLOGICAL FACTORS**
Electromechanical and electronic cockpit displays effectiveness in terms of aircraft control and psychological/physiological factors relating to pilot performance and workload
02 p0136 A73-11666
- Psychological and physiological components of biorhythm cycles governing periodic variations in physical, emotional and intellectual performance
05 p0544 A73-16720

- Naval aviator training program dropouts identification in terms of physiological, safety, security, social, self-esteem and self-actualization needs
14 p1722 A73-30513
- U-2 and SR-71 aircrews physiological training for high altitude and supersonic flight hazards, discussing pressure suits, ejection seats, parachutes and survival and life support equipment
16 p1974 A73-32657
- Physiological factors and optical parameters as bases of vegetation discrimination and stress analysis.
16 p2003 A73-33355
- A frequency response approach to flying qualities criteria and flight control system design.
17 p2105 A73-35073
- Sudden incapacitation in flight.
18 p2279 A73-36847
- Pilot workload and performance measures in terms of physiological activity in flight deck environment for reduced aircraft accidents due to human error
19 p2398 A73-37732
- Individual physiological differences in evoked potential reactions to light sources, discussing latent periods, potential amplitude distribution and EEG measurement techniques
22 p2812 A73-41888
- PHYSIOLOGICAL INDEXES**
U PHYSIOLOGICAL TESTS
PHYSIOLOGICAL RESPONSES
NT HEMODYNAMIC RESPONSES
Cardiorespiratory responses to exercise in air and underwater.
01 p0007 A73-10161
- Changes in ventilatory patterns after ablation of various respiratory feedback mechanisms.
01 p0007 A73-10162
- Utility of heat stress indices and effect of humidity and temperature on single physiologic strains.
01 p0007 A73-10163
- Oxygen uptake, heart rate and pulmonary ventilation during swimming for different speeds and styles, comparing to running and cycling data
01 p0008 A73-10171
- Temporary threshold shift caused by combined steady-state and impulse noises.
01 p0077 A73-10785
- Microvascular responses to alterations in oxygen tension.
01 p0009 A73-11010
- The role of the vagus nerves in the respiratory response to CO₂ under hyperoxic conditions.
01 p0010 A73-11501
- Atrioventricular block response to exercise and intraventricular conduction at rest.
01 p0010 A73-11506
- Importance of the Lohmann reaction in the response of the heart to anoxic aggression
02 p0133 A73-12152
- Analysis of the response characteristics of optic tract and geniculate units and their mutual relationship.
02 p0134 A73-12162
- Hepatic lipogenesis in fasted, re-fed rats and mice - Response to dietary fats of differing fatty acid composition.
03 p0258 A73-13054
- Exercise electrocardiography and vasoregulatory abnormalities.
03 p0260 A73-13541
- Perceived exertion, heart rate, oxygen uptake and blood lactate in different work operations.
03 p0267 A73-13698
- Correlation between the voltage-time curves of H- and M-responses of a human muscle during various functional states of the spinal center
03 p0262 A73-13819
- Cardiovascular reflexes evoked by potassium ion stimulation of the heart under conditions of spinal deafferentation and intact innervation
03 p0262 A73-13820
- Recording and discrimination of pulsed neuron activity responses to stimulus application and removal
03 p0268 A73-13823
- Response of single units of the posterior hypothalamus to thermal stimulation.
03 p0262 A73-14111
- Multiple hormonal responses to graded exercise in relation to physical training.
03 p0263 A73-14116
- Multiple hormonal responses to prolonged exercise in relation to physical training.
03 p0263 A73-14117
- Absence of appreciable cardiovascular and respiratory responses to muscle vibration.
03 p0263 A73-14119
- Design and function of sweat sensor to monitor motion sickness sweat response
03 p0269 A73-14160
- Derivation of a function of nerve-fiber distribution according to fiber diameters on the basis of electrophysiological measurements
04 p0413 A73-15787
- Changes in whole body force transmission of dogs exposed repeatedly to vibration.
[ASME PAPER 72-WA/BHF-11]

- 04 p0410 A73-15878
- The stereoscopic frame of reference in asymmetric convergence of the eyes - Response to 'point' stimulation of the retina.
05 p0573 A73-16149
- Genesis mechanism of slow cortical after-discharges during brain injury by radiation
05 p0539 A73-16331
- Effect of hypoxia on free fatty acid metabolism during exercise.
05 p0540 A73-16609
- Intercortical functional connections in lower monkeys, *Macacus rhesus*, exhibited by evoked responses
05 p0540 A73-16693
- Visual evoked responses elicited by rapid stimulation.
06 p0654 A73-18350
- Human endocrine-metabolic responses to graded oxygen pressures.
07 p0785 A73-19479
- Influence of a low-intensity ultrahigh-frequency electromagnetic field on the bioelectrical activity of the brain in rabbits
09 p1044 A73-22367
- Influence of ultrasound and of a superhigh-frequency electromagnetic field in the three-centimeter band on the oxidative phosphorylation of liver and kidney mitochondria
09 p1044 A73-22368
- Adaptive hormone action and nonspecific adaptive function of steroid hormones, discussing stress resistance mechanisms of steroids pharmacologically classified as syntoxic and catatoxic
09 p1045 A73-22536
- Polysensory responses and sensory interaction in pulvinar and related postero-lateral thalamic nuclei in cat.
09 p1040 A73-22696
- Light evoked responses in invertebrate photoreceptor cells, considering cell organization, microvilli, lateral eye of *Limulus*, generator potentials, visual responses, etc
09 p1042 A73-23307
- Limulus photoreceptor response to single photon stimulation, discussing flash intensity, dim lights, discrete waves and subliminal responses
09 p1042 A73-23308
- Caloric vestibular stimulation via UHF-microwave irradiation.
10 p1178 A73-23650
- Examination of responses evoked in the sensory cortex by thalamic stimulation.
10 p1178 A73-23772
- Effect of respiration stabilization on hemodynamic reactions during acute hypoxic hypoxia
10 p1180 A73-23938
- Sinusoidal stimuli induced electrical activity of hippocampus in waking *rhesus* monkeys and baboons
10 p1180 A73-24330
- Physiological studies of human organism adaptation to high altitudes in temporary and permanent mountain inhabitants, discussing oxygen uptake, lung ventilation and cardiac ventricle hypertrophy
10 p1181 A73-24514
- Physiological responses of rats to intermittent high-altitude stress - Effects of age.
10 p1182 A73-24564
- Laddermil and ergometry - A comparative summary.
11 p1322 A73-25183
- Physiological response to exercise after space flight - Apollo 7 to Apollo 11.
11 p1314 A73-25326
- Single unit and evoked potential responses in cat optic tract to paired light flashes.
11 p1317 A73-25647
- Laser speckle for determining ametropia and accommodation response of the eye.
11 p1377 A73-26232
- Mammalian tissue response to subcutaneous and intraperitoneal injection of aqueous suspensions of lunar fine material, noting insolubility in tissue and irritant action
11 p1320 A73-26484
- Human visual evoked response signal decomposition by complex demodulation in terms of after-discharge time, envelope and frequency parameters
11 p1324 A73-26497
- Single unit reactions in the visual cortex of the unanesthetized rabbit to the light flashes of different intensities.
11 p1321 A73-26719
- Estimation of the variability of the latency of responses to brief flashes.
11 p1321 A73-26720
- Spectral sensitivities of colour mechanisms isolated by the human visual evoked response.
12 p1461 A73-26919
- Physiological effect of air nitrogen replacement by inert gases under high and low temperature conditions
12 p1465 A73-27701
- Dynamics of certain characteristics of the evoked potential of the optic cortex in rabbits under conditions of increasing hypoxia
12 p1463 A73-27709

PHYSIOLOGICAL TELEMETRY

Physiological time zone entrainment and stressor effects during prolonged C-141 transmeridian flights, using endocrine-metabolic indices in urine specimens 13 p1574 A73-28283

Scotopic visibility curve in man obtained by the VER. 13 p1575 A73-28356

A clinical method for obtaining pattern visual evoked responses. 13 p1575 A73-28357

Scotopic electroretinography and visual evoked responses under adaptive illumination, comparing blind spot stray light with parafoveal stimulation 13 p1575 A73-28361

Threshold Pco₂ as a chemical stimulus for ventilation during acute hypoxia in dogs. 13 p1576 A73-28534

Step-wise changes in thermoregulatory responses to slowly changing thermal stimuli. 13 p1576 A73-28535

Late visual cortical region reactions during the convergence of light stimulation and electrocutaneous stimulation 13 p1576 A73-29073

Human hematologic responses to 4 hr of isobaric hyperoxic exposure /100% oxygen at 760 mm Hg/. 14 p1714 A73-29751

Posthyperventilation breathing - Different effects of active and passive hyperventilation. 14 p1714 A73-29752

The effect of iontophoretically applied acetylcholine upon the cat's retinal ganglion cells. 14 p1715 A73-30061

Saccadic eye movement control system, investigating response characteristics to variously timed pulse stimuli 14 p1716 A73-30389

Pupil movements to light and accommodative stimulation - A comparative study. 14 p1717 A73-30395

Towards an objective assessment of cockpit workload. I - Physiological variables during different flight phases. 14 p1718 A73-30515

Role of peripheral chemoreceptors in reactions of rats to short and lasting hypoxia 14 p1719 A73-30840

Evoked negative electrical potentials due to auditory zone stimulation by local cooling, mechanical trauma and potential recording, observing reaction regeneration variations 15 p1833 A73-31159

Reactivity and certain metabolic indices during prolonged sustenance of animals in artificial nutrient conditions 15 p1833 A73-31162

Cerebellar responses of animals under varied rotation conditions in a centrifuge 15 p1834 A73-31506

Influence of restricted motor activity on the resistance of animals to acute action of carbon monoxide 15 p1835 A73-31519

Self-estimates of distractibility as related to performance decrement on a task requiring sustained attention. 15 p1839 A73-32394

Relationship of physiological strain to change in heart rate during work in the heat. 15 p1836 A73-32548

Sleep behaviour as a biorhythm. 16 p1972 A73-33158

Damage-risk criteria - The trading relation between intensity and the number of nonreverberant impulses. 16 p1973 A73-33678

Roentgenographic study of relative heart motion during vibration in water-immersed cats. 16 p1973 A73-34039

Impact acceleration effects on rabbit central nervous system, noting changes in nerve tissue elements and cerebral vessels 17 p2111 A73-34227

Heat acclimatization while wearing vapor-barrier clothing. 17 p2115 A73-34742

Effects of oxygen-augmented atmosphere on the immune response. 17 p2115 A73-34743

Opponent-colors responses in the visually evoked potential in man. 17 p2112 A73-34844

Stereoscopic vision - Cortical limitations and a disparity scaling effect. 18 p2269 A73-35922

Metabolic responses of monkeys to increased gravitational fields. 18 p2270 A73-35982

Optokinetic stimulation of an immobilized eye in the monkey. 18 p2273 A73-36457

Role of arterial and venous vessels of limbs in the process of cardiovascular reflex responses 18 p2277 A73-36578

Cardiorespiratory transients in exercising man. I - Tests of superposition. II - Linear models. 18 p2278 A73-36656

Body fluid volume changes during a 14-day continuous exposure to 5.2% O₂ in N₂ at pressure equivalent to 100 FSW /4 ata/. 18 p2279 A73-36796

Human physiological responses to high speed aerial tow. 18 p2286 A73-36939

Study of the heart rate of humans exposed to heat 18 p2280 A73-36942

Regional serotonin content variations in the brain of cats during a prolonged absence of sleep 19 p2393 A73-37394

Non-linearity of visual signals in relation to shape-sensitive adaptation responses. 19 p2394 A73-37418

Orientation specificity and response variability of cells in the striate cortex. 19 p2394 A73-37421

Book - Pathological effects of radio waves. 19 p2395 A73-37774

Role of specific and nonspecific thalamic nuclei in the genesis of certain slow rhythms on the human electrocorticogram 19 p2395 A73-37939

Functional characteristics of different neurons in the auditory cortex 19 p2395 A73-37940

Evoked potentials in the hypothalamus in response to stimulation of the vagus and sciatic nerves 19 p2395 A73-37941

Model of evaporation responses to heat load increases 19 p2395 A73-38150

Physiological cost in 36- and 48-hour simulated flights. 20 p2512 A73-39101

Circadian variations in presumably healthy men under conditions of peace-time army reserve unit training. 20 p2513 A73-39482

Altered susceptibility to motion sickness as a function of subgravity level. 20 p2518 A73-39486

A study of evoked slow activities in man which follow a voluntary movement and articulated speech 20 p2514 A73-39759

Visually evoked cortical potentials to patterned stimuli in monkey and man. 20 p2514 A73-39760

Correlation of ventilatory responses to hypoxia and hypercapnia. 20 p2514 A73-39776

Transient ventilatory response to hypoxia with and without controlled alveolar PCO₂. 20 p2515 A73-39777

Formation of various functional states in the symmetrical structures of the brain as a function of the intensity of unconditioned excitation 20 p2516 A73-39801

Effects of repeated simulated sonic booms of 1.0 PSF on the sleep behavior of young and old subjects. 21 p2644 A73-41151

Physiologic cost of prolonged double-crew flights in C-5 aircraft. 21 p2644 A73-41152

Physiological and operational state of a group of aeroplane pilots under the conditions of stressing tracking tests. 21 p2645 A73-41157

Response delays and the timing of discrete motor responses. 21 p2645 A73-41177

Evoked potentials in the hypothalamus and mesencephalic reticular formation upon stimulation of the vagus nerve 21 p2640 A73-41263

Skylab 1 medical experiments concerning astronaut physiological responses and work capability as affected by exposure to space flight environment 21 p2778 A73-41519

Mathematics of interaction between blood and electromagnetic fields. 22 p2802 A73-41788

Estimate of integrative cerebral activity using an orientation response example 22 p2807 A73-42651

Statistical treatment of evoked cerebral potentials during experiments on a Dnepr-1 computer 22 p2814 A73-42657

Investigation of complex and hypercomplex receptive fields of visual cortex of the cat as spatial frequency filters. 22 p2810 A73-42958

Rectifier-like color dependent phase shifts in electrophysiological responses to different colored stimuli at evoked potential and single neuron levels 22 p2810 A73-42961

Human reactions to whole-body transverse angular vibrations compared to linear vertical vibrations. 23 p2948 A73-43216

Physiological study of dynamics and evolution of chimpanzee complex behavior, considering motor reactions, group behavior and nerve mechanisms of voluntary acts 23 p2947 A73-43928

Neuronal activity of the sensorimotor and visual cortex in rabbits during development of a summation focus in the reticular formation 24 p3058 A73-44550

The energetic metabolism and some reactions of the cardiovascular system during multichannel electrical stimulation and voluntary stressing of muscles 24 p3059 A73-44670

Comparison of visual evoked potentials to stationary and to moving patterns. 24 p3061 A73-45168

PHYSIOLOGICAL TELEMETRY

U BIOTELEMETRY

PHYSIOLOGICAL TESTS

NT BODY SWAY TEST

NT CARBOXYHEMOGLOBIN TEST

NT EAR PRESSURE TEST

NT VESTIBULAR TESTS

Exercise testing for evaluation of cardiac performance. 03 p0259 A73-13538

Practical exercise test for physical fitness and cardiac performance. 03 p0259 A73-13540

Exercise testing for detecting changes in cardiac rhythm and conduction. 03 p0260 A73-13542

Correlation of computer-quantitated treadmill exercise electrocardiogram with arteriographic location of coronary artery disease. 03 p0260 A73-13543

Cardiac dysrhythmias associated with exercise stress testing. 03 p0260 A73-13544

Variability of normal glabellar and supraorbital reflexes in man 03 p0261 A73-13748

An evaluation of sinus arrhythmia as a measure of mental load. 05 p0543 A73-16718

Uses and limitations of stress testing in the evaluation of ischemic heart disease. 05 p0552 A73-17278

Evaluation of the state of the cardiovascular system from polycardiographic test data 06 p0650 A73-17749

Visual-motor coordination characteristics of parachute jumpers 06 p0657 A73-17750

Physiological tests for hypothalamus regions stimulation effects on coronary circulation, noting hypoxia and emotional stress effects 06 p0650 A73-17770

On-line computer analysis and breath-by-breath graphical display of exercise function tests. 08 p0935 A73-21511

Thirty-month follow-up of maximal treadmill stress test and double Master's test in normal subjects. 08 p0932 A73-21803

Work-heat test comparisons of dry and wet heat and exercise programs for heat acclimatization 09 p1041 A73-22932

Thermoregulatory behavior of man during rest and exercise. 10 p1178 A73-23572

Changes in the cardiac rhythm during a hypoxic functional test 10 p1179 A73-23820

Cardiac arrhythmias during exercise testing in healthy men. 11 p1315 A73-25336

Kinetics of oxygen uptake and recovery for supramaximal work of short duration. 11 p1323 A73-25648

Maximal oxygen intake and nomographic assessment of functional aerobic impairment in cardiovascular disease. 11 p1319 A73-26362

German monograph - Investigation concerning a consideration of the human circadian rhythm by means of a variable working time. 13 p1580 A73-29283

Inflated air bag head restraints for prevention of brain injuries due to whiplash acceleration during crash landings or ejection 16 p1965 A73-32654

A monkey metabolism pod for space-flight weightlessness studies. 18 p2270 A73-35963

The significance of pendulum nystagmography in aviation medicine 18 p2286 A73-36941

Skylab medical experiments altitude test crew observations. [ASME PAPER 73-ENAS-30] 19 p2400 A73-37985

Exercise during hyperoxia and hyperbaric oxygenation. 19 p2396 A73-38160

- Changes in whole body force transmission of dogs exposed repeatedly to vibration. 20 p2512 A73-39106
- Effect of skin wetting on finger cooling and freezing. 20 p2518 A73-39779
- Automatic apparatus for the study of conditioned reflexes in a monkey seated in the primatological chair. 21 p2644 A73-41140
- Functional aging - Present status of assessments regarding airline pilot retirement. 21 p2645 A73-41161
- Ischemic heart disease prediction via exercise ECG tests, discussing work load standardization. 22 p2809 A73-42835
- PHYSIOLOGY**
- NT AUDIOLOGY
- NT BODY COMPOSITION [BIOLOGY]
- NT ELECTROPHYSIOLOGY
- NT HEMATOPOIETIC SYSTEM
- NT MENSTRUATION
- NT NEUROPHYSIOLOGY
- NT PSYCHOPHYSIOLOGY
- NT RESPIRATORY PHYSIOLOGY
- Book - How man moves: Kinesiological studies and methods. 03 p0268 A73-13993
- Book - Principles of biological regulation: An introduction to feedback systems. 15 p1840 A73-32576
- Book on comparative physiology of thermoregulation covering primitive and aquatic mammals, torpidity aspects, evolution and newborns. 22 p2809 A73-42859
- PI-ELECTRONS**
- Projected states of open shell molecules - The pi-electron states of the cyclopentadienyl cation. 06 p0726 A73-18775
- Spin contamination in unrestricted Hartree-Fock calculations. 22 p2889 A73-42442
- PIASECKI MILITARY AIRCRAFT**
- U MILITARY AIRCRAFT
- PICKLING**
- U CHEMICAL CLEANING
- PICKOFFS**
- U SENSORS
- PICTURE TUBES**
- Properties of magnetic focusing systems for picture tubes. 10 p1194 A73-23850
- PIERCING**
- Metal barrier maximum puncturable thickness dependence on high velocity meteorite particle impact parameters. 12 p1554 A73-27642
- Estimation of corrosion damage levels in thin-walled structural elements by the punching method. 18 p2320 A73-36825
- PIEZOELECTRIC CRYSTALS**
- Optimum operation conditions of thyatron generator circuit in electroacoustic system for excitation of quartz piezoelectric vibrators in ultrasonic NDT. 02 p0168 A73-12147
- Rayleigh wave propagation at the boundary between a piezoelectric insulator and a semiconductor. 03 p0350 A73-14037
- Anisotropy of piezoelectrical scattering in semiconductors with a wurtzite structure. 06 p0738 A73-18648
- Polynomial solutions to the plane problem of electroelasticity theory. 11 p1434 A73-25394
- The elastic dielectric as oriented elastic continuum. 13 p1658 A73-28163
- Generation and detection of sound by distributed piezoelectric sources. 13 p1661 A73-29289
- Analog transducers based on monocrystalline silicon semiconductors piezoresistivity properties, describing various piezo-FET circuits. 14 p1751 A73-29728
- A sandwich-transducer technique for measurement of internal dynamic stress. 14 p1751 A73-29773
- Bleustein-Gulyaev shear surface waves in piezoelectric-dielectric-perfect conductor layered system, applying theoretical results to lithium iodate crystals. 14 p1783 A73-30259
- Study of excitation conditions for a piezo-semiconductor oscillator by the electron modeling method. 14 p1737 A73-30946
- Interaction of nearly monochromatic LA phonons with excitons in CdS crystals. 15 p1924 A73-31718
- Response of thermally controlled, vibrating piezoelectric quartz to the deposition of multiple metal layers. 15 p1924 A73-31843
- High speed serial multiplexed holographic recording for large capacity random access memories, using piezoelectric deflector and ferroelectric ceramic array modulators. 16 p2013 A73-32872
- Remote measurement of the thickness, distance and velocity of objects by means of a piezoelectric laser beam deflector. 16 p2023 A73-32877
- Nonlinear light scattering in crystals. 19 p2462 A73-38539
- Theory of quantum oscillations of the Nernst-Ettingshausen thermomagnetic coefficient in semiconductors. 20 p2599 A73-39397
- Study of self-excitation conditions in an acoustic oscillator in relation to the type of boundary conditions. 22 p2886 A73-41900
- The development of the quartz resonator as a digital temperature sensor with a precision of .0001. 22 p2854 A73-41992
- Bending of a rectangular piezoelectric plate clamped over its edge. 23 p3043 A73-43923
- PIEZOELECTRIC GAGES**
- Piezoelectric gages for fluid dynamic multicomponent force measurements, discussing quartz transducers, measurement accuracy and capability for rapidly fluctuating forces measurement. 12 p1499 A73-27871
- Impact gages for detecting meteoroid and other orbital debris impacts on space vehicles. 17 p2238 A73-34606
- Shock wave structure in liquid/gas bubble medium from theoretical two-phase model and experimental piezoelectric pressure profile measurements. 20 p2547 A73-39283
- PIEZOELECTRIC TRANSDUCERS**
- NT PIEZOELECTRIC GAGES
- Piezoelectric matrices for reception of acoustic images and holograms. 01 p0051 A73-10930
- Dynamic errors in force measuring transducers, simulating unsteady processes by analog model with varying step function input signals. 02 p0170 A73-12540
- Piezoelectric material constants, vibration mode, radiation directivity and VHF and UHF operation of ultrasonic transducers. 03 p0306 A73-12954
- An electronic method of temperature compensation in hydrostatic pressure transducers with semiconductor p-n junctions. 03 p0308 A73-13784
- A quick and inexpensive method of monitoring on tape the heart rate during exposure of the human head to pulsed magnetic fields. 03 p0270 A73-14289
- Piezoelectric transducers for the study of short-duration mechanical loads. 04 p0448 A73-15374
- Convolution and correlation by nonlinear interaction in a diode-coupled tapped delay line. 06 p0678 A73-18746
- Load amplifiers for vibration and shock measurements. 07 p0808 A73-19009
- Diffraction effects from cylindrical transducers in a piezo-electric medium of hexagonal symmetry/class C6v/6mm//. 07 p0822 A73-19108
- Theory of excitation of microwave elastic waves by multilayer transducers /considering the effect of metallic and insulator layers/. 07 p0801 A73-20139
- Differentiators and integrators with RC circuits for piezoelectric transducer signals, noting instrument errors and SNR. 07 p0827 A73-20534
- On the mechanical response of a non-uniform piezoelectric transducer with elastic compliances having damping characteristics. 08 p0994 A73-20875
- Development and application of a 0.14 gm piezoelectric accelerometer. 09 p1083 A73-22507
- Thickness dependence of effective coupling factors of ZnO thin-film surface-wave transducers. 09 p1086 A73-23097
- Radar direction measurements by phase comparison of ultrasonic echo pulses reflected from targets in water tank, using piezoelectric sensors for receiving antennas simulation. 10 p1194 A73-23736
- Micromovement servocontrollers in closed loop system, using piezoelectric device, ceramic element actuators and rotary switch derived logic control signal. 10 p1199 A73-24027
- Piezoelectric matrices for the reception of acoustic images and holograms. 10 p1218 A73-24190
- Single mode ion laser tuning over entire emission range via intracavity etalon tilting by piezoelectric drive. 11 p1376 A73-26104
- The dependence of piezo-electric accelerometer response on method of attachments. 12 p1496 A73-26974
- Anisotropic piezoelectric heterogeneous acoustic surface waveguides of arbitrary cross section computing mode spectrum by efficient and accurate numerical techniques. 12 p1480 A73-27568
- Correction for angle of incidence of meteoric particle with penetration and piezoelectric sensors in estimates of spatial density of meteoric matter. 12 p1554 A73-27644
- Laser beam scanned 1.1 GHz acoustic microscope based on photoconductive CdS piezoelectric transducer. 13 p1614 A73-28580
- Method of recording elastoplastic stress waves in solids with a dielectric sensor. 13 p1618 A73-29059
- Piezoelectric sound pressure sensor for damping measurement of structural element coatings under intense acoustic loads. 13 p1618 A73-29060
- The features of disk shape piezoelectric ceramic transducer equivalent circuit. 14 p1754 A73-30892
- Structure-dependent transfer parameters of interdigital transducers for surface waves. I. 14 p1754 A73-30895
- A method of recording elastoplastic stress waves in solids by means of a dielectric pickup. 18 p2317 A73-36891
- Piezoelectric sound pressure sensor for damping measurement of structural element coatings under intense acoustic loads. 18 p2317 A73-36892
- RF sputtering of ZnO shear-wave transducers. 21 p2702 A73-40952
- Linear signal processing by acoustic surface-wave transversal filters. 21 p2705 A73-41426
- Monograph - Generation of acoustic waves in piezoelectric devices. 22 p2861 A73-42700
- PIEZOELECTRICITY**
- Influence of nonlinear polarization on the ultrasonic gain factor in piezosemiconductors. 05 p0605 A73-16821
- The low temperature strain sensitivity of MOS transistors. 08 p0948 A73-21476
- Perturbation theory for multistrip acoustoelectric surface-wave amplifier. 11 p1337 A73-25362
- Polynomial solutions to the plane problem of electroelasticity theory. 11 p1434 A73-25394
- Crystal lattice dynamics, elasticity and piezoelectricity theories covering linear, Cosserat and strain gradient theories, acoustic and optical properties, etc. 11 p1409 A73-26276
- Thin piezoelectric plate bending deformation and polarization theory in terms of piezoelectricity, electrostatics and elasticity equations for anisotropic body. 12 p1552 A73-27371
- Electrooptical and piezoelectric alignment of a composite resonator in a semiconductor laser. 13 p1627 A73-28764
- Parametric excitation of ultrasonic waves in piezoelectric semiconductors. 14 p1783 A73-29916
- Spectral determination of rare-earth components in Seignette-ceramic and piezoceramic materials. 21 p2752 A73-40555
- PIEZOMETERS**
- Anomalous lower dynamic pressure in piezometer of pitot tube in liquid flow containing solid particles, using seeds in aqueous solution of calcium chloride. 11 p1367 A73-26476
- Measurement of pulsating pressure with a piezometer. 13 p1612 A73-28449
- PIEZORESISTIVE TRANSDUCERS**
- NT PIEZOELECTRIC GAGES
- Miniature pressure transducers with a silicon diaphragm. 09 p1084 A73-22692
- An IC piezoresistive pressure sensor for biomedical instrumentation. 10 p1183 A73-23649
- Piezoresistive semiconductor strain gage optimum applications and practical merits comparison with wire or foil resistance types, considering stability, accuracy and temperature compensation. 10 p1195 A73-24571
- Implantable transducer for in vivo measurement of bone strain. 12 p1464 A73-27443
- Analog transducers based on monocrystalline silicon semiconductors piezoresistivity properties, describing various piezo-FET circuits. 14 p1751 A73-29728
- Use of cellulose crystallite structures with solid state strain gages for humidity and moisture measurement. 17 p2166 A73-34621
- PIGMENTS**
- NT CHLOROPHYLLS

PILOT ERROR

NT CYTOCHROMES

NT MELANIN

NT VISUAL PIGMENTS

Rod vision chemistry in terms of rhodopsin, visual cycle and pigment-vision relations, considering dark and light adaptation

05 p0540 A73-16479

Light enhanced decarboxylations by proteinoids.

06 p0661 A73-17941

Polarization dependence of a photoelectric current during the modulated illumination of a system composed of an electrolyte, a porous pigment film, and a metal

07 p0851 A73-19473

Organic coating technology review, discussing binders, pigments and various processing techniques

11 p1388 A73-25848

Response of tobacco tissue cultures growing in contact with lunar fines.

11 p1320 A73-26483

Effect of iron and salt on prodigiosin synthesis in *Serratia marcescens*.

17 p2112 A73-34399

PILOT ERROR

Identifying pilot error potential in the F-4 aircraft.

05 p0545 A73-16731

Personal life changes and health stresses in contrast to accident proneness as factors in pilot error

05 p0545 A73-16732

Realistic pilot training and aircraft handling qualities in pilot error risk minimization for military, commercial and general aviation

05 p0545 A73-16733

Human factor role in flying personnel errors, noting man machine system performance and medical service engagement

06 p0659 A73-18258

Safety in operation and human error.

17 p2097 A73-34077

Pilot error evaluation in aircraft accidents, discussing human failure factors and flight and cockpit voice recorder evidence

17 p2115 A73-34748

Internal operational environment effects on pilot errors in commercial aircraft flights in terms of man machine interface and flight deck design

19 p2384 A73-37728

Systems for collision avoidance - An overview.

19 p2453 A73-38467

A flight evaluation of pilotage error in area navigation with vertical guidance.

21 p2733 A73-40029

PILOT PERFORMANCE

Pilot incapacitation as cause of aircraft accidents, noting age connected cardiovascular disease as leading cause for loss of pilot license

01 p0013 A73-11238

Electromechanical and electronic cockpit displays effectiveness in terms of aircraft control and psychological/physiological factors relating to pilot performance and workload

[DGLR PAPER 72-097] 02 p0136 A73-11666

Favorable effect of flight on pilots exhibiting degenerative arteriopathy of the lower limbs

02 p0137 A73-12151

Reorganization of airplane manual flight control dynamics.

05 p0595 A73-16707

Critical skills and procedures isolation within replacement air group (RAG) training for F-4 pilot performance prediction

05 p0544 A73-16723

A statistical analysis of pilot control during a simulation of STOL landing approaches.

[ALAA PAPER 73-182] 05 p0536 A73-16922

Transinformation and real time identification applied to the study of pilot workload

05 p0545 A73-17195

Reactions of the cardiovascular system of pilots with atherosclerosis symptoms under professional activity conditions

06 p0657 A73-17689

Functional state alteration of the visual analyzer in pilots

06 p0659 A73-18257

Case histories of valvular cardiopathies in military pilots, determining tolerance to flight

07 p0784 A73-19209

Civil aviation medicine in the coming decade.

07 p0785 A73-19484

Recent advances and applications in the prediction of pilot acceptance of aircraft flying qualities.

07 p0777 A73-20586

AH-56A rigid rotor compound helicopter configuration and handling qualities under autorotation conditions, discussing flight test program, piloting descent performance

09 p1030 A73-22179

Pilot incapacitation as cause for aircraft operational risks, discussing flight crews education for emergency situations handling

10 p1185 A73-24717

Aviation medicine assessment of environment effects on pilot responsiveness, task performance and flight safety predictability, considering temperature,

oxygen, gravity, acceleration, pressure and stress effects

11 p1321 A73-25039

Implications of psychoanalytic factors for Air Force operations.

11 p1323 A73-25340

Effects of ethyl alcohol on pilot performance.

13 p1579 A73-28501

Manual vs fully automatic landing concepts, discussing pilots abilities and limitations and primary requirements for displays

13 p1656 A73-28905

Role of the air line pilot in air transportation.

13 p1570 A73-29105

Towards an objective assessment of cockpit workload. I - Physiological variables during different flight phases.

14 p1718 A73-30515

Medical diagnosis of pilot performance disturbances from viewpoint of flight surgeon responsibilities

15 p1837 A73-31171

Special physical training of pilots as a prophylactic measure against obesity

15 p1837 A73-31172

Work-rest cycle effects on airline pilots performance, considering central nervous system changes measurement techniques

15 p1839 A73-32059

Pilot-electronics-control surfaces as feedback loop for aircraft flight control, discussing instruments, pilot training and aircraft flying qualities

15 p1830 A73-32472

Electronic integrated flight data displays for pilot workload reduction at takeoff, approach and landing, considering head-up and head-down and colored systems

15 p1831 A73-32506

VTOL and STOL projects flight simulation trials for autostabilization, head-up displays and flight controls effectiveness in handling qualities improvement and pilot workload reduction

16 p1996 A73-33209

Annual Scientific Meeting, Las Vegas, Nev., May 7-10, 1973, Preprints.

16 p1973 A73-33421

Pilot operation practices for helicopter noise level reduction, with emphasis on flight altitude increase and routing over noise insensitive areas

17 p2099 A73-34442

Flight control problems during STOL landing approaches, considering navigation aids, pilot work load and flight safety

17 p2207 A73-34483

General aviation pilot operational profile study, discussing implications for airman certification standards, flight safety regulations and aircraft design

[SAE PAPER 730334] 17 p2115 A73-34687

Lone woman pilot sleep patterns and sleep disruptions on global flight across time zones

17 p2115 A73-34745

Self destructive behavior of aircraft pilot due to stress accumulation, discussing man machine relationship, coping mechanisms, competence and invulnerability myth

17 p2115 A73-34746

Military aircraft pilot in-flight consciousness loss etiologies, discussing rapid decompression, hypoxia, dysbarism, seizure, improper maneuver, vasovagal syncope, acceleration sensitivity, etc

17 p2115 A73-34747

V/STOL aircraft pilot-in-loop flight control/display system to overcome pilot limitations with performance and decision making flexibility enhancement

[AHS PREPRINT 722] 17 p2105 A73-35063

A frequency response approach to flying qualities criteria and flight control system design.

[AHS PREPRINT 740] 17 p2105 A73-35073

Intellectual performance during prolonged exposure to noise and mild hypoxia.

18 p2283 A73-36783

Hypoglycemia in airline pilots.

18 p2278 A73-36790

Further sleep problems in airline pilots on worldwide schedules.

18 p2283 A73-36792

Sudden incapacitation in flight.

18 p2279 A73-36847

Study of Indian naval aircrew experiences and psychic factors in disorientation.

18 p2285 A73-36919

Some characteristics of pilot's performance under complicated flight conditions.

18 p2285 A73-36921

Management of cataract in commercial flight personnel.

18 p2285 A73-36927

The significance of pendulum nystagmography in aviation medicine

18 p2286 A73-36941

Estimation of hypoxia tolerance in a decompression chamber

18 p2280 A73-36945

Ambient temperature rise effects on pilot performance in a flight simulator

18 p2287 A73-36948

Problems related to high-performance flight in the Arctic regions

18 p2287 A73-36953

Symposium on Flight Deck Environment and Pilot Workload, London, England, March 15, 1973, Proceedings.

19 p2383 A73-37726

Transport aircraft external operational environmental factors, discussing navigation, ATC, airspace, flight and pilot workload conditions

19 p2450 A73-37727

Two man crew cockpit design for commercial jet transport aircraft, discussing pilot vision, control and display panels and avionics disposition

19 p2384 A73-37729

STOL pilot functional requirements on air transportation system in terms of airport design, aircraft, ATC route selection, navigation and communications

19 p2450 A73-37730

Flight deck management and pilot operation priorities in high pressure and emergency situations, using integrated aircraft-environment mental model

19 p2384 A73-37731

Pilot workload and performance measures in terms of physiological activity in flight deck environment for reduced aircraft accidents due to human error

19 p2398 A73-37732

Cockpit layout effects on pilot and flight crew activities, using in-flight observation, photography and pilot eye movement evaluation

19 p2384 A73-37733

Pilot workload immediate, duty day and long term period evaluation from heart rate, subjective, psychological, biochemical stress and sleep pattern measurements

19 p2398 A73-37734

Cockpit mock-ups and simulator design for pilot workload assessment for Concorde program and V/STOL research

19 p2384 A73-37735

Aircrew workload during the approach and landing.

19 p2401 A73-38005

Fixed base simulation of variable stability T-33 handling qualities, considering pilot performance in pitch tracking during atmospheric turbulence

19 p2386 A73-38072

The prediction of pilot acceptance for a large aircraft.

19 p2453 A73-38073

A Lie algebra of visual piloting

20 p2590 A73-39038

Aircraft pilot spatial disorientation and illusory perceptual break-off sensations during flight associated with minor vestibular asymmetry

20 p2512 A73-39111

Sudden incapacitation in flight - 1 Jan. 1966-30 Nov. 1971.

20 p2512 A73-39112

Crew discipline factors in aircraft accident statistics, linking pilot-related accidents to crew carelessness, flight regulation infractions and unfamiliarity with flight conditions

20 p2509 A73-39216

Ocular tension in flying personnel

21 p2637 A73-40347

Carrier landing simulation for pilot visual perception, describing Fresnel lens optical landing system, periscopes, cockpit equipment and glide paths

[ALAA PAPER 73-917] 21 p2634 A73-40865

Touchdown performance with a computer graphics night visual attachment.

[ALAA PAPER 73-927] 21 p2673 A73-40874

Studies of pilot performance. III - Validation of objective performance measures for rotary-wing aircraft.

21 p2644 A73-41154

Physiological and operational state of a group of aeroplane pilots under the conditions of stressing tracking tests.

21 p2645 A73-41157

Frequency of anti-collision observing responses by solo pilots as a function of traffic density, ATC traffic warnings, and competing behavior.

21 p2645 A73-41158

Barotrauma in United States Air Force accidents/incidents.

21 p2645 A73-41160

Functional aging - Present status of assessments regarding airline pilot retirement.

21 p2645 A73-41161

Monocular pilot ability in securing and retaining license as compared to controls

21 p2639 A73-41163

Development of pilot-in-the-loop analysis.

[ALAA PAPER 73-898] 22 p2817 A73-43110

PILOT SELECTION

Toward the development of a criterion for fleet effectiveness in the F-4 fighter community.

13 p1579 A73-28512

Naval aviator training program dropouts identification in terms of physiological, safety, security, social, self-esteem and self-actualization needs

14 p1722 A73-30513

Jet procedures trainer for pilot transition from straight wing propeller plane to swept wing jets, discussing pilot instruction and selection

15 p1837 A73-31095

PILOT TRAINING

Flight simulator development in parallel with aircraft flight test A case study of the American Airlines DC-10 program. [SAE PAPER 720858] 05 p0562 A73-16664

Critical skills and procedures isolation within replacement air group /RAG/ training for F-4 pilot performance prediction 05 p0544 A73-16723

Computer-assisted instruction in pilot training and certification. 05 p0544 A73-16724

The isolation of critical elements within selected maneuvers during primary flight training. 05 p0544 A73-16727

Realistic pilot training and aircraft handling qualities in pilot error risk minimization for military, commercial and general aviation 05 p0545 A73-16733

Toward the development of a criterion for fleet effectiveness in the F-4 fighter community. 13 p1579 A73-28512

Aircraft accident prevention problems, considering pilot judgement errors, factory skill degradation, training, lightning and structure factors and air bag use 13 p1570 A73-29349

Night search and rescue techniques over sea in poor visibility by helicopter, discussing automatic flight control systems, radar, plotting facility and pilot training 15 p1825 A73-31094

Jet procedures trainer for pilot transition from straight wing propeller plane to swept wing jets, discussing pilot instruction and selection 15 p1837 A73-31095

Training simulator for civil aviation schools 15 p1859 A73-32511

Flight Simulation Symposium, 2nd, London, England, May 16, 17, 1973, Proceedings. 16 p1995 A73-33201

Specific Behavior Objective approach to airline flight simulation, featuring duplicate training elimination and education time reduction 16 p1995 A73-33202

Airline flight simulator programs for aircraft type conversion training, outlining flight instructor training, certification and instructional aids 16 p1995 A73-33203

Airline flight simulation program, examining visual system capacity for replacement of in-flight training with pilot learning transfer estimation and simulation effectiveness appraisal 16 p1995 A73-33204

Flight simulation visual image innovations, including closed circuit television, motion pictures and computer generated imagery with wide angle presentation and day/night realizations 16 p1995 A73-33205

The simulator industry and its contribution to military training requirements. 16 p1996 A73-33208

Royal Aircraft Establishment Aerodynamics Flight Division flight simulators for V/STOL and helicopters, emphasizing handling, aircraft mathematical models and cockpit simulation 16 p1996 A73-33211

BOAC computer aided flight simulators, detailing simulator systems history, Boeing 747 training adaptation, and simulation types 16 p1996 A73-33212

British Airline Pilots Association and RAF Institute of Aviation Medicine questionnaire results on training simulator effectiveness, analyzing auditory and visual aids 16 p1996 A73-33213

Visual scene simulation with computer generated images. 17 p2147 A73-34820

Objectives of training in relation to accident prevention. 18 p2284 A73-36850

A visual detection simulator /VDS/ for pilot warning instrument evaluation. 21 p2672 A73-40864

The Large Amplitude Multi-Mode Aerospace Research /LAMAR/ Simulator. [AIAA PAPER 73-922] 21 p2673 A73-40870

Design and application of a part-task trainer to teach formation flying in USAF Undergraduate Pilot Training. [AIAA PAPER 73-935] 21 p2674 A73-40881

Studies of pilot performance. III - Validation of objective performance measures for rotary-wing aircraft. 21 p2644 A73-41154

Stress and strain in student helicopter pilots. 21 p2644 A73-41155

PILOTED CENTRIFUGES

U HUMAN CENTRIFUGES

PILOTLESS AIRCRAFT

NT DRONE AIRCRAFT

NT JINDIVIK TARGET AIRCRAFT

High altitude remotely piloted vehicle /RPV/ platforms for tactical pseudo-satellite multichannel relay transponder systems 22 p2826 A73-42423

PILOTS [PERSONNEL]

NT AIRCRAFT PILOTS

NT TEST PILOTS

PINCH EFFECT

NT PLASMA PINCH

NT THETA PINCH

Magnetospheric quasi-stationary pinch effect and filamentary structure due to electron streams parallel to geomagnetic field lines 07 p0816 A73-19464

Earth magnetosphere pinch effect related to geomagnetic field pulsations and polar aurora luminosity fluctuations 10 p1212 A73-24228

Linear Z pinch magnetohydrodynamic instability mode and characteristic wavelength determined by discharge tube radius and current buildup rate 15 p1918 A73-31703

High enthalpy supersonic ionized gas flow in shock tube experiment, investigating pinch effect on flow acceleration and setup performance 19 p2415 A73-37168

Classical diffusion of free boundary plasma in plane and cylindrical slab geometries, calculating belt pinch effect and pressure decay rate 21 p2750 A73-41679

Free point method finite difference solution for two dimensional nonstationary hydrodynamic problem of continuous media, demonstrating feasibility by plasma pinch effect calculation 23 p2968 A73-43799

PINEAL GLAND

Hydroxyindole-O-methyl transferases in rat pineal, retina and Harderian gland. 02 p0136 A73-12644

Control of pineal indole biosynthesis by changes in sympathetic tone caused by factors other than environmental lighting. 19 p2393 A73-37300

PINHOLES

Evaluation of pinholes in unbaked metal film filters to be used in rocket- and satellite-borne XUV spectroheliographs. 19 p2429 A73-37262

Semiconductor failures due to oxide defects and diffusion faults, describing nematic liquid crystals application to pinholes detection in oxide layers 19 p2410 A73-38447

PION BEAMS

Interaction lengths of energetic pions and protons in iron. 08 p0990 A73-21523

Pion-nucleon interaction structure based on negative pion beam data from Serpukhov accelerator, showing secondary particle energy distribution asymmetry 23 p3021 A73-43537

PIIONEER F SPACE PROBE

U PIIONEER 10 SPACE PROBE

PIIONEER PROJECT

SNAP 19/Pioneer radioisotope thermoelectric generator program status report, stressing Jupiter first mission converters performance prediction 09 p1118 A73-22800

PIIONEER SPACE PROBES

NT PIIONEER 6 SPACE PROBE

NT PIIONEER 8 SPACE PROBE

NT PIIONEER 9 SPACE PROBE

NT PIIONEER 10 SPACE PROBE

Pioneer Jupiter spacecraft magnetic field control with periodically updated magnetic model for tradeoffs in subsystem moments within allowed magnetic budget [IEEE PAPER 41,4] 07 p0905 A73-19364

Mission building blocks for outer solar system exploration. 14 p1805 A73-30527

Heat shielding for Venus entry probes. [AIAA PAPER 73-712] 18 p2368 A73-36332

Electric propulsion interactive effects with spacecraft science payloads. [AIAA PAPER 73-559] 18 p2353 A73-36497

Pioneer Venus mission plan for atmospheric probes and an orbiter. [AIAA PAPER 73-579] 18 p2353 A73-36499

Pioneer spacecraft for atmospheric entry missions to the outer planets. 18 p2360 A73-36500

Radio occultation experiments planned for Pioneer and Mariner missions to the outer planets. 22 p2912 A73-42980

PIIONEER 6 SPACE PROBE

Pioneer 6 crossing of earth bow shock on 16 December 1965 reexamined and reinterpreted by magnetic field measurement combination with plasma data 02 p0155 A73-11729

PIIONEER 8 SPACE PROBE

Pioneers 8 and 9 cosmic dust data reliability, presenting sensor geometry, field of view, response function, instrument control and sensitivity 21 p2775 A73-41411

PIIONEER 9 SPACE PROBE

The Pioneer 9 electric field experiment. III - Radial gradients and storm observations. 17 p2230 A73-34513

PIPE FLOW

Pioneers 8 and 9 cosmic dust data reliability, presenting sensor geometry, field of view, response function, instrument control and sensitivity 21 p2775 A73-41411

PIIONEER 10 SPACE PROBE

Observations of galactic cosmic-ray intensity at heliocentric radial distances of from 1.0 to 2.0 astronomical units. 01 p0093 A73-11044

Pioneer 10 spacecraft spin-scan imaging photopolarmetric optical system for Jupiter mapping 15 p1880 A73-32385

Pioneer 10 space probe measurement of interplanetary particulates and aggregates via reflected and scattered sunlight, with emphasis on distribution in asteroid belt [AIAA PAPER 73-546] 18 p2350 A73-36095

Probing the structure and composition of the Jupiter atmosphere from Pioneer 10/11. [AIAA PAPER 73-561] 18 p2353 A73-36498

Observations of zodiacal light from the Pioneer 10 Asteroid-Jupiter probe - Preliminary results. 21 p2776 A73-41423

Pioneer 10 flyby trajectory relationship to analogy between earth and Jupiter bow shocks with emphasis on oblique shock structure 22 p2906 A73-41942

PIONS

Nuclear-electron cascades longitudinal evolution calculation in ionization calorimeter for primary nucleons and pions, using Monte Carlo method 02 p0171 A73-12654

Ionization calorimeter study of cosmic ray hadrons inelastic collision cross sections and partial K-neutral pion inelasticity factor 02 p0208 A73-12656

High energy cosmic ray pions and nucleons interactions with atomic nuclei, using ionization calorimeter and spark chambers system 02 p0209 A73-12661

K-neutral pion inelasticity factor measurement for nucleon interactions in carbon corresponding to primary neutron energy transferred to pions 02 p0209 A73-12663

Inelastic pionization cross section of cosmic ray hadrons with carbon nuclei at energies of 100 to 300 GeV 02 p0209 A73-12665

Secondary particles in pion-nucleon and coherent interactions, measuring momentum from multiple Coulomb scattering 02 p0209 A73-12666

Nuclear photoemulsions under bombardment by pion beam of 60 GeV/c momentum, investigating pion-nucleon interactions involving recoil protons 02 p0195 A73-12667

Pion-nucleon high energy interactions, determining inelasticity coefficient distribution 02 p0195 A73-12668

Spark calorimeter calibration by particle accelerator induced high energy pions, noting neutral and charged particles track detectors high geometric resolution 02 p0171 A73-12686

K-neutral pion energy fractions and inelasticity coefficients at primary energies of 100-1500 GeV during cosmic ray hadron-target interaction 02 p0210 A73-12689

Elastic scattering of negative pions from O-16 in the region of the /3, 3/ resonance. 04 p0477 A73-16037

Interaction contributions to the solar proton-proton reaction. 05 p0612 A73-17339

Energy spectra of cosmic pions and nucleons at the top of the atmosphere. 07 p0872 A73-20015

Contribution of pion production by primary cosmic-ray nucleons to the interstellar electron-positron flux. 10 p1269 A73-24348

Delta ray particle track structure theory for radiation dosimetry and biological cell response to heavy ions, fast neutrons, stopped pions and mixed radiation fields 11 p1323 A73-25423

Charged stopping pions from nuclear-electromagnetic cascades in rock, calculating number and energy spectra by Monte Carlo method 13 p1671 A73-29667

Electrically neutral condensate of pions arises in nuclear matter at neutron star densities, discussing phase transitions 21 p2771 A73-41022

Inelastic interaction between pions and emulsion nuclei at an energy of 60 GeV 23 p3021 A73-43541

PIPE FLOW

Heat transfer and hydraulic resistance of single banks and systems of tubes in cross flow of gases and viscous liquids 01 p0120 A73-10289

Natural convective heat transfer in cavities and horizontal circular tubes, considering boundary layer and core flow interaction effects 01 p0120 A73-10290

Liquid- and wall-temperature calculations for a flow in tubes with allowance for heat losses into the ambient medium and for axial heat conductivity

01 p0122 A73-10860

Gasdynamics calculations for a pulsating flow in pipelines

02 p0152 A73-11610

Molecular transmission probability through duct connecting two large vessels calculated from data on cylindrical tubes, comparing with Monte Carlo data for error correction

03 p0341 A73-12905

Measurements of pressure and velocity fluctuations in turbulent pipe flow

03 p0290 A73-12963

Steady flow of neutrally buoyant flat-faced rigid cylindrical capsules along pipeline under hydraulic pressure gradient effect, noting toroidal vortices

03 p0293 A73-13528

Magnetogasdynamic characteristics, transonic and compression regions and pressure losses of conducting gas flow in circular tube within axisymmetric magnetic field

03 p0346 A73-13620

Hydrodynamics and heat transfer in a fluid with an asymmetrical stress tensor

03 p0398 A73-13722

On a heat transfer problem in the laminar flow in a tube

03 p0398 A73-13772

Quasi-frozen flow of a thermodynamically relaxing gas

03 p0295 A73-13791

Influence of distributed grit-type roughness on the spectrum of wall pressure fluctuations of turbulent flow in a tube.

03 p0295 A73-14038

Singular characteristics of turbulent wall pressure fluctuations associated with flow in a tube.

03 p0295 A73-14041

Arterial wick heat pipes self filling capability theoretical and experimental investigation, deriving expressions for mesh size, artery radius and stem height relationships

[ASME PAPER 72-WA/HT-36] 04 p0518 A73-15819

An experimental investigation of naturally developing turbulent flow and flow with fixed transition in a parallel pipe.

[ASME PAPER 72-WA/FE-38] 04 p0435 A73-15855

The effects of compressibility in multi-element hydraulic lines.

[ASME PAPER 72-WA/FE-43] 04 p0435 A73-15857

Heat and mass transfer laws for fully turbulent wall flows.

04 p0520 A73-15935

Forced convective heat transfer to supercritical water flowing in tubes.

04 p0520 A73-15945

Combined free and forced laminar convection in inclined tubes.

05 p0564 A73-16173

Numerical solutions of the Navier-Stokes equations in inlet regions.

[ASME PAPER 72-APM-DD] 05 p0564 A73-16526

Study of local heat transfer coefficients in a tube in the case of a local flow swirling by swirl vanes

05 p0639 A73-16768

A momentum integral solution for pulsatile flow in a rigid tube with and without longitudinal vibration.

05 p0567 A73-17273

Transient heat transfer through a thin-walled circular pipe.

06 p0766 A73-17443

Associated mass of a simple doubly periodic lattice

06 p0643 A73-17465

Investigation of friction drag during gas flow in a tube with wall temperatures up to 2800 K

06 p0686 A73-18126

Asymptotic analysis of turbulent channel and boundary-layer flow.

06 p0687 A73-18528

Approximate calculations of the hydrodynamic characteristics of a turbulent flow of liquid in annular channels

06 p0688 A73-18562

Dynamics of axial heat transfer in turbulent duct flow

06 p0770 A73-18831

Intermittent behavior of a plasma discharge in turbulent gas flow.

07 p0856 A73-19517

Spiral flows in finite rotating annular tubes.

07 p0812 A73-20435

Reduction of the thermal flux through a cylindrical pipe containing an ionized gas flow

07 p0860 A73-20617

Unsteady laminar flow in a pipe with arbitrarily changing flow rate.

08 p0954 A73-20867

Blood vessels simulation by muscle pump represented by elastically deformable pipe with valves, solving Navier-Stokes equation for viscous fluid flow

08 p0934 A73-21375

Some extremum principles for pipe flow in magnetohydrodynamics.

08 p0993 A73-21403

Swirl injector driven air flow in cylindrical tube, measuring flow velocity and turbulent stress tensor components

08 p0956 A73-21601

Heat transfer for turbulent flow with suction in a porous tube.

08 p1024 A73-21637

Velocity distribution in tubes of circular cross section

09 p1072 A73-22846

Optimal measurement location for integrating pipe flowmeters, exemplifying by linearly integrating ultrasonic flowmeter

09 p1086 A73-23114

Temperature recovery coefficients during turbulent flow of liquid in a circular pipe

10 p1204 A73-23509

Influence of the Reynolds number on nonstationary convective heat transfer in a pipe during a change in the thermal load

10 p1204 A73-23511

Experimental investigation of turbulent flow structure in a circular pipe with delivery through a porous wall

10 p1204 A73-23512

An approximate analysis of the diffusing flow in a self-controlled heat pipe.

[ASME PAPER 72-HT-M] 10 p1295 A73-23776

Variable-property turbulent flow in a horizontal smooth tube during uniform heating and constant surface-temperature cooling.

10 p1295 A73-23779

An experimental study of turbulent flow in pipes with artificial wall roughness

10 p1206 A73-24460

Unsteady uniform-length turbulent flow of incompressible fluid in circular pipe studied via Reynolds and turbulence energy balance equations

10 p1210 A73-24851

Errors in the velocity-area method of measuring asymmetric flows in circular pipes.

10 p1221 A73-24861

Turbulence in a conical diffuser with fully developed flow at entry.

11 p1345 A73-25057

Interaction of free and forced convection in horizontal tubes in the transition regime.

11 p1448 A73-25153

Numerical study of a viscous flow through a pipe orifice.

11 p1346 A73-25213

Unsteady laminar convection in uniformly heated vertical pipes.

11 p1449 A73-25221

Laminar incompressible fluid steady secondary flow in circular cross section curved tube at various Reynolds numbers

11 p1346 A73-25225

Spectra of turbulent pulsations in velocity, temperature, and their correlations for air flow in a circular pipe

11 p1301 A73-25744

The force acting from the direction of a flow of liquid on a thin curved body of circular cross section

11 p1348 A73-26427

Mathematical description of the turbulent isobaric flow of a chemically reacting gas in a heated pipe

11 p1453 A73-26428

Turbulence intensity and turbulent transfer characteristics behind grids in tubes

11 p1349 A73-26431

The limits and the nature of the onset of influence of thermogravitational forces on turbulent flow and heat transfer in vertical tubes

12 p1487 A73-27313

Liquid and wall temperature during flow in tubes with heat loss to the surrounding medium and axial heat conduction.

12 p1560 A73-27909

Integral properties of viscous channel or pipe flow satisfying mixed no-slip and no-shear conditions from total momentum flux considerations

13 p1599 A73-28417

Interpretation of hot-film anemometer response in a non-isothermal field.

13 p1620 A73-29256

The unpolarized electrode in a pulsating Poiseuille pipe flow.

13 p1620 A73-29258

Energy relations for turbulent flow in rough pipes.

13 p1604 A73-29265

Phase velocities and angle of inclination for frequency components in fully developed turbulent flow through pipes.

13 p1604 A73-29266

The flow of highly rarefied gases.

14 p1744 A73-29997

Rotating flow evolution in long circular tubes, deriving mathematical formulation for laminar and turbulent flow

14 p1745 A73-30296

The calculation of low-Reynolds-number phenomena with a two-equation model of turbulence.

14 p1746 A73-30606

Uses of the equation of pulsation energy balance in the theory of MHD flows in channels and tubes

15 p1917 A73-31404

Trapped wave vortex breakdown model for long weakly nonlinear wave propagation on critical flows in tubes of variable cross sections

16 p1998 A73-32796

Swirl decay in circular pipe air flow in terms of angular and axial momenta, dimensionless parameter and velocity profiles

16 p1999 A73-32825

Identification and coding of fluid and electrical piping system functions.

[SAE AIR 1273] 16 p1970 A73-33019

Thermal creep of rarefied gas in a circular tube.

16 p2039 A73-33328

Approximate calculations of the hydrodynamic characteristics of turbulent fluid flow in annular ducts.

16 p2000 A73-33587

Heat-transfer regimes during mixed convection in vertical pipes

17 p2253 A73-34133

Pulsatile Newtonian frictional losses in a rigid tube.

17 p2151 A73-34532

Out-of-plane vibration and stability of curved tubes conveying fluid.

[ASME PAPER 72-WA/APM-36] 17 p2248 A73-35101

Temperature restitution coefficients for turbulent flow in a circular pipe.

17 p2155 A73-35189

Effect of Reynolds number on nonstationary convective heat exchange in a tube with variable heat load.

17 p2255 A73-35191

Experimental investigation of turbulent flow structure in a circular tube with expansion through a porous wall.

17 p2155 A73-35192

Light beam absorption correlation with axial dispersion of ink injected into turbulent water flow in pipe

17 p2156 A73-35509

Swirling flows in streamtubes of variable cross section.

18 p2298 A73-36314

Investigation of laminar flow in a porous pipe with variable wall suction.

[AIAA PAPER 73-725] 18 p2299 A73-36342

On the convective diffusion in tubes of circular section

18 p2299 A73-36489

Numerical calculation of heat exchange and frictional resistance for a turbulent flow in a tube in the case of a gas with variable physical characteristics

18 p2301 A73-36816

Incompressible potential flow past axisymmetric bodies in cylindrical pipes.

19 p2376 A73-37489

Experimental study of turbulent flow in pipes with artificially roughened walls.

19 p2421 A73-38130

Turbulent flow development characteristics in channel inlets.

19 p2421 A73-38184

Vibration of tubes containing flowing fluid.

[MERL-TN-72-2] 20 p2616 A73-39147

Coaxial jet mixing in confined tube simulating combustion chamber, considering Reynolds number, stream functions, recirculation, lip condition, vorticity and inlet conditions

20 p2548 A73-39518

An approach to the determination of conditions impairing heat transfer under supercritical pressure

20 p2628 A73-39614

Hankel transforms and boundary layer solutions for pulsating laminar flow in curved circular tube under sinusoidal pressure gradients

20 p2549 A73-39809

Motion of a two-component stratified gas-liquid flow in a horizontal pipe

21 p2677 A73-40989

Unsteady convective heat transfer attending the cooling of gas in tubes.

21 p2791 A73-41053

Heat pipe theory and design, discussing typical operating conditions and heat transfer capacity from flow equations solution by finite difference method

21 p2792 A73-41059

The dynamic stability of a pipe conveying a pulsatile flow.

21 p2678 A73-41671

Dispersion of a harmonic signal within a turbulent pipe flow.

21 p2678 A73-41687

Some results of experimental investigations of turbulent flow in flexible tubes

22 p2841 A73-42120

Experimental investigations of the effects of polymer additions on the kinematic characteristics of a plane turbulent flow in a tube with variable wall roughness

22 p2841 A73-42121

Influence of suction on the supercavitation flow behind a body in a porous tube
22 p2841 A73-42125

German monograph - A contribution to the investigation of the stability of pipelines with flowing liquids according to the method of finite elements.
22 p2924 A73-42737

The dynamic behavior of articulated pipes conveying fluid with periodic flow rate.
[ASME PAPER 73-APMW-32] 22 p2925 A73-42892

Some effects of pipe flow generated entry conditions on the performance of straight walled conical diffusers with high sub-sonic entry Mach number.
23 p2939 A73-43294

Laminar flow of a viscous barotropic gas through a circular pipe
23 p2968 A73-43721

Technically oriented algorithms for unsteady pipe flow.
23 p2968 A73-43800

Space-time autocorrelation and cross correlation coefficients for transverse turbulent velocity fluctuations in pipe flow
24 p3080 A73-45451

A method of calculating a chemically nonequilibrium flow of gas in a heated tube under conditions close to the equilibrium or frozen state
24 p3081 A73-45527

Experimental investigation of the viscosity of lubricating oil containing air
24 p3094 A73-45548

PIPELINES

Steady flow of neutrally buoyant flat-faced rigid cylindrical capsules along pipeline under hydraulic pressure gradient effect, noting toroidal vortices
03 p0293 A73-13528

Large payload aircraft for Alaskan and Canadian gas-oil transportation, examining alternative pipeline economic factors and possible new North Canadian island fuel fields
16 p2088 A73-33183

Studies on the hydraulic loss in pipe bends - Results for 90-deg screw type elbows.
19 p2420 A73-37672

Floating superport.
19 p2418 A73-37748

Failure stress levels of flaws in pressurized cylinders.
22 p2921 A73-42156

German monograph - A contribution to the investigation of the stability of pipelines with flowing liquids according to the method of finite elements.
22 p2924 A73-42737

Theory and design of pipelined fast Fourier transform processors.
23 p2956 A73-43325

Fracture control - Past, present and future.
23 p3039 A73-43383

PIPES (TUBES)

NT GAS PIPES

Theoretical and experimental analysis of plane and cylindrical reinforced-plastic structures
02 p0185 A73-12794

A numerical solution of an elastoplastic thick-walled tube subjected to thermal loading.
[AIAA PAPER 73-256] 05 p0635 A73-16978

Prevention of pollution in hydraulic circuits.
06 p0649 A73-17845

Thin-walled pipe designs with a curvilinear axis
09 p1158 A73-22362

A note on the arrangement of strain gauges and the sensitivity of strain measurement.
10 p1219 A73-24572

Determination of the turbulent exchange coefficients in the case of tube bundles in crossflow
11 p1448 A73-25109

Considerations concerning the inadequacy of the classical concept of equivalent diameter in calculations of heat transfer in elliptical pipes
12 p1557 A73-26796

Deterioration of impermeable alumina tubes in inert atmospheres at elevated temperatures.
12 p1515 A73-27032

Large elastic flexural and elongation strains in a portion of tube prepared from a material with different resistance to tensile and compressive strains
12 p1552 A73-27369

Production of a niobium-stainless steel bimetal by explosion welding
14 p1755 A73-30386

Stress concentration in tubes with a hole of star-shaped profile
19 p2494 A73-37185

Welded titanium tubes and their applications
19 p2433 A73-37834

Hot fluomachining of Ti alloy tubes and turbine casings, noting dimensional accuracy dependence on temperature
19 p2441 A73-37835

Book - Criteria for current and advanced aircraft hydraulic tubing.
[SAE SP-378] 19 p2434 A73-37863

Commercial jet transport aircraft hydraulic fuel distribution tubing systems, discussing maintenance,

fabrication problems, fittings, quality control and materials
[SAE SP-378] 19 p2434 A73-37864

The application of Armco 21-6-9 steel tubing to the DC-10 hydraulic system.
[SAE SP-378] 19 p2389 A73-37865

Aircraft hydraulic tubing permissible defects in Cr-Ni-Mn, Al and Ti tubes and return lines, noting wall thickness, chafing, denting, weld seam cracks and impulse tests
[SAE SP-378] 19 p2434 A73-37866

Defects in high quality aircraft tubing and inspection methods.
[SAE SP-378] 19 p2434 A73-37867

Quality requirements for Ti-3Al-2.5V annealed and cold worked hydraulic tubing.
[SAE SP-378] 19 p2434 A73-37868

Production of extruded tube hollows for titanium 3Al-2.5V hydraulic tubing.
[SAE SP-378] 19 p2434 A73-37869

The development and control of crystallographic texture in 3Al-2.5V titanium alloy tubing.
[SAE SP-378] 19 p2434 A73-37870

The effects of crystallographic texture on the mechanical and fracture properties of Ti-3Al-2.5V hydraulic tubing.
[SAE SP-378] 19 p2434 A73-37871

Surface conditioning of titanium alloy tubing.
[SAE SP-378] 19 p2434 A73-37872

Application of the hydrostatic extrusion process toward production of 3Al-2.5V titanium alloy hydraulic tubing.
[SAE SP-378] 19 p2434 A73-37873

Heat release by free convection from horizontal cylinders to CO₂ under near-critical conditions
20 p2628 A73-39613

Steady-state creep of a thin-walled tube in the general case of applied forces
21 p2787 A73-41194

Phase-sensitive method of electromagnetic flaw detection.
24 p3093 A73-44696

Experimental investigations regarding optimally designed three-layer wound glass fiber/plastic tubes under internal pressure
24 p3147 A73-44882

PISTON ENGINES

NT DIESEL ENGINES

Piston engine turbocharging system based on split low and high pressure exhaust gas discharge porting, discussing different turbine staging arrangements
10 p1263 A73-24925

The development of reciprocating engine installation data for general aviation aircraft.
[SAE PAPER 730325] 17 p2102 A73-34681

Design of a piston-driven shock tube
21 p2675 A73-41552

PISTON THEORY

Rise time and pressure measurements in transient flow during quasi-steady gas injection into vacuum with piston valve, using fast ionization gage
02 p0168 A73-11963

Quasi-frozen flow of a thermodynamically relaxing gas
03 p0295 A73-13791

Rates of change of flutter Mach number and flutter frequency.
03 p0395 A73-14188

Fluid undercutting in the successive channel flow of two gases.
[AIAA PAPER 73-214] 05 p0566 A73-16944

Piston motion in semiclosed tube under high initial pressure, using gas-to-piston mass ratio as perturbation parameter in analysis based on Lagrange solution [DFVLR-SONDDR-255] 06 p0685 A73-17739

Movement of viscous incompressible fluids through annular interstices with walls in relative alternating translational motion
12 p1486 A73-26795

Cauchy problem solution for motion of piston generating shock wave after fast impact under influence of one dimensional gas flow
15 p1822 A73-31289

Permeable elastic piston models of shock wave formation before flame front during inflammable gas mixture combustion in channels
15 p1957 A73-31868

Stability of the general plane membrane adjacent to a supersonic airstream.
[ASME PAPER 72-APM-UUU] 17 p2248 A73-35103

Nonlinear gas oscillations in pipes, I - Theory.
18 p2299 A73-36505

Exact solutions of some problems of the Stefan type
20 p2627 A73-39335

A numerical study of the explosion of a supernova into the interstellar magnetic field.
22 p2914 A73-43007

PISTONS

Expanding split ring seal types for pistons, discussing straight cut, step, two piece and three piece rings and pressure and friction effects
22 p2865 A73-41777

PITCH

Some kinematic considerations of tone generation in axial turbomachinery.
22 p2899 A73-41710

Mathematical model of human pitch perception based on acoustic stimulus Fourier transformation by sense organ into peripheral neural activity pattern recognition
22 p2811 A73-41816

Multiple pure tone noise generation and control.
[AIAA PAPER 73-1021] 24 p3122 A73-44853

PITCH (INCLINATION)

Magnetospheric tail plasma sheet near earth structure explained via tangential magnetic field gradient drift velocity coupling to strong pitch-angle diffusion
02 p0157 A73-11898

Shadowing of electron azimuthal-drift motions near the noon magnetopause.
02 p0164 A73-12442

Stability characteristics of re-entry wing shapes and their measurement.
03 p0244 A73-13567

Characteristics of magnetosheath plasma observed at low altitudes in the dayside magnetospheric cusps.
03 p0302 A73-13857

Observations suggesting weak pitch angle diffusion of protons.
04 p0493 A73-15532

Accelerations of points on a flight vehicle during short-period motion
07 p0777 A73-20095

A laser optical lever system for measuring the pitch and yaw of a ground-launched rocket.
08 p0974 A73-20669

Electron pitch angle distributions throughout the magnetosphere as observed on Ogo 5.
10 p1213 A73-24732

Time optimal control of satellite pitching motions by variable mass distribution, solving nonlinear optimization problem via maximum principle
16 p2072 A73-33233

Synchrotron radiation sources with relativistic particles moving at small pitch angles in magnetic field, discussing emission properties and degrees of polarization
19 p2484 A73-37617

Inner zone population of trapped 2.14-9.0 MeV alpha particles, noting strong peak in pitch angle and intensity decrease with L value decrease
22 p2901 A73-41910

Application of harmonic analysis to the calculation of staturs with variable blade pitch
23 p3019 A73-43734

Magnetically trapped charged particle pitch angle diffusion and lifetime calculation for radiation belts, taking into account geomagnetic dipole geometry
24 p3127 A73-45138

PITCH ANGLES

U PITCH (INCLINATION)

PITCH ATTITUDE CONTROL

U LONGITUDINAL CONTROL

PITCHING MOMENTS

Pitch amplitude stabilization in a spacecraft carrier body
09 p1155 A73-23107

Some effects of camber on swept-back wings.
[SAE PAPER 730298] 17 p2094 A73-34661

Flight simulator evaluation of control moment usage and requirements for V/STOL aircraft.
[AHS PREPRINT 743] 17 p2147 A73-35076

Prediction of the lift and moment on a slender cylinder-segment wing-body combination.
19 p2377 A73-38007

On the aerodynamic damping moment in pitch of a rigid helicopter rotor in hovering, I - Experimental phase.
19 p2387 A73-38281

On the aerodynamic damping moment in pitch of a rigid helicopter rotor in hovering, II - Analytical phase.
21 p2631 A73-40087

Closed-form lift and moment for Osborne's unsteady thin-airfoil theory.
21 p2632 A73-40442

PITOT STATIC TUBES

U PITOT TUBES

U SPEED INDICATORS

PITOT TUBES

Anomalous lower dynamic pressure in piezometer of pitot tube in liquid flow containing solid particles, using seeds in aqueous solution of calcium chloride
11 p1367 A73-26476

Maintenance of pitot-static systems of transport aircraft.
[SAE AIR 975] 16 p2014 A73-33014

Aerodynamic interference of pitot tubes in a turbulent boundary layer at supersonic speed.
22 p2796 A73-42552

Dynamic range and frequency response of the vortex rate sensor.
23 p2942 A73-43406

PITS

On the nature of films over corrosion pits in stainless steel.
11 p1378 A73-24975

PITTING

PITTING

Surface preparation and pit propagation in stainless steels.

03 p0325 A73-13726

Study of pitting corrosion and stress corrosion in stainless steels with the aid of alloys of very high purity

07 p0838 A73-19114

Composition of anolyte within pit anode of austenitic stainless steels in chloride solution.

07 p0840 A73-20352

Temperature dependent pitting corrosion tests of Mo containing austenitic stainless steels

07 p0840 A73-20354

Distinguishing characteristics of pitting and crevice corrosion.

08 p0980 A73-21775

Study on the superposition of intergranular corrosion and pitting corrosion by fatigue cracking of stainless steels.

11 p1383 A73-25831

On the relationship between grainboundary corrosion and stress corrosion cracking of Al-Zn-Mg alloys.

12 p1511 A73-27059

Pitting corrosion - A review of recent advances in testing methods and interpretation.

15 p1889 A73-31741

Pitting of titanium. I - Titanium-foil experiments. II - One-dimensional pit experiments.

23 p2991 A73-43521

PITUITARY GLAND

Participation of the hypophysis and adrenal glands in intra-ocular pressure regulation

22 p2807 A73-42661

PITUITARY HORMONES

Relation between the frequency-amplitude characteristics of cerebral electrical activity and gonadotropic hormone excretion levels at various stages of ontogenesis

08 p0930 A73-21319

High altitude chamber effect on thyroid stimulating hormone and thyroxine concentrations, noting shift from extra to intravascular

09 p1041 A73-22926

Hypothalamo-adenohypophysis-adrenal neurosecretory system under hyperthermia

14 p1719 A73-30847

Mechanisms of secretion of neurohypophyseal hormones - Cellular and subcellular aspects

15 p1836 A73-32286

PIVOTED WING AIRCRAFT

U TILT WING AIRCRAFT

PIVOTS

Determination of directional corrections and the time required for passage through the meridian on the basis of 'pivot irregularities' obtained with the aid of 'pivot deviations'

03 p0307 A73-13244

PLAGES [FACULAE]

U FACULAE

PLAINES

NT FLOOD PLAINS

PLAN POSITION INDICATORS

A proposal on automatic tracking of an aircraft for the radar.

14 p1728 A73-30471

Pulsed-Doppler velocity isotach displays of storm winds in real time.

18 p2333 A73-36707

PLANAR STRUCTURES

Current spreading at contacts to planar Gunn devices.

07 p0799 A73-19343

Drift of the breakdown voltage in highly doped planar junctions.

09 p1064 A73-23047

Computational estimate of applicability of infinite-array theory.

09 p1065 A73-23099

Application of the finite element method to the study of the stability of plane structures

10 p1287 A73-23618

Directivities of planar arrays with triangular arrangement of elements.

11 p1333 A73-26699

Planar dipole antenna arrays directivity evaluation from spatial radiation density distribution, considering arbitrary aperture shape and amplitude loading

12 p1469 A73-27040

Mean value and variance of the directivity of randomly thinned array antennas

16 p1979 A73-33093

Elastic semiinfinite cylindrical shell stress-strain state after axial impact against static rigid plane, obtaining solutions for small time values

17 p2244 A73-34740

Substrate effect estimation for space charge limited current in intrinsic materials and planar structures, discussing I-V curves

20 p2543 A73-39593

Planar phased array beam steering methods, emphasizing electronic driver and logic circuit sharing between phase shifters for cost reduction

21 p2652 A73-40666

Planar conductance transistor based on charge carrier accumulation due to n-n junction, featuring steep negative resistance characteristics and low sustaining voltage

21 p2655 A73-41048

Plane strain and generalized plane stress problems for fibre-reinforced materials.

21 p2788 A73-41546

Investigation of temperature pulsations accompanying the heating of a laminar sample by alternating and pulsating currents

23 p3048 A73-43446

PLANCKS CONSTANT

Error minimization methods for Planck law remote measurements of single and two color temperature, considering multiple wavelengths

04 p0445 A73-15773

Quantum and relativity theories compatibility based on hypothesis of matter tensor delta structure and Plancks constant for action singularity

14 p1775 A73-30425

PLANE WAVES

Application of the averaging method to the problem of plane wave propagation in a dissipative heat conducting medium

01 p0075 A73-10086

Kinetic theory of scattering by a plasma cylinder.

01 p0081 A73-10136

Nonlinear magnetic sound in a gravitational field

01 p0016 A73-10202

Incidence of a plane electromagnetic wave on a moving shock wave in an ionized gas

01 p0016 A73-10205

Interaction of opposed beams of electromagnetic waves in a transparent nonlinear medium

01 p0016 A73-10208

Incident plane wave fluctuations effect on diffraction pattern formed by scattering on reflecting sphere, calculating amplitude distribution in Fresnel and Fraunhofer regions

01 p0016 A73-10211

Reflection of plane stress waves in an elastoplastic medium with a variable yield limit

01 p0114 A73-10570

Wave propagation in elastic laminates using a multi-continuum theory.

01 p0117 A73-11364

Conical solutions for diffraction of plane pulse wave by three dimensional trihedron corner via boundary conditions reduction to eigenvalue problem, presenting sonic boom example

01 p0019 A73-11424

The velocity of a wave packet in an anisotropic absorbing medium.

01 p0079 A73-11494

Quasimonochromatic whistler mode packets of slowly varying amplitude.

02 p0140 A73-11920

Plane electromagnetic wave diffraction by periodic grid of dielectric cylindrical filaments, determining reflection and transmission coefficients of radome composite materials

02 p0141 A73-12024

An analysis of thermally-induced plane waves in elastic-plastic single crystals.

03 p0394 A73-13980

The effect of polarity on the diffraction of plane elastic waves by a cylindrical cavity.

03 p0396 A73-14627

Total reflection of a plane wave by a semi-infinite random medium.

04 p0480 A73-15198

Net-field polarization in a magnetically biased plasma.

04 p0422 A73-15481

Plane time-harmonic wave propagation through periodically arranged composite material, determining displacement mode shapes and dispersion relations by variational method

[ASME PAPER 72-WA/APM-10]

04 p0516 A73-15902

Diagnostic procedures for nonhomogeneous plasma based on geometrical optics approximation, irradiating plasma by plane wave at oblique incidence

05 p0601 A73-16070

Outer-scale effects in turbulence-degraded light-beam spectra.

05 p0597 A73-16498

Approximate method for solving wave propagation problems in viscoelastic materials

05 p0636 A73-17088

Stream instabilities in a cold plasma in the presence of a magnetic field.

06 p0728 A73-17793

Wave propagation in a micro-isotropic, micro-elastic solid.

06 p0762 A73-17990

A new approach to the problem of wave fluctuations in localized smoothly varying turbulence.

06 p0665 A73-18183

Monte Carlo computer technique for one-dimensional random media.

06 p0665 A73-18188

Source excited dielectric wedge surface magnetic field local mode solution compared with plane wave method, noting inaccuracy near surface wave cutoff

06 p0666 A73-18197

Diffraction of an arbitrary plane electromagnetic wave by a half-plane.

06 p0667 A73-18203

Diffraction of electromagnetic plane wave by an infinite slit embedded in an anisotropic plasma.

06 p0668 A73-18356

Propagation of one-dimensional, plane waves in a physically nonlinearly-elastic medium

06 p0765 A73-18691

On the reflection of harmonic waves in fiber-reinforced materials.

07 p0909 A73-19096

Transverse hydromagnetic plane waves in the presence of a temperature gradient.

07 p0856 A73-19339

E-polarized plane wave diffraction by conducting wedge loaded with thin dielectric slab, obtaining Fresnel integral solution with application to cylindrical wave excitation

07 p0792 A73-19383

Diffraction of a plane electromagnetic wave at an array of circular cylinders with a spiral slot

07 p0793 A73-19917

The plane-wave method in the study of helium atoms physisorbed on graphite

07 p0843 A73-20000

On the transmission of the energy in an incompressible magnetohydrodynamic wave into a conducting solid.

07 p0858 A73-20029

Diffraction of a plane wave by a random phase screen.

07 p0793 A73-20056

Diffraction of plane electromagnetic wave at anisotropic halfspace in free space and in planar waveguide.

07 p0793 A73-20126

Influence of radiation damping on the motion of a charge in a uniform magnetic field and in the field of a plane electromagnetic wave

08 p0989 A73-21516

Propagation of a transverse harmonic wave in a plate with a statistically rough circular hole

08 p1020 A73-21770

Resonant excitation of a circular cylinder with a longitudinal slit by a plane wave

09 p1048 A73-21905

Momentum method extension to thermal conduction laser heating of nonhomogeneous plasma, obtaining closed form solutions for plane waves

09 p1126 A73-22171

On the definitions of parameters in ferrite-electromagnetic wave interactions.

09 p1062 A73-22323

Scattering by perfectly conducting rotational bodies of arbitrary form excited by an obliquely incident plane wave or by a linear antenna.

09 p1052 A73-22959

Simultaneous diffusion of photons and particles in a semiinfinite space. II - Concentration of excited atoms before a shock wavefront

09 p1123 A73-23069

Conversion of the wave spectrum in a medium with smooth spatial-temporal fluctuations

09 p1052 A73-23082

Strong irradiance fluctuations in turbulent air - Plane waves.

10 p1248 A73-23837

The energy-momentum tensor for an electromagnetic wave in plasma.

10 p1254 A73-24115

Restoring the orthogonality of two polarizations in radio communication systems. II.

10 p1190 A73-24623

Study of the Rayleigh zone of circular radiating apertures

11 p1328 A73-25283

Calculation of the radiation diagram of an antenna in the presence of a radome

11 p1328 A73-25285

Near field of scattering by a hollow semi-infinite cylinder and its application to sensor booms.

11 p1328 A73-25658

Near-field analysis by the plane-wave spectrum approach.

11 p1329 A73-25674

Reflection and transmission of radio waves at a dielectric slab with variable permittivity.

11 p1329 A73-25675

Size determination of a perfectly conducting sphere from the extrema of Mie scattering intensities.

11 p1329 A73-25679

Inverse scattering method application to plane wave incident on perfectly conducting sphere, comparing results to simulation experiments

11 p1329 A73-25680

Plane wave expansion approximation for wave field on dielectric wedge representing tapered antenna, considering lateral wave contribution

11 p1329 A73-25681

Time-dependent electromagnetic field scattering and diffraction by half plane during illumination by impulsive plane cylindrical or spherical wave
11 p1330 A73-25683

The wave length dependence of the transfer properties of photographic materials for holography.
11 p1370 A73-26536

Electromagnetic wave scattering by an inhomogeneous magnetoplasma column moving in the axial direction.
11 p1407 A73-26700

An existence proof for permanent capillary gravity waves with general vortex distributions
11 p1349 A73-26747

Changes in the mean energy of an electron in the field of a plane wave with allowance for radiation damping
12 p1526 A73-26969

On the momentum of quasi-monochromatic waves in a plasma.
[IPPCZ-167] 12 p1529 A73-27435

Application of series to an investigation of a plane electromagnetic wave in a ferromagnetic half-space
12 p1474 A73-27804

Reflection of plane heterogeneous and uniform electromagnetic waves and the reflected wave displacement
13 p1658 A73-28072

Scattering from a periodic corrugated surface - Semi-infinite alternately filled plates.
13 p1659 A73-28484

Extension of the hodograph method for the one-dimensional elastic-plastic wave propagation.
13 p1696 A73-28646

Plane and cylindrical electromagnetic waves diffraction on infinitely long cylindrical bodies, calculating induced currents, diffraction patterns and near fields
13 p1582 A73-28654

Diffraction of a plane wave at an array of planar waveguides with projecting dielectric plates.
13 p1582 A73-28655

Plane TE polarized electromagnetic wave diffraction on infinite conducting cylinder in nonhomogeneous medium, calculating far field diffraction patterns
13 p1582 A73-28656

Conditions for stability of incompressible elastic material obtained from small-amplitude plane sinusoidal waves superposed on finitely deformed state of material
13 p1696 A73-28753

Planar shear wave motions polarized in plane of bonded elastic orthotropic layered plates with each layer having distinct mechanical and inertial properties and thickness
13 p1697 A73-28820

Asymptotic pressure calculation of plane acoustic wave diffraction by infinitely long isotropic solid elastic circular cylinder in viscous liquid medium
13 p1583 A73-28863

Upper and lower stability limits criterion for plane shock waves, based on Hugoniot curve positive slope
15 p1860 A73-31090

General properties of electromagnetic scattering by inhomogeneous anisotropic composite obstacles of arbitrary shape.
15 p1844 A73-31930

Obliquely incident plane wave scattering from moving perfectly conducting cylinder, discussing mode coupling, Doppler shift and far field scattered power
15 p1845 A73-32238

Resonant excitation of a circular cylinder with a longitudinal slot by a plane wave.
15 p1847 A73-32630

Planar pressure waves propagation across wall with elastically supported and damped edges, considering induced gas flow characteristics behind wall
16 p2000 A73-33257

Correlation measurements on the complex amplitude of stellar plane waves perturbed by atmospheric turbulence.
16 p2037 A73-33684

Hydrodynamic equilibrium structure of plane shock waves in arbitrary liquid or gas at large distance behind shock front
16 p2001 A73-34059

Diffraction of a plane electromagnetic wave on arrays of periodically spaced cylinders
17 p2121 A73-34583

Plane finite amplitude viscoelastic wave propagation, deriving expressions for nonlinear, dispersion and dissipation effects
17 p2244 A73-34792

Plane monochromatic electromagnetic waves in general relativity theory
17 p2212 A73-35562

Book - Acoustic fields and waves in solids. Volumes 1 & 2.
17 p2213 A73-35597

Book - Electromagnetic wave propagation.
17 p2130 A73-35857

Two dimensional wave problems in rotating elastic media.
19 p2460 A73-38183

Boltzmann equation with Gross-Krook type model for investigation of steady plane shock wave structure in fully ionized gas
20 p2596 A73-38968

Wave equation solutions for free plane standing wave fields formation in unbounded elastic media
21 p2740 A73-40794

Reflection and transmission of plane waves at a boundary between two conducting media.
21 p2655 A73-41047

Diffraction of a plane electromagnetic wave by a slit in a thick screen placed between two different media.
22 p2821 A73-41744

Diffraction of a plane electromagnetic wave by a perfectly conducting elliptic cylinder.
22 p2822 A73-41749

Plane transient electromagnetic wave propagation in a generalized conducting medium.
22 p2886 A73-41965

Energy propagation lines in the diffraction of a plane electromagnetic wave by a slot in a conductive plane
22 p2826 A73-42353

Computer simulation of the acceleration of charged particles captured by plane electromagnetic waves
22 p2826 A73-42378

Plane shock wave propagation, reflection and transmission in subsonic flow regime through T-junctions, predicting pressure variation upstream and downstream for comparison with experiment
23 p2967 A73-43295

Damping of a plane shock wave during high-velocity impact
24 p3076 A73-44712

Similarity of flows arising during reflection of weak shock waves from a rigid wall and from a free surface
24 p3076 A73-44713

Electromagnetic wave interaction with moving bounded plasmas.
24 p3069 A73-45409

PLANET EPHEMERIDES
Synoptic Jupiter visual observation during 1966-1968, noting band activity and Red Spot longitude change
01 p0101 A73-10849

The role of occultations in the improvement of the lunar ephemeris.
03 p0369 A73-13107

Resonances and encounters in the inner solar system.
04 p0500 A73-15519

Choosing the optimal distribution of radar and optical observations of Venus
09 p1142 A73-22091

Normal matrix equations for major planet orbital element corrections from optical observations, testing by numerical experiment for Mercury
09 p1143 A73-22096

Analytical solution of lunar ephemerides, considering sun-earth-moon problem and required corrections and perturbation methods
09 p1147 A73-22710

Position and velocity components for Jupiter VIII-XII.
11 p1429 A73-26684

Positions of minor planets Baumeia 813, Triberga 619, and Jessonda 459.
11 p1429 A73-26687

Some preliminary conclusions from the available observation results of the International Saturn Patrol of 1966
16 p2070 A73-33847

Mars physical ephemeris elements and aerographic coordinate system for Mariner 9 mapping
19 p2479 A73-37228

Mars almanac /ephemerides, rotation data, coordinate data, etc/ for Viking lander position definition and stellar and planetary observations from Mars surface
21 p2733 A73-40031

Apollo asteroid discovery, orbital peculiarities, future earth approaches, Apollo group ephemerides and distribution
21 p2765 A73-40299

Simultaneous determination of pole coordinates and the nonuniformity of the earth's rotation
21 p2768 A73-40727

PLANET ORIGINS
PLANETARY EVOLUTION
PLANETARIUMS
Starry sky energetic simulator design, analyzing comparative brightness of stars
13 p1598 A73-29321

PLANETARY ATMOSPHERES
NT JUPITER ATMOSPHERE
NT MARS ATMOSPHERE
NT VENUS ATMOSPHERE
A solution to the auxiliary equation of radiative transfer for a planetary atmosphere with molecular anisotropy.
01 p0097 A73-10352

Synthetic spectra production via solution of radiative transfer equation at frequencies across absorption

PLANETARY ATMOSPHERES
line for homogeneous and inhomogeneous atmospheres
01 p0097 A73-10362

Nongray theory for temperature wave propagation without turbulent or convective motions, discussing diurnal waves simulation for planetary atmospheres
01 p0039 A73-10396

Homogeneous gas sphere model light scattering for different energy source distributions in planetary and stellar atmospheres
01 p0100 A73-10704

Estimation of the global circulation characteristics of planetary atmospheres with various hypotheses concerning the nature of dissipation
01 p0040 A73-10868

The spherical albedo of a planetary atmosphere
01 p0102 A73-10942

Similarity theory of planetary atmosphere circulations applied to solar atmosphere in terms of radius and rotational Mach number
01 p0106 A73-11316

Absorption line profile and equivalent line width derivation for planetary atmosphere with low and high optical thicknesses, assuming arbitrary scattering coefficients
01 p0106 A73-11321

Molecular beam simulation of planetary atmospheric entry - Some recent results.
03 p0287 A73-13564

Titan atmosphere composition of methane hydrate with ammonia impurity, discussing hydrogen and hydrocarbon production, liquid water existence and greenhouse effects
04 p0497 A73-14973

Two layer model for diurnal temperature variations analysis of radiative heat transfer between planetary lower atmosphere and underlying
04 p0473 A73-15574

Complete spectrum of pulsation frequencies for a polytropic atmosphere.
04 p0504 A73-16029

Study of accuracy requirements for autonomous trajectory measurements providing conditions for entering planetary atmospheres
05 p0619 A73-17001

Radiation transfer in a single-layer spherical planetary atmosphere
05 p0620 A73-17015

Calculation of light scattering in planetary atmospheres with allowance for refraction
05 p0599 A73-17358

Symposium on Planetary Atmospheres and Surfaces, Madrid, Spain, May 10-13, 1972, Proceedings.
06 p0743 A73-17427

Review of surface and atmosphere studies of Venus and Mercury.
06 p0743 A73-17428

Stabilization concepts for a spherical planetary entry probe configuration.
06 p0756 A73-17653

[ALAA PAPER 73-184] The atmospheres of the earth and the terrestrial planets - Their origin and evolution.
06 p0749 A73-17868

Uranus atmosphere - Structure and composition.
07 p0874 A73-19068

Potential atmospheric composition of smaller bodies in the solar system and some aspects of planetary evolution.
07 p0875 A73-19249

Determination of the transfer function for the spectral albedo of the surface-atmosphere system of the planet
07 p0818 A73-19659

Cross sections for emission of Lyman-alpha radiation in collisions of 1-25 keV protons and hydrogen atoms with constituents of planetary atmospheres.
08 p0957 A73-20660

Theorems on symmetries and flux conservation in radiative transfer using the matrix operator theory.
08 p1020 A73-20791

Intensity variation across Uranus disk during limb darkening-brightening cycles observations to test cloud absence theory, predicting limb brightening in methane bands
08 p1003 A73-20889

On the He-H2 thermal opacity in planetary atmospheres.
08 p1003 A73-20890

Measurements on the infrared lines of planetary gases at low temperatures. I - Nu-3 fundamental of methane.
08 p1003 A73-20891

Investigation of molecular absorption in the atmospheres of the giant planets
08 p1007 A73-21064

Remote sensing of the turbulence characteristics of a planetary atmosphere by radio occultation of a space probe.
09 p1146 A73-22427

Determination of the transfer function of a planet atmosphere by spectrophotometry of the planet surface from space
09 p1077 A73-22488

Spherical albedo of a planetary atmosphere.
09 p1147 A73-22737

- Planetary atmospheres 09 p1152 A73-23471
- Light flux vertical distribution in spherical multilayer cloud and gas scattering planetary atmosphere, calculating radiation intensity 10 p1276 A73-23891
- Light scattering functions in the atmospheric ground layer for a range of large scattering angles 11 p1393 A73-25616
- Logarithmic wind profile in neutral barotropic planetary boundary layers, discussing von Karman constant 11 p1394 A73-25717
- An explicit form of the Mie phase matrix for multiple scattering calculations in the I, Q, U and V representation. 11 p1390 A73-25718
- Phase equilibria in fluid mixtures at high pressures - The He-CH₄ system. 11 p1399 A73-25889
- Ultra-violet argon dayglow lines in the atmosphere of Mercury. 11 p1421 A73-25916
- Ionospheric currents induced by solar wind interaction with planetary atmospheres. 11 p1412 A73-25921
- The effect of a uniform external pressure on the ionospheric boundary of a non-magnetic planet in a steady solar wind. 11 p1421 A73-25925
- General theory of optimal trajectory for rocket flight in a resisting medium. 12 p1538 A73-27119
- Luminosity levels in deep planetary atmosphere layers 12 p1536 A73-27858
- Optical properties and structure of the atmosphere of Saturn. II - Latitudinal variations of absorption in the CH₄ 0.62-micron line and the characteristic features of the planet in the near ultraviolet 12 p1546 A73-27862
- Formation of spectral lines in planetary atmospheres. V - Collision narrowed profiles of quadrupole lines in hydrogen atmospheres. 13 p1680 A73-28456
- Formation of spectral lines and study of growth curves in a semiinfinite scattering atmosphere 13 p1680 A73-28458
- Estimates of global circulation characteristics of planetary atmospheres. 13 p1607 A73-28692
- Gaseous ring mechanism of Titan atmosphere, considering atmospheric particle outgassing and recapture under Saturn gravitational field to form torus at Titan orbit 14 p1788 A73-29719
- Planetary atmospheres chemistry, discussing physical factors, atomic oxygen reactions, ozone, airglow and mathematical models 14 p1723 A73-30128
- Elemental and isotopic abundances of the volatile elements in the outer planets. 14 p1799 A73-30529
- Outer planet satellites and atmospheres composition and structure from low temperature condensation accretion models 14 p1724 A73-30530
- The significance of atmospheric measurements for interior models of the major planets. 14 p1799 A73-30532
- The dynamics of the atmospheres of the major planets. 14 p1799 A73-30534
- Jupiter, Saturn, Uranus and Neptune upper atmospheric ionization equilibrium distribution, emphasizing ionosphere 14 p1799 A73-30535
- Imaging as primary exploration tool for outer planets and satellites, considering flyby and orbital imaging for planetary atmospheres 14 p1800 A73-30536
- Long wave measurements of brightness temperature for thermal structure of major planet atmospheres at great depths, discussing Jupiter and Saturn microwave spectra 14 p1800 A73-30537
- Scaling laws for outer planet magnetospheres, noting energetic trapped particles radiation belts possibility 14 p1800 A73-30538
- Remote sensing of LF nonthermal radio emission for composition and dynamic processes of interplanetary and interstellar media and planetary magnetospheres 14 p1800 A73-30539
- Outer solar system, including planetary atmospheres, natural satellites, solar wind, interstellar cosmic rays and spacecraft missions 14 p1800 A73-30616
- Calculation of light scattering in planetary atmospheres with allowance for refraction. 15 p1912 A73-31008
- Observational constraint on the structure of hydrogen planets. 15 p1936 A73-31565
- Water vapor from a lunar breccia - Implications for evolving planetary atmospheres. 16 p2060 A73-33124
- Radiation transport theory for anisotropic light scattering in planetary atmospheres, formulating transmission and reflection coefficients 16 p2066 A73-33790
- Jupiter and Saturn optical observations, discussing atmospheric composition, cloud layers and temperature distribution 16 p2069 A73-33837
- Book - Space physics and space astronomy. 17 p2230 A73-34575
- Saturn - A study of the 3 nu sub 3 methane band. 17 p2231 A73-34765
- The escape of H₂ from Titan. 17 p2232 A73-34861
- Scientific considerations for a common Saturn/Uranus atmospheric entry probe. [ALAA PAPER 73-594] 18 p2350 A73-36080
- Plasma physics phenomena in the outer planet magnetospheres. [ALAA PAPER 73-566] 18 p2345 A73-36097
- Solar wind-Mercury atmosphere interaction - Determination of the planet's atmospheric density. 18 p2352 A73-36294
- Reflecting heat-shield entry analysis computer program for planetary probes. [ALAA PAPER 73-714] 18 p2368 A73-36333
- Planetary atmospheric entry vehicles shock layer energy transport with nongray radiation, using optical thick-thin approximation for radiative transfer in temperature distribution calculation 18 p2369 A73-36334
- Pioneer spacecraft for atmospheric entry missions to the outer planets. [ALAA PAPER 73-595] 18 p2360 A73-36500
- Molecular absorption in the atmospheres of the giant planets. 18 p2355 A73-36865
- Path-length distributions of photons diffusely reflected from a semi-infinite atmosphere. 18 p2314 A73-37110
- Effect of noble gases on an atmospheric greenhouse /Titan/. 19 p2487 A73-38173
- Planetary boundary-layer turbulence studies from acoustic echo sounder and in-situ measurements. 19 p2448 A73-38223
- Light flux vertical distribution in spherical multilayer cloud and gas scattering planetary atmosphere, calculating radiation intensity 20 p2603 A73-38910
- Radiation field in the deep layers of planetary atmospheres. 20 p2602 A73-39232
- Optical properties and structure of Saturn's atmosphere. II - Latitudinal variations of absorption in the 0.62-micron CH₄ band and characteristics of the planet in the near ultraviolet. 20 p2608 A73-39236
- Absorption line contours in homogeneous plane-parallel semiinfinite aerosol layers and planetary atmosphere overcloud gas layers for nonspherical scattering 21 p2768 A73-40723
- Use of the numerical method of Estoque and Bhumalkar for the planetary boundary layer. 21 p2732 A73-41572
- Russian book - Light scattering in planetary atmospheres. 22 p2906 A73-41877
- Limb scanning as a method for measuring the temperature structure of a planetary atmosphere. 22 p2883 A73-42058
- The inference of temperature from the infrared spectra of planets. 22 p2906 A73-42065
- Interaction of the solar wind with the outer planets. 22 p2903 A73-42937
- The origin and evolution of the atmospheres of the terrestrial planets. 22 p2912 A73-42976
- The radio occultation method for the study of planetary atmospheres. 22 p2912 A73-42979
- Radio occultation experiments planned for Pioneer and Mariner missions to the outer planets. 22 p2912 A73-42980
- Atmospheric Uranus and Neptune models with massive atmospheres above solid cores, discussing Uranus solid methane cloud layer 22 p2913 A73-42987
- Radiative transfer within the atmospheres of the major planets. 22 p2913 A73-42991
- Planetary spectrum formation in atmospheric model with lower and upper layers of infinite and small optical thickness respectively 23 p3029 A73-43623
- Weakly-shocked flows of the solar wind plasma through atmospheres of comets and planets. 23 p3024 A73-43682
- Scattering and transmission functions of radiation by finite atmospheres with reflecting surfaces. 23 p3030 A73-43755
- Jupiter Red Spot photographic, IR image, spectral, photometric, polarimetric and chemical studies, comparing with earth and Mars atmospheric data 23 p3032 A73-43940
- A first look at atmospheric dynamics and temperature variations on Titan. 24 p3128 A73-44433
- Planetary Atmosphere Experiments Test vehicle reentry into earth atmosphere for flight experience, discussing onboard instrumentation 24 p3088 A73-44440
- Analysis of spikes in occultation curves - A critique of Brinkmann's method. 24 p3129 A73-44444
- Methane absorption in the atmosphere of Saturn - Rotational temperature and abundance from the 3 nu sub 3 band. 24 p3129 A73-44445
- Disk integrated polarization observation for Titan at small phase angles, noting optically thin Rayleigh atmosphere on opaque cloud deck 24 p3130 A73-44451
- A numerical method for determining the temperature structure of planetary atmospheres. 24 p3130 A73-44456
- Greenhouse effect for Titanian atmospheric models with different methane, hydrogen, helium and ammonia proportions, deriving brightness temperature spectrum and surface pressure 24 p3130 A73-44457
- Model for radiative dynamic instability of cloudy planetary atmosphere from coupling for case of radiative heating rate dependent cloud properties 24 p3132 A73-44534
- Parameterization of baroclinicity effects in the planetary boundary layer. 24 p3088 A73-45366
- ### PLANETARY COMPOSITION
- Relation between solar and planetary neon in carbonaceous chondrites. 02 p0211 A73-11744
- Mercury - Surface composition from the reflection spectrum. 02 p0218 A73-12420
- The internal structure of planetary bodies. 04 p0495 A73-14772
- Deuterium-hydrogen ratio in Jupiter. 05 p0623 A73-17182
- An alpha particle experiment for chemical analysis of the Martian surface and atmosphere. 09 p1048 A73-22190
- Ground based spectroscopic observation of carbon dioxide distribution on Mars surface, noting Tharsis region pressure anomaly, ridge slope and dust storm activity 09 p1144 A73-22262
- Natural radioactive element contents in Venusian rock - Results of a Venus-8 station experiment 11 p1418 A73-25635
- High pressure physical model of hydrogen planets Jupiter, Saturn, Uranus and Neptune 11 p1419 A73-25877
- Isentropic compression of fused quartz and liquid hydrogen to several Mbar. 11 p1398 A73-25884
- Deep planetary interior models and internal structure evidence from lunar magnetism, considering planetary magnetic field studies from flyby and orbiting satellite measurements 11 p1420 A73-25893
- Planetary and lunar surface color as geochemical history indicator in terms of oxidation state, solar wind access to atmosphere and planetary moisture content 12 p1541 A73-27484
- Elemental and isotopic abundances of the volatile elements in the outer planets. 14 p1799 A73-30529
- Outer planet satellites and atmospheres composition and structure from low temperature condensation accretion models 14 p1724 A73-30530
- Jupiter He abundance determination methods, considering mean density, spectral line broadening and stellar occultations with emphasis on far IR emission 14 p1799 A73-30533
- Terrestrial planetary core model concerning mantle-core iron oxide composition to avoid phase transition theory difficulties 15 p1867 A73-31100
- Internal structure and chemical composition of Mercury 16 p2066 A73-33796
- Planet Mars atmospheric physics covering optical parameters, brightness distributions, pressure, aerosol, chemical composition, photometric and surface layer properties and topography 16 p2069 A73-33830
- Figures and internal structure of hydrogen-helium planets 16 p2069 A73-33838

Results of observations of methane /6190 A/ and ammonia /6441 and 6478 A/ absorption bands on the Jovian disk over a period of three years 16 p2070 A73-33840

Two layer cores in terrestrial planets with emphasis on Mars and Venus, discussing pressure at earth mantle-core boundary, equations of state and composition 17 p2235 A73-35743

Content of natural radioactive elements in Venusian rock Results of experiment with Venera-8 station. 19 p2486 A73-38142

Numerical model for cold gaseous planets /Jupiter, Saturn, Uranus, Neptune/ as remnants of star formation attempts, taking into account density fluctuations in collapse region 21 p2766 A73-40374

Cosmogonic prerequisites for the accumulation of volatile substances in the upper mantle of the earth 22 p2912 A73-42972

High altitude infrared spectroscopic evidence for bound water on Mars. 24 p3127 A73-44395

On the process of accretion in the formation of the planets and comets. 24 p3128 A73-44400

PLANETARY ENTRY
U ATMOSPHERIC ENTRY
PLANETARY ENVIRONMENTS
NT JUPITER ATMOSPHERE
NT MARS ATMOSPHERE
NT MARS ENVIRONMENT
NT PLANETARY ATMOSPHERES
NT VENUS ATMOSPHERE

In-depth exploration of the solar system and its utilization for the benefit of Earth. 06 p0751 A73-18029

PLANETARY EVOLUTION
Solar system origin and variable gravitational constant theory from earth history viewpoint 01 p0101 A73-10874

Solar system origin and evolution theory, describing planets and satellites condensation from embryo grains captured in particle streams 01 p0109 A73-11481

Nonstellar origin of Jupiter from tidal instability considerations, discussing binary star formation 02 p0216 A73-12377

On the formation of Saturn's rings. 02 p0225 A73-12805

Lunar and planetary topography formation by exogenous and endogenous mechanisms, considering fluidization by volcanism 03 p0369 A73-13109

Book - Evolution of the protoplanetary cloud and formation of the earth and the planets. 05 p0615 A73-16356

Natural remanent magnetizations of carbonaceous chondrites and the magnetic field in the early solar system. 05 p0619 A73-16839

Protoplanet formation models with floccule accumulation, discussing momentum considerations and supersonically turbulent collapsing gas cloud 05 p0625 A73-17318

The atmospheres of the earth and the terrestrial planets - Their origin and evolution. 06 p0749 A73-17868

Surface topography of the inner planets as related to planetary origins. 06 p0749 A73-18005

Solar system planets spin rate change and core growth, discussing Mars geology and earth evolution 06 p0749 A73-18006

Mars surface volcano and canyon features from Mariner 9 photographs and geological map, suggesting internal heating, water erosion, atmospheric evolution and life problem solution 06 p0754 A73-18672

Mariner spacecraft photographed Mars surface volcanic mountains and water in polar caps, suggesting recurring rainfall and rivers during successive interglacial periods 07 p0875 A73-19166

Potential atmospheric composition of smaller bodies in the solar system and some aspects of planetary evolution. 07 p0875 A73-19249

Structure and evolution of the asteroid ring 07 p0902 A73-20324

The role of the satellite swarm in the origin of the earth's rotation. 08 p1012 A73-21579

Galactic dust region molecular cloud effects on cloud chemical evolution, star and planetary formation and life development on planets 09 p1140 A73-21975

On the accretion mechanism for the formation of a protoplanetary disc. 09 p1143 A73-22110

Mars surface ellipticity discrepancy with dynamic value obtained from satellite orbital precession explained by solid state convection in deep interior and Martian evolution 09 p1144 A73-22268

A new cosmological model - Formation of organic molecules, planets, and comets. 09 p1151 A73-23147

Stellar evolutionary calculation for Jupiter, considering gravitational contraction 11 p1420 A73-25892

The origin and chemical composition of the earth's core. 11 p1355 A73-25896

Bode law rationalization based on Dole computer-generated planetary system with constant spacing ratio generated by random number sequence and accretion process closeness constraints 11 p1428 A73-26665

Structure and evolution of the asteroid belt. 12 p1540 A73-27296

Polar wandering and the earth's dynamical evolution cycle. 13 p1679 A73-28403

Ejection of bodies from the solar system in the course of the accumulation of the giant planets and the formation of the cometary cloud. 14 p1793 A73-29825

Comets and cometsimals formation from icy material during solar system evolution from collapsing dust and gas cloud 14 p1794 A73-29835

The origin and evolution of the comets and other small bodies in the solar system. 14 p1794 A73-29837

Prebiological synthesis of organic compounds. 14 p1724 A73-30129

Outer planet formation from gaseous solar nebula with absence of magnetic effects, discussing gravitational instabilities, gas capture onto planetary core and model construction 14 p1799 A73-30528

Solar system evolution and planets configuration regularity and geometrical shape considerations in terms of tidal dissipation, stray body collision and close approach 15 p1937 A73-31776

Water vapor from a lunar breccia - Implications for evolving planetary atmospheres. 16 p2060 A73-33124

Planetary cosmogony theory review emphasizing cold evolution through dust-gas protoplanetary cloud nucleosynthesis, discussing iron fractionation, organic compounds and planetary thermal history 16 p2066 A73-33793

Growth features of the embryos of planets 16 p2066 A73-33794

Thermal history of the terrestrial planets 16 p2066 A73-33795

Solar system origin models in terms of cataclysmic theories, solar nebula concept, planetary accumulation, protoplanets, etc 17 p2226 A73-34402

Magnetohydrodynamics, hydrodynamics and dynamics of solar system model as contracting rotating cloud, discussing effects of turbulence 17 p2226 A73-34403

Numerical model construction for primitive solar nebula and physical accumulation processes within collapsing interstellar gas cloud 17 p2227 A73-34405

Some remarks on solar nebula type theories of the origin of the solar system. 17 p2227 A73-34406

Small grain aggregates created by equalized grain orbits on Kepler trajectories, with low collisional frequency in early state of solar system planetary evolution 17 p2227 A73-34407

Protoplanetary gas-dust cloud evolution and planetary formation, investigating earth initial state 17 p2227 A73-34408

Models comparison for heavy elements segregation mechanism from gaseous hydrogen and helium for terrestrial planets formation from primordial granular matter 17 p2228 A73-34422

Planetary accretion from grains in intersecting solar orbits, investigating velocity impact behavior of silicate particles 17 p2228 A73-34423

Pallas evolution on basis of orbital eccentricity and inclination, discussing accumulation in asteroid belt in quiescent solar nebula, collisions and planetary gravitational encounters 17 p2229 A73-34428

Revision of initial size, mass and angular momentum of the solar nebula and the problem of its origin. 17 p2229 A73-34431

Iron core age end in terrestrial planets via Ramsey phase change onset producing metallic state core with growth via radioactive heating 17 p2236 A73-35745

Cometary exploration - A case for Encke. 18 p2353 A73-36501

[AIAA PAPER 73-596] A generalized geologic map of Mars. 19 p2477 A73-37201

Water and processes of degradation in the Martian landscape. 19 p2477 A73-37202

Martian volcanic and tectonic features from Mariner 9 photography, comparing evolutionary phases with lunar and terrestrial morphology 19 p2477 A73-37203

Mars troughs from Mariner 9 pictures, interpreting evolutionary origin in terms of surface and core processes 19 p2477 A73-37204

Martian lowland terrains fretted and chaotic characteristics, hypothesizing evolutionary processes based on escarpment recession, subsurface ground ice and magma collapse 19 p2477 A73-37205

Martian cratering. IV - Mariner 9 initial analysis of cratering chronology. 19 p2477 A73-37207

Possible trend of the earth's evolution 19 p2481 A73-37242

Circularity of Martian craters. 19 p2486 A73-37800

Reports of fourth Lunar Science Conference concerning lunar rock chemical composition assessment as information source on early solar system, lunar early geologic history, etc 19 p2487 A73-38293

Four-stage planetesimal accretion from solar nebula describing dust particle condensation, disk formation, gas drag, orbital decay and particle collisions 19 p2489 A73-38524

Inclination of the moon's orbit - The early history. 20 p2605 A73-39055

Numerical model for cold gaseous planets /Jupiter, Saturn, Uranus, Neptune/ as remnants of star formation attempts, taking into account density fluctuations in collapse region 21 p2766 A73-40374

Correction to calculation of temperature rise in connection with gravitational energy release accompanying rapid core formation from undifferentiated earth 22 p2848 A73-42499

Cosmogonic prerequisites for the accumulation of volatile substances in the upper mantle of the earth 22 p2912 A73-42972

Lunar and planetary chemical composition dependence on condensation temperature in solar nebula 23 p0300 A73-43760

Extrasolar planetary systems. 24 p3127 A73-44391

Radial and vertical force balance in primitive solar nebula, describing techniques for gravitational potential and gas opacity computation for energy transport 24 p3127 A73-44392

Planetary formation processes in primitive solar nebula analyzed from collapse phase for accumulation time 24 p3127 A73-44393

On the process of accretion in the formation of the planets and comets. 24 p3128 A73-44400

Mars surface evolution from analysis of Mariner 6 and 7 equatorial photographs, discussing internal dynamic activity 24 p3128 A73-44432

Chondrites - Initial strontium-87/strontium-86 ratios and the early history of the solar system. 24 p3137 A73-44688

PLANETARY EXPLORATION
U SPACE EXPLORATION
PLANETARY EXPLORER
U OUTER PLANETS EXPLORERS
PLANETARY GRAVITATION

Axisymmetrical planet gravitational field potential expression in spherical function series, noting expansion coefficient decrease in power law for smooth density body 01 p0099 A73-10691

Neptune model calculation from mass, radius and rotation period, comparing with gravitational moment 01 p0101 A73-10844

Wolf number solar activity and planetary tidal force correlation during 1770-1970, noting 11-year cycle relation 01 p0101 A73-10848

Gravitational fields of Jupiter and Saturn. 01 p0107 A73-11332

Estimation of gravity field harmonics in the presence of spin-axis direction error using radio tracking data. 02 p0164 A73-12373

Sunspot number relationship to planetary tides on sun, considering earth-Venus conjunctions and opposition 02 p0219 A73-12436

Trajectory analysis for swingby technique using Jovian gravitational field for leaving plane of ecliptic along heliocentric orbit and for solar flyby at specified distance 03 p0378 A73-14552

Error sources in numerical integration of spacecraft equations of motion in solar and planetary gravitational fields, suggesting methods for improving accuracy 03 p0379 A73-14553

Satellite motion near the equatorial plane of a slowly rotating planet 05 p0617 A73-16468

Alteration of the Laplace spheres of planetary influence during the application of a new intermediate orbit

Venus - Radar determination of gravity potential.
05 p0620 A73-17022
07 p0875 A73-19167

Cometary parent bodies transfer to short period orbits by Jupiter caused gravitational disturbances, noting qualitative analysis of orbits evolution

Perturbation function expansion in series of orbital elements for satellite motion in rotating oblate planet gravitational field with two fixed centers
08 p1012 A73-21576

Large scale surface structure of Mars.
10 p1282 A73-24493

Gravity field of Mars from Mariner 9 tracking data.
11 p1417 A73-25268

Borelly periodic comet motion, including secular acceleration due to nongravitational forces and orbital elements perturbations by planets from Venus to Pluto
11 p1425 A73-26138

Periodic comet Stephan-Oterma orbit, taking into account perturbations by major planets
14 p1791 A73-29805

The major planets as powerful transformers of cometary orbits.
14 p1792 A73-29808

Meteoritic particles orbits secular evolution under planetary perturbation and Poynting-Robertson effects, considering osculating orbital elements long term variations via simplified model
14 p1794 A73-29834

Major planets gravitational fields models from flyby spacecraft measurements, discussing Red Spot and Jupiter effect on Galilean satellites
14 p1795 A73-29842

Neptune model calculation from mass, radius and rotation period, comparing computed gravitational moments with observation
14 p1799 A73-30531

Wolf number solar activity and planetary tidal force correlation during 1770-1970, noting 11-year cycle relation
15 p1928 A73-30984

Canonical elements of the translational-rotational motion of a planet satellite
15 p1928 A73-30984

Mariner 9 celestial mechanics experiment - A status report.
19 p2476 A73-37199

Secular perturbations of third order with respect to oblateness from all zonal harmonics of the gravitational potential of a planet
19 p2479 A73-37223

Satellite intermediate orbit and secular perturbations due to second zonal harmonics of planetary potential and outer body attraction
23 p3037 A73-44253

23 p3037 A73-44254

PLANETARY LANDING

The facsimile camera - Its potential as a planetary lander imaging system.
12 p1495 A73-26875

Linear filtering of ballistic-entry-probe data for atmospheric reconstruction.
[AIAA PAPER 73-904]
20 p2589 A73-38838

PLANETARY LONGITUDE

U PLANET EPHEMERIDES

PLANETARY MAGNETIC FIELDS

Soviet Venus probes data on planetary atmosphere composition, temperature and pressure profiles, magnetic field, diameter, mass density and rotation period
01 p0102 A73-10992

Extensive air showers on Jupiter, and its sporadic decimeter radio emission.
01 p0106 A73-11323

Non-dipole terms in the magnetic fields of Jupiter and the earth.
02 p0212 A73-11897

Inner planets of the solar system - A comparative study.
06 p0749 A73-18007

The magnetic field in the immediate vicinity of Mars according to Mars 2 and Mars 3 satellite data.
10 p1281 A73-24461

Electrical conductivity of condensed molecular hydrogen in the giant planets.
11 p1420 A73-25885

Deep planetary interior models and internal structure evidence from lunar magnetism, considering planetary magnetic field studies from flyby and orbiting satellite measurements
11 p1420 A73-25893

Outer solar system planetary and subplanetary objects magnetic field existence, discussing internal dynamo fields, externally driven dynamos and fossil fields
14 p1800 A73-30540

Jupiter's radiation belts and the sweeping effect of its satellites.
16 p2062 A73-33429

Radio astronomical, radar and interplanetary probe measurements of Venus rotation, dimensions, atmosphere and magnetic field
16 p2066 A73-33798

On limits to Jupiter's magnetospheric diffusion rates.
17 p2224 A73-34511

Magnetic field in the near vicinity of Mars from data of the Mars-2 and Mars-3 satellites.
19 p2486 A73-38127

Magnetic field in the very close neighborhood of Mars according to data from the Mars 2 and Mars 3 spacecraft.
20 p2604 A73-38959

Jupiter magnetospheric interaction with innermost satellite Io, noting magnetic field annihilation enhancement in neutral point by LF MHD waves
21 p2764 A73-40166

Jupiter and terrestrial upper atmospheres comparison, discussing solar wind interactions with planetary magnetic fields, Jovian Van Allen belt and cold plasma distribution
22 p2913 A73-42985

Jupiter magnetic dipole offset along rotation axis from 11 cm radio centroid measurements with Parkes telescope
24 p3130 A73-44459

PLANETARY MASS

The mass and figure of Saturn by photographic astrometry of its satellites.
01 p0096 A73-10316

Soviet Venus probes data on planetary atmosphere composition, temperature and pressure profiles, magnetic field, diameter, mass density and rotation period
01 p0102 A73-10992

Evidence for objects of lunar mass in the early solar system and for capture as a general process for the origin of satellites.
02 p0217 A73-12394

Earth-moon system mass and angular momentum distribution anomaly, considering light gases association with Jupiter, Saturn, Uranus and Neptune satellites
11 p1419 A73-25793

Solar system planets and satellites fundamental properties, considering observational uncertainty in masses and dimensions
11 p1419 A73-25878

A survey of dynamical data for the major planets and satellites.
11 p1420 A73-25880

Planetary masses, dynamic flattening and orbital elements determination by perturbation analysis for disturbed planet, space probe and satellite
11 p1420 A73-25882

Determination of planetary masses from the motions of comets.
14 p1792 A73-29809

The determination of Jupiter's mass from large perturbations on cometary orbits in Jupiter's sphere of action.
14 p1792 A73-29810

Determination of the mass of Jupiter from observations of 10 Hygiea during 1932-1969.
14 p1792 A73-29811

Hidalgo orbit near Saturn, discussing resemblance to extinct comet nucleus, nongravitational forces effects and planetary mass determination
14 p1792 A73-29812

Saturn mass determination from Hidalgo orbit trajectory and variational equation, obtaining probable error from fitted parabola
14 p1792 A73-29813

Isochronous derivatives of certain spacecraft-trajectory parameters
14 p1796 A73-29857

Determination of the mass of Saturn from the motion of Trojans.
17 p2234 A73-35615

Some considerations about the upper and the lower limits of the planetary dimensions.
19 p2486 A73-38152

Mass and position limits for an hypothetical tenth planet of the solar system.
22 p2907 A73-42209

PLANETARY MOTION

U SOLAR ORBITS

PLANETARY NEBULAE

Planetary nebulae NGC 7635, 7008, 1514, 650-1, 7139, 3587, 6781 and 6543 monochromatic images, centering filters on H alpha, N II and O III forbidden lines
02 p0221 A73-12703

Polarimeter search for optical circular polarization in eclipsing binaries, magnetic Ap stars, planetary nebula, Hubble and Orion nebulae, M87 and Sirius
03 p0366 A73-12939

On the stationary mass outflow from stars. I - The computational method and the results for a 1 solar mass star.
03 p0370 A73-13195

Hydrodynamic calculations for novae origin and mass ejection from luminous red giants, considering planetary nebulae and plausible models
07 p0903 A73-20628

Nebular Fabry-Perot, Pepsios, and Sissam monochromators.
08 p0964 A73-21039

Spatial spectroscopic diagnostic of planetary nebulae. III - Numerical investigation of local absolute monochromatic energies and local absolute energies in spherically symmetric models.
08 p1010 A73-21313

Image tube spectra of planetary nebulae for relative line intensities and radial velocities, considering nebulae properties
09 p1141 A73-22015

The influence of dust upon the dynamics and thermal stability of planetary nebulae.
09 p1142 A73-22032

Spectral observations of southern planetary nebulae. I.
11 p1415 A73-25070

The spatial distribution of the 11.7 micron radiation of NGC 7027.
11 p1415 A73-25071

Fabry-Perot interferometer with etalon for studying gas movements and planetary nebulae in Large Magellanic Cloud by spectral analysis from pressure scanning
11 p1361 A73-25176

Late stage nonrotating star evolution, discussing giant models, planetary nebulae, degenerate carbon cores, supernova explosions and pulsars
12 p1543 A73-27748

8-13-micron spectra of NGC 7027, BD + 30.3639 deg, and NGC 6572.
18 p2357 A73-37104

Planetary nebula evolution model to explain FG Sagittae luminosity changes due to thermal pulse in He burning shell
19 p2489 A73-38530

IR astronomical objects, methods and instruments, discussing galactic and extragalactic sources, early and late stars, planetary nebulae, interstellar dust and hydrogen ion clouds
20 p2605 A73-39060

Investigation of the planetary nebula NGC 1360 and its nucleus
21 p2768 A73-40715

Detection of radio emission from M1-11 and HD37806.
21 p2780 A73-41646

Observation of 9.0-micron line emission from Ar III in NGC 7027 and NGC 6572.
22 p2910 A73-42704

Planetary nebulae nuclei emission line spectral features similarity to spectra of Population I Wolf-Rayet and O-type stars
23 p3026 A73-43199

PLANETARY ORBITS

Gravity thrust Jupiter orbiter trajectories generated by encountering the Galilean satellites.
01 p0095 A73-10103

Approximate method to determine collision probabilities, hyperbolas, and direct and retrograde ellipses during single close encounters in three body planetary problem
01 p0099 A73-10693

Theoretical model for tidal evolution induced capture of natural satellite pairs into orbit-orbit resonance, discussing Titan and Hyperion relationship with Saturn
02 p0219 A73-12421

Expansions of the derivatives of the disturbing function in planetary problems.
03 p0377 A73-14272

Spacecraft optimal control after transfer from hyperbolic trajectory to planetary orbit by atmospheric drag, minimizing engine thrust
03 p0340 A73-14570

Optimal correction of a planetary-approach trajectory for transfer to an artificial-satellite orbit
05 p0616 A73-16428

Satellite motion near the equatorial plane of a slowly rotating planet
05 p0617 A73-16468

On the origin of the commensurabilities amongst the satellites of Saturn.
06 p0752 A73-18238

The effects of trajectory characteristics on scientific objectives for major planetary orbiters.
06 p0757 A73-18376

Perturbed satellite motion differential equations, on basis of fixed center problem and perturbing forces with no force function
10 p1274 A73-23721

Perturbation function expansion in series of orbital elements for satellite motion in rotating oblate planet gravitational field with two fixed centers
10 p1282 A73-24493

Planetary masses, dynamic flattening and orbital elements determination by perturbation analysis for disturbed planet, space probe and satellite
11 p1420 A73-25882

Least squares method for satellite motion parameters determination in orbital plane, using altimeter distance to planet surface measurements
12 p1543 A73-27627

Optimization of descent maneuvers for a section of a satellite in a planetary orbit
15 p1931 A73-31227

Horseshoe and Trojan orbits associated with Jupiter and Saturn.

15 p1937 A73-31948

Contribution to the dynamic study of the Galilean system of Jupiter. I - The intermediate solution in the nonresonant case

16 p2059 A73-32839

Bode's law and the preference for near-commensurability among pairs of orbital periods in the solar system.

17 p2229 A73-34429

Barnard star multiplanet system, discussing inclinations of planetary orbits and cosmogonic implications

17 p2229 A73-34430

Technology requirements for ballistic mode Mercury orbiter mission, discussing performance potential with Venus gravity assist and conventional spacecraft propulsion techniques

[ALAA PAPER 73-581]

18 p2350 A73-36073

Pioneer Venus mission plan for atmospheric probes and an orbiter.

[ALAA PAPER 73-579]

18 p2353 A73-36499

Perturbed satellite motion differential equations derivation on basis of fixed center problem and perturbing forces with no force function, obtaining intermediate orbital elements

18 p2355 A73-36746

Utilization of tangential trajectories for lowering high-altitude elliptic orbits of artificial satellites of planets

23 p3027 A73-43265

Investigations of Mars from the Soviet automatic stations Mars 2 and 3.

24 p3128 A73-44431

PLANETARY QUARANTINE

Quarantine necessity, protocol and effectiveness for Mars samples, emphasizing risks of foreign replicating agent introduction to earth biosphere

03 p0272 A73-14321

Sterilization technology in the United States space program.

16 p1976 A73-33697

Ten years of development of the Planetary Quarantine Program of the United States.

18 p2281 A73-35966

Planetary quarantine constraints for outer planet satellite encounter missions, determining spacecraft impact probability in terms of trajectory analysis and navigation error numerical integration

18 p2349 A73-35976

Terrestrial quarantine considerations for unmanned sample return missions.

18 p2349 A73-35977

Lunar sample quarantine procedures - Interaction with non-quarantine experiments.

18 p2281 A73-35978

The significance of outer planet satellite quarantine constraints on aim-point selection.

[ALAA PAPER 73-553]

18 p2359 A73-36096

Life sciences and space research XI; Proceedings of the Fifteenth Plenary Meeting, Madrid, Spain, May 10-24, 1972.

22 p2803 A73-42158

Developments in the analysis of planetary quarantine requirements.

22 p2803 A73-42159

Safety margins in the implementation of planetary quarantine requirements.

22 p2803 A73-42161

Soil microbiological tests to evaluate Antarctica as Mars environment model for quarantine standards

22 p2803 A73-42162

PLANETARY RADIATION

Time variations of the ultraviolet absorption in the continuous spectrum of Jupiter and Saturn

01 p0101 A73-10843

P, T invariance of electromagnetic interaction and the circular polarization of planetary emission

01 p0092 A73-10940

Polarimetric investigations of the giant planets. II - Phase variation of the polarization of selected regions on the Saturn disk

01 p0102 A73-10941

The spherical albedo of a planetary atmosphere

01 p0102 A73-10942

Extensive air showers on Jupiter, and its sporadic decimeter radio emission.

01 p0106 A73-11323

Thickness of Saturn's rings from observations in 1966.

01 p0107 A73-11325

Measurement of Jupiter's radio emission at 2.94 m.

01 p0107 A73-11330

The possibilities of determining the temperature profile in the Venusian atmosphere from the thermal radio emission of the planet

02 p0219 A73-12463

The radioastronomy of the planets

03 p0372 A73-13273

Observations of planets, nebulae, and galaxies at 350 microns.

03 p0374 A73-13716

Jovian spectrum at 8-13 microns from 60 inch IR telescope, discussing surface brightness of central disk and brightness temperature spectrum

03 p0374 A73-13850

Decameter-wave radiation from Jupiter and solar activity.

04 p0491 A73-14956

Circular polarization of Saturn.

04 p0499 A73-15368

Brightness temperature of Mars thermal emission in two orthogonal polarizations by microwave radiometry from Mars 2 and 3 orbiters

06 p0747 A73-17490

Mars microwave spectra computation by improved thermal model with seasonal polar cap effects and accurate aspect geometry, noting lunar-like planetary subsurface nature

06 p0747 A73-17492

Fine structure of the Jupiter radio bursts.

08 p1013 A73-21646

P, T invariance of electromagnetic interaction, and circular polarization of planetary radiation.

09 p1138 A73-22735

Polarimetric observations of the major planets. II - Phase dependence of the polarization for selected areas on the disk of Saturn.

09 p1147 A73-22736

Spherical albedo of a planetary atmosphere.

09 p1147 A73-22737

The radiation regime of the Martian surface and dusty atmosphere

11 p1418 A73-25628

Preliminary results of measurements of the infrared temperature of the Mars surface by the Mars 3 interplanetary spacecraft

11 p1418 A73-25629

Major planets nonthermal radio emission observations, noting powerful decametric sources related to Jupiter rotation and Io orbital motion

11 p1420 A73-25879

Thermal radio emission from Jupiter and Saturn.

11 p1420 A73-25883

Estimate of the mean size of cloud layer particles in the Jovian atmosphere

11 p1423 A73-26080

Saturn 49.5 and 94.3 cm brightness temperature, considering magnetic field effects, synchrotron emission and atmosphere

11 p1424 A73-26127

Jupiter radio observations at 13 cm during 1969 and 1971 oppositions for circular polarization and flux density

11 p1424 A73-26128

Jovian decametric emission origin in cyclotron instability of weakly relativistic electrons trapped in magnetic field, considering group velocity in magnetospheric plasma

11 p1424 A73-26129

Jupiter radiation reception at decametric wavelengths by Yagi antenna and radiometer, taking into account Io modulation effect

11 p1424 A73-26131

Simple model for scanning-angle distribution of planetary albedo gamma-rays.

11 p1414 A73-26475

The geometry and dynamic spectra of Io-modulated Jovian decametric radio emissions.

12 p1540 A73-27327

Preliminary results of observations at the 2-cm wavelength of discrete sources and Jupiter at Pulkovo

12 p1546 A73-27855

Polarimetric studies of the giant planets. III - Jupiter

12 p1546 A73-27861

Interpretation of hydrogen quadrupole and methane observations of Jupiter and the radiative properties of the visible clouds.

13 p1673 A73-28280

Spectra of star and planet scintillation and dependence of their characteristics on meteorological conditions

13 p1683 A73-29097

Temporal variation of ultraviolet absorption in continuous spectra of Jupiter and Saturn.

15 p1928 A73-30979

The possibilities of determining the temperature profile in Venus' atmosphere from the planet's thermal radio emission.

15 p1942 A73-32613

Upper limit to the 11.4 m flux of Saturn using VLBI.

16 p2061 A73-33221

Monochromatic and radiometric albedo of Mars and Venus

16 p2067 A73-33811

Distribution of radio brightness across the disk of Venus at the 8-mm wavelength

16 p2068 A73-33816

Radio emission from Venus and Jupiter at 2 and 8 mm wavelengths

16 p2068 A73-33817

High-resolution interferometric observations of Venus at the 3.1-cm wavelength

16 p2068 A73-33818

Statistical brightness distributions for photometric planetary image improvement, considering telescope

resolution, diaphragm diffraction and atmospheric turbulence

16 p2069 A73-33832

Continuing activity of Jupiter and comparison of the 1871-1880 and 1961-1965 flare-ups

16 p2057 A73-33842

Results of Jupiter observations in the centimeter wavelength range

16 p2070 A73-33844

On limits to Jupiter's magnetospheric diffusion rates.

17 p2224 A73-34511

Radio interferometry of moving sources in the presence of confusion - An application to Mercury at 21-centimeter wavelength.

17 p2231 A73-34763

Saturn - A study of the 3 nu sub 3 methane band.

17 p2231 A73-34765

New infrared spectra of the Jovian planets from 12,000 to 4000/cm by Fourier transform spectroscopy. I - Study of Jupiter in the 3 nu-sub 3 CH4 band.

17 p2234 A73-35617

An upper limit on the 4.9-micron flux from Titan.

18 p2357 A73-37112

Preliminary report on infrared radiometric measurements from the Mariner 9 spacecraft.

19 p2479 A73-37221

Martian south polar region albedo map from Mariner 9 photographs, comparing with earth-based telescopic observations

19 p2480 A73-37232

Fine structure of Jupiter's decametric source B.

19 p2482 A73-37389

Arizona-NASA Atlas of the Infrared Solar Spectrum. X.

19 p2483 A73-37576

Analysis of the Jovian electron radiation belts. II - Observations of the decimetric radiation.

19 p2475 A73-37622

Radiation regime of the surface and dust-filled atmosphere of Mars.

19 p2486 A73-38140

Preliminary results of infrared temperature measurements of the surface of Mars by the Mars-3 automatic interplanetary station.

19 p2486 A73-38141

Jupiter atmosphere discrete source maps of 5 micron radiation distribution, correlating brightness temperature and photographically recorded colors

19 p2489 A73-38525

The brightness temperature of Venus at 70 centimeters.

19 p2489 A73-38526

The brightness temperature of Venus and the absolute flux-density scale at 608 MHz.

19 p2489 A73-38527

Ground based photometry of planets, stars and galactic nebulae at 34 microns

19 p2489 A73-38529

Preliminary results of observations of discrete sources and of Jupiter with 2-cm wavelength at Pulkovo.

20 p2608 A73-39229

Polarimetric observations of the giant planets. III.

20 p2608 A73-39235

Jupiter satellite Io controlled decametric Alfvén wave emission pattern, considering relationship to coherent cyclotron radiation growth rate

21 p2764 A73-40168

Calculations of the limb radiance of Venus in the 600 to 700 per cm region and their application to spacecraft navigation.

21 p2767 A73-40693

Possibilities of calculating the spectral albedo of Venus in the near infrared

21 p2770 A73-40914

Pluto polarimetric measurements showing degree and position angle of polarization and probable error

22 p2905 A73-41763

The far-ultraviolet spectrum of Jupiter.

22 p2905 A73-41769

The source and structure of the Jovian radiation belt.

22 p2903 A73-42986

Observation of the Raman effect in the spectrum of Uranus.

22 p2916 A73-43126

Planetary spectrum formation in atmospheric model with lower and upper layers of infinite and small optical thickness respectively

23 p3029 A73-43623

Looking at the solar system in the far-ultraviolet.

23 p3034 A73-44220

Absolute measurements and computed values for Martian irradiance between 10.5 and 12.5 microns.

24 p3127 A73-44394

Mars and Jupiter - Radio emission at 1.35 cm.

24 p3128 A73-44399

The effects of scattering and conduction upon radiative transfer in lunar and Mercurian surfaces.

24 p3133 A73-44541

Martian surface albedo compared with Mariner-observed topography, noting dark-band correlation with maximum topographic irregularity regions

24 p3133 A73-44551

PLANETARY ROTATION

- H2 pressure-induced lines in the spectra of the major planets. 24 p3138 A73-45050
- High-angular-resolution observations of Saturn at 21.1-centimeter wavelength. 24 p3138 A73-45051
- ## PLANETARY ROTATION
- Neptune model calculation from mass, radius and rotation period, comparing with gravitational moment 01 p0101 A73-10844
- Estimation of the global circulation characteristics of planetary atmospheres with various hypotheses concerning the nature of dissipation 01 p0040 A73-10868
- Possibility of determining the lunar rotation elements with a narrow-angle television camera 01 p0051 A73-10944
- Soviet Venus probes data on planetary atmosphere composition, temperature and pressure profiles, magnetic field, diameter, mass density and rotation period 01 p0102 A73-10992
- The role of occultations in the improvement of the lunar ephemeris. 03 p0369 A73-13107
- Motion stability of librational points in gravitational field of rotating triaxial ellipsoid, applying to planets of solar system 03 p0376 A73-14266
- Resonance rotation of celestial bodies and Cassini's laws. 03 p0377 A73-14275
- Application of a narrow-angle television camera for determining the rotation elements of the moon. 09 p1084 A73-22739
- Martian spin axis wandering resulting from equatorial volcanic convections and gravity field non-hydrostatic low order components 09 p1151 A73-23172
- Summary of Jovian latitude and rotation period observations from 1898 to 1970. 11 p1415 A73-25134
- Major planets nonthermal radio emission observations, noting powerful decametric sources related to Jupiter rotation and to orbital motion 11 p1420 A73-25879
- Jupiter's decametric rotation period and the Source-A emission beam. 11 p1420 A73-25881
- The elastic energy and character of quakes in solid stars and planets. 11 p1420 A73-25894
- Asteroidal rotational properties interpreted in terms of model with collisional breakup into irregular fragments 11 p1425 A73-26136
- Estimates of global circulation characteristics of planetary atmospheres. 13 p1607 A73-28692
- Determination of the motion and rotation parameters of an asteroid by the measurement of distances to a space station situated on the asteroid surface 14 p1796 A73-29858
- Neptune model calculation from mass, radius and rotation period, comparing computed gravitational moments with observation 15 p1928 A73-30980
- Clairaut equation solution for determination of equilibrium configuration of corotating masses, considering density distribution of fluid rotating planet 15 p1939 A73-32006
- Photographic measurements of the rotation of Mercury 16 p2066 A73-33797
- Radio astronomical, radar and interplanetary probe measurements of Venus rotation, dimensions, atmosphere and magnetic field 16 p2066 A73-33798
- Computer analysis of reflected signals obtained during radar sounding of Venus 16 p2067 A73-33807
- Determination of elements of Venusian rotational motion and of coordinates of surface regions with higher reflectivity at radio frequencies 16 p2067 A73-33808
- Comparison of determinations of the rotational velocity of Venus by radar, optical Doppler effect, and spot measurement methods 16 p2067 A73-33809
- Figures and internal structure of hydrogen-helium planets 16 p2069 A73-33838
- Venus upper atmosphere four-day retrograde rotation derived from statistical analysis of telephotographic observation of Y-shaped feature 21 p2767 A73-40566
- A possible connection between variation in the rotational period of Jupiter's central zone and variation in its equatorial diameter. 21 p2779 A73-41545
- Upper Venusian atmosphere four-day retrograde zonal circulation, discussing moving flame phenomenon, convective instability to mean shear and tidal forcing 22 p2913 A73-42983

- Venus upper atmosphere retrograde rotation above main cloud cover, investigating equatorial bulge from pressure surfaces at high elevations 23 p3029 A73-43604
- Initial development of the June 1971 South Equatorial Belt disturbance on Jupiter. 23 p3033 A73-43945
- Observations of the South Equatorial Belt disturbance on Jupiter in 1971. 23 p3033 A73-43946
- Rotation period for a subsurface source in the NNTeB of Jupiter. 23 p3033 A73-43947
- Short-term Jovian rotation profiles, 1970-1972. 24 p3110 A73-44562
- ## PLANETARY SATELLITES
- ### U NATURAL SATELLITES
- ## PLANETARY SPACE FLIGHT
- ### U INTERPLANETARY FLIGHT
- ## PLANETARY SPACECRAFT
- ### U INTERPLANETARY SPACECRAFT
- ## PLANETARY STRUCTURE
- Interior of Jupiter and Saturn. 17 p2226 A73-34357
- Mars crustal structure model from analysis of surface markings with Mariner 9 data, showing petrologic distinctions between dark and light regions 24 p3133 A73-44543
- Metallic hydrogen concept and experimental investigations, considering high temperature superconductivity and role in outer planets structure 24 p3110 A73-45225
- ## PLANETARY SURFACES
- ### NT MARS SURFACE
- Mercury - Surface composition from the reflection spectrum. 02 p0218 A73-12420
- Lunar and planetary topography formation by exogenous and endogenous mechanisms, considering fluidization by volcanism 03 p0369 A73-13109
- Venus atmospheric parameters below critical refraction and surface refractive index from signal amplitude measurement by radio holographic occultation techniques 03 p0379 A73-14567
- Review of surface and atmosphere studies of Venus and Mercury. 06 p0743 A73-17428
- Cartography of the surface markings of Mercury. 06 p0743 A73-17429
- Mercury - Interpretation of optical observations. 06 p0743 A73-17430
- Some characteristics of the Venus surface. 06 p0744 A73-17439
- Radar brightness mapping of Venus surface, noting roughness of terrain from polarization studies and signal processing for extraction of echo power 06 p0744 A73-17440
- Surface topography of the inner planets as related to planetary origins. 06 p0749 A73-18005
- Radar techniques for planetary mapping with orbiting vehicle. 06 p0664 A73-18011
- Planets geometric figure via visible site photography from spacecraft, noting coordinate transformation for conical projection surface 06 p0751 A73-18152
- Determination of the transfer function for the spectral albedo of the surface-atmosphere system of the planet 07 p0818 A73-19659
- Albedo and illuminance of the surface of a planet with an inhomogeneous, purely scattering atmosphere. 07 p0820 A73-20345
- The development of light tracked vehicles for lunar and planetary exploration 08 p0952 A73-20781
- Jupiter surface maps for 1965-70 from drawings obtained with astrophot, noting high activity and eruptive changes after 1961-63 outburst 08 p1012 A73-21583
- Jupiter surface maps from synoptic observations with refracting telescope, considering white cloud formations and atmosphere motions 08 p1012 A73-21584
- Influence of atmospheric haze on the color of the underlying surface observed from a manned spacecraft 09 p1077 A73-22484
- Determination of the transfer function of a planet atmosphere by spectrophotometry of the planet surface from space 09 p1077 A73-22488
- Terrain-vehicle dynamic interaction studies of a mobility concept /ELMS/ for planetary surface exploration. [AIAA PAPER 73-407] 11 p1343 A73-25536
- Determination of the polarization transfer function in space-based spectrophotometric observations of natural formations on a planetary surface 12 p1488 A73-26965

- Planetary and lunar surface color as geochemical history indicator in terms of oxidation state, solar wind access to atmosphere and planetary moisture content 12 p1541 A73-27484
- Radar observations of Venus at 3.8 cm 16 p2067 A73-33806
- Continuing activity of Jupiter and comparison of the 1871-1880 and 1961-1965 flare-ups 16 p2057 A73-33842
- Remote control of planetary surface vehicles. 17 p2148 A73-35316
- Landmark navigational and topographical mapping techniques for planetary surface exploration using unmanned vehicles and earth based computers 17 p2210 A73-35383
- Mission planning for remote exploration of the surface of Venus. [AIAA PAPER 73-580] 18 p2350 A73-36072
- Optical properties of the Mercury surface layer 19 p2480 A73-37233
- Venus upper atmosphere four-day retrograde rotation derived from statistical analysis of telephotographic observation of Y-shaped feature 21 p2767 A73-40566
- Circular polarization of light reflected from the planets 21 p2769 A73-40732
- Results of direct measurements of the illumination in the atmosphere and on the surface of the planet Venus during the flight of the Venera 8 interplanetary probe 21 p2773 A73-41274
- Use of the numerical method of Estoque and Bhunkar for the planetary boundary layer. 21 p2732 A73-41572
- The International Planetary Patrol Program - An assessment of the first three years. 22 p2912 A73-42978
- Planetary surface reflectivity and topography mapping by ground based radar with emphasis on observational methods 23 p2953 A73-43353
- Venera 8 - Measurements of solar illumination through the atmosphere of Venus. 23 p3029 A73-43603
- Rotation period for a subsurface source in the NNTeB of Jupiter. 23 p3033 A73-43947
- Asteroid reflectivities from polarization curves - Calibration of the 'slope-albedo' relationship. 24 p3129 A73-44437
- Topography on satellite surfaces and the shape of asteroids. 24 p3129 A73-44446
- ## PLANETARY TEMPERATURE
- Gas-liquid hydrogen mixture and helium adiabatic model of Jupiter temperature and pressure distribution, estimating planet center temperature 01 p0107 A73-11324
- The abundance of NH3 on Jupiter inferred from UHF radiometry data. [AIAA PAPER 73-128] 05 p0619 A73-16881
- Mars 3 onboard optical measurements of Mars surface and lower atmosphere, considering temperatures, water vapor content, dust cloud and particle characteristics 06 p0746 A73-17481
- Temperatures of Uranus and Neptune at 24 microns. 07 p0874 A73-19067
- Terrestrial thermal history from mathematical model of earth formation with low temperature dust and gas accumulation 07 p0818 A73-19997
- On the He-H2 thermal opacity in planetary atmospheres. 08 p1003 A73-20890
- Ground based radar measurement of Martian topography, surface temperature and thermal properties by microwave and IR radiometry and spectral reflectivity observation 09 p1144 A73-22259
- The present thermal state of the terrestrial planets. 11 p1421 A73-25905
- Thermal history of the terrestrial planets 16 p2066 A73-33795
- An upper limit on the 4.9-micron flux from Titan. 18 p2357 A73-37112
- The brightness temperature of Venus and the absolute flux-density scale at 608 MHz. 19 p2489 A73-38527
- A correlation between colors of Jovian clouds and their 5-micron temperatures. 23 p3033 A73-43948
- Jupiter radiative greenhouse model overestimation of lower cloud level temperature due to convective heat transport neglect, discussing rejection of water cumulus cloud possibility 24 p3129 A73-44439
- Methane absorption in the atmosphere of Saturn - Rotational temperature and abundance from the 3 nu sub 3 band. 24 p3129 A73-44445

Planetary brightness temperature measurements at 8.6 mm and 3.1 mm wavelengths. 24 p3130 A73-44458

General atmospheric circulation driven by polar and diurnal surface temperature variations. 24 p3131 A73-44463

PLANETOCENTRIC COORDINATES

NT GEOCENTRIC COORDINATES

PLANETOLOGY

Mercury thermal stress and strain fields of elastic deformation from solar heating variations due to resonance rotation 02 p0223 A73-12721

The internal structure of planetary bodies. 04 p0495 A73-14772

Venus gravity anomalies and physical properties arising from convection currents and topography deduced from geodetic aspects derived from mass, radius and surface temperature. 04 p0496 A73-14812

Selenodesy and planetary geodesy progress review, discussing gravitational fields and topography variations, outer planets oblateness and mass determinations, lunar body tides, etc 04 p0496 A73-14813

An earlier generation of long-enduring south temperate ovals on Jupiter. 06 p0745 A73-17441

Interplanet variations in scale of crater morphology - Earth, Mars, Moon. 06 p0745 A73-17442

Mariner 9 map analysis of Mars geology, covering cratering, circular basins, volcanism, canyons, chaotic terrain, channels and eolian activity 06 p0745 A73-17476

Conference on Planetology and Space Mission Planning, 3rd, New York, N.Y., October 28-30, 1970, Proceedings. 06 p0749 A73-18001

Planets geometric figure via visible site photography from spacecraft, noting coordinate transformation for conical projection surface 06 p0751 A73-18152

Earth-moon system mass and angular momentum distribution anomaly, considering light gases association with Jupiter, Saturn, Uranus and Neptune satellites 11 p1419 A73-25793

Critique of missing planet theory of asteroidal origin, considering mass required, Bode law and disruption forces 11 p1419 A73-25861

High pressure physics and planetary interiors; Proceedings of the Conference, Houston, Tex., March 1-3, 1972. 11 p1419 A73-25876

Shock wave determination of shear velocity at high pressures for understanding of planetary interior behavior with abrupt change in density from seismic interpretation 11 p1355 A73-25898

The present thermal state of the terrestrial planets. 11 p1421 A73-25905

Evidence for convection in planetary interiors from first-order topography. 12 p1542 A73-27492

Equations of planet figures solved for third order accuracy, covering flattening, density distribution, Jupiter and Saturn models and gravitational moments corrections for radii 12 p1546 A73-27860

Xenoliths in maars and diatremes with inferences for the moon, Mars, and Venus. 13 p1681 A73-28848

Numerical integration of orbits for evolution of different configurations, discussing Titius-Bode law and stability limits of planetoid and hypothetical planet orbits 13 p1686 A73-29366

Motions of perfect incompressible homogeneous fluid planets surrounded by rigid oscillating rings, noting application to two-satellite planets 15 p1860 A73-31049

Observational constraint on the structure of hydrogen planets. 15 p1936 A73-31565

Solar system evolution and planets configuration regularity and geometrical shape considerations in terms of tidal dissipation, stray body collision and close approach 15 p1937 A73-31776

Polarimetric observation of moon and planets via imaging system consisting of slot scanner, telescope, condenser lens, rotating disk analyzer and photomultiplier tube 15 p1876 A73-31960

Clairaut equation solution for determination of equilibrium configuration of corotating masses, considering density distribution of fluid rotating planet 15 p1939 A73-32006

Russian book - Physics of the moon and planets. 16 p2063 A73-33751

Growth features of the embryos of planets 16 p2066 A73-33794

The current level of volcanic activity on Venus 16 p2068 A73-33813

Papers on earth and planetary sciences, volume I covering earth planetary structure, red beds, planetary interiors, mineral deposits and order-disorder relationship in silicates 17 p2158 A73-34356

Iron core age end in terrestrial planets via Ramsey phase change onset producing metallic state core with growth via radioactive heating 17 p2236 A73-35745

Probing the structure and composition of the Jupiter atmosphere from Pioneer 10/11. [AIAA PAPER 73-561] 18 p2353 A73-36498

Jupiter and Saturn interior structure models based on state equations and transport properties of hydrogen and helium at high pressures and temperatures 18 p2354 A73-36644

A three-level model for calculating vertical motions generated by planetary orography. 18 p2314 A73-37073

An overview of geological results from Mariner 9. 19 p2477 A73-37200

Approximations to the mean surface of Mars and Mars atmosphere using Mariner 9 occultations. 19 p2479 A73-37226

Some considerations about the upper and the lower limits of the planetary dimensions. 19 p2486 A73-38152

Equations of planet figures solved for third order accuracy, covering flattening, density distribution, Jupiter and Saturn models and gravitational moments corrections for radii 20 p2608 A73-39234

Spacecraft television image comparison between earth and Mars surface features and geology, discussing mountain chains, deserts and tectonic mapping techniques 20 p2613 A73-39897

A possible connection between variation in the rotational period of Jupiter's central zone and variation in its equatorial diameter. 21 p2779 A73-41545

Mass and position limits for an hypothetical tenth planet of the solar system. 22 p2907 A73-42209

Very-long-baseline interferometry techniques applied to problems of geodesy, geophysics, planetary science, astronomy, and general relativity. 23 p2980 A73-43354

Jupiter Red Spot photographic, IR image, spectral, photometric, polarimetric and chemical studies, comparing with earth and Mars atmospheric data 23 p3032 A73-43940

Polarimetric instrument of moon and planets via imaging system consisting of slot scanner, telescope, condenser lens, rotating disk analyzer and photomultiplier tube 24 p3089 A73-44485

High-angular-resolution observations of Saturn at 21.1-centimeter wavelength. 24 p3138 A73-45051

PLANETS

NT EARTH [PLANET]

NT EXTRASOLAR PLANETS

NT JUPITER [PLANET]

NT MARS [PLANET]

NT MERCURY [PLANET]

NT NEPTUNE [PLANET]

NT PLUTO [PLANET]

NT SATURN [PLANET]

NT URANUS [PLANET]

NT VENUS [PLANET]

Photographic techniques for earth based planet observation, discussing optical equipment, atmospheric disturbance effects and photointerpretation methods 01 p0051 A73-10991

Planetary observation by earth based photography, discussing resolution limitation and improvement in terms of modulation transfer function 02 p0216 A73-12330

High resolution limitations and improvement for earth based visual and photographic planetary observation, considering atmospheric boundary layer and use of elevated stations 02 p0169 A73-12331

Brady trans-Plutonian planet existence rejection from dynamical considerations, noting disruption of coplanar configuration in outer solar system 02 p0276 A73-12833

Trans-Plutonian planet calculations by Brady, discussing Halley, Olbert and Pons-Brook comet trajectories and perturbation and planet parameters 03 p0370 A73-13199

Limits of possible position of tenth planet at 50-100 AU from analysis of Neptune orbit 05 p0622 A73-17180

Note on Brady's hypothetical trans-Plutonian planet. 10 p1275 A73-23847

Solar system planets and satellites fundamental properties, considering observational uncertainty in masses and dimensions 11 p1419 A73-25878

A survey of dynamical data for the major planets and satellites. 11 p1420 A73-25880

Russian book - Physics of the moon and planets. 16 p2063 A73-33751

New determinations of the diameters of planets and satellites 16 p2066 A73-33792

Distribution of satellite bodies according to their mean distances in the systems of the sun, Jupiter, Saturn and Uranus 17 p2231 A73-34598

Planetary elements for 10 000 000 years. 18 p2352 A73-36418

The Lunar and Planetary Laboratory and its telescopes. 19 p2417 A73-37580

Trajectory of a solar-electric propelled vehicle passing through the shadow cone of a celestial body 21 p2779 A73-41556

Mass and position limits for an hypothetical tenth planet of the solar system. 22 p2907 A73-42209

PLANIFORMS

NT ARROW WINGS

NT CARET WINGS

NT DELTA WINGS

NT RECTANGULAR PANELS

NT RECTANGULAR PLANFORMS

NT RECTANGULAR PLATES

NT RECTANGULAR WINGS

NT SWEPTBACK TAIL SURFACES

NT SWEPTBACK WINGS

NT TRAPEZOIDAL WINGS

NT VARIABLE SWEEP WINGS

NT WING PLANFORMS

Influence of geometrical parameters on propeller performance at low advance ratios 21 p2635 A73-41582

PLANIMETRY

U AREA

U DIMENSIONAL MEASUREMENT

PLANISPHERES

A cartographic projection of photographs of celestial bodies obtained from space 21 p2769 A73-40860

PLANNING

NT AIRPORT PLANNING

NT MANAGEMENT PLANNING

NT MISSION PLANNING

NT PRODUCTION PLANNING

NT PROJECT PLANNING

NT REGIONAL PLANNING

NT URBAN PLANNING

PLANOTRONS

NT CATHODE RAY TUBES

NT CELESTROSCOPES

NT HELIOTRONS

NT THERMIONIC DIODES

NT THYRATRONS

Amplifier stability in optimal frequency regime, relating cut-off voltage and plate current as function of magnetic field, input power and geometrical parameters 03 p0284 A73-14068

PLANTS [BOTANY]

NT ALGAE

NT AUTOTROPHS

NT AZOTOBACTER

NT BACILLUS

NT BACTERIA

NT BLUE GREEN ALGAE

NT CHLORELLA

NT CORN

NT FOLIAGE

NT FUNGI

NT GRASSES

NT LEAVES

NT NITROBACTER

NT PHOTOPHILIC PLANTS

NT RHIZOPUS

NT STAPHYLOCOCCUS

NT THERMOPHILIC PLANTS

NT TOBACCO

NT TREES [PLANTS]

NT YEAST

The evolution of ferredoxins from primitive life to higher organisms. 03 p0265 A73-14318

Interpretation of wetlands imagery based on spectral reflectance characteristics of selected plant species. 09 p1077 A73-22388

Biochemical and morphological studies of lunar material effects on plant tissue culture cells, noting nonpathological increased cellular activity and chloroplast and cytoplasm changes 11 p1320 A73-26482

Plant growth response to low temperature and UV treatment, discussing chlorophyll synthesis, carbohydrate levels, ion balance and enzyme characteristics 11 p1320 A73-26486

The effects of mercury compounds on the growth and orientation of cucumber seedlings. 12 p1462 A73-27274

The evolution of lignin - Experiments and observations.

13 p1577 A73-29649

Monitoring for microbial flora contamination on spacecraft surface, discussing cultural techniques and sampling methods for microorganisms detection and sterilization

16 p1976 A73-33698

Cytogenetic analysis of diploid and autotetraploid *Crepis capillaris* seeds following space travel on the 'Cosmos-368' artificial earth satellite

18 p2271 A73-36117

The usefulness of ERTS-1 and supporting aircraft data for monitoring plant development in rangeland environments.

20 p2563 A73-39911

Effects of space flight factors on the heredity of higher and lower plants.

22 p2804 A73-42168

Free fall effects on differential growth and radiation sensitivity of higher plants in space flight and ground based clinostat experiments

22 p2804 A73-42172

Theoretical study of primary photosynthesis processes in higher plants and algae

23 p2946 A73-43707

PLANTS [INDUSTRIES]

U INDUSTRIAL PLANTS

PLASMA ACCELERATION

Possibility of accelerating the matter of hot stars by absorption in spectral lines

01 p0100 A73-10706

Plasma jet acceleration by plasma injectors with capacitive and inductive energy storage for instantaneous breaking of charging circuit, noting energy conversion efficiency

02 p0196 A73-11712

Plasma heating and acceleration due to Landau damping of hydromagnetic waves.

04 p0480 A73-15197

Investigation of the gun aspects of a rotating plasma source.

06 p0732 A73-18779

Analytical model of electron velocity, resonance and potential of plasma accelerated in crossed electric and magnetic fields

10 p1253 A73-23577

Population inversion calculations using near-resonant charge exchange as a pumping mechanism.

13 p1627 A73-28549

Particle acceleration by a moving laser focus, focusing front or ultrashort laser pulse front.

14 p1757 A73-30338

MHD acceleration in the unsteady expansion of a shock tube driver.

15 p1917 A73-31376

Application of a Thomson mass spectrograph with an electron-optical recorder to the investigation of the mechanism of plasmoid acceleration

19 p2467 A73-37370

Solar wind velocity investigation based on solar corona and interplanetary plasma data, analyzing possible acceleration mechanisms

21 p2755 A73-40533

Possibility of radiative acceleration of the gas in stellar atmospheres

21 p2767 A73-40534

Investigation of plasma acceleration in crossed electric and magnetic fields

24 p3115 A73-44751

PLASMA ACCELERATORS

NT COAXIAL PLASMA ACCELERATORS

Influence of the parameters of the accelerating circuit of an injector with inductive energy storage on the process of plasma-cluster acceleration

02 p0196 A73-11633

Device for measuring the instantaneous value of current and voltage in the operation of a pulsed plasma accelerator

02 p0196 A73-11792

Current near the insulator wall in plasma accelerators.

03 p0348 A73-14437

Electromagnetic thrust from magnetic dc arc discharge plasma accelerators, noting MHD experiments and reentry simulation

04 p0489 A73-15728

Structure of the current front in an unsteady plasma accelerator, and turbulent acceleration of the ions. I

09 p1124 A73-21881

Structure of the current front in an unsteady plasma accelerator, and turbulent acceleration of the ions. II

09 p1124 A73-21882

Hypersonic wind tunnel MHD accelerator design and operating principles, discussing flux density, I-V characteristics, cooling losses, plasma temperature, gas pressure and velocity, etc

14 p1743 A73-30295

Investigation of forced oscillations of the plasma potential in a closed electron-drift accelerator/CDA/

15 p1920 A73-32310

The influence of a feedback system on the plasma flux in a closed-drift accelerator/CDA/

15 p1920 A73-32311

Experimental investigation of the plasma focus in erosion-source plasma accelerators. I

15 p1921 A73-32325

Structure of the current front and turbulent acceleration of ions in a pulsed plasma accelerator. I.

17 p2215 A73-34305

Structure of current front and turbulent acceleration of ions in a plasma accelerator. II.

17 p2215 A73-34306

Theoretical and experimental research on the electromagnetic acceleration of shock-induced flow in argon.

19 p2419 A73-37174

Russian papers on physical processes in plasma accelerators covering types, diagnostic methods, gas dynamics, control and space studies

19 p2466 A73-37352

Plasma accelerators design, discussing physical principles, acceleration techniques, plasma conductivity and optimization

19 p2466 A73-37353

Plasma accelerators in gas dynamics, discussing ion propulsion systems, high velocity wind tunnels with electric arc heating and electromagnetic shock tubes

19 p2466 A73-37354

Plasma acceleration techniques in space studies, discussing simulation experiments, solar wind-geomagnetic field interaction and astronomical models

19 p2482 A73-37355

Closed Hall current accelerators for physical and technological applications involving ion acceleration

19 p2466 A73-37356

Study of plasma systems with a closed electron drift and a distributed electric field

19 p2466 A73-37357

Stationary high-current plasma accelerators

19 p2466 A73-37359

Analysis and investigation of cathode processes in a high-current arc discharge

19 p2466 A73-37360

Two cascade plasma accelerator with conical and ring electrodes, investigating plasma jet-cascade current interaction dynamics via magnetic probes and I-V characteristics

19 p2467 A73-37362

Effect of near-electrode processes on plasma behavior in electrodynamic accelerators

19 p2467 A73-37365

Experimental determination of the velocity characteristics of a pulsed erosion-type accelerator

19 p2467 A73-37366

Control of the dynamic characteristics of a plasma jet of a given composition by selecting the parameters of a pulsed accelerator

19 p2467 A73-37368

Thrust stand performance measurements of a lithium fueled applied field MPD arcjet.

19 p2473 A73-38320

Technical and experimental investigations of a plasma focus neutron source

21 p2744 A73-39976

Principal properties of plasma oscillations in an accelerator with closed drift and an extended zone of acceleration/ACDE/

21 p2746 A73-40523

Formation of a plasma focus in erosion-type plasma accelerators. I

21 p2746 A73-40525

Ions bombarding the cathode of a pulsed plasma accelerator and their participation in the development of thermal fluxes

23 p3014 A73-44343

Driven electrostatic plasma oscillations in a closed electron drift accelerator.

24 p3114 A73-44618

Effect of a feedback system on the plasma flux in an accelerator with closed electron drift.

24 p3115 A73-44619

Experiments on the Polytron, a toroidal Hall accelerator employing cusp confinement.

24 p3116 A73-45239

PLASMA ARC SPRAYING

U ARC SPRAYING

U PLASMA SPRAYING

PLASMA ARC WELDING

Electrode phenomena with plasma-MIG welding.

01 p0055 A73-10114

Plasma-MIG arc welding with deposition from automatic reel fed wire via rotating arc, noting suitability for stainless steel sheet

09 p1089 A73-22693

PLASMA ARCS

U PLASMA JETS

PLASMA CHEMISTRY

Stationary composition of a nonisothermal plasma in chemically active media

13 p1664 A73-28420

Plasma chemical synthesis of higher oxides of cesium and rubidium.

13 p1581 A73-29599

PLASMA CLOUDS

Radio emission source picture from observed Cygnus X-3 outburst, suggesting expanding cloud with traveling relativistic electrons and protons

02 p0211 A73-11870

Effect of Thomson scattering on the emission spectrum of an optically semiopaque plasma.

04 p0493 A73-16024

Solar outer atmospheric eruption from photographic recording by OSO 7 spacecraft borne coronagraph, noting ejected gas and plasma clouds caused by flare

06 p0753 A73-18374

Moment equations of temperature and high latitude spread F instability in presence of north-south electric field, relating to maximum Pedersen current and barium cloud deformation

07 p0814 A73-19242

Heating of charged particles by electric waves.

08 p0993 A73-21233

Deformation and striation of plasma clouds in the ionosphere. I, II.

09 p1074 A73-22006

Investigation of the motion of artificially ionized clouds in the upper atmosphere.

10 p1212 A73-24225

A diffusion model for the electron density distribution along the earth's magnetic field in an F-region plasma cloud.

11 p1354 A73-25768

A cylindrical shell model of the NASA-MPE barium ion cloud experiment.

12 p1492 A73-27607

Diffusive motion of initially ellipsoidal plasma irregularities or ion clouds in upper atmosphere, considering space charge electric field effects

17 p2160 A73-34787

High resolution television imaging of barium cloud release in magnetosphere, discussing cloud shape development, striation patterns, core behavior and diffusion characteristics

22 p2845 A73-41936

Computer model of Ba ion cloud expansion in magnetosphere, taking into account self-consistent electric and magnetic field interactions

22 p2846 A73-41938

Small angle multiple backscattering from randomly spaced cylindrical plasma cloud striations, obtaining ray density via Fokker-Planck transport equation

22 p2896 A73-43182

Neutron emission from laser produced plasmas and collisionless electrostatic shock waves.

24 p3116 A73-45242

PLASMA COMPOSITION

Radiation and conductivity of a high current constricted discharge plasma.

01 p0081 A73-10119

Diffusion of weak inhomogeneities in a magnetoelectroactive two-ion plasma

06 p0727 A73-17536

Stationary composition of a nonisothermal plasma in chemically active media

13 p1664 A73-28420

Effect of Debye shielding on the ionization energy of air plasma components

13 p1667 A73-29164

Possibility of electron concentration determination in a plasma with the aid of a gas laser with a nonlinearly rotating absorption cell

14 p1781 A73-30465

Limitation of beam instability as a result of the capture of plasma electrons by the wave

15 p1920 A73-32320

The electric field and structure of a weakly ionized plasma in the vicinity of a small charged body

15 p1921 A73-32322

Diffusion of weak inhomogeneities in a magnetically active plasma consisting of two ions.

16 p2039 A73-32760

Book - Equilibrium compositions and thermodynamic properties of mixed plasmas. III - Argon-hydrogen plasmas at .01 to 1000 atmospheres between 2,000 and 35,000 K.

16 p2042 A73-33420

Parametric instabilities in a plasma containing two types of ions

16 p2043 A73-34057

Effect of finite resistivity on the dynamic stability of a composite plasma.

17 p2214 A73-34074

Experiment and observation of isotope and element separation in a plasma with cosmic applications.

17 p2216 A73-34420

Sensitivity of the numerical analysis of the three-fluid plasma mixed initial-boundary value problem.

18 p2338 A73-36160

Calculation of components, electrical conductivity, and total radiative source strength of nitrogen plasma in local thermodynamic equilibrium.

18 p2339 A73-36360

Experimental investigation of a fast ion-acoustic wave in a multicomponent plasma

18 p2339 A73-36564

Shock waves within the two fluid model in the presence of the magnetic field.

19 p2464 A73-37160

Application of a Thomson mass spectrograph with an electron-optical recorder to the investigation of the mechanism of plasmoid acceleration

19 p2467 A73-37370

A tensor surface harmonic expansion of the collision integral for a weakly ionized plasma. I
20 p2596 A73-39193
Mass-spectrometric investigation of the ion composition of potassium and cesium discharge plasmas
21 p2746 A73-40526
Cyclotron resonance in a weakly ionized hydrogen plasma with nitrogen, oxygen and air impurities
22 p2890 A73-41864
Shielding of moving test particles in warm, isotropic plasma.
22 p2893 A73-42392
Hydromagnetic stability of a composite plasma in the presence of Hall currents.
22 p2894 A73-42439
One-component two dimensional plasma, calculating equilibrium pair correlation function by Debye approximation for particle interaction via Coulomb potential
23 p3013 A73-44172

PLASMA CONDUCTIVITY

Electrical conductivity and total radiant power of air plasma.
01 p0081 A73-10121
The electron diffusion scattering cross section of cesium atoms
01 p0080 A73-10852
Periodic structure of the electric field in a stratified plasma with tensor conductivity
01 p0085 A73-10955
Stability of a plasma with an axial current surrounded by a cold gas with a pressure gradient.
02 p0198 A73-12108
Electron-ion collision frequency and electrical conductivity of non-Debye plasma formed in high pressure discharge from Ar, Kr and Xe tubes
03 p0345 A73-13176
Kinetic theory for calculation of low temperature homogeneous plasma electric conductivity in magnetic field, noting monotonic decrease
03 p0346 A73-13177
The diffusion-driven current in a toroidal resistive plasma.
03 p0348 A73-14433
Hydromagnetic stability of closed plasma configurations
04 p0478 A73-15020
Measurement of the dc plasma electric resistivity perpendicular to the magnetic surface.
04 p0482 A73-15959
Ion-acoustic oscillations effect on turbulent plasma electric conductivity within weak external electric field
06 p0729 A73-17973
Instability of a current-carrying plasma at cyclotron harmonics, and anomalous resistance
06 p0729 A73-18113
Isotropic conducting plasma dynamic behavior near rotating magnetized sphere, showing electric field-produced meridional convective currents
07 p0856 A73-19430
Hydromagnetic waves excited by transverse magnetic dipole in finite-conductivity plasma
07 p0816 A73-19462
Effects of collisions with neutrals on the dynamic stability of a finitely conducting hydromagnetic composite plasma in the presence of Hall currents.
07 p0858 A73-19600
Electrodynamic mathematical model for electroconductivity of nonuniform plasma with Hall effect, calculating current distribution from Riemann problem solution
08 p0992 A73-20863
One-dimensional numerical experiment on anomalous plasma resistivity
09 p1127 A73-22482
Conductivity tensor and dispersion equation for collisional magnetoactive plasma.
09 p1131 A73-22922
Thermal conductivity of the plasma electron component across the magnetic field
10 p1258 A73-24890
Collective interactions and electrical conductivity of plasma in strong electric fields.
11 p1406 A73-26554
The frequency dispersion of the transverse electrical conductivity of ionospheric plasma
12 p1491 A73-27357
The periodic structure of an electric field in stratified plasma with tensor conductivity.
12 p1529 A73-27531
The diffusion cross section for scattering of electrons by cesium atoms.
12 p1526 A73-27902
Particle trapping effect on conductivity of toroidal plasma with like-particle collisions taken into account, obtaining results applicable to all aspect ratios
14 p1778 A73-29687
Equatorial spread F formation convective electric fields generation by neutral winds and conductivity caused by metallic ion concentrations
14 p1749 A73-29988
Quantum correction to the electrical conductivity of a Coulomb plasma
14 p1781 A73-30584

A generalized flux-vorticity theorem. I.
15 p1916 A73-31088
Screened potential Lorentz model for electrical conductivity of non-Debye plasma, investigating electron energy distribution function
17 p2214 A73-34127
Heat conductivity measurements for a hydrogen plasma in a stabilized electric arc
17 p2214 A73-34129
Current distribution at the zero line of the magnetic field and the turbulent resistance of a plasma
18 p2339 A73-36550
Structure of almost collisionless shocks in a magneto-plasma and the ion-acoustic instability.
19 p2464 A73-37158
Plasma accelerators design, discussing physical principles, acceleration techniques, plasma conductivity and optimization
19 p2466 A73-37353
Experimental study of conductivity, velocity, and temperature distributions in a submerged jet of low-temperature plasma
21 p2747 A73-40575
Conductivity tensor of a collisional plasma in a magnetic field.
21 p2749 A73-41628
Transverse electron thermal conductivity for a plasma in a magnetic field.
21 p2749 A73-41665
Role of nonlinear effects in the problem of the anomalous resistance of plasma.
22 p2890 A73-41723
Nature of the anomaly of the electrical conductivity of a magnetized plasma
22 p2892 A73-42381
Frequency dispersion of transverse electrical conductivity of ionospheric plasma.
23 p2971 A73-43256
Electrical conductivity of a plasma during collective interactions in a high-current gas discharge
23 p3009 A73-43652
Instability of a current-carrying plasma at cyclotron harmonics and the anomalous resistance.
24 p3114 A73-44502
Plasma conductivity model of current structure of MHD waves propagating from electric dipole source in magnetosphere in relation to geomagnetic pulsations
24 p3084 A73-44805
Gaseous plasma thermal conductivity in dynamic equilibrium, relating particle binary correlation to shielding distance under temperature gradients
24 p3116 A73-45243
Wave-wave contribution to the high-frequency resistivity of nonequilibrium plasma.
24 p3117 A73-45457
Spectroscopic measurements of plasma temperatures and density at X type magnetic neutral points, suggesting ion acoustic instability role in turbulent conductivity
24 p3118 A73-45461

PLASMA CONFINEMENT
U PLASMA CONTROL
PLASMA CONTROL
Radiation and conductivity of a high current constricted discharge plasma.
01 p0081 A73-10119
Two-dimensional investigation of absolute instabilities in mirror plasmas.
01 p0083 A73-10458
Use of the virtual-casing principle in calculating the containing magnetic field in toroidal plasma systems.
01 p0084 A73-10464
A 12-coil superconducting 'bumpy torus' magnet facility for plasma research.
02 p0150 A73-11839
Purification of hydrogen plasmoids by the magnetic field in an injector-diverter.
02 p0198 A73-12113
Shadowing of electron azimuthal-drift motions near the noon magnetopause.
02 p0164 A73-12442
Injection of an electron beam into a plasma confined by a conducting shell.
03 p0347 A73-14093
Plasma confinement in a racetrack magnetic field with a diverter.
03 p0347 A73-14094
Methods of plasma injection into closed magnetic confinement systems
04 p0479 A73-15041
Confinement in a magnetic mirror of a plasma generated by laser radiation
04 p0482 A73-15620
Measurement of the dc plasma electric resistivity perpendicular to the magnetic surface.
04 p0482 A73-15959
Transverse and longitudinal heat flow in a laser-heated magnetically confined plasma.
05 p0603 A73-17162
Surrounding wall electrical resistivity effects on plasma pinch stabilized by outer region force-free current flow, deriving instability growth rate
05 p0604 A73-17363

Fusion plasma confined by nonpenetrating uniform magnetic field, calculating temperature and density effects on energy balance instabilities from particle conservation equations
05 p0604 A73-17366
Contribution of Coulomb collisions to plasma relaxation in the DECA mirror machine.
05 p0604 A73-17367
Confined plasma diffusion due to growing or nonlinearly saturated LF ion waves causing energy transfer from electrons to ions in slabs
05 p0604 A73-17368
Motion of plasmoids in a toroidal magnetic multipole.
06 p0727 A73-17421
Instability of a magnetoactive plasma with a transverse ion beam.
06 p0731 A73-18602
Conversion of trapped charged particles into untrapped particles in a high-frequency electric field.
06 p0732 A73-18608
Modified negative mass mode stabilization in finite magnetic mirror confined plasmas with highly anisotropic velocity distribution, considering bounce harmonic effects and gyrofrequency
07 p0856 A73-19522
Feedback control of ionization instability in MHD generators.
07 p0779 A73-20395
Radiative and collisional effects in a cylindrically confined plasma. I - Optically thin considerations. II - Absorption effects.
08 p1021 A73-20793
Steady state hot toroidal Tokamaks plasma, calculating seed current density for bootstrap effect produced by neutral particle injection parameters control
08 p0991 A73-20814
Non-local asymptotic treatment of the stability of an inhomogeneous confined plasma.
08 p0991 A73-20819
Particle and energy fluxes across magnetic field in axisymmetric toroidal magnetic traps and plasmas with weak collisions, calculating radial electric field
08 p0993 A73-21695
Influence of magnetic field curvature on the stability of a plasma confined by a dense shell of neutral gas
09 p1124 A73-21902
Excitation of low-frequency oscillations by an electron beam in a hot plasma confined in a magnetic mirror
09 p1125 A73-21907
Application of a system of orthogonalized windings with automatically regulated current for plasma stabilization in Tokamak systems
09 p1125 A73-21908
Investigation of the heating mechanism for the electron component of a plasma under beam-instability conditions in a mirror confinement system
09 p1130 A73-22703
Propagation of discharges and confinement of a dense plasma by electromagnet fields
09 p1132 A73-23327
Injection of a laser-produced plasma into a magnetic trap.
10 p1254 A73-24210
Internal instabilities derived for electron plasma with electrons rotating about axis of symmetry parallel to confining external magnetic field
10 p1256 A73-24449
Particle kinetic energy vs number density in equilibrium E layer under external and self magnetic fields related to plasma confinement in astron device
11 p1404 A73-25259
Numerical studies of charged particle trapping in a time varying magnetic mirror field.
11 p1404 A73-25273
Magneto-viscous effects on the ideal and resistive gravitational instabilities in Cartesian geometry.
11 p1406 A73-26553
Influence of electric drift on the cone instability of a plasma in adiabatic traps
12 p1527 A73-26930
Effect of a high frequency magnetic field on plasma diffusion in a Q-machine.
13 p1664 A73-28348
Experiments on the containment of an alkali plasma in a corrugated magnetic field.
13 p1664 A73-28612
Suppression of the flute instability of a dense plasma by a magnetic system of feedbacks in an open trap
13 p1666 A73-28953
German book on plasma physics covering plasma containment, magnetohydrostatics, gravitational effects, plasma pinch, toroidal plasmas, plasma waves and MHD instabilities
13 p1667 A73-29288
Averaged equations of cumulative laser heating of a plasma focus with consideration of the heat of nuclear fusion.
13 p1667 A73-29389
Partial trapping of a low-density plasma by an RF quasipotential well.
14 p1779 A73-29917

Plasma produced by lasers on solid targets
14 p1779 A73-30025

General radio-frequency properties of bounded plasma systems in connection with the production and heating of dense plasmas.
14 p1780 A73-30120

Experiments on CO₂-laser heating of magnetically confined underdense plasmas.
14 p1780 A73-30123

Determination of electromagnetic field correlators for a contained plasma
15 p1916 A73-31037

Experimental study of the interaction of a plasma with a magnetic field in the case of a plasma generated by laser irradiation of solids
15 p1917 A73-31249

Effect of laser pulse rise time on heating of a magnetically confined plasma.
15 p1919 A73-31929

Coulomb drift of electrons from a mirror confinement system in the case of a positive plasma potential
15 p1920 A73-32306

Intensity of thermal fluctuations of plasma flute instabilities in open confinement systems in the presence of a feedback system
15 p1920 A73-32307

The influence of a feedback system on the plasma flux in a closed-drift accelerator/CDA/
15 p1920 A73-32311

Experimental investigation of the plasma focus in erosion-source plasma accelerators. I
15 p1921 A73-32325

Equilibrium of a plasma contained between two parallel plates by a magnetic field
15 p1921 A73-32333

Effect of magnetic field curvature on the stability of a plasma confined by a dense neutral gas.
15 p1921 A73-32627

Electron-beam excitation of low-frequency waves in a hot plasma confined in a mirror machine.
15 p1922 A73-32632

Magnetic feedback stabilization in a Tokamak.
15 p1922 A73-32633

Magnetic multipole containment of large uniform collisionless quiescent plasmas.
17 p2215 A73-34271

Wave transformation due to oblique incidence on the boundary of a magnetoactive plasma
18 p2289 A73-36553

Nonlinear excitation of an ion-acoustic wave in a bounded plasma
18 p2340 A73-36675

Study of plasma systems with a closed electron drift and a distributed electric field
19 p2466 A73-37357

Energy characteristics of a coaxial plasma source
19 p2467 A73-37363

Control of the dynamic characteristics of a plasma jet of a given composition by selecting the parameters of a pulsed accelerator
19 p2467 A73-37368

Stability of plasma flows in multipolar magnetic fields
19 p2467 A73-37372

Formation of a plasma focus in erosion-type plasma accelerators. I
21 p2746 A73-40525

Directional plasma transport equations derived from Boltzmann equation by averaging of velocity space subset, applying to plasma confinement by external time dependent electromagnetic fields
21 p2748 A73-41127

Numerical methods for solving some problems of the theory of plasma equilibrium in toroidal configurations.
21 p2750 A73-41680

Anomalous transport due to the dissipative trapped-ion instability.
21 p2750 A73-41682

Effect of electric drift on the loss-cone plasma instability.
22 p2891 A73-42264

Longitudinal polarization and focusing of plasmoids in a linear multipole magnetic field
22 p2893 A73-42383

Polarizing interaction between colliding plasma flows in a toroidal magnetic field. II
22 p2893 A73-42384

Investigation of the dynamics of plasma flows in the field of a pulsed magnetic barrier
23 p3010 A73-43658

Shaping of plasma clusters moving in a longitudinal magnetic field
23 p3010 A73-43659

Motion of a plasma in curvilinear magnetic fields of constant and alternating curvature
23 p3010 A73-43661

Suppression of the flute instability in a dense plasma in an open system by magnetic feedback.
23 p3013 A73-44305

Investigation of neoclassical diffusion in toroidal systems with a three-dimensional magnetic axis
23 p3014 A73-44337

Investigation of the efficiency of laser-plasma trapping by a magnetic field
23 p3014 A73-44341

Coulomb loss of electrons from a mirror device with a positive plasma potential.
24 p3114 A73-44614

Thermal flute perturbations in an open plasma device with feedback.
24 p3114 A73-44615

Effect of a feedback system on the plasma flux in an accelerator with closed electron drift.
24 p3115 A73-44619

Experiments on the Polytron, a toroidal Hall accelerator employing cusp containment.
24 p3116 A73-45239

PLASMA CYLINDERS

Kinetic theory of scattering by a plasma cylinder.
01 p0081 A73-10136

Kinetic theory of surface waves in a cylindrical plasma waveguide.
02 p0198 A73-12106

The excitation of resonances by a dipole antenna inside a hollow cylindrical plasma.
03 p0346 A73-13695

Pulse discharge plasma in Ar with gas ionization level near unity, noting plasma cylinder parameters, electron temperature and I-V characteristics
03 p0347 A73-14091

Ion distribution function in plasma cylinder flow around thin plate in magnetic field under ionospheric conditions
04 p0481 A73-15617

Scattering by nonconcentric circular plasma cylinders with axial magnetic fields.
06 p0729 A73-18204

Screw instability of a plasma with a distributed current
07 p0855 A73-19280

Numerical analysis of magnetohydrodynamic instabilities by the finite element method.
07 p0856 A73-19515

Spatial distributions of plasma density in a high-frequency discharge with a superimposed static magnetic field.
07 p0856 A73-19518

Radiative and collisional effects in a cylindrically confined plasma. I - Optically thin considerations. II - Absorption effects.
08 p1021 A73-20793

Tokamak axisymmetric toroidal plasma filament equilibrium in conducting circular and elliptic cylinder for pressure and current distributions, using numerical MHD equation integration
09 p1123 A73-21877

Rotation of the ion component of a plasma from a hot-cathode Penning discharge
09 p1125 A73-21955

Enhanced energy transfer to a cylindrical plasma by an Alfvén wave.
09 p1128 A73-22629

Ion distribution function in plasma cylinder flow around thin plate in magnetic field under ionospheric conditions
10 p1254 A73-24207

Straight plasma column confined by static axial and oscillating transverse magnetic fields, deriving stability criteria via viscous fluid model
10 p1255 A73-24264

Conducting medium flow in cylinder with nonconducting walls, solving nonlinear elliptic equation /Dirichlet problem/ by projective-iterative method
10 p1256 A73-24509

Stability of a plasma rotating in crossed electric and magnetic fields
11 p1403 A73-25240

Electromagnetic wave scattering by an inhomogeneous magnetoplasma column moving in the axial direction.
11 p1407 A73-26700

Nonlinear helical waves formation due to Kelvin-Helmholtz instability in type 1 comet tail modeled as plasma cylinder immersed in solar wind
12 p1542 A73-27609

Screw instability in a plasma with a distributed current.
13 p1665 A73-28680

Stability of a plasma cylinder containing axisymmetric opposite currents
13 p1666 A73-28952

Influence of longitudinal thermal conductivity on the ohmic heating of plasma in the Tuman-I facility
13 p1666 A73-28959

Investigation of the radial structure of the oscillations of a plasma column situated in crossed fields in the presence of resonant cyclotron instability
14 p1781 A73-30579

Comprehensive theory of r.f. energy absorption by a hot ion-electron plasma cylinder excited by an arbitrary electromagnetic field.
15 p1916 A73-31080

Intensity of thermal fluctuations of plasma flute instabilities in open confinement systems in the presence of a feedback system
15 p1920 A73-32307

Steady state arc discharge physical properties, discussing boundary geometry of plasma column, and stabilities in gas flow and high current and vacuum conditions
16 p2040 A73-32939

Reflection coefficient of an electromagnetic wave by a plasma column of variable electron density in a waveguide.
16 p1984 A73-33994

Tokamak axisymmetric toroidal plasma filament equilibrium in conducting circular and elliptic cylinder for pressure and current distributions, using numerical MHD equation integration
17 p2215 A73-34301

Investigation of scattering of microwaves in a plasma-beam discharge.
17 p2217 A73-35716

Electron temperature and density in the He-CdII positive column used for an I/+ laser.
17 p2186 A73-35798

Ion cyclotron instability of a rotating plasma
18 p2340 A73-36671

Oscillations of the earth's magnetic field
19 p2482 A73-37349

Low-frequency flute instabilities of a bounded plasma column.
20 p2595 A73-38889

Dynamics of plasma column constriction and electromagnetic acceleration of ions
21 p2745 A73-40362

Theory of a steady-state nonisothermal positive column in a magnetic field.
21 p2748 A73-40954

Narrow-beam antennas using cylindrical columns of isotropic plasma.
21 p2665 A73-41124

Investigation of the waveguide properties of a plasma cylinder for axially asymmetric waves
22 p2892 A73-42379

Stability of a plasma cylinder with counterstreaming axisymmetric currents.
23 p3013 A73-44304

Effect of longitudinal thermal conductivity on ohmic heating in Tuman-1.
23 p3013 A73-44311

Thermal flute perturbations in an open plasma device with feedback.
24 p3114 A73-44615

PLASMA DECAY

Vapour density variations in a pulsed mercury discharge.
05 p0601 A73-16432

Instability limits of an isothermal weakly ionized plasma in a magnetic field
07 p0855 A73-19282

Electron heat conductivity along a magnetic field in a decaying plasma
09 p1124 A73-21887

Experimental study of the relaxation of excited states in a decaying alkaline plasma
10 p1256 A73-24576

Thermal conductivity of the plasma electron component across the magnetic field
10 p1258 A73-24890

Stability of a weakly ionized isothermal plasma in a magnetic field.
13 p1665 A73-28682

Partial trapping of a low-density plasma by an RF quasipotential well.
14 p1779 A73-29917

Nonstationary theory of decay instability in a weakly inhomogeneous plasma
15 p1918 A73-31704

Arc discharge properties in ionized gases, discussing interruption and reignition in terms of instabilities, decay processes, and circuit breaker problem
16 p2040 A73-32940

Nonlinear evolution of the decay instability in a plasma with comparable electron and ion temperatures.
16 p2041 A73-33324

Decay of a high temperature helium plasma - Validity of local thermodynamic equilibrium and estimation of recombination coefficients for He+ + I, He+ + I, and He2+ /-.
16 p2043 A73-33867

Electron thermal conductivity along the magnetic field in an afterglow.
17 p2215 A73-34310

Cooling and heating of electrons during the decay and development of a cesium discharge plasma
19 p2469 A73-37962

Experimental results concerning the time decay of the line emission in luminescent plasmas of medium-pressure inert-gas discharges
20 p2596 A73-39191

Afterglow studies in helium-cesium mixtures.
21 p2745 A73-40223

Electron density in a locally ionized plasma afterglow.
21 p2748 A73-40970

Transverse electron thermal conductivity for a plasma in a magnetic field.
21 p2749 A73-41665

Classical diffusion of free boundary plasma in plane and cylindrical slab geometries, calculating belt pinch effect and pressure decay rate
21 p2750 A73-41679

Experimental observation of the decay of high-frequency waves in a plasma
22 p2826 A73-42389

Thermonuclear laser synthesis and parametric instabilities 23 p2988 A73-44091

A 337-micron HCN laser interferometer for plasma diagnostics. 24 p3097 A73-45410

Plasma decay instability nonlinear saturation spectrum in small spontaneous emission limit for comparable ion and electron temperatures from kinetic equation numerical solution 24 p3118 A73-45460

PLASMA DENSITY

Plasma density measurement by a Langmuir probe in the presence of a magnetic field 01 p0082 A73-10428

Fluctuation characteristics of dense plasmas from high-current discharges produced by electric explosion of metallic wires in vacuum 01 p0086 A73-11283

Energy spectra of modulated relativistic electron beam as function of plasma density at beam-plasma interaction region boundary 01 p0086 A73-11284

Long-lived sectors of enhanced density irregularities in the solar wind. 02 p0205 A73-11911

Spherical probe measurements of dense weakly ionized plasma parameters, noting ionization, recombination and secondary surface effects on probe characteristics 02 p0198 A73-12109

Determination of the ionospheric density and temperature using a double probe electric field detector. 02 p0164 A73-12310

Investigation of a dense plasma produced by an electron beam in a magnetic mirror 04 p0479 A73-15040

The dispersion diagram of the plasma waves on the plasma branch in a beam-created plasma. 04 p0482 A73-15949

Resonance coupling of a transverse magnetic response to a transverse electric excitation by the axial density gradient of a bounded plasma. 05 p0601 A73-16364

A neutral-potassium-beam measurement of plasma density. 05 p0604 A73-17364

Boundary-value problem for a Langmuir probe in a dense plasma. 06 p0727 A73-17420

Determination of the spatial distribution of a plasma with a microwave resonator. 06 p0727 A73-17423

Controlled nuclear fusion process based on laser heating of deuterium-tritium pellets, considering laser energy reduction by pulse induced plasma compression 06 p0699 A73-17752

Density and electric field oscillations of plasma in stellarator, considering magnetic field strength effect, stabilization by ionic collisions and energy pumping mechanism 06 p0728 A73-17968

The equation of state of a dense metal vapor plasma and electron mobility 06 p0730 A73-18552

Scattering of microwaves by a stratified overdense plasma at high collision frequencies. 06 p0732 A73-18780 [AD-756733]

Production of hot plasmas of solid-state density by ultrashort laser pulses. 06 p0733 A73-18783

Contribution of 1- and 5-nsec frame-type motion-picture photography to the study of dense plasmas 06 p0696 A73-18857

Screw instability of a plasma with a distributed current 07 p0855 A73-19280

Instability limits of an isothermal weakly ionized plasma in a magnetic field 07 p0855 A73-19282

Measurement of plasma density in a torsatron by a multimode resonator technique 07 p0855 A73-19283

Intermittent behavior of a plasma discharge in turbulent gas flow. 07 p0856 A73-19517

Spatial distributions of plasma density in a high-frequency discharge with a superimposed static magnetic field. 07 p0856 A73-19518

Kelvin-Helmholtz instability in a high-beta collisionless plasma. 07 p0856 A73-19520

Thermonuclear reactor model with core surrounded by dense cold plasma, noting temperature profile effects on fusion and energy release locations 08 p0991 A73-20818

Measurement of spatial plasma-density distributions with the aid of an open barrel-shaped resonant cavity 09 p1124 A73-21879

Solar plasma electron density and temperature measurement by Mars 2 and Mars 3 orbiter-borne retarding potential analyzers, considering solar wind shock front interaction role 09 p1126 A73-22263

Wave transformation in warm magnetoplasma slab with parabolic density profile and two lower hybrid layers, discussing long wavelength energy tunneling and conversion efficiency 09 p1129 A73-22637 [TTU-SR-2]

Nonlinear theory of the interaction of a monoenergetic beam with a dense plasma 09 p1130 A73-22706

Drift-like instability in density modulated plasmas in a static magnetic field. 09 p1131 A73-22904

A plasma laser operating on molecular electronic transitions 10 p1228 A73-24454

Numerical modeling of laser produced plasmas - The dynamics and neutron production in dense spherically symmetric plasmas. 11 p1404 A73-25272

Plasma low density regions caused by Langmuir turbulence, discussing energy dissipation of long wave oscillations and wave collapse 11 p1406 A73-26185

Current and fields reduced in plasmas by relativistic electron beams with arbitrary radial and axial density profiles. 11 p1407 A73-26560

Inhomogeneous plasma density distribution relation to ambipolar diffusion and ionization balance processes of electron cooling, particle recombination and ground state, step wise and Penning ionization 12 p1527 A73-26932

Interplanetary scintillations observations from solar wind plasma density fluctuations power spectrum 12 p1533 A73-26980

Screw instability in a plasma with a distributed current. 13 p1665 A73-28680

Stability of a weakly ionized isothermal plasma in a magnetic field. 13 p1665 A73-28682

Multimode cavity measurements of plasma density in a torsatron. 13 p1665 A73-28683

Rayed auroral structures and their relation to the drift current instability in a plasma blob. 13 p1607 A73-28705

Ignition condition in Tokamak experiments and role of neutral injection heating. 14 p1777 A73-29684

'Drift' instabilities distorting the magnetic surfaces of Tokamak-type toroidal systems. 14 p1778 A73-29690

Electric field and plasma density oscillations due to the high-frequency Hall current two-stream instability in the auroral E region. 14 p1748 A73-29971

Diffusion of plasma density and temperature perturbations in a magnetic field 14 p1749 A73-30264

Correlation between the potential and density fluctuations of a plasma, and the convective transport of particles across the magnetic field in a Penning discharge in the presence of rotational instability 14 p1781 A73-30581

Ionization oscillations in a plasma in the presence of negative ions 15 p1920 A73-32319

Hydrodynamic theory of high-amplitude ionization waves 15 p1921 A73-32326

Use of emissive probes in plasma density measurements. 16 p2011 A73-32725

Influence of diffusion on plasma parameters - A qualitative estimate and a physical interpretation. 16 p2040 A73-32941

Remote feedback stabilization of ion acoustic type instability in plasma with LF density modulation, noting Van der Pol approach agreement and crossed field diffusion decrease 16 p2041 A73-33327

Early-time model of laser plasma expansion. 16 p2042 A73-33340

Equation of state of a plasma of a dense metal vapor and the electron mobility. 16 p2042 A73-33577

Measurement of plasma density distribution using an open barrel-shaped cavity. 17 p2215 A73-34303

Transformation of high-frequency waves and vanishing of low-frequency instabilities in a radially-inhomogeneous beam-plasma discharge. 17 p2217 A73-35525

Corner expansion flow of ionized argon, calculating electron density, plasma density and recombination rate constant for comparison with measurements 19 p2465 A73-37177

Quenching of the beam-plasma instability by mode mixing at a density discontinuity. 19 p2469 A73-37859

Electron transitions of molecules in a plasma laser. 19 p2438 A73-38135

ULF excitation of plasmopause sinusoidal oscillations by magnetic disturbances exterior to plasma-

sphere boundary, inferring plasma density from wave frequency and damping rate 21 p2650 A73-40507

Nonlinear and nonstationary effects in the solar wind 21 p2757 A73-40594

Maintenance of the F-region at night - Incoherent scatter measurements at a mid-latitude station. 21 p2683 A73-40776

A numerical investigation of the current and density distributions for a non-equilibrium plasma in a segmented electrode duct. 21 p2748 A73-40926

Nonlinear interacting longitudinal and transverse electron oscillations due to plasma density inhomogeneity in HF hybrid resonance region 21 p2750 A73-41683

Mariner 5 observations of solar wind shock-like structures including density, velocity, and proton temperature increases, suggesting nonlinear magnetoacoustic waves under steepening process 22 p2901 A73-41902

New dispersion relation for a strongly magnetized degenerate electron plasma with anisotropic pressure. 22 p2890 A73-42237

Inhomogeneous plasma density distribution relation to ambipolar diffusion and ionization balance processes of electron cooling, particle recombination and ground state, step wise and Penning ionization 22 p2891 A73-42266

The effect of nonstationarity in the chemical composition of plasma flows from the sun. 23 p3027 A73-43252

Fluctuation characteristics of a dense plasma of high current discharges produced by electric explosion of metallic wires. 23 p3009 A73-43504

Energy spectra of modulated relativistic electron beam as function of plasma density at beam-plasma interaction region boundary 23 p3009 A73-43505

Langmuir wave attenuation in collisionless plasma of variable density due to field generated by resonant particle currents moving toward lower density region 23 p3015 A73-44349

Direct-display plasma density and temperature meter by the use of Langmuir probe. 23 p3015 A73-44367

Large-scale inhomogeneities in the sector structure of the solar wind 24 p3124 A73-44779

Vela 3 proton data analysis for compressions and rarefactions effects on solar wind density, temperature and velocity behavior 24 p3125 A73-45106

MilliHertz plasma oscillations associated with strong gradients in density and temperature 24 p3087 A73-45139

Computerized simulation of electrostatic instabilities development in underdense plasmas during heating by high output lasers with frequencies above electron plasma frequency 24 p3118 A73-45466

PLASMA DIAGNOSTICS

Measurement of the macroscopic velocity of the neutral component of weakly ionized gas in the crossed fields. 01 p0081 A73-10116

Theoretical and experimental study of the H.F. current associated with a plasma wave. 01 p0081 A73-10118

CO2 plasma emissivity at temperatures from 7000 to 9000 K in the spectral range of 2100 to 10,000 Å 01 p0085 A73-10854

Electron temperature measurement in collisional plasma with double probe, noting electron and ion density distribution near isolated electrode under floating potential 01 p0085 A73-10866

X-ray fine structure of dense plasma in a co-axial accelerator. 01 p0086 A73-11493

The plasma diagnostics experiments of the Aeros satellite [DGLR PAPER 72-070] 02 p0166 A73-11669

A large double plasma device for plasma beam and wave studies. 02 p0168 A73-11964

Spherical probe measurements of dense weakly ionized plasma parameters, noting ionization, recombination and secondary surface effects on probe characteristics 02 p0198 A73-12109

Purification of hydrogen plasmoids by the magnetic field in an injector-diverter. 02 p0198 A73-12113

Electric fields and conductivities derived from wake measurements on a rocket. 02 p0164 A73-12311

Uniform low temperature gas discharge plasma diagnostics in shielded volume, noting application of stable plasma generation effect for isotope analysis 02 p0199 A73-12693

Measurement of electron distribution function in a cesium plasma. 02 p0199 A73-12815

Pumping rate in He-Cd laser from metastable atoms concentration measurement and plasma diagnostics, noting upper level population dependence on Penning effect 03 p0319 A73-13753

Injun 5 observations of magnetospheric electric fields and plasma convection. 03 p0303 A73-13875

Spectroscopic investigation of turbulent plasma parameters. 03 p0347 A73-14095

Measurement of temperature by recording the absolute line intensity with apparent increase of plasma optical thickness. 03 p0348 A73-14439

Racetrack configuration design of Uragan stellarator for plasma diagnostics and heating, noting shear and rotational angle of magnetic system 04 p0432 A73-15038

Electron density and temperature measurements in the lower ionosphere as deduced from the warm plasma theory of the H.F. quadrupole probe. 04 p0480 A73-15199

Electric field and plasma observations in the magnetosphere. 04 p0442 A73-15334

Use of an electron beam for low-temperature plasma measurement in the magnetosphere and interplanetary space. 04 p0450 A73-15553

A technique for making dispersion relation measurements of electrostatic waves. 04 p0450 A73-15554

Plasma diagnostics in overcompensation operated Knudsen thermionic converter with Cs-Ba filler, noting W cathode surface properties 04 p0481 A73-15614

Measurement of the electron energy distribution function in a plasma with periodically varying parameters 04 p0481 A73-15615

Diagnostic procedures for nonhomogeneous plasma based on geometrical optics approximation, irradiating plasma by plane wave at oblique incidence 05 p0601 A73-16070

Evaluation of an orifice probe for plasma diagnostics. 05 p0601 A73-16431

Characteristics of an argon RF plasma - Active discharge and laminar sonic flow region. 05 p0602 A73-16559

Measurement of continuum radiation from an argon plasma. 05 p0602 A73-16564

Determination of plasma electron temperature from the reversal of radial ambipolar electric field in a longitudinal magnetic field. 05 p0602 A73-16584

The measurement of plasma transport properties in a free-burning electric arc. 05 p0603 A73-16763

A simple bakeable hollow cathode device for the direct study of plasma constituents. 05 p0563 A73-17262

Boundary-value problem for a Langmuir probe in a dense plasma. 06 p0727 A73-17420

Determination of the spatial distribution of a plasma with a microwave resonator. 06 p0727 A73-17423

Possibility of observing the decay interaction of plasma waves in top-side sounding experiments 06 p0689 A73-17551

Gain correlation with sidelight and plasma impedance properties of a CO₂ laser discharge. 06 p0700 A73-18137

Experimental investigations on the impedance behavior of a cylindrical antenna in a collisional magnetoplasma. 06 p0729 A73-18186

Effects of non-Maxwellian electron energy distributions on the orbital limited current-voltage characteristics of cylindrical and spherical Langmuir probes under collisionless conditions. 06 p0730 A73-18463

Heating of a magnetized plasma under parametrically unstable conditions 06 p0731 A73-18574

Sharp focused short pulse X ray source with laser flash synchronization for radiographic plasma diagnostics 06 p0732 A73-18609

Determination of parameters of laser-induced plasma in air by a scattering method. 06 p0732 A73-18610

Contribution of 1- and 5-nsec frame-type motion-picture photography to the study of dense plasmas 06 p0696 A73-18857

Measurement of plasma density in a torsatron by a multimode resonator technique 07 p0855 A73-19283

Experimental and numerical studies of flush electrostatic probes in hypersonic ionized flows. II - Theory. 07 p0858 A73-19961

Continuum electrostatic probe theory with magnetic field. 07 p0860 A73-20476

Correlation of ground-based measurements of structured Pc 1 micropulsations withOGO-V plasmopause observations. 08 p0937 A73-20652

Ar plasma diagnostics from stabilized arc emission spectra, noting thermodynamic equilibrium in central zone of arc channel 08 p0992 A73-20855

Plasma diagnostics with open microwave cavities 08 p0963 A73-21014

Characteristics of a spherical electrostatic probe in a weakly ionized plasma. 08 p0993 A73-21390

A comparative experimental study of electron and positive-ion current collection by a cylindrical Langmuir probe under orbital-limited conditions. 08 p0967 A73-21598

Accuracy of interferometric plasma investigations involving heating of the optical elements 09 p1131 A73-22883

Use of magnetic probes for diagnostics of pulse plasma. 09 p1086 A73-23149

Plasma self radiation and absorption, schlieren signals and lasing levels recording methods based on diode lasers, using Mach-Zehnder IR interferometer 10 p1253 A73-23517

Plasma diagnostics in overcompensation operated Knudsen thermionic converter with Cs-Ba filler, noting W cathode surface properties 10 p1177 A73-24204

Measurement of electron energy distribution in a plasma with periodically varying parameters. 10 p1254 A73-24205

Microwave cavity measurements of electron densities in a shock tube. 10 p1220 A73-24620

Electrostatic probe theories and measurements in flame plasmas. 10 p1220 A73-24621

A simple device for measuring the characteristics of double Langmuir probes in a periodic pulse discharge 10 p1257 A73-24691

Light scattering from weakly ionized nonhomogeneous plasmas. 11 p1405 A73-25971

Aspects of the application of Rogovskii's coil to the measurement of steady currents in a plasma 12 p1528 A73-27306

ARC discharge plasma diagnostics for nonuniform nonequilibrium turbulent sources, including automatic methods for control applications 12 p1528 A73-27322

The radiative capacity of a CO₂ plasma at temperatures 7000-9000 K in the spectral interval 2100-10,000 Å. 12 p1529 A73-27904

Probe device for measuring local parameters of ionized gas flow. 12 p1499 A73-27915

Electron temperature measurement in recombination collisional plasma with double probe, noting electron and ion density distribution near isolated electrode under floating potential 12 p1499 A73-27916

Laser interaction and related plasma phenomena; Proceedings of the Second Workshop, Rensselaer Polytechnic Institute of Connecticut, Hartford, Conn., August 30-September 3, 1971. Volume 2. 12 p1508 A73-27922

A device for experiments on high-beta plasmas in a toroidal geometry 13 p1663 A73-28120

Multimode cavity measurements of plasma density in a torsatron. 13 p1665 A73-28683

Integral relations for an equilibrium toroidal plasma filament with a noncircular cross section 13 p1665 A73-28951

Experimental study of a conical theta-pinch plasma gun. 14 p1779 A73-29928

Contributions to the mechanism and the plasma diagnostics at the negative glow light in the case of the cylindrical hollow cathode discharge 14 p1780 A73-30427

Investigation of a low-pressure arc erosion plasma 14 p1781 A73-30459

Possibility of electron concentration determination in a plasma with the aid of a gas laser with a nonlinearly rotating absorption cell 14 p1781 A73-30465

Spectral diagnostics of a plasma flare during well-developed vaporization of metals by laser radiation 14 p1782 A73-30804

Q switched ruby laser optical diagnostic system for plasma shock waves and plasmoid observation, noting schlieren photographs of exploding wire experiments 14 p1782 A73-30925

The determination of plasma electron density from refraction measurements. 15 p1916 A73-31085

Wide-band power amplifier for studying the high-frequency properties of plasmas 15 p1850 A73-31497

Current extension from a quasi-steady MPD arcjet. 15 p1918 A73-31550

Dynamic pressure transducer system for pulsed plasma flow diagnosis. 15 p1876 A73-31977

Test for detection of fine structure of the solar wind velocity. 15 p1927 A73-32015

Measurement of density and temperature of a hydrogen plasma using an argon laser. 15 p1920 A73-32257

Quasi-monochromatic measurements of homogeneous arc plasmas. 15 p1841 A73-32393

Possibility of observing the decay interaction of plasma waves in topside sounding experiments. 16 p2002 A73-32775

Transient current overshoot to electrostatic probes in continuum, slightly ionized plasmas. 16 p2041 A73-33331

Heating of magnetized plasma under conditions of parametric instability. 16 p2042 A73-33599

Applicability of an adiabatic compression method to the study of a cesium plasma 17 p2214 A73-34130

Antenna admittance determination of electron density. 17 p2121 A73-34187

Multiring probe in a flowing ionospheric plasma. 17 p2214 A73-34199

Plasma self radiation and absorption, schlieren signals and lasing levels recording methods based on carbon dioxide lasers, using Mach-Zehnder IR interferometer 17 p2217 A73-35197

Theory of the excitation of the lower oblique resonance in the magnetospheric plasma. 18 p2302 A73-35939

Investigation of the discharge structure in a noble gas alkali MHD generator plasma. I. 18 p2338 A73-36303

Investigation of the discharge structure in a rare gas alkali MHD generator plasma. II. 18 p2339 A73-36304

Procedure for measuring plasma electron energies from the bremsstrahlung with the aid of Cerenkov detectors 18 p2339 A73-36566

Recent developments in strong shock wave research. 19 p2415 A73-37155

A review of electrostatic probe response in a flowing, low density plasma. 19 p2465 A73-37165

Measurement of nonisotropic electron velocity distributions by laser scattering. 19 p2465 A73-37166

Electromagnetic interactions with turbulent plasmas. 19 p2465 A73-37167

Quasi-steady plasma wind tunnel for Alfvén wave measurements of MHD flow involving shock waves and wakes, using Langmuir probes 19 p2465 A73-37172

Russian papers on physical processes in plasma accelerators covering types, diagnostic methods, gas dynamics, control and space studies 19 p2466 A73-37352

Methods of corpuscular plasma diagnostics in a pulsed coaxial accelerator 19 p2467 A73-37371

Use of charged particle beams for low temperature plasma measurement in magnetosphere and interplanetary space. 19 p2429 A73-37381

Russian book on satellite measurement of magnetic fields and plasmas in interplanetary medium, magnetosphere, moon and Venus vicinity and geomagnetic field-solar wind interaction region 19 p2486 A73-37772

Application of cylindrical Langmuir probes to streaming plasma diagnostics. 19 p2469 A73-37862

Comparison of Langmuir double probe and laser scattering measurements of plasma parameters. 20 p2595 A73-38880

Gas discharge plasma diagnostics based on polarization plane rotation of submillimeter laser radiation 20 p2598 A73-39622

Application of image-converter technique in quantum radiophysics and nonlinear optics [Survey paper]. 21 p2709 A73-39940

Schlieren-optic and interferometric methods using TEA-CO₂ lasers and thermal liquid crystal IR image converters in the diagnostics of fast processes 21 p2744 A73-39998

Probability distribution of electric fields in thermal and nonthermal plasmas. 21 p2744 A73-40216

Three-wavelength holographic diagnostics of an optical flare at a potassium target
21 p2700 A73-40529

An argon ion laser with a gas-discharge tube of relatively large diameter
21 p2714 A73-40556

An appraisal of the mass spectrometer diagnostic technique in the study of afterglow plasmas.
21 p2702 A73-40792

Studies of collisional preionization in large pinch vessels.
21 p2748 A73-40927

On the reflection of transverse waves from a cold plasma.
21 p2748 A73-40930

Phase method of investigation of short time scale disturbances and motions in space plasma.
21 p2748 A73-41373

Investigation of the electron concentration behind strong shock waves
22 p2893 A73-42385

Langmuir probe signal analysis of root-mean-square electron density fluctuations in turbulent Ar plasma jet
22 p2893 A73-42394

Experimental investigation of the interaction between plasma fluxes and a spatially-periodic magnetic field
23 p3010 A73-43656

Local measurements of plasma parameters by a microwave interferometer with a moving emitter
23 p3011 A73-43666

Some diagnostic methods for dense plasmas from high-pressure pulse discharges
23 p3011 A73-43667

Investigation of a turbulent plasma in a reflex discharge with the aid of a double electric probe
23 p3011 A73-43668

Problem of increasing the effectiveness of laser usage in experiments on light scattering in a plasma
23 p2987 A73-43670

Application of cybernetic means and methods in studies of plasma physics and controlled thermonuclear synthesis
23 p3011 A73-43671

Equilibrium of a toroidal plasma with noncircular cross section.
23 p3013 A73-44303

Volt-ampere characteristics of double electrical plasma probe measuring ionization level in low temperature dense plasma under interelectrode gap near-breakdown conditions
23 p2983 A73-44344

The inadequate reference electrode, a widespread source of error in plasma probe measurements.
24 p3115 A73-44873

Picosecond framing photography of a laser-produced plasma.
24 p3090 A73-44920

Heos I plasma and magnetic field experiments during bow shock crossings for turbulent bow structure, discussing proton velocity distribution
24 p3125 A73-45111

Spectroscopic measurements of plasma temperatures and density at X type magnetic neutral points, suggesting ion acoustic instability role in turbulent conductivity
24 p3118 A73-45461

PLASMA DIFFUSION

Amplitude modulation of electromagnetic waves by acoustic waves in a dispersive plasma - Modified theory.
01 p0083 A73-10455

Inward diffusion of Tokamak-trapped particles by slow magnetic pumping.
01 p0083 A73-10461

Floating potential and diffusion coefficients of viscosity damping of convective cells in stellarator for confined He, Ar and Xe plasmas
01 p0083 A73-10462

Magnetic pumping of electrons in ohmic dissipation mechanism responsible for neoclassical plasma diffusion rate increase in banana regime
01 p0084 A73-10467

Quasi-linear theory of plasma waves resonant diffusion, proceeding from Vlasov equation to derive frequency, wavenumber and velocity by quantum methods
01 p0086 A73-11492

Electromagnetic dispersion relation for two equidense counterstreaming ion beams in warm electron background oscillating plasma, considering ion instability criteria
02 p0197 A73-12066

Diffusion approximation for kinetic equation of repeatedly ionized plasma, calculating direct transitions between excited ion states
03 p0344 A73-13180

The diffusion-driven current in a toroidal resistive plasma.
03 p0348 A73-14433

Magnetically coupled transport of a cold plasma in the outer ionosphere at low latitudes.
05 p0567 A73-16094

Confined plasma diffusion due to growing or nonlinearly saturated LF ion waves causing energy transfer from electrons to ions in alabs
05 p0604 A73-17368

Diffusion time of charged particles in a plasma with volume ionization.
06 p0726 A73-17417

Diffusion of weak inhomogeneities in a magnetoactive two-ion plasma
06 p0727 A73-17536

Macroscopic instability and anomalous diffusion in a glow discharge plasma
07 p0854 A73-19047

Theory and simulation of turbulent heating by the modified two-stream instability.
07 p0857 A73-19526

Effect of collision frequency on the characteristics of waveguide filled with homogeneous anisotropic plasma.
07 p0857 A73-19533

Plasma diffusion across a magnetic field due to thermal vortices.
09 p1126 A73-22217

Microwave heating and resonant diffusion of electron plasmas, considering relativistic theory and Fokker-Planck equation
09 p1129 A73-22641

Pulsed probe studies on the diffusion coefficient of an afterglow plasma across a magnetic field.
09 p1132 A73-23250

Computer simulation of two dimensional plasma diffusion via wave interactions descriptions by nonlinear differential equations, considering electric field and particle velocity correlations
10 p1255 A73-24266

Ambipolar drift, deformation, and diffusion of a plasma in a magnetic field.
11 p1402 A73-24989

Brownian motion of electrons in time-dependent magnetic fields.
11 p1403 A73-25124

Numerical simulation and theory of plasma diffusion across magnetic field at thermal equilibrium, noting collective mode domination at moderate and high fields
11 p1403 A73-25257

Ambipolar diffusion in the F1-region of the ionosphere.
11 p1357 A73-25928

Integral equation for electromagnetic field in diffuse boundary plasma, noting anomalous skin effect
11 p1405 A73-26184

Powerful laser beam and material interaction, investigating gas dynamics of plasma heating and ejection
12 p1506 A73-27138

Effect of a high frequency magnetic field on plasma diffusion in a Q-machine.
13 p1664 A73-28348

Diffusion of plasma density and temperature perturbations in a magnetic field
14 p1749 A73-30264

Investigation of low-frequency instabilities in a linear plasma betatron
14 p1782 A73-30805

Diffusion of weak inhomogeneities in a magnetically active plasma consisting of two ions.
16 p2039 A73-32760

Influence of diffusion on plasma parameters - A qualitative estimate and a physical interpretation.
16 p2040 A73-32941

On the magnetogravitational instability of a plasma which possesses an anisotropic pressure in uniform movement of rotation and under the influence of the Hall current - The equation of dispersion. I
17 p2215 A73-34250

Instability of transverse electromagnetic waves in a drifting electron-hole plasma
21 p2751 A73-40368

Principal properties of plasma oscillations in an accelerator with closed drift and an extended zone of acceleration /ACDE/
21 p2746 A73-40523

Classical diffusion of free boundary plasma in plane and cylindrical slab geometries, calculating belt pinch effect and pressure decay rate
21 p2750 A73-41679

Dense argon plasma expansion into vacuum or low density partially ionized hydrogen plasma, examining momentum transfer, electron density and electric field effects
22 p2891 A73-42239

Anomalous diffusion in a magnetized plasma.
22 p2894 A73-42483

On the determination of electron temperature in diffusion-dominated non-L.T.E. plasmas.
22 p2896 A73-43167

Investigation of neoclassical diffusion in toroidal systems with a three-dimensional magnetic axis
23 p3014 A73-44337

PLASMA DIODES

Characteristics of ionization-recombination processes in a plasma discharge diode
09 p1124 A73-21884

PLASMA DYNAMICS

Calculation of the Knudsen-arc ignition potential in a gas-filled diode with cylindrical and spherical electrode geometries
09 p1061 A73-21912

Microwave oscillations and the visible radiation spectrum of a cesium plasma diode
12 p1527 A73-26938

Ignition potential of a Knudsen arc in a gas-filled diode with cylindrical and spherical electrodes.
15 p1922 A73-32637

Ionization and recombination in a plasma diode.
17 p2215 A73-34308

Dynamic characteristics of a plasma diode under conditions of a low-voltage arc discharge. I - Theory of the dynamic characteristics
18 p2339 A73-36557

Microwave oscillations and visible emission in a cesium diode.
22 p2892 A73-42272

Dynamic characteristics of a plasma diode with a low-voltage arc discharge. II - Experimental study of dynamic characteristics
22 p2833 A73-42386

PLASMA DISCHARGES

U PLASMA JETS

PLASMA DISPERSION

U PLASMA DIFFUSION

PLASMA DYNAMICS

Book - An introduction to the theory of plasma turbulence.
01 p0081 A73-10124

A method for nonlinear plasma wave kinetics.
01 p0082 A73-10419

One-fluid MHD model for beta and flow effects on stationary axisymmetric self consistent toroidal equilibria, using Bennett relation
01 p0083 A73-10460

Quantum kinetics equations for a nonideal gas and a nonideal plasma
01 p0086 A73-11286

Numerical model and computational results for earth bow shock structure, discussing linear dispersion relation for magnetized plasma with counterstreaming ion beams
02 p0155 A73-11728

Role of trapped particles in plasma waves and instabilities.
02 p0197 A73-12067

The kinematical behaviour of the plasma tail of Comet Tago-Sato-Kosaka 1969 IX.
02 p0221 A73-12704

Description of classical homogeneous systems in terms of dressed particles. II - Application to the Debye plasma
02 p0199 A73-12722

Plasma inhomogeneity in crossed electromagnetic fields, comparing motion velocity to ion component transverse drift rate in polarized electric field
03 p0346 A73-13178

Ring current effect on plasma convection in magnetosphere, assuming pressure due to proton population
03 p0302 A73-13854

Plasma convection in the vicinity of the geosynchronous orbit.
03 p0303 A73-13878

Comparison of wave propagation in the stationary and moving plasma - Motion and wave propagation along the magnetic field.
04 p0479 A73-15190

Behavior of thermal plasma in the magnetosphere and topside ionosphere.
04 p0442 A73-15336

Remarks on the steady and time dependent mathematical convection models.
04 p0443 A73-15341

Gas-dynamic description of a plasma in a corrugated magnetic field.
05 p0603 A73-17360

Mechanism of motion of inhomogeneities in a nonequilibrium plasma in a magnetic field.
06 p0726 A73-17401

Polarization interaction of opposed plasma streams in a linear magnetic octupole.
06 p0727 A73-17422

Fast radial displacement of a toroidal plasma by a transverse magnetic field.
06 p0732 A73-18620

Astrophysical masers. II - Polarization properties.
07 p0873 A73-19059

Isotropic conducting plasma dynamic behavior near rotating magnetized sphere, showing electric field-produced meridional convective currents
07 p0856 A73-19430

Magnetosphere tail internal plasma boundary layer dynamics during substorms based on aurora data
07 p0816 A73-19463

Neutron flux anisotropy from plasma focus measured by gamma spectroscopy of activated Ag target, discussing axial concentration
07 p0857 A73-19529

Influence of the thermal effect of the gas on the motion of an electric arc in a transverse magnetic field
07 p0858 A73-20081

PLASMA ELECTRODES

Thermomagnetic effect in plasma located in an inhomogeneous magnetic field.

07 p0859 A73-20135

Electromagnetic loss-cone instability of a plasma.

07 p0859 A73-20196

Gauge invariant and covariant description of plasma response to electromagnetic disturbances, deriving waves dispersion properties in arbitrary reference frame

07 p0859 A73-20234

Transport equations for dilute plasma in a magnetic field.

07 p0860 A73-20479

Classification, orientational characteristics, and some examples of rotational discontinuities in the solar wind

08 p0998 A73-21278

Ion saturation currents to planar Langmuir probes in a collision-dominated flowing plasma.

08 p0993 A73-21597

Kinetic theory of a two-dimensional magnetized plasma. II - Balescu-Lenard limit.

09 p1126 A73-22282

Kinetic theory of a two-dimensional magnetized plasma. III - Limit of very large magnetic field.

09 p1127 A73-22283

Influence of the Hall effect on current structure in a plasma flow through a spatially periodic magnetic field

09 p1127 A73-22606

Fluctuation theory for isothermal and nonisothermal semibounded plasma, obtaining correlation functions, dispersion laws and damping coefficients

09 p1129 A73-22689

Electric arc motion during initiation by plasma injection between static electrodes in dc circuit, applying to pulsed arc commutator design

09 p1131 A73-22938

Stability of a gravitating fluid layer in the presence of a uniform magnetic field perpendicular to its boundary.

10 p1253 A73-23832

Frequency entrainment of a drift instability by nonlinear effects in a plasma.

10 p1253 A73-24114

Auroral absorption and magnetospheric plasma dynamics pattern from arctic stations atmospheric opacity data

10 p1212 A73-24220

Kinetic equations for time behavior of electron concentration and proton, electron and H I atom temperatures in ionized hydrogen medium

10 p1282 A73-24492

On the origin of the electric field of polarization in a gravitational plasma.

11 p1350 A73-24990

Effect of electron-electron collisions on the thermal conductivity of a dense plasma.

11 p1402 A73-25120

Collisional transverse MHD shock wave structure within magnetic field inducing anisotropic plasma transport properties, using singular perturbation approach

11 p1403 A73-25254

Rotational discontinuities in an anisotropic plasma. II.

11 p1405 A73-25922

Boltzmann kinetic equation for nonideal plasma with allowance for polarization effects, noting collision integral convergence

11 p1406 A73-26187

Temporal development of longitudinal plasma current radial profile, obtaining effective collision frequency estimation for electron heating, hot plasma production conditions and stability restoration force

14 p1777 A73-29685

Interplanetary plasma inhomogeneities effect on Alfvén wave propagation direction from Pioneer 6 magnetic measurements

14 p1796 A73-29957

Nonlinear plasma oscillations in terms of Van Kampen modes.

14 p1780 A73-30350

Plasma fine velocity structure and dynamics from diffraction pattern of interplanetary radio sources scintillation

15 p1919 A73-31959

Interplanetary gas dynamics, discussing solar atmospheric structure, plasma kinetics, continuous flows, collective particle behavior, hydrodynamic coronal and free expansions

15 p1939 A73-31975

Reflection of electromagnetic waves from a moving plasma

15 p1846 A73-32303

An investigation of the reflection of electromagnetic pulses from moving plasmas.

16 p2041 A73-33199

Dynamic stabilization of plasmas by means of a high-frequency-modulated electron beam.

16 p2041 A73-33326

Early-time model of laser plasma expansion.

16 p2042 A73-33340

Plasma hydrodynamics in high frequency electromagnetic field, discussing hydrodynamic equa-

tions, small perturbations, plasma equilibrium and movement in field

17 p2216 A73-34341

Wave-trains in the solar wind. I - General theory and its application to an ideal, isotropic, one-fluid plasma.

17 p2224 A73-34505

ESRO Geos geostationary satellite for measurement of magnetospheric plasma electric and magnetic fields and drift rate at various frequency regions via electron injection

17 p2176 A73-35816

Fluctuations in plasma and nonlinear susceptibilities.

17 p2217 A73-35817

Transition probability approach to the theory of plasmas.

17 p2218 A73-35819

Dynamic characteristics of a plasma diode under conditions of a low-voltage arc discharge. I - Theory of the dynamic characteristics

18 p2339 A73-36557

Dynamics of ionized gases; Proceedings of the International Symposium, Tokyo, Japan, September 13-17, 1971.

19 p2463 A73-37151

Expansion of a plasma from a spherical source into a vacuum.

19 p2465 A73-37176

Interaction of plasma streams with a neutral gas cloud.

19 p2466 A73-37179

Control of the dynamic characteristics of a plasma jet of a given composition by selecting the parameters of a pulsed accelerator

19 p2467 A73-37368

Effect of collisions on the random electron density fluctuations in a plasma.

19 p2468 A73-37519

Ionosphere, magnetosphere and interplanetary plasma instabilities effects on magnetosphere dynamics

19 p2476 A73-37758

Ion trajectories in plasma focusing devices based on numerical integration of three dimensional equations of motion

19 p2468 A73-37856

Classification, characteristics of orientation, and some examples of rotational discontinuities in the solar wind.

19 p2476 A73-37907

Instability of electromagnetic surface waves supported by a bounded plasma stream.

20 p2595 A73-38891

Non-turbulent electric fields in soliton and shock-like structures in magnetized plasmas.

20 p2596 A73-38967

Dynamics of ionization inhomogeneities in the ionosphere

20 p2553 A73-39152

Technical and experimental investigations of a plasma focus neutron source

21 p2744 A73-39976

Plasmaspheric quasistatic electric fields and plasma convection, discussing dynamic electric fields and magnetospheric field penetration to low latitudes

21 p2679 A73-40075

Dynamics of plasma column constriction and electromagnetic acceleration of ions

21 p2745 A73-40362

Russian book on low temperature plasmatron-generated plasmas covering physical and transport properties, optical, thermophysical and gasdynamic analytic methods, etc

21 p2746 A73-40516

Self-similar solutions of the plasma equations

21 p2747 A73-40553

The optimal number of soundings for a complete investigation of the ionization-neutralization and dynamic characteristics of the middle ionosphere

21 p2686 A73-40911

Comparison of the plane, cylindrical and spherical one-dimensional models of the free expansion of a collisionless plasma.

21 p2748 A73-40929

Perturbation of the magnetic configuration of a stellarator by a longitudinal current in the plasma.

21 p2750 A73-41678

Theoretical and experimental investigations of the electron temperature in laser-produced plasmas.

22 p2891 A73-42249

On the stability of a class of plasma flows with helical flow and field lines.

22 p2892 A73-42351

Longitudinal polarization and focusing of plasmoids in a linear multipole magnetic field

22 p2893 A73-42383

Thermodynamic expansion processes for argon plasma in a convergent-divergent nozzle.

22 p2894 A73-42632

Quantum kinetic equations for a nonideal gas and a nonideal plasma.

23 p3009 A73-43507

Investigation of the dynamics of plasma flows in the field of a pulsed magnetic barrier

23 p3010 A73-43658

Shaping of plasma clusters moving in a longitudinal magnetic field

23 p3010 A73-43659

Plasma cluster movements in guides using straight stellarator magnetic fields and axisymmetric-straight rod produced field combination

23 p3010 A73-43660

Motion of a plasma in curvilinear magnetic fields of constant and alternating curvature

23 p3010 A73-43661

Single particle approximation analysis of particle velocity changes influence on plasma motion across nonhomogeneous magnetic field, examining energy exchange between particles

23 p3010 A73-43662

Induced currents in a stationary plasma flow in an axially-symmetric magnetic field

23 p3010 A73-43663

Magnetospheric plasma motion during a sudden commencement.

23 p2972 A73-43689

Ionosphere dynamic process investigations, describing wind models, E region drift velocity curves and energy distribution chart

23 p2978 A73-43978

Investigation of the efficiency of laser-plasma trapping by a magnetic field

23 p3014 A73-44341

Plasma fine velocity structure and dynamics from diffraction pattern of interplanetary radio sources scintillation

24 p3132 A73-44484

Reflection of electromagnetic waves from a moving plasma.

24 p3067 A73-44611

Computerized simulation of plasma particle collisions, using electric dipole expansion method for grid charge density and electrostatic force determination with Fourier transformation

24 p3116 A73-45027

Hot plasma in contact with cold wall, calculating dynamic behavior in magnetic field from numerical solution of one-fluid two-temperature equations

24 p3117 A73-45456

Experimental determination of the nonlinear interaction in a one dimensional beam-plasma system.

24 p3117 A73-45458

PLASMA ELECTRODES

Electrode phenomena with plasma-MIG welding.

01 p0055 A73-10114

Push-pull ac modulator design allowing balanced thermal load on plasma electrodes in pulsed high power short arc Xe flash lamps

03 p0282 A73-13933

Potential drops near the electrodes in a pulsed plasma accelerator.

03 p0347 A73-14096

Investigation of a coaxial plasma accelerator with a uniform gas pressure distribution in the electrode gap

04 p0481 A73-15616

Theoretical analysis of a time-of-flight mass spectrometer with spherical electrodes and radial ion paths.

06 p0693 A73-18270

Pressed cathodes made from barium scandate and refractory metals mixture, investigating operation in plasma discharge of He-Ne lasers

06 p0703 A73-18601

Electrode and gasdynamic effects in a large nonequilibrium MHD generator.

08 p0928 A73-20713

Parallel plate electromagnetic shock tube, investigating drive current, gas pressure and electrode material effects on electrode ablation and current sheet velocity

08 p0953 A73-21632

Calculation of the Knudsen-arc ignition potential in a gas-filled diode with cylindrical and spherical electrode geometries

09 p1061 A73-21912

Calculation of the boundary layers of a fully ionized two-temperature plasma for given temperatures of components at the electrodes

09 p1127 A73-22605

Relationship between adsorption processes on the cathode surface and processes in the region near the electrode in a high-current plasma discharge

09 p1127 A73-22608

Low temperature plasma electric arc discharge generators, noting electrode interaction, energy losses and high enthalpy efficiencies

10 p1253 A73-23516

Coaxial plasma accelerator with uniform pressure distribution.

10 p1254 A73-24206

Dependence of the parameters of a plasma cluster obtained from a coaxial source on the polarity of the central electrode

10 p1257 A73-24878

Electric field in the plasma sheath at the electrodes and the Bohm condition

10 p1258 A73-24879

Influence of initial gas conditions in a coaxial accelerator on plasma parameters

13 p1666 A73-28956

- Relaxation to Maxwellian distribution of electrons near low voltage Cs arc plasma discharge cathode 13 p1666 A73-28962
- Effect of plasma inhomogeneity on the relaxation of the electron distribution function in the electrode area of a low voltage arc 13 p1667 A73-28963
- Investigation of the steady-state temperature field in a composite cathode of a plasmatron 15 p1917 A73-31192
- Ignition potential of a Kaudsen arc in a gas-filled diode with cylindrical and spherical electrodes. 15 p1922 A73-32637
- Investigation of plasma inhomogeneities between coaxial electrodes in a magnetic field 17 p2214 A73-34128
- Characteristics of the electrode-adjointing potential layer in an alkali metal plasma in the presence of adsorption 17 p2214 A73-34131
- Low temperature plasma electric arc discharge generators, noting electrode interaction, energy losses and high enthalpy efficiencies 17 p2217 A73-35196
- Stationary high-current plasma accelerators 19 p2466 A73-37359
- Two cascade plasma accelerator with conical and ring electrodes, investigating plasma jet-cascade current interaction dynamics via magnetic probes and I-V characteristics 19 p2467 A73-37362
- Energy characteristics of a coaxial plasma source 19 p2467 A73-37363
- Effect of near-electrode processes on plasma behavior in electrodynamic accelerators 19 p2467 A73-37365
- MHD boundary layers on a segmented electrode-wall of a nonequilibrium generator. 19 p2470 A73-38314
- The breakdown condition of the electrode layer in an ionized gas flow 20 p2597 A73-39278
- Microarc current flow and potential drop through cold boundary layer near plasma electrodes in MHD generators 20 p2598 A73-39604
- Numerical experiment in a study of the separation of a laminar boundary layer in an MHD channel 20 p2598 A73-39611
- Experimental investigation of the performance of a porous electrode in an MHD converter during the injection of argon with potassium addition 20 p2511 A73-39619
- Pulsed Langmuir probe measurements of hollow cathode plasma discharge electron emission in terms of secondary, thermionic and field components 21 p2747 A73-40793
- Dependence of the parameters of a plasmoid obtained from a coaxial source on the polarity of the central electrode. 21 p2749 A73-41653
- Electric field in an electrode sheath and the Bohm criterion. 21 p2749 A73-41654
- Effect of initial gas conditions in a coaxial accelerator on the plasma parameters. 23 p3013 A73-44308
- Relaxation to Maxwellian distribution of electrons near low voltage Cs arc plasma discharge cathode 23 p3013 A73-44314
- Effect of plasma inhomogeneity on the relaxation of the electron distribution near the electrodes in a low-voltage arc. 23 p3013 A73-44315
- Ions bombarding the cathode of a pulsed plasma accelerator and their participation in the development of thermal fluxes 23 p3014 A73-44343
- Self-sustaining Penning avalanche discharge in crossed electric and magnetic fields, discussing anode surface boundary effects and maximum discharge intensity conditions 23 p3015 A73-44345
- The inadequate reference electrode, a widespread source of error in plasma probe measurements. 24 p3115 A73-44873
- PLASMA ENGINES**
- Electric propulsion and its space applications; Workshop, 2nd, Toulouse, France, June 21-23, 1972, Proceedings 04 p0487 A73-15712
- Low power pulsed ablation plasma thruster design for satellite attitude control and stationkeeping, describing operating principle and performance measurements 04 p0489 A73-15731
- Description of power conditioning systems intended for satellite stabilization thrusters 04 p0489 A73-15732
- Performance of a modified downstream-cathode MPD thruster. 07 p0867 A73-19492
- Theoretical and experimental study of the performance of quasi-steady MPD thrusters 10 p1262 A73-24499
- Thrust stand performance measurements of a lithium fueled applied field MPD arcjet. 19 p2473 A73-38320
- PLASMA FLOW**
- U MAGNETOHYDRODYNAMIC FLOW**
- PLASMA FLUX MEASUREMENTS**
- Solar wind observations on the lunar surface with the Apollo-12 ALSEP. 02 p0205 A73-11903
- The influence of a feedback system on the plasma flux in a closed-drift accelerator /CDA/ 15 p1920 A73-32311
- Plasma columnar content measurement between earth and Mariner 9 at small solar elongations by phase-group velocity difference technique 19 p2479 A73-37224
- Effect of a feedback system on the plasma flux in an accelerator with closed electron drift. 24 p3115 A73-44619
- PLASMA FREQUENCIES**
- Anomalous absorption of electromagnetic radiation at double the plasma frequency. 01 p0082 A73-10425
- Influence of the degree of uniformity of the magnetic field on the emission of electron cyclotron frequency harmonics from a plasma 04 p0478 A73-15036
- Multicomponent plasmas with cations or anions in presence of Coriolis force, determining crossover frequencies for polarization reversal and mode coupling of waves 05 p0603 A73-16594
- Excitation of parametric instabilities by microwave pumping in a magnetoactive plasma 06 p0729 A73-18108
- Difference frequency generation using non-linear interaction between a modulated electron beam and a collisionless plasma. 06 p0733 A73-18839
- Oblique electromagnetic wave propagation with respect to double stream in plasma, calculating unstable wave oscillation frequency and growth rate dependence on stream direction 08 p0993 A73-21633
- Nonlinear frequency correction to plasma instability at half harmonics of electron gyrofrequency as observed by OGO 5 near geomagnetic equator outside plasmopause 09 p1075 A73-22069
- Amplifier design for continuous recording of plasma frequency, using dipolar resonance signal obtained from parallel whip antennas surrounded by plasma sheath 10 p1216 A73-23747
- Low-frequency parametric instabilities of magnetized plasmas with two ion species. 10 p1255 A73-24261
- Strong plasma turbulence at helicon frequencies 10 p1257 A73-24757
- Nose extension method based on approximate dispersion function for calculating ducted whistler frequency and associated travel time, discussing ionosphere-magnetosphere interactions 11 p1358 A73-26704
- Absorption of waves by a two-dimensionally inhomogeneous plasma in the vicinity of singularity points 13 p1666 A73-28960
- Plasma chemical synthesis of higher oxides of cesium and rubidium. 13 p1581 A73-29599
- Electrostatic waves in warm random plasmas. 14 p1779 A73-29708
- High frequency discharges sustained either on a cavity resonance or on a plasma resonance 14 p1779 A73-29923
- Structured discharges in high frequency plasmas. 14 p1782 A73-30770
- Ion-acoustic turbulence as MHD wave damping mechanism in weakly turbulent magnetosphere plasma at high and low frequencies 15 p1919 A73-31893
- Nonlinear evolution of the decay instability in a plasma with comparable electron and ion temperatures. 16 p2041 A73-33324
- Nonlinear wave interaction and fluctuations in plasma. 17 p2217 A73-35818
- Low-frequency flute instabilities of a hollow cathode arc discharge - Theory and experiment. 19 p2468 A73-37858
- Hot-electron production and anomalous microwave absorption near the plasma frequency. 19 p2469 A73-38289
- Potential oscillations with frequencies higher than the gyrofrequency in a plasma containing a cone of losses 20 p2597 A73-39207
- Contribution to the theory of parametric instability of a bounded homogeneous plasma 22 p2892 A73-42380
- Determination of valence electron plasma frequencies and optical permittivity in single crystals of trisulfide of antimony 22 p2897 A73-42648
- Wave absorption near singular points in a two-dimensional inhomogeneous plasma. 23 p3013 A73-44312
- Excitation of parametric instabilities in a magnetoactive plasma by a microwave pumping wave. 24 p3114 A73-44497
- Wave-wave contribution to the high-frequency resistivity of nonequilibrium plasma. 24 p3117 A73-45457
- PLASMA GENERATION**
- U PLASMA GENERATORS**
- PLASMA GENERATORS**
- NT DUOPLASMATRONS
- NT PLASMA GUNS
- NT PLASMATRONS
- NT TOKAMAK FUSION REACTORS
- Pulsed UV-radiation source for producing highly ionized low-density initial plasmas 01 p0082 A73-10325
- A large double plasma device for plasma beam and wave studies. 02 p0168 A73-11964
- The feasibility of producing laser plasmas via photoionization. 02 p0177 A73-12572
- Uniform low temperature gas discharge plasma diagnostics in shielded volume, noting application of stable plasma generation effect for isotope analysis. 02 p0199 A73-12693
- End effects in Faraday type MHD generators with nonequilibrium plasmas. 03 p0254 A73-14185
- Investigation of a dense plasma produced by an electron beam in a magnetic mirror 04 p0479 A73-15040
- Confinement in a magnetic mirror of a plasma generated by laser radiation 04 p0482 A73-15620
- Laser plasma generation with high electron densities by photoionization from flashlamp or coherent UV source from harmonic generation or gas lasers 05 p0603 A73-16362
- The formation of primary gas discharge zones in electrical wire explosions 06 p0723 A73-17911
- Plasma generation by nanosecond and picosecond laser pulses, discussing Raman scattering from solid hydrogen and deuterium targets 06 p0731 A73-18581
- High power laser generation and heating of plasma in solid targets due to radiation damage, discussing liquid lasers as light amplifiers 06 p0731 A73-18582
- Determination of parameters of laser-induced plasma in air by a scattering method. 06 p0732 A73-18610
- Production of hot plasmas of solid-state density by ultrashort laser pulses. 06 p0733 A73-18783
- Microchannel electron multipliers application to X ray cinematography of laser generated plasma 06 p0697 A73-18861
- Collision effects on electromagnetic wave propagation in a plasma generated by a moving ionization source 07 p0858 A73-19906
- Laser microspectral analyzer operation in Q switched mode, discussing microplasma generation under inert gas at variable pressure 07 p0836 A73-20162
- German monograph - Observation of stimulated Raman-Anti-Stokes radiation of higher order and its significance for the starting phase of plasma generation by laser. 07 p0837 A73-20383
- Plasma production by laser, discussing basic equations, dimensional analysis, heating, focusing lens and targets 09 p1125 A73-22050
- The problem of laser sources of radiation in the far-ultraviolet and X-ray regions of the spectrum 09 p1094 A73-22600
- Low temperature plasma electric arc discharge generators, noting electrode interaction, energy losses and high enthalpy efficiencies 10 p1253 A73-23516
- Injection of a laser-produced plasma into a magnetic trap. 10 p1254 A73-24210
- Rotational instability of a plasma from a hot-cathode Penning discharge 11 p1403 A73-25243
- Numerical modeling of laser produced plasmas - The dynamics and neutron production in dense spherically symmetric plasmas. 11 p1404 A73-25272
- Harmonic generation and parametric excitation of waves in a laser-created plasma. 11 p1405 A73-25972
- Operating properties of a helical microwave plasma source in high density high magnetic field regime. 11 p1407 A73-26562
- Investigation of the feasibility of the injection of electrons into heliotron-type closed magnetic mirror configurations 13 p1666 A73-28957

- Studies of plasma production at hypervelocity microparticle impact. 13 p1667 A73-29424
- High frequency discharges sustained either on a cavity resonance or on a plasma resonance 14 p1779 A73-29923
- Plasma produced by lasers on solid targets 14 p1779 A73-30025
- General radio-frequency properties of bounded plasma systems in connection with the production and heating of dense plasmas. 14 p1780 A73-30120
- The use of fast magnetic compression for the production and heating of plasma in Tokamak-like geometries. 14 p1780 A73-30121
- Self-igniting pulsed optical discharge in an erosion laser plasma. 14 p1757 A73-30334
- Investigation of a low-pressure arc erosion plasma 14 p1781 A73-30459
- Comparison of the hot-electron plasmas produced using two different plasma sources in a magnetic mirror compression experiment. 14 p1781 A73-30657
- Experimental study of the interaction of a plasma with a magnetic field in the case of a plasma generated by laser irradiation of solids 15 p1917 A73-31249
- Numerical analysis of the averaged equations of concentric laser cumulation of plasma with consideration of nuclear fusion energy. 17 p2216 A73-34323
- Book - Principles of plasma physics. 17 p2216 A73-34467
- Momentum transfer to laser-irradiated targets, indicating the nonlinear interaction force. 17 p2184 A73-34897
- High-energy pulsed CO₂-laser-target interactions in air. 17 p2184 A73-34914
- Low temperature plasma electric arc discharge generators, noting electrode interaction, energy losses and high enthalpy efficiencies 17 p2217 A73-35196
- Energy characteristics of a coaxial plasma source 19 p2467 A73-37363
- Plasma characteristics with TEA-CO₂ laser and wavelength scaling law. 19 p2468 A73-37520
- Magnetically induced collisionless coupling between counterstreaming laser-produced plasmas. 19 p2469 A73-38290
- Thrust stand performance measurements of a lithium fueled applied field MPD arcjet. 19 p2473 A73-38320
- Off-resonance microwave-created plasmas. 20 p2597 A73-39196
- Ionization of a neutral medium by an electron beam. 20 p2597 A73-39279
- Theoretical and experimental investigations of the electron temperature in laser-produced plasmas. 22 p2891 A73-42249
- The production of plasma by lasers on targets in the gaseous state 22 p2892 A73-42350
- Shaping of plasma clusters moving in a longitudinal magnetic field 23 p3010 A73-43659
- Investigation of the possibility of developing a wide-aperture injector of fast neutral atoms 23 p3010 A73-43665
- Electron injection through the diverter in a heliotron. 23 p3013 A73-44309
- Investigation of the efficiency of laser-plasma trapping by a magnetic field 23 p3014 A73-44341
- PLASMA GUNS**
- Investigation of the gun aspects of a rotating plasma source. 06 p0732 A73-18779
- Dynamic viscosity and current distribution model of inhomogeneous Cs plasma flow in coaxial plasma gun with thermionic cathode 10 p1258 A73-24886
- Experimental study of a conical theta-pinch plasma gun. 14 p1779 A73-29928
- Dynamic viscosity and current distribution model of inhomogeneous Cs plasma flow in coaxial plasma gun with thermionic cathode 21 p2749 A73-41661
- PLASMA HEATING**
- Theory of turbulent heating of an isothermal plasma with a transverse current. 01 p0083 A73-10456
- Neoclassical theory of Landau damping and ion and electron transit-time magnetic pumping /ITMP/ in toroidal geometry. 01 p0083 A73-10459
- Electron-ion recombination in cryogenic helium plasmas. 01 p0084 A73-10565
- Interaction between intense optical radiation and free electrons /Nonrelativistic case/ 01 p0061 A73-11248
- Heating of plasma by high-energy electrons, and nonthermal X-ray emission in solar flares. 01 p0093 A73-11313
- Number density estimation for neutral hydrogen hot component required for solar wind heating to satisfy observed proton temperature relationship to wind velocity 02 p0205 A73-11745
- A 12-coil superconducting 'bumpy torus' magnet facility for plasma research. 02 p0150 A73-11839
- Collisionless plasma compression shock waves thermodynamics, noting entropy variations along shock adiabat under plasma heating in magnetic field 02 p0198 A73-12552
- Parametric instability and anomalous heating due to electromagnetic waves in plasma. 03 p0345 A73-13060
- Averaged equations of cumulative-laser heating of plasma in Z-pinch with consideration of the recovery of the energy of nuclear fusion. 03 p0347 A73-13782
- Averaged equations of cumulative-laser heating of two-temperature plasma in Z-pinch taking into account the nuclear fusion energy. 03 p0347 A73-13783
- Theory of electron cyclotron resonance heating. I-Short time and adiabatic effects. 03 p0345 A73-14434 [AD-759528]
- Estimates of dense plasma heating by stable intense electron beams. 03 p0348 A73-14438
- Influence of external high-frequency modulation of the electron beam on ion heating during beam-plasma interaction 04 p0478 A73-15032
- Racetrack configuration design of Uragan stellarator for plasma diagnostics and heating, noting shear and rotational angle of magnetic system 04 p0432 A73-15038
- Plasma heating and acceleration due to Landau damping of hydromagnetic waves. 04 p0480 A73-15197
- Equations of laser heating of plasma in a system of the 'focus' type, the recovered energy of nuclear fusion being taken into consideration. 04 p0480 A73-15593
- Averaged equations of laser heating of two-temperature plasma in Z-pinch, the thermonuclear fusion energy being taken into consideration. 04 p0480 A73-15594
- Cumulation-laser heating of two-temperature plasma, the recovered energy of nuclear fusion being taken into consideration. 04 p0480 A73-15596
- Radiation energy distribution in laser pulse heating of moving plasma without reflection, noting thermal wave propagation 04 p0481 A73-15605
- Ferrous and nonferrous metal alloys melting and remelting in plasma induction and beam furnaces, noting cost reduction and ingots homogeneity 04 p0455 A73-15748
- Possible mechanisms of turbulent heating of a plasma by ultrashort pulses of laser radiation. 05 p0603 A73-16792
- Experimental observation of heating of a hydrogen plasma by a relativistic electron beam. 05 p0603 A73-17161
- Transverse and longitudinal heat flow in a laser-heated magnetically confined plasma. 05 p0603 A73-17162
- High intensity CO₂ laser-plasma interaction. 05 p0603 A73-17224
- Numerical simulation of high Mach number supercritical magnetosonic collisionless shock wave propagation perpendicular to magnetic field, considering cause of anomalous ion heating 05 p0604 A73-17365
- Character of acoustic dispersion in plasma. 06 p0726 A73-17403
- Some averaged properties of wave solutions for a hypersonic thermal wave. 06 p0728 A73-17890
- Ionization-relaxation time measurements upon krypton and xenon in a shock-wave heated plasma 06 p0728 A73-17912
- Combined plasma heating by an electron beam and an intense ion-cyclotron wave 06 p0729 A73-18106
- Plasma heating, emission spectrum distortion and light pressure effects under stimulated Compton scattering, noting upper bound of cosmic maser brightness temperature 06 p0729 A73-18110
- Anomalous ion heating in a laser heated plasma. 06 p0730 A73-18461
- Heating of a magnetized plasma under parametrically unstable conditions 06 p0731 A73-18574
- Heating of a plasma in stimulated scattering of laser radiation /Review/. 06 p0731 A73-18578
- High power laser generation and heating of plasma in solid targets due to radiation damage, discussing liquid lasers as light amplifiers 06 p0731 A73-18582
- Measurement of the polarization of the radiation reflected backward from a laser-heated plasma. 06 p0731 A73-18589
- Anode sheath plasma current instabilities, examining electron and ion turbulent heating, plasma particle limiting energies and unsteady oscillation spectra 06 p0731 A73-18604
- Microwave heating of a plasma and longitudinal electronic thermal conductivity in a magnetic field. 06 p0732 A73-18606
- Current induced drift rate of plasma electrons in electric and magnetic fields, noting electron velocities in turbulent heating of plasma 06 p0732 A73-18621
- Observation of laser oscillation in a 1-atm CO₂-N₂-He laser pumped by an electrically heated plasma generated via photoionization. 06 p0703 A73-18649 [AD-759094]
- Stochastic ion heating by ion-acoustic turbulence. 06 p0733 A73-18850
- High-frequency heating of a plasma under lower hybrid-resonance conditions 07 p0855 A73-19290
- Ionospheric electron density changes caused by strong radio waves induced plasma heating 07 p0816 A73-19457
- Electron cyclotron off-resonance heating rate in hot electron plasmas, comparing numerical calculation in terms of harmonic resonance with computerized simulation 07 p0856 A73-19519
- Theory and simulation of turbulent heating by the modified two-stream instability. 07 p0857 A73-19526
- Steady state dense arc plasma heating by inverse bremsstrahlung process with IR carbon dioxide laser, calculating maximum attainable temperature 07 p0857 A73-19531
- Thermal behavior of a plasma-heated tungsten probe in the presence of tungsten vapor. 07 p0788 A73-20447 [ECS PAPER 88]
- Anomalous plasma ion heating by parametric excitation of lower hybrid instabilities, using long wavelength oscillating electric field 07 p0860 A73-20482 [AD-759477]
- Lower-hybrid-resonance heating of a plasma in a parallel-plate waveguide. 08 p0991 A73-20816
- Electrostatic turbulence at colliding plasma streams as the source of ion heating in the solar wind. 08 p0997 A73-20886
- Heating of astrophysical plasma due to rotation. 08 p1007 A73-20957
- Turbulent heating of colliding streams in the solar wind. 08 p0998 A73-21164
- Heating of charged particles by electric waves. 08 p0993 A73-21233
- Plasma-ion beam nonlinear interaction for beam velocity exceeding electrons thermal velocity, noting plasma heating and beam energy dissipation 08 p0994 A73-21696
- Parametric heating of a dense arc plasma with 0.337 mm laser radiation. 09 p1125 A73-21944
- Heating of laser-induced plasmas in helium. 09 p1125 A73-21998
- Momentum method extension to thermal conduction laser heating of nonhomogeneous plasma, obtaining closed form solutions for plane waves 09 p1126 A73-22171
- Structure of a collisionless boundary layer and the turbulent braking of ions 09 p1127 A73-22607
- Topical Conference on RF Plasma Heating, 1st, Texas Tech University, Lubbock, Tex., July 6-8, 1972, Proceedings. 09 p1128 A73-22626
- Radio-frequency heating of a collisionless plasma. [TTU-SR-2] 09 p1128 A73-22627
- RF plasma heating by the modified two stream instability. [TTU-SR-2] 09 p1128 A73-22628
- Cyclotron heating of plasmas with finite amplitude waves. [TTU-SR-2] 09 p1128 A73-22630
- Operating features of an ion-cyclotron-wave plasma apparatus running in the RF-sustained mode. [TTU-SR-2] 09 p1128 A73-22632
- Nonlinear theory of plasma heating by parametric instabilities. [TTU-SR-2] 09 p1128 A73-22633
- Measurement of effective collision frequency in RF heating through parametric instabilities. [TTU-SR-2] 09 p1128 A73-22634
- Electromagnetic fields in electrodeless discharges of arbitrary length. [TTU-SR-2] 09 p1128 A73-22635

Particle seeded RF hydrogen plasma opacity, emission spectra, heat transfer and temperature profile at high temperatures
[TTU-SR-2] 09 p1128 A73-22636

Lower-hybrid-resonance heating of a plasma in a parallel-plate waveguide.
[TTU-SR-2] 09 p1129 A73-22639

Analytical and computer simulation of two ion species RF heated magnetoplasmas response to driving electric fields near lower hybrid frequency, observing parametric instabilities
[TTU-SR-2] 09 p1129 A73-22640

Microwave heating and resonant diffusion of electron plasmas, considering relativistic theory and Fokker-Planck equation
[TTU-SR-2] 09 p1129 A73-22641

Computer simulation of ion heating by pulsed microwaves.
[TTU-SR-2] 09 p1129 A73-22642

Investigation of the heating mechanism for the electron component of a plasma under beam-instability conditions in a mirror confinement system
09 p1130 A73-22703

Wave-wave interactions in turbulent plasma and ion sound turbulence enhancement of three wave interaction processes, considering plasma heating experiments
09 p1131 A73-22901

Anomalous nonlinear dissipation of high-frequency radio waves in a plasma
09 p1053 A73-23330

Dense air plasma compression and heating by TNT explosive charge, noting shock tube flow patterns
10 p1203 A73-23515

Collisionless plasma compression shock waves thermodynamics, noting entropy variations along shock adiabat under plasma heating in magnetic field
10 p1254 A73-24179

Radiation energy distribution in laser pulse heating of moving plasma without reflection, noting thermal wave propagation
10 p1254 A73-24195

Heating of theta-pinch plasmas by pulsed CO₂ lasers.
10 p1256 A73-24527

Solar wind He nuclei kinetic temperature, considering resonant heating and proton temperature
10 p1269 A73-24723

Electrostatic turbulence parametric excitation by electric field with frequency near plasma frequency, accounting for saturation electric field in anomalous plasma heating via electron trapping theory
11 p1403 A73-25256

Measurement of the ion energy distribution resulting from the turbulent heating of a plasma.
11 p1404 A73-25269

Thermal cumulation equations for concentric conductive laser heating of two temperature D-T plasma with nuclear fusion energy recovery
11 p1406 A73-26411

Laser concentric conduction heating of two-temperature D-T plasma.
11 p1406 A73-26412

A note on the heating of magnetoplasma by magnetic perturbations.
11 p1407 A73-26659

Powerful laser beam and material interaction, investigating gas dynamics of plasma heating and ejection
12 p1506 A73-27138

Development of acoustic and overheat instabilities in a plasma with molecular impurities
12 p1528 A73-27303

Applied electrical potential effect on heat transfer to tube immersed in highly ionized flow of atmospheric pressure Ar plasma
12 p1529 A73-27696

Investigation of the heating of electrons of a dense beam-plasma discharge in strong magnetic fields
12 p1529 A73-27942

Two-stream instability heating of plasmas by relativistic electron beams.
13 p1663 A73-28186

Role of stimulated Compton scattering in the interaction of laser radiation with a superdense plasma.
13 p1664 A73-28615

Variation of parameters in a shock-heated argon plasma flow.
13 p1665 A73-28624

Plasma heating at the lower hybrid resonance.
13 p1665 A73-28690

Influence of longitudinal thermal conductivity on the ohmic heating of plasma in the Tuman-1 facility
13 p1666 A73-28959

Averaged equations of cumulative laser heating of a plasma focus with consideration of the heat of nuclear fusion.
13 p1667 A73-29389

Concentric laser cumulation of plasma with consideration of the heat of nuclear fusion.
13 p1667 A73-29393

Theory of turbulent plasma heating by anomalous absorption of magnetosonic waves.
14 p1777 A73-29683

Ignition condition in Tokamak experiments and role of neutral injection heating.
14 p1777 A73-29684

Problems associated with the injection of a high-energy neutral beam into a plasma.
14 p1778 A73-29688

Alfvén waves in a two-fluid model of the solar wind.
14 p1787 A73-30005

Symposium on Plasma Heating and Injection, Varenna, Italy, September 21-October 4, 1972, Lectures and Seminars.
14 p1779 A73-30117

Parametric instabilities and anomalous absorption and heating of plasmas.
14 p1779 A73-30118

General radio-frequency properties of bounded plasma systems in connection with the production and heating of dense plasmas.
14 p1780 A73-30120

The use of fast magnetic compression for the production and heating of plasma in Tokamak-like geometries.
14 p1780 A73-30121

Experiments on CO₂-laser heating of magnetically confined underdense plasmas.
14 p1780 A73-30123

Investigation of the heating of a plasma ion component by a collisionless shock wave.
14 p1780 A73-30336

Ion acoustic wave scattering effects on stochastic ion heating in turbulent plasma
14 p1780 A73-30340

Plasma heating by an intense electron beam.
14 p1781 A73-30553

The turbulent heating of ions and related efficiencies in a current carrying plasma.
15 p1916 A73-31081

Ignition and maintenance of a CW plasma in atmospheric-pressure air with CO₂ laser radiation.
15 p1884 A73-31398

Stochastic heating of a plasma during development of a Langmuir turbulence instability
15 p1918 A73-31705

Kinetics of stimulated scattering of Langmuir waves by plasma ions
15 p1919 A73-31708

Earth magnetosphere ion acoustic turbulence generation by longitudinal currents and electric fields, relating turbulence induced current dissipation to plasma heating
15 p1872 A73-31894

Effect of laser pulse rise time on heating of a magnetically confined plasma.
15 p1919 A73-31929

Heating of a high-density plasma with the aid of powerful electron beams
15 p1920 A73-32308

Influence of saturation effects on stimulating scattering in laser heating of a plasma.
16 p2041 A73-33079

Lagrangian description of phase space flow - Turbulent heating.
16 p2041 A73-33322

Saturation in cyclotron resonance heating of plasma.
16 p2042 A73-33339

Heating of magnetized plasma under conditions of parametric instability.
16 p2042 A73-33599

Two fluid models for solar wind heating under boundary conditions, considering enhanced energy transfer between electrons and protons in kinetic theory calculations
17 p2224 A73-34515

Dense air plasma compression and heating by TNT explosive charge, noting shock tube flow patterns
17 p2147 A73-35195

Laser energy absorption by plasma for controlled thermonuclear fusion, comparing uses of electrically pumped gas, chemical and solid state lasers
17 p2185 A73-35379

Damping of Alfvén and magnetoacoustic waves at high beta.
17 p2217 A73-35524

Anomalous heating of dense plasma by laser radiation.
17 p2218 A73-35823

Experimental investigations on arc-heated steady plasma flow.
19 p2415 A73-37169

Study of plasma systems with a closed electron drift and a distributed electric field
19 p2466 A73-37357

Plasma heat source and heat exchanger design for liquid potassium circulation system, using air-kerosene aviation gas turbine combustion chamber
20 p2545 A73-39617

Generation of high-power light pulses at wavelengths 1.06 and 0.53 micron and their application in plasma heating. I - Experimental investigations of reflection of light of two wavelengths in laser heating of plasma.
20 p2573 A73-39684

Non-thermal solar wind heating by supra-thermal ions.
21 p2763 A73-41499

Parametric instabilities and turbulent heating of a plasma in the field of a fast magneto-acoustic wave.
21 p2750 A73-41677

Role of nonlinear effects in the problem of the anomalous resistance of plasma.
22 p2890 A73-41723

Generation of high-power light pulses at wavelengths 1.06 and 0.53 microns and their application in plasma heating. II - Neodymium-glass laser with a second-harmonic converter.
22 p2869 A73-42248

Theoretical and experimental investigations of the electron temperature in laser-produced plasmas.
22 p2891 A73-42249

Interaction of intense optical radiation with free electrons /nonrelativistic case/.
22 p2892 A73-42346

The production of plasma by lasers on targets in the gaseous state
22 p2892 A73-42350

Ion temperature in the case of ohmic heating of the plasma in the 'Uragan' stellarator
22 p2893 A73-42382

German monograph - Investigation of relaxation effects behind secondary shock fronts in shock-wave heated and partially ionized argon plasmas.
22 p2895 A73-42850

Observation of extraordinary wave propagation near the lower hybrid resonance frequency.
22 p2895 A73-43023

Current-induced heating of a dense plasma during collective interactions in a high-current gas discharge
23 p3009 A73-43651

Effect of longitudinal thermal conductivity on ohmic heating in Tuman-1.
23 p3013 A73-44311

Combined heating of a plasma by an electron beam and an intense ion-cyclotron wave.
24 p3114 A73-44495

Plasma heating, emission spectrum distortion and light pressure effects under stimulated Compton scattering, noting upper bound of cosmic maser brightness temperature
24 p3114 A73-44499

Heating of a dense plasma by a powerful electron beam.
24 p3114 A73-44616

Heat current and anisotropy-driven instabilities in connection with the solar wind.
24 p3126 A73-45126

Simplified averaged equations of concentric laser compression of plasma.
24 p3117 A73-45427

Optimization of compression constants for cumulated plane shock waves in a closed tube.
24 p3117 A73-45428

Transformation of shock compression into isentropic compression in a nonhomogeneous body.
24 p3117 A73-45429

Magnetically induced electrothermal instability in unseeded partially ionized shock heated argon plasma
24 p3117 A73-45454

Computerized simulation of electrostatic instabilities development in underdense plasmas during heating by high output lasers with frequencies above electron plasma frequency
24 p3118 A73-45466

PLASMA INSTABILITY
U MAGNETOHYDRODYNAMIC STABILITY
PLASMA INTERACTIONS
NT PLASMA-ELECTROMAGNETIC INTERACTION
Collisionless plasma flow over a conducting sphere.
02 p0158 A73-11919

Momentum transfer interaction of a laser-produced plasma with a low-pressure background.
02 p0197 A73-12062

Spectral characteristics in visible and UV regions of laser plasma-air interaction, using focused beams on metal targets at atmospheric pressure and vacuum
02 p0176 A73-12351

Geomagnetic field variations caused by changes in the quiet-time solar wind pressure.
03 p0298 A73-12885

A phenomenological study of the steady-state current sheet speed in a magnetically driven shock tube.
03 p0288 A73-13809

Physical mechanisms of magnetospheric processes, discussing matter and energy exchange between solar wind and magnetosphere, substorms, interaction with ionosphere, etc
03 p0302 A73-13853

Solar wind interaction with geomagnetic field, discussing magnetosphere polar cap region and geomagnetic tail neutral sheet structure
03 p0302 A73-13871

Atmospheric model for substorm triggering mechanism, plasma sheath behavior and substorm recovery, noting solar wind interaction with magnetosphere
03 p0304 A73-13886

Solar wind plasma entry into earth magnetosphere, reviewing major uncertainties in light of current observational knowledge

04 p0442 A73-15330

Comparison of theory with experiment for electron density distribution in the near wake of an ionospheric satellite.

04 p0444 A73-15541

Observation of the region of interaction between the solar-wind plasma and Mars.

05 p0608 A73-16095

Polarization interaction of opposed plasma streams in a linear magnetic octupole.

06 p0727 A73-17422

Quasi-hydrodynamic equations for transverse quanta in inhomogeneous plasma, using geometric optics approximation

06 p0728 A73-17969

Density-matrix method for a weakly ionized plasma.

06 p0730 A73-18373

Interaction of singly charged interstellar helium ions with the solar wind.

07 p0870 A73-19253

Ionospheric plasma interaction with neutral meridional wind, noting effects of east-west gradients in electron concentration

07 p0819 A73-20057

Heating of charged particles by electric waves.

08 p0993 A73-21233

Partially ionized nonideal plasma model electron-ion interactions, equilibrium, equations of state and thermodynamic quantities

10 p1252 A73-23501

Nonlinear interactions between Langmuir waves in a weakly inhomogeneous plasma

10 p1253 A73-23576

Ionospheric currents induced by solar wind interaction with planetary atmospheres.

11 p1412 A73-25921

Precise calculation of the magnetosphere surface for a tilted dipole.

11 p1421 A73-25923

The effect of the earth's bow shock and magnetosheath on the interaction of a discontinuity in the solar wind with the magnetosphere.

11 p1357 A73-25924

Collective interactions and electrical conductivity of plasma in strong electric fields.

11 p1406 A73-26554

Solar wind-lunar limb interaction from viscous MHD approach including continuum fluids, kinetic plasma and magnetic boundary layer

12 p1534 A73-27003

Photoelectrons and solar wind/lunar limb interaction.

12 p1534 A73-27495

Solar wind properties near and beyond Jupiter orbit, considering steady state wind extrapolation to large distances, cosmic ray modulation and interactions with planetary bodies

14 p1787 A73-30541

Interaction of the interstellar medium with the solar wind.

14 p1787 A73-30543

Mars 3 solar wind probe of upper Mars atmosphere, showing plasma interaction with ionosphere measured by energy spectra

15 p1930 A73-31150

Kinetics of stimulated scattering of Langmuir waves by plasma ions

15 p1919 A73-31708

Interaction between an ionized metal vapor flow and a body at Mach numbers equal to or larger than unity

15 p1919 A73-31863

Interaction of the geomagnetic field with the antiparallel solar-wind field

15 p1926 A73-31891

Kinetic instability of a plasma located in an SHF field

15 p1921 A73-32332

Single-fluid model of the distant solar wind.

16 p2056 A73-33459

On the extent of the Martian ionosphere.

16 p2062 A73-33462

Partially ionized nonideal plasma model electron-ion interactions, equilibrium equations of state and thermodynamic quantities

17 p2216 A73-35181

Characteristics of the influence of the solar wind on cosmic-ray intensity during 1969

18 p2345 A73-36108

On solar wind interaction with the earth's magnetosphere.

18 p2346 A73-36184

Solar wind interaction with the earth's magnetic field. I - Magnetosheath.

18 p2346 A73-36270

Solar wind interaction with the earth's magnetic field. II - Magnetohydrodynamic bow shock.

18 p2346 A73-36271

Solar wind interaction with the earth's magnetic field. III - On the earth's bow shock structure.

18 p2346 A73-36272

Solar wind-Mercury atmosphere interaction - Determination of the planet's atmospheric density.

18 p2352 A73-36294

Streaming plasma interaction with variable longitudinal magnetic fields.

19 p2465 A73-37171

Magnetic measurements in laboratory model tests of solar wind-geomagnetic field interactions

19 p2481 A73-37338

Solar wind-geomagnetic field interaction simulation by plasma flow and magnetic dipole, proving collisionless dissipation presence

19 p2481 A73-37339

Plasma acceleration techniques in space studies, discussing simulation experiments, solar wind-geomagnetic field interaction and astronomical models

19 p2482 A73-37355

Two cascade plasma accelerator with conical and ring electrodes, investigating plasma jet-cascade current interaction dynamics via magnetic probes and I-V characteristics

19 p2467 A73-37362

Ionosphere, magnetosphere and interplanetary plasma instabilities effects on magnetosphere dynamics

19 p2476 A73-37758

Numerical simulation of counterstreaming high Mach number plasma laminar interactions, using one dimensional model based on Vlasov equation

19 p2469 A73-37861

Second-order plasma interaction in the Crab Nebula.

20 p2610 A73-39579

Nonlinear theory of a quasi-monochromatic electrostatic wave packet in an inhomogeneous plasma

21 p2745 A73-40363

Nonlinear interacting longitudinal and transverse electron oscillations due to plasma density inhomogeneity in HF hybrid resonance region

21 p2750 A73-41683

Effects of electrostatic instabilities on planetary and interstellar ions in the solar wind.

22 p2902 A73-41940

Polarizing interaction between colliding plasma flows in a toroidal magnetic field. II

22 p2893 A73-42384

Interaction of the solar wind with the outer planets.

22 p2903 A73-42937

Interactions of plasmas with magnetic field boundaries.

22 p2851 A73-42977

Jupiter and terrestrial upper atmospheres comparison, discussing solar wind interactions with planetary magnetic fields, Jovian Van Allen belt and cold plasma distribution

22 p2913 A73-42985

Experimental investigation of the interaction between plasma fluxes and a spatially-periodic magnetic field

23 p3010 A73-43656

Cyclotron oscillations of a plasma in an inhomogeneous magnetic field

23 p3012 A73-44090

Investigation of the efficiency of laser-plasma trapping by a magnetic field

23 p3014 A73-44341

Solar wind interaction modes with lunar magnetic fields, discussing moon surface charging, magnetic field compression and wind deflection

24 p3126 A73-45127

Collisionless magnetospheric-solar wind plasmas interactions, noting boundary stability and tail instability

24 p3127 A73-45213

PLASMA JET WIND TUNNELS

Transverse ion temperature measurements in plasma stream wind tunnel simulating ionospheric conditions, using cylindrical Langmuir probe and collimator-collection device

[ONERA, TP NO. 1180]

02 p0151 A73-12813

Quasi-steady plasma wind tunnel for Alfvén wave measurements of MHD flow involving shock waves and wakes, using Langmuir probes

19 p2465 A73-37172

PLASMA JETS

Radiation and conductivity of a high current constricted discharge plasma.

01 p0081 A73-10119

Electron density measurements in time varying plasmas with a microwave reflectometer system.

01 p0044 A73-10120

Time variable dynamics of plasma beam discharge oscillations frequency spectra

01 p0084 A73-10633

Investigation of the temporal-spatial distribution of optical density in a plasma of high-current Li and In discharges

01 p0085 A73-10853

Computation of the axisymmetrical free expansion of a nonequilibrium hydrogen plasma

02 p0196 A73-11604

Plasma jet acceleration by plasma injectors with capacitive and inductive energy storage for instantaneous breaking of charging circuit, noting energy conversion efficiency

02 p0196 A73-11712

Oscillation modes and cathode potential drop in plasma generated by continuous electric discharge at low pressure between anode and cold cathode

03 p0346 A73-13603

Investigation of the stability of plasma-jet motion in the magnetic field of a diverter

04 p0479 A73-15045

Polarization interaction of opposed plasma streams in a linear magnetic octupole.

06 p0727 A73-17422

Gasdynamic structure of a plasma flame arising during vaporization of metals by strong optical radiation

06 p0729 A73-18107

Macroscopic instability and anomalous diffusion in a glow discharge plasma

07 p0854 A73-19047

Choosing the parameters for plasma anodizing of aluminum

07 p0830 A73-19293

Numerical calculations for the turbulent arc constrictor.

07 p0858 A73-19960

Influence of boundaries of the ionization instability of a plasma in a discharge of coaxial geometry.

08 p0992 A73-20851

Investigation of the operation of a coaxial plasma injector employing preionization of the gas

09 p1124 A73-21880

Characteristics of ionization-recombination processes in a plasma discharge diode

09 p1124 A73-21884

Features of the flow of a nonisothermal plasma, obtained in a beam-plasma discharge, through a magnetic nozzle

09 p1124 A73-21890

Acceleration of ions during the formation of an electron beam from a stationary vacuum-arc plasma

09 p1125 A73-21909

Investigation of the azimuthal symmetry of the discharge in a coaxial plasma injector

09 p1125 A73-21911

Relationship between adsorption processes on the cathode surface and processes in the region near the electrode in a high-current plasma discharge

09 p1127 A73-22608

Measurement of the electron temperature of a quasi-stationary pulsed glow-discharge plasma in highly overcharged gaps

09 p1129 A73-22663

Niobium and tungsten cementation in a glow-discharge plasma

09 p1089 A73-23197

Propagation of discharges and confinement of a dense plasma by electromagnetic fields

09 p1132 A73-23327

Local transient phenomena induced in an inert gas plasma by a short pulse.

10 p1257 A73-24626

Effectiveness of using the energy of a plasma jet in powder coating deposition

10 p1226 A73-24689

Experimental investigation oscillations in a synthesized plasma jet

10 p1257 A73-24877

Spectroscopic measurement method for the electron temperature and density of a focusing discharge of the 'plasma focusing' type

11 p1404 A73-25270

A plasma-beam discharge laser.

11 p1377 A73-26181

Steady conditions of a radiating self-constricted high-current discharge in a plasma

11 p1406 A73-26333

Charged particle production and plasma electron/ion current discharges from W targets under laser beam, noting dependence on electric field strength, pressure and operation mode

11 p1378 A73-26522

Transient processes in an inductive energy storage element for a plasma injector

12 p1460 A73-26931

High speed corotating plasma streams in solar wind from time dependent radial MHD flow model

12 p1533 A73-26979

ARC discharge plasma diagnostics for nonuniform nonequilibrium turbulent sources, including automatic methods for control applications

12 p1528 A73-27322

Investigation of the space-time distribution of the optical density of the plasma in high-current Li-In discharges.

12 p1529 A73-27903

Investigation of the heating of electrons of a dense beam-plasma discharge in strong magnetic fields

12 p1529 A73-27942

High pressure plasma torch to heat air for high temperature chemical reactions and hypersonic wind tunnels for reentry vehicle ablation studies

13 p1597 A73-28479

Influence of initial gas conditions in a coaxial accelerator on plasma parameters

13 p1666 A73-28956

Relaxation to Maxwellian distribution of electrons near low voltage Cs arc plasma discharge cathode

13 p1666 A73-28962

Effect of plasma inhomogeneity on the relaxation of the electron distribution function in the electrode area of a low voltage arc
13 p1667 A73-28963

Measurements of the electronic recombination coefficient in a helium plasma jet.
14 p1780 A73-30245

Temperature distribution and ionization characteristics of sodium and rubidium chlorides, silicon dioxide and atomized carbon jets generated by plasmatron
14 p1781 A73-30464

Current extension from a quasi-steady MPD arcjet.
15 p1918 A73-31550

Contact methods of measuring temperatures in low-temperature plasma jets from stationary sources
15 p1876 A73-31871

Ion acceleration in the formation of an electron beam in a vacuum arc.
15 p1922 A73-32634

Azimuthal symmetry in a coaxial plasma injector.
15 p1922 A73-32636

Operational aspects of coaxial plasma accelerator with gas preionization by induction electric field introduced into interelectrode gap via longitudinal slits in external electrode
17 p2215 A73-34304

Ionization and recombination in a plasma diode.
17 p2215 A73-34308

Flow of nonisothermal plasma through a magnetic nozzle.
17 p2215 A73-34313

Investigation of scattering of microwaves in a plasma-beam discharge.
17 p2217 A73-35716

Transient flow and expansion of a pinch discharge plasma in self-induced magnetic fields.
[AIAA PAPER 73-689]
18 p2338 A73-36240

Experimental investigations on arc-heated steady plasma flow.
19 p2415 A73-37169

Linearized MPD jet and channel flows in external magnetic fields with the Hall effect.
19 p2465 A73-37175

Interaction of plasma streams with a neutral gas cloud.
19 p2466 A73-37179

Generation of energetic ion fluxes from a high temperature electron discharge in an inhomogeneous magnetic field
19 p2466 A73-37358

Coaxial hydrogen and erosion pulsed plasma accelerators in vacuum, discussing experiment design, discharge characteristics and practical applications
19 p2466 A73-37361

Two cascade plasma accelerator with conical and ring electrodes, investigating plasma jet-cascade current interaction dynamics via magnetic probes and I-V characteristics
19 p2467 A73-37362

Effect of near-electrode processes on plasma behavior in electrodynamic accelerators
19 p2467 A73-37365

Experimental determination of the velocity characteristics of a pulsed erosion-type accelerator
19 p2467 A73-37366

Control of the dynamic characteristics of a plasma jet of a given composition by selecting the parameters of a pulsed accelerator
19 p2467 A73-37368

Excitation of an open resonator by initial emission from a high current discharge
19 p2469 A73-37963

The magnetic channeling of a supersonic axisymmetric plasma jet.
19 p2470 A73-38318

Thrust stand performance measurements of a lithium fueled applied field MPD arcjet.
19 p2473 A73-38320

Low-frequency vibrations of a high-frequency E-discharge plasma in a magnetic field
20 p2598 A73-39398

The application of high-speed photography and spectrography for investigations of erosive pulsed plasma streams.
21 p2744 A73-39999

Mass-spectrometric investigation of the ion composition of potassium and cesium discharge plasmas
21 p2746 A73-40526

Experimental study of conductivity, velocity, and temperature distributions in a submerged jet of low-temperature plasma
21 p2747 A73-40575

Pulsed Langmuir probe measurements of hollow cathode plasma discharge electron emission in terms of secondary, thermionic and field components
21 p2747 A73-40793

Investigation of conditions for the formation of a beam-plasma discharge without a magnetic field
21 p2748 A73-41516

Oscillations in a synthesized plasma jet.
21 p2749 A73-41652

Changes in the characteristics of giant laser radiation pulses and of luminous plasma during formation

of damage regions on the surface or in the bulk of transparent dielectrics.
22 p2869 A73-42250

Transients in inductive energy-storage devices for plasma injectors.
22 p2891 A73-42265

Ion temperature in the case of ohmic heating of the plasma in the 'Uragan' stellarator
22 p2893 A73-42382

Polarizing interaction between colliding plasma flows in a toroidal magnetic field. II
22 p2893 A73-42384

Dynamic characteristics of a plasma diode with a low-voltage arc discharge. II - Experimental study of dynamic characteristics
22 p2833 A73-42386

Langmuir probe signal analysis of root-mean-square electron density fluctuations in turbulent Ar plasma jet
22 p2893 A73-42394

Measurement of arc radiation for selected spectral regions.
22 p2861 A73-42569

Diamagnetism of Penning discharge plasma as function of gas pressure, magnetic field strength and applied voltage, discussing plasma energetic lifetime and current characteristics
23 p3009 A73-43653

Structure of currents in a stationary plasma jet in the presence of the Hall effect
23 p3010 A73-43664

Investigation of a turbulent plasma in a reflex discharge with the aid of a double electric probe
23 p3011 A73-43668

Effect of initial gas conditions in a coaxial accelerator on the plasma parameters.
23 p3013 A73-44308

Relaxation to Maxwellian distribution of electrons near low voltage Cs arc plasma discharge cathode
23 p3013 A73-44314

Effect of plasma inhomogeneity on the relaxation of the electron distribution near the electrodes in a low-voltage arc.
23 p3013 A73-44315

Ion acceleration by relativistic electron beam extracted from discharge plasma, discussing proton acceleration and beam composition and energy distribution
23 p3014 A73-44339

Plasma-electromagnetic wave interactions in toroidal discharge chamber, noting possibility of collisionless wave absorption due to conversion to longitudinal plasma waves at hybrid resonance
23 p3014 A73-44340

Gas-dynamic structures of a plasma flare produced during the evaporation of metals by high-intensity optical radiation.
24 p3114 A73-44496

PLASMA LAYERS

NT PLASMA SHEATHS

Stimulated Raman scattering of microwaves in a layer of collisionless plasma.
01 p0082 A73-10423

Periodic structure of the electric field in a stratified plasma with tensor conductivity
01 p0085 A73-10955

On the plasma sheet contribution to the force balance requirements in the geomagnetic tail.
02 p0156 A73-11746

Infinite set of velocity fields to describe geomagnetic field lines and interpret discrepancy in plasma sheet motion observations during substorms
02 p0157 A73-11754

Magnetospheric tail plasma sheet near earth structure explained via tangential magnetic field gradient drift velocity coupling to strong pitch-angle diffusion
02 p0157 A73-11898

The international magnetospheric study 1975-1977 - Scientific fundamentals and objectives.
02 p0164 A73-12313

Ion acceleration in a plasma boundary layer formed by two electron groups
03 p0347 A73-13755

Magnetospheric charged particle populations in magnetosheath, plasma sheet, extraterrestrial ring current, electron trough and trapping regions
03 p0302 A73-13856

Electron intensity measurements by sounding rockets over auroral arcs at magnetospheric plasma boundary
03 p0362 A73-13865

Geomagnetic tail plasma sheet thinning and auroral zone negative bays development during magnetospheric substorms, suggesting auroral particles acceleration along magnetic field lines
03 p0304 A73-13887

The self-consistent geomagnetic tail under static conditions.
04 p0440 A73-14957

On the equilibrium configuration of the geomagnetic tail.
05 p0568 A73-16140

Vertical electric dipole excited electromagnetic fields in triple layer medium with plane boundaries,

noting waveguide thickness effect on electromagnetic wave propagation
05 p0549 A73-16386

Influence of magnetic-field nonuniformity on the fluctuations of the plasma layer in the magnetospheric tail
06 p0690 A73-17559

Kinetic theory of longitudinal wave dispersion in nonuniform plasma layer in HF electromagnetic field, noting plasma instability for electron parametric resonance
06 p0729 A73-18109

Scattering by nonconcentric circular plasma cylinders with axial magnetic fields.
06 p0729 A73-18204

Substorm variations of the magnetotail plasma sheet at geocentric distances measured along the solar magnetospheric x-axis from -6 to -60 earth radii.
07 p0813 A73-19235

Absorption of light at oblique incidence on a plasma layer.
07 p0854 A73-19262

Dispersion equations for E and H waves in multilayer plasma, defining amplitudes correlation for incident, transmitted and reflected waves
07 p0855 A73-19278

Noncoherent reflection of electromagnetic waves from a plasma layer
07 p0855 A73-19281

Magnetosphere tail internal plasma boundary layer dynamics during substorms based on aurora data
07 p0816 A73-19463

On the radio optical depth of the layer where the temperature equals the brightness temperature.
08 p1002 A73-20761

One-dimensional line radiative transfer.
08 p1021 A73-20792

The diffraction of fast magneto-acoustic waves by a plasma layer of a periodically varying density.
08 p0993 A73-21459

Quasi-static ion acoustic surface wave propagation along warm plasma layer-dielectric boundary
08 p0993 A73-21460

Ionospheric and plasma sheet particle densities, fluxes and bulk velocities along auroral magnetic field line for collisionless ion-exosphere model
09 p1079 A73-22842

Obliquely incident electromagnetic wave propagation through plane-stratified weakly ionized plasma with electron density inhomogeneity scale length comparable with mean free path
09 p1052 A73-23077

Stability of a gravitating fluid layer in the presence of a uniform magnetic field perpendicular to its boundary.
10 p1253 A73-23832

Heating of a substance by short laser pulses
10 p1230 A73-24885

Particle kinetic energy vs number density in equilibrium E layer under external and self magnetic fields related to plasma confinement in astron device
11 p1404 A73-25259

Reflection of electromagnetic waves from non-homogeneous anisotropic plasma layers /normal incidence/
12 p1470 A73-27356

The periodic structure of an electric field in stratified plasma with tensor conductivity.
12 p1529 A73-27531

Dipole antenna radiation in homogeneous plasma layer magnetized by normal uniform magnetic field, calculating radiation pattern
13 p1583 A73-28661

Dispersion equations for E and H waves in multilayer plasma, defining amplitudes correlation for incident, transmitted and reflected waves
13 p1665 A73-28678

Incoherent reflection of electromagnetic waves from a plasma layer.
13 p1665 A73-28681

Parametric instabilities and harmonic generation in Tonks-Datner resonances in inhomogeneous bounded electron plasma layer
13 p1665 A73-28791

Self consistent one dimensional plasma layer model with current layer at center described by Vlasov equation and nonexistent normal magnetic field component
14 p1796 A73-29870

Electron current estimation along auroral zone-plasma neutral sheet field line from steady state one dimensional model
15 p1866 A73-31065

Frequency dependence of radio-wave absorption in a reflecting layer
15 p1844 A73-31884

Absorption of hydromagnetic waves in the plasma layer of the magnetospheric tail
15 p1872 A73-31902

Effect of magnetic field inhomogeneity on oscillations of the plasma sheet of the magnetospheric tail.
16 p2002 A73-32783

Selective properties and form of a signal transmitted through a statistically nonhomogeneous layer of arbitrary thickness
16 p1978 A73-32896

Axial compression of the astron E-layer during neutralization.

16 p2042 A73-33337

Theory of the anomalous skin effect in a plasma with a diffuse boundary

16 p2043 A73-34060

Propagation of frequency-modulated pulses in a randomly stratified plasma.

17 p2214 A73-34095

Characteristics of the electrode-adjointing potential layer in an alkali metal plasma in the presence of adsorption

17 p2214 A73-34131

Convection dominated electrons in auroral zone, discussing plasma sheet as magnetospheric electron source, convection electron spatial distribution and convection-precipitation coupling

17 p2223 A73-34358

One-dimensional model for nonlinear reflection of laser radiation by an inhomogeneous plasma layer.

17 p2218 A73-35824

ULF magnetic fluctuations in the plasma sheet as recorded by the Explorer 34 satellite.

18 p2352 A73-36276

Absorption and transformation of electrostatic surface waves in the transition layer of a magneto-active plasma.

19 p2467 A73-37438

Development of a turbulent boundary layer in MHD channel.

19 p2470 A73-38316

Thermal model for streamers in nonequilibrium plasmas.

19 p2470 A73-38317

The theory of parametric excitation of electrostatic surface waves in a plasma layer

20 p2597 A73-39194

Raman scattering of SHF radiation in a bounded plasma of a solid

21 p2657 A73-41509

Heating with short laser pulses.

21 p2717 A73-41660

Electromagnetic wave diffraction by a metallic cylinder surrounded by a plasma layer

22 p2892 A73-42336

Characteristics of the fast and slow magnetosonic waves in layered plasmas.

22 p2894 A73-42397

Reflection of electromagnetic waves from inhomogeneous anisotropic plasma sheets /normal incidence/.

23 p2952 A73-43255

Kinetic theory of longitudinal wave dispersion in nonuniform plasma layer in HF electromagnetic field, noting plasma instability for electron parametric resonance

24 p3114 A73-44498

Role of the neutral sheet in the illumination of polar caps by solar protons.

24 p3086 A73-45132

Life-time of ion waves in unstable and turbulent plasmas.

01 p0084 A73-10463

Plasma confinement in a racetrack magnetic field with a diverter.

03 p0347 A73-14094

Charged-particle lifetime measurements in a helium plasma

07 p0855 A73-19284

Lifetime of charged particles in a helium plasma.

13 p1665 A73-28684

End effects in Faraday type MHD generators with nonequilibrium plasmas.

03 p0254 A73-14185

Electrostatic waves with frequencies above the gyrofrequency in a plasma with a loss-cone.

17 p2218 A73-35831

Potential oscillations with frequencies higher than the gyrofrequency in a plasma containing a cone of losses

20 p2597 A73-39207

Theoretical and numerical results in the case of the nonlinear Vlasov equation

01 p0069 A73-10073

Reductive perturbation theory application to nonlinear Schroedinger equation for plasma of cold ions and isothermal electrons, investigating ion oscillation mode automodulation

01 p0082 A73-10420

Time variable dynamics of plasma beam discharge oscillations frequency spectra

01 p0084 A73-10633

Fluctuation characteristics of dense plasmas from high-current discharges produced by electric explosion of metallic wires in vacuum

01 p0086 A73-11283

Natural oscillations of type-I comet tails.

01 p0107 A73-11331

Electromagnetic dispersion relation for two equidense counterstreaming ion beams in warm electron background oscillating plasma, considering ion instability criteria

02 p0197 A73-12066

Low-frequency oscillations in a bounded low-density plasma.

02 p0198 A73-12105

Spectral characteristics of nonlinear plasma oscillations near collapse limit, discussing wave interaction, energy exchange and velocity corrections

02 p0198 A73-12486

Oscillation modes and cathode potential drop in plasma generated by continuous electric discharge at low pressure between anode and cold cathode

03 p0346 A73-13603

Instability of a weakly ionized plasma at wavelengths of the order of the Debye radius.

03 p0347 A73-14092

Ion-cyclotron instability of a plasma produced by a fast-ion beam.

03 p0347 A73-14101

Incoherent excitation of plasma oscillations by an almost-monoenergetic relativistic beam.

03 p0347 A73-14102

Multiple soliton excitation by ion acoustic square pulse wave in double plasma device in frame of Korteweg-de Vries equation

04 p0477 A73-14771

A mechanism of steady-turbulence development in a plasma

04 p0477 A73-14876

Effect of plasma oscillations on the process of ionizational relaxation

04 p0477 A73-14878

Quasi-linear equations for uniform plasma instabilities connected with potential oscillations, noting non-relativistic electron beam relaxation and abnormal plasma resistance

04 p0477 A73-15017

Hydrodynamic and kinetic instability and oscillations of plasma with non-Maxwellian particle velocity distribution, noting laboratory and cosmic plasmas

04 p0478 A73-15018

Nonlinear monochromatic Langmuir standing waves in a plasma

04 p0478 A73-15033

LF spectrum of plasma oscillations from amplitude modulation of plasma SHF radiation, noting Langmuir and magnetoacoustic waves interaction

04 p0478 A73-15034

Spatial echo and nonlinear interaction of waves in a plasma

04 p0478 A73-15035

Influence of the degree of uniformity of the magnetic field on the emission of electron cyclotron frequency harmonics from a plasma

04 p0478 A73-15036

Cyclotron resonance instability in a rotating plasma

04 p0479 A73-15042

Multifrequency modulation of electron beam for instability oscillations control and energy transfer to plasma particles

04 p0479 A73-15044

Plasma ion and electron modes nonlinear damping, presenting solution for Vlasov-Poisson system

04 p0480 A73-15195

Stationary turbulence of a parametrically unstable plasma.

04 p0480 A73-15474

Stable electron density fluctuations in a plasma in the presence of a high-frequency electric field.

04 p0444 A73-15539

Parametric excitation of high-frequency potential oscillations in a cold magnetoactive plasma by the field of an electromagnetic wave

04 p0481 A73-15612

Non-linear damping of longitudinal ion oscillations in a collisionless non-isothermal plasma.

04 p0482 A73-16042

Character of acoustic dispersion in plasma.

06 p0726 A73-17403

Influence of magnetic-field nonuniformity on the fluctuations of the plasma layer in the magnetospheric tail

06 p0690 A73-17559

Physical principles in incompressible fluid and plasma turbulence comparison, noting quasi-linear approximation for nonlinear particle diffusion in turbulent oscillations

06 p0728 A73-17924

Density and electric field oscillations of plasma in stellarator, considering magnetic field strength effect, stabilization by ionic collisions and energy pumping mechanism

06 p0728 A73-17968

Stationary nonlinear ion acoustic oscillations in dense weakly ionized current carrying plasma, considering wave propagation velocity and instability process

06 p0728 A73-17971

Ion-acoustic oscillations effect on turbulent plasma electric conductivity within weak external electric field

06 p0729 A73-17973

Current-induced nonlinear ion oscillations in a plasma

06 p0729 A73-18112

High-frequency instabilities in a plasma with a nonlinear ion-acoustic wave.

06 p0731 A73-18603

Anode sheath plasma current instabilities, examining electron and ion turbulent heating, plasma particle limiting energies and unsteady oscillation spectra

06 p0731 A73-18604

Theory of parametric resonance in an inhomogeneous plasma

07 p0855 A73-19279

Spectra of potential ion-cyclotron plasma oscillations

07 p0855 A73-19289

Alternating current instability produced by the two-stream instability.

07 p0857 A73-19528

Nonlinear longitudinal oscillations of relativistic plasma.

07 p0859 A73-20217

Ion acceleration in the current sheath of a solar flare

07 p0872 A73-20320

On the instability of longitudinal oscillations in an inhomogeneous isotropic plasma.

08 p0992 A73-20956

Electron plasma oscillation due to beam plasma interaction with standing wave formation between electrodes, observing temporal growth rate during beam modulation removal

08 p0992 A73-21005

The diffraction of fast magneto-acoustic waves by a plasma layer of a periodically varying density.

08 p0993 A73-21459

Ultrarelativistic electrons beam steady injection into plasma filled half space, using weak turbulence theory for assumed beam excited oscillations interaction

08 p0994 A73-21698

Low threshold unstable nonpotential oscillations of weakly ionized rotating plasma in crossed field centrifuge, noting MHD generator and ionospheric implications

09 p1124 A73-21891

Surface oscillations of a weakly ionized plasma in a magnetic field

09 p1124 A73-21901

Influence of magnetic field curvature on the stability of a plasma confined by a dense shell of neutral gas

09 p1124 A73-21902

The instability of hydrodynamic longitudinal oscillations in a non-uniform magnetoactive plasma.

09 p1127 A73-22285

Direct current and voltage effects on plasma longitudinal oscillations, discussing frequency dependence and waves in semiconductors with ionic lattices

09 p1129 A73-22681

Excitation of long-wave oscillations by a secondary electron stream in a plasma generated by an ion beam

09 p1129 A73-22684

Fluctuation theory for isothermal and nonisothermal semibounded plasma, obtaining correlation functions, dispersion laws and damping coefficients

09 p1129 A73-22689

Relaxation processes in a parametrically unstable plasma

09 p1130 A73-22707

Damping of plasma waves in the lower hybrid frequency range.

09 p1131 A73-22908

Parametric excitation of high-frequency electrostatic oscillations in a cold magnetoactive plasma by an electromagnetic wave.

10 p1254 A73-24202

Experimental investigation oscillations in a synthesized plasma jet

10 p1257 A73-24877

Stability of a plasma rotating in crossed electric and magnetic fields

11 p1403 A73-25240

Parametric excitation of Langmuir oscillations in the ionosphere in a field of powerful radio waves

11 p1331 A73-26153

Plasma low density regions caused by Langmuir turbulence, discussing energy dissipation of long wave oscillations and wave collapse

11 p1406 A73-26185

Nonlinear ion sound in a fully ionized current-carrying plasma.

11 p1406 A73-26186

Parametric instability in a plasma placed in non-homogeneous magnetic field.

11 p1407 A73-26563

Parametric instability in an inhomogeneous plasma containing hot ions

12 p1526 A73-26926

HF radio wave enhanced electron cyclotron frequency lines and ion plasma fluctuations due to artificial ionospheric excitation

12 p1490 A73-27008

Ion acceleration in the current layer of a solar flare.

12 p1534 A73-27292

Development of acoustic and overheat instabilities in a plasma with molecular impurities

12 p1528 A73-27303

Oscillations of the earth's magnetic tail in a quasi-hydrodynamics approximation

12 p1491 A73-27347

Asymmetric eigenmodes in a simple model plasmasphere with non-uniform Alfvén speed.

12 p1529 A73-27613

The influence of the scattering by plasma oscillation on the spectrum of emission from semi-opaque plasma 12 p1529 A73-27869

Interaction of a high-frequency magnetic field with plasma potential oscillations in a Q machine 12 p1530 A73-27976

Effect of a high frequency magnetic field on plasma diffusion in a Q-machine. 13 p1664 A73-28348

Intermittent generation of microwave oscillations through a plasma-beam interaction. 13 p1583 A73-28664

Electrostatic ion-cyclotron plasma oscillations. 13 p1665 A73-28689

Stability of flute disturbances in a plasma of toroidal geometry 13 p1666 A73-28954

Interaction between a monoenergetic nonrelativistic electron beam and the surface potential oscillations of a plasma 13 p1666 A73-28955

Parametric instability in the region of low-frequency hybrid resonances. 14 p1778 A73-29686

Wave periodic structure solution instability and unstable oscillation growth rates for nonlinear drift waves and solitons in collisionless plasma 14 p1778 A73-29692

A nonlinear theory for the parametric instability with comparable electron and ion temperatures. 14 p1779 A73-30119

Interaction between a plasma and an electron beam modulated by low-frequency oscillations. 14 p1780 A73-30335

Nonlinear plasma oscillations in terms of Van Kampen modes. 14 p1780 A73-30350

Investigation of the radial structure of the oscillations of a plasma column situated in crossed fields in the presence of resonant cyclotron instability 14 p1781 A73-30579

Correlation between the potential and density fluctuations of a plasma, and the convective transport of particles across the magnetic field in a Penning discharge in the presence of rotational instability 14 p1781 A73-30581

Detection of a feedback in a plasma-electron beam system 14 p1781 A73-30585

Wake past an obstacle in a magnetized plasma flow. 15 p1916 A73-31089

Allowance for the influence of the space charge in the kinematic theory of microwave devices 15 p1850 A73-31491

Stochastic heating of a plasma during development of a Langmuir turbulence instability 15 p1918 A73-31705

Kinetics of stimulated scattering of Langmuir waves by plasma ions 15 p1919 A73-31708

Magnetopause plasma oscillations excitation and transformation into electromagnetic waves, estimating magnetic bremsstrahlung and X ray emission intensities 15 p1926 A73-31892

Dispersion equation for nonpotential oscillations and hydrodynamic instabilities in hot ion plasma with transverse current in magnetic field 15 p1920 A73-32304

Investigation of forced oscillations of the plasma potential in a closed electron-drift accelerator/CDA/ 15 p1920 A73-32310

Ionization oscillations in a plasma in the presence of negative ions 15 p1920 A73-32319

Kinetic instability of a plasma located in an SHF field 15 p1921 A73-32332

Surface oscillations of a weakly ionized plasma in a magnetic field. 15 p1921 A73-32626

Effect of magnetic field curvature on the stability of a plasma confined by a dense neutral gas. 15 p1921 A73-32627

Effect of magnetic field inhomogeneity on oscillations of the plasma sheet of the magnetospheric tail. 16 p2002 A73-32783

Application of the Kubo-Mori theory to the line shape of plasma oscillations. 16 p2041 A73-33332

Lineshape of stable electrostatic fluctuations in a beam plasma system. 16 p2042 A73-33338

Theory of the oscillations and stability of a semiconductor plasma with a small number of carriers in a strong electric field 16 p2042 A73-33734

The effect of plasma resonance on the propagation of surface waves along plasma-vacuum channel. 16 p2043 A73-34023

Parametric instabilities in a plasma containing two types of ions 16 p2043 A73-34057

Low threshold unstable nonpotential oscillations of weakly ionized rotating plasma in crossed field cen-

trifuge, noting MHD generator and ionospheric implications 17 p2215 A73-34314

Waves in a plasma amid magnetic and gravitational fields 17 p2226 A73-34373

Surface oscillations of a magneto-active plasma. 17 p2217 A73-35522

Transformation of high-frequency waves and vanishing of low-frequency instabilities in a radially-inhomogeneous beam-plasma discharge. 17 p2217 A73-35525

Hydromagnetic eigenoscillations in the magneto-spheric tail. 18 p2352 A73-36295

Interaction between a tubular electron beam and a plasma 18 p2339 A73-36555

Parametric excitation of surface waves in an inhomogeneous magnetized plasma 18 p2339 A73-36556

Perturbation of a plasma by a focused CO₂ laser beam. 18 p2339 A73-36623

Oscillations of the earth's magnetic tail 19 p2482 A73-37349

Stability of plasma flows in multipolar magnetic fields 19 p2467 A73-37372

Wavenumber space analysis of oscillations in weakly non-uniform magnetoplasmas. 19 p2468 A73-37442

Potential oscillations with frequencies higher than the gyrofrequency in a plasma containing a cone of losses 20 p2597 A73-39207

Influence of scattering by plasma oscillations on the spectrum of a semitransparent plasma. 20 p2597 A73-39243

Low-frequency vibrations of a high-frequency E-discharge plasma in a magnetic field 20 p2598 A73-39398

A new type of ionizational instability in a plasma with negative ions 20 p2598 A73-39621

Nonlinear ion surface oscillations in a semibounded current-carrying plasma 21 p2745 A73-40361

Electron-acoustic and drift instabilities in a finite-pressure plasma with a transverse current 21 p2745 A73-40364

Parametric excitation of oscillations in an electron plasma 21 p2746 A73-40518

Parametric excitation of ion-acoustic oscillations in a plasma situated in an alternating electric field and a constant magnetic field 21 p2746 A73-40519

Electron-acoustic and ion-cyclotron parametric instabilities of a plasma in an alternating electric field. I, II 21 p2746 A73-40520

Linear theory of transverse-current instability in a plasma 21 p2746 A73-40521

Instability of an azimuthal ion beam in a dense plasma 21 p2746 A73-40522

Principal properties of plasma oscillations in an accelerator with closed drift and an extended zone of acceleration /ACDE/ 21 p2746 A73-40523

Nonlinear conversion of electromagnetic waves at the boundary of a magnetoactive plasma 21 p2658 A73-41517

Oscillations in a synthesized plasma jet. 21 p2749 A73-41652

Nonlinear interacting longitudinal and transverse electron oscillations due to plasma density inhomogeneity in HF hybrid resonance region 21 p2750 A73-41683

Role of nonlinear effects in the problem of the anomalous resistance of plasma. 22 p2890 A73-41723

Wave spectrum analysis of electron beam-plasma longitudinal electrostatic fluctuations, finding triplet wave line shape and intensity and dispersion relations. 22 p2891 A73-42240

Parametric instability in an inhomogeneous plasma with hot ions. 22 p2891 A73-42260

Self-action of electromagnetic wave in plasma under parametric instability. 22 p2895 A73-43022

Oscillations of the earth's magnetic tail in the approximation of quasi-hydrodynamics. 23 p2970 A73-43244

Fluctuation characteristics of a dense plasma of high current discharges produced by electric explosion of metallic wires. 23 p3009 A73-43504

Theta-pinch instability of plasma beam, relating plasma oscillation frequency to microwave emission and electromagnetic wave scattering 23 p3011 A73-43710

Backward ionization waves linear evolution to nonlinear saturated state from gaseous plasma self oscillation instability viewpoint, noting electron temperature and density increase 23 p3011 A73-43829

Nonlinear dissipation of electromagnetic waves in a plasma 23 p3012 A73-44017

Cyclotron oscillations of a plasma in an inhomogeneous magnetic field 23 p3012 A73-44090

Flute stability in a toroidal plasma. 23 p3013 A73-44306

Interaction of a monoenergetic nonrelativistic electron beam with electrostatic surface oscillations in a plasma. 23 p3013 A73-44307

Physical principles in incompressible fluid and plasma turbulence comparison, noting quasi-linear approximation for nonlinear particle diffusion in turbulent oscillations 23 p3013 A73-44326

Influence of Langmuir electron oscillations on the degree of neutralization of an ion beam 23 p3014 A73-44342

Nonpotential gravitationally-dissipative instability of a plasma in toroidal systems 23 p3015 A73-44348

Nonlinear plasma ion oscillations excited by a current. 24 p3114 A73-44501

Dispersion equation for nonpotential oscillations and hydrodynamic instabilities in hot ion plasma with transverse current in magnetic field 24 p3114 A73-44612

Driven electrostatic plasma oscillations in a closed electron drift accelerator. 24 p3114 A73-44618

On coupled fields in stratified plasmas with tensor pressure perturbations. 24 p3115 A73-44625

MilliHertz plasma oscillations associated with strong gradients in density and temperature 24 p3087 A73-45139

On the instability of magnetohydrodynamic Couette flow via non-axisymmetric, oscillatory critical modes. 24 p3116 A73-45241

PLASMA PERTURBATION

U PLASMA OSCILLATIONS

PLASMA PHYSICS

Radio emission from traveling disturbances in solar corona, considering contributions of interplanetary observations, plasma theory and ground observations 01 p0091 A73-10058

Book - An introduction to the theory of plasma turbulence. 01 p0081 A73-10124

Collisionless magnetoactive plasma nonlinear responses tensors symmetry properties, stressing Onsager relations generalization 01 p0083 A73-10454

Equations of state and dissociation equilibrium for CsCl plasma, noting thermodynamic model for phase transitions of liquid metal into nonideal ion plasma. 01 p0084 A73-10851

Concentration distribution and effective lifetimes of excited atoms at small optical thicknesses of the plasma 01 p0085 A73-11083

Distribution function of atomic level populations in a plasma 02 p0196 A73-11603

Influence of the parameters of the accelerating circuit of an injector with inductive energy storage on the process of plasma-cluster acceleration 02 p0196 A73-11633

German book on plasma physics covering MHD equations for incompressible and compressible flow, shock waves, electrical and thermal conductivity, viscosity, flow stability, turbulence, etc 02 p0196 A73-11894

Magnetization currents effect on linear hydromagnetic instabilities development in collisionless anisotropic plasmas 02 p0196 A73-11899

Consistency of fields and particle motion in the 'speiser' model of the current sheet. 02 p0157 A73-11901

Time correlation between current sheet collapse in plasma focus and X ray production, investigating radiation intensity and distribution 02 p0197 A73-12061

Electron-ion collision frequency and electrical conductivity of non-Debye plasma formed in high pressure discharge from Ar, Kr and Xe tubes 03 p0345 A73-13176

Wave scattering in collisionless magnetoactive plasma, taking into account magnetic field effects, spiral motion of scattering particle and shielding fields 03 p0346 A73-13357

Velocity distribution of plasma electrons in the negative H₂- and He-glow with superimposed longitudinal magnetic field. 04 p0477 A73-14897

Low pressure plasma equilibrium in helitron device with stellarator confinement system, calculating plasma pressure from MHD equations

04 p0479 A73-15039

Double layer formation in homogeneous plasma with constant current, considering occurrence in ionosphere and solar atmosphere

05 p0601 A73-16146

German book - Deutsche Gesellschaft für Luft- und Raumfahrt, 1971 Yearbook.

05 p0528 A73-16755

Quantum theory of the dielectric constant of a magnetized plasma and astrophysical applications. I.

05 p0624 A73-17310

Plasma parameters in gas discharges for positive-column He-Se/+ lasers.

06 p0701 A73-18360

Zero and first velocity moments of Boltzmann equation with complications placed on Ohm Law in plasmas, considering momentum exchange

06 p0730 A73-18462

Electrical characteristics of the plasma in a CO laser.

06 p0703 A73-18614

Nonphysical noises and instabilities in plasma simulation due to a spatial grid.

07 p0854 A73-19267

Use of Olver's algorithm to evaluate certain definite integrals of plasma physics involving Chebyshev polynomials.

07 p0854 A73-19270

Magnetic field effects on effective thermal conductivity of partially ionized plasmas, indicating neutral component role in solar magnetoplasma heat transport

08 p1001 A73-20755

Electrical and thermal conductivities of a relativistic degenerate plasma.

08 p0992 A73-21161

Dissipation of hydromagnetic waves with application to the outer solar corona. I - Collisionless protons and collisionless electrons. II - Transition from collisional to collisionless electrons.

09 p1142 A73-22038

Coulomb collision induced mean-energy variations in homogeneous nonrelativistic plasma components, discussing two-component plasma and energy transfer rates

10 p1257 A73-24760

Photon rest mass limit determination from Galactic magnetic field measurements, utilizing maximum current density capability of plasmas

11 p1415 A73-25121

Electron-neutral particle collisions effect on potential of test charge moving at velocity lower than plasma electrons, using BGK model and Lorentz collision operator

11 p1404 A73-25260

Feedback stabilization of a multimode two-stream instability.

11 p1406 A73-26556

Long wavelength instability in a perpendicular shock.

11 p1406 A73-26557

Equations of state and dissociation equilibrium for CsCe plasma, noting thermodynamic model for phase transitions of liquid metal into nonideal ion plasma

12 p1529 A73-27901

Radiative transfer through carbon ablation layers.

13 p1705 A73-28457

Distribution of flux of charge-exchange atoms from a plasma over the cross section of the plasma filament in the Tokamak-4 apparatus.

13 p1664 A73-28611

Concerning one exact solution of the theory of quasilinear relaxation of a parametrically unstable plasma in the field of powerful radiation.

13 p1664 A73-28613

Stellar magnetism origin via fossil, battery and dynamo theories, discussing two fluid plasma model and turbulence

13 p1683 A73-28992

German book on plasma physics covering plasma containment, magnetohydrostatics, gravitational effects, plasma pinch, toroidal plasmas, plasma waves and MHD instabilities

13 p1667 A73-29288

Energy variational principle formulation for stability determination of scalar-pressure toroidal plasma, writing potential energy as one dimensional integral

14 p1778 A73-29689

Consideration on the 'equilibrium' electrons distribution function for a homogeneous, high-frequency, fully ionized plasma.

14 p1779 A73-29998

Energy partitioning of gaseous ions in an electric field.

14 p1776 A73-30246

Comprehensive theory of r.f. energy absorption by a hot ion-electron plasma cylinder excited by an arbitrary electromagnetic field.

15 p1916 A73-31080

Russian book - Plasma astrophysics.

15 p1936 A73-31579

Maximum equilibrium pressure of a plasma in a three-dimensional system with helical geometry

15 p1920 A73-32305

Physics of ionized gases 1972; Proceedings of the Sixth Yugoslav Symposium and Summer School, Miljevac, Yugoslavia, July 16-21, 1972.

16 p2040 A73-32938

Axial distribution for a hot electron plasma.

16 p2041 A73-33325

Free surface shape of MHD flow due to constant mass source expansion into uniform magnetic field as function of time

16 p2041 A73-33329

Crossover frequencies in multicomponent plasma.

16 p2041 A73-33333

Ion-ion instability induced by ac electric fields.

16 p2042 A73-33336

Saturation in cyclotron resonance heating of plasma.

16 p2042 A73-33339

Nonlinear theory of wave interaction in a plasma

16 p2042 A73-33735

Anomalous penetration of a magnetic pulse into a plasma.

17 p2214 A73-34098

Acoustic instability of a bounded weakly ionized plasma

17 p2214 A73-34135

Continuous uniform excitation of medium-pressure CO₂ laser plasmas by means of controlled avalanche ionization.

17 p2183 A73-34207

Book - Principles of plasma physics.

17 p2216 A73-34467

Equations for a plasma consisting of matter and antimatter.

17 p2216 A73-34508

Nonphysical self forces removal from electromagnetic plasma models by simulation algorithm, discussing optimization of particle orbit equations integration

17 p2216 A73-34895

Book - Plasma engineering.

17 p2217 A73-35475

Structure and evolutionary history of the solar system. III.

17 p2236 A73-35784

Transition probability approach to the theory of plasmas.

17 p2218 A73-35819

Plasma physics phenomena in the outer planet magnetospheres.

[AIAA PAPER 73-566]

18 p2345 A73-36097

Russian book - Interplanetary medium and the physics of the magnetosphere.

19 p2481 A73-37336

Constitutive equations of a plasma with bound charges.

19 p2468 A73-37521

Engineering aspects of magnetohydrodynamics; Proceedings of the Thirteenth Symposium, Stanford University, Stanford, Calif., March 26-28, 1973.

19 p2469 A73-38310

The electron kinetics of a weakly ionized Lorentz plasma in arbitrarily oriented external electric and magnetic fields

20 p2596 A73-39192

Russian book - Physical bases of thermionic energy conversion.

22 p2890 A73-41876

Interferometric measurement of thermodynamic variables of rare gas plasmas produced by shock waves

22 p2896 A73-43168

Experimental investigation of a 'poloidal' current in a plasma flow in an inhomogeneous axially-symmetric magnetic field

23 p3010 A73-43657

Application of cybernetic means and methods in studies of plasma physics and controlled thermonuclear synthesis

23 p3011 A73-43671

Maximum equilibrium pressure of a plasma in a spatial system with helical symmetry.

24 p3114 A73-44613

Allowance for electron degeneration in a pseudopotential model of a nonideal plasma

24 p3115 A73-44759

The ion-sound instability and its associated multimode phenomena.

24 p3115 A73-44874

Transfer of energy to light ions from the ion-acoustic-wave instability developed in a heavy-ion plasma.

24 p3117 A73-45406

Thermodynamics of white dwarf matter in crystal-line phase.

24 p3143 A73-45435

PLASMA PINCH

NT THETA PINCH

Averaged equations of cumulative-laser heating of plasma in Z-pinch with consideration of the recovery of the energy of nuclear fusion.

03 p0347 A73-13782

Averaged equations of cumulative-laser heating of two-temperature plasma in Z-pinch taking into account the nuclear fusion energy.

03 p0347 A73-13783

Equations of laser heating of plasma in a system of the 'focus' type, the recovered energy of nuclear fusion being taken into consideration.

04 p0480 A73-15593

Averaged equations of laser heating of two-temperature plasma in Z-pinch, the thermonuclear fusion energy being taken into consideration.

04 p0480 A73-15594

Instability of a relativistically strong electromagnetic wave of circular polarization.

[AD-759478]

04 p0482 A73-15960

Hydrodynamic instability of the boundary of a viscous plasma in a magnetic field.

05 p0603 A73-16793

Surrounding wall electrical resistivity effects on plasma pinch stabilized by outer region force-free current flow, deriving instability growth rate

05 p0604 A73-17363

Kadomtsev-Nedospasov helical instability during a strong pinch effect in an electron-hole plasma

06 p0729 A73-18119

Plasma sheath capacitance and resistance in double inverse pinch device from I-V measurements with Langmuir probe, noting relationship to plasma temperature and density

[AD-760249]

06 p0696 A73-18784

Necessary and sufficient condition for hydromagnetic stability of the Bennett pinch.

06 p0733 A73-18648

Hydromagnetic instabilities of current carrying pinch in magnetic field, noting thin walled resistive liner effect on nonlocal modes stabilization

08 p0991 A73-20821

Development and properties of the halo in pinch plasmas

10 p1253 A73-23673

X-ray and electron spectra from the double inverse pinch device.

10 p1251 A73-24258

Pinch effect in a germanium electron-hole plasma.

11 p1409 A73-26189

Rayed auroral structures and their relation to the drift current instability in a plasma blob.

13 p1607 A73-28705

Magnetohydrodynamic simulation of toroidal belt-pinch experiments.

14 p1778 A73-29694

Linear Z pinch magnetohydrodynamic instability mode and characteristic wavelength determined by discharge tube radius and current buildup rate

15 p1918 A73-31703

Experimental observation of the high-density plasma-beam formation by continuous-flow Z-pinch.

17 p2217 A73-35523

Transient flow and expansion of a pinch discharge plasma in self-induced magnetic fields.

[AIAA PAPER 73-689]

18 p2338 A73-36240

High enthalpy supersonic ionized gas flow in shock tube experiment, investigating pinch effect on flow acceleration and setup nonrecurrence

19 p2415 A73-37168

Study of a linear noncylindrical discharge by holographic interferometry

20 p2597 A73-39198

Dynamics of plasma column constriction and electromagnetic acceleration of ions

21 p2745 A73-40362

Studies of collisional preionization in large pinch vessels.

21 p2748 A73-40927

Classical diffusion of free boundary plasma in plane and cylindrical slab geometries, calculating belt pinch effect and pressure decay rate

21 p2750 A73-41679

Free point method finite difference solution for two dimensional nonstationary hydrodynamic problem of continuous media, demonstrating feasibility by plasma pinch effect calculation

23 p2968 A73-43799

Kadomtsev-Nedospasov helical instability in a strong pinch effect in an electron-hole plasma.

24 p3114 A73-44503

PLASMA POTENTIALS

Floating potential and diffusion coefficients of viscosity damping of convective cells in stellarator for confined He, Ar and Xe plasmas

01 p0083 A73-10462

Potential drops near the electrodes in a pulsed plasma accelerator.

03 p0347 A73-14096

Special features of Debye screening and the equation of state of a partially ionized plasma

06 p0730 A73-18551

Experimental investigation of the electrical conductivity of a coaxial high-temperature jet with dispersed particles of Ti

07 p0858 A73-20010

Continuum electrostatic probe theory with magnetic field.

07 p0860 A73-20476

Features of the flow of a nonisothermal plasma, obtained in a beam-plasma discharge, through a magnetic nozzle

09 p1124 A73-21890

Analytical model of electron velocity, resonance and potential of plasma accelerated in crossed electric and magnetic fields

10 p1253 A73-23577

Electric field in the plasma sheath at the electrodes and the Bohm condition

10 p1258 A73-24879

Measurement of the potential distribution in the vicinity of an electron beam with the aid of a thermal probe

10 p1258 A73-24889

Probe device for measuring local parameters of ionized gas flow.

12 p1499 A73-27915

Interaction of a high-frequency magnetic field with plasma potential oscillations in a Q machine

12 p1530 A73-27976

Interaction between a monoenergetic nonrelativistic electron beam and the surface potential oscillations of a plasma

13 p1666 A73-28955

Temperature distribution and ionization characteristics of sodium and rubidium chlorides, silicon dioxide and atomized carbon jets generated by plasmatron

14 p1781 A73-30464

Correlation between the potential and density fluctuations of a plasma, and the convective transport of particles across the magnetic field in a Penning discharge in the presence of rotational instability

14 p1781 A73-30581

Coulomb drift of electrons from a mirror confinement system in the case of a positive plasma potential

15 p1920 A73-32306

Investigation of forced oscillations of the plasma potential in a closed electron-drift accelerator (CDA)

15 p1920 A73-32310

Debye screening and equation of state of a partially ionized plasma.

16 p2042 A73-33576

Screened potential Lorentz model for electrical conductivity of non-Debye plasma, investigating electron energy distribution function

17 p2214 A73-34127

Characteristics of the electrode-adjointing potential layer in an alkali metal plasma in the presence of adsorption

17 p2214 A73-34131

Flow of nonisothermal plasma through a magnetic nozzle.

17 p2215 A73-34313

Analysis of methods for measuring electric field intensities in the magnetosphere

19 p2481 A73-37340

Potential created by a test particle in one-, two- and three-dimensions in a flowing ion-electron plasma.

20 p2596 A73-38969

Microarc current flow and potential drop through cold boundary layer near plasma electrodes in MHD generators

20 p2598 A73-39604

Shielding of a moving test charge in a turbulent plasma.

20 p2599 A73-39722

Electric field in an electrode sheath and the Bohm criterion.

21 p2749 A73-41654

Measurement of the potential distribution near an electron beam using a thermionic probe.

21 p2749 A73-41664

Propagation mode with fine structure interpreted as quasi-cylindrical electrostatic wave interference with cold plasma field from potential measurements near point source antenna

22 p2895 A73-43021

Interaction of a monoenergetic nonrelativistic electron beam with electrostatic surface oscillations in a plasma.

23 p3013 A73-44307

Transition of a low-pressure plasma into a highly ionized state

23 p3013 A73-44335

Coulomb loss of electrons from a mirror device with a positive plasma potential.

24 p3114 A73-44614

Driven electrostatic plasma oscillations in a closed electron drift accelerator.

24 p3114 A73-44618

Determination of the voltage distribution in the interelectrode space of a grid probe immersed in a Maxwellian plasma

24 p3116 A73-45328

Plasma density measurement by a Langmuir probe in the presence of a magnetic field

01 p0082 A73-10428

Electron temperature measurement in collisional plasma with double probe, noting electron and ion density distribution near isolated electrode under floating potential

01 p0085 A73-10866

Boltzmann transport equation for plasma probe detector characteristics for Maxwellian and non-Maxwellian distribution functions of electrons in dc and ac electric fields

04 p0480 A73-15602

Evaluation of an orifice probe for plasma diagnostics.

05 p0601 A73-16431

Recent results of plasma-wall heat transfer studies in highly ionized, dense plasmas.

05 p0603 A73-16762

Electric probe performance in weakly ionized dense plasma flow for lower ionosphere measurements, considering stagnation point and particle distribution-potential effects

06 p0689 A73-17538

Use of magnetic probes for diagnostics of pulse plasma.

09 p1086 A73-23149

Boltzmann transport equation for plasma probe detector characteristics for Maxwellian and non-Maxwellian distribution functions of electrons in dc and ac electric fields

10 p1254 A73-24192

Measurement of the potential distribution in the vicinity of an electron beam with the aid of a thermal probe

10 p1258 A73-24889

A noise-immune ionizational manometer for pressures between 1 millitorr and 1 nanotorr

12 p1497 A73-27213

Electron temperature measurement in recombination collisional plasma with double probe, noting electron and ion density distribution near isolated electrode under floating potential

12 p1499 A73-27916

Contact methods of measuring temperatures in low-temperature plasma jets from stationary sources

15 p1876 A73-31871

Use of emissive probes in plasma density measurements.

16 p2011 A73-32725

Electric probe performance in weakly ionized dense plasma flow for lower ionosphere measurements, considering stagnation point and particle distribution-potential effects

16 p2001 A73-32762

Effect of a sheath on the fields of a probe in a hot magnetized plasma.

16 p2041 A73-33330

An evaluation of ionospheric probe performance. I - Evidence of contamination and clean-up of probe surfaces. II - The influence of vehicle wake effects on electron density and temperature measurements.

17 p2160 A73-34786

Double-probe measurements of electron temperatures on low pressure diffusion flames - Criticism of the methods for determining the electron temperature from the double-probe current voltage characteristic.

18 p2317 A73-37097

Analysis of methods for measuring electric field intensities in the magnetosphere

19 p2481 A73-37340

Methods of corpuscular plasma diagnostics in a pulsed coaxial accelerator

19 p2467 A73-37371

Cavity perturbation technique for determining the presence of molecular ions of helium in a dc discharge plasma.

19 p2469 A73-37901

Effect of an isotropic nonequilibrium plasma on electron temperature measurements.

20 p2552 A73-38947

Determination of electron density and electron collision frequency in a plasma by an RF nonimmersive probe.

21 p2748 A73-40953

Measurement of the potential distribution near an electron beam using a thermionic probe.

21 p2749 A73-41664

Satellite-borne swept frequency impedance probe /gyroplasma probe/ for ionospheric plasma parameters including electron density and ion composition, noting PCM telemetry system

22 p2917 A73-42571

Investigation of a turbulent plasma in a reflex discharge with the aid of a double electric probe

23 p3011 A73-43668

Volt-ampere characteristics of double electrical plasma probe measuring ionization level in low temperature dense plasma under interelectrode gap near-breakdown conditions

23 p2983 A73-44344

Experimental study of shocked-plasma flows with a double search-coil conductivity probe.

24 p3113 A73-44402

Equipment for measuring local plasma flow parameters by a thermoanemometer probe

24 p3089 A73-44761

Determination of the voltage distribution in the interelectrode space of a grid probe immersed in a Maxwellian plasma

24 p3116 A73-45328

PLASMA PROPULSION

Resistojet and plasma propulsion system technology.

[ALAA PAPER 72-1124] 03 p0355 A73-13436

Continuing development of the short-pulsed ablative space propulsion system.

[ALAA PAPER 72-1154] 03 p0356 A73-13457

Electromagnetic thrust from magnetic dc arc discharge plasma accelerators, noting MHD experiments and reentry simulation

04 p0489 A73-15728

Quasi-steady MPD thruster research at Rome University.

04 p0489 A73-15730

A low-power MPD thruster of Duoplasmatron type.

18 p2342 A73-36154

Coaxial Ar plasma accelerator for spacecraft propulsion, discussing quasi-steady state I-V characteristics and exhaust velocity

19 p2466 A73-37180

PLASMA RADIATION

A simple method for calculating nongray radiation.

01 p0119 A73-10109

Radiation and conductivity of a high current constricted discharge plasma.

01 p0081 A73-10119

Electrical conductivity and total radiant power of air plasma.

01 p0081 A73-10121

Dispersion relation for Cerenkov radiation of moving test particles in a magnetoplasma.

01 p0083 A73-10453

Energy and mass analysis of neutral particles emitted from a toroidal theta-pinch plasma.

01 p0084 A73-10466

Ultrasonic waves generation by plasma of activated flame, presenting sound pressure and light emission graphs

01 p0086 A73-11272

Possibilities of using organic compound lasers in spectral analysis

02 p0176 A73-12095

UV light intensities calibration in astrophysics and high temperature metrology with thermal arc plasma as radiation sources, discussing intensity standard establishment

02 p0199 A73-12715

Radiation from a magnetic line source in a compressible and anisotropic plasma half-space.

03 p0345 A73-12996

Changes in the distribution function of magnetospheric particles associated with gyroresonant interactions.

03 p0303 A73-13882

EUV emitting plasma structure of solar quiet and active atmospheres, noting extreme departures from LTE

03 p0363 A73-13952

The transient highly excited solar flare plasma.

03 p0364 A73-13960

The light emission of the column plasma in current-modulated noble-gas discharges at intermediate pressures

03 p0348 A73-14621

Low current mercury vapor discharge positive column plasma continuous radiation measurements as function of pressure, current density and temperature at 2300-14,000 A

03 p0348 A73-14624

Influence of the degree of uniformity of the magnetic field on the emission of electron cyclotron frequency harmonics from a plasma

04 p0478 A73-15036

H emission line shape of plasma radiation under anisotropic electric microfields, calculating field distribution function, dispersion and frequency

04 p0480 A73-15601

Radiation energy distribution in laser pulse heating of moving plasma without reflection, noting thermal wave propagation

04 p0481 A73-15605

Continuum radiation from nonisothermal hydrogen plasmas.

05 p0602 A73-16558

An estimate of radiative emission from an isothermal xenon plasma at temperatures up to 50,000 K.

05 p0602 A73-16561

Measurement of continuum radiation from an argon plasma.

05 p0602 A73-16564

Soft X-ray spectra of the Cygnus Loop and Cygnus X-2 in the energy range of 0.16-6.7 keV.

05 p0612 A73-17332

Quantum electrodynamical models of coherent plasma electron-positron pair production and pulsed radiation in electric field, relating to pulsars

05 p0626 A73-17383

PLASMA POWER SOURCES

NT PLASMA ENGINES

PLASMA PROBES

NT ELECTROSTATIC PROBES

Possibilities of measuring the velocity of circulation of the magnetospheric plasma with the help of a quadrupole probe used in the vicinity of the low hybrid frequency

01 p0035 A73-10326

PLASMA RESONANCE

Electromagnetic radiation caused by the two-stream instability in a bounded plasma. 06 p0726 A73-17416

Excitation of parametric instabilities by microwave pumping in a magnetoactive plasma 06 p0729 A73-18108

Gain correlation with sidelight and plasma impedance properties of a CO₂ laser discharge. 06 p0700 A73-18137

Comparison of exact and mean beam length results for a radiating hydrogen plasma. 07 p0859 A73-20221

The effect of a metallic reflector upon cyclotron radiation. 08 p0990 A73-20813

Some questions on the evidence of laser X-ray emission from CuS₀₄ doped gelatin. 08 p0975 A73-21061

Observation of beam-plasma interaction in a toroidal plasma in a large electric field. 08 p0993 A73-21631

Relativistic electron bremsstrahlung suppression in isotropic plasma, noting analogy to synchrotron radiation 10 p1252 A73-23476

Plasma self radiation and absorption, schlieren signals and lasing levels recording methods based on dioxide lasers, using Mach-Zehnder IR interferometer 10 p1253 A73-23517

Plasma excitation by HF field in carbon dioxide-argon flow under low pressure, noting disappearance of striations 10 p1253 A73-24072

Micrometeoroid mass, velocity and composition from Heos 2 and Helios satellite experiments, using hypervelocity dust particle impacting plasma emission 10 p1218 A73-24119

H emission line shape of plasma radiation under anisotropic electric microfields, calculating field distribution function, dispersion and frequency 10 p1254 A73-24191

Radiation energy distribution in laser pulse heating of moving plasma without reflection, noting thermal wave propagation 10 p1254 A73-24195

Optical orientation of metastable He-3 atoms and its influence on the electron density and on the emission of helium atoms in a plasma 10 p1257 A73-24755

Harmonic structure of flare related type 5 burst, suggesting plasma wave emission 11 p1412 A73-25856

Nonthermal radiation from a magnetoactive plasma in the field of a microwave pumping wave. 11 p1405 A73-26182

Steady conditions of a radiating self-constricted high-current discharge in a plasma 11 p1406 A73-26333

Study of the effect of a plasma on the microwave radiation of a helical beam in a waveguide 12 p1527 A73-26935

Microwave oscillations and the visible radiation spectrum of a cesium plasma diode 12 p1527 A73-26938

Study on ionizing shock waves in argon. III - Thermodynamic properties of the plasma. 12 p1527 A73-27173

Effect of a magnetic field on the soft X-ray radiation of a laser plasma 12 p1530 A73-27977

Investigation of the absorption and emission of electron-beam-induced waves in an inhomogeneous magnetoactive plasma 13 p1666 A73-28958

Focused high power CW carbon dioxide laser sustained Xe, Kr and Ar continuous plasmas, investigating plasma radiative properties by calorimetric techniques 14 p1779 A73-29922

Plasma radiation from collisionless MHD shock waves and the high-frequency waves in the upstream solar wind. 14 p1786 A73-29978

Nonstationary emission from dipole sources in a plasma with a diagonal permittivity tensor 14 p1780 A73-30263

Electrical conductivity and total emission coefficient of air plasma. 15 p1918 A73-31657

Magnetopause plasma oscillations excitation and transformation into electromagnetic waves, estimating magnetic bremsstrahlung and X ray emission intensities 15 p1926 A73-31892

Heating of a high-density plasma with the aid of powerful electron beams 15 p1920 A73-32308

Electromagnetic emission during surface wave excitation by a relativistic electron beam in a plasma 15 p1921 A73-32321

The radiative properties of high density argon plasma in explosively driven shock waves. 16 p2040 A73-32907

Arc plasmas as radiation standards in the vacuum ultraviolet. 16 p2036 A73-32942

An investigation of the reflection of electromagnetic pulses from moving plasmas. 16 p2041 A73-33199

Excitation of electromagnetic waves in a plasma with a relativistic electron beam. 17 p2216 A73-35159

Plasma self radiation and absorption, schlieren signals and lasing levels recording methods based on carbon dioxide lasers, using Mach-Zehnder IR interferometer 17 p2217 A73-35197

A method for solving the problem of irradiation in anisotropic plasma. 17 p2217 A73-35724

Normal Doppler shifted cyclotron radiation from a cold plasma. 18 p2338 A73-36189

Calculation of components, electrical conductivity, and total radiative source strength of nitrogen plasma in local thermodynamic equilibrium. [ALAA PAPER 73-744] 18 p2339 A73-36360

Magnetic modulation of the optical emission intensity of a plasma from a high-frequency H-discharge 18 p2339 A73-36565

Continuum emission from recombining oxygen and nitrogen plasmas. 18 p2338 A73-36799

Investigation of the performance of a coaxial accelerator in the production of a dense high-energy plasma 19 p2467 A73-37367

X-ray emission in laser-produced plasmas. 20 p2595 A73-38890

The interaction of a laser with matter as an intense source of UV and soft X-ray radiation - Application to X-ray cinematography 21 p2709 A73-39944

Dynamics of plasma column constriction and electromagnetic acceleration of ions 21 p2745 A73-40362

Near-infrared radiation intensity from restriks of exploding wires. 21 p2740 A73-40955

Basic method for realization of temperature scale at 10,000 K by photometric comparison between vacuum-UV-blackbody radiation of a plasma and synchrotron radiation. 22 p2852 A73-41978

Structure of ionizing shock waves with radiative energy loss. 22 p2841 A73-42200

Changes in the characteristics of giant laser radiation pulses and of luminous plasma during formation of damage regions on the surface or in the bulk of transparent dielectrics. 22 p2869 A73-42250

Effect of a plasma on the microwave radiation from a helical beam in a waveguide. 22 p2892 A73-42269

Microwave oscillations and visible emission in a cesium diode. 22 p2892 A73-42272

Possible emission of transverse electromagnetic waves in an isotropic plasma 22 p2893 A73-42390

Measurement of arc radiation for selected spectral regions. 22 p2861 A73-42569

On the emission coefficient of uranium plasmas. 23 p3005 A73-43388

Theta-pinch instability of plasma beam, relating plasma oscillation frequency to microwave emission and electromagnetic wave scattering 23 p3011 A73-43710

UV radiation measurements of Ar-Hg gas discharge plasma as function of temperature and pressure with emphasis on fluorescent light design 23 p3011 A73-43830

Absorption and emission of waves generated by an electron beam in an inhomogeneous magnetoplasma. 23 p3013 A73-44310

Excitation of parametric instabilities in a magnetoactive plasma by a microwave pumping wave. 24 p3114 A73-44497

Heating of a dense plasma by a powerful electron beam. 24 p3114 A73-44616

A theory of the origin of the split pair burst emission from the solar corona. 24 p3123 A73-44646

Solar coronal radio spectra emitted by synchrotron process, computing radio wave suppression due to isotropic and anisotropic plasma 24 p3118 A73-45484

PLASMA RESONANCE

Local hydromagnetic toroidal equilibria without symmetry. 01 p0083 A73-10457

Quasi-linear theory of plasma waves resonant diffusion, proceeding from Vlasov equation to derive frequency, wavenumber and velocity by quantum methods 01 p0086 A73-11492

frequency, wavenumber and velocity by quantum methods 01 p0086 A73-11492

Ionospheric resonance signal envelope and waveform observation by rocket-borne RF sounder, noting electron gyrofrequency third harmonic due to beating waves 02 p0140 A73-11750

Ionospheric VLF and ELF electric field observation by Alouette 2 satellite, obtaining ion mass distribution from lower hybrid resonance hiss during geomagnetic storm 02 p0164 A73-12623

The excitation of resonances by a dipole antenna inside a hollow cylindrical plasma. 03 p0346 A73-13695

Reconstitution of signals deformed by a fast AGO application to plasma resonances. 04 p0417 A73-15297

Resonance coupling of a transverse magnetic response to a transverse electric excitation by the axial density gradient of a bounded plasma. 05 p0601 A73-16364

Book - Geophysics 3. Part 4. 06 p0688 A73-17501

Resonance and propagation theory for all electromagnetic wave types in plasmas of ionosphere and interplanetary space, discussing stability and oscillations 06 p0689 A73-17505

Kinetic theory of longitudinal wave dispersion in nonuniform plasma layer in HF electromagnetic field, noting plasma instability for electron parametric resonance 06 p0729 A73-18109

Theory of parametric resonance in an inhomogeneous plasma 07 p0855 A73-19279

High-frequency heating of a plasma under lower hybrid-resonance conditions 07 p0855 A73-19290

The sideband instability of electrostatic waves in an inhomogeneous medium. 07 p0858 A73-19667

Parametric action of high-power radiation on a plasma near the electron cyclotron frequencies 09 p1123 A73-21876

Absorption of electromagnetic waves by a magnetoactive plasma at parametric-resonance frequencies 09 p1124 A73-21889

Cold collisionless plasma equations for electromagnetic waves absorption near lower hybrid resonance in inhomogeneous magnetized plasma contained in ideally conducting cylinder 09 p1125 A73-21906

Characteristics of the electric field far from and close to a radiating antenna around the lower hybrid resonance in the ionospheric plasma. 09 p1049 A73-22277

Lower-hybrid-resonance heating of a plasma in a parallel-plate waveguide. 09 p1129 A73-22639

Analytical and computer simulation of two ion species RF heated magnetoplasmas response to driving electric fields near lower hybrid frequency, observing parametric instabilities 09 p1129 A73-22640

Analytical model of electron velocity, resonance and potential of plasma accelerated in crossed electric and magnetic fields 10 p1253 A73-23577

Amplifier design for continuous recording of plasma frequency, using dipolar resonance signal obtained from parallel whip antennas surrounded by plasma sheath 10 p1216 A73-23747

Parametric instability in a plasma placed in non-homogeneous magnetic field. 11 p1407 A73-26563

Satellite-borne electrostatic wave topside ionosphere sounder for electron plasma resonance measurement, discussing data spectra preservation, frequency synthesizer and gain-change mechanism features 11 p1339 A73-26629

Parametric instability in an inhomogeneous plasma containing hot ions 12 p1526 A73-26926

Observations of noise bands associated with the upper hybrid resonance by the Imp 6 radio astronomy experiment. 12 p1468 A73-26995

Excitation and damping-mechanism of waves and resonances in bounded magnetoactive media. [IPPCZ-167] 12 p1528 A73-27431

Parametric resonance in an inhomogeneous plasma. 13 p1665 A73-28679

Plasma heating at the lower hybrid resonance. 13 p1665 A73-28690

Parametric instabilities and harmonic generation in Tonks-Dattner resonances in inhomogeneous bounded electron plasma layer 13 p1665 A73-28791

High frequency discharges sustained either on a cavity resonance or on a plasma resonance

14 p1779 A73-29923

General radio-frequency properties of bounded plasma systems in connection with the production and heating of dense plasmas.

14 p1780 A73-30120

Self-induced effects of radio waves in the vicinity of plasma resonance

15 p1918 A73-31706

Anomalous absorption of superhigh-frequency waves in a plasma at frequencies close to the upper hybrid frequency

15 p1846 A73-32323

Cold collisionless plasma equations for electromagnetic waves absorption near lower hybrid resonance in inhomogeneous magnetized plasma contained in ideally conducting cylinder

15 p1922 A73-32631

The effect of plasma resonance on the propagation of surface waves along plasma-vacuum channel.

16 p2043 A73-34023

Absorption of electromagnetic waves at parametric resonances in a magnetoactive plasma.

17 p2215 A73-34312

Theory of the excitation of the lower oblique resonance in the magnetospheric plasma.

18 p2302 A73-35939

Resonant absorption of an electromagnetic wave by an inhomogeneous magnetoactive plasma at electron cyclotron frequency harmonics

18 p2289 A73-36563

Parametric decay of obliquely incident electromagnetic waves into ion acoustic and electron plasma waves in vicinity of resonance

20 p2595 A73-38874

Off-resonance microwave-created plasmas.

20 p2597 A73-39196

Nonlinear theory of a quasi-monochromatic electrostatic wave packet in an inhomogeneous plasma

21 p2745 A73-40363

Interference structure of oscillating point charge near resonance cone in warm magnetized collisionless plasma, relating structure location to cyclotron frequency and plasma parameters

22 p2891 A73-42242

Parametric instability in an inhomogeneous plasma with hot ions.

22 p2891 A73-42260

Observation of extraordinary wave propagation near the lower hybrid resonance frequency.

22 p2895 A73-43023

The shape of the cyclotron absorption line in a weakly ionized plasma

23 p3011 A73-43794

Cyclotron oscillations of a plasma in an inhomogeneous magnetic field

23 p3012 A73-44090

Theory of parametric resonance in a spatially modulated plasma

23 p3013 A73-44334

Plasma-electromagnetic wave interactions in toroidal discharge chamber, noting possibility of collisionless wave absorption due to conversion to longitudinal plasma waves at hybrid resonance

23 p3014 A73-44340

Kinetic theory of longitudinal wave dispersion in nonuniform plasma layer in HF electromagnetic field, noting plasma instability for electron parametric resonance

24 p3114 A73-44498

Generation of VLF waves in the ionosphere near the low-frequency plasma resonance. I

24 p3115 A73-44788

Simultaneous in situ electron temperature comparison of Alouette 2-probe and plasma resonance data.

24 p3086 A73-45129

PLASMA RINGS

U TOROIDAL PLASMAS

PLASMA ROCKETS

U PLASMA ENGINES

PLASMA SHEATHS

Magnetospheric structure studies during 1969-1971, discussing bow shock magnetosheath, magnetopause, polar cusps, electric fields and trapped particle composition

03 p0302 A73-13852

Acceleration of auroral particles by electric double layers.

03 p0303 A73-13877

Atmospheric model for substorm triggering mechanism, plasma sheath behavior and substorm recovery, noting solar wind interaction with magnetosphere

03 p0304 A73-13886

Magnetotail plasma leakage into magnetosheath during magnetospheric substorms from Vela satellites proton flux measurements

04 p0443 A73-15530

Anode sheath plasma current instabilities, examining electron and ion turbulent heating, plasma particle limiting energies and unsteady oscillation spectra

06 p0731 A73-18604

Experimental investigation of the transient formation of a microwave-generated ionized sheath in air.

06 p0732 A73-18781

Plasma sheath capacitance and resistance in double inverse pinch device from I-V measurements with Langmuir probe, noting relationship to plasma temperature and density

06 p0696 A73-18784

Structure of the current front in an unsteady plasma accelerator, and turbulent acceleration of the ions. I

09 p1124 A73-21881

Dynamics of the current sheath in a pulsed electrodynamic plasma accelerator

09 p1125 A73-21910

Measurement of ion-rich sheath thickness by ion acoustic wave.

09 p1126 A73-22279

Two dimensional model of solar wind passage past magnetosphere, assuming hot plasma current sheath in geomagnetic tail

09 p1077 A73-22485

Electric field in the plasma sheath at the electrodes and the Bohm condition

10 p1258 A73-24879

The kinetic reflection coefficient in a formula for the current at a plasma/semiconductor interface in the case of an inelastic mechanism of electron energy relaxation

12 p1527 A73-26928

Equilibrium of a plasma contained between two parallel plates by a magnetic field

15 p1921 A73-32333

Current-shell dynamics in a pulsed electrodynamic plasma accelerator.

15 p1922 A73-32635

Effect of a sheath on the fields of a probe in a hot magnetized plasma.

16 p2041 A73-33330

Structure of the current front and turbulent acceleration of ions in a pulsed plasma accelerator. I.

17 p2215 A73-34305

Plasma channel flow theoretical and experimental review, considering heat transfer studies, turbulent nonequilibrium plasma boundary layers and plasma sheaths

19 p2464 A73-37161

Continuum thick sheath probe studies in hypersonic ionized boundary layers.

19 p2375 A73-37164

Formation and decay of vortex filaments in a plasma current sheath.

19 p2465 A73-37173

Boundary-layer plasma of a re-entry vehicle - A comparison of prediction models and flight measurements.

21 p2632 A73-40420

Electric field in an electrode sheath and the Bohm criterion.

21 p2749 A73-41654

Impedance and large signal excitation of satellite-borne antennas in the ionosphere.

22 p2831 A73-41835

Kinetic reflection coefficient at a plasma-semiconductor boundary for inelastic electron energy relaxation.

22 p2891 A73-42262

E-polarized electromagnetic scattering by conducting circular cylinder coated with plasma sheath during spacecraft reentry flight under plane wave incidence

22 p2827 A73-42466

Interactions of plasmas with magnetic field boundaries.

22 p2851 A73-42977

Experimental investigation of the low-frequency capacitive response of a plasma sheath.

24 p3117 A73-45408

PLASMA SLABS

Nonlinear radio-frequency response of a non-uniform plasma slab-condenser system with realistic density and velocity profiles.

04 p0479 A73-15189

Reflection and transmission of electromagnetic waves obliquely incident on a relativistically moving uniaxial plasma slab.

06 p0665 A73-18185

Measurement of the attenuation of an electromagnetic wave in a bounded hot electron plasma.

07 p0860 A73-20478

Wave transformation in warm magnetoplasma slab with parabolic density profile and two lower hybrid layers, discussing long wavelength energy tunneling and conversion efficiency

09 p1129 A73-22637

Propagation through a slab of irregularities in a magneto-ionic medium.

09 p1051 A73-22647

Reflection and transmission of electromagnetic waves obliquely incident on a relativistically moving isotropic plasma slab.

15 p1919 A73-31947

Self-consistent calculation of the motion of a sheet of ions in the magnetosphere.

16 p2003 A73-33433

Ellipsoidal coordinates - A natural coordinate system for calculations of laser irradiations of slabs.

20 p2572 A73-38972

Magnetic field effects on slab surface plasmons in the local limit.

20 p2599 A73-39720

Classical diffusion of free boundary plasma in plane and cylindrical slab geometries, calculating belt pinch effect and pressure decay rate

21 p2750 A73-41679

Magnetotail plasma flow observation with Vela 4A oriented perpendicular to ecliptic plane, considering plasma sheet recovery relation to auroral electrojet poleward shift

22 p2844 A73-41907

Electromagnetic wave interaction with moving bounded plasmas.

24 p3069 A73-45409

PLASMA SOUND WAVES

U MAGNETOHYDRODYNAMIC WAVES

U PLASMA WAVES

PLASMA SPECTRA

Book - An introduction to the theory of plasma turbulence.

01 p0081 A73-10124

CO₂ plasma emissivity at temperatures from 7000 to 9000 K in the spectral range of 2100 to 10,000 Å

01 p0085 A73-10854

Spectral characteristics of nonlinear plasma oscillations near collapse limit, discussing wave interaction, energy exchange and velocity corrections

02 p0198 A73-12486

Ultraviolet and X-ray spectroscopy of astrophysical and laboratory plasmas; Proceedings of the Third Symposium, Utrecht, Netherlands, August 24-26, 1971.

03 p0363 A73-13951

Spectroscopic investigation of turbulent plasma parameters.

03 p0347 A73-14095

Low current mercury vapor discharge positive column plasma continuous radiation measurements as function of pressure, current density and temperature at 2300-14,000 Å

03 p0348 A73-14624

Induced enhancement of the plasma line in the backscatter spectrum by ionospheric heating.

04 p0445 A73-15555

Ion sound turbulence in dense plasma within magnetic fields, representing global equilibrium spectrum

04 p0480 A73-15563

H emission line shape of plasma radiation under anisotropic electric microfields, calculating field distribution function, dispersion and frequency

04 p0480 A73-15601

Effect of Thomson scattering on the emission spectrum of an optically semiopaque plasma.

04 p0493 A73-16024

The influence of spatial temperature distribution and measuring configuration on line-reversal temperature.

05 p0602 A73-16563

Search for coronal line emission from the Cygnus Loop.

05 p0626 A73-17380

Spectrum of small-scale inhomogeneities in the interplanetary plasma

06 p0747 A73-17529

Determination of parameters of laser-induced plasma in air by a scattering method.

06 p0732 A73-18610

Charged-particle lifetime measurements in a helium plasma

07 p0855 A73-19284

Spectra of potential ion-cyclotron plasma oscillations

07 p0855 A73-19289

The radial amplification profile of the 4880-Å ionic laser line and the distribution of the charge carriers in the wall-stabilized Ar low-pressure arc column

08 p0989 A73-20786

Spectroscopic measurement of the source function as a test for deviations from local thermodynamic equilibrium (L.T.E.) in arc plasmas.

08 p0992 A73-21018

H emission line shape of plasma radiation under anisotropic electric microfields, calculating field distribution function, dispersion and frequency

10 p1254 A73-24191

Microwave oscillations and the visible radiation spectrum of a cesium plasma diode

12 p1527 A73-26938

HF radio wave enhanced electron cyclotron frequency lines and ion plasma fluctuations due to artificial ionospheric excitation

12 p1490 A73-27008

Ultraviolet spectrum emitted from a laser-produced uranium plasma.

12 p1527 A73-27123

The influence of the scattering by plasma oscillation on the spectrum of emission from semi-opaque plasma

12 p1529 A73-27869

PLASMA SPRAYING

The radiative capacity of a CO₂ plasma at temperatures 7000-9000 K in the spectral interval 2100-10,000 Å.

12 p1529 A73-27904

Lifetime of charged particles in a helium plasma.

13 p1665 A73-28684

Electrostatic ion-cyclotron plasma oscillations.

13 p1665 A73-28689

Determination of magnetic fields in a plasma from the contour of hydrogen spectral lines.

14 p1780 A73-30339

Spectral diagnostics of a plasma flare during well-developed vaporization of metals by laser radiation

14 p1782 A73-30804

Quasi-monochromatic measurements of homogeneous arc plasmas.

15 p1841 A73-32393

Spectrum of small-scale interplanetary plasma inhomogeneities.

16 p2058 A73-32753

Stark broadening and shift of singly ionized aluminum lines.

16 p2040 A73-32845

Satellite waves effects on dynamic behavior of resonant wave-triplet coupling from comparison with isolated triplet in explosive and decay instabilities

16 p2041 A73-33334

Theory of optical polarization measurements of the turbulence spectrum in a plasma

17 p2216 A73-34627

Investigation of the performance of a coaxial accelerator in the production of a dense high-energy plasma

19 p2467 A73-37367

Application of a Thomson mass spectrograph with an electron-optical recorder to the investigation of the mechanism of plasmoid acceleration

19 p2467 A73-37370

Influence of scattering by plasma oscillations on the spectrum of a semitransparent plasma.

20 p2597 A73-39243

Photoelectric plasma arc measurements of Si oscillator line intensities in 2500-8000 Å range, relating with transition probabilities

20 p2595 A73-39590

The interaction of a laser with matter as an intense source of UV and soft X-ray radiation - Application to X-ray cinematography

21 p2709 A73-39944

The application of high-speed photography and spectroscopy for investigations of erosive pulsed plasma streams.

21 p2744 A73-39999

Spectral discharge plasma emission analysis with controlled electrical synchronization of laser vaporized microsamples of steel and wolframite

21 p2711 A73-40302

Theory of Stark broadening of hydrogen spectral lines in a plasma

21 p2745 A73-40365

An appraisal of the mass spectrometer diagnostic technique in the study of afterglow plasmas.

21 p2702 A73-40792

Magnetic pulsation spectra in a nonisothermal plasma.

22 p2890 A73-41725

Microwave oscillations and visible emission in a cesium diode.

22 p2892 A73-42272

Measurement of arc radiation for selected spectral regions.

22 p2861 A73-42569

Level populations in plasmas - RF discharges and sonic channel.

22 p2895 A73-42994

Vacuum-UV radiation of laser-produced plasmas.

23 p3008 A73-43340

The shape of the cyclotron absorption line in a weakly ionized plasma

23 p3011 A73-43794

Some electric and spectroscopic properties of the radiofrequency plasma in a steady magnetic field.

23 p3012 A73-43831

Temperature and ion energy spectra of laser plasma produced by giant-pulse ruby laser heating metallic targets

23 p3012 A73-43849

Plasma temperature measurement by a spectroscopic technique with continuous automatic recording

24 p3115 A73-44757

Turbulent motions in an artificial plasma inhomogeneity released in the ionosphere.

24 p3088 A73-45238

Calculation of the Lyman-alpha asymmetry in a dense, partially-ionized hydrogen plasma.

24 p3116 A73-45323

Plasma decay instability nonlinear saturation spectrum in small spontaneous emission limit for comparable ion and electron temperatures from kinetic equation numerical solution

24 p3118 A73-45460

PLASMA SPRAYING

Cermet-oxide plasma jet spray coating of metal surfaces, determining thermal performance characteristics by calorimetric measurements

06 p0714 A73-18448

Synthesis of reverse osmosis membranes by plasma polymerization of allylamine.

07 p0780 A73-19169

Measurements of the emissivity of materials fabricated by powder- and plasma-metallurgy techniques

09 p1103 A73-22472

Thermal conductivity of mixed-composition plasma-sprayed coatings.

09 p1111 A73-23464

Temperature dependence of the adhesive strength and elasticity of some high-melting coatings

10 p1225 A73-24371

Effectiveness of using the energy of a plasma jet in powder coating deposition

10 p1226 A73-24689

The spray deposition of oxide-free coatings consisting of special metals with a high affinity to oxygen

11 p1372 A73-25411

Plasma sprayed boron fiber reinforced titanium oxide and Al matrix composites, discussing temperature control for particle size and SiC coating effects on strength

11 p1388 A73-25413

Investigation of the heat conductivity of aluminum oxide deposited by plasma spraying

11 p1373 A73-25731

Part manufacturing with plasma arc torch by extending plasma spray coating technology to mandrel design and machining with consideration for base materials

13 p1624 A73-28907

Dependence of some physicochemical properties of plasma-deposited aluminum oxide on sputtering conditions

15 p1881 A73-31211

Effect of base material on the formation of thin plasma coatings

15 p1881 A73-31590

The technology of plasma arc spraying.

16 p2017 A73-32698

Plasma sprayed coatings

18 p2318 A73-35882

Comparative evaluation of the wear resistance of electrolytic and plasma chromium coatings

18 p2318 A73-35883

Ferrite thick film deposition by arc plasma spraying, discussing apparatus, process and film properties after annealing

19 p2435 A73-38096

Investigation of the effective heat conductivity of plasma-sprayed alumina coatings subject to radiative heating in the temperature range from 100 to 900 °C

21 p2792 A73-41220

International Metal Spraying Conference, 7th, London, England, September 10-14, 1973, Proceedings.

22 p2879 A73-42591

Fibre-reinforced metallic and ceramic composites produced by thermal spraying.

22 p2866 A73-42592

Alloy or metal coated composite powder thermal spraying applications, discussing bonding properties, wear resistance, low friction applications and abrasibility

22 p2866 A73-42593

Reactive kinetic observations for spraying with Ni-Al powder.

22 p2879 A73-42594

PLASMA STABILITY

U MAGNETOHYDRODYNAMIC STABILITY

PLASMA TEMPERATURE

The application of Langmuir probes to the measurement of very low electron temperatures.

02 p0158 A73-11912

Effect of ion viscosity on the stability of a finite-pressure plasma.

02 p0198 A73-12104

Study of the boundary layers of a completely ionized two-temperature plasma on the nonconducting wall of an MHD channel

03 p0346 A73-13610

Averaged equations of cumulative-laser heating of two-temperature plasma in Z-pinch taking into account the nuclear fusion energy.

03 p0347 A73-13783

Measurement of temperature by recording the absolute line intensity with apparent increase of plasma optical thickness.

03 p0348 A73-14439

Induced enhancement of the plasma line in the backscatter spectrum by ionospheric heating.

04 p0445 A73-15555

Averaged equations of laser heating of two-temperature plasma in Z-pinch, the thermonuclear fusion energy being taken into consideration.

04 p0480 A73-15594

Characteristics of waveguides containing anisotropic warm plasma in the presence of transverse magnetic field.

04 p0480 A73-15600

Temperature distribution in a plasma filament in the presence of turbulent heat conduction

04 p0482 A73-15621

The influence of spatial temperature distribution and measuring configuration on line-reversal temperature.

05 p0602 A73-16563

New procedure for measuring the radial temperature distribution in inhomogeneous and unsteady plasma columns with considerable self-absorption

06 p0728 A73-17913

Heat removal in a sectioned channel of an electric arc plasmatron

06 p0731 A73-18372

Pressure, temperature, current density and potential difference fluctuations in subsonic flow of combustion products plasma, noting steadiness, ergodicity and distribution functions

06 p0732 A73-18616

Steady state dense arc plasma heating by inverse bremsstrahlung process with IR carbon dioxide laser, calculating maximum attainable temperature

07 p0857 A73-19531

Limiting factors of plasma temperature measurement by spectral line reversal method

07 p0859 A73-20152

Temperature determination of rare gas plasmas seeded with alkali, considering oscillator forces of K excited states in He plasma

08 p0990 A73-20649

X-ray temperature measurements of laser produced plasmas in large radiation fields.

09 p1125 A73-22024

Ogo 6 measurements of supercooled plasma in the equatorial exosphere.

09 p1074 A73-22066

Ion cyclotron instability in current-carrying plasmas with anisotropic temperatures.

09 p1127 A73-22284

Relaxation in a two-temperature plasma with directed motion of electrons

09 p1127 A73-22601

Calculation of the boundary layers of a fully ionized two-temperature plasma for given temperatures of components at the electrodes

09 p1127 A73-22605

Measurement of the electron temperature of a quasi-stationary pulsed glow-discharge plasma in highly overcharged gaps

09 p1129 A73-22663

Effects of plasma temperature on the frequency shift in resonant cavities.

09 p1131 A73-22907

Determination of the electron temperature of a plasma by sounding with an extraordinary wave along a magnetic field

10 p1253 A73-23504

Temperature distribution in a plasma with turbulent thermal conductivity.

10 p1255 A73-24211

Measurement of plasmoid energy in a time-variable magnetic field

10 p1258 A73-24881

IR spectrum line reversal for measurement of CO and gas mixture laser plasma vibrational temperatures as function of discharge current and gas pressure

10 p1230 A73-24884

The transport coefficients and material functions of a plasma with different electron and gas temperatures.

11 p1404 A73-25343

Application of the collisionless absorption of an extraordinary wave to the determination of plasma electron temperatures

12 p1528 A73-27302

Influence of a transverse electron-temperature gradient on the plasma flow in an axisymmetric magnetic field

12 p1528 A73-27305

Electrostatic waves in warm random plasmas.

14 p1779 A73-29708

Collisionless magnetized unstable plasma two dimensional adiabatic compression, calculating gamma from temperature distributions

14 p1779 A73-29984

Diffusion of plasma density and temperature perturbations in a magnetic field

14 p1749 A73-30264

Hypersonic wind tunnel MHD accelerator design and operating principles, discussing flux density, I-V characteristics, cooling losses, plasma temperature, gas pressure and velocity, etc

14 p1743 A73-30295

Temperature distribution and ionization characteristics of sodium and rubidium chlorides, silicon dioxide and atomized carbon jets generated by plasmatron

14 p1781 A73-30464

Observation of stable, high Mach number collisionless electrostatic shocks.

15 p1916 A73-31079

Contact methods of measuring temperatures in low-temperature plasma jets from stationary sources

15 p1876 A73-31871

Measurement of density and temperature of a hydrogen plasma using an argon laser.

15 p1920 A73-32257

Intensity of thermal fluctuations of plasma flute instabilities in open confinement systems in the presence of a feedback system 15 p1920 A73-32307

Influence of diffusion on plasma parameters - A qualitative estimate and a physical interpretation. 16 p2040 A73-32941

Heat removal in the sectionalized channel of an electrode-type plasmatron. 16 p2042 A73-33597

Heat conductivity measurements for a hydrogen plasma in a stabilized electric arc 17 p2214 A73-34129

Applicability of an adiabatic compression method to the study of a cesium plasma 17 p2214 A73-34130

Determination of electron temperature of a plasma by probing the extraordinary wave along a magnetic field. 17 p2217 A73-35184

X-ray emission in laser-produced plasmas. 20 p2595 A73-38890

Effect of an isotropic nonequilibrium plasma on electron temperature measurements. 20 p2552 A73-38947

Experimental investigation of the characteristics of a nonequilibrium MHD generator 20 p2511 A73-39618

Electron temperature and ionization state in laser produced plasmas. 21 p2745 A73-40470

Inhomogeneous structure of plasma near sun due to drift, slipping and anisotropic temperature distribution instabilities, noting association with radio astronomy observed fine structure 21 p2767 A73-40537

Experimental study of conductivity, velocity, and temperature distributions in a submerged jet of low-temperature plasma 21 p2747 A73-40575

Rotating cylinder model for plasma gradient-temperature instability in gravitational field, showing heat convection due to Coriolis-caused particle drift 21 p2769 A73-40730

Studies of collisional preionization in large pinch vessels. 21 p2748 A73-40927

Theory of a steady-state nonisothermal positive column in a magnetic field. 21 p2748 A73-40954

Measurement of plasmoid energy in a time-varying magnetic field. 21 p2749 A73-41656

IR spectrum line reversal for measurement of CO and gas mixture laser plasma vibrational temperatures as function of discharge current and gas pressure 21 p2717 A73-41659

Effects of interhemisphere transport on plasma temperatures at low latitudes. 22 p2844 A73-41919

Chromospheric hydrogen and helium spectral lines investigation in solar flares determining plasma and ionization temperatures, energy spectra and electron density 22 p2903 A73-42066

Solar corona plasma temperature estimation from ground observations based on ionization theory, line width, radio and radar measurements and hydrostatic equilibrium assumption 22 p2906 A73-42067

Shielding of moving test particles in warm, isotropic plasma. 22 p2893 A73-42392

Electrostatic waves with frequencies exceeding the gyrofrequency in the magnetosphere. 22 p2851 A73-42933

Temperature and ion energy spectra of laser plasma produced by giant-pulse ruby laser heating metallic targets 23 p3012 A73-43849

Relaxation of longitudinal and transverse temperatures in a plasma with directional motion of electrons 23 p3014 A73-44336

Direct-display plasma density and temperature meter by the use of Langmuir probe. 23 p3015 A73-44367

Thermal flute perturbations in an open plasma device with feedback. 24 p3114 A73-44615

Plasma temperature measurement by a spectroscopic technique with continuous automatic recording 24 p3115 A73-44757

X-ray flare plasma temperature - A comment on a paper by Deshpande and Tandon. 24 p3124 A73-45047

Vela 3 proton data analysis for compressions and rarefactions effects on solar wind density, temperature and velocity behavior 24 p3125 A73-45106

MilliHertz plasma oscillations associated with strong gradients in density and temperature 24 p3087 A73-45139

PLASMA TURBULENCE

Transport phenomena in turbulent plasma with electromagnetic waves. 01 p0081 A73-10117

Book - An introduction to the theory of plasma turbulence. 01 p0081 A73-10124

Discussion of radiative-transfer methods applied to electromagnetic reflection from turbulent plasma. 01 p0081 A73-10196

Theory of turbulent heating of an isothermal plasma with a transverse current. 01 p0083 A73-10456

Life-time of ion waves in unstable and turbulent plasmas. 01 p0084 A73-10463

Onset of turbulence in the interaction between a 'monoenergetic' beam and a plasma 01 p0086 A73-11285

Sawtooth, solitary, and turbulent waves in a weakly ionized plasma. 02 p0196 A73-12058

Spectroscopic investigation of turbulent plasma parameters. 03 p0347 A73-14095

A mechanism of steady-turbulence development in a plasma 04 p0477 A73-14876

Electron-ion density fluctuations in turbulent weakly ionized Ar plasma, comparing experimental results with theory based on quasi-static formulation of Boltzmann equation 04 p0479 A73-15192

Turbulent wave field growth rate and saturation amplitude for nonresonant instability in weak cold beam plasma system, using Dupree plasma turbulence theory 04 p0479 A73-15193

Stationary turbulence of a parametrically unstable plasma. 04 p0480 A73-15474

Ion sound turbulence in dense plasma within magnetic fields, representing global equilibrium spectrum 04 p0480 A73-15563

Helicon /whistler/ turbulence spectra in collisionless plasma, noting ion scattering relation to self trapping and concentration along magnetic field with Landau absorption decay 04 p0480 A73-15564

Turbulent plasma 'piles' in the nuclei of galaxies. 04 p0504 A73-16022

Ionospheric propagation effects on riometer recorded cosmic radio emission spectra, noting temporal and frequency spectra dependence on ionospheric plasma turbulence scale 05 p0573 A73-16266

Radiative modes of a weakly ionized, collision-dominated, turbulent plasma. 05 p0624 A73-17309

Mechanism of motion of inhomogeneities in a nonequilibrium plasma in a magnetic field. 06 p0726 A73-17401

Physical principles in incompressible fluid and plasma turbulence comparison, noting quasi-linear approximation for nonlinear particle diffusion in turbulent oscillations 06 p0728 A73-17924

Ion-acoustic oscillations effect on turbulent plasma electric conductivity within weak external electric field 06 p0729 A73-17973

Scattering of electromagnetic waves from a turbulent plasma slab. 06 p0729 A73-18120

Conservation of quasiparticles in weakly turbulent plasmas. 06 p0730 A73-18273

Steady-state charged and neutral particle densities in a bounded turbulent high-temperature plasma. 06 p0732 A73-18607

Propagation of a nonlinear wave in a weakly turbulent plasma 07 p0854 A73-19276

Turbulence spectra of collisionless magnetized plasma produced in high voltage theta pinch, considering initial magnetic field orientation and instability theories tests 07 p0857 A73-19527

Wave propagation in a stratified turbulent magnetized plasma. II. 07 p0858 A73-19534

Electrostatic turbulence at colliding plasma streams as the source of ion heating in the solar wind. 08 p0997 A73-20886

Structure of the current front in an unsteady plasma accelerator, and turbulent acceleration of the ions. I 09 p1124 A73-21881

Structure of the current front in an unsteady plasma accelerator, and turbulent acceleration of the ions. II 09 p1124 A73-21882

Structure of a collisionless boundary layer and the turbulent braking of ions 09 p1127 A73-22607

Wave-wave interactions in turbulent plasma and ion sound turbulence enhancement of three wave interaction processes, considering plasma heating experiments 09 p1131 A73-22901

Anomalous nonlinear dissipation of high-frequency radio waves in a plasma 09 p1053 A73-23330

Influence of ionizational turbulence on the operation of an MHD generator with nonequilibrium plasma 10 p1253 A73-23502

Electrostatic turbulence and ion thermalization in modified Penning discharge, investigating ion heating processes 10 p1251 A73-24259

Electron-cyclotron drift instability in high-beta plasmas, developing nonlinear theory based on wave kinetic equation for weak turbulence 10 p1255 A73-24263

Strong plasma turbulence at helicon frequencies 10 p1257 A73-24757

Turbulent plasma dynamo mechanisms of magnetic field origin in astrophysics, noting Steenbeck and Parker theories 10 p1285 A73-24942

Plasma low density regions caused by Langmuir turbulence, discussing energy dissipation of long wave oscillations and wave collapse 11 p1406 A73-26185

On the evolution of turbulent magnetic fields in a collision dominated plasma. 11 p1406 A73-26559

Braking of electron beams in a plasma with a high level of Langmuir turbulence 12 p1527 A73-26956

Optimization of the power of a Faraday-type MHD-generator operating with a nonequilibrium plasma 12 p1460 A73-27320

Propagation of a nonlinear wave in a weakly turbulent plasma. 13 p1665 A73-28676

Threshold of appearance of anomalous resistance for field-aligned currents in the magnetosphere. 13 p1608 A73-28726

Theory of turbulent plasma heating by anomalous absorption of magnetosonic waves. 14 p1777 A73-29683

Solar wind velocity fluctuations with heliocentric distance beyond one AU via nonlinear fluid dynamic equations numerical solution, considering interplanetary plasma turbulence effects 14 p1786 A73-29956

Observation of a current-driven plasma instability at the outer zone-plasma sheet boundary. 14 p1747 A73-29966

Ion acoustic wave scattering effects on stochastic ion heating in turbulent plasma 14 p1780 A73-30340

Universality of the power spectra of relativistic electrons generated in a turbulent plasma 14 p1782 A73-30808

Transport effects in a turbulent flowing plasma - The moment relations. 15 p1916 A73-31082

Russian book - Plasma astrophysics. 15 p1936 A73-31579

Stochastic heating of a plasma during development of a Langmuir turbulence instability 15 p1918 A73-31705

Kinetics of stimulated scattering of Langmuir waves by plasma ions 15 p1919 A73-31708

Solar surface and atmosphere activity due to magnetic field production, transport and dissipation, discussing flares, sunspots, corona, dynamo, plasma turbulence and prominences 15 p1937 A73-31848

Ion-acoustic turbulence as MHD wave damping mechanism in weakly turbulent magnetosphere plasma at high and low frequencies 15 p1919 A73-31893

On electron trapping in ion sound waves in turbulent plasma. 16 p2040 A73-32800

Lagrangian description of phase space flow - Turbulent heating. 16 p2041 A73-33322

Theory and computer simulation of whistler turbulence and velocity space diffusion in the magnetospheric plasma. 16 p2003 A73-33439

Structure of the current front and turbulent acceleration of ions in a pulsed plasma accelerator. I. 17 p2215 A73-34305

Structure of current front and turbulent acceleration of ions in a plasma accelerator. II. 17 p2215 A73-34306

Theory of optical polarization measurements of the turbulence spectrum in a plasma 17 p2216 A73-34627

Effect of ionization turbulence on the operation of an MHD generator operating with a nonequilibrium plasma. 17 p2217 A73-35182

PLASMA WAVES

Current distribution at the zero line of the magnetic field and the turbulent resistance of a plasma 18 p2339 A73-36550

Interaction between an ion beam and a turbulent low-pressure theta-pinch plasma 18 p2340 A73-36667

Weakly ionized continuum plasma turbulent shear flow and transport properties calculation, noting ratio of Debye shielding length to local integral scale 19 p2463 A73-37153

Rarefied collisionless plasma turbulence and dissipation process due to instability, examining magnetic field effects on shock wave front nature 19 p2464 A73-37154

Electromagnetic interactions with turbulent plasmas. 19 p2465 A73-37167

High-frequency plasma turbulence in outer-space 19 p2481 A73-37341

Deceleration of electron beams in a plasma with a high level of Langmuir turbulence. 19 p2469 A73-38133

Hydrogen plasma compression producing collisionless shock waves, measuring turbulence intensity as function of cut-off angle and anisotropy 20 p2596 A73-38966

Modification of weak turbulence theory due to perturbed orbit effects. II - Nonlinear Landau damping of electron plasma waves. 20 p2598 A73-39302

Shielding of a moving test charge in a turbulent plasma. 20 p2599 A73-39722

Electron-acoustic and drift instabilities in a finite-pressure plasma with a transverse current 21 p2745 A73-40364

Annual review of astronomy and astrophysics. Volume 11. 21 p2771 A73-41234

Turbulence and scintillations in the interplanetary plasma. 21 p2748 A73-41235

Trapped-particle scattering by electrostatic turbulence in toroidal plasmas. 21 p2749 A73-41675

Parametric instabilities and turbulent heating of a plasma in the field of a fast magneto-acoustic wave. 21 p2750 A73-41677

Parametric instabilities of weakly turbulent plasma, determining collision frequencies characterizing high frequency electric field energy absorption 21 p2750 A73-41681

Propagation of electromagnetic waves through turbulent plasma using transport theory. 22 p2824 A73-41860

Experimental investigation of current-driven ion wave turbulence in plasma. 22 p2890 A73-42224

German monograph - Model of a parallel shock wave with turbulent dissipation in a hot plasma. 22 p2895 A73-42718

Collisionless shock wave propagation parallel to magnetic field for large plasma/magnetic pressure ratio, discussing shock structure in developing turbulence 22 p2851 A73-42932

Appearance of turbulence during the interaction of a 'monoenergetic' beam with a plasma. 23 p3009 A73-43506

Investigation of a turbulent plasma in a reflex discharge with the aid of a double electric probe 23 p3011 A73-43668

Measurement of turbulent HF fields in a high-current rectilinear gas discharge from the intensity of forbidden HeI lines 23 p3011 A73-43669

Theta-pinch instability of plasma beam, relating plasma oscillation frequency to microwave emission and electromagnetic wave scattering 23 p3011 A73-43710

Spectroscopic polarization analysis of turbulent plasma noise produced by the annihilation of opposite magnetic fields 23 p3012 A73-44016

Physical principles in incompressible fluid and plasma turbulence comparison, noting quasi-linear approximation for nonlinear particle diffusion in turbulent oscillations 23 p3013 A73-44326

Heos I plasma and magnetic field experiments during bow shock crossings for turbulent bow structure, discussing proton velocity distribution 24 p3125 A73-45111

Turbulent motions in an artificial plasma inhomogeneity released in the ionosphere. 24 p3088 A73-45238

Spectroscopic measurements of plasma temperatures and density at X type magnetic neutral points, suggesting ion acoustic instability role in turbulent conductivity 24 p3118 A73-45461

Strong plasma turbulence theory, discussing convergence of perturbation series formed with renormalized particle propagator 24 p3118 A73-45462

Current driven ion acoustic plasma instability based on ion orbit perturbation by turbulent waves, calculating angular spectrum for comparison with computerized simulation 24 p3118 A73-45463

PLASMA WAVES

NT ELECTROSTATIC WAVES

Theoretical and experimental study of the H.F. current associated with a plasma wave. 01 p0081 A73-10118

A method for nonlinear plasma wave kinetics. 01 p0082 A73-10419

Anomalous absorption of electromagnetic radiation at double the plasma frequency. 01 p0082 A73-10425

Capture of plasma electrons by the field of a wave that is excited by an ion beam 01 p0084 A73-10632

Energy balance in the current sheath of a solar flare and the acceleration of cosmic rays by plasma waves 01 p0092 A73-10936

Onset of turbulence in the interaction between a 'monoenergetic' beam and a plasma 01 p0086 A73-11285

Quasi-linear theory of plasma waves resonant diffusion, proceeding from Vlasov equation to derive frequency, wavenumber and velocity by quantum methods 01 p0086 A73-11492

On the stability of nonlinear cold plasma waves. 01 p0087 A73-11497

Ionospheric effects on the transmission of ultralow-frequency plasma waves. 02 p0155 A73-11520

Momentum formulae derived for quasi-mono-chromatic wave packets of transverse and longitudinal waves in plasma without magnetic field 02 p0195 A73-11522

Sawtooth, solitary, and turbulent waves in a weakly ionized plasma. 02 p0196 A73-12058

Oblique shock waves heating of high beta plasma ions, suggesting Landau damping of wave energy 02 p0197 A73-12059

Third order collisionless electron plasma echo signal wavelength and rise and fall rate about central position, comparing experiment with Vlasov equation theory 02 p0197 A73-12064

Free streaming electrons effect on spatial ballistic electron plasma wave echoes response, calculating echo electric fields and electron distribution function 02 p0197 A73-12065

Nonrelativistic collisionless plasma ion acoustic waves modulation by hf electromagnetic oscillation, calculating wave complex frequency [AD-753362] 02 p0197 A73-12069

Nonlinear waves in a multicomponent plasma with weak dissipation. 02 p0198 A73-12103

Spectral characteristics of nonlinear plasma oscillations near collapse limit, discussing wave interaction, energy exchange and velocity corrections 02 p0198 A73-12486

Collisionless plasma compression shock waves thermodynamics, noting entropy variations along shock adiabat under plasma heating in magnetic field 02 p0198 A73-12552

Parametric instability and anomalous heating due to electromagnetic waves in plasma. 03 p0345 A73-13060

Shock wave and isentropic compression/expansion in plasma with anomalous thermodynamic properties due to strong particle interactions, discussing phase transitions types 03 p0346 A73-13190

Magnetospheric observations inOGO-5 plasma wave experiment, emphasizing electrostatic wave particles interaction with plasma 03 p0303 A73-13883

Parametric instability of a spatially modulated plasma. 03 p0347 A73-14089

Surface drift waves in a weakly ionized plasma. 03 p0347 A73-14090

Instability of a weakly ionized plasma at wavelengths of the order of the Debye radius. 03 p0347 A73-14092

Spatial plasma echoes of ion acoustic waves in low pressure He and Ne discharges in anode direction 03 p0348 A73-14622

Propagation of ion acoustic waves in a weakly ionized plasma 03 p0348 A73-14625

Multiple soliton excitation by ion acoustic square pulse wave in double plasma device in frame of Korteweg-de Vries equation 04 p0477 A73-14771

Nonlinear monochromatic Langmuir standing waves in a plasma 04 p0478 A73-15033

LF spectrum of plasma oscillations from amplitude modulation of plasma SHF radiation, noting Langmuir and magnetoacoustic waves interaction 04 p0478 A73-15034

Spatial echo and nonlinear interaction of waves in a plasma 04 p0478 A73-15035

Comparison of wave propagation in the stationary and moving plasma - Motion and wave propagation along the magnetic field. 04 p0479 A73-15190

Instability of a large-amplitude plasma wave due to inverted trapped particle population. 04 p0480 A73-15194

Short-life mode of electrostatic electron cyclotron harmonic waves. 04 p0477 A73-15196

The importance of wave-particle interactions in the magnetosphere. 04 p0492 A73-15339

Influence of carrier drift on the propagation of electromagnetic wave in a solid-state plasma. 04 p0480 A73-15473

Morphology and interpretation of magnetospheric plasma waves at conjugate points during December solstice. 04 p0443 A73-15535

Stability of a plasma with inequilibrium ions with respect to the generation of magneto-sonic waves 04 p0481 A73-15603

Excitation of electromagnetic waves in a plasma with the aid of longitudinal electric fields 04 p0481 A73-15606

One dimensional analysis of saturation spectral lines for energy transfer in plasma waves interaction, noting Landau damping effect on parametric instability 04 p0482 A73-15650

The dispersion diagram of the plasma waves on the plasma branch in a beam-created plasma. 04 p0482 A73-15949

Landau attenuation in a plasma excited by a monochromatic electron beam 05 p0601 A73-16394

Multicomponent plasmas with cations or anions in presence of Coriolis force, determining crossover frequencies for polarization reversal and mode coupling of waves 05 p0603 A73-16594

Possibility of radar observation of nonlinear wave interaction in ionospheric plasma 05 p0570 A73-17023

Monochromatic plasma wave instability due to induced scattering on thermal plasma electrons and ions with and without magnetic field 05 p0604 A73-17361

Cosmic-ray evolution due to interactions with self-excited plasma waves. 05 p0612 A73-17385

Electromagnetic radiation caused by the two-stream instability in a bounded plasma. 06 p0726 A73-17416

Evolutionary aspects of shock waves in the Chew, Goldberg, and Low approximation 06 p0727 A73-17471

Book - Geophysics 3. Part 4. 06 p0688 A73-17501

Magnetospheric plasma waves propagation effects on rapid geomagnetic field variations, noting magnetic pulsations and ionospheric propagation 06 p0747 A73-17504

Possibility of observing the decay interaction of plasma waves in top-side sounding experiments 06 p0689 A73-17551

Nonequilibrium plasma wave scattering cross section dependence on energy bands shape and field orientation in semiconductors 06 p0735 A73-17975

Kinetic theory of longitudinal wave dispersion in nonuniform plasma layer in HF electromagnetic field, noting plasma instability for electron parametric resonance 06 p0729 A73-18109

Damping of an ion acoustic wave in a weakly ionized plasma 06 p0730 A73-18460

A specific feature of surface waves at the boundary of inhomogeneous plasma. 06 p0730 A73-18466

Propagation of a nonlinear wave in a weakly turbulent plasma 07 p0854 A73-19276

Dispersion equations for E and H waves in multilayer plasma, defining amplitudes correlation for incident, transmitted and reflected waves 07 p0855 A73-19278

Instability of surface ion-acoustic waves of finite amplitude 07 p0855 A73-19291

Investigation of the temperature dependence of the anisotropy parameter K in n-Si and n-Ge by using magneto-plasma waves 07 p0861 A73-19327

Nonlinear wave modulation in cold magnetized plasmas. 07 p0855 A73-19338

Wave pattern of three dimensional hydromagnetic perturbations produced by harmonic magnetic dipole in anisotropic plasma 07 p0816 A73-19461

- Wave propagation in a stratified turbulent magnetized plasma. II. 07 p0858 A73-19534
- Collision absorption of a rapid hydromagnetic wave in a plasma of two kinds of ions - Experiment 07 p0859 A73-20149
- Parametric excitation of circularly polarized and Langmuir waves in a magnetized plasma. 07 p0859 A73-20197
- Trapped electrons instability in Tokamak configuration, calculating plasma wave propagation modes via Fokker-Planck equation 08 p0991 A73-20815
- Lower-hybrid-resonance heating of a plasma in a parallel-plate waveguide. 08 p0991 A73-20816
- Ion cyclotron wave generation in a two-ion plasma. 08 p0991 A73-20817
- Electromagnetic effects on electrostatic modes in a magnetized plasma. 08 p0991 A73-20820
- Possible explanation for nonthermal radio noise from binary stars. 08 p1003 A73-20883
- Landau damping of type III solar radio bursts. 08 p0997 A73-20902
- Buildup of a narrow plasma channel by microwaves. 08 p0992 A73-20954
- Simultaneous suppression of an electron plasma wave and an ion acoustic wave by beam modulation. 08 p0992 A73-21006
- Focusing of EM waves in plasmas by inhomogeneous magnetic fields. 08 p0993 A73-21205
- Quasi-static ion acoustic surface wave propagation along warm plasma layer-dielectric boundary 08 p0993 A73-21460
- Book - Theory of ionospheric waves. 08 p0962 A73-21838
- Parametric excitation of surface waves in a non-homogeneous magnetized plasma 09 p1124 A73-21892
- Waves in magnetoactive plasma in the presence of a distinct transverse ion velocity 09 p1125 A73-21904
- Propagation of backward surface wave along an annular plasma guide with azimuthal electron density variation. 09 p1125 A73-21930
- Collisional effect on the saturation amplitude of nonlinearly excited plasma waves. 09 p1125 A73-22023
- Momentum method extension to thermal conduction laser heating of nonhomogeneous plasma, obtaining closed form solutions for plane waves 09 p1126 A73-22171
- Propagation of electronic longitudinal modes in a non-Maxwellian plasma. 09 p1126 A73-22278
- Effects of collisions and gyroviscosity on gravitational instability in a two-component plasma. 09 p1127 A73-22286
- Ultrarelativistic pulsar plasmas with one dimensional distribution functions in strong magnetic fields, considering dispersion ratios of plasma waves along magnetic lines 09 p1145 A73-22294
- Wave number space analysis of propagation in nonuniform media. 09 p1120 A73-22474
- Incident radio wave resonance effect on stationary electric and magnetic fields and standing magnetoplasma wave excitation in Bi plates 09 p1127 A73-22604
- Mathematical model for nonlinear interactions between HF waves and LF acoustic waves applied to electromagnetic wave stability in plasmas and dielectrics 09 p1128 A73-22614
- Cyclotron heating of plasmas with finite amplitude waves. 09 p1128 A73-22630
- Fast wave propagation and damping at the second harmonic of the ion cyclotron frequency. 09 p1128 A73-22631
- Operating features of an ion-cyclotron-wave plasma apparatus running in the RF-sustained mode. 09 p1128 A73-22632
- Coupled waves and particle scattering processes in ferromagnetic semiconductors and metals 09 p1133 A73-22677
- Influence of dispersion on the nonlinear evolution of quasi-monochromatic spiral waves in a magnetoactive plasma 09 p1130 A73-22708
- Energy balance in the current sheet of a solar flare, and the acceleration of cosmic rays by plasma waves. 09 p1138 A73-22731
- Drift-like instability in density modulated plasmas in a static magnetic field. 09 p1131 A73-22904
- Propagation of surface waves and instability wave growth in an ion beam-plasma system. 09 p1131 A73-22906
- Damping of plasma waves in the lower hybrid frequency range. 09 p1131 A73-22908
- Conductivity tensor and dispersion equation for collisional magnetoactive plasma. 09 p1131 A73-22922
- Collisional absorption of the fast hydromagnetic wave in a plasma with two ion species - Theory 09 p1131 A73-23029
- The energy-momentum tensor for an electromagnetic wave in a plasma. 10 p1254 A73-24115
- Stability of a plasma with nonequilibrium ions with respect to magnetosonic waves. 10 p1254 A73-24193
- Excitation of electromagnetic waves in a plasma by longitudinal electric fields. 10 p1254 A73-24196
- Electromagnetic instability for plasma waves propagating perpendicular to uniform magnetic field in counterstreaming electron-ion plasmas based on linearized Vlasov-Maxwell equations 10 p1255 A73-24262
- Computer simulation of two dimensional plasma diffusion via wave interactions descriptions by nonlinear differential equations, considering electric field and particle velocity correlations 10 p1255 A73-24266
- Electromagnetic wave instability characteristics during propagation oblique to electron stream in cold electron-ion plasma 10 p1255 A73-24268
- Negative energy mode loss to positive energy mode in positive-negative energy wave interactions within magnetized plasma, considering ion acoustic waves 11 p1402 A73-25123
- Harmonic structure of flare related type 5 burst, suggesting plasma wave emission 11 p1412 A73-25856
- Transitions between Zeeman atomic sublevels in a medium 11 p1405 A73-26155
- Contribution to the nonlinear theory of kinetic instability of an electron beam in plasma. 11 p1405 A73-26183
- Temperature-waves in connection with drift type instabilities in a Q-plasma. 11 p1406 A73-26558
- Plasma research in space and in the laboratory. 12 p1526 A73-26849
- Cosmic dilute collisionless plasma physical properties, discussing plasma wave turbulence characteristics, particle acceleration, relativistic plasmas, synchrotron emission, pulsars and galactic nuclei 12 p1537 A73-26850
- Czechoslovak Seminar on Plasma Physics, 6th, Liblice, Czechoslovakia, May 10-12, 1972, Research Report. 12 p1528 A73-27430
- [IPPCZ-167] Excitation and damping-mechanism of waves and resonances in bounded magnetoactive media. 12 p1528 A73-27431
- [IPPCZ-167] The theoretical situation with the investigations of parametric instabilities in gaseous plasmas. 12 p1528 A73-27432
- [IPPCZ-167] On the momentum of quasi-monochromatic waves in a plasma. 12 p1529 A73-27435
- [IPPCZ-167] Nonlinear helical waves formation due to Kelvin-Helmholtz instability in type I comet tail modeled as plasma cylinder immersed in solar wind 12 p1542 A73-27609
- Nonlinear ion sound waves in a plasma with three-dimensional random inhomogeneities 12 p1530 A73-27980
- Nonlinear theory of parametric wave instability in a plasma 12 p1530 A73-27981
- Monoenergetic particle beam instabilities in homogeneous plasma due to secondary emission wave interactions 13 p1664 A73-28289
- Propagation of a nonlinear wave in a weakly turbulent plasma. 13 p1665 A73-28676
- Dispersion equations for E and H waves in multilayer plasma, defining amplitudes correlation for incident, transmitted and reflected waves 13 p1665 A73-28678
- Instability of ion-acoustic surface waves of finite amplitude. 13 p1665 A73-28691
- Investigation of the absorption and emission of electron-beam-induced waves in an inhomogeneous magnetoactive plasma 13 p1666 A73-28958
- Shock wave large particle model of ion density discontinuity decay in nonisothermal plasma, assuming high electron temperature and Boltzmann distribution 13 p1667 A73-29171
- Receiving characteristics of antennas in an isotropic compressible plasma. 13 p1594 A73-29230
- German book on plasma physics covering plasma containment, magnetohydrostatics, gravitational effects, plasma pinch, toroidal plasmas, plasma waves and MHD instabilities 13 p1667 A73-29288
- Wave periodic structure solution instability and unstable oscillation growth rates for nonlinear drift waves and solitons in collisionless plasma 14 p1778 A73-29692
- Study of two types of turnstile aerial immersed in a warm plasma. 14 p1731 A73-29712
- Ionospheric plasma waves instabilities induced by energetic electron beam fired perpendicular to magnetic field 14 p1747 A73-29967
- Existence conditions for magnetoactive plasma longitudinal waves with phase velocity near light velocity, investigating increments during synchrotron instability due to relativistic particles 14 p1780 A73-30337
- Quasi-linear theory of a parametrically unstable magnetoactive plasma 14 p1782 A73-30806
- Q switched ruby laser optical diagnostic system for plasma shock waves and plasmoid observation, noting schlieren photographs of exploding wire experiments 14 p1782 A73-30925
- The effect of temperature perturbations on ion-acoustic and drift waves in a weakly collisional plasma. 15 p1916 A73-31087
- Nonstationary theory of decay instability in a weakly inhomogeneous plasma 15 p1918 A73-31704
- Electromagnetic instability in a counterstreaming plasma. 15 p1919 A73-31928
- Electromagnetic wave propagation in p-type Ge and Si semiconductor plasmas, studying dispersion, cyclotron resonance, and kinetic equations 15 p1925 A73-32214
- Structure of the current front of an electron-acoustic wave in a plasma 15 p1920 A73-32301
- Formation of fast electrons in a plasma under the influence of SHF power near harmonics of the electron cyclotron frequency 15 p1920 A73-32309
- Nonlinear ion-acoustic and electron-acoustic waves of a plasma in a magnetic field 15 p1921 A73-32324
- Hydrodynamic theory of high-amplitude ionization waves 15 p1921 A73-32326
- Waves in a magnetoplasma with an isolated transverse ion velocity component. 15 p1922 A73-32629
- Possibility of observing the decay interaction of plasma waves in topside sounding experiments. 16 p2002 A73-32775
- Satellite waves effects on dynamic behavior of resonant wave-triplet coupling from comparison with isolated triplet in explosive and decay instabilities 16 p2041 A73-33334
- Ion cyclotron waves observed in the polar cusp. 16 p2003 A73-33437
- Satellite studies of magnetospheric substorms on August 15, 1968. VIII - Ogo 5 plasma wave observations. 16 p2004 A73-33456
- Nonlinear frequency shift and damping stabilization mechanisms of unstable plasma waves in hot beam-cold plasma system 16 p2043 A73-34058
- Instability of plasma waves with nonlinear Landau effect. 17 p2215 A73-34296
- Parametric excitation of surface waves in an inhomogeneous magnetized plasma. 17 p2215 A73-34315
- Transformation of high-frequency waves and vanishing of low-frequency instabilities in a radially-inhomogeneous beam-plasma discharge. 17 p2217 A73-35525
- Nonlinear wave interaction and fluctuations in plasma. 17 p2217 A73-35818
- On the explosive instabilities of waves in plasmas with special regard to dissipation and phase effects. 17 p2218 A73-35820
- Five wave interaction - A possibility for enhancement of optical or microwave radiation by nonlinear coupling to explosively unstable plasma waves. 17 p2218 A73-35821
- On the stabilization of explosive instabilities by nonlinear frequency shifts. 17 p2218 A73-35822
- Transformation, transmission, and reflection of plasma waves in the presence of a tangential velocity discontinuity 18 p2339 A73-36551
- Permittivity of a plasma with transverse nonazimuthal fluxes 18 p2339 A73-36552

Wave transformation due to oblique incidence on the boundary of a magnetoactive plasma 18 p2289 A73-36553

Nonlinear transformation of an electromagnetic wave at the boundary of a magnetoactive plasma 18 p2289 A73-36562

Experimental investigation of a fast ion-acoustic wave in a multicomponent plasma 18 p2339 A73-36564

Cold collisionless plasma flow along magnetic field, deriving quasi-shock wave characteristics from Vlasov-Maxwell equations 19 p2463 A73-37152

High-frequency plasma turbulence in outer-space 19 p2481 A73-37341

Wavenumber space analysis of oscillations in weakly non-uniform magnetoplasmas. 19 p2468 A73-37442

Quenching of the beam-plasma instability by mode mixing at a density discontinuity. 19 p2469 A73-37859

Influence of thermal effects and particle capture by plasma waves on the dispersion characteristics of nonlinear waves 19 p2469 A73-37960

Interaction of parametrically coupled waves in nonequilibrium media /Survey/ 19 p2406 A73-38326

Emission of longitudinal waves from a charge in an external high-frequency electric field in a magnetoactive plasma 19 p2470 A73-38331

Parametric decay of obliquely incident electromagnetic waves into ion acoustic and electron plasma waves in vicinity of resonance 20 p2595 A73-38874

Low-frequency flute instabilities of a bounded plasma column. 20 p2595 A73-38889

Plasma wave observations near the plasmopause with the S3-A satellite. 20 p2552 A73-38956

Magnetospheric implications of the nonlinear whistler instability obtained in a computer experiment. 20 p2553 A73-38961

Non-turbulent electric fields in soliton and shock-like structures in magnetized plasmas. 20 p2596 A73-38967

The theoretical situation with the investigations of parametric instabilities in gaseous plasmas. 20 p2597 A73-39195

Unsteady shock waves in a rarefied plasma 20 p2597 A73-39277

Excitation of transverse extraordinary mode in an inhomogeneous magnetoplasma. 20 p2598 A73-39300

Electron plasma wave shocks in a collisionless plasma. 20 p2598 A73-39301

Modification of weak turbulence theory due to perturbed orbit effects. II - Nonlinear Landau damping of electron plasma waves. 20 p2598 A73-39302

The role of Korteweg-de Vries equation in plasma physics. 20 p2599 A73-39625

High-speed camera study of the shock wave propagation. 21 p2697 A73-39993

Rocket experiments on nonlinear wave-wave interaction in the ionospheric plasma. 21 p2685 A73-40823

Refraction of plasma waves in the ionosphere /in connection with topside sounding of the ionosphere/ 21 p2691 A73-41507

Monoenergetic particle beam bunching instabilities in homogeneous plasma due to secondary emission wave interactions 22 p2890 A73-41813

Instabilities of drift magnetosonic waves due to the magnetic drift resonance. 22 p2894 A73-42395

Characteristics of the fast and slow magnetosonic waves in layered plasmas. 22 p2894 A73-42397

Large amplitude electromagnetic waves in hot relativistic plasmas. 22 p2895 A73-43024

Appearance of turbulence during the interaction of a 'monoenergetic' beam with a plasma. 23 p3009 A73-43506

Backward ionization waves linear evolution to nonlinear saturated state from gaseous plasma self oscillation instability viewpoint, noting electron temperature and density increase 23 p3011 A73-43829

Nonlinear interaction of high-amplitude Langmuir waves in a collisionless plasma 23 p3012 A73-44015

Hydrodynamic equations for nonlinear stability of plasma ionization wave interactions in absence of magnetic field 23 p3012 A73-44040

Non-linear propagation of VLF waves in a magnetoplasma including the effect of ions. 23 p3012 A73-44143

Absorption and emission of waves generated by an electron beam in an inhomogeneous magnetoplasma. 23 p3013 A73-44310

Kinetic theory of longitudinal wave dispersion in nonuniform plasma layer in HF electromagnetic field, noting plasma instability for electron parametric resonance 24 p3114 A73-44498

Structure of the current front of an electron-acoustic wave in a plasma. 24 p3114 A73-44609

Production of fast plasma electrons by microwave power at harmonics of the electron cyclotron frequency. 24 p3114 A73-44617

A theory of the origin of the split pair burst emission from the solar corona. 24 p3123 A73-44646

Parametric instability of strong circularly polarized electromagnetic wave in plasma producing relativistic electrons and backscattered light 24 p3117 A73-45459

PLASMA-ELECTROMAGNETIC INTERACTION

Transport phenomena in turbulent plasma with electromagnetic waves. 01 p0081 A73-10117

Electron density measurements in time varying plasmas with a microwave reflectometer system. 01 p0044 A73-10120

Radiation resistance of small electric and magnetic antennas in a cold uniaxial plasma. 01 p0081 A73-10194

Incidence of a plane electromagnetic wave on a moving shock wave in an ionized gas 01 p0016 A73-10205

Propagation of electromagnetic waves in a plasma with a sheared magnetic field 01 p0081 A73-10206

Excitation of electromagnetic waves in a plasma by a flux of phased oscillators 01 p0082 A73-10207

Nonlinear interaction of two monochromatic Langmuir waves 01 p0016 A73-10209

Stimulated Raman scattering of microwaves in a layer of collisionless plasma. 01 p0082 A73-10423

Anomalous absorption of electromagnetic radiation at double the plasma frequency. 01 p0082 A73-10425

Theory of turbulent heating of an isothermal plasma with a transverse current. 01 p0083 A73-10456

Neoclassical theory of Landau damping and ion and electron transit-time magnetic pumping /TTP/ in toroidal geometry. 01 p0083 A73-10459

Subsonic plasma motion in continuous laser light. 01 p0084 A73-10472

Propagation of submillimeter-band electromagnetic waves in the drifting plasma of a solid 01 p0017 A73-10976

Second harmonic generation in an inhomogeneous laser plasma 01 p0086 A73-11288

VLF-ELF radiation characteristics of a 90 degree-phased crossed-dipole array in a cold multicomponent magnetoplasma. 02 p0140 A73-11739

Earth atmosphere He isotopes abundance based on calculation of ionization rates and solar wind interaction during geomagnetic dipole reversal 02 p0156 A73-11741

Electromagnetic dispersion relation for two equidense counterstreaming ion beams in warm electron background oscillating plasma, considering ion instability criteria 02 p0197 A73-12066

Propagation of surface waves along a plane boundary between two magnetoactive plasmas. 02 p0198 A73-12107

Electromagnetic and electroacoustic mode radiation resistance of linear antennas in compressible electron plasma. 02 p0199 A73-12858

Radiation from a magnetic line source in a compressible and anisotropic plasma half-space. 03 p0345 A73-12996

Coupled wave equations for propagation in generally inhomogeneous compressible magnetoplasma. 03 p0345 A73-13069

The excitation of resonances by a dipole antenna inside a hollow cylindrical plasma. 03 p0346 A73-13695

Changes in the distribution function of magnetospheric particles associated with gyroresonant interactions. 03 p0303 A73-13882

Parametric instability of a spatially modulated plasma. 03 p0347 A73-14089

Numerical and analytic solutions for dispersion equation for flute-like ion cyclotron instabilities in

high beta plasma, noting magnetic field inhomogeneity effect 03 p0348 A73-14436

Kinetic and dispersion equations for collisionless plasma interaction with HF magnetic and electric fields, noting conical, drift and cyclotron instabilities prevention 04 p0478 A73-15019

Nonlinear radio-frequency response of a non-uniform plasma slab-condenser system with realistic density and velocity profiles. 04 p0479 A73-15189

Input resistance of a short dipole antenna in a warm uniaxial plasma. 04 p0429 A73-15480

Net-field polarization in a magnetically biased plasma. 04 p0422 A73-15481

The integral equation and boundary conditions for a cylindrical antenna in a warm plasma. 04 p0429 A73-15482

Equatorial region radio wave enhanced absorption by resonant coupling to electrojet irregularities and damped upper hybrid modes 04 p0423 A73-15548

Application of the Stark effect to the determination of the fields in the region of microwave/plasma interaction 04 p0423 A73-15611

Parametric excitation of high-frequency potential oscillations in a cold magnetoactive plasma by the field of an electromagnetic wave 04 p0481 A73-15612

Instability of a relativistically strong electromagnetic wave of circular polarization. 04 p0482 A73-15960

Parametric amplification of a UHF signal by plasma-beam interaction in the presence of a magnetic field of finite amplitude 04 p0424 A73-15996

Electromagnetic wave propagation in a medium with two-dimensionally periodic variations of the refractive index 05 p0548 A73-16268

Resonance coupling of a transverse magnetic response to a transverse electric excitation by the axial density gradient of a bounded plasma. 05 p0601 A73-16364

Determination of plasma electron temperature from the reversal of radial ambipolar electric field in a longitudinal magnetic field. 05 p0602 A73-16584

High intensity CO2 laser-plasma interaction. 05 p0603 A73-17224

Stochastic kinetic theory of strong wave-plasma interaction. I - Kinetic equations. 05 p0603 A73-17323

Propagation of electromagnetic waves in a rarefied plasma which has been placed in an alternating magnetic field. 06 p0726 A73-17402

Boundary conditions for penetration of an electromagnetic wave into a plasma. 06 p0727 A73-17418

Nonlinear damping of potential monochromatic waves in inhomogeneous plasma, obtaining resonance particle distribution function 06 p0728 A73-17967

Plasma instability in terms of electron oscillations due to parametric interaction with UHF electric field, noting inverse Cerenkov effect for electrons 06 p0729 A73-18111

Scattering of electromagnetic waves from a turbulent plasma slab. 06 p0729 A73-18120

Reflection and transmission of electromagnetic waves obliquely incident on a relativistically moving uniaxial plasma slab. 06 p0665 A73-18185

Experimental investigations on the impedance behavior of a cylindrical antenna in a collisional magnetoplasma. 06 p0729 A73-18186

Thin walled open ended cylindrical antenna in cold magnetoplasma, calculating current distribution by approximations based on Wiener-Hopf procedure 06 p0729 A73-18193

Diffraction of electromagnetic plane wave by an infinite slit embedded in an anisotropic plasma. 06 p0668 A73-18356

Anomalous ion heating in a laser heated plasma. 06 p0730 A73-18461

Argon plasma density and energy distribution development during microwave radiation absorption at upper hybrid resonance 06 p0732 A73-18605

Fast radial displacement of a toroidal plasma by a transverse magnetic field. 06 p0732 A73-18620

Current induced drift rate of plasma electrons in electric and magnetic fields, noting electron velocities in turbulent heating of plasma 06 p0732 A73-18621

Surface absorption coefficient of electromagnetic wave incident on plasma boundary, considering particle specular reflection and density-frequency relation 06 p0732 A73-18642

Scattering of microwaves by a stratified overdense plasma at high collision frequencies. [AD-756733] 06 p0732 A73-18780

Microwave power absorption by a plasma outside the electron cyclotron resonance region. 06 p0733 A73-18795

Self trapping modulational instability of electron cyclotron wave whistler in cold and hot dense plasmas, discussing relevance to phenomena in magnetosphere 07 p0814 A73-19239

Variational algorithms for numerical simulation of collisionless plasma with point particles including electromagnetic interactions. 07 p0854 A73-19264

Nonlinear propagation theory for electromagnetic waves in a weakly ionized plasma 07 p0854 A73-19277

Dispersion equations for E and H waves in multilayer plasma, defining amplitudes correlation for incident, transmitted and reflected waves 07 p0855 A73-19278

Noncoherent reflection of electromagnetic waves from a plasma layer 07 p0855 A73-19281

Transient radiation in homogeneous anisotropic cold plasmas. 07 p0856 A73-19381

Isotropic conducting plasma dynamic behavior near rotating magnetized sphere, showing electric field-produced meridional convective currents 07 p0856 A73-19430

Equilibrium and stability of large-amplitude magnetic Bernstein-Greene-Kruskal waves. 07 p0857 A73-19524

Intrinsic bandwidth of cyclotron resonance in the geomagnetic field. 07 p0792 A73-19532

Collision effects on electromagnetic wave propagation in a plasma generated by a moving ionization source 07 p0858 A73-19906

Lateral expansion of a laser-supported detonation wave in a gas. 07 p0920 A73-19979

The theory of a coaxial gas-discharge oscillator loaded by a helical line. 07 p0801 A73-20138

Gauge invariant and covariant description of plasma response to electromagnetic disturbances, deriving waves dispersion properties in arbitrary reference frame 07 p0859 A73-20234

The complete iso-thermalization by collective electromagnetic interactions of strongly anisotropic magnetized collisionless plasmas. 07 p0859 A73-20235

Waves in a hot uniaxial plasma excited by a current source. 07 p0860 A73-20477

Measurement of the attenuation of an electromagnetic wave in a bounded hot electron plasma. 07 p0860 A73-20478

Anomalous plasma ion heating by parametric excitation of lower hybrid instabilities, using long wavelength oscillating electric field [AD-759477] 07 p0860 A73-20482

Buildup of a narrow plasma channel by microwaves. 08 p0992 A73-20954

Oblique electromagnetic wave propagation with respect to double stream in plasma, calculating unstable wave oscillation frequency and growth rate dependence on stream direction 08 p0993 A73-21633

Parametric action of high-power radiation on a plasma near the electron cyclotron frequencies 09 p1123 A73-21876

Absorption of electromagnetic waves by a magnetoactive plasma at parametric-resonance frequencies 09 p1124 A73-21889

Cold collisionless plasma equations for electromagnetic waves absorption near lower hybrid resonance in inhomogeneous magnetized plasma contained in ideally conducting cylinder 09 p1125 A73-21906

Parametric heating of a dense arc plasma with 0.337 mm laser radiation. 09 p1125 A73-21944

Collisional effect on the saturation amplitude of nonlinearly excited plasma waves. 09 p1125 A73-22023

X-ray temperature measurements of laser produced plasmas in large radiation fields. 09 p1125 A73-22024

Impedance of an ion-sheathed spherical probe in a warm, isotropic plasma. 09 p1127 A73-22431

Wave number space analysis of propagation in nonuniform media. 09 p1120 A73-22474

One-dimensional numerical experiment on anomalous plasma resistivity 09 p1127 A73-22482

Solution of equations for one-dimensional propagation of a monochromatic light pulse in absorbing media 09 p1095 A73-22623

Certain properties of an electron plasma in a strong electromagnetic field 09 p1130 A73-22704

Relaxation processes in a parametrically unstable plasma 09 p1130 A73-22707

Obliquely incident electromagnetic wave propagation through plane-stratified weakly ionized plasma with electron density inhomogeneity scale length comparable with mean free path 09 p1052 A73-23077

Kinetic theory for the reflection of waves obliquely incident on the boundary of a magnetoactive plasma 09 p1052 A73-23078

Propagation of discharges and confinement of a dense plasma by electromagnetic fields 09 p1132 A73-23327

Anomalous nonlinear dissipation of high-frequency radio waves in a plasma 09 p1053 A73-23330

Problems of linear and nonlinear theory of cosmic ray modulation 10 p1266 A73-23913

Plasma excitation by HF field in carbon dioxide-argon flow under low pressure, noting disappearance of striations 10 p1253 A73-24072

Determination of field strength in a microwave-plasma interaction by means of the Stark effect. 10 p1254 A73-24201

Parametric excitation of high-frequency electrostatic oscillations in a cold magnetoactive plasma by an electromagnetic wave. 10 p1254 A73-24202

Electromagnetic wave reflection at interface between anisotropic Vlasov plasma and vacuum with external magnetic field, deriving electric and magnetic field characteristics 10 p1255 A73-24260

Low-frequency parametric instabilities of magnetized plasmas with two ion species. 10 p1255 A73-24261

Efficiency of the microwave energy absorption in a plasma at high magnetic fields. 10 p1257 A73-24627

Kinetic equations describing thermalization of anisotropic solar wind plasma via linear and nonlinear wave-particle interaction 10 p1270 A73-24912

Brownian motion of electrons in time-dependent magnetic fields. 11 p1403 A73-25124

Nonlinear hydrodynamic VLF wave scattering in the earth's magnetosphere. 11 p1331 A73-25913

Enhanced laser-light absorption by optical resonance in inhomogeneous plasma. 11 p1405 A73-25970

Refraction by the electromagnetic pump of parametrically generated electrostatic waves. 11 p1405 A73-25973

Absorption and amplification of electromagnetic waves in a nonstationary magnetoactive plasma with allowance for spatial dispersion 11 p1405 A73-26151

Nonthermal radiation from a magnetoactive plasma in the field of a microwave pumping wave. 11 p1405 A73-26182

Integral equation for electromagnetic field in diffuse boundary plasma, noting anomalous skin effect 11 p1405 A73-26184

Electromagnetic wave scattering by an inhomogeneous magnetoplasma column moving in the axial direction. 11 p1407 A73-26700

Absorption of microwaves by a plasma in a magnetic field in the presence of a large effect due to longitudinal inhomogeneity 12 p1467 A73-26934

Facility to determine spectra of light scattered at free plasma electrons during single laser pulse, obtaining electron component profiles with high speed streak camera 12 p1506 A73-27301

Influence of a SHF field on the inhomogeneities of a nonequilibrium plasma from a low-pressure gas discharge 12 p1528 A73-27304

Reflection of electromagnetic waves from non-homogeneous anisotropic plasma layers /normal incidence/ 12 p1470 A73-27356

Absorption of the microwave energy in a magnetoactive plasma. 12 p1529 A73-27433

Laser interaction and related plasma phenomena; Proceedings of the Second Workshop, Rensselaer Polytechnic Institute of Connecticut, Hartford, Conn., August 30-September 3, 1971. Volume 2. 12 p1508 A73-27922

Investigation of the heating of electrons of a dense beam-plasma discharge in strong magnetic fields 12 p1529 A73-27942

Interaction of a high-frequency magnetic field with plasma potential oscillations in a Q machine 12 p1530 A73-27976

Electron temperature in a weakly ionized plasma during a nonlinear skin effect 12 p1530 A73-27979

Nonlinear behavior of stimulated Brillouin and Raman scattering in laser-irradiated plasmas. 13 p1664 A73-28187

Laser light pulse absorption in transient dense hot plasma generated around metallic anode tip by fast capacitive discharge in vacuum 13 p1664 A73-28460

Role of stimulated Compton scattering in the interaction of laser radiation with a superdense plasma. 13 p1664 A73-28615

Numerical solution of the problem of transmission of ELF waves through the lower ionosphere. 13 p1582 A73-28651

Nonlinear propagation of electromagnetic waves in a weakly ionized plasma. 13 p1665 A73-28677

Dispersion equations for E and H waves in multilayer plasma, defining amplitudes correlation for incident, transmitted and reflected waves 13 p1665 A73-28678

Incoherent reflection of electromagnetic waves from a plasma layer. 13 p1665 A73-28681

Absorption of waves by a two-dimensionally inhomogeneous plasma in the vicinity of singularity points 13 p1666 A73-28960

Determination of the parameters of a fluctuating plasma from the modulation of microwave signals 13 p1666 A73-28961

Theory of surface wave dispersion in an inhomogeneous plasma situated in a strong HF field 13 p1667 A73-29161

Radiation from travelling wave circular loop antenna in compressible electron plasma. 14 p1731 A73-29709

Study of two types of turnstile aerial immersed in a warm plasma. 14 p1731 A73-29712

Partial trapping of a low-density plasma by an RF quasipotential well. 14 p1779 A73-29917

Observation of a current-driven plasma instability at the outer zone-plasma sheet boundary. 14 p1747 A73-29966

Complex radiation effects of sources moving in a plasma 14 p1780 A73-30262

Direct nonlinear coupling of electromagnetic waves and electrostatic waves in a plasma - Theory. 14 p1781 A73-30656

Effect of induced axial electric field on a relativistic electron beam pulse propagating through a plasma. 14 p1777 A73-30661

On the absorption of microwave through laboratory plasma. 14 p1782 A73-30800

Quasi-linear theory of a parametrically unstable magnetoactive plasma 14 p1782 A73-30806

Determination of electromagnetic field correlators for a contained plasma 15 p1916 A73-31037

Electromagnetic instabilities of finite pressure anisotropic plasma with hot electrons. 15 p1916 A73-31084

Longitudinal force exerted by circularly polarized high-powered laser radiation in a dense electron plasma. 15 p1917 A73-31091

Experimental study of the interaction of a plasma with a magnetic field in the case of a plasma generated by laser irradiation of solids 15 p1917 A73-31249

Numerical study of the interaction of a shock-wave caused, supersonic, ionized-argon flow with electric and magnetic fields, using the method of characteristics 15 p1918 A73-31571

Zone of Poynting vector rotation toward the direction of an applied magnetic field for a wave incident on an inhomogeneous plasma 15 p1919 A73-31707

Transport phenomena in a fully ionized ultrarelativistic plasma 15 p1919 A73-31709

The possible nature of the fine structure of sporadic radio emission from the sun and other cosmic sources having a high density of electromagnetic radiation 15 p1926 A73-31876

Reflection and transmission of electromagnetic waves obliquely incident on a relativistically moving isotropic plasma slab. 15 p1919 A73-31947

PLASMA-PARTICLE INTERACTIONS

Pulsar radio emission limiting polarization resulting from passage through magnetoactive plasma, discussing electron density effects

15 p1844 A73-32003

Reflection of electromagnetic waves from a moving plasma

15 p1846 A73-32303

Investigation of the absorption of laser radiation in a laser spark in air

15 p1885 A73-32313

Anomalous absorption of superhigh-frequency waves in a plasma at frequencies close to the upper hybrid frequency

15 p1846 A73-32323

German monograph - Investigations regarding the structure of planar boundary layers between magnetic field and plasma.

15 p1921 A73-32584

Cold collisionless plasma equations for electromagnetic waves absorption near lower hybrid resonance in inhomogeneous magnetized plasma contained in ideally conducting cylinder

15 p1922 A73-32631

An investigation of the reflection of electromagnetic pulses from moving plasmas.

16 p2041 A73-33199

Nonlinear theory of wave interaction in a plasma

16 p2042 A73-33735

Reflection coefficient of an electromagnetic wave by a plasma column of variable electron density in a waveguide.

16 p1984 A73-33994

Parametric instabilities in a plasma containing two types of ions

16 p2043 A73-34057

Theory of the anomalous skin effect in a plasma with a diffuse boundary

16 p2043 A73-34060

A high-temperature plasma state in a high-power microwave discharge

17 p2214 A73-34136

Antenna admittance determination of electron density.

17 p2121 A73-34187

Edge instability of transverse electromagnetic waves in a weakly ionized plasma

17 p2214 A73-34249

Absorption of electromagnetic waves at parametric resonances in a magnetoactive plasma.

17 p2215 A73-34312

Plasma hydrodynamics in high frequency electromagnetic field, discussing hydrodynamic equations, small perturbations, plasma equilibrium and movement in field

17 p2216 A73-34341

Scattering of a spherical wave by spherical inhomogeneity with arbitrary refractive index distribution along the radius.

17 p2123 A73-35163

One-dimensional model for nonlinear reflection of laser radiation by an inhomogeneous plasma layer.

17 p2218 A73-35824

Transformation, transmission, and reflection of plasma waves in the presence of a tangential velocity discontinuity

18 p2339 A73-36551

Parametric excitation of surface waves in an inhomogeneous magnetized plasma

18 p2339 A73-36556

Nonlinear transformation of an electromagnetic wave at the boundary of a magnetoactive plasma

18 p2289 A73-36562

Resonant absorption of an electromagnetic wave by an inhomogeneous magnetoactive plasma at electron cyclotron frequency harmonics

18 p2289 A73-36563

Perturbation of a plasma by a focused CO₂ laser beam.

18 p2339 A73-36623

Nonlinear excitation of an ion-acoustic wave in a bounded plasma

18 p2340 A73-36675

Nonlinear expansion of arbitrarily polarized electromagnetic waves in gyrotropic media

18 p2340 A73-36961

Electromagnetic interactions with turbulent plasmas.

19 p2465 A73-37167

Penetration and crossing of transverse magnetic field barrier by a purely ionic plasma.

19 p2465 A73-37170

Theoretical and experimental research on the electromagnetic acceleration of shock-induced flow in argon.

19 p2419 A73-37174

Quenching of the beam-plasma instability by mode mixing at a density discontinuity.

19 p2469 A73-37859

Direct nonlinear coupling of electromagnetic waves and electrostatic waves in a plasma - Experiment.

19 p2469 A73-37860

The propagation of an intense electromagnetic wave in a plasma.

19 p2469 A73-38087

Excitation of the earth-ionosphere waveguide by point dipoles at satellite heights.

20 p2528 A73-38846

Parametric decay of obliquely incident electromagnetic waves into ion acoustic and electron plasma waves in vicinity of resonance

20 p2595 A73-38874

Instability of electromagnetic surface waves supported by a bounded plasma stream.

20 p2595 A73-38891

Theory of radio wave incoherent scattering by a plasma and the application of the theory in ionospheric studies

20 p2554 A73-39164

Second harmonic amplitude modulation of an electromagnetic wave by an acoustic wave in a dispersive plasma.

20 p2597 A73-39199

Radiative and convective heat transfer in a magnetic field

20 p2628 A73-39608

The application of high-speed photography and spectrography for investigations of erosive pulsed plasma streams.

21 p2744 A73-39999

Contribution to the theory of electromagnetic fluctuations of a plasma situated in a weak SHF electric field

21 p2746 A73-40517

Wave absorption by a plasma with a nonmonotonic longitudinal distribution of the concentration

21 p2746 A73-40524

Nonlinear parametric electron plasma instability due to cyclotron harmonic Bernstein wave interaction in strong electric field

21 p2747 A73-40791

On the reflection of transverse waves from a cold plasma.

21 p2748 A73-40930

Raman scattering of SHF radiation in a bounded plasma of a solid

21 p2657 A73-41509

Nonlinear conversion of electromagnetic waves at the boundary of a magnetoactive plasma

21 p2658 A73-41517

Parametric instabilities of weakly turbulent plasma, determining collision frequencies characterizing high frequency electric field energy absorption

21 p2750 A73-41681

Magnetic pulsation spectra in a nonisothermal plasma.

22 p2890 A73-41725

Impedance and large signal excitation of satellite-borne antennas in the ionosphere.

22 p2831 A73-41835

On input impedance of an arbitrarily oriented small loop antenna in a cold collisionless magnetoplasma.

22 p2824 A73-41858

Propagation of electromagnetic waves through turbulent plasma using transport theory.

22 p2824 A73-41860

Kinesonde observations of ionosphere modification by intense electromagnetic fields from Platteville, Colorado.

22 p2844 A73-41921

Steady-state solutions for relativistically strong electromagnetic waves in plasmas.

22 p2891 A73-42238

Microwave absorption by a magnetoplasma with a strong longitudinal inhomogeneity.

22 p2891 A73-42268

Kinetic theory of electromagnetic waves in an electron plasma characterized by slowly changing parameters

22 p2892 A73-42327

Incident electromagnetic wave reflection in inhomogeneous plasma with local nonlinearity, discussing reflection point shift and dielectric permittivity effect

22 p2892 A73-42328

Contribution to the theory of parametric instability of a bounded homogeneous plasma

22 p2892 A73-42380

Experimental observation of the decay of high-frequency waves in a plasma

22 p2826 A73-42389

Nonlinear propagation of electromagnetic waves in a plasma containing random irregularities.

22 p2894 A73-42398

E-polarized electromagnetic scattering by conducting circular cylinder coated with plasma sheath during spacecraft reentry flight under plane wave incidence

22 p2827 A73-42466

The efficient inject of high microwave powers into the overdense magnetoactive plasma in the waveguide.

22 p2827 A73-42517

Self-action of electromagnetic wave in plasma under parametric instability.

22 p2895 A73-43022

Large amplitude electromagnetic waves in hot relativistic plasmas.

22 p2895 A73-43024

Reflection and transmission of electromagnetic waves at a moving magnetoplasma half-space.

22 p2896 A73-43179

Reflection of electromagnetic waves from inhomogeneous anisotropic plasma sheets /normal incidence/.

23 p2952 A73-43255

Second-harmonic generation in an inhomogeneous laser plasma.

23 p3009 A73-43509

Current-induced heating of a dense plasma during collective interactions in a high-current gas discharge

23 p3009 A73-43651

Electric polarization of a plasma beam in an axially symmetrical magnetic field

23 p3009 A73-43655

Plasma cluster movements in guides using straight stellarator magnetic fields and axisymmetric-straight rod produced field combination

23 p3010 A73-43660

VLF input impedance of a loop antenna embedded in the magnetosphere.

23 p2954 A73-43700

Nonlinear dissipation of electromagnetic waves in a plasma

23 p3012 A73-44017

Thermonuclear laser synthesis and parametric instabilities

23 p2988 A73-44091

Wave propagation through a highly restrained solid-state plasma.

23 p3012 A73-44141

Wave absorption near singular points in a two-dimensional inhomogeneous plasma.

23 p3013 A73-44312

Determination of the parameters of a fluctuating plasma from modulation of a microwave signal.

23 p3013 A73-44313

Plasma-electromagnetic wave interactions in toroidal discharge chamber, noting possibility of collisionless wave absorption due to conversion to longitudinal plasma waves at hybrid resonance

23 p3014 A73-44340

Excitation of parametric instabilities in a magnetoactive plasma by a microwave pumping wave.

24 p3114 A73-44497

Plasma instability in terms of electron oscillations due to parametric interaction with UHF electric field, noting inverse Cerenkov effect for electrons

24 p3114 A73-44500

Reflection of electromagnetic waves from a moving plasma.

24 p3067 A73-44611

Absorption of laser radiation in a laser spark in air.

24 p3095 A73-44621

Determination of the transmittance of an optically not dense plasma by an intracavity method

24 p3115 A73-44762

Lunar electromagnetic scattering. I - Propagation parallel to the diamagnetic cavity axis.

24 p3139 A73-45109

Electromagnetic wave interaction with moving bounded plasmas.

24 p3069 A73-45409

Redistribution of charged particles and self-distortion of high-amplitude electromagnetic waves in a plasma.

24 p3117 A73-45413

Theory of a corner-driven loop antenna immersed in a warm plasma.

24 p3070 A73-45486

PLASMA-PARTICLE INTERACTIONS

Life-time of ion waves in unstable and turbulent plasmas.

01 p0084 A73-10463

Capture of plasma electrons by the field of a wave that is excited by an ion beam

01 p0084 A73-10632

Polarization of relativistic-electron emission in the case of Compton scattering at turbulent plasma oscillations

01 p0085 A73-10949

Transition radiation from a plasma boundary.

01 p0085 A73-11063

Energy spectra of modulated relativistic electron beam as function of plasma density at beam-plasma interaction region boundary

01 p0086 A73-11284

Onset of turbulence in the interaction between a 'monoenergetic' beam and a plasma

01 p0086 A73-11285

Electric potential and particle concentration of a plasma in the proximity of a projectile moving rapidly toward the plasma

01 p0086 A73-11289

Heating of plasma by high-energy electrons, and nonthermal X-ray emission in solar flares.

01 p0093 A73-11313

Quasimonochromatic whistler mode packets of slowly varying amplitude.

02 p0140 A73-11920

Quasi-linear interaction of whistler-mode waves and nonthermal electrons.

02 p0141 A73-12390

Shock wave and isentropic compression/expansion in plasma with anomalous thermodynamic properties due to strong particle interactions, discussing phase transitions types

03 p0346 A73-13190

Magnetospheric observations in OGO-5 plasma wave experiment, emphasizing electrostatic wave particles interaction with plasma

03 p0303 A73-13883

Injection of an electron beam into a plasma confined by a conducting shell.

03 p0347 A73-14093

Ion-cyclotron instability of a plasma produced by a fast-ion beam.

03 p0347 A73-14101

Incoherent excitation of plasma oscillations by an almost-monoenergetic relativistic beam.

03 p0347 A73-14102

Estimates of dense plasma heating by stable intense electron beams.

03 p0348 A73-14438

Hypersonic solar wind flow interactions with comet emitted gas forming tails, discussing contact surface with stagnation point and bow shock front

04 p0494 A73-14758

Interaction of an intense electron beam with a homogeneous and a nonhomogeneous plasma

04 p0478 A73-15031

Influence of external high-frequency modulation of the electron beam on ion heating during beam-plasma interaction

04 p0478 A73-15032

Parametric electron-beam instability in a spatially periodic electric field

04 p0479 A73-15043

Turbulent wave field growth rate and saturation amplitude for nonresonant instability in weak cold beam plasma system, using Dupree plasma turbulence theory

04 p0479 A73-15193

Plasma ion and electron modes nonlinear damping, presenting solution for Vlasov-Poisson system

04 p0480 A73-15195

The importance of wave-particle interactions in the magnetosphere.

04 p0492 A73-15339

Influence of carrier drift on the propagation of electromagnetic wave in a solid-state plasma.

04 p0480 A73-15473

Relation of Pc 1 micropulsations to the ring current and geomagnetic storms.

04 p0444 A73-15536

Electromagnetic-emission energy flux during the development of beam instability in a magnetically confined plasma

04 p0481 A73-15607

Vibrational and energy spectra of welding electron beam interacting with beam produced plasma, noting interaction length effect on instability

04 p0454 A73-15609

Landau attenuation in a plasma excited by a monochromatic electron beam

05 p0601 A73-16394

Relaxation of ion beam injected into a plasma transversely to a magnetic field.

05 p0602 A73-16550

A neutral-potassium-beam measurement of plasma density.

05 p0604 A73-17364

Electromagnetic radiation caused by the two-stream instability in a bounded plasma.

06 p0726 A73-17416

Boundary conditions for penetration of an electromagnetic wave into a plasma.

06 p0727 A73-17418

Nonlinear theory of interaction between restricted relativistic particle beam and plasma, determining field amplitudes and beam radii

06 p0728 A73-17972

Combined plasma heating by an electron beam and an intense ion-cyclotron wave

06 p0729 A73-18106

High-frequency instabilities in a plasma with a nonlinear ion-acoustic wave.

06 p0731 A73-18603

Collective processes in the passage of high-current relativistic beams through a gas and a plasma.

06 p0732 A73-18714

Difference frequency generation using non-linear interaction between a modulated electron beam and a collisionless plasma.

06 p0733 A73-18839

Observed relationships between electric fields and auroral particle precipitation.

07 p0814 A73-19237

Variational algorithms for numerical simulation of collisionless plasma with point particles including electromagnetic interactions.

07 p0854 A73-19264

Mode-coupling and wave-particle interactions for unstable ion-acoustic waves.

07 p0856 A73-19521

Alternating current instability produced by the two-stream instability.

07 p0857 A73-19528

The behaviour of ULF waves and particles in the magnetosphere.

07 p0792 A73-19666

The sideband instability of electrostatic waves in an inhomogeneous medium.

07 p0858 A73-19667

Large-amplitude stabilization of the drift instability.

07 p0860 A73-20481

Energy loss of charged particles in Maxwellian plasmas.

08 p0992 A73-20823

Electron plasma oscillation due to beam plasma interaction with standing wave formation between electrodes, observing temporal growth rate during beam modulation removal

08 p0992 A73-21005

Simultaneous suppression of an electron plasma wave and an ion acoustic wave by beam modulation.

08 p0992 A73-21006

Validity criteria for local thermodynamic equilibrium and coronal equilibrium.

08 p0992 A73-21007

Observation of beam-plasma interaction in a toroidal plasma in a large electric field.

08 p0993 A73-21631

Plasma-ion beam nonlinear interaction for beam velocity exceeding electrons thermal velocity, noting plasma heating and beam energy dissipation

08 p0994 A73-21696

Ultrarelativistic electrons beam steady injection into plasma filled half space, using weak turbulence theory for assumed beam excited oscillations interaction

08 p0994 A73-21698

Quasi-linear relaxation of a monoenergetic relativistic electron beam in an external magnetic field

09 p1124 A73-21903

Excitation of low-frequency oscillations by an electron beam in a hot plasma confined in a magnetic mirror

09 p1125 A73-21907

Plasma effects and the acceleration of charged particles in pulsar fields.

09 p1141 A73-22016

Ion velocity temperature observation at Mars surface boundary, suggesting solar plasma interaction with outer atmosphere from ion flux disturbance ahead of shock wave

09 p1126 A73-22264

Electron-beam excitation of finite-sized plasma near the lower-hybrid frequency.

09 p1129 A73-22638

Kinetic theory of the spatial instability of a radially bounded plasma-electron beam system with a given radially nonhomogeneous plasma configuration

09 p1129 A73-22688

Investigation of the heating mechanism for the electron component of a plasma under beam-instability conditions in a mirror confinement system

09 p1130 A73-22703

High-frequency instability of an electromagnetic wave in a nonequilibrium magnetized plasma

09 p1130 A73-22705

Nonlinear theory of the interaction of a monoenergetic beam with a dense plasma

09 p1130 A73-22706

Polarized radiation of relativistic electrons scattered by plasma turbulence.

09 p1130 A73-22743

Nonequilibrium transport process calculation by theoretical microscopic model for interaction between ionized gas and solid particles in suspension, noting free electron concentration change

09 p1130 A73-22826

Propagation of surface waves and instability wave growth in an ion beam-plasma system.

09 p1131 A73-22906

Excitation of magnetosonic waves in a plasma with nonequilibrium ions

09 p1131 A73-23076

Electromagnetic energy in the two-stream instability in a magnetized plasma.

10 p1254 A73-24197

Vibrational and energy spectra of welding electron beam interacting with beam produced plasma, noting interaction length effect on instability

10 p1224 A73-24199

Computer simulation of two dimensional plasma diffusion via wave interactions descriptions by nonlinear differential equations, considering electric field and particle velocity correlations

10 p1255 A73-24266

Disturbance of a magnetized plasma by a fast traveling charge

10 p1257 A73-24758

Experimental investigation oscillations in a synthesized plasma jet

10 p1257 A73-24877

Relativistic particle beam stability and electromagnetic oscillations in plasma rectangular waveguide under longitudinal magnetic field

10 p1258 A73-24887

Observation of stationary acceleration of ions to energies of 2 to 20 keV in a nonisothermal plasma

10 p1258 A73-24888

Measurement of the potential distribution in the vicinity of an electron beam with the aid of a thermal probe

10 p1258 A73-24889

Stimulated emission due to the interaction between a relativistic high-current beam and a plasma

11 p1403 A73-25241

On nonlinear transformation and stabilization of beam-plasma instability.

11 p1404 A73-25274

A plasma-beam discharge laser.

11 p1377 A73-26181

Contribution to the nonlinear theory of kinetic instability of an electron beam in plasma.

11 p1405 A73-26183

Current and fields reduced in plasmas by relativistic electron beams with arbitrary radial and axial density profiles.

11 p1407 A73-26560

Macroscopic equilibria of relativistic electron beams in plasmas.

11 p1407 A73-26561

Stability of a magneto-active plasma with a relativistic electron beam, situated in a high-frequency electric field

12 p1527 A73-26927

Analysis of the behavior of the electron velocity distribution function of beam interacting with a plasma

12 p1527 A73-26933

Study of the effect of a plasma on the microwave radiation of a helical beam in a waveguide

12 p1527 A73-26935

Braking of electron beams in a plasma with a high level of Langmuir turbulence

12 p1527 A73-26956

Czechoslovak Seminar on Plasma Physics, 6th, Liblice, Czechoslovakia, May 10-12, 1972, Research Report.

[IPPCZ-167]

12 p1528 A73-27430

Dynamics of strongly nonlinear beam-plasma interaction.

[IPPCZ-167]

12 p1529 A73-27434

The influence of the scattering by plasma oscillation on the spectrum of emission from semi-opaque plasma

12 p1529 A73-27869

Two-stream instability heating of plasmas by relativistic electron beams.

13 p1663 A73-28186

Monoenergetic particle beam instabilities in homogeneous plasma due to secondary emission wave interactions

13 p1664 A73-28289

Intermittent generation of microwave oscillations through a plasma-beam interaction.

13 p1583 A73-28664

Interaction between a monoenergetic nonrelativistic electron beam and the surface potential oscillations of a plasma

13 p1666 A73-28955

Investigation of the feasibility of the injection of electrons into heliotron-type closed magnetic mirror configurations

13 p1666 A73-28957

Investigation of the absorption and emission of electron-beam-induced waves in an inhomogeneous magnetoactive plasma

13 p1666 A73-28958

Problems associated with the injection of a high-energy neutral beam into a plasma.

14 p1778 A73-29688

Effect of radial profile of a charged particle pulse on the electromagnetic wake in a plasma.

14 p1779 A73-29710

Observation of a current-driven plasma instability at the outer zone-plasma sheet boundary.

14 p1747 A73-29966

Symposium on Plasma Heating and Injection, Varenna, Italy, September 21-October 4, 1972, Lectures and Seminars.

14 p1779 A73-30117

Instabilities in a system of a plasma and an intense relativistic electron beam.

14 p1780 A73-30122

Interaction between a plasma and an electron beam modulated by low-frequency oscillations.

14 p1780 A73-30335

Plasma heating by an intense electron beam.

14 p1781 A73-30553

Detection of a feedback in a plasma-electron beam system

14 p1781 A73-30585

Investigation of low-frequency instabilities in a linear plasma betatron

14 p1782 A73-30805

Magnetic neutralization and discharge neutralization of an electron beam injected into a magnetoactive plasma

14 p1782 A73-30807

Interaction of solar wind with interstellar neutral gas at the heliospheric boundary.

15 p1926 A73-31380

Interaction between the interstellar medium and solar wind plasma.

15 p1927 A73-32001

Contribution to the theory of electron-beam stability in an inhomogeneous dielectric medium 15 p1920 A73-32302

Limitation of beam instability as a result of the capture of plasma electrons by the wave 15 p1920 A73-32320

Electromagnetic emission during surface wave excitation by a relativistic electron beam in a plasma 15 p1921 A73-32321

Quasilinear relaxation of a monoenergetic relativistic electron beam in an external magnetic field. 15 p1922 A73-32628

Electron-beam excitation of low-frequency waves in a hot plasma confined in a mirror machine. 15 p1922 A73-32632

The problem of interaction between a relativistic electron beam and plasma in a waveguide 16 p2040 A73-32899

Dynamic stabilization of plasmas by means of a high-frequency-modulated electron beam. 16 p2041 A73-33326

Nonlinear radial electron beam focusing in plasma under beam-plasma instability, showing irreversibility conditions dependence on electromagnetic wave propagation mode 16 p2043 A73-34056

Excitation of electromagnetic waves in a plasma with a relativistic electron beam. 17 p2216 A73-35159

A three-dimensional picture of the development of instability during the interaction of a modulated electron beam with a plasma. 17 p2216 A73-35170

Entry of a high-frequency longitudinal field into a nonequilibrium plasma 18 p2339 A73-36554

Interaction between a tubular electron beam and a plasma 18 p2339 A73-36555

Interaction between an ion beam and a turbulent low-pressure theta-pinch plasma 18 p2340 A73-36667

Probe measurement of the electrostatic field in the ionosphere and magnetosphere 18 p2314 A73-37026

Interaction of plasma streams with a neutral gas cloud. 19 p2466 A73-37179

Deceleration of electron beams in a plasma with a high level of Langmuir turbulence. 19 p2469 A73-38133

Excitation of electromagnetic waves propagating along a magnetic field in a cold plasma by a beam of phased oscillators 19 p2406 A73-38330

Emission of longitudinal waves from a charge in an external high-frequency electric field in a magnetoactive plasma 19 p2470 A73-38331

Influence of scattering by plasma oscillations on the spectrum of a semitransparent plasma. 20 p2597 A73-39243

Extraction of electrons from a plasma in the presence of a gas in the high-voltage gap 20 p2598 A73-39606

Numerical calculation for polar ionospheric current under realistic electric field and conductivity distributions, considering solar wind effect on charged particles in magnetosphere 21 p2681 A73-40155

Instability of an azimuthal ion beam in a dense plasma 21 p2746 A73-40522

Role of plasma effects in the propagation and isotropization of cosmic rays in the Galaxy 21 p2756 A73-40579

Investigation of conditions for the formation of a beam-plasma discharge without a magnetic field 21 p2748 A73-41516

Oscillations in a synthesized plasma jet. 21 p2749 A73-41652

Relativistic particle beam stability and electromagnetic oscillations in plasma rectangular waveguide under longitudinal magnetic field 21 p2749 A73-41662

Steady-state acceleration of ions to 2-20 keV in a nonisothermal plasma. 21 p2749 A73-41663

Measurement of the potential distribution near an electron beam using a thermionic probe. 21 p2749 A73-41664

Trapped-particle scattering by electrostatic turbulence in toroidal plasmas. 21 p2749 A73-41675

Ion acceleration upon expansion of a rarefied plasma. 22 p2890 A73-41724

Monoenergetic particle beam bunching instabilities in homogeneous plasma due to secondary emission wave interactions 22 p2890 A73-41813

Wave spectrum analysis of electron beam-plasma longitudinal electrostatic fluctuations, finding triplet wave line shape and intensity and dispersion relations 22 p2891 A73-42240

Stability of a magnetoactive plasma with a relativistic electron beam in an RF electric field. 22 p2891 A73-42261

Variation of electron velocity distribution function in the beam-plasma interaction. 22 p2891 A73-42267

Effect of a plasma on the microwave radiation from a helical beam in a waveguide. 22 p2892 A73-42269

Particle streams along the force lines of a magnetic field in a multicomponent ionospheric plasma in the presence of longitudinal currents 22 p2892 A73-42329

Kinetics of impact-radiation ionization and recombination. 22 p2892 A73-42344

Possible emission of transverse electromagnetic waves in an isotropic plasma 22 p2893 A73-42390

Turbulence generation by supersonic nozzle gas flow interaction with plasmas, discussing high current electric arc in axis 22 p2895 A73-43166

Energy spectra of modulated relativistic electron beam as function of plasma density at beam-plasma interaction region boundary 23 p3009 A73-43505

Appearance of turbulence during the interaction of a 'monoenergetic' beam with a plasma. 23 p3009 A73-43506

Electric potential and particle concentration of a plasma in the vicinity of a rapidly moving charge. 23 p3009 A73-43510

Electrical conductivity of a plasma during collective interactions in a high-current gas discharge 23 p3009 A73-43652

Single particle approximation analysis of particle velocity changes influence on plasma motion across nonhomogeneous magnetic field, examining energy exchange between particles 23 p3010 A73-43662

Two level atomic inelastic transitions in plasma with damping for static, Weisskopf, adiabatic, exponential and Purcell/Born particle regions 23 p3008 A73-44014

Pair production near energy threshold by electron oscillation and acceleration to relativistic velocities at laser beam focus with plasma wave excitation 23 p2899 A73-44121

One-component two dimensional plasma, calculating equilibrium pair correlation function by Debye approximation for particle interaction via Coulomb potential 23 p3013 A73-44172

Interaction of a monoenergetic nonrelativistic electron beam with electrostatic surface oscillations in a plasma. 23 p3013 A73-44307

Electron injection through the diverter in a heliotron. 23 p3013 A73-44309

Absorption and emission of waves generated by an electron beam in an inhomogeneous magnetoplasma. 23 p3013 A73-44310

Equilibrium configurations of electron beams in a plasma 23 p3014 A73-44338

Combined heating of a plasma by an electron beam and an intense ion-cyclotron wave. 24 p3114 A73-44495

Stability of an electron beam in an inhomogeneous dielectric medium. 24 p3114 A73-44610

Excitation of electron-cyclotron waves by high-current counter-streaming electron beams. 24 p3115 A73-44620

Generation of VLF waves in the ionosphere near the low-frequency plasma resonance. I 24 p3115 A73-44788

Plasma instabilities in the region in front of a body moving rapidly in the ionosphere 24 p3115 A73-44790

Electron beam concentration enhanced by a laser-produced plasma. 24 p3115 A73-44921

Experimental determination of the nonlinear interaction in a one dimensional beam-plasma system. 24 p3117 A73-45458

Nonlinear saturation of the relativistic beam-plasma instability in the presence of ion density fluctuations. 24 p3118 A73-45465

PLASMAGUIDES

Kinetic theory of surface waves in a cylindrical plasma waveguide. 02 p0198 A73-12106

Characteristics of waveguides containing anisotropic warm plasma in the presence of transverse magnetic field. 04 p0480 A73-15600

Buildup of a narrow plasma channel by microwaves. 08 p0992 A73-20954

Propagation of backward surface wave along an annular plasma guide with azimuthal electron density variation. 09 p1125 A73-21930

Characteristics of waveguides filled with homogeneous lossy anisotropic drifting plasma. 10 p1192 A73-23574

Electromagnetic energy in the two-stream instability in a magnetized plasma. 10 p1254 A73-24197

Properties of plane asymmetric plasma waveguides as applied to short-wave propagation along inhomogeneities of the topside ionosphere. 10 p1188 A73-24216

Study of the effect of a plasma on the microwave radiation of a helical beam in a waveguide 12 p1527 A73-26935

The problem of interaction between a relativistic electron beam and plasma in a waveguide 16 p2040 A73-32899

Dispersion relations for parallel-plane waveguide containing transversely magnetized uniaxial and warm plasma in relative motion. 22 p2824 A73-41857

Effect of a plasma on the microwave radiation from a helical beam in a waveguide. 22 p2892 A73-42269

Investigation of the waveguide properties of a plasma cylinder for axially asymmetric waves 22 p2892 A73-42379

The efficient inject of high microwave powers into the overdense magnetoactive plasma in the waveguide. 22 p2827 A73-42517

Plasma cluster movements in guides using straight stellarator magnetic fields and axisymmetric-straight rod produced field combination 23 p3010 A73-43660

Local measurements of plasma parameters by a microwave interferometer with a moving emitter 23 p3011 A73-43666

PLASMAPAUSE

Ring current proton injection instability for ion loss cone and electromagnetic ion cyclotron waves in low beta low density region outside plasmapause 02 p0156 A73-11748

Recent satellite measurements of the morphology and dynamics of the plasmasphere. 03 p0301 A73-13709

Behavior of thermal plasma in the magnetosphere and topside ionosphere. 04 p0442 A73-15336

The light-ion trough, the main trough, and the plasmapause. 04 p0493 A73-15533

Earth magnetosphere essential processes, discussing outermost atmosphere, solar wind theory and sector structure, models, plasmapause, polar cusps, tail theory and ionospheric currents 06 p0688 A73-17502

Whistler observations of the depletion of the plasmasphere during a magnetospheric substorm. 09 p1074 A73-22060

On what ionospheric workers should know about the plasmapause-plasmasphere. 10 p1215 A73-24781

An association of magnetospheric whistler dispersion characteristics with changes in local plasma density. 12 p1488 A73-26985

Satellite studies of magnetospheric substorms on August 15, 1968. III - Some features of magnetospheric convection. 16 p2004 A73-33451

The plasmasphere during a magnetic recovery period - A combined study of the OGO 4 and OGO 5 satellite data and of whistlers received at the ground 16 p2008 A73-33876

VLF goniometer observations at Halley Bay, Antarctica. I - The equipment and the measurement of signal bearing. II - Magnetospheric structure deduced from whistler observations. 17 p2159 A73-34777

Predawn enhancement of 6300-A emission observed near the plasmapause from the Isis-2 spacecraft. 20 p2551 A73-38945

Explorer 45 /S3-A/ symmetrical floating probes for plasmapause dc electric fields, discussing plasma sheaths, noise storms, whistlers, electric field strength and orbit configuration 20 p2552 A73-38954

Proton flux density and differential energy spectra recorded by solid state proton detectors and three-axis fluxgate magnetometer aboard Explorer 45 at plasmapause 20 p2552 A73-38955

Plasma wave observations near the plasmapause with the S3-A satellite. 20 p2552 A73-38956

ULF excitation of plasmapause sinusoidal oscillations by magnetic disturbances exterior to plasmasphere boundary, inferring plasma density from wave frequency and damping rate 21 p2650 A73-40507

Relationship of the sporadic F2 layer with certain features of the ionosphere and magnetosphere at subauroral latitudes 24 p3083 A73-44792

PLASMAS [PHYSICS]

NT ARGON PLASMA
NT BETA PARTICLES
NT CESIUM PLASMA
NT COLD PLASMAS
NT COLLISIONAL PLASMAS
NT COLLISIONLESS PLASMAS
NT COSMIC PLASMA
NT DENSE PLASMAS
NT DEUTERIUM PLASMA
NT ELECTRON PLASMA
NT HELIUM PLASMA
NT HIGH TEMPERATURE PLASMAS
NT HYDROGEN PLASMA
NT LASER PLASMAS
NT METALLIC PLASMAS
NT MICROPLASMAS
NT NITROGEN PLASMA
NT NONEQUILIBRIUM PLASMAS
NT NONUNIFORM PLASMAS
NT OXYGEN PLASMA
NT RAREFIED PLASMAS
NT RELATIVISTIC PLASMAS
NT ROTATING PLASMAS
NT SOLAR WIND
NT STELLAR WINDS
NT THERMAL PLASMAS
NT URANIUM PLASMAS

Partial differential equations with random coefficients and boundary conditions for stochastic processes in plasma, using parabolic equations for distribution function

High-speed stereoscopic investigation of paths of luminous objects

Measurement of plasmoid energy in a time-variable magnetic field

Continuum theory of a slightly ionized plasma, diamagnetic effects.

Measurement of plasmoid energy in a time-varying magnetic field.

PLASMATRONS

NT DUOPLASMATRONS
Russian book on plasma cutting covering electrophysical and thermophysical principles of arc discharges application for metal cutting, arc I-V characteristics, plasmatrons and operation

Heat removal in a sectioned channel of an electric-arc plasmatron

Effectiveness of a gas screen in plasmatrons of axial configuration

Investigation of the steady-state temperature field in a composite cathode of a plasmatron

Heat removal in the sectioned channel of an electrode-type plasmatron.

Russian book on low temperature plasmatron-generated plasmas covering physical and transport properties, optical, thermophysical and gasdynamic analytic methods, etc

PLASMOIDS

U PLASMAS [PHYSICS]

PLASMONS

Many-body effects at metal-semiconductor junctions. I - Surface plasmons and the electron-electron screened interaction.

Two quantum induced photon-plasmon transition probability for hydrogen atom in processes of nebulas and stellar chromospheres

Dynamics of the non-linear interaction of magneto-hydrodynamic waves.

Magnetic field effects on slab surface plasmons in the local limit.

PLASTIC AIRCRAFT STRUCTURES

Age control evaluation of Buna N elastomers by ANA Bulletin 438, using shelf aging and crashed aircraft case studies

Advantage of reinforced plastics for helicopter blades and hubs

Polyimide composites development for aircraft structures.

High modulus organic fibre composites in aircraft applications.

Feasibility evaluation of graphite/epoxy composite materials to helicopter transmission housing.

Fiberglass-reinforced plastics for glider laminate wing spars, describing elastic properties and strength characteristics

Lightning protection for boron and graphite reinforced plastic composite aircraft structures, discussing zonal design concept and channel intermittent contact with protrusions on surface

F-14 aircraft boron-epoxy and graphite-epoxy composite structure production protection against degradation by lightning discharges, discussing design, processing and tests

Glass fabric structures, properties and designs of reinforced polyester and epoxy laminates for aerospace applications

High strength low density Hyfil carbon fiber prepreg sheet properties and production for aircraft applications

Cost/weight tradeoff ratios for fiber reinforced plastic aircraft structural components [SAE PAPER 730338]

Reinforced plastics for aerospace applications covering history of laminates, use of cellulose, asbestos, boron, glass and oriented carbon fibers, whisker composites and resin matrices

Buffalo aircraft fiberglass laminated polyester nose boom for mounting horizontal and vertical wind sensing probes, describing instruments and measurement procedures

Development and problems of testing prepregs for the purposes of the Czechoslovakian aircraft industry

Feasibility study of skirt configurations and materials for an ACLS aircraft.

Composite fabrication and structural design for commercial aircraft, discussing graphite post installation and testing and pultrusion and autoclave molding processes [SME PAPER EM 73-717]

Aircraft windshield stretched acrylic plastic, chemically strengthened glass, and clad polycarbonate curved composite materials

Low-pressure prepregs as structural material for light-construction designs

PLASTIC ANISOTROPY

NT ELASTIC ANISOTROPY

Plastic strain anisotropy changes in single crystals of beryllium following programmed load application

Anisotropic material characteristics due to plastic deformation during fabrication processes, presenting tensor analysis

Plastic anisotropy of low-carbon, low-manganese steels containing niobium.

Yield surface equation derivation for plastically prestrained anisotropic material from simple tension and compression tests

Transient response of a plastically anisotropic cylinder in plane strain.

Investigation of the strong anisotropy and resistance of fiber-strengthened plastics to interlayer shearing and compression normal to the fibers

Biharmonic solutions of problems for elastoplastic bodies in the presence of nonuniformity of the stress field

The effect of plastic anisotropy in the low-cycle fatigue behavior of Zircaloy.

Work hardened plastic material mechanical properties changes manifested by Bauschinger effect defined as acquired anisotropy, examining plastic deformation conditions

The anisotropy of creep behaviour in oriented thermoplastics.

Anisotropic nature of strain hardening during unsteady creep of alloy AK4-I subject to combined tension and torsion

Round bars of an anisotropically hardening material in torsion

Strain-hardening anisotropy and original anisotropy in creep

Anisotropy of the mechanical properties of aluminum hardened by a stainless steel grid

PLASTIC DEFORMATION

General two-dimensional problem in the theory of ideal plasticity of anisotropic materials

Plastic deformation and anisotropy of sapphire crystals via nonbasal plane slip under bending, obtaining stress-strain curves and flow stresses temperature dependence

PLASTIC COATINGS

Resin powder coating technology, describing fluidized bed, electrostatic and plasma spray processes

Russian papers on metal corrosion and protection covering additives, annealing, polymer coatings, anodic polarization, electrodeposition, magnetic alloy coatings, etc

An intumescent coating for improved fuel fire protection of heat sensitive articles.

Selection and application of the protective coating system for the AWACS radome.

HF transverse resonant vibrations of annular Al plates with polychlorovinyl and polyamide base coatings, noting damping and strain relationship to energy dissipation

The experimental determination of wall-fluid mass transfer coefficients using plasticized polymer surface coatings.

Asbestos-textolite coating required thickness calculation with allowance for aerodynamic heating, discussing softening mechanisms

Study of the structural and mechanical properties of polyvinyl-chloride pastes used as anticorrosion coatings

Elastomeric and ceramic coatings for aircraft and missile radomes protection in subsonic and supersonic rain erosion environments

Cross-linking ambient curing mechanisms for air-drying oxidizable coatings, involving chemical film-forming reactions

Thin film temperature sensor with polymer coating for medical research providing good sensitivity and stability for rapid temperature changes in biochemical reactions

PLASTIC DEFORMATION

Combined heating and irradiation effects on body elastoplastic stress-strain state, deriving thermoradiative plasticity equations

Shell designs by the theory of small elastoplastic deformations with allowance for the compressibility of material

Investigation of a deformation process in a heated elastoplastic cylindrical shell

Use of a plastic deformation design model of polycrystalline material in the analysis of loading surface transformation

Thermal cycle influence in heat resistant materials plastic strain and time to failure for different stress and temperature conditions

Book - Deformations of fibre-reinforced materials.

Structural changes during the deformation of molybdenum alloys

Role of the crystalline structure and orientation of single crystals in the formation of the external friction process

Mathematical model for the buildup of imperfections in plastic isotropic materials

Deformation and failure of heat-resistant materials under conditions of thermal fatigue and creep as functions of the nature of the temperature change cycle and of the boundary conditions

Dislocation density in Mo single crystals subject to uniaxial tensile stress or sphere-produced indentation, evaluating plastic strain level

Plastic strain anisotropy changes in single crystals of beryllium following programmed load application

Textures of deformation and of primary and secondary recrystallization in high-purity nickel

Axisymmetric plastic response of rings to short-duration pressure pulses.

Investigation of creep in Kh18N10T steel at varying temperatures 01 p0066 A73-11094

Elastic-plastic analysis on the structural elements with different values of stress concentration factor. 01 p0117 A73-11222

Unit for fatigue testing with a pulsating load at a specified force and deflection. 01 p0054 A73-11299

Austenite deformation effect on thermal stability and hardness of Ni steels at various C and Ni concentrations 01 p0067 A73-11349

Assessment of the stressed state of a material from the strain nomogram 02 p0229 A73-11618

Characteristics of the process of plastic deformation of bcc metals in the microyield zone 02 p0179 A73-11622

Numerical solution to the problem of the elastoplastic stability of doubly connected plates with curvilinear boundaries 02 p0231 A73-11813

Thin walled shells strength dependence on residual stresses, noting stress analysis of shallow spherical shell with variable residual deformations 02 p0232 A73-11932

Surfaces of constant rate of energy dissipation and deformation velocity for arbitrary thin walled shell under steady creep with given strain hardening 02 p0233 A73-11937

Plastic limit behavior and failure of filament reinforced materials. 02 p0234 A73-12074

Relation between plasticity characteristics and geometrical dimensions of cylindrical specimens under tension. 02 p0235 A73-12140

Study of the effect of small elastoplastic deformations on the load-bearing capacity of specimens with stress concentrators under repeated variable loading. I. 02 p0235 A73-12202

Study of the effect of small elastoplastic deformations on the load-bearing capacity of specimens with stress concentrators under repeated variable loading. II. 02 p0181 A73-12203

The effect of a preliminary plastic strain on the form of a mechanical hysteresis loop. 02 p0235 A73-12208

On approximate solutions for rigid-plastic structures subjected to dynamic loading. 02 p0236 A73-12520

Direct observation of the magnetic microstructure in niobium-based superconducting alloys subject to deformation 02 p0201 A73-12554

Experimental investigation of the influence of initial flexures on the stability of smooth conical shells loaded by external pressure 02 p0236 A73-12576

Elastic and plastic deformations of circular ring with initial machining produced stresses distributed across thickness, calculating critical load for static stability 02 p0236 A73-12581

Stress concentration in a plane weakened by two different circular holes in the presence of small elastoplastic strains 02 p0237 A73-12585

Elastoplastic stressed state of cylindrical shells weakened by a circular hole 02 p0237 A73-12590

The effect of prior deformation on the strength and annealing of reverted austenite. 02 p0183 A73-12766

High resolution marker transport sintering study. 02 p0175 A73-12771

Elasto-plastic analysis of three-dimensional structures using the isoparametric element. 03 p0383 A73-12874

The post-buckled behaviour of a thin-walled box beam in pure bending. 03 p0384 A73-13114

On the influence of acceleration stresses on the yielding of disks of uniform thickness. 03 p0384 A73-13118

Finite plastic deformation of pressurized membranes of revolution. 03 p0384 A73-13120

Effect of a single plastic deformation on the fatigue behavior of metals 03 p0322 A73-13136

Dynamic plastic tensile stress analysis based on equation of motion, kinematic equation and material law with conditions regarding disturbance propagation velocity 03 p0385 A73-13142

Stress-strain diagrams for stability of structures under plastic bending, noting differential equations for rigidity characteristics 03 p0386 A73-13144

An experimental investigation of a rigid-plastic state of deformation with the aid of the Moire method 03 p0306 A73-13148

Impulsive loading of rectangular plates with finite plastic deformations. 03 p0389 A73-13322

Triaxial plastic compression soil theory generalization to three dimensional complex stress fields, discussing yield surface for granular materials 03 p0390 A73-13332

Inhomogeneity of the structure and deformability of aluminum and aluminum-magnesium alloys 03 p0324 A73-13506

Influence of deformations on the mechanical properties of magnesium alloys containing yttrium 03 p0324 A73-13509

Plane strain limit analysis of plastic material described by piecewise analytic nonlinear yield condition and associated flow rule 03 p0393 A73-13778

Microstructure and plastic deformation of the Ni4Mo alloy. 03 p0325 A73-13804

Substructural changes during high-temperature creep deformation of aluminum single crystals 03 p0327 A73-13978

Sn alloying effect on heat resistant Ni-Cr alloys plastic strain resistance and strength at room and high temperatures 03 p0327 A73-14003

Determination of critical stresses for elements of cylindrical shells in the plastic state 03 p0396 A73-14619

Large elasto-plastic deflection of a circular plate of mild steel under cyclic loading. 03 p0396 A73-14626

Metal deformation processes, discussing hot working, fracture, hydrostatic extrusion, superplastic forming, diffusion bonding and powder fabrication 04 p0452 A73-14742

Dynamic response of nonlinear media at large strains. 04 p0509 A73-14947

Frequency spectra of acoustic emissions generated by deforming metals and ceramics. 04 p0448 A73-15122

Plastic deformations and crack propagation in cylindrical and spherical shells under uniform pressure, calculating stress intensity factor 04 p0512 A73-15239

Grain boundary interface and crystal structure effect on elastic and plastic deformation and mechanical properties of metals at low and high temperatures 04 p0462 A73-15301

Dislocation dynamics in niobium-oxygen solid solutions. 04 p0462 A73-15303

Optimal temperature and strain rate for deformation in superplastic state for alpha-beta Ti alloy 04 p0464 A73-15498

Influence of hydrogen on the technological plasticity of the alloy Ti + 9% Al 04 p0464 A73-15499

Temperature dependence of the elastic micro- and macro-stiffness of dispersion hardenable Co-Ni-Ti and Co-Ni-Ti-Al alloys. II 04 p0465 A73-15640

Influence of cold deformation and subsequent heating on the structure and properties of dispersion-strengthened nickel 04 p0466 A73-15666

Compression tests for plastic deformation and fracturing of Al alloy powder at hot working temperatures, noting limiting deformations in forging [ASME PAPER 72-WA/MAT-5] 04 p0456 A73-15808

Elastic-plastic deformation in edge-notched tension specimens under plane stress conditions. [ASME PAPER 72-WA/MAT-3] 04 p0514 A73-15809

Boron fiber-aluminum alloy matrix composite structure Charpy impact energy absorbing capacity explained via energy dissipation of matrix by plastic deformation 03 p0588 A73-16111

A plastic-strip specimen for fatigue crack propagation studies in low yield strength alloys. 03 p0581 A73-16127

On the similarity conditions in the phototheological method of stress analysis. 03 p0632 A73-16430

Deformation, displacement, and work bounds for structures in a state of creep and subject to variable loading. [ASME PAPER 72-APM-U] 03 p0632 A73-16529

Two types of loss of stability and strength in cylindrical shells 03 p0634 A73-16747

Material deformations determined with the aid of X rays in the case of elongations remaining after a uniaxial tensile test involving titanium and TiAl6V4 03 p0588 A73-17243

Minimum principles in the dynamics of isotropic rigid-plastic and rigid-viscoplastic continuous media. 06 p0757 A73-17396

Limit analysis of plates with piecewise linear yield surface. 06 p0758 A73-17398

Evaluation of multiaxial theories for room-temperature plasticity and elevated-temperature creep and relaxation of several metals. 06 p0759 A73-17599

A new approach to the mode approximation for impulsively loaded rigid-plastic structures. 06 p0760 A73-17764

Lagrange description of equations for finite deflections of incompressible plastic shells, classifying stress-strain relations 06 p0760 A73-17778

Structural design with allowance for shakedown in the case of temperature-dependent elastic constants 06 p0760 A73-17780

Truncated conical shell buckling and stability beyond elastic limit, deriving lower critical loads by orthogonalization method 06 p0760 A73-17781

Dynamic plastic deformation of rings under impulsive load. 06 p0761 A73-17817

Observations on the deformation properties of sand-wich materials. 06 p0761 A73-17819

Plastic deformation magnitude and direction /sign/ for maraging steels under heat treatment, noting optimal conditions for maximum hardening 06 p0697 A73-17878

Surface effects in solid bodies undergoing deformation and fracture 06 p0734 A73-17922

Deformation by Poirier-Luders bands observed on composites of oriented solidification [ONERA, TP NO. 1192] 06 p0708 A73-18099

The martensitic transformation during deformation of titanium alloys with metastable beta phase. 06 p0708 A73-18207

Extremum principles on time independent elastoplastic solids nonisothermal deformation properties based on yield function dependence on temperature 06 p0763 A73-18456

An experimental investigation into the mechanics of deep semielliptical surface cracks in mode I loading. 06 p0763 A73-18478

Influence of local variations of yield strength on plastic zones at crack tips. 06 p0709 A73-18480

Stress analysis of sharply notched plates and measurement of notch tip blunting. 06 p0764 A73-18487

Mathematical model for plastic deformation of polycrystalline materials with Hooke's Law elastic strains 06 p0765 A73-18641

Microtwinning factors in plastic deformation, volume changes and carbon solution content of Ni martensite 06 p0710 A73-18645

Application of the finite element method to the solution of elastoplastic problems 06 p0766 A73-18726

On the convergence of the method of homogeneous linear approximations in problems of the theory of plasticity of inhomogeneous bodies. 07 p0906 A73-19022

FORTAN sequence with economical computer storage requirement for matrix method application to rigid plastic collapse analysis of frame, considering bounded variable problem 07 p0907 A73-19034

Decohesive load carrying capacity of elastoplastic bodies based on permissible discontinuities due to strain increase, relating to structural strength determination 07 p0908 A73-19082

Behavior of austenitic stainless steels under continuous or repeated strain 07 p0838 A73-19115

Axisymmetric buckling of uniformly loaded spherical caps undergoing plastic deformation. 07 p0913 A73-19971

Body centered cubic transition metal stage 3 electrical resistivity recovery mechanism from experiment on recrystallized and stress-relieved plastically deformed Nb wire 07 p0839 A73-20112

Rheological materials thermodynamics with plastic deformations, discussing thermoplastic boundary value problems, thermal shock and heat generation 07 p0914 A73-20180

Nonlinear effect of initial stress on crack propagation between similar and dissimilar orthotropic media. 07 p0915 A73-20334

Investigation of the plastic state of disks by the hardness measurement method 07 p0917 A73-20514

Self-compensating strain measurement in rotating disks subjected to elastic and plastic deformation 07 p0826 A73-20516

Use of chromoplastic models for the study of the behaviour of rectangular plates after buckling. 08 p0107 A73-20946

The diffusion coefficient during plastic deformation in AlMg₅ 08 p0977 A73-21019

Effects of thermal loading on foil and sheet composites with constituents of differing thermal expansivities. 08 p0979 A73-21572
[ASME PAPER 72-MAT-E]

Effects of thermal loading on fiber-reinforced composites with constituents of differing thermal expansivities. 08 p0979 A73-21573
[ASME PAPER 72-MAT-F]

A recovery creep model based on dislocation distributions. 08 p0980 A73-21777

On dynamic plasticity. I 08 p1020 A73-21823

Parametrization of low-temperature deformation characteristics in single crystals of molybdenum. 09 p1099 A73-21928

Thermal-activation parameters of plastic deformation in alpha-titanium single crystals 09 p1099 A73-21964

Features of the structure and of plastic deformation in zirconium saturated with nitrogen and oxygen 09 p1099 A73-21967

Annealing of discontinuities in deformed aluminum 09 p1100 A73-21973

On the influence of deformation rate on intergranular crack propagation in Type 304 stainless steel. 09 p1100 A73-22000

Certain regularities in the deformation and rupture of molybdenum-, niobium-, and tantalum-based high-melting-point alloys under programmed temperature changes 09 p1100 A73-22151

Deformation and rupture of molybdenum under conditions of creep 09 p1100 A73-22161

Grain size effects on strength and ductility of two phase Ni-Cr and Ni-Mo alloys at high and low deformation temperatures 09 p1101 A73-22164

Rigidly plastic shells yield point, deriving yield surface in generalized stress space 09 p1158 A73-22360

A strain criterion for failure of materials subjected to stress and temperature cycles 09 p1159 A73-22570

An investigation into the relationships of fatigue fracture and inelastic deformation of metals in torsion. 09 p1161 A73-23052

Plasticity and failure of heat-resistant materials at a low number of cycles of simultaneous fluctuations of temperature and load. 09 p1105 A73-23154

Plane stress rupture criterion for age hardening materials during plastic deformation, calculating resistance to shear and torsion of solid and hollow round bars 09 p1106 A73-23157

Influence of the combined effect of plastic deformation and high temperatures on the diffusion mobility of carbon 09 p1108 A73-23241

Fatigue crack initiation and propagation in part through crack metal specimens under cyclic loading, discussing plasticity effects and surface wave interaction 09 p1163 A73-23253

Plastic strain rates within discrete crack tip zones at running brittle cracks in mild steel plates, identifying twinning as main deformation mode 09 p1163 A73-23258

Cantilever cylindrical shells of rigid-plastic material, determining collapse loads under external pressure combined with end moment by numerical solution to limit analysis 09 p1164 A73-23271
[ASME PAPER 72-PVP-B]

On the elastoplastic problem of cantilever subject to combined bending and twisting. 09 p1164 A73-23320

Some investigations on the methods of measuring 3-dimensional plastic deformations by laser. 09 p1086 A73-23321

Ductile fracture strain criteria from known stress-strain relationships, predicting microscopic crack and void nucleation strain 09 p1164 A73-23322

Elastoplastic deformation and stresses in clamped multilayer cylinders 10 p1287 A73-23593

Influence of the degree of deformation and annealing temperature on the recovery of 99.999% pure nickel after plastic deformation at -196 C and 25 C, respectively 10 p1231 A73-23690

Plastic strain and zero stress concepts as specific properties of materials with long range memory, formulating functional plasticity and moving dislocations theory 10 p1289 A73-24159

Difference of the plastic deformation of the surface and internal layers of polycrystalline iron under fatigue loading. 10 p1233 A73-24183

Direct observation of magnetic microstructure in deformed niobium-based superconducting alloys. 10 p1259 A73-24186

The analysis of dislocation systems by the finite element method. 10 p1290 A73-24298

Design stability of composite samples with a soft interlayer in static tension 10 p1291 A73-24352

Plastic strain as factor in crack propagation rate smoothing and branching rate reduction in elastic and elastoplastic materials 10 p1291 A73-24362

Investigation of the load-carrying capacity of rotating disks by the method of optically sensitive coatings 10 p1291 A73-24364

Study of the effectiveness of various thermomechanical methods of hardening alpha + beta titanium alloys 10 p1234 A73-24425

Investigation of the durability of metals under conditions of transition from brittle to plastic failure 10 p1235 A73-24456

Cylindrical metal projectile impact induced elastoplastic deformation, determining dynamic yield point by computer simulation of Taylor stress wave propagation model 10 p1292 A73-24529

An upper bound solution for rectangular plate in plane stress compression. 10 p1292 A73-24640

On the identification of the unknown functions in Drucker's work-hardening relation for plastic deformation of crystalline materials. 10 p1292 A73-24652

Thin walled elastoplastic cylindrical shells deformations investigation by elliptic quasi-linear equation systems 11 p1433 A73-25044

Upper bounds to plastic strains in shake-down of structures subjected to cyclic loads. 11 p1434 A73-25216

Experimental verification of the applicability of small elastoplastic deformation theory to the calculation of rotating disks 11 p1434 A73-25392

Discontinuous fibres alignment in metal composites by plastic deformation. 11 p1372 A73-25409

Influence of small local deviations in specimen diameter on conventional strain at maximum load in tensile test 11 p1380 A73-25448

The influence of environment and the surface layer on crack propagation and cyclic behavior. 11 p1380 A73-25807

The soft surface effect in plastic deformation and fatigue of metals and alloys. 11 p1381 A73-25808

Application of some aspects of low-cycle fatigue research in structural design. 11 p1443 A73-25846

An elastic-plastic buckling solution using the incremental theory. 11 p1443 A73-26089

Plane strain plastic yielding due to bending of end-loaded cantilevers containing circular, triangular or diamond-shaped holes. 11 p1443 A73-26091

The role of plastic deformation in metal powder compaction. 11 p1374 A73-26270

Gradient decomposition and kinematic constitutive equations for elastoplastic material behavior under large strains 11 p1445 A73-26410

Antiplane deformation near a cut in a hardening elastoplastic material 11 p1445 A73-26458

Amplitude-dependent anelasticity in aluminum and copper single crystals. II - Studies in amplitude range III during and after plastic deformation 11 p1385 A73-26567

Influence of deformation and heat treatment on the structural changes of the OKh12N13M alloy 12 p1508 A73-26836

Plastic deformation, martensite transformation and temperature effects on shape memory of nitinol and other alloys 12 p1509 A73-26896

Influence of impact deformation on the strengthening and aging kinetics of austenitic steel 4Kh12N8G8MBF 12 p1510 A73-26901

Improving the properties of the MA5 magnesium alloy by high-temperature thermomechanical treatment 12 p1510 A73-26910

Deformation and recrystallization of twin crystals in aluminum and magnesium alloys 12 p1510 A73-26913

Deformation of zero-moment shells subjected to internal pressure under creep conditions 12 p1551 A73-27179

Continuum mechanics analysis of local rupture and plastic strains near cracks and fractures, noting elastoplastic applications 12 p1551 A73-27251

Kinetic strain criteria of cyclic failure at high temperatures 12 p1552 A73-27252

Influence of plastic deformation on the electrical resistance of molybdenum single crystals 12 p1512 A73-27260

Ideal plasticity theory for solid bodies of isotropic materials with different yield points in extension and compression 12 p1553 A73-27374

Conditional margin of plastic strength for shaft-type elements subjected to torsion at low temperatures 12 p1554 A73-27478

Deformation and strength characteristics of carbon-fiber strengthened plastics in compression 13 p1644 A73-27991

Deformable body with reticular structure, studying microstructural transitions using physical model with isolated-valence bond coupling 13 p1690 A73-27992

Solution of the problem of plane deformation for a tube consisting of a physically nonlinear quadratic viscoelastic material 13 p1690 A73-27995

Dislocation structure and low-temperature plasticity of chromium alloys with rare earth metals 13 p1630 A73-28011

Influence of deformation history on the yield locus and stress-strain behavior of aluminum and copper. 13 p1632 A73-28130

Ferritic stainless steel transverse tension ridging mechanism in terms of CF and CC mixed texture bands, contradicting plastic buckling theory 13 p1633 A73-28147

On a finite strain theory of elastic-inelastic materials. 13 p1692 A73-28167

Mechanical behavior of plastically deformed polycrystalline metal subjected to hydrostatic pressure soaking. 13 p1634 A73-28196

Weak-beam high-resolution electron micrographs of plastic deformation-generated extended dislocations in Ge single crystals 13 p1668 A73-28222

Plastically deformed Fe-Si and Al alloys surface layer crystal dislocation density and plastic flow onset determination as function of depth 13 p1635 A73-28264

Dynamically possible finite deformations of isotropic, incompressible, elastic-inelastic solids with temperature independent response. 13 p1695 A73-28416

Elastic and creep limits of heteroplastic micrograin metallic (duralumin) materials in terms of stress-strain curve, sliding plane and stress hardening and relaxation 13 p1635 A73-28471

Strain gage measurements of elastoplastic deformations under biaxial and triaxial stresses with application to cylindrical steel container 13 p1617 A73-28843

Multiphase composite material models for elastoplastic beam bending under loading and unloading, using stress-strain diagram in tension and compression 13 p1698 A73-29052

Method of recording elastoplastic stress waves in solids with a dielectric sensor 13 p1618 A73-29059

Titanium flow curves in octahedral coordinates for various conditions of deformation 13 p1636 A73-29132

The effect of strain rate and heat developed during deformation on the stress-strain curve of plastics. [SESA PAPER 2088A] 13 p1646 A73-29303

Inelastic column buckling of internally pressurized tubes. [SESA PAPER 2049] 13 p1699 A73-29305

Theoretical interpretation of residual lattice strains induced in polycrystalline metals by plastic deformation. 13 p1639 A73-29460

Effects of specimen geometry and loading conditions on the crack tip plastic zone. 13 p1701 A73-29474

The interaction of material and geometric aspects in the fracture of aluminum alloys. 13 p1640 A73-29475

Plane strain elastic-plastic state and fracture in cracked blunt notched steel plates under tensile loads 13 p1701 A73-29477

Fatigue crack initiation and propagation in low stacking fault energy austenite steel related to plastic deformation induced gamma alpha transformation and martensite failure 13 p1640 A73-29481

Choice of materials on the basis of random vibration and structural fatigue. 13 p1641 A73-29495

Machine parts fatigue life and linear cumulative damage at stresses below endurance limit, including plastic strain, microcracking and S-N curves
13 p1641 A73-29496

Cumulative damage and behavior of plastic strain in high and low cycle fatigue.
13 p1641 A73-29500

Life prediction of metals subjected to high temperature fatigue.
13 p1708 A73-29503

Some observations on grain boundary sliding in aluminum bicrystals deformed at elevated temperatures.
13 p1641 A73-29508

Stress-strain state of thin circular perforated Cu plate under uniform tensile load, showing applicability of small elastoplastic finite deformation theory
13 p1703 A73-29601

Hysteresis loop equation for calculation of elastoplastic deformations caused by forced vibrations, taking into account medium compressibility and inertial forces
13 p1703 A73-29609

A method of elastic-plastic analysis of largely deformed plate problems.
14 p1808 A73-30194

Stability criteria for rigid plastic cylindrical shells at yield point load as function of deformation rate and geometry changes
14 p1809 A73-30257

Minimum potential and complementary energy rate principle formulation for finite plastic deformation, applying to cylindrical shell under uniformly distributed internal load
14 p1809 A73-30258

Deformation and destruction of heat-resistant materials in conditions of thermal fatigue and creep as a function of the nature of the cyclic change in temperature and boundary conditions.
14 p1759 A73-30303

Assessment of the degree of plastic deformation in a crater with ball imprint.
14 p1810 A73-30309

The Portevin-Le Chatelier effect in the case of alloys of copper with aluminum, gallium, germanium, arsenic, and indium
14 p1760 A73-30443

A comparison of theory and experiments on the dynamic plastic behavior of shells.
14 p1811 A73-30476

Yield conditions for plastic deformation of anisotropic bodies, using stress tensor invariants and Tresca form
14 p1811 A73-30480

Linearized constitutive equations for thin viscoplastic shell deflection under dynamic loads
14 p1811 A73-30488

Some thermodynamic considerations of phenomenological theory of non-isothermal elastic-plastic deformations.
14 p1811 A73-30490

Initial plastic deformations due to surface defects, deriving corresponding elastic distortions and velocity fields of medium from equilibrium equations
14 p1812 A73-30544

Extremum principles in the dynamics of rigid-plastic bodies and mathematical programming.
14 p1813 A73-30547

Dislocation structure of Ni3Al intermetallic compound during various stages of deformation
14 p1760 A73-30591

German monograph - Elevation of the yield point and pronounced yield range of multicrystalline aluminum-magnesium alloys.
14 p1762 A73-30673

Rotating turbine disks ultimate strength relation to stress-strain state, material mechanical properties and plastic deformation
14 p1814 A73-30684

Fatigue failure of a two-phase titanium alloy in vacuum
14 p1763 A73-30713

Mechanical deformation and failure of metals under the action of a 0.01-sec laser light pulse
14 p1758 A73-30714

Some plastic deformation laws for titanium under static and alternating loads
14 p1763 A73-30723

Study of the elastoplastic stressed state and plastic zones of a plate with a circular hole under tension
14 p1815 A73-30794

Kinetics of changes in deformability of a heat-resistant nickel-base alloy
14 p1764 A73-30861

Mechanism of plastic deformation and low-temperature brittleness of a Cr alloy containing 45 at.% Fe
14 p1764 A73-30866

Aluminum structure effects on thermal activation parameters of plastic deformation, proposing strain rate control mechanism
14 p1764 A73-30867

Stacking fault energy in iron-nickel and iron-nickel-chromium alloys
14 p1764 A73-30869

Influence of alpha- and beta-stabilizers on the plastic deformation mechanism of titanium
14 p1765 A73-30888

Note on volume integrals of the elastic field around an ellipsoidal inclusion.
15 p1946 A73-31104

Designs of statically undeterminable elastoplastic systems under complex loads
15 p1946 A73-31141

Constitutive equations and directors in plastic and viscoplastic media
15 p1947 A73-31368

The dynamic plastic behavior of simply supported spherical shells.
15 p1948 A73-31369

Characteristics of dynamic hot pressing with high deformation rates
15 p1881 A73-31589

Superplasticity of the Kh18Ni9Ti steel
15 p1890 A73-31816

Work hardened plastic material mechanical properties changes manifested by Bauschinger effect defined as acquired anisotropy, examining plastic deformation conditions
15 p1952 A73-32079

Displacements and elastoplastic deformations at a crack edge under tension
15 p1954 A73-32105

Transition theory application to creep deformation, considering spherical shells
15 p1954 A73-32117

Behaviour of aluminium during the passage of large-amplitude plastic waves.
15 p1891 A73-32164

Influence of plastic deformation and of alloying with small additions of oxygen on the decomposition of the metastable beta phase in the Ti6Al4V alloy
15 p1894 A73-32526

Influence of plastic deformation and of phase transformations at negative temperatures on the properties of titanium alloys
15 p1894 A73-32531

Investigation of friction behavior in titanium alloy with 3.8% Al
15 p1894 A73-32535

Deformation of a multilayer shell of revolution under nonisothermal loading
16 p2074 A73-32684

Forming energy in rigid-plastic materials unsteady molding processes, obtaining nonlinear equations system solution by iterative procedure
16 p2037 A73-33237

Hypoelastic approximation for plastic media axisymmetric deformation, determining grid for numerical analysis from orthogonality relations
16 p2079 A73-33239

Thin shell elastoplastic deformation theory development for small strains, using Hooke's law to analyze hardening, stress and unloading
16 p2084 A73-34033

Enhanced ductility in metals/Superplasticity/
17 p2240 A73-34113

Investigation of thermal deformations by methods of holographic interferometry
17 p2164 A73-34172

Inelastic buckling of eccentrically loaded columns.
17 p2240 A73-34180

Method of recording the deformation diagram in thermal-fatigue tests.
17 p2165 A73-34278

Mechanism of the micrononhomogeneous deformation of metals throughout a wide interval of temperature
17 p2186 A73-34330

Theory of disclinations. II - Continuous and discrete disclinations in anisotropic elasticity.
17 p2242 A73-34500

Effects of cold plastic deformation and aging temperature on the mechanical properties of dispersively hardening Cr-Ni-Co-Mo steel
17 p2188 A73-34559

Characteristics of deformation texture development in austenitic steel in a plane stressed state
17 p2188 A73-34564

On the stress analysis of creeping structures subject to variable loading.
[ASME PAPER 72-APM-NNN] 17 p2250 A73-35115

Acoustic emission instrumentation and application for plastic deformation, flaw detection monitoring of fatigue crack growth, stress corrosion and hydrogen embrittlement
17 p2175 A73-35670

Elastic-plastic expansion of 6061-T6 aluminum rings.
18 p2362 A73-36320

Contact problem for infinite elastic isotropic plane weakened by rectilinear cut with free, slipping and adhesive segments and uniformly distributed load at infinity
18 p2363 A73-36415

Polymers fatigue life under cyclic deformation, discussing stress-strain and failure behavior as function of reversed stress cycle frequency
18 p2328 A73-36587

Cyclic inelastic deformation and the fatigue notch factor.
18 p2364 A73-36590

Cumulative fatigue damage under complex strain histories.
18 p2364 A73-36593

A numerical method for creep deformation of solids.
18 p2365 A73-36612

Torsional rigidities for bars under fully plastic torsion.
18 p2365 A73-36695

Influence of plastic strain on the paramagnetic susceptibility of molybdenum single crystals
18 p2324 A73-36802

Some characteristics of the microplastic deformation of the surface layers of semiconductor crystals at temperatures below and above the thermal brittleness threshold
18 p2341 A73-36805

Multiphase composite material models for elastoplastic beam bending under loading and unloading, using stress-strain diagram in tension and compression
18 p2366 A73-36884

A method of recording elastoplastic stress waves in solids by means of a dielectric pickup.
18 p2317 A73-36891

Effect of temperature on the effectiveness of hardening components made of heat-resistant alloys
19 p2439 A73-37268

Some studies of the influence of localized and gross plasticity on the monotonic and cyclic concentration factors.
19 p2497 A73-37589

Plastic state of disks studied from hardness measurements.
19 p2499 A73-37789

Autocompensatory strain measurement of rotating disks subjected to elastic and plastic deformation.
19 p2430 A73-37792

Some details concerning plastic deformation mechanism of commercial titanium between -100 and 400 C
19 p2441 A73-37839

Investigation of the durability of metals under conditions of a transition from brittle fracture to plastic flow.
19 p2442 A73-38138

Plastic deformation anisotropy and work-hardening of composite materials.
19 p2444 A73-38261

Influence of non-singular stress terms and specimen geometry on small-scale yielding at crack tips in elastic-plastic materials.
19 p2501 A73-38264

Metal fatigue studies of nucleation and crack propagation through plastic and elastic regimes
19 p2502 A73-38548

On the relationship of stress crazing and yielding of polymethyl methacrylate.
20 p2579 A73-38641

Propagation of stress wave with plastic deformation in metal obeying the constitutive equation of the Johnson-Gilman type.
20 p2615 A73-38888

The problem of wave propagation in physically nonlinear rods of finite length
20 p2618 A73-39315

Group properties of the equations of strain theory of thermoplasticity
20 p2618 A73-39329

Method of studying thermal fatigue from the parameters of the hysteresis loop in temperature-force coordinates
20 p2619 A73-39362

Anisotropy of low-temperature plasticity and the tendency of deformed molybdenum toward exfoliation
20 p2578 A73-39377

Finite difference technique for elastic-plastic buckling of edge-loaded rectangular plates, finding bifurcation stresses via Hill and Prandtl-Reuss expressions
20 p2623 A73-39560

Study of elastoplastic deformations in a two-layer shell under dynamic loads
20 p2625 A73-39653

Grain boundary destruction mechanisms in pure nickel polycrystals following plastic deformation, discussing annealing, fault concentration, microscopic techniques and critical loads
20 p2578 A73-39735

Effect of iron on the phase composition and mechanism of plastic deformation of titanium
20 p2579 A73-39737

Structural changes during plastic deformation and annealing of tungsten single crystals
20 p2579 A73-39738

Study of the mechanism of plastic deformation of aging nickel-aluminum alloys with a large volume fraction of gamma prime phase
20 p2579 A73-39740

Effect of the degree of plastic deformation on the structure and mechanical properties of low-alloy molybdenum 20 p2579 A73-39741

Electrical resistance variation kinetics in deformed beryllium after annealing 20 p2579 A73-39746

Velocity of a stress wave superimposed on the initial plastic stress state of a rod. 21 p2784 A73-40436

Finite plasticity theory in acoustic tensor calculation for elastic, viscoplastic and plastic wave propagation 21 p2740 A73-40947

Influence of nonuniform heating on the stability of plates beyond the elastic limit 21 p2786 A73-40983

Plastic deformation, martensite transformation and temperature effects on shape memory of nitinol and other alloys 21 p2720 A73-41029

Effect of explosive impact on hardening and kinetics of aging of austenitic steel 4Kh12N8G8MFB. 21 p2720 A73-41034

Experimental investigation of a cylindrical shell loaded by a concentrated tangential force and a bending moment 21 p2787 A73-41193

Residual-stress measurement using surface displacements around an indentation. 21 p2704 A73-41265

The Bauschinger effect and its role in mechanical anisotropy. 21 p2722 A73-41547

A finite-element representation of stable crack-growth. 21 p2788 A73-41549

Torsional elasticity of human skin in vivo. 21 p2642 A73-41625

Plastic collapse of steep conical shells under axial compression. 21 p2789 A73-41684

Field-ion-microscopic study of interstitial plasticity of tungsten microcrystals. 22 p2872 A73-41726

Deformation and microfracture characteristics of two-phase tungsten-composite materials sintered with the liquid phase 22 p2872 A73-41948

Acoustic emission measurements during plastic deformation of metals. 22 p2919 A73-41975

Effect of the superplasticity of titanium and its alloys, and the use of this phenomenon for welding in a solid state 22 p2866 A73-42093

Phase diagrams and composition selections for strengthening of multicomponent deformable Mg alloys with rare earth and transition elements 22 p2874 A73-42094

Some patterns of deformation and failure of refractory alloys of molybdenum, niobium and tantalum during a programmed change of temperature. 22 p2874 A73-42101

The deformation and fracture of molybdenum under creep conditions. 22 p2874 A73-42109

Grain size effects on strength and ductility of two phase Ni-Cr and Ni-Mo alloys at high and low deformation temperatures 22 p2875 A73-42112

Some further results of J-integral analysis and estimates. 22 p2920 A73-42144

A comparison of the J-integral fracture criterion with the equivalent energy concept. 22 p2920 A73-42145

Effects of strain gradients on the gross strain crack tolerance of A 533-B steel. 22 p2876 A73-42153

Accelerating the convergence of elastic-plastic stress analysis. 22 p2922 A73-42481

The cyclic elastoplastic torsion of the circular cylinder in the case of finite deformations 22 p2922 A73-42527

Response function class for constitutive equations in nonlinear isothermal theory of elastic-plastic metals, discussing free energy and stress response as measure of deformation 22 p2925 A73-42890

[ASME PAPER 73-APMW-30] Elastic-plastic wave reflection and refraction obtained by method of singular surfaces, discussing interface and plastic deformation effects 22 p2926 A73-42895

[ASME PAPER 73-APMW-38] The effect of stacking fault energy on the plastic deformation of polycrystalline Ni-Co alloys. 22 p2879 A73-43074

Effective application of double exposure holographic interferometry to the study of deformations of ceramics due to the impact of a projectile 22 p2863 A73-43096

Procedure and device for the study of the behavior of metals subjected to dynamic torsional stresses 22 p2868 A73-43171

Limit pressures for cylindrical shells with two adjacent circular cut outs. 22 p2929 A73-43175

Microplasticizing mechanism of hydrogen embrittlement due to stress activated chemisorption, noting association with temperature dependent hydrogen-metal atomic interaction 23 p3039 A73-43465

Compressive strength and plastic deformation of monocrystal bismuth telluride, polycrystal lead telluride, Cu-Te compounds and Pb-Sn-Te solid solution 23 p3015 A73-43480

Microstructural characteristics of the plastic deformation and recrystallization of an aluminum alloy of various heterophase structure 23 p2991 A73-43489

Designing a slender-wing-type cantilever plate under conditions of unsteady creep 23 p3042 A73-43728

Plastic deformation and anisotropy of sapphire crystals via nonbasal plane slip under bending, obtaining stress-strain curves and flow stresses temperature dependence 23 p2997 A73-43772

The plastic deformation of NiAl single crystals between 300 K and 1050 K. I - Experimental evidence on the role of kinking and uniform deformation in crystals compressed along the 001 direction. II - The mechanism of kinking and uniform deformation. 23 p2991 A73-43773

Certain methods in the physically nonlinear theory of three-layer plates 23 p3043 A73-43921

Postcritical deformations in a multilayer plate under edge pressure 23 p3043 A73-43925

Experimental bases and models for the study of the overall behavior of metals 23 p2993 A73-43964

Elementary mechanisms and physical models in plasticity and viscoplasticity 23 p3043 A73-43965

Constitutive equations of elastoplastic and elastoviscoplastic bodies based on thermodynamic state, considering deformation velocity and stress relaxation 23 p3043 A73-43967

Classical viscoplasticity and Mandel plasticity theories comparison with emphasis on strain hardening, acceleration wave propagation and plastic and elastic deformations 23 p3043 A73-43968

Thermodynamic treatment of plastic media with application to viscoplastic materials, elastoplastic deformation and entropy jump across weak shock waves 23 p3043 A73-43969

Mandel viscoplasticity theory constitutive equations satisfying causality principle, considering finite deformations tensor representation by partial differentials. 23 p3044 A73-43970

Order of magnitude of the differences between theory and experiment in viscoplasticity under varying stress and temperature 23 p3044 A73-43971

Plasticity theory algebraic structure with emphasis on plastic flow laws formulation by adjoint functions and elastoplastic media finite deformations 23 p3044 A73-43972

Study of a dynamic problem in viscoelastoplasticity and ideal plasticity with conditions of friction at the boundary 23 p3044 A73-43973

Uniqueness theorems and variational principles derivation for free viscoplastic flow and constrained plastic deformation, obtaining Castigliano theorem from boundary value problem solution 23 p3044 A73-43974

Orientation dependent slip in polycrystalline titanium. 23 p2993 A73-44028

Microstrain gage for plastic deformation measurements of crystalline solids in compression, obtaining stress-strain diagrams for Ta single crystals 23 p2986 A73-44036

Potential theory-based relationships between plastic deformation and strain hardening properties of elastoviscoplastic and elastoplastic media, considering specific entropy and free energy contributions 23 p3045 A73-44099

Complex elastoplastic torsion of cylindrical shafts 23 p3045 A73-44184

Creep buckling stability for deformable rod with initial deflection, determining perturbed and unperturbed motion of random and deterministic components 23 p3046 A73-44188

Determination of the strained state of a thick elastoplastic plate with an elliptical hole 23 p3046 A73-44201

Dislocation plasticity theory for slip system in terms of constitutive equations for dislocation speeds and densities, extending to rigid viscoplastic body 23 p3046 A73-44226

Surface phenomena in solids during the course of their deformation and failure. 23 p3018 A73-44322

Deformation of molten glass in the zone where a hollow glass fiber is formed 24 p3102 A73-44520

Investigation of the elastic stiffness of niobium low-alloys subjected to small plastic strains 24 p3099 A73-44572

Deformation characteristics and ductility of two-phase titanium alloys of laminated structure 24 p3099 A73-44573

A lower bound theorem for dynamically loaded rigid-viscoplastic structures. 24 p3146 A73-44680

On the description of cyclic deformation processes using a more general elasto-plastic constitutive law. 24 p3147 A73-44683

Experimental investigations regarding optimally designed three-layer wound glass fiber/plastic tubes under internal pressure 24 p3147 A73-44882

Fracture criteria for a unidirectional glass fiber/plastic material under planar short-term and long-term stress 24 p3103 A73-44884

Plastic plate bending under concentrated forces, defining stress and strain principles at yield limit 24 p3148 A73-44919

Displacements and rotations in micropolar elastic body with external loading and permanent distortions 24 p3149 A73-45004

Memory effect on mechanical properties of plastically prestrained Al-Mg alloy sheets 24 p3100 A73-45247

Hardening and softening of aluminum alloys under load at 135-150 C. 24 p3100 A73-45271

Superplasticity of steel Kh18N10T. 24 p3100 A73-45279

Plastic relaxation of a shear crack near a planar interface. 24 p3152 A73-45403

Laser-induced deformation modes in thin metal targets. 24 p3097 A73-45417

Materials testing by sonic emission analysis /SEA/ 24 p3094 A73-45445

Martensitic transformations in Fe-Cr-Ni austenitic stainless steels - Relation between the parameters of the epsilon phase and the transformation mechanisms 24 p3101 A73-45522

Plastic deformation of Co-Ni-Cr and Co-Ni-Cr-Mo alloys 24 p3101 A73-45525

PLASTIC FILMS

U POLYMERIC FILMS

PLASTIC FLOW

NT TRESCA FLOW

The early stages of the mechanism of sintering. 01 p0062 A73-10277

Certain generalizations of load-limit theorems for a Cosserat medium 01 p0114 A73-10573

Yield and plastic flow theory for porous metal powder compacts and preforms, discussing stress-strain and deformation-densification relations 03 p0388 A73-13260

Plane strain limit analysis of plastic material described by piecewise analytic nonlinear yield condition and associated flow rule 03 p0393 A73-13778

Determination of constants in the equation for the fatigue-crack propagation rate with allowance for properties of the plastic zone 06 p0761 A73-17847

Tresca-type plastic materials in the theory of hypoeasticity. I Mechanical constitutive equations and simple shear deformation. 07 p0909 A73-19161

Photoelastic investigation of serrated plastic flow in 6061 Al alloy, considering Luders bands effects relative to type A and B serrations 09 p1101 A73-22408

Stress-strain relations for materials with different tension, compression yield strengths. 09 p1166 A73-23452

Tensorial expansions for the plastic flow of partially compressible media. 10 p1290 A73-24325

On the formulation of the traction problem for the flow theory of plasticity. 12 p1551 A73-27046

Plastically deformed Fe-Si and Al alloys surface layer crystal dislocation density and plastic flow onset determination as function of depth 13 p1635 A73-28264

Coupled thermoplasticity model of two stress-strain regions characterized by nonevolutionary plastic flow equations and simple wave collapse, with and without thermal conductivity 13 p1698 A73-29087

Titanium flow curves in octahedral coordinates for various conditions of deformation 13 p1636 A73-29132

Study of plasticity laws of polycrystalline metals at elevated temperatures - Specifically the influence of hydrostatic stress on creep. 13 p1641 A73-29506

Rate-type constitutive equations for plateau predictions in dynamic plasticity for stress, strain and particle velocity functions 14 p1812 A73-30492

Flow stress of metals and its application in metal forming analyses. [ASME PAPER 73-PROD-4] 16 p2019 A73-33534

Chemo-rheology of two high temperature epoxy resins. 17 p2197 A73-35347

A procedure for solving problems of elasto-plastic flow. 19 p2496 A73-37484

Coupled thermoplasticity model of two stress-strain regions characterized by nonevolutionary plastic flow equations and simple wave collapse, with and without thermal conductivity 19 p2498 A73-37637

Study of the phenomenon of stress relaxation of flow in the case of titanium 19 p2442 A73-37840

Capillarity induced stresses effects on dislocations generation during early stage sintering, predicting plastic flow via modified Hirth method of surface nucleation 20 p2576 A73-39221

Equations of motion for ideal isotropic viscoplastic medium in axisymmetric space, determining conditions for flow core existence 20 p2619 A73-39336

General two-dimensional problem in the theory of ideal plasticity of anisotropic materials 20 p2624 A73-39643

Plasticity theory algebraic structure with emphasis on plastic flow laws formulation by adjoint functions and elastoplastic media finite deformations 23 p3044 A73-43972

Uniqueness theorems and variational principles derivation for free viscoplastic flow and constrained plastic deformation, obtaining Castigliano theorem from boundary value problem solution 23 p3044 A73-43974

Influence of high hydrostatic pressure on the flow stress of 18-8 stainless steel. 23 p2994 A73-44161

Discontinuous flow in steady-state creep of Al-Mg alloys at high temperatures. 23 p2995 A73-44162

Fracture micromechanism characteristics and crack tip plastic zone formation effects on metal embrittlement, using elastoplasticity theory 23 p3047 A73-44277

Strip weakened by array of holes, investigating plastic zone initiation and propagation under uniaxial tension for load bearing capacity estimation 24 p3147 A73-44685

Fundamentals of the theory of plastic flow in discretized bodies 24 p3110 A73-44917

PLASTIC MATERIALS

U PLASTICS

PLASTIC MEMORY

Ultrasonic attenuation measurement of a microplastic memory effect in aluminum single crystals. 03 p0323 A73-13331

The Castigliano variational equation in the theory of nonlinearly hereditary creep 07 p0912 A73-19322

Plastic strain and zero stress concepts as specific properties of materials with long range memory, formulating functional plasticity and moving dislocations theory 10 p1289 A73-24159

Plastic deformation, martensite transformation and temperature effects on shape memory of nitinol and other alloys 12 p1509 A73-26896

Design of zero-moment axisymmetric tanks made of a reinforced hereditary-elastic material 12 p1551 A73-27181

Boundary value problem solution uniqueness in dynamic linear theory of hereditary-elastic rheologically composite media 12 p1555 A73-27793

Memory effects associated with bulk viscosity on the spectrum of stimulated Brillouin scattering. 13 p1626 A73-28372

Nickel-titanium memory material stress measurement methods, energy absorption capacity and cyclic response, discussing nickel foil surface temperature sensing devices 17 p2166 A73-34616

Plastic deformation, martensite transformation and temperature effects on shape memory of nitinol and other alloys 21 p2720 A73-41029

Memory effect on mechanical properties of plastically pretrained Al-Mg alloy sheets 24 p3100 A73-45247

PLASTIC PROPELLANTS

Induced plasticization - An inner bore surface treatment technique for solid-propellant rocket motors. 22 p2897 A73-42626

Ignition and flame spreading over a solid fuel - Non-similar theory for a hot oxidizing boundary layer. 22 p2936 A73-42809

PLASTIC PROPERTIES

NT ELASTOPLASTICITY

NT PHOTOPLASTICITY

NT SUPERPLASTICITY

NT THERMOPLASTICITY

NT VISCOPLASTICITY

NT YIELD POINT

Superplasticity in two phase compositions based on refractory compounds, noting creep rate dependence on concentration and electroconductivity 01 p0066 A73-11339

C and Re effects on brittleness threshold temperature and plasticity of Mo-Re alloy 01 p0066 A73-11342

Impurities effect on Mo plastic properties and toughness, suggesting lower vacuum arc welding rates and increased electron beam zone refining runs 01 p0066 A73-11343

Asymptotic analysis of nonlinearly elastic and plastic thin rectilinear panels under combined bending and tensile stress 01 p0119 A73-11442

Influence of fiber/matrix interfaces on the plasticity and strength of fiber-reinforced composites 02 p0184 A73-11623

Rigidly plastic cylindrical shell design for axial-load and lateral-pressure combinations with allowance for large deflections 02 p0231 A73-11808

Calculus of variations and finite difference method for equilibrium equations in axisymmetric plastic shell design 02 p0232 A73-11821

The effect of tin on the strength and plasticity of titanium at low temperatures. 02 p0181 A73-12212

A numerical method considering the Bauschinger effect for large deflection analysis of elastic-plastic circular plates. 02 p0236 A73-12522

Constitutive equation for shock waves under dynamic load in prismatic bar axially prestressed to plastic range 03 p0383 A73-12903

Mechanical properties and stress analysis of elastoplastic body, noting yield conditions and Bauschinger effect 03 p0386 A73-13155

Elastic-plastic analysis of Saint-Venant torsion problem by a hybrid stress model. 03 p0390 A73-13338

Experiments on shell stability in air-driven shock tubes. 03 p0288 A73-13836

Loading-rate dependence of the deformation mechanism in a Zn-22% Al superplastic alloy 03 p0326 A73-13970

An analysis of thermally-induced plane waves in elastic-plastic single crystals. 03 p0394 A73-13980

Constitutive analysis of elastic-plastic crystals at arbitrary strain. 03 p0394 A73-13983

The dynamic growth of a void in a plastic material and an application to fracture. 03 p0394 A73-13984

Large deflection calculation of circular and annular strain hardenable rigid plastic plates under axisymmetric load, using Kirchhoff-Love hypothesis and Tresca flow condition 03 p0394 A73-14022

Minimum-weight plastic design of continuous beams subjected to one single moveable load. 04 p0510 A73-15030

Safety factor calculation procedure for perfectly plastic body under given plane stress based on complex variable functions 04 p0511 A73-15175

Influence of the composition and structure on the mechanical properties of ultraplasic alloys of the Al-Zn system 04 p0464 A73-15497

Plastic behavior of two-layer sandwich structures. [ASME PAPER 72-WA/APM-11] 04 p0516 A73-15901

The load carrying capacities of symmetrically loaded shallow shells. 05 p0631 A73-16120

Numerical solution of elastoplastic problems by the method of local variations 06 p0760 A73-17777

Interaction curves for bending and axial forces of perfectly plastic curved I-beams. 06 p0762 A73-18339

A unified formulation of the theory of optimal plastic design with convex cost function. 06 p0763 A73-18343

Tresca type plastic material shear, considering hypocoelastic yield interrelation to Tresca yields 06 p0763 A73-18457

Method of plasticity enhancement in aluminum and nickel-aluminum diffusion coatings on medium-carbon steel 06 p0711 A73-18665

High strength and plastic properties of two phase austenitic-martensitic Fe alloys after aging in alpha and gamma states 07 p0841 A73-20522

The phenomenon of superplasticity of polymorphous metals and alloys and its use for welding and hardening in the solid state. 08 p0978 A73-21242

Optimal superplasticity model of metallic material involving interphase surface of new phase fluctuation nuclei in framework of Frenkel theory 09 p1099 A73-21960

An analysis of plastic instability in pure shear in high strength AISI 4340 steel. 09 p1101 A73-22405

High strength TRIP /transformation induced plasticity/ steels hydrogen embrittlement susceptibility under cathodic charging, gaseous hydrogen environment and loading conditions 09 p1102 A73-22410

Metal fcc polycrystals macroscopic plasticity theory based on discrete aggregate model, predicting stress-strain curves for partial load cycles 09 p1160 A73-22896

Electrothermal annealing via electrical heating in vacuum for improved plasticity of thin walled molybdenum alloy elements after cold working 09 p1107 A73-23196

Temperature dependent combined hardening theory within plasticity formulations for finite element analysis of aerospace vehicle engines under plastic strain and cyclic fatigue 09 p1166 A73-23463

Plasticity theory, strength-differential /SD/ phenomenon, and volume expansion in metals and plastics. 10 p1234 A73-24428

Application of the fluctuation model of superplasticity to calculate the surface tension of metals during phase transformations 10 p1235 A73-24455

Ultrasonic treatment of alloy MA2-1 during solidification. 10 p1236 A73-24930

Asymptotic analysis of nonlinearly elastic and plastic thin rectilinear panels under combined bending and tensile stress 11 p1443 A73-26060

Elastic-plastic fracture by homogeneous microvoid coalescence tearing along alternating shear planes. 13 p1633 A73-28142

A theory of an elastic-plastic continuum with special emphasis to artificial graphite. 13 p1644 A73-28168

Plane strain slip line theory for anisotropic rigid/plastic materials. 13 p1697 A73-28793

The relations between superplasticity and high temperature resistance alloys of metallic systems. 13 p1639 A73-29457

Statistical criteria of ultimate strength and plasticity of materials in the complex stress state. 13 p1703 A73-29620

Investigation of the strength of construction materials for different ratios of the main stresses. 13 p1703 A73-29622

Energy methods in plasticity theory extension to creep mechanics with respect to stress-strain rate tensors relationships 14 p1811 A73-30478

Stress convexity domains for rigid perfectly plastic continuum, using directional derivative and distance function 14 p1811 A73-30483

Duality of limit theorems for a structure of a standard rigid-plastic material 14 p1812 A73-30491

Finite bending of incompressible hyperelastic plastic strip, analyzing stress and stored energy function 14 p1812 A73-30496

Book - A course in continuum mechanics. Volume 4 - Elastic and plastic solids and the formation of cracks. 14 p1813 A73-30595

Plastic crystals structural, thermodynamic and mechanical properties, noting high deformability due to molecular rotational freedom 15 p1923 A73-31415

Superplasticity of the Kh18N10T steel 15 p1890 A73-31816

Failure retardation mechanism in plastic titanium alloys 15 p1894 A73-32529

Nonlinear behavior of shells of revolution under cyclic loading. 16 p2075 A73-32791

Influence of in-plane displacements at the boundaries of rigid-plastic beams and plates.

16 p2083 A73-33973

Enhanced ductility in metals [Superplasticity/].

17 p2240 A73-34113

A steadily moving longitudinal-shear crack with an infinitely narrow plastic zone

17 p2241 A73-34266

Strength and plasticity of tantalum in rapid tests

17 p2188 A73-34561

Investigation of molybdenum-rich Mo-Ni-C, Mo-Ni-Zr, and Mo-Zr-Ni-C alloys

17 p2188 A73-34569

Determination of the carrying capacity of axisymmetric shells under piecewise linear plasticity conditions

17 p2244 A73-34738

Study of a stationary flow of rigidly plastic material by the numerical finite element method

17 p2244 A73-34796

Inertial motion of a plastic ring under the action of a pulsed load

17 p2244 A73-34797

Fracture toughness parameters and elastic-plastic analysis of non-moderate fracture conditions using finite element methods.

17 p2245 A73-34877

An experimental study of the heat generated in the plastic region of a running crack in different polymeric materials.

17 p2195 A73-34878

Evaluation of finite-plasticity theories for torsion-tension members made of Tresca materials.

[SESA PAPER 2109]

17 p2251 A73-35447

Limiting equilibrium of reinforced cylindrical shells

18 p2363 A73-36412

The plastic bending of beams and their failure by low cycle fatigue.

18 p2365 A73-36617

Optimal plastic design for partially preassigned strength distribution.

18 p2365 A73-36638

Influence of temperature and strain rate on the load-elongation curve and plastic properties of molybdenum

18 p2324 A73-36801

Low temperature tensile tests for strength and plasticity of pure bcc, hcp and fcc polycrystalline metals, indicating stacking fault energy role

18 p2324 A73-36804

Fluctuation model of superplasticity and surface tension of a metal at a phase transition.

19 p2442 A73-38137

General theory of constrained continuous media and plastic materials, deriving Huber-Mises yield condition by finite element method

19 p2501 A73-38304

Yield surfaces of metals at elevated temperatures.

20 p2615 A73-38640

Rigid-plastic collapse of compression-bent shallow shells.

20 p2616 A73-39114

Investigation of the plasticity of coatings on heat-resistant alloys

20 p2566 A73-39367

Motion of a rigid-plastic beam in a resistant medium under the action of a local load

20 p2620 A73-39470

Work hardening of copper, nickel, and alloy H31 by compression and explosion

21 p2707 A73-40705

Russian book on structural and functional plasticity of interneuron synapses during readjustment to chemical and physical damage covering degenerative and regenerative changes

21 p2640 A73-41280

Application of strip model to crack tip resistance and crack closure phenomena.

22 p2875 A73-42132

Unified plastic yield criterion for ductile solids.

22 p2923 A73-42555

The effect of plasticity and crack blunting on the stress distribution in orthotropic composite materials. [ASME PAPER 73-APMW-2]

22 p2924 A73-42876

Evolution of the stress state and hardening for certain materials with positive hardening

23 p3044 A73-43975

Turbine wheel strength, lifetime and safety margin calculations based on classical elasticity and plasticity theories

23 p3020 A73-44225

Critical equilibrium of cylindrical shells made from an ideal rigid-plastic material with different yield points in tension and compression

23 p3047 A73-44280

Influence of the offset on the experimental yield surfaces of metals - A theoretical evaluation.

24 p3147 A73-44747

An elastoplastic strain-hardening material - Quasi-static evolution of the stress distribution

24 p3147 A73-44748

Superplasticity of steel Kh18NiOT.

24 p3100 A73-45279

The governing equations and extremum principles of elasticity and plasticity generated from a single functional. I.

24 p3152 A73-45315

Book - Solid-state mechanics 3.

24 p3153 A73-45495

Continuity equation and equations of motion for ideal plastic body based on von Mises yield condition, considering stress discontinuity and boundary value problems

24 p3153 A73-45499

Plasticity theory development taking into account thermodynamics of elastoplastic materials, considering existence theorems for plastic flow and variational principle for equilibrium problems solution

24 p3153 A73-45500

PLASTIC YIELDING

U PLASTIC DEFORMATION

PLASTICITY

U PLASTIC PROPERTIES

PLASTICIZERS

Influence of a mixture of plasticizers, exhibiting a different mechanism of action, on the deformation of cellulose triacetate over a wide range of temperatures

21 p2647 A73-40264

Induced plasticization - An inner bore surface treatment technique for solid-propellant rocket motors.

22 p2897 A73-42626

PLASTICS

NT ACRYLIC RESINS

NT ADDITION RESINS

NT CARBON FIBER REINFORCED PLASTICS

NT EPOXY RESINS

NT NYLON [TRADEMARK]

NT PERSPEX [TRADEMARK]

NT PHENOLIC RESINS

NT POLYAMIDE RESINS

NT POLYBUTADIENE

NT POLYESTER RESINS

NT POLYETHER RESINS

NT POLYETHYLENE TEREPHTHALATE

NT POLYETHYLENES

NT POLYMETHYL METHACRYLATE

NT POLYPROPYLENE

NT POLYSTYRENE

NT POLYTETRAFLUOROETHYLENE

NT POLYVINYL ALCOHOL

NT POLYVINYL CHLORIDE

NT REINFORCED PLASTICS

NT SYNTHETIC RESINS

NT TEFLON [TRADEMARK]

NT THERMOPLASTIC RESINS

NT THERMOSETTING RESINS

Double discharge TEA carbon dioxide laser trigger circuit, using plastic materials with selected dielectric constant and resistivity for trigger current increase

02 p0175 A73-11958

Plastic material turbine blades adaptability under nonsteady start-stop thermal and mechanical stress cycle conditions, noting residual stress effects

02 p0235 A73-12129

The relationship between dielectric and mechanical properties of polymers.

03 p0332 A73-13036

Cracking and corrosion of plastic materials under stress

03 p0334 A73-13592

Laser irradiation testing - A new method for the nondestructive study of plastic material

04 p0458 A73-15324

Causes of defects arising in semiconductor devices encapsulated with plastic

04 p0427 A73-15350

Russian book on ultrasonic welding of metals and plastics covering equipment, transducers, welded joints stabilization, quality control and efficiency

04 p0457 A73-15970

Optical constitutive equation derivation for Tresca type plastic dielectrics, calculating birefringence and extinction angle in simple shear

06 p0723 A73-18458

Self lubricating bearing materials strength, friction, wear, thermal and dimensional stability properties, considering plastic, metal matrix and carbon graphite composites

07 p0842 A73-19555

Reliability aspects of plastic encapsulated integrated circuits.

08 p0944 A73-20739

Features of the influence of the ambient medium on the friction of plastics against metal during intermittent travel

09 p1089 A73-22855

Relaxation of diagonal length and indentation depth of Vickers microhardness measurements on plastics

11 p1388 A73-25449

Skyhook plastic balloons for transporting scientific instruments to high altitudes for long durations

11 p1306 A73-26348

Tresca-type plastic materials in the theory of hypoplasticity. II [Optical constitutive equations and birefringence in simple shear.

11 p1447 A73-26649

The effects of radiation sterilization on plastics.

16 p2030 A73-33693

Society of Plastics Engineers, Annual Technical Conference, 31st, Montreal, Canada, May 7-10, 1973, Proceedings.

17 p2196 A73-35339

A bonding-wire failure mode in plastic encapsulated integrated circuits.

19 p2410 A73-38442

High-reliability plastic package for integrated circuits.

19 p2411 A73-38455

Glass and plastic optical fiber properties, performance, limitations and applications

23 p3007 A73-44211

PLASTISOLS

NT SMOKE

PLATE [METAL]

U METAL PLATES

PLATE THEORY

Construction of finite-difference schemes in engineering theory of elasticity on the basis integral representations of the resolvent functions

01 p0114 A73-10483

Rectangular plates with unidirectionally variable rigidity

01 p0114 A73-10572

Fourier analysis of laminated anisotropic rectangular plates with strong cross elasticity effects, presenting deflection, bending moments and buckling data

01 p0115 A73-10735

Thermal bending of moderately thick rectangular plate.

01 p0115 A73-10739

Mesh subdivision type influence on convergence properties of mixed triangular elements in plate bending analysis

01 p0115 A73-10745

Plane stress analysis of an annular disk with distorted inner hole.

01 p0115 A73-10754

Nonlinear axisymmetric flexural vibration equations of a cylindrically anisotropic circular plate.

01 p0115 A73-10756

Bending of a uniformly loaded clamped sector plate.

01 p0116 A73-11006

Stress concentration in disk with radial slot and with outer boundary subject to arbitrary continuous load, using plane elasticity theory

01 p0117 A73-11095

Approximate relationships between the behavior of plates under destabilizing and non-destabilizing loads.

01 p0117 A73-11120

Radiation heat transfer in isothermal adjacent plate system with directionally emitting and nondiffuse reflecting surfaces, considering surface roughness effects

01 p0123 A73-11140

Interaction of thermal radiation with laminar free convection from a heated vertical plate.

01 p0123 A73-11141

Some exact solutions in the design of technically orthotropic axisymmetric plates.

01 p0118 A73-11365

The deformations and stresses in floating ice plates.

01 p0118 A73-11366

Equilibrium equations in theory of anisotropic shells and plates with arbitrary boundary conditions under external loads, noting thin walled reinforced shells

02 p0231 A73-11807

Integration of a differential equation describing the bending of a physically nonlinear plate of variable thickness

02 p0231 A73-11811

Perturbed bifurcation and buckling of circular plates.

02 p0186 A73-11973

Shell and plate theory covering constitutive and equilibrium equations, Cosserat surfaces and uniqueness theorem

02 p0234 A73-11981

Analysis of unbalanced angle-ply rectangular plates.

02 p0234 A73-12073

General non-linear plate theory applied to a circular plate with large deflections.

02 p0236 A73-12517

Vibration of a square plate symmetrically supported at four points.

02 p0237 A73-12605

Resonant frequencies of free vibrating plate via finite difference method, noting difference equations for plate equilibrium

03 p0391 A73-13345

Vibration and buckling of a rectangular plate with an internal support.

03 p0391 A73-13372

A simple finite element model for elastic-plastic plate bending.

03 p0391 A73-13680

On the conforming cubic triangular element for plate bending.

03 p0391 A73-13682

Stress intensity factor for an elliptical crack approaching the surface of a plate in bending.

04 p0505 A73-14677

PLATE THEORY

- Plate bending analysis using 12 degrees of freedom isoparametric and assumed-stress hybrid plate element theory 04 p0508 A73-14943
- Modified shear-flexible orthotropic plate theory application to simply supported rectangular sandwich plates buckling problem, comparing results with Reissner theory and experimental data 04 p0509 A73-14946
- Matrix displacement analysis of shells and plates including transverse shear strain effects. 04 p0509 A73-15005
- Finite element analysis of finite sized plates bonded to an elastic half space. 04 p0510 A73-15012
- Velocity corrected theory of laminated plates applied to free plate strip vibrations. 04 p0513 A73-15588
- Low order spatial modes principal resonance region of in-plane loaded skew stiffened plate, obtaining equation of motion by Hamilton principle [ASME PAPER 72-WA/APM-32] 04 p0515 A73-15887
- Governing equations for vibrating constrained-layer damping sandwich plates and beams. [ASME PAPER 72-WA/APM-24] 04 p0515 A73-15892
- Stress analysis of thick laminated composite and sandwich plates. 05 p0631 A73-16110
- Some remarks concerning heterogeneous anisotropic plates. 05 p0631 A73-16117
- Convergence and error estimation of Svirskii approximation method for determining circular plate deflections 05 p0635 A73-17081
- Vibration of thermally stressed plates with various boundary conditions. 05 p0636 A73-17101
- Analytical and experimental methods in composite mechanics. [ASCE PREPRINT 1655] 06 p0758 A73-17448
- Linearized theory of dynamically loaded thin rigid viscoplastic rectangular plates transient response, investigating strain rate effect 06 p0760 A73-17760
- Monograph - Grid analysis of orthotropic plates. 06 p0761 A73-17873
- Bending theory of rectangular plates loaded along curve, obtaining solutions by Fourier single and double series 06 p0763 A73-18451
- Dynamic stress intensity factor for an unbounded plate having collinear cracks. [AD-758426] 06 p0764 A73-18492
- Tensor-linear approach to the stability problem of nonlinearly elastic isotropic plates 06 p0765 A73-18690
- Dioptric powers of transparent plates in a plane state of tension 06 p0765 A73-18697
- Plate stretching and plane strain and plate bending. 06 p0765 A73-18723
- A finite element tensor approach to plate buckling and postbuckling. 07 p0907 A73-19028
- The quadratic programming approach to the finite element method. 07 p0907 A73-19030
- Homogeneous flat elastic plate theory in Cosserat surface context, considering application of general constitutive equations and extension to right circular cylindrical shells 07 p0908 A73-19085
- Postbuckling analysis of rectangular orthotropic plates. 08 p1015 A73-20673
- Bending of nonuniform plates with asymmetric thickness variation inclusion of shear deformation. 08 p1015 A73-20716
- Free vibrations of an infinite strip of variable thickness. 08 p1016 A73-20940
- Weight optimization for multilayered plates and shells with given load, end conditions and middle surface shape and dimension 08 p1019 A73-21762
- Secondary terms of thin multilayer plate equations, involving edge and stress-strain state fluctuation effects on boundary condition formulation 08 p1019 A73-21766
- Application of the finite element method to the study of the elastic buckling of thin plates of any form 09 p1157 A73-22214
- Large deflection analysis of plates and shallow shells using the finite element method. 09 p1158 A73-22396
- Stacked membrane elements for plate and shell analysis, noting spurious shear components suppression 09 p1159 A73-22401
- Book - Vibration of solids and structures under moving loads. 09 p1159 A73-22526
- Difference iterative solution for two dimensional boundary value problem for rectangular elastic plate with rectangular cutout 09 p1159 A73-22584
- Computerized two dimensional boundary value problem solutions for bounded multiply connected structural regions with periodic inclusions, using three step R-functions and Rvachev method 09 p1120 A73-22586
- Muskhelishvili boundary value problem of plate bending and point deformation for round and annular plates under uniform loads 09 p1159 A73-22854
- Biharmonic coupling solutions of Saint Venant equation for elastoplastic plane under unequal loads, using Kolosov-Muskhelishvili functions and conformal mapping 09 p1165 A73-23350
- Bifurcation of the equilibrium of a randomly inhomogeneous nonlinearly elastic plate 09 p1165 A73-23356
- Mathematical analogy between the bending of a plate and the circulating motion of a liquid in a geometrically similar region 10 p1205 A73-23598
- Elastic deformation of an orthotropic semi-infinite plate with straight boundary asymmetric with respect to the elastic axes of the material under uniform partial loading. 10 p1293 A73-24922
- Reissner's edge effect in three-layer plates with filler 11 p1433 A73-25030
- Probable collapse mechanisms in indefinite plates on an elastoplastic continuum. 11 p1434 A73-25217
- Finite element method for structural analysis, discussing theory for isoparametric stress quadrilateral plate bending elements with curved boundaries 11 p1435 A73-25437
- Incremental deformations in orthotropic laminated plates under initial stress. [ASME PAPER 72-APM-VV] 11 p1441 A73-25707
- Application of double trigonometric series to the calculation of shell plates of variable thickness 11 p1446 A73-26600
- Eigenfunction analysis for bending of clamped rectangular, orthotropic plates. 11 p1447 A73-26653
- Creep analysis of a thin-walled wing on the basis of the plate analogy 12 p1551 A73-27086
- Boundary value problems in elastoplastic plate theory, obtaining solution through reduction to operator equations 12 p1552 A73-27370
- Thin piezoelectric plate bending deformation and polarization theory in terms of piezoelectricity, electrostatics and elasticity equations for anisotropic body 12 p1552 A73-27371
- Study of the rigidity of rectangular plates during bending by the finite-element method 12 p1553 A73-27461
- Application of the method of power series to derive solutions for one-dimensional problems of thermophysically nonhomogeneous media 12 p1560 A73-27808
- On moderately large deflection of multiply connected plates. 12 p1557 A73-27933
- On the unity of the constant strain/constant moment finite element methods. 13 p1691 A73-28079
- Triangular finite elements for plate bending with constant and linearly varying bending moments. 13 p1692 A73-28230
- The local solution approach in the finite element method. 13 p1692 A73-28232
- Finite element theory of plates and shells including transverse shear strain effects. 13 p1693 A73-28235
- The mechanical interpretation of high accuracy multipoint difference methods for plates and shells. 13 p1694 A73-28255
- Axissymmetric vibrations of circular plates of linearly varying thickness. 13 p1695 A73-28415
- Generalized Green function for infinite plate strip with free edges, noting application to elastic boundary value problems 13 p1695 A73-28560
- Plate theory boundary value problems algorithm from Fourier transformation of ultradistribution functions 13 p1695 A73-28561
- Elastic circular inclusion in an infinite plane containing two cracks. 13 p1696 A73-28749
- Clamped orthotropic triangular plates free nonlinear vibrations, solving equations of motion in first order approximation by von Karman plate theory 13 p1697 A73-28808
- A finite element study of the vibration of trapezoidal plates. 13 p1700 A73-29378
- The optimum distribution of diagonal stiffeners reinforcing a clamped infinitely long plate buckling under shear. 13 p1700 A73-29386
- Ritz method application to structural eigenvalue problems, considering plate buckling in box beams 14 p1805 A73-29741
- Effect on the stresses around a crack due to the presence of circular inclusion. 14 p1806 A73-30042
- Equivalent finite element model derivation from plate bending triangular element, assumed stress hybrid method and elements with polynomial deflection function 14 p1807 A73-30184
- Matrix method analysis of stiffened plates free vibrations, deriving governing equation in stiffness matrix form by combining plane stress theory and lateral vibration equation 14 p1807 A73-30186
- A method of elastic-plastic analysis of largely deformed plate problems. 14 p1808 A73-30194
- Construction of finite difference diagrams of the engineering theory of elasticity, on the basis of integral representations of the resolvent functions. 14 p1810 A73-30308
- Boundary value problem solutions for parallelogram and elliptical thin plates vibration frequencies and mode shapes based on eigenvalues domain dependence and parameter differentiation technique 14 p1810 A73-30408
- Limit state solution to equilibrium equation of elliptical plate with Johansen yield condition under uniform load, using Abel differential equation 14 p1811 A73-30486
- Unsymmetric wrinkling of circular plates. 14 p1812 A73-30522
- Study of the elastoplastic stressed state and plastic zones of a plate with a circular hole under tension 14 p1815 A73-30794
- Equilibrium equations for static computations of symmetrical plates with large number of rods, point supports or holes 14 p1815 A73-30814
- Internal stress-strain boundary layer theory of shells and orthotropic plates with zero stress conditions at upper and lower planes and edge distance dependent attenuation 14 p1815 A73-30815
- Natural oscillations of multilayer shells and plates with fillers 15 p1944 A73-30970
- Use of the surface of influence of the clamping couple on a circular plate for design calculation under an asymmetrical load 15 p1944 A73-30974
- Derivation of a normal displacement function for the triangular finite element of plates and shells 15 p1945 A73-31032
- General solution of an equation system on plate equilibrium 15 p1945 A73-31033
- The large deflection and post-buckling behaviour of some laminated plates. 15 p1946 A73-31117
- Harmonic vibrations of inclined plate in separated free surface flow of ideal fluid in terms of weak perturbation flow theory 15 p1946 A73-31157
- Discrete element development for anisotropic plates via bicubic Hermite interpolation functions, considering patch generation from boundary geometry data 15 p1951 A73-32033
- Determination of stress intensity factors in cracked plates by the finite element method. 15 p1951 A73-32034
- Finite deflections of transversally-isotropic plates and shallow shells 15 p1953 A73-32089
- Stress distribution near holes 15 p1953 A73-32097
- Elastic buckling instability of rotating rods and plates due to compressive stress under critical speed 15 p1955 A73-32161
- Stress concentration in plates with holes for large curvatures at the points of inflection 16 p2074 A73-32688
- Small parameter series convergence evaluation in geometrically nonlinear problems by Cauchy majorants, applying to flat curvilinear beam deflection 16 p2074 A73-32689
- Estimates of the eigenvalues of a difference problem for a plate 16 p2074 A73-32690
- Variational principles for plate bending - A unified approach. 16 p2077 A73-32983
- Galerkin variational method combination with least squares error distribution technique for application in plate and shell theory 16 p2077 A73-32992
- Solution of equations of Reissner's theory of plates by application of Hajdin's method. 16 p2078 A73-33004

Stress calculation for plates and beams via finite element method, improving accuracy by smoothing stress and strain distributions at element boundaries
16 p2080 A73-33262

Influence of in-plane displacements at the boundaries of rigid-plastic beams and plates.
16 p2083 A73-33973

Free vibrations of multilayered composite plates.
17 p2241 A73-34192

Layered composite plate theory with interlaminar transverse shear stress as unknown variables, demonstrating agreement with elasticity solutions
17 p2250 A73-35116

Boundary layer concept /attenuating stress-strain state with homogeneous boundary conditions/ incorporation into internal stress-strain state theory for orthotropic rectangular elastic plates
19 p2499 A73-37763

Nonlinear bending of rectangular orthotropic plates.
19 p2500 A73-38116

The state of stress produced in a quadrant shaped plate by concentrated forces acting in its plane.
19 p2501 A73-38305

The vibrations of a circular plate with uniformly distributed load around the outer periphery.
19 p2502 A73-38348

Dispersion curve computation for elastic acoustic waves propagation in /001/-cut cubic free anisotropic plate, noting relationship with slowness curves for bulk waves
20 p2616 A73-39050

Temperature field calculation for a plate of a complex shape with systems of double-periodic holes, inclusions, and energy sources
20 p2627 A73-39255

Method for determining the unsteady thermal field of piecewise homogeneous plates of complex shape
20 p2627 A73-39256

Determination of kinetic stress functions in elastodynamic problems of plates
20 p2617 A73-39262

Certain approximations in the solution of shell and plate bending problems with allowance for physical and geometrical nonlinearity
20 p2618 A73-39311

Investigation of the free vibrations of sectorial plates and conical panels by a theoretical-experimental method
20 p2618 A73-39314

Improved relations in the dynamics of moderately thick shells and plates under the action of massive moving loads
20 p2618 A73-39316

Moderate-thickness plate equilibrium equations and boundary value problems, discussing successive approximation method, static bending and potential energy
20 p2618 A73-39317

Application of the Peaceman-Rochford method to the solution of the deflection problem for a plate strengthened by a square grid
20 p2620 A73-39496

Determination of the stress strain state of closed cylindrical shells and infinite plates with cracks
20 p2624 A73-39645

The boundary theory of strength and nonlinear programming of boundary value problems of plate bending
20 p2625 A73-39821

Mindlin theory extension to transverse shear effects in laminate plates, taking into account continuous stress across thickness and discontinuous shear strain
21 p2784 A73-40432

Deflection function for the asymmetrical bending of circular plates.
21 p2784 A73-40435

Influence of nonuniform heating on the stability of plates beyond the elastic limit
21 p2786 A73-40983

Application of R-functions to a calculation of the dynamic stability of plates with a complex planform geometry
21 p2786 A73-40984

Russian book on R-function method for solving boundary value problems of bending and vibration of thin plates with complex configurations
21 p2787 A73-41250

Complementary variational principles and error bounds for biharmonic boundary value problems.
22 p2921 A73-42433

Large deflection theory for viscoelastic anisotropic thin plates, deriving constitutive, plane stress, plate and nonlinear integrodifferential equations
22 p2923 A73-42638

On the behavior of a numerical approximation to the rotatory inertia and transverse shear plate.
[ASME PAPER 73-APMW-7] 22 p2924 A73-42880

Asymptotic method for approximate elastodynamic plate theories derivation from elasticity equations with application to plate free extensional and forced flexural vibration frequency spectrum
[ASME PAPER 73-APMW-44] 22 p2926 A73-42900

Transformation of a symmetric wave-type process of deformation into an asymmetric process in a plate during the development of a shock wave
22 p2927 A73-42930

A higher order theory for extensional motion of laminated composites.
22 p2929 A73-43139

Certain methods in the physically nonlinear theory of three-layer plates
23 p3043 A73-43921

Bending of a rectangular piezoelectric plate clamped over its edge
23 p3043 A73-43923

Postcritical deformations in a multilayer plate under edge pressure
23 p3043 A73-43925

Solution of plane problems of elasticity utilizing partitioning concepts.
[ASME PAPER 73-APM-C] 23 p3047 A73-44378

Power series solution to Volterra equations in nonlinear viscoelastic dynamic plate and shell theory with application to flexible cylindrical shell vibrations under periodic loads
24 p3145 A73-44518

Plastic plate bending under concentrated forces, defining stress and strain principles at yield limit
24 p3148 A73-44919

Bending of transversely isotropic plates with a reinforced edge
24 p3149 A73-45174

Three-dimensional axisymmetric problem of a normal load concentrated on an elastic free-underface plate of constant thickness - Expression for the stresses in the vicinity of the load
24 p3149 A73-45218

Mixed finite-difference scheme for analysis of simply supported thick plates.
24 p3150 A73-45226

Influence of initial deflections on the work of a rectangular plate subject to bending in its plane
24 p3150 A73-45244

Operator of thin plate reinforced with thin-walled ribs.
24 p3152 A73-45440

PLATELETS
Effect of heparin on blood platelet aggregation and thrombosis under the action of direct electric current
08 p0931 A73-21321

Intravascular platelet aggregation in the heart induced by stress.
08 p0933 A73-21805

PLATES [STRUCTURAL MEMBERS]
NT ANISOTROPIC PLATES
NT ANNULAR PLATES
NT CANTILEVER PLATES
NT CIRCULAR PLATES
NT CORRUGATED PLATES
NT ELASTIC PLATES
NT ORTHOTROPIC PLATES
NT PERFORATED PLATES
NT POROUS PLATES
NT REINFORCED PLATES

Orthogonal function approximation of uniform thickness plate temperature distribution, using reduced two dimensional unsteady heat conduction equations
01 p0119 A73-10010

A study of the kinematic and dynamic characteristics in the wake behind a plate in an unbounded flow
01 p0032 A73-10620

Boundary layer growth of a micropolar fluid.
02 p0154 A73-12093

On the unbonded contact between a beam and a semi-infinite plate.
03 p0389 A73-13324

The modal density for flexural vibration of thick plates and bars.
03 p0393 A73-13839

Perturbation and harmonic balance methods for nonlinear panel flutter.
03 p0395 A73-14182

Crack shapes and stress intensity factors for edge-cracked specimens.
04 p0506 A73-14681

Fatigue crack growth data for various materials deduced from the fatigue lives of precracked plates
04 p0506 A73-14684

Free convection along the downward-facing surface of a heated horizontal plate.
04 p0520 A73-15943

Influence of a moving load on the vibrational characteristics of plates
05 p0636 A73-17093

Limit analysis of plates with piecewise linear yield surface.
06 p0758 A73-17398

Collocated interfacial stress intensity factors for finite bi-material plates.
06 p0763 A73-18477

An experimental investigation into the mechanics of deep semielliptical surface cracks in mode I loading.
06 p0763 A73-18478

PLATES [STRUCTURAL MEMBERS]

Natural frequencies and vibration modes determination for skew plates with different edge conditions involving support and clamping based on Ritz variational method
07 p0909 A73-19094

Multiparameter optimal design of plates and shells.
07 p0912 A73-19367

Corner supported equilateral triangular plates.
08 p1016 A73-20827

The application of nodal stress concepts to the bending of plates and shells.
08 p1019 A73-21691

Stability of a ferromagnetic plate within a gas flow in the presence of a magnetic field
08 p0989 A73-21723

Bending and vibration of multilayer sandwich beams and plates.
10 p1289 A73-24290

Beam and plate flexural vibration damping by free or uncompressed rigid viscoelastic coatings applied on sides
10 p1293 A73-24794

The temperature field and thermal stresses in a symmetrical system of three infinite plates
10 p1293 A73-24795

On unsteady magnetohydrodynamic boundary layers in a rotating flow.
10 p1257 A73-24841

A numerical study of unsteady laminar combined convective flow over vertical plates.
10 p1296 A73-24848

Method of solving heat conduction problems with nonideal thermal contact
11 p1450 A73-25624

Dynamic moire methods for the bending of plates.
12 p1550 A73-27023

Selection of optimal parameters for unidirectionally compressed three-layer plates
12 p1555 A73-27795

Triangular elements descriptive of sandwich panels for finite element analysis of symmetric panels, comparing numerical solutions to experimental data and analytical results
13 p1693 A73-28238

Study of kinematic and dynamic characteristics in a wake behind a plate in an unbounded flow.
13 p1601 A73-28739

Stress-singularities due to uniformly distributed loads along straight boundaries.
13 p1696 A73-28757

Interaction of elasto-plastic cracks subjected to a uniform tensile stress in an infinite or a semi-infinite plate.
13 p1701 A73-29471

Acoustic field produced in a gas by arbitrary disturbances on a moving plate
14 p1775 A73-30834

Reduction of noise generated by flow of fluid over plate.
14 p1746 A73-30915

Apparent added masses of a plate array in an incompressible liquid
15 p1861 A73-31281

Application of an irregular mesh finite difference approximation to the plate buckling problem.
16 p2079 A73-33008

The optimization of the cross-sectional profile of rods and plates subjected to dynamic stress
16 p2080 A73-33241

Similarity in the flow of a magnetized plasma around a plate and cylinder
17 p2215 A73-34260

Diffraction of an acoustic wave at a moving plate
18 p2265 A73-37012

Studies on the impact resistance of composite plates.
18 p2367 A73-37093

Monograph on optimal structure design by linear programming and calculus of variations covering pin jointed frameworks, beams, circular sandwich plates, Michell continua, etc
19 p2502 A73-38364

Dynamics of structural systems subjected to moving loads. II - Half-spaces, plates, and shells under the action of moving loads
20 p2617 A73-39304

In-plane and lateral displacements triangular elements represented by cubic and quintic polynomials for folded plate structural analysis
20 p2622 A73-39545

Russian book on elasticity theory for multilayer media covering plate compression and bending under boundary contact conditions, Algol programming, tensile stress, functional equations, etc
21 p2782 A73-40175

A mixture theory of the response of a laminated plate to impulsive loads.
21 p2783 A73-40291

Fracture control - Past, present and future.
23 p3039 A73-43383

Sound field created in a gas by arbitrary perturbations on a moving plate.
23 p3006 A73-43584

PLATFORMS

Calculation of the thermal field of an inhomogeneous plate of complex composition with energy sources 24 p3157 A73-45361

PLATFORMS

NT OFFSHORE PLATFORMS

PLATING

NT ELECTROPLATING

Semihydrostatic hot extrusion for Ti plated Cu anode bar, noting metal bonding and current distribution 03 p0312 A73-13583

Mechanical properties of base and coating metals for explosive plating, noting heat treatment for strain hardening prevention 03 p0312 A73-13584

The deposition of multicomponent phases by ion plating. 04 p0456 A73-15758

PLATINUM

Impurities effect on platinum resistance thermometer temperature reading accuracy, presenting empirical formula for approximate error estimate as function of operational conditions 03 p0307 A73-13193

Hydrogen/proton adsorption behavior on fuel cell Pt electrode, considering surface roughness factor, Pt sites number and equilibrium data 04 p0407 A73-15104

Influence of structural perturbations applied to platinum and gold on kinetic processes at the electrode. 04 p0407 A73-15105

Carbon-PtFE fuel cell electrode for hydrogen-KOH-air batteries for operation over long time periods, discussing rolling technique and industrialization possibilities 04 p0407 A73-15114

The adsorption and decomposition of CO on Pt(111). 08 p0937 A73-21617

Aircraft engine fuel and oil differential temperature measurement via platinum probes, specifying sensor sensitivity, calibration, circuit operation and data reduction 17 p2165 A73-34607

Theory of successive electron transfer steps in cyclic voltammetry Application to oxygen pseudocapacitance on platinum. 21 p2636 A73-40843

Platinum resistance thermometry below 13.81 K. 22 p2854 A73-42002

Intercomparison of standard platinum thermometers calibrated on IPTS-68 between 13.81 and 273.15 K. 22 p2854 A73-42003

High temperature platinum resistance thermometry. 22 p2855 A73-42005

Platinum resistance thermometry up to the gold point. 22 p2855 A73-42006

Stability of 25 ohm platinum thermometer up to 1100 C. 22 p2855 A73-42007

The high temperature stability of platinum resistance thermometers. 22 p2855 A73-42008

The influence of crystal defects in platinum on platinum resistance thermometry. 22 p2855 A73-42009

Platinum resistance thermometer as standard instrument for interpolation on International Practical Temperature Scale, discussing design development, operational characteristics and errors 22 p2855 A73-42010

Calibration of platinum resistance thermometers. 22 p2855 A73-42011

Unique platinum resistance temperature sensors for lunar heat flow measurements. 22 p2855 A73-42013

Calibration of capsule platinum resistance thermometers at the triple point of water. 22 p2857 A73-42027

The use of operational amplifiers to generate precise current ratios for platinum resistance thermometry. 22 p2832 A73-42028

Diffusion in thin film couples of platinum-gold. 23 p3015 A73-43528

PLATINUM ALLOYS

X ray diffraction measurement of ordering kinetics in Ni-Pt alloy at annealing temperatures, showing disorder-order transitions relation to nucleation and growth 04 p0467 A73-15982

The vibrational frequency of Fe-57 atoms in Pt-Fe solid solution from measurements of the second-order Moessbauer Doppler shift. 13 p1634 A73-28258

The homogeneity regions of superconducting phases in the molybdenum-platinum system 21 p2717 A73-40320

PLAYA LAKES

U LAKES

A-1340

PLAYBACKS

Technique for measuring time-base errors of magnetic instrumentation recorders/reproducers. 08 p0965 A73-21084

PLENUM CHAMBERS

From theory to practical use of air cushions for transport of heavy loads in the factory 05 p0535 A73-16753

Filling tests in single and double arm plenum configuration models used in gasdynamic laser systems, noting wave controlled unsteady flow processes 09 p1030 A73-23447

Static performance of plenum and peripheral jet air cushions. 19 p2377 A73-37703

PLETHYSMOGRAPHY

NT ELECTROPLETHYSMOGRAPHY

Studies in stress-relaxation and distensibility characteristics of small skin veins in vivo by a combined photoelectric-photographic and plethysmographic technique. 05 p0541 A73-17098

Ventilation measured by body plethysmography in hibernating mammals and in poikilotherms. 08 p0932 A73-21612

Characteristics of vasomotor alterations during brief arbitrary hyperventilation according to data from rheographic and plethysmographic studies 11 p1314 A73-25041

Angiotensinography using an air plethysmograph 18 p2282 A73-36575

A multiplex cathode-ray-tube display with digital readout for a body plethysmograph. 22 p2815 A73-42666

A new method of measuring arterial dilation and its application. 22 p2815 A73-42669

Comparison of plethysmographic and electromagnetic flow measurements. 23 p2950 A73-44215

Fundamental frequency analysis of pulmonary mechanical resistance and compliance. 24 p3060 A73-45067

PLEURAE

Regional lung volumes with positive pressure inflation in erect humans. 06 p0653 A73-18334

Peak expiratory flow rate and rate of change of pleural pressure. 21 p2642 A73-41636

PLEXIGLASS [TRADEMARK]

U POLYMETHYL METHACRYLATE

PLIES

U LAYERS

PLOTTERS

Point plot recording instrument for instantaneous signal values measurement, discussing dynamic characteristics of constant plotting rate devices 06 p0693 A73-18168

Automation of plotting root-locus curves for automatic control systems 13 p1596 A73-29142

Kinoform production method combining pen-drum plotter with low pass spatial filter converting binary transmittance of precursive mask. 22 p2862 A73-43088

PLOTTING

Computerized normal loci plotting by orthogonal Chebyshev approximation, using minimum variance principle and Fisher test for regression curve selection 09 p1143 A73-22094

A computer program for plotting exponentially smoothed average control charts. 13 p1588 A73-29299

National Center for Atmospheric Research utility plotting programs for computer graphics, two and three dimensional fields display and movie generation 24 p3070 A73-45089

Three dimensional computer plots of zero velocity contours for restricted three and four body problems, discussing motion stability near equilibrium points 24 p3142 A73-45297

PLOTTING INSTRUMENTS

U PLOTTERS

FLOWED FIELDS

U FARMLANDS

PLSS

U PORTABLE LIFE SUPPORT SYSTEMS

PLUG NOZZLES

Annular truncated plug nozzle flowfield and base pressure characteristics. [AIAA PAPER 73-137] 05 p0530 A73-16887

PLUGS

A photoelastic and finite-element investigation of a nonsymmetrical plug-hatch configuration. 10 p1293 A73-24721

PLUMBANE

U LEAD COMPOUNDS

U METAL HYDRIDES

PLUMES

NT ROCKET EXHAUST

Space simulation experiments on reaction control system thruster plumes. [AIAA PAPER 72-1071] 03 p0354 A73-13398

Implementing the design of airplane engine exhaust systems. [AIAA PAPER 72-1112] 03 p0355 A73-13427

Atmospheric dispersion of air pollutants, analyzing buoyant plumes and wakes 10 p1205 A73-23857

Instability, transition, and turbulence in buoyancy-induced flows. 10 p1205 A73-23859

A study of convective elements in the atmospheric surface layer. 11 p1393 A73-25692

Observation of Raman scattering by SO₂ in a generating plant stack plume. 13 p1607 A73-28547

Exhaust cloud rise and growth for Apollo Saturn engines. 15 p1906 A73-31920

Aircraft exhaust plume dispersion and flight corridor concentration profiles in stratosphere as function of flight frequency and scale dependent diffusion [AIAA PAPER 73-532] 16 p2046 A73-33565

Mass flux measurements and correlations in the back flow region of a nozzle plume. [AIAA PAPER 73-731] 18 p2342 A73-36348

Some laboratory observations on convective plumes. 18 p2333 A73-36711

Jet engine exhaust plume effects on solid bodies, examining nozzle drag effects, nozzle geometry, plume entrainment and shape, wind tunnel tests and pressure effects 20 p2626 A73-38651

Plume boundary jump of an underexpanded jet exhausting counter to a freestream. 21 p2790 A73-40433

PLUNGERS

Minimum pressure zone determination for pressure field at axial plunger pump inlet during cavitation onset, discussing working fluid temperature and composition 02 p0172 A73-11800

PLUTO [PLANET]

Survey of the outer planets Jupiter, Saturn, Uranus, Neptune, Pluto, and their satellites. 11 p1417 A73-25315

Mercury, Venus and Pluto satellite system elimination by tidal friction, discussing possible erosion of earth and Mars small satellites 11 p1419 A73-25778

Pluto polarimetric measurements showing degree and position angle of polarization and probable error 22 p2905 A73-41763

PLUTONIUM

NT PLUTONIUM ISOTOPES

NT PLUTONIUM 238

PLUTONIUM COMPOUNDS

NT PLUTONIUM OXIDES

PLUTONIUM ISOTOPES

NT PLUTONIUM 238

Uranium and extinct Pu-244 effects in Apollo 14 materials. 07 p0888 A73-19784

On Pu-244 in lunar rocks from Fra Mauro and implications regarding their origin. 23 p2951 A73-43771

PLUTONIUM OXIDES

Thermoelectric nuclear batteries fabrication in milliwatt power range combining bismuth telluride thermopiles with plutonia fuel capsules 19 p2455 A73-38410

PLUTONIUM 238

Comparison of strontium-90 and plutonium-238 milliwatt thermoelectric generators. 09 p1037 A73-23277

Operational safety experience and advances of space nuclear power systems fueled with Pu-238, discussing modular heat sources 09 p1119 A73-23287

Cost-effective radioisotope thermoelectric generator designs involving Cm-244 and Pu-238 heat sources. 19 p2455 A73-38389

Multihundred watt radioisotope thermoelectric generator design for on-pad and orbital conditions, discussing configurations, Pu-238 heat source and operating characteristics 19 p2456 A73-38419

The MHW heat source - An advance in radioisotope heat source technology for space applications. 19 p2456 A73-38420

Multihundred watt power supply with Si-Ge thermoelectric couples for Pu-238 source heat energy conversion into electric power, discussing computer model for performance projection 19 p2456 A73-38422

PLUVIOGRAPHS

U RAIN GAGES

U RECORDING INSTRUMENTS

FLYWOOD

High frequency load tests for fatigue properties of glass and carbon fiber reinforced plastics and epoxy impregnated wood laminates 12 p1515 A73-26879

PNEUMATIC CIRCUITS

Jet element output impedance for pneumatic circuits transients determination considering load dynamic properties influence

02 p0133 A73-12120
Systematic method of designing fluidic-pneumatic control circuits.

02 p0133 A73-12646
An application of pneumatic phase shifting to stabilization of externally pressurized journal gas bearings.

[ASME PAPER 72-LUB-4] 03 p0313 A73-14327
Pneumosomatic data transmission and processing based on pressurized gases and dynamic body interactions

12 p1460 A73-26771
Accuracy of switching pressure of fluidic OR-NOR device.

13 p1571 A73-29044
Dynamic structural model of transient processes of discrete jet element chain with duct joints

15 p1832 A73-31145
Use of fluidic and pneumatic elements to determine the composition of a gas mixture

16 p1970 A73-33025
Application of fluidic shift-register modules for sequential control of pneumatic sequential circuits.

23 p2943 A73-43412
Pneumatic sequential circuits assembly method involving modules with switching elements and shift register, considering control valves and operation modes

23 p2943 A73-43416
Punched card controlled program units including readers, comparator circuits, pneumomechanical counters and fluidic feedback oscillators

23 p2944 A73-43424
PNEUMATIC CONTROL
Systematic method of designing fluidic-pneumatic control circuits.

02 p0133 A73-12646
Fluidic ignition system with two-component aerodynamic resonance heating /pneumatic match/ and hand pump for solid propellant sounding rocket engine

[AIAA PAPER 72-1197] 03 p0252 A73-13486
An application of pneumatic phase shifting to stabilization of externally pressurized journal gas bearings.

[ASME PAPER 72-LUB-4] 03 p0313 A73-14327
Pneumatic controller with two cascade amplification stages and mechanical solid state gain adjustment variable feedback system

10 p1177 A73-24020
Sequential pneumatic distribution system /Biselector/ with logic control by leakage obstruction, describing industrial pressure perforated card programmer

11 p1307 A73-25377
Pneumatic and fluidic automatic controls, investigating peripheral elements and systems feed

11 p1308 A73-25380
Book on fluid power control covering servovalve orifices discharge characteristics, flow forces, hydraulic and pneumatic servomechanisms, fluid logic and sequential circuits

11 p1313 A73-26258
Diagnostic simulation of a pneumatically controlled blowdown wind tunnel.

11 p1344 A73-26546
Problems in constructing aerodynamically active elements - Converters of input and output signals in automatic control systems

12 p1459 A73-26769
Turbulence amplifier with transition process control for multi-input fluid logic OR device operation at very low pressures and flow rates

23 p2942 A73-43399
Systems engineering approach to pneumatic hybrid automatic/manual control system with fluid logical elements and reduced air consumption

23 p2943 A73-43413
Fluidic logic circuit universal block with turbulence amplifiers for control of servomechanisms, comparing with use of conventional fluid logical elements

23 p2943 A73-43414
PNEUMATIC EQUIPMENT

NT GAS VALVES

NT PNEUMATIC CIRCUITS
Experimental investigations concerning pneumatic ejectors, with special reference to the effect of dimensional parameters on performance characteristics.

03 p0297 A73-14503
Pneumatic torque generator subsystem of French D2 satellite, discussing engineering technical difficulties

07 p0778 A73-18925
Satellite-equipment compartment separation system.

07 p0905 A73-18997
Determination of the hydraulic resistance of throttles by short unsteady blowing

07 p0779 A73-20083
Speed control for an air motor using fluidic techniques.

[ASME PAPER 73-DE-35] 14 p1713 A73-30824

Study of the static and dynamic characteristics of a family of discrete pneumatic jet modules

16 p1971 A73-33670
Digital control of a pneumatic isolation system for inertial instrument testing.

[AIAA PAPER 73-830] 20 p2543 A73-38775
A gasdynamic test stand and its use in studying sprayer nozzles for spraying metallic solutions.

24 p3075 A73-44742
PNEUMATIC PROBES

An infrared pneumatic transducer with capacitive detection.
[ONERA, TP NO. 1150] 08 p0968 A73-21682
Pneumatic sensors without contact

11 p1308 A73-25381
Level and density sensors using pneumatic repeaters

11 p1364 A73-26099
Total pressure tube measurements in turbomachine-simulating pulsating nozzle flow generator supplemented by pneumatic tube probes for averaging error comparison

17 p2166 A73-34608
Dynamic range and frequency response of the vortex rate sensor.

23 p2942 A73-43406
PNEUMATIC RESET

U PNEUMATIC CONTROL

PNEUMATICS
Russian book - Aerohydrodynamic methods for measuring input parameters of automatic systems: Fluidic measuring elements.

21 p2704 A73-41288
PNEUMOGRAPHY

U PNEUMOGRAPHY
PNEUMOGRAPHY
Respiratory air flow telemetry during exercise, discussing flowmeter working conditions and equipment testing

03 p0270 A73-14286
Heated Fleisch pneumotachometer - A calibration procedure.

08 p0935 A73-21509
Technique for the implantation of long-term diagnostic electrodes in the amygdaloid complex of the human brain

09 p1046 A73-22857
Electrical operational and pneumatic /variometer/ differentiation recording of displaced volume derivative from pneumotachograph in spontaneous breathing

09 p1046 A73-22937
POCKELS EFFECT

U BIREFRINGENCE

POGO

Equatorial electrojet characteristics observation during 1967-1970 with POGO satellite-borne magnetometers, noting anomaly characterized by sharp negative V-signature in width and variable amplitude

15 p1870 A73-31768
POGO satellite observed electrojet signature data comparison with daily geomagnetic variation amplitude measurement at equatorial ground station in India

15 p1870 A73-31769
POGO satellite observed electrojet current data comparison with ground measurement at Ibadan, discussing data ratios variation by upper earth mantle conductivity structure

15 p1870 A73-31772
POGO satellite observation of electrojet profiles compared with H variation around measurements, interpreting data by classical band current model

15 p1871 A73-31773
POGO EFFECTS

Analysis of the vibrational characteristics of a liquid contained in a tank
[ONERA, TP NO. 1197] 07 p0812 A73-20074

The dynamic behavior and compliance of a stream of cavitating bubbles.
[ASME PAPER 73-FE-34] 17 p2153 A73-35025

Influence of combustion phenomena on the Pogo effect
21 p2754 A73-41551

POIKILOTHERMIA

NT AMPHIBIA

NT FROGS

Ventilation measured by body plethysmography in hibernating mammals and in poikilotherms.
08 p0932 A73-21612

POINCARE PROBLEM

Periodic solutions of piecewise-continuous systems with a small parameter
13 p1661 A73-29084

Critique of Poincare technique for construction of global solution of resonance of dynamical system, considering procedure using secular terms and regularizing function

15 p1930 A73-31111
Periodic solutions of the restricted three-body problem encompassing a large number of revolutions about the smaller body

15 p1931 A73-31240
Resonances and some cases of integrability of the motion of a heavy rigid body about a fixed point.

15 p1914 A73-32068
POINT SOURCES

Lagrange function based Poincare mechanics of inertial relativity, using Mach-Einstein inertia principle for gravitational potential

16 p2036 A73-33072
A perturbation method for obtaining approximate solutions of an equation with two small parameters

17 p2201 A73-35046
Poincare-Lighthill and linear-time-scales methods for linear perturbation problems.

19 p2445 A73-37752
A global solution in the resonance problem of Poincare.

24 p3141 A73-45288
POINCARE SPHERES

Restoring the orthogonality of two polarizations in radio communication systems. II.

10 p1190 A73-24623
Poincare sphere representation of partially polarized electromagnetic field, calculating power reception by antenna for field intensity measurement

17 p2128 A73-35681
Receiving antenna optimum polarization determination by mapping on Poincare sphere for maximum ratio of signal to summed external interference and internal noise

24 p3068 A73-44943
POINT DEFECTS

NT FRENKEL DEFECTS

NT VACANCIES [CRYSTAL DEFECTS]

The diffusion of point defects to a propagating crack tip.
01 p0116 A73-11000

Dislocation-point defect interactions in fatigued pure aluminum
05 p0588 A73-17231

On the point defect production in electron-irradiated molybdenum.
06 p0705 A73-17832

Atomic modeling of internal friction in solids, considering paraelastic point defects relaxation time
16 p2037 A73-33227

POINT IMPACT

Steady state solution for moving point force on solid-solid interface for supersonic load velocities, using DeHoop modification of Cagniard technique

14 p1812 A73-30493
POINT MATCHING METHOD [MATHEMATICS]

U BOUNDARY VALUE PROBLEMS

POINT SOURCES

The detection of a point source in the presence of nongaussian background noise.
01 p0017 A73-10832

An analysis of the acoustic power radiated by a point dipole source into a rectangular reverberation chamber.
02 p0194 A73-12603

Power spectrum due to point source convection at uniform subsonic speed along round jet flow axis
03 p0246 A73-13841

Maxwell equations in a spherically symmetric black-hole background and radiation by a radially moving charge.
05 p0597 A73-16470

Fluctuations in the level and phase of a field in a waveguide with a random boundary
07 p0793 A73-19916

Spectra of the Becklin-Neugebauer point source and the Kleinmann-Low nebula from 2.8 to 13.5 microns.
08 p1008 A73-21157

Optimum holographic recording of complex light fields generated by diffusive objects in presence of point sources, maximizing SNR or distortion-free diffraction level
09 p1084 A73-22880

Friedmann expanding cosmological model with superimposed spherically symmetric inhomogeneity for gravitational lens and point light sources dispersion and motion effects on images
11 p1418 A73-25747

Preliminary results of observations at the 2-cm wavelength of discrete sources and Jupiter at Pulkovo
12 p1546 A73-27855

Conditions of anastigmatization for Rowland assemblies fitted with concave holographic networks
13 p1613 A73-28567

Acoustic imaging by Bragg diffraction using point sources and spherical optics
13 p1616 A73-28594

Traveling wave solutions of differential equations describing thin elastic shell oscillations due to point source
14 p1815 A73-30951

Homographic motions of Newtonian point mass system interacting through two body forces, considering relativistic interactions
15 p1930 A73-31110

Gradient instabilities in a system of gravitating point masses
15 p1938 A73-31954

A three-dimensional stratospheric point-source tracer experiment and its implications for dispersion of effluent from a fleet of supersonic aircraft.
16 p2007 A73-33562

The path independence of orbit inclination momentum.
17 p2234 A73-35661

POINT TO POINT COMMUNICATIONS

Short-wave asymptotics of the Green's function in the problem of diffraction at a plane layer

18 p2290 A73-36987

Waveguide channel point source electric field level and phase derived by Rytov smooth perturbation technique, obtaining correlation functions, energy spectra and phase fluctuations

19 p2406 A73-38338

Preliminary results of observations of discrete sources and of Jupiter with 2-cm wavelength at Pulkov.

20 p2608 A73-39229

A numerical diffusion model for continuous releases.

21 p2732 A73-41568

The reflexion of an acoustic pulse by a plane vortex sheet.

22 p2842 A73-42348

Resolution of point sources of light as analyzed by quantum detection theory.

23 p2987 A73-43523

Traveling wave solutions of differential equations describing thin elastic shell oscillations due to point source

23 p3047 A73-44327

POINT TO POINT COMMUNICATIONS

CO2 laser communication through an urban atmosphere.

13 p1582 A73-28481

POINTING CONTROL SYSTEMS

Dynamical interaction in biaxial control systems.

01 p0075 A73-11198

Azimuthal pointing control system for balloon observations of celestial bodies, analyzing suspension rope twisting method

01 p0075 A73-11207

Radio telescope for high resolution radio source mapping, discussing system design, computerized control and calibration

02 p0150 A73-18869

Moving vehicle borne automatic sighting device pointing problem mathematical analysis and applications to aircraft and camera aiming for airborne photography

03 p0277 A73-13913

Position and rate aided tracking for conventional pointing systems.

04 p0430 A73-15256

Certain states of rotation of a magnetized spin-stabilized satellite in the geomagnetic field

05 p0627 A73-16291

An amplitude-type position sensor for an optical sun-tracking system

06 p0692 A73-17766

Eole satellite gravity gradient stabilized pointing control system, discussing implementation by eddy current, inertia and magnetic hysteresis devices

07 p0904 A73-18936

Mobile ground station for sounding balloons remote control, telemetry and localization, noting antenna pointing control, tracking receiver and trajectory recording

07 p0790 A73-18972

Sun sensors for D-2B scientific satellite spin axis alignment and attitude stabilization with pointing control accuracy, discussing tests, compensatory tracking and solar simulation

07 p0821 A73-18986

The double gimbaled 'DRALLRAD' and its possible use for three-axis-stabilization of application satellites.

07 p0849 A73-19143

A method for the analysis of optical tracking systems.

07 p0822 A73-19194

Experimental verification and assessment of an infra-red radiation modulator based on a Fabry-Perot etalon.

07 p0825 A73-20373

Attitude control of the AEROS aeronomy satellite during the acquisition phase.

08 p1014 A73-21660

Offset guiding through large space telescopes.

08 p0970 A73-21731

Image integration and display system for guiding on stars beyond the visual detection limit.

08 p0987 A73-21748

Balloon-borne UV stellar spectrometer telescope pointing and stabilization, discussing in-house feasibility studies by small scale test payload experiments

08 p0971 A73-21750

Passive solar array orientation devices for terrestrial application.

09 p1033 A73-22440

UK5 X ray astronomy satellite, discussing structural design, attitude sensing for pointing control, data handling, attitude control and power supply systems

09 p1155 A73-22920

STRAP IV - High accuracy, low drift attitude control system.

[AIAA PAPER 73-288]

09 p1116 A73-23208

Two concepts for the reduction of payload attitude slewing times.

[AIAA PAPER 73-290]

09 p1155 A73-23209

An attitude control system for a stellar X-ray source mapping payload.

[AIAA PAPER 73-291]

09 p1116 A73-23210

A digital attitude control system for orientation of rocket launched scientific payloads.

[AIAA PAPER 73-292]

09 p1116 A73-23211

An apparatus for the orientation of stratospheric-balloon payloads

11 p1304 A73-25355

A simple stabilized antenna platform for maritime satellite communications.

12 p1481 A73-27673

Relationship between pointing precision, spread functions and modulation transfer functions.

12 p1501 A73-27969

Aided tracking as applied to high accuracy pointing systems.

15 p1854 A73-31726

Astronomic follow-up systems with mismatch signal buildup

15 p1877 A73-32134

Television in the control system of an optical telescope

15 p1877 A73-32135

Attitude determination-attitude control in the case of the satellite Aeros

15 p1943 A73-32179

Investigations of the Intelsat IV bearing and power transfer assembly.

17 p2238 A73-34867

Selection of a direct-transmission television satellite system from the point of view of stringent pointing requirements

[DGLR PAPER 73-047]

17 p2126 A73-35483

The multi-moded remote manipulator system.

19 p2416 A73-37314

On the stabilization of aided track pointing systems.

19 p2404 A73-38070

A precision control system for a large astronomical telescope.

19 p2430 A73-38079

An attitude control system for earth observation spacecraft.

[AIAA PAPER 73-854]

20 p2585 A73-38792

Precision pointing control thruster design for satellite experiment to test relativistic precession of gyroscope moving through gravitational field, determining gyro orientation via superconducting circuitry

[AIAA PAPER 73-858]

20 p2586 A73-38796

Large scale telescope pointing stability augmentation system, using control moment gyro gimbal servo error signal to command momentum augmentation system

[AIAA PAPER 73-868]

20 p2587 A73-38806

Fine pointing performance characteristics of the Orbiting Astronomical Observatory /OAO-3/.

[AIAA PAPER 73-869]

20 p2587 A73-38807

Precision gimbal rate control for single gimbal control moment gyro /CMG/ pointing control systems, designing for high frequency response, bandwidth and output torque dynamic range

[AIAA PAPER 73-871]

20 p2587 A73-38808

Assessment of fine stabilization problems for the LST.

[AIAA PAPER 73-881]

20 p2587 A73-38817

Large orbiting telescopes fine guidance system for ultrahigh pointing stability based on disturbance accommodation standard deviation optimal controller design

[AIAA PAPER 73-882]

20 p2588 A73-38818

Achieving ultrahigh accuracy with a body pointing CMG/RW control system.

[AIAA PAPER 73-883]

20 p2588 A73-38819

Development and test of a double gimbaled momentum wheel stabilization system for communication satellites.

[AIAA PAPER 73-906]

20 p2614 A73-38840

Dual spin gas bearing reaction wheel for spacecraft fine pointing applications requiring long component life, describing manufacturing methods, safety factors and testing

[AIAA PAPER 73-907]

20 p2568 A73-38841

Gyroscopes as prime attitude references for the large space telescope.

[AIAA PAPER 73-870]

21 p2700 A73-40506

Considerations about the atmospheric background and the technique of differential modulation in infrared astronomy.

21 p2740 A73-40690

POINTS [MATHEMATICS]

NT FIXED POINTS [MATHEMATICS]

Classical mechanics and field theory derivation based on material points motion in space, discussing space-time metric, electromagnetic and gravitational fields and quantum mechanics

01 p0076 A73-10599

Boundary value problems with a turning point.

03 p0336 A73-13066

Existence theorem for integral manifolds of point mappings in resonant and nonresonant cases for differential equations systems with fast rotating phases

05 p0560 A73-16290

Application of the characteristics of singular points to the determination of the period of quantization in time

11 p1340 A73-25009

Convergence of distributions of point complexes in Z/super m/ to Poisson processes

12 p1523 A73-27191

Zero tangential acceleration points on bodies moving in three dimensional Euclidean space, considering helical-spherical and rotating-spherical motion

14 p1775 A73-30707

Solution of a multipoint problem about the eigenvalues and eigenfunctions of an ordinary linear differential operator using a decomposition technique

20 p2582 A73-39251

POISEUILLE FLOW

U LAMINAR FLOW

POISONING

Hydrazine derivative poisoning in industry and clinical medicine treatments, noting causes of vitamin B6 deficiency

10 p1183 A73-23819

POISONING [TOXICOLOGY]

U TOXIC DISEASES

POISONS

NT ENDOTOXINS

NT URETHANES

POISSON DENSITY FUNCTIONS

Survival probability of a system with a Poisson flow of losses in life-sustaining elements

01 p0028 A73-11422

Poisson model of atmospheric noise from lightning discharges as function of thunderstorm distribution and propagation conditions, calculating statistics for narrow band receiver

02 p0142 A73-12528

Mathematical model for information search and retrieval under Poisson process requests, discussing data processing time minimization sorting algorithms

06 p0670 A73-17856

Atmospheric turbulence effects on laser beam transmitted signals, considering filtering and detection based on doubly stochastic Poisson process

09 p1067 A73-22229

On-board registration and redundancy reduction method for quasi-stationary Poisson processes.

09 p1058 A73-23420

Convergence of distributions of point complexes in Z/super m/ to Poisson processes

12 p1523 A73-27191

A study of integral pulse frequency modulation of a random carrier.

14 p1729 A73-30502

Application of the Poisson stochastic process for collision relaxation calculations in a nonequilibrium gas

15 p1915 A73-30968

An empirical Bayes approach for the Poisson life distribution.

15 p1901 A73-32262

Distribution of the response of linear systems to Poisson distributed random pulses.

16 p2035 A73-32918

Sequential analysis algorithm for data channel detection of received signal represented by Poisson sequence of quantum transitions under large SNR

17 p1219 A73-35711

On the identifiability of finite mixtures of Laguerre distributions.

18 p2330 A73-36984

Bispectrum synthesizer by using multiple Poisson processes.

23 p2965 A73-44089

Pseudorandom Poisson process binary pulse generator, discussing digital hardware implementation and test results

24 p3069 A73-45256

POISSON EQUATION

Russian book - Study of the theory of differentiable functions of many variables and its applications. IV.

02 p0187 A73-12176

Weighted estimates of the error in the grid method of solving the Laplace and Poisson equations

02 p0187 A73-12177

Calculation of the potential created and the velocity induced by a uniform source distribution on a polygon and on a periodic distribution of polygons for the solution of two-dimensional Poisson fields

03 p0241 A73-12910

Transformation group theory for Poisson equation solutions to boundary value problem of steady heat conduction with generation

03 p0400 A73-14631

The finite element method in domains with curved boundaries.

07 p0907 A73-19029

A direct method for solving Poisson's equation.

07 p0845 A73-19574

Differential solutions of the biharmonic Poisson and first order Stokes equations.

08 p0983 A73-21203

The continuity and Poisson's equations for semiconductors with many coexisting kinds of multiple energy-level defects.

09 p1133 A73-22306

Axisymmetric triangular finite elements for the scalar Helmholtz equation. 09 p1120 A73-22392

Numerical solution of mixed boundary value problems using numerical Green's functions. 09 p1112 A73-22394

Newtonian aerodynamic forces from Poisson's equation. 11 p1303 A73-26382

On the numerical treatment of the Navier-Stokes equations for an incompressible fluid. 13 p1599 A73-28090

Approximate solution of the Laplace and Poisson equations in weighted Hoelder spaces 13 p1647 A73-28340

Nonlinear plasma oscillations in terms of Van Kampen modes. 14 p1780 A73-30350

Poisson formula analogs for a class of higher-order elliptic-type differential equations with a singular line in the case of a half-space 15 p1898 A73-31020

Variational principle with penalty for finite element solution of model Poisson equation with homogeneous Dirichlet boundary conditions, noting convergence 17 p2199 A73-34209

The Laplace and Poisson equations in Schwarzschild's space-time. 23 p3005 A73-43345

An iteration method of alternating directions for the Poisson difference equation in curvilinear orthogonal coordinates 24 p3105 A73-44650

POISSON PROCESS

U POISSON DENSITY FUNCTIONS

U STOCHASTIC PROCESSES

POISSON RATIO

On the unbonded contact between a beam and a semi-infinite plate. 03 p0389 A73-13324

Determination of Young's modulus and of the Poisson coefficient by a method of resonant bars 04 p0462 A73-15247

Studies of the elastic properties of molybdenum 04 p0464 A73-15372

Study on fracture mechanism for composite materials based on the concept of the change in Poisson's ratio. 07 p0915 A73-20328

Parameters governing load transfer for single reinforcing members. 08 p1016 A73-20799

Influence of Poisson's ratio on the condition of the finite element stiffness matrix. 09 p1160 A73-22892

Ultrasonic measurement of elastic moduli in slender specimens using extensional and torsional wave pulses. 11 p1365 A73-26171

Determining elasticity constants of disc-shaped specimens of material. 13 p1613 A73-28521

Interpretation of mechanical behavior of pure aluminum in terms of microstructure. 13 p1639 A73-29459

Stress differentiation procedure for screen technique studies in dynamic photoelasticity, giving expressions for elastic modulus and Poisson ratio 13 p1703 A73-29613

Effect of Poisson's ratio strains in adherends on stresses of an idealized lap joint. 15 p1948 A73-31620

Symmetric vector-type tensor functions of elastic bodies related to strain measure invariants, formulating limited hardness principle in terms of Poisson ratio 15 p1954 A73-32123

Poisson's Ratio and the deflection of a viscoelastic plate. 15 p1956 A73-32342

Calculation of the physicochemical constants of metals associated with the strength of interatomic bonds 22 p2874 A73-42097

On the integral equations of three-dimensional multiple inclusion problems. 22 p2924 A73-42682

POLAR AURORAS

U AURORAS

POLAR CAP ABSORPTION

Mesospheric nitric oxide concentrations during a PCA. 01 p0041 A73-10881

Solar flare development particle acceleration phase model, noting association with white light emission, hard X-rays and PCA 04 p0490 A73-14833

Solar flare effects in ionosphere, discussing long term variability, sudden ionospheric disturbances, PCA and magnetic storms 04 p0491 A73-14839

Solar electrons and alpha particles during polar-cap absorption events. 04 p0493 A73-15558

The time-latitude distribution of solar flares accompanied by type IV radio bursts during the period 1956 to 1969. 08 p0997 A73-20770

Solar cosmic ray flare of 11-18 April 1969, investigating effect on polar cap absorption in lower ionosphere 08 p1000 A73-21348

Ionospheric magnetic disturbances during March 1970 related to solar flare corpuscular and proton fluxes, generating ring current and PCA absorption 10 p1211 A73-24218

Millimeter wave burst mean duration relation to PCA event intensity derived from relationship between impulsive single frequency microwave bursts and solar proton events 12 p1543 A73-27616

Ionospheric D region dissociation-recombination reaction constants derived from ion production rate data compiled during polar cap absorption 15 p1872 A73-31887

A rocket-borne riometer for the study of lower ionosphere. 18 p2315 A73-36046

Atomic hydrogen and water vapour in the lower arctic thermosphere during geomagnetic storm and PCA event. 18 p2310 A73-36141

Satellite and ground-based observations during the onset phase of the 2 November 1969 PCA event. 19 p2426 A73-38016

Axial symmetry of the magnetosphere and the noon recovery of polar cap absorption 21 p2759 A73-40608

Rocket measurements of electric field and optical aurora during weak PCA event, noting rocket passage through discrete auroral forms 21 p2684 A73-40781

Penetration of solar cosmic rays into the earth's polar caps 21 p2760 A73-40920

Rocket measurements of production and ionization during a PCA event. 21 p2760 A73-41371

Steady state coefficients in the D region during solar particle events. 21 p2760 A73-41372

Midday recovery of HF absorption during PCA events relationship to satellite observation of solar proton latitudinal variations 22 p2846 A73-41943

The solar radio patrol network of the USAF and its application. 23 p2958 A73-43371

POLAR CAPS

Mars polar caps formation at aerographic latitudes, assuming water vapor condensation on ground and water presence in carbon dioxide snow 01 p0106 A73-11322

On the types of current patterns of weak geomagnetic disturbances at the polar caps. 02 p0158 A73-11915

Mars exploration by spacecraft, discussing erosional processes, atmospheric pressure and composition, heat absorption and radiation and polar caps formation 02 p0221 A73-12575

North/south asymmetric entry of solar protons during the November 18, 1968 event. 03 p0360 A73-12878

Bombardment of the polar-cap ionosphere by solar cosmic rays. 03 p0301 A73-13710

Preferential particle arrival at polar caps during solar events, noting north pole flux increase from ESRO 1 measurements 03 p0362 A73-13861

Mars microwave spectra computation by improved thermal model with seasonal polar cap effects and accurate aspect geometry, noting lunar-like planetary subsurface nature 06 p0747 A73-17492

Mariner spacecraft photographed Mars surface volcanic mountains and water in polar caps, suggesting recurring rainfall and rivers during successive interglacial periods 07 p0875 A73-19166

Strong pitch angle diffusion and magnetospheric solar protons. 07 p0869 A73-19229

Ionograms for slant sporadic E layer under continuous sunlight inside polar cap, noting occurrence probability and auroral activity 07 p0819 A73-20065

Response of a general circulation model of the atmosphere to removal of the arctic ice-cap. 07 p0848 A73-20122

German monograph - Investigations of the behavior of high energetic protons and electrons in the inner magnetosphere. 07 p0872 A73-20385

Penetration of solar protons into the geomagnetic tail 08 p0998 A73-21276

Nonadiabatic particle motion in the magnetosphere. 09 p1073 A73-22052

Low-energy solar protons in the pseudo-trapping region of the magnetosphere. 09 p1137 A73-22053

New optical measurements of planetary diameters. IV - Size of the North polar cap of Mars. 09 p1145 A73-22273

A possible current system associated with the Sqg variation. 11 p1356 A73-25910

Pulsar magnetospheres, braking index, polar caps, and period-pulse-width distribution. 11 p1428 A73-26618

Magnetic field signatures of substorms on high-latitude field lines in the nighttime magnetosphere. 12 p1488 A73-26981

Mars photographic observations during opposition, analyzing polar caps, surface reliefs, dust storms and atmospheric optical thickness 12 p1542 A73-27498

Polar cap E layer conductivity difference effects on ring currents associated with vertical current along lines of force at conjugate points 13 p1608 A73-28717

Polar cap magnetic variations and their relationship with the interplanetary magnetic sector structure. 14 p1747 A73-29959

Correspondence of solar field sector direction and polar cap geomagnetic field changes for 1965. 14 p1747 A73-29960

The altitude of the scattering layer near the mesopause over the summer poles. 14 p1750 A73-30768

Model of dayside magnetopause displacement relation to convection currents feeding polar cap ionosphere to estimate electric field and flux return as function of displacement 16 p2003 A73-33432

Role of water vapor in the meteorology of Mars 16 p2069 A73-33831

Mariner 9 observations of the surface of Mars in the north polar region. 19 p2478 A73-37213

Penetration of solar protons into the geomagnetic tail. 19 p2476 A73-37905

Structural and dynamic features of solar cosmic-ray penetration into polar regions 21 p2758 A73-40606

Jupiter satellite Europa polar cap from photoelectric observation of occultations by satellite Io 21 p2687 A73-41077

Uneven illumination of the polar caps by solar protons - Comparison of different particle entry models. 22 p2901 A73-41906

Short-period interplanetary and polar magnetic field variations. 23 p3029 A73-43691

Mariner 9 ultraviolet spectrometer experiment - 1971 Mars' dust storm. 24 p3127 A73-44396

Role of the neutral sheet in the illumination of polar caps by solar protons. 24 p3086 A73-45132

Polar cap electric field measurements by balloons indicating ionospheric convection control by interplanetary magnetic field 24 p3086 A73-45135

Seasonal variations of the south polar cap of Mars according to measurements made on photographs taken near the time of the 1971 opposition. 24 p3143 A73-45439

POLAR COORDINATES

Cartesian coordinates for panoramic perspective position of point on conical map, noting relationship to semipolar coordinates of object point 02 p0166 A73-11644

Dipolar coordinate system for geomagnetic field dipole approximation in studies of diffusion and heat conduction in F region and outer ionosphere 07 p0816 A73-19452

Geometrical dynamics method for orbit geometry in configuration space of dynamical system, using polar coordinates as generalized coordinates for circular restricted three body problem 09 p1148 A73-22911

Simultaneous determination of pole coordinates and the nonuniformity of the earth's rotation 21 p2768 A73-40727

Ischemic polarcardiographic changes induced by exercise - A new criterion. 24 p3060 A73-44946

Canonical elements based on polar coordinates in Kustanheimo-Stiefel space and applications to satellite motion perturbation from oblate bodies 24 p3111 A73-45293

POLAR GASES

Investigation of heat transfer in a rarefied molecular gas with the aid of the Sentfleben effect 11 p1453 A73-26445

Electric field interaction with polar molecules at varying density diffusing through solid body surface.

POLAR IONOSPHERE BEACON

- deriving dispersion law for density and potential fluctuations 12 p1526 A73-27939
- Momentum transfer and total scattering cross sections for ions with polar molecules. 17 p2213 A73-35178
- POLAR IONOSPHERE BEACON**
- U BEACON SATELLITES**
- POLAR METEOROLOGY**
- On the maintenance of the polar front jet stream. 17 p2205 A73-34854
- Structure variations in the winter polar atmosphere. 21 p2685 A73-40827
- POLAR ORBIT GEOPHYSICAL OBSERVATORY**
- U POGO**
- POLAR ORBITS**
- Global nitric oxide and gamma emission measurements with Ebert-Fastie scanning spectrometer on-board polar orbiting OGO 4 satellite 01 p0040 A73-10878
- Multifrequency radio beacon on polar orbiting satellite for wideband transmission through ionosphere without significant signal distortion 03 p0275 A73-13627
- Earth geodetic mapping with rotating torsional gravity gradiometers onboard spin stabilized satellite in low polar orbit 04 p0446 A73-14806
- Environmental data transmission from arctic data buoys via polar orbiting satellite. 04 p0421 A73-15431
- A system of four geosynchronous satellites for global observations 15 p1903 A73-31605
- Transit satellite-borne radioisotope thermoelectric generators launch aboard Scout missile into circular polar orbit, obtaining electrical and thermal data 19 p2494 A73-38394
- POLAR REGIONS**
- NT ANTARCTIC REGIONS**
- NT ARCTIC REGIONS**
- Isis 1 observations of the high-latitude ionosphere during a geomagnetic storm. 02 p0155 A73-11735 [AD-759885]
- Probe measurements of positive ions and electron temperatures in high latitude rocket flights. 02 p0159 A73-12032
- Upper atmospheric dust concentrations in polar regions. 02 p0215 A73-12260
- High-latitude precipitation of low-energy particles as observed by ESRO IA. 02 p0206 A73-12312
- Latitude-time variations of the total number of electrons and of its gradients in the ionosphere at high latitudes 02 p0164 A73-12474
- Transmission and reflection of magnetospheric whistlers in the ionosphere and lower exosphere at high latitudes. 03 p0298 A73-12884
- Some results about the satellite scintillation on 150/400 MHz and the horizontal gradient of the total electron content in the polar ionosphere. 03 p0300 A73-13648
- Inferring the interplanetary magnetic field by observing the polar geomagnetic field. 03 p0373 A73-13712 [AD-755684]
- ESRO IA/B observations at high latitudes of trapped and precipitating protons with energies above 100 keV. 03 p0362 A73-13863
- Ground based goniometric observations of medium and high latitude VLF emissions due to transverse resonance instability and auroral oval Cerenkov radiation from magnetosheath 03 p0276 A73-13884
- Precipitation of low-energy electrons at high latitudes - Effects of interplanetary magnetic field and dipole tilt angle. 04 p0493 A73-15531
- Polar ionospheric ion escape /polar wind/ hydrodynamic model equations, discussing singularities and critical points in terms of reduced Mach number 04 p0444 A73-15546
- Equatorward shift of the polar F layer irregularity zone as a function of the Kp index. 04 p0445 A73-15557
- Study of the effect of the east-west component of the interplanetary magnetic field on the currents equivalent to the magnetic perturbations of high latitude regions 04 p0502 A73-16000
- Nonuniformities of the ion density at an altitude of 600 km in the ionosphere. 05 p0567 A73-16083
- The effect of photoelectrons on kinetic polar wind models. 05 p0572 A73-17159
- Geological framework of the south polar region of Mars. 06 p0745 A73-17477

- Moment equations of temperature and high latitude spread F instability in presence of north-south electric field, relating to maximum Pedersen current and barium cloud deformation 07 p0814 A73-19243
- Spatial-temporal distribution of E/s formations associated with visible forms of polar aurorae 08 p0958 A73-21283
- Simultaneous observations of low energy electron fluxes and the polar red emission at 6300 A. 09 p1075 A73-22137
- Field-aligned currents between 400 and 3000 km in auroral and polar latitudes. 09 p1078 A73-22834
- Esro 4 performance of abandoned TD-2 experiments for particle measurements over polar regions, describing satellite construction, thermal control, power supply, attitude control and measurement 10 p1285 A73-23748
- Observation of the entrance of solar protons in the magnetosphere at very high latitudes 10 p1211 A73-23769
- Sector structure of the interplanetary magnetic field, and magnetic disturbances in the circumpolar region 10 p1276 A73-23896
- A model for the polar transition layer and corona for November 1967. 10 p1279 A73-24139
- Sporadic ionization of the ionospheric E-region at high latitudes as a function of magnetic activity. 10 p1212 A73-24221
- Energetic solar proton observations by Explorer 33 and 35 /interplanetary medium/ and Injun 5 /polar caps/, comparing proton fluxes in space and poles 10 p1269 A73-24729
- Effects of interplanetary magnetic sector structure on auroral zone and polar cap magnetic activity. 10 p1213 A73-24730
- OGO 5 observation of ULF geomagnetic fluctuation at polar cusp boundaries in terms of ionospheric drift wave and Kelvin-Helmholtz instabilities 10 p1214 A73-24744
- On empirical models of the upper atmosphere in the polar regions. 11 p1356 A73-25915
- Distributions and characteristics of high-latitude field-aligned electron precipitation. 12 p1534 A73-26988
- Cosmic ray storm effect on midlatitude and polar neutron monitors, noting comparison with underground mu-meson telescopic observations at high rigidities 12 p1534 A73-27001
- Heos 2 magnetometer observations of magnetosheath high and low energy electron flux during magnetopause boundary crossings in polar regions 12 p1489 A73-27004
- Solar prominences during period between sunspot minimum and maximum, investigating secondary polar zone coronal activity phase shift relationship to main zone anomaly 12 p1545 A73-27837
- International polar experiment /POLEX/ program for global circulation research and long range weather forecasting improvement 13 p1654 A73-28933
- Influence of the interplanetary magnetic field on the magnetic perturbations of high latitude regions - Demonstration of an asymmetry in relation to the earth-sun direction 13 p1611 A73-29563
- Mars polar regions layered deposits annual solar insolation variations due to eccentricity 13 p1687 A73-29674
- Field-aligned currents, plasma waves, and anomalous resistivity in the disturbed polar cusp. 14 p1747 A73-29964
- Polar ionospheric electron density distribution near closed field line boundaries for ISIS 1 dayside passes, discussing geomagnetic storm effects 14 p1748 A73-29980
- Average high latitude magnetic field: Variation with interplanetary sector and with season. I - Disturbed conditions. 15 p1866 A73-31073
- Isis-2 observations of auroral emissions characteristics in polar region during December 1971 magnetic storm recovery phase 15 p1866 A73-31076
- Diurnal variations of the vertical component of the magnetic field in high latitude regions as a function of the east-west component of the interplanetary magnetic field 15 p1868 A73-31570
- Zonal nature of some micropulsation disturbances at the geomagnetic pole 15 p1872 A73-31897
- Latitudinal and time variations of total electron number and its gradients in the ionosphere at high latitudes. 15 p1874 A73-32625
- Ion cyclotron waves observed in the polar cusp. 16 p2003 A73-33437

- Wave polarizations of geomagnetic pulsations observed in high latitudes on the earth's surface. 16 p2003 A73-33440
- F 2 critical frequency and maximum height at high southern latitudes explained via additional ionization provided by energetic particles 16 p2009 A73-33911
- Enhancements of the electron concentration in the F2-layer at magnetic noon. 16 p2010 A73-33914
- Russian monograph on polar auroras and magnetospheric geomagnetic disturbances from rocket, balloon and ground station soundings covering magnetic storms, solar wind and geoelectric fields. 18 p2302 A73-35873
- OGO-5 observations of the physical processes occurring in the disturbed polar cusp and the cusp-magnetosheath interface. 18 p2303 A73-35943
- Estimation of H/+ / fluxes at the polar regions. 18 p2304 A73-35969
- Ionospheric electron content and its horizontal gradients at high and middle latitudes from radiowave propagation from satellites. 18 p2304 A73-35972
- Rocket investigation of the intensity and composition of the corpuscular radiation at altitudes 180 km up to the polar region. 18 p2345 A73-36137
- Temperature and wind velocity variations in winter mesosphere of polar regions. 18 p2310 A73-36140
- Mass spectrometric investigations of the night polar ionospheric structure. 18 p2310 A73-36145
- Meteor ions in the polar ionosphere according to the rocket mass-spectrometric measurements and theoretical calculations. 18 p2311 A73-36146
- Dependence of the polar cusp on the north-south component of the interplanetary magnetic field. 18 p2351 A73-36273
- Mariner 9 observations of the surface of Mars in the north polar region. 19 p2478 A73-37213
- Wind erosion in the Martian polar regions. 19 p2478 A73-37214
- Martian south polar region pitted and etched terrain features, interpreting surface layered blanketing material as due to wind action 19 p2478 A73-37215
- Nature and origin of layered deposits of the Martian polar regions. 19 p2478 A73-37216
- Martian polar stacked laminae interpreted in terms of conditions for carbon dioxide liquefaction, considering atmosphere history 19 p2478 A73-37217
- Mars atmosphere during the Mariner 9 Extended Mission - Television results. 19 p2478 A73-37218
- Martian south polar region albedo map from Mariner 9 photographs, comparing with earth-based telescopic observations 19 p2480 A73-37232
- Sector-patterned structure of interplanetary magnetic field and magnetic disturbances in the circumpolar region. 20 p2603 A73-38915
- Correlational relations between F2 critical frequency deviations and the solar activity cycle according to a number of high-latitude stations 20 p2555 A73-39176
- Numerical calculation for polar ionospheric current under realistic electric field and conductivity distributions, considering solar wind effect on charged particles in magnetosphere 21 p2681 A73-40155
- Limit of the region of low-energy solar proton irruption into the polar ionosphere 21 p2758 A73-40607
- Polar region soil moisture content remote sensing based on electromagnetic backscattering and depolarization by ice and terrain, considering radar, microwave and IR sensors 21 p2654 A73-40814
- A study of geoelectrocorpuscles and photoelectrons on the Cosmos 261 satellite. VI - Epithelial electrons in the energy range from 30 to 150 eV in the region of the dayside and nightside polar cusps 21 p2686 A73-40909
- Rocket measurements of electron concentration and electron temperature in the polar ionosphere. 21 p2690 A73-41367
- High energy electrons at the magnetopause above the north pole - Preliminary results from the HEOS 2 satellite. 21 p2761 A73-41376
- A current mechanism for the formation of inhomogeneities resulting in the ionospheric spread F region at high latitudes 21 p2692 A73-41508
- Latitude and local time dependence of precipitated low-energy electrons at high latitudes. 22 p2901 A73-41914

Sudden commencement and sudden impulse absorption events at high latitudes.

22 p2845 A73-41928

Polar magnetic storm temporal properties and distribution patterns, discussing solar activity, annual and twenty-seven day variations and sudden commencement

22 p2851 A73-42749

Short-time fluctuations of the VLF field along polar paths

24 p3067 A73-44809

High-latitude proton precipitation and light ion density profiles during the magnetic storm initial phase.

24 p3126 A73-45114

Polar wind measurements by electrically neutral luminous by-product clouds from Ba ion releases, discussing ion drag

24 p3085 A73-45120

POLAR SUBSTORMS

Variations of the auroral electron energy spectra during substorms.

01 p0036 A73-10339

Multidiscipline study of perturbations observed on March 8, 1970 in the midnight sector

01 p0036 A73-10343

Infinite set of velocity fields to describe geomagnetic field lines and interpret discrepancy in plasma sheet motion observations during substorms

02 p0157 A73-11754

Atmospheric model for substorm triggering mechanism, plasma sheath behavior and substorm recovery, noting solar wind interaction with magnetosphere

03 p0304 A73-13886

Geomagnetic tail plasma sheet thinning and auroral zone negative bays development during magnetospheric substorms, suggesting auroral particles acceleration along magnetic field lines

03 p0304 A73-13887

Interpretation of magnetic field variations during substorms.

03 p0304 A73-13888

Local time variations of X ray substorm activity observed at auroral zone station, including atmospheric passage and energy spectrum measurements

03 p0363 A73-13889

Excitation of polar substorms by northward interplanetary magnetic field.

03 p0304 A73-13890

Precipitation of low-energy electrons at high latitudes - Effects of interplanetary magnetic field and dipole tilt angle.

04 p0493 A73-15531

Resonance acceleration of low-energy protons in the earth's radiation belts

06 p0742 A73-17526

Magnetosphere tail internal plasma boundary layer dynamics during substorms based on aurora data

07 p0816 A73-19463

Relationships between the equatorial electrojet and polar magnetic variations.

07 p0818 A73-19662

Some statistical characteristics of the spectra of polar magnetic substorms

08 p0959 A73-21293

Relationship of magnetospheric substorms on the ground and in the distant magnetotail.

08 p0961 A73-21392

Electron and proton acceleration in the outer regions of the magnetosphere during polar substorms.

10 p1268 A73-24227

VLF radio signals propagational effects relationship to ionospheric polar substorm different phases

11 p1330 A73-25765

The day-sector polar F-layer during a magnetospheric substorm.

11 p1356 A73-25918

Enhancements of ionospheric total electron content in the southern auroral zone associated with magnetospheric substorms.

11 p1359 A73-26715

Dayside polar aurorae during various substorm phases from IGY data, noting time of glow intensity maximum

12 p1490 A73-27343

Midday aurora behavior during auroral substorms from all sky photographs at south pole, considering modification of Starkov-Feldstein model

12 p1493 A73-27614

Analogies between substorm phenomena of the visual polar aurora and the radio aurora

12 p1493 A73-27757

Perpendicular and parallel electric fields in the ionosphere during a magnetospheric substorm

12 p1494 A73-27776

On the longitudinal extension of electron precipitation during magnetospheric substorms.

13 p1606 A73-28152

The effect of polar magnetic sub-storms on the equatorial sporadic E.

15 p1874 A73-32596

Resonance acceleration of low-energy protons in the radiation belts of the earth.

16 p2051 A73-32751

An instrument for real-time determination of polar electrojet position and current parameters.

17 p2176 A73-35768

Synoptic survey for the neutral line in the magnetotail during the substorm expansion phase.

18 p2352 A73-36275

Some statistical characteristics of the spectra of polar magnetic substorms.

19 p2425 A73-37922

Bremsstrahlung X ray measurements over subauroral latitudes during substorms, noting c folding energy correlated with local electrojet and anticorrelated with conjugate electrojet

21 p2760 A73-41366

Response of the polar electrojets in the evening sector to polar magnetic substorms.

22 p2902 A73-41916

Current flow in auroral loops and surges inferred from ground-based magnetic observations.

22 p2902 A73-41917

Dayside polar aurorae during various substorm phases from IGY data, noting time of glow intensity maximum

23 p2970 A73-43240

Short-wave propagation along several paths during auroral storm periods

24 p3067 A73-44796

Correlation between the excitation of p1 and pc1 geomagnetic pulsations and magnetospheric substorms

24 p3084 A73-44811

POLARIMETERS

Light polarization measurement with multichannel polarimeters, considering achromatic modulators to convert polarization information into intensity modulation before light beam split into constituent wavelengths

01 p0050 A73-10542

Some new satellite sensors and applications.

01 p0052 A73-11161

Polarimeter search for optical circular polarization in eclipsing binaries, magnetic Ap stars, planetary nebula, Hubble and Orion nebulae, M87 and Sirius

03 p0366 A73-12939

A dual polarization laser backscatter system for water quality studies.

06 p0700 A73-18306

Polarimeter-photometer to study solar corona or disk over wide photon arrival rate range, measuring magnitude of polarization effects

08 p0971 A73-21746

Imaging photopolarimeter for measuring orthogonal, sky glow and gegenschein brightness and polarization in sky mapping mode

11 p1415 A73-25177

Astronomical polarimeter design, polarization sensitivity and 5 and 10 micron analyzers efficiency

11 p1369 A73-26513

Pioneer 10 spacecraft spin-scan imaging photopolarimetric optical system for Jupiter mapping

15 p1880 A73-32385

Polarization observations of variable stars and extragalactic objects. I - Instruments and methods of observation and data processing. II - Polarization of the EV Lac flare

16 p2057 A73-32708

Intercompos satellite-borne X ray polarimeter measurements of solar flares

18 p2345 A73-36144

Investigation of the gain instability of a semiconductor radiometer

21 p2700 A73-40539

High precision photoelectric azimuthal polarimeter design, construction and operation for determining angular rotation of polarized light beam

21 p2704 A73-41258

Polarimetric instrument of moon and planets via imaging system consisting of slot scanner, telescope, condenser lens, rotating disk analyzer and photomultiplier tube

24 p3089 A73-44485

A double image chopping polarimeter.

24 p3091 A73-45185

POLARIMETRY

Upward short wave radiation polarization characteristics observation by airborne polarimeter over grey sand desert, dense altocumulus liquid drops and cumulonimbus clouds and seas

02 p0169 A73-12269

A polarimetric method of measuring radial velocities.

02 p0171 A73-12830

A photometric and polarimetric study of the moon's surface.

04 p0497 A73-15183

Photography of the zodiacal light outside the ecliptic in quadrature and in opposition with the sun

09 p1073 A73-22001

Precision spectropolarimetry of starlight - Development of a wide-band version of the Dollfus polarization modulator.

09 p1084 A73-22866

Measurements of the magnetic field vector of a sunspot.

10 p1275 A73-23827

Possibility of polarimetric monitoring of the optical stability of the atmosphere

11 p1392 A73-25609

Photometric and polarimetric analysis of the coronal streamers observed at the March 7, 1970 Mexican eclipse.

11 p1425 A73-26263

Polarigraphic observations of the solar corona at the total eclipse on March 7, 1970 in Mexico.

11 p1425 A73-26264

Twilight circular polarization due to Mie scattering, analyzing polarimeter measurements in IR and UV spectral bands

12 p1490 A73-27150

Polarimetric studies of the giant planets. III - Jupiter

12 p1546 A73-27861

Polarimetric observation of moon and planets via imaging system consisting of slot scanner, telescope, condenser lens, rotating disk analyzer and photomultiplier tube

15 p1876 A73-31960

Equipment for infrared photometric and polarimetric observations

15 p1878 A73-32138

Galactic X-ray polarimetry and high-resolution X-ray spectroscopy.

16 p2058 A73-32736

Aerological investigation of the volcanic beds of Kamchatka by polarizational and spectral methods

16 p1977 A73-33760

Polarimetric observations of the giant planets. III.

20 p2608 A73-39235

The Synthesis Radio Telescope at Westerbork - Methods of polarization measurement.

20 p2566 A73-39581

Polarimetric mapping techniques using multichannel digital photometry via remote sensors, discussing terrain types, lunar topographic analysis and soil and vegetation mapping

20 p2568 A73-39860

Pluto polarimetric measurements showing degree and position angle of polarization and probable error

22 p2905 A73-41763

Disk integrated polarization observation for Titan at small phase angles, noting optically thin Rayleigh atmosphere on opaque cloud deck

24 p3130 A73-44451

Titan satellite optical polarization observation in three spectral regions, noting inconsistency with scattering from planetary surface or pure molecular atmosphere

24 p3130 A73-44452

POLARIS MISSILES

Book - The Polaris system development: Bureaucratic and programmatic success in government.

12 p1561 A73-27400

POLARISCOPES

A dynamic polariscope for stress wave analysis.

08 p0962 A73-20668

Dual-beam polariscope and framing camera for dynamic photoelasticity.

12 p1496 A73-27025

POLARITY

The effect of polarity on the diffraction of plane elastic waves by a cylindrical cavity.

03 p0396 A73-14627

Dependence of the parameters of a plasma cluster obtained from a coaxial source on the polarity of the central electrode

10 p1257 A73-24878

Geomagnetic field polarity reversal mechanism, interpreting frequency distribution by energy exchange between dynamo models and conversion between kinetic and magnetic energies

11 p1355 A73-25792

Effects of target-electrode polarity and the position of the focal plane of the lens on the characteristics of a discharger with laser ignition

13 p1627 A73-28964

Dependence of the parameters of a plasmoid obtained from a coaxial source on the polarity of the central electrode.

21 p2749 A73-41653

Effects of target-electrode polarity and focal-plane position on a laser-triggered gap.

23 p2989 A73-44316

Observation of a possible neutral sheet in the corone.

24 p3136 A73-44636

POLARIZATION [CHARGE SEPARATION]

NT DIELECTRIC POLARIZATION

NT ELECTROLYTIC POLARIZATION

Study of polarization during electrodeposition of tungsten simultaneously with nickel

02 p0174 A73-12539

Pre-threshold conductance and polarization effects in amorphous semiconductor switches.

04 p0427 A73-15343

A new method to measure non-uniformity in the intact heart.

04 p0412 A73-15645

Influence of an external electric field on the initial phase of the explosion of wires in a vacuum

09 p1119 A73-21883

POLARIZATION [SPIN ALIGNMENT]

Variational determination of electric field induced by charge separation in near wake of negatively charged body moving at mesothermal speeds in collisionless plasma

10 p1254 A73-24116

On the origin of the electric field of polarization in a gravitational plasma.

11 p1350 A73-24990

Boltzmann kinetic equation for nonideal plasma with allowance for polarization effects, noting collision integral convergence

11 p1406 A73-26187

Mono- and polycrystalline bismuth titanate structural and physical properties, discussing thermally induced structural changes effects on polarization, permittivity and loss tangent

15 p1924 A73-31775

Calculations on the radio emission resulting from geomagnetic charge separation in an extensive air shower.

17 p2223 A73-34244

Effect of an external electric field on exploding wires in vacuum.

17 p2211 A73-34307

Polarization operator of a superconducting electron gas - The Kohn anomalies and charge screening in superconductors

18 p2337 A73-36666

Changes in some behavioral reactions and in the bioelectric activity of the brain in cats during the development of sleep under polarization of individual brain structures

19 p2393 A73-37393

Attempt at an interpretation of thermal reversals in the spontaneous polarization of ferroelectric microdomains

19 p2470 A73-37537

High power density hydrazine-oxygen fuel cell, discussing cell polarization, critical resistance losses and efficiency

19 p2390 A73-38398

Polarizability of interacting atoms - Relation to collision-induced light scattering and dielectric models.

21 p2742 A73-40211

Polarization of rare gas atoms in the successive layers adsorbed on graphite

21 p2724 A73-41599

Polarizing interaction between colliding plasma flows in a toroidal magnetic field. II

22 p2893 A73-42384

Polarizable particle entrainment in electromagnetic field consisting of wave packets propagating in opposite directions

22 p2889 A73-43099

Thunderstorm electrification by the inductive charging mechanism. I - Particle charges and electric fields. II - Possible effects of updraft on the charge separation process.

23 p3002 A73-43599

Electric polarization of a plasma beam in an axially symmetrical magnetic field

23 p3009 A73-43655

Local resistance variations caused by membrane potential shifts in the interior of the horizontal retina cell

24 p3061 A73-45250

POLARIZATION [SPIN ALIGNMENT]

Fermions spin polarization reversal for HF high intensity gravitational waves generation and detection, suggesting superconducting metals for waves receiver

04 p0476 A73-15633

He odd parity states computed via Hylleraas trial wave function with nonlinear parameters, considering mass-polarization correction and electron transitions

05 p0600 A73-16599

Atomic nuclei physical properties for space navigation system gyroscopes, noting nuclear magnetic resonance and nuclei polarization

06 p0692 A73-17774

A general formula for free-free absorption on highly-polarizable neutral atoms.

16 p2039 A73-33740

POLARIZATION [WAVES]

NT CIRCULAR POLARIZATION

NT ELLIPTICAL POLARIZATION

Supernova remnants descriptions, distance and hydrodynamic evolution, considering galactic nonthermal radio sources, radio maps, and X ray and radio polarization

01 p0094 A73-10057

Holographic image polarization recording and sum wave simulation on photoanisotropic materials, using Weigert effect

01 p0052 A73-11086

Experimental study of the inverse Faraday effect in plasmas

02 p0196 A73-11587

Extensive air showers radio emission polarization, spatial distribution and electric field strength, noting geomagnetic mechanism effect

02 p0209 A73-12672

Possibility of emission-line polarization in diffuse nebulae with a C + E spectrum

05 p0617 A73-16462

On the location of the source of Weber's gravitational events.

05 p0625 A73-17330

Holographic recording and reproduction of wave polarization information by correlation matrix and Stokes parameter method

09 p1087 A73-23333

Instrumental polarization concerning magnetographic measurements.

10 p1218 A73-24148

Polarization of radio waves reflected from an inhomogeneous ionosphere

12 p1468 A73-26971

Absorption of the microwave energy in a magnetoactive plasma.

12 p1529 A73-27433

A null-reading method of measuring the complex reflection coefficient in the short-wave end of the millimeter band

14 p1728 A73-30271

Generation of opposed waves polarized in different planes in a ring laser

14 p1757 A73-30368

Ionospherically propagated backscatter from Pacific Ocean via swept frequency continuous wave recordings, noting sky wave polarization rotation modulation of received signal

15 p1845 A73-32228

Wave polarizations of geomagnetic pulsations observed in high latitudes on the earth's surface.

16 p2003 A73-33440

Microwave propagation in atmosphere with oblate spheroidal raindrops, discussing linear and circular cross-polarization effectiveness statistical analysis with allowance for raindrop orientation

16 p1983 A73-33724

Some results of a theoretical study of radio emission polarization on a rough moon

16 p2064 A73-33770

Raindrops in satellite communications.

18 p2289 A73-36515

Scattering properties of oblate raindrops and cross polarization of radio waves due to rain - Calculations at 19.3 and 34.8 GHz.

18 p2290 A73-36880

Airborne remote sensing of cloud particle size and shapes via IR polarimeter, obtaining polarization vs phase angle curve for thick tropical cirrus clouds

20 p2567 A73-39859

Ultrahigh frequency radar scattering by perfectly conducting conical pyramidal noded bodies, deriving polarized radar cross sections via wedge diffracted field integration

22 p2824 A73-41854

Gravitational-wave observations as a tool for testing relativistic gravity.

22 p2887 A73-42709

Use of cancellation techniques in the measurement of atmospheric crosspolarisation.

23 p2955 A73-44111

Determination of the vertical parameters of wavelike ionospheric disturbances

24 p3083 A73-44797

Vector wave field hologram generation via polarization contrast method, described by correlation matrix formalism

24 p3091 A73-44957

POLARIZATION CHARACTERISTICS

NT GYROTROPISM

Off-axis polarization characteristics of Cassegrainian and front-fed paraboloidal antennas.

01 p0022 A73-10177

Influence of the polarization of phonons on the thermal conductivity of single crystals of indium phosphide between 300 and 800 K

01 p0087 A73-10430

Comparison of the linear polarization and albedo of volcanic rocks in the spectral region between 0.75 and 3.0 microns with the values of these parameters for the moon

01 p0101 A73-10841

Polarization of the inner corona during the solar eclipse of March 7, 1970

01 p0102 A73-10939

Polarimetric investigations of the giant planets. II - Phase variation of the polarization of selected regions on the Saturn disk

01 p0102 A73-10941

Polarization of relativistic-electron emission in the case of Compton scattering at turbulent plasma oscillations

01 p0085 A73-10949

Backward Monte Carlo calculations of the polarization characteristics of the radiation emerging from spherical-shell atmospheres.

01 p0078 A73-11233

Relative polarization of type III solar radio bursts at 23.5 and 30 MHz.

01 p0093 A73-11315

The results of coronal investigation at the September 22, 1968 solar eclipse.

01 p0108 A73-11383

A search of a connection between the polarization of Decam-type III bursts and magnetic fields in different heights of the solar atmosphere.

01 p0093 A73-11392

Effect of temperature and polarization rate on the electrochemical behavior of titanium alloys in a sulfuric medium

02 p0178 A73-11523

Spectrum and polarization of the Cygnus X-3 outburst.

02 p0210 A73-11556

Three-dimensional polarization characteristics of high-latitude Pc 5 geomagnetic micropulsations.

02 p0156 A73-11738

FLux density and linear polarization measurements of radio outburst from Cygnus X-3, suggesting synchrotron radiation from expanding cloud of relativistic particles

02 p0205 A73-11871

Radioastronomical measurements of ionospheric electron content.

02 p0159 A73-12031

Upward short wave radiation polarization characteristics observation by airborne polarimeter over grey sand desert, dense altocumulus liquid drops and cumulonimbus clouds and seas

02 p0169 A73-12269

Filters for solar corona polarization observations, deriving equations for arbitrary settings to obtain data reduction with simplified polarization direction calculation

02 p0170 A73-12370

Second virial coefficients for polar molecules in steam based on PVT data, using Stockmayer potential for curve fitting at 100-1000 C

02 p0238 A73-12643

Electromagnetic field, polarization and population inversion equations for spiked emission operation analysis in single mode laser

02 p0177 A73-12694

Atmospheric aerosol Mie scattering calculation as function of polarization parameters based on models for three laser wavelengths and two materials

03 p0341 A73-12900

Atmospheric wave perturbations of total electron content.

03 p0299 A73-13633

Problems in estimating the total electron content from Faraday rotation observations on geostationary satellites.

03 p0300 A73-13638

Radially conducting cone wave spectrum calculation for noncophasal excitation, noting circularly polarized TEM and elliptically polarized TM wave amplitudes

03 p0278 A73-14058

Degree and direction of polarization of multiple scattered light. I - Homogeneous cloud layers.

03 p0344 A73-14427

Results of precipitation backscatter measurements at 1.8 cm with a polarization diversity radar.

03 p0338 A73-14509

Cosmic radio wave anomalous absorption height dependence on zenith distance in midlatitude ionosphere during solar flare emission from ionization study

03 p0365 A73-14561

Net-field polarization in a magnetically biased plasma.

04 p0422 A73-15481

Receiving antenna polarization parameters selection in side-looking synthetic aperture radars

04 p0423 A73-15914

Parabolic, Cassegrain, spherical and horn-parabolic axisymmetric mirror antennas, calculating primary radiating element orientation effects on radiation polarization characteristics

05 p0547 A73-16052

Application of the method of least squares to the determination of optical constants of uniaxial isotropic and anisotropic substances, and of the rate of polarization of monochromators in the far UV

05 p0597 A73-16148

Implications of a quadratic stream definition in radiative transfer theory.

05 p0592 A73-16196

Multicomponent plasmas with cations or anions in presence of Coriolis force, determining crossover frequencies for polarization reversal and mode coupling of waves

05 p0603 A73-16594

Influence of nonlinear polarization on the ultrasonic gain factor in piezosemiconductors

05 p0605 A73-16821

The directivity and polarisation of thick target X-ray bremsstrahlung from solar flares.

05 p0610 A73-17045

Study of the scattering properties of the atmosphere by light polarization measurements in a twilight sky

05 p0572 A73-17355

Polarization interaction of opposed plasma streams in a linear magnetic octupole.

06 p0727 A73-17422

Polarization characteristics of partially scattered radio waves for turbulent ionosphere vertical sounding applications

06 p0662 A73-17533

Dielectric constant and molar polarizability of compressed gaseous and liquid fluorine.

06 p0661 A73-18124

Cross polarization definitions in terms of antenna pattern measurement coordinate system and source current distribution, considering relative merits

06 p0666 A73-18199

Electric vector peak and rms magnitude determination for near field polarization ellipse, relating to radiation hazard criteria

06 p0667 A73-18202

Nonlinear polarization coefficients of proustite and tellurium.

06 p0738 A73-18596

Polarization properties of a traveling-wave laser.

06 p0703 A73-18611

Resonator polarization parameters effect on backward wave attenuation in three and four mirror TW ring laser, noting colliding waves intensity dependence on polarization angle

06 p0703 A73-18619

Amplitude-time and polarization characteristics of the subpulses of pulsar CP 1133.

06 p0754 A73-18633

Polarization of radio sources. IV - The compact source PKS 2134+004.

07 p0873 A73-19052

Astrophysical masers. II - Polarization properties.

07 p0873 A73-19059

Fractional polarization constancy in pulsars to critical frequency with subsequent falloff

07 p0874 A73-19070

HD 215441 and 53 Camelopardalis - Intrinsic polarization of H-beta and the continuum.

07 p0874 A73-19075

Stress-induced rotation of polarization directions of elastic waves in slightly anisotropic materials.

07 p0908 A73-19083

Preliminary observations of variable polarization in epsilon Aurigae.

07 p0875 A73-19118

Measurements of the integrated Stokes parameters of compact radio sources.

07 p0876 A73-19354

Radio wave reflection from ionosphere, determining polarization and fluctuation characteristics via Stokes parameters

07 p0815 A73-19436

Polarization dependence of a photoelectric current during the modulated illumination of a system composed of an electrolyte, a porous pigment film, and a metal

07 p0851 A73-19473

Polarization measurement of clear sky light and comparison with theoretical data

07 p0818 A73-19590

Polarimetric properties of the lunar surface and its interpretation. V - Apollo 14 and Luna 16 lunar samples.

07 p0897 A73-19891

Fourier transformations and statistical analysis for spectral content of geomagnetic micropulsations, noting polarization sense preference

07 p0819 A73-20064

Frequency dependent synchrotron emission polarization variation in cosmic radio source models, allowing for cold plasma and relativistic distribution nonuniformities

07 p0872 A73-20307

Stokes polarization parameters of optical emission scattered in absorbing medium calculated for Galaxy and M 82 galaxy, assuming thermal IR radiation from nucleus

07 p0901 A73-20312

VLF ion cyclotron whistler propagation in upper ionosphere, noting polarization reversal and mode coupling from satellite observation

08 p0937 A73-20653

Polarization structure of a solar flare region at 9.5 mm wavelength.

08 p0997 A73-20767

Horizontal-polarization biconical horn antenna excited by TE/sub-11/ mode in circular waveguide.

08 p0945 A73-20805

Polarization of the total coronal emission during the solar eclipse of March 7, 1970

08 p1007 A73-21070

Application of the method of polarizational ultraviolet fluorescence microscopy to study giant muscle fibers Balanus rostratus Hock

08 p0930 A73-21135

Magnetic field effect on laser radiation intensity and polarization, noting Zeeman component change

09 p1095 A73-22666

Electrically controlled microwave polarization transformer

09 p1064 A73-22675

Polarization of the inner corona at the total eclipse of March 7, 1970.

09 p1147 A73-22734

Polarimetric observations of the major planets. II - Phase dependence of the polarization for selected areas on the disk of Saturn.

09 p1147 A73-22736

Polarized radiation of relativistic electrons scattered by plasma turbulence.

09 p1130 A73-22743

Study of antenna cross-polarization characteristics by using microwave holography

09 p1065 A73-23087

Problem of the time dependence of the polarization level of Type III solar radio bursts

10 p1264 A73-23719

Spatial distributions of intensity and polarization over the source of microwave impulsive bursts.

10 p1275 A73-23828

Preliminary interpretation of the polarization measurements performed on 'Intercoms-4' during three X-ray solar flares.

10 p1268 A73-24142

Latitudinal rotation direction daytime characteristics of Pc 5 pulsation polarization based on global magnetic observations

10 p1212 A73-24231

Investigation of the polar and protective properties of magnesium salts of organic acids

10 p1239 A73-24248

On the origin of the electric field of polarization in a gravitational plasma.

11 p1350 A73-24990

OJ 287 and BL Lacertae with rapid radio, IR and optical variability, high IR luminosity, line free optical spectra and varying polarization

11 p1416 A73-25179

Polarization of the cloudless daytime sky in the 1.25- to 2.42-micron range

11 p1353 A73-25645

Linear polarization and spectrum of PSR0833-45 and the effects of scattering.

11 p1416 A73-25748

Performance studies on a rechargeable hydrogen-oxygen fuel cell.

11 p1309 A73-25988

Astronomical polarimeter design, polarization sensitivity and 5 and 10 micron analyzers efficiency

11 p1369 A73-26513

Polarization measurements in the green coronal line.

11 p1428 A73-26623

Solar corona streamers polarization, intensity and electron density and temperature during 22 September 1968 total eclipse

12 p1533 A73-26861

Evaluation of the efficiency of the polarization selection method in suppressing fluctuating polarization noise

12 p1468 A73-26946

Determination of the polarization transfer function in space-based spectrophotometric observations of natural formations on a planetary surface

12 p1488 A73-26965

Means of measuring the linear polarization of cosmic gamma quanta by means of the Compton effect

12 p1496 A73-27204

Frequency dependent synchrotron emission polarization variation in cosmic radio source models, allowing for cold plasma and relativistic electron distribution nonuniformities

12 p1534 A73-27279

Stokes polarization parameters of optical emission scattered in absorbing medium calculated for Galaxy and M 82 galaxy, assuming thermal IR radiation from nucleus

12 p1539 A73-27284

Solar limb Ca I Fraunhofer line polarization rate computation, considering radiation field anisotropy effects and depolarizing collisions in wings

12 p1544 A73-27826

Solar corona anomalous polarization degree and E vector vibration direction, interpreting discrepancy from Thomson scattering prediction by scattered electron velocity effects

12 p1545 A73-27845

Solar radio burst of 7 August 1972, discussing peak flux density, magnetic field intensity, energy distribution and polarization degree

12 p1536 A73-27850

Altitudinal variations of the brightness indicatrices and angular characteristics of polarization levels in daytime skies in the 1.27-micron oxygen emission band

13 p1609 A73-29157

Effects of polarization on the transmission of coude-spectrometer systems.

13 p1621 A73-29351

Rainfall crosspolarization at microwave frequencies with differential phase shift and attenuation, considering rain models

13 p1587 A73-29670

Calculation of the nonlinear polarizability of a gas at a lasing transition with allowance for capture of resonance emission

14 p1757 A73-30367

POLARIZATION CHARACTERISTICS

Pulsar positions, polarization characteristics, intensity and fine structure, considering models explaining rotating neutron stars, galactic magnetic fields and electron densities and temperature

14 p1800 A73-30549

Comparison of linear polarization and albedo of igneous rocks in the spectral region 0.75-3.0 mu and lunar values of those parameters.

15 p1928 A73-30977

Derivation of scattering properties of the atmosphere from polarization measurements on the light of the twilight sky.

15 p1865 A73-31005

Investigations of Pi2 micropulsations. I - Frequency spectra and polarisation. II - Relevance of observations to generation theories.

15 p1866 A73-31064

Polarization-dependent intensity transmittance of optical systems.

15 p1913 A73-31125

Cross polarization in radomes - A program for its computation.

15 p1851 A73-31730

Pulsar radio emission limiting polarization resulting from passage through magnetoactive plasma, discussing electron density effects

15 p1844 A73-32003

Quasistatic generation of harmonics in a ferroelectric crystal with a second order transition above the Curie point.

15 p1924 A73-32157

Application of the perturbation method in a polarization analysis of anisotropic laser resonators

15 p1886 A73-32334

Polarization characteristics of partially scattered radio waves for turbulent ionosphere vertical sounding applications

16 p1978 A73-32757

Monochromatic field frequency mismatch effect on polarization and population ratio instabilities of single frequency traveling wave laser with broadened active medium

16 p2024 A73-32894

Non-existence of linear polarization in type III solar bursts at 80 MHz.

16 p2053 A73-32962

Scattering of electromagnetic radiation from a black hole.

16 p2060 A73-33120

Helical antenna for satellite transmission.

16 p1980 A73-33686

Linear cross-polarisation and attenuation measurements at 11 and 36 GHz.

16 p1982 A73-33723

Italian SIRIO satellite cross polarization signal measurements aided by ground station antenna system using narrow bandwidth

16 p1983 A73-33725

Atmospheric refractivity variation, precipitation and wind effects on two orthogonal linearly polarized microwave signals transmission over radio link at 22 and 37 GHz

16 p1983 A73-33733

Moonlight polarization study and the nature of the lunar surface

16 p2063 A73-33758

Investigation of the lunar surface with the aid of a polarivisor-discriminator

16 p2063 A73-33759

Simultaneous observations of Pci micropulsation polarization at four low latitude sites.

16 p2008 A73-33877

Polarization charge capture dependence of two layer dielectric metal-silicon nitride-silica-silicon semiconductor structures on pulse duration and temperature

16 p1991 A73-34003

Polarization properties of lidar backscattering from clouds.

17 p1225 A73-35416

Accurate measurement of antenna gain and polarization at reduced distances by an extrapolation technique.

17 p1217 A73-35676

A practical method for measuring the complex polarization ratio of arbitrary antennas.

17 p1217 A73-35677

Poincare sphere representation of partially polarized electromagnetic field, calculating power reception by antenna for field intensity measurement

17 p1218 A73-35681

Use of a stable polarization modulator in a scanning spectrophotometer and ellipsometer.

17 p1217 A73-35751

Forecasting of proton flares.

18 p2344 A73-35974

Time dependence of the polarization of type III solar radio bursts.

18 p2347 A73-36744

Polarization of the resultant emission of the corona during the solar eclipse of March 7, 1970.

18 p2355 A73-36871

Injection currents in semiconductors with deep polarizable impurity centers

18 p2341 A73-37046

POLARIZATION CHARTS

Synchrotron radiation sources with relativistic particles moving at small pitch angles in magnetic field, discussing emission properties and degrees of polarization

19 p2484 A73-37617

2.2- and 3.5-micron polarization measurements of the Becklin-Neugebauer object in the Orion Nebula.

19 p2489 A73-38528

Polarization of signals which are reflected from a group of independently fluctuating targets.

20 p2529 A73-38927

Minor planets and related objects. IX - Photometry and polarimetry of 1685/ Toro.

20 p2607 A73-39119

Lowering of average directive gain caused by cross-polarization radiation in an aperture antenna

20 p2537 A73-39456

The nature of the polarization of geomagnetic micropulsations of Pi 2 type

21 p2681 A73-40108

Evaluation of the magnitude of the magnetic field in the solar corona from measurements of the linear polarization of solar radio bursts

21 p2755 A73-40538

Pulsar polarization measurements by multielement interferometer dipole antenna and DKR-1000 cross array radio telescope

21 p2662 A73-40546

Polarization characteristics of phased arrays of elliptically polarized elementary radiators

21 p2664 A73-41082

Gravity wave nonlinear interactions producing secondary waves of opposite polarization, discussing tide polarization

21 p2688 A73-41343

Polarization inversions in the radio emission at 237 MHz of McMath zone 11482/Research note/.

21 p2657 A73-41495

Pluto polarimetric measurements showing degree and position angle of polarization and probable error

22 p2905 A73-41763

Scale model development of a high efficiency dual polarized line feed for the Arecibo spherical reflector.

22 p2831 A73-41830

Longitudinal polarization and focusing of plasmoids in a linear multipole magnetic field

22 p2893 A73-42383

E-polarized electromagnetic scattering by conducting cylinder coated with plasma sheath during spacecraft reentry flight under plane wave incidence

22 p2827 A73-42466

German monograph - Polarization measurements in galactic latitudes b less than -45 deg.

22 p2910 A73-42698

Polarization characteristics of a regenerative laser with a Faraday cell and a partial polarizer

22 p2870 A73-42721

Further observations of Cygnus X-3 at 8 GHz during the September 1972 outbursts.

22 p2915 A73-43026

The effect of change of polarisation of the illuminating beam on the microstructure of speckles produced by a random diffuser.

22 p2871 A73-43095

Matrix method evaluating an internal radiation field in a plane-parallel atmosphere.

23 p3030 A73-43754

Spectroscopic polarization analysis of turbulent plasma noise produced by the annihilation of opposite magnetic fields

23 p3012 A73-44016

Optical and polarization study of magnetization processes around individual dislocations in yttrium-iron garnet single crystals

23 p3017 A73-44024

Oversize waveguide polarization diplexers based on metal grating or dielectric plate at Brewster angle, measuring performances in microwave circuit and with HCN IR laser

23 p2960 A73-44071

Solar U burst radio source spectrographic and polarization observations, using Waldeimer corona model for particle exciter in magnetic field

23 p3036 A73-44247

Polarization variations in the emission of some M-type supergiants

23 p3037 A73-44357

Asteroid reflectivities from polarization curves - Calibration of the 'slope-albedo' relationship.

24 p3129 A73-44437

The optical properties of Venus and the Jovian planets. I - The atmosphere of Jupiter according to polarimetric observations.

24 p3129 A73-44442

Asteroid belt white light polarization curve measurements, indicating surface texturizing and albedo dispersion

24 p3131 A73-44462

Photometric and polarimetric properties of the Bruderheim chondritic meteorite.

24 p3133 A73-44557

Solar coronal Fe XIII 10747 A emission line resonance polarization observations during 12 November 1966 eclipse, discussing magnetic field effects

24 p3135 A73-44633

On the observation of linear polarization of solar microwave bursts.

24 p3136 A73-44644

Receiving antenna optimum polarization determination by mapping on Poincare sphere for maximum ratio of signal to summed external interference and internal noise

24 p3068 A73-44943

Influence of the microstructure of water aerosol on the phase function, its asymmetry, and polarization of scattered light

24 p3084 A73-44963

Generation of nonunidirectionally polarized modes by a gas laser oscillator with a mode selector.

24 p3096 A73-45031

Theory of the polarisation of the ordinary wave reflected from the ionosphere in the limit of vertical incidence and vertical magnetic field.

24 p3069 A73-45202

Some data for the design of low-crosspolarisation feeds.

24 p3069 A73-45255

High resolution observations of the radio galaxy NGC5128 at 10.7 GHz.

24 p3143 A73-45489

POLARIZATION CHARTS

U GRAPHS [CHARTS]

U POLARIZATION [WAVES]

POLARIZED ELASTIC WAVES

Utilization of polarized ultrasound in stress investigations

02 p0166 A73-11645

Effect of orthotropy on singular stresses produced near a crack tip by incident SH-waves.

21 p2786 A73-40933

POLARIZED ELECTROMAGNETIC RADIATION

NT POLARIZED LIGHT

NT SYNCHROTRON RADIATION

Propagation of electromagnetic waves in a plasma with a sheared magnetic field

01 p0081 A73-10206

Antenna synthesis via inverse electrodynamic problem solution for infinite impedance cylinder excited by traveling wave, noting directional antenna with rotating polarization

01 p0017 A73-10217

The consequences of grains in the atmospheres of late-type stars. I - Intrinsic polarization, infrared excesses, and emission lines.

01 p0103 A73-11035

Rain attenuation of vertically and horizontally polarized signals of 18 GHz communication system

04 p0419 A73-15395

Instability of a relativistically strong electromagnetic wave of circular polarization.

04 p0482 A73-15960

A model of the Crab Nebula derived from dual-frequency radio measurements.

05 p0622 A73-17075

Diffraction of an arbitrary plane electromagnetic wave by a half-plane.

06 p0667 A73-18203

Lunar polarized 1420 MHz thermal radio emission aperture synthesis maps evaluation

06 p0752 A73-18237

Iterative formula for wave functions related to sources situated on prism symmetry plane with application to electromagnetically polarized wave diffraction by dielectric wedge

06 p0669 A73-18841

Antenna design for Eole satellite radio communications with balloons, noting wave polarization and sea reflection effects

07 p0797 A73-18963

Fractional polarization constancy in pulsars to critical frequency with subsequent falloff

07 p0874 A73-19070

Preliminary observations of variable polarization in epsilon Aurigae.

07 p0875 A73-19118

E-polarized plane wave diffraction by conducting wedge loaded with thin dielectric slab, obtaining Fresnel integral solution with application to cylindrical wave excitation

07 p0792 A73-19383

R and L modes of ion cyclotron whistler propagation in ionosphere, noting refractive indexes and wave polarization for multicomponent plasma

07 p0819 A73-20060

Faraday rotation of polarized extragalactic radio sources interpretation as plasmas of mixed matter and antimatter

07 p0900 A73-20277

Radio sources with variable circular polarization, noting synchrotron radiation theory applicability

08 p1006 A73-20936

Multifrequency polarization observations of eight extragalactic sources.

08 p1008 A73-21156

Evidence for polarised radiation from the sun in the far infrared.

08 p1000 A73-21419

Resonant excitation of a circular cylinder with a longitudinal slit by a plane wave

09 p1048 A73-21905

Magnetic field effect on laser radiation intensity and polarization, noting Zeeman component change

09 p1095 A73-22666

Kinetic theory for the reflection of waves obliquely incident on the boundary of a magnetoactive plasma

09 p1052 A73-23078

The interpretation of continuum and line absorption and radiation by circumstellar dust.

09 p1150 A73-23132

Circular polarization of the emission of cosmic objects

09 p1151 A73-23329

Compton effect in charged particle under intense circularly polarized electromagnetic wave, noting application to Crab pulsar

10 p1271 A73-23485

A method for determining the polarization and energy spectrum of cosmic-ray gamma quanta

10 p1266 A73-23914

Measurement of the integral parameters of the nighttime ionosphere from observations of Intercomos-2 signals.

10 p1212 A73-24238

Restoring the orthogonality of two polarizations in radio communication systems. II.

10 p1190 A73-24623

Radio polarization and variability of pulsar NP 0532.

11 p1417 A73-25582

Frequency dependence of circular polarization in three compact radio sources.

11 p1419 A73-25777

Polarization interferometer for 2800 MHz solar noise studies with a 0.5-min fan beam.

11 p1422 A73-25943

Consideration of the different wave paths of the ordinary and extraordinary component in the calculation of electron density and collision frequency with the aid of the Faraday experiment

12 p1494 A73-27773

Measurements and interpretation of the polarization of radiation emerging from the atmosphere at an altitude of 28 km over south-western New Mexico /USA/.

13 p1652 A73-28269

Observation of linear polarization of the Crab nebula during an occultation by the solar corona.

13 p1586 A73-29247

Solution of a boundary value problem for the oblique incidence of a plane E-polarized wave on a metallic strip array with an optically active medium

13 p1623 A73-29682

Amplification of cylindrical electromagnetic waves reflected from a rotating body.

14 p1728 A73-30333

Resonant excitation of a circular cylinder with a longitudinal slot by a plane wave.

15 p1847 A73-32630

Klein-Gordon equation for a charged particle interacting with an electromagnetic wave.

16 p1979 A73-33164

Reliability of diversity reception by antennas with different polarizations.

16 p1991 A73-33984

Doppler radar with polarization diversity.

17 p2122 A73-34862

Poincare sphere representation of partially polarized electromagnetic field, calculating power reception by antenna for field intensity measurement

17 p2128 A73-35681

Nonlinear transformation of an electromagnetic wave at the boundary of a magnetoactive plasma

18 p2289 A73-36562

Nonlinear expansion of arbitrarily polarized electromagnetic waves in gyrotropic media

18 p2340 A73-36961

Load currents in missile circuits excited by a plane polarized field.

19 p2409 A73-37272

Electromagnetic wave propagation in inhomogeneous multilayered structures of arbitrary thickness - Full wave solutions.

19 p2461 A73-38380

Faraday rotation patterns in Crab Nebula pulsar radio spectra for average signal and giant pulses, noting difference in linear polarization percentage

19 p2488 A73-38516

Circular polarized emission from solar active regions at millimeter wavelengths.

20 p2601 A73-39070

The Synthesis Radio Telescope at Westerbork - Methods of polarization measurement.

20 p2566 A73-39581

Brightness and polarization distributions of head-tail galaxies at 1415 MHz.

20 p2610 A73-39583

Linear polarization in the Orion Nebula.

22 p2908 A73-42313

The efficient inject of high microwave powers into the overense magnetoactive plasma in the waveguide.

22 p2827 A73-42517

Periodic variations in geostationary satellite polarisation observations.

24 p3082 A73-44735

Parametric instability of strong circularly polarized electromagnetic wave in plasma producing relativistic electrons and backscattered light

24 p3117 A73-45459

POLARIZED LIGHT

Polarization of near-infrared sunlight reflected by terrestrial clouds.

01 p0073 A73-10363

Light polarization measurement with multichannel polarimeters, considering achromatic modulators to convert polarization information into intensity modulation before light beam split into constituent wavelengths

01 p0050 A73-10542

General solution for polarized radiation in a homogeneous-slab atmosphere.

01 p0078 A73-10333

Polarization of light by circumstellar material.

02 p0226 A73-12828

Intensity and polarization of the solar light scattered by an isolated volume of interplanetary matter

03 p0380 A73-14611

Tunable polarized violet light pulse emission from anthracene doped organic molecular fluorene crystal laser pumped with nitrogen laser, noting pulse amplitude and duration

04 p0458 A73-14873

Circular polarization of Saturn.

04 p0499 A73-15368

Study of the scattering properties of the atmosphere by light polarization measurements in a twilight sky

05 p0572 A73-17355

Ellipsometric polarized light methods application to corrosion technology, discussing surface film optical properties and measurement techniques

06 p0704 A73-17508

Emission of metals under the action of non-relativistic electrons

06 p0725 A73-18102

Connection of the linear polarization level of atmosphere-air scattered light with the light reduction in the infrared spectral region

06 p0691 A73-18733

Fraunhofer line depth in daytime airglow

07 p0817 A73-19471

Analysis of light polarization variations in a twilight sky in terms of upper atmosphere effects

07 p0817 A73-19588

Polarization of the total coronal emission during the solar eclipse of March 7, 1970

08 p1007 A73-21070

Imaging photopolarimeter for measuring orthogonal, sky glow and gegenschein brightness and polarization in sky mapping mode

11 p1415 A73-25177

Polarization of continuous-spectrum emission in the Larger Orion Nebula

11 p1416 A73-25227

Twisted nematic liquid-crystal electro-optic devices with areas of reverse twist.

11 p1337 A73-25357

Possibility of polarimetric monitoring of the optical stability of the atmosphere

11 p1392 A73-25609

Spectroelectrophotometer for atmospheric optical measurements in the near infrared region of the spectrum

11 p1362 A73-25610

Optical properties of polydisperse media with different size distributions of particles

11 p1398 A73-25611

Estimate of the mean size of cloud layer particles in the Jovian atmosphere

11 p1423 A73-26080

Polarization of the emission from the solar corona in the 5303 A line

12 p1538 A73-26859

Effects of polarization on the transmission of coude-spectrometer systems.

13 p1621 A73-29351

Derivation of scattering properties of the atmosphere from polarization measurements on the light of the twilight sky.

15 p1865 A73-31005

Polarization-dependent intensity transmittance of optical systems.

15 p1913 A73-31125

Depth of the Fraunhofer lines in the spectrum of the daytime sky.

15 p1873 A73-32061

Transmission of isotropic light across a dielectric surface in two and three dimensions.

16 p2037 A73-33685

Moonlight polarization study and the nature of the lunar surface

16 p2063 A73-33758

Laser spectrometer for combination scattering, recording polarized spectra with thermoelectrically cooled photomultiplier by photon count

17 p2164 A73-34164

Polarization of the resultant emission of the corona during the solar eclipse of March 7, 1970.

18 p2355 A73-36871

Polarization of stellar light between the two Magellanic clouds

20 p2606 A73-39063

Calculation of the power of polarized emission from a laser with an anisotropic resonator

21 p2712 A73-40312

Circular polarization of light reflected from the planets

21 p2769 A73-40732

Observations in linearly polarized light of the intensity of the diffuse 6180 A absorption band in 49 O, B, and A stars.

22 p2908 A73-42308

Polarization - A key to an airborne optical system for the detection of oil on water.

23 p2979 A73-43225

Two-phonon absorption in SbSI single crystals

23 p3016 A73-43713

Scattered-light phenomena in interstellar space

24 p3137 A73-44824

POLARIZED RADIATION

NT POLARIZED ELASTIC WAVES

NT POLARIZED ELECTROMAGNETIC RADIATION

NT POLARIZED LIGHT

NT SYNCHROTRON RADIATION

A survey of linear polarization at 1415 MHz. III - Method of reduction and results for the galactic spurs.

01 p0096 A73-10319

Pitch-angle distributions of polarized hard X-radiation from solar flares, assuming electron-proton bremsstrahlung mechanism

01 p0093 A73-11390

Study of the dispersion curve of polaritons excited by Raman diffusion in the presence of damping

04 p0476 A73-15997

New results of solar X-ray flare studied

05 p0609 A73-16372

Measurement of the polarization of the radiation reflected backward from a laser-heated plasma.

06 p0731 A73-18589

Daytime cloudless sky glow, atmospheric transmittance, neutral polarization and aerosol optical characteristics in solar almucantar and vertical

11 p1353 A73-25608

Twilight circular polarization due to Mie scattering, analyzing polarimeter measurements in IR and UV spectral bands

12 p1490 A73-27150

Polarization observations of variable stars and extragalactic objects. I - Instruments and methods of observation and data processing. II - Polarization of the EV Lac flare

16 p2057 A73-32708

Radiometric measurements of temperature of the ocean surface - Improvement brought by use of a polarizing radiometer

17 p2161 A73-34946

Polarimetric observations of the giant planets. III.

20 p2608 A73-39235

Polarization phenomena in multiphoton ionization of atoms.

21 p2743 A73-40468

POLARIZERS

Coherent production of electron-positron pairs and bremsstrahlung on a corundum crystal

11 p1410 A73-26447

Printed circuit meander line polarizer for converting microwaves in 1-20 GHz range from linear to circular polarization, describing construction and performance

14 p1735 A73-30221

A wide-band square-waveguide array polarizer.

14 p1735 A73-30228

POLAROGRAPHY

U POLAROGRAPHY

POLAROGRAPHY

Determination of the value of blood oxygen capacity and of the oxyhemoglobin dissociation curves by polarographic coulombometry

03 p0267 A73-13750

Oxygen partial pressure measurement in respiratory air via radio telemetry system with polarographic catheter electrode pressure sensor

03 p0270 A73-14287

Methodical studies concerning the polarographic measurement of respiration and 'critical oxygen pressure' in mitochondria and isolated cells with the aid of the membrane-covered platinum electrode

03 p0272 A73-14647

The determination of iron, titanium, and nickel in Apollo 14 samples by cathode ray polarography.

06 p0660 A73-17899

Investigation of the operation of a polarographic sensor under the action of surge-type polarizing voltage, using an electric analog

08 p0965 A73-21107

Determination of oxidized and reduced pyridine nucleotides in human and rabbit blood with the aid of the polarographic cycling technique

09 p1044 A73-21871

Procedures for polarocochleography and for pressure measurement in the inner ear perilymph in acute experiments on animals

11 p1314 A73-25043

Polarization of continuous-spectrum emission in the Larger Orion Nebula

11 p1416 A73-25227

AC polarographic determination of sulfur in molybdenum-rhenium alloy.

17 p2118 A73-34276

POLARONS

Giant polaritons and selfinduced transparency of Frenkel-excitons.

10 p1249 A73-24694

POLITIES

NT PROCUREMENT POLICY

Book - Civil aviation development - A policy and operations analysis.

08 p1026 A73-21837

The attitude of the public towards the Space Programme - Its assessment and its influence as a guiding policy factor.

11 p1454 A73-26275

The transatlantic charter policy of the United States.

24 p3158 A73-44575

POLISHED METALS

U METAL POLISHING

POLISHING

NT ELECTROPOLISHING

NT METAL POLISHING

NT VIBRATORY POLISHING

Certain results of studies of the accuracy in grinding shaped surfaces by the method of nontemplate shaping of the cutting surface of an abrasive ribbon

02 p0172 A73-11798

The polished surface of a telescope mirror as seen in an electron microscope

14 p1752 A73-30060

POLITICS

Social, economic and political factors associated with earth resources observation and information analyses.

05 p0642 A73-17137

POLLEN

Reactions of singlet oxygen with pine pollen.

19 p2402 A73-38295

POLLUTANTS

U CONTAMINANTS

POLLUTION

NT AIR POLLUTION

NT ENVIRONMENT POLLUTION

NT NOISE POLLUTION

NT THERMAL POLLUTION

NT WATER POLLUTION

ERTS-1 satellite-borne multispectral scanner remote sensor for global pollution monitoring, geological and heat balance surveys, and storm and earthquake caused damage

21 p2692 A73-41520

POLONIUM

NT POLONIUM 210

POLONIUM ISOTOPES

NT POLONIUM 210

POLONIUM 210

Alpha spectrometry of a surface exposed lunar rock.

07 p0870 A73-19796

Detection of a nonuniform distribution of polonium-210 on the moon with the Apollo 16 alpha particle spectrometer.

15 p1941 A73-32266

Radon emanation from the moon - Spatial and temporal variability.

18 p2349 A73-36033

POLYACRYLATES

U ACRYLIC RESINS

POLYAMIDE RESINS

NT NYLON (TRADEMARK)

Polyamide compounds stress corrosion properties and chemical resistance in different test fluids, discussing fluid effect on flaw development rate

02 p0184 A73-11583

Flame resistant and nonflammable textile fibers.

17 p2198 A73-35839

The effect of a fiberglass reinforcement on the properties of laminates with a polyamide binder

18 p2328 A73-36481

Polyquinoxalines, thermostable polymers with thermoplastic properties [ONERA, TP NO. 1228]

22 p2881 A73-42218

POLYATOMIC GASES

NT DIATOMIC GASES

Thermal conductivity in vibrationally excited gases.

05 p0600 A73-16048

Far IR molecular lasers evaluation, discussing excitation, line assignment, relaxation, frequency measurement and development predictions

07 p0835 A73-19636

Application of the method of Bhatnagar-Gross-Krook-Morse to the Knudsen layer of a polyatomic gas which is solidified or in equilibrium - Expression of discontinuities of wall temperatures

09 p1072 A73-23033

Vibrational relaxation theory of diatomic and multiatomic single component and gas mixture systems for molecular laser mechanisms, using oscillator simulation

09 p1097 A73-23331

POLYATOMIC MOLECULES

- Kinetic equations for vibrational energy relaxation in a polyatomic gas mixture 10 p1250 A73-23579
- POLYATOMIC MOLECULES**
 NT DIATOMIC MOLECULES
 NT TRIATOMIC MOLECULES
 Use of translational energy measurements in the evaluation of the energetics for dissociative attachment processes. 10 p1251 A73-24244
 Molecular abundances in stellar atmospheres. II. 11 p1417 A73-25265
 Collective spontaneous emission of polyatomic systems 23 p2988 A73-44010
 Theoretical study of a photodissociation model in polyatomic molecules 24 p3113 A73-45326
- POLYBENZIMIDAZOLE**
 Thermal resistance and aging properties of polybenzimidazoles, polyimides and polyamides-imides used for Mach 3 aircraft radomes 11 p1335 A73-25291
- POLYBUTADIENE**
 Carbonyl terminated polybutadiene polymer binder development for solid propellant, describing properties, manufacturing processes and performance reproducibility 01 p0089 A73-11111
 Non polar thermosetting resins for high temperature electrical/electronic components. 03 p0332 A73-13035
 Thermal cyclization of 1,2-polybutadiene and 3,4-polyisoprene. 17 p2119 A73-34925
- POLYCARBONATES**
 Growth of fatigue cracks in polycarbonate. 02 p0185 A73-12430
 Brittle crack initiation at the elastic-plastic interface. 02 p0182 A73-12752
 Creep and recovery of polycarbonate. 17 p2194 A73-34525
 Polycarbonate as a model material for three-dimensional photoplasticity. [ASME PAPER 73-APM-4] 17 p2247 A73-35029
 Cold rolling of polymers. II - Toughness enhancement in amorphous polycarbonates. 17 p2197 A73-35350
 Cold rolling of polymers. III - Properties of rolled crystallized polycarbonates. 17 p2197 A73-35351
 Mechanical characteristics of thermoplastic materials reinforced with short glass fibers, taking into account various degrees of reinforcement 18 p2327 A73-36479
 A critical examination of the impact test for glassy polymers. 19 p2444 A73-38093
 Effect of gas diffusion on creep behavior of polycarbonate. 20 p2580 A73-39403
 Influence of chemical composition on the structure and mechanical properties of polycarbonate films and the possibility of using them as a substrate for moving-picture films 21 p2646 A73-40259
 Dynamic fracture criteria for a polycarbonate. 21 p2723 A73-40956
- POLYCRYSTALS**
 Use of a plastic deformation design model of polycrystalline material in the analysis of loading surface transformation 01 p0112 A73-10008
 Mosaic-angle and dislocation-density variations in polycrystalline aluminum alloys under tension 01 p0064 A73-10609
 Metallographic macro- and microstructural study of semiconductor compounds, discussing single crystal imperfections, polycrystals and semiconducting films. 02 p0199 A73-11582
 Polycrystalline organic compounds effect on second harmonic generation of neodymium laser, noting relation between nonlinear susceptibility and intramolecular charge transport 02 p0176 A73-12097
 Stress shock waves effect on polycrystalline metals grain structure, discussing strain rate critical value zones 03 p0386 A73-13147
 A fourth-order nonlinear equation of state - Application to the determination of the elastic moduli of single-crystal and polycrystalline solids 03 p0350 A73-14601
 Metallographic orientation determinations on hexagonal polycrystals with the aid of the quantitative polarization equipment of the Neophot. 05 p0577 A73-16752
 Calculation of X-ray elastic constants on the basis of single crystal coefficients of metals with a hexagonal structure 05 p0588 A73-17244
 Resistivity of doped polycrystalline silicon films. 06 p0733 A73-17745

- Mathematical model for plastic deformation of polycrystalline materials with Hooke's Law elastic strains 06 p0765 A73-18641
 Influence of a constant electric field on the dielectric properties of polycrystalline BaTiO₃ 08 p0995 A73-21273
 Electric resistance of hydraulically extruded and annealed beryllium 09 p1098 A73-21847
 Metal fcc polycrystals macroscopic plasticity theory based on discrete aggregate model, predicting stress-strain curves for partial load cycles 09 p1160 A73-22896
 Networks of polycrystalline metal whiskers for composite materials 11 p1379 A73-25408
 Service failures and fracture mechanisms under cyclic load at high temperature. 11 p1442 A73-25845
 Change in the dislocation structure during fatigue of nickel prestrained by tension 11 p1386 A73-26732
 Variational treatment of the elastic constants of disordered materials. 13 p1692 A73-28169
 Mechanical behavior of plastically deformed polycrystalline metal subjected to hydrostatic pressure soaking. 13 p1634 A73-28196
 Interpretation of mechanical behavior of pure aluminum in terms of microstructure. 13 p1639 A73-29459
 Theoretical interpretation of residual lattice strains induced in polycrystalline metals by plastic deformation. 13 p1639 A73-29460
 Study of plasticity laws of polycrystalline metals at elevated temperatures - Specifically the influence of hydrostatic stress on creep. 13 p1641 A73-29506
 Some characteristics of the failure by fatigue of mild steel in vacuum 14 p1763 A73-30681
 Mechanism of the micrononhomogeneous deformation of metals throughout a wide interval of temperature 17 p2186 A73-34330
 Spatial distributions of H₂ desorbed from Fe, Pt, Cu, Nb, and stainless steel surfaces. 19 p2402 A73-37951
 Influence of electric field strength on effective carrier mobility in polycrystalline CdSe thin films 20 p2536 A73-39200
 Diagrams of cumulative damage during tension of polycrystalline metals 20 p2577 A73-39371
 Grain boundary destruction mechanisms in pure nickel polycrystals following plastic deformation, discussing annealing, fault concentration, microscopic techniques and critical loads 20 p2578 A73-39735
 Investigation of the imperfect structure of polycrystalline aluminum after low-temperature rolling and annealing 20 p2579 A73-39747
 The effect of stacking fault energy on the plastic deformation of polycrystalline Ni-Co alloys. 22 p2879 A73-43074
 Orientation dependent slip in polycrystalline titanium. 23 p2993 A73-44028
 Influence of ion ordering on the induced anisotropy in Li-Fe ferrites 23 p3018 A73-44175
 The Portevin-Le Chatelier effect in compression tests of polycrystalline aluminum 24 p3148 A73-44914
- POLYCYTHERMIA**
 Cobalt compound administration effects on hypoxic stress control, testing polycythemic response and cobalt retention in rats 17 p2115 A73-34744
- POLYESTER RESINS**
 Carbon fibre adhesion to organic matrices. [ONERA, TP NO. 1173] 01 p0068 A73-11499
 Glass bead reinforced epoxy and polyester resins mechanical properties as function of volume fraction and interfacial bond strength, discussing beads chemical surface treatment effects 02 p0185 A73-12428
 Properties of pultruded composites containing high modulus graphite fibers. 03 p0332 A73-13032
 Glass fiber reinforced polyester laminates, testing layer base material and molding condition effects on tensile and bending strengths and other mechanical properties 07 p0843 A73-20326
 The fracture toughness and crack propagation properties of polyester resin casts and laminates. 08 p0983 A73-21595
 Critical stress intensity factors applied to glass reinforced polyester resin. 15 p1897 A73-31676

- Factors affecting the impact strength of glass-fibre-reinforced polyester composites. 16 p2031 A73-33987
 Relations between the hardening conditions and the degree of hardening of unsaturated polyester resins 18 p2327 A73-36466
 Initiator composition and glass content effects on polyester resin hardening in glass laminate fabrication 18 p2327 A73-36467
 Study of the hardening and mechanical properties of polyester resins 18 p2327 A73-36468
 Concepts from the realization of the development of the technology and assembly lines for the fabrication of polyester glass laminates 18 p2320 A73-36472
 Self extinguishing properties of polyester-glass laminates with reduced flammability due to polyvinyl chloride and antimony trioxide additives 18 p2327 A73-36478
 Water damage in polyester/glass laminates. II - Microscopic evidence. 21 p2723 A73-40921
 Creep and aging characteristics of glass-fiber-reinforced plastics 24 p3104 A73-44885
 Hardening with UV radiation in the manufacture of glass-fiber-reinforced unsaturated polyester resin molding materials 24 p3093 A73-44889
 Mechanical properties of glass fiber reinforced plastic laminate formed by spraying unsaturated polyester resin on fiber rovings 24 p3094 A73-44890
- POLYESTERS**
 Rheological equation for expansion rate effects on stress-strain relation of polyester binders hardened thermochemically and by gamma radiation 08 p1019 A73-21764
 Studies on testing methods and weatherability of plastics. 13 p1646 A73-29532
 Mechanism of breakdown in the interface region of glass reinforced polyester by artificial weathering. 15 p1898 A73-31838
- POLYETHER RESINS**
 NT POLYMETHYL METHACRYLATE
 Low temperature dynamic mechanical properties of polyurethane-polyether block copolymers. 02 p0185 A73-12426
- POLYETHYLENE TEREPHTHALATE**
 Influence of proton irradiation in vacuum on the properties of polymer films 11 p1389 A73-26740
 Investigation of the crystallization of polyethylene terephthalate 21 p2647 A73-40260
- POLYETHYLENES**
 NT POLYETHYLENE TEREPHTHALATE
 Balloon polyethylene film materials orthotropic mechanical properties, considering temperature effects on brittle fracture by transverse tension 01 p0005 A73-11206
 Investigations in connection with the preliminary development of a FLOX-polyethylene hybrid propulsion system [DGLR PAPER 72-086] 02 p0202 A73-11676
 Thermal conductivity of polyethylene - The effects of crystal size, density and orientation on the thermal conductivity. 02 p0185 A73-12431
 Feasibility of a fluidized powder demand mode gas generator. [AIAA PAPER 72-1194] 03 p0352 A73-13484
 Measurement of zincate permeation in a polyethylene battery separator with controlled external hydrodynamic conditions. 11 p1307 A73-24974
 Reinforcing glass fiber preparation effect on fiber wetting by polyethylene melt, analyzing adhesion strength relationship to residual stresses 12 p1516 A73-27178
 Determination of the diffusion length of excess carriers in semiconductors under a polyethylene film 13 p1668 A73-28462
 Long-life, high energy Ni-Cd aerospace cells. 13 p1572 A73-29585
 Combined tension-torsion creep of polyethylene with abrupt changes of stress. 15 p1897 A73-31613
 The role of a porous filler structure in strengthening polymers 16 p2030 A73-33929
 Investigation of the thermophysical and antifurcation characteristics of polyethylene composites. III - The effect of fillers on the heat conductivity of polyethylene 16 p2030 A73-33930
 Flows with and without suspensions in channels with curvilinear segments 22 p2842 A73-42229
- POLYGONIZATION**
 Mechanical properties of strip molybdenum with a polygonized single-crystal structure 12 p1513 A73-27265

POLYGONS

NT HEXAGONS
NT TRIANGLES

Calculation of the potential created and the velocity induced by a uniform source distribution on a polygon and on a periodic distribution of polygons for the solution of two-dimensional Poisson fields

03 p0241 A73-12910

A unified method for determination of fundamental natural frequency of orthotropic plate with arbitrary boundary.

20 p2622 A73-39546

POLYHEDRONS

NT PARALLELEPIPEDS
NT PYRAMIDS
NT RHOMBOHEDRONS
NT TETRAHEDRONS

PRADIS - An advanced programming system for 3-D-display.

09 p1059 A73-22225

POLYIMIDE RESINS

Development and evaluation of graphite and boron polyimide composites.

03 p0329 A73-13003

General purpose autoclave processable polyimide laminating resin selection, evaluating molding process techniques

03 p0329 A73-13004

Polyimide 2080 molded composites mechanical, thermal and electrical properties, discussing processing techniques

03 p0329 A73-13005

Light weight graphite-polyimide composite honeycomb core and sandwich panel design, fabrication and tests for shuttle orbiter thermal protection system

03 p0333 A73-13051

Polyimide composites development for aircraft structures.

06 p0715 A73-18720

Graphite fiber reinforced polyimide resin composites for structural applications in long duration high temperature environments, discussing fabrication with match-metal die

[SME PAPER EM 72-107] Low void composites based on NR-150 polyimide binders.

07 p0832 A73-20448

The effect of long-time thermal exposure on the mechanical properties of graphite/polyimide composites.

10 p1237 A73-23953

High temperature creep properties of P10P polyimide - HMS graphite composites.

10 p1238 A73-23970

Preparation and performance characteristics of flammable and inflammable polyimide foams as sandwich fillers

10 p1239 A73-23975

Thermal resistance and aging properties of polybenzimidazoles, polyimides and polyamides-imides used for Mach 3 aircraft radomes

11 p1335 A73-25291

Low void polyimide/glass and graphite reinforced composite properties and fabrication, showing improved interlaminar shear and wet strength

16 p2029 A73-33048

Effect of prepregging solvent on high-temperature stability of KERIMID 601 composites.

16 p2029 A73-33049

Polyimide resin dielectric and mechanical properties, discussing syntactic foam composite with aluminum filler for radome construction

17 p2195 A73-34804

POLYIMIDES

Lubricating characteristics of polyimide bonded graphite fluoride and polyimide thin films. [ASLE PREPRINT 72LC-7C-3]

03 p0317 A73-14372

Processing and properties of composites based on NR-150 polyimide binders.

16 p2029 A73-33047

POLYISOPRENES

Thermal cyclization of 1,2-polybutadiene and 3,4-polyisoprene.

17 p2119 A73-34925

POLYMER CHEMISTRY

Carbonyl terminated polybutadiene polymer binder development for solid propellant, describing properties, manufacturing processes and performance reproducibility

01 p0089 A73-11111

Mechanical properties of glassy carbon fibres derived from phenolic resin.

01 p0068 A73-11498

Physical and chemical aspects of aging of polymer-base composite materials

03 p0273 A73-13590

Stereo-enriched poly-alpha-amino acids - Synthesis under postulated prebiotic conditions.

06 p0661 A73-17940

Syntheses and conformational studies of polyacidic amino acids containing optical active side chains.

06 p0661 A73-17942

Chemical volatilization as a technique for the detection of extraterrestrial biopolymers and possible metabolic products.

11 p1319 A73-26479

Diffraction spectra and electron density distributions of interatomic graphitizing carbon molecule bonds as polymer combinations, using diffractometer and scintillation counter recording

14 p1767 A73-30839

Thermochemical and thermo-oxidative reactions of polyacrylonitrile fibers.

16 p1976 A73-33038

Hydrolytic stability of electrical insulation materials.

17 p2197 A73-35348

Hydrolytic degradation of polymer electrical insulating materials in warm humid environments, noting relation to ester and ether linkage presence

17 p2197 A73-35349

Relations between the hardening conditions and the degree of hardening of unsaturated polyester resins

18 p2327 A73-36466

Evaluation of hazard presented by gas-off products from polymeric materials intended for use in space cabins.

18 p2286 A73-36931

Investigation of the photosensitivity of polyvinyl-cinnamate

21 p2646 A73-40255

Advantages of using polymer bases as fixing agents in hydrotype printing

21 p2646 A73-40258

Photographic nuclear emulsions with total replacement of gelatin by synthetic polymers

21 p2647 A73-40269

Synthesis and characterization of isomeric cis- and trans-pyrone model compounds.

21 p2648 A73-41215

Pyrolysis and oxidation of polymers at high heating rates.

22 p2936 A73-42806

Linear pyrolysis of various polymers under combustion conditions.

22 p2898 A73-42807

Combustion of thermoplastic polymer particles in various oxygen atmospheres - Comparison of theory and experiment.

22 p2937 A73-42822

On the dimensions of intramolecularly crosslinked polymer molecules. I - The synthesis and chemical characterization of intramolecularly crosslinked polystyrene molecules having a narrow distribution of molecular weight. II - The theoretical prediction of the dimensions in solution of intramolecularly crosslinked polystyrene molecules. III - The measurement of the dimensions of intramolecularly crosslinked polystyrene.

23 p3008 A73-43795

POLYMER PHYSICS

Prediction of strength of a polymer body with allowance for solar radiation

01 p0068 A73-11078

Carbonyl terminated polybutadiene polymer binder development for solid propellant, describing properties, manufacturing processes and performance reproducibility

01 p0089 A73-11111

Development of internal damage in silicate glasses and polymers under the action of laser radiation

02 p0184 A73-11616

Extended chain crystals of linear high polymers.

02 p0139 A73-12650

Biaxial stress relaxation in glassy polymers - Polymethylmethacrylate.

02 p0186 A73-12811

Polyporphazene fluoroelastomers preparation, properties and potential applications.

03 p0331 A73-13029

Physical and chemical aspects of aging of polymer-base composite materials

03 p0273 A73-13590

Viscoelastic properties of amorphous polymers employed in stress investigations by the optical polarization method

03 p0335 A73-13737

Investigation of gas sorption and desorption in polymer materials in the process of gaseous sterilization of such materials

06 p0656 A73-17681

Theory of one-dimensional Mott semiconductors and electronic structure of long molecules with conjugate bonds

06 p0734 A73-17923

Effects of hardening conditions on the physicochemical and frictional properties of polyvinyl fufural

08 p0982 A73-21591

Combustion products of polymeric materials containing nitrogen in their chemical structure.

08 p0983 A73-21821

Polymer chain model with internal rotations for elastic body stress-strain state, internal work, elastic energy and equations of motion

10 p1240 A73-24307

Thermostable polymers for freezing and cryogenic temperatures, noting theory, methodology and preparation for science and industry

10 p1241 A73-24675

Theory of cooperative defect formation in a biopolymer molecule under the action of radiation

11 p1323 A73-25637

The micro-structural approach toward a kinetic theory of polymer fracture.

13 p1646 A73-29529

Nonlinear thermodynamics of irreversible processes for polymer microfracture process under mechanical, thermal, diffusion and chemical actions

14 p1766 A73-30479

Determination of the temperature of a sample undergoing pulsed irradiation by sunlight

15 p1896 A73-30997

Intensity of mechanical influences and mechanical degradation of hard polymers

16 p2030 A73-33940

Cold rolling of polymers. II - Toughness enhancement in amorphous polycarbonates.

17 p2197 A73-35350

Cold rolling of polymers. III - Properties of rolled crystallized polycarbonates.

17 p2197 A73-35351

New fire resistant polymers - Poly(phosphazenes).

17 p2197 A73-35356

Thermoplastic temperature range extended up to 260 C by polysulphones.

18 p2326 A73-36068

Interfacial, mechanical and fracture properties of fibre reinforced polycaprolactam.

18 p2328 A73-36480

A critical examination of the impact test for glassy polymers.

19 p2444 A73-38093

Mechanical properties of polymeric solids.

19 p2444 A73-38549

Changes in the physicomechanical properties of structural polymers after heat treatment

20 p2580 A73-39333

Ionic dissociation energy in polymeric electrical conductivity behavior, taking into account conductivity, viscosity, dissociation energy, dielectric constant, gas constant and absolute temperature

20 p2581 A73-39667

Physical nature of gelatin as polymer material, emphasizing low temperature restoration of collagen structure, supermolecular structure formation capability and glassy-elastic state transition temperature

21 p2647 A73-40265

Approximate estimation of the possibility of using the viscoelasticity hypothesis for the formulation of an equation of motion for a liquid with polymer additions

22 p2841 A73-42122

Structure of polymers and fatigue crack propagation.

22 p2880 A73-42152

Finite amplitude dynamic motion of viscoelastic materials.

23 p3038 A73-43273

Theory of one-dimensional Mott semiconductors and the electronic structure of long molecules having conjugated bonds.

23 p3018 A73-44323

Mathematical model for fracture strength of material undergoing molecular orientation during tensile strain, accounting for anomalous polymer characteristics

24 p3144 A73-44508

The relationship of certain mechanical and thermophysical properties of polymer composites with the reduced filler concentration

24 p3102 A73-44512

POLYMERIC FILMS

Balloon polyethylene film materials orthotropic mechanical properties, considering temperature effects on brittle fracture by transverse tension

01 p0005 A73-11206

The relationship between dielectric and mechanical properties of polymers.

03 p0332 A73-13036

Thin films durability increase of poly(n-alkyl methacrylate) polymers with alkyl group length, noting friction coefficient behavior [ASLE PREPRINT 72LC-7C-4]

03 p0317 A73-14373

Continuous ultrasonic joining of thin plastic films

07 p0828 A73-18902

Thermally stable heterocyclic ladder polymer films preparation techniques in manufacture of solar cells with CdS or CdTe thin films for space applications

07 p0841 A73-18903

Synthesis of reverse osmosis membranes by plasma polymerization of allylamine.

07 p0780 A73-19169

Changes in the durability and lifetime of polymer films under simultaneous exposures to an electric field and mechanical loading

07 p0842 A73-19394

The experimental determination of wall-fluid mass transfer coefficients using plasticized polymer surface coatings.

08 p1023 A73-21261

POLYMERIZATION

Experimental study of the damping of bending vibrations in supported square plates with coatings.

09 p1161 A73-23153

The use of electret films as time-of-arrival detectors for shock and detonation waves.

10 p1218 A73-24122

The mechanism responsible for luminescence of polymer films during their formation by ion-beam bombardment of solids

10 p1252 A73-24762

Transfer function model for analog simulation of transient unsteady heat conduction through flat and cylindrical walls, optimizing moving polymer film heating

11 p1451 A73-25732

IR spectroscopic study of polydimethylsiloxane thin film structure and polymerization under glow discharge

11 p1400 A73-26144

Influence of proton irradiation in vacuum on the properties of polymer films

11 p1389 A73-26740

Determination of the diffusion length of excess carriers in semiconductors under a polyethylene film

13 p1668 A73-28462

Indoline series spirochromene polymer matrices for holographic recordings with argon and helium-neon lasers in green and UV spectral regions

14 p1753 A73-30365

Low loss light guiding polymer thin film with continuously adjustable refractivity, discussing fabrication and refractivity and scattering loss measurements

17 p2172 A73-35423

Causes of changes in the properties of resite in aqueous and alkaline media

18 p2328 A73-36822

Oxygen index flammability test relationship to flame spread model for polystyrene film burning rate as function of gas velocity and film thickness

19 p2504 A73-38274

Cross-linking ambient curing mechanisms for air-drying oxidizable coatings, involving chemical film-forming reactions

20 p2580 A73-39636

Investigation of the hypervelocity impact on thin plastics and metal foils

21 p2696 A73-39990

Russian book - High-molecular-weight compounds in photographic processes.

21 p2646 A73-40252

High-molecular compounds and recording of information on thermoplastic films

21 p2646 A73-40253

Physicochemical principles of the photographic process on vesicular films and the high-molecular-weight compounds used for these films

21 p2646 A73-40254

Certain features of sensitive layers containing bifunctional polymers/fixatives on a blank film

21 p2646 A73-40257

Influence of chemical composition on the structure and mechanical properties of polycarbonate films and the possibility of using them as a substrate for moving-picture films

21 p2646 A73-40259

Investigation of the crystallization of polyethylene terephthalate

21 p2647 A73-40260

Influence of a mixture of plasticizers, exhibiting a different mechanism of action, on the deformation of cellulose triacetate over a wide range of temperatures

21 p2647 A73-40264

Photographic nuclear emulsions with total replacement of gelatin by synthetic polymers

21 p2647 A73-40269

Physico-mechanical properties and damage mechanism of moving-picture photographic materials as film systems

21 p2699 A73-40270

Pyrolysis and oxidation of polymers at high heating rates.

22 p2936 A73-42806

Comment on 'Film reinforced multifastened mechanical joints in fibrous composites.'

22 p2928 A73-43115

Study of low-energy heavy-nucleus track regression in plastic detectors /cellulose triacetate and polyethylene terephthalate/ and in low-sensitivity nuclear photoemulsion

23 p2981 A73-43567

A megarad plastic film dosimeter.

23 p2949 A73-44212

POLYMERIZATION

NT COPOLYMERIZATION

Synthesis of reverse osmosis membranes by plasma polymerization of allylamine.

07 p0780 A73-19169

Polymerization of amino acids under primitive earth conditions.

07 p0787 A73-19217

IR spectroscopic study of polydimethylsiloxane thin film structure and polymerization under glow discharge

11 p1400 A73-26144

Polyimidazopyrrolone model compounds.

15 p1840 A73-31572

Origin of terrestrial polypeptides - A theory based on data from discharge-tube experiments.

20 p2513 A73-39484

Experimental investigation of the strength and deformability of vacuum-prepared fiberglass-reinforced plastic shells

22 p2881 A73-43062

POLYMERS

NT POLYISOPRENES

Drag reduction in non-Newtonian turbulent flow, considering viscosity change with strain in long-chain molecules /polymers/ fluid solutions

01 p0034 A73-11134

Thermogravimetry of thermally stable aromatic and heterocyclic polymers.

01 p0015 A73-11447

Analysis of volatile combustion products and a study of their toxicological effects.

02 p0138 A73-12429

Application of optical methods to the verification of microscopic data on polymer materials

04 p0468 A73-15693

Russian book - Strength of viscoelastic materials relative to solid-propellant rocket-motor charges.

04 p0517 A73-15967

Predicting failures with conducting-polymer fatigue-damage indicators.

06 p0759 A73-17598

Reliability tests on miniature ceramic capacitors encapsulated by epoxy-novolac block polymer compounds

06 p0677 A73-18398

Elastic behavior of polymer-impregnated porous ceramics.

07 p0842 A73-19198

Application of simultaneous DTA/TGA and DTA/MS analysis for predicting the flammability of composite textile fabrics and polymers.

09 p1110 A73-22515

Solid polymer electrolyte fuel cell technology application to space shuttle orbiter requirements, noting 2000 hours maintenance free life and thermal stability

09 p1035 A73-22786

Preparation and thermomechanical properties of pyrrone moldings.

10 p1237 A73-23961

Calculation of the shear strength of an axisymmetric joint constructed out of Locitite

10 p1224 A73-24091

Damping of an aerial photo camera with the aid of polymeric materials

10 p1219 A73-24478

Linearized hydrodynamic instability initiation in polymer melts extrusion, examining Weissenberg number role in melt fracture onset

10 p1241 A73-24655

Experimental models of communication at the molecular and microsystemic levels.

11 p1324 A73-25140

Double spiral DNA-like polynucleotide analog in carbonaceous chondrite, indicating organic compound synthesis at low temperature

11 p1423 A73-26053

Effect of polymer additions on some energy balance components in a turbulent flow

11 p1349 A73-26433

The thermal expansion of composites based on polymers.

12 p1515 A73-27030

Evaluation of the smoke and flammability characteristics of polymer systems.

12 p1515 A73-27143

The effect of strain rate and heat developed during deformation on the stress-strain curve of plastics.

[SESA PAPER 2088A]

13 p1646 A73-29303

Natural and synthetic thermally stable polymers, discussing pyrolysis, structure-property relationships and bond strengths

14 p1724 A73-30132

Low-temperature relaxations in amorphous polymers.

14 p1765 A73-30134

Quantitative measurement of aluminum film adhesion to polymers, noting influence of substrate nature on adhesion strength

14 p1755 A73-30724

Design criteria for inert or consumable polymer cartridge materials.

15 p1925 A73-31919

Finite amplitude dynamic motion of viscoelastic materials.

15 p1956 A73-32223

The development and properties of a polyacrylonitrile /PAN/ fiber based carbon felt

16 p2028 A73-33041

Prediction of the deformation properties of polymer materials

17 p2194 A73-34268

Mechanical and optical characterization of an anelastic polymer at large strain rates and large strains. [SESA PAPER 2198A]

17 p2198 A73-35458

Book - Stress analysis of polymers.

17 p2253 A73-35861

Polymers fatigue life under cyclic deformation, discussing stress-strain and failure behavior as function of reversed stress cycle frequency

18 p2328 A73-36587

Evaluation of hazard presented by gas-off products from polymeric materials intended for use in space cabins.

18 p2286 A73-36931

Modulus reinforcement in elastomer composites. II - Polymeric fillers.

18 p2328 A73-36981

Book - Flame retardancy of polymeric materials. Volume 1.

18 p2287 A73-37123

Mechanical, thermal and electrical properties of polymers as functions of temperature, radiation and frequency for cryogenic environment material and design selection

19 p2443 A73-37525

Electrolytic hydrogen fuel production with solid polymer electrolyte technology.

19 p2391 A73-38413

Experimental investigations of the effects of polymer additions on the kinematic characteristics of a plane turbulent flow in a tube with variable wall roughness

22 p2841 A73-42121

An application of topographical analysis to the wear of polymers.

22 p2881 A73-42355

Recent results in nonlinear viscoelastic wave propagation.

24 p3151 A73-45305

POLYMETHYL METHACRYLATE

Biaxial stress relaxation in glassy polymers - Polymethylmethacrylate.

02 p0186 A73-12811

Fracture criteria in quasi-viscoelastic analysis of crack initiation and propagation in polymethyl methacrylate, noting thermal effects on stress intensity factor

04 p0512 A73-15237

Stress intensity factor for axially stressed thin polymethyl methacrylate plate with cracks, noting fracture angle prediction

04 p0512 A73-15240

Carbon replicas for fracture failure electron fractography by two stage Lucite technique

05 p0586 A73-16134

Growth of part-through thickness fatigue cracks in sheet polymethylmethacrylate.

06 p0714 A73-18481

Crack propagation measurements by surface gage of polymethyl methacrylate, epoxy resin and glass reinforced epoxy composites, conforming with Mott energy balance equation

06 p0714 A73-18499

Durability and fracture mechanics of polymethylmethacrylate under the action of liquid, surface-active media

06 p0715 A73-18670

Effects of a high-pressure gas medium on the mechanical properties of polymethylmethacrylate

06 p0715 A73-18671

Large scintillation counter with a high amplitude resolution

09 p1085 A73-23003

Energy resolution of scintillation counters employing a light guide

09 p1085 A73-23004

The determination of Mode I stress-intensity factors by holographic interferometry.

12 p1550 A73-27021

Symmetrical crack branching in polymethyl methacrylate plates, using method of caustics for stress intensity factor evaluation

13 p1645 A73-28842

Surface temperature measurement of regressing polymethyl methacrylate slabs burning in oxygen-nitrogen mixtures, discussing chemical mechanism for condensed phase depolymerization

13 p1707 A73-28994

Studies on testing methods and weatherability of plastics.

13 p1646 A73-29532

Laser-induced shock effects in Plexiglas and 6061-T6 aluminum.

15 p1956 A73-32259

Intensity of mechanical influences and mechanical degradation of hard polymers

16 p2030 A73-33940

Investigation of the dynamic modulus of polymethyl methacrylate saturated by carbon dioxide

16 p2031 A73-33943

An experimental study of the heat generated in the plastic region of a running crack in different polymeric materials.

17 p2195 A73-34878

Acceleration wave propagation in a nonlinear viscoelastic solid.

[ASME PAPER 73-APM-2]

17 p2247 A73-35028

Crack resistance tests of polymethyl methacrylate specimens under tensile stress

18 p2366 A73-36824

The compression yield behaviour of polymethyl methacrylate over a wide range of temperatures and strain-rates. 19 p2444 A73-38097

The motion of a brittle crack. 19 p2444 A73-38263

On the relationship of stress crazing and yielding of polymethyl methacrylate. 20 p2579 A73-38641

Combustion of a solid fuel in a gaseous oxidizer flow. 21 p2754 A73-40701

Propagation of steady shock waves in non-linear thermoviscoelastic solids. 21 p2724 A73-41548

The response of viscoelastic materials to slow cyclic stresses. 21 p2789 A73-41689

Laminar combustion of polymethylmethacrylate in O₂/N₂ mixtures. 22 p2898 A73-42805

Linear viscoelasticity theory application to high polymers mechanical properties determination via relaxation spectrum with emphasis on polymethyl methacrylate. 22 p2881 A73-43170

Investigation of the initial stage of crack development during compression and tension of polymethylmethacrylate samples. 23 p2998 A73-44278

Free vibrational development of laser-induced cracks. 24 p3095 A73-44510

POLYMORPHISM

A note on the hypothesis - Protein polymorphism as a phase of molecular evolution. 04 p0410 A73-16033

Polymorphous transformation mechanism in thallium. 06 p0735 A73-18045

Phase dependence of positron annihilation in tristearin. 06 p0661 A73-18267

The phenomenon of superplasticity of polymorphous metals and alloys and its use for welding and hardening in the solid state. 08 p0978 A73-21242

Some characteristics of the influence of alloying elements on the polymorphous transformation temperature of zirconium. 14 p1765 A73-30886

Investigation of cobalt molybdate polymorphism. 15 p1887 A73-31207

Quartz transformation to stishovite in shock loaded quartz-copper mixture, discussing relationship to short range order phase. 22 p2848 A73-42497

POLYNOMIALS

NT BINOMIALS

NT DYADICS

NT HERMITIAN POLYNOMIAL

Additions and multiplications number required for fast evaluation of polynomials, investigating savings through preconditioning. 01 p0068 A73-10043

Stress analysis for two stamps impression into linearly deformable base, solving integral stress equation by orthogonal polynomials method. 01 p0118 A73-11411

Polynomial traces and smoothness moduli of functions of many variables. 02 p0187 A73-12179

Approximate solution of the Cauchy problem by the method of polynomial operators. 04 p0470 A73-14936

A new numerical method for the inversion of the Laplace transform. 04 p0471 A73-15229

The use of interval arithmetic to bound the zeros of real polynomials. 04 p0471 A73-15232

Mathematical analysis of body surface potentials. 04 p0412 A73-15646

Existence of analytic solutions of partial differential equations with constant coefficients in an arbitrary number of variables. 05 p0591 A73-17246

Absolute minima determination for homogeneous polynomial real valued goal function under equality constraints, solving nonlinear programming problem by penalty function method. 06 p0716 A73-17851

A method for solving moving boundary problems in heat flow using cubic splines or polynomials. 06 p0768 A73-17979

Polynomial weights and code constructions. 06 p0671 A73-18143

Approximate perturbation solution in Chebyshev polynomials for partial differential equation of heat conduction with cylindrical, spherical or hyperspherical symmetry. 06 p0769 A73-18503

Matrices, polynomials, and linear time-invariant systems. 06 p0719 A73-18863

Use of Olver's algorithm to evaluate certain definite integrals of plasma physics involving Chebyshev polynomials. 07 p0854 A73-19270

Synthesis of functions for polynomial linear-phase amplifiers with feedback. 08 p0947 A73-21396

Orthogonal polynomials for computerized construction of equations of state for substances under thermodynamic restrictions. 10 p1293 A73-23505

Polynomial solutions to the plane problem of electroelasticity theory. 11 p1434 A73-25394

Geometric programming with signomial transformation into equivalent polynomials minimized under inequality constraints and generalization by equilibrium solutions to reverse programs in larger class. 11 p1391 A73-26576

Spline representation by finite functions. 12 p1518 A73-27238

Use of approximating polynomials in the determination of correction parameters for pulsed amplifiers. 13 p1591 A73-28732

Algorithms for finding the coefficients of polynomials of matrix determinants. 13 p1587 A73-28864

The application of Gegenbauer polynomials to antenna array synthesis. 14 p1725 A73-29747

Construction of a uniformly converging sequence of algebraic polynomials by the generalized method of least squares for a class of continuous functions. 14 p1768 A73-30249

Group data handling theorems on uniqueness of mathematical model for regression curve reconstruction in polynomial domain with small number of points. 14 p1738 A73-30288

Numerical solutions by the continuation method. 14 p1769 A73-30454

An equivalence theorem on best approximation of continuous functions by algebraic polynomials. 15 p1902 A73-32376

Nonlinear algebraic equations in continuum mechanics. 17 p2199 A73-34102

Iteration methods for finding all zeros of a polynomial simultaneously. 17 p2200 A73-34215

A scheme for estimating aircraft velocity directly from airborne range measurements. 17 p2209 A73-34873

Orthogonal polynomials for computerized construction of equations of state for substances under thermodynamic restrictions. 17 p2255 A73-35185

Computation of the exponential of a matrix. I - Theoretical considerations. 17 p2203 A73-35521

Umbral /finite operator/ calculus in combinatorial theory of special polynomial sequences as technique for expressing one polynomial set in terms of another. 17 p2204 A73-35732

Polynomial estimators for systems with polynomial nonlinearities. 19 p2445 A73-38042

Synthesis of the functions of polynomial linear-phase feedback amplifiers. 19 p2410 A73-38354

In-plane and lateral displacements triangular elements represented by cubic and quintic polynomials for folded plate structural analysis. 20 p2622 A73-39545

Recursive formulas for the partial fraction expansion of a rational function with multiple poles. 21 p2660 A73-40097

The existence and convergence of subsequences of Padé approximants. 21 p2725 A73-40296

An approximate analysis of non-linear, non-conservative systems using orthogonal polynomials. 21 p2740 A73-40755

Polynomial approximations of the characteristics of low-sensitivity filters. 21 p2666 A73-41315

Germanium resistance thermometers - Resistance vs. temperature and thermal time constant characteristics. 22 p2854 A73-42000

Comparison of a suggested polynomial method with the method of F. M. Perelman in the calculation of the solidus surface of the W-Ta-Mo-Nb system. 22 p2877 A73-42456

Solving linear boundary value problems by approximating the coefficients. 22 p2882 A73-42519

Topology of linear operators in Banach space generalized to invariant polynomials for minimum Schatten ideals in Hilbert space. 24 p3105 A73-45008

Curve fitting by application of splines under tension, discussing polynomial interpolation drawbacks and linear system solution for unknown second derivatives. 24 p3070 A73-45090

POLYPHENYL ETHER

Elastohydrodynamic traction characteristics of 5P4E polyphenyl ether. [ASME PAPER 72-LUB-40] 03 p0335 A73-14347

POLYPHENYLS

Polyphenylquinoxaline/graphite composite laminates tests for flexure, shear and tensile strength at 316 C. 16 p2029 A73-33050

POLYPROPYLENE

Thin polypropylene window proportional counters for the observation of cosmic soft X-rays. 01 p0046 A73-10433

Solid phase stretch forming of thermoplastic polypropylene at temperatures below crystalline melting point. 03 p0332 A73-13034

Glass fiber reinforced polypropylene composites fabrication technology and physico-mechanical properties. 19 p2444 A73-38162

The response of viscoelastic materials to slow cyclic stresses. 21 p2789 A73-41689

POLYQUINOXALINES

Polyphenylquinoxaline/graphite composite laminates tests for flexure, shear and tensile strength at 316 C. 16 p2029 A73-33050

POLYSACCHARIDES

NT CELLULOSE

NT DEXTRANS

NT GLYCOCENS

NT STARCHES

POLYSTYRENE

Stimulated Brillouin scattering for hypersound speed measurement as function of temperature in polystyrene, observing pulsed laser induced damage. 01 p0068 A73-11232

Studies on testing methods and weatherability of plastics. 13 p1646 A73-29532

Intensity of mechanical influences and mechanical degradation of hard polymers. 16 p2030 A73-33940

The yielding of a two-dimensional void assembly in an organic glass. 19 p2444 A73-38090

Oxygen index flammability test relationship to flame spread model for polystyrene film burning rate as function of gas velocity and film thickness. 19 p2504 A73-38274

On the dimensions of intramolecularly crosslinked polymer molecules. I - The synthesis and chemical characterization of intramolecularly crosslinked polystyrene molecules having a narrow distribution of molecular weight. II - The theoretical prediction of the dimensions in solution of intramolecularly crosslinked polystyrene molecules. III - The measurement of the dimensions of intramolecularly crosslinked polystyrene. 23 p3008 A73-43795

POLYSULFIDES

Thermally conducting alumina and boron nitride filled silicone and polysulfide elastomer sheet materials for electrical insulation and heat sink applications. 03 p0331 A73-13028

POLYTETRAFLUOROETHYLENE

Investigation of the friction and wear behavior of polytetrafluoro-ethylene composite materials as compared to synthetic carbon and sintered metal. I. 06 p0714 A73-18449

Polytetrafluoroethylene friction and wear properties as function of heat treatment, speed and temperature, attributing high wear rate to slippage in banded fine structure. 10 p1224 A73-24164

Investigation of the friction and wear behavior of polytetrafluoroethylene composite materials as compared with that of artificial coal and sintered metal. II. 13 p1647 A73-29652

Polytetrafluoroethylene and fluorinated ethylene-propylene grease lubricants. [ASLE PREPRINT 73AM-1A-2] 17 p2195 A73-34977

A reliable Teflon cell with many electrical leads for pressures up to 40 kilobars. 17 p2175 A73-35761

POLYTROPIC PROCESSES

Two-dimensional, unsteady, self-similar flows in gas dynamics. 02 p0152 A73-11569

Radial and nonradial oscillation modes of gaseous polytrope with toroidal magnetic field, using variational principle. 02 p0217 A73-12400

Equations of motion for steady state spherically symmetric flow of polytropic gases into or out of neutron stars, black holes or Schwarzschild singularities. 02 p0223 A73-12729

Polytropic subsonic stellar winds with magnetic fields. 03 p0361 A73-13368

POLYURETHANE FOAM

Differential rotation of polytropic stellar models from structural equations, disproving Porfiriev theory
04 p0504 A73-16025

Complete spectrum of pulsation frequencies for a polytropic atmosphere.
04 p0504 A73-16029

Nonsynchronous uniformly rotating binary system polytrope models computed and compared to Roche model
05 p0624 A73-17307

The hydromagnetic oscillations and stability of self-gravitating masses. III - Magnetic polytropes.
08 p1005 A73-20917

Small amplitude hydromagnetic waves for a plasma with a generalized polytrope law.
11 p1406 A73-26555

Implicit finite difference scheme for Eulerian fluid dynamics of time dependent one dimensional polytropic gas flow, noting numerical stability
17 p2151 A73-34894

Hypersonic polytropic transformations of an ideal fluid. II
19 p2420 A73-37645

Equilibrium structure of polytropes with toroidal magnetic fields.
22 p2912 A73-42941

POLYURETHANE FOAM

Wind tunnel and flight tests for Saturn S-2 stage polyurethane spray foam insulation erosion under aerodynamic heating, shear stress and static pressure. [AIAA PAPER 73-740]
18 p2326 A73-36357

Transient and steady state sound absorption coefficients of fiberglass and polyurethane foam.
19 p2459 A73-37286

Spacecraft polyurethane foam jacket sterilization by gas method, discussing ethylene oxide and methyl bromide sorption and desorption
22 p2803 A73-42160

POLYURETHANE RESINS

Low temperature dynamic mechanical properties of polyurethane-polyether block copolymers.
02 p0185 A73-12426

The fracture energy and some mechanical properties of a polyurethane elastomer.
02 p0185 A73-12641

Selection and application of the protective coating system for the AWACS radome.
03 p0329 A73-13008

Modeling, identification and prediction of a class of nonlinear viscoelastic materials. I.
16 p2082 A73-33904

Stress field in a sphere subjected to large deformations.
19 p2500 A73-38111

POLYVINYL ALCOHOL

Effects of hardening conditions on the physicochemical and frictional properties of polyvinyl furfural
08 p0982 A73-21591

Method allowing biological and biochemical studies of vacuum-exposed bacteria.
20 p2513 A73-39483

Investigation of the photosensitivity of polyvinylcinnamate
21 p2646 A73-40255

Investigation of the spectral properties of sensitized polyvinylcinnamate
21 p2646 A73-40256

POLYVINYL CHLORIDE

Experiments on shell stability in air-driven shock tubes.
03 p0288 A73-13836

Measurement of the dielectric constant of polyvinyl chloride at very low frequencies, and influence of the superposition of a continuous voltage
08 p0942 A73-20648

Influence of proton irradiation in vacuum on the properties of polymer films
11 p1389 A73-26740

Studies on testing methods and weatherability of plastics.
13 p1646 A73-29532

Study of the structural and mechanical properties of polyvinyl-chloride pastes used as anticorrosion coatings
14 p1766 A73-30377

Fire retardation of polyvinyl chloride and related polymers.
18 p2329 A73-37126

Experiments on free vibration of shells of revolution.
23 p3039 A73-43384

PONTRYAGIN PRINCIPLE

Optimal processes theory, discussing Pontryagin principle, special controls, dynamic programming, discrete systems, algorithms, identification and controllability
01 p0028 A73-11072

A fast computational algorithm for optimum digital control systems.
01 p0021 A73-11463

Pontryagin maximum principle application to optimal linear filtration for multivariable systems with signal processing
03 p0286 A73-14082

Pontryagin maximum principle for optimal terminal velocity control of automatic space probe descent in Mars atmosphere
03 p0383 A73-14556

Linear and nonlinear systems dynamic stability conditions for incomplete coefficients data, determining worst disturbance from Pontryagin principle
04 p0475 A73-14887

Optimal trajectory control system synthesis via Pontryagin maximum principle, taking into account system dynamics, control constraints and boundary conditions
04 p0429 A73-15201

Pontryagin principle for variational problem of controllability region in three dimensional pursuit tracking, noting rendezvous optimal control system
05 p0560 A73-16403

The maximum principle in the identification of distributed-parameter systems
05 p0562 A73-17283

Optimal processes theory, discussing Pontryagin principle, special controls, dynamic programming, discrete systems, algorithms, identification and controllability
09 p1069 A73-22997

Formulation of Pontryagin's maximality principle in a problem of structural mechanics.
11 p1434 A73-25185

A proof of the Pontryagin maximum principle for initial-value problems.
12 p1517 A73-27117

Application of Pontryagin's maximum principle for minimum weight design of rigid-plastic circular plates.
13 p1696 A73-28754

Optimal control of discrete systems
14 p1738 A73-30348

Optimal curved pursuit trajectories of point mass in three dimensional space, establishing search technique via Pontryagin principle calculations and equations of state
16 p2061 A73-33269

Straightforward design of a three-layer cylindrical shell
19 p2494 A73-37183

The maximum principle in problems of optimal control of systems having a nonsmooth right side
20 p2593 A73-39323

Convex approximation of the control process and a method for constructing generalized optimum regimes
21 p2727 A73-41064

German monograph - Principles concerning proofs regarding optimality conditions in the case of time-dependent processes.
22 p2888 A73-42853

Classical mechanics Noether theorem and variational calculus for optimal control, noting Pontryagin maximum principle equations first integral solution existence condition
22 p2837 A73-43073

POPULATION INVERSION

Electric discharge CO mixing gas dynamic laser, noting nitrogen molecules vibrational excitation and mixing with cold CO in supersonic expansion with population inversion
02 p0175 A73-12050

Gain distribution in a CO₂ TEA laser.
02 p0177 A73-12434

Dynamics of the CO₂ atmospheric pressure laser with transverse pulse excitation.
02 p0177 A73-12435

[AD-760231] Simultaneous population inversions observation at Zeeman levels in ruby paramagnetic microwave quantum amplifier, noting pumping efficiency
02 p0177 A73-12499

Electromagnetic field, polarization and population inversion equations for spiked emission operation analysis in single mode laser
02 p0177 A73-12694

Ion density and electron temperature calculations for metallic plasma population inversion possibility by near resonant charge exchange with inert gas ions
02 p0194 A73-12847

Relaxation of excess populations in the lower laser level CO₂/100/.
03 p0318 A73-13278

Chemical lasers population inversion mechanism and excitation energy comparison with other molecular gas lasers including carbon dioxide systems, considering efficiency
04 p0458 A73-14749

Instability of a large-amplitude plasma wave due to inverted trapped particle population.
04 p0480 A73-15194

The role of CO in CO₂ lasers.
04 p0459 A73-16039

Study of excitation transfer in a flowing helium afterglow pumped with a tuneable dye laser. II - Measurement of the rate coefficient for the rotational relaxation of He2/3p 3Pi-g.
05 p0600 A73-16045

Population inversion by mixing in a shock tube flow.
05 p0600 A73-16556

Cavity detuning and multimode operation of an optically pumped gas laser.
05 p0585 A73-16598

Chemical lasers with molecular gas excitation and population inversion by chemical reactions, discussing lasing conditions, vibrational transition and pumping mechanism
05 p0585 A73-16602

Carbon dioxide-nitrogen gasdynamic lasers, predicting population inversion from numerical model of vibrational relaxation of anharmonic diatomic oscillators in supersonic expansions
07 p0834 A73-19511

CW and pulsed deuterium fluoride-carbon dioxide transfer chemical laser with molecular vibrational energy transfer for population inversion to obtain high power output
07 p0834 A73-19630

Relaxation and pumping processes in thermally excited carbon dioxide lasers.
08 p0975 A73-21194

Problem of the nuclear pumping of molecular gas lasers
09 p1096 A73-22702

Optically pumped gas laser steady state solution for population inversion, gain coefficient, radiative intensity and power output, noting Doppler broadening role
09 p1097 A73-23070

Analytic approximation for the saturation behavior of OH emission regions.
10 p1272 A73-23542

Population inversion and radiation density in a Q-switched CO₂ laser
10 p1227 A73-23578

Nuclear laser realizability for gamma quanta production from population inversion during radiative capture of neutrons, considering constraints imposed on heating of active medium
10 p1229 A73-24754

Relationship between macroinhomogeneity of the field and the kinetics of free regular emission from a ruby laser
11 p1376 A73-26140

Hg vapor laser with He, Ne, Kr, H or N additions, investigating population inversion and lasing properties for optimal performance conditions
12 p1504 A73-26887

Vibrational level populations in diatomic molecules during steady pumping
12 p1504 A73-26888

Operation of a laser with a planar resonator at high pumping levels.
12 p1507 A73-27507

Gasdynamic laser with a high water vapor content.
12 p1507 A73-27510

Influence of the inversion inhomogeneity on the transverse structure of oscillations in solid-state lasers.
12 p1507 A73-27518

Population inversion calculations using near-resonant charge exchange as a pumping mechanism.
13 p1627 A73-28549

Chemical laser research survey covering device performance, reaction kinetics, theoretical modeling for population inversion and bibliography
13 p1628 A73-29112

Investigation of the inversion medium of a quasi-stationary CO₂ laser with 'pulsed' excitation
13 p1628 A73-29162

Quantization effects in semiconductor inversion and accumulation layers.
13 p1669 A73-29291

Gas discharge CW and pulsed CO laser population inversion mechanism, noting high output and efficiency in CW and Q switched modes
13 p1629 A73-29428

Theoretical study of the mechanism of the population inversion and of the efficiency in an ionized argon laser operating in the continuous mode
14 p1755 A73-29729

Performance comparison of pulsed discharge and E-beam controlled CO₂ lasers.
14 p1756 A73-29918

Influence of CO on the population inversion in CO₂ lasers.
14 p1756 A73-29921

Evolution of the CO vibrational energy distribution in a transverse flow laser.
15 p1884 A73-31313

High power chemical laser technology.
16 p2022 A73-32724

Chemical laser power output prediction by laminar analysis modification with conventional gross mixing concept of turbulent flow in population inversion
17 p2183 A73-34193

Effect of temperature and composition of gas mixture on population inversion in pulsed CO₂ laser.
17 p2183 A73-34295

Chemical laser and molecular amplifiers characteristics covering population inversion and vibrational energy generation, storage, distribution and transfer
18 p2321 A73-35902

Calculation of the generation of inversion and the laser output power for expanding combustion gases /CO₂-N₂-He/
19 p2504 A73-38157

Amplified spontaneous emission comparison with laser stimulated emission during He-Ne transitions, noting threshold condition relation to population inversion density 20 p2570 A73-38619

Approximate determination of the inverted population and amplification factor of a gas expanding adiabatically in a nozzle 20 p2572 A73-39280

Probability balance equations for energy level population analysis of ultrashort pulse solid state laser generation and amplification 21 p2712 A73-40309

The carbon monoxide laser - Mechanism of formation of population inversion 21 p2712 A73-40444

Gasdynamic processes in obtaining inversion in shock tubes 21 p2677 A73-40696

Self-termination of free oscillations in ruby at low temperatures. 22 p2896 A73-42251

Maximum inversion measurement above threshold as function of pump power for Nd glass laser operating in transverse mode 22 p2871 A73-43081

N₂+/- Meinel and O₂+/- second negative bands laser theory. 22 p2871 A73-43144

A kinetic model of population inversion generation in a gas-discharge carbon monoxide laser 23 p2988 A73-44012

POPULATION THEORY

Second-level population of a hydrogen atom in a plasma medium 01 p0085 A73-10950

Distribution function of atomic level populations in a plasma 02 p0196 A73-11603

Collisional-radiative coefficients and population coefficients of hydrogen plasma. 02 p0198 A73-12347

A method for phenomenological analysis of ecological data. 02 p0188 A73-12629

Pumping rate in He-Cd laser from metastable atoms concentration measurement and plasma diagnostics, noting upper level population dependence on Penning effect 03 p0319 A73-13753

An instrument for the simultaneous detection of the OI ground state [2p4 3P] and first metastable state [2p4 1D] populations. 05 p0580 A73-17258

Two dimensional jet stream dynamics from simulation particle population evolution in different collision models 05 p0623 A73-17301

Population of the second level of the hydrogen atom in a plasma medium. 09 p1130 A73-22744

Experimental study of the relaxation of excited states in a decaying alkaline plasma 10 p1256 A73-24576

Ionization, recombination, and population of excited levels in hydrogen plasmas. 11 p1407 A73-26584

Kinetic equations solved for population of different molecular quantum states via quasi-steady state approximation 12 p1526 A73-27307

Analysis of early failures in unequal size samples. 16 p2020 A73-33622

Asteroidal dust population model coinciding with spatial density demonstrating distribution below astrodynamical mass limit and larger time for distribution function extrapolation 21 p2776 A73-41422

Dynamics of a laser with regulated cavity Q 21 p2716 A73-41510

Longitudinal alignment of working levels in a helium-neon laser 22 p2870 A73-42412

Dissociation of diatomic molecules. I. 22 p2889 A73-42443

Level populations in plasmas - RF discharges and sonic channel. 22 p2895 A73-42994

POPULATIONS

Gas discharge efficiency from populations comparison of Ne absorbing levels in hollow cathode and positive column discharges, measuring laser output power peak 02 p0176 A73-12096

PORCELAIN

Porcelain enamels for heat resistant alloys low temperature fatigue strength and high temperature vibration damping increase [SAE PAPER 720809] 05 p0633 A73-16629

Resistance to crack propagation in ceramics subjected to thermal shock. 23 p2997 A73-44031

PORES

U POROSITY

POROSITY

NT MICROPOROSITY

Porosity measurement of porous bronze, nichrome and steel sintered specimens by fluid displacement technique 02 p0178 A73-11540

An observation of the effect of grain structure on the appearance of Kirkendall porosity. 02 p0184 A73-12772

Porous cellular structure materials, investigating porosity effects on modulus of elasticity based on central monoporous model 03 p0394 A73-14015

Morphology and capacity of a cadmium electrode - Studies on a simulated pore. 06 p0649 A73-17744

A photometric investigation of the packing state of Apollo 11 lunar regolith samples. 07 p0878 A73-19669

Cylindrical pores in viscous incompressible liquid film, considering existence duration and pore wall motion under surface tension forces 07 p0923 A73-20420

Possibility of argon-nitrogen gas metal-arc welding of some non-ferrous metals. 08 p0973 A73-21237

Deterioration of impermeable alumina tubes in inert atmospheres at elevated temperatures. 12 p1515 A73-27032

Dependence of some physicochemical properties of plasma-deposited aluminum oxide on sputtering conditions 15 p1881 A73-31211

Effect of porosity on creep in niobium carbide and other powder materials under uniaxial loads 20 p2578 A73-39381

POROUS BOUNDARY LAYER CONTROL

Experimental investigation of flow stability during intense injection 06 p0643 A73-17462

Two-dimensional turbulent jets at a porous wall. 07 p0811 A73-19613

Heat transfer and friction in the turbulent boundary layer of a compressible gas on a permeable surface 08 p0926 A73-20992

Solution of the Cauchy problem for a nonlinear equation describing a gas flow in the presence of strong blowing 09 p1029 A73-23352

Approximate method for solving a boundary value problem describing gas flow during strong blowing 12 p1458 A73-27811

Transpiration nose tip coolant flow control. 18 p2371 A73-36382

[AIAA PAPER 73-767] Study of turbulent transfer with strong injection, longitudinal pressure gradient and nonisothermicity. 20 p2547 A73-39421

Burnout of a graphite surface during the blowing of an inert gas through it 21 p2790 A73-40698

Experimental investigation of the filtration characteristics of porous materials used in boundary-layer control systems 22 p2841 A73-42119

POROUS MATERIALS

Pressure distribution vs porosity and load variation with permeability for squeeze fluid films in porous metal journal bearings [ASME PAPER 72-LUB-P] 01 p0055 A73-10219

Fabrication of porous tungsten foils for contact ionization of cesium [ONERA, TP NO. 1113] 01 p0055 A73-10234

Properties and fabrication of cermet fibers from refractory compounds and of porous materials based on these fibers 02 p0178 A73-11538

Porosity measurement of porous bronze, nichrome and steel sintered specimens by fluid displacement technique 02 p0178 A73-11540

Effect of vacuum solidification on the porosity of wound fiberglass-reinforced plastics 02 p0174 A73-12577

Yield and plastic flow theory for porous metal powder compacts and preforms, discussing stress-strain and deformation-densification relations 03 p0388 A73-13260

Porous cellular structure materials, investigating porosity effects on modulus of elasticity based on central monoporous model 03 p0394 A73-14015

Electric and thermal conductivity, elastic properties, and resistance to bending of porous tungsten throughout the porosity range 04 p0464 A73-15371

Thermal conductivity measurements of porous materials in several gaseous environments at subatmospheric pressures. 05 p0640 A73-16858

Theory of steady-state burning of porous propellants by means of a gas-penetrative mechanism. [AIAA PAPER 73-221] 06 p0767 A73-17663

Heat exchange between gas and air cooled porous metal plate prepared from stainless steel powder under induction and resistance heating 06 p0768 A73-18129

Dynamics of moisture diffusion through a partially liquid filled porous matrix. 06 p0649 A73-18259

On the series solution to the laminar boundary layer with stationary origin on a continuous, moving porous surface. 06 p0687 A73-18505

Low Reynolds number flow past a porous spherical shell. 06 p0687 A73-18506

Description of the transfer of heat by natural convection in a horizontal porous layer with the help of a solid-fluid transfer coefficient 06 p0769 A73-18538

Elastic behavior of polymer-impregnated porous ceramics. 07 p0842 A73-19198

Flow characteristics in air injection through porous surface of blunt bodies, noting blowing parameter effect on boundary layer flow 07 p0774 A73-19622

Lunar soil porosity and its variation as estimated from footprints and boulder tracks. 07 p0898 A73-19903

Review of theories and experimental results pertaining to the dynamic behavior of porous bodies 07 p0912 A73-19905

Convective combustion of porous explosives 07 p0920 A73-19990

Supersonic-hypersonic motion around a porous circular cone 07 p0776 A73-20615

Bielayev's point in poroelastic bodies in contact. 08 p1016 A73-20829

Visualization of thermal fields in saturated porous media by the Christiansen effect. 08 p0963 A73-21030

Theoretical calculation of the compressibility of porous media. 09 p1157 A73-22144

Solute rejection by porous glass membranes. II - Pore size distributions and membrane permeabilities. 09 p1048 A73-22525

Physical characteristics of sponge titanium of a hardness below 100 HB units, obtained by heat treatment with magnesium 09 p1107 A73-23227

Natural convection in a sloping porous layer. 11 p1449 A73-25220

Performance studies on a rechargeable hydrogen-oxygen fuel cell. 11 p1309 A73-25988

Flow of viscous fluid at small Reynolds numbers past a porous body. 13 p1601 A73-28625

On the flow between two independently rotating disks of variable distance with blowing. 13 p1605 A73-29295

Sponge rubber absorption coefficient of sound and acoustic impedance measurements to test porous material sound absorption theories 14 p1767 A73-30894

Enhancement of the electrical strength of deposited aluminum oxide coatings by electrophoretically filling the pores 15 p1881 A73-31212

Preparation of porous electrodes from titanium nitrides 15 p1881 A73-31592

Efficiency of the recovery of high thermal energy densities during porous vaporization of alkali metals 15 p1957 A73-31864

Russian book - Transition of burning of compacted systems to detonation. 15 p1959 A73-32420

The role of a porous filler structure in strengthening polymers 16 p2030 A73-33929

Thermal contact conductance of porous metallic materials in a vacuum environment. 18 p2323 A73-36363

[AIAA PAPER 73-747] Small angle X ray scattering study of submicroscopic voids in glassy carbon, using two density theory 19 p2444 A73-38091

Shape of porous cooled region for surface heat flux and temperature both specified. 19 p2505 A73-38482

The thermal and electrical conductivities of porous copper and stainless steel to elevated temperatures. [ASME PAPER 73-HT-47] 20 p2575 A73-38572

The effect of the porous material characteristics on the internal heat and mass transfer. [ASME PAPER 73-HT-49] 20 p2626 A73-38573

Experimental investigation of the performance of a porous electrode in an MHD converter during the injection of argon with potassium addition 20 p2511 A73-39619

Experimental investigation of the filtration characteristics of porous materials used in boundary-layer control systems 22 p2841 A73-42119

On some further applications of the variational formulation based on local potential to the solution of diffusion equation. I - Temperature distribution in a transpiration cooled half-space with variable thermal properties. II - Heat conduction in an ablating solid with variable thermal properties.

22 p2931 A73-42468
Porous and dense layers in Nb-Ti-O system analyzed by X-ray spectroscopy, finding element content influence

23 p2990 A73-43481
Investigation of the dross molding process for titanium carbide

23 p2991 A73-43490
Effect of secondary oxidizer supply through a porous solid fuel on the hybrid combustion process

23 p3019 A73-43783
Kinetics of shrinkage during the sintering of porous glass/metal composites

24 p3092 A73-44415
Influence of porosity on the effective heat conductivity of graphite

24 p3104 A73-45082

POROUS PLATES

Skin friction on porous surfaces calculated by a simple integral method.

01 p0057 A73-10726

Temperature field and heat transfer equation of unsteady conducting fluid motion on porous plate within magnetic field, allowing for Joule dissipation

01 p0085 A73-11079

Applying quasilinearization to the steady laminar flow between two parallel porous plates.

03 p0292 A73-13307

Measurement of the velocity profile in a turbulent boundary layer on a permeable plate.

06 p0643 A73-17409

Application of the integral balance method to the solution of the problem of interrelated heat and mass transfer in an unbounded plate

07 p0921 A73-20011

Flow of a viscous incompressible fluid between a fixed porous disk and a rotating nonporous disk, with radial discharge

07 p0811 A73-20069

Thermal state of a porous plate cooled by intense blowing under conditions of radiative-convective heating

08 p1021 A73-20993

Turbulent incompressible boundary layer on porous heat insulated plate with uniform suction, calculating ratio of friction drag coefficients

08 p0954 A73-21178

Boundary layers calculation for nonporous surface extended to porous with suction by replacing velocity distribution with longitudinal pressure gradient

08 p0954 A73-21179

Variable properties laminar gas flow heat transfer in the entry region of parallel porous plates.

08 p1024 A73-21640

Kochin hydrodynamic equation solutions for gas injection through plate for intense blowing at constant and changing rates

08 p0927 A73-21772

Unsteady flow between a fixed porous disk and a rotating disk

10 p1209 A73-24837

Porous layer strongly nonlinear heat transfer curve bounds numerical computation by variational method, using boundary layer analysis

11 p1448 A73-25055

On MHD flow along an infinite flat wall with constant suction.

11 p1405 A73-25975

Approximate calculation of the incompressible laminar boundary layer on a plate with suction

13 p1600 A73-28446

The heat and mass transfer of a binary laminar boundary layer in the presence of simultaneous convection at a vertical permeable flat surface

13 p1708 A73-29350

Construction of solutions for the equations of a compressible laminar boundary layer on a plate with abruptly changing boundary conditions

13 p1567 A73-29408

Heat transfer by fluctuating flow of an elastico-viscous liquid past an infinite plate with time varying suction.

14 p1816 A73-29999

Boundary layer about a plate assuming an arbitrary gas injection law

14 p1711 A73-30017

Free convection effects on the oscillatory flow past an infinite, vertical, porous plate with constant suction. I, II.

14 p1816 A73-30049

Experimental investigation of a turbulent boundary layer on a porous plate with intense injection

15 p1824 A73-31858

Investigation of boundary layer flow on a flat porous plate with a regulated pressure gradient in the outer flow

15 p1864 A73-31873

On the solution of magnetohydrodynamic elastico-viscous flow past a plane porous plate.

16 p2042 A73-33370

Some effects of variable surface temperature on heat transfer to a partially porous flat plate.

[ASME PAPER 73-GT-4] 16 p2086 A73-33482

Bounding flow existence for turbulent convection in fluid and porous layers analysis between parallel plates based on calculus of variations in Banach spaces

20 p2626 A73-39012

Energy spectra of velocity pulsations in a turbulent boundary layer on a permeable plate

20 p2547 A73-39286

The turbulent boundary layer with stepwise varying boundary conditions at a permeable surface.

20 p2628 A73-39423

Investigation of the laminar boundary layer at a permeable surface.

21 p2678 A73-41054

Hot-wire anemometer investigation of turbulent boundary layers at a permeable plate with injection.

21 p2678 A73-41055

On unsteady flow of an elastico-viscous fluid past an infinite plate with variable suction.

22 p2840 A73-41747

Variable mass flow rate air injection from porous flat plate into uniform incompressible air flow, obtaining laminar flow velocity profile and pressure measurements

23 p2940 A73-43932

Asymptotic suction boundary layer profile past porous plane surface, obtaining upper and lower bounds on energy stability limit

23 p2969 A73-44381

Heat and mass transfer in a turbulent layer above permeable plates

24 p3081 A73-45528

POROUS WALLS

The steady state performance of an externally pressurized gas lubricated porous thrust bearing with a uniform film.

03 p0311 A73-13203

A study of the stability of externally pressurized gas bearings with porous wall by Liapunov's direct method.

03 p0314 A73-14333

Production of porous tungsten thin walls intended for cesium ionization by contact

04 p0454 A73-15721

Supersonic boundary layer on a permeable surface

05 p0534 A73-17268

Unsteady laminar boundary layers calculation for arbitrary velocity distributions at inner boundary in presence of suction/blowing through porous surface

08 p0954 A73-21176

Heat transfer for turbulent flow with suction in a porous tube.

08 p1024 A73-21637

Experimental investigation of turbulent flow structure in a circular pipe with delivery through a porous wall

10 p1204 A73-23512

Calculation of the gas parameters in the injection region for the flow at an angle of incidence past a porous cone

10 p1172 A73-24505

Unsteady flow of a conducting viscous fluid between parallel porous walls with heat transfer

10 p1256 A73-24587

Development of unsteady boundary layers under variable suction.

10 p1209 A73-24831

Heat and mass transfer during the evaporation of liquids from capillary porous bodies situated in a hot air flow

12 p1559 A73-27474

Wind tunnel interference on oscillating airfoils in low supersonic flow.

13 p1563 A73-28166

Application of small perturbation method in calculations of turbulent boundary layers on a curvilinear surface with suction

13 p1600 A73-28447

Experimental investigation of the convection inversion process in the viscous sublayer of a turbulent boundary layer during blowing of carbon dioxide through a vertical porous heated surface under conditions of natural convection

13 p1708 A73-29407

Experimental investigation of longitudinal flow over a flat plate during strong blowing of a foreign gas under isothermal conditions

15 p1957 A73-31856

Interferometric and thermoanemometric methods of studying binary boundary layers

15 p1876 A73-31859

Determination of the thickness of a wall layer by an approximate method in the presence of intense injection

15 p1876 A73-31861

A procedure for simultaneous measurement of convective and radiant thermal fluxes in permeable walls

15 p1957 A73-31866

Example of utilization of a wind tunnel with perforated variable-geometry walls

16 p1993 A73-32818

Pressure distributions in porous ducts of arbitrary cross section.

[ASME PAPER 73-FE-9] 17 p2152 A73-35008

Experimental investigation of turbulent flow structure in a circular tube with expansion through a porous wall.

17 p2155 A73-35192

Investigation of laminar flow in a porous pipe with variable wall suction.

[AIAA PAPER 73-725] 18 p2299 A73-36342

Porous cooling in a supersonic turbulent boundary layer

20 p2628 A73-39609

Influence of suction on the supercavitation flow behind a body in a porous tube

22 p2841 A73-42125

Stability criteria for two phase transpiration, cooling system with equilibrium phase transition inside porous wall

24 p3156 A73-45079

PORPHYRINS

Abiogenic formation of porphyrin, chlorin and bacteriochlorin.

06 p0651 A73-17934

PORPHYRINS

NT CHLOROPHYLLS

Interstellar matter. II - Diffuse interstellar lines and porphyrins.

06 p0750 A73-18013

Cosmochemical evolution of large organic molecules - Illustrative laboratory simulations for porphyrins.

06 p0752 A73-18235

Apollo 11, 12 and 14 surface fines analysis by fluorescent technique for porphyrins content

06 p0753 A73-18419

Porphyrins analysis in Apollo 11, 12 and 14 soils via analytical demetallation followed by recovery and recomplexing with divalent cations

06 p0753 A73-18420

Spectrofluorometric search for porphyrins in Apollo 14 surface fines.

07 p0891 A73-19823

Spectroscopy of tetrabenzoporphyrin molecules and possible astrophysical implications.

09 p1048 A73-23136

A search for porphyrin biomarkers in Nonesuch Shale and extraterrestrial samples.

11 p1319 A73-26481

Investigation by the laser photolysis method of the spectral and time characteristics of tetrapyrrole molecules in a triplet state

13 p1628 A73-29050

PORTABLE EQUIPMENT

Portable self contained computerized in-aircraft engine analyzer with cassette tape resident program control and digital display and punched card indicators

[AIAA PAPER 72-1080] 03 p0307 A73-13403

Portable electronic thermometer for temperature measurement during exercise elevation of body temperature in heat acclimatization experiment

10 p1185 A73-24567

Portable electro-phonocardiograph using magnetic tape recorder equipped with patient's voice print.

11 p1323 A73-25475

Solar array concept for a portable retractable oriented power system.

11 p1310 A73-26007

Portable radio communication system for guided tours in industrial plants, construction sites and museums, discussing transmitter, receiver, earphones and rechargeable battery power supply

16 p1987 A73-33165

A portable millisecond-integration-time photoelectric photometer.

17 p2165 A73-34273

Compact carbon monoxide sensor utilizing a confo-cal optical cavity.

[ASME PAPER 73-ENAS-20] 19 p2400 A73-37976

Portable respirable dust monitor for continuous concentration measurement by light scattering of gas laser cavity beam

21 p2708 A73-39923

A high vacuum, low temperature specimen transfer device for use in measuring optical properties of thin films

21 p2693 A73-39925

Portable pulse X-ray micro and nanosecond range apparatus for studying fast-going processes in opaque media.

21 p2696 A73-39977

Inexpensive portable vibration-insensitive wave front shearing interferometer developed at NBS for lens testing

21 p2704 A73-41259

Geociever passive Doppler receiver precision capabilities and accuracy experience, noting portability, commercial availability, error sources enumerated and quantified

21 p2705 A73-41329

PORTABLE LIFE SUPPORT SYSTEMS

Influence of the packing and of certain conditions of usage on the medications in portable emergency medicine stores

12 p1465 A73-27720

Mercury, Gemini and Apollo space suits, discussing glove development, boot design, portable life support equipment and extravehicular mobility 16 p1976 A73-34025

PORTS [OPENINGS]
The acoustic response of rooms with open windows to airborne sounds. 05 p0537 A73-17369
The transmission of sonic boom signals into rooms through open windows. 05 p0537 A73-17370

POSEIDON MISSILES
Predicting the service life of neoprene launch tube liner pads for the Poseidon missile. 04 p0468 A73-14861
Data quality assurance in a shipboard computer-controlled telemetry system. 09 p1057 A73-23410
Safety aspects in documentation system for orientation, training and maintenance of equipment for Poseidon Missile System 16 p2073 A73-33639

POSITION [LOCATION]
NT SOLAR POSITION
Stellar positions and proper motions representation of fundamental reference system, improving and extending to faint objects and radio sources. 01 p0094 A73-10056
Determination of the location of a moving object with the aid of navigation systems using information on the cruising speed of the object 02 p0190 A73-11779
Position locus by measurement of the ascension speed of a real or fictitious star 02 p0190 A73-12011
Adjustment of large observation systems in networks of satellite triangulation. 02 p0159 A73-12169
Photographic satellite tracking instrument technology and data reduction methods, describing various camera types and for photogrammetric and astrometric position determination 03 p0274 A73-13252
Method and equipment for localizing satellites by laser range and direction finding. [ONERA, TP NO. 1149] 04 p0417 A73-15096
Limits of possible position of tenth planet at 50-100 AU from analysis of Neptune orbit 05 p0622 A73-17180
Accurate localization by the Geole Project satellite 05 p0623 A73-17192
Positions and some identifications for 111 sources of about 1 flux unit at 408 MHz. 06 p0754 A73-18628
Radio sources identified with stellar objects using precise radio and optical positions. 07 p0900 A73-20281
Frequency of star eliminations in the meridian catalogues constitutive of the Melchior-Dejaiffe ILS stars catalogue. 09 p1141 A73-22011
One dimensional supersonic shock front location by sonic circle involute point by point plotting, using geometric considerations 09 p1030 A73-23467
Independence of the recognition of an object's orientation and position in the field of vision 10 p1180 A73-24331
Optical identifications of radio sources from the B2 catalogue - Quasi stellar sources. 10 p1280 A73-24403
Algorithm for locating a moving object 11 p1394 A73-26097
Positions of minor planets Baumeia 813, Triberga 619, and Jessonda 459. 11 p1429 A73-26687
Observations of the satellites Jupiter VI and VII. 12 p1540 A73-27429
Complex measuring device for moving object location from multiple autonomous and nonautonomous information sources with different noise spectral compositions 12 p1484 A73-27447
Pole position studied with artificial earth satellites. 13 p1656 A73-28393
Pulsar positions and periods with He cooled parametric receiver at 11 cm, confirming PSR 0355 position at 218 cm 13 p1681 A73-28920
Comet orbit and ephemeris calculations with reference to position and magnitude to facilitate reobservation with long focus telescopes 14 p1789 A73-29782
X-ray pulse profile and celestial position of Hercules X-1. 15 p1936 A73-31563
Results and problems of a theory of final-position control systems with a nonstationary singular feedback 20 p2540 A73-38707
Three dimensional transponders array for exact solution to positioning problem, discussing large measurements sequential interrogation effects on accuracy 21 p2734 A73-40034

A survey of satellite-based systems for navigation, position surveillance, traffic control and collision avoidance. 21 p2736 A73-40052
Arctic-Antarctic geodetical survey program, discussing length and direction determination for lines connecting eight principal locations 21 p2685 A73-40813
Optical identifications of radio sources using accurate radio and optical positions. 24 p3135 A73-44579

POSITION ERRORS
Precise positions of radio sources measured at 2695 MHz. 01 p0098 A73-10580
Improved positions and some identifications for 108 radio sources between declinations -33 and +27 deg. 03 p0372 A73-13348
Short term bounds for the effect of oblateness on ballistic trajectories. 03 p0373 A73-13495
Asymmetries related to cerebral dominance in returning the eyes to specified target positions in the dark. 03 p0261 A73-13760
Two-channel direction finding with point source emission and spaced antennas reception, investigating cross correlation and background noise interference effects on accuracy 03 p0278 A73-14062
Modeling of the radar scattering characteristics of aircraft. 04 p0416 A73-15057
Optimal optical measurement for two dimensional object position on plane in Gaussian background noise, calculating mean square error for false identification probability determination 05 p0547 A73-16055
Modeling of aircraft position errors with independent surveillance. [AIAA PAPER 73-162] 05 p0595 A73-16908
Analytical approach to orbit determination in the presence of model errors. [AIAA PAPER 73-170] 05 p0619 A73-16915
Determination of the true course and instantaneous position of an aircraft from aerial pictures 06 p0721 A73-18467
Numerical position deviation and release delay time estimates for gyroscope motion in gimbal suspension during rotor start-up 09 p1081 A73-22345
Low level wind measurement error as it affects sounding rocket dispersion. [AIAA PAPER 73-296] 09 p1116 A73-23215
A new VHF-interferometer with three steerable high-gain-antennas for satellite-tracking. 09 p1070 A73-23434
Optimum strategy for the correction of orbit-injection errors of arbitrary orientation. 09 p1151 A73-23451
LORAN range difference location system, deriving exact straight line of position on plane or spherical surface with computer-generated error maps 11 p1333 A73-26642
Inertial air navigation system error minimization, using discrete-sampled position fixing and star sighting data in computerized calculations 12 p1522 A73-26821
Spacecraft local vertical estimation and error limits in meridional and equatorial planes based on terrestrial IR radiation measuring instruments 12 p1543 A73-27630
Analytical estimates of the accuracy of spacecraft autonomous navigation based on measurements of flight altitude and zenith-distance inertial-space reference point. 12 p1523 A73-27647
Relationship between pointing precision, spread functions and modulation transfer functions. 12 p1501 A73-27969
The effects of scanning position and motion errors on hologram resolution. 13 p1615 A73-28590
Geometric dilution of position /GDOP/ in spherical or hyperbolic system determination, noting position error relationship to collinearity between platform and radio sources pair 13 p1585 A73-29121
Kalman filter design considerations for space-stable inertial navigation systems. 13 p1657 A73-29220
A kinematically designed mount for the precise location of specimens for holographic interferometry. 14 p1753 A73-30414
Aided tracking as applied to high accuracy pointing systems. 15 p1854 A73-31726
Tilt-table alignment for inertial-platform maintenance without a surveyed site. 15 p1858 A73-31728
Convergence criteria for reverse error coefficient expansion under transient conditions for tracking servo system with open loop transfer function 15 p1854 A73-31735

Potentialities of lunar laser ranging for measuring tectonic motions. 15 p1873 A73-32201
Geodetic control point accurate position determination by Navy navigation Doppler satellite observations with geocenter and teletype tape 15 p1873 A73-32268
Multiple path induced position errors in microwave landing systems, considering beating beam and Doppler systems based on time and frequency division multiplexing respectively 15 p1910 A73-32471
Altitude damping of space-stable inertial navigation systems. 16 p2034 A73-33403
Gated phase locked loop tracking device for maximum likelihood estimation of pulsed sinusoid imbedded in noise, predicting phase noise performance 16 p1980 A73-33408
Faraday rotation based total ionospheric electron content information for correction of near real time satellite position determination errors, using spherically stratified ionospheric model 16 p2035 A73-33414
Venus and Jupiter telescopic observation aiming errors using Wanschaff vehicle circle, suggesting error sources and correction procedures 17 p2230 A73-34593
Strapdown air navigation with dry inertial instruments and high speed general purpose digital computer predicting system performance by position error analysis 17 p2210 A73-35211
Shop level maintenance of inertial platforms without a surveyed site. 17 p2148 A73-35644
An in-flight investigation of the influence of flying qualities on precision weapons delivery. [AIAA PAPER 73-783] 19 p2378 A73-37453
A hybrid fluidic directional gyro. 19 p2430 A73-38055
Sensor concept and algorithms for a completely strapdown autonomous navigation approach. 19 p2452 A73-38057
Precise positions of radio sources. IV - Improved solutions and error analysis for 59 sources. 19 p2488 A73-38510
Combined determination of the turn value and screw errors of the position micrometer of an astronomical universal instrument 19 p2432 A73-38553
GX5-1 X ray source position determination from lunar observation observations by Copernicus satellite, noting error bounds 20 p2605 A73-39014
Imaging system pointing precisions, deriving ground target size relationships to spread function and modulation transfer function respectively 20 p2567 A73-39672
Communications and position fixing experiments using the ATS satellites. 21 p2733 A73-40024
Three dimensional transponders array for exact solution to positioning problem, discussing large measurements sequential interrogation effects on accuracy 21 p2734 A73-40034
Navy Transit Navigation System precision improvements for stationary and nonstationary users, considering uncertainties due to satellite position and instrumentation errors and user motion 21 p2734 A73-40039
Accuracy of coordinate measurements with the aid of a variable-profile antenna 21 p2667 A73-41472
Determination of nongravitational forces in the motion of comets. I - Analysis of observation errors 22 p2910 A73-42643
Evaluation of the accuracy of predicting the motion parameters of low-orbit artificial earth satellites 23 p3027 A73-43266
Impulse application for optimal correction of angular position of orbital plane line of apsides, expressing axis angle of rotation as linear function 23 p3027 A73-43269
Laser range measurement to lunar surface retroreflector, discussing initial Apollo 11 observations and achieved lunar orbit and selenophysical information accuracy improvement 24 p3137 A73-44686
Extremal search method errors in determining azimuthal position of gyro-stabilized platform relative to meridian plane, comparing with gyrocompasses 24 p3109 A73-45022

POSITION INDICATORS
NT PLAN POSITION INDICATORS
NT RADIO DIRECTION FINDERS
NT SPACECRAFT POSITION INDICATORS
Astronomical position detector with image disector tube at Cassegrain telescope focus for automatic guiding by illumination distribution analysis 01 p0029 A73-10544
A small model of the Nusi-Fric diazenithal and position determination 03 p0307 A73-13245

POSITIONING

Apparatus note - A system for detecting and recording movements of the head.

06 p0656 A73-17522

Observations of Jupiter with Danjon astrolabes in 1965, 1966, and 1967

08 p1005 A73-20911

Jupiter astrolabe observations analysis, investigating corrections for defective illumination, instrumental comparisons and systematic errors

09 p1140 A73-22002

Precision hover sensor for heavy-lift helicopter.

10 p1216 A73-23784

Geometric dilution of position (GDOP) in spherical or hyperbolic system determination, noting position error relationship to collinearity between platform and radio sources pair

13 p1585 A73-29121

Ship positioning by sonar group and ultrasonic transponder beacons with tracking station axis direction definition capability

14 p1741 A73-30083

A priori evaluation of the position finding system of the Guiana Space Center /CSG/ by the application of Kalman's algorithm

14 p1727 A73-30092

French launching base real time trajectory system for rocket space location information, investigating evolution towards maximum reliability

14 p1773 A73-30094

Decatron indicator for a micromanipulator controlled by a stepping motor

14 p1722 A73-30850

PRS-system for determination of position of flight inspection aircraft for control of ILS- and VOR facilities.

15 p1909 A73-32449

Microwave guidance system for aircraft landing, discussing civil and military requirements, position measurement capability, shadowing in propagation, and ground reflection induced signal fading

15 p1910 A73-32468

Integrated image and symbolic display hierarchy with increasing horizontal and vertical information content for superposition as helicopter aid in approach and precision hovering

[AHS PREPRINT 724]

17 p2168 A73-35065

Measurement of change in a cross section and position of small particles by diffraction techniques.

21 p2695 A73-39959

Indicator and setting devices for circular-mirror sections of the RATAN-600 radio telescope

21 p2675 A73-41451

Reference indication and setting devices for circular mirror sections of the RATAN-600 radio telescope

21 p2675 A73-41452

POSITIONING

Auxiliary instruments for 4-m reflectors related to astronomical telescope focal positions, discussing correlators, cameras, sensitometers, film, rotator-adaptor, guider, echelle spectrograph and photometers

01 p0046 A73-10504

Basic instrumentation components for prime, Cassegrain and coude focal positions of Anglo-Australian telescope, discussing acquisition and guiding, photography, photometry and spectrography

01 p0046 A73-10506

Positioning accuracy with binary selective and fixed gain manual control systems, using finger stick control for operator performance tests

15 p1840 A73-32583

POSITIONING DEVICES [MACHINERY]

NT BOOMS [EQUIPMENT]
Fluidic system for precision positioning of cylindrical machine parts and length and angle measurements, using nozzle jet impingement system for pressure symmetry sensing

05 p0538 A73-17248

Variable-reluctance stepping motor performance capabilities for point-to-point positional control.

10 p1199 A73-24024

An adaptive, time-suboptimal position servomechanism

20 p2511 A73-39664

German monograph - Theoretical and experimental investigation of digital hydraulic positioning devices.

22 p2801 A73-42848

Compensation of an underdamped fluidic position control system by a digital pulse compensator.

23 p2944 A73-43420

Optimal parameters on fluidic noncontact sensors for drives of exact positioning.

23 p2945 A73-43427

POSITIVE FEEDBACK

Low noise regenerative amplifier with direct coupling to load, noting optimal use at moderately high frequencies

03 p0284 A73-14033

Selectivity evaluation for reflection and transmission regenerative amplifiers of complex design

03 p0284 A73-14034

Continuous measurement of internal friction and modulus with a regenerative feedback loop and composite oscillator.

05 p0559 A73-17255

Phase-amplitude and amplitude characteristics of a regenerative parametric amplifier

08 p0948 A73-21555

Effect of nonlinearity in the feedback loop of a recirculation comb filter.

10 p1203 A73-24935

Oscillatory operational amplifiers for control systems and computer technology

12 p1477 A73-26773

Coherent optical signal superregenerative amplification in Q switched gas laser, calculating sensitivity of He-Ne laser light amplifier

13 p1627 A73-28663

SNR improvement by negative feedback and deterioration by positive feedback in amplifiers, discussing input circuit thermal noise

13 p1591 A73-28735

Synthesis of regenerative amplifiers with isothermal approximation of the amplitude-frequency characteristics

13 p1592 A73-28896

Application of the superregeneration principle to a ferromagnetic amplifier

13 p1592 A73-28910

Automatic control of positive feedback depth and its application for stabilization of high Q-factor circuit characteristics

15 p1853 A73-31494

Self organizing behavior of multivariable stochastic extremal control systems with environmental or intrinsic positive feedback under perturbation

20 p2539 A73-38689

POSITRON ANNIHILATION

Phase dependence of positron annihilation in tristearin.

06 p0661 A73-18267

Positron-annihilation radiation from neutron stars.

14 p1788 A73-30738

POSITRONIUM

Galactic positronium annihilation gamma ray spectrum with 476 keV photon peak, indicating possible origin in supernova explosive nucleosynthesis of positrons

21 p2770 A73-40941

POSITRONS

The stopping power of atomic matter for relativistic ions, mesons, electrons and positrons.

07 p0852 A73-19036

Contribution of pion production by primary cosmic-ray nucleons to the interstellar electron-positron flux.

10 p1269 A73-24348

Vacuum state of a relativistic system interacting with an external field

11 p1397 A73-25245

Low-energy positrons from metallic moderators in a back scattering mode.

11 p1402 A73-26544

Solar radio bursts of 4 and 7 August 1972, deducing positron synchrotron process effects on radio spectrum from gamma ray measurements

12 p1535 A73-27785

On the energy spectrum of relativistic electrons in the Crab Nebula.

19 p2475 A73-37619

POSTURE

Electromyographic study on human standing posture in experimental hypogravic state.

01 p0013 A73-11211

Muscular activity control mechanism interactions in vertical posture maintenance from stabilogram, mechanogram and electromyogram data

02 p0137 A73-12119

The role of muscle stiffness in meeting the changing postural and locomotor requirements for force development by the ankle extensors.

02 p0138 A73-12166

Vertical posture control after Souiez 6, 7 and 8 flights and 120-day hypokinesia

08 p0933 A73-20985

The interaction between muscle groups in a complex motor act in humans

08 p0930 A73-21320

Effects of some antinotion sickness drugs and secobarbital on postural equilibrium functions at sea level and at 12,000 feet/simulated/.

09 p1045 A73-22529

Posture responses of upper limb muscles during electric stimulation of the vestibular apparatus

11 p1317 A73-26087

Polarcardiographic responses to maximal exercise and to changes in posture in healthy middle-aged men.

16 p1972 A73-33114

Postural effects on respiration, pulmonary ventilation, oxygen uptake and inhalation and exhalation volumes during asana (yoga gymnastics) exercises executed by athletes

18 p2276 A73-36573

Intracranial hemodynamic changes in pilots to tilting.

18 p2279 A73-36916

Effects of posture on exercise performance - Measurement by systolic time intervals.

19 p2396 A73-38260

A descriptive model of multi-sensor human spatial orientation with applications to visually induced sensations of motion.

[AIAA PAPER 73-915]

The relationship between left ventricular ejection time and stroke volume during passive cardiovascular stress.

21 p2644 A73-40863

Effect of lateral body tilts and visual frames on perception of the apparent vertical.

21 p2641 A73-41565

Human sensorimotor coordination following space flights.

22 p2811 A73-41736

22 p2814 A73-42170

POTABLE LIQUIDS

NT POTABLE WATER

POTABLE WATER
Development of sulfonated polyphenylene oxide membranes for the reverse osmosis purification of wash water at sterilization temperatures /165 F/.

[ASME PAPER 73-ENAS-16]

19 p2399 A73-37973

POTASSIUM

NT LIQUID POTASSIUM

NT POTASSIUM ISOTOPES

Molecular beam study of the K+CH3I reaction - Energy dependence of the detailed differential reactive cross section.

05 p0546 A73-16047

Uranium and potassium fractionation in pre-Irbrian lunar crustal rocks.

07 p0880 A73-19695

Temperature determination of rare gas plasmas seeded with alkali, considering oscillator forces of K excited states in He plasma

08 p0990 A73-20649

Partitioning of potassium between alkalis and sulphide melts - Experiments relevant to the earth's core.

11 p1355 A73-25902

Investigation of the discharge structure in a rare gas alkali MHD generator plasma. II.

18 p2339 A73-36304

Experimental investigation of the characteristics of a nonequilibrium MHD generator

20 p2511 A73-39618

Experimental investigation of the performance of a porous electrode in an MHD converter during the injection of argon with potassium addition

20 p2511 A73-39619

Mass-spectrometric investigation of the ion composition of potassium and cesium discharge plasmas

21 p2746 A73-40526

Three-wavelength holographic diagnostics of an optical flare at a potassium target

21 p2700 A73-40529

Breakdown potential of potassium-seeded combustion products.

24 p3121 A73-45164

POTASSIUM CHLORIDES

KCl ionization and diffusion in premixed flames with uniform temperature and composition, studying gas velocity and photometry

13 p1707 A73-28995

Nutritional circulation in the heart. IV - Effect of calcium chloride and potassium chloride on myocardial hemodynamics and clearance of rubidium-86.

16 p1973 A73-33990

Recording of diffraction patterns by X-ray pulses of materials subjected to a shock wave compression

21 p2695 A73-39967

POTASSIUM CHROMATES

A mass spectrometric investigation of reactions involving vanadium and chromium with potassium-seeded H2/O2 flames.

10 p1186 A73-23555

POTASSIUM COMPOUNDS

NT POTASSIUM CHLORIDES

NT POTASSIUM CHROMATES

NT POTASSIUM IODIDES

NT POTASSIUM NITRATES

NT POTASSIUM OXIDES

NT POTASSIUM PHOSPHATES

Phenomenological theory of antiferroelectricity and ferroelectricity applied to NaNbO3 and the system KNbO3-NaNbO3.

06 p0737 A73-18354

Conductivity and solubility measurements and potentiometry for composition of yttrium nitrate-potassium metaniobate/potassium niobate/-water system

09 p1134 A73-22979

Spectroscopic and lasing studies of a new laser crystal, KY(WO4)2-Nd3+/

09 p1134 A73-22984

Stability of micromorphology of carbon fibres and their interstitial compounds.

11 p1389 A73-25858

Biaxial potassium niobate single crystal nonlinear optical coefficients determination by Marker fringe pattern method, using CW Nd doped yttrium-aluminum garnet laser

23 p3018 A73-44369

POTASSIUM IODIDES

Infrared absorption and local symmetry of negative ClO4 and ReO4 impurity ions in KI and CsI crystals

18 p2340 A73-36673

POTASSIUM ISOTOPES

Sodium Na-24 and potassium K-42 availability for sweat production after intravenous injection and their handling by sweat glands.

19 p2395 A73-37757

POTASSIUM NITRATES

Inhibition of stress corrosion cracking of AISI 4340 steel in 10% potassium nitrate solution at 100 C.

01 p0061 A73-10138

POTASSIUM OXIDES

Atmospheric regeneration in closed chambers by potassium superoxide

18 p2287 A73-36951

POTASSIUM PHOSPHATES

Fracture of nonlinear crystals /KDP and LiNbO3/ by radiation from a ruby laser.

02 p0176 A73-12112

Electro-optical multiple transit laser beam deflection system using KDP crystals and quadrupolar electrode arrangements

03 p0319 A73-14066

Light signal modulation by traveling wave in circular waveguide with coaxial KDP crystal

05 p0558 A73-16781

Maximum permissible pulse duration in second-harmonic generation in a KDP crystal.

06 p0703 A73-18595

Noncollinear second harmonic generation in KDP.

22 p2871 A73-43078

POTENTIAL ENERGY

NT BIOELECTRIC POTENTIAL

NT CONTACT POTENTIALS

NT COULOMB POTENTIAL

NT ELECTRIC POTENTIAL

NT GEOPOTENTIAL HEIGHT

NT IONIZATION POTENTIALS

NT LOW VOLTAGE

NT PHOTOVOLTAGES

NT PLASMA POTENTIALS

NT SPIKE POTENTIALS

Square well fluid liquid-vapor interface density profiles from perturbation expansion in chemical potential, comparing to BGYB and excess free energy minimization approaches

03 p0342 A73-13277

On the maximum value of the mass of a star.

04 p0500 A73-15525

Studies of the potential-curve-crossing problem. II - General theory and a model for close crossings.

06 p0726 A73-18263

The quadratic programming approach to the finite element method.

07 p0907 A73-19030

Influence of the Schottky effect and the peculiarities in the distribution of the applied voltage on the thickness of the depletion layer and the volt-ampere characteristics of a semiconductor with blocking contact.

07 p0802 A73-20191

Solution to a time-dependent Schroedinger equation in the case of a specific potential

09 p1122 A73-22021

Finite element methods for elastic bodies containing cracks.

09 p1162 A73-23186

Optimization of finite element grids based on minimum potential energy.

[ASME PAPER 72-PVP-3]

09 p1163 A73-23268

Intermolecular potential energy curve crossing probabilities and associated phases determination for low energy elastic scattering cross section of He cations by Ne, noting rainbow effect

10 p1250 A73-23670

Use of translational energy measurements in the evaluation of the energetics for dissociative attachment processes.

10 p1251 A73-24244

Russian book on linear truss systems potential strain energy and displacements covering matrix and graph-analytic methods, influence functions, simple and complex strains, etc

11 p1442 A73-25775

A general theory of harmonic wave propagation in linear periodic systems with multiple coupling.

13 p1658 A73-28066

Energy variational principle formulation for stability determination of scalar-pressure toroidal plasma, writing potential energy as one dimensional integral

14 p1778 A73-29689

Empirical intermolecular potentials for N2 and CO2 from crystal data.

15 p1915 A73-31272

Solution uniqueness for elasticity problem with modulus diversity based on deformation potential energy as convex function

15 p1950 A73-31826

Finite element methods in continuum mechanics.

15 p1950 A73-31973

Superexchange potential and kinetic energy theory in molecular orbital and configurational interaction approximation for three center four electron model of ferrimagnetic materials

15 p1924 A73-32156

Theory of satellite structures on spectral-line profiles.

15 p1915 A73-32289

Thermal dissociation and recombination of hydrogen according to the reversible reactions $H_2 + H \rightarrow H + H + H$.

16 p1977 A73-33674

Optimum finite element idealization characterization based on displacement formulation, system potential energy true minimum, stiffness matrix gradients and geometry considerations

16 p2082 A73-33909

The role of surface states in the formation of a Schottky barrier at a metal/gallium arsenide contact

18 p2341 A73-36717

Thermodynamic heat concept, discussing kinetic and potential particle energy, internal energy, heat absorption and release and thermal energy

20 p2627 A73-39293

Moderate-thickness plate equilibrium equations and boundary value problems, discussing successive approximation method, static bending and potential energy

20 p2618 A73-39317

Bifurcation and stability of steady motions of complex mechanical systems

21 p2738 A73-40176

Hartree-Fock equation with allowance for the correlation

22 p2889 A73-42647

Solution of boundary value problems in thermoviscoelasticity with allowance for mass forces exhibiting a potential

23 p3046 A73-44196

POTENTIAL FIELDS

A solution to the problem of the third integral of motion. I.

01 p0106 A73-11318

Equations of motion of solid body about fixed point with nonholonomic constraint, noting potential forces field effect

02 p0193 A73-12195

Analysis of internally generated sound in continuous materials. III - The momentum potential field description of fluctuating fluid motion as a basis for a unified theory of internally generated sound.

07 p0909 A73-19097

Minimum magnetic field energy of two dimensional magnetosphere with neutral sheet for arbitrary dipole inclination to solar wind as function of potential difference on boundary points

07 p0816 A73-19443

Characteristic functions of potential distribution on sphere with longitude dependent conductivity for application to ionosphere electrodynamics

07 p0816 A73-19444

Experimental investigation of the parameters of a statistical Gaussian model of the field below the radio horizon at centimeter wavelengths.

07 p0794 A73-20131

On the analysis of glory scattering data for the extraction of information on the interatomic potential well.

09 p1122 A73-22072

Measurement of the potential distribution in the vicinity of an electron beam with the aid of a thermal probe

10 p1258 A73-24889

Magnetic and gravitational potential anomalies due to uneven nonuniform material layers, using Fourier transforms

13 p1607 A73-28623

Superposition method for potential distribution in plane tetrode field with unipotential and bipotential grids, noting electro-optical effect in cylindrical lenses

13 p1591 A73-28667

Computational algorithm for three dimensional mixed boundary value problem for perturbing potential in earth figure theory

13 p1609 A73-29130

Potential distribution in a two-gas thermionic converter at current saturation.

15 p1832 A73-32638

Electron gun with concentric hemispherical anode and space charge limited thermionic emitter for potential field simulation, measuring electron energy distribution for comparison with calculation

17 p2143 A73-35764

Third integral of motion and the velocity field for a quasi-Newtonian potential. I

19 p2486 A73-37848

Measurement of the potential distribution near an electron beam using a thermionic probe.

21 p2749 A73-41664

Improvement of the electron optics of X-ray image-intensifiers.

23 p2982 A73-43678

Velocity field determination in meridional plane of potential field using third isolating integral of motion

23 p3035 A73-44238

POTENTIAL FLOW

NT EQUIPOTENTIALS

Three dimensional potential flow past arbitrarily shaped aerodynamic configurations, using Hess-Smith numerical method

[DGLR PAPER 72-105]

02 p0127 A73-11657

Integral transformations and conformal mapping for velocity distribution of steady two dimensional potential flow along given profile curve

03 p0241 A73-12904

Ponderable barotropic fluid irrotational flow in horizontal cylindrical channel, noting solitary depression waves possibility

03 p0289 A73-12911

A variational principle for the nonrotational flow of a perfect compressible liquid in a flexible tank [ONERA, TP NO. 1178]

03 p0294 A73-13601

Numerical solution for a flat plate experiencing a ground effect

03 p0245 A73-13721

Mathematical prediction for pressure distribution over arbitrary thin airfoil in inviscid potential and real fluid flows, determining velocity increment at leading edge

05 p0527 A73-16593

Solution of some boundary-value problems in the theory of potential flows of a gas and the propagation of weak shock waves.

05 p0565 A73-16790

Unsteady compressible potential flow around lifting bodies - General theory.

[AIAA PAPER 73-196]

05 p0531 A73-16931

Finite element model for discontinuous potential flow field analysis leading to Dirichlet, Neumann and mixed boundary value problems solution

06 p0644 A73-17514

Eddy cavitation flow past a wedge

06 p0686 A73-18071

Velocity distribution of quasi-steady and steady flow of ideal incompressible fluids with congruent streamlines, investigating conditions for vortex and irrotational flow

07 p0809 A73-19017

Conformal mapping for potential flow about airfoils with attached flap.

07 p0773 A73-19192

Calculation of the potential flow about axisymmetrical fuselages, annular profiles, and propulsion system inlets

[DFVLR-SONDDR-265]

07 p0773 A73-19205

German monograph - An iteration procedure for the calculation of planar compressible flows around circular profiles.

07 p0774 A73-19580

Special relativity theory for steady irrotational ideal gas flow, noting subsonic, supersonic and transonic flow calculations based on small perturbation theory

08 p0926 A73-21128

Some remarks on the behaviour of surface source distributions near the edge of a body.

08 p0926 A73-21437

Graphoanalytic method of calculating plane potential flows

09 p1029 A73-23106

Potential flow past axisymmetric ring wing profiles via singularity method, applying source and vortex distributions to curved thick profiles

[DFVLR-SONDDR-271]

11 p1300 A73-25348

Higher order numerical solution of the integral equation for the two-dimensional Neumann problem.

11 p1300 A73-25434

Unsteady subsonic compressible flow around finite thickness wings.

[AIAA PAPER 73-313]

11 p1301 A73-25544

A linearized potential flow theory for airfoils with spoilers.

11 p1301 A73-25853

Aerodynamics of wake vortices.

11 p1303 A73-26385

Conformal mapping method application to unsteady motion of arbitrary deformable contour in potential flow of ideal incompressible fluid

11 p1348 A73-26426

Potential flow of an inviscid incompressible liquid around a profile in the presence of solid rectilinear boundaries

12 p1487 A73-27797

Flows with wakes about a zero-incidence symmetric profile

13 p1599 A73-28069

A direct integral equation method for the potential flow about arbitrary bodies.

13 p1563 A73-28083

Subsynoptic rainbands within precipitation ahead of surface warm front, discussing midtropospheric large-scale dynamic ascent interaction with upper boundary potential instability

13 p1651 A73-28265

Two dimensional incompressible steady potential electrohydrodynamic flows past flat dielectric plate, using quasi one dimensional and boundary layer approximation

13 p1664 A73-28442

Potential flow about arbitrary thick blades of large camber in cascade.

13 p1565 A73-29009

A comparison between potential flow studies through blade cascade by theoretical and rheo-electric analogy methods.

13 p1565 A73-29010

POTENTIAL GRADIENTS

Approximate solutions and applications of hodograph equations in elliptic diabolic flow.
14 p1745 A73-30428

Book - A course in continuum mechanics. Volume 3 - Fluids, gases and the generation of thrust.
14 p1745 A73-30594

Using the singularity method in studies of potential flow about bulbous streamline bodies
14 p1712 A73-30706

Approximate solution of a stream problem of subsonic gasdynamics
15 p1821 A73-31152

Vertical submersion of a floating cylindrical solid
15 p1861 A73-31283

Pressure distribution on multicomponent airfoils in two dimensional incompressible potential flow, using Martensen-Jacob vorticity distribution method to derive Fredholm type circulation equation
15 p1823 A73-31637

Potential flow induced aerodynamic forces and moments on triaxial ellipsoids, using Lagally theorem based on source, sink and doublet distribution imaging method
15 p1823 A73-31641

Local potential variational method for analytic approximation of stagnation in plane flow, discussing generalized entropy method for accuracy improvement
15 p1957 A73-31665

Special relativity theory for steady irrotational ideal gas flow, noting subsonic, supersonic and transonic flow calculations based on small perturbation theory
15 p1864 A73-32060

Subcritical and supercritical compressible shock-free flows in blade cascades
16 p1962 A73-32812

Computerized three dimensional calculations of hypersustained aircraft in viscous potential flow in terms of boundary layers and wakes
16 p1962 A73-32816

The computation and utilization of Busemann's analysis of potential flow in an impeller.
[ASME PAPER 73-GT-45] 16 p1964 A73-33506

A wake and an eddy in a rotating, radial-flow passage. I - Experimental observations.
[ASME PAPER 73-GT-57] 16 p1964 A73-33512

A wake and an eddy in a rotating, radial-flow passage. II - Flow model.
[ASME PAPER 73-GT-58] 16 p1964 A73-33513

Plane unsteady irrotational flow of ideal incompressible fluid through turbomachine stage due to interaction between stationary and moving grids
16 p2001 A73-34015

Method for calculating the steady irrotational isentropic flow in a two-dimensional supercritical turbine cascade.
17 p2093 A73-34390

Vortex-lift prediction for complex wing planforms.
17 p2094 A73-34438

Book - Lectures on fluid mechanics.
17 p2150 A73-34457

Foppl vortices stability for two dimensional inviscid irrotational steady flow past circular cylinder
17 p2154 A73-35117

Turbulent flow research, discussing time domain analysis of velocity, displacement and pressure, potential flow models of vortices, and shear flow turbulence
17 p2155 A73-35330

Prediction of turbulent separated boundary layers.
[AIAA PAPER 73-663] 18 p2261 A73-36214

Three dimensional jet flap potential flow theory based on vortex lattice method, comparing iterative solution with slatted unswept blown flapped wing experimental results
[AIAA PAPER 73-653] 18 p2263 A73-36260

On viscous and wind tunnel wall effects in transonic flows over airfoils.
[AIAA PAPER 73-660] 18 p2263 A73-36261

Forces acting on a small body in an arbitrary incompressible fluid flow and equations of motion of a two-phase medium
18 p2302 A73-37008

Incompressible potential flow past axisymmetric bodies in cylindrical pipes.
19 p2376 A73-37489

Interference between a wing and a surface of velocity discontinuity.
19 p2376 A73-37490

On the Oseen limiting movements around a rectilinear profile placed under a free line
19 p2459 A73-37526

Incompressible potential flow past sphere parallel to contact plane tangent as model to determine critical velocity for dissipation onset in superfluid liquid He II
19 p2421 A73-37853

Thin steady two dimensional potential flow with free and/or rigid boundaries in presence of gravity, determining outer and inner expansions characteristics
20 p2546 A73-39085

The Lagrange function for a gas bubble in an inhomogeneous flow
21 p2676 A73-40206

Thermodynamic conditions of conservation of irrotational or oligotropic motions across a shock wave
21 p2677 A73-40948

High Reynolds number flow in a moving corner.
22 p2840 A73-41746

Nozzle design for subsonic flow in axisymmetric contractions based on potential flow theory and visual observation, obtaining velocity distribution along wall
22 p2798 A73-43029

Numerical solution of Fredholm integral equation describing incompressible inviscid potential flow past three dimensional bodies
23 p2939 A73-43474

Analytic solutions for potential flow over a class of semi-infinite two-dimensional bodies having circular-arc noses.
23 p2940 A73-43931

POTENTIAL GRADIENTS

Potential drops near the electrodes in a pulsed plasma accelerator.
03 p0347 A73-14096

Sources of spurious background in the Spectracon.
14 p1732 A73-29907

POTENTIAL PROBLEMS

U POTENTIAL THEORY

Potential theory
Solution to certain boundary value problems of a generalized axisymmetric theory of potential
01 p0070 A73-10092

Plane flow past vortex of inviscid incompressible fluid jets bound by free surface and horizontal wall, considering complex potential function and submerged lifting airfoils
01 p0031 A73-10304

Axisymmetrical planet gravitational field potential expression in spherical function series, noting expansion coefficient decrease in power law for smooth density body
01 p0099 A73-10691

Analytical model potential function application to Ar, Kr, Xe, nitrogen, methane and carbon dioxide, applying to different properties
01 p0122 A73-10850

Second virial coefficients for polar molecules in steam based on PVT data, using Stockmayer potential for curve fitting at 100-1000 C
02 p0238 A73-12643

Calculation of the potential created and the velocity induced by a uniform source distribution on a polygon and on a periodic distribution of polygons for the solution of two-dimensional Poisson fields
03 p0241 A73-12910

Hilbert space and calculus of variations for eigenvalue bounds of integral equations of elasticity and potential theories
03 p0387 A73-13162

Minimum potential principles application to elastic-plastic analysis of nonhardening materials, using quadratic programming
04 p0509 A73-14948

Potential methods in the linear couple-stress theory of elasticity.
04 p0514 A73-15676

Jacobi-Hamilton equation of motion of mass point, using elliptic functions for harmonic potential
05 p0597 A73-16467

Further exact and approximate considerations of the barrier problem.
06 p0716 A73-17981

Electromagnetic radiation from charges in weak gravitational fields.
07 p0852 A73-20179

Boundary value problem solution method for hyperbolic partial differential equations based on theory of retarded potentials
07 p0845 A73-20440

Calculation of the magnetic properties of a hydrogen molecule with the aid of the method of varying the vector potential and the method of varying the induced current
09 p1122 A73-22017

Elastic potentials application to second axisymmetric problem solution in micropolar elasticity, considering moments loaded semifinite elastic body deformation and stress tensor components
09 p1157 A73-22170

Work function measurements by the field emission retarding potential method.
09 p1133 A73-22196

Calculation of the transonic flow around an airfoil, taking account of the exact law of compressibility
09 p1027 A73-22210

Isotropic homogeneous elastic medium internal crack analysis based on Laurent series expansions of complex potentials consistent with displacements and stress-strain single valuedness
09 p1162 A73-23179

Book on boundary value problems in physics and engineering covering Fourier series and integrals, heat, wave and potential equations, Laplace transforms and numerical methods
09 p1113 A73-23300

Oscillator strength and photoionization cross section computation for Cs ground state during photoab-

sorption, using semiempirical model potential with adjustable parameters
10 p1250 A73-23672

Potential operator theory in Hilbert spaces applied to rigorous definition of conservative loading, examining pressure loading case
11 p1434 A73-25212

Nonlinear plane cavity flow past flexible barrier, deriving uniqueness theorem by variational operator formulation in terms of potentialness conditions
11 p1391 A73-26547

Stability of the solutions of differential equations with a nonlinear potential operator in a Hilbert space
12 p1516 A73-26959

Magnetic field line velocity associated with Euler potentials set, considering flux preservation properties of particle motion
12 p1489 A73-27000

Inverse problems of a logarithmic potential with analytic closeness
12 p1518 A73-27729

On Maxwell-type equations in the theory of inertial-gravitational field.
13 p1657 A73-28025

Generalization of the integral balance method in problems of correlated heat and mass transfer
13 p1705 A73-28464

Role of exchange in shifted scattering of light for a double hole
13 p1660 A73-28760

Downwash-velocity potential method for oscillating surfaces.
13 p1564 A73-28803

Gas molecule-solid surface interactions, considering rainbow scattering, roughness at molecular scale, potential well and statistical analysis procedures
13 p1663 A73-28912

Application of the regularization method to the solution of the inverse problem in potential theory for electron-optical systems
13 p1662 A73-29681

Static electromagnetic field structure in elastic homogeneous medium for sources distributed by simple and double layers in terms of scalar and vector potentials
14 p1774 A73-30030

Dispersion relation derivation and approximation applications for generalized optical potential use in analysis of energy dependence of empirical potential strength
14 p1774 A73-30237

Some computation-steeples in fluid mechanics.
14 p1745 A73-30412

Some comments on the importance of third order contributions to the screening of the ionic potential and to the structural energy of metals.
14 p1783 A73-30432

Stellar resonant motion in axisymmetric galactic potential, deriving invariant energy mappings from Hamiltonian system of differential equations
14 p1770 A73-30772

Hilbert space of states, considering variational principles, linear elasticity pointwise bounds for homogeneous/inhomogeneous problems and potential theory
15 p1954 A73-32112

Thin rectangular lifting wing investigation at small angle of attack in parallel flow based on Prandtl acceleration potential theory
15 p1955 A73-32126

Dolapchiev-Mangeron-Tsenov analytical mechanics equations extension to potential force systems, applying to electric charge motion in electromagnetic field
16 p2035 A73-32681

Mixed variational principles based on stationary potential energy concept applied to finite element method in thin shell theory
16 p2077 A73-32986

Initial-value problems in potential theory.
16 p2032 A73-33304

Quaternion equations and hypercomplex potentials in continuous medium mechanics
17 p2201 A73-34793

Transonic flow analysis using a streamline coordinate transformation procedure.
[AIAA PAPER 73-657] 18 p2261 A73-36211

Stresses and strains in a rotating disk
19 p2497 A73-37555

Eigenstate localization parameter calculation for wave functions in one dimensional disordered potential chain, considering extension to coupled oscillators and electromagnetic waves in stratified media
21 p2750 A73-40227

Wave potentials for an elastic transversely isotropic medium
22 p2921 A73-42285

The panel method for the calculation of the pressure distribution on missiles in the subsonic range
22 p2797 A73-43028

Potential theory-based relationships between plastic deformation and strain hardening properties of elastoviscoplastic and elastoplastic media, considering specific entropy and free energy contributions
23 p3045 A73-44099

Solvable pair potential for the Bogoliubov-de Gennes equations of space-dependent superconductivity.

23 p3018 A73-44275

Computation of plane-meridional fields of non-homogeneous coaxial cables

24 p3067 A73-44598

The momentum potential field description of fluctuating fluid motion as a basis for a unified theory of internally generated sound.

[AIAA PAPER 73-1000]

24 p3077 A73-44835

POTENTIOMETERS [INSTRUMENTS]

Quick-response automatic range switch for electronic potentiometers

01 p0045 A73-10257

Single automatic potentiometer based maximum-minimum temperature control unit, noting elimination of dual temperature regulators

03 p0309 A73-14026

POTENTIOMETRIC ANALYSIS

Concentrational dependence of resistivity in solid disordered binary alloys of nontransition metals

09 p1104 A73-22687

POTENTIOMETRY

U POTENTIOMETRIC ANALYSIS

POTTING COMPOUNDS

Hydrolytic reversion of elastomeric potting compounds.

13 p1646 A73-29274

POWDER [PARTICLES]

NT FINES

NT METAL POWDER

NT POWDERED ALUMINUM

Aluminizing process improvement by CaAl and ammonium chloride contents increase in powder

01 p0057 A73-11350

Resin powder coating technology, describing fluidized bed, electrostatic and plasma spray processes

01 p0058 A73-11513

Electron-microscopic investigations of metal oxide powders

02 p0178 A73-11543

Diffusive boronizing of molybdenum and niobium in boron carbide powder

02 p0178 A73-11544

Relation of the diffuse reflectance emission function to the fundamental optical parameters.

02 p0193 A73-12350

Feasibility of a fluidized powder demand mode gas generator.

03 p0352 A73-13484

Freeze drying - A unique approach to the synthesis of ultrafine powders.

04 p0455 A73-15753

Investigation in the sintering of Y2O3 powders in the temperature range 1000 to 1400 C.

04 p0457 A73-15987

Electron microscopic investigation of lubricating mechanism of dry and oil-suspended molybdenum disulfide powder, discussing physical and chemical properties effects

05 p0589 A73-17067

Necessary conditions of stable combustion of powder in a semiclosed chamber

10 p1294 A73-23588

Radiative heat transport models for evacuated powder to specify IR radiation environment on lunar surface

10 p1282 A73-24645

Effectiveness of using the energy of a plasma jet in powder coating deposition

10 p1226 A73-24689

Effect of porosity on creep in niobium carbide and other powder materials under uniaxial loads

20 p2578 A73-39381

Lunar surface fine-rock powders seismic measurements in terms of Q factor and acoustic propagation velocity under various temperatures and pressures

20 p2612 A73-39712

Similarity relations derived for unsteady powder burning with light irradiation or occurrence in semiclosed volume

21 p2791 A73-40700

Temperature dependence of dc electroconductivity of CdSe single crystals and compressed micron particle size powders, noting pressure and annealing effects on powder conductivity

23 p3018 A73-44372

A self-similar regime of powder combustion with variable optical constants

24 p3154 A73-44706

Experimental study of the critical conditions of powder ignition and combustion

24 p3155 A73-44707

POWDER METALLURGY

Powder metallurgy for high-performance applications; Proceedings of the Eighteenth Sagamore Army Materials Research Conference, Raquette Lake, N.Y., August 31-September 3, 1971.

01 p0062 A73-10276

Fundamental principles of powder preform forging.

01 p0056 A73-10278

Processing and properties of powder forgings.

01 p0056 A73-10279

Hot isostatic pressing of high-performance materials.

01 p0056 A73-10280

Fabrication of high-strength aluminum products from powder.

01 p0063 A73-10281

Cold rolling of dispersion-strengthened nickel.

01 p0063 A73-10282

Development of IN-100 powder-metallurgy disks for advanced jet engine application.

01 p0063 A73-10283

Hot extrusion and filled billet techniques to process superalloy powder metallurgy products into complex shapes, bars or wire

01 p0056 A73-10284

Potential titanium airframe applications.

01 p0063 A73-10285

Processing of high-performance alloys by powder metallurgy.

01 p0063 A73-10286

Book - Research in powder metallurgy.

01 p0065 A73-10812

Hydrogenation as a means of utilization of industrial titanium scrap.

01 p0065 A73-10821

Metal vapor crystallization in rare gas atmosphere for powder production, noting particle size distribution control

02 p0172 A73-11545

National Powder Metallurgy Conference, Chicago, Ill., April 17-19, 1972, Proceedings.

03 p0322 A73-13259

Mechanical properties of Fe, Al, Ti and heat resistant alloys consolidated powders, establishing coupling between fundamental concepts and engineering application

03 p0322 A73-13261

Consolidation of tungsten and molybdenum powders.

03 p0322 A73-13262

Titanium powder properties, production, alloying, costs and hardware fabrication by pressing, casting, molding, coining and forging

03 p0322 A73-13263

Mechanical properties of pressed and sintered titanium powder.

03 p0322 A73-13264

Metal deformation processes, discussing hot working, fracture, hydrostatic extrusion, superplastic forming, diffusion bonding and powder fabrication

04 p0452 A73-14742

High speed tool steel, Ti alloys and vanadium carbide products manufacturing by powder metallurgy, using vacuum and high pressure techniques

04 p0460 A73-14745

Powder metallurgy production of structural shapes.

04 p0461 A73-15022

Heat resistant Ni and Cr alloys powder metallurgy, discussing inert and solute gas atomization, rotating electrode and gatorizing processes for powder fabrication

04 p0461 A73-15023

Trace phase analysis as an aid in the study of heterogeneous raw material impurities in powder metallurgy

04 p0464 A73-15370

The role of pore size in the ultimate densification achievable during P/M forging.

04 p0456 A73-15799

The properties of 18Ni 350 maraging steel produced from elemental and prealloyed powders.

04 p0466 A73-15800

Nature of anisotropy in half-cells made of cold-pressed Bi-Te-Se-Sb alloys

06 p0738 A73-18653

Electronic mechanism of the basic technological processes in the powder metallurgy of high temperature materials.

08 p0982 A73-21825

Measurements of the emissivity of materials fabricated by powder- and plasma-metallurgy techniques

09 p1103 A73-22472

Creep associated with hot pressing titanium carbide powders

10 p1224 A73-24315

Development of a production technology for high-density metal-ceramic materials by the method of impregnating porous preforms with low-melting iron boride alloys

10 p1224 A73-24316

Composite material production by grinding Ni-Al-Ti alloy powder with other mixed powders, noting alloying elements effects on corrosion resistance and ductility

11 p1372 A73-25406

Silicon carbide whisker reinforced Al composite production by powder metallurgy, discussing mechanical strength and extrusion process for fiber orientation

11 p1373 A73-25414

The role of plastic deformation in metal powder compaction.

11 p1374 A73-26270

Ni-base alloy powder metallurgy from production waste cuttings by oxidation and subsequent oxide reduction with hydrogen and calcium hydride

12 p1503 A73-27553

Superalloys processing technology for aircraft gas turbine applications, discussing developments in eutectics and powder metallurgy for increased operating temperatures

13 p1636 A73-28931

Investigation of the friction and wear behavior of polytetrafluoroethylene composite materials as compared with that of artificial coal and sintered metal. II

13 p1647 A73-29652

Thermophysical properties of high temperature electrical insulating materials on the basis of non-metallic compounds with high melting point [ECTP PAPER D2-3]

14 p1766 A73-30436

Technical note on some mechanical properties of a magnesium-25 vol% boron particulate composite.

14 p1765 A73-30935

Powder metallurgical preparation (sintering) of conventional maraging steel and similar alloys with Ni and/or Mo replacement by Mn and Ti, considering age hardening characteristics

14 p1765 A73-30936

Book - Forging of powder metallurgy preforms.

15 p1891 A73-32195

Structure of powdered solders with a Ni-Cr-Si-Fe-B-C/Mo base

15 p1892 A73-32245

Techniques for fabrication of composite materials.

16 p2017 A73-32699

Silicon nitride materials for gas turbine components. [ASME PAPER 73-GT-47]

16 p2048 A73-33508

Hot isostatic pressing of titanium alloys for turbine engine components.

16 p2019 A73-33516

Investigation of the effect of pressed-powder grain composition on the physico-mechanical properties of magnesia refractory materials

17 p2187 A73-34337

Effect of autoclave heat treatments on the mechanical properties of the prealloyed-powder cobalt-base alloy HS-31.

19 p2443 A73-38248

The fabrication of fiber-reinforced composites with the aid of high-speed extrusion presses

19 p2435 A73-38272

Nitride inclusions in titanium ingots - A study of possible sources in the production of magnesium-reduced sponge.

20 p2576 A73-39026

Explosive and electrohydraulic forming techniques cost effectiveness in metal technology, considering welding methods and metal powder compaction

22 p2865 A73-41779

Compacting of metallic powders by plane high-explosive charges. I

24 p3092 A73-44414

Temperature range for centrifugal thermal diffusion sintering in Cr-Ni powder coatings, relating upper and lower bounds to heating rate

24 p3092 A73-44419

POWDERED ALUMINUM

Ammonium perchlorate/aluminum powder propellant rocket engine feasibility evaluation, considering test firing results on performance and stability characteristics for various injector configurations

03 p0357 A73-13463

Propane-oxygen pilot flame ignition of steady flowing Al powder stream in oxygen

07 p0865 A73-20362

Dispersivity of the combustion products of a mechanical mixture of aluminum and cadmium powders

07 p0923 A73-20421

Foamed Al production from Al powder mixture with aluminum hydroxide and orthophosphoric acid, discussing mechanical, thermal conductivity and electrical insulating properties

10 p1236 A73-24919

The pressing of profiles of aluminum casting alloys from granules and the study of their mechanical properties

12 p1503 A73-27560

Application of a scanning electron microscope in powder investigations

15 p1892 A73-32239

Ignition temperature of conglomerates which form by burnout of the binder in a suspension of aluminum powder in kerosene

18 p2372 A73-37118

POWDERED METALS

U METAL POWDER

POWER AMPLIFIERS

M/W power transistors and MIC amplifiers - State-of-the-art.

01 p0024 A73-10719

High-power avalanche IMPATT reflection amplifier using the Rucker combining circuit.

03 p0282 A73-13894

Time-averaged power stage models transient and frequency responses characterization and circuit component values derivation for switched dc-dc converters design

03 p0282 A73-13927

High power SHF transmitter experiment using TWT depressed collector beam microwave amplifier for flight testing on communications technology satellite /CTS/

04 p0428 A73-15447

Gunn diodes oscillating circuit with waveguide cavity in push-pull mode at 42 GHz for high power parametric amplifier pump applications

05 p0558 A73-16807

Large-signal behaviour of R.F. power transistors. I - Analysis of the equivalent circuit.

05 p0559 A73-17125

Book - Transistor circuit design.

06 p0673 A73-17672

Regenerative amplifier based on multiple IMPATT diodes

07 p0802 A73-20295

Electrodynamic exciter power amplifier with pulse width modulation and Schmitt trigger output stage for structural vibration tests

07 p0803 A73-20535

Integrated electrically tuned X-band power amplifier utilizing Gunn and IMPATT diodes.

07 p0803 A73-20551

Waveguide cavity multistage Gunn reflection amplifiers for FM-CW systems, discussing stabilization techniques, bandwidth, noise, power variation with temperature and group delay distortion

07 p0803 A73-20552

Wideband class-C Trapatt amplifiers.

08 p0947 A73-21145

1-2 GHz high-power linear transistor amplifier.

08 p0947 A73-21146

Two stage microwave monolithic integrated circuit power amplifier design with matched transistors, calculating distributed matching network

08 p0950 A73-21826

Microstrip solid state power amplifiers with transistors and varactors for spaceborne applications in L and S band ranges

09 p1066 A73-23428

Analysis and synthesis of automatic control systems with controlled converters.

10 p1198 A73-24019

Microwave transistor power amplifier.

11 p1338 A73-26149

Considerations about jump effect in microwave power amplifier.

12 p1478 A73-27073

Output characteristics of high frequency transistor power amplifiers.

12 p1479 A73-27169

Self-stabilizing power amplifiers with combination-type negative feedback

14 p1736 A73-30564

Dual mode microwave tube parameters for ECM power amplifiers based on systems rationale analysis, considering TWT and injected-beam crossed field amplifier

14 p1736 A73-30621

Wide-band power amplifier for studying the high-frequency properties of plasmas

15 p1850 A73-31497

Performance and advantages of FET's as microwave solid state amplifiers.

17 p2141 A73-35322

A pulse-width modulator operating on dc integral amplifiers

18 p2293 A73-36855

Regenerative multidiode IMPATT amplifier.

18 p2294 A73-37132

Pulsed RF life of an L-band power transistor.

19 p2411 A73-38460

High power transistor amplifier thermal design with heat sink convective and radiant cooling for low junction temperature and long service life

19 p2411 A73-38474

Satellite-borne power amplifier state of art, comparing TWT development to different technological solutions

20 p2538 A73-39772

A 50-W VHF amplifier with transistors

21 p2664 A73-41088

Reduction of noise in high-power crossed-field amplifiers.

21 p2665 A73-41114

Russian book on semiconductor radio transmitter design covering power amplifiers, frequency multipliers, oscillators and Gunn effect devices for sub-microwave frequencies

21 p2666 A73-41424

Pulse push-pull power amplifier

22 p2833 A73-42361

POWER CONDITIONING

Optical power handling capacity of low loss optical fibers as determined by stimulated Raman and Brillouin scattering.

01 p0078 A73-11216

A sequenced PWM controlled power conditioning unit for a regulated bus satellite power system.

03 p0252 A73-13930

Push-pull ac modulator design allowing balanced thermal load on plasma electrodes in pulsed high power short arc Xe flash lamps

03 p0282 A73-13933

The IHTS - A new building block for power conditioners.

03 p0282 A73-13934

Switching stepdown dc-to-dc converter with analog signal to discrete interval converter, hybrid micromodule and two-loop control subsystem, discussing circuitry and performance

03 p0283 A73-13935

High power inverter with commutator of single LC network and steering SCR capable of multiple high voltage dc bridge operation

03 p0253 A73-13936

Processing power for a low voltage source-pulse load system.

03 p0253 A73-13939

Circuit design of triode thyristors and companion rectifiers for high frequency power conditioning, discussing emitter selection, lifetime control, encapsulation and interdigitation optimization

03 p0283 A73-13943

The performance of recently developed high voltage high current power transistors.

03 p0283 A73-13944

Electric power processing, distribution and control for advanced aerospace vehicles.

03 p0253 A73-13947

Analog signal to discrete time interval converter /ASDTC/ feedback control for high performance aerospace power supply conditioning

04 p0486 A73-14901

Description of power conditioning systems intended for satellite stabilization thrusters

04 p0489 A73-15732

High voltage fuel supplies intended for ion thrusters

04 p0489 A73-15734

Switch transistor control using an intensity transformer

04 p0489 A73-15736

Space station solar array-energy storage-power control and distribution system based on regenerative fuel cell integrated with life support system

09 p1153 A73-22784

Modularised power conditioning units for high power satellite applications.

09 p1035 A73-22806

X4 scientific satellite subsystems development status, discussing solar array, attitude control, data handling, power conditioning and antenna systems

09 p1154 A73-22919

AC impedance of silicon solar cells.

11 p1310 A73-26000

Concept for a high voltage solar array with integral power conditioning.

11 p1310 A73-26001

Power system for a 4.1 kilowatt synchronous satellite.

11 p1312 A73-26023

Sealed aircraft battery with integral power conditioner.

13 p1573 A73-29589

Microwave power transistors - The present and the future.

15 p1852 A73-32275

A low noise, very low power charge sensitive amplifier for space applications.

17 p2134 A73-34272

The cause and effects of dc offset voltage in solid state ac power controllers.

17 p2109 A73-35255

Extending the useful life of radioisotope thermoelectric generators through active power control.

19 p2455 A73-38392

Reduction of power requirements in dynamic elements based on bipolar transistor

21 p2660 A73-40022

Thermal response of microwave transistors under pulsed power operation.

21 p2663 A73-40774

CODYMOS frequency dividers achieve low power consumption and high frequency.

21 p2670 A73-41111

Power Electronics Specialists Conference, California Institute of Technology, Pasadena, Calif., June 11-13, 1973, Record.

22 p2801 A73-42901

High voltage waveform generation at low power levels by circuit techniques and system configurations involving parallel series chains of light triggered bilateral switches

22 p2834 A73-42907

Linearized stability analysis and design of a flyback dc-dc boost regulator.

22 p2801 A73-42910

Bilateral power conditioner with common filters and transistor control circuits for battery charge and discharge functions onboard near earth orbit spacecraft

22 p2802 A73-42916

A symmetry correcting pulse-width modulator for power conditioning applications.

22 p2802 A73-42919

POWER CONVERSION

U ELECTRIC GENERATORS

U FLUX DENSITY

POWER EFFICIENCY

High-efficiency Ga_{1-x}Al_x/x-Al_x-GaAs solar cells.

01 p0005 A73-10132

The radiation efficiency of a dipole antenna located above an imperfectly conducting ground.

01 p0015 A73-10185

High efficiency dc-to-dc converter with second non-saturable transformer for eliminating collector current spike to reduce electromagnetic interference and transistor damage

01 p0005 A73-10247

Effect of heterogeneity and Hall current on the MHD power generator.

01 p0005 A73-10434

Superconducting magnet ac generators development, emphasizing conversion efficiency, manufacturing, relative costs, machine geometry and interwinding coupling factor effects

02 p0132 A73-11833

TWT power gain, efficiency and output variations compensation methods during electron beam switching between pulsed and CW modes

02 p0148 A73-12570

High pressure stage efficiency of the turbines of modern turbopumps

03 p0359 A73-14137

Laser energy conversion into electrical energy with photovoltaic cells, noting Si and GaAs cells power efficiencies improvement compared to operation in sunlight

03 p0254 A73-14210

Minority carrier lifetime and diffusion constant as function of impurity concentration in double junction vertical solar cell, determining power efficiency

03 p0254 A73-14213

Spin saturation and pump depletion in continuous spin-flip Raman oscillation.

03 p0319 A73-14452

Chemical lasers population inversion mechanism and excitation energy comparison with other molecular gas lasers including carbon dioxide systems, considering efficiency

04 p0458 A73-14749

Quadrature amplitude-shift key satellite communication feasibility based on SNR and transmitter power efficiency comparison with multiphase-shift key system

04 p0420 A73-15411

Investigation of a gallium arsenide laser pumped by an electron beam

05 p0584 A73-16553

Silicon X band oscillation TRAPATT diodes with high power efficiency, presenting electric field variation with distance

05 p0559 A73-16809

GaAs transferred electron /Gunn/ device microwave oscillator with harmonic tuning, noting reactive termination and bias voltage effects on efficiency optimization

05 p0559 A73-16813

Heterojunction injection lasers with high efficiency and low threshold currents, discussing amplification, emission, epitaxial layers, and performance superiority over homostructures

05 p0586 A73-17266

Equivalent circuits for microwave frequency converter design, noting small and large signal operation and power efficiency of variable capacity diode circuit

06 p0673 A73-17578

On some noise properties of high frequency solid-state oscillators.

06 p0673 A73-17714

Low power thermoelectric cascade for cooling substrates to 145 K, discussing materials electrical and thermal properties, design optimization, computerized performance simulation, fabrication and testing

06 p0683 A73-18316

CW Q band Gunn diode microwave oscillator fabricated by integral heat sink technique for high power output and efficiency

06 p0677 A73-18345

Theoretical and experimental study of GaAs IMPATT oscillator efficiency.

06 p0678 A73-18789

IMPATT diode microwave oscillator performance analysis for I-V characteristics, output power, efficiency and starting current from equivalent circuit

08 p0943 A73-20707

IMPATT diode anomalous microwave oscillation mode performance analysis, calculating I-V variation, power and efficiency from equivalent circuit

08 p0943 A73-20708

Electrode and gasdynamic effects in a large nonequilibrium MHD generator.

08 p0928 A73-20713

Conditions derived for reactive two-terminal-pair matching transformer networks operation at maximum power transfer efficiency

09 p1061 A73-22046

Gradual degradation of GaAs double-heterostructure lasers.

09 p1092 A73-22241

Laser system output mirrors alignment for beam quality and power performance optimization and ex-

ternal optical component premature degradation prevention, using autocollimator 09 p1094 A73-22445

Nonlinear properties of microwave avalanche diodes operated in IMPATT mode, discussing current density effect and power efficiency 09 p1063 A73-22489

Computer calculation of the characteristics of multistage gas turbines 09 p1136 A73-22567

Radioisotope thermoelectric generator SiGe thermopile power degradation and operating temperature changes, discussing performance prediction model 09 p1117 A73-22763

SNAP 19 thermoelectric generator long term performance tests, attributing output degradation to sublimation and hot junction bond loss due to internal gas cover depletion 09 p1118 A73-22765

Lundell solid rotor brushless alternator windage power losses, measuring aerodynamic drag coefficient over Reynolds number and gap width range 09 p1034 A73-22772

Isotope Brayton electric power system for the 500 to 2500 watt range. 09 p1118 A73-22793

Performance improvement of cesium thermionic converters by addition of oxygen. 09 p1036 A73-22818

Radiophotovoltaic devices power and energy conversion efficiency limits, investigating phosphors deterioration and nuclide layer optimal thickness 09 p1037 A73-23280

Boundary layer efficiency as working fluid in ram-jets for high aircraft speeds, obtaining external efficiency as function of boundary layer parameters and flow rate 09 p1073 A73-23360

Influence of a change in the throughput of the power turbine on the parameters of a dual-shaft gas turbine engine 10 p1262 A73-23599

Aircraft turboengine noise, discussing noise level/power output relations 10 p1262 A73-23861

Research and technology assessment of high power short wavelength molecular lasers, emphasizing carbon dioxide laser efficiency 10 p1229 A73-24654

Efficiency transition point for inductively loaded monopole. 11 p1337 A73-25364

The calculated long-term performance characteristics of a typical silicon-germanium RTG. 11 p1312 A73-26030

The long term performance characteristics of a SNAP-19 generator operating under vacuum conditions. 11 p1396 A73-26038

Output characteristics of high frequency transistor power amplifiers. 12 p1479 A73-27169

Nitrogen laser with a longitudinal discharge and high power density 12 p1506 A73-27214

Optimization of the power of a Faraday-type MHD-generator operating with a nonequilibrium plasma 12 p1460 A73-27320

Continuous-wave laser with a vortex-stabilized lamp. 12 p1506 A73-27503

Gas discharge CW and pulsed CO laser population inversion mechanism, noting high output and efficiency in CW and Q switched modes 13 p1629 A73-29428

Optimizing power efficiency of hydrazine-oxygen fuel cells. 13 p1574 A73-29598

Charge transfer semiconductor devices operational principles and possible structures with two or three phases, discussing efficiency, regeneration circuitry and noise and dissipation problems 14 p1731 A73-29727

Theoretical study of the mechanism of the population inversion and of the efficiency in an ionized argon laser operating in the continuous mode 14 p1755 A73-29729

Circuits for power density reduction in TRAPATT diodes. 14 p1732 A73-29927

Shaping of subreflectors in Cassegrainian antennas for maximum aperture efficiency. 14 p1734 A73-30207

Compressor or fan location at intake or outflow side of compressible flow plant, considering power and size requirements with and without heat exchange 14 p1711 A73-30297

TWT for air-to-air missile fire control radar transmitter application, considering high average power, RF gain and PPM focusing requirements 14 p1737 A73-30624

A comparison of silicon and gallium arsenide large signal IMPATT diode behaviour between 10 and 100 GHz. 15 p1850 A73-31131

Emission characteristics of a tube-shaped laser oscillator. 15 p1885 A73-31940

X band oscillators for microwave generation based on silicon avalanche diodes, presenting power and efficiency dependence on frequency and bias current 15 p1851 A73-32160

Experiments on the design of a small axial turbine. 17 p2092 A73-34379

Microwave amplifier design with discrete variable components, testing power output and efficiency, bandwidth, and temperature, vacuum and vibration effects on performance 17 p2141 A73-35324

Corrugated horn antenna with high efficiency and monotonic amplitude in microwave pattern ranges applicable as calibrating standard 17 p2143 A73-35693

Designing high efficiency TWT's. 18 p2293 A73-36777

Ion implanted X-band IMPATT/TRAPATT back-to-back diodes. 19 p2408 A73-37146

The development of propulsion systems in the case of airliners 19 p2473 A73-38120

NaK-nitrogen liquid metal MHD converter tests at 30 kW. 19 p2389 A73-38311

High power density hydrazine-oxygen fuel cell, discussing cell polarization, critical resistance losses and efficiency 19 p2390 A73-38398

Development of a lightweight body-mounted solar cell array with a high power to weight ratio. 19 p2391 A73-38408

Design and testing of a 150 watt SNAP 19 high performance generator. [IECEC PAPER 739090] 19 p2458 A73-38437

Book - Hydraulic systems and maintenance. 20 p2510 A73-39142

Summation of the output power from two Gunn diodes 21 p2659 A73-40008

Investigation of the influence of the leading-edge configuration on the efficiency of cooled rotor- and guide-vane cascades 21 p2632 A73-40406

Scale model development of a high efficiency dual polarized line feed for the Arecibo spherical reflector. 22 p2831 A73-41830

Approximate nonlinear theory of orotron as SHF hybrid-type monotron oscillator, calculating output power and efficiency as function of tube electrical parameters and geometry 22 p2826 A73-42338

Boost klystron efficiency with three-cavity design. 22 p2833 A73-42400

Quenching effects in flashlamp-excited polymethine dye lasers. 22 p2871 A73-43083

POWER GAIN

New design concepts for microwaves power transistor. 01 p0024 A73-10721

Resonant feedback loops and impedance matching network analysis of pulsed and CW transistor microwave power oscillators 01 p0024 A73-10722

The superconductor maser - A calculation of the gain from the two-level model and the BCS theory, and some new experimental results. 02 p0175 A73-11848

Gain distribution in a CO₂ TEA laser. 02 p0177 A73-12434

TWT power gain, efficiency and output variations compensation methods during electron beam switching between pulsed and CW modes 02 p0148 A73-12570

Gain and frequency characteristics of a 20 mW C.W. water vapour laser oscillating at 118.6 microns. 02 p0177 A73-12724

Laser oscillation and anisotropic gain in the 1 to 0 vibrational band of optically pumped HF gas. 02 p0177 A73-12747

Some aspects of radiation from a circular loop antenna. 02 p0148 A73-12854

Analysis of an asymmetric dipole antenna with displaced feed points. 02 p0148 A73-12856

Combined nonlinear amplification and absorption role in ultrashort pulse generation of mode locked quasi-continuous dye laser in absence of short relaxation time 03 p0318 A73-12870

Influence of satellite antenna gain on a satellite communications system. 03 p0277 A73-14027

Statistical characteristics of antenna gain threshold as function of link trajectory during radiation pattern shift with respect to fixed orientation 03 p0278 A73-14061

Optimal output power of tunnel drift diode oscillator in millimeter band as function of electric field and diode geometry 03 p0284 A73-14086

Carbon dioxide laser output signature calculation as function of cavity length based on homogeneously broadened line with dispersion 03 p0320 A73-14455

Transient analysis of an electronically tunable dye laser. I - Simulation study. 03 p0320 A73-14457

Effect of surface states on surface-wave amplification in a composite structure of CdSe film on LiNbO₃. 05 p0559 A73-17073

Nonreciprocal circulator coupled reflection type microwave amplifier gain and stability characteristics, presenting scattering matrix and signal flow diagram. 06 p0673 A73-17590

Gain correlation with sidelight and plasma impedance properties of a CO₂ laser discharge. 06 p0700 A73-18137

Errors in the predicted gain of pyramidal horns. 06 p0676 A73-18180

The 'Paradise' antenna - A novel technique to improve the axial ratio of a circularly polarized high gain antenna system. 06 p0676 A73-18195

Class I OH emission sources structure and variability, considering variable gain maser models. 06 p0751 A73-18227

On the theory of the avalanche transit-time diode reflection amplifier. 06 p0678 A73-18838

Interactions among multiple lines in the 8446-A atomic-oxygen laser. 07 p0834 A73-19336

An analysis of an arbitrary n-element adaptive array. 07 p0795 A73-20583

Interdigitated power junction transistor technology assessment for power gain, bandwidth and frequency performance, noting packaging effect and thin film module advantage 08 p0949 A73-21648

High energy and power carbon dioxide laser with nitrogen and He mixtures, transverse electric discharge excitation and modular construction, noting efficiency and gain 09 p1090 A73-22081

High gain gas laser oscillators saturation, verifying with 3.51 micron Xe oscillator having unsaturated single pass intensity gain of ten million 09 p1091 A73-22086

Application of four methods for approximating optimal feedback gains. 09 p1067 A73-22234

Gain-current relation for GaAs lasers with n-type and undoped active layers. 09 p1091 A73-22239

Design criteria for high gain, wide band, microwave amplifiers. 09 p1062 A73-22304

A high pressure gas-dynamic laser powered by a slow compression heater [ONERA, TP NO. 1184] 09 p1096 A73-22712

A laser amplifier with resonator natural frequencies misaligned with respect to the gain profile of the active medium 09 p1096 A73-22969

Optically pumped gas laser steady state solution for population inversion, gain coefficient, radiative intensity and power output, noting Doppler broadening role 09 p1097 A73-23070

Performance of multifrequency parametric converter with resonant circuits as function of input and parametric diode characteristics, using gain and noise temperature coefficients 10 p1196 A73-24605

Carbon dioxide laser active medium excitation by ionizing radiation from external source during electric current passage, discussing gain dependence on pressure and mixture 10 p1229 A73-24756

Computerized large signal model of IMPATT diode, calculating output power and admittance as function of frequency and amplitude 11 p1336 A73-25320

Active electromagnetic horn antenna with tunnel diode. 11 p1331 A73-26124

High power microwave tubes design trends, considering output capacity and quality, bandwidth, gain, linearity, low noise and intermodulation performance factors 11 p1339 A73-26691

Performance characteristics of a TEA double-discharge grid amplifier. 12 p1505 A73-27015

The significance of the elementary radiator directivity for the determination of the directive gain of linear arrays 12 p1468 A73-27039

Design and performance of deflected-beam electron-bombarded semiconductor amplifiers. 12 p1478 A73-27113

Some features of the application of controlled-gain transistors.

12 p1480 A73-27271

A shipboard satellite communication experiment.

12 p1473 A73-27675

Pulse amplifier with active gain adjustment for constant bandwidth

13 p1590 A73-28571

High power microwave nanosecond pulse generator with waveguide standing wave resonator, noting power gain and pulse shape

13 p1583 A73-28672

Injection phase locked microwave oscillator for FM amplifier, calculating frequency drift caused gain limitation in terms of diode and circuit properties temperature effects

13 p1593 A73-29116

Radiating waveguide antenna elliptical beam off-axis gain maximization, applying to geostationary satellite

13 p1587 A73-29671

Log periodic dipole antenna design procedure, discussing gain as function of transmission line characteristic impedance, half length/dipole radius ratio and geometric parameters

14 p1734 A73-30206

Gain-bandwidth limitations of microwave transistor amplifiers.

14 p1735 A73-30247

A high-power oscillator triode with zero bias

15 p1850 A73-31259

Time-resolved gain of a volume-excited TEA CO₂ laser amplifier.

15 p1885 A73-31945

Several parallel-plate guides with screen as phased array - Effect of the coupling on the directive gain

16 p1979 A73-33374

Si transistor amplifier design for power gain stability against temperature variations, considering emitter and collector base voltage as stability parameters

16 p1988 A73-33399

Atmospheric refractivity effects on maximum antenna gain and correlation coefficient in design of microwave line of sight links for high reliability

16 p1981 A73-33704

Gain and energy measurements on an HF/DF electrically pulsed chemical laser.

17 p2183 A73-34203

A self-stabilized 3.5-micron waveguide He-Xe laser.

17 p2183 A73-34206

Effect of upper sideband impedance on a lower sideband up-converter.

17 p2123 A73-34971

Experimental gain and noise parameters of microwave GaAs FET's in the L and S bands.

17 p2136 A73-34972

Multifield high-frequency broadband constant index lens antenna with high power and variable polarization handling capabilities and low manufacturing cost advantage

17 p2137 A73-35206

Accurate measurement of antenna gain and polarization at reduced distances by an extrapolation technique.

17 p2127 A73-35676

Antenna gain calibration on a ground reflection range.

17 p2128 A73-35688

On the relative response and absolute gain toward the zenith of HF field-expedient antennas - measured with an ionospheric sounder.

17 p2129 A73-35698

Vacuum UV radiation of electron beam excited high pressure Xe laser, measuring optical gain due to diatomic state-repulsive ground state transitions

17 p1986 A73-35794

Two dimensional Mach 5 supersonic nozzle configurations with hot nitrogen expansion for mixing carbon dioxide gasdynamic laser, calculating and measuring gain distribution

[AIAA PAPER 73-622]

18 p2321 A73-36170

Experimental test of optical antenna-gain reciprocity.

19 p2439 A73-38487

Technique for gain determinations in pulsed CO₂ TEA lasers.

20 p2572 A73-38885

Lowering of average directive gain caused by cross-polarization radiation in an aperture antenna

20 p2537 A73-39456

Limitation of the axial gain of large antennas under partial coherent illumination.

21 p2660 A73-40098

Diffuse parasitics gain thresholds of laser modes for rectangular geometries, discussing radiation field and boundary conditions

21 p2710 A73-40145

Small arrays - Their analysis and their use for the design of array elements.

21 p2652 A73-40656

Laser resonator mode structure during interaction with active medium, considering combined effects of gain and refractivity variations for arbitrary mirror configurations

21 p2714 A73-40761

Sealed-off waveguide carbon dioxide laser, investigating gas mixture and pressure effects on power gain and output and optical properties effects on losses

21 p2715 A73-40763

Cw degradation at 300 K of GaAs double-heterostructure junction lasers. I - Emission spectra. II - Electronic gain.

21 p2715 A73-40964

Laser gain characterization of near-atmospheric CO₂:N₂:He glows in a planar electrode geometry.

21 p2715 A73-40965

A new method for calculating correction factors for near-field gain measurements.

22 p2830 A73-41829

High loop gain operational amplifiers voltage changes as slewing rates using nonlinear circuit model, discussing equivalent circuits, frequency characteristics and bandwidth

22 p2832 A73-41896

Comparison of theory and experiment for nanosecond-pulse amplification in high-gain CO₂ amplifier systems.

22 p2870 A73-42521

Stability circle criteria extended to signal power gain mean-square criteria for nonlinear feedback distributed parameter system defined by transfer function

22 p2837 A73-43066

Microchannel image intensifiers for detection at low light levels

23 p2979 A73-43222

Junction or Schottky gate type FET power gain and high frequency limitations from γ parameters calculation, using analog RC transmission line as equivalent network

23 p2963 A73-43452

Optimum design of electron beam-semiconductor linear low-pass amplifiers. II - Output capabilities.

23 p2958 A73-43454

A method for the study of the gain and the oscillating modes of a CO₂ laser.

23 p2989 A73-44176

Aspects of field-effect transistor applications in amplifier stages with feedback

24 p3072 A73-44936

Darlington composite transistor frequency properties concerning alpha and beta cut-off points and high frequency power gain in common-emitter configuration

24 p3073 A73-45481

Longitudinal inhomogeneity of gain in the active element of a helium-neon laser pumped by direct current

24 p3097 A73-45517

POWER GENERATORS

U ELECTRIC GENERATORS

POWER LIMITERS

Satellite frequency division multiple access communication net, examining channel monitoring and self regulating downlink power output for performance improvement

09 p1053 A73-23363

Semiconductor diodes for controlling microwave power.

12 p1480 A73-27266

Mathematical description and calculation of the static mode of operation of a microwave power regulator with a semiconductor attenuator.

15 p1849 A73-30993

POWER LINES

High voltage phase meter with electrostatic logometer for loss angle measurements in capacitors and power cables during operation

12 p1495 A73-26790

Application of multiplexing to the B-1 aircraft.

17 p2107 A73-35247

POWER PLANTS

Application of heat pipes to unmanned space power systems.

11 p1452 A73-25994

POWER SERIES

NT TAYLOR SERIES

Expansion of the force function of two homogeneous spheroids with noncoincident symmetry planes.

04 p0503 A73-16021

Power series method for accurate solution of eigenvalue problems and simultaneous equations representing static, dynamic and stability responses to structural design parameter changes

07 p0906 A73-19027

Construction of exact solutions to certain systems of linear and nonlinear Volterra integral equations by using a power series

07 p0844 A73-19129

Sundman power series convergence enhancement in three body problem by Poincare transformation

07 p0852 A73-20042

Conformal mapping of two airfoil profiles symmetric with respect to real axis onto circles, using rational function power series

07 p0812 A73-20200

Studies in the application of recurrence relations to special perturbation methods.

09 p1149 A73-22914

Application of series to an investigation of a plane electromagnetic wave in a ferromagnetic half-space

12 p1474 A73-27804

Power series solution of quasi-linear parabolic heat conduction equation for temperature wave propagation in soil

12 p1560 A73-27807

Application of the method of power series to derive solutions for one-dimensional problems of thermophysically nonhomogeneous media

12 p1560 A73-27808

Unsteady temperature condition of a conductor with a nonlinear source of heat

13 p1705 A73-28466

Vertical free vibrations of rectangular vessel partially filled with perfect incompressible liquid analyzed by power series

15 p1860 A73-31045

Method for calculating the steady irrotational isentropic flow in a two-dimensional supercritical turbine cascade.

17 p2093 A73-34390

An application of truncated power series controllers for optimization of dynamic systems.

19 p2413 A73-38040

On Blasius's equation governing flow in the boundary layer on a flat plate.

19 p2421 A73-38101

Study of methods of computing transition matrices /Computer-program description/.

20 p2532 A73-39129

Asymptotic expansion of random processes depending on a small parameter

20 p2582 A73-39387

Chapman-Enskog-Hilbert expansion for a Markovian model of the Boltzmann equation.

20 p2549 A73-39627

POWER SPECTRA

Operator remnant power spectral density measurement during compensatory tracking task by serial segments method, noting Fourier coefficient processing

01 p0011 A73-10324

Pi 2 type geomagnetic pulsation spectra from simultaneous meridional measurements at equatorial, middle and auroral latitudes, noting secondary amplitude maximum and HF augmentation

01 p0039 A73-10414

Numerical analysis of spontaneous electric activity of the brain - Study of the statistical properties of the power density spectra

02 p0138 A73-12160

Further studies of the aeroacoustics of jets perturbed by screens.

02 p0154 A73-12200

Digital simulation of random processes and its applications.

02 p0144 A73-12607

Some results on zero crossing distribution of non-stationary random noise.

02 p0143 A73-12857

Inlet sound power of axial compressors.

03 p0241 A73-12956

Correlation analysis as applied to the observation of fluctuations of laser light diffracted on an ultrasonic wave in an inhomogeneous medium.

03 p0318 A73-12994

Atmospheric wave perturbations of total electron content.

03 p0299 A73-13633

Power spectrum due to point source convection at uniform subsonic speed along round jet flow axis

03 p0246 A73-13841

Application of the spatial spectral power density to the calculation of resolution limits.

03 p0277 A73-13916

Acoustic power spectrum of a subsonic jet.

03 p0295 A73-14040

Study of the influence of the volumetric mass of a jet on acoustic sound emission

03 p0359 A73-14143

Atmospheric turbulence information in signal backscattered from pulsed radar, discussing Doppler power spectrum variance determination

03 p0279 A73-14528

Observation and spectral analysis of instantaneous signals of velocity fluctuation in the laminar boundary layer

03 p0297 A73-14602

Power spectral density estimation by spline smoothing in the frequency domain.

04 p0471 A73-15254

A possible new interpretation of power spectra of solar-granulation brightness fluctuations.

04 p0499 A73-15367

Cosmic-ray scintillations. I - Inside the magnetosphere.

04 p0492 A73-15526

Line existence in H component magnetic power spectra of geomagnetic field LF components

04 p0445 A73-15552

Correlation analysis of the continuum radio emission of noise storms.

04 p0504 A73-16028

Incoherent radiation from relativistic electrons with power energetic spectrum.

05 p0611 A73-17313

Deformation of the power spectrum of a random function during frequency translation
06 p0664 A73-17807

Coherent and non-coherent optical processing of analog signals.
06 p0667 A73-18313

On the variance spectra and spatial coherences of equatorial winds.
07 p0846 A73-19038

Time spectra and cross-spectra of kinetic energy in the planetary boundary layer.
07 p0847 A73-19044

Turbulent transport measurements with a laser Doppler velocimeter.
07 p0826 A73-20462

The effect of a nonlinearity upon signals in the presence of noise.
07 p0795 A73-20499

Clusters of galaxies and the cosmic light.
08 p1002 A73-20876

Power reduction and fluctuations caused by narrow laser beam motion in the far field.
08 p0975 A73-21059

Linear FM pulses in chirp radar transmitter, calculating and plotting bounds on amplitude, energy and power spectra for electromagnetic compatibility analysis
08 p0949 A73-21665

On the use of running means in the power spectrum analysis of ionospheric data.
09 p1078 A73-22831

Solar oscillatory phenomenon at 9.6 mm with atmospheric absorption effects minimized, discussing power spectra
09 p1149 A73-22962

Conversion of the wave spectrum in a medium with smooth spatial-temporal fluctuations
09 p1052 A73-23082

Bandwidth as measure of dimensions added to signal space per unit time in digital transmission power spectral density computation, presenting comparison for telemetry signals
09 p1054 A73-23384

Direct measurements of solar-wind fluctuations between 0.0048 and 13.3 Hz.
10 p1264 A73-23539

Experimental properties of injection lasers - Modal distribution of laser power.
10 p1228 A73-24530

Bistatic-radar estimation of surface-slope probability distributions with applications to the moon.
10 p1190 A73-24892

Spectra of short-term fluctuations of line-of-sight signals - Electromagnetic and acoustic.
10 p1190 A73-24893

Estimate of the spectral density of a stationary random process by an indirect method
11 p1341 A73-25017

Radome insertion phase delay errors due to element impedance, frequency uncertainty, power instability and heat effects
11 p1327 A73-25278

Huygens principle, power spectrum and photon and photographic noise intensities effects in holography, discussing optical information transmission by eigen-solutions
11 p1369 A73-26529

Interplanetary scintillations observations from solar wind plasma density fluctuations power spectrum
12 p1533 A73-26980

Steady ELF plasmaspheric hiss, studying whistler mode turbulence, band limitation, power spectra and peak intensities
12 p1488 A73-26984

Solar surface photospheric oscillation spatiotemporal power spectrum observation, considering long-period oscillation correlation with chromospheric flare
12 p1544 A73-27828

Temporal intensity fluctuation measurements in K line wing near solar disk center, noting power spectrum peaks and brightness relationship to Fe I line displacement
12 p1544 A73-27830

Power spectral analysis of Chandler wobble latitude variations over 70 year period, showing doubtfulness of two-peak resonance pattern in wobble
13 p1678 A73-28381

Effect of randomly fluctuating pressure gradients, with arbitrarily specified power spectrum and probability density, on flow in channels.
13 p1604 A73-29263

Calculation of phase difference power spectrum for slant-path propagation.
13 p1661 A73-29327

Angle-of-arrival difference spectrum of a simple interferometer in turbulent air.
13 p1621 A73-29330

Electron density phase velocity, drift rate and ion temperatures from radar echoes power spectrum near equatorial electrojet
14 p1748 A73-29972

Theory of the nonlinear power resonances in gas lasers
14 p1758 A73-30803

Universality of the power spectra of relativistic electrons generated in a turbulent plasma
14 p1782 A73-30808

Quasi-classical calculation of the power output of a cyclotron resonance maser
14 p1758 A73-30944

Software design and implementation for real time power spectral analysis on IBM-1130 8K-core computer, discussing coherence and cross spectra estimation and arithmetic errors
15 p1848 A73-32032

High pass filter and power spectral analysis of periodicity in solar activity time series, applying statistical tests to sunspot and flare indices
16 p2060 A73-32955

Angle-of-arrival difference spectrum of a simple interferometer in turbulent air.
16 p2037 A73-33683

Comparing bandwidth requirements for binary baseband signals.
16 p1984 A73-33745

A search for periodic variations in geomagnetic activity and their solar cycle dependence.
17 p2157 A73-34073

Fine structure in the sunspot spectrum - 2 to 70 years.
17 p2230 A73-34514

Time-domain analysis of intermodulation effects caused by nonlinear amplifiers.
17 p2136 A73-34868

Decomposition of pulse-type data by cepstrum techniques.
17 p2127 A73-35635

ULF geomagnetic power near $L = 4$. I - Quiet day power spectra at conjugate points during December solstice.
18 p2352 A73-36278

Short term gyro drift measurements.
19 p2430 A73-38081

Nonlinear transformation by a travelling wave tube and power spectral density of a PSK-signal.
20 p2522 A73-38718

ULF geomagnetic power near $L = 4$. II - Temporal variation of the radial diffusion coefficient for relativistic electrons.
20 p2551 A73-38936

Power spectrum of small-scale irregularities in the solar wind.
21 p2755 A73-40163

Research of short-period variations in cosmic rays at Moscow's latitude
21 p2759 A73-40610

Study of excitation transfer in dye mixtures by measurements of gain spectra.
21 p2716 A73-40968

Noise in solid travelling-wave tubes using coupled-mode analysis.
21 p2665 A73-41122

Relative sunspot number periodicities determination, using power spectral analysis
21 p2777 A73-41489

Signal and noise in the human oculomotor system.
22 p2810 A73-42964

Bispectrum synthesizer by using multiple Poisson processes.
23 p2965 A73-44089

Studies on a band limited white noise with a uniform bispectrum.
23 p2965 A73-44135

Noise generation by turbulent combustion, discussing sound power, spectral content, enclosure effect, and importance in turbopropulsion system core engine noise
24 p3155 A73-44855

Calculation of the spectrum of a sinusoidal signal modulated by phase displacement with one, two, or three states for any values of phase jumps
24 p3068 A73-44972

A mathematical model of real signal spectra
24 p3068 A73-45005

Correlation length for interplanetary magnetic field fluctuations.
24 p3139 A73-45125

Power spectra of solar wind parameters at 20 solar radii derived from Mariner 5 data.
24 p3126 A73-45133

POWER SUPPLIES

Hydraulic system on de Havilland Twin Otter STOL aircraft for flaps, wheel brakes and nose wheel steering, noting power supply mounting
03 p0252 A73-13350

Logic network design for digital waveform shaping of polyphase voltage generator, noting application for airborne and marine gyroscope power supply
03 p0258 A73-14618

Self regulated transistorized voltage and frequency converters for multiple motor drives power supply, discussing circuit design, performance characteristics and overload protection
05 p0556 A73-16074

Aircraft power supply alternators with superconductive field windings, calculating specific weights and performance characteristics
07 p0779 A73-20408

A system for the evaluation of solar cell samples.
09 p1033 A73-22438

Development of a plutonium-fueled miniature power supply based on thermionic conversion.
11 p1396 A73-26028

Power Sources Symposium, 25th, Atlantic City, N.J., May 23-25, 1972, Proceedings.
13 p1572 A73-29581

Megawatt fuel cells for aerospace applications.
13 p1573 A73-29597

Methods of calculating high-power rectifier and inverter circuits
15 p1832 A73-31696

POWER SUPPLY CIRCUITS

Reignition characteristics of low current a.c. TIG welding arcs.
01 p0055 A73-10115

Russian book on electrical power supply devices for radio systems covering design of rectifiers, transformers, current limiters, voltage regulators, filters, converters and inverters
02 p1033 A73-12863

Thermal design and tests of transcendent solid state power thyristor, rectifier and transistor devices, using heat pipe-silicon wafer construction
03 p0283 A73-13940

Advanced aerospace power distribution and control techniques.
04 p0408 A73-15389

A switching circuit for a low voltage, medium current dc power supply.
06 p0649 A73-18847

Battery charge regulator for Eole meteorological balloons power supply, describing printed circuit design and construction
07 p0778 A73-18970

High-frequency converter for power supply applications. [IEEE PAPER 17,3]
07 p0779 A73-19363

Calculation of series and shunt resistances on the basis of the current-voltage characteristics of a solar cell
09 p1033 A73-22720

Intelsat 3 power system design and orbital performance, discussing solar arrays, cell bypass, output, conversion efficiency, regulation, reliability and testing
09 p1153 A73-22787

A time-optimal response inverter.
11 p1308 A73-25981

An electrochemical cell equivalent circuit for storage battery/power system calculations by digital computer.
11 p1309 A73-25985

Nitrogen laser with a transverse discharge
12 p1506 A73-27215

Analysis of primary currents and voltages in single-modulation frequency converters
13 p1593 A73-28942

Special features of the suppression of low-frequency modulation in a direct-coupled frequency converter
13 p1593 A73-28943

The influence of Auger recombination on the forward characteristic of semiconductor power rectifiers at high current densities.
15 p1850 A73-31130

Electronically-regulated power supplies for microwave backward-wave oscillators.
17 p2142 A73-35643

Electron beam current fluctuation reduction by placing hot filament into Wheatstone bridge arm for temperature regulation in power supply for electron gun
17 p2176 A73-35776

Hybrid biological power cells for cardiac pacemakers - Materials evaluation.
20 p2520 A73-39823

Electrical design requirements for electrolytic capacitors used in regulated low voltage DC power supplies.
21 p2663 A73-40772

Power Electronics Specialists Conference, California Institute of Technology, Pasadena, Calif., June 11-13, 1973, Record.
22 p2801 A73-42901

A failure tolerant power subsystem for outer planet spacecraft.
22 p2801 A73-42902

Power subsystem for Skylab radiometer/scatterometer/altimeter experiment.
22 p2801 A73-42903

Flight performance of the ERTS-1 spacecraft power system.
22 p2801 A73-42904

Decentralized power processing for large-scale systems.
22 p2801 A73-42905

High voltage waveform generation at low power levels by circuit techniques and system configurations involving parallel series chains of light triggered bilateral switches
22 p2834 A73-42907

Four terminal, optically isolated, zero crossing arc relay.
22 p2834 A73-42913

- Sequence amplitude modulated inverters.
22 p2802 A73-42917
- The application of standardized control and interface circuits to three dc to dc power converters.
22 p2802 A73-42918
- POWER TRANSMISSION**
- Irreversible thermodynamics and losses in energy conversion, discussing N-port storage representation, flux rate, power flow and electro-caloric and state space relations
07 p0779 A73-20396
- Satellite solar power station for solar energy conversion into electricity and transmission to ground receiving stations via microwave beams
09 p1035 A73-22791
- Satellite electric power station for conversion of solar energy to microwaves beamed to earth, discussing structural design, flight control, transportation and technology assessment
10 p1178 A73-24554
- Investigations of the Intelsat IV bearing and power transfer assembly.
17 p2238 A73-34867
- Grease lubrication of helicopter transmissions.
[ASLE PREPRINT 73AM-2A-1]
17 p2178 A73-34980
- Helicopter power transfer systems analysis in terms of weight reduction and reliability improvement
[AHS PREPRINT 773]
17 p2106 A73-35091
- Effect of aerosols on the transfer of solar energy through realistic model atmospheres. I - Non-absorbing aerosols.
18 p2333 A73-36704
- The Satellite Nuclear Power Station - An option for future power generation.
19 p2455 A73-38412
- Helicopter transmission research.
22 p2798 A73-41750
- Random vibration of distributed systems strongly coupled at discrete points.
22 p2918 A73-41820
- Prediction and measurement of the proportionality constant in statistical energy analysis of structures.
22 p2918 A73-41821
- POYNTING THEOREM**
- Zone of Poynting vector rotation toward the direction of an applied magnetic field for a wave incident on an inhomogeneous plasma
15 p1919 A73-31707
- Eddy power flow of electromagnetic waves.
16 p1980 A73-33690
- Alfvén waves in the solar wind - Wave pressure, Poynting flux, and angular momentum.
18 p2346 A73-36264
- Green function and Poynting vector calculation of solid angles of radiation outside and inside anisotropic crystal in laser light scattering experiments
20 p2591 A73-38617
- The upward propagation of LF waves /electron whistlers/ into the ionosphere and the turning of the Poynting vector towards the earth's magnetic field.
21 p2654 A73-40782
- Second order cross stress study of elastic shear deformation, considering rotation invariant Cauchy tensor and Poynting effect
23 p3039 A73-43306
- POYNTING-ROBERTSON EFFECT**
- Meteoritic particles orbits secular evolution under planetary perturbation and Poynting-Robertson effects, considering osculating orbital elements long term variations via simplified model
14 p1795 A73-29842
- Influence of nongravitational effects on the evolution of dust particles moving along elliptic orbits around the sun
23 p3036 A73-44251
- PPI (POSITION INDICATORS)**
- U PLAN POSITION INDICATORS
- PPM (MODULATION)**
- U PULSE POSITION MODULATION
- PRAESEPE STAR CLUSTERS**
- Solar neutrino deficiency related to solar core periodic expansion, considering Martian river-like channel formation and Praesepe cluster distribution through main sequence
17 p2229 A73-34434
- PRANDTL NUMBER**
- Infinite Prandtl number fluids with constraint characterized by Taylor number heated from below, choosing boundary conditions for laminar convection
03 p0293 A73-13329
- A model for eddy conductivity and turbulent Prandtl number.
[ASME PAPER 72-WA/HT-13]
04 p0434 A73-15834
- Natural convection in annular horizontal space
08 p1024 A73-21498
- Euler, Lagrange and time turbulence scales for Prandtl mixing length, relating with velocity and pressure pulsations in steady turbulent gas flow
10 p1204 A73-23474
- Temperature recovery coefficients during turbulent flow of liquid in a circular pipe
10 p1204 A73-23509
- Temperature restitution coefficients for turbulent fluid flow in a circular pipe.
17 p2155 A73-35189

- Calculation of turbulent boundary layers over flat plates with different phenomenological theories of turbulence and variable turbulent Prandtl number.
18 p2301 A73-36699
- Second-approximation boundary layer equations in Prandtl-Mises variables
20 p2549 A73-39610
- Euler, Lagrange and time turbulence scales for Prandtl mixing length, relating with velocity and pressure pulsations in steady turbulent gas flow
21 p2678 A73-41321
- Nonisothermal surface cooling for arbitrary temperature distribution and Prandtl number approaching zero, solving thermal boundary layer equations by series expansion
21 p2792 A73-41323
- Approximate calculation of the optimal section of a compressible gas on a thermally insulated surface at Prandtl numbers other than unity
22 p2795 A73-42118
- Unsteady stagnation point heat transfer due to unsteady free stream temperature.
22 p2931 A73-42290
- Experimental determination of the turbulent Prandtl number near a smooth wall
22 p2937 A73-42952
- Forced convective heat transfer from isothermal sphere in steady incompressible flow at low Reynolds and various Prandtl numbers, obtaining mean Nusselt number
23 p3049 A73-43934
- The linear spin-up of a strongly stratified fluid of small Prandtl number.
24 p3079 A73-45312
- PRANDTL-MEYER EXPANSION**
- NT THERMAL BUCKLING**
- Applications of shock expansion theory to the flow over non-conical delta wings.
06 p0645 A73-18512
- PREAMPLIFIERS**
- A programmable four channel system for long-time radio telemetry of biomedical parameters.
03 p0270 A73-14280
- Low noise VHF preamplifier design for backscatter radar, presenting circuit diagram
07 p0801 A73-19536
- VHF preamplifier with FET for resolving crosstalk and overload problems comparing designed and observed specifications
09 p1066 A73-23429
- Parameters and energy resolution of the KP303 field effect transistors at low temperatures
17 p2133 A73-34162
- Optical communication channel optimization with binary signals preamplified in optical parametric amplifier, noting amplifier gain and SNR
17 p2123 A73-35155
- Cryogenic preamplifier with cooled GaAs junction FET in input stage, discussing application to sensor systems using high impedance cryogenically cooled optical detectors
17 p2137 A73-35219
- A universal preamplifier for bioelectric signals
21 p2643 A73-40345
- PRECAMBRIAN PERIOD**
- Organic inclusions within hydrothermal minerals from S.W. Africa and elsewhere.
11 p1352 A73-25472
- Late Precambrian microfossils - A new stromatolitic biota from Boorthanna, South Australia.
14 p1713 A73-29723
- Possible stratotype sequences for the basal Paleozoic in North America.
15 p1865 A73-31025
- PRECAUTIONS**
- U ACCIDENT PREVENTION
- PRECESSION**
- NT LARMOR PRECESSION**
- NT PROTON PRECESSION**
- Stellar proper motion effects on precession and galactic rotation constants determination, considering star velocity fields in solar neighborhood
01 p0098 A73-10583
- A theory of perturbations in angle-action variables: Application to the motion of a solid about a fixed point - Precession-nutation
01 p0107 A73-11362
- Regular gyrostator precession in a central Newtonian field of forces
02 p0192 A73-11771
- Existence conditions of precessional motions of gyroscope with fixed point, assuming constant time function and unit vector coincident with gravity force direction
02 p0192 A73-11772
- Precession equations of a triaxial power-driven gyrostabilizer
02 p0167 A73-11775
- The effects of viscous friction on the precession and nutation of celestial bodies.
02 p0217 A73-12396
- Earth polar motion from revised station coordinates and data from additional Doppler satellite tracking stations
04 p0439 A73-14800

- Stability of the motion of a nonautonomous gyrostator
04 p0475 A73-14932
- Equations of motion for precession theory of two rotor gyroscopes on earth satellites for orbit plane determination, noting noise spectrum transformation
05 p0628 A73-16407
- Theory of diurnal fluctuations of the earth's magnetic tail
05 p0620 A73-17011
- Anisotropic flexible bearings mounted rotors backward and forward precessional motion excitation, noting internal viscous damping forces effect on vibration amplitude
06 p0758 A73-17515
- On a relation between the variations of the rotational velocity of the earth and the anomalous behavior of the polar wobble around 1930.
07 p0877 A73-19603
- Computerized precession and nutation matrix calculations of rectangular equatorial coordinates with longitude and inclination allowance for radar data processing
09 p1142 A73-22092
- Ponderous nutational motion of gyroscope in gimbal suspension, calculating precession rate from reduced equations of motion
09 p1081 A73-22351
- Precession motion stability and drift rates of gimbal gyroscope under angular and translational resonant base vibration
09 p1087 A73-23343
- Investigation of the influence of precession, nutation, and yearly aberration on the average equatorial coordinates, azimuth, and elevation of the North Star
10 p1281 A73-24476
- Stability of the regular precession of a symmetrical solid with an ellipsoidal cavity
11 p1401 A73-26469
- Artificial satellites to test general relativity theory
11 p1431 A73-26590
- Nutation dampers vs precession dampers for asymmetric spinning spacecraft.
11 p1432 A73-26670
- Rotation of the earth; Proceedings of the Symposium, Morioka, Japan, May 9-15, 1971.
13 p1677 A73-28376
- Chandler polar motion due to elastic earth free nutation using models based on historical data
13 p1678 A73-28380
- Power spectral analysis of Chandler wobble latitude variations over 70 year period, showing doubtfulness of two-peak resonance pattern in wobble
13 p1678 A73-28381
- Analysis of the Chandler period of polar coordinates calculated by the Orlov method.
13 p1678 A73-28383
- Vortex core precession in water or air high swirl flows above critical Reynolds number
13 p1602 A73-29017
- Effects of motion of the equatorial plane on the orbital elements of an earth satellite.
15 p1930 A73-31112
- Forward precession motion of the moon caused by attraction to the earth and the sun
15 p1939 A73-31966
- Strapdown electrostatic gyroscope spin axis precession drift rate calibration, using virtual work technique for modeling bearing torques on rotor
17 p2137 A73-35210
- Precession rate matching for a space station in orbit about an oblate planet.
18 p2351 A73-36153
- The precession of unsymmetric spin-stabilized satellites.
18 p2361 A73-36878
- Precision pointing control thruster design for satellite experiment to test relativistic precession of gyroscope moving through gravitational field, determining gyro orientation via superconducting circuitry [AIAA PAPER 73-858]
20 p2586 A73-38796
- Some linear problems in the theory of gyroscopes
20 p2565 A73-38983
- Core coupling to mantle precession, discussing model with quantitative consideration of inertial and dissipative coupling torque superposition
21 p2764 A73-39929
- Precession damping of solar probes by radiative forces.
21 p2737 A73-40767
- The precession of unsymmetric spin-stabilized satellites.
22 p2916 A73-42190
- Moments acting on a spherical rotor with magnetically suspended bearings
22 p2860 A73-42360
- Mars precession scheme for prolonged equinoctial habitable spring in terms of Sagan model extension
24 p3131 A73-44464
- Translational-precessional motion of the moon in the gravitational field of the earth and sun.
24 p3132 A73-44491

PRECIOUS METALS

U NOBLE METALS

PRECIPITATION

Mathematical models for yield point dependence on statistical arrangements of ordered precipitated phases, noting crystal dislocations interaction effect
06 p0735 A73-18044

PRECIPITATION [CHEMISTRY]

Inter-crystalline structures effect on precipitation reactions in supersaturated solid solutions, noting Widmanstatten structure growth in U alloy
04 p0467 A73-15953

Ir catalysts for high performance hydrazine decomposition, discussing preparation by coprecipitation of active metallic element with support in chloroiridic acid solution
07 p0865 A73-18928

Struvite precipitation from evaporating sea water with added ammonia, considering importance for pre-biotic phosphorylation
07 p0787 A73-19168

The effect of carbon and oxygen on the brittleness characteristics of molybdenum
08 p0978 A73-21417

Intergranular precipitation in the oriented bicrystals of aluminum-copper
09 p1105 A73-23039

Precipitation processes in Nb microalloyed converter steel
12 p1514 A73-27685

Study of precipitates formed by internal oxidation in cobalt-nickel-chromium alloys with a cobalt base. I - Precipitates formed by oxidation in air
14 p1759 A73-29750

AC polarographic determination of sulfur in molybdenum-rhenium alloy.
17 p2118 A73-34276

On the process of precipitation in Mg-Ce alloy.
23 p2994 A73-44155

PRECIPITATION [METEOROLOGY]

NT DEW
NT HAIL
NT RAIN
NT SNOW
NT SNOW COVER

Precipitable water vapor temperature-geopotential height profiles from satellite IR spectrometer (SIRS)/measurements, using stepwise regression technique
01 p0073 A73-10380

Observations of precipitation zones from satellites using microwave radiometers.
02 p0160 A73-12267

Precipitation detection over the ocean using microwave satellite radiometry.
02 p0188 A73-12268

Two dimensional deep convection primitive model of pressure perturbation in cumulus cloud with precipitation
02 p0189 A73-12781

Terminal velocity equations for ice crystal growth forms and precipitation rates calculation in clouds, using drag coefficients, aspect ratios and densities
02 p0189 A73-12783

Particle size spectra measurement in cirrus generating cells, deriving particle concentration, crystal length, ice water content, reflectivity and precipitation rate
02 p0189 A73-12784

Multiple contrail streamers observed by radar.
03 p0279 A73-14519

Numerical simulation of precipitation development in supercooled cumuli. I, II.
05 p0594 A73-16572

Form of the spectrum of radar signals due to precipitation
05 p0552 A73-17356

Use of numerical guidance at the National Weather Service's National Meteorological Center.
06 p0720 A73-18703

Updating of numerical precipitation guidance.
06 p0720 A73-18709

Doppler radar characteristics of precipitation at vertical incidence.
10 p1190 A73-24778

Asymmetric positively skewed distributions family for precipitation data analysis, using two-sample non-parametric test
12 p1520 A73-26804

Precipitation drops initial growth and final size limits due to collision mechanism, investigating drop interactions by wind tunnel experiments
12 p1520 A73-26807

Precipitation patterns effective fall velocity determination from three dimensional radar scan data, discussing interpolation/extrapolation technique to improve coarse sampling time effects
12 p1520 A73-26808

An experimental investigation of the nature of changes in the intensity of precipitations from stratiform and cumuloform clouds
12 p1522 A73-27747

Mechanisms influencing the distribution of precipitation within baroclinic disturbances.
13 p1652 A73-28266

The orientations of ice crystal models during a fall in an electric field
13 p1654 A73-28882

Heavy precipitation from mixed phase composition cloud systems vs light precipitation from droplet and crystal containing clouds
13 p1654 A73-28887

Precipitation forecasting by numerical scheme using dew point depression as moisture parameter and gradual onset techniques
13 p1655 A73-29336

Definition and radar measurement of the parameters characterizing the cloud environment of a launch base
14 p1743 A73-30114

The shape of the spectrum of radar echoes from precipitation.
15 p1842 A73-31006

Statistical properties of precipitation patterns.
15 p1903 A73-31316

The global distribution of the maximum 24-hour totals of precipitation
15 p1906 A73-32346

Artificial inducement of drizzling rain in an uncloudy atmosphere at relatively high humidity
16 p2034 A73-33109

The respective influences of multi-path configurations and precipitation rates for frequencies lying between 10 GHz and 30 GHz.
16 p1981 A73-33710

Scheme for evaluating the influence of convective-cloud modifications aimed at controlling precipitations artificially, and the results of cumulus cloud structure investigations from aircraft
18 p2332 A73-35917

Water and processes of degradation in the Martian landscape.
19 p2477 A73-37202

Long term weather forecasting techniques, criteria and implementation, discussing statistical weather analysis, cloud types, air masses, sunspot activity, precipitation and pressure systems
20 p2584 A73-39628

Russian book on UHF meteorological radar techniques and applications covering precipitation and cloud monitoring radiolocation stations, lidar, sonar, echo signals and meteorological satellites
20 p2584 A73-39758

Effect of coagulation and spatial redistribution of cloud particles on the precipitation spectrum
21 p2730 A73-40120

The investigation of the periodicity of hydrometeorological phenomena according to the autocorrelation method of Fuhrich
22 p2883 A73-42449

PRECIPITATION HARDENING

NT MARAGING

Structural changes following annealing in a dispersion-strengthened tungsten alloy
01 p0062 A73-10261

Cold rolling of dispersion-strengthened nickel.
01 p0063 A73-10282

Structure changes during aging in aluminum 4 wt. % copper alloy studied by the channeling technique.
01 p0063 A73-10310

Effect of various methods of oxide introduction on the properties of dispersion-hardened nickel.
01 p0065 A73-10814

Thermogravimetry system designed for use in dispersion strengthening studies.
01 p0015 A73-11449

Structural studies of Laves intermetallic phase precipitation in Fe-Ta alloys by microscopic, X ray diffraction and electron probe techniques
02 p0182 A73-12754

Electron-vacancy prediction methods for sigma phase precipitation in residual matrix compositions of austenitic Niand Co-base superalloys
02 p0183 A73-12757

Two phase recrystallization temperatures and structural inhomogeneity of dispersion hardened Ni after cold working and annealing at 1300-1400 C
03 p0324 A73-13508

Disordered precipitation effect on steady state creep rate of gamma prime Ni-Al-Ti single crystals
03 p0326 A73-13963

The effect of small magnesium additions on microstructure and high-temperature properties of nickel-2-1/2 vol. % alumina.
03 p0326 A73-13966

Carbide hardening of chromium-molybdenum-vanadium steel.
03 p0327 A73-14005

Hardness-controlling additions in transition metal-beryllium alloys
03 p0328 A73-14655

A study of precipitation at elevated temperatures in a Mg-8.7 pct Y alloy.
04 p0463 A73-15318

Characterization of age-hardenable and stress-rupture properties of some cobalt-base alloys.
04 p0465 A73-15579

Characteristics of secondary phases in heat-resisting alloys.
04 p0465 A73-15580

Precipitation hardening effect on Co-Ni-Ti-Al alloys stress-strain, grain size and strain resistance behavior in micro- and macrodeformation yield point region
04 p0465 A73-15639

PRECIPITATION HARDENING

Temperature dependence of the elastic micro- and macro-stiffness of dispersion hardenable Co-Ni-Ti and Co-Ni-Ti-Al alloys. II
04 p0465 A73-15640

Influence of cold deformation and subsequent heating on the structure and properties of dispersion-strengthened nickel
04 p0466 A73-15666

Freeze drying - A unique approach to the synthesis of ultrafine powders.
04 p0455 A73-15753

Temperature effects on intragranular sigma phase precipitation in low carbon superrefractory alloys
04 p0467 A73-15956

Aging kinetics of maraging nickel and chromium steels
06 p0705 A73-17877

Plastic deformation magnitude and direction/sign/for maraging steels under heat treatment, noting optimal conditions for maximum hardening
06 p0697 A73-17878

Investigation of precipitation morphology in Cu-Ti alloys
06 p0707 A73-18037

Structure and properties of nickel-phosphorus coatings in relation to annealing temperature and time.
06 p0698 A73-18214

Substructure and dispersion hardening in aged, cold worked, and annealed Al-4 wt pct Cu alloy.
06 p0711 A73-18754

Morphology of gamma prime and gamma double prime precipitates and thermal stability of Inconel 718 type alloys.
06 p0711 A73-18755

Creep of precipitation-hardened nickel-base alloy single crystals at high temperatures.
06 p0713 A73-18768

The formation and structure of precipitates in a dilute magnesium-neodymium alloy.
07 p0838 A73-19121

A specific type of carbide phase precipitation during the aging of KHN77TiAl alloy
07 p0841 A73-20640

Stress rupture behavior of a dispersion strengthened superalloy.
08 p0978 A73-21570

[ASME PAPER 72-MAT-G] The effect of niobium carbide on the creep rupture properties of austenitic stainless steels.
08 p0981 A73-21790

The ageing and creep behaviour of a Cr-Ni-Mn austenitic steel.
08 p0981 A73-21791

The influence of some structural factors on the creep strength of wrought precipitation-hardened Ni-Cr alloys.
08 p0982 A73-21793

The influence of structure upon the notched creep strength of a nickel-base alloy.
08 p0982 A73-21795

Strengthening mechanisms in ferritic creep resistant steels.
08 p0982 A73-21797

Investigation of partially dissolved secondary-phase precipitates in a molybdenum-based alloy
09 p1098 A73-21849

Young modulus anomaly in precipitation-hardening subjected Invars
09 p1099 A73-21962

Recrystallization in Ti-15 Mo base beta titanium alloys.
09 p1103 A73-22423

Short time aging characteristics of Inconel X-750.
10 p1230 A73-23631

An electron microscopy study of precipitation in Cu-Ti sideband alloys.
10 p1234 A73-24434

The effect of environmental relative humidity upon the ultrasonic fatigue endurance of an age hardening aluminum alloy.
11 p1382 A73-25825

Alpha phase lattice constant curves and composition effects of Cr-Ni-Co-Mo steels on microstress rate reduction during age hardening
12 p1509 A73-26840

Laminar precipitation hardening in Al alloy during aging by microscopic, X ray and Widmanstatten structure analyses
12 p1510 A73-26912

Tensile behaviors of high Cr-low Ni two-phase stainless steels at room and low temperatures.
12 p1511 A73-27056

Precipitation and its hardening effect in Ni-rich NiTi.
12 p1511 A73-27057

Hardening by tempering of Fe-Ni-Mo and Fe-Ni-Co-Mo martensites
12 p1514 A73-27987

The lattice heat conductivity of aluminum alloys during age-hardening.
13 p1636 A73-29068

Recent developments in precipitation hardenable stainless steels.
13 p1637 A73-29271

PRECIPITATION PARTICLE MEASUREMENT

Dynamic and static strain aging in Al-Mg solid solution alloys. 13 p1639 A73-29458

Properties and structure of Ti-Nb-base superconducting alloys 13 p1643 A73-29644

Precipitation and dispersion hardened alloys, fiber reinforced metal matrix composites, carbon-carbon composites, and dispersed system, eutectics application in aerospace industry 14 p1759 A73-30067

Precipitation in EB welded beryllium ingot sheet. 14 p1759 A73-30146

Precipitation of iron in rapidly solidified aluminum-iron alloys 14 p1760 A73-30439

Anomalous creep behavior of crystal bar alpha-Zr during dynamic strain aging at 723-823 K as function of temperature, stress and oxygen content 14 p1760 A73-30626

Radiation-induced strengthening and embrittlement in aluminum. 14 p1761 A73-30628

A theoretical model for the elevated temperature deformation of dispersion hardened metals. 14 p1761 A73-30636

Solute aluminum strengthening and strain aging in Ti-Al alloys at 78-810 K 14 p1761 A73-30639

Activation energy measurement for static strain aging rate controlling process in ferritic chromium steel 14 p1762 A73-30642

German monograph - Investigations concerning the hot working of heterogeneous iron-molybdenum alloys with differing precipitation distribution. 14 p1762 A73-30670

Electron-microscopic investigation of the spatial distribution parameters of second-phase precipitation in aging nickel-base alloys 14 p1764 A73-30862

Powder metallurgical preparation /sintering/ of conventional maraging steel and similar alloys with Ni and/or Mo replacement by Mn and Ti, considering age hardening characteristics 14 p1765 A73-30936

Kinetics of gamma-prime phase precipitation in steel N36T2lu2 15 p1887 A73-31322

The effect of stacking-fault energy on the stress-strain curve of dispersion-hardened Ni-Co alloys. 15 p1887 A73-31351

Hard WC-Co alloys as dispersion strengthened materials 15 p1887 A73-31591

Hardening and softening of aluminum alloys under an applied load at 135 to 150 C 15 p1889 A73-31808

High strength Ti alloy cracking and brittle fracture prevention during aging by high heat rate treatment at 250-500 C 15 p1889 A73-31814

Enhanced strain aging of niobium by cyclic deformation. 15 p1890 A73-31990

Properties of HSLA steels, with and without molybdenum. 15 p1891 A73-32169

Study of multiple surface compound precipitation during passivation of D6AC-steel. 15 p1895 A73-32566

Effect of thermomechanical treatment on the stress corrosion cracking of metastable beta III titanium. 15 p1896 A73-32574

Phenomena of precipitation observed in carburized tantalum in the vapor phase 15 p1896 A73-32645

Techniques for fabrication of composite materials. 16 p2017 A73-32699

Electric contact materials technology, discussing intermetallics, ordered alloys, metal matrix composites and silver, gold and platinum based dispersion hardened alloys manufacture and properties 16 p2027 A73-32946

Diffusional creep and creep-degradation in dispersion-strengthened Ni-Cr base alloys. 16 p2025 A73-33111

Eutectic superalloys strengthened by aligned delta, Ni3Cb lamellae, gamma-prime, Ni3Al precipitates and reduced interlamellar spacing. 16 p2026 A73-33425

The precipitation behavior of a commercial aluminum-copper-lithium alloy. I - The microstructure after isothermal heat treatment 16 p2026 A73-33954

The influence of vacancies on the nucleation of incoherent germanium precipitates in aluminum-germanium alloys. III - The effect of germanium nuclei on precipitation at higher temperatures 16 p2026 A73-33959

Effects of cold plastic deformation and aging temperature on the mechanical properties of dispersively hardening Cr-Ni-Co-Mo steel 17 p2188 A73-34559

Behavior of hafnium dioxide particles in dispersively hardened nickel during isothermal annealing 17 p2188 A73-34560

Stress relaxation measurements for strain rate sensitivity of dispersion hardened thoriated Ni alloys as function of applied stress concentration 17 p2190 A73-34647

Second phase particle redistribution in dispersion-hardened alloys by directed particle diffusion via chemical potential control 18 p2325 A73-36807

The influence of primary precipitates on the tensile strength of unidirectionally solidified /Fe, Cr-/Cr, Fe/7C3 in-situ grown composites containing 30 wt % Cr. 19 p2442 A73-38088

Influence of coherency strains on precipitate shape in a Fe-Ni-Ta alloy. 20 p2577 A73-39223

Ti, Al, W and Mo concentrations effect on heat resistance of precipitation hardened Ni-based alloys 21 p2720 A73-41035

Properties and structure of superconducting Ti-Nb alloys. 21 p2720 A73-41037

Weldability and weld metal capabilities of a new precipitation-hardenable alloy. 21 p2708 A73-41255

Influence of the method of preparing a Ni + ThO2 composite and of its strengthening-oxide content on heat resistance 23 p2990 A73-43486

Precipitation and magnetic hardening in sintered WC-Co composite materials. 23 p2997 A73-43776

Recrystallization and X-ray fine structure studies of the age-hardening characteristics of the metastable titanium alloy Ti-13V-11Cr-3Al 23 p2992 A73-43913

Study of precipitates in an aged Mg-3.6 wt%Zn alloy by an X-ray method. 23 p2993 A73-44124

On the age-hardening of Fe-Pt-Mn ternary alloys. 23 p2994 A73-44139

Influence of small beryllium, titanium, and zirconium additions on the structure and properties of Al9 alloy 24 p3098 A73-44571

Hardening and softening of aluminum alloys under load at 135-150 C. 24 p3100 A73-45271

High strength Ti alloy cracking and brittle fracture prevention during aging by high heat rate treatment at 250-500 C 24 p3100 A73-45277

Dynamic strain ageing in creep of beta-NiAl. 24 p3100 A73-45331

The precipitation of titanium in copper and copper-nickel base alloys. 24 p3100 A73-45473

Influence of boron on the precipitation of carbides in Fe-Ni-Cr austenitic matrices 24 p3101 A73-45523

Recrystallization and precipitation induced by high temperature deformation - Case of a weldable construction steel containing niobium 24 p3101 A73-45524

PRECIPITATION PARTICLE MEASUREMENT Results of precipitation backscatter measurements at 1.8 cm with a polarization diversity radar. 03 p0338 A73-14509

Simultaneous quantitative measurements of rainfall rate and drop size distribution by X-band radar and drop distrometer /system Joss-Waldvogel/ at two rain gauge equipped places near to Bonn/West Germany. 03 p0338 A73-14520

Satellite data and estimates of precipitation for hydrologic applications. 04 p0473 A73-15774

Form of the spectrum of radar signals due to precipitation 05 p0552 A73-17356

Doppler radar characteristics of precipitation at vertical incidence. 10 p1190 A73-24778

Precipitation drops initial growth and final size limits due to collision mechanism, investigating drop interactions by wind tunnel experiments 12 p1520 A73-26807

The shape of the spectrum of radar echoes from precipitation. 15 p1842 A73-31006

Russian book - Scattering and attenuation of electromagnetic radiation by atmospheric particles. 15 p1843 A73-31586

Doppler radar measurements and observations of precipitation velocity fields. 17 p2125 A73-35361

Integral moisture content determination in rain clouds by simultaneous thermal radiation and radar measurements 20 p2584 A73-39190

Rainfall estimation from satellite visible and IR imagery, discussing calibration and accuracy requirements 21 p2730 A73-40093

Photographic investigation of hailstone form, size and structure, determining layer growth from air bubble shape and spectrum 21 p2730 A73-40116

Cumulus-scale vertical transport of mass, heat and momentum calculated from radar and rain gauge precipitation measurement 23 p3002 A73-43596

PRECISION

Machining precision in deep-hole boring by a feed-division technique 02 p0174 A73-12578

Efficiency estimates of methods for analyzing the precision of nonlinear control systems 11 p1342 A73-26094

PREDICTION ANALYSIS TECHNIQUES

In situ prediction techniques for solar wind velocity at earth based on probability theory, statistical correlation coefficients and autocorrelation analysis 04 p0491 A73-14836

Quantitative short-term prediction of proton and nonproton flares. 04 p0491 A73-14844

Aircraft flight plan data processing in FORTRAN program to predict altitude and time conflicts, noting short CPU time 05 p0595 A73-16618

Random forcing effects on numerical weather predictability, assessing atmospheric variables computational space truncation impact 06 p0720 A73-18701

Air traffic volume prediction by 1985, determining passenger growth factors for terminal pairs 07 p0923 A73-19348

Optimal estimation of operator-valued stochastic processes and applications to distributed parameter systems. 07 p0805 A73-20580

Techniques for short-term predictions of atmospheric noise levels. 08 p0940 A73-21662

Comparison of grids and difference approximations for numerical weather prediction over a sphere. 12 p1519 A73-26803

A self starting predictor corrector algorithm of arbitrary order having exact stability. 12 p1517 A73-27170

Toward the development of a criterion for fleet effectiveness in the F-4 fighter community. 13 p1579 A73-28512

Some aspects of nonorthogonal data analysis. I. Developing prediction equations. 13 p1650 A73-29298

Predicting coronary heart disease. 14 p1716 A73-30351

Attempted prediction of the superconducting transition temperature for some metallic compounds with the aid of a computer 15 p1922 A73-31177

On the existence of extended range predictability. 15 p1903 A73-31320

German book - Long-term weather forecaster: Fundamentals of a new experiment with monthly predictions. 15 p1903 A73-31473

Prediction and measurement of aircraft noise. 16 p2014 A73-33133

Book - A handbook series on electromagnetic interference and compatibility. 17 p2121 A73-34462

Automated prediction of light aircraft performance and riding and handling qualities. [SAE PAPER 730305] 17 p2101 A73-34666

Performance of low-aspect-ratio diffusers with fully developed turbulent inlet flows. II - Development and application of a performance prediction method. [ASME PAPER 73-FE-13] 17 p2152 A73-35010

A probabilistic approach to the design of heat pipes. [AIAA PAPER 73-754] 18 p2370 A73-36370

Leidenfrost temperature - Its correlation for liquid metals, cryogenics, hydrocarbons, and water. [ASME PAPER 73-HT-F] 19 p2504 A73-37641

Fixed base simulation of variable stability T-33 handling qualities, considering pilot performance in pitch tracking during atmospheric turbulence 19 p2386 A73-38072

Dynamics and stability of the algorithm of a digital adaptive system using a prediction technique 20 p2532 A73-38688

Signal filtering using hard-limited digital processing. II - Performance with a single target in a coloured-noise background. 20 p2530 A73-39126

Evaluation of various analytical models for buckling and vibration of stiffened shells. 21 p2784 A73-40424

Solar flare prediction objective baseline calculation, applying regression analysis to sunspot, magnetic field, calcium plage and radio brightness temperature data 21 p2762 A73-41392

- A model of the human in a cognitive prediction task. 22 p2814 A73-42223
- The numerical prediction of streamer growth in MHD ducts. 22 p2894 A73-42558
- Estimation of general aviation air traffic. [ASCE PREPRINT 2041] 22 p2839 A73-42866
- Theoretical studies of sound emission from aircraft ducts. [AIAA PAPER 73-1012] 24 p3078 A73-44844
- Numerical weather prediction and analysis in isentropic coordinates. 24 p3108 A73-45091

PREDICTIONS

- NT IMPACT PREDICTION
- NT LINEAR PREDICTION
- NT PERFORMANCE PREDICTION

PREFIRING TESTS

- Nondestructive and impulsive testing of electroexplosive devices. 05 p0606 A73-17207

PREFLIGHT ANALYSIS

- Three point check method of solar panel characteristics for satellite. 01 p0006 A73-11162
- Computer and interactive graphics as applied to mission analysis. [AIAA PAPER 73-112] 05 p0554 A73-16870
- Closed loop preflight qualification testing of a reentry vehicle roll rate control system. [AIAA PAPER 73-878] 20 p2587 A73-38815

PREFLIGHT OPERATIONS

- NT COUNTDOWN
- The pre-flight handling of inertial navigation systems. 07 p0849 A73-19347

PREFORMS

- Fundamental principles of powder preform forging. 01 p0056 A73-10278
- Processing and properties of powder forgings. 01 p0056 A73-10279
- Hot deformation of metal ceramic titanium preforms 10 p1225 A73-24321
- Investigation of the dross molding process for titanium carbide 23 p2991 A73-43490

PREGNANCY

- Aircraft cabin altitude hypoxia effects on mother, embryo and fetus during first trimester of pregnancy in air hostesses and women passengers 14 p1718 A73-30519

PREHEATERS

- U HEATING EQUIPMENT

PREHEATING

- U HEATING

PREIMPREGNATION

- Effect of prepregging solvent on high-temperature stability of KERIMID 601 composites. 16 p2029 A73-33049
- High strength low density Hyfil carbon fiber prepreg sheet properties and production for aircraft applications 16 p2021 A73-33986
- The processability of unidirectional prepregs in aerospace applications. 17 p2195 A73-34808
- Development and problems of testing prepregs for the purposes of the Czechoslovakian aircraft industry 18 p2327 A73-36469
- Low-pressure prepregs as structural material for light-construction designs 24 p3104 A73-44887

PRELAUNCH TESTS

- NT STATIC FIRING
- Computerized ground support acceptance checkout systems for space shuttle program, discussing capabilities, future goal and unified test equipment 04 p0432 A73-15458
- Solar cell dark I-V characteristics and their applications. 11 p1310 A73-26003
- Problems related to the development and firing of launchers 14 p1742 A73-30102

PRELOADING

- U PRESTRESSING

PREMIXED FLAMES

- Turbulent flame velocities in premixed sprays. I - Experimental study. 01 p0121 A73-10635
- Turbulent flame velocities in premixed sprays. II - Theoretical analysis. 01 p0121 A73-10636
- The production of nitric oxide in ammonia oxidation flames. 01 p0121 A73-10640
- Asymptotic analysis of premixed burning with large activation energy. 03 p0397 A73-13531
- Kinetics of the sulphur dioxide catalyzed recombination of radicals in hydrogen flames. 03 p0352 A73-14393
- Fuel-rich and stoichiometric carbon monoxide-nitrous oxide premixed laminar flames with varying

- water contents, determining flame temperature by line reversal method 03 p0399 A73-14396

- Flame propagation in premixed propane /air or propane/ oxygen vortex rings, describing normal and schlieren photographic techniques 03 p0399 A73-14399

- Combustion effectiveness in high speed swirling flow tested in chamber with premixed air-kerosene mixture injected tangentially in annular channel [ONERA, TP NO. 1076] 04 p0517 A73-15098

- The stability of lifted turbulent diffusion and premixed flames. [WSCI PAPER 72-39] 05 p0638 A73-16678

- Flame structure and flame reaction kinetics. VIII - Structure, properties and mechanism of a rich hydrogen + nitrogen + oxygen flame at low pressure. 07 p0918 A73-19154

- Nitric oxide formation and radical overshoot in premixed hydrogen flames. 10 p1294 A73-23558

- KCl ionization and diffusion in premixed flames with uniform temperature and composition, studying gas velocity and photometry 13 p1707 A73-28995

- Flame quenching, extinction, propagation, convection and ignition limits in premixed gas mixtures 13 p1707 A73-29003

- Mechanism of decay of ammonia in flame gases from an NH3/O2 flame. 16 p1976 A73-33345

- Nitric oxide emissions from tube combustor burning premixed gaseous propane-air mixture, considering inlet conditions for equivalence ratios 17 p2222 A73-35468

- Experimental investigation of premixed swirling jet flames - Combustion characteristics. 19 p2504 A73-37946

- Ambipolar diffusion generator based on self generated electric fields in premixed ionized methane-air flame, comparing with opposite electroelectric effects 22 p2895 A73-42773

- Kinetics of nitric oxide formation in premixed laminar flames. 22 p2820 A73-42792

- Formation of nitric oxide in fuel-lean and fuel-rich flames. 22 p2820 A73-42794

- Electrical control of particulate pollutants from flames. 22 p2935 A73-42799

PREPARATION

- NT PRESTRESSING

- NT PRETREATMENT

PREPOLYMERS

- NT DIMERS
- Synthetic foam from Pyrrone prepolymer and hollow carbon microsphere mixtures, discussing low curing shrinkage and high thermal stability 16 p2029 A73-33051

PRESBYOPIA

- The problem of early presbyopia in aircrew. 18 p2285 A73-36923
- Visual problems among senior flight personnel. 18 p2285 A73-36924

PRESELECTORS

- U PREAMPLIFIERS

PRESINTERING

- U SINTERING

PRESESSES

- NT RAMS [PRESSES]

PRESSING

- Observations on the deformation properties of sandwich materials. 06 p0761 A73-17819

PRESSING [FORMING]

- NT STAMPING
- Mechanical properties of pressed and sintered titanium powder. 03 p0322 A73-13264

- The nature of slated cleavage planes in pressed VAD 23 alloy 12 p1511 A73-26915

- Strain ratio data for commercial Al alloys in various temper conditions as drawability criterion for sheet press performance, discussing single tensile test method 14 p1762 A73-30643

- Mechanical treatment of tungsten powder compacts 15 p1892 A73-32246

- Process anisotropy of randomly reinforced fiberglass plastics 24 p3102 A73-44515

PRESSURE

- NT ATMOSPHERIC PRESSURE
- NT BASE PRESSURE
- NT BLOOD PRESSURE
- NT CRITICAL PRESSURE
- NT DENSIIFICATION
- NT DYNAMIC PRESSURE
- NT ELECTRON PRESSURE
- NT GAS PRESSURE
- NT HIGH ALTITUDE PRESSURE
- NT HIGH PRESSURE

- NT HIGH VACUUM
- NT HYDROSTATIC PRESSURE
- NT HYPERTENSION
- NT HYPOTENSION
- NT HYPOXEMIA
- NT ILLUMINANCE
- NT IMPACT LOADS
- NT INLET PRESSURE
- NT INTERNAL PRESSURE
- NT INTRACRANIAL PRESSURE
- NT INTRAOCULAR PRESSURE
- NT ISOSTATIC PRESSURE
- NT LOW PRESSURE
- NT LUMINANCE
- NT LUMINOUS INTENSITY
- NT OVERPRESSURE
- NT OXYGEN TENSION
- NT PARTIAL PRESSURE
- NT RADIATION PRESSURE
- NT SOUND PRESSURE
- NT STAGNATION PRESSURE
- NT STATIC PRESSURE
- NT SUPERCRITICAL PRESSURES
- NT SYSTOLIC PRESSURE
- NT TRANSIENT PRESSURES
- NT ULTRAHIGH VACUUM
- NT VACUUM
- NT VAPOR PRESSURE
- NT WALL PRESSURE
- NT WATER PRESSURE
- NT WIND PRESSURE

PRESSURE BREATHING

- Human respiration under increased pressures. 12 p1461 A73-26924
- Analysis of the mechanism of the therapeutic action of pressurized oxygen in organic phosphorus poisoning 14 p1722 A73-30848
- Hematological, biochemical, and immunological studies during a 14-day continuous exposure to 5.2% O2 in N2 at pressure equivalent to 100 FSW /4 ata/. 18 p2278 A73-36794
- Endocrine studies during a 14-day continuous exposure to 5.2% O2 in N2 at pressure equivalent to 100 FSW /4 ata/. 18 p2279 A73-36795
- Body fluid volume changes during a 14-day continuous exposure to 5.2% O2 in N2 at pressure equivalent to 100 FSW /4 ata/. 18 p2279 A73-36796
- Comparative value of both hypoxic and positive pressure breathing tests for detection of premature beats. 18 p2280 A73-36944
- Positive-pressure breathing as a protective technique during +Gz acceleration. 20 p2519 A73-39793

PRESSURE BROADENING

- Calculation of pressure-broadened linewidths of SO2 and NO2. 04 p0414 A73-14815
- Pressure broadening of magnetically-tuned infrared absorption spectrum of NO using a CO laser. 07 p0833 A73-19145

PRESSURE CABINS

- U PRESSURIZED CABINS

PRESSURE CHAMBERS

- NT HYPERBARIC CHAMBERS

- NT VACUUM CHAMBERS

- Two chamber adiabatic test compression system design with controlled throttle for high temperature nitrogen- and nitrous oxide-type gases with exothermal reactions 06 p0683 A73-17413
- Stress corrosion cracking and corrosion fatigue for hydraulic aluminum pressure cylinders used for landing gear, stabilizers and aircraft systems 11 p1383 A73-25827
- Procedure for preparing an oxygen-nitrogen gas mixture for respiration in a pressure chamber 13 p1580 A73-29409
- High-pressure chamber for optical studies at low temperatures 17 p2164 A73-34174
- Assembly for optical studies of semiconductors under pressures up to 10 kbar at 77 K 17 p2145 A73-34175
- Estimation of hypoxia tolerance in a decompression chamber 18 p2280 A73-36945
- Method of selecting particles formed during the burning of metallized compacted systems in a constant-pressure chamber 19 p2503 A73-37518

PRESSURE COEFFICIENT

- U AERODYNAMIC COEFFICIENTS

PRESSURE DISTRIBUTION

- The estimation of ground-level pressure fields from computer analyses and their application to large-scale atmospheric mass transfer. 01 p0072 A73-10144
- On the general solution of externally pressurized gas journal bearings. [ASME PAPER 72-LUB-Q] 01 p0055 A73-10218

PRESSURE DISTRIBUTION

Pressure distribution vs porosity and load variation with permeability for squeeze fluid films in porous metal journal bearings
[ASME PAPER 72-LUB-P] 01 p0055 A73-10219

Elastohydrodynamic lubrication in rolling and sliding contacts
[ASME PAPER 72-LUB-K] 01 p0055 A73-10222

An elastohydrodynamic analysis of the sleeve type high pressure seal
[ASME PAPER 72-LUB-M] 01 p0055 A73-10224

Comparative study of free jets and jets emitted in the wake of a cylinder with axis parallel to a hyper-sonic flow
01 p0002 A73-10417

A nonlinear analysis of pulsatile flow in arteries.
01 p0011 A73-10449

Load carrying capacity of ceramic spherical shells under external pressure
01 p0114 A73-10481

Pressure distributions in manifolds with return ducts.
01 p0032 A73-10699

Gas-liquid hydrogen mixture and helium adiabatic model of Jupiter temperature and pressure distribution, estimating planet center temperature
01 p0107 A73-11324

Combustion chamber pressure calculation for a pulsed air jet engine in the process of filling
02 p0203 A73-11708

Minimum pressure zone determination for pressure field at axial plunger pump inlet during cavitation onset, discussing working fluid temperature and composition
02 p0172 A73-11800

Rigidly plastic cylindrical shell design for axial-load and lateral-pressure combinations with allowance for large deflections
02 p0231 A73-11808

The pressure on flat and anhedral delta wings with attached shock waves.
02 p0128 A73-12501

Separation of turbulent boundary layer - Wall pressure distribution near separation.
02 p0154 A73-12523

Experimental investigation of the influence of initial flexures on the stability of smooth conical shells loaded by external pressure
02 p0236 A73-12576

Sound propagation in a combustion can with axial temperature and density gradients.
02 p0238 A73-12608

Evaluation of the method of characteristics applied to a pressure transient analysis of the B.A.C./S.N.I.A.S. Concorde refuelling system.
02 p0133 A73-12645

Finite element technique application for determining velocity field of three dimensional fluid continuum and pressure distribution of lubrication film described by Reynolds equation
03 p0289 A73-12872

A search for density and pressure inversions in high-temperature, low-gravity model atmospheres.
03 p0366 A73-12935

Separated flow noise.
03 p0291 A73-12975

Cs vapors thermal conductivity at various temperatures and pressures, using low emissivity Ni cylinders
03 p0396 A73-13181

A method of analysing the effect of inertia and compressibility in an externally pressurized gas lubricated thrust bearing.
03 p0312 A73-13209

Some details of the pressure and velocity fields near the nozzle of a round turbulent jet.
03 p0293 A73-13311

Solution of the wedge entry problem by numerical conformal mapping.
03 p0244 A73-13537

Pressure distribution and shock wave intensity variations in supersonic flow past two plane wings forming dihedral angle
03 p0245 A73-13623

Experimental investigation of the base pressure on slender circular cylinders
03 p0245 A73-13674

Plateau pressure in hypersonic turbulent boundary-layer interactions.
03 p0296 A73-14200

Thermohydrodynamic phenomena in fluid film lubrication.
[ASME PAPER 72-LUB-25] 03 p0314 A73-14338

Theoretical and experimental pressure distribution in supersonic domain for an inherently compensated circular thrust bearing.
[ASME PAPER 72-LUB-43] 03 p0315 A73-14349

Elastohydrodynamic lubrication in rolling and sliding contacts.
[ASME PAPER 72-LUB-K] 03 p0315 A73-14351

The prediction of airfoil pressure distributions for subcritical viscous flow and for supercritical inviscid flow.
03 p0247 A73-14378

Buffet boundaries for arrow wings in transonic flow, presenting methods for pressure distribution and

three dimensional turbulent boundary layer calculation
[DGLR PAPER 72-123] 03 p0248 A73-14382

Plastic deformations and crack propagation in cylindrical and spherical shells under uniform pressure, calculating stress intensity factor
04 p0512 A73-15239

Investigation of a coaxial plasma accelerator with a uniform gas pressure distribution in the electrode gap
04 p0481 A73-15616

An extension of the Grubin theory of elastohydrodynamic lubrication.
05 p0581 A73-16433

Mathematical prediction for pressure distribution over arbitrary thin airfoil in inviscid potential and real fluid flows, determining velocity increment at leading edge
05 p0527 A73-16593

Isentropic compressible flow equations for pressure and velocity distributions across vortex in axial core mass flow, noting atmospheric circulation and pressure effects
05 p0529 A73-16866

Unsteady transonic flow analysis for low aspect ratio, pointed wings.
05 p0530 A73-16878

Experimental results on the intermittent properties of the boundary layer pressure field during transition.
[AIAA PAPER 73-243] 05 p0566 A73-16967

Optimal and stiffened simply supported circular plates comparison under uniform pressure and uniform compression loads
[AIAA PAPER 73-254] 05 p0635 A73-16976

Nose pressure distribution and separation on an inclined axisymmetric body.
05 p0533 A73-17123

Calculation of stagnation-point pressure during shock-wave incidence on a body moving at supersonic velocity
06 p0643 A73-17459

Pressure surfaces and flow lines geometry of three dimensional parallel steady flow, noting geodesics formation on surfaces of constant pressure
06 p0686 A73-18174

Deformation of an elastic spherical shell with random initial imperfections
07 p0911 A73-19319

German monograph - Free convection of air in a horizontal circular gap in the case of temperature- and pressure-dependent density.
07 p0920 A73-19579

Supersonic flow past large-angle pointed cones.
07 p0775 A73-19981

Turbulent boundary layer separation in supersonic air flow around flat rectangular plate, calculating flow geometry and pressure distribution
07 p0775 A73-20082

Pressure distribution measurement at surface of aerodynamic body by pneumatically activated inductive sensor
08 p0965 A73-21180

Stability of the state of moment stress of a three-layer orthotropic cylindrical shell under uniform and nonuniform external pressure
08 p1018 A73-21374

Steady nonviscous nonheat-conducting plane flow of compressible fluid, calculating entropy, speed and pressure under assumption of variable pressure along streamlines
09 p1071 A73-22419

Coaxial plasma accelerator with uniform pressure distribution.
10 p1254 A73-24206

Stimulated emission of acoustic power as analog to lasers and masers, noting nonpreservation of phase between incident and stimulated pressure
10 p1249 A73-24388

Dynamic viscous pressure interaction on a cone.
10 p1173 A73-24821

Pressure distributions on circular cylinders at critical Reynolds numbers.
11 p1300 A73-25151

The diurnal and semidiurnal barometric oscillations, global distribution and annual variation.
11 p1351 A73-25167

Aerodynamic noise field associated with pressure distributions generated by local protuberance on launch vehicle during atmospheric flight
11 p1300 A73-25384

An exploratory investigation of the unsteady aerodynamic response of a two-dimensional airfoil at high reduced frequency.
[AIAA PAPER 73-309] 11 p1301 A73-25540

Buffeting pressures on a swept wing in transonic flight - Comparison of model and full scale measurements.
[AIAA PAPER 73-311] 11 p1305 A73-25542

Numerical method for predicting unsteady aerodynamic loadings caused by control surface motions in subsonic flow.
[AIAA PAPER 73-315] 11 p1301 A73-25546

Computerized maritime sea level atmospheric pressure field analysis, using pressure and wind velocity data
12 p1519 A73-26802

Stratospheric geopotential pressure field numerical prediction based on quasi-geostrophic atmosphere model, considering stratospheric heating period.
12 p1521 A73-27742

Design of an infinite beam with an elastic base in a nonclassical formulation
12 p1555 A73-27796

The pressure and velocity fields of convected vortices.
13 p1599 A73-28067

Incipient separation pressure rise for a Mach 3.8 turbulent boundary layer.
13 p1601 A73-28827

An approximate method for calculating the interaction between shock wave and turbulent boundary layer.
13 p1602 A73-29018

Response of a jet to a pressure gradient and its relation to edgetones.
13 p1603 A73-29035

Study of the effects of geometrical parameters on the characteristics of air jet flow by some optical methods.
13 p1618 A73-29039

Tensometric strain gage evaluation of stress analysis methods for hollow cylindrical shells under uniform internal pressure
13 p1698 A73-29057

Turbulent velocity and pressure fields in boundary-layer flows over rough surfaces.
13 p1604 A73-29264

Experimental investigation of the pressure distribution in constrained MHD flows past cylinders
15 p1917 A73-31401

Two dimensional unsteady vortex flow of ideal fluid past inflating decelerating wedge, obtaining pressure distribution on wedge surface
[AIAA PAPER 73-449] 15 p1823 A73-31435

Pressure distribution on multicomponent airfoils in two dimensional incompressible potential flow, using Martensen-Jacob vorticity distribution method to derive Fredholm type circulation equation
15 p1823 A73-31637

Reynolds equation solutions for transverse velocity and pressure variations in incompressible fluids within journal bearings and between rotating eccentric cylinders
15 p1882 A73-31639

A pseudo shock theory of pressure depression in externally pressurized circular thrust gas bearings.
15 p1882 A73-31699

Longitudinal evolution of the velocity and pressure in a circular duct in pulsating flow
16 p1998 A73-32805

Supersonic laminar wakes past wedge, determining pressure distribution, velocity profiles and stream line patterns in recirculation region
16 p1962 A73-32905

Circular elastic membrane stability against wrinkling under radial peripheral tension and transverse pressure loading, considering solutions via Foeppl-Hencky theory
16 p2080 A73-33246

Experimental results in the case of the Nonweiler wave-rider in the subsonic, transonic, and supersonic regimes
16 p1963 A73-33265

Procedure for the simulation of sonic fields, particularly for fatigue tests
16 p1997 A73-33384

Lift and measurements in an aerofoil in unsteady flow.
[ASME PAPER 73-GT-41] 16 p1964 A73-33503

Pressure measurements on the rotating blades of an axial-flow compressor.
[ASME PAPER 73-GT-79] 16 p2049 A73-33524

Flexural wave mechanics - An analytical approach to the vibration of periodic structures forced by convected pressure fields.
16 p2083 A73-33947

Low-speed performance of a compressor cascade designed for prescribed velocity distribution and tested with variable axial velocity ratio.
17 p2093 A73-34393

Solving some contact problems by electrical modeling
17 p2244 A73-34795

Recent developments on noncontacting face seals.
[ASLE PREPRINT 73AM-8B-3] 17 p2179 A73-34995

Analytical study of pressure balancing in gas film seals.
17 p2180 A73-35000

Pressure distributions in porous ducts of arbitrary cross section.
[ASME PAPER 73-FE-9] 17 p2152 A73-35008

Three-dimensional flow field in rocket pump inducers. I - Measured flow field inside the rotating blade passage and at the exit.
[ASME PAPER 73-FE-33] 17 p2095 A73-35024

Shock wave pattern visualization and static pressure distribution in supersonic diffusers for mixed flow supersonic compressors, using closed Freon loop test rig
[ASME PAPER 73-FE-35] 17 p2095 A73-35026

On the possibilities of improving the accuracy of the evaluation of inertia forces in laminar and turbulent films.
 [ASME PAPER 73-LUBS-3] 17 p2181 A73-35389
 Experimental study on the interference of inertia and friction forces in turbulent lubrication.
 [ASME PAPER 73-LUBS-12] 17 p2181 A73-35393
 Solution for the pressure and temperature in thrust bearings operating in the thermohydrodynamic turbulent regime.
 [ASME PAPER 73-LUBS-14] 17 p2181 A73-35394
 Calculation of pressure, shear, and flow in lubricating films for high speed bearings.
 [ASME PAPER 73-LUBS-21] 17 p2182 A73-35399
 Supersonic flow around concave and convex blunt bodies.
 17 p2097 A73-35865
 A prediction of the phenomena that take place during so called 'sudden warnings'.
 18 p2308 A73-36038
 Inviscid supersonic far wake flow past pointed bodies using the method of integral relations.
 [AIAA PAPER 73-671] 18 p2262 A73-36222
 Forces acting on conical diffusers and their relation to integral performance parameters.
 [AIAA PAPER 73-686] 18 p2262 A73-36237
 A contact problem for a transversely isotropic cylindrical shell of finite length
 18 p2363 A73-36404
 Tensometric strain gage evaluation of stress analysis methods for hollow cylindrical shells under uniform internal pressure
 18 p2366 A73-36889
 Effect of yaw on supersonic and hypersonic flow over delta wings.
 19 p2377 A73-38008
 Aerodynamic sound and the low-wavenumber wall-pressure spectrum of nearly incompressible boundary-layer turbulence.
 20 p2545 A73-39053
 Shock wave structure in liquid/gas bubble medium from theoretical two-phase model and experimental piezoelectric pressure profile measurements
 20 p2547 A73-39283
 The effect of the wedge angle on the similarity parameter of the turbulent mixing region in the case of an incompressible flow
 20 p2547 A73-39408
 Rigid viscoplastic thin circular plate under uniformly distributed transverse pressure, deriving Mises and Tresca yield surface conditions
 20 p2624 A73-39567
 Pressure fields over hypersonic wing-bodies at moderate incidence.
 20 p2508 A73-39808
 Determination of the wind field from the pressure field and the latitudinal effect of the geomagnetic field in the ionosphere
 21 p2681 A73-40105
 Numerical integration method for Navier-Stokes equation of time dependent flow past impulsively started circular cylinder, calculating length of separated wake and pressure distribution
 21 p2631 A73-40248
 Analysis of gas flow in multinozzle jets
 21 p2631 A73-40393
 Pressure distribution and boundary layer separation measurement on circular cylinder at critical subsonic velocities for various Reynolds and Mach numbers
 21 p2632 A73-40476
 Classical diffusion of free boundary plasma in plane and cylindrical slab geometries, calculating belt pinch effect and pressure decay rate
 21 p2750 A73-41679
 Acoustic wave fronts in ideal membrane transversely by steady pressure distribution, noting abrupt displacement gradient changes across pressure front
 22 p2918 A73-41823
 Quantitative analysis of sonic fields during their visualization by holographic methods
 22 p2852 A73-41899
 Local deformations arising in the contact between a cylindrical shell and a solid
 22 p2921 A73-42281
 Effect of a Griffith crack on the distribution of stress in a semi-infinite two-dimensional medium.
 22 p2922 A73-42470
 Correlation of hypersonic zero-lift drag data.
 22 p2797 A73-42635
 High pressure burning rates of liquid alcohol and hydrocarbon fuels with droplet simulation by porous spheres, deriving surface temperature, pressure distribution and critical burning conditions
 22 p2937 A73-42817
 Electric analogy method for subsonic wind tunnel contraction cone design providing uniform velocity distribution in test section, obtaining pressure distribution in cone boundary
 22 p2797 A73-43000
 The panel method for the calculation of the pressure distribution on missiles in the subsonic range
 22 p2797 A73-43028

Contact pressure problem solution for circular cylindrical shell resting on circular Winklerian bases under external load in terms of Fourier expansion
 22 p2928 A73-43053
 An experimental investigation of a jet issuing from a wing in crossflow.
 22 p2798 A73-43111
 Plane shock wave propagation, reflection and transmission in subsonic flow regime through T-junctions, predicting pressure variation upstream and downstream for comparison with experiment
 23 p2967 A73-43295
 Output pressure-displacement and flow pattern characteristics of digital limit Schrenk, wall attachment and nozzle receiver fluidic switches
 23 p2945 A73-43426
 Approximate method for calculating the turbulent boundary layer in front of a recess
 23 p2968 A73-43732
 Investigation of some theoretical point-explosion problems by the difference method
 24 p3076 A73-44656
 Total pressure loss distribution in viscous gas flow through annular cascades of axial flow compressors, examining three dimensional flow effects on boundary layer development
 24 p3054 A73-44916
 Some results from tests in the NAE high Reynolds number two-dimensional test facility on shockless and other airfoils.
 24 p3054 A73-44995
 Supersonic laminar flow over wedge or backward-facing step for large Reynolds number and small base or step height, predicting pressure distribution at reattachment
 24 p3055 A73-45314
PRESSURE DRAG
NT WAVE DRAG
 Experiments on flow about a yawed circular cylinder.
 [ASME PAPER 72-FE-2] 05 p0527 A73-16546
PRESSURE DROP
 Pressure drop, gas content, liquid drop size and nozzle length effects on flow velocity and heat transfer in two phase nozzle flow
 01 p0033 A73-10863
 Numerical predictions of some three-dimensional boundary layers in ducts.
 04 p0433 A73-15006
 Pressure changes produced by sudden expansion of a two-phase flow
 08 p0955 A73-21197
 Optimum operational flow characteristics derivation for control valves based on frequency distribution of relative pressure drop occurring in practical applications
 10 p1223 A73-24015
 Calculation of single phase pressure drop in heat exchangers considering the change of fluid properties along the flow path.
 12 p1559 A73-27694
 Pressure drop, gas content, liquid drop size and nozzle length effects on flow velocity and heat transfer in two phase nozzle flow
 12 p1560 A73-27912
 Control by pressure drop of the radial distribution of the Mach number behind a subsonic annular cascade [ONERA, TP NO. 1220] 13 p1565 A73-28838
 Fluidic strain gages based on detection of flow resistance or pressure drop changes due to elongation, comparing various type gage factors
 20 p2564 A73-38873
 Flows with and without suspensions in channels with curvilinear segments
 22 p2842 A73-42229
 Vapor flow in cylindrical heat pipes.
 [ASME PAPER 73-HT-P] 22 p2931 A73-42289
 Total pressure loss distribution in viscous gas flow through annular cascades of axial flow compressors, examining three dimensional flow effects on boundary layer development
 24 p3054 A73-44916
PRESSURE EFFECTS
 Effect of increased atmospheric pressure on the dynamics of free oxygen content in animal muscle tissues
 01 p0007 A73-10156
 Reflection of plane stress waves in an elastoplastic medium with a variable yield limit
 01 p0114 A73-10570
 French monograph - Experimental study of the thermal conductivity of rare gases and helium-argon mixtures as functions of temperature and pressure.
 01 p0120 A73-10604
 Adsorption equilibria at high pressures in the helium-nitrogen-activated carbon system.
 01 p0014 A73-10725
 Detonation in a medium of variable density with allowance for variable back pressure
 01 p0034 A73-10956
 Optimal thickness of a cylindrical shell under external pressure
 01 p0116 A73-10964

Pressure and temperature effects on carbon dioxide extinction coefficients, tabulating absorption cross sections
 02 p0191 A73-11758
 Problem of the influence of an instantaneous change in normal pressure on the magnitude of contact friction force
 02 p0172 A73-11796
 Similarity solutions for spherically and cylindrically symmetric gas expansions in rarefied atmospheres, taking into account ambient pressure effect
 02 p0154 A73-12055
 Apparatus for testing reinforced plastics during nonuniform heating, with due allowance for the gas permeability of the material.
 02 p0150 A73-12143
 Fatigue strength of constructional materials and components of GTD-type compressors under conditions of fretting corrosion.
 02 p0181 A73-12217
 Gain distribution in a CO₂ TEA laser.
 02 p0177 A73-12434
 Prediction of the response of a cylindrical shell to arbitrary or boundary-layer-induced random pressure fields.
 02 p0237 A73-12601
 Performance characteristics of a helical TEA CO₂ laser.
 02 p0177 A73-12745
 Finite plastic deformation of pressurized membranes of revolution.
 03 p0384 A73-13120
 Effect of injection velocity ratio and combustion chamber pressure on experimental performance of throttleable LO₂/GH₂-rocket engines with coaxial injectors.
 [AIAA PAPER 72-1079] 03 p0354 A73-13402
 Pressure exponent of controllable solid rocket propellants.
 [AIAA PAPER 72-1135] 03 p0352 A73-13442
 Secondary jet interaction with emphasis on outflow and jet location.
 03 p0243 A73-13496
 Compressible boundary layer formation on shock tube walls after bursting of diaphragm separating gases at different pressures
 03 p0293 A73-13527
 Steady flow of neutrally buoyant flat-faced rigid cylindrical capsules along pipeline under hydraulic pressure gradient effect, noting toroidal vortices
 03 p0293 A73-13528
 Human thresholds for perceiving sudden changes in atmospheric pressure.
 03 p0260 A73-13554
 Circular orifice flow of monatomic rarefied gas between two reservoirs, observing pressure ratio effect
 03 p0295 A73-13773
 Medical considerations for aircraft passengers.
 03 p0267 A73-13802
 Tubular materials plane stress-strain test facility for combined axial load and internal pressure effects
 03 p0288 A73-14024
 Studies leading to the realization of supersonic combustion in propulsion applications.
 03 p0398 A73-14141
 Viscous interaction in integrated supersonic intakes.
 03 p0246 A73-14149
 Transient interaction of a flexible ring-reinforced shell and a fluid medium.
 03 p0395 A73-14197
 The role of compressional viscoelasticity in the lubrication of rolling contacts.
 [ASME PAPER 72-LUB-O] 03 p0315 A73-14354
 Laser frequency fluctuations due to mechanical vibrations.
 03 p0319 A73-14451
 The role of atmospheric pressure variations above the mesopause in the phenomena of winter anomaly and variability of the lower ionosphere.
 04 p0441 A73-15290
 The effects of radiation pressure from resonance scattering in a quasar cloud.
 04 p0499 A73-15355
 I-V characteristics and luminescence changes in Cs vapor arc discharge at various spark gap widths, noting pressure effect on gas stratification
 04 p0481 A73-15613
 Rb87 vapor maser with optical pumping, measuring nitrogen or nitrogen argon mixture buffer gas partial pressure effect on power output
 04 p0459 A73-15920
 Effect of H₂ pressure on pulsed H₂ + F₂ laser - Experiment and theory.
 05 p0583 A73-16043
 Solid-state sliding friction and wear in the case of iron, cobalt, copper, silver, magnesium, and aluminum, kept in an oxygen-nitrogen mixture at pressures from 760 torr to 0.2 microtorr
 05 p0581 A73-16107
 Extent of engagement of various cardiovascular effectors to alterations of carotid sinus pressure.
 05 p0539 A73-16250

Solidification pressure effect on hydrogen in Al ingots, noting blister formation correlation to pressure 05 p0587 A73-16579

Computing pressure cure viscoelastic effects in solid propellants. 05 p0606 A73-17208

Nonzero radiation pressure inclusion into Einstein cosmological equations, discussing Friedmann models evolution from radiation state epoch to matter domination 05 p0624 A73-17304

Dynamic behaviour of thin cylindrical shells subjected to high-speed travelling inner pressures. 06 p0758 A73-17518

Aerial photograph distortion due to sealed compartment temperature and pressure effects in terms of internal refraction 06 p0693 A73-18156

Magnetic transitions observed in sulfide minerals at elevated pressures and their geophysical significance. 06 p0691 A73-18576

Effects of a high-pressure gas medium on the mechanical properties of polymethylmethacrylate 06 p0715 A73-18671

Laser-induced gas breakdown initiated by ultraviolet photoionization. 06 p0703 A73-18749

Environmental hydrogen embrittlement of an alpha-beta titanium alloy - Effect of hydrogen pressure. 06 p0713 A73-18769

Vibrational relaxation times of oxygen in the pressure range 10-110 atm. 07 p0853 A73-19927

Stroboscopic investigation of the effect of standing acoustic waves on turbulent flames 07 p0920 A73-19992

The effect of variable temperature on creep collapse of a cylindrical shell under external pressure 07 p0913 A73-20070

Fiber reinforced plastics with adhesive bonded elements, investigating ply number and adhesive pressure effects on shear, bending and impact strengths 07 p0844 A73-20330

Influence of liquid lubricant properties on their performance. 07 p0844 A73-20464

On the He-H₂ thermal opacity in planetary atmospheres. 08 p1003 A73-20890

Combined gravitational and solar radiation pressure effects on the semimajor axis of the earth's satellite. 08 p1010 A73-21314

Characteristics of a spherical electrostatic probe in a weakly ionized plasma. 08 p0993 A73-21390

The oxidation of tantalum and niobium in the temperature range 400-600 C. 08 p0978 A73-21416

Dependence of He-Ne laser output power on discharge current, gas pressure and tube radius. 08 p0976 A73-21462

Electrical properties of InAs to very high pressures. 08 p0995 A73-21533

Studies in molecular dynamics by collision-induced infrared absorption in H₂-rare gas mixtures. I - Profile analysis and the intercollisional interference effect. 08 p0990 A73-21630

Influence of the surface microstructure on the evolution of the combustion velocity of ammonium perchlorate composite solid propellants as a function of pressure [ONERA, TP NO. 1167] 08 p0995 A73-21678

Dependence of the base pressure on the ratio of specific heats at supersonic velocities 09 p1027 A73-21917

Pressure-induced optical distortion in laser windows. 09 p1090 A73-21937

Shock wave compression of iron-silicate garnet. 09 p1076 A73-22146

Pathophysiological and clinical aspects of aeroinfarctus and frontal sinus neumatoma formation due to barometric pressure changes from pilot case history studies 09 p1039 A73-22538

Optical breakdown of compressed gases by carbon dioxide laser emission 09 p1094 A73-22594

Mathematical model for extinguishing gunpowder combustion via pressure variations, assuming gunpowder surface dependence on combustion rates 09 p1167 A73-22617

A high pressure gas-dynamic laser powered by a slow compression heater [ONERA, TP NO. 1184] 09 p1096 A73-22712

Necessary conditions of stable combustion of powder in a semiclosed chamber 10 p1294 A73-23588

Experimental determination of the temperature and pressure dependence of the absolute viscosity of mineral oils 10 p1237 A73-23661

Influence of pressure anisotropy on the fluctuations of the magnetospheric tail 10 p1276 A73-23884

The Elbrus cosmic ray spectrograph 10 p1203 A73-23926

Acoustic emission studies of large advanced composite rocket motor cases. 10 p1288 A73-23967

I-V characteristics and luminescence changes in Cs vapor arc discharge at various spark gap widths, noting pressure effect on gas stratification 10 p1254 A73-24203

Quantitative characterization of the substructure of AISI 316 stainless steel resulting from creep. 10 p1234 A73-24436

Methyl nitrite photolysis reaction products under various ambient gas mixture environments, noting irradiation time and gas pressure effects 10 p1186 A73-24656

Carbon dioxide laser active medium excitation by ionizing radiation from external source during electric current passage, discussing gain dependence on pressure and mixture 10 p1229 A73-24756

Influence of pressure on VT14 alloy wear and friction against 30KhGSA steel 10 p1226 A73-24797

Vitamin metabolism alteration under increased atmospheric pressure 11 p1321 A73-25036

Potential operator theory in Hilbert spaces applied to rigorous definition of conservative loading, examining pressure loading case 11 p1434 A73-25212

EEG activity of rats compressed by inert gases to 700 feet and oxygen-helium to 4000 feet. 11 p1314 A73-25327

Strength and weight optimization of strengthened spherical shells under external pressure 11 p1434 A73-25389

Stability of cylindrical shells with filler under axial compression and external pressure 11 p1435 A73-25396

A finite element method for nonaxisymmetric vibrations of pressurized shells of revolution partially filled with liquid. 11 p1440 A73-25528

[ALAA PAPER 73-399] Earth mantle rutile-structure germanium dioxide elastic properties as function of pressure and temperature in single crystals 11 p1352 A73-25585

Surface damage under fretting fatigue as function of applied normal load and clamping pressure 11 p1383 A73-25836

Determination of the resistivity of nickel and of some of its alloys as a function of pressure up to 60 kbar 11 p1384 A73-25873

Correlation of theory and experiment for high-pressure hydrogen. 11 p1398 A73-25887

Shock wave determination of shear velocity at high pressures for understanding of planetary interior behavior with abrupt change in density from seismic interpretation 11 p1355 A73-25898

The effect of a uniform external pressure on the ionospheric boundary of a non-magnetic planet in a steady solar wind. 11 p1421 A73-25925

Thermochemical calculation for high temperature and pressure formation of interstellar molecules in compact H II regions, considering prestellar and late stellar atmospheres 11 p1423 A73-26105

Pressure effects on contact potential in diode p-n junction, discussing potential barrier height variation, minority carrier concentration changes and relative position of energy bands 11 p1338 A73-26520

NASA use of liquid and gaseous oxygen under extreme pressure, temperature and flow rate conditions, discussing safety requirements in terms of structural and chemical compatibility 11 p1410 A73-26525

The physics and chemistry of high pressures. 12 p1523 A73-26923

Reactions of O/ID/ with methane and ethane. 12 p1466 A73-27126

Deformation of zero-moment shells subjected to internal pressure under creep conditions 12 p1551 A73-27179

Flattening and creep stability loss of nonlinear viscoelastic ring under external pressure 12 p1551 A73-27180

Pressure sensitization relation to electrical conductivity relaxation during isothermal isobaric annealing of CdTe crystals 12 p1531 A73-27196

Condensation of cesium from an incident shock wave in cesium vapors 12 p1528 A73-27323

Elastoplastic bending of a cylindrical shell according to the Prandtl-Reuss theory 12 p1554 A73-27472

Explosion in a variable-density medium in the presence of variable counterpressure. 12 p1487 A73-27532

On optimal thickness of a cylindrical shell loaded by external pressure. 12 p1554 A73-27540

Mechanical behavior of plastically deformed polycrystalline metal subjected to hydrostatic pressure soaking. 13 p1634 A73-28196

Contribution to the study of the behavior of liquid cobaltous oxide in an oxidizing atmosphere 13 p1634 A73-28204

The effect of processing on the microstructure of CFRP. 13 p1645 A73-28779

Solid propellant ballistic properties from pressure changes due to combustion, considering transient effects 13 p1669 A73-28997

The input characteristic due to the interaction of jets of beam-deflection amplifier. 13 p1571 A73-29037

Accuracy of switching pressure of fluidic OR-NOR device. 13 p1571 A73-29044

Effect of randomly fluctuating pressure gradients, with arbitrarily specified power spectrum and probability density, on flow in channels. 13 p1604 A73-29263

German monograph - A contribution to the stability calculation and the test of cylindrical shells of glass-fiber reinforced plastics under uniform external pressure. 13 p1646 A73-29280

Reaction H + C₂H₄ - Investigation into the effects of pressure, stoichiometry, and the nature of the third body species. 13 p1581 A73-29426

Forced vibration solution and wind tunnel investigation of shallow cylindrical shells under moving pulsating pressure discontinuities, noting compression shock effects 13 p1703 A73-29602

A nongravitational effect in the simulation of cometary phenomena. 14 p1793 A73-29824

The shear strength of thin lubricant films. 14 p1754 A73-30050

Influence of flow and pressure on wave propagation in the canine aorta. 14 p1715 A73-30066

Rapid gas-phase reactions - The reaction of ammonia and the methylamines with boron trifluoride. III - Pressure dependence of rate constant. 14 p1723 A73-30068

Nonlinear stability of a liquid film adjacent to a supersonic stream. 14 p1711 A73-30166

Load-bearing capacity of ceramic spherical shells under external pressure. 14 p1810 A73-30306

Microwave pulse excited argon ion laser. 14 p1758 A73-30472

Nonlinear toroidal curved elastic sheet inflated by fluid at constant pressure, discussing existence, uniqueness and asymptotic behavior 14 p1812 A73-30520

Some relations for high pressure flows with and without heat transfer. 14 p1817 A73-30604

The influence of back pressure on the point of instability of axisymmetric shells deformed by fluid pressure. 14 p1813 A73-30662

The contact problem of two coaxial cylindrical shells. 14 p1813 A73-30663

Critical rpm of conical shells incorporated in turbine rotors 14 p1814 A73-30686

Influence of air pressure on the brittle fracture of graphite 14 p1766 A73-30715

Influence of increased air atmosphere pressure on the excitability of the neuro-motor apparatus in man 14 p1719 A73-30845

Procedure for recording the rate of pressure changes in heart cavities 15 p1837 A73-31167

Temperature dependence of the electrical resistance of superconducting Ti-Nb and Ti-Nb-Zr alloys subjected to working by hydrostatic pressure 15 p1887 A73-31186

High-temperature electrical conductivity relaxations induced in CdTe crystals by variations in cadmium vapor pressure 15 p1923 A73-31201

Influence of a longitudinal pressure gradient on turbulent diffusion in ducts 15 p1862 A73-31297

Effect of a crack in an infinite plane containing a circular hole under uniform normal pressure. 15 p1947 A73-31333

Current extension from a quasi-steady MPD arcjet. 15 p1918 A73-31500

Buckling analysis of elastically constrained stiffened conical shells under hydrostatic pressure by the collocation method.

Method for measuring the collision-induced broadening of spectral lines

Decomposition of hydrazine on Shell 405 catalyst at high pressure.

Determination of atmospheric water-vapor densities from measurements of the 6943.8-A absorption line strength.

Maximum equilibrium pressure of a plasma in a three-dimensional system with helical geometry

Phase and structural changes in titanium under impulsive loads

Bottom pressure and specific-heat ratio at supersonic velocities.

Solar radiation pressure on Mariner 9 Mars orbiter from mathematical model of luminance and reflectivity characteristics

High pressure-sintering preparation of barium ferrites, discussing temperature and compression effects on density and magnetic properties

An experimental study of the low pressure limit for steady deflagration of ammonium perchlorate.

Climate simulation via environmental test chambers examining mechanical, thermal and pressure effects to determine functional component suitability

Experimental studies and applications of vanadium oxides.

Sodium chloride electrolyte data at high temperatures and pressures.

[ASME PAPER 73-PROD-1] Equivalent widths of the oxygen A-band absorption lines at different pressures

The kinetics of the dissolution of oxygen in niobium at low oxygen pressures and high temperatures

Effects of high omnidirectional pressures and residual stresses on the superconductivity of alloys of the V3/Si1-xGex/ system

Cylindrical probe in a glowing-discharge nitrogen plasma at medium pressures

The dynamic behavior and compliance of a stream of cavitating bubbles.

[ASME PAPER 73-FE-34] A detailed experimental analysis of dynamic stall on an unsteady two-dimensional airfoil.

[AHS PREPRINT 702] Elasticity of water-saturated rocks as a function of temperature and pressure.

Burnett cell design and fabrication for error reduction in high precision P-V-T data generation without volume or mass measurements

Pressure dependency of the NF3-H2 transverse-discharge pulse-initiated HF chemical laser.

The prediction of turbulent heat transfer and pressure on a swept leading edge near its intersection with a vehicle.

[ALAA PAPER 73-677] Thin clamped hemispherical shell nonlinear dynamic response to suddenly applied pressure, deriving finite difference formulation of fourth order coupled nonlinear equations

Stability of truncated conical shells under dynamic external pressure

The effect of hydrostatic pressure environment on the low cycle fatigue properties of a maraging steel.

[ASME PAPER 73-MAT-K] Atmospheric regeneration in closed chambers by potassium superoxide

Some observations of the relationship between film thickness and load in high Hertz pressure sliding elastohydrodynamic contacts.

[ASME PAPER 73-LUB-D] Evaluation of F-15 inlet dynamic distortion.

[ALAA PAPER 73-784] Flow film boiling heat transfer correlations - Parametric study with data comparisons.

[ASME PAPER 73-HT-50] Effect of pressure anisotropy on oscillations of magnetotail.

Vibration of tubes containing flowing fluid.

[MERL-TN-72-2]

System of experimentally verified equations for calculating the thermodynamic characteristics of some technologically important gases at temperatures ranging from the normal boiling point to 1300 K at pressures up to 1000 bar

Experimental investigation of the stability of oblique conical panels under the action of uniform external pressure

Heat transfer through free convection of air between vertical plates, obtaining Nusselt and Grashof numbers, and temperature and pressure effects

Tungsten inert gas arc welding for refractory or active metals working in gas-tight chamber, noting effects of reduced pressure on cathode zone energy density

CW laser action from acetylene oxidation, noting sensitivity to total pressure and helium, oxygen and acetylene partial pressure changes

Correlation between output power and composition of discharge products in a water vapor laser.

Analysis of ground tests of a microwave, earth-occultation, pressure-reference-level system.

Seasonal variations of the barometric effect of the cosmic ray neutron component intensity

Possibilities of barotherapy in ophthalmology

Determination of the thermodynamic characteristics of a liquid-propellant rocket engine with nonisobaric combustion

Sealed-off waveguide carbon dioxide laser, investigating gas mixture and pressure effects on power gain and output and optical properties effects on losses

Effect of high pressure on the superconducting transition temperature of Pd-H.

Oxygen uptake during maximal work at lowered and raised ambient air pressures.

Steady-state creep of a thin-walled tube in the general case of applied forces

Noise caused by supersonic jet shock waves as function of jet pressure ratio, determining spectral characteristics

Expanding split ring seal types for pistons, discussing straight cut, step, two piece and three piece rings and pressure and friction effects

Acoustic wave fronts in ideal membrane transversely by steady pressure distribution, noting abrupt displacement gradient changes across pressure front

Buckling of segments of toroidal shells.

Buckling of toroidal shells under hydrostatic pressure.

Radiative transfer within the atmospheres of the major planets.

A survey of compatibility of materials with high pressure oxygen service.

Diamagnetism of Penning discharge plasma as function of gas pressure, magnetic field strength and applied voltage, discussing plasma energetic lifetime and current characteristics

Effect of pressure on the flame propagation velocity in a turbulent flow

Uniaxial pressure effects on diode structures volt-ampere characteristics, examining potential barrier height and photo emf changes

Postcritical deformations in a multilayer plate under edge pressure

Influence of high hydrostatic pressure on the flow stress of 18-8 stainless steel.

Optically pumped 33-atm CO2 laser.

Low-pressure gas breakdown with CO2 laser radiation.

Maximum equilibrium pressure of a plasma in a spatial system with helical symmetry.

A self-similar regime of powder combustion with variable optical constants

Transient process due to pressure increase during combustion of condensed material, using fractional-differentiation operator method to determine unsteady burning velocity

Critical heat flux for two-phase flow of helium I.

The use of glass-fiber-reinforced plastics for containers which are subjected to external pressure

HF and molecular fluorine refractive indices in visible spectral region computed from interferometer fringe shift vs pressure measurements

H2 pressure-induced lines in the spectra of the major planets.

Burning rate studies of fuel air mixtures at high pressures.

PRESSURE FIELDS

U PRESSURE DISTRIBUTION

PRESSURE GAGES

NT IONIZATION GAGES

NT KNUDSEN GAGES

NT MANOMETERS

NT OSMOMETERS

NT PHILIPS IONIZATION GAGES

NT PIEZOELECTRIC GAGES

NT PIEZOMETERS

NT VACUUM GAGES

Pressure gage performance tests for air turbine through flow static pressure measurement

PRESSURE GAUGES

U PRESSURE GAGES

PRESSURE GRADIENTS

Stability of a plasma with an axial current surrounded by a cold gas with a pressure gradient.

Peripheral turbocompressors for high pressure rise with small mass flow rate, discussing operational principles, design and performance

Linear schlieren photography with concave mirror and variable ultrasonic source for high resolution display of acoustic free field pressure gradient on TV screen

Plane Poiseuille flow with small amplitude modulated pressure gradient, noting disturbance shear wave and stability from energy transfer calculation

Heat transfer in the turbulent boundary layer of an incompressible fluid flow past a surface when the pressure gradient and temperature on the surface are variable

Aircraft reference altitude computation from air data inputs, deriving algorithm for pressure gradient errors correction

Free turbulent mixing in axial pressure gradients.

[ASME PAPER 72-WA/APM-31]

The transpired turbulent boundary layer in an adverse pressure gradient.

Boundary layer characteristics with radiant energy transfer under adverse pressure gradient.

[ALAA PAPER 73-117] Unsteady compressible boundary layers with arbitrary pressure gradients.

[ALAA PAPER 73-132] Calculations of turbulent shear stress in supersonic turbulent boundary layer zero and adverse pressure gradient flow.

[ALAA PAPER 73-166] Turbulence measurements in a compressible boundary layer subjected to a shock-wave-induced adverse pressure gradient.

[ALAA PAPER 73-167] Plane equilibrium turbulent boundary layer with longitudinal pressure gradient

Determination of the hydraulic resistance of throttles by short unsteady blowing

Kinetic theory of suction flow, discussing slip coefficient determination for perturbation boundary conditions in Chapman-Enskog-Hilbert method and pressure gradient effects

A zero-streamwise-pressure-gradient, three-dimensional turbulent boundary layer in a 90 deg curved rectangular duct.

Steady turbulent boundary layer of compressible perfect gas on heat insulated surface with suction and longitudinal pressure gradient

Boundary layers calculation for nonporous surface extended to porous with suction by replacing velocity distribution with longitudinal pressure gradient

A two-layer model of high speed two- and three dimensional turbulent boundary layers with pressure gradient, surface mass injection and entropy layer swallowing. 08 p0956 A73-21800 [AIAA PAPER 73-135]

Low velocity wind tunnel design with adjustable pressure gradient, determining contraction section wall contour to avoid boundary layer separation via velocity distribution improvement. 11 p1347 A73-25714

Investigation of the transition of a turbulent boundary layer into a laminar boundary layer in the presence of deep negative pressure gradients. 11 p1347 A73-25737

Calculation of turbulent boundary layers and wall jets over curved surfaces. 11 p1348 A73-26383

Prediction of heat transfer for turbulent boundary layer with pressure gradient. 11 p1453 A73-26393

Linear viscoelastic fluid parallel flow in straight duct of uniform cross section under axial pressure gradient. 13 p1602 A73-28918

Investigation of the influence of compressibility and the pressure gradient on the value of the permissible Reynolds number of roughness. 13 p1567 A73-29406

Effect of radial total pressure gradients on the Mach number distribution in turbomachines. 13 p1567 A73-29450

Gas flow properties in curvilinear turbine ducts, considering pressure gradient, outer flow shear and Coriolis force on boundary layer. 14 p1712 A73-30649

Free stream vorticity effect on incompressible boundary layer stability via Orr-Sommerfeld equation, considering self-similar flows with pressure gradients. 14 p1712 A73-30651

Bulk elastic properties of excised lungs and the effect of a transpulmonary pressure gradient. 15 p1832 A73-31128

Transpulmonary pressure gradient and ventilation distribution in excised lungs. 15 p1833 A73-31129

Investigation of boundary layer flow on a flat porous plate with a regulated pressure gradient in the outer flow. 15 p1864 A73-31873

Low-density jets behind a sonic nozzle at large pressure gradients. 17 p2150 A73-34263

Pulsatile Newtonian frictional losses in a rigid tube. 17 p2151 A73-34532

Jet boundary and a free surface behind a body of revolution in the presence of a longitudinal pressure gradient. 17 p2094 A73-34774

Effect of adverse pressure gradient on film cooling effectiveness. 18 p2368 A73-36246 [AIAA PAPER 73-697]

An integral procedure for estimating boundary layer parameters and heat transfer in arbitrary pressure gradients. 18 p2298 A73-36249 [AIAA PAPER 73-700]

Turbulent mixing of gas flows in the presence of a pressure gradient. 18 p2266 A73-37016

Numerical solution existence for three dimensional boundary layer equations governing corner flow in symmetry plane with critical pressure gradients. 19 p2419 A73-37492

A comparison between axisymmetric and slab-symmetric cumulus cloud models. 19 p2447 A73-37659

Single axis analog fluoric accelerometer using mercury as solid proof mass, describing differential gas pressure outputs, porous cylindrical configuration and hydrostatic pressure gradients. 19 p2389 A73-38076

Transonic laminar boundary layers with surface curvature. 19 p2423 A73-38480

Study of turbulent transfer with strong injection, longitudinal pressure gradient and nonisothermicity. 20 p2547 A73-39421

Hankel transforms and boundary layer solutions for pulsating laminar flow in curved circular tube under sinusoidal pressure gradients. 20 p2549 A73-39809

French monograph - Study of the behavior of the laminar boundary layer in the presence of a positive or negative pressure gradient in hypersonic flow around obstacles. 22 p2797 A73-42744

Rarefied gas flow through an orifice at low pressure gradients. 23 p2969 A73-44347

Investigation of the flow pattern in the wall region of a turbulent boundary layer during injection with a positive pressure gradient. 24 p3079 A73-45080

Boundary layer on flat plate in shear flow, calculating induced pressure gradients near leading edge and far downstream. 24 p3080 A73-45369

PRESSURE MEASUREMENTS

Experimental study of the saturated-vapor pressure of rubidium and cesium. 01 p0080 A73-10858

Alternating-pressure measurements involving mushroom-nozzle flows with regard to dynamic stresses in the case of the skin structures of reusable carrier rockets. 02 p0128 A73-11686 [DGLR PAPER 72-076]

Rise time and pressure measurements in transient flow during quasi-steady gas injection into vacuum with piston valve, using fast ionization gage. 02 p0168 A73-11963

Ultrahigh vacuum quartz spring microbalance for determination of evaporation rate and vapor pressure. 02 p0168 A73-11965

Molecular fluorine concentration and pressure change monitor based on UV absorption spectrum during chemical reactants mixing, noting measurement accuracy. 02 p0168 A73-11967

Ocular tonus measurements for glaucoma detection in flying personnel, discussing subsequent test procedures in case of abnormal findings. 02 p0134 A73-12158

Total-pressure averaging in pulsating flows. 02 p0171 A73-12618

A new variant of the Knudsen vacuumeter as a measurement standard for low pressures. 03 p0306 A73-12898

Oxygen partial pressure measurement in respiratory air via radio telemetry system with polarographic catheter electrode pressure sensor. 03 p0270 A73-14287

Radiotelemetry of direct bloodpressure measurements in aorta, pulmonary artery and heart. 03 p0271 A73-14291

Digital readout top-loading balance adaptation as micromanometer, discussing accuracy, sensitivity and repeatability characteristics. 03 p0309 A73-14471

A method for transonic wind-tunnel corrections. 05 p0563 A73-17105

Determination of the pass band of a system of measurement of rapidly variable pressures in the air. 05 p0579 A73-17228

Investigation of the vapor pressure of cesium by the boiling-point method. 06 p0722 A73-17404

Measurements of base pressure upon a plate and a wedge in the 2.8 to 6.8 Mach number range [DFVLR-SONDDR-256]. 06 p0645 A73-17740

Motion of a fluid outside a turbulent jet system. 07 p0812 A73-20091

Pressure gage performance tests for air turbine through flow static pressure measurement. 07 p0824 A73-20100

Measurement of dynamic mechanical quantities; Scientific-Engineering Conference, 3rd, Warsaw, Poland, October 26-28, 1972, Summaries. 07 p0826 A73-20526

Servomanometer designs with two membrane sensing elements for absolute and excess pressure measurements. 07 p0827 A73-20542

A charge amplifier for pressure measurements. 07 p0827 A73-20543

A new probe for measurement of velocity and flow direction in separated flows. 08 p0963 A73-20871

Pressure distribution measurement at surface of aerodynamic body by pneumatically activated inductive sensor. 08 p0965 A73-21180

Photo-optic instrumentation of magnetic flyer plate facility for pressure-time response measurement of impact loaded test specimens, using streak and high speed framing cameras. 09 p1083 A73-22512

Experimental determination of the transonic flow on circular cones at angle of attack. 10 p1172 A73-24496

Low gas pressure measurement with ionization and extractor gages, discussing methods for suppressing or eliminating disturbance effects. 11 p1361 A73-25400

The theoretical and experimental methods used in France for flutter prediction. 11 p1305 A73-25558 [AIAA PAPER 73-329]

Three dimensional gas flow noncollinear total impulse normal and tangential components calculation leading to pressure force determination. 12 p1486 A73-27089

A noise-immune ionizational manometer for pressures between 1 millitorr and 1 nanotorr. 12 p1497 A73-27213

Dynamic measurement of the basic quantities of fluids. 12 p1461 A73-27596

High-fidelity left ventricular pressure measurements for the assessment of cardiac contractility in man. 12 p1464 A73-27888

Experimental investigation of the pressure of the saturated vapor of rubidium and cesium. 12 p1526 A73-27907

Measurement of pulsating pressure with a piezometer. 13 p1612 A73-28449

Atmosphere Explorer pressure measurements - Ion gage and capacitance manometer. 13 p1688 A73-28632

Base pressures in flow expansions by hydraulic analogy. 13 p1564 A73-28811

Detection of flight vehicle transition from base measurements. 13 p1706 A73-28834

Interaction position and static pressure measurements of two opposing plane turbulent wall jets in still air in terms of frozen flow. 15 p1863 A73-31342

Method for the interpretation of surface pressure measurements under rarefied hypersonic conditions. 16 p1963 A73-33316

Pressure measurements on the rotating blades of an axial-flow compressor. 16 p2049 A73-33524 [ASME PAPER 73-GT-79]

Pressure measurements for establishing inlet/engine compatibility. 17 p2221 A73-34609

A performance data acquisition and analysis system for turbine engine component testing. 17 p2146 A73-34610

A reliable Teflon cell with many electrical leads for pressures up to 40 kilobars. 17 p2175 A73-35761

Supersonic, turbulent boundary layer separation measurements at Reynolds number of 10,000,000 to 100,000,000. 18 p2261 A73-36216 [AIAA PAPER 73-665]

Measurements of surface pressure on an elliptic airfoil oscillating in uniform flow. 19 p2375 A73-37374

Determination of a combustion wave in a conical supersonic flow. 19 p2503 A73-37551

New vapour pressure measurements for argon and nitrogen and a new method for establishing rational vapour pressure equations. 19 p2461 A73-38200

Application of the semiconductor p-n junction to measurements of rapidly varying pressures. 19 p2432 A73-38308

Frequency response of short pressure probes. 20 p2564 A73-38872

Trimming and checking aircraft gas-turbine engines with the aid of the ratio of total pressure behind the turbine to total pressure in front of the compressor. 21 p2754 A73-40403

Influence of the wall temperatures of gauges on the measurement of limit pressures. 22 p2852 A73-41870

Experiments on radiatively driven harmonic acoustic waves in a confined gas. 22 p2930 A73-42236

French monograph - Contribution to the experimental study of a boundary layer trap in a supersonic air inlet. 22 p2797 A73-42740

Combustion in high speed swirling flow in gas turbine combustion chamber, discussing flame stability, pressure measurements and chamber configuration. 22 p2935 A73-42790

Combustion noise radiation by open turbulent flames. 24 p3156 A73-44856 [AIAA PAPER 73-1025]

PRESSURE MICROPHONES
U MICROPHONES
PRESSURE OSCILLATIONS

Alternating-pressure measurements involving mushroom-nozzle flows with regard to dynamic stresses in the case of the skin structures of reusable carrier rockets. 02 p0128 A73-11686 [DGLR PAPER 72-076]

Two dimensional deep convection rimitive model of pressure perturbation in cumulus cloud with precipitation. 02 p0189 A73-12781

Turbulent pressure fluctuations on smooth and rough walls. 03 p0289 A73-12960

Measurements of pressure and velocity fluctuations in turbulent pipe flow. 03 p0290 A73-12963

Experimental investigation of the pressure and velocity fluctuations in a sound-affected free jet. 03 p0290 A73-12965

Characteristics of pressure fluctuations in the subsonic free jet. 03 p0290 A73-12966

Measuring combustion response by a forced oscillation method. 03 p0397 A73-13385 [AIAA PAPER 72-1054]

Aircraft engine inlets total pressure fluctuations and distortion factors, presenting extreme-value statistical method for maximum distortion level probability estimate. 03 p0354 A73-13419 [AIAA PAPER 72-1100]

TF-30-P1 engine mixed flow augmentor test for combustion instability under operation with abnormal

fuel zone combination, comparing with predicted pressure oscillations from model
[AIAA PAPER 72-1206] 03 p0358 A73-13489

Decoding of thermocouple data for a flow with velocity, pressure, and temperature pulsations
03 p0308 A73-13667

Sonic boom induced underwater pressure oscillations, noting strong attenuation with depth
03 p0250 A73-13835

Influence of distributed grit-type roughness on the spectrum of wall pressure fluctuations of turbulent flow in a tube.
03 p0295 A73-14038

Singular characteristics of turbulent wall pressure fluctuations associated with flow in a tube.
03 p0295 A73-14041

The starting transient of solid-propellant rocket motors with high internal gas velocities.
[AIAA PAPER 72-1119] 04 p0486 A73-14909

Turbulence effect on wall pressure fluctuations.
04 p0403 A73-14939

Effect of an oscillating free stream on the unsteady pressure on a circular cylinder.
[ASME PAPER 72-WA/FE-12] 04 p0434 A73-15843

Experimental investigation of hypersonic buzz on a high cross-range shuttle configuration.
[AIAA PAPER 73-137] 05 p0531 A73-16904

Role of condensed phase details in the oscillatory combustion of composite propellants.
[AIAA PAPER 73-218] 05 p0641 A73-16948

Nonlinearity of Helmholtz resonators
05 p0599 A73-17269

Noise characteristics of combustion augmented high speed jets.
[AIAA PAPER 73-189] 06 p0767 A73-17655

Interaction of sound and flow in T-burners - Experiments compared with theory.
[AIAA PAPER 73-220] 06 p0741 A73-17662

Screen and porous absorbing liner design for damping pressure oscillations in ramjet combustors based on acoustic absorption efficiency and combustion instability calculation
06 p0767 A73-17665

Acoustic amplification during solid propellant combustion.
07 p0865 A73-19390

Microsensor measurement of spatial correlation between pressure fluctuations of turbulent boundary layer
08 p0965 A73-21188

Thermo-acoustic oscillations in forced convection heat transfer to supercritical pressure water.
08 p1022 A73-21253

Diagram of the shock wave processes in the unsteady interaction between a jet and an obstacle
08 p0927 A73-21607

Characteristics of unsteady interaction between a supersonic jet and an infinite obstacle
08 p0927 A73-21609

Nozzle-target system geometry and gas dynamics parameters effect on supersonic underexpanded jets interaction with walls, noting frequency response and pressure oscillations
08 p0927 A73-21610

Prediction of pressure fluctuation in sounding rockets and manifolded recovery systems.
[AIAA PAPER 73-286] 09 p1155 A73-23206

Study of the fluctuations of wall pressures in transonic flow on a cone-cylinder group presenting a constriction
10 p1173 A73-24825

Measurement of pulsating pressure with a piezometer
13 p1612 A73-28449

Calculation of the unsteady subsonic aerodynamic pressures on compressor blades
[ONERA, TP NO. 1221] 13 p1565 A73-28839

Effect of randomly fluctuating pressure gradients, with arbitrarily specified power spectrum and probability density, on flow in channels.
13 p1604 A73-29263

Experimental investigations regarding the behavior of turbulent boundary layers in the case of small periodic pressure changes
14 p1745 A73-30299

Nonlinear dynamic problem concerning a cylinder with a slowly changing internal boundary
16 p2082 A73-33932

Dielectric impulse pressure recorders consisting of organic glass, cellulose-ether film and muscovite mica, investigating shock wave profiles and electrode voltage amplitude
18 p2317 A73-36764

Flow properties fluctuations in a convergent-divergent nozzle.
19 p2375 A73-37402

Shock oscillation associated with Hartmann resonance tubes excited by underexpanded sonic jets, using schlieren streak photography
21 p2677 A73-40616

Interpretation of hot-wire anemometer readings in a flow with velocity, pressure and temperature fluctuations.
21 p2705 A73-41317

Pressure waves generated by constant velocity deflagration flame in explosive hydrocarbon-air mixture for self-similar flow field
22 p2936 A73-42808

Forced vibrations of a cylindrical shell in the presence of gas pressure fluctuations
22 p2928 A73-43057

Signal transmission in analog fluidic systems mainly with respect to noise influence.
23 p2944 A73-43421

Nonlinear parametric vibrations of cylindrical shells prepared from composite materials
24 p3145 A73-44517

Response of panels to turbulence-induced, surface-pressure fluctuations and resulting acoustic radiation to the flow field.
[AIAA PAPER 73-993] 24 p3077 A73-44828

Pressure fluctuations underlying attached and separated supersonic turbulent boundary layers and shock waves.
[AIAA PAPER 73-996] 24 p3053 A73-44831

Surface pressure fluctuations in hypersonic turbulent boundary layers.
[AIAA PAPER 73-997] 24 p3053 A73-44832

Solid propellants with a pulsating burning rate
24 p3121 A73-45200

Study of the field of fluctuating pressures at the surface of a circular cylinder
24 p3079 A73-45220

PRESSURE PROBES

U PRESSURE SENSORS

PRESSURE PULSES

Axissymmetric plastic response of rings to short-duration pressure pulses.
01 p0115 A73-10759

Transient response of a plastically anisotropic cylinder in plane strain.
07 p0908 A73-19081

Possibility of improving the erosive activity of a cavitation bubble by the combined effect of continuous and pulsed sound
08 p0955 A73-21448

Investigation of the deformation of a hollow sphere under an impulsive load on the basis of three-dimensional elasticity theory and shell theory
08 p1019 A73-21761

Nonlinear wave propagation processes in elastic tubes
13 p1692 A73-28165

Buckling of viscoplastic cylindrical shells loaded by radial pressure impulse.
14 p1811 A73-30481

Nonlinear vibrations of rectangular plates.
15 p1944 A73-31000

Possibility of enhancing the erosive activity of a cavitation void under the simultaneous action of continuous and pulsed sound.
15 p1860 A73-31012

Sinusoidal pulse flow through an axial flow gas turbine.
17 p2093 A73-34395

Inertial motion of a plastic ring under the action of a pulsed load
17 p2244 A73-34797

Nonlinear response of plates subjected to inplane and lateral pressure pulses.
20 p2622 A73-39547

Emission of sound from a rectangular plate vibrating under the action of pressure pulsations in a turbulent boundary layer
24 p3109 A73-44899

PRESSURE RECORDERS

The use of telemetry to study the physiological and clinical variations of intracranial pressure in man.
03 p0271 A73-14300

Method of recording elastoplastic stress waves in solids with a dielectric sensor
13 p1618 A73-29059

Dielectric impulse pressure recorders consisting of organic glass, cellulose-ether film and muscovite mica, investigating shock wave profiles and electrode voltage amplitude
18 p2317 A73-36764

A method of recording elastoplastic stress waves in solids by means of a dielectric pickup.
18 p2317 A73-36891

PRESSURE RECOVERY

Effects of transverse ribs on pressure recovery in two-dimensional subsonic diffusers.
[AIAA PAPER 72-1141] 03 p0243 A73-13447

Performance of truncated conical diffusers with compressible flow.
03 p0249 A73-14641

Inverse problem approach to the design of short two-dimensional diffusers.
[ASME PAPER 72-WA/GT-6] 04 p0404 A73-15870

Mach numbers up to 30 obtained in a continuous operating wind tunnel
05 p0533 A73-17194

Diffuser static pressure recovery coefficient for varying turbulence intensity at inlet, considering performance correlation with geometrical and/or velocity profile parameters
12 p1488 A73-27930

A pseudo shock theory of pressure depression in externally pressurized circular thrust gas bearings.
15 p1882 A73-31699

Further data on the pressure recovery performance of straight-channel, plane-divergence diffusers at high subsonic Mach numbers.
[ASME PAPER 73-FE-5] 17 p2152 A73-35005

PRESSURE REDUCTION

Depressurization extinguishment of composite solid propellants - Influence of composition and catalysts.
[AIAA PAPER 72-1136] 03 p0352 A73-13443

Medical considerations for aircraft passengers.
03 p0267 A73-13802

The effect of time of electrical stimulation of the carotid sinus on the amount of reduction in arterial pressure.
03 p0265 A73-14648

Theoretical trans-respiratory pressure during rapid decompression. I Model experiment. II - Animal experiments.
09 p1045 A73-22530

Sustained human skin and muscle vasoconstriction with reduced baroreceptor activity.
15 p1833 A73-31344

Changes in cardiac activity and in the latter's phase structure during decompression of the lower half of the body
15 p1835 A73-31513

Influence of lower-body decompression on the state of the human cardiovascular system /according to roentgenokymographic data/
17 p2111 A73-34234

Utilization of miniature diaphragm-leakport devices in fluidic applications.
20 p2511 A73-39752

Free surface profile of wedge-shaped cavity in metal during collapse due to incident shock wave with decreasing pressure behind shock front
24 p3093 A73-44711

PRESSURE SENSORS

Digital apparatus for telemetry of pressure
01 p0044 A73-10034

Dynamic study of a very-low-pressure sensor
02 p0165 A73-11591

Device signaling unsteady modes of compressor operation
02 p0166 A73-11635

An electronic method of temperature compensation in hydrostatic pressure transducers with semiconductor p-n junctions.
03 p0308 A73-13784

Oxygen partial pressure measurement in respiratory air via radio telemetry system with polarographic catheter electrode pressure sensor
03 p0270 A73-14287

The use of telemetry to study the physiological and clinical variations of intracranial pressure in man.
03 p0271 A73-14300

Automated calibration of blood pressure signal conditions.
04 p0411 A73-14846

Fluidic system for precision positioning of cylindrical machine parts and length and angle measurements, using nozzle jet impingement system for pressure symmetry sensing
05 p0538 A73-17248

New method of measuring rapidly varying pressures in the range below 500 atm
07 p0827 A73-20541

Pressure distribution measurement at surface of aerodynamic body by pneumatically activated inductive sensor
08 p0965 A73-21180

Microsensor measurement of spatial correlation between pressure fluctuations of turbulent boundary layer
08 p0965 A73-21188

Instrument Society of America, Annual Conference, 27th, New York, N.Y., October 9-12, 1972, Proceedings, Part 2.
09 p1082 A73-22501

Digital pressure transducer based on vibrating cylinder frequency response to pressure changes, discussing operational principles and applications
09 p1082 A73-22502

Digital quartz pressure transducer for FM signal output to interface with digital computer and telemetry, noting insensitivity to temperature and vibration interference effects
09 p1082 A73-22503

Miniature pressure transducers with a silicon diaphragm.
09 p1084 A73-22692

An IC piezoresistive pressure sensor for biomedical instrumentation.
10 p1183 A73-23649

Flat circular acoustic transducer for pressure spectrum analysis, deriving flow noise response correction factor in terms of polynomial coefficients and frequency-dependent constants
13 p1613 A73-28492

Piezoelectric sound pressure sensor for damping measurement of structural element coatings under intense acoustic loads
13 p1618 A73-29060

PRESSURE SUITS

Design and development of Manganin and other wire sensors together with a resistance strain gauge transducer for use at pressures up to 200 000 lbf/sq in /1.38 GN/sq m.

14 p1750 A73-29702

Technique for measuring the vessel blood pressure in long continued experiments

15 p1838 A73-31394

Dynamic pressure transducer system for pulsed plasma flow diagnosis.

15 p1876 A73-31977

Development and employment of a measurement transformer for a difference in pressure. I

16 p2014 A73-33224

Total pressure tube measurements in turbomachine-simulating pulsating nozzle flow generator supplemented by pneumatic tube probes for averaging error comparison

17 p2166 A73-34608

A solid state bonding and packaging technique for integrated sensor transducers.

17 p2166 A73-34618

Performance and economic advantages offered by a diffused semiconductor strain gage pressure transducer.

17 p2167 A73-34626

Wind measurement by magnetometers, optical and static pressure sensors.

18 p2310 A73-36136

Piezoelectric sound pressure sensor for damping measurement of structural element coatings under intense acoustic loads

18 p2317 A73-36892

Jet engine noise reduction technology and design, discussing sonic pressure probes, high bypass turbofan engines, noise source fluctuations and far field measurements

19 p2472 A73-37287

Measurements of surface pressure on an elliptic airfoil oscillating in uniform flow.

19 p2375 A73-37374

Application of the semiconductor p-n junction to measurements of rapidly varying pressures

19 p2432 A73-38308

Frequency response of short pressure probes.

20 p2564 A73-38872

PRESSURE SUITS

NT SPACE SUITS

Nutrition systems for pressure suits.

20 p2517 A73-39105

Effects of tilting on pulmonary capillary blood flow in normal man.

20 p2519 A73-39786

PRESSURE TRANSDUCERS

U PRESSURE SENSORS

PRESSURE VESSEL DESIGN

Limit pressures for cylindrical shells with two adjacent circular cut outs.

22 p2929 A73-43175

PRESSURE VESSELS

Acoustic emission during burst tests of filament wound composite pressure bottles as function of pressure, microscopic damage and winding parameters

03 p0331 A73-13031

Computers and the analysis of pressure vessels.

03 p0391 A73-13678

Stress intensity factors for internally pressurized thick-wall cylinders.

04 p0505 A73-14680

Ductile fracture initiation, propagation, and arrest in cylindrical vessels.

04 p0506 A73-14697

Postirradiation notch ductility and fracture strength of pressure vessel steel plate by Charpy V tests

04 p0460 A73-14702

Relationship between material fracture toughness using fracture mechanics and transition temperature tests.

04 p0506 A73-14703

Verification of structural integrity of pressure vessels by acoustic emission and periodic proof testing.

04 p0453 A73-14859

Theoretical-experimental studies and research concerning the technical safety of the casing of a high-pressure cylindrical tank. I

04 p0454 A73-15657

Pressure vessel proof test variables and flaw growth.

05 p0581 A73-16129

Influence of thermal nonstationarity on convective heat-transfer intensity

05 p0640 A73-16773

Partial yielding of cylindrical pressure vessel with elastic modulus and yield function as arbitrary functions of radial coordinate, assuming elastoplastic strain hardening material

06 p0761 A73-17895

Stress intensity factors for nozzle corner cracks.

07 p0912 A73-19564

Temper embrittlement of pressure vessel steels.

07 p0839 A73-20271

An approximate rigid-plastic analysis of shell intersections loaded dynamically.

[ASME PAPER 72-WA/DE-1] 09 p1164 A73-23272

Filament-wound vessel from an organic fiber-epoxy system.

10 p1237 A73-23958

A comparison of the effects of explosive forming and static deformation on the mechanical properties of pressure vessel steels.

10 p1225 A73-24426

Three-dimensional photoelastic tests of thin shell pressure vessels.

13 p1699 A73-29307

Guide to a quality control system for Code vessels.

14 p1755 A73-30144

Pressure vessels filament winding with inflatable mandrel in reinforced elastomer, discussing use of balloon as liner

16 p2018 A73-33068

Acoustic emission coincidence detector for monitoring high residual stress areas in symmetrical pressure vessels.

17 p2166 A73-34620

High modulus filament wound vessels for cryogenic containers in spacecraft.

17 p2238 A73-34807

A unique method of leak-rate measurements.

18 p2316 A73-36714

Random loading on a spherical pressure vessel of Hooke-Norton material.

19 p2501 A73-38252

Fracture mechanics technology for optimum pressure vessel design.

22 p2920 A73-42155

Failure stress levels of flaws in pressurized cylinders.

22 p2921 A73-42156

Experimentally determined shape factors for deep part-through cracks in a thick-walled pressure vessel.

22 p2866 A73-42157

Acoustic emission produced during burst tests of filament-wound bottles.

24 p3094 A73-45146

PRESSURE WAVES

U ELASTIC WAVES

PRESSURE WELDING

NT DIFFUSION WELDING

NT EXPLOSIVE WELDING

NT ULTRASONIC WELDING

A comparison of the capabilities of continuous drive friction and inertia welding.

[SME PAPER AD 73-221] 19 p2436 A73-38493

Human thresholds for perceiving sudden changes in atmospheric pressure.

03 p0260 A73-13554

Theoretical trans-respiratory pressure during rapid decompression. I Model experiment. II - Animal experiments.

09 p1045 A73-22530

Russian book on passenger aircraft high altitude equipment covering cabin pressurization, air conditioning and temperature and pressure control, human tolerances, reliability factors, etc

14 p1712 A73-30355

Pressurized fuselage design studies for short haul transport aircraft, discussing sandwich structures and bonding techniques for Al and Ti alloy construction materials

16 p2018 A73-33069

PRESSURIZING

NT FUEL TANK PRESSURIZATION

Externally pressurized bearings; Proceedings of the Conference, London, England, November 17, 18, 1971.

03 p0311 A73-13201

Computer-aided design of externally pressurized bearings.

03 p0311 A73-13202

The steady state performance of an externally pressurized gas lubricated porous thrust bearing with a uniform film.

03 p0311 A73-13203

Externally pressurized gas bearings development and applications, considering design, control systems and manufacture

03 p0311 A73-13205

Externally pressurized gas-lubricated journal bearings with herringbone grooves - Load capacity and stability analysis.

03 p0311 A73-13208

Characteristics of supercharge devices in gas bearings

15 p1881 A73-31296

PRESTON TUBES

U PILOT TUBES

U SPEED INDICATORS

PRESTRAINING

U PRESTRESSING

Certain regularities in the influence of preliminary loading by alternating tensile stress on the long-term strength of Kh18N10T steel

02 p0180 A73-11928

The effect of a preliminary plastic strain on the form of a mechanical hysteresis loop.

02 p0235 A73-12208

Constitutive equation for shock waves under dynamic load in prismatic bar axially prestressed to plastic range

03 p0383 A73-12903

On optimal design of prestressed elastic structures.

03 p0384 A73-13119

Effect of a single plastic deformation on the fatigue behavior of metals

03 p0322 A73-13136

Yield surface equation derivation for plastically prestrained anisotropic material from simple tension and compression tests

06 p0763 A73-18455

Tensile and compressive prestressing effects on notched steel cantilever beam specimens low cycle fatigue life

06 p0764 A73-18490

A new relationship between pre-strain and yield stress drop due to Bauschinger effect.

06 p0713 A73-18772

Design of lowest-cost prestressed combined metallic systems

11 p1371 A73-25035

Effects of prestressing boron/epoxy prepreg on composite strength properties.

[AIAA PAPER 73-382] 11 p1388 A73-25512

Cumulative creep formulas for construction steels at stepwise increasing temperatures

12 p1510 A73-26900

Effect of prestraining on the brittleness of molybdenum.

12 p1511 A73-27058

Design optimization of prestressed concrete spans for high speed ground transportation.

12 p1554 A73-27735

A study of the effects of prestrain on the tensile properties of filamentary composites.

[ASME PAPER 72-MAT-K] 13 p1699 A73-29198

Effect of tensile prestrain on fatigue strength of aluminum alloy in high cycle fatigue.

[ASME PAPER 72-MAT-N] 13 p1636 A73-29199

Monotonic and cyclic prestrain influence on alpha-Ti fatigue life, suggesting twin/grain boundary dislocation interactions

13 p1640 A73-29486

Some effects of prestraining nickel at various rates on its subsequent tensile properties.

14 p1761 A73-30637

On dynamic response of prestressed cylindrical shells - Green's tensor technique.

15 p1947 A73-31367

Design for bending of a clamped infinite strip with a prestressed stiffness rib along the edge

16 p2075 A73-32695

Effect of prestress levels on the long term strength of 1Kh18N9T steel at elevated temperatures

18 p2323 A73-36761

Influence of stresses on the nature of the distribution of dislocations in Kh18N10T steel at a temperature of 650 C

18 p2325 A73-36820

Some results in the erosion of prestressed materials due to water-jet impact.

19 p2443 A73-38299

Nonlinear response of plates subjected to inplane and lateral pressure pulses.

20 p2622 A73-39547

Two-dimensional contact problem for a prestressed elastic body

20 p2625 A73-39652

Nonsymmetric buckling of cylinders with axisymmetric thermal discontinuities.

21 p2784 A73-40425

Influence of preloading on the sustained load cracking behavior of maraging steels in hydrogen.

21 p2719 A73-40924

Cumulative creep formulas for construction steels at stepwise increasing temperatures

21 p2720 A73-41033

Book - Prestressed pavements of airports and roads.

21 p2675 A73-41287

The Bauschinger effect and its role in mechanical anisotropy.

21 p2722 A73-41547

Improvement of thermal shock resistance by surface prestressing.

22 p2921 A73-42462

Prestressing force and tendon configuration optimization for indeterminate structure with prescribed cross sectional dimensions, using linear programming and design variable transformation

22 p2922 A73-42476

Memory effect on mechanical properties of plastically prestrained Al-Mg alloy sheets

24 p3100 A73-45247

PRETESTS

U TESTS

PRETREATMENT

NT PRESTRESSING

Cyclic endurance and alteration nature of the dislocation structure in nickel before and after programmed strengthening

06 p0707 A73-17906

The effect of thermomechanical pretreatment on the allotropic transformation in cobalt.

17 p2190 A73-34645
Filiform corrosion associated with commonly applied aircraft metal pretreatments and finishes. [SAE PAPER 730311]
17 p2177 A73-34671

PRETWISTING

U PRESTRESSING

U TWISTING

PREVENTION

NT ACCIDENT PREVENTION
NT CORROSION PREVENTION
NT FIRE PREVENTION
NT ICE PREVENTION

PRIMARY BATTERIES

NT ALKALINE BATTERIES
NT NICKEL ZINC BATTERIES

Power Sources Symposium, 25th, Atlantic City, N.J., May 23-25, 1972, Proceedings.

13 p1572 A73-29581
Primary cells hybridization with sealed nickel cadmium batteries for power supply operation over wide temperature ranges and discharge rates
13 p1573 A73-29588

PRIMARY COSMIC RAYS

NT SOLAR COSMIC RAYS

High energy muons /not less than 150 GeV/ in extensive air showers.

01 p0092 A73-10788
Primary proton-air atom nuclei interaction study of negative and positive cosmic ray muon coupling coefficients with angular distribution allowance

02 p0205 A73-12173
Study of energy spectra of primary cosmic rays at very high energies on the proton series of satellites.

02 p0207 A73-13238
Midlatitude excess radiation energy density relation to primary cosmic ray background from spectrum measurement data

02 p0208 A73-12460
Inelastic nuclear interactions between 200-GeV cosmic ray particles and polyethylene targets, correlating similarity property, momentum spectra and secondary particle pairs

02 p0208 A73-12652
Scintillation and anticoincidence Cerenkov counters for recording heavy nonrelativistic single charge particles in cosmic rays at sea level

02 p0209 A73-12670
Energy spectrum, composition and anisotropy study of cosmic radiation from extensive air showers observation, using scintillation and Cerenkov detectors

02 p0209 A73-12671
Primary cosmic radiation energy spectrum approximation from air showers, high-energy hadrons and Proton 4 data

02 p0209 A73-12675
Extensive air shower spectra based on electron and muon number for given shower development mechanism and primary cosmic ray chemical composition

02 p0209 A73-12677
Extensive air shower characteristics and muon counts at different level observations relative to particle number and primary energy spectra

02 p0209 A73-12678
K-neutral pion energy fractions and inelasticity coefficients at primary energies of 100-1500 GeV during cosmic ray hadron-target interaction

02 p0210 A73-12689
Studies of the chemical composition of cosmic rays with $Z = 3-30$ at high and low energies.

02 p0210 A73-12737
Adiabatic propagation of cosmic rays in the Galaxy.

03 p0360 A73-12929
Rigidity spectrum of helium nuclei above 17 GV and a search for high energy anti-nuclei in primary cosmic rays.

04 p0493 A73-15980
High energy primary cosmic ray particles total energy and mass spectra measurement

05 p0609 A73-16370
Unorthodox ideas concerning the origin of cosmic radiation.

05 p0611 A73-17175
Nuclear gamma rays from Li-7 in the galactic cosmic radiation.

05 p0612 A73-17329
Cosmic ray electrons of E greater than 1 Gev - Some new measurements and interpretations.

07 p0869 A73-19226
Coupling function for the vertical muon telescope at 60-meters-water-equivalent depth.

07 p0869 A73-19251
Composition of radiation excess over primary cosmic ray background recorded by Cosmos satellites below midlatitude belt region

07 p0870 A73-19426
Predicting light flashes due to alpha-particle flux on SST planes.

07 p0777 A73-20157
Energy dependence of primary cosmic ray nuclei abundance ratios.

07 p0873 A73-20564

Primary cosmic rays energy spectrum at .100-1000 TeV from Proton 4 satellite data

08 p0999 A73-21329
Primary cosmic ray particles disappearance and proton spectrum slope rise in 1 TeV energy region from Proton satellites data

08 p0999 A73-21330
Primary cosmic rays alpha particles and protons energy spectra similarity and intensity difference at .05 to 1.6 TeV, using Proton satellites data

08 p0999 A73-21331
Primary cosmic radiation antiproton flux, finding .005 ratio upper limit to proton flux with balloon-borne-magnetic spectrometer

08 p0999 A73-21333
Probabilistic integral multiplicity of generation of primary cosmic ray particles from count rate and primary spectrum relationship, using definition for neutron component calculations

08 p1000 A73-21352
A possible cosmic ray primary particle energy spectrum above 10 TeV and its astrophysical implications.

08 p1000 A73-21824
Semiautomatic photometer for determining the charge of heavy cosmic-ray nuclei in photonuclear emulsions

09 p1085 A73-23001
Large scintillation counter with a high amplitude resolution

09 p1085 A73-23003
Primaries of extensive air showers of cosmic radiation.

09 p1138 A73-23170
Manganese-54 and the lifetime of relativistic cosmic rays.

10 p1264 A73-23541
Upper limit of the antinucleus abundance in primary cosmic rays

10 p1265 A73-23899
Certain data concerning heavy primary nuclei /Z above 33/ obtained outside the earth's magnetosphere

10 p1266 A73-23915
Methods for determining the charges of heavy primary nuclei /Z greater than 26/ in photonuclear emulsions of different sensitivities

10 p1267 A73-23922
Capture of primary cosmic rays in the upper atmosphere as a source of excess radiation

10 p1268 A73-23931
Contribution of pion production by primary cosmic-ray nucleons to the interstellar electron-positron flux.

10 p1269 A73-24348
On the secondary production of galactic cosmic ray electrons.

10 p1270 A73-24910
Gamma-gamma total hadronic cross section and absorption of extragalactic gamma-rays.

11 p1413 A73-26107
Low momentum integral muon spectrum at sea level near the geomagnetic equator.

13 p1670 A73-28211
Iron energy spectra due to acceleration at neutron star surface vs primary cosmic rays

14 p1787 A73-30618
Null correlation method for estimation of the primary energies of cosmic ray jets.

15 p1927 A73-32149
Midlatitude excess radiation energy density relation to primary cosmic ray background from spectrum measurement data

15 p1927 A73-32610
International Conference on Cosmic Rays, 12th, University of Tasmania, Hobart, Tasmania, Australia, August 16-25, 1971, Papers. Volume 7 & Invited and Rapporteur Papers.

16 p2054 A73-33276
Superconducting magnetic spectrometer technique application to charged primary cosmic rays, discussing calibration, experiments and electron-positron and isotopic separation

16 p2014 A73-33277
Solar electrons, Galactic electron radiation modulation and spectrum of high energy cosmic ray electrons

16 p2055 A73-33293
Cosmic antiproton production in interstellar pp collisions.

17 p2223 A73-34099
Apollo 14 and Apollo 16 heavy-particle dosimetry experiments.

19 p2396 A73-37150
Investigation of cosmic radiation about the moon aboard the Luna 10, 11, and 12 artificial lunar satellites

19 p2474 A73-37344
Isotopic composition measurements of cosmic-ray nuclei with Z greater than or equal to 10 made using a new technique.

19 p2475 A73-37628
Upper limit of antinuclei content in primary cosmic rays.

20 p2601 A73-38918
Differential energy spectra of low-energy /less than 8.5 MeV per nucleon/ heavy cosmic rays during solar quiet times.

21 p2755 A73-40509

Investigation of primary gamma radiation from the northern polar region of the Galaxy

21 p2756 A73-40578
The Forbush effect in the nuclear component of primary cosmic rays in August 1972

21 p2757 A73-40588
Acoustical spark chamber in a telescope designed for investigations of primary cosmic gamma radiation

21 p2701 A73-40612
High energy cosmic rays and elementary particles, discussing detection, sources, nature and properties

21 p2764 A73-41611
The multiplicity distribution of shower particles underground and the cosmic-ray primary spectrum.

21 p2764 A73-41633
Biological effects due to single accelerated heavy particles and the problems of nervous system exposure in space.

22 p2814 A73-42181
Apollo 16 Biostack experiment for biological effects of cosmic ray heavy primaries on cell and tissue development and mutations of bacilli, Artemia and plant seeds

22 p2805 A73-42185
Size spectra of extensive air showers and primary cosmic-ray spectrum.

22 p2903 A73-42427
Galactic nuclei, pulsars and supernovae as sources of primary cosmic rays from ground based and satellite observations, relating chemical composition to origin

22 p2904 A73-43116
Events in a photoemulsion indicating the formation of superheavy fireballs

23 p3021 A73-43535
Observation of cosmic-ray particles with Z of 50 or greater and interpretation of the charge spectrum.

23 p3024 A73-43610
The solar coronal green line as an index of cosmic ray modulation.

23 p3024 A73-43683

PRIMATES

NT CHIMPANZEES

PRIMERS [COATINGS]

Aircraft surface primers and finishes composition, pretreatment and application, discussing epoxy, acrylic and polyurethane primers mechanical and chemical properties

10 p1237 A73-23522

PRIMING

Arterial wick heat pipes self filling capability theoretical and experimental investigation, deriving expressions for mesh size, artery radius and stem height relationships [ASME PAPER 72-WA/HT-36]

04 p0518 A73-15819

PRINTED CIRCUITS

NT LARGE SCALE INTEGRATION

Design and fabrication of helix-like strip meander line delay equalizer in printed circuit technology, noting group delay and insertion loss frequency responses

02 p0145 A73-11823

Printed circuit and electronic component solderability tests subsequent to adverse environment exposure, comparing electroplated materials with pressure leveled solder and Cu and Be coatings

03 p0333 A73-13046

An advanced printed circuit board system having outstanding resistance to humid environments.

03 p0281 A73-13047

Multilayer thin film microcircuit and printed circuit conductors partial capacitance and potential coefficients, using matrix method for approximate calculation

03 p0284 A73-14070

Reversing the trend - Infrared testing is simplicity itself.

08 p0952 A73-20685

Microwave bandpass filters formed by shunt and series stubs with quarter wave matching strip lines, noting advantage of equal lengths

09 p1063 A73-22463

Forced air cooling of dual-in-line packages.

10 p1193 A73-23607

Printed circuit meander line polarizer for converting microwaves in 1-20 GHz range from linear to circular polarization, describing construction and performance

14 p1735 A73-30221

Influence of tolerances on printed directional-coupler circuit parameters

15 p1850 A73-31498

The role of temperature in the environmental acceptance testing of electronic equipment.

16 p1989 A73-33606

Microwave energy absorbing elements based on Pd/Ag

17 p2141 A73-35549

Statistical analysis of the influence of various factors on the quality of photolithographic operations in the production of integrated circuits

20 p2534 A73-38851

A method of computer design of microelectronic equipment

20 p2534 A73-38852

PRINTED RESISTORS

IR test data evaluation for printed circuits using computer techniques, discussing testing time reduction and efficiency optimization, programming language and error analysis

20 p2567 A73-39769

Some considerations on solder flow-up into plated-through holes.

23 p2986 A73-44002

PRINTED RESISTORS

Proton irradiation at 30 K and isochronal annealing of reactively sputtered Ta thin-film resistors.

06 p0737 A73-18352

Adjustment of thick-film resistors by laser and new pastes for the thick-film technology

13 p1627 A73-28574

PRINTERS

Failure analysis and reliability estimation methodology for electromechanical mosaic printer

07 p0800 A73-19419

IR scanner for aerial stereoscopic photography, discussing use of computer controlled orthophoto printer for image distortion reduction by rectification

20 p2566 A73-39671

PRINTING

NT LITHOGRAPHY

The use of the electronic computer for the urgent publication of astronomical material.

14 p1730 A73-29791

Advantages of using polymer bases as fixing agents in hydrotype printing

21 p2646 A73-40258

PRINTOUTS

Automation of the print-out of strips of flight plans for air traffic control

15 p1847 A73-32441

PRIORITIES

Allowance for the correlation of factors in the method of priorities for electrical system optimization

05 p0560 A73-16272

Control algorithm for digital computer operations organization in real time processing of variable priority assignment tasks, estimating memory storage requirements

07 p0796 A73-20049

PRISMATIC BARS

Constitutive equation for shock waves under dynamic load in prismatic bar axially prestressed to plastic range

03 p0383 A73-12903

Torsion of certain prismatic bars.

03 p0395 A73-14198

Torsion of prismatic bars made of various materials

04 p0510 A73-15077

Investigation of the stressed state of a rod with a cut under elastoplastic torsion

07 p0911 A73-19308

Torsion of a viscoelastic prismatic rod under the action of a vibrational load

07 p0911 A73-19315

Inequalities for torsion rigidity of a prismatic rod with steady creep

07 p0912 A73-19323

Bending of an orthotropic prismatic beam by a transverse force in a geometrically nonlinear formulation

08 p1020 A73-21769

Thin reinforcing coatings effect on mechanical behavior of homogeneous isotropic prismatic bars under torsion, obtaining stress-strain expressions

09 p1165 A73-23358

Elasto-plastic stress analysis of prismatic bar under combined bending and torsion.

10 p1289 A73-24160

Torsional stress on micropolar prismatic nonsymmetrically elastic rotating cylindrical shaft with six degrees of freedom evaluated in terms of Saint Venant function

11 p1445 A73-26409

Elastoplastic torsion of a cylindrical bar of multiconnected section

14 p1805 A73-29762

Oblique bending of a homogeneous orthotropic prismatic beam by a force couple in the quadratic theory of elasticity

14 p1815 A73-30785

A method for studying the stressed state during torsion of hollow prismatic beams

14 p1815 A73-30790

Nonlinear differential equation solutions for prismatic body elastic equilibria in terms of deformation and stress tensor relations by small parameter method

15 p1945 A73-31042

Saint Venant problem for a continuously inhomogeneous anisotropic beam

15 p1953 A73-32103

Experimental study of the stressed state of an elastic beam undergoing transverse impact

20 p2620 A73-39385

The description of vortex-excited oscillations of prismatic bodies by means of a sequence of pulses having random time differences

20 p2594 A73-39770

Pure torsion of prismatic rods composed of different materials

21 p2787 A73-40990

Book - Dynamics in engineering structures.

22 p2922 A73-42491

Determination of heat flow shape factors for hollow, regular polygonal prisms.

23 p3049 A73-44164

PRISMS

NT PRISMATIC BARS

Parameter calculation and design of synchronization circuit for firing pumping lamp of laser with modulator employing total internal reflection prism for Q switching

01 p0059 A73-10831

Iterative formula for wave functions related to sources situated on prism symmetry plane with application to electromagnetically polarized wave diffraction by dielectric wedge

06 p0669 A73-18841

Two-pass-internal second-harmonic generation using a prism coupler.

07 p0834 A73-19539

Temperature distribution in a wedge-shaped prism

08 p1022 A73-21098

Astronomical spectroscopy with prism in front of Schmidt correcting plate, considering spectral resolution and light loss characteristics in plate field

08 p0966 A73-21359

A proposal for a flint objective prism for the ESO Schmidt camera.

08 p0966 A73-21360

Frequency selection schemes based on combined use of dispersive prism and interferometer in laser resonator

09 p1097 A73-23012

A chart for the computation of the gravitational attraction of a right rectangular prism.

11 p1351 A73-25160

A non-stroboscopic system for examining high speed rotating objects.

14 p1750 A73-29704

Interferograms of high optical quality by double exposure.

21 p2695 A73-39963

PRIVATE AIRCRAFT

U GENERAL AVIATION AIRCRAFT

PRIVATE AVIATION

U CIVIL AVIATION

U GENERAL AVIATION AIRCRAFT

PROBABILITY

U PROBABILITY THEORY

PROBABILITY DENSITY FUNCTIONS

NT NORMAL DENSITY FUNCTIONS

NT RAYLEIGH DISTRIBUTION

NT WEIBULL DENSITY FUNCTIONS

Accuracy of the determination of the spectral density of a vibrational process with the aid of a spectrum analyzer

01 p0077 A73-10677

Some results on zero crossing distribution of non-stationary random noise.

02 p0143 A73-12857

Random fatigue of 2024-T3 aluminum under two spectra with identical peak-probability density functions.

03 p0322 A73-13235

Conditionally sampled measurements near the outer edge of a turbulent boundary layer.

03 p0293 A73-13526

Concentration probability of a passive admixture in turbulent shear flows

03 p0294 A73-13614

A Bayes analysis of availability for a system consisting of several independent subsystems.

03 p0336 A73-13732

Binary noncoherent FSK communication under influence of bandpass Gaussian noise and linear FM jamming waveform, deriving error probability

03 p0276 A73-13905

Optimum detection and signal design for channels with non- but near-Gaussian additive noise.

04 p0415 A73-14988

Nonlinear analysis of double feedback loop tracking system with coupling, obtaining steady state phase error probability density functions with application to satellite transponder

04 p0429 A73-14994

Functional analysis approach of the partial differential equation arising from non-linear filtering theory.

04 p0472 A73-15263

Digital simulation of imperfect second-order hybrid phase locked loop operating in RF interference background, determining phase error variance and probability density function

04 p0422 A73-15438

Sinusoidal signal and stationary quasi-white Gaussian noise mixture effects on stochastic phase locked AFC system operation, noting phase error probability density function

05 p0547 A73-16060

Optical anemometers applicability to steady atomized fuel sprays, obtaining particle velocity profiles and probability density distributions

05 p0565 A73-16761

Propellant requirements for midcourse velocity corrections.

[AIAA PAPER 73-172]

05 p0630 A73-16916

Total number and mass of Pultusk meteorite shower fragments, using spatial distribution rule

06 p0748 A73-17838

Error incidence probability for system control reliability determination, assuming error function as Markov process

06 p0680 A73-17956

The probability density function for the output of a cross-correlator with bandpass inputs.

06 p0665 A73-18139

Nonstationary envelope process and first excursion probability.

06 p0762 A73-18341

The plane-wave method in the study of helium atoms physisorbed on graphite

07 p0843 A73-20000

Estimate of the probability density and distribution function of a scalar product of vectors with independent, normally distributed components

07 p0845 A73-20050

Comparative study of methods of analysis of nonlinear systems subjected to random input

08 p0938 A73-20969

Statistical approach to the prediction of M.O.S.-device performance.

08 p0946 A73-21116

Statistical properties of two sine waves in Gaussian noise.

09 p1120 A73-22115

Solution of the Fokker-Planck-Kolmogorov equation for a dynamic system with analytical characteristics

09 p1068 A73-22563

A probabilistic approach to a differential-difference equation arising in analytic number theory.

10 p1241 A73-23643

Determination of changes in the properties and recognition of random processes with a complicated structure.

10 p1201 A73-24057

Measurement of certain one-dimensional characteristics describing the evolution of the two-dimensional probability density of random processes when changing the interval between readings

11 p1340 A73-25004

Asymptotic behavior of some statistical estimates. II - Limit theorems for a-posteriori density and Bayesian estimates

12 p1517 A73-27188

Probability density characteristics of elapsed time interval to synchronization disruption in phase locked AFC systems

13 p1584 A73-28890

Calculation of probability of detection with target scintillation.

13 p1586 A73-29219

The effect of limiting upon the mean cross section of log-normal radar clutter.

13 p1586 A73-29224

Effect of randomly fluctuating pressure gradients, with arbitrarily specified power spectrum and probability density, on flow in channels.

13 p1604 A73-29263

Finding the approximate angular probability density function of wave arrival by using a directional antenna

14 p1727 A73-30210

Solutions of a class of random differential equations.

16 p2032 A73-33308

Generalized random forces in time domain for rectangular panels under subsonic and supersonic boundary layer turbulence, investigating probabilistic nature by Monte Carlo method

17 p2241 A73-34182

Effect of bandlimiting on the noncoherent detection of Amplitude-Shift Keying /ASK/ signals.

17 p2125 A73-35377

The effects of cycle slips and phase jitter on the probability of bit error in suppressed carrier phase-shift keyed communications.

17 p2126 A73-35628

Probabilistic analysis of a two-unit system with a warm standby and a single repair facility.

17 p2149 A73-35809

Probability distributions and correlations in a turbulent boundary layer.

18 p2300 A73-36626

The domain analysis of intersymbol interference effects on phase shift keyed /PSK/ and quadrature phase shift keyed /QPSK/ communication systems.

20 p2524 A73-38734

The structure of internal intermittency in turbulent flows at large Reynolds number - Experiments on scale similarity.

20 p2546 A73-39090

Combined density of the probability distribution of instantaneous values for the phase difference of two oscillations and for the phase difference derivatives

20 p2593 A73-39390

Probabilistic and deterministic solutions of random vibration response problems.

21 p2783 A73-40294

Linear fire control predictor with non-Gaussian inputs, calculating on-target probability lower bounds for verification by digital simulation

21 p2649 A73-40332

Phase-locked loop operation in the presence of impulsive and Gaussian noise.

21 p2656 A73-41166

Phase-tracking performance of direct-detection optical receivers.

21 p2656 A73-41169

First-order probability densities of laser speckle patterns observed through finite-size scanning apertures.

22 p2872 A73-43188

Probability displacement and modal cross spectral density parameters of two span beam random vibrations under white noise

23 p3039 A73-43304

An existence and uniqueness theorem for the solution of a stochastic integrodifferential equation

23 p2999 A73-44101

PROBABILITY DISTRIBUTION FUNCTIONS

Classes of limiting distributions for the sums of a random number of independent equally distributed random quantities

01 p0071 A73-11247

Some exact statistics of two-dimensional viscous flow with random forcing.

02 p0153 A73-12041

Worst inputs and a bound on the highest peak statistics of a class of non-linear systems.

02 p0188 A73-12602

Estimation of the cumulative amplitude probability distribution function of ionospheric scintillations. [AD-756247]

03 p0275 A73-13644

Failure probability distribution models for reliability analysis, considering selection criteria based on application

04 p0507 A73-14708

Limit analysis of structures with stochastic strength variations.

04 p0510 A73-15027

Estimates of reliability functions for systems with redundancy.

04 p0471 A73-15210

Estimation of the cumulative amplitude probability distribution function of ionospheric scintillations.

04 p0443 A73-15477

Vertical scintillation propagation from ground characterized by log normal probability distribution, universal spectral function and variance behavior dependent on near ground meteorological conditions

05 p0569 A73-16625

Pulse and monochromatic short wave signals phase/amplitude autocorrelation functions and probability distributions during oblique incidence reflection from ionosphere

05 p0550 A73-16776

Numerical calculation of cumulative probability from the moment-generating function.

05 p0591 A73-16815

Mathematical model for independent operations complex with rectangular probability distribution of random parameters, noting time optimal control

05 p0562 A73-17282

Transmission of a GaAs laser beam through the atmosphere.

06 p0699 A73-17495

Performance of M-ary PSK systems in Gaussian noise and intersymbol interference.

06 p0665 A73-18140

Estimate of the probability density and distribution function of a scalar product of vectors with independent, normally distributed components

07 p0845 A73-20050

Frequency response of a dynamic system with statistical damping.

08 p0950 A73-20715

Numerical experiments on probability distribution of random force in stellar gravitational systems, noting agreement with Chandrasekhar and von Neumann theory

08 p1003 A73-20884

A special purpose computer for the study of fading signals.

08 p0939 A73-21139

Statistical phenomena during shock wave formation

08 p0955 A73-21447

Measurement of log-irradiance fluctuation of He-Ne laser in the atmosphere.

09 p1096 A73-22750

Opacity probability distribution functions for application to non-grey late-type stars model atmospheres.

09 p1149 A73-23131

A probabilistic evaluation of helicopter lift capability.

10 p1175 A73-23775

Bi-static-radar estimation of surface-slope probability distributions with applications to the moon.

10 p1190 A73-24892

Use of simple test signals in experimental investigations of devices for measuring the one-dimensional probability characteristics of random signals

11 p1360 A73-25019

Shaping of the one-dimensional distribution and correlation function of a reference signal when checking statistical analyzers

11 p1360 A73-25022

Error analysis of a generator with a uniform probability distribution of instantaneous values

11 p1331 A73-26100

Ruby and Nd-YAG pulsed laser induced surface damage probability comparison at 1.06 and 0.69 micron wavelengths by breakdown starting time distribution measurement

11 p1377 A73-26226

Rate of convergence of the distribution of the maximum of successive sums of independent random variables

12 p1516 A73-26958

Regularity of conditional probabilities for random processes

12 p1518 A73-27192

Inequalities for the large deviation probabilities of sums of independent random quantities in the case of a limiting stable law

12 p1518 A73-27221

Equations for finitely-dimensional probability distributions of pulsating variables in a turbulent flow

13 p1599 A73-28287

Accuracy of switching pressure of fluidic OR-NOR device.

13 p1571 A73-29044

Correlated clutter and resultant properties of binary signals.

13 p1585 A73-29208

Statistical effects in the generation of shock waves.

15 p1860 A73-31011

Probability distribution of the concentration and intermittency in turbulent jets

15 p1862 A73-31286

Maximum likelihood M-ary detection theory application to incoherent optical system model based on photodetectors governed by Laguerre counting statistics, deriving error probability

15 p1875 A73-31734

Solar radiation fluxes at the earth's surface in the presence of cumulus clouds

15 p1905 A73-31794

Probability distribution function of cloud spectral brightness for IR range based on 1966-1969 observations

15 p1905 A73-31821

Error probability of binary optical communications in turbulent atmosphere - Experimental results.

16 p1984 A73-33995

A projection model for Bayesian estimation of distributed functions.

17 p2202 A73-35373

Asymptotic methods for the effectiveness computation of a sampling scheme of active sub-channels in an adaptive, multi-channel communication system.

17 p2129 A73-35712

Estimates of unknown parameter from quantized observations given as sequence of evenly distributed random values, noting optimal grouping equations for general distribution function

17 p2130 A73-35722

Density of the radiation of the earth/atmosphere system into space

18 p2309 A73-36112

Detection probability of laser radars for satellite ranging.

18 p2290 A73-36882

Distribution of peaks in atmospheric radio noise.

19 p2403 A73-37269

Methods for calculating and enhancing the efficiency of automatic systems

20 p2540 A73-38705

Probabilistic statistical methods for analysis of impulse flows in nerves

20 p2516 A73-39002

Latitudinal distribution change in the conditions for F1 layer occurrence from the solar-activity maximum to minimum

20 p2554 A73-39170

Smoothed distribution function of equilibrium states and probability of particle occurrence in thermodynamic systems, using Liouville equation

20 p2627 A73-39294

Frequency distribution of the parameters of the diurnal variation of the cosmic ray intensity

21 p2755 A73-40112

Determination of the root-mean-square and mean intensity of the atmospheric radio noise field

21 p2648 A73-40208

Probability distribution of electric fields in thermal and nonthermal plasmas.

21 p2744 A73-40216

Risk of estimation by data obtained via communication channel.

21 p2654 A73-40689

Equations for the finite-dimensional probability distributions of pulsating variables in a turbulent flow.

22 p2840 A73-41810

The theory of distribution of elastic deformations in two-component composites

24 p3102 A73-44521

PROBABILITY THEORY

Mean error probability during diversity reception at extremal group frequencies under random noise conditions

01 p0019 A73-11262

Experimental determination of the probability characteristics of perturbations relative to the principal axis of a gyroscope

01 p0054 A73-11414

Survival probability of a system with a Poisson flow of losses in life-sustaining elements

01 p0028 A73-11422

Stability characteristics of thin elastic plate with time varying temperature under transversal magnetic field, calculating buckling probability

02 p0234 A73-12016

Conjoint-measurement framework for the study of probabilistic information processing.

02 p0138 A73-12545

A variational principle for wave propagation in random media.

02 p0194 A73-12732

Russian book on machine-based determination of random process characteristics covering correlation, moment functions, spectral features, probability functions, etc

02 p0149 A73-12866

Molecular transmission probability through duct connecting two large vessels calculated from data on cylindrical tubes, comparing with Monte Carlo data for error correction

03 p0341 A73-12905

Probabilistic aspects of fatigue; Proceedings of the Symposium, Atlantic City, N.J., June 27-July 2, 1971.

03 p0387 A73-13228

New method for the statistical evaluation of constant stress amplitude fatigue-test results.

03 p0387 A73-13229

Estimating the median fatigue limit for very small up-and-down quantal response tests and for S-N data with runouts.

03 p0387 A73-13230

Regression models for the effect of stress ratio on fatigue crack growth rate.

03 p0387 A73-13231

Comparison of scatter under program and random loading and influencing factors. [DFVLR-SONDDR-259]

03 p0387 A73-13232

Investigation of fatigue life and residual strength of wing panel for reliability purposes.

03 p0387 A73-13233

A reliability approach to the fatigue of structures.

03 p0387 A73-13234

Random fatigue of 2024-T3 aluminum under two spectra with identical peak-probability density functions.

03 p0322 A73-13235

On the probabilistic determination of scatter factors using Miner's rule in fatigue life studies.

03 p0388 A73-13237

An exact analysis of the Method-One maintainability demonstration plan in MIL-STD-471.

03 p0336 A73-13731

Multilayer debugging process / A new method of screening/.

03 p0336 A73-13734

Effects of test capability on system reliability and availability.

03 p0313 A73-13736

Error probabilities estimates for digital communication systems using orthogonal multiposition signals in data transmission

03 p0278 A73-14029

Structural reliability definition and determination in terms of survival probability concept, discussing analytical errors effect on design and applications to aerospace vehicles

04 p0508 A73-14724

Recent studies towards the development of procedures for design of brittle materials.

04 p0508 A73-14725

Static analysis of beams with random material or environmental characteristics, deriving probability functions for beam descriptors

04 p0509 A73-14945

Probability model and causal approach to failure mechanisms and reliability of control system elements applied to IC

04 p0424 A73-15208

Structural reliability under cumulative fatigue damage and chance overload interaction, postulating kinetic fracture model based on probabilistic service load histories

04 p0512 A73-15243

Low error rate transmission by iterative probabilistic threshold decoding, noting performance improvement over sequential and low density parity check code techniques from simulation

04 p0425 A73-15399

Information theory mathematical models applied to different visual function activity phases, covering Shannon and Fisher probability models, Shreider semantic theory and Kolmogorov algorithm
04 p0412 A73-15784

Radar sequential detector for digital processing of signal masked by noise, determining false alarm and detection probabilities and mean sampling time
04 p0423 A73-15917

Indeterminacy functions side maxima for phase manipulated signals with low sidelobe levels in autocorrelation functions, noting Doppler frequency shift effect
04 p0423 A73-15925

Attempt at the application of the theory for linear extrapolation of probabilistic processes in long-range temperature forecasts
05 p0593 A73-16235

Probability of short-wave signal transmission over a medium-range path
05 p0548 A73-16263

Analytical techniques for the determination of equipment probability of survival to radiation stress.
05 p0596 A73-16509

On the probability of error and the expected Bhat-tacharyya distance in multiclass pattern recognition.
05 p0554 A73-16814

Determination of the average duration of a machining process on automatic production lines
05 p0582 A73-16997

The probability of fracture as parameter of crack propagation under cyclic stress
05 p0635 A73-17065

The limiting theorems for certain functionals of multidimensional additive processes
05 p0591 A73-17226

Probabilistic minimum weight limit design of one dimensional pin jointed structures with random continuous variables, using stochastic programming
06 p0757 A73-17397

Cosmic-ray particle density
06 p0742 A73-17771

Optimal sampling and quantization rates for analog signal by mean-square-error estimates and information content quantitative measure, describing probabilistic properties estimation
06 p0664 A73-17854

Transmission quality in noiseless multiple-access systems with feedback
06 p0679 A73-17855

Method for planning systems with prescribed design reliability
06 p0670 A73-17857

Probability estimate for visual target detection in terms of luminance threshold and target size and duration
06 p0658 A73-18242

Noise figures, detection probabilities and scintillation energy distributions in second generation image intensifier tubes
06 p0676 A73-18299

Electromagnetic interactions of cosmic ray muons in iron. II - Momentum dependence of the interaction probabilities.
06 p0743 A73-18387

Scalar and vector partitions of the probability score. II - N-state situation.
06 p0720 A73-18704

Failure causes probability and accelerated life test conditions for ceramic capacitors, noting product selection by modified quality control procedures
07 p0799 A73-19405

Flawless operation probability for information transmission reliability of electronic logic circuits with binary data inputs
07 p0801 A73-20040

Ionograms for slant sporadic E layer under continuous sunlight inside polar cap, noting occurrence probability and auroral activity
07 p0819 A73-20065

Flight vehicle equations of motion with variable information, noting flight control algorithm for random variable with given probability
07 p0849 A73-20077

Arithmetic of probability laws defined on a separable Hilbert space
07 p0845 A73-20148

Probability theory for vibrational strength of turbomachine parts, calculating statistical maximum stress for given stress distribution conditions
07 p0917 A73-20502

Calculation of probabilities of energy transfer - Application to the vibrational relaxation of the CS radical in the presence of argon
07 p0854 A73-20608

Theory and application of the optimal linear approximation of linear processes
08 p0983 A73-20645

The oscillation probability of self-excited multimode oscillators.
08 p0945 A73-20803

Probability estimates of the accuracy of a solution to the problem of antenna synthesis in the case of an

experimental determination of the direct operator of the problem
08 p0946 A73-21104

Thermodynamic probability and statistical interpretations of entropy, with particular attention to information theory, negentropy and Boltzmann-Gibbs theory
08 p1022 A73-21234

Probabilistic analysis of the statistical accuracy of a transistor blocking generator with a common emitter
08 p0949 A73-21590

On degenerate elliptic-parabolic operators of second order and their associated diffusions.
09 p1111 A73-21996

Digital FM signal receiver with postdetector integration, determining error probability as function of input SNR and noise stability
09 p1049 A73-22044

Resonant enhancement of photoexcited nitrogen trap n-type GaAs laser electron-hole recombination probability by crystal composition variation and gamma conduction band degeneration
09 p1093 A73-22255

Probability characteristics of complex systems with a hierarchical control
09 p1068 A73-22559

A reliability and comparative analysis of two standby system configurations.
09 p1112 A73-22643

Probabilistic model for the resolvent kernel in diffusion problems in spherical-shell media.
09 p1121 A73-23071

L orthogonal signaling scheme transmission bandwidth tradeoff with error probability performance of associated receiver used for data detection
09 p1054 A73-23383

Ordinal relationships between measures of the 'accuracy' and 'value' of probability forecasts - Preliminary results.
10 p1244 A73-23646

Universal methods for estimating probabilities of cloud-free lines-of-sight through the atmosphere.
10 p1245 A73-23981

Hedging, proper and improper skill scoring rules for meteorological probability forecasts
10 p1246 A73-23992

On the normality and accuracy of simulated random processes.
10 p1292 A73-24395

Evaluation of the characteristics of the boundary layer in transitional flow on a flat plate
10 p1296 A73-24497

Description of random processes with allowance for irregularity of changes in their properties
11 p1340 A73-25008

A probabilistic model of an optical-field and the statistical properties of a videosegment from a vidicon target
11 p1360 A73-25025

Probabilistic fragmentation model for collapsing interstellar cloud, predicting stellar mass spectrum
11 p1415 A73-25171

Approximate log normal distribution of normalized power antenna patterns, relating first sidelobe level and antenna size to 0.5 probability level
11 p1337 A73-25668

Influence of control periodicity on the reliability of repairable devices
12 p1502 A73-26760

Book - Fourier analysis in probability theory.
12 p1517 A73-27051

Unified approach to the performance analysis of linear modulation systems with coherent detection.
12 p1469 A73-27072

Some general questions in the theory of probability measures in linear spaces
12 p1517 A73-27187

Optimal control with probabilistic quadratic performance criterion and constraints, using stochastic principle for reduction to time derivative maximization problem
12 p1485 A73-27897

Kalman filtering of systems with parameter uncertainties - A survey.
13 p1597 A73-29569

Probabilistic properties and spectral characteristics of the duobinary code in the baseband
14 p1729 A73-30897

Central limiting theorem in the 'noncommutative' probability theory
15 p1899 A73-31215

Description of the $I_{\text{sub } \alpha}$ class in a special subgroup of probabilistic measures
15 p1899 A73-31243

Evolution of the CO vibrational energy distribution in a transverse flow laser.
15 p1884 A73-31313

Probability series weak uniform convergence based on Billingsley-Topsoe uniformity theorem, using Borel set theory for separable metric space
16 p2031 A73-33107

Reliability estimate of a Space Deployable Antenna.
16 p1989 A73-33620

Statistical and probabilistic MTBF models for parts, sockets and systems reliability
16 p2020 A73-33628

Probabilistic analysis of sequential test plans.
16 p1986 A73-33636

Probabilistic fatigue design alternative to Miner's cumulative damage rule.
16 p2061 A73-33643

Probabilistic radiative transfer - Mean number of scatterings.
16 p2038 A73-33739

Application of the random walk method for solving problems in the theory of elasticity
17 p2241 A73-34332

Probabilistic model for radiative transfer problems in cylindrical shell media with complete redistribution in frequency.
17 p2236 A73-35781

A probabilistic approach to the design of heat pipes. [AIAA PAPER 73-754]
18 p2370 A73-36370

Optimal control with probabilistic quadratic performance criterion and constraints, using stochastic principle for reduction to time derivative maximization problem
18 p2294 A73-36602

Vector partition of probability [Brier] score providing reliability and resolution measures of weather forecasts
18 p2332 A73-36703

Heat detector signal transients during time constant fluctuations in terms of mathematical expectation of ambient temperature
18 p2317 A73-36857

A topology on a group of measurements of probability defined on a Borelian tribe with an enumerable base, and an associated Glivenko-Cantelli theorem
19 p2444 A73-37534

Probability theory for vibrational strength of turbomachine parts, calculating statistical maximum stress for given stress distribution conditions
19 p2499 A73-37777

Probability of error in binary communication systems with causal band-limiting filters. I - Non-return-to-zero signal. II - Split-phase signal.
19 p2415 A73-38384

Probabilistic automata minimization for system states reduction by deterministic matrix method
19 p2408 A73-38564

Pulse-position modulation based on energy detection.
21 p2649 A73-40329

Probability of error in a bandlimited quadriphase communication system.
21 p2649 A73-40334

Degradation of probability of error due to IF filtering.
21 p2649 A73-40335

Considerations concerning the evaluation of the detection probability in radar systems
21 p2650 A73-40500

The quantity of initial-parameter information contained in trajectory measurements
21 p2726 A73-40916

A probabilistic algorithm for grouped handling of arguments with sequential discrimination of input features
21 p2658 A73-40994

Russian book on probabilistic computer simulation and statistical processing techniques covering linear algebra and partial differential equations, Markov chains, random numbers, automata, and analog modeling
21 p2659 A73-41432

Risk analysis and reliability based design for probabilistic approach implementation for safety and performance of structures and structural components
21 p2788 A73-41650

Safety margins in the implementation of planetary quarantine requirements.
22 p2803 A73-42161

A few error detection codes for decision feedback system and error characteristics of channels.
22 p2835 A73-42192

Probabilistic analysis of random and deterministic phase coding for lowering Fourier transform spectrum dynamic range in digitally generated hologram and kinoform memories
22 p2864 A73-43149

Statistical analysis of two dimensional turbulence, noting probability characteristics ergodicity with respect to class of two dimensional characteristic functions with converging mean squares
23 p2968 A73-43475

Resolution of point sources of light as analyzed by quantum detection theory.
23 p2987 A73-43523

Bayes theorem for probabilistic analysis of logic circuits applied to reliability estimation of switching circuits
23 p2965 A73-44107

A model for estimating joint probabilities of cloud-free lines-of-sight through the atmosphere.
23 p3004 A73-44260

Probabilistic molecular contact rupture strength at solid-solid adhesive joint interface

24 p3092 A73-44516

Revision of the probability laws of sunspot variations.

24 p3137 A73-44648

Reliability estimation for repairable and nonrepairable flight vehicles, considering nomographs for failure rate and probability of defined requirements satisfaction

24 p3057 A73-45197

PROBLEM SOLVING

NT ASYMPTOTIC METHODS

NT ITERATIVE SOLUTION

NT THEOREM PROVING

PLANEX I plan executor program for robot system, creating plan for sequence of actions via problem solving program STRIPS

01 p0020 A73-11452

Reasoning by analogy as an aid to heuristic theorem proving.

01 p0020 A73-11453

Intellectual ability and performance on a non-verbal problem-solving task.

03 p0260 A73-13553

Book on passive IR sensing devices design and use in industrial and manufacturing problems solution covering detector types, display devices and reliability analysis

03 p0283 A73-13994

Procedural formalization and methodology for automated problem solving in terms of digital program systems for algorithms generation, describing operational procedures

06 p0669 A73-17594

Studies in interactive communication. I - The effects of four communication modes on the behavior of teams during cooperative problem-solving.

06 p0658 A73-18241

Critique of Poincare technique for construction of global solution of resonance of dynamical system, considering procedure using secular terms and regularizing function

15 p1930 A73-31111

A computer program to find analytical solutions of second order linear differential equations.

17 p2132 A73-35611

Monograph on Question-Answerer 4 /QA4/ programming language for artificial intelligence application to problem solving covering pattern matching, built-in functions and robot work tasks

22 p2830 A73-42745

PROCEDURES

NT FINITE ELEMENT METHOD

NT OPTICAL CORRECTION PROCEDURE

PROCESSORS (COMPUTERS)

U CENTRAL PROCESSING UNITS

U COMPUTERS

PROCUREMENT

NT GOVERNMENT PROCUREMENT

PROCUREMENT MANAGEMENT

C-5 program developments and alterations in terms of defense requirements and cost problems, discussing objectives and management policies in F-15 and B-1 projects

01 p0124 A73-11069

Book - Applied maintainability engineering.

02 p0238 A73-18883

Reducing the cost of the R&D proposal process.

02 p0239 A73-12349

Quality control in Concerto reliable space components procurement program for multilayer ceramic capacitors and thermistors manufacture

07 p0829 A73-18920

French Concerto aerospace part procurement program contribution to mass produced electronic component reliability assessment, control and improvement based on tin oxide resistor experience

07 p0829 A73-18923

French Concerto program for component reliability and quality assurance in manufacturing and procurement controls for Symphonic satellite

07 p0790 A73-18975

Electronic display devices for command, monitoring, surveillance, simulation and training in military applications, considering reliability, cost and performance specifications in procurement decision making

08 p0965 A73-21245

Government request to industry to propose product or service for buyer, discussing procurement role and centralized vs decentralized control

09 p1168 A73-21946

USAF experience in lightweight fighter aircraft acquisition as illustration of requests for industrial proposals simplification and source selection process streamlining

09 p1168 A73-21947

Government request to industry to propose product or service to buyer, discussing communications effectiveness, technical and management requirements and procurement

09 p1168 A73-21948

Mobile satellite communication systems constraints imposed by international institution disagreements on management, procurement and operation, considering US and European conflicts on Aerosat project

12 p1471 A73-27653

Two approaches to aircraft development - The USA and Europe.

13 p1568 A73-28177

Testing and evaluation community role in weapon system acquisition, describing R and D philosophy

13 p1569 A73-28902

Resources management logistics support of research and development laboratories.

13 p1709 A73-29574

Developing country industrial product reliability from buying and manufacturing viewpoints, considering local methods, customs, attitudes and working conditions effects on management techniques

16 p2089 A73-33646

The financing of aircraft procurement.

17 p2257 A73-34534

Computerized approach for aerospace electronic components standardization for procurement cost, logistics and warehousing problems reduction and reliability improvement

17 p2140 A73-35260

PROCUREMENT POLICY

Financial problems related to aircraft and ships development and production for Defense Department, stressing C-5A, Cheyenne helicopter and DD-963 class of automated destroyers

03 p0401 A73-13897

Statistical expectation application to risk density functions and fee/incentive-element relationships for contract incentive structuring, considering C-5A procurement

08 p1025 A73-20958

PRODUCT DESIGN

U PRODUCT DEVELOPMENT

PRODUCT DEVELOPMENT

NT WEAPONS DEVELOPMENT

C-5 program developments and alterations in terms of defense requirements and cost problems, discussing objectives and management policies in F-15 and B-1 projects

01 p0124 A73-11069

Aircraft industry design and development costs prediction, using Monte Carlo model to determine effect of poor estimates

02 p0238 A73-11860

Data acquisition, processing and retrieval in information system for product design and development, noting storage system for spring material data

03 p0400 A73-13238

Aircraft engine development in terms of money, manpower, facilities and knowledge, discussing project organization and scheduling

03 p0251 A73-14469

ESKA ion thrusters - Development and application for geocentric missions.

04 p0489 A73-15739

Army 1500 shp advanced technology engine development program, discussing in components design and fabrication, air leakage losses, environmental testing and maintainability oriented design

05 p0606 A73-16627

Air and naval gyroscopic instruments development in Germany during 1927-1945, discussing inertial platforms, antiaircraft fire control, gas bearings and accelerometers

05 p0577 A73-16766

Economically viable and socially acceptable second-generation SST, discussing technological developments for range/payload, airport noise and sonic boom improvements

06 p0646 A73-17608

A business man views commercial ventures in space.

06 p0771 A73-17640

High reliability semiconductors development, discussing research in Si single crystals growth, epitaxial films, photoengraving, oxidation/passivation and large-scale integration techniques

07 p0829 A73-18919

Quality control in Concerto reliable space components procurement program for multilayer ceramic capacitors and thermistors manufacture

07 p0829 A73-18920

An innovation index based on factor analysis.

08 p1026 A73-21700

U.S. industry R and D fund cutback caused problems survey by questionnaire, discussing problem minimization with consideration for economic market conditions

10 p1298 A73-24632

Boeing 727 design and development in response to airline market requirements, emphasizing profitability

10 p1176 A73-24875

Two approaches to aircraft development - The USA and Europe.

13 p1568 A73-28177

Product liability prevention via a controlled system.

16 p2088 A73-33617

PRODUCTION ENGINEERING

NT PRODUCTION PLANNING

Investigation of the influence of technological factors on the endurance of gas-turbine engine rotor blades

01 p0114 A73-10477

Book - Forging design handbook.

02 p0173 A73-11884

Applying surface integrity principles in jet engine production.

03 p0312 A73-13272

Metal ions implantation to produce alloy or semiconductor, discussing transmission electron microscopy use for viewing target material defect clusters

03 p0350 A73-13794

Extreme value methods for design, production, testing and maintenance of components and system with low failure probability

04 p0507 A73-14709

Powder metallurgy production of structural shapes.

04 p0461 A73-15022

Russian book - Organization and planning of production at aircraft-construction plants.

04 p0524 A73-15965

Determination of the average duration of a machining process on automatic production lines

05 p0582 A73-16997

Product quality concept definition in terms of use requirements, characteristic properties reproducibility/quality control and cost, discussing steel metallurgy and fabrication methods

05 p0582 A73-16999

Explosive forming for axisymmetric dished shells without clamped blank around edge, discussing design parameters, formability limits and optimization techniques

06 p0698 A73-18095

The use of model building in a production environment.

06 p0698 A73-18514

Assembling by welding and bonding - Introductory report on assemblies

06 p0698 A73-18692

MOS production line with individual manufacturing operation reliability assurance based on failure analysis, process perfection, material control and experimental verification

07 p0829 A73-18917

High reliability technology assessment for metal film resistors production, discussing qualification tests

07 p0829 A73-18921

Reliability dynamism at the Deutsch Company.

07 p0829 A73-19008

Lost-model method of precision casting - Its possibilities, limitations and present trends

07 p0831 A73-20160

The casting of titanium and its alloys by the lost-model method

07 p0831 A73-20161

Effect of engineering-design factors on the parameters of microstrip transmission lines

08 p0951 A73-21109

Design and development of a lightweight flexible solar array compatible with mass production techniques.

09 p1036 A73-22813

Photoresist technology for passive ICs production with optical waveguides, describing vaporization deposition and processing for glass films

09 p1086 A73-23075

Equipment for casting directionally solidified parts.

09 p1089 A73-23294

Reliability and quality control of production engineering computer programs.

11 p1373 A73-25493

Automation considerations in technological methods for microcircuit fabrication, emphasizing electron-ion technology

12 p1477 A73-26783

Book - Reliability concepts in engineering manufacture.

12 p1502 A73-27398

Ni-base alloy powder metallurgy from production waste cuttings by oxidation and subsequent oxide reduction with hydrogen and calcium hydride

12 p1503 A73-27553

Part manufacturing with plasma arc torch by extending plasma spray coating technology to mandrel design and machining with consideration for base materials

13 p1624 A73-28907

Study of the effect of technical factors on the fatigue limit of the working blades of gas turbine motors.

14 p1810 A73-30302

Application of human engineering principles and techniques in the design of electronic production equipment.

14 p1722 A73-30497

Processability/mechanical properties trade-off for reinforced plastics.

17 p2197 A73-35353

Concepts from the realization of the development of the technology and assembly lines for the fabrication of polyester glass laminates

18 p2320 A73-36472

PRODUCTION MANAGEMENT

- Computer aided design-drafting /CADD/- Engineering/manufacturing tool. 19 p2407 A73-37460 [AIAA PAPER 73-793]
- Explosive metal forming, considering energy cost, operational speed, achievable tolerances in symmetrical or nonsymmetrical shapes, production quantities and lead time for die preparation 20 p2569 A73-39405
- Dynamic model of economically efficient multipurpose plants 21 p2793 A73-40386
- Certain problems in determining the capacity of digital computers 22 p2829 A73-41953

PRODUCTION MANAGEMENT

- Organization and management for adhesive bonding aircraft structures. 03 p0333 A73-13048
- Russian book - Organization and planning of production at aircraft-construction plants. 04 p0524 A73-15965
- Guide to a quality control system for Code vessels. 14 p1755 A73-30144
- Product liability prevention via a controlled system. 16 p2088 A73-33617
- Management and control of flight test programs of the Western Region FAA. 23 p3050 A73-44053

PRODUCTION METHODS

U PRODUCTION ENGINEERING

PRODUCTION PLANNING

- Dynamic prediction model and optimal control of a commercial plant 12 p1561 A73-27081
- Unit batch size optimization in mass production, discussing labor efficiency, operational cycle length, unfinished volume and total cost 12 p1562 A73-27477
- Study of the static and dynamic characteristics of a family of discrete pneumatic jet modules 16 p1971 A73-33670
- Helicopter design and production cost target and tradeoff considerations based on past programs, supplier quotations, government documents, estimating practices and functional requirements [AHS PREPRINT 712] 17 p2257 A73-35058
- Management and control of commercial flight test programs. 23 p3050 A73-44057
- Technological change measurement methodology for cost and production estimates with application to aircraft turbine engine development 23 p3020 A73-44219

PRODUCTIVITY

- Management systems for quality cost accounting, time control and productivity analysis based on random time sampling technique 06 p0771 A73-17866
- Productivity estimates of the strategic airlift system by the use of simulation. 10 p1297 A73-23774
- Justification and calculation of the lifetimes and efficiency of new equipment 12 p1562 A73-27468

PROFICIENCY MEASUREMENT

U HUMAN PERFORMANCE

U PERFORMANCE TESTS

PROFILES

- Approximate shock-free transonic solution for a symmetric profile at zero incidence. 13 p1564 A73-28823

PROFILERES

- Acousto-optical profilometer system with two diffracted laser beams for surface topography holographic measurements 06 p0694 A73-18290

PROGNOSIS

- Economic-mathematics approaches to prognostic air traffic computations 11 p1455 A73-26724
- Prediction of the outcomes of myocardial infarction from formulas derived by the dynamic programming method 20 p2516 A73-39000
- Ischemic heart disease prediction via exercise ECG tests, discussing work load standardization 22 p2809 A73-42835

PROGRAM MANAGEMENT

U PROJECT MANAGEMENT

PROGRAMMED INSTRUCTION

- Liquid crystal approach to integrated programmable digital displays and aircraft control, considering flat panel digital-matrix display 17 p2139 A73-35234

PROGRAMMING

NT QUADRATIC PROGRAMMING

- Programmed control of a two-level hierarchical system 01 p0027 A73-10665
- Programming and correcting control effects for prescribed interrelationship between variable states of dynamic control, noting system synthesis for programmed motion 01 p0027 A73-10667

- Preparation of information for programming machining operations during grinding of a blade profile by the continuous-shaping method 02 p0172 A73-11799

- Nonlinear heat transfer systems design optimization based on physical properties cost functionals, presenting geometric programming method [ASME PAPER 72-WA/HT-15] 04 p0519 A73-15833
- Book on nonlinear optimization covering search, iteration, gradient, algorithmic and computer techniques, mathematical and dynamic programming, calculus of variations, Pontryagin maximum principle, etc 06 p0717 A73-18401

- A unified approach to the problem of optimization in the design of structures. 11 p1436 A73-25477 [AIAA PAPER 73-337]

- Mathematical programming techniques of dimensionless index solutions for optimal structural design by iterative search on computer, applying to beam column steel structures 11 p1436 A73-25483 [AIAA PAPER 73-344]
- Geometric programming with signomial transformation into equivalent posynomials minimized under inequality constraints and generalization by equilibrium solutions to reverse programs in larger class 11 p1391 A73-26576

- Selection of optimal parameters for unidirectionally compressed three-layer plates 12 p1555 A73-27795

- Modified quasilinearization method for mathematical programming problems and optimal control problems. 17 p2200 A73-34362

- The use of singularity programming in finite-difference and finite-element computations of temperature. 22 p2930 A73-42287 [ASME PAPER 73-HT-K]

PROGRAMMING (SCHEDULING)

NT THRUST PROGRAMMING

- Electronic programming timer with crystal oscillator, IC counters and memory core matrix for event sequence radio control during spacecraft or rocket launchings 01 p0020 A73-11167

PROGRAMMING LANGUAGES

NT ALGOL

NT FORTRAN

NT MACHINE ORIENTED LANGUAGES

- Satellite orbit inclination function computation as representative problem in symbolic programming applied to celestial mechanics 01 p0099 A73-10688

- Simulation aids for designing integrated information systems - The ECSS language. 02 p0144 A73-12600

- The solution of linear, constant-coefficient, ordinary differential equations with APL. 04 p0470 A73-15008

- GAELIC - Grumman Aerospace Engineering Language for Instructional Checkout. 08 p0941 A73-20689

- Spring Joint Computer Conference, Atlantic City, N.J., May 16-18, 1972, Proceedings. 09 p1059 A73-22221

- Automaton external and internal languages linking by computer programming languages discussing structure and operation relation to language structure and realization 12 p1485 A73-27893

- German monograph - The design of digital filters with minimal storage word length for coefficients and state parameters. 14 p1737 A73-30667

- Small digital computer program packet organization for central processor productivity and use coefficient improvement, discussing graph-algorithm language for program splicing 15 p1848 A73-31694

- Digital simulation of physical systems using CSMP. 16 p1985 A73-33129

- An integrated, modular approach to automatic testing and data monitoring. 16 p1986 A73-33632

- Easing international language difficulties via an accommodating software design. 18 p2288 A73-36092 [AIAA PAPER 73-614]

- Command language for supervisory control of remote manipulation. 19 p2403 A73-37329

- Monograph on Question-Answerer 4 /QA4/ programming language for artificial intelligence application to problem solving covering pattern matching, built-in functions and robot work tasks 22 p2830 A73-42745

- GASP simulation of terminal air traffic system. [ASCE PREPRINT 2059] 22 p2839 A73-42868

- PEARL middle level programming language for process control, discussing algorithms, structure, time behavior and input/output of real time operation 23 p2956 A73-44388

PROGRAMS

NT APOLLO APPLICATIONS PROGRAM

NT APOLLO PROJECT

NT COMSAT PROGRAM

NT DEFENSE PROGRAM

- NT EARTH RESOURCES PROGRAM
- NT EARTH RESOURCES SURVEY PROGRAM
- NT EUROPEAN SPACE PROGRAMS
- NT JUPITER PROJECT
- NT LUNAR PROGRAMS
- NT MARINER PROGRAM
- NT MARS 71 PROJECT
- NT NASA PROGRAMS
- NT PIONEER PROJECT
- NT QUIET ENGINE PROGRAM
- NT ROVER PROJECT
- NT SATURN PROJECT
- NT SKYLAB PROGRAM
- NT SPACE PROGRAMS
- NT U.S.S.R. SPACE PROGRAM

PROJECT MANAGEMENT

- Budgeting role in development and implementation of five year plan of operations at French space research center 01 p0124 A73-11233

- Physical contents and financial underpinning of future French and European space research programs, noting meteorology, satellite communication and R and D planning 01 p0125 A73-11254

- Experience obtained so far in connection with the German scientific spacecraft program [DGLR PAPER 72-052] 02 p0227 A73-11654

- Book - Applied maintainability engineering. 02 p0238 A73-11883

- A method for re-allocating funds to meet a reduced budget. 02 p0239 A73-12348

- Aerothermodynamics R and D for space shuttle configurational design, discussing program organization and wind tunnel testing to generate design technology base 06 p0755 A73-17632

- Management and cost of European-U.S. Aerost program based on geostationary satellites for air/ground voice and data messages relay and aircraft position determination 07 p0905 A73-19174

- Apollo project management techniques transfer to socio-economic programs, discussing systems oriented approach to city planning, mass transportation, pollution control, public hygiene, etc 09 p1167 A73-21898

- Management aspects of the development of the Ariel 4 satellite. 09 p1168 A73-22915

- Project analysis - An evaluation tool for positive development direction. 10 p1298 A73-24634

- Project management and installation of the Arvi satellite communication earth station. 11 p1344 A73-26147

- The role of the Project Manager in the management of satellite projects. 11 p1454 A73-26262

- ELDO and ESRO space research activities review, stressing increased European cooperation, negotiations with U.S. and project budgeting vs national priorities 11 p1455 A73-26420

- Book - The Polaris system development: Bureaucratic and programmatic success in government. 12 p1561 A73-27400

- Two approaches to aircraft development - The USA and Europe. 13 p1568 A73-28177

- AEROS satellite launching from Western Test Range, describing time sequence of satellite and rocket countdwns and communication system activities coordinated by project management 13 p1689 A73-28781

- Engineering management for the Dallas/Fort Worth Airport. 13 p1708 A73-29110

- Multi-Role Combat Aircraft Program management, discussing international cooperation, industrial arrangements and governmental objectives 13 p1709 A73-29384

- Sortie lab experiment management, integration and operational techniques, discussing airborne science/shuttle experiment system simulation /AS-SESS/ program 14 p1803 A73-29942

- Aerospace industry project managers and support personnel authority perceptions based on assessment of situational factors surrounding decision making, tabulating empirical investigation statistics 17 p2257 A73-35214

- Project form of organization adoption for managing innovation, stressing impact of technology on career progression of scientist engineers 17 p2258 A73-35217

- A fundamental methodology for planning and management of research and development programmes. 17 p2258 A73-35836

- The Netherlands astronomical satellite /ANSI/. 22 p2917 A73-42291

Society of Flight Test Engineers, National Symposium, 3rd, Arlington, Tex., September 11-14, 1972, Proceedings.

23 p3050 A73-44052
Management and control of flight test programs of the Western Region FAA.

23 p3050 A73-44053
Management and control of flight test programs at U.S. Army Aviation Systems Command.

23 p3050 A73-44054
Management and control of commercial flight test programs.

23 p3050 A73-44057
Air Force Prototype Program management.

23 p3051 A73-44061
The role of a military flight test engineer in test management.

23 p3051 A73-44062
The capabilities of government test facilities at the Air Force Systems Command.

23 p2966 A73-44065

PROJECT PLANNING

GREMEX - A management game for the new public administration.

01 p0124 A73-11007
Scientific mission and German and U.S. plans/design for Helios cooperative solar probe, stressing advanced technology requirements

01 p0110 A73-11103
The ground operations system for the AEROS research satellite.

08 p0953 A73-21661
Logistics planning with cost reduction for NASA phased programs in conducting R and D and real time inventory control, discussing major activities and objectives

11 p1454 A73-25450
Space shuttle orbiter system planning and operational modes, considering propulsion into orbit, automated observatories, sortie workshop and European cooperation

14 p1803 A73-29943
A procedure for the minimization of the costs of a project in the case of a given project duration

15 p1959 A73-31224
Design considerations for offshore airports.

15 p1856 A73-31527
Denmark offshore airport projects progress reports covering historical background, present status, political efforts, legislation, market retention, access problem and technical design considerations

15 p1960 A73-31537
Canadian government planning for second land based or offshore jet airport in Toronto area, considering environmental and community factors

15 p1858 A73-31545
A fundamental methodology for planning and management of research and development programmes.

17 p2258 A73-35836
Indian national educational communications program for information dissemination on health, family planning, hygiene and agriculture, discussing satellite TV development project

20 p2629 A73-38576
[AAS PAPER 73-106]
Management and control of flight test programs of the Naval Air Systems Command.

23 p3050 A73-44056
Management and control of military and commercial flight test programs at Bell Helicopter Company.

23 p3050 A73-44058
Flight test programs management and control, considering weapon systems performance tests relative to contractual requirements, personnel allocation and supporting facilities

23 p3051 A73-44060

PROJECTED AREAS

U AREA
U PROJECTIVE GEOMETRY

PROJECTILE CRATERING

Fracture due to damage from projectile impact.

06 p0763 A73-18484
Investigation of the Canyon Diablo metallic spheroids and their relationship to the breakup of the Canyon Diablo meteorite.

09 p1144 A73-22145
Close range photogrammetry of objects moving at high speed.

09 p1081 A73-22377
French monograph - Study of craters formed on glass surfaces by the impact of artificial micrometeoroids.

15 p1898 A73-32591
Investigation of the hypervelocity impact on thin plastics and metal foils

21 p2696 A73-39990
Ceramic component strength degradation by projectile impacts in terms of momentum and elasticity relation

21 p2723 A73-40892

PROJECTILES

NT HYPERVELOCITY PROJECTILES
NT SABOT PROJECTILES

On the higher approximations of the supersonic projectile theory.

[AIAA PAPER 73-669] 18 p2262 A73-36220

PROJECTION

The role of interpolation and approximation theory in variational and projectional methods for solving partial differential equations.

01 p0071 A73-11458
Central projection parameter determination of photographed objects

06 p0693 A73-18153
Two direct methods for reconstructing pictures from their projections - A comparative study.

09 p1080 A73-22224
Continuous best approximation projections in certain Banach spaces

09 p1113 A73-23027
Chebyshev projections properties, determining method for minimum linear distortion in class of conformal mappings of given region

10 p1212 A73-24300

PROJECTIVE DIFFERENTIAL GEOMETRY

U DIFFERENTIAL GEOMETRY

U PROJECTIVE GEOMETRY

PROJECTIVE GEOMETRY

Cartesian coordinates for panoramic perspective position of point on conical map, noting relationship to semipolar coordinates of object point

02 p0166 A73-11644
The reconstruction of three-dimensional objects from two orthogonal projections and its application to cardiac cineangiography.

06 p0657 A73-17801
Parallel algorithms for plotting profiles, projections, and cross sections with the aid of receptor matrices on a digital computer

08 p0941 A73-21588
Collinear theory of photogrammetry developed from projective equations in three dimensional space through singular transformation with 11 independent parameters

09 p1082 A73-22383
Analytical transformation of photographs for plotting topographic and photographic maps in prescribed projections

10 p1219 A73-24483
Projective properties of an anamorphic bundle of projecting beams

10 p1219 A73-24484
Projection method in the shell theory and its realization on a computer

15 p1944 A73-30971
Theory of conjugate projections in finite element analysis.

17 p2201 A73-34828
Almost projective mapping of gravitational fields - Degenerate case

17 p2212 A73-35564
Use of the azimuthal equal-area projection to display radiation patterns of complex antennas

21 p2661 A73-40202
A cartographic projection of photographs of celestial bodies obtained from space

21 p2769 A73-40860
Motion of a solid with a nonholonomic constraint at a fixed point

23 p3007 A73-44200

PROJECTORS

Servo-controlled moving stimulus generator for single unit studies in vision.

14 p1722 A73-30401
Astronomical educational aids design and application, including photometers for star cluster detection, ocular comparators and projection devices for photograph examination

16 p2014 A73-32950

PROJECTS

NT APOLLO PROJECT

NT APOLLO SOYUZ TEST PROJECT

NT JUPITER PROJECT

NT MARS 71 PROJECT

NT ORBITER PROJECT

NT PIONEER PROJECT

NT ROVER PROJECT

NT SATURN PROJECT

PROLATE SPHEROIDS

The extended boundary condition solution of the dipole antenna of revolution.

01 p0016 A73-10186
Closed form analytical solution for secondary flow in viscoelastic liquids axisymmetric flow past oblate and prolate ellipsoids

06 p0687 A73-18507
Correction to 'The echo area of a perfectly conducting prolate spheroid.'

11 p1330 A73-25684

PROMETHIUM

Triply ionized Pm in lithium yttrium fluoride laser, calculating crystal field split energy levels and radiative transition probabilities

21 p2715 A73-40764

PROMINENCES

NT SOLAR PROMINENCES

PRONY SERIES

Inversion of Prony series characterization for viscoelastic stress analysis.

09 p1158 A73-22393

PROPAGATION [EXTENSION]

NT CRACK PROPAGATION

NT FLAME PROPAGATION

PROPAGATION MODES

Helical gas lenses for guiding optical beam over long distances, calculating irradiance patterns for various propagation mode numbers and temperatures

01 p0053 A73-11218
Studies of the lower ionosphere by means of VLF propagation over long distances

01 p0044 A73-11515
Quasimonochromatic whistler mode packets of slowly varying amplitude.

02 p0140 A73-11920
An analysis of multi-station ground observations of VLF Hiss.

03 p0274 A73-12950
Mathematical treatment of long wave sound propagation in curved ducts and junctions, obtaining principal mode from linearized equation of motion solved for eigenvalues

03 p0343 A73-13832
Space-modulated side radiation from an ultrasonic beam in a solid.

03 p0344 A73-14042
Attenuation of spiral modes in a circular and annular lined duct.

04 p0487 A73-15591
Characteristics of waveguides containing anisotropic warm plasma in the presence of transverse magnetic field.

04 p0480 A73-15600
Higher-order evanescent modes on slow-wave structures.

05 p0547 A73-16160
Mirror corner for use with overmoded circular waveguide.

05 p0548 A73-16165
Pulse propagation in a two-mode waveguide.

05 p0548 A73-16365
Higher-order loss processes and the loss penalty of multimode operation.

05 p0549 A73-16367
Nonducted whistlers observed in the plasmasphere.

05 p0572 A73-17165
Radiative modes of a weakly ionized, collision-dominated, turbulent plasma.

05 p0624 A73-17309
Resonance and propagation theory for all electromagnetic wave types in plasmas of ionosphere and interplanetary space, discussing stability and oscillations

06 p0689 A73-17505
Eigenvalues of a class of spherical wave functions.

06 p0665 A73-18177
Aperture fields and gain of open-ended parallel-plate waveguides.

06 p0676 A73-18178
A comparison of mode match, geometrical theory of diffraction, and Kirchhoff radiation.

06 p0666 A73-18192
Normal-mode analysis of anisotropic and gyrotropic thin-film waveguides for integrated optics.

06 p0702 A73-18365
Nonlinear mode-mode coupling of Alfvén waves in the interstellar medium.

06 p0730 A73-18465
Cut-off frequency calculation for TE and TM modes in doubly ridged circular and elliptical microwave waveguides, using Mathieu function and eigenfunctions

06 p0669 A73-18736
Satellite S-band telemetry evanescent mode waveguide diplexer design with foreshortened band-pass filters to eliminate I junction and connecting flanges

06 p0678 A73-18741
Quartz optical waveguide by ion implantation.

06 p0703 A73-18745
Pulse broadening in multimode fibres excited by GaAs lasers.

07 p0833 A73-19155
Propagation and radiation characteristics of corrugated horns.

07 p0798 A73-19156
Effect of collision frequency on the characteristics of waveguide filled with homogeneous anisotropic plasma.

07 p0857 A73-19533
Surface wave characteristics of circular cylindrical corrugated and uniform dielectric rod excited in E sub 0-mode.

07 p0792 A73-19545
Corrugated and uniform dielectric rod aerial excited in E sub 0-mode.

07 p0792 A73-19547
Application of the Lorentz lemma to the calculation of diffraction mode excitation coefficients

07 p0793 A73-19918
Wave transformation by a phase corrector

07 p0793 A73-19923

- VLF modal interference effects observed on transequatorial paths. 07 p0793 A73-20059
- R and L modes of ion cyclotron whistler propagation in ionosphere, noting refractive indexes and wave polarization for multicomponent plasma 07 p0819 A73-20060
- The computation of critical frequencies of waves of higher types in a hollow elliptical waveguide. 07 p0802 A73-20141
- Refraction of acoustic duct waveguide modes by exhaust jets. 07 p0812 A73-20338
- Propagation modes of radio whistlers and gyroelectric echoes received in middle latitudes 08 p0937 A73-20651
- VLF ion cyclotron whistler propagation in upper ionosphere, noting polarization reversal and mode coupling from satellite observation 08 p0937 A73-20653
- Horizontal-polarization biconical horn antenna excited by TE/sub-11/ mode in circular waveguide. 08 p0945 A73-20805
- Trapped electrons instability in Tokamak configuration, calculating plasma wave propagation modes via Fokker-Planck equation 08 p0991 A73-20815
- Electromagnetic effects on electrostatic modes in a magnetized plasma. 08 p0991 A73-20820
- Circular electric waveguide of minimum loss and elastic flexibility. 08 p0938 A73-20838
- Simultaneous suppression of an electron plasma wave and an ion acoustic wave by beam modulation. 08 p0992 A73-21006
- Band-splitting filters in oversized rectangular waveguide. 08 p0946 A73-21119
- Laser oscillation in leaky corrugated optical waveguides. 08 p0975 A73-21206
- The design, analysis, and performance of resonant and nonresonant microwave transmission devices with theoretically infinite rejection. 09 p1080 A73-22103
- Nighttime midionosphere dynamical perturbations on ionizations from solutions of time dependent continuity equation with charge transport effects, considering semidiurnal atmospheric tide propagation mode 09 p1075 A73-22130
- Phase and amplitude variations of 40-kHz radio waves propagating over a 7.1-Mm path. 09 p1049 A73-22134
- Investigation of the dielectric waveguide modes in homostructure GaAs laser. 09 p1091 A73-22238
- Propagation of electronic longitudinal modes in a non-Maxwellian plasma. 09 p1126 A73-22278
- Design criteria for high gain, wide band, microwave amplifiers. 09 p1062 A73-22304
- Transmission zeros in microstrip discontinuities, considering structure effective width for TEM and higher modes 09 p1049 A73-22315
- Propagation in periodically loaded waveguides with higher symmetries. 09 p1063 A73-22490
- Nonducted whistlers observed in the plasmasphere. 09 p1078 A73-22748
- Propagational mode deduced from signal strengths in the VHF band on the trans-equatorial path. 09 p1051 A73-22749
- Conductivity tensor and dispersion equation for collisional magnetoactive plasma. 09 p1131 A73-22922
- Transmission loss at high frequencies on 3260 km temperate-latitude path. 09 p1052 A73-22958
- Near-field technique for inferring aperture antenna radiation patterns. 09 p1052 A73-22960
- Fundamental and parasitic modes of a shielded microstrip transmission line 09 p1052 A73-23085
- Book - Optical waveguides. 09 p1066 A73-23274
- Characteristics of waveguides filled with homogeneous lossy anisotropic drifting plasma. 10 p1192 A73-23574
- General cavity analysis for corrugation in rectangular waveguide microwave filters, using admittance method with consideration for propagation modes 10 p1192 A73-23606
- Analysis of electromagnetic-wave modes in lens-like media. 10 p1248 A73-23834
- Tube waveguide for optical transmission. 10 p1196 A73-24624
- Half-harmonic modes for different frequency ranges and wave vectors from infinite homogeneous plasma model for high frequency electrostatic wave propagation in magnetosphere 10 p1213 A73-24733
- Group velocity and nonlinear dispersive wave propagation. 10 p1249 A73-24775
- The transition from locked to leaky modes in tropospheric radio propagation. 11 p1327 A73-25122
- Negative energy mode loss to positive energy mode in positive-negative energy wave interactions within magnetized plasma, considering ion acoustic waves 11 p1402 A73-25123
- Two mode rectangular waveguide longitudinal and transverse narrow half wave slots properties, discussing measurement apparatus and techniques and radiation patterns 11 p1328 A73-25661
- Radiation pattern produced by open ended radial waveguide with TM mode excitation, comparing computed with measured patterns 11 p1329 A73-25677
- Physical interpretation of the diurnal behavior of the TM and TE components of VLF fields in the far zone 11 p1331 A73-26152
- Small amplitude hydromagnetic waves for a plasma with a generalized polytrope law. 11 p1406 A73-26555
- Calculation of the statistical characteristics of a long waveguide line in a two-wave model 12 p1469 A73-27189
- IMCON reflection mode dispersive delay line in large time-bandwidth product pulse compression systems, deriving operational characteristics from transfer function 12 p1480 A73-27565
- Anisotropic piezoelectric heterogeneous acoustic surface waveguides of arbitrary cross section computing mode spectrum by efficient and accurate numerical techniques 12 p1480 A73-27568
- Measurements of wave normal direction of whistler mode signals in the ionosphere by means of the rocket-Doppler technique. 12 p1492 A73-27610
- Employment of mode theory and ray theory for the interpretation of very-long-wave measurements at medium distances 12 p1474 A73-27769
- Flare-produced coronal MHD-fast-mode wavefronts and Moreton's wave phenomenon. 12 p1536 A73-27848
- VLF atmospheric measurement and geophysical analysis, discussing meteorological, geoelectric and propagation aspects 13 p1582 A73-28151
- A mode theory of radio wave propagation in an inhomogeneous atmosphere with jointed-segment N-profile. 13 p1586 A73-29227
- Critical frequencies of electromagnetic wave propagation in H waveguides with a dielectric cross-piece 13 p1595 A73-29411
- Acoustic-gravity modes and large-scale traveling ionospheric disturbances of a realistic, dissipative atmosphere. 14 p1748 A73-29977
- Radial mode analysis of electromagnetic wave propagation on slotted cylindrical structures. 14 p1727 A73-30208
- The Stiles-Crawford effect - Explanation and consequences. 14 p1717 A73-30396
- Analysis of EH inhomogeneities and singular H inhomogeneities in a rectangular-section waveguide 14 p1729 A73-30560
- Monomode optical fiber waveguide propagation attenuation due to random curvature, analyzing radiation losses for clad cores with uniform and gradient refractive index profiles 14 p1729 A73-30695
- Study in curvature of long distance wave guides - The case of helicoidal guides. I 15 p1842 A73-31360
- Dispersion of gravitational waves by a collisionless gas. 16 p2036 A73-33122
- Wave propagation in the magnetosphere of Jupiter. 17 p2229 A73-34506
- Parasitic mode conversion loss measurement for circular waveguide section quality evaluation, determining transmission coefficient from signal envelope 17 p2121 A73-34588
- Design of second-order phase circuits constructed with TEM-line segments 17 p2144 A73-34592
- On the optimum design of tapered waveguide transitions. 17 p2136 A73-34970
- Dielectric properties of ferrites in the microwave band 17 p2141 A73-35548
- Papers on integrated optics covering waveguides, mode launching, radiation losses, lasers, parametric devices, light deflectors and thin film deposition 17 p2185 A73-35599
- Propagation of VLF waves in the earth-ionosphere waveguide under nighttime ionospheres. 17 p2126 A73-35629
- Results of numerical solution of the complex dispersion equation for the HE/11/ wave in a two-layer circular waveguide. 17 p2143 A73-35718
- Ducted propagation of VLF waves through the magnetosphere. 18 p2288 A73-35995
- Note regarding the propagation of electromagnetic fields through slots in cylinders. 19 p2403 A73-37273
- A unified picture of the parallel whistler mode instability. 19 p2403 A73-37440
- Wave propagation between two plane, parallel reactive walls. 19 p2404 A73-37721
- Waveguide transitions especially for excitation of the H sub 11 mode in a circular waveguide 19 p2404 A73-37722
- An approximation method for calculating the attenuation characteristic of dielectric-lined circular waveguides. 19 p2404 A73-37723
- Magnetodynamic and magnetostatic surface waves in a ferrite layered structure 19 p2470 A73-37724
- Ducted propagation of low-latitude whistlers deduced from simultaneous observations at multi-stations. 19 p2404 A73-38019
- The effect of geomagnetic disturbance on the duct propagation of low-latitude whistlers. 19 p2426 A73-38020
- Electromagnetic wave propagation in inhomogeneous multilayered structures of arbitrary thickness - Full wave solutions. 19 p2461 A73-38380
- Whistler-mode hiss at low and medium frequencies in the dayside-cusp ionosphere. 20 p2529 A73-38935
- Wave guide propagation of micropulsations out of the plane of the geomagnetic meridian. 20 p2529 A73-38937
- Magnetospheric implications of the nonlinear whistler instability obtained in a computer experiment. 20 p2553 A73-38961
- Gravity waves in the F region of the ionosphere 20 p2554 A73-39173
- Collisionless damping of hydromagnetic waves in relativistic plasma. I - Weak Landau damping - Heating of the Crab Nebula. 20 p2609 A73-39442
- Corrugated circular waveguide boundary value problem solution to predict lower attenuation for HE sub 11 mode 20 p2538 A73-39598
- Elaborated attenuation computation for elliptic waveguide with corrected expressions for axial and transverse surface impedances and TE and TM modes 21 p2656 A73-41112
- Modulation of spectrum and amplitude of VLF signal in the magnetosphere. 21 p2657 A73-41381
- On inhomogeneously filled rectangular waveguides. 21 p2657 A73-41430
- Statistical model for phase relations derived from observations of photospheric oscillations, criticizing horizontal propagation theory for phase propagation 21 p2777 A73-41482
- Attenuation of spiral modes in a circular and annular lined duct. 22 p2839 A73-41714
- New dispersion relation for a strongly magnetized degenerate electron plasma with anisotropic pressure. 22 p2890 A73-42237
- Instabilities of drift magnetosonic waves due to the magnetic drift resonance. 22 p2894 A73-42395
- An exact solution on the propagation of small disturbances in a radiating grey gas with isotropic scattering. 22 p2932 A73-42570
- Absorption of vlf and elf waves in whistler mode - Sunrise and sunset effects. 22 p2849 A73-42622
- Absorption of whistler waves during night. 22 p2850 A73-42623
- Finite difference scheme for wave equation solution for wave propagation in layered composite materials, obtaining matrix eigenvalues with Floquet condition for various methods [ASME PAPER 73-APMW-40] 22 p2926 A73-42897
- Modes of one-dimensional wave propagation in an infinite thermoelastic medium with finite heat propagation rates 22 p2927 A73-42928

- Propagation mode with fine structure interpreted as quasi-cylindrical electrostatic wave interference with cold plasma field from potential measurements near point source antenna
22 p2895 A73-43021
- Self-focusing and self-trapping of light beams in a nonlinear medium.
22 p2888 A73-43050
- Propagation of optical pulses through clad fibers - Modified theory.
22 p2828 A73-43163
- TEM-TE coupled transmission line model for microstrip, calculating frequency-dependent wave dispersion curves for comparison with experiment
23 p2964 A73-44073
- Optical directional coupler tolerance improvement by tapered propagation coefficients based on numerical model
23 p2955 A73-44113
- The eigenvalue solution of asymmetric-ridge waveguides using the mode-matching method.
23 p2955 A73-44146
- On coupled fields in stratified plasmas with tensor pressure perturbations.
24 p3115 A73-44625
- Guided propagation of very low frequency electromagnetic waves in irregularities of electronic density in the vicinity of the constant velocity mode
24 p3067 A73-44726
- Unsteady aerodynamic loads on slender cones at free-stream Mach numbers from 0 to 22.
[AIAA PAPER 73-998] 24 p3053 A73-44833
- The ion-sound instability and its associated multimode phenomena.
24 p3115 A73-44874
- Extension of Kirchhoff's theory to coupled strip lines - Application to the calculation of band line couplers
24 p3068 A73-44975
- Dielectric coaxial waveguide modal cut-off, dispersion and attenuation characteristics, discussing guide geometry and dielectric properties effects
24 p3069 A73-45407
- PROPAGATION VELOCITY**
Linear solutions for heat propagation in relativistic fluid dynamics
01 p0076 A73-10266
- On self-similar blast waves headed by the Chapman-Jouguet detonation.
01 p0120 A73-10441
- Turbulent flame velocities in premixed sprays. I - Experimental study.
01 p0121 A73-10635
- Turbulent flame velocities in premixed sprays. II - Theoretical analysis.
01 p0121 A73-10636
- Analysis of the problem of the thermal propagation of a flame by the method of joining asymptotic expansions
01 p0123 A73-10958
- Relativistic cosmic rays propagation, calculating abundances of Pt, Pb, actinides and superheavy groups as function of cosmic ray leakage time
01 p0092 A73-11027
- Normal flame velocity in aerodisperse systems
01 p0123 A73-11245
- MHD detonation waves properties and propagation velocities within relativistic theory, discussing shock equations nontrivial solution existence and uniqueness
01 p0085 A73-11260
- The velocity of a wave packet in an anisotropic absorbing medium.
01 p0079 A73-11494
- Wave front propagation velocity definition valid for classical and relativistic fluid dynamics
02 p0152 A73-11572
- Small disturbance propagation in infinitely extended thermoelastic medium with initial finite homogeneous deformation, determining longitudinal and transverse wave propagation velocities
02 p0234 A73-12018
- The effects of frequency of loading and of nonreactive external media on growth of fatigue cracks.
02 p0235 A73-12132
- Limiting crack propagation rates during a quasi-brittle failure
02 p0236 A73-12582
- The propagation of small disturbances in radiative magnetogasdynamics.
03 p0345 A73-12923
- Amplification of turbulence level by a flame and turbulent flame velocity.
03 p0399 A73-14391
- Microfracture effects on seismic wave propagation velocity and Q factor in lunar rocks by Rayleigh ultrasonic surface wave technique
04 p0497 A73-15125
- Fatigue crack propagation in terms of fracture mechanics concepts
04 p0462 A73-15298
- The influence of atmospheric oxygen on velocity of flame spread along a solid.
[ASME PAPER 72-WA/HT-23] 04 p0519 A73-15831
- Lunar seismic wave velocity change at 25 km interpreted in terms of fine rock powder undergoing final densification
05 p0622 A73-17181
- Dynamic behaviour of thin cylindrical shells subjected to high-speed travelling inner pressures.
06 p0758 A73-17518
- Speed of propagation of shock waves responsible for geomagnetic storms and Forbush decreases
06 p0689 A73-17548
- Stationary nonlinear ion acoustic oscillations in dense weakly ionized current carrying plasma, considering wave propagation velocity and instability process
06 p0728 A73-17971
- Method of analysis and prediction for variable amplitude fatigue crack growth.
06 p0709 A73-18482
- Subcritical crack growth of TRIP steels in air under static loads.
06 p0710 A73-18485
- Materials cracking resistance characterization by fracture toughness determination as function of crack front speed
06 p0764 A73-18491
- P and S waves propagation velocity distribution for lunar mantle and crust composition, noting petrological models with differentiated mantle
07 p0894 A73-19849
- Elastic wave velocities and thermal diffusivities of Apollo 14 rocks.
07 p0894 A73-19851
- Elastic velocity and Q factor measurements on Apollo 12, 14, and 15 rocks.
07 p0894 A73-19852
- Ultrasonic P and S waves velocity of Apollo 14 and 15 lunar igneous and breccia rocks for elastic properties determination, noting cracks distribution function
07 p0894 A73-19853
- Apollo 12 soil sample strength, compressibility, bulk density, porosity and shear wave velocity
07 p0898 A73-19901
- Fatigue crack growth under C.O.D. cycling.
09 p1163 A73-23252
- Influence of material properties on dynamic fracture toughness of steels.
09 p1109 A73-23259
- Research and application problems in fracture of materials and structures in the United States Air Force.
09 p1163 A73-23261
- Computation of time-dependent laminar flame structure.
10 p1294 A73-23552
- Normal flame velocity in aerosol systems.
10 p1295 A73-24185
- Determination of the velocity of shock waves in the interplanetary medium.
10 p1279 A73-24236
- Ionization front propagation velocity as function of microwave power density, showing dependence on precursor electron density profiles
10 p1251 A73-24257
- Plastic strain as factor in crack propagation rate smoothing and branching rate reduction in elastic and elastoplastic materials
10 p1291 A73-24362
- Gaseous environments compatibility with structural alloys under fatigue loading, presenting crack growth rate data
11 p1381 A73-25816
- Geometric interpretation of conditions for resonant wave interactions valid under nondispersive conditions, noting relevance for acoustic waves in crystals and slowness vectors
11 p1400 A73-26278
- Compressional wave velocity profile of lunar near-surface and crust derived from seismic refraction data at Apollo 14 and 16 sites
12 p1541 A73-27486
- Analysis of the problem of thermal flame propagation by the method of matched asymptotic expansions.
12 p1559 A73-27534
- Asymmetric eigenmodes in a simple model plasma-sphere with non-uniform Alfvén speed.
12 p1529 A73-27613
- Relative transit time measurements of high-frequency signals using an FM-CW technique
12 p1474 A73-27763
- An inversion method for the determination of the electron density profile of the ionosphere on the basis of satellite tracking data
12 p1494 A73-27772
- Wave propagation in the two temperature theory of thermoelasticity.
13 p1691 A73-28162
- Wave propagation aspects of the generalized theory of heat conduction.
13 p1704 A73-28414
- Propagation of a brittle crack at constant and accelerating speeds.
13 p1635 A73-28755
- Instability of hydromagnetic perpendicular shocks in inhomogeneous fluids.
13 p1601 A73-28775
- Asymptotic analysis of the steady propagation of a successive two-stage exothermal reaction front in a condensed medium
13 p1707 A73-29166
- Extension of Mandel inequalities to plastic acceleration wave velocities in a finitely deformed medium
13 p1703 A73-29553
- Automatic measurement of intervals of shock wave transit across a base section
15 p1876 A73-31862
- Crack growth resistance curves [R-curves] - Literature review.
15 p1950 A73-31983
- R-curve determination using a crack-line-wedge-loaded [CLWL] specimen.
15 p1950 A73-31984
- Fracture extension resistance [R-curve] characteristics for three high-strength steels.
15 p1951 A73-31986
- Comparison of R-curves determined from different specimen types.
15 p1951 A73-31988
- Nonlinear acoustics of inviscid fluid in duct with varying cross section, obtaining propagation velocity potential as power series for reduction to Neumann problem
15 p1865 A73-32154
- Quasi-monochromatic viscoelastic waves energy velocity equivalence to phase velocity for medium represented by standard linear solid or Maxwell model
15 p1955 A73-32176
- Propagation velocity of shock waves causing geomagnetic storms and Forbush decreases.
16 p2002 A73-32772
- Apollo 17 seismic profiling - Probing the lunar crust.
16 p2059 A73-32903
- A steadily moving longitudinal-shear crack with an infinitely narrow plastic zone
17 p2241 A73-34266
- Possible role of faster-than-light radiation under pulsar conditions
17 p2226 A73-34370
- Rotating stall in an isolated rotor row and a single-stage compressor.
17 p2093 A73-34386
- Elasticity of water-saturated rocks as a function of temperature and pressure.
17 p2163 A73-35271
- Recent developments in strong shock wave research.
19 p2415 A73-37155
- Argon laser application in a study of velocity in flames
20 p2573 A73-39620
- Propagation velocities and amplitudes of thermoacoustical waves in thermo-plastic materials.
21 p2789 A73-40088
- Velocity of a stress wave superimposed on the initial plastic stress state of a rod.
21 p2784 A73-40436
- Acceleration waves in ideal fluid mixtures with several temperatures.
22 p2929 A73-41772
- Prior to failure extension of flaws in a rate sensitive Tresca solid.
22 p2880 A73-42136
- Characteristics of the fast and slow magnetosonic waves in layered plasmas.
22 p2894 A73-42397
- On detonation waves supported by diffusive flames.
22 p2936 A73-42810
- Radio astronomical problems due to pulsar radiation dispersal by frequency dependent propagation velocity in interstellar medium, discussing signal reception and data recording techniques
23 p2953 A73-43368
- Effect of pressure on the flame propagation velocity in a turbulent flow
23 p3019 A73-43730
- Propagation velocity of picosecond pulse from mode locked Nd-glass laser investigated by optically induced birefringence, self phase modulation and self focused light
23 p2988 A73-44120
- Guided propagation of very low frequency electromagnetic waves in irregularities of electronic density in the vicinity of the constant velocity mode
24 p3067 A73-44726
- Velocity of hypersonic waves in liquid oxygen.
24 p3110 A73-44984
- Vortex model for flames and free jets characteristic velocities based on three dimensional turbulent combustible flow
24 p3158 A73-45387
- PROPANE**
Nitric oxide emissions from tube combustor burning premixed gaseous propane-air mixture, considering inlet conditions for equivalence ratios
17 p2222 A73-35468
- Branched-chain mechanism of propane-oxygen-fluorine explosions.
22 p2819 A73-42778
- PROPELLANT ADDITIVES**
NT PROPELLANT BINDERS
NT SOLID ROCKET BINDERS

- Additives for heat transfer reduction in the propellant combinations N2O4-MMH and N2O4-A-50.
[AIAA PAPER 72-1132] 03 p0352 A73-13439
- Depressurization extinguishment of composite solid propellants - Influence of composition and catalysts.
[AIAA PAPER 72-1136] 03 p0352 A73-13443
- Gas-releasing additives to jet fuels
21 p2754 A73-41070
- Contribution to the phase stabilization of ammonium nitrate
24 p3066 A73-45201

PROPELLANT BINDERS

NT SOLID ROCKET BINDERS

- Propellants and combustion. I - Role of binder in solid propellant combustion.
[AIAA PAPER 72-1121] 04 p0485 A73-14910
- Ignition temperature of conglomerates which form by burnout of the binder in a suspension of aluminum powder in kerosene
18 p2372 A73-37118
- Pyrolysis and oxidation of polymers at high heating rates.
22 p2936 A73-42806
- Effects of copper chromite and iron oxide catalysts on AP/CTPB sandwiches.
22 p2899 A73-42812

PROPELLANT CHEMISTRY

- Simulation of the compounder in a single base propellant (SBP) process.
17 p2220 A73-34819

PROPELLANT COMBUSTION

NT SOLID PROPELLANT IGNITION

- The role of impurity particles in the combustion of double-base propellants.
01 p0089 A73-10639
- Ignition of nonhypergolic rocket fuels with fuming nitric acid under suitable conditions.
01 p0089 A73-10736
- Development of a small end-burning type motor by using pellet impregnated propellant.
01 p0090 A73-11108
- Multi-droplet combustion of liquid propellants.
01 p0089 A73-11114
- Recent developments in testing unstable burning characteristics of solid propellants.
01 p0089 A73-11115

- Solid propellant combustion instability suppression devices.
[AIAA PAPER 72-1051] 03 p0353 A73-13382

- Survey of ONERA and SNPE work on combustion instability in solid propellant rockets.
[AIAA PAPER 72-1052] 03 p0353 A73-13383

- Measuring combustion response by a forced oscillation method.
[AIAA PAPER 72-1054] 03 p0397 A73-13385

- Erosive burning rate perturbation in colloidal propellant slab combustor channel as function of lateral velocity gradient and chamber pressure
[AIAA PAPER 72-108] 03 p0351 A73-13423

- Determination of solid-propellant transient regression rates using a microwave Doppler shift technique.
[AIAA PAPER 72-1118] 03 p0351 A73-13433

- Catalytic effects of copper chromite and iron oxide on AP-HTPB binder sandwich combustion to 3200 psia by cinematomicrography
[AIAA PAPER 72-1120] 03 p0352 A73-13434

- Pressure exponent of controllable solid rocket propellants.
[AIAA PAPER 72-1135] 03 p0352 A73-13442

- Combustion theory of hybrid rocket propellant-oxidizer combinations based on heat transfer limited model, discussing chemical kinetics and temperature effects on regression rate
[AIAA PAPER 72-1143] 03 p0397 A73-13449

- A nonlinear model of combustion instability in liquid propellant rocket engines.
[AIAA PAPER 72-1146] 03 p0356 A73-13451

- Supersonic mixing and combustion of a hydrogen jet in a coaxial high-temperature test gas.
[AIAA PAPER 72-1179] 03 p0397 A73-13474

- Gas generator system with continuously burning driver propellant and demand propellant combustion during exposure to driver gas flow, testing performance
[AIAA PAPER 72-1193] 03 p0358 A73-13483

- Asymptotic analysis of premixed burning with large activation energy.
03 p0397 A73-13531

- Decomposition and hybrid combustion of hydrazine, MMH and UDMH as droplets in a combustion gas environment.
03 p0352 A73-14392

- The starting transient of solid-propellant rocket motors with high internal gas velocities.
[AIAA PAPER 72-119] 04 p0486 A73-14909

- Propellants and combustion. I - Role of binder in solid propellant combustion.
[AIAA PAPER 72-1121] 04 p0485 A73-14910

- Combustion mechanisms of fuel rich propellants in flow fields.
[AIAA PAPER 72-1145] 04 p0485 A73-14915

- Effect of the guidance reserve of the Europa II third stage on the consumption of propellants for stationing
04 p0504 A73-15294

- Transport phenomena of reactive fluid flow in heterogeneous combustion processes.
[ASME PAPER 72-WA/HT-30] 04 p0519 A73-15825

- Extinguishment of composite propellants at low pressures.
[AIAA PAPER 73-175] 05 p0640 A73-16918

- Role of condensed phase details in the oscillatory combustion of composite propellants.
[AIAA PAPER 73-218] 05 p0641 A73-16948

- A novel high area ratio T-burner for characterizing metalized propellants.
[AIAA PAPER 73-219] 05 p0563 A73-16949

- Interaction of sound and flow in T-burners - Experiments compared with theory.
[AIAA PAPER 73-220] 06 p0741 A73-17662

- Theory of steady-state burning of porous propellants by means of a gas-penetrative mechanism.
[AIAA PAPER 73-221] 06 p0767 A73-17663

- German book - Solid rocket propulsion systems II: Theory and technology.
06 p0740 A73-18074

- Direct mixing and combustion measurements in ducted, particle-laden jets.
[AIAA PAPER 72-1177] 06 p0769 A73-18400

- Acoustic amplification during solid propellant combustion.
07 p0865 A73-19390

- Combustion catalysis model of a single-component fuel/as applied to ammonium perchlorate/
07 p0865 A73-19991

- An experimental study of ammonium perchlorate-binder sandwich combustion in standard and high acceleration environments.
07 p0866 A73-20363

- An asymptotic analysis of radiant and hypergolic heterogeneous ignition of solid propellants.
07 p0866 A73-20364

- Critical mass of cryogenic rocket propellants.
07 p0866 A73-20415

- Influence of the surface microstructure on the evolution of the combustion velocity of ammonium perchlorate composite solid propellants as a function of pressure
[ONERA, TP NO. 1167] 08 p0995 A73-21678

- Mathematical model for extinguishing gunpowder combustion via pressure variations, assuming gunpowder surface dependence on combustion rates
09 p1167 A73-22617

- The gas-phase reaction of perchloric acid with ethylene.
10 p1186 A73-23556

- The influence of diameter on the burning velocity of strands of solid propellant.
10 p1261 A73-23560

- Necessary conditions of stable combustion of powder in a semiclosed chamber
10 p1294 A73-23588

- Heterogeneity effect on L instability of solid rocket propellant combustion, using sideways sandwich model
11 p1450 A73-25373

- A mechanistic model for analysis of pulse-mode engine operation.
[AIAA PAPER 72-1184] 12 p1533 A73-27100

- Solid propellant ballistic properties from pressure changes due to combustion, considering transient effects
13 p1669 A73-28997

- Linear nonstationary effects - A source of information on the kinetics of reactions on the surface of a solid fuel
14 p1818 A73-30873

- Temperature and velocity profiles measurement in hybrid rocket engine combustion, using optical method based on Na line reversal technique
15 p1957 A73-31636

- Effects of composition on acceleration induced burning-rate augmentation.
15 p1925 A73-31661

- Explosive behavior of aluminized ammonium perchlorate.
16 p2045 A73-33346

- An experimental study of the low pressure limit for steady deflagration of ammonium perchlorate.
16 p2045 A73-33347

- Deflagration in the combustion of hydrogen-fluorine mixtures.
16 p2045 A73-33349

- Influence of acceleration on the combustion of solid propellants - Measurement and prediction of the effects
16 p2045 A73-33391

- Experimental study of the condensed phase in the combustion products of metalized solid propellants
16 p2086 A73-33965

- Effects of additions of metals and metal borides on the burning rates of mixture systems
19 p2503 A73-37509

- Mechanism of burning in condensed systems with solid additions in a field of mass forces
19 p2472 A73-37510

- Contribution to the theory of high-frequency pulsations caused by instability of the combustion process in a solid-propellant rocket engine
21 p2753 A73-40391

- Determination of the thermodynamic characteristics of a liquid-propellant rocket engine with nonisobaric combustion
21 p2754 A73-40402

- Quasi-steady gas-phase flame theory in unsteady burning of a homogeneous solid propellant.
21 p2790 A73-40430

- Burning gunpowder interaction with an acoustic field in the presence of balanced chemical reactions behind the flame
21 p2791 A73-40699

- Effects of copper chromite and iron oxide catalysts on AP/CTPB sandwiches.
22 p2899 A73-42812

- Ammonium perchlorate gasification and combustion at high heating rates and low pressures.
22 p2899 A73-42815

- A method for calculating the burning rates of solid fuels in a turbulent gaseous oxidizer flow at Le unequal to unity
23 p3049 A73-43729

- Formation of a pseudoliquefied layer during combustion of condensed systems with solid nonagglomerating additives in a field of mass forces
24 p3121 A73-44705

- Solid propellants with a pulsating burning rate
24 p3121 A73-45200

- Mechanism of erosive burning of solid rocket propellants.
24 p3121 A73-45385

PROPELLANT DECOMPOSITION

- The thermal decomposition of nitroglycerin and its relation to the stability of CMDB propellants.
[WSCI PAPER 72-30] 05 p0605 A73-16685

- Factor of fuel pyrolysis in injector design.
05 p0606 A73-17109

- Ir catalysts for high performance hydrazine decomposition, discussing preparation by coprecipitation of active metallic element with support in chloridic acid solution
07 p0865 A73-18928

- Propulsion system for space applications, based on the catalytic decomposition of hydrazine
07 p0866 A73-18929

- Specific characteristics of the high-temperature decomposition of ammonium perchlorate and of ammonium perchlorate-based heterogeneous systems
19 p2471 A73-37503

- Kinetics of the catalytic reactions of the thermal decomposition of perchloric acid and ammonium perchlorate
19 p2402 A73-37505

- Effect of composite propellant catalysts on the stabilities of HClO4 and the HClO4-NH3 system.
22 p2899 A73-42814

- Ammonium perchlorate gasification and low pressures.
22 p2899 A73-42815

PROPELLANT EVAPORATION

- Suppression of evaporation of hydrocarbon liquids and fuels by aqueous films.
[WSCI PAPER 72-27] 05 p0639 A73-16687

- Gas-phase ignition model for some solid fuels in a shock tube
07 p0865 A73-19989

PROPELLANT GRAINS

- Photoelastic stress analysis of solid propellant grains.
01 p0090 A73-11118

- Solid propellant rocket service life prediction based on propellant grain structural failure analysis, discussing surveillance program rationale for various conditions
[AIAA PAPER 72-1085] 03 p0354 A73-13407

- Prediction of the critical diameter of composite propellants.
[AIAA PAPER 72-1117] 03 p0351 A73-13432

- Propellant grain surface contamination effect on ignition transient characteristics of solid rocket motor
[AIAA PAPER 72-1198] 04 p0487 A73-14920

- Computing pressure cure viscoelastic effects in solid propellants.
05 p0606 A73-17208

- U.S. double-base solid propellant tactical rockets of the 1940-1955 era.
[AIAA PAPER 73-274] 09 p1135 A73-23248

- Strain measurements in the solid propellant of a large booster structural test vehicle.
13 p1669 A73-29304

- Russian book - Solid-propellant rocket engines.
22 p2900 A73-41880

- Contribution to the phase stabilization of ammonium nitrate
24 p3066 A73-45201

PROPELLANT OXIDIZERS

U ROCKET OXIDIZERS

PROPELLANT PROPERTIES

NT PROPELLANT STORABILITY

- Measuring apparatus for residual effective stabilizer content in single and double base propellants by passing nitrogen dioxide through ground sample
09 p1135 A73-22300

- The acute inhalation toxicology of chlorine pentafluoride.
15 p1839 A73-32173

PROPELLANT STORABILITY

Extending the life and recycle capability of earth storable propellant systems.
[SAE PAPER 720837] 05 p0629 A73-16631

PROPELLANT STORAGE

Considerations concerning the service life, handling and storage of double base solid propellant rocket motors.
[AIAA PAPER 72-1086] 03 p0351 A73-13408
Cape Kennedy Space Center ground support equipment welding machines and techniques, emphasizing propellant storage tanks and mobile launcher transporters
16 p1995 A73-33195

PROPELLANT TANKS

Apollo 14 mission, discussing extravehicular activities time and payload increase via enlarged propellant tanks
03 p0368 A73-13085
Natural frequencies, forces and moments for liquid propellant sloshing in tilted cylindrical tank as function of tilt angle and liquid depth
03 p0293 A73-13314
German monograph - Propagation of ion acoustic waves in a weakly ionized plasma.
03 p0398 A73-13814
An experimental investigation of some heat transfer characteristics on an orbiter/HO-tank/SRM Space Shuttle configurations, freestream Mach number equal to 8.0.
[AIAA PAPER 73-92] 05 p0640 A73-16856
Zero-g propellant gauging
06 p0755 A73-17573
Space shuttle external tank, discussing Orbiter engine, propellant conditioning, solid rocket boosters structural support, environment effects and safe disposals
19 p2492 A73-37598

PROPELLANT TESTS

Selection of a surface tension propellant management system for the Viking 75 Orbiter.
[AIAA PAPER 72-1042] 03 p0381 A73-13377
The T-burner test method for determining the combustion response of solid propellants.
[AIAA PAPER 72-1053] 03 p0353 A73-13384
Determination of solid-propellant transient regression rates using a microwave Doppler shift technique.
[AIAA PAPER 72-1118] 03 p0351 A73-13433
Failure detection in solid propellants.
[AIAA PAPER 72-1087] 04 p0485 A73-14906
The influence of combustor parameters on the combustion of particle-laden fuels in ducted flows.
[AIAA PAPER 73-177] 05 p0640 A73-16919
A novel high area ratio T-burner for characterizing metalized propellants.
[AIAA PAPER 73-219] 05 p0563 A73-16949
Investigation of a single spraying site of a colloid thruster.
08 p0996 A73-21599
Perchlorate degradation of ethyl oleate in solid propellants.
10 p1262 A73-23758
Influence of acceleration on the combustion of solid propellants - Measurement and prediction of the effects
16 p2045 A73-33391

PROPELLANT TRANSFER

Rocket propellant handling personnel protective clothing, describing head gear, ventilated underwear and airtight external suit
07 p0784 A73-18949
Development of propellant loading systems and checkout systems for the TD-1A and AEROS satellite projects
11 p1430 A73-25354
Cryogenic propellants in rocket engines.
16 p2045 A73-33118

PROPELLANTS

NT CASE BONDED PROPELLANTS
NT COLLOIDAL PROPELLANTS
NT COMPOSITE PROPELLANTS
NT CRYOGENIC ROCKET PROPELLANTS
NT DOUBLE BASE PROPELLANTS
NT DOUBLE BASE ROCKET PROPELLANTS
NT GASEOUS ROCKET PROPELLANTS
NT GUN PROPELLANTS
NT HYPERGOLIC ROCKET PROPELLANTS
NT LIQUID ROCKET PROPELLANTS
NT MONOPROPELLANTS
NT PLASTIC PROPELLANTS
NT ROCKET PROPELLANTS
NT SOLID PROPELLANTS
NT SOLID ROCKET PROPELLANTS
NT STORABLE PROPELLANTS
Space science terrestrial applications in biomedical data exchange and telediagnosis, propellant technology, life support atmospheres without fire hazard, industrial mixers and nozzle materials
[AAS PAPER 73-133] 20 p2629 A73-38589

PROPELLER BLADES

Fatigue and impact tests on composite propeller blades made of glass- and carbon fiber reinforced plastics, noting comparison with measured vibratory strains
12 p1458 A73-26881

Deformation equations of a propeller blade and the orthogonality characteristics of its normal mode shapes of vibration

The influence of pitch and twist on blade vibrations.
12 p1458 A73-27085
17 p2099 A73-34440
Hovercraft propeller and turbine engine fan blades with glass and carbon fiber reinforced plastics respectively, discussing design and constructions
17 p2103 A73-34813
Rotating blades and aerodynamic sound.
17 p2096 A73-35333
Application of the method of integrating matrices to the calculation of the natural vibrations of a propeller blade with allowance for deflection in two planes and for torsion
21 p2783 A73-40389
Calculation of the deformations of a propeller blade in flight
23 p3041 A73-43724
Spectral trends in rotor noise generation.
[AIAA PAPER 73-1033] 24 p3056 A73-44862
Natural, flexural and torsional vibration frequencies and modes for helicopter tail rotor blades
24 p3057 A73-45245

PROPELLER DRIVE

NT HELICOPTER PROPELLER DRIVE
Status of international noise certification standards for business aircraft.
[SAE PAPER 730286] 17 p2101 A73-34651
PROPELLER EFFICIENCY
Influence of geometrical parameters on propeller performance at low advance ratios
21 p2635 A73-41582

PROPELLER FANS

Radiation properties of propeller and helicopter /free field/ rotors and fans and gas turbine compressors /ducted rotors/
02 p0131 A73-12611
Variable pitch fan experimental design for quiet STOL propulsion, testing blade designs for aerodynamic and acoustic performance
03 p0359 A73-14147
Low vs high speed propeller fan noise, discussing pseudosound generation by rotating aerodynamic pressure fields
13 p1603 A73-29030
Shrouded Q-FAN propulsor for light aircraft, discussing propulsion system performance, weight, noise and cost trends
[SAE PAPER 730323] 17 p2221 A73-34680
Hovercraft propeller and turbine engine fan blades with glass and carbon fiber reinforced plastics respectively, discussing design and constructions
17 p2103 A73-34813
Aircraft installation requirements and considerations for variable pitch fan engines.
[AIAA PAPER 73-807] 19 p2379 A73-37465
PROPELLER SLIPSTREAMS
Theoretical determination of the characteristics of helicopter rotors
09 p1027 A73-22205

PROPELLER SYNCHRONIZERS

U PROPELLERS
U SYNCHRONIZERS
PROPELLERS
NT PROPELLER FANS
NT SHROUDED PROPELLERS
NT VARIABLE PITCH PROPELLERS
Optimum performance of static propellers and rotors.
03 p0242 A73-13308
Corrections for response errors in a three-component propeller anemometer.
18 p2316 A73-36710

PROPHYLAXIS

Use of sodium hydrocarbonate for medication and prophylaxis of motion sickness
08 p0933 A73-20990
Special physical training of pilots as a prophylactic measure against obesity
15 p1837 A73-31172
Development of effective means for desaturation of the human organism as a prophylactic measure against altitude decompression disturbances
17 p2111 A73-34231
Preventive value of early diagnosis of coronary heart disease, noting importance of screening populations for genetic and environmental risk factors
22 p2808 A73-42828

PROPORTIONAL CONTROL

The dimensioning of resistance thermometers with an output parameter which is proportional to the temperature
14 p1754 A73-30922
Simultaneous control of temperature and humidity in a confined space. III Feedback control synthesis via optimal control theory.
15 p1855 A73-32549
System performance prediction by modeling test data in digital simulations.
[AIAA PAPER 73-880] 20 p2543 A73-38816
Pneumatic fluidic operational amplifier application to proportional position servocontrol with hydraulic

actuator for high force output, considering working fluid and Reynolds number effects
23 p2941 A73-43397

PROPORTIONAL COUNTERS

Monograph - Satellite-borne instrument for the measurement of soft solar X-rays.
01 p0045 A73-10150
Thin polypropylene window proportional counters for the observation of cosmic soft X-rays.
01 p0046 A73-10433
Spectroscopic techniques in X-ray astronomy.
03 p0375 A73-13961
A position-sensitive X-ray detector for the HEAO-A satellite.
11 p1364 A73-25963
A multiwire proportional counter with integral readout delay line.
11 p1364 A73-25964
High spatial resolution MWPC systems using electromagnetic delay line readouts.
11 p1364 A73-25966
Coaxial anode for background suppression in X-ray proportional counters.
13 p1612 A73-28367
A position sensitive proportional counter with high spatial resolution.
13 p1622 A73-29643
Proportional counter energy deposition spectral quality prediction from experimental data, using folding procedure to produce composite energy absorption distributions for biological materials
15 p1839 A73-31549
A gas density control system for X-ray proportional counters in space.
22 p2851 A73-41699
Identification of hadrons with 500 GeV energies in cosmic rays by using transitional emission
23 p2981 A73-43566

PROPRICEPTION

NT AUTOKINESIS
Vestibular influences on orientation in zero gravity, produced by parabolic flight.
06 p0653 A73-18032
Role of visual and articular afferentation in the implementation of motor reactions involving complex coordination and precision
06 p0653 A73-18164

PROPULSION

NT ASCENT PROPULSION SYSTEMS
NT AUXILIARY PROPULSION
NT CHEMICAL PROPULSION
NT ELECTRIC PROPULSION
NT ELECTROMAGNETIC PROPULSION
NT ELECTROSTATIC PROPULSION
NT ION PROPULSION
NT JET PROPULSION
NT LOW THRUST PROPULSION
NT MAN OPERATED PROPULSION SYSTEMS
NT MARINE PROPULSION
NT NUCLEAR ELECTRIC PROPULSION
NT NUCLEAR PROPULSION
NT PHOTONIC PROPULSION
NT PLASMA PROPULSION
NT SOLAR PROPULSION
NT SPACECRAFT PROPULSION
NT UNDERWATER PROPULSION
PROPULSION CALCULATIONS
U MATHEMATICAL MODELS
PROPULSION SYSTEM CONFIGURATIONS
Secondary low thrust propulsion systems technology requirements and parameters, covering electrothermal, radioisotope and ion bombardment thrusters
01 p0090 A73-11109
M-4 S four-stage solid propellant rocket launch vehicle for scientific satellites, detailing design and performance characteristics
01 p0111 A73-11158
The Delta launch vehicle for scientific and applications satellites.
01 p0111 A73-11159
Synerjet composite rocket-air breathing propulsion system for reusable spacecraft mission profile optimization, discussing multimode operation and performance capabilities
01 p0112 A73-11300
Criteria concerning the adaptation of the rear components of a propulsion system to the subsonic and transonic altitude flight
[DGLR PAPER 72-065] 02 p0128 A73-11690
Comparison of modern aircraft engines with other power plants used in transportation
03 p0352 A73-13072
Engine technology for large subsonic nuclear powered aircraft.
[AIAA PAPER 72-1062] 03 p0353 A73-13391
Prospects for rocket propulsion with laser-induced fusion microexplosions.
[AIAA PAPER 72-1063] 03 p0353 A73-13392
High performance reactorless nuclear propulsion of reusable orbital space tug by laser rocket engine
[AIAA PAPER 72-1095] 03 p0341 A73-13415
Propulsion unit, components, environmental tests and development problems of Swedish air to ground missile rocket engine operating on liquid propellants
[AIAA PAPER 72-1102] 03 p0355 A73-13421

Detonation propulsion system for missile/spacecraft maneuvering, determining performance characteristics by one dimensional computer calculations for various configurations
[AIAA PAPER 72-1161] 03 p0357 A73-13462

Solar escape achievement by solid propulsion augmentation system and design independent of multiplanetary swingby, analyzing cost effectiveness of different programs
[AIAA PAPER 72-1163] 03 p0382 A73-13464

Installation effects on performance of multiple model V/STOL lift fans.
[AIAA PAPER 72-1175] 03 p0250 A73-13471

Comparison of propulsion system concepts for V/STOL commercial transports.
[AIAA PAPER 72-1176] 03 p0250 A73-13472

Development of aft inlets for a ramjet powered missile.
03 p0246 A73-14133

Viscous interaction in integrated supersonic intakes.
03 p0246 A73-14149

Engine concepts for space applications.
03 p0360 A73-14475

Stratospheric airship propulsion system using electric engine, hydrogen-air fuel cells and liquid hydrogen
04 p0408 A73-15119

Terrestrial prototype of a lunar hopping transporter.
[ASME PAPER 72-WA/AUT-7] 04 p0433 A73-15882

Solid rocket motors for the Space Shuttle booster.
[SAE PAPER 72-0804] 05 p0607 A73-16648

NASA lift fan V/STOL transport technology status.
[SAE PAPER 72-0856] 05 p0535 A73-16663

Principle of operations and characteristics of electric propulsion devices - Application to satellite stabilization. I
05 p0608 A73-17193

Air breathing hypersonic aircraft technology developments in propulsion systems and structures with emphasis on use of hydrogen fuel
[AIAA PAPER 73-58] 06 p0647 A73-17631

Nuclear pulse propulsion system for interplanetary space flight, describing operational principles and design concepts
06 p0722 A73-18022

Geostationary satellites stabilization by microthrusters based on solid sublimation or hydrazine monopropellant, describing propulsion system development
07 p0866 A73-18926

Operational principle and characteristics of electric propulsion systems. II - Application to satellite stabilization
07 p0906 A73-20247

Flowfield calculations for some supersonic sections with ducted heat addition.
09 p1028 A73-23089

Program objectives and propulsive, equipment case, attitude control, interstage, separation skirt and nose cone subassemblies of French Diamant B-P4 launch vehicle
10 p1285 A73-23654

Development program of medium range winged design helicopter, describing wing-fuselage structure, propulsion and power transmission systems and combustion, electrical and hydraulic plants
12 p1459 A73-27383

Multibladed shrouded fan /Q-fan/ with rotary or piston engines as propulsion system for light/medium business aircraft, noting noise and drag reduction
14 p1785 A73-29996

Theoretical and practical design aspects on spacecraft propellant and pressurant loading systems.
14 p1742 A73-30107

Propulsion system optimization for interstellar probes.
15 p1943 A73-32217

Design considerations for supersonic V/STOL aircraft.
[ASME PAPER 73-GT-65] 16 p1969 A73-33517

V/STOL airframe/propulsion integration problem
[ASME PAPER 73-GT-76] 16 p2048 A73-33522

New low-pressure-ratio fans for quiet business aircraft propulsion.
[SAE PAPER 73-0288] 17 p2221 A73-34653

Turbine powerplants for missiles - Cost improvement requirements.
[SAE PAPER 73-0364] 17 p2222 A73-34709

Utilization of electric propulsion systems in communications satellites
[DGLR PAPER 73-048] 17 p2126 A73-35484

Titan/Centaur launch vehicle for high payload escape missions and large synchronous orbit spacecraft, describing propulsion, control/guidance and telemetry systems
[AIAA PAPER 73-617] 18 p2359 A73-36094

Propulsion by absorption of laser radiation.
[AIAA PAPER 73-624] 18 p2342 A73-36172

Engine-over-the-wing noise research.
[AIAA PAPER 73-631] 18 p2267 A73-36190

Thermal control and structures approach for fluorinated propulsion.
[AIAA PAPER 73-772] 18 p2360 A73-36386

The Dolphin airship with an undulating propulsion system - Surface and width of the fuselage
19 p2387 A73-38122

Rumanian contributions regarding the application of the Coanda effect
19 p2387 A73-38303

Aircraft economics and its effect on propulsion system design.
[AIAA PAPER 73-808] 19 p2388 A73-38372

German book on rocket propulsion theory covering orbital mechanics, equations of motion, performance parameters and nuclear, electric and chemical propulsion types
22 p2909 A73-42493

Aerial-survey aircraft of the new generation
22 p2799 A73-42590

PROPULSION SYSTEM PERFORMANCE

Synerjet composite rocket-air breathing propulsion system for reusable spacecraft mission profile optimization, discussing multimode operation and performance capabilities
01 p0112 A73-11300

The construction of an operational model of the high-frequency ionic propulsion system RIT 10 M
[DGLR PAPER 72-088] 02 p0202 A73-11672

Propulsion system performance for satellite attitude and orbit correction, discussing hydrogen, ammonia and hydrazine resistojets
[DGLR PAPER 72-078] 02 p0203 A73-11697

Chemical and nuclear space tugs in the earth orbital shuttle mission.
02 p0216 A73-12372

Mission performance of a 360 mw nuclear rocket engine.
[AIAA PAPER 72-1064] 03 p0381 A73-13393

Performance potential of the colloid core reactor concept in near-earth applications.
[AIAA PAPER 72-1065] 03 p0340 A73-13394

Scaling of performance and thermal environment in fuel-cooled rocket engines.
[AIAA PAPER 72-1075] 03 p0354 A73-13399

Effect of injection velocity ratio and combustion chamber pressure on experimental performance of throttleable LO2/GH2-rocket engines with coaxial injectors.
[AIAA PAPER 72-1079] 03 p0354 A73-13402

High performance reactorless nuclear propulsion of reusable orbital space tug by laser rocket engine
[AIAA PAPER 72-1095] 03 p0341 A73-13415

Durability tests of a five-centimeter diameter ion thruster system.
[AIAA PAPER 72-1151] 03 p0356 A73-13455

One-millipound colloid thruster system development.
[AIAA PAPER 72-1153] 03 p0356 A73-13456

Continuing development of the short-pulsed ablative space propulsion system.
[AIAA PAPER 72-1154] 03 p0356 A73-13457

Hydrogen-oxygen Space Shuttle ACPs thruster technology review.
[AIAA PAPER 72-1158] 03 p0356 A73-13460

Detonation propulsion system for missile/spacecraft maneuvering, determining performance characteristics by one dimensional computer calculations for various configurations
[AIAA PAPER 72-1161] 03 p0357 A73-13462

Ammonium perchlorate/aluminum powder propellant rocket engine feasibility evaluation, considering test firing results on performance and stability characteristics for various injector configurations
[AIAA PAPER 72-1162] 03 p0357 A73-13463

From earth to Mars orbit - Mariner 9 propulsion flight performance with analytical correlations.
[AIAA PAPER 72-1185] 03 p0382 A73-13478

Gas generator system with continuously burning driver propellant and demand propellant combustion during exposure to driver gas flow, testing performance
[AIAA PAPER 72-1193] 03 p0358 A73-13483

Investigation of damping methods for low frequency augmentor combustion instability.
[AIAA PAPER 72-1207] 03 p0358 A73-13490

Variable pitch fan experimental design for quiet STOL propulsion, testing blade designs for aerodynamic and acoustic performance
03 p0359 A73-14147

Spacecraft low thrust propulsion systems applications to earth orbital and planetary missions, discussing payload capabilities vs flight time
[AIAA PAPER 72-1125] 04 p0486 A73-14911

Electrothermal hydrazine thruster analyses and performance evaluation.
[AIAA PAPER 72-1152] 04 p0486 A73-14917

Linear slit colloid electrostatic thruster development and testing, discussing emitter geometry, gap design, exhaust velocity, operating voltage and power efficiency relationships
04 p0488 A73-15725

Transfer from a standby to a stationary orbit using electric propulsion
04 p0505 A73-15740

Considerations on transfer into geostationary orbit using ion propulsion - Application to the Europa III booster
04 p0505 A73-15742

Potential operating advantages of a variable area turbine turbojet.
[ASME PAPER 72-WA/AERO-4] 04 p0490 A73-15906

Small turbine advanced gas generator for future propulsion requirements.
[SAE PAPER 72-0831] 05 p0537 A73-16634

Principle of operations and characteristics of electric propulsion devices - Application to satellite stabilization. I
05 p0608 A73-17193

Comparison of advanced propulsion concepts for deep space exploration.
05 p0608 A73-17201

Propulsion by impinging laser beams.
05 p0585 A73-17211

Rapid continuous evaluation of thruster performance dependence on system parameters using thrust balance for measurement, noting suitability for electric microthruster characterization
05 p0579 A73-17253

Technology applied to the Space Shuttle Main Engine.
[AIAA PAPER 73-60] 06 p0741 A73-17633

Monopropellant and bipropellant thruster systems with afterburning for geostationary satellite orbital control, evaluating performance and reliability based on calculation and test data
07 p0866 A73-18930

Ion thruster thermal characteristics and performance.
07 p0867 A73-19488

Performance of a modified downstream-cathode MPD thruster.
07 p0867 A73-19492

Performance of recoverable single and multiple Space Tugs for missions beyond earth escape.
07 p0906 A73-20471

Gas turbine engine transient performance presentation for digital computer programs.
[SAE ARP 1257] 08 p0996 A73-20696

Potentials and problems of hydrogen fueled supersonic and hypersonic aircraft.
09 p1032 A73-22830

ARIES, the Minuteman I second stage as a controlled sound rocket.
[AIAA PAPER 73-287] 09 p1155 A73-23207

Theoretical and experimental study of the performance of quasi-steady MPD thrusters
10 p1262 A73-24499

Certain considerations concerning a magnetoplasma-dynamic flux in the one-dimensional hypothesis
12 p1527 A73-27061

Analysis of the operational parameters of a bypass turbojet
12 p1532 A73-27069

Influence of the turbine air cooling system on the characteristics of a turbojet engine during regulation of the latter
12 p1532 A73-27091

German monograph on bypass turbojet propulsion systems with jet mixing covering engine parts, thrust characteristics and fuel consumption
14 p1785 A73-30671

Possibility of utilizing the ERIDAN rocket probe as an experimental vehicle
16 p2071 A73-32817

High bypass fan engines for quiet propulsion and optimal aircraft performance in military and commercial applications
16 p2046 A73-33190

NASA research commercial VTOL transport propulsion system specifications and components development, discussing lift fan propulsion method for aircraft attitude control
[ASME PAPER 73-GT-24] 16 p2047 A73-33498

Comparative analysis of turbine loss parameters.
[ASME PAPER 73-GT-91] 16 p1964 A73-33529

Potential payoffs of variable geometry engines in fighter aircraft.
17 p2099 A73-34436

Shrouded Q-FAN propulsor for light aircraft, discussing propulsion system performance, weight, noise and cost trends
[SAE PAPER 73-0323] 17 p2221 A73-34680

Integrated Propulsion Control System program.
[SAE PAPER 73-0359] 17 p2222 A73-34707

Status of current development activity related to STOL propulsion noise reduction.
[SAE PAPER 73-0377] 17 p2222 A73-34716

The role of the auxiliary power unit in future airplane secondary power systems.
[SAE PAPER 73-0381] 17 p2108 A73-34720

Pulsejet engines operational characteristics compared to turbojet engines, noting flight speed limit due to interaction between unsteady gas flow and combustion process
18 p2342 A73-36063

Solid propellant rocket burning rate optimization at constant thrust by imbedded inert heat conducting fibers, analyzing flight performance
18 p2342 A73-36064

A low-power MPD thruster of Duoplasmatron type.
18 p2342 A73-36154

Propulsion system optimisation for a single-stage constant-thrust relativistic rocket.
18 p2361 A73-37037

On the role of the radiation directivity in noise reduction for STOL aircraft.
19 p2378 A73-37277

F-12 series aircraft propulsion system performance and development.
[AIAA PAPER 73-821] 19 p2380 A73-37473
Optimum propulsion system design for advanced technology commercial transport, emphasizing low noise and emission, performance, reliability, maintainability and economics
[AIAA PAPER 72-760] 20 p2600 A73-38648
RB-211 turbofan engine development, in-service problems and modifications for performance improvement
20 p2600 A73-39660
Airframe/propulsion system interactions - An important factor in supersonic aircraft flight control.
[AIAA PAPER 73-831] 21 p2634 A73-40501
Manned and unmanned aerospace launch vehicle liquid and solid rocket propulsion system effectiveness survey questionnaire response data concerning various tests
21 p2781 A73-41202
German book on rocket propulsion theory covering orbital mechanics, equations of motion, performance parameters and nuclear, electric and chemical propulsion types
22 p2909 A73-42493
German monograph - A method for the calculation of mixing and combustion processes in a rocket propulsion system with air-augmentation.
22 p2900 A73-42851
Potential of hydrogen fuel for future air transportation systems.
[ASME PAPER 73-ICT-104] 23 p3019 A73-43499
Effect of secondary oxidizer supply through a porous solid fuel on the hybrid combustion process
23 p3019 A73-43783

PULSIVE EFFICIENCY
NT PROPELLER EFFICIENCY
Space charge neutralized Hall ion microthrusters, discussing ion exhaust velocity, thrust and efficiency relationships
04 p0489 A73-15729
Electron bombardment ion rocket engine with large diameter and divergent magnetic field for efficiency improvement, considering application as source in plasma wind tunnel
07 p0868 A73-20486
Thermodynamic performance analysis of gas turbine power plants with intercooler. II - Performance of intercooling-regeneration-reheat type and precise calculation method.
11 p1411 A73-26343
Investigation of the aerodynamic performance of small axial turbines.
[ASME PAPER 73-GT-3] 16 p1963 A73-33481
Subsonic aircraft turbojet engines, discussing thermodynamic cycles, entry temperature increase, propulsion efficiency and economy improvements and ecological requirements
18 p2343 A73-36994

PROPYLENE
Nitrogen quadrupole coupling constants in cis-propyleneimine.
23 p2950 A73-43272

PROSTHETIC DEVICES
The mathematics of coordinated control of prosthetic arms and manipulators.
[ASME PAPER 72-WA/AUT-4] 04 p0414 A73-15884
Periodic conditions in artificial-muscle autopulsators
14 p1721 A73-30289
The effects of the Westinghouse active magnetometer /WD-4/ on implanted cardiac pacemakers.
18 p2286 A73-36936
Some aspects of the inverted pendulum problem for modelling of locomotion systems.
19 p2460 A73-38035

PROTECTION
NT ACCELERATION PROTECTION
NT CIRCUIT PROTECTION
NT CORROSION PREVENTION
NT ENVIRONMENT PROTECTION
NT EYE PROTECTION
NT METEOROID PROTECTION
NT RADIATION PROTECTION
NT RADIATION SHIELDING
NT SOLAR RADIATION SHIELDING
NT THERMAL PROTECTION
Computer protection mechanisms design principles for operating system and hardware architecture implementation, considering access matrix storage, efficiency and subject and object selection
09 p1059 A73-22223

PROTECTIVE CLOTHING
NT HELMETS
NT PRESSURE SUITS
NT SPACE SUITS
Rocket propellant handling personnel protective clothing, describing head gear, ventilated underwear and airtight external suit
07 p0784 A73-18949
Thermal protective garment using independent regional control of coolant temperature.
07 p0785 A73-19481

Carbon monoxide content in the exhaled air and carboxyhemoglobin in the blood of subjects equipped with an isolating protective garment
12 p1463 A73-27712
Protective helmets performance evaluation for design optimization, considering failure analysis from aircraft accident reports
16 p1973 A73-32655
Bioassay method for thermal protective clothing fabrics evaluation, measuring skin damage with various fabric combinations under exposure to calibrated flame source
16 p1974 A73-32671
Ventilated wet suit for naval aircrews protection against water exposure in aircraft accidents, describing neoprene foam and nylon liner construction with air ventilation
16 p1974 A73-32672
Helmets effectiveness evaluation from acceleration and impact tests, discussing test criteria and civilian and military standards
16 p1975 A73-33132
Heat acclimatization while wearing vapor-barrier clothing.
17 p2115 A73-34742
Comparative study of patches for liquid cooled garments.
19 p2398 A73-37404

PROTECTIVE COATINGS
NT ANODIC COATINGS
NT CERAMIC COATINGS
NT PRIMERS [COATINGS]
The effect of oxide thickness on the hot salt stress corrosion susceptibility of Ti-6Al-4V.
01 p0061 A73-10137
Fatigue strength and stress-rupture strength of KhN77TiU and KhN70VMTiU steels with a protective coating
02 p0180 A73-11628
Investigation of the possibility for ultrasonic dispersion of certain corrosion inhibitors introduced in easily removable film coatings
02 p0184 A73-11643
Russian papers on metal corrosion and protection covering additives, annealing, polymer coatings, anodic polarization, electrodeposition, magnetic alloy coatings, etc
02 p0174 A73-12534
An intumescent coating for improved fuel fire protection of heat sensitive articles.
02 p0185 A73-12642
Selection and application of the protective coating system for the AWACS radome.
03 p0329 A73-13008
An advanced printed circuit board system having outstanding resistance to humid environments.
03 p0281 A73-13047
Book - Corrosion and corrosion control: An introduction to corrosion science and engineering /2nd edition/.
03 p0321 A73-13125
Design and practical aspects of maximum efficiency silicon solar cells for satellite applications.
03 p0254 A73-14205
Some aspects of the metallurgy and wear resistance of surface coatings.
05 p0580 A73-16102
Effect of boundary conditions on the radiative reflectance of dielectric coatings.
[AIAA PAPER 73-148] 05 p0598 A73-16896
Microorganisms induced biological corrosion, considering oxidizing agents, inhibitors, protective coatings and cathodic protection
06 p0704 A73-17507
Maraging steels galvanic corrosion reduction by two layer Fe-Cu protective coatings, presenting salt water stress corrosion/time-to-failure test results
06 p0705 A73-17799
Evaluation of protective coatings for prevention of corrosion of high strength steels when subjected to extreme environments.
06 p0711 A73-18717
Influence of thermal-diffusion coatings on the physicochemical properties of heat-resistant metals
07 p0840 A73-20512
The effect of metal gripping during dynamic loading
08 p0973 A73-21132
Borating kinetics and coating phase composition and thickness on cobalt and cobalt base alloys by metallographic, microhardness and X ray analyses
09 p1103 A73-22467
Utilization of the detonation phenomenon for the deposition of coatings /Survey/
09 p1088 A73-22468
The emissivity of a system consisting of a semitransparent isothermal coating and a flat opaque substrate
10 p1294 A73-23514
The effect of surface films on fatigue crack initiation.
11 p1381 A73-25810
Metal surfaces corrosion fatigue due to environmentally induced localized attack, discussing protective

film growth, crack propagation hydrogen interaction and stresses
11 p1381 A73-25811
Oxygen and temperature effects on Ni base superalloys fatigue fracture, discussing trans- and intergranular crack propagation and initiation in single and polycrystals and surface coatings
11 p1382 A73-25818
Ti alloy coating and surface treatment to prolong fatigue life by eliminating fretting damage, discussing design parameters selection, screening and strength tests and performance evaluation
11 p1383 A73-25838
Metallic, nonmetallic, inorganic and organic protective coatings for metals against mechanical and chemical damage, discussing processing methods and applications
11 p1374 A73-25847
Organic coating technology review, discussing binders, pigments and various processing techniques
11 p1388 A73-25848
Influence of welding parameters on the strength properties of spot welds of MST1X steel with protective coatings
11 p1374 A73-26293
Chromium coated steels corrosion fatigue in normal conditions, aggressive media and high temperature environments
11 p1386 A73-26733
'Glazes' produced on nickel-base alloys during high temperature wear.
12 p1513 A73-27598
Surface preparation, protective coatings, materials selection and equipment used in soldering, discussing quality control
12 p1504 A73-27990
Improved corrosion protection for solid rocket propulsion systems.
13 p1645 A73-29273
Protective coating systems for Navy aircraft turbine engines.
[NACE PAPER 113] 13 p1637 A73-29313
Compatible coatings for corrosion resistant aerospace fasteners.
[NACE PAPER 116] 13 p1638 A73-29316
Critical properties of exterior aircraft finish systems to protect fastener areas.
[NACE PAPER 117] 13 p1638 A73-29317
New inhibited elastomeric finish system designed by corrosion engineers to solve acute corrosion problems on military aircraft.
[NACE PAPER 118] 13 p1638 A73-29318
Use of soft X-ray spectroscopy to study corrosion and oxidation products on metals and alloys.
[NACE PAPER 124] 13 p1638 A73-29319
Influence of stress concentrations on the mechanical properties of cast molybdenum with protective coatings
14 p1763 A73-30688
Thin dielectric films as protective coatings for metallic mirrors and antireflective coatings for semiconductors and active laser materials
15 p1884 A73-31416
The passivation behaviour of the Ti-6Al-4V alloy.
15 p1895 A73-32567
Sand erosion tests and protective coatings for aircraft jet and turbojet engines and helicopter compressor airfoils
16 p2046 A73-33029
Elastomeric and ceramic coatings for aircraft and missile radomes protection in subsonic and supersonic rain erosion environments
16 p2027 A73-33031
Lightweight coatings for protecting boron filament and graphite fiber reinforced plastic composites from structural damage by lightning
16 p2028 A73-33033
Coating development of Martin Marietta's reusable surface insulation /MAR-SI/ for Space Shuttle applications.
16 p2071 A73-33059
Comparative testing and evaluation of conformal coating materials and processes.
16 p2018 A73-33062
Filiform corrosion associated with commonly applied aircraft metal pretreatments and finishes.
[SAE PAPER 730311] 17 p2177 A73-34671
Radiating power of a system consisting of a semitransparent isothermal coating and a flat non-transparent substrate.
17 p2212 A73-35194
High-temperature protective coatings; All-Union Conference on Heat Resistant Coatings, 5th, Kharkov, Ukrainian SSR, May 12-16, 1970, Transactions
18 p2318 A73-35876
Certain mechanisms of the solid-phase interaction arising during the formation and operation of high-temperature coatings
18 p2322 A73-35877
High temperature coatings on graphite
18 p2318 A73-35885
Some physicochemical and technological aspects of obtaining annealed coatings from melts and semimelts
18 p2318 A73-35887

PROTECTORS

Protection of certain borides from oxidation in air at 1200 C 18 p2318 A73-35888

Protective coating-metal adhesion dependence on chemical bonds, double electric layers at interface and thermoelastic stresses 18 p2319 A73-35893

Applications in aerospace construction and fallout of ONERA thermochemical techniques [ONERA, TP NO. 1246] 18 p2320 A73-36688

Effect of thermomodification coatings on the physicochemical properties of refractory metals. 19 p2440 A73-37787

Investigation of the plasticity of coatings on heat-resistant alloys 20 p2566 A73-39367

Performance of a water-repellent radome coating in an airport surveillance radar. 21 p2648 A73-40101

Investigation of the antistatic properties of lacquer coatings based on quaternary polyvinylpyridine salts 21 p2647 A73-40261

Russian book - High-temperature strain gauges based on heat-resistant oxides. 21 p2704 A73-41286

Catalytic activity in platinum group temperature sensors, discussing elimination by noncatalytic coatings 22 p2857 A73-42034

High reliability protective coatings for high temperature technology. 22 p2879 A73-42596

Wear resistant abrasive and dry lubricant cobalt-chromium carbide composite material coatings obtained by electrolytic codeposition 24 p3094 A73-45073

PROTECTORS

NT EAR PROTECTORS

PROTEIN METABOLISM

NT LIPID METABOLISM

Brain serotonin content - Physiological regulation by plasma neutral amino acids. 01 p0008 A73-10408

Cytochemical-luminescence study of adrenal cortex proteins under the influence of ionizing radiation 02 p0134 A73-12354

Accelerated chromatographic method for determination of hydroxyproline. 03 p0273 A73-13600

Differential housing /isolation vs aggregation/ as factor in postnatal development of mouse brain cell specificity and metabolism, noting relation to sleep behavior 03 p0264 A73-14259

Oxidation effects on rate of C 14-labeled leucine incorporation into rat skeletal muscle protein 05 p0538 A73-16152

Oxidation of amino acids by diaphragms from fed and fasted rats. 05 p0538 A73-16153

Research on the displacement of blood-plasma proteins and on the nerve conduction velocity in rats subjected to accelerations and hypokinesia 06 p0650 A73-17769

Adenonucleotides, NAD+, and NADN in skeletal muscles during intensive work and at rest 07 p0780 A73-19475

Thermal factor and dehydration influences on protidic and lipidic catabolisms of young men with partial food deprivation in hot climate, discussing metabolic balances 08 p0934 A73-21248

Changes in total plasma content of electrolytes and proteins with maximal exercise. 08 p0934 A73-21507

Proteinuria and civil aviation aircrew 08 p0931 A73-21538

Proteinuria and military aircrew 08 p0931 A73-21539

Effect of light deprivation on the metabolic reaction development in retinal ganglion cells 10 p1178 A73-23681

Autoradiographic study of protein synthesis in perikaryons and of nitrogen migration into the axons of hypertrophic sympathetic neurons 13 p1574 A73-28296

Reactivity and certain metabolic indices during prolonged sustenance of animals in artificial nutrient conditions 15 p1833 A73-31162

Protein and nucleic acid contents in animal tissues under hypokinesia 15 p1834 A73-31503

Effect of protein quality in the diet of rats on their tolerance to severe hypoxia 15 p1835 A73-31511

Protein synthesis in lung - Recovery from exposure to hyperoxia. 18 p2277 A73-36653

Protein synthesis in the neurons and glial cells of the stellate ganglia of rats during the adaptation to the effects of high altitude hypoxia 19 p2393 A73-37396

Effect of convulsions on certain aspects of the biosynthesis of proteins in the brain cortex 21 p2638 A73-40750

Microchemical urinalysis. IX - Determination of hydroxyproline in urine. 21 p2648 A73-41213

Ribonucleic acid /RNA/ polymerase and adenyl cyclase in cardiac hypertrophy and cardiomyopathy. 22 p2808 A73-42687

PROTEINOIDS

Evolution from amino acids - Lunar occurrence of their precursors. 01 p0008 A73-10249

Concepts related to the origin of the genetic apparatus. 03 p0265 A73-14317

On the electrophoretic behavior of thermal polymers of amino acids. 06 p0661 A73-17939

Light enhanced decarboxylations by proteinoids. 06 p0661 A73-17941

Conjugation of proteinoid microspheres - A model of primordial recombination. 06 p0652 A73-17952

Experimental models of communication at the molecular and microsystemic levels. 11 p1324 A73-25140

Organic inclusions within hydrothermal minerals from S.W. Africa and elsewhere. 11 p1352 A73-25472

Book - Molecular evolution and the origin of life. 12 p1461 A73-27049

PROTEINS

NT ADENOSINE DIPHOSPHATE [ADP]

NT ADENOSINE TRIPHOSPHATE [ATP]

NT ADENOSINES

NT ALBUMINS

NT CARBOXYHEMOGLOBIN

NT FIBRIN

NT FIBRINOGEN

NT LIPOPROTEINS

NT MELANIN

NT NUCLEASE

NT NUCLEOTIDES

NT OXYHEMOGLOBIN

NT PEPTIDES

NT PROTEINOIDS

NT PYRIDINE NUCLEOTIDES

Corticosterone level and the binding capacity of blood plasma proteins under thermal effects 03 p0261 A73-13749

The evolution of ferredoxins from primitive life to higher organisms. 03 p0265 A73-14318

Body temperature effect on protein conformation stability in healthy and diseased organisms, noting blood plasma albumin fractions 04 p0409 A73-14822

A note on the hypothesis - Protein polymorphism as a phase of molecular evolution. 04 p0410 A73-16033

Myosin ATPase and fiber composition from trained and untrained rat skeletal muscle. 05 p0538 A73-16155

Proteins and nucleic acids in prebiotic evolution. 06 p0652 A73-17937

Model experiments on the prebiological formation of protein. 06 p0652 A73-17938

Dependence of poly U-directed cell-free system on ratios of divalent and monovalent cations. 06 p0652 A73-17945

Protein-lipid films as prototypes of biological membranes. 06 p0652 A73-17949

Quantitative gas-liquid chromatography of non-protein amino acids in the presence of the twenty protein amino acids. 06 p0661 A73-18175

Silk fibroin, collagen, glycoproteins, keratin and protamines formation in single evolutionary event by de novo synthesis of DNA 07 p0780 A73-19219

Action of a serum protein on muscular contraction. 08 p0930 A73-21200

Protein molecules peptide groups excitation interpretation by quantum theory, noting application to muscle contraction 09 p1046 A73-23297

Study of the possibilities of histone-RNA complex formation in experiments in vitro 10 p1181 A73-24513

Gas-liquid chromatographic resolution of several protein amino acid enantiomers on a packed column. 10 p1186 A73-24658

X ray data refinement on proteins, discussing backbone and side chain dihedral angles adjustment by least squares fitting to relieve atomic overlaps 17 p2112 A73-34893

The nature of chemoreception in posterior hypothalamic structures 21 p2636 A73-40279

PROTOBIOLOGY

Chemical evolution under the bion hypothesis. 03 p0265 A73-14316

Concepts related to the origin of the genetic apparatus. 03 p0265 A73-14317

Protobiochemical developments in terms of extraterrestrial life search and roles of nitriles and urea in prebiological chemical evolution 03 p0265 A73-14319

Modelling of structure and functional unity on coacervate systems. 06 p0652 A73-17950

Coacervate systems and evolution of matter on the earth. 06 p0652 A73-17951

PROTON BEAMS

Proton beam effect on carbon dioxide laser discharge I-V characteristics and emission power 04 p0458 A73-15559

Interaction lengths of energetic pions and protons in iron. 08 p0990 A73-21523

Use of electron and proton beams for production of very low frequency and hydromagnetic emissions. 09 p1074 A73-22061

Proton beam measurement of absolute cross section for neutron knockout reaction on C 12 at pion-nucleon resonance, correcting for muon and electron contamination 21 p2743 A73-40686

Reaction Li-6/p, pt/ at 590 MeV. 21 p2743 A73-41018

PROTON BELTS

Effects of the secular magnetic variation on the distribution function of inner-zone protons. 02 p0155 A73-11731

Radiation belt low energy protons intensity and spectrum variations during geomagnetic storms from Molniya 1 satellite measurements, interpreting results in terms of electric field effects 02 p0206 A73-12318

Observations of low-energy protons with the Molniya 1 satellite in July-August, 1970. 05 p0608 A73-16084

Resonance acceleration of low-energy protons in the earth's radiation belts 06 p0742 A73-17526

Influence of a variable ionospheric-protonospheric plasma flow on the nighttime F region of the ionosphere 12 p1490 A73-27336

Exponential distributions of protons according to adiabatic invariants in the outer radiation belt 15 p1926 A73-31898

Resonance acceleration of low-energy protons in the radiation belts of the earth. 16 p2051 A73-32751

Cosmic ray albedo neutron decay injection theory for proton belt, considering radial diffusion, atmospheric losses, geomagnetic models, atmospheric density, etc 21 p2755 A73-40071

Influence of nonadiabatic effects during magnetic storms on the dynamics of proton belts 21 p2760 A73-40907

Secular geomagnetic variation consequences for steady state inner zone of energetic protons, discussing minimum altitude decrease and mirror point field magnitude increase 21 p2761 A73-41375

Energetic protons at low L-values of the equatorial magnetosphere. 21 p2761 A73-41379

Effect of changing ionospheric-protonospheric plasma flow on the nighttime F-region of the ionosphere. 23 p2970 A73-43234

Steady state exponential distribution function of outer radiation belt low energy protons in terms of adiabatic invariants 24 p3124 A73-44807

PROTON DAMAGE

Defect structure introduced during operation of heterojunction GaAs lasers. 24 p3096 A73-44923

PROTON DENSITY [CONCENTRATION]

NT MAGNETOSPHERIC PROTON DENSITY

Ring current effect on plasma convection in magnetosphere, assuming pressure due to proton population 03 p0302 A73-13854

Observations of low-energy protons with the Molniya 1 satellite in July-August, 1970. 05 p0608 A73-16084

Low-energy electron experiment for Atmosphere Explorer-C and -D. 13 p1689 A73-28642

Exponential distributions of protons according to adiabatic invariants in the outer radiation belt 15 p1926 A73-31898

The effect of nonstationarity in the chemical composition of plasma flows from the sun. 23 p3027 A73-43252

- Proton dosimeter design for distributed body or
23 p2949 A73-43389
- PROTON ENERGY**
- Energetic protons detection below radiation belt at equatorial latitudes from Azur satellite measurements, hypothesizing exospheric and upper atmospheric charge exchange processes
01 p0043 A73-11514
- Number density estimation for neutral hydrogen hot component required for solar wind heating to satisfy observed proton temperature relationship to wind velocity
02 p0205 A73-11745
- Radio emission source picture from observed Cygnus X-3 outburst, suggesting expanding cloud with traveling relativistic electrons and protons
02 p0211 A73-11870
- Measurements of energetic particle fluxes during a slowly varying absorption event by two co-ordinated rocket flights.
02 p0206 A73-12314
- Proton energy spectra from recent rocket measurements in the night and morning time auroral zone.
02 p0206 A73-12315
- Flux and energy spectra of solar protons observed aboard the ESRO 2 satellite in 1968-1969.
02 p0206 A73-12316
- ESRO IA/B observations at high latitudes of trapped and precipitating protons with energies above 100 keV.
03 p0362 A73-13863
- High energy proton model for the inner radiation belt.
03 p0363 A73-13880
- Propagation of solar cosmic rays in the solar wind.
04 p0491 A73-14837
- A solar-wind model including proton thermal anisotropy.
04 p0492 A73-15365
- Anisotropy of low-energy solar protons at the boundary of the magnetotail.
04 p0493 A73-15544
- Backward elastic proton-deuteron differential cross sections at different energies, describing experimental setup
05 p0601 A73-17322
- Propagation anisotropies of solar flare protons and electrons at low energies in interplanetary space.
07 p0869 A73-19227
- German monograph - Investigations of the behavior of high energetic protons and electrons in the inner magnetosphere.
07 p0872 A73-20385
- Primary cosmic ray particles disappearance and proton spectrum slope rise in 1 TeV energy region from Proton satellites data
08 p0999 A73-21330
- Primary cosmic rays alpha particles and protons energy spectra similarity and intensity difference at .05 to 1.6 TeV, using Proton satellites data
08 p0999 A73-21331
- Energy evaluation of protons responsible for Pc 1 emissions based on sources drift determination
08 p0961 A73-21494
- Low-energy solar protons in the pseudo-trapping region of the magnetosphere.
09 p1137 A73-22053
- Cosmic ray bursts in 1970-1971 according to measurements in the stratosphere
10 p1266 A73-23916
- Solar proton energy spectra recorded in stratosphere during two solar cycles, approximating generation spectra by power law
10 p1266 A73-23917
- The asymptotic behavior of the supersonic solutions of the two-fluid solar wind equations.
10 p1268 A73-24147
- Electron and proton acceleration in the outer regions of the magnetosphere during polar substorms.
10 p1268 A73-24227
- Solar wind He nuclei kinetic temperature, considering resonant heating and proton temperature
10 p1269 A73-24723
- Dependence of the light yield of a plastic scintillator on the energy of protons and electrons
12 p1496 A73-27206
- Influence of initial gas conditions in a coaxial accelerator on plasma parameters
13 p1666 A73-28956
- Solar wind proton temperature anomalies relation to interplanetary shock waves, considering solar flare induced material ejection and magnetic bottle formation
14 p1786 A73-29952
- Solar wind velocity and proton temperature time dependent relations, considering interplanetary medium nonlinear unsteady processes effects
14 p1786 A73-29955
- A new test for solar modulation theory - The 1972 May-July low-energy galactic cosmic-ray proton and helium spectra.
17 p2224 A73-34769
- Decay of the magnetic storm ring current by the charge-exchange mechanism.
17 p2159 A73-34782
- Particle entry into the equatorial magnetosphere.
18 p2344 A73-35928
- Differential energy spectrum of low-energy protons in the inner regions of the radiation belt
18 p2345 A73-36110
- Equatorial and auroral zone geomagnetic indices and micropulsations variations relation to 11-18keV protons occurrence in interplanetary space
18 p2345 A73-36120
- Sounding balloon nuclear emulsion chamber recording of energy spectra and angular distribution of incoming and outgoing proton fluxes in atmosphere
18 p2310 A73-36124
- Solar wind heat transport in the vicinity of the earth's bow shock.
18 p2346 A73-36269
- Low-energy protons of solar origin and interplanetary medium studies
19 p2474 A73-37345
- Energy spectra and pitch angle distributions of storm-time and substorm injected protons.
20 p2552 A73-38953
- Particle and field observations from Explorer 45 during the December 1971 magnetic storm period.
20 p2552 A73-38958
- Laboratory studies of collisions of energetic H⁺ and hydrogen with atmospheric constituents.
21 p2679 A73-40072
- Effects of nuclear reactions with fast protons in a supernova shell and the origin of cosmic rays
21 p2756 A73-40581
- Energetic protons at low L-values of the equatorial magnetosphere.
21 p2761 A73-41379
- Mariner 5 observations of solar wind shock-like structures including density, velocity, and proton temperature increases, suggesting nonlinear magnetoacoustic waves under steepening process
22 p2901 A73-41902
- Effect of initial gas conditions in a coaxial accelerator on the plasma parameters.
23 p3013 A73-44308
- Solar wind proton thermal anisotropy association with moments of proton velocity distribution and dependence on temperature decrease
24 p3125 A73-45105
- Heos 1 plasma and magnetic field experiments during bow shock crossings for turbulent bow structure, discussing proton velocity distribution
24 p3125 A73-45111
- Energy deposition of protons in molecular nitrogen and applications to proton auroral phenomena.
24 p3126 A73-45116
- PROTON FLUX DENSITY**
- Spectral behaviour and proton effects of the type IV broad-band continua.
01 p0093 A73-11394
- Measurements of energetic particle fluxes during a slowly varying absorption event by two co-ordinated rocket flights.
02 p0206 A73-12314
- Flux and energy spectra of solar protons observed aboard the ESRO 2 satellite in 1968-1969.
02 p0206 A73-12316
- Radiation belt low energy protons intensity and spectrum variations during geomagnetic storms from Molniya 1 satellite measurements, interpreting results in terms of electric field effects
02 p0206 A73-12318
- Interplanetary anisotropy measurements of energetic solar proton entry into geomagnetic tail by ESRO 2 satellite
03 p0362 A73-13860
- New observations of the proton population of the radiation belt between 1.5 and 104 MeV.
03 p0362 A73-13862
- Solar proton intensity structures in the magnetosphere during interplanetary anisotropies.
04 p0492 A73-14962
- 12.5-minute periodicity in solar proton fluxes at balloon altitude and in magnetic micropulsations.
04 p0492 A73-15527
- Magnetotail plasma leakage into magnetosheath during magnetospheric substorms from Vela satellites proton flux measurements
04 p0443 A73-15530
- Observations suggesting weak pitch angle diffusion of protons.
04 p0493 A73-15532
- Fokker-Planck equation for solar atmosphere modulation of galactic proton and electron flux at earth, including convection, diffusion and adiabatic deceleration effects
07 p0870 A73-19576
- Coupling between the F-region and protonosphere - Numerical solution of the time-dependent equations.
07 p0818 A73-19665
- Galactic cosmic ray particle intensity decrease relationship to low energy proton flux increase based on interplanetary Zond 3 and Venera probes measurements
08 p0999 A73-21326
- Primary cosmic radiation antiproton flux, finding .005 ratio upper limit to proton flux with balloon-borne-magnetic spectrometer
08 p0999 A73-21333
- Proton scattering in the region near the earth's bow shock.
09 p1137 A73-22054
- Anisotropies in the interplanetary intensity of solar protons with energies greater than 0.3 MeV.
10 p1269 A73-24728
- Energetic solar proton observations by Explorer 33 and 35 /interplanetary medium/ and Injun 5 /polar caps/, comparing proton fluxes in space and poles
10 p1269 A73-24729
- Satellite measurement of variable intensities for geomagnetically trapped protons during magnetic storms, noting ring current source of low-altitude protons
10 p1213 A73-24731
- A charged-particle scintillation spectrometer with large geometric factor.
11 p1364 A73-25965
- The results of measurements of the intensity of cosmic rays by the automatic station 'Venera-7'.
12 p1535 A73-27638
- The first results of balloon measurements during the solar proton events in the period from August 2 to August 10, 1972
12 p1535 A73-27777
- Study of the directional distribution of energetic electrons and protons in the morning sector of the auroral zone during enhanced particle flux
13 p1606 A73-28153
- Solar flare ejected protons intensity increase during July 1970 from Pioneer 6 and 8 and Explorer 41 data
14 p1786 A73-29859
- Interplanetary radial gradients of galactic cosmic ray protons and helium nuclei - Pioneer 8 and 9 measurements from 0.75 to 1.10 AU.
14 p1786 A73-29951
- On the generation of high-energy particles in solar flares.
15 p1925 A73-31068
- Estimate of the probability of observing solar cosmic-ray proton fluxes at the earth orbit
15 p1926 A73-31877
- French monograph - Interpretation of particle measurements carried out aboard rocket probes during the solar event of Jan. 28 1967.
15 p1927 A73-32586
- Satellite studies of magnetospheric substorms on August 15, 1968. VII - Ogo 5 energetic proton observations - Spatial boundaries.
16 p2056 A73-33455
- Observation of trapped and solar particles since 2 October 1972.
18 p2344 A73-35931
- Intensity variations of low-energy protons and electrons in the outer magnetosphere at the sudden onset of a magnetic storm
18 p2309 A73-36109
- Sounding balloon nuclear emulsion chamber recording of energy spectra and angular distribution of incoming and outgoing proton fluxes in atmosphere
18 p2310 A73-36124
- Solar cosmic ray alpha particles and protons flux measurement after events in 1967-1969 for 1-10 MeV particles
18 p2347 A73-36289
- Low-energy protons of solar origin and interplanetary medium studies
19 p2474 A73-37345
- Inner belt equilibrium equatorial proton flux computation from albedo neutron measurements, including effects of atmospheric collisions, radial diffusion and geomagnetic secular decrease
20 p2601 A73-38943
- Ring current particle distributions during the magnetic storms of December 16-18, 1971.
20 p2552 A73-38952
- Proton flux density and differential energy spectra recorded by solid state proton detectors and three-axis fluxgate magnetometer aboard Explorer 45 at plasmopause
20 p2552 A73-38955
- Propagation of protons injected near 1 AU in a medium with a constant transport length
21 p2756 A73-40583
- Determination and interpretation of solar proton spectra at the earth and in the source
21 p2756 A73-40584
- Satellite counting of excess radiation measured as ionospheric electron and proton intensity dependent on geomagnetic activity, discussing proton energy spectra and electron albedo
21 p2758 A73-40604
- Structural and dynamic features of solar cosmic-ray penetration into polar regions
21 p2758 A73-40606
- Limit of the region of low-energy solar proton intrusion into the polar ionosphere
21 p2758 A73-40607
- Influence of nonadiabatic effects during magnetic storms on the dynamics of proton belts
21 p2760 A73-40907
- Penetration of solar cosmic rays into the earth's polar caps
21 p2760 A73-40920

PROTON IMPACT

- Rocket measurements of production and ionization during a PCA event. 21 p2760 A73-41371
- Steady state coefficients in the D region during solar particle events. 21 p2760 A73-41372
- Enhancement of 0.24- to 0.96-MeV trapped protons during the May 25, 1967, magnetic storm. 22 p2901 A73-41909
- Low-energy cosmic ray protons from nuclear interactions of cosmic rays with the interstellar medium. 22 p2902 A73-41927
- Steady state exponential distribution function of outer radiation belt low energy protons in terms of adiabatic invariants 24 p3124 A73-44807
- Satellite measurement of magnetopause location, speed and thickness during satellite immersion within adjacent steep proton flux gradient 24 p3126 A73-45113
- ### PROTON IMPACT
- Further observed degradation on the LES-6 synchronous solar cell experiment. 03 p0258 A73-14247
- Cross sections for emission of Lyman-alpha radiation in collisions of 1-25 keV protons and hydrogen atoms with constituents of planetary atmospheres. 08 p0957 A73-20660
- Proton-impact dissociation and ionization of H₂+ molecular ions. 10 p1250 A73-23671
- Vibrational excitation of H₂ by proton impact. 14 p1777 A73-30957
- Detailed balance as check on impact parameter calculations, discussing proton-hydrogen collisions with small transition amplitudes and interpolation errors 21 p2743 A73-40467
- Proton collisional excitation in the ground configuration of Fe I+12/. 24 p3123 A73-44634
- Solar Fe 13 coronal lines relative intensity calculation as function of electron density from cross sections for collisional excitation by protons 24 p3136 A73-44635
- ### PROTON IRRADIATION
- Luminescence excitation by protons and electrons, applied to Apollo lunar samples. 03 p0369 A73-13098
- Irradiation of solar cell candidates for the ATS-F solar cell flight experiment. 03 p0257 A73-14245
- Effects of 10-150 keV proton bombardment on silicon solar cells. 04 p0406 A73-14984
- Effects of proton irradiation on several spacecraft science components. 05 p0596 A73-16513
- Effect of irradiation on the absolute thermal emf of metals and alloys 06 p0706 A73-17901
- Proton irradiation at 30 K and isochronal annealing of reactively sputtered Ta thin-film resistors. 06 p0737 A73-18352
- Optical and electrical properties of proton-bombarded p-type GaAs. 06 p0739 A73-18786
- Thermoluminescence of Apollo 14 lunar samples following irradiation at -196 C. 07 p0897 A73-19879
- Influence of the substrate and the structure of the metal film on the nature of the annealing treatment of defects formed in the film by proton bombardment 07 p0864 A73-20524
- Silicon solar cells radiation damage from orbital flight and electron and proton irradiation laboratory test data, discussing radiation hardening by Li doping 09 p1036 A73-22811
- Influence of proton irradiation in vacuum on the properties of polymer films 11 p1389 A73-26740
- Study of lymphocyte chromosome aberrations in human peripheral blood under in vitro exposures to 645-MeV protons and X-rays 15 p1835 A73-31517
- Experimental results on combined ultraviolet-proton excitation of moon rock luminescence. 17 p2233 A73-35273
- Darkening of silicate rock powders by solar wind sputtering. 17 p2235 A73-35740
- Reaction Li-6/p, pt/ at 590 MeV. 21 p2743 A73-41018
- Complete hydrogen and helium particle spectra from 30- to 60-MeV proton bombardment of nuclei with A = 12 to 209 and comparison with the intranuclear cascade model. 21 p2744 A73-41019
- A radially streaming proton model for the broad component of hydrogen emission in Seyfert galaxies. 24 p3138 A73-45039
- He and Ne cross sections in natural Mg, Al, and Si targets and radionuclide cross sections in natural Si, Ca, Ti, and Fe targets bombarded with 14- to 45-MeV protons. 24 p3125 A73-45103

PROTON MAGNETIC RESONANCE

- A study of the secondary structure of ilamycin B1 by 300 MHz proton magnetic resonance. 11 p1326 A73-25572
- ### PROTON PRECESSION
- Magnetic anomalies in New Guinea-New Zealand region from proton magnetometer measurements, noting effects of andesite-basalt volcanic processes and nuclear precession signal variations 13 p1608 A73-28727
- ### PROTON PRECIPITATION
- Ring current proton injection instability for ion loss cone and electromagnetic ion cyclotron waves in high beta low density region outside plasmapause 02 p0156 A73-11748
- Auroral particle precipitation patterns from satellite observations, discussing electron and proton penetration from magnetosheath plasma and magnetotail 02 p0163 A73-12308
- High-latitude precipitation of low-energy particles as observed by ESRO IA. 02 p0206 A73-12312
- Precipitation of auroral and ring current particles by artificial plasma injection. 03 p0301 A73-13711
- ESRO IA/B observations at high latitudes of trapped and precipitating protons with energies above 100 keV. 03 p0362 A73-13863
- Low energy auroral electron and proton precipitation patterns from polar orbiting ESRO IA satellite, noting discontinuities, flux distribution valleys, latitudinal crossover and Kp dependence 03 p0362 A73-13864
- Observations suggesting weak pitch angle diffusion of protons. 04 p0493 A73-15532
- Observation of the entrance of solar protons in the magnetosphere at very high latitudes 10 p1211 A73-23769
- Turbulent loss mechanism of ring current protons in plasmapause vicinity via electrostatic drift cyclotron loss cone waves 10 p1270 A73-24743
- A uniform belt of diffuse auroral emission seen by the ISIS-2 scanning photometer. 15 p1866 A73-31069
- French monograph - Interpretation of particle measurements carried out aboard rocket probes during the solar event of Jan. 28 1967. 15 p1927 A73-32586
- An example of anticorrelation of auroral particles and electric fields. 18 p2312 A73-36297
- Occurrence of IPDP events accompanied by cosmic noise absorption in the course of proton aurora substorms. 18 p2312 A73-36298
- Satellite and ground-based observations during the onset phase of the 2 November 1969 PCA event. 19 p2426 A73-38016
- Magnetic storm inflation analysis from Explorer 45 and ground observation data, noting proton penetration into magnetosphere evening quadrant 20 p2552 A73-38951
- Auroral arc mechanism of solar wind intrusion and electron and proton energization and precipitation in magnetosphere from Isis photometric and spectrometric observations 20 p2553 A73-39124
- Precipitating protons with E greater than 12.4 keV to 500 keV near the midnight trapping boundary. 21 p2760 A73-40822
- Auroral electron and proton flux density, energy spectra, acceleration and precipitation mechanisms and turbulent diffusion from rocket and satellite measurements 22 p2850 A73-42748
- Radiation production and energy deposition by ring current protons precipitated into the mid-latitude upper atmosphere. 23 p3024 A73-43685
- Critique of Lukina theory of number of auroral arc orientations related to characteristic precipitation zone 24 p3084 A73-44799
- High-latitude proton precipitation and light ion density profiles during the magnetic storm initial phase. 24 p3126 A73-45114
- Simultaneous growth of high-latitude positive bay and DR-field in the course of proton aurora substorm. 24 p3127 A73-45215
- ### PROTON RESONANCE
- Resonance acceleration of low-energy protons in the earth's radiation belts 06 p0742 A73-17526
- Resonance acceleration of low-energy protons in the radiation belts of the earth. 16 p2051 A73-32751
- ### PROTON SATELLITES
- NT PROTON 2 SATELLITE
- NT PROTON 3 SATELLITE
- NT PROTON 4 SATELLITE
- Study of energy spectra of primary cosmic rays at very high energies on the proton series of satellites. 02 p0207 A73-12328

- Primary cosmic ray particles disappearance and proton spectrum slope rise in 1 TeV energy region from Proton satellites data 08 p0999 A73-21330
- The effect of aerodynamic moments on the rotational motion of Proton satellites 12 p1548 A73-26820
- Parameter estimation for a specular-diffusion reflection model from the motion of 'Proton' series satellites about their centers of mass 14 p1803 A73-29851
- ### PROTON SCATTERING
- Primary proton-air atom nuclei interaction study of negative and positive cosmic ray muon coupling coefficients with angular distribution allowance 02 p0205 A73-12173
- Backward elastic proton-deuteron differential cross sections at different energies, describing experimental setup 05 p0601 A73-17322
- Penetration of solar protons into the geomagnetic tail 08 p0998 A73-21276
- Solar protons propagation from instantaneous injection source and inhomogeneities interaction description by mean free path and scattering angle specification 08 p0999 A73-21327
- Nonadiabatic particle motion in the magnetosphere. 09 p1073 A73-22052
- Low-energy solar protons in the pseudo-trapping region of the magnetosphere. 09 p1137 A73-22053
- Proton scattering in the region near the earth's bow shock. 09 p1137 A73-22054
- Dissipation of hydromagnetic waves with application to the outer solar corona. III - Transition from collisional to collisionless protons. 11 p1428 A73-26619
- Balmer-line emission from auroral protons. 17 p2213 A73-34766
- Coronal propagation of low-energy solar protons. 18 p2347 A73-36290
- Penetration of solar protons into the geomagnetic tail. 19 p2476 A73-37905
- Measurement of the effective cross section of inelastic interaction between protons and carbon nuclei in the energy range 0.1 TeV to 1.0 TeV, on the Proton-4 space station 23 p3021 A73-43539
- He and Ne cross sections in natural Mg, Al, and Si targets and radionuclide cross sections in natural Si, Ca, Ti, and Fe targets bombarded with 14- to 45-MeV protons. 24 p3125 A73-45103
- ### PROTON TELESCOPES
- #### U PARTICLE TELESCOPES
- ### PROTON 2 SATELLITE
- Rarefied gas interaction with spacecraft surface, calculating aerodynamic forces and accommodation coefficient for Proton 2 satellite 03 p0383 A73-14574
- ### PROTON 3 SATELLITE
- Solar cosmic ray burst on July 7, 1966 and its measurement on the Proton-3 artificial earth satellite 02 p0208 A73-12461
- Solar cosmic-ray burst of July 7, 1966 and its measurement by Proton-3 satellite. 15 p1927 A73-32611
- ### PROTON 4 SATELLITE
- Primary cosmic rays energy spectrum at .100-1000 TeV from Proton 4 satellite data 08 p0999 A73-21329
- ### PROTON-PROTON REACTIONS
- Interaction contributions to the solar proton-proton reaction. 05 p0612 A73-17339
- Effect of rapidly rising proton-proton total cross sections on idealized extensive air showers. 11 p1412 A73-25745
- Pulsational instability of a star of 0.5 solar mass during core hydrogen burning. 13 p1685 A73-29362
- ### PROTONS
- #### NT RECOIL PROTONS
- #### NT SOLAR PROTONS
- Gas-phase acidities of binary hydrides. 02 p0139 A73-12632
- Inelastic scattering calculations with projected Hartree-Fock wave functions. II - Coupled-channel treatment. 03 p0345 A73-13806
- Hydrogen/proton adsorption behavior on fuel cell Pt electrode, considering surface roughness factor, Pt sites number and equilibrium data 04 p0407 A73-15104
- Line broadening of Lyman alpha wings due to protons calculated via positive molecular hydrogen ion wave functions 08 p0997 A73-20892
- On the theory of tunnelling in electron and proton transfer reactions. 09 p1133 A73-22199

PROTOPLASM

Activated oxygen ashing of biological specimens for the microdetermination of Na, K, Mg, and Ca by atomic absorption spectrophotometry.
02 p0139 A73-12546

PROTOSTARS

NT T TAURI STARS
Condensation and protostar expansion hypotheses of stellar and galactic evolution in view of discoveries of quasars, central bodies and stellar associations
03 p0365 A73-12902

A numerical experiment in the accretion problem.
04 p0503 A73-16004

Star formation from interstellar clouds gravitational collapse, discussing protostars evolution based on model calculations
07 p0878 A73-19675

Spectra of the Becklin-Neugebauer point source and the Kleinmann-Low nebula from 2.8 to 13.5 microns.
08 p1008 A73-21157

Carbon monoxide rotational transitions as dark cloud cooling mechanism during protostar formation
08 p1013 A73-21814

Condensation of stars and magnetic field formation in protogalaxies
12 p1547 A73-27868

Dynamical contraction of rotating gaseous spheroids.
13 p1680 A73-28774

Interstellar cloud collapse into protostellar objects and star formation, discussing young stellar objects observation
13 p1681 A73-28946

Collapse calculations and their implications for the formation of the solar system.
17 p2227 A73-34411

IR and molecular radio emissions from interstellar clouds representing formation stage of normal stars, discussing dust screening effects
17 p2229 A73-34433

Water masers in a protostellar gas cloud.
19 p2483 A73-37573

Star contraction and magnetic-field generation in protogalaxies.
20 p2608 A73-39242

PROTOTYPES

Prototype development for Army personnel and equipment airborne mobility, considering various aircraft conceptual designs feasibility relative to logistics requirements
[SAE PAPER 720846] 05 p0534 A73-16658

Choices for the future - An industry viewpoint on prototyping.
[SAE PAPER 720848] 05 p0534 A73-16659

Prototype distance measuring instrument for modulated light beam transit time determination
11 p1367 A73-26308

Air Force Prototype Program management.
23 p3051 A73-44061

PROTOZOA

Racemization of amino acids in marine sediments determined by gas chromatography.
23 p2973 A73-43843

PROTUBERANCES

Steady state aerodynamic characteristics of cylinders with spanwise protrusions, presenting wind tunnel drag and lift measurements in Reynolds number transition range
04 p0403 A73-14949

Visualization of boundary layer flow patterns around protuberances using an optical-surface indicator technique.
07 p0808 A73-19530

Aerodynamic noise field associated with pressure distributions generated by local protuberance on launch vehicle during atmospheric flight
11 p1300 A73-25384

PROUSTITE

Nonlinear polarization coefficients of proustite and tellurium.
06 p0738 A73-18596

High-power broadly tunable difference-frequency generation in proustite.
13 p1626 A73-28548

Difference frequency generation by optical mixing of two dye lasers in proustite.
19 p2438 A73-38165

PROVING

NT THEOREM PROVING

PRUSSIC ACID

U HYDROCYANIC ACID

PSEUDONOISE

Synthesis of an optimal receiver structure for amplitude modulated pseudo-noise signals.
04 p0415 A73-14982

Acquisition time evaluation at different input SNR values for pseudonoise signal demodulation, noting common bandwidth detection system advantage
04 p0421 A73-15427

Common-bandwidth transmission of data signals and wide-band pseudonoise synchronization waveforms.
07 p0790 A73-19200

Limits of suitability of pseudorandom signals for statistical tests
08 p0938 A73-20835

Hadamard transform spectrometer designed for airborne IR astronomical observations of Mars, using binary orthogonal pseudonoise codes in multiplexing scheme
08 p0972 A73-21753

PSEUDORANDOM SEQUENCES

Pseudorandom noise for telemetry error rate measurement applications and limitations.
04 p0449 A73-15457

Auto and cross correlation functions of combined binary pseudorandom sequences in digital space communication systems
04 p0423 A73-15916

Limits of suitability of pseudorandom signals for statistical tests
08 p0938 A73-20835

Noiselike FM signals shaping by numerical periodic pseudoeven sequences, analyzing FSK signals
09 p1049 A73-22049

Noise immunity in detection of pseudorandom PSK signals with allowance for synchronization errors, noting reception fidelity dependence on signal to noise ratio
09 p1050 A73-22455

Suboptimal input signal synthesis for linear control system identification based on output SNR maximization, bandwidth matching and pseudorandom binary noise nature
11 p1327 A73-25197

Pseudo random modulation - An effective means of enhancing PSK signal transmission in a diffuse multipath environment.
17 p2125 A73-35376

Pseudorandom Poisson process binary pulse generator, discussing digital hardware implementation and test results
24 p3069 A73-45256

PSYCHIATRY

Psychiatric and psychometric predictability of test pilot school performance.
[AD-754148] 03 p0269 A73-14165

Alpha-delta sleep as replacement for delta sleep in various psychiatric patients with chronic fatigue and depression
09 p1045 A73-22694

Psychopharmacology in treating psychiatric diseases, negative emotions, and nerve stimulation, discussing tranquilizers synthesis and effects
12 p1465 A73-27497

PSYCHOACOUSTICS

A note on the quantity /effective/ perceived noisiness and units of perceived noise level.
04 p0406 A73-15587

Behavioural awakening and subjective reactions to indoor sonic booms.
04 p0412 A73-15592

Effects of aircraft noise on human sleep.
06 p0659 A73-18546

German monograph - The objectivization of the effect of load and stress on an information-reception process of man with the aid of acoustically evoked potentials.
07 p0786 A73-20389

Study of the peripheral auditory adaptation in a psycho-acoustic experiment
10 p1179 A73-23807

Book - Foundations of modern auditory theory. Volume 2.
14 p1715 A73-30276

Psychoacoustic theory of signal detectability based on mathematical input-output mapping model and memory role in human auditory system
14 p1721 A73-30278

Interaural difference thresholds in binaural perception of signals nonexistent in normal acoustic environment, considering beats, memory, learning, and stereophony
14 p1716 A73-30285

Sonic booms and sleep - Affect change as a function of age.
18 p2282 A73-36780

Pure-tone equal-loudness contours for standard tones of different frequencies.
21 p2645 A73-41176

Cognitions and 'placebos' in behavioral research on ambient noise.
22 p2816 A73-42950

PSYCHOLOGICAL EFFECTS

NT MOON ILLUSION

NT OCULOGRAPHIC ILLUSIONS

Mathematical description of certain properties of human sensitivity to vibration
01 p0012 A73-10659

Space-time relations - The effects of variations in stimulus and interstimulus interval duration on perceived visual extent.
05 p0545 A73-17199

Psychological and psychophysiological factors of human performance in manned space missions, considering environmental effects of space flight and man-machine system
06 p0650 A73-17775

PSYCHOLOGICAL TESTS

Visual after-images in athletes and coaches as a prestart condition index
06 p0658 A73-18161

Effect of mild acute hypoxia on a decision-making task.
14 p1717 A73-30514

Physical and psychological effects of electromagnetic fields on human and animal central nervous system
14 p1718 A73-30571

A model of psychological annoyance of noise.
17 p2118 A73-35627

Some characteristics of pilot's performance under complicated flight conditions.
18 p2285 A73-36921

Human noise sensitivity, discussing personality effects, Maplin airport planning and population separation into sensitive and imperturbable groups
24 p3062 A73-44770

PSYCHOLOGICAL FACTORS

Electromechanical and electronic cockpit displays effectiveness in terms of aircraft control and psychological/physiological factors relating to pilot performance and workload
[DGLR PAPER 72-097] 02 p0136 A73-11666

Psychological and medical viewpoint for hijacker handling, discussing air crew training program
[AD-757130] 02 p0138 A73-12564

Effects of intermittent and continuous noise on serial search performance.
03 p0267 A73-13560

Identification and adjustment of psychological factors to improve solar patrol observing.
04 p0411 A73-14841

Vestibular adaptation in man - Effects of increased acceleration during different phases of adaptation.
04 p0411 A73-15218

Reflex act structural components interaction in terms of reflection, creativity and organism-environment relations, noting subjective and objective perception and attitude formation
04 p0410 A73-15798

Psychological and physiological components of biorhythm cycles governing periodic variations in physical, emotional and intellectual performance
05 p0544 A73-16720

Personal life changes and health stresses in contrast to accident proneness as factors in pilot error
05 p0545 A73-16732

Community response to aircraft noise.
10 p1298 A73-24562

Implications of psychoanalytic factors for Air Force operations.
11 p1323 A73-25340

Effects of prolonged dark adaptation on autokinetic movement.
11 p1324 A73-26322

Changes in blood-flow distribution during acute emotional stress in dogs.
13 p1576 A73-28533

Naval aviator training program dropouts identification in terms of physiological, safety, security, social, self-esteem and self-actualization needs
14 p1722 A73-30513

Psychological factors influencing the relationship between cardiac arrhythmia and mental load.
14 p1720 A73-30877

Russian book - Engineering psychology in aviation and astronautics.
15 p1838 A73-31375

Daytime human performance and temperament rhythms as function of individual introversion-extroversion rating
16 p1972 A73-33157

Nonadjectival rating scales in human response experiments.
17 p2117 A73-35400

Sudden incapacitation in flight.
18 p2279 A73-36847

Study of Indian naval aircrew experiences and psychic factors in disorientation.
18 p2285 A73-36919

Russian book - Psychological problems of activity regulation.
22 p2812 A73-41884

Some psychological and engineering aspects of the extravehicular activity of astronauts.
22 p2814 A73-42167

Myocardial infarction susceptibility correlated with psychosocial factors in life change measurement studies
22 p2809 A73-42833

PSYCHOLOGICAL INDEXES

U PSYCHOLOGICAL TESTS

PSYCHOLOGICAL TESTS

Conjoint-measurement framework for the study of probabilistic information processing.
02 p0138 A73-12545

Psychological test for relative contributions of specific and nonspecific components to intersensory transfer between vision and touch
03 p0266 A73-13525

Verbal estimates of perceived time of flashing lights interval, relating to lights separation distance
03 p0260 A73-13552

Intellectual ability and performance on a non-verbal problem-solving task.

03 p0260 A73-13553

Clairvoyant perception of target material in three states of consciousness.

03 p0260 A73-13555

Multidimensional judgments in design of ideal organisms with integral number of resource units allocated among characteristics such as memory, vision, resourcefulness, etc

03 p0261 A73-13559

Human performance measures relationship determination across sense modes under visual, auditory and combined stimulus conditions by controlling for task difficulty on individual basis

06 p0658 A73-18244

Step input tracking experiment for testing human psychological refractory period, noting directional error correcting reaction time similarities with keyboard tasks

06 p0659 A73-18470

Central nervous system stresses effects estimation, discussing ocular positioning movements functional significance and psychological processes

08 p0935 A73-21542

Proposed new test for aptitude screening of air traffic controller applicants.

09 p1045 A73-22535

Psychic stress detection and measurement, discussing psychological test methods and physiological correlates

10 p1183 A73-23684

Adaptation-level and theory of signal detection - An examination and integration of two judgment models for voluntary stimulus generalization.

12 p1464 A73-26749

Properties of human visual orientation detectors - A new approach using patterned afterimages.

13 p1579 A73-29124

Effect of stimulus uncertainty on the pupillary dilation response and the vertex evoked potential.

14 p1714 A73-29991

Conditioned reflex switching effects in higher nervous system reactions as function of experimental stimuli background conditions /arousal, diurnal rhythms, test conditions, physiological condition/

14 p1718 A73-30567

Formation of conditioned responses to symbolic stimulations in healthy individuals of different age

15 p1833 A73-31158

Intellectual performance during prolonged exposure to noise and mild hypoxia.

18 p2283 A73-36783

Initial results of a psychophysiological study of certified parachutists

18 p2284 A73-36917

Relation between vibratory sensibility and electric signal of living body.

22 p2816 A73-42680

Clinical psychology diagnostic methods in military aviation medicine, considering neurotic symptoms and psychosomatic disorders in flight fitness examinations

22 p2817 A73-43129

Individual personality variability difficulties in measurement of human psychophysiological reactions to flight stress, emphasizing psychological interview and evaluation methods

22 p2817 A73-43130

PSYCHOLOGY

NT MILITARY PSYCHOLOGY

NT PSYCHOACOUSTICS

NT PSYCHOPHYSICS

Psychopharmacology in treating psychiatric diseases, negative emotions, and nerve stimulation, discussing tranquilizers synthesis and effects

12 p1465 A73-27497

Book - The psychology of visual perception.

17 p2117 A73-35474

PSYCHOMETRICS

Conjoint-measurement framework for the study of probabilistic information processing.

02 p0138 A73-12545

Psychiatric and psychometric predictability of test pilot school performance.

03 p0269 A73-14165

German monograph - Vigilance prognosis with the aid of a computer analysis of the spontaneous electroencephalogram.

07 p0786 A73-20391

Psychic stress detection and measurement, discussing psychological test methods and physiological correlates

10 p1183 A73-23684

Visual temporal integration for threshold, signal detectability, and reaction time measures.

13 p1578 A73-28097

Psychotechnical selection of flight crews in South Vietnam

18 p2284 A73-36918

Sentography - Dynamic forms of communication of emotion and qualities.

23 p2949 A73-44180

PSYCHOMOTOR PERFORMANCE

NT PSYCHOSOMATICS

Prediction of flight safety hazards from drug induced performance decrements with alcohol as reference substance.

[DFVLR-SONDDR-268] 03 p0269 A73-14158

Behavioural awakening and subjective reactions to indoor sonic booms.

04 p0412 A73-15592

Utilization extent of the muscle apparatus capabilities during maximum voluntary force exertion

05 p0541 A73-16696

Effects of noise and response complexity upon vigilance performance.

06 p0656 A73-17523

Vertical posture control after Soiz 6, 7 and 8 flights and 120-day hypokinesia

08 p0933 A73-20985

The interaction between muscle groups in a complex motor act in humans

08 p0930 A73-21320

Simultaneous motor and verbal processing of visual information in a modified Stroop test.

09 p1044 A73-21896

A study of Halon 1301 /CBRF3/ toxicity under simulated flight conditions.

09 p1045 A73-22537

Self-imposed timeouts under increasing response requirements.

10 p1185 A73-24625

Forced guidance and distribution of practice in sequential information processing.

11 p1323 A73-26319

Target-detection performance as a function of noise intensity and task difficulty.

11 p1323 A73-26320

Formation of conditioned responses to symbolic stimulations in healthy individuals of different age

15 p1833 A73-31158

Work-rest cycle effects on airline pilots performance, considering central nervous system changes measurement techniques

15 p1839 A73-32059

Informative parameters of the psychophysiological state of flight personnel when working with indicators

17 p2114 A73-34237

Psychotechnical selection of flight crews in South Vietnam

18 p2284 A73-36918

Physiological cost in 36- and 48-hour simulated flights.

20 p2512 A73-39101

Effects of single exposures of carbon monoxide on sensory and psychomotor response.

21 p2637 A73-40409

Individual and simultaneous tracking of a step input by the horizontal saccadic eye movement and manual control systems.

22 p2811 A73-41735

Cognitions and 'placebos' in behavioral research on ambient noise.

22 p2816 A73-42950

Physiological study of dynamics and evolution of chimpanzee complex behavior, considering motor reactions, group behavior and nerve mechanisms of voluntary acts

23 p2947 A73-43928

Sentography - Dynamic forms of communication of emotion and qualities.

23 p2949 A73-44180

PSYCHOPHYSICS

NT PSYCHOACOUSTICS

Cat optic tract and geniculate unit responses corresponding to human visual masking effects.

02 p0134 A73-12161

Psychophysical effects of night vision perceptual contrast in terms of central visual receptive field organization

03 p0261 A73-13759

Psychophysical studies of visual image normalization mechanisms in man

04 p0413 A73-15791

Angular velocity magnitude conversion into visually perceived apparent velocity, using psychophysical mathematical model based on axisymmetric annular visual field perception

04 p0413 A73-15796

Inter-hemispheric transfer of meaningful visual information in normal human subjects.

07 p0782 A73-20123

Human receptive visual field adaptation characteristics for stabilized retinal images by psychophysical probe detection technique

07 p0782 A73-20252

Psychophysical areal summation and stimulus contour and threshold visibility effects on size selective adaptation in human vision for single- and multichannel models

08 p0931 A73-21563

Forced guidance and distribution of practice in sequential information processing.

11 p1323 A73-26319

Estimation of the variability of the latency of responses to brief flashes.

11 p1321 A73-26720

Implications of measurement of eye fixations for a psychophysics of form perception.

13 p1577 A73-28092

Brightness functions for a complex field with changing illumination and background.

13 p1578 A73-28100

A comparison of electrophysiological and psychophysical temporal modulation transfer functions of human vision.

13 p1575 A73-28360

Retinal receptive fields - Correlations between psychophysics and electrophysiology.

14 p1717 A73-30397

Human cone optical density estimation implications of conflicting results for luminosity at bleaching intensities in dichromats related to use of psychophysical data

14 p1717 A73-30402

On the perception of a class of bilaterally symmetric forms.

17 p2118 A73-35495

Bioelectric and vegetative components of conditioned reflexes of 'negative-emotional type'

20 p2515 A73-39797

Contingent negative variation expectancy waveform relation to human psychic state in response to visual and imperative acoustic stimuli

20 p2516 A73-39804

Visually perceived motion in depth resulting from proximal changes. I, II.

21 p2640 A73-41186

The psychophysical inquiry into binocular summation.

21 p2640 A73-41187

Experimental substantiation of the optimal method for scaling the duration of acoustic stimuli

22 p2814 A73-42654

PSYCHOPHYSIOLOGY

Development and adjustment of a multi-channel miniaturized FM/AM telemetering system adapted to the primates.

03 p0270 A73-14284

Multidimensional coding for telemetric transmission of work load factors in ergonomics research.

03 p0272 A73-14307

Technology for man 72; Proceedings of the Sixteenth Annual Meeting, Los Angeles, Calif., October 17-19, 1972.

05 p0542 A73-16701

The interaction of auditory noise and subjective noise annoyance sensitivity with peripheral visual sensitivity.

05 p0543 A73-16703

Psychological and psychophysiological factors of human performance in manned space missions, considering environmental effects of space flight and man-machine system

06 p0650 A73-17775

The operational control of the alpha component in the electroencephalogram by means of auditory feedback

11 p1324 A73-26549

Work movement performance of the astronaut in flight.

12 p1465 A73-27645

Electrophysiological evidence that abnormal early visual experience can modify the human brain.

15 p1838 A73-31371

Memory fixation during sleep, discussing EEG, EOG, EMG and ECG recordings for differences between light and paradoxal sleep

15 p1835 A73-31749

A device for the continuous measurement of subjective changes

16 p1975 A73-33090

A standard psychophysiological preparation for the study of environmental stress.

16 p1975 A73-33130

Informative parameters of the psychophysiological state of flight personnel when working with indicators

17 p2114 A73-34237

Determination of the type of higher nervous activity from the aftereffect characteristics of multidimensional stimuli

18 p2277 A73-36577

Initial results of a psychophysiological study of certified parachutists

18 p2284 A73-36917

Psychophysiological characteristic of the activity of military-transport-aviation flight crews during low-altitude flights

19 p2397 A73-37196

The problem of spiritual requirements and the theory of human higher nervous activity

20 p2515 A73-39796

High-frequency synchronized activity of the amygdaloid complex as an EEG indicator of certain psychophysiological states

21 p2636 A73-40277

Ability of a human operator to estimate the probability characteristics of alternative stimuli

22 p2813 A73-41893

Individual personality variability difficulties in measurement of human psychophysiological reactions to

flight stress, emphasizing psychological interview and evaluation methods 22 p2817 A73-43130

PSYCHOSES

Role of associations in the formation of evoked potentials from the human cerebral cortex 20 p2515 A73-39798

PSYCHOSOMATICS

Clinical psychology diagnostic methods in military aviation medicine, considering neurotic symptoms and psychosomatic disorders in flight fitness examinations 22 p2817 A73-43129

PTM [MODULATION]

U PULSE TIME MODULATION

PUBLIC RELATIONS

The attitude of the public towards the Space Programme - Its assessment and its influence as a guiding policy factor. 11 p1454 A73-26275

Airline pilots problems in terms of job security, working conditions, management relations, public relations, flight safety due to noise abatement rules, etc 12 p1562 A73-27599

PUBLICATIONS

U DOCUMENTS

PUERTO RICO

Semi-annual variation in the true height of the F2-peak in low latitudes /at Puerto Rico/. 15 p1869 A73-31762

PULMONARY CIRCULATION

Effect of interstitial edema on distribution of ventilation and perfusion in isolated lung. 01 p0008 A73-10167

Hemodynamic effects of physical maneuvers /Valsalva, effort, respiration/ and of pharmacodynamic tests - Their clinical application 02 p0138 A73-12159

Gas-blood CO₂ equilibration in dog lungs during rebreathing. 03 p0263 A73-14115

Radiotelemetry of direct bloodpressure measurements in aorta, pulmonary artery and heart. 03 p0271 A73-14291

Effects of cardiac output on /O-18/2 lung diffusion in normal resting man. 06 p0654 A73-18335

Time course of pulmonary vascular response to hypoxia in dogs. 07 p0782 A73-20168

Sinus venosus atrial septal defect - Analysis of fifty cases. 07 p0784 A73-20368

Pathogenesis of some respiration and circulation reactions to barometric pressure gradients 08 p0929 A73-20980

Significance of the Bohr and Haldane effects in the pulmonary capillary. 08 p0935 A73-21614

A model of time-varying gas exchange in the human lung during a respiratory cycle at rest. 08 p0936 A73-21615

Changes in the vascular tone of certain organs during experimental embolism of pulmonary circulation 09 p1039 A73-22366

Red cell flexibility and pressure-flow relations in isolated lungs. 09 p1041 A73-22927

Distribution of systemic blood flow during cardiopulmonary bypass. 09 p1041 A73-22930

Effect of physical exercises on the lung rheogram 10 p1182 A73-24524

Independent effects of changes in H+ and CO₂ concentrations on hypoxic pulmonary vasoconstriction. 10 p1182 A73-24565

Comparison of blood and alveolar gas composition during rebreathing in the dog lung. 11 p1318 A73-26218

Book on echocardiography covering examination of mitral, aortic, tricuspid and pulmonic valves, ventricles, atrium, pericardial effusion, coronary artery disease and tumors 14 p1721 A73-30358

Determination of diffusive capacity components in lungs and of alveoloarterial oxygen gradients for the estimation of oxygen transport conditions in lungs 14 p1719 A73-30849

Effects of tilting on pulmonary capillary blood flow in normal man. 20 p2519 A73-39786

Oxygen delivery and oxygen return to the lungs at onset of exercise in man. 20 p2519 A73-39788

Effect of stimulation of the hypothalamus on the pH of arterial and venous blood 21 p2637 A73-40281

Effect of stimulation of certain hypothalamic structures on systemic and pulmonary circulation 21 p2637 A73-40282

Circulatory reflexes from mechanoreceptors in the cardio-aortic area. 21 p2638 A73-40637

Morphometry of the human pulmonary arterial tree. 21 p2638 A73-40639

Cardiopulmonary responses of male and female swine to simulated high altitude. 24 p3060 A73-45058

Model experiments on apparent blood viscosity and hematocrit in pulmonary alveoli. 24 p3064 A73-45064

PULMONARY FUNCTIONS

Insensitivity of the alveolar septum to local hypoxia. 01 p0006 A73-10134

Cardiorespiratory responses to exercise in air and underwater. 01 p0007 A73-10161

Arterial oxygen increase by high-carbohydrate diet at altitude. 01 p0007 A73-10164

Effect of interstitial edema on distribution of ventilation and perfusion in isolated lung. 01 p0008 A73-10167

Bronchial tree model simulation of pressure-flow-volume relationships during expiration, using gas physics and lung physiology and anatomy data 01 p0011 A73-10169

Oxygen uptake, heart rate and pulmonary ventilation during swimming for different speeds and styles, comparing to running and cycling data 01 p0008 A73-10171

A system for continuous measurement of gas exchange and respiratory functions. 01 p0011 A73-10172

High altitude adaptation in mountain inhabitants of Tian Shan and Pamir, discussing effects on hemodynamic and pulmonary functions 02 p0133 A73-11922

Relationship of anginal symptoms to lung mechanics during myocardial ischemia. 02 p0136 A73-12820

Normal pulmonary pressure-flow relationship during exercise in the sitting position. 03 p0266 A73-13124

Indexes of ventilation distribution before/after airway occlusion in dogs, indicating collateral channel inspired gas distribution reduction 03 p0262 A73-14113

Prediction tests for pulmonary elasticity model of expansion stresses in lung region restricted by obstructed airways 03 p0262 A73-14114

Finite element displacement analysis of a lung. 03 p0273 A73-14661

A new method for simultaneous measurement of total respiratory resistance and compliance. 05 p0545 A73-16799

Regional lung volumes with positive pressure inflation in erect humans. 06 p0653 A73-18334

Effects of cardiac output on /O-18/2 lung diffusion in normal resting man. 06 p0654 A73-18335

Predictions of the dynamic response of the lung. 07 p0785 A73-19477

Respiration mechanics during weightlessness simulation in an immersion medium 08 p0929 A73-20986

Effects of lung volume and disease on the lung nitrogen decay curve. 08 p0934 A73-21501

Cardiovascular changes in middle-aged men during two years of training. 08 p0934 A73-21504

Effects of anesthesia and muscle paralysis on respiratory mechanics in normal man. 08 p0934 A73-21505

Ventilation measured by body plethysmography in hibernating mammals and in poikilotherms. 08 p0932 A73-21612

Pulmonary respiration and acid-base state in hibernating marmots and hamsters. 08 p0932 A73-21613

Theoretical trans-respiratory pressure during rapid decompression. I Model experiment. II - Animal experiments. 09 p1045 A73-22530

Influence of developmental adaptation on aerobic capacity at high altitude. 09 p1041 A73-22928

'Closing volumes' and decreased maximum flow at low lung volumes in young subjects. 09 p1041 A73-22929

Single breath nitrogen washout method for measurement of functional residual capacity. 11 p1315 A73-25332

Effect of acute exposure to CO₂ on lung mechanics in normal man. 11 p1318 A73-26216

Mechanics of breathing in high altitude and sea level subjects. 11 p1318 A73-26217

Method of PaCO₂ determination in men with functional disorders of external respiration 13 p1579 A73-29075

Hypoxic pulmonary steady-state diffusing capacity for CO and cardiac output in rats born at a simulated altitude of 3500 m. 14 p1720 A73-30911

Transpulmonary pressure gradient and ventilation distribution in excised lungs. 15 p1833 A73-31129

Breath to breath cyclical variations in functional residual capacity, oxygen uptake, carbon dioxide release, tidal volume, respiratory period, alveolar gas tension and heart rate 15 p1834 A73-31346

Some compensatory adjustment reactions of the blood circulation system in pulmonary pathology 15 p1835 A73-31623

Validity of Haldane calculation for estimating respiratory gas exchange. 17 p2113 A73-35463

Postural effects on respiration, pulmonary ventilation, oxygen uptake and inhalation and exhalation volumes during asana /yoga gymnastics/ exercises executed by athletes 18 p2276 A73-36573

Gas mixing during breath holding studied by intrapulmonary gas sampling. 18 p2277 A73-36651

Use of the single-breath method of estimating cardiac output during exercise-stress testing. 18 p2283 A73-36788

A study of Halon 1301 /CBrF₃/ toxicity under simulated flight conditions. 18 p2285 A73-36930

Pulmonary volume, respiration rate and alveolar air carbon dioxide content measurements in pilots during flight, noting hyperventilation occurrence 19 p2392 A73-37197

Phase IV volume of the single-breath nitrogen washout curve on exposure to altitude. 20 p2518 A73-39783

A system for automatic end-tidal gas sampling at rest and during exercise. 20 p2519 A73-39794

Pulmonary function in man after short-term exposure to ozone. 21 p2642 A73-40001

Effect of acceleration on distribution of lung perfusion and on respiratory gas exchange. 21 p2643 A73-40274

Advantage or disadvantage of a decrease of blood oxygen affinity for tissue oxygen supply at hypoxia - A theoretical study comparing man and rat. 21 p2641 A73-41620

Control of the duration of expiration. 21 p2642 A73-41635

Peak expiratory flow rate and rate of change of pleural pressure. 21 p2642 A73-41636

Rebreathing and steady state pulmonary diffusing capacity for O₂ in the dog and in inhomogeneous lung models. 21 p2645 A73-41639

External airway resistance effects on ventilation and carbon dioxide response during human steady state exercise 22 p2806 A73-42417

Gas transport in the human lung. 22 p2806 A73-42421

Influence of expiratory flow limitation on the pattern of lung emptying in normal man. 22 p2807 A73-42422

Respiratory work minimization during exercise, using respiratory frequency, functional residual capacity and air flow pattern effects as controlled variables 24 p3060 A73-45066

Fundamental frequency analysis of pulmonary mechanical resistance and compliance. 24 p3060 A73-45067

PULMONARY LESIONS

Thoracic X ray photography technique for tubercular lesion detection in flight personnel, comparing to standard radiography and roscoposcopy 02 p0137 A73-12155

Cat and rat lung damage due to hyperbaric oxygen exposure and head injury, discussing alveolar surfactants, sympathetic stimulation and monkey injuries [AD-759298] 13 p1576 A73-28507

Development and reversibility of pulmonary oxygen poisoning in the rat. 14 p1718 A73-30516

Experimental studies on the production of pulmonary infarction. IV - Effects of UK, heparin, t-AMCHA or ellagic acid. 22 p2805 A73-42319

PULSARS

Pulsar structure theory with respect to rotating neutron star hypothesis, discussing evolutionary elements 01 p0095 A73-10065

Short-term pulsar intensity variation in the frequency range 70-115 MHz. I - Correlation measurements. 01 p0106 A73-11306

Pulsar glitches and the metastability of the superfluid core. 02 p0211 A73-11895

Self consistent model of closed field lines of pulsar magnetosphere valid for oblique rotators and unipolar inductors 02 p0216 A73-12382

- The nature of radio emission from pulsars.
02 p0218 A73-12407
- Very long baseline interferometer observations of Taurus A and other sources at 121.6 MHz.
03 p0366 A73-12933
- Periodicities in seismic response caused by pulsar CP1133.
03 p0367 A73-13056
- Search for seismic signals from gravitational radiation of pulsar CP1133.
03 p0367 A73-13058
- Frequency independent characteristic time scales in meter wave intensity structure of pulsars CP 0950 and 1133, using predetection dispersion removal technique
03 p0374 A73-13715
- Thermal conductivity and hot magnetic poles of pulsars.
03 p0374 A73-13796
- Detection of 10-100 MeV gamma-rays from the Crab Nebula pulsar NP 0532.
03 p0362 A73-13847
- Pulsar associated with the supernova remnant IC 443.
03 p0374 A73-13848
- Positions, periods, period derivatives, dispersion measures and pulse widths of twenty two weak pulsars
03 p0380 A73-14635
- A search for isolated radio pulses from the Crab Nebula at 151.5 MHz.
04 p0500 A73-15493
- The period and light curve of HZ Herculis.
04 p0501 A73-15683
- The pulse shape of the Crab Nebula pulsar NP 0532 as a function of color.
04 p0501 A73-15685
- Pulsars and the evolution of supernova remnants.
04 p0501 A73-15686
- Pulsars spectrum measurements with 100 m radio telescope, using 2.8 cm receiver in prime focus and cryogenically cooled parametric amplifier
04 p0502 A73-15977
- Frequency correlation measurement of pulsar spectral fine structure due to radio emission scattering by interstellar plasma
04 p0503 A73-16002
- Crab Nebula evolution from 1054 supernova to neutron star and nebula expansion, discussing pulsar properties
05 p0614 A73-16304
- The excitation mechanism for the filaments in the Crab Nebula.
05 p0617 A73-16471
- Time-dependent radiation transfer and a possible explanation of the interpulse in CP 0950.
05 p0623 A73-17302
- Mechanisms of optical, X-ray and gamma-radiation from Crab pulsar.
05 p0611 A73-17314
- Quantum electrodynamical models of coherent plasma electron-positron pair production and pulsed radiation in electric field, relating to pulsars
05 p0626 A73-17383
- Pulsar timing techniques for planet discovery, interstellar electron density measurement, braking mechanism and neutron star structure investigation and gravitational red shift verification
06 p0750 A73-18008
- Pulsars as rotating magnetic neutron stars created during catastrophic collapses of old stars, discussing radiation mechanism
06 p0750 A73-18012
- Multiple and intrinsic variable stars, considering pulsars, binary systems, Cepheids, stellar structure and evolution
06 p0750 A73-18014
- Amplitude-time and polarization characteristics of the subpulses of pulsar CP 1133.
06 p0754 A73-18633
- Fractional polarization constancy in pulsars to critical frequency with subsequent falloff
07 p0874 A73-19070
- Gravitational energy conversion into rotational energy in contraction process for pulsars, quasars and galactic radio emission energy sources
07 p0898 A73-19934
- Soft X-ray pulsations from PSR 0833-45.
07 p0872 A73-20153
- The generation of the highest cosmic ray energies.
07 p0872 A73-20193
- Recent supernova in NGC 5253 and the supernova rate.
07 p0900 A73-20238
- Pulsar magnetosphere evolution, discussing electron and positive ion supply at surface, plasma flow and Crab Nebula characteristics
07 p0900 A73-20276
- Isotropic X ray and optical emissions from supernovae and pulsars, deriving pulsar synchrotron emission evolution formulas
07 p0900 A73-20304
- Earth as gravitational waves detector, discussing pulsar CP 1133 emission
08 p1000 A73-20675
- Ultrarelativistic cosmic plasma analysis of high density electron beams transport across strong magnetic fields with application to pulsar NP 0532 spectrum
08 p0999 A73-21334
- Application of statistics to results in gamma ray astronomy.
08 p1012 A73-21644
- Very long baseline interferometry techniques for Crab Nebula pulsar observation at meter wavelengths
08 p1013 A73-21812
- Plasma effects and the acceleration of charged particles in pulsar fields.
09 p1141 A73-22016
- Ultrarelativistic plasma momentum loss perpendicular to pulsar magnetic field, considering synchrotron compression of electrons leading to emission mechanisms
09 p1144 A73-22172
- Ultrarelativistic pulsar plasmas with one dimensional distribution functions in strong magnetic fields, considering dispersion ratios of plasma waves along magnetic lines
09 p1145 A73-22294
- Radio halos around old pulsars - Ghost supernova remnants.
09 p1148 A73-22871
- The structure of the Crab Nebula. III - The radio filamentary radiation.
09 p1151 A73-23291
- Compton effect in charged particle under intense circularly polarized electromagnetic wave, noting application to Crab pulsar
10 p1271 A73-23485
- Pulsed gamma ray emission at 5-25 MeV from Crab Nebula pulsar, noting time-averaged energy flux with consideration for telescope efficiency
10 p1272 A73-23535
- Short-term temporal studies of the X-ray emission from Cassiopeia A, Tycho, and Scorpius X-1.
10 p1264 A73-23547
- Formation of neutron star spots and its connection with pulsars. II - Close similarities between radiation from the sun and pulsars.
10 p1275 A73-23829
- Generalized electromagnetic torque on a vacuum pulsar model.
10 p1284 A73-24914
- Radio polarization and variability of pulsar NP 0532.
11 p1417 A73-25582
- The 1969 solar occultation of the Crab Nebula pulsar.
11 p1417 A73-25583
- Linear polarization and spectrum of PSR0833-45 and the effects of scattering.
11 p1419 A73-25748
- Pulsar decametric radiation reception hindrance by SNR deterioration caused by bandwidth decrease and background radiation, discussing signal processing methods
11 p1426 A73-26474
- Equations derived for magnetic field line configuration and plasma flow about rotating object having axisymmetric field with emphasis on pulsar magnetosphere
11 p1427 A73-26614
- Pulsar magnetospheres, braking index, polar caps, and period-pulse-width distribution.
11 p1428 A73-26618
- Isotropic X ray and optical emissions from supernovae and pulsars, deriving pulsar synchrotron emission evolution formulas
12 p1539 A73-27276
- Late stage nonrotating star evolution, discussing red giant models, planetary nebulae, degenerate carbon cores, supernova explosions and pulsars
12 p1543 A73-27748
- Supernova outbursts and the formation of relativistic objects. I
12 p1546 A73-27853
- Path length distribution of cosmic rays from pulsar nebula complexes.
12 p1536 A73-27880
- Pulsar positions and periods with He cooled parametric receiver at 11 cm, confirming PSR 0355 position at 218 cm
13 p1681 A73-28920
- Radio emission from pulsars and surface temperature of neutron stars.
13 p1681 A73-28925
- Papers on stellar evolution from main sequence to white dwarf stage covering pulsars, supernovae luminosity, neutron stars, nucleosynthesis, etc
13 p1681 A73-28976
- Gamma-ray emission above 20 MeV from the Crab Nebula and NP 0532.
14 p1785 A73-29737
- Rotation effects in stellar and quasi-stellar relativistic objects models required for pulsars and quasars explanation, discussing gravitation theories
14 p1798 A73-30141
- Cosmic ray properties and origin, discussing pulsars and superstrong magnetic fields existence effects
14 p1787 A73-30233
- Rotating neutron star matter and model properties with emphasis on pulsar observations, discussing equations of state, transport processes and relativistic effects
14 p1798 A73-30234
- Pulsar positions, polarization characteristics, intensity and fine structure, considering models explaining rotating neutron stars, galactic magnetic fields and electron densities and temperature
14 p1800 A73-30549
- Slow variations of pulsar intensities.
14 p1802 A73-30750
- Pulsar detections at frequencies of 8.4 and 15.1 GHz.
14 p1802 A73-30751
- Pulsar fluctuation spectra and the generalized drifting-subpulse phenomenon.
15 p1936 A73-31558
- The possible nature of the fine structure of sporadic radio emission from the sun and other cosmic sources having a high density of electromagnetic radiation
15 p1926 A73-31876
- Anticipated variability of Pulsar NP 0532 emission in the Crab nebula associated with angular velocity jumps
15 p1938 A73-31964
- Pulsar radio emission limiting polarization resulting from passage through magnetoactive plasma, discussing electron density effects
15 p1844 A73-32003
- Crab Nebula pulsar electromagnetic radiation emission model based on high energy electron circular motion around magnetic field lines
15 p1942 A73-32649
- Pulsar X ray emission relation to general X ray sources, considering NP 0532, Sco X-1 and Cen X-3
16 p2050 A73-32740
- High energy gamma ray discrete source identification in Crab Nebula, pulsar NP 0532 and galactic regions from Apollo and TD-1 satellite measurements
16 p2051 A73-32750
- Continuum radio emission from the vicinity of pulsars.
16 p2061 A73-33219
- Wide integrated pulse profiles of pulsars.
16 p2071 A73-34036
- Measurement of relaxation time during acceleration of rotation of vessels containing helium II, and superfluidity in pulsars
16 p2038 A73-34065
- Magnetic moment generation in pulsars based on baryon model with superconducting proton fluid and normal electron field
17 p2226 A73-34365
- Possible role of faster-than-light radiation under pulsar conditions
17 p2226 A73-34370
- The beaming of radiation from an accreting magnetic neutron star and the X-ray pulsars.
17 p2225 A73-35618
- Synchrotron model limitations for optical pulsars and compact extragalactic objects, considering NP 0532, PKS 2134+004, OQ 208 and NGC 10608
19 p2485 A73-37618
- On the energy spectrum of relativistic electrons in the Crab Nebula.
19 p2475 A73-37619
- Periodic analysis of arrival times in delayed cosmic-ray coincidences.
19 p2476 A73-38086
- The X-ray structure of the Vela X region observed from Uhuru.
19 p2488 A73-38514
- Pulsar model magnetosphere for uniformly rotating infinitely conducting magnetized neutron star with aligned magnetic field
19 p2488 A73-38515
- Faraday rotation patterns in Crab Nebula pulsar radio spectra for average signal and giant pulses, noting difference in linear polarization percentage
19 p2488 A73-38516
- The optical polarization of the Crab Nebula pulsar. I - A relativistic vector model.
19 p2488 A73-38517
- Optical polarization of the Crab Nebula pulsar. II - Observational results and fits by the relativistic vector model.
19 p2488 A73-38518
- Tables and graphs for characteristics and pulse profiles of pulsars discovered in low Galactic latitude radio telescope survey
20 p2605 A73-39017
- Supernova outbursts and the formation of relativistic objects. I.
20 p2608 A73-39227
- Stimulated linear acceleration radiation - A pulsar radio emission mechanism.
20 p2602 A73-39444
- Radiative corrections and soft-photon emission in magnetic bremsstrahlung.
20 p2602 A73-39445
- Solar radio frequency radiation characteristics, considering flare stars, pulsars, X ray sources, Antares

types, novae, red supergiants and stars with gas and dust envelopes

Variations of pulsar intensity as a result of scintillations at an inhomogeneous plasma

Pulsar polarization measurements by multielement interferometer dipole antenna and DKR-1000 cross array radio telescope

A system for the photographic recording of pulsar pulses

Evolution of supermassive stars with a strong magnetic field

Magnetized and nonmagnetized rotating neutron star reactions to applied torques for pulsar slowdown, discussing magnetosphere and wind zone

Pulsar searches at 408 MHz with Northern Cross radio telescope, comparing discovered objects with previously known pulsars

Measurements of neutral-hydrogen absorption in the spectra of eight pulsars.

Pulsed high-energy gamma rays from the Crab Nebula.

Origin of cosmic rays, atomic nuclei, and pulsars in explosions of massive stars.

Pulsar search in Galactic nucleus region at 430 MHz with 140 foot telescope, discussing data reduction and results

Neutrino losses effects on 4-8 solar mass stars leading to collapse of degenerate carbon-oxygen cores, discussing type II supernovae and pulsar formation

Frequency distribution functions of pulsars, supernovae and sunspot groups relationship to age and lifetime, considering stellar mass and initial luminosity

Galactic nuclei, pulsars and supernovae as sources of primary cosmic rays from ground based and satellite observations, relating chemical composition to origin

Pulsar properties covering galactic distribution, pulse periodicity computed from arrival time measurements, models, emission mechanisms, total intensity pulse shapes, etc

Radio astronomical problems due to pulsar radiation dispersal by frequency dependent propagation velocity in interstellar medium, discussing signal reception and data recording techniques

Pulsars radio observations of magnetic field, electron density and neutral hydrogen atoms in interstellar space

Microwave emission mechanism of frequency dependent pulse profile changes in pulsar, using cooled parametric amplifier observations

Statistical correlation between pulsar and supernova remnant distribution along galactic longitudes, noting difference due to relative motions

Expected radiative variability of Crab-Nebula pulsar NP 0532, related to abrupt changes in angular velocity.

On self-consistent models for the pulsar magnetosphere.

FULSATING FLOW U UNSTEADY FLOW PULSE AMPLITUDE

Signal amplitude ratios measurement in automatic control applications by digital differential logometer, using time-pulse dividing circuits

Semiconductor device degradation by high amplitude current pulses.

Large amplitude waves in bounded media. I - Reflexion and transmission of large amplitude shockless pulses at an interface.

Amplitude-time and polarization characteristics of the subpulses of pulsar CP 1133.

A digital instrument for measuring amplitude-time parameters of nanosecond-duration pulses

Amplitude selector for linear transistorized devices

Linearization limits for optimal pulse controller adjustments, using comparison with continuous controller and extrapolation

Amplitude discriminator with variable effective range design for use with/without digital computer in neuron pulsed activity analysis

Subnanosecond pulse-front shaping with the aid of switches based on chalcogenide glass

Instrument providing dc voltage corresponding to amplitude of uniform pulse train, using differential comparator as sensing element and closed loop control scheme

Design of sinusoidal and pulsed signal amplification stages with emitter high-frequency compensation.

Use of approximating polynomials in the determination of correction parameters for pulsed amplifiers.

Alpha wave peak amplitude dependence on blocking pattern after stimulation during habituation-pseudoconditioning, conditioning and extinction

Incidence of pulsation wind velocities exceeding a given value

A generator of rectangular voltage pulses with 50 kV amplitude

Laser pulse shape measurement by successive oscillographing of pulse front areas and concurrent signal amplitude variation

Control of laser-pulse shape with the aid of an organic dye switch

Higher conservation laws and coherent pulse propagation.

Amplitude stabilization of pulses from a Q-switched ruby laser by means of interaction with a non-linear medium.

Peak height measurement system for pulsed laser experiments.

Impact generated elastic strain low amplitude pulses propagating in filamentary composite rods, using Fourier transform technique and viscoelastic relation

Influence of semiconductor laser heating on the parameters of the output pulses

Influence of vibrational, rotational, and reorientational relaxation on pulse amplification in molecular amplifiers.

Protection of radiometers from pulse interference

Amplification of short pulses in CO₂ laser amplifiers.

Microwave emission mechanism of frequency dependent pulse profile changes in pulsar, using cooled parametric amplifier observations

PULSE AMPLITUDE MODULATION

Absolute instability of nonlinear pulse-amplitude control systems - Frequency criteria.

Adaptive maximum-likelihood sequence estimation for digital signaling in the presence of intersymbol interference.

Kalman filtering theory application to optimal causal demodulator for pulse amplitude modulated signals in white Gaussian noise

Pulse amplitude modulation of a CO₂ laser in an electro-optic thin-film waveguide.

Analysis of the stochastic stability of pulsed control systems in the frequency domain

The estimate feedback equalizer - A suboptimum nonlinear receiver.

Optimum mean-square decision feedback equalization.

PULSE CODE MODULATION

NT DELTA MODULATION

Conditions for the absence of periodic conditions in multivariable pulse-coded systems

Active terminal devices for wide band time multiplexed laser PCM communication systems.

Design of communication systems using short-constraint-length convolutional codes.

A DPCM codec using edge coding and line replacement.

Pulsed random process energy spectra methods for spectral distribution of signal power in multichannel

PULSE CODE MODULATION

AM, FM and PM PCM systems with time division multiplexing

Atmospheric conditions effects on line-of-sight microwave PCM data transmission system performance, comparing predicted error probability vs predetection SNR with measurement

Electro-optical multiplexers and demultiplexers for time-multiplexed PCM laser communication systems.

Bandpass error free wideband PCM communications system response to pulse signal

A study on accumulation of waveform distortions in PCM hybrid transmission.

8-phase and 16-phase high speed PSK modems for PCM-TDMA satellite communication.

Double heterojunction [GaAl]As laser pulse modulation at 200 Mbits/sec continuous operation at room temperature, considering lasing delay time and damped oscillations problems

640 Mbit/sec waveguide transmitter at 38 GHz.

Video signals differential pulse code modulation, improving SNR by quantizing characteristics modification via nonlinear coding

Pretransmission normalization procedure to suppress transmission error accumulation in receivers of differential PCM systems

Delta modulation and differential PCM systems performance comparison at high sampling rates for color video signal coding

Matched filters for extracting synchronization in signaling, nonreturn-to-zero and split phase PCM systems, using finite-time-duration trigonometric pulse synthesis

A new type of PSK anti-ambiguity system for satellite applications.

PCM and DPCM digital modulators design and performance comparison for sampling rate effects on quantizing noise, noting tradeoffs between cost and system efficiency

A method for substantially improving the reliability of multistable pulse-phase-coded elements

Amplitude-modulated pulse code sequence demodulation using physically realizable linear filter for reconstruction of discrete sample message at optimum mean-square error level

A simple method for converting a pulse code into a phase code by using parametrons

PCM multiplexing system for incorporation into telemetry systems of large ballistic missiles or spacecraft launch vehicles

Measurement equipment for the PCM transmission system KFK 30/32

Remote feed, control, and signalization in transmission lines of multichannel systems with pulse code modulation

Spectral analysis of optical pulse signals in application to the problem of synchronizing PCM laser communications lines

Tapped delay line filter for optimal single pulse detection in band-limited PCM/NRZ system in presence of Gaussian noise

Direct modulation of a double heterostructure laser at a rate of 2.3 Gbit/s

Decision-directed detector for overlapping PCM/NRZ signals.

Pulse coded scanning beam microwave landing system technology assessment for civil aviation application, describing ground equipment and procedures

Application of data compression techniques to spacecraft imaging systems.

French book - Theory of communication: Signals, noises, and modulations.

Maximum likelihood synchronizer for binary overlapping PCM/NRZ signals.

Range and range-rate measuring equipments for communication satellites.

- An error correction method for DPCM picture transmission 19 p2432 A73-38268
- Sampling, quantization and channel errors in differential pulse code modulation systems, discussing SNR, quantizer levels, standard PCM systems, reconstruction filters and bit errors 19 p2407 A73-38383
- An adaptive scheme for PCM transmission. 20 p2523 A73-38728
- Application of some data compression systems to ESRO satellite data. 20 p2524 A73-38735
- Applications of error-correcting codes to TDMA satellite communications. 20 p2526 A73-38751
- Low pass filter design for FDM and PCM systems, discussing active RC realization techniques and microelectronics model tests 22 p2832 A73-42293
- Signal analysis using stochastic-ergodic principles, discussing PCM correlation procedures, analog-digital signal conversion and measurement methods 23 p2983 A73-44149
- ### PULSE COMMUNICATION
- #### NT DIGITAL SPACECRAFT TELEVISION
- Correlation and structure functions for pulse propagation in a turbulent atmosphere. 01 p0016 A73-10195
- Pulse communication at microwave bit rates using Gunn domains. 02 p0145 A73-11534
- Effects of a finite-width decision threshold on binary CPSK and FSK communication systems. 03 p0277 A73-13911
- Standard deviation of thresholding time during detection of pulse perturbed by Gaussian noise 03 p0277 A73-13912
- Error probabilities estimates for digital communication systems using orthogonal multiposition signals in data transmission 03 p0278 A73-14029
- Satellite digital communications over domestic and international networks for data, voice and video signal transmission 04 p0415 A73-14739
- Differentially encoded multiple phase shift keyed signals transmission and detection, analyzing digital communication system performance 04 p0415 A73-14991
- Auto and cross correlation functions of combined binary pseudorandom sequences in digital space communication systems 04 p0423 A73-15916
- Pulse propagation in a two-mode waveguide. 05 p0548 A73-16365
- Higher-order loss processes and the loss penalty of multimode operation. 05 p0549 A73-16367
- Discrete frequency modulated signals with frequency shifted identical-envelope pulses, discussing transmission, construction and correlation functions 05 p0550 A73-16778
- Inductance and magnetic reversal losses in pulse operated communication, describing bridge circuit for comparing test sample current with capacitor voltage/time characteristics 05 p0559 A73-17241
- Bandpass error free wideband PCM communications system response to pulse signal 06 p0668 A73-18391
- Applications for quantum amplifiers in simple digital optical communication systems. 06 p0668 A73-18404
- German monograph - Synchronization of digital telephone networks by means of phase averaging with parameter transfer. 07 p0794 A73-20386
- The effect of impulsive noise on FSK digital communication. 08 p0938 A73-20834
- A special purpose computer for the study of fading signals. 08 p0939 A73-21139
- Bandwidth efficiency for digital communication via a hard limiting channel. 09 p1054 A73-23382
- Signal synthesis based on desired autocorrelation function for pulse shaping applications in radar and communications, discussing nonlinear equations solution by decomposition into source polynomials 10 p1187 A73-23730
- Linear codes and transverse equalization for limiting the effects of intersymbolic interference in the transmission of digital signals 10 p1189 A73-24416
- Optimal passband of a double-tuned selective amplifier during the simultaneous passage of rectangular radio pulses and white noise 12 p1477 A73-26874
- Increasing the capacity of a discrete communications channel by additional modulation of a carrier parameter 12 p1467 A73-26941
- An optimal electrooptical method of signal processing in coherent pulse reception 12 p1468 A73-26947
- Phase discriminator of a nonregular signal. 12 p1480 A73-27270
- Information transmission reliability enhancement via digital code group symbol transmission by wide-band linear FM radio signals 12 p1471 A73-27593
- Pulse amplifier with active gain adjustment for constant bandwidth 13 p1590 A73-28571
- Calculation of the amplitude of pulse signals at the output of linear filters in optical communications systems. 13 p1583 A73-28671
- Shaping circuit for complex RF pulse consisting of simultaneous equilength square pulses with different frequencies, discussing carrier frequencies selection 13 p1583 A73-28730
- Evaluation of the noise immunity of pulsed systems for transmission of continuous messages with allowance for quantization and interpolation errors. I 13 p1584 A73-28891
- Modified Kalman filter for digital communication channel equalization with tap gains and initial state variable estimated by decision feedback and prediction process respectively 13 p1593 A73-29118
- Multipaths by diffusion on the ground and application to the transmission of digital messages affected by jumps of the carrier frequency 14 p1725 A73-29732
- U.S. civil and military air-ground communications development history and expectations, considering information exchange, radar beacon transponders, digital communication and data links 14 p1725 A73-29880
- Multipath propagation in aircraft digital communication with ground terminal, modeling received signal for detection and estimation theories applications 14 p1726 A73-29902
- Application of acoustic surface-wave technology to spread spectrum communications. 14 p1733 A73-29934
- Distortions of UHF pulse signals propagating along the earth at distances below the radio horizon 14 p1729 A73-30559
- Spectral-energy dispersal in digital communication-satellite systems. 15 p1842 A73-31096
- Optimal reception of digital signals on an additive noise background 15 p1843 A73-31493
- The influence of pulsed noise on the performance of incoherent digital communications systems 15 p1843 A73-31567
- Digital transmission techniques for ATC satellite system, considering technical and economic aspects of various coding systems 15 p1846 A73-32427
- Selective properties and form of a signal transmitted through a statistically nonhomogeneous layer of arbitrary thickness 16 p1978 A73-32896
- Decomposition of pulse-type data by cepstrum techniques. 17 p2127 A73-35635
- Multimode glass fiber as transmission medium for digital signals. 20 p2521 A73-38659
- Evaluation of the noise immunity of pulse systems for continuous message transmission allowing for quantization and interpolation errors. II 20 p2531 A73-39462
- Communications and position fixing experiments using the ATS satellites. 21 p2733 A73-40024
- Russian monograph on linear signal system models covering steady state, variance and transducers of continuous and discrete signals and random and nonstationary estimates 21 p2669 A73-40798
- Sudden ionospheric disturbance effects on LF radio pulse train amplitude during reception from Loran-C transmitters, comparing with VLF sudden phase anomaly 22 p2825 A73-42188
- Losses and impulse response of a parabolic index fiber with random bends. 23 p2987 A73-43989
- Noise immunity of quasi-optimal noncoherent reception during resynchronization with respect to time and frequency 24 p3067 A73-44590
- ### PULSE COMPRESSION
- Correction of the dynamic distortions of signals resulting from measurement information compression 05 p0577 A73-16986
- Theory of incoherent-scatter measurements using compressed pulses. 09 p1050 A73-22429
- Optimum bandlimited signal synthesis with pulse compression for transionospheric propagation along vertical path, considering statistical effects of total ionospheric electron content variations 11 p1330 A73-25689
- The design and applications of highly dispersive acoustic surface-wave filters. 12 p1484 A73-27564
- IMCON reflection mode dispersive delay line in large time-bandwidth product pulse compression systems, deriving operational characteristics from transfer function 12 p1480 A73-27565
- The use of surface-elastic-wave reflection gratings in large time-bandwidth pulse-compression filters. 12 p1480 A73-27566
- Improvements in surface-acoustic-wave pulse-compression filters. 13 p1595 A73-28048
- Echo signal spectral compression in airborne FM Doppler radar measurement, allowing for flight trajectory and target surface characteristics 13 p1584 A73-28889
- Ionospheric and pulse compression induced distortions in chirped Gaussian electromagnetic pulses 14 p1728 A73-30232
- Huffman binary codes for pulse compression radar, evaluating ambiguity or cross correlation by computer program for replicas formation performance 17 p2131 A73-35221
- Digital step transform for airborne radar linear FM signal pulse compression, reducing data memory requirements 17 p2123 A73-35237
- Application of surface acoustic wave devices to radar. 17 p2140 A73-35319
- Use of pulse compression in mapping-type radars. 17 p2127 A73-35632
- VM 256 - Experimental system of a 3-D radar installation 18 p2335 A73-37040
- Surface acoustic wave devices and applications. II - Pulse compression systems. 21 p2703 A73-41137
- ### PULSE DIFFRACTION
- Time-dependent electromagnetic field scattering and diffraction by half plane during illumination by impulsive plane cylindrical or spherical wave 11 p1330 A73-25683
- ### PULSE DOPPLER RADAR
- #### NT MONOPULSE RADAR
- #### NT PULSE RADAR
- Mathematical algorithm using invariant imbedding method for accurate range and range rate estimates in terms of pulse Doppler radar ambiguity resolution 03 p0276 A73-13902
- Pulse Doppler radar observations of hailstone maximum diameters as function of time 03 p0337 A73-14506
- Pulse pair estimation of Doppler spectrum parameters. 03 p0279 A73-14527
- Use of a surface-acoustic-wave delay line to provide pseudocoherence in a clutter-reference pulse doppler radar. 08 p0939 A73-21113
- A semicoherent detection and Doppler estimation statistic. 13 p1585 A73-29202
- Side-looking pulse Doppler radar data presuming prior to correlation to obtain desired resolution performance with minimal digital storage 13 p1585 A73-29203
- Clutter spectra of low PRF AMTI pulse-Doppler radar. 16 p1980 A73-33413
- The structure of an inversion above a convective boundary layer as observed using high-power pulsed Doppler radar. 19 p2447 A73-38205
- Doppler spectrum turbulence spreading updraft velocity estimation from observation by pulsed radar, noting average value and standard deviation in small thunderstorm 21 p2728 A73-40058
- The effect of weighting upon signal-to-noise ratio in pulse bursts. 21 p2649 A73-40327
- Optimum cross-coupled tracker for pulse-Doppler radar. 21 p2649 A73-40328
- ### PULSE DURATION
- An optical bridge for the assessment of mode-locked CO2 lasers. 01 p0058 A73-10471
- Nd glass and ruby lasers in mode locking operation for picosecond light pulses emission, noting pulse duration measurement 01 p0059 A73-10713
- Axisymmetric plastic response of rings to short-duration pressure pulses. 01 p0115 A73-10759
- Multichannel differential coincidence circuit in the nanosecond range 01 p0024 A73-10792

Ultrashort light pulse generation in lasers with bleachable filters, covering mode formation, secondary effects and two photon recording of emission time structures

01 p0061 A73-11354
Russian book on nanosecond multiphase multivibrators covering transistorized single- and dual-stage amplifiers and wave shaping circuits for digital control and computer logic applications

02 p0146 A73-11887
Mode-locked high-pressure waveguide CO₂ laser.

02 p0178 A73-12748
Combined nonlinear amplification and absorption role in ultrashort pulse generation of mode locked quasi-continuous dye laser in absence of short relaxation time

03 p0318 A73-12870
Continuing development of the short-pulsed ablative space propulsion system.
[AIAA PAPER 72-1154]

03 p0356 A73-13457
Multiple overlapping signal decomposition in noisy environment by inverse filtering, considering tradeoff between resolution and output SNR, and optimum pulse duration

03 p0277 A73-13908
Distortion of laser pulses in resonant media

04 p0458 A73-14883
Possibility of generating ultrashort laser pulses on combination vibrational-rotational transitions of molecular hydrogen.

04 p0458 A73-15472
Mode locked laser system generated picosecond pulses envelope and phase structure measurement methods

05 p0583 A73-16339
Direct measurement of pulse broadening in the second harmonic of mode-locked Nd:glass laser.

05 p0585 A73-17221
Picosecond pulses from a passively mode-locked cw dye laser.

05 p0585 A73-17222
Short pulse laser based on versatile 60 kV fast switching circuit, noting application as pump source for organic dye molecule solutions

05 p0586 A73-17252
Plasma generation by nanosecond and picosecond laser pulses, discussing Raman scattering from solid hydrogen and deuterium targets

06 p0731 A73-18581
External self focusing of converging short duration pulsed light beams, analyzing resultant focal points trebling, nonlinear focus motion and intensity distribution

06 p0702 A73-18590
Maximum permissible pulse duration in second-harmonic generation in a KDP crystal.

06 p0703 A73-18595
Production of hot plasmas of solid-state density by ultrashort laser pulses.

06 p0733 A73-18783
Pulse broadening in multimode fibres excited by GaAs lasers.

07 p0833 A73-19155
Radio pulse shaping network synthesis composed of lumped elements, noting pulse duration limitation by network efficiency

07 p0805 A73-20134
A digital instrument for measuring amplitude-time parameters of nanosecond-duration pulses

08 p0949 A73-21711
A new approach to picosecond laser pulse analysis shaping and coding.

09 p1090 A73-22077
Measuring the off-duty factor of chaotic pulsed interference on a Gaussian noise background

09 p1050 A73-22338
A picosecond single-pulse laser

09 p1095 A73-22661
Microinhomogeneous active medium effects on laser monopulse duration and energy, noting luminescence band random shift and directional diversity in dipole moments

09 p1097 A73-23083
Nanosecond pulse amplification in electron-beam-pumped CO₂ amplifiers.

09 p1097 A73-23336
Powerful nanosecond pulses by stable passive mode-locking of TEA CO₂ lasers.

09 p1098 A73-23340
Transverse discharge pulsed CO₂ chemical transfer laser.

10 p1227 A73-23840
Resonator parameters effect on stability characteristics of ultrashort pulse produced by ruby laser, using mirror and thin reflector

10 p1227 A73-24070
Study of the behavior of a monostable transistor circuit in the avalanche mode

10 p1195 A73-24413
Electron-optical investigations of discharge in air and carbon dioxide in the nanosecond range

10 p1219 A73-24469
Rise time of the spike potential in fast and slowly contracting muscle of man.

10 p1181 A73-24500

Neodymium-glass laser with tunable pulse width

11 p1376 A73-25433
Influence of saturable-absorber transmission and optical pumping on the reproducibility of passive mode locking.

12 p1505 A73-27013
Short time constant limits of pulse duration on electromagnetic energy emission as function of frequency, applying to extragalactic radio astronomy observations

12 p1547 A73-27884
Transient processes in second harmonic excitation by ultrashort laser light pulse train related to crystal length and phase matching

13 p1629 A73-29433
Formation of an ultrashort pulse of light in a ruby laser with resonant modulation of losses

14 p1757 A73-30265
Investigation of the shape of radiation pulses emitted by a self-mode-locked laser.

14 p1757 A73-30329
Injection of a short light pulse into a laser with extensive length of the resonator

15 p1884 A73-31247
Detection of short CO₂ laser pulses using the optical Kerr effect.

16 p2024 A73-34027
Wide integrated pulse profiles of pulsars.

16 p2071 A73-34036
Laser pulse shape measurement by successive oscillography of pulse front areas and concurrent signal amplitude variation

17 p2183 A73-34201
Dependence of laser-induced breakdown field strength on pulse duration.

17 p2186 A73-35796
Investigation of the characteristics of a mode-locked Nd:glass laser with the aid of a picosecond streak camera.

17 p2186 A73-35796
Control of laser-pulse shape with the aid of an organic dye switch

18 p2322 A73-36558
Parametric measurements on a CO₂ TEA laser with electrodes which have a Rogowsky profile

19 p2438 A73-37999
Generation of fifth picosecond laser harmonic.

20 p2574 A73-39700
Flashlamp pumped CW mode-locked dye laser picosecond light pulse duration measurement by electro-optical streak camera

21 p2694 A73-39946
A multichannel-discharge of high light intensity and short duration

21 p2695 A73-39971
Influence of semiconductor laser heating on the parameters of the output pulses

21 p2710 A73-40134
Thermal defocusing avoidance by short pulse duration reduction to permit IR laser window operation before temperature rise, considering changes in index of refraction

21 p2710 A73-40134
The mechanism responsible for shortening of the stimulated Mandelstam-Brillouin scattering light-pulse duration and for generation of nanosecond-duration pulses

21 p2739 A73-40355
Excitation of ultrashort light pulses in a ruby ring laser with resonant Q-switching

21 p2712 A73-40356
Generation of microsecond pulses with controllable pulse width in a ruby laser

21 p2713 A73-40527
An automatic sweep generator for a strobed oscilloscope

21 p2664 A73-41098
Ultrasonic pulse techniques based on acoustic velocity for inert gas thermometry, discussing electroacoustic transducer response time, temperature sensitivity and momentary contact coupling technique

22 p2854 A73-41994
Changes in the characteristics of giant laser radiation pulses and of luminous plasma during formation of damage regions on the surface or in the bulk of transparent dielectrics.

22 p2869 A73-42250
Self-termination of free oscillations in ruby at low temperatures.

22 p2896 A73-42251
Rotational relaxation effects in short-pulse CO₂ amplifiers.

22 p2870 A73-42520
Radiation pulse development time instability in electrooptically Q switched lasers due to flash lamp output fluctuations

22 p2870 A73-42722
Ultrashort pulses from mode-locked cw dye lasers.

22 p2871 A73-43079
Calorimeter for picosecond laser pulses.

22 p2872 A73-43153
Interpolation using finite duration impulse response digital filters.

23 p2952 A73-43313

PULSE FREQUENCY MODULATION

Diaphragm ejector pulse shortener for transforming periodic input signal into sharp pulses by adjusting vent areas of two fluid amplifiers

23 p2942 A73-43408
Compensation of an underdamped fluidic position control system by a digital pulse compensator.

23 p2944 A73-43420
Propagation velocity of picosecond pulse from mode locked Nd-glass laser investigated by optically induced birefringence, self phase modulation and self focused light

23 p2988 A73-44120
Pulse generator for testing and measurement, describing pulse frequency, duration and sequence capacity, digital design and normal and alarm sequences

23 p2955 A73-44150
Choice of the duration of an elementary signal in the presence of fluctuations in the synchronization channel

24 p3067 A73-44605
Pulsed argon laser discharge oscillographic electron temperature and time variations measurement, obtaining short and long pulse regime emission characteristics

24 p3097 A73-45516

PULSE DURATION MODULATION

Influence of additive and multiplicative noise on the accuracy in measuring the angular position of a source of radiation by systems with pulse-width modulation

01 p0017 A73-10212
Linear characteristics of transistorized Schmitt trigger pulse width regulators in response to sinusoidal and sawtooth signals for automatic control systems

02 p0149 A73-12343
Magnetic pulse width modulator and power switch subsystem of switching-mode dc regulator, deriving describing function from transfer functions

03 p0282 A73-13928
A sequenced PWM controlled power conditioning unit for a regulated bus satellite power system.

03 p0252 A73-13930
Processing power for a low voltage source-pulse load system.

03 p0253 A73-13939
Pulse duration-frequency modulation multichannel biotelemetry system for physiological parameter assessment during exercise, noting circuit diagrams of radio transmitter and receiver

03 p0270 A73-14281
Global asymptotic stability of two classes of control systems with pulse duration and pulse frequency modulations.

06 p0680 A73-17957
Periodic oscillations in feedback systems with combined pulse modulation.

06 p0680 A73-18518
Electrodynamic exciter power amplifier with pulse width modulation and Schmitt trigger output stage for structural vibration tests

07 p0803 A73-20535
Frequency criteria for the absolute stability and instability of pulse-width modulated control systems

08 p0951 A73-21544
Some limitations on the use of fluidic pulse width and pulse position modulation for phase measurement.

08 p0929 A73-21832
Miniature single channel narrow-band differential pulse width modulation-FM crystal controlled transmitter for biomedical telemetry system

09 p1047 A73-23381
A pulse-width modulator operating on dc integral amplifiers

18 p2293 A73-36855
Fundamentals of the theory of nonlinear control systems with pulsed frequency and width modulation

20 p2539 A73-38696
A general quadratic criterion for absolute stability of nonlinear automatic control systems and its application to sampled-data systems with pulse-width modulation

20 p2541 A73-38988
Pulse push-pull power amplifier

22 p2833 A73-42361
A symmetry correcting pulse-width modulator for power conditioning applications.

22 p2802 A73-42919

PULSE FREQUENCY MODULATION

Investigation of a class of nonsearching extremal-control systems with pulse frequency modulation

01 p0027 A73-10594
Investigation of the dissipativity of a pulse-frequency modulated system of stabilizing an unsteady plant

01 p0027 A73-10596
Application of frequency-pulse modulation to adaptive automatic control systems

01 p0027 A73-10597
Global asymptotic stability of two classes of control systems with pulse duration and pulse frequency modulations.

06 p0680 A73-17957
Periodic oscillations in feedback systems with combined pulse modulation.

06 p0680 A73-18518

PULSE FREQUENCY MODULATION TELEMETRY

Demodulation of pulse modulated signals using Kalman filtering techniques.

06 p0669 A73-18809

Satellite attitude control by reaction jet frequency modulation.

07 p0906 A73-19489

Linear FM pulses in chirp radar transmitter, calculating and plotting bounds on amplitude, energy and power spectra for electromagnetic compatibility analysis

08 p0949 A73-21665

Mathematical model of equilibrium and steady state stability of pulse frequency modulation feedback systems of second kind with time delay filters

09 p1069 A73-22723

A study of integral pulse frequency modulation of a random carrier.

14 p1729 A73-30502

Mathematical model of equilibrium and steady state stability of pulse frequency modulation feedback systems of second kind with time delay filters

14 p1740 A73-30956

Study of the frequency impulse system of spacecraft orientation control

18 p2359 A73-36102

Fundamentals of the theory of nonlinear control systems with pulsed frequency and width modulation

20 p2539 A73-38696

PULSE FREQUENCY MODULATION TELEMETRY

Digital apparatus for telemetry of pressure

01 p0044 A73-10034

Multichannel PDM-FM biomedical radio telemetry system for ECG, respiratory rate and oxygen consumption during exercise, considering transmitter and receiver design

03 p0269 A73-14278

Multichannel telemetry of physiological parameters /body temperature eeg, eeg/ in the rat. I - Design and methods.

03 p0272 A73-14305

PULSE GENERATORS

High-repetition-rate optical pulse generator using a Fabry-Perot electro-optic modulator.

01 p0058 A73-10127

Linear characteristics of transistorized Schmitt trigger pulse width regulators in response to sinusoidal and sawtooth signals for automatic control systems

02 p0149 A73-12343

Three channel transistorized pulse generator for electric stimuli used in electrophysiological studies

05 p0545 A73-16739

Programmable digital pulse generator for NMR applications based on master clock, several counters and inexpensive ICs

05 p0559 A73-17256

Time difference measuring instrument for asynchronous and synchronized positive pulses in automatic control system, noting pulse generator and switching, trigger and logic circuits

06 p0677 A73-18384

Electronics associated with ultrahigh-speed photographic equipment

06 p0679 A73-18855

Russian book on pulse radar circuits covering signal and device characteristics, shaping circuits, amplifiers, limiters, frequency dividers and generators

07 p0794 A73-20231

Dynamic response of digital-analog flow measurement system based on turbine driven pulse generator as sensor element

07 p0828 A73-20545

High efficiency microwave avalanche diode capability for digital applications, describing GHz rate 100 V pulse generator circuit

07 p0804 A73-20556

Probabilistic analysis of the statistical accuracy of a transistor blocking generator with a common emitter

08 p0949 A73-21590

A magnetic thyristor pulse generator with shock-wave generation in the transmission line

08 p0949 A73-21712

Operating conditions of a triggered pulse generator with a limiter diode

10 p1195 A73-24380

Transistor sawtooth voltage generator design for accelerated rise time piecewise linear leading edge, using capacitor charge/discharge acceleration

10 p1196 A73-24604

Experimental verification of new Gunn-effect reflection-insensitive pulse regenerator.

11 p1337 A73-25361

Electro-optical transient sampling analyzer with neon laser and hydrogen thyatron pulse generator and minimum optical and electrical jitter

11 p1377 A73-26244

Selection of the parameters of a rectangular-pulse generator with quartz-crystal controlled frequency

12 p1481 A73-27587

High power microwave nanosecond pulse generator with waveguide standing wave resonator, noting power gain and pulse shape

13 p1583 A73-28672

Blocking oscillator multipulse mode operation digital control by supply voltage regulation

13 p1593 A73-29119

Inexpensive fast solid state current drive circuit for injection lasers, using parallel conventional transistor switches operated at avalanche breakdown for pulse generation

16 p2024 A73-33400

A generator of rectangular voltage pulses with 50 kV amplitude

17 p2120 A73-34153

Sinusoidal pulse flow through an axial flow gas turbine.

17 p2093 A73-34395

Probability method and algorithm for analyzing the dynamic precision of pulse generators

18 p2294 A73-37024

Ion implanted X-band IMPATT/TRAPATT back-to-back diodes.

19 p2408 A73-37146

Versatile logic system for use in nuclear experiments on scientific satellites.

19 p2412 A73-37147

A technique for gating short microwave pulses.

19 p2410 A73-38000

A pulse-regenerating optical transmission line.

20 p2522 A73-38668

Approaches to the design of low-voltage pulse generators using avalanche semiconductor devices

20 p2538 A73-39467

A square-wave generator with digital frequency setting

21 p2662 A73-40346

The mechanism responsible for shortening of the stimulated Mandelstam-B Brillouin scattering light-pulse duration and for generation of nanosecond-duration pulses

21 p2739 A73-40355

Parametric amplification and generation of pulses in nonlinear distributed systems

22 p2826 A73-42333

Pulse generator for testing and measurement, describing pulse frequency, duration and sequence capacity, digital design and normal and alarm sequences

23 p2955 A73-44150

Pseudorandom Poisson process binary pulse generator, discussing digital hardware implementation and test results

24 p3069 A73-45256

PULSE HEATING

Temperature stresses in an elastic infinite strip due to sudden heating and heat transfer at the boundary of the strip

01 p0113 A73-10091

Unalloyed and alloyed steels hardening by pulse heating methods, noting hardness and ductility characteristics due to fine-grained structure

01 p0056 A73-10307

Radiation energy distribution in laser pulse heating of moving plasma without reflection, noting thermal wave propagation

04 p0481 A73-15605

Nondestructive screening and pulse damage mechanism for thermal second breakdown of semiconductor junction diodes

05 p0557 A73-16504

Adaptation of the P-N junction burnout model to circuit analysis codes.

05 p0557 A73-16506

Possible mechanisms of turbulent heating of a plasma by ultrashort pulses of laser radiation.

05 p0603 A73-16792

Radiation energy distribution in laser pulse heating of moving plasma without reflection, noting thermal wave propagation

10 p1254 A73-24195

Measurement of a set of thermal properties of metals at high temperatures by the periodic-heating method

11 p1379 A73-25426

Analytical investigation of heat transfer in bodies with moving boundaries

11 p1450 A73-25622

Energy transfer from a pulsed thermal source to He II below 0.3 K.

13 p1658 A73-28191

Dynamic yield strength determination at elevated temperatures after nanosecond pulse heating.

[SESA PAPER 2141A]

17 p2148 A73-35450

Measurement of the heat capacity of graphite in the range 1500 to 3000 K by a pulse heating method.

22 p2881 A73-42510

Determination of thermal contact resistance using a pulse technique.

22 p2878 A73-42511

PULSE HEIGHT

U PULSE AMPLITUDE

PULSE MODULATION

NT DELTA MODULATION

NT PULSE AMPLITUDE MODULATION

NT PULSE CODE MODULATION

NT PULSE DURATION MODULATION

NT PULSE FREQUENCY MODULATION

NT PULSE FREQUENCY MODULATION

TELEMETRY

NT PULSE POSITION MODULATION

NT PULSE TIME MODULATION

Two component magnetic pulsed modulator for electroluminescent and laser diodes, using ac source with nonresonance input capacitance charge

01 p0059 A73-10793

Principles of synthetic-aperture radar

05 p0552 A73-17267

Russian book on pulse radar circuits covering signal and device characteristics, shaping circuits, amplifiers, limiters, frequency dividers and generators

07 p0794 A73-20231

Short-pulse modulation of gallium-arsenide lasers with TRAPATT diodes.

13 p1626 A73-28050

Narrowband time domain reflectometer uses pulse modulated Gunn-oscillator to measure small reflections in 6 and 7.5 GHz band waveguides.

14 p1733 A73-30005

Protecting a quantum amplifier from saturation by pulsed modulation of the pumping.

17 p1284 A73-35157

Pulse modulation of Gunn-effect oscillator.

17 p1242 A73-35652

First order theory of steady state single optical pulses /solitons/ phase modulation during propagation in nonlinear absorbers, predicting nonchirped and chirped pulse trains

20 p2591 A73-38626

Modulation of gallium arsenide laser diodes

20 p2572 A73-38665

Dynamic properties of transistor current switches

22 p2833 A73-42369

PULSE POSITION MODULATION

Energy spectra of mixed discrete random processes in statistical multiplexing systems with pulse position, delta and pulse code modulation

06 p0668 A73-18390

Demodulation of pulse modulated signals using Kalman filtering techniques.

06 p0669 A73-18809

Some limitations on the use of fluidic pulse width and pulse position modulation for phase measurement.

08 p0929 A73-21832

Information in the time of arrival of a photon packet - Capacity of PPM channels.

10 p1188 A73-23836

A technique of modulating pulsed semiconductor lasers.

12 p1505 A73-27009

Designing high efficiency TWT's.

18 p2293 A73-36777

PPM pulse waveform synthesis with SNR performance improvement while retaining bandwidth-mean-square error properties inherent in wideband modulation system

20 p2524 A73-38736

Pulse-position modulation based on energy detection.

21 p2649 A73-40329

A semiconductor-laser communication system using differential pulse position modulation.

21 p2656 A73-41094

PULSE RADAR

NT MONOPULSE RADAR

Computerized airborne multilateration radar with wide-beam antenna and narrow pulsewidth for high resolution terrain image mapping

01 p0019 A73-11479

Atmospheric turbulence information in signal backscattered from pulsed radar, discussing Doppler power spectrum variance determination

03 p0279 A73-14528

Satellite borne Ku-band pulsed radar altimeter for altitude measurement above ocean surface, evaluating random and bias errors due to instrument, propagation and geometry

04 p0446 A73-14805

The University of Oklahoma acoustic radar.

04 p0475 A73-15067

Passive clutter region and reflecting area calculation for ground surface illuminated by pulse radar antenna

06 p0668 A73-18389

Optimal and suboptimal systems for detecting fluctuating optical radar pulses.

06 p0668 A73-18393

Russian book on pulse radar circuits covering signal and device characteristics, shaping circuits, amplifiers, limiters, frequency dividers and generators

07 p0794 A73-20231

Range-azimuth-coupling aberrations in pulse-scanned imaging systems.

10 p1188 A73-23833

Signal accumulation efficiency for single-site coherent pulse radar moving over earth surface, using Tarasikin approximation of signal/ground clutter ratio for monopulse radars

12 p1467 A73-26944

Faraday effect of incoherently scattered radar signals.

13 p1583 A73-28712

Fluctuation loss and diversity gain for in-phase systems with post-detection integration.

13 p1586 A73-29218

Crossed field amplifier selection for application to pulsed radar transmitters, considering system opera-

- tion effects, power supply regulation and droop limitation method
16 p1991 A73-33899
- Use of pulse compression in mapping-type radars.
17 p2127 A73-35632
- The staggering of pulse sequences in the case of a pulsed radar providing moving target indication
18 p2289 A73-36399
- A technique for gating short microwave pulses.
19 p2410 A73-38000
- Nonbiased rule for detection of radar signals in noise of unknown power.
20 p2529 A73-38928
- The effect of staggered PRF's on MTI signal detection.
21 p2650 A73-40344
- Basic principles and the theory of operation of the equipment for the identification-friend or foe /SIF/ in military aircraft
21 p2650 A73-40348
- Surface acoustic wave devices and applications. II - Pulse compression systems.
21 p2703 A73-41137
- Russian book - Digital methods and systems in radar technology.
21 p2657 A73-41433
- Measurement of short distances with optical pulse radars
24 p3069 A73-45467
- PULSE RATE**
High-repetition-rate optical pulse generator using a Fabry-Perot electro-optic modulator.
01 p0058 A73-10127
- A limitation on repetition rate of pulsations of junction lasers due to the repetitively Q-switched mechanism.
09 p1093 A73-22253
- Clutter spectra of low PRF AMTI pulse-Doppler radar.
16 p1980 A73-33413
- Continuous radio telemetric recording of pulse rate in radar controllers while on duty
20 p2517 A73-39208
- PULSE RECORDERS**
U COUNTERS
PULSE TIME MODULATION
NT PULSE DURATION MODULATION
NT PULSE POSITION MODULATION
Increasing the capacity of a discrete communications channel by additional modulation of a carrier parameter
12 p1467 A73-26941
- PULSE WIDTH**
U PULSE DURATION
PULSE WIDTH AMPLITUDE CONVERTERS
Pulse width amplitude converter design and performance for ion engine high voltage power supply, noting oscillator, modulator and circuit protection
04 p0489 A73-15733
- PULSE WIDTH MODULATION**
U PULSE DURATION MODULATION
PULSED JET ENGINES
Development of pulsed hydrogen/oxygen attitude-control engines
[DGLR PAPER 72-077] 02 p0202 A73-11689
- Low power pulsed ablation plasma thruster design for satellite attitude control and stationkeeping, describing operating principle and performance measurements
04 p0489 A73-15731
- Pulsed electric thrusters theoretical and experimental radiation intensities and spectra, estimating interference with onboard satellite communication systems
[ALAA PAPER 73-263] 05 p0608 A73-16984
- PULSED LASERS**
NT Q SWITCHED LASERS
Passive mode locking of the cw dye laser.
01 p0058 A73-10129
- Synchronously pulsed high repetition rate IR up converter based on Nd-YAG pump laser and proustite nonlinear crystal, describing experimental arrangement and operation
01 p0044 A73-10133
- Nd glass and ruby lasers in mode locking operation for picosecond light pulses emission, noting pulse duration measurement
01 p0059 A73-10713
- Organic dye lasers tuning by diffraction gratings and prisms, noting CW, pulsed and mode locking operations
01 p0059 A73-10716
- Coaxial gas discharge tubes for pulsed lasers
01 p0059 A73-10796
- On the mechanism of particle emission from graphite during pulsed laser heating.
01 p0068 A73-10923
- Investigation of the statistical properties of ultrashort light pulses with the aid of two-photon absorption in semiconductors
01 p0061 A73-11282
- Coherence of the radiation of a pulsed single-mode injection semiconductor laser.
01 p0061 A73-11335
- Ultrashort light pulse generation in lasers with bleachable filters, covering mode formation, secondary effects and two photon recording of emission time structures
01 p0061 A73-11354
- Optical properties of the Apollo laser ranging retroreflector arrays.
02 p0141 A73-12250
- Dynamics of the CO₂ atmospheric pressure laser with transverse pulse excitation.
[AD-760231] 02 p0177 A73-12435
- Fiber-dispersion measurements using a mode-locked krypton laser.
02 p0177 A73-12574
- Laser oscillation and anisotropic gain in the 1 to 0 vibrational band of optically pumped HF gas.
02 p0177 A73-12747
- Mode-locked high-pressure waveguide CO₂ laser.
02 p0178 A73-12748
- Power output of a pulsed Raman laser with saturable excitation.
03 p0319 A73-14453
- Submicrosecond pulses from a hydrogen-fluorine laser with high energy density and quantum efficiency.
03 p0320 A73-14454
- Phase space trajectory analysis of pulsed laser spot pursuit tracking problem for autonomous line-of-sight interceptor missile with flip-flop controls
03 p0287 A73-14483
- Calorimetric measurement of optical power from pulsed lasers.
03 p0310 A73-14494
- Supersonic electrical-discharge copper vapor laser.
04 p0457 A73-14746
- Tunable polarized violet light pulse emission from anthracene doped organic molecular fluorene crystal laser pumped with nitrogen laser, noting pulse amplitude and duration
04 p0458 A73-14873
- Distortion of laser pulses in resonant media
04 p0458 A73-14883
- Method and equipment for localizing satellites by laser range and direction finding.
[ONERA, TP NO. 1149] 04 p0417 A73-15096
- Possibility of generating ultrashort laser pulses on combination vibrational-rotational transitions of molecular hydrogen.
04 p0458 A73-15472
- Time history of laser power pulses from molecular gas lasers.
04 p0459 A73-16041
- Effect of H₂ pressure on pulsed H₂ + F₂ laser - Experiment and theory.
05 p0583 A73-16043
- Mode locked laser system generated picosecond pulses envelope and phase structure measurement methods
05 p0583 A73-16339
- Operational characteristics of a volume excited TEA CO₂ laser.
05 p0584 A73-16436
- Atmospheric pressure CO₂ pulsed laser with semiconducting plastic electrodes.
05 p0585 A73-16567
- Possible mechanisms of turbulent heating of a plasma by ultrashort pulses of laser radiation.
05 p0603 A73-16792
- Short pulse laser based on versatile 60 kV fast switching circuit, noting application as pump source for organic dye molecule solutions
05 p0586 A73-17252
- Fog droplet vaporization and fragmentation by a 10.6-micron laser pulse.
[AD-758948] 06 p0698 A73-17494
- Transmission of a GaAs laser beam through the atmosphere.
06 p0699 A73-17495
- Review of controlled fusion research using laser heating.
[ALAA PAPER 73-258] 06 p0728 A73-17667
- Controlled nuclear fusion process based on laser heating of deuterium-tritium pellets, considering laser energy reduction by pulse induced plasma compression
06 p0699 A73-17752
- Kinetics of a pulsed chemical CO laser with photostimulation based on the carbon disulfide oxidation reaction
06 p0700 A73-18103
- Mode locking picosecond pulse Nd glass laser design for reliable and reproducible operation as function of pump power, mirror alignment and saturable absorber
06 p0700 A73-18293
- CO₂ laser-induced gas breakdown in hydrogen.
06 p0701 A73-18355
- Five temperature model of pumping and output power pulse shape predictions for carbon dioxide-nitrogen-helium TEA lasers
06 p0701 A73-18362
- High-frequency electro-optic prism deflector with application to optical demultiplexing and multiplexing.
06 p0701 A73-18363
- A note on fatigue crack starter defects produced by a pulsed laser.
06 p0710 A73-18500
- Emission spectrum of a polyhedral-resonator laser pumped by long pulses.
06 p0702 A73-18580
- Plasma generation by nanosecond and picosecond laser pulses, discussing Raman scattering from solid hydrogen and deuterium targets
06 p0731 A73-18581
- Pulsed nitrogen laser emitting at 3371 Å.
06 p0702 A73-18587
- Laser-radiation-induced damage to the surface of lithium niobate and tantalate single crystals.
06 p0738 A73-18591
- Sharp focused short pulse X ray source with laser flash synchronization for radiographic plasma diagnostics
06 p0732 A73-18609
- 110-J pulsed laser using a solution of rhodamine 6G in ethyl alcohol.
06 p0703 A73-18612
- Laser-induced gas breakdown initiated by ultraviolet photoionization.
06 p0703 A73-18749
- An efficient electrical CO₂ laser using preionization by ultraviolet radiation.
06 p0704 A73-18797
- Ultrafast photodiode for mode locked laser pulses detection, estimating rise time
06 p0678 A73-18851
- Propagation characteristics of collimated, pulsed laser beams through an absorbing atmosphere.
07 p0833 A73-19272
- CW and pulsed deuterium fluoride-carbon dioxide transfer chemical laser with molecular vibrational energy transfer for population inversion to obtain high power output
07 p0834 A73-19630
- Exothermic deuterium-fluorine chain reaction pumping of high pressure pulsed carbon dioxide chemical transfer laser
07 p0835 A73-19631
- A kinetic model and computer simulation for a pulsed DF-CO₂ chemical transfer laser.
07 p0835 A73-19632
- Pulsed CO laser vibrational distribution function time dependent evolution, considering V-V and V-T processes, spontaneous and stimulated emission, electron impact excitation and kinetic heating
07 p0835 A73-19635
- Electron-beam-controlled CO₂ laser amplifiers.
07 p0835 A73-19639
- Parametric studies of pulsed HF lasers using transverse excitation.
07 p0835 A73-19641
- Some characteristics of a miniature pulsed laser with electron excitation.
07 p0836 A73-20136
- Interaction of TEA-CO₂-laser pulses with metals enhanced by liquid layers.
07 p0836 A73-20195
- German monograph - Observation of stimulated Raman-anti-Stokes radiation of higher order and its significance for the starting phase of plasma generation by laser.
07 p0837 A73-20383
- Chemical lasers - A comprehensive literature survey.
08 p0974 A73-21026
- Low cost nitrogen laser design for dye laser pumping.
08 p0974 A73-21027
- Numerical solutions to wave and hydrodynamic equations for thermal blooming of pulsed focused Gaussian laser beams in heated gas medium
08 p0974 A73-21029
- Pulsed laser produced holograms with iron doped lithium niobate, noting application in high capacity information storage
08 p0964 A73-21051
- Photoinitiated transversely sustained CO₂ laser.
08 p0975 A73-21208
- A new approach to picosecond laser pulse analysis shaping and coding.
09 p1090 A73-22077
- Efficient parametric conversion in cesium vapor irradiated by 3470-Å mode-locked pulses.
09 p1090 A73-22079
- Variation of spontaneous emission with current in GaAs homostructure and double-heterostructure injection lasers.
09 p1091 A73-22236
- Room temperature pulsed n-type GaAs cleaved platelet lasers bulk optically pumped near band gap by tunable parametric oscillator, noting emission peak at threshold
[AD-758950] 09 p1092 A73-22240
- Theory of second-order mode locking in semiconductor lasers.
09 p1092 A73-22244
- Feasibility analysis of MIS sandwich structure for pulsed laser based on calculation for field distribution and TE and TM modes in optical cavity
09 p1093 A73-22254

Holographic laboratory practice for NDT, discussing data reduction, display and pulse laser development 09 p1083 A73-22513

Luminescence of a molecular gas under the action of a carbon dioxide laser pulse 09 p1094 A73-22595

Gasdynamic and thermal processes during giant laser pulse impingement on target material, considering heat wave propagation at supersonic and subsonic velocities 09 p1127 A73-22610

A picosecond single-pulse laser 09 p1095 A73-22661

Deformation of laser pulses in resonant media. 09 p1096 A73-22902

Microinhomogeneous active medium effects on laser monopulse duration and energy, noting luminescence band random shift and directional diversity in dipole moments 09 p1097 A73-23083

Performance of an unstable repetitive pulsed CO₂ laser oscillator. 09 p1098 A73-23338

Powerful nanosecond pulses by stable passive mode-locking of TEA CO₂ lasers. 09 p1098 A73-23340

Pulsed GaAs illuminators for night-vision systems. 10 p1216 A73-23785

Obtaining beams of singly charged metal ions with the aid of giant ruby laser pulses 10 p1227 A73-23815

Resonator parameters effect on stability characteristics of ultrashort pulse produced by ruby laser, using mirror and thin reflector 10 p1227 A73-24070

Some characteristics of transition processes in He-Ne lasers operating at the 0.63-micron wavelength 10 p1227 A73-24073

Distance measurement by laser based on reflected pulse time measurement, discussing operating principle and military applications 10 p1228 A73-24174

Heating of theta-pinch plasmas by pulsed CO₂ lasers. 10 p1256 A73-24527

New method of increasing the emission frequency of high-power laser pulses. 10 p1229 A73-24769

Heating of a substance by short laser pulses 10 p1230 A73-24885

Retinal damage thresholds for multiple pulse lasers. [AD-758330] 11 p1315 A73-25341

Neodymium-glass laser with tunable pulse width 11 p1376 A73-25433

Laser beam welding technology review, discussing technical and economic aspects of pulse and CW techniques 11 p1374 A73-25850

Ruby and Nd-YAG pulsed laser induced surface damage probability comparison at 1.06 and 0.69 micron wavelengths by breakdown starting time distribution measurement 11 p1377 A73-26226

Hydrogen fluoride chemical laser with high voltage pulse initiation in simple transverse discharge geometry, measuring maximum energy output and corresponding efficiency 11 p1378 A73-26323

Stabilized two-pulse operation of the phase-modulated, frequency-doubled laser. 12 p1504 A73-26831

Improving the angular divergence of the emission from a neodymium-glass laser with a high pulse energy level 12 p1505 A73-26963

A technique of modulating pulsed semiconductor lasers. 12 p1505 A73-27009

Influence of saturable-absorber transmission and optical pumping on the reproducibility of passive mode locking. 12 p1505 A73-27013

An analysis of pulsation in coupled-cavity structure semiconductor lasers. 12 p1505 A73-27014

Commutation of spark gaps with the aid of a pulsed gas laser emitting in the ultraviolet range 12 p1506 A73-27211

Temporal characteristics of spark gaps with discharge initiation by a laser flare 12 p1506 A73-27212

Nitrogen laser with a longitudinal discharge and high power density 12 p1506 A73-27214

Nitrogen laser with a transverse discharge 12 p1506 A73-27215

Electron-beam ionized pulsed CO₂ laser 12 p1506 A73-27216

Pulsed gas laser employing substances of low volatility 12 p1506 A73-27218

Possible utilization of a vapor, formed by the action of a high-power electron beam on a target, as an active medium for stimulated emission of light. 12 p1507 A73-27517

KGP-2 - An electron-beam pumped cadmium sulfide laser. 12 p1507 A73-27520

Electron-beam tube with a semiconductor target - An electron-beam-pumped scanning laser. 12 p1508 A73-27526

Quantum oscillations and pump depletion effects in an efficient high-power tunable spin-flip laser. 13 p1626 A73-28216

Characteristics of a high-pressure carbon dioxide laser with a transverse discharge 13 p1627 A73-28966

Heterodyne detection of frequency sweeping in the output of transverse-excitation CO₂ lasers. 13 p1628 A73-29186

Transient processes in second harmonic excitation by ultrashort laser light pulse train related to crystal length and phase matching 13 p1629 A73-29433

Pulsed laser utilizing a fluorine and hydrogen mixture. 13 p1629 A73-29434

Theory of the shape of pulses produced by transient parametric generation of light. 13 p1629 A73-29438

Transient self focusing theory of high power laser pulse for homogeneous isotropic transparent solid dielectric with allowance for electrostriction and thermal effects 13 p1629 A73-29440

Thermal deformation of an injection laser crystal during the passage of pumping current pulses. 13 p1630 A73-29443

Propagation of ultrashort light pulses in a semiconductor under two-photon resonance conditions. 13 p1630 A73-29445

Analysis of the first laser echoes obtained on the reflector of Luna 21 13 p1686 A73-29561

Performance comparison of pulsed discharge and E-beam controlled CO₂ lasers. 14 p1756 A73-29918

High resolution spectroscopy with lasers. 14 p1756 A73-29925

Plasma produced by lasers on solid targets 14 p1779 A73-30025

Lunar range measurements with a high-radiance frequency-doubled neodymium-glass laser system. 14 p1756 A73-30152

Effect of laser pulse shape on the form of holographic velocity fringes. 14 p1752 A73-30153

High-pressure CO₂-N₂ laser excited by electric discharge controlled by means of electron beam. 14 p1757 A73-30260

Formation of an ultrashort pulse of light in a ruby laser with resonant modulation of losses 14 p1757 A73-30265

A controlled single-pulse neodymium-glass laser 14 p1757 A73-30369

Spectral analysis of optical pulse signals in application to the problem of synchronizing PCM laser communications lines 14 p1729 A73-30556

Heterojunction laser diode fabrication procedures operation and details, considering peak power levels, wavelengths and operating temperatures for CW and pulsed operations 14 p1736 A73-30575

Mechanical deformation and failure of metals under the action of a 0.01-sec laser light pulse 14 p1758 A73-30714

Injection of a short light pulse into a laser with extensive length of the resonator 15 p1884 A73-31247

Pulsed holographic interferometry at 10.6 microns. 15 p1875 A73-31400

Role of laser radiation self-focusing during breakdown in liquid He4 15 p1884 A73-31701

Effect of laser pulse rise time on heating of a magnetically confined plasma. 15 p1919 A73-31929

Emission characteristics of a tube-shaped laser oscillator. 15 p1885 A73-31940

Laser transit-time measurements between the earth and the moon with a transportable system. 15 p1873 A73-32265

Unsteady processes in multimode lasers with a nonuniformly widening line of lasing 15 p1886 A73-32329

Holographic method for measuring spatial coherence functions 15 p1879 A73-32339

High power chemical laser technology. 16 p2022 A73-32724

Nitrogen pulsed ultraviolet laser. 16 p2023 A73-32861

Pulsed interferometric holography of laser-produced air breakdown. 16 p2014 A73-33175

Detection of short CO₂ laser pulses using the optical Kerr effect. 16 p2024 A73-34027

Chemical lasers and chemical reactions induced by lasers. 17 p2182 A73-34112

Laser pulse shape measurement by successive oscillographing of pulse front areas and concurrent signal amplitude variation 17 p2183 A73-34168

Gain and energy measurements on an HF/DF electrically pulsed chemical laser. 17 p2183 A73-34209

Effect of temperature and composition of gas mixture on population inversion in pulsed CO₂ laser. 17 p2183 A73-34295

Thermal blooming of pulsed laser radiation. 17 p2184 A73-34890

High-energy pulsed CO₂-laser-target interactions in air. 17 p2184 A73-34914

Experimental studies of pulse lasers using organic-dye solutions covering the spectral range from 7,100 to 11,000 Å - Analysis of optimal generation conditions 17 p2184 A73-34918

Light pulse structure and bandwidth bounds in ruby laser with delay line inside variable effective length resonator 17 p2185 A73-35169

Pulsed HCN laser output power enhancement with auxiliary dc discharge, noting low gas flow rate and nonmultiple pulsing advantages 17 p2185 A73-35406

Pulse time of flight measurements using mode locked laser ranging systems consisting of image converter tubes with deflection plates 17 p2185 A73-35411

Repetitively pulsed high power nitrogen laser for UV radiation at room temperature, discussing electrical design and construction 17 p2185 A73-35767

Effect of rotational level coupling on pulse sharpening in CO₂ amplifiers. 17 p2143 A73-35791

Investigation of the characteristics of a mode-locked Nd:glass laser with the aid of a picosecond streak camera. 17 p2186 A73-35796

Self-focusing of CO₂ laser radiation in resonantly absorbing gases. 17 p2186 A73-35811

Russian book on solid state pulsed laser design and construction covering optical, electronic and cooling elements, amplifiers, energy storage, illuminators and semiconductor instruments 18 p2321 A73-35875

Electron-beam irradiated discharges for initiating high-pressure pulsed chemical lasers. [ALAA PAPER 73-645] 18 p2322 A73-36259

Perturbation of a plasma by a focused CO₂ laser beam. 18 p2339 A73-36623

Effect of particle collisions in a resonance gas medium on the deformation of laser pulses 18 p2322 A73-36677

Measurement of nonisotropic electron velocity distributions by laser scattering. 19 p2465 A73-37166

Parametric measurements on a CO₂ TEA laser with electrodes which have a Rogowsky profile 19 p2438 A73-37999

Shock and compression by TEA-CO₂-laser pulses drastically enhanced by liquid layers spread on surfaces of solids. 19 p2438 A73-38024

Formation of a periodic wave structure on the dry surface of a solid by TEA-CO₂-laser pulses. 19 p2438 A73-38025

Improving the angular divergence of a neodymium glass laser beam having a high radiation energy per pulse. 19 p2438 A73-38146

Material processing with solid-state laser. [SME PAPER EM 73-213] 19 p2436 A73-38495

First order theory of steady state single optical pulses /solitons/ phase modulation during propagation in nonlinear absorbers, predicting nonchirped and chirped pulse trains 20 p2591 A73-38626

Self-pulsing in laser amplification of broadband noise. 20 p2571 A73-38635

Peak height measurement system for pulsed laser experiments. 20 p2572 A73-38876

Low power laser-triggered switching at voltages greater than 500 kV. 20 p2572 A73-38883

Technique for gain determinations in pulsed CO₂ TEA lasers. 20 p2572 A73-38885

Intensity limitation and energy spreading in an optical field under transient thermal defocusing conditions. 20 p2574 A73-39689

Pulsed lead vapor laser with high peak and average output powers. 20 p2574 A73-39693

Application of a pulsed laser for measurements of bathymetry and algal fluorescence.

20 p2574 A73-39863

Short interval double-pulsed holography of reflecting objects.

21 p2695 A73-39960

Repetitive recording of stress waves in a photoelastic material using a multi-pulsed laser and an inexpensive streak camera.

21 p2695 A73-39970

Utilization of the laser as a source in ultrahigh-speed cinematography

21 p2709 A73-39972

Holographic investigations and measurements in a cloud of moving microparticles

21 p2696 A73-39979

High-speed photography of laser damage in solids.

21 p2709 A73-39987

Satellite borne diffused pulsed laser with scattered light detection by optical receiver on ground for applications to wide range geodetic survey

21 p2681 A73-40133

Degree of coherence mapping of single ruby laser pulses using holographic interferometry, discussing self-coherence, length and photographic recording

21 p2710 A73-40146

Probability balance equations for energy level population analysis of ultrashort pulse solid state laser generation and amplification

21 p2712 A73-40309

Relative performance of a variety of NF3+/hydrogen-donor transverse-discharge HF chemical-laser systems.

21 p2714 A73-40757

Generation of reproducible giant pulses with an optically regenerative Q switch.

21 p2715 A73-40959

Impulse reaction resulting from the in-air irradiation of aluminum by a pulsed CO2 laser.

21 p2715 A73-40960

Red-light-emitting Al_xGa_{1-x}As heterojunction laser diodes.

21 p2716 A73-40971

Parametric study of a helical TEA CO2 laser.

21 p2716 A73-41050

Heating with short laser pulses.

21 p2717 A73-41660

A parametric study of the performance of a TEA CO2 laser.

22 p2868 A73-41700

Generation of high-power light pulses at wavelengths 1.06 and 0.53 microns and their application in plasma heating. II - Neodymium-glass laser with a second-harmonic converter.

22 p2869 A73-42248

Comparison of theory and experiment for nanosecond-pulse amplification in high-gain CO2 amplifier systems.

22 p2870 A73-42521

The influence of electron plasma formation on superbroadening in light filaments.

22 p2871 A73-43077

Ultrashort pulses from mode-locked cw dye lasers.

22 p2871 A73-43079

Pulsed laser saturation spectroscopy - Observation of power broadening by optical nutations.

22 p2871 A73-43082

N2+/Meinel and O2+/second negative bands laser theory.

22 p2871 A73-43144

Nonlinear transmission loss in Ge beam splitter in pulsed HF and DF lasers operating at 2.5 to 4 microns.

22 p2897 A73-43145

Calorimeter for picosecond laser pulses.

22 p2872 A73-43153

Investigation of the statistical properties of ultrashort light pulses by two-photon absorption in semiconductors.

23 p2987 A73-43503

Temperature and ion energy spectra of laser plasma produced by giant-pulse ruby laser heating metallic targets

23 p3012 A73-43849

Study of light amplification in a pulsed gas-dynamic laser with burning acetylene-air mixtures

23 p2988 A73-44011

High-pressure CO2 laser with a transverse discharge.

23 p2989 A73-44318

Optically pumped 33-atm CO2 laser.

24 p3095 A73-44587

Rapidly fading absorption induced in polymethine dyes by nanosecond pulses of ruby laser radiation

24 p3096 A73-44959

Pulsed argon laser discharge oscillographic electron temperature and time variations measurement, obtaining short and long pulse regime emission characteristics

24 p3097 A73-45516

Pulsed high output double discharge TEA carbon dioxide laser with multiple electrodes and gas preionization in cavity, noting energy conversion efficiency

24 p3098 A73-45551

Pulsed Nd-YAG laser output spiking for control of materials machining parameters

24 p3098 A73-45552

PULSED RADIATION

NT ELECTROMAGNETIC PULSES

Pulsed UV-radiation source for producing highly ionized low-density initial plasmas

01 p0082 A73-10325

Short period pulsating radio auroras properties, determining apparent Doppler characteristics of long period echo sequences

01 p0017 A73-10340

High voltage square pulse oscillator and recording circuit for negative and positive autoelectron emission properties

01 p0024 A73-10795

Higher conservation laws for coherent optical pulse propagation in an inhomogeneously broadened medium.

01 p0078 A73-11221

Investigation of the statistical properties of ultrashort light pulses with the aid of two-photon absorption in semiconductors

01 p0061 A73-11282

The velocity of a wave packet in an anisotropic absorbing medium.

01 p0079 A73-11494

Design and operation of high power pulsed X ray tube with photocathode and nitrogen laser illumination for electron beam generation

02 p0175 A73-11960

Electron density measurement in a pulsed ablation accelerator plasma.

02 p0198 A73-12110

Breakdown thresholds in rare and molecular gases using pulsed 10.6-micron radiation.

02 p0195 A73-12859

FM Gaussian electromagnetic pulse distortion during reflection from ionospheric model with linear electron density profile and constant collision frequency

04 p0422 A73-15479

Error analysis of ionospheric parameter measurement by satellite transmitted or reflected multiple frequency pulsed radiation signal, using perturbation method

05 p0547 A73-16051

Pulse and monochromatic short wave signals phase/amplitude autocorrelation functions and probability distributions during oblique incidence reflection from ionosphere

05 p0550 A73-16776

Light flash induced by a pulsed X-ray source in the upper atmosphere

05 p0610 A73-17016

Geomagnetic field perturbation by gamma quanta pulsating source, studying accompanying radio emission behavior

07 p0816 A73-19445

Microwave or acoustic holographic synthetic aperture interferometry with pulsed techniques, noting single scan, resolution and fringe number advantages

07 p0824 A73-20110

Visualization of pulsed ultrasound using stroboscopic photoelasticity.

08 p0973 A73-21078

Radial pulsations of a white dwarf in the case of nonuniform rotation

09 p1145 A73-22290

Solution of equations for one-dimensional propagation of a monochromatic light pulse in absorbing media

09 p1095 A73-22623

Holographic photography of high-speed processes with the aid of paired radiation pulses

09 p1085 A73-23014

Pulsed gamma ray emission at 5-25 MeV from Crab Nebula pulsar, noting time-averaged energy flux with consideration for telescope efficiency

10 p1272 A73-23535

Quasi-radial pulsations of rotating white dwarfs and neutron stars in the relativistic theory of gravitation

10 p1274 A73-23711

Quasi-periodic /wave/ motions in the solar photosphere. I - Preliminary results

10 p1274 A73-23718

Ionization vacuum chambers for radiation measurement, discussing secondary emission, Greening theory and dosimeters, electron beam monitors, pulse measurement, energy spectrometers and interface dosimetry applications

11 p1362 A73-25422

Thermal limitations of CW and pulsed silicon TRAPATT diodes.

12 p1478 A73-27110

An optimal algorithm for the detection of radar signals on a noise background of unknown power level

12 p1471 A73-27588

Intermittent generation of microwave oscillations through a plasma-beam interaction.

13 p1583 A73-28664

A digital measurement converter of pulsed flows

13 p1591 A73-28872

Photoresistor synchronous detector circuits with rectangular light pulse switching elements for capacitive and resistive loads

13 p1592 A73-28900

Optical fibre guide measurements with short coherent light pulses.

14 p1756 A73-30056

Effect of induced axial electric field on a relativistic electron beam pulse propagating through a plasma.

14 p1777 A73-30661

Determination of the temperature of a sample undergoing pulsed irradiation by sunlight

15 p1896 A73-30997

Pulsar fluctuation spectra and the generalized drifting-subpulse phenomenon.

15 p1936 A73-31558

Harmonic and impulsive acoustic source-produced sound propagation across vortex sheet separating two subsonic fluids, investigating instability waves

17 p2151 A73-34825

Doppler radar with polarization diversity.

17 p2122 A73-34862

VLF pulse ionosounder measurements of the reflection properties of the lower ionosphere.

18 p2305 A73-36010

Quasiradial pulsation of rotating white dwarfs and neutron stars in general relativity.

18 p2354 A73-36736

Quasiperiodic /wavelike/ motions in the solar photosphere. I - Preliminary results.

18 p2355 A73-36743

Optical pulses interaction with two level atom spins, determining sub-cooperation limit in resonant absorbers

20 p2591 A73-38625

A high resolution pulse transmission technique for determining ultrasonic velocities.

20 p2564 A73-38881

Statistics of a pulse signal reflected from an inhomogeneous ionosphere

20 p2530 A73-39157

Portable pulse X-ray micro and nanosecond range apparatus for studying fast-going processes in opaque media.

21 p2696 A73-39977

On the derivation of Zone I spectra for a pulsed finite-amplitude source operating in a nonviscous non-dispersive fluid medium.

22 p2885 A73-41819

Plane transient electromagnetic wave propagation in a generalized conducting medium.

22 p2886 A73-41965

Dynamic effects on ignitability limits of solid propellants subjected to radiative heating.

22 p2899 A73-42813

Computer simulation of light pulse propagation for communication through thick clouds.

22 p2828 A73-43156

Experiments on light pulse communication and propagation through atmospheric clouds.

22 p2828 A73-43157

Investigation of the statistical properties of ultrashort light pulses by two-photon absorption in semiconductors.

23 p2987 A73-43503

Sensitive search for microwave pulses from the galactic centre.

23 p3033 A73-43961

PULSEJET ENGINES

Pulsejet engines operational characteristics compared to turbojet engines, noting flight speed limit due to interaction between unsteady gas flow and combustion process

18 p2342 A73-36063

Fuel combustion rate and turbulent diffusion induced self ignition in pulsejet engine combustion chamber from schlieren photography and pressure distribution measurements

24 p3123 A73-45377

PULSES

NT ELECTRIC PULSES

NT ELECTROMAGNETIC PULSES

NT GEOMAGNETIC MICROPULSATIONS

NT GEOMAGNETIC PULSATIONS

NT MICROPULSATIONS

NT PRESSURE PULSES

PUMP IMPELLERS

Improvement of the calculation of the guide vanes of centrifugal pumps

09 p1028 A73-22569

Calculation of the pumping characteristic of a turbomolecular vacuum pump

12 p1461 A73-27475

Possibility of using an axial-flow impeller designed according to the law $c \cdot \text{sub } u/r = \text{const}$ as the primary pump

21 p2754 A73-40394

Synchronized operation of a positive-displacement gear pump and a vane pump within the lubricant oil delivery system of a jet engine

23 p3020 A73-43742

PUMPING

Electron beam pumped super radiant light source.

01 p0058 A73-10311

Simultaneous population inversions observation at Zeeman levels in ruby paramagnetic microwave quantum amplifier, noting pumping efficiency

02 p0177 A73-12499

- Access to uncombined titanium through an inhibiting film in sublimation pumping of deuterium. 02 p0194 A73-12844
- Investigation of a gallium arsenide laser pumped by an electron beam 05 p0584 A73-16553
- Chemical lasers with molecular gas excitation and population inversion by chemical reactions, discussing lasing conditions, vibrational transition and pumping mechanism 05 p0585 A73-16602
- Waveguide resonator structure of an electron-beam-pumped semiconductor laser. 06 p0702 A73-18584
- Observation of laser oscillation in a 1-atm CO₂-N₂-He laser pumped by an electrically heated plasma generated via photoionization. 06 p0703 A73-18649 [AD-759094]
- Steady nonlinear Ekman-Hartmann boundary layer on flat surface, evaluating pumping and electric current as functions of Rossby number and magnetic interaction parameter 07 p0856 A73-19512
- Some characteristics of a miniature pulsed laser with electron excitation. 07 p0836 A73-20136
- Problem of the nuclear pumping of molecular gas lasers 09 p1096 A73-22702
- Nanosecond pulse amplification in electron-beam-pumped CO₂ amplifiers. 09 p1097 A73-23336
- KGP-2 - An electron-beam pumped cadmium sulfide laser. 12 p1507 A73-27520
- Electron-beam tube with a semiconductor target - An electron-beam-pumped scanning laser. 12 p1508 A73-27526
- Semiconductor lasers pumped by pulsed electric discharge in vacuum. 13 p1626 A73-28545
- Quenching of lasing and the short wave fluorescence in a 3,3 diethylthiatricarbocyanine dye laser 14 p1757 A73-30462
- Protecting a quantum amplifier from saturation by pulsed modulation of the pumping. 17 p2184 A73-35157
- Variable pulse-length electron beam CO₂ laser. 21 p2716 A73-40973
- Divergence of the output radiation of electron-beam-pumped 'radiating mirror' lasers. 22 p2869 A73-42258
- Maximum inversion measurement above threshold as function of pump power for Nd glass laser operating in transverse mode 22 p2871 A73-43081
- Measurement of the gain distribution in a helium-neon laser /0.63-micron wavelength/ cell during high-frequency pumping 24 p3096 A73-44956
- Longitudinal inhomogeneity of gain in the active element of a helium-neon laser pumped by direct current 24 p3097 A73-45517

PUMPS

- NT AXIAL FLOW PUMPS
- NT CENTRIFUGAL PUMPS
- NT CONDENSATION PUMPS
- NT DIFFUSION PUMPS
- NT FUEL PUMPS
- NT ION PUMPS
- NT JET PUMPS
- NT MOLECULAR PUMPS
- NT RAMS [PUMPS]
- NT TURBINE PUMPS
- NT VACUUM PUMPS
- Some refinements of the theory of the viscous screw pump. [ASME PAPER 72-LUB-24] 03 p0314 A73-14337
- The tolerance of fluid machinery to contaminant wear. 13 p1571 A73-29031
- The scale effect and design method of the regenerative pump with non-radial vanes. 23 p2986 A73-44274

PUNCHED CARDS

- Punched card controlled program units including readers, comparator circuits, pneumomechanical counters and fluidic feedback oscillators 23 p2944 A73-43424

PUNCHED TAPES

- A punched tape recorder for observation data 15 p1878 A73-32142
- A flexible automatic typewriting system using three tape readers. 23 p2944 A73-43422

PUNCTURING

U PIERCING

PUPIL SIZE

- Effect of stimulus uncertainty on the pupillary dilation response and the vertex evoked potential. 14 p1714 A73-29991

- Pupil movements to light and accommodative stimulation - A comparative study. 14 p1717 A73-30395

- Visual acuity dependence on background brightness, object contrast, pupil diameter and visual time lag 17 p2114 A73-34639

- Visual field defects after missile injuries to the geniculo-striate pathway in man. 21 p2641 A73-41600

PUPILS

- Photoelectric servo simulator for pupil, using Wheatstone bridge with CdS light dependent resistor 14 p1722 A73-30399

PURIFICATION

NT AIR PURIFICATION

- Purification, crystallization, and subunit structure of allosteric adenosine 5'-monophosphate nucleosidase. 03 p0273 A73-13807

- Alkali metal purification and handling for advanced space power systems. 11 p1310 A73-26004

- NS-1 membranes - Potentially effective new membranes for treatment of wastewater in space cabins. [ASME PAPER 73-ENAS-19] 19 p2400 A73-37975

PURIFIERS

U PURIFICATION

PURINES

- Gamma irradiation induced abiogenic radiochemical synthesis of deoxynucleosides from dry mixtures of purine bases with deoxyribose and ribose 22 p2803 A73-42166

- Chlorination studies. IV - The reaction of aqueous hypochlorous acid with pyrimidine and purine bases. 23 p2950 A73-43274

PURSUIT TRACKING

- Optimal control problems in differential games of pursuit and evasion involving deterministic, random and controlled motion 01 p0028 A73-11071

- Pursuit-evasion reconnaissance game with evader reconnoitering target from close distance with guaranteed safe escape from pursuer 03 p0336 A73-13523

- Phase space trajectory analysis of pulsed laser spot pursuit tracking problem for autonomous line-of-sight interceptor missile with flip-flop controls 03 p0287 A73-14483

- Pontryagin principle for variational problem of controllability region in three dimensional pursuit tracking, noting rendezvous optimal control system 05 p0560 A73-16403

- Pursuit/evasion game problem with two pursuers to one evader, discussing coalition tactic based on open loop and closed loop conjugate points difference [AIAA PAPER 73-230] 05 p0536 A73-16955

- A new illusion - The underestimation of distance during pursuit eye movements. 06 p0656 A73-17575

- Heuristic response strategies and operator performance errors as function of practice in cross coupled pursuit tracking control tasks 07 p0785 A73-19548

- Approach and evasion games in conflict controlled system with nonlinear control, deriving necessary condition for winning 09 p1068 A73-22355

- Optimal control problems in differential games of pursuit and evasion involving deterministic, random and controlled motion 09 p1113 A73-22996

- Necessary termination conditions for difference-differential rendezvous /pursuit with evasion/ game with functional goal set 12 p1524 A73-27401

- Existence solution to linear differential rendezvous game of dynamic system with pursuit and evasion 12 p1524 A73-27402

- Apparent motion of stimuli presented stroboscopically during pursuit movement of the eye. 13 p1577 A73-28093

- Extremal controls in a nonlinear differential game 13 p1660 A73-29077

- Differential game estimate of phase point pursuit of evading closed convex set for feedback control in irregular case 13 p1660 A73-29079

- Optimal stochastic guidance laws for tactical missiles. 15 p1908 A73-31917

- Memorization and model change, alpha-beta, adaptive model and Kalman type radar pursuit tracking techniques efficiency comparison 15 p1908 A73-32443

- Optimal curved pursuit trajectories of point mass in three dimensional space, establishing search technique via Pontryagin principle calculations and equations of state 16 p2061 A73-33269

- Optimal pursuit-evasive conflicts with guidance systems containing time delays. 17 p2145 A73-35380

- Optimum minimax strategy in pursuit game with observation of evading player phase vector at fixed times 21 p2724 A73-40180

- Maneuvering target motion modeling with binary random variable in state equation, obtaining optimal tracking solution as weighted combination of two Kalman filter estimates 21 p2649 A73-40331

PUSH-PULL AMPLIFIERS

- Gunn diodes oscillating circuit with waveguide cavity in push-pull mode at 42 GHz for high power parametric amplifier pump applications 05 p0558 A73-16807

- Pulse push-pull power amplifier 22 p2833 A73-42361

PWM [MODULATION]

U PULSE DURATION MODULATION

PYRAMIDAL BODIES

- Errors in the predicted gain of pyramidal horns. 06 p0676 A73-18180

- Ultrahigh frequency radar scattering by perfectly conducting conical pyramidally noded bodies, deriving polarized radar cross sections via wedge diffracted field integration 22 p2824 A73-41854

PYRAMIDS

- HF microwave scattering by perfectly conducting four-sided involuted pyramid, deriving principally polarized radar cross section at small aspect angles [AD-753370] 01 p0016 A73-10193

- Diffraction effects encountered in the measurement of bidirectional reflectance from square pyramids. [AIAA PAPER 73-150] 05 p0598 A73-16898

- Investigations on 'doping stacking fault' pyramids. 08 p0995 A73-21479

PYRANOMETERS

- Pyranometer calibration by substandard and working instrument comparison on X-Y recorder, using computerized statistical analysis 08 p0966 A73-21264

- A method for the determination of the multiplicative constants of thermoelectric pyranometers 15 p1879 A73-32350

- Instrumentation for remote sensing solar radiation from light aircraft. 22 p2864 A73-43161

PYRAZINES

NT AZINES

PYREX [TRADEMARK]

U BOROSILICATE GLASS

PYRIDINE NUCLEOTIDES

- Determination of oxidized and reduced pyridine nucleotides in human and rabbit blood with the aid of the polarographic cycling technique 09 p1044 A73-21871

- Influence of certain brain structures on the sulphydryl-group, diphosphopyridine-nucleotide, and serotonin contents of the blood 09 p1040 A73-22856

PYRIDINES

- Investigation of the antistatic properties of lacquer coatings based on quaternary polyvinylpyridine salts 21 p2647 A73-40261

- A search for interstellar acrylonitrile, pyrimidine, and pyridine. 22 p2821 A73-43004

PYRIDOXINE

- Hydrazine derivative poisoning in industry and clinical medicine treatments, noting causes of vitamin B6 deficiency 10 p1183 A73-23819

PYRIMIDINES

NT MITOCHONDRIA

- Heterocyclic compounds extraction and identification from carbonaceous meteorites by gas chromatography and mass spectrometry, noting pyrimidine distribution and absence of biological heterocycles 10 p1277 A73-24101

- A search for interstellar acrylonitrile, pyrimidine, and pyridine. 22 p2821 A73-43004

- Chlorination studies. IV - The reaction of aqueous hypochlorous acid with pyrimidine and purine bases. 23 p2950 A73-43274

PYRITES

- Atmospheric moisture effects on hematitic sandstone, pyrite and galena electrical resistivity, noting comparison with semiconductors and insulators 13 p1609 A73-28847

- Oscillations of the magnetic susceptibility in n-type semiconductors with a chalcopyrite lattice 16 p2044 A73-34008

PYROELECTRICITY

- Pyroelectric IR detector materials thermal and electric properties, discussing applications in thermographs, focal plane reticle scanners, linear array thermal imaging, radiometers and laser detectors 06 p0694 A73-18317

- Response of edge- and face-electroded pyroelectric detectors to infrared laser signals. 06 p0704 A73-18798

- Pyroelectric tubes for thermal imaging system, discussing materials, electron beam read-out, SNR

and performance limit compared with scanned photon detectors

07 p0798 A73-19224

Analysis of thermal spread in a pyroelectric imaging system.

08 p0967 A73-21420

Optical damage and internal fields in pyroelectrics.

10 p1260 A73-24531

Opto-thermal gas concentration detector operation by measuring temperature variations caused by chopped laser beam in sample cell, using pyroelectric material as temperature sensor

21 p2701 A73-40691

PYROGRAPHALLOY

U COMPOSITE MATERIALS

U PYROLYTIC GRAPHITE

U REFRACTORY MATERIALS

PYROHELIOMETERS

The third international comparisons of pyrheliometers and a comparison of radiometric scales.

08 p0966 A73-21266

Active cavity radiometer as pyrheliometer for accurate radiation scale definition, determining measurement uncertainty through error analysis on quasi-equilibrium of power balance

11 p1365 A73-26236

Instrumentation for remote sensing solar radiation from light aircraft.

22 p2864 A73-43161

Angstrom pyrheliometer scale correction for ratio of incident circumsolar radiation to electric current heating power derived from nonuniform painted surface strip illumination

23 p3025 A73-43985

PYROHYDROLYSIS

An electrochemical model for hot-salt stress-corrosion of titanium alloys.

17 p2189 A73-34643

PYROLYSIS

On the mechanism of particle emission from graphite during pulsed laser heating.

01 p0068 A73-10923

Mechanical properties of glassy carbon fibres derived from phenolic resin.

01 p0068 A73-11498

Methane pyrolysis in a low current DC discharge.

03 p0398 A73-13798

Pyrolysis of kerosene and mechanism of formation of carbon deposits

[ONERA, TP NO. 1157]

04 p0485 A73-15989

Competitive oxidation and pyrolysis of ethane in the presence of low concentrations of oxygen

05 p0641 A73-17050

Factor of fuel pyrolysis in injector design.

05 p0606 A73-17109

An evaluation of pyrolytic techniques with regard to the Apollo 11, 12 and 14 lunar samples analyses.

06 p0753 A73-18411

Aromatic and heteroatom-containing organic compounds in the lunar samples.

06 p0662 A73-18424

Pyrolysis system with high sensitivity medium-resolution mass spectroscopy to quantify ions pyrolyzed in lunar fines, confirming presence of indigenous lower hydrocarbons

06 p0662 A73-18431

Comparison of four simple models of steady flow combustion of pyrolyzed methane and air.

07 p0865 A73-20360

Passivation of gallium arsenide with silicon nitride.

07 p0864 A73-20571

Thermal fragmentation of quinoline and isouquinoline N-oxides in the ion source of a mass spectrometer.

09 p1048 A73-23470

An experimental method for determining the characteristics of ablative materials

12 p1557 A73-27068

Natural and synthetic thermally stable polymers, discussing pyrolysis, structure-property relationships and bond strengths

14 p1724 A73-30132

Stresses in molybdenum coatings obtained by thermal decomposition of Mo/CO/6

18 p2319 A73-35892

Investigation of failure of a fiberglass plastic due to differential carbon burnup

18 p2328 A73-36813

Heat and mass transfer processes during thermal decomposition of resin binders in fiberglass reinforced plastics

18 p2328 A73-36814

Inorganic flame retardants and their mode of action.

18 p2288 A73-37125

Fire retardation of polyvinyl chloride and related polymers.

18 p2329 A73-37126

Specific characteristics of the high-temperature decomposition of ammonium perchlorate and of ammonium perchlorate-based heterogeneous systems

19 p2471 A73-37503

Kinetics of the catalytic reactions of the thermal decomposition of perchloric acid and ammonium perchlorate

19 p2402 A73-37505

Sulfur hexafluoride pyrolysis and subsequent oxidation in mixtures with oxygen atoms and molecules, measuring decomposition rate at high temperature in shock tube experiment

22 p2818 A73-42767

Pyrolysis and oxidation of polymers at high heating rates.

22 p2936 A73-42806

Linear pyrolysis of various polymers under combustion conditions.

22 p2898 A73-42807

Combustion of thermoplastic polymer particles in various oxygen atmospheres - Comparison of theory and experiment.

22 p2937 A73-42822

PYROLYTIC GRAPHITE

Weave geometry effects on pyrolytic infiltration of carbon-carbon /graphite-graphite/ composite structures for nose tip and thermal shield materials

03 p0332 A73-13044

Carbon and pyrolytic graphite isothermal chemical vapor deposited /CVD/ composite coated and free standing products fluid bed manufacturing and applications

03 p0333 A73-13053

Study of electronic spectroscopy at low energy on graphite

[ONERA, TP NO. 1181]

03 p0336 A73-14607

Directional dependence of the thermal conductivity of crystal-oriented pyrolytic graphite at high temperatures.

06 p0713 A73-17405

Solid propellant rocket engines - Design and development of components in refractory and stratified materials.

07 p0867 A73-18992

The anisotropy of carrier lifetime in graphite.

08 p0982 A73-21220

Soot oxidation kinetics at combustion temperatures.

12 p1557 A73-26844

The relationship between thermal history, X-ray crystallographic structure and thermal properties of rayon precursor carbon-carbon composites A literature review.

16 p2028 A73-33045

Certain thermophysical properties of isotropic pyrolytic graphite

17 p2253 A73-34132

PYROLYTIC MATERIALS

NT PYROLYTIC GRAPHITE

Scanning electron microscope investigation of interaction between pyrolytic carbon fibers and oxidizer, noting periodic variations of carbon chemical activity in radial direction

02 p0185 A73-12556

High temperature coatings on graphite

18 p2318 A73-35885

PYROMETALLURGY

Preparation of zirconium-niobium alloy by carbide-oxide reaction.

21 p2717 A73-40321

PYROMETERS

NT RADIATION PYROMETERS

NT THERMOCOUPLE PYROMETERS

Pyrometer for measurement of surface temperature distribution on a rotating turbine blade.

02 p0171 A73-12617

Pyrometric obturation devices effect on sample temperature level during high temperature tests with radiant heating

03 p0306 A73-13189

High speed pyrometer for high temperature measurement of thermophysical properties, presenting experiment computer program outline

14 p1753 A73-30438

Measuring transient high temperatures by optical pyrometry.

22 p2853 A73-41989

PYROMETRY

U TEMPERATURE MEASUREMENT

PYROPHYLLITE

Possibility of obtaining mullite at high dynamic pressures

02 p0178 A73-11542

PYROTECHNICS

Ignition system development for end-burning solid propellant rocket motor, describing tubular, orifice and perforated type igniter configurations experiments

[ALAA PAPER 72-1137]

03 p0355 A73-13444

Pyrotechnic shock synthesis using nonstationary broad band noise.

[ASME PAPER 72-WA/APM-19]

04 p0516 A73-15897

Satellite-equipment compartment separation system.

07 p0905 A73-18997

Pyrotechnic explosive power devices and systems for aerospace applications.

16 p2045 A73-33106

PYROXENES

NT ENSTATITE

Apollo 14 lunar rock ultrabasic fragments chemical analysis, noting pyroxene and olivine compositions

02 p0219 A73-12441

The valence states of 3d - Transition elements in Apollo 11 and 12 rocks.

03 p0369 A73-13097

Site preferences of Ni²⁺ and Co²⁺ in clinopyroxene and olivine - Limitations of the statistical approach.

06 p0690 A73-18268

Crystallography and chemical trends of orthopyroxene-pigeonite from rock 14310 and coarse fine 12033.

07 p0881 A73-19703

Pyroxenes as recorders of lunar basalt petrogenesis - Chemical trends due to crystal-liquid interaction.

07 p0881 A73-19704

Pyroxenes from breccia 14303.

07 p0881 A73-19705

Fe²⁺/Mg site distribution in Apollo 12021 clinopyroxenes - Evidence for bias in Moessbauer measurements, and relation of ordering to exsolution.

07 p0881 A73-19706

Distinct subsolidus cooling histories of Apollo 14 basalts.

07 p0881 A73-19707

Clinopyroxenes from Apollo 12 and 14 - Exsolution, domain structure, and cation order.

07 p0881 A73-19708

Crystal field spectra of lunar pyroxenes.

07 p0881 A73-19709

Lunar plagioclase and pyroxene observation for lamella thicknesses by X ray diffraction, noting twinning, exsolution and crystal disorder effects

07 p0788 A73-19711

Charge assignment to cosmic ray heavy ion tracks in lunar pyroxenes.

07 p0872 A73-19877

Electronic spectra of pyroxenes and interpretation of telescopic spectral reflectivity curves of the moon.

07 p0897 A73-19885

Petrography, mineralogy and composition of plagioclase and pyroxenes of Washougal hardwite by density and refraction measurements

09 p1139 A73-21853

Luna 20 pyroxenes - Exsolution and phase transformation as indicators of petrologic history.

13 p1675 A73-28313

Apollo 15 sample 15597 vitrophyric nature, pyroxene segregation and textural appearance as evidence for arrival on lunar surface in entirely liquid state

17 p2230 A73-34518

Anisotropy of absorption bands in some lunar, meteoritic, and terrestrial pyroxenes.

17 p2235 A73-35738

Electrical conductivity, internal temperatures and thermal evolution of the moon.

17 p2235 A73-35741

PYROXYLIN

U CELLULOSE NITRATE

PYRRHOTITE

NT TROILITE

PYRROLES

NT INDOLES

NT TRYPTOPHAN

Abiogenic formation of porphyrin, chlorin and bacteriochlorin.

06 p0651 A73-17934

Investigation by the laser photolysis method of the spectral and time characteristics of tetrapyrrole molecules in a triplet state

13 p1628 A73-29050

Synthesis and characterization of isomeric cis- and trans-pyrone model compounds.

21 p2648 A73-41215

PYRRONES [TRADEMARK]

Preparation and thermomechanical properties of pyrrone moldings.

10 p1237 A73-23961

Polyimidazopyrrolone model compounds.

15 p1840 A73-31572

Synthetic foam from Pyrrone prepolymer and hollow carbon microsphere mixtures, discussing low curing shrinkage and high thermal stability

16 p2029 A73-33051

PIRUVATES

Studies on acid production during carbohydrate metabolism by extremely halophilic bacteria.

07 p0780 A73-19500

Sterically controlled syntheses of optically active organic compounds. XVI - Temperature dependence of hydrolytic asymmetric transamination.

12 p1467 A73-27974

P3V AIRCRAFT

U P-3 AIRCRAFT

Q

Q DEVICES

Resonances of an antenna associated with the excitation of ion Bernstein modes.

02 p0198 A73-12071

Radio-frequency heating of a collisionless plasma.

[TTU-SR-2]

09 p1128 A73-22627

Measurement of effective collision frequency in RF heating through parametric instabilities.

09 p1128 A73-22634

Q FACTORS

Temperature-waves in connection with drift type instabilities in a Q-plasma. 11 p1406 A73-26558

Interaction of a high-frequency magnetic field with plasma potential oscillations in a Q machine 12 p1530 A73-27976

Effect of a high frequency magnetic field on plasma diffusion in a Q-machine. 13 p1664 A73-28348

Wake past an obstacle in a magnetized plasma flow. 15 p1916 A73-31089

Q FACTORS

Integral equations for current distribution and input impedances of curved thin symmetrical dipole antenna, noting Q factor of fourth wave antennas 01 p0017 A73-10216

Stable optico-mechanical Q-factor modulator for a laser resonator 01 p0059 A73-10797

A feasibility study for definition of inlet flow quality and development criteria. [AIAA PAPER 72-1098] 03 p0243 A73-13418

Quartz self-oscillator short term frequency instability lower limit estimation by calculating Q values and nonlinearity and resonator parameter fluctuation effects 03 p0284 A73-14064

Low-sensitivity, frequency-selective amplifier circuits for hybrid and bipolar fabrication. 04 p0427 A73-15054

Wideband microwave device with diode and single component correction circuits Q factors measurement from frequency dependence of input traveling wave coefficients 04 p0429 A73-15927

Design of selective third-order active RC filters exhibiting high Q values at low Q sensitivities 07 p0796 A73-18896

Elastic velocity and Q factor measurements on Apollo 12, 14, and 15 rocks. 07 p0894 A73-19852

High-Q toroidal cavities for high frequency klystrons. 07 p0803 A73-20550

X band Gunn oscillator FM noise spectrum dependence on quality factor of resonant circuit 09 p1062 A73-22322

Equivalent resistance, Q factor and winding capacitance of air-core coils with coplanar spiral winding intended for bandpass filters 09 p1065 A73-23073

Inductance and Q factor measurements of inductive p-n-p transistor element in IC circuit as function of frequency, temperature and junction capacitance 10 p1196 A73-24613

Theory of spontaneous and stimulated electroluminescence of ZnS-Mn layers 10 p1261 A73-24766

High Q bandpass low sensitivity RC amplifier-filter networks, discussing two-step decomposition of denominator polynomial of second order filter transfer function 11 p1338 A73-26417

Constant-Q pulsed feedback electronics for strapped-down gyro systems. 11 p1342 A73-26635

Automatic measurement of the Q factor of stationary bipolar networks and multiports 13 p1589 A73-28123

Microwave filters physical volume relation to losses, discussing intrinsic and loaded Q factors from frequency attenuation curves and graphical design procedures 15 p1850 A73-31252

Automatic control of positive feedback depth and its application for stabilization of high Q-factor circuit characteristics 15 p1853 A73-31494

Measurement of external Q factor of microwave oscillators using frequency pulling or frequency locking. 15 p1852 A73-32646

Three layer concentric sphere microwave filter resonators, considering eigenvalue equation for arbitrary conductivity and complex permittivity and permeability effects on resonant frequencies and Q factors 16 p1987 A73-33092

Properties of microwave cavities containing magnetic resonant samples. 17 p2130 A73-35758

An integral transistor model using the quality parameters of a technological process 19 p2409 A73-37400

Investigation of the transient process quality of automatic control systems with variable parameters using the method of the biased characteristic equation 20 p2541 A73-39036

Real laser cavity with nonideal reflecting mirrors, showing Q factor increase relation to mode order for plane monochromatic linearly polarized waves 23 p2987 A73-43650

Electromagnetic resonances and Q-factors of lossy dielectric spheres. 23 p2960 A73-44067

Short-term frequency stability of an L band oscillator with a superconducting cavity. 23 p2961 A73-44117

Q SWITCHED LASERS

Study of the conditions of the breakdown threshold of argon at high pressure under the effect of laser radiation 01 p0058 A73-10175

Parameter calculation and design of synchronization circuit for firing pumping lamp of laser with modulator employing total internal reflection prism for Q switching 01 p0059 A73-10831

Frequency stabilization of Q factor modulated ruby laser with mode selection, using rotating prism and quartz selecting element 01 p0060 A73-11087

Q-switching of a CO2 laser with the aid of an active gas cell 02 p0175 A73-11617

Fracture of nonlinear crystals /KDP and LiNbO3/ by radiation from a ruby laser. 02 p0176 A73-12112

Holograms of spark discharges produced by nanosecond electrical pulses. 03 p0309 A73-14100

Pulse pumped Q switched Nd-YAG and ruby lasers single longitudinal mode selection by providing intracavity resonator with active medium 03 p0320 A73-14464

Q switched carbon dioxide laser based on PM by rotating mirror in one arm of Michelson interferometer, establishing phase relationships 05 p0583 A73-16062

Crystal transverse modulators for laser Q-switching, discussing electro-optical properties of various materials 06 p0699 A73-17753

Optimization of the parameters of a quasi-CW YAG:Nd3+/ laser with a nonlinear element in the resonator. 06 p0703 A73-18599

Remote probing by laser radar. 07 p0793 A73-19947

Laser microspectral analyzer operation in Q switched mode, discussing microplasma generation under inert gas at variable pressure 07 p0836 A73-20162

Effect of impurity gradient on the time delays and Q-switching in junction lasers. 07 p0836 A73-20189

The powering and synchronization of a solid-state laser operating at a repetition rate of several Hertz 08 p0976 A73-21716

Mode-locking of high power lasers by a combination of intensity and time dependent Q-switching. 09 p1090 A73-21999

Megawatt power IR output of Nd-YAG 50 micron pulse laser, using antireflection coated lithium niobate crystal for Q switch with high polarization contrast ratio 09 p1091 A73-22088

Time behavior of the internal Q switching in GaAs lasers under electron-beam excitation. 09 p1092 A73-22245

Time delays and Q switching in homostructure and heterostructure injection lasers. 09 p1092 A73-22246

A limitation on repetition rate of pulsations of junction lasers due to the repetitively Q-switched mechanism. 09 p1093 A73-22253

Peak-mode operation and self-Q-switching in a solid state laser 09 p1094 A73-22487

Holographic photography of high-speed processes with the aid of paired radiation pulses 09 p1085 A73-23014

Resonant multiphoton ionization of a cesium atomic beam by a tunable-wavelength Q-switched neodymium-glass laser. 09 p1098 A73-23472

Population inversion and radiation density in a Q-switched CO2 laser 10 p1227 A73-23578

The application of holography to sonic boom investigations. 11 p1371 A73-26633

Single-frequency ruby laser with electrooptical Q switching and smooth frequency tuning 12 p1504 A73-26886

Single-frequency neodymium-glass lasers under nonspiking free-oscillation and Q-switched conditions. 12 p1506 A73-27502

Investigation of a pulsed laser utilizing an exploding-film Q switch. 12 p1507 A73-27504

Measuring the positions of satellites with the aid of laser pulses. 13 p1582 A73-28149

Coherent optical signal superregenerative amplification in Q switched gas laser, calculating sensitivity of He-Ne laser light amplifier 13 p1627 A73-28663

Gas discharge CW and pulsed CO laser population inversion mechanism, noting high output and efficiency in CW and Q switched modes 13 p1629 A73-29428

Damping time of a ruby laser with flat mirrors 13 p1630 A73-29556

Spike operation and self Q-switching in a solid-state laser. 14 p1757 A73-30323

Investigation of the shape of radiation pulses emitted by a self-mode-locked laser. 14 p1757 A73-30329

Burst-mode frequency-doubled YAG:Nd3+/ laser for time-sequenced high-speed photography and holography. 15 p1886 A73-32384

Current status of Nd:YAG lasers. 16 p2022 A73-32855

Electrooptical Q-switching /EQQS/ in solid-state laser resonators 17 p2184 A73-34917

Control of laser-pulse shape with the aid of an organic dye switch 18 p2322 A73-36558

Amplitude stabilization of pulses from a Q-switched ruby laser by means of interaction with a non-linear medium. 20 p2570 A73-38614

Effect of ionizing radiation on second breakdown. 20 p2599 A73-39007

Ruby laser with a wide emission spectrum. 20 p2574 A73-39696

Switching of the resonator Q factor by stimulated Mandel' shtam-Brillouin scattering. 20 p2574 A73-39703

Threshold minima in the superhigh-pressure gas breakdown by Q-switched lasers. 20 p2574 A73-39721

Application of image-converter technique in quantum radiophysics and nonlinear optics /Survey paper/. 21 p2709 A73-39940

Short interval double-pulsed holography of reflecting objects. 21 p2695 A73-39960

Flash photography using laser excited fluorescent tracers. 21 p2709 A73-39969

Practical lasers for photographic and holographic recording. 21 p2709 A73-39973

Automatic surface mapping via holographic system, describing Q switched ruby laser holograms, image dissector, computer video signal analysis and scan signals 21 p2699 A73-40150

Emission spectrum of a Q-switched ruby laser and its dependence on the density of the bleachable filter 21 p2711 A73-40304

Slow electron scattering near focused beam of Q-switched ruby laser, investigating scattering probability dependence on electron impact parameter 21 p2712 A73-40354

Excitation of ultrashort light pulses in a ruby ring laser with resonant Q-switching 21 p2712 A73-40356

GaAs two-photon absorption coefficient obtained from transmission measurements with Q switched Nd-YAG laser, noting thermal self focusing 21 p2713 A73-40459

Generation of microsecond pulses with controllable pulse width in a ruby laser 21 p2713 A73-40527

Q switched carbon dioxide laser pulse forms and spectrum, covering mirror and prism configurations, sodium chloride plate irradiation, laser wavelengths and pressure effects 21 p2714 A73-40572

Generation of reproducible giant pulses with an optically regenerative Q switch. 21 p2715 A73-40959

Dynamics of a laser with regulated cavity Q 21 p2716 A73-41510

Laser-induced gas breakdown in superhigh pressure region. 22 p2869 A73-42227

Radiation pulse development time instability in electrooptically Q switched lasers due to flash lamp output fluctuations 22 p2870 A73-42722

Experiments on light pulse communication and propagation through atmospheric clouds. 22 p2828 A73-43157

A possible Q-factor modulation mechanism in a ruby laser with a misaligned resonator 23 p2988 A73-44047

Q switched Nd-YAG laser third harmonic for pumping dye laser, extending tunable output range to blue region 23 p2989 A73-44373

The possibility of field emission from metal surface with a Q-switched laser pulse. 24 p3095 A73-44404

Laser-induced deformation modes in thin metal targets. 24 p3097 A73-45417

QSO [RADIO SOURCES]

U QUASARS

QUADRANTID METEORIODS

Radio-echo measurements of the flux of the Quadrantid, Perseid and Geminid meteor streams.

11 p1415 A73-25169

QUADRANTS

The state of stress produced in a quadrant shaped plate by concentrated forces acting in its plane.

19 p2501 A73-38305

QUADRATIC EQUATIONS

Lapapunov functions for quadratic differential equations with applications to adaptive control.

03 p0336 A73-13520

On a quadratic first integral for the charged particle orbits in the charged Kerr solution.

06 p0725 A73-17889

Matrix Riccati differential and quadratic algebraic equations in optimal control and filtering theory, discussing stabilizing solutions, asymptotic properties and computational techniques

09 p1069 A73-23102

Higher-order numerical differentiation of experimental information.

10 p1244 A73-24719

Maximal finite groups of $n \times n$ integral matrices and complete groups of integral automorphisms of positive quadratic forms /Bravais types/

13 p1648 A73-28342

Extendibility over the entire plane and the functional equation of a scalar product of Hecke L-series of two quadratic fields

13 p1648 A73-28344

Minimization of quadratic functionals in the presence of quadratic constraints and the necessity of a frequency condition in the quadratic criterion of absolute stability for nonlinear control systems

16 p2034 A73-34071

Book - Variational analysis: Critical extremals and sturmian extensions.

17 p2203 A73-35598

A theory of gravitation incorporating the quadratic action principle of relativity.

19 p2459 A73-37446

Linearization of Cauchy's problem for quadratic semilinear partial differential equations.

20 p2581 A73-38865

The variable metric algorithm for non-definite quadratic functions.

21 p2727 A73-40999

QUADRATIC PROGRAMMING

Mathematical formulation of linear programming problem, reducing vector valued optimal management plan determination to quadratic programming problem.

02 p0144 A73-12126

Data processing method for optimal prediction of spacecraft orbital elements, using dynamic and quadratic programming

03 p0379 A73-14555

Minimum potential principles application to elastic-plastic analysis of nonhardening materials, using quadratic programming

04 p0509 A73-14948

The quadratic programming approach to the finite element method.

07 p0907 A73-19030

Bayes criteria and previous test data for industrial equipment test optimization, using linear and quadratic programming

07 p0831 A73-20076

An adaptive convex feedback method for linear control systems with quadratic performance index.

10 p1199 A73-24038

Integral action in the optimal control of linear systems with some inaccessible state variables.

15 p1854 A73-31631

Optimal control in a finite time interval for discrete systems in the minimization problem of an inhomogeneous quadratic functional /a case of fixed terminals/

15 p1854 A73-31802

Book - Mathematical programming and the numerical solution of linear equations.

15 p1901 A73-32300

Mathematical programming methods in structural analysis.

16 p2078 A73-33001

Curved rotational shell elements by the constraint method.

16 p2078 A73-33002

An approach to nonlinear programming.

16 p2032 A73-33301

Extensions of Newton's method and Simplex methods for solving quadratic programs.

16 p2033 A73-33856

Book - Optimum structural design: Theory and applications.

17 p2242 A73-34350

A comparison of the complex method of optimization with the penalty function approach using Zangwill's method for constrained optimization problems.

17 p2202 A73-35385

An optimal feedback control law for regulator problems with linear state inequality constraints.

19 p2413 A73-38060

Performance of LQG control systems using optimal k-step-ahead control laws.

19 p2413 A73-38062

A new approach to the 'inverse problem of optimal control theory' by use of a generalized performance index /GPI/.

19 p2414 A73-38063

Complementary variational principle existence condition and duality in linear and quadratic programming in Hilbert space setting, considering relationship to Kuhn-Tucker saddle point theory

21 p2774 A73-40296

Possibilities of suboptimal control in a linear-quadratic problem

21 p2671 A73-41606

Failure diagnosis using quadratic programming.

22 p2867 A73-42966

Optimal feedback control solution existence and uniqueness conditions for asymptotic stability, discussing relationships with Pontryagin equations and linear regulator problem with quadratic cost functionals

22 p2837 A73-43070

Optimal control over a finite time-interval for discrete systems in the problem of minimizing an inhomogeneous quadratic functional /The case of fixed end-points/.

23 p2965 A73-44331

QUADRATURE APPROXIMATION

U QUADRATURES

QUADRATURES

Quadrature phase splitter with indications of the quadrature and equality of output voltage amplitudes

01 p0022 A73-10081

Accelerated convergence of sequences of quadrature approximations.

01 p0072 A73-11471

Damping perturbation of high order nonlinear autonomous Liapunov system, reducing system equations integration to quadratures via transformation to lower order quasi-linear nonautonomous system

03 p0344 A73-14054

Discrete Galerkin and related one-step methods for ordinary differential equations.

05 p0590 A73-16375

Numerical solution of Volterra integral equations.

09 p1113 A73-23020

Exact analytical solutions basic to a class of two-body orbits.

11 p1423 A73-26072

Gaussian quadrature formula derivation by integration of linear interpolation operator replacing Hermitian polynomial with vanishing derivative for error minimization

13 p1647 A73-28194

Quadrature errors upper bound estimates for Gauss-Legendre, Newton-Cotes and Gauss-Laguerre formulas

13 p1649 A73-28603

A quadrature-iterative method of solving linear and nonlinear integral equations

13 p1651 A73-29679

Quadrature errors effect on finite element method solutions accuracy, considering stiffness matrix numerical stability

14 p1806 A73-30179

A simple integration method for the momentum and energy theorem of boundary layer theory

14 p1745 A73-30300

Note on error bounds for numerical integration.

17 p2200 A73-34214

Numerical evaluation of integrals around simple closed curves.

21 p2725 A73-40378

Quadrature solution for the general relativistic motion of a satellite or a planet.

24 p3142 A73-45291

QUADRUPOLE LENSES

U MAGNETIC LENSES

QUADRUPOLE NETWORKS

Use of matrix eigenvalues in the synthesis of symmetrical two terminal pair networks

08 p0947 A73-21397

Reduction of nonlinear distortions in a two-port network exhibiting a small nonlinearity

13 p1592 A73-28894

Analysis of the dynamic operation of a four-terminal network with slight nonlinearity.

16 p1993 A73-33979

Use of the eigenvalues of a matrix to synthesize symmetrical four-terminal networks.

19 p2415 A73-38355

Approximation of the characteristics of two-port networks with a complex nonlinearity

20 p2537 A73-39464

Method of calculating the amplitude and phase-amplitude characteristics of high-frequency amplifiers

21 p2666 A73-41314

Noise factor of a multiple-circuit input device

23 p2953 A73-43518

A quantitative estimate of the electromagnetic compatibility of high-frequency leads in electronic equipment

24 p3071 A73-44596

QUADRUPOLES

Possibilities of using a quadrupole probe in the 0 to 1000-Hz range to measure the collision frequencies of charged particles in the ionosphere

08 p0957 A73-20654

On the quadrupole interaction in the diamond structure.

13 p1667 A73-28213

Interpretation of hydrogen quadrupole and methane observations of Jupiter and the radiative properties of the visible clouds.

13 p1673 A73-28280

Formation of spectral lines in planetary atmospheres. V - Collision narrowed profiles of quadrupole lines in hydrogen atmospheres.

13 p1680 A73-28456

Differential equations for digital model of linear quadrupole, discussing digital simulation of analog radio equipment circuits

13 p1591 A73-28659

Temperature effects in quadrupole interaction in NbHf alloys

15 p1923 A73-31710

Noise from an isolated rotor due to inflow turbulence.

22 p2795 A73-41711

Dipole-quadrupole dispersion coefficient calculation for interactions of atomic pairs formed from hydrogen, alkali and rare gas atoms, using perturbation and variation methods

23 p3007 A73-43522

On the level of H₂ quadrupole absorption in the Jovian atmosphere.

24 p3129 A73-44443

Deflecting moments in magnetic suspensions of gyroscopic devices

24 p3089 A73-44546

Reorientation /collision/ cross sections for hydrogen intermolecular potentials, taking into account quadrupole-quadrupole interaction effects

24 p3113 A73-44980

QUALITATIVE ANALYSIS

Methane pyrolysis in a low current DC discharge.

03 p0398 A73-13798

Qualitative analysis of MHD energy conversion efficiency

12 p1460 A73-27321

QUALITY CONTROL

Development and present state of the non-destructive testing of semi-finished products

01 p0056 A73-10587

An electromagnetic comparator system with improved possibilities in regard of sorting and recording of absolute test parameters

01 p0056 A73-10588

Mathematical formulation for classification, realization and evaluation of electronic components and systems reliability tests

01 p0023 A73-10647

Book on functional pavements design covering support condition, quality control and construction tolerance, environmental and landing gear effects, mathematical models, etc

02 p0150 A73-11879

Hot worked Al alloy machine elements mechanical properties scattering, discussing quality control procedures

03 p0327 A73-14004

Concept and conduct of proof test of F-111 production aircraft.

03 p0317 A73-14467

Information criterion for optimal planning of reliability control tests, maximizing average effect

04 p0430 A73-15211

Quantitative materials evaluation and inspection with the image analysing computer.

05 p0575 A73-16288

Product quality concept definition in terms of use requirements, characteristic properties reproducibility /quality control/ and cost, discussing steel metallurgy and fabrication methods

05 p0582 A73-16999

Management systems for quality cost accounting, time control and productivity analysis based on random time sampling technique

06 p0771 A73-17866

Economic performance and cost problems in civil air transport maintenance and engineering quality control related to selling price trends

06 p0647 A73-17888

MOS production line with individual manufacturing operation reliability assurance based on failure analysis, process perfection, material control and experimental verification

07 p0829 A73-18917

Quality control in Concerto reliable space components procurement program for multilayer ceramic capacitors and thermistors manufacture

07 p0829 A73-18920

French Concerto aerospace part procurement program contribution to mass produced electronic component reliability assessment, control and improvement based on tin oxide resistor experience

07 p0829 A73-18923

Circuit design, manufacture and testing of static memory for D2 satellite computer, considering test equipment, quality control and fabrication 07 p0796 A73-18958

Satellite electronic equipment reliability and quality control at preproject, project, fabrication and mission levels, noting electric welding quality specification 07 p0904 A73-18974

French Concerto program for component reliability and quality assurance in manufacturing and procurement controls for Symphonie satellite 07 p0790 A73-18975

Reliability dynamism at the Deutsch Company. 07 p0829 A73-19008

Failure causes probability and accelerated life test conditions for ceramic capacitors, noting product selection by modified quality control procedures 07 p0799 A73-19405

Quality control of semiconductor elements manufactured in low-run series production - Ultrahigh frequency components 07 p0801 A73-19422

Determination of the extent of ultrasonically detected defects - Application to welded butt joint quality control 07 p0831 A73-19904

The use of automatic test equipment for performing screening and production reliability verification testing. 08 p0942 A73-20681

A laser scanner for integrated circuit testing. 08 p0974 A73-20731

Electronic equipment burn-in for repairable equipment. 08 p0945 A73-20949

Bayesian MFR life test sampling plans. 08 p0973 A73-20950

Measuring apparatus for residual effective stabilizer content in single and double base propellants by passing nitrogen dioxide through ground sample 09 p1135 A73-22300

Optimal control system design with respect to vector quality criterion, noting linear system described by differential equations 09 p1068 A73-22560

Value engineering methodology for quality control and reliability, noting cost effectiveness 09 p1168 A73-22644

Solar cell interconnections with different weld types, discussing semiautomatic and automatic ultrasonic processes, solder thickness control and quality inspection methods and criteria 09 p1035 A73-22807

A quality criterion test for tubes intended for measurement of acoustic absorption and impedance coefficients 09 p1121 A73-23105

Management of a magnetic tape dubbing and evaluation station. 09 p1087 A73-23408

Cu annealability tests for assessing suitability for applications requiring low softening temperature, discussing recrystallization behavior and softness measures 11 p1379 A73-25130

Reliability and quality control of production engineering computer programs. [AIAA PAPER 73-356] 11 p1373 A73-25493

Electronic equipment computerized radiation hardness assurance program for retaliatory or deterrent missile system, discussing supplier data monitoring, verification test and radiation shield assurance 11 p1342 A73-26637

Graphs, tables and discussion to aid in the design and evaluation of an acceptance sampling procedure based on cumulative sums. 13 p1709 A73-29297

Guide to a quality control system for Code vessels. 14 p1755 A73-30144

Russian book on ionizing radiation introspective methods for nondestructive flaw detection in non-transparent objects covering imaging techniques and quality control equipment 15 p1883 A73-31580

Techniques and equipment for thermal nondestructive quality control of products and materials. 15 p1882 A73-31692

Truncated sequential life tests for a 3-way decision procedure. 15 p1883 A73-32260

Development of a data-processing installation for the automatic quality control of spot-welding joints 16 p2019 A73-33222

Organization of a reliability study on an electromechanical product 16 p1970 A73-33271

Integral transform theory for derivation of compound binomial beta, uniform, and gamma distributions with applications to series-parallel systems reliability determination in manufacturing 16 p2020 A73-33604

Quality assurance for the data processing industry. 16 p1985 A73-33614

Magnetic-tape qualification and acceptance testing. 16 p2016 A73-33616

Product liability prevention via a controlled system. 16 p2088 A73-33617

Analysis of early failures in unequal size samples. 16 p2020 A73-33622

Lower confidence bounds determination for component or system reliability by sampling with and without replacement, censored, truncated and mixed sampling test programs 16 p2033 A73-33629

Microcomputer programs for data reduction and quality control chart work, using Olivetti P-101, HP 9100-B and Wang 700-A calculators 16 p1986 A73-33642

Developing country industrial product reliability from buying and manufacturing viewpoints, considering local methods, customs, attitudes and working conditions effects on management techniques 16 p2089 A73-33646

System effectiveness and the one error per man per day expectation. 16 p2020 A73-33647

Nuclear hardness assurance and radiation specifications for overall system assurance, listing electronic component failure modes 16 p2035 A73-33651

Prolonged monitoring of experimental equipment with the aid of semiconductor emitters 17 p2133 A73-34152

Failure analysis used to vindicate JANTX components. 17 p2135 A73-34791

Military and civil jet aircraft fuel specifications, discussing additives types, test procedures and quality control complexity 17 p2220 A73-34848

The human side of quality assurance /as viewed from helicopter manufacturing experiences/. [AHS PREPRINT 751] 17 p2180 A73-35079

Book - Handbook of adhesive bonding. 17 p2180 A73-35337

Aircraft radio equipment manufacture, assembling, mounting, installing and testing, discussing hangar installation, bundle elements, castings, printed circuits and welding techniques 19 p2433 A73-37767

The influence of fabrication and structure processes on the result of control by ultrasonics of semifinished products of titanium alloys 19 p2441 A73-37830

Book - Criteria for current and advanced aircraft hydraulic tubing. 19 p2434 A73-37863

[SAE SP-378] Commercial jet transport aircraft hydraulic fuel distribution tubing systems, discussing maintenance, fabrication problems, fittings, quality control and materials 19 p2434 A73-37864

[SAE SP-378] Aircraft hydraulic tubing permissible defects in Cr-Ni-Mn, Al and Ti tubes and return lines, noting wall thickness, chafing, denting, weld seam cracks and impulse tests 19 p2434 A73-37866

[SAE SP-378] Defects in high quality aircraft tubing and inspection methods. 19 p2434 A73-37867

[SAE SP-378] Quality requirements for Ti-3Al-2.5V annealed and cold worked hydraulic tubing. 19 p2434 A73-37868

[SAE SP-378] High reliability manufacturing technology for COS/MOS IC devices, discussing failure mechanisms and MIL-STD-883 and MIL-M-38510 tests for quality control 20 p2534 A73-38656

Uses of image recognition methods without teaching, in product quality control and lost observation estimations 20 p2568 A73-38712

Statistical analysis of the influence of various factors on the quality of photolithographic operations in the production of integrated circuits 20 p2534 A73-38851

Transient process quality assessment for dynamic systems with variable parameters 20 p2541 A73-39035

An experimental model for the automated detection, measurement, and quality control of low-level cloud motion vectors from geosynchronous satellite data. 20 p2533 A73-39853

Inspecting thin tubes by ultrasounds - Choice of examination frequency 21 p2707 A73-41068

The testing of varnishing products used in aeronautics 21 p2724 A73-41557

Assuring reliability program effectiveness. 22 p2938 A73-42199

Product reliability management, providing MTBF charts for relationships between part count, laboratory test results and operational performance 22 p2867 A73-42969

Eye movements of trained inspectors recorded during visual inspection of colored slides of IC chips, determining performance with emphasis on speed 23 p2947 A73-43212

Glass fiber reinforced casting plastics mechanical properties dependence on processing quality fluctuations, considering laminates with unsaturated polyesters and fiber glass mats 24 p3103 A73-44878

Determination of the point at which damage occurs in glass-reinforced laminates - New nondestructive methods and their suitability as production control procedures 24 p3103 A73-44879

QUALITY FACTORS

U Q FACTORS

QUANTITATIVE ANALYSIS

NT KJELDAHL METHOD

Quantitative gas-liquid chromatography of non-protein amino acids in the presence of the twenty protein amino acids. 06 p0661 A73-18175

Quantitative evaluation of superficial organic contaminants, soluble in halogenated solvents, discussing sampled surface solvent extraction method and subsequent IR absorption spectrographic analysis 06 p0660 A73-18547

An automated gas chromatographic analysis of phenylalanine in serum. 11 p1326 A73-25571

Carbon compounds in pyrolysates and amino acids in extracts of Apollo 14 lunar samples. 11 p1426 A73-26471

Quantitative analysis of specific gases by means of a microwave cavity spectrometer. 13 p1612 A73-28224

Measurement of gas quantities by liquid displacement. 14 p1723 A73-30048

QUANTIZATION

U MEASUREMENT

QUANTIZER

U COUNTERS

QUANTUM AMPLIFIERS

Simultaneous population inversions observation at Zeeman levels in ruby paramagnetic microwave quantum amplifier, noting pumping efficiency 02 p0177 A73-12499

Signal detection in ruby element quantum paramagnetic amplifier operating at liquid nitrogen temperature 03 p0319 A73-14085

Applications for quantum amplifiers in simple digital optical communication systems. 06 p0668 A73-18404

A dual-resonator quantum amplifier operating at a wavelength of 1.35 cm for radio-astronomical observations 15 p1851 A73-31832

Protecting a quantum amplifier from saturation by pulsed modulation of the pumping. 17 p2184 A73-35157

Natural fluctuations in linear quantum amplifiers. 20 p2574 A73-39699

Influence of vibrational, rotational, and reorientational relaxation on pulse amplification in molecular amplifiers. 21 p2742 A73-40217

Carrier-frequency distance dependence of a pulse propagating in a two-level system. 21 p2649 A73-40224

Frequency-locking band of a traveling-wave laser. 22 p2869 A73-42255

QUANTUM COUNTERS

Channel electron multiplier prepared from shaped glass tubing with inner conductive coating, discussing electron and photon detection characteristics 02 p0146 A73-11954

Marine quantum Cs Z-magnetometer design and compensation for onboard nonmagnetic schooner operation, using vertical gyro mount 06 p0691 A73-17547

Photon counting statistics of the superposition of coherent and chaotic light of arbitrary spectrum passed through the turbulent atmosphere or a Gaussian medium. 08 p0987 A73-20952

Two dimensional photon counting - A design based on the Aerospace-NASA videomagnetograph. 08 p0972 A73-21756

Laser optical double resonance and efficient infrared quantum counter upconversion in LaCl₃:Pr³⁺/+ and LaF₃:Pr³⁺/+. 09 p1090 A73-21936

Automatic stellar electrophotometer with photon counting 15 p1878 A73-32136

A three-channel reversible data converter and its possible applications in astronomy 15 p1878 A73-32146

Marine quantum Cs Z-magnetometer design and compensation for onboard nonmagnetic schooner operation, using vertical gyro mount 16 p2011 A73-32771

Optimum astronomical photoelectric photometry - Terrestrial operations in the UV-IR band up to 1 micron wavelength. 16 p2011 A73-32829

Gamma detectors using mercuric iodide and other heavy metal compounds as semiconductors with charge carriers for current surge in quantum energy resolution

17 p2134 A73-34247

An investigation of the statistical properties of the radiation of a laser, operating in several axial modes, by the photon counting method.

17 p2184 A73-35156

Two-photon time distributions in mixed light beams.

20 p2570 A73-38615

Optimum detection of an optical image on a photoelectric surface.

21 p2650 A73-40338

QUANTUM ELECTRODYNAMICS

Quantum kinetic equation for monatomic and molecular gases optical characteristics calculation, considering spontaneous emission spectrum of atoms

04 p0459 A73-15565

Quantum electrodynamical models of coherent plasma electron-positron pair production and pulsed radiation in electric field, relating to pulsars

05 p0626 A73-17383

CW operation in some CO lines below 5.0 microns.

06 p0704 A73-18892

Differential light scattering cross section derivation for photon interaction with relativistic electrons, comparing with quantum electrodynamic calculation and Thomson scattering experiment

07 p0851 A73-19516

Soviet papers on quantum radio physics covering injection lasers, high intensity beam and material interactions, laser dynamics and masers

12 p1505 A73-27135

Theory for the susceptibility of quantum systems with degenerate levels

13 p1659 A73-28759

Survey of the present status of neoclassical radiation theory.

20 p2590 A73-38604

Quantum signal superposition in radio communication, discussing Glauber convolution formula limitations and minimum three signal rule

20 p2529 A73-38924

Photon retinue and infra-red divergence problem in quantum electrodynamics.

22 p2889 A73-42426

QUANTUM GENERATORS

U STIMULATED EMISSION DEVICES

QUANTUM MECHANICS

NT QUANTUM ELECTRODYNAMICS

Classical mechanics and field theory derivation based on material points motion in space, discussing space-time metric, electromagnetic and gravitational fields and quantum mechanics

01 p0076 A73-10599

Equations for matrix elements in Euclidean quantum electrodynamics

01 p0076 A73-10621

Quantum mechanical interpretation for low intensity optical interference experiments with independent light sources and modulated light beams

01 p0078 A73-11250

Quantum kinetics equations for a nonideal gas and a nonideal plasma

01 p0086 A73-11286

A simple illustration of the principle of correspondence in quantum mechanics

02 p0193 A73-12542

Conduction electrons collective wave properties in metals, discussing energy structure, ground state, Fermi surface and quasi-particle concept for crystal conductivity.

06 p0739 A73-18674

Book - Introduction to quantum electronics.

08 p0994 A73-20951

Optimal binary quantum signal detection in two dimensional Hilbert space by a priori probability vector projection method, using randomized decision strategy

09 p1049 A73-22230

Quantum mechanical operator for photon flux density passing through spatial point over infinite time, interpreting photon wave functions

09 p1094 A73-22598

Certain properties of an electron plasma in a strong electromagnetic field

09 p1130 A73-22704

Dielectric modulation of single mode CW gas laser by acoustic wave, solving equations for creation and annihilation operators to obtain quantum number

09 p1096 A73-22973

Statistical characteristics of phase variable states and phase operators in optical quantum fields by intrinsic state factorization method

10 p1228 A73-24151

Quantum mechanical formalism for unitary transformations of wave functions, gauge transformations and current conservation, discussing use of gauge invariant atomic orbitals

10 p1251 A73-24245

Correlation of theory and experiment for high-pressure hydrogen.

11 p1398 A73-25887

Ground state energy of solid molecular hydrogen at high pressure.

11 p1401 A73-25891

Kinetic equations solved for population of different molecular quantum states via quasi-steady state approximation

12 p1526 A73-27307

Raman scattering from phonon bath using quantum mechanical model with random and stochastic Stokes and anti-Stokes coupled modes in light fields

13 p1658 A73-28209

Light scattering in coherent systems for Stokes and anti-Stokes impurity centers in terms of classical and quantum mechanical theories

13 p1660 A73-28770

The stochastic and deterministic aspects of the 'classical' approach to problems of quantum mechanics.

13 p1661 A73-29388

Quantum irreversible statistical thermodynamics with allowance for occurrence of many temperatures based on principle of isentropic motion, applying to laser action

14 p1756 A73-30150

Classical mechanics-quantum mechanics relations and analogies, considering symmetry groups, Casimir invariants, energy levels and quantization

14 p1774 A73-30239

Quantum correction to the electrical conductivity of a Coulomb plasma

14 p1781 A73-30584

Central limiting theorem in the 'noncommutative' probability theory

15 p1899 A73-31215

Calculation of the electron density in heterogeneous mixtures with allowance for the tunneling effect and for super-barrier reflection

15 p1915 A73-31854

Quantum scattering theory of rotational relaxation and spectral line shapes in H₂-He gas mixtures.

17 p2119 A73-35175

Coherence and quantum optics; Proceedings of the Third Rochester Conference, University of Rochester, Rochester, N.Y., June 21-23, 1972.

20 p2569 A73-38601

Master equations in the theory of incoherent and coherent spontaneous emission.

20 p2570 A73-38608

Orthogonal operators and phase space distributions in quantum optics.

20 p2591 A73-38629

On the diffraction of dense electron beams in quantum mechanics.

20 p2595 A73-39766

Quantum mechanics /semiclassical/ theory investigation of shot and thermal noise effects on laser behavior, deriving Fokker-Planck equations for field probability distribution

21 p2711 A73-40215

Quantum-beat g-value measurements on transitions from levels of aligned fast ions.

22 p2890 A73-42974

Quantum kinetic equations for a nonideal gas and a nonideal plasma.

23 p3009 A73-43507

Gravitational red shift - A simple quantum field-theoretical consideration in a curved space.

23 p3006 A73-43607

QUANTUM NUMBERS

Interstellar organic molecules millimeter wave line spectra and transition rotational quantum numbers

09 p1150 A73-23141

Sulfur dioxide infrared-active vibration-rotation combination spectral band, examining quantum numbers, infrared absorption, centrifugal distortion effects and dipole moments

19 p2402 A73-37896

Stark broadening of high quantum number delta n = 1 transitions of carbon V and VI in a laser-produced plasma.

21 p2745 A73-40471

QUANTUM STATISTICS

Formula approximating Fermi-Dirac integrals for electron gas density, pressure and internal energy, discussing pressure ionization effect on equation of state in stellar interiors

11 p1417 A73-25261

Quantum statistical mechanics of dense partially ionized hydrogen.

11 p1405 A73-25886

Book on statistical mechanics, covering thermodynamics, canonical ensembles, quantum statistics, simple gases, ensemble theory, phase transitions, cluster expansions and interacting systems

14 p1775 A73-30360

Bose-Einstein condensation of dipole-active excitons and photons

16 p2039 A73-34064

Quasi-averages for Green functions construction in solving quantum statistical mechanics problems with degenerate equilibrium states

21 p2741 A73-41297

Hartree-Fock equation with allowance for the correlation

22 p2889 A73-42647

QUANTUM THEORY

Image photon counting technique nature, performance, merits, implementation and applications, noting photoelectronic components and image information treatment at quantum level

01 p0048 A73-10529

Integral of collisions for a rarefied plasma /Quantum theory/

01 p0086 A73-11287

Linear synchrotron instability theory results via quantum method with Einstein coefficients, obtaining synchrotron radiation growth rate in relativistic electrons with anisotropic momentum distribution

02 p0223 A73-12726

Arrhenius rate law for thermally activated processes, deriving master equation based on rates of transition between quantum states

03 p0397 A73-13289

Quantum cosmology for universe beginning and first microseconds, treating quantum gravitation, time and cycles, superspace and quantum foam

05 p0614 A73-16310

Quantum theory of the dielectric constant of a magnetized plasma and astrophysical applications. I.

05 p0624 A73-17310

Momentum constraints as integrability conditions for the Hamiltonian constraint in general relativity.

05 p0599 A73-17350

Geomagnetic field perturbation by gamma quanta pulsating source, studying accompanying radio emission behavior

07 p0816 A73-19445

Nonstationary radiation diffusion in a semiinfinite isotropically scattering medium

08 p0985 A73-21453

Protein molecules peptide groups excitation interpretation by quantum theory, noting application to muscle contraction

09 p1046 A73-23297

Conformal invariance of the equations of motion in curved spaces.

10 p1241 A73-23637

Quantum theory of line formation in a magnetic field.

10 p1249 A73-24134

Certain quantum-gravitational effects in central classical fields

12 p1538 A73-26970

Soviet papers on quantum radio physics covering injection lasers, high intensity beam and material interactions, laser dynamics and masers

12 p1505 A73-27135

Russian book on quantum radio physics, Volume 1 covering photons and nonlinear media, matter-radiation interaction, electromagnetic fields, relaxation, emission, solid state physics, etc

12 p1508 A73-27924

Continuous-discrete and probability-deterministic theory of space-time and matter, considering resolution of antagonism between relativity and quantum theories

13 p1658 A73-28373

Spontaneous-emission feedback in a three-level quantum system - A case of conflict between semiclassical and quantum theories of radiation.

13 p1659 A73-28375

Thermodynamics relativistic and quantum structure, considering Lorentz transformation relationship to first principle for entropy and action

13 p1706 A73-28550

Mode locking in quantum optics.

13 p1627 A73-28928

The employment of an extended theorem of corresponding conditions in the computation of the surface tension of pure substances

14 p1776 A73-30124

Normalization properties of resonance wave functions of quantum systems associated with poles of Green function in terms of Siegert and Kapur-Peierls energy definitions

14 p1776 A73-30244

Group theory generalization of Dicke quantum theory for spontaneous coherent radiation of multilevel molecules, noting angular distribution of photon echo effects

14 p1757 A73-30332

Quantum theory of a high energy gas laser

14 p1757 A73-30363

Quantum and relativity theories compatibility based on hypothesis of matter tensor delta structure and Planck's constant for action singularity

14 p1775 A73-30425

Quantum theory of nonlinear oscillators interacting with a medium

14 p1775 A73-30812

Quantum theory of frequency conversion in nonlinear optics

15 p1886 A73-32330

The variation of the electronic transition moment, Re, in the intensity theory of diatomic molecules.

15 p1916 A73-32392

Third Kepler law application to quanta hypothesis of two body systems of physical nature involving centers of attraction

16 p2071 A73-34004

QUARKS

- Theory of electromagnetic field scattering in gases
16 p1984 A73-34007
- Existence of thermodynamic limits in some models of quantum field theory
17 p2254 A73-34633
- Quantum theory of the spinor field in the two-dimensional space-time of de Sitter
17 p2213 A73-35571
- A quantum treatment of spontaneous emission without photons.
20 p2594 A73-38611
- Theory of quantum oscillations of the Nernst-Ettingshausen thermomagnetic coefficient in semiconductors
20 p2599 A73-39397
- Turbulent diffusion in Schwinger formulation of quantum field theory, deriving transition probabilities from Dyson and Saffman equations
20 p2599 A73-39674
- Van der Waals energy calculation from electromagnetic mode quantum energy in spheres and cylinders, considering finite boundary conditions, Green function techniques, and periodic lattices
20 p2538 A73-39706
- Laser transient behavior analysis by quantum theory, obtaining density matrix equation solution in terms of exponentially decaying eigenmodes by truncation method
21 p2711 A73-40214
- Quantum theory of nonlinear optical processes with time-dependent pump amplitude and phase - Frequency conversion.
21 p2711 A73-40222
- Quantum interference effects due to singlet-spin pairing in superconductors, considering normal metal, electron correlations, single particle excitations, thermodynamic properties and ideal superconductors
21 p2752 A73-40642
- Russian book - Statistical physics and quantum field theory.
21 p2741 A73-41296
- Collision integral for a low-density plasma/quantum theory/.
23 p3009 A73-43508
- Resolution of point sources of light as analyzed by quantum detection theory.
23 p2987 A73-43523
- Quantum transport theory of high-field conduction in semiconductors.
23 p3016 A73-43775

QUARKS

- Hadron number density model to predict fossil quark abundance in big bang cosmology
01 p0104 A73-11098
- A search for the quark in extensive air showers, using a counter-controlled cloud chamber.
01 p0093 A73-11249
- Sea level search for leptonic quarks in cosmic rays.
11 p1414 A73-26660
- Search for quarks using a flash-tube chamber.
13 p1670 A73-28210
- Quark search positive results, discussing mathematical models, magnetic monopole searches and existence debate
16 p2054 A73-33289

QUARRIES U MINES [EXCAVATIONS]

QUARTZ

- Quartz light pipe for scanning electron microscope, noting photomultiplier voltage reduction and indefinite service life
05 p0580 A73-17259
- Quartz optical waveguide by ion implantation.
06 p0703 A73-18745
- Optical constants measurement for far IR materials of crystalline quartz, sapphire, Ge and Si at room temperature and 1.5 K
08 p0994 A73-21049
- Isentropic compression of fused quartz and liquid hydrogen to several Mbar.
11 p1398 A73-25884
- A comparison of quasi-static uniaxial-strain and Hugoniot tests for quartz-phenolic composite.
12 p1550 A73-27024
- Quartz transformation to stishovite in shock loaded quartz-copper mixture, discussing relationship to short range order phase
22 p2848 A73-42497
- An electrostatic suspension method for determining photoionization energies of solids.
23 p3015 A73-43447
- Venus carbon dioxide production kinetics involving quartz reaction with calcite to form wollastonite and carbon dioxide
24 p3133 A73-44540

QUARTZ CRYSTALS

- Quartz self-oscillator short term frequency instability lower limit estimation by calculating Q values and nonlinearity and resonator parameter fluctuation effects
03 p0284 A73-14064
- High level quartz resonators and oscillators
07 p0798 A73-19177

- Investigation of the fluctuation characteristics of quartz-crystal harmonic generators
07 p0802 A73-20300
- Selection of the parameters of a rectangular-pulse generator with quartz-crystal controlled frequency
12 p1481 A73-27587
- Response of thermally controlled, vibrating piezoelectric quartz to the deposition of multiple metal layers
15 p1924 A73-31843
- Investigation of the fluctuation characteristics of quartz harmonic oscillators.
18 p2294 A73-37137
- The development of the quartz resonator as a digital temperature sensor with a precision of .0001.
22 p2854 A73-41992
- Complementary MOS transistor inverter application to quartz oscillator in terms of frequency, temperature and supply voltage
23 p2960 A73-44112
- Some experiments to crystallize the metal thin films on quartz plates.
23 p3018 A73-44136
- Equivalent circuits for differential bridge quartz filter inductance evaluation in mass production
24 p3071 A73-44600

QUARTZ TRANSDUCERS

- Velocity measurements of microwave ultrasonic waves in quartz.
06 p0724 A73-18776
- Digital quartz pressure transducer for FM signal output to interface with digital computer and telemetry, noting insensitivity to temperature and vibration interference effects
09 p1082 A73-22503
- Piezoelectric gages for fluid dynamic multicomponent force measurements, discussing quartz transducers, measurement accuracy and capability for rapidly fluctuating forces measurement
12 p1499 A73-27871
- A sandwich-transducer technique for measurement of internal dynamic stress.
14 p1751 A73-29773

QUASARS

- Observational data on galaxies with UV continuum, listing objects with emission lines, s-sd classification and quasar spectral energy distribution
01 p0099 A73-10701
- Autocorrelation function of the 'rapid' brightness variations of the 3C 273 quasar
01 p0101 A73-10932
- Hypothetical process of galaxy or quasar formation by material outflow from singularity, discussing expansion velocity, stellar light concentration, interstellar lines and universe density
01 p1012 A73-10968
- Optical identifications and positions of blue stellar radio sources without UV excess, comparing with N-galaxies and quasars with red shift
01 p1013 A73-10997
- Single gaseous object and stellar cluster models of quasars and galactic nuclei stability, noting neutron and collapsing star lifetimes
01 p1016 A73-11302
- The mass and angular momentum losses from spinars.
02 p0217 A73-12384
- Blue objects in the vicinity of M31. I - Discovery probability of newly found blue objects
02 p0226 A73-12837
- Long time optical variability model of quasars and Seyfert galaxies in terms of grain extinction variations in intervening clouds due to thermal and atom impact evaporation
02 p0226 A73-12839
- Condensation and protostar expansion hypotheses of stellar and galactic evolution in view of discoveries of quasars, central bodies and stellar associations
03 p0365 A73-12902
- Theoretical models of photoionized intergalactic hydrogen.
03 p0365 A73-12926
- Statistical analysis of galaxy counts in small red shift quasar fields, comparing to number of galaxies around randomly chosen point
03 p0370 A73-13194
- Improved positions and some identifications for 108 radio sources between declinations -33 and +27 deg.
03 p0372 A73-13348
- The redshifts of quasi-stellar objects and associated galaxies.
03 p0375 A73-13896
- Radio source counts and redshifts in steady state cosmology.
04 p0497 A73-15048
- The redshift-distance relation. II - The Hubble diagram and its scatter for first-ranked cluster galaxies: A formal value for q-sub 0. III Photometry and the Hubble diagram for radio sources and the possible turn-on time for QSOs.
04 p0498 A73-15351
- The effects of radiation pressure from resonance scattering in a quasar cloud.
04 p0499 A73-15355

- NGC 2992 and the blue stellar object Weedman No. 2.
04 p0502 A73-15690
- Extragalactic objects state of knowledge including galaxy definition and classification systems and quasar characteristics
05 p0614 A73-16307
- Cygnus X-3 radio source - Lower limit on size and upper limit on distance.
05 p0623 A73-17185
- The distribution of redshifts of quasi-stellar objects and related emission-line objects.
05 p0626 A73-17376
- Absorption lines in the spectrum of the quasar Ton 1530.
05 p0626 A73-17377
- The red-shifts and the patterns of electromagnetic waves in quasistellar objects.
06 p0750 A73-18015
- Absorption-line profiles in the quasi-stellar object PHL 957.
06 p0751 A73-18125
- Long-term variations of total and polarized fluxes, absolute energy distribution, and line strength of BL Lacertae and four quasi-stellar sources.
07 p0873 A73-19051
- Polarization of radio sources. IV - The compact source PKS 2134+004.
07 p0873 A73-19052
- Yale Observatory photographic monitoring program for quasar observation, presenting light curves and magnitudes for 25 objects
07 p0876 A73-19356
- Gravitational energy conversion into rotational energy in contraction process for pulsars, quasars and galactic radio emission energy sources
07 p0898 A73-19934
- Preliminary quasar model based on the Yilmaz exponential metric.
07 p0899 A73-20178
- Search for 3C 191 ionization potential-red shift correlations to other quasar absorption lines
07 p0900 A73-20237
- Observational discrepancies of redshift-distance relationships associated with galaxies and quasars
07 p0904 A73-20639
- Hubble diagram construction for optically luminous quasars, noting relation between red shift and apparent magnitude
08 p1002 A73-20877
- A search for hard X-rays from extragalactic objects.
08 p0997 A73-21153
- Quasars as events in the nuclei of galaxies - The evidence from direct photographs.
08 p1009 A73-21168
- The role of Schmidt telescopes in the study of external galaxies.
08 p1011 A73-21361
- Schmidt telescopes for quasars and blue stars radio astronomy in southern sky survey, considering UV filtering-out for image quality improvement
08 p1011 A73-21362
- Models for extragalactic objects with very high IR and X-ray luminosity.
09 p1141 A73-22007
- Galactic absorbing material effects on quasar apparent distribution, noting brightness decrease with red shift
09 p1147 A73-22572
- Autocorrelation function for the 'rapid' light variations of the quasar 3C 273.
09 p1147 A73-22727
- Galactic nuclei and QSO far IR radiation luminosity explanation by nonthermal maser emission due to gas molecules in dense clouds
09 p1150 A73-23145
- Invalidity of quasar-nearby galaxy angular distance dependence on galaxy red shift from investigation of larger sampling of pairing systems
10 p1273 A73-23702
- Quasar characteristics, considering emission or absorption lines, red shift, optical intensity variation, unipolar generator representation and relativistic particle production
10 p1280 A73-24322
- A statistical investigation of the properties of quasars.
10 p1280 A73-24401
- A first 1415 MHz survey with the Westerbork Synthesis Radio Telescope An attempt to detect radio emission from quasi stellar objects.
10 p1280 A73-24402
- Optical identifications of radio sources from the B2 catalogue - Quasi stellar sources.
10 p1280 A73-24403
- The equilibrium, stability and evolution of a rotating magnetized gaseous disk.
10 p1284 A73-24903
- Statistical analysis of multiple absorption spectra in QSO.
10 p1284 A73-24905
- Quasar classes to explain radio, optical and X ray observations, considering models for local quasar intrinsic red shift
11 p1417 A73-25262

The redshift-distance relation. IV - The composite nature of N galaxies, their Hubble diagram, and the validity of measured redshifts as distance indicators.

Simplified photoionization analysis of quasar emission spectra.

IR spectra of quasars and Seyfert galaxies interpreted as thermal radiation from dust envelopes around cores, considering graphite and silica dust particles.

Blue OB stars detection by flicker comparison, astronomical photography and two color diagrams, discussing classification as quasars and white dwarfs.

Quasar optical luminosities compared to Seyfert galaxies and radio-quiet objects showing broad emission lines of permitted transitions and sharp lines of forbidden transitions.

Hypothesis postulating two types of quasars, considering cosmologically distant quasars /type I/ and type II branch produced by explosions in nearby galaxies.

Redshift-magnitude bands, quasi-stellar sources, and systems of redshift.

Black holes and absorption redshifts in quasi-stellar objects.

Rotation effects in stellar and quasi-stellar relativistic objects models required for pulsars and quasars explanation, discussing gravitation theories.

A list of quasi-stellar radio sources and quasi-stellar radio-source candidates from the 3C and 4C catalogs between declination -7 deg and +40 deg.

Quasar red shift mechanism based on atomic energy levels and particle rest masses variations in scalar gravitational field.

Double structure characterization in ideal model by two extended radio emitting regions near nucleus of optical galaxy or quasar.

The properties of extragalactic X-ray sources from visible light observations.

Spectral characteristics of quasar OQ172 with large red shift, considering absorption and emission spectra and Lyman alpha radiation.

Evidence for luminosity evolution of quasars.

Interplanetary-scintillation observations of 203 sources identified as radio galaxies or quasars.

On the apparent association of quasi-stellar objects with clusters or groups of galaxies with about the same redshift.

Optical and UV astronomical telescopes and instrumentation for quasar detection, emphasizing observational requirements and emission line red shift problem.

Faraday depolarization of radio galaxies and quasars with simple spectra.

Invalidity of quasar-nearby galaxy angular distance dependence on galaxy red shift from investigation of larger sampling of pairing systems.

The luminosity function of quasars and its evolution - A comparison of optically selected quasars and quasars found in radio catalogs.

The redshift-magnitude relation for quasi-stellar objects.

Optical and near IR absorption line spectra of quasar 1331+170, discussing red shift and line locking process.

A search for high-ionization redshift systems in the absorption spectra of five quasars.

Coude spectroscopy for quasar Markarian 132 absorption lines wavelengths and profiles and red shift systems.

A search for 21-centimeter absorption in quasars and other sources near to spiral galaxies.

Quasar and galactic nuclei energy source models, considering supermassive rotating magnetoplasma body, black hole and compact star cluster with flares and collisions.

Quasar scintillations at an inhomogeneous interstellar plasma.

Evolution of supermassive stars with a strong magnetic field.

On the interpretation of the redshift-angular size diagram for quasars.

Extragalactic radio sources identification with galaxies and quasars by high sensitivity and resolution astronomical telescopes, obtaining angular structure maps and radio spectra.

Radio spectra and mapping of extragalactic radio sources including radio galaxies and quasars with high angular resolution, noting energy sources and red shift.

Optical identifications of radio sources using accurate radio and optical positions.

QUASI-STEADY STATES

Quasi-stationary theory of hydrocarbon droplet ignition. I - Moment and limit of ignition.

Quasi-stationary emission from ruby and neodymium-glass lasers.

Theoretical, quasi-static analysis of cavitation compliance in turbopumps.

Stellar evolution as succession of quasi-equilibrium states, investigating dynamic stability via hydrodynamic and state equations.

QUASI-STELLAR RADIO SOURCES

U QUASARS

QUASILINEARITY

U NONLINEARITY

QUATERNARY ALLOYS

New magnesium alloys intended for operation at elevated temperatures.

Influence of the degree of decomposition of a solid solution of zirconium in aluminum on the recrystallization temperature of an aluminum-zinc-magnesium-zirconium system alloy.

Fractographic observations of fatigue crack tip behavior of age hardened Al-Zn-Mg-Cu alloy during static loading.

Bivariant eutectic alloys located on liquidus surface within Ni-Nb-Cr-Al quaternary, permitting production of aligned delta Ni-Nb lamellae within nichrome matrix containing Ni-Al fcc precipitate.

Equilibrium of vanadium carbide with an alpha or gamma solid solution in the iron-rich Fe-Cr-V-C system at temperatures from 700 to 1150 C and at a carbon concentration of 0.30%.

Hardening by tempering of Fe-Ni-Mo and Fe-Ni-Co-Mo martensites.

Structure and properties of alloys of the V3Si-V3Ga-V3Al system.

Investigation of the structure of electron bands in In1-x/Ga1-x/As1-y/P1-y on the basis of luminescence.

Oxidizability of AN-type beta titanium alloys and their protection from gaseous corrosion.

The influence of prior thermal treatment of cast blocks on the coarse grain characteristics in extruded bars and profiles of alloys of the type AlCuSiMn.

Ti-Ta-V-Mo system phase diagram in Ti corner region for 600-900 C, investigating solubility, electrical resistivity and hardness.

Russian book - The structure of zirconium alloys.

Comparison of a suggested polynomial method with the method of F. M. Perelman in the calculation of the solidus surface of the W-Ta-Mo-Nb system.

Influence of dislocation density and aging on the yield point of Al-Cu-Mg-Mn alloys.

QUATERNIONS

A four-component hypermass equation possibly applying to unstable neutrinos.

Errors associated with Rodrigues-Hamilton parameters /vector space basis quaternions/ calculation by numerical integration of kinematic equations of moving body orientation.

Quaternion equations and hypercomplex potentials in continuous medium mechanics.

Geometric interpretation of spinor representations for groups of motions in quasi-elliptic 5-spaces.

Certain theorems concerning functions of an incomplete quaternion variable.

QUENCHING

Quenching of vibrationally excited N2 by atomic oxygen.

Photoionization of vibrationally excited N2. II - Quenching by CO2 and N2O.

Nonequilibrium crystallization of Al-Ru alloys.

Quenching of lasing and the short wave fluorescence in a 3,3 diethylthiatricarbocyanine dye laser.

QUENCHING [COOLING]

Physical nature of the processes of formation of the set of mechanical properties of quench-hardened alloyed structural steel during tempering.

Comment on the nature of the disaccommodation in HCP Co-C alloys.

Low-cycle fatigue behavior of quenched and tempered UNI 38NiCrMo4 steel.

Impurities and cooling rate effects on cast W structure during crystallization from optical metallography.

Phase transformations in Al-rich Al-W alloys rapidly quenched from the melt.

A method for performing high precision lattice parameter change measurements on quenched aluminum.

Observation of Bardeen-Herring sources in quenched magnesium.

Austenite stabilization in Kh17N6M3 transition-type steel.

Interpretation of quench-sensitivity in Al-Zn-Mg-Cu alloys.

Effect of atomic oxygen on the N2 vibrational temperature in the lower thermosphere.

Zr additions effect on quenched and aged Al-Mg-Li alloy having phases in equilibrium with solid solution.

Investigation of the hardening process of alloy D16 in liquid nitrogen.

Diffusion layer structure and phase composition during quenched and annealed steel saturation by Cr at high heating rates.

The effect of an addition of molybdenum on the quenched and aged structure of a Ti-1 wt % Si alloy.

Use of high cooling rates to obtain aluminum alloys with special properties.

Temperature conditions of aluminum alloy crystallization at cooling rates of 10,000 to 1,000,000 deg/sec.

Crystallization of nickel-based alloys and indium-lithium system alloys at ultrahigh cooling rates.

Serrated flow in quenched duralumin alloy.

Internal friction in niobium quenched from premelting temperatures.

Ultrahigh-speed quenching of niobium and vanadium.

Effect of structural and mechanical factors on the nature of cold shortness curves for steels.

Vacancy precipitation in quenched and aged Zr-Al alloys and Zircaloy 2, obtaining evidence by transmission electron microscopy for detailed dislocation structure examination.

The influence of crystal defects in platinum on platinum resistance thermometry.

Structural transformations in molybdenum-carbon alloys during quenching and aging.

Metastable phase diagrams of eutectic and peritectic alloys crystallization during rapid cooling from liquid state.

Metastable phases produced by laser melt quenching.

Investigation of the structure and properties of annealed alloys of the Ti-Mo system.

QUEUEING THEORY

- Phase transformations in beta-Cu-Al during extremely rapid cooling from the melt
23 p2992 A73-43914
- Diagram of continuous cooling transformation of a titanium alloy with 6 per cent Al, 6 per cent V, and 2 per cent Sn /TA 6-V 6-E 2/ homogenized in the beta /sub 0/ phase
23 p2995 A73-44177

QUEUEING THEORY

- Air-terminal queues under time-dependent conditions.
07 p0850 A73-20375
- Estimations for queueing and reliability theory
13 p1649 A73-28796
- Multiple queueing system of control plants, determining optimal order and initiation moments for minimized total time for all requests
20 p2530 A73-38989

QUIET ENGINE PROGRAM

- Jet aircraft engine noise reduction.
10 p1263 A73-24555

QUINOLINE

- Thermal fragmentation of quinoline and isoquinoline N-oxides in the ion source of a mass spectrometer.
09 p1048 A73-23470

QUOTIENTS

- Certain properties of functions with a non-zero difference quotient
09 p1112 A73-22887
- The existence and convergence of subsequences of Pade approximants.
21 p2725 A73-40298

R

RACE FACTORS

- Unacclimatized male Caucasians lower critical temperature determination for subsequent investigation of ethnic variability in acute cold exposure responses
01 p0008 A73-10166

RACETRACKS [PARTICLE ACCELERATORS]

- Plasma confinement in a racetrack magnetic field with a diverter.
03 p0347 A73-14094
- Racetrack configuration design of Uranan stellarator for plasma diagnostics and heating, noting shear and rotational angle of magnetic system
04 p0432 A73-15038
- Influence of longitudinal thermal conductivity on the ohmic heating of plasma in the Tuman-1 facility
13 p1666 A73-28959
- Effect of longitudinal thermal conductivity on ohmic heating in Tuman-1.
23 p3013 A73-44311

RACON BEACONS

U RADAR BEACONS

RADAR

- NT COHERENT RADAR
- NT CONTINUOUS WAVE RADAR
- NT DOPPLER RADAR
- NT METEOROLOGICAL RADAR
- NT MONOPULSE RADAR
- NT MOVING TARGET INDICATORS
- NT OPTICAL RADAR
- NT PULSE DOPPLER RADAR
- NT PULSE RADAR
- NT RADAR MEASUREMENT
- NT RANGE AND RANGE RATE TRACKING
- NT SEARCH RADAR
- NT SECONDARY RADAR
- NT SIDE-LOOKING RADAR
- NT SURVEILLANCE RADAR
- NT TRACKING RADAR
- Reliability tests on fire control airborne radars prototypes, measuring MTBF
07 p0800 A73-19416

RADAR ALTIMETERS

U RADIO ALTIMETERS

RADAR ANTENNAS

- Aperture matching of wideband phased array radar antennas, using digital ferrite phase shifters and dielectric transformer with magnetic resonance limiting
01 p0022 A73-10178
- Meteorological radar site selection factors, discussing antenna towers installation
03 p0288 A73-14514
- Remote sensor for atmospheric physical properties with FM-CW scanning radar, parabolic antennas and waveguide feeds for linear and circular polarization
03 p0339 A73-14544
- Computation of element patterns of an E plane sectoral-horn planar phased array.
04 p0415 A73-14987
- Airborne synthetic aperture /hologram/ radar maximum ambiguity range extension by using additional receive-only antenna ahead of transmit-recvie unit
05 p0577 A73-16817
- The use of a simulator in a synthetic aperture radar data processing tradeoff study.
05 p0554 A73-17149

Principles of synthetic-aperture radar

- 05 p0552 A73-17267
- An initialization technique for improved MTI performance in phased array radars.
06 p0664 A73-17790

- Aircraft radome design mechanical, electrical and aerodynamic requirements, taking into account lightning hazards, electrostatic surface charges and plastic components deformations
06 p0648 A73-17997

- Passive clutter region and reflecting area calculation for ground surface illuminated by pulse radar antenna
06 p0668 A73-18389

- Ground and angel clutter in radar systems - The two-beam antenna solution.
07 p0794 A73-20250

- TRAPATT amplifiers for phased-array radar systems.
09 p1051 A73-22497

- Wideband squintless linear arrays.
10 p1192 A73-23605

- Radar direction measurements by phase comparison of ultrasonic echo pulses reflected from targets in water tank, using piezoelectric sensors for receiving antennas simulation
10 p1194 A73-23736

- Influence of the illumination law on the radioelectric performance of radomes - Contribution to the determination of apparent illumination of the antenna
11 p1328 A73-25284

- Study on the limit efficiency of lightning conductors on aircraft radomes.
11 p1336 A73-25303

- A brief survey of monopulse techniques.
11 p1331 A73-26148

- Radar technology applied to air traffic control.
14 p1725 A73-29895

- Frequency-selective surfaces for multiple-frequency antennas Design data plus experimental results.
14 p1737 A73-30625

- Bringing data processing to projects and tests of large antennas
15 p1846 A73-32430

- Light aircraft-borne low cost phased array X band radar and display design requirements for weather detection and ground mapping
15 p1909 A73-32451

- Coaxial cable fed dipole antenna array for observation of coherent backscatter radar signal from ionospheric electron density irregularities in electrojet region
16 p1987 A73-33117

- On the angular resolution of a search radar with a mechanically rotated antenna.
17 p2125 A73-35369

- Spatial statistics of instrument-limited angular measurement errors in phased array radars.
17 p2128 A73-35687

- Circular synthetic radar with interferometer elements mounted at ends of horizontal boom rotating about vertical mast, predicting echo response to point and multiple targets
21 p2650 A73-40342

- BMD requirements for phased array radars.
21 p2651 A73-40644

- Phased array antennas in ground based remote sensor system, assessing technologies of AN/FPS-85, HAPDAR and APTPN-19 radar systems
21 p2672 A73-40645

- Development programs status report on airborne planar, conformal and distributed aperture phased array antennas for use in radar and communication systems
21 p2662 A73-40646

- Design, performance, and cost considerations for solid-state arrays.
21 p2662 A73-40648

- On the effects of eliminating the passive elements from a thinned array.
21 p2652 A73-40655

- Phased array antenna feed systems developments, discussing relative merits, problems and design choices for air surveillance radar applications in microwave region
21 p2672 A73-40664

- Time scanned array radar with time delay or phase gradient for electronic beam steering control by signal
21 p2652 A73-40669

- High resolution beam steering phased array radar antenna design by subarray techniques, using time delay circuit for cost effective driver control simplification
21 p2653 A73-40672

- A single-plane electronically scanned antenna for airborne radar applications.
21 p2653 A73-40684

- Synthesis of antennas with minimum mean sidelobe level of the radiation pattern.
24 p3068 A73-44939

RADAR APPROACH CONTROL

- Automatic runway and aircraft approach path surveillance system /CORAIL/ consisting of Doppler radar, signal extractor and data processing, alarm, display and control equipment
14 p1773 A73-30444

- The Corail radar - Automatic equipment for runway surveillance
15 p1846 A73-32431

RADAR ASTRONOMY

- Lunar topography - First radar-interferometer measurements of the Alphonsus-Ptolemaeus-Arzachel region.
03 p0378 A73-14446

- Fourier analysis of Mars radar topographic data for magnitude and direction of center of mass/center of figure offset, comparing to earth and moon
11 p1419 A73-25862

- Stationary target identification with radar beam for comet nucleus within coma, noting echo spatial extent and Doppler bandwidth effects on data processing
17 p2174 A73-35634

- The figure of Mars and its effect on radar-ranging.
20 p2611 A73-39588

- Comparison of Apollo and earth-based observations - Definition of surface units in Mare Serenitatis.
21 p2769 A73-40821

- Measurement of antenna parameters and calibration of the sensitivity of the RATAN-600 radio telescope in the radar mode of operation at the 8-mm wavelength
21 p2667 A73-41467

- Sampling phase rotator for removal of Doppler shift in a lunar radar.
21 p2658 A73-41590

- Russian book on radio astronomy with electronic engineering emphasis covering observation and equipment, cosmic source characteristics, radio telescope antenna systems, radar techniques, coordinate measurement, etc
22 p2905 A73-41875

- Planetary surface reflectivity and topography mapping by ground based radar with emphasis on observational methods
23 p2953 A73-43353

- Results of delay-time and Doppler-correction measurements obtained in radar observations of Venus during 1962, 1964, 1969, 1970, and 1972
23 p3037 A73-44252

RADAR ATTENUATION

- A comparison of precipitation attenuation and radar backscatter along earth-space paths.
01 p0015 A73-10183

- Venus - Radar determination of gravity potential.
07 p0875 A73-19167

- Ionization of the atmosphere and attenuation of radar waves after a nuclear explosion.
15 p1844 A73-32198

RADAR BACKSCATTER

U BACKSCATTERING

U RADAR SCATTERING

RADAR BEACONS

- Automated radar terminal systems /ARTS/.
07 p0849 A73-19184

- Signal processing in the Air Traffic Control Radar Beacon System.
12 p1469 A73-27165

- U.S. civil and military air-ground communications development history and expectations, considering information exchange, radar beacon transponders, digital communication and data links
14 p1725 A73-29880

- The development of the ATC radar beacon system - Past, present, and future.
14 p1725 A73-29881

- Bit synchronized discrete address radar beacon system with ground based U.S. civil interrogator complex for compatibility with ATC and aircraft operator services
14 p1772 A73-29882

- FAA air traffic control systems projected improvements, including microwave landing system, aeronautical satellites, electronic voice switching and discrete address radar beacon
16 p2087 A73-33179

- Automated discrete address radar beacon system and data link for ATC, describing simultaneous message decoding capacity, system specifications and implementation prognosis
17 p2208 A73-34612

RADAR BEAMS

- A note on the use of airborne 30-millimetre radar at long ranges.
04 p0423 A73-15699

- Antenna beam focusing and deflection with the aid of a digital phase computer, in a radiation-fed electronically controlled antenna
06 p0673 A73-17580

- Quantizer functions and their use in the analyses of digital beamformer performance.
13 p1582 A73-28496

- Mean square and reflectivity variance decrease due to radar beam smoothing and post-detection integration in terms of reflectivity fields autocorrelation function
18 p2333 A73-36706

RADAR CLUTTER MAPS

- Passive clutter region and reflecting area calculation for ground surface illuminated by pulse radar antenna
06 p0668 A73-18389

RADAR CROSS SECTIONS

Backscatter from snow and ice surfaces at near incident angles.

01 p0016 A73-10191
HF microwave scattering by perfectly conducting four-sided involuted pyramid, deriving principally polarized radar cross section at small aspect angles [AD-753370]

01 p0016 A73-10193
Geometrical optics calculation of radar cross sections.

04 p0416 A73-15058
Spaced radar observation of auroral scattering cross sections, noting radar backscattering intensity peak and echo detection probability relationship to aspect angle

08 p0957 A73-20661
A theory of tracking for a dynamic radar scatterer ensemble.

10 p1189 A73-24532
Radar cross section measurements for right circular cones with spherically blunted noses, presenting as functions of diameter/wavelength ratio and aspect angle

11 p1330 A73-25682
Radar angels cross section statistical distribution model based on radar measurement and direct ornithological data on bird populations density

11 p1332 A73-26630
Probability of detecting aircraft targets.

11 p1333 A73-26634
Calculation of probability of detection with target scintillation.

13 p1586 A73-29219
The effect of limiting upon the mean cross section of log-normal radar clutter.

13 p1586 A73-29224
Modified radar cross section of a dielectric cylinder with conducting circumferential loop loading.

14 p1729 A73-30699
Remote sensing of complex permittivity with multiple resonances in RCS.

17 p2128 A73-35692
Reflection characteristics of quasi-tapered anechoic chamber at VHF and EHF, evaluating broadband response, radar cross sections and field in quiet zone

17 p2129 A73-35701
Ultrahigh frequency radar scattering by perfectly conducting conical pyramidal noded bodies, deriving polarized radar cross sections via wedge diffracted field integration

22 p2824 A73-41854

RADAR DATA

Investigation of fading radio echoes from meteor trails. I

01 p0016 A73-10201
Application of pattern recognition techniques to digitized radar data.

03 p0279 A73-14517
Project Cloud Catcher weather radar data system revisions in radar set, echo pulse integrator, data logging and analysis and graphic displays

03 p0289 A73-14523
High resolution radar target recognition, discussing effects of transfer curves of radar signal strength vs display luminance on operator performance

05 p0550 A73-16716
Signal synthesis based on desired autocorrelation function for pulse shaping applications in radar and communications, discussing nonlinear equations solution by decomposition into source polynomials

10 p1187 A73-23730
Applications of vector and parallel computers to radar defense systems.

12 p1476 A73-27822
[ALAA PAPER 73-428]

RAPID - A system for online radar data reduction and performance analysis.

12 p1476 A73-27825
[ALAA PAPER 73-438]
Calculation of the growth and melting of ice particles and the radar signal reflection profiles in cumulonimbus clouds

13 p1653 A73-28878
Side-looking pulse Doppler radar data presuming prior to correlation to obtain desired resolution performance with minimal digital storage

13 p1585 A73-29203
Radar data digital relay from outlying stations to ATC centers for air traffic image integration, discussing computerized plotting and alphanumeric display techniques

15 p1847 A73-32435
ATC radar information processing systems optimization, discussing hard- and software selection criteria

15 p1847 A73-32440
ATC system with radar data processing, discussing hardware and software organization, programmed logic integration possibilities and functional flexibility

15 p1909 A73-32445
Digitized weather radar data models of intense storm cells with 1-2 km resolution and 10 dBZ reflectivity

16 p1983 A73-33727
Holography, radar data and interpreter performance.

17 p2165 A73-34286

Method of detecting meteor streams and associations

19 p2480 A73-37236
Airborne multimode radar digital data system using high transfer rate magnetic tape recording, discussing 8 track tape storage capacity, coding and logic circuits

19 p2431 A73-38198
NAS enroute automated flight and radar data processing, describing communication facilities, computer complex, software, data entry, display function and ATC personnel interface

19 p2453 A73-38464

RADAR DETECTION

Low cost monolithic range gated radar moving target indicator using bucket brigade delay line circuits

02 p0141 A73-12360
Bistatic-radar detection of high-altitude clear-air atmospheric targets.

02 p0142 A73-12526
Equivalence of the likelihood ratio processor, the maximum signal-to-noise ratio filter, and the Wiener filter.

03 p0282 A73-13917
Evaluation of a dual-wavelength radar hail detector.

03 p0337 A73-14505
Radar sequential detector for digital processing of signal masked by noise, determining false alarm and detection probabilities and mean sampling time

04 p0423 A73-15917
Generation of small-scale irregularities in the equatorial electrojet.

07 p0814 A73-19245
Compact laser radar probes the upper atmosphere.

07 p0834 A73-19573
Complex target resolution with the random signal radar.

10 p1189 A73-24560
Electromagnetic window for a trajectory radar

11 p1327 A73-25280
Signal accumulation efficiency for single-site coherent pulse radar moving over earth surface, using Tarasnik approximation of signal/ground clutter ratio for monopulse radars

12 p1467 A73-26944
Range-gated moving target indicator with digital filters.

12 p1469 A73-27161
An optimal algorithm for the detection of radar signals on a noise background of unknown power level

12 p1471 A73-27588
A semicoherent detection and Doppler estimation statistic.

13 p1585 A73-29202
Radar system with spatial/antenna pattern/ and temporal/Doppler filter/ responses adaptively controlled for optimum SNR and detection performance

13 p1586 A73-29213
Fluctuation loss and diversity gain for in-phase systems with post-detection integration.

13 p1586 A73-29218
Book - Introduction to defense radar systems engineering.

13 p1587 A73-29677
Radar technology applied to air traffic control.

14 p1725 A73-29895
Automatic detection radar with false alarm rate regulation capability in log-normal and Weibull clutter under severe environments

16 p1980 A73-33412
Simulation of a multiple element test environment.

16 p1985 A73-33417
USAF Airborne Warning and Control System with overland downlook Doppler radar for low-fly aircraft detection in severe clutter environment, discussing design and performance

17 p1211 A73-34371
Coherent optical processing of linear phased array radar signals.

17 p2132 A73-35649
The Apollo 17 Lunar Sounder.

18 p2288 A73-35959
North polar aurora oval detection by high frequency sounder radar aided by all sky photography and statistical auroral data, discussing backscatter and auroral echoes

18 p2312 A73-36282
Detection probability of laser radars for satellite ranging.

18 p2290 A73-36882
Incoherent radar target extraction in clutter of unknown level by recursive integration for signal and threshold.

18 p2290 A73-37089
Radar and sodar probing of waves and turbulence in statically stable clear-air layers.

19 p2405 A73-38204
The structure of an inversion above a convective boundary layer as observed using high-power pulsed Doppler radar.

19 p2447 A73-38205
Effect of wind shear on atmospheric wave instabilities revealed by FM/CW radar observations.

19 p2447 A73-38206
New developments in FM-CW radar sounding.

19 p2405 A73-38210

Nonbiased rule for detection of radar signals in noise of unknown power.

20 p2529 A73-38928
Oil spill radar scatterometer detection at 13.3 GHz through backscattering cross sections, discussing ground truth, data correlation and wind velocity

20 p2560 A73-39892
Dual wavelength synchronized and slaved radars for hail shaft boundaries detection based on average echo power ratio logarithm range derivative computation

21 p2728 A73-40061
Considerations concerning the evaluation of the detection probability in radar systems

21 p2650 A73-40500
Russian book - Digital methods and systems in radar technology.

21 p2657 A73-41433
Autocorrelation functions for meteorological scatterer velocity measurements in Doppler spectrum from linear, quadratic and logarithmic radar signal detectors

23 p2955 A73-44268

RADAR DIRECTION FINDERS

U RADIO DIRECTION FINDERS

RADAR DISPLAYS

U RADARS COPIES

RADAR ECHOES

NT ANGELS

NT CLUTTER

NT LUNAR RADAR ECHOES

NT VENUS RADAR ECHOES

Simultaneous measurements of radar reflectivity and refractive index spectra in clear air convection.

01 p0018 A73-11060
Results of precipitation backscatter measurements at 1.8 cm with a polarization diversity radar.

03 p0338 A73-14509
Kinematic and thermodynamic structure of thunderstorm, considering updraft, upper air environment, surface features and radar echoes

03 p0338 A73-14511
Use of airborne radar to evaluate hurricane modification experiments.

03 p0338 A73-14513
Echo top height characteristics based on convection cloud reflectivity structures measured by radar

03 p0338 A73-14516
Uncertainties in coherent measurement of the mean frequency and variance of the Doppler spectrum from meteorological echoes.

03 p0279 A73-14525
Coherent signal from incoherent meteorological radar echoes for atmospheric turbulence intensity measurement, noting autocorrelation function for average frequency

03 p0338 A73-14531
An analysis of coexistent waves and turbulence near clear air echoes.

03 p0339 A73-14535
Radar echo in clear air convection shown due to backscattering from fine refractivity fluctuations caused by turbulent mixing

03 p0280 A73-14543
Meteorological echoes movement and evolution measurement potential of conventional radars connected to programmable real time processor

03 p0280 A73-14549
Average return pulse form and bias for the S193 radar altimeter on Skylab as a function of wave conditions.

04 p0446 A73-14804
Atmospheric diffusion, radio meteor trail radius and electron density distribution effects on radar echoes time position, noting recorder resolution increase

05 p0617 A73-16613
Form of the spectrum of radar signals due to precipitation

05 p0552 A73-17356
Updating of numerical precipitation guidance.

06 p0720 A73-18709
Electron drift instabilities in turbulent equatorial electrojet from radar echo observations at 50 MHz

07 p0814 A73-19244
Sierra Nevada mountain lee waves atmospheric structure from lidar, rawinsonde and aircraft observations, delineating atmospheric flow patterns from particulate matter concentrations induced echoes

10 p1245 A73-23988
Field-aligned ionospheric E-region irregularities and sporadic E.

10 p1191 A73-24897
Correction to 'The echo area of a perfectly conducting prolate spheroid.'

11 p1330 A73-25684
VHF Doppler spectra of radar echoes associated with a visual auroral form - Observations and implications.

12 p1468 A73-26996
Quantization and roundoff errors in a digital MTI filter.

13 p1590 A73-28478
Echo signal spectral compression in airborne FM Doppler radar measurement, allowing for flight trajectory and target surface characteristics

13 p1584 A73-28889

RADAR EQUIPMENT

- Radar echo from a 'clear sky' in the decimeter radio wave range 13 p1585 A73-29156
- Correlated clutter and resultant properties of binary signals. 13 p1585 A73-29208
- Electron density phase velocity, drift rate and ion temperatures from radar echoes power spectrum near equatorial electrojet 14 p1748 A73-29972
- Unified theory of type I and II irregularities in the equatorial electrojet. 14 p1748 A73-29973
- The shape of the spectrum of radar echoes from precipitation. 15 p1842 A73-31006
- Radar clutter elimination techniques, considering antenna radiation patterns, resolution cells and Doppler filters 15 p1846 A73-32432
- Real-time estimates of mean velocity by averaging quantized phase displacements of Doppler radar echoes. 17 p2125 A73-35362
- The composite scattering model for radar sea return. 17 p2163 A73-35364
- Stationary target identification with radar beam for comet nucleus within coma, noting echo spatial extent and Doppler bandwidth effects on data processing 17 p2174 A73-35634
- Decomposition of pulse-type data by cepstrum techniques. 17 p2127 A73-35635
- Coherent optical processing of linear phased array radar signals. 17 p2132 A73-35649
- Drift measurement with spectral analysis during period of chemical releases into the ionosphere. 18 p2314 A73-35955
- Analysis and interpretation of aspect-dependent ionospheric radar scatter. 18 p2289 A73-36283
- The staggering of pulse sequences in the case of a pulsed radar providing moving target indication 18 p2289 A73-36399
- The structure of an inversion above a convective boundary layer as observed using high-power pulsed Doppler radar. 19 p2447 A73-38205
- VHF radar aurora echo Doppler spectral properties, discussing electron density irregularities, echo power spectra, drift velocity, two stream instability and convection hypothesis 20 p2553 A73-38962
- Dual wavelength synchronized and slaved radars for hail shaft boundaries detection based on average echo power ratio logarithm range derivative computation 21 p2728 A73-40061
- Basic principles and the theory of operation of the equipment for the identification-friend or foe (SIF) in military aircraft 21 p2650 A73-40348
- Electronic moving-target selection systems 21 p2651 A73-40512
- The comparison of sensitivities of atmospheric echo-sounders. 22 p2862 A73-42727
- ## RADAR EQUIPMENT
- NT PLAN POSITION INDICATORS
- NT RADAR ANTENNAS
- NT RADAR BEACONS
- NT RADAR FILTERS
- NT RADAR RECEIVERS
- NT RADAR REFLECTORS
- NT RADAR TRANSMITTERS
- NT RADARSCOPES
- Recent advances in diode and ferrite phaser technology for phased-array radars. II. 01 p0024 A73-10720
- Radar engineering developments, discussing microwave and optical systems, plan position indicators, antennas, displays, receivers, transmitters, solid state IC devices and signal processing 06 p0668 A73-18440
- Tracking radar equipment evolution in connection with French space program development, describing reliability technology 07 p0807 A73-18943
- Minimum performance standards - Airborne distance measuring equipment /DME/ operating within the radio-frequency range of 960-1215 megahertz. 07 p0849 A73-19575
- Russian book on pulse radar circuits covering signal and device characteristics, shaping circuits, amplifiers, limiters, frequency dividers and generators 07 p0794 A73-20231
- Use of a surface-acoustic-wave delay line to provide pseudocoherence in a clutter-reference pulse doppler radar. 08 p0939 A73-21113
- Radar systems development under solid state electronics advances impact, discussing silicon ICs, HF transistors, hybrid microwave circuits, parametric amplifiers and p-i-n diodes applications 08 p0949 A73-21650

- Computer control of a multifunction radar. 13 p1587 A73-28619
- Automatic checkout and monitoring in the AN TPQ-27 radar system. 13 p1585 A73-29210
- Book - Introduction to defense radar systems engineering. 13 p1587 A73-29677
- Vibration and shock qualification testing of an airborne early warning radar. 16 p1987 A73-33137
- AEGIS AN/SPY-1 radar system - Design for availability. 16 p1980 A73-33607
- Airborne air to air and air to ground fire control radar systems for all-weather fighter aircraft, emphasizing cost effectiveness through modularity and commonality 16 p1985 A73-34041
- Techniques for digital-microwave hybrid real-time radar simulation. 17 p2131 A73-35303
- VM 256 - Experimental system of a 3-D radar installation 18 p2335 A73-37040
- Noise processes in a homing radar seeker. 18 p2290 A73-37088
- Secondary surveillance radar - Current usage and improvements. 19 p2451 A73-37808
- Evaluation of effects of the microwave oven /915 and 2450 MHz/ and radar /2810 and 3050 MHz/ electromagnetic radiation on noncompetitive cardiac pacemakers. 20 p2520 A73-39824
- Monopulse radar equipment 21 p2651 A73-40511
- Surface acoustic wave devices and applications. II - Pulse compression systems. 21 p2703 A73-41137
- ## RADAR FILTERS
- Theory and practice of the signal processor in surveillance radars 05 p0550 A73-16473
- Recursive MTI radar filter design for sharp spectrum rolloff and flat pass band, investigating clutter rejection performance vs spectral spread 05 p0558 A73-16808
- Moving-target-indicator recursive radar filter using bucket-brigade circuits. 09 p1065 A73-23096
- Radar filter asymptotic efficiency analysis for pass-band and impulse response duration increase, considering realization of approximate Urkowitz filter with controlled memory 10 p1194 A73-23737
- Optimal control theory for constant gain radar filter design with weighted variance average minimization comparable with Kalman filter performance 11 p1339 A73-26643
- The design and applications of highly dispersive acoustic surface-wave filters. 12 p1484 A73-27564
- Potential applications of acoustic matched filters to air-traffic control systems. 12 p1522 A73-27572
- Improvements in surface-acoustic-wave pulse-compression filters. 13 p1595 A73-28048
- Optimum mismatched filters for sidelobe suppression. 13 p1593 A73-29209
- Radar system with spatial /antenna pattern/ and temporal /Doppler filter/ responses adaptively controlled for optimum SNR and detection performance 13 p1586 A73-29213
- MTI radar filter with adaptively controlled double canceller for frequency shifted clutter spectra effects minimization 13 p1594 A73-29222
- Radar clutter elimination techniques, considering antenna radiation patterns, resolution cells and Doppler filters 15 p1846 A73-32432
- Application of surface acoustic wave devices to radar. 17 p2140 A73-35319
- Signal filtering using hard-limited digital processing. II - Performance with a single target in a coloured-noise background. 20 p2530 A73-39126

RADAR IMAGERY

- Computerized airborne multilateration radar with wide-beam antenna and narrow pulsewidth for high resolution terrain image mapping 01 p0019 A73-11479
- Side-look radar provides a new tool for topographic and geological surveys. 02 p0140 A73-11850
- Imaging radar techniques for remote sensing applications. 03 p0278 A73-14486
- Automated procedures for mapping and display of digitized radar data. 03 p0281 A73-14522

- Lunar maps from CW radar imagery by aperture synthesis method at long wavelengths, noting depolarized return from highland regions 04 p0417 A73-15178
- Topographic earth observations using radar techniques with a single flight. 04 p0419 A73-15403
- Applications of the discriminant function in automatic pattern recognition of side-looking radar imagery. 05 p0553 A73-16289
- Visual time compression. II - Detecting moving targets in dense radar ground clutter. [AD-753746] 05 p0550 A73-16715
- Synthetic aperture SLAR systems and their application for regional resources analysis. 05 p0578 A73-17133
- The use of a simulator in a synthetic aperture radar data processing tradeoff study. 05 p0554 A73-17149
- Principles of synthetic-aperture radar 05 p0552 A73-17267
- Coherent optical processing and display techniques for microwave imagery generation from synthetic aperture radar system data, discussing hologram and side-looking radar 06 p0667 A73-18279
- Radar imagery and aerial photography for geological remote sensing applications in coastal mapping, land-form analysis, engineering and reconnaissance 06 p0667 A73-18282
- Radar imagery and supporting aerial photography tests for topographic mapping capabilities and metric quality of side-looking stereo radar system 06 p0667 A73-18283
- Similarities and differences in the interpretation of air photos and SLAR imagery. 06 p0693 A73-18284
- Clustering phenomena in side-looking radar /SLR/ microtexture. 06 p0667 A73-18285
- Analysis and interpretation of air-borne multi-frequency side-looking radar sea ice imagery. 09 p1080 A73-22150
- Imaging properties of monostatic and bistatic troposcatter radars. 09 p1050 A73-22426
- Range-azimuth-coupling aberrations in pulse-scanned imaging systems. 10 p1188 A73-23833
- Toros side-looking radar system for sea-ice distribution and geomorphological mapping and agricultural soil studies 12 p1474 A73-27962
- Mapping of mangrove and perpendicular-oriented shell reefs in southeastern Panama with side-looking radar. 13 p1606 A73-28170
- Cloud research by radar, describing tracking, imaging and Doppler techniques 15 p1904 A73-31748
- Radiogoniometric vectors superposition on ATC Doppler radar image, noting direction finding display availability and echoes identification 15 p1847 A73-32438
- Application of the visualization of radar information in television 15 p1911 A73-32484
- Mapping with coherent-radiation focused synthetic-aperture side-looking radar. 16 p2015 A73-33357
- Controlled-quality images from synthetic-aperture radar data. 16 p2015 A73-33358
- Holography, radar data and interpreter performance. 17 p2165 A73-34286
- On radar mapping of sea surface. 17 p2123 A73-35153
- Pattern recognition techniques suggested from psychological correlates of a model of the human visual system. 17 p2116 A73-35241
- Mission planning for remote exploration of the surface of Venus. [AIAA PAPER 73-580] 18 p2350 A73-36072
- Hologram matrix and its application to a novel radar. 19 p2428 A73-37145
- Two-dimensional statistic analysis of radar imagery of sea ice. 20 p2556 A73-39843
- Relationship between sea wave parameters and the spectra of aerial photography and radar imagery of sea surface. 20 p2531 A73-39891
- Polar region soil moisture content remote sensing based on electromagnetic backscattering and depolarization by ice and terrain, considering radar, microwave and IR sensors 21 p2654 A73-40814
- Radio techniques applied to oceanography and earth science - Oceanic wind measurement and overland imaging as examples. 21 p2654 A73-40817

An improved single flight technique for radar stereo.
23 p2953 A73-43449
Book - The surveillant science: Remote sensing of the environment.
23 p2971 A73-43605

RADAR MAPS
NT RADAR IMAGERY
Computerized airborne multilateration radar with wide-beam antenna and narrow pulsewidth for high resolution terrain image mapping
01 p0019 A73-11479
Lunar radar mapping at 162.4 MHz from Jodrell Bank observations in January and February 1970, discussing depolarized returns
03 p0368 A73-13084
Lunar topography - Global determination by radar.
03 p0378 A73-14445
Radar brightness mapping of Venus surface, noting roughness of terrain from polarization studies and signal processing for extraction of echo power
06 p0744 A73-17440
Radar techniques for planetary mapping with orbiting vehicle.
06 p0664 A73-18011
Radar imagery and supporting aerial photography tests for topographic mapping capabilities and metric quality of side-looking stereo radar system
06 p0667 A73-18283
Light aircraft-borne low cost phased array X band radar and display design requirements for weather detection and ground mapping
15 p1909 A73-32451
Mapping with coherent-radiation focused synthetic-aperture side-looking radar.
16 p2015 A73-33357
On radar mapping of sea surface.
17 p2123 A73-35153
Monopulse radar equipment
21 p2651 A73-40511
Mapping of North Atlantic winds by HF radar sea backscatter interpretation.
22 p2882 A73-41836
Planetary surface reflectivity and topography mapping by ground based radar with emphasis on observational methods
23 p2953 A73-43353

RADAR MEASUREMENT
Simultaneous measurements of radar reflectivity and refractive index spectra in clear air convection.
01 p0018 A73-11060
Daytime laser radar measurements of the atmospheric sodium layer.
02 p0157 A73-11875
E region electromagnetic east-west drift velocity measurement at magnetic equator by incoherent scatter radar
02 p0161 A73-12285
Radar measurement of ionosphere motion in the presence of current-induced spectral asymmetries.
02 p0143 A73-12532
Radio aurora aspect sensitivity from radar VHF measurement error analysis
03 p0300 A73-13692
Frequency discriminator use for range measurements with FM radar systems, deriving reflecting target distance relationship to output voltage
03 p0278 A73-14028
Lunar topography - First radar-interferometer measurements of the Alphonsus-Ptolemaeus-Arzachel region.
03 p0378 A73-14446
Pulse Doppler radar observations of hailstone maximum diameters as function of time
03 p0337 A73-14506
Doppler radar evidence of severe storm high-reflectivity cores acting as obstacles to airflow.
03 p0337 A73-14507
Measurement of wind gradients in convective storms by Doppler radar.
03 p0278 A73-14508
Echo top height characteristics based on convection cloud reflectivity structures measured by radar
03 p0338 A73-14516
Radar measurement errors due to rain attenuation compensation and improper system calibration, discussing error reduction procedures
03 p0279 A73-14518
Multiple contrail streamers observed by radar.
03 p0279 A73-14519
Simultaneous quantitative measurements of rainfall rate and drop size distribution by X-band radar and drop distrometer /system Joss-Waldvogel/ at two rain gauge equipped places near to Bonn/West Germany.
03 p0338 A73-14520
A modified coefficient for the weather radar equation.
03 p0279 A73-14526
High power radar for measurement of refractivity inhomogeneities in clear air turbulence from backscattered energy Doppler shift
03 p0338 A73-14530
Coherent signal from incoherent meteorological radar echoes for atmospheric turbulence intensity measurement, noting autocorrelation function for average frequency
03 p0338 A73-14531

Doppler radar measurements of the velocity field associated with a turbulent clear air layer.
03 p0338 A73-14532
Measurement of small-scale turbulence and thermal stability in the lower atmosphere by radar.
03 p0279 A73-14536
Radar measurement of the atmospheric turbulence structure function.
03 p0279 A73-14537
Inverse problem in the theory of turbulence filtering by the radar pulse volume.
03 p0279 A73-14538
The effects of a finite radar pulse volume on turbulence measurements.
03 p0279 A73-14540
Simultaneous FM-CW radar and lidar observations of climatological regions, convective activity, cloud echoes, layered structures, insects and breaking Kelvin-Helmholtz waves
03 p0280 A73-14545
Meteorological echoes movement and evolution measurement potential of conventional radars connected to programmable real time processor
03 p0280 A73-14549
Geos-C mini arc orbit determination from radar altimeter observations under perturbations from gravitational anomalies
04 p0437 A73-14784
Martian topography from radar observations and the Mariner 6 and 7 and ground-based CO2 measurements.
04 p0503 A73-16016
Interferometric CW radar for group delay difference measurement of reflected signal components in ionospheric sounding
05 p0548 A73-16253
Acoustic sounding of meteorological phenomena in the planetary boundary layer.
06 p0721 A73-18710
Venus - Radar determination of gravity potential.
07 p0875 A73-19167
Two-beam observations of ionospheric irregularity structure and velocity at Arecibo.
07 p0791 A73-19379
Determination of the velocity of a radio meteor with minimum rms error.
08 p1012 A73-21581
Modulation Langmuir probe and incoherent scatter radar measurements of ionospheric electron temperature.
09 p1075 A73-22128
Ground based radar measurement of Martian topography, surface temperature and thermal properties by microwave and IR radiometry and spectral reflectivity observation
09 p1144 A73-22259
Radar measurement of altitude profiles and reflected power for Martian topography and surface properties, noting heavy cratering
09 p1144 A73-22260
High resolution radar observation of Martian surface topography and scattering properties, noting dielectric constant and rms surface slope variations
09 p1144 A73-22261
Radar direction measurements by phase comparison of ultrasonic echo pulses reflected from targets in water tank, using piezoelectric sensors for receiving antennas simulation
10 p1194 A73-23736
Multistatic incoherent scatter measurements of ionospheric drift velocity.
10 p1188 A73-24274
Bistatic-radar estimation of surface-slope probability distributions with applications to the moon.
10 p1190 A73-24892
Remote measurement of wind speed by laser Doppler systems.
11 p1375 A73-25062
Radio-echo measurements of the flux of the Quadrantid, Perseid and Geminid meteor streams.
11 p1415 A73-25169
Large scale surface structure of Mars.
11 p1417 A73-25268
Utilization of the Doppler effect to measure the drift angle and the ground speed of an aircraft
11 p1305 A73-25797
Optimum processor accuracy for radar altimetry for geodesy over sea, considering surface reflectivity, height variation additive noise and pointing errors
11 p1371 A73-26631
Measurements of distributed targets with the random signal radar.
11 p1332 A73-26632
Observation of Raman scattering by SO2 in a generating plant stack plume.
13 p1607 A73-28547
Definition and radar measurement of the parameters characterizing the cloud environment of a launch base.
14 p1743 A73-30114
Millstone Hill Thomson scatter results for 1966 and 1967.
15 p1866 A73-31067
Observations of aerosol layers in the upper atmosphere by laser radar.
15 p1868 A73-31383

Incoherent scatter observations of the ionosphere over Chatanika, Alaska.
16 p2004 A73-33442
Radar observations of Venus at 3.8 cm
16 p2067 A73-33806
Computer analysis of reflected signals obtained during radar sounding of Venus
16 p2067 A73-33807
Certain results of a combined treatment of the Venera 4 interplanetary probe and ground-based radio-astronomical and radar measurements
16 p2068 A73-33819
Interpretation of radar measurements of Venus in the microwave range
16 p2068 A73-33820
Doppler radar measurements and observations of precipitation velocity fields.
17 p2125 A73-35361
Atmospheric density values from radar-determined low altitude satellite orbit decay and accelerometer data
18 p2302 A73-35942
Meteor radar observations of long period waves in the 80-100 km altitudes range.
18 p2304 A73-35968
Results of simultaneous wind velocity profile measurements in the lower thermosphere by the meteor radar and rocket methods.
18 p2310 A73-36130
Results of air temperature, density and pressure measurements obtained with the aid of foil cloud sensors in the height region between 80 and 95 km.
18 p2311 A73-36179
Comparison of satellite-measured and radar-observed cloud-top heights.
18 p2334 A73-37066
HF radar observations of cesium plasma cloud released from the rocket K-9 M-39.
19 p2423 A73-37378
Capabilities of radar, sodar and lidar for measuring the structure and motion of the stably stratified atmosphere.
19 p2405 A73-38239
Minor planets and related objects. XII - Radar observations of /1685/ Toro.
20 p2607 A73-39122
Tall buildings induced microwave scattering coefficient measurement with helicopter-borne bistatic pulse radar, explaining coefficient dependence on azimuth, elevation and range
20 p2530 A73-39127
Integral moisture content determination in rain clouds by simultaneous thermal radiation and radar measurements
20 p2584 A73-39190
Dual frequency bistatic radar lunar investigations from Apollo 14 and 15 echo spectra
20 p2612 A73-39714
Locating large masses of ground ice with an impulse radar system.
20 p2556 A73-39841
High resolution measurements of snowpack stratigraphy using a short pulse radar.
20 p2556 A73-39842
Satellite based ATC system with radar range and rate measurements, analyzing errors due to ground station position, transponder delay time and atmospheric refraction uncertainties
21 p2735 A73-40042
Daytime applications of Raman technique of laser backscatter to measure atmospheric composition profiles
21 p2729 A73-40067
Bounds estimation for normalized second spectral moment of random radar signal process in terms of measured quantities statistics without weighting
21 p2650 A73-40343
Basic principles and the theory of operation of the equipment for the identification-friend or foe /SIF/ in military aircraft
21 p2650 A73-40348
Comparison of Apollo and earth-based observations - Definition of surface units in Mare Serenitatis.
21 p2769 A73-40821
Measurements of thermospheric temperatures by incoherent scatter radar.
21 p2688 A73-41346
Waves and tides and their observation from ground and space.
21 p2689 A73-41356
Results of radar experiments performed on automatic stations Luna 16 and Luna 17.
21 p2774 A73-41401
Two frequency radar interferometry applied to the measurement of ocean wave height.
22 p2843 A73-41832
The combined use of satellite differential Doppler and ground-based measurements for ionospheric studies.
22 p2843 A73-41837
Solar corona plasma temperature estimation from ground observations based on ionization theory, line width, radio and radar measurements and hydrostatic equilibrium assumption
22 p2906 A73-42067

RADAR NAVIGATION

Radar altimeter signal propagation delay estimation, calculating and plotting noise fluctuation characteristics as function of aircraft ground speed, altitude and other parameters

22 p2828 A73-43067

Forward scatter CW radar effectiveness for cross path wind velocity profile measurements compared with radiosonde and pilot balloon observations

23 p3004 A73-44261

A comparison of radar-determined cloud height and reflected solar radiance measured from the geosynchronous satellite ATS-3.

23 p3005 A73-44269

On the variation with height of the top brightness of precipitating convective clouds.

23 p3005 A73-44270

Optical radar measurements of meteorological parameters and air pollution related to environment protection, using Raman effect and resonance and Mie scattering

24 p3096 A73-44896

Electric field observations by incoherent scatter radar in the auroral zone.

24 p3085 A73-45117

Nighttime sporadic E layer measurements and integrated content measurements at Arecibo Observatory, using Barker coded incoherent scatter radar pulses

24 p3087 A73-45142

Measurement of short distances with optical pulse radars

24 p3069 A73-45467

RADAR NAVIGATION

Radar correlation navigation map matching systems for civilian and military application, noting preprocessing aspects

06 p0721 A73-18280

Radio navigation review, discussing Decca, Loran, Omega, VOR/DME, satellite, inertial, integrated, area, approach and landing, collision avoidance and space navigation systems

10 p1246 A73-23636

A new approach to Doppler-inertial navigation /Doppler Beam Sampling/.

12 p1522 A73-27162

Aircraft terminal approach and entry spacing systems supported by automated terminal radar using area navigation techniques

17 p2210 A73-35852

United States en route air traffic control systems.

19 p2451 A73-37810

ARTS II automated air traffic control systems.

19 p2453 A73-38463

RADAR OBSERVATION

U RADAR TRACKING

RADAR PHOTOGRAPHY

Lunar photography - Global determination by radar.

03 p0378 A73-14445

Computerized analyses of radar photographs.

03 p0281 A73-14524

Aerial radar photograph restitution for photogrammetric application, discussing geometric qualities and methods and instruments for partial removal of distortion

12 p1502 A73-27972

RADAR RANGE

Solar-planetary system mechanical parameters determination based on astronomical unit, discussing conversion into terrestrial units via radar distance measurements

03 p0376 A73-14174

FM-CW radar range measurement at 10-micron wavelength.

03 p0278 A73-14459

Multiple target CW FM Doppler radar with solid state devices and CRT indicator, noting range resolution advantage over pulse radar

12 p1469 A73-27164

Optimum mismatched filters for sidelobe suppression.

13 p1593 A73-29209

Atmospheric lens effect - Another loss for the radar range equation.

16 p1980 A73-33407

Effects of modulation nonlinearity on the range response of FM radars.

21 p2650 A73-40341

RADAR RECEIVERS

Phase and amplitude balance - Key to image rejection mixers.

02 p0148 A73-12571

Cell averaging constant-false-alarm-rate radar receiver with noise estimated from logarithmic detector output, determining performance in Gaussian noise by Monte Carlo simulation

03 p0277 A73-13910

A modified coefficient for the weather radar equation.

03 p0279 A73-14526

Theory and practice of the signal processor in surveillance radars

05 p0550 A73-16473

Optimal and suboptimal systems for detecting fluctuating optical radar pulses.

06 p0668 A73-18393

Dynamic AGC correction for angle signal variations in monopulse radar receivers with reference signal, analyzing signal statistics

12 p1469 A73-27163

Detection of Doppler signals by a receiver which incorporates a counter of the number of excursions of additive noise.

13 p1583 A73-28728

Application of surface acoustic wave devices to radar.

17 p2140 A73-35319

RADAR RECEPTION

Receiving antenna polarization parameters selection in side-looking synthetic aperture radars

04 p0423 A73-15914

The effect of weighting upon signal-to-noise ratio in pulse bursts.

21 p2649 A73-40327

RADAR REFLECTIONS

U RADAR ECHOES

RADAR REFLECTORS

Surveillance radar cosecant reflectors electromagnetic energy emission distribution, discussing design and directional characteristics

05 p0550 A73-16474

RADAR RESOLUTION

Application of the spatial spectral power density to the calculation of resolution limits.

03 p0277 A73-13916

Microwave remote sensor technology review, discussing target-sensor interaction, spatial resolution concepts and meteorological applications of radiometric and radar systems

06 p0667 A73-18278

Lidar illuminator/sensor system for range and/or angle spatial resolution enhancement, discussing pulse shape, optical characteristics and atmospheric effects on performance

06 p0667 A73-18303

Imaging properties of monostatic and bistatic troposcatter radars.

09 p1050 A73-22426

Theory of incoherent-scatter measurements using compressed pulses.

09 p1050 A73-22429

FM laser noise effects on optical Doppler radar systems.

11 p1333 A73-26639

Multiple target CW FM Doppler radar with solid state devices and CRT indicator, noting range resolution advantage over pulse radar

12 p1469 A73-27164

Side-looking pulse Doppler radar data presuming prior to correlation to obtain desired resolution performance with minimal digital storage

13 p1585 A73-29203

Radar clutter elimination techniques, considering antenna radiation patterns, resolution cells and Doppler filters

15 p1846 A73-32432

On the angular resolution of a search radar with a mechanically rotated antenna.

17 p2125 A73-35369

Use of pulse compression in mapping-type radars.

17 p2127 A73-35632

Analysis of optimal recognition of space-time signals.

17 p2130 A73-35721

Mean square and reflectivity variance decrease due to radar beam smoothing and post-detection integration in terms of reflectivity fields autocorrelation function

18 p2333 A73-36706

RADAR SCANNING

Mobile FM-CW radar sounder with scanning capability for high resolution remote sensing in lower troposphere, discussing design and performance

02 p0140 A73-11959

Remote sensor for atmospheric physical properties with FM-CW scanning radar, parabolic antennas and waveguide feeds for linear and circular polarization

03 p0339 A73-14544

The concentric double spherical reflector as an antenna for simple scanning over a limited angular range

10 p1187 A73-23739

Determination of the maximum scan-gain contours of a beam-scanning paraboloid and their relation to the Petzval surface.

11 p1328 A73-25651

Radar scatterer ensemble cross section centroid tracking by raster scan observation technique, estimating mean-squared dimensions

11 p1333 A73-26644

Optimal search scanning for electronic surveillance radar based on antenna beam position with highest echo signal for maximum likelihood target acquisition

13 p1581 A73-27999

Pulse coded scanning beam microwave landing system technology assessment for civil aviation application, describing ground equipment and procedures

15 p1910 A73-32469

Clutter spectra of low PRF AMTI pulse-Doppler radar.

16 p1980 A73-33413

Reflection coefficients for wires, cables, ropes and chains from scanning laser radar, discussing wire avoidance system for airplanes and helicopters

17 p2210 A73-35421

Ultraviolet, panchromatic, infrared and radar remote sensing of Mesabi Range /Minnesota/, discussing Precambrian rock formations, geological faults, predawn and daytime photography and vegetation patterns

20 p2561 A73-39894

RADAR SCATTERING

A comparison of precipitation attenuation and radar backscatter along earth-space paths.

01 p0015 A73-10183

Backscatter from snow and ice surfaces at near incident angles.

01 p0016 A73-10191

Acoustic-Doppler-radar scattering equation and general solution.

03 p0276 A73-13830

Meteorological structure of thin clear air scatter layers observed by ultra-high resolution radar.

03 p0338 A73-14529

Modeling of the radar scattering characteristics of aircraft.

04 p0416 A73-15057

Doppler spectral width of radar signal reflected from sea surface as function of illuminated region dimensions, waviness scale and emission factors

04 p0423 A73-15913

Form of the spectrum of radar signals due to precipitation

05 p0552 A73-17356

Comparison of Te and Ti from Ogo 6 and from various incoherent scatter radars.

07 p0790 A73-19241

Low noise VHF preamplifier design for backscatter radar, presenting circuit diagram

07 p0801 A73-19536

Influence of the geometrical parameters of a lidar on the applicability of single-scattering approximation

08 p0986 A73-21457

High resolution radar observation of Martian surface topography and scattering properties, noting dielectric constant and rms surface slope variations

09 p1144 A73-22261

A theory of tracking for a dynamic radar scatterer ensemble.

10 p1189 A73-24532

Measurements of distributed targets with the random signal radar.

11 p1332 A73-26632

Radar scatterer ensemble cross section centroid tracking by raster scan observation technique, estimating mean-squared dimensions

11 p1333 A73-26644

Faraday effect of incoherently scattered radar signals.

13 p1583 A73-28712

Detection of oil spills using a 13.3-GHz radar scatterometer.

13 p1610 A73-29196

Amplitude modulation effects of the Doppler return at low altitudes.

13 p1586 A73-29223

The shape of the spectrum of radar echoes from precipitation.

15 p1842 A73-31006

Incoherent scatter observations of the ionosphere over Chatanika, Alaska.

16 p2004 A73-33442

The composite scattering model for radar sea return.

17 p2163 A73-35364

Analysis and interpretation of aspect-dependent ionospheric radar scatter.

18 p2289 A73-36283

Limits of applicability of the Delano model for describing the process of wave scattering by a complex-shaped body

19 p2407 A73-38343

Multipath channel characterization for Aerosat.

20 p2526 A73-38755

Tall buildings induced microwave scattering coefficient measurement with helicopter-borne bistatic pulse radar, explaining coefficient dependence on azimuth, elevation and range

20 p2530 A73-39127

Ultrahigh frequency radar scattering by perfectly conducting conical pyramidal noded bodies, deriving polarized radar cross sections via wedge diffracted field integration

22 p2824 A73-41854

Low albedo lunar areas, discussing spectral reflectivity, radar backscatter characteristics and Apollo 17 landing site

22 p2909 A73-42495

Autocorrelation functions for meteorological scatterer velocity measurements in Doppler spectrum from linear, quadratic and logarithmic radar signal detectors

23 p2955 A73-44268

RADAR SIGNATURES
Correction to 'The echo area of a perfectly conducting prolate spheroid.'

11 p1330 A73-25684

Doppler radar measurements and observations of precipitation velocity fields. 17 p2125 A73-35361

Use of pulse compression in mapping-type radars. 17 p2127 A73-35632

RADAR TARGETS

High resolution radar target recognition, discussing effects of transfer curves of radar signal strength vs display luminance on operator performance 05 p0550 A73-16716

Microwave remote sensor technology review, discussing target-sensor interaction, spatial resolution concepts and meteorological applications of radiometric and radar systems 06 p0667 A73-18278

Measurements of distributed targets with the random signal radar. 11 p1332 A73-26632

Fluctuation loss and diversity gain for in-phase systems with post-detection integration. 13 p1586 A73-29218

Calculation of probability of detection with target scintillation. 13 p1586 A73-29219

Accuracy of target angular coordinate estimates by the maximum likelihood method on a correlated noise background 14 p1729 A73-30557

Air traffic control, discussing man machine systems, multipath with ILS, target indicator radars and flight progress strip preparation 17 p2206 A73-34086

Polarization of signals which are reflected from a group of independently fluctuating targets. 20 p2529 A73-38927

Circular synthetic radar with interferometer elements mounted at ends of horizontal boom rotating about vertical mast, predicting echo response to point and multiple targets 21 p2650 A73-40342

The effect of staggered PRF's on MTI signal detection. 21 p2650 A73-40344

Use of a digital computer for studying velocity judgements of radar targets. 23 p2948 A73-43213

Octave bandwidth microwave spectral response. 24 p3068 A73-44996

RADAR TRACKING

Influence of selectivity on the observed orbital-parameter distribution of radio meteors 01 p0101 A73-10846

Radar observations of intense undulance in an evaporating cloud layer. 03 p0339 A73-14541

Intensive probing of clear air convective fields by radar and instrumented drone aircraft. 03 p0339 A73-14542

Digital modeling of multipath induced monopulse angle tracking errors. 04 p0416 A73-15056

Tunable dye laser radar observation for Na layer nocturnal vertical distribution, suggesting meteor shower effect on layer content increase 04 p0444 A73-15543

Russian book on aircraft control systems covering radio communication and navigation, automatic guidance and landing and homing and radar tracking. 04 p0474 A73-15964

Apparatus replicating and extending development work on real-time time-compressed radar observation processor and display system 05 p0576 A73-16714

Possibility of radar observation of nonlinear wave interaction in ionospheric plasma 05 p0570 A73-17023

Electronically controlled phased arrays for radar tracking systems, considering military, earth resources and planetary topography applications 06 p0677 A73-18447

Earth-moon mass ratio from Mariner 9 radio tracking data. 07 p0899 A73-20156

Adaptive nonlinear filtering for tracking with measurements of uncertain origin. 07 p0805 A73-20584

Choosing the optimal distribution of radar and optical observations of Venus 09 p1142 A73-22091

A mobile tone range/RDF system for telemetry tracking of sounding rockets. 09 p1057 A73-23412

Determination of upper atmosphere parameters from measurements of the ambipolar diffusion coefficient by radar observations of meteor trails. 10 p1212 A73-24223

A brief survey of monopulse techniques. 11 p1331 A73-26148

Radar scatterer ensemble cross section centroid tracking by raster scan observation technique, estimating mean-squared dimensions 11 p1333 A73-26644

Balloon-aircraft ranging, data, and voice experiment. 12 p1473 A73-27680

Space geodetic techniques since 1957 covering photography, radar and laser uses in satellite observations with geodetic applications 13 p1671 A73-28006

Wind profile measurements in proximity of a moderate storm. 13 p1651 A73-28205

Corrugated circular waveguide horn as monopulse antenna feed for optimal tracking performance, using difference-sum patterns with hybrid modes 14 p1731 A73-29705

Meteor streams and comet orbital statistics from radar observations during 1967-1968 14 p1795 A73-29847

A proposal on automatic tracking of an aircraft for the radar. 14 p1728 A73-30471

Effect of selectivity on the observed distribution of orbital parameters for radio meteors. 15 p1928 A73-30982

Automatic radar terminal system /ARTS/ for high density ATC centers, noting improved target identification and alphanumeric data display 15 p1907 A73-31133

Cloud research by radar, describing tracking, imaging and Doppler techniques 15 p1904 A73-31748

Use of associative processors for radar data processing in air traffic control systems. 15 p1849 A73-32434

Memorization and model change, alpha-beta, adaptive model and Kalman type radar pursuit tracking techniques efficiency comparison 15 p1908 A73-32443

The London Air Traffic Control Centre radar data processing system. 15 p1911 A73-32485

Simulation results for a radar multipath angle error reduction method. 17 p2127 A73-35633

FM-CW ground and aircraft radar observations of clear air echo strata, examining turbulence levels, Richardson number, turbulent scattering, radar reflectance and power spectra 19 p2427 A73-38203

ATC enroute automation program using radar tracking and computer readout system, describing terminal traffic control, wake vortices and aircraft spacing 19 p2453 A73-38439

Suboptimal algorithms for nonlinear smoothing. 21 p2669 A73-40333

Electronic moving-target selection systems 21 p2651 A73-40512

A method of optimization of algorithms for secondary processing of radio signals 21 p2656 A73-41129

Results of simultaneous wind measurements in the stratosphere, mesosphere and low thermosphere. 21 p2732 A73-41340

Octave-bandwidth, acoustic M/W frequency-memory loop. 22 p2834 A73-42873

The accuracy of phase-comparison angle tracking by phased-array antennas 24 p3071 A73-44594

RADAR TRANSMISSION

A study of tropospheric radar propagation characteristics during an unusual spell of persistent dust haze followed by thunderstorm over Delhi during May 1966. 03 p0280 A73-14547

High power latching ferrite phase shifters for AEGIS. 13 p1591 A73-28620

Opto-acoustic signal processors extend radar and communication system capabilities. 14 p1729 A73-30675

Cross polarization in radomes - A program for its computation. 15 p1851 A73-31730

Huffman binary codes for pulse compression radar, evaluating ambiguity or cross correlation by computer program for replicas formation performance 17 p2131 A73-35221

Russian book on radar signal synthesis optimization problems covering proximity criterion, ambiguity and autocorrelation functions and FM and PSK signals 21 p2650 A73-40419

Interplanetary radar time delays in different theories of gravitation. 23 p3032 A73-43842

RADAR TRANSMITTERS

Linear FM pulses in chirp radar transmitter, calculating and plotting bounds on amplitude, energy and power spectra for electromagnetic compatibility analysis 08 p0949 A73-21665

Microwave transmitter tubes for surface-based and airborne radar applications, considering ATC, output power, stability, spectrum, size, weight, reliability, maintainability and cost requirements 13 p1590 A73-28532

TWT for air-to-air missile fire control radar transmitter application, considering high average power, RF gain and PPM focusing requirements 14 p1737 A73-30624

Crossed field amplifier selection for application to pulsed radar transmitters, considering system operation effects, power supply regulation and droop limitation method 16 p1991 A73-33899

Mobile IC coherent radar with computerized display and calibration, incorporating cold cathode crossed field amplifier tube in transmitter amplifier stage 20 p2528 A73-38871

High power airborne radar CW tube-transmitter interface failures due to design, maintenance, handling and environment effects 22 p2834 A73-42875

RADARSOPES

NT PLAN POSITION INDICATORS

Human factors evaluation of labelled radar displays. 03 p0268 A73-14155

Visual time compression. II - Detecting moving targets in dense radar ground clutter. 05 p0550 A73-16715

Techniques for simulation of radar displays. 12 p1475 A73-27132

Automatic radar terminal system /ARTS/ for high density ATC centers, noting improved target identification and alphanumeric data display 15 p1907 A73-31133

Mobile IC coherent radar with computerized display and calibration, incorporating cold cathode crossed field amplifier tube in transmitter amplifier stage 20 p2528 A73-38871

RADIAL DISTRIBUTION

Radial density distribution and luminosity functions for stars in alpha Persei cluster 01 p0106 A73-11320

Optimum performance of static propellers and rotors. 03 p0242 A73-13308

Infrared observations of Comets Ikeya-Seki /1965f/ and Bennett /1969i/. 04 p0494 A73-14755

Radial concentration profiles of NO and combustion products formation in laminar diffusion flames, using vertical coaxial burner and quartz microprobe 06 p0740 A73-17730

New procedure for measuring the radial temperature distribution in inhomogeneous and unsteady plasma columns with considerable self-absorption 06 p0728 A73-17913

Radial anode current density distribution measurement in high current pulsed arcs in air on copper split anode, using Rogowski coils 06 p0723 A73-18357

Earth electrical conductivity radial distribution effect on solar quiet day geomagnetic field variations 07 p0816 A73-19466

The heliocentric radial gradient in cosmic ray density and the 'Swinson' sidereal time variation. 07 p0870 A73-19671

Flow equation for axisymmetric compressible fluid flow in conical turbine stage, calculating radial distribution of flow velocity 07 p0868 A73-20088

The radial amplification profile of the 4880-A ionic laser line and the distribution of the charge carriers in the wall-stabilized Ar low-pressure arc column 08 p0989 A73-20786

Radial pulsations of a white dwarf in the case of nonuniform rotation 09 p1145 A73-22290

Method of calculating yield for LSI arrays considering radial distribution of defects on wafers. 10 p1193 A73-23668

Three phase alternators with two/four poles superconducting inductors and with outer/inner induction winding, determining magnetic field radial distribution 10 p1177 A73-24411

Measurement of the potential distribution in the vicinity of an electron beam with the aid of a thermal probe 10 p1258 A73-24889

Structural design errors resulting from conventional treatment of distribution law for local radial and torque loads 11 p1433 A73-25028

Properties of a radial mode CO2 laser. 12 p1505 A73-27016

Further evidence for a complex limb structure in the solar radial brightness distribution at mm wavelengths. 12 p1545 A73-27841

Improved three-dimensional mapping of the electron density distribution of the solar corona. 12 p1536 A73-27843

Control by pressure drop of the radial distribution of the Mach number behind a subsonic annular cascade. 13 p1565 A73-28838

Temporal development of longitudinal plasma current radial profile, obtaining effective collision frequency estimation for electron heating, hot plasma production conditions and stability restoration force 14 p1777 A73-29685

Effect of radial profile of a charged particle pulse on the electromagnetic wake in a plasma.

14 p1779 A73-29710

Interplanetary radial gradients of galactic cosmic ray protons and helium nuclei - Pioneer 8 and 9 measurements from 0.75 to 1.10 AU.

14 p1786 A73-29951

Asymptotic behavior of a kinetic model of the solar wind

14 p1787 A73-30424

Nonlinear radial electron beam focusing in plasma under beam-plasma instability, showing irreversibility conditions dependence on electromagnetic wave propagation mode

16 p2043 A73-34056

Transformation of high-frequency waves and vanishing of low-frequency instabilities in a radially-inhomogeneous beam-plasma discharge.

17 p2217 A73-35525

Observation of the absolute intensity and the centre-to-limb variations of the sun in the vacuum ultraviolet region.

19 p2482 A73-37376

Measurement of the potential distribution near an electron beam using a thermionic probe.

21 p2749 A73-41664

Experimental study of shocked-plasma flows with a double search-coil conductivity probe.

24 p3113 A73-44402

RADIAL DRAINAGE PATTERNS U DRAINAGE PATTERNS

RADIAL FLOW

Problems regarding the use of electronic data processing for the calculation of diagonal cascades in turbomachines

03 p0242 A73-13169

Steady transverse plane magnetogasdynamic flows.

03 p0346 A73-13693

On the solution of the Navier-Stokes equations for a spherically symmetric expanding flow.

06 p0684 A73-17707

Flow of a viscous incompressible fluid between a fixed porous disk and a rotating nonporous disk, with radial discharge

07 p0811 A73-20069

A radial diffuser with a rotating boundary layer at the throat.

08 p0953 A73-20795

A hydrodynamic theory of radial-face mechanical seals.

10 p1223 A73-23698

Inertia effects in laminar radial flow of power law fluids.

10 p1206 A73-24660

A reappraisal of design methods for inward flow radial gas turbines.

11 p1411 A73-26370

High speed corotating plasma streams in solar wind from time dependent radial MHD flow model

12 p1533 A73-26979

A new approach to the problem of predicting the performance of centrifugal compressors.

13 p1565 A73-29012

Fundamental study on compressible transient flow and leakage in partially admitted axial and radial flow turbines.

13 p1566 A73-29025

Critical rpm of a radial-flow turbine wheel of the closed type

14 p1814 A73-30685

Approximation nature and error magnitude in radial radiative heat flux within optically thin nongray isothermal gas cylinder

15 p1959 A73-32282

Restrictions on radial magnetic field and flow solutions for the solar wind.

16 p2053 A73-32967

A wake and an eddy in a rotating, radial-flow passage. I - Experimental observations.

[ASME PAPER 73-GT-57] 16 p1964 A73-33512

A wake and an eddy in a rotating, radial-flow passage. II - Flow model.

[ASME PAPER 73-GT-58] 16 p1964 A73-33513

Viscous flow in radial turbomachine blade passages.

17 p2093 A73-34389

Flow studies in radial inflow turbines interspace between nozzles and rotors.

17 p2093 A73-34392

High speed cinematographic study of mass flow rate of pressurized subcooled liquid nitrogen inward choked flow through radial gap at various stagnation pressures

21 p2740 A73-40634

The effects of speed and radial flow on the axial force on an enclosed rotating disc.

21 p2754 A73-41685

Heat transfer from an enclosed rotating disk with uniform suction and injection.

22 p2938 A73-42998

RADIAL VELOCITY

Some features of the Leiden radial velocity instrument.

01 p0047 A73-10516

Photoelectric determination of radial velocities.

01 p0047 A73-10517

The interaction of primordial gravitational waves with groups of galaxies.

01 p0098 A73-10585

White dwarfs gravitational red shifts, radial velocities and mass-radius relationships, considering colors and luminosities

01 p0104 A73-11036

Physical reality of apparent carbon star group in Auriga from radial velocity measurements, spectral classification and V/R photometry observations

01 p0104 A73-11039

Laser Doppler anemometer theory and application to radial flow velocity measurements in oscillating boundary layer in front of blunt body

02 p0171 A73-12559

A polarimetric method of measuring radial velocities.

02 p0171 A73-12830

Radial velocity and microturbulence dependence on excitation potential and time in A type supergiants atmosphere, deriving chemical composition

03 p0371 A73-13215

Measurement of radial velocities with coude spectrograph of the 152-cm telescope of the Haute Provence Observatory

03 p0371 A73-13223

A-type supergiants - A list of line intensities and radial velocity measurements

03 p0375 A73-13950

Use of airborne radar to evaluate hurricane modification experiments.

03 p0338 A73-14513

Possible cause of the variations of the intensity of an interstellar maser.

04 p0493 A73-16023

Mean radial velocity of Virgo galactic cluster from red shift data, approximating velocity distribution of elliptical-lenticular and spiral galaxies

05 p0622 A73-17074

Fast radial displacement of a toroidal plasma by a transverse magnetic field.

06 p0732 A73-18620

Violet shift of the H alpha absorption line of the hydrogen-depleted star HD 30353

07 p0877 A73-19598

Time dependent hydrodynamics of meridional circulation in rotating star radiative zone, confirming Eddington-Sweet velocity formulation

07 p0877 A73-19599

Determination of the type of motion in spherically symmetric systems of galaxies

07 p0901 A73-20313

Magnetic fields and the vibrational motions of the solar photosphere

07 p0901 A73-20319

Shakhbazian I - A distant cluster of compact galaxies.

08 p1004 A73-20897

Study of the galactic structure from observations of interstellar calcium. I - Analysis of radial velocities

08 p1004 A73-20909

Galactic differential rotation derived from the radial velocities of some population I objects.

08 p1005 A73-20912

Spectral variations of 53 Cam /AX Cam/.

08 p1006 A73-20931

Properties and nature of shell stars. III - Periodic radial-velocity changes of 4 Hercules.

09 p1140 A73-22003

Image tube spectra of planetary nebulae for relative line intensities and radial velocities, considering nebulae properties

09 p1141 A73-22015

On the nature of X Persei - Evidence from the 1957 outburst.

10 p1275 A73-23845

Additional observations of supergiants and foreground stars in the direction of the Large Magellanic Cloud.

10 p1279 A73-24167

Kinematics of the Huyghenian region of the Orion Nebula.

11 p1427 A73-26605

Determination of the type of motion in spherically symmetric clusters of galaxies.

12 p1539 A73-27285

Magnetic fields and oscillatory motion in the solar photosphere.

12 p1540 A73-27291

On a correlation between the magnitude and the radial velocity of hot stars.

13 p1672 A73-28036

Cepheid variables model characteristics, determining luminosity, radial velocity and radius time dependent variations

13 p1682 A73-28981

On the kinematics of a local component of the interstellar hydrogen gas possibly related to Gould's Belt.

13 p1686 A73-29369

On the kinematical and spatial coincidence of optical and radio spiral arms in our galaxy.

15 p1929 A73-31055

Aperture synthesis study of neutral hydrogen in NGC 2403 and NGC 4236. I - Observations.

15 p1929 A73-31056

The spectrum variable a Centauri /HD 125 823/.

15 p1935 A73-31485

Radial velocity, light and colour curves of RZ Cep, an RR Lyrae star.

15 p1937 A73-31700

The large-scale velocity field, the magnetic fields, and the brightness of the solar atmosphere

16 p2057 A73-32701

Velocity field in the active regions of the sun

16 p2057 A73-32702

Fabry-Perot interferometric studies on H II regions.

16 p2058 A73-32831

The radial velocity variations of HD 125823 a Centauri.

16 p2059 A73-32843

A method of measuring three-dimensional rotating wakes behind turbomachinery rotors.

[ASME PAPER 73-FE-31] 17 p2095 A73-35023

A technique for measuring small displacements in digital spectra.

17 p2170 A73-35297

Interferometry of the Medusa nebula A21 /YM 29/.

18 p2354 A73-36729

Radial velocity measurements of the Cetus Arc nebula around Loop II.

19 p2483 A73-37571

Profiles of emission lines in Be stars. II - Interpretation of the long-period V/R variation.

19 p2484 A73-37615

The suitability of the microdensitometer PDS 1000 for the measurement of radial velocities

20 p2565 A73-39065

Radial velocity fluctuations of the Ap star HD 224801

20 p2607 A73-39083

Study of the redshift structure of the Coma cluster.

20 p2610 A73-39580

Residual velocities of clusters and indications of the existence of a local cluster

21 p2768 A73-40713

Investigation of the planetary nebula NGC 1360 and its nucleus

21 p2768 A73-40715

On the possibility of determining stellar radial velocities to 0.01 km per sec.

22 p2907 A73-42207

Simeiz 59 /Sharpless 104/ nebula radial and expansion velocity indicating type I supernova origin, discussing spectral and interferometric measurements and relativistic electron energy and density

23 p3035 A73-44233

Study of the kinematics of O and B spectral type stars

23 p3036 A73-44241

RADIANCE

Electron beam pumped super radiant light source.

01 p0058 A73-10311

Atmospheric temperature profile determination by limb radiance inversion radiometer, discussing radiative transfer, instrument parameters and inversion process effects on retrievable information content

01 p0072 A73-10354

An improved algorithm for the inversion of limb radiance measurements.

01 p0072 A73-10355

The global distribution of outgoing long-wave radiation derived from SIRS radiance measurements.

01 p0038 A73-10391

Photopic luminous efficiency measured by critical flicker frequency method, noting dependence on intermittence frequency of light stimulus or overall radiance level

[AD-754344] 02 p0137 A73-12076

Direct determination of the thickness of stratospheric layers from single-channel satellite radiance measurements.

05 p0569 A73-16574

Global time and space changes of satellite radiances received from the stratosphere and lower mesosphere.

09 p1076 A73-22149

The altitude of the scattering layer near the mesopause over the summer poles.

14 p1750 A73-30768

Operational radiance maps of the stratosphere, with preliminary details of a major stratospheric warming.

18 p2303 A73-33950

Photometric variability of counter glow radiance as evidence for dust cloud presence in earth-moon system region

18 p2351 A73-36183

Satellite radiances and clear air turbulence probabilities.

19 p2448 A73-38218

Stratospheric temperature profiles from limb radiance measurement by Aerobee rocket, comparing with rocket sounding and radiosonde data

21 p2729 A73-40064

A comparison of radar-determined cloud height and reflected solar radiance measured from the geosynchronous satellite ATS-3.

23 p3005 A73-44269

Interior radiances in optically deep absorbing media. II - Rayleigh scattering.

24 p3111 A73-45319

RADIANT COOLING

- Model analysis for heat radiation effect on development and evolution of single buoyant thermal rising in neutrally stratified atmosphere, noting radiative relaxation time
[AD-755499] 01 p0039 A73-10398
- Computer programs for radiative heat transfer and thermal equilibrium equations, noting transient temperature distribution measurement of two stage radiant cooler
01 p0111 A73-11151
- Magnitude estimate for long wave radiative cooling effects for isolated buoyant thermal rising in uniform ambient atmosphere
[AD-755500] 02 p0224 A73-12779
- Fabrication of a lightweight circular orbit passive radiative cooler.
03 p0329 A73-13010
- Russian book on space flight radiative heat transfer problems covering spacecraft thermal conditions, solar and planetary heat flux, radiant cooling and vacuum tests
09 p1166 A73-22348
- Infrared radiative heating and cooling in the Venusian mesosphere. II - Day-to-night variation.
11 p1418 A73-25719
- Diurnal thermospheric heat budget in terms of electron-ion recombination, photodissociation and neutral wind energy transfer and conductive and radiative cooling
12 p1492 A73-27604
- Transient cooling of a solid cylinder by combined convection and radiation at its surface.
13 p1704 A73-28086
- Thermal wet representation of cloud layer from radiative cooling and weak dependence on thickness, deriving approximate formulas for radiant fluxes
15 p1904 A73-31784
- Cooling of the heated region formed during breakdown of air by laser radiation
17 p2183 A73-34262
- Time-dependent radiative cooling of a hot low-density cosmic gas.
17 p2231 A73-34756
- Aerosol influence on atmospheric radiative cooling, calculating long wave flux divergence dependence on particle size, relative humidity and refractivity
23 p2978 A73-43984
- Cloud destabilization due to long wave radiative cooling resulting from IR radiative heat transfer in cloudy atmosphere, considering temperature inversion effects and cyclogenesis mechanism
24 p3108 A73-45016

RADIANT FLUX DENSITY

- NT ELECTRON FLUX DENSITY
NT ILLUMINANCE
NT IRRADIANCE
NT LUMINANCE
NT LUMINOUS INTENSITY
NT NEUTRON FLUX DENSITY
NT PARTICLE FLUX DENSITY
NT PROTON FLUX DENSITY
NT RADIANCE
NT SOLAR CONSTANT
NT SOLAR FLUX DENSITY
- A simple method for calculating nongray radiation.
01 p0119 A73-10109
- Preliminary report on the infrared spectrum of Nova Serpentis 1970.
01 p0095 A73-10269
- Intensity variation of CN bands with temperature in active nitrogen methylene chloride chemiluminescent reaction.
01 p0014 A73-10333
- The infrared spectrum of nitrogen excited by fast electrons.
01 p0036 A73-10338
- Research of the emission at 5577 Å in the period of 1958-1967 in Ashkhabad.
01 p0036 A73-10345
- Airglow 6300 Å emission predawn enhancement amplitude variation with geomagnetic and solar activity
01 p0037 A73-10347
- Precise positions of radio sources measured at 2695 MHz.
01 p0098 A73-10580
- French monograph - Contribution to the experimental study of the integrated intensity of the translational absorption bands induced in pressurized rare-gas mixtures.
01 p0080 A73-10601
- Observations of galactic cosmic-ray intensity at heliocentric radial distances of from 1.0 to 2.0 astronomical units.
01 p0093 A73-11044
- 21-micron observations of H II regions.
01 p0104 A73-11045
- Short-term pulsar intensity variation in the frequency range 70-115 MHz. I - Correlation measurements.
01 p0106 A73-11306
- Observations at 408 MHz of the Cyg X-3 radio outburst.
02 p0204 A73-11552

- Time dependence of Cygnus X-3 8 GHz flux density and spectral index during outburst decay, describing source model
02 p0204 A73-11553
- X ray intensity observations of Cygnus X-3 by Uhuru satellite before/during September 1972 radio flare
02 p0210 A73-11554
- 15.5 GHz observations at the Haystack Observatory of the Cygnus X-3 outburst.
02 p0210 A73-11555
- Radio observations of Cygnus X-3 and the surrounding region.
02 p0210 A73-11557
- Discovery of infrared emission from the radio source near Cygnus X-3.
02 p0210 A73-11558
- 21 cm and 18 cm observations of the Cygnus X-3 radio outburst.
02 p0204 A73-11559
- Radiant flux densities of Cygnus X-3, observing OH and formaldehyde absorption
02 p0210 A73-11560
- Observations of Cygnus X-3 at the Mullard Radio Astronomy Observatory.
02 p0210 A73-11561
- Cygnus X-3 intensity drop and principal period observation by X ray instrument onboard OAO Copernicus
02 p0204 A73-11563
- Cross sections for the production of excited products in the photoionization of N₂, O₂, CO, and N₂O by 58.4-nm radiation.
02 p0157 A73-11752
- FLUX density and linear polarization measurements of radio outburst from Cygnus X-3, suggesting synchrotron radiation from expanding cloud of relativistic particles
02 p0205 A73-11871
- Time correlation between current sheet collapse in plasma focus and X ray production, investigating radiation intensity and distribution
02 p0197 A73-12061
- Solar UV spectra with high angular resolution from rocket observations, obtaining center to limb intensity variations
02 p0207 A73-12325
- Cosmic diffuse soft X rays intensity distribution, taking interstellar absorption into account
02 p0207 A73-12402
- Energy spectrum of muon formed electromagnetic cascades in vertical cosmic radiation flux
02 p0209 A73-12681
- UV light intensities calibration in astrophysics and high temperature metrology with thermal arc plasma as radiation sources, discussing intensity standard establishment
02 p0199 A73-12715
- Thermal radio source DR 21 centimeter flux density measurements for antenna aperture calibration, comparing with standard sources
03 p0366 A73-12932
- Energy flux intensity in IR bands of selectively radiating molecular gas nonisothermal layer from radiative transfer equation and mathematical model
03 p0396 A73-13183
- Properties of the Red Spot of Jupiter in 1971.
03 p0371 A73-13216
- Frequency independent characteristic time scales in meter wave intensity structure of pulsars CP 0950 and 1133, using predetection dispersion removal technique
03 p0374 A73-13715
- Solar cyclic intensity variation of excess radiation with respect to galactic radiation background at low altitudes from satellite data analysis
03 p0365 A73-14575
- Granularity produced by a diffuser illuminated in partially coherent light
03 p0320 A73-14606
- An interferometric survey of the areas surrounding four intense radio sources.
03 p0380 A73-14637
- Extreme ultraviolet observations of solar flares.
04 p0490 A73-14831
- The residual cosmic ray modulation at the 1954 solar minimum.
04 p0492 A73-14968
- Distances and absolute luminosities of galactic X-ray sources.
04 p0492 A73-15358
- Observations of extragalactic variable sources at 2.8 and 4.5 cm wavelength.
04 p0500 A73-15515
- Modulation of low-energy galactic cosmic rays over solar maximum /cycle 20/.
04 p0493 A73-15549
- Possible cause of the variations of the intensity of an interstellar maser.
04 p0493 A73-16023
- Anomalous recurrent diurnal anisotropy in cosmic ray intensity with maximum along the garden hose direction.
05 p0608 A73-16142

RADIANT FLUX DENSITY

- Variations of cosmic ray intensity in consequence of the corotation effect.
05 p0609 A73-16371
- Influence of refractive index on emittance from semi-infinite absorbing scattering media.
[ALAA PAPER 73-147] 05 p0598 A73-16895
- A Green Bank sky survey in search of radio sources at 1400 MHz. III - Positions and flux densities of the GB radio sources.
05 p0622 A73-17070
- Radio galaxies luminosity function from radio power range at 178 MHz with known red shift, using 3C catalog galaxies
05 p0622 A73-17071
- Radio astronomy receiver with digital integrator for weak radio source detection, noting minimum detectable flux density
05 p0552 A73-17166
- High frequency observations of the second radio flare in Cygnus X-3.
05 p0623 A73-17184
- Cygnus X-3 radio source - Lower limit on size and upper limit on distance.
05 p0623 A73-17185
- Small Magellanic Cloud X-1 X ray source binary nature, occultation, energy spectrum and intensity from Uhuru satellite observation
05 p0626 A73-17345
- Temporal and spatial changes in cosmic ray intensity increases preceding Forbush decreases
06 p0742 A73-17531
- A general study of the effect of collision parameters on the cosmic ray fluxes in the atmosphere.
06 p0743 A73-17831
- Long-term variations of total and polarized fluxes, absolute energy distribution, and line strength of BL Lacertae and four quasi-stellar sources.
07 p0873 A73-19051
- Physics of the X-radiation from clusters of galaxies.
07 p0874 A73-19074
- Centimeter waves radio sources survey, tabulating position coordinates, 5 GHz flux densities, spectral index and optical identification
07 p0876 A73-19353
- Measurements of the integrated Stokes parameters of compact radio sources.
07 p0876 A73-19354
- 7.8-GHz flux density measurements of variable radio sources.
07 p0876 A73-19355
- Brightness temperatures in the southern sky at 408 MHz
07 p0876 A73-19357
- Observations of periodic variations in the X-ray intensity of Cygnus X-3.
07 p0872 A73-20240
- Radio brightness distribution in the Crab Nebula at the 3.55-cm and 1.28-cm wavelengths
07 p0901 A73-20309
- Cyg X-3 flux density measurements at 365 MHz with broadband synthesis interferometer, comparing radio flares with Laan model
07 p0902 A73-20559
- H flux density observations for 21 cm absorption spectrum in front of Cyg X-3
07 p0902 A73-20560
- Heat flux contours on a plane for parallel radiation specularly reflected from a cone, a hemisphere and a paraboloid.
08 p1022 A73-21255
- Time dependence of cosmic ray intensity during the anisotropic phase of solar flares
08 p0998 A73-21279
- Spatial spectroscopic diagnostic of planetary nebulae. III - Numerical investigation of local absolute monochromatic energies and local absolute energies in spherically symmetric models.
08 p1010 A73-21313
- High energy electrons and gamma quantum flux in upper atmospheric layers from high altitude balloon measurements
08 p0999 A73-21337
- Solar modulation of cosmic ray intensity in stratosphere, examining relationship to sunspots group number and heliographic latitudes over 11 year period
08 p0999 A73-21339
- Three dimensional cosmic ray anisotropy and density distribution at earth orbit and in interplanetary space with allowance for primary particle and nucleon energy spectrum
08 p1000 A73-21343
- Stratospheric cosmic ray short period variations at 30 km by spectral density method
08 p1000 A73-21351
- The X-ray surface brightness of the Cygnus Loop.
08 p1013 A73-21811
- The transfer of radiation from a flame to its fuel.
08 p1025 A73-21822
- Surface and body vaporization mechanisms during intense energy flux interaction with substance, relating flux density to mean depth of surface-to-bulk vaporization shift
09 p1095 A73-22611

Magnetic field effect on laser radiation intensity and polarization, noting Zeeman component change
09 p1095 A73-22666

Periodic components in the flux-density variation of the radio source VRO 42.22.01 /BL Lacertae/.
09 p1147 A73-22728

Anisotropic model of gravitational radiation enhancement from relativistic disk located in Galactic nucleus
09 p1149 A73-22946

Characteristics of the diffuse /tenuous/ interstellar medium determined from radio recombination lines.
09 p1150 A73-23137

The Eddington factor for radiative transfer in spherical geometry.
09 p1121 A73-23289

Performance of an unstable repetitive pulsed CO₂ laser oscillator.
09 p1098 A73-23338

Interstellar and interplanetary dust grains orientation distribution function in anisotropic corpuscular or radiation fluxes
10 p1271 A73-23482

Energy spectrum and time variations of hard X-rays from Cyg X-1.
10 p1263 A73-23488

On the calibration of flux densities and the determination of spectra at radio frequencies.
10 p1272 A73-23527

Gamma-ray emission from the region of the Galactic center.
[AD-759042] 10 p1264 A73-23530

Population inversion and radiation density in a Q-switched CO₂ laser
10 p1227 A73-23578

D-2A satellite experiments for sky mapping and radiation intensity measurement, discussing attitude correction processing
10 p1285 A73-23623

Problem of the time dependence of the polarization level of Type III solar radio bursts
10 p1264 A73-23719

Restrictions on the intensity of cosmic masers and the possibility of detecting new OH and H₂O sources in a rapid sky survey
10 p1275 A73-23725

Light flux vertical distribution in spherical multilayer cloud and gas scattering planetary atmosphere, calculating radiation intensity
10 p1276 A73-23891

Detection of a flux of gamma quanta in the direction of the Cygnus constellation
10 p1265 A73-23906

Frequency spectrum of cosmic ray intensity and solar activity variations
10 p1267 A73-23924

A mathematical model of the optimization of cosmic ray intensity observation data
10 p1268 A73-23935

Probability model of mode interactions, radiation density and output gain of gas laser channels with common lower energy level in active medium
10 p1227 A73-24071

Suggested interpretation of the correlations in intensity fluctuations in the lines Ca II H and K, magnesium b, and hydrogen H beta /Research note/.
10 p1278 A73-24132

Low energy solar proton events intensity increase near time of magnetic storm sudden commencement and Forbush decrease, using propagation shock wave model
10 p1268 A73-24146

North-south asymmetry in the increase of cosmic-ray intensity before magnetic storms.
10 p1268 A73-24212

Radio pulses from the direction of the galactic centre.
10 p1280 A73-24272

Solar quiet long-term modulation of cosmic ray intensity diurnal variation explained via interplanetary sector pattern changes
10 p1269 A73-24448

OJ 287 and BL Lacertae with rapid radio, IR and optical variability, high IR luminosity, line free optical spectra and varying polarization
11 p1416 A73-25179

Gamma-gamma total hadronic cross section and absorption of extragalactic gamma-rays.
11 p1413 A73-26107

Jupiter radio observations at 13 cm during 1969 and 1971 oppositions for circular polarization and flux density
11 p1424 A73-26128

Gaussian light beam transmitted intensity derivation for thermal lensing in solids by vector Kirchhoff approach, obtaining time dependent shift in diffraction focus
11 p1377 A73-26228

First results from the Texas interferometer - Positions of 605 discrete sources.
11 p1428 A73-26676

Laser beam evaporation of dense substances, examining luminous flux densities with gasdynamic equations
12 p1506 A73-27137

Radio-brightness distribution over the Crab Nebula at 3.55 and 1.28 cm.
12 p1539 A73-27281

31.4-GHz flux density measurements of variable radio sources.
12 p1540 A73-27426

Space distribution of the intensity of excess radiation at low altitudes.
12 p1535 A73-27637

Solar radio burst of 7 August 1972, discussing peak flux density, magnetic field intensity, energy distribution and polarization degree
12 p1536 A73-27850

Identification and radio spectra of bright galaxies in the second Bologna Catalogue of radio sources and their radio luminosity function.
13 p1671 A73-28034

An absolute method of measuring energy outputs from CO₂ lasers.
13 p1626 A73-28369

Statistical analysis of Forbush decreases and of cosmic-ray intensity increases preceding them.
13 p1670 A73-28701

Variation of the cosmic-ray gradient during the solar activity cycle.
13 p1670 A73-28721

A digital measurement converter of pulsed flows
13 p1591 A73-28872

Radio star MWC 349 observations at 10.52 and 6.63 GHz, obtaining angular size from flux density and IR temperature
13 p1681 A73-28924

The cloud bright spot.
13 p1619 A73-29238

Multibeam satellite Effective Isotropic Radiative Power /EIRP/ for aeronautical communications, discussing carrier-to-noise density increase and communication load per channel decrease
14 p1726 A73-29900

Log-intensity correlations of a laser beam in a turbulent medium.
14 p1757 A73-30162

Galactic origin, distance and flux estimates of transient X ray sources, rejecting extragalactic and supernova event hypotheses
14 p1788 A73-30732

Slow variations of pulsar intensities.
14 p1802 A73-30750

Interplanetary scintillations of cosmic rays.
14 p1788 A73-30752

Investigation of high-voltage photoelectric converters at low radiation intensities
14 p1713 A73-30948

Calculation of radiant energy transfer by the Galerkin method
15 p1956 A73-30963

Flux density for ray propagation in discrete index media expressed in terms of the intrinsic geometry of the deflecting surface.
15 p1913 A73-31135

High radio frequency observations of the Omega nebula.
15 p1932 A73-31268

Accurate flux densities at 8.87 GHz of 195 radio sources.
15 p1933 A73-31379

Cosmological information from surveys of radio source spectra.
15 p1933 A73-31396

Pulsar fluctuation spectra and the generalized drifting-subpulse phenomenon.
15 p1936 A73-31558

Features of the long-wave radiant influx in the presence of stratified cloudiness /A numerical experiment/
15 p1904 A73-31783

Estimation of errors arising in calculations of the fluxes and influxes of thermal radiation due to errors in the initial meteorological parameters
15 p1905 A73-31786

Short wave radiation flux calculation method for cloudless and cloudy atmospheres, computing geographic distribution of daily absorbed solar radiation
15 p1905 A73-31787

Certain methodological aspects of measurements of the average short-wave radiation fluxes in the presence of cloudiness
15 p1905 A73-31790

Accuracy of averaging total-radiation fluxes
15 p1905 A73-31791

Yearly and trimonthly variations in solar activity and cosmic-ray intensity
15 p1926 A73-31879

Field spectroradiometer system to measure incident and reflected radiation intensity, discussing optical equipment, detectors, electronics and reference blackbodies
15 p1876 A73-31979

Optical thickness of Saturn rings along cross section from intensity of radiation transmitted through rings, considering dark side illumination sources
15 p1939 A73-32008

Laser-induced shock effects in Plexiglas and 6061-T6 aluminum.
15 p1956 A73-32259

Time and space variations of cosmic-ray intensity increases prior to Forbush decreases.
16 p2052 A73-32755

Theory of transient radiation in a waveguide with a piecewise-homogeneous dielectric filler
16 p1978 A73-32898

Absolute calibration of solar radio flux density in the microwave region.
16 p1993 A73-32968

Observation of excess gamma-radiation fluxes from the region of the northern galactic pole.
16 p2054 A73-33078

The velocity of separation of the components of extragalactic radio sources.
16 p2062 A73-33572

Luminosity of thermal X-ray sources with a strong magnetic field.
16 p2062 A73-33574

Measurement of cosmic rays and searches for radiation belts near Venus
16 p2057 A73-33829

Spatial correlation functions of the field and intensity of laser radiation
16 p2024 A73-34053

High peak power from /GaAl/As-GaAs double-heterostructure injection lasers.
17 p2183 A73-34202

Cosmic radiation intensity constancy from observations of cosmic ray induced transmutations in meteorites
17 p2223 A73-34419

Observations of soft X-rays - Upper limits on the flux from SN 1972E and measurements of the diffuse background in Centaurus.
17 p2224 A73-34754

Observations of gamma-ray bursts of cosmic origin.
17 p2224 A73-34770

Cylindrical X ray source with Al K-alpha radiation production for spherical photoelectron spectrometer, discussing radiation intensity with minimum bremsstrahlung
17 p2176 A73-35765

Experimental verification of the effective photon theory of laser induced gas ionization.
17 p2186 A73-35832

Characteristics of the influence of the solar wind on cosmic-ray intensity during 1969
18 p2345 A73-36108

Simultaneous measurements of ion concentration and corpuscular stream intensity at altitudes ranging from 10 to 79 km
18 p2345 A73-36121

Time dependence of the polarization of type III solar radio bursts.
18 p2347 A73-36744

Constraints on cosmic maser intensity, and the possibility of detecting new OH and H₂O radio sources by a rapid sky survey.
18 p2355 A73-36750

Observation of the absolute intensity and the centre-to-limb variations of the sun in the vacuum ultraviolet region.
19 p2482 A73-37376

Observations of further outbursts in the radio galaxy 3C 120.
19 p2485 A73-37625

Time dependence of cosmic-ray intensity at the anisotropic stage of solar flares.
19 p2476 A73-37908

The effect of solar activity on temperatures in the equatorial mesosphere.
19 p2426 A73-38015

Effect of the solar wind on geomagnetic activity
19 p2476 A73-38154

The brightness temperature of Venus and the absolute flux-density scale at 608 MHz.
19 p2489 A73-38527

Light flux vertical distribution in spherical multilayer cloud and gas scattering planetary atmosphere, calculating radiation intensity
20 p2603 A73-38910

Radio luminosity function of galaxies.
20 p2606 A73-39062

A catalog of data on optically visible H II regions.
20 p2607 A73-39084

Spatial distribution of outgoing long wave radiation fluxes according to Cosmos-320 satellite data
20 p2555 A73-39188

Plane unsteady dispersion of gas behind deflagration wave moved by laser radiation with high flux density
20 p2573 A73-39281

The 27-day variations of the hard cosmic ray component and the atmospheric ozone X-layer according to IGY data
21 p2755 A73-40109

The relation between cosmic ray intensity variations and effects due to the electromagnetic complex
21 p2755 A73-40110

Frequency distribution of the parameters of the diurnal variation of the cosmic ray intensity
21 p2755 A73-40112

X-ray studies of the Crab nebula occultations, 1974-75.
21 p2765 A73-40300

- Long wave radiation flux, water content and temperature measurements in stratus and cumulostratus clouds by aircraft radiometry 21 p2731 A73-40496
- Variations of pulsar intensity as a result of scintillations at an inhomogeneous plasma 21 p2767 A73-40536
- Cosmic ray intensity over the past 100,000 to 1,000,000 years and the Kr-81 isotope content in the atmosphere 21 p2756 A73-40586
- Cosmic ray intensity variation observation during August 2-8, 1972, suggesting complex interactions with interplanetary shock waves and magnetic field and magnetosphere 21 p2757 A73-40590
- The 11-year cycle of cosmic ray intensity in the stratosphere and its dependence on solar activity 21 p2758 A73-40597
- Differences in the correlations of 27-day and 11-year cosmic ray variations with solar activity parameters 21 p2758 A73-40598
- Research of short-period variations in cosmic rays at Moscow's latitude 21 p2759 A73-40610
- X ray background radiation intensity fluctuations from random discrete point sources, indicating extragalactic origin 21 p2759 A73-40710
- Latitudinal distributions and composition of the radiation on nonclosed drift shells in the altitude range from 200 to 400 km 21 p2686 A73-40908
- Near-infrared radiation intensity from restrikes of exploding wires. 21 p2740 A73-40955
- Results of direct measurements of the illumination in the atmosphere and on the surface of the planet Venus during the flight of the Venera 8 interplanetary probe 21 p2773 A73-41274
- The impulsive increase in the intensity of solar X-rays. 21 p2761 A73-41388
- Correlation and spectral analysis of daily solar radio flux. 21 p2762 A73-41494
- Dynamics of a laser with regulated cavity Q 21 p2716 A73-41510
- Angular effects in the propagation of cosmic rays in the atmosphere. 21 p2764 A73-41629
- Detection of radio emission from M1-11 and HD37806. 21 p2780 A73-41646
- Size spectra of extensive air showers and primary cosmic-ray spectrum. 22 p2903 A73-42427
- Measurements of absolute intensities of cosmic-ray muons in the vertical and greatly inclined directions at geomagnetic latitudes 16 N. 22 p2903 A73-42437
- Measurement of the absolute vertical integral and differential cosmic-ray single-muon flux at 3.6 GeV and a measurement of the showerless penetrating particle-pair flux above 3.6 GeV. 22 p2903 A73-42440
- Further observations of Cygnus X-3 at 8 GHz during the September 1972 outbursts. 22 p2915 A73-43026
- The wall condition of the specific density of a radiation field 22 p2888 A73-43046
- Calorimeter for picosecond laser pulses. 22 p2872 A73-43153
- Pulsar properties covering galactic distribution, pulse periodicity computed from arrival time measurements, models, emission mechanisms, total intensity pulse shapes, etc 23 p3028 A73-43351
- Airglow hydroxyl emission IR spectral bands intensity measurements with allowance for atmospheric extinction, deriving vibrational level excitation rates from spontaneous emission transition probabilities 23 p2972 A73-43690
- Statistical properties of radio sources at centimeter wavelengths in a range of terminally weak flux densities 23 p3034 A73-44229
- Posteclipse brightening of Io observed at 3500 and 4000 A suggested as transient partial covering of high-albedo material 24 p3134 A73-44564
- Clusters of galaxies with a wide range of X-ray luminosities. 24 p3139 A73-45055
- A method for studying the radiant flux distribution in the circumfocal area of a concentrator with the aid of an asymptotic calorimeter 24 p3058 A73-45253
- Infrared and X-ray variability of Cyg X-3. 24 p3143 A73-45347
- High resolution observations of the radio galaxy NGC5128 at 10.7 GHz. 24 p3143 A73-45489
- Observations of Cyg X-1 and Cyg X-3 above 7 keV from OSO-7. 24 p3144 A73-45494
- An all-sky catalogue of strong radio sources at 408 MHz. 24 p3144 A73-45560
- RADIANT HEATING**
- Kinetics of heating a light-scattering field by radiant heat transfer 02 p0238 A73-12098
- Pyrometric obturation devices effect on sample temperature level during high temperature tests with radiant heating 03 p0306 A73-13189
- Analysis of sublimation-cooled coated mirrors in convective and radiative environments. 05 p0641 A73-17108
- Some limits on cosmic-ray heating of H I clouds by magnetic stars. 10 p1263 A73-23487
- Metal foil panels for radiant heating, describing historical development, design, fabrication methods and applications 10 p1177 A73-24175
- Principles of evacuated cryogenic insulations. 11 p1450 A73-25623
- Modification of the two-flow approximation in radiant-transfer calculations 11 p1450 A73-25623
- Infrared radiative heating and cooling in the Venusian mesosphere. II - Day-to-night variation. 11 p1418 A73-25719
- Heating effects due to radiative energy loss from acoustic waves in solar atmosphere, estimating temperature difference between radiative equilibrium and empirical model 11 p1421 A73-25931
- Vapor chamber fin radiator study for the potassium Rankine cycle. 11 p1451 A73-25991
- Motion of a heated gas layer and the asymptotic characteristics of the gas layer 15 p1958 A73-32107
- Thermal shielding by subliming volume reflectors in convective and intense radiative environments. 17 p2253 A73-34183
- Investigation of the effective heat conductivity of plasma-sprayed alumina coatings subject to radiative heating in the temperature range from 100 to 900 C. 21 p2792 A73-41220
- Dynamic effects on ignitability limits of solid propellants subjected to radiative heating. 22 p2899 A73-42813
- The ignition of hydrocarbon-air mixtures with laser radiation 22 p2938 A73-43190
- RADIANT INTENSITY**
- U RADIANT FLUX DENSITY**
- RADIATION**
- NT X RAY SOURCES**
- RADIATION ABSORPTION**
- NT ATMOSPHERIC ATTENUATION**
- NT AURORAL ABSORPTION**
- NT ELECTROMAGNETIC ABSORPTION**
- NT MOLECULAR ABSORPTION**
- NT PHOTOABSORPTION**
- NT POLAR CAP ABSORPTION**
- NT SELF ABSORPTION**
- NT ULTRAVIOLET ABSORPTION**
- NT X RAY ABSORPTION**
- Book - Emission, absorption, and transfer of radiation in heated atmospheres. 01 p0119 A73-10125
- Extraterrestrial solar flux attenuation and photodissociation cross sections effects on errors in photochemical kinetic model calculations 01 p0014 A73-10369
- Simultaneous measurements of solar radiation from aircraft and satellites during BOMEX. 01 p0038 A73-10377
- Possibility of accelerating the matter of hot stars by absorption in spectral lines 01 p0100 A73-10706
- Computed total radiation properties of compressed oxygen between 100 and 1000 K. 01 p0122 A73-10809
- Calculation of the spectral, angular and altitudinal distributions of the thermal radiation field of the atmosphere and the earth's surface 01 p0040 A73-10871
- Atmospheric absorption and scattering as radiation extinction mechanisms, discussing attenuation coefficient wavelength and weather dependence 01 p0102 A73-10993
- Direct Monte Carlo simulation of two-dimensional radiative heat transfer in absorbing-emitting medium bounded by the non-isothermal gray walls. 01 p0123 A73-11139
- Absorbing boundary propagation model for solar cosmic rays energy spectrum kink type behavior, using Gleeson-Ng theory 02 p0205 A73-11753
- [AD-756355]
- Gas discharge efficiency from populations comparison of Ne absorbing levels in hollow cathode and positive column discharges, measuring laser output power peak 02 p0176 A73-12096
- The spectral characteristics of radiation extinction and the effects of the relative humidity on these characteristics 02 p0189 A73-12368
- Free-free absorption of gyrosynchrotron radiation in solar microwave bursts. 04 p0492 A73-15366
- Q switched ruby laser emission absorption by diatomic Rb vapor, noting molecular fluorescence intensity changes 04 p0458 A73-15560
- Thermal defocusing of high intensity continuous Ar laser radiation in absorbing medium with allowance for spherical aberrations 04 p0458 A73-15562
- Dielectric layers in the radiation field of microwave antennas 05 p0550 A73-16475
- CO2 laser radiation absorption in SF6-air boundary layers. 05 p0585 A73-16983
- [AIAA PAPER 73-262]
- Infrared measurements of R. Coronae Borealis through its 1972 March-June minimum. 05 p0627 A73-17391
- Argon plasma density and energy distribution development during microwave radiation absorption at upper hybrid resonance 06 p0732 A73-18605
- Radiation absorption calculation for nonisothermal gas containing combustion products, noting approximation for water vapor radiation 08 p1021 A73-20860
- Ultraviolet photometry from the Orbiting Astronomical Observatory. VII alpha squared Canum Venaticorum. 08 p1008 A73-21158
- Direct measurement of water vapor absorption of solar radiation in the free atmosphere. 08 p0985 A73-21389
- Stagnation region radiative heating with steady-state ablation during Venus entry. 08 p1025 A73-21817
- The thermal future of the universe. 09 p1143 A73-22109
- Radiative transfer model for simulation of airborne remote sensing scanner data under flight conditions in hazy atmosphere with scattering and absorption effects 09 p1077 A73-22386
- Luminescence of a molecular gas under the action of a carbon dioxide laser pulse 09 p1094 A73-22595
- Intensities and half-widths of lines in the A and B bands of the red atmospheric system of O2 bands 09 p1077 A73-22664
- Influence of absorption on the optical properties of solids - Propagation of uniform, plane, heterogeneous electromagnetic waves in isotropic and homogeneous mediums 09 p1121 A73-22963
- Rotating neutron star gas cocoon heating by LF radiation absorption, noting X ray emission 10 p1263 A73-23481
- Modulation of infrared and sub-mm waves with crossed forward-biased junction diodes. 10 p1194 A73-24171
- Investigation of the diffuse glow of the clouds of dark absorbing matter in the region of the Aquila constellation 11 p1416 A73-25229
- Solar microwave burst radiation spectrum, explaining burst intensity decreasing phase by gyromagnetic absorption model 11 p1413 A73-25946
- Gamma-gamma total hadronic cross section and absorption of extragalactic gamma-rays. 11 p1413 A73-26107
- Simultaneous radiative and conductive heat transfer in non-gray media. 11 p1453 A73-26583
- Simplification of one-dimensional heat-conduction problems in the case of impulsive radiative heating of flat bodies 12 p1558 A73-27317
- Radiative transfer through carbon ablation layers. 13 p1705 A73-28457
- The spectral, angular, and altitudinal distributions of the earth and sky thermal radiation field. 13 p1607 A73-28695
- Stellar opacity and energy transport based on radiation-matter interactions, discussing radiative transfer, absorption and scattering cross sections, quantum mechanical methods, etc 13 p1682 A73-28987
- Absorption saturation effects on high-power CO2 laser beam transmission. 13 p1628 A73-29329
- An analytic formula for heating due to ozone absorption. 14 p1750 A73-30767

- Relationship between T-associations and the interstellar medium in the northern region of the Monoceros complex
15 p1934 A73-31421
- Short wave radiation flux calculation method for cloudless and cloudy atmospheres, computing geographic distribution of daily absorbed solar radiation
15 p1905 A73-31787
- Radiation absorption in stellar atmospheres due to photoionization in magnetic field, discussing frequency relation to propagation direction and Larmor frequency
15 p1872 A73-31955
- Absorption and production of soft X-rays in the Galaxy.
16 p2051 A73-32746
- A general formula for free-free absorption on highly-polarizable neutral atoms.
16 p2039 A73-33740
- Self-focusing of CO₂ laser radiation in resonantly absorbing gases.
17 p2186 A73-35811
- Propulsion by absorption of laser radiation.
[AIAA PAPER 73-624] 18 p2342 A73-36172
- An approximation for combined heat transfer in a radiatively absorbing and emitting gas.
[AIAA PAPER 73-750] 18 p2370 A73-36366
- Infrared absorption and local symmetry of negative ClO₄ and ReO₄ impurity ions in KI and CsI crystals
18 p2340 A73-36673
- Absorber theory of radiation and the future of the universe.
19 p2460 A73-38172
- Heat transfer in an absorbing, emitting and scattering slug flow between parallel plates.
[ASME PAPER 73-HT-13] 20 p2625 A73-38568
- 18-cm OH absorption of W 49 A and W 49 B.
20 p2610 A73-39575
- Absorption of CO₂ laser radiation by carbonyl fluoride.
21 p2715 A73-40958
- Self-similar flows with increasing energy. III - Radiation-driven shock wave.
21 p2793 A73-41673
- The ignition of hydrocarbon-air mixtures with laser radiation
22 p2938 A73-43190
- Note on the modified two-stream approximation of Sagan and Pollack.
24 p3123 A73-44438
- Radiation absorption in stellar atmospheres due to photoionization in magnetic field, discussing frequency relation to propagation direction and Larmor frequency
24 p3081 A73-44480
- A self-similar regime of powder combustion with variable optical constants
24 p3154 A73-44706
- Magnitude-redshift and count-magnitude relations in presence of a uniform intergalactic absorption.
24 p3143 A73-45436
- RADIATION BELTS**
NT INNER RADIATION BELT
NT OUTER RADIATION BELT
NT PROTON BELTS
- New observations of the proton population of the radiation belt between 1.5 and 104 MeV.
03 p0362 A73-13862
- Some parameters affecting the poleward boundary of trapped electrons.
03 p0363 A73-13869
- The importance of wave-particle interactions in the magnetosphere.
04 p0492 A73-15339
- Steady axisymmetric ring current models computed with energy density distribution parameters variations for effects on magnetic field and particle belt parameters
05 p0609 A73-16144
- Book - Geophysics 3. Part 4.
06 p0688 A73-17501
- Energy dependent time lag in the long-term modulation of cosmic rays.
07 p0869 A73-19252
- DR ring current belt formation due to electron and proton gradient drift in inhomogeneous geomagnetic field, calculating charged particles trajectories
07 p0816 A73-19446
- German monograph - Investigations of the behavior of high energetic protons and electrons in the inner magnetosphere.
07 p0872 A73-20385
- Rapid injection of energetic particles into the gap between the inner and outer radiation belts
08 p0998 A73-21300
- Pulsed magnetic system /terrella/ for model of earth radiation belts and geomagnetic field-solar wind interaction
08 p0960 A73-21309
- Distribution of radiation doses in the earth's radiation belts during years of maximum solar activity
10 p1264 A73-23889
- Energetic electron production and loss model for Jupiter radiation belt, considering drive mechanisms for electron diffusion from solar wind
11 p1424 A73-26130
- Super-Alfven displacement of hydromagnetic pulses in the earth's radiation belt
12 p1491 A73-27349
- Earth radiation belts energetic electrons quiet equilibrium structure based on balance between pitch angle scattering loss and inward radial diffusion
14 p1786 A73-29965
- Scaling laws for outer planet magnetospheres, noting energetic trapped particles radiation belts possibility
14 p1800 A73-30538
- Jupiter's radiation belts and the sweeping effect of its satellites.
16 p2062 A73-33429
- Results of Jupiter observations in the centimeter wavelength range
16 p2070 A73-33844
- The electron energy and number densities of the Jovian radiation belt. I.
19 p2475 A73-37621
- Analysis of the Jovian electron radiation belts. II - Observations of the decimetric radiation.
19 p2475 A73-37622
- Fast injection of energetic particles into the gap between the inner and outer radiation belts.
19 p2476 A73-37929
- Generation and decay of a narrow belt of energetic electrons in the earth's magnetosphere.
19 p2476 A73-37934
- Effect of secondary emission of the potential of a metallic body in the electron radiation belts of the earth.
20 p2601 A73-38875
- Radiation dose distribution in the earth's radiation belts during year of maximum solar activity.
20 p2601 A73-38908
- Study of cosmic rays by the Prognoz satellites
21 p2756 A73-40577
- Experimental test to determine the origin of geomagnetically trapped radiation.
22 p2846 A73-41944
- The source and structure of the Jovian radiation belt.
22 p2903 A73-42986
- Super-Alfven displacement of hydromagnetic pulses in the radiation belt of the earth.
23 p2970 A73-43246
- Drift of radiation-belt particles during substorms
24 p3124 A73-44804
- Relativistic electron belt formation mechanism hypothesis based on Cosmos 137 data on electron intensity near geomagnetic shell L equal to 2.8
24 p3124 A73-44808
- High-angular-resolution observations of Saturn at 21.1-centimeter wavelength.
24 p3138 A73-45051
- Magnetically trapped charged particle pitch angle diffusion and lifetime calculation for radiation belts, taking into account geomagnetic dipole geometry
24 p3127 A73-45138
- RADIATION CONTROL**
U RADIATION PROTECTION
RADIATION COUNTERS
NT CERENKOV COUNTERS
NT ELECTRON COUNTERS
NT GEIGER COUNTERS
NT NEUTRON COUNTERS
NT PARTICLE TELESCOPES
NT PROPORTIONAL COUNTERS
NT QUANTUM COUNTERS
NT SCINTILLATION COUNTERS
NT SPARK CHAMBERS
- Image photon counting technique nature, performance, merits, implementation and applications, noting photoelectronic components and image information treatment at quantum level
01 p0048 A73-10529
- A measurement of the atmospheric neutron flux in the energy range 50 less than E less than 350 MeV.
03 p0298 A73-12886
- Papers on radiation dosimetric instruments and problems covering nuclear track recorders, ionization chambers, proportional counters, radiophotoluminescence, thermoluminescence, X rays, neutron equivalents, etc
11 p1362 A73-25420
- A high resolution position sensitive detector for ultraviolet and X-ray photons.
11 p1363 A73-25958
- Electrostatic toroidal analyzer for studying charged particle fluxes in outer space
12 p1496 A73-27203
- Two descriptions for the photocounting detection of radiation passed through a random medium - A comparison for the turbulent atmosphere.
15 p1914 A73-32291
- Charge and energy spectra of cosmic rays with Z equal to or greater than 30.
16 p2054 A73-33279
- Charge and energy spectra of particles with E from 0.2 to 30 MeV/nuc in the January 25, 1971 solar flare.
16 p2054 A73-33281
- Spectrophotometric setup with a detector for individual photon count
17 p2164 A73-34165
- The lateral distribution of muons in near vertical EAS.
17 p2223 A73-34243
- The University College London image photon counting system - Performance and observing configuration.
17 p2169 A73-35279
- Digital pulse counting astronomical spectrograph system with TV camera tube, image intensifier and minicomputer for camera scan control and video data processing
17 p2169 A73-35282
- Photon counting with a self-scanned diode array.
17 p2169 A73-35283
- Small hypervelocity particle in-flight detection against background noise using forward scattering from laser illuminated particle distribution
17 p2172 A73-35415
- Electron calibration of a high-energy cosmic ray detector.
21 p2703 A73-41150
- A gas density control system for X-ray proportional counters in space.
22 p2851 A73-41699
- Latitude and local time dependence of precipitated low-energy electrons at high latitudes.
22 p2901 A73-41914
- Solid state AgCl detectors for nuclear tracks with on- and off-response at choice - Applications to life sciences.
22 p2814 A73-42179
- Investigation of the intensity distribution in a molecular beam expelled from a conical ring source
22 p2889 A73-42387
- The assembly edge effect and the spatial distribution of extensive air shower particles in an assembly with widely spaced detectors
23 p3022 A73-43547
- Results of radio emission studies at frequencies of 32 and 58 MHz in extensive air showers on the assembly of Moscow State University
23 p3022 A73-43550
- Study of low-energy heavy-nucleus track regression in plastic detectors /cellulose triacetate and polyethylene terephthalate/ and in low-sensitivity nuclear photoemulsion
23 p2981 A73-43567
- Charged particle track detector design with electric field control of nuclear photoemulsion sensitivity, discussing microcrystals, trajectory recording and proton irradiation
23 p2982 A73-43569
- Physical characteristics of the set of scientific devices used to record the cosmic-ray ionizing component on 'Prognoz' satellites
24 p3089 A73-44784
- RADIATION DAMAGE**
Influence of strong external factors on the characteristics of semiconductor devices sensitive to the state of the surface /Review/
01 p0022 A73-10036
- Influence of gamma-radiation on the electrical properties of a real germanium surface
01 p0087 A73-10039
- The Bauschinger effect in annealed and irradiated titanium
01 p0064 A73-10495
- The destruction of reflecting dielectric coatings by laser radiation.
01 p0059 A73-10836
- Effects of chemical impurities, oxygen and dopant, on the gamma and neutron damage of silicon solar cells.
01 p0006 A73-11163
- The accurate prediction of radiation environment and solar cell degradation.
01 p0006 A73-11164
- Electron spin resonance of ultraviolet radiation induced defects in ZnO thermal control coating pigment.
01 p0088 A73-11276
- Investigation of laser radiation self-focusing by alkali halide single crystals according to data on the damage-focus displacement effect
01 p0061 A73-11443
- Development of internal damage in silicate glasses and polymers under the action of laser radiation
02 p0184 A73-11616
- Fracture of nonlinear crystals /KDP and LiNbO₃/ by radiation from a ruby laser.
02 p0176 A73-12112
- Analogies in the laser-induced destruction of the surface and interior of transparent glass.
02 p0176 A73-12115
- Investigation of the disintegration of semiconductors exposed to laser radiation
03 p0349 A73-13660
- Book - Fundamentals of nuclear hardening of electronic equipment.
03 p0283 A73-13990

- Summary of results of JPL lithium-doped solar cell development program. 03 p0257 A73-14240
- Further observed degradation on the LES-6 synchronous solar cell experiment. 03 p0258 A73-14247
- The effect of boron concentration on radiation damage in silicon solar cells. 03 p0258 A73-14249
- The mechanism of stage III recovery of electron irradiated molybdenum. 04 p0461 A73-14870
- Radiation damage effects in microwave dielectric substrate materials. 05 p0557 A73-16507
- Analytical techniques for the determination of equipment probability of survival to radiation stress. 05 p0596 A73-16509
- The radiation environments of outer-planet missions. 05 p0617 A73-16511
- Effects of proton irradiation on several spacecraft science components. 05 p0596 A73-16513
- Permanent and transient radiation effects in BARITT microwave oscillators. 05 p0558 A73-16518
- Neutron irradiation effects on microwave transistor amplifiers. 05 p0558 A73-16520
- Beta irradiation of silicon junction devices - Effects on diffusion length. 05 p0537 A73-16522
- Neutron damage in GaAs laser diodes - At and above laser threshold. 05 p0584 A73-16523
- On the point defect production in electron-irradiated molybdenum. 06 p0705 A73-17832
- Effect of gamma irradiation on carbon redistribution processes in the martensite lattice. 06 p0706 A73-17902
- Investigation of molybdenum after exposure to single-charge helium atom radiation. 06 p0707 A73-17909
- Proton irradiation at 30 K and isochronal annealing of reactively sputtered Ta thin-film resistors. 06 p0737 A73-18352
- High power laser generation and heating of plasma in solid targets due to radiation damage, discussing liquid lasers as light amplifiers. 06 p0731 A73-18582
- Laser-radiation-induced damage to the surface of lithium niobate and tantalate single crystals. 06 p0738 A73-18591
- Prevention of damage to the science instruments of Mariner-Mars '71 spacecraft due to accidental viewing of the sun during sun-acquisition following exit from earth shadow. 06 p0696 A73-18829
- Effects of ionizing radiations on MOS components. 07 p0860 A73-18914
- Influence of the substrate and the structure of the metal film on the nature of the annealing treatment of defects formed in the film by proton bombardment. 07 p0864 A73-20524
- UV-induced lipid peroxidation in human epidermis, dermis, and hypodermis in vitro. 09 p1038 A73-21873
- Alloying elements effects on voids nucleation in irradiated Al alloys, tabulating defect concentration. 09 p1101 A73-22175
- Silicon solar cells radiation damage from orbital flight and electron and proton irradiation laboratory test data, discussing radiation hardening by Li doping. 09 p1036 A73-22811
- Energetic and structural models of microdefects in germanate glasses. 10 p1240 A73-24465
- Optical damage and internal fields in pyroelectrics. 10 p1260 A73-24531
- Retinal damage thresholds for multiple pulse lasers. [AD-758530] 11 p1315 A73-25341
- Investigation of self-focusing of laser radiation with alkali halide single crystals from data concerning the displacement of the focus of damage. 11 p1376 A73-26065
- The analytically determined response of silicon detectors to a polyenergetic neutron beam. 11 p1365 A73-26210
- Ruby and Nd-YAG pulsed laser induced surface damage probability comparison at 1.06 and 0.69 micron wavelengths by breakdown starting time distribution measurement. 11 p1377 A73-26226
- Confirmation of an electron avalanche causing laser-induced bulk damage at 1.06 micron. 11 p1377 A73-26227
- Investigation of radiation defects in silicon and germanium single crystals irradiated by 50-MeV electrons. 11 p1410 A73-26449
- An experimental basis for carcinogenic effects of ultraviolet radiation. 11 p1320 A73-26485
- Solar flare heavy ion damage in Luna 20 soil sample, producing angular amorphous micron-sized grains via accumulated radiation damage. 13 p1676 A73-28327
- Influence of gate metal on gamma-ray induced defects in MOS structures. 13 p1589 A73-28421
- Mechanism of damage of the surface of a transparent dielectric during illumination with short light pulses. 13 p1629 A73-29429
- The effect of neutron irradiation damage on the low temperature deformation characteristics of b.c.c. metals and their alloys. 13 p1638 A73-29454
- Bauschinger effect in annealed and irradiated titanium. 14 p1759 A73-30320
- Aftereffects in IMPATT oscillators with transient ionizing radiation. 15 p1851 A73-32187
- Electrical properties of semiconductors with non-spherical radiation damage regions. 16 p2044 A73-33198
- The effects of radiation sterilization on plastics. 16 p2030 A73-33693
- Dependence of laser-induced breakdown field strength on pulse duration. 17 p2183 A73-34201
- Stellar wind radiation damage in cosmic dust grains - Implications for the history of early accretion in the solar nebula. 17 p2228 A73-34424
- Effect of dynamic factors of space flights on green alga *Chlorella vulgaris*. 18 p2270 A73-36098
- Retinal change induced in the primate/Macaca mulatta by oxygen nuclei radiation. 18 p2271 A73-36125
- Nature of the damage caused by laser radiation on the surfaces or in the bulk of transparent glasses. 20 p2573 A73-39687
- High-speed photography of laser damage in solids. 21 p2709 A73-39987
- Ocular hazard from viewing the sun unprotected and through various windows and filters. 21 p2698 A73-40143
- Surface and bulk laser-damage statistics and the identification of intrinsic breakdown processes. 21 p2714 A73-40758
- Chemical protection from genetic damages induced by radiation in the period of aftereffect of acceleration. 21 p2643 A73-40815
- Changes in the peripheral blood of the rat exposed to microwave radiation /2400 MHz/ in conditions of chronic exposure. 21 p2645 A73-41159
- RF fields as new ecological factor in environment pollution, considering radiation interaction with biological systems and increased use of electromagnetic spectrum. 22 p2811 A73-41787
- Damage produced by laser radiation in optical materials. II. 22 p2868 A73-41824
- Frequency of heavy ions in space and their biologically important characteristics. 22 p2805 A73-42178
- Estimation of the biological danger of the very high energy component of space radiation. 22 p2805 A73-42180
- The radiobiological effects of heavy ions on mammalian cells and bacteria. 22 p2805 A73-42182
- Probability cross sections of heavy ion single hit inactivation paths for human cells using nitrogen ion accelerator experiments. 22 p2805 A73-42183
- Changes in the characteristics of giant laser radiation pulses and of luminous plasma during formation of damage regions on the surface or in the bulk of transparent dielectrics. 22 p2869 A73-42250
- German monograph - The back-scattering method as a procedure for the determination of the radiation damage profile in silicon doped by ion implantation. 22 p2897 A73-42852
- Effects of electromagnetic waves of the millimeter range on a cell and on some structural elements of a cell. 23 p2949 A73-44095
- Bulk and surface damage mechanisms of laser crystalline and nonlinear optical materials and thin films, noting plasma thresholds and surface polishing. 23 p2989 A73-44210
- Laser-induced deformation modes in thin metal targets. 24 p3097 A73-45417
- Monograph - Satellite-borne instrument for the measurement of soft solar X-rays. 01 p0045 A73-10150
- Analysis of a nonisothermal, spherical detector for monitoring the earth's radiative energy budget. 01 p0045 A73-10382
- Search for gravitational radiation of extraterrestrial origin. 01 p0097 A73-10424
- Positive detection of an excess of low-energy diffuse X-rays at high galactic latitude. 01 p0092 A73-11029
- Rocket stages separation distance measurement by monitoring gamma ray flux variation, noting separation mechanisms and retromotor performances. 01 p0052 A73-11166
- Weakly superconducting, thin-film structures as radiation detectors. 02 p0167 A73-11849
- Computer analyses of gravitational radiation detector coincidences. 02 p0144 A73-12222
- Energy spectrum, composition and anisotropy study of cosmic radiation from extensive air showers observation, using scintillation and Cerenkov detectors. 02 p0209 A73-12671
- Russian book on color recognition methods and devices covering algorithms for radiation color identification and optimal spectra of photosensitive radiation detector. 02 p0144 A73-12862
- A versatile Moessbauer spectrometer and its applications in structural mechanics. 03 p0305 A73-12875
- Cosmic gravitational waves detection and measurement, describing Weber experimental apparatus and theoretical foundations based on Einstein relativity theory. 03 p0341 A73-12924
- Side-viewing detector for a vacuum ultraviolet reflectometer. 03 p0309 A73-14430
- Frequency modulated laser radiation detection, studying photomultiplier current harmonics, phase/amplitude detector nonlinearities and noise-resonator coupling effects. 05 p0585 A73-16782
- Possibility of detecting weak solar cosmic ray fluxes by ground-based radio engineering methods. 06 p0742 A73-17532
- Characteristics of recombination centers defining the high sensitivity of n-CdSb photoresistors. 06 p0675 A73-18082
- Star sensor of spin stabilized Uhuru satellite for detection and location of stellar X ray sources with accuracies of one arc-minute. 06 p0695 A73-18323
- Macroscopic systems response to gravitational radiation for detector design and calibration, noting accessibility to people unfamiliar with general relativity. 06 p0724 A73-18549
- Photomultipliers for UV radiation detection, discussing high sensitivity and speed features, components, photon detection, tube types and applications. 07 p0821 A73-18981
- Semiconductor radiation detectors fabrication methods, discussing p-n junctions diffusion and ion implantation techniques and surface barrier, dE/dx, chessboard and rod type counters. 07 p0822 A73-19172
- Recent studies of magnetospheric electric field emissions above the electron gyrofrequency. 07 p0815 A73-19254
- An image intensifier spectrometer for remote sensing applications. 07 p0824 A73-19943
- Millimeter and submillimeter wave detection and mixing with superconducting weak links. 07 p0863 A73-20102
- Josephson junction millimeter microwave source and homodyne detector. 07 p0863 A73-20104
- Comparative studies of noise limitations in superconducting thin-film radiation detectors. 07 p0863 A73-20105
- Submillimeter radio telescope employing an n-InSb detector. 07 p0825 A73-20311
- Earth as gravitational waves detector, discussing pulsar CP 1133 emission. 08 p1000 A73-20675
- The macroscopic high-frequency quantum generator and detector of the gravitational radiation. 08 p0987 A73-21017
- An infrared pneumatic transducer with capacitive detection. [ONERA, TP NO. 1150] 08 p0968 A73-21682
- Use of open-structure channel electron multipliers in sounding rocket experiments. 09 p1080 A73-22105
- A high resolution position sensitive detector for ultraviolet and X-ray photons. 11 p1363 A73-25958

RADIATION DETECTORS
NT DOSIMETERS
NT SILICON RADIATION DETECTORS
NT THRESHOLD DETECTORS [DOSIMETERS]

RADIATION DISTRIBUTION

High spatial resolution wire spark chamber system using electromagnetic delay line readout.
11 p1363 A73-25962

A position-sensitive X-ray detector for the HEAO-A satellite.
11 p1364 A73-25963

Submillimeter radio telescope with an n-InSb detector.
12 p1497 A73-27283

A telescope for soft gamma ray astronomy.
12 p1499 A73-27892

The illumination distribution in the image plane from the radiation of a plane-parallel plate with the actual ray paths taken into consideration.
13 p1621 A73-29325

Experimental studies of a method of detecting microwave-modulated laser radiation in a photosensitive detector
13 p1628 A73-29415

Cd doped CdTe microwave film detectors sensitivity, frequency response, thermal characteristics and stability
14 p1737 A73-30855

Possibility of using semiconductor photocells as receivers of ultraviolet radiation
14 p1713 A73-30949

The effect of unmodulated sunlight on the integral voltage sensitivity of some radiation detectors.
14 p1754 A73-30954

Large area focusing collector for the observation of cosmic X rays.
15 p1876 A73-31976

Russian book on elementary particle counters covering gas discharge (Geiger-Mueller), scintillation, Cerenkov and semiconductor counters and matter-radiation interactions
15 p1880 A73-32418

Possibility of detecting weak solar-cosmic-ray fluxes by ground-based radio methods.
16 p2052 A73-32756

The fine solar sensor of the Astronomical Netherlands Satellite.
16 p2012 A73-32852

A magnetic spectrometer for recording particles in a range up to 4 GeV/c
17 p2164 A73-34151

Prolonged monitoring of experimental equipment with the aid of semiconductor emitters
17 p2133 A73-34152

The KP303 field transistor in a soft gamma radiation spectrometer
17 p2133 A73-34163

Gamma detectors using mercuric iodide and other heavy metal compounds as semiconductors with charge carriers for current surge in quantum energy resolution
17 p2134 A73-34247

Experimental use of self-scanned photodiode arrays in astronomy.
17 p2169 A73-35287

Flexural vibration frequencies of right circular cylindrical tensor gravitational wave detectors in regime with sound wavelength comparable to diameter
17 p2176 A73-35763

Detection of optical and infrared radiation with dc-biased electron-tunneling metal-barrier-metal diodes.
17 p2143 A73-35792

AgCl detectors in the Biostack II experiment aboard Apollo 17.
18 p2314 A73-35986

The charge spectrum of heavy cosmic ray nuclei measured on board of Apollo 16 (Biostack) using plastic detectors.
18 p2344 A73-35987

IMP and Pioneer satellite-borne sensors for cataloging solar particle events, discussing onset time, multiple flare injections, enhancement differentiation and contamination problems
18 p2345 A73-36061

Electron calibration on a high-energy cosmic ray detector.
18 p2317 A73-36979

The sensitivity of optoelectronic scanning systems with out-of-phase connection of the radiation detector elements.
20 p2564 A73-38850

Optimization and data analysis of the Frascati gravitational-wave detector.
20 p2565 A73-39013

The interaction of a laser with matter as an intense source of UV and soft X-ray radiation - Application to X-ray cinematography
21 p2709 A73-39944

A photoneutron antimony-124-beryllium system for fissile materials assay.
21 p2738 A73-40769

First results of the solar hard X-ray spectrometer on board the ESRO TD-1 A satellite.
21 p2761 A73-41386

Gravitational radiation detection via computerized delay-dependent coincidence comparisons of squared time derivatives of output powers of Argonne and Maryland cylindrical antenna detectors
22 p2885 A73-41734

Spectrum sensitive high amplification solar blind UV sensor for flame surveillance in jet engine environments at 1000 F, using miniature Geiger-Mueller tube
22 p2861 A73-42694

Heavy elements in surface materials - Determination by alpha particle scattering.
23 p2981 A73-43529

Fast linear detection system for TE CO₂ lasers.
24 p3096 A73-44922

RADIATION DISTRIBUTION

NT ANTENNA RADIATION PATTERNS

NT DIFFRACTION PATTERNS

NT RAINBOWS

NT SIDELOBES

The global distribution of outgoing long-wave radiation derived from SIRS radiance measurements.
01 p0038 A73-10391

Spatial distribution of charge carriers and radiant energy in single and double heterostructure semiconductor lasers, noting technology of potential barriers formation
01 p0059 A73-10715

CO₂ plasma emissivity at temperatures from 7000 to 9000 K in the spectral range of 2100 to 10,000 Å
01 p0085 A73-10854

Calculation of the spectral, angular and altitudinal distributions of the thermal radiation field of the atmosphere and the earth's surface
01 p0040 A73-10871

Spinorial solution associated to a radially symmetric radiation field in general relativity.
01 p0079 A73-11257

On quasi-periodic components with periods from 30 to 60 min of amplitude fluctuations of X-band solar radio emission.
01 p0108 A73-11382

Pitch-angle distributions of polarized hard X-radiation from solar flares, assuming electron-proton bremsstrahlung mechanism
01 p0093 A73-11390

Angular distributions of auroral electrons in the energy range 0.8 to 16 keV.
02 p0155 A73-11734

Time correlation between current sheet collapse in plasma focus and X ray production, investigating radiation intensity and distribution
02 p0197 A73-12061

Radial gradients and anisotropies due to galactic cosmic rays.
02 p0207 A73-12378

Cosmic diffuse soft X rays intensity distribution, taking interstellar absorption into account
02 p0207 A73-12402

Transfer of resonance radiation and photon random walks.
02 p0207 A73-12403

Nonlinear interaction between a spontaneous radiation field and the active media of high-gain gas laser amplifiers
02 p0177 A73-12489

Radiation properties of propeller and helicopter (free field) rotors and fans and gas turbine compressors (ducted rotors)
02 p0131 A73-12611

North/south asymmetric entry of solar protons during the November 18, 1968 event.
03 p0360 A73-12878

On the altitude dependence of the atmospheric X-rays in the energy range 0.1-1 MeV.
03 p0365 A73-14441

Infrared observations of Comets Ikeya-Seki (1965f) and Bennett (1969i).
04 p0494 A73-14755

Diurnal and annual behavior of the radiation balance
05 p0609 A73-16218

Calculation of averaged values for short- and long-wave fluxes and influxes in a real atmosphere
05 p0593 A73-16243

Measurements of flux fluctuation in solar radiation emission at a wavelength of 3 cm
05 p0573 A73-16270

Isotropic and incoherent light scattering by atomic slab, calculating Doppler effect induced diffuse radiation energy partial redistribution by Monte Carlo method
05 p0597 A73-16562

Angular distribution of radiation reflected from roughened brass - Experiment and analysis.
[ALAA PAPER 73-151]
05 p0598 A73-16899

Radiation balance mapping with multispectral scanner data.
05 p0572 A73-17158

The possibility that nongaseous hydrogen supplies the missing cosmological mass.
05 p0625 A73-17328

The formation of diatomic molecules in interstellar clouds.
05 p0625 A73-17333

Radiation field in a scattering medium after a long time interval following exposure to a light pulse
05 p0599 A73-17354

A comparison of mode match, geometrical theory of diffraction, and Kirchhoff radiation.
06 p0666 A73-18192

Photochemistry chemical kinetics in the interstellar medium.
06 p0752 A73-18236

Influence of waveguide properties of heterojunction layers on the principal characteristics of injection lasers.
06 p0702 A73-18585

Optically thin stellar winds in early-type stars.
07 p0873 A73-19061

Use of nonstationary holography to improve the directivity of laser radiation.
07 p0834 A73-19275

Parametric radiation of relativistic electron bundles in a waveguide with a stratified dielectric filling.
07 p0802 A73-20145

On near-field distributions along the leaky coaxial cable.
08 p0937 A73-20804

Severe self-induced beam distortion in laboratory simulated laser propagation at 10.6 microns.
08 p0974 A73-21031

Light distribution in photographic meters by means of multicolour photometry.
08 p1010 A73-21316

Solar active regions effects on galactic cosmic ray distribution and interplanetary magnetic field structure
08 p1000 A73-21344

On the near- and far-field radiation patterns generated by the non-linear interaction of two separate and non-planar monochromatic sources.
08 p0988 A73-21469

X-ray temperature measurements of laser produced plasmas in large radiation fields.
09 p1125 A73-22024

Diffusion of charged particles in a random magnetic field.
09 p1137 A73-22035

The thermal future of the universe.
09 p1143 A73-22109

Lateral distribution of u.h.f. radio emission associated with cosmic ray showers.
09 p1137 A73-22174

/GaAl/As lasers with a heterostructure for optical confinement and additional heterojunctions for extreme carrier confinement.
09 p1092 A73-22243

Spectral behavior and linewidth of /GaAl/As-GaAs double-heterostructure lasers at room temperature with stripe geometry configuration.
09 p1093 A73-22252

Measurement of log-irradiance fluctuation of He-Ne laser in the atmosphere.
09 p1096 A73-22750

Effect of a laser field on the gain line profile of an adjacent transition in an argon laser
09 p1096 A73-22968

Distribution of diffuse solar radiation over regions of the sky for various regions of the spectrum in the absence of cloudiness
09 p1138 A73-22994

Sco X-1 hard X rays and optical emission time variations from simultaneous observations, using balloon-borne counter telescopes
10 p1263 A73-23493

Relationship between the 27-day cosmic-ray variations and various solar-activity indices during the period from 1957 to 1970
10 p1266 A73-23918

Polar coupling coefficients and generalization of the spectrographic method for studying cosmic-ray variations of magnetospheric and interplanetary origin
10 p1267 A73-23927

A simulation of the directivity effect to be expected in hard X-ray flares.
10 p1268 A73-24143

Effect of heating water droplets by optical radiation.
10 p1246 A73-24181

Extraction of energy and charge from a black hole.
10 p1280 A73-24342

The three-ring effect in flexible bunches of optical fibers
10 p1228 A73-24585

Anisotropies in the interplanetary intensity of solar protons with energies greater than 0.3 MeV.
[AD-759099]
10 p1269 A73-24728

Electron pitch angle distributions throughout the magnetosphere as observed on Ogo 5.
10 p1213 A73-24732

The radio diameter of the sun from interferometer measurements at 9 mm wavelength.
10 p1284 A73-24773

The spatial distribution of the 11.7 micron radiation of NGC 7027.
11 p1415 A73-25071

The distribution of X-ray sources in our galaxy.
11 p1415 A73-25178

Radiation pattern produced by open ended radial waveguide with TM mode excitation, comparing computed with measured patterns
11 p1329 A73-25677

Size determination of a perfectly conducting sphere from the extrema of Mie scattering intensities.
11 p1329 A73-25679

Relationship between macroinhomogeneity of the field and the kinetics of free radical emission from a ruby laser

Density distribution of radiation from a source of limited size in a scattering medium.

Some effects of magnetospheric acceleration mechanisms on variations in ultraviolet intensity height profiles, and on consequent rocket spectrograph sensitivities.

Improving the angular divergence of the emission from a neodymium-glass laser with a high pulse energy level

Properties of unstable resonators with large equivalent Fresnel numbers.

Influence of the inversion inhomogeneity on the transverse structure of oscillations in solid-state lasers.

Space distribution of the intensity of excess radiation at low altitudes.

Luminosity levels in deep planetary atmosphere layers

The radiative capacity of a CO₂ plasma at temperatures 7000-9000 K in the spectral interval 2100-10,000 Å.

Emission field structure during transverse mode synchronization in a laser

Galactic continuum loops and the diameter-surface brightness relation for supernova remnants.

The spectral, angular, and altitudinal distributions of the earth and sky thermal radiation field.

East-west asymmetry of cosmic rays at sea level at geomagnetic latitudes from 50 N to 20 S.

Plane electromagnetic wave diffraction by ideally conducting circular cylinder in far and bright spot zones, using Green theorem for field calculation

German monograph on signal transmission and radiation distribution in optical waveguide consisting of glass fibers with refractive index gradient and optically dense envelope

Two-bladed large rotor mounted on tower in inverted mode to overcome recirculation effects, analyzing broadband noise spectra and directivity pattern

Waveguide laser mode patterns in the near and far field.

Radiation from line vortex filaments exhausting from a two-dimensional semi-infinite duct.

Magnetospheric dayside cusp - A topside view of its 6300-angstrom atomic oxygen emission.

The annual radiation balance of the earth-atmosphere system during 1969-70 from Nimbus 3 measurements.

The light field existing in a scattering medium long after its illumination by a light pulse.

Redistribution of resonance radiation. II - The effect of magnetic fields.

Comparison of methods for calculating long-wave radiation fields

Accuracy of averaging total-radiation fluxes

Spatial structure of the short-wave radiation field in stratocumulus and cumulus clouds

Radiation configuration factors for annular rings and hemispherical sectors.

Field properties and losses in a three-mirror optical ring resonator with a Gaussian diaphragm

Solutions of certain difference equations describing transformation of the temporal characteristics of radiation in a laser

Acoustic radiation from the end of a two-dimensional duct - Effects of uniform flow and duct lining.

Angular quadrature perturbations in radiative transfer theory.

Transient radiation in a shortened waveguide

Visual observation of the picture of a CO₂-laser radiation field

Search for small-scale anisotropy in the 2.7 K cosmic background radiation at a wavelength of 3.56 centimeters.

Satellite monitoring of climate parameters, discussing energy transfer in atmosphere, energy distribution, radiation balance, climatic models

Radiation efficiency of an X-band waveguide antenna

Measurement of near fields of antennas and scatterers.

Density of the radiation of the earth/atmosphere system into space

On the role of the radiation directivity in noise reduction for STOL aircraft.

Investigation of cosmic radiation about the moon aboard the Luna 10, 11, and 12 artificial lunar satellites

Calculation of the radiation field in a semiinfinite medium in the presence of isotropic scattering

Improving the angular divergence of a neodymium-glass laser beam having a high radiation energy per pulse.

Frequency spectra of strong fluctuations of laser radiation in a turbulent atmosphere

Jupiter atmosphere discrete source maps of 5 micron radiation distribution, correlating brightness temperature and photographically recorded colors

The radiation balance of the earth's surface and inclinations of isodiptic surfaces

Nonlinear radiation reaction field effects on operator self-field and oscillating dipole, taking into account one-atom spontaneous emission and superradiance theories

Green function and Poynting vector calculation of solid angles of radiation outside and inside anisotropic crystal in laser light scattering experiments

Coupled superradiance master equations - Application to fluctuations in coherent signal propagation in resonant media.

Intensity modulated laser with expansion and contraction of absorbing medium for thermoacoustic broadside array with highly directional acoustic propagation

Radiation field in the deep layers of planetary atmospheres.

Cosmic ray muon zenith angle distribution during horizontal air showers, discussing kaon and pion decay, spectrum characteristics, bremsstrahlung effects and flux upper limits

The arrival of solar radiation on variously oriented inclined surfaces

A survey on the recent measurements of the absolute vertical cosmic-ray muon flux at sea level.

Diffuse parasitics gain thresholds of laser modes for rectangular geometries, discussing radiation field and boundary conditions

Russian book - The stochastic structure of cloud and radiation fields.

Investigation of isotropic and anisotropic effects of cosmic rays during October through November 1968

Finite aperture waveguide laser resonators with external reflectors by matrices coupling linearly polarized modes, calculating power efficiency, resonant frequencies and radiation patterns

Latitudinal distributions and composition of the radiation on nonclosed drift shells in the altitude range from 200 to 400 km

Surface wave radiation pattern determination for solid state lasers, taking into account dielectric interface presence

Angular effects in the propagation of cosmic rays in the atmosphere.

Radiation field frequency dependent source function for two level atom, noting different stimulated emission and absorption line profiles

Divergence of the output radiation of electron-beam-pumped 'radiating mirror' lasers.

Ideal laser amplifier as a phase measuring system of a microscopic radiation field.

Measurements of the energy exchange between earth and space from satellites during the 1960's.

Investigation of the radiation properties of a laser without external feedback

The wall condition of the specific density of a radiation field

First-order probability densities of laser speckle patterns observed through finite-size scanning apertures.

Radio astronomical problems due to pulsar radiation dispersal by frequency dependent propagation velocity in interstellar medium, discussing signal reception and data recording techniques

An arrangement for studying horizontal air showers - Initial results

Results of radio emission studies at frequencies of 32 and 58 MHz in extensive air showers on the assembly of Moscow State University

Matrix method evaluating an internal radiation field in a plane-parallel atmosphere.

A method for the study of the gain and the oscillating modes of a CO₂ laser.

Radiation transfer in a multilayer plane-parallel system with nonisotropic scattering

Calculation of the mode structure in the Fabry-Pérot cavity of a laser with a high flow rate

Measurements of the distribution of sound source intensities in turbulent jets.

Microphone radiated acoustic power directivity measurement enhancement by integral transform, matrix inversion and relaxation techniques, considering application limits, resolution, noise sensitivity and computation

Variations of three-dimensional anisotropy of cosmic rays during Forbush decreases.

Performance of a large-bore high-power argon ion laser.

RADIATION DOSAGE

A shielding application of perturbation theory to determine changes in neutron and gamma doses due to changes in shield layers.

Uncertainties in determining the effective UV radiation at various altitudes.

Gamma ray dose and energy absorption buildup factors approximation based on geometrical progression formula as function of source energy and medium atomic number

Influence of the dose of neutron irradiation on the anelastic behavior of an aluminum deformed at 80 K

Cosmic radiation and research carried out on board the 001 prototype Concorde

Distribution of radiation doses in the earth's radiation belts during years of maximum solar activity

Radiation protection at the work site: Scientific, technical and organizational aspects; Annual Scientific Conference, 6th, Karlsruhe, West Germany, May 17-19, 1972, Reports

Papers on radiation dosimetric instruments and problems covering nuclear track recorders, ionization chambers, proportional counters, radiophotoluminescence, thermoluminescence, X rays, neutron equivalents, etc

Dose equivalent determinations in neutron fields by means of moderator techniques.

Geomagnetic latitude variation of cosmic radiation rates measured onboard Concorde SST prototypes, investigating solar flares

Radiation doses during a prolonged orbital space flight about the earth

Electronic safety test replaces radioactive test source.

Experimental methods of correlation between the trajectories of cosmic heavy ions and biological ob-

RADIATION EFFECTS

- jects: Dosimetric results - Experiment Biostack on Apollo XVI and XVII. 18 p2270 A73-35946
 - Radiation dose distribution in the earth's radiation belts during year of maximum solar activity. 20 p2601 A73-38908
 - Proton dosimeter design for distributed body organs. 23 p2949 A73-43389
 - A megarad plastic film dosimeter. 23 p2949 A73-44212
- RADIATION EFFECTS**
- NT RADIATION DAMAGE
 - NT RADIATION INJURIES
 - NT RADIOLYSIS
 - Combined heating and irradiation effects on body elastoplastic stress-strain state, deriving thermoradiative plasticity equations 01 p0112 A73-10004
 - Study of the conditions of the breakdown threshold of argon at high pressure under the effect of laser radiation 01 p0058 A73-10175
 - Model analysis for heat radiation effect on development and evolution of single buoyant thermal rising in neutrally stratified atmosphere, noting radiative relaxation time [AD-755499] 01 p0039 A73-10398
 - Radiation in the reacting boundary layer. 01 p0121 A73-10642
 - Prediction of strength of a polymer body with allowance for solar radiation 01 p0068 A73-11078
 - Interaction of thermal radiation with laminar free convection from a heated vertical plate. 01 p0123 A73-11141
 - Kinetics of the deactivation of the vibrations of highly excited oscillators in an inert gas medium with allowance for spontaneous emission 02 p0194 A73-11607
 - Cross sections for the production of excited products in the photoionization of N₂, O₂, CO, and N₂O by 58.4-nm radiation. 02 p0157 A73-11752
 - Gravitational radiation effects on cosmological time scale and models from matter fractional conversion and mass loss rate profile analysis 02 p0205 A73-11873
 - Saturation of stimulated ruby laser radiation under the action of CO-60 gamma rays 02 p0176 A73-12353
 - Cytochemical-luminescence study of adrenal cortex proteins under the influence of ionizing radiation 02 p0134 A73-12354
 - Spectroscopic properties of ruby and neodymium lasers under the action of a Co-60 gamma ray 02 p0176 A73-12355
 - Lunar rock C 14 production rate as function of depth, discussing solar and galactic cosmic radiation induced nuclear reactions 02 p0220 A73-12479
 - Russian monograph on radioactive isotopes effects on organisms covering metabolism, elimination acceleration methods, pathogenesis and treatment of damage, toxicity, biological action, etc 02 p0138 A73-12865
 - Solar corpuscular irradiation induced latent and etched nuclear particle tracks in lunar dust grains, presenting electron microscopic studies of Apollo 11/12 lunar soil samples 03 p0361 A73-13099
 - Low energy solar nuclear particle irradiation of lunar and meteoritic breccias. 03 p0361 A73-13100
 - Influence of gamma irradiation on the surface properties of metal-dielectric-semiconductor structures 03 p0349 A73-13661
 - Response of motoneurons of the spinal cord to gamma radiation - A cytochemical study. 03 p0262 A73-13808
 - Photovoltaic and I-V characteristics of integral diode solar cells as function of temperature and radiation exposure 03 p0256 A73-14231
 - Electron irradiated float-zone Si solar cell I-V performance degradation due to photon irradiation, noting base region minority carrier lifetime role 03 p0257 A73-14246
 - Internal friction in polycrystalline copper foils after alpha-irradiation at 78 K 03 p0328 A73-14653
 - Postirradiation notch ductility and fracture strength of pressure vessel steel plate by Charpy V tests 04 p0460 A73-14702
 - Observed effects of earth-reflected radiation and hydrogen drag on the orbital accelerations of balloon satellites. 04 p0439 A73-14802
 - Effects of 10-150 keV proton bombardment on silicon solar cells. 04 p0406 A73-14984
 - Thermally induced stress waves in an elastic layer. [ASME PAPER 72-WA/AFM-22] 04 p0516 A73-15894
 - Heat transfer in static packed beds - Effects of radiation on temperature distribution. 05 p0638 A73-16219
 - Annual Conference on Nuclear and Space Radiation Effects, 9th, University of Washington, Seattle, Wash., July 24-27, 1972, Proceedings. 05 p0557 A73-16501
 - Effect of ionizing radiation on Gunn diode amplifiers. 05 p0557 A73-16502
 - Aging effects on electrical and radiation characteristics of discrete semiconductors. 05 p0557 A73-16510
 - Electrical properties of electron-irradiated GaAs. 05 p0604 A73-16516
 - Transient ionizing radiation effects on IMPATT diode oscillators. 05 p0558 A73-16519
 - Radiation produced trapping effects in devices. 05 p0605 A73-16521
 - Effects of ionizing radiation on dielectrically isolated junction field effect transistors. 05 p0558 A73-16524
 - De Gaston decharger with ionizing radiation for temporary jet fuel conductivity increase and charge density reduction, discussing theory, design and tests [SAE PAPER 720864] 05 p0537 A73-16673
 - Nonsteady heat conduction of multilayer cylindrical and conical shells in periodic radiation flux, calculating temperature distribution 05 p0640 A73-16798
 - Effect of irradiation on the absolute thermal emf of metals and alloys 06 p0706 A73-17901
 - Amplification factor of light in a CO₂ + N₂ + He mixture expanding in a supersonic jet. 06 p0723 A73-17964
 - Metal atom migration acceleration under radioactive radiation, showing diffusion coefficient dependence on free and coupling electron interactions 06 p0735 A73-18038
 - Physiological effects of microwave electromagnetic fields on human and animal organisms, considering etiology, diagnostics and prophylaxis 06 p0659 A73-18256
 - A radiative-conductive model for the prediction of radiation fog. 06 p0720 A73-18327
 - Superlattice of voids in neutron-irradiated tungsten. 06 p0709 A73-18353
 - Postirradiation mechanical properties of Types 304 and 304 + 0.15% titanium stainless steel. 06 p0710 A73-18545
 - White and black paints for satellite thermal control coatings, discussing space environment radiation effects on emissivity and solar absorptance 07 p0841 A73-18909
 - Improving the performance of M.I.S. circuits under radiation. 07 p0797 A73-18918
 - Radiation effects on state of gas behind strong shock wave, representing power density of non-relativistic fully ionized hydrogen plasma 07 p0920 A73-19508
 - Co-60 source gamma irradiation of Mo-Au doped p-type Si MOS transistors, noting threshold voltage increase and current carrier mobility decrease 07 p0862 A73-19541
 - Lunar rocks age determination by Ar isotopes technique, noting plagioclase gas retention and cosmic ray exposure characteristics 07 p0888 A73-19782
 - Rare-gas analyses on neutron irradiated Apollo 12 samples. 07 p0889 A73-19798
 - Collision controlled radiation history of the lunar regolith. 07 p0871 A73-19870
 - Radiation and shock effects on Apollo 14 and 15 breccias substructure history, reporting optical microscope observations of solar flares and cosmic ray tracks 07 p0896 A73-19872
 - Radiation effects in soils from five lunar missions. 07 p0896 A73-19875
 - Thermoluminescence of Apollo 14 lunar samples following irradiation at -196 C. 07 p0897 A73-19879
 - Far infrared properties of lunar rock. 07 p0897 A73-19886
 - The generation of the highest cosmic ray energies. 07 p0872 A73-20193
 - Radiative transfer theory application to stellar images in photographic emulsions, deriving theoretical relation between star brightness and photographic effective radius 08 p1006 A73-20926
 - Radiation-induced oxidation of impurities in the water obtained from human moisture-containing bioactivity products 08 p0933 A73-20984
 - The Iarkovskii-Radzievskii effect and the evolution of condensations in a meteor stream 08 p1007 A73-21066
 - Influence of radiation damping on the motion of a charge in a uniform magnetic field and in the field of a plane electromagnetic wave 08 p0989 A73-21516
 - Neutron bombardment radiative effects on thin metal plate stability, considering compressive force, lattice defects and critical flux relations 08 p1020 A73-21771
 - Irradiation creep in some austenitic stainless steels, nimonic PE16 alloy and nickel. 08 p0982 A73-21794
 - Neutrino hindrance of density irregularities growth in expanding radiation dominated cosmological model from numerical integration of perturbation equations 09 p1141 A73-22026
 - Influence of a low-intensity ultrahigh-frequency electromagnetic field on the bioelectrical activity of the brain in rabbits 09 p1044 A73-22367
 - Influence of ultrasound and of a superhigh-frequency electromagnetic field in the three-centimeter band on the oxidative phosphorylation of liver and kidney mitochondria 09 p1044 A73-22368
 - Assessment of temperature rise suppression by edge losses during irradiation. 09 p1045 A73-22533
 - Optical breakdown of compressed gases by carbon dioxide laser emission 09 p1094 A73-22594
 - Influence of changes in the contact region on the basic characteristics of a semiconductor in the illuminated mode 09 p1134 A73-22685
 - Study of the influence of weak electromagnetic field gradients on man 09 p1046 A73-22850
 - Ultraviolet effects on the chemical composition and optical properties of interstellar grains. 09 p1150 A73-23138
 - Isotopic and crystalline structure changes in lunar rock and meteorite constituents for cosmic ray nuclear intensity and energy spectrum 09 p1138 A73-23169
 - Caloric vestibular stimulation via UHF-microwave irradiation. 10 p1178 A73-23650
 - Color centers in gamma-irradiated ruby with vanadium additions 10 p1259 A73-24069
 - EASCON '72; Electronics and Aerospace Systems Convention, Washington, D.C., October 16-18, 1972, Record. 10 p1298 A73-24551
 - Methyl nitrite photolysis reaction products under various ambient gas mixture environments, noting irradiation time and gas pressure effects 10 p1186 A73-24656
 - Pressure shocks in thermally and electrically conducting viscous gas, discussing growth equation and radiation effects 11 p1403 A73-25164
 - Nd laser radiation thermochemical effects on oxide formation on thin Cr films, Fe-Ni-Co and Cr-SiO alloys and MgO-MnO ferrites, noting resistance and etching rates 11 p1376 A73-25636
 - Theory of cooperative defect formation in a biopolymer molecule under the action of radiation 11 p1323 A73-25637
 - Influence of radiation on the conditions in the atmospheric boundary layer 11 p1393 A73-25641
 - Neutron irradiation effects on room and high temperature fatigue behavior of stainless steel, noting fatigue life enhancement at low temperature and strains 11 p1383 A73-25832
 - Radiation effects on multiplier phototubes. 11 p1363 A73-25960
 - Influence of a powerful electromagnetic wave on the electrical conductivity of a semiconductor 11 p1409 A73-26165
 - The effect of direct solar radiation on the attitude of the SKYNET spacecraft. 11 p1431 A73-26261
 - Spatial-temporal structure of emission from a ruby laser irradiated by gamma rays 11 p1378 A73-26523
 - Solar radiation effects on terrestrial electromagnetic environment, considering interplanetary space, earth internal structure, geomagnetism, upper atmosphere, dynamo action, energetic particles and magnetospheric storms 12 p1538 A73-27053
 - Laser beam evaporation of dense substances, examining luminous flux densities with gasdynamic equations 12 p1506 A73-27137
 - Effect of neutron irradiation on the structure and properties of zirconium carbide 12 p1512 A73-27200

Output radiation influence on catastrophic and slow degradation process in heterojunction injection lasers, noting service life dependence on current density 12 p1508 A73-27525

Photoisomerization of 2-isocyanato- and 2,x'-diisocyanobiphenyls in cyclohexane. 12 p1466 A73-27600

Effects of chronic irradiation of dogs with Co-60 gamma rays on the level of auto-antibodies 12 p1462 A73-27706

Morphological changes in the liver of dogs induced by chronic gamma irradiation 12 p1463 A73-27707

Proliferative activity of bone marrow cells in dogs exposed to chronic and repeated acute gamma irradiation 12 p1463 A73-27708

On the Aller's admixture radiation effect during the compression process in the solar corona and generation of coronal formations. 12 p1536 A73-27844

Possibility of atom displacements in solids under the action of laser light pulses 13 p1626 A73-28003

UV radiation effects on gamma irradiated Cr ions spin lattice relaxation rate in ruby and on resonant phonon scattering 13 p1668 A73-28219

Concerning one exact solution of the theory of quasilinear relaxation of a parametrically unstable plasma in the field of powerful radiation. 13 p1664 A73-28613

Specific characteristics of interband luminescence in crystals in the presence of intense laser radiation 13 p1628 A73-29049

Overview of the biological effects of electromagnetic radiation. 13 p1580 A73-29211

Possibility of a superconducting transition in a semiconductor subjected to high-power laser radiation. 13 p1629 A73-29439

Relaxation spectra of niobium irradiated at low temperature. 13 p1638 A73-29455

Optoelectronic semiconductor components under the influence of ionizing radiation 14 p1733 A73-30070

High pressure, radiation, high temperature and vacuum chemistries, discussing planetary matter, solar and cosmic radiation effects, plasma temperatures, solar winds and molecular populations 14 p1723 A73-30127

Spacecraft decontamination and sterilization by formaldehyde, beta-propiolactone, ethylene oxide, radiation and dry heat, noting effects on polymers 14 p1721 A73-30137

Complex radiation effects of sources moving in a plasma 14 p1780 A73-30262

Valency transfers of vanadium ions in ruby 14 p1783 A73-30582

Radiation-induced strengthening and embrittlement in aluminum. 14 p1761 A73-30628

The effect of unmodulated sunlight on the integral voltage sensitivity of some radiation detectors. 14 p1754 A73-30954

Changes in the quantity of overall sulphydryl groups in the blood of persons coming in contact with microwave radiation sources 15 p1837 A73-31169

The combined influence of microwave radiation and an adverse climate on the organism 15 p1837 A73-31170

Characteristics of the narcotic action of hexenal in combination with aminothyl-series radioprotective drugs in irradiated animals 15 p1838 A73-31391

Duplicity and its consequences among variable stars in general. 15 p1935 A73-31484

Study of lymphocyte chromosome aberrations in human peripheral blood under in vitro exposures to 645-MeV protons and X-rays 15 p1835 A73-31517

The dynamical effects of cosmic rays in the Galaxy and the generation of the galactic magnetic field. 16 p2054 A73-33287

Thermal stability of radiating fluids - Asymmetric slot problem. 16 p2085 A73-33314

Industrial sterilization; Proceedings of the International Symposium, Amsterdam, Netherlands, September 1972. 16 p1975 A73-33691

The effects of radiation sterilization on plastics. 16 p2030 A73-33693

The synergistic inactivation of biological systems by thermoradiation. 16 p1976 A73-33696

Sterilization technology in the United States space program. 16 p1976 A73-33697

Changes in the optical properties of minerals and their atomization caused by ion bombardment 16 p1977 A73-33756

Morphological and electron-microscopic alterations of the myocardium in dogs subjected to lasting chronic gamma irradiation 17 p2111 A73-34230

Momentum transfer to laser-irradiated targets, indicating the nonlinear interaction force. 17 p2184 A73-34897

Laser emission spectral theory, calculating cross relaxation in three and four level systems, monochromatic radiation effects on matter and laser action in inhomogeneous media 17 p2184 A73-34923

Experimental results on combined ultraviolet-proton excitation of moon rock luminescence. 17 p2233 A73-35273

Darkening of silicate rock powders by solar wind sputtering. 17 p2235 A73-35740

Russian book - Primary and initial processes of the biological action of radiation. 18 p2269 A73-35896

AgCl detectors in the Biostack II experiment aboard Apollo 17. 18 p2314 A73-35986

The charge spectrum of heavy cosmic ray nuclei measured on board of Apollo 16 /Biostack/ using plastic detectors. 18 p2344 A73-35987

Preliminary results of the action of cosmic heavy ions on development of eggs of Artemia salina. 18 p2271 A73-36129

Ablation and radiation coupled viscous hypersonic shock layers. 18 p2264 A73-36315

Yarkovskii-Radzievskii effect and the evolution of meteor swarms. 18 p2355 A73-36867

Pulsed RF life of an L-band power transistor. 19 p2411 A73-38460

Effect of ionizing radiation on second breakdown. 20 p2599 A73-39007

Apollo diet evaluation - A comparison of biological and analytical methods including bioisolation of mice and gamma radiation of diet. 20 p2517 A73-39103

Apparatus for creep and long-term strength testing of materials in aggressive media under irradiation 20 p2544 A73-39368

Threshold minima in the superhigh-pressure gas breakdown by Q-switched lasers. 20 p2574 A73-39721

Variation of the electrical resistance of ordered Ni3Mn alloy during irradiation by fission fragments 20 p2600 A73-39733

Russian book on radiation effects on ferroelectric crystals and ceramic materials covering changes in dielectric, piezoelectric and optical properties, structure and phase transitions 20 p2600 A73-39757

Heat conduction in blackened skin accompanying pulsatile heating with a xenon flash lamp. 20 p2519 A73-39791

Evaluation of effects of the microwave oven /915 and 2450 MHz/ and radar /2810 and 3050 MHz/ electromagnetic radiation on noncompetitive cardiac pacemakers. 20 p2520 A73-39824

Dissociation and bleaching of a multilevel molecular gas under the influence of radiation from a powerful CO2 laser 21 p2712 A73-40357

Similarity relations derived for unsteady powder burning with light irradiation or occurrence in semiclosed volume 21 p2791 A73-40700

A study of the properties of stimulated ruby laser emission during the action of Co-60 gamma rays 21 p2715 A73-40796

Interaction between radiation effects, gravity and other environmental factors in Tribolium confusum. 21 p2643 A73-40808

Amorphous alloy resistance thermometer development. 22 p2856 A73-42015

Development of a thermistor type temperature probe for use at low absolute pressures. 22 p2856 A73-42016

Measured drift of irradiated and unirradiated W3%Re/W25%Re thermocouples at a nominal 2000 K. 22 p2858 A73-42046

Gamma irradiation induced abiogenic radiochemical synthesis of deoxynucleosides from dry mixtures of purine bases with deoxyribose and ribose 22 p2803 A73-42166

Effects of space flight factors on the heredity of higher and lower plants. 22 p2804 A73-42168

Results of cytogenetic studies of seeds after their extended orbital flight aboard the Salyut orbital scientific station. 22 p2804 A73-42169

Heavy ion irradiation effects on bacteria mutations in balloon flight and accelerator experiments, comparing with cosmic rays 22 p2805 A73-42184

Apollo 16 Biostack experiment for biological effects of cosmic ray heavy primaries on cell and tissue development and mutations of bacilli, Artemia and plant seeds 22 p2805 A73-42185

Radiatively driven harmonic acoustic waves in vibrational equilibrium in closed cylindrical tube, deriving pressure response, radiative absorption coefficient and spectral detail 22 p2930 A73-42235

Viscous laminar Hartmann flow of electrically conducting liquid between parallel walls in transverse magnetic field, assessing thermal radiation effects and temperature distribution 23 p3008 A73-43207

Interstellar grain temperature fluctuations due to interstellar radiation field, discussing H atom recombination problem 23 p3029 A73-43747

Angstrom pyroheliometer scale correction for ratio of incident circumsolar radiation to electric current heating power derived from nonuniform painted surface strip illumination 23 p3025 A73-43985

Structural changes caused in glassy arsenic trisulfide and triselenide by penetrating radiation 23 p3017 A73-44042

Reactions of living organisms to the action of electromagnetic waves in the millimeter range 23 p2949 A73-44094

Prospects for studying mechanisms responsible for the nonthermal effects of millimeter- and submillimeter-band electromagnetic radiation on biologically active compounds 23 p2949 A73-44096

The effect of low X-ray doses on the central nervous system 23 p2947 A73-44179

Measurement of optically induced refractive-index changes with sharp edged illumination pattern. 23 p2984 A73-44371

Radiative damping of trapped gravity waves in the solar atmosphere. 24 p3135 A73-44629

Hardening with UV radiation in the manufacture of glass-fiber-reinforced unsaturated polyester resin molding materials 24 p3093 A73-44889

Influence of radiation on the current-voltage characteristic of tunnel diodes /Survey/ 24 p3072 A73-44926

The shapes of neutral globules associated with diffuse nebulae. 24 p3141 A73-45194

Effects of thermal conductivity in radiative magnetohydrodynamic channel flow. 24 p3117 A73-45370

Clearing of a cloudy atmosphere containing water drops by intense monochromatic radiation 24 p3108 A73-45520

RADIATION EXPOSURE

U RADIATION DOSAGE

RADIATION FIELDS

U RADIATION DISTRIBUTION

RADIATION HARDENING

Book - Fundamentals of nuclear hardening of electronic equipment. 03 p0283 A73-13990

Performance of hardened P-MOS devices in severe neutron environments. 05 p0557 A73-16517

Thin film nickel-chromium resistor failures in integrated circuits. 08 p0944 A73-20746

Rheological equation for expansion rate effects on stress-strain relation of polyester binders hardened thermochemically and by gamma radiation 08 p1019 A73-21764

Silicon solar cells radiation damage from orbital flight and electron and proton irradiation laboratory test data, discussing radiation hardening by Li doping 09 p1036 A73-22811

Electronic equipment computerized radiation hardness assurance program for retaliatory or deterrent missile system, discussing supplier data monitoring, verification test and radiation shield assurance 11 p1342 A73-26637

Nuclear hardness assurance and radiation specifications for overall system assurance, listing electronic component failure modes 16 p2035 A73-33651

He, Ne and Ar in chondritic Ni-Fe as irradiation hardness sensors. 17 p2120 A73-35801

Electromagnetic radiation hazard test facility, instrumentation, and weapon system susceptibility evaluation for providing environment protection and military standards 22 p2822 A73-41791

RADIATION HAZARDS

Influence of neutron bombardment on the mechanical properties of titanium and the magnitude of the programmed-hardening effect

23 p2995 A73-44284

RADIATION HAZARDS

Radioactive isotope powered thermoelectric generators operation and performance characteristics and design trends, discussing radiation hazards

01 p0005 A73-10475

Accuracy limitation in measurements of HF field intensities for protection against radiation hazards.

03 p0310 A73-14491

Russian book on radiation genetics of microorganisms covering lethal and mutagenic action of radiation on fungi, microscopic algae, bacteria and viruses

04 p0410 A73-15701

Radiation problems of supersonic flight - The operators' viewpoint.

05 p0542 A73-16624

Electric vector peak and rms magnitude determination for near field polarization ellipse, relating to radiation hazard criteria

06 p0667 A73-18202

Radiation protection at the work site: Scientific, technical and organizational aspects; Annual Scientific Conference, 6th, Karlsruhe, West Germany, May 17-19, 1972, Reports

11 p1322 A73-25310

Biophysical hazards of microwave radiation.

16 p1974 A73-32723

Cosmic rays airborne dosimetry from Concorde aircraft, noting passenger and crew radiobiological hazards at supersonic flight altitudes

18 p2348 A73-36908

Microwave radiation hazards around large microwave antenna.

19 p2397 A73-37274

Laser hazards and safety performance standards, discussing ocular and skin damage and exposure limits and operational regulation

20 p2517 A73-39205

Overview of Department of Defense Electromagnetic Radiation Hazards Standardization Program.

22 p2822 A73-41790

Frequency of heavy ions in space and their biologically important characteristics.

22 p2805 A73-42178

RADIATION HEATING

U RADIANT HEATING

RADIATION INDICATORS

U DOSIMETERS

U INDICATING INSTRUMENTS

RADIATION INJURIES

Russian book - Information macromolecules during radiation injury to cells.

04 p0410 A73-15707

Effect of lunar soil on radiation injuries in mice.

05 p0538 A73-16090

Genesis mechanism of slow cortical afterdischarges during brain injury by radiation

05 p0539 A73-16331

Deficits in visual function associated with laser irradiation.

10 p1182 A73-24563

Retinal damage from repeated subthreshold exposures using a ruby laser photocoagulator.

13 p1576 A73-28508

Book - Pathological effects of radio waves.

19 p2395 A73-37774

RADIATION INTENSITY

U RADIANT FLUX DENSITY

RADIATION LAWS

NT KIRCHHOFF LAW OF RADIATION

NT STEFAN-BOLTZMANN LAW

Influence of the surface-radiation law on the calculation of the aerodynamic coefficients in the near free molecular flow transient regime

12 p1487 A73-27391

RADIATION MEASUREMENT

Influence of additive and multiplicative noise on the accuracy in measuring the angular position of a source of radiation by systems with pulse-width modulation

01 p0017 A73-10212

An improved algorithm for the inversion of limb radiance measurements.

01 p0072 A73-19355

Inference of stratospheric temperature structure from limb radiance profiles.

01 p0072 A73-10356

Simultaneous measurements of solar radiation from aircraft and satellites during BOMEX.

01 p0038 A73-10377

A method for calculating atmospheric thicknesses directly from satellite radiation measurements.

01 p0073 A73-10378

The effect of solar radiation reflected from water surfaces on airborne and surface measurements in the thermal infrared.

01 p0038 A73-10385

Apparatus PG-1 for the study of the radiation characteristics in the neighbourhood of the earth by satellite Intercosmos 3.

01 p0051 A73-11021

Photomultiplier tubes nonlinear response in radiation measurements, suggesting fatigue avoidance through pulsed operation

01 p0053 A73-11222

Solar wind observations on the lunar surface with the Apollo-12 ALSEP.

02 p0205 A73-11903

Solar cosmic ray burst on July 7, 1966 and its measurement on the Proton-3 artificial earth satellite

02 p0208 A73-12461

Scintillation and anticoincidence Cerenkov counters for recording heavy nonrelativistic single charge particles in cosmic rays at sea level

02 p0209 A73-12670

Vertical resolution of temperature profiles obtained from remote radiation measurements.

02 p0165 A73-12778

A measurement of the atmospheric neutron flux in the energy range 50 less than E less than 350 MeV.

03 p0298 A73-12886

Measurements of the ultraweak bioluminescence phenomena as a new biotelemetric method.

03 p0272 A73-14304

Solar radio emission measurement and interpretation, discussing source mapping, coronal density, magnetic field and flare and particle events predictions

04 p0496 A73-14830

Vertical distribution of minor atmospheric constituents as derived from air-borne measurements of atmospheric emission and absorption infrared spectra. [AIAA PAPER 73-103]

05 p0570 A73-16863

New method for determining the total radiating power of partially transparent materials at high temperatures.

06 p0722 A73-17414

Measurement of the polarization of the radiation reflected backward from a laser-heated plasma.

06 p0731 A73-18589

Composition of radiation excess over primary cosmic ray background recorded by Cosmos satellites below midlatitude belt region

07 p0870 A73-19426

Night sky background radiation measurement by far IR radiometer carried on rocket launched from Hawaii

07 p0825 A73-20187

Measurement of the vertical transparency of the atmosphere in the infrared using an artificial source.

07 p0848 A73-20349

Measurements of the solar spectrum between 30 and 128 Å.

[AD-757958]

08 p1002 A73-20760

Detection of radon emanation from the crater Aristarchus by the Apollo 15 alpha particle spectrometer.

08 p1009 A73-21222

Solar energy outside the earth's atmosphere.

08 p1010 A73-21265

The third international comparisons of pyrheliometers and a comparison of radiometric scales.

08 p0966 A73-21266

Measurements of absorbed short-wave energy in a tropical atmosphere.

08 p0958 A73-21267

Measurements of solar energy reflected by the earth and atmosphere from meteorological satellites.

08 p0958 A73-21268

New radiometric techniques and solar constant measurements.

08 p0966 A73-21270

Direct measurement of water vapor absorption of solar radiation in the free atmosphere.

08 p0985 A73-21389

Statistical analysis of continuous neutron component intensity measurements in cosmic rays

09 p1137 A73-22020

Saint Severin meteorite irradiation data from thermoluminescence measurements, considering saturation of natural thermoluminescence from calibration curves

09 p1148 A73-22875

Large scintillation counter with a high amplitude resolution

09 p1085 A73-23003

Determination of emission spectra of the sky in the infrared between 45 and 500 micrometer using an interferometer aboard an airplane

10 p1210 A73-23749

Fluxes of electrons with energies above 80 MeV at the equator on the basis of measurements by the Cosmos 490 satellite

10 p1265 A73-23897

Some aspects of measuring the differential cosmic-ray spectrum.

10 p1268 A73-24213

Measurement of the absorption of solar ultraviolet radiation with the aid of a photoelectron analyzer

11 p1350 A73-25080

Nuclear track etching in radiation and fast neutron dosimetry and health physics, discussing counter materials and fission and alpha particles and recoil nucleus recordings

11 p1362 A73-25421

Ionization vacuum chambers for radiation measurement, discussing secondary emission, Greening theory

and dosimeters, electron beam monitors, pulse measurement, energy spectrometers and interface dosimetry applications

11 p1362 A73-25422

Delta ray particle track structure theory for radiation dosimetry and biological cell response to heavy ions, fast neutrons, stopped pions and mixed radiation fields

11 p1323 A73-25423

Radiophotoluminescence dosimetry for personnel monitoring, discussing thermoluminescence of phosphate and silver activated glasses, energy compensation filters and measurement techniques

11 p1362 A73-25425

Haven View project for atmospheric visibility and radiation measurements, describing airborne and ground based instrumentation and measurement results

11 p1352 A73-25444

Equipment and procedures for measurement of atmospheric spectral transmittance in the infrared region of the spectrum

11 p1363 A73-25643

Experimental determination of the integral radiative capacity of nickel

11 p1398 A73-25739

Lunar composition from Apollo orbital measurements.

11 p1422 A73-25956

Photoemission diode standards with high sensitivity, time stability and response uniformity for accurate measurement of monochromatic UV light, discussing design and construction

11 p1365 A73-26234

Active cavity radiometer as pyroheliometer for accurate radiation scale definition, determining measurement uncertainty through error analysis on quasi-equilibrium of power balance

11 p1365 A73-26236

Total irradiance calibrations using electrically calibrated radiometer, discussing lamp detector alignment procedures

11 p1366 A73-26252

Investigations of atmospheric extinction using direct solar radiation measurements made with a multiple wavelength radiometer.

12 p1520 A73-26810

Dependence of the light yield of a plastic scintillator on the energy of protons and electrons

12 p1496 A73-27206

Book - Microwave power measurement.

12 p1480 A73-27425

Collimator corrections to the measured diffuse X-ray background.

12 p1537 A73-27885

The estimation of extratropical cyclone parameters from satellite radiation measurements.

15 p1903 A73-31315

Certain methodological aspects of measurements of the average short-wave radiation fluxes in the presence of cloudiness

15 p1905 A73-31790

Certain parameters of cumulus clouds as determined from sky photographs and from ground-based actinometric measurements

15 p1905 A73-31793

Field spectroradiometer system to measure incident and reflected radiation intensity, discussing optical equipment, detectors, electronics and reference blackbodies

15 p1876 A73-31979

Measuring earth-to-space contrast transmittance from ground stations.

15 p1914 A73-32386

Solar cosmic-ray burst of July 7, 1966 and its measurement by Proton-3 satellite.

15 p1927 A73-32611

Detection and measurement of low-level backscattering of laser radiation

16 p1978 A73-32893

Properties of the satellite photoelectron sheath derived from photoemission laboratory measurements.

16 p2062 A73-33435

The abnormal stratosphere studied with the aid of satellite radiation measurements. [AIAA PAPER 73-493]

16 p2005 A73-33537

Observations of soft X-rays - Upper limits on the flux from SN 1972E and measurements of the diffuse background in Centaurus.

17 p2224 A73-34754

Rapid interferometric technique for MTF measurements in the visible or infrared region.

17 p2171 A73-35404

Measurement of near fields of antennas and scatterers.

17 p2142 A73-35679

Bandpass filter with cooled InSb detector for measurement of far IR radiation and temperature-wavelength characteristics of Hg arc lamp

17 p2176 A73-35774

Methods of measurements and some results of lower ionosphere by using VLF and LF radio waves.

18 p2302 A73-35926

Rocket investigation of the intensity and composition of the corpuscular radiation at altitudes 180 km up to the polar region. 18 p2345 A73-36137

Temperature determination of the upper atmosphere by the low-level detection of artificial luminous cloud radiation. 18 p2311 A73-36149

IR spectral measurements of reusable surface insulations via radiative four flux model [AIAA PAPER 73-745] 18 p2370 A73-36361

Solar proton and galactic background radiation measurements project Cold Flare at SST cruising altitudes, using high altitude radiation instrument system /HARIS/ 18 p2347 A73-36905

Statistical structure of the brightness field of reflected radiation in the 0.6-0.8 micron spectral interval. 18 p2314 A73-37063

Assessment of characteristics of the atmospheric moisture distribution with the aid of satellite measurements. 18 p2334 A73-37064

Utilization of satellite radiation measurements in analyzing the temperature near the ground. 18 p2334 A73-37067

Effect of cloud cover on the variability of outgoing radiation. 18 p2314 A73-37069

Measurements of the log-irradiance distribution of a laser wave propagated through the turbulent atmosphere. 19 p2405 A73-38222

Electron fluxes with energies greater than 80 MeV at the equator based on measurement data from the Cosmos-490 satellite. 20 p2601 A73-38916

The Synthesis Radio Telescope at Westerbork - Methods of polarization measurement. 20 p2566 A73-39581

The arrival of solar radiation on variously oriented inclined surfaces 20 p2555 A73-39818

Solar proton measurements during August 1972 chromos ray and magnetic field events caused by chromospheric flares associated with sunspots on east limb 21 p2757 A73-40592

Satellite counting of excess radiation measured as ionospheric electron and proton intensity dependent on geomagnetic activity, discussing proton energy spectra and electron albedo 21 p2758 A73-40604

Flux measurements of galactic cosmic-ray albedo neutrons by the Molnia 1 satellite in 1972 21 p2758 A73-40605

Remote sounding of water surface conditions from aboard artificial satellites. 21 p2657 A73-41333

Lunar orbital gamma ray measurements from Apollo 15 and Apollo 16. 21 p2762 A73-41397

Theory and measurement of emittance properties for radiation thermometry applications. 22 p2886 A73-41982

The determination of surface temperature from satellite 'window' radiation measurements. 22 p2846 A73-42057

Measurement of arc radiation for selected spectral regions. 22 p2861 A73-42569

UV radiation measurements of Ar-Hg gas discharge plasma as function of temperature and pressure with emphasis on fluorescent light design 23 p3011 A73-43830

The Nimbus-4 backscatter ultraviolet /BUV/ atmospheric ozone experiment Two years' operation. 23 p2975 A73-43877

Aerosols - A limitation on the determination of ozone from BUV observations. 23 p2975 A73-43879

RADIATION MEASURING INSTRUMENTS

NT ACTINOMETERS

NT BOLOMETERS

NT CERENKOV COUNTERS

NT DICKE RADIOMETERS

NT DOSIMETERS

NT ELECTRON COUNTERS

NT ELECTROPHOTOMETERS

NT ELECTROSTATIC PROBES

NT FABRY-PEROT SPECTROMETERS

NT GEIGER COUNTERS

NT HODOSCOPES

NT INFRARED DETECTORS

NT INFRARED INSTRUMENTS

NT INFRARED SCANNERS

NT INFRARED SPECTROMETERS

NT INFRARED SPECTROPHOTOMETERS

NT MICROWAVE RADIOMETERS

NT NEUTRON COUNTERS

NT PARTICLE TELESCOPES

NT PHOTOMETERS

NT PROPORTIONAL COUNTERS

NT PYRANOMETERS

NT QUANTUM COUNTERS

NT RADIATION COUNTERS

NT RADIATION DETECTORS

NT RADIOMETERS

NT RIOMETERS

NT SCINTILLATION COUNTERS

NT SILICON RADIATION DETECTORS

NT SOLAR SPECTROMETERS

NT SPARK CHAMBERS

NT SPECTROHELIOGRAPHS

NT SPECTROPHOTOMETERS

NT SPECTROPHOTOMETERS

NT THRESHOLD DETECTORS [DOSIMETERS]

NT ULTRAVIOLET SPECTROMETERS

NT ULTRAVIOLET SPECTROPHOTOMETERS

Inexpensive solar radiation measuring instruments comparison to standard solarimeter for mean and weekly errors 01 p0044 A73-10146

The design of broad-band resistive radiation probes. 03 p0310 A73-14492

Hot wire probe applications to radiation, fluid flow, vacuum and temperature measurements, deriving mathematical expressions for physical laws 08 p0962 A73-20750

Nuclear Science Symposium, 19th, and Nuclear Power Systems Symposium, 4th, Miami, Fla., December 6-8, 1972, Proceedings. 11 p1363 A73-25955

A digital measurement converter of pulsed flows 13 p1591 A73-28872

Russian book - Radiation receivers of automatic electron optics devices. 15 p1875 A73-31588

Photometer for detection of sodium day airglow. 19 p2428 A73-37261

Ideal laser amplifier as a phase measuring system of a microscopic radiation field. 22 p2870 A73-42516

Scientific equipment for studying cosmic rays on Prognoz satellites. I 24 p3144 A73-44783

Antenna design for intergalactic gravitational wave detection, discussing binary star and pulsar sources, Weber wave receiver and Zeldovich-Braginsky dumb-bell antenna 24 p3071 A73-44900

RADIATION MEDICINE

NT RADIOBIOLOGY

Observations concerning the combined radiation-protective effect of pantothenic acid and aminoethylisothionium 02 p0136 A73-11586

Russian book on auto-antibodies of X ray irradiated animal and human blood and organisms covering cell formation, isolation, preparations, sickness treatment and auto-immune reactions 04 p0410 A73-15711

RADIATION METERS

U RADIATION MEASURING INSTRUMENTS

RADIATION NOISE

U ELECTROMAGNETIC NOISE

RADIATION PRESSURE

NT ELECTRON PRESSURE

NT ILLUMINANCE

NT LUMINANCE

NT LUMINOUS INTENSITY

NT SOUND PRESSURE

Use of light pressure for selective evacuation of gases 01 p0059 A73-10627

Diffusion of radiation in a stellar shell expanding at a constant rate 01 p0100 A73-10707

Periodic perturbation of the libration points of the restricted three-body problem due to presence of a resisting medium and both gravitational and radiative fields of a fourth body. 01 p0103 A73-11018

Evolution of a satellite orbit under the influence of light pressure 02 p0211 A73-11777

New interpretations of extraterrestrial Lyman-alpha observations. 02 p0206 A73-12323

Extensive cosmic ray shower production by relativistic dust grain accelerated in interstellar space by galactic radiation pressure and subsequent magnetic processes 02 p0207 A73-12388

Re-calculation of efficiency factors for radiation pressure. 02 p0225 A73-12804

On the formation of Saturn's rings. 02 p0225 A73-12805

Geomagnetic field variations caused by changes in the quiet-time solar wind pressure. 03 p0298 A73-12885

On the stationary mass outflow from stars. I - The computational method and the results for a 1 solar mass star. 03 p0370 A73-13195

Chromospheric heating of very hot stars by radiation driven sound waves. 03 p0371 A73-13222

RADIATION PROTECTION

Pressure of radiation due to the absorption of resonant light 03 p0318 A73-13604

The effects of radiation pressure from resonance scattering in a quasar cloud. 04 p0499 A73-15355

Nonzero radiation pressure inclusion into Einstein cosmological equations, discussing Friedmann models evolution from radiation state epoch to matter domination 05 p0624 A73-17304

Radiation-driven efflux and circulation of dust in spiral galaxies. 07 p0875 A73-19345

A redshift magnitude relation for radiation universes. 08 p1007 A73-21002

Combined gravitational and solar radiation pressure effects on the semimajor axis of the earth's satellite. 08 p1010 A73-21314

Application of Gauss' method to the determination of secular radiational perturbations of artificial earth satellites 09 p1143 A73-22100

Chromospheric heating of very hot stars by radiation driven sound waves. II. 09 p1148 A73-22868

Influence of pressure anisotropy on the fluctuations of the magnetospheric tail 10 p1276 A73-23884

The effect of a uniform external pressure on the ionospheric boundary of a non-magnetic planet in a steady solar wind. 11 p1421 A73-25925

Radiation pressure effects on close binary mass loss and luminosity in terms of Roche potential, using contact surface model 12 p1537 A73-27881

Zero order approximation for attitude angle of stabilized satellite at high orbits under solar pressure perturbation, using trigonometric polynomials based on magnetometer data 15 p1943 A73-31241

Gravity oriented satellite librational damping by solar radiation pressure, comparing WKB method with numerical integration results 15 p1943 A73-31640

Solar radiation pressure on Mariner 9 Mars orbiter from mathematical model of illuminance and reflectivity characteristics 16 p2052 A73-32906

Earth radiation pressure and the determination of density from atmospheric drag. 18 p2308 A73-36051

Alfven waves in the solar wind - Wave pressure, Poynting flux, and angular momentum. 18 p2346 A73-36264

Effect of pressure anisotropy on oscillations of magnetotail. 20 p2603 A73-38903

Acceleration of heavy ions by radiation pressure. 22 p2900 A73-41759

The stability of rotating supermassive stars. 22 p2907 A73-42304

Solar pressure induced librations of spinning axisymmetric satellites. 22 p2910 A73-42633

Relationships between forces acting on bodies moving in a rarefied gas, in a light flux, and in hypersonic Newtonian flow 24 p3055 A73-45532

RADIATION PROTECTION

NT RADIATION SHIELDING

NT SOLAR RADIATION SHIELDING

Observations concerning the combined radiation-protective effect of pantothenic acid and aminoethylisothionium 02 p0136 A73-11586

Radiation protective effect of a mixture of ATP, AET, and serotonin on yields of 600-R X-ray-induced chromosome aberrations in the rat. 02 p0134 A73-12187

Electron-microscopic investigations regarding the protective effect of hypothermia on cell organelles in the case of whole-body X-irradiation 03 p0262 A73-13824

Further observed degradation on the LES-6 synchronous solar cell experiment. 03 p0258 A73-14247

Accuracy limitation in measurements of HF field intensities for protection against radiation hazards. 03 p0310 A73-14491

Antiradial properties of DNA and of its denaturation products 06 p0656 A73-18875

Radiation protection at the work site: Scientific, technical and organizational aspects; Annual Scientific Conference, 6th, Karlsruhe, West Germany, May 17-19, 1972, Reports 11 p1322 A73-25310

New norms and standardization trends for dosimetry and protection against radiation 11 p1322 A73-25311

Personnel radiation protection technology and criteria review, discussing dosimeter specifications and automatic data processing

11 p1322 A73-25314

Book - An introduction to radiation protection.

12 p1464 A73-27048

Mechanism of the action of radiation protecting agents - A biochemical shock hypothesis

12 p1465 A73-27499

Russian book on ionizing radiation protection covering shielding design, radiation source characteristics, maximum permissible levels, neutron, alpha, beta and gamma radiation, albedo, etc

18 p2336 A73-35872

Effect of secondary emission of the potential of a metallic body in the electron radiation belts of the earth.

20 p2601 A73-38875

RADIATION PYROMETERS

Turbine blade radiation pyrometer system.

06 p0692 A73-17844

Optical pyrometers with dual spectral ratios to eliminate instrument error due to selective radiation

08 p0962 A73-20862

Apparatus for measuring spectral emissivity of metals.

08 p0962 A73-20868

Multichannel quick-response photoelectric micropycnometer

17 p2164 A73-34173

Theory and measurement of emittance properties for radiation thermometry applications.

22 p2886 A73-41982

Radiation pyrometric probe /homogeneous thermally insulated rod/ for measuring body surface thermal loads and heat transfer coefficients

24 p3089 A73-44758

RADIATION RESISTANCE

U RADIATION TOLERANCE

RADIATION SHIELDING

NT SOLAR RADIATION SHIELDING

A shielding application of perturbation theory to determine changes in neutron and gamma doses due to changes in shield layers.

01 p0075 A73-10244

Evaluation of cerium stabilised microsheet coverslips for higher solar cell outputs.

03 p0256 A73-14229

Possible role of antitissular autoantibodies in the protective mechanism of local shielding during total radiation exposure

06 p0657 A73-17685

The process of reinforcement of lead shields in electroradiography

07 p0822 A73-19330

Evaluation of gamma-ray shielding calculations and determination of shielding parameters with bremsstrahlung radiation.

07 p0850 A73-20232

On the self-shielding coefficient of plates against neutron fluxes.

09 p1117 A73-22018

Attenuation of 15 MeV neutrons in multilayer shields composed of steel, polyethylene and borated materials.

10 p1248 A73-23571

Radiation doses during a prolonged orbital space flight about the earth

14 p1721 A73-29867

Space radiation environment effects on Intelsat 4 design, emphasizing trapped electrons and protons influences on solar cell shielding requirements

17 p2108 A73-34864

RADIATION SOURCES

NT MONOCHROMATORS

NT NEUTRON SOURCES

NT POINT SOURCES

Influence of additive and multiplicative noise on the accuracy in measuring the angular position of a source of radiation by systems with pulse-width modulation

01 p0017 A73-10212

Spatial-temporal processing of thermal radio signals from emitters moving in the near zone of an interferometer

01 p0017 A73-10213

Pulsed UV-radiation source for producing highly ionized low-density initial plasmas

01 p0082 A73-10325

Diffusion of radiation in a stellar shell expanding at a constant rate

01 p0100 A73-10707

Galactic and extragalactic X and gamma ray sources identification from satellite, rocket and high altitude balloon observations, discussing radiation generation theories

01 p0092 A73-10990

Observations of soft X-rays - Two supernova remnants in the constellation Lupus and the diffuse background.

01 p0103 A73-11031

Infrared stars with strong 1665/1667-MHz OH microwave emission.

01 p0104 A73-11040

21-micron observations of H II regions.

01 p0104 A73-11045

Antennas for measurement of microwave electromagnetic field by a light-modulated scattering technique.

01 p0025 A73-11055

Transfer equations for high-energy electrons and photons in magnetic fields.

01 p0080 A73-11309

International Conference on Cosmic Rays, 12th, University of Tasmania, Hobart, Tasmania, Australia, August 16-25, 1971, Papers. Volumes 1, 2, 3, 4, 5 & 6.

01 p0093 A73-11375

Composition of relativistic cosmic rays near the earth and at the sources.

02 p0207 A73-12327

Cosmic soft X rays observations by rocket-borne polypropylene window proportional counters, analyzing X ray sources spectra and intensity distributions

02 p0207 A73-12404

UV light intensities calibration in astrophysics and high temperature metrology with thermal arc plasma as radiation sources, discussing intensity standard establishment

02 p0199 A73-12715

Possibility of continuous monitoring of celestial X-ray sources through their ionization effects in the nocturnal D-region ionosphere.

03 p0361 A73-13361

A balloon-borne observation of the X-ray source Cygnus XR-1.

03 p0361 A73-13367

Observation of a correlated X-ray-radio transition in Cygnus X-1.

03 p0361 A73-13714

GX 17 + 2 X ray source optical counterpart identification, noting interstellar absorption role in magnitude estimation

03 p0374 A73-13795

Solar X-ray source unassociated with sunspots.

03 p0363 A73-13955

IR observations of comets Bennett and Tago-Sato-Kosaka, noting thermal origin of flux, source structure and material temperature, emissivity and composition

04 p0494 A73-14754

Distances and absolute luminosities of galactic X-ray sources.

04 p0492 A73-15358

Infra-red sources in the H II region W3.

04 p0499 A73-15485

Light flash induced by a pulsed X-ray source in the upper atmosphere

05 p0610 A73-17016

IR radiation source shape and size effects on aerial IR surveys at various flight altitudes, noting spectral composition change with height

05 p0578 A73-17140

Unorthodox ideas concerning the origin of cosmic radiation.

05 p0611 A73-17175

The Uhuru catalog of X-ray sources.

05 p0625 A73-17326

Observations of the extended X-ray sources in the Perseus and Coma clusters from Uhuru.

05 p0625 A73-17327

On the location of the source of Weber's gravitational events.

05 p0625 A73-17330

Hard X-ray observations of Hercules X-1 by OSO-7.

05 p0612 A73-17343

Positional evidence of Virgo X ray source correspondence with spiral galaxy IC 3576, noting optical and radio data incompatibility

05 p0626 A73-17346

A soft X-ray survey of the galactic plane from Cygnus to Norma.

05 p0612 A73-17389

Observations of Vela XR-1 by the UCSD X-ray telescope on OSO-7.

05 p0627 A73-17390

Arbitrary source emitted electromagnetic radiation in anisotropic stratified media, evaluating transverse and scattered fields and plane wave response

07 p0791 A73-19382

Geomagnetic field perturbation by gamma quanta pulsating source, studying accompanying radio emission behavior

07 p0816 A73-19445

Josephson junction millimeter microwave source and homodyne detector.

07 p0863 A73-20104

Spectral energy distribution and IR radiation source size of M8 star cluster, determining stellar dust temperature

08 p1003 A73-20893

Some questions on the evidence of laser X-ray emission from CuSO4 doped gelatin.

08 p0975 A73-21061

Nonprimordial hypothesis for cosmic microwave background radiation generation by ordinary astronomical processes and subsequent thermalization by interaction with dust grains

08 p1008 A73-21152

Cosmic ray source composition calculated from diffusion-produced path length spreads

08 p0998 A73-21232

On the near- and far-field radiation patterns generated by the non-linear interaction of two separate and non-planar monochromatic sources.

08 p0988 A73-21469

Application of statistics to results in gamma ray astronomy.

08 p1012 A73-21644

A possible cosmic ray primary particle energy spectrum above 10 TeV and its astrophysical implications.

08 p1000 A73-21824

Emission spectrum of a source moving along a stable circular orbit near a rotating 'black hole'

09 p1145 A73-22295

Balloon observations of galactic and extragalactic objects at 100 microns.

09 p1150 A73-23134

Primaries of extensive air showers of cosmic radiation.

09 p1138 A73-23170

Circular polarization of the emission of cosmic objects

09 p1151 A73-23329

Synchrotron emission amplification by magnetic field in cosmic sources from analysis of relativistic electron system, noting pulsars and UV Ceti stars

10 p1264 A73-23708

Faraday pulsations and circular polarization of optical radiation from cosmic sources in terms of angle between interstellar dust orientation vector and galactic plane

10 p1273 A73-23709

Analysis of the variations of cosmic rays of magnetospheric and interplanetary origins according to spectrographic data

10 p1267 A73-23928

Capture of primary cosmic rays in the upper atmosphere as a source of excess radiation

10 p1268 A73-23931

The circular polarization of sources of synchrotron radiation.

10 p1270 A73-24901

Radiation source motion at superluminal speed in vacuum, defining conditions for Vavilov-Cerenkov and Doppler effects

10 p1250 A73-24943

Acoustic dipole source strength on flat plate and simple airfoil surfaces from local surface and far field acoustic pressure cross correlation

11 p1345 A73-24982

OJ 287 and BL Lacertae with rapid radio, IR and optical variability, high IR luminosity, line free optical spectra and varying polarization

11 p1416 A73-25179

IR sources at 1-5 microns, discussing Betelgeuse, R Doradus, dying stars, new stars and galaxies

11 p1422 A73-25974

Quasi-optical diffraction-type radiation generator

11 p1331 A73-26159

The generation of tunable coherent radiation in the wavelength range 2300-3000 A using lithium formate monohydrate.

12 p1504 A73-26826

Confined optical and radio source image reconstruction from spatial frequency components of source not passed by imaging system

13 p1671 A73-28030

Source altitude for experiments to simulate space-to-earth laser propagation.

14 p1756 A73-30151

Complex radiation effects of sources moving in a plasma

14 p1780 A73-30262

Nonstationary emission from dipole sources in a plasma with a diagonal permittivity tensor

14 p1780 A73-30263

Transition radiation production by relativistic electrons traversing cosmic grains as source of celestial X rays, discussing formation zone effect

14 p1787 A73-30730

Primordial cosmic ray abundance from rotating magnetic A stars with accelerating ionized interstellar gas particles

15 p1925 A73-31059

Gamma and cosmic ray astronomy review, covering balloon and rocket measurements, galactic and metagalactic source locations and radio source information

15 p1926 A73-31148

Small perturbation method study of nonlinear weak D-type unsteady ionization front geometry with radiation source in interstellar incompressible gas medium

15 p1932 A73-31295

Pulsed holographic interferometry at 10.6 microns.

15 p1875 A73-31400

Infrared emission from the OH/H2O sources in W49.

15 p1940 A73-32196

An electronically gated gamma and X-ray calibration scheme.

15 p1879 A73-32222

Sco X 1, Cygnus and galactic center X ray sources radio observations, discussing identification, properties and variabilities

16 p2050 A73-32733

High energy gamma ray discrete source identification in Crab Nebula, pulsar NP 0532 and galactic regions from Apollo and TD-1 satellite measurements
16 p2051 A73-32750

Preparation of high-level alpha-particle sources for the Surveyor Alpha Scattering Experiment.
16 p2035 A73-32975

Gamma ray astronomical state-of-art, discussing cosmic gamma ray sources observation and diffuse radiation measurement
16 p2055 A73-33290

Galactic sources and the propagation of cosmic rays - A review of the light isotopes and the odd-Z elements.
16 p2055 A73-33295

Grazing incidence X ray telescope lens design for radio and optical identifications of radiation sources by satellites
17 p2171 A73-35409

Antenna array facility with small digital computer and multichannel tape recorder for real time simulation of radiation source movement through view field
17 p2149 A73-35755

Calculation of components, electrical conductivity, and total radiative source strength of nitrogen plasma in local thermodynamic equilibrium.
[AIAA PAPER 73-744]
18 p2339 A73-36360

Synchrotron radiation stimulated amplification by magnetic field in cosmic sources from analysis of relativistic electron system, noting pulsars and UV Ceti stars
18 p2347 A73-36733

Faraday pulsations and circular polarization of optical radiation from cosmic sources in terms of angle between interstellar dust orientation vector and galactic plane
18 p2354 A73-36734

Zeeman effect in the X-ray star candidates HD 77581 and theta super 2 Orionis.
19 p2482 A73-37399

Synchrotron radiation sources with relativistic particles moving at small pitch angles in magnetic field, discussing emission properties and degrees of polarization
19 p2484 A73-37617

Evidence for an interstellar or interplanetary source of diffuse He I 584 A radiation.
19 p2475 A73-37629

Jupiter atmosphere discrete source maps of 5 micron radiation distribution, correlating brightness temperature and photographically recorded colors
19 p2489 A73-38525

2.2- and 3.5-micron polarization measurements of the Becklin-Neugebauer object in the Orion Nebula.
19 p2489 A73-38528

IR astronomical objects, methods and instruments, discussing galactic and extragalactic sources, early and late stars, planetary nebulae, interstellar dust and hydrogen ion clouds
20 p2605 A73-39060

Cosmic sources of X rays and gamma rays
20 p2601 A73-39061

Quantized magnetic bremsstrahlung from white dwarfs surface layer as possible source of Galactic center infrared radiation
20 p2611 A73-39709

The effect of comparison source reflectance on gas temperature measurement by Kuribau's method and line reversal methods.
21 p2692 A73-39916

All-Union Conference on the Physics of Cosmic Rays, Apatity, USSR, December 12-15, 1972, Proceedings
21 p2755 A73-40576

Investigation of primary gamma radiation from the northern polar region of the Galaxy
21 p2756 A73-40578

Nova and supernova stars as sources of relativistic particles
21 p2756 A73-40580

Effects of nuclear reactions with fast protons in a supernova shell and the origin of cosmic rays
21 p2756 A73-40581

Variability of high-energy gamma-radiation sources
21 p2759 A73-40707

X ray background radiation intensity fluctuations from random discrete point sources, indicating extragalactic origin
21 p2759 A73-40710

A two-dimensional field induced by travelling sources.
21 p2740 A73-41016

Infrared maps of the galactic nucleus.
22 p2904 A73-41757

Electromagnetic radiation excited by electric or magnetic line source near inhomogeneous dielectric layer, evaluating reflected and transmitted fields by saddle point technique
22 p2824 A73-41831

Radiation field frequency dependent source function for two level atom, noting different stimulated emission and absorption line profiles
22 p2907 A73-42205

Cerenkov-effect based standard radiation source designed for the calibration of space experiments - Spectral energy distribution measurement
22 p2860 A73-42307

Investigation of the intensity distribution in a molecular beam expelled from a conical ring source
22 p2889 A73-42387

Charged black hole collisions as gravitational radiation sources in terms of conservation of mass and surface area
22 p2908 A73-42428

The H II region G333.6-0.2, a very powerful 1-20 micron source.
23 p3028 A73-43527

Role of constraining forces for ultrarelativistic particle motion as a source of gravitational radiation.
23 p3006 A73-43606

Galactic and extragalactic gamma ray bursts contribution to diffuse cosmic X ray flux, noting superposition of supernovae outbursts
23 p3025 A73-43957

RADIATION SPECTRA

NT ABSORPTION SPECTRA
NT BALMER SERIES
NT D LINES
NT ELECTROMAGNETIC SPECTRA
NT ELECTRONIC SPECTRA
NT EMISSION SPECTRA
NT FRAUNHOFER LINES
NT H ALPHA LINE
NT H BETA LINE
NT H GAMMA LINE
NT H LINES
NT HERZBERG BANDS
NT INFRARED SPECTRA
NT K LINES
NT LINE SPECTRA
NT LYMAN SPECTRA
NT MICROWAVE SPECTRA
NT PASCHEN SERIES
NT RADIO SPECTRA
NT RAMAN SPECTRA
NT RYDBERG SERIES
NT SOLAR SPECTRA
NT STELLAR SPECTRA
NT TELLURIC LINES
NT ULTRAVIOLET SPECTRA
NT VIBRATIONAL SPECTRA

The fluctuation spectrum of laser radiation in a turbulent atmosphere in the presence of rain
01 p0060 A73-10872

Extensive air shower spectra based on electron and muon number for given shower development mechanism and primary cosmic ray chemical composition
02 p0209 A73-12677

Russian book on color recognition methods and devices covering algorithms for radiation color identification and optimal spectra of photosensitive radiation detector
02 p0144 A73-12862

The Fermi mechanism and the source spectrum of cosmic ray nuclei.
03 p0361 A73-13365

Quasi-hydrodynamic equations for transverse quanta in inhomogeneous plasma, using geometric optics approximation
06 p0728 A73-17969

Interstellar matter. II - Diffuse interstellar lines and porphyrins.
06 p0750 A73-18013

Interstellar extinction curve structure via photographic techniques, considering optical observation extension into UV with OAO-C telescope
06 p0751 A73-18228

Charge dependence of the energy spectra of cosmic rays.
07 p0873 A73-20561

Optical pyrometers with dual spectral ratios to eliminate instrument error due to selective radiation
08 p0962 A73-20862

Apparatus for measuring spectral emissivity of metals.
08 p0962 A73-20868

Study of the galactic structure from observations of interstellar calcium. I - Analysis of radial velocities
08 p1004 A73-20909

Primary cosmic ray particles disappearance and proton spectrum slope rise in 1 TeV energy region from Proton satellites data
08 p0999 A73-21330

The directivities and spectral contents of radiation of multidiode injection lasers.
09 p0197 A73-23049

An estimate of the energy spectrum of gamma rays from the central region of the Galaxy and some implications.
10 p1263 A73-23486

Luminosity and frequency spectrum of radiation from spherically symmetric steady state accretion of interstellar gas onto nonrotating black hole at rest
10 p1272 A73-23534

Some aspects of measuring the differential cosmic-ray spectrum.
10 p1268 A73-24213

Spectral shift between components of homogeneous /radiation or shock/ line, using ring laser spatial and frequency burnout effects
10 p1228 A73-24464

The thermal radiation spectra of supermassive stars and X-ray sources.
10 p1270 A73-24902

Development of spark chambers for use in measurements of the charge spectrum of high energy cosmic rays.
11 p1363 A73-25961

The spectrum of the extranuclear regions of Ton 256.
11 p1428 A73-26624

Microwave oscillations and the visible radiation spectrum of a cesium plasma diode
12 p1527 A73-26938

Ring cavity for analyzing the spectral composition of CO₂-laser radiation
12 p1506 A73-27217

Selection of a propagation model for computing the solar-proton injection spectrum
12 p1534 A73-27333

The spectrum of fluctuations of laser radiation in a turbulent atmosphere during rain.
13 p1627 A73-28696

Investigation of the shape of radiation pulses emitted by a self-mode-locked laser.
14 p1757 A73-30329

Gas absorption lines detection based on multiple light passage through absorbing medium during generation process, noting radiation spectra of neodymium glass laser
14 p1757 A73-30331

Black holes in binary systems, discussing radiation spectrum, disk formation, optical luminosity, X rays, UV regions and temperature distribution
15 p1928 A73-31051

Calculations of neutron flux spectra induced in the earth's atmosphere by galactic cosmic rays.
16 p2055 A73-33426

Some results of lunar surface luminescence studies at the Kharkov Astronomical Observatory
16 p2063 A73-33762

Spectral shift between components of homogeneous /radiation or shock/ line, using ring laser spatial and frequency burnout effects
19 p2438 A73-38136

Remote sensing of terrestrial resources
19 p2426 A73-38176

The multiplicity distribution of shower particles underground and the cosmic-ray primary spectrum.
21 p2764 A73-41633

Inner zone population of trapped 2.14-9.0 MeV alpha particles, noting strong peak in pitch angle and intensity decrease with L value decrease
22 p2901 A73-41910

Frequency of heavy ions in space and their biologically important characteristics.
22 p2805 A73-42178

Microwave oscillations and visible emission in a cesium diode.
22 p2892 A73-42272

Size spectra of extensive air showers and primary cosmic-ray spectrum.
22 p2903 A73-42427

Selection of a propagation model for calculating the injection spectrum of solar protons.
23 p3020 A73-43231

Vacuum-UV radiation of laser-produced plasmas.
23 p3008 A73-43340

Planetary spectrum formation in atmospheric model with lower and upper layers of infinite and small optical thickness respectively
23 p3029 A73-43623

Role of hydromagnetic waves in cosmic-ray confinement in the disk. I - Theory of behavior in general wave spectra.
24 p3124 A73-45040

RADIATION THERAPY

Attenuation of 15 MeV neutrons in multilayer shields composed of steel, polyethylene and borated materials.
10 p1248 A73-23571

RADIATION TOLERANCE

Progress in the development of radiation-resistant aluminum-doped silicon solar cells.
03 p0258 A73-14248

Radiation sensitivity of silicon imaging sensors on missions to the outer planets.
05 p0557 A73-16512

Sensitivity to oxygen at high pressure of radioreistant and radiosensitive strains of bacteria.
07 p0780 A73-19483

Morphological changes in the testicles of dogs exposed to chronic and combined gamma-radiation
08 p0929 A73-20981

Effects of boron density on radiation resistance of copper-contaminated n/p type silicon solar cells.
08 p0928 A73-21114

Retinal damage from repeated subthreshold exposures using a ruby laser photocoagulator.
13 p1576 A73-28508

Preparation of CdS single crystals with a radiation-stable sensitivity to ionizing emissions
15 p1923 A73-31208

RADIATIVE HEAT TRANSFER

- Biophysical hazards of microwave radiation.
16 p1974 A73-32723
- Biological indicators and the effectiveness of sterilization procedures.
16 p1976 A73-33692
- Book - Pathological effects of radio waves.
19 p2395 A73-37774
- Free fall effects on differential growth and radiation sensitivity of higher plants in space flight and ground based clinostat experiments
22 p2804 A73-42172

RADIATIVE HEAT TRANSFER

- Tropical atmosphere radiative heating estimates for BOMEX /Barbados Oceanographic and Meteorological Experiment/ from direct radiation measurements, satellite images and surface and rawinsonde data
01 p0038 A73-10387
- Rigid and free boundaries effects on radiative heat transfer stabilization of fluid layer against Benard thermal convection
01 p0120 A73-10397
- Numerical simulation of radiative-conductive heat transfer in the Martian atmosphere-polar cap utilizing Mariner 9 Iris data.
01 p0097 A73-10401
- Radiation in the reacting boundary layer.
01 p0121 A73-10642
- Radiative and convective heating during Venus entry.
01 p0003 A73-10757
- Direct Monte Carlo simulation of two-dimensional radiative heat transfer in absorbing-emitting medium bounded by the non-isothermal gray walls.
01 p0123 A73-11319
- Radiation heat transfer in isothermal adjoint plate system with directionally emitting and nondiffuse reflecting surfaces, considering surface roughness effects
01 p0123 A73-11440
- Computer programs for radiative heat transfer and thermal equilibrium equations, noting transient temperature distribution measurement of two stage radiant cooler
01 p0111 A73-11151
- A design study of thermal louver system.
01 p0111 A73-11152
- Nonstationary interaction of thermal radiation with surfaces of pure metals
01 p0124 A73-11434
- Kinetics of heating a light-scattering field by radiant heat transfer
02 p0238 A73-12098
- Apparatus for investigations into long-term strength and creep of coated materials at temperatures above 1400 C in air.
02 p0150 A73-12219
- Magnitude estimate for long wave radiative cooling effects for isolated buoyant thermal rising in uniform ambient atmosphere
[AD-755500] 02 p0224 A73-12779
- Radiation base heating from solid propellant launch vehicle exhaust plumes.
[ALAA PAPER 72-1168] 03 p0397 A73-13466
- Radiative and convective heat transfer occurring in the hypersonic flow past a blunted body.
03 p0244 A73-13617
- Two layer model for diurnal temperature variations analysis of radiative heat transfer between planetary lower atmosphere and underlying
04 p0473 A73-15574
- Combustion chamber temperature profiles analytical derivation from simultaneous radiative and turbulent diffusion heat transfer of turbulent flame front
[ASME PAPER 72-WA/HT-27] 04 p0519 A73-15827
- Application of Olfe's modified differential approximation to the radiation-layer problem on a flat plate.
[DFVLR-SONDDR-254] 04 p0520 A73-15946
- Insulating materials fireproofing effectiveness prediction by finite element method for combined time dependent convective-radiative boundary conditions
05 p0637 A73-16132
- Heat transfer in static packed beds - Effects of radiation on temperature distribution.
05 p0638 A73-16219
- Numerical tests of atmospheric circulation and climate theory and accuracy conditions for atmospheric models, noting temperature dependence on radiative and nonradiative heat transfer
05 p0593 A73-16242
- Gas flow temperature determination in the presence of radiation heat exchange between the heat sensor and some surrounding structures
05 p0578 A73-16996
- Investigation of convective and radiative heating of blunted bodies in hypersonic flow
06 p0644 A73-17469
- Approximate analytical solution of an asymmetrical problem of unsteady heat conduction with nonlinear boundary conditions
06 p0768 A73-18128
- Integral equations for temperature distribution in radiative and conductive heat transfer in semitransparent medium, noting temperature oscillation propagation
06 p0769 A73-18565

- Determination of the sensitivity of an infrared pyrometer with a thermocouple
06 p0695 A73-18567
- Combustion molecular gases radiative heat transfer, emissivity and absorptivity calculation, presenting high speed computer routine
06 p0770 A73-18832
- Integral method for nonlinear transient heat transfer in a semi-infinite solid.
07 p0919 A73-19493
- Characteristics of the calculation of radiant transfer in a system of diathermic bodies separated by an absorbing and scattering medium
07 p0921 A73-20080
- Comparison of exact and mean beam length results for a radiating hydrogen plasma.
07 p0859 A73-20221
- The applicability of an approximate expression for radiative heating.
07 p0921 A73-20222
- Electrical components heat dissipation via thermal radiation, determining nonlinear temperature dependence from Stefan-Boltzmann law
08 p1020 A73-20775
- Non-gray radiative heat transfer in the picket-fence approximation.
08 p1020 A73-20790
- Radiation between finite surfaces with variable radiative characteristics.
08 p1021 A73-20794
- Radiative heat transfer in fiberglass insulation.
08 p1021 A73-20866
- Thermal state of a porous plate cooled by intense blowing under conditions of radiative-convective heating
08 p1021 A73-20993
- Short-wave spectral radiant heat influx in the atmosphere
08 p0984 A73-21133
- Spectral reflection of heat radiation from an arbitrary reflector surface to an arbitrary receiver surface.
08 p1022 A73-21254
- Quasi isothermal, transonic flow of radiating gases
08 p1024 A73-21497
- Stagnation region radiative heating with steady-state ablation during Venus entry.
08 p1025 A73-21817
- The transfer of radiation from a flame to its fuel.
08 p1025 A73-21822
- Russian book on space flight radiative heat transfer problems covering spacecraft thermal conditions, solar and planetary heat flux, radiant cooling and vacuum tests
09 p1166 A73-22348
- Study of the radiative properties of the atmosphere between cloud layers
09 p1114 A73-22371
- Some results of investigations programmed according to the complex atmospheric energetics experiment /1970-1972/
09 p1115 A73-22989
- Radiant heat flux distribution on the surface of a sphere in hypersonic flow of an inviscid radiating gas
10 p1171 A73-23581
- Radiative heat transport models for evacuated powder to specify IR radiation environment on lunar surface
10 p1282 A73-24645
- Integral transform and heat conduction in a hollow cone with radiation.
10 p1297 A73-24920
- Influence of radiation on the conditions in the atmospheric boundary layer
11 p1393 A73-25641
- Radiative slip between two adjacent absorbing-emitting gases and its application to air pollution.
11 p1353 A73-25722
- Nonstationary interaction of thermal radiation with surfaces of pure metals.
11 p1452 A73-26061
- Simultaneous radiative and conductive heat transfer in non-gray media.
11 p1453 A73-26583
- Simplification of one-dimensional heat-conduction problems in the case of impulsive radiative heating of flat bodies
12 p1558 A73-27317
- Spectral and boundary effects on coupled conduction-radiation heat transfer through semitransparent solids.
12 p1559 A73-27695
- Nonlinear problems for a system of two heat-radiating gray bodies separated by a diathermic medium
12 p1560 A73-27810
- Iterative-zonal method for studying and calculating the local characteristics of radiative heat transfer.
12 p1560 A73-27913
- The transient temperature distribution in a slab subjected to radiative and convective heating calculated by variational method.
13 p1704 A73-28429
- Modified separable kernel method for heat conduction with a nonlinear boundary condition.
13 p1706 A73-28819

- Screen effect on the radiation heat transfer in an area of penetrating radiation
14 p1816 A73-30013
- The stability of a thermally radiating stratified shear layer.
14 p1816 A73-30169
- Radiant heat transfer on circular-finned cylinders.
14 p1817 A73-30574
- The thermal analysis of a belt type radiator by the method of matched asymptotic expansions.
14 p1817 A73-30609
- An analytic formula for heating due to ozone absorption.
14 p1750 A73-30767
- Study of the effect of heat influxes on the formation of lower and higher baric fields in the Northern Hemisphere
15 p1903 A73-31602
- Experimental assembly for complex heat transfer studies
15 p1858 A73-31860
- A procedure for simultaneous measurement of convective and radiant thermal fluxes in permeable walls
15 p1957 A73-31866
- Radiative heat transfer through semitransparent solid plane layer, measuring temperature profile and heat flux for comparison with rectangular multiband model calculation
[ASME PAPER 72-WA/HT-6] 15 p1958 A73-32276
- Approximation nature and error magnitude in radial radiative heat flux within optically thin nongray isothermal gas cylinder
15 p1959 A73-32282
- Photochemical, radiative and dynamic modeling of the stratosphere.
[AIAA PAPER 73-527] 16 p2007 A73-33561
- Integral equations for temperature distribution in radiative and conductive heat transfer in semitransparent medium, noting temperature oscillation propagation
16 p2086 A73-33590
- Determination of sensitivity of infrared pyrometer with a thermopile.
16 p2016 A73-33592
- The thermal regime and convective motions in the lower layers of the Venusian atmosphere
16 p2068 A73-33825
- Thermal shielding by subliming volume reflectors in convective and intense radiative environments.
17 p2253 A73-34183
- Radiative heat transfer with no temperature jump at interface of media
17 p2254 A73-34773
- Russian book on radiative and complex heat transfer covering electromagnetic energy-matter interaction, modeling, convective and conductive transfer and thermodynamic equilibrium radiation
17 p2254 A73-34899
- Nearly spherical constant-power detonation waves as driven by focused radiation.
[AIAA PAPER 73-674] 18 p2322 A73-36225
- Radiation heat transfer in multilayer insulation having perforated shields.
[AIAA PAPER 73-718] 18 p2369 A73-36337
- Approximate configuration factors for a gray nonisothermal gas-filled conical enclosure.
[AIAA PAPER 73-752] 18 p2370 A73-36368
- Radiative heat transfer through composite materials.
18 p2371 A73-36621
- Computation of heat flux in numerical weather forecasting.
18 p2334 A73-37059
- Experiments on incorporating radiative heat influx in numerical forecasting.
18 p2334 A73-37077
- Experimental measurement of heat transfer to a cylinder immersed in a large aviation-fuel fire.
[ASME PAPER 73-HT-2] 20 p2625 A73-38565
- Heat transfer in an absorbing, emitting and scattering slug flow between parallel plates.
[ASME PAPER 73-HT-13] 20 p2625 A73-38568
- Combined forced convection and radiation heat transfer in the thermal entrance region of a non-isothermal parallel plate channel - Optical thin gases.
[ASME PAPER 73-HT-14] 20 p2625 A73-38569
- Study of heat transfer in boundary layer taking into account the radiation at the surface.
20 p2507 A73-39420
- Radiative and convective heat transfer in a magnetic field
20 p2628 A73-39608
- Multispectral remote sensing of elements of water and radiation balances.
20 p2558 A73-39864
- Small surface plate calorimeter for convection and radiation heat transfer measurements from heated body in air
21 p2692 A73-39920
- Radiative-convective heat transfer in flows of hot air past a flat plate.
21 p2791 A73-41056
- Structure of ionizing shock waves with radiative energy loss.
22 p2841 A73-42200

- Spaced annular ring shell-to-shell and shell-to-tube view factors for finite difference radiative heat transfer solutions 22 p2923 A73-42564
- An exact solution on the propagation of small disturbances in a radiating grey gas with isotropic scattering. 22 p2932 A73-42570
- Book - Thermal radiative properties: Coatings. 22 p2937 A73-42857
- Radiation heat transmission from human underlying and surface skin effect on epidermal temperature gradient 23 p2950 A73-44217
- An unsteady heat-conduction problem in a system of diathermally separated bodies 24 p3154 A73-44422
- A first look at atmospheric dynamics and temperature variations on Titan. 24 p3128 A73-44433
- Model for radiative dynamic instability of cloudy planetary atmosphere from coupling for case of radiative heating rate dependent cloud properties 24 p3132 A73-44534
- Radiant-conductive heat transfer in a plane layer of an absorbing and scattering medium 24 p3155 A73-44754
- RADIATIVE LIFETIME**
- Measurements of the upper and lower level lifetime in He-Se lasers. 22 p2871 A73-43086
- Metastable oxygen atoms radiative lifetime quenching rate as function of altitude in lower ionosphere based on auroral observations and atmospheric model 23 p2972 A73-43692
- RADIATIVE RECOMBINATION**
- Three component static thermosphere model for oxygen radiative recombination and thermal diffusion dependence on underlying layers and solar UV radiation 06 p0689 A73-17539
- Infrared and microwave emission from nebulae in the galaxy. 09 p1150 A73-23133
- Semiconductor injection lasers, discussing optical transitions threshold effects, radiative recombination, coherent emission, etc 12 p1506 A73-27136
- Stimulated emission of light from solid solutions of tin and lead chalcogenides in the region of 10 microns. 12 p1507 A73-27519
- Observations of formamide at 6 cm in Sagittarius B2. 15 p1933 A73-31377
- Recombination of doubly ionized atoms in the afterglow of a helium plasma produced by laser. 15 p1915 A73-31675
- Three component static thermosphere model for oxygen radiative recombination and thermal diffusion dependence on underlying layers and solar UV radiation 16 p2001 A73-32763
- Radiative and dielectronic recombination coefficients for complex ions. 16 p2038 A73-32842
- Non-thermal ionization and recombination processes during solar flares. 16 p2052 A73-32958
- Approximation to the collisional-radiative recombination coefficient in a partially ionized gas. 17 p2213 A73-34197
- Continuum emission from recombining oxygen and nitrogen plasmas. 18 p2338 A73-36799
- Location in magnetic latitude and local time of the tropical ultraviolet bands seen from Apollo 16. 21 p2684 A73-40788
- Kinetics of impact-radiation ionization and recombination. 22 p2892 A73-42344
- Air afterglow radiative recombination reaction of NO with O yielding nitrogen dioxide, considering pressure dependence in chemiluminescence spectral region 22 p2819 A73-42772
- Theory of donor-acceptor radiative and Auger recombination in simple semiconductors. 23 p3016 A73-43796
- RADIATIVE TRANSFER**
- NT RADIATIVE HEAT TRANSFER**
- Book - Emission, absorption, and transfer of radiation in heated atmospheres. 01 p0119 A73-10125
- Discussion of radiative-transfer methods applied to electromagnetic reflection from turbulent plasma. 01 p0081 A73-10196
- IR radiative energy transfer in gases, applying spectroscopic band absorption information 01 p0120 A73-10291
- A solution to the auxiliary equation of radiative transfer for a planetary atmosphere with molecular anisotropy. 01 p0097 A73-10352
- Radiative calculation models for infrared transfer through cloud, aerosol and the continuum. 01 p0073 A73-10358
- Global mean radiative equilibrium model for Venusian mesosphere, determining horizontal variation of thermal heating and cooling 01 p0097 A73-10361
- Synthetic spectra production via solution of radiative transfer equation at frequencies across absorption line for homogeneous and inhomogeneous atmospheres 01 p0097 A73-10362
- Atmospheric radiative transfer by carbon dioxide. 01 p0037 A73-10366
- The infrared spectrum of Jupiter - Structure and radiative properties of the clouds. 01 p0097 A73-10370
- Multispectral cloud type identification based on Nimbus 3 medium resolution IR radiometer measurements, using radiative transfer theory 01 p0073 A73-10381
- Nongray atmospheric model to assess radiative effects of water vapor and carbon dioxide layer injected into lower stratosphere by SST and HST exhaust gases 01 p0038 A73-10388
- Condensation trail effects on atmospheric radiation budget from model calculation for ice particle layer near tropopause, using Mie scattering and radiative transfer approximation 01 p0038 A73-10389
- A detailed radiation model for climate studies - Comparisons with a general circulation model radiation subroutine. 01 p0039 A73-10393
- Radiation transfer within spectral line in symmetric isothermal medium, assuming spherical incoherent scattering characteristic and scattering angle-independent redistribution law 01 p0100 A73-10705
- An approximation to radiative transfer in a nongray gas. 01 p0121 A73-10733
- General solution for polarized radiation in a homogeneous-slab atmosphere. 01 p0078 A73-11033
- Book - Radiation transport in spectral lines. 02 p0194 A73-11876
- Collisional-radiative coefficients and population coefficients of hydrogen plasma. 02 p0198 A73-12347
- On combined operations method for transfer problems in homogeneous, cylindrical media. 02 p0193 A73-12383
- Invariant imbedding and Chandrasekhar's planetary problem of radiative transfer. 02 p0207 A73-12389
- Transfer of resonance radiation and photon random walks. 02 p0207 A73-12403
- Optimization of spectral intervals for remote sensing of atmospheric temperature profiles. 02 p0171 A73-12774
- Seasonal and monthly global atmosphere radiative profiles of thermal and solar heating due to ozone and cooling due to carbon dioxide 02 p0165 A73-12780
- Energy flux intensity in IR bands of selectively radiating molecular gas nonisothermal layer from radiative transfer equation and mathematical model 03 p0396 A73-13183
- Compression shock formation in arbitrary medium described by first order quasi-linear partial differential equations, considering strongly radiating and emission dominated gases 03 p0400 A73-14629
- The interaction between ground reflecting power and celestial brightness 04 p0441 A73-15292
- Cloudiness as a global climatic feedback mechanism - The effects on the radiation balance and surface temperature of variations in cloudiness. 05 p0591 A73-16187
- Implications of a quadratic stream definition in radiative transfer theory. 05 p0592 A73-16196
- Solution on a BESM-3M electronic computer of the equation for transfer of diffuse radiation in two-layer plane-parallel models of galaxies 05 p0617 A73-16461
- Continuum radiation from nonisothermal hydrogen plasmas. 05 p0602 A73-16558
- Boundary layer characteristics with radiant energy transfer under adverse pressure gradient. [AIAA PAPER 73-117] 05 p0530 A73-16874
- Effect of boundary conditions on the radiative reflectance of dielectric coatings. 05 p0598 A73-16896
- Radiation transfer in a single-layer spherical planetary atmosphere 05 p0620 A73-17015
- Variational solution to the radiative equation by the use of a step function. II - Extension to nonlinear case by iteration method. 05 p0641 A73-17102
- Annual fluctuation in atmospheric transmission of normal incidence solar radiation 05 p0611 A73-17183
- Time-dependent radiation transfer and a possible explanation of the interpulse in CP 0950. 05 p0623 A73-17302
- Radiative modes of a weakly ionized, collision-dominated, turbulent plasma. 05 p0624 A73-17309
- Solution of the transfer equation for interlocked multiplets by probabilistic method. 05 p0599 A73-17320
- Transfer and moment equations obtained for radiation transfer in spherically moving medium with relativistic corrections, discussing matter-radiation coupling and energy conservation 05 p0612 A73-17382
- A transformation of the radiative transfer equation useful for problems with steep source gradients. 07 p0918 A73-19265
- Radiating-conducting thick-transparent normal shock solution. 07 p0919 A73-19507
- Application of the theory of multiple wave scattering to the derivation of the radiative transfer equation for a statistically inhomogeneous medium 07 p0792 A73-19913
- A direct solution of the radiative transfer equation - Application to Rayleigh and Mie atmospheres. 07 p0852 A73-20220
- Effects of Compton scattering in a moving gas 07 p0853 A73-20308
- Theorems on symmetries and flux conservation in radiative transfer using the matrix operator theory. 08 p1020 A73-20791
- One-dimensional line radiative transfer. 08 p1021 A73-20792
- Radiative and collisional effects in a cylindrically confined plasma. I - Optically thin considerations. II - Absorption effects. 08 p1021 A73-20793
- Radiative transfer theory application to stellar images in photographic emulsions, deriving theoretical relation between star brightness and photographic effective radius 08 p1006 A73-20926
- Matrix operator theory of radiative transfer for Rayleigh scattering and radiance calculation of multilayered atmospheres with large optical depths 08 p0958 A73-21040
- Hemispherical reflectivity and transmissivity of an absorbing, isotropically scattering slab with a reflecting boundary. 08 p1025 A73-21643
- Nonlinear acoustics of a radiating gas. I - General analysis of the equations 09 p1119 A73-21920
- Heating of laser-induced plasmas in helium. 09 p1125 A73-21998
- Radiative transfer model for simulation of airborne remote sensing scanner data under flight conditions in hazy atmosphere with scattering and absorption effects 09 p1077 A73-22386
- An effective cross section method of accounting for the selectivity of emission and absorption in a hot gas 09 p1123 A73-22613
- Simultaneous diffusion of photons and particles in a semiinfinite space. I - Distribution of excited atoms in a semiinfinite space 09 p1123 A73-23068
- Equivalence relationships between diffuse radiation fields for finite slabs bounded by a perfect specular reflector and a perfect absorber. 09 p1121 A73-23072
- The Eddington factor for radiative transfer in spherical geometry. 09 p1121 A73-23289
- Analytic approximation for the saturation behavior of OH emission regions. 10 p1272 A73-23542
- Energy balance in the chromosphere-corona transition region. 10 p1279 A73-24138
- The radiation balance of the earth-atmosphere system - Recent results from satellite measurements 10 p1213 A73-24599
- Radiative losses in a magnetostatic and intense electromagnetic field. 10 p1270 A73-24908
- An explicit form of the Mie phase matrix for multiple scattering calculations in the I, Q, U and V representation. 11 p1390 A73-25718
- Implicit difference method of temperature determination in problems of radiative gasdynamics 11 p1348 A73-26329
- Transfer of solar irradiance through cirrus cloud layers. 11 p1357 A73-26345

RADIATORS

Radiative transfer in a nongray spherical layer - Simplified rectangular model. 11 p1401 A73-26585

Radiative transfer theory model of isotropic monochromatic scattering of light in plane layer of finite optical thickness 12 p1538 A73-26862

Compton-scattering effects in a moving gas. 12 p1526 A73-27280

General relativistic effects detection experiments for supernova and collapsed objects, noting gravitational radiation transfer of energy equal to entire energy generation during thermonuclear evolution 12 p1542 A73-27550

Luminosity levels in deep planetary atmosphere layers 12 p1536 A73-27858

Nongray radiative transfer and simultaneous turbulent diffusion in layer of molecular gas enclosed by parallel black walls, presenting temperature profiles 13 p1705 A73-28433

Radiative transfer through carbon ablation layers. 13 p1705 A73-28457

Stellar opacity and energy transport based on radiation-matter interactions, discussing radiative transfer, absorption and scattering cross sections, quantum mechanical methods, etc 13 p1682 A73-28987

Radiative transport in stars, considering radiation field, transfer equation and radiative heat equation 13 p1683 A73-28988

Lyman alpha radiation transfer in spherically symmetric hydrogen nebula from Monte Carlo techniques, computing for different optical depths 13 p1685 A73-29358

Matrix operator theory of radiative transfer. II - Scattering from maritime haze. 14 p1749 A73-30163

Calculation of radiant energy transfer by the Galerkin method 15 p1956 A73-30963

UV dayglow in 750-1050 A region at 100-800 km observed with rocket-borne thin film filter photometer, solving radiative transfer problem for excitation process 15 p1867 A73-31077

Redistribution of resonance radiation. II - The effect of magnetic fields. 15 p1913 A73-31559

Transmission of solar radiation by stratified cloudiness as a function of the statistical characteristics of its structure 15 p1905 A73-31796

An improved separability approximation for line radiative transport in nonhomogeneous media. 15 p1959 A73-32391

Radiative transfer considerations for kinetic modeling and sensitivity studies. 16 p2005 A73-33545

The characteristics of the solar ultraviolet radiation at Arosa. [AIAA PAPER 73-523] 16 p2056 A73-33558

Angular quadrature perturbations in radiative transfer theory. 16 p2037 A73-33738

Probabilistic radiative transfer - Mean number of scatterings. 16 p2038 A73-33739

Radiation transport theory for anisotropic light scattering in planetary atmospheres, formulating transmission and reflection coefficients 16 p2066 A73-33790

A new numerical technique for solving the time-dependent radiation transport equation. 17 p2255 A73-35595

Numerical techniques in two- and three-dimensional radiation hydrodynamics. 17 p2255 A73-35596

Non-coherent scattering in transfer problems in spherical shell media. I - Frequency-independent source function. 17 p2236 A73-35780

Probabilistic model for radiative transfer problems in cylindrical shell media with complete redistribution in frequency. 17 p2236 A73-35781

Curvature effects in extended stellar atmospheres - Pure absorption. 17 p2237 A73-35788

Non-coherent scattering in transfer problems in spherical shell media. II - Frequency-dependent source function. 17 p2237 A73-35789

The dynamic-bias in radiation intergradation of two-phase flow. 17 p2256 A73-35846

Book - Radiative transfer and interactions with conduction and convection. 17 p2256 A73-35864

Fully coupled nongray radiating gas flows with ablation product effects about planetary entry bodies. [AIAA PAPER 73-672] 18 p2368 A73-36223

Engineering approximations for radiating nonequilibrium shock layers. [AIAA PAPER 73-673] 18 p2297 A73-36224

Planetary atmospheric entry vehicles shock layer energy transport with nongray radiation, using optical thick-thin approximation for radiative transfer in temperature distribution calculation [AIAA PAPER 73-715] 18 p2369 A73-36334

Effect of downstream massive blowing on Jovian entry heating. [AIAA PAPER 73-717] 18 p2264 A73-36336

Spherical harmonics approximation for radiative transfer in polluted atmospheres. [AIAA PAPER 73-749] 18 p2313 A73-36365

Comparison of three techniques for solving the radiative transport equation. [AIAA PAPER 73-751] 18 p2337 A73-36367

Radiative equilibrium of a gray medium in a rectangular enclosure. 18 p2371 A73-36800

Book - Physics of stellar interiors. 18 p2356 A73-36965

Nonlinear acoustics of a radiating gas. II - Weak shock waves 18 p2337 A73-36989

Path-length distributions of photons diffusely reflected from a semi-infinite atmosphere. 18 p2314 A73-37110

Time dependent radiative transfer. III - Development of the formalism. 19 p2503 A73-37565

Water masers in a protostellar gas cloud. 19 p2483 A73-37573

Multiple scattering theory of radiative transfer in inhomogeneous atmospheres. 19 p2423 A73-37586

An analysis of linear focused collectors for solar power. 19 p2391 A73-38409

Radiative transfer in homogeneous, nongray gases with non-isotropic particle scattering. [ASME PAPER 73-HT-9] 20 p2625 A73-38566

Comparison of the Beckmann model with bidirectional reflectance measurements. [ASME PAPER 73-HT-11] 20 p2563 A73-38567

Radiation field in the deep layers of planetary atmospheres. 20 p2602 A73-39232

Atmospheric radiative transfer model for correction of Apollo photographic remote imagery data degradation due to radiation scattering 20 p2559 A73-39881

Numerical solution of nonlinear resonant wave equation of radiating gas between parallel walls by parametric differentiation 21 p2790 A73-40250

Possibility of radiative acceleration of the gas in stellar atmospheres 21 p2767 A73-40554

Numerical solution of the radiative transfer equation in spherical shells. 21 p2727 A73-41000

The effects of departures from LTE in stellar spectra. 21 p2772 A73-41243

On the possibility of constructing a radiative sunspot model in magnetohydrostatic equilibrium. 21 p2777 A73-41486

Russian book - Light scattering in planetary atmospheres. 22 p2906 A73-41877

Inversion techniques for remote sensing of atmospheric temperature profiles. 22 p2883 A73-42056

Radiatively driven harmonic acoustic waves in vibrational equilibrium in closed cylindrical tube, deriving pressure response, radiative absorption coefficient and spectral detail 22 p2930 A73-42235

Unsteady, combined radiation and conduction in an absorbing, scattering, and emitting medium. [ASME PAPER 73-HT-J] 22 p2930 A73-42288

Coupling between thermal conduction and radiative transfer in a moving atmosphere. 22 p2907 A73-42305

Effect of line or band shape on the radiative flux of an isothermal spherical layer. 22 p2938 A73-42990

Radiative transfer within the atmospheres of the major planets. 22 p2913 A73-42991

Curvature effects in extended stellar atmospheres - Absorption and scattering. 23 p3030 A73-43751

Scattering and transmission functions of radiation by finite atmospheres with reflecting surfaces. 23 p3030 A73-43755

Collisional radiative processes and molecular lasers 23 p2988 A73-44013

Radiation transfer equations for atomic spectra lines in stellar magnetic field, allowing for nonequilibrium population of atomic ground state and excited atom-particle collisions 23 p3036 A73-44242

Note on the modified two-stream approximation of Sagan and Pollack. 24 p3123 A73-44438

The effects of scattering and conduction upon radiative transfer in lunar and Mercurian surfaces. 24 p3133 A73-44541

Density variation and radiative exchange effects on convective instability of plane-parallel polytropic atmosphere heated from below with application to solar granulation 24 p3135 A73-44628

Radiation transfer in a multilayer plane-parallel system with nonisotropic scattering. 24 p3154 A73-44659

The formation of resonance lines in multidimensional media. II - Radiation operators and their numerical representation. 24 p3113 A73-45041

The formation of resonance lines in multidimensional media. III Interpolation functions, accuracy and stability. 24 p3138 A73-45042

Lyman alpha 1216 A intensity behavior for atomic hydrogen density distribution below 200 km on Mars, calculating radiative transfer 24 p3139 A73-45108

Interior radiances in optically deep absorbing media. I - Exact solutions for one-dimensional model. 24 p3111 A73-45318

Radiative transfer through a Compton-scattering atmosphere with continuous energy dependence. 24 p3111 A73-45321

Spectral data for the nu sub 2 bands of ammonia with applications to radiative transfer in the atmosphere of Jupiter. 24 p3142 A73-45324

Radiating optically thick gas boundary layer based on approximation of gray gas in LTE, noting similarity to Knudsen layer 24 p3158 A73-45535

RADIATORS

Cerenkov shower spectrometer with a conical radiator made of TF-5 glass 09 p1085 A73-23002

Influence of the shape of radiators on the energy resolution of Cerenkov shower spectrometers 12 p1496 A73-27205

A new flush mounted antenna element for phased array application. 21 p2663 A73-40662

RADICALS

Nitric oxide formation and radical overshoot in premixed hydrogen flames. 10 p1294 A73-23558

Reactions of HO2 with carbon monoxide and nitric oxide and of O/I D/ with water. 14 p1723 A73-30069

Study of the dependence of the properties of radicals on the characteristics of the initial hydrazine structure 17 p2220 A73-34638

Reaction of HO2 with O3. 19 p2402 A73-37674

Organic compounds oxidation and combustion reactions, discussing hydrogen dioxide radical role and reaction rate 22 p2933 A73-42753

Relation between ion creation and C2, CH, and OH formation in the combustion of hydrocarbons. 22 p2819 A73-42771

RADIO ALTIMETERS

Phase switched FM-CW radio altimeter, noting error reduction by controlled switching of phase difference between emitted and echo signals 02 p0165 A73-11526

Average return pulse form and bias for the S193 radar altimeter on Skylab as a function of wave conditions. 04 p0446 A73-14804

Satellite borne Ku-band pulsed radar altimeter for altitude measurement above ocean surface, evaluating random and bias errors due to instrument, propagation and geometry 04 p0446 A73-14805

Optimum processor accuracy for radar altimetry for geodesy over sea, considering surface reflectivity, height variation additive noise and pointing errors 11 p1371 A73-26631

Study of the integrity of an equipment - Application to radio altimeters for category III landing 15 p1880 A73-32493

Microwave landing system elevation data or altimeter information for flare-out guidance, considering airport, aircraft autopilot and ground equipment and cost factors 21 p2736 A73-40050

Results of radar experiments performed on automatic stations Luna 16 and Luna 17. 21 p2774 A73-41401

Radar altimeter signal propagation delay estimation, calculating and plotting noise fluctuation characteristics as function of aircraft ground speed, altitude and other parameters 22 p2828 A73-43067

RADIO ANTENNAS

The quasi-linear intensity interferometer. 01 p0045 A73-10184

Optical modeling of antenna radiation patterns by radio holograms of aperture fields
02 p0146 A73-12020

Receiving characteristics of antennas in the case of coherent and incoherent radiation
04 p0427 A73-14775

Input impedance of a thin biconical antenna vertically buried near the air-ground interface.
05 p0548 A73-16162

Low-frequency loop antenna arrays - Ground reaction and mutual interaction.
06 p0665 A73-18176

Mobile ground station for sounding balloons remote control, telemetry and localization, noting antenna pointing control, tracking receiver and trajectory recording
07 p0790 A73-18972

Noise immunity of diversity reception with threshold switching of antennas
07 p0802 A73-20291

A surface-wave antenna integrated with the excitation device
07 p0802 A73-20294

Project management and installation of the Arvi satellite communication earth station.
11 p1344 A73-26147

Influence of phase fluctuations of the received radiation on the performance of a synthetic antenna
11 p1331 A73-26158

Evaluation of the efficiency of the polarization selection method in suppressing fluctuating polarization noise
12 p1468 A73-26946

Spiral top-loaded antenna /STLA/ characteristics and design procedure derivation via self consistent field method, noting VLF applications
14 p1734 A73-30204

Finding the approximate angular probability density function of wave arrival by using a directional antenna.
14 p1727 A73-30210

Absolute calibration of solar radio flux density in the microwave region.
16 p1993 A73-32968

Reliability of diversity reception by antennas with different polarizations.
16 p1991 A73-33984

Electronic location finder radio antenna homing system for helicopter search and rescue of downed air crewmen
[AHS PREPRINT 720]
17 p2116 A73-35061

The measurement of large antennas with cosmic radio sources.
17 p2127 A73-35680

Absolute calibration of antennas at extremely low frequencies.
17 p2128 A73-35686

Measurement of the radiation patterns of full-scale HF and VHF antennas.
17 p2128 A73-35689

A comparison of time- and frequency-domain measurement techniques in antenna theory.
17 p2129 A73-35702

Antenna impedance measurement with Weissfloch transformer between terminals and point in input transmission line for achieving high precision
17 p2129 A73-35704

Noise immunity of diversity reception with antenna threshold switching.
18 p2290 A73-37128

A surface-wave antenna matched to the exciter.
18 p2291 A73-37131

Ground stations in Intelsat 4 communication satellite radio relay system, discussing all-solid-state equipment design, carrier frequency assignment and antenna installation
20 p2523 A73-38723

Design of coincident dual-frequency mirror antennas
21 p2661 A73-40194

Russian book - Stellar atmospheres and interplanetary plasma.
21 p2671 A73-40531

Phased array antennas for applications on spacecraft.
21 p2662 A73-40647

Operation of a variable profile antenna with a plane periscopic reflector
21 p2666 A73-41444

Main-mirror aberrations in a variable-profile antenna and beam scanning by displacement of the primary radiating element
21 p2667 A73-41446

Adjustment of a variable-profile antenna
21 p2675 A73-41456

Experimental study of an autocollimation method for alignment of a variable-profile antenna
21 p2675 A73-41457

Computer processing of RF neutral-hydrogen line observations carried out with a fixed antenna
21 p2659 A73-41468

Experimental verification of the possibility of beam scanning in a variable profile antenna by radial displacement of the primary radiating element
21 p2667 A73-41469

Sensitivity of an intensity radio interferometer
21 p2705 A73-41471

Accuracy of coordinate measurements with the aid of a variable-profile antenna
21 p2667 A73-41472

Antenna coupling induced intersystem electromagnetic interference prediction, discussing tradeoffs between analysis level, input information, measurements, cost results and user requirements
22 p2822 A73-41795

Broad-band antenna array with application to radio astronomy.
22 p2831 A73-41840

Modification of antenna radiating characteristics with multi-impedance loading.
22 p2831 A73-41848

Russian book on radio astronomy with electronic engineering emphasis covering observation and equipment, cosmic source characteristics, radio telescope antenna systems, radar techniques, coordinate measurement, etc
22 p2905 A73-41875

Results of radio emission studies at frequencies of 32 and 58 MHz in extensive air showers on the assembly of Moscow State University
23 p3022 A73-43550

Receiving antenna optimum polarization determination by mapping on Poincare sphere for maximum ratio of signal to summed external interference and internal noise
24 p3068 A73-44943

RADIO ASTRONOMY

Spatial-temporal processing of thermal radio signals from emitters moving in the near zone of an interferometer
01 p0017 A73-10213

Observations at 750, 1400, and 2700 MHz of radio sources in the Vermilion River Observatory survey.
01 p0096 A73-10312

A survey of linear polarization at 1415 MHz. III - Method of reduction and results for the galactic spurs.
01 p0096 A73-10319

High frequency radio observations of optically interacting galaxies.
01 p0099 A73-10586

Low frequency, high resolution observations of Virgo A.
01 p0100 A73-10791

Observation of compact objects of cosmic radio emission with maximum angular resolution at the 3.55-cm wavelength
01 p0092 A73-10931

Periodic components of the density variations of the radio source VRO 42.22.01 /BL Lacertae/
01 p0101 A73-10933

Short-term pulsar intensity variation in the frequency range 70-115 MHz. I - Correlation measurements.
01 p0106 A73-11306

International Conference on Cosmic Rays, 12th, University of Tasmania, Hobart, Tasmania, Australia, August 16-25, 1971, Papers. Volumes 1, 2, 3, 4, 5 & 6.
01 p0093 A73-11375

Data processing for radioastronomy and cosmic ray air shower arrays.
01 p0020 A73-11455

Observations at 408 MHz of the Cyg X-3 radio outburst.
02 p0204 A73-11552

Radio observations of Cygnus X-3 and the surrounding region.
02 p0210 A73-11557

Results of an experimental investigation of a two-mirror antenna with a modified counter reflector
02 p0146 A73-12019

Radioastronomical measurements of ionospheric electron content.
02 p0159 A73-12031

Differential interferometry for radio astronomy applications, discussing earth-based tracking of lunar rover relative to module, moon libration determination, Venus wind measurement, etc
02 p0218 A73-12416

The radioastronomy of the planets
03 p0372 A73-13273

Hydrogen recombination line and continuum observations at 5000 MHz of 13 southern HII regions.
03 p0372 A73-13347

Observation of a correlated X-ray-radio transition in Cygnus X-1.
03 p0361 A73-13714

A review of microwave parametric amplifiers with particular reference to satellite communications and radio astronomy.
03 p0284 A73-13999

Radio evidence of twisted bi-polar magnetic fields in the solar corona.
03 p0378 A73-14417

Positions, periods, period derivatives, dispersion measures and pulse widths of twenty two weak pulsars
03 p0380 A73-14635

An interferometric survey of the areas surrounding four intense radio sources.
03 p0380 A73-14637

Solar radio emission measurement and interpretation, discussing source mapping, coronal density, magnetic field and flare and particle events predictions
04 p0496 A73-14830

A search for isolated radio pulses from the Crab Nebula at 151.5 MHz.
04 p0500 A73-15493

A revised low-frequency cosmic noise spectrum.
04 p0500 A73-15516

Measurements of flux fluctuation in solar radio emission at a wavelength of 3 cm
05 p0573 A73-16270

A neutral hydrogen survey of the galaxy M 33. I.
05 p0618 A73-16740

Coronal abundance of elements and a model of the quiet sun from radio observations.
05 p0621 A73-17034

A model of the Crab Nebula derived from dual-frequency radio measurements.
05 p0622 A73-17075

Expansion hypothesis and assumption of invisible intergalactic matter in galactic clusters stability theory, noting IR spectroscopy and radio observation
05 p0623 A73-17196

High resolution interferometric observations of Venus at three radio wavelengths.
06 p0744 A73-17437

Interferometric observations of Mars at 21-cm wavelength.
06 p0747 A73-17491

Radio telescope identification of interstellar isocyanic acid, methylacetylene and hydrogen isocyanide molecules from pure rotational transitions
06 p0751 A73-18229

Observations of the radio source PKS0123-01 at 5000, 408, and 80 MHz.
06 p0754 A73-18627

Positions and some identifications for 111 sources of about 1 flux unit at 408 MHz.
06 p0754 A73-18628

Amplitude-time and polarization characteristics of the subpulses of pulsar CP 1133.
06 p0754 A73-18633

7.8-GHz flux density measurements of variable radio sources.
07 p0876 A73-19355

5 GHz observations of the infrared star MWC 349, and the H II condensation W3/OH/
07 p0899 A73-20121

Radio brightness distribution in the Crab Nebula at the 3.55-cm and 1.28-cm wavelengths
07 p0901 A73-20309

Results of radio source observations at short millimeter wavelengths
07 p0901 A73-20310

Submillimeter radio telescope employing an n-InSb detector
07 p0825 A73-20311

A thermal calibrator for radiometers used in radioastronomy.
08 p0963 A73-20873

Virgo A nucleus compact radio source observation from February 1971 to August 1972, noting absence of intensity or size variations
08 p1004 A73-20898

Microwave background radiation in terms of isotropy, universe mass density, sky brightness temperature spectra investigations and H distribution in intergalactic space
08 p1010 A73-21229

Schmidt telescopes for quasars and blue stars radio astronomy in southern sky survey, considering UV filtering-out for image quality improvement
08 p1011 A73-21362

Observations of compact radio-emitting objects at 3.55 cm with maximum angular resolution.
09 p1147 A73-22726

Recent progress in infrared and microwave techniques of astronomical interest.
09 p1086 A73-23128

Venus - New microwave measurements show no atmospheric water vapor.
09 p1151 A73-23171

Interferometric investigations of the A21 nebula /YM29, Medusa/
10 p1273 A73-23704

The Parkes 2700 MHz survey. IV - Catalogue for the south polar cap zone, declinations -75 deg to -90 deg.
10 p1275 A73-23751

Culgoora /Australia/ solar radio observatory site, facilities, instrumentation and research activities
10 p1203 A73-24150

Quantization circuit for radio astronomical signals conversion into binary code and bit blocks recording on magnetic tape via Razdan-3 computer
10 p1220 A73-24698

Optical and radio observations of the Orion Nebula.
11 p1425 A73-26265

Infrared and radio observations of the nucleus of NGC 253.
11 p1428 A73-26625

Observations of noise bands associated with the upper hybrid resonance by the Imp 6 radio astronomy experiment.
12 p1468 A73-26995

Radio-brightness distribution over the Crab Nebula at 3.55 and 1.28 cm. 12 p1539 A73-27281

Observations of radio sources at short millimeter wavelengths. 12 p1539 A73-27282

Submillimeter radio telescope with an n-InSb detector. 12 p1497 A73-27283

31.4-GHz flux density measurements of variable radio sources. 12 p1540 A73-27426

Parabolic 10 m antenna-8.4 mm wavelength radiometer system for radio astronomy 12 p1498 A73-27724

Interstellar molecules and radio spectroscopy in the cm- and mm-wave range 12 p1544 A73-27779

Galactic and extragalactic radio emission and satellite observations of RF cosmic radiation and noise intensity 12 p1544 A73-27783

Remote sensing of LF nonthermal radio emission for composition and dynamic processes of interplanetary and interstellar media and planetary magnetospheres 14 p1800 A73-30539

High radio frequency observations of the Omega nebula. 15 p1932 A73-31268

A dual-resonator quantum amplifier operating at a wavelength of 1.35 cm for radio-astronomical observations 15 p1851 A73-31832

Two-component equilibrium model of the HI regions of the interstellar medium satisfying a set of radio observations 15 p1938 A73-31965

The Berkeley low-latitude survey of neutral hydrogen. I - Profiles. 16 p2063 A73-33600

Radio astronomical, radar and interplanetary probe measurements of Venus rotation, dimensions, atmosphere and magnetic field 16 p2066 A73-33798

Distribution of radio brightness across the disk of Venus at the 8-mm wavelength 16 p2068 A73-33816

Radio emission from Venus and Jupiter at 2 and 8 mm wavelengths 16 p2068 A73-33817

Certain results of a combined treatment of the Venera 4 interplanetary probe and ground-based radio-astronomical and radar measurements 16 p2068 A73-33819

Estimates of water content in the atmosphere of Venus on the basis of radio-astronomical measurements and space probe data 16 p2068 A73-33823

Interferometry of the Medusa nebula A21 (YM 29). 18 p2334 A73-36729

A low temperature bolometer heterodyne receiver for millimeter wave astronomy. 20 p2564 A73-38878

Tables and graphs for characteristics and pulse profiles of pulsars discovered in low Galactic latitude radio telescope survey 20 p2605 A73-39017

Optical and radio observations of NGC 4258 anomalous arms indicating eruptive processes in galactic nucleus as possible source of spiral structure 20 p2605 A73-39057

Radio luminosity function of galaxies. 20 p2606 A73-39062

Russian book - Stellar atmospheres and interplanetary plasma. 21 p2671 A73-40531

Inhomogeneous structure of plasma near sun due to drift, slipping and anisotropic temperature distribution instabilities, noting association with radio astronomy observed fine structure 21 p2767 A73-40537

Method and results of observations of the occultation of the source 3C144 by the solar corona with the DKR-1000 FIAN cross-array radio telescope 21 p2767 A73-40545

Pulsar polarization measurements by multielement interferometer dipole antenna and DKR-1000 cross array radio telescope 21 p2662 A73-40546

Temperature gradient in gaseous nebulae 21 p2768 A73-40716

Radio astronomy millimeter wave receiver techniques and atmospheric restrictions for coherent /radio/ detection 21 p2771 A73-41237

Methods of radio-astronomical utilization of the RATAN-600 21 p2666 A73-41442

A radio-astronomical method of adjusting variable-profile antennas 21 p2667 A73-41458

Astrophysical problems to be solved with the RATAN-600 radio telescope 21 p2776 A73-41465

Possibility of obtaining radio images of celestial bodies with a resolution greater than .01 arc sec 21 p2667 A73-41466

A method of reducing the influence of interference on the operation of a correlation interferometer 21 p2667 A73-41511

Pulsar searches at 408 MHz with Northern Cross radio telescope, comparing discovered objects with previously known pulsars 21 p2778 A73-41532

Interactive processing of map data produced by the Westerbork supersynthesis radio telescope. 21 p2778 A73-41534

Broad-band antenna array with application to radio astronomy. 22 p2831 A73-41840

Russian book on radio astronomy with electronic engineering emphasis covering observation and equipment, cosmic source characteristics, radio telescope antenna systems, radar techniques, coordinate measurement, etc 22 p2905 A73-41875

Pulsar search in Galactic nucleus region at 430 MHz with 140 foot telescope, discussing data reduction and results 22 p2909 A73-42484

The radio occultation method for the study of planetary atmospheres. 22 p2912 A73-42979

Further observations of Cygnus X-3 at 8 GHz during the September 1972 outbursts. 22 p2915 A73-43026

Spectral line radio astronomy observations of interstellar molecular clouds in Galaxy, relating to stellar and life evolution 23 p3028 A73-43350

Very-long-baseline interferometry techniques applied to problems of geodesy, geophysics, planetary science, astronomy, and general relativity. 23 p2980 A73-43354

Fixed baseline millimeter wave interferometer with aperture synthesis telescope of antenna array for interstellar and planetary water vapor and radio sources mapping 23 p2980 A73-43364

An 8-mm interferometer for solar radio astronomy at Bordeaux, France. 23 p2980 A73-43365

Computer controlled steerable radio telescope construction and performance for decimeter and centimeter wavelength observations 23 p2958 A73-43367

Radio astronomical problems due to pulsar radiation dispersal by frequency dependent propagation velocity in interstellar medium, discussing signal reception and data recording techniques 23 p2953 A73-43368

The solar radio patrol network of the USAF and its application. 23 p2958 A73-43371

Multifrequency meter wave Culgoora radioheliograph design, picture format and operation, using automatic switching and track-scan computer 23 p2958 A73-43372

Radio astronomical traveling wave maser with ruby or doped rutile single crystals, superconducting magnet, cryogenic equipment and low noise temperature 23 p2953 A73-43375

Radio astronomy interferometer receiver IF control for centimeter wave polarized signal processing and parabolic antenna instrumentation 23 p2980 A73-43377

Sensitive search for microwave pulses from the galactic centre. 23 p3033 A73-43961

Microwave emission mechanism of frequency dependent pulse profile changes in pulsar, using cooled parametric amplifier observations 23 p3034 A73-43963

Galactic protocluster radio emission detection, using adiabatic density perturbation theory of galactic evolution 23 p3037 A73-44256

Statistical correlation between pulsar and supernova remnant distribution along galactic longitudes, noting difference due to relative motions 23 p3037 A73-44359

Jupiter magnetic dipole offset along rotation axis from 11 cm radio centroid measurements with Parkes telescope 24 p3130 A73-44459

Two-component equilibrium model of interstellar HI regions that satisfy the overall radio observations. 24 p3132 A73-44490

Communication possibilities between earth and technologically advanced galactic civilizations, discussing radio astronomy requirements, technology differences and communication distance estimates 24 p3133 A73-44555

High resolution observations of the radio galaxy NGC5128 at 10.7 GHz. 24 p3143 A73-45489

RADIO ASTRONOMY EXPLORER SATELLITE
Radio Astronomy Explorer /RAE/. I - Observations of terrestrial radio noise. 11 p1356 A73-25920

RADIO ATTENUATION
NT MANDELSTAM REPRESENTATION
Influence of an important region of the ionospheric layer on ELF propagation characteristics 01 p0016 A73-10203

Winter anomaly in ionospheric absorption of radio waves on 1.725 MHz during sunspot minimum. 01 p0043 A73-10910

Atmospheric water vapor absorption coefficient in 0.73 mm transmittance window as function of humidity from monochromatic RF radiation measurements 02 p0142 A73-12488

Russian book on radio wave propagation covering ground, ionospheric and tropospheric propagation, radio attenuation, scattering and ionospheric and tropospheric reflection 02 p0143 A73-12775

Cosmic radio wave anomalous absorption height dependence on zenith distance in midlatitude ionosphere during solar flare emission from polarization study 03 p0365 A73-14561

E region electron collision frequency vertical distribution from ground and rocket measurements of radio wave absorption and electron density respectively 03 p0304 A73-14562

D region HF radio wave nighttime absorption correlation to winds and temperature in Northern Hemisphere during IQSY 03 p0304 A73-14593

The role of atmospheric pressure variations above the mesopause in the phenomena of winter anomaly and variability of the lower ionosphere. 04 p0441 A73-15290

Equatorial region radio wave enhanced absorption by resonant coupling to electrojet irregularities and damped upper hybrid modes 04 p0423 A73-15548

Electrodynamic models for radio attenuation in ice by electromagnetic absorption and reflection from ice sheet interfaces, noting radar sounding 04 p0445 A73-15572

Passage of medium-frequency radio waves through the ionosphere 05 p0550 A73-16395

Some characteristics of the Venus surface. 06 p0744 A73-17439

Omega v.l.f. wave propagation and the 1922-23 Marconi expedition. 06 p0668 A73-18442

Ionospheric attenuation of 3-100 MHz radio waves, interpreting scatter mode propagation mechanism as total reflection from lower ionizational irregularities 07 p0792 A73-19458

On the collisional absorption of radio waves in cosmology. 07 p0877 A73-19602

Problem of the influence of absorption on the amplitude fluctuations of submillimeter radio waves in the atmosphere 07 p0793 A73-19922

Determination of the apparatus constant during multifrequency measurements of radio-wave absorption by the A1 method 08 p0939 A73-21303

Transmission loss at high frequencies on 3260 km temperate-latitude path. 09 p1052 A73-22958

Signal reflection height seasonal variations effect on radio waves absorption estimation from vertical ionospheric sounding 10 p1188 A73-24242

Ionospheric radio wave absorption coefficient correlation with solar activity Wolf number in IGY, IGC and IQSY 11 p1327 A73-25083

Vertical distribution of absorption of cosmic radio emission and radio waves in ionosphere and lower ionosphere based on electron density profiles 11 p1327 A73-25084

Relationship of the sporadic Es layer parameters with the absorption of radio waves in the ionosphere 11 p1350 A73-25085

Latitudinal and longitudinal auroral radio wave absorption in Arctic during IQSY, noting comparison with geomagnetic field disturbances 11 p1350 A73-25086

Radome material technology in UK, summarizing permittivity, loss tangent, internal phase difference, attenuation, aberration, cross polarization and pattern distortion measurements and environmental tests 11 p1336 A73-25308

On the solar Lyman alpha control of the ionospheric absorption at 2775 kHz. 11 p1412 A73-25770

Results of ship-borne ionospheric absorption measurements on the North Atlantic during winter. 11 p1359 A73-26713

Daily altitude variations of medium frequency radio waves reflection in ionosphere over Tsumeb, SW

Africa, examining attenuation correlation with solar zenith angle 12 p1494 A73-27767

Rain-attenuation measurements of millimetre waves over short paths. 15 p1848 A73-32647

Fading correlation on terminal point and spaced microwave paths, discussing switched path diversity to overcome rain attenuation effects 16 p1983 A73-33732

Experimental results of radio wave absorption measurements in Southwest Europe. 18 p2288 A73-35940

Unusual LF radio absorption events during a major meteor shower. 18 p2289 A73-36302

Measurement of the attenuation of 9.303 MHz waves from ISIS-II through the ionosphere. 18 p2289 A73-36876

Determination of the instrument constant in multifrequency measurements of radio wave absorption by the A1 method. 19 p2404 A73-37932

Relationship between anomalous radio absorption and the solar zenith angle during periods of sudden ionospheric disturbances 19 p2406 A73-38327

Ionospheric inhomogeneity parameters and geoelectromagnetic field variations 20 p2553 A73-39156

B-2 installation for radio wave absorption measurements in the ionosphere at two frequencies simultaneously by the A1/pulse method 20 p2566 A73-39165

Method for the computation of radio paths up to 4000 km long 20 p2530 A73-39180

A radio signal shaping device with large signal attenuation in the intervals between signals 21 p2661 A73-40174

Phase integral corrections to radio wave absorption and virtual height for model ionospheric layers. 21 p2654 A73-40777

A comparison of the latitudinal variation of auroral absorption at different longitudes. 21 p2684 A73-40785

Electromagnetic interference in military transport aircraft, discussing RF terminal voltage and current, radiated field, fuselage attenuation and power supply impedance measurements 22 p2821 A73-41693

The effect of snow on antenna radiation patterns - A presentation of results. 22 p2831 A73-41850

Measurement of attenuation of 9.303 MHz waves from ISIS-II through the ionosphere. 22 p2825 A73-42193

An iterative mathematical technique for deriving electron-density profiles from multifrequency riometer data. 22 p2828 A73-43177

RADIO AURORAS

Short period pulsating radio auroras properties, determining apparent Doppler characteristics of long period echo sequences 01 p0017 A73-10340

Radio aurora aspect sensitivity from radar VHF measurement error analysis 03 p0300 A73-13692

Analogies between substorm phenomena of the visual polar aurora and the radio aurora 12 p1493 A73-27757

Radio aurora occurrence data from statistical data on radio echo occurrence, comparing radio zone to optical auroral belts 16 p2009 A73-33893

Radar aurora type III spectra with phase velocities exceeding ion acoustic velocity, discussing relation to current-excited ionospheric electrostatic ion cyclotron oscillations 18 p2312 A73-36299

Radio aurora, storm sudden commencements, and hydromagnetic waves. 18 p2313 A73-36646

Radio auroral measurements near an auroral electrojet. 20 p2550 A73-38862

VHF radar aurora echo Doppler spectral properties, discussing electron density irregularities, echo power spectra, drift velocity, two stream instability and convection hypothesis 20 p2553 A73-38962

RADIO BEACONS

Symposium on the Future Application of Satellite Beacon Measurements, Graz, Austria, May 29-June 2, 1972, Proceedings. 03 p0299 A73-13626

Multifrequency radio beacon on polar orbiting satellite for wideband transmission through ionosphere without significant signal distortion 03 p0275 A73-13627

Atmospheric wave perturbations of total electron content. 03 p0299 A73-13633

ATS-F satellite borne radio beacon transmitter experiment for obtaining ionospheric electron content, discussing design, in-orbit performance, calibration information dissemination and propagation measurement 03 p0275 A73-13639

A receiver design for the ATS-F radio beacon experiment. 03 p0275 A73-13640

Computed effects of the ionosphere/protonosphere distribution on VHF signals from ATS-F/G. 03 p0275 A73-13641

Application of satellite radio beacons for measurement of small-scale ionospheric irregularities. 03 p0300 A73-13642

Russian book on aircraft landing control automation covering radio beacons, communications equipment, instrument landing trajectories, flight control, autopilot, atmospheric disturbances and display systems 04 p0474 A73-15966

Autonomous hydrogen/air fuel cell for long-life missions. 09 p1033 A73-22752

First order effects of terrain on the radiation pattern of a non-directional LF beacon. 11 p1332 A73-26204

Radiation pattern of a low-frequency beacon antenna in the presence of a semi-elliptic terrain irregularity. 16 p1979 A73-32913

Radiation pattern of a low-frequency beacon antenna located on a semi-elliptic terrain irregularity. 19 p2409 A73-37716

ASTRO-DABS communication system with hybrid satellite and terrestrial discrete address beacon system for accurate aerial surveillance and navigation with reliable data link 20 p2527 A73-38759

The use of radio beacons in geophysics and their applications. 21 p2657 A73-41331

RADIO BLACKOUT

U BLACKOUT [PROPAGATION]

RADIO BROADCASTING

U BROADCASTING

RADIO BURSTS

NT SOLAR RADIO BURSTS

NT TYPE 2 BURSTS

NT TYPE 3 BURSTS

NT TYPE 4 BURSTS

NT TYPE 5 BURSTS

Extensive air showers on Jupiter, and its sporadic decimeter radio emission. 01 p0106 A73-11323

15.5 GHz observations at the Haystack Observatory of the Cygnus X-3 outburst. 02 p0210 A73-11555

Radio outbursts observation in X ray source Cyg X-3, showing relativistic electrons sporadic injection dominance of synchrotron radio emission characteristics 02 p0210 A73-11564

Radio emission source picture from observed Cygnus X-3 outburst, suggesting expanding cloud with traveling relativistic electrons and protons 02 p0211 A73-11870

Flux density and linear polarization measurements of radio outburst from Cygnus X-3, suggesting synchrotron radiation from expanding cloud of relativistic particles 02 p0205 A73-11871

Cygnus X-3 radio outburst as consequence of synchrotron radiation due to expanding relativistic plasma ejection, considering polarization, flux densities and spectral index 02 p0211 A73-11872

High frequency observations of the second radio flare in Cygnus X-3. 05 p0623 A73-17184

Fine structure of the Jupiter radio bursts. 08 p1013 A73-21646

Radio pulses from the direction of the galactic centre. 10 p1280 A73-24272

Particle injection in the Cygnus X-3 radio outburst. 11 p1419 A73-25859

Search for sporadic radio emission from space at centimeter and decimeter wavelengths 14 p1798 A73-30261

Limit to pulses of radiofrequency emission from the galactic centre. 14 p1800 A73-30600

Intense outburst S/ of radio radiation detected with the Goldstone-Haystack interferometer. 19 p2485 A73-37624

Observations of further outbursts in the radio galaxy 3C 120. 19 p2485 A73-37625

RADIO COMMUNICATION

NT PULSE FREQUENCY MODULATION

TELEMETRY

NT RADIO RELAY SYSTEMS

NT RADIO TELEGRAPHY

NT RADIO TELEMETRY

NT TELEPHONY

Results of the World Conference of Space Telecommunications, Geneva, 1971 04 p0523 A73-15150

Russian book on aircraft control systems covering radio communication and navigation, automatic guidance and landing and homing and radar tracking 04 p0474 A73-15964

Optimal planning of technological systems maintenance according to a reliability criterion 07 p0830 A73-19126

The average duration of the failed state in the interval between adjacent tests of a periodically verified standby radio system with z-multiple redundancy 09 p1051 A73-22464

Some effects of the equatorial ionosphere on terrestrial HF radiocommunication. 09 p1051 A73-22500

Educational radio and television satellite networks, considering computer networks, cable TV and NASA Applications Technology Satellites (ATS)/utilization 09 p1056 A73-23397

Restoring the orthogonality of two polarizations in radio communication systems. II. 10 p1190 A73-24623

Factors affecting the frequency chosen for aircraft to satellite communications. 12 p1472 A73-27667

A shipboard satellite communication experiment. 12 p1473 A73-27675

The operational requirements for a maritime satellite communication service. 12 p1473 A73-27676

Engineering economic considerations for a maritime-satellite service. 12 p1473 A73-27677

Arbeitsgemeinschaft Ionosphaere, URSL, and Nachrichtentechnische Gesellschaft, General Session, Kleinheubach, West Germany, October 9-14, 1972, Reports 12 p1493 A73-27750

Radio noise contaminated area avoidance by vehicles dependent on navigation or communication radio receivers, giving equations and curves for navigational problem 12 p1523 A73-27887

Shaping circuit for complex RF pulse consisting of simultaneous equallength square pulses with different frequencies, discussing carrier frequencies selection 13 p1583 A73-28730

Evaluation of the noise immunity of pulsed systems for transmission of continuous messages with allowance for quantization and interpolation errors. I 13 p1584 A73-28891

RF spectrum utilization for optimum communication capacity, considering tradeoff between bandwidth and interference, antenna directivity and wave reflection and scattering effects 13 p1584 A73-29113

Aeronautical communication technology for civil ATC system development through 1990s, discussing SNR design and need for radio channel models 14 p1725 A73-29890

Theory of short radio wave propagation over very great distances 15 p1844 A73-31888

VOLMET transmission automation with the aid of the 'DECLAM' system using a speech synthesizer 15 p1846 A73-32429

Portable radio communication system for guided tours in industrial plants, construction sites and museums, discussing transmitter, receiver, earphones and rechargeable battery power supply 16 p1987 A73-33165

Multiple access techniques for the Canadian domestic satellite communications systems. 17 p2124 A73-35305

Communications systems of television-radio satellites [DGLR PAPER 73-053] 17 p2126 A73-35487

Distribution of peaks in atmospheric radio noise. 19 p2403 A73-37269

Satellites for maritime applications. 19 p2494 A73-38099

The ARINC plan for implementing air/ground DATALINK. 20 p2527 A73-38758

Quantum signal superposition in radio communication, discussing Glauber convolution formula limitations and minimum three signal rule 20 p2529 A73-38924

The susceptibility of modern aircraft instrument systems to interference in the HF band. 22 p2851 A73-41694

Short wave radio signal fadeout due to ionospheric disturbances, obtaining experimental equation on magnitude relationship with solar zenith angle and operating frequency 22 p2825 A73-42194

Interstellar radio communication and the frequency selection problem. 24 p3068 A73-44992

RADIO CONTROL

Electronic programming timer with crystal oscillator, IC counters and memory core matrix for event

sequence radio control during spacecraft or rocket launchings
01 p0020 A73-11167

Radio-guidance algorithms applied to the control of spacecrafts descending in the earth's atmosphere
10 p1247 A73-23880

Mean risk determination in radio-electronic device control
14 p1735 A73-30291

Russian book - Radio devices for flight vehicle control systems.
15 p1908 A73-32421

Noise immunity of optical communications links with radio and optical AGC systems.
16 p1984 A73-33977

Algorithms for radio guidance with application to control of landing of spacecraft in the earth's atmosphere.
20 p2590 A73-38899

RADIO DIRECTION FINDERS

Target angular characteristics of direction finding antenna in sidelobe region for wideband signals, using single coordinate measurement and amplitude scanning
02 p0146 A73-12023

Multipole sine-cosine azimuth patterns for wide aperture Adcock direction finders, determining spacing and reradiation errors and array pickup factor
02 p0142 A73-12529

Two-channel direction finding with point source emission and spaced antennas reception, investigating cross correlation and background noise interference effects on accuracy
03 p0278 A73-14062

Most convenient intervals of amplitude quantization in direction finding
08 p0939 A73-21394

A mobile tone range/RDF system for telemetry tracking of sounding rockets.
09 p1057 A73-23412

Radio direction finders error compensation in air navigation, considering flight speed, polarization, near field and ground effects and great circle deviation
10 p1246 A73-23686

The dual-aperture counterwound log-spiral antenna direction-finder system.
11 p1338 A73-25669

Miniature phase/amplitude tracking RF receiver frontends.
14 p1737 A73-30623

Radiogoniometric vectors superposition on ATC Doppler radar image, noting direction finding display availability and echoes identification
15 p1847 A73-32438

Radiation pattern of a low-frequency beacon antenna in the presence of a semi-elliptic terrain irregularity.
16 p1979 A73-32913

Wideband monopulse radio direction finding measurement improvement, using receiver with log video IF amplifier, multiplexing filters and detectors to provide signal normalization
16 p1990 A73-33850

Radio direction finder of increased accuracy with a moving antenna.
16 p1991 A73-33976

Book - Recommended basic characteristics for airborne radio homing and alerting equipment for use with emergency locator transmitters (ELT).
17 p2207 A73-34475

VLF goniometer observations at Halley Bay, Antarctica. I - The equipment and the measurement of signal bearing. II - Magnetospheric structure deduced from whistler observations.
17 p2159 A73-34777

Electronic location finder radio antenna homing system for helicopter search and rescue of downed air crewmen
[AHS PREPRINT 720]
17 p2116 A73-35061

The most advantageous amplitude quantization intervals for direction finding.
19 p2407 A73-38352

A goniometer for use with high-frequency circularly disposed aerial arrays.
21 p2703 A73-41207

Synthetic radio direction defining methods with virtual antenna patterns.
21 p2658 A73-41649

RADIO ECHOES

Investigation of fading radio echoes from meteor trails. I
01 p0016 A73-10201

Synoptic studies of D-region ionization changes and electron densities by the partial reflection differential absorption experiment.
01 p0042 A73-10904

Comparative study of monthly and diurnal occurrences of whistlers and gyroelectric echoes in conjugate regions of Europe and South Africa
01 p0403 A73-11274

Conjugate ducted echoes observed on Alouette II ionograms.
02 p0143 A73-12624

The theory of the reflection of low frequency radio waves in the ionosphere near critical coupling conditions.
05 p0551 A73-17052

Conjugate ducted echoes observed on Alouette II ionograms.
05 p0572 A73-17164

Radio wave reflection from ionosphere, determining polarization and fluctuation characteristics via Stokes parameters
07 p0815 A73-19436

On the unequal accuracy of radio range finder measurements in the reflection of radio waves from an underlying surface.
07 p0793 A73-20041

Radio-echo measurements of the flux of the Quadrantid, Perseid and Geminid meteor streams.
11 p1415 A73-25169

A method for smoothing level fluctuations caused by echoes in the case of FM directional radio links
11 p1328 A73-25344

Reflection and transmission of radio waves at a dielectric slab with variable permittivity.
11 p1329 A73-25675

Polarization of radio waves reflected from an inhomogeneous ionosphere
12 p1468 A73-26971

Disturbances of directional radio due to echoes caused by high buildings
12 p1473 A73-27753

The concept of an installation for measuring partial reflections with the aid of the FM-CW procedure and the principle of measurement involved
12 p1486 A73-27764

D layer electron density long term continuous monitoring, comparing FM-CW method application to partial reflection technique with conventional pulse method
12 p1474 A73-27765

Daily altitude variations of medium frequency radio waves reflection in ionosphere over Tsumeb, SW Africa, examining attenuation correlation with solar zenith angle
12 p1494 A73-27767

Investigation of the signal-to-noise ratio of ionospheric reflection by the method of coherent reception
15 p1844 A73-31890

Some characteristics of the ionospheric irregularities associated with Esq layers.
16 p2004 A73-33443

Determination of the lunar albedo at the 6-m wavelength
16 p2064 A73-33772

Determination of elements of Venusian rotational motion and of coordinates of surface regions with higher reflectivity at radio frequencies
16 p2067 A73-33808

The Budrio station of the meteoric radar system of the CNR for the systematic study of the upper atmosphere
17 p2147 A73-34959

Radio anechoic chamber reflectivity level evaluation, comparing antenna pattern method and free space voltage standing wave ratio technique
17 p2128 A73-35684

Reflection of powerful radio waves from the lower ionosphere
19 p2406 A73-38334

Measurement of the dispersion of waves in the ionosphere.
21 p2682 A73-40232

Kinesonde observations of ionosphere modification by intense electromagnetic fields from Platteville, Colorado.
22 p2844 A73-41921

Fading characteristics and drift and anisotropy parameters of the ground diffraction pattern of the radio waves reflected from the equatorial ionosphere during spread F conditions.
22 p2825 A73-41929

Theoretical and experimental investigations of the coefficients of reflection from plant foliage at small slip angles
22 p2847 A73-42332

Parameter behavior in mass distribution analysis of overdense Geminid trail radio echoes
22 p2915 A73-43041

Determination of the vertical parameters of wavelike ionospheric disturbances
24 p3083 A73-44797

Theory of the polarisation of the ordinary wave reflected from the ionosphere in the limit of vertical incidence and vertical magnetic field.
24 p3069 A73-45202

RADIO ELECTRONICS

Russian book on electrical power supply devices for radio systems covering design of rectifiers, transformers, current limits, voltage regulators, filters, converters and inverters
02 p0133 A73-12863

Harmonic balance method for spectral investigation of periodic and disturbing functions of nonlinear systems in radio engineering, using autofiltration hypothesis
14 p1739 A73-30555

Application of the describing-function approach to radio engineering problems. II
15 p1853 A73-31254

Oscillographic equipment for research in the field of semiconductor microwave electronics
17 p2218 A73-34160

Discrete reproduction of a random parameter change process in standard automation equipment elements
20 p2543 A73-39393

Automated systems for designing electronic circuits
21 p2265 A73-41304

Optimization of electronic circuits with characteristics depending on a continuously varying parameter
21 p2666 A73-41311

Russian book on radio astronomy with electronic engineering emphasis covering observation and equipment, cosmic source characteristics, radio telescope antenna systems, radar techniques, coordinate measurement, etc
22 p2905 A73-41875

Russian monograph on signal transmission channel identification systems in statistical communication theory covering mathematical models, design principles, radio electronic systems, etc
22 p2827 A73-42600

Conference on Electron Device Techniques, New York, N.Y., May 1, 2, 1973, Record.
22 p2833 A73-42691

A quantitative estimate of the electromagnetic compatibility of high-frequency leads in electronic equipment
24 p3071 A73-44596

Performance efficiency of systems employing information from radio-electronic means of observation
24 p3071 A73-44599

RADIO EMISSION

NT RADIO BURSTS
NT SOLAR RADIO BURSTS
NT SOLAR RADIO EMISSION
NT TYPE 2 BURSTS
NT TYPE 3 BURSTS
NT TYPE 4 BURSTS
NT TYPE 5 BURSTS

Brightness temperature measurement of Callisto satellite thermal radio emission, using ice layer model
01 p0101 A73-10845

Measurement of Jupiter's radio emission at 2.94 m.
01 p0107 A73-11330

Very long baseline interferometry observations of radio emissions from geostationary satellites.
02 p0215 A73-12270

The nature of radio emission from pulsars.
02 p0218 A73-12407

Relativistic electron radio emission models, calculating magnetic bremsstrahlung spectra from galactic electron space-energy distributions
02 p0208 A73-12459

The possibilities of determining the temperature profile in the Venusian atmosphere from the thermal radio emission of the planet
02 p0219 A73-12463

Extensive air showers radio emission polarization, spatial distribution and electric field strength, noting geomagnetic mechanism effect
02 p0209 A73-12672

Thermal radio source DR 21 centimeter flux density measurements for antenna aperture calibration, comparing with standard sources
03 p0366 A73-12932

The radioastronomy of the planets
03 p0372 A73-13273

The absorption by the interstellar medium of 80 MHz radio emission from galactic supernova remnants.
03 p0372 A73-13346

Physical phenomena of controlled experiments in earth magnetosphere using test particles, radio emission and electron and ion beams
04 p0443 A73-15342

Pulsars and the evolution of supernova remnants.
04 p0501 A73-15686

Observations of maser radio sources with an angular resolution of 0.0002 sec.
04 p0503 A73-16001

Investigations of high-energy charged particles and VLF radiation with the Interkosmos 3 satellite.
05 p0608 A73-16085

Ionospheric propagation effects on riometer recorded cosmic radio emission spectra, noting temporal and frequency spectra dependence on ionospheric plasma turbulence scale
05 p0573 A73-16266

Surveillance radar cosecant reflectors electromagnetic energy emission distribution, discussing design and directional characteristics
05 p0550 A73-16474

A satellite study of the mid-latitude trough in electron density and VLF radio emissions during the magnetic storm of 25-27 May 1967.
05 p0571 A73-17060

Lunar polarized 1420 MHz thermal radio emission aperture synthesis maps evaluation
06 p0752 A73-18237

Geomagnetic field perturbation by gamma quanta pulsating source, studying accompanying radio emission behavior

07 p0816 A73-19445
2.8 cm radio emission from alpha Orionis, HBV 475 and MWC 349.

07 p0899 A73-20120
Properties of the radio continuum emission from interacting galaxies.

07 p0900 A73-20280
Possible explanation for nonthermal radio noise from binary stars.

08 p1003 A73-20883
A numerical model of the structure and evolution of young supernova remnants.

09 p1143 A73-22111
Lateral distribution of u.h.f. radio emission associated with cosmic ray showers.

09 p1137 A73-22174
Formamide rotational transition microwave emission detection in interstellar medium in Sgr B2 and Sgr A direction

09 p1150 A73-23140
Probabilities of infrared and RF transitions in OH and CH molecules

10 p1250 A73-23710
A first 1415 MHz survey with the Westerbork Synthesis Radio Telescope An attempt to detect radio emission from quasi stellar objects.

10 p1280 A73-24402
Anomalous absorption of cosmic radio emission in the auroral zone during the IQSY

11 p1411 A73-25087
Continuum radio emission from NGC 4656/7 and NGC 891 at 408 MHz.

11 p1415 A73-25170
The geometry and dynamic spectra of Io-modulated Jovian decametric radio emissions.

12 p1540 A73-27327
Galactic radio emission at 38 MHz using steerable reflector telescope with defined beam and small sidelobes

13 p1673 A73-28278
Radio emission from pulsars and surface temperature of neutron stars.

13 p1681 A73-28925
Limit to pulses of radiofrequency emission from the galactic centre.

14 p1800 A73-30600
Brightness temperature measurement of Callisto thermal radio emission, using ice layer model

15 p1928 A73-30981
High-resolution survey of thermal sources of radio emission at the 8.2-mm wavelength

15 p1938 A73-31952
Continuum galactic background radio emission, considering rarefied ionized hydrogen gas with filaments due to dense inhomogeneities

15 p1938 A73-31953
Anticipated variability of Pulsar NP 0532 emission in the Crab nebula associated with angular velocity jumps

15 p1938 A73-31964
Pulsar radio emission limiting polarization resulting from passage through magnetoactive plasma, discussing electron density effects

15 p1844 A73-32003
Relativistic electron radio emission models, calculating magnetic bremsstrahlung spectra from galactic electron space-energy distributions

15 p1927 A73-32609
The possibilities of determining the temperature profile in Venus' atmosphere from the planet's thermal radio emission.

15 p1942 A73-32613
X-ray and radio emission from stellar coronae.

16 p2052 A73-32827
Variable radio emission from the extragalactic supernova 1970g in M101.

16 p2060 A73-33094
Continuum radio emission from the vicinity of pulsars.

16 p2061 A73-33219
Upper limit to the 11.4 m flux of Saturn using VLBI.

16 p2061 A73-33221
Extragalactic radio phenomena.

16 p2054 A73-33288
Radio emission of the moon at millimeter and sub-millimeter wavelengths

16 p2064 A73-33769
Some results of a theoretical study of radio emission polarization on a rough moon

16 p2064 A73-33770
Investigation of the lunar surface by the method of the scattering of radio waves emitted by lunar satellites

16 p2064 A73-33773
Calculations on the radio emission resulting from geomagnetic charge separation in an extensive air shower.

17 p2223 A73-34244
Absorption of ultrahigh energy photons in the universe

17 p2223 A73-34368

Possible role of faster-than-light radiation under pulsar conditions

17 p2226 A73-34370
Observations at 1415 MHz of radio sources in the field of the double-galaxy system NGC 2798/99.

17 p2234 A73-35614
Infrared and radio transition probabilities of OH and CH.

18 p2338 A73-36735
The brightness temperature of Venus at 70 centimeters.

19 p2489 A73-38526
Stimulated linear acceleration radiation - A pulsar radio emission mechanism.

20 p2602 A73-39444
Continuum centimeter wave radiometers circuits, parameters, sensitivity and atmospheric radio emission fluctuations

21 p2705 A73-41460
Detection of radio emission from V1016 Cygni.

21 p2780 A73-41644
Radio emission from HD167362 and Vy2-2.

21 p2780 A73-41645
Detection of radio emission from M1-11 and HD37806.

21 p2780 A73-41646
Root-mean-square signal amplitude variation measurements of LF radio emission from extensive air showers by whip antenna

22 p2827 A73-42486
The source and structure of the Jovian radiation belt.

22 p2903 A73-42986
Some statistical characteristics of active regions with the yellow coronal line.

22 p2915 A73-43037
Pulsar properties covering galactic distribution, pulse periodicity computed from arrival time measurements, models, emission mechanisms, total intensity pulse shapes, etc

23 p3028 A73-43351
Results of radio emission studies at frequencies of 32 and 58 MHz in extensive air showers on the assembly of Moscow State University

23 p3022 A73-43550
Mars and Jupiter - Radio emission at 1.35 cm.

24 p3128 A73-44399
High-resolution survey of thermal radio sources at 8.2 mm.

24 p3131 A73-44477
Continuum galactic background radio emission, considering rarefied ionized hydrogen gas with filaments due to dense inhomogeneities

24 p3131 A73-44478
Expected radiative variability of Crab-Nebula pulsar NP 0532, related to abrupt changes in angular velocity.

24 p3132 A73-44489
A theory of the origin of the split pair burst emission from the solar corona.

24 p3123 A73-44646
Two types of radio emission from the auroral ionosphere and ionospheric disturbances

24 p3083 A73-44798
Physical conditions in nuclei of spiral galaxies. I - Study of galaxies with a nuclear radio-component.

24 p3141 A73-45192

RADIO ENERGY

U RADIANT FLUX DENSITY

U RADIO WAVES

RADIO EQUIPMENT

NT IONOSONDES

NT RADIO ANTENNAS

NT RADIO BEACONS

NT RADIO FILTERS

NT RADIO RECEIVERS

NT RADIO TELESCOPES

NT RADIO TRANSMITTERS

NT RADIOSONDES

NT RADIOTELEPHONES

NT RAWINSONDES

NT RECEPTION DIVERSITY

NT SPACECRAFT ANTENNAS

NT SUPERHETERODYNE RECEIVERS

NT TRANSMITTER RECEIVERS

NT TRANSPONDERS

NT VERY HIGH FREQUENCY RADIO EQUIPMENT

Lunar surface SEP transmitter-receiver ground wave experiment, discussing electronic equipment, multifrequency antennas and signal variation

04 p0428 A73-15391
Equipment for observation of fast fluctuations in the solar radio emission flux

05 p0573 A73-16269
The limiting advantage derived from the compounding of information-extracting devices in the presence of wideband Gaussian noise

12 p1482 A73-26867
Differential equations for digital model of linear quadrupole, discussing digital simulation of analog radio equipment circuits

13 p1591 A73-28659

RADIO FREQUENCY DISCHARGE

Taking into account correlation when forecasting the parameters of failure-free operation of radio equipment.

15 p1849 A73-30994
Linear theory of an IMPATT diode distributed microwave amplifier.

16 p1991 A73-33983
Aircraft radio equipment manufacture, assembling, mounting, installing and testing, discussing hangar installation, bundle elements, castings, printed circuits and welding techniques

19 p2433 A73-37767
B-2 installation for radio wave absorption measurements in the ionosphere at two frequencies simultaneously by the /A1/ pulse method

20 p2566 A73-39165
German book on HF technology, Volume 1, covering coupling filters, transmission lines, antennas, Lecher waves, waveguides, etc

24 p3073 A73-44999

RADIO FILTERS

Channel filters with longitudinally coupled flexural mode resonators.

04 p0427 A73-15320
A three-cavity ring type filter.

07 p0804 A73-20572
Preliminary frequency selection for signal matched filtering.

12 p1469 A73-27268
The use of selective RC amplifiers in the RF amplifier of a superheterodyne receiver.

16 p1991 A73-33982
High performance surface wave bandpass filters for signal processing applications.

17 p2140 A73-35320
Total power filter spectrometer for radio astronomy, featuring local oscillators with commutation for removing output instabilities to reduce instrument errors

21 p2703 A73-41149
Approximation of transfer functions for filters with equalized group-delay characteristics.

23 p2960 A73-43676

RADIO FREQUENCIES

NT C BAND

NT EXTREMELY HIGH FREQUENCIES

NT EXTREMELY LOW RADIO FREQUENCIES

NT HIGH FREQUENCIES

NT LOW FREQUENCIES

NT LOW FREQUENCY BANDS

NT MICROWAVE FREQUENCIES

NT SUPERHIGH FREQUENCIES

NT ULTRAHIGH FREQUENCIES

NT VERY HIGH FREQUENCIES

NT VERY LOW FREQUENCIES

Nonlinear radio-frequency response of a non-uniform plasma slab-condenser system with realistic density and velocity profiles.

04 p0479 A73-15189
Role of the sporadic E layer in short radio wave propagation at frequencies exceeding the maximum usable frequencies of the F2 layer

05 p0548 A73-16264
Large-signal behaviour of R.F. power transistors. I - Analysis of the equivalent circuit.

05 p0559 A73-17125
Radio oscillators short term frequency instability, examining relations between time domain and frequency domain sample variance definitions

07 p0798 A73-19176
Single point thunderstorm ranging method based on two radio frequencies field intensity spectral components ratio

07 p0847 A73-19439
Result of medium- and long-wave observations at distances of about 7500 km

12 p1474 A73-27768
RF field space-time modulation devices to obtain molecular beam velocity distribution and Zeeman pattern components shift

13 p1662 A73-28345
Partial trapping of a low-density plasma by an RF quasipotential well.

14 p1779 A73-29917
Comprehensive theory of r.f. energy absorption by a hot ion-electron plasma cylinder excited by an arbitrary electromagnetic field.

15 p1916 A73-31080
Frequency dependence of radio-wave absorption in a reflecting layer

15 p1844 A73-31884
Television sound subcarrier transmission in space communication.

20 p2524 A73-38737
Electroexplosive device pin-pin firing frequency mathematical modeling and prediction based on RF impedance data obtained nondestructively by automatic network analyzer

22 p2822 A73-41793

RADIO FREQUENCY DISCHARGE

Spectroscopic investigation of turbulent plasma parameters.

03 p0347 A73-14095

RADIO FREQUENCY HEATING

The RIT engine family. - From microthruster to main propulsion units. 04 p0488 A73-15716

Characteristics of an argon RF plasma - Active discharge and laminar sonic flow region. 05 p0602 A73-16559

Spatial distributions of plasma density in a high-frequency discharge with a superimposed static magnetic field. 07 p0856 A73-19518

A model for the kinetics of oxygen dissociation in a microwave discharge. 07 p0789 A73-20643

Plasma excitation by HF field in carbon dioxide-argon flow under low pressure, noting disappearance of striations 10 p1253 A73-24072

Digital electrode breakdown potential controller for spark source mass spectrometer automation, using radio frequency pulse amplitude sensing 11 p1367 A73-26315

Structured discharges in high frequency plasmas. 14 p1782 A73-30770

A high-temperature plasma state in a high-power microwave discharge 17 p2214 A73-34136

Recombination and negative ion role in high-frequency gas discharges 21 p2743 A73-40366

Level populations in plasmas - RF discharges and sonic channel. 22 p2895 A73-42994

Influence of the magnetic field on electrodeless-discharge plasmas 23 p3009 A73-43654

An MHD generator with a nonequilibrium plasma produced by VHF ionization 23 p3011 A73-43714

Some electric and spectroscopic properties of the radiofrequency plasma in a steady magnetic field. 23 p3012 A73-43831

Tuned loop antenna for radio observation of electrostatic spark and corona discharges generated during oil tanker cleaning operations 23 p2945 A73-43960

RADIO FREQUENCY HEATING

Stable electron density fluctuations in a plasma in the presence of a high-frequency electric field. 04 p0444 A73-15539

Further ionosonde observations of ionospheric modification by a high-powered HF transmitter. 04 p0444 A73-15540

Microwave heating of a plasma and longitudinal electron thermal conductivity in a magnetic field. 06 p0732 A73-18606

High-frequency heating of a plasma under lower hybrid-resonance conditions 07 p0855 A73-19290

Topical Conference on RF Plasma Heating, 1st, Texas Tech University, Lubbock, Tex., July 6-8, 1972, Proceedings. [TTU-SR-2] 09 p1128 A73-22626

Radio-frequency heating of a collisionless plasma. [TTU-SR-2] 09 p1128 A73-22627

RF plasma heating by the modified two stream instability. [TTU-SR-2] 09 p1128 A73-22628

Operating features of an ion-cyclotron-wave plasma apparatus running in the RF-sustained mode. [TTU-SR-2] 09 p1128 A73-22632

Nonlinear theory of plasma heating by parametric instabilities. [TTU-SR-2] 09 p1128 A73-22633

Measurement of effective collision frequency in RF heating through parametric instabilities. [TTU-SR-2] 09 p1128 A73-22634

Electromagnetic fields in electrodeless discharges of arbitrary length. [TTU-SR-2] 09 p1128 A73-22635

Particle seeded RF hydrogen plasma opacity, emission spectra, heat transfer and temperature profile at high temperatures [TTU-SR-2] 09 p1128 A73-22636

Lower-hybrid-resonance heating of a plasma in a parallel-plate waveguide. [TTU-SR-2] 09 p1129 A73-22639

Analytical and computer simulation of two ion species RF heated magnetoplasmas response to driving electric fields near lower hybrid frequency, observing parametric instabilities [TTU-SR-2] 09 p1129 A73-22640

Microwave heating and resonant diffusion of electron plasmas, considering relativistic theory and Fokker-Planck equation [TTU-SR-2] 09 p1129 A73-22641

Computer simulation of ion heating by pulsed microwaves. [TTU-SR-2] 09 p1129 A73-22642

Anomalous nonlinear dissipation of high-frequency radio waves in a plasma 09 p1653 A73-23330

Plasma heating at the lower hybrid resonance. 13 p1665 A73-28690

Isothermal ionization of the lower ionosphere under the effect of radio waves. 13 p1608 A73-28709

Microwave heating of electrons of a dense plasma column at frequencies higher than electron cyclotron frequency. 14 p1782 A73-30771

Saturation in cyclotron resonance heating of plasma. 16 p2042 A73-33339

Evaluation of effects of the microwave oven /915 and 2450 MHz/ and radar /2810 and 3050 MHz/ electromagnetic radiation on noncompetitive cardiac pacemakers. 20 p2520 A73-39824

The thermospheric heating function. III - The function describing the heating of the thermosphere by short-wave solar radiation during a period of high solar activity 24 p3084 A73-44800

RADIO FREQUENCY IMPEDANCE PROBES

Measurement of admittances of microwave oscillators with injection locking. 03 p0310 A73-14497

Measurement of electron temperature in the ionosphere by the high-frequency probe method 14 p1746 A73-29861

Radio-frequency size effect in a normal metal layer adjacent to a superconducting phase 14 p1784 A73-30810

Oriental dependence of certain RF impedance probes in the ionosphere. 18 p2288 A73-36188

Determination of electron density and electron collision frequency in a plasma by an RF nonimmersive probe. 21 p2748 A73-40953

RADIO FREQUENCY INTERFERENCE

NT ATMOSPHERICS

NT BLACKOUT [PROPAGATION]

NT CHIRP SIGNALS

NT COSMIC NOISE

NT DAWN CHORUS

NT ELECTROMAGNETIC NOISE

NT HISS

NT IONOSPHERIC NOISE

NT IONOSPHERICS

NT SHOT NOISE

NT SUDDEN ENHANCEMENT OF ATMOSPHERICS

NT THERMAL NOISE

NT WHISTLERS

Digital simulation of imperfect second-order hybrid phase locked loop operating in RF interference background, determining phase error variance and probability density function 04 p0422 A73-15438

System design, hardware and software of RF interference measurement experiment regarding microwave frequency optimal sharing between ATS-F satellite and terrestrial relay telecommunication 04 p0422 A73-15460

Correlation analysis of the continuum radio emission of noise storms. 04 p0504 A73-16028

Pulse interference suppression during noise signal intensity measurements with a modulation radiometer 07 p0792 A73-19911

VLF modal interference effects observed on transequatorial paths. 07 p0793 A73-20059

Interference protection of regenerative parametric amplifiers. 09 p1061 A73-22042

Frequency correlation of fluctuations of radio waves reflected from the ionosphere. 10 p1188 A73-24240

Zero-steering antenna system for receiving a signal close to the direction of strong interference. 11 p1332 A73-26284

Investigation of the permissible power level of FM radio interference at the input of the frequency converter in an FM-signal receiver 12 p1477 A73-26873

Disturbances of directional radio due to echoes caused by high buildings 12 p1473 A73-27753

Determination of the height of ionospheric irregularities with the holographic method. 13 p1606 A73-28155

Measurement of an energy-independent parameter of a radio signal in the presence of high-level additive and modulating interference. 13 p1583 A73-28729

Correlation of random noise levels in short-wave radio channels 13 p1584 A73-28888

RF spectrum utilization for optimum communication capacity, considering tradeoff between bandwidth and interference, antenna directivity and wave reflection and scattering effects 13 p1584 A73-29113

A study of frequency sharing between satellite and terrestrial broadcasting systems. 14 p1725 A73-29748

Payload/launcher radio compatibility, discussing RF link parameters choice, terminal devices quality and test schedule 14 p1742 A73-30113

Statistical computation of compatibility of tropospheric and satellite communication lines. 15 p1842 A73-30986

Microwave radiometer measurement at 17 GHz to investigate atmospheric attenuation and radio noise and interference sources for optimal satellite communication systems design 16 p1982 A73-33718

Interference into angle-modulated systems carrying multichannel telephony signals. 16 p1983 A73-33742

Radio interferometry of moving sources in the presence of confusion - An application to Mercury at 21-centimeter wavelength. 17 p2231 A73-34763

Effects of cochannel interference and Gaussian noise in M-ary PSK systems. 17 p2122 A73-34871

Effect of modulating /multiplicative/ interference on signal processing in a system consisting of a phased array antenna and a receiver. 17 p2129 A73-35710

Probability of reception of discrete information with a specified reliability under conditions of random radio interference. 17 p2129 A73-35713

SID effects as observed in intensities of LF radio waves. 18 p2290 A73-36879

Radio noise from towns - Measured from an airplane. 19 p2404 A73-37675

Secondary surveillance radar - Current usage and improvements. 19 p2451 A73-37808

Error rate of a 4-phase coherent PSK satellite channel with non-Gaussian interference. 20 p2523 A73-38721

Adjacent-channel interference between unfiltered and filtered QPSK signals. 20 p2526 A73-38754

ILS technology assessment, considering landing glide path determination, interference due to multipath propagation and ground effects, and operating frequency range problem 21 p2737 A73-41075

Protection of radiometers from pulse interference 21 p2705 A73-41463

A method of reducing the influence of interference on the operation of a correlation interferometer 21 p2667 A73-41511

Electromagnetic interference and compatibility control in aircraft communication, discussing RF current, voltage, impedance and SNR measurement techniques 22 p2821 A73-41692

The susceptibility of modern aircraft instrument systems to interference in the HF band. 22 p2851 A73-41694

RF fields as new ecological factor in environment pollution, considering radiation interaction with biological systems and increased use of electromagnetic spectrum 22 p2811 A73-41787

A modified composite wave technique for OMEGA. 22 p2884 A73-42325

Spectrum control procedures for the National Radio Astronomy Observatory. 23 p2953 A73-43381

Evaluation of the correctness of Gaussian approximation in noise immunity theory 23 p2954 A73-43519

Adaptive array based on feedback concept for interference rejection, discussing processing of modulated signal with CW reference system 24 p3067 A73-44737

RADIO FREQUENCY NOISE

U ELECTROMAGNETIC NOISE

RADIO FREQUENCY RADIATION

U RADIO WAVES

RADIO FREQUENCY SHIELDING

Effect of engineering-design factors on the parameters of microstrip transmission lines 08 p0951 A73-21109

Electromagnetic shielding techniques and testing for environment and instrument protection from radio emission and noise 22 p2823 A73-41804

Optical identifications and positions of blue stellar radio sources without UV excess, comparing with N-galaxies and quasars with red shift 01 p0103 A73-10997

Stellar gas injection into nucleus of radio galaxy NGC 4486, estimating energy release during gas accretion 01 p0106 A73-11301

A preferred orientation of extragalactic double radio sources. 02 p0217 A73-12405

Improved positions and some identifications for 108 radio sources between declinations -33 and +27 deg.

03 p0372 A73-13348

Radio source counts and redshifts in steady state cosmology.

04 p0497 A73-15048

Radio galaxies luminosity function from radio power range at 178 MHz with known red shift, using 3C catalog galaxies

05 p0622 A73-17071

The distribution of redshifts of quasi-stellar objects and related emission-line objects.

05 p0626 A73-13736

The interpretation of the X-ray emission detected from some nearby radio galaxies.

07 p0872 A73-19940

Optical variability of the nuclei of Seyfert galaxies

07 p0901 A73-20306

Cyg X-3 flux density measurements at 365 MHz with broadband synthesis interferometer, comparing radio flares with Laan model

07 p0902 A73-20559

Neutral hydrogen in Markarian galaxies.

08 p1006 A73-20933

Observational data and interpretation of infrared spectra and microwaves of galaxies and the intergalactic matter

09 p1150 A73-23143

Optical variability of the nuclei of Seyfert galaxies.

12 p1539 A73-27278

A survey of elliptical galaxies at 6 cm.

13 p1685 A73-29361

Redshifts for 51 galaxies identified with radio sources in the 4C catalog.

15 p1936 A73-31562

The properties of extragalactic X-ray sources from visible light observations.

16 p2050 A73-32742

Interplanetary-scintillation observations of 203 sources identified as radio galaxies or quasars.

17 p2225 A73-34289

Paraday depolarization of radio galaxies and quasars with simple spectra.

17 p2234 A73-35621

Intense outburst /S/ of radio radiation detected with the Goldstone-Haystack interferometer.

19 p2485 A73-37624

Observations of further outbursts in the radio galaxy 3C 120.

19 p2485 A73-37625

The redshift-distance relation. VI - The Hubble diagram from S20 photometry for rich clusters and sparse groups - A study of residuals.

19 p2487 A73-38505

Brightness and polarization distributions of head-tail galaxies at 1415 MHz.

20 p2610 A73-39583

Extragalactic radio sources identification with galaxies and quasars by high sensitivity and resolution astronomical telescopes, obtaining angular structure maps and radio spectra

23 p3028 A73-43347

Radio spectra and mapping of extragalactic radio sources including radio galaxies and quasars with high angular resolution, noting energy sources and red shift

23 p3029 A73-43625

Optical identifications of radio sources using accurate radio and optical positions.

24 p3135 A73-44579

High resolution observations of the radio galaxy NGC5128 at 10.7 GHz.

24 p3143 A73-45489

RADIO HORIZONS

Diurnal variation of the effective earth's radius factor /k/ over India and its influence on microwave propagation.

04 p0423 A73-15599

Diurnal variation of the effective earth's radius factor /k/ over India and its influence on microwave propagation.

04 p0423 A73-15928

Experimental investigation of the parameters of a statistical Gaussian model of the field below the radio horizon at centimeter wavelengths.

07 p0794 A73-20131

Centimeter wave propagation beyond horizon, considering terrestrial surface curvature and mountain effects on deflection and atmospheric refractivity inhomogeneity caused scattering

12 p1473 A73-27754

Distortions of UHF pulse signals propagating along the earth at distances below the radio horizon

14 p1729 A73-30559

RADIO INTERFERENCE

U RADIO FREQUENCY INTERFERENCE

RADIO INTERFEROMETERS

The quasi-linear intensity interferometer.

01 p0045 A73-10184

Spatial-temporal processing of thermal radio signals from emitters moving in the near zone of an interferometer

01 p0017 A73-10213

Radio interferometry observation of extragalactic radio sources for geodetic survey of baseline between antenna sites in Massachusetts and West Virginia

01 p0039 A73-10405

Three station interferometric observation of TAC-SAT synchronous communications satellite radio signals for orbit determination, discussing method feasibility for tracking and geodesy applications

01 p0097 A73-10407

Low frequency, high resolution observations of Virgo A.

01 p0100 A73-10791

Observation of compact objects of cosmic radio emission with maximum angular resolution at the 3.55-cm wavelength

01 p0092 A73-10931

Very long baseline interferometer observations of Taurus A and other sources at 121.6 MHz.

03 p0366 A73-12933

Australian east-west baseline interferometer observations at 2.3 GHz.

03 p0372 A73-13349

Lunar topography - First radar-interferometer measurements of the Alphonsus-Ptolemaeus-Arzachel region.

03 p0378 A73-14446

Observations of maser radio sources with an angular resolution of 0.0002 sec.

04 p0503 A73-16001

Determination of the effective angular distance between the reflection points of an ordinary ray and an extraordinary ray by the interference method

05 p0548 A73-16259

Observations of radio sources with an interferometer of 24-km baseline. I - The angular structures at 408 MHz of 106 sources from the Parkes catalogue.

07 p0899 A73-19937

Interferometer observations of W 3/OH/ at 2.695 GHz and 8.085 GHz.

08 p1006 A73-20929

Very long baseline interferometry techniques for Crab Nebula pulsar observation at meter wavelengths

08 p1013 A73-21812

Observations of compact radio-emitting objects at 3.55 cm with maximum angular resolution.

09 p1147 A73-22726

Interferometric observations of formaldehyde absorption in front of strong galactic sources.

09 p1150 A73-23139

A new VHF-interferometer with three steerable high-gain-antennas for satellite-tracking.

09 p1070 A73-23434

The radio diameter of the sun from interferometer measurements at 9 mm wavelength.

10 p1284 A73-24773

Accuracy of statistical measurements of random field characteristics in interferometric systems

11 p1360 A73-25020

Polarization interferometer for 2800 MHz solar noise studies with a 0.5-min fan beam.

11 p1422 A73-25943

First results from the Texas interferometer - Positions of 605 discrete sources.

11 p1428 A73-26676

Baseline arrangement of radio interferometer array for tracking artificial satellites.

13 p1586 A73-29233

Radio interferometry of moving sources in the presence of confusion - An application to Mercury at 21-centimeter wavelength.

17 p2231 A73-34763

Radio interferometer for the range from 136 to 138 MHz in the central German ground station

19 p2432 A73-38273

Precise positions of radio sources. IV - Improved solutions and error analysis for 59 sources.

19 p2488 A73-38510

Circular synthetic radar with interferometer elements mounted at ends of horizontal boom rotating about vertical mast, predicting echo response to point and multiple targets

21 p2650 A73-40342

Direct determination of universal time based on east-west interferometer observations of radio sources using 5 km radio telescope

21 p2739 A73-40373

Pulsar polarization measurements by multielement interferometer dipole antenna and DKR-1000 cross array radio telescope

21 p2662 A73-40546

Application of long-baseline radio interferometers to astrometric tasks

21 p2701 A73-40726

A study of planar deployment control and libration damping of a tethered orbiting interferometer satellite.

21 p2781 A73-40900

Sensitivity of an intensity radio interferometer

21 p2705 A73-41471

A method of reducing the influence of interference on the operation of a correlation interferometer

21 p2667 A73-41511

Long baseline interferometry with high angular resolution widely separated radio telescopes and video signal magnetic recording tapes, discussing coherence and timing requirements and calibration

23 p2980 A73-43349

Very-long-baseline interferometry techniques applied to problems of geodesy, geophysics, planetary science, astronomy, and general relativity.

23 p2980 A73-43354

High angular resolution very long baseline interferometry for emission spectra and angular size determination and structure mapping of galactic and extragalactic radio sources

23 p2980 A73-43355

Spectral-line analysis of very-long-baseline interferometric data.

23 p2980 A73-43357

National Radio Astronomy Observatory interferometer system with rotating head video tape recording and computerized sampled data processing equipment for use with radio telescope

23 p2980 A73-43358

Stanford radio telescope array with five paraboloid antennas for fast image forming interferometry, using earth rotation synthesis to produce sky continuous radiation brightness map

23 p2957 A73-43359

Radio telescope array of interferometers formed by fixed and movable antennas operating on rotational aperture synthesis for radiation observation, emphasizing electronic system stability

23 p2957 A73-43360

Southern Hemisphere earth rotational synthesis radio telescope array with paraboloids arranged as compound grating interferometer for astronomical radio sources mapping

23 p2958 A73-43361

Radio astronomy interferometer receiver IF control for centimeter wave polarized signal processing and parabolic antenna instrumentation

23 p2980 A73-43377

Analog scale model of radio interferometry depth sounding at centimeter wavelengths, examining glacier layer boundaries

24 p3082 A73-44750

RADIO METEOROLOGY

Theoretical possibilities for determining the moisture content of the atmosphere through the thermal radio emission in the submillimeter range.

07 p0848 A73-20347

Russian book - Scattering and attenuation of electromagnetic radiation by atmospheric particles.

15 p1843 A73-31586

Waves and turbulence in stable layers and their effects on EM propagation; Proceedings of the Third Symposium, La Jolla, Calif., June 5-15, 1972. Parts 1 & 2.

19 p2447 A73-38202

RADIO METEORS

Influence of selectivity on the observed orbital-parameter distribution of radio meteors

01 p0101 A73-10846

Upper-atmosphere motion, as determined by observations of radio echoes from meteor trails.

02 p0159 A73-12145

Atmospheric diffusion, radio meteor trail radius and electron density distribution effects on radar echoes time position, noting recorder resolution increase

05 p0617 A73-16613

Determination of the velocity of a radio meteor with minimum rms error.

08 p1012 A73-21581

Statistical model of meteor streams. III - Stream search among 19303 radio meteors.

11 p1425 A73-26135

Effect of selectivity on the observed distribution of orbital parameters for radio meteors.

15 p1928 A73-30982

Meteor radar study of tides in the 80 to 100 km altitude range.

18 p2305 A73-35999

Upper atmospheric turbulence kinetic energy spectrum from radio meteor trails observations, noting relationship to structure function for isotropic turbulence

18 p2312 A73-36288

Parameter behavior in mass distribution analysis of overdense Geminid trail radio echoes

22 p2915 A73-43041

RADIO NAVIGATION

NT DECCA NAVIGATION

NT HYPERBOLIC NAVIGATION

NT LORAN

NT LORAN C

NT TACAN

NT VHF OMNIRANGE NAVIGATION

Future of exclusive measurements of distances

02 p0190 A73-12012

Review of radio navigation of civil aircraft - Current and future outlook

02 p0191 A73-12015

Radio navigation review, discussing Decca, Loran, Omega, VOR/DME, satellite, inertial, integrated, area, approach and landing, collision avoidance and space navigation systems

10 p1246 A73-23636

Air navigation evolution and current state of art, discussing MF four axis and nondirectional beacons, VOR, DECCA, DME, TACAN, VOR-Doppler, terminal and landing systems

14 p1773 A73-30445

Russian book - Air navigation: Application of radio navigational aids and automated navigation complexes.

15 p1908 A73-31471

RADIO OBSERVATION

Exclusive distance measurements as substitute to combined distance difference and angular measurements in radio navigation, considering system accuracy and electromagnetic wave transmission

15 p1909 A73-32450

Radio navigation and landing aid equipment for major airports and airlines, noting simplified equipment for minor airports

15 p1912 A73-32559

Mixed CTOL-QTOL traffic effects on air traffic controller tasks, microwave landing and radio navigation systems, airport operation and ground equipment [MBB-UH-05-73]

17 p2207 A73-34487

Aircraft VLF radio navigation, discussing propagation characteristics, Omega and Global Navigation systems and historical development [SAE PAPER 730313]

17 p2209 A73-34673

VLF navigation development at NAE.

17 p2209 A73-34849

Prospects of automation of air traffic control systems using satellites for radio navigation

17 p2209 A73-34961

Low cost data processor and display for ICNI, DME/TACAN, LORAN or range/range difference radio navigation systems in aerospace applications

17 p2210 A73-35213

Operational global navigation system development program with repeater satellites deployed over continental USA to provide radio links for digital communication, surveillance and ATC

21 p2735 A73-40041

Russian book on design and operational principles of monopulse and moving target radar, atomic time and frequency measuring devices, radio navigation and optical processing

21 p2650 A73-40510

Aircraft and spacecraft radio navigation systems, discussing Doppler, inertial and VHF omnirange techniques, Apollo spacecraft guidance systems, TACAN, Harrier and Swedish SAA337 aircraft navigation

21 p2736 A73-40514

A linear method of autonomous space navigation and guidance

21 p2737 A73-40906

A modified composite wave technique for OMEGA.

22 p2884 A73-42325

RADIO OBSERVATION

The short-wavelength spectrum of the microwave background.

01 p0015 A73-10062

Low frequency radio observations of the Andromeda Galaxy.

01 p0096 A73-10313

Prototype solid state radio sounder with digitization concept of multipulse integration for LF sounding of lower ionosphere, noting performance

01 p0043 A73-10909

Radio sensors for the three-axis attitude fine measurement of geostationary communication satellites

02 p0228 A73-11822

Beyond the horizon ionospheric propagation experiment from an equatorial orbiting satellite to a middle latitude station.

03 p0274 A73-12892

An analysis of multi-station ground observations of VLF hiss.

03 p0274 A73-12950

Venus atmospheric parameters below critical refraction and surface refractive index from signal amplitude measurement by radio holographic occultation techniques

03 p0379 A73-14567

Possibility of detecting weak solar cosmic ray fluxes by ground-based radio engineering methods

06 p0742 A73-17532

Investigation of the motion of artificially ionized clouds in the upper atmosphere.

10 p1212 A73-24225

Measurement of the integral parameters of the nighttime ionosphere from observations of Intercomos-2 signals.

10 p1212 A73-24238

Geometric dilution of position (GDOP) in spherical or hyperbolic system determination, noting position error relationship to collinearity between platform and radio sources pair

13 p1585 A73-29121

Possibility of detecting weak solar-cosmic-ray fluxes by ground-based radio methods.

16 p2052 A73-32756

High resolution radio observation of sun at 3.71 and 11.1 cm with three-element interferometer, noting flare near east limb

16 p2060 A73-33097

Traveling regions of high solar wind density observed in early August 1972.

16 p2056 A73-33460

Fast pulse VHF background noise measurements in site selection for radio detection of cosmic ray air showers

16 p1984 A73-33924

VLF pulse ionosounder measurements of the reflection properties of the lower ionosphere.

18 p2305 A73-36010

Electron-density profiles obtained from MF sounding at Tsuamb.

18 p2306 A73-36012

Drift velocity measurements for small-scale inhomogeneities at various levels of the F2 layer

20 p2553 A73-39158

The use of radio beacons in geophysics and their applications.

21 p2657 A73-41331

RADIO OCCULTATION

Mariner 9 S-band radio occultation measurements of Mars shape and atmospheric parameters, discussing global dust storm and equatorial surface pressure

06 p0746 A73-17487

Observation of linear polarization of the Crab nebula during an occultation by the solar corona.

13 p1586 A73-29247

Atmosphere and ionosphere of Venus on the basis of data obtained by Mariner 5 in the S band during radio occultation

16 p2067 A73-33801

Radio-occultation measurements of the Venusian atmosphere conducted by Mariner 5 in the 10-centimeter band

16 p2067 A73-33802

Influence of horizontal inhomogeneity in the Venusian atmosphere on the accuracy of measurements of its parameters by a radio occultation method

16 p2068 A73-33824

S band radio occultation measurements of the atmosphere and topography of Mars with Mariner 9 - Extended mission coverage of polar and intermediate latitudes.

19 p2479 A73-37225

Approximations to the mean surface of Mars and Mars atmosphere using Mariner 9 occultations.

19 p2479 A73-37226

Method and results of observations of the occultation of the source 3C144 by the solar corona with the DKR-1000 FIAN cross-array radio telescope

21 p2767 A73-40545

The radio occultation method for the study of planetary atmospheres.

22 p2912 A73-42979

Radio occultation experiments planned for Pioneer and Mariner missions to the outer planets.

22 p2912 A73-42980

RADIO PHYSICS

Soviet papers on quantum radio physics covering injection lasers, high intensity beam and material interactions, laser dynamics and masers

12 p1505 A73-27135

Russian book on quantum radio physics, Volume 1 covering photons and nonlinear media, matter-radiation interaction, electromagnetic fields, relaxation, emission, solid state physics, etc

12 p1508 A73-27924

RADIO PROBING

A comparison of two ground-based techniques for measuring D-region electron densities. I.

01 p0042 A73-10905

A comparison of two ground-based techniques for measuring D-region electron densities. II.

01 p0042 A73-10906

Automatic N/h, t/ profiles of the ionosphere with a digital ionosonde.

02 p0143 A73-12530

Minimized calculation errors in phase ionosonde true height reduction technique for electron density profile, noting lowest observable radio frequency

02 p0143 A73-12531

A comparison of total electron content determined by the differential Doppler and the Faraday effects using radio signals from a geostationary satellite.

03 p0300 A73-13637

Broad-band isotropic electromagnetic radiation monitor.

03 p0310 A73-14493

Parameter optimization technique for remote radio probing and diagnostics of inhomogeneous media with properties variation along single dimension

04 p0422 A73-15478

The ionospheric effects of geomagnetic sudden commencements as measured with an HF Doppler sounder at Hawaii.

05 p0571 A73-17062

Impedance of an ion-sheathed spherical probe in a warm, isotropic plasma.

09 p1127 A73-22431

Results of volley flights of radio probes on the Kolsk peninsula during periods of magnetic disturbances in March and April 1971

10 p1267 A73-23929

Use of reflection-coefficient amplitude-phase diagrams for choosing and analyzing the operating modes of a radio defektoscope.

11 p1375 A73-26363

Vertical profiles of small-scale temperature structure in the atmosphere.

19 p2448 A73-38209

Measurements of the dielectric properties of seawater and NaCl solutions at 2.65 GHz.

22 p2849 A73-42549

RADIO PROPAGATION

U RADIO TRANSMISSION

RADIO RANGE

Microwave range-difference measurements on 65-km slanted overwater path, interpreting tropospheric noise power spectra and rms values as function of baseline length

11 p1330 A73-25685

Effect of multipath on ranging error for an airplane-satellite link.

14 p1725 A73-29892

Satellite-aircraft multipath and ranging experiment results at L band.

14 p1726 A73-29898

RADIO RANGES

U RADIO BEACONS

RADIO RECEIVERS

NT SUPERHETERODYNE RECEIVERS

NT TRANSMITTER RECEIVERS

Satellite-borne HF ionospheric noise meter receiver system with narrow band monolithic crystal filters, comparing with Ariel 3

01 p0026 A73-11175

A receiver design for the ATS-F radio beacon experiment.

03 p0275 A73-13640

A system for the precise calibration of air navigational receivers.

03 p0310 A73-14501

Synthesis of an optimal receiver structure for amplitude modulated pseudo-noise signals.

04 p0415 A73-14982

The performance of a noncoherent FSK receiver preceded by a bandpass limiter.

04 p0416 A73-14992

OMEGA time transmissions and receiver design.

04 p0416 A73-15063

Modulating /multiplicative/ noise effects on output signal characteristics of receiver designed for optimal reception against background of Gaussian noise

04 p0423 A73-15915

Radio astronomy receiver with digital integrator for weak radio source detection, noting minimum detectable flux density

05 p0552 A73-17166

Design and performance of VHF telemetry transmitter and remote controlled radio receiver for Eole satellite, noting production technology and block diagram

07 p0790 A73-18961

Design and performance of UHF transmitter and receiver system for two way links between Eole satellite and constant ceiling balloons

07 p0790 A73-18962

Height-gain experimental data for groundwave propagation. I - Homogeneous paths.

07 p0791 A73-19377

Detection of signals using receivers with processing of moduli.

07 p0794 A73-20133

Characteristics of the adaptive optimal detection of Gaussian signals on a pulse-noise background in receivers with a logarithmic amplifier

08 p0940 A73-21554

Modulation type microwave receiver with selective filter and ferrite resonator in waveguide coupling

08 p0949 A73-21561

Some perspectives on receiver noise performance and its measurement.

08 p0940 A73-21624

Microwave and millimeter wave receiver noise performance state of art and acoustic measurement methods, discussing traveling wave maser, parametric and transistor amplifiers and tunnel diodes

08 p0940 A73-21625

Algorithm for optimal radio signals detection under narrow band anisotropic noise, noting two channel space diversity receiver system

09 p1050 A73-22454

Recent development results on the HELIOS S-band command receiver.

09 p1057 A73-23416

Digital microwave receiver with passive discriminator for precise and instantaneous pulsed RF signal frequency measurement

10 p1188 A73-24168

Tunnel diodes in receivers to reduce noise level and improve selectivity, discussing distortions, crosstalk and passband dependence on signal amplitude

10 p1195 A73-24385

Investigation of the permissible power level of FM radio interference at the input of the frequency converter in an FM-signal receiver

12 p1477 A73-26873

Optimal passband of a double-tuned selective amplifier during the simultaneous passage of rectangular radio pulses and white noise

12 p1477 A73-26874

Effectiveness of analog storage in the detection of signals on a background of noise and strong random pulsed interference

12 p1467 A73-26942

The first two receivers for the radio astronomy programme on the 100 meter radiotelescope - An assessment of performance.

13 p1581 A73-28000

Theoretical and experimental investigations of a phase-coordinate second-order receiver.

13 p1591 A73-28658

Influence of the nonlinearity of the phase characteristic of the RF signal path in an FM receiver on the signal distortions

13 p1584 A73-28897

Miniature phase/amplitude tracking RF receiver front ends.

14 p1737 A73-30623

Wideband monopulse radio direction finding measurement improvement, using receiver with log video IF amplifier, multiplexing filters and detectors to provide signal normalization

16 p1990 A73-33850

Book - Recommended basic characteristics for airborne radio homing and alerting equipment for use with emergency locator transmitters (ELT).

17 p2207 A73-34475

Effect of modulating /multiplicative/ interference on signal processing in a system consisting of a phased array antenna and a receiver.

17 p2129 A73-35710

SID effects as observed in intensities of LF radio waves.

18 p2290 A73-36879

A low temperature bolometer heterodyne receiver for millimeter wave astronomy.

20 p2564 A73-38878

Application of the method of equivalent nonlinear systems to noise rejection analysis in FM tracking receivers

20 p2537 A73-39451

Sensitivity and resolution of panoramic analyzers

20 p2537 A73-39455

Radio receiver intermodulation characteristics description by generic model, discussing frequency/distance separation criteria to avoid interference, signal measurement procedure and application to equipment standards

22 p2823 A73-41801

Low-noise microwave receiving systems in a worldwide network of large antennas.

23 p2958 A73-43376

Noise factor of a multiple-circuit input device

23 p2953 A73-43518

RADIO RECEPTION

Mean error probability during diversity reception at extremal group frequencies under random noise conditions

01 p0019 A73-11262

HF radio signal reception behavior near maximum usable frequency during evening and at midnight, noting SNR

07 p0792 A73-19456

Noise immunity of diversity reception with threshold switching of antennas

07 p0802 A73-20291

Noise immunity of quasi-coherent reception of phase-shift keyed signals with respect to additive fluctuation noise.

10 p1191 A73-24938

Jupiter radiation reception at decametric wavelengths by Yagi antenna and radiometer, taking into account to modulation effect

11 p1424 A73-26131

Influence of phase fluctuations of the received radiation on the performance of a synthetic antenna

11 p1331 A73-26158

Atmospheric refractivity fluctuation caused transit time variation effects on propagation noise and frequency stability in microwave radio link signal reception at 36 GHz

16 p1982 A73-33714

Reliability of diversity reception by antennas with different polarizations.

16 p1991 A73-33984

Probability of reception of discrete information with a specified reliability under conditions of random radio interference.

17 p2129 A73-35713

Noise immunity of diversity reception with antenna threshold switching.

18 p2290 A73-37128

Determination of the difference in group paths by the method of frequency-diversity reception

24 p3068 A73-44810

RADIO REFLECTION

U RADIO ECHOES

U RADIO RELAY SYSTEMS

A study of frequency sharing between satellite and terrestrial broadcasting systems.

01 p0018 A73-11179

Signal relay systems using large space arrays.

04 p0415 A73-14990

Moored radio telemetering buoy relay stations for North Pacific climatological data acquisition, noting optimum channel frequency for data transmission error rate reduction

04 p0421 A73-15429

Radio set design requirements for communication link between meteorological sensor platforms and spacecraft in Geostationary Operational Environmental Satellite System

04 p0421 A73-15432

System design, hardware and software of RF interference measurement experiment regarding microwave frequency optimal sharing between ATS-F satellite and terrestrial relay telecommunication

04 p0422 A73-15460

Design of modern semiconductor senders for frequency-modulated directional radio systems.

06 p0663 A73-17585

Noise of local oscillators of high capacity radio links

07 p0798 A73-19179

Path diversity for mm-wave earth-to-satellite links.

07 p0791 A73-19376

Selectively faded nondiversity and space diversity narrowband microwave radio channels.

08 p0939 A73-21086

Satellite design considerations.

12 p1549 A73-27659

ESRO Aerosat L-band communication techniques experiments with stratospheric balloon-borne transponders relaying ground station signals to aircraft flying over sea

12 p1498 A73-27672

Technical factors determining the choice of frequency bands for the links between satellite and coast stations of a maritime communications satellite service.

12 p1473 A73-27674

Disturbances of directional radio due to echoes caused by high buildings

12 p1473 A73-27753

Optimal digital modulation techniques for aeronautical communications via satellite, considering air navigational systems for transoceanic flight

15 p1847 A73-32480

Propagation of radio waves at frequencies above 10 GHz; Proceedings of the Conference, London, England, April 10-13, 1973.

16 p1980 A73-33701

Propagation studies and the development of terrestrial microwave radio relay systems above 10 GHz in the UK.

16 p1980 A73-33702

Single and dual path propagation at 18 GHz with application to the design of digital radio relay systems.

16 p1981 A73-33703

Atmospheric refractivity effects on maximum antenna gain and correlation coefficient in design of microwave line of sight links for high reliability

16 p1981 A73-33704

EHF radio wave limitations and potentialities for high speed data communications systems, considering applications in urban short range relays

16 p1981 A73-33705

The characteristics of millimeter wavelength satellite-to-ground space diversity links.

16 p1981 A73-33707

Methods for investigating the effects of multipath fading on 2-phase digital radio systems.

16 p1981 A73-33708

Atmospheric refractivity variation, precipitation and wind effects on two orthogonal linearly polarized microwave signals transmission over radio link at 22 and 37 GHz

16 p1983 A73-33733

Domestic communication satellite systems with microwave transmission links and coast-to-coast earth stations and receivers, detailing design and interference problems

18 p2289 A73-36776

Ground stations in Intelsat 4 communication satellite radio relay system, discussing all-solid-state equipment design, carrier frequency assignment and antenna installation

20 p2523 A73-38723

Adaptive ground implemented phased arrays.

20 p2523 A73-38729

Operational global navigation system development program with repeater satellites deployed over continental USA to provide radio links for digital communication, surveillance and ATC

21 p2735 A73-40041

Satellite techniques for automatic platforms location and data relay.

21 p2737 A73-41335

Low-noise microwave down-converter with optimum matching at idle frequencies.

21 p2666 A73-41428

High altitude remotely piloted vehicle (RPV) platforms for tactical pseudo-satellite multichannel relay transponder systems

22 p2826 A73-42423

An aperture-synthesis interferometer at Ooty for operation at 327 MHz.

23 p2980 A73-43366

RADIO SCATTERING

Characteristics of radio wave scattering by the lunar surface at the landing sites of the Luna 16 and Luna 17 automatic stations

02 p0220 A73-12473

Fraunhofer zone distribution functions for azimuth and elevation angles of radio waves reflected from inhomogeneous ionospheric scattering layer

03 p0278 A73-14071

Note on solar plasma irregularities and plasma instabilities.

03 p0378 A73-14420

Frequency correlation measurement of pulsar spectral fine structure due to radio emission scattering by interstellar plasma

04 p0503 A73-16002

Spectrum of small-scale inhomogeneities in the interplanetary plasma

06 p0747 A73-17529

Polarization characteristics of partially scattered radio waves for turbulent ionosphere vertical sounding applications

06 p0662 A73-17533

Space wave field produced by a vertical electric dipole above a perfectly conducting sinusoidal ocean surface.

06 p0665 A73-18181

Signal level fluctuations line spectra energy characteristics comparison for oblique and oblique-backscatter sounding, noting changes in harmonics intensity and period

07 p0792 A73-19438

Spaced radar observation of auroral scattering cross sections, noting radio backscattering intensity peak and echo detection probability relationship to aspect angles

08 p0957 A73-20661

Some problems in methods for determining the parameters of scattering inhomogeneities

08 p0959 A73-21284

Frequency dependence of losses by radio-wave scattering at turbulent discontinuities in the troposphere

08 p0939 A73-21398

Energy characteristics of radio signals scattered by statistically uneven surface, proposing statistical variables substitution

10 p1191 A73-24934

Possibilities and some results of studying the ionosphere by the method of 'incoherent' scattering of radio waves

11 p1350 A73-25088

Two-position scattering of radio waves by the sea surface at small slip angles

11 p1331 A73-26154

Specific effective scattering area of the surface of the moon, Mars, and Venus in the radio-frequency range.

12 p1543 A73-27639

Radio-wave scattering characteristics of the moon's surface at the landing sites of Luna 16 and Luna 17.

15 p1942 A73-32624

Spectrum of small-scale interplanetary plasma inhomogeneities.

16 p2058 A73-32753

Polarization characteristics of partially scattered radio waves for turbulent ionosphere vertical sounding applications

16 p1978 A73-32757

Average intensity of the normal wave during super-refraction

16 p1978 A73-32897

Investigation of the lunar surface by the method of the scattering of radio waves emitted by lunar satellites

16 p2064 A73-33773

Some problems concerning the method of determining the parameters of scattering inhomogeneities.

19 p2424 A73-37913

Frequency dependence of the loss when radio waves are scattered by turbulent inhomogeneities in the troposphere.

19 p2407 A73-38356

Theory of radio wave incoherent scattering by a plasma and the application of the theory in ionospheric studies

20 p2554 A73-39164

On separating aberrant effects from random scattering effects in radio telescopes.

23 p2958 A73-43379

Changes in the distribution of density and radio scattering in the solar corona in 1971.

24 p3138 A73-45049

RADIO SIGNAL ABSORPTION

U ELECTROMAGNETIC ABSORPTION

U RADIO TRANSMISSION

RADIO SIGNAL PROPAGATION

U RADIO TRANSMISSION

RADIO SIGNALS

Three station interferometric observation of TAC-SAT synchronous communications satellite radio signals for orbit determination, discussing method feasibility for tracking and geodesy applications

01 p0097 A73-10407

Superconducting time variant filter tracking test for RF signal amplitude modulation, using photoelectric perturbation in semiconductor cavity resonator frequency

02 p0146 A73-11847

Clock comparisons by short wave, ULF and VLF signals, Loran C and Omega methods, onboard aircraft atomic clocks and TV synchronizing pulses

03 p0307 A73-13246

Maximum likelihood estimate of carrier frequency and arrival direction of radio signals in background noise for large aperture antennas

03 p0278 A73-14081

RADIO SOURCES [ASTRONOMY]

- Mars shape determination from radio occultation measurements by Mariner 9 probe of signal extinction time and spacecraft ephemeris 06 p0747 A73-17488
- Ionospheric radio signal reflection fields verified via quantitative statistical reliability criterion 07 p0815 A73-19434
- Radio pulse shaping network synthesis composed of lumped elements, noting pulse duration limitation by network efficiency 07 p0805 A73-20134
- Wideband multiphase radio signal processing with given ambiguity function via sequential synthesis 07 p0794 A73-20292
- Noise immunity in the reception of binary radio signals on a correlated-noise background 08 p0939 A73-21553
- Noiselike FM signals shaping by numerical periodic pseudospectrum sequences, analyzing FSK signals 09 p1049 A73-22049
- Algorithm for optimal radio signals detection under narrow band anisotropic noise, noting two channel space diversity receiver system 09 p1050 A73-22454
- The accuracy of an approximate representation of the correlation functions of complex signals distorted in the linear stages of a radio channel 09 p1051 A73-22461
- Investigation of nonstationary processes in the ionosphere and space with quantum frequency standards. 10 p1211 A73-24214
- Measurement of the integral parameters of the nighttime ionosphere from observations of Intercomos-2 signals. 10 p1212 A73-24238
- Energy characteristics of radio signals scattered by statistically uneven surface, proposing statistical variables substitution 10 p1191 A73-24934
- Noise immunity of quasi-coherent reception of phase-shift keyed signals with respect to additive fluctuation noise. 10 p1191 A73-24938
- Nonlinear hydrodynamic VLF wave scattering in the earth's magnetosphere. 11 p1331 A73-25913
- A spectral analysis method for single radio signals 11 p1331 A73-26101
- Investigation of the phase variation of a NWC signal /22.3 kHz/ along a transequatorial path 12 p1469 A73-27339
- Long duration radio signals reception on noise background, recording signal/noise mixture on photographic film 12 p1470 A73-27578
- Correlation and indeterminate functions of signals with discrete frequency-time structure, noting linear frequency modulation of signal element 13 p1583 A73-28669
- Detection of Doppler signals by a receiver which incorporates a counter of the number of excursions of additive noise. 13 p1583 A73-28728
- Measurement of an energy-independent parameter of a radio signal in the presence of high-level additive and modulating interference. 13 p1583 A73-28729
- Thermal IR radiation receiver with ferroelectric capacitor for amplification and transformation of signals from RF oscillator 13 p1618 A73-29133
- Effect of nonlinearity in a coherent pulse integrator on signal-to-noise gain. 15 p1842 A73-30988
- Automatic recording method for the moments of exact-time radio signals 15 p1878 A73-32143
- Experimental investigation of microwave signal fluctuations for propagation above the sea at low slip angles 16 p1978 A73-32889
- Two-phase radio-frequency generators employing phase-lock AFC 17 p2135 A73-34590
- Bayes theorem for radio signals parameter estimation on random noise background, using rectangular function of losses 17 p2123 A73-35167
- Wideband multiphase radio signal processing with given ambiguity function via sequential synthesis 18 p2290 A73-37129
- Self calibrating automatic equipment for pulsed and CW RF testing of phase, amplitude and frequency characteristics of pulsed electronic devices 20 p2535 A73-38870
- Geomagnetic field effects in Martin theory of radio wave propagation in ionosphere with oblique and vertical signal incidence 20 p2555 A73-39181
- Study of phase changes of the NWC signal /22.3 kHz/ on a transequatorial path. 23 p2952 A73-43237

RADIO SOURCES [ASTRONOMY]

- NT CASSIOPEIA A
- NT EXTRAGALACTIC RADIO SOURCES

- NT PULSARS
- NT QUASARS
- NT RADIO GALAXIES
- NT RADIO STARS
- Stellar positions and proper motions representation of fundamental reference system, improving and extending to faint objects and radio sources 01 p0094 A73-10056
- Supernova remnants descriptions, distance and hydrodynamic evolution, considering galactic nonthermal radio sources, radio maps, and X ray and radio polarization 01 p0094 A73-10057
- Application of ultrastable oscillators to aerospace [ONERA, TP NO. 1114] 01 p0045 A73-10235
- Observations at 750, 1400, and 2700 MHz of radio sources in the Vermilion River Observatory survey. 01 p0096 A73-10312
- An upper limit on the OH abundance in the intercloud medium. 01 p0096 A73-10314
- Precise positions of radio sources measured at 2695 MHz. 01 p0098 A73-10580
- High frequency radio observations of optically interacting galaxies. 01 p0099 A73-10586
- Space maser with feedback 01 p0060 A73-10934
- Study of the angular structure of radio sources from their lunar occultations. II 01 p0102 A73-10951
- Investigation of the faint nebula identified with radio source HB-21. 01 p0106 A73-11304
- The nature of the first Cygnus X-3 radio outburst. 02 p0204 A73-11551
- Time dependence of Cygnus X-3 8 GHz flux density and spectral index during outburst decay, describing source model 02 p0204 A73-11553
- X ray intensity observations of Cygnus X-3 by Uhuru satellite before/during September 1972 radio flare 02 p0210 A73-11554
- 15.5 GHz observations at the Haystack Observatory of the Cygnus X-3 outburst. 02 p0210 A73-11555
- Spectrum and polarization of the Cygnus X-3 outburst. 02 p0210 A73-11556
- Radio observations of Cygnus X-3 and the surrounding region. 02 p0210 A73-11557
- Discovery of infrared emission from the radio source near Cygnus X-3. 02 p0210 A73-11558
- 21 cm and 18 cm observations of the Cygnus X-3 radio outburst. 02 p0204 A73-11559
- Radiant flux densities of Cygnus X-3, observing OH and formaldehyde absorption 02 p0210 A73-11560
- Observations of Cygnus X-3 at the Mullard Radio Astronomy Observatory. 02 p0210 A73-11561
- Search for a visible counterpart of the September 2, 1972 radio outburst in Cygnus. 02 p0204 A73-11562
- Cygnus X-3 intensity drop and principal period observation by X ray instrument onboard OAO Copernicus 02 p0204 A73-11563
- Radio emission source picture from observed Cygnus X-3 outburst, suggesting expanding cloud with traveling relativistic electrons and protons 02 p0211 A73-11870
- Long-lived sectors of enhanced density irregularities in the solar wind. 02 p0205 A73-11911
- Energy distribution of relativistic electrons generated within radio sources with constant magnetic field and diffusion coefficient, discussing simplified model representation for Crab nebula 02 p0207 A73-12379
- The radio emission of NGC 4258 and the possible origin of spiral structure. 02 p0221 A73-12701
- Blue objects in the vicinity of M31. I - Discovery probability of newly found blue objects 02 p0226 A73-12837
- Thermal radio source DR 21 centimeter flux density measurements for antenna aperture calibration, comparing with standard sources 03 p0366 A73-12932
- Very long baseline interferometer observations of Taurus A and other sources at 121.6 MHz. 03 p0366 A73-12933
- A radio map of the spiral galaxy Maffei 2 at 1415 MHz. 03 p0370 A73-13210
- 4830 MHz observations of the formaldehyde molecule in the direction of discrete radio sources. 03 p0371 A73-13214

- Improved positions and some identifications for 108 radio sources between declinations -33 and +27 deg. 03 p0372 A73-13348
- Australian east-west baseline interferometer observations at 2.3 GHz. 03 p0372 A73-13349
- Photometric search for H alpha optical emission in Sco X-1 nebulosity region for linking companion radio sources to X ray source 03 p0373 A73-13374
- The self absorption of gyro-synchrotron emission in a magnetic dipole field - Microwave impulsive burst and hard X-ray burst. 03 p0364 A73-14416
- An interferometric survey of the areas surrounding four intense radio sources. 03 p0380 A73-14637
- Radio sources in decimeter wave range from astronomical model and radio observations, noting spectral characteristics dependence on electron energy spectra 04 p0496 A73-14824
- The redshift-distance relation. II - The Hubble diagram and its scatter for first-ranked cluster galaxies: A formal value for q-sub 0. III Photometry and the Hubble diagram for radio sources and the possible turn-on time for QSOs. 04 p0498 A73-15351
- Observed anisotropy in the distribution of radio sources. 04 p0499 A73-15352
- Infra-red sources in the H II region W3. 04 p0499 A73-15485
- Observations of maser radio sources with an angular resolution of 0.0002 sec. 04 p0503 A73-16001
- Recombination radio lines in H I regions. 04 p0504 A73-16026
- Universe evolution model, considering quasar number density, radio source counts and big-bang cosmologies 05 p0614 A73-16309
- A Green Bank sky survey in search of radio sources at 1400 MHz. III - Positions and flux densities of the GB radio sources. 05 p0622 A73-17070
- Radio astronomy receiver with digital integrator for weak radio source detection, noting minimum detectable flux density 05 p0552 A73-17166
- High frequency observations of the second radio flare in Cygnus X-3. 05 p0623 A73-17184
- Cygnus X-3 radio source - Lower limit on size and upper limit on distance. 05 p0623 A73-17185
- 3C 120, BL Lacertae, and OJ 287 - Coordinated optical, infrared, and radio observations of intraday variability. 05 p0625 A73-17342
- Polarization of radio sources. IV - The compact source PKS 2134+004. 07 p0873 A73-19052
- Extended X-ray and radio observations of Scorpius X-1. 07 p0874 A73-19069
- Centimeter waves radio sources survey, tabulating position coordinates, 5 GHz flux densities, spectral index and optical identification 07 p0876 A73-19353
- Measurements of the integrated Stokes parameters of compact radio sources. 07 p0876 A73-19354
- Observations of radio sources with an interferometer of 24-km baseline. I - The angular structures at 408 MHz of 106 sources from the Parkes catalogue. 07 p0899 A73-19937
- Observations of radio sources with an interferometer of 24-km baseline. II - The angular structures at 151 and 408 MHz of 46 unidentified radio sources from the revised 3C catalogue. 07 p0899 A73-19938
- Observations of radio sources with an interferometer of 24-km baseline. III - The angular structures at 408 and 1423 MHz of 44 relatively intense radio sources. 07 p0872 A73-20153
- Soft X-ray pulsations from PSR 0833-45. 07 p0899 A73-19939
- Radio sources identified with stellar objects using precise radio and optical positions. 07 p0900 A73-20281
- Frequency dependent synchrotron emission polarization variation in cosmic radio source models, allowing for cold plasma and relativistic distribution nonuniformities 07 p0872 A73-20307
- Results of radio source observations at short millimeter wavelengths 07 p0901 A73-20310
- Cellular or filamentary structure of galactic magnetic fields, noting correlations between rotations of radio sources and angular separation 08 p1002 A73-20880

Interferometer observations of W 3/OH/ at 2.695 GHz and 8.085 GHz.

Radio sources with variable circular polarization, noting synchrotron radiation theory applicability

Redshifts of a BSO and galaxies in the vicinity of the radio source RN 8.

Jupiter southern equatorial band eruptive centers and decametric radio sources interrelationship, discussing reanimations responsible for Red Spot displacement sense

RCW 117 and DR 15 observed in the far infrared.

H I absorption in the galactic center region and between galactic longitudes 350 deg and 359 deg.

Cosmic maser generator model with resonance scattering feedback for galactic clouds OH molecule radio emission

Lunar occultations of radio sources as a technique for investigating their angular structure. II.

Interferometric observations of formaldehyde absorption in front of strong galactic sources.

On the calibration of flux densities and the determination of spectra at radio frequencies.

Restrictions on the intensity of cosmic masers and the possibility of detecting new OH and H₂O sources in a rapid sky survey

Spatial distributions of intensity and polarization over the source of microwave impulsive bursts.

Reply to criticism of local fluctuation interpretation of radio source counts deviation from Euclidean distribution

Optical identifications of radiosources from the B2 catalogue - Quasi stellar sources.

Remarks on the soft X-ray emission from the galactic radio spurs.

OJ 287 and BL Lacertae with rapid radio, IR and optical variability, high IR luminosity, line free optical spectra and varying polarization

Frequency dependence of circular polarization in three compact radio sources.

Major planets nonthermal radio emission observations, noting powerful decametric sources related to Jupiter rotation and Io orbital motion

X ray source identified with galaxy NGC 5128 located at center of radio source Cen A, noting 3.4 keV low energy cutoff in X ray spectrum

First results from the Texas interferometer - Positions of 605 discrete sources.

Frequency dependent synchrotron emission polarization variation in cosmic radio source models, allowing for cold plasma and relativistic electron distribution nonuniformities

Observations of radio sources at short millimeter wavelengths.

Preliminary results of observations at the 2-cm wavelength of discrete sources and Jupiter at Pulkovo

Analysis of the non-Gaussian spectra of interplanetary scintillations.

High resolution space-time structure and centre-limb distribution of solar type I sources observed at 169 MHz.

A measurement of the gravitational deflection of radio waves by the sun during 1972 October.

RY Sct detection from search for binary systems with early type star and mass exchange for radio source candidacy

A list of quasi-stellar radio sources and quasi-stellar radio-source candidates from the 3C and 4C catalogs between declination -7 deg and +40 deg.

Interferometric observations of formaldehyde absorption in front of strong galactic sources.

Gamma and cosmic ray astronomy review, covering balloon and rocket measurements, galactic and metagalactic source locations and radio source information

Low energy X-ray map of Puppis A supernova remnant.

Accurate flux densities at 8.87 GHz of 195 radio sources.

Russian book - Plasma astrophysics.

High-resolution survey of thermal sources of radio emission at the 8.2-mm wavelength

Plasma fine velocity structure and dynamics from diffraction pattern of interplanetary radio sources

On a possible mechanism responsible for the differential energy spectrum of relativistic electrons and non-linear low-frequency spectra of cosmic radio sources.

Culgoora-1 list of radio source measurements at 80 MHz.

Infrared emission from the OH/H₂O sources in W49.

Scatter X-1 noncorrelation of radio with optical or X ray intensities, noting paucity of simultaneous observations of other X ray sources

A test for revealing the fine-scale velocity structure of the solar wind

Methylacetylene and isocyanic acid data from April 1972 and February 1973 observation of interstellar media in direction of Galactic center source Sgr B2

Continuum radio emission from the vicinity of pulsars.

Atmospheric attenuation measurement for nine millimeter wavelength signal from radio source, discussing solar power, radiosonde, emission temperature and nodding solar methods

Compact radio source associated with the OH source ON-1 /OH69.5-1.0/.

Measurement of the displacement of the electrical axis of an antenna with respect to its geometrical axis by using extraterrestrial radio emission sources

Observations at 1415 MHz of radio sources in the field of the double-galaxy system NGC 2798/99.

The measurement of large antennas with cosmic radio sources.

A comparison between Compton-synchrotron and Compton black-body emission in radio sources.

Time dependent radio sources scintillation spectra with allowance for interplanetary plasma discontinuities velocity dispersion at small solar distances

Constraints on cosmic maser intensity, and the possibility of detecting new OH and H₂O radio sources by a rapid sky survey.

Fine structure of Jupiter's decametric source B.

Observations of galactic supernova remnants at 1.7 and 2.7 GHz.

The luminosity function of quasars and its evolution - A comparison of optically selected quasars and quasars found in radio catalogs.

Radio maps of sources around spiral galaxies and associated peculiar companion galaxies

Precise positions of radio sources. IV - Improved solutions and error analysis for 59 sources.

A catalog of data on optically visible H II regions.

Investigation of the inhomogeneous structure of the ionosphere using observations of discrete cosmic radio emission sources and vertical soundings

Preliminary results of observations of discrete sources and of Jupiter with 2-cm wavelength at Pulkovo.

A Green Bank sky survey in search of radio sources at 1400 MHz. IV - Anisotropy and counts of radio sources.

18-cm OH absorption of W 49 A and W 49 B.

Dynamical models of tailed radio sources in clusters of galaxies.

Power spectrum of small-scale irregularities in the solar wind.

Direct determination of universal time based on east-west interferometer observations of radio sources using 5 km radio telescope

Method and results of observations of the occultation of the source 3C144 by the solar corona with the DKR-1000 FIAN cross-array radio telescope

A new estimate of the fluctuation of relic radiation in the universe

H II region OH maser source pumping by far IR radiation-induced population inversions between Lambda doublet levels

Application of long-baseline radio interferometers to astrometric tasks

Monitoring antenna parameters from radio-astronomical directions

Scanning the sky with the aid of the RATAN-600 radio telescope

Measurement of antenna parameters and calibration of the sensitivity of the RATAN-600 radio telescope in the radar mode of operation at the 8-mm wavelength

Experimental verification of the possibility of beam scanning in a variable profile antenna by radial displacement of the primary radiating element

Accuracy of coordinate measurements with the aid of a variable-profile antenna

Russian book on radio astronomy with electronic engineering emphasis covering observation and equipment, cosmic source characteristics, radio telescope antenna systems, radar techniques, coordinate measurement, etc

Radio source signal scintillation correlation with high power HF transmitter caused F region electron density fluctuations

Linear array radio telescope for large aperture synthesis by using earth rotation to change relative orientation to radio source, discussing design and performance

High angular resolution very long baseline interferometry for emission spectra and angular size determination and structure mapping of galactic and extragalactic radio sources

Spectral-line analysis of very-long-baseline interferometric data.

Computer controlled steerable array of multiple conical log spiral antennas for solar and discrete radio source studies

Enhanced scintillation sectors outside the plane of the ecliptic.

Statistical properties of radio sources at centimeter wavelengths in a range of terminally weak flux densities

Count of radio sources at a frequency of 86 MHz. I - Method of processing observations in the radio source survey by the East-West arm of the DKR-1000

Distribution of interstellar hydroxyl in the Cyg X region

Solar U burst radio source spectrographic and polarization observations, using Waldmeier corona model for particle exciter in magnetic field

Approximate formula for completeness estimation of radio source distributions in spherical zones in terms of distance to system central source

High-resolution survey of thermal radio sources at 8.2 mm.

A search for narrow band 21-cm wavelength signals from ten nearby stars.

Radio SPECTRA

NT MICROWAVE SPECTRA

Optical, far UV and radio spectra observations and results for solar spicules, considering morphology, spectroscopic properties and dynamic models

Radio spectrum analysis of loop prominence development, temperature and H atom density on May 13, 1971, noting consistency with Jefferies-Orrall model

RADIO SPECTROSCOPY

Investigation of the radio wave absorption spectrum of atmospheric water vapor in the 1.15 to 1.5-mm range

02 p0142 A73-12487

I Zw 1727+50 energy distribution relationship to lacerid spectra, noting featureless optical spectrum, flat or inverted radio spectrum and fast irregular variations

03 p0380 A73-14636

High resolution interferometric observations of Venus at three radio wavelengths.

06 p0744 A73-17437

Venus - Measurements of brightness temperatures in the 7-15 cm wavelength range and theoretical radio and radar spectra for a two-layer subsurface model.

06 p0744 A73-17438

The radio continuum of the Large Magellanic Cloud. I - The sources at 6 cm wavelength.

06 p0754 A73-18629

The radio continuum of the Large Magellanic Cloud. II - Continuum observations at 11 cm wavelength.

06 p0754 A73-18630

The radio continuum of the Large Magellanic Cloud. III - The sources at 11 cm wavelength.

06 p0754 A73-18631

The radio continuum of the Large Magellanic Cloud. IV - Spectra of sources.

06 p0754 A73-18632

H flux density observations for 21 cm absorption spectrum in front of Cyg X-3

07 p0902 A73-20560

Meter-wavelength observations of the solar radio burst storm of August 17-22, 1968.

08 p0997 A73-20768

Interferometer observations of W 3 OH/ at 2.695 GHz and 8.085 GHz.

08 p1006 A73-20929

X-ray emission of coronal condensations during the eclipse on 20 May 1966 and its connection with optical and radio observations.

08 p0998 A73-21310

Galactic interstellar molecules, discussing physical, chemical and spectral characteristics, hydroxyl emission, occurrence regions, hydrogen clouds, isotope ratios, interstellar masers and probes

09 p1146 A73-22446

On the calibration of flux densities and the determination of spectra at radio frequencies.

10 p1272 A73-23527

Galactic background spectrum at 230-2600 kHz from IMP-6 radio astronomy, discussing ambient plasma effects on synchrotron emission in galactic models

10 p1272 A73-23529

Isotopic combination identification in interstellar clouds through radio spectral line observations, discussing millimeter wave astronomy, molecular clouds, excitation mechanisms, galactic structure, etc

10 p1280 A73-24323

VHF Doppler spectra of radar echoes associated with a visual auroral form - Observations and implications.

12 p1468 A73-26996

Type IV bursts on August 4 and 7, 1972

12 p1535 A73-27784

Solar radio bursts of 4 and 7 August 1972, deducing positron synchrotron process effects on radio spectrum from gamma ray measurements

12 p1535 A73-27785

Identification and radio spectra of bright galaxies in the second Bologna Catalogue of radio sources and their radio luminosity function.

13 p1671 A73-28034

NASA computer generated 136/400-MHz radio sky maps covering whole celestial sphere for earth-based receiver noise temperature determination in satellite communication

13 p1585 A73-29115

Pulsar detections at frequencies of 8.4 and 15.1 GHz.

14 p1802 A73-30751

High radio frequency observations of the Omega nebula.

15 p1932 A73-31268

Cosmological information from surveys of radio source spectra.

15 p1933 A73-31396

The possible nature of the fine structure of sporadic radio emission from the sun and other cosmic sources having a high density of electromagnetic radiation

15 p1926 A73-31876

Radar aurora type III spectra with phase velocities exceeding ion acoustic velocity, discussing relation to current-excited ionospheric electrostatic ion cyclotron oscillations

18 p2312 A73-36299

Time dependent radio sources scintillation spectra with allowance for interplanetary plasma discontinuities velocity dispersion at small solar distances

18 p2355 A73-36741

Faraday rotation patterns in Crab Nebula pulsar radio spectra for average signal and giant pulses, noting difference in linear polarization percentage

19 p2488 A73-38516

Dual frequency bistatic radar lunar investigations from Apollo 14 and 15 echo spectra

20 p2612 A73-39714

Radiospectrographs for the RATAN-600 radio telescope

21 p2705 A73-41461

Computer processing of RF neutral-hydrogen line observations carried out with a fixed antenna

21 p2659 A73-41468

Correlation and spectral analysis of daily solar radio flux.

21 p2762 A73-41494

Microwave radiometric systems.

22 p2859 A73-42059

Wolf-Rayet stars UV spectra from OAO-2 satellite-borne spectrometer measurements, considering radio spectra of W stars with symmetrical nebulae from ground based observations

23 p3025 A73-43194

Extragalactic radio sources identification with galaxies and quasars by high sensitivity and resolution astronomical telescopes, obtaining angular structure maps and radio spectra

23 p3028 A73-43347

Radio spectra and mapping of extragalactic radio sources including radio galaxies and quasars with high angular resolution, noting energy sources and red shift

23 p3029 A73-43625

Observations of Type I bursts at 169 MHz and coronal scattering.

24 p3140 A73-45182

Solar coronal radio spectra emitted by synchrotron process, computing radio wave suppression due to isotropic and anisotropic plasma

24 p3118 A73-45484

RADIO SPECTROSCOPY

Monograph - A multi-channel solar radio spectrograph.

01 p0044 A73-10149

Electromagnetic measurement at submillimeter wavelengths for solids and liquids absorption and refraction and atmospheric gases and plasmas emission based on Fourier transform spectrometry

03 p0310 A73-14496

Radio spectroscopy superiority for interstellar cloud chemical composition studies, detecting formaldehyde, X-ogen, HNC and other exotic molecular species

05 p0546 A73-16305

A solar radio spectrograph with high time resolution.

05 p0621 A73-17039

Interstellar molecules and radio spectroscopy in the cm- and mm-wave range

12 p1544 A73-27779

A broadband antenna and multiplexer system in the decimeter-wave range for solar radio astronomy

12 p1481 A73-27782

D region electron density profiles from radio broadcast field strength measurements by rocket-borne passive RF spectrometers, using ray theory for wave propagation

18 p2303 A73-35956

Saturation effect in RF spectroscopy for transverse optical pumping.

21 p2713 A73-40473

Total power filter spectrometer for radio astronomy, featuring local oscillators with commutation for removing output instabilities to reduce instrument errors

21 p2703 A73-41149

A 21-cm radio spectrograph

21 p2705 A73-41462

Electrooptical radio spectrograph design for high resolution in time and frequency based on photographic film recording density and coherent optical processing data rate

23 p2980 A73-43374

A new ion and electron detector for ion cyclotron resonance spectroscopy.

24 p3089 A73-44816

RADIO STARS

NT PULSARS

Periodic components of the density variations of the radio source VRO 42.22.01 /BL Lacertae/

01 p0101 A73-10933

Optical identifications and positions of blue stellar radio sources without UV excess, comparing with N-galaxies and quasars with red shift

01 p0103 A73-10997

MWC 349 - A new radio star.

03 p0374 A73-13849

Beta Persei decimetric-centimetric radio emission variations, relating observational data to discontinuous structural adjustment model based on starquakes hypothesis

05 p0627 A73-17392

2.8 cm radio emission from alpha Orionis, HBV 475 and MWC 349.

07 p0899 A73-20120

Radio sources identified with stellar objects using precise radio and optical positions.

07 p0900 A73-20281

Heat conductivity, plasma instabilities, and radio star scintillations in the solar wind.

08 p0998 A73-21165

Periodic components in the flux-density variation of the radio source VRO 42.22.01 /BL Lacertae/.

09 p1147 A73-22728

Time dependent radio stars scintillation spectra with allowance for interplanetary plasma discontinuities velocity dispersion at small solar distances

10 p1274 A73-23716

Radio star MWC 349 observations at 10.52 and 6.63 GHz, obtaining angular size from flux density and IR temperature

13 p1681 A73-28924

Radio counterparts of X-ray sources and X-ray counterparts of radio stars.

16 p2050 A73-32734

Upper limits to the X-ray emission from Beta Persei during radio flares.

19 p2475 A73-37630

Solar radio frequency radiation characteristics, considering flare stars, pulsars, X ray sources, Antares types, novae, red supergiants and stars with gas and dust envelopes

20 p2613 A73-39749

Radio binaries observation, noting black hole, large magnetic field or thermal bremsstrahlung as possible origin of strong X-ray radiation

21 p2770 A73-40940

Optical identifications of radio sources using accurate radio and optical positions.

24 p3135 A73-44579

Nature of the peculiar emission object V1016 Cygni.

24 p3143 A73-45490

RADIO TELEGRAPHY

A high-power oscillator triode with zero bias

15 p1850 A73-31259

RADIO TELEMETRY

NT PULSE FREQUENCY MODULATION TELEMETRY

A three channel telemetry system, compatible with the British medical and biological telemetry regulations.

03 p0269 A73-14277

A time-division multiplexed telemetry system using delta-modulation.

03 p0270 A73-14279

A programmable four channel system for long-time radio telemetry of biomedical parameters.

03 p0270 A73-14280

Blood flow and pressure and ECG data acquisition and transmission via radio telemetry system with electromagnetic flowmeter

03 p0270 A73-14283

Telemetry and ergometry associated to the measure of oxygen consumption during sports events.

03 p0270 A73-14285

Oxygen partial pressure measurement in respiratory air via radio telemetry system with polarographic catheter electrode pressure sensor

03 p0270 A73-14287

Radio telemetric measurements of oxygen consumption during exercise via respiratory air flow and oxygen partial pressure monitors, considering water vapor and temperature

03 p0270 A73-14288

Radiotelemetry of direct bloodpressure measurements in aorta, pulmonary artery and heart.

03 p0271 A73-14291

Voltage controlled subcarrier oscillator design and performance for FM/FM multiplex telemetry system for ECG recording during exercise

03 p0271 A73-14293

A compact low-cost electronic time division multiplexer.

04 p0417 A73-15295

The Mariner Venus Mercury flight data subsystem.

04 p0425 A73-15423

Moored radio telemetering buoy relay stations for North Pacific climatological data acquisition, noting optimum channel frequency for data transmission error rate reduction

04 p0421 A73-15429

An IRIG FM-FM telemetry system for the Petrel sounding rocket.

05 p0551 A73-16850

Miniature four-channel radiotelemetry system for the transmission of cerebral biopotentials

06 p0658 A73-18167

Satellite S-band telemetry evanescent mode waveguide diplexer design with foreshortened band-pass filters to eliminate I junction and connecting flanges

06 p0678 A73-18741

Telemetry data acquisition, transmission lines and delayed time processings onboard spacecraft and at ground receiving stations and center, discussing multiplexing and computer control

07 p0795 A73-18953

Mechanical and electrical performance of satellite-borne magnetic tape recording system for computer data storage in radio telemetry

07 p0820 A73-18960

Design and performance of VHF telemetry transmitter and remote controlled radio receiver for Eole satellite, noting production technology and block diagram 07 p0790 A73-18961

Increasing the traffic-capacity utilization factor of a telemetry channel 07 p0794 A73-20297

Preemphasis for an S-band constant bandwidth FM/FM system. 08 p0939 A73-21085

Radio telemetering trends in post-Apollo space programs, emphasizing service lifetimes and orbiting space station data bit generation rate 09 p1053 A73-23362

Missile and spacecraft radio telemetry data acquisition site polarization diversity signal combiner transient response requirements, comparing bench test with flight test data 09 p1057 A73-23414

A telecommunications link model for deep space - With applications to the HELIOS probe. 09 p1058 A73-23419

Reconstruction of analog signals and choice of sampling rates in telemetry. 09 p1058 A73-23421

Long life 100 W triode for ATC and telemetry transponders. 09 p1066 A73-23427

Radio telemetry for strain measurements in turbines. 14 p1752 A73-30064

Sounding rocket range facilities at Esrange /Sweden/ for auroral studies, discussing telemetry support for simultaneous launchings 14 p1741 A73-30085

The German Central-Ground-Station concept motivation and its multipurpose and automation aspects. 14 p1742 A73-30099

Solid-state transmitter for VHF/UHF space telemetry. 16 p1979 A73-33104

Evolution of the satellite telemetry data processing facility at the Goddard Space Flight Center. 17 p2123 A73-35300

Increasing the utilization factor of the carrying capacity of a telemetry channel. 18 p2291 A73-37134

Continuous radio telemetric recording of pulse rate in radar controllers while on duty 20 p2517 A73-39208

Russian book on radio telemetry systems analysis and theory covering analog and digital data, signal processing, algebraic and trigonometric polynomials and discrete representations 22 p2824 A73-41879

An evaluation of experimental errors in electromagnetic wave measurements aboard satellites. 22 p2844 A73-41911

RADIO TELESCOPES

Monograph - A multi-channel solar radio spectrograph. 01 p0044 A73-10149

Radio telescope for high resolution radio source mapping, discussing system design, computerized control and calibration 02 p0150 A73-11869

Algorithm for automatic optimal control of radio telescope parabolic antenna with extremal characteristic in radiation pattern, noting quasi-steady and steady operation 02 p0147 A73-12497

Pulsars spectrum measurements with 100 m radio telescope, using 2.8 cm receiver in prime focus and cryogenically cooled parametric amplifier 04 p0502 A73-15977

Observations of radio sources with an interferometer of 24-km baseline. I - The angular structures at 408 MHz of 106 sources from the Parkes catalogue. 07 p0899 A73-19937

Submillimeter radio telescope employing an n-InSb detector 07 p0825 A73-20311

The 15 m Cracow radiotelescope. I - Technical description and observational possibilities. 08 p0952 A73-20850

Neutral hydrogen in Markarian galaxies. 08 p1006 A73-20933

Radio spectrographs operating at wavelengths between 0.3 and 3 m 08 p0969 A73-21714

A first 1415 MHz survey with the Westerbork Synthesis Radio Telescope An attempt to detect radio emission from quasi stellar objects. 10 p1280 A73-24402

The 73.5-cm wavelength radio interferometer of the Biurakan Observatory 12 p1479 A73-27226

Submillimeter radio telescope with an n-InSb detector. 12 p1497 A73-27283

Cryogenically cooled parametric amplifiers for 100 meter radio telescope low noise operation, describing system design and performance 12 p1481 A73-27780

Radio astronomy telescope all sky survey procedure and data acquisition systems development for use with parametric amplifiers 12 p1544 A73-27781

The first two receivers for the radio astronomy programme on the 100 meter radiotelescope - An assessment of performance. 13 p1581 A73-28000

Determination of the collimation error of a radio telescope 15 p1849 A73-31021

The measurement of large antennas with cosmic radio sources. 17 p2127 A73-35680

The Synthesis Radio Telescope at Westerbork - Methods of polarization measurement. 20 p2566 A73-39581

Direct determination of universal time based on east-west interferometer observations of radio sources using 5 km radio telescope 21 p2739 A73-40373

Beam steering system of the north-south array of the DKR-1000 FIAN radio telescope 21 p2662 A73-40542

Linear scan receiver for electronic beam steering of the north-south array of the DKR-1000 radio telescope 21 p2662 A73-40543

New multiple-support radially-symmetric design of the parabolic-reflector suspension for a radio telescope 21 p2672 A73-40547

Transverse displacements of the radiating element of the parabolic antenna of a mobile radio telescope 21 p2672 A73-40548

Changes in the geometrical parameters of a radio-telescope parabolic mirror experiencing radially symmetric deformations 21 p2672 A73-40549

Longitudinal displacements of the secondary mirror of a parabolic antenna 21 p2672 A73-40550

Computerized simulation of radio telescope control for minimum rms error and system parameter optimization 21 p2672 A73-40551

Observation of solar submillimeter-band emission at sea level with the aid of a Fourier spectrometer 21 p2760 A73-40731

The RATAN-600 radio telescope 21 p2675 A73-41441

Methods of radio-astronomical utilization of the RATAN-600 21 p2666 A73-41442

Choice of the dimensions of the reflecting elements and calculation of the electrical characteristics of the RATAN-600 radio telescope 21 p2666 A73-41443

Calculation of the antenna noise temperature in the RATAN-600 radio telescope 21 p2667 A73-41448

Design of the reflecting elements and secondary mirror of the RATAN-600 radio telescope 21 p2675 A73-41449

Use of two-stage condenser braking of the single-motor drive for the mirror sections of the RATAN-600 radio telescope 21 p2675 A73-41450

Indicator and setting devices for circular-mirror sections of the RATAN-600 radio telescope 21 p2675 A73-41451

Reference indication and setting devices for circular mirror sections of the RATAN-600 radio telescope 21 p2675 A73-41452

Errors arising in the RATAN-600 radio telescope due to temperature effects 21 p2675 A73-41453

Geodetic tasks during the construction and alignment of the RATAN-600 radio telescope 21 p2675 A73-41454

Laying out the foundations for circular-mirror sections of the RATAN-600 radio telescope 21 p2675 A73-41455

Experimental study of an autocollimation method for alignment of a variable-profile antenna 21 p2675 A73-41457

Monitoring antenna parameters from radio-astronomical directions 21 p2667 A73-41459

Radiospectrographs for the RATAN-600 radio telescope 21 p2705 A73-41461

Protection of radiometers from pulse interference 21 p2705 A73-41463

Scanning the sky with the aid of the RATAN-600 radio telescope 21 p2776 A73-41464

Astrophysical problems to be solved with the RATAN-600 radio telescope 21 p2776 A73-41465

Possibility of obtaining radio images of celestial bodies with a resolution greater than .01 arc sec 21 p2667 A73-41466

Measurement of antenna parameters and calibration of the sensitivity of the RATAN-600 radio telescope in the radar mode of operation at the 8-mm wavelength 21 p2667 A73-41467

Experimental study of the distribution of irradiation on the variable-profile reflector of the large Pulkovo radio telescope using electronic methods 21 p2667 A73-41470

Russian book on radio astronomy with electronic engineering emphasis covering observation and equipment, cosmic source characteristics, radio telescope antenna systems, radar techniques, coordinate measurement, etc 22 p2905 A73-41875

Long baseline interferometry with high angular resolution widely separated radio telescopes and video signal magnetic recording tapes, discussing coherence and timing requirements and calibration 23 p2980 A73-43349

Linear array radio telescope for large aperture synthesis by using earth rotation to change relative orientation to radio source, discussing design and performance 23 p3028 A73-43352

National Radio Astronomy Observatory interferometer system with rotating head video tape recording and computerized sampled data processing equipment for use with radio telescope 23 p2980 A73-43358

Stanford radio telescope array with five paraboloid antennas for fast image forming interferometry, using earth rotation synthesis to produce sky continuous radiation brightness map 23 p2957 A73-43359

Radio telescope array of interferometers formed by fixed and movable antennas operating on rotational aperture synthesis for radiation observation, emphasizing electronic system stability 23 p2957 A73-43360

Southern Hemisphere earth rotational synthesis radio telescope array with paraboloids arranged as compound grating interferometer for astronomical radio sources mapping 23 p2958 A73-43361

A supersynthesis radio telescope for neutral hydrogen spectroscopy at the Dominion Radio Astrophysical Observatory. 23 p2958 A73-43362

Fixed baseline millimeter wave interferometer with aperture synthesis telescope of antenna array for interstellar and planetary water vapor and radio sources mapping 23 p2980 A73-43364

An aperture-synthesis interferometer at Ooty for operation at 327 MHz. 23 p2980 A73-43366

Computer controlled steerable radio telescope construction and performance for decimeter and centimeter wavelength observations 23 p2958 A73-43367

Millimeter wave radio telescope with high resolution for obtaining heliograph, discussing fast rotational synthesis and array redundancy design features 23 p2958 A73-43373

A digital correlation spectrometer employing multiple-level quantization. 23 p2981 A73-43378

On separating aberrant effects from random scattering effects in radio telescopes. 23 p2958 A73-43379

FORTH computer program for National Radio Astronomy Observatory telescope observed millimeter wave spectral line data reduction, summarizing language capabilities 23 p2956 A73-43380

Spectrum control procedures for the National Radio Astronomy Observatory. 23 p2953 A73-43381

Beam characteristics of the 300-ft telescope. 24 p3066 A73-44580

A method for accurately compensating for the effects of the error beam of the NRAO 300-ft radio telescope at 21-cm wavelength. 24 p3067 A73-44581

Interstellar radio communication and the frequency selection problem. 24 p3068 A73-44992

RADIO TRACKING

NT WILDLIFE RADIOLOCATION

Very long baseline interferometry observations of radio emissions from geostationary satellites. 02 p0215 A73-12270

Estimation of gravity field harmonics in the presence of spin-axis direction error using radio tracking data. 02 p0164 A73-12373

Differential interferometry for radio astronomy applications, discussing earth-based tracking of lunar rover relative to module, moon libration determination, Venus wind measurement, etc 02 p0218 A73-12416

RADIO TRANSMISSION

- Atmospheric correction for the troposphere and stratosphere in radio ranging of satellites.
04 p0439 A73-14808
- Conditions for termination of tracking in electronic servo systems
10 p1202 A73-24610
- Miniature phase/amplitude tracking RF receiver front ends.
14 p1737 A73-30623
- Application of the method of equivalent nonlinear systems to noise rejection analysis in FM tracking receivers
20 p2537 A73-39451
- Tracking the Apollo Lunar Rover with interferometry techniques.
23 p2953 A73-43356
- RADIO TRANSMISSION**
NT DOUBLE SIDEBAND TRANSMISSION
NT IONOSPHERIC F-SCATTER PROPAGATION
NT IONOSPHERIC PROPAGATION
NT MANDELSTAM REPRESENTATION
NT MICROWAVE ATTENUATION
NT MICROWAVE TRANSMISSION
NT MULTIPATH TRANSMISSION
NT SHORT WAVE RADIO TRANSMISSION
NT SINGLE SIDEBAND TRANSMISSION
NT TRANSEQUATORIAL PROPAGATION
NT TRANSHORIZON RADIO PROPAGATION
Towards faithful radio transmission of very wide bandwidth signals.
01 p0015 A73-10176
- The theory of coupling of characteristic radio waves in the ionosphere.
02 p0141 A73-12030
- Scintillation phenomenon due to radio wave propagation through ionospheric and tropospheric regions with irregularities in refractive index
02 p0162 A73-12300
- Poisson model of atmospheric noise from lightning discharges as function of thunderstorm distribution and propagation conditions, calculating statistics for narrow band receiver
02 p0142 A73-12528
- Russian book on radio wave propagation covering ground, ionospheric and tropospheric propagation, radio attenuation, scattering and ionospheric and tropospheric reflection
02 p0143 A73-12775
- An analysis of multi-station ground observations of VLF Hiss.
03 p0274 A73-12950
- Sporadic E cloud focusing of radio waves as interpretation of observed short duration bursts accompanied by rapid phase variation
03 p0280 A73-14592
- Tropospheric refraction effects on satellite range measurements.
04 p0415 A73-14750
- The production and analysis of transmission ionograms.
04 p0440 A73-14953
- Omega navigation system.
04 p0474 A73-15061
- Electromagnetic wave propagation in a medium with two-dimensionally periodic variations of the refractive index
05 p0548 A73-16268
- Book - Calculation of wave propagation by nomograms - Frequencies above 30 MHz.
05 p0548 A73-16325
- Propagation of radio waves in a triple-layer medium with spheroidal boundary surfaces
05 p0549 A73-16388
- A theoretical and experimental study of non-ducted VLF waves after propagation through the magnetosphere.
05 p0551 A73-17054
- Radio wave propagation in stratified media with nonuniform boundaries and varying electromagnetic parameters - Full wave analysis.
07 p0791 A73-19261
- Propagation modes of radio whistlers and gyroelectric echoes received in middle latitudes
08 p0937 A73-20651
- On near-field distributions along the leaky coaxial cable.
08 p0937 A73-20804
- Ionospheric electron density profile observation by partial reflection experiment, discussing radio signal amplitude and phase data recording sensitivity requirement
09 p1075 A73-22071
- Phase and amplitude variations of 40-kHz radio waves propagating over a 7.1-Mm path.
09 p1049 A73-22134
- Ionogram traces production by mode coupling process in thin sporadic E layers, using calculated reflection and transmission coefficients for radio waves incidence
09 p1076 A73-22139
- Type variation of solar sudden field anomaly (SFA) on 164 kHz as an indicator of seasonal structure changes in the D-region.
09 p1076 A73-22141

- Remote sensing of the turbulence characteristics of a planetary atmosphere by radio occultation of a space probe.
09 p1146 A73-22427
- Study of ionospheric phase distortion at Ahmedabad.
10 p1188 A73-24170
- Propagating radio wave field strength from double knife edge diffraction signals
10 p1189 A73-24335
- The transition from locked to leaky modes in tropospheric radio propagation.
11 p1327 A73-25122
- Hypervelocity tactical missile radome materials with noncharring ablator and fiberglass substructure for thermal protection against aerodynamic heating with negligible effects on radio transmission
11 p1336 A73-25307
- Reflection and transmission of radio waves at a dielectric slab with variable permittivity.
11 p1329 A73-25675
- VLF radio signals propagational effects relationship to ionospheric polar substorm different phases
11 p1330 A73-25765
- Midlatitude bremsstrahlung X rays, VLF propagation disturbances and electron precipitation during magnetospheric substorm
12 p1468 A73-26983
- Information transmission reliability enhancement via digital code group symbol transmission by wide-band linear FM radio signals
12 p1471 A73-27593
- Methods for the comparison and the propagation of time scales
12 p1498 A73-27751
- Shimazaki formula corrected for F 2 layer altitude estimation for 2-30 MHz field intensity and transmission losses calculations
12 p1493 A73-27762
- Result of medium- and long-wave observations at distances of about 7500 km
12 p1474 A73-27768
- Employment of mode theory and ray theory for the interpretation of very-long-wave measurements at medium distances
12 p1474 A73-27769
- Ground-wave perturbation over a transition zone between two different sections.
13 p1583 A73-28798
- A mode theory of radio wave propagation in an inhomogeneous atmosphere with jointed-segment N-profile.
13 p1586 A73-29227
- Post-occultation reception of lunar ship America radio transmission.
14 p1725 A73-29733
- Aircraft-satellite multipath communication characteristics, considering surface scatter, ionospheric scintillation and refraction and tropospheric refraction and scatter
14 p1725 A73-29891
- Distortions of UHF pulse signals propagating along the earth at distances below the radio horizon
14 p1729 A73-30559
- Modeling of pulsed propagation problems of radio waves excited by an infinite electric current filament in homogeneous dispersing media
15 p1853 A73-31496
- Propagation of radio waves at frequencies above 10 GHz; Proceedings of the Conference, London, England, April 10-13, 1973.
16 p1980 A73-33701
- Analysis of radio-wave propagation in the Venusian atmosphere
16 p1984 A73-33822
- Earth-flattening approximations in the theory of radio wave propagation near the surface of the earth.
16 p1984 A73-33916
- Radio-TV satellite ground support systems, discussing frequency ranges, satellite orbit, transponder signal amplification and ground reception systems
17 p2126 A73-35488
- Ionospheric electron content and its horizontal gradients at high and middle latitudes from radiowave propagation from satellites.
18 p2304 A73-35972
- Occurrence and features of ducted modes of internal gravity waves over Western Europe and their influence on microwave propagation.
19 p2405 A73-38225
- Calculation of structurally compressed satellite radio lines
20 p2531 A73-39469
- A radio signal shaping device with large signal attenuation in the intervals between signals
21 p2661 A73-40174
- Determination of the root-mean-square and mean intensity of the atmospheric radio noise field
21 p2648 A73-40208
- Sudden ionospheric disturbance effects on LF radio pulse train amplitude during reception from Loran-C transmitters, comparing with VLF sudden phase anomaly
22 p2825 A73-42188

- Use of cancellation techniques in the measurement of atmospheric crosspolarisation.
23 p2955 A73-44111
- Short-time fluctuations of the VLF field along polar paths
24 p3067 A73-44809
- Fluctuation characteristics of the electric component of the troposphere.
24 p3084 A73-44940
- RADIO TRANSMITTERS**
NT IONOSONDES
NT RADIO BEACONS
NT RADIOSONDES
NT RADIOTELEPHONES
NT RAWINSONDES
NT TRANSMITTER RECEIVERS
Noise characteristics, channel capacities, power requirements and transmission efficiencies of various semiconductor transmitter designs for FM directional radio systems
03 p0284 A73-14125
- Radio set design requirements for communication link between meteorological sensor platforms and spacecraft in Geostationary Operational Environmental Satellite System
04 p0421 A73-15432
- High power SHF transmitter experiment using TWT depressed collector beam microwave amplifier for flight testing on communications technology satellite (CTS)
04 p0428 A73-15447
- Design of modern semiconductor senders for frequency-modulated directional radio systems. I
06 p0663 A73-17585
- Design and performance of UHF transmitter and receiver system for two way links between Eole satellite and constant ceiling balloons
07 p0790 A73-18962
- Intelsat 4 communications system, discussing radio transponders, earth stations, and multiple access, modulation and multiplexing methods
09 p1051 A73-22700
- 640 Mbit/sec waveguide transmitter at 38 GHz.
09 p1065 A73-23095
- Miniature single channel narrow-band differential pulse width modulation-FM crystal controlled transmitter for biomedical telemetry system
09 p1047 A73-23381
- High power radio transmitter for structural investigation and electron concentration profiles of ionospheric D and E regions
13 p1583 A73-28725
- Ionospheric echoes due to sideland and harmonic radiation from Isis topside sounder transmitters, discussing effects of satellite spread and ion sheath distortions
14 p1752 A73-29974
- Technologies applicable to the development of an onboard L-band transmitter
15 p1852 A73-32481
- Solid-state transmitter for VHF/UHF space telemetry.
16 p1979 A73-33104
- Book - Recommended basic characteristics for airborne radio homing and alerting equipment for use with emergency locator transmitters (ELT).
17 p2207 A73-34475
- Microwave radiation hazards around large microwave antenna.
19 p2397 A73-37274
- Russian book on semiconductor radio transmitter design covering power amplifiers, frequency multipliers, oscillators and Gunn effect devices for sub-microwave frequencies
21 p2666 A73-41424
- RADIO WAVE REFRACTION**
Critical frequency gradients-geometric parameters equivalence coefficients for ionospheric layer with parabolic vertical ionization distribution for radio wave path determination
06 p0690 A73-17555
- Second-order corrections for ionospheric radio-wave propagation
08 p0939 A73-21287
- Critical frequency gradients-geometric parameters equivalence coefficients for ionospheric layer with parabolic vertical ionization distribution for radio wave path determination
16 p2002 A73-32779
- Average intensity of the normal wave during super-refraction
16 p1978 A73-32897
- Spectroscopic measurement of material samples refractive index at submillimeter wavelengths
17 p2120 A73-34157
- Second-order corrections for radio-wave propagation through the ionosphere.
19 p2404 A73-37916
- Statistics of a pulse signal reflected from an inhomogeneous ionosphere
20 p2530 A73-39157
- Some results and accuracy of satellite measurements of the electron content in the ionosphere
20 p2554 A73-39166

RADIO WAVES

NT DECA-METRIC WAVES
NT DECIMETER WAVES
NT EXTRATERRESTRIAL RADIO WAVES
NT GALACTIC RADIO WAVES
NT IONOSPHERIC NOISE
NT LONG WAVE RADIATION
NT MICROWAVES
NT MILLIMETER WAVES
NT RADIO BURSTS
NT RADIO EMISSION
NT SHORT WAVE RADIATION
NT SKY WAVES
NT SOLAR RADIO BURSTS
NT SOLAR RADIO EMISSION
NT SUBMILLIMETER WAVES
NT TYPE 2 BURSTS
NT TYPE 3 BURSTS
NT TYPE 4 BURSTS
NT TYPE 5 BURSTS
NT WHISTLERS

Book - Cosmic rays: Selected readings in physics.
01 p0091 A73-10122
Universal dimensionless formulas for physical property and trajectory computation in cosmic spherical media, applying to Kepler orbits, particle motions and radio wave paths

01 p0103 A73-11019
Time-dependent characteristics of radio waves passing through the irregular ionosphere.

03 p0275 A73-13645
The Doppler frequency shift in ionospheric propagation of radio waves

05 p0548 A73-16260
Ionospheric electron density changes caused by strong radio waves induced plasma heating

07 p0816 A73-19457
Nighttime ionospheric wave propagation curves in the broadcast band

08 p0939 A73-21286
Incident radio wave resonance effect on stationary electric and magnetic fields and standing magnetoplasma wave excitation in Bi plates

09 p1127 A73-22604
Parametric excitation of Langmuir oscillations in the ionosphere in a field of powerful radio waves

11 p1331 A73-26153
The measurement of winds in the D-region of the ionosphere by the use of partially reflected radio waves.

11 p1358 A73-26707
HF radio wave enhanced electron cyclotron frequency lines and ion plasma fluctuations due to artificial ionospheric excitation

12 p1490 A73-27008
A measurement of the gravitational deflection of radio waves by the sun during 1972 October.

13 p1673 A73-28281
Analytic ray trajectory model of radio wave lateral incidence on traveling large scale ionospheric inhomogeneities as function of location and departure angle

13 p1583 A73-28724
Modeling of pulsed propagation problems of radio waves excited by an infinite electric current filament in homogeneous dispersing media

15 p1853 A73-31496
Self-induced effects of radio waves in the vicinity of plasma resonance

15 p1918 A73-31706
Book - Pathological effects of radio waves.

19 p2395 A73-37774
Propagation curves of an ionospheric wave at night for the broadcasting range.

19 p2404 A73-37915
Winds and wave motions 70-100 km/ as measured by a partial reflection radiowave system.

24 p3088 A73-45212

RADIOACTIVE AGE DETERMINATION

Radioactive crystallization ages of Apollo 14 basaltic rocks from Fra Mauro formation, comparing with Apollo 11 samples

02 p0213 A73-12231
The Rb-Sr age of a crystalline rock from Apollo 16.

02 p0220 A73-12483
Fossil particle tracks in lunar materials, discussing track densities implications, production rates via cosmic ray spallation and interpretation for rock ages and erosion rates

03 p0361 A73-13102
Moon and solar system origin in view of chemical evidence and Apollo lunar rock RB-87/SR-87 ages and remelting conditions

03 p0370 A73-13111
Cosmogenic rare gas production rates in chondritic meteorites.

03 p0375 A73-14107
Rb-87/Sr-87 'ages' of the soil and rock fragments brought back from the lunar mountains by the automatic probe Luna 20 /Apollonius crater region/

05 p0546 A73-16830
U-Th-Pb systematics in lunar highland samples from the Luna 20 and Apollo 16 missions.

05 p0618 A73-16832

Moon geochronology from U-Pb systematics applied to lunar basalt data, discussing two and three stage evolutionary models based on Pb isotope ratios

05 p0618 A73-16834
Isotopic abundance ratios and concentrations of selected elements in Apollo 14 samples.

07 p0887 A73-19773
Apollo 14 mineral ages and the thermal history of the Fra Mauro formation.

07 p0887 A73-19776
Apollo 14 and 15 samples - Rb-Sr ages, trace elements, and lunar evolution.

07 p0887 A73-19777
The ages of lunar material from Fra Mauro, Hadley Rille, and Spur Crater.

07 p0888 A73-19780
K-Ar dating of lunar fines - Apollo 12, Apollo 14, and Luna 16.

07 p0888 A73-19781
Lunar rocks age determination by Ar isotopes technique, noting plagioclase gas retention and cosmic ray exposure characteristics

07 p0888 A73-19782
Ar-40/Ar-39 ages of Apollo 14 and 15 samples.

07 p0888 A73-19783
Uranium and extinct Pu-244 effects in Apollo 14 materials.

07 p0888 A73-19784
Study on the cosmic ray produced long-lived Mn-53 in Apollo 14 samples.

07 p0870 A73-19795
Apollo 14 and 15 lunar rocks and soils rare gas content via fast neutron irradiation, noting radioactive age determination

07 p0889 A73-19802
Track studies of Apollo 14 rocks, and Apollo 14, Apollo 15, and Luna 16 soils.

07 p0896 A73-19873
Rb-Sr ages and initial strontium in basalts from Apollo 15.

08 p0936 A73-20839
Nucleocosmochronology and stellar nucleosynthesis models for Galaxy origin and solar system formation

08 p1010 A73-21231
Saint Severin meteorite irradiation age from thermoluminescence measurements, considering saturation of natural thermoluminescence from calibration curves

09 p1148 A73-22875
Argon 40-argon 39 chronology of four calcium-rich achondrites.

10 p1278 A73-24110
Lunar Rb-Sr age correction according to stable isotope tracer /spike/ recalibration, using stoichiometric salts

10 p1278 A73-24112
New data on the cosmic history of the Sikhote-Alin meteorite

10 p1281 A73-24462
Lunar 20 lunar soil samples Pb-207/Pb-206 age determination by ion microprobe mass analysis, determining U, Th and radiogenic Pb concentrations

13 p1674 A73-28304
The age and petrography of two Luna 20 fragments and inferences for widespread lunar metamorphism.

13 p1675 A73-28319
Cenozoic coral and aragonitic fossil age determination by He, U, Th and Ru isotope retentivity consistency checks

13 p1609 A73-29178
Orgueil chondrite magnetite age via I 129/Xe 129 method compared to Karoonda magnetite age

13 p1684 A73-29250
Apollo 17 landing site crystalline rock age determinations for coarse grained basalt and anorthositic gabbro samples via Ar isotope ratios

14 p1788 A73-29720
Time differences in the formation of meteorites as determined from the ratio of lead-207 to lead-206.

17 p2225 A73-34096
Lunar volcanism - Age of the glass in the Apollo 17 orange soil.

17 p2230 A73-34522
Pb isotopic composition measurement in chondrites and achondrite for model ages, noting 50 My variations

17 p2233 A73-35265
Radioactivities and He, Ne and Ar stable isotopes measured in meteorites for cosmic ray exposure ages

17 p2233 A73-35267
North American microtektites from the Caribbean Sea and their fission track age.

18 p2354 A73-36511
A response to a comment on U-Pb systematics in lunar basalts.

18 p2354 A73-36512
New data on the cosmic history of the Sikhote-Alin meteorite.

19 p2486 A73-38128
Thermal track fading factor in Georgia tektite stratigraphy and fission track ages, noting agreement with K/Ar ages

20 p2612 A73-39717

Lead isotopic composition ages of carbonaceous chondritic meteorites with correction for terrestrial lead contamination

21 p2765 A73-40239
Trapped solar wind noble gases and exposure age of Luna 16 lunar fines.

21 p2770 A73-41001
Rb-87 - Sr-87 age of fragments and soils from the lunar Sea of Fertility.

21 p2770 A73-41005
Variability of the He-3 and Ne-21 production rates in ordinary chondrites.

21 p2771 A73-41008
Al-26 and Na-22 measurements on Luna 16 samples by non-destructive gamma-gamma coincidence spectrometry.

21 p2774 A73-41405
Galactic nucleosynthesis time interval from birth to solar system formation /Galactic age/ from radioactive decay nuclear yield ratios

22 p2916 A73-43049
Crater Copernicus age determination using mass spectrometric Ar isotope ratio dating of KREEP glasses from lunar soil

23 p3031 A73-43763
On Pu-244 in lunar rocks from Fra Mauro and implications regarding their origin.

23 p2951 A73-43771
Chondrites - Initial strontium-87/strontium-86 ratios and the early history of the solar system.

24 p3137 A73-44688

RADIOACTIVE CONTAMINANTS

Nuclear meteorology as branch of atmospheric physics, examining natural and artificial fission products, nuclear explosion effects, atmospheric purification and radioactive tracers for meteorological process investigation

21 p2730 A73-40115

RADIOACTIVE DATING

U RADIOACTIVE AGE DETERMINATION

RADIOACTIVE DECAY

NT ALPHA DECAY

NT NEUTRON EMISSION

Neutrino archaeology - The simulation of double beta-decay by solar neutrinos.

03 p0344 A73-13293
Superheavy element fissionability on r-process path, considering experimental search methods and doubly magic nucleus concept

10 p1272 A73-23536
Manganese-54 and the lifetime of relativistic cosmic rays.

10 p1264 A73-23541
Radioactive spallation induced scintillator errors in satellite measurements of diffuse cosmic X ray spectrum, considering astrophysical implications

12 p1537 A73-27882
Re-187, recycling r-process elements through stars, and the age of the Galaxy.

15 p1939 A73-32014
Muon decay/transmission ratios at 60 and 850 mwe measured by scintillation counter

23 p3023 A73-43563

RADIOACTIVE ELEMENTS

U RADIOACTIVE ISOTOPES

RADIOACTIVE FALLOUT PARTICLES

U FALLOUT

RADIOACTIVE ISOTOPES

NT CARBON 14
NT COBALT 60
NT CURIUM ISOTOPES
NT CURIUM 244
NT PLUTONIUM ISOTOPES
NT PLUTONIUM 238
NT POLONIUM 210
NT SODIUM 22
NT SODIUM 24
NT STRONTIUM 90
NT TRITIUM
NT URANIUM 238

Radioactive isotope powered thermoelectric generators operation and performance characteristics and design trends, discussing radiation hazards

01 p0005 A73-10475
Luna 16 rock composition, gamma radiation and natural radioactive element content determination by neutron activation and radiometric analysis

02 p0213 A73-12230
Meteorite aphebia calculation from activity levels of accumulated cosmogenic radioisotope due to cosmic ray irradiation

02 p0221 A73-12690
Russian monograph on radioactive isotopes effects on organisms covering metabolism, elimination acceleration methods, pathogenesis and treatment of damage, toxicity, biological action, etc

02 p0138 A73-12865
Possible thermal history of the moon.

03 p0369 A73-13106
Design point characteristics of a 500 - 2500 watt isotope-Brayton power system.

[ATAA PAPER 72-1059] 03 p0252 A73-13388
Development of a radioisotope-fueled thruster for satellite propulsion.

[ATAA PAPER 72-1066] 03 p0354 A73-13395

RADIOACTIVE MATERIALS

Utilization of radioactive isotopes as tracers in the investigation of general atmospheric circulation
05 p0593 A73-16234

Investigation of the gamma-emission of lunar soil delivered by the automatic station Luna 16
05 p0620 A73-17020

U-Th-Pb and Rb-Sr measurements on some Apollo 14 lunar samples.
07 p0888 A73-19779

Abundances of primordial and cosmogenic radionuclides in Apollo 14 rocks and fines.
07 p0888 A73-19787

Primordial radionuclides and cosmogenic radionuclides in lunar samples from Apollo 15.
07 p0888 A73-19788

Gamma-ray measurements of Apollo 12, 14, and 15 lunar samples.
07 p0888 A73-19789

Lunar surface processes and cosmic ray characterization from Apollo 12-15 lunar sample analyses.
07 p0870 A73-19790

Cosmic-ray produced radioisotopes in Apollo 12 and Apollo 14 samples.
07 p0870 A73-19791

Radionuclides in lunar rocks from solar and galactic cosmic ray bombardment, examining long and short-lived isotopes activity
07 p0889 A73-19793

Solar flare intensity estimation based on measurements for Ar 37 radioactivities and depth dependence of tritium in Apollo 11 and 12 lunar rock samples
07 p0889 A73-19794

A target design for irradiation of NaI at high beam current.
07 p0853 A73-20469

Nuclear particle fluxes and radioactive isotopes production rate distribution from cosmic rays data along orbits, calculating iron meteorite dimensions prior to atmosphere entry
08 p1012 A73-21582

Half life and activity of cosmogenic radionuclides in Haverro /Finland/ achondrite determined by non-destructive gamma ray spectrometry
09 p1139 A73-21861

Isotope Brayton electric power system for the 500 to 2500 watt range.
09 p1118 A73-22793

Development of an actinium fueled thermionic converter.
09 p1038 A73-23282

Natural radioactive element contents in Venusian rock - Results of a Venus-8 station experiment
11 p1418 A73-25635

Radioisotope heater design and optimization for manned spacecraft thermal control and life support systems and various mission times
11 p1310 A73-25996

An integrated radiation physics computer code system.
11 p1334 A73-25997

An isotope heat source integrated with a 7 kW/e/ to 25 kW/e/ Brayton cycle space power supply.
11 p1312 A73-26019

Application of lasers, radioisotopes, and the correlation method for measuring flow velocity
12 p1495 A73-26847

Russian book - Accelerated wear-resistance tests for machine components and machinery.
15 p1881 A73-31582

An electronically gated gamma and X-ray calibration scheme.
15 p1879 A73-32222

Video instrumentation for radionuclide angiocardiology.
19 p2399 A73-37796

Content of natural radioactive elements in Venusian rock Results of experiment with Venera-8 station.
19 p2486 A73-38142

Atmospheric entry and impact behavior of modular disk shaped radioactive isotope heat source for space nuclear power
19 p2454 A73-38387

Isotope organic Rankine cycle electric power systems for the 150 to 1500 watt range.
19 p2456 A73-38414

Multihundred watt radioactive isotope heat source wind tunnel tests to obtain aerodynamic coefficients, heating rate, stability and ablation for reentry protection design
19 p2456 A73-38425

Multihundred watt radioactive isotope heat source assembly for multiple space missions, discussing aerodynamic heating, shield ablation and thermal stress performance during reentry
19 p2456 A73-38426

Multihundred watt radioisotope thermoelectric generator heat source materials compatibility with thermochemical environment, considering maximum operational and reentry temperatures
19 p2457 A73-38427

Design of a nuclear isotope heat source assembly for a spaceborne mini-Brayton power module.
19 p2457 A73-38431

Nuclear safety considerations for the design of a shuttle launched 500 to 2000 watt isotope Brayton power system.
19 p2457 A73-38432

Nuclide production rates in stone meteorites and lunar samples by galactic cosmic radiation.
20 p2612 A73-39716

Fuel capsule vent system development for the Viking radioisotope thermoelectric generator.
21 p2737 A73-40766

Gamma-spectrometric analysis of lunar samples from Luna 16.
21 p2774 A73-41404

He and Ne cross sections in natural Mg, Al, and Si targets and radionuclide cross sections in natural Si, Ca, Ti, and Fe targets bombarded with 14- to 45-Mev protons.
24 p3125 A73-45103

RADIOACTIVE MATERIALS

Influence of rare-earth metal dust containing radioactive components on the development of reticulosa of the lungs
10 p1183 A73-23680

Spatial variations of cosmic rays on the basis of data for the radioactivity of meteorites with known orbits
10 p1266 A73-23910

RADIOACTIVE NUCLIDES

U RADIOACTIVE ISOTOPES

RADIOACTIVE WASTES

The transportation of highly active nuclear waste: products to the sun
20 p2590 A73-39148

RADIOACTIVITY

Thallium isotope analysis of terrestrial chondrites and achondrite and lunar soil, noting lunar chronology information from lead isotope extinct radioactivity
03 p0375 A73-14109

Argon, radon, and tritium radioactivities in the sample return container and the lunar surface.
07 p0870 A73-19792

A first look at the lunar orbital gamma-ray data.
07 p0871 A73-19824

Lunar surface radioactivity - Preliminary results of the Apollo 15 and Apollo 16 gamma-ray spectrometer experiments.
08 p1009 A73-21224

Argon-37, argon-39, and tritium radioactivities in the Haverro meteorite.
09 p1140 A73-21865

Tillaberi /Niger/ stony meteorite elements abundance and radioactivity determination by gamma ray spectrometry
09 p1149 A73-23032

Tracks from extinct radioactivity, ancient cosmic rays, and calibration ions.
10 p1269 A73-24271

Detection of a nonuniform distribution of polonium-210 on the moon with the Apollo 16 alpha particle spectrometer.
15 p1941 A73-32266

RADIOBIOLOGY

Russian book on radiation genetics of microorganisms covering lethal and mutagenic action of radiation on fungi, microscopic algae, bacteria and viruses
04 p0410 A73-15701

Possible role of antitissular autoantibodies in the protective mechanism of local shielding during total radiation exposure
06 p0657 A73-17685

Sensitivity to oxygen at high pressure of radioreistant and radiosensitive strains of bacteria.
07 p0780 A73-19483

Mechanism of the action of radiation protecting agents - A biochemical shock hypothesis
12 p1465 A73-27499

Russian book on ionizing radiation protection covering shielding design, radiation source characteristics, maximum permissible levels, neutron, alpha, beta and gamma radiation, albedo, etc
18 p2336 A73-35872

Russian book - Primary and initial processes of the biological action of radiation.
18 p2269 A73-35896

Solid state AgCl detectors for nuclear tracks with on- and off-response at choice - Applications to life sciences.
22 p2814 A73-42179

The radiobiological effects of heavy ions on mammalian cells and bacteria.
22 p2805 A73-42182

Measurement of coronary blood flow by radiocardiography - Study of 116 cases.
22 p2809 A73-42838

RADIOCHEMISTRY

Gamma irradiation induced abiotic radiochemical synthesis of deoxynucleosides from dry mixtures of purine bases with deoxyribose and ribose
22 p2803 A73-42166

RADIOGENIC MATERIALS

U-Th-Pb systematics in lunar highland samples from the Luna 20 and Apollo 16 missions.
05 p0618 A73-16832

RADIOGONIOMETERS

Radiogoniometric vectors superposition on ATC Doppler radar image, noting direction finding display availability and echoes identification
15 p1847 A73-32438

VLF goniometer observations at Halley Bay, Antarctica. I - The equipment and the measurement of signal bearing. II - Magnetospheric structure deduced from whistler observations.
17 p2159 A73-34777

RADIOGRAPHY

NT ANGIOGRAPHY

NT AUTORADIOGRAPHY

The influence of X-ray parameters on crack detection capability.
02 p0173 A73-11985

Thoracic X ray photography technique for tubercular lesion detection in flight personnel, comparing to standard radiography and radioscopy
02 p0137 A73-12155

Dynamic radiography - A new imaging technique using penetrating radiation.
05 p0573 A73-16278

Imaging techniques for low-flux neutron radiography.
05 p0573 A73-16279

Improvements in solid state radiographic converter screens.
05 p0574 A73-16280

Pulsed X-ray photography of a shock wave in cesium vapor using two X-ray tubes
06 p0731 A73-18554

Microchannel electron multipliers application to X ray cinematography of laser generated plasma
06 p0697 A73-18861

The use of a compartmental hypothesis for the estimation of cardiac output from dye-dilution curves and the analysis of radiocardiograms.
07 p0784 A73-19124

The process of reinforcement of lead shields in electroradiography
07 p0822 A73-19330

Moving radiography for photographic recording and display of transient or cyclic motion, emphasizing application to aircraft gas turbines under dynamic conditions
07 p0832 A73-20451

Some new developments in nondestructive testing.
08 p0963 A73-20869

Radiography and ultrasonic tests for weldment and flaw inspection, discussing choice based on economic, technical and application considerations
08 p0952 A73-21076

Non-destructive testing in industry - Non-ferrous metals.
08 p0973 A73-21077

Left ventricular performance after myocardial infarction assessed by radioisotope angiocardiology.
08 p0932 A73-21801

Neutron radiography as a diagnostic tool in the study of corrosion in lithium-filled heat pipes.
09 p1079 A73-21991

Regional myocardial dynamics from single-plane coronary cineangiograms.
10 p1185 A73-24771

Application of an electronic image analyzer to dimensional measurements from neutron radiographs.
11 p1371 A73-26743

Tomosynthesis - A holographic method for variable depth display.
12 p1495 A73-26829

A method for ingredient composition control in binary and quasi-binary systems
15 p1881 A73-31222

Russian book on ionizing radiation isotropic methods for nondestructive flaw detection in non-transparent objects covering imaging techniques and quality control equipment
15 p1875 A73-31580

Determination of fatigue strength of welded joints with artificial flaws by radiographic examination
15 p1882 A73-32051

Pulse X-ray photography of a shock wave in cesium vapor using two X-ray tubes.
16 p2042 A73-33579

Flaw detection and characterization using acoustic emission.
16 p2022 A73-34013

Roentgenographic study of relative heart motion during vibration in water-immersed cats.
16 p1973 A73-34039

Biplane roentgen videometric system for dynamic, 60/sec, studies of the shape and size of circulatory structures, particularly the left ventricle.
19 p2399 A73-37798

Ti rich corner of Ti-Al alloys phase diagrams investigated by differential thermal analysis and radiography for thermal resistance and intermetallic compounds existence
19 p2441 A73-37838

Slit electronic camera with scanned memory used in high speed cineradiography
21 p2694 A73-39942

The interaction of a laser with matter as an intense source of UV and soft X-ray radiation - Application to X-ray cinematography

21 p2709 A73-39944

Recording of diffraction patterns by X-ray pulses of materials subjected to a shock wave compression

21 p2695 A73-39967

New tubes and techniques for flash X-ray diffraction and high contrast radiography.

21 p2696 A73-39974

Portable pulse X-ray micro and nanosecond range apparatus for studying fast-going processes in opaque media.

21 p2696 A73-39977

A wave propagation method for conversion of grey pictures into line figures.

21 p2654 A73-40688

Electrofluoroplanigraphy for human body layer single-plane sections synchronization, using X ray tomography and TV imaging followed by roentgenogram electronic summation

21 p2645 A73-41216

Electroradiography technique involving photoproduction of free electrons via Townsend avalanche amplification in diode/triode/ gap, noting increased quantum efficiency

23 p2950 A73-44214

RADIOISOTOPE BATTERIES

NT SNAP 19

NT SNAP 27

NT SNAP 29

Thermoelectric radioisotope generators and nuclear thermoelectronic reactors, noting anaerobic self contained reliable operation and suitability for underwater energy sources

09 p1032 A73-22203

Silicon-germanium technology program of the Jet Propulsion Laboratory.

09 p1117 A73-22759

Vaporization and compatibility of SiGe radioisotope thermoelectric generators.

09 p1117 A73-22761

Radioisotope thermoelectric generator SiGe thermopile power degradation and operating temperature changes, discussing performance prediction model

09 p1117 A73-22763

Co-60 fueled tubular radioisotope thermoelectric generator, correlating long term test data with performance prediction model results

09 p1117 A73-22764

Radioisotope thermoelectric converter for Navy TRANSIT navigational satellite 5 year power supply, describing design and performance test data

09 p1034 A73-22767

Computer program for the transient analysis of radioisotope thermoelectric generators.

09 p1060 A73-22768

Radioisotope thermoelectric generators for Nimbus 3 weather satellite, Pioneer 10 Jupiter probe and SNAP 27 powered ALSEP station missions, summarizing operational experience

09 p1154 A73-22795

Spacecraft nuclear power source optimization, considering radioisotope and reactor heat sources, cryogenic cooler cycle types and spacecraft design

09 p1118 A73-22799

SNAP 19/Pioneer radioisotope thermoelectric generator program status report, stressing Jupiter first mission converters performance prediction

09 p1118 A73-22800

Power from radioisotopes; International Symposium, 2nd, Madrid, Spain, May 29-June 1, 1972, Proceedings

09 p1037 A73-23276

Comparison of strontium-90 and plutonium-238 milliwatt thermoelectric generators.

09 p1037 A73-23277

Radioisotopic energy conversion by radiovoltaic effect, describing titanium-tritium sources and semiconductor converter

09 p1037 A73-23278

A model of a thermophotovoltaic radionuclide battery.

09 p1037 A73-23279

Development of thermionic radioisotope batteries.

09 p1038 A73-23281

The Gicodyne 400 power generator using a radioisotopic source with thermodynamic conversion

09 p1038 A73-23283

Five year lifetime space radioisotope thermoelectric generator with lead telluride panels and plutonium 238 dioxide heat source, analyzing reliability, design and performance

09 p1038 A73-23284

Testing of the improved SNAP 19-primary power for advanced space missions.

09 p1038 A73-23285

A review of radioisotope power source development at Atomic Energy of Canada Limited.

09 p1038 A73-23286

Leak testing of tritium fuelled experimental batteries.

09 p1038 A73-23288

SNAP-27/ALSEP power subsystem used in the Apollo program.

11 p1312 A73-26021

Unmanned interplanetary spacecraft power systems with nickel-cadmium batteries, solar panels or radioisotope thermoelectric generators

11 p1312 A73-26022

Multi-Hundred Watt converter design considerations.

11 p1396 A73-26029

The calculated long-term performance characteristics of a typical silicon-germanium RTG.

11 p1312 A73-26030

Analytical model for radioisotope thermoelectric generator performance prediction in air and vacuum, taking into account modified heat transfer rates

11 p1312 A73-26031

Detailed mathematical models of a radioisotope thermoelectric generator.

11 p1396 A73-26033

TRANSIT radioisotope thermoelectric generator technology, discussing structural design, thermal efficiency, performance prediction, panel configurations and life test data

11 p1312 A73-26034

Five-year lifetime thirty-watt radioisotope thermoelectric generator for NAVY Transit Navigational Satellite, discussing system design, major components, reliability and performance tests

11 p1397 A73-26041

Solar independent power source with radioisotope thermoelectric generator for Grand Tour missions, discussing radiation and thermal interfaces

11 p1313 A73-26042

An evolutionary approach for a compact-split-core reactor.

17 p2211 A73-35470

Improved technology for multiwatt radioisotope heater units.

18 p2336 A73-36681

The behavior of xenon when used as a fill-gas in a silicon germanium radioisotope thermoelectric generator.

19 p2455 A73-38388

Cost-effective radioisotope thermoelectric generator designs involving Cm-244 and Pu-238 heat sources.

19 p2455 A73-38389

High temperature material interactions of thermoelectric systems using silicon germanium.

19 p2455 A73-38390

Analytical model for long term performance prediction of multihundred watt radioisotope thermoelectric generator with Si-Ge alloy as thermoelectric material, noting degradation mechanisms

19 p2390 A73-38391

Extending the useful life of radioisotope thermoelectric generators through active power control.

19 p2455 A73-38392

Transit satellite-borne radioisotope thermoelectric generators launch aboard Scout missile into circular polar orbit, obtaining electrical and thermal data

19 p2494 A73-38394

Thermoelectric nuclear batteries fabrication in milliwatt power range combining bismuth telluride thermopiles with plutonia fuel capsules

19 p2455 A73-38410

The multi-hundred watt RTG - Technology background and flight systems program.

19 p2456 A73-38418

Multihundred watt radioisotope thermoelectric generator design for on-pad and orbital conditions, discussing configurations, Pu-238 heat source and operating characteristics

19 p2456 A73-38419

Multihundred watt radioisotope thermoelectric generator full scale thermal performance, vibration, shock, acoustic, acceleration and magnetic field tests

19 p2456 A73-38421

Multilayer foil insulated Si-Ge thermopile design for multihundred watt radioisotope thermoelectric generator to withstand launch environments, evaluating performance under shock and vibration loads

19 p2392 A73-38424

Curium 244 heat source design for multihundred watt radioisotope thermoelectric generator with Si-Ge thermocouples for energy conversion, noting low cost

19 p2457 A73-38429

Theory and performance of a tritium battery for the microwatt range.

21 p2737 A73-39922

High-efficiency converter and battery charger for an RTG power source.

22 p2801 A73-42906

RADIOLOGY

Gas management system for control, bleeding, evacuating and radiological and pressure monitoring of He atmosphere in multihundred watt heat source

19 p2457 A73-38428

Radiological assessment of the vertebral column from the point of view of aviation medicine

22 p2817 A73-43131

The frequency of barotraumas as determined by nasal findings and X-rays of the paranasal sinuses

22 p2817 A73-43132

RADIOLYSIS

An investigation of the possible differential radiolysis of amino acid optical isomers by C-14 betas.

06 p0660 A73-17935

RADIOMETERS

NT DICKE RADIOMETERS

NT INFRARED DETECTORS

NT INFRARED SCANNERS

NT MICROWAVE RADIOMETERS

NT SPECTRORADIOMETERS

Atmospheric temperature profile determination by limb radiation inversion radiometer, discussing radiative transfer, instrument parameters and inversion process effects on retrievable information content

01 p0072 A73-10354

Multispectral cloud type identification based on Nimbus 3 medium resolution IR radiometer measurements, using radiative transfer theory

01 p0073 A73-10381

A high-precision computer-controlled dual-channel polarizing radiometer.

01 p0045 A73-10383

Theory and design of economical net solar flux radiometer adaptable to conventional short wave radiosonde system, discussing prototype instrument tests and modifications

01 p0045 A73-10386

Radiometric techniques for observing the atmosphere from aircraft.

01 p0073 A73-10404

Remote sensing of the near-surface moisture profile of specular soils with multi-frequency microwave radiometry.

04 p0446 A73-15782

Accurate measurements of and corrections for nonlinearities in radiometers.

06 p0693 A73-17898

Pyroelectric IR detector materials thermal and electric properties, discussing applications in thermographs, focal plane reticle scanners, linear array thermal imaging, radiometers and laser detectors

06 p0694 A73-18317

Optics, image scanning mechanism and response characteristics of visible/IR radiometer onboard stationary satellite for earth imagery

07 p0822 A73-18988

Pulse interference suppression during noise signal intensity measurements with a modulation radiometer

07 p0792 A73-19911

Balloon measurements of the far-infrared background radiation.

[AD-757848]

07 p0825 A73-20177

A thermal calibrator for radiometers used in radioastronomy.

08 p0963 A73-20873

Image formation radiometers for blind landing, aerial reconnaissance over land and sea, horizon detection and detection of obstacles at sea

08 p0986 A73-21087

The third international comparisons of pyrhielometers and a comparison of radiometric scales.

08 p0966 A73-21266

New radiometric techniques and solar constant measurements.

08 p0966 A73-21270

Active cavity radiometer as pyrhielometer for accurate radiation scale definition, determining measurement uncertainty through error analysis on quasi-equilibrium of power balance

11 p1365 A73-26236

Total irradiance calibrations using electrically calibrated radiometer, discussing lamp detector alignment procedures

11 p1366 A73-26252

An interference filter radiometer with cooled optics and a cooled PbS detector for rocket application.

11 p1368 A73-26507

Dual channel high resolution radiometer of French synchronous meteorological satellite Meteosat for full time cloud coverage of earth in visible and IR ranges

11 p1368 A73-26508

Real time quantitative display for visible and IR scanning radiometer in ITOS-D satellite-borne automatic picture transmission system with stations access to computers

12 p1520 A73-26811

Comments on the determination of the total heat flux from the sea with a two-wavelength radiometer system as developed by McAlister.

13 p1610 A73-29197

Photosensor aperture shaping to reduce aliasing in optical-mechanical line-scan imaging systems.

14 p1753 A73-30161

Instrumental theory in absolute radiometry

15 p1875 A73-31500

High-resolution atmospheric-transmission measurement using a laser heterodyne radiometer.

15 p1886 A73-32378

Radiometric observations of atmospheric water vapor injection by thunderstorms.

[AIAA PAPER 73-512]

16 p2006 A73-33550

Monochromatic and radiometric albedo of Mars and Venus

16 p2067 A73-33811

RADIONUCLIDES

- Remote sensing with VHRR satellite imagery.
18 p2308 A73-36041
- Design and performance characteristics of the Vertical Temperature Profile Radiometer (VTPR) for atmospheric temperature soundings.
20 p2567 A73-39852
- Improvements brought to the measurement of the ocean surface temperature by utilization of a polarizing infrared radiometer
21 p2698 A73-40142
- Influence of the resolution of television cameras and radiometers on the accuracy of determining the quantity of clouds from satellites
21 p2731 A73-40493
- Amplifier with distributed gain for use in radiometry
21 p2700 A73-40540
- Radio techniques applied to oceanography and earth science - Oceanic wind measurement and overland imaging as examples.
21 p2654 A73-40817
- Protection of radiometers from pulse interference
21 p2705 A73-41463
- Remote sounding of atmospheric temperature from satellites. IV - The selective chopper radiometer for Nimbus 5.
21 p2706 A73-41601
- Effect of radiometric errors on accuracy of temperature-profile measurement by the spectral-scanning method.
22 p2853 A73-41988
- Power subsystem for Skylab radiometer/scatterometer/altimeter experiment.
22 p2801 A73-42903
- Instrumentation for remote sensing solar radiation from light aircraft.
22 p2864 A73-43161
- Picture of the month - NOAA 2 scanning radiometer visual and infrared imagery received real-time over a 50,000-mile transmission link.
24 p3085 A73-45020

RADIONUCLIDES

U RADIOACTIVE ISOTOPES

RADIOPHOSPHORS

- Radiophotovoltaic devices power and energy conversion efficiency limits, investigating phosphors deterioration and nucleic layer optical thickness
09 p1037 A73-23280

RADIOPROTECTIVE AGENTS

U ANTIRADIATION DRUGS

RADIOSENSITIVITY

U RADIATION TOLERANCE

RADIOSOONES

NT IONOSONDES

NT RAWINSONDES

- Theory and design of economical net solar flux radiometer adaptable to conventional short wave radiosonde system, discussing prototype instrument tests and modifications
01 p0045 A73-10386

- Electrodynamic models for radio attenuation in ice by electromagnetic absorption and reflection from ice sheet interfaces, noting radar sounding
04 p0445 A73-15572

- Radiosonde soundings for typhoons and hurricanes isobaric surfaces heights, temperatures and humidities, calculating correlation coefficients between sea level pressure and other parameters
10 p1245 A73-23985

- Effective 'radius of operation' of a system for measuring ionospheric drifts
12 p1490 A73-27341

- Statistics of a pulse signal reflected from an inhomogeneous ionosphere
20 p2530 A73-39157

- Increase of error in range correction with elapsed time, evaluated by ray tracing through radiosonde-generated atmospheric models.
22 p2828 A73-43176

- Effective 'radius of action' of a device for measuring ionospheric drifts.
23 p2970 A73-43239

- Radiosonde ground station ozone concentration measurements as stratospheric motions Lagrangian tracer, noting sonde data inadequacy and alternative measurement possibilities
23 p2975 A73-43873

RADIOTELEPHONES

- Engineering economic considerations for a maritime-satellite service.
12 p1473 A73-27677

- Canadian space programs in communications, navigation and atmospheric science, considering telephony, data transmission, TV broadcasting and remote sensing
20 p2584 A73-38580

- System aspects of the initial Telesat Thin Route satellite communication system.
20 p2523 A73-38720

RADIOTHERAPY

U RADIATION THERAPY

RADOME MATERIALS

- Plane electromagnetic wave diffraction by periodic grid of dielectric cylindrical filaments, determining

- reflection and transmission coefficients of radome composite materials
02 p0141 A73-12024

- Selection and application of the protective coating system for the AWACS radome.
03 p0329 A73-13008

- Loaded and artificial dielectric materials with variable permittivity for sandwich radomes, discussing weight saving, multiband coverage and cross polarization reduction
11 p1335 A73-25281

- Influence of the illumination law on the radioelectric performance of radomes - Contribution to the determination of apparent illumination of the antenna
11 p1328 A73-25284

- The state of technology of ceramic radomes, their use and possibilities for the future.
11 p1335 A73-25286

- Electrically stabilized alumina as ceramic material for radome applications, tabulating dielectric, thermal and mechanical properties and firing conditions
11 p1408 A73-25287

- Fabrication and physical, mechanical and electrical properties of inorganic composite material for aircraft radomes
11 p1387 A73-25288

- Contribution to the study and perfecting of materials for radomes in the field of refractory ceramics
11 p1387 A73-25289

- Thermal resistance and aging properties of polybenzimidazoles, polyimides and polyamides-imides used for Mach 3 aircraft radomes
11 p1335 A73-25291

- Rain-erosion resistance and other properties of Schott infrared-transmitting glasses.
11 p1387 A73-25299

- Military aircraft radome design technology developments in Sweden, discussing use of glass fiber reinforced plastics, manufacturing method, computerized optimization and measurement techniques
11 p1335 A73-25300

- Aircraft and missile radomes technology in France, discussing materials, antenna radiation pattern calculation, computer programming for transmission and angular aberrations, and raindrop erosion tests
11 p1336 A73-25301

- Raindrop impact erosion damage on ceramic radome materials, discussing Rayleigh wave mathematical model comparison with sled test data, and laboratory simulation
11 p1336 A73-25306

- Hypervelocity tactical missile radome materials with noncharring ablator and fiberglass substructure for thermal protection against aerodynamic heating with negligible effects on radio transmission
11 p1336 A73-25307

- Radome material technology in UK, summarizing permittivity, loss tangent, internal phase difference, attenuation, aberration, cross polarization and pattern distortion measurements and environmental tests
11 p1336 A73-25308

- Cross polarization in radomes - A program for its computation.
15 p1851 A73-31730

- Elastomeric and ceramic coatings for aircraft and missile radomes protection in subsonic and supersonic rain erosion environments
16 p2027 A73-33031

- Rigid lightweight honeycomb core radome development from materials and processes standpoint, discussing cost reduction and fabrication [SAE PAPER 730310]
17 p2177 A73-34670

- Polyimide resin dielectric and mechanical properties, discussing syntactic foam composite with aluminum filler for radome construction
17 p2195 A73-34804

RADOMES

- Dielectric layers in the radiation field of microwave antennas
05 p0550 A73-16475

- Aircraft radome design mechanical, electrical and aerodynamic requirements, taking into account lightning hazards, electrostatic surface charges and plastic components deformations
06 p0648 A73-17997

- Internal equation numerical solution for excitation of multilayer arbitrary shape dielectric body of revolution, considering radome curvature effects on antenna radiation pattern
09 p1052 A73-23084

- International Conference on Electromagnetic Windows, 2nd, Ecole Nationale Supérieure de Techniques Avancées, Paris, France, September 8-10, 1971, Proceedings. Volume 1, 2 & 3
11 p1334 A73-25276

- Radome precision testing for fire control, missile aiming, Doppler navigation and bombing
11 p1335 A73-25277

- Radome insertion phase delay errors due to element impedance, frequency uncertainty, power instability and heat effects
11 p1327 A73-25278

- Electromagnetic window for a trajectory radar
11 p1327 A73-25280

- Method of calculation of radioelectric performances of airborne radomes
11 p1327 A73-25282

- Study of the Rayleigh zone of circular radiating apertures
11 p1328 A73-25283

- Calculation of the radiation diagram of an antenna in the presence of a radome
11 p1328 A73-25285

- Experimental study of electrical reflectors equipped with thin radomes
11 p1335 A73-25292

- Development of loaded resin one-piece radomes
11 p1387 A73-25294

- Influence of fabrication inaccuracies on the axis deviation of an airborne radome
11 p1328 A73-25295

- Airliner radomes erosion by atmospheric precipitation, water penetration, icing, bird and stone impact and lightning
11 p1335 A73-25297

- Determination of criteria for rain erosion testing of the standard arm radome.
11 p1335 A73-25298

- Military aircraft radome design technology developments in Sweden, discussing use of glass fiber reinforced plastics, manufacturing method, computerized optimization and measurement techniques
11 p1335 A73-25300

- Calculation of the temperature distribution within an ogival radome in supersonic flight
11 p1336 A73-25302

- Study on the limit efficiency of lightning conductors on aircraft radomes.
11 p1336 A73-25303

- Thick walled multilayer wideband radomes for supporting high hydrostatic pressures and protecting weakly directional submarine antennas with circular polarization
11 p1336 A73-25305

- Electrical characteristics of hardenable metallic lens or radome with near unity refractive index at off-band frequencies
11 p1338 A73-25670

- Large antennas and radomes boresight measurement with angular accuracy by laser mirror system incorporated into pattern range for antenna tower alignment
17 p2143 A73-35696

- Performance of a water-repellent radome coating in an airport surveillance radar.
21 p2648 A73-40101

RADON

NT RADON ISOTOPES

- Argon, radon, and tritium radioactivities in the sample return container and the lunar surface.
07 p0870 A73-19792

- Observation of lunar radon emanation with the Apollo 15 alpha particle spectrometer.
07 p0891 A73-19826

RADON ISOTOPES

- Detection of radon emanation from the crater Aristarchus by the Apollo 15 alpha particle spectrometer.
08 p1009 A73-21222

- Determination of coefficients of vertical diffusion between 0 and 100 m with the help of radon and of ThB
13 p1655 A73-29342

- Radon emanation from the moon - Spatial and temporal variability.
18 p2349 A73-36033

RAFTS

NT LIFE RAFTS

RAIL TRANSPORTATION

- Experimental aerodynamic studies for intra-urban trains traveling in tunnels.
[AIAA PAPER 73-155]
05 p0566 A73-16903

- On the application of parameter identification to high-speed ground transportation systems.
07 p0808 A73-20433

- Drag effectiveness of aerodynamic brakes in series on high speed train-like vehicle, considering fixed and moving model testing techniques
15 p1828 A73-31460

- Subway system vertical tunnel simulation facility including plenum assembly, instrumentation, model launcher, subway car simulation models, tube scaffolding and data acquisition
16 p1994 A73-33148

RAILROADS

U RAIL TRANSPORTATION

- A comparison of precipitation attenuation and radar backscatter along earth-space paths.
01 p0015 A73-10183

- The fluctuation spectrum of laser radiation in a turbulent atmosphere in the presence of rain
01 p0060 A73-10872

- Simultaneous quantitative measurements of rainfall rate and drop size distribution by X-band radar and drop distrometer /system Joas-Waldvogel/ at two rain gauge equipped places near to Bonn/West Germany.
03 p0338 A73-14520

Rain attenuation of vertically and horizontally polarized signals of 18 GHz communication system 04 p0419 A73-15395

On the reduction of rainfall outages by space diversity for millimeter-wave earth-satellite communications systems. 06 p0668 A73-18712

Tests of coherence for the empirical laws of distribution of raindrops 08 p0938 A73-20966

Subsynoptic rainbands within precipitation ahead of surface warm front, discussing midtropospheric large-scale dynamic ascent interaction with upper boundary potential instability 13 p1651 A73-28265

Rain fall deceleration effect on flow velocity of infinitely deep water mass, solving Navier-Stokes equations via Laplace transforms 13 p1600 A73-28419

The spectrum of fluctuations of laser radiation in a turbulent atmosphere during rain. 13 p1627 A73-28696

Rainfall crosspolarization at microwave frequencies with differential phase shift and attenuation, considering rain models 13 p1587 A73-29670

Rain-attenuation measurements of millimetre waves over short paths. 15 p1848 A73-32647

Rain attenuation and fade duration statistics for design of satellite-based communication system, predicting outage for 16 GHz path diversity system 16 p1981 A73-33706

On rainfall and space diversity for millimeter-wave earth-satellite communications systems. 18 p2289 A73-36709

Effect of scattering on radiometer measurements of attenuation in rain. 19 p2403 A73-37426

A method of providing rain margins for 18/30 GHz communications satellites without increasing the solar power requirement. 20 p2524 A73-38731

Rainfall estimation from satellite visible and IR imagery, discussing calibration and accuracy requirements 21 p2730 A73-40093

Design of a phased array radiating face for prevention of performance degradation in the presence of rain. 21 p2663 A73-40663

Mediterranean, south Sahara and northwest India rainfall records analysis, correlating general circulation changes with winter-spring and monsoon rainfall fluctuations 23 p3003 A73-39594

Upper tropospheric disturbances of the equatorial atmosphere and their influence on rainfall near the equator. 23 p3004 A73-44104

Use of cancellation techniques in the measurement of atmospheric crosspolarization. 23 p2955 A73-44111

On the variation with height of the top brightness of precipitating convective clouds. 23 p3005 A73-44270

RAIN EROSION **U WATER EROSION** **RAIN GAGES**

An experimental investigation of the nature of changes in the intensity of precipitations from stratiform and cumuloform clouds 12 p1522 A73-27747

RAIN IMPACT DAMAGE

The state of technology of ceramic radomes, their use and possibilities for the future. 11 p1335 A73-25286

Test rails possibilities for rain erosion phenomena study on aircraft or missile structures 11 p1335 A73-25296

Airliner radomes erosion by atmospheric precipitation, water penetration, icing, bird and stone impact and lightning 11 p1335 A73-25297

Rain-erosion resistance and other properties of Schott infrared-transmitting glasses. 11 p1387 A73-25299

Aircraft and missile radomes technology in France, discussing materials, antenna radiation pattern calculation, computer programming for transmission and angular aberrations, and raindrop erosion tests 11 p1336 A73-25301

Space shuttle lightweight thermal protective insulation materials rain erosion resistance determination at 200-400 MPH and various angles of attack, using rotating arm test apparatus 16 p2071 A73-33030

Elastomeric and ceramic coatings for aircraft and missile radomes protection in subsonic and supersonic rain erosion environments 16 p2027 A73-33031

Rain erosion of reinforced plastics for aerospace applications in terms of drop size, impact angle and velocity effects and protective coatings 17 p2195 A73-34806

Performance of a water-repellent radome coating in an airport surveillance radar. 21 p2648 A73-40101

RAINBOWS
Atmospheric optical phenomena, discussing physical origin of rainbows and halos 04 p0445 A73-15629

Vector theory of the glory and rainbow 21 p2731 A73-40742

RAINDROPS

Thermal effect of optical radiation on water drops of small size 01 p0074 A73-11244

A new Monte-Carlo simulation model for the temporal development of cloud droplet spectra. 02 p0144 A73-12782

Effect of heating water droplets by optical radiation. 10 p1246 A73-24181

Determination of criteria for rain erosion testing of the standard arm radome. 11 p1335 A73-25298

Raindrop impact erosion damage on ceramic radome materials, discussing Rayleigh wave mathematical model comparison with sled test data, and laboratory simulation 11 p1336 A73-25306

Radiative properties of terrestrial clouds at visible and infra-red thermal window wavelengths. 13 p1652 A73-28274

Heavy precipitation from mixed phase composition cloud systems vs light precipitation from droplet and crystal containing clouds 13 p1654 A73-28887

The effect of the size distribution of the rain drops on the standard visibility 15 p1902 A73-31139

Linear cross-polarisation and attenuation measurements at 11 and 36 GHz. 16 p1982 A73-33723

Microwave propagation in atmosphere with oblate spheroidal raindrops, discussing linear and circular cross-polarization effectiveness statistical analysis with allowance for raindrop orientation 16 p1983 A73-33724

Raindrops in satellite communications. 18 p2289 A73-36515

Scattering properties of oblate raindrops and cross polarization of radio waves due to rain - Calculations at 19.3 and 34.8 GHz. 18 p2290 A73-36880

Numerical model of a two-phase stratiform cloud taking its microstructure into account 20 p2583 A73-39185

Structure of cumulus clouds during various development phases 20 p2583 A73-39186

Water condensation coefficient for 3-micron radius droplets, noting expected error confirmation with standard deviation in experiment 22 p2883 A73-42548

RAINSTORMS

NT THUNDERSTORMS
Results of precipitation backscatter measurements at 1.8 cm with a polarization diversity radar. 03 p0338 A73-14509

ATS-3 observed cloud brightness field related to a meso-to-synoptic scale rainfall pattern. 06 p0720 A73-17867

Statistical properties of precipitation patterns. 15 p1903 A73-31316

RAISED REEFS

U REEFS

RAMAN EFFECT

U RAMAN SPECTRA

RAMAN LASERS

Power output of a pulsed Raman laser with saturable excitation. 03 p0319 A73-14453

Remote measurement of atmospheric temperatures by Raman lidar. 17 p2163 A73-35467

Laser-pumped tunable spin-flip InSb Raman lasers in terms of low field operation, linewidth measurement technique, power output and applications 20 p2571 A73-38623

Daytime applications of Raman technique of laser backscatter to measure atmospheric composition profiles 21 p2729 A73-40067

Interference filter laser Raman spectrometry of gases and volatile liquids, discussing instrument sensitivity and response linearity, signal to noise ratios, and bandwidths 21 p2698 A73-40140

RAMAN SCATTERING

U RAMAN SPECTRA

RAMAN SPECTRA

Stimulated Raman scattering of microwaves in a layer of collisionless plasma. 01 p0082 A73-10423

Gas density measurements in a jet using Raman scattering. 01 p0050 A73-10763

Optical power handling capacity of low loss optical fibers as determined by stimulated Raman and Brillouin scattering. 01 p0078 A73-11216

Spectral composition of thermal and stimulated light scattering in the wing of the Rayleigh line 02 p0194 A73-11945

Raman scattering by phonons and magnons and phonon-magnon interactions in NiO. 02 p0201 A73-12640

Morphic effects. V - Time reversal symmetry and the mode properties of long wavelength optical phonons. 03 p0349 A73-12901

Laser Raman spectrum of crystalline cyclopentane-d/sub 0/ and -d/sub 10/. 03 p0318 A73-13282

Spin saturation and pump depletion in continuous spin-flip Raman oscillation. 03 p0319 A73-14452

Investigation of certain characteristics of induced Raman scattering produced in a plane-parallel ruby-laser resonator 04 p0458 A73-14882

Study of the dispersion curve of polaritons excited by Raman diffusion in the presence of damping 04 p0476 A73-15997

Absolute Raman scattering cross-section of molecular hydrogen. 05 p0601 A73-17340

Angular distribution of first Stokes component for stimulated combinational Raman scattering investigated under various excitation conditions 06 p0700 A73-17965

Plasma generation by nanosecond and picosecond laser pulses, discussing Raman scattering from solid hydrogen and deuterium targets 06 p0731 A73-18581

Rayleigh scattering influence on stimulated Raman effect, determining occurrence conditions for absolute instability due to feedback 06 p0702 A73-18593

Structure of lunar glasses by Raman and soft X-ray spectroscopy. 07 p0788 A73-19737

Far infrared and Raman spectroscopic investigations of lunar materials from Apollo 11, 12, 14, and 15. 07 p0897 A73-19889

German monograph - Observation of stimulated Raman-anti-Stokes radiation of higher order and its significance for the starting phase of plasma generation by laser. 07 p0837 A73-20383

Efficient parametric conversion in cesium vapor irradiated by 3470-A mode-locked pulses. 09 p1090 A73-22079

New method of increasing the emission frequency of high-power laser pulses. 10 p1229 A73-24769

Characteristics of the vibrational spectrum of laminar As₂S₃ semiconductors 11 p1408 A73-25244

Nonlinear behavior of stimulated Brillouin and Raman scattering in laser-irradiated plasmas. 13 p1664 A73-28187

Raman scattering from phonon bath using quantum mechanical model with random and stochastic Stokes and anti-Stokes coupled modes in light fields 13 p1658 A73-28209

Quantum oscillations and pump depletion effects in an efficient high-power tunable spin-flip laser. 13 p1626 A73-28216

Observation of Raman scattering by SO₂ in a generating plant stack plume. 13 p1607 A73-28547

Vibrational spectra of substituted hydrazines. IV - Raman and far-infrared spectra and structure of tetramethylhydrazine. 15 p1841 A73-32220

Vibrational spectrum of bis(trifluoromethyl) trioxide. 15 p1841 A73-32221

Rotational temperature measurement of gases using laser Raman scattering techniques. 17 p2166 A73-34623

Gas concentration measurement by coherent Raman anti-Stokes scattering. 18 p2315 A73-36251

[AIAA PAPER 73-702] Measurements of F₂, NO, and ONF Raman cross sections and depolarization ratios for diagnostics in chemical lasers. 18 p2322 A73-36978

Spatial coherence characteristics of noise emission in active waveguide channel, considering Raman scattering of focused beam 19 p2437 A73-37247

Theory of resonant light scattering processes in solids. 20 p2570 A73-38612

Relative Raman cross section of O₃ for four Ar+ laser frequencies. 20 p2595 A73-38893

Stimulated Raman scattering in sulfur hexafluoride. 20 p2574 A73-39688

RAMAN SPECTROSCOPY

Remote measurement of subsurface sea water temperature by airborne Raman scattering with cross polarizer in front of light source and detector, noting precision 20 p2568 A73-39889

Amplification of stimulated Raman scattering of light in various nonlinear amplifier pumping circuits 21 p2711 A73-40306

On the possibility of measuring gas concentrations by stimulated anti-Stokes scattering. 21 p2699 A73-40458

Three-wavelength holographic diagnostics of an optical flare at a potassium target 21 p2700 A73-40529

Raman spectrum of PbZrO₃. 21 p2752 A73-40894

Far infrared and Raman spectra of gaseous carbon suboxide and the potential function for the low frequency bending mode. 21 p2740 A73-40935

Raman scattering of SHF radiation in a bounded plasma of a solid 21 p2657 A73-41509

Observation of the Raman effect in the spectrum of Uranus. 22 p2916 A73-43126

Light scattering intermolecular and Raman spectra in liquid and solid hydrogen, showing short wave collective excitations in relation to phonon processes 23 p3007 A73-44171

RAMAN SPECTROSCOPY

Laser applications to spectroscopic analysis, Raman, maximum resolution and excited state spectroscopies, and spectral instruments manufacture 02 p0177 A73-12725

Infrared and Raman spectroscopic studies of structural variations in minerals from Apollo 11, 12, 14, and 15 samples. 07 p0897 A73-19887

Comparison between a double and triple monochromator in Raman laser spectrometry 07 p0836 A73-20166

Laser spectroscopy of stimulated Raman scattering of weakly interacting molecules, and its applications 09 p1097 A73-23326

Spectroscopic laser methods of automatic gas analysis based on Raman backscattering, resonance fluorescence or absorption measurements for atmospheric pollutant and exhaust gas detection 16 p2023 A73-32876

Application of laser Raman spectroscopy to the study of factors that influence turbulent gas mixing rates. 17 p2185 A73-35510

Interference filter laser Raman spectrometry of gases and volatile liquids, discussing instrument sensitivity and response linearity, signal to noise ratios, and bandwidths 21 p2698 A73-40140

Low-noise instrumentation for Raman and luminescence spectrometry with ruby and argon laser excitation. 22 p2868 A73-41783

RAMJET ENGINES

NT PULSEJET ENGINES

NT SUPERSONIC COMBUSTION RAMJET ENGINES

Propellants selection to provide an air simulant for hot gas testing or ramjets. 03 p0351 A73-13397

Screen and porous absorbing liner design for damping pressure oscillations in ramjet combustors based on acoustic absorption efficiency and combustion instability calculation [AIAA PAPER 73-226] 06 p0767 A73-17665

Boundary layer efficiency as working fluid in ramjets for high aircraft speeds, obtaining external efficiency as function of boundary layer parameters and flow rate 09 p1073 A73-23360

Magnetic intake limitations on interstellar ramjets. 10 p1262 A73-24539

RAMJET MISSILES

Development of aft inlets for a ramjet powered missile. 03 p0246 A73-14133

RAMS [PRESSES]

Fuel tank wall response to hydraulic ram during the shock phase. 22 p2843 A73-43114

RAMS [PUMPS]

Ram air turbine with hydraulic pitch change servo regulated speed as emergency power source for aircraft control in event of main engine failure 24 p3058 A73-45475

RANDOM ACCESS MEMORY

NT CORE STORAGE

N-type Si MNOS random access memory devices for data storage without applied voltage, noting threshold shifts vs writing pulse width for various oxide thicknesses 05 p0553 A73-16166

An integrated random access memory with full-current recording and readout 14 p1730 A73-30290

Block organized holographic read only optical memory /ROOM/ model for random access large storage capacities with electro-optical or acousto-optical light deflection system 16 p2012 A73-32869

Fast random access permanent storage read only optical memory, using light emitting diode matrix addressing, semiconductor laser and holographic lens system 16 p2012 A73-32870

Holographic read-write memory, optical organization and capacity enhancement by three-dimensional storage. 16 p2013 A73-32871

High speed serial multiplexed holographic recording for large capacity random access memories, using piezoelectric deflector and ferroelectric ceramic array modulators 16 p2013 A73-32872

Integrated semiconductor storage devices, discussing bipolar transistor, Schottky diode and MOS memories and RAM, ROM and PROM types with circuit compatibility considerations 16 p1991 A73-33960

Block oriented random access and read-only archival holographic memories design, considering relationships between lens geometric parameters, laser power and packing density requirements 17 p2173 A73-35432

RANDOM DISTRIBUTIONS

U STATISTICAL DISTRIBUTIONS

RANDOM ERRORS

Algorithms for spacecraft trajectory optimization programs for orbit perturbations caused by random measurement errors and minimum mathematical expectancy of energy dissipation 02 p0220 A73-12468

Error incidence probability for system control reliability determination, assuming error function as Markov process 06 p0680 A73-17956

Optimization of antenna parameters in the presence of random errors. 07 p0801 A73-20128

Method of utilizing structural redundancy in a measuring system for processing experimental data with systematic errors 12 p1494 A73-26776

An analysis of the effectiveness of ways of increasing the accuracy of a treatment 12 p1503 A73-27467

Errors in the absolute method of measuring the frequency of difference oscillations 15 p1853 A73-31256

Algorithms for spacecraft trajectory optimization programs for orbit perturbations caused by random measurement errors and minimum mathematical expectancy of energy dissipation 15 p1942 A73-32618

Gyroscopic orbit errors caused by random perturbations 18 p2317 A73-36853

Transmission strategy and optimal block size in high-speed data communication. 20 p2530 A73-39128

A few error detection codes for decision feedback system and error characteristics of channels. 22 p2835 A73-42192

RANDOM LOADS

NT GUST LOADS

Random stresses effect on dynamic creep properties of Ti alloy in high temperature air flow 02 p0180 A73-11625

Response of helicopter rotor blades to random loads near hover. 02 p0129 A73-12503

Correlation theory for equations of motion of constant thickness shallow shell vibration under random loads 03 p0387 A73-13158

Comparison of scatter under program and random loading and influencing factors. 03 p0387 A73-13232

Application of the Monte Carlo technique to fatigue-failure analysis under random loading. 03 p0388 A73-13236

Impact loading on structures with random properties. 04 p0510 A73-15028

Prediction of failure for a multiple load-path system under random loading. 04 p0510 A73-15075

Choice of a rational control law for control systems for delayed objects subjected to random load disturbances. 04 p0429 A73-15202

Design criteria for structural elements subjected to stationary random loads. [ASME PAPER 72-WA/DE-19] 04 p0514 A73-15837

Probability of stress-corrosion fracture under random loading. 06 p0763 A73-18483

Random forcing effects on numerical weather predictability, assessing atmospheric variables computational space truncation impact 06 p0720 A73-18701

Stability of a multivariable discrete system for controlling a fatigue testing process with random loading 12 p1557 A73-27949

Generalized random forces in time domain for rectangular panels under subsonic and supersonic boundary layer turbulence, investigating probabilistic nature by Monte Carlo method 17 p2241 A73-34182

Fatigue life of structural components under random loading 17 p2242 A73-34520

Effect of load sequences on crack propagation under random and program loading. 17 p2190 A73-34879

Computer based analyses of the response of box type structures to random pressures. 19 p2497 A73-37485

Random loading on a spherical pressure vessel of Hooke-Norton material. 19 p2501 A73-38252

Functional reliability of structures. 19 p2501 A73-38279

Fatigue life under random loading with varying mean stress and rms value. 20 p2622 A73-39553

Fatigue-crack growth under variable-amplitude loading in ASTM A514-B steel. 22 p2875 A73-42140

Monograph - Fatigue and stochastic loadings. 22 p2923 A73-42673

Stability of nonlinearly elastic plates in the presence of random initial stresses 22 p2928 A73-43060

On response of initially stressed structures to random excitations. 24 p3150 A73-45229

RANDOM NOISE

NT RANDOM SIGNALS

Influence of additive and multiplicative noise on the accuracy in measuring the angular position of a source of radiation by systems with pulse-width modulation 01 p0017 A73-10212

Mean error probability during diversity reception at extremal group frequencies under random noise conditions 01 p0019 A73-11262

Investigation of the effectiveness of the variable-step simplex optimization method in a noise environment 01 p0028 A73-11420

Some results on zero crossing distribution of non-stationary random noise. 02 p0143 A73-12857

Standard deviation of thresholding time during detection of pulse perturbed by Gaussian noise 03 p0277 A73-13912

Neumann-Pearson-optimal signal detection procedure invariant with respect to amplitude and random noise intensity 03 p0278 A73-14073

Mathematical expectation of angularly modulated signal in unsteady linear random noise, using Marchenko formula 03 p0278 A73-14074

Optimal risk equation and solution existence and uniqueness of dual control problems with unknown parameter and additive noise 04 p0429 A73-15203

An adaptive Kalman filter using decomposition of the innovations sequence. 04 p0431 A73-15258

Performance of correlation receivers in the presence of impulse noise. 04 p0419 A73-15406

Pseudorandom noise for telemetry error rate measurement applications and limitations. 04 p0449 A73-15457

Modulating /multiplicative/ noise effects on output signal characteristics of receiver designed for optimal reception against background of Gaussian noise 04 p0423 A73-15915

Optimal distribution of resources in automatic detector-meters determining number of random concentrated radio noises in assigned frequency range 04 p0423 A73-15926

Variance reduction in remotely sensed multispectral data caused by random noises and systematic variations in system angular response and in apparent scene radiance 05 p0554 A73-17148

Noise magnitude calculation for intensity quantized hologram based on Laplace transform for nonlinear device analysis and Gaussian random process 05 p0579 A73-17220

Performance of M-ary PSK systems in Gaussian noise and intersymbol interference. 06 p0665 A73-18140

High resolution infrared spectrometer with multiplex advantage. 06 p0695 A73-18318

Identification of multivalued nonlinearities in a class of noisy time invariant dynamic systems. 06 p0681 A73-18811

Some problems of statistical estimation of a signal source in a dispersive medium 07 p0792 A73-19912

The resistance of discrete phase modulation to random interference 07 p0793 A73-20023

Adaptive algorithms for reducing a random field to a prescribed set of states with constraints on the elements of the approximating sequences 07 p0796 A73-20079

The oscillation probability of self-excited multimode oscillators. 08 p0945 A73-20803

Characteristics of the adaptive optimal detection of Gaussian signals on a pulse-noise background in receivers with a logarithmic amplifier 08 p0940 A73-21554

Statistical properties of two sine waves in Gaussian noise. 09 p1120 A73-22115

Kalman filtering theory application to optimal causal demodulator for pulse amplitude modulated signals in white Gaussian noise 09 p1067 A73-22116

Measuring the off-duty factor of chaotic pulsed interference on a Gaussian noise background 09 p1050 A73-22338

Algorithm for optimal radio signals detection under narrow band anisotropic noise, noting two channel space diversity receiver system 09 p1050 A73-22454

Estimation of noise covariance matrices for a linear time-varying stochastic process. 10 p1201 A73-24053

Transient characteristics of simple systems to modulated random noise. [ASME PAPER 72-APM-FFF] 11 p1398 A73-25703

The limiting advantage derived from the compounding of information-extracting devices in the presence of wideband Gaussian noise 12 p1482 A73-26867

Nonparametric signal detectors in the case of dependent sampled magnitudes 12 p1467 A73-26868

Effectiveness of analog storage in the detection of signals on a background of noise and strong random pulsed interference 12 p1467 A73-26942

Second-order phase-lock-loop acquisition time in the presence of narrow-band Gaussian noise. 12 p1468 A73-27010

Quantizer functions and their use in the analyses of digital beamformer performance. 13 p1582 A73-28496

Detection of Doppler signals by a receiver which incorporates a counter of the number of excursions of additive noise. 13 p1583 A73-28728

Correlation of random noise levels in short-wave radio channels 13 p1584 A73-28888

Evaluation of the noise immunity of pulsed systems for transmission of continuous messages with allowance for quantization and interpolation errors. I 13 p1584 A73-28891

Noise immunity evaluation for noncoherent demodulators or FSK and PSK signals in short wave channels, using minimum a priori information on additive noise properties 13 p1592 A73-28899

Atmospheric effects on ocean surface temperature sensing from the NOAA satellite scanning radiometer. 13 p1610 A73-29195

A minimax filter for systems with large plant uncertainties using measurements corrupted by colored noise. 13 p1593 A73-29205

An asymptotically optimal rank detection algorithm for a signal in noise of unknown distribution 15 p1842 A73-31490

Optimal reception of digital signals on an additive noise background 15 p1843 A73-31493

Signal interference and improvement of signal-to-noise ratios in a half-wave linear detector. 15 p1843 A73-31729

Optimal receiver design for discrete information in the presence of non-Gaussian noise 16 p1990 A73-33669

Effects of cochannel interference and Gaussian noise in M-ary PSK systems. 17 p2122 A73-34871

Bayes theorem for radio signals parameter estimation on random noise background, using rectangular function of losses 17 p2123 A73-35167

Unsupervised learning of the optimal linear signal estimator in the presence of unknown multiplicative, additive, and message generating noise. 17 p2144 A73-35374

Dependence of sidelobe level on random phase error in a linear array antenna. 17 p2129 A73-35697

Probability of reception of discrete information with a specified reliability under conditions of random radio interference. 17 p2129 A73-35713

Effect of the random disturbances in the principal gyro axis on the readings of a ground gyrocompass 18 p2317 A73-36854

Reliability estimation for integral logical elements from intermittent failures under noise effects 18 p2292 A73-37045

A practical filter for noisy dynamic systems with unknown time-varying parameters. 19 p2410 A73-38047

Methods of adaptation in problems involving nonparametric detection and resolution of signals 20 p2540 A73-38700

FM distortion of a TV signal and subcarriers due to bandpass filtering and additive Gaussian noise. 20 p2523 A73-38722

ML receiver for binary signals with intersymbol interference in Gaussian noise. 20 p2524 A73-38733

Detection of weak signals in narrowband noises. 20 p2529 A73-38921

Nonbiased rule for detection of radar signals in noise of unknown power. 20 p2529 A73-38928

Optimal Markov sequence signal detection in correlated FM random electronic countermeasure background noise 20 p2529 A73-38929

Approximate solution of Bellman's equation for a class of problems involving optimal terminal control 21 p2668 A73-40179

A conservative bound on the estimation error covariance matrix in the presence of correlated driving noise and correlated discrete measurement noise. 21 p2724 A73-40295

Digital communication channel with noisy errors, discussing statistical analysis of binary burst sequences for coding design 21 p2655 A73-41090

Phase-locked loop operation in the presence of impulsive and Gaussian noise. 21 p2656 A73-41166

Combined effects of intersymbol, interchannel, and co-channel interferences in M-ary CPSK systems. 21 p2656 A73-41167

Radar altimeter signal propagation delay estimation, calculating and plotting noise fluctuation characteristics as function of aircraft ground speed, altitude and other parameters 22 p2828 A73-43067

Evaluation of the correctness of Gaussian approximation in noise immunity theory 23 p2954 A73-43519

An innovations approach to least-squares estimation. V - Innovations representations and recursive estimation in colored noise. 23 p2954 A73-43819

Gilbert burst noise model for statistical analysis of nonindependent errors in digital data transmission systems, noting performance and utility in communication theory 23 p2954 A73-43986

RANDOM NUMBERS

Bode law rationalization based on Dole computer-generated planetary system with constant spacing ratio generated by random number sequence and accretion process closeness constraints 11 p1428 A73-26665

RANDOM PROCESSES

NT RANDOM WALK

Canonical expansions of random processes, discussing discrete and continuous set transformations for spectral representation and shaping filters in time domain 01 p0068 A73-10027

Periodically correlated random processes to model additive and multiplicative rhythmical phenomena, discussing structural properties and theorems 01 p0075 A73-10028

Steady creep bending in a beam with random material parameters. 01 p0113 A73-10198

A systematic approach to the problem of crossings by a random process. 01 p0070 A73-10577

Accuracy of the determination of the spectral density of a vibrational process with the aid of a spectrum analyzer 01 p0077 A73-10677

Velocity variation of a star as a purely discontinuous random process. III Stars with different masses in an open cluster 01 p0100 A73-10711

Analog computer regression line and correlation ratio determination for random stationary processes with time lag 01 p0028 A73-10928

Optimal control problems in differential games of pursuit and evasion involving deterministic, random and controlled motion 01 p0028 A73-11071

Application of random time and frequency multiplexing to a data collection satellite. 01 p0018 A73-11182

Some exact statistics of two-dimensional viscous flow with random forcing. 02 p0153 A73-12041

Optimization of control and observation processes in dynamic systems under random perturbations. 02 p0149 A73-12118

Statistical theory of light propagation in a turbulent medium /Survey/ 02 p0141 A73-12485

Digital simulation of random processes and its applications. 02 p0144 A73-12607

Some results on zero crossing distribution of non-stationary random noise. 02 p0143 A73-12857

Russian book on machine-based determination of random process characteristics covering correlation, moment functions, spectral features, probability functions, etc 02 p0149 A73-12866

Monte Carlo solution of structural dynamics. 03 p0391 A73-13681

Variance estimate of random process second order moment by nonlinear correlator in presence of additive amplitude and phase modulated and normal noise processes 03 p0278 A73-14075

Optimal equalization of discrete signals passed through a random channel. 04 p0420 A73-15418

Reliability of systems with shifting redundancy in servicing a random demand flow 05 p0560 A73-16274

Automatic control system synthesis for optimal correction, maximum accuracy and stability of linear unsteady final action systems under deterministic and random actions 05 p0561 A73-16420

On the transport properties of charged particles in one dimension in random electric fields. 05 p0612 A73-17384

Structure of the pulsations of the earth's electromagnetic field as a random function of time 06 p0689 A73-17541

A new approach to the problem of wave fluctuations in localized smoothly varying turbulence. 06 p0665 A73-18183

Monte Carlo computer technique for one-dimensional random media. 06 p0665 A73-18188

Energy spectra of mixed discrete random processes in statistical multiplexing systems with pulse position, delta and pulse code modulation 06 p0668 A73-18390

On the convergence of random search algorithms in continuous time with applications to adaptive control. 06 p0671 A73-18623

Approximate method for the synthesis of the optimal control of a dynamic system subjected to random disturbances 06 p0725 A73-18879

An actively adaptive control for linear systems with random parameters via the dual control approach. [AD-751587] 07 p0806 A73-20601

Kalman-Bucy method solution to time-space dependent random fields optimal filtration under additive white noise 07 p0804 A73-20635

Comparative study of methods of analysis of non-linear systems subjected to random input 08 p0938 A73-20969

Passage of useful and noise signals through a non-linear circuit containing a p-n junction capacitance 08 p0946 A73-21111

Internal additive noise generated by a random pulse process 08 p0939 A73-21395

Correlation techniques in the analysis of transient processes. 08 p0988 A73-21466

Random coding bound of information theory providing upper bound to decoding error probability for best code of given rate and block length 09 p1111 A73-22117

Self-synchronization of mechanical vibrators in the event of random disturbances 09 p1120 A73-22356

Weak convergence of stepwise random processes 09 p1112 A73-22886

Optimal control problems in differential games of pursuit and evasion involving deterministic, random and controlled motion 09 p1113 A73-22996

Signal processing in a randomly time varying system. 10 p1197 A73-23800

Determination of changes in the properties and recognition of random processes with a complicated structure. 10 p1201 A73-24057

Analog computer regression line and correlation ratio determination for random stationary processes with time lag 10 p1201 A73-24188

RANDOM SAMPLING

On the normality and accuracy of simulated random processes.

10 p1292 A73-24395

Methods of representation and machine analysis of random fields and processes; All-Union Symposium, 5th, Vilnius, Lithuanian SSR, May 1972, Transactions, Sections 1, 2, 3 & 4

11 p1339 A73-25001

Measurement of certain one-dimensional characteristics describing the evolution of the two-dimensional probability density of random processes when changing the interval between readings

11 p1340 A73-25004

Error analysis of correlation method for determining directional characteristics [angular power density] of homogeneous random wave field

11 p1359 A73-25005

A structural model of random processes and its invariant properties

11 p1340 A73-25007

Description of random processes with allowance for irregularity of changes in their properties

11 p1340 A73-25008

A representation of uncorrelated random processes by stochastic integrals

11 p1340 A73-25010

Simulation of random processes with the aid of piecewise linear transformations of unit interval

11 p1340 A73-25012

Problem of forming classes of input processes in the study of errors in devices for statistical measurements

11 p1359 A73-25014

Effect of time-quantization errors on the accuracy in periodogram analysis of random processes

11 p1360 A73-25015

Effect of measuring-device error on the accuracy of the determination of the mathematical expectation and dispersion of a stationary random process

11 p1360 A73-25016

Estimate of the spectral density of a stationary random process by an indirect method

11 p1341 A73-25017

Errors in the determination of random process characteristics with the aid of measuring converters with randomly varying parameters

11 p1341 A73-25024

Launch vehicle response to inflight winds during ascent, modeling wind velocity as nonstationary random process

[AIAA PAPER 73-398]

11 p1392 A73-25527

The spatial correlation method and a time-varying flexible structure.

[AIAA PAPER 73-406]

11 p1440 A73-25535

Statistically orthogonal functions for finite intervals of a random process

11 p1390 A73-25642

Field scattered by rough surface generated by stationary random process, constructing two dimensional density from given marginals and correlation coefficient

11 p1328 A73-25656

On the random nature of the eruption of magnetic flux at the solar surface.

11 p1422 A73-25939

On the mapping associated with the complex representation of functions and processes.

11 p1333 A73-26645

Temperature field in front of or behind gas turbine with additive white noise, deriving optimal filter for dynamic programming technique in random fields analysis

12 p1483 A73-27080

On optimal nonlinear estimation. I - Continuous observation.

12 p1517 A73-27147

Absolute continuity of estimates corresponding to uniform Gaussian fields

12 p1523 A73-27185

Regularity of conditional probabilities for random processes

12 p1518 A73-27192

Canonical representations of random processes with multiplicities of one and two

12 p1518 A73-27193

Stochastic equations of nonlinear filtering of random processes

12 p1518 A73-27222

Determining the trend of a random sequence

12 p1518 A73-27224

Random failure process similarity in redundant schemes for systems with binary elements, noting statistical modeling on specialized Monte Carlo machines

12 p1485 A73-27620

Approximate calculation of the moments of the distribution of the maxima of correlated Gaussian random sequences

12 p1485 A73-27621

Optimal estimation of the phase coordinates for a linear dynamic system

12 p1485 A73-27898

Earth mantle-core mechanical and electromagnetic interactions influencing rotation rate random variations

13 p1679 A73-28396

Earth polar motion and angular velocity sequential estimation in presence of unmodelled random accelerations, via Gauss-Markov process representation

13 p1679 A73-28397

Estimations for queueing and reliability theory

13 p1649 A73-28796

Maximum information compression and minimum entropy of random process, using Karhunen-Loeve basis

13 p1596 A73-28869

Statistical definition of fatigue behavior of strength of low alloy steels.

13 p1641 A73-29492

Random and program fatigue tests of Cr-Mo steel specimen with V-grooved notch.

13 p1641 A73-29494

Electrostatic waves in warm random plasmas.

14 p1779 A73-29708

Diffusion of comets from parabolic into nearly parabolic orbits.

14 p1793 A73-29828

Determination of some characteristics of random processes describing the operation of transient action systems with allowance for reliability

14 p1730 A73-30037

Random yield limit of stochastically non-homogeneous elements in tension.

14 p1811 A73-30489

A study of integral pulse frequency modulation of a random carrier.

14 p1729 A73-30502

Central limiting theorem in the 'noncommutative' probability theory

15 p1859 A73-31215

Random /turbulent/ excitation of flutter in wind tunnel dynamic models and flight test aircraft, comparing prediction and damping measurement results [ONERA, TP NO. 1234]

15 p1830 A73-31638

Kalman-Bucy method for optimal filtering of time and space dependent random fields in Hilbert space in presence of additive white noise

15 p1854 A73-31689

Some properties of the amplitude frequency characteristics of linear automatic control systems and their control quality under random influences

15 p1854 A73-31695

Output signal-to-noise ratio for a random-access repeater link with an ideal hard limiter.

15 p1844 A73-31733

Sporadic E random electron concentration due to wind shift spectral composition, determining empirical autocorrelation functions for frequency parameters

15 p1871 A73-31885

Approximate determination of the reliability function of a digital computer

15 p1848 A73-31912

Problems of reliability theory in the mechanics of deformable solids

15 p1914 A73-32082

Macroscopic elastic constant determination for randomly reinforced composite materials by equilibrium method

15 p1954 A73-32115

Certain aspects of the asymptotic behavior of generalized random systems with complete connections

15 p1901 A73-32208

Two descriptions for the photocounting detection of radiation passed through a random medium - A comparison for the turbulent atmosphere.

15 p1914 A73-32291

Approximate synthesis method for optimal control of a system subjected to random perturbations.

15 p1915 A73-32404

Structure of pulsations of the electromagnetic field of the earth as a random function of time.

16 p2001 A73-32765

Repairable electronic system random failure and repair time related to simulator time available for operation, analyzing MTBF and repair rates

16 p1996 A73-33207

Bode's law and the preference for near-commensurability among pairs of orbital periods in the solar system.

17 p2229 A73-34429

A generalization of the equations governing the evolution of a particle distribution in a random force field.

17 p2213 A73-34449

Nonstationary response of linear time-varying dynamical systems to random excitation.

[ASME PAPER 73-APM-6]

17 p2247 A73-35031

Ionspheric drift measurements. I - A new method for ionospheric drift measurements. II - The effect of random drift velocities upon the determination of ionospheric drift velocities.

18 p2304 A73-35989

The asymptotic dispersion characteristics of the best unbiased linear estimate obtained by the uniform division of the observation interval for the unknown mathematical expectation of a stationary random process

18 p2329 A73-36162

Optimal estimation of the phase coordinates of a linear dynamic system.

18 p2294 A73-36603

On the kinetic theory of wave propagation in random media.

19 p2460 A73-38103

Internal additive interference produced by a pulsed random process.

19 p2407 A73-38353

Convergence of learning and adaptation algorithms

20 p2532 A73-38711

Choice of optimal parameters for flight-vehicle control systems in the presence of random disturbances

20 p2590 A73-38991

A programmed control task in a two-level hierarchical system under conditions of uncertainty

20 p2541 A73-39034

A nonsearching system of identification with a model, synthesized according to the hyperstability criterion

20 p2532 A73-39347

Combined density of the probability distribution of instantaneous values for the phase difference of two oscillations and for the phase difference derivatives

20 p2593 A73-39390

Development of a program basis for statistical data processing on an analog-digital complex

20 p2532 A73-39392

Discrete reproduction of a random parameter change process in standard automation equipment elements

20 p2543 A73-39393

Correlation of random phases spaced over oscillation frequencies

20 p2531 A73-39457

Investigation of the motion of a gyroscopic pendulum on a randomly vibrating base

20 p2566 A73-39504

Dynamic systems stability under influence of white noise-Gaussian random processes, discussing optical control, Markov processes, linear equations and vector fields

20 p2583 A73-39768

The description of vortex-excited oscillations of prismatic bodies by means of a sequence of pulses having random time differences

20 p2594 A73-39770

Antenna system design for detection of random gravitational waves with separation from effects of antenna random fluctuations

21 p2662 A73-40315

Use of gyro technology to measure small random angular motion.

[AIAA PAPER 73-839]

21 p2700 A73-40504

Russian book - Introduction to the statistical dynamics of systems with possible disturbances.

21 p2686 A73-40775

Nonlinear elasticity of random inhomogeneous materials reinforced by grains or oriented fibers, using Kauderer stress relation

21 p2787 A73-40987

Contribution to the theory of wave propagation in a one-dimensional randomly inhomogeneous medium

22 p2826 A73-42334

Short-wave propagation in a randomly inhomogeneous medium with an arbitrary law of permittivity fluctuations

22 p2826 A73-42335

Small angle multiple backscattering from randomly spaced cylindrical plasma cloud striations, obtaining ray density via Fokker-Planck transport equation

22 p2896 A73-43182

Problem of synthesizing a control system in the case of a plant involving random jerky forces

23 p2963 A73-43577

Non-linear creep buckling with random temperature variations.

23 p3045 A73-44166

Singular approximation in the calculation of the elastic properties of reinforced systems

24 p3145 A73-44514

An empirical Bayes estimator for the scale parameter of the two-parameter Weibull distribution.

24 p3105 A73-44577

Correlometry of ergodic nonstationary random processes

24 p3074 A73-45095

RANDOM SAMPLING

Almost sure exponential bounds for stochastic operator systems, with applications to randomly sampled control.

01 p0027 A73-10426

Management systems for quality cost accounting, time control and productivity analysis based on random time sampling technique

06 p0771 A73-17866

Bayesian MFR life test sampling plans.

08 p0973 A73-20950

Graphs, tables and discussion to aid in the design and evaluation of an acceptance sampling procedure based on cumulative sums.

13 p1709 A73-29297

High-density image-storage holograms by sampling and random phase shifter method.

15 p1876 A73-31946

Solution of the three-parameter Weibull equations by constrained modified quasilinearization /progressively censored samples/.

15 p1901 A73-32263

A consistent shape parameter estimator for the Weibull distribution. 16 p2032 A73-33602

Lower confidence bounds determination for component or system reliability by sampling with and without replacement, censored, truncated and mixed sampling test programs 16 p2033 A73-33629

Speckle reduction in holography by means of random spatial sampling. 17 p2172 A73-35429

RANDOM SIGNALS

Output signal-to-noise ratios in frequency measurement system using correlation detector. 01 p0018 A73-11183

Spatial-temporal coherent processing technique application to thermal radio emission random signal reception, deriving ambiguity function 05 p0547 A73-16057

PM signal cross-correlated receiver output SNR in presence of random misalignments with respect to carrier frequency and signal arrival time 05 p0547 A73-16058

On the dynamics of randomly excited nonlinear systems. 06 p0715 A73-17393

Limits of suitability of pseudorandom signals for statistical tests 08 p0938 A73-20835

Autocorrelation function synthesis from arbitrary function on finite interval for case of random signals 08 p0951 A73-21102

Internal additive noise generated by a random pulse process 08 p0939 A73-21395

Characteristics of the adaptive optimal detection of Gaussian signals on a pulse-noise background in receivers with a logarithmic amplifier 08 p0940 A73-21554

An optimal algorithm for measuring the dispersion of a random process in the case of separate allowance for the influence of external and internal additive noise 09 p1051 A73-22462

Equivalence of systems that follow a stochastic principle of computation 09 p1059 A73-22554

Operational algorithms for probabilistic digital integrators for Stieltjes integral and nonhypertranscendental functions 09 p1060 A73-22555

Linear decision rule for probabilistic signal estimation in image recognition problems with sampling 09 p1060 A73-22556

Complex target resolution with the random signal radar. 10 p1189 A73-24560

Optimal reconstruction of a stationary random process from discrete readings 10 p1202 A73-24611

Application of the characteristics of singular points to the determination of the period of quantization in time 11 p1340 A73-25009

Random analog signal quantization and reconstruction from discrete sample values by optimal filtration according to statistical criteria 11 p1341 A73-25013

Use of simple test signals in experimental investigations of devices for measuring the one-dimensional probability characteristics of random signals 11 p1360 A73-25019

Accuracy of statistical measurements of random field characteristics in interferometric systems 11 p1360 A73-25020

Measurements of distributed targets with the random signal radar. 11 p1332 A73-26632

Comparison of different methods of reconstitution of a signal furnished under a sampled form 13 p1582 A73-28475

Reliability estimation technique for data transmission processes in remote control systems with redundancy, assuming Markovian randomness of signal input 15 p1854 A73-31806

Isolation and sampling of random signals transmitted by several hot-wire anemometers 16 p2017 A73-34016

Transient response in a receiving system with AGC under the influence of fluctuating signals 17 p2121 A73-34591

Linear filtering of random signals according to the criterion of maximum signal-to-noise ratio. 17 p2145 A73-35719

Analysis of the operation of devices for normalizing random signals 18 p2293 A73-36851

Internal additive interference produced by a pulsed random process. 19 p2407 A73-38353

Spectral analysis and a synthesis of linear systems with variable and random parameters in finite time intervals. 20 p2540 A73-38704

Nonparametric properties of detectors optimized for Gaussian interference of unknown intensity. 20 p2529 A73-38923

Transformation of random signals by circuits containing a majoritarian element 20 p2542 A73-39046

Approximate methods for the mathematical description and analysis of processes controlling the spectral characteristics of random vector signals 20 p2542 A73-39047

Study of a correlator using two auxiliary noise sources 20 p2532 A73-39203

Antenna system design for detection of random gravitational waves with separation from effects of antenna random fluctuations 21 p2662 A73-40315

Bounds estimation for normalized second spectral moment of random radar signal process in terms of measured quantities statistics without weighting 21 p2650 A73-40343

Russian monograph on linear signal system models covering steady state, variance and transducers of continuous and discrete signals and random and nonstationary estimates 21 p2669 A73-40798

The filtering of random sequences with gaps by optimal discrete filters with a constant memory volume 21 p2658 A73-40857

Level transgressions and extremal values of continuous stochastic signals 23 p2952 A73-43310

Bispectrum synthesizer by using multiple Poisson processes. 23 p2965 A73-44089

Studies on a band limited white noise with a uniform bispectrum. 23 p2965 A73-44135

Pseudorandom Poisson process binary pulse generator, discussing digital hardware implementation and test results 24 p3069 A73-45256

Reliability estimation technique for data transmission processes in remote control systems with redundancy, assuming Markovian randomness of signal input 24 p3075 A73-45350

RANDOM VARIABLES

Asymptotic properties of eigenvalues in the Sturm-Liouville problem of a class of equations with random coefficients 01 p0070 A73-10099

Proof for sigma algebra of asymptotic events represented as sequence of partial sums of series of independent and essentially divergent random variables 01 p0070 A73-10411

Classes of limiting distributions for the sums of a random number of independent equally distributed random quantities 01 p0071 A73-11247

Steady ergodic Markovian random function construction 01 p0071 A73-11271

The behavior of a self-excited system acted upon by a sequence of random impulses. 04 p0469 A73-14664

Static analysis of beams with random material or environmental characteristics, deriving probability functions for beam descriptors 04 p0509 A73-14945

Total reflection of a plane wave by a semi-infinite random medium. 04 p0480 A73-15198

Mathematical model for independent operations complex with rectangular probability distribution of random parameters, noting time optimal control 05 p0562 A73-17282

Deformation of the power spectrum of a random function during frequency translation 06 p0664 A73-17807

Microinhomogeneous plane with a circular hole in tension 07 p0911 A73-19320

Optimal control of stochastic systems with continuous and discontinuous random disturbances, obtaining problem solution conditions for linear system via dynamic programming 07 p0805 A73-20038

Flight vehicle equations of motion with variable information, noting flight control algorithm for random variable with given probability 07 p0849 A73-20077

Randomized solutions in stochastic-programming problems 09 p1112 A73-22845

Convergence to logarithmic distribution laws 09 p1112 A73-22884

Evaluation of the convergence rate in an integral limit theorem 09 p1112 A73-22885

Random function theory method for estimation of tensile, compressive and shear strength and elastic constants of monodirectional fiberglass reinforced plastics 09 p1110 A73-23056

Bifurcation of the equilibrium of a randomly inhomogeneous nonlinearly elastic plate 09 p1165 A73-23356

Problems of accuracy in the representation of values by stochastic sequences 10 p1202 A73-24418

Normalization of stochastic system analog of linear determinate system with combined normal distribution of input/output signal, noting theorems for random variable distributions 11 p1341 A73-25632

Second order approximation to autocorrelation matrix of random variable nonlinear transformation, discussing application to Poisson process and monopulse radar receiver AGC effects 11 p1333 A73-26695

Rate of convergence of the distribution of the maximum of successive sums of independent random variables 12 p1516 A73-26958

Book - Fourier analysis in probability theory. 12 p1517 A73-27051

Asymptotic behavior of some statistical estimates. II - Limit theorems for a-posteriori density and Bayesian estimates 12 p1517 A73-27188

Strengthening of Liapunov-type estimates /case where the distributions of members are close to the normal distribution/ 12 p1517 A73-27190

Inequalities for the large deviation probabilities of sums of independent random quantities in the case of a limiting stable law 12 p1518 A73-27221

On the robustness of properties characterizing the normal distribution. 13 p1650 A73-28797

Optimal harmonic synthesis of generalized Fourier series and integrals with randomly perturbed coefficients 13 p1650 A73-28893

Exponential bounds for error and equivocation based on Markov chain observations. 13 p1651 A73-29600

Damped lateral vibration in an axially creeping beam with random material parameters. 16 p2082 A73-33902

Estimates of unknown parameter from quantized observations given as sequence of evenly distributed random values, noting optimal grouping equations for general distribution function 17 p2130 A73-35722

Normalization of stochastic system analog of linear determinate system with combined normal distribution of input/output signal, noting theorems for random variable distributions 19 p2414 A73-38143

Rate of convergence of the distribution of the maximum of successive sums of independent variously distributed random vectors toward the limiting law 20 p2583 A73-39476

Thermoelastic wave propagation in a random medium and some related problems. 21 p2789 A73-41667

Concentration functions of finite-dimensional and infinite-dimensional random vectors 22 p2882 A73-42649

RANDOM VIBRATION

A digital system for shaping, analysis and control of a random vibration spectrum 01 p0027 A73-10598

Partial optical coherence theory based Greenspon modification for calculation of sound power radiation from statistically vibrating flat surfaces 03 p0384 A73-12991

Correlation theory for equations of motion of constant thickness shallow shell vibration under random loads 03 p0387 A73-13158

Parametric vibration of simply supported rectangular plate and cylindrical shell under random excitation, using Markov process theory and Fokker-Planck equation 03 p0388 A73-13318

Analysing vibration and shock data. II - Processing and presentation of results. 05 p0637 A73-17234

Methods and techniques in spectral analysis of random-vibration data 05 p0637 A73-17271

Randomly separated ends scattering effect on linear and nonlinear coherent oscillations of elastic string by perturbation technique 06 p0723 A73-17900

Nonstationary envelope process and first excursion probability. 06 p0762 A73-18341

Response of nonlinear beam to random excitation. 07 p0916 A73-20436

Rytov method to predict random vibration amplitude and phase fluctuations range and frequency dependence in Mintzer region, noting applicability domain 08 p0988 A73-21193

- First-excursion probability in non-stationary random vibration. 13 p1691 A73-28064
- Choice of materials on the basis of random vibration and structural fatigue. 13 p1641 A73-29495
- Book - Theory of vibration with applications. 13 p1703 A73-29676
- A numerical integration method for the determination of flutter speeds. 15 p1955 A73-32163
- Distribution of the response of linear systems to Poisson distributed random pulses. 16 p2035 A73-32918
- Performance and methodology of a digital random vibration control system. 16 p1993 A73-33134
- Ranges of instability of the first and the second kind for vibrational systems with random parameter excitation. 16 p2080 A73-33264
- A statistical analysis of product reliability due to random vibration. 16 p2020 A73-33637
- Computerized finite difference method with reduced core storage requirements for solving boundary value problem of forced random vibration of rotating beam. 17 p2204 A73-35830
- Simulation of complex excitation of structures in random vibration by one-point excitation. 20 p2617 A73-39269
- Asymptotic expansion of random processes depending on a small parameter. 20 p2582 A73-39387
- Optimal control of stochastic systems with random shocks and discontinuous trajectories, using functional minimization. 20 p2582 A73-39388
- Probabilistic and deterministic solutions of random vibration response problems. 21 p2783 A73-40294
- Technical progress on new vibration and acoustic tests for proposed MIL-STD-810C, 'environmental test methods.' 21 p2674 A73-41200
- Random vibration of distributed systems strongly coupled at discrete points. 22 p2918 A73-41820
- Prediction and measurement of the proportionality constant in statistical energy analysis of structures. 22 p2918 A73-41821
- Tuned dampers for randomly excited dynamic systems. [ASME PAPER 73-DET-70] 22 p2919 A73-42070
- Automatic control theory application to random vibration passive and active isolators synthesis, considering vehicle suspension systems and electrohydraulic damper. 22 p2927 A73-42922
- Probability displacement and modal cross spectral density parameters of two span beam random vibrations under white noise. 23 p3039 A73-43304
- Eigenfunction expansions for randomly excited non-linear systems. 24 p3151 A73-45265
- Random vibrations of elastic nonlinear nonautonomous systems with variable parameters. 24 p3112 A73-45502
- RANDOM WALK**
- Transfer of resonance radiation and photon random walks. 02 p2027 A73-12403
- Application of the random walk method for solving problems in the theory of elasticity. 17 p2241 A73-34332
- The rate of separation of magnetic lines of force in a random magnetic field. 19 p2489 A73-38522
- Monte Carlo method for biharmonic boundary value problems solution, using isotropic random walk and mean value relation. 20 p2581 A73-39094
- A model of diffusion in the respiratory unit. 21 p2645 A73-41638
- RANEY NICKEL**
- U CATALYSTS
- U NICKEL
- RANGE (EXTREMES)**
- NT FREQUENCY RANGES
- NT OCTAVES
- NT RADIO RANGE
- NT ROCHE LIMIT
- Upper limits on the lunar atmosphere determined from solar-wind measurements. 02 p0211 A73-11727
- Upper bounds for long range numerical weather forecasts errors due to inadequate knowledge of frictional constants, heating and initial conditions. 02 p1918 A73-12777
- Bounds for eigenvalues in some vibration and stability problems. 03 p0390 A73-13341

The use of interval arithmetic to bound the zeros of real polynomials. 04 p0471 A73-15232

Limits of possible position of tenth planet at 50-100 AU from analysis of Neptune orbit. 05 p0622 A73-17180

Asymptotic motion stability analysis with respect to part of variables, using Liapunov functions for solution boundedness conditions. 07 p0850 A73-19012

Bounds upon the growth rate of errors in quasi-non-divergent prediction models. 13 p1652 A73-28271

Exponential bounds for error and equivocation based on Markov chain observations. 13 p1651 A73-29600

Computation of upper and lower bounds to the frequencies of elastic systems by the method of Lehmann and Maehly. 15 p1951 A73-32027

Liapunov functions and boundedness and global existence of solutions. 15 p1901 A73-32375

Upper limit to the 11.4 m flux of Saturn using VLBI. 16 p2061 A73-33221

An upper bound on the stress in plane Couette flow. [ASME PAPER 73-FE-8] 17 p2152 A73-35007

Quiet-time solar neutron flux upper limit from OGO-6 neutron detector, evaluating solar cosmic ray acceleration, nuclear reaction and energy region. 21 p2763 A73-41498

Extremum principles and error bound for a non-linear boundary value problem in the theory of laminar boundary layers. 24 p3080 A73-45340

RANGE AND RANGE RATE TRACKING

Mathematical algorithm using invariant imbedding method for accurate range and range rate estimates in terms of pulse Doppler radar ambiguity resolution. 03 p0276 A73-13902

Tropospheric refraction effects on satellite range measurements. 04 p0415 A73-14750

Position and rate aided tracking for conventional pointing systems. 04 p0430 A73-15256

Relative motion of near orbiting satellites. 10 p1283 A73-24662

Preliminary orbit determination for lunar satellites. 11 p1426 A73-26396

Ranging and data transmission using digital encoded FM-'chirp' surface acoustic wave filters. 12 p1470 A73-27571

ATS-F and Nimbus-E satellites use for range and range rate determination, earth gravity anomaly detection and orbital position determination. 13 p1656 A73-28391

Aided tracking as applied to high accuracy pointing systems. 15 p1854 A73-31726

Range and range-rate measuring equipments for communication satellites. 17 p2130 A73-35813

Satellite based ATC system with radar range and rate measurements, analyzing errors due to ground station position, transponder delay time and atmospheric refraction uncertainties. 21 p2735 A73-40042

Optimum cross-coupled tracker for pulse-Doppler radar. 21 p2649 A73-40328

RANGE CONTROL

U TRAJECTORY CONTROL

RANGE ERRORS

Missile range dispersions produced by meteorological factors, drag differences and mass changes during passive ballistic flight. 02 p0211 A73-11787

Influence of ephemerides errors on various determinations using laser lunar ranging. 11 p1417 A73-25266

LORAN range difference location system, deriving exact straight line of position on plane or spherical surface with computer-generated error maps. 11 p1333 A73-26642

An analysis of helicopter rotor modulation interference. 15 p1843 A73-31731

Correction of electrical path length by passive microwave radiometry. 16 p1983 A73-33729

Increase of error in range correction with elapsed time, evaluated by ray tracing through radiosonde-generated atmospheric models. 22 p2828 A73-43176

RANGE FINDERS

NT LASER RANGE FINDERS

NT OPTICAL RANGE FINDERS

Frequency discriminator use for range measurements with FM radar systems, deriving reflecting target distance relationship to output voltage. 03 p0278 A73-14028

On the unequal accuracy of radio range finder measurements in the reflection of radio waves from an underlying surface. 07 p0793 A73-20041

Range-azimuth-coupling aberrations in pulse-scanned imaging systems. 10 p1188 A73-23833

LORAN range difference location system, deriving exact straight line of position on plane or spherical surface with computer-generated error maps. 11 p1333 A73-26642

A scheme for estimating aircraft velocity directly from airborne range measurements. 17 p2209 A73-34873

RANGE INDICATORS

U INDICATING INSTRUMENTS

U RANGE FINDERS

RANGE MEASUREMENT

U RANGEFINDING

RANGE SAFETY

Selected analytic procedures for range safety analysis. 01 p0117 A73-11200

RANGEFINDING

NT LUNAR RANGEFINDING

A technique for synoptic measurement of ionospheric propagation delays by ranging from geostationary satellites to a network of unmanned transponders. 03 p0308 A73-13629

Application of electron content observations in navigational ranging. 03 p0275 A73-13654

Singularity solutions to critical configurations of geodetic range networks with distributed and in plane ground stations and target satellites. 04 p0436 A73-14777

Geometric accuracy obtainable from simultaneous range measurements to satellites. 04 p0436 A73-14778

Survey improvement and calibration analysis for the Air Force Eastern Test Range with Geos C. 04 p0437 A73-14786

Single point thunderstorm ranging method based on two radio frequencies field intensity spectral components ratio. 07 p0847 A73-19439

Orbit determination by range-only data. 08 p1013 A73-21816

Range instrumentation system timing error sources classification and uncertainty reduction for comparison of telemetry inertial guidance data with radar and optical data. 09 p1057 A73-23413

Ranging and data transmission using digital encoded FM-'chirp' surface acoustic wave filters. 14 p1733 A73-29935

Nonlinear filter evaluation for estimating vehicle position and velocity using satellites. 16 p1988 A73-33410

Hybrid-inertial navigation with range updates in a relative grid. [AIAA PAPER 73-873] 20 p2587 A73-38810

Communications and position fixing experiments using the ATS satellites. 21 p2733 A73-40024

Three dimensional transponders array for exact solution to positioning problem, discussing large measurements sequential interrogation effects on accuracy. 21 p2734 A73-40034

RANGELANDS

The usefulness of ERTS-1 and supporting aircraft data for monitoring plant development in rangeland environments. 20 p2563 A73-39911

RANGES (FACILITIES)

NT BALLISTIC RANGES

NT MISSILE RANGES

NT TEST RANGES

Present and future plans for the development of Sriharikota satellite launching range. 14 p1741 A73-30081

Andoya Rocket Range facilities in northern Norway, discussing rocket launching for auroral research. 14 p1741 A73-30082

Sounding rocket range facilities at Esrange /Sweden/ for auroral studies, discussing telemetry support for simultaneous launchings. 14 p1741 A73-30085

RANK TESTS

Classification of weak signals on a non-Gaussian noise background. 09 p1051 A73-22557

An asymptotically optimal rank detection algorithm for a signal in noise of unknown distribution. 15 p1842 A73-31490

Effectiveness of certain easily realizable rank algorithms for detections of signals against a background of noise. 17 p2130 A73-35720

State-space matrix rank test in locating zeros of linear multivariable systems, noting application to feedforward regulators. 23 p2964 A73-43828

RANKINE CYCLE

- 3000 hour endurance test of a 6 kWe organic Rankine cycle power system. 09 p1034 A73-22769
- Low peak temperatures and hydrodynamic bearings - Key to long life organic Rankine cycle systems. 09 p1034 A73-22770
- Experimental operation of constant temperature heat pipes. 11 p1451 A73-25989
- Vapor chamber fin radiator study for the potassium Rankine cycle. 11 p1451 A73-25991
- The design of components for an advanced Rankine cycle test facility. 11 p1344 A73-25995
- A 6 kWe organic Rankine power conversion system for space applications. 11 p1310 A73-26006
- 66 kWe ZrH reactor-organic Rankine power systems for large manned orbiting space systems. 11 p1311 A73-26014
- Isotope organic Rankine cycle electric power systems for the 150 to 1500 watt range. 19 p2456 A73-38414

RANKINE TEMPERATURE SCALE

U TEMPERATURE SCALES

RANKINE-HUGONIOT RELATION

- MHD partial differential equations solution via hyperbolic system indicating shock wave structure existence satisfying Rankine-Hugoniot relation and entropy condition 24 p3116 A73-45221

RAPCON [CONTROL]

U RADAR APPROACH CONTROL

RAPID EYE MOVEMENT STATE

- Spontaneous middle ear muscle activity in man - A rapid eye movement sleep phenomenon. 02 p0134 A73-12423
- Wakefulness and sleep states in developing organism, discussing REM sleep deprivation effects on behavior, brain excitability, pharmacology and biochemistry 03 p0265 A73-14265
- Rapid eye movement state beneficial effects on memory refuted in favor of delta wave slumber, emphasizing stage 4 sleep 06 p0653 A73-18225
- Rapid eye movement analyzer. 09 p1045 A73-22697
- A vecto-oculographic approach to fast sleep eye movements in man. 14 p1715 A73-29994
- Cholinergic activation of vestibular neurons leading to rapid eye movements in the mesencephalic cat. 18 p2272 A73-36439
- Variations of heart rate during sleep as a function of the sleep cycle. 20 p2514 A73-39762
- Similarities and differences concerning the sleep of two baboons, Papio hamadryas and Papio papio 20 p2514 A73-39764
- Spiral aftereffect durations following awakening from REM sleep and non-REM sleep. 21 p2639 A73-41179

RAPID TRANSIT SYSTEMS

- Short haul air travel with Intermodal Automated Transfer system for integrating ground transportation to allow passenger to stay in seat from origin to destination 10 p1174 A73-23653
- Subway system vertical tunnel simulation facility including plenum assembly, instrumentation, model launcher, subway car simulation models, tube scaffolding and data acquisition 16 p1994 A73-33148
- Air-ground transportation interface at airports, examining baggage handling, ticketing, security procedures, rapid transit access, in-airport time and walking distances 16 p1995 A73-33178
- Seattle-Tacoma's unconventional concept. 22 p2839 A73-42315
- The role ground transportation can play in the airport site selection process. [ASME PAPER 73-JCT-70] 23 p2966 A73-43497

RARE EARTH ALLOYS

- NT ERBIUM ALLOYS
- NT NEODYMIUM ALLOYS
- Effect of rare-earth metals on mechanical characteristics of chromium. 02 p0181 A73-12214
- Temper embrittlement response and toughness of a rare earth treated Ni-Cr-Mo steel. 02 p0183 A73-12762
- Influence of rare-earth metals on the grain growth process during recrystallization of heat-resistant steels 06 p0706 A73-17887
- Zone refining of chromium alloys with rare-earth metals 06 p0707 A73-18042
- Amorphous thin films of rare earth transition metal alloys for magneto-optic applications, noting SNR in thermomagnetically written film 11 p1409 A73-26325

Rare earth-rhodium systems intermediate phase equilibria and crystal structures, using powder X ray diffraction technique 11 p1410 A73-26569

Dislocation structure and low-temperature plasticity of chromium alloys with rare earth metals 13 p1630 A73-28011

Phase diagrams and composition selections for strengthening of multicomponent deformable Mg alloys with rare earth and transition elements 22 p2874 A73-42094

Influence of deformation on the strength and ductility of low-alloy chromium 23 p2996 A73-44290

RARE EARTH COMPOUNDS

- NT CERIUM COMPOUNDS
- NT EUROPIUM COMPOUNDS
- NT NEODYMIUM COMPOUNDS
- NT SAMARIUM COMPOUNDS
- NT SCANDIUM COMPOUNDS
- NT SCANDIUM OXIDES
- NT THULIUM COMPOUNDS
- NT YTTERBIUM COMPOUNDS
- Phase equilibria in V-N-Sc/Y, Ce, Pr/ alloys 09 p1108 A73-23238
- Some physicochemical properties of compounds formed by oxides of rare-earth elements and barium 11 p1410 A73-26673
- Lattice constants vs compositions of body centered tetragonal solid solutions of mixed rare earth dicarbides according to Vegard law 21 p2751 A73-40322
- Preparation of lanthanum sulfides using carbon disulfide as a sulfurizing agent and the change of these sulfides on heating in air. 23 p3018 A73-44130

RARE EARTH ELEMENTS

- NT CERIUM
- NT DYSPROSIUM
- NT ERBIUM
- NT EUROPIUM
- NT EUROPIUM ISOTOPES
- NT GADOLINIUM
- NT HOLMIUM
- NT LANTHANUM
- NT NEODYMIUM
- NT PROMETHIUM
- NT SAMARIUM
- NT SCANDIUM
- NT YTTERBIUM
- NT YTTRIUM
- Effects of rare earth elements on the oxidation resistance of iron and nickel base alloys. 04 p0465 A73-15584
- The chemical composition of soil from the Apollo 16 and Luna 20 sites. 05 p0546 A73-16831
- Rare earths and other trace elements in Apollo 14 samples. 07 p0886 A73-19760
- Precise determination of rare-earth elements in the Apollo 14 and 15 samples. 07 p0886 A73-19762
- Electron-hole processes in CaF2 crystals doped with rare-earth ions 07 p0837 A73-20208
- Fine structures of mutually normalized rare-earth patterns of chondrites. 07 p0789 A73-20620
- Influence of rare-earth metal dust containing radioactive components on the development of reticulosarcoma of the lungs 10 p1183 A73-23680
- Variation in the kinetics of the natural aging process for Mg-Li-Al alloys as a function of the presence of impurities and small additions of rare-earth elements 12 p1510 A73-26911
- Distribution coefficients and solubility curves of certain rare-earth elements in GaAs 12 p1531 A73-27194
- Luna 20 and Apollo 16 lunar soil samples rare earth, iron and other trace elements contents from neutron activation analysis, noting Eu anomaly 13 p1675 A73-28317
- Application of an extended method of calculation to rare-earth atoms and ions in the 4fN configuration 14 p1784 A73-30852
- Effect of rare earth metal additions on the recrystallization of nickel 14 p1765 A73-30887
- Rare-earth elements, Co, Sc and Hf in the Steens Mountain basalts. 15 p1874 A73-32389
- Effect of chemically activated elements on the properties of electron-beam-melted nickel 21 p2718 A73-40482
- Spectral determination of rare-earth components in Seignette-ceramic and piezoceramic materials 21 p2752 A73-40555
- Chromium-rare-earth energy transfer in YAlO3. 21 p2752 A73-40957
- Ternary systems: Rare earth metal - iron family metal - silicon /Component interaction and crystal structures of compounds/ 22 p2873 A73-42084

Stimulation of two-valent rare earth ion luminescence in CaF2 crystals by ruby and neodymium lasers 22 p2870 A73-42725

Rare-earth elements in matrix, inclusions, and chondrules of the Allende meteorite. 24 p3133 A73-44539

RARE GASES

- NT ARGON
- NT ARGON ISOTOPES
- NT HELIUM
- NT HELIUM ATOMS
- NT HELIUM FILM
- NT HELIUM ISOTOPES
- NT LIQUID HELIUM
- NT LIQUID HELIUM 2
- NT NEON
- NT NEON ISOTOPES
- NT RADON
- NT RADON ISOTOPES
- NT XENON
- NT XENON ISOTOPES
- NT XENON 129
- Theoretical treatment of the translational absorption spectrum induced in mixtures of rare gases 01 p0079 A73-10500
- French monograph - Contribution to the experimental study of the integrated intensity of the translational absorption bands induced in pressurized rare-gas mixtures. 01 p0080 A73-10601
- French monograph - Experimental study of the thermal conductivity of rare gases and helium-argon mixtures as functions of temperature and pressure. 01 p0120 A73-10604
- Analytical model potential function application to Ar, Kr, Xe, nitrogen, methane and carbon dioxide, applying to different properties 01 p0122 A73-10850
- Metal vapor crystallization in rare gas atmosphere for powder production, noting particle size distribution control 02 p0172 A73-11545
- Kinetics of the deactivation of the vibrations of highly excited oscillators in an inert gas medium with allowance for spontaneous emission 02 p0194 A73-11607
- Thermal energy charge transfer reactions of rare-gas ions to methane, ethane, propane, and silane - The importance of Franck-Condon factors. 02 p0195 A73-12084
- Rare gases in the regolith from the Sea of Fertility. 02 p0212 A73-12229
- A device for working with extraterrestrial material in an inert-gas medium 02 p0151 A73-12465
- Ion density and electron temperature calculations for metallic plasma population inversion possibility by near resonant charge exchange with inert gas ions 02 p0194 A73-12847
- Breakdown thresholds in rare and molecular gases using pulsed 10.6-micron radiation. 02 p0195 A73-12859
- Cosmogenic rare gas production rates in chondritic meteorites. 03 p0375 A73-14107
- The light emission of the column plasma in current-modulated noble-gas discharges at intermediate pressures 03 p0348 A73-14621
- Rare-gas analyses on neutron irradiated Apollo 12 samples. 07 p0889 A73-19798
- Noble gas studies on regolith materials from Apollo 14 and 15. 07 p0889 A73-19799
- Trapped solar wind noble gases in Apollo 12 lunar fines 12001 and Apollo 11 breccia 10046. 07 p0871 A73-19800
- Inert gases from Apollo 12, 14, and 15 fines. 07 p0889 A73-19801
- Apollo 14 and 15 lunar rocks and soils rare gas content via fast neutron irradiation, noting radioactive age determination 07 p0889 A73-19802
- Classification and source of lunar soils; clastic rocks; and individual mineral, rock, and glass fragments from Apollo 12 and 14 samples as determined by the concentration gradients of the helium, neon, and argon isotopes. 07 p0889 A73-19804
- A comparison of noble gases released from lunar fines /no. 15601.64/ with noble gases in meteorites and in the earth. 07 p0889 A73-19806
- Noble gases concentration profiles in lunar fines and minerals, investigating thermal release patterns 07 p0889 A73-19807
- The use of the thermal accommodation coefficients of a rare gas for studying the adsorption of an active gas on a metal, such as in the case of nitrogen and oxygen on tungsten 07 p0839 A73-20150

Noble gas measurement in powdered aliquots of eleven H-chondrites, using Reynolds type mass spectrometer

07 p0789 A73-20623

Inert-gas transport in liquid metals during boiling experiments.

08 p1023 A73-21263

Studies in molecular dynamics by collision-induced infrared absorption in H₂-rare gas mixtures. I - Profile analysis and the intercollisional interference effect.

08 p0990 A73-21630

Fire retardance of mixtures of inert gases and oxygen.

09 p1045 A73-22532

An approximate analysis of the diffusing flow in a self-controlled heat pipe.

[ASME PAPER 72-HT-M]

10 p1295 A73-23776

Noble gas and carbon abundances of the Haverro, Dingo Pup Donga, and North Haig urelites.

10 p1277 A73-24104

Calculation of electron energy flux distributions in noble gases.

11 p1401 A73-25144

EEG activity of rats compressed by inert gases to 700 feet and oxygen-helium to 4000 feet.

11 p1314 A73-25327

Depth variation of cosmogenic noble gases in the approximately 120-kg Keyes chondrite.

11 p1418 A73-25587

Vibrational relaxation in hydrogen-rare-gases mixtures.

11 p1402 A73-25969

Photoabsorption cross sections of H₂, D₂, N₂, O₂, Ar, Kr, and Xe at the 584-A line of neutral helium.

12 p1465 A73-26989

Deterioration of impermeable alumina tubes in inert atmospheres at elevated temperatures.

12 p1515 A73-27032

Inert gas injection for W-Re thermocouple wire corrosion protection during temperature measurement in aggressive media

12 p1497 A73-27319

Physiological effect of air nitrogen replacement by inert gases under high and low temperature conditions

12 p1465 A73-27701

Inert gases in a terra sample - Measurements in six grain-size fractions and two single particles from Lunar 20.

13 p1675 A73-28318

Studies of noble-gas lasers for continuous operation

13 p1627 A73-28790

Solubilities of noble gases in magnetite - Implications for planetary gases in meteorites.

13 p1684 A73-29182

Russian book - Geochemistry and cosmochemistry of inert gas isotopes.

15 p1840 A73-31585

Quantum oscillators employing the luminescence of self-localized excitons in condensed inert gases

15 p1885 A73-31714

An apparatus for work with extraterrestrial water in an inert gas atmosphere.

15 p1859 A73-32615

Noble gas isotopes abundances for solar wind and outer convective zone of sun, emphasizing isotopic abundance of deuterium

17 p2228 A73-34416

The A, B, C's of trapped helium, neon, and argon in meteorites and lunar samples.

17 p2228 A73-34417

Experiment and observation of isotope and element separation in a plasma with cosmical applications.

17 p2216 A73-34420

Apollo 17 mass spectrometer indication of rare gases and molecular hydrogen in lunar atmosphere, confirming noncondensable gas model

18 p2349 A73-35973

Investigation of the discharge structure in a noble gas alkali MHD generator plasma. I.

18 p2338 A73-36303

Infrared spectrum and geometry of ozone isolated in inert gas matrices at 20.4 K.

19 p2463 A73-37904

Effect of noble gases on an atmospheric greenhouse /Titan/.

19 p2487 A73-38173

A possibility of creating a new type of thermionic converter

19 p2392 A73-38560

Experimental results concerning the time decay of the line emission in luminescent plasmas of medium-pressure inert-gas discharges

20 p2596 A73-39191

Evidence for solar flare rare gases in the Khor Temiki aubrite.

21 p2764 A73-40231

Stimulated emission in multiple-photon-pumped xenon and argon excimers.

21 p2713 A73-40456

Trapped solar wind noble gases and exposure age of Luna 16 lunar fines.

21 p2770 A73-41001

Helium, neon and argon in Level C of Luna 16 fines.

21 p2770 A73-41004

Polarization of rare gas atoms in the successive layers adsorbed on graphite

21 p2724 A73-41599

State variables and transport coefficients of binary gaseous mixtures. II - The binary interaction between identical and nonidentical molecules

[DFVLR-SONDDR-279]

22 p2931 A73-42374

Experimental study of the thermal conductivity coefficient of noble gas mixtures at low and moderate densities.

22 p2932 A73-42503

The temperature dependence of viscosity and thermal conductivity of dilute noble gases at moderate and high temperatures.

22 p2932 A73-42504

Interferometric measurement of thermodynamic variables of rare gas plasmas produced by shock waves

22 p2896 A73-43168

Influence of the magnetic field on electrodeless-discharge plasmas

23 p3009 A73-43654

Track density gradient and light noble gas isotope analysis of lunar breccia, postulating higher solar flux densities during early brecciation history

23 p2950 A73-43766

Rare gas diffusion studies in individual lunar soil particles and in artificially implanted glasses.

23 p3031 A73-43769

RAREFACTION

A study of the rarefaction of the interaction between an exhaust plume and a hypersonic external flow.

[AIAA PAPER 73-199]

06 p0645 A73-17657

Vela 3 proton data analysis for compressions and rarefactions effects on solar wind density, temperature and velocity behavior

24 p3125 A73-45106

RAREFACTION WAVES

U ELASTIC WAVES

RAREFIED GAS DYNAMICS

Cryoprobe with truncated circular cross sectioned Cu cone with copper slug heat sink for momentum flow rate measurement in hypersonic low density flow

01 p0003 A73-10755

Hypersonic spherical source flow expansion into rarefied atmosphere of same gas, using kinetic model and asymptotic solution of Boltzmann equation

02 p0154 A73-12054

Similarity solutions for spherically and cylindrically symmetric gas expansions in rarefied atmospheres, taking into account ambient pressure effect

02 p0154 A73-12055

Investigation of the effect of the nozzle cone angle on the parameters of a rarefied gas flow

03 p0245 A73-13624

Circular orifice flow of monatomic rarefied gas between two reservoirs, observing pressure ratio effect

03 p0295 A73-13773

Hypersonic rarefied flow past an insulated flat plate with suction/injection.

04 p0520 A73-15939

Effect of accommodation coefficient on thermal creep flow of rarefied gas.

04 p0436 A73-15973

Book - Progress in aerospace sciences.

05 p0627 A73-16176

Some problems of gas-solid surface interaction.

05 p0638 A73-16177

Measured axial and normal force coefficients for 9-deg cones in rarefied, hypersonic flow.

[AIAA PAPER 73-154]

05 p0531 A73-16902

Mean free path of molecules from a surface in rarefied flow with application to correlating drag data.

[AIAA PAPER 73-198]

05 p0531 A73-16933

Numerical computation of the hypersonic rarefied flow near the sharp leading edge of a flat plate.

[AIAA PAPER 73-200]

05 p0531 A73-16934

Numerical solution to kinetic equations of rarefied supersonic steady gas flow normal to plate by method of characteristics

06 p0643 A73-17461

Use of a paraboloidal layer to study gas-wall interaction

06 p0685 A73-17772

Effects of Compton scattering in a moving gas

07 p0853 A73-20308

Free molecular flow past a flat plate in the presence of a nontrivial gas-surface interaction.

08 p0926 A73-21401

Investigation of the applicability of some statistical models to the shock-wave structure problem

08 p0956 A73-21606

Error analysis of approximate formula for transform of rarefied gas particle reflection from homogeneous anisotropic random surface

09 p1123 A73-22615

Flow of a supersonic nitrogen jet and of a low-density nitrogen-hydrogen mixture around a blunt body

10 p1171 A73-23582

Molecular gas dynamics, considering molecules in internal degrees of freedom, Navier-Stokes and Knud-

sen layer boundary conditions, heterogeneous reactions, evaporation, condensation and surface shocks

10 p1251 A73-23865

Weakly rarefied gas flow described by simplified Barnett equations, analyzing boundary layer structure

10 p1172 A73-24491

Fluid turbulence equations for large molecular drift velocity gradients in rarefied gas, near surface and stellar system motions, using Predvoditelev hydrodynamic equations

11 p1347 A73-25733

Compton-scattering effects in a moving gas.

12 p1526 A73-27280

Kinetic phenomena in a Knudsen gas with rotational degrees of freedom

12 p1530 A73-27982

Translational temperature and atomic velocity distribution functions in rarefied binary gas jets by electron beam excited Doppler line measurement

13 p1618 A73-29163

Measurement of rarefied gas flow rates from the drift of an ion mark produced by an electron beam

13 p1619 A73-29167

Diffusion processes in the mixing zone of a low-density supersonic jet

13 p1567 A73-29170

The flow of highly rarefied gases.

14 p1744 A73-29997

Test of statistical models for gases with and without internal energy states.

14 p1818 A73-30653

Application of the Poisson stochastic process for collision relaxation calculations in a nonequilibrium gas

15 p1915 A73-30968

Solution of the plane problem of rarefied-gas aerodynamics on the basis of the Boltzmann kinetic equation

15 p1822 A73-31244

Longitudinal rarefied diatomic and monatomic gas flows past elongated plates

15 p1822 A73-31293

Book - Advances in applied mechanics. Volume 12.

15 p1950 A73-31972

Interplanetary gas dynamics, discussing solar atmospheric structure, plasma kinetics, continuous flows, collective particle behavior, hydrodynamic coronal and free expansions

15 p1939 A73-31975

Dynamic pressure transducer system for pulsed plasma flow diagnosis.

15 p1876 A73-31977

Dispersion of gravitational waves by a collisionless gas.

16 p2036 A73-33122

Poiseuille flow and thermal creep of a rarefied gas between parallel plates.

16 p2085 A73-33315

Thermal creep of rarefied gas in a circular tube.

16 p2039 A73-33328

The interaction of a transient exhaust plume with a rarefied atmosphere.

16 p2086 A73-33873

Low-density jets behind a sonic nozzle at large pressure gradients

17 p2150 A73-34263

Three dimensional dynamo theory in the magnetosphere.

17 p2158 A73-34503

Applications of a ray reflection model in the problem of highly rarefied gas flow past bodies.

17 p2094 A73-34549

Nonlinear radial wave propagation in low density expanding flows with application to the free jet.

18 p2300 A73-36630

Cylindrical Poiseuille flow and thermal creep of a rarefied gas.

18 p2300 A73-36635

Expansion of a plasma from a spherical source into a vacuum.

19 p2465 A73-37176

A modulation technique for measuring small disturbances in the upstream flow field of a sharp leading edge in a rarefied hypersonic flow.

19 p2377 A73-37714

Unique solution of boundary value problem of Boltzmann equation for unsteady rarefied gas flow of formless particles past arbitrary surface

19 p2462 A73-37843

Analysis of rarefied gas flow through an arbitrary cross section by the finite element method.

20 p2549 A73-39528

Simulation of the flow past a high-altitude ion-concentration sensor

21 p2633 A73-41223

Rarefied gas flows based on variational principle.

22 p2840 A73-41741

Dynamical evolution of an expanding gas cloud.

22 p2840 A73-41758

Rarefied-gas heat transfer in Knudsen layer using ellipsoidal model.

22 p2932 A73-42471

The temperature dependence of viscosity and thermal conductivity of dilute noble gases at moderate and high temperatures. 22 p2932 A73-42504

Gaskinetic treatment of the Rayleigh problem in the case of moderately to greatly diluted gases 22 p2843 A73-42529

Heat transfer in plane Couette flow of rarefied gas between parallel plates, determining temperature jumps at plates from transfer equations 23 p3048 A73-43206

Rarefied gas flow through an orifice at low pressure gradients 23 p2969 A73-44347

Expansion of a plane rarefied gas layer into a vacuum 24 p3076 A73-44655

A variant of the Monte-Carlo method for solving the linear dynamics problems of a rarefied gas 24 p3076 A73-44660

New kind of boundary layer over a convex solid boundary in a rarefied gas. 24 p3080 A73-45453

RAREFIED GASES

NT COSMIC GASES

NT INTERPLANETARY GAS

NT INTERSTELLAR GAS

Heat transfer from a circular cylinder in a rarefied gas stream. 01 p0122 A73-10761

Effect of gas-surface interaction on the transmission of sound through a collisionless gas. 01 p0077 A73-10972

Influence of roughness on the process of interaction between a rarefied gas and the surface of a solid 02 p0194 A73-11608

Rarefied gas interaction with spacecraft surface, calculating aerodynamic forces and accommodation coefficient for Proton 7 satellite 03 p0383 A73-14574

Investigation of heat transfer in a rarefied molecular gas with the aid of the Senftleben effect 11 p1453 A73-26445

Diameter reduction rate and time dependence of corresponding temperature variation of liquid drop unsteady evaporation in rarefied ambient gas 12 p1558 A73-27392

State variables and transport coefficients of binary gaseous mixtures. III - The calculation of transport coefficients with the aid of consistent potential parameters [DFVLR-SONDDR-280] 22 p2931 A73-42375

Experimental study of the thermal conductivity coefficient of noble gas mixtures at low and moderate densities. 22 p2932 A73-42503

Relationships between forces acting on bodies moving in a rarefied gas, in a light flux, and in hypersonic Newtonian flow 24 p3055 A73-45532

RAREFIED PLASMAS

Pulsed UV-radiation source for producing highly ionized low-density initial plasmas 01 p0082 A73-10325

Integral of collisions for a rarefied plasma/Quantum theory/ 01 p0086 A73-11287

Low-frequency oscillations in a bounded low-density plasma. 02 p0198 A73-12105

Comparison of theory with experiment for electron density distribution in the near wake of an ionospheric satellite. 04 p0444 A73-15541

Propagation of electromagnetic waves in a rarefied plasma which has been placed in an alternating magnetic field. 06 p0726 A73-17402

Damping of an ion acoustic wave in a weakly ionized plasma 06 p0730 A73-18460

Transport equations for dilute plasma in a magnetic field. 07 p0860 A73-20479

Heating of a substance by short laser pulses 10 p1230 A73-24885

Cosmic dilute collisionless plasma physical properties, discussing plasma wave turbulence characteristics, particle acceleration, relativistic plasmas, synchrotron emission, pulsars and galactic nuclei 12 p1537 A73-26850

Partial trapping of a low-density plasma by an RF quasipotential well. 14 p1779 A73-29917

Solar wind interpenetrating ion streams from Imp 6 electrostatic analyzer measurements, considering origin due to interplanetary high velocity filaments merging into rarefied plasma regions 14 p1786 A73-29954

Experiments on CO2-laser heating of magnetically confined underdense plasmas. 14 p1780 A73-30123

Plasma and fields in the vicinity of a rapidly moving body in the presence of an external magnetic field 15 p1919 A73-31880

Structure of the current front of an electron-acoustic wave in a plasma 15 p1920 A73-32301

German monograph - Investigations regarding the structure of planar boundary layers between magnetic field and plasma. 15 p1921 A73-32584

Similarity in the flow of a magnetized plasma around a plate and cylinder 17 p2215 A73-34260

Rarefied collisionless plasma turbulence and dissipation process due to instability, examining magnetic field effects on shock wave front nature 19 p2464 A73-37154

Laminar boundary layers in low pressure argon plasma. 19 p2464 A73-37163

A review of electrostatic probe response in a flowing, low density plasma. 19 p2465 A73-37165

System for calibrating on-board instruments and for laboratory simulation of low-density plasma flows past models 19 p2417 A73-37351

Unsteady shock waves in a rarefied plasma 20 p2597 A73-39277

MPD annular duct flows in crossed external fields for arbitrary values of the Hall parameter 20 p2599 A73-39675

Magnetohydrodynamic waves in the solar wind plasma 21 p2763 A73-41506

Heating with short laser pulses. 21 p2717 A73-41660

Ion acceleration upon expansion of a rarefied plasma. 22 p2890 A73-41724

Electron wave excitation and propagation in low density large volume plasmas near electron Langmuir frequency 22 p2891 A73-42241

Collision integral for a low-density plasma/quantum theory/. 23 p3009 A73-43508

Structure of the current front of an electron-acoustic wave in a plasma. 24 p3114 A73-44609

RASERS

U MASERS

RATE METERS

U MEASURING INSTRUMENTS

RATE OF CLIMB INDICATORS

Glider soaring flight energy budget analysis, discussing rate of climb indicator error compensation 08 p0968 A73-21656

Electronic systems for time constant and altitude error compensation of rate of climb indicator used in high performance glider flight 10 p1222 A73-24916

RATES [PER TIME]

NT ACCELERATION [PHYSICS]

NT ACOUSTIC VELOCITY

NT AIRSPEED

NT ANGULAR ACCELERATION

NT ANGULAR VELOCITY

NT ARRHYTHMIA

NT BRADYCARDIA

NT BURNING RATE

NT COLLISION PARAMETERS

NT COLLISION RATES

NT CRITICAL VELOCITY

NT CURRENT DENSITY

NT DECAY RATES

NT DECELERATION

NT DRIFT RATE

NT ELECTRON DECAY RATE

NT ELECTRON FLUX DENSITY

NT ESCAPE VELOCITY

NT EVAPORATION RATE

NT EXHAUST VELOCITY

NT FLOW VELOCITY

NT FLUX [RATE]

NT FLUX DENSITY

NT GROUND SPEED

NT GROUP VELOCITY

NT HEART RATE

NT HEAT FLUX

NT HIGH ACCELERATION

NT HIGH GRAVITY ENVIRONMENTS

NT HIGH SPEED

NT HYPERSONIC SPEED

NT HYPOVENTILATION

NT ILLUMINANCE

NT IMPACT ACCELERATION

NT ION PRODUCTION RATES

NT IRRADIANCE

NT LANDING SPEED

NT LIGHT SPEED

NT LOADING RATE

NT LOW SPEED

NT LUMINANCE

NT LUMINOUS INTENSITY

NT MAGNETIC FLUX

NT MASS FLOW RATE

NT NEUTRON FLUX DENSITY

NT ORBITAL VELOCITY

NT PARTICLE ACCELERATION

NT PARTICLE FLUX DENSITY

NT PHASE VELOCITY

NT PHOTON DENSITY

NT PHYSIOLOGICAL ACCELERATION

NT PLASMA ACCELERATION

NT PROPAGATION VELOCITY

NT PROTON FLUX DENSITY

NT PULSE RATE

NT RADIAL VELOCITY

NT RADIANCE

NT RADIANT FLUX DENSITY

NT RECOMBINATION COEFFICIENT

NT RELATIVISTIC VELOCITY

NT RESPIRATORY RATE

NT ROTOR SPEED

NT SOLAR CONSTANT

NT SOLAR FLUX

NT SOLAR FLUX DENSITY

NT SOLAR VELOCITY

NT SOUND INTENSITY

NT SPIN REDUCTION

NT STRAIN RATE

NT SUBSONIC SPEED

NT SUPERSONIC SPEEDS

NT SYSTOLE

NT TACHYCARDIA

NT TERMINAL VELOCITY

NT TIP SPEED

NT TRANSONIC SPEED

NT WIND VELOCITY

RATINGS

Book - ASTM manual for rating motor, diesel, and aviation fuels. 06 p0740 A73-18402

Nonadjectival rating scales in human response experiments. 17 p2117 A73-35400

RATIONAL FUNCTIONS

Choice of a rational control law for control systems for delayed objects subjected to random load disturbances. 04 p0429 A73-15202

Conformal mapping of two airfoil profiles symmetric with respect to real axis onto circles, using rational function power series 07 p0812 A73-20200

Features of the application of the root-locus method to the study of sampled-data automatic systems on the basis of the w-transform 09 p1068 A73-22341

Degeneracy phenomenon in minimax rational approximation behavior in neighborhood of approximating function pole 13 p1650 A73-29396

Algebraic criteria for positive realness relative to the unit circle. 16 p2032 A73-33162

On the generation of rational function approximations for Laplace transform inversion with an application to viscoelasticity. 16 p2032 A73-33307

Contribution to the theory of biplane wing sections. 17 p2091 A73-34325

Algebraic algorithm for positive realness of real rational functions and matrices relative to unit circle in complex plane, determining real polynomial zeros distribution 19 p2446 A73-38488

Recursive formulas for the partial fraction expansion of a rational function with multiple poles. 21 p2660 A73-40097

RATIOS

NT ASPECT RATIO

NT DIMENSIONLESS NUMBERS

NT FROUDE NUMBER

NT FUEL-AIR RATIO

NT GRASHOF NUMBER

NT HIGH ASPECT RATIO

NT INDEXES [RATIOS]

NT LEWIS NUMBERS

NT LIFT DRAG RATIO

NT LOW ASPECT RATIO

NT MACH NUMBER

NT MASS RATIOS

NT NUSSELT NUMBER

NT OPTICAL REFLECTION

NT PECLET NUMBER

NT PERVEANCE

NT POISSON RATIO

NT PRANDTL NUMBER

NT RAYLEIGH NUMBER

NT REYNOLDS NUMBER

NT RICHARDSON NUMBER

NT SCALE [RATIO]

NT SIGNAL TO NOISE RATIOS

NT SIMILARITY NUMBERS

NT STANDING WAVE RATIOS

NT STANTON NUMBER

NT STRESS RATIO

NT STROUHAL NUMBER

NT THICKNESS RATIO

NT THRUST-WEIGHT RATIO

NT VOID RATIO

Uniqueness of Chebyshev approximation representation by ratios of exponential functions with restricted number of zeros 13 p1651 A73-29400

RAWINSONDES

Life cycle of brief CAT episodes determined by mesoscale analysis. 03 p0338 A73-14533

High-level circulation studies based on rawinsonde, rocketsonde and satellite observations. 18 p2350 A73-36040

Clear air turbulence mesoscale history from sequential analysis of rawinsonde stations network observed data 21 p2728 A73-40057

RAY TRACING

Ray optical procedure to obtain scalar Green function for polygonal waveguides by image diagram identification from rectangular guide equivalent combinations 01 p0024 A73-10684

Infrasound in the ionosphere generated by severe thunderstorms. 01 p0040 A73-10826

Beam spread of laser light propagating through the atmosphere. 01 p0060 A73-11056

Satellite transmitted impulse response transfer function evaluation by ray tracing technique for ionospheric model with Chapman ionization vertical profile 03 p0299 A73-13630

Propagation of electromagnetic waves in media which vary slowly with position and time. 04 p0423 A73-15483 [AD-75394]

Determination of the effective angular distance between the reflection points of an ordinary ray and an extraordinary ray by the interference method 05 p0548 A73-16259

Passage of medium-frequency radio waves through the ionosphere 05 p0550 A73-16395

Wave normal and ray propagation in lossless positive bianisotropic media. 06 p0723 A73-17875

Triangular obstacle caused microwave shadow zone diffraction pattern calculation by ray optics theory, comparing with scale model test results 06 p0666 A73-18201

Evaluation of the wavefront aberration in holography. 08 p0963 A73-21013

Three-dimensional acoustic-ray tracing in an inhomogeneous anisotropic atmosphere using Hamilton's equations. 08 p0988 A73-21190

Second-order corrections for ionospheric radio-wave propagation 08 p0939 A73-21287

Further studies of backscattering from a finite cone. 10 p1191 A73-24898

Small scale loop structuring of F region ionogram traces due to HF ray propagation through irregularities 11 p1354 A73-25766

Automatic sensor with parabola null test and ray intercept error measurement for optical system wave front error determination, noting interferometric sensitivity 11 p1365 A73-26242

Employment of mode theory and ray theory for the interpretation of very-long-wave measurements at medium distances 12 p1474 A73-27769

Eikonal properties for real rays chromatic aberration formulas in terms of path length, image space and lens parameters 13 p1660 A73-28768

The illumination distribution in the image plane from the radiation of a plane-parallel plate with the actual ray paths taken into consideration. 13 p1621 A73-29325

Ionospheric model impulse response transfer functions phase and amplitude dependence on profile parameters and TE C, using ray tracing technique 14 p1728 A73-30231

Flux density for ray propagation in discrete index media expressed in terms of the intrinsic geometry of the deflecting surface. 15 p1913 A73-31135

Angular diameter calculation of Ellis atmospheric window via ionospheric wave ray tracing technique 15 p1844 A73-32048

Ray models for sound propagation and attenuation in ducts, in the absence of mean flow. 15 p1865 A73-32153

Three dimensional ionograms synthesis method, considering quasi-parabolic layer ionospheric model application and ray path parameters 15 p1845 A73-32232

Angle-of-arrival difference spectrum of a simple interferometer in turbulent air. 16 p2037 A73-33683

The influence of the sea evaporation duct on the phase of the received field on a line-of-sight path. 16 p1981 A73-33713

Correction formulas for aerial photograph distortions due to internal refraction of light rays in separation of gas media by lateral surface of circular cylinder 16 p2038 A73-34050

Wavefront investigation of a Fourier transform lens with the fan trace interferometer. 17 p2172 A73-35427

Second-order corrections for radio-wave propagation through the ionosphere. 19 p2404 A73-37916

Passage of pulses through an inhomogeneous plasma medium 19 p2406 A73-38329

Electromagnetic scattering by discontinuities in weakly inhomogeneous parallel plane waveguides or ducts, noting edge diffraction singularities role from ray optical calculation 20 p2528 A73-38847

Effects of collisions on whistler-mode ray tracing. 20 p2531 A73-39404

Analysis of ground tests of a microwave, earth-occultation, pressure-reference-level system. 21 p2729 A73-40065

Wave amplitude calculation for propagation in inhomogeneous isotropic media by optical ray tracing consisting of integration of first and second order differential equations 22 p2885 A73-41817

Increase of error in range correction with elapsed time, evaluated by ray tracing through radiosonde-generated atmospheric models. 22 p2828 A73-43176

Small angle multiple backscattering from randomly spaced cylindrical plasma cloud striations, obtaining ray density via Fokker-Planck transport equation 22 p2896 A73-43182

Propagation of shock waves in anisotropic composite plates. 24 p3149 A73-45149

RAYLEIGH DISTRIBUTION

Best linear unbiased estimator of the parameter of the Rayleigh distribution. I - Small sample theory for censored order statistics. 09 p1112 A73-22645

Fluctuation loss and diversity gain for in-phase systems with post-detection integration. 13 p1586 A73-29218

RAYLEIGH EQUATIONS

A variational solution of the Rayleigh problem for a power law non-Newtonian conducting fluid. 03 p0347 A73-13790

RAYLEIGH NUMBERS

Longitudinal rolls and Benard cells in water layer natural convection, predicting wavelength-depth relations and Rayleigh numbers for comparison with experiments [AIAA PAPER 73-42] 06 p0684 A73-17623

Certain feedbacks generated during turbulent cellular convection in the atmosphere 08 p0986 A73-21456

Periodic semi-integral solutions of secondary unsteady convective flows in external force field for critical Rayleigh numbers by Liapunov-Schmidt method 10 p1204 A73-23584

Natural convection in a sloping porous layer. 11 p1449 A73-25220

A model for investigating eddy viscosity effects on mesoscale cellular convection. 11 p1393 A73-25716

Convection near critical Rayleigh numbers in the case of an almost vertical temperature gradient 11 p1453 A73-26435

Numerical experiments for the determination of characteristic dimensions and intensities of convection cells 15 p1902 A73-31138

Experimental study of the stability of differentially heated inclined air layers. 17 p2256 A73-35847

Some further studies on the transition to turbulent convection. 23 p3003 A73-43935

Air flow in circular convection chamber, investigating transition to turbulence by simultaneous measurements of heat flux and temperature field at low Rayleigh number 24 p3157 A73-45311

The effect of rotation on nonlinear thermal convection. 24 p3158 A73-45559

RAYLEIGH SCATTERING

Spectral composition of thermal and stimulated light scattering in the wing of the Rayleigh line 02 p0194 A73-11945

Scattering of a light pulse by a spherical particle 03 p0345 A73-13752

Rayleigh and Brillouin scattering from fluids in thermal equilibrium and light scattering from macromolecules in solution, discussing light and medium properties interrelationship 05 p0583 A73-16345

Scattering of a transverse elastic wave by an elastic sphere in a solid medium. 06 p0737 A73-18351

Rayleigh scattering influence on stimulated Raman effect, determining occurrence conditions for absolute instability due to feedback 06 p0702 A73-18593

Determination of parameters of laser-induced plasma in air by a scattering method. 06 p0732 A73-18610

Polarization measurement of clear sky light and comparison with theoretical data 07 p0818 A73-19590

A direct solution of the radiative transfer equation - Application to Rayleigh and Mie atmospheres. 07 p0852 A73-20220

Matrix operator theory of radiative transfer for Rayleigh scattering and radiance calculation of multilayered atmospheres with large optical depths 08 p0958 A73-21040

Investigation of long-chain molecule dynamics in condensed state by the IR-spectroscopy and Rayleigh-scattering methods 09 p1122 A73-21956

Light scattering from weakly ionized nonhomogeneous plasmas. 11 p1405 A73-25971

Light scattering from independent particles - Non-gaussian correction to the clipped intensity correlation function. 13 p1658 A73-28208

Role of exchange in shifted scattering of light for a double hole 13 p1660 A73-28760

Matrix operator theory of radiative transfer. II - Scattering from maritime haze. 14 p1749 A73-30163

Rayleigh-fast Fourier transformation techniques for electromagnetic scattering over rough sinusoidal surface, comparing numerical validity with perturbation, physical optics and integral equation methods 14 p1728 A73-30230

Generalisation and application of Rayleigh's theory of sound scattering 14 p1775 A73-30893

Experimental studies on the scattering pattern from a ruby laser rod. 16 p2023 A73-32875

Non-critical Rayleigh scattering from pure liquids. 20 p2570 A73-38618

Self consistent microscopic theory of Rayleigh light scattering by molecular aggregates based on random phase modulation and stochastic theories 21 p2739 A73-40219

Variations in the stratospheric ozone field inferred from Nimbus satellite observations. 23 p2975 A73-43878

Interior radiances in optically deep absorbing media. II - Rayleigh scattering. 24 p3111 A73-45319

RAYLEIGH WAVES

Generation and detection of helical surface waves at cylindrical bodies by means of contactless electrodynamic transducers 01 p0051 A73-10974

Rayleigh wave propagation at the boundary between a piezoelectric insulator and a semiconductor. 03 p0350 A73-14037

Rayleigh waves for continuous monitoring of a propagating crack front. 04 p0452 A73-14691

Microfracture effects on seismic wave propagation velocity and Q factor in lunar rocks by Rayleigh ultrasonic surface wave technique 04 p0497 A73-15125

Helmholtz-Rayleigh instability of nondivergent horizontal flows in a barotropic atmosphere 04 p0441 A73-15287

Resonant coupling of ocean Rayleigh waves to atmospheric shock waves from Apollo rockets. [AD-755609] 05 p0569 A73-16380

Elastic velocity and Q factor measurements on Apollo 12, 14, and 15 rocks. 07 p0894 A73-19852

Some results of a study of the interaction between Rayleigh pulses and edge cracks 10 p1287 A73-23591

Raindrop impact erosion damage on ceramic radome materials, discussing Rayleigh wave mathematical model comparison with sled test data, and laboratory simulation 11 p1336 A73-25306

Building a dynamic test complex near an inertial test facility and general test pad considerations. [AIAA PAPER 73-827] 20 p2543 A73-38772

Dispersed signal filtering and filtered signal duration relation to filter bandwidth and dispersiveness, isolating fundamental mode of Rayleigh waves from earthquake 650 km deep 21 p2648 A73-39931

On the surface-to-bulk mode conversion of Rayleigh waves. 21 p2705 A73-41429

RAYLEIGH-RITZ METHOD

A finite element analogue of the modified Rayleigh-Ritz method for vibration problems. 03 p0390 A73-13336

Eigenproblems condensation techniques consisting of combined finite element, Rayleigh-Ritz and power methods

03 p0337 A73-14190

Variational methods in solid media linear theory of elasticity, discussing Rayleigh-Ritz method application to linear static, harmonic response and linearized stability problems

06 p0765 A73-18724

On the generalization of stress function procedure for dynamic analysis of plates.

09 p1158 A73-22395

Rayleigh-Ritz solution of boundary value problem for plane compressible subsonic flow past aerofoil noting convergence

09 p1028 A73-22954

Rayleigh quotient minimization and eigenvalue/eigenvector errors of mode convergence in dynamic structural analysis, using gradient algorithm and scaling transformation

11 p1438 A73-25497

Ritz method extension to mechanics problems by introducing artificial spring parameters at boundary and using Legendre functions as coordinate functions

12 p1555 A73-27740

Rayleigh-Ritz method for approximate solutions to nonlinear ordinary differential equations with nonlinear boundary conditions

13 p1650 A73-29399

Rayleigh-Ritz coefficient application in variational principle calculations of instability and flutter load of nonconservative systems

16 p2031 A73-32980

Discrete approximations of elastic-plastic bodies by variational methods.

16 p2078 A73-32994

Combined Rayleigh-Ritz and Lagrange multiplier technique for investigation of free vibrations of constrained cylindrical shell, considering axisymmetric mode

17 p2241 A73-34198

Book - An analysis of the finite element method.

20 p2581 A73-39139

A unified method for determination of fundamental natural frequency of orthotropic plate with arbitrary boundary.

20 p2622 A73-39546

Variational principles in dynamic thermoviscoelasticity.

24 p3151 A73-45306

RAYON

The relationship between thermal history, X-ray crystallographic structure and thermal properties of Pyco-bond rayon precursor carbon-carbon composites.

16 p2028 A73-33044

The relationship between thermal history, X-ray crystallographic structure and thermal properties of rayon precursor carbon-carbon composites A literature review.

16 p2028 A73-33045

RB-57 AIRCRAFT

U B-57 AIRCRAFT

RELATIVE BIOLOGICAL EFFECTIVENESS (RBE)

RC CIRCUITS

Application of the asymptotic method to third-order oscillatory systems

01 p0021 A73-10030

Synthesis of active RC circuits by means of equivalent circuits of impedance converters

02 p0148 A73-11549

Mathematical model for spectral distribution function of brain waves, noting analogy with RC oscillator

02 p0135 A73-12557

Feedback networks for RC oscillators with maximum frequency stability

06 p0673 A73-17581

A diode model with a current-dependent series resistance

06 p0674 A73-17828

Design of selective third-order active RC filters exhibiting high Q values at low Q sensitivities

07 p0796 A73-18896

Analysis of active RC circuits with nonhomogeneously distributed parameters in the time domain

07 p0805 A73-20024

Differentiators and integrators with RC circuits for piezoelectric transducer signals, noting instrument errors and SNR

07 p0827 A73-20534

RC planar distributed networks one and two dimensional analysis techniques and frequency response characterization, noting FORTRAN program use

09 p1067 A73-22309

Theoretical fundamentals of constructing parametric filters equivalent to linear filters

09 p1063 A73-22451

Synthesis of gyrator RC filters from the cascaded model

10 p1193 A73-23729

Active RC filter synthesis with decoupling stage and third order element for minimizing impedance mismatching and overall capacitance

10 p1193 A73-23734

Active RC filter circuit design based on Pukhov generalized two subcircuit model, determining complex transfer function

10 p1195 A73-24511

Transistor sawtooth voltage generator design for accelerated rise time piecewise linear leading edge, using capacitor charge/discharge acceleration

10 p1196 A73-24604

Synthesis of RC gyrator circuits with a constant characteristic resistance

10 p1196 A73-24608

Design procedures for matched and broadbanding filters for scanning tests.

11 p1341 A73-25074

High Q bandpass low sensitivity RC amplifier-filter networks, discussing two-step decomposition of denominator polynomial of second order filter transfer function

11 p1338 A73-26417

A new zero-beat indicator and its use in frequency measurements

13 p1617 A73-28859

Evaluation of the noise and dynamic range of transistorized selective RC amplifiers with controlled tuning

13 p1591 A73-28868

Active analog bandpass RC and LC filters design calculation by wave parameters

13 p1592 A73-28875

Dynamic losses in a transistorized switch operating on an active-capacitance load

13 p1593 A73-28944

Selectivity enhancement of certain low-sensitivity RC active networks.

14 p1738 A73-29711

Active LC, RC and C/gyrator/ filters design, operation, tolerance, cost and noise characteristics

14 p1736 A73-30375

Phase effect in RC transistor oscillator with single transistor or tube as amplifying element, determining vibration frequency, reverse communication amplification and frequency dependence

14 p1737 A73-30793

The use of selective RC amplifiers in the RF amplifier of a superheterodyne receiver.

16 p1991 A73-33982

Near-harmonic integrated oscillators in the 10 MHz to 40 MHz range.

19 p2412 A73-38538

Signal to noise ratios of inertial detector of mixture of stationary, normal, random and harmonic voltages, varying RC circuit time constants

20 p2537 A73-39459

Operation, design and applications of inductorless digital IC selective N-path filters

21 p2664 A73-41099

The approximation problem in the synthesis of circuits with distributed RC parameters

21 p2670 A73-41128

The accuracy and operational stability of a transistorized time-delay relay with an RC network

21 p2668 A73-41640

Low pass filter design for FDM and PCM systems, discussing active RC realization techniques and microelectronics model tests

22 p2832 A73-42293

Junction or Schottky gate type FET power gain and high frequency limitations from γ parameters calculation, using analog RC transmission line as equivalent network

23 p2963 A73-43452

The effect of amplifier gain-bandwidth product on the performance of active filters.

24 p3073 A73-45393

REACTANCE

Conditions derived for reactive two-terminal-pair matching transformer networks operation at maximum power transfer efficiency

09 p1061 A73-22046

Substrates with end effect in shorted slot, measuring normalized inductive reactance dependence on thickness to wavelength ratio

23 p2954 A73-44068

REACTION CONTROL

Space simulation experiments on reaction control system thruster plumes.

[AIAA PAPER 72-1071] 03 p0354 A73-13398

Cryogenic liquid O₂/H₂ reaction control systems for Space Shuttle.

[AIAA PAPER 72-1155] 03 p0382 A73-13458

Space shuttle bipropellant reaction control system /RCS/ engine design, characteristics and tests, emphasizing reusability and minimum servicing

[SAE PAPER 720839] 05 p0607 A73-16668

Aerothermodynamics of the Space Shuttle reaction control system.

[AIAA PAPER 73-93] 05 p0629 A73-16857

Satellite attitude control by reaction jet frequency modulation.

07 p0906 A73-19489

Spacecraft single-turn reorientation optimization with respect to fuel expenditure depending on maneuver duration and reaction control torque constraints

14 p1803 A73-29852

Lift engine bleed flow management for a VSTOL fighter reaction control system.

[ASME PAPER 73-GT-70] 16 p2048 A73-33521

Attitude control of a large flexible spacecraft using three-axis mass expulsion control.

[AIAA PAPER 73-893] 20 p2588 A73-38829

REACTION JET ATTITUDE CONTROL

U ATTITUDE CONTROL

U JET THRUST

REACTION JETS

U JET FLOW

U JET THRUST

REACTION KINETICS

Review of laboratory measurements of aerodynamic ion-neutral reactions.

01 p0014 A73-10335

Extraterrestrial solar flux attenuation and photodissociation cross sections effects on errors in photochemical kinetic model calculations

01 p0014 A73-10369

Interaction of chromium carbide with copper-nickel melts

02 p0178 A73-11539

Relative rate measurements for oxygen atom addition to simple olefins in liquid Ar at 87.5 K, noting activation energies during reactions

02 p0139 A73-12086

Rate coefficient calculation for near resonant charge transfer reaction between oxygen cations and hydrogen atoms as function of temperature at thermal energies

02 p0217 A73-12391

Arrhenius rate law for thermally activated processes, deriving master equation based on rates of transition between quantum states.

03 p0397 A73-13289

Effect of reagent vibrational excitation on reaction rate and product energy distribution in F + HCl yields HF + Cl.

03 p0273 A73-13290

Neutrino archaeology - The simulation of double beta-decay by solar neutrinos.

03 p0344 A73-13293

Combustion theory of hybrid rocket propellant-oxidizer combinations based on heat transfer limited model, discussing chemical kinetics and temperature effects on regression rate

03 p0397 A73-13449

Properties of phosphoribulokinase from *Thiobacillus neapolitanus*.

03 p0261 A73-13597

Ionization balance for ions of Na, Al, P, Cl, A, K, Ca, Cr, Mn, Fe and Ni.

03 p0345 A73-13949

Kinetics of the sulphur dioxide catalyzed recombination of radicals in hydrogen flames.

03 p0352 A73-14393

Electrode kinetic studies on the anodic oxidation of methanol.

04 p0406 A73-15102

Mechanisms and kinetics of absorption and desorption reactions in systems of refractory metals with nitrogen, oxygen or carbon.

04 p0462 A73-15302

X ray diffraction measurement of ordering kinetics in Ni-Pt alloy at annealing temperatures, showing disorder-order transitions relation to nucleation and growth

04 p0467 A73-15982

Study of excitation transfer in a flowing helium afterglow pumped with a tuneable dye laser. I. Measurement of the rate coefficient for selected quenching reactions involving He/5-3P/.

05 p0600 A73-16044

Chemical kinetics equations of lower ionosphere and D region particle interactions for aerodynamic problems

05 p0569 A73-16396

Solutions of the chemical kinetic equations for initially inhomogeneous mixtures.

[AIAA PAPER 73-101] 05 p0546 A73-16861

Numerical solution of viscous reacting blunt body flows of a multicomponent mixture.

[AIAA PAPER 73-202] 05 p0532 A73-16936

Competitive oxidation and pyrolysis of ethane in the presence of low concentrations of oxygen

05 p0641 A73-17050

Influence of the degree of purity on the kinetics of the recrystallization of deformed magnesium

05 p0587 A73-17216

Current kinetic modeling techniques for continuous flow combustors.

06 p0767 A73-17728

Some observations on flows described by coupled mixing and kinetics.

06 p0767 A73-17729

Investigation of NO formation kinetics in combustion processes - The methane-oxygen-nitrogen reaction.

06 p0767 A73-17731

REACTION KINETICS

Kinetics of a pulsed chemical CO laser with photostimulation based on the carbon disulfide oxidation reaction

06 p0700 A73-18103

The hydroperoxyl radical in atmospheric chemical dynamics - Reaction with carbon monoxide.

06 p0661 A73-18224

Diatomic molecule formation in interstellar medium via two body collision, calculating rate coefficients for radiative association

06 p0752 A73-18231

Photochemistry chemical kinetics in the interstellar medium.

06 p0752 A73-18236

Chemisorption and catalysis of hydrogen on polycrystalline wires of tungsten and nickel.

06 p0661 A73-18253

The synthesis and characterization of tin complexes using inert atmosphere techniques - An advanced laboratory experiment.

06 p0661 A73-18272

Dissociative recombination at elevated temperatures. III - O₂+/ dominated afterglows.

07 p0852 A73-19148

Flame structure and flame reaction kinetics. VIII - Structure, properties and mechanism of a rich hydrogen + nitrogen + oxygen flame at low pressure.

07 p0918 A73-19154

Reaction kinetics of nitric oxide positive ion with ozone yielding nitrogen dioxide positive ion and oxygen, noting impact on ionospheric chemistry

07 p0787 A73-19258

The cool-flame oxidation of n-heptane. I - The kinetic features of the reaction.

07 p0918 A73-19385

Kinetics and convection in the combustion of alkane droplets.

07 p0919 A73-19391

Disturbed ionospheric electron and ion kinetics, detailing dissociative recombination as regulating process for temporal evolution

07 p0816 A73-19454

Contribution to the study of the effect of molybdenum on the ageing kinetics of maraging steels.

07 p0838 A73-19499

A kinetic model and computer simulation for a pulsed DF-CO₂ chemical transfer laser.

07 p0835 A73-19632

Distribution of reaction products (theory). VIII - Cl + HI, Cl + DI.

07 p0788 A73-19926

Study of the ignition reaction in an oxygen-hydrogen mixture at relatively high pressures and low temperatures in the shock tube

07 p0920 A73-19993

Upper self-ignition limit of hydrogen in oxygen

07 p0921 A73-19994

Oxygen D line collisional quenching by atmospheric oxygen, nitrogen, carbon monoxide and dioxide, water vapor and ozone, determining absolute rate constants

07 p0788 A73-20239

The photochemical oxidation of iodide to iodine in the presence of oxygen.

07 p0788 A73-20398

A model for the kinetics of oxygen dissociation in a microwave discharge.

07 p0789 A73-20643

Internal oxidation of silver-beryllium and silver-lithium alloys.

08 p0977 A73-21022

Reaction of graphite with carbon dioxide at temperatures from 1200 to 2400 C

08 p0982 A73-21095

Analytical predictions of emissions from and within an Allison J-33 combustor.

08 p1025 A73-21670

Valence-bond study of the /H₂, D₂/ exchange reaction mechanism.

09 p1047 A73-22074

Borating kinetics and coating phase composition and thickness on cobalt and cobalt base alloys by metallographic, microhardness and X ray analyses

09 p1103 A73-22467

Effect of excited states of atomic oxygen ions on the reaction rates and thermal balance in the F-region.

09 p1078 A73-22832

Kinetics of transformation of carbon- and nitrogen-enriched austenite by carbonitriding in the gas phase

09 p1105 A73-23038

Criteria for oscillations in closed isothermal reacting systems.

10 p1294 A73-23561

Photoionization and charge exchange reaction kinetics inadequacy for explanation of observed positive nitrogen dioxide ion concentration in lower ionosphere, considering alternative mechanism

10 p1214 A73-24749

Nb nitriding kinetics and external effects observations, noting nitrogen diffusion through crystal lattices

10 p1236 A73-24955

Reactivity and interface characteristics of titanium-alumina composites.

11 p1384 A73-26043

Phenolic binder decomposition in silica-phenolic ablator, determining reaction mechanism from Arrhenius rate equations for various temperatures

11 p1452 A73-26376

Soot oxidation kinetics at combustion temperatures.

12 p1557 A73-26844

Ionospheric production and loss processes of atomic sulfur ions, considering dissociative ionization sources

12 p1489 A73-26999

An approximate estimate of the reaction coefficient during the motion of a vaporizing droplet of fuel in a gas flow

12 p1532 A73-27088

Investigation of the ferroniobium oxidation process

13 p1630 A73-28010

Al, Sr or Co effects on kinetics of grain boundary ferrite allotriomorphic formation relative to iron alloys, noting displacement of TTT curve

13 p1632 A73-28129

Mechanism and kinetics of the formation of intermediate products in an auxiliary mixture and the effect of such products on the combustion of the working mixture

13 p1704 A73-28293

Nitric oxide formation in gas turbine combustors.

13 p1670 A73-28805

Reduction kinetics and phase transformations of tungsten and molybdenum oxides

13 p1636 A73-28938

Chemical laser research survey covering device performance, reaction kinetics, theoretical modeling for population inversion and bibliography

13 p1628 A73-29112

Classical dynamical investigations of reaction mechanism in three-body hydrogen-halogen systems.

13 p1581 A73-29427

Chlorine trifluoride chemical laser emission, discussing output power dependence on partial pressures and chemical reaction kinetics

13 p1630 A73-29444

Rapid gas-phase reactions - The reaction of ammonia and the methylamines with boron trifluoride. III - Pressure dependence of rate constant.

14 p1723 A73-30068

Rate constants for the reactions of hydroxyl and hydroperoxyl radicals with ozone.

14 p1724 A73-30619

Layered and aggregate product displacement reaction kinetics in solid state /metal-metal oxide/ couples for metal matrix composites at 1000 C from thermodynamic and diffusion data

14 p1783 A73-30634

Linear nonstationary effects - A source of information on the kinetics of reactions on the surface of a solid fuel

14 p1818 A73-30873

The reaction of a titanium alloy with hydrogen gas at low temperatures.

15 p1890 A73-31993

Kinetics of physicochemical processes in a shock wave in mercury vapors. II - The relaxation zone: Region of initial ionization

15 p1916 A73-32314

Na₂SO₄-induced attack of Ni-20Cr-2ThO₂.

15 p1896 A73-32575

Exo-electron emission during heterogeneous catalysis /the effect of external electric potentials/.

15 p1842 A73-32599

Critical behaviour in chemically reacting systems. I - Difficulties with the Semenov theory. II - An exactly soluble model.

16 p1976 A73-33342

Shock-tube measurements of soot oxidation rates.

16 p2085 A73-33344

The production of nitric oxide in the stratosphere by oxidation of nitrous oxide.

16 p2008 A73-33885

The kinetics of the dissolution of oxygen in niobium at low oxygen pressures and high temperatures

16 p2026 A73-33955

New rate measurements on the reaction of O₃/P₂, O₃, and OH.

[ALAA PAPER 73-501]

16 p1977 A73-34045

A study of the process of oxidation of zirconium-oxygen alloys

17 p2188 A73-34558

Two dimensional half-jet mixing of dissociated air, investigating chemical rate and diffusion processes in interaction effects on mixing layer thermodynamics

17 p2156 A73-35503

New methods for studying gas solid reaction kinetics using automated resistance monitoring.

17 p2175 A73-35756

Photochemical reactions in the Jovian atmosphere.

17 p2237 A73-35835

Effect of interphase boundaries on the kinetics of molybdenum siliconizing

18 p2318 A73-35881

The combustibility of aluminum-nickel powders

18 p2325 A73-36862

Experimental study of the heat transfer in the vicinity of the critical point during nonequilibrium

physicochemical transformations and determination of the nitrogen recombination rate constant

18 p2287 A73-37013

Investigation of the kinetics of high-temperature aluminum/oxygen interaction by the ignition method

19 p2503 A73-37504

Kinetics of the catalytic reactions of the thermal decomposition of perchloric acid and ammonium perchlorate

19 p2402 A73-37505

The hydrogen evolution reaction on Ti-6Al-4V in acidic solutions of NaCl-HCl.

19 p2402 A73-37585

Reaction of HO₂ with O₃.

19 p2402 A73-37674

High-temperature gas-solid reactions.

19 p2403 A73-38552

Equilibrium point asymptotic stability for nonlinear generalization of Onsager theory for entropy functions construction with applications to chemical reaction kinetics

20 p2627 A73-39338

Stabilized gamma phase U-Nb-Zr alloy observation by electron microscopy, noting displacement reaction role in transition phase formation

20 p2578 A73-39489

Reactive kinetic observations for spraying with Ni-Al powder.

22 p2879 A73-42594

International Symposium on Combustion, 14th, Pennsylvania State University, University Park, Pa., August 20-25, 1972, Proceedings.

22 p2933 A73-42751

Elementary reactions in the combustion of small inorganic molecules.

22 p2818 A73-42752

Organic compounds oxidation and combustion reactions, discussing hydrogen dioxide radical role and reaction rate

22 p2933 A73-42753

Some reactions and hydroperoxyl and hydroxyl radicals at high temperatures.

22 p2898 A73-42754

Elementary reaction rates from post-induction-period profiles in shock-initiated combustion.

22 p2933 A73-42755

High-temperature oxidation of hydrogen by nitrous oxide in shock waves.

22 p2933 A73-42756

A single-pulse shock-tube study of the reaction between nitrous oxide and carbon monoxide.

22 p2933 A73-42757

Reaction rate constants for carbon monoxide-hydrogen-oxygen and hydrogen-nitrogen-oxygen systems at high temperatures, modeling hydrocarbon combustion for product distribution

22 p2933 A73-42758

Estimation of rate constants of elementary processes - A review of the state of the art.

22 p2933 A73-42759

High-temperature fast-flow reactor studies of metal-atom oxidation kinetics.

22 p2898 A73-42761

Catalytic efficiencies of atoms in the vibrational relaxation of HF and DF.

22 p2818 A73-42763

Precise measurements of diatomic dissociation rates in shock waves.

22 p2818 A73-42765

Shock tube kinetics of NO decomposition in mixtures with Ar, measuring ground state atomic oxygen formation rate by resonance absorption spectrophotometry

22 p2818 A73-42766

Sulfur hexafluoride pyrolysis and subsequent oxidation in mixtures with oxygen atoms and molecules, measuring decomposition rate at high temperature in shock tube experiment

22 p2818 A73-42767

Atomic oxygen reaction with acetylene in low pressure fast flow system, measuring free radical formation rate by photoionization mass spectrometer

22 p2818 A73-42768

Nitrogen dioxide and ozone photolysis as oxygen atom sources for high pressure addition reaction rate studies, discussing quantum yields and photolysis dependence on pressure

22 p2819 A73-42769

Inhibition of the first limit of the hydrogen-oxygen reaction by ethyl bromide.

22 p2898 A73-42777

Reaction of H atoms with CH₂Cl₂ - Application to the inhibition of flames.

22 p2819 A73-42779

Mathematical modeling of combustors based on turbulent mixing, droplet evaporation and chemical kinetics, considering stirred reactor heat balance and combustor performance prediction

22 p2935 A73-42789

Nitric oxide formation kinetics in combustion processes, discussing formation from nitrogen-containing compounds

22 p2819 A73-42791

- Experimental and theoretical studies of NO/x/ formation in a jet-stirred combustor. 22 p2820 A73-42793
- The effects of imperfect fuel-air mixing in a burner on NO formation from nitrogen in the air and the fuel. 22 p2820 A73-42795
- Effects of turbulent mixing and chemical kinetics on nitric oxide production in a jet-stirred reactor. 22 p2820 A73-42796
- Kinetics of carbon monoxide oxidation in postflame gases. 22 p2820 A73-42803
- Turbulent flow reactor for oxidation of moist CO and postinduction phase oxidation of methane, using chemical sampling and gas chromatographic analysis. 22 p2820 A73-42804
- Linear pyrolysis of various polymers under combustion conditions. 22 p2898 A73-42807
- Time variation in the reaction-zone structure of two-phase spray detonations. 22 p2936 A73-42811
- Effect of composite propellant catalysts on the stabilities of HClO₄ and the HClO₄-NH₃ system. 22 p2899 A73-42814
- German monograph - The tribology of solid lubricants of the type of the alkaline-earth hydroxides in the system Fe-Me/OH/2. 22 p2881 A73-42846
- Corrosion and deposition of steels and nickel-base alloys in liquid sodium. 23 p2990 A73-43456
- A discussion of the chemistry of some minor constituents in the stratosphere and troposphere. 23 p2951 A73-43893
- Quantum yield of metastable oxygen atoms and molecules via ozone photolysis by UV absorption, noting uncertainties in secondary reaction kinetics. 23 p2951 A73-43899
- Nitrogen oxides role in global stratospheric ozone balance demonstrated by observed instantaneous photochemical rates comparison with Chapman ozone formation theory. 23 p2952 A73-43900
- Venus carbon dioxide production kinetics involving quartz reaction with calcite to form wollastonite and carbon dioxide. 24 p3133 A73-44540
- Numerical integration of the equations of chemical kinetics. 24 p3065 A73-44703
- Ignition of metal particles in the case of a logarithmic oxidation law. 24 p3154 A73-44704
- Determination of the rate coefficients of ionospheric reactions from experimental data for electron concentration. 24 p3083 A73-44787
- Kinetics of formation of chloride ions in atmospheric pressure flames by way of the reversible reaction HCl+e/- yields H+Cl/-/. 24 p3085 A73-44991
- Study of the spatial development of oxidation and combustion reactions by means of image photoelectric receivers, and of a thermometric method. 24 p3091 A73-45398
- REACTION TIME**
- Color effects in visual discrimination, measuring response times in letter matching task. 02 p0135 A73-12525
- Possibility of the occurrence of self-oscillations in a circuit containing a constant source of current and a homogeneous semiconductor specimen with small response times. 03 p0349 A73-12907
- Test field surround effects on onset and offset reaction time to foveal stimulation. 03 p0261 A73-13558
- EMG measurement on male adults for muscular relaxation reaction time interval from light stimulus onset to elbow flexor response. 03 p0267 A73-13699
- Reaction time as a measure of the temporal response properties of individual colour mechanisms. 03 p0267 A73-13757
- Effects of 24-hour sleep deprivation on rate of decrement in a 10-minute auditory reaction time task. 04 p0411 A73-15220
- Step input tracking experiment for testing human psychological refractory period, noting directional error correcting reaction time similarities with keyboard tasks. 06 p0659 A73-18470
- Response time of metal-insulator-metal tunnel junctions. 08 p0945 A73-20844
- Reaction time method using EEG monitored paroxysm controlled auditory stimuli for responsiveness /consciousness/ evaluation of spike wave burst onset during epileptic seizures. 09 p1040 A73-22695
- Charged particle thermonuclear reactions in nucleosynthesis. 10 p1271 A73-23479
- Effect of passive 70-deg head-up tilt on peripheral visual response time. 10 p1185 A73-24566
- Effect of whole-body vibration on peripheral nerve conduction time in the Rhesus monkey. 11 p1315 A73-25335
- Forced guidance and distribution of practice in sequential information processing. 11 p1323 A73-26319
- The dependence of the negative afterimage on the duration of the stimulus and the stimulus intensity. 11 p1321 A73-26550
- Estimation of the variability of the latency of responses to brief flashes. 11 p1321 A73-26720
- Visual temporal integration for threshold, signal detectability, and reaction time measures. 13 p1578 A73-28097
- Flashblindness recovery following exposure to constant energy adaptive flashes. 13 p1579 A73-28505
- Saccadic eye movement control system, investigating response characteristics to variously timed pulse stimuli. 14 p1716 A73-30389
- The Mach-Dvorak phenomenon and binocular fusion of moving stimuli. 14 p1717 A73-30392
- Brain alpha rhythm activity relationship to perceptual and motor performance, correlating with reaction time and computer cycle time analogy. 16 p1972 A73-33159
- Probabilistic Monte Carlo computerized simulation of surface to air missile systems reaction time from aircraft attack in non-jamming environment and over flat terrain. 16 p1985 A73-33418
- Temporal factors of movements in visual aftereffects. 17 p2115 A73-34843
- The effect of colour on time delays in the human oculomotor system. 17 p2112 A73-34847
- On the rate of acquisition of visual information about space, time, and intensity. 17 p2118 A73-35496
- The control of eye movements in the saccadic system. 18 p2273 A73-36453
- Nonequilibrium velocity distributions and reaction rates in fast highly exothermic reactions. 19 p2402 A73-37897
- Monte Carlo calculations of reaction rates and energy distributions among reaction products. IV - F + HF/nu/ yields HF/nu-prime/ + F and F + DF/nu/ yields DF/nu-prime/ + F. 19 p2463 A73-37898
- Sleep deprivation effects on accuracy and speed of response selection and execution. 21 p2644 A73-40853
- Response delays and the timing of discrete motor responses. 21 p2645 A73-41177
- Reaction times for focal and nonfocal /peripheral/ processing of simultaneously presented color and form stimuli. 21 p2639 A73-41182
- Individual and simultaneous tracking of a step input by the horizontal saccadic eye movement and manual control systems. 22 p2811 A73-41735
- Effect of exercise on the response time in an identification problem. 22 p2813 A73-41894
- Reaction time to changes in the tempo of acoustic pulse trains. 22 p2816 A73-42705
- REACTION WHEELS**
- Satellite attitude control estimators and observers, discussing applications to reaction wheel, spinning attitude and drag-free satellite translation control systems. 01 p0075 A73-11193
- The double gimbal 'DRALLRAD' and its possible use for three-axis-stabilization of application satellites. 07 p0849 A73-19143
- The use of a spinning dissipator for attitude stabilization of earth-orbiting satellites. 13 p1690 A73-29216
- Communication satellites attitude control methods, considering conventional attitude gyros, control moment gyroscopes, reaction wheels and optimal solar cell utilization. 17 p2239 A73-35476
- The design of a two wheel momentum bias system for the attitude control of spacecraft in low altitude orbits. 20 p2585 A73-38793
- Achieving ultrahigh accuracy with a body pointing CMG/RW control system. 20 p2588 A73-38819
- Dual spin gas bearing reaction wheel for spacecraft fine pointing applications requiring long component life, describing manufacturing methods, safety factors and testing. 20 p2568 A73-38841
- [AIAA PAPER 73-907] 20 p2568 A73-38841
- On the use of a dual spin vehicle for scanning a celestial body. 20 p2614 A73-38844
- [AIAA PAPER 73-910] 20 p2614 A73-38844
- German monograph - Passive and active satellite attitude control with the aid of rod-like torsion pendula. 22 p2917 A73-42599
- REACTOR CHEMISTRY**
- U RADIOCHEMISTRY**
- REACTOR CORES**
- Performance potential of the colloid core reactor concept in near-earth applications. 03 p0340 A73-13394
- [AIAA PAPER 72-1065] 03 p0340 A73-13394
- An analysis of the operating characteristics of the Colloid Core Reactor. 03 p0341 A73-13414
- [AIAA PAPER 72-1094] 03 p0341 A73-13414
- Post impact behavior of mobile reactor core containment systems. 07 p0850 A73-20468
- Thermionic fuel elements for in-core reactor power plant space applications, summarizing operating and environmental requirements and technology development. 09 p1036 A73-22819
- An out-of-core version of a six-cell heat-pipe heated thermionic converter array. 09 p1036 A73-22820
- Exploratory investigation of an electric power plant utilizing a gaseous core reactor with MHD conversion. 09 p1119 A73-22829
- In-core 100 kWe thermionic power system design to meet manned spacecraft shielding requirements, discussing waste heat removal and integration with space base. 11 p1395 A73-26026
- An evolutionary approach for a compact-split-core reactor. 17 p2211 A73-35470
- Exploratory study of several advanced nuclear-MHD power plant systems. 19 p2455 A73-38411
- High temperature core thermocouple development for the Nuclear Rocket Engine Program /Rover/. 22 p2885 A73-42047
- A model of the dynamic behavior of the coaxial-flow gaseous-core nuclear reactor. 23 p3005 A73-43387
- REACTOR DESIGN**
- Technology assessment of nuclear rocket engines based on solid core reactors for space propulsion. 02 p0191 A73-11995
- An analysis of the operating characteristics of the Colloid Core Reactor. 03 p0341 A73-13414
- [AIAA PAPER 72-1094] 03 p0341 A73-13414
- Engineering problems in the design of controlled thermonuclear reactors. 05 p0596 A73-16980
- [AIAA PAPER 73-259] 05 p0596 A73-16980
- Zirconium hydride space power reactor design and fabrication technology evaluation, emphasizing requirements for coupling with power conversion and applications for thermoelectric power generation. 09 p1118 A73-22801
- The optimization of nuclear reactor energy supply installations with turbogenerators. 11 p1395 A73-25352
- ZrH space power reactors design, discussing long life fuel elements, high temperature hard vacuum irradiation environment control drive components and shield fabrication. 11 p1395 A73-26011
- Preliminary design of reactor power systems for the manned space base. 11 p1395 A73-26018
- Unmanned reactor-thermoelectric systems for applications in the 1970's. 11 p1395 A73-26024
- Thermionic reactor systems for electric propulsion. 11 p1395 A73-26025
- Nuclear thermionic power plants in the 50-300 kWe range. 11 p1396 A73-26027
- Development costs for a nuclear electric propulsion stage. 19 p2458 A73-38434
- REACTOR FUELS**
- U NUCLEAR FUELS**
- REACTOR MATERIALS**
- Acoustic emission weld monitoring of nuclear components. 07 p0832 A73-20274
- Device for investigating the mechanical characteristics of materials in a complex stressed state. 09 p1070 A73-22167
- Apparatus for creep and long-term strength testing of materials in aggressive media under irradiation. 20 p2544 A73-39368
- A system for continuous remote measurements and automatic recording of nonlinear displacements in testing structural materials in the field of reactor emission. 20 p2566 A73-39369

REACTOR SAFETY

A device for the investigation of the mechanical characteristics of materials under a complex stress system.

22 p2838 A73-42115

Real-time X-ray inspection system for fast flux test facility fuel.

23 p2966 A73-44169

REACTOR SAFETY

Optimal control problems of spacecraft mass minimization and nuclear power engine operation under uncontrollable perturbations due to errors and external field interactions

05 p0596 A73-16414

Navy transit RTG safety and test integration from users viewpoint.

09 p1118 A73-22796

REACTOR TECHNOLOGY

AEC/NASA thermionic reactor program with emphasis on technology utilization, comparing with French, German and Soviet programs

09 p1036 A73-22815

An out-of-core version of a six-cell heat-pipe heated thermionic converter array.

09 p1036 A73-22820

Exploratory investigation of an electric power plant utilizing a gaseous core reactor with MHD conversion.

09 p1119 A73-22829

Reactor-thermoelectric power systems for NASA Space Station/Space Base.

11 p1395 A73-26012

Low temperature-reactor Brayton cycle for Space Station/Base application.

11 p1311 A73-26013

The Satellits Nuclear Power Station - An option for future power generation.

19 p2455 A73-38412

REACTORS

NT TOKAMAK FUSION REACTORS

READERS

Study of a read-only optical memory addressed by an array of electroluminescent diodes

14 p1755 A73-29726

A flexible automatic typewriting system using three tape readers.

23 p2944 A73-43422

Punched card controlled program units including readers, comparator circuits, pneumomechanical counters and fluidic feedback oscillators

23 p2944 A73-43424

READING MACHINES

U READERS

READJUSTMENT

U ADJUSTING

READOUT

Design of a search memory using elements with reluctance modulation

08 p0941 A73-21108

The image-readout system of the combination photographic and television scanners of the Mars-2 and Mars-3 automatic interplanetary space probes.

09 p1086 A73-23050

High spatial resolution wire spark chamber system using electromagnetic delay line readout.

11 p1363 A73-25962

A multiwire proportional counter with integral readout delay line.

11 p1364 A73-25964

Recorder adapter operational circuit design for continuous logarithmic readout recording of atomic absorption double beam spectrophotometers

11 p1367 A73-26313

Spacecraft attitude gyro reference system and readout accuracy, discussing strapdown guidance, electrical suspension, instrument errors, spin and damping coils and degrees of freedom

21 p2733 A73-40026

REAL GASES

Thermodynamic equilibrium and relaxation models of ideal and real high temperature gas flows for reversible and irreversible processes

04 p0517 A73-15678

A universal method of calculation of the state of a real gas behind primary and reflected shock waves.

06 p0684 A73-17700

Some relations for the ultrasonic region of flow of a real gas in the presence of heat transfer.

14 p1817 A73-30603

Some relations for high pressure flows with and without heat transfer.

14 p1817 A73-30604

Calculations of real gas properties from tables of thermodynamic functions

18 p2372 A73-36817

Real gas turbocompressor calculations based on equations of state for fundamental thermodynamic processes in ideal gas

22 p2797 A73-42645

REAL NUMBERS

Evaluations of matrix functions by real similarity transformation.

06 p0718 A73-18536

Torsional vibrations of a bar of variable cross-section.

16 p2079 A73-33075

A note on pairs of matrices and matrices of monotone kind.

21 p2725 A73-40377

REAL TIME OPERATION

Minicomputer for real time sequential decoding of convolutional code transmission in space communication, discussing system design, performance and metric bias effect

01 p0020 A73-11185

Comparison of Kalman filter and stepwise methods for real time orbit determination.

01 p0105 A73-11187

Real-time computer for monitoring a rapid-scanning Fourier spectrometer.

01 p0020 A73-11231

Data processing for radioastronomy and cosmic ray air shower arrays.

01 p0020 A73-11455

Digital filters applicable to electroencephalographic pattern recognition.

01 p0013 A73-11464

Real time tracking radar for radio guidance system, obtaining algorithm for rocket motor direction and ignition time for satellite orbit optimization

03 p0339 A73-13067

Pulsar associated with the supernova remnant IC 443.

03 p0374 A73-13848

Real time linear and nonlinear motion desmearing of imagery telemetered from airborne platform, discussing inverse filter error analysis and analog simulation

03 p0276 A73-13907

Meteorological echoes movement and evolution measurement potential of conventional radars connected to programmable real time processor

03 p0280 A73-14549

Command and control for a missile air defense system. II - Implementation of system requirements.

04 p0418 A73-15378

An electronic multiband camera film viewer.

04 p0450 A73-15771

Bragg-diffraction imaging and it's application for non destructive testing.

05 p0574 A73-16281

Apparatus replicating and extending development work on real-time time-compressed radar observation processor and display system

05 p0576 A73-16714

Data processing remote terminals for real time on-line computer communication systems, discussing design, characteristics and applications

05 p0551 A73-16801

Computerized airlines reservations systems with real time conversational interactive characteristics, discussing initial design, simulation, measurement, stability, reliability and data processing techniques

05 p0551 A73-16806

Interactive real time simulation for scheduling and monitoring of STOL aircraft in the terminal area.

[AIAA PAPER 73-163] 05 p0535 A73-16909

Soft constraint trajectory optimization formulation as real time optimal feedback guidance method for multiborn orbital maneuvers

[AIAA PAPER 73-249] 05 p0596 A73-16972

Measurement of vibration characteristics by impact testing.

05 p0637 A73-17233

Methods and techniques in spectral analysis of random-vibration data

05 p0637 A73-17271

Real time coherent electro-optic two dimensional on-line spatial light modulator role in optical data processing system

06 p0693 A73-18286

Display of microwave pulse response via the real-time Fourier transform of the transfer function.

06 p0677 A73-18346

Adaptive real time control for defense systems - A minimum risk algorithm.

06 p0682 A73-18823

Control algorithm for digital computer operations organization in real time processing of variable priority assignment tasks, estimating memory storage requirements

07 p0796 A73-20049

Scheduling algorithms for multiprogramming in a hard-real-time environment.

08 p0941 A73-20961

Real time 3-D holographic display, discussing reusable thermoplastic photoconducting recording film and frequency compensation with short laser pulses and acousto-optic modulator

08 p0965 A73-21246

Nucleation film/electron beam recorder - Near-real-time display system.

08 p0965 A73-21247

Modal control applied to the real-time figure control of a spaceborne telescope mirror.

08 p0969 A73-21729

Real time display, processing and image-data products production system for supporting Mariner 9 TV experiment, discussing computer algorithms

09 p1080 A73-22266

Real-time analysis and ground command control to achieve accurate vehicle and payload event functions. [AIAA PAPER 73-298] 09 p1117 A73-23217

Digital coherent demodulator techniques for moderate data rate PSK signal reception in real time, describing synchronous bandpass sampling receiver with IF signal A/D conversion

09 p1053 A73-23371

Design philosophy and operation of hardware and data flow of TELFILE real time multiprogrammed telemetry system, discussing support of Minuteman III Weapons Systems

09 p1057 A73-23415

Real time digital computer algorithm for linear and nonlinear electronic circuit modeling in state variable form for static and dynamic regimes

10 p1196 A73-24607

Holographic motion picture camera allows front surface detail to be recorded in real time using a continuous wave laser.

11 p1366 A73-26249

Holographic approach to real time correction of optical instruments images, discussing restoration by spatial frequency filtering

11 p1370 A73-26535

Real time quantitative display for visible and IR scanning radiometer in ITOS-D satellite-borne automatic picture transmission system with stations access to computers

12 p1520 A73-26811

Redundant central processor system for fault tolerant real time operation in space applications, describing systems organization

12 p1476 A73-27821

Real-time reconstruction of images from hydroacoustic holograms.

13 p1614 A73-28578

Real time high resolution 100 MHz acoustic image or holograph microscope using optical measurement of boundary displacement by incident angular sound wave

13 p1614 A73-28579

Foil-electret transducer arrays for real-time acoustical holography.

13 p1614 A73-28583

Real time microwave hologram data acquisition by double circular scanning of single sensor over recording aperture, presenting optical bench simulation

13 p1618 A73-29122

Self adaptive filter algorithm for automatic tracking of high performance maneuvering targets in real time surveillance systems in changing environments

13 p1596 A73-29207

The data processing architecture on the launch bases of the Directorate of Research and Test Methods

14 p1742 A73-30091

French launching base real time trajectory photography system for rocket space location information, investigating evolution towards maximum reliability

14 p1773 A73-30094

Suboptimal adaptive control of a class of non-linear systems.

15 p1853 A73-31628

Software design and implementation for real time power spectral analysis on IBM-1130 8K-core computer, discussing coherence and cross spectra estimation and arithmetic errors

15 p1848 A73-32032

Use of associative processors for radar data processing in air traffic control systems.

15 p1849 A73-32434

MADAP - Implementation of a large size real time data processing system.

15 p1849 A73-32448

Real time information processing automated systems for ATC, considering reliability based on redundancy

15 p1910 A73-32483

French monograph on numerical data processing organs for real time process control, describing modular computer design project

15 p1849 A73-32590

Speckle reference beam /by retro reflection/ holography for the real time visualisation of vibration patterns.

16 p2012 A73-32847

Faraday rotation based total ionospheric electron content information for correction of near real time satellite position determination errors, using spherically stratified ionospheric model

16 p2035 A73-33414

Evaluation of machinery characteristics through on-line vibration spectrum monitoring.

[ASME PAPER 73-GT-68] 16 p2048 A73-33520

A real-time simulator for image data systems.

17 p2147 A73-34903

Real time digital videomagnetograph at the Aerospace San Fernando Solar Observatory.

17 p2168 A73-34909

Techniques for digital-microwave hybrid real-time radar simulation.

17 p2131 A73-35303

Real-time estimates of mean velocity by averaging quantized phase displacements of Doppler radar echoes.

17 p2125 A73-35362

Vibration analysis of plates by real-time stroboscopic holography.

[SESA PAPER 2111] 17 p2173 A73-35448

Remote sensing of chlorophyll and temperature in marine and fresh waters.

17 p2164 A73-35664

Computerized processing system with real time control, data analysis and display capabilities for space shuttle checkout, servicing, launching and landing to reduce cost

[AIAA PAPER 73-601] 18 p2295 A73-36083

A real-time software operating system for a computer-controlled acoustic emission flaw monitor.

18 p2316 A73-36679

Pulsed-Doppler velocity isotach displays of storm winds in real time.

18 p2333 A73-36707

Hidden-line removal at 20 pictures/second through hybrid techniques.

18 p2291 A73-36830

Real-time, three-dimensional, visual scene generation with computer generated images.

18 p2291 A73-36831

Real-time hybrid hardware-in-the-loop simulation of a terminal homing missile.

18 p2291 A73-36834

Technological survey of machine intelligence for real time autonomous manipulation with computer recognition sensory feedback and programmed task control to eliminate human operator

19 p2417 A73-37330

A precision control system for a large astronomical telescope.

19 p2430 A73-38079

Data collection platforms, ground receiving and processing equipment for environmental study and management

[AAAS PAPER 73-122] 20 p2520 A73-38583

Rapid in situ processing for real-time holographic interferometry.

21 p2692 A73-39918

Real time nitrogen dioxide and nitric oxide pollution measurement by molecular fluorescence induced by argon laser beam

21 p2671 A73-40135

Two wavelength variable sensitivity interferometry, extending static technique to real time dynamic testing

21 p2698 A73-40138

Optical processing of radar signals

21 p2651 A73-40515

GDC/EOS - Real-time visual and motion simulators for evaluation of fire control and electro-optical guidance systems.

[AIAA PAPER 73-919] 21 p2673 A73-40867

Real-time identification using adaptive discrete model.

23 p2962 A73-43286

Dual lane runway configuration design and operational characteristics investigation by real time computer simulation for solution to airport capacity problem

[ASME PAPER 73-ICT-61] 23 p2966 A73-43496

Real-time X-ray inspection system for fast flux test facility fuel.

23 p2966 A73-44169

PEARL middle level programming language for process control, discussing algorithms, structure, time behavior and input/output of real time operation

23 p2956 A73-44388

Elastomechanical model measurements conducted with the aid of holographic approaches in the case of a mirror cell

24 p3090 A73-44897

REAL VARIABLES

NT ABEL FUNCTION

NT ASYMPTOTES

NT ASYMPTOTIC SERIES

NT BESSEL FUNCTIONS

NT BIHARMONIC EQUATIONS

NT BINARY INTEGRATION

NT BLASIUS EQUATION

NT BOREL SETS

NT BURGER EQUATION

NT CALCULUS OF VARIATIONS

NT CAUCHY-RIEMANN EQUATIONS

NT CHANDRASEKHAR EQUATION

NT COLLINEARITY

NT COPLANARITY

NT CURL (VECTORS)

NT DELTA FUNCTION

NT DIFFERENTIAL EQUATIONS

NT DUFFING DIFFERENTIAL EQUATION

NT EINSTEIN EQUATIONS

NT ELLIPTIC DIFFERENTIAL EQUATIONS

NT EXISTENCE THEOREMS

NT EXTREMUM VALUES

NT FALKNER-SKAN EQUATION

NT FOKKER-PLANCK EQUATION

NT FOURIER SERIES

NT FUNCTIONAL INTEGRATION

NT GAUSS EQUATION

NT GREEN FUNCTION

NT HANKEL FUNCTIONS

NT HELMHOLTZ VORTICITY EQUATION

NT HYPERBOLIC DIFFERENTIAL EQUATIONS

NT HYPERBOLIC FUNCTIONS

NT HYPERPLANES

NT INTEGRAL CALCULUS

NT JACOBI INTEGRAL

NT JACOBI MATRIX METHOD

NT KERNEL FUNCTIONS

NT LAME WAVE EQUATIONS

NT LEBESGUE THEOREM

NT LLAPUNOV FUNCTIONS

NT LIMITS [MATHEMATICS]

NT LINEAR EQUATIONS

NT LIQUVILLE EQUATIONS

NT LIPSCHITZ CONDITION

NT MAXIMA

NT MEASURE AND INTEGRATION

NT NEUMANN PROBLEM

NT NONLINEAR EQUATIONS

NT NUMERICAL INTEGRATION

NT PADE APPROXIMATION

NT PARABOLIC DIFFERENTIAL EQUATIONS

NT PARTIAL DIFFERENTIAL EQUATIONS

NT PERIODIC FUNCTIONS

NT POISSON EQUATION

NT POWER SERIES

NT PRONY SERIES

NT QUADRATIC EQUATIONS

NT RUNGE-KUTTA METHOD

NT SERIES [MATHEMATICS]

NT STIELTJES INTEGRAL

NT STURM-LIOUVILLE THEORY

NT TAYLOR SERIES

NT TRIGONOMETRIC FUNCTIONS

NT VECTOR ANALYSIS

NT VLASOV EQUATIONS

NT VORTICITY

NT WEIERSTRASS FUNCTIONS

NT WEIGHTING FUNCTIONS

NT WHITTAKER FUNCTIONS

Approximation by functions of fewer variables.

02 p0186 A73-11969

Algebraic algorithm for positive realness of real rational functions and matrices relative to unit circle in complex plane, determining real polynomial zeros distribution

19 p2446 A73-38488

Proposal of a new criterion for evaluating the adequacy of models

21 p2669 A73-40499

The variable metric algorithm for non-definite quadratic functions.

21 p2727 A73-40999

On quasi-concave and strictly quasi-concave functions on a convex set relative to one of its nonvacant subsets

21 p2727 A73-41023

Convergence rate of two-real-parameter iterative solution of linear equations system based on matrix eigenvalues relationship

24 p3106 A73-45442

REATTACHED FLOW

Theoretical analysis of the flow through a particular wall-attachment fluidic component.

03 p0295 A73-13767

Jet interaction in a simplified model of a bistable fluid amplifier.

[ASME PAPER 72-WA/FLCS-6] 04 p0409 A73-15863

Heat transfer downstream of attachment of a turbulent supersonic shear layer.

05 p0533 A73-17112

Some incompressible jet flow and reattachment effects in fluid control elements.

06 p0687 A73-18513

Unsteady aerodynamics of separating and reattaching flow on bodies of revolution.

10 p1173 A73-24816

Base pressures in flow expansions by hydraulic analogy.

13 p1564 A73-28811

The switching of wall-reattachment fluidic devices.

13 p1571 A73-29041

Qualitative study of flow deviation by a wall cavity

16 p1962 A73-32811

Reattachment of a separated boundary layer to a convex surface.

22 p2843 A73-42554

Some investigation on base flow behind cylindrical bodies in incompressible flow.

22 p2797 A73-42997

Supersonic laminar flow over wedge or backward-facing step for large Reynolds number and small base or step height, predicting pressure distribution at reattachment

24 p3055 A73-45314

REBREATHING

Gas-blood CO₂ equilibration in dog lungs during rebreathing.

03 p0263 A73-14115

Mixed-venous oxygen tension by nitrogen rebreathing - A critical, theoretical analysis.

06 p0654 A73-18336

The influence of age, sex, body size and lung size on the control and pattern of breathing during CO₂ inhalation in Caucasians.

06 p0654 A73-18337

Comparison of blood and alveolar gas composition during rebreathing in the dog lung.

11 p1318 A73-26218

Studies of alveolar-mixed venous CO₂ and O₂ gradients in the rebreathing dog lung.

11 p1318 A73-26219

Assessment of left heart function by noninvasive exercise test in normal subjects.

15 p1834 A73-31345

Rebreathing and steady state pulmonary diffusing capacity for O₂ in the dog and in inhomogeneous lung models.

21 p2645 A73-41639

Rebreathing equilibration of CO₂ during exercise.

24 p3060 A73-45068

RECEIVERS

NT LINEAR RECEIVERS

NT LOGARITHMIC RECEIVERS

NT RADAR RECEIVERS

NT RADIO RECEIVERS

NT RADIOTELEPHONES

NT SUPERHETERODYNE RECEIVERS

NT TELEVISION RECEIVERS

Conversion coefficients of optical heterodyne receiver mixer for various amplitude-phase distributions of interfering signal

03 p0319 A73-14067

Sensitivity of optical autodyne quantum receiver in presence of output noise, using photomultiplier signal model

03 p0319 A73-14076

Optimal receiver design for discrete information in the presence of non-Gaussian noise

16 p1990 A73-33669

Optimal processing of signals in systems with multiple elements /channels/ of reception.

17 p2130 A73-35723

Geocover passive Doppler receiver precision capabilities and accuracy experience, noting portability, commercial availability, error sources enumerated and quantified

21 p2705 A73-41329

RECEIVING SYSTEMS

U RECEIVERS

RECEPTACLES [CONTAINERS]

U CONTAINERS

RECEPTION DIVERSITY

Three dimensional summer time sporadic E layer structure and electron concentration during 1966-1969 by ionospheric space diversity sounding

06 p0689 A73-17553

On the reduction of rainfall outages by space diversity for millimeter-wave earth-satellite communications systems.

06 p0668 A73-18712

Algorithm for optimal radio signals detection under narrow band anisotropic noise, noting two channel space diversity receiver system

09 p1050 A73-22454

Frequency correlation of fluctuations of radio waves reflected from the ionosphere.

10 p1188 A73-24240

Three dimensional summer time sporadic E layer structure and electron concentration during 1966-1969 by ionospheric space diversity sounding

16 p2002 A73-32777

On rainfall and space diversity for millimeter-wave earth-satellite communications systems.

18 p2289 A73-36709

Noise immunity of diversity reception with antenna threshold switching.

18 p2290 A73-37128

UHF airborne antenna diversity combiner for signal reception using correlation technique for phase variation removal to improve SNR and gain

20 p2523 A73-38725

Interpretation of the results of drift measurements by the space diversity reception method

20 p2555 A73-39819

Determination of the difference in group paths by the method of frequency-diversity reception

24 p3068 A73-44810

RECEPTORS [PHYSIOLOGY]

Activity relation between internal organ receptors and skeletal muscles in terms of laws controlling process coordination

01 p0007 A73-10154

Left ventricular receptors activated by severe asphyxia and by coronary artery occlusion.

01 p0008 A73-10549

Orientation: Sensory basis; Proceedings of the Conference, New York, N.Y., February 8-10, 1971.

06 p0653 A73-18030

Book - Sensory coding in the mammalian nervous system.

11 p1317 A73-25799

Electrical and metabolic manifestations of receptor and higher-order neuron activity in vertebrate retina.

13 p1574 A73-28353

RECIPROCAL THEOREMS

Reciprocity theorem for antenna directivity pattern measurement of optical superheterodyne receiver for carbon dioxide laser radiation

03 p0284 A73-14084

A note on a general linear initial-boundary value problem.

06 p0716 A73-17980

Globally equivalent representations for reciprocal stationary nonlinear systems in equilibrium or steady state conditions, considering electric circuits and thermodynamic system examples

06 p0716 A73-17993

Book - Applications of the electromagnetic reciprocity principle.

15 p1915 A73-32577

RECIPROCATING ENGINES

U PISTON ENGINES

RECIRCULATION

U CIRCULATION

RECIRCULATIVE FLUID FLOW

Optimal stabilization conditions of turboreactor combustor initial recirculation zone determined by hydraulic analogy technique, describing vorticity generation and mass flow rates [ONERA, TP NO. 1105]

03 p0359 A73-14126

Pollutant formation in reacting turbulent jet flow field with recirculation, presenting methane-air system pointwise properties determination by numerical analysis

[WSCIPAPER 72-21]

05 p0638 A73-16676

Upwelling of a stratified fluid in a rotating annulus - Steady state. I - Linear theory.

06 p0684 A73-17702

Unsteady two dimensional flow within circular cavity with arbitrary velocity distribution on cylinder wall, investigating recirculating flow initiation

10 p1210 A73-24838

Base drag reduction on blunt based axisymmetric bodies by base burning, calculating inviscid flow field with heat addition around recirculating bubble

11 p1449 A73-25347

Thermosiphon technology advances covering open and closed single-phase natural convection and mixed convection systems, two phase systems and turbine blade cooling

17 p2254 A73-34352

Linearized implicit schemes for the computation of viscous incompressible flow - with applications.

17 p2155 A73-35141

Recirculation and mixing characteristics prediction for enclosed turbulent jet flames in flow regions, using similarity parameters

22 p2934 A73-42782

Analytical modeling of a spherical combustor including recirculation.

22 p2934 A73-42783

RECLAMATION

NT MATERIALS RECOVERY

NT WATER RECLAMATION

Machinery to be developed for an offshore airport constructed by reclamation.

19 p2418 A73-37746

RECOGNITION

NT CHARACTER RECOGNITION

NT PATTERN RECOGNITION

NT SPEECH RECOGNITION

NT TARGET RECOGNITION

Determination of changes in the properties and recognition of random processes with a complicated structure.

10 p1201 A73-24057

RECOIL PROTONS

Nuclear photoemulsions under bombardment by pion beam of 60 GeV/c momentum, investigating pion-nucleon interactions involving recoil protons

02 p0195 A73-12667

Reaction Li-6/p, p/t at 590 MeV.

21 p2743 A73-41018

RECOILINGS

Possible cause of the variations of the intensity of an interstellar maser.

04 p0493 A73-16023

RECOMBINATION COEFFICIENT

Ion composition dependent recombination coefficient loss rate changes in D region during solar flares, using electron density and X ray flux measurements

01 p0042 A73-10903

The effect of surface recombination velocity on the performance of vertical multi-junction solar cell.

03 p0255 A73-14214

Temporal variations of the recombination coefficient and electron density profile in the lower ionosphere

05 p0568 A73-16261

Temperature dependence of the ion recombination coefficient in a hydrocarbon flame plasma

06 p0731 A73-18553

Atomic recombination rate determination through heat-transfer measurement.

09 p1048 A73-23449

Recombination coefficient, heat flux, ionization balance and photoelectron kinetic energy from iono-

spheric electron temperature and density profiles and solar UV absorption data

11 p1350 A73-25081

D-region recombination coefficients and the short wavelength X-ray flux during a solar flare.

11 p1356 A73-25914

Ionization, recombination, and population of excited levels in hydrogen plasmas.

11 p1407 A73-26584

Effective recombination coefficient in the ionospheric D-region.

13 p1608 A73-28711

Measurements of the electronic recombination coefficient in a helium plasma jet.

14 p1780 A73-30245

The influence of Auger recombination on the forward characteristic of semiconductor power rectifiers at high current densities.

15 p1850 A73-31130

Radiative and dielectronic recombination coefficients for complex ions.

16 p2038 A73-32842

Non-thermal ionization and recombination processes during solar flares.

16 p2052 A73-32958

Temperature dependence of the ion recombination coefficient for a hydrocarbon flame.

16 p2042 A73-33578

Recombination rate measurements in nitrogen.

16 p2039 A73-33673

Decay of a high temperature helium plasma - Validity of local thermodynamic equilibrium and estimation of recombination coefficients for He/ $+I$, He/ $+II$, and He2/ $+I$.

16 p2043 A73-33867

Approximation to the collisional-radiative recombination coefficient in a partially ionized gas.

17 p2213 A73-34197

D region electron and ion density profiles, recombination coefficient and electron detachment rate changes during solar eclipse

18 p2310 A73-36127

Simultaneous measurements of some ionospheric parameters at altitudes 100-170 km.

18 p2310 A73-36131

Measurement of electron-ion recombination rate of a dense high-temperature cesium plasma.

18 p2339 A73-36622

Experimental study of the heat transfer in the vicinity of the critical point during nonequilibrium physicochemical transformations and determination of the nitrogen recombination rate constant

18 p2287 A73-37013

Temperature dependence for dissociative recombination of NO/ $+I$ in E- and F-region models.

21 p2684 A73-40787

Effective recombination levels in N- and P-type silicon irradiated by 4.5 MeV electrons.

21 p2753 A73-41558

Measurements of recombination of electrons with HCO $+$ ions.

23 p3007 A73-43530

Determination of the rate coefficients of ionospheric reactions from experimental data for electron concentration

24 p3083 A73-44787

Magnetic resonance spectrometer measurements of atomic hydrogen surface recombination.

24 p3113 A73-45425

RECOMBINATION REACTIONS

NT ATOMIC RECOMBINATION

NT ELECTRON RECOMBINATION

NT ELECTRON-ION RECOMBINATION

NT HYDROGEN RECOMBINATIONS

NT ION RECOMBINATION

NT OXYGEN RECOMBINATION

NT RADIATIVE RECOMBINATION

Low-frequency oscillations in a bounded low-density plasma.

02 p0198 A73-12105

Spherical probe measurements of dense weakly ionized plasma parameters, noting ionization, recombination and secondary surface effects on probe characteristics

02 p0198 A73-12109

Calculation of the diffusion current of a finite-base semiconductor diode

03 p0284 A73-14322

Recombination radio lines in H I regions.

04 p0504 A73-16026

Flow of a two-temperature plasma in the duct of a disk-type magnetohydrodynamic generator with allowance for nonequilibrium ionization and recombination reactions

06 p0727 A73-17464

Characteristics of recombination centers defining the high sensitivity of n-CdSb photoresistors

06 p0675 A73-18082

Influence of low-temperature heat treatment on the electrical and recombination properties of silicon-silicon dioxide systems

06 p0736 A73-18085

Photodiode structure performance dependence on surface properties in static and kinetic operations, noting surface recombination and photoeffect relaxation

06 p0676 A73-18086

Dissociative recombination at elevated temperatures. III - O2/ $+I$ dominated afterglows.

07 p0852 A73-19148

Disturbed ionospheric electron and ion kinetics, detailing dissociative recombination as regulating process for temporal evolution

07 p0816 A73-19454

Problem of the selective mechanism for the excitation of the C III 5696-A line in the spectra of certain stars. I

08 p1012 A73-21549

Spontaneous emission and stimulated recombination of p-n-n double heterojunction AlGaAs-GaAs laser diodes above and below threshold currents

09 p1093 A73-22256

Nitric oxide formation and radical overshoot in premixed hydrogen flames.

10 p1294 A73-23558

Electron impact ionization, three body recombination and thermal energy balance effects on gas discharge positive column between plane parallel walls

10 p1255 A73-24265

A plasma laser operating on molecular electronic transitions

10 p1228 A73-24454

Determination of the parameters of r-type recombination centers in germanium-doped GaTe single crystals

11 p1410 A73-26587

Analytical model of the unsteady nighttime F2 region of the ionosphere at mid-latitudes

12 p1490 A73-27337

Surface effects on trapping and recombination processes in Bi13 single crystals

12 p1531 A73-27938

Molecule formation. I - In normal H I clouds. II - In interstellar shock waves.

12 p1547 A73-27973

Liquid propellant rockets, discussing effective exhaust velocity, nozzle expansion, chamber pressure effects on equilibrium performance and kinetic recombinations

14 p1784 A73-30136

The Li donor, and binding of excitons at neutral donors and acceptors in crystals

15 p1924 A73-31722

Ionospheric D region dissociation-recombination reaction constants derived from ion production rate data compiled during polar cap absorption

15 p1872 A73-31887

Thermal and ionization equilibrium in a dense hydrogen cloud.

16 p2059 A73-32841

Laboratory methods for study of aeronautical reactions of excited ions.

16 p2009 A73-33894

Recombination effects in chemical laser nozzles. [AIAA PAPER 73-643]

18 p2287 A73-36258

Parameters of fast recombination centers in CdS single crystals and the effect of the parameters on photosensitivity

18 p2340 A73-36669

Comparison of electron and electronic temperatures in recombining nozzle flow of ionized nitrogen-hydrogen mixture. I, II.

19 p2462 A73-37441

Electron transitions of molecules in a plasma laser.

19 p2438 A73-38135

Search for solar recombination lines in the frequency range 110-115 GHz.

19 p2488 A73-38521

The photolytic stability of the Martian atmosphere.

21 p2764 A73-40159

The optimal number of soundings for a complete investigation of the ionization-neutralization and dynamic characteristics of the middle ionosphere

21 p2686 A73-40911

Elementary reaction rates from post-induction-period profiles in shock-initiated combustion.

22 p2933 A73-42755

Analytical model of the nocturnal nonstationary F2-region of the ionosphere at middle latitudes.

23 p2970 A73-43235

Photoelectric methods of determining the electrical characteristics of MDS systems

23 p3006 A73-43616

Eigenfunction calculation of injected carrier density in doped semiconductor filaments, relating negative eigenvalues to Suhl effect and lifetime dependence to bulk and surface recombination

23 p3016 A73-43674

Electron temperature of regions of the formation of recombinational continua on the sun - Temperature of the carbon emission regions

23 p3036 A73-44246

RECOMPRESSION

U COMPRESSING

RECONNAISSANCE

NT AERIAL RECONNAISSANCE

NT PHOTORECONNAISSANCE

NT SPECTRAL RECONNAISSANCE

Pursuit-evasion reconnaissance game with evader reconnoitering target from close distance with guaranteed safe escape from pursuer

03 p0336 A73-13523

RECONNAISSANCE AIRCRAFT

NT CL-84 AIRCRAFT

NT EARTH RESOURCES SURVEY AIRCRAFT
Electronic warfare tactics against remotely piloted unmanned aircraft used for reconnaissance or weapons delivery, considering onboard countermeasures

04 p0418 A73-15379

Experimental autostabilized tethered rotor platform for reconnaissance, communications and ECM, discussing control system effectiveness from flight test results

16 p1969 A73-33736

Aerodynamic unmanned wingless reconnaissance aircraft, covering hovering capacity, internal flow duct for conventional flight, flight test results and stability characteristics

17 p2098 A73-34255

Aerial-survey aircraft of the new generation

22 p2799 A73-42590

RECONNAISSANCE DRONE AIRCRAFT

U DRONE AIRCRAFT

U RECONNAISSANCE AIRCRAFT

RECONSTRUCTION

NT WAVE FRONT RECONSTRUCTION

RECORDING

NT DATA RECORDING

NT DATA SMOOTHING

NT MAGNETIC RECORDING

NT PHOTOGRAPHIC RECORDING

RECORDING HEADS

Ultrawideband longitudinal magnetic tape recording of 120 MHz biased LF/HF signal frequencies, describing high velocity tape transport and recording heads design

09 p1087 A73-23366

Record/reproduce process induced phase distortion in magnetic tape recorders as function of record head gap length

09 p1087 A73-23368

RECORDING INSTRUMENTS

NT FLIGHT LOAD RECORDERS

NT FLIGHT RECORDERS

NT LUNAR SEISMOGRAPHS

NT MECHANOGRAMS

NT OSCILLOGRAPHS

NT PLOTTERS

NT PRESSURE RECORDERS

NT SEISMOGRAPHS

NT WEATHER DATA RECORDERS

NT X-Y PLOTTERS

Quick-response automatic range switch for electronic potentiometers

01 p0045 A73-10257

On-line digital recording of stellar spectrum with photoelectron-counting spectrophotometer, noting discrimination against spurious signals from noise and pulse height distribution measurements

01 p0048 A73-10531

Automatic pulse count recorder, discussing circuit, performance and applications to laboratory and clinic

01 p0012 A73-10663

Sensitometric instruments for black and white and color photographic material and image measurements, including recording microdensitometer, reflection goniodensitometer, automatic granulometer and projection resoluometer

01 p0051 A73-10837

Ceramic film indicator for determining and recording of temperatures on space vehicle heat shield.

01 p0052 A73-11168

Two coordinate oscillograph recording device with automatic reversing for stress-strain tests under static and cyclic loads

02 p0168 A73-12144

Magnetograph instrumentation and measurements, presenting solar magnetic field fine structure observations

04 p0496 A73-14829

Two beam optical recording instrument for atmospheric IR transmissivity, discussing spectrophotometers with changeable NaCl, KBr and LiF prisms

04 p0450 A73-15575

Atmospheric diffusion, radio meteor trail radius and electron density distribution effects on radar echoes time position, noting recorder resolution increase

05 p0617 A73-16613

Apparatus note - A system for detecting and recording movements of the head.

06 p0656 A73-17522

High bandwidth and resolution laser scanners and recorders for imagery transmission, discussing component constraints and integrated optics utilization in modulator and scanner development

06 p0701 A73-18310

High data rate holographic recorder with six-channel acousto-optical modulator array as input composer and mode locked Ar laser as light source

06 p0694 A73-18311

Experimental results on the application of an x-y acousto-optic deflection system to wide band laser recorders.

06 p0701 A73-18312

The influence of recording speed on apexcardiographic timing - A multi-observer study of precision and performance utilizing randomized tracings in multiple subjects.

07 p0785 A73-19932

Design and performance of multichannel current ink jet recording instruments with galvanometers, noting mercury lamp light source, sensitivity and temperature effects

07 p0828 A73-20547

Recording and reconstruction method for image plane hologram multiplexed tenfold in small area, using He-Cd laser

08 p0964 A73-21052

Nucleation film/electron beam recorder - Near-real-time display system.

08 p0965 A73-21247

A method for electrocardiogram recording in Rhesus monkeys

08 p0934 A73-21324

Photomultiplier pairs arrays operation as solar magnetograph detector using fiber optics, comparing to photographic methods

08 p0970 A73-21737

Modification of the electroencephalograph 4EEG-1 for polygraphy

09 p1044 A73-22370

A new method for thermographic investigation of high-speed crystallization processes in high-melting-point metals

09 p1103 A73-22483

Apparatus for recording acoustic signals from cracks initiated in brittle materials.

09 p1086 A73-23165

Amplifier design for continuous recording of plasma frequency, using dipolar resonance signal obtained from parallel whip antennas surrounded by plasma sheath

10 p1216 A73-23747

Continuously recording cloud nuclei counter, describing diffusion chamber with separate functions of sample supersaturation and photoelectric droplets recording

10 p1217 A73-23990

Recorder adapter operational circuit design for continuous logarithmic readout recording of atomic absorption double beam spectrophotometers

11 p1367 A73-26313

An ultrasonic technique for the inspection of magnetic and explosive welds, using a facsimile recording system.

12 p1502 A73-27037

Multi-information recording and reproduction in the ultrasono-cardio-tomography.

13 p1579 A73-28581

Phase and amplitude only scanned acoustical holograms, noting Fraunhofer diffraction region reconstructed images

13 p1615 A73-28592

Triggering apparatus for optimal recording of slowly evolving phenomena using electrical impulse or mechanical contact signal

13 p1617 A73-28840

Video-to-film color-image recorder.

13 p1619 A73-29240

New method of thermographic investigation of rapid processes of crystallization of refractory metals.

15 p1891 A73-32070

Equipment for recording and computer input of solar magnetograph data

15 p1878 A73-32139

Automatic recording method for the moments of exact-time radio signals

15 p1878 A73-32143

ARINC-573 recording system - Application to maintenance

15 p1883 A73-32462

System of recording based on partial on-board processing

15 p1880 A73-32494

A device for the continuous measurement of subjective changes

16 p1975 A73-33090

Real time digital videomagnetograph at the Aerospace San Fernando Solar Observatory.

17 p2168 A73-34909

Third generation Aircraft Recording Instrumentation System /ARIS III/, consisting of digitizer and logic, analog interface and hybrid instrumentation recorder

17 p2174 A73-35581

A low-cost system for reproducing ERTS imagery.

18 p2315 A73-36018

A photometric system for automatic recording of optical absorption spectra

21 p2700 A73-40561

A comparison of predicted skin temperatures with thermographic measurements.

22 p2813 A73-42053

A new automatic ozone recorder for near-surface measurements working at 19 stations on a meridional chain between Norway and South Africa.

23 p2982 A73-43863

RECOVERABILITY

Drone launch and recovery reliability requirements for target, reconnaissance, air-to-air combat, high altitude endurance and defense suppression missions

19 p2381 A73-37681

The Jindivik Drone Program to demonstrate air cushion launch and recovery.

19 p2382 A73-37697

RECOVERABLE LAUNCH VEHICLES

Performance of recoverable single and multiple Space Tugs for missions beyond earth escape.

07 p0906 A73-20471

Space shuttle solid rocket boosters ocean recovery, discussing mission requirements, parachute configurations, tradeoff studies and model testing

18 p2358 A73-36084

RECOVERABLE SATELLITES

U RECOVERABLE SPACECRAFT

RECOVERABLE SPACECRAFT

NT APOLLO SPACECRAFT

NT REUSABLE SPACECRAFT

NT SPACE SHUTTLES

Two stage recoverable space shuttle structural design, discussing configurations, costs and orbiter and booster materials and thermal protection systems

23 p0308 A73-43786

RECOVERY

Prediction of the landing point of a balloon payload.

01 p0005 A73-11208

Air cushion landing system /ACLS/ application to Jindivik target drone aircraft for recovery improvement, considering flight performance degradation

19 p2383 A73-37698

RECOVERY PARACHUTES

Decelerator parachute systems for heavy loads recovery, discussing stress, stability and reliability assessment

03 p0251 A73-14638

Recovery of sounding rocket payloads by center-of-gravity position control.

09 p1155 A73-23213

Cost effective space shuttle solid rocket booster recovery parachute system planning, discussing model drop and structural load testings

15 p1825 A73-31427

Performance/stability of midair recovery system with tandem parachute configuration, discussing gliding and nongliding systems

15 p1827 A73-31447

Drone recovery surface impact and midair techniques involving parachutes and/or hot-air balloons, considering TALOS/Low Altitude Supersonic Target recovery capability

15 p1827 A73-31451

Aircraft recovery by inflatable wing canopy with steel cable or fiber suspension lines, discussing aerodynamic characteristics, suspension system and centrifugal compressor performance

15 p1828 A73-31454

An airdrop system for testing large parachutes for recovery of loads in excess of 50,000 lb.

15 p1828 A73-31455

A 14.2-ft-Do variable-porosity conical ribbon chute for supersonic application.

15 p1828 A73-31456

F/R-101 ejection seat upgrade kit for performance improvement, discussing propulsion, trajectory control, snubber system and rapid recovery parachute opening

16 p1966 A73-32667

Space shuttle solid rocket boosters ocean recovery, discussing mission requirements, parachute configurations, tradeoff studies and model testing

18 p2358 A73-36084

RECOVERY TEMPERATURE

U SKIN TEMPERATURE [NON-BIOLOGICAL]

RECOVERY ZONES

Sounding rocket payload recovery systems

14 p1804 A73-30088

RECRYSTALLIZATION

Textures of deformation and of primary and secondary recrystallization in high-purity nickel

01 p0064 A73-10614

Two phase recrystallization temperatures and structural inhomogeneity of dispersion hardened Ni after cold working and annealing at 1300-1400 C

03 p0324 A73-13508

Secondary maximum grain size and even-grained texture in the region of low and moderate deformations during recrystallization of certain nickel- and iron-based alloys

03 p0326 A73-13967

Influence of the degree of decomposition of a solid solution of zirconium in aluminum on the recrystallization temperature of an aluminum-zinc-magnesium-zirconium system alloy

03 p0327 A73-13972

Hardness-controlling additions in transition metal-beryllium alloys

03 p0328 A73-14655

Influence of the degree of purity on the kinetics of the recrystallization of deformed magnesium
05 p0587 A73-17216

Electron microscopic investigation of cold worked and annealed thin V and Mo foils recrystallization characteristics, considering effect of grain boundaries pinning at surface
05 p0588 A73-17245

Effect of recovery on recrystallization of aluminum
99.85
06 p0705 A73-17849

Influence of rare-earth metals on the grain growth process during recrystallization of heat-resistant steels
06 p0706 A73-17887

Regeneration and recrystallization of austenite in low-carbon stainless steel 18-10 after rolling at room temperature
07 p0837 A73-19113

Determination of some kinetic recrystallization parameters of thin films by mathematical and graphical analysis of crystallite boundary shapes
07 p0861 A73-19329

Body centered cubic transition metal stage 3 electrical resistivity recovery mechanism from experiment on recrystallized and stress-relieved plastically deformed Nb wire
07 p0839 A73-20112

Havero ureilite - Evidence for recrystallization and partial reduction.
09 p1140 A73-21869

Recrystallization in Ti-15 Mo base beta titanium alloys.
09 p1103 A73-22423

Structural features of surface layers in molybdenum alloy sheets
09 p1106 A73-23188

Recrystallization of electron-beam-melted tungsten with tantalum and zirconium carbide additions
09 p1106 A73-23189

Recrystallization of the IVT-1 beta titanium alloy
09 p1107 A73-23192

Ductility of recrystallized molybdenum as a function of oxygen concentration and grain size
09 p1108 A73-23231

Determination of the composition of Ni-NiMo eutectic by the zone recrystallization method
09 p1108 A73-23239

Influence of the degree of deformation and annealing temperature on the recovery of 99.999% pure nickel after plastic deformation at -196 C and 25 C, respectively
10 p1231 A73-23690

Mechanical properties of recrystallized molybdenum containing vanadium microadditions
10 p1233 A73-24361

Ultrasonic treatment of alloy MA2-1 during solidification.
10 p1236 A73-24930

Cu annealability tests for assessing suitability for applications requiring low softening temperature, discussing recrystallization behavior and softness measures
11 p1379 A73-25130

Additives alloying with cobalt, discussing allotropic transformation dependence, recrystallization, mobile dislocations, and iron deformation by twinning
11 p1408 A73-25322

Possibility of silicon carbide recrystallization in the process of reactive sintering
12 p1503 A73-27555

The role of annealing twins in the primary recrystallization of nickel 270 work hardened in tension
12 p1514 A73-27988

Influence of recovery and recrystallization on the Young's modulus and its temperature dependence in Invar-type iron-nickel alloys
14 p1760 A73-30586

Characteristics of the decomposition of an interstitial-impurities solid solution in molybdenum during recrystallization
14 p1760 A73-30589

German monograph - The effect of interstitial elements and recrystallization on the defined yield point of titanium.
14 p1762 A73-30665

Effect of rare earth metal additions on the recrystallization of nickel
14 p1765 A73-30887

Carbonyl nickel recrystallization characteristics from hardness-temperature graphs and X ray analyses
14 p1765 A73-30891

Grain-boundary sliding and recrystallization of Nimonic 108 during creep.
15 p1887 A73-31352

Inter-crystalline failure in recrystallized low-alloyed molybdenum alloys
17 p2189 A73-34577

Relation between the brittle-viscous transition temperature and structural characteristics in certain low-alloyed chromium alloys
17 p2189 A73-34579

The effect of thermomechanical pretreatment on the allotropic transformation in cobalt.
17 p2190 A73-34645

Fine structure of rolled annealed tungsten sheet, discussing subsurface layer recrystallization and deformation effects based on radiographic examinations
19 p2440 A73-37443

Influence of alloying with elements of group VIII on the mechanical properties of a molybdenum alloy containing carbon in the cast and recrystallized states
20 p2577 A73-39366

Microstructure of recrystallized alloy Kh20N80.
21 p2721 A73-41042

Microstructural characteristics of the plastic deformation and recrystallization of an aluminum alloy of various heterophase structure
23 p2991 A73-43489

Recrystallization and X-ray fine structure studies of the age-hardening characteristics of the metastable titanium alloy Ti-13V-11Cr-3Al
23 p2992 A73-43913

Investigation of the softening processes in molybdenum and its alloys under conditions of creep
23 p2995 A73-44281

Transformation of meteorite material in experiments on explosively produced shock compression at pressures of 500 and 1000 kbar
24 p3137 A73-44710

The Canyon Diablo meteorite.
24 p3137 A73-44949

Recrystallization and precipitation induced by high temperature deformation - Case of a weldable construction steel containing niobium
24 p3101 A73-45524

RECTANGULAR BEAMS

Application of the Dirac delta function in the calculation of the bending of a rectangular beam with shear strain
03 p0384 A73-13130

Minimum weight rectangular beam grillages and reinforced plates of given strength or stiffness, presenting solutions for various boundary conditions
04 p0508 A73-14937

Bending-produced cracks, stresses and fracture of rectangular cross section beam from brittle body homogeneous model
12 p1552 A73-27255

Modal synthesis technique for natural frequencies and mode shapes of bent rectangular beam in flexure-torsion oscillation under six boundary constraint conditions
16 p2075 A73-32792

The plastic bending of beams and their failure by low cycle fatigue.
18 p2365 A73-36617

Creep relaxation approximations and exact solutions, discussing rectangular beam pure bending, spherical shell internal pressure loading and thin circular tube bending
20 p2616 A73-39115

Optimum tapering design of vibrating cantilever beams, considering geometrically similar and rectangular cross sections and degenerated end mass case
21 p2785 A73-40839

RECTANGULAR DRAINAGE

U DRAINAGE PATTERNS

RECTANGULAR GUIDES

Ray optical procedure to obtain scalar Green function for polygonal waveguides by image diagram identification from rectangular guide equivalent combinations
01 p0024 A73-10684

Microwave-power attenuation in Gunn diodes
01 p0025 A73-10979

Natural frequencies of a rectangular waveguide filled with a piecewise-homogeneous dielectric
04 p0417 A73-15076

Characteristics of waveguides containing anisotropic warm plasma in the presence of transverse magnetic field.
04 p0480 A73-15600

Computer analysis of latching phase shifters in rectangular waveguide.
06 p0678 A73-18743

Effect of collision frequency on the characteristics of waveguide filled with homogeneous anisotropic plasma.
07 p0857 A73-19533

Application of impedance treatment to diffraction problems for rectangular waveguide.
07 p0802 A73-20143

Reflection of a microwave signal from a semiconductor plate of finite thickness
08 p0995 A73-21517

General cavity analysis for corrugation in rectangular waveguide microwave filters, using admittance method with consideration for propagation modes
10 p1192 A73-23606

A measurement stand for reciprocal circuits in a waveguide
10 p1189 A73-24417

Relativistic particle beam stability and electromagnetic oscillations in plasma rectangular waveguide under longitudinal magnetic field
10 p1258 A73-24887

Two mode rectangular waveguide longitudinal and transverse narrow half wave slots properties, discussing measurement apparatus and techniques and radiation patterns
11 p1328 A73-25661

Design and performance of electrically regulated phase shifter comprising rectangular waveguide section containing two ferrite resonators magnetized at ferromagnetic-resonance frequency
12 p1477 A73-26945

Synthesis of a reflection-type broadband Esaki-diode amplifier using rectangular waveguide.
13 p1594 A73-29229

Electromagnetic wave reflection and transmission by slant air/dielectric interface in rectangular waveguide investigated by Green function technique
14 p1724 A73-29706

The scattering matrix of a double truncated corner in a waveguide
14 p1726 A73-30073

Broad-band impedance matching of rectangular waveguide phased arrays.
14 p1734 A73-30205

A wide-band square-waveguide array polarizer.
14 p1735 A73-30228

Analysis of EH inhomogeneities and singular H inhomogeneities in a rectangular-section waveguide
14 p1729 A73-30560

Transient radiation in a shortened waveguide
17 p2120 A73-34116

An experimental investigation of the propagation of electromagnetic waves in a rectangular waveguide, partially filled with n-InSb in a transverse magnetic field.
17 p2123 A73-35166

Analysis of thick rectangular waveguide windows with finite conductivity.
18 p2292 A73-36605

A circular waveguide 'hybrid-T' and its applications.
18 p2292 A73-36606

Rectangular waveguide loaded by a semiinfinite chain of ferrite spheres
19 p2406 A73-38341

Phase characteristics of a rectangular waveguide with symmetrically arranged, transversely magnetized ferrite layers
19 p2407 A73-38342

Equivalent conductivity of a longitudinal slot on the broad wall of a uniformly curved rectangular waveguide
21 p2648 A73-40199

Tilted, off-center, matched slots on the broad wall of a uniformly curved rectangular waveguide
21 p2648 A73-40200

Analysis of infinite planar array of rectangular waveguides by generalized scattering matrix approach.
21 p2651 A73-40652

Realized gain function for a cylindrical array of open-ended waveguides.
21 p2653 A73-40677

On inhomogeneously filled rectangular waveguides.
21 p2657 A73-41430

Relativistic particle beam stability and electromagnetic oscillations in plasma rectangular waveguide under longitudinal magnetic field
21 p2749 A73-41662

Impedance properties of a longitudinal slot antenna in the broad face of a rectangular waveguide.
22 p2831 A73-41845

Coupling coefficient/frequency characteristics of rectangular dielectric waveguide channel dropping coupled line filter for millimeter wave
23 p2961 A73-44118

Wave propagation through a highly restrained solid-state plasma.
23 p3012 A73-44141

Optical information transmission over rectangular waveguide communication channels in terms of geometry-wavelength ratio, transparency and repeater functions
23 p2955 A73-44296

The damping of electromagnetic waves in smooth, superconductive waveguides.
24 p3068 A73-44945

RECTANGULAR PANELS

Flutter of flat rectangular sandwich type panels in a supersonic, coplanar gas flow, with arbitrary direction.
03 p0392 A73-13768

On the weight optimization problem for supersonic rectangular flat panels with specified flutter speed.
04 p0511 A73-15170

The stability of simply supported rectangular surfaces in uniform subsonic flow.
11 p1441 A73-25702

Generalized random forces in time domain for rectangular panels under subsonic and supersonic boundary layer turbulence, investigating probabilistic nature by Monte Carlo method
17 p2241 A73-34182

Weight reduction in stiffened panels with specified initial buckling load in uniform longitudinal compression by stiffeners utilization 21 p2787 A73-41190

Response of panels to turbulence-induced, surface-pressure fluctuations and resulting acoustic radiation to the flow field. [AIAA PAPER 73-993] 24 p3077 A73-44828

RECTANGULAR PLANFORMS

NT RECTANGULAR PANELS

NT RECTANGULAR PLATES

NT RECTANGULAR WINGS

Study of the far wake vortex field generated by a rectangular airfoil in a water tank. [AIAA PAPER 73-682] 18 p2262 A73-36233

Free oscillations of a double layer in a turning rectangular basin of constant depth 19 p2419 A73-37530

Integral equation in the theory of lifting surfaces 19 p2377 A73-37846

Stress-strain state of stiffened shallow shells of rectangular planform 22 p2928 A73-43054

RECTANGULAR PLATES

Iterative solution of thermal bending problem for nonuniformly heated thin rectangular plate with discrete boundary conditions 01 p0113 A73-10020

Rectangular plates with unidirectionally variable rigidity 01 p0114 A73-10572

Fourier analysis of laminated anisotropic rectangular plates with strong cross elasticity effects, presenting deflection, bending moments and buckling data 01 p0115 A73-10735

Thermal bending of moderately thick rectangular plate. 01 p0115 A73-10739

Buckling of laterally loaded plates having initial curvature. 01 p0115 A73-10768

Phase plane analysis of free vibration of rectangular plate loaded by in-plane compressive load, calculating critical load and amplitude in postbuckling region 01 p0115 A73-10770

Elasticity theory contact problem for rectangle under compression loads, using Airy stress function for reduced linear algebraic equations system 01 p0117 A73-10990

Approximate relationships between the behavior of plates under destabilising and non-destabilising loads. 01 p0117 A73-11120

Rectangular plate stability under compression by uniformly distributed loads applied to two opposite simply supported edges with mixed boundary conditions at other edges 02 p0230 A73-11640

Solution to the bending problem and to the plane problem of an anisotropic rectangular plate with arbitrary boundary conditions and the application of the solution to composite structure designs 02 p0230 A73-11715

Analysis of unbalanced angle-ply rectangular plates. 02 p0234 A73-12073

Bending of a physically nonlinear viscoelastic rectangular plate under the action of a transversely distributed load 02 p0237 A73-12587

Vibration of a square plate symmetrically supported at four points. 02 p0237 A73-12605

Effect of residual or characteristic stresses on the deformation of plates 03 p0385 A73-13143

Parametric vibration of simply supported rectangular plate and cylindrical shell under random excitation, using Markov process theory and Fokker-Planck equation 03 p0388 A73-13318

Impulsive loading of rectangular plates with finite plastic deformations. 03 p0389 A73-13322

Effect of membrane forces on large deflection of simply supported rectangular plates. 03 p0389 A73-13323

Vibration and buckling of a rectangular plate with an internal support. 03 p0391 A73-13372

Minimum weight rectangular beam grillages and reinforced plates of given strength or stiffness, presenting solutions for various boundary conditions 04 p0508 A73-14937

On the forced vibration of a rectangular plate. [ASME PAPER 72-WA/DE-20] 04 p0514 A73-15838

Linearized theory of dynamically loaded thin rigid viscoplastic rectangular plates transient response, investigating strain rate effect 06 p0760 A73-17760

Monograph - Grid analysis of orthotropic plates. 06 p0761 A73-17873

Thermal shock induced transverse vibrations in rectangular plate with combined simple and clamped edge supports, deriving infinite series solutions 06 p0761 A73-17896

Two-dimensional temperature fields in straight rectangular fins 06 p0768 A73-17921

Bending theory of rectangular plates loaded along curve, obtaining solutions by Fourier single and double series 06 p0763 A73-18451

Nonlinear natural vibrations of rectangular plates and cylindrical panels. 06 p0765 A73-18640

Steady state vibrational frequencies of grid stiffened rectangular plates with monolithic connection at node points for simply supported case 07 p0909 A73-19095

Notch induced stress concentrations at elastic rectangular core /inclusion/ in extended rectangular plate with rigidly supported edges, using finite element method 07 p0910 A73-19196

Nonlinear vibrations of rectangular plates with cutouts. 07 p0913 A73-19978

Stability of clamped rectangular plates in uniform subsonic flow. 07 p0913 A73-19982

Turbulent boundary layer separation in supersonic air flow around flat rectangular plate, calculating flow geometry and pressure distribution 07 p0775 A73-20082

Finite element displacement method for large amplitude free flexural vibrations of beams and plates. 07 p0914 A73-20212

Three dimensional analysis in series form for statics and dynamics of simply supported rectangular plates of micropolar elastic material, obtaining free vibration frequencies 07 p0917 A73-20565

Postbuckling analysis of rectangular orthotropic plates. 08 p0105 A73-20673

Free vibrations of square plates with stiffened square openings. 08 p0106 A73-20826

Vibration of four point-supported plates by a finite element method. 08 p0107 A73-20945

Use of chromoplastic models for the study of the behaviour of rectangular plates after buckling. 08 p0107 A73-20946

Acoustic radiation from plates excited by flow noise. 08 p0988 A73-21470

Calculation of the stability of rectangular plates in an air flow by the finite-element method 08 p0108 A73-21512

A theoretical study of natural convection heat transfer from downward-facing horizontal surfaces with uniform heat flux. 08 p1024 A73-21638

Difference iterative solution for two dimensional boundary value problem for rectangular elastic plate with rectangular cutout 09 p1159 A73-22584

Experimental study of the damping of bending vibrations in supported square plates with coatings. 09 p1161 A73-23153

Post-buckling behaviour of rectangular orthotropic plates. 10 p1288 A73-23699

Vibration analysis of clamped, rectangular plates of generalized orthotropy. 10 p1291 A73-24387

An upper bound solution for rectangular plate in plane stress compression. 10 p1292 A73-24640

Buckling and vibration of unsymmetrically laminated cross-ply rectangular plates. [AIAA PAPER 73-368] 11 p1438 A73-25503

Incremental deformations in orthotropic laminated plates under initial stress. [ASME PAPER 72-APM-VV] 11 p1441 A73-25707

On the vibration of shear deformable curved anisotropic composite plates. 11 p1442 A73-25711

An elastic-plastic buckling solution using the incremental theory. 11 p1443 A73-26089

Influence of a small bending stiffness on the lateral vibrations of a clamped rectangular membrane [DFVLR-SONDDR-226] 11 p1445 A73-26425

Eigenfunction analysis for bending of clamped rectangular, orthotropic plates. 11 p1447 A73-26653

Stability of rectangular plates under mixed boundary conditions 12 p1552 A73-27372

Study of the rigidity of rectangular plates during bending by the finite-element method 12 p1553 A73-27461

Discrete flexural analyses of rectangular plates of abruptly varying stiffnesses. 12 p1556 A73-27926

Shape function generation for high order conforming rectangular plate element in bending theory, noting rapid convergence of deflection and bending moments 13 p1691 A73-28087

Elastic structures nonlinear free vibrations theory based on Hamilton principle and perturbation method, applying to beams and rectangular plates 13 p1696 A73-28751

Analysis of self-excited and forced vibrations of a rectangular plate on many supports in supersonic flow. 13 p1700 A73-29392

Effects of specimen geometry and loading conditions on the crack tip plastic zone. 13 p1701 A73-29474

Finite element analysis with improved accuracy for rectangular plate bending element. 14 p1810 A73-30456

Bending of rectangular plates of variable thickness with edges reinforced by elastic ribs 14 p1815 A73-30796

Nonlinear vibrations of rectangular plates. 15 p1944 A73-31000

Buckling of eccentrically stiffened rectangular plates subjected to linearly varying longitudinal compression. 15 p1952 A73-32043

Thermal stress in and bending of elastic rectangular plates from Kantorovich method combined with iterative techniques 16 p2077 A73-32993

Buckling of rectangular plates with general variation in thickness. [ASME PAPER 73-APM-10] 17 p2247 A73-35035

Vibration of plates subject to arbitrary in-plane loads - A perturbation approach. [ASME PAPER 73-APM-26] 17 p2248 A73-35042

Nonlinear vibration of a rectangular plate arbitrarily laminated of anisotropic material. [ASME PAPER 73-APM-F] 17 p2249 A73-35105

Approximate method for determining the natural frequencies of flexible rectangular plates 18 p2363 A73-36408

Photoelastic study of rectangular plates under bending. 19 p2498 A73-37667

Two-dimensional problem in elasticity theory for a rectangle with mixed boundary conditions 19 p2499 A73-37761

Free harmonic vibrations of thin pretwisted rectangular plates analyzed in terms of torsional and bending vibration coupling based on shell theory 19 p2500 A73-38115

Nonlinear bending of rectangular orthotropic plates. 19 p2500 A73-38116

A difference-energy method of studying the stability of rectangular plates in shear 20 p2617 A73-39306

Nonlinear response of plates subjected to inplane and lateral pressure pulses. 20 p2622 A73-39547

An approximate solution for bending of anisotropic laminated plates. 20 p2623 A73-39554

Finite difference technique for elastic-plastic buckling of edge-loaded rectangular plates, finding bifurcation stresses via Hill and Prandtl-Reuss expressions 20 p2623 A73-39560

Large deflection of shallow paraboloid shells. 21 p2782 A73-40005

Square plate symmetrically supported at four diagonal points, evaluating fundamental vibration frequency with accuracy by finite element method 21 p2783 A73-40293

Sinusoidal response of composite-material plates with material damping. [ASME PAPER 73-DET-120] 22 p2919 A73-42082

The theory of elasticity of flexural-stiffness exhibiting, planar particle systems with a rectangular net 22 p2922 A73-42526

Bending of a rectangular piezoelectric plate clamped over its edge 23 p3043 A73-43923

Large amplitude vibrations of elastically restrained rectangular plates. 23 p3048 A73-44380

Nonlinear transverse vibration analysis of a rectangular plate with lumped M-S-D systems. 23 p3048 A73-44384

Solution of physically nonlinear quasi-static problems of viscoelasticity 24 p3145 A73-44519

Transverse coupled thermoelastic vibrations of elastically supported rectangular and circular plates under nonstationary harmonic temperature field 24 p3147 A73-44682

Emission of sound from a rectangular plate vibrating under the action of pressure pulsations in a turbulent boundary layer 24 p3109 A73-44899

Influence of initial deflections on the work of a rectangular plate subject to bending in its plane 24 p3150 A73-45244

Free vibration of square plates under different boundary conditions, determining opening geometry

RECTANGULAR WIND TUNNELS

effects on fundamental frequencies by grid framework model with finite difference operators
24 p3151 A73-45266

Vibration of rectangular plates with mixed boundary conditions.
24 p3151 A73-45268

RECTANGULAR WIND TUNNELS

A general solution for lift interference in rectangular ventilated wind tunnels.
05 p0563 A73-16940

RECTANGULAR WINGS

Vortex sheath formalism based on coupled integral equations for rectangular wing-slipstream aerodynamic interference
03 p0244 A73-13562

The effects of leading-edge serrations on reducing flow unsteadiness about airfoils.
05 p0529 A73-16853

Calculation of the aerodynamic characteristics of a rectangular wing with tip plates moving at a low subsonic speed in the proximity of a screen
07 p0775 A73-20094

Downwash-velocity potential method for oscillating surfaces.
13 p1564 A73-28803

A theory for rectangular wings with small tip clearance in a channel.
15 p1821 A73-31120

Thin rectangular lifting flow investigation at small angle of attack in parallel flow based on Prandtl acceleration potential theory
15 p1955 A73-32126

On the application of a new version of lifting surface theory to nonslender and kinked wings.
23 p2939 A73-43210

RECTIFICATION

Electric power generation on earth via satellite solar power station, assessing technologies of energy collection and conversion, microwave transmission and rectification
17 p2110 A73-35313

RECTIFIERS

NT AVALANCHE DIODES

NT GERMANIUM DIODES

NT THYRATRONS

NT THYRISTORS

Circuit design of triode thyristors and companion rectifiers for high frequency power conditioning, discussing emitter selection, lifetime control, encapsulation and interdigitation optimization
03 p0283 A73-13943

Multiphase even harmonic frequency multipliers using nonlinear magnetic reactors with bridge rectifiers, considering output signal waveforms
12 p1477 A73-26788

The influence of Auger recombination on the forward characteristic of semiconductor power rectifiers at high current densities.
15 p1850 A73-31130

Methods of calculating high-power rectifier and inverter circuits
15 p1832 A73-31696

Semiconductor rectifiers and thyristor devices, discussing transistor switching, Zener diode, controlled and light activated p-n-p diodes
21 p2668 A73-41619

Theory of power rectification and harmonic generation processes at super-high frequencies
22 p2800 A73-42213

Impulse analysis of subharmonic oscillations in control systems with thyristor converters.
22 p2835 A73-42299

Semiconductor rectifiers analysis, considering triac and thyristor tetrode circuits, trigger devices and circuit diagrams
22 p2835 A73-43128

RECUPERATORS

U REGENERATORS

RECURSION FORMULAS

U RECURSIVE FUNCTIONS

RECURSIVE FUNCTIONS

A non-parametric method with applications to pattern recognition and mode estimation.
06 p0672 A73-18805

An efficient parallel algorithm for the solution of a tridiagonal linear system of equations.
08 p0983 A73-20960

Tree-manipulating systems and Church-Rosser theorems.
08 p0941 A73-20962

Recursive solution for steady forced vibration modes of tensed string under concentrated harmonic forces
09 p1120 A73-22583

On a method of adaptive control under conditions of great uncertainty.
10 p1199 A73-24036

Study of recurrence relationships and their applications by the Laboratoire d'Automatique et de ses Applications Spatiales.
10 p1200 A73-24042

An analytical iterative algorithm for the prediction of special satellite orbit points with the Brouwer orbit theory.
11 p1423 A73-26075

Counting operation based recursive digital filter hardware design in canonic and direct forms, emphasizing low cost, low speed and high flexibility
12 p1483 A73-27116

Algebraic criteria for positive realness relative to the unit circle.
16 p2032 A73-33162

A class of particular solutions to three-dimensional equations of dynamics in the theory of elasticity
17 p2251 A73-35587

Convergence of learning and adaptation algorithms
20 p2532 A73-38711

Recursive formulas for the partial fraction expansion of a rational function with multiple poles.
21 p2660 A73-40097

A practical means of calculating normal forms in problems involving nonlinear oscillations
21 p2738 A73-40178

Recursive methods in photogrammetric data reduction.
22 p2862 A73-42825

Design and structure of a flexible recursive digital filter
23 p2957 A73-43315

Adaptive equalization with recursive noncanonical scanning filters
23 p2953 A73-43323

An innovations approach to least-squares estimation. V - Innovations representations and recursive estimation in colored noise.
23 p2954 A73-43819

Perturbation method applications to elasticity theory three-dimensional problems, discussing differential operator construction via recursion relations
23 p3046 A73-44190

RECYCLING

U CIRCULATION

RED ARCS

Simultaneous occurrences of hydrogen arcs and mid-latitude stable auroral red arcs.
10 p1214 A73-24740

Stable auroral red arc equatorial edge observation with photometer during recovery phase of magnetic storm on 18 December 1971 in Southern Africa
12 p1492 A73-27611

Red arc data from Richland /WA/ and by Ogo 6 satellite observations, discussing thermal conduction formation theory
14 p1749 A73-30500

Red auroras in the morning sector.
16 p2004 A73-33446

On the motion of the tropical red arc north boundary.
16 p2008 A73-33882

F-layer and 6300-A measurements in the day sector of the auroral oval.
18 p2312 A73-36281

RED BLOOD CELLS

U ERYTHROCYTES

RED SHIFT

Optical identifications and positions of blue stellar radio sources without UV excess, comparing with N-galaxies and quasars with red shift
01 p0103 A73-10997

White dwarfs gravitational red shifts, radial velocities and mass-radius relationships, considering colors and luminosities
01 p0104 A73-11036

Statistical analysis of galaxy counts in small red shift quasar fields, comparing to number of galaxies around randomly chosen point
03 p0370 A73-13194

The redshifts of quasi-stellar objects and associated galaxies.
03 p0375 A73-13896

Hubble law from constant light velocity in Euclidean space, noting red shift equation and Einstein gravitational shift
03 p0379 A73-14577

Schwarzschild interior metric singularity for ideal fluid sphere radius relation to Schwarzschild radius, noting conditions for emitted light red shift
03 p0380 A73-14588

Radio source counts and redshifts in steady state cosmology.
04 p0497 A73-15048

The redshift-distance relation. II - The Hubble diagram and its scatter for first-ranked cluster galaxies: A formal value for q-sub 0. III Photometry and the Hubble diagram for radio sources and the possible turn-on time for QSOs.
04 p0498 A73-15351

Cosmological deceleration parameter differences prediction from light evolution correction on diameter-red shift relation of cluster elliptical galaxies
04 p0502 A73-15689

Radio galaxies luminosity function from radio power range at 178 MHz with known red shift, using 3C catalog galaxies
05 p0622 A73-17071

Mean radial velocity of Virgo galactic cluster from red shift data, approximating velocity distribution of elliptical-lenticular and spiral galaxies
05 p0622 A73-17074

The distribution of redshifts of quasi-stellar objects and related emission-line objects.
05 p0626 A73-17376

The red-shifts and the patterns of electromagnetic waves in quasistellar objects.
06 p0750 A73-18015

Search for 3C 191 ionization potential-red shift correlations to other quasar absorption lines
07 p0900 A73-20237

Observational discrepancies of redshift-distance relationships associated with galaxies and quasars
07 p0904 A73-20639

Hubble diagram construction for optically luminous quasars, noting relation between red shift and apparent magnitude
08 p1002 A73-20877

Shakhbazian I - A distant cluster of compact galaxies.
08 p1004 A73-20897

A redshift magnitude relation for radiation universes.
08 p1007 A73-21002

Redshifts of a BSO and galaxies in the vicinity of the radio source RN 8.
08 p1009 A73-21171

Galactic absorbing material effects on quasar apparent distribution, noting brightness decrease with red shift
09 p1147 A73-22572

Invalidity of quasar-nearby galaxy angular distance dependence on galaxy red shift from investigation of larger sampling of pairing systems
10 p1273 A73-23702

Quasar characteristics, considering emission or absorption lines, red shift, optical intensity variation, unipolar generator representation and relativistic particle production
10 p1280 A73-24322

Statistical analysis of multiple absorption spectra in QSO.
10 p1284 A73-24905

Quasar classes to explain radio, optical and X ray observations, considering models for local quasar intrinsic red shift
11 p1417 A73-25262

The redshift-distance relation. IV - The composite nature of N galaxies, their Hubble diagram, and the validity of measured redshifts as distance indicators.
11 p1427 A73-26602

The spectrum of the extranuclear regions of Ton 256.
11 p1428 A73-26624

List of clusters of galaxies with published redshifts.
11 p1428 A73-26677

A survey of elliptical galaxies at 6 cm.
13 p1685 A73-29361

Redshift-magnitude bands, quasi-stellar sources, and systems of redshift.
14 p1797 A73-30004

Black holes and absorption redshifts in quasi-stellar objects.
14 p1797 A73-30006

Quasar red shift mechanism based on atomic energy levels and particle rest masses variations in scalar gravitational field
15 p1929 A73-31062

Cosmological information from surveys of radio source spectra.
15 p1933 A73-31396

Mariner 9 ultraviolet spectrometer experiment - Upper limits on the Lyman-alpha flux from clusters of galaxies.
15 p1936 A73-31551

Redshifts for 51 galaxies identified with radio sources in the 4C catalog.
15 p1936 A73-31562

The possibility of measuring gravitational redshift by means of earth satellites.
15 p1940 A73-32074

Spectral characteristics of quasar OQ172 with large red shift, considering absorption and emission spectra and Lyman alpha radiation
16 p2070 A73-33925

Evidence for luminosity evolution of quasars.
17 p2225 A73-34287

On the apparent association of quasi-stellar objects with clusters or groups of galaxies with about the same redshift.
17 p2231 A73-34767

Optical and UV astronomical telescopes and instrumentation for quasar detection, emphasizing observational requirements and emission line red shift problem
17 p2233 A73-35277

Invalidity of quasar-nearby galaxy angular distance dependence on galaxy red shift from investigation of larger sampling of pairing systems
18 p2354 A73-36727

The redshift-distance relation. V - Galaxy colors as functions of galactic latitude and redshift - Observed colors compared with predicted distributions for various world models.
19 p2487 A73-38504

The redshift-distance relation. VI - The Hubble diagram from S20 photometry for rich clusters and sparse groups r A study of residuals. 19 p2487 A73-38505

The redshift-distance relation. VII - Absolute magnitudes of the first three ranked cluster galaxies as functions of cluster richness and Bautz-Morgan cluster type - The effect on q sub 0. 19 p2487 A73-38506

The redshift-magnitude relation for quasi-stellar objects. 19 p2487 A73-38507

Optical and near IR absorption line spectra of quasar 1331+170, discussing red shift and line locking process 19 p2487 A73-38508

A search for high-ionization redshift systems in the absorption spectra of five quasars. 20 p2609 A73-39435

Coude spectroscopy for quasar Markarian 132 absorption lines wavelengths and profiles and red shift systems 20 p2609 A73-39436

Study of the redshift structure of the Coma cluster. 20 p2610 A73-39580

Gravitational red shift, Mercury perihelion, light deflection and signal delay tests of Einstein relativity vs Jordan-Brans-Dicke theory 20 p2613 A73-39751

Centrosymmetrical nonstatic pulsating metric development, discussing minipulsar particles, perihelion displacement, gravitational energy, red shift, luminous ray curvature and Schwarzschild metric 20 p2594 A73-39765

On the interpretation of the redshift-angular size diagram for quasars. 22 p2907 A73-42211

Shakhbazian I compact galactic cluster, discussing red shift, angular size, galactic type, velocity dispersion, mass/light ratio and photographic plates 22 p2909 A73-42586

Gravitational red shift - A simple quantum field-theoretical consideration in a curved space. 23 p3006 A73-43607

The relation between redshift and surface brightness for normal galaxies in systems of galaxies. 24 p3141 A73-45193

Magnitude-redshift and count-magnitude relations in presence of an uniform intergalactic absorption. 24 p3143 A73-45436

REDUCED GRAVITY

Heat transfer as function of temperature on small horizontal wires in water and organic liquids noting application for heater low gravity behavior prediction 01 p0122 A73-10801

Biomechanics of locomotion via jumping on lunar surface, discussing subgravity effects on energy requirements, body potential and kinetic energy, muscular work, etc 22 p2804 A73-42175

REDUCTION [CHEMISTRY]

NT DEOXIDIZING

NT HYDROGENATION

Thermogravimetry system designed for use in dispersion strengthening studies. 01 p0015 A73-11449

The magnetic properties and morphology of metallic iron produced by subsolidus reduction of synthetic Apollo 11 composition glasses. 05 p0619 A73-16837

A study of germanium monoxide at high temperatures 06 p0739 A73-18659

Metallic mounds produced by reduction of material of simulated lunar composition and implications on the origin of metallic mounds on lunar glasses. 07 p0884 A73-19738

The kinetics of ulvoespinel reduction - Synthetic study and applications to lunar rocks. 08 p0936 A73-20840

Titanium alloys corrosion resistance modification relative to nonoxidizing acid media by hydrogen reduction conditions or anodic dissociation curve alteration 09 p1104 A73-22965

Comparative estimation of thermodynamic characteristics for reduction of tungsten and molybdenum oxides 09 p1107 A73-23226

Molybdenum metal by the aluminothermic reduction of calcium molybdate. 10 p1234 A73-24430

Vapor-phase deposition of elementary boron at substrate temperatures in the range from 1100 to 1400 C 13 p1645 A73-28181

The chemical stage in the mechanism of metal oxide reduction 13 p1581 A73-28937

Reduction kinetics and phase transformations of tungsten and molybdenum oxides 13 p1636 A73-28938

Prebiological synthesis of organic compounds. 14 p1724 A73-30129

The use of nitride intermediates in the preparation of metals - A study of the reduction of Nb2O5 with NH3. 14 p1761 A73-30629

Reduction of oxygen compounds of cobalt by methane 14 p1724 A73-30828

Sampling nitric oxide from combustion gases. 16 p2085 A73-33348

Procedure for preparation of metallic titanium by direct reduction of oxides under flux 19 p2441 A73-37829

Adsorption of spacecraft contaminants on Bosch carbon. 19 p2399 A73-37972

[ASME PAPER 73-ENAS-15] Nitride inclusions in titanium ingots - A study of possible sources in the production of magnesium-reduced sponge. 20 p2576 A73-39026

Preparation of zirconium-niobium alloy by carbide-oxide reaction. 21 p2717 A73-40321

Molybdenum sintering and the molybdenum-oxygen-carbon system. 21 p2722 A73-41585

The effect of halide impurities on the mass production of metal whiskers by reduction. 24 p3098 A73-44401

Specific surface changes in tungsten and molybdenum oxides during reduction processes 24 p3099 A73-44738

REDUNDANCY

Least square approach for system reliability optimization. 06 p0681 A73-18524

The average duration of the failed state in the interval between adjacent tests of a periodically verified standby radio system with z-multiple redundancy 09 p1051 A73-22464

A reliability and comparative analysis of two standby system configurations. 09 p1112 A73-22643

Reliability estimation technique for data transmission processes in remote control systems with redundancy, assuming Markovian randomness of signal input 15 p1854 A73-31806

A unified method for analyzing mission reliability for fault tolerant computer systems. 15 p1901 A73-32261

The safety, the reliability, and redundancy in the automatic flight control system of the A300-B Airbus 15 p1830 A73-32459

Onboard electronic equipment optimization and redundancy 15 p1852 A73-32460

High reliability solid state force sensors for flight control systems. 17 p2165 A73-34603

Redundant system design for advanced digital flight control. 20 p2585 A73-38785

[AIAA PAPER 73-846] Optimal stabilization of moving control plants during multichannel measurement of their coordinates 20 p2542 A73-39039

Redundant independent guidance, navigation and control system application to space shuttle, estimating channel output divergence due to sensor bias and scale factor errors 21 p2735 A73-40043

Optimal utilization of redundant information in thermal radiation in thermophysical measurements. 22 p2931 A73-42408

[ECTP PAPER II-2] Reliability estimation technique for data transmission processes in remote control systems with redundancy, assuming Markovian randomness of signal input 24 p3075 A73-45350

REDUNDANCY ENCODING

Redundant area encoding for relieving integration time requirement in airborne reconnaissance photograph transmission, discussing algorithms, display technique, data reduction and pictorial simulation 09 p1054 A73-23386

Convolutional coding for multiple-access satellite communication. 09 p1056 A73-23399

Block coding for digital computer error detection and correction, considering applications for arithmetic operations, storage media and permanent hardware failure recognition 09 p1061 A73-23400

Concatenated and hybrid coding system performance and implementation complexity for moderate speed deep space communication 09 p1056 A73-23401

Concatenated coding for deep space interplanetary communication with low data rate and SNR, comparing performance of three binary codes 09 p1058 A73-23424

Run length code for redundancy encoding of black-white facsimile picture data transmission to allow channel or storage capacity reduction and hardware simplification 10 p1188 A73-23741

Design principles for control systems of digital computers 14 p1730 A73-30035

A digital communications system for manned spaceflight applications. 20 p2527 A73-38763

Digital codings of multi-dimensional information sources and applications to image coding. 21 p2655 A73-41043

Data transmission system based on voice channels time division into blocks using cyclic code redundancy without appreciable loss in error correcting capability 21 p2655 A73-41044

Symbol set for multiregenerated digital transmission featuring highly redundant timing for low frequency phase noise suppression 21 p2656 A73-41110

Error-correcting codes in computer arithmetic. 22 p2830 A73-42713

Redundant speckle free hologram production without spurious background patterns, blocking intensity by cutting of lower order frequencies 22 p2862 A73-43089

REDUNDANT COMPONENTS

Stochastic behaviour of a complex system with standby redundancy. 01 p0023 A73-10649

The optimum allocation of redundancy - An application of mathematical programming to system design. 01 p0071 A73-11199

Study of the nonstationary characteristics of a doubled system with an unreliable servicing device 02 p0188 A73-12588

Estimates of reliability functions for systems with redundancy. 04 p0471 A73-15210

Reliability of systems with shifting redundancy in servicing a random demand flow 05 p0560 A73-16274

Avionics systems redundancy and complexity, suggesting component design with guaranteed operational life [AIAA PAPER 73-28] 06 p0673 A73-17617

Design of a fault-tolerant, modular computer with dynamic redundancy. 06 p0671 A73-18064

Calculation of the reliability of hierarchical systems with quorum redundancy 09 p1088 A73-22552

Electronic system reliability improvement by partitioning into functional parallel redundant blocks 10 p1193 A73-23651

A computer method of optimal redundancy allocation in satellite communication system. 10 p1188 A73-23753

The concept of coverage and its effect on the reliability model of a repairable system. 10 p1226 A73-24871

Parallel-redundant flight control systems, discussing sensor bias and combined control computer input effects on controllability and steady state modal response 11 p1342 A73-25783

Method of utilizing structural redundancy in a measuring system for processing experimental data with systematic errors 12 p1494 A73-26776

Mean time of the failure-free operation of a redundant system with allowance for monitoring of operational efficiency 12 p1504 A73-27619

Random failure process similarity in redundant schemes for systems with binary elements, noting statistical modeling on specialized Monte Carlo machines 12 p1485 A73-27620

Redundant central processor system for fault tolerant real time operation in space applications, describing systems organization [AIAA PAPER 73-424] 12 p1476 A73-27821

Calculation of redundant equipment recovery time when only failures of entire systems are detected by inspection 14 p1754 A73-30036

Reliability analysis of time to failure distribution of redundant system with failing elements number as periodic function of time 15 p1880 A73-30998

Multidigit switching circuit synthesis for functionally complete redundant systems with incomplete splicing correlation 15 p1853 A73-31038

Expected value and variance of failure time in redundant systems. 15 p1901 A73-32264

Quad redundant fly by wire servocontrol system design and tests in F-8C high speed jet aircraft, using fail/safe hydraulic actuators 16 p1970 A73-33080

Operational behaviour of a complex system with two out of M failed components. 16 p2022 A73-34030

Complex system reliability with general repair time distributions under preemptive repeat repair discipline. 16 p2022 A73-34031

REDUNDANT STRUCTURES

Redundant system design and flight test evaluation for the TAGS digital control system.

[AHS PREPRINT 721] 17 p2131 A73-35062
Digital fly by wire flight control system with airborne digital processor for increased aircraft survivability, determining redundancy level to satisfy system performance

17 p2138 A73-35222
Optimal modular redundancy over a set of configurations for attaining specified system availability and reliability requirements.

17 p2139 A73-35257
Failure detection and isolation methods for redundant gimbaled inertial measurement units.

[AIAA PAPER 73-851] 20 p2585 A73-38790
A design problem for redundant systems with recovery

20 p2568 A73-38996
Use of switching circuits as redundant multiplier elements in canonic digital networks.

21 p2658 A73-41209
Failure detection and isolation techniques for gimbaled and strapdown inertial systems examining redundant system reliability relationship to MTBF

[AIAA PAPER 73-852] 22 p2884 A73-41969
Triple Modular Redundancy Single Single voter-switch with majority voting of three parallel data channels or converters, estimating reliability for short and long missions

22 p2825 A73-42294
The robustness of reliability predictions for series systems of identical components.

22 p2867 A73-42667
Reliability of some redundant systems with repair.

22 p2867 A73-42668
Equivalence of redundant systems with respect to time to failure.

22 p2867 A73-42970
Hybrid fluid logic systems for integrated circuits using static and dynamic logical elements, considering fluidic circuits design with redundancy

23 p2943 A73-43411
Probability estimate models for reliable function of redundant systems with adaptable and inadaptably neuron-like restoration organs

24 p3063 A73-44904

REDUNDANT STRUCTURES U REDUNDANT COMPONENTS

REEFS
Mapping of mangrove and perpendicular-oriented shell reefs in southeastern Panama with side-looking radar.

13 p1606 A73-28170
Honolulu International Airport reef runway.

15 p1857 A73-31538

REENTRY

NT HYPERBOLIC REENTRY
NT HYPERSONIC REENTRY
NT MANEUVERABLE REENTRY
NT SPACECRAFT REENTRY

REENTRY ANGLE
U ANGLES (GEOMETRY)
U REENTRY TRAJECTORIES

REENTRY BODIES

U REENTRY VEHICLES

REENTRY EFFECTS

A Chebyshev minimax technique oriented to aerospace trajectory optimization problems.

01 p0100 A73-10729
Radiative and convective heating during Venus entry.

01 p0003 A73-10757
Systems analysis applied to a hybrid computer simulation of a missile reentering the atmosphere.

08 p0941 A73-20825
Atmospheric braking of a manned spacecraft after interplanetary flight

10 p1286 A73-23879
A mechanism for ablation-induced spin-up.

11 p1431 A73-26402
Derivation of shape change equations for asymmetrically heated ablating reentry vehicles.

13 p1706 A73-28750
Spatial oscillations of a vehicle with a nonlinear stabilization system during reentry

14 p1803 A73-29853
Impact of space shuttle orbiter reentry on mesospheric NOx.

[AIAA PAPER 73-525] 16 p2007 A73-33559
Angle of attack tests for graphite ablation models simulating spacecraft reentry using arc heating, showing temperature and pressure effects, model size and flow field characteristics

[AIAA PAPER 73-736] 18 p2295 A73-36353
Three-dimensional nosetip shape changes in hypersonic flow. I - Illustration of a mathematical model-characteristic method.

[AIAA PAPER 73-762] 18 p2264 A73-36377
A method for computing roughwall heat transfer rates on reentry nosetips.

[AIAA PAPER 73-763] 18 p2264 A73-36378
Multihundred watt radioactive isotope heat source wind tunnel tests to obtain aerodynamic coefficients, heating rate, stability and ablation for reentry protection design

19 p2456 A73-38425

Multihundred watt radioactive isotope heat source assembly for multiple space missions, discussing aerodynamic heating, shield ablation and thermal stress performance during reentry

19 p2456 A73-38426

Multihundred watt radioisotope thermoelectric generator heat source materials compatibility with thermochemical environment, considering maximum operational and reentry temperatures

19 p2457 A73-38427

Atmospheric deceleration of a manned spacecraft returning from an interplanetary flight.

20 p2614 A73-38898

E-polarized electromagnetic scattering by conducting circular cylinder coated with plasma sheath during spacecraft reentry flight under plane wave incidence

22 p2827 A73-42466

REENTRY GLIDERS

U LIFTING REENTRY VEHICLES

REENTRY GUIDANCE

Atmospheric reentry optimal lateral guidance for low lift/drag ratio space shuttle vehicle, presenting formulation as optimal stochastic control problem

[AIAA PAPER 71-914] 01 p0074 A73-10106
Synthesis of a nonlinear control law for the motion of a space vehicle in the earth's atmosphere.

05 p0627 A73-16077

Aerodynamic entry vehicle autopiots.

06 p0721 A73-18515

The conjugate gradient method and its application to aerospace vehicle guidance and control. II - Mars entry guidance and control.

08 p0986 A73-21429

Guidance methods for heat-optimal three-dimensional descent paths of aerodynamic reentry bodies

11 p1430 A73-25350

REENTRY PHYSICS

Electrical power source for spacecraft reentry trajectory control system, thermal protection and radio communication based on reentry vehicle external surfaces utilization as generator electrodes

01 p0111 A73-11174

Electromagnetic thrust from magnetic dc arc discharge plasma accelerators, noting MHD experiments and reentry simulation

04 p0489 A73-15728

Evaluation of turbulent heating predictions with flight data.

05 p0532 A73-16943

Mass spectroscopic investigation of dissociation and ionization in a simulated re-entry plasma.

09 p1130 A73-22843

Russian book - Nonequilibrium physicochemical processes in aerodynamics.

09 p1029 A73-23225

Radiative transfer through carbon ablation layers.

13 p1705 A73-28457

Inflight electrostatic probe measurements of the effect of chemical injection on the properties of the reentry flow field.

[AIAA PAPER 73-692] 18 p2338 A73-36243

Boundary-layer plasma of a re-entry vehicle - A comparison of prediction models and flight measurements.

21 p2632 A73-40420

A theoretical and experimental study of sound attenuation in an annular duct.

[AIAA PAPER 73-1005] 24 p3077 A73-44838

Aeroballistic range facilities development and application to reentry physics, discussing program for turbulent wake properties of hypersonic projectiles

24 p3054 A73-44993

REENTRY RANGE

Analytical estimate of the landing range of a spacecraft for hyperbolic return-flight paths.

05 p0627 A73-16078

Investigation of the range interval of the landing phase for hyperbolic velocities of re-entry into the earth's atmosphere.

05 p0627 A73-16079

REENTRY SHIELDING

Surface materials ablation cooling for thermal protection during reentry, discussing chemical reactions, plastics pyrolysis and propulsion chemistry

14 p1724 A73-30133

Graphite oxidation at low temperature in subsonic air.

[AIAA PAPER 73-735] 18 p2326 A73-36352

REENTRY TRAJECTORIES

The optimum reentry trajectory of a lifting vehicle.

01 p0105 A73-11126

Reentry trajectory optimization at supersonic velocities by aerodynamic lift control, using Pontryagin maximum principle

01 p0105 A73-11127

Multistep three-parameter algorithm for spacecraft stabilization on an atmospheric reentry trajectory

02 p0229 A73-12451

Minimization of spacecraft maximum acceleration in atmosphere after reentry, applying results to reentry trajectory optimization and associated optimal control problems

02 p0219 A73-12457

Design of a digital adaptive control system for reentry vehicles.

03 p0286 A73-14482

Application of adaptive tuning of filters to exoatmospheric target tracking.

04 p0498 A73-15275

Prediction in control of re-entry into the atmosphere.

05 p0627 A73-16076

Analytical estimate of the landing range of a spacecraft for hyperbolic return-flight paths.

05 p0627 A73-16078

Investigation of the range interval of the landing phase for hyperbolic velocities of re-entry into the earth's atmosphere.

05 p0627 A73-16079

Flight-path characteristics for few re-entry trajectories.

05 p0623 A73-17297

Impulsive deboost analysis for maximum and minimum atmospheric entry angles for hyperbolically orbiting rocket vehicles

07 p0875 A73-19207

Russian book - Mechanics of optimal spatial motion of flight vehicles in the atmosphere.

07 p0777 A73-20380

Free flight and re-entry of a missile with a high ballistic coefficient.

09 p1147 A73-22625

Russian book on earth satellite, lunar, interplanetary and reentry trajectory analysis and optimal control covering motions under low thrust, aerodynamic heating and ablation

10 p1286 A73-23949

Guidance methods for heat-optimal three-dimensional descent paths of aerodynamic reentry bodies

11 p1430 A73-25350

An algorithm for controlling the descent of a spacecraft from an artificial earth satellite orbit.

12 p1543 A73-27631

Three-parameter multistep algorithms for stabilization of a spacecraft on the descent trajectory through the atmosphere.

15 p1944 A73-32601

Minimization of spacecraft maximum acceleration in atmosphere after reentry, applying results to reentry trajectory optimization and associated optimal control problems

15 p1941 A73-32607

Sighting methods during flights from the moon to the earth

18 p2351 A73-36107

Computerized trajectory estimation for maneuvering reentry vehicles, obtaining minimum variance trajectory parameters by Kalman filtering of radar, optical and inertial reference measurements

[AIAA PAPER 73-902] 20 p2589 A73-38836

REENTRY VEHICLES

NT APOLLO SPACECRAFT
NT LIFTING REENTRY VEHICLES
NT MANEUVERABLE REENTRY BODIES
NT RECOVERABLE SPACECRAFT
NT REUSABLE SPACECRAFT

Electrical power source for spacecraft reentry trajectory control system, thermal protection and radio communication based on reentry vehicle external surfaces utilization as generator electrodes

01 p0111 A73-11174

Thermal stress analysis of reentry vehicle nosetips at angle of attack.

03 p0392 A73-13688

Design of a digital adaptive control system for reentry vehicles.

03 p0286 A73-14482

Full scale reentry vehicle laminar to turbulent wake transition characteristics from electrostatic probe inflight measurements of charged particle density fluctuations

[AIAA PAPER 73-109] 05 p0529 A73-16868

Reentry vehicle finned roll rate control - Aerodynamic and flight dynamic analysis.

[AIAA PAPER 73-183] 05 p0531 A73-16923

A study of fin-induced laminar interactions on sharp and spherically blunted cones.

[AIAA PAPER 73-235] 05 p0532 A73-16960

Transition effects on slender vehicle stability and trim characteristics.

[AIAA PAPER 73-126] 06 p0756 A73-17646

Reentry vehicle dynamic stability mechanism during boundary layer transition, using angle of attack divergence dependence on fluctuating pressure

[AIAA PAPER 73-180] 06 p0756 A73-17652

Effect of low heat-shield ablation rates on flight test turbulent base pressure.

07 p0920 A73-19975

Unsteady three-dimensional motion of a flight vehicle during hypersonic reentry in the atmosphere

10 p1286 A73-24304

A mechanism for ablation-induced spin-up.

11 p1431 A73-26402

Flight test correlation technique for turbulent base heat transfer with low ablation.

11 p1453 A73-26671

Beta estimation accuracy for reentry vehicles using a priori target information with 6-component state vectors to reduce computation time

12 p1548 A73-27131

Derivation of shape change equations for asymmetrically heated ablating reentry vehicles.

13 p1706 A73-28750

Spatial oscillations of a vehicle with a nonlinear stabilization system during reentry

14 p1803 A73-29853

Computerized six degree of freedom parachute deployment model for predicting entry vehicle-decelerator dynamic response to aerodynamic forces and physical property changes

[AIAA PAPER 73-460]

15 p1827 A73-31446

The operational performance of reentry vehicle heatshield thermodynamic instrumentation

17 p2238 A73-34605

Linear and nonlinear filtering techniques for estimating the state of reentry vehicles from optical tracking data.

17 p2125 A73-35371

Experimental evaluation of a roll control system for a shrouded cone.

17 p2239 A73-35500

Fully coupled nongray radiating gas flows with ablation product effects about planetary entry bodies.

[AIAA PAPER 73-672]

18 p2368 A73-36223

Reentry vehicle ablating control surface gap and slot regions flow characteristics prediction based on quasi-one-dimensional compressible flow finite difference solution

[AIAA PAPER 73-742]

18 p2265 A73-36663

Composition of the earth's atmosphere by shock-layer radiometry during the PAET entry probe experiment.

18 p2313 A73-36797

Computation of the nonlinear dynamic stability functions of a reentry body in hypersonic flight

18 p2361 A73-37081

Lifting body configurations for sustained hypersonic flight.

19 p2377 A73-37710

Closed loop preflight qualification testing of a reentry vehicle roll rate control system.

[AIAA PAPER 73-878]

20 p2587 A73-38815

An aerodynamic entry control technique utilizing the yaw flap concept.

[AIAA PAPER 73-888]

20 p2588 A73-38824

Optimal guidance for aerodynamically controlled reentry vehicles.

[AIAA PAPER 73-891]

20 p2588 A73-38827

REFLECTANCE ATMOSPHERES

Reproduction of sound propagation in the standard atmosphere

03 p0342 A73-12993

Upper atmosphere structure from rocket and satellite observations, considering COSPAR International Reference Atmosphere /CIRA 1972/

07 p0813 A73-19221

Parametric description of thermospheric ion composition results.

07 p0815 A73-19255

The standard electron density profile of the F2-layer at noon.

09 p1078 A73-22746

Variations of the global values of F2-layer thickness and the parameters of the neutral atmosphere.

13 p1608 A73-28722

Results of air temperature, density and pressure measurements obtained with the aid of foil cloud sensors in the height region between 80 and 95 km.

18 p2311 A73-36179

CIRA 1972: COSPAR international reference atmosphere 1972.

21 p2683 A73-40626

COSPAR mean international reference atmosphere for 25-500 km region, considering 25-75, 75-120 and regions above 120 km

21 p2683 A73-40627

REFLECTION STARS

Determination of lunar orbital elements by the method of equal altitudes.

03 p0372 A73-13247

Hyades stellar flux parallaxes for cosmic scale photometric distance determinations and calibration

03 p0372 A73-13248

Zonal spectrophotometric standards - Energy distribution in the spectra of 109 stars in absolute units

05 p0617 A73-16465

Image integration and display system for guiding on stars beyond the visual detection limit.

08 p0987 A73-21748

Analytical estimates of the accuracy of spacecraft autonomous navigation based on measurements of flight altitude and zenith-distance inertial-space reference point.

12 p1523 A73-27647

Determination of the absolute intrinsic motions of stars with respect to galaxies in area 32 of a special Kapteyn map

15 p1938 A73-31961

The application of the method of equal heights to the determination of astronomical azimuth

19 p2490 A73-38557

Determination of absolute stellar proper motions relative to galaxies in selected area 32 of the special Kapteyn plan.

24 p3132 A73-44486

REFERENCE SYSTEMS

Stellar positions and proper motions representation of fundamental reference system, improving and extending to faint objects and radio sources

01 p0094 A73-10056

Schwarzschild coordinate system identification with frames of reference within exterior gravitational field of spherical nonrotating star

02 p0211 A73-11896

Analog simulation and design of single- and multiple input/output model reference adaptive systems, using hyperstability concept

[ASME PAPER 72-WA/AUT-13]

04 p0432 A73-15881

An all-earth inertial navigation scheme.

06 p0721 A73-18255

A precision position and time service for the air traffic of the future.

07 p0849 A73-19350

Instrument axes trihedron orientation relative to reference, deriving expressions for angular misalignment statistical estimation

09 p1115 A73-22353

Kinematic problem of orientation in a rotating coordinate system

09 p1116 A73-22354

On the demonstration and interpretation of the Coriolis effect.

09 p1120 A73-22475

Lunar surface reference points requirements for selenodetic coordinate system, analyzing coordinate transformations precision

10 p1277 A73-24087

Thermal reference system with linear temperature profile down fin axis for thermography, using scanning IR camera as image detector

11 p1366 A73-26305

Speckle reference beam /by retro reflection/ holography for the real time visualisation of vibration patterns.

16 p2012 A73-32847

Deformation of a selenodetic reference system due to errors in lunar rotation constants

17 p2230 A73-34595

Digital attitude reference system for three-axis-stabilized earth oriented satellites, using gyrocompasses with solar and horizon sensors

17 p2209 A73-34875

Spacecraft attitude gyro reference system and readout accuracy, discussing strapdown guidance, electrical suspension, instrument errors, spin and damping coils and degrees of freedom

21 p2733 A73-40026

Indoor azimuth reference systems specifications, characteristics and results, discussing optical windows, theodolites, reflectors, bulk monument structure measurements and rocket applications

[AIAA PAPER 73-842]

21 p2671 A73-40505

Astronomical constants and cataloging from 1964 International Astronomical Union, discussing inadequacies and different specific reference systems

21 p2780 A73-41612

Design of discrete model reference adaptive systems using the positivity concept.

23 p2962 A73-43287

Design of multivariable adaptive model following control systems.

23 p2962 A73-43288

The inadequate reference electrode, a widespread source of error in plasma probe measurements.

24 p3115 A73-44873

REFERENCES [STANDARDS]

U STANDARDS

REFINING

NT ELECTROREFINING

NT ELECTROSLAG REFINING

Refinement of primary silicon crystals in a hyperpure Al-20% Si alloy by sulphur addition.

02 p0179 A73-11597

Means of improving the quality of heat-resistant metals and their alloys

03 p0324 A73-13504

Evaluation of the lubricating properties of chemically upgraded MoS2.

07 p0842 A73-19553

Fine grained weld structures.

07 p0832 A73-20273

Microstructural control of Ti-6Al-4V forgings.

09 p1088 A73-22495

Grain refinement by titanium in the unidirectionally solidified aluminum alloys.

19 p2442 A73-37949

REFLECTANCE

NT SPECTRAL REFLECTANCE

Light scattering by cirrus cloud layers.

01 p0038 A73-10376

Simultaneous measurements of radar reflectivity and refractive index spectra in clear air convection.

01 p0018 A73-11060

Radiation heat transfer in isothermal adjoint plate system with directionally emitting and nondiffuse reflecting surfaces, considering surface roughness effects

01 p0123 A73-11140

Reflection and transmission coefficients for stratified media, considering total optical reflection at attenuator and metal film reflector

01 p0078 A73-11229

Thermochromic cuprous mercuric iodide for IR recording applications, observing phase transition hysteresis from reflectance-vs-temperature, specific heat and sensitivity measurements

01 p0054 A73-11230

Relation of the diffuse reflectance remission function to the fundamental optical parameters.

02 p0193 A73-12350

Some optical properties of solid solutions in the 2GaAs-ZnSiAs2 section

05 p0605 A73-16612

Effect of boundary conditions on the radiative reflectance of dielectric coatings.

[AIAA PAPER 73-148]

05 p0598 A73-16896

Weak normal shock wave interactions with materials, investigating incident pressure ratio, thickness, perforation diameter, close area and flow resistance effects on acoustic reflectance

[AIAA PAPER 73-244]

05 p0598 A73-16968

Effects of leaf age for four growth stages of cotton and corn plants on leaf reflectance, structure, thickness, water and chlorophyll concentrations and selection of wavelengths for crop discrimination.

05 p0571 A73-17128

Mars UV reflectance properties from Mariner 9 spectrometer, giving topographic map based on ultraviolet light scattering from atmosphere

06 p0746 A73-17483

Scattering of electromagnetic waves from a turbulent plasma slab.

06 p0729 A73-18120

Reflectance and absorption spectra of Apollo 11 and Apollo 12 samples.

07 p0897 A73-19890

Comparative study of reflectivity measurements performed in the visible and infrared wavelengths.

07 p0824 A73-19945

Ionogram traces production by mode coupling process in thin sporadic E layers, using calculated reflection and transmission coefficients for radio waves incidence

09 p1076 A73-22139

Thermionic constants and electron reflection for Ta/100/ by the Shelton retarding field method.

10 p1259 A73-23695

Coefficients of hydromagnetic wave reflection from conjugate ionospheres

10 p1211 A73-23895

An analytical expression for the limits of error in the measurement of reflection-coefficient phase.

10 p1190 A73-24867

Coated laser windows characterized by strong surface absorption, calculating absorptivity, transmittance and reflectivity under assumption of insignificant interference effects within substrate

11 p1377 A73-26243

The kinetic reflection coefficient in a formula for the current at a plasma/semiconductor interface in the case of an inelastic mechanism of electron energy relaxation

12 p1527 A73-26928

Precise measurement of reflection coefficients by means of tuned microwave reflectometers.

12 p1478 A73-27047

Visible and near-infrared transmission and reflectance measurements of the Luna 20 soil.

13 p1674 A73-28303

Reflectance and optical constants of evaporated osmium in the vacuum ultraviolet from 300 to 2000 A.

13 p1660 A73-28936

A null-reading method of measuring the complex reflection coefficient in the short-wave end of the millimeter band

14 p1728 A73-30271

Characteristics of the reflection spectra of CdS(x)/Se(1-x)/ mixed crystals in their exciton absorption region

14 p1783 A73-30578

Solar radiation pressure on Mariner 9 Mars orbiter from mathematical model of illuminance and reflectivity characteristics

16 p2052 A73-32906

Effects of mirror reflectivity in a distributed-feedback laser.

16 p2024 A73-33081

Radar observations of Venus at 3.8 cm

16 p2067 A73-33806

Spectrophotometry of individual regions of Venus

16 p2068 A73-33814

Frequency analysis of calculated ionospheric reflection coefficients.

16 p1984 A73-33920

Reflection coefficient of an electromagnetic wave by a plasma column of variable electron density in a waveguide.

16 p1984 A73-33994

Determination of changes in the reflection coefficient of absorbing coatings in the millimeter wavelength band

17 p2120 A73-34156

REFLECTED RADIATION

Aqueous ammonium sulfate aerosol optical properties via attenuated total reflectance (ATR) spectroscopy 17 p2171 A73-35402

Reflection coefficients for wires, cables, ropes and chains from scanning laser radar, discussing wire avoidance system for airplanes and helicopters 17 p2210 A73-35421

Radio anechoic chamber reflectivity level evaluation, comparing antenna pattern method and free space voltage standing wave ratio technique 17 p2128 A73-35684

Reflection characteristics of quasi-tapered anechoic chamber at VHF and EHF, evaluating broadband response, radar cross sections and field in quiet zone 17 p2129 A73-35701

Radiative property degradation of water impinging on thermally-controlled surfaces under space conditions. [AIAA PAPER 73-733] 18 p2336 A73-36350

Mean square and reflectivity variance decrease due to radar beam smoothing and post-detection integration in terms of reflectivity fields autocorrelation function 18 p2333 A73-36706

Comparison of the Beckmann model with bidirectional reflectance measurements. [ASME PAPER 73-HT-11] 20 p2563 A73-38567

Reflection coefficients of hydromagnetic waves from conjugate ionospheres. 20 p2551 A73-38914

The effect of comparison source reflectance on gas temperature measurement by Kurlbaum's method and line reversal methods. 21 p2692 A73-39916

Electromagnetic radiation excited by electric or magnetic line source near inhomogeneous dielectric layer, evaluating reflected and transmitted fields by saddle point technique 22 p2824 A73-41831

Kinetic reflection coefficient at a plasma-semiconductor boundary for inelastic electron energy relaxation. 22 p2891 A73-42262

Theoretical and experimental investigations of the coefficients of reflection from plant foliages at small slip angles 22 p2847 A73-42332

Asteroid reflectivities from polarization curves - Calibration of the 'slope-albedo' relationship. 24 p3129 A73-44437

Terrestrial rock optical constants, finding refractive index and reflectivity for andesite, basalt, basaltic glass, obsidian and obsidian glass through spectrophotometric analysis 24 p3081 A73-44558

Electromagnetic wave interaction with moving bounded plasmas. 24 p3069 A73-45409

REFLECTED RADIATION

U REFLECTED WAVES

REFLECTED RAYS

U REFLECTED WAVES

REFLECTED WAVES

Some aspects of radiation from a circular loop antenna. 02 p0148 A73-12854

Fraunhofer zone distribution functions for azimuth and elevation angles of radio waves reflected from inhomogeneous ionospheric scattering layer 03 p0278 A73-14071

On the Napier method for the photometric reflection effect in close binary stars. 03 p0379 A73-14583

Determination of the effective angular distance between the reflection points of an ordinary ray and an extraordinary ray by the interference method 05 p0548 A73-16259

Diffraction effects encountered in the measurement of bidirectional reflectance from square pyramids. [AIAA PAPER 73-150] 05 p0598 A73-16898

Angular distribution of radiation reflected from roughened brass - Experiment and analysis. [AIAA PAPER 73-151] 05 p0598 A73-16899

Measurement of the polarization of the radiation reflected backward from a laser-heated plasma. 06 p0731 A73-18589

Reflection spectra of lunar dust grains with amorphous coatings. 07 p0876 A73-19583

Algorithm for numerical calculation of transmitted and reflected electromagnetic waves, noting multiple reflections for inertial inhomogeneities 09 p1063 A73-22458

Backscattering of a scalar wave field by an ideally reflecting object situated near the caustic surface 09 p1052 A73-23081

Microwave reflection from detonation waves in equimolar C₂H₂-O₂ at low pressures. 10 p1294 A73-23557

Optically active materials light reflection polarization characteristics, comparing theories based on wave vector and permittivity tensor and on polarization/magnetization current constitutive equations 10 p1261 A73-24693

The measurement of winds in the D-region of the ionosphere by the use of partially reflected radio waves. 11 p1358 A73-26707

Polarization of radio waves reflected from an inhomogeneous ionosphere 12 p1468 A73-26971

Reflection of plane heterogeneous and uniform electromagnetic waves and the reflected wave displacement 13 p1658 A73-28072

Amplification of cylindrical electromagnetic waves reflected from a rotating body. 14 p1728 A73-30333

The annual radiation balance of the earth-atmosphere system during 1969-70 from Nimbus 3 measurements. 14 p1750 A73-30762

Flux density for ray propagation in discrete index media expressed in terms of the intrinsic geometry of the deflecting surface. 15 p1913 A73-31135

Self-induced effects of radio waves in the vicinity of plasma resonance 15 p1918 A73-31706

Calculation of the parameters of a chemically reacting gas behind an incident and reflected shock wave 15 p1840 A73-31855

Influence of a reflected signal on the operation of a laser 16 p1978 A73-32892

Time dependent one dimensional Navier-Stokes differential equations solved via difference scheme, determining reflected shock wave structure and end wall pressure 16 p1999 A73-33251

Asymptotic development method for the determination of the field reflected by a random surface 16 p1984 A73-33966

Dissociation of carbon dioxide behind reflected shock waves. 17 p2119 A73-35173

Progress in remote optical analysis of lunar surface composition. 17 p2119 A73-35747

Limits of applicability of the Delano model for describing the process of wave scattering by a complex-shaped body 19 p2407 A73-38343

Spallation and fracture resulting from reflected and intersecting stress waves. 21 p2782 A73-39989

Evanescent fields produced by totally reflected beams. 22 p2824 A73-41853

Contribution to the theory of wave propagation in a one-dimensional randomly inhomogeneous medium 22 p2826 A73-42334

Analysis of the self-ignition of fuel droplets behind a reflected shock wave 24 p3121 A73-45390

REFLECTING TELESCOPES

Auxiliary instruments for 4-m reflectors related to astronomical telescope focal positions, discussing correlators, cameras, sensitometers, film, rotator-adaptor, guider, echelle spectrograph and photometers 01 p0046 A73-10504

Instrumentation and some principal programs of the McDonald Observatory 2.75-meter /107-inch/ reflector. 01 p0046 A73-10505

A computer-controlled digital spectrum scanner for La Silla. 01 p0047 A73-10515

Grating mosaic for use in conjunction with coude focus of 3.6 meter reflecting telescope, discussing optical and optomechanical implementation methods 01 p0047 A73-10521

Blank pupil arrangement of coude spectrograph with echelle for 1.52 meter reflector, describing dispersions obtained, receivers used and electronic camera adaptation 01 p0048 A73-10523

The coude of the 1.2 meter telescope at Victoria. 01 p0048 A73-10527

The lunar regolith as a site for an astronomical observatory. 01 p0105 A73-11204

General analysis of aplantic Cassegrain, Gregorian, and Schwarzschild telescopes. 03 p0309 A73-14426

Multiple mirror telescope consisting of six Cassegrainian telescopes combined for common focal surface, noting light gathering power equivalent to 180 inch standard telescope 08 p0970 A73-21738

Some design aspects of a multiple-mirror telescope. 08 p0970 A73-21739

Galactic radio emission at 38 MHz using steerable reflector telescope with defined beam and small sidelobes 13 p1673 A73-28278

The polished surface of a telescope mirror as seen in an electron microscope 14 p1752 A73-30060

The 2.2-m telescope of the Max-Planck Institute for Astronomy 14 p1743 A73-30273

Akademiia Nauk SSSR, Astronomicheskii Sovet, Meeting of the Commission on Astronomical Instrument Engineering, Sverdlovsk, USSR, July 1-3, 1970, Proceedings 15 p1877 A73-32128

The universal automatic reflector AZT-12 15 p1877 A73-32129

The automatic telescope AZT-11 15 p1877 A73-32130

Grazing incidence X ray telescope lens design for radio and optical identifications of radiation sources by satellites 17 p2171 A73-35409

Determination of the centering conditions of two-mirror systems with the aid of Hartmann photographs 20 p2565 A73-39067

Changes in the geometrical parameters of a radio-telescope parabolic mirror experiencing radially symmetric deformations 21 p2672 A73-40549

Large telescope design, discussing optical telescope efficiency as function of aperture, exposure time auxiliary instrumental parameters 21 p2703 A73-41245

Choice of the dimensions of the reflecting elements and calculation of the electrical characteristics of the RATAN-600 radio telescope 21 p2666 A73-41443

Design of the reflecting elements and secondary mirror of the RATAN-600 radio telescope 21 p2675 A73-41449

Use of two-stage condenser braking of the single-motor drive for the mirror sections of the RATAN-600 radio telescope 21 p2675 A73-41450

Indicator and setting devices for circular-mirror sections of the RATAN-600 radio telescope 21 p2675 A73-41451

Reference indication and setting devices for circular mirror sections of the RATAN-600 radio telescope 21 p2675 A73-41452

Errors arising in the RATAN-600 radio telescope due to temperature effects 21 p2675 A73-41453

Geodetic tasks during the construction and alignment of the RATAN-600 radio telescope 21 p2675 A73-41454

Laying out the foundations for circular-mirror sections of the RATAN-600 radio telescope 21 p2675 A73-41455

Experimental study of an autocollimation method for alignment of a variable-profile antenna 21 p2675 A73-41457

Monitoring antenna parameters from radio-astronomical directions 21 p2667 A73-41459

Experimental study of the distribution of irradiation on the variable-profile reflector of the large Pulkovo radio telescope using electronic methods 21 p2667 A73-41470

REFLECTION

NT INFRARED REFLECTION

NT RETROREFLECTION

NT SIGNAL REFLECTION

NT SPECTULAR REFLECTION

NT ULTRAVIOLET REFLECTION

NT WAVE REFLECTION

Narrow band and broadband light curves for Algol eclipsing binary from differential photometry, calculating reflection effect 03 p0366 A73-12940

REFLECTION COEFFICIENT

U REFLECTANCE

REFLECTIVITY

U REFLECTANCE

REFLECTOMETERS

NT MICROWAVE REFLECTOMETERS

Side-viewing detector for a vacuum ultraviolet reflectometer. 03 p0309 A73-14430

An automatic reflectometer for the upper shortwave range 13 p1590 A73-28569

Narrowband time domain reflectometer uses pulse modulated Gunn-oscillator to measure small reflections in 6 and 7.5 GHz band waveguides. 14 p1733 A73-30057

Improvement of absolute accuracy for a multiple bounce reflectometer through a detailed effort to reduce systematic errors. 17 p2172 A73-35420

The generalized multiprobe reflectometer and its application to automated transmission line measurements. 17 p2143 A73-35691

Application of the 'differential reflectometer' to materials research in corrosion, ordering and alloying. 21 p2719 A73-40897

Evaluation of a high accuracy reflectometer for specular materials. 22 p2864 A73-43160

REFLECTORS

NT FRESNEL REFLECTORS
NT PARABOLIC REFLECTORS
NT PARABOLOID MIRRORS
NT RADAR REFLECTORS

A comparison of geometrical theory of diffraction and integral equation formulation for analysis of reflector antennas.

01 p0022 A73-10179

Graphite-epoxy composite properties, fabrication and tests for light weight low distortion spacecraft antenna reflector applications

03 p0331 A73-13023

Metalized fiberglass antenna meshes for spacecraft deployable reflectors, discussing low mass/area, long term stability and performance characteristics and degradation tests

03 p0333 A73-13045

Small nuclear light bulb engines with cold beryllium reflectors.

[AIAA PAPER 72-1093]

04 p0475 A73-14907

The effect of a metallic reflector upon cyclotron radiation.

08 p0990 A73-20813

Experimental study of electrical reflectors equipped with thin radomes

11 p1335 A73-25292

Depolarisation with Cassegrainian and front-fed reflectors.

14 p1728 A73-30448

Thermal shielding by subliming volume reflectors in convective and intense radiative environments.

17 p2253 A73-34183

Design techniques for multiple beam reflector antennas.

17 p2142 A73-35636

Multiple-beam spherical-reflector antenna systems for satellite communications.

20 p2525 A73-38739

Choice of the dimensions of the reflecting elements and calculation of the electrical characteristics of the RATAN-600 radio telescope

21 p2666 A73-41443

Operation of a variable profile antenna with a plane periscopic reflector

21 p2666 A73-41444

Operational features of variable-profile antennas during near-zenith observations

21 p2666 A73-41445

Adjustment of a variable-profile antenna

21 p2675 A73-41456

Scale model development of a high efficiency dual polarized line feed for the Arecibo spherical reflector.

22 p2831 A73-41830

REFLEXES

NT CAROTID SINUS REFLEX
NT RESPIRATORY REFLEXES

Polysynaptic pathways role in tonic vibration and monosynaptic reflexes due to muscle vibratory or nerve electric stimulation, respectively, discussing tetanization effects

01 p0008 A73-10409

Peripheral electromyography spike and ventral root unit discharge intervals during tonic vibration reflex of cat soleus motoneuron

01 p0008 A73-10410

Study of the acoustic reflex in human beings. I - Dynamic characteristics.

01 p0013 A73-10828

The role of muscle stiffness in meeting the changing postural and locomotor requirements for force development by the ankle extensors.

02 p0138 A73-12166

Variability of normal glabellar and supraorbital reflexes in man

03 p0261 A73-13748

Phasic discharge activity and localization of sheep medullary neurons in relation to swallowing reflex after superior laryngeal nerve stimulation

03 p0262 A73-13786

Correlation between the voltage-time curves of H- and M-responses of a human muscle during various functional states of the spinal center

03 p0262 A73-13819

Cardiovascular reflexes evoked by potassium ion stimulation of the heart under conditions of spinal deafferentation and intact innervation

03 p0262 A73-13820

Patterns of reflex excitability during the ontogenesis of sleep and wakefulness.

03 p0264 A73-14264

Reflex act structural components interaction in terms of reflection, creativity and organism-environment relations, noting subjective and objective perception and attitude formation

04 p0410 A73-15798

The dynamic properties of the acoustic middle ear reflex in nonanesthetized rabbits - Quantitative aspects of a polysynaptic reflex system.

05 p0539 A73-16249

A robot conditioned reflex system modeled after the cerebellum.

06 p0658 A73-18065

Participation of the hippocampal structures in the formation of external inhibition

06 p0653 A73-18162

Functional alterations in the auditory and visual analyzer systems of monkeys during experimental neurosis

06 p0653 A73-18163

Statistical distribution methods for analyzing formation of reflexes conditioned to time intervals between periodic unconditioned stimuli

06 p0653 A73-18166

Ontogenic cerebrospinal reflex activity studies, covering spinal cord morphology, reflex arches, inhibition, intracranial responses and post-tetanic potentiation

07 p0784 A73-20366

Effect of copper ions on the functional state of the neuromuscular apparatus

09 p1039 A73-22369

Organization of spontaneous muscular activity in man

09 p1040 A73-22863

Reflex bradycardia elicited from left ventricular receptors during acute severe hypoxia in cats.

09 p1042 A73-23244

Features of supraspinal control of the reflex paths of the spinal cord during walking

10 p1178 A73-23677

Hippocampus contribution to conditioned reflexes, memory, voluntary motions, orientation and emotional reactions, noting theta rhythm in stimuli response

10 p1180 A73-24326

Reflex excitability of spinal motor neurons in man under high atmospheric pressure

10 p1182 A73-24525

Reflex reaction of antagonist muscles during an evoked tendon reflex

10 p1182 A73-24598

Useful future action models of instrumental reflexes and voluntary actions based on memory role in engraving storage of received stimuli

11 p1314 A73-25199

The role of analyzers of conditional and unconditional stimuli in the functional system of the behavioral conditioned-reflex action

12 p1461 A73-27105

Conditioned reflex switching effects in higher nervous system reactions as function of experimental stimuli background conditions /arousal, diurnal rhythms, test conditions, physiological condition/

14 p1718 A73-30567

Forward and backward conditional link formation as physiological mechanism for reinforcement conditioning connection

14 p1718 A73-30568

Vestibular and spinal control of eye movements.

18 p2272 A73-36440

Role of arterial and venous vessels of limbs in the process of cardiovascular reflex responses

18 p2277 A73-36578

Human miniature eye movement relationship to visibility and saccades position-correcting reflex function and suppression

21 p2637 A73-40411

Automatic apparatus for the study of conditioned reflexes in a monkey seated in the primatological chair

21 p2644 A73-41140

Loudness changes resulting from an electrically induced middle-ear reflex.

22 p2811 A73-41815

Reflex arch lability in rabbits at synchronous maximum frequency of electromyographic and muscle stretching vibration measurement

22 p2807 A73-42659

Human phasic reflex response to parameters of a mechanical stimulus as an index of muscle-spindle sensitivity.

22 p2816 A73-42679

Use of the conditioned reflex method to study the motor analyzer during hygienic evaluation of working conditions in the presence of vibrations

24 p3062 A73-44673

REFRACTED RADIATION

U REFRACTED WAVES

REFRACTED RAYS

U REFRACTED WAVES

REFRACTED WAVES

Refraction of whistler-mode waves by large-scale gradients in the middle-latitude ionosphere.

21 p0017 A73-10328

The laws of reflection and refraction of incompressible magnetohydrodynamic waves at a fluid-solid interface.

07 p0858 A73-20028

On the transmission of the energy in an incompressible magnetohydrodynamic wave into a conducting solid.

07 p0858 A73-20029

Refraction of acoustic duct waveguide modes by exhaust jets.

07 p0812 A73-20338

Refraction by the electromagnetic pump of parametrically generated electrostatic waves.

11 p1405 A73-25973

Single reflection Fresnel rhomb for quarter-wave retardation in the infrared.

11 p1400 A73-26251

Flux density for ray propagation in discrete index media expressed in terms of the intrinsic geometry of the deflecting surface.

15 p1913 A73-31135

Shadow zone effect of electromagnetic wave propagation in stratified layer with vertical dipole source and square law dependent refractive index profile

16 p1978 A73-32890

Book - Acoustic fields and waves in solids. Volumes 1 & 2.

17 p2213 A73-35597

Sound propagation in rotating vortex flow downstream from delta wing in wind tunnel, discussing acoustic ray refraction by flow

22 p2839 A73-41715

Elastic-plastic wave reflection and refraction obtained by method of singular surfaces, discussing interface and plastic deformation effects

[ASME PAPER 73-APMW-38]

22 p2926 A73-42895

Losses and impulse response of a parabolic index fiber with random bends.

23 p2987 A73-43989

REFRACTING TELESCOPES

Long focal length refractor telescopes for high resolution stellar photography, describing follower drive construction and control

10 p1218 A73-24275

REFRACTION

NT ATMOSPHERIC REFRACTION

NT BIREFRINGENCE

NT RADIO WAVE REFRACTION

German monograph - Spatial oscillations of light in the refraction and image field of rough objects.

03 p0319 A73-13817

Peak subsonic noise level reduction by jet refraction, showing directivity patterns as function of jet velocities and temperature ratios

21 p2754 A73-40753

REFRACTIVE INDEX

U REFRACTIVITY

REFRACTIVITY

An inversion technique developed to determine characteristics of mie scatterers differing in index of refraction interspersed in the stratosphere.

01 p0037 A73-10353

IR absorption and refraction index of atmospheric aerosol, using KBr disk transmittance and specular reflection measurements

01 p0038 A73-10373

Measurement of the complex index of refraction of atmospheric aerosols using optical spectral analysis techniques.

01 p0045 A73-10375

Relation of the equation of state of compressed gases with the optical complex and the specific refraction - Virial coefficients of carbon dioxide

01 p0080 A73-10856

Simultaneous measurements of radar reflectivity and refractive index spectra in clear air convection.

01 p0018 A73-11060

Major, minor and trace elements, specific gravities and refraction indices of Ivory Coast tektites, comparing composition to Bosumtwi crater glasses and Apollo lunar materials

01 p0109 A73-11475

Electromagnetic wave propagation in a medium with two-dimensionally periodic variations of the refractive index

05 p0548 A73-16268

The refractive index profile in a glass-fiber light waveguide

05 p0584 A73-16472

Beam trajectory distortions due to turbulent air refractive index fluctuations in optical waveguides

05 p0551 A73-16785

Influence of refractive index on emittance from semi-infinite absorbing scattering media.

[AIAA PAPER 73-147]

05 p0598 A73-16895

Waveguide properties, modes and optical pumping effects on thin film organic dye lasers, noting temperature effects on refractivity and laser modes

06 p0699 A73-17808

Bismuth germanate and silicate single crystals refractive index and electro-optic coefficient measurement

06 p0737 A73-18367

Use of nonstationary holography to improve the directivity of laser radiation.

07 p0834 A73-19275

Wave propagation in a stratified turbulent magnetized plasma. II.

07 p0858 A73-19534

Apollo 14 glasses of impact origin and their parent rock types.

07 p0883 A73-19735

Intensity fluctuations of a light beam propagating through a wave guide channel with random refraction-index inhomogeneities

07 p0792 A73-19915

REFRACTOMETERS

R and L modes of ion cyclotron whistler propagation in ionosphere, noting refractive indexes and wave polarization for multicomponent plasma
07 p0819 A73-20060

High-resolution study of anomalous dispersion in the ruby R lines.
09 p1090 A73-21940

Tube waveguide for optical transmission.
10 p1196 A73-24624

Optical constants of water in the 200-nm to 200-micron wavelength region.
11 p1350 A73-25060

Electrical characteristics of hardenable metallic lens or radome with near unity refractive index at out-of-band frequencies
11 p1338 A73-25670

Integral equation numerical solution by minimum mean-squared estimator for atmospheric electromagnetic refractivity profile from satellite radio tracking data, noting iterative procedure convergence
11 p1330 A73-25686

Connection between the equation of state of compressed gases with an optical complex and the specific refraction - The virial coefficients of carbon dioxide.
12 p1526 A73-27906

Exciton absorption band splitting in the PbI₂ spectrum
12 p1532 A73-27945

Reflectance and optical constants of evaporated osmium in the vacuum ultraviolet from 300 to 2000 Å.
13 p1660 A73-28936

A mode theory of radio wave propagation in an inhomogeneous atmosphere with jointed-segment N-profile.
13 p1586 A73-29227

German monograph on signal transmission and radiation distribution in optical waveguide consisting of glass fibers with refractive index gradient and optically dense envelope
13 p1628 A73-29282

Measurement of the temperature coefficient of the refractive index of infrared materials with the aid of a carbon dioxide laser
14 p1757 A73-30371

The determination of plasma electron density from refraction measurements.
15 p1916 A73-31085

Electromagnetic wave propagation through a gas lens.
15 p1913 A73-31136

Shadow zone effect of electromagnetic wave propagation in stratified layer with vertical dipole source and square law dependent refractive index profile
16 p1978 A73-32890

Analysis of radio-wave propagation in the Venusian atmosphere
16 p1984 A73-33822

Coherent light propagation and scattering in vaporized alkali metal atmosphere as function of refractive index and coherent to incoherent transformation
16 p2086 A73-34002

Spectroscopic measurement of material samples refractive index at submillimeter wavelengths
17 p2120 A73-34157

Scattering of a spherical wave by spherical inhomogeneity with arbitrary refractive index distribution along the radius.
17 p2123 A73-35163

Low loss light guiding polymer thin film with continuously adjustable refractivity, discussing fabrication and refractivity and scattering loss measurements
17 p2172 A73-35423

A reflectance analog computer for the determination of thin film optical properties.
17 p2132 A73-35773

Apparent reflectance from a semi-infinite absorbing-scattering medium.
[AIAA PAPER 73-753]
18 p2337 A73-36369

Dynamics of the emission of semiconductor lasers whose refractive index depends on the emission intensity
18 p2322 A73-36560

The interaction between atmospheric microstructure and acoustic and electromagnetic waves.
19 p2406 A73-38242

Double heterostructure lasers for optical communications systems
20 p2572 A73-38664

Refractive index of n-type gallium arsenide.
20 p2599 A73-38892

Acoustical radiation reaction by conservation of energy and Dirac prescription methods and derivation of acoustic index of refraction for system of soft spheres
20 p2592 A73-39049

Thermal defocusing avoidance by short pulse duration reduction to permit IR laser window operation before temperature rise, considering changes in index of refraction
21 p2710 A73-40134

Laser resonator mode structure during interaction with active medium, considering combined effects of

gain and refractivity variations for arbitrary mirror configurations
21 p2714 A73-40761

Measurements of refractive index step and of carrier confinement at /AlGa/As-GaAs heterojunctions.
21 p2752 A73-40962

Optical waveguide refractive index control process for glass film during deposition by sputtering power density variance
21 p2665 A73-41116

Computer simulation of the acceleration of charged particles captured by plane electromagnetic waves
22 p2826 A73-42378

Determination of the size and the imaginary part of the refractive index of Al₂O₃ drops in a flame
22 p2932 A73-42724

The influence of electron plasma formation on superbroadening in light filaments.
22 p2871 A73-43077

Holographic thin-beam reconstruction technique for the study of 3-D refractive-index field.
22 p2862 A73-43087

Measurement of optically induced refractive-index changes with sharp edged illumination pattern.
23 p2984 A73-44371

Terrestrial rock optical constants, finding refractive index and reflectivity for andesite, basalt, basaltic glass, obsidian and obsidian glass through spectrophotometric analysis
24 p3081 A73-44558

Fluctuation characteristics of the electric component of the troposphere.
24 p3084 A73-44940

Radon transform application in holographic interferometry for reconstructing two and three dimensional spatial distribution of refractivity in object
24 p3091 A73-44944

HF and molecular fluorine refractive indices in visible spectral region computed from interferometer fringe shift vs pressure measurements
24 p3113 A73-44983

Chromatic photosensitization of a variable-index material for the recording of high-efficiency phase holograms
24 p3091 A73-45011

REFRACTOMETERS

Optical wavelengths and microwaves operated holographic refractometers and reflectometers based on dielectric microwaveguides
09 p1085 A73-23013

REFRACTORYS

Development of special graphites for lithium hydride/fluorine rocket engines
09 p1110 A73-23019

REFRACTORY MATERIALS

NT CHROMIUM
NT IRIDIUM
NT MOLYBDENUM
NT MOLYBDENUM ALLOYS
NT NIOBIUM
NT NIOBIUM ALLOYS
NT OSMIUM
NT PORCELAIN
NT REFRACTORIES
NT REFRACTORY METAL ALLOYS
NT REFRACTORY METALS
NT RENE 41
NT RHENIUM
NT RHENIUM ALLOYS
NT RHENIUM ISOTOPES
NT TANTALUM
NT TANTALUM ALLOYS
NT TUNGSTEN
NT TUNGSTEN ALLOYS

Thermal cycle influence in heat resistant materials plastic strain and time to failure for different stress and temperature conditions
01 p0112 A73-10009

Superplasticity in two phase compositions based on refractory compounds, noting creep rate dependence on concentration and electroconductivity
01 p0066 A73-11339

Properties and fabrication of cermet fibers from refractory compounds and of porous materials based on these fibers
02 p0178 A73-11538

Apparatus for investigations into long-term strength and creep of coated materials at temperatures above 1400 C in air.
02 p0150 A73-12219

Electron beam heating test arrangement for high temperature testing of refractory materials in vacuum, describing temperature control systems
02 p0150 A73-12220

Metal-metal laminar composites for high-temperature applications.
02 p0182 A73-12620

Material and structural studies of metal and polymer matrix composites.
02 p0182 A73-12621

High melting point transition metals carbides, nitrides, borides, silicides and oxides thermal conductivity as function of characteristic temperature
03 p0322 A73-13191

Book on surface ionization covering atomic and molecular ionization during thermal desorption from high melting point solid surfaces
03 p0345 A73-13996

Solid propellant rocket engines - Design and development of components in refractory and stratified materials.
07 p0867 A73-18992

Ignition of systems having refractory reaction products
07 p0920 A73-19988

The influence of a thorium dispersion on preferred orientation in nickel alloys.
08 p0977 A73-21012

Electronic mechanism of the basic technological processes in the powder metallurgy of high temperature materials.
08 p0982 A73-21825

Measurements of the emissivity of materials fabricated by powder- and plasma-metallurgy techniques
09 p1103 A73-22472

Refractory materials cyclic elastoplastic tests under shear with holding creep, showing relationship between creep rate and recurrent static deformation
09 p1161 A73-23155

Temperature dependent heat conductivity, Lorentz number and electrical resistivity of high melting Ti, Zr, Nb, Cr, Mo and W carbides and borides at 300-1200 K
10 p1230 A73-23519

Temperature dependence of the adhesive strength and elasticity of some high-melting coatings
10 p1225 A73-24371

Thermophysical and electrical properties of powdered boron carbonitride as high temperature insulating and refractory material at 1800-2020 C
10 p1241 A73-24687

Heat resistant and refractory materials contact eutectic melting for surface coating production
10 p1227 A73-24967

Tests concerning the production of gas turbine blades with directionally solidified structure
11 p1372 A73-25104

Russian book on thermal stability of refractory ceramics covering strength and thermophysical characteristics, high temperature thermal fracture and facilities for normal and cyclic load tests
11 p1386 A73-25174

Contribution to the study and perfecting of materials for radomes in the field of refractory ceramics
11 p1387 A73-25289

Investigation of the preparation of high-temperature strain gauges based on heat-resistant oxides
11 p1362 A73-25455

Investigation of heatproof materials under unsteady operating conditions
11 p1450 A73-25730

New phenomena during the burning of condensed systems
12 p1559 A73-27454

Sintering of refractory titanium carbide with varied bound nitrogen content, discussing crystal dislocation effects on initial stage compaction intensification in nonstoichiometric specimens
12 p1503 A73-27556

Obtaining of carbide and nitride dispersions in iron
13 p1633 A73-28182

Thermionic emission properties of refractory metal borides
13 p1634 A73-28201

Investigation of some principles in the processes of creep and fracture in heat-resistant materials.
13 p1643 A73-29626

Test equipment for thermal stability determination of brittle refractory material, noting data processing procedure and formulas for temperature distribution and thermal stress
13 p1599 A73-29629

Thermophysical properties of high temperature electrical insulating materials on the basis of non-metallic compounds with high melting point
[ECTP PAPER D2-3]
14 p1766 A73-30436

Compatibility of components in metal-ceramics composites
14 p1766 A73-30442

Single crystal mechanical and electrophysical properties in refractory compounds, including temperature effects, microhardness, resistivity, heat transfer, deformation and Hall effect
15 p1898 A73-32241

Void free high temperature resistant bismaleimide/woven fiberglass composite laminates, discussing synthesis, processing and fabrication
16 p2028 A73-33046

Investigation of the effect of pressed-powder grain composition on the physico-mechanical properties of magnesia refractory materials
17 p1287 A73-34337

Temperature dependent heat conductivity, Lorentz number and electrical resistivity of high melting Ti, Zr, Nb, Cr, Mo and W carbides and borides at 300-1200 K
17 p1291 A73-35199

Chemo-rheology of two high temperature epoxy resins.
17 p1297 A73-35347

Certain mechanisms of the solid-phase interaction arising during the formation and operation of high-temperature coatings

18 p2322 A73-35877

Application of refractory oxide coatings in extensometry

18 p2314 A73-35886

Solid refractory metal and nonmetal alloys for machine structural components under dynamic and steady cumulative stresses

18 p2326 A73-37000

Analysis and investigation of cathode processes in a high-current arc discharge

19 p2466 A73-37360

Method for determining the heat conductivity coefficient of high-temperature materials during unsteady heating

20 p2629 A73-39616

Russian book - High-temperature strain gauges based on heat-resistant oxides.

21 p2704 A73-41286

Improvement of thermal shock resistance by surface prestressing.

22 p2921 A73-42462

High concentration of refractory elements in lunar crust explained by melting and differentiation model

23 p3033 A73-43958

Influence of cooling on surface dispersion during the friction process

24 p3092 A73-44417

REFRACTORY METAL ALLOYS

NT MOLYBDENUM ALLOYS

NT NIOBIUM ALLOYS

NT RENE 41

NT RHENIUM ALLOYS

NT TANTALUM ALLOYS

NT TUNGSTEN ALLOYS

Some aspects of the instability of superrefractory alloys rich in nickel

01 p0062 A73-10270

Diffusive boronizing of molybdenum and niobium in boron carbide powder

02 p0178 A73-11544

Refractory alloys fatigue life up to 950 C under non-stationary loading, noting log-normal law distribution

03 p0327 A73-14010

Phase diagrams and properties of binary alloys of refractory metals, taking into account the electronic structure of the atoms of the components

03 p0328 A73-14652

Superrefractory Ni-based alloys mechanical properties enhancement through unidirectional solidification, considering grain boundary structure

07 p0838 A73-19116

Heat conductivity of cermet with titanium carbide as function of temperature and metal content

09 p1103 A73-22471

Influence of environment on the appearance of fatigue striations in various alloys

09 p1104 A73-22716

Electrical resistance and emissivity of certain transition metals and alloys in the high-temperature range

10 p1230 A73-23520

Microstructure, microhardness and mechanical strength of ingots and granules of Al alloys with high refractory metal contents

12 p1511 A73-26917

Strength characteristics of layers obtained by spark-alloying steels with high-melting metals

12 p1512 A73-27264

Strengthening and fracture of Ta, Nb, Mo and W binary solid solutions with short range order.

13 p1638 A73-29452

Investigation of titanium alloys containing refractory elements

15 p1889 A73-31813

Electrical resistivity and emissivity of some transition metals and alloys in the high-temperature range.

17 p2191 A73-35200

Solid refractory metal and nonmetal alloys for machine structural components under dynamic and steady cumulative stresses

18 p2326 A73-37000

X-ray investigation of the mechanism of effects of alloying on defect formation in refractory metal alloys

22 p2877 A73-42454

Alloys of titanium with refractory elements.

24 p3100 A73-45276

REFRACTORY METALS

NT CHROMIUM

NT IRIIDIUM

NT MOLYBDENUM

NT NIOBIUM

NT OSMIUM

NT RHENIUM

NT RHENIUM ISOTOPES

NT TANTALUM

NT TUNGSTEN

Cold shortness of W and related refractory metals, noting oxide phases and impurities effects on mechanical properties temperature dependence

01 p0066 A73-11341

Metallic materials developments in aircraft construction and gas turbine engine applications,

discussing superalloys, refractory metals, composites and directionally solidified alloys

04 p0460 A73-14741

Mechanisms and kinetics of absorption and desorption reactions in systems of refractory metals with nitrogen, oxygen or carbon.

04 p0462 A73-15302

Trace phase analysis as an aid in the study of heterogeneous raw material impurities in powder metallurgy

04 p0464 A73-15370

Metallurgical, chemical and electrochemical production and refining of refractory metals, including titanium, fluorotitanates and artificial rutile

04 p0465 A73-15660

Stability of reactive and refractory metal borides in ternary chromium-base alloys.

07 p0838 A73-19122

Influence of thermal-diffusion coatings on the physicomechanical properties of heat-resistant metals

07 p0840 A73-20512

A new method for thermographic investigation of high-speed crystallization processes in high-melting-point metals

09 p1103 A73-22483

Effect of heat treatment on the structure and properties of NV10M5T3Ts alloy

09 p1106 A73-23190

Recent materials compatibility studies in refractory metal-alkali metal systems for space power applications.

11 p1310 A73-26005

Investigation of diffused titanium coatings on refractory metals

13 p1630 A73-28015

The partitioning of refractory metal elements in hafnium-modified cast nickel-base superalloys.

13 p1633 A73-28138

Investigation at the Moscow University of the thermal characteristics of material

13 p1704 A73-28426

Allende carbonaceous chondrite Ca-Al rich inclusion refractory trace metals condensation temperature calculation, indicating high temperature primitive solar nebula condensates

13 p1684 A73-29176

The use of nitride intermediates in the preparation of metals - A study of the reduction of Nb2O5 with NH3.

14 p1761 A73-30629

Mechanism of the lubricating action of sulfides and selenides of refractory metals

14 p1755 A73-30717

The interaction of gases and carbon with refractory metals

15 p1890 A73-31925

New method of thermographic investigation of rapid processes of crystallization of refractory metals.

15 p1891 A73-32070

Electrophysical properties of TiC-Nb, TiC-Ta, TiC-Mo, and TiC-W cermet

15 p1892 A73-32242

Effect of some activators on the molybdenum and niobium siliciding process

15 p1892 A73-32247

Russian book on single crystals of high melting and rare metals and alloys covering structure, interatomic bonds, growth, plastic deformation, heat treatment, etc

15 p1893 A73-32297

Prediction of the heat-resistance characteristics of high melting materials

18 p2323 A73-36757

Effect of thermomodification coatings on the physicomechanical properties of refractory metals.

19 p2440 A73-37787

An arrangement for carrying out metal creep and stress-rupture strength tests under high vacuum conditions

20 p2545 A73-39384

Experimental investigation of the integral hemispherical emissivity of refractory metals and alloys.

20 p2593 A73-39426

Tungsten inert gas arc welding for refractory or active metals working in gas-tight chamber, noting effects of reduced pressure on cathode zone energy density

20 p2569 A73-39666

Determination of work functions near melting points of refractory metals by using a direct-current arc.

21 p2722 A73-41563

Long-term drift of some noble and refractory-metal thermocouples at 1600 K in air, argon, and vacuum.

22 p2857 A73-42033

Material preparation and fabrication techniques for the production of high reliability thermocouple devices.

22 p2858 A73-42040

Kinetics of gas absorption by refractory metals in dissociated environments - The nitrogen/tantalum system.

22 p2879 A73-42583

The nature of the high microhardness of surfaces strain-hardened by friction

23 p2984 A73-43467

Intensity of charged particle recombination on the surface of certain borides of high-melting-point metals in a weakly ionized hydrogen plasma

24 p3098 A73-44418

REFRACTORY PERIOD

Step input tracking experiment for testing human psychological refractory period, noting directional error correcting reaction time similarities with keyboard tasks

06 p0659 A73-18470

REFRASIL (TRADEMARK)

U FIBERS

U SILICON DIOXIDE

REFRIGERANTS

A shock tube study on condensation kinetics.

21 p2792 A73-41143

REFRIGERATING

Refrigeration of lunar samples destined for thermoluminescence studies.

02 p0219 A73-12439

REFRIGERATING MACHINERY

NT REFRIGERATORS

Miniature Stirling cycle refrigerators to cool IR detectors, discussing refrigerators with rhombic drive, thermal coupling to detector, triple expansion and Vuilleumier cycle

13 p1707 A73-29066

DC9-30 refrigeration system diagnosis by computer.

16 p1969 A73-33654

Development of a direct condensing radiator for use in a spacecraft vapor compression refrigeration system.

[ASME PAPER 73-ENAS-5] 19 p2493 A73-37967

Experimental investigation of the antifiric properties of Teflon-base materials at low temperatures

21 p2724 A73-41197

REFRIGERATORS

Investigation of cryogenic stability and reliability of operation of Nb3Sn coils in helium gas environment.

02 p0200 A73-11838

Cryogenic cooling systems technology for spacecraft applications, comparing passive and phase-change coolers and closed cycle refrigerator for capacity and service life

10 p1285 A73-23790

Thermodynamic optimization of current leads into low temperature regions.

13 p1707 A73-29067

50 kG gas cooled superconducting solenoid operated at 13 K.

21 p2702 A73-41103

REFUELING

Extraterrestrial propellant resupply for advanced manned missions.

02 p0221 A73-12599

Evaluation of the method of characteristics applied to a pressure transient analysis of the B.A.C./S.N.I.A.S. Concorde refuelling system.

02 p0133 A73-12645

Space shuttle orbiter applications to manned high energy missions from low earth orbit, considering refueling requirements, aerobraking and overall mission capability

[AIAA PAPER 73-206] 05 p0630 A73-16939

New developments in aircraft refuelling vehicles.

22 p2838 A73-41861

REGENERATION [ENGINEERING]

Interference protection of regenerative parametric amplifiers.

09 p1061 A73-22042

A tunnel diode regenerative frequency multiplier with a high multiplication factor.

13 p1591 A73-28734

Low emissions combustion for the regenerative gas turbine. I - Theoretical and design considerations.

[ASME PAPER 73-GT-11] 16 p2086 A73-33489

Low emissions combustion for the regenerative gas turbine. II - Experimental techniques, results, and assessment.

[ASME PAPER 73-GT-12] 16 p2086 A73-33490

Atmospheric regeneration in closed chambers by potassium superoxide

18 p2287 A73-36951

Regenerative multidiode IMPATT amplifier.

18 p2294 A73-37132

The scale effect and design method of the regenerative pump with non-radial vanes.

23 p2986 A73-44274

REGENERATION [PHYSIOLOGY]

Evoked negative electrical potentials due to auditory zone stimulation by local cooling, mechanical trauma and potential recording, observing reaction regeneration variations

15 p1833 A73-31159

Effect of steady magnetic fields up to 4,500 Oe on the mitotic activity of the corneal epithelium in mice

15 p1838 A73-31510

Russian book on structural and functional plasticity of interneuron synapses during readjustment to chemical and physical damage covering degenerative and regenerative changes

21 p2640 A73-41280

REGENERATIVE COOLING

REGENERATIVE COOLING

The Viking Orbiter 1975 beryllium INTERGEN rocket engine assembly. 03 p0382 A73-13438 [AIAA PAPER 72-1131]
Algorithm for calculating unsteady heat transfer in liquid-propellant rocket-engine chambers with regenerative cooling 07 p0868 A73-20087

Spacecraft dynamic solar electric power/thermal control system with cold liquid flow and regenerator cooling for energy conversion efficiency and weight characteristics improvements 09 p1153 A73-22785

Thermodynamic performance analysis of gas turbine power plants with intercooler. II - Performance of intercooling-regeneration-reheat type and precise calculation method. 11 p1411 A73-26343

REGENERATIVE CYCLES

U REGENERATION [ENGINEERING]

REGENERATIVE FEEDBACK

U POSITIVE FEEDBACK

REGENERATIVE FUEL CELLS

Space station solar array-energy storage-power control and distribution system based on regenerative fuel cell integrated with life support system 09 p1153 A73-22784

High-temperature batteries. 17 p2110 A73-35594

A regenerative fuel cell system for modular space station integrated electrical power. 19 p2390 A73-38402

REGENERATORS

NT THERMOSIPHONS

Time jitter in line regenerators with pattern dependent pulse waveforms. 09 p1062 A73-22301

REGIONAL PLANNING

NT URBAN PLANNING

Remote sensing applications in the Metropolitan Washington Council of Governments. 20 p2556 A73-39833

Remote sensing to detect regional change in land use characteristics, using aerial photo mosaics and high altitude photography 20 p2557 A73-39846

REGIONS

NT ANTARCTIC REGIONS

NT ARCTIC REGIONS

NT AURORAL ZONES

NT BRILLOUIN ZONES

NT D REGION

NT E REGION

NT F REGION

NT FRESNEL REGION

NT POLAR REGIONS

NT REMOTE REGIONS

NT SUBARCTIC REGIONS

NT TEMPERATE REGIONS

NT TROPICAL REGIONS

REGISTERS [COMPUTERS]

Optimization of register length in a control algorithm for a nonstationary plant 05 p0561 A73-17280

REGRESSION [STATISTICS]

U REGRESSION ANALYSIS

REGRESSION ANALYSIS

NT REGRESSION COEFFICIENTS

Analog computer regression line and correlation ratio determination for random stationary processes with time lag 01 p0028 A73-10928

Regression models for the effect of stress ratio on fatigue crack growth rate. 03 p0387 A73-13231

Interdependence of oxygen uptake, heart rate and ventilation during treadmill exercise from regression slope analysis of lag logarithms 03 p0263 A73-14118

Book - Sequential analysis and optimal design. 05 p0590 A73-16352

Double cross-validation of video cartographic symbol location performance. 05 p0543 A73-16719

One- and multistage multivariable function max-min problem solution by random search type method through regression curve construction based on statistical test and root determination 06 p0715 A73-17563

The use of model output statistics /MOS/ in objective weather forecasting. 06 p0720 A73-18706

Dynamic system model identification computational considerations, discussing equation error methods based on regression analysis, maximum likelihood estimates and gradient dependent algorithms for optimization 07 p0845 A73-20428

Calibration of resistance strain gauges 07 p0827 A73-20538

Mathematical analysis of the responses of the human respiratory system to hypoxia and hypercapnia 08 p0931 A73-21322

Computerized normal loci plotting by orthogonal Chebyshev approximation, using minimum variance principle and Fisher test for regression curve selection 09 p1143 A73-22094

Correlation analysis of the accuracy of the machining of micromachine components 09 p1088 A73-22660

Analog computer regression line and correlation ratio determination for random stationary processes with time lag 10 p1201 A73-24188

Linear regression filtering and prediction for tracking maneuvering aircraft targets. 11 p1333 A73-26640

Determination of the type of motion in spherically symmetric clusters of galaxies. 12 p1539 A73-27285

Some aspects of nonorthogonal data analysis. I - Developing prediction equations. 13 p1650 A73-29298

Group data handling theorems on uniqueness of mathematical model for regression curve reconstruction in polynomial domain with small number of points 14 p1738 A73-30288

The estimation of extratropical cyclone parameters from satellite radiation measurements. 15 p1903 A73-31315

Parachute-payload system performance prediction for cause and effect relationships by parametric sensitivity and regression analysis for optimal design with computer simulation [AIAA PAPER 73-487] 15 p1829 A73-31469

The regression relations for turbulence parameters in the air layer near the ground in the case of an inhomogeneous base 15 p1907 A73-32359

Difference between even and odd 11-year solar activity cycles 16 p2056 A73-33658

Book - Statistical design and analysis of engineering experiments. 17 p2200 A73-34456

Solar flare prediction objective baseline calculation, applying regression analysis to sunspot, magnetic field, calcium plage and radio brightness temperature data 21 p2762 A73-41392

Response surface methodology analysis of training transfer in pursuit rotor tracking task, relating three independent variables through multiple-regression prediction equations 24 p3063 A73-44774

Prediction equation validity for response surface methodology analysis of surveillance tracking by human operators, comparing variance and regression procedures 24 p3063 A73-44776

REGRESSION COEFFICIENTS

Determining the trend of a random sequence 12 p1518 A73-27224

REGULARITY

On the regularity of solutions of two-dimensional variational problems with obstructions. 01 p0069 A73-10044

REGULATIONS

Effect of aircraft reliability regulations on takeoff and landing performance of QSTOL aircraft [DGLR PAPER 72-056] 02 p0130 A73-11658

U.S.S.R. laws and regulations regarding civil air transport equipment operations and maintenance, considering personnel training and safety 19 p2435 A73-38119

REGULATORS

NT AUTOMATIC FREQUENCY CONTROL

NT CURRENT REGULATORS

NT FLOW REGULATORS

NT FREQUENCY CONTROL

NT FUEL FLOW REGULATORS

NT OXYGEN REGULATORS

NT SPEED REGULATORS

NT THERMOSTATS

NT VOLTAGE REGULATORS

Magnetic pulse width modulator and power switch subsystem of switching-mode dc regulator, deriving describing function from transfer functions 03 p0282 A73-13928

Computerized design and algorithm for linear and nonlinear regulators by mathematical programming approach involving vector determination for objective function minimization 03 p0286 A73-14480

Logidyn analog components regulator systems for industrial current and speed control, amplifier output voltage control, digital-analog converters, analog storage devices, etc 05 p0556 A73-16075

Fuzzy multi-stage decision-making, fuzzy state and terminal regulators and their relationship to non-fuzzy quadratic state and terminal regulators. 06 p0681 A73-18523

A computational algorithm for design of regulators for linear jump parameter systems. 19 p2408 A73-38066

Nonlinear regulator theory and an inverse optimal control problem. 23 p2963 A73-43820

REHEATING

U HEATING

REIGNITION

U IGNITION

REINFORCED MATERIALS

U COMPOSITE MATERIALS

REINFORCED PLASTICS

NT GLASS FIBER REINFORCED PLASTICS

Investigation of the macroscopic rheonomic properties of a monodirectional fiberglass-reinforced plastic 01 p0067 A73-10002

Highly-stressed centrifuge and rotor drums made of reinforced plastics 01 p0056 A73-10308

Crack formation in orthogonally reinforced fiberglass plastics 01 p0067 A73-10482

Carbon fibre adhesion to organic matrices. [ONERA, TP NO. 1173] 01 p0068 A73-14999

Possibility of using the method of time characteristics for solving applied problems concerning the bending of sandwich plates with allowance for creep of the materials 02 p0230 A73-11641

Physicomechanical properties of a structural cold-hardened fiberglass-reinforced plastic 02 p0184 A73-11719

Crack initiation and propagation in glass fiber reinforced plastic materials, noting rod bending 02 p0231 A73-11810

Glass reinforced epoxy structure for a lightweight superconducting dipole magnet. 02 p0232 A73-11836

Plastic limit behavior and failure of filament reinforced materials. 02 p0234 A73-12074

Glass laminates and high strength oriented fiberglass reinforced plastics failure mechanism in tension and bending, noting equalizing effect through proper cohesion characteristics between layers 02 p0185 A73-12134

Apparatus for testing reinforced plastics during nonuniform heating, with due allowance for the gas permeability of the material. 02 p0150 A73-12143

Randomly oriented glass fiber reinforced epoxy composites tensile strength properties as function of fiber volume fraction 02 p0185 A73-12427

Glass bead reinforced epoxy and polyester resins mechanical properties as function of volume fraction and interfacial bond strength, discussing beads chemical surface treatment effects 02 p0185 A73-12428

Axial compression buckling of single metal fiber embedded in plastic matrix, using photoelastic stress analysis and finite element method 02 p0236 A73-12432

Effect of vacuum solidification on the porosity of wound fiberglass-reinforced plastics 02 p0174 A73-12577

Material and structural studies of metal and polymer matrix composites. 02 p0182 A73-12621

Theoretical and experimental analysis of plane and cylindrical reinforced-plastic structures 02 p0185 A73-12794

Moisture effects on the high-temperature strength of fiber-reinforced resin composites. 03 p0328 A73-13002

Development and evaluation of graphite and boron polyimide composites. 03 p0329 A73-13003

Polyimide 2080 molded composites mechanical, thermal and electrical properties, discussing processing techniques 03 p0329 A73-13005

Advances in glass fiber fabrics for plastic reinforcement. 03 p0330 A73-13014

Tensile, compressive and shear strength and absolute modulus of PRD fibers from reinforced plastic honeycomb and filament wound strand tests 03 p0330 A73-13015

Fiber strength of S-glass/epoxy composites under biaxial loading. 03 p0330 A73-13017

Design, development, fabrication and qualification load testing of high modulus graphite-epoxy reflector support truss for ATSF and G 03 p0330 A73-13021

Graphite-epoxy composite missile adapter design, fabrication, tooling, bonded assembly and costs, comparing with boron-aluminum material 03 p0331 A73-13022

Graphite-epoxy composite properties, fabrication and tests for light weight low distortion spacecraft antenna reflector applications 03 p0331 A73-13023

Filament wound boron/epoxy rocket motor chamber fabrication and hydroproof, burst and firing tests, including failure and deformation evaluation
03 p0331 A73-13024

Response of boron/epoxy composite materials to simulated lightning current.
03 p0331 A73-13025

Glass reinforced structural components for the synchronous meteorological satellite.
03 p0331 A73-13030

Properties of pultruded composites containing high modulus graphite fibers.
03 p0332 A73-13032

Recent advances in automated manufacture of composite structures, e.g., tape laying and pultrusion.
03 p0332 A73-13033

Reinforced all-plastic quadrant molded missile airframes design, fabrication and flight testing
03 p0333 A73-13052

Advantage of reinforced plastics for helicopter blades and hubs
03 p0250 A73-13586

Preparations and properties of boron and silicon carbide filaments
03 p0334 A73-13588

Physical and chemical aspects of aging of polymer-base composite materials
03 p0273 A73-13590

Mechanical properties and applications of reinforced plastics for cast alloy elements, machine parts and noncorrosive light structures production, emphasizing glass fiber reinforcement
03 p0334 A73-13593

Selective reinforcement of wing structure for flutter prevention.
03 p0392 A73-13705

Effect of the glass fiber diameter on the compressive strength of glass fiber reinforced plastics
03 p0335 A73-13738

Deformation characteristics of plastics reinforced by high-modulus anisotropic fibers
03 p0335 A73-13739

Compensation, by the layer winding method, for thermal stresses in articles manufactured from reinforced plastics
03 p0313 A73-13740

Algorithm for stress tensor and stability analysis of glass fiber reinforced plastic shells under hydrostatic pressure
03 p0392 A73-13741

Creep of wound orthotropic glass fiber reinforced plastic
03 p0335 A73-13745

High frequency fatigue test assembly for glass fiber reinforced plastics specimens under symmetric tension-compression
03 p0288 A73-13747

Effects of process and test variables on the properties of carbon-fibre/epoxide-resin composites.
03 p0335 A73-13800

Speed brake in carbon fibre composite construction.
03 p0393 A73-13920

The effects of matrix and interface modification on local fractures of carbon fibers in epoxy.
03 p0335 A73-13982

Failure phenomena relationship to kinetic equation for defect buildup from brittle fracture analysis of composite glass fiber reinforced plastic in uniaxial eccentric tension
03 p0394 A73-14008

The application of adhesive bonded structures and composite materials on advanced turbofan engines.
03 p0359 A73-14134

The influence of temperature on the wear of carbon fiber reinforced resins.
[ASLE PREPRINT 72LC-5B-3]
03 p0335 A73-14363

Nonlinear physical stress-strain relation for reticular polymers and fiberglass plastics under conditions of microcreep and elastic aftereffect
04 p0468 A73-15508

The energy of crack propagation in carbon fibre-reinforced resin systems.
04 p0469 A73-15981

Improvements in the transverse properties of composites. I - Fracture surface energy and mechanism of transverse fracture in glass fibre composites.
04 p0469 A73-15984

On the re-inforcement of thermoplastics by imperfectly aligned discontinuous fibres.
04 p0469 A73-15986

Optimal experimental measurements of anisotropic failure tensors.
05 p0631 A73-16113

The vibration of cantilever beams of fiber reinforced material.
05 p0631 A73-16115

A simple procedure for experimental determination of the longitudinal shear modulus of unidirectional composites.
05 p0588 A73-16119

Effect of specimen geometry on fatigue strength of boron and glass epoxy composites.
05 p0588 A73-16139

The mechanical properties of thermoplastics strengthened by short discontinuous fibres.
05 p0589 A73-16434

Heat conductivity of system composed of a silicor-ganic elastomer and a powdered mineral filler
05 p0589 A73-16771

Response of a cylindrical fiberglass-reinforced plastic shell to the action of an explosive load
05 p0635 A73-17079

Glass fiber reinforced thermoplastic molding materials mechanical and thermal-dimensional stability properties, considering time dependent behavior under static and dynamic loads
06 p0714 A73-18450

Crack propagation measurements by surface gage of polymethyl methacrylate, epoxy resin and glass reinforced epoxy composites, conforming with Mott energy balance equation
06 p0714 A73-18499

Properties of pultruded composites containing high modulus graphite fibers.
06 p0715 A73-18719

Polyimide composites development for aircraft structures.
06 p0715 A73-18720

Reinforced plastics role in construction and shielding of Diamant B satellite booster main components
07 p0905 A73-18995

Industrial manufacturing of stratospheric balloons.
07 p0829 A73-18998

Effect of additives on ablation of phenolic-silica composites.
07 p0842 A73-19486

The Kaiser effect in stress wave emission testing of carbon fibre composites.
07 p0843 A73-20185

The erosion of carbon fibre reinforced plastic by repeated liquid impact.
07 p0843 A73-20224

Glass fiber reinforced polyester laminates, testing layer base material and molding condition effects on tensile and bending strengths and other mechanical properties
07 p0843 A73-20326

Hybrid composite of carbon and glass fiber reinforced epoxy resin, testing mechanical properties and optimal fibrous modulus ratios and volume fraction
07 p0844 A73-20327

A visco-plasto-elastic expression for stress-strain diagram of fiber reinforced plastics subjected to repeated low frequency loads.
07 p0915 A73-20329

Fiber reinforced plastics with adhesive bonded elements, investigating ply number and adhesive pressure effects on shear, bending and impact strengths
07 p0844 A73-20330

Flat laminated FRP-FRTP and carbon FRP-FRTP composites, testing lamination effects on bending and impact strengths
07 p0844 A73-20331

Graphite fiber reinforced polyimide resin composites for structural applications in long duration high temperature environments, discussing fabrication with match-metal die
[SME PAPER EM 72-107]
07 p0832 A73-20448

Friction and wear of graphite fiber composites.
07 p0833 A73-20500

Plastic analysis of filled, reinforced, circular cylindrical shells.
08 p1015 A73-20672

Large deflections and stability of a long cylindrical panel prepared from an orthotropic fiberglass plastic under the action of piecewise-uniform loading
08 p1017 A73-21370

Deformation of a frame coupled to a fiberglass-plastic shell under the action of local loads
08 p1017 A73-21372

The influence of orthotropy on the stability of some multi-plate structures in compression.
08 p1018 A73-21435

Measurement of the flexural damping capacity and dynamic Young's modulus of metals and reinforced plastics.
08 p0967 A73-21594

Flammability comparisons of glass-reinforced unsaturated polyester moldings in various laboratory-scale tests.
08 p0983 A73-21820

Thermal expansion at elevated temperatures. IV - Carbon-fibre composites.
09 p1110 A73-22121

High modulus organic fibre composites in aircraft applications.
09 p1110 A73-22519

Random function theory method for estimation of tensile, compressive and shear strength and elastic constants of monodirectional fiberglass reinforced plastics
09 p1110 A73-23056

The thermal expansion coefficients of some glass-reinforced plastics and their components at low and high temperatures.
09 p1111 A73-23063

Brittle fracture of orthogonally reinforced glass-fiber plastics during tension
09 p1111 A73-23349

Evaluation of static test methods for determining the fundamental mechanical properties of fiberglass-reinforced plastics
10 p1237 A73-23663

Reinforced plastics - Ever new; Proceedings of the Twenty-eighth Annual Conference, Washington, D.C., February 6-9, 1973.
10 p1237 A73-23951

Polyester fiber/glass fiber composite sandwich structural design, considering thickness loss during abrasion test, physical properties and flexural strength
10 p1237 A73-23954

A theoretical study of the effect of the interface on composite toughness.
10 p1288 A73-23955

Effect of fiber-matrix adhesion on the properties of short fiber reinforced ABS.
10 p1237 A73-23956

Gear and bearing designs with lubricated and reinforced thermoplastics.
10 p1223 A73-23957

Filament-wound vessel from an organic fiber-epoxy system.
10 p1237 A73-23958

Analysis, test, and comparison of composite material laminates configured for isotropic low thermal expansion.
10 p1237 A73-23960

Fiberglass reinforced plastics dynamic models, discussing stress-strain relationship, Poisson ratio and fatigue
10 p1288 A73-23962

Mineral filler reinforcement value in polyolefins, stressing composite properties at high temperatures
10 p1237 A73-23963

Ballistic-tolerant helicopter flight control components from plastic composite materials.
10 p1237 A73-23964

Fatigue and creep testing of unidirectional carbon fibre reinforced plastics.
10 p1238 A73-23965

Criteria for selecting resin matrices for improved composite strength.
10 p1238 A73-23966

Acoustic emission studies of large advanced composite rocket motor cases.
10 p1288 A73-23967

Feasibility evaluation of graphite/epoxy composite materials to helicopter transmission housing.
10 p1238 A73-23969

The effect of long-time thermal exposure on the mechanical properties of graphite/polyimide composites.
10 p1238 A73-23970

Energy dissipation sources during reinforced plastic fracture, investigating fiber debonding energetics, toughness and crack propagation resistance
10 p1238 A73-23971

Impact strength and fracture of carbon fiber composite beams.
10 p1238 A73-23972

Bearing materials from graphite fiber composites.
10 p1238 A73-23974

High temperature creep properties of P10P polyimide - HMS graphite composites.
10 p1239 A73-23975

The influence of interfacial bonding on the properties of carbon fiber composites.
10 p1239 A73-23976

High modulus graphite fiber-epoxy composite shear strength and structural observation by X ray and electron diffraction and surface dark field electron microscopy
10 p1239 A73-23977

The dynamic properties of unidirectional fibre reinforced composites in flexure and torsion.
10 p1240 A73-24279

Effects of shear damage on the torsional behaviour of carbon fibre reinforced plastics.
10 p1240 A73-24280

The effect of specimen and testing variables on the fracture of some fibre reinforced epoxy resins.
10 p1240 A73-24281

Interlaminar shear strength of a carbon fibre reinforced composite material under impact conditions.
10 p1240 A73-24286

Bulk compressibility of carbon fibre reinforced plastics.
10 p1240 A73-24288

Investigation of the strong anisotropy and resistance of fiber-strengthened plastics to interlayer shearing and compression normal to the fibers
10 p1240 A73-24353

Creep-rupture strength criterion in the case of inter-layer shearing of oriented fiberglass plastics
10 p1240 A73-24355

Limiting deformability of lengthwise-crosswise wound fiberglass-reinforced plastics under conditionally instantaneous and prolonged biaxial compression
11 p1386 A73-25034

Effect of heat treatment on the fatigue properties of unweaved fiberglass-reinforced plastics
11 p1386 A73-25047

Military aircraft radome design technology developments in Sweden, discussing use of glass fiber reinforced plastics, manufacturing method, computerized optimization and measurement techniques
11 p1335 A73-25300

Experimental investigation of oscillation damping in shells with holes
11 p1435 A73-25398

Effects of prestressing boron/epoxy prepreg on composite strength properties.
[AIAA PAPER 73-382]
11 p1388 A73-25512

The elastic constants of carbon-fibre composites.
11 p1389 A73-26045

The impact toughness of discontinuous boron-reinforced epoxy composites.
11 p1389 A73-26046

Property control in reinforced plastics through interface tailoring.
11 p1389 A73-26296

Glass fiber reinforced polyester laminates mechanical properties evaluation for structural design, considering failure criteria in terms of fiber debonding and resin and gel coat cracking
12 p1515 A73-26877

Carbon fiber reinforced epoxy resins mechanical properties, correlating test parameters with observed failure mechanism
12 p1515 A73-26878

High frequency load tests for fatigue properties of glass and carbon fiber reinforced plastics and epoxy impregnated wood laminates
12 p1515 A73-26879

Fatigue resistant design with fiber reinforced plastics /FRP/, discussing stress analysis, failure criteria, material anisotropy, multiaxial stress conditions and cumulative damage
12 p1515 A73-26880

Fatigue and impact tests on composite propeller blades made of glass- and carbon fiber reinforced plastics, noting comparison with measured vibratory strains
12 p1458 A73-26881

Fiber strength, fracture types and material elastic properties relationship to impact resistance in carbon fiber reinforced plastics
12 p1515 A73-26882

The effect of fibre-matrix interface strength on the impact and fracture properties of carbon-fibre-reinforced epoxy resin composites.
12 p1515 A73-26922

A comparison of quasi-static uniaxial-strain and Hugoniot tests for quartz-phenolic composite.
12 p1515 A73-27024

Temperature sensitivity of CFRP honey-comb structures under holographic ndt.
12 p1496 A73-27036

Reinforcing glass fiber preparation effect on fiber wetting by polyethylene melt, analyzing adhesion strength relationship to residual stresses
12 p1516 A73-27178

Design of zero-moment axisymmetric tanks made of a reinforced hereditary-elastic material
12 p1511 A73-27181

Realization of the mechanical properties of the fibers in high-modulus polymeric composites
12 p1516 A73-27183

Statistical characteristics of the mechanical constants of glass-fiber-reinforced plastics
12 p1516 A73-27184

Deformation and strength characteristics of carbon-fiber strengthened plastics in compression
13 p1644 A73-27991

Probability characteristics of the shear modulus of fiberglass-strengthened plastics
13 p1644 A73-27997

Determination of the mechanical characteristics of fiberglass-strengthened plastics in the winding state
13 p1644 A73-27998

High strength glass fibre-resin composites.
13 p1645 A73-28498

Glass fiber reinforced plastics optimum glass volume fraction for maximum flexural rigidity and strength
13 p1645 A73-28777

Determination of the nominal strength characteristics of fiberglass-strengthened plastics in the stress-concentration zones
13 p1645 A73-29051

German monograph - A contribution to the stability calculation and the test of cylindrical shells of glass-fiber reinforced plastics under uniform external pressure.
13 p1646 A73-29280

Three-dimensional scattered-light stress analyses of discontinuous fiber reinforced composites.
[SESA PAPER 2033]
13 p1699 A73-29306

Heat and mass transfer on the surface of a fiberglass-reinforced plastic in a high-temperature air flow
13 p1708 A73-29403

Interfiber failure of unidirectional composite material.
13 p1702 A73-29538

Internal fracture and acoustic emission of fiberglass reinforced plastics.
13 p1647 A73-29544

On fatigue damage and debonding of glass fiber reinforced plastics.
13 p1647 A73-29546

Book - Fibre-reinforced materials technology.
13 p1644 A73-29675

Fiberglass-reinforced plastics for glider laminate wing spars, describing elastic properties and strength characteristics
14 p1809 A73-30241

Crack formation in orthogonally reinforced glass-fiber ware.
14 p1765 A73-30307

Fracture strength of fiber reinforced plastics, investigating crack propagation susceptibility, stress concentration and fracture mechanics
[ASME PAPER 73-DE-20]
14 p1767 A73-30821

Conditionally-instantaneous and long term strength of a longitudinally-transversely wound glass-fiber-reinforced plastic under biaxial compression
15 p1896 A73-30975

Critical stress intensity factors applied to glass reinforced polyester resin.
15 p1897 A73-31676

Dynamic mechanical properties of graphite-epoxy and carbon-epoxy composites.
15 p1897 A73-31677

Theoretical post-yielding behavior of composite laminates. I - Inelastic micromechanics.
15 p1897 A73-31678

Tensile and compressive strength tensor prediction for anisotropic boron-epoxy composites from off axis tests
15 p1897 A73-31682

Mechanism of breakdown in the interface region of glass reinforced polyester by artificial weathering.
15 p1898 A73-31838

Theory for cylindrical wavy shells via fiberglass-plastic models, noting application to wavy rod torsion problem
15 p1952 A73-32083

Two component glass fiber reinforced plastic model describing stress-strain state via elastic properties analysis, internal energy production and Hookes Law application
15 p1952 A73-32085

Light weight impact protective helmet shell materials and designs, noting E- or S-glass and polyimide resin for oxygen rich space station/shuttle applications
16 p2027 A73-32677

Lightweight coatings for protecting boron filament and graphite fiber reinforced plastic composites from structural damage by lightning
16 p2028 A73-33033

Lightning protection for boron and graphite reinforced plastic composite aircraft structures, discussing zonal design concept and channel intermittent contact with protrusions on surface
16 p1968 A73-33034

F-14 aircraft boron-epoxy and graphite-epoxy composite structure production protection against degradation by lightning discharges, discussing design, processing and tests
16 p2028 A73-33035

Low void polyimide/glass and graphite reinforced composite properties and fabrication, showing improved interlaminar shear and wet strength
16 p2029 A73-33048

Effect of prepregging solvent on high-temperature stability of KERIMID 601 composites.
16 p2029 A73-33049

Polyphenylquinoxaline/graphite composite laminates tests for flexure, shear and tensile strength at 316 C
16 p2029 A73-33050

Glass fabric structures, properties and designs of reinforced polyester and epoxy laminates for aerospace applications
16 p2030 A73-33064

Pressure vessels filament winding with inflatable mandrel in reinforced elastomer, discussing use of balloon as liner
16 p2018 A73-33068

Nonlinear creep in glassfiber-reinforced plastics in the presence of some types of complex stress conditions
16 p2030 A73-33926

Stresses in plastics reinforced by anisotropic fibers in the presence of transversal normal loads
16 p2030 A73-33928

Experimental investigation of the effect of vibrations on the creep of glassfiber-reinforced plastics in the presence of complex stress conditions
16 p2030 A73-33939

High strength low density Hyfil carbon fiber prepreg sheet properties and production for aircraft applications
16 p2021 A73-33986

Factors affecting the impact strength of glass-fibre-reinforced polyester composites.
16 p2031 A73-33987

The effects of adverse environmental conditions on the resin-glass interface of epoxy composites.
16 p2031 A73-33989

Boron composites - Status in the USA.
16 p2031 A73-34042

Monograph - Fibre reinforcement.
17 p2240 A73-34125

Investigation of the bond strength between layers of textile materials
17 p2194 A73-34333

Cost/weight tradeoff ratios for fiber reinforced plastic aircraft structural components
[SAE PAPER 730338]
17 p2257 A73-34689

Reinforced plastics for aerospace applications covering history of laminates, use of cellulose, asbestos, boron, glass and oriented carbon fibers, whisker composites and resin matrices
17 p2194 A73-34801

High strength organic fiber PRD-49 reinforced plastics compared to materials reinforced with glass, graphite and boron, discussing weight required to achieve Al faced sandwich performance
17 p2194 A73-34802

Development of advanced composite rocket motor chambers using boron and graphite fibers.
17 p2194 A73-34803

Reinforced plastics under ablative conditions for thermal insulation and structural applications.
17 p2195 A73-34805

Rain erosion of reinforced plastics for aerospace applications in terms of drop size, impact angle and velocity effects and protective coatings
17 p2195 A73-34806

Edgewise tape wound reinforced plastic ablative components for rocket motors to provide balance between optimum char strength, heat flow and insulation characteristics
17 p2195 A73-34809

Hovercraft propeller and turbine engine fan blades with glass and carbon fiber reinforced plastics respectively, discussing design and constructions
17 p2103 A73-34813

Aircraft structural applications of filamentary composites, discussing fiberglass, boron-epoxy and graphite-epoxy composites
17 p2103 A73-34814

Shock unloading phenomena in fiber-reinforced composites.
17 p2247 A73-34916

Low cost manufacturing methods for highly reliable ballistic-tolerant composite helicopter flight control components.
[AHS PREPRINT 754]
17 p2180 A73-35082

Performance, structural reliability and fatigue life of glass fiber-epoxy twin beam helicopter rotor blades
[AHS PREPRINT 782]
17 p2106 A73-35095

The anisotropy of creep behaviour in oriented thermoplastics.
17 p2196 A73-35342

Short- and long-term strength characteristics of particulate-filled cast epoxy resin.
17 p2197 A73-35343

Tensile creep in short fibre reinforced thermoplastics.
17 p2197 A73-35344

Processability/mechanical properties trade-off for reinforced plastics.
17 p2197 A73-35353

Exploratory development of composite missile fuselages.
17 p2181 A73-35354

Non-destructive testing of plastics by means of holographic interferometry.
17 p2181 A73-35355

Micromechanic stresses in photoelastic composite coupons.
[SESA PAPER 2175A]
17 p2251 A73-35456

Carbon, boron and glass fiber-epoxy resin composites fracture processes, predicting fracture strength of aligned fibrous composites via linear elastic fracture mechanics concepts
17 p2198 A73-35530

Tensile fracture of boron-epoxy composites with ordered filament packing geometry.
17 p2198 A73-35535

High modulus fiber reinforced metal and plastic matrix composites fracture within linear elastic fracture mechanics framework, reviewing standard notch toughness test
17 p2192 A73-35536

Failure mechanisms in impact loaded carbon and glass fiber reinforced plastics, discussing specimen geometry, notch presence, fiber type, fiber orientation and hybridization effects
17 p2198 A73-35538

Fiber orientation effects on fatigue failure of aligned short fiber composite materials.
17 p2198 A73-35546

Surface ablation of silica-reinforced composites.
18 p2368 A73-36316

The strength prediction problem of unidirectional fiberglass-reinforced plastics under transverse tension and shear

18 p2326 A73-36409
Reinforced plastics; Conference, Karlovy Vary, Czechoslovakia, May 15-17, 1973, Lectures

18 p2326 A73-36464
Development and problems of testing prepregs for the purposes of the Czechoslovakian aircraft industry

18 p2327 A73-36469
Rational winding of vessels with nonlinear winding program

18 p2319 A73-36470
Optimal cutting conditions for working of reinforced plastic laminates, comparing with metals

18 p2319 A73-36471
Concepts from the realization of the development of the technology and assembly lines for the fabrication of polyester glass laminates

18 p2320 A73-36472
On stress concentration factors in orthotropic glass-fiber reinforced plastics.

18 p2327 A73-36474
Matrix method for the determination of the elastic and mechanical properties of reinforced plastics

18 p2327 A73-36475
Studies of fiberglass plastic under tensile load with the aid of transparency measurements

18 p2327 A73-36476
Nondestructive testing of fiberglass reinforced plastic plates by means of holographic interferometry

18 p2316 A73-36477
Self extinguishing properties of polyester-glass laminates with reduced flammability due to polyvinyl chloride and antimony trioxide additives

18 p2327 A73-36478
Mechanical characteristics of thermoplastic materials reinforced with short glass fibers, taking into account various degrees of reinforcement

18 p2327 A73-36479
Interfacial, mechanical and fracture properties of fibre reinforced polycaprolactam.

18 p2328 A73-36480
The effect of a fiberglass reinforcement on the properties of laminates with a polyamide binder

18 p2328 A73-36481
Adhesion effect on the tensile properties of fibre reinforced composite materials.

18 p2328 A73-36683
High current lightning simulation testing of composite materials.

18 p2296 A73-36713
Evaluation of the carrying capacity of reinforced plastics subjected to nonuniform heating

18 p2328 A73-36760
Investigation of failure of a fiberglass plastic due to differential carbon burnup

18 p2328 A73-36813
Heat and mass transfer processes during thermal decomposition of resin binders in fiberglass reinforced plastics

18 p2328 A73-36814
Determination of rated strength characteristics of fiberglass in zones of stress concentration.

18 p2328 A73-36883
Modulus reinforcement in elastomer composites. I - Inorganic fillers.

18 p2328 A73-36980
Modulus reinforcement in elastomer composites. II - Polymeric fillers.

18 p2328 A73-36981
An improved method of production for high strength fibre-reinforced thermoplastics.

18 p2329 A73-37092
Studies on the impact resistance of composite plates.

18 p2367 A73-37093
Fatigue of fibre-reinforced plastics - A review.

18 p2329 A73-37094
The elastic properties of carbon fibres and their composites.

18 p2329 A73-37095
Boron epoxy, polyimide and aluminum composite materials for cost effective high performance aircraft and turbine engine structures, assessing development and application status

19 p2443 A73-37892
[SAWE PAPER 992]
Studies on glass-reinforced epoxy resin using either Vulkadur A or a mixture of Vulkadur A and triethanolamine as crosslinking agent.

19 p2444 A73-38092
A critical examination of the impact test for glassy polymers.

19 p2444 A73-38093
Glass fiber reinforced polypropylene composites fabrication technology and physico-mechanical properties

19 p2444 A73-38162
Boron-stiffened longerons on the B-1.

19 p2436 A73-38499
[SME PAPER EM 73-719]
A study on the dynamical behaviors of composite materials by dynamical model.

20 p2580 A73-38643

Influence of cycle ratio on the elastic modulus of glassfiber reinforced plastics subjected to repeated tensile load.

20 p2580 A73-38644
The impact resistance of glassfiber reinforced plastics under accumulation of fatigue damage.

20 p2580 A73-38645
Changes in the physicochemical properties of structural polymers after heat treatment

20 p2580 A73-39333
Method of studying the resistivity to external effects in fiberglass plastic structural elements with highly dispersed initial-state properties

20 p2580 A73-39380
Plane crack problems for ideal fibre-reinforced materials.

21 p2787 A73-41014
Fiber glass reinforced plastics measurement for ratio of elastic modulus to mean thermal conduction for use in cryostat to resist large forces

21 p2723 A73-41106
Upper bounds to in-plane shear strength of unidirectional fiber-reinforced composites.

23 p3048 A73-44383
The strength of unidirectionally reinforced plastics subjected to tension at an angle to the direction of reinforcement

24 p3102 A73-44511
The relationship of certain mechanical and thermophysical properties of polymer composites with the reduced filler concentration

24 p3102 A73-44512
The strength of orthogonally reinforced plastics during uniaxial tension

24 p3145 A73-44522
Whiskers as reinforcing component of composite materials, process-technical alignment methods

24 p3104 A73-44888

REINFORCED PLATES

Grillages of maximum strength and maximum stiffness.

01 p0115 A73-10767
Matrix analysis of local instability in plates, stiffened panels and columns.

03 p0390 A73-13339
Minimum weight rectangular beam grillages and reinforced plates of given strength or stiffness, presenting solutions for various boundary conditions

04 p0508 A73-14937
Minimum weight design of plastic and elastic grillages and fiber reinforced plates of given strength or stiffness, presenting optimal solutions for various boundary conditions

04 p0509 A73-15011
Low order spatial modes principal resonance region of in-plane loaded skew stiffened plate, obtaining equation of motion by Hamilton principle

[ASME PAPER 72-WA/APM-32]
Analysis of transverse cracks in an orthotropic strip with edge stiffeners.

04 p0516 A73-15904
[ASME PAPER 72-WA/APM-4]
Lateral rigidity of longitudinally stiffened plates.

05 p0633 A73-16543
Optimal and stiffened simply supported circular plates comparison under uniform pressure and uniform compression loads

05 p0635 A73-16976
[AIAA PAPER 73-254]
Plate stretching and plane strain and plate bending.

06 p0765 A73-18723
Imperfection-sensitivity of a wide integrally stiffened panel under compression.

07 p0908 A73-19087
Steady state vibrational frequencies of grid stiffened rectangular plates with monolithic connection at node points for simply supported case

07 p0909 A73-19095
Some contact problems for an infinite plate strengthened by elastic cover pieces

07 p0910 A73-19305
Elastic wedge whose apex section is reinforced with a rod of variable cross section

07 p0911 A73-19313
Two dynamic contact problems for a half-plane with elastic cover pieces

07 p0911 A73-19314
Transmission of the load from an annular cover piece to a plane with a circular hole

07 p0911 A73-19321
Free vibrations of square plates with stiffened square openings.

08 p1016 A73-20826
On the theory of optimal, constant thickness fibre-reinforced plates. II.

08 p1016 A73-20830
Thermoelastic bending theory based on structural analysis of multilayer reinforced shells and plates

08 p1017 A73-21373
Stresses and displacements in reinforced orthotropic panels under static loads, obtaining differential equations solution as numerically derived transfer matrices

09 p1161 A73-23091

Post-buckling behaviour of rectangular orthotropic plates.

10 p1288 A73-23699
Influence of an intermediate stiffener on the vibration frequency spectrum of a cantilever plate

10 p1291 A73-24357
Reissner's edge effect in three-layer plates with filler

11 p1433 A73-25030
Linear elastic behavior of laminated plate with ribs reinforced by continuous unidirectional fibers under surface distributed loads orthogonal and parallel to plane

11 p1435 A73-25403
Synthesis of compression panels having non-uniform stiffener sections.

11 p1437 A73-25485
[AIAA PAPER 73-347]
Statistical method for fiber-reinforced plate design optimization for important boundary conditions, noting topographies associated with piecewise linear specific cost functions

11 p1443 A73-26092
Compressive buckling analysis and design of stiffened flat plates with multilayered composite reinforcement.

12 p1554 A73-27736
Equilibrium of an anisotropic plane reinforced by an isotropic circular ring

13 p1698 A73-29131
The optimum distribution of diagonal stiffeners reinforcing a clamped infinitely long plate buckling under shear.

13 p1700 A73-29386
Matrix method analysis of stiffened plates free vibrations, deriving governing equation in stiffness matrix form by combining plane stress theory and lateral vibration equation

14 p1807 A73-30186
Finite element analysis with improved accuracy for rectangular plate bending element.

14 p1810 A73-30456
Bending of rectangular plates of variable thickness with edges reinforced by elastic ribs

14 p1815 A73-30796
Buckling of eccentrically stiffened rectangular plates subjected to linearly varying longitudinal compression.

15 p1952 A73-32043
Alleviation of stress concentration with analogue reinforcement.

17 p2250 A73-35446
[SESA PAPER 2102]
A method for determining the stressed state of anisotropic plates with a nonsymmetrically reinforced edge

18 p2363 A73-36407
Transverse bending of an annular slab with supporting ribs

18 p2367 A73-36960
Flexural wave fields in infinite beam-reinforced plates under point excitation.

19 p2498 A73-37725
Application of the Peaceman-Rochford method to the solution of the deflection problem for a plate strengthened by a square grid

20 p2620 A73-39496
Limiting zero and infinite edge beam stiffness effect on natural vibrational frequencies of reinforced annular plates

20 p2622 A73-39548
Temperature stresses in a partly reinforced orthotropic plate

21 p2787 A73-40991
Plane crack problems for ideal fibre-reinforced materials.

21 p2787 A73-41014
Fatigue behavior of stiffened flat panels

21 p2788 A73-41555
Analysis of stress intensity factors for the tension of a centrally cracked strip with stiffened edges.

23 p2992 A73-43812
Vibration characteristics of aluminum plates reinforced with boron-epoxy composite material.

24 p3149 A73-45148
Bending of transversely isotropic plates with a reinforced edge

24 p3149 A73-45174
Stress wave calculations in composite plates using the fast Fourier transform.

24 p3150 A73-45232
Optimal force transmission by flexure-clamped boundaries.

24 p3152 A73-45317
Operator of thin plate reinforced with thin-walled ribs.

24 p3152 A73-45440

REINFORCED SHELLS

A semimomentless theory of asymmetrically structured cylindrical sandwich shells with a rigid compressible filler

01 p0118 A73-11406
Stability of orthotropic circular cylindrical shells reinforced by annular ribs under external pressure

01 p0118 A73-11409

Stress analysis of cantilever thin walled cylindrical shell with concentrated force on free reinforcement ring, noting members rigidity relationship to internal stress concentration

02 p0230 A73-11718

Equilibrium equations in theory of anisotropic shells and plates with arbitrary boundary conditions under external loads, noting thin walled reinforced shells

02 p0231 A73-11807

Stability of a cylindrical shell under the action of concentrated axial compression loads

02 p0231 A73-11815

On bending and vibration of reinforced and bireinforced elastic and viscoelastic shells.

03 p0387 A73-13160

Algorithm for stress tensor and stability analysis of glass fiber reinforced plastic shells under hydrostatic pressure

03 p0392 A73-13741

Stability of fiberglass-reinforced cylindrical shell under the action of axial dynamic loads

03 p0392 A73-13746

A consistent approximation in the linear theory of elastic lattice-type shells.

03 p0393 A73-13780

Transient interaction of a flexible ring-reinforced shell and a fluid medium.

03 p0395 A73-14197

Russian book on orthotropic laminated cylindrical shells strength and optimal design covering glass ribbon reinforced zero moment shells and interlayer shear theory

04 p0514 A73-15702

Equations for the oscillations of multilayer shells with allowance for shear deformation and for fiber pressing in the filler

05 p0634 A73-16749

Response of a cylindrical fiberglass-reinforced plastic shell to the action of an explosive load

05 p0635 A73-17079

Static-geometric analogy and complex transformation in the theory of three-layer shells with a light-weight filler

07 p0912 A73-19470

Axisymmetric deformation of a laminar, orthotropic, cylindrical shell

08 p1017 A73-21368

Thermoclastic bending theory based on structural analysis of multilayer reinforced shells and plates

08 p1017 A73-21373

Stability of a shallow three-layer shell with a linearly viscoelastic filler

09 p1157 A73-21994

Stability analysis of axially compressed closed circular cylindrical shells with reinforcement rings

10 p1290 A73-24301

Strength and weight optimization of strengthened spherical shells under external pressure

11 p1434 A73-25389

Stability of cylindrical shells with filler under axial compression and external pressure

11 p1435 A73-25396

Stress, stability, and vibration of complex, branched shells of revolution.

11 p1437 A73-25496

Vibration and flutter of cylindrical shells including the effects of stringer stiffening.

11 p1441 A73-25543

Contribution to the theory of the finite element method applied to the overall stress analysis of a fuselage

12 p1551 A73-27084

Elastic and viscoelastic zero moment reinforced and weakened shells of composite materials, calculating deformation mode characteristics

12 p1553 A73-27375

Certain fatigue phenomena in aeronautical structures with stiffened shells

12 p1553 A73-27394

Stability of a reinforced cylindrical shell during axial compression

12 p1553 A73-27463

Stresses in a pressurized ribbed cylindrical shell with a reinforced hole.

15 p1948 A73-31621

Buckling analysis of elastically constrained stiffened conical shells under hydrostatic pressure by the collocation method.

15 p1948 A73-31642

Stringer stiffened cylindrical shells stability characteristics under axial compression, using Donnell thin-shell and Vlasov thin-walled beam theories

15 p1949 A73-31656

Stability of a spherical shell containing an elastic filler

15 p1950 A73-31828

Design of stiffened cylinders to resist axial compression.

15 p1950 A73-31921

Static-geometric analogy and complex transformation in the theory of three-layered shells with light fillers.

15 p1952 A73-32072

Effect of transverse shear on the stability of an orthotropic cylindrical shell with an elastic filler under axial compression

16 p2082 A73-33931

Application of a technical theory to the calculation of three-layered vaulted shells with a continuous middle layer of polymer material

16 p2083 A73-33935

Combined Rayleigh-Ritz and Lagrange multiplier technique for investigation of free vibrations of constrained cylindrical shell, considering axisymmetric mode

17 p2241 A73-34198

Further experimental studies on buckling of integrally ring-stiffened cylindrical shells under axial compression.

17 p2250 A73-35441

Limiting equilibrium of reinforced cylindrical shells

18 p2363 A73-36412

Symmetrical three-layer shells with a light-weight elastic filler

20 p2618 A73-39328

Calculation of joint shells differing in their material and thickness

20 p2619 A73-39365

Buckling analysis of deformation and stress distribution in axially compressed longitudinally stiffened cylindrical shells, considering prebuckling deformation effects

20 p2621 A73-39539

Large deformations of cord-reinforced multilayered axisymmetric shells.

20 p2621 A73-39542

Response of a cylindrical shell with filler to the action of a moving load

20 p2624 A73-39648

Evaluation of various analytical models for buckling and vibration of stiffened shells.

21 p2784 A73-40424

Critical pressure and vibration frequencies of cylindrical shells with edges elastically reinforced in the axial direction

21 p2786 A73-40980

Stress-strain state of stiffened shallow shells of rectangular planform

22 p2928 A73-43054

Experimental investigation of the strength and deformability of vacuum-prepared fiberglass-reinforced plastic shells

22 p2881 A73-43062

Experimental evaluation of the load capacity of smooth fiberglass-reinforced plastic shells under external hydrostatic pressure

23 p2998 A73-44191

Investigation of the stress-strain state at a strengthened hole in an orthotropic cylindrical shell

23 p3046 A73-44193

Dynamic buckling of an axially compressed cylindrical shell with discrete rings and stringers.

23 p3047 A73-44377

Dynamic stability of a viscoelastic orthotropic cylindrical shell

24 p3146 A73-44532

Skylab complex stiffened structure shell instability analysis by computer program, discussing convergence of finite difference formulation and eigenvalue calculation

24 p3144 A73-45234

REINFORCEMENT [PSYCHOLOGY]

Learning ability of rats to regulate hypoxic ambient atmosphere by instrumental response, discussing motivation and reinforcement factors

06 p0655 A73-18439

Behavioral and electrophysiological correlates during flash-frequency discrimination learning in monkeys.

14 p1714 A73-29989

Forward and backward conditional link formation as physiological mechanism for reinforcement conditioning connection

14 p1718 A73-30568

Motivation in vigilance - A test of the goal-setting hypothesis of the effectiveness of knowledge of results.

17 p2113 A73-34149

REINFORCEMENT [STRUCTURES]

Stress determination below thin elastic stiffeners partially braced to finite boundary of elastic half space

01 p0117 A73-11091

Selective reinforcement of wing structure for flutter prevention.

03 p0392 A73-13705

Integrodifferential equation for three dimensional contact problem of elastic half space strengthened by elastic stringer, solving by Fourier series

06 p0766 A73-18876

Parameters governing load transfer for single reinforcing members.

08 p1016 A73-20799

Thin reinforcing coatings effect on mechanical behavior of homogeneous isotropic prismatic bars under torsion, obtaining stress-strain expressions

09 p1165 A73-23358

Isogrid as integral stiffened waffle with triangular pattern to allow simple graphical solution for optimizing spherical caps or cylinders under various buckling loads

11 p1438 A73-253

[AIAA PAPER 73-365]

Elastic deformation of thin walled U-bars lateral stiffeners under torsion, eccentric tension and bending loads, determining vaulting stiffness by finite element method

15 p1950 A73-319

Macroscopic elastic constant determination for randomly reinforced composite materials by equilibrium method

15 p1954 A73-321

Integrodifferential equation for three dimensional contact problem of elastic half space strengthened by elastic stringer, using Fourier series

15 p1956 A73-32402

Design for bending of a clamped infinite strip with prestressed stiffness rib along the edge

16 p2075 A73-32402

Weight reduction in stiffened panels with specified initial buckling load in uniform longitudinal compression by stiffeners utilization

21 p2787 A73-411

REINFORCEMENT RINGS

Stress concentration near a circular hole reinforced with a wide ring in the case of a nonlinear law of elasticity

02 p0236 A73-12588

Transient interaction of a flexible ring-reinforced shell and a fluid medium.

03 p0395 A73-14151

Stability analysis of axially compressed closed cylindrical shells with reinforcement rings

10 p1290 A73-24301

Buckling of unstiffened and ring stiffened cylindrical shells under axial compression.

13 p1696 A73-28757

Ring finite elements for axisymmetric and non axisymmetric thin shell analysis.

16 p2077 A73-32984

Further experimental studies on buckling of integrally ring-stiffened cylindrical shells under axial compression.

17 p2250 A73-35441

Limiting equilibrium of reinforced cylindrical shells

18 p2363 A73-36412

Calculation of joint shells differing in their material and thickness

20 p2619 A73-39365

Evaluation of various analytical models for buckling and vibration of stiffened shells.

21 p2784 A73-40424

Numerical integration of shell equations using the field method.

[ASME PAPER 73-APMW-27] 22 p2925 A73-42888

REINFORCING FIBERS

NT CARBON FIBERS

Book - Deformations of fibre-reinforced materials.

01 p0113 A73-10148

Highly-stressed centrifuge and rotor drums made of reinforced plastics

01 p0056 A73-10308

Experimental investigation of the thermal expansion of filamentary composite materials

01 p0068 A73-10859

Discontinuous or short fiber reinforced composites properties, manufacturing procedures and aircraft structural applications

01 p0057 A73-11240

Spiral wrap - A technique for fabricating thick-wall carbon composites.

01 p0057 A73-11294

Phenolic resin char-formation during hyperthermal ablation.

01 p0124 A73-11448

PRD 49 high modulus organic fibre as aluminium replacement.

01 p0068 A73-11510

Influence of fiber/matrix interfaces on the plasticity and strength of fiber-reinforced composites

02 p0184 A73-11623

Physicomechanical properties of a structural cold-hardened fiberglass-reinforced plastic

02 p0184 A73-11719

Crack initiation and propagation in glass fiber reinforced plastic materials, noting rod bending

02 p0231 A73-11810

Plastic limit behavior and failure of filament reinforced materials.

02 p0234 A73-12074

Creep and durability of tungsten wire.

02 p0180 A73-12137

Axial compression buckling of single metal fiber embedded in plastic matrix, using photoelastic stress analysis and finite element method

02 p0236 A73-12432

Effect of vacuum solidification on the porosity of wound fiberglass-reinforced plastics

02 p0174 A73-12577

Theoretical and experimental analysis of plane and cylindrical reinforced-plastic structures

02 p0185 A73-12794

Failure mechanisms in transversely loaded boron-aluminum. 02 p0184 A73-12861

Moisture effects on the high-temperature strength of fiber-reinforced resin composites. 03 p0328 A73-13002

Advances in glass fiber fabrics for plastic reinforcement. 03 p0330 A73-13014

Tensile, compressive and shear strength and absolute modulus of PRD fibers from reinforced plastic honeycomb and filament wound strand tests 03 p0330 A73-13015

Properties of pultruded composites containing high modulus graphite fibers. 03 p0332 A73-13032

Stress redistribution model for anisotropic fiber reinforced laminates with internal cracks, assuming preferred directions to bonding planes and fiber orientation 03 p0334 A73-13333

Composite materials of today and tomorrow: New materials and conventional industries; International Conference, 1st, Lyons, France, September 22-24, 1971, Proceedings 03 p0334 A73-13579

Stockings, extensible plane structures and three dimensional textile fiber blocks reinforced materials, noting application to structures of revolution under external pressure 03 p0334 A73-13585

Structure-property relationships for composites. 03 p0334 A73-13587

Preparations and properties of boron and silicon carbide filaments 03 p0334 A73-13588

Mechanical properties and applications of reinforced plastics for cast alloy elements, machine parts and noncorrosive light structures production, emphasizing glass fiber reinforcement 03 p0334 A73-13593

Effect of the glass fiber diameter on the compressive strength of glass fiber reinforced plastics 03 p0335 A73-13738

Deformation characteristics of plastics reinforced by high-modulus anisotropic fibers 03 p0335 A73-13739

Creep of wound orthotropic glass fiber reinforced plastic 03 p0335 A73-13745

High frequency fatigue test assembly for glass fiber reinforced plastics specimens under symmetric tension-compression 03 p0288 A73-13747

Aluminum-stainless steel and Ni-Mo composites prepared by dynamic hot pressing, determining bond strength between fibers and reinforced metal matrix 03 p0328 A73-14013

Weibull flaw distribution models for fracture strength and failure analysis of brittle materials and fiber reinforced composites 04 p0468 A73-14726

On the re-inforcement of thermoplastics by imperfectly aligned discontinuous fibers. 04 p0469 A73-15986

On the effective moduli of composite materials - Slender rigid inclusions at dilute concentrations. 05 p0630 A73-16099

Factors affecting coefficient of friction and wear of friction materials for brakes, discussing fillers use as reinforcements and friction modifiers 05 p0580 A73-16106

Axial impact response of semiinfinite cylindrical membrane shell of helically oriented linearly elastic orthotropic fiber reinforced material, solving motion equations 05 p0631 A73-16112

Geometric dispersion of acoustic waves by a fibrous composite. 05 p0597 A73-16114

The vibration of cantilever beams of fiber reinforced material. 05 p0631 A73-16115

Effective stiffness of randomly oriented fibre composites. 05 p0631 A73-16116

Tensile properties of PRD-49 fiber in epoxy matrix. 05 p0588 A73-16118

Elastic wave propagation in filamentary composite materials. 05 p0631 A73-16122

Bright future forecast for composites in aerospace. 05 p0589 A73-16185

Aircraft tire improvements and possible developments, discussing fibers, rubber compounds, tread, carcass and retreading [SAE PAPER 720869] 05 p0581 A73-16653

Equations for the oscillations of multilayer shells with allowance for shear deformation and for fiber pressing in the filler 05 p0634 A73-16749

On the establishment of a diffusion barrier between a boron fiber and its tungsten substrate 05 p0589 A73-17049

Response of a cylindrical fiberglass-reinforced plastic shell to the action of an explosive load 05 p0635 A73-17079

Analytical and experimental methods in composite mechanics. [ASCE PREPRINT 1655] 06 p0758 A73-17448

Book - Electronic properties of composite materials. 06 p0714 A73-17872

Deformation by Pöbner-Lueders bands observed on composites of oriented solidification [ONERA, TP NO. 1192] 06 p0708 A73-18099

Glass fiber reinforced thermoplastic molding materials mechanical and thermal-dimensional stability properties, considering time dependent behavior under static and dynamic loads 06 p0714 A73-18450

Composite Al- and Ni-base alloys strengthened by B and W/Mo fibers respectively for reduced weight wing spars and high temperature applications 06 p0710 A73-18638

High strength and low density graphite fiber yarn for reinforcement in structural composite components on heavily loaded flight vehicles 06 p0715 A73-18716

Properties of pultruded composites containing high modulus graphite fibers. 06 p0715 A73-18719

On the reflection of harmonic waves in fiber-reinforced materials. 07 p0909 A73-19096

Fracture mechanics application to initial notch extension under tension in quasi-isotropic fiberglass reinforced laminates, noting transplanar buckling effects on fracture toughness 07 p0841 A73-19186

A visco-plasto-elastic expression for stress-strain diagram of fiber reinforced plastics subjected to repeated low frequency loads. 07 p0915 A73-20329

Fiber reinforced plastics with adhesive bonded elements, investigating ply number and adhesive pressure effects on shear, bending and impact strengths 07 p0844 A73-20330

On the torsional strength of composite materials reinforced with glass fabric laminates and the effect of the voids in matrix. 07 p0915 A73-20332

On the theory of optimal, constant thickness fibre-reinforced plates. II. 08 p1016 A73-20830

Effects of thermal loading on fiber-reinforced composites with constituents of differing thermal expansivities. [ASME PAPER 72-MAT-F] 08 p0979 A73-21573

Experimental investigation of the failure mechanism of fiber-reinforced composites subjected to uniaxial tension. 09 p1156 A73-21874

Variational bounds of unidirectional fiber-reinforced composites. 09 p1157 A73-21931

Unidirectional filament reinforced metal matrix composites compositional changes due to temperature induced interatomic diffusion, using diffusion equation finite difference solutions superposition technique 09 p1101 A73-22404

Investigation of the compatibility of boron fibers with tungsten substrates and titanium matrices 09 p1103 A73-22469

High modulus organic fiber/epoxide properties for reinforced composites, including strands, rings and filament wound vessels 09 p1110 A73-22518

High modulus organic fibre composites in aircraft applications. 09 p1110 A73-22519

Random function theory method for estimation of tensile, compressive and shear strength and elastic constants of monodirectional fiberglass reinforced plastics 09 p1110 A73-23056

Effective use of composite materials directionally reinforced with hollow fibers. 09 p1111 A73-23151

Fracture mechanics of brittle matrix ductile fiber composites. 09 p1111 A73-23251

Determination of the modulus of elasticity of metallic and nonmetallic fibers based on bending oscillations 10 p1231 A73-23691

Fiber reinforced metal matrix composites mixing rule, determining tensile strength, deformation energy and flow curve 10 p1231 A73-23694

Polyester fiber/glass fiber composite sandwich structural design, considering thickness loss during abrasion test, physical properties and flexural strength 10 p1237 A73-23954

Effect of fiber-matrix adhesion on the properties of short fiber reinforced ABS. 10 p1237 A73-23956

On the elastic properties of fiber composite laminates with statistically dispersed fiber and ply orientations. 10 p1288 A73-23959

Fiber reinforced composite design and application within performance and cost parameters, considering composite structure cost reduction and functional redesign increase 10 p1238 A73-23968

Energy dissipation sources during reinforced plastic fracture, investigating fiber debonding energetics, toughness and crack propagation resistance 10 p1238 A73-23971

Carbon-felt, carbon-matrix composites - Dependence of thermal and mechanical properties on fiber volume percent. 10 p1240 A73-24278

The dynamic properties of unidirectional fibre reinforced composites in flexure and torsion. 10 p1240 A73-24279

The effect of specimen and testing variables on the fracture of some fibre reinforced epoxy resins. 10 p1240 A73-24281

The propagation of waves from a cylindrical cavity. 10 p1289 A73-24282

Elastic properties of materials strengthened by short unidirectional fibers 10 p1240 A73-24306

Investigation of the strong anisotropy and resistance of fiber-strengthened plastics to interlayer shearing and compression normal to the fibers 10 p1240 A73-24353

Creep and creep-rupture-strength of titanium strengthened by molybdenum fibers 10 p1233 A73-24356

Failure analysis and heat resistance optimization factors of reinforced metal sheet under thermal cycling 10 p1233 A73-24369

Reinforcement of magnesium with boron and tantalum filaments. 10 p1234 A73-24437

Experimental observations of tensile fracture in unidirectional boron filament reinforced aluminum sheet. 10 p1235 A73-24439

Effect of heat treatment on the fatigue properties of unwoven fiberglass-reinforced plastics 11 p1386 A73-25047

Direct nondestructive prediction of engineering properties. 11 p1372 A73-25129

Fiber reinforced metal production by explosive welding, discussing fiber winding upon metal foils 11 p1372 A73-25353

Composite materials; Meeting, 2nd, Konstanz, West Germany, March 15, 16, 1972, Technical Reports 11 p1372 A73-25401

Boron filament reinforced Al and Ti matrices manufactured by pressure-sintering method, investigating filament external silicon carbide effects on mechanical properties 11 p1379 A73-25402

Linear elastic behavior of laminated plate with ribs reinforced by continuous unidirectional fibers under surface distributed loads orthogonal and parallel to plane 11 p1435 A73-25403

Production and properties of tungsten-wire reinforced NiCr 80 20 11 p1379 A73-25407

Discontinuous fibres alignment in metal composites by plastic deformation. 11 p1372 A73-25409

Ag- or Cu-based fiber reinforced composite materials for springs in electrical contact devices, investigating mechanical strength and contact and wear resistances 11 p1387 A73-25410

Plasma sprayed boron fiber reinforced titanium oxide and Al matrix composites, discussing temperature control for particle size and SiC coating effects on strength 11 p1388 A73-25413

Silicon carbide whisker reinforced Al composite production by powder metallurgy, discussing mechanical strength and extrusion process for fiber orientation 11 p1373 A73-25414

The joining of fiber-reinforced composite-metal components with similar or different components 11 p1373 A73-25418

Possibilities regarding the development and the employment of fiber-reinforced composites in comparison with conventional materials 11 p1454 A73-25419

Effects of prestressing boron/epoxy prepreg on composite strength properties. [AIAA PAPER 73-382] 11 p1388 A73-25512

Dynamic properties of graphite fiber honeycomb panels. [AIAA PAPER 73-326] 11 p1388 A73-25556

Effect of water vapor on fatigue behavior of an aluminum-boron composite. 11 p1383 A73-25828

REINFORCING FIBERS

- The impact toughness of discontinuous boron-reinforced epoxy composites. 11 p1389 A73-26046
- Statistical method for fiber-reinforced plate design optimization for important boundary conditions, noting topographies associated with piecewise linear specific cost functions 11 p1443 A73-26092
- Saint Venant principle for plane deformation of anisotropic elastic solid extended to analysis of fiber reinforced transversely isotropic composites 11 p1444 A73-26280
- Property control in reinforced plastics through interface tailoring. 11 p1389 A73-26296
- Universal solutions for fiber-reinforced incompressible isotropic elastic materials. 11 p1447 A73-26656
- Carbon fiber reinforced epoxy resins mechanical properties, correlating test parameters with observed failure mechanism 12 p1515 A73-26878
- High frequency load tests for fatigue properties of glass/carbon fiber reinforced plastics and epoxy impregnated wood laminates 12 p1515 A73-26879
- Fatigue resistant design with fiber reinforced plastics (FRP), discussing stress analysis, failure criteria, material anisotropy, multiaxial stress conditions and cumulative damage 12 p1515 A73-26880
- Reinforcing glass fiber preparation effect on fiber wetting by polyethylene melt, analyzing adhesion strength relationship to residual stresses 12 p1516 A73-27178
- Realization of the mechanical properties of the fibers in high-modulus polymeric composites 12 p1516 A73-27183
- Statistical characteristics of the mechanical constants of glass-fiber-reinforced plastics 12 p1516 A73-27184
- Damping properties of a composite material with monodirectional continual fibers 12 p1516 A73-27258
- Experimental investigation of thermal expansion in composite fibrous materials. 12 p1516 A73-27908
- Deformation and strength characteristics of carbon-fiber strengthened plastics in compression 13 p1644 A73-27991
- Probability characteristics of the shear modulus of fiberglass-strengthened plastics 13 p1644 A73-27997
- Determination of the mechanical characteristics of fiberglass-strengthened plastics in the winding state 13 p1644 A73-27998
- High strength glass fibre-resin composites. 13 p1645 A73-28498
- A study of the effects of prestrain on the tensile properties of filamentary composites. [ASME PAPER 72-MAT-K] 13 p1699 A73-29198
- Three-dimensional scattered-light stress analyses of discontinuous fiber reinforced composites. [SESA PAPER 2033] 13 p1699 A73-29306
- Fiber composite materials properties, technological assessment and future development and application for aerospace flight structures, considering manufacturing cost, tailorability and stiffness requirements 13 p1699 A73-29346
- Metal-filament-reinforced materials and their mechanical behaviour. 13 p1642 A73-29537
- Theory and experiments of compressive strength of unidirectionally fiber-reinforced composite materials. 13 p1702 A73-29539
- Conditions for rational arrangement of reinforcing fibres in materials and structures. 13 p1702 A73-29540
- Carbon fibre reinforced ceramics. 13 p1646 A73-29541
- Mechanical properties of titanium reinforced with unidirectional molybdenum wires. 13 p1643 A73-29604
- Book - Fibre-reinforced materials technology. 13 p1644 A73-29675
- Steel reinforcement fiber arrangement and volume content influence on aluminum composites strength and fatigue resistance at room and elevated temperatures 14 p1766 A73-30710
- Fracture strength of fiber reinforced plastics, investigating crack propagation susceptibility, stress concentration and fracture mechanics [ASME PAPER 73-DE-20] 14 p1767 A73-30821
- Thin flexible inextensible fiber reinforced compressible isotropic elastic materials under large elastic deformations, obtaining solutions to equilibrium and constitutive equations 15 p1946 A73-31101
- Compatibility of silicon carbide fiber with a tungsten base and a titanium matrix 15 p1888 A73-31595
- Stresses in a fiber-reinforced elastic sheet containing a circular hole. 15 p1949 A73-31655
- Techniques for fabrication of composite materials. 16 p2017 A73-32699
- Deformation and fracture behaviours of composites of copper and copper-chromium alloys reinforced with tungsten or molybdenum fibres. 16 p2025 A73-33022
- Lightning protection for boron and graphite fibers in epoxy resins for aircraft composite structures 16 p1967 A73-33032
- Lightweight coatings for protecting boron filament and graphite fiber reinforced plastic composites from structural damage by lightning 16 p2028 A73-33033
- Thermochemical and thermo-oxidative reactions of polyacrylonitrile fibers. 16 p1976 A73-33038
- Processing aerospace textiles into fabric composite reinforcements 'The weaver's viewpoint.' 16 p2018 A73-33065
- Boron fiber coating by chemical vapor deposition of boron carbide for improved mechanical properties and incorporation in Al alloy matrices 16 p2030 A73-33070
- Stresses in plastics reinforced by anisotropic fibers in the presence of transversal normal loads 16 p2030 A73-33928
- Monograph - Fibre reinforcement. 17 p2240 A73-34125
- Investigation of the bond strength between layers of textolite materials 17 p2194 A73-34333
- Room temperature creep of Borsic-aluminum composites. 17 p2189 A73-34644
- Fatigue and fracture of advanced composite materials. [SAE PAPER 730337] 17 p2194 A73-34688
- Cost/weight tradeoff ratios for fiber reinforced plastic aircraft structural components [SAE PAPER 730338] 17 p2257 A73-34689
- Reinforced plastics for aerospace applications covering history of laminates, use of cellulose, asbestos, boron, glass and oriented carbon fibers, whisker composites and resin matrices 17 p2194 A73-34801
- High strength organic fiber PRD-49 reinforced plastics compared to materials reinforced with glass, graphite and boron, discussing weight required to achieve Al faced sandwich performance 17 p2194 A73-34802
- Development of advanced composite rocket motor chambers using boron and graphite fibers. 17 p2194 A73-34803
- Hovercraft propeller and turbine engine fan blades with glass and carbon fiber reinforced plastics respectively, discussing design and constructions 17 p2103 A73-34813
- The successful use of composites in the L-1011 TriStar commercial transport. 17 p2103 A73-34815
- Shock unloading phenomena in fiber-reinforced composites. 17 p2247 A73-34916
- Composite materials structure, describing component interactions, major constituents, determinants of mechanical properties, particulate composites, materials applications and fiber types 17 p2195 A73-34974
- Anisotropic laminated fiber composite plates under short duration impact line forces, calculating one dimensional transient stress and displacement waves by fast Fourier transform [ASME PAPER 73-APM-L] 17 p2249 A73-35108
- Stress analysis of composite materials with strong fibers in weak matrix, obtaining tensile stress boundary layer equations via elasticity theory and perturbation methods [ASME PAPER 72-APM-TTT] 17 p2249 A73-35110
- On the transverse strength of fiber-reinforced materials. [ASME PAPER 72-APM-EEE] 17 p2249 A73-35111
- Ultimate tensile properties and composite structure of flow-molded short fiber composites. 17 p2197 A73-35352
- Processability/mechanical properties trade-off for reinforced plastics. 17 p2197 A73-35353
- A nondestructive measurement of the elastic constants of unidirectional borsic fiber reinforced aluminum composites. [SC-DC-72-1644] 17 p2182 A73-35439
- Alleviation of stress concentration with analogue reinforcement. [SESA PAPER 2102] 17 p2250 A73-35446
- Borsic/Ti-Al-V composite properties, fracture modes and fabrication, discussing tensile strength and temperature dependence of longitudinal strength 17 p2192 A73-35532
- Tension-tension low cycle fatigue failure mechanism in uniaxially and biaxially reinforced boron fiber-aluminum alloy composites, considering matrix plasticity role 17 p2193 A73-35544
- High modulus graphite fabrics production processes for applications in composite aerospace materials reinforcement, discussing winding, creeling, sizing, drawing, reeling and weaving 17 p2182 A73-35840
- Reinforced plastics; Conference, Karlovy Vary, Czechoslovakia, May 15-17, 1973, Lectures 18 p2326 A73-36464
- Surface properties of carbon and graphite fibers 18 p2327 A73-36465
- Interfacial, mechanical and fracture properties of fibre reinforced polycaprolactam. 18 p2328 A73-36480
- Adhesion effect on the tensile properties of fibre reinforced composite materials. 18 p2328 A73-36683
- Selection of the composition for the matrix of a composite material, which will not dissolve the reinforcing fibers 18 p2328 A73-36860
- Isochromatic and isoclinic parameters for fiber reinforced birefringent composite materials, discussing mechanical and optical characterization 19 p2495 A73-37195
- Longitudinal shear waves in a fiber-reinforced composite. 19 p2500 A73-38113
- Production techniques for advanced composites fabrication by tape machine automation. [SME PAPER EM 73-718] 19 p2436 A73-38498
- Impact generated elastic strain low amplitude pulses propagating in filamentary composite rods, using Fourier transform technique and viscoelastic relation 20 p2623 A73-39557
- Three-dimensional problem of the stability of fibers in a matrix in the presence of highly elastic strains 20 p2581 A73-39642
- An improved test for interfacial shear strength. 21 p2719 A73-40922
- Nonlinear elasticity of random inhomogeneous materials reinforced by grains or oriented fibers, using Kauderer stress relation 21 p2787 A73-40987
- Plane strain and generalized plane stress problems for fibre-reinforced materials. 21 p2788 A73-41546
- Possible reinforcement of the tungsten-nickel-iron composite with tungsten fibers. 21 p2722 A73-41586
- Interaction of cracks with rigid inclusions in longitudinal shear deformation. II - Further results. 22 p2920 A73-42134
- Fibre-reinforced metallic and ceramic composites produced by thermal spraying. 22 p2866 A73-42592
- Comment on 'Film reinforced multifastened mechanical joints in fibrous composites.' 22 p2928 A73-43115
- A higher order theory for extensional motion of laminated composites. 22 p2929 A73-43139
- Statistical theory of solid heterogeneous materials, discussing constant elastic bounds, fiber reinforced cell model, thermal expansion and stress-strain relations 23 p3038 A73-43303
- Analysis of the test methods for high modulus fibers and composites; Proceedings of the Symposium, San Antonio, Tex., April 12, 13, 1972. 23 p2996 A73-43626
- Fracture mechanics and composite materials - A critical analysis. 23 p3040 A73-43628
- Fiber reinforced composite crack model performance prediction and tests, noting fiber volume fraction for maximum fracture toughness 23 p3040 A73-43629
- Method for estimating fracture strength of specially orthotropic composite laminates. 23 p3040 A73-43630
- Compressive strength and failure modes of unidirectional composites. 23 p3041 A73-43634
- Influence of the free edge upon the strength of angle-ply laminates. 23 p3041 A73-43635
- Deformation behaviour and deviation from the simple rule of mixture for the ultimate tensile strength in the cold rolled fibre-reinforced composites. 23 p2998 A73-44151
- Testing of composite materials with the aid of annular samples 23 p2998 A73-44295
- Load capacity of rings formed by winding of composites reinforced with high-modulus anisotropic fibers 24 p3093 A73-44528
- Theoretical post-yielding behavior of composite laminates. II - Inelastic macromechanics. 24 p3104 A73-45145
- Acoustic emission produced during burst tests of filament-wound bottles. 24 p3094 A73-45146

Load concentration factors for circular holes in composite laminates. 24 p3149 A73-45151

Optimization of fiber reinforced composite structures. 24 p3151 A73-45304

Optimal force transmission by flexure-clamped boundaries. 24 p3152 A73-45317

REISSNER THEORY

Nonlinear shell theory with finite rotation and stress-function vectors. [ASME PAPER 72-APM-CC] 05 p0633 A73-16533

Reissner's edge effect in three-layer plates with filler 11 p1433 A73-25030

Finite element methods by variational principles with relaxed continuity requirement. 16 p2031 A73-32985

Solution of equations of Reissner's theory of plates by application of Hajdin's method. 16 p2078 A73-33004

RELATIVE BIOLOGICAL EFFECTIVENESS (RBE)

Estimation of the biological danger of the very high energy component of space radiation. 22 p2805 A73-42180

Probability cross sections of heavy ion single hit inactivation paths for human cells using nitrogen ion accelerator experiments 22 p2805 A73-42183

RELATIVISTIC EFFECTS

White dwarfs gravitational red shifts, radial velocities and mass-radius relationships, considering colors and luminosities 01 p0104 A73-11036

The deflection of light at the sun and the change of its velocity and wavelength 02 p0225 A73-12809

Gravitation theory - Empirical status from solar system experiments. 04 p0498 A73-15249

Transfer and moment equations obtained for radiation transfer in spherically moving medium with relativistic corrections, discussing matter-radiation coupling and energy conservation 05 p0612 A73-17382

Motional effects in retardation plates and mode locking in ring lasers. 06 p0699 A73-17496

Reflection and transmission of electromagnetic waves obliquely incident on a relativistically moving uniaxial plasma slab. 06 p0665 A73-18185

Collisional effect on the saturation amplitude of nonlinearly excited plasma waves. 09 p1125 A73-22023

Electromagnetic field configuration about aligned rotating magnetic star from relativistic model of rotating magnetosphere 09 p1142 A73-22034

Quasi-radial pulsations of rotating white dwarfs and neutron stars in the relativistic theory of gravitation 10 p1274 A73-23711

Gravitational radiation from a mass projected into a Schwarzschild black hole. 10 p1280 A73-24343

Relativistic effects on gyromagnetic ratio of massive rotating body with uniform charge density and with shell large in comparison to Schwarzschild radius 10 p1252 A73-24345

Polarization of synchrotron radiation from relativistic Schwarzschild circular geodesics. 10 p1252 A73-24347

Production of metagalactic X-rays by relativistic dust grains. 10 p1270 A73-24907

Compressible magnetorelativistic flow character in subsonic, supersonic and transonic regions, obtaining pressure coefficient, free stream Mach number and Alfvén speed interrelationships 10 p1210 A73-24921

Sagnac effect on clock synchronization of two clocks moving under equal equatorial westward and eastward velocities 11 p1398 A73-25860

General relativistic effects detection experiments for supernova and collapsed objects, noting gravitational radiation transfer of energy equal to entire energy generation during thermoneutral evolution 12 p1542 A73-27550

Relativistic astrophysics. III - Gravitational collapse, singularities, and black holes 12 p1543 A73-27749

Supernova outbursts and the formation of relativistic objects. I 12 p1546 A73-27853

Integral parameters and pulsation frequencies for equilibrium configurations of rotating neutron stars, expanding energy characteristics into series of relativistic members 12 p1546 A73-27854

Thermodynamics of relativistic rotating perfect fluids. 12 p1525 A73-27886

Airborne clock change from synchronized stationary clock after circumnavigation of earth, discussing directional dependence 13 p1660 A73-28922

German book on physical foundations of electronics covering charged particle motions in electric and magnetic fields, relativistic effects, electron and ion optics, etc 14 p1736 A73-30597

Variation of the antenna radiation pattern during motion of the medium 17 p2122 A73-34924

Newtonian method of relativistic gas dynamics for steady gas, shock wave, nozzle, Prandtl-Meyer flow and photon gas applications 18 p2300 A73-36632

Quasiradial pulsation of rotating white dwarfs and neutron stars in general relativity. 18 p2354 A73-36736

Propulsion system optimization for a single-stage constant-thrust relativistic rocket. 18 p2361 A73-37037

On the propagation of relativistic thermo-magneto-viscoelastic waves in a material of Voigt-type. 19 p2459 A73-37648

Precision pointing control thruster design for satellite experiment to test relativistic precession of gyroscope moving through gravitational field, determining gyro orientation via superconducting circuitry [AIAA PAPER 73-858] 20 p2586 A73-38796

Supernova outbursts and the formation of relativistic objects. I. 20 p2608 A73-39227

Integral parameters and pulsation frequencies for equilibrium configurations of rotating neutron stars, expanding energy characteristics into series of relativistic members 20 p2608 A73-39228

Relativistic baryon effective masses and thresholds for strongly interacting superdense matter. 21 p2766 A73-40318

Experiments to determine satellite orbit geometry in spherically symmetric gravitational field, discussing aging asymmetry in clock paradox 21 p2739 A73-40623

The stability of rotating supermassive stars. 22 p2907 A73-42304

The relativistic Roche problem. I - Equilibrium theory for a body in equatorial, circular orbit around a Kerr black hole. 24 p3138 A73-45035

Quadrature solution for the general relativistic motion of a satellite or a planet. 24 p3142 A73-45291

Ergosphere concept extended to classical mechanics from relativistic black hole mechanics 24 p3142 A73-45341

Relativistic torque detection on freely spinning rotor, obtaining phenomenological expression by incremental Hubble law 24 p3142 A73-45342

RELATIVISTIC PARTICLES

Polarization of relativistic-electron emission in the case of Compton scattering at turbulent plasma oscillations 01 p0085 A73-10949

Relativistic cosmic rays propagation, calculating abundances of Pt, Pb, actinides and superheavy groups as function of cosmic ray leakage time 01 p0092 A73-11027

Energy spectra of modulated relativistic electron beam as function of plasma density at beam-plasma interaction region boundary 01 p0086 A73-11284

Transfer equations for high-energy electrons and photons in magnetic fields. 01 p0080 A73-11309

The nature of the first Cygnus X-3 radio outburst. 02 p0204 A73-11551

Radio outbursts observation in X ray source Cyg X-3, showing relativistic electrons sporadic injection dominance of synchrotron radio emission characteristics 02 p0210 A73-11564

Radio emission source picture from observed Cygnus X-3 outburst, suggesting expanding cloud with traveling relativistic electrons and protons 02 p0211 A73-11870

FLUX density and linear polarization measurements of radio outburst from Cygnus X-3, suggesting synchrotron radiation from expanding cloud of relativistic particles 02 p0205 A73-11871

Cygnus X-3 radio outburst as consequence of synchrotron radiation due to expanding relativistic plasma ejection, considering polarization, flux densities and spectral index 02 p0211 A73-11872

Equilibrium model for force-free relativistic electron beam, obtaining solution with maximum beam radius and maximum axial current 02 p0198 A73-12070

Composition of relativistic cosmic rays near the earth and at the sources. 02 p0207 A73-12327

Energy distribution of relativistic electrons generated within radio sources with constant magnetic field and diffusion coefficient, discussing simplified model representation for Crab nebula 02 p0207 A73-12379

Extensive cosmic ray shower production by relativistic dust grain accelerated in interstellar space by galactic radiation pressure and subsequent magnetic processes 02 p0207 A73-12388

Relativistic electron radio emission models, calculating magnetic bremsstrahlung spectra from galactic electron space-energy distributions 02 p0208 A73-12459

Linear synchrotron instability theory results via quantum method with Einstein coefficients, obtaining synchrotron radiation growth rate in relativistic electrons with anisotropic momentum distribution 02 p0223 A73-12726

Circular polarization of synchrotron radiation in the presence of hydromagnetic waves. 02 p0224 A73-12739

Incoherent excitation of plasma oscillations by an almost-monoenergetic relativistic beam. 03 p0347 A73-14102

Trapped and precipitated electron energy spectra in relativistic electron precipitation events /REP/, discussing bremsstrahlung measurements deductions 03 p0304 A73-14591

Electromagnetic-emission energy flux during the development of beam instability in a magnetically confined plasma 04 p0481 A73-15607

Instability of a relativistically strong electromagnetic wave of circular polarization. 04 p0482 A73-15960

Turbulent plasma 'piles' in the nuclei of galaxies. 04 p0504 A73-16022

Experimental observation of heating of a hydrogen plasma by a relativistic electron beam. 05 p0603 A73-17161

Incoherent radiation from relativistic electrons with power energetic spectrum. 05 p0611 A73-17313

Nonlinear theory of interaction between restricted relativistic particle beam and plasma, determining field amplitudes and beam radii 06 p0728 A73-17972

Collective processes in the passage of high-current relativistic beams through a gas and a plasma. 06 p0732 A73-18714

The stopping power of atomic matter for relativistic ions, mesons, electrons and positrons. 07 p0852 A73-19036

Parametric radiation of relativistic electron bundles in a waveguide with a stratified dielectric filling. 07 p0802 A73-20145

Detection of relativistic solar particles before the H alpha maximum of a solar flare. 08 p0996 A73-20666

Ultrarelativistic electrons beam steady injection into plasma filled half space, using weak turbulence theory for assumed beam excited oscillations interaction 08 p0994 A73-21698

Quasi-linear relaxation of a monoenergetic relativistic electron beam in an external magnetic field 09 p1124 A73-21903

Polarized radiation of relativistic electrons scattered by plasma turbulence. 09 p1130 A73-22743

A computational study of the non-linear stage of the development of radiation instability in relativistic electron rings. 09 p1131 A73-22909

Nonlinear theory of a relativistic monotron 09 p1065 A73-23086

A synchrotron radiation model of the infrared radiation from the nucleus of NGC 1068. 09 p1150 A73-23144

The structure of the Crab Nebula. II - The spatial distribution of the relativistic electrons. 09 p1151 A73-23290

Relativistic electron bremsstrahlung suppression in isotropic plasma, noting analogy to synchrotron radiation 10 p1252 A73-23476

Manganese-54 and the lifetime of relativistic cosmic rays. 10 p1264 A73-23541

Synchrotron emission amplification by magnetic field in cosmic sources from analysis of relativistic electron system, noting pulsars and UV Ceti stars 10 p1264 A73-23708

Electromagnetic energy in the two-stream instability in a magnetized plasma. 10 p1254 A73-24197

Vector and tensor radiation from Schwarzschild relativistic circular geodesics. 10 p1249 A73-24346

Relativistic particle beam stability and electromagnetic oscillations in plasma rectangular waveguide under longitudinal magnetic field 10 p1258 A73-24887

RELATIVISTIC PLASMAS

Production of metagalactic X-rays by relativistic dust grains. 10 p1270 A73-24907

Motion of fast particles in a spherically-symmetric gravitational field 11 p1416 A73-25239

Stimulated emission due to the interaction between a relativistic high-current beam and a plasma 11 p1403 A73-25241

Vacuum state of a relativistic system interacting with an external field 11 p1397 A73-25245

Jovian decametric emission origin in cyclotron instability of weakly relativistic electrons trapped in magnetic field, considering group velocity in magnetospheric plasma 11 p1424 A73-26129

Nonlinear theory of Ubitron microwave oscillator device using fast electromagnetic wave-fast electron beam interaction in spatially periodic magnetostatic field 11 p1332 A73-26164

Current and fields reduced in plasmas by relativistic electron beams with arbitrary radial and axial density profiles. 11 p1407 A73-26560

Macroscopic equilibria of relativistic electron beams in plasmas. 11 p1407 A73-26561

Preliminary Pioneer-10 intensity gradients of galactic cosmic rays. 11 p1414 A73-26622

Sea level search for leptonic quarks in cosmic rays. 11 p1414 A73-26660

Stability of a magneto-active plasma with a relativistic electron beam, situated in a high-frequency electric field 12 p1527 A73-26927

Nonadiabatic condition effects on ultrarelativistic electron energy losses in geomagnetic trap in remote magnetosphere regions 12 p1535 A73-27649

Two-stream instability heating of plasmas by relativistic electron beams. 13 p1663 A73-28186

Instabilities in a system of a plasma and an intense relativistic electron beam. 14 p1780 A73-30122

Existence conditions for magnetoactive plasma longitudinal waves with phase velocity near light velocity, investigating increments during synchrotron instability due to relativistic particles 14 p1780 A73-30337

Effect of induced axial electric field on a relativistic electron beam pulse propagating through a plasma. 14 p1777 A73-30661

Transition radiation production by relativistic electrons traversing cosmic grains as source of celestial X rays, discussing formation zone effect 14 p1787 A73-30730

Universality of the power spectra of relativistic electrons generated in a turbulent plasma 14 p1782 A73-30808

Production of astrophysical X-rays by transition radiation. 15 p1926 A73-31553

On a possible mechanism responsible for the differential energy spectrum of relativistic electrons and non-linear low-frequency spectra of cosmic radio sources. 15 p1927 A73-32005

Electromagnetic emission during surface wave excitation by a relativistic electron beam in a plasma 15 p1921 A73-32321

Relativistic electron radio emission models, calculating magnetic bremsstrahlung spectra from galactic electron space-energy distributions 15 p1927 A73-32609

Quasilinear relaxation of a monoenergetic relativistic electron beam in an external magnetic field. 15 p1922 A73-32628

The problem of interaction between a relativistic electron beam and plasma in a waveguide 16 p2040 A73-32899

Axial compression of the astron E-layer during neutralization. 16 p2042 A73-33337

Radiation emitted by a charge in a stack of plates at frequencies approaching the Bragg frequencies 17 p2120 A73-34114

Transition radiation from interstellar dust grains. 17 p2231 A73-34755

Excitation of electromagnetic waves in a plasma with a relativistic electron beam. 17 p2216 A73-35159

Synchrotron radiation stimulated amplification by magnetic field in cosmic sources from analysis of relativistic electron system, noting pulsars and UV Ceti stars 18 p2347 A73-36733

Statistical acceleration of ultrarelativistic electrons by random electromagnetic waves. 19 p2462 A73-37558

Synchrotron radiation sources with relativistic particles moving at small pitch angles in magnetic field, discussing emission properties and degrees of polarization 19 p2484 A73-37617

On the energy spectrum of relativistic electrons in the Crab Nebula. 19 p2475 A73-37619

ULF geomagnetic power near $L = 4$. II - Temporal variation of the radial diffusion coefficient for relativistic electrons. 20 p2551 A73-38936

Nova and supernova stars as sources of relativistic particles 21 p2756 A73-40580

Relativistic particle beam stability and electromagnetic oscillations in plasma rectangular waveguide under longitudinal magnetic field 21 p2749 A73-41662

Stability of a magnetoactive plasma with a relativistic electron beam in an RF electric field. 22 p2891 A73-42261

Possible emission of transverse electromagnetic waves in an isotropic plasma 22 p2893 A73-42390

Energy spectra of modulated relativistic electron beam as function of plasma density at beam-plasma interaction region boundary 23 p3009 A73-43505

Role of constraining forces for ultrarelativistic particle motion as a source of gravitational radiation. 23 p3006 A73-43606

Distribution function of relativistic electrons in a strong magnetic field. 23 p3011 A73-43753

Ion acceleration by relativistic electron beam extracted from discharge plasma, discussing proton acceleration and beam composition and energy distribution 23 p3014 A73-44339

Relativistic electron belt formation mechanism hypothesis based on Cosmos 137 data on electron intensity near geomagnetic shell L equal to 2.8 24 p3124 A73-44808

Electron beam concentration enhanced by a laser-produced plasma. 24 p3115 A73-44921

Role of hydromagnetic waves in cosmic-ray confinement in the disk. I - Theory of behavior in general wave spectra. 24 p3124 A73-45040

Nonlinear saturation of the relativistic beam-plasma instability in the presence of ion density fluctuations. 24 p3118 A73-45465

RELATIVISTIC PLASMAS

Relativistic gas dynamics problems reduction to equivalent Newtonian flow via transformation of governing equations 01 p0034 A73-11138

An action principle in general relativistic magnetohydrodynamics. 01 p0079 A73-11258

Nonlinear longitudinal oscillations of relativistic plasma. 07 p0859 A73-20217

The disc model of gaseous accretion on a relativistic star in a close binary system 07 p0901 A73-20305

Electrical and thermal conductivities of a relativistic degenerate plasma. 08 p0992 A73-21161

Ultrarelativistic cosmic plasma analysis of high density electron beams transport across strong magnetic fields with application to pulsar NP 0532 spectrum 08 p0999 A73-21334

Ultrarelativistic plasma momentum loss perpendicular to pulsar magnetic field, considering synchrotron compression of electrons leading to emission mechanisms 09 p1144 A73-22172

Ultrarelativistic pulsar plasmas with one dimensional distribution functions in strong magnetic fields, considering dispersion ratios of plasma waves along magnetic lines 09 p1145 A73-22294

Relativistic MHD formulation in terms of non-holonomic tetrad field for rotating plasma coupled to frozen-in magnetic field, noting Alfven waves propagation velocity 09 p1131 A73-22921

Cosmic dilute collisionless plasma physical properties, discussing plasma wave turbulence characteristics, particle acceleration, relativistic plasmas, synchrotron emission, pulsars and galactic nuclei 12 p1537 A73-26850

Disk model of gas accretion on a relativistic star in a close binary system. 12 p1539 A73-27277

A generalized flux-vorticity theorem. I. 15 p1916 A73-31088

Transport phenomena in a fully ionized ultrarelativistic plasma 15 p1919 A73-31709

Reflection and transmission of electromagnetic waves obliquely incident on a relativistically moving isotropic plasma slab. 15 p1919 A73-31947

On an initial value problem for a nonlinear system of Vlasov-Maxwell equations. 17 p2200 A73-34320

Extragalactic radio sources modeled as bubbles of relativistic plasma rising through hot gas, producing galactic clusters X ray emission 18 p2353 A73-36508

High temperature relativistic plasmas, calculating post-shock properties for steady hydromagnetic shock wave production 19 p2464 A73-37156

The propagation of an intense electromagnetic wave in a plasma. 19 p2469 A73-38087

Collisionless damping of hydromagnetic waves in relativistic plasma. I - Weak Landau damping - Heating of the Crab Nebula. 20 p2609 A73-39442

Second-order plasma interaction in the Crab Nebula. 20 p2610 A73-39579

Parametric excitation of oscillations in an electron plasma 21 p2746 A73-40518

Steady-state solutions for relativistically strong electromagnetic waves in plasmas. 22 p2891 A73-42238

Large amplitude electromagnetic waves in hot relativistic plasmas. 22 p2895 A73-43024

Energy conversion between longitudinal and transverse waves by mode-mode coupling in a relativistic plasma. 24 p3116 A73-45240

RELATIVISTIC THEORY

NT MANDELSTAM REPRESENTATION

Relativistic dispersion equation for a circular waveguide with a rotating tubular electron beam, allowing for the effect of the space charge 01 p0017 A73-10982

MHD detonation waves properties and propagation velocities within relativistic theory, discussing shock equations nontrivial solution existence and uniqueness 01 p0085 A73-11260

Calculation of the perihelion advance of planets in a field approach to gravitation. 02 p0225 A73-12802

Relativistic spheres of hadron gas with zero baryon number constructed from Hagedorn hadronic equation of state, considering sphere stability properties 03 p0370 A73-13211

On the apparent visual forms of relativistically moving objects. 03 p0343 A73-13294

Relativistic equations of balance in continuum mechanics. 04 p0476 A73-15223

Relativistic thermodynamics of simple heat conducting fluids. 05 p0641 A73-17235

Similarity solution for equations of nonplanar relativistic flow from point energy source, applying to spherical shock propagation and cosmic ray generation 07 p0810 A73-19506

Anisotropic model of gravitational radiation enhancement from relativistic disk located in Galactic nucleus 09 p1149 A73-22946

Anisotropic and isotropic descriptions of physical process speeds in special relativity theory space-time metric 10 p1250 A73-24944

Planck relativistic equations of moving body heat and absolute temperature transformation (1907) and alternative equations by Ott (1963), comparing validity 12 p1557 A73-26973

Conservation laws and preferred frames in relativistic gravity. I Preferred-frame theories and an extended PPN formalism. II - Experimental evidence to rule out preferred-frame theories of gravity. 12 p1540 A73-27326

Lorentz contraction and transformation of equilibrium forces and moments in inertial reference systems transition, discussing special relativity theory 12 p1525 A73-27733

Entropy supply for classical and relativistic heat conducting fluids, assuming linearity for momentum and energy supplies 13 p1704 A73-28286

The general form of constitutive equations in relativistic physics. 13 p1658 A73-28374

Thermodynamics relativistic and quantum structure, considering Lorentz transformation relationship to first principle for entropy and action 13 p1706 A73-28550

Relativistic stars and gravitational waves - An account for non-relativists. 13 p1683 A73-28991

Stellar structure deviation from neutron star models, deriving equations for relativistic models with deviation from Einstein principle of equivalence 13 p1686 A73-29655

Rotation effects in stellar and quasi-stellar relativistic objects models required for pulsars and quasars explanation, discussing gravitation theories 14 p1798 A73-30141

Relativistic stellar stability - An empirical approach. 14 p1801 A73-30740

Homographic motions of Newtonian point mass system interacting through two body forces, considering relativistic interactions 15 p1930 A73-31110

Relativistic elasticity theory for solids based on Cattaneo definitions for Riemann metric, considering hyper- and hypoelastic media 16 p2036 A73-33108

A new theory of gravity. 16 p2036 A73-33123

On an initial value problem for a nonlinear system of Vlasov-Maxwell equations. 17 p2200 A73-34320

Y-covariant formulation of the relativistic electrodynamics of material media 17 p2213 A73-35569

Local Y-transformations in the electrodynamics of inhomogeneous accelerated media 17 p2213 A73-35570

The applications of relativistic kinetic theory to cosmological models - Some observational consequences. 17 p2234 A73-35616

A theory of gravitation incorporating the quadratic action principle of relativity. 19 p2459 A73-37446

The optical polarization of the Crab Nebula pulsar. I - A relativistic vector model. 19 p2488 A73-38517

Optical polarization of the Crab Nebula pulsar. II - Observational results and fits by the relativistic vector model. 19 p2488 A73-38518

The effect of magnetic mass on Alfvén waves. 21 p2701 A73-40624

Gravitational-wave observations as a tool for testing relativistic gravity. 22 p2887 A73-42709

On a criterion for the occurrence of a Dedekind-like point of bifurcation along a sequence of axisymmetric systems. I - Relativistic theory of uniformly rotating configurations. 24 p3110 A73-45032

Relativistic gravity in the solar system. III - Experimental disproof of a class of linear theories of gravitation. 24 p3138 A73-45034

RELATIVISTIC VELOCITY

Linear solutions for heat propagation in relativistic fluid dynamics 01 p0076 A73-10266

The effects of drag on relativistic spacelike. 01 p0095 A73-10274

Wave front propagation velocity definition valid for classical and relativistic fluid dynamics 02 p0152 A73-11572

On the apparent visual forms of relativistically moving objects. 03 p0343 A73-13294

Possibility for observational verification of the relativistic motion of the periselenium of artificial satellites of the moon 06 p0748 A73-17765

Vector and tensor radiation from Schwarzschild relativistic circular geodesics. 10 p1249 A73-24346

Superrelativistic interstellar flight or cracks in the light barrier. 17 p2234 A73-35658

Relativistic rocket motion tensor equations analogous to particle motion in electromagnetic fields, discussing Hamiltonian functions, Lagrangian coordinates and variable mass body mechanics 18 p2356 A73-37038

The asynchronous formulation of relativistic states and thermodynamics. 22 p2931 A73-42436

RELATIVITY

The equations of motion of gyroscopes in general relativity 01 p0098 A73-10559

A non-uniform relativistic cosmological model. 01 p0098 A73-10581

Cosmological evolution from initial inhomogeneous and anisotropic universe to present structure, using general relativity for free gravitational field and waves 01 p0106 A73-11242

On space-time, reference frames and the structure of relativity groups. 01 p0079 A73-11255

Newtonian dynamics canonical formulation in Galilean relativity framework, representing motions of bodies as integral manifolds of 2-form characteristic distribution 01 p0079 A73-11256

Propagation of the discontinuities of the covariant derivative of the electromagnetic and of the curvature tensor in an electromagnetic and gravitational wave 01 p0079 A73-11261

Hydrodynamic motions and the vacuum stage in an anisotropic cosmological model 01 p0108 A73-11432

Schwarzschild coordinate system identification with frames of reference within exterior gravitational field of spherical nonrotating star 02 p0211 A73-11896

Neutrino contribution to relativistic interacting matter-radiation cosmological models, presenting cosmological interpretation of quasars 02 p0218 A73-12410

Exact cosmological solutions in Brans and Dicke's scalar-tensor theory. II. 02 p0224 A73-12743

International system of units applicability to constitutive equations of four dimensional relativistic electrodynamics 03 p0341 A73-12896

Cosmic gravitational waves detection and measurement, describing Weber experimental apparatus and theoretical foundations based on Einstein relativity theory 03 p0341 A73-12924

Cosmological vacuum solutions in Brans and Dicke's scalar-tensor theory. 03 p0373 A73-13356

Astronomical applications of general relativity, considering energy and matter outbursts, black holes and Kerr and Schwarzschild metrics 03 p0374 A73-13895

Gravitational origin of high energy interactions and general relativity equivalence principle for unitary symmetry, noting quantum geometrodynamics cosmological model 04 p0501 A73-15632

Invariant criterion generalization for pure gravitational waves in tetrad formulation of general relativity theory, noting electromagnetic field energy tensor 04 p0476 A73-15638

Russian monograph on relativistic celestial mechanics covering celestial and solar system bodies motion, Riemann geometry, tensor analysis, N body problem and cosmology 04 p0502 A73-15969

Relativistic stress tensor in general relativity theory 05 p0597 A73-16469

Harmonic frames of reference in Einstein's theory of gravitation. 05 p0598 A73-16791

A comparative study of Brans-Dicke and general relativistic cosmologies in terms of observationally measurable quantities. 05 p0624 A73-17303

Momentum constraints as integrability conditions for the Hamiltonian constraint in general relativity. 05 p0599 A73-17350

Newtonian and relativistic gravitational theories, discussing gravitational waves generating mechanism and black holes formation 06 p0753 A73-18274

Gravitation finite range evidence presentation of major theoretical problem for general relativity, discussing continuity and invariance 06 p0724 A73-18548

General relativity in the equal proper time formalism. 06 p0724 A73-18626

Determination of properties of cold stars in general relativity by a variational method. 07 p0874 A73-19065

Gravitation theory harmonic condition equations to separate relativity-valid subclass of extremal manifolds from class of m-dimensional pseudo-Riemannian manifolds 08 p0987 A73-20700

Special relativity theory for steady irrotational ideal gas flow, noting subsonic, supersonic and transonic flow calculations based on small perturbation theory 08 p0926 A73-21128

Construction of the spinor field equations in cosmological space 08 p1010 A73-21271

A classification of particle motions in the equatorial plane of a gravitational monopole-quadrupole field in Newtonian mechanics and general relativity. 09 p1148 A73-22910

Zero-mass scalar and electrostatic fields with the central symmetry in the general relativity. 09 p1121 A73-23148

Cosmological evolution from initial inhomogeneous and anisotropic universe to present structure, using general relativity for free gravitational field and waves 10 p1279 A73-24178

Gravitational waves - A progress report. 10 p1280 A73-24324

Gravitational collapse with a physical singularity on an isotropic hypersurface. 10 p1283 A73-24751

Model universe generalization to minisuperspace with Einstein equation solution and nondiagonal met-

ric replacing wave equation, considering commutation relations for quantization in curved space 11 p1397 A73-25309

Hydrodynamic motions and the vacuum stage in an anisotropic cosmological model. 11 p1423 A73-26052

Gravitational instability of regular model-universes in a modified theory of general relativity. 11 p1431 A73-26106

Artificial satellites to test general relativity theory 11 p1431 A73-26590

Combined electromagnetic and gravitational field equations derivation with explicit interaction term and tensors for curved space-times unrestrained in Einstein-Maxwell equations framework 11 p1401 A73-26658

A characteristic initial value problem in general relativity in the case of a perfect fluid with axial symmetry. 13 p1658 A73-28199

Continuous-discrete and probability-deterministic theory of space-time and matter, considering resolution of antagonism between relativity and quantum theories 13 p1658 A73-28373

On the concepts of viscous fluids, of elastic solids, and of heat conduction in relativity 13 p1661 A73-29555

Mach principle incorporation into general relativity, discussing application as selection rule in Einstein field equations solution and other gravitation theories 14 p1798 A73-30238

Quantum and relativity theories compatibility based on hypothesis of matter tensor delta structure and Planck's constant for action singularity 14 p1775 A73-30425

Dyadic formalism in two dimensional distributions in general relativity theory, discussing gravitational, diffusive, wave, Einstein and preservation equations 14 p1776 A73-30942

Painlevé metric replacement for Schwarzschild metric in tests of general relativity, considering problem of supermassive celestial body gravitational collapse 15 p1937 A73-31650

Evaluation of the directivity of gravitational wave radiators. 15 p1914 A73-31944

Relativistic cosmology of interacting hadronic matter-radiation models, discussing compatibility with Hagedorn equation of state based on statistical mechanics 15 p1939 A73-32002

Special relativity theory for steady irrotational ideal gas flow, noting subsonic, supersonic and transonic flow calculations based on small perturbation theory 15 p1864 A73-32060

Rigid motion of relativistic surfaces 15 p1914 A73-32095

Local structure of space-time singularity and gravitational collapse. 15 p1940 A73-32177

Lagrange function based Poincaré mechanics of inertial relativity, using Mach-Einstein inertia principle for gravitational potential 16 p0206 A73-33072

Electric dipole motion in Einstein unitary field with electrostatic potential as function of polar coordinates, deriving law of motion from Clausen integral formula 16 p2037 A73-33371

Electromagnetic emission in the general relativity theory. I 16 p1984 A73-34006

German book - The physics of the scientist: Mechanics, relativity, gravitation. 17 p2229 A73-34465

Gravitational and electromagnetic shock waves 17 p2212 A73-35048

Superposition of Schwarzschild solutions and metric of a gravitational dipole 17 p2212 A73-35561

Plane monochromatic electromagnetic waves in general relativity theory 17 p2212 A73-35562

Gravitational-inertial waves in the general theory of relativity 17 p2212 A73-35563

Type-III Einsteinian void spaces with a G/2 Abelian group of motions and solvable G/3 groups 17 p2212 A73-35565

Bireductive spaces, Jordanian algebras, and spinor representations of non-Euclidean and quasi-non-Euclidean motions 17 p2212 A73-35566

Nonconformally plane relativistic recurrent-curvature spaces 17 p2212 A73-35567

Geometric interpretation of spinor representations for groups of motions in quasi-elliptic 5-spaces 17 p2213 A73-35568

Quantum theory of the spinor field in the two-dimensional space-time of de Sitter 17 p2213 A73-35571

Book on large scale structure of space-time covering gravity roles, differential geometry, general relativity, gravitational collapse, black holes, spatially homogeneous cosmological models, etc
18 p2336 A73-35901

Medium-velocity and electric-current concepts in restricted relativity
19 p2459 A73-37535

Precise attitude control of the Stanford relativity satellite.
19 p2494 A73-38080

Mars internal structure computed via general relativity application to earth-like model
20 p2612 A73-39711

Gravitational red shift, Mercury perihelion, light deflection and signal delay tests of Einstein relativity vs Jordan-Brans-Dicke theory
20 p2613 A73-39751

Centrosymmetrical nonstatic pulsating metric development, discussing minipulsar particles, perihelion displacement, gravitational energy, red shift, luminous ray curvature and Schwarzschild metric
20 p2594 A73-39765

The rod contraction-clock retardation ether theory and the special theory of relativity.
21 p2739 A73-40622

Schwarzschild solution indeterminacy as indicator of physical singularity analogous to intrinsically singular vertex of cone in Euclidean space
21 p2741 A73-41630

On the impossibility of the first-order relativity test.
21 p2742 A73-41632

Transformation between orbital parameters in different coordinate systems of the general relativistic Schwarzschild problem.
22 p2886 A73-41967

General relativistic gravitation theories based space-time curvature tests near sun from interplanetary probe motion analysis using probe-borne laser light transmission
[ONERA, TP NO. 1210] 22 p2907 A73-42216

Nonsingular unified field model for charged particle described by interrelation of gravitational mass, global energy and effective charge, considering comparison with Reissner metric
22 p2887 A73-42432

Matter representation in general theory of relativity in terms of sourceless metric tensor and Einstein matter tensor, examining Mach principle status
22 p2887 A73-42435

On the problem of the initial state in the isotropic scalar-tensor cosmology of Brans-Dicke.
22 p2911 A73-42931

General relativistic time analysis leading to scalar Hamiltonian formalism for particle mass based on Riemannian metric, considering Hamilton-Jacobi equation in particle dynamics
22 p2888 A73-43048

Very-long-baseline interferometry techniques applied to problems of geodesy, geophysics, planetary science, astronomy, and general relativity.
23 p2980 A73-43354

Gravitational red shift - A simple quantum field-theoretical consideration in a curved space.
23 p3006 A73-43607

Unaccelerated-returning-twin paradox in flat space-time.
23 p3006 A73-43608

On a possible repulsive interaction in universal gravitation.
24 p3110 A73-45038

RELAXATION [MECHANICS]

NT SPIN-LATTICE RELAXATION

NT STRESS RELAXATION

Quasi-frozen flow of a thermodynamically relaxing gas
03 p0295 A73-13791

Effect of plasma oscillations on the process of ionizational relaxation
04 p0477 A73-14878

Development and use of relaxation tests for study of the long-term creep of metals
[ONERA, TP NO. 1146] 04 p0511 A73-15095

Study on ionizing shock waves in argon. II - Ionization relaxation.
04 p0436 A73-15975

Relaxation of ion beam injected into a plasma transversely to a magnetic field.
05 p0602 A73-16550

The influence of anisotropy and crystalline slip on relaxation at a crack tip.
06 p0709 A73-18331

Behavior of austenitic stainless steels under continuous or repeated strain
07 p0838 A73-19115

Nature of localized states in amorphous semiconductors - A study by electron spin resonance.
07 p0863 A73-20174

Carre method for optimum overrelaxation factor determination in electron gun performance analysis by digital simulation, discussing choice of parameters for rapid iterative convergence
08 p0990 A73-20836

Relaxation in a two-temperature plasma with directed motion of electrons
09 p1127 A73-22601

Relaxation processes in a parametrically unstable plasma
09 p1130 A73-22707

Recent experimental and theoretical investigations of infrared and microwave molecular spectra of astronomical interest [Introductory report].
09 p1123 A73-23127

Rotating galaxies gravothermal catastrophe via violent relaxation leading to black hole core and halo system
10 p1284 A73-24911

Relaxation of diagonal length and indentation depth of Vickers microhardness measurements on plastics
11 p1388 A73-25449

Calculation of the relaxed one-dimensional flow of a gas in a convergent-divergent sonic nozzle
11 p1348 A73-25869

Relaxation processes in metastable beta titanium alloys.
11 p1385 A73-26498

Pressure sensitization relation to electrical conductivity relaxation during isothermal isobaric annealing of CdTe crystals
12 p1531 A73-27196

Boltzmann-Volterra constitutive law for viscoelastic linear materials, investigating criteria for relaxation properties
13 p1659 A73-28562

Two-dimensional calculation of revolution of the relaxed flow of a gas in a convergent-divergent sonic nozzle
13 p1563 A73-28563

Theory for the susceptibility of quantum systems with degenerate levels
13 p1659 A73-28759

Relaxation to Maxwellian distribution of electrons near low voltage Cs arc plasma discharge cathode
13 p1666 A73-28962

Effect of plasma inhomogeneity on the relaxation of the electron distribution function in the electrode area of a low voltage arc
13 p1667 A73-28963

Application of holographic interferometry to predict long time torsional relaxation.
13 p1620 A73-29301

Low-temperature relaxations in amorphous polymers.
14 p1765 A73-30134

The use of elastic relaxation for testing aerospace equipment.
[AIAA PAPER 73-478] 15 p1948 A73-31462

Finite element methods by variational principles with relaxed continuity requirement.
16 p2031 A73-32985

Geometry of relaxing gas flows.
18 p2299 A73-36330

Calculation of structures by superrelaxation iterations over moments
19 p2497 A73-37549

Relaxation to Maxwellian distribution of electrons near low voltage Cs arc plasma discharge cathode
23 p3013 A73-44314

Effect of plasma inhomogeneity on the relaxation of the electron distribution near the electrodes in a low-voltage arc.
23 p3013 A73-44315

Plastic relaxation of a shear crack near a planar interface.
24 p3152 A73-45403

An inverse torsion pendulum with continuous frequency variation for studies of elastic relaxation and fatigue
24 p3076 A73-45554

RELAXATION [PHYSIOLOGY]

EMG measurement on male adults for muscular relaxation reaction time interval from light stimulus onset to elbow flexor response
03 p0267 A73-13699

Volume-pressure characteristics of rib cage-diaphragm interaction in standing subjects during voluntary relaxation
20 p2518 A73-39778

RELAXATION METHOD [MATHEMATICS]

Buckling of laterally loaded plates having initial curvature.
01 p0115 A73-10768

Application of relaxed solutions to minimum sensitivity optimal control.
02 p0149 A73-12509

Relaxation algorithms for nonlinear system modal trajectory estimation by approximate step with lower triangular matrix inversions sequence, comparing convergence with Gauss-Newton method
04 p0472 A73-15265

High subsonic flow past airfoils at 2 deg angle of attack, describing relaxation method for hyperbolic Euler equations conversion to parabolic form
06 p0645 A73-17738

Clamped orthotropic skew plates under uniformly distributed transverse load, considering nonlinear

analysis based on numerical technique of dynamic relaxation involving critically damped vibration
11 p1444 A73-26380

Convergence of the upper relaxation method for solving variational-difference equations for elliptic equations in an arbitrary plane
15 p1898 A73-30960

On the choice of relaxation parameters for nonlinear problems.
17 p2199 A73-34100

Relaxation solutions for inviscid axisymmetric transonic flow over blunt or pointed bodies.
17 p2095 A73-35122

Uniqueness requirements for calculated jump conditions across embedded shock waves based on relaxation methods, comparing to time dependent finite difference calculation
17 p2154 A73-35133

Relaxation factors for supercritical flows.
17 p2154 A73-35133

Inconsistencies and S.O.R. convergence for the discrete Neumann problem.
17 p2202 A73-35519

Chattering arcs and chattering controls.
18 p2294 A73-36639

Use of a relaxation technique in nozzle wave propagation problems.
[AIAA PAPER 73-1011] 24 p3078 A73-44842

Microphone radiated acoustic power directivity measurement enhancement by integral transform matrix inversion and relaxation techniques, considering application limits, resolution, noise sensitivity and computation
[AIAA PAPER 73-1040] 24 p3090 A73-44866

RELAXATION OSCILLATORS

Weakly superconducting, thin-film structures as radiation detectors.
02 p0167 A73-118494

Stabilization of relaxation oscillators based on devices with an S-type current-voltage characteristic.
10 p1197 A73-24933

Inductive relaxation oscillator design using common emitter avalanche transistors with N-shaped I-V characteristics at base input
17 p2133 A73-34154

The effect of a magnetic field on the operation of a dual-base-diode oscillator.
17 p2136 A73-35166

RELAXATION TIME

Model analysis for heat radiation effect on development and evolution of single buoyant thermal rising in neutrally stratified atmosphere, noting radiative relaxation time
[AD-755499] 01 p0039 A73-103900

Vibrational relaxation in CO₂ with selected collisional partners. I - H₂O and D₂O.
01 p0080 A73-10775

Multiphonon transition theory for electron transitions probability between conduction and forbidden bands, noting semiconductor surface states with long relaxation time
01 p0089 A73-11430

Relaxation of excess populations in the lower laser level CO₂/100.
03 p0318 A73-13278

Quasi-frozen flow of a thermodynamically relaxing gas
03 p0295 A73-13792

Passage of electric current through an illuminated semiconductor under conditions where the anisotropy parameters, the electrical conductivity, and the relaxation time are nonuniform. I
04 p0484 A73-15641

Thermodynamic equilibrium and relaxation models of ideal and real high temperature gas flows for reversible and irreversible processes
[DFVLR-SONDDR-282] 04 p0517 A73-15678

Contribution of Coulomb collisions to plasma relaxation in the DECA mirror machine.
05 p0604 A73-17367

Hydrogen maser frequency stability dependence on signal output, magnetic polarization field and relaxation effects, describing automated relaxation rate measurement and atomic line spectrum registration
06 p0699 A73-17588

Ionization-relaxation time measurements upon krypton and xenon in a shock-wave heated plasma
06 p0728 A73-17912

Atomic oxygen formation times obtained from measurements of electron density profiles behind shock waves in air.
07 p0853 A73-19510

Vibrational relaxation times of oxygen in the pressure range 10-110 atm.
07 p0853 A73-19927

Hydrogen maser amplifier performance characteristics, discussing relaxation time measurements, frequency stability and performance enhancement via resonator cavity magnetic shielding improvement
08 p0974 A73-20774

Quasi-linear relaxation of a monoenergetic relativistic electron beam in an external magnetic field
09 p1124 A73-21903

- Spin relaxation times in ferromagnetic materials with magnetic anisotropy, discussing temperature effects and energy considerations
09 p1134 A73-22686
- Direct measurements of the electrical conductivity and relaxation time of ionized air in the stratosphere and mesosphere
10 p2121 A73-23890
- Relaxation time measurements by an electronic method.
10 p2127 A73-23998
- Viscosity of the moon. I - After mare formation. II - During mare formation.
10 p1277 A73-24081
- Experimental study of the relaxation of excited states in a decaying alkaline plasma
10 p1256 A73-24576
- Atmospheric convection and its effect on relaxation time and charge distribution.
11 p1394 A73-25759
- Ultrasonic investigation of the nematic-isotropic phase transition in MBBA.
11 p1409 A73-26213
- Relaxation stability of iron and nickel alloys at high temperatures
12 p1509 A73-26898
- Measurements of free stream velocity and ionization relaxation behind a shock in xenon.
12 p1527 A73-27172
- Relaxation rates of lower laser levels in CO₂.
13 p1626 A73-28544
- Relaxation of the bending vibration of CO₂ in pure CO₂ and in mixtures of CO₂ with noble gases.
13 p1662 A73-28553
- Maxwell kinetic theory of gases with elasticity of shape /modulus of rigidity/ and obeying Hooke's law, deriving expressions for simple shear and relaxation time
14 p1745 A73-30477
- Linearization of the relaxation time control of a transistor multivibrator.
15 p1849 A73-30992
- High-temperature electrical conductivity relaxations induced in CdTe crystals by variations in cadmium vapor pressure
15 p1923 A73-31201
- Kinetics of physicochemical processes in a shock wave in mercury vapors. II - The relaxation zone: Region of initial ionization
15 p1916 A73-32314
- Quasilinear relaxation of a monoenergetic relativistic electron beam in an external magnetic field.
15 p1922 A73-32628
- Vibrational relaxation measurements in CO₂ employing an incremental TEA laser gain technique.
16 p2024 A73-33083
- Atomic modeling of internal friction in solids, considering paraelastic point defects relaxation time
16 p2037 A73-33227
- Measurement of relaxation time during acceleration of rotation of vessels containing helium II, and superfluidity in pulsars
16 p2038 A73-34065
- Scattering of a nonlocalized exciton on phonons in thin quantized semiconductor films
17 p2218 A73-34118
- Prediction of the deformation properties of polymer materials
17 p2194 A73-34268
- Kinetics of bleaching in polymethylene cyanine dyes.
17 p2186 A73-35793
- Third- and higher-order intensity correlations in laser light.
20 p2571 A73-38630
- Direct measurements of the electrical conductivity and relaxation time of ionized air in the stratosphere and mesosphere.
20 p2551 A73-38909
- Nd doped YAG laser crystal relaxation time, describing population inversion, beam gain time dependence and phonon spectra
20 p2574 A73-39695
- Relaxation resistance of alloys based on iron and nickel at high temperatures.
21 p2720 A73-41031
- Relaxation time in disk galaxy simulations.
22 p2904 A73-41754
- Vibrational relaxation of oxygen in an unsteady expansion wave.
22 p2889 A73-42441
- German monograph - Investigation of relaxation effects behind secondary shock fronts in shock-wave heated and partially ionized argon plasmas.
22 p2895 A73-42850
- Fireball spectral data reduction for self absorption, Fe abundance, excitation temperatures, relaxation time and optical thickness effects
22 p2915 A73-43043
- CW single mode He-Ne laser intensity fine structure fluctuations correlation measurement near threshold by digital correlator, obtaining higher order relaxation rates
22 p2871 A73-43085
- Linear viscoelasticity theory application to high polymers mechanical properties determination via relaxation spectrum with emphasis on polymethyl methacrylate
22 p2881 A73-43170
- ## RELAY SATELLITES
- AEROSAT - An aeronautical communications satellite for oceanic areas.
[AIAA PAPER 73-46]
06 p0771 A73-17624
- An efficient multiplexing approach for adaptive aircraft communications via a relay satellite.
14 p1726 A73-29899
- The application of simulation to mission planning for communications and data relay satellites.
18 p2291 A73-36424
- ## RELIABILITY
- NT AIRCRAFT RELIABILITY
NT CIRCUIT RELIABILITY
NT COMPONENT RELIABILITY
NT SPACECRAFT RELIABILITY
NT STRUCTURAL RELIABILITY
- Autonomous hydrogen/air fuel cell for long-life missions.
09 p1033 A73-22752
- ## RELIABILITY ANALYSIS
- Mathematical formulation for classification, realization and evaluation of electronic components and systems reliability tests
01 p0023 A73-10647
- Stochastic behaviour of a complex system with standby redundancy.
01 p0023 A73-10649
- Application of the algorithm of a median for accuracy and reliability improvement in data processing.
01 p0020 A73-10678
- Reliability-performance comparisons between tube and transistor power modules for ground-based and airborne radar applications
01 p0024 A73-10718
- M/W power transistors and MIC amplifiers - State-of-the-art.
01 p0024 A73-10719
- Reliability and failure sequence characteristics of automatic system, using input rarefaction of Markov renewal process
01 p0058 A73-11423
- The system approach to the design of engineering systems from the standpoint of reliability and efficiency
02 p0145 A73-11547
- The generalized gamma distribution and the power distribution as element lifetime distributions
02 p0145 A73-11584
- Generalized gamma distribution with a negative shape parameter as a model of the lifetime distribution of electrical elements with a single-maximum failure rate
02 p0145 A73-11585
- Onboard ILS equipment reliability in integrated airborne all-weather landing system
02 p0190 A73-11855
- Book - Applied maintainability engineering.
02 p0238 A73-11883
- Application of the device of linear programming to solve certain optimal problems of reliability theory.
02 p0187 A73-12121
- Investigation of fatigue life and residual strength of wing panel for reliability purposes
03 p0387 A73-13233
- A reliability approach to the fatigue of structures.
03 p0387 A73-13234
- Book on passive IR sensing devices design and use in industrial and manufacturing problems solution covering detector types, display devices and reliability analysis
03 p0283 A73-13994
- Statistical analysis applied to solar cell shorting caused by reverse bias voltage stress.
03 p0255 A73-14223
- Statistical considerations for structural reliability analysis.
04 p0507 A73-14707
- Failure probability distribution models for reliability analysis, considering selection criteria based on application
04 p0507 A73-14708
- Reliability analysis methods for metallic structures.
04 p0452 A73-14714
- Evaluation of a reliability analysis method for fatigue life of aircraft structures.
04 p0452 A73-14715
- Structural reliability definition and determination in terms of survival probability concept, discussing analytical errors effect on design and applications to aerospace vehicles
04 p0508 A73-14724
- Estimates of reliability functions for systems with redundancy.
04 p0471 A73-15210
- Reliability of electromyographic measurements by means of surface electrodes
04 p0412 A73-15520
- Monograph on structural element and structures reliability covering structural design, failure analysis and reinforced element collapse under moment and force loads
04 p0472 A73-15694
- Reliability of systems with shifting redundancy in servicing a random demand flow
05 p0560 A73-16274
- Synthesis of optimal control problems with allowance for a prescribed reliability
05 p0561 A73-16416
- Solar electric space mission risk analysis, describing computerized multistage failure process simulation procedure with application to Encke comet rendezvous mission
[AIAA PAPER 73-208]
06 p0748 A73-17660
- Comparison of the Powell 1, Powell 2, and Zangwill static optimization methods
06 p0670 A73-17859
- Error incidence probability for system control reliability determination, assuming error function as Markov process
06 p0680 A73-17956
- Automation of reliability evaluation procedures through CARE - The computer-aided reliability estimation program.
06 p0670 A73-18058
- Reliability tests on miniature ceramic capacitors encapsulated by epoxy-novolac block polymer compounds
06 p0677 A73-18398
- Scalar and vector partitions of the probability score. II - N-state situation.
06 p0720 A73-18704
- Scanning electron microscope operation and application to technology research and electronic components and circuits failure and reliability analysis
07 p0797 A73-18922
- Computer for automatic equipment monitoring, operation control and breakdown diagnosis in telemetry data processing, discussing management routines and reliability
07 p0795 A73-18956
- Design, production, reliability analysis and testing of Eole satellite decoder for balloon sounding data, noting performance tests
07 p0790 A73-18966
- Satellite electronic equipment reliability and quality control at preproject, project, fabrication and mission levels, noting electric welding quality specification
07 p0904 A73-18974
- Optimal planning of technological systems maintenance according to a reliability criterion
07 p0830 A73-19126
- National Congress on Reliability, Perros-Guirec, Cotes-du-Nord, France, September 20-22, 1972, Text of the Lectures
07 p0799 A73-19401
- Calculation of the reliability of electronic components in an 'aeronautics' environment shaped by the operational service routines of onboard equipment devices used by Air France
07 p0799 A73-19403
- Help derivable from failure analyses for the definition of a reliability evaluation model applicable to large-scale integrated circuits
07 p0800 A73-19411
- Statistical diagnostics and information synthesis relating to the reliability and maintenance of an equipment
07 p0830 A73-19414
- Estimation of reliability in storage - Optimal test procedure
07 p0830 A73-19415
- Reliability tests on fire control airborne radars prototypes, measuring MTBF
07 p0800 A73-19416
- Influence of repeated voltage applications on the reliability of a system
07 p0800 A73-19417
- Operational reliability of onboard equipment subjected to very long idling periods
07 p0831 A73-19418
- Failure analysis and reliability estimation methodology for electromechanical mosaic printer
07 p0800 A73-19419
- Stress and strength theory application to mechanical failure of electronic equipment, showing Weibull law use in reliability analysis
07 p0800 A73-19420
- Reliability of sealed reed switches /SRS/
07 p0801 A73-19423
- Reliability of thin nickel-chromium resistance layers deposited by sublimation under vacuum on a glass substrate
07 p0862 A73-19424
- Ionospheric radio signal reflection fields verified via quantitative statistical reliability criterion
07 p0815 A73-19434
- Failure analysis of semiconductor device bonds under on-off operation, noting fatigue testing machine for accelerated life tests
08 p0972 A73-20744
- Bayesian MFR life test sampling plans.
08 p0973 A73-20950

Bayesian prior distributions for multi-component systems. 09 p1111 A73-22374

Reliability of a self-repairing system with scheduled maintenance. 09 p1088 A73-22443

Calculation of the reliability of hierarchical systems with quorum redundancy 09 p1088 A73-22552

A reliability and comparative analysis of two standby system configurations. 09 p1112 A73-22643

Best linear unbiased estimator of the parameter of the Rayleigh distribution. I - Small sample theory for censored order statistics. 09 p1112 A73-22645

Five year lifetime space radioisotope thermoelectric generator with lead telluride panels and plutonium 238 dioxide heat source, analyzing reliability, design and performance 09 p1038 A73-23284

Electronic system reliability improvement by partitioning into functional parallel redundant blocks 10 p1193 A73-23651

Development of maintenance policies in the operation of aircraft 10 p1174 A73-23655

Tensile creep modulus, creep lateral contraction ratio and torsional creep measurements on small non-rigid specimens. 10 p1218 A73-24120

Comparative analysis of optimal failure search procedures, considering criteria, failure extent, initial data, reliability and compatibility 10 p1226 A73-24696

Variable area, positive displacement, turbine type, electromagnetic and pressure difference flowmeters, noting reliability, repeatability and accuracy 10 p1221 A73-24853

Aircraft design and reliability analysis method based on accidents occurrence investigation by Franco-British airworthiness authorities, noting applicability to Concorde aircraft 11 p1306 A73-26589

Reliability analysis of helicopter mechanical transmission components and reduction gearboxes 11 p1306 A73-26596

Two component system reliability model, taking into account stress effects under failure normal distribution assumption 11 p1448 A73-26730

Influence of control periodicity on the reliability of repairable devices 12 p1502 A73-26760

Information transmission reliability enhancement via digital code group symbol transmission by wide-band linear FM radio signals 12 p1471 A73-27593

A confidence estimate of the reliability of a system from the results of tests of its components 12 p1503 A73-27618

Mean time of the failure-free operation of a redundant system with allowance for monitoring of operational efficiency 12 p1504 A73-27619

Reliability considerations in hybrid microcircuits. 13 p1588 A73-28045

Estimations for queuing and reliability theory 13 p1649 A73-28796

Analytical elasticity methods for airfield pavement structural stress-strain, failure and reliability performance evaluation 13 p1598 A73-29106

A reliability analysis of fatigue limits based on large sample quantal response data. 13 p1702 A73-29548

Automatic evaluation of strain gage data reliability by comparison with a preset parameter and determination of a statistical yield strength. 13 p1622 A73-29549

Calculation of redundant equipment recovery time when only failures of entire systems are detected by inspection 14 p1754 A73-30036

Determination of some characteristics of random processes describing the operation of transient action systems with allowance for reliability 14 p1730 A73-30037

Launching operations organization and optimization and information supply, discussing vehicle reliability impact 14 p1741 A73-30086

Matrix, pyramid and rectangular decoder reliability and operational probability during short circuit/cut-off failures 14 p1736 A73-30566

Prediction of failures and efficiency characteristics of a system 14 p1740 A73-30799

Reliability analysis of time to failure distribution of redundant system with failing elements number as periodic function of time 15 p1880 A73-30998

Reliability estimation technique for data transmission processes in remote control systems with redundancy, assuming Markovian randomness of signal input 15 p1854 A73-31806

A critical study on the reliability of electron temperature measurements with a Langmuir probe. 15 p1871 A73-31835

Approximate determination of the reliability function of a digital computer 15 p1848 A73-31912

Reliability testing functions for memory elements 15 p1848 A73-31914

A method of assigning noise-resistant analog-to-digital converters 15 p1848 A73-31915

Problems of reliability theory in the mechanics of deformable solids 15 p1914 A73-32082

Reliability testing of high-perveance three-electrode guns 15 p1851 A73-32215

Truncated sequential life tests for a 3-way decision procedure. 15 p1883 A73-32260

A unified method for analyzing mission reliability for fault tolerant computer systems. 15 p1901 A73-32261

An empirical Bayes approach for the Poisson life distribution. 15 p1901 A73-32262

Expected value and variance of failure time in redundant systems. 15 p1901 A73-32264

The safety, the reliability, and redundancy in the automatic flight control system of the A300-B Airbus 15 p1830 A73-32459

Onboard electronic equipment optimization and redundancy 15 p1852 A73-32460

Study of the integrity of an equipment - Application to radio altimeters for category III landing 15 p1880 A73-32493

Analysis of the reliability of airborne material in an airline company - Objectives and methods 15 p1831 A73-32495

Organization of a reliability study on an electromechanical product 16 p1970 A73-33271

The analysis of defects and the possibilities brought by the scanning electron microscope 16 p2019 A73-33272

Fluidic component performance and circuit reliability. 16 p1971 A73-33475

Hydrofluidic component and system reliability. 16 p1971 A73-33478

A current turbine engine maintenance program and the experience and logic upon which it is based. [ASME PAPER 73-GT-81] 16 p2049 A73-33526

Annual Reliability and Maintainability Symposium, Philadelphia, Pa., January 23-25, 1973, Proceedings. 16 p2020 A73-33601

Some statistical techniques useful in system aging studies. 16 p2020 A73-33603

Integral transform theory for derivation of compound binomial beta, uniform, and gamma distributions with applications to series-parallel systems reliability determination in manufacturing 16 p2020 A73-33604

Universal operating characteristic curves for sequential probability ratio tests. 16 p2020 A73-33611

Computerized analysis of reliability or failure rate function data from electronic component and equipment operation and testing, using hazard plotting technique 16 p1989 A73-33613

The Kolmogorov-Smirnov test modified for censored data. 16 p2033 A73-33619

Reliability estimate of a Space Deployable Antenna. 16 p1989 A73-33620

Reliability of GaAs/1-x/P/x light emitting diodes. 16 p1990 A73-33623

Data sample analysis of anomalous in-flight behavior incidents for spacecraft reliability covering incident causes and occurrence time, effects on mission and corrective actions 16 p2073 A73-33625

Lower confidence bounds determination for component or system reliability by sampling with and without replacement, censored, truncated and mixed sampling test programs 16 p2033 A73-33629

Specifying maintainability-demonstration-test parameters. 16 p2020 A73-33635

Integrated reliability and safety analysis of the DC-10 all-weather landing system. 16 p1969 A73-33641

Probabilistic fatigue design alternative to Miner's cumulative damage rule. 16 p2081 A73-33643

Computer program for Equipment Improvement Recommendation /EIR/ evaluation relative to reliability, availability, inventory cost and total annual expenditure in Army engineering management decision making 16 p2089 A73-33653

Operational behaviour of a complex system with two out of M failed components. 16 p2022 A73-34030

Complex system reliability with general repair rate distributions under preemptive repeat repair discipline. 16 p2022 A73-34031

The development of a turbine engine maintenance program from a new reliability model. [SAE PAPER 730374] 17 p2177 A73-34713

Review of engine maintenance concepts applied to wide body jets. [SAE PAPER 730375] 17 p2178 A73-34714

New relationships between stress testing, failure and reliability. 17 p2178 A73-34730

Interdisciplinary communications problems of metal physicists, fracture mechanists, structural designers and reliability analysts for fatigue crack generation and growth 17 p2246 A73-34886

Helicopter power transfer systems analysis in terms of weight reduction and reliability improvement [AHS PREPRINT 773] 17 p2106 A73-35091

Monte Carlo simulation on CRT display for training and learning system reliability and early decision effects on life cycle cost effectiveness 17 p2140 A73-35261

Book - Graph theory in modern engineering: Computer aided design, control, optimization, reliability analysis. 17 p2132 A73-35600

Probabilistic analysis of a two-unit system with a warm standby and a single repair facility. 17 p2149 A73-35809

Bayesian estimation of life parameters in the Weibull distribution. 17 p2204 A73-35810

A reliability, cost and risk analysis of establishing and maintaining a space communications satellite network. [AIAA PAPER 73-582] 18 p2288 A73-36074

Matrix formulation of reliability analysis and reliability-based design. 19 p2496 A73-37479

Functional reliability of structures. 19 p2501 A73-38279

ATC enroute automation program using radar tracking and computer readout system, describing terminal traffic control, wake vortices and aircraft spacing 19 p2453 A73-38439

A design problem for redundant systems with recovery 20 p2568 A73-38996

Electric connector reliability assessment model based on operating conditions and failure modes analysis without using MTBF 21 p2665 A73-41208

Pioneers 8 and 9 cosmic dust data reliability, presenting sensor geometry, field of view, response function, instrument control and sensitivity 21 p2775 A73-41411

Triple Modular Redundancy Single Single voter-switch with majority voting of three parallel data channels or converters, estimating reliability for short and long missions 22 p2825 A73-42294

The robustness of reliability predictions for series systems of identical components. 22 p2867 A73-42967

Reliability of some redundant systems with repair. 22 p2867 A73-42968

Equivalence of redundant systems with respect to time to failure. 22 p2867 A73-42970

Characterization of composites for the purpose of reliability evaluation. 23 p3040 A73-43627

Sequential determination of inspection epochs for reliability systems with general lifetime distributions. 24 p3093 A73-44576

Information seeking with multiple sources of conflicting and unreliable information. 24 p3063 A73-44778

Reliability estimation for repairable and nonrepairable flight vehicles, considering nomographs for failure rate and probability of defined requirements satisfaction 24 p3057 A73-45197

Reliability estimation technique for data transmission processes in remote control systems with redundancy, assuming Markovian randomness of signal input 24 p3075 A73-45350

RELIABILITY CONTROL
U QUALITY CONTROL
U RELIABILITY ENGINEERING

RELIABILITY ENGINEERING

Superconducting magnetic systems reliability engineering and design, noting combined conductors for uncontrolled transition prevention in normal state under subcritical currents

01 p0005 A73-10616

The optimum allocation of redundancy - An application of mathematical programming to system design.

01 p0071 A73-11199

A method for computing complex system reliability.

03 p0336 A73-13733

Multilayer debugging process /A new method of screening/.

03 p0336 A73-13734

Reliability optimization of a series-parallel system.

03 p0336 A73-13735

Effects of test capability on system reliability and availability.

03 p0313 A73-13736

Extreme value methods for design, production, testing and maintenance of components and system with low failure probability

04 p0507 A73-14709

The design and development of fracture resistant structures.

04 p0507 A73-14712

Information criterion for optimal planning of reliability control tests, maximizing average effect

04 p0430 A73-15211

Hydraulic and flight control system for Space Shuttle Orbiter.

[SAE PAPER 720838]

05 p0537 A73-16630

Computer communication networks with programmable concentrators for combining multiple terminals, discussing structure, message handling and transmission, routing and reliability

05 p0551 A73-16805

Method for planning systems with prescribed design reliability

06 p0670 A73-17857

Fault insertion techniques and models for digital logic simulation.

06 p0671 A73-18062

Design of a fault-tolerant, modular computer with dynamic redundancy.

06 p0671 A73-18064

Describing functions, circle criteria and multiple-loop feedback systems.

06 p0680 A73-18444

Least square approach for system reliability optimization.

06 p0681 A73-18524

A general model for the study of fault tolerance and diagnosis.

06 p0672 A73-18808

French spacecraft electronic components reliability program, considering failure characteristics, operating limits, environmental conditions and confidence level

07 p0797 A73-18915

MOS production line with individual manufacturing operation reliability assurance based on failure analysis, process perfection, material control and experimental verification

07 p0829 A73-18917

High reliability semiconductors development, discussing research in Si single crystals growth, epitaxial films, photoengraving, oxidation/passivation and large-scale integration techniques

07 p0829 A73-18919

High reliability technology assessment for metal film resistors production, discussing qualification tests

07 p0829 A73-18921

Tracking radar equipment evolution in connection with French space program development, describing reliability technology

07 p0807 A73-18943

Third generation satellite PCM telemetry data processing with computer control for optimization and supervision, discussing system reliability, automatic control and diagnostic routine

07 p0795 A73-18954

Reliability dynamism at the Deutsch Company.

07 p0829 A73-19008

Reliability design of type 2N 3966 field effect elements

07 p0801 A73-19421

The use of automatic test equipment for performing screening and production reliability verification testing.

08 p0942 A73-20681

Reliability physics; Proceedings of the Tenth Annual Symposium, Las Vegas, Nev., April 5-7, 1972.

08 p0943 A73-20729

Design and fabrication of MOS/LSI circuits for reliability, discussing layout rules and protective circuitry

08 p0943 A73-20733

Electronic equipment burn-in for repairable equipment.

08 p0945 A73-20949

Thermoelectric radioisotope generators and nuclear thermoelectric reactors, noting anaerobic self contained reliable operation and suitability for underwater energy sources

09 p1032 A73-22203

Computer protection mechanisms design principles for operating system and hardware architecture implementation, considering access matrix storage, efficiency and subject and object selection

09 p1059 A73-22223

Reliability of a self-repairing system with scheduled maintenance.

09 p1088 A73-22443

Value engineering methodology for quality control and reliability, noting cost effectiveness

09 p1168 A73-22644

Optimization of system reliability using a parametric approach.

09 p1112 A73-22646

Hydrogen-oxygen fuel cell as reliable electric power supply for space shuttle mission requirements, assessing technological developments

09 p1035 A73-22777

Isotope Brayton electric power system for the 500 to 2500 watt range.

09 p1118 A73-22793

Autonomous power subsystem design for an Outer Planet Spacecraft.

09 p1154 A73-22805

Block coding for digital computer error detection and correction, considering applications for arithmetic operations, storage media and permanent hardware failure recognition

09 p1061 A73-23400

LSI computer design and fabrication for Space Ultrareliable Modular Computer Demonstration Vehicle, discussing assembly, physical and electrical characteristics and electronic testing procedures

10 p1191 A73-23794

Figure of merit for fault-tolerant space computers.

10 p1192 A73-24870

The concept of coverage and its effect on the reliability model of a repairable system.

10 p1226 A73-24871

Modeling of a bubble-memory organization with self-checking translators to achieve high reliability.

10 p1192 A73-24872

Reliability and quality control of production engineering computer programs.

[ALAA PAPER 73-356]

11 p1373 A73-25493

Experimental evaluation of the single-cell concept for a lightweight, rechargeable hydrogen-oxygen fuel cell.

11 p1309 A73-25987

Holographic optical memory superiority over conventional localized computer storage devices, considering capacity, access time, immunity to local imperfections, and crosstalk problem

11 p1370 A73-26538

Book - Engineering means in automatic control.

12 p1481 A73-26751

The quorum element and its application in the design of adaptive automatic control systems

12 p1482 A73-26758

Features of the engineering theory for combined estimates of automatic control system reliability and lifetime

12 p1482 A73-26763

Fault-tolerance in the modular spacecraft computer.

12 p1475 A73-27130

Improvements in the use of FAA resources for system performance assurance.

12 p1561 A73-27364

Book - Reliability concepts in engineering manufacture.

12 p1502 A73-27398

Shuttle payloads - Saving dollars by offsetting risks.

12 p1549 A73-27438

Random failure process similarity in redundant schemes for systems with binary elements, noting statistical modeling on specialized Monte Carlo machines

12 p1485 A73-27620

Microwave transmitter tubes for surface-based and airborne radar applications, considering ATC, output power, stability, spectrum, size, weight, reliability, maintainability and cost requirements

13 p1590 A73-28532

Fundamentals of the theory of combined reliability and service life estimates for machines and instruments

13 p1624 A73-29134

High-reliability strapdown platforms using two-degree-of-freedom gyros.

13 p1657 A73-29214

Graphs, tables and discussion to aid in the design and evaluation of an acceptance sampling procedure based on cumulative sums.

13 p1709 A73-29297

General aviation aircraft technology developments based on military and transport aircraft design, considering cost, complexity and reliability

13 p1570 A73-29348

Long-life light weight reliable fuel cell development for long term space missions power supplies, describing system components and construction materials

13 p1573 A73-29596

Russian papers on cybernetic systems reliability and accuracy covering analog, hybrid and digital computers, electronic modeling, nonlinear control systems, computer and complex system design, etc

14 p1730 A73-30031

Techniques and equipment for thermal nondestructive quality control of products and materials.

15 p1882 A73-31692

Real time information processing automated systems for ATC, considering reliability based on redundancy

15 p1910 A73-32483

Limitations in the use of all-electric systems for vital application in civil aircraft.

15 p1852 A73-32492

Utilization of realization to optimize the choices of reliability from the economic point of view

16 p2088 A73-33270

Annual Reliability and Maintainability Symposium, Philadelphia, Pa., January 23-25, 1973, Proceedings.

16 p2020 A73-33601

AEGIS AN/SPY-1 radar system - Design for availability.

16 p1980 A73-33607

AEGIS Operational Readiness Test System - Design for system effectiveness.

16 p2073 A73-33609

Approach to reliability for the SM-2 missile.

16 p2073 A73-33610

Time dependent stress-strength models for non-electrical and electrical systems. I.

16 p2020 A73-33621

Tactical weapon system final test for random failures, discussing electronic component defects effects and semiconductor device screening for system reliability improvement

16 p1990 A73-33624

Statistical and probabilistic MTBF models for parts, sockets and systems reliability

16 p2020 A73-33628

A statistical analysis of product reliability due to random vibration.

16 p2020 A73-33637

Mathematical modeling technique for marketing reliability programs in terms of cost/performance assurance for use in management decision making

16 p2089 A73-33638

Developing country industrial product reliability from buying and manufacturing viewpoints, considering local methods, customs, attitudes and working conditions effects on management techniques

16 p2089 A73-33646

A synergistic reliability and maintainability prediction package.

16 p1986 A73-33652

Organization of checks of the central control unit in a digital process-control computer operating with fixed word length

16 p1986 A73-33665

Synthesis of a universal cell with increased reliability for the realization of an iterative automatic system

16 p1986 A73-33667

Atmospheric refractivity effects on maximum antenna gain and correlation coefficient in design of microwave line of sight links for high reliability

16 p1981 A73-33704

Book - Optimum structural design: Theory and applications.

17 p2242 A73-34350

L-1011 aircraft hydraulic system layout and installation techniques with modular design and plug-in cartridges for Murphy law error reduction during servicing

17 p2108 A73-34523

High reliability solid state force sensors for flight control systems.

17 p2165 A73-34603

Prototype TDMA system design for Intelsat 4 satellite, discussing separate synchronization and data bursts transmission feature for service quality and reliability improvement

17 p2122 A73-34967

A dynamics approach to helicopter transmission noise reduction and improved reliability.

[AHS PREPRINT 772]

17 p2106 A73-35090

Unconventional digital avionics black box approach for cost reduction and reliability improvement in terms of packaging, component coding and hardware qualification programs multiplicity

17 p2137 A73-35205

Optimal modular redundancy over a set of configurations for attaining specified system availability and reliability requirements.

17 p2139 A73-35257

CPU design for command and control system with programmable read-only control memory, discussing self microdiagnostics for control store error detection

17 p2144 A73-35258

Time Division Multiple Access for the defense satellite communications system.

17 p2124 A73-35307

Microwave equipment reliability design for aerospace environment applications, considering vibration, shock, humidity and temperature effects and frequency stability

18 p2293 A73-36778

RELIEF MAPS

Book on mechanical reliability from engineering standpoint covering statistical probability, performance quality, systems design and manufacturer and user roles

18 p2321 A73-36970

Matrix formulation of reliability analysis and reliability-based design.

19 p2496 A73-37479

U.S. instrument landing system performance improvements, considering terrain and weather effects, installation requirements, airport limitations, accuracy, reliability and maintainability

19 p2450 A73-37805

Multilayer foil insulated Si-Ge thermopile design for multihundred watt radioisotope thermoelectric generator to withstand launch environments, evaluating performance under shock and vibration loads

19 p2392 A73-38424

Computer program using successive system reduction on basis of calculation of reliability of pure parallel and series arrangements

20 p2533 A73-39632

Russian book on reliability optimization in complex automatic control system information transfer and processing covering performance criteria, noise immunity, error sources and types, etc

21 p2670 A73-41293

Risk analysis and reliability based design for probabilistic approach implementation for safety and performance of structures and structural components

21 p2788 A73-41650

Failure detection and isolation techniques for gimbaled and strapdown inertial systems examining redundant system reliability relationship to MTBF [AIAA PAPER 73-852]

22 p2884 A73-41969

Fracture mechanics technology for optimum pressure vessel design.

22 p2920 A73-42155

Assuring reliability program effectiveness.

22 p2938 A73-42199

Triple Modular Redundancy Single Single voter-switch with majority voting of three parallel data channels or converters, estimating reliability for short and long missions

22 p2825 A73-42294

Toward reliable composites - An examination of design methodology.

24 p3094 A73-45144

Total In-Flight Simulator for X-22A aircraft based on variable stability-and-control system concept for reliability design

24 p3057 A73-45153

Aircraft gas turbine engines with single crystal blades to avoid conventional casting grain boundary weakness and premature damage

24 p3094 A73-45155

RELIEF MAPS

Martian topography from radar observations and the Mariner 6 and 7 and ground-based CO₂ measurements.

04 p0503 A73-16016

Hypsometric properties of the near side of the moon.

04 p0503 A73-16018

A first look at the lunar orbital gamma-ray data.

07 p0871 A73-19824

Far IR mapping of lunar surface during 19 December 1964 eclipse, discussing thermal contours and Apollo observed regions

10 p1282 A73-24644

Optical and radio observations of the Orion Nebula.

11 p1425 A73-26265

The growth and decay of the main phase of the September 21-23, 1963 magnetic storm.

12 p1490 A73-27275

Experiment in stereophotogrammetric processing of aerial photographs with decentrations on an STD-2 stereometer

14 p1753 A73-30417

Photometric relief of the lunar continent cover

16 p2064 A73-33766

Lunar surface hypsographic curve plotting from point absolute height measurements

16 p2065 A73-33777

Systematic elevation errors in maps of the lunar edge zone

17 p2230 A73-34594

The precision of contour lines and contour intervals of large- and medium-scale maps.

23 p2979 A73-44123

RELIEVING

NT STRESS RELIEVING

RELUCTANCE

Design of a search memory using elements with reluctance modulation

08 p0941 A73-21108

Variable-reluctance stepping motor performance capabilities for point-to-point positional control.

10 p1199 A73-24024

RELUCTIVITY

U RELUCTANCE

REMAGNETIZATION

U MAGNETIZATION

REMANENCE

Natural remanent magnetizations of carbonaceous chondrites and the magnetic field in the early solar system.

05 p0619 A73-16839

Natural remanent magnetization and thermomagnetic properties of the Allende meteorite.

05 p0619 A73-16840

Metallic Fe-Ni-S lunar core as source of remanent magnetism in lunar rocks, consistent with thermal models

07 p0877 A73-19654

Lunar magnetic field measurements with Apollo 15 subsatellite, discussing surface remanent magnetization, solar wind interactions and limb shocks

07 p0892 A73-19833

Iron-titanium-chromite, a possible new carrier of remanent magnetization in lunar rocks.

07 p0892 A73-19836

Remanent magnetization of Apollo 14 rocks and fines, discussing iron contribution and early internal magnetic field

07 p0892 A73-19837

On the remanent magnetism of lunar samples with special reference to 10048.55 and 14053.48.

07 p0892 A73-19838

Lunar breccia 14321 natural remanent magnetization characteristics from alternating field and thermal demagnetization tests, describing magnetic measurement procedures

07 p0893 A73-19841

Lunar surface rock remanent magnetization, considering breccia, igneous samples, thermal demagnetization and Apollo landing sites

07 p0893 A73-19843

Astronomical, geochemical and geophysical data and constraints for lunar evolution, considering remanent magnetization, electrical conductivity and early evolution model

12 p1541 A73-27491

A determination of the intensity of the ancient lunar magnetic field.

12 p1542 A73-27494

Memory of early magnetic fields in carbonaceous chondrites.

17 p2228 A73-34421

Geomagnetic field, cosmic rays, and radiocarbon content in the earth's atmosphere

21 p2756 A73-40585

REMELTING

U MELTING

REMOTE CONSOLES

Data processing remote terminals for real time on-line computer communication systems, discussing design, characteristics and applications

05 p0551 A73-16801

REMOTE CONTROL

NT RADIO CONTROL

Electrostatic autopilot using atmosphere electric field lines for stabilization and guidance, applying to remotely piloted vehicles

02 p0191 A73-12595

A remotely operated ECG telemeter for chronic implantation in rats.

03 p0272 A73-14303

NTC '72; National Telecommunications Conference, Houston, Tex., December 4-6, 1972, Record.

04 p0417 A73-15376

The mathematics of coordinated control of prosthetic arms and manipulators.

[ASME PAPER 72-WA/AUT-4]

04 p0414 A73-15884

Aircraft and spacecraft guidance and remote and automatic control of moving objects, using calculus of variations for systems synthesis

05 p0560 A73-16402

Design and performance of VHF telemetry transmitter and remote controlled radio receiver for Eole satellite, noting production technology and block diagrams

07 p0790 A73-18961

Sounding balloon system SITTTEL for upper atmosphere physical parameters measurement, noting PCM telemetry, remote control and vehicle localization

07 p0790 A73-18971

Mobile ground station for sounding balloons remote control, telemetry and localization, noting antenna pointing control, tracking, receiver and trajectory recording

07 p0790 A73-18972

Apollo 15 and 16 ground-commanded television assembly.

07 p0823 A73-19375

An automated two-channel scanning spectrophotometer system.

08 p0970 A73-21740

Aerodyne flight vehicle testing for hover flight characteristics during remote control by radio with pilot commands, noting reliability and attitude control

13 p1569 A73-28785

The contribution of the German Telecommand Station to the overall command safety in the Helios project.

14 p1727 A73-30101

Remote feed, control, and signalization in transmission lines of multichannel systems with pulse code modulation

14 p1728 A73-30374

Russian book on remote guidance control systems covering theory, optimization and constraints for steady, unsteady, linear and nonlinear automatic control systems

15 p1853 A73-31374

Development of an improved midair-retrieval parachute system for drone/RPV aircraft.

[AIAA PAPER 73-469]

15 p1828 A73-31453

An omnidirectional gliding ribbon parachute and control system.

[AIAA PAPER 73-486]

15 p1829 A73-31468

Reliability estimation technique for data transmission processes in remote control systems with redundancy, assuming Markovian randomness of signal input

15 p1854 A73-31806

Independently targeted short haul individual rotorcraft for air taxi service, considering traffic control system, market possibilities, environmental impact and projected utilization

16 p2088 A73-33186

Teleoperators - Manual/automatic system requirements.

17 p2180 A73-35315

Remote control of planetary surface vehicles.

17 p2148 A73-35316

X-reference frame bilateral control for the Shuttle Attached Manipulator System.

17 p2180 A73-35317

Remotely manned systems: Exploration and operation in space; Proceedings of the First National Conference, California Institute of Technology, Pasadena, Calif., September 13-15, 1972.

19 p2415 A73-37301

Simulation concepts for a full-sized Shuttle manipulator system.

19 p2416 A73-37310

Science aspects of a remotely controlled Mars surface roving vehicle.

19 p2416 A73-37311

Planetary surface rover/remotely manned system concepts and applications from lunar and Mars mission studies

19 p2416 A73-37312

A study of remote guidance and control for planetary surface vehicles.

19 p2403 A73-37313

The multi-moded remote manipulator system.

19 p2416 A73-37314

Some preliminary correlations between control modes of manipulator systems and their performance indices.

19 p2416 A73-37315

Man-machine interface for controllers and end effectors.

19 p2397 A73-37325

Terminal pointer hand controller and other recent teleoperator controller concepts - Technology summary and application to earth orbital missions.

19 p2397 A73-37326

Command language for supervisory control of remote manipulation.

19 p2403 A73-37329

Performance improvement in remote manipulation with time delay by means of a learning system.

19 p2417 A73-37331

Application of self-organizing control to remote piloting of vehicles.

19 p2449 A73-37332

Hierarchical hybrid control of manipulators - Artificial intelligence in LSI.

19 p2407 A73-37334

Learning control in remote manipulator and robot systems.

19 p2412 A73-37754

Design and evaluation of a backhoe model with a master slave control.

19 p2401 A73-38085

Risk of estimation by data obtained via communication channel.

21 p2654 A73-40689

Telecontrol system for particle accelerator target displacement via micrometer electronic control with emphasis on adaptation to ultrahigh vacuum chamber simulating ionospheric plasma

22 p2838 A73-41868

Reliability estimation technique for data transmission processes in remote control systems with redundancy, assuming Markovian randomness of signal input

24 p3075 A73-45350

REMOTE HANDLING

Operation of spacecraft in orbit with the aid of remote-controlled manipulators - A joint project of ERNA, KYBERTRONIK, KLERA

[DGLR PAPER 72-098]

02 p0136 A73-11659

Experimental evaluation of remote manipulator systems.

19 p2416 A73-37305

- Shuttle Payload Accommodation System teleoperator. 19 p2491 A73-37308
- Developments in Canada related to remotely manned systems. 19 p2416 A73-37317
- A survey study of teleoperators, robotics, and remote systems technology. 19 p2417 A73-37335
- Design and evaluation of a backhoe model with a master slave control. 19 p2401 A73-38085
- A high vacuum, low temperature specimen transfer device for use in measuring optical properties of thin films. 21 p2693 A73-39925
- Teleoperator monoscopic television system and stereoscopic TV system with Fresnel display, using static simulations to investigate camera locations and depth alignment [AIAA PAPER 73-920] 21 p2673 A73-40868
- REMOTE REGIONS**
- NT ANTARCTIC REGIONS
- NT ARCTIC REGIONS
- Digital data acquisition and processing from a remote magnetic observatory. 17 p2175 A73-35667
- Public air transportation service needs for nonurban areas, considering low traffic density problem, operational requirements and future trend [ASME PAPER 73-ICT-72] 23 p3050 A73-43498
- Aerosol ice nuclei concentration measurements in remote regions of Southern Hemisphere near Australia by shipborne membrane filters, noting land or stratospheric sources 23 p3002 A73-43598
- REMOTE SENSORS**
- Influence of haze layers upon remotely-sensed surface properties. 01 p0037 A73-10360
- Atmospheric ozone distribution from remote sensing with spaceborne IR interferometer spectrometer, estimating error due to cloud cover 01 p0038 A73-10384
- Compact laser radar for remote atmospheric probing. 01 p0060 A73-11059
- Some new satellite sensors and applications. 01 p0052 A73-11161
- Test of horizon sensor for the ionosphere sounding satellite. 01 p0053 A73-11172
- Spacecraft-borne IR optical remote sensor for detection, identification and distribution measurement of asteroid and meteoroid particles 01 p0105 A73-11205
- Some new techniques for processing remotely obtained images by self-generated spectral masks. 01 p0078 A73-11219
- Digital image-processing activities in remote sensing for earth resources. 01 p0021 A73-11476
- Earth resources remote survey methods capability assessment, considering radar and passive microwave imaging, IR and multispectral scanning and photographic and absorption spectrometric methods [DGLR PAPER 72-072] 02 p0155 A73-11703
- Mobile FM-CW radar sounder with scanning capability for high resolution remote sensing in lower troposphere, discussing design and performance 02 p0140 A73-11959
- Remotely sensing strain-rate meter based on the Doppler shift of laser light. 02 p0168 A73-11961
- National reports on earth resources surveys at 1971 COSPAR meeting, including remote sensing techniques application in agriculture, forestry, geology and oceanography 02 p0160 A73-12264
- Aircraft measurements of microwave emission from Arctic Sea ice. 02 p0171 A73-12773
- Optimization of spectral intervals for remote sensing of atmospheric temperature profiles. 02 p0171 A73-12774
- Vertical resolution of temperature profiles obtained from remote radiation measurements. 02 p0165 A73-12778
- Status of remote sensing of the troposphere. 03 p0299 A73-13061
- Diagnostic instrumentation on J-85 engines for gas path and vibration analysis, noting flight test program and installation of remote pressure transducers and signal conditioners [AIAA PAPER 72-1081] 03 p0308 A73-13404
- Urban-change detection systems - Remote-sensing inputs. 03 p0301 A73-13845
- Parametric and nonparametric classification techniques for pattern recognition in remote sensed data processing, noting crop identification 03 p0281 A73-14485
- Imaging radar techniques for remote sensing applications. 03 p0278 A73-14486
- Automatic digital image processing for remote sensing with ERTS, Skylab and NASA survey aircraft, considering image registration, projective transformation and ground truth information 03 p0309 A73-14487
- Linear integral equation, wave function and parameter optimization for numerical analysis of remote sensing problem 03 p0337 A73-14488
- Remote sensor for atmospheric physical properties with FM-CW scanning radar, parabolic antennas and waveguide feeds for linear and circular polarization 03 p0339 A73-14544
- The evaluation, conservation, and international development of terrestrial resources from outer space 04 p0523 A73-15143
- Spectroscopic remote sensing of lunar surface composition. 04 p0448 A73-15181
- Autonomous satellite navigation from strapdown landmark measurements. 04 p0474 A73-15266
- Data handling and analysis for the 1971 corn blight watch experiment. 04 p0443 A73-15402
- Information transfer satellite system/ITSS/ design for earth resource and meteorological data collection and relay from remote sensing platforms 04 p0419 A73-15404
- Earth resources sensing technology - 24-channel multispectral sensor system development. 04 p0449 A73-15463
- Parameter optimization technique for remote radio probing and diagnostics of inhomogeneous media with properties variation along single dimension 04 p0422 A73-15478
- Remote sensing of earth resources and the environment; Proceedings of the Seminar-in-Depth, Palo Alto, Calif., November 8, 9, 1971. 04 p0450 A73-15766
- Remote CAT detection by IR scanning of atmospheric temperature profiles, discussing flight tests design and results 04 p0450 A73-15767
- Large ruby laser radar for remote detection and recording of atmospheric scattering data, describing tracking mount, optics, electronic signal processing and display features 04 p0433 A73-15768
- Tunable dye lidar techniques for measurement of atmospheric constituents. 04 p0423 A73-15769
- Electro-optical multiband cameras for spaceborne remote sensing, discussing optical multiplexing, return beam vidicon, intensifier vidicon storage tube, image spectrophotometer and dissector 04 p0450 A73-15770
- Error minimization methods for Planck law remote measurements of single and two color temperature, considering multiple wavelengths 04 p0445 A73-15773
- Prototype data processing system design for automatic correlation of earth resources image data collected from remote sensors and gyrating vehicle platforms 04 p0426 A73-15776
- Surface winds from sun-glitter measurements from a spacecraft. 04 p0474 A73-15777
- Ocean color measurements utilizing a noon orbit for earth resources satellite applications. 04 p0445 A73-15778
- High altitude remote spectroscopy of the ocean. 04 p0451 A73-15779
- Optical design of an imaging spectral radiometer for earth resources applications. 04 p0451 A73-15780
- Satellite-borne solid state multispectral image remote sensors with photodiode linear arrays for data acquisition, noting system performance and reliability advantages 04 p0451 A73-15781
- Remote sensing of the near-surface moisture profile of specular soils with multi-frequency microwave radiometry. 04 p0446 A73-15782
- An airborne Ka-band microwave radiometric measurement mapping system. 04 p0451 A73-15783
- Measuring rocket attitude by starlight. 05 p0594 A73-16300
- Remote sensing for healthier crops. 05 p0569 A73-16745
- Remote sensing of earth resources; Proceedings of the Conference on Earth Resources Observation and Information Analysis Systems, Tullahoma, Tenn., March 13, 14, 1972. Volume 1. 05 p0571 A73-17126
- Considerations and techniques for incorporating remotely sensed imagery into the land resource management process. 05 p0642 A73-17127
- A critique of remote sensing evaluation techniques. 05 p0571 A73-17129
- Earth resources remote sensors operation and potential, explaining atmospheric transmission and scattering and radiation polarization 05 p0578 A73-17130
- Remote sensing techniques in evaluating earth resources - A study of potential uses of remote sensing for Southeastern U.S. 05 p0642 A73-17131
- Remote sensing applications in urban and regional planning in the Los Angeles metropolis - Problems and accomplishments. 05 p0642 A73-17132
- Legal aspects of water pollution detection through remote sensing. 05 p0642 A73-17138
- Diffusion coefficients and current velocities in coastal waters by remote sensing techniques. 05 p0572 A73-17141
- A digital processing and analysis system for multispectral scanner and similar data. 05 p0554 A73-17147
- Variance reduction in remotely sensed multispectral data caused by random noises and systematic variations in system angular response and in apparent scene radiance 05 p0554 A73-17148
- Texture dependent features recognition in terms of spatial frequencies of remotely sensed multispectral data small sections 05 p0555 A73-17152
- Automatic classification by sequential statistical variance and K-means clustering techniques for remote multispectral earth resource observation data 05 p0555 A73-17154
- Experience with the cross-beam photometer system. 05 p0579 A73-17156
- Luminescence signatures induced by lasers with enhanced specificity for remote active sensing. 05 p0585 A73-17157
- Satellite oceanographic measurements and observations and required sensors assessment, noting benefits to marine and coastal interests and to weather forecasting [AIAA PAPER 73-11] 06 p0690 A73-17605
- Remote sensing application to the fisheries environment. 06 p0690 A73-17606
- Microwave remote sensor technology review, discussing target-sensor interaction, spatial resolution concepts and meteorological applications of radiometric and radar systems 06 p0667 A73-18278
- Radar imagery and aerial photography for geological remote sensing applications in coastal mapping, landform analysis, engineering and reconnaissance 06 p0667 A73-18282
- Lidar illuminator/sensor system for range and/or angle spatial resolution enhancement, discussing pulse shape, optical characteristics and atmospheric effects on performance 06 p0667 A73-18303
- Global and local scale satellite surveillance of atmospheric pollution. 06 p0691 A73-18305
- Apollo 17 spacecraft telemetered IR scanner remote sensing data, reduction, discussing use of interpolating and smoothing splines for restored image resolution improvement 06 p0696 A73-18807
- Lunar geology developments by remotely sensed earth-based, moon satellite and unmanned and manned lunar lander observations, discussing moon structure and evolution 07 p0875 A73-19223
- Compact laser radar probes the upper atmosphere. 07 p0834 A73-19573
- An image intensifier spectrometer for remote sensing applications. 07 p0824 A73-19943
- A four-channel scanning photometer for remote sensing. 07 p0824 A73-19944
- Remote probing by laser radar. 07 p0793 A73-19947
- Economical system design for remote data acquisition. 07 p0824 A73-19948
- Natural resources information system. 08 p0961 A73-21707
- Ground based photometric observations of Mars during 1971 opposition, using conventional photography, multichannel spot photometry and dual channel area scanning 09 p1145 A73-22272
- Mandelstam-Brillouin laser light scattering theory and application to atmospheric parameters remote sensing 09 p1094 A73-22327
- Remote sensing of lunar color differences using isoluminous enhancement techniques. 09 p1082 A73-22384
- Radiative transfer model for simulation of airborne remote sensing scanner data under flight conditions in

REMOTE SENSORS

hazy atmosphere with scattering and absorption effects 09 p1077 A73-22386

Remote sensing of the turbulence characteristics of a planetary atmosphere by radio occultation of a space probe. 09 p1146 A73-22427

Remote measurement of wind speed by laser Doppler systems. 11 p1375 A73-25062

Laser application for remote analysis of gaseous air pollutants emission based on Raman scattering, resonance fluorescence or absorption measurements 11 p1375 A73-25399

Near field of scattering by a hollow semi-infinite cylinder and its application to sensor booms. 11 p1328 A73-25658

Microwave radiometric observations of simulated sea surface conditions. 11 p1355 A73-25774

Lunar composition from Apollo orbital measurements. 11 p1422 A73-25956

Level and density sensors using pneumatic repeaters 11 p1364 A73-26099

Remote sensing capability development program planning, discussing world participation in ERTS and alternatives 12 p1500 A73-27951

Remote sensor dynamic imageries produced by stereo systems, discussing line-by-line and section-by-section orientation methods and triple channel recording scheme 12 p1500 A73-27956

Spaceborne imaging sensors planimetric resolution characteristics, describing Apollo, Mariner, ERTS, Jupiter Pioneer, Skylab and Viking imaging systems 12 p1500 A73-27957

Electronic image enhancement in remote sensing by information content reduction before computer read-in, discussing electronic image transformations 12 p1501 A73-27961

Apparatus and techniques for electron beam fluorescence probe measurements. 13 p1612 A73-28365

Cylindrical scan acoustical holographic transmitter/sensor system for ultrasonic under ocean surveillance and NDT applications 13 p1615 A73-28588

ERAF - Proposal for a European Earth Resources Aircraft. 13 p1569 A73-28786

The cloud bright spot. 13 p1619 A73-29238

Spatially filtered helium-neon laser link operation parallel to IR radiometer for real time atmospheric propagation monitoring over short path 13 p1661 A73-29328

Solution of linear equations in remote sensing and picture reconstruction. 14 p1767 A73-29767

A VOR sensor of advanced design - The Bendix RVA-33A. 15 p1909 A73-32454

An ILS sensor for fail operative automand systems - The Bendix RIA-32A. 15 p1880 A73-32461

Carbon dioxide laser technological advances and applications including frequency stability systems, remote sensing, air pollution detection, optical heterodyning and pumping 16 p2023 A73-32860

Remote sensing and photointerpretation, discussing black and white, color and IR photography, microwave imagery, atmospheric attenuation, reflectance and potential application for ERTS satellites 16 p2014 A73-33100

Operational remote sensing; Proceedings of the Seminar, Houston, Tex., February 1-4, 1972. 16 p2002 A73-33351

Improved Tiros Operational Satellite and future near-polar orbiting environmental system, discussing scanning radiometer and vidicon and automatic picture transmission camera remote sensors 16 p2015 A73-33352

Physiological factors and optical parameters as bases of vegetation discrimination and stress analysis. 16 p2003 A73-33355

Remote sensing in a circulatory survey of Boston Harbor. 16 p2003 A73-33356

Airborne remote sensing of Georgia tidal marshes. 16 p2003 A73-33359

Thermal mapping at electrical power generating sites for outfall from fossil or nuclear fuel plants, considering airborne application 16 p2015 A73-33360

Airborne photography with multispectral scanners for remote sensing of large area features, discussing cost and feasibility of computerized pattern recognition and automatic identification 16 p2015 A73-33361

Cartographic applications of high-altitude aircraft photographs. 16 p2016 A73-33362

Utility of remote-sensing data for urban land use planning. 16 p2003 A73-33363

Applications of high-altitude remote sensing to coastal zone ecological studies. 16 p2003 A73-33364

Evaluation of remote sensor imagery for military geographic information. 16 p2016 A73-33365

Remote sensing of atmosphere and ocean by lidar, radar, bistatic radio, IR optics, microwave radiometry, crossed-beam correlation, etc 16 p2003 A73-33368

High altitude aircraft water vapor measurements using aluminum oxide hygrometer, noting comparison with remote sounders [AIAA PAPER 73-511] 16 p2006 A73-33549

Monitoring earth's resources from space. 17 p2157 A73-34279

Aircraft wake vortex avoidance system for safety management and capacity optimization in airport operations related to ATC, considering various sensors and display subsystem requirements 17 p2166 A73-34613

The control of the terrestrial environment from space: International collaboration, methods and technologies; International Conference on Space, 13th, Rome, Italy, March 22-24, 1973, Proceedings 17 p2160 A73-34926

The use of remote sensing for the detection of natural resources - Definition of the platforms, technical-organizational considerations 17 p2160 A73-34930

Satellite remote monitoring of earth environment and natural resources by high resolution multispectral scanners for European requirements 17 p2160 A73-34931

Airborne remote sensing for forestry and agricultural land imagery and water pollution detection, discussing use of color films and picture processing 17 p2161 A73-34933

Critical analysis of the results obtained by SIRS-A in remote sensing of the temperature field over the Mediterranean 17 p2205 A73-34936

Key technological challenges of the Earth Resources Technology Satellite program. 17 p2161 A73-34943

Airborne and satellite remote sensing of Anacapa Island for hydrology and aquatic biology. 17 p2161 A73-34944

Remote sensing applications in agriculture and forestry including land inventories, soil classification and water resources detection 17 p2162 A73-34948

The use of satellites for remote sensing of the sea surface 17 p2162 A73-34956

IR line scanners using stereoscopic techniques for aerial remote sensing of topography, discussing pivoting mechanism, scanner cameras and scan planes 17 p2168 A73-34957

Passive microwave radiometry and its potential applications to earth resources surveys. 17 p2162 A73-34958

Solid state null tracking Doppler radar ground velocity sensor for supersonic weapon delivery aircraft precision bombing, discussing design and test with computer simulation 17 p2137 A73-35209

Modular MOS LSI digital data bus system design for integrated avionics and remote sensors interconnection in aerospace vehicles 17 p2139 A73-35232

Astronomical observations with television-type sensors; Proceedings of the Symposium, University of British Columbia, Vancouver, Canada, May 15-17, 1973. 17 p2168 A73-35276

Exploration of Mars by Mariner 9 - Television sensors and image processing. 17 p2170 A73-35298

On the measuring of soil moisture by microwave radiometric techniques. 17 p2170 A73-35363

Remote sensing technology - The 24-channel multispectral scanner. 17 p2171 A73-35365

Microwave signatures of first-year and multiyear sea ice. 17 p2163 A73-35466

Spacecraft systems design trade-offs for the Earth Resources Technology Satellite. 17 p2239 A73-35631

Remote sensing using microwave radiometry. 17 p2174 A73-35639

Remote sensing of chlorophyll and temperature in marine and fresh waters. 17 p2164 A73-35664

Remote sensing of complex permittivity by multipole resonances in RCS. 17 p2128 A73-35692

Teledetection experiments using balloons 17 p2176 A73-35815

The preparatory phase of the German Earth Resources program. 18 p2372 A73-35934

Remote sensing techniques for support of coastal zone resource management. 18 p2306 A73-36020

Prospects for physical oceanography from space. 18 p2306 A73-36021

Applications of the ERTS-1 satellite in remote sensing of water resource data in Canada. 18 p2307 A73-36024

Hydrological phenomena teledetection based on multispectral band scanners for IR and visible frequency ranges 18 p2307 A73-36027

A review of some possible uses of remote sensing techniques in fishery research and commercial fisheries. 18 p2307 A73-36031

Remote sensing with VHRR satellite imagery. 18 p2308 A73-36041

Mission planning for remote exploration of the surface of Venus. 18 p2350 A73-36072

Theoretical analysis of improvements in remote sensing of atmospheric and pollutant gases through high resolution detection of individual infrared emission lines. 18 p2315 A73-36252

Teledetection of terrestrial resources by satellites 18 p2373 A73-36390

Use of continuous simulation models in application of remote sensing to hydrology. 18 p2292 A73-36840

Remote viewing system with TV cameras to duplicate human visual field and acuity functions, featuring operator command and data link bandwidth minimization 19 p2416 A73-37319

The oculometer in remote viewing systems. 19 p2397 A73-37320

Application of self-organizing control to remote piloting of vehicles. 19 p2449 A73-37332

A survey study of teleoperators, robotics, and remote systems technology. 19 p2417 A73-37335

Remote sensing - The application of space technology to the survey of the earth and its environment. 19 p2423 A73-37497

The growth of remote sensing through the Nimbus and ERTS spacecraft. 19 p2430 A73-37712

Sensor concept and algorithms for a completely strapdown autonomous navigation approach. 19 p2452 A73-38057

Remote sensing of terrestrial resources 19 p2426 A73-38176

Equipment for checking of terrestrial resources 19 p2431 A73-38177

Remote sensing experiments with balloons 19 p2431 A73-38180

The remote sensing of wind velocity in the lower troposphere using an acoustic sounder. 19 p2427 A73-38208

A note on the FM-CW radar as a remote probe of the Pacific Trade-Wind Inversion. 19 p2448 A73-38211

Remote sensing of the ocean. 19 p2405 A73-38240

The interaction between atmospheric microstructure and acoustic and electromagnetic waves. 19 p2406 A73-38242

Sensor development - An overview of recent Canadian experience. 20 p2533 A73-38578

The use of remote sensing in the USSR for the study of natural resources. 20 p2520 A73-38579

Canadian space programs in communications, navigation and atmospheric science, considering telephony, data transmission, TV broadcasting and remote sensing [AAS PAPER 73-115] 20 p2584 A73-38580

Atmospheric sounding by satellite-borne remote sensors, discussing radiometric measurements of temperature, composition, and reflected and emitted radiance in visible, IR and microwave bands [AAS PAPER 73-125] 20 p2550 A73-38585

Management looks at the Canadian program of remote sensing, phase I, 1971-1975. 20 p2521 A73-38587

Study of laser remote sensing techniques from space platforms. 20 p2521 A73-38591

IR quasi-synoptic global sensing of ocean surface temperature, covering IR theory, airborne radiation thermometry and single band satellite data analysis techniques [AAS PAPER 73-146] 20 p2550 A73-38595

Remote sensing data management from a user's viewpoint. [AAS PAPER 73-152] 20 p2521 A73-38598

A system for continuous remote measurements and automatic recording of nonlinear displacements in testing structural materials in the field of reactor emission

20 p2566 A73-39369

Long range fluidic acoustic sensors cross air currents and temperature gradient effects on operational characteristics and resolution, and prototype design for industrial applications

20 p2511 A73-39753

International Symposium on Remote Sensing of Environment, 8th, University of Michigan, Ann Arbor, Mich., October 2-6, 1972, Proceedings. Volumes 1 & 2.

20 p2556 A73-39829

Development of a practical remote sensing water quality monitoring system.

20 p2567 A73-39830

Organizational design for South Dakota state government to apply remote sensing technology to resources research and management, emphasizing hardware and information dissemination

20 p2629 A73-39831

Remote sensing applications in the Metropolitan Washington Council of Governments.

20 p2556 A73-39833

An integrated resource survey using orbital imagery - An example from south-east Spain.

20 p2556 A73-39834

Enhancement of Earth Resources Technology Satellite (ERTS) and aircraft imagery using atmospheric corrections.

20 p2567 A73-39835

Corn blight epiphytotic remote sensing, data acquisition and crop identification by photointerpretation and computer aided multispectral band scanner data analysis

20 p2556 A73-39836

Remote sensor role in international environmental management, considering monitoring of biosphere, atmosphere and oceans and UN action plan for natural resources

20 p2629 A73-39837

High resolution measurements of snowpack stratigraphy using a short pulse radar.

20 p2556 A73-39842

Remote sensing to detect regional change in land use characteristics, using aerial photo mosaics and high altitude photography

20 p2557 A73-39846

A comprehensive remote sensing legend system for the ecological characterization and annotation of natural and altered landscapes.

20 p2557 A73-39851

Structure of dust storms fromITOS-I T.V. images obtained over Iraq and the Gulf of Persia.

20 p2584 A73-39854

Remote sensing of atmospheric O3 and H2O to 70 km by aircraft measurements of radiation at 1.64 mm wavelength.

20 p2557 A73-39855

Mesospheric ozone concentration night and day variations comparison, describing microwave radiometer and remote sensing and photochemical theories

20 p2557 A73-39857

Airborne remote sensing of cloud particle size and shapes via IR polarimeter, obtaining polarization vs phase angle curve for thick tropical cirrus clouds

20 p2567 A73-39859

Polarimetric mapping techniques using multichannel digital photometry via remote sensors, discussing terrain types, lunar topographic analysis and soil and vegetation mapping

20 p2568 A73-39860

Eutrophication assessment using remote sensing techniques.

20 p2558 A73-39861

Application of a pulsed laser for measurements of bathymetry and algal fluorescence.

20 p2574 A73-39863

Multispectral remote sensing of elements of water and radiation balances.

20 p2558 A73-39864

Remote sensing application to habitat of mosquito vectors of disease, considering St. Louis and Venezuelan encephalitis strains and human filariasis

20 p2520 A73-39866

Water quality determinations in the Virgin Islands from ERTS-A data.

20 p2558 A73-39867

Utilization of thermal infra-red ground measurements for determination of adequate surveying periods in remote sensing.

20 p2558 A73-39868

Thermal structure of the sand desert from the data of IR aerophotography.

20 p2558 A73-39869

Progress report on aircraft gamma-ray surveys for soil-moisture detection at a NOAA test site near Phoenix, Arizona.

20 p2558 A73-39871

Test flight and configuration of Skylark based SL 1081 earth resources rocket prototype with two photographic cameras and earth albedo sensors

20 p2615 A73-39874

Performance evaluation of multispectral scanner classification methods.

20 p2559 A73-39876

Unsupervised maximum likelihood classification technique multispectral remote sensing data, using two-part statistical clustering technique of sequential variance analysis

20 p2559 A73-39879

Atmospheric radiative transfer model for correction of Apollo photographic remote imagery data degradation due to radiation scattering

20 p2559 A73-39881

Remotely sensed multispectral scanner data collection over agricultural area, discussing spatial resolution modification for crops and unresolved objects classification

20 p2559 A73-39882

Environment models and algorithm for obtaining statistically optimal proportions estimates for category mixtures in multispectral sensor data processing

20 p2559 A73-39883

A new method for evaluating and mapping colours in aerial photographs.

20 p2568 A73-39884

Time sensing and analysis of coastal water dynamic features obtained from aircraft and satellite provided sequential photographic data

20 p2560 A73-39885

Southern California coastal processes as analyzed from multi-sensor data.

20 p2560 A73-39886

A statistical-temporal image merging technique for automatic bathymetry applied to southern California coastal waters.

20 p2560 A73-39887

Isothermal mapping of temperature patterns from thermal discharges in Italian coastal waters.

20 p2560 A73-39888

Remote measurement of subsurface sea water temperature by airborne Raman scattering with cross polarizer in front of light source and detector, noting precision

20 p2568 A73-39889

NOAA environmental satellites with IR remote sensors for detection of upwelling off Mexican Pacific Coast and cold water eddies in Sargasso Sea

20 p2560 A73-39890

Remote sensor geological mapping of Rio Grande rift zone/Colorado/ using aerial color infrared photography for compilation of tectonic and geomorphic histories

20 p2560 A73-39893

Ultraviolet, panchromatic, infrared and radar remote sensing of Mesabi Range /Minnesota/, discussing Precambrian rock formations, geological faults, predawn and daytime photography and vegetation patterns

20 p2561 A73-39894

Thermal activity of the Uson Caldera based on infrared and photographic aerial survey.

20 p2561 A73-39895

Crop identification by microwave remote sensing obtained spectral response data from fields with corn, sorghum, soybeans and alfalfa

20 p2562 A73-39902

A comparison of four remote sensing media for assessing salt marsh primary productivity.

20 p2562 A73-39903

Photodensity and the impact of shifting agriculture on subtropical vegetation - A case study in the Bahamas.

20 p2562 A73-39905

Remote mapping of standing crop biomass for estimation of the productivity of the shortgrass prairie, Pawnee National Grasslands, Colorado.

20 p2562 A73-39907

Monitoring levels of existing environmental impact utilizing remote sensing techniques.

20 p2562 A73-39908

The usefulness of ERTS-1 and supporting aircraft data for monitoring plant development in rangeland environments.

20 p2563 A73-39911

Canadian remote sensing programs for ERTS data, describing receiving stations, data acquisition and processing facilities and techniques, digital system and aerial photography

20 p2545 A73-39913

Satellite borne diffused pulsed laser with scattered light detection by optical receiver on ground for applications to wide range geodetic survey

21 p2681 A73-40133

Phased array antennas in ground based remote sensor system, assessing technologies of AN/FPS-85, HAPDAR and AP/TPN-19 radar systems

21 p2672 A73-40645

Polar region soil moisture content remote sensing based on electromagnetic backscattering and depolarization by ice and terrain, considering radar, microwave and IR sensors

21 p2654 A73-40814

Earth surveys by remote sensing in Israel.

21 p2685 A73-40816

Integration of remote sensing data into spatial information systems, discussing data specification, acquisition, storage, retrieval, processing, etc

21 p2658 A73-40820

Assessment of applications of space-borne remote sensing to hydrology and water resources - An overview.

21 p2686 A73-40832

Space research XIII; Proceedings of the Fifteenth Plenary Meeting, Madrid, Spain, May 10-24, 1972. Volumes 1 & 2.

21 p2687 A73-41325

Remote sounding of water surface conditions from aboard artificial satellites.

21 p2657 A73-41333

ERTS-1 satellite-borne multispectral scanner remote sensor for global pollution monitoring, geological and heat balance surveys, and storm and earthquake caused damage

21 p2692 A73-41520

ERTS-1 satellite-borne TV cameras and multispectral band scanners for remote sensing and data collection with applications in agriculture, forestry, and water resources survey

21 p2692 A73-41521

Remote sounding of atmospheric temperature from satellites. IV - The selective chopper radiometer for Nimbus 5.

21 p2706 A73-41601

Inversion techniques for remote sensing of atmospheric temperature profiles.

22 p2883 A73-42056

Remote sensing of atmospheric and surface temperatures with microwaves.

22 p2825 A73-42060

Spectroscopic measurement of upper atmospheric temperature.

22 p2846 A73-42062

Diffraction techniques for vibration measurement. [ASME PAPER 73-DET-116]

22 p2859 A73-42081

Remote probing of atmospheric turbulence.

22 p2884 A73-42620

A direct comparison of satellite and aircraft infrared /10 to 12 microns/ remote measurements of surface temperature.

22 p2850 A73-42729

Remote measurement of salinity in an estuarine environment.

22 p2850 A73-42730

Remote sensing of estuarine circulation dynamics.

22 p2851 A73-42823

Computer techniques for scatterer shape from far field data /inverse scattering/ via remote sensing, with application to antenna radiation pattern synthesis and holography

22 p2828 A73-42845

Instrumentation for remote sensing solar radiation from light aircraft.

22 p2864 A73-43161

Book - The surveillance science: Remote sensing of the environment.

23 p2971 A73-43605

Use of earth resources satellites for supranational inventories of forests and agricultural areas

23 p2972 A73-43779

Remote sensing of the global distribution of total ozone and the inferred upper-tropospheric circulation from Nimbus IRIS experiments.

23 p2975 A73-43876

REMOTELY PILOTED VEHICLES

Electronic warfare tactics against remotely piloted unmanned aircraft used for reconnaissance or weapons delivery, considering onboard countermeasures

04 p0418 A73-15379

Application of self-organizing control to remote piloting of vehicles.

19 p2449 A73-37332

A technology tool for urban applications - The remotely piloted blimp.

22 p2799 A73-42533

Remotely piloted vehicle /RPV/ for reconnaissance, electronic warfare systems, target acquisition, weapon delivery, air-air combat and different combinations

24 p3057 A73-45399

RENES U RAPID EYE MOVEMENT STATE

RENAL FUNCTION

Renal vascular response to saline infusion from radioactive Xe washout and sodium excretion concentration data

01 p0008 A73-10170

Renal component of the antigravitation function of the organism

08 p0929 A73-20976

Morphological changes in the juxtaglomerular apparatus of rat kidneys exposed to the action of diversely directed accelerations for many hours

08 p0929 A73-20978

Effect of ultrafiltration and plasma osmolality upon the flow properties of blood - A possible mechanism for control of blood flow in the renal medullary Vasa recta.

08 p0930 A73-21199

RENDEZVOUS

- Renal lithiasis among civil operating aircrew
08 p0931 A73-21536
- Renal lithiasis among military operating aircrew
08 p0931 A73-21537
- Role of mineralocorticoids in the natriuresis of water immersion in man.
09 p1040 A73-22676
- Activity variations of some renal enzymes during stepwise increased hypoxia
18 p2277 A73-36582
- Russian book - Mutual relationship of water and salt secretion functions in digestive and excretory organs under conditions of high temperature.
21 p2641 A73-41438
- Effect of hypothermia on renal sodium reabsorption.
21 p2641 A73-41623
- Mechanism of 'readjustment' of aorta baroreceptors during hypertonia
22 p2807 A73-42655
- An analogue-computer simulation of the facultative water-reabsorption process in the human kidney - A vascular role for a.d.h.
22 p2815 A73-42668

RENDEZVOUS

- NT ORBITAL RENDEZVOUS
NT SPACE RENDEZVOUS
- Dynamic programming method for constructing stable bridges based on mixed strategies in differential games of rendezvous-evasion
21 p2669 A73-40856

RENDEZVOUS GUIDANCE

- Trajectory optimization of pursuer vehicle for multitarget rendezvous, noting algorithm for dynamic programming
01 p0105 A73-11124
- Optimal energetic characteristics of the parallel guidance method in satellite rendezvous
02 p0219 A73-12456
- Nonlinear stochastic optimal control theory application to guidance policies determination of nonmaneuvering target interception or rendezvous and goal-tending game
03 p0286 A73-14478
- Pontryagin principle for variational problem of controllability region in three dimensional pursuit tracking, noting rendezvous optimal control system
05 p0560 A73-16403
- Constrained low thrust guidance algorithms for three axis and spin stabilized constant power solar electric propelled spacecraft on fixed time rendezvous missions
[ALAA PAPER 73-173] 05 p0595 A73-16917
- Optimum energetic characteristics of the parallel-guidance method of bringing satellites into proximity.
15 p1941 A73-32606
- Results and problems of a theory of final-position control systems with a nonstationary singular feedback
20 p2540 A73-38707
- Study of a method of exponential control of a spacecraft rendezvous
21 p2781 A73-40905

RENDEZVOUS TRAJECTORIES

- Game problem of impulse controlled soft rendezvous of two material points under attraction and control forces
03 p0344 A73-14044
- Earth-based orbit determination for solar electric spacecraft with application to a Comet Encke rendezvous.
[ALAA PAPER 73-174] 06 p0748 A73-17651
- Extremal targeting in a nonlinear rendezvous game
09 p1112 A73-22476
- Necessary termination conditions for difference-differential rendezvous /pursuit with evasion/ game with functional goal set
12 p1524 A73-27401
- Existence solution to linear differential rendezvous game of dynamic system with pursuit and evasion
12 p1524 A73-27402
- Comet exploration - Scientific objectives and mission strategy for a rendezvous with comet Encke.
[ALAA PAPER 73-550] 18 p2353 A73-36496
- Realisation of rendezvous by the transfer orbit which is tangential to the original and terminal orbits.
21 p2779 A73-41550

RENE 41

- Comparison and analysis of residual stress measuring techniques and the effect of post-weld heat treatment on residual stresses in Inconel 600, Inconel X-750 and Rene 41 weldments.
03 p0313 A73-13596
- Stretch formed corrugated Rene 41 panel development for space shuttle booster nose section hot area skin, discussing tooling and formation techniques
[SAE PAPER 720873] 05 p0582 A73-16670
- Eleven ribs and spars made of flat Rene 41 caps based on hot structure concept for thermal environment
16 p2072 A73-33061

REPAIRING

U MAINTENANCE

REPEATERS

- Microwave varactor upconverter in radio repeater for domestic wideband communication satellite, emphasizing transmission characteristics design
01 p0006 A73-11177
- Symphonic satellite radio link equipment design and performance, noting transmission characteristics and frequency response of repeater
07 p0821 A73-18965
- A study on accumulation of waveform distortions in PCM hybrid transmission.
07 p0791 A73-19369
- Time jitter in line regenerators with pattern dependent pulse waveforms.
09 p1062 A73-22301
- 640 Mbit/sec waveguide transmitter at 38 GHz.
09 p1065 A73-23095
- Output signal-to-noise ratio for a random-access repeater link with an ideal hard limiter.
15 p1844 A73-31733
- Multiple-beam satellite repeater tradeoffs applied to a multifunctional system.
20 p2524 A73-38732
- Design of the 14/11 GHz repeater for the European Orbital Test Satellite.
20 p2525 A73-38745
- Communication system with self limiting multiple access repeaters, calculating critical intermodulation power levels resulting from N equal amplitude carriers for comparison with measurements
20 p2526 A73-38750
- High-bit-rate transmissions through a channelized repeater.
20 p2526 A73-38753
- Utilization of miniature diaphragm-leakport devices in fluidic applications.
20 p2511 A73-39752
- Operational global navigation system development program with repeater satellites deployed over continental USA to provide radio links for digital communication, surveillance and ATC
21 p2735 A73-40041
- ATS-1 borne Random Access Discrete Address System for multiple access satellite communication, discussing repeater performance concerning CW signal transmission efficiency, intermodulation and SNR
22 p2825 A73-42187
- Octave-bandwidth, acoustic M/W frequency-memory loop.
22 p2834 A73-42873

REPLACING

- Optimal time calculation for aging complex control system replacement with allowance for downtime losses
05 p0554 A73-16989
- Prediction for a park of helicopters of the same type
12 p1561 A73-27077
- Prediction of optimal maintenance for devices
13 p1625 A73-29136

REPLICAS

- Carbon replicas for fracture failure electron fractography by two stage Lucite technique
05 p0586 A73-16134

REPORTS

- Apollo Experience Reports contents and development, detailing engineering, life sciences, flight crew operations, flight control safety and applications
17 p2256 A73-34300

REPRODUCTION (COPYING)

- NT XEROGRAPHY
Modulated laser beam photographic recorder/reproducer system bandwidth and SNR tradeoff alternatives consideration for high dynamic range performance, suggesting FM recording technique superiority
06 p0701 A73-18309
- Characteristics of interference pattern formation during a self-reproduction process
09 p1096 A73-22858

REPRODUCTIVE SYSTEMS

- NT TESTES
Regulation of testis function in golden hamsters - A circadian clock measures photoperiodic time.
02 p0134 A73-12422

REPUBLIC MILITARY AIRCRAFT

U MILITARY AIRCRAFT

- REQUIREMENTS
General requirements for aerospace powered mobile ground support equipment.
[SAE ARP 1247] 08 p0952 A73-20694

RESCUE OPERATIONS

- Some of the more important problems of international space rescue.
01 p0110 A73-11106
- Unmanned rendezvous applications for space rescue.
01 p0105 A73-11156
- Human threats to air safety; Proceedings of the Twenty-fifth Annual International Air Safety Seminar, Washington, D.C., October 16-18, 1972.
10 p1176 A73-24707

- Post-crash survival planning and procedures, discussing passenger instructions and control, crew training and rescue signalling devices
10 p1176 A73-24711

- Significant elements of an effective search, rescue, and survival system.
10 p1176 A73-24712

- Night search and rescue techniques over sea in poor visibility by helicopter, discussing automatic flight control systems, radar, plotting facility and pilot training
15 p1825 A73-31094

- Performance/stability of midair recovery system with tandem parachute configuration, discussing gliding and nongliding systems
15 p1827 A73-31447

- Aircraft recovery by inflatable wing canopy with steel cable or fiber suspension lines, discussing aerodynamic characteristics, suspension system and centrifugal compressor performance
[ALAA PAPER 73-470] 15 p1828 A73-31454

- Survival and Flight Equipment Association, Annual Symposium, 10th, Phoenix, Ariz., October 2-5, 1972, Proceedings.
16 p1965 A73-32653

- Stowable deployable autogyro aircrew vehicle escape rotoseat /SAVER/ conversion to flight vehicle for advanced escape rescue capability /AERCAB/ from hostile areas
16 p1966 A73-32674

- Electronic location finder radio antenna homing system for helicopter search and rescue of downed aircrewmembers
[AHS PREPRINT 720] 17 p2116 A73-35061

- All-wheel drive fire fighting equipment evolution under impact of wide bodied aircraft introduction
20 p2545 A73-39661

- Skylab flight schedule emphasizing Command Service, Module, discussing meteoroid shield deployment difficulties and rescue team development of solar heat shield
21 p2767 A73-40415

- Skylab 26 day rescue mission diary, describing docking, communications, extravehicular activity, repair work, medical checkouts, physical exercises, solar array problems, etc
23 p3038 A73-43992

RESEARCH

- NT CRITICAL PATH METHOD
NT DYNAMIC PROGRAMMING
NT GAME THEORY
NT HIGH TEMPERATURE RESEARCH
NT LINEAR PROGRAMMING
NT MARKET RESEARCH
NT NONLINEAR PROGRAMMING
NT NUCLEAR RESEARCH
NT OPERATIONS RESEARCH
NT SADDLE POINTS [GAME THEORY]
- Papers on chemistry in space research covering planetary atmospheres, organic compounds, carbonaceous meteorites, liquid and solid propellant rockets, and spacecraft sterilization
14 p1723 A73-30126

RESEARCH AIRCRAFT

- NT B-70 AIRCRAFT
NT X-22 AIRCRAFT
- A description of the NAE T-33 turbulence research aircraft, instrumentation and data analysis.
11 p1306 A73-26269

- NASA research commercial VTOL transport propulsion system specifications and components development, discussing lift fan propulsion method for aircraft attitude control
[ASME PAPER 73-GT-24] 16 p2047 A73-33498

- Measurement of high-altitude air quality using aircraft.
[ALAA PAPER 73-517] 16 p2006 A73-33554

- Testing noise-reducing approach techniques with the HFB 320 research aircraft of the DFVLR
19 p2387 A73-38265

RESEARCH AND DEVELOPMENT

- Bell Laboratories optical communications research and development on lasers, transmission media, principles, methods and components for systems
01 p0060 A73-11212

- Laser related Bell Laboratories research on light scattering, solid state physics, nonlinear optics, materials science, quantum electronics and ultrashort light pulses
01 p0060 A73-11214

- A method for re-allocating funds to meet a reduced budget.
02 p0239 A73-12348

- Reducing the cost of the R&D proposal process.
-02 p0239 A73-12349

- Russian book on jet engines testing covering tests in research and development, design, production and maintenance, test laboratories and stands and automation
04 p0487 A73-15708

- Choices for the future - An industry viewpoint on prototyping.
[SAE PAPER 720848] 05 p0534 A73-16659

Aerothermodynamics R and D for space shuttle configurational design, discussing program organization and wind tunnel testing to generate design technology base
[AIAA PAPER 73-59] 06 p0755 A73-17632
Military contributions to civil aviation.
[AIAA PAPER 73-67] 06 p0647 A73-17635
Space technology transfer to community and industry; Proceedings of the Eighteenth Annual Meeting and Tenth Goddard Memorial Symposium, Washington, D.C., March 13, 14, 1972.
06 p0771 A73-17673
Work carried out by Societe Bertin under contract to CNES in the field of fluidic control
07 p0904 A73-18938
The role of basic research in the total R&D process.
07 p0923 A73-19185
Ducts, nacelles, power source components and cabin noise sources identified for aircraft noise control research, considering prerequisites for quiet operations
[SAE AIR 1079] 08 p0928 A73-20698
The use of dynamic programming techniques for determining resource allocations among R/D projects - An example.
08 p1025 A73-20970
Performance control in government R&D projects - The measurable effects of performing required management and engineering techniques.
08 p1025 A73-20971
A dynamic model of some multistage aspects of research and development portfolios.
08 p1025 A73-20972
R and D organizational resource allocation, discussing attributes of formal evaluation and selection model for management decision processes
08 p1025 A73-20973
Book - Civil aviation development - A policy and operations analysis.
08 p1026 A73-21837
Modular space station operation as general purpose laboratory with attached or free flying R and D modules for specific projects
09 p1152 A73-22325
Research and application problems in fracture of materials and structures in the United States Air Force.
09 p1163 A73-23261
The DOT/NASA Civil Aviation Research and Development Policy Study.
10 p1298 A73-24552
U.S. industry R and D fund cutback caused problems survey by questionnaire, discussing problem minimization with consideration for economic market conditions
10 p1298 A73-24632
Maintaining vitality and productivity in R & D - Steps to maintain high level staff performance.
10 p1298 A73-24633
Project analysis - An evaluation tool for positive development direction.
10 p1298 A73-24634
Research and technology assessment of high power short wavelength molecular lasers, emphasizing carbon dioxide laser efficiency
10 p1229 A73-24654
General aviation requirements within National Aviation System, discussing basic services, facilities, federal spending and R and D
12 p1459 A73-27361
Testing and evaluation community role in weapon system acquisition, describing R and D philosophy
13 p1569 A73-28902
A simple approach to post-evaluation of research.
13 p1708 A73-28926
Aircraft-airport system R and D program in terms of efficient planning, lighting and marking, geometric design, safety and pavements
13 p1598 A73-29103
The air traffic control R & D program of the Federal Aviation Administration.
15 p1908 A73-32437
Civil aviation research patterns, discussing effects of nonregular carrier competition and Boeing 747 introduction
15 p1859 A73-32557
The financing of aircraft procurement.
17 p2257 A73-34534
A survey of behavioral science contributions to laboratory management.
17 p2257 A73-35216
A fundamental methodology for planning and management of research and development programmes.
17 p2258 A73-35836
Emerging aerospace materials and fabrication techniques.
17 p2198 A73-35841
The preparatory phase of the German Earth Resources program.
18 p2372 A73-35934
A new approach to aircraft design education.
19 p2505 A73-37457

Sensor development - An overview of recent Canadian experience.
[AAS PAPER 73-114] 20 p2533 A73-38578
Weather modification activities, discussing state and local funding, research, federal programs, precipitation, hail and warm fog
21 p2729 A73-40092
Management and control of commercial flight test programs.
23 p3050 A73-44057
Research and development of aerospace adhesive bonded systems and concepts.
24 p3093 A73-44763
R and D efforts for various aircraft construction materials, considering steels, alloys and fiber-containing laminates
24 p3100 A73-45198
RESEARCH FACILITIES
German book - Deutsche Forschungs- und Versuchsanstalt fur Luft- und Raumfahrt, Annual Report 1971.
02 p0150 A73-11877
The space environment simulation chamber of Toulouse.
07 p0807 A73-19000
The Toulouse centre's space environment simulator - 'The sun.'
07 p0807 A73-19002
French CNES and Toulouse space center organization and activities, describing installation history
07 p0808 A73-19006
Incoherent ionospheric scatter sounding facility for ionospheric energy balance, neutral atmospheric structure and upper atmosphere dynamics studies
07 p0817 A73-19550
Wind tunnel facilities in India for subsonic, transonic and supersonic aeronautical R and D, describing design layouts, power requirements, operational functions and instrumentation
07 p0808 A73-20249
Performance of a 12-coil superconducting 'bumpy torus' magnet facility.
07 p0809 A73-20460
Culgoora /Australia/ solar radio observatory site, facilities, instrumentation and research activities
10 p1203 A73-24150
The RAE 5m low-speed wind tunnel.
11 p1344 A73-26499
Facility to determine spectra of light scattered at free plasma electrons during single laser pulse, obtaining electron component profiles with high speed streak camera
12 p1506 A73-27301
Resources management logistics support of research and development laboratories.
13 p1709 A73-29574
Sounding rocket and satellite launcher facilities at Kagoshima Space Center, considering physical plant for assembling, launching, tracking and data acquisition
14 p1741 A73-30079
Andoya Rocket Range facilities in northern Norway, discussing rocket launching for auroral research
14 p1741 A73-30082
Water towing tank facility for studies of boundary layers, aircraft ground effects, wakes and unsteady and stratified fluid flows
15 p1858 A73-32041
The shock wind tunnel of the Institute of Aerodynamics and Gasdynamics of Stuttgart University
15 p1858 A73-32042
Monograph - Development of hotshot wind tunnels for hypersonic aerodynamic studies.
15 p1859 A73-32595
Zero Gravity Facility for space vehicle fluid systems research.
16 p1994 A73-33151
Langley Research Center shuttle-compatible spaceborne advanced technology laboratory concept with sortie flight operation mode
18 p2358 A73-36089
Photographic instrumentation in Hyperballistic Range /G/ of the von Karman Gas Dynamics Facility.
22 p2864 A73-43189
NAFEC test facilities.
23 p2966 A73-44063
The capabilities of government test facilities at the Air Force Systems Command.
23 p2966 A73-44065
Aeroballistic range facilities development and application to reentry physics, discussing program for turbulent wake properties of hypersonic projectiles
24 p3054 A73-44993
Research Aviation Facility collected aircraft data processing, merging and enhancement problems, software development and future resource requirements
24 p3070 A73-45088
RESEARCH MANAGEMENT
GREMEX - A management game for the new public administration.
01 p0124 A73-11007

SAGESS /Analytical System for Managing Space Assemblies and Systems/ - A management system applicable to CNES
01 p0124 A73-11252
German book - Deutsche Forschungs- und Versuchsanstalt fur Luft- und Raumfahrt, Annual Report 1971.
02 p0150 A73-11877
The role of basic research in the total R&D process.
07 p0923 A73-19185
The use of dynamic programming techniques for determining resource allocations among R/D projects - An example.
08 p1025 A73-20970
Performance control in government R&D projects - The measurable effects of performing required management and engineering techniques.
08 p1025 A73-20971
A dynamic model of some multistage aspects of research and development portfolios.
08 p1025 A73-20972
R and D organizational resource allocation, discussing attributes of formal evaluation and selection model for management decision processes
08 p1025 A73-20973
Book - Civil aviation development - A policy and operations analysis.
08 p1026 A73-21837
U.S. industry R and D fund cutback caused problems survey by questionnaire, discussing problem minimization with consideration for economic market conditions
10 p1298 A73-24632
Maintaining vitality and productivity in R & D - Steps to maintain high level staff performance.
10 p1298 A73-24633
Project analysis - An evaluation tool for positive development direction.
10 p1298 A73-24634
A simple approach to post-evaluation of research.
13 p1708 A73-28926
A survey of behavioral science contributions to laboratory management.
17 p2257 A73-35216
Management and control of flight test programs of the Western Region FAA.
23 p3050 A73-44053
Management of Air Force test and evaluation activities.
23 p3050 A73-44055
Management and control of flight test programs of the Naval Air Systems Command.
23 p3050 A73-44056
Naval test and evaluation capabilities for aircraft, emphasizing organizational relationships
23 p3051 A73-44066
RESEARCH PROJECTS
Astronomical telescope research programs, emphasizing spectrographic instrumentation to detect and record extragalactic light sources spectra
01 p0046 A73-10502
German book - Deutsche Forschungs- und Versuchsanstalt fur Luft- und Raumfahrt, Annual Report 1971.
02 p0150 A73-11877
ESRO electric propulsion research program, discussing colloid and field emission thruster concepts for different exhaust velocity ranges
04 p0487 A73-15714
Quasi-steady MPD thruster research at Rome University.
04 p0489 A73-15730
Research and applications modules /RAM/ program for manned space research satellites transportation and support, discussing mission requirements and design concepts
[AIAA PAPER 73-72] 06 p0755 A73-17637
Fasp - A student developed application program.
06 p0671 A73-18265
Fatigue and fracture basic research at the Langley Research Center.
06 p0764 A73-18486
French scientific space research progress assessment, noting ionospheric rocket sounding, plasma wave propagation study and absorption technique for upper atmosphere millimetric radiation measurement
09 p1168 A73-23275
U.S., UK and French research programs on conditions encountered by civil aviation and supersonic transports in stratosphere
11 p1455 A73-26594
NASA in general aviation research: Past - present - future
[SAE PAPER 730317] 17 p2257 A73-34675
Water resources systems modelling today and its research opportunities.
19 p2426 A73-38074
Project Cyclops investigation of extraterrestrial civilization signal detection, discussing microwave apparatus, frequency bands, antenna arrays and research implementation proposals
24 p3134 A73-44561

RESEARCH VEHICLES

A rocket system for hypersonic, high Reynolds number aerothermodynamic research.
[AIAA PAPER 73-304] 09 p1156 A73-23223
Possibility of utilizing the ERIDAN rocket probe as an experimental vehicle 16 p2071 A73-32817

Automatic control of the Skylab Astronaut Maneuvering Research Vehicle.
[AIAA PAPER 73-857] 20 p2586 A73-38795

RESERVOIRS

ERTS-1 multispectral scanner analysis of Kansas reservoirs color and water content, discussing turbidity, gray coloration levels, water management possibilities and water sample data 20 p2563 A73-39912

RESIDUAL GAS

Calculation of the pumping characteristic of a turbo-molecular vacuum pump 12 p1461 A73-27475

The VAK-2 unit with heated condenser pumps for obtaining a vacuum better than 0.1 pm Hg 23 p2966 A73-43672

RESIDUAL STRESS

Utilization of polarized ultrasound in stress investigations 02 p0166 A73-11645

Thin walled shells strength dependence on residual stresses, noting stress analysis of shallow spherical shell with variable residual deformations 02 p0232 A73-11932

Plastic material turbine blades adaptability under nonsteady start-stop thermal and mechanical stress cycle conditions, noting residual stress effects 02 p0235 A73-12129

Effect of diamond smoothing on the surface finish and fatigue strength of El961 steel 02 p0174 A73-12141

The influence of oxygen concentration on the internal stress and dislocation arrangements in alpha titanium 02 p0184 A73-12768

Effect of residual or characteristic stresses on the deformation of plates 03 p0385 A73-13143

Investigation of fatigue life and residual strength of wing panel for reliability purposes 03 p0387 A73-13233

Comparison and analysis of residual stress measuring techniques and the effect of post-weld heat treatment on residual stresses in Inconel 600, Inconel X-750 and Rene 41 weldments 03 p0313 A73-13596

Dynamic singularity in the continuum theory of dislocations 03 p0343 A73-13775

Heated rolls application in hot rolling of metals, estimating residual thermal stresses and heat transfer [ASME PAPER 72-WA/MAT-2] 04 p0457 A73-15810
Internal stress and dislocation structure of aluminum in high-temperature creep 04 p0467 A73-15930

Load-time dependent relaxation of residual stresses 05 p0636 A73-17214

Application of elastoplastic modeling studies in determining optimal shapes for plane structures 06 p0760 A73-17782

Sectioning method for residual stress measurement in structural members, describing test procedure, specimen preparation, tools and measuring devices and working conditions 09 p1156 A73-21875

A theoretical study of the effect of the interface on composite toughness 10 p1288 A73-23955

Character and magnitude determination of residual stresses in surface layers of rolling bodies 10 p1289 A73-24068

Heat resistant Ni alloys residual stresses from machining operations, considering cutting rates, temperature, work piece blanks and cutting tools parameter effects 10 p1226 A73-24798

Reinforcing glass fiber preparation effect on fiber wetting by polyethylene melt, analyzing adhesion strength relationship to residual stresses 12 p1516 A73-27178

Theoretical interpretation of residual lattice strains induced in polycrystalline metals by plastic deformation 13 p1639 A73-29460

Further consideration of crack propagation by oscillating crystal X-ray microbeam diffraction technique 13 p1625 A73-29483

Residual surface stress changes dependence on fatigue life and steel specimen size during rotating bending fatigue tests from X ray diffraction study 13 p1625 A73-29485

Machine parts fatigue life and linear cumulative damage at stresses below endurance limit, including plastic strain, microcracking and S-N curves 13 p1641 A73-29496

Thermal stress analysis of metals with temperature dependent mechanical properties 13 p1701 A73-29507

A sandwich-transducer technique for measurement of internal dynamic stress 14 p1751 A73-29773

Minimum potential and complementary energy rate principle formulation for finite plastic deformation, applying to cylindrical shell under uniformly distributed internal load 14 p1809 A73-30258

Optimal conditions for residual stress reduction in a cylindrical shell by local annealing 14 p1814 A73-30721

Internal stress-strain boundary layer theory of shells and orthotropic plates with zero stress conditions at upper and lower planes and edge distance dependent attenuation 14 p1815 A73-30815

A simple model of uniaxial creep recovery and stress relaxation based on residual-stress redistribution 15 p1948 A73-31615

Residual stress measurement and analysis using ultrasonic techniques 15 p1879 A73-32249

Effects of high omnidirectional pressures and residual stresses on the superconductivity of alloys of the V3Si1-xGex system 16 p2027 A73-34062

Acoustic emission coincidence detector for monitoring high residual stress areas in symmetrical pressure vessels 17 p2166 A73-34620

Recognition and control of abusive machining effects on helicopter components 17 p2180 A73-35078

Development and qualification of a magnetic technique for the nondestructive measurement of residual stress in CH-47 A rotor blade spars 17 p2180 A73-35080

The application of strip strain gages for measuring residual surface stresses in beryllium 17 p2191 A73-35438

Residual stresses and mechanical properties of circumferentially wrapped metal-metal composite cylinders fabricated from plasma sprayed Al reinforced with steel filaments 17 p2251 A73-35534

The effect of load interaction and sequence on the fatigue behavior of notched coupons 18 p2364 A73-36589

High strength steel strain hardening residual stresses, discussing rolling treatment, complex strengthening, fatigue strength, asymmetric stress cycles and torsional stress 18 p2323 A73-36762

Residual stress relaxation stability in 13Kh12NVM-FA steel 18 p2323 A73-36763

Measurement of residual stresses in a cylinder. III - On the effect of eccentricity of holes bored out in Sachs method 19 p2501 A73-38345

Calculation of shear-sensitive orthotropic shells with residual stresses 21 p2786 A73-40977

Possibility of predicting the residual stress pattern in boronized steels 21 p2721 A73-41229

Residual-stress measurement using surface displacements around an indentation 21 p2704 A73-41265

Application of strip model to crack tip resistance and crack closure phenomena 22 p2875 A73-42132

Prediction and control of macroscopic fabrication stresses in hoop wound, fiberglass rings 23 p3041 A73-43638

Additive distribution and formation of internal stress in fired magnesias 23 p2998 A73-44133

Some results of the application of the nondestructive ultrasonic method to the measurement of residual stresses 23 p2996 A73-44289

Effect of the characteristics of diamond grinding on the stressed state and strength of hard alloy VK6 24 p3094 A73-44968

A numerical, thermo-mechanical model for the welding and subsequent loading of a fabricated structure 24 p3150 A73-45231

Computational assessment of the numerical influence of the cutting step size and evaluation equation on the precision of experimental and analytical residual-stress determinations 24 p3153 A73-45446

RESIN BONDING

On some relation between the mechanical properties and the bond strength of elastomer to solid inclusion in solid propellant 01 p0090 A73-11117

The influence of interfacial bonding on the properties of carbon fiber composites 10 p1239 A73-23976

Natural and synthetic thermally stable polymers, discussing pyrolysis, structure-property relationships and bond strengths 14 p1724 A73-30132

Competitive processes in joining; Proceedings of the Twenty-sixth Autumn Review Course, Eastbourne, England, October 27-29, 1972 16 p2021 A73-33859

Joining of plastics to plastics and to metals 16 p2021 A73-33861

Enhancement of polymer adhesion to metals by means of additives with crosslink systems 16 p2030 A73-33941

RESINS

NT ACRYLIC RESINS

NT ADDITION RESINS

NT EPOXY RESINS

NT ION EXCHANGE RESINS

NT NYLON [TRADEMARK]

NT PHENOLIC RESINS

NT POLYAMIDE RESINS

NT POLYESTER RESINS

NT POLYETHER RESINS

NT POLYIMIDE RESINS

NT POLYMETHYL METHACRYLATE

NT POLYURETHANE RESINS

NT SYNTHETIC RESINS

NT THERMOPLASTIC RESINS

NT THERMOSETTING RESINS

Resin powder coating technology, describing fluidized bed, electrostatic and plasma spray processes 01 p0058 A73-11513

RESISTANCE COEFFICIENTS

U COEFFICIENTS

RESISTANCE HEATING

Bibliography on Resistance Welding, 1950-1971 01 p0058 A73-11374

Quiet time magnetosphere-thermosphere couplings, describing global wind system model and convection and auroral Joule heating 02 p0162 A73-12292

Character of acoustic dispersion in plasma 06 p0726 A73-17403

Heat exchange between gas and air cooled porous metal plate prepared from stainless steel powder under induction and resistance heating 06 p0768 A73-18129

Adaptation of resistance welding techniques to hot staking 07 p0831 A73-20268

Investigation of the failure characteristics of electrically heated samples of heat-resistant steels and alloys in a high-pressure oxidizing flow 09 p1069 A73-21980

The load life characteristics of thick-film resistors 09 p1065 A73-23048

Electrothermal annealing via electrical heating in vacuum for improved plasticity of thin walled molybdenum alloy elements after cold working 09 p1107 A73-23196

Methods and means of studying the characteristics of heat-resistant strain gauges by means of devices heated by electric current 11 p1362 A73-25457

Iron silicate disproportionation by ruby laser and static heating in resistance furnace, discussing X ray diffraction patterns 11 p1409 A73-25901

Joule heating effect due to currents in the equatorial electrojet as observed by rocket borne probes 18 p2310 A73-36128

Dynamic thermal properties of IMPATT diodes 19 p2411 A73-38459

Temperature and stress fields in a cylindrical shell subjected to induction heat treatment 21 p2787 A73-41233

Ion temperature in the case of ohmic heating of the plasma in the 'Uragan' stellarator 22 p2893 A73-42382

Investigation of temperature pulsations accompanying the heating of a laminar sample by alternating and pulsating currents 23 p3048 A73-43446

A square-law voltmeter based on elements with a thermal coupling 24 p3071 A73-44544

RESISTANCE THERMOMETERS

Intermediate resistance standards for low resistivity resistance thermometer calibration, discussing accuracy requirements and error analysis 02 p0167 A73-11866

Impurities effect on platinum resistance thermometers temperature reading accuracy, presenting empirical formula for approximate error estimate as function of operational conditions 03 p0307 A73-13193

The design of broad-band resistive radiation probes 03 p0310 A73-14492

An improved thin-film gauge for shock-tube thermal studies 06 p0696 A73-18845

Copper resistance thermoanemometer for channel unsteady air flow rate measurement, discussing design, operation principles and maximum error
07 p0823 A73-19623

Transient functions to estimate thermal inertia of gas temperature sensors with film resistance thermometer mounted on wedge shape insulating base
09 p1081 A73-22346

Sensitive platinum film resistance thermometers for heat transfer measurement.
09 p1083 A73-22509

An empirical function between the resistance and the temperature of a carbon thermometer for 0.3 to 4.2 K.
13 p1618 A73-29071

The dimensioning of resistance thermometers with an output parameter which is proportional to the temperature
14 p1754 A73-30922

Self balancing ac resistance bridge design with digital readout for low temperature carbon resistance thermometers
21 p2659 A73-39921

A survey of thermometric characteristics of recently produced Allen-Bradley/Ohmite resistors.
22 p2854 A73-41996

Mixed particle sizes in fast carbon thermometry.
22 p2854 A73-41997

Thermistors as cryogenic thermometers.
22 p2854 A73-41998

Germanium resistance thermometers for cryogenic temperature precision measurement, discussing design technology, resistance-temperature characteristics types, installation and measurement methods
22 p2854 A73-41999

Germanium resistance thermometers - Resistance vs. temperature and thermal time constant characteristics.
22 p2854 A73-42000

Representation of the temperature-resistance characteristic of germanium thermometers below 30 K.
22 p2854 A73-42001

Platinum resistance thermometry below 13.81 K.
22 p2854 A73-42002

Intercomparison of standard platinum thermometers calibrated on IPTS-68 between 13.81 and 273.15 K.
22 p2854 A73-42003

A rhodium-iron resistance thermometer for use below 20 K.
22 p2855 A73-42004

High temperature platinum resistance thermometry.
22 p2855 A73-42005

Platinum resistance thermometry up to the gold point.
22 p2855 A73-42006

Stability of 25 ohm platinum thermometer up to 1100 C.
22 p2855 A73-42007

The high temperature stability of platinum resistance thermometers.
22 p2855 A73-42008

The influence of crystal defects in platinum on platinum resistance thermometry.
22 p2855 A73-42009

Platinum resistance thermometer as standard instrument for interpolation on International Practical Temperature Scale, discussing design development, operational characteristics and errors
22 p2855 A73-42010

Calibration of platinum resistance thermometers.
22 p2855 A73-42011

Reproducibility, stability and linearization of thermistor resistance thermometers.
22 p2855 A73-42012

Unique platinum resistance temperature sensors for lunar heat flow measurements.
22 p2855 A73-42013

Amorphous alloy resistance thermometer development.
22 p2856 A73-42015

Low temperature thermometry in high magnetic fields.
22 p2856 A73-42017

A fixed point calibration procedure for precision platinum resistance thermometers.
22 p2857 A73-42026

Calibration of capsule platinum resistance thermometers at the triple point of water.
22 p2857 A73-42027

The use of operational amplifiers to generate precise current ratios for platinum resistance thermometry.
22 p2832 A73-42028

Comparison of temperature sensors for space instrumentation.
22 p2859 A73-42064

RESISTIVITY
U ELECTRICAL RESISTIVITY
RESISTOJET ENGINES
Propulsion system performance for satellite attitude and orbit correction, discussing hydrogen, ammonia and hydrazine resistojets
[DGLR PAPER 72-078] 02 p0203 A73-11697

Resistojet and plasma propulsion system technology.
[AIAA PAPER 72-1124] 03 p0355 A73-13436

Hydrogen resistojets for primary propulsion of communications satellites.
04 p0489 A73-15741

Ammonia resistojet development for satellite stabilization and position control with 5-year service life, discussing dissociation catalysis research and high efficiency heat exchanger design
07 p0867 A73-18932

RESISTOJET
U RESISTOJET ENGINES
RESISTORS
NT PRINTED RESISTORS
NT THERMISTORS
Thin film and thick metal film technology comparison and production cost analysis, emphasizing thin film resistors application in hybrid circuits
01 p0026 A73-11399

Loss compensation in the case of filters with additional resistors
03 p0284 A73-14124

High reliability technology assessment for metal film resistors production, discussing qualification tests
07 p0829 A73-18921

French Concerto aerospace part procurement program contribution to mass produced electronic component reliability assessment, control and improvement based on tin oxide resistor experience
07 p0829 A73-18923

Thin film nickel-chromium resistor failures in integrated circuits.
08 p0944 A73-20746

Tantalum-glass cermet thin-film resistors.
08 p0945 A73-20809

The load life characteristics of thick-film resistors.
09 p1065 A73-23048

Topological design of thin-film resistors with the aid of a digital computer
09 p1066 A73-23119

Integrated neuristor lines based on p-n-p-n structures with diffused resistors
10 p1193 A73-23727

Analog voltage squaring circuits with series-connected resistors shunted by semiconductor diodes or ladder network, discussing design, construction and operation principles
12 p1481 A73-27591

Photoelectric servo simulator for pupil, using Wheatstone bridge with CdS light dependent resistor
14 p1722 A73-30399

An elusive open-circuit failure mode in thin-film chip resistors.
19 p2410 A73-38444

Ion implanted megohm silicon monolithic IC resistors with buried n-guard layer protection against sice-to-slice variations of fixed surface charge
20 p2537 A73-39416

The Ebers-Moll effect transistor used as a low-value controlled resistor in ACC and other variable-gain applications.
21 p2661 A73-40229

A bilevel thin film hybrid circuit containing crossovers, resistors, capacitors, and integrated circuits.
21 p2669 A73-40773

Fluid pad resistor for linear laminar flow resistance between parallel plates with emphasis on fluidic circuits application
23 p2945 A73-43425

RESOLUTION
NT ANGULAR RESOLUTION
NT HIGH RESOLUTION
NT RADAR RESOLUTION
NT SPECTRAL RESOLUTION
Determination of chromatographic resolution for peaks of vast concentration differences.
01 p0014 A73-10225

The resolution of flaw depth of angle probes for ultrasonic testing
01 p0056 A73-10589

The prediction of resolving power of air and space photographic systems.
02 p0171 A73-12567

Multiple overlapping signal decomposition in noisy environment by inverse filtering, considering tradeoff between resolution and output SNR, and optimum pulse duration
03 p0277 A73-13908

Optical resolution of aspartic acid by using copper complexes of optically active amino acids.
07 p0789 A73-20457

Establishment of a relationship between the frequency and contrast characteristics of objects on aerial photographs and the resolving power
08 p0963 A73-21024

The use of image quality criteria in designing a diffraction limited large space telescope.
08 p0969 A73-21730

Energy resolution of scintillation counters employing a light guide
09 p1085 A73-23004

Subgrid resolution achievement by spline fitting during flow and force field sources conversion from

Lagrangian distribution onto Eulerian grid and interpolation
10 p1248 A73-23603

The detection and resolution of incoherent objects by an aberrated optical system in the presence of background noise.
10 p1229 A73-24618

Gas-liquid chromatographic resolution of several protein amino acid enantiomers on a packed column.
10 p1186 A73-24658

Spaceborne imaging sensors planimetric resolution characteristics, describing Apollo, Mariner, ERTS, Jupiter Pioneer, Skylab and Viking imaging systems
12 p1500 A73-27957

The resolving power and the modulation transfer function of terrestrial and aerial cameras in working conditions.
12 p1501 A73-27963

Influence of illumination on the temporal resolution of photomultipliers
16 p1988 A73-33273

Characteristics of the U.B.C. television systems.
17 p2169 A73-35288

Influence of the resolution of television cameras and radiometers on the accuracy of determining the quantity of clouds from satellites
21 p2731 A73-40493

Chromatic aberration effects on inelastic image resolution for high voltage electron microscopes
21 p2702 A73-40789

Characteristics of thin-film metal arrays for laser-beam information storage.
22 p2869 A73-42254

Optical system imaging in partially coherent light, noting Rayleigh criterion insensitivity to aberration as characteristic of two-point resolution criteria
22 p2889 A73-43187

The Saturn rings in 1969: Morphological and photometric study. II - Deconvolution of the raw photometric curves
24 p3128 A73-44435

RESOLUTONS
U PROBLEM SOLVING
RESOLVING POWER
U RESOLUTION
RESONANCE
NT CYCLOTRON RESONANCE
NT ELECTRON PARAMAGNETIC RESONANCE
NT FERROMAGNETIC RESONANCE
NT MAGNETIC RESONANCE
NT MAGNETOSONIC RESONANCE
NT MICROWAVE RESONANCE
NT NUCLEAR MAGNETIC RESONANCE
NT NUCLEAR QUADRUPOLE RESONANCE
NT OPTICAL RESONANCE
NT PARAMAGNETIC RESONANCE
NT PLASMA RESONANCE
NT PROTON MAGNETIC RESONANCE
NT PROTON RESONANCE
NT RESONANT VIBRATION
NT SPIN RESONANCE
Normality condition derivation for algorithm of first order solution to ideal resonance problem, applying to critical inclination of oblate planet satellite
01 p0077 A73-10686

Resonance, particle trapping, and Landau damping in finite amplitude obliquely propagating waves.
02 p0197 A73-12068

Resonances of an antenna associated with the excitation of ion Bernstein modes.
02 p0198 A73-12071

Steady state conditions for maximal and minimal energy transfer between any load form and any system displacement shape, examining coincidence and resonance
02 p0194 A73-12604

Pressure of radiation due to the absorption of resonant light
03 p0318 A73-13604

Single circuit amplifier design characterized by cascade connections of transistors to resonance network
03 p0284 A73-14036

Resonance rotation of celestial bodies and Cassini's laws.
03 p0377 A73-14275

Amplification of signal by Cerenkov resonance interaction.
04 p0415 A73-14958

Resonances and encounters in the inner solar system.
04 p0500 A73-15519

Application possibilities of atomic resonance absorption spectroscopy in vacuum metallurgy.
04 p0455 A73-15754

Low order spatial modes principal resonance region of in-plane loaded skew stiffened plate, obtaining equation of motion by Hamilton principle
[ASME PAPER 72-WA/APM-32] 04 p0515 A73-15887

Stability analysis of gyroscopic systems for parametric resonance case, allowing for viscous friction at gimbal axes
05 p0578 A73-17085

Three dimensional self oscillating motion study of roll and pitch stabilized vehicle with thrust vector control under resonance, using averaging method
05 p0599 A73-17086

Multiplicity link to transverse momenta in ultrahigh energy nucleon-nucleon interaction processes, considering resonance formation and expected average elasticity
06 p0743 A73-17830

Thermal conductivity and resonant multipole interactions.
06 p0725 A73-18121

Saturation resonances by magnetic mode crossing in optical pumping with a multimode gas laser.
07 p0837 A73-20606

Solar neutrino problem - No low energy He-3 + He-3 resonance.
08 p1000 A73-21530

Satellite resonance with longitude-dependent gravity. III - Inclination changes for close satellites.
09 p1154 A73-22837

Satellite orientation relative to force center, considering condition for maximum lock strength of resonance rotation
09 p1149 A73-22912

Parallel perturbation solution for ideal resonance problem characterized by one degree of freedom Hamiltonian system, considering singularities at separatrix
10 p1283 A73-24666

Resonances in circular arrays with dielectric sheet covers.
11 p1337 A73-25654

Loaded multiport electromagnetic scatterer modal analysis, presenting current resonating procedure
11 p1328 A73-25659

Ionosphere spatial resonance as result of internal gravity wave phase velocity equal to ionization irregularity drift rate
11 p1356 A73-25908

Resonances and librations of some Apollo and Amor asteroids with the Earth.
11 p1429 A73-26688

Point matching /collocation/ computation of transverse resonances by complex valued solutions of Helmholtz equation with Neumann or Dirichlet problems, applying to electromagnetic waveguides
13 p1581 A73-28076

Resonant bipolar linear networks representation by matched equivalent circuits
13 p1589 A73-28121

Measurement by double resonance of Lande factors of the 3 s/2 and 2 p/4 of neon pumped optically by a laser beam
13 p1627 A73-28568

Classification theorem for analytical transformations of second order differential equations of motion at arbitrary resonance based on group theory
13 p1661 A73-29081

Critique of Poincare technique for construction of global solution of resonance of dynamical system, considering procedure using secular terms and regularizing function
15 p1930 A73-31111

Evolution of satellite resonances by tidal dissipation.
15 p1938 A73-31950

Convergence of periodic solutions of differential equations for resonance circuits with nonlinear semiconductor capacitance
17 p2144 A73-34585

Classification theorem for analytical transformations of second order differential equations of motion at arbitrary resonance based on group theory
19 p2445 A73-37632

Coupled superradiance master equations - Application to fluctuations in coherent pulse propagation in resonant media.
20 p2571 A73-38627

AM radio receiver diode resonance circuit design for large signal processing, considering FET pinch-off voltage effects and correct circuit parameter selection
21 p2664 A73-41089

Contribution to the rotorcraft ground resonance theory
22 p2800 A73-43056

The global solution of the problem of the critical inclination.
23 p3031 A73-43836

The formation of resonance lines in multidimensional media. II - Radiation operators and their numerical representation.
24 p3113 A73-45041

The formation of resonance lines in multidimensional media. III Interpolation functions, accuracy, and stability.
24 p3138 A73-45042

Ideal resonance problem for dynamic system of N degrees of freedom, obtaining global solution covering libration and circulation regimes under normality condition
24 p3141 A73-45287

A global solution in the resonance problem of Poincare.
24 p3141 A73-45288

RESONANCE CHARGE EXCHANGE

Rate coefficient calculation for near resonant charge transfer reaction between oxygen cations and hydrogen atoms as function of temperature at thermal energies
02 p0217 A73-12391

RESONANCE PROBES

Electron density profiles in the equatorial lower ionosphere at Thumba.
01 p0043 A73-10908

Measurement of spatial plasma-density distributions with the aid of an open barrel-shaped resonant cavity
09 p1124 A73-21879

Measurement of plasma density distribution using an open barrel-shaped cavity.
17 p2215 A73-34303

RESONANCE SCATTERING

Space maser with feedback
01 p0060 A73-10934

Observation of upper atmospheric constituents by laser radar systems.
01 p0018 A73-11202

Backscatter of solar resonance radiation. II.
02 p0205 A73-11917

Transfer of resonance radiation and photon random walks.
02 p0207 A73-12403

The effects of radiation pressure from resonance scattering in a quasar cloud.
04 p0499 A73-15355

Elastic scattering of negative pions from O-16 in the region of the β , β /3 resonance.
04 p0477 A73-16037

Cosmic maser generator model with resonance scattering feedback for galactic clouds OH molecule radio emission
09 p1147 A73-22729

Observation of the effects of rotational transitions in the resonant scattering of electrons from N₂.
14 p1776 A73-29696

Normalization properties of resonance wave functions of quantum systems associated with poles of Green function in terms of Siegert and Kapur-Peierls energy definitions
14 p1776 A73-30244

Resonant scattering from inhomogeneous nonspherical targets.
14 p1775 A73-30906

Electron impact excitation of N₂. I, II.
16 p2039 A73-33866

Resonance scattering from interstellar and planetary helium.
24 p3140 A73-45188

RESONANCE TESTING

Resonance methods for the dynamic study of deformable structures
19 p2497 A73-37556

Reconciliation of calculated and measured natural frequencies and normal modes.
22 p2929 A73-43136

RESONANT CAVITIES

U CAVITY RESONATORS

RESONANT FREQUENCIES

Determination of attenuation factors from experimental vibrograms of multifrequency attenuating oscillations
02 p0233 A73-11942

A method of estimating the probability of faults in material on cyclic loading.
02 p0236 A73-12221

Free vibrations of elastic systems with discrete dynamic systems attached.
03 p0384 A73-12983

Natural frequencies, forces and moments for liquid propellant sloshing in tilted cylindrical tank as function of tilt angle and liquid depth
03 p0293 A73-13314

A computational method for optimal structural design. I - Piecewise uniform structures.
03 p0390 A73-13337

Resonant frequencies of free vibrating plate via finite difference method, noting difference equations for plate equilibrium
03 p0391 A73-13345

German monograph - Contributions to the calculation of natural frequencies of undamped oscillator chains by the transfer method.
03 p0343 A73-13815

Natural frequencies of a hemispherical shell.
03 p0395 A73-14474

N degrees of freedom system resonant vibration mode and frequencies determination from forced vibration of complementary body
04 p0509 A73-14979

Natural frequencies of a rectangular waveguide filled with a piecewise-homogeneous dielectric
04 p0417 A73-15076

Determination of the natural oscillation frequencies of three-layer circular cylindrical shells by a numerical method
04 p0510 A73-15081

Numerical determination of the sound field and the characteristic frequencies in a circular enclosure by the discretization method
04 p0476 A73-15375

Equations of motion for mathematical models of turbine rotors with elastic shaft in unsteady operation, calculating resonant angular velocity
04 p0514 A73-15654

The vibration of cantilever beams of fiber reinforced material.
05 p0631 A73-16115

Free vibration of a beam with one end spring-hinged and the other free.
05 p0633 A73-16542

The calculation of the natural vibration parameters of a damped system on the basis of the results of a vibration test in an exciter configuration
05 p0634 A73-16758

Use of associated matrices in deriving frequency equations for rods with variable rigidities and masses
05 p0636 A73-17082

Measurement of vibration characteristics by impact testing.
05 p0637 A73-17233

Two dimensional cascade acoustic resonant frequencies estimation by variational method, presenting results for three cavity modes
05 p0599 A73-17372

Group theory application to in-plane vibrations natural frequencies of nth order polygonal particle elastic system, obtaining analytical solution through eigenvalue problem simplification
05 p0599 A73-17373

Zero-g propellant gauging
06 p0755 A73-17573

On the analysis of scattering and antenna problems using the singularity expansion technique.
06 p0665 A73-18184

Resonance characteristics of semiconductor mechanical components.
06 p0676 A73-18344

Natural frequencies and vibration modes determination for skew plates with different edge conditions involving support and clamping based on Ritz variational method
07 p0909 A73-19094

Three dimensional analysis in series form for statics and dynamics of simply supported rectangular plates of micropolar elastic material, obtaining free vibration frequencies
07 p0917 A73-20565

Microwave filters with single crystal YIG sample as ferrimagnetic resonators, determining magnetic field and temperature effects on resonator cut-off frequency
08 p0942 A73-20705

IMPATT diode microwave oscillator performance analysis based on model with ac current and voltage superposition on dc, determining avalanche frequency and negative resistance
08 p0942 A73-20706

A remark on the sloshing frequencies for a half-space.
08 p0953 A73-20788

Free vibrations of square plates with stiffened square openings.
08 p1016 A73-20826

Stability of a gyroscope on a vibrating base under resonance conditions
08 p0972 A73-21763

Absorption of electromagnetic waves by a magnetoactive plasma at parametric-resonance frequencies
09 p1124 A73-21889

The instability of hydrodynamic longitudinal oscillations in a non-uniform magnetoactive plasma.
09 p1127 A73-22285

Development and application of a 0.14 gm piezoelectric accelerometer.
09 p1083 A73-22507

Optimal beam frequencies by the finite element displacement method.
09 p1160 A73-22898

Determination of the modulus of elasticity of metallic and nonmetallic fibers based on bending oscillations
10 p1231 A73-23691

Performance of multifrequency parametric converter with resonant circuits as function of input and parametric diode characteristics, using gain and noise temperature coefficients
10 p1196 A73-24605

Vibrations of segmented shells.
10 p1293 A73-24720

Solar wind He nuclei kinetic temperature, considering resonant heating and proton temperature
10 p1269 A73-24723

Structure statistical identification method based on experimental measurements of natural frequencies and mode shapes to modify finite element model structural parameters
11 p1436 A73-25479

Multiple shaker resonance testing for structural dynamic characteristics, considering natural frequencies, mode shapes, damping and generalized masses [AIAA PAPER 73-402]
11 p1440 A73-25531

European contribution to structural response to noise, [AIAA PAPER 73-332]
11 p1305 A73-25561

On the vibration of shear deformable curved anisotropic composite plates.

11 p1442 A73-25711

Dynamical system of N degrees of freedom reduced to ideal resonance problem involving Hamiltonian function, presenting algorithm for calculating ignorable coordinates

11 p1423 A73-26071

Geometric interpretation of conditions for resonant wave interactions valid under nondispersive conditions, noting relevance for acoustic waves in crystals and slowness vectors

11 p1400 A73-26278

Minimum-mass design of multielement structures under a frequency constraint.

11 p1444 A73-26380

Effect on shell dynamics of a shell mass distributed within a shell surface area

11 p1446 A73-26461

Dynamic stiffness matrix method for determining natural frequencies of plane frame with axially loaded Timoshenko members of uniform mass distribution

11 p1446 A73-26494

In-flight flutter testing methods for determining aircraft structure natural frequencies and vibration damping ratios with air flow
[ONERA, TP NO. 1224]

11 p1306 A73-26593

Autonomous second order system model for nonlinear disturbances of multifrequency systems at resonance, using group properties of differential equation

12 p1524 A73-27404

Asymptotic distribution of the natural frequencies of elastic shells

12 p1524 A73-27452

Selection of optimal rigidities for elastic regions of a mechanical system with resonance oscillations

12 p1524 A73-27473

Optimum design of composite shells subject to natural frequency constraints.

12 p1554 A73-27734

Mathematical observations in structural dynamics.

12 p1555 A73-27739

Approximate dependences for the vibration frequencies of smooth cylindrical shells and for ones with concentrated inclusions

12 p1555 A73-27789

Transverse vibration of membranes of arbitrary shape by the method of constant-deflection contours.

13 p1690 A73-28058

Natural frequencies of a beam considering support characteristics.

13 p1691 A73-28065

Natural vibrations of thin, prismatic flat-walled structures.

13 p1694 A73-28247

Power spectral analysis of Chandler wobble latitude variations over 70 year period, showing doubtfulness of two-peak resonance pattern in wobble

13 p1678 A73-28381

Free and forced vibration analysis of laminated ring structure with elastic inner, outer layers and core, obtaining natural frequency response by variational method

13 p1695 A73-28486

Two coupled nonlinear oscillators driven by sinusoidal input, calculating fractional harmonic frequency pairs relationship to driving and resonance frequencies

13 p1659 A73-28487

Complex resonant frequencies calculation in external diffraction problems for arbitrary shaped bodies, noting Green function poles correspondence to eigenvalue zeros of integral equation

13 p1582 A73-28652

Wave resistance determination in synthesis of oscillatory circuits with homogeneous line segments for given resonant frequencies spectrum

13 p1591 A73-28660

Calculation of the low natural frequencies of clamped cylindrical shells by asymptotic methods.

13 p1696 A73-28752

Use of narrow resonances in methane for frequency stabilization of a 3.39-micron He-Ne laser

13 p1627 A73-28763

Axisymmetric inertial oscillations of a fluid in a rotating spherical shell.

13 p1601 A73-28916

Experimental study by resonance method of unsteady aerodynamic forces acting on cascading blades.

13 p1566 A73-29028

Small perturbation evolutionary motion equations for forced vibrations of quasi-linear two frequency autonomous systems at resonance

13 p1661 A73-29082

Quadratically coupled oscillators interaction at semiresonant frequencies, considering time dependent Duffing equation and frequency divider application

13 p1661 A73-29375

A finite element study of the vibration of trapezoidal plates.

13 p1700 A73-29378

Resonant frequency, fatigue and energy dissipation relations for endurance limit determination in Al alloy specimens under vibrational loads

13 p1643 A73-29618

Free vibrations of shells of revolution with variable thickness.

14 p1805 A73-29768

Tunnel diode oscillator synchronization by external harmonic force with frequency close to generator natural frequency, discussing loading effects

14 p1728 A73-30267

Russian book on elastic structures vibration in aircraft covering integral equations for beams, damping principles and transcendental equations for flexural and torsional vibrations natural frequencies

14 p1810 A73-30354

Optimal shapes of simply supported vibrating elastic beams for maximum fundamental frequency under axial compressive load

14 p1812 A73-30494

Coupled twist-bending waves and natural frequencies of multispan curved beams.

14 p1815 A73-30914

Calculation of natural frequencies and modes of steadily rotating systems - A teaching note.

15 p1946 A73-31123

Mass and stiffness matrices reduction in determining linearly elastic structure natural modes and frequencies with computational accuracy improvement

15 p1949 A73-31672

Lower bounds to the frequencies of continuous elastic systems.

15 p1954 A73-32125

Modal synthesis technique for natural frequencies and mode shapes of bent rectangular beam in flexure-torsion oscillation under six boundary constraint conditions

16 p2075 A73-32792

Application of stress functions to dynamic analysis of shallow shells.

16 p2077 A73-32987

Three layer concentric sphere microwave filter resonators, considering eigenvalue equation for arbitrary conductivity and complex permittivity and permeability effects on resonant frequencies and Q factors

16 p1987 A73-33092

Elastic viscously damped ten degree of freedom system with two torsion-elastically mutually pivotally joined rotors, determining eigenfrequencies by equations of motion numerical evaluation

16 p1968 A73-33235

Effects of attenuation on the stability characteristics in the case of combination resonances

16 p2080 A73-33260

Flexural vibrations of clamped orthotropic plates.

16 p2081 A73-33680

Natural frequencies and normal modes of a four plate structure.

16 p2083 A73-33948

Absorption of electromagnetic waves at parametric resonances in a magnetoactive plasma.

17 p2215 A73-34312

Statistics calculation method for natural frequencies and mode shapes of vibration for structures under external static loads

17 p2242 A73-34527

Quenched-domain mode oscillation in waveguide circuits.

17 p2136 A73-34969

Vibration of plates subject to arbitrary in-plane loads - A perturbation approach.

[ASME PAPER 73-APM-26]

17 p2248 A73-35042

Out-of-plane vibration and stability of curved tubes conveying fluid.

[ASME PAPER 72-WA/APM-36]

17 p2248 A73-35101

Large amplitude forced vibrations of simply supported thin cylindrical shells.
[ASME PAPER 73-APM-Q]

17 p2249 A73-35107

Use of the Singularity Expansion Method in electromagnetic transient scattering problems.

17 p2124 A73-35360

Mass condensation and simultaneous iteration for vibration problems.

17 p2252 A73-35605

Remote sensing of complex permittivity by multipole resonances in RCS.

17 p2128 A73-35692

Properties of microwave cavities containing magnetic resonant samples.

17 p2130 A73-35758

Book - Vibration of linear mechanical systems.

18 p2361 A73-35900

Approximate method for determining the natural frequencies of flexible rectangular plates

18 p2363 A73-36408

Effect of particle collisions in a resonance gas medium on the deformation of laser pulses

18 p2322 A73-36677

Calculation of the natural frequencies and the principal modes of helicopter blades.

18 p2367 A73-37090

Influence of the structure of the material of a three-layered cylindrical shell on the natural frequencies

19 p2494 A73-37184

Three models of the vibrating ulna

19 p2398 A73-37543

Calculation of the eigenfrequencies for a shaft/bearing system with the aid of transfer matrices

19 p2433 A73-37548

Small perturbation evolutionary motion equations for forced vibrations of quasi-linear two frequency autonomous systems at resonance

19 p2445 A73-37633

A quantitative estimate of the effect of the parameters of oscillatory systems on the natural frequencies

19 p2498 A73-37653

Stability of an almost periodic solution to a generalized Duffing equation

20 p2593 A73-39493

Transverse oscillations of a beam lying on an elastic base under the action of a perturbation force which has several harmonics with frequencies close to the first natural frequency

20 p2620 A73-39512

A unified method for determination of fundamental natural frequency of orthotropic plate with arbitrary boundary.

20 p2622 A73-39546

Limiting zero and infinite edge beam stiffness effect on natural vibrational frequencies of reinforced annular plates

20 p2622 A73-39548

Second-harmonic resonance in the interaction of an air stream with capillary-gravity waves.

20 p2550 A73-39816

Free vibration of arches flexible in shear.

21 p2782 A73-40002

Numerical solution of nonlinear resonant wave equation of radiating gas between parallel walls by parametric differentiation

21 p2790 A73-40250

Computer program for determining system resonance frequencies and damping via numerical analysis of vector modal response loci plots

21 p2783 A73-40290

Square plate symmetrically supported at four diagonal points, evaluating fundamental vibration frequency with accuracy by finite element method

21 p2783 A73-40293

A natural frequency analogy between spherically curved panels and flat plates.

21 p2785 A73-40754

Determination of equations of conditions between harmonics of resonance of the order of 14 starting with observations from the Eole satellite

21 p2781 A73-41327

Energy of an equilibrium fluctuating electromagnetic field in matter

21 p2741 A73-41515

Interwire coupling noise and cable resonance equations for fast rise time signal switching at resonant frequencies

22 p2823 A73-41800

Asymptotic distribution of the eigenfrequencies of elastic shells.

22 p2881 A73-41811

In-plane free vibrations of tapered oval rings, determining normal modes and resonant frequencies from differential force and moment equilibrium equations

22 p2918 A73-41818

Random vibration of distributed systems strongly coupled at discrete points.

22 p2918 A73-41820

Free flexural vibrations of elliptical thin plate with free edge, calculating mode shapes and frequencies by use of Mathieu function

22 p2918 A73-41822

Self-resonant LSA oscillator diode of rectangular cross-section.

22 p2832 A73-41895

Effect of support flexibility on the fundamental frequency of vibrating beams.

22 p2918 A73-41966

Cylindrical circular shell vibrational frequencies, examining free surface or solid plane influence on shell natural vibrations in incompressible fluids

22 p2920 A73-42130

Combinational parametric resonance in a gyro-pendulum mounted on a mobile base

22 p2860 A73-42367

Exact hydroelastic solution for an ideal fluid in a hemispherical container.

22 p2843 A73-42631

German monograph on microwave filters for communication channels separation at millimeter wavelengths covering coupling circuits design and resonant frequencies of coaxial resonator

22 p2827 A73-42701

German monograph - Lifetime detection in the case of acoustically loaded structures on the basis of the appropriate form of vibration.

22 p2924 A73-42741

Observation of extraordinary wave propagation near the lower hybrid resonance frequency.

22 p2895 A73-43023

RESONANT VIBRATION

- Critical analysis of the method of M. A. Biot for determining natural torsional frequencies 22 p2867 A73-43047
- Reconciliation of calculated and measured natural frequencies and normal modes. 22 p2929 A73-43136
- Resonance conditions for nonlinear interaction of acoustic gravity waves with viscous damping taken into account 22 p2828 A73-43178
- Experiments on free vibration of shells of revolution. 23 p3039 A73-43384
- An analog investigation of the gas jet resonance tube. 23 p2967 A73-43401
- Electromagnetic resonances and Q-factors of lossy dielectric spheres. 23 p2960 A73-44067
- In-plane vibration of continuous curved beams. 23 p3045 A73-44165
- Linear system resonance effects in single loop controlled frequency tank circuit with variable capacitor under variable or constant emf 24 p3074 A73-44591
- Hydrodynamics in weak gravitational fields - Plane oscillation problems of an ideal liquid in a vessel 24 p3076 A73-44653
- Manufacture and properties of compressor blades made of plastics reinforced with carbon filaments 24 p3122 A73-44880
- Thunderstorm excited cavity resonances between earth and ionosphere measured by solenoidal coil antenna, finding diurnal frequency variations related to solar and geomagnetic effects 24 p3088 A73-45211
- Free vibration of square plates under different boundary conditions, determining opening geometry effects on fundamental frequencies by grid framework model with finite difference operators 24 p3151 A73-45266
- Boundaries of natural frequency variations during the longitudinal oscillations of rods 24 p3152 A73-45360

RESONANT VIBRATION

- Vibrational resonance modes of balanced gyroscope on fixed base, determining gimbal vibration amplitude and gyro drift rate as function of perturbation frequency 01 p0054 A73-11401
- Acoustic resonance during the vibrations of a plate cascade in subsonic gas flow 03 p0294 A73-13619
- HF transverse resonant vibrations of annular Al plates with polychlorovinyl and polyamide base coatings, noting damping and strain relationship to energy dissipation 03 p0394 A73-14009
- N degrees of freedom system resonant vibration mode and frequencies determination from forced vibration of complementary body 04 p0509 A73-14979
- On the phenomenon of parametric resonance of a nonlinear vibrator under the action of electromagnetic force. 04 p0429 A73-15598
- Resonance characteristics of semiconductor mechanical components. 06 p0676 A73-18344
- Small amplitude viscous similarity solution for vertical two dimensional internal wave production by circular cylinder resonant oscillation in incompressible stratified fluid 06 p0646 A73-18527
- Non-linear resonant attitude motions in gravity-stabilized gyrostat satellites. 07 p0905 A73-19162
- Resonances and certain cases of integrability of the motion of a heavy solid about a fixed point 07 p0851 A73-19469
- Monofrequent resonance oscillations with external excitation. 07 p0851 A73-19544
- Determination of the frequency and amplitude of an external force that induces resonance in a linear system with variable parameters 07 p0792 A73-19908
- Calculation of the natural and forced vibrations of circular plates with allowance for energy dissipation in the material 07 p0917 A73-20501
- Contribution to the theory of the resonant thermal self-stabilization in ferroelectric vibrational systems 08 p0948 A73-21519
- Resonant excitation of a circular cylinder with a longitudinal slit by a plane wave 09 p1048 A73-21905
- Digital pressure transducer based on vibrating cylinder frequency response to pressure changes, discussing operational principles and applications 09 p1082 A73-22502
- Cantilever beam dynamic stability under follower force, investigating divergence, flutter and autoparametric resonance relations 09 p1161 A73-23088

- Defect detection in solid materials with the aid of holographic vibration analysis 09 p1089 A73-23115
- Precession motion stability and drift rates of gimbal gyroscope under angular and translational resonant base vibration 09 p1087 A73-23343
- Resonance phenomena associated with nonlinear vibrations of solid bodies 10 p1249 A73-24303
- Subharmonic resonance of order 1/2 with an asymmetrical restoring force. 10 p1292 A73-24649
- Resonant oscillations of conservative system with nonlinear component, obtaining differential equations of motion solution 11 p1448 A73-26731
- Contribution to the theory of the natural vibration spectra of a nonequilibrium resonant cavity 13 p1589 A73-28290
- Normal coordinates in the analysis of the principal resonances of nonlinear vibrating systems with multiple degrees of freedom 13 p1695 A73-28557
- Resonances and some cases of integrability of the motion of a heavy rigid body about a fixed point. 15 p1914 A73-32068
- Resonant excitation of a circular cylinder with a longitudinal slot by a plane wave. 15 p1847 A73-32630
- Satellite waves effects on dynamic behavior of resonant wave-triplet coupling from comparison with isolated triplet in explosive and decay instabilities 16 p2041 A73-33334
- Oscillations of a system with two degrees of freedom during resonance 17 p2213 A73-35591
- Superharmonic resonance in piecewise-linear system - Effect of damping and stability problem. 19 p2459 A73-37669
- Calculation of forced and free oscillations of round plates taking into account the dissipation of energy in the material. 19 p2499 A73-37776
- Simulation of complex excitation of structures in random vibration by one-point excitation. 20 p2617 A73-39269
- Excitation of parametric vibrations in stochastic systems with two degrees of freedom 20 p2594 A73-39641
- Theory of eigenmode spectra of a nonequilibrium resonator. 22 p2830 A73-41814
- Resonant oscillations of intermediate frequency in a stratified atmosphere. 22 p2848 A73-42539
- The dynamic behavior of articulated pipes conveying fluid with periodic flow rate. [ASME PAPER 73-APMW-32] 22 p2925 A73-42892
- Nonlinear gas vibrations maintained in a closed tube by a heat source 23 p2968 A73-43719
- Study and calculation of the vibrations of a rotating rotor with allowance for clearances in the bearings 23 p3041 A73-43725
- Application of harmonic analysis to the calculation of stators with variable blade pitch 23 p3019 A73-43734
- Stability of a biaxial gyroframe on a vibrating base in resonance conditions 23 p3007 A73-44186
- Vibrations of a three-degree-of-freedom gyroscope in transition through resonance 23 p2983 A73-44199
- On the stability limit of nonlinear resonances in multiple-degree-of-freedom vibrating systems. 24 p3146 A73-44681

RESONATORS

- NT CAVITY RESONATORS
- NT MULTIMODE RESONATORS
- NT OPTICAL RESONATORS
- Spectrum of stimulated radiation in a flat-mirror resonator. 02 p0177 A73-12695
- Channel filters with longitudinally coupled flexural mode resonators. 04 p0427 A73-15320
- High level quartz resonators and oscillators 07 p0798 A73-19177
- Optimized design - Characteristic vibration shapes and resonators. 08 p1017 A73-21191
- Equation of motion derived for laser resonator with frequency dispersion effect on emission kinetics and spectral features, analyzing unsteady /transient/ processes 09 p1094 A73-22596
- High power microwave nanosecond pulse generator with waveguide standing wave resonator, noting power gain and pulse shape 13 p1583 A73-28672
- Calculation of dispersion in delay systems composed of resonator sequences with mixed excitation 14 p1733 A73-30028

Three layer concentric sphere microwave filter resonators, considering eigenvalue equation for arbitrary conductivity and complex permittivity and permeability effects on resonant frequencies and Q factors 16 p1987 A73-33092

Parallel resonator with a resistance and a frequency dependent negative resistance realized with a single operational amplifier. 19 p2411 A73-38536

Experimental characteristics of certain types of semi-open, multi-circuit microwave ferrite filters. 20 p2535 A73-38920

Analysis of a resonant amplifier with stagger-tuned circuits at the input and output 20 p2538 A73-39466

Russian book on wideband microwave oscillatory systems covering stepwise and smoothly irregular stripline and coaxial line resonators for radio receivers, multipliers, etc 22 p2832 A73-41881

Use of edge-tone resonators as gas temperature sensing devices. 22 p2853 A73-41991

The development of the quartz resonator as a digital temperature sensor with a precision of .0001. 22 p2854 A73-41992

Ultrasonic thermometry using resonance techniques. 22 p2854 A73-41993

RESOURCE ALLOCATION

- A method for re-allocating funds to meet a reduced budget. 02 p0239 A73-12348
- Multidimensional judgments in design of ideal organisms with integral number of resource units allocated among characteristics such as memory, vision, resourcefulness, etc 03 p0261 A73-13559
- The use of dynamic programming techniques for determining resource allocations among R/D projects - An example. 08 p1025 A73-20970
- A dynamic model of some multistage aspects of research and development portfolios. 08 p1025 A73-20972
- R and D organizational resource allocation, discussing attributes of formal evaluation and selection model for management decision processes 08 p1025 A73-20973
- An innovation index based on factor analysis. 08 p1026 A73-21700
- Optimal sequence for introducing elements of large system into operation, using resource allocation cost criterion 09 p1068 A73-22551
- Design of control and display panels using computer algorithms. 11 p1361 A73-25180
- Improvements in the use of FAA resources for system performance assurance. 12 p1561 A73-27364
- Book - The economics of airborne emissions: The case for an air rights market. 12 p1561 A73-27399
- Resources management logistics support of research and development laboratories. 13 p1709 A73-29574
- Rational distribution of meteorological stations as a problem of operation studies 15 p1903 A73-31604
- Air Force Increase Reliability of Operational Systems computer program and mathematical models for economic logistic resource allocations and cost effective system modification 16 p2088 A73-33627
- Resource exchange and allocation /a generalized thermodynamic approach/. I 20 p2629 A73-39349
- Resource exchange and allocation /a generalized thermodynamic approach/. II 20 p2629 A73-39351
- Use of earth resources satellites for supranational inventories of forests and agricultural areas 23 p2972 A73-43779
- Optimal macroscopic control and resource exchange model for open market-like systems in economic and thermodynamic terms 24 p3154 A73-44665

RESOURCES

- NT EARTH RESOURCES
- NT EXTRATERRESTRIAL RESOURCES
- RESOURCES MANAGEMENT
- NT LAND MANAGEMENT
- Remote sensing techniques in evaluating earth resources - A study of potential uses of remote sensing for Southeastern U.S. 05 p0642 A73-17131
- International space station program for global resources and ecological monitoring and management, reviewing US Skylab and Space Shuttle and USSR Soyuz projects 06 p0757 A73-18026

Apollo program review on resources and technologies utilization, considering budget, radiation and meteoroid hazards, lunar surface, flight design and reliability and Saturn 5 testing 17 p2239 A73-35575

Remote sensing techniques for support of coastal zone resource management. 18 p2306 A73-36020

A review of some possible uses of remote sensing techniques in fishery research and commercial fisheries. 18 p2307 A73-36031

Natural resources research and development in Lesotho using ERTS imagery. 18 p2308 A73-36045

Organizational design for South Dakota state government to apply remote sensing technology to resources research and management, emphasizing hardware and information dissemination 20 p2629 A73-39831

A comprehensive remote sensing legend system for the ecological characterization and annotation of natural and altered landscapes. 20 p2557 A73-39851

RESPIRATION

NT HIGH ALTITUDE BREATHING
NT PRESSURE BREATHING

Cardiorespiratory responses to exercise in air and underwater. 01 p0007 A73-10161

Arterial oxygen increase by high-carbohydrate diet at altitude. 01 p0007 A73-10164

Studies of the electron transport chain of extremely halophilic bacteria. VIII - Respiration-dependent detergent dissolution of cell envelopes. 01 p0009 A73-10625

Control of exercise hyperpnea under varying durations of exposure to moderate hypoxia. 03 p0259 A73-13499

Dynamic aspects of regulation of ventilation in man during acclimatization to high altitude. 03 p0259 A73-13500

Interdependence of oxygen uptake, heart rate and ventilation during treadmill exercise from regression slope analysis of lag logarithms 03 p0263 A73-14118

Absence of appreciable cardiovascular and respiratory responses to muscle vibration. 03 p0263 A73-14119

Respiratory air flow telemetry during exercise, discussing flowmeter working conditions and equipment testing 03 p0270 A73-14286

Oxygen partial pressure measurement in respiratory air via radio telemetry system with polarographic catheter electrode pressure sensor 03 p0270 A73-14287

Radio telemetric measurements of oxygen consumption during exercise via respiratory air flow and oxygen partial pressure monitors, considering water vapor and temperature 03 p0270 A73-14288

Augmentation of chemosensitivity during mild exercise in normal man. 05 p0540 A73-16610

Biological role of atmospheric oxygen in the mechanism of blood coagulation 06 p0650 A73-17678

Electrical operational and pneumatic /variometer/ differentiation recording of displaced volume derivative from pneumotachograph in spontaneous breathing 09 p1046 A73-22937

Threshold Pco₂ as a chemical stimulus for ventilation during acute hypoxia in dogs. 13 p1576 A73-28534

Procedure for preparing an oxygen-nitrogen gas mixture for respiration in a pressure chamber. 13 p1580 A73-29409

Blood pressure and body temperature dynamic control systems and respiration relationship to heart rate variability 14 p1720 A73-30878

Intracardiac heart murmurs and sounds influenced by respiration. 15 p1836 A73-32546

Effect of stepwise adaptation to high-mountain areas on the respiratory function and the acid-alkali equilibrium of blood in subjects with different motor activity stresses 17 p2111 A73-34232

Validation of open-circuit method for the determination of oxygen consumption. 17 p2117 A73-35462

Validity of Haldane calculation for estimating respiratory gas exchange. 17 p2113 A73-35463

Postural effects on respiration, pulmonary ventilation, oxygen uptake and inhalation and exhalation volumes during asana /yoga gymnastics/ exercises executed by athletes 18 p2276 A73-36573

Steady-state equality of respiratory gaseous N₂ in resting man. 18 p2278 A73-36660

Pulmonary volume, respiration rate and alveolar air carbon dioxide content measurements in pilots during flight, noting hyperventilation occurrence 19 p2392 A73-37197

Respiratory changes in the stroke volume of the left ventricle in healthy humans 19 p2393 A73-37397

RESPIRATORS

Respirator cartridge filter efficiency under cyclic- and steady-flow conditions. 21 p2643 A73-40408

RESPIRATORY DISEASES

NT AEROSINUSITIS
NT TUBERCULOSIS

Effects of lung volume and disease on the lung nitrogen decay curve. 08 p0934 A73-21501

Influence of rare-earth metal dust containing radioactive components on the development of reticulosaeroma of the lungs 10 p1183 A73-23680

Age-related characteristics of pulmonary edema development during acute hypoxic hypoxia 10 p1180 A73-23939

Method of PaCO₂ determination in men with functional disorders of external respiration 13 p1579 A73-29075

Development and reversibility of pulmonary oxygen poisoning in the rat. 14 p1718 A73-30516

Evaluation of positive end-expiratory pressure in hypoxemic dogs. 20 p2515 A73-39781

RESPIRATORY IMPEDANCE

Prediction tests for pulmonary elasticity model of expansion stresses in lung region restricted by obstructed airways 03 p0262 A73-14114

A new method for simultaneous measurement of total respiratory resistance and compliance. 05 p0545 A73-16799

Correlation between the impulse activity of bulbar respiratory neurons, the electrical activity of respiratory muscles, and pulmonary respiration volume during obstructed respiration 06 p0650 A73-17683

Mechanics of breathing in high altitude and sea level subjects. 11 p1318 A73-26217

Control of the duration of expiration. 21 p2642 A73-41635

External airway resistance effects on ventilation and carbon dioxide response during human steady state exercise 22 p2806 A73-42417

Submaximal exercise with increased inspiratory resistance to breathing. 22 p2806 A73-42419

Fundamental frequency analysis of pulmonary mechanical resistance and compliance. 24 p3060 A73-45067

RESPIRATORY PHYSIOLOGY

Changes in ventilatory patterns after ablation of various respiratory feedback mechanisms. 01 p0007 A73-10162

Bronchial tree model simulation of pressure-flow-volume relationships during expiration, using gas physics and lung physiology and anatomy data 01 p0011 A73-10169

Biochemical processes during the maturation of erythrocytes - Further results with regard to the action site of the respiratory inhibitor F from reticulocytes in the respiratory chain 02 p0134 A73-12510

Relationship of anginal symptoms to lung mechanics during myocardial ischemia. 02 p0136 A73-12820

Methodical studies concerning the polarographic measurement of respiration and 'critical oxygen pressure' in mitochondria and isolated cells with the aid of the membrane-covered platinum electrode 03 p0272 A73-14647

Responses of bulbar respiratory neurons to apparatus-aided artificial respiration 05 p0541 A73-16699

Correlation between the impulse activity of bulbar respiratory neurons, the electrical activity of respiratory muscles, and pulmonary respiration volume during obstructed respiration 06 p0650 A73-17683

Regional lung volumes with positive pressure inflation in erect humans. 06 p0653 A73-18334

The influence of age, sex, body size and lung size on the control and pattern of breathing during CO₂ inhalation in Caucasians. 06 p0654 A73-18337

Predictions of the dynamic response of the lung. 07 p0785 A73-19477

Mediator systems and respiratory function during an acute lethal loss of blood 07 p0781 A73-19645

Digital computer studies of respiratory control. 07 p0787 A73-20577

A model to predict respiration from VCG measurements. 07 p0787 A73-20578

Respiration mechanics during weightless simulation in an immersion medium 08 p0929 A73-20986

High altitude acclimatization and mountain climbing effects on human organism, considering oculomotor, cardiovascular and respiratory responses and endurance 08 p0930 A73-20991

Mathematical analysis of the responses of the human respiratory system to hypoxia and hypercapnia 08 p0931 A73-21322

Effects of anesthesia and muscle paralysis on respiratory mechanics in normal man. 08 p0934 A73-21505

On-line computer analysis and breath-by-breath graphical display of exercise function tests. 08 p0935 A73-21511

Ventilation measured by body plethysmography in hibernating mammals and in poikilotherms. 08 p0932 A73-21612

Pulmonary respiration and acid-base state in hibernating marmots and hamsters. 08 p0932 A73-21613

A model of time-varying gas exchange in the human lung during a respiratory cycle at rest. 08 p0936 A73-21615

Neuroendocrine, cardiorespiratory, and performance reactions of hypoxic men during a monitoring task. 09 p1044 A73-22527

'Closing volumes' and decreased maximum flow at low lung volumes in young subjects. 09 p1041 A73-22929

Oxygen consumption and its 'critical' tension for the cerebral cortex in situ 10 p1179 A73-23801

Role of the medial area of the medulla oblongata in the rhythmic activity of respiratory-center neurons 10 p1179 A73-23804

Physiological studies of human organism adaptation to high altitudes in temporary and permanent mountain inhabitants, discussing oxygen uptake, lung ventilation and cardiac ventricle hypertrophy 10 p1181 A73-24514

Single breath nitrogen washout method for measurement of functional residual capacity. 11 p1315 A73-25332

Kinetics of oxygen uptake and recovery for supramaximal work of short duration. 11 p1323 A73-25648

Effect of acute exposure to CO₂ on lung mechanics in normal man. 11 p1318 A73-26216

Mechanics of breathing in high altitude and sea level subjects. 11 p1318 A73-26217

Comparison of blood and alveolar gas composition during rebreathing in the dog lung. 11 p1318 A73-26218

Human respiration under increased pressures. 12 p1461 A73-26924

Posthyperventilation breathing - Different effects of active and passive hyperventilation. 14 p1714 A73-29752

Effects of altitude stress on mitochondrial function. 14 p1717 A73-30430

Role of peripheral chemoreceptors in reactions of rats to short and lasting hypoxia 14 p1719 A73-30840

Ventilatory responses to transient hypoxia and hypercapnia in man. 15 p1832 A73-31126

Bulk elastic properties of excised lungs and the effect of a transpulmonary pressure gradient. 15 p1832 A73-31128

Effects of vagotomy on the impulse activity of respiratory neurons 15 p1833 A73-31160

Aspects of air flow to the olfactory region of the human nose 15 p1833 A73-31163

Changes in respiration effectiveness during muscular activity 18 p2277 A73-36580

Gas mixing during breath holding studied by intrapulmonary gas sampling. 18 p2277 A73-36651

Molecular diffusion model of cardiogenic gas mixing during inspiration at alveolar boundary in dogs. 18 p2277 A73-36652

Cardiorespiratory transients in exercising man. I - Tests of superposition. II - Linear models. 18 p2278 A73-36656

Adequacy of the Haldane transformation in the computation of exercise oxygen consumption in man. 18 p2278 A73-36658

Human calorimeter with a new type of gradient layer. 18 p2282 A73-36662

Use of the single-breath method of estimating cardiac output during exercise-stress testing. 18 p2283 A73-36788

- Correlation of ventilatory responses to hypoxia and hypercapnia. 20 p2514 A73-39776
- Force output of the diaphragm as a function of phrenic nerve firing rate and lung volume. 20 p2515 A73-39780
- Ventilatory and hemodynamic responses to acute hypoxia and hypercapnia in Hereford calf, comparing with man 20 p2515 A73-39782
- Anaerobic threshold and respiratory gas exchange during exercise. 20 p2519 A73-39785
- Changes in respiration accompanying a diencephalic vegetative-vascular syndrome under the action of a hypoxic mixture 21 p2636 A73-40280
- A model of diffusion in the respiratory unit. 21 p2645 A73-41638
- Gas transport in the human lung. 22 p2806 A73-42421
- Influence of expiratory flow limitation on the pattern of lung emptying in normal man. 22 p2807 A73-42422
- Differences between inspired and expired minute volumes of nitrogen in man. 24 p3060 A73-45069
- ## RESPIRATORY RATE
- ### NT HYPOVENTILATION
- Passive and active warm-up effects on track athletes heart and respiration rates 03 p0266 A73-13123
- Multichannel PDM-FM biomedical radio telemetry system for ECG, respiratory rate and oxygen consumption during exercise, considering transmitter and receiver design 03 p0269 A73-14278
- Investigations concerning the coordination of heart rate and respiration rate /pulse-respiration quotient/ during exercise 07 p0782 A73-20034
- A respirometer for the continuous measurement of respiration volume with remote transmission 07 p0785 A73-20035
- Respiratory nitrogen elimination - A potential source of error in closed-circuit spirometry. 20 p2512 A73-39113
- Transient ventilatory response to hypoxia with and without controlled alveolar PCO₂. 20 p2515 A73-39777
- Human intrapair twin differences, examining age, height, weight, heart volume, metabolism, respiratory rate and monozygous/dizygous differences 20 p2519 A73-39792
- A system for automatic end-tidal gas sampling at rest and during exercise. 20 p2519 A73-39794
- The significance of an increased RQ after sucrose ingestion during prolonged aerobic exercise. 21 p2641 A73-41621
- Control of the duration of expiration. 21 p2642 A73-41635
- Peak expiratory flow rate and rate of change of pleural pressure. 21 p2642 A73-41636
- Respiratory work minimization during exercise, using respiratory frequency, functional residual capacity and air flow pattern effects as controlled variables 24 p3060 A73-45066
- ### RESPIRATORY REFLEXES
- The role of the vagus nerves in the respiratory response to CO₂ under hyperoxic conditions. 01 p0010 A73-11501
- The role of the carotid chemoreceptors in the CO₂-hyperpnea under hyperoxia. 01 p0010 A73-11502
- Pathogenesis of some respiration and circulation reactions to barometric pressure gradients 08 p0929 A73-20980
- Ventilation at transition from rest to exercise. 24 p3061 A73-45375
- ## RESPIRATORY SYSTEM
- ### NT BRONCHI
- ### NT DIAPHRAGM [ANATOMY]
- ### NT LUNGS
- ### NT NOSE [ANATOMY]
- A system for continuous measurement of gas exchange and respiratory functions. 01 p0011 A73-10172
- Formalization of certain functional aspects of the external respiration system 01 p0012 A73-10657
- Indexes of ventilation distribution before/after airway occlusion in dogs, indicating collateral channel inspired gas distribution reduction 03 p0262 A73-14113
- Effect of hypercapnia on the electrical discharges of the bulbar respiratory neurons and motor neuron ganglia of respiratory muscles 05 p0541 A73-16735
- The influence of change in the functional state of the central nervous system on the course of asphyxia 10 p1179 A73-23937

- Effect of respiration stabilization on hemodynamic reactions during acute hypoxic hypoxia 10 p1180 A73-23938
- The occurrence of nitrate on the early earth and its role in the evolution of the prokaryotes. 11 p1320 A73-26490
- Breath to breath cyclical variations in functional residual capacity, oxygen uptake, carbon dioxide release, tidal volume, respiratory period, alveolar gas tension and heart rate 15 p1834 A73-31346
- On correlation between the changes in cerebellar bioelectric activity and the adaptive reactions under the effect of accelerations. 18 p2279 A73-36915
- Nonthermal metabolic response of rats to He-O₂, N₂-O₂, and Ar-O₂ at 1 atm. 22 p2805 A73-42201
- ## RESPIROMETERS
- A respirometer for the continuous measurement of respiration volume with remote transmission 07 p0785 A73-20035
- A rapid method for determining the CO₂ transport characteristics in man by using a capnograph and a multichannel respirator 22 p2815 A73-42665
- ## RESPONDERS
- ### U TRANSPONDERS
- ### RESPONSE TIME [COMPUTERS]
- Response time in the application of interactive graphics in structural analysis. 13 p1693 A73-28244
- ## RESPONSES
- ### NT DYNAMIC RESPONSE
- ### NT FREQUENCY RESPONSE
- ### NT GALVANIC SKIN RESPONSE
- ### NT HEMODYNAMIC RESPONSES
- ### NT MODAL RESPONSE
- ### NT PHYSIOLOGICAL RESPONSES
- ### NT TIME RESPONSE
- ### NT TRANSIENT RESPONSE
- ## REST
- ### NT BED REST
- A model of time-varying gas exchange in the human lung during a respiratory cycle at rest. 08 p0936 A73-21615
- Oscillations in oxygen consumption of man at rest. 14 p1714 A73-29755
- Steady-state equality of respiratory gaseous N₂ in resting man. 18 p2278 A73-36660
- Plasma insulin and carbohydrate metabolism after sucrose ingestion during rest and prolonged aerobic exercise. 21 p2641 A73-41622
- ## RESTARTABLE ROCKET ENGINES
- Hypergol rocket engines restart difficulties investigation via cold flow and hot firing tests, simulating worst case environmental conditions [AIAA PAPER 72-1160] 03 p0357 A73-13461
- Restart transients of hybrid rocket engines. 11 p1411 A73-26669
- ## RESTRAINTS
- ### U CONSTRAINTS
- ## RESTRICTIONS
- ### U CONSTRICTIONS
- ## RESUSCITATION
- Responses of bulbar respiratory neurons to apparatus-aided artificial respiration 05 p0541 A73-16699
- Organism-machine interactions in hybrid control systems for cardiac stimulation, artificial breathing apparatus and intelligence assignments 09 p1047 A73-23298
- ## RETARDERS [DEVICES]
- UPSTARS - A single escape subsystem providing stabilization, retardation, and separation. 16 p1966 A73-32668
- ## RETENTION [PSYCHOLOGY]
- Effect of ethimazol on short term memory and mental working capacity 06 p0653 A73-18160
- Rapid eye movement state beneficial effects on memory refuted in favor of delta wave slumber, emphasizing stage 4 sleep 06 p0653 A73-18225
- A method for the investigation of interpolated information and time effects in short term retention. 06 p0659 A73-18475
- Retention of information in the iconic visual memory during recognition of images of varying complexity 11 p1323 A73-26084
- Eye movements during visual search and memory search. 13 p1579 A73-29125
- ## RETICULOCYTES
- Biochemical processes during the maturation of erythrocytes - Further results with regard to the action site of the respiratory inhibitor F from reticulocytes in the respiratory chain 02 p0134 A73-12510
- ## RETINA
- ### NT FOVEA
- ### NT VISUAL PIGMENTS

- Airline flight and ground personnel fatigue and orthostatic hypotension syndrome manifested by variations in retinal arterial pressure and brain circulation 02 p0134 A73-12156
- A minor perturbing effect of retinal locus on dot pattern recognition - Rejection of a possible artifact. 02 p0135 A73-12524
- Hydroxyindole-O-methyl transferases in rat pineal, retina and Harderian gland. 02 p0136 A73-12644
- Electrooptical model of the first retina layers of a visual analyzer 03 p0267 A73-13657
- A relationship between the detection of size, rate, orientation and direction in the human visual system. 03 p0261 A73-13758
- Idiopathic central serous retinopathy /choroidopathy/ in flying personnel. 03 p0269 A73-14164
- An optical model of a detector of oriented segments of the visual analyzer in animals 04 p0413 A73-15795
- Visual function as sum of visual acuity and visual field, considering role of resolution and detection tasks in retinal function examinations 05 p0539 A73-16478
- Rod vision chemistry in terms of rhodopsin, visual cycle and pigment-vision relations, considering dark and light adaptation 05 p0540 A73-16479
- Photochemical receptor mechanism of chromatic vision and scotopic contrast hue sensation due to cone and rod activity interaction 07 p0783 A73-20261
- Modified rhodopsin in the pigment epithelium. 07 p0783 A73-20263
- Contrast and assimilation effects analysis based on receptive field models of vertebrate retinal function 08 p0929 A73-20812
- The morphological organization of the vertebrate retina. 09 p1042 A73-23304
- The structure and reactions of visual pigments. 09 p1042 A73-23306
- Inhibitory interaction in the retina of Limulus. 09 p1043 A73-23311
- Frog retinal metabolism in photoreceptors during dark and light adaptation, using ERG, radiopirrometry, oxygen uptake polarography and pyridine spectrophotometric assay 09 p1044 A73-23319
- Effect of light deprivation on the metabolic reaction development in retinal ganglion cells 10 p1178 A73-23681
- Visual acuity as a function of exposure duration. 10 p1184 A73-23838
- Investigation of the infrastructural organization of interdisk spaces and photoreceptor membranes of the retina in vertebrates during aldehyde fixations, delipidization, and pronase treatment 10 p1181 A73-24458
- Deficits in visual function associated with laser irradiation. 10 p1182 A73-24563
- Retinal damage thresholds for multiple pulse lasers. [AD-758530] 11 p1315 A73-25341
- The ultrastructural organization of the photoreceptor membranes and the intradisk spaces of the vertebrate retina as revealed by various experimental treatments. 11 p1321 A73-26717
- Changes caused by illumination in the Na⁺, K⁺ adenosine-triphosphatase and n-nitrophenylphosphatase activities of the external segments of the retina 13 p1574 A73-28294
- Light adaptation of the late receptor potential in the cat retina. 13 p1574 A73-28352
- Electrical and metabolic manifestations of receptor and higher-order neuron activity in vertebrate retina. 13 p1574 A73-28353
- Theoretical models of the generation of steady-state evoked potentials, their relation to neuroanatomy and their relevance to certain clinical problems. 13 p1574 A73-28354
- Retinal damage from repeated subthreshold exposures using a ruby laser photocoagulator. 13 p1576 A73-28508
- Anatomical and neurophysiological investigations of centrifugal control of retinal activity via efferent optic nerve fibers 14 p1714 A73-29875
- The effect of iontophoretically applied acetylcholine upon the cat's retinal ganglion cells. 14 p1715 A73-30061
- Oscillatory waves in intraretinally recorded electroretinograms in primates, considering electrode depth, stimulus duration and intensity and background illumination, anesthesia and tetrodotoxin effects 14 p1717 A73-30393
- Retinal receptive fields - Correlations between psychophysics and electrophysiology. 14 p1717 A73-30397

Servo-controlled moving stimulus generator for single unit studies in vision. 14 p1722 A73-30401

Human cone optical density estimation implications of conflicting results for luminosity at bleaching intensities in dichromats related to use of psychophysical data 14 p1717 A73-30402

Vein wall changes as the main cause of acute disturbance of blood circulation in the Vena centralis retinae system 15 p1833 A73-31173

Retinal vessel reactions and intraocular tension in humans staying in a horizontal position for 120 days 15 p1835 A73-31514

Retinal change induced in the primate /Macaca mulatta/ by oxygen nuclei radiation. 18 p2271 A73-36125

Comparative physiology of movement-detecting neuronal systems in lower vertebrates /anura and urodela/. 18 p2273 A73-36454

Rabbit optokinetic reactions and retinal direction-selective cells /A preliminary model/. 18 p2273 A73-36455

The significance of retinal pathology in ageing aircrew. 18 p2285 A73-36925

Ribes Nigrum anthocyanosides in ophthalmology 18 p2280 A73-36935

Investigation of the geometry of the dendritic tree of retinal ganglion cells 19 p2395 A73-37944

Ocular hazard from viewing the sun unprotected and through various windows and filters. 21 p2698 A73-40143

Possibilities of barotherapy in ophthalmology 21 p2637 A73-40349

Glycogen content in the rabbit retina in relation to blood circulation. 22 p2802 A73-41732

Recovery of cone receptor activity in the frog's isolated retina. 22 p2810 A73-42962

Frog red rod dark adaptation from recorded receptor potentials of isolated retina, examining permanent sensitivity loss due to pigment bleaching 22 p2810 A73-42963

Fluorescent angiographic technique for fundus oculi 23 p2946 A73-43788

Inhibition by selenium of the free-radical states of the retina of the eye 24 p3059 A73-44724

Local resistance variations caused by membrane potential shifts in the interior of the horizontal retina cell 24 p3061 A73-45250

RETINAL ADAPTATION

NT DARK ADAPTATION

NT LIGHT ADAPTATION

Reaction time as a measure of the temporal response properties of individual colour mechanisms. 03 p0267 A73-13757

Visual work duration and intensity effects on optic papillae expansions and shape alterations, noting differences between trained and untrained subjects 05 p0540 A73-16694

Human receptive visual field adaptation characteristics for stabilized retinal images by psychophysical probe detection technique 07 p0782 A73-20252

Psychophysical areal summation and stimulus contour and threshold visibility effects on size selective adaptation in human vision for single- and multichannel models 08 p0931 A73-21563

On neural inhibition, contrast effects and visual sensitivity. 11 p1318 A73-26197

Apparent contraction and disappearance of moving objects in the peripheral visual field. 11 p1318 A73-26198

The influence of wavelength on visual adaptation to spatially periodic stimuli. 11 p1318 A73-26199

After-effects of movement contingent on direction of gaze. 11 p1324 A73-26721

Spectral sensitivities of colour mechanisms isolated by the human visual evoked response. 12 p1461 A73-26919

Cone spectral sensitivity studied with an ERG method. 13 p1575 A73-28358

Monocular contribution to binocular vision in normals and amblyopes. 13 p1575 A73-28359

The macular and paramacular local electroretinograms of the human retina and their clinical application. 13 p1575 A73-28364

Linear summation of spatial harmonics in human vision. 19 p2393 A73-37411

Spatial frequency channels in human vision and the threshold for adaptation. 19 p2394 A73-37416

Non-linearity of visual signals in relation to shape-sensitive adaptation responses. 19 p2394 A73-37418

Disparity detectors in human depth perception - Evidence for directional selectivity. 21 p2637 A73-40413

Comparison of tilt and displacement adaptation in visual perception, establishing qualitative differences by interocular transformation magnitude and exposure time methods 21 p2640 A73-41188

The effect of atmospheric and physiological conditions on the homogeneity of observations of noctilucent clouds 22 p2847 A73-42448

Optimal input rates for tilt adaptation. 22 p2814 A73-42500

Stimulus specificity in the human visual system. 22 p2810 A73-42960

Increment thresholds for multiple identical flashes in the peripheral retina. 23 p2946 A73-43343

Apparatus for measurement of vision acuity restoration time after brief macula lutea exposures to light 23 p2949 A73-43791

RETINAL IMAGES

Extraretinal feedback and visual localization. 01 p0008 A73-10437

Induced retinal image blurring effects on rabbit mid-brain single cell trigger features and response efficiencies, noting receptive field responsive area 01 p0010 A73-11503

Vernier acuity as affected by target length and separation. 03 p0266 A73-13063

Cortical area of neural loci involved in monoptic and dichoptic metacontrast occurring for target and masking stimuli imaged on different retinal regions 03 p0261 A73-13764

Axiomatic mathematical model for human visual edge contrast based on additivity, one-dimensionality and contrast continuity parameters 04 p0413 A73-15788

Visual field image analysis via investigation of receptor-furnished signal analysis by network of neuron-like structures 04 p0413 A73-15789

The stereoscopic frame of reference in asymmetric convergence of the eyes - Response to 'point' stimulation of the retina. 05 p0573 A73-16149

Visibility, resolution and spatial acuities in terms of target-background contrast, diffraction, luminance, stimuli wavelength and anatomical variations effects on retinal images 05 p0542 A73-16477

A model of image-shape analysis based on fiber-optics elements and on the principle of photoelectric conversion 06 p0671 A73-18084

The control of sensitivity in the retina. 06 p0655 A73-18673

Predicting light flashes due to alpha-particle flux on SST planes. 07 p0777 A73-20157

Vernier alignment acuity task accuracy related to retinal image line position location, noting effect of high contrast grating background 07 p0782 A73-20159

Human receptive visual field adaptation characteristics for stabilized retinal images by psychophysical probe detection technique 07 p0782 A73-20252

Intrinsic light brightness and intensity estimation tests for foveal and peripheral retina under photopic and scotopic stimuli 07 p0783 A73-20257

Cyclofusional stimulation effects on retinal image disparity in terms of central component and Panum fusional areas 07 p0783 A73-20265

Saccadic suppression for structured background as function of visual image pattern and threshold detection elevation in central nervous system 07 p0783 A73-20267

Human retina-patterned ideal perceiving machine to calculate visual acuities for spatial arrangement in line figures 08 p0932 A73-21564

Single cell analysis of saturation discrimination in the macaque. 08 p0932 A73-21568

Polarity cue for visual accommodation response of trained subjects to target motion direction change, considering retinal image blur and feedback relation 08 p0932 A73-21569

Peripheral threshold of perceived contrast of the human eye. 09 p1046 A73-22964

Receptive fields of retinal ganglion cells. 09 p1043 A73-23315

RETROREFLECTION

Retinal mechanisms of colour vision. 09 p1043 A73-23316

Pattern recognition based on visual perception relation to transformations and identification by coded sentences 11 p1334 A73-25621

Foveal contrast sensitivity edge effect dependence on test stimulus size, form and duration 11 p1321 A73-26716

Apparent motion of stimuli presented stroboscopically during pursuit movement of the eye. 13 p1577 A73-28093

Scotopic visibility curve in man obtained by the VER. 13 p1575 A73-28356

A clinical method for obtaining pattern visual evoked responses. 13 p1575 A73-28357

Scotopic electroretinography and visual evoked responses under adaptive illumination, comparing blind spot stray light with parafoveal stimulation 13 p1575 A73-28361

New method of stimulation for the study of photoreceptors. 13 p1578 A73-28362

Evidence for non-linear response processes in the human visual system from measurements on the thresholds of spatial heat frequencies. 17 p2112 A73-34839

Extended border enhancement during intermittent illumination - Binocular effects. 17 p2112 A73-34842

Stabilized target visibility as a function of contrast and flicker frequency. 17 p2112 A73-34846

Distance perception and the ambiguity of visual stimulation - A theoretical note. 17 p2117 A73-35492

Stereoscopic vision - Cortical limitations and a disparity scaling effect. 18 p2269 A73-35922

Investigations of the eye tracking system through stabilized retinal images. 18 p2273 A73-36456

Eye movements necessary for continuous perception during stabilization of retinal images. 18 p2273 A73-36461

Visual perception of direction and voluntary saccadic eye movements. 18 p2274 A73-36463

Spatial characteristics of chromatic induction - The segregation of lateral effects from straylight artefacts. 19 p2394 A73-37419

Invariance of visual receptive-field size and visual acuity with viewing distance. 19 p2396 A73-38484

Effect of eye movements on backward masking and perceived location. 21 p2639 A73-41184

Performance decrement, under prolonged testing, across the visual field. 22 p2802 A73-41730

Soviet book on visual image formation on retina covering perception, stabilization, manipulative ability, etc 22 p2810 A73-42869

RETIREMENT

Functional aging - Present status of assessments regarding airline pilot retirement. 21 p2645 A73-41161

RETRACTABLE EQUIPMENT

Solar array concept for a portable retractable oriented power system. 11 p1310 A73-26007

RETRACTABLE LANDING GEAR

U LANDING GEAR

U RETRACTABLE EQUIPMENT

RETRIEVAL

NT DATA RETRIEVAL

NT INFORMATION RETRIEVAL

RETROREFLECTION

The laser telemetry station of the Pic-du-Midi Observatory and the acquisition of the French retroreflectors of Luna 17 02 p0151 A73-12247

Ruby laser ranging experiment for lunar returned signal from Apollo 11 retroreflector package, using multichannel pulse height counter and CRT 02 p0141 A73-12248

Optical properties of the Apollo laser ranging retroreflector arrays. 02 p0141 A73-12250

Structural and thermal design and fabrication of Lunokhod retroreflecting panel mounted on lunar surface for earth-moon distance determination by laser telemetry 02 p0176 A73-12251

Speckle reference beam /by retro reflection/ holography for the real time visualisation of vibration patterns. 16 p2012 A73-32847

A hologram interferometer with a retro-reflected speckle reference beam for the real time visualization of vibration patterns. 16 p2013 A73-32880

RETROCKET ENGINES

Laser range measurement to lunar surface retroreflector, discussing initial Apollo 11 observations and achieved lunar orbit and selenophysical information accuracy improvement

24 p3137 A73-44686

RETROCKET ENGINES

Penetration of retrorocket exhausts into subsonic counterflows.

07 p0773 A73-19491

RETROSEQUENCING

U SEQUENTIAL CONTROL

RETURN BEAM VIDCONS

ERTS two-inch RBV cameras performance characteristics.

05 p0579 A73-17144

ERTs return beam vidicon TV cameras and ground based electron beam recording system resolution and distortion characteristics from preflight and in-flight simulation and calibration studies

09 p1082 A73-22385

Photogrammetric solution for precision processing of E.R.T.S. images.

12 p1501 A73-27964

Monitoring earth's resources from space.

17 p2157 A73-34279

Ultra high resolution electronic imaging and storage with the return beam vidicon.

17 p2136 A73-34904

Key technological challenges of the Earth Resources Technology Satellite program.

17 p2161 A73-34943

A low-cost system for reproducing ERTS imagery.

18 p2315 A73-36018

ERTS-1 satellite return beam vidicon and multispectral scanner comparative evaluation for image quality, considering response functions, resolution, measurability, detectability and image motion effects

20 p2563 A73-39909

RETURN TO EARTH SPACE FLIGHT

Selection of a trajectory for the return to earth from lunar orbit of an artificial satellite

18 p2351 A73-36106

REUSABLE LAUNCH VEHICLES

The effect of the precooling of the air before compression in the case of air-breathing propulsion systems of boosters for space vehicles

02 p2002 A73-11673

Space shuttle liquid propellant reusable rocket engine design, discussing regenerative cooling, fuel pump, oxidizer turbopumps and electronic control systems

19 p2492 A73-37597

REUSABLE ROCKET ENGINES

Space shuttle bipropellant reaction control system (RCS) engine design, characteristics and tests, emphasizing reusability and minimum servicing

05 p0607 A73-16668

High pressure dual fuel chemical LOX/hydrocarbon rocket vehicle concepts for reusable one stage to orbit shuttles

16 p2072 A73-33085

Economic tradeoff study of design criteria cost effectiveness, applying to reusable nuclear shuttle (RNS) engine concepts

16 p2035 A73-33650

REUSABLE SPACECRAFT

NT SPACE SHUTTLES

Synerjet composite rocket-air breathing propulsion system for reusable spacecraft mission profile optimization, discussing multimode operation and performance capabilities

01 p0112 A73-11300

Alternating-pressure measurements involving mushroom-nozzle flows with regard to dynamic stresses in the case of the skin structures of reusable carrier rockets

02 p0128 A73-11686

Design of low-cost, refurbishable spacecraft for use with the Shuttle.

06 p0756 A73-17638

Reusable space tug system study for space shuttle payload delivery, retrieval and support capability augmentation, discussing mission requirements, costs and program scheduling

06 p0756 A73-17639

Earth orbital, lunar, and planetary missions of the space tug.

06 p0750 A73-18019

A fracture control program for the reusable Space Shuttle booster.

06 p0764 A73-18493

Thermal performance evaluation of REI panel gaps for Space Shuttle Orbiter.

07 p0919 A73-19487

Structural testing of ceramic nose cap and leading edge components for a reusable entry vehicle.

11 p1388 A73-25507

Refurbishable spacecraft - Modules and components for the Shuttle era.

12 p1549 A73-27437

Aerodynamic studies of spacecraft in the freestream Mach number range of 3 to 10 at high Reynolds numbers

13 p1567 A73-29447

Space cost effectiveness through space shuttle orbiter programs based on payload recovery and reuse in routine round trip operations

14 p1803 A73-29941

Reusable space tug system and missions for space shuttle operations with 1980s planned payloads, discussing interfaces and configuration alternatives

18 p2358 A73-36088

REVERBERATION

Model study of aircraft noise reverberation in a city street.

02 p0130 A73-12199

An analysis of the acoustic power radiated by a point dipole source into a rectangular reverberation chamber.

02 p0194 A73-12603

A mathematical analysis concerning the edge effect of sound absorbing materials.

08 p0987 A73-21124

A closed-loop automatic control system for high-intensity acoustic test systems.

16 p1994 A73-33147

Design and construction of a reverberation chamber for high-intensity acoustic testing.

16 p1998 A73-33677

Damage-risk criteria - The trading relation between intensity and the number of nonreverberant impulses.

16 p1973 A73-33678

Comparison of aircraft noise measured in flight test and in the NASA Ames 40-by 80-foot wind tunnel.

24 p3056 A73-44871

REVERSE TIME

U REACTION TIME

REVERSED FLOW

On some solutions of the Falkner-Skan equation.

02 p0154 A73-12797

Reverse flow solutions of the Falkner-Skan equation for a lambda greater than one.

02 p0154 A73-12799

The applicability of Stokes expansions to reversed flow.

05 p0565 A73-16606

Flow of an ideal fluid past a body with a reverse-stream.

11 p1348 A73-26056

The prevention of separation and flow reversal in the corners of compressor blade cascades.

17 p2094 A73-34448

An investigation of supersonic swirling jets.

19 p2376 A73-37488

Numerical investigation of unsteady boundary-layer separation.

19 p2420 A73-37852

Investigation of the mechanism of reverse jet flame stabilization for a heterogeneous mixture.

24 p3158 A73-45388

REYNOLDS EQUATION

Reynolds equation time dependent numerical integration errors due to phase shifts, indicating correction by extrapolated Crank-Nicolson scheme

[ASME PAPER 72-LUB-L] 01 p0055 A73-10223

Reynolds stresses and turbulent kinetic energy production in wall jets on flat and concave walls

01 p0034 A73-11357

Finite element technique application for determining velocity field of three dimensional fluid continuum and pressure distribution of lubrication film described by Reynolds equation

03 p0289 A73-12872

The performance of a four-pocket conical hydrostatic bearing.

03 p0311 A73-13206

A brief comparison of the accuracy of time-dependent integration schemes for the Reynolds equation.

[ASME PAPER 72-LUB-L] 03 p0297 A73-14352

The Reynolds tensor in a homogeneous turbulence associated with a mean shearing flow

04 p0436 A73-15995

Pointwise bounds for smooth film profiles Reynolds equation solution based on elliptic equations maximum principle, considering journal bearings

07 p0845 A73-20484

Unsteady uniform-length turbulent flow of incompressible fluid in circular pipe studied via Reynolds and turbulence energy balance equations

10 p1210 A73-24851

A survey of the mean turbulent field closure models.

13 p1601 A73-28801

Turbulent flow energy transfer paths and irreversible dissipation as internal thermal energy analyzed by Reynolds convention for turbulent velocity

13 p1605 A73-29267

The origin of secondary flow in turbulent flow along a corner.

14 p1744 A73-30164

Reynolds equation solutions for transverse velocity and pressure variations in incompressible fluids within journal bearings and between rotating eccentric cylinders

15 p1882 A73-31639

Two-point correlation model and the redistribution of Reynolds stresses.

18 p2300 A73-36627

Ratio of Reynolds shear stress to turbulence kinetic energy in a boundary layer.

18 p2300 A73-36633

An explanation of anomalously large Reynolds stresses within the convective planetary boundary layer.

23 p3002 A73-43593

Measurements of the structure of the Reynolds stress in a turbulent boundary layer.

24 p3079 A73-45310

REYNOLDS LAW

U REYNOLDS EQUATION

REYNOLDS NUMBER

The applicability of Stokes expansions to reversed flow.

05 p0565 A73-16606

Kinematic eddy viscosity at low Reynolds numbers.

05 p0567 A73-17111

Negative Magnus forces in the critical Reynolds number regime.

05 p0533 A73-17212

Hartmann flow stability of conducting incompressible viscous fluid between parallel plates at arbitrary Reynolds numbers under transverse magnetic field

06 p0727 A73-17453

Experimental studies of a Ludwieg tube high Reynolds number transonic tunnel.

06 p0645 A73-17661

Monatomic gas flow around uniformly heated sphere for small Reynolds numbers, noting drag decrease due to thermal stresses

06 p0646 A73-18884

Lundell solid rotor brushless alternator windage power losses, measuring aerodynamic drag coefficient over Reynolds number and gap width range

09 p1034 A73-22772

High Reynolds number experimental data for forebody axial force.

09 p1030 A73-23453

Influence of the Reynolds number on nonstationary convective heat transfer in a pipe during a change in the thermal load

10 p1204 A73-23511

Lift forces on an oscillating cylinder at low Reynolds number.

10 p1173 A73-24822

Unsteady wakes of bluff and streamlined bodies with screens behind them.

10 p1173 A73-24823

Long bore thick plate orifices performance in flow velocity measurement at low Reynolds numbers, calculating uncalibrated uncertainty in discharge coefficient

10 p1221 A73-24860

Pressure distributions on circular cylinders at critical Reynolds numbers.

11 p1300 A73-25151

Flow at the trailing edges of a blade cascade at variable M and Re numbers

12 p1457 A73-27096

Boundary layer due to sphere rotation in a medium at rest

13 p1599 A73-28068

High Reynolds number fluid dynamics and heat and mass transfer in real concentrated particulate two-phase systems.

13 p1704 A73-28427

Effects of sweepback angle and unit Reynolds number on boundary layer transition at supersonic velocities

13 p1567 A73-29172

Investigation of the influence of compressibility and the pressure gradient on the value of the permissible Reynolds number of roughness

13 p1567 A73-29406

Natural convection in a sound field giving large streaming Reynolds numbers.

14 p1817 A73-30613

Unbounded nondiffusive high Reynolds number stratified flow with lee waves over vertical barrier investigated for Froude number range on basis of Oseen-Boussinesq approximation

15 p1863 A73-31341

Monatomic gas flow around uniformly heated sphere for small Reynolds numbers, noting drag decrease due to thermal stresses

15 p1824 A73-32409

Computational program for calculating the Re-number-dependent polar of a glider with arbitrary double trapezoidal wing

16 p1967 A73-33024

Critical Reynolds number for nonlaminar transition in environmental testing for internal and external fluid flows

16 p1999 A73-33146

Numerical solution method for Navier-Stokes equations of a compressible gas over a wide range of Reynolds numbers

17 p2151 A73-34632

Oscillatory flow phenomena in diffusers at low Reynolds numbers.

[ASME PAPER 73-FE-14] 17 p2152 A73-35011

Effect of Reynolds number on nonstationary convective heat exchange in a tube with variable heat load. 17 p2255 A73-35191

Supersonic, turbulent boundary layer separation measurements at Reynolds number of 10,000,000 to 100,000,000. [AIAA PAPER 73-665] 18 p2261 A73-36216

Separation of a supersonic turbulent boundary layer at moderate to high Reynolds numbers. [AIAA PAPER 73-666] 18 p2261 A73-36217

Determination of the heat transfer coefficient for bodies of arbitrary shape at Re tending to 0 18 p2372 A73-37121

Mach number and Reynolds number effect on orbiter/tank interference heating. 19 p2491 A73-37403

Velocity distributions of rough wall turbulent boundary layers without pressure gradient. 19 p2422 A73-38284

Some transient MHD-flows with finite magnetic Reynolds numbers. 19 p2470 A73-38319

The structure of internal intermittency in turbulent flows at large Reynolds number - Experiments on scale similarity. 20 p2546 A73-39090

Herschel-type venturimeter discharge coefficients at low Reynolds number. 20 p2566 A73-39116

Study of the stability of a perturbed conducting gas flow in a magnetic field at arbitrary Reynolds magnetic numbers 20 p2597 A73-39276

Hydrodynamic bearing damping in infinitely broad gap between oppositely oscillating parallel boundary surfaces, discussing inertia, Reynolds number and coefficient of friction 20 p2547 A73-39409

Some integral characteristics of an MHD channel at finite magnetic Reynolds numbers 21 p2747 A73-40889

Eddies development downstream a pipe orifice. 22 p2840 A73-41738

High Reynolds number flow in a moving corner. 22 p2840 A73-41746

Turbulent line vortex decay dependence on Reynolds number, suggesting triple vortex structure with outer and inner regions and viscous core with varying circulation distribution 22 p2842 A73-42230

Flow stability of viscous homogeneous incompressible electrically conducting fluid between nonconducting walls at large magnetic Reynolds numbers 22 p2894 A73-42639

Laminar and turbulent mixing of compressible jets at low Reynolds numbers. 23 p2967 A73-43403

Oil hydraulic button vortex valve optimization experiment for power consumption reduction, noting Reynolds number effects on turn down and pressure ratios 23 p2942 A73-43404

Tetrahedral Mylar plastic balloon drag coefficient measurement as function of Reynolds numbers from experimental free flight test data 23 p3004 A73-44263

Applicability of difference methods for solving Navier-Stokes equations at large Reynolds numbers 24 p3076 A73-44426

A Method for solving problems involving viscous flows past bodies at large Reynolds numbers 24 p3081 A73-45530

RF-4 AIRCRAFT

U F-4 AIRCRAFT

RF-8 AIRCRAFT

U F-8 AIRCRAFT

RH-2 HELICOPTER

U UH-1 HELICOPTER

RHENIUM

NT RHENIUM ISOTOPES

Carbon content relationship to rhenium microhardness, determining cast specimens phase composition by X ray analysis and microstructure observations 10 p1234 A73-24424

States of absorption, velocities of absorption, of desorption of oxygen on rhenium, and mechanisms of atomization and oxidation at high temperature and low pressure 13 p1580 A73-28451

Thermal properties of rhenium single crystals at high temperatures. 16 p2026 A73-33581

Thermionic properties of zirconium carbide/rhenium composites 21 p2751 A73-40530

Structure of lanthanum-hexaboride-coated rhenium filaments. 24 p3105 A73-45401

RHENIUM ALLOYS

Preparation and sintering of tungsten-rhenium alloy powders. 01 p0065 A73-10820

C and Re effects on brittleness threshold temperature and plasticity of Mo-Re alloy 01 p0066 A73-11342

Quadrilateral packet structure and lattice atom positions in single crystal ternary Re-Co-B alloy by X ray analysis 02 p0181 A73-12198

Phase diagrams of ternary Ni-Re alloys with La, Y, Sc, Hf, Si and Mo for cathode applications in electronic vacuum devices 03 p0325 A73-13516

Heat conductivity and the Lorentz number of tungsten-rhenium alloys within the solid-solution limits from 0 to 27% Re at temperatures between 1200 and 3000 K 06 p0710 A73-18556

Observations on the interaction of twins with grain boundaries in Mo-35 at.% Re alloy. 09 p1100 A73-21982

Temperature range of maximum aging of Mo-Re-C alloys after quenching and tempering, noting carbon solubility effects due to Re content 09 p1106 A73-23187

Study of the W-Ta-Re phase diagram by the diffusion layer method 09 p1108 A73-23236

Work function of the principal faces of single crystals of rhenium solutions in molybdenum 10 p1231 A73-23818

Phase equilibria and crystal structure of intermediate phases in Er-Rh binary alloys 10 p1260 A73-24435

Characteristics of martensite decomposition during the tempering of rhenium steels 12 p1509 A73-26894

Temperature dependence of the hardness and estimation of the creep of the Rh-18% Re alloy 12 p1509 A73-26899

Rhenium solubility determination for deformed and annealed Re-Al alloy at 500 and 600 C by microstructural analysis and hardness and electrical resistance measurements 12 p1510 A73-26907

Inert gas injection for W-Re thermocouple wire corrosion protection during temperature measurement in aggressive media 12 p1497 A73-27319

Grain growth of chemical vapour deposited tungsten-22 wt % rhenium alloy. 13 p1636 A73-28927

Molybdenum-rhenium alloy microstructure changes due to nitriding in ammonia vapors from metallographic and X ray structural analysis 15 p1887 A73-31206

Electrical resistance of tungsten-rhenium cermet alloys 15 p1892 A73-32243

Thermal conductivity and Lorenz number of tungsten-rhenium alloys in the solid-solution region 0-27% Re/at temperatures of 1200-3000 K. 16 p2026 A73-33582

Certain physical properties of a new alloy of the nickel-rhenium-molybdenum system 17 p2186 A73-34137

Certain law controlling the temperature dependence of the microdeformation of Fe-Cu-Ti, W, and W-Re bcc alloys 18 p2324 A73-36803

Some electron structure characteristics of W-Re solid solutions 18 p2325 A73-36809

Mechanical properties of electron-beam-melted molybdenum and dilute Mo-Re alloys. 20 p2576 A73-39032

Experimental investigation of the integral hemispherical emissivity of refractory metals and alloys. 20 p2593 A73-39426

Decomposition of martensite during tempering of rhenium steels. 21 p2720 A73-41027

Temperature dependence of hardness and creep of alloy Rh 18Re. 21 p2720 A73-41032

Tungsten-rhenium thermocouple, describing alloys behavior, fabrication, insulation sheaths, calibration, stability and applications 22 p2857 A73-42037

Thermal properties of tungsten-rhenium alloys used in high temperature thermocouples. 22 p2858 A73-42038

Studies of the performance of W-Re type thermocouples. 22 p2858 A73-42039

Measured drift of irradiated and unirradiated W3%Re/W25%Re thermocouples at a nominal 2000 K. 22 p2858 A73-42046

Anomalous concentration dependence of thermal expansion coefficients of tungsten-rhenium and tungsten-niobium alloys. 22 p2878 A73-42509

RHENIUM ISOTOPES

Isotopic anomalies in lunar rhenium. 07 p0889 A73-19805

Re-187, recycling r-process elements through stars, and the age of the Galaxy. 15 p1939 A73-32014

RHEOELECTRICAL SIMULATION

Application of electrical modeling in the analysis of the dynamic properties of temperature sensors 02 p0166 A73-11637

Mathematical models for elastic solid bodies via similarity theory, noting rheoelectrical simulation for thermal stress analysis 03 p0386 A73-13146

The application of electrical analogy to the solution of problems of continuum mechanics 03 p0342 A73-13161

A comparison between potential flow studies through blade cascade by theoretical and rheo-electric analogy methods. 13 p1565 A73-29010

Solution of the problem of unsteady heat transfer for a body and the liquid flow around it 14 p1744 A73-30018

Electric analogy method for subsonic wind tunnel contraction cone design providing uniform velocity distribution in test section, obtaining pressure distribution in cone boundary 22 p2797 A73-43000

RHEOENCEPHALOGRAPHY

Application of multichannel rheography to physiological studies on a centrifuge 06 p0657 A73-17693

Characteristics of vasomotor alterations during brief arbitrary hyperventilation according to data from rheographic and plethysmographic studies 11 p1314 A73-25041

RHEOGRAPHY

U RECORDING INSTRUMENTS

U RHEOMETERS

RHEOLOGY

Investigation of the macroscopic rheonomic properties of a monodirectional fiberglass-reinforced plastic 01 p0067 A73-10002

Investigation of the rheological properties of a model material based on the 'Epidian 2' epoxy resin 01 p0068 A73-10571

Vibratory loads effect on metal microstructure under sliding friction, noting rheological criteria for fretting corrosion wear resistance 02 p0180 A73-11934

Nonclassical flow theory for continuum mechanics with asymmetrical stress concentration, noting rheological problems in laminar high polymers flow, hydrodynamic instability and turbulent flow 03 p0291 A73-13152

On the similarity conditions in the photorheological method of stress analysis. 05 p0632 A73-16430

Laminar liquid jets thrust measurement apparatus for dilute polymer solutions rheological characteristics determination, using air bearing suspended rotor with discharge capillary 05 p0562 A73-16441

Optimization of the rheological properties of s-triazine derivatives. 07 p0787 A73-19561

Rheological materials thermodynamics with plastic deformations, discussing thermoplastic boundary value problems, thermal shock and heat generation 07 p0914 A73-20180

Approximation of experimental rheological curves by distribution functions 08 p1019 A73-21592

Rheological equation for expansion rate effects on stress-strain relation of polyester binders hardened thermochemically and by gamma radiation 08 p1019 A73-21764

Boundary value problem solution uniqueness in dynamic linear theory of hereditary-elastic rheologically composite media 12 p1555 A73-27793

Finite amplitude dynamic motion of viscoelastic materials. 15 p1956 A73-32223

Chemo-rheology of two high temperature epoxy resins. 17 p2197 A73-35347

Rheology of steady turbulent flows of an incompressible fluid 18 p2301 A73-37001

Finite amplitude dynamic motion of viscoelastic materials. 23 p3038 A73-43273

Solution of boundary value problems in thermoviscoelasticity with allowance for mass forces exhibiting a potential 23 p3046 A73-44196

Influence of temperature on the behavior of the rheological properties of plastic carbon-black systems 24 p3101 A73-44471

RHEOMETERS

Electro-rheocardiotelemetric device for complex monitoring of the dynamics and efficiency of cardiac contraction. 03 p0271 A73-14292

RHIZOPUS

- Modification of the electroencephalograph 4EEG-1 for polygraphy 09 p1044 A73-22370
- Effect of physical exercises on the lung rheogram 10 p1182 A73-24524
- Stroke volume measurement from an integral rheogram of human body 24 p3062 A73-44719

RHIZOPUS

- Total lipid and sterol components of Rhizopus arrhizus - Identification and metabolism. 16 p1973 A73-33900

RHODIUM ALLOYS

- Rare earth-rhodium systems intermediate phase equilibria and crystal structures, using powder X ray diffraction technique 11 p1410 A73-26569
- Temperature dependence of the hardness and estimation of the creep of the Rh-18% Re alloy 12 p1509 A73-26899
- Temperature dependence of hardness and creep of alloy Rh 18Re. 21 p2720 A73-41032
- A rhodium-iron resistance thermometer for use below 20 K. 22 p2855 A73-42004
- Phase diagrams of ruthenium and rhodium systems with carbon 22 p2878 A73-42461

RHOMBOHEDRONS

- Symmetry properties of energy zones in rhombohedral-system crystals 09 p1134 A73-22682
- Preparation of a rhombohedral boron carbide of the composition of B13C2 13 p1645 A73-28185

RHYTHM [BIOLOGY]

- NT CIRCADIAN RHYTHMS
- Vector summation dial for analysis of time-nonstationary cyclic biological data, applying to peak time change detection and random walks 03 p0263 A73-14120

- Psychological and physiological components of biorhythm cycles governing periodic variations in physical, emotional and intellectual performance 05 p0544 A73-16720

- Study of the influence of weak electromagnetic field gradients on man 09 p1046 A73-22850

- Role of the medial area of the medulla oblongata in the rhythmic activity of respiratory-center neurons 10 p1179 A73-23804

- Investigation of the sleep and wakefulness rhythms in the crewmembers of Soyuz-3 through Soyuz-9 spacecraft prior to, during, and after space flight 10 p1182 A73-24697

- Physiological time zone entrainment and stressor effects during prolonged C-141 transmeridian flights, using endocrine-metabolic indices in urine specimens 13 p1574 A73-28283

- Effects of flying and of time changes on menstrual cycle length and on performance in airline stewardesses. 13 p1576 A73-28509

- Oscillations in oxygen consumption of man at rest. 14 p1714 A73-29755

- Circaseptan 7-day/ oviposition rhythm and growth of *Spring Tail*, *Folsomia candida* /*Collembola*: *Isotomidae*. 15 p1836 A73-32185

- Book - Biological rhythms and human performance. 16 p1972 A73-33154

- The explanation and investigation of biological rhythms. 16 p1972 A73-33155

- Brain alpha rhythm activity relationship to perceptual and motor performance, correlating with reaction time and computer cycle time analogy 16 p1972 A73-33159

- Industrial work rhythm and between-day fluctuation studies 1920-1969, emphasizing industrial record and between-day fluctuations 16 p1975 A73-33160

- Visual responsiveness repeat variability magnitude during prolonged sessions and time of day 20 p2513 A73-39479

- Investigation of the nature of biological rhythm sensors by means of automatic networks 22 p2812 A73-41865

- Some physiological mechanisms of alpha-rhythm frequency fluctuations in man under conditions of relative rest 24 p3059 A73-44717

- The nature and significance of the dynamics of electrical activity in the neocortex and hippocampus during the paradoxal phase of sleep 24 p3059 A73-44718

RIBBON PARACHUTES

- Analysis of deployment and inflation of large ribbon parachutes. [AIAA PAPER 73-451] 15 p1826 A73-31437
- A 14.2-ft-Do variable-porosity conical ribbon chute for supersonic application. [AIAA PAPER 73-472] 15 p1828 A73-31456

- Drag and stability characteristics of high-speed parachutes in the transonic range. 15 p1828 A73-31457

- [AIAA PAPER 73-473] An omnidirectional gliding ribbon parachute and control system. 15 p1829 A73-31468

- [AIAA PAPER 73-486] Several computerized techniques to aid in the design and optimization of parachute deceleration and aerial-delivery systems. 15 p1829 A73-31470

- [AIAA PAPER 73-488] Reinforcement of aluminum alloys by high strength steel ribbons 03 p0312 A73-13581

- The edge-defined, film-fed growth (EFG) of silicon single crystal ribbon for solar cell applications. 03 p0258 A73-14254

- An elastic ribbon under the action of a nonuniform load 09 p1165 A73-23348

- Spatial amplitude distribution of vibrating ribbon two dimensional wake mean, periodic and random velocity components measured in uniform flow by hot-wire anemometry 10 p1173 A73-24828

- RIBONUCLEIC ACIDS
- Topochemical differences in RNA content in spinal cord motoneurons during hypoxia and hypokinesia 02 p0135 A73-12558

- Evolution of ribonuclease in relation to polypeptide folding mechanisms. 04 p0409 A73-15047

- Dependence of poly U-directed cell-free system on ratios of divalent and monovalent cations. 06 p0652 A73-17945

- Informational biopolymer structure in early living forms. 06 p0652 A73-17946

- Ribosomal RNA base composition and molecular evolution in plants and animals of various taxonomic groups 07 p0780 A73-19220

- Effect of actinomycin D on aldosterone-mediated changes in electrolyte excretion. 09 p1040 A73-22650

- Study of the possibilities of histone-RNA complex formation in experiments in vitro 10 p1181 A73-24513

- RNA and DNA of internal organs during a remote postreanimation period in animals with complete and incomplete functional recovery of the central nervous system 14 p1719 A73-30842

- Influence of ribonuclease on changes in the membrane potential of muscle fibers evoked by stimulation of the sympathetic nerve 15 p1833 A73-31166

- Protein and nucleic acid contents in animal tissues under hypokinesia 15 p1834 A73-31503

- Effect of convulsions on certain aspects of the biosynthesis of proteins in the brain cortex 21 p2638 A73-40750

- Biosynthesis of RNA in the brain cortex during various functional states 21 p2640 A73-41262

- Ribonucleic acid /RNA/ polymerase and adenylyl cyclase in cardiac hypertrophy and cardiomyopathy. 22 p2808 A73-42687

- RIBS [SUPPORTS]
- Effects of transverse ribs on pressure recovery in two-dimensional subsonic diffusers. 03 p0243 A73-13447

- [AIAA PAPER 72-1141] Piecewise linear approximation of thin walled rib and diaphragm reinforced conical beams under thermal field and axial loads, using limit stress-strain diagrams 07 p0913 A73-20096

- Linear elastic behavior of laminated plate with ribs reinforced by continuous unidirectional fibers under surface distributed loads orthogonal and parallel to plane 11 p1435 A73-25403

- Bending of rectangular plates of variable thickness with edges reinforced by elastic ribs 14 p1815 A73-30796

- Design for bending of a clamped infinite strip with a prestressed stiffness rib along the edge 16 p2075 A73-32695

- Eleven ribs and spars made of flat Rene 41 caps based on hot structure concept for thermal environment 16 p2072 A73-33061

- Incremental forging of parts with cross-ribs. [SME PAPER MF 73-164] 19 p2437 A73-38503

- Series analysis of cylindrical shells - New look at an old problem. 20 p2622 A73-39550

- Thin wall rib structured fan shaped wing design for arbitrary air loads, using strain compatibility conditions 21 p2784 A73-40390

- Weight reduction in stiffened panels with specified initial buckling load in uniform longitudinal compression by stiffeners utilization 21 p2787 A73-41190

- Asymptotic behavior of the solutions to the Navier-Stokes equations near ribs 21 p2678 A73-41275

- Operator of thin plate reinforced with thin-walled ribs. 24 p3152 A73-45440

- The motion of a body containing a liquid-filled cavity with elastic radial ribs and exhibiting perturbations relative to the longitudinal axis 24 p3112 A73-45513

- RICCATTI EQUATION
- Stability analysis of Riccati covariance equations of Kalman filter. 04 p0472 A73-15273

- A boundary layer method for the matrix Riccati equation. 06 p0719 A73-18864

- Matrix Riccati differential and quadratic algebraic equations in optimal control and filtering theory, discussing stabilizing solutions, asymptotic properties and computational techniques 09 p1069 A73-23102

- Optimal control for functional differential systems through Krasovskii generalization for time delay systems and resulting Riccati equations numerical solution 11 p1392 A73-26581

- Riccati transformation for optimal control linear two-point boundary value problems formulated from first order numerical integration methods 15 p1908 A73-31666

- Second-order optimality conditions for the Bolza problem with variable endpoints and separated end conditions. 19 p2445 A73-38039

- Laguerre transform of a continuous signal - Application to the study of the asymptotic regime of a Kalman filter 22 p2832 A73-42352

- An innovations approach to least-squares estimation. V - Innovations representations and recursive estimation in colored noise. 23 p2954 A73-43819

- Adiabatic variance. I - Exponential property for the simple oscillator. 24 p3112 A73-45543

- RICHARDSON NUMBER
- Atmospheric stratification stability at heights of 30-90 km from grenade test determined wind and temperature data, presenting Richardson number latitudinal and seasonal distribution 02 p0160 A73-12273

- Direct temperature measurements for rotating annulus experiments, showing symmetric baroclinic instability and Richardson number for baroclinic wave 02 p0189 A73-12788

- Turbulence and tropopause evolution in northeast jet stream over Treviso airport, noting Richardson criterion value as diagnostic and short range prognosis tool 08 p0986 A73-21487

- Linear stability to axisymmetric perturbations of compressible nondissipative swirling flow, noting Richardson number role 13 p1605 A73-29374

- Effect of wind shear on atmospheric wave instabilities revealed by FM/CW radar observations. 19 p2447 A73-38206

- Turbulence spectra, length scales and structure parameters in the stable surface layer. 19 p2448 A73-38216

- Richardson number profiles through shear instability wave regions observed in the lower planetary boundary layer. 19 p2448 A73-38228

- Eddy heat/momentum diffusivity ratio dependence on Richardson number relationship between Deacon numbers of wind and temperature profiles in Antarctic surface layer 23 p3003 A73-43983

- RICHARDSON-DUSHMAN EQUATION
- U TEMPERATURE EFFECTS
- U THERMIONIC EMISSION

- RIDGES
- Lunar mare ridge formation with broad gentle arch overlaid by sharper contorted ridge, discussing ring structures and volcanic ring complexes 03 p0368 A73-13091

- Radiation pattern of a low-frequency beacon antenna in the presence of a semi-elliptic terrain irregularity. 16 p1979 A73-32913

- RIEMANN INTEGRAL
- U MEASURE AND INTEGRATION
- RIEMANN MANIFOLD

- Gravitation theory harmonic condition equations to separate relatively-valid subclass of extremal manifolds from class of m-dimensional pseudo-Riemannian manifolds 08 p0987 A73-20700

Relativistic elasticity theory for solids based on Cattaneo definitions for Riemann metric, considering hyper- and hypoelastic media 16 p2036 A73-33108

Almost projective mapping of gravitational fields - Degenerate case 17 p2212 A73-35564

General relativistic time analysis leading to scalar Hamiltonian formalism for particle mass based on Riemannian metric, considering Hamilton-Jacobi equation in particle dynamics 22 p2888 A73-43048

RIEMANN PROBLEM

U CAUCHY PROBLEM

RIEMANN SPACE

U RIEMANN MANIFOLD

RIEMANN WAVES

Statistical phenomena during shock wave formation 08 p0955 A73-21447

Statistical effects in the generation of shock waves. 15 p1860 A73-31011

RIFT VALLEYS

U VALLEYS

RIFTS

U GEOLOGICAL FAULTS

RIGID BODIES

U RIGID STRUCTURES

RIGID ROTOR HELICOPTERS

Stability of elastic bending and torsion of uniform cantilevered rotor blades in hover. [AIAA PAPER 73-405] 11 p1440 A73-25534

On the aerodynamic damping moment in pitch of a rigid helicopter rotor in hovering. II - Analytical phase. 21 p2631 A73-40087

RIGID ROTORS

AH-56A rigid rotor compound helicopter configuration and handling qualities under autorotation conditions, discussing flight test program, piloting descent performance 09 p1030 A73-22179

Influence of the rotor weight on the changes in the axial rigidity of gyromotors 13 p1572 A73-29146

Self induced vibration of friction bearing mounted rigid rotor, considering oscillation damping or enhancing effect of oil film 16 p1968 A73-33236

Future technical developments and efficiency of helicopters and their derivatives 17 p2098 A73-34252

An economical method of analyzing transient motion of gas-lubricated rotor-bearing systems. [ASLE PREPRINT 73AM-2B-2] 17 p2178 A73-34982

A study of stall-induced flap-lag instability of hingeless rotors. [AHS PREPRINT 730] 17 p2095 A73-35066

Effect of torsion-flap-lag coupling on hingeless rotor stability. [AHS PREPRINT 731] 17 p2105 A73-35067

On the question of adequate hingeless rotor modeling in flight dynamics. [AHS PREPRINT 732] 17 p2105 A73-35068

Investigation of reactionless mode stability characteristics of a stiff inplane hingeless rotor system. [AHS PREPRINT 734] 17 p2105 A73-35070

Handling qualities comparison of two hingeless rotor control system designs. [AHS PREPRINT 741] 17 p2105 A73-35074

Longitudinal-torsional vibrations of rotors 20 p2569 A73-39374

Balance threshold of rigid rotors with nonideal bearings 20 p2569 A73-39639

German monograph - Characteristics of motion of an elastically supported rotor with interior damping. 22 p2867 A73-42849

Non-linear flap-lag dynamics of hingeless helicopter blades in hover and in forward flight. 22 p2800 A73-43134

RIGID STRUCTURES

NT RIGID ROTORS

Stability of a spinning body containing an elastic membrane via Liapunov's direct method. 01 p0077 A73-10728

Rigidly plastic cylindrical shell design for axial-load and lateral-pressure combinations with allowance for large deflections 02 p0231 A73-11808

Diffraction of elastic waves by two coplanar and parallel rigid strips. 02 p0234 A73-12088

On approximate solutions for rigid-plastic structures subjected to dynamic loading. 02 p0236 A73-12520

Flight-mechanical analysis of various flight states of conventional aircraft. VII - Mechanical principles: Rigid-body dynamics 03 p0250 A73-13074

Stress-strain diagrams for stability of structures under plastic bending, noting differential equations for rigidity characteristics 03 p0386 A73-13144

Transient response of inelastic shells of revolution. 03 p0392 A73-13686

A new approach to the mode approximation for impulsively loaded rigid-plastic structures. 06 p0760 A73-17764

Facility for studying the strength and rigidity of circular plates prepared from an anisotropic material 07 p0809 A73-20517

Rigidly plastic shells yield point, deriving yield surface in generalized stress space 09 p1158 A73-22360

Longitudinal impact of a rigid body against a clamped rod 09 p1158 A73-22361

Explicit addition of rigid-body motions in curved finite elements. 09 p1165 A73-23441

Reduction of a gyrostat problem to that of a rigid body. [ASME PAPER 72-APM-QQ] 11 p1398 A73-25704

Solution of kinematical differential equations for a rigid body. [ASME PAPER 72-APM-AAA] 11 p1398 A73-25705

Experimental investigation of hydrodynamic stability at rigid and elastic-damping surfaces 11 p1349 A73-26440

Impact interaction of an absolutely hard body and an elastic two-mass system 11 p1400 A73-26455

Anholonomic constraints imposed on mechanical systems which have rigid solid bodies as constituent elements. II - Anholonomic constraints realized by nonsliding roller bearings 12 p1523 A73-26794

A contribution to Hertz's theory of elastic impact. 13 p1696 A73-28748

Plane strain slip line theory for anisotropic rigid/plastic materials. 13 p1697 A73-28793

Inelastic column buckling of internally pressurized tubes. [SESA PAPER 2049] 13 p1699 A73-29305

Duality of limit theorems for a structure of a standard rigid-plastic material 14 p1812 A73-30491

Optimisation theory of elastic-rigid bodies under repeated variable deformation. 14 p1812 A73-30495

Extremum principles in the dynamics of rigid-plastic bodies and mathematical programming. 14 p1813 A73-30547

Numerical solution to the problem of elastic ring impact at a rigid obstacle 14 p1815 A73-30798

Characteristic matrix method for automatic recognition and extraction of rigid body modes from inconsistent to natural force-deformation relationship of stress and strain elements 16 p2077 A73-32990

Book - Flight dynamics of rigid and elastic airplanes. Parts 1 & 2. 17 p2099 A73-34451

Elastic semiinfinite cylindrical shell stress-strain state after axial impact against static rigid plane, obtaining solutions for small time values 17 p2244 A73-34740

An appreciation of the design of carbon fibre rigid solar panels for spacecraft. 17 p2238 A73-34812

A nonlinear oscillator analog of rigid body dynamics. 18 p2337 A73-36416

Nonlinear bending problem for a beam of variable rigidity 18 p2366 A73-36959

The method of plane-axial vector coordinates in the determination of velocities in the general motion of a rigid solid 19 p2459 A73-37643

Application of the Gauss principle in the dynamics of systems having rigid solids of variable mass as constituent elements 19 p2459 A73-37652

Device for studying the strength and rigidity of round plates of anisotropic material. 19 p2418 A73-37793

Flight-mechanics analysis of various flight conditions of conventional aircraft. VIII/1 - Mechanical foundations: Kinematic equations of motion of a rigid body 19 p2387 A73-38123

Coefficients of stress intensity near rigid acute-angled inclusions 20 p2619 A73-39370

RIGIDITY

Rectangular plates with unidirectionally variable rigidity 01 p0114 A73-10572

Lateral rigidity of longitudinally stiffened plates. 05 p0633 A73-16543

Maxwell equation for equilibrium force in electromagnetic suspension system of force measuring instrument, noting rigidity dependence on system parameters 05 p0577 A73-16995

Inequalities for torsion rigidity of a prismatic rod with steady creep 07 p0912 A73-19323

Study of the rigidity of rectangular plates during bending by the finite-element method 12 p1553 A73-27461

Torsional rigidities for bars under fully plastic torsion. 18 p2365 A73-36695

RILLS

U VALLEYS

RIMS

Geometric interpretation of the ratio of overall diameter to rim crest diameter for lunar and terrestrial craters. 22 p2909 A73-42498

RING CURRENTS

Magnetic field strength change in equatorial plasmasphere, considering quiet ring current as equatorial sheet current extension of neutral sheet current in magnetospheric tail 02 p0155 A73-11732

Ring current proton injection instability for ion loss cone and electromagnetic ion cyclotron waves in high beta low density region outside plasmopause 02 p0156 A73-11748

Precipitation of auroral and ring current particles by artificial plasma injection. 03 p0301 A73-13711

Ring current effect on plasma convection in magnetosphere, assuming pressure due to proton population 03 p0302 A73-13854

Magnetospheric charged particle populations in magnetosheath, plasma sheet, extraterrestrial ring current, electron trough and trapping regions 03 p0302 A73-13856

The effect of an electric field induced by a time-dependent ring current on the particle drift motion. 04 p0440 A73-14954

Magnetospheric field distortion relation to ring currents based on satellite-borne magnetometer measurements of magnetic field topology 04 p0442 A73-15338

Relation of Pc 1 micropulsations to the ring current and geomagnetic storms. 04 p0444 A73-15536

On the distinction between the auroral electrojet and partial ring current systems. 04 p0444 A73-15550

Steady axisymmetric ring current models computed with energy density distribution parameters variations for effects on magnetic field and particle belt parameters 05 p0609 A73-16144

Magnetic current annular ring near belt, noting application to coaxially driven parallel monopole arrays analysis 06 p0666 A73-18198

DR ring current belt formation due to electron and proton gradient drift in inhomogeneous geomagnetic field, calculating charged particles trajectories 07 p0816 A73-19446

A series expansion of a magnetic vector-potential calculated for a ring with a current 08 p0959 A73-21298

Ionospheric magnetic disturbances during March 1970 related to solar flare corpuscular and proton fluxes, generating ring current and PCA absorption 10 p1211 A73-24218

Satellite measurement of variable intensities for geomagnetically trapped protons during magnetic storms, noting ring current source of low-altitude protons 10 p1213 A73-24731

Simultaneous occurrences of hydrogen arcs and mid-latitude stable auroral red arcs. 10 p1214 A73-24740

Turbulent loss mechanism of ring current protons in plasmopause vicinity via electrostatic drift cyclotron loss cone waves 10 p1270 A73-24743

Polar cap E layer conductivity difference effects on ring currents associated with vertical current along lines of force at conjugate points 13 p1608 A73-28717

Correlation of reported gravitational radiation events with terrestrial phenomena. 14 p1749 A73-30554

Energy and momentum theorems in magnetospheric processes. 15 p1871 A73-31846

Interplanetary magnetic field and geomagnetic Dst variations. 17 p2158 A73-34507

Decay of the magnetic storm ring current by the charge-exchange mechanism. 17 p2159 A73-34782

Particle entry into the equatorial magnetosphere. 18 p2344 A73-35928

Comparison of the two-dipole and empirical magnetospheric models. 18 p2310 A73-36135

Series expansion of the magnetic vector-potential computed for a current carrying ring. 19 p2425 A73-37927

Explorer 45 mission objectives discussing magnetospheric ring current, magnetic storm detection, parti-

RING LASERS

- cle energy and interactions, electric and magnetic fields measurements, etc 20 p2614 A73-38949
- Ring current particle distributions during the magnetic storms of December 16-18, 1971. 20 p2552 A73-38952
- Energy spectra and pitch angle distributions of storm-time and substorm injected protons. 20 p2552 A73-38953
- Heating of the low-latitude upper atmosphere caused by the decaying magnetic storm ring current. 21 p2684 A73-40786
- Precipitating protons with E greater than 12.4 keV to 500 keV near the midnight trapping boundary. 21 p2760 A73-40822
- Narrow-beam antennas using cylindrical columns of isotropic plasma. 21 p2665 A73-41124
- Equivalent filamentary current derivation for bi-static field diffracted by ring singularity based on geometrical theory 22 p2824 A73-41838
- Periodically structured Pc 1 micropulsations during the recovery phase of intense magnetic storms. 22 p2844 A73-41913
- Radiation production and energy deposition by ring current protons precipitated into the mid-latitude upper atmosphere. 23 p3024 A73-43685
- Influence of the conductivity of the ionosphere on the pulsations of DP1 and DP2 current systems 24 p3084 A73-44806
- Diffusion of ring current particles by low-frequency long-wavelength electrostatic oscillations. 24 p3126 A73-45128
- ### RING LASERS
- Effect of a magnetic field on emission fluctuations in a ring gas laser 01 p0060 A73-11089
- Gas and solid state lasers amplitude and phase fluctuations calculated from Langevin equations, noting spectral line width and ring laser wave coupling 01 p0061 A73-11355
- Motional effects in retardation plates and mode locking in ring lasers. [AD-757833] 06 p0699 A73-17496
- Polarization properties of a traveling-wave laser. 06 p0703 A73-18611
- Resonator polarization parameters effect on backward wave attenuation in three and four mirror TW ring laser, noting colliding waves intensity dependence on polarization angle 06 p0703 A73-18619
- A tunable flashlamp-pumped dye ring laser of extremely narrow bandwidth. 09 p1091 A73-22083
- Spectral shift between components of homogeneous /radiation or shock/ line, using ring laser spatial and frequency burnout effects 10 p1228 A73-24464
- Steady state lasing stability in ring-type gas laser with symmetrical distribution of three longitudinal modes 10 p1228 A73-24580
- Ring laser output calculation in the region of capture 12 p1504 A73-26885
- Ring cavity for analyzing the spectral composition of CO₂-laser radiation 12 p1506 A73-27217
- Mode locking in quantum optics. 12 p1506 A73-27442
- Competition between longitudinal modes in a ring laser with an anisotropic resonator. 12 p1507 A73-27508
- Time characteristics of a ring laser with a bleachable filter. 12 p1507 A73-27509
- Effect of an external magnetic field on the beat frequency of opposite waves in a ring laser with a noninteracting phase-shifting device 13 p1627 A73-28965
- Formation of an ultrashort pulse of light in a ruby laser with resonant modulation of losses 14 p1757 A73-30265
- Generation of opposed waves polarized in different planes in a ring laser 14 p1757 A73-30368
- Laser mode locking using saturable absorbers. 15 p1885 A73-31941
- Dependence of the locking zone of a gas ring laser on the emission frequency 15 p1885 A73-32316
- Investigation of longitudinal-mode selection and frequency stabilization of the emission from a helium-neon laser with a ring resonator 15 p1886 A73-32335
- Field properties and losses in a three-mirror optical ring resonator with a Gaussian diaphragm 15 p1886 A73-32341
- Geometric magnification and collimation of traveling wave unidirectional unstable ring lasers, comparing with standing wave resonators 15 p1886 A73-32382

- Detection and measurement of low-level backscattering of laser radiation 16 p1978 A73-32893
- Experimental study of fluctuations of the difference frequency in a ring laser 16 p2024 A73-32895
- Periodic Faraday bias and lock-in phenomena in a laser gyro. 17 p2172 A73-35413
- Reproducibility of the frequency of a stabilized laser employing a ring cavity 19 p2437 A73-37246
- Spectral shift between components of homogeneous /radiation or shock/ line, using ring laser spatial and frequency burnout effects 19 p2438 A73-38136
- General method for the calculation of the frequency of beats in a single-mode ring laser. 20 p2573 A73-39678
- Excitation of ultrashort light pulses in a ruby ring laser with resonant Q-switching 21 p2712 A73-40356
- Russian book - The laser gyroscope. 21 p2704 A73-41295
- Effect of external magnetic field on the beat frequency in a ring laser with nonreciprocal phase shifter. 23 p2989 A73-44317
- Frequency dependence of locking in a ring laser. 24 p3095 A73-44622

RING STRUCTURES

- ### NT REINFORCEMENT RINGS
- ### NT RING WINGS
- Initial postbuckling of circular rings under pressure loads. 01 p0115 A73-10744
- Axisymmetric plastic response of rings to short-duration pressure pulses. 01 p0115 A73-10759
- Elastic and plastic deformations of circular ring with initial machining produced stresses distributed across thickness, calculating critical load for static stability 02 p0236 A73-12581
- Lunar mare ridge formation with broad gentle arch overlaid by sharper contorted ridge, discussing ring structures and volcanic ring complexes 03 p0368 A73-13091
- The relative validity of the concepts of coefficient of friction and interface friction shear factor for use in metal deformation studies. [ASLE PREPRINT 72LC-7A-3] 03 p0316 A73-14368
- Theoretical structure and spectrum of a shock wave in the interstellar medium - The Cygnus Loop. 04 p0499 A73-15359
- An evolutionary thermal model for the Cygnus Loop. 04 p0499 A73-15361
- The liquid metal slip ring experiment for the Communications Technology Satellite. 04 p0408 A73-15449
- Bifurcation of rings under concentrated centrally directed loads. [ASME PAPER 72-WA/APM-37] 04 p0515 A73-15885
- Spinning satellite with partially filled viscous ring damper, solving equations of motion for nutation-synchronous and spin-synchronous modes [ALAA PAPER 73-143] 05 p0629 A73-16892
- Comparison of eigenvalues and characteristic vibration modes of circular ring bars, circular ring disks, and circular ring fibers 06 p0758 A73-17584
- Comparison of the characteristic values and characteristic vibration forms of a circular ring beam, a circular ring disk, and a circular ring fiber. II 06 p0759 A73-17586
- Dynamic plastic deformation of rings under impulse load. 06 p0761 A73-17817
- Thin-walled pipe designs with a curvilinear axis 09 p1158 A73-22362
- Action of a concentrated force on an elastic ring pressed into a circular hole in an isotropic plate 09 p1165 A73-23357
- Three layered sandwich rings damped vibrations under time-harmonic radial concentrated load, comparing experimental and theoretical mechanical impedance data 09 p1165 A73-23440
- Deformation of shells of revolution with attached rings under different local loads, deriving approximate expressions for stressed state 10 p1287 A73-23592
- Elastic circular ring stability under uniformly distributed equal radial concentrated forces 10 p1287 A73-23594
- Friction, wear, and noise of slip ring and brush contacts for synchronous satellite use. 11 p1374 A73-26211
- Thin uniform circular rings axial and radial bending vibrations under perturbing effect of circumferentially attached small cylinder, comparing theoretical with experimental results 11 p1444 A73-26290

- Hamilton variational principle for deriving equations of motion for small elastic displacements of thin circular rings, noting twist equation occurrence 11 p1446 A73-26493
- Flattening and creep stability loss of nonlinear viscoelastic ring under external pressure 12 p1551 A73-27180
- Improvement of damping characteristics of structural members with high damping elastic inserts. 13 p1690 A73-28056
- Free and forced vibration analysis of laminated ring structure with elastic inner, outer layers and core, obtaining natural frequency response by variational method 13 p1695 A73-28486
- Unbalance vibration of a rotor-bearing system supported by floating-ring journal bearings. 13 p1623 A73-28647
- Equilibrium of an anisotropic plane reinforced by an isotropic circular ring 13 p1698 A73-29131
- Numerical solution to the problem of elastic ring impact at a rigid obstacle 14 p1815 A73-30798
- Motions of perfect incompressible homogeneous fluid planets surrounded by rigid oscillating rings, noting application to two-satellite planets 15 p1860 A73-31049
- Photoelastic analysis of an orthotropic ring under diametral compression. 15 p1949 A73-31653
- Radiation configuration factors for annular rings and hemispherical sectors. 15 p1959 A73-32281
- Inertial motion of a plastic ring under the action of a pulsed load 17 p2244 A73-34797
- Tradeoff studies for feasibility of multiblade ring rotor configuration for helicopter design, discussing ring drag [AHS PREPRINT 714] 17 p2104 A73-35060
- Elastic-plastic expansion of 6061-T6 aluminum rings. 18 p2362 A73-36320
- Postbuckling behavior of circular rings with two or four concentrated loads. 19 p2501 A73-38251
- Use of turning ring electrodes for study of the transport of matter in fluid in a laminar or turbulent hydrodynamic regime 19 p2432 A73-38481
- Operational temperature and frequency effects on radial driving point mechanical impedance of damped thin walled ring with mass segments attached by viscoelastic material 20 p2616 A73-39051
- Approximate solutions for heat conduction and thermal stresses in thermoelasticity of solids and beam and ring structures, considering dynamic, coupling, melting and solidification effects 20 p2620 A73-39514
- Distances of 26 stars of the stellar ring 58. 20 p2610 A73-39576
- Micropolar elasticity solution for static plane boundary value problems in circular ring shaped region, considering Volterra dislocation example 21 p2789 A73-41670
- In-plane free vibrations of tapered oval rings, determining normal modes and resonant frequencies from differential force and moment equilibrium equations 22 p2918 A73-41818
- Spaced annular ring shell-to-shell and shell-to-tube view factors for finite difference radiative heat transfer solutions 22 p2923 A73-42564
- Stress amplification in a ring caused by dynamic instability. [ASME PAPER 73-APMW-35] 22 p2925 A73-42893
- Prediction and control of macroscopic fabrication stresses in hoop wound, fiberglass rings. 23 p3041 A73-43638
- Load capacity of rings formed by winding of composites reinforced with high-modulus anisotropic fibers 24 p3093 A73-44528
- ### RING WINGS
- Calculation of the potential flow about axisymmetric critical fuselages, annular profiles, and propulsion system inlets [DFVLR-SONDDR-265] 07 p0773 A73-19205
- Potential flow past axisymmetric ring wing profiles via singularity method, applying source and vortex distributions to curved thick profiles [DFVLR-SONDDR-271] 11 p1300 A73-25348
- ### RINGS [MATHEMATICS]
- Symbol ring as alphabetic element in information processing technique, defining address substitution operation 02 p0143 A73-11642
- A new fundamental system of modified cylindrical functions for an annular region. 17 p2200 A73-34248
- Splittability of radically semisimple torsion over local and commutative Noetherian rings 24 p3144 A73-44423

RIMETERS

Satellite-borne HF ionospheric noise meter receiver system with narrow band monolithic crystal filters, comparing with Ariel 3

01 p0026 A73-11175

Ionospheric propagation effects on riometer recorded cosmic radio emission spectra, noting temporal and frequency spectra dependence on ionospheric plasma turbulence scale

05 p0573 A73-16266

Observations of the entry of solar protons into the magnetosphere by use of riometers.

18 p2344 A73-35930

A rocket-borne riometer for the study of lower ionosphere.

18 p2315 A73-36046

An iterative mathematical technique for deriving electron-density profiles from multifrequency riometer data.

22 p2828 A73-43177

RIMETRY

U MEASUREMENT

U RIMETERS

RISK

Management system for aviation safety.

01 p0005 A73-10825

Information-loss and risk-increase estimation during observational data reduction in successive estimation problems

05 p0589 A73-16299

Impulse noise damage risk criteria.

17 p2117 A73-35327

RITZ AVERAGING METHOD

Non-linear vibration of rotating cantilever blades treated by the Ritz averaging process.

02 p0232 A73-11859

Determination of root locus for nonlinear multi-variable system.

[ASME PAPER 72-WA/AUT-21]

04 p0472 A73-15879

Calculation of eigenvalues and eigenvectors of normal matrix couples with the aid of Ritz iteration

11 p1392 A73-26726

The Ritz-Galerkin procedure for nonlinear control problems.

13 p1649 A73-28607

Ritz method application to structural eigenvalue problems, considering plate buckling in box beams

14 p1805 A73-29741

Error investigations regarding the solution of the inhomogeneous natural boundary value problem by means of a Ritz approach with standardized coordinate functions

15 p1899 A73-31364

Lower bounds to the frequencies of continuous elastic systems.

15 p1954 A73-32125

The Ritz-Galerkin procedure for parabolic control problems.

19 p2446 A73-38375

Large deflection of shallow paraboloid shells.

21 p2782 A73-40005

RIVERS

High-altitude photographs of the Oregon coast.

09 p1078 A73-22719

Statistical uniformity of hydrological data from series of river drainage pattern observations

19 p2446 A73-38546

RIVETED JOINTS

Weldbonding/rivetbonding - Application testing of thin gauge aircraft components.

[AIAA PAPER 73-805]

19 p2433 A73-37464

RIVETING

Adaptation of resistance welding techniques to hot staking.

07 p0831 A73-20268

Effect of rivet spacing on crippling loads of joined aluminium angles.

19 p2499 A73-38009

RLC CIRCUITS

NT RLC CIRCUITS

Engineering technique for secondary-medium parameter calculation in the substitution circuits of flat, linear induction MHD machines with side busbars

15 p1832 A73-31411

Inductive relaxation oscillator design using common emitter avalanche transistors with N-shaped I-V characteristics at base input

17 p2133 A73-34154

RLC CIRCUITS

Determination of the frequency and amplitude of an external force that induces resonance in a linear system with variable parameters

07 p0792 A73-19908

Requirements specification for ac and dc current carrying filter networks for electromagnetic interference reduction, noting RLC circuits

[SAE ARP 1172]

08 p0942 A73-20697

Designing electrical analogs for solving a hyperbolic energy equation

08 p1022 A73-20999

Analysis of the nonlinearity of the modulation characteristic of a single-circuit phase modulator employing a varactor

10 p1195 A73-24382

Analysis of the distortions of an FM signal in a servo loop with external control

12 p1470 A73-27576

Optimization of the operating conditions of planar transistors in stages with inductive correction.

13 p1591 A73-28733

Resonant RLC tank circuit design with coupled stripline segments, using lumped and distributed parameter system synthesis theory

13 p1592 A73-28895

The features of disk shape piezoelectric ceramic transducer equivalent circuit.

14 p1754 A73-30892

Convergence of periodic solutions of differential equations for resonance circuits with nonlinear semiconductor capacitance

17 p2144 A73-34585

Distortions of signal frequency in FM oscillators.

17 p2136 A73-35154

Means of improving the effectiveness of designing nonlinear electronic circuits on a digital computer by the method of nodular potentials

21 p2666 A73-41310

Noise factor of a multiple-circuit input device

23 p2953 A73-43518

Linear system resonance effects in single loop controlled frequency tank circuit with variable capacitor under variable or constant emf

24 p3074 A73-44591

RLC NETWORKS

U RLC CIRCUITS

RNA

U RIBONUCLEIC ACIDS

ROADS

NT HIGHWAYS

German book - Soil mechanics of retaining structures, roads, and runways.

11 p1344 A73-26255

Book - Prestressed pavements of airports and roads.

21 p2675 A73-41287

ROBOTS

PLANEX 1 plan executor program for robot system, creating plan for sequence of actions via problem solving program STRIPS

01 p0020 A73-11452

Striding devices for astronautical application areas

04 p0433 A73-15630

A robot conditioned reflex system modeled after the cerebellum.

06 p0658 A73-18065

Descriptions and plans in an interactive robot simulation system.

06 p0672 A73-18891

Mars surface exploration by self-guided stereo TV equipped roving vehicle /robot/, describing computerized object and scene ranging and recognition

19 p2429 A73-37321

Depth sensing, camera and touch/force sensing systems for autonomous industrial robotics and planetary exploration

19 p2429 A73-37322

A survey study of teleoperators, robotics, and remote systems technology.

19 p2417 A73-37335

Learning control in remote manipulator and robot systems.

19 p2412 A73-37754

Digital processing of stereoscopic image pairs.

19 p2432 A73-38534

Monograph on Question-Answer 4 /QA4/ programming language for artificial intelligence application to problem solving covering pattern matching, built-in functions and robot work tasks

22 p2830 A73-42745

ROCHE LIMIT

The stability of certain model binary stellar systems in galactic gravitational fields.

07 p0898 A73-19935

Roche model application to close binary systems, emphasizing geometrical properties of limiting equipotentials for configuration breakup

10 p1282 A73-24642

Radiation pressure effects on close binary mass loss and luminosity in terms of Roche potential, using contact surface model

12 p1537 A73-27881

The relativistic Roche problem. I - Equilibrium theory for a body in equatorial, circular orbit around a Kerr black hole.

24 p3138 A73-45035

ROCKET BOOSTERS

U BOOSTER ROCKET ENGINES

ROCKET CATAPULTS

F/RF-101 ejection seat upgrade kit for performance improvement, discussing propulsion, trajectory control, snubber system and rapid recovery parachute opening

16 p1966 A73-32667

ROCKET CHAMBERS

U COMBUSTION CHAMBERS

U THRUST CHAMBERS

ROCKET COMBUSTORS

U COMBUSTION CHAMBERS

U THRUST CHAMBERS

ROCKET ENGINE CASES

A description of the design, testing and application of the 'Waxwing' apogee boost motor for the 'Black Arrow' satellite launcher, with particular reference to development problems.

[AIAA PAPER 72-1134]

03 p0355 A73-13441

Anisotropic structures reliability in terms of design safety factor, analyzing composite rocket motor cases under plane stress

04 p0452 A73-14723

Pressure vessel proof test variables and flaw growth.

05 p0581 A73-16129

Solid propellant rocket engines - Design and development of components in refractory and stratified materials.

07 p0867 A73-18992

Acoustic emission studies of large advanced composite rocket motor cases.

10 p1288 A73-23967

On the ultrasonic inspection of separation in solid propellant rocket motors.

20 p2568 A73-38646

ROCKET ENGINE CONTROL

Thrust modulation of solid propellant rocket motors [ONERA, TP NO. 1155]

02 p0203 A73-11990

Real time tracking radar for radio guidance system, obtaining algorithm for rocket motor direction and ignition time for satellite orbit optimization

03 p0339 A73-13067

Monopropellant and bipropellant thruster systems with afterburning for geostationary satellite orbital control, evaluating performance and reliability based on calculation and test data

07 p0866 A73-18930

Work carried out by Societe Bertin under contract to CNES in the field of fluidic control

07 p0904 A73-18938

Fluidic circuits fabrication and design technology for rocket guidance and attitude control

07 p0778 A73-18939

Russian book - Dynamics of rocket control systems with onboard digital computers.

07 p0906 A73-20229

Russian book on aircraft, rocket and spacecraft control systems design methods covering ground and onboard systems synthesis, performance estimates, system effectiveness, etc

14 p1773 A73-30353

Fluidic programmer for nuclear engine application.

19 p2454 A73-38054

Fluidic logic circuits applications under adverse environmental conditions, considering sequential control devices and rocket engine roll axis numerical control

23 p2941 A73-43394

ROCKET ENGINE DESIGN

Lambda-4S solid propellant four-stage sounding rocket and scientific satellite launcher, describing design, operational and performance features

01 p0091 A73-11157

M-4 S four-stage solid propellant rocket launch vehicle for scientific satellites, detailing design and performance characteristics

01 p0111 A73-11158

The construction of an operational model of the high-frequency ionic propulsion system RIT 10 M [DGLR PAPER 72-088]

02 p0202 A73-11672

Investigations in connection with the preliminary development of a FLOX-polyethylene hybrid propulsion system

[DGLR PAPER 72-086]

02 p0202 A73-11676

Investigation of the fitness for space travel of the electric propulsion plant ESKA 18

[DGLR PAPER 72-087]

02 p0131 A73-11694

Prospects for rocket propulsion with laser-induced fusion microexplosions.

[AIAA PAPER 72-1063]

03 p0353 A73-13392

Development of a radioisotope-fueled thruster for satellite propulsion.

[AIAA PAPER 72-1066]

03 p0354 A73-13395

Scaling of performance and thermal environment in fuel-vortex cooled rocket engines.

[AIAA PAPER 72-1075]

03 p0354 A73-13399

Optimum design of space storable gas/liquid coaxial injectors.

[AIAA PAPER 72-1076]

03 p0354 A73-13400

Unmanned outer planets and round trip mission nuclear rocket engine design for carrying payload into orbit by single earth orbital shuttle

[AIAA PAPER 72-1090]

03 p0340 A73-13411

High performance reactorless nuclear propulsion of reusable orbital space tug by laser rocket engine

[AIAA PAPER 72-1095]

03 p0341 A73-13415

Propulsion unit, components, environmental tests and development problems of Swedish air to ground missile rocket engine operating on liquid propellants

[AIAA PAPER 72-1102]

03 p0355 A73-13421

Evaluation of acoustic cavities for combustion stabilization.

[AIAA PAPER 72-1147]

03 p0356 A73-13452

Hydrogen-oxygen Space Shuttle ACPS thruster technology review.

[AIAA PAPER 72-1158]

03 p0356 A73-13460

Material evaluation under direct rocket exhaust impingement. 03 p0287 A73-13465

A procedure for optimum rocket engine system/turbopump integration. 03 p0357 A73-13477

Analytical correlation technique for air breathing and rocket engines combustor design and performance prediction based on hydrogen oxygen engines test data [AIAA PAPER 72-1074] 04 p0486 A73-14904

Experimental evaluation of a 600 lbf spacecraft rocket engine. 04 p0486 A73-14914

Electrothermal hydrazine thruster analyses and performance evaluation. 04 p0486 A73-14917

Hydrogen oxygen propulsion component design and hot firing tests for space shuttle auxiliary systems and upper stage applications [AIAA PAPER 72-1156] 04 p0486 A73-14918

Long life contact-ionized cesium low thrust engine design, considering ionizer working temperatures and neutralizer ion current densities 04 p0488 A73-15720

Low power pulsed ablation plasma thruster design for satellite attitude control and stationkeeping, describing operating principle and performance measurements 04 p0489 A73-15731

ESKA ion thrusters - Development and application for geocentric missions. 04 p0489 A73-15739

Maintainability of the Space Shuttle Orbiter main engine. 05 p0606 A73-16642

Space Shuttle Orbiter main engine design. [SAE PAPER 720807] 05 p0607 A73-16644

Maneuvering engines for Space Shuttle Orbiter. [SAE PAPER 720806] 05 p0607 A73-16646

Space shuttle bipropellant reaction control system /RCS/ engine design, characteristics and tests, emphasizing reusability and minimum servicing [SAE PAPER 720839] 05 p0607 A73-16668

Technology applied to the Space Shuttle Main Engine. [AIAA PAPER 73-60] 06 p0741 A73-17633

German book - Hybrid rocket propulsion systems: An introduction to theoretical and technical problems. 06 p0741 A73-17669

Subliming solid propellant microthruster for satellite stabilization, discussing operational principles and design features 07 p0866 A73-18927

Ammonia resistojet development for satellite stabilization and position control with 5-year service life, discussing dissociation catalysis research and high efficiency heat exchanger design 07 p0867 A73-18932

Performance of a modified downstream-cathode MPD thruster. 07 p0867 A73-19492

Electron bombardment ion rocket engine with large diameter and divergent magnetic field for efficiency improvement, considering application as source in plasma wind tunnel 07 p0868 A73-20486

Astrobac F sounding rocket system design and development, describing advanced propulsion technology test program and results [AIAA PAPER 73-300] 09 p1156 A73-23219

Rocket motor, Dart vehicle, booster and launcher design and instruments and payload description for Super Loki meteorological rocket systems [AIAA PAPER 73-303] 09 p1156 A73-23222

Russian book - Fundamentals of the theory of operational processes in solid-propellant rocket systems. 10 p1262 A73-23948

Effect of solidity on rocket pump inducer performance. 13 p1624 A73-29011

Problems related to the development and firing of launchers 14 p1742 A73-30102

Russian book - Solid-fuel ballistic rockets. 14 p1804 A73-30356

Russian book - Physical principles of rocket weaponry. 15 p1944 A73-32419

The scope and methods of environmental testing of double-base propellant rocket motors - Choice of conditions and interpretation of results. 16 p2047 A73-33390

Economic tradeoff study of design criteria cost effectiveness, applying to reusable nuclear shuttle /RNS/ engine concepts 16 p2035 A73-33650

Development of advanced composite rocket motor chambers using boron and graphite fibers. 17 p2194 A73-34803

Edgewise tape wound reinforced plastic ablative components for rocket motors to provide balance between optimum char strength, heat flow and insulation characteristics 17 p2195 A73-34809

High strength continuous filament wound carbon fiber reinforced plastic performance evaluation for use in light weight rocket motors 17 p2195 A73-34810

Rocket power, Redstone to Saturn V, now Space Shuttle, 20 years of development. 19 p2493 A73-37886

Precision pointing control thruster design for satellite experiment to test relativistic precession of gyroscope moving through gravitational field, determining gyro orientation via superconducting circuitry [AIAA PAPER 73-858] 20 p2586 A73-38796

Test flight and configuration of Skylark based SL 1081 earth resources rocket prototype with two photographic cameras and earth albedo sensors 20 p2615 A73-39874

Russian book - Solid-propellant rocket engines. 22 p2900 A73-41880

ROCKET ENGINE NOISE

Determination of maximum ground noise during a rocket launch - Discussion and simple prediction method. 16 p2072 A73-33142

ROCKET ENGINES

NT BOOSTER ROCKET ENGINES
NT ELECTRIC ROCKET ENGINES
NT ELECTROSTATIC ENGINES
NT HYBRID PROPELLANT ROCKET ENGINES

NT HYDRAZINE ENGINES
NT HYDROGEN OXYGEN ENGINES
NT LIQUID PROPELLANT ROCKET ENGINES
NT LITHERGOL ROCKET ENGINES
NT MICROROCKET ENGINES

NT NUCLEAR ENGINE FOR ROCKET VEHICLES
NT NUCLEAR LIGHTBULB ENGINES
NT NUCLEAR ROCKET ENGINES

NT RESTARTABLE ROCKET ENGINES
NT RETOROCKET ENGINES
NT REUSABLE ROCKET ENGINES

NT SOLID PROPELLANT ROCKET ENGINES
NT TURBOROCKET ENGINES
NT UPPER STAGE ROCKET ENGINES

NT VERNIER ENGINES
Unmanned planetary spacecraft chemical rocket propulsion. 01 p0090 A73-10102

Photoelastic stress analysis of solid propellant grains. 01 p0090 A73-11118

Guidance of spacecraft controlled by low-thrust rocket engines and evolving in the plane of the initial trajectory 02 p0227 A73-11580

Filament wound boron/epoxy rocket motor chamber fabrication and hydroproof, burst and firing tests, including failure and deformation evaluation 03 p0331 A73-13024

The service life of rocket motors filled with double base propellants. [AIAA PAPER 72-1109] 03 p0351 A73-13424

The Viking Orbiter 1975 beryllium INTEREGEN rocket engine assembly. [AIAA PAPER 72-1131] 03 p0382 A73-13438

Additives for heat transfer reduction in the propellant combinations N2O4-MMH and N2O4-A-50. [AIAA PAPER 72-1132] 03 p0352 A73-13439

One-millipound colloid thruster system development. [AIAA PAPER 72-1153] 03 p0356 A73-13456

Ammonium perchlorate/aluminum powder propellant rocket engine feasibility evaluation, considering test firing results on performance and stability characteristics for various injector configurations [AIAA PAPER 72-1162] 03 p0357 A73-13463

Experimental evolution of an earth-storable bimodal rocket engine. [AIAA PAPER 72-1128] 04 p0486 A73-14913

German book - Flight propulsion systems: Principles, systematics, and technology of aeronautical and astronautical propulsion systems. 05 p0606 A73-16355

Nonlinear longitudinal combustion instability in rocket motors. [AIAA PAPER 73-217] 05 p0641 A73-16947

Rapid continuous evaluation of thruster performance dependence on system parameters using thrust balance for measurement, noting suitability for electric microthruster characterization 05 p0579 A73-17253

Ion thrusters with cesium contact ionization - Study of the main elements. 07 p0867 A73-18933

Certain results of flight tests of a model ion thruster employing contact ionization of cesium on tungsten 10 p1262 A73-23892

Homogeneous and composite solid propellants, discussing rocket motor performance, energetics, smokeless exhaust, energy-weight relations and cost 14 p1784 A73-30135

Russian book - Pioneers rocket engineering: Selected works /1929-1945/. 15 p1943 A73-31576

The geometry and physical properties of exhaust clouds generated during the static firing of large rocket engines. 17 p2253 A73-34349

Three-dimensional flow field in rocket pump inducers. I - Measured flow field inside the rotating blade passage and at the exit. [ASME PAPER 73-FE-33] 17 p2095 A73-35024

Experimental evaluation of a roll control system for a shrouded cone. 17 p2239 A73-35500

Some results of flight tests of an ion-engine model using surface ionization of cesium on tungsten. 20 p2600 A73-38911

Structure of the base flow in a four-nozzle cluster rocket engine 21 p2754 A73-40392

Experimental investigation of a gas-liquid thruster model with a ballasting-reinforced thrust 22 p2841 A73-42127

German book on rocket propulsion theory covering orbital mechanics, equations of motion, performance parameters and nuclear, electric and chemical propulsion types 22 p2909 A73-42493

German monograph - A method for the calculation of mixing and combustion processes in a rocket propulsion system with air-augmentation. 22 p2900 A73-42851

Russian book on rocketry principles covering jet propulsion, jet engine combustion chambers, rocket propellants, design, aerodynamics, flight control and anti-aircraft rockets 23 p3038 A73-43334

Experimental and theoretical determination of the admittances of a family of nozzles subjected to axial instabilities. 24 p3122 A73-45267

ROCKET EXHAUST

The removal of impurities from hydrazine for control of contamination caused by rocket engine exhaust. [AIAA PAPER 72-1046] 03 p0351 A73-13379

Space simulation experiments on reaction control system thruster plumes. [AIAA PAPER 72-1071] 03 p0354 A73-13398

Material evaluation under direct rocket exhaust impingement. [AIAA PAPER 72-1167] 03 p0287 A73-13465

Radiation base heating from solid propellant launch vehicle exhaust plumes. [AIAA PAPER 72-1168] 03 p0397 A73-13466

Titan III convective base heating from solid rocket motor exhaust plumes. [AIAA PAPER 72-1169] 03 p0382 A73-13467

A study of the plume impingement environment experienced by the booster during the space shuttle nominal staging maneuver. [AIAA PAPER 72-1171] 03 p0273 A73-13468

Solid propellant rocket motors exhaust smoke minimization, discussing smoke formation mechanism and optical properties relationship to propellant characteristics [AIAA PAPER 72-1192] 03 p0352 A73-13482

The optical temperature of the Apollo 15 exhaust plume. [AD-757298] 03 p0358 A73-13497

Effect of nozzle boundary layers on rocket exhaust plumes. 03 p0247 A73-14193

Rocket exhaust plume ground test facilities and scaling for in-flight conditions simulation and separation in supersonic flow [AIAA PAPER 72-1072] 04 p0414 A73-14903

A study of the rarefaction of the interaction between an exhaust plume and a hypersonic external flow. [AIAA PAPER 73-199] 06 p0645 A73-17657

Exhaust plume prediction model for a low-altitude supersonic missile. [AIAA PAPER 72-1170] 06 p0741 A73-18399

Penetration of retrorocket exhausts into subsonic counterflows. 07 p0773 A73-19491

Detachment of the outer shock from underexpanded rocket plumes. 07 p0920 A73-19977

An analytical model for the prediction of liquid rocket plume contamination effects on sensitive surfaces. [AIAA PAPER 72-1172] 12 p1532 A73-27099

Homogeneous and composite solid propellants, discussing rocket motor performance, energetics, smokeless exhaust, energy-weight relations and cost 14 p1784 A73-30135

Exhaust cloud rise and growth for Apollo Saturn engines. 15 p1906 A73-31920

The interaction of a transient exhaust plume with a rarefied atmosphere. 16 p2086 A73-33873

The geometry and physical properties of exhaust clouds generated during the static firing of large rocket engines. 17 p2253 A73-34349

Multiphase underexpanded plume computational technique including turbulent mixing and nonequilibrium chemistry.
 [AIAA PAPER 73-695] 18 p2368 A73-36244
 Impingement of small, very high pressure solid rocket motor plumes upon nearby surfaces.
 [AIAA PAPER 73-730] 18 p2342 A73-36347
 Plume boundary jump of an underexpanded jet exhausting counter to a freestream.
 21 p2790 A73-40433
 Determination of disturbances acting on a space vehicle from the liquid-disposal nozzle.
 21 p2781 A73-41199

ROCKET FIRING

Hypergol rocket engines restart difficulties investigation via cold flow and hot firing tests, simulating worst case environmental conditions.
 [AIAA PAPER 72-1160] 03 p0357 A73-13461
 Ammonium perchlorate/aluminum powder propellant rocket engine feasibility evaluation, considering test firing results on performance and stability characteristics for various injector configurations.
 [AIAA PAPER 72-1162] 03 p0357 A73-13463
 The starting transient of solid-propellant rocket motors with high internal gas velocities.
 [AIAA PAPER 72-1119] 04 p0486 A73-14909
 Red fuming nitric acid suitability for nonhypergolic rocket fuel ignition in presence of chromate and dichromate catalysts.
 07 p0865 A73-19986
 Launching base creation process and economic factors, considering rocket firing safety, scientific requirements and financial investments criteria.
 14 p1741 A73-30080
 Problems related to the development and firing of launchers.
 14 p1742 A73-30102
 Deleterious vibrations development in support structure of launch pad during initial firing of launch vehicle, noting frequency spectrum dependence on soil characteristics and structural design.
 14 p1742 A73-30105
 Meteorological lidar for determining aerological data above launching base prior to rocket firing.
 14 p1771 A73-30115

ROCKET FLIGHT

Gravity selection by animals in fields of centrifugal acceleration superimposed on weightlessness during sounding rocket flights.
 01 p0009 A73-11209
 Rocket flight in rarefied layers of the atmosphere.
 02 p0227 A73-11579
 Minimum fuel rocket maneuvers in horizontal flight.
 08 p1014 A73-20714
 Rocket rectilinear motion, comparing Meshcherskii and Gantmacher-Levin equations in light of contact interaction hypothesis.
 08 p1014 A73-21181
 A method for the analysis of artificial clouds in the upper atmosphere.
 08 p0961 A73-21391
 Controlling the angular motions of a flight vehicle with the aid of flywheels.
 12 p1522 A73-27083
 General theory of optimal trajectory for rocket flight in a resisting medium.
 12 p1538 A73-27119
 Influence of structural flexibility on the dynamic stability of rockets.
 14 p1803 A73-30043
 Russian book - Physical principles of rocket weaponry.
 15 p1944 A73-32419
 Intermediate-thrust arcs and their optimality in a central, time-invariant force field.
 16 p2062 A73-33305
 The rocket motion in resisting medium on a given trajectory.
 18 p2353 A73-36490
 Relativistic rocket motion tensor equations analogous to particle motion in electromagnetic fields, discussing Hamiltonian functions, Lagrangian coordinates and variable mass body mechanics.
 18 p2356 A73-37038

ROCKET FUEL TANKS

U PROPELLANT TANKS

ROCKET LAUNCHERS

NT ROCKET CATAPULTS

Gun launched sounding rockets and sabot projectiles for low cost meteorological and geophysical data acquisition, considering cost advantages.
 06 p0756 A73-18020
 The operational facilities of the French Guyana Space Center.
 07 p0807 A73-18946
 The influence of the concept of a launcher on the layout of a launch base, and on the organization of test flights and operational launches.
 14 p1804 A73-30103

ROCKET LAUNCHING

NT ORBITAL LAUNCHING

Space rocket/ launch vehicle computer guidance and targeting equations, discussing Q, Delta, explicit,

linear tangent, optimal, numerical integration and parameter optimization techniques.

06 p0721 A73-18824
 Launching base telelimiter apparatus with image superposition on TV screen for controlling missile or rocket from going beyond security limits during initial flight.
 07 p0789 A73-18950
 A laser optical lever system for measuring the pitch and yaw of a ground-launched rocket.
 08 p0974 A73-20669

Tibere rocket launched Electre nose cones reentry impact safety optimization policy based on probabilistic viewpoint.
 [ONERA, TP NO. 1152] 08 p1014 A73-21679
 Stabilizing the elastic modes of the Space Shuttle vehicle during launch.
 [AIAA PAPER 73-319] 11 p1430 A73-25550

Explanation of the accident to the Europa II F 11 launcher by phenomena of electrostatic origin.
 11 p1431 A73-25749
 Andoya Rocket Range facilities in northern Norway, discussing rocket launching for auroral research.
 14 p1741 A73-30082

DFVLR Mobile Rocket Base use of foreign ranges to launch sounding rockets.
 14 p1741 A73-30084
 Sounding rocket range facilities at Esrange /Sweden/ for auroral studies, discussing telemetry support for simultaneous launchings.
 14 p1741 A73-30085

The problem of launching bases in the meteorological rocket network.
 14 p1743 A73-30116
 Exhaust cloud rise and growth for Apollo Saturn engines.
 15 p1906 A73-31920

Determination of maximum ground noise during a rocket launch - Discussion and simple prediction method.
 16 p2072 A73-33142
 Vibration and shock stresses in the case of ballistic rockets. III - Evaluation of the results and comparison with the specifications available.
 16 p2073 A73-33389

Russian book on rocket weapon systems safety handling covering HF electromagnetic, noise and vibration effects, ionizing radiation, fire, etc.
 22 p2812 A73-41874

ROCKET LININGS

Stability of combustors with partial length acoustic liners.
 01 p0090 A73-10641
 On the ultrasonic inspection of separation in solid propellant rocket motors.
 20 p2568 A73-38646

ROCKET MOTOR CASES

U ROCKET ENGINE CASES

ROCKET NOSE CONES

Program objectives and propulsive, equipment case, attitude control, interstage, separation skirt and nose cone subassemblies of French Diamant B-P4 launch vehicle.
 10 p1285 A73-23654
 Electre nose cones reentry impact safety policy, discussing launcher trajectory, cost and performance indices and ascent optimization.
 14 p1804 A73-30097
 Experimental evaluation of a roll control system for a shrouded cone.
 17 p2239 A73-35500

ROCKET NOZZLES

Theoretical consideration on the supersonic axisymmetrical nozzle.
 01 p0003 A73-11131
 Review of nozzle damping in solid rocket instabilities.
 [AIAA PAPER 72-1050] 03 p0353 A73-13381
 Rocket nozzle design and analysis techniques, considering requirements for high energy propellants, multiple pulse operation and long duration high temperature exposure.
 [AIAA PAPER 72-1190] 03 p0358 A73-13480
 Rocket nozzles fabrication technology, discussing construction materials and manufacturing processes.
 [AIAA PAPER 72-1191] 03 p0358 A73-13481
 Experimental determination of three-dimensional liquid rocket nozzle admittances.
 09 p1167 A73-23438
 Flow properties fluctuations in a convergent-divergent nozzle.
 19 p2375 A73-37402
 Structure of the base flow in a four-nozzle cluster rocket engine.
 21 p2754 A73-40392

ROCKET OXIDIZERS

NT FLOX

Corrosion tests for rocket propulsion system components materials for use with nitric acid-nitrogen tetroxide blend oxidizer.
 03 p0329 A73-13007
 The acute inhalation toxicology of chlorine pentafluoride.
 15 p1839 A73-32173

Effect of secondary oxidizer supply through a porous solid fuel on the hybrid combustion process.
 23 p3019 A73-43783

ROCKET PROPELLANT TANKS

U PROPELLANT TANKS

ROCKET PROPELLANTS

NT CRYOGENIC ROCKET PROPELLANTS
 NT DOUBLE BASE ROCKET PROPELLANTS
 NT GASEOUS ROCKET PROPELLANTS
 NT HYPERGOLIC ROCKET PROPELLANTS
 NT LIQUID ROCKET PROPELLANTS
 NT MONOPROPELLANTS
 NT SOLID ROCKET PROPELLANTS

The service life of rocket motors filled with double base propellants.
 [AIAA PAPER 72-1109] 03 p0351 A73-13424

Rocket propellant handling personnel protective clothing, describing head gear, ventilated underwear and airtight external suit.
 07 p0784 A73-18949

Investigation of a single spraying site of a colloid thruster.
 08 p0996 A73-21599
 Russian book - Fuels and lubricants for flight vehicles.
 19 p2472 A73-37769

Russian book on rocketry principles covering jet propulsion, jet engine combustion chambers, rocket propellants, design, aerodynamics, flight control and aircraft rockets.
 23 p3038 A73-43334

ROCKET PROPELLED SLEDS

Rocket sled facility for impact tests with friable balloon platforms, describing braking and accelerating jet configurations, vibration damping measures and telemetry system.
 07 p0808 A73-19004

ROCKET SONDES

U SOUNDING ROCKETS

ROCKET SOUNDING

Rocket measurements of low energy electrons and optical emissions in the dayglow and aurora.
 01 p0036 A73-10346
 A vertical profile of OH in the mesosphere.
 01 p0041 A73-10883
 Rocket measurements of electron fluxes in the upper atmosphere at midlatitudes.
 01 p0041 A73-10887
 Positive ion composition measurements in the D and E regions of the equatorial ionosphere.
 01 p0041 A73-10889
 Negative-ion composition measurements in the D and lower E regions.
 01 p0042 A73-10896
 Rocket payload designs simulated by Monte Carlo method for aerodynamic properties during D region composition measurements.
 02 p0156 A73-11740

Ionospheric resonance signal envelope and waveform observation by rocket-borne RF sounder, noting electron gyrofrequency third harmonic due to beating waves.
 02 p0140 A73-11750
 Probe measurements of positive ions and electron temperatures in high latitude rocket flights.
 02 p0159 A73-12032

Neutral wind measurement during daytime in the thermosphere.
 02 p0159 A73-12224
 Mesospheric cosmic dust concentration measurements from particle collection rocket flights, discussing interference from uplifted aerosols of terrestrial or cosmic origin.
 02 p0215 A73-12259

Upper atmospheric dust concentrations in polar regions.
 02 p0215 A73-12260
 Commencement of routine meteorological rocket observation at Ryori, Japan.
 02 p0188 A73-12271

Rocket photometric observations of dayglow sky radiation in O green line, noting aerosol scattering coefficient and particle concentration.
 02 p0161 A73-12277

E and F regions ion composition measurement with rockets, noting nitric oxide variation with molecular/atomic oxygen cations ratios at different solar activity phases.
 02 p0206 A73-12305

Electron density and wind structure observations in lower ionosphere by rocket, noting sporadic E layer due to wind shear.
 02 p0163 A73-12307

Rocket sounding of ionospheric electron density and temperature profiles during moderate auroral event, noting field-aligned motion of irregularities in F region.
 02 p0163 A73-12309

Electric fields and conductivities derived from wake measurements on a rocket.
 02 p0164 A73-12311

Measurements of energetic particle fluxes during a slowly varying absorption event by two co-ordinated rocket flights.
 02 p0206 A73-12314

Proton energy spectra from recent rocket measurements in the night and morning time auroral zone.
02 p0206 A73-12315

Preliminary findings of a petrel rocket experiment to investigate the VLF emission 'chorus' in the ionosphere.
02 p0141 A73-12319

Recent results of the Goddard rocket program for observing stars.
02 p0215 A73-12324

High angular resolution observations from rockets - Solar XUV observations.
02 p0216 A73-12336

Rocket sounding and grenade experiments for stratosphere-mesosphere interaction, showing simultaneous winter temperature changes of opposite sign.
02 p0163 A73-12789

Rocket-ultraviolet spectra of eight stars in Ophiuchus and Scorpius.
03 p0366 A73-12942

Rocket-ultraviolet spectra of six stars in Perseus.
03 p0366 A73-12943

Asymmetry of soft X-ray emission near M87.
03 p0361 A73-13713

Electron intensity measurements by sounding rockets over auroral arcs at magnetospheric plasma boundary.
03 p0362 A73-13865

A revised low-frequency cosmic noise spectrum.
04 p0500 A73-15516

Rocket sounding for space charge distribution and electric field strength in stratosphere and mesosphere, noting vertical distribution of atmospheric conductivity.
05 p0570 A73-17013

Rocket-borne measurement of UV background radiation at 1115, 1425 and 1446 Å, setting upper limit to flux from Coma galactic cluster.
07 p0868 A73-19057

Observations of the He II 304-Å radiation in the night sky.
07 p0869 A73-19232

Dawn airglow far UV spectrum observed by scanning Ebert spectrophotometer aboard Aerobee rocket, obtaining altitude profiles at 100-244 km.
07 p0814 A73-19247

Lower ionospheric electron densities from rocket measurements employing LF radio propagation and DC probe techniques.
07 p0818 A73-19670

Photography of a lithium vapor trail during the daytime.
07 p0820 A73-20068

Night sky background radiation measurement by far IR radiometer carried on rocket launched from Hawaii.
07 p0825 A73-20187

Auroral particle influx behavior and electric field aligned electron precipitation observation by Ba release and electrostatic probe in rocket and satellite experiments.
08 p0957 A73-20662

Measurements of the solar spectrum between 30 and 128 Å.
[AD-757958] 08 p1002 A73-20760

A soft X-ray survey from the galactic center to Cassiopeia.
08 p1008 A73-21163

Measurement of auroral Birkeland currents and energetic particle fluxes.
09 p1073 A73-22057

Electron intensities over auroral arcs from rocket flight, noting electron phase-space density increase with northward progress.
09 p1078 A73-22833

Short-term temporal studies of the X-ray emission from Cassiopeia A, Tycho, and Scorpius X-1.
10 p1264 A73-23547

A comparative study of the wind structure in the stratosphere at Sonmiani vis-a-vis CIRA 1965.
10 p1244 A73-23647

Comparative characteristics of the soft component of solar and galactic cosmic rays on the basis of rocket and stratospheric measurements at Heis Island and Apatite Station.
10 p1267 A73-23920

Twilight airglow. I - Photoelectrons and forbidden O I 5577-angstrom radiation.
10 p1214 A73-24737

Some results of ionospheric measurements based on observations of geophysical rocket signals from spaced points and observations of signals reflected by space objects.
11 p1350 A73-25077

Vertical electron density and temperature data from geophysical rocket borne Langmuir probes and electrode traps.
11 p1350 A73-25078

Ionospheric vertical electron density profiles from geophysical rocket-borne microwave dispersing interferometer.
11 p1350 A73-25079

Formation of the density profile of charged particles at heights from 10 to 90 km.
11 p1411 A73-25082

The distribution of X-ray sources in our galaxy.
11 p1415 A73-25178

Rocket measurements of particle flux during the April 1969 solar cosmic ray event.
12 p1535 A73-27651

Fraunhofer line data reduction and wavelengths identification in solar UV spectra recorded during flight of Skylark rocket SL 601.
12 p1544 A73-27827

Study of the directional distribution of energetic electrons and protons in the morning sector of the auroral zone during enhanced particle flux.
13 p1606 A73-28153

Metal ion density measurement in sporadic E layer during beta Taurids shower by rocket-borne mass spectrometry, noting origin in cosmic debris ablation.
13 p1673 A73-28277

Fe XVII emission from the solar corona.
13 p1685 A73-29356

Rocket-based mass spectrometric measurements of midlatitude and north polar region ionospheric ion composition, discussing ionization of water and heavy water vapors.
14 p1747 A73-29864

Auroral electrons of energy less than 1 keV observed at rocket altitudes.
14 p1748 A73-29969

The concept of the flight safeguard interferometer for rocket probes of the French Guiana Space Center.
14 p1773 A73-30090

Interstellar gas abundances from rocket observations of ultraviolet absorption lines.
14 p1801 A73-30734

UV dayglow in 750-1050 Å region at 100-800 km observed with rocket-borne thin film filter photometer, solving radiative transfer problem for excitation process.
15 p1867 A73-31077

Rocket flight observations of solar UV chromosphere at 1190-1320 Å, considering spectral and angular resolutions.
15 p1936 A73-31564

French monograph - Interpretation of particle measurements carried out aboard rocket probes during the solar event of Jan. 28 1967.
15 p1927 A73-32586

Charge and energy spectra of particles with E from 0.2 to 30 MeV/nuc in the January 25, 1971 solar flare.
16 p2054 A73-33281

Mesospheric and lower thermospheric ozone concentration measurement at sunset via occultation technique from rocket payloads.
17 p2159 A73-34780

Skylark rocket measurement of earth atmosphere and ionosphere, examining payload capacity, camera image quality, cost, use of smaller rockets and practical applications.
17 p2239 A73-34953

Global meridional cross sections and charts for mesospheric circulation and temperature variability via meteorological rocket network.
18 p2302 A73-35925

Experimental results of radio wave absorption measurements in Southwest Europe.
18 p2288 A73-35940

Combined temperature, diffusion coefficient and density measurements of photoluminescent A10 releases.
18 p2303 A73-35949

Some features of the equatorial D-region as revealed from the Langmuir probe experiments conducted at Thumba.
18 p2303 A73-35954

Ion and neutral composition measurements in the lower ionosphere.
18 p2303 A73-35960

Extreme temperature deviations from the climatological mean in the upper stratosphere - observed by rockets, confirmed by satellites.
18 p2304 A73-35962

Accuracy of rocket measurements of lower ionosphere electron concentrations.
18 p2304 A73-35965

Electron density profiles from ionograms - Comparisons with rocket profiles.
18 p2306 A73-36017

Recent stratospheric temperature measurement compatibility tests at Wallops Island.
18 p2307 A73-36035

High-level circulation studies based on rawinsonde, rocketsonde and satellite observations.
18 p2350 A73-36040

Electron temperature profile and its solar activity dependence in the middle latitude region.
18 p2308 A73-36047

A rocket observation of the disturbed mid-latitude nighttime ionosphere.
18 p2308 A73-36048

Rocket sounding of upper atmosphere vertical wind profiles, shear, temperature distribution and diffusion coefficient for model atmosphere calculation.
18 p2309 A73-36057

Joule heating effect due to currents in the equatorial electrojet as observed by rocket borne probes.
18 p2310 A73-36128

Rocket investigation of the intensity and composition of the corpuscular radiation at altitudes 180 km up to the polar region.
18 p2345 A73-36137

Ion composition measurements at altitudes 100-180 km in 1972.
18 p2310 A73-36143

Mass spectrometric investigations of the night polar ionospheric structure.
18 p2310 A73-36145

Rocket measurements of electron density and electron temperature at sunset.
18 p2311 A73-36148

Ionospheric magnetic field measurements at auroral latitudes.
18 p2313 A73-36647

HF radar observations of cesium plasma cloud released from the rocket K-9 M-39.
19 p2423 A73-37378

Rocket measurement of photoelectrons in the ionosphere by K-9 M-40.
19 p2474 A73-37379

Measurement of the ionospheric electron density by using S-210-6 rocket.
19 p2423 A73-37380

A comparison of geostrophic and rocket winds at stratospheric levels, measured from a small network of rocket sounding stations.
19 p2424 A73-37604

Diurnal and annual temperature variations in the 30-60 km region as indicated by statistical analysis of rocketsonde temperature data.
19 p2424 A73-37662

On the propagation of ionospheric whistlers at low latitude.
19 p2404 A73-38018

Skylark rocket magnetometer measurement of sporadic E layer magnetic fields, testing wind shear theory of ionization redistribution at midlatitudes.
19 p2426 A73-38022

Electron flux variation measurements in the upper atmosphere at altitudes of 200 to 500 km.
20 p2554 A73-39168

Test flight and configuration of Skylark based SL 1081 earth resources rocket prototype with two photographic cameras and earth albedo sensors.
20 p2615 A73-39874

Stratospheric temperature profiles from limb radiance measurement by Aerobee rocket, comparing with rocket sounding and radiosonde data.
21 p2729 A73-40064

Thermal electron energy distribution measurements in the ionosphere.
21 p2681 A73-40156

Rocket measurements of electric field and optical aurora during weak PCA event, noting rocket passage through discrete auroral forms.
21 p2684 A73-40781

Ground based and rocket techniques for vertical ionospheric electron density distribution measurement, considering incoherent scatter, partial reflection, wave interaction, and Faraday rotation.
21 p2685 A73-40809

Rocket experiments on nonlinear wave-wave interaction in the ionospheric plasma.
21 p2685 A73-40823

Mean D-region electron density profiles derived by combination of rocket and radio wave propagation data.
21 p2686 A73-40831

The optimal number of soundings for a complete investigation of the ionization-neutralization and dynamic characteristics of the middle ionosphere.
21 p2686 A73-40911

Complex studies of corpuscular radiation in the upper atmosphere at midlatitudes during geomagnetic perturbations.
21 p2760 A73-40918

Results of simultaneous wind measurements in the stratosphere, mesosphere and low thermosphere.
21 p2732 A73-41340

Study of neutral composition of lower thermosphere at Fort Churchill.
21 p2688 A73-41344

Estimates of thermospheric neutral constituents from ion composition measurements.
21 p2688 A73-41350

Investigation of mid-latitude ionospheric currents by combined rocket techniques.
21 p2689 A73-41359

Diurnal and seasonal variations of neutral winds and electric fields above 90 km in the vicinity of the auroral electrojet.
21 p2690 A73-41365

Rocket measurements of electron concentration and electron temperature in the polar ionosphere.
21 p2690 A73-41367

Rocket measurements of production and ionization during a PCA event.
21 p2760 A73-41371

Preliminary results from the noctilucent sampling from Kiruna in 1970.
21 p2775 A73-41413

Noctilucent cloud sampling by a multi-experiment payload.

21 p2775 A73-41414

Near-earth micrometeorite flux measurement by rocket-borne acoustic detectors, noting consistency with previous observations

21 p2775 A73-41415

Dust measurements in the upper atmosphere during and in the absence of noctilucent cloud display.

21 p2691 A73-41417

The far-ultraviolet spectrum of Jupiter.

22 p2905 A73-41769

Rocket observations of electron precipitation in a westward-traveling surge.

22 p2902 A73-41915

Atmospheric temperature measurement using balloons and rockets.

22 p2883 A73-42061

Cerenkov-effect based standard radiation source designed for the calibration of space experiments - Spectral energy distribution measurement

22 p2860 A73-42307

Postsunset oxygen emission observation by radiometer on rocket launched at Natal, Brazil, observing 10-km thick emission layer

22 p2848 A73-42536

Rocket-borne magnetometer measurement of magnetic field changes associated with electron density fluctuations and wind structure, testing wind shear theory of sporadic E formation

23 p3024 A73-43701

The mean ozone distribution from several series of rocket soundings to 52 km at latitudes from 58 deg S to 64 deg N.

23 p2975 A73-43880

Comet Kohoutek earth orbit properties and rocket and satellite observations, including parent molecule and inner solar system measurements

23 p3034 A73-44222

Rocket-borne spectrometer measurement of solar UV flux for thermospheric vertical distribution of molecular oxygen

24 p3135 A73-44632

Comparative analysis of rocket measurements of n sub e/h and of ground-based vertical sounding data

24 p3083 A73-44795

Ionospheric electric field measurements with a spin stabilized detector.

24 p3090 A73-44818

Probe electric field measurements near a midlatitude ionospheric barium release.

24 p3085 A73-45119

ROCKET TEST FACILITIES

Rocket exhaust plume ground test facilities and scaling for in-flight conditions simulation and separation in supersonic flow

04 p0414 A73-14903

Space missile test center development for checkout, launch and data processing for space boosters, intermediate and intercontinental range ballistic missiles and supersonic aircraft

16 p1993 A73-33087

Test stand for the propulsion systems of the 'Symphonie' communications satellite in vacuum

19 p2419 A73-38271

ROCKET THRUST

A one-dimensional flow model for an air-augmented rocket.

05 p0607 A73-16848

Book - A course in continuum mechanics. Volume 3 - Fluids, gases and the generation of thrust.

14 p1745 A73-30594

Solid propellant rocket burning rate optimization at constant thrust by imbedded inert heat conducting fibers, analyzing flight performance

18 p2342 A73-36064

Propulsion by absorption of laser radiation. [AIAA PAPER 73-624]

18 p2342 A73-36172

Experimental investigation of a gas-liquid thruster model with a ballasting-reinforced thrust

22 p2841 A73-42127

Pulsated over-heated water rocket /POHWARD/ thrust augmentation system for combat aircraft takeoff runs from short runways under severe weather conditions

24 p3057 A73-45391

ROCKET VEHICLES

NT AEROBEE ROCKET VEHICLE
NT AGENA ROCKET VEHICLES
NT ASTROBEE ROCKET VEHICLES
NT ATLAS CENTAUR LAUNCH VEHICLE
NT BLACK KNIGHT ROCKET VEHICLE
NT CENTAUR LAUNCH VEHICLE
NT DIAMANT LAUNCH VEHICLE
NT ELDO LAUNCH VEHICLE
NT LAMBDA ROCKET VEHICLES
NT MULTISTAGE ROCKET VEHICLES
NT SATURN LAUNCH VEHICLES
NT SATURN 5 LAUNCH VEHICLES
NT SINGLE STAGE ROCKET VEHICLES
NT SKYLARK ROCKET VEHICLE
NT SOUNDING ROCKETS
NT TITAN 3 LAUNCH VEHICLE
NT VIKING ROCKET VEHICLE

Analysis of the orbit of Cosmos 268 rocket /1969-20B/.

04 p0496 A73-14964

Optimum flight paths of rocket powered vehicles for general thrust law.

06 p0756 A73-17742

Impulsive deboost analysis for maximum and minimum atmospheric entry angles for hyperbolically orbiting rocket vehicles

07 p0875 A73-19207

Pitch amplitude stabilization in a spacecraft carrier body

09 p1155 A73-23107

Stiletto air-launched supersonic aerial target design, development and capabilities, describing configuration, propulsion and control systems and operational envelope

09 p1032 A73-23121

Stability of symmetric flight vehicles in oblique flow

12 p1548 A73-27076

Rocket vehicle concepts for global transport application, discussing space shuttle technology use, commercial markets, international fleets, single stage feasibility, etc

[AAS PAPER 73-163]

20 p2613 A73-38600

A streak technique for measuring the initial movement of a rocket with four unknown and two known degrees of motion.

21 p2696 A73-39986

ROCKET-BORNE INSTRUMENTS

Neutral composition measurements of the mesosphere and lower thermosphere.

01 p0040 A73-10879

Rocket infrared observations of H II regions.

01 p0103 A73-11026

Positive detection of an excess of low-energy diffuse X-rays at high galactic latitude.

[AD-760197]

01 p0092 A73-11029

Atmospheric atomic oxygen density vertical distribution measurement by rocket-borne cryocooled mass spectrometer ion source

02 p0157 A73-11756

Rocket-borne instrumentation to measure ionospheric electron temperature with good spatial resolution.

02 p0167 A73-11953

Ionospheric electron and ion temperature profile measurements with satellite- and rocket-borne probes, comparing merits and discrepancies

02 p0163 A73-12303

Cosmic soft X rays observations by rocket-borne polypropylene window proportional counters, analyzing X ray sources spectra and intensity distributions

02 p0207 A73-12404

Dc electric field measurement with rocket-borne double probes and by satellite and balloon observation, noting ionospheric fields, magnetospheric plasma and auroras

03 p0302 A73-13874

Solar UV Lyman alpha radiation intensity measurements, using Vertikal-1 rocket-borne photometer and photoelectron analyzer

03 p0379 A73-14565

A compact low-cost electronic time division multiplexer.

04 p0417 A73-15295

Measuring rocket attitude by starlight.

05 p0594 A73-16300

An IRIG FM-FM telemetry system for the Petrel sounding rocket.

05 p0551 A73-16850

Rocket-borne instruments for cosmic dust particles detection in extraterrestrial space, noting collector foils and plates fabrication

06 p0748 A73-17768

High resolution accelerometer for sounding rocket, describing calibration methods

[ONERA, TP NO. 1215]

10 p1219 A73-24398

The evacuating and outgassing of a vacuum UV spectrophotometer for rockets

10 p1220 A73-24683

High resolution rocket EUV solar spectrograph.

11 p1360 A73-25059

Measurement of the absorption of solar ultraviolet radiation with the aid of a photoelectron analyzer

11 p1350 A73-25080

Rocket-borne high spatial resolution solar L alpha photographs during 10 July 1972 eclipse, describing instrumentation and photographic details

11 p1422 A73-25935

A light and compact X-ray image read-out system for space applications.

11 p1364 A73-26050

An interference filter radiometer with cooled optics and a cooled PbS detector for rocket application.

11 p1368 A73-26507

Atomic oxygen loss in ion source of sounding rocket-borne mass spectrometer for determining lower thermosphere neutral composition

12 p1489 A73-26991

Coaxial anode for background suppression in X-ray proportional counters.

13 p1612 A73-28367

Rocket-borne scientific experiment program Sun-Atmosphere 1971, using meteorological rockets for meteor trail, atmospheric and ionospheric observations during geomagnetic disturbances

13 p1609 A73-29188

Split Langmuir probe measurements of current density and electric fields in an aurora.

14 p1748 A73-29970

A thermosphere composition measurement using a quadrupole mass spectrometer with a side energy focusing quasi-open ion source.

14 p1748 A73-29976

Large area focusing collector for the observation of cosmic X rays.

15 p1876 A73-31976

A sequential programme for rocket payloads.

16 p1992 A73-33105

A rocket-borne instrument for the measurement of nighttime atmospheric densities.

17 p2164 A73-34270

D region electron density profiles from radio broadcast field strength measurements by rocket-borne passive RF spectrometers, using ray theory for wave propagation

18 p2303 A73-35956

Recent stratospheric temperature measurement compatibility tests at Wallops Island.

18 p2307 A73-36035

A rocket-borne riometer for the study of lower ionosphere.

18 p2315 A73-36046

Wind measurement by magnetometers, optical and static pressure sensors.

18 p2310 A73-36136

Evaluation of pinholes in unbaked metal film filters to be used in rocket- and satellite-borne XUV spectroheliographs.

19 p2429 A73-37262

Russian book on gyroscope theory covering maritime, aircraft, rocket and spacecraft applications, instrument error, differential equations of motion, rotor precession and degrees of freedom

21 p2705 A73-41437

Crystal spectrometry of active regions on the sun.

21 p2706 A73-41602

French monograph - Preparation of a space experiment intended for high resolution study of the far ultraviolet spectrum of the star gamma Gemini.

22 p2910 A73-42714

Micrometeoroid flux measurement during the 1970 Geminid meteor shower.

22 p2915 A73-43035

Experimental test of the wind-shear theory: A reply - Rocket-borne magnetometers do measure B.

23 p3024 A73-43702

ROCKET-BORNE PHOTOGRAPHY

Stellar sources UV photography from sounding rocket, obtaining mean interstellar absorption, stars magnitudes and distribution and UVB spectrum

02 p0216 A73-12326

Rocket-borne high spatial resolution solar L alpha photographs during 10 July 1972 eclipse, describing instrumentation and photographic details

11 p1422 A73-25935

UV photography of star field by Eridan rocket-borne wide angle camera, noting inertial guidance system pointing errors data reduction problems

18 p2315 A73-35994

Test flight and configuration of Skylark based SL 1081 earth resources rocket prototype with two photographic cameras and earth albedo sensors

20 p2615 A73-39874

ROCKETRY

U ROCKETS

ROCKETS

Russian book on rocketry principles covering jet propulsion, jet engine combustion chambers, rocket propellants, design, aerodynamics, flight control and anti-aircraft rockets

23 p3038 A73-43334

ROCKS

NT ANDESITE
NT ANORTHOSITE
NT BASALT
NT BRECCIA
NT CARBONACEOUS ROCKS
NT COAL
NT DUNITE
NT GRANITE
NT IGNEOUS ROCKS
NT LUNAR ROCKS
NT MOLDAVITE
NT OBSIDIAN
NT PERIDOTITE
NT SANDSTONES
NT SEDIMENTARY ROCKS
NT SHALES

Hornblendes from calc-alkaline volcanic rocks of island arcs and continental margins.

02 p0165 A73-12635

Geothermal energy extraction from hot rocks via deep dry wells by pressurized water circulation, solving numerically fluid flow, heat transport and rock fracture equations

05 p0569 A73-16382

RODENTS

A technique for extracting Radiolaria from radiolarian cherts. 11 p1324 A73-25141

Deformation and transformation of rock-forming minerals by natural and experimental shock processes. I - Behavior of minerals under shock compression. 14 p1750 A73-30958

Investigation of the dielectric properties of terrestrial rocks at super-high frequencies for the purpose of improving accuracy for the composition of lunar material. 16 p2064 A73-33771

Whole rock Th-Pb age for the Masuke and Dembe-Divula complexes, Rhodesia. 17 p2159 A73-34519

Elasticity of water-saturated rocks as a function of temperature and pressure. 17 p2163 A73-35271

Two probable astroblemes in Brazil, considering meteorite impact origin by discovery of diagnostic shock-metamorphic effects in rocks from ERTS-1 satellite and aerial photographs. 21 p2771 A73-41078

Terrestrial rock optical constants, finding refractive index and reflectivity for andesite, basalt, basaltic glass, obsidian and obsidian glass through spectrophotometric analysis. 24 p3081 A73-44558

RODENTS

NT MICE

RODS

Dynamic edge effect in rods - Formulation of shortened problems. 01 p0118 A73-11405

Long-wave approximation in problems of stability loss by impact. 01 p0118 A73-11410

Rods theory covering constitutive equations, boundary value problems, variational formulation of equilibrium problems and uniqueness theorems. 02 p0234 A73-11982

Stability and uniqueness of initially straight elastic rods undergoing three dimensional deformations. 04 p0514 A73-15682

Short-term longitudinal dynamic stability of rods with allowance for clamping methods and for previous transverse deflection. 05 p0632 A73-16329

Rod vision chemistry in terms of rhodopsin, visual cycle and pigment-vision relations, considering dark and light adaptation. 05 p0540 A73-16479

Use of associated matrices in deriving frequency equations for rods with variable rigidities and masses. 05 p0636 A73-17082

Application of the variational-difference method in solving the problems of torsion for rods of complex form. 05 p0636 A73-17094

Vibration theory optimization problems for rectilinear rods, noting Lagrange multipliers continuity in linear hyperbolic equations. 06 p0766 A73-18886

Photochemical receptor mechanism of chromatic vision and scotopic contrast hue sensation due to cone and rod activity interaction. 07 p0783 A73-20261

Longitudinal impact of a rigid body against a clamped rod. 09 p1158 A73-22361

Vertebrate photoreceptor cell /rods and cones/ development and structure, discussing light pathway, ciliary connective and microtubules, outer and inner segments, etc. 09 p1042 A73-23303

Transient compressional wave propagation in a two-layered circular rod with imperfect bonding. 10 p1291 A73-24390

The free surface on a liquid between cylinders rotating at different speeds. II. 10 p1207 A73-24790

Acoustically induced vibrations of slender rods in a cylindrical duct with parallel flow. 11 p1432 A73-24983

Random yield limit of stochastically non-homogeneous elements in tension. 14 p1811 A73-30489

Elastic buckling instability of rotating rods and plates due to compressive stress under critical speed. 15 p1955 A73-32161

Vibration theory optimization problems for rectilinear rods, noting Lagrange multipliers continuity in linear hyperbolic equations. 15 p1956 A73-32411

Solution on a digital computer of boundary value problems for three-dimensional rod systems with branchings. 16 p2075 A73-32692

The optimization of the cross-sectional profile of rods and plates subjected to dynamic stress. 16 p2080 A73-33241

Transverse vibrations of variable rectangular cross section rod, reducing fourth order differential equation to second order via Kirchhoff relation. 16 p2080 A73-33259

Assembly for studying oscillation damping in rod elements in the field of centrifugal forces. 17 p2145 A73-34340

The problem of wave propagation in physically nonlinear rods of finite length. 20 p2618 A73-39315

Velocity of a stress wave superimposed on the initial plastic stress state of a rod. 21 p2784 A73-40436

Pure torsion of prismatic rods composed of different materials. 21 p2787 A73-40990

Thermal response of a viscoelastic rod under cyclic loading. [ASME PAPER 73-APMW-39] 22 p2926 A73-42896

Creep buckling stability for deformable rod with initial deflection, determining perturbed and unperturbed motion of random and deterministic components. 23 p3046 A73-44188

Boundaries of natural frequency variations during the longitudinal oscillations of rods. 24 p3152 A73-45360

ROGALLO WINGS

U FLEXIBLE WINGS

U FOLDING STRUCTURES

ROLL CONTROL

U LATERAL CONTROL

ROLL FORMING

Development of a process utilizing heated rolls for hot rolling metals. 04 p0454 A73-15001

Carbon-PTFE fuel cell electrode for hydrogen-KOH-air batteries for operation over long time periods, discussing rolling technique and industrialization possibilities. 04 p0407 A73-15114

Raney-Ni catalysts preparation for carbon-PTFE fuel cell electrodes from Ni-Al alloy, discussing rolling technique suitability and electrode characteristics. 04 p0407 A73-15115

Heated rolls application in hot rolling of metals, estimating residual thermal stresses and heat transfer. [ASME PAPER 72-WA/MAT-2] 04 p0457 A73-15810

Three-roll flow turning. 06 p0697 A73-17827

Influence of hot rolling on the mechanical properties of unstable austenitic chromium-manganese steels. 09 p1098 A73-21848

ROLLER BEARINGS

Hybrid fluid film and rolling element bearings for long fatigue life and gas bearings for high temperature operation in gas turbine applications. [SAE PAPER 720739] 02 p0173 A73-12005

Inlet shear heating in elastohydrodynamic lubrication. [ASME PAPER 72-LUB-21] 03 p0314 A73-14336

Facility for roller bearing parameters testing during high speed rotation in ultrahigh vacuum, discussing circuitry and principal elements. 07 p0807 A73-18908

Anholonomic constraints imposed on mechanical systems which have rigid solid bodies as constituent elements. II - Anholonomic constraints realized by nonsliding roller bearings. 12 p1523 A73-26794

German monograph - Investigations regarding the elastohydrodynamic lubricant film thickness in the case of elliptical Hertzian contact surfaces. 13 p1625 A73-29287

Choice of the geometrical parameters, R, r, and r₁, of a roller-ring mechanism as a function of maximum load capacity. 15 p1832 A73-31277

Failure modes and accelerated life test methods for despun antenna bearings. [ASLE PREPRINT 73AM-1A-4] 17 p2178 A73-34979

Analysis of sudden death tests of bearing endurance. [ASLE PREPRINT 73AM-3B-2] 17 p2179 A73-34984

Airframe ball, roller and spherical plain bearing designs for flight control, landing gear and wing mechanisms. 21 p2707 A73-41125

ROLLERS

Heated rolls application in hot rolling of metals, estimating residual thermal stresses and heat transfer. [ASME PAPER 72-WA/MAT-2] 04 p0457 A73-15810

ROLLING

Bending and rolling methods for tensile testing of metals without local necking, considering fracture under reduced axial stress. 05 p0581 A73-16130

Observations on the deformation properties of sandwich materials. 06 p0761 A73-17819

Regeneration and recrystallization of austenite in low-carbon stainless steel 18-10 after rolling at room temperature. 07 p0837 A73-19113

Mechanism of plastic deformation and low-temperature brittleness of a Cr alloy containing 45 at. % Fe. 14 p1764 A73-30866

Faulty structure in niobium single crystals deformed by rolling at 77 K. 20 p2579 A73-39743

ROLLING CONTACT BEARINGS

U ANTI-FRICTION BEARINGS

ROLLING CONTACT LOADS

The role of compressional viscoelasticity in the lubrication of rolling contacts. [ASME PAPER 72-LUB-O] 01 p0055 A73-10220

Test facility for determination of S-3A aircraft landing gear behavior during critical pulse loads while rolling over carrier deck, discussing moving platform components. 02 p0150 A73-11999

Shear stresses below asperities in Hertzian contact as measured by photoelasticity. [ASME PAPER 72-LUB-14] 03 p0314 A73-14330

A new criterion for predicting rolling-element fatigue lives of through-hardened steels. [ASME PAPER 72-LUB-32] 03 p0328 A73-14342

Elastohydrodynamic traction characteristics of 5P4E polyphenyl ether. [ASME PAPER 72-LUB-40] 03 p0335 A73-14347

Elastohydrodynamic lubrication in rolling and sliding contacts. [ASME PAPER 72-LUB-K] 03 p0315 A73-14351

The role of compressional viscoelasticity in the lubrication of rolling contacts. [ASME PAPER 72-LUB-O] 03 p0315 A73-14354

The assessment of recently developed lubricants for rolling elements. [ASLE PREPRINT 72LC-4C-2] 03 p0316 A73-14361

The application of elastohydrodynamic lubrication in gear tooth contacts. 03 p0317 A73-14375

Non-steady-state thermal analysis of a rolling aircraft tire. [SAE PAPER 720871] 05 p0535 A73-16667

Effects of surface roughness and form factor on rolling contact fatigue. 07 p0831 A73-20119

Metal tongues in trailing edge of surface pits near fracture path end in rolling contact fatigue of failed ball bearings. 07 p0831 A73-20158

Influence of the nonlinear compliance of rolling contact bearings on the vibrations of a balanced shaft. 09 p1088 A73-22479

Dependence of the coefficient of external friction on a normal load during elastic saturated contact. 10 p1222 A73-23596

Character and magnitude determination of residual stresses in surface layers of rolling bodies. 10 p1289 A73-24068

Frictional traction in elastohydrodynamic lubrication. 13 p1623 A73-28198

Choice of the geometrical parameters, R, r, and r₁, of a roller-ring mechanism as a function of maximum load capacity. 15 p1832 A73-31277

Effect of nonlinear compliance in rolling motion bearings on the vibrations of a balanced shaft. 15 p1883 A73-32066

Spherical debris - Its occurrence, formation and significance in rolling contact fatigue. 16 p2022 A73-34029

An analysis and prediction of lubricant film starvation in rolling contact systems. [ASLE PREPRINT 73AM-3B-4] 17 p2179 A73-34985

The role of physicochemical processes in surface wear under rolling friction in low-molecular hydrocarbon media. 18 p2343 A73-36821

ROLLING MOMENTS

German monograph - The steady and unsteady aerodynamic coefficients for the rolling motion of slender wings. 07 p0774 A73-19578

Roll coupling moment of deflected wing-body combination. 15 p1823 A73-31573

Finite chord effects on vortex induced large aspect ratio wing loads, noting rolling moment magnitude overestimate from lifting line solution. 15 p1823 A73-31670

Flight simulator evaluation of control moment usage and requirements for V/STOL aircraft. [AHS PREPRINT 743] 17 p2147 A73-35076

ROLLUP SOLAR ARRAYS

U SOLAR ARRAYS

ROOFS

Geometric nonlinearity effects on rigid joint deformation of three dimensional skeletal structures, including roofing, cable and shallow dome systems. 06 p0762 A73-18342

ROOM TEMPERATURE

Processing conditions and sample dimensions and shapes effects on Ti alloy creep characteristics at room temperature. 01 p0064 A73-10487

The relation between creep at room temperature and the characteristics of the stress-strain diagram in the case of metallic materials

02 p0181 A73-12366

Room temperature pulsed n-type GaAs cleaved platelet lasers bulk optically pumped near band gap by tunable parametric oscillator, noting emission peak at threshold

[AD-758950] 09 p1092 A73-22240

Spectral behavior and linewidth of /GaAl/As-GaAs double-heterostructure lasers at room temperature with stripe geometry configuration.

09 p1093 A73-22252

Processing conditions and sample dimensions and shapes effects on Ti alloy creep characteristics at room temperature

14 p1759 A73-30312

Miniaturized Nd-YAG laser end pumped by single incoherent gallium-arsenide-phosphide light emitting diode to achieve threshold at room temperature

21 p2713 A73-40457

ROOMS

NT CLEAN ROOMS

The acoustic response of rooms with open windows to airborne sounds.

05 p0537 A73-17369

The transmission of sonic boom signals into rooms through open windows.

05 p0537 A73-17370

ROOT-MEAN-SQUARE ERRORS

Influence of additive and multiplicative noise on the accuracy in measuring the angular position of a source of radiation by systems with pulse-width modulation

01 p0017 A73-10212

Determination of the mean square errors of functions of variables in uniquely determinate geodetic constructions

04 p0443 A73-15511

Optimal optical measurement for two dimensional object position on plane in Gaussian background noise, calculating mean square error for false identification probability determination

05 p0547 A73-16055

Numerical solution of integral equations of the first kind using a priori information on the function to be determined.

05 p0591 A73-16789

Optimal sampling and quantization rates for analog signal by mean-square-error estimates and information content quantitative measure, describing probabilistic properties estimation

06 p0664 A73-17854

Estimation of the precision of presentation of gravimetric, magnetic and other geophysical and experimental data.

07 p0817 A73-19542

Determination of the velocity of a radio meteor with minimum rms error.

08 p1012 A73-21581

Spacecraft transmitted TV picture geometrical distortion in terms of root-mean-square errors, considering applications to ESSA-7, Surveyor-7 and Mariner 4 data samples

10 p1219 A73-24485

Analytical and Monte Carlo analysis of rms beam pointing errors of planar phased arrays with isotropic elements

11 p1328 A73-25660

Light velocity from Io eclipse times observation by Picard and Roemer, noting rms deviation with present value

11 p1429 A73-26685

Amplitude-modulated pulse code sequence demodulation using physically realizable linear filter for reconstruction of discrete sample message at optimum mean-square error level

12 p1467 A73-26943

Mean risk determination in radio-electronic device control

14 p1735 A73-30291

An empirical Bayes approach for the Poisson life distribution.

15 p1901 A73-32262

Validation of digital radar landmass simulation utilizing terrain elevation data compression.

18 p2292 A73-36842

Determination of an optimal dynamic system according to complex statistical criteria in the presence of constraints

20 p2539 A73-38680

Evaluation of the noise immunity of pulse systems for continuous message transmission allowing for quantization and interpolation errors. II

20 p2531 A73-39462

Fatigue life under random loading with varying mean stress and rms value.

20 p2622 A73-39553

Root-mean-square signal amplitude variation measurements of LF radio emission from extensive air showers by whip antenna

22 p2827 A73-42486

Comparison of the Kryloff-Bogoliuboff method and the refined elliptic function method.

22 p2882 A73-43071

An optimality condition for assessing systematic errors

23 p2999 A73-43264

ROOTS OF EQUATIONS

Asymptotic estimates for solutions of linear systems of ordinary differential equations having multiple characteristic roots.

02 p0188 A73-12625

Russian book - Fundamentals of the general theory for the root loci of automatic control systems.

02 p0149 A73-12750

Boundary value problems with a turning point.

03 p0336 A73-13066

The use of interval arithmetic to bound the zeros of real polynomials.

04 p0471 A73-15232

Roots of the circular cylindrical shell characteristic equation.

05 p0632 A73-16499

The existence and the numerical evaluation of generalized solutions of semilinear initial value problems

07 p0845 A73-20288

Synthesis of nonsearching self-adjusting systems by the root-locus method. II

07 p0807 A73-20637

Features of the application of the root-locus method to the study of sampled-data automatic systems on the basis of the w-transform

09 p1068 A73-22341

Second order differential equations with complex-valued coefficients.

09 p1112 A73-22425

Sturm-Liouville problem monotone proper function zeros lower and upper bounds evaluation using Barta inequality and Schwartz iteration

09 p1113 A73-23026

Application of Krylov's method to the solution of the frequency equation describing the weak vibrations of a truss structure

10 p1288 A73-23624

Speed active multipole filter design with a flexible computer program that calculates the component values for optimum performance.

10 p1191 A73-23755

Positive solutions of infinite equation and inequality systems and Lagrange multipliers for infinite differentiable optimization problems

10 p1243 A73-24163

Synthesis of searchless self-adjusting systems based on the root locus method. I.

12 p1484 A73-27460

Determination of the equilibrium positions of mechanisms with two degrees of freedom

12 p1524 A73-27465

Automation of plotting root-locus curves for automatic control systems

13 p1596 A73-29142

Degeneracy phenomenon in minimax rational approximation behavior in neighborhood of approximating function pole

13 p1650 A73-29396

Uniqueness of Chebyshev approximation representation by ratios of exponential functions with restricted number of zeros

13 p1651 A73-29400

Asymptotic stability and perturbations for linear Volterra integrodifferential systems.

14 p1770 A73-30757

Stability in the critical case of purely imaginary roots for neutral functional differential equations.

14 p1771 A73-30773

Hodograph construction by root trajectory method to provide maximum information on linear feedback systems dynamics

14 p1740 A73-30945

Asymptotic solution of a system of linear differential equations with slowly varying coefficients of the neutral type

15 p1898 A73-31036

Analysis of stability and periodic motions in nonlinear sampled-data systems by the root locus method.

15 p1854 A73-31690

Synthesis of searchless selfadjusting systems on the basis of the root-locus method. II.

15 p1854 A73-31691

Crossover frequencies in multicomponent plasma.

16 p2041 A73-33333

Iteration methods for finding all zeros of a polynomial simultaneously.

17 p2200 A73-34215

On an accurate theory for circular cylindrical shells. [ASME PAPER 73-APM-E]

17 p2250 A73-35114

Aerodynamic coefficients determination for nonlinear equations of motion solution to fit experimental free flight data, obtaining starting solution by noniterative continuation method

18 p2263 A73-36307

Solving M. A. Aizerman's first problem of absolute stability of nonlinear systems on the basis of the general theory of root trajectories

18 p2337 A73-37025

Algebraic algorithm for positive realness of real rational functions and matrices relative to unit circle in

complex plane, determining real polynomial zeros distribution

19 p2446 A73-38488

Root trajectories method for stability analysis of two channel automatic control systems with antisymmetric and symmetric cross couplings

20 p2541 A73-38980

Nonlinear boundary value problem with permissible zeros on the contour

20 p2582 A73-39206

Recursive formulas for the partial fraction expansion of a rational function with multiple poles.

21 p2660 A73-40097

Linear Kalman filter triangular square root formulation guaranteeing positive covariance matrix, computation and time savings and core storage requirement standardization

21 p2736 A73-40422

Transfer function root method for synthesis of multiply connected determinate automatic control systems with asymmetrical channels and limited nonautonomous control elements

22 p2836 A73-42614

Root locus analysis of stability of a class of nonlinear systems.

22 p2837 A73-42624

A galvanomagnetic analog device for extracting square roots

24 p3070 A73-45101

ROSSBY REGIMES

The effect of radiative and viscous dissipation of the propagation of forced planetary waves in the vicinity of critical levels.

01 p0039 A73-10395

Adiabatic inviscid quasi-geostrophic planetary scale perturbations forced by stratospheric disturbance, obtaining vertical propagation from layered models representation for zonal wind

05 p0591 A73-16189

Asymptotic solution for vertical propagation of equatorial planetary waves in shear, noting gravity-Rossby and Kelvin waves and wind effects on diurnal tides

05 p0591 A73-16190

Steady nonlinear Ekman-Hartmann boundary layer on flat surface, evaluating pumping and electric current as functions of Rossby number and magnetic interaction parameter

07 p0856 A73-19512

Rossby wave barotropic instability effects on errors leading to large scale atmosphere predictability experiments by numerical simulation of two dimensional turbulence

08 p0985 A73-21386

On the simplest example of the barotropic instability of Rossby wave motion.

08 p0985 A73-21388

On hydromagnetic Rossby waves excited by travelling forcing effects.

11 p1403 A73-25154

Evidence and characteristics of internal and planetary waves within the D-region plasma.

18 p2304 A73-35967

Waves and tides and their observation from ground and space.

21 p2689 A73-41356

Allowance for the effects of the relief and of the Coriolis force in forecasting meteorological elements

22 p2883 A73-41954

Numerical study of the unstable modes of a hyperbolic-tangent barotropic shear flow.

23 p3002 A73-43591

The effect of dissipation on the vertical propagation of planetary waves in the vicinity of critical levels.

23 p3032 A73-43906

Spectral analysis of traveling planetary scale waves - Vertical structure in middle latitudes of Northern Hemisphere.

23 p2978 A73-43982

Hydromagnetic gradient waves in the ionosphere

24 p3083 A73-44789

ROTARY DRIVES

U MECHANICAL DRIVES

ROTARY GYROSCOPES

NT FLUID ROTOR GYROSCOPES

Experimental determination of the probability characteristics of perturbations relative to the principal axis of a gyroscope

01 p0054 A73-11414

Effect of friction in suspension bearings on the motion of a gyroscope with a forced rotation of its base

01 p0054 A73-11415

Existence conditions of precessional motions of gyroscope with fixed point, assuming constant time function and unit vector coincident with gravity force direction

02 p0192 A73-11772

Theory of a single-rotor gyro orbit of a satellite stabilized with respect to roll angle

05 p0628 A73-16408

Electric forces in electrostatic gyroscope for rotor gravity center displacement, taking into account mutual effects of electrode pairs

05 p0577 A73-16994

ROTARY STABILITY

Numerical position deviation and release delay time estimates for gyroscope motion in gimbal suspension during rotor start-up

09 p1081 A73-22345

Construction of the frequency spectrum of a three-degree-of-freedom gyroscope with a flexible rotor shaft and elastic gimbal mountings

09 p1084 A73-22656

Systematic drift of a gyroscope with variable angular momentum in the gimbal suspension during vibrations of the frame

09 p1084 A73-22657

A condition for drift invariance with respect to acting accelerations in a two-degree-of-freedom gyroscope having arbitrary gas lubricated bearings on the main axis

09 p1084 A73-22658

Periodic small parameter solutions of rotary gyroscope motions about axis of ellipsoid of inertia, using Euler-Poisson equations

10 p1220 A73-24678

Stability of the steady motions of a gyroscope with spring limiters on a revolving platform in a Newtonian central force field

11 p1364 A73-26095

Calculation of the rotor potential of an electrostatic gyroscope

11 p1364 A73-26098

Drift moments produced by rotor nonsphericity in a suspension system with an axially-symmetric field

11 p1367 A73-26453

Nonlinear effects of axial load and rigidity changes on ball bearings of gyroscopes with symmetrical gyromotor design

13 p1618 A73-29145

Influence of the rotor weight on the changes in the axial rigidity of gyromotors

13 p1572 A73-29146

Influence of the orthogonal axes of the suspension of an electrostatic gyroscope at zero rotor potential

13 p1618 A73-29148

Analytical description of the three-dimensional distribution of the scattering of a gyromotor magnetic field

13 p1618 A73-29149

Some problems of orientation accuracy for a gyroscopic orbit with nonlinear control laws

18 p2335 A73-36118

The position of the axis of rotation of a free gyroscope ball rotor

18 p2317 A73-36852

Gyroscopic orbit errors caused by random perturbations

18 p2317 A73-36853

The impact of space navigation on the spherical gas bearing gyro.

21 p2697 A73-40025

Effect of the elastic deformation of a gimbal suspension on the nutation oscillation frequency of a gyroscope

22 p2860 A73-42359

Moments acting on a spherical rotor with magnetically suspended bearings

22 p2860 A73-42360

Stability of an indicator gyro stabilizer during the rotation of a three-stage gyroscope

22 p2860 A73-42368

Stability of a biaxial gyroframe on a vibrating base in resonance conditions

23 p3007 A73-44186

Vibrations of a three-degree-of-freedom gyroscope in transition through resonance

23 p2983 A73-44199

Deflecting moments in magnetic suspensions of gyroscopic devices

24 p3089 A73-44546

Effect of the gyromotor torque on the dynamics of a gyroscope

24 p3091 A73-45021

Calculation of the force characteristics of the external spherical suspension of a cryogenic gyroscope

24 p3091 A73-45023

ROTARY STABILITY

NT GYROSCOPIC STABILITY

Automatic impulse frequency stabilization of space vehicle rotation angle with respect to inertial coordinates by Liapunov discrete method

01 p0110 A73-1C595

Optimization of hybrid gas lubricated conical bearings.

01 p0057 A73-10698

Stability of a spinning body containing an elastic membrane via Liapunov's direct method.

01 p0077 A73-10728

Instability of rotation about a centroidal axis of maximum moment of inertia.

01 p0077 A73-10743

The effect of the Coriolis force on the stability of rotating magnetic stars.

01 p0103 A73-11034

Theory for the stability of a star with a toroidal magnetic field.

01 p0106 A73-11312

Dynamics of a rotating free system of bodies with an oriented axis of rotation

02 p0192 A73-11774

Equilibrium equations for rotating conical shells under centrifugal forces and compression loads, calculating revolutions number and stability limits

02 p0232 A73-11819

An application of pneumatic phase shifting to stabilization of externally pressurized journal gas bearings.

[ASME PAPER 72-LUB-4] 03 p0313 A73-14327

Experiments on the stability of various water-lubricated fixed geometry hydrodynamic journal bearings at zero load.

[ASME PAPER 72-LUB-46] 03 p0315 A73-14350

Equilibrium shape and stability conditions of rotating inviscid liquid drop in electric field

04 p0476 A73-15165

Stability of a rotating inhomogeneous star

09 p1145 A73-22293

Improving reliability and eliminating maintenance with elastomeric dampers for rotor systems.

10 p1175 A73-23950

Stability of transverse waves in a spinning membrane disk.

[ASME PAPER 72-APM-MM] 11 p1441 A73-25706

Rotating flexible shaft stability criterion development by perturbation method, considering internal and external friction and rotor inertia loading moments effects

11 p1444 A73-26368

The role of the Coriolis force on the stability of rotating magnetic stars and the origin of convective motions.

12 p1547 A73-27883

Newkirk effect - Thermally induced dynamic instability of high-speed rotors.

[ASME PAPER 73-GT-26] 16 p2047 A73-33499

Self excited whirl stability limits and frequencies of continuous rotors under gyroscopic, damping and hydrodynamic bearing film forces

16 p2022 A73-34035

Transient response simulation model for stability analysis of flexible high speed rotor-bearing system dynamics, examining nonlinear effects

[ASME PAPER 73-DET-102] 22 p2865 A73-42079

The stability of gravitating systems with a quadratic potential. II - The stability of models of spherically symmetric and axisymmetric clusters with elliptic orbits of particles

23 p3035 A73-44236

Decomposition and determination of the parameters of a system for angular motion stabilization in an asymmetric solid body

24 p3074 A73-45099

ROTARY WING AIRCRAFT

NT AUTOGYROS

NT CH-46 HELICOPTER

NT CH-47 HELICOPTER

NT COMPOUND HELICOPTERS

NT H-53 HELICOPTER

NT H-56 HELICOPTER

NT HELICOPTERS

NT HH-43 HELICOPTER

NT MILITARY HELICOPTERS

NT P-531 HELICOPTER

NT RIGID ROTOR HELICOPTERS

NT S-61 HELICOPTER

NT UH-1 HELICOPTER

Prediction of height-velocity boundaries for rotorcraft by application of optimization techniques.

12 p1459 A73-27175

Wind tunnel tests as part of rotary wing aircraft development, discussing technical and economic aspects

14 p1743 A73-30469

Rotary wing aircraft ecological advantages in logging, off shore oil exploration and short haul passenger transport for airport size reduction

16 p2088 A73-33185

Test techniques for high lift, two-dimensional airfoils with boundary layer and circulation control for application to rotary wing aircraft.

17 p2091 A73-34292

Digital control of rotary wing aircraft landing approach based on spatially variable preassigned flight path

[MBB-UFE-1021] 17 p2207 A73-34486

Investigation of reactionless mode stability characteristics of a stiff inplane hingeless rotor system.

[AHS PREPRINT 734] 17 p2105 A73-35070

A consistent crashworthiness design approach for rotary-wing aircraft.

[AHS PREPRINT 781] 17 p2106 A73-35094

Rotorcraft stability augmentation and gust alleviation by collective and cyclical rotor blade pitch angle changes, discussing nonlinear dynamic effects

18 p2267 A73-36397

Rotary and fixed wing aircraft growth factors from implicit differentiation of gross weight relative to fixed weight

[SAWE PAPER 952] 19 p2385 A73-37880

Contribution to the rotorcraft ground resonance theory

22 p2800 A73-43056

ROTARY WINGS

NT LIFTING ROTORS

NT RIGID ROTORS

NT TILTING ROTORS

NT TIP DRIVEN ROTORS

Random gust response statistics for coupled torsion-flapping rotor blade vibrations.

01 p0004 A73-10046

Flutter analysis method for unsteady aerodynamic forces on wings and rotating blades under harmonic vibrations and uniform flow

[ONERA, TP NO. 1099] 01 p0001 A73-10230

Calculation and measurement of the aerodynamic forces on an oscillating airfoil profile with and without stall

[ONERA, TP NO. 1132] 01 p0002 A73-10240

The pressure-jet helicopter propulsion system.

02 p0130 A73-11858

Response of helicopter rotor blades to random loads near hover.

02 p0129 A73-12503

Radiation properties of propeller and helicopter /free field/ rotors and fans and gas turbine compressors /ducted rotors/

02 p0131 A73-12611

Optimum performance of static propellers and rotors.

03 p0242 A73-13308

Advantage of reinforced plastics for helicopter blades and hubs

03 p0250 A73-13586

Aeroelastic instabilities of hingeless helicopter blades.

[AIAA PAPER 73-193] 05 p0536 A73-16929

Boundary-layer separation on rotating blades in forward flight.

07 p0774 A73-19955

Theoretical determination of the characteristics of helicopter rotors

09 p1027 A73-22205

Helicopter main-rotor blade flutter in steady inclined flight

10 p1174 A73-23662

Synthesis of helicopter rotor tips for less noise.

11 p1299 A73-24981

Analysis of stall flutter of a helicopter rotor blade.

[AIAA PAPER 73-403] 11 p1305 A73-25532

The spatial correlation method and a time-varying flexible structure.

[AIAA PAPER 73-406] 11 p1440 A73-25535

Twin-engined Anglo-French Lynx helicopter main rotor head, blade and drive train with conformal gearing, discussing design and material features

11 p1374 A73-25790

An analysis of helicopter rotor modulation interference.

15 p1843 A73-31731

Some findings from a preliminary fatigue experiment with model light-alloy specimens

15 p1955 A73-32191

Three dimensional flow analysis for helicopter rotor aerodynamic design, considering Mach number, inclination, angle of attack, trajectory, Reynolds number and vortex shedding

16 p1962 A73-32973

The application of circulation control aerodynamics to a helicopter rotor model.

[AHS PREPRINT 704] 17 p2104 A73-35055

Heavy lift helicopter rotor blade design including airfoils, fiberglass skin, titanium spar, fail-safety and aerodynamic and structural features

[AHS PREPRINT 710] 17 p2104 A73-35056

Sikorsky CH-53D helicopter main rotor head design, considering spherical elastomeric bearing, microstructural analysis, flight and ground fatigue tests and forging techniques

[AHS PREPRINT 713] 17 p2104 A73-35059

Tradeoff studies for feasibility of multiblade ring rotor configuration for helicopter design, discussing ring drag

[AHS PREPRINT 714] 17 p2104 A73-35060

An investigation of the vibratory and acoustic benefits obtainable by the elimination of the blade tip vortex.

[AHS PREPRINT 735] 17 p2105 A73-35071

Handling qualities comparison of two hingeless rotor control system designs.

[AHS PREPRINT 741] 17 p2105 A73-35074

Tail rotor performance in presence of main rotor, ground, and winds.

[AHS PREPRINT 764] 17 p2106 A73-35087

Performance, structural reliability and fatigue life of glass fiber-epoxy twin beam helicopter rotor blades

[AHS PREPRINT 782] 17 p2106 A73-35095

CH-53D titanium main rotor blade, describing spar, fiberglass cover and honeycomb core, fabrication methods, ground and flight tests and vibrational characteristics

[AHS PREPRINT 783] 17 p2106 A73-35096

Heavy lift helicopter rotor hub design and fatigue test technology, using fail-safe criteria, finite element analysis and fracture mechanics

[AHS PREPRINT 784] 17 p2180 A73-35097

Analysis of the use of an auxiliary wing on a helicopter

18 p2268 A73-37021

Calculation of the natural frequencies and the principal modes of helicopter blades. 18 p2367 A73-37090

A parametric weights study of a composite material prop/rotor blade. [SAWE PAPER 950] 19 p2385 A73-37878

On the aerodynamic damping moment in pitch of a rigid helicopter rotor in hovering. I - Experimental phase. 19 p2387 A73-38281

Rotorcraft design concepts, considering economics, propulsion, control, trim devices, advancing blade concept, materials and rotor aerodynamics 21 p2635 A73-41189

Effects of certain flight parameters and of certain structural parameters on helicopter main-rotor blade flutter 21 p2635 A73-41581

Perceived noise level ratings for helicopter noise, discussing blade slap, tail rotor whine, broadband noise and PNL rating shortcomings 22 p2798 A73-41708

Non-linear flap-lag dynamics of hingeless helicopter blades in hover and in forward flight. 22 p2800 A73-43134

Spectral trends in rotor noise generation. [AIAA PAPER 73-1033] 24 p3056 A73-44862

Natural, flexural and torsional vibration frequencies and modes for helicopter tail rotor blades 24 p3057 A73-45245

A comparison of the overall and broadband noise characteristics of full-scale and model helicopter rotors. 24 p3057 A73-45264

ROTATING

U ROTATION

ROTATING BODIES

NT COMPRESSOR ROTORS

NT FLYWHEELS

NT IMPELLERS

NT LIFTING ROTORS

NT LUNAR ROTATION

NT PUMP IMPELLERS

NT RIGID ROTORS

NT ROTARY WINGS

NT ROTATING CYLINDERS

NT ROTATING DISKS

NT ROTATING SPHERES

NT ROTORS

NT TILTING ROTORS

NT TIP DRIVEN ROTORS

NT TURBINE WHEELS

Moments of inertia for fluid-filled rotating bodies, solving Laplace and Navier-Stokes equations for cylinder and sphere 01 p0030 A73-10089

Stability of a spinning body containing an elastic membrane via Liapunov's direct method. 01 p0077 A73-10728

Turbulent swirling wake behind spinning axisymmetric body of revolution having axis aligned with free stream direction, obtaining velocity profiles variations 01 p0004 A73-11136

Experimental satellite for attitude control. IV - Nutational damping of a spinning satellite. 01 p0112 A73-11191

Ultraelliptic integrals degeneration to elliptic integrals in Goriachev-Chaplygin equation of rotating body, noting asymptotic approach to limiting motion 02 p0191 A73-11761

Time dependence of the basic variables in the symmetric solution to the problem of the motion of a body having a fixed point 02 p0191 A73-11763

Equations of motion for Kovalevskaja gyroscopic uniform rotation about axes differing from inertia ellipsoid principal axes, noting sufficient stability conditions 02 p0167 A73-11765

New solutions of the problem of the motion of a gyroscope in a central Newtonian force field 02 p0192 A73-11770

Dynamics of a rotating free system of bodies with an oriented axis of rotation 02 p0192 A73-11774

Equilibrium equations for rotating conical shells under centrifugal forces and compression loads, calculating revolutions number and stability limits 02 p0232 A73-11819

Equations of motion of solid body about fixed point with nonholonomic constraint, noting potential forces field effect 02 p0193 A73-12195

The effects of viscous friction on axial rotation of celestial bodies. 02 p0216 A73-12376

Pyrometer for measurement of surface temperature distribution on a rotating turbine blade. 02 p0171 A73-12617

The equilibrium and stability of uniformly rotating gaseous systems in hydromagnetics. I. 02 p0225 A73-12806

Axial and transverse wave motions of inviscid perfect gas in isothermal solid-body rotation in cylinder 04 p0434 A73-15163

Rotating paraboloid of revolution in viscous conducting fluid, calculating flow velocity and magnetic field from MHD equations 05 p0601 A73-16172

Numerical integration of rotating body dynamic and kinematic equations, noting orthogonalization, normalization and error minimization methods 05 p0595 A73-16423

Relativistic stress tensor in general relativity theory 05 p0597 A73-16469

Magnus force and moment coefficients for spinning ogive and cone cylinders and conical bodies in laminar compressible flow, including boundary layer and radial pressure gradient effects 05 p0530 A73-16879

[AIAA PAPER 73-124] Optimal control of a combined propulsion system of a rotating spacecraft 05 p0630 A73-17003

Rotating black holes - Locally nonrotating frames, energy extraction, and scalar synchrotron radiation. 05 p0625 A73-17331

First-order perturbations of the two finite body problem. 07 p0877 A73-19594

Gravitational energy conversion into rotational energy in contraction process for pulsars, quasars and galactic radio emission energy sources 07 p0898 A73-19934

The Iarkovskii-Radzievskii effect and the evolution of condensations in a meteor stream 08 p1007 A73-21066

Emission spectrum of a source moving along a stable circular orbit near a rotating 'black hole' 09 p1145 A73-22295

Scattering by perfectly conducting rotational bodies of arbitrary form excited by an obliquely incident plane wave or by a linear antenna. 09 p1052 A73-22959

Differential equations in terms of the osculatory elements of a solid for the motion of the solid about its center of mass 09 p1121 A73-23355

Incomplete/complete feedback and off-on control moments for prescribed orientation of solid body in rotational motion 10 p1248 A73-23744

Electromagnetic field of rotating charged oblate ellipsoid of revolution with infinite conductivity and vacuum or infinite magnetic susceptibility 10 p1252 A73-24344

Relativistic effects on gyromagnetic ratio of massive rotating body with uniform charge density and with shell large in comparison to Schwarzschild radius 10 p1252 A73-24345

Attitude stability of two elastically coupled spinning bodies. 10 p1286 A73-24543

Reduction of a gyrostator problem to that of a rigid body. [ASME PAPER 72-APM-QQ] 11 p1398 A73-25704

Laminar symmetry-plane boundary layer on a sharp spinning body at incidence. 11 p1303 A73-26397

A mechanism for ablation-induced spin-up. 11 p1431 A73-26402

Instability of equilibrium figures consisting of several isolated components rotating jointly 13 p1684 A73-29141

A non-stroboscopic system for examining high speed rotating objects. 14 p1750 A73-29704

Rotation effects in the nongravitational parameters of comets. 14 p1793 A73-29821

Amplification of cylindrical electromagnetic waves reflected from a rotating body. 14 p1728 A73-30333

Sound radiation from a body moving in a circle near a sphere. 15 p1912 A73-31009

Calculation of natural frequencies and modes of steadily rotating systems - A teaching note. 15 p1946 A73-31123

Clairaut equation solution for determination of equilibrium configuration of corotating masses, considering density distribution of fluid rotating planet 15 p1939 A73-32006

Elastic buckling instability of rotating rods and plates due to compressive stress under critical speed 15 p1955 A73-32161

Laminar film condensation on the inside of slender, rotating truncated cones. 15 p1958 A73-32279

Theory for the flexural vibrations of a rotating viscoelastic cantilever 16 p2083 A73-33936

Resonance damping of oscillations in a model of a spherical stellar cluster 17 p2226 A73-34367

Disk formation by collapsing rotating gas cloud, considering free turbulence and intermittency effects on gravitational instability 17 p2227 A73-34413

Viscous flow over spinning cones at angle of attack. 17 p2096 A73-35132

Computerized finite difference method with reduced core storage requirements for solving boundary value problem of forced random vibration of rotating beam 17 p2204 A73-35830

Motion of a free solid body about its center of mass when the body is stabilized by rotation about a non-principal axis of inertia 18 p2336 A73-36163

Yarkovskii-Radzievskii effect and the evolution of meteor swarms. 18 p2355 A73-36867

Analysis of some functional parameters of rotary hydrostatic engines under dynamic conditions by modeling on a computer 19 p2388 A73-37557

Use of turning ring electrodes for study of the transport of matter in fluid in a laminar or turbulent hydrodynamic regime 19 p2432 A73-38481

Mathematical modeling of spinning elastic bodies for modal analysis. 21 p2784 A73-40421

Finite element analysis of rotating shells. [ASME PAPER 73-DET-94] 22 p2919 A73-42074

On the behavior of a numerical approximation to the rotatory inertia and transverse shear plate. [ASME PAPER 73-APMW-7] 22 p2924 A73-42880

About the stability of the libration points of a rotating triaxial ellipsoid in a degenerate case. 23 p3032 A73-43838

Dynamics of the rotary motions with respect to the center of mass of a system of solids with a variable geometry of the masses 23 p3007 A73-44187

Decomposition and determination of the parameters of a system for angular motion stabilization in an asymmetric solid body 24 p3074 A73-45099

The restricted problem of three bodies with rigid dumb-bell satellite. 24 p3142 A73-45300

Relativistic torque detection on freely spinning rotor, obtaining phenomenological expression by incremental Hubble law 24 p3142 A73-45342

ROTATING CONES

U CONICAL BODIES

U ROTATING BODIES

ROTATING CYLINDERS

Convective transport terms effect on laminar flow-field of Newtonian fluid between rotating cylinders, using adapted finite difference solution technique 03 p0298 A73-14643

Stability of nonrotationally symmetric disturbances for inviscid flow between rotating cylinders in the presence of an axial magnetic field. 04 p0433 A73-14899

Negative Magnus forces in the critical Reynolds number regime. 05 p0533 A73-17212

Spiral flows in finite rotating annular tubes. 07 p0812 A73-20435

A subsonic diffuser with moving walls for boundary-layer control. 08 p0953 A73-20723

The free surface on a liquid between cylinders rotating at different speeds. I. 10 p1207 A73-24789

The free surface on a liquid between cylinders rotating at different speeds. II. 10 p1207 A73-24790

Transient Ekman and Stewartson layers in a rotating tank with a spinning cover. 10 p1210 A73-24840

The dynamical effect of inertial waves on the gyroscopic motion of a body containing several eccentrically located liquid-filled cylinders. 11 p1346 A73-25224

A note on the unsteady motion of a viscous conducting liquid between two porous concentric circular cylinders acted on by a radial magnetic field. 11 p1404 A73-25368

The free vibrations of a thin circular finite rotating cylinder. 11 p1443 A73-26088

Study of flow around a rotating circular cylinder. 11 p1302 A73-26337

Influence of rotational inertia on the frequency spectrum of the natural vibrations of a cylindrical shell 12 p1556 A73-27801

Analysis of centrifugal stresses in anisotropic viscoelastic cylinder. 13 p1697 A73-28810

The thick turbulent boundary layers on rotating cylinders in axial flow. 13 p1602 A73-29016

Determination, by a wall probe, of the changing regime of the flow between two off-center cylinders with very close radii 15 p1863 A73-31568

On the establishment and solution of equations of motion of an electrically conducting fluid set in motion by the slow and uniform rotation of walls of a ring-shaped receiver, in the presence of an axial magnetic

ROTATING DISKS

field, in the case where the mean value of the intensity of the currents induced in a straight section takes a nonzero value

15 p1918 A73-31569

Reynolds equation solutions for transverse velocity and pressure variations in incompressible fluids within journal bearings and between rotating eccentric cylinders

15 p1882 A73-31639

Wavelength and cell size determination of steady supercritical Taylor vortex flow for long rotating cylinders with radius, viscosity and end boundary variations

16 p1998 A73-32798

Analysis of flow separation in an annular expansion - Contraction with inner cylinder rotating. [ASME PAPER 73-FE-7]

17 p2152 A73-35006

The Taylor vortex regime in the flow between eccentric rotating cylinders.

[ASME PAPER 73-LUBS-8] Spectral characteristics of the scatter field from a rotating impedance cylinder in uniform motion.

17 p2181 A73-35391

17 p2129 A73-35707

Stresses and strains in a rotating disk

19 p2497 A73-37555

Boundary value problem of steady MHD flow in rotating cylindrical pipe under uniform magnetic field

19 p2468 A73-37647

Heat transfer in rotating cylindrical enclosures with axial inflow and outflow of coolant.

19 p2504 A73-37877

Taylor vortex occurrences between rotating eccentric cylinders

20 p2547 A73-39284

Ultrahigh speed cinematography with rotating Ti drums bound by monocrySTALLINE boron fibers, noting prototype performance

21 p2693 A73-39937

Investigation of secondary flows between coaxial rotating cylinders

21 p2676 A73-40574

Rotating cylinder model for plasma gradient-temperature instability in gravitational field, showing heat convection due to Coriolis-caused particle drift

21 p2769 A73-40730

Rotation of a cylinder in a conducting fluid in an axial magnetic field

21 p2747 A73-40883

Vibrations of a rotating solid body with a cavity partly filled with an arbitrary viscous fluid

21 p2677 A73-40988

An electronically synchronized drum-type film camera

21 p2706 A73-41580

Vibrations of a rotating solid body containing a cavity partially filled with a viscous fluid

22 p2843 A73-43058

Large amplitude baroclinic waves generation via instabilities of two layer fluid in rapidly rotating cylinder compared with mathematical model based on quasi-geostrophic equations

23 p3001 A73-43590

Gradient instabilities in a system of gravitating point masses.

24 p3132 A73-44479

Study of the steady flow of an incompressible viscous fluid around a cylinder in rotation

24 p3079 A73-45219

ROTATING DISKS

Navier-Stokes equations numerical solution for steady state axisymmetric flow of incompressible Newtonian fluid between two parallel infinite rotating disks

01 p0122 A73-10805

Direction of winding in spiral galaxies.

01 p0106 A73-11317

Approximate solutions of laminar flow between two rotating coaxial disks.

02 p0151 A73-11527

Non-linear vibration of rotating cantilever blades treated by the Ritz averaging process.

02 p0232 A73-11859

On the influence of acceleration stresses on the yielding of disks of uniform thickness.

03 p0384 A73-13118

Effect of the thickness on the stressed state of rotating disks

03 p0384 A73-13128

Calculation of the stress distribution in rotating disks in the case of unsteady creep with the aid of a digital computer

03 p0385 A73-13140

Flow parameter iterative formulas for laminar incompressible viscous fluid flow between two parallel disks rotating at same angular velocity

03 p0295 A73-13625

Current distribution prediction in transient response of rotating disk electrode, noting mass transfer for cathodic reduction of ferriyanide

03 p0273 A73-13728

The effects of wall conductance on torque of the MHD viscous coupler and hydrostatic thrust bearing. [ASME PAPER 72-LUB-1]

03 p0313 A73-14326

On unsteady forced flow against a rotating disk.

06 p0643 A73-17394

Flow of a viscous incompressible fluid between a fixed porous disk and a rotating nonporous disk, with radial discharge

07 p0811 A73-20069

Investigation of the plastic state of disks by the hardness measurement method

07 p0917 A73-20514

Self-compensating strain measurement in rotating disks subjected to elastic and plastic deformation

07 p0826 A73-20516

The stress intensity factor of an edge crack in a finite rotating elastic disc.

07 p0918 A73-20566

Stress concentration in rotating orthotropic elliptic disks solution via Chen-Hsu modification of stress function for bounded plates

08 p1017 A73-20943

Experiments on a shrouded, parallel disk system with rotation and coolant throughflow.

08 p1023 A73-21256

Design of rotating discs of irregular outline.

09 p1161 A73-23051

Flexural vibrations of a cantilever strut mounted on a rotating disk

10 p1290 A73-24308

Investigation of the load-carrying capacity of rotating disks by the method of optically sensitive coatings

10 p1291 A73-24364

Unsteady flow between a fixed porous disk and a rotating disk

10 p1209 A73-24837

The equilibrium, stability and evolution of a rotating magnetized gaseous disk.

10 p1284 A73-24903

Experimental verification of the applicability of small elastoplastic deformation theory to the calculation of rotating disks

11 p1434 A73-25392

Stability of transverse waves in a spinning membrane disk.

[ASME PAPER 72-APM-MM]

11 p1441 A73-25706

Calculation of turbulent skin friction on a rotating disk.

11 p1348 A73-26387

Anholonomic constraints imposed on mechanical systems which have rigid solid bodies as constituent elements. II - Anholonomic constraints realized by nonsliding roller bearings

12 p1523 A73-26794

Hydrogen ignition in flat rotating disk phase of stellar formation, determining central conditions from total mass and adiabatic constant

12 p1542 A73-27575

On the flow between two independently rotating disks of variable distance with blowing.

13 p1605 A73-29295

Rotating turbine disks ultimate strength relation to stress-strain state, material mechanical properties and plastic deformation

14 p1814 A73-30684

Turbulent source flow between parallel stationary and co-rotating disks.

15 p1862 A73-31337

Optimal structural design of elastic rotating disks by dynamic programming

16 p2079 A73-33009

Calculation of temperature distribution in multistage axial gas turbine rotor assemblies when blades are uncooled.

[ASME PAPER 73-GT-8]

16 p2047 A73-33486

The transverse vibration of spinning aeolotropic disk.

16 p2084 A73-34026

Electrochemical thinning of a metal disk rotating on a floating self-moulded cathode.

17 p2182 A73-35766

Laminar mixed convection from a horizontal rotating disc.

17 p2256 A73-35848

Strength of nonuniformly heated rotating disks

18 p2366 A73-36755

Elastic stresses in rotating orthotropic discs of variable thickness.

19 p2496 A73-37436

Theoretical and experimental study, for different electrical conditions, of the laminar motion of an incompressible and electrically conducting fluid drawn along in a confined medium, and in the presence of an axial magnetic field, by the uniform rotation of a disk

19 p2468 A73-37531

Stresses and strains in a rotating disk

19 p2497 A73-37555

Plastic state of disks studied from hardness measurements.

19 p2499 A73-37789

Autocompensatory strain measurement of rotating disks subjected to elastic and plastic deformation.

19 p2430 A73-37792

Heat transfer in rotating cylindrical enclosures with axial inflow and outflow of coolant.

19 p2504 A73-37877

The effects of speed and radial flow on the axial force on an enclosed rotating disc.

21 p2754 A73-41685

Heat transfer from an enclosed rotating disk with uniform suction and injection.

22 p2938 A73-42994

Dynamic stability of rotating disks loaded by a concentrated force

22 p2928 A73-43066

Thickness of liquid film on a rotating disk.

23 p2969 A73-44142

Analysis of the heat transfer associated with the evaporation of a fluid film on a rotating disk

24 p3156 A73-45070

ROTATING ELECTRICAL MACHINES

Rotating electrical machine superconducting field winding design requirements in terms of size, magnetic energy storage, power level, rotation speed and pole number

02 p0132 A73-11870

Computer technique for automated acoustical inspection of rotating machines

03 p0311 A73-129595

Superconducting a.c. machines - An approach to development.

07 p0779 A73-20460

ROTATING ENVIRONMENTS

Moving visual scenes influence the apparent direction of gravity.

04 p0411 A73-152505

On the demonstration and interpretation of the Coriolis effect.

09 p1120 A73-224750

Differential effects of central versus peripheral vision on egocentric and exocentric motion perception.

11 p1318 A73-262212

Features of the influence of hypergravitation on the motor activity of the chicken embryo amnion developing under normal conditions and under conditions of constant rotation

14 p1715 A73-300229

Calculation of a Coriolis acceleration acting on semicircular canal receptors of man in rotating systems

15 p1835 A73-315184

The derivation of the mechanical balance equations of the Cosserat continuum on the basis of the energy equation and its behavior at the transition to rotating systems

16 p2080 A73-332404

Visual-vestibular interaction and motion perception.

18 p2273 A73-364604

ROTATING FLUIDS

NT ROTATING LIQUIDS

An experimental and analytical investigation of angular momentum exchange in a rotating fluid.

01 p0073 A73-104444

Boundary layer formation on hollow circular cylinder walls aligned with axial motion of incompressible rotating fluid as function of Rossby and Reynolds numbers

01 p0032 A73-104511

Stability of rotating stratified flow produced by tangential injection of high pressure gas into closed cylindrical vessel filled with gas of different density

01 p0033 A73-107522

An asymmetrically rotating fluid disc with applications.

[AD-751727]

02 p0217 A73-123939

Numerical simulation of initial value problem of axisymmetric equatorially trapped oscillation modes of constant density viscous fluid in rotating spherical shell

03 p0384 A73-130644

Oscillatory point force generated motion in inviscid incompressible rotating stratified fluid, obtaining closed form solutions via Fourier transforms

03 p0296 A73-143133

Calculation methods of three-dimensional boundary layers with and without rotation of the walls.

[ONERA, TP NO. 1135]

04 p0403 A73-150933

The motion of a plate in a rotating fluid at an arbitrary angle of attack.

04 p0404 A73-151611

The oscillatory boundary layer growth over the top and bottom plates of a rotating channel.

[ASME PAPER 72-WA-FE-5]

04 p0434 A73-158422

MHD-rotation of a conducting fluid in a rotationally symmetric electromagnetic field

05 p0603 A73-165900

Upwelling of a stratified fluid in a rotating annulus - Steady state. I - Linear theory.

06 p0684 A73-177022

Effects of spanwise rotation on the structure of two-dimensional fully developed turbulent channel flow.

06 p0685 A73-177088

Asymptotic formulas for the thickness of the Ekman boundary layer

06 p0691 A73-18730

Hall current effects on waves in an electrically conducting rotating fluid.

07 p0854 A73-19104

On unsteady magnetohydrodynamic boundary layers in a rotating flow.

07 p0859 A73-20290

A radial diffuser with a rotating boundary layer at the throat.

08 p0953 A73-20795

Turbulent hydrodynamics and heat transfer in rotating flows of incompressible fluid

08 p0954 A73-21184

Mathematical analogy between the bending of a plate and the circulating motion of a liquid in a geometrically similar region

10 p1205 A73-23598

Oscillation of axisymmetric bodies in a stratified fluid.

10 p1205 A73-23625

Putting an electrically conducting fluid in rotation by a rotating magnetic field

10 p1254 A73-24125

Transonic gas flow in rotating turbomachine cascade channels, reducing flow equations to second order differential equation

10 p1172 A73-24507

Flow twisting in front of rotor for centrifugal blower operation control, predicting efficiency criteria

10 p1173 A73-24671

Calculation of a three-dimensional boundary layer in revolving channels of centrifugal rotors

10 p1173 A73-24672

Unsteady boundary layer flow, considering Stokes, Rayleigh and Heisenberg-Tollmien theories application to oscillatory, fluctuating, impulsive and rotational effects

10 p1207 A73-24802

Prominent vertical shear layers and zonal currents in axisymmetric fluid filled spherical/conical rotating container due to nonlinear interactions in boundary layers

10 p1210 A73-24839

On unsteady magnetohydrodynamic boundary layers in a rotating flow.

10 p1257 A73-24841

Equations for nonlinear Benard convection with rotation for fluid layer, investigating asymptotic solution for two dimensional cells at large Rayleigh and Taylor numbers

11 p1448 A73-25052

Axisymmetric flow model of rotating inviscid incompressible fluid into point sink at low Rossby numbers, discussing selective withdrawal and blocking

11 p1345 A73-25053

On hydromagnetic Rossby waves excited by travelling forcing effects.

11 p1403 A73-25154

Nonlinear hydrodynamic and hydromagnetic spin-up driven by Ekman-Hartmann boundary layers.

11 p1403 A73-25156

Convection in a rotating annulus uniformly heated from below. II - Nonlinear results.

11 p1449 A73-25159

Nonlinear resistive boundary layer in rotating hydromagnetic flow related to earth dynamo theory, discussing steady solution uniqueness and numerical temporal stability

11 p1355 A73-25794

Report on the NATO Advanced Study Institute on magnetohydrodynamic phenomena in rotating fluids.

11 p1404 A73-25851

Hydrodynamic stability of density-stratified spiral flows.

11 p1348 A73-26388

Stability of the regular precession of a symmetrical solid with an ellipsoidal cavity

11 p1401 A73-26469

Motion of a conducting gas with variable properties between rotating cylinders

12 p1487 A73-27798

Thermodynamics of relativistic rotating perfect fluids.

12 p1525 A73-27886

Instability of density-stratified incompressible inviscid rotary Couette flow between corotating coaxial vertical cylinders due to gravitational effects

13 p1600 A73-28439

Axisymmetric inertial oscillations of a fluid in a rotating spherical shell.

13 p1601 A73-28916

Instability of equilibrium figures consisting of several isolated components rotating jointly

13 p1684 A73-29141

Study of a new family of solutions of Navier-Stokes equations

14 p1744 A73-29758

Valve effect of inhomogeneities on anisotropic wave propagation.

14 p1780 A73-30165

Rotating flow evolution in long circular tubes, deriving mathematical formulation for laminar and turbulent flow

14 p1745 A73-30296

Further investigations on the nonlinear behavior of a system of parallel line vortices.

14 p1746 A73-30652

Korteweg-de Vries equation solution for long nonlinear wave amplification and decay in rotating and stratified fluids with application to shallow water waves

16 p1998 A73-32795

Stratified Taylor column model for topography effect on slow rotating baroclinic flow, considering Jupiter Red Spot and oceanic observations

16 p1998 A73-32797

The variational principle and the virial theorem for uniformly rotating magnetohydrodynamic systems.

16 p2040 A73-32926

Hagen-Poiseuille flow stability with superimposed rigid rotation, deriving perturbed differential flow equations from Navier-Stokes and continuity equations

16 p1999 A73-33253

A wake and an eddy in a rotating, radial-flow passage. I - Experimental observations.

16 p1964 A73-33512

On unsteady Stokes, Ekman and Rayleigh layers in a rotating fluid.

17 p2150 A73-34322

A numerical study in three space dimensions of Benard convection in a rotating fluid.

17 p2151 A73-34855

Generalized expressions for secondary vorticity using intrinsic co-ordinates.

18 p2299 A73-36506

Velocity profiles in steady and unsteady rotating flows for a finite cylindrical geometry. II.

18 p2300 A73-36629

On the torsional oscillations of a sphere placed at the axis of a rotating viscous incompressible fluid.

19 p2419 A73-37422

Theoretical and experimental study, for different electrical conditions, of the laminar motion of an incompressible and electrically conducting fluid drawn along in a confined medium, and in the presence of an axial magnetic field, by the uniform rotation of a disk

19 p2468 A73-37531

Boundary value problem of steady MHD flow in rotating cylindrical pipe under uniform magnetic field

19 p2468 A73-37647

Laboratory vortices in rotating, sheared flow.

19 p2420 A73-37664

Taylor vortex occurrences between rotating eccentric cylinders

20 p2547 A73-39284

Rotation of an electrically conducting fluid with a free surface in a rotating field

21 p2747 A73-40885

Experimental study of rotational MHD Couette flow in a coplanar field

21 p2747 A73-40886

Sound propagation in rotating vortex flow downstream from delta wing in wind tunnel, discussing acoustic ray refraction by flow

22 p2839 A73-41715

Dynamics of quasigeostrophic flows and instability theory.

22 p2842 A73-42450

Study of hydromagnetic stability of a hot rotating layer of fluid by Liapunov method.

22 p2894 A73-42474

Vibrations of a rotating solid body containing a cavity partially filled with a viscous fluid

22 p2843 A73-43058

Experimental investigation of turbulent flow characteristics in a rotating channel

23 p2968 A73-43443

Numerical study of the unstable modes of a hyperbolic-tangent barotropic shear flow.

23 p3002 A73-43591

Thermal convection in a large rotating fluid annulus - Some effects of varying the aspect ratio.

23 p3002 A73-43597

On a criterion for the occurrence of a Dedekind-like point of bifurcation along a sequence of axisymmetric systems. I - Relativistic theory of uniformly rotating configurations.

24 p3110 A73-45032

On a criterion for the occurrence of a Dedekind-like point of bifurcation along a sequence of axisymmetric systems. II - Newtonian theory for differentially rotating configurations.

24 p3110 A73-45033

Stability of a potential vortex with a non-rotating and rigid-body rotating top-hat jet core.

24 p3055 A73-45309

The linear spin-up of a strongly stratified fluid of small Prandtl number.

24 p3079 A73-45312

Boundary value problem concerning the oscillations of a rotating ideal fluid

24 p3081 A73-45531

The effect of rotation on nonlinear thermal convection.

24 p3158 A73-45559

ROTATING GENERATORS

NT AC GENERATORS

NT DYNAMOMETERS

NT TURBOGENERATORS

Three-phase-synchronous alternator with a superconducting field winding.

02 p0132 A73-11832

Effect of linear load graduation in the end zones of an inductor on the longitudinal side effect in induction machines

15 p1832 A73-31410

ROTATING LIQUIDS

Flow stability of ideal compressible and incompressible fluids, solving Navier-Stokes equation for rotating liquid with free boundary in gravitational field

02 p0154 A73-12692

Equilibrium shape and stability conditions of rotating inviscid liquid drop in electric field

04 p0476 A73-15165

A possible application of large orbiting space laboratories - An artificial moon

05 p0613 A73-16201

Newtonian and non-Newtonian liquids rotating adjacent to a stationary surface.

11 p1346 A73-25369

Flow regimes for a magnetic suspension under a rotating magnetic field.

14 p1774 A73-29924

Measurement of relaxation time during acceleration of rotation of vessels containing helium II, and superfluidity in pulsars

16 p2038 A73-34065

Free oscillations of a double layer in a turning rectangular basin of constant depth

19 p2419 A73-37530

On the effects of uniform high suction on the rotationally symmetric flow of a conducting liquid near a stationary disc in the presence of a transverse magnetic field.

19 p2469 A73-38186

ROTATING MATTER

Rotational perturbations in anisotropic cosmology.

01 p0107 A73-11328

Evidence for elliptical galaxy rotation, considering flattening, orbital statistics and interactions of external and internal forces

05 p0616 A73-16453

Stochastic wave model of spiral galaxy rotation based on weak interaction, obtaining frequency spectrum integrals for Milky Way Galaxy

05 p0616 A73-16454

Open spiral density wave propagation and distortion due to differential rotation in Lindblad resonance region

05 p0616 A73-16455

Neutral hydrogen cloud rotation and recurrent eflux from central region of Galaxy, considering material and energy resources limitation

05 p0616 A73-16457

Time evolution of rotating incoherent matter with vanishing internal pressure by Einstein field equations

09 p1151 A73-23342

Dynamical contraction of rotating gaseous spheroids.

13 p1680 A73-28774

Two dimensional wave problems in rotating elastic media.

19 p2460 A73-38183

Amplification of electromagnetic and gravitational waves during scattering on a rotating black hole

23 p3034 A73-44008

ROTATING MIRRORS

Q switched carbon dioxide laser based on PM by rotating mirror in one arm of Michelson interferometer, establishing phase relationships

05 p0583 A73-16062

Error in the interferometric measurement of length by the rotational movement of a mirror and multipass corner cube arrangement.

11 p1365 A73-26240

Gas bearing technique for ultrahigh speed rotating mirror mounted on opto-mechanical camera

21 p2693 A73-39936

Visualization of the shape and symmetry of detonation waves by a slit camera - Application to hollow charges

21 p2697 A73-39992

ROTATING PLASMAS

Measurement of the macroscopic velocity of the neutral component of weakly ionized gas in the crossed fields.

01 p0081 A73-10116

Cyclotron resonance instability in a rotating plasma

04 p0479 A73-15042

Investigation of the stability of plasma-jet motion in the magnetic field of a diverter

04 p0479 A73-15045

Resultant value of the inertial emf during thermal convection in a rotating plasma

04 p0481 A73-15604

Experimental investigation of the kinetic instabilities in Gabor's alternative magnetron

04 p0481 A73-15610

Investigation of the gun aspects of a rotating plasma source.

06 p0732 A73-18779

Heating of astrophysical plasma due to rotation.

08 p1007 A73-20957

Classification, orientational characteristics, and some examples of rotational discontinuities in the solar wind

08 p0998 A73-21278

Low threshold unstable nonpotential oscillations of weakly ionized rotating plasma in crossed field centrifuge, noting MHD generator and ionospheric implications

09 p1124 A73-21891

ROTATING SHAFTS

Rotation of the ion component of a plasma from a hot-cathode Penning discharge 09 p1125 A73-21955

Relativistic MHD formulation in terms of non-holonomic tetrad field for rotating plasma coupled to frozen-in magnetic field, noting Alfvén waves propagation velocity 09 p1131 A73-22921

Inertial emf due to thermal convection in a rotating plasma. 10 p1254 A73-24194

Experimental investigation of kinetic instabilities in the Gabor magnetron. 10 p1254 A73-24200

Internal instabilities derived for electron plasma with electrons rotating about axis of symmetry parallel to confining external magnetic field 10 p1256 A73-24449

Stability of a plasma rotating in crossed electric and magnetic fields 11 p1403 A73-25240

Rotational instability of a plasma from a hot-cathode Penning discharge 11 p1403 A73-25243

High speed corotating plasma streams in solar wind from time dependent radial MHD flow model 12 p1533 A73-26979

Intensive chromospheric flares and rotational discontinuities in the solar wind 12 p1534 A73-27330

Interplanetary medium rotational discontinuities polarization, vorticity transport and angular momentum properties, implying solar wind velocity jump from magnetic field transverse perturbation 14 p1796 A73-29961

Investigation of the radial structure of the oscillations of a plasma column situated in crossed fields in the presence of resonant cyclotron instability 14 p1781 A73-30579

Existence of a new type of rotating equilibrium ellipsoids in the presence of a toroidal magnetic field 14 p1782 A73-30816

On the magnetogravitational instability of a plasma which possesses an anisotropic pressure in uniform movement of rotation and under the influence of the Hall current - The equation of dispersion. I 17 p2215 A73-34250

Low threshold unstable nonpotential oscillations of weakly ionized rotating plasma in crossed field centrifuge, noting MHD generator and ionospheric implications 17 p2215 A73-34314

Ion cyclotron instability of a rotating plasma 18 p2340 A73-36671

Classification, characteristics of orientation, and some examples of rotational discontinuities in the solar wind. 19 p2476 A73-37907

Low-frequency flute instabilities of a bounded plasma column. 20 p2595 A73-38889

Quasar and galactic nuclei energy source models, considering supermassive rotating magnetoplasma body, black hole and compact star cluster with flares and collisions 20 p2609 A73-39570

Powerful chromospheric flares and rotational discontinuities in the solar wind. 23 p3020 A73-43228

Influence of the magnetic field on electrodeless-discharge plasmas 23 p3009 A73-43654

ROTATING SHAFTS

NT SHAFTS [MACHINE ELEMENTS]

NT TURBOSHAFTS

Feasibility study of a slanted 'O-ring' as a high pressure rotary seal. [ASME PAPER 72-WA/DE-14] 04 p0457 A73-15873

Rotating shafts dynamic stability, analyzing eigenvalue problem derived via energy equations based on virtual work principle 06 p0697 A73-17517

A fluidic transducer of rotor-shaft torque 06 p0692 A73-17836

Quasi-static load acting on a rotating shaft in the presence of creep 07 p0830 A73-19309

A contactless method of measuring the radial deformations of rotating shafts 07 p0827 A73-20533

Influence of the nonlinear compliance of rolling contact bearings on the vibrations of a balanced shaft 09 p1088 A73-22479

Rotating flexible shaft stability criterion development by perturbation method, considering internal and external friction and rotor inertia loading moments effects 11 p1444 A73-26368

Torsional stress on micropolar prismatic nonsymmetrically elastic rotating cylindrical shaft with six degrees of freedom evaluated in terms of Saint Venant function 11 p1445 A73-26409

Low speed of sound modeling of a high pressure ratio centrifugal compressor. 13 p1566 A73-29020

Gyroscopic moment effect on rotating shafts lowest critical velocity, plotting convergence characteristics 15 p1949 A73-31668

Effect of nonlinear compliance in rolling motion bearings on the vibrations of a balanced shaft. 15 p1883 A73-32066

Whirling shafts motion stability necessary and sufficient conditions analysis based on Liapunov method, taking into account internal and external damping effects 15 p1955 A73-32166

On the vibrations of a rotor with rotating inequality and with variable rotating speed. 15 p1883 A73-32216

Book - Vibration of linear mechanical systems. 18 p2361 A73-35900

Critical speeds for cantilever shafts. 18 p2320 A73-36700

Calculation of the eigenfrequencies for a shaft/bearing system with the aid of transfer matrices 19 p2433 A73-37548

Mechanical face seal between rotating shaft and surrounding member using stationary and rotating ultraflat radial sealing faces, discussing temperature and chemical considerations 22 p2865 A73-41775

Dynamic shaft seal types for high speed continuous shaft rotation, considering service life, failure modes and materials selection 22 p2865 A73-41776

The load transfer problem in shafts coupled through a sleeve. [ASME PAPER 73-APMW-3] 22 p2867 A73-42877

Solid friction oscillation characteristics of self excited rotational shaft-spring system with sliding contact surfaces 23 p2986 A73-44273

Increasing the critical rotational speed of the tail rotor drive shaft in SM-1 and SM-2 helicopters 24 p3057 A73-45195

ROTATING SPHERES

Isotropic conducting plasma dynamic behavior near rotating magnetized sphere, showing electric field-produced meridional convective currents 07 p0856 A73-19430

Equivalent gravity wave mode approximation for main solar diurnal tide in rotating spherical dissipative atmosphere modeled by Newtonian cooling and Rayleigh friction 08 p0958 A73-20959

Boundary layer due to sphere rotation in a medium at rest 13 p1599 A73-28068

The computation of the flow in the gap between two concentrically rotating spherical surfaces 16 p2000 A73-33255

Non-steady, stratified Couette flow between concentric rotating spheres. 20 p2548 A73-39521

The influence of rotation on the heat transfer from a sphere to an air stream. 22 p2938 A73-42955

ROTATING STALLS

Unstable operation and rotating stall in axial flow compressors. [ONERA, TP NO. 1090] 01 p0001 A73-10228

Unstable operation and rotating stall in axial flow compressors. 13 p1566 A73-29024

Conditions of rotating stall suppression in axial compressors 16 p2049 A73-33964

Rotating stall in an isolated rotor row and a single-stage compressor. 17 p2093 A73-34386

ROTATING VEHICLES

U ROTATING BODIES

ROTATION

NT AUTOROTATION

NT EARTH ROTATION

NT MOLECULAR ROTATION

NT PLANETARY ROTATION

NT SATELLITE ROTATION

NT SOLAR ROTATION

NT STELLAR ROTATION

Intersection line of axes cone with sphere and locus of angular velocity vectors for uniform gyroscopic rotation with different moments of inertia 02 p0191 A73-11764

Algorithms for equations of oscillatory motion about moving center, noting disturbing force effect on vibrational frequency 02 p0193 A73-12196

Constancy and illusion of apparent direction of rotary motion in depth - Tests of a theory. 13 p1577 A73-28094

Canonical elements of the translational-rotational motion of a planet satellite 19 p2476 A73-37199

Displacements and rotations in micropolar elastic body with external loading and permanent distortions 24 p3149 A73-45004

ROTATIONAL FLOW

U FLUID FLOW

U VORTICES

ROTOR AERODYNAMICS

Random gust response statistics for coupled torsion-flapping rotor blade vibrations. 01 p0004 A73-10046

Flexible rotor balancing of a high-speed gas turbine engine. [SAE PAPER 720741] 02 p0203 A73-12007

Rotor unsteady wakes three dimensional flow analysis by wave front averaging technique, using constant temperature hot-wire anemometer 02 p0129 A73-12504

Experimental rotor unbalance response using hydrostatic gas lubrication. [ASME PAPER 72-LUB-31] 03 p0315 A73-14341

Anisotropic flexible bearings mounted rotors backward and forward precessional motion excitation, noting internal viscous damping forces effect on vibration amplitude 06 p0758 A73-17515

Model tests on unsteady rotor wake effects. 07 p0773 A73-19191

The use of averaged flow equations of motion in turbomachinery aerodynamics. 13 p1603 A73-29047

Two-bladed large rotor mounted on tower in inverted mode to overcome recirculation effects, analyzing broadband noise spectra and directivity pattern 13 p1570 A73-29380

Three dimensional flow analysis for helicopter rotor aerodynamic design, considering Mach number, inclination, angle of attack, trajectory, Reynolds number and vortex shedding 16 p1962 A73-32973

A method of measuring three-dimensional rotating wakes behind turbomachinery rotors. [ASME PAPER 73-FE-31] 17 p2095 A73-35023

Aerodynamic design parameters effects on static performance of short ducted fans for helicopter tail rotor applications, comparing theoretical analysis and experimental results 17 p2104 A73-35052

On the question of adequate hingeless rotor modeling in flight dynamics. [AHS PREPRINT 732] 17 p2105 A73-35068

Reduction of helicopter control system loads with fixed system damping. [AHS PREPRINT 733] 17 p2105 A73-35069

ABC helicopter stability, control, and vibration evaluation on the Princeton Dynamic Model Track. [AHS PREPRINT 744] 17 p2105 A73-35077

Design of axial flow fans by cascade method. 21 p2631 A73-40124

Rotorcraft design concepts, considering economics, propulsion, control, trim devices, advancing blade concept, materials and rotor aerodynamics 21 p2635 A73-41189

Sound generation by open supersonic rotors. 22 p2795 A73-41712

An aeroelastic whirl phenomenon in turbomachinery rotors. [ASME PAPER 73-DET-97] 22 p2900 A73-42076

Transient response simulation model for stability analysis of flexible high speed rotor-bearing system dynamics, examining nonlinear effects [ASME PAPER 73-DET-102] 22 p2865 A73-42079

Non-linear flap-lag dynamics of hingeless helicopter blades in hover and in forward flight. 22 p2800 A73-43134

Study and calculation of the vibrations of a rotating rotor with allowance for clearances in the bearings 23 p3041 A73-43725

Spectral trends in rotor noise generation. [AIAA PAPER 73-1033] 24 p3056 A73-44862

ROTOR BLADES

Investigation of an axial-flow blower during variation of axial clearance and of blade mounting angles in the stator and rotor sections 02 p0131 A73-11791

Design and test of a small, high-pressure ratio, axial compressor with tandem and swept stators. [SAE PAPER 720713] 02 p0203 A73-12010

Helicopter main-rotor blade flutter in steady inclined flight 10 p1174 A73-23662

Calculation of a three-dimensional boundary layer in revolving channels of centrifugal rotors 10 p1173 A73-24672

Analysis of stall flutter of a helicopter rotor blade. [AIAA PAPER 73-403] 11 p305 A73-25532

Sensitivity of rotor blade vibration characteristics to torsional oscillations. [AIAA PAPER 73-404] 11 p1440 A73-25533

Stability of elastic bending and torsion of uniform cantilevered rotor blades in hover. [AIAA PAPER 73-405] 11 p1440 A73-25534

Twinned-engine Anglo-French Lynx helicopter main rotor head, blade and drive train with conformal gearing, discussing design and material features 11 p1374 A73-25790

Periodic gust and wake induced unsteady air flow, calculating velocity variation with distance from rotor blade for cascade effect 13 p1566 A73-29026

- Two-bladed large rotor mounted on tower in inverted mode to overcome recirculation effects, analyzing broadband noise spectra and directivity pattern 13 p1570 A73-29380
- Helicopter rotor blade passing close to tip vortex, calculating fluctuating lift induced harmonic blade loads and generated cyclic banging noise 13 p1570 A73-29382
- Three bladed model rotor gust induced impulsive discrete noise characteristics prediction by point dipole and rotational noise theories for comparison with measurement 16 p1967 A73-32917
- An algebraic method for linear dynamical systems with stationary excitations. 16 p2076 A73-32919
- Effect of rotor design tip speed on aerodynamic performance of a model VTOL lift fan under static and crossflow conditions. [ASME PAPER 73-GT-2] 16 p1963 A73-33480
- The unsteady response of a blade row from measurements of the time-mean total pressure. [ASME PAPER 73-GT-94] 16 p1964 A73-33531
- Nonstationary response of linear time-varying dynamical systems to random excitation. [ASME PAPER 73-APM-6] 17 p2247 A73-35031
- On the question of adequate hingeless rotor modeling in flight dynamics. [AHS PREPRINT 732] 17 p2105 A73-35068
- Development and qualification of a magnetic technique for the nondestructive measurement of residual stress in CH-47 A rotor blade spars. [AHS PREPRINT 752] 17 p2180 A73-35080
- Wind tunnel test technique to establish rotor system aeroelastic characteristics. [AHS PREPRINT 760] 17 p2095 A73-35083
- Rotorcraft stability augmentation and gust alleviation by collective and cyclical rotor blade pitch angle changes, discussing nonlinear dynamic effects 18 p2267 A73-36397
- Design method of the axial-flow blade row on modified isolated aerofoil theory with interference coefficient. II - The influence of the aerodynamic parameter on the fan performance at low flow rate. 19 p2377 A73-37671
- The axial flow molecular pump. IV - Performance of a rotor with a single blade row in the transition flow regime. 19 p2433 A73-37673
- The interaction of creep and fatigue for a rotor steel /The William M. Murray Lecture, 1972/. 21 p2722 A73-41264
- The effects of modulated blade spacing on static rotor acoustics and performance. [AIAA PAPER 73-1020] 24 p3121 A73-44852
- Multiple pure tone noise generation and control. [AIAA PAPER 73-1021] 24 p3122 A73-44853
- ROTOR BLADES (TURBOMACHINERY)**
- Investigation of the influence of technological factors on the endurance of gas-turbine engine rotor blades 01 p0114 A73-10477
- Gas velocity measurements within a compressor rotor passage using the laser Doppler velocimeter. [ASME PAPER 72-WA/GT-2] 04 p0451 A73-15866
- High temperature gas turbine engines rotor blades cooling, deriving generalized dimensionless relations for heat transfer data extension from static tests to operational conditions 05 p0607 A73-16797
- Approximate analysis of containment/deflection ring responses to engine rotor fragment impact. 07 p0910 A73-19188
- Designing turbomachine blades for forced vibrations under various excitation conditions 07 p0917 A73-20503
- Study of the effect of technical factors on the fatigue limit of the working blades of gas turbine motors. 14 p1810 A73-30302
- Critical rpm of conical shells incorporated in turbine htuors 14 p1814 A73-30686
- Calculation of temperature distribution in multistage axial gas turbine rotor assemblies when blades are uncooled. [ASME PAPER 73-GT-8] 16 p2047 A73-33486
- The use of a finite difference technique to predict cascade, stator, and rotor deviation angles and optimum angles of attack. [ASME PAPER 73-GT-10] 16 p1963 A73-33488
- A contribution to the theoretical and experimental examination of the flow through plane supersonic deceleration cascades and supersonic compressor rotors. [ASME PAPER 73-GT-17] 16 p2047 A73-33494
- Conditions of rotating stall suppression in axial compressors 16 p2049 A73-33964
- Rotating stall in an isolated rotor row and a single-stage compressor. 17 p2093 A73-34386
- Viscous flow in radial turbomachine blade passages. 17 p2093 A73-34389
- The determination of the static pressure and relative velocity distribution in a two-dimensional radially bladed rotor. 17 p2093 A73-34396
- Rotating blades and aerodynamic sound. 17 p2096 A73-35333
- Rotor noise due to inflow turbulence. 18 p2259 A73-36191
- Calculating the fundamental oscillations in turboengine blades with different types of excitation. 19 p2499 A73-37778
- Longitudinal-torsional vibrations of rotors 20 p2569 A73-39374
- Blade synchronous rotation about pitch axis in single stage axial compressor at front of gas turbine engine during fan rotation 20 p2601 A73-39663
- Investigation of the influence of the leading-edge configuration on the efficiency of cooled rotor- and guide-vane cascades 21 p2632 A73-40406
- Some kinematic considerations of tone generation in axial turbomachinery. 22 p2899 A73-41710
- Noise from an isolated rotor due to inflow turbulence. 22 p2795 A73-41711
- An aeroelastic whirl phenomenon in turbomachinery rotors. [ASME PAPER 73-DET-97] 22 p2900 A73-42076
- Evaluation of slip factor of centrifugal impellers. 22 p2796 A73-42625
- Heat release from turbine rotor blades 23 p3020 A73-43744
- Transonic equation for flow in apertures between compressor and turbine blades, examining gas dynamic and geometric parameter influence on near-sonic flow 24 p3054 A73-45024
- ROTOR DISKS**
- U TURBINE WHEELS**
- ROTOR HUBS**
- U HUBS**
- U ROTORS**
- ROTOR LIFT**
- Helicopter rotor blade passing close to tip vortex, calculating fluctuating lift induced harmonic blade loads and generated cyclic banging noise 13 p1570 A73-29382
- Upstream attenuation and quasi-steady rotor lift fluctuations in asymmetric flows in axial compressors. [ASME PAPER 73-GT-30] 16 p2048 A73-33501
- ROTOR SPEED**
- Generalized mathematical model for gas turbine dynamic behavior simulation based on one dimensional flow theory with functional integration for rotor speed time derivative 15 p1925 A73-31629
- Newkirk effect - Thermally induced dynamic instability of high-speed rotors. [ASME PAPER 73-GT-26] 16 p2047 A73-33499
- Flow studies in radial inflow turbines interspace between nozzles and rotors. 17 p2093 A73-34392
- Gas bearing technique for ultrahigh speed rotating mirror mounted on opto-mechanical camera 21 p2693 A73-39936
- Vibration tests with rotors as a rotor identification problem 21 p2707 A73-40395
- Studies of pilot performance. III - Validation of objective performance measures for rotary-wing aircraft. 21 p2644 A73-41154
- Further experiments on balancing of a high-speed flexible rotor. [ASME PAPER 73-DET-99] 22 p2865 A73-42077
- ROTORCRAFT**
- U ROTARY WING AIRCRAFT**
- ROTORCRAFT AIRCRAFT**
- Independently targeted short haul individual rotorcraft for air taxi service, considering traffic control system, market possibilities, environmental impact and projected utilization 16 p2088 A73-33186
- Military VTOL combat and commercial efficiency considerations, including convertiplane substitution, Mach number effects and reverse flow on blades, rotor design and speed limitations 17 p2098 A73-34256
- Rotorcraft design concepts, considering economics, propulsion, control, trim devices, advancing blade concept, materials and rotor aerodynamics 21 p2635 A73-41189
- ROTORS**
- NT COMPRESSOR ROTORS**
- NT FLYWHEELS**
- NT IMPELLERS**
- NT LIFTING ROTORS**
- NT PUMP IMPELLERS**
- NT RIGID ROTORS**
- NT ROTARY WINGS**
- NT TILTING ROTORS**
- NT TIP DRIVEN ROTORS**
- NT TURBINE WHEELS**
- Dynamics of angular motions of a solid body carrying a rotating rotor, with allowance for energy dissipation 01 p0075 A73-10087
- A rapid matching procedure for twin-spool turbobfans. 02 p0202 A73-11593
- Drift rate of the rotor axis in the generalized problem of the gyroscope with a Cardan mounting 02 p0167 A73-11768
- Flooded rotor, direct current acyclic motor, with superconducting field winding. 02 p0132 A73-11829
- Linearized Kalman filtering for turbopump rotating assembly inertial and bearing parameter identification and state estimation, noting state-space model feasibility 03 p0313 A73-13904
- Rotors and turbine disks fracture resistance optimization at high temperatures from plane strain toughness criteria 14 p1813 A73-30679
- On the vibrations of a rotor with rotating inequality and with variable rotating speed. 15 p1883 A73-32216
- Simultaneous flexural and torsional vibrations of multidisk rotors 16 p2075 A73-32691
- Application of the finite element method to cases requiring the combination of elements possessing different numbers of degrees of freedom. 16 p2077 A73-32991
- Balancing equipment for jet engine components, compressors, and turbine - Rotating type for measuring unbalance in one or more than one transverse planes. [SAE ARP 587A] 16 p1993 A73-33013
- Elastic viscously damped ten degree of freedom system with two torsion-elastically mutually pivotally joined rotors, determining eigenfrequencies by equations of motion numerical evaluation 16 p1968 A73-33235
- Military VTOL combat and commercial efficiency considerations, including convertiplane substitution, Mach number effects and reverse flow on blades, rotor design and speed limitations 17 p2098 A73-34256
- VTOL and helicopter design considerations, including nonsymmetrical rotor flow characteristics, rotor types, airspeed capacities, compound helicopters, tilt wing and tilt rotor aircraft 17 p2099 A73-34259
- Experimental investigation of model variable-geometry and ogee tip rotors. [AHS PREPRINT 703] 17 p2104 A73-35054
- Helicopter tail rotor teeter hinge with Teflon conical journal bearing allowing axial and radial preload inservice adjustment, discussing oscillatory loads and temperature effects [AHS PREPRINT 762] 17 p2180 A73-35085
- Problems of minimum-weight turbomachine rotor designs 18 p2367 A73-37140
- Helicopter and fixed wing aircraft design consideration comparison, examining maintenance and reliability requirements, rigid, hinged and tilted rotors and load characteristics 21 p2634 A73-40225
- Application of simultaneous iteration method to torsional vibration problems. 21 p2783 A73-40289
- Vibration tests with rotors as a rotor identification problem 21 p2707 A73-40395
- Experimental investigation of a simple squeeze film damper. [ASME PAPER 73-DET-101] 22 p2865 A73-42078
- Increasing the critical rotational speed of the tail rotor drive shaft in SM-1 and SM-2 helicopters 24 p3057 A73-45195
- ROUGHNESS**
- NT SEA ROUGHNESS**
- NT SURFACE ROUGHNESS**
- ROUND TRIP TRAJECTORIES**
- Unmanned outer planets and round trip mission nuclear rocket engine design for carrying payload into orbit by single earth orbital shuttle [AIAA PAPER 72-1090] 03 p0340 A73-13411
- Earth-orbit mission considerations and Space Tug requirements. 19 p2490 A73-37302
- ROUNDED LEADING EDGES**
- U LEADING EDGES**
- ROUTES**
- Collection and processing of data for the establishment of route charges. 07 p0796 A73-19182
- International regional rental system for air transportation ground installations and route services, discussing ICAO recommendations 16 p2087 A73-32971
- ROUTINES**
- A computer-aided design procedure to approximate aircraft area curve shapes. [SAWE PAPER 982] 19 p2385 A73-37888

ROVER PROJECT

ROVER PROJECT

High temperature core thermocouple development for the Nuclear Rocket Engine Program (Rover/ 22 p2885 A73-42047

ROVING VEHICLES

NT LUNAR ROVING VEHICLES

System modeling and optimal design of a Mars-roving vehicle.

07 p0906 A73-20593
Retroflecting satellite with laser range finder for Martian roving vehicle navigation, discussing error analysis and minimization by measurement geometry choice through nonlinear programming

10 p1247 A73-24005
Terrain-vehicle dynamic interaction studies of a mobility concept (ELMS) for planetary surface exploration.

11 p1343 A73-25336
[AIAA PAPER 73-407]
Remote control of planetary surface vehicles.

17 p2148 A73-35316
Science aspects of a remotely controlled Mars surface roving vehicle.

19 p2416 A73-37311
Planetary surface rover/remotely manned system concepts and applications from lunar and Mars mission studies

19 p2416 A73-37312
Mars surface exploration by self-guided stereo TV equipped roving vehicle (robot), describing computerized object and scene ranging and recognition

19 p2429 A73-37321
ROVINGS
Mechanical properties of glass fiber reinforced plastic laminate formed by spraying unsaturated polyester resin on fiber rovings

24 p3094 A73-44890

RPV

U REMOTELY PILOTED VEHICLES

RUBBER

NT BUNA (TRADEMARK)

NT CHLOROPRENE RESINS

NT ELASTOMERS

NT SILICONE RUBBER

NT SYNTHETIC RUBBERS

NT THIOPLASTICS

NT VITON RUBBER (TRADEMARK)

Rubber friction effect on vehicle tire force-slip and breaking behavior in terms of peripheral and sideslip components and structural and operational parameters

03 p0251 A73-13242
Bending rigidity of an inflated circular cylindrical membrane of rubbery materials.

03 p0395 A73-14183
Antifriction bearing with lubricated rubber and metal laminations for wear elimination in limited rotation applications, discussing design guidelines and advantages

03 p0317 A73-14424
Influence of the nonlinear thermomechanical effect on the thermal stability of rubber-metallic couplings of vibration machines

04 p0509 A73-14981
A closed-form solution of the propagation problem of an unloading shock wave in a bilinear elastic body

04 p0513 A73-15395
Aircraft tire improvements and possible developments, discussing fibers, rubber compounds, tread, carcass and retreading

05 p0581 A73-16653
[SAE PAPER 720869]
Liquid rubber formulation for cold and hot urethane casting of photoelastic models, including membranes and thin walled structures

07 p0843 A73-19566
Layer strength and vulcanization effects on rubber/metal bonding with MEGUM agent

10 p1239 A73-24095
Corrosive aspects of the fatigue of rubber.

11 p1388 A73-25841
Sponge rubber absorption coefficient of sound and acoustic impedance measurements to test porous material sound absorption theories

14 p1767 A73-30894
Magnetic rubber inspection to extend NDT capabilities for locating cracks and defects on or near magnetic material surface

21 p2708 A73-41324

RUBIDIUM

NT RUBIDIUM ISOTOPES

Experimental study of the saturated-vapor pressure of rubidium and cesium

01 p0080 A73-10858
Cation exchange binding of rubidium and cesium by rat liver cell microsomes.

02 p0135 A73-12549

Q switched ruby laser emission absorption by diatomic Rb vapor, noting molecular fluorescence intensity changes

04 p0458 A73-15560
Lunar highlands soil analysis from Luna 20 and Apollo 16 samples, estimating lunar crust differentiation process age from Rb-Sr concentrations

05 p0618 A73-16833
A search for the solar Sr-87 content and the solar Rb/Sr ratio.

05 p0620 A73-17027

Experimental investigation of the pressure of the saturated vapor of rubidium and cesium.

12 p1526 A73-27907
The absorption spectrum of Rb I between 350 and 810 Å.

19 p2462 A73-37623
A test of Jaynes' neoclassical theory - Incoherent resonance fluorescence from a coherently excited state.

20 p2570 A73-38605
Adiabatic following and the self-defocusing of light in rubidium vapor.

20 p2571 A73-38632

RUBIDIUM COMPOUNDS

Plasma chemical synthesis of higher oxides of cesium and rubidium.

13 p1581 A73-29599

RUBIDIUM ISOTOPES

Rb87 vapor maser with optical pumping, measuring nitrogen or nitrogen argon mixture buffer gas partial pressure effect on power output

04 p0459 A73-15920
Rb-87/Sr-87 'ages' of the soil and rock fragments brought back from the lunar mountains by the automatic probe Luna 20 /Apollo crater region/

05 p0546 A73-16830
Solar Rb isotopic ratio from Rb I resonance lines at 7800 and 7947 Å in photospheric spectrum

05 p0620 A73-17026
Rb-Sr ages and initial strontium in basalts from Apollo 15.

08 p0936 A73-20839
Lunar Rb-Sr age correction according to stable isotope tracer (spike) recalibration, using stoichiometric salts

10 p1278 A73-24112
Light shift and light broadening in the Rb-87 maser.

20 p2572 A73-38861
Rb-87 - Sr-87 age of fragments and soils from the lunar Sea of Fertility.

21 p2770 A73-41005

RUBY

Simultaneous population inversions observation at Zeeman levels in ruby paramagnetic microwave quantum amplifier, noting pumping efficiency

02 p0177 A73-12499

Bottleneck of 29/cm phonons in ruby.

04 p0484 A73-15471
Influence of lattice defects on EPR line-shapes in ruby.

06 p0734 A73-17794
Microwave method of investigating the quality of ruby boules.

06 p0734 A73-17813
E resonance line broadening due to superhyperfine interactions in ruby, noting angular dependence of mosaic structure mechanism

09 p1132 A73-21954
Color centers in gamma-irradiated ruby with vanadium additions

10 p1259 A73-24069
Ultraviolet luminescence and nonlinear extinction in ruby

10 p1260 A73-24579
UV radiation effects on gamma irradiated Cr ions spin lattice relaxation rate in ruby and on resonant phonon scattering

13 p1668 A73-28219
Valency transfers of vanadium ions in ruby

14 p1783 A73-30582
Quantum losses during excitation of ruby luminescence

15 p1924 A73-31721
Ruby coloring centers and orange coloration dependence in corundum crystals on additive Mg, Cr, V and Ti ions

21 p2752 A73-40560
Cathodoluminescence of ruby (0.05 wt %/ at high temperatures

21 p2752 A73-40797
EPR-line splitting in irradiated ruby containing impurities

23 p3017 A73-44039

RUBY LASERS

Frequency stabilization of Q factor modulated ruby laser with mode selection, using rotating prism and quartz selecting element

01 p0060 A73-11087
Accumulation of the light sum in alkali halide crystals under the action of laser emission

01 p0060 A73-11088
Analogies in the laser-induced destruction of the surface and interior of transparent glass.

02 p0176 A73-12115
The laser telemetry station of the Pic-du-Midi Observatory and the acquisition of the French retroreflectors of Luna 17

02 p0151 A73-12247
Ruby laser ranging experiment for lunar returned signal from Apollo 11 retroreflector package, using multichannel pulse height counter and CRT

02 p0141 A73-12248
Saturation of stimulated ruby laser radiation under the action of CO-60 gamma rays

02 p0176 A73-12353

Signal detection in ruby element quantum paramagnetic amplifier operating at liquid nitrogen temperature

03 p0319 A73-14085
Pulse pumped Q switched Nd-YAG and ruby lasers single longitudinal mode selection by providing intracavity resonator with active medium

03 p0320 A73-14464
Investigation of certain characteristics of induced Raman scattering produced in a plane-parallel ruby-laser resonator

04 p0458 A73-14882
A dynamic holographic grating for a mode of operation with peaks

04 p0447 A73-14884
Q switched ruby laser emission absorption by diatomic Rb vapor, noting molecular fluorescence intensity changes

04 p0458 A73-15560
Large ruby laser radar for remote detection and recording of atmospheric scattering data, describing tracking mount, optics, electronic signal processing and display features

04 p0433 A73-15768
Ruby laser radiation removal of glowing spot from Kron electronograph image tube

05 p0580 A73-17260
Design and characteristics of a single pass normal mode ruby oscillator-amplifier laser for hole drilling in metals.

06 p0700 A73-18277
Quasi-stationary emission from ruby and neodymium-glass lasers

08 p0976 A73-21718
High-resolution study of anomalous dispersion in the ruby R lines.

09 p1090 A73-21940
Efficient parametric conversion in cesium vapor irradiated by 3470-Å mode-locked pulses.

09 p1090 A73-22079
The effect of an external signal on a ruby laser in the free-emission mode

09 p1095 A73-22667
Generation spectra of a ruby laser with frequency scanning

09 p1095 A73-22680
Deformation of laser pulses in resonant media.

09 p1096 A73-22902
Production of a coherent submillimetric radiation by a heterodyne method

09 p1097 A73-23030
Obtaining beams of singly charged metal ions with the aid of giant ruby laser pulses

10 p1227 A73-23815
Resonator parameters effect on stability characteristics of ultrashort pulse produced by ruby laser, using mirror and thin reflector

10 p1227 A73-24070
Relationship between macroinhomogeneity of the field and the kinetics of free regular emission from a ruby laser

11 p1376 A73-26140
Influence of elastic deformations on the lasing-threshold characteristics of a ruby laser

11 p1376 A73-26141
Spatial-temporal structure of emission from a ruby laser irradiated by gamma rays

11 p1378 A73-26523
Programmed radiation spectrum control in a ruby laser

12 p1504 A73-26883
Single-frequency ruby laser with electrooptical Q switching and smooth frequency tuning

12 p1504 A73-26886
Angular distribution of induced combinational light scattering in liquid nitrogen

12 p1505 A73-26889
Luminescence line width in ruby crystals of a laser resonator

12 p1505 A73-26892
Emission of a ruby laser with a moving mirror in the presence of a selector in the resonator

12 p1505 A73-26955
A cooled illuminator for studying ruby lasers

12 p1506 A73-27219
Operation of a laser with a planar resonator at high pumping levels.

12 p1507 A73-27507
Measuring the positions of satellites with the aid of laser pulses.

13 p1582 A73-28149
High-power broadly tunable difference-frequency generation in proustite.

13 p1626 A73-28548
Damping time of a ruby laser with flat mirrors

13 p1630 A73-29556
Formation of an ultrashort pulse of light in a ruby laser with resonant modulation of losses

14 p1757 A73-30265
Temperature stability of the disperse phase component of the output emission of an optical quantum amplifier

14 p1758 A73-30576

Q switched ruby laser optical diagnostic system for plasma shock waves and plasmoid observation, noting schlieren photographs of exploding wire experiments 14 p1782 A73-30925

The laser - A unique tool for /for the time being/ unique applications 15 p1884 A73-31325

Holographic method for measuring spatial coherence functions 15 p1879 A73-32339

Experimental studies on the scattering pattern from a ruby laser rod. 16 p2023 A73-32875

Light pulse structure and bandwidth bounds in ruby laser with delay line inside variable effective length resonator 17 p2185 A73-35169

Investigation of 'external' self-focusing of ruby laser emission in CdS crystals 18 p2322 A73-36674

Ruby laser light spark ion-electron currents in gap between copper plates under electric field 18 p2322 A73-37047

Generation in a ruby laser with moving mirror and a selector in the resonator. 19 p2438 A73-38132

Material processing with solid-state laser. [SME PAPER EM 73-213] 19 p2436 A73-38495

Amplitude stabilization of pulses from a Q-switched ruby laser by means of interaction with a non-linear medium. 20 p2570 A73-38614

Ruby laser with a wide emission spectrum. 20 p2574 A73-39696

Automatic surface mapping via holographic system, describing Q switched ruby laser holograms, image dissector, computer video signal analysis and scan signals 21 p2699 A73-40150

Emission spectrum of a Q-switched ruby laser and its dependence on the density of the bleachable filter 21 p2711 A73-40304

Slow electron scattering near focused beam of Q-switched ruby laser, investigating scattering probability dependence on electron impact parameter 21 p2712 A73-40354

Excitation of ultrashort light pulses in a ruby ring laser with resonant Q-switching 21 p2712 A73-40356

Generation of microsecond pulses with controllable pulse width in a ruby laser 21 p2713 A73-40527

Generation of internal modes and its influence on the operation of a tunable ruby laser 21 p2714 A73-40558

Surface and bulk laser-damage statistics and the identification of intrinsic breakdown processes. 21 p2714 A73-40758

A study of the properties of stimulated ruby laser emission during the action of Co-60 gamma rays 21 p2715 A73-40796

Low-noise instrumentation for Raman and luminescence spectrometry with ruby and argon laser excitation. 22 p2868 A73-41783

Self-termination of free oscillations in ruby at low temperatures. 22 p2896 A73-42251

A possible Q-factor modulation mechanism in a ruby laser with a misaligned resonator 23 p2988 A73-44047

Rapidly fading absorption induced in polymethine dyes by nanosecond pulses of ruby laser radiation 24 p3096 A73-44959

RUBBLES

A short description of the NAE airborne simulator feel system. 21 p2672 A73-40854

RULES

NT FLIGHT RULES

NT INSTRUMENT FLIGHT RULES

NT SUM RULES

NT WHITHAM RULE

RUMBLE INSTABILITY

U ACOUSTIC INSTABILITY

RUN TIME [COMPUTERS]

Minimum variance linear filter with partial state elimination by linear transformation for reduction of computational burden and storage requirements in Kalman filter 04 p0431 A73-15268

On the number of operations simultaneously executable in Fortran-like programs and their resulting speedup. 05 p0553 A73-16450

Noisy data filtering of linear steady state control problems based on nearest neighbor interaction, discussing dimensionality reduction model for saving computer time 06 p0682 A73-18868

A direct method for solving Poisson's equation. 07 p0845 A73-19574

An efficient parallel algorithm for the solution of a tridiagonal linear system of equations. 08 p0983 A73-20960

Computer simulation of semiconductor devices. 08 p0948 A73-21534

FORTTRAN IV program and recursive matrix partitioning algorithm for solution of photogrammetric simultaneous equations, noting computation time 09 p1059 A73-22382

A comparison of first and second order axially symmetric finite elements. 09 p1158 A73-22399

Finite difference programs with grid self adjustment for steady or unsteady problems with arbitrary boundaries and without coordinate hierarchy, noting computer time saving 09 p1071 A73-22400

Finite element method for solution of two dimensional flow equations with applications to passive advection and nonlinear gravity wave problems, noting computing time 09 p1113 A73-22955

Alternative algorithmic scheme for spherical harmonics series summation, noting high speed and precision loss at high resolution in comparison with conventional methods 10 p1246 A73-23993

Viscous flow over a cone at moderate incidence. I - Hypersonic tip region. 11 p1300 A73-25114

A numerical solution of the Navier-Stokes equations using the finite element technique. 11 p1345 A73-25116

Beta estimation accuracy for reentry vehicles using a priori target information with 6-component state vectors to reduce computation time 12 p1548 A73-27131

Dynamic structural response analysis with eigenvalue problem solution in terms of stiffness and mass matrices, discussing algorithm selection for efficient computation 13 p1691 A73-28081

Automatic system for kinematic analysis /ASKA/ computer programs for structural finite element solution, discussing design concepts, element types, user interface and computation time 13 p1693 A73-28243

Computational efficiency of equilibrium models in eigenvalue analysis. 13 p1694 A73-28248

An efficient algorithm for calculation of the Luenberger canonical form. 14 p1769 A73-30508

A new method for the Lebedev-Ufliand integral equation for contact problems of elasticity. 15 p1946 A73-31103

Computational efficiency comparison for discrete linear filtering Kalman algorithms and information matrix methods, noting Householder square-root implementation identity with Potter technique 16 p2032 A73-33404

Some aspects of numerical integration. 17 p2202 A73-35372

Comparison of three techniques for solving the radiative transport equation. 18 p2337 A73-36367

[AIAA PAPER 73-751] A numerical integration scheme for the N-body gravitational problem. 20 p2604 A73-38973

Numerical and analytical prediction methods for time dependent reactions in homogeneous gas mixtures, considering accuracy and computing times 20 p2626 A73-39095

A comparison of the times of computation required by two approaches for determining a shortest route in a network - A contribution to the economy of programming 20 p2533 A73-39631

Large deflection of shallow paraboloid shells. 21 p2782 A73-40005

Iterative and matrix inversion techniques for antenna electromagnetic radiation and scattering prediction compared for computer storage and execution time 22 p2823 A73-41799

A method for numerically solving second-order non-homogeneous linear differential equations with variable coefficients. 22 p2882 A73-42482

A simplified minimal-realization algorithm for a symmetric transfer-function matrix. 23 p2999 A73-43382

The role of computers in the development of numerical weather prediction. 24 p3108 A73-45085

Parallel and string array processor hardware design and computer programs for computing speed increase over conventional series computers 24 p3070 A73-45086

RUNGE-KUTTA METHOD

Improved sixth-order Runge-Kutta formulas and approximate continuous solution of ordinary differential equations. 02 p0188 A73-12822

Optimum Runge-Kutta-Fehlberg methods for second-order differential equations. 04 p0471 A73-15231

Contribution to the numerical solution of differential equations by means of Runge-Kutta formulas with Newton-Cotes numbers weights. 09 p1113 A73-22988

A self starting predictor corrector algorithm of arbitrary order having exact stability. 12 p1517 A73-27170

Analysis of gas flow through a multilayer insulation system. 17 p2149 A73-34184

Some aspects of numerical integration. 17 p2202 A73-35372

Stability and convergence of streamline curvature flow analysis procedures. 19 p2421 A73-38190

A method for numerically solving second-order non-homogeneous linear differential equations with variable coefficients. 22 p2882 A73-42482

A Runge-Kutta Nystrom algorithm. 24 p3142 A73-45290

Multistep-multistage-multiderivative methods for ordinary differential equations. 24 p3106 A73-45334

RUNWAY ALIGNMENT

An instrument approach system for Hong-Kong International Airport. 15 p1910 A73-32464

RUNWAY CONDITIONS

Airport requirements for air traffic safety, considering runway drainage and lighting, ILS, rescue and fire services, communications and weather reporting networks 01 p0030 A73-11239

Airfield requirements for flight safety enhancement, considering approach and takeoff path obstructions, runway conditioning, glide slope information and radio aids 10 p1203 A73-24713

Aquaplaning prevention during take-off and landing, discussing friction loss factors, aircraft tires and runway surface treatment by antiskid overlays and grooving 11 p1343 A73-25209

Fog frequency and characteristics at the site of the proposed New York offshore airport, as compared with those at J. F. Kennedy International Airport - A preliminary report. 15 p1903 A73-31546

Fully automatic assessment of RVR, and comparison with observers. 15 p1910 A73-32466

Technical studies and research on airport infrastructure 15 p1859 A73-32561

Air cushion landing systems for aircraft mobility on unprepared surfaces, considering refraction, vertical energy absorption, braking, steering and weight and power reduction 19 p2380 A73-37677

LA-4 aircraft air cushion landing system ACLS development tests covering static and mobile ground tests, flight tests and performance from and to various surfaces 19 p2382 A73-37692

Runway condition effects on landing safety, discussing surface friction, approach control, skidding, directional control, water and ice conditions, tires and brakes 20 p2509 A73-39220

Pulsated over-heated water rocket /POHWARO/ thrust augmentation system for combat aircraft takeoff runs from short runways under severe weather conditions 24 p3057 A73-45391

RUNWAY LIGHTS

Airport runway lights system location and use for aircraft takeoff operations and visual indication of landing approach angle 14 p1743 A73-30242

Operational considerations in the design of offshore airports. 15 p1856 A73-31532

Airport lighting systems as visual landing aids, discussing runway disposition, brightness levels, beam orientation, visibility factors and flashing light 16 p1993 A73-32974

Runway lighting emergency power supplies for low visibility, comparing single supply backed by automatic generator with separate cable and duplicate supplies 22 p2839 A73-42318

RUNWAYS

Airfield pavement full scale performance tests under simulated C-5A load conditions, evaluating construction joint systems 01 p0029 A73-10823

Airport layout planning, considering air traffic, conventional and STOL aircraft, runway requirements, passenger and baggage processing facilities, environmental factors, etc 02 p0150 A73-11704

The capacity of a single-runway S.T.O.L./R.T.O.L. airport. 07 p0849 A73-19352

RUPTURING

- German book - Soil mechanics of retaining structures, roads, and runways. 11 p1344 A73-26255
- Subgrade strengthening of existing airfield runways. 15 p1856 A73-31388
- Honolulu International Airport reef runway. 15 p1857 A73-31538
- Runway visual range equation derivation, taking into account background luminance, atmospheric absorption and illumination 15 p1906 A73-32351
- Book - Aircraft noise: Selection of runway sites for Maplin Airport. 15 p1859 A73-32415
- The Corail radar - Automatic equipment for runway surveillance 15 p1846 A73-32431
- Runway VHF localizer antenna array for Norwegian airports ILS, taking into account difficulties due to course bends and snow 15 p1859 A73-32498
- Floating offshore airport in Osaka Bay, Japan - Digest of preliminary engineering study. 19 p2418 A73-37747
- Operational considerations in the design of airports. 19 p2418 A73-37820
- Runway configuration improvement programming model. [ASCE PREPRINT 2034] 22 p2839 A73-42864
- Dual lane runway configuration design and operational characteristics investigation by real time computer simulation for solution to airport capacity problem [ASME PAPER 73-ICT-61] 23 p2966 A73-43496
- Airport runway and taxiway surfaces modifications for heavy and supersonic aircraft demonstrated by aircraft static and dynamic landing loads and physical dimensions 24 p3075 A73-45199

RUPTURING

- Inter- and transcrystallite breakdown of steels and alloys under the action of various media [A review/ 01 p0062 A73-10258
- Creep rupture under multi-axial states of stress. 03 p0327 A73-13981
- Continuum mechanics analysis of local rupture and plastic strains near cracks and fractures, noting elastoplastic applications 12 p1551 A73-27251
- A molecular theory of elastomer deformation and rupture. 13 p1646 A73-29528

RUSTING

- Composition and structure of rust layers and corrosion rate of chromium steels exposed to a marine atmosphere. 05 p0586 A73-16137

RUTHENIUM ALLOYS

- Nonequilibrium crystallization of Al-Ru alloys 09 p1108 A73-23228
- Microstructure and hardness investigations of alpha prime, alpha double prime and omega metastable phases formed during quenching of Ti-Ru alloys 17 p2188 A73-34567
- Phase diagrams of ruthenium and rhodium systems with carbon 22 p2878 A73-42461
- Exceptional hardness and corrosion resistance of Mo5Ru3 and W3Ru2 films. 22 p2866 A73-42581

RUTILE

- Metallurgical, chemical and electrochemical production and refining of refractory metals, including titanium, fluorotitanates and artificial rutile 04 p0465 A73-15660
- Electron microprobe chemical analysis and structural formula of niobian rutile in Apollo 14 microbreccia sample KREEP fragment 09 p1139 A73-21856
- Moessbauer spectroscopic studies of iron-doped rutile. 10 p1258 A73-23567
- Earth mantle rutile-structure germanium dioxide elastic properties as function of pressure and temperature in single crystals 11 p1352 A73-25585
- Luna 20 - Mineral chemistry of spinel, pleonaste, chromite, ulvöspinel, ilmenite and rutile. 13 p1675 A73-28316

RVAN MILITARY AIRCRAFT U MILITARY AIRCRAFT RYDBERG SERIES

- Theoretical assignments of the low-lying electronic states of carbon dioxide. 19 p2462 A73-37583

S

S BAND

- U SUPERHIGH FREQUENCIES
U ULTRAHIGH FREQUENCIES

A-1528

S GLASS

- Fiber strength of S-glass/epoxy composites under biaxial loading. 03 p0330 A73-13017

S MATRIX THEORY

- Statistical method of calculating scattering matrix elements and parameter deviations of SHF octupole networks /square bridge, hybrid ring or directional junction/ 02 p0146 A73-12025

- On the analysis of scattering and antenna problems using the singularity expansion technique. 06 p0665 A73-18184

- S matrix method featuring eigenenergy and eigenfunction trials number reduction for rapid numerical determination of bound states of partial-wave-projected Schroedinger equation 10 p1248 A73-23669

- A measurement stand for reciprocal circuits in a waveguide 10 p1189 A73-24417

- An explicit form of the Mie phase matrix for multiple scattering calculations in the I, Q, U and V representation. 11 p1390 A73-25718

- Atmospheric air characteristics classification as haze, foggy haze, fog and drizzle from light scattering matrix on basis of aerosol condensation 13 p1654 A73-29159

- The scattering matrix of a double truncated corner in a waveguide 14 p1726 A73-30073

- Resonant scattering from inhomogeneous nonspherical targets. 14 p1775 A73-30906

- Scattering of waves at a step in a circular multiwave waveguide. 17 p2123 A73-35152

- Analysis of infinite planar array of rectangular waveguides by generalized scattering matrix approach. 21 p2651 A73-40652

- Numerical solution of edge effects of external coupling between elements in linear phased array of slots covered by dielectric slab, using scattering matrix 21 p2651 A73-40654

- Conformal arrays on surfaces with rotational symmetry. 21 p2653 A73-40676

- On the evaluation of the principal value integral in the scattering problems. 21 p2728 A73-41475

- Photon retinue and infra-red divergence problem in quantum electrodynamics. 22 p2889 A73-42426

- Scattering and transmission functions of radiation by finite atmospheres with reflecting surfaces. 23 p3030 A73-43755

S WAVES

- Shear waves and perturbations in linearized steady plane flows of a thermally nonconducting compressible ideal fluid [ONERA, TP NO. 1169] 01 p0034 A73-11359

- Utilization of polarized ultrasound in stress investigations 02 p0166 A73-11645

- Extension of an interface flaw under the influence of transient waves. 07 p0908 A73-19080

- P and S waves propagation velocity distribution for lunar mantle and crust composition, noting petrological models with differentiated mantle 07 p0894 A73-19849

- Elastic wave velocities and thermal diffusivities of Apollo 14 rocks. 07 p0894 A73-19851

- Apollo 12 soil sample strength, compressibility, bulk density, porosity and shear wave velocity 07 p0898 A73-19901

- Scattering of a cylindrical wave in an elastic plate in the presence of an absolutely rigid cylindrical inclusion 12 p1551 A73-27240

- Planar shear wave motions polarized in plane of bonded elastic orthotropic layered plates with each layer having distinct mechanical and inertial properties and thickness 13 p1697 A73-28820

- Representative shear wave passage through plane flame front, determining wave refraction and modification, flame generated turbulence and noise and perturbation of front 13 p1707 A73-28993

- Bleustein-Gulyaev shear surface waves in piezoelectric-dielectric-perfect conductor layered system, applying theoretical results to lithium iodate crystals 14 p1783 A73-30259

- Dynamic stress concentration at an elliptic hole due to plane SH-waves 15 p1947 A73-31331

- Shear waves in infinitely extended double walls with coupling rods of circular cross section. I - Shear waves in the infinitely extended disk 17 p2241 A73-34246

- Effect of orthotropy on singular stresses for a finite crack. [ASME PAPER 72-APM-VVV] 17 p2249 A73-35109

- Elasticity of water-saturated rocks as a function of temperature and pressure. 17 p2163 A73-35271

- New seismic data on the state of the deep lunar interior. 17 p2237 A73-35805

- Longitudinal shear waves in a fiber-reinforced composite. 19 p2500 A73-38113

- Linear dispersive shear waves in two-layer elastic medium. 19 p2461 A73-38185

- Richardson number profiles through shear instability wave regions observed in the lower planetary boundary layer. 19 p2448 A73-38228

- Thermal structure and stability study of internal and Kelvin-Helmholtz waves in low Reynolds number flows by sampling and stratified wind tunnel methods 19 p2422 A73-38235

- Effect of orthotropy on singular stresses produced near a crack tip by incident SH-waves. 21 p2786 A73-40933

- RF sputtering of ZnO shear-wave transducers. 21 p2702 A73-40952

- Gravity wave nonlinear interactions producing secondary waves of opposite polarization, discussing tide polarization 21 p2688 A73-41343

- A higher order theory for extensional motion of laminated composites. 22 p2929 A73-43139

- Gravity-shear waves in jet flow near tropopause with arbitrary temperature-wind stratification 23 p3001 A73-43462

- Transmission of anti-plane shear waves past an interface crack in dissimilar media. 23 p3043 A73-43815

S-N DIAGRAMS

- Vibrational strength of structural members from Woehler lines, calculating service life from S-N diagrams 03 p0385 A73-13138

- New method for the statistical evaluation of constant stress amplitude fatigue-test results. 03 p0387 A73-13229

- Estimating the median fatigue limit for very small up-and-down quantal response tests and for S-N data with runouts. 03 p0387 A73-13230

- Accelerated method of estimating the growth rate of fatigue cracks. 04 p0514 A73-15671

- Low cycle fatigue tests of medium strength Al alloys, showing agreement with Manson-Halford fatigue life-strain relation 05 p0586 A73-16135

- S-N fatigue curve analysis from ultimate tensile strength to cyclic elastic limit below fatigue limit, discussing load cycle zones and discontinuities 07 p0910 A73-19214

- Welded structural components fatigue behavior representation by characteristic curves derived from S-N diagrams, describing data reduction procedure 07 p0910 A73-19216

- Evaluating the variation in fatigue properties of aluminum alloys due to variable loads by using secondary fatigue curves. 08 p0977 A73-21147

- Surface work hardening as a means of increasing the resistance of machine parts to low cycle fatigue. 09 p1089 A73-23162

- The effect of the structure of the titanium alloys VT3-1 and VT-18 on their fatigue resistance under asymmetrical cyclic loading. 09 p1106 A73-23164

- The effect of coatings on the fatigue characteristics of notched aluminum alloy sheet specimens. 11 p1383 A73-25829

- Fretting fatigue strength of several materials combinations. 11 p1385 A73-26335

- High-cyclic fatigue curves for annealed metals from investigation of defect buildups, lattice distortions, microcrack nucleation and fatigue crack growth 12 p1552 A73-27253

- Relationship between the strain curves of a material subjected to static and to cyclic loads 13 p1698 A73-29055

- Statistical definition of fatigue behavior of strength of low alloy steels. 13 p1641 A73-29492

- Machine parts fatigue life and linear cumulative damage at stresses below endurance limit, including plastic strain, microcracking and S-N curves 13 p1641 A73-29496

Low carbon steel S-N diagram for stresses ranging to fatigue limit, noting cyclic creep, macroplastic cyclic stress and fatigue failure 13 p1703 A73-29603

Investigation of the thermal fatigue of type Kh18N10T steel under complex stress distributions, 13 p1643 A73-29623

Wing spar static and fatigue tests and S-N curve for lifetime measurement of root sections of small trainer and passenger aircraft 15 p1955 A73-32190

Relation of strain curves of material in static and cyclical loading. 18 p2366 A73-36887

Investigation of fatigue strength of D1T alloy with due regard to dispersion of results. 19 p2440 A73-37791

The effect of stress amplitude below the fatigue limit on cumulative fatigue lives in perforated round specimens. 19 p2501 A73-38344

The fretting fatigue of titanium and some titanium alloys in a corrosive environment. 22 p2876 A73-42356

Monograph - Fatigue and stochastic loadings. 22 p2923 A73-42673

German monograph on cyclic stress-strain curves and fracture strength of steels with various compositions covering plastic strain energy, S-N diagrams and test equipment 22 p2879 A73-42739

Fatigue test apparatus for metals at ultrasonic frequencies consisting of transducers, strain amplitude monitor, cooling circuit and static stress mechanism, discussing S-N response 22 p2867 A73-43169

S-18 SATELLITE
U OAO

S-3 AIRCRAFT
Test facility for determination of S-3A aircraft landing gear behavior during critical pulse loads while rolling over carrier deck, discussing moving platform components 02 p0150 A73-11999

S-3A aircraft systems, performance and design, discussing flight simulation, wind tunnel tests, weapons systems, flutter tests, avionics, TF-34 engine, stalls and computer programming [ALAA PAPER 73-778] 19 p2387 A73-38367

S-61 HELICOPTER
S-61N helicopter all-weather IFR operation for North Sea oil rigs supply and harbor pilots transportation, describing onboard instrumentation, navigation and communication systems 05 p0535 A73-16847

SABOT PROJECTILES
Gun launched sounding rockets and sabot projectiles for low cost meteorological and geophysical data acquisition, considering cost advantages 06 p0756 A73-18020

SABOTILIVER AIRCRAFT
U T-39 AIRCRAFT

SACCHARIDES
U CARBOHYDRATES

SADDLE POINTS
NT SADDLE POINTS [GAME THEORY]
Book - Mathematical problems in wave propagation theory. 12 p1524 A73-27625

Distribution of the response of linear systems to Poisson distributed random pulses. 16 p2035 A73-32918

A note on saddle point behavior for ordinary and functional differential equations. 17 p2204 A73-35733

Complementary variational principle existence condition and duality in linear and quadratic programming in Hilbert space setting, considering relationship to Kuhn-Tucker saddle point theory 21 p2724 A73-40296

SADDLE POINTS [GAME THEORY]
Zero sum differential game theory for two players, discussing strategies, stochastic versions and saddle value and points existence 13 p1651 A73-29650

Optimality and lower and upper bound conditions for multistep games with saddle point and minimax/maximin strategies, extending to differential games 20 p2539 A73-38678

Optimal stopping time for stochastic games corresponding to diffusion process, obtaining saddle point characterization via elliptical variational inequality solution 23 p2999 A73-44083

SADDLES [SUPPORTS]
Design and model tests for a 5 Tesla superconducting saddle magnet. 02 p0132 A73-11837

SAFETY
NT AIRCRAFT SAFETY
NT FLIGHT SAFETY
NT INDUSTRIAL SAFETY
NT RANGE SAFETY
NT REACTOR SAFETY

SAFETY DEVICES
NT ABORT APPARATUS
NT ARRESTING GEAR
NT EJECTION SEATS
NT ESCAPE CAPSULES
NT ESCAPE ROCKETS
NT HELMETS
NT SEAT BELTS
NT SPACE SUITS

Fail-safe aircraft composite structures, achieving crack arrestment by integral buffer strips in primary load carrying laminates 06 p0764 A73-18494

Modulated light transmission for electrical isolation in a multichannel physiological monitoring system. 07 p0785 A73-19482

Airborne fire protection equipment. 13 p1568 A73-28171

Relative merit of the disc-gap-band parachute applied to individual aircrew member escape. 15 p1829 A73-31465

[ALAA PAPER 73-483]

Multiple occupant flotation devices for commercial transport aircraft survivors sea ditching, discussing slide/raft design improvement for high density loading 16 p1974 A73-32658

Aircraft in-flight visibility /conspicuity/ during daytime, discussing exterior paints, tapes and high intensity lighting effectiveness for midair collision avoidance 16 p1965 A73-32661

Lightning protection for aircraft canopy, discussing simulation tests, safety margins, side puncture, corona streamering and pilot physiological reactions 16 p1968 A73-33036

Helmets effectiveness evaluation from acceleration and impact tests, discussing test criteria and civilian and military standards 16 p1975 A73-33132

All-wheel drive fire fighting equipment evolution under impact of wide bodied aircraft introduction 20 p2545 A73-39661

VAK 191B. 22 p2798 A73-41752

SAFETY FACTORS
Hazard and interference avoidance in implant telemetry, discussing leakage currents, muscle interference, magnetic influence, high frequency noise, electrode and respiratory artifacts, etc 03 p0271 A73-14295

Distribution functions with fatigue analysis laws and safety predictions, noting life length and fleet assurance models 04 p0507 A73-14710

Anisotropic structures reliability in terms of design safety factor, analyzing composite rocket motor cases under plane stress 04 p0452 A73-14723

Airframe structural testing and safety design for military aircraft, discussing static, dynamic and fatigue tests and environmental effects 04 p0454 A73-14865

Safety factor calculation procedure for perfectly plastic body under given plane stress based on complex variable functions 04 p0511 A73-15175

Theoretical-experimental studies and research concerning the technical safety of the casing of a high-pressure cylindrical tank. I 04 p0454 A73-15657

Time-temperature safety thresholds for human epidermal injury related to materials thermal properties 05 p0637 A73-16138

Operational safety experience and advances of space nuclear power systems fueled with Pu-238, discussing modular heat sources 09 p1119 A73-23287

NASA use of liquid and gaseous oxygen under extreme pressure, temperature and flow rate conditions, discussing safety requirements in terms of structural and chemical compatibility 11 p1410 A73-26525

Launching base creation process and economic factors, considering rocket firing safety, scientific requirements and financial investments criteria 14 p1741 A73-30080

Composite material design criteria, discussing fatigue, stress concentration, safety factors, scaling effects and load characteristics 16 p1967 A73-33028

Safety aspects in documentation system for orientation, training and maintenance of equipment for Poseidon Missile System 16 p2073 A73-33639

Integrated reliability and safety analysis of the DC-10 all-weather landing system. 16 p1969 A73-33641

Technical and safety aspects of maintenance work on commercial aircraft wing fuel tanks, considering wing deformation effects and sealant materials and reapplications 18 p2286 A73-36932

Laser hazards and safety performance standards, discussing ocular and skin damage and exposure limits and operational regulation 20 p2517 A73-39205

Safe flying, skilled personnel and aircraft maintenance assurance via safety equipment, initial and recurrent training, protective clothing and shelter from inclement weather, maintenance scheduling, etc 20 p2518 A73-39212

Fire protection and insurance in airport hangars, discussing governmental safety codes, fire prevention systems, aircraft vs building values and legislative proposals 20 p2544 A73-39214

Russian book on rocket weapon systems safety handling covering HF electromagnetic, noise and vibration effects, ionizing radiation, fire, etc 22 p2812 A73-41874

Safety margins in the implementation of planetary quarantine requirements. 22 p2803 A73-42161

SAFETY HAZARDS
U HAZARDS

SAFETY MANAGEMENT
Tibere rocket launched Electre nose cones reentry impact safety optimization policy based on probabilistic viewpoint 08 p1014 A73-21679

[ONERA, TP NO. 1152] Human threats to air safety; Proceedings of the Twenty-fifth Annual International Air Safety Seminar, Washington, D.C., October 16-18, 1972. 10 p1176 A73-24707

Airlines flight safety management, discussing visual systems simulator /VSS/ for Tristar systems environmental and cycling endurance ground tests 10 p1176 A73-24710

Airport design and management for safe aircraft ground handling, discussing FAA rules on pavement and safety areas, marking and lighting, fire fighting, etc 10 p1204 A73-24714

Aircraft and ground equipment damage during ground handling operations, discussing repair costs and out-of-service time 10 p1176 A73-24715

Civil aviation medicine functional standardization and expansion, emphasizing preventive medicine, health education and operational safety 10 p1185 A73-24718

Aircraft airport system R and D program in terms of efficient planning, lighting and marking, geometric design, safety and pavements 13 p1598 A73-29103

Research on ignition and combustion in oxygen systems. 13 p1708 A73-29402

Electre nose cones reentry impact safety policy, discussing launcher trajectory, cost and performance indices and ascent optimization 14 p1804 A73-30097

Operational considerations in the design of offshore airports. 15 p1856 A73-31532

The role of testing in achieving aerospace systems effectiveness. 16 p2020 A73-33605

Safety management of air to surface nuclear short range attack missile /SRAM/ at fabrication, testing and operation levels 16 p2073 A73-33640

Aircraft wake vortex avoidance system for safety management and capacity optimization in airport operations related to ATC, considering various sensors and display subsystem requirements 17 p2166 A73-34613

Nuclear safety considerations for the design of a shuttle launched 500 to 2000 watt isotope Brayton power system. 19 p2457 A73-38432

Book - The role of testing in achieving aerospace systems effectiveness. 21 p2675 A73-41201

SAHA EQUATIONS
Saha's equation under deviation from thermodynamic equilibrium. 22 p2915 A73-43040

SAILPLANES
U GLIDERS

SAILS
Experimental investigation of the supersonic two-dimensional flow past a sail at small angles of attack 01 p0004 A73-11371

Equilibrium equation for weightless flexible two dimensional sail in inviscid supersonic airstream, noting centred isentropic compression 03 p0246 A73-13789

SAINT VENANT FLEXURE PROBLEM
U SAINT VENANT PRINCIPLE

SAINT VENANT PRINCIPLE
Elastic-plastic analysis of Saint-Venant torsion problem by a hybrid stress model. 03 p0390 A73-13338

On the determination of the centers of twist and of shear for cylindrical shell beams. 05 p0633 A73-16534

[ASME PAPER 72-APM-XX] Finite element stress field solution of the problem of Saint Venant torsion. 09 p1158 A73-22390

SALINITY

Biharmonic coupling solutions of Saint Venant equation for elastoplastic plane under unequal loads, using Kolosov-Muskhelishvili functions and conformal mapping 09 p1165 A73-23350

Saint Venant principle for plane deformation of anisotropic elastic solid extended to analysis of fiber reinforced transversely isotropic composites 11 p1444 A73-26280

Saint Venant principle investigation for plane problem of linear elastostatics for anisotropic media by energy method, calculating exponential stress decay constant lower bound 15 p1946 A73-31102

Saint Venant problem for a continuously inhomogeneous anisotropic beam 15 p1953 A73-32103

Book - Elasticity. 23 p0309 A73-43434

Saint Venant continuity equation for identical formulation of Lamé equations and elasticity theory problem of stress-strain state in bodies of revolution 23 p3045 A73-44185

SALINITY

Salinity surveys using an airborne microwave radiometer. 20 p2558 A73-39865

Remote measurement of salinity in an estuarine environment. 22 p2850 A73-42730

SALT BATHS

Effects of hot-salt stress corrosion on titanium alloys. 03 p0323 A73-13268

Synergistic effects of anions in the corrosion of aluminum alloys. 03 p0325 A73-13729

Influence of microstructure on the corrosion behavior of Ti-2% Ni in hot acidic chloride solutions with particular reference to weld regions. 03 p0325 A73-13730

Study by autoradiography at high resolution power of the role of hydrogen in the mechanism of cracking of TA6V titanium alloy in salt water 04 p0461 A73-15097

Subcritical crack growth measurement during static loading of precracked Ti alloys in salt water, discussing arrested crack propagation at different stress intensities 10 p1234 A73-24429

Fused salt techniques for metal diffusion coatings with beryllium, boron, silicon, aluminum, titanium and chromium 16 p2017 A73-32697

SALT MARSHES

U MARSHLANDS

SALT SPRAY TESTS

The effect of oxide thickness on the hot salt stress corrosion susceptibility of Ti-6Al-4V. 01 p0061 A73-10137

Corrosion fatigue of type 4140 high strength steel. 02 p0183 A73-12764

Exfoliation corrosion testing of 7178 and 7075 aluminum alloys. 15 p1889 A73-31742

An electrochemical model for hot-salt stress-corrosion of titanium alloys. 17 p2189 A73-34643

Filiform corrosion associated with commonly applied aircraft metal pretreatments and finishes. [SAE PAPER 730311] 17 p2177 A73-34671

Solid film lubricant corrosion study employing salt spray test with sulfur dioxide and synthetic sea water, examining molybdenum disulfide, antimony trioxide and graphite films [ASLE PREPRINT 73AM-3C-4] 17 p2196 A73-34989

Long term life tests for thermal shock cycles effects on plastic encapsulated semiconductor device reliability, presenting salt atmosphere testing data for silicone package 19 p2471 A73-38454

Cloud microphysics spaceborne laboratory experimentation under zero-gravity conditions, discussing salt nuclei distribution mechanism due to spray breakup as task for Apollo-Soyuz program [AAS PAPER 73-135] 20 p2583 A73-38590

SALTS

Water-salt homeostasis mathematical model, solving equations with analog and digital computers 10 p1184 A73-23941

Investigation of the polar and protective properties of magnesium salts of organic acids 10 p1239 A73-24248

Temperature dependence of the Na-23 quadrupole coupling constants in Rochelle salt. 11 p1409 A73-25875

A comparison of four remote sensing media for assessing salt marsh primary productivity. 20 p2562 A73-39903

Nuclear magnetic resonance thermometry. 22 p2856 A73-42022

SALYUT SPACE STATION

Alpha Lyra and beta Cen spectrograms from Merseid system telescope aboard Salyut space station, demonstrating viability of space observatories 03 p0375 A73-13953

Investigation of charged-particle fluxes at altitudes of 200 to 300 km with the aid of the Saliut orbital station 10 p1267 A73-23930

Visual observations of the earth and of the circumterrestrial space environment from manned orbital stations 23 p2971 A73-43331

SAMARIUM

Stimulation of nonradiating transitions during intense excitation by light 15 p1885 A73-31720

SAMARIUM COMPOUNDS

Samarium oxide neodymium oxide activated glass fiber output power under lasing conditions 14 p1766 A73-30468

SAMARIUM ISOTOPES

Apollo 16 neutron stratigraphy. 18 p2354 A73-36514

SAMPLED DATA

U DATA SAMPLING

SAMPLED DATA SYSTEMS

U DATA SAMPLING

SAMPLES

Viking lander-borne gas chromatograph mass spectrometer for Martian atmosphere sampling and soil analyses 02 p0168 A73-12000

Sampling circuit for HF repetitive waveforms reproduction on standard x-y recorder, noting SNR improvement by signal averaging 11 p1366 A73-26304

SAMPLING

NT AIR SAMPLING

NT CORE SAMPLING

NT DATA SAMPLING

NT PARTICULATE SAMPLING

NT RANDOM SAMPLING

Conditionally sampled measurements near the outer edge of a turbulent boundary layer. 03 p0293 A73-13526

Gas concentration profiles in combustion gas sampling probes, using IR absorption technique 03 p0399 A73-14397

Linear aperture distribution synthesis by pattern sampling for arbitrary sampling points location and edge exponent alpha choice, using nonharmonic Fourier series theory 11 p1328 A73-25657

HF CW ultrasonics, discussing elimination of electromagnetic leakage or crosstalk between transmitter and receiver by sampling technique 13 p1612 A73-28483

Sampling nitric oxide from combustion gases. 16 p2085 A73-33348

SAMPLING DEVICES

U SAMPLERS

SAN MARCO SATELLITE

Density measurements in the equatorial atmosphere by means of the San Marco 3 satellite 19 p2426 A73-38151

SANDS

Sand erosion tests and protective coatings for aircraft jet and turbojet engines and helicopter compressor airfoils 16 p2046 A73-33029

Thermal structure of the sand desert from the data of IR aerophotography. 20 p2558 A73-39869

Reversing barchan dunes in lower Victoria Valley, Antarctica. 21 p2687 A73-41214

SANDSTONES

Atmospheric moisture effects on hematitic sandstone, pyrite and galena electrical resistivity, noting comparison with semiconductors and insulators 13 p1609 A73-28847

SANDWICH CONSTRUCTION

U SANDWICH STRUCTURES

SANDWICH PLATES

U PLATES [STRUCTURAL MEMBERS]

U SANDWICH STRUCTURES

SANDWICH STRUCTURES

Photoelastic model analysis of sandwich beams. 01 p0050 A73-10737

Axisymmetric buckling and stability of annular sandwich panel under radially varying in-plane stresses 01 p0115 A73-10740

A semimomentless theory of asymmetrically structured cylindrical sandwich shells with a rigid compressible filler 01 p0118 A73-11406

Possibility of using the method of time characteristics for solving applied problems concerning the bending of sandwich plates with allowance for creep of the materials 02 p0230 A73-11641

Light weight graphite-polyimide composite honeycomb core and sandwich panel design, fabrication and tests for shuttle orbiter thermal protection system 03 p0333 A73-13051

Finite element analysis of thick, thin and sandwich plates, considering quadrilateral elements with allowance for transverse shear effect 03 p0390 A73-13344

Selective reinforcement of wing structure for flutter prevention. 03 p0392 A73-13705

Flutter of flat rectangular sandwich type panels in a supersonic, coplanar gas flow, with arbitrary direction. 03 p0392 A73-13768

Stability of an idealized circular three-layer plate beyond the elastic limit 03 p0393 A73-13777

Modified shear-flexible orthotropic plate theory application to simply supported rectangular sandwich plates buckling problem, comparing results with Reissner theory and experimental data 04 p0509 A73-14946

Determination of the natural oscillation frequencies of three-layer circular cylindrical shells by a numerical method 04 p0510 A73-15081

Governing equations for vibrating constrained-layer damping sandwich plates and beams. [ASME PAPER 72-WA/APM-24] 04 p0515 A73-15892

Plastic behavior of two-layer sandwich structures. [ASME PAPER 72-WA/APM-11] 04 p0516 A73-15901

Stress analysis of thick laminated composite and sandwich plates. 05 p0631 A73-16110

Classical and nonlinear buckling analyses of spherical sandwich shells. 05 p0631 A73-16121

Nondestructive eddy current tests of Al bronze alloy fillet size and flatwise distribution in Ti honeycomb sandwich panels 05 p0581 A73-16131

Sandwich beams of unsymmetrical structure. 06 p0759 A73-17699

Buckling of a circular sandwich plate beyond the elastic limit 06 p0760 A73-17784

Observations on the deformation properties of sandwich materials. 06 p0761 A73-17819

Effects of electropolishing on the tunneling current in aluminum-aluminum-oxide-aluminum diodes. 06 p0678 A73-18744

Highly-rigid sandwich structures for interstages. 07 p0906 A73-18994

Tunneling observation of bound states in a normal metal-superconductor sandwich. 07 p0862 A73-19606

Theory of excitation of microwave elastic waves by multilayer transducers /considering the effect of metallic and insulator layers/. 07 p0801 A73-20139

An experimental study of ammonium perchlorate-binder sandwich combustion in standard and high acceleration environments. 07 p0866 A73-20363

Feasibility analysis of MIS sandwich structure for pulsed laser based on calculation for field distribution and TE and TM modes in optical cavity 09 p1093 A73-22254

Izod impact properties of carbon-fibre/glass-fibre sandwich structures. 09 p1110 A73-22517

Thermal limitation for CW output power of a Gunn diode. 09 p1064 A73-23043

Book - Structural analysis of shells. 09 p1164 A73-23273

Three layered sandwich rings damped vibrations under time-harmonic radial concentrated load, comparing experimental and theoretical mechanical impedance data 09 p1165 A73-23440

High-damping measurements and a preliminary evaluation of an equation for constrained-layer damping. 09 p1166 A73-23458

Technology of production of bonded sandwich structures 10 p1224 A73-24096

Fatigue properties of sandwich material with a honeycomb filler 10 p1289 A73-24097

Preparation and performance characteristics of flammable and inflammable polyimide foams as sandwich fillers 10 p1239 A73-24098

Bending and vibration of multilayer sandwich beams and plates. 10 p1289 A73-24290

Stress-strain state in the filler of a three-layer strip under local loading 10 p1291 A73-24354

Reissner's edge effect in three-layer plates with filler 11 p1433 A73-25030

Loaded and artificial dielectric materials with variable permittivity for sandwich radomes, discussing weight saving, multiband coverage and cross polarization reduction 11 p1335 A73-25281

Minimum-mass design of multielement structures under a frequency constraint. 11 p1444 A73-26380

Differential equations for asymmetric bending of circular sandwich plates. 11 p1445 A73-26406

Selection of optimal parameters for unidirectionally compressed three-layer plates 12 p1555 A73-27795

Triangular elements descriptive of sandwich panels for finite element analysis of symmetric panels, comparing numerical solutions to experimental data and analytical results 13 p1693 A73-28238

Epoxy adhesive bonding of Concorde light alloy sandwich structure elevons, discussing surface treatment, polymerization and ultrasonic testing 13 p1623 A73-28468

Photoelasticity - An improvement in the sandwich technique. 14 p1765 A73-29703

Vibration analysis of sandwich beam with constrained viscoelastic layers on both sides. 14 p1806 A73-30046

Natural oscillations of multilayer shells and plates with fillers 15 p1944 A73-30970

Static-geometric analogy and complex transformation in the theory of three-layered shells with light fillers. 15 p1952 A73-32072

Deformation of a multilayer shell of revolution under nonisothermal loading 16 p2074 A73-32684

Adhesive viscoelasticity effects on sandwich structure performance, presenting mathematical model for adhesive behavior and time dependent loading 16 p2029 A73-33053

Epoxy resin adhesive for metal-to-metal and honeycomb sandwich bonding, featuring high flow during cure for high structural strength 16 p2029 A73-33054

Application of a technical theory to the calculation of three-layered vaulted shells with a continuous middle layer of polymer material 16 p2083 A73-33935

Matrix analysis of multilayered and sandwich shells by the finite element method 16 p2083 A73-33968

Lagrangian formulation of sandwich shell theory. 17 p2242 A73-34526

Variational methods for vibratory bending equations of asymmetrical sandwich plates with mode families in terms of displacement ratios, taking into account inertia effects 17 p2243 A73-34548

Use of honeycomb and bonded structures in light aircraft. [SAE PAPER 730307] 17 p2101 A73-34667

Wave propagation in uniform laminar cylindrical shells, discussing group and phase velocities on wave numbers in sandwich walls 17 p2243 A73-34734

High strength organic fiber PRD-49 reinforced plastics compared to materials reinforced with glass, graphite and boron, discussing weight required to achieve Al faced sandwich performance 17 p2194 A73-34802

An advanced composite tailboom for the AH-1G helicopter. [AHS PREPRINT 785] 17 p2107 A73-35098

Phase velocity dispersion for transverse normal elastic wave propagation through sandwiched CdS and molten quartz or germanium layers 18 p2340 A73-36672

Natural transverse vibrations of sandwich beams of unsymmetrical structure. 18 p2367 A73-37141

Straightforward design of a three-layer cylindrical shell 19 p2494 A73-37183

Influence of the structure of the material of a three-layered cylindrical shell on the natural frequencies 19 p2494 A73-37184

Monograph on optimal structure design by linear programming and calculus of variations covering pin jointed frameworks, beams, circular sandwich plates, Michell continua, etc 19 p2502 A73-38364

Symmetrical three-layer shells with a light-weight elastic filler 20 p2618 A73-39328

Numerical solution of problems of stability of three-layer cylindrical shells 20 p2620 A73-39503

Sandwich plates minimum volume design for elliptic, triangular and annular structures, discussing Mises criterion and bending coordinates 20 p2623 A73-39559

Calculation of three-layer minimum-weight panels as a problem of mathematical programming 20 p2625 A73-39651

Optimum design of three-layer shells 20 p2625 A73-39655

British X4 spacecraft mechanical design configuration with honeycomb sandwich panels, on yo-yo principle based despin system and flexible solar array 20 p2615 A73-39774

A numerical study of damping in viscoelastic sandwich beams. [ASME PAPER 73-DET-73] 22 p2919 A73-42071

Free-edge effects in the characterization of composite materials. 23 p3040 A73-43632

Effects of specimen geometry on the strength of composite materials. 23 p2996 A73-43633

Vibrations of turbojet-engine components containing structural dampers of the type of sandwich rods 23 p3020 A73-43735

Certain methods in the physically nonlinear theory of three-layer plates 23 p3043 A73-43921

Aluminum brazed titanium honeycomb sandwich structure - A new system. 23 p2985 A73-44000

Procedure development for brazing Inconel 718 honeycomb sandwich structures. 23 p2985 A73-44001

Sandwich shells nonlinear theory with stress-strain relations in tensor notation, using Hamilton principle for equations of motion and boundary conditions 23 p3044 A73-44078

Shrinkage of reinforced sandwich-type materials during hot pressing 24 p3092 A73-44416

Experimental investigations regarding optimally designed three-layer wound glass fiber/plastic tubes under internal pressure 24 p3147 A73-44882

Structural design optimization by iterative analysis using proper stiffness matrix with applications to sandwich plate and frame problems 24 p3150 A73-45236

SAPPHIRE

Influence of vacuum conditions in fabrication on the structure and electrophysical properties of epitaxial silicon films on sapphire 06 p0736 A73-18089

Optical constants measurement for far IR materials of crystalline quartz, sapphire, Ge and Si at room temperature and 1.5 K [AD-760151] 08 p0994 A73-21049

Reactivity and interface characteristics of titanium-alumina composites. 11 p1384 A73-26043

Stability of nickel coated sapphire whiskers. 11 p1389 A73-26044

Complementary MOS/silicon on sapphire LSI technology for high speed digital multiplier and correlator logical building blocks design, fabrication and subsystem array implementations 17 p2140 A73-35318

Silicon-on-sapphire thin film junction diodes, investigating second breakdown onset delay time and minimum energy dependence on high resistivity side heating 20 p2536 A73-39415

Improvement of thermal shock resistance by surface prestressing. 22 p2921 A73-42462

Plastic deformation and anisotropy of sapphire crystals via nonbasal plane slip under bending, obtaining stress-strain curves and flow stresses temperature dependence 23 p2997 A73-43772

The creep of sapphire filament with orientations close to the c-axis 23 p2997 A73-44029

The stability of sapphire whiskers in nickel at elevated temperatures. I - General morphological and chemical stability. II - The kinetics of morphological changes over the temperature range 1100 to 1400 C. 23 p2986 A73-44032

SARCOMA

U CANCER

SAS

U SMALL ASTRONOMY SATELLITES

SATAN (SENSOR)

U TERRAIN ANALYSIS

SATELLITE ANTENNAS

Omnidirectional satellite antennas with radiation pattern distortion minimization by adjustment of antenna inclination, height above spacecraft structure and angle with metallic objects 01 p0111 A73-11173

SATELLITE ATTITUDE CONTROL

Orientation accuracy of the Symphonie communication antennas [DGLR PAPER 72-063] 02 p0140 A73-11684

Influence of satellite antenna gain on a satellite communications system. 03 p0277 A73-14027

Signal relay systems using large space arrays. 04 p0415 A73-14990

An amplitude-steered, electronically despun antenna for the synchronous meteorological satellite. 04 p0428 A73-15453

Series diode SP4T switch for satellite applications. 04 p0428 A73-15455

A novel VHF turnstile antenna for the SMS satellite. 04 p0428 A73-15456

Antenna design for Eole satellite radio communications with balloons, noting wave polarization and sea reflection effects 07 p0797 A73-18963

Antenna design for meteorological Meteosat satellite, noting transmitting and receiving radiation patterns 07 p0797 A73-18964

X4 scientific satellite subsystems development status, discussing solar array, attitude control, data handling, power conditioning and antenna systems 09 p1154 A73-22919

Canadian domestic ANIK communication satellite with all-microwave 12-channel repeater, discussing system components, antenna design and performance parameters 09 p1059 A73-23437

Symphonie satellite communication equipment payload, discussing mission requirements, receiving and transmitting antennas, transponder and ground testing methods and arrangements 11 p1417 A73-25356

Satellite systems for mobile communications and surveillance; Proceedings of the International Conference, London, England, March 13-15, 1973. 12 p1471 A73-27652

Satellite design considerations. 12 p1549 A73-27659

A maritime communications concept using spaceborne phased arrays. 12 p1472 A73-27665

Maritime Satellite System with broadband and multibeam dish antennas, assessing FDM communication capability as function of channel quality and ship terminal antenna gain 12 p1473 A73-27679

Support scattering effects on low-gain satellite antenna pattern measurements. 14 p1735 A73-30218

Synchronous communication satellite crosslink antenna design and tracking and acquisition procedures for Ka band frequencies, describing reflectors, paraboloids, and five horn feed system 16 p1977 A73-32721

Helical antenna for satellite transmission. 16 p1980 A73-33686

Electron depletion in the wake of ionospheric spacecraft - A comparison between results from Langmuir probes and antennas. 17 p2159 A73-34783

Oscillations of a spinning satellite due to small deflections of its dipole antennae. 21 p2780 A73-40089

Impedance and large signal excitation of satellite-borne antennas in the ionosphere. 22 p2831 A73-41835

A cavity-backed dipole antenna with wide-bandwidth characteristics. 22 p2831 A73-41851

Power subsystem for Skylab radiometer/scatterometer/altimeter experiment. 22 p2801 A73-42903

Theory of a corner-driven loop antenna immersed in a warm plasma. 24 p3070 A73-45486

SATELLITE ATTITUDE CONTROL

Gravitational interaction effects between parts of gravity stabilized satellite on attitude dynamics and control 01 p0095 A73-10110

Digital attitude sun sensor for ionosphere sounding satellite. 01 p0053 A73-11171

Test of horizon sensor for the ionosphere sounding satellite. 01 p0053 A73-11172

Experimental satellite for attitude control. I - System design. 01 p0111 A73-11188

Experimental satellite for attitude control. II - Measurement of low thrust gas jet performance. 01 p0111 A73-11189

Experimental satellite for attitude control. II - Numerical analysis and a test of a yo-yo de-spinner. 01 p0111 A73-11190

Experimental satellite for attitude control. IV - Nutational damping of a spinning satellite. 01 p0112 A73-11191

Experimental satellite for attitude control. V - Attitude control electronics.

01 p0112 A73-11192

Satellite attitude control estimators and observers, discussing applications to reaction wheel, spinning attitude and drag-free satellite translation control systems

01 p0075 A73-11193

Attitude dynamics of a 'nearly-spherical' dual-spin satellite and orbital results for OSO-7.

02 p0227 A73-11600

The attitude-measuring and attitude-control system of the satellite Aeros and its employment in the acquisition phase

[DGLR PAPER 72-062]

02 p0227 A73-11653

Propulsion system performance for satellite attitude and orbit correction, discussing hydrogen, ammonia and hydrazine resistojets

[DGLR PAPER 72-078]

02 p0203 A73-11697

Contributions to the standardization of control systems for satellites and peak payloads

02 p0228 A73-11705

Radio sensors for the three-axis attitude fine measurement of geostationary communication satellites

02 p0228 A73-11822

Dynamics of flexible satellites with active attitude control.

02 p0228 A73-11994

An operational satellite propulsion system providing for vernier velocity, high and low level attitude control and spin trim.

[AIAA PAPER 72-1130]

04 p0486 A73-14916

The attitude stabilization and control system for the Communications Technology Satellite.

04 p0504 A73-15450

Development of electrical propulsion in the Federal Republic of Germany.

04 p0487 A73-15713

Cs ion bombardment engines for communication satellites stationkeeping and attitude control, noting mission life and test facilities

04 p0488 A73-15718

Orbit transfer, -corrections, and attitude control of a lightweight direct broadcasting satellite for Europe.

04 p0505 A73-15738

Study of the dynamics of the preliminary-damping system of a gravitationally stable satellite with allowance for constraints on its sensors and on the flexural vibrations of the stabilizer

05 p0628 A73-16406

An experimental investigation of attitude control systems for astronaut maneuvering units.

[AIAA PAPER 73-250]

05 p0563 A73-16973

A quasi-inertial attitude mode for orbiting spacecraft.

05 p0630 A73-17203

An optimization technique for the transient response of passively stable satellites.

06 p0755 A73-17566

French Monograph - Contribution to the study of the stabilization of gyroscopic satellites - Conception and development of an active nutation damper.

06 p0757 A73-18097

Attitude dynamics of a three-axis stabilized satellite with a large flexible solar array.

06 p0757 A73-18379

A simple method for precise attitude determination of a spinning spacecraft.

06 p0722 A73-18827

Subliming solid propellant microthruster for satellite stabilization, discussing operational principles and design features

07 p0866 A73-18927

Ammonia resistojets development for satellite stabilization and position control with 5-year service life, discussing dissociation catalysis research and high efficiency heat exchanger design

07 p0867 A73-18932

Eole satellite gravity gradient stabilized pointing control system, discussing implementation by eddy current, inertia and magnetic hysteresis devices

07 p0904 A73-18936

French satellites attitude stabilization and control systems, describing electronic sensor and servocontrol circuitry

07 p0904 A73-18967

High performance three axis attitude control system of TD1/A European scientific satellite, describing control circuits, logic, ancillaries and packaging procedure

07 p0904 A73-18968

Optical instrumentation for satellite attitude control, solar direction and earth magnetic field sensors, thermal detection, star tracking and Lunokhod 1 laser reflector

07 p0821 A73-18979

Thermopile IR static horizon sensor for Synchronic satellite three axis attitude stabilization in geostationary orbit

07 p0821 A73-18985

Sun sensors for D-2B scientific satellite spin axis alignment and attitude stabilization with pointing control accuracy, discussing tests, compensatory tracking and solar simulation

07 p0821 A73-18986

The double gimbaled 'DRALLRAD' and its possible use for three-axis-stabilization of application satellites.

07 p0849 A73-19143

Non-linear resonant attitude motions in gravity-stabilized gyrostats satellites.

07 p0905 A73-19162

Satellite attitude control by reaction jet frequency modulation.

07 p0906 A73-19489

Operational principle and characteristics of electric propulsion systems. II - Application to satellite stabilization

07 p0906 A73-20247

Experimental verification and assessment of an infra-red radiation modulator based on a Fabry-Perot etalon.

07 p0825 A73-20373

Satellites elastic structures equations of state for stability and attitude control systems analysis, deriving translational and rotational momentum equations for moving coordinate systems

08 p1014 A73-20779

Attitude control of the AEROS aeronomy satellite during the acquisition phase.

08 p1014 A73-21660

X4 scientific satellite subsystems development status, discussing solar array, attitude control, data handling, power conditioning and antenna systems

09 p1154 A73-22919

UK5 X ray astronomy satellite, discussing structural design, attitude sensing for pointing control, data handling, attitude control and power supply systems

09 p1155 A73-22920

D-2A satellite experiments for sky mapping and radiation intensity measurement, discussing attitude correction processing

10 p1285 A73-23623

Precision and economy estimates for manual control of spacecraft orientation

10 p1286 A73-23893

The effect of direct solar radiation on the attitude of the SKYNET spacecraft.

11 p1431 A73-26261

Equilibrium attitude transitions of a three-rotor gyrostatt in a circular orbit.

11 p1431 A73-26379

Monopropellant hydrazine system for satellite attitude control, reporting catalysts properties, decomposition mechanisms and activities

12 p1532 A73-27064

Quasi time-optimal spacecraft reorientation maneuvers using single gimbal control moment gyros /SG CMG's/.

12 p1548 A73-27153

AEROS research satellite acquisition phase performance, considering injection, attitude determination and control, trajectory measurement and correction, nutation reduction, solar alignment, etc

13 p1689 A73-28782

AEROS aeronomy satellite successfully completes acquisition phase.

13 p1689 A73-28783

The use of a spinning dissipator for attitude stabilization of earth-orbiting satellites.

13 p1690 A73-29216

Errors of the gravitational stabilization system of a satellite with gyrodampping

14 p1803 A73-29869

Theoretical and practical design aspects on spacecraft propellant and pressurant loading systems.

14 p1742 A73-30107

Effects of flexibility on a momentum-stabilised communication-satellite attitude-control system.

15 p1942 A73-31099

Requirements regarding the position and the attitude of future application satellites

15 p1907 A73-31134

Attitude determination-attitude control in the case of the satellite Aeros

15 p1943 A73-32179

Gravity-gradient stabilization of synchronous orbiting satellites - Additional considerations of attitude stability.

15 p1944 A73-32218

Infra-red detection for satellite attitude sensing - The ANS horizon sensor.

16 p2012 A73-32853

Time optimal control of satellite pitching motions by variable mass distribution, solving nonlinear optimization problem via maximum principle

16 p2072 A73-33233

Estimation and correction of electric thruster misalignment effects on a geostationary satellite.

17 p2238 A73-34866

Investigations of the Intelsat IV bearing and power transfer assembly.

17 p2238 A73-34867

Digital attitude reference system for three-axis-stabilized earth oriented satellites, using gyrocompasses with solar and horizon sensors

17 p2209 A73-34875

Influence of structural flexibility on attitude control of spacecraft

17 p2162 A73-34950

State space attitude control synthesis for a satellite with flexible appendages.

17 p2239 A73-34951

Communication satellites attitude control methods, considering conventional attitude gyros, control moment gyroscopes, reaction wheels and optimal solar cell utilization

17 p2239 A73-35476

Control laws of magnetic attitude stabilization systems of earth satellites

18 p2359 A73-36103

Spinning HEOS-A2 satellite active deconing with pulse sequence from attitude reorientation system, discussing optimal control pulse number and timing

18 p2361 A73-36957

Dynamic passivation of a spinning and tumbling satellite using free-flying teleoperators.

19 p2490 A73-37306

Precise attitude control of the Stanford relativity satellite.

19 p2494 A73-38080

An attitude control system for earth observation spacecraft.

[AIAA PAPER 73-854]

20 p2585 A73-38792

The design of a two wheel momentum bias system for the attitude control of spacecraft in low altitude orbits.

[AIAA PAPER 73-855]

20 p2585 A73-38793

Attitude measurement and control system of the aeronomy satellite AEROS.

[AIAA PAPER 73-856]

20 p2585 A73-38794

Precision pointing control thruster design for satellite experiment to test relativistic precession of gyroscope moving through gravitational field, determining gyro orientation via superconducting circuitry

[AIAA PAPER 73-858]

20 p2586 A73-38796

Techniques for flat-spin recovery of spinning satellites.

[AIAA PAPER 73-859]

20 p2614 A73-38797

Three-axis attitude control system air-bearing tests with flexible dynamics.

[AIAA PAPER 73-866]

20 p2543 A73-38804

Large scale telescope pointing stability augmentation system, using control moment gyro gimbal servo error signal to command momentum augmentation system

[AIAA PAPER 73-868]

20 p2587 A73-38806

Large orbiting telescopes fine guidance system for ultrahigh pointing stability based on disturbance accommodation standard deviation optimal controller design

[AIAA PAPER 73-882]

20 p2588 A73-38818

Achieving ultrahigh accuracy with a body pointing CMG/RW control system.

[AIAA PAPER 73-883]

20 p2588 A73-38819

Development and test of a double gimbaled momentum wheel stabilization system for communication satellites.

[AIAA PAPER 73-906]

20 p2614 A73-38840

Energy-sink analysis for asymmetric dual-spin spacecraft.

[AIAA PAPER 73-909]

20 p2614 A73-38843

On the use of a dual spin vehicle for scanning a celestial body.

[AIAA PAPER 73-910]

20 p2614 A73-38844

Evaluation of precision and economy of systems of manual spacecraft orientation.

20 p2614 A73-38912

Geostationary injection dispersions and thrusting error elimination by apogee motor firing attitude optimization

21 p2780 A73-40614

Mathematical model for ISIS satellite attitude and spin rate computerized predictions during electromagnetic torque control operation

21 p2781 A73-40615

German monograph - Passive and active satellite attitude control with the aid of rod-like torsion pendula.

22 p2917 A73-42599

French paper on satellite attitude stabilization by gyroscopes covering autonomous activator systems, kinetic moment principles and control in roll-yaw for flexible panels

22 p2917 A73-42743

Russian book on satellite attitude stabilization systems design covering gravity gradients, linear and nonlinear control laws, spin stabilization, high torque control moment gyros, etc

23 p3038 A73-43335

Attitude control for the Netherlands astronomical satellite /ANS/.

24 p3144 A73-45558

SATELLITE ATTITUDE DISTURBANCE

U ATTITUDE STABILITY

U SPACECRAFT STABILITY

SATELLITE COMMUNICATIONS

U SPACECRAFT COMMUNICATION

SATELLITE COMMUNICATIONS SHIPS

The effects of multipath on the design of ship board satellite communications antennas.

20 p2523 A73-38726

Small ship antennas for fleet satellite communications.

20 p2523 A73-38727

Maritime communications via satellites employing phased arrays. 21 p2649 A73-40330

SATELLITE CONFIGURATIONS

About the motion of a heavy flexible string attached to the satellite in the central field of attraction. 03 p0376 A73-14267

Low altitude orbit feasibility study of integrated SNAP 29/Agena satellite configuration, comparing with solar cell power system 11 p1396 A73-26040

Meteosat - Project of a European geostationary meteorological satellite - Status: 9/15/1972 13 p1689 A73-28743

Equilibrium configurations and attitude stability criteria for articulated satellite idealized as point-connected rigid two gyrost problem 14 p1802 A73-29757

Gravitational stabilization of a two-body satellite. 15 p1943 A73-31916

Mission, project profile, and description of the Symphonic satellite [DGLR PAPER 73-043] 17 p2126 A73-35480

Solar arrays for the next generation of communication satellites. 18 p2269 A73-37036

Concepts of high-capacity communications satellites. 20 p2613 A73-38714

The restricted problem of three bodies with rigid dumb-bell satellite. 24 p3142 A73-45300

SATELLITE CONTROL

NT SATELLITE ATTITUDE CONTROL

Some problems of the optimal angular stabilization of an artificial earth satellite 05 p0628 A73-16413

Control of a maneuver involving rotation of the plane of a circular satellite orbit while ensuring passage through a prescribed point 05 p0595 A73-16426

Selection of the measurement frequency in the determination of satellite orientation 05 p0630 A73-17007

Electric propulsion systems for satellite station-keeping, discussing developments in colloid thrusters and diagnostic equipment for performance measurement 07 p0867 A73-19222

Communications, despin control, electrical power, telemetry and command, positioning and orientation subsystems of Intelsat 4 satellite 09 p1152 A73-22698

Utilization of electric propulsion systems in communications satellites [DGLR PAPER 73-048] 17 p2126 A73-35484

Impulse application for optimal correction of angular position of orbital plane line of apsides, expressing axis angle of rotation as linear function 23 p3027 A73-43269

Orbit osculation control algorithm guaranteeing satellite repeated passage over given point of earth surface, deriving functional for satellite thrust control 23 p3027 A73-43271

SATELLITE DESIGN

The structure of scientific satellites developed by the University of Tokyo. 01 p0110 A73-11119

Three point check method of solar panel characteristics for satellite. 01 p0006 A73-11162

Experimental satellite for attitude control. I - System design. 01 p0111 A73-11188

TV satellite system feasibility and design study for Germany, discussing technical and economic aspects [DGLR PAPER 72-051] 02 p0140 A73-11664

Wearher satellite Meteosat operational features and objectives, describing instrumentation, communication, data acquisition and processing facilities [DGLR PAPER 72-082] 02 p0227 A73-11695

Design principles for contamination abatement in scientific satellites. 02 p0136 A73-11991

Glass reinforced structural components for the synchronous meteorological satellite. 03 p0331 A73-13030

Aeros satellite component tests for design and manufacturing error detection and failure prevention, using structural, thermal and electrical integration models 03 p0288 A73-13918

Yo-yo system despin mechanism for the Aeros aeronomy satellite. 03 p0382 A73-13919

Design and practical aspects of maximum efficiency silicon solar cells for satellite applications. 03 p0254 A73-14205

Evaluation and reduction on the electromagnetic fields associated with a solar array. 03 p0256 A73-14233

Preliminary study for the design of a satellite thermal-control heat pipe. 07 p0918 A73-18913

Star sensor/mapper for the Small Astronomy Satellites. 08 p0970 A73-21733

UK5 X ray astronomy satellite, discussing structural design, attitude sensing for pointing control, data handling, attitude control and power supply systems 09 p1155 A73-22920

Intelsat communication satellites global network analysis, investigating technical factors affecting design options 09 p1059 A73-23436

Intercoms 2 satellite design, construction, on-board scientific instrumentation, ionospheric experiments and data processing equipment 10 p1217 A73-23886

The role of the Project Manager in the management of satellite projects. 11 p1454 A73-26262

Satellite design considerations. 12 p1549 A73-27659

L-band satellite systems for mobile applications. 12 p1472 A73-27664

Atmosphere Explorer for satellite observation of the thermosphere, discussing design goals, spacecraft components and data system 13 p1687 A73-28627

The feasibility of a satellite solar power station. 16 p1970 A73-32718

Microwave radiometer measurement at 17 GHz to investigate atmospheric attenuation and radio noise and interference sources for optimal satellite communication systems design 16 p1982 A73-33718

Space radiation environment effects on Intelsat 4 design, emphasizing trapped electrons and protons influences on solar cell shielding requirements 17 p2108 A73-34864

Influence of structural flexibility on attitude control of spacecraft 17 p2162 A73-34950

Realization of a geostationary orbit by means of an electromagnetic propulsion system /quasi-steady MPD/ 17 p2239 A73-34954

Canadian domestic satellite system applications. 17 p2124 A73-35311

The orbital test satellite for the European Communication Satellites Programme - Performance and growth capability. [DGLR PAPER 73-044] 17 p2126 A73-35481

Spacecraft systems design trade-offs for the Earth Resources Technology Satellite. 17 p2239 A73-35631

Concepts of high-capacity communications satellites. 20 p2613 A73-38714

Communication satellite history and present developments, discussing Intelsat and ATS programs and TDMA techniques 20 p2526 A73-38747

Fine pointing performance characteristics of the Orbiting Astronomical Observatory /OAO-3/. [AIAA PAPER 73-869] 20 p2587 A73-38807

Intercoms 2 satellite design, construction, on-board scientific instrumentation, ionospheric experiments and data processing equipment 20 p2565 A73-38905

Helios probe design for solar wind acceleration mechanism, magnetic and electric fields, interplanetary dust and cosmic radiation 21 p2780 A73-40449

The telecommunication payload of the satellite Symphonic 21 p2655 A73-41081

Attitude stability conditions of multiple spin satellites. 22 p2916 A73-42189

The Netherlands astronomical satellite /ANS/. 22 p2917 A73-42291

Flight performance of the ERTS-1 spacecraft power system. 22 p2801 A73-42904

SATELLITE DRAG

Satellite attitude control estimators and observers, discussing applications to reaction wheel, spinning attitude and drag-free satellite translation control systems 01 p0075 A73-11193

Satellite drag data for analysis of semiannual atmospheric density variations, showing latitudinal dependence of amplitude 02 p0161 A73-12281

Observed effects of earth-reflected radiation and hydrogen drag on the orbital accelerations of balloon satellites. 04 p0439 A73-14802

Solution of the low-altitude satellite equations. 06 p0757 A73-18072

Satellite-caused energy dissipation via tides in spinning planet leading to orbital decay induced destruction or escape or to stable synchronism 09 p1142 A73-22041

Exact analytical solutions for orbits of bodies with atmospheric drag. 09 p1152 A73-23454

Variations of the structural parameters of the thermosphere from satellite braking data 11 p1350 A73-25076

Lower thermosphere density and composition model from satellite drag and accommodation coefficients 12 p1488 A73-26990

Systematic analysis of perturbations of orbits - The case of drag. 14 p1788 A73-29717

Atmospheric density values from radar-determined low altitude satellite orbit decay and accelerometer data 18 p2302 A73-35942

Earth radiation pressure and the determination of density from atmospheric drag. 18 p2308 A73-36051

Air density at heights near 200 km from the orbit of 1970-65D. 18 p2309 A73-36052

Drag density data from the Cannon Ball II and Musket Ball satellites. 18 p2309 A73-36053

A study of the diurnal variation in the thermosphere as derived by satellite drag. 18 p2309 A73-36059

An analysis of the solar-activity effects in the upper atmosphere. 18 p2309 A73-36060

Interpretation of short period density changes shown by the drag of satellites. 18 p2310 A73-36133

Density scale height and geopotential coefficients evaluations from analysis of Cosmos 54 rocket orbit perturbations due to drag and odd-zonal harmonics 18 p2351 A73-36176

Problems of the aerodynamics of satellites with uniaxial orientation 21 p2781 A73-40902

Thermospheric density diurnal and seasonal variations from cosmos drag data, discussing amplitude, density distribution, coefficients of expansion, summer solstice spherical functions 21 p2689 A73-41351

Structure of the neutral atmosphere between 150 and 500 km. 21 p2689 A73-41352

Evaluation of the accuracy of predicting the motion parameters of low-orbit artificial earth satellites 23 p3027 A73-43266

Densities deduced from perturbations at high altitudes. 23 p2972 A73-43688

SATELLITE GROUND SUPPORT

Prospero satellite orbital/operational performance and control, describing ground-satellite telemetry and data processing operations 07 p0905 A73-19142

SATELLITE GROUND TRACKS

Orbit analysis for coastal zone oceanography observations. [AIAA PAPER 73-207] 06 p0748 A73-17659

SATELLITE GUIDANCE

Real time tracking radar for radio guidance system, obtaining algorithm for rocket motor direction and ignition time for satellite orbit optimization 03 p0339 A73-13067

Effect of the guidance reserve of the Europa II third stage on the consumption of propellants for stationing 04 p0504 A73-15294

Communications, despin control, electrical power, telemetry and command, positioning and orientation subsystems of Intelsat 4 satellite 09 p1152 A73-22698

SATELLITE INSTRUMENTS

NT LASER ALTIMETERS

German-NASA joint Aeros aeronomy satellite project, discussing mission objectives and related instrumentation 01 p0109 A73-10470

Some new satellite sensors and applications. 01 p0052 A73-11161

Heos 2 satellite instrumentation and space exploration objectives, considering earth and interplanetary magnetic fields, electron and proton energies, solar radiation and wind, cosmic dust and micrometeoroids 02 p0228 A73-11949

Skylab instrumentation and solar observation objectives in coordinated program of correlative ground based, rocketborne and other spaceborne observations 02 p0169 A73-12337

Star sensor of spin stabilized Uhuru satellite for detection and location of stellar X ray sources with accuracies of one arc-minute 06 p0695 A73-18323

Satellite electronic equipment reliability and quality control at preproject, project, fabrication and mission levels, noting electric welding quality specification 07 p0904 A73-18974

Optical instrumentation for satellite attitude control, solar direction and earth magnetic field sensors, thermal detection, star tracking and Lunokhod 1 laser reflector 07 p0821 A73-18979

SATELLITE LAUNCHING

Infra-red detection for satellite attitude sensing - The ANS horizon sensor. 16 p2012 A73-32853

Thin film thermopile for Symphonie geostationary satellite attitude determination based on absorbed energy transformation into heat, discussing design and applications 16 p1988 A73-33275

Dynamic behavior of satellites with large-area solar cell panels [DGLR PAPER 73-049] 17 p2239 A73-35485

A cryogenic heat pipe for satellite sensor cooling. [ASME PAPER 73-ENAS-50] 19 p2494 A73-37997

SATELLITE LAUNCHING

U SPACECRAFT LAUNCHING

SATELLITE LIFETIME

Prediction of the density of the upper atmosphere for the duration of artificial earth satellites. 05 p0567 A73-16091

ESRO TD-1A satellite signal hibernation in sky-scanning experiments after successful performance during first orbital life, noting tape recorder failure 11 p1431 A73-25750

Economic models for satellite system effectiveness. 16 p2073 A73-33618

SATELLITE MANEUVERS

U SPACECRAFT MANEUVERS

SATELLITE NAVIGATION SYSTEMS

Autonomous satellite navigation from strapdown landmark measurements. 04 p0474 A73-15266

Radio navigation review, discussing Decca, Loran, Omega, VOR/DME, satellite, inertial, integrated, area, approach and landing, collision avoidance and space navigation systems 10 p1246 A73-23636

Circular, hyperbolic, hybrid and angular measurement procedures of satellite navigation, describing Transit system 10 p1246 A73-23660

Retroflecting satellite with laser range finder for Martian roving vehicle navigation, discussing error analysis and minimization by measurement geometry choice through nonlinear programming 10 p1247 A73-24005

Autonomous satellite navigation - An historical summary and current status. 19 p2452 A73-38056

System error analysis and algorithms for a strap-down navigation system. 19 p2452 A73-38058

Aerosat program for civil aviation needs established by Seventh Air Navigation Conference of ICAO, discussing airborne equipments specification development [AAS PAPER 73-120] 20 p2520 A73-38581

The impact of space navigation on the spherical gas bearing gyro. 21 p2697 A73-40025

Navy Transit Navigation System precision improvements for stationary and nonstationary users, considering uncertainties due to satellite position and instrumentation errors and user motion 21 p2734 A73-40039

Navy Transit navigation satellite system, discussing flight test for feasibility of military application to YP-3C Antisubmarine Warfare Weapons System aircraft 21 p2735 A73-40040

Operational global navigation system development program with repeater satellites deployed over continental USA to provide radio links for digital communication, surveillance and ATC 21 p2735 A73-40041

Satellite based ATC system with radar range and rate measurements, analyzing errors due to ground station position, transponder delay time and atmospheric refraction uncertainties 21 p2735 A73-40042

A survey of satellite-based systems for navigation, position surveillance, traffic control and collision avoidance. 21 p2736 A73-40052

SATELLITE NETWORKS

Multisatellite systems for transoceanic aircraft communications and ATC, discussing day and night operations, cost-benefit optimization and adaptive techniques for capacity augmentation 01 p0018 A73-11201

Progress in commercial satellite communications. 03 p0381 A73-13200

The adjustment of a spatial terrestrial net according to the method of satellite geodesy 03 p0299 A73-13257

Satellite educational TV systems for underdeveloped countries, discussing installation problems, capital investments requirements and potential benefits 03 p0401 A73-14173

Current and near future data transmission via satellites of the Intelsat network. 03 p0280 A73-14659

Juridical problems connected with European network of telecommunication satellites, discussing satellite direct transmission 04 p0497 A73-15146

Permanent arrangements for the global commercial communications satellite system of INTELSAT. 04 p0523 A73-15148

Single channel per carrier FCM FDMA demand assignment satellite communications system /SPADEF/ for INTELSAT, discussing hardware and software introduction at first terminal 04 p0420 A73-15414

Synchronous meteorological satellite /SMS/ system responsibilities of NASA and Commerce Department, discussing program objectives, payload, spacecraft subsystems and ground systems 04 p0504 A73-15451

Orbital parameters optimization of circular orbit earth satellites network for continuous earth observation, using group theory 05 p0620 A73-17004

Management and cost of European-U.S. Aerosat program based on geostationary satellites for air/ground voice and data messages relay and aircraft position determination 07 p0905 A73-19174

Multiple access analog and digital satellite telecommunication systems, discussing Intelsat /FM/ and Spade /frequency division/ systems 07 p0790 A73-19181

Weather forecasting with the aid of satellite data. [AIAA PAPER 73-21] 07 p0848 A73-19582

Educational radio and television satellite networks, considering computer networks, cable TV and NASA Applications Technology Satellites /ATS/ utilization 09 p1056 A73-23397

Intelsat communication satellites global network analysis, investigating technical factors affecting design options 09 p1059 A73-23436

Problem of continuous survey of the earth, and kinematically correct satellite systems. II 10 p1276 A73-23882

Configuration control of dual satellite systems in earth orbit, obtaining equations of motion, deployment paths and force functions 10 p1276 A73-24008

Canadian telecommunications satellite system for TV, voice and analog or digital data transmission, describing space segment, satellite control and ground station network 11 p1431 A73-26259

The satellite system as an integrated telecommunications switching center. 12 p1468 A73-27011

Replacement of a system of aeronautical satellites. 12 p1549 A73-27678

The impact of satellites on military communications. 14 p1729 A73-30874

Spectral-energy dispersal in digital communication-satellite systems. 15 p1842 A73-31096

Operational utilization of an aeronautical satellite system for air traffic control over the North Atlantic. 15 p1911 A73-32487

Small earth terminals for satellite communications. 16 p1979 A73-33084

Efficient utilization of orbit/frequency for satellite broadcasting. 16 p1979 A73-33401

Rain attenuation and fade duration statistics for design of satellite-based communication system, predicting outage for 16 GHz path diversity system 16 p1981 A73-33706

Book - Satellite broadcasting. 17 p1211 A73-34473

Low altitude satellite networks for recording programmable earth atmosphere parameters related to terrestrial environment control 17 p2205 A73-34929

Demand-assignment multiple-access control techniques. 17 p2144 A73-35304

Synchronous satellite systems for civilian air, ship and land vehicle traffic control, communication, navigation and surveillance, discussing technology requirements for continental and oceanic systems [AIAA PAPER 73-583] 18 p2288 A73-36075

Domestic communication satellite systems with microwave transmission links and coast-to-coast earth stations and receivers, detailing design and interference problems 18 p2289 A73-36776

Technological trends in commercial satellite communications. 18 p2290 A73-37034

Future communication satellite technology improvement, market expansion and cost effectiveness, considering foreign domestic, and international light-to-medium and high density systems 20 p2522 A73-38715

Orbital design strategy for domestic communication satellite systems. 20 p2527 A73-38761

The problem of continuous earth coverage and kinematically regular satellite networks. II. 20 p2603 A73-38901

Operational global navigation system development program with repeater satellites deployed over con-

tinental USA to provide radio links for digital communication, surveillance and ATC 21 p2735 A73-40041

Analysis of the results of the geometric satellite world network 22 p2849 A73-42589

Geostationary meteorological satellite network development for static and cinematographic image transmission based on international cooperation 22 p2884 A73-43118

Telesat Canada-Anik - Canada's domestic satellite communications system 24 p3069 A73-45392

SATELLITE OBSERVATION

Radio emission from traveling disturbances in solar corona, considering contributions of interplanetary observations, plasma theory and ground observations 01 p0091 A73-10058

Transmittance functions for satellite temperature sounding. 01 p0037 A73-10367

Atmospheric solid and liquid water particles IR spectral properties, interpreting Nimbus 4 IR spectroscopic cloud observations 01 p0037 A73-10371

Atmospheric moisture and wind field synoptic analysis based on Nimbus 4 temperature-humidity IR radiometer /THIR/ measurements 01 p0073 A73-10379

Precipitable water vapor temperature-geopotential height profiles from satellite IR spectrometer /SIRS/ measurements, using stepwise regression technique 01 p0073 A73-10380

Atmospheric ozone distribution from remote sensing with spaceborne IR interferometer spectrometer, estimating error due to cloud cover 01 p0038 A73-10384

Natural variation of the radiation budget of the earth-atmosphere system as measured from satellites. 01 p0038 A73-10390

Three station interferometric observation of TACSAT synchronous communications satellite radio signals for orbit determination, discussing method feasibility for tracking and geodesy applications 01 p0097 A73-10407

German monograph - Short-period transverse variations in the magnetic field data from the Azur research satellite. 01 p0040 A73-10603

High-energy cosmic gamma-ray observations from the OSO-3 satellite. 01 p0092 A73-11028

The Earth Resources Program - International benefits from space. 01 p0043 A73-11107

Some new satellite sensors and applications. 01 p0052 A73-11161

Energetic protons detection below radiation belt at equatorial latitudes from Azur satellite measurements, hypothesizing exospheric and upper atmospheric charge exchange processes 01 p0043 A73-11514

X ray intensity observations of Cygnus X-3 by Uhuru satellite before/during September 1972 radio flare 02 p0210 A73-11554

Use of space techniques in the detection and monitoring of climate parameters and air pollutants [DGLR PAPER 72-081] 02 p0188 A73-11668

Pioneer 6 crossing of earth bow shock on 16 December 1965 reexamined and reinterpreted by magnetic field measurement combination with plasma data 02 p0155 A73-11729

Magnetopause motions at lunar distance determined from the Explorer 35 plasma experiment. 02 p0155 A73-11730

Satellite observations of energetic heavy ions during a geomagnetic storm. 02 p0204 A73-11733

Isis 1 observations of the high-latitude ionosphere during a geomagnetic storm. [AD-759885] 02 p0155 A73-11735

Inner magnetosphere distortions during magnetic storm development phase from Explorer 26 observations, comparing with Williams-Mead, ring current and compression models 02 p0156 A73-11747

Adjustment of large observation systems in networks of satellite triangulation. 02 p0159 A73-12169

Processing of results of observations of the satellite 65-011-04 carried out within the framework of INTEROS program 1966. 02 p0159 A73-12170

Cosmic dust distribution measurement by satellites, relating accuracy to sensor calibration conditions and region characteristics 02 p0215 A73-12258

The zodiacal light as seen from the Pioneer F/G and Helios probes. 02 p0215 A73-12263

Meteorological and atmospheric physics observations by Soyuz manned spacecraft, analyzing spec-

trphotometry, photography and visual observation data of twilight, night and day horizons

02 p0160 A73-12265

The radiation budget of the earth-atmosphere system as measured from the Nimbus 3 satellite /1969-1970/.

02 p0160 A73-12266

Observations of precipitation zones from satellites using microwave radiometers.

02 p0160 A73-12267

Precipitation detection over the ocean using microwave satellite radiometry.

02 p0188 A73-12268

Very long baseline interferometry observations of radio emissions from geostationary satellites.

02 p0215 A73-12270

High-latitude precipitation of low-energy particles as observed by ESRO I A.

02 p0206 A73-12312

Radiation belt low energy protons intensity and spectrum variations during geomagnetic storms from Molniya 1 satellite measurements, interpreting results in terms of electric field effects

02 p0206 A73-12318

Plasmasphere hydrogen, helium, oxygen and nitrogen ions inbound and outbound profiles from OGO 5 mass spectrometric measurements

02 p0164 A73-12320

New interpretations of extraterrestrial Lyman-alpha observations.

02 p0206 A73-12323

Study of energy spectra of primary cosmic rays at very high energies on the proton series of satellites.

02 p0207 A73-12328

Satellite-borne radio telescope observation of traveling solar radio bursts for energetic solar particle propagation in interplanetary space, discussing wind density and magnetic field

02 p0208 A73-12419

Solar cosmic ray burst on July 7, 1966 and its measurement on the Proton-3 artificial earth satellite

02 p0208 A73-12461

Ionospheric VLF and ELF electric field observation by Alouette 2 satellite, obtaining ion mass distribution from lower hybrid resonance hiss during geomagnetic storm

02 p0164 A73-12623

Conjugate ducted echoes observed on Alouette II ionograms.

02 p0143 A73-12624

On the application of satellite data on cloud brightness to the study of tropical wave disturbances.

02 p0190 A73-12790

North/south asymmetric entry of solar protons during the November 18, 1968 event.

03 p0360 A73-12878

Symposium on the Future Application of Satellite Beacon Measurements, Graz, Austria, May 29-June 2, 1972, Proceedings.

03 p0299 A73-13626

Ionospheric total electron content measurements from the Australian zone.

03 p0299 A73-13632

Atmospheric wave perturbations of total electron content.

03 p0299 A73-13633

The use of Faraday rotation measurements on geostationary satellites.

03 p0300 A73-13635

Determination of exospheric electron content from group delay and Faraday rotation observations of geostationary satellite signals.

03 p0300 A73-13636

A comparison of total electron content determined by the differential Doppler and the Faraday effects using radio signals from a geostationary satellite.

03 p0300 A73-13637

Problems in estimating the total electron content from Faraday rotation observations on geostationary satellites.

03 p0300 A73-13638

A receiver design for the ATS-F radio beacon experiment.

03 p0275 A73-13640

Computed effects of the ionosphere/protonosphere distribution on VHF signals from ATS-F/G.

03 p0275 A73-13641

Time-dependent characteristics of radio waves passing through the irregular ionosphere.

03 p0275 A73-13645

Recent satellite measurements of the morphology and dynamics of the plasmasphere.

03 p0301 A73-13709

Observation of a correlated X-ray-radio transition in Cygnus X-1.

03 p0361 A73-13714

Auroral flux enhancements due to solar proton injection at medium energies during flares from ESRO 2 satellite measurements

03 p0362 A73-13859

Interplanetary anisotropy measurements of energetic solar proton entry into geomagnetic tail by ESRO 2 satellite

03 p0362 A73-13860

Preferential particle arrival at polar caps during solar events, noting north pole flux increase from ESRO 1 measurements

03 p0362 A73-13861

ESRO IA/B observations at high latitudes of trapped and precipitating protons with energies above 100 keV.

03 p0362 A73-13863

Low energy auroral electron and proton precipitation patterns from polar orbiting ESRO 1A satellite, noting discontinuities, flux distribution valleys, latitudinal crossover and Kp dependence

03 p0362 A73-13864

Dc electric field measurement with rocket-borne double probes and by satellite and balloon observation, noting ionospheric fields, magnetospheric plasma and auroras

03 p0302 A73-13874

Injun 5 observations of magnetospheric electric fields and plasma convection.

03 p0303 A73-13875

Plasma convection in the vicinity of the geosynchronous orbit.

03 p0303 A73-13878

Magnetospheric observations in OGO-5 plasma wave experiment, emphasizing electrostatic wave particles interaction with plasma

03 p0303 A73-13883

Automated procedures for mapping and display of digitized radar data.

03 p0281 A73-14522

Soyuz 9 spectrophotometry of earth surface features, comparing manned spacecraft-obtained and conventional spectrographs

03 p0304 A73-14564

Solar cyclic intensity variation of excess radiation with respect to galactic radiation background at low altitudes from satellite data analysis

03 p0365 A73-14575

L alpha photometry of Comet Bennett.

04 p0494 A73-14757

The use of artificial satellites for geodesy; Proceedings of the Third International Symposium, Washington, D.C., April 15-17, 1971.

04 p0436 A73-14776

Status of data reduction and analysis methods for the worldwide geometric satellite triangulation program.

04 p0437 A73-14780

Geometrical adjustment with simultaneous laser and photographic observations on the European datum.

04 p0437 A73-14781

Analysis of methods for computing an earth gravitational model from a combination of terrestrial and satellite data.

04 p0437 A73-14787

Isostatic reduction potential of earth mass distribution for spherical harmonic solutions of satellite determined gravity anomalies

04 p0437 A73-14788

Interior point mass earth potential model for satellite geodesy, considering geoid heights, gravity anomalies and spherical harmonics

04 p0438 A73-14791

Improvement of zonal harmonics by the use of observations of low-inclination satellites Dial, SAS, and Peole.

04 p0438 A73-14795

Detailed gravimetric geoid computation for U.S. area from satellite spherical harmonic and surface gravity data, comparing with astrogeodetic geoid

04 p0439 A73-14798

Earth polar motion from revised station coordinates and data from additional Doppler satellite tracking stations

04 p0439 A73-14800

Tracking stations interdistances and solid-earth tidal perturbations determination by laser ranging to satellites

04 p0439 A73-14801

Auroral-zone X-ray measurements at Kiruna in 1970.

04 p0492 A73-15100

Electric field and plasma observations in the magnetosphere.

04 p0442 A73-15334

Magnetospheric field distortion relation to ring currents based on satellite-borne magnetometer measurements of magnetic field topology

04 p0442 A73-15338

Millimeter wave propagation measurement for attenuation probability statistics by ATS-5 satellite, considering impact on space communication system design

04 p0418 A73-15387

A revised low-frequency cosmic noise spectrum.

04 p0500 A73-15516

Satellite data and estimates of precipitation for hydrologic applications.

04 p0473 A73-15774

Ocean color measurements utilizing a noon orbit for earth resources satellite applications.

04 p0445 A73-15778

Martian topography from radar observations and the Mariner 6 and 7 and ground-based CO2 measurements.

04 p0503 A73-16016

Nonuniformities of the ion density at an altitude of 600 km in the ionosphere.

05 p0567 A73-16083

Observations of low-energy protons with the Molniya 1 satellite in July-August, 1970.

05 p0608 A73-16084

Observation of the region of interaction between the solar-wind plasma and Mars.

05 p0608 A73-16095

Prospects for the utilization of satellite information in studies of the general atmospheric circulation

05 p0593 A73-16244

Utilization of meteorological data from satellites in studies of the general atmospheric circulation

05 p0593 A73-16245

Utilization of meteorological data from earth satellites in the analysis of global weather maps and in studies of planetary atmospheric circulation

05 p0593 A73-16246

Significant vortex structures occurrences from ESSA 3 and 5 global cloud observations, discussing source and formation patterns over Northern and Southern Hemisphere regions

05 p0593 A73-16346

Direct determination of the thickness of stratospheric layers from single-channel satellite radiance measurements.

05 p0569 A73-16574

The measurement of environmental pollution with the aid of aircraft and satellites

05 p0570 A73-16767

Vertical-ray structure/horizontal inhomogeneity/ of emission from the earth's upper atmosphere on the basis of observations from the Sioiz 3 spacecraft

05 p0570 A73-16845

Orbital parameters optimization of circular orbit earth satellites network for continuous earth observation, using group theory

05 p0620 A73-17004

Solar X-ray emission in July 1964 and in November-December 1965 according to data from the 'Elektron-4' satellite and the 'Venera-2' station

05 p0610 A73-17017

Martian dust storm from photometric observations on board the Automatic Interplanetary Station Mars 3

05 p0620 A73-17018

Sunspot fine structure from photographs taken on U.S.S.R. Stratospheric Solar Station, noting high Rayleigh resolution of small elements

05 p0621 A73-17031

Solar flares EUV observations by OSO 5 three band grating spectrophotometer, discussing flare intensity time dependence with superimposed impulsive bursts

05 p0610 A73-17044

Type 3 radio bursts correlation with solar flares and electron events from OGO 5, IMP 5 and Explorer 35 observations

05 p0610 A73-17047

A satellite study of the mid-latitude trough in electron density and VLF radio emissions during the magnetic storm of 25-27 May 1967.

05 p0571 A73-17060

Study of VLF and ELF noises observed by Alouette 2.

05 p0552 A73-17163

Conjugate ducted echoes observed on Alouette II ionograms.

05 p0572 A73-17164

Nonducted whistlers observed in the plasmasphere.

05 p0572 A73-17165

Assessment of ISS topside sounder system by computer simulation.

05 p0579 A73-17168

Cosmic ray number density modulation by off-ecliptic phenomena to explain interplanetary magnetic field measurements onboard Heos 1 and 2

05 p0611 A73-17186

Interpretation of numerical observations of meteorological satellites with infrared and monochromatic vision by means of high resolution satellites - The case of storm cloud systems

05 p0594 A73-17232

The Uhuru catalog of X-ray sources.

05 p0625 A73-17326

Observations of the extended X-ray sources in the Perseus and Coma clusters from Uhuru.

05 p0625 A73-17327

Satellite oceanographic measurements and observations and required sensors assessment, noting benefits to marine and coastal interests and to weather forecasting

06 p0690 A73-17605

Possibility for observational verification of the relativistic motion of the periselenium of artificial satellites of the moon

06 p0748 A73-17765

Electron-proton spectrometer for the GEOS satellite.

06 p0692 A73-17826

Lunar shape parameter extraction from Apollo 15 and 16 laser altimeter measurements of CSM to surface distance
06 p0751 A73-18223

Mapping of atmospheric and sea ice parameters with an imaging microwave radiometer from the Nimbus 5 satellite.
06 p0667 A73-18281

Global and local scale satellite surveillance of atmospheric pollution.
06 p0691 A73-18305

Observations of Taurus X-1 by the 1-60 keV X-ray detector on the OSO-7.
07 p0868 A73-19064

Lunar geology developments by remotely sensed earth-based, moon satellite and unmanned and manned lunar lander observations, discussing moon structure and evolution
07 p0875 A73-19223

Interpretation of Ogo 5 Lyman alpha measurements in the upper geocorona.
07 p0813 A73-19233

Substorm variations of the magnetotail plasma sheet at geocentric distances measured along the solar magnetospheric x-axis from -6 to -60 earth radii.
07 p0813 A73-19235

Observed relationships between electric fields and auroral particle precipitation.
07 p0814 A73-19237

Recent studies of magnetospheric electric field emissions above the electron gyrofrequency.
07 p0815 A73-19254

Composition of radiation excess over primary cosmic ray background recorded by Cosmos satellites below midlatitude belt region
07 p0870 A73-19426

The ABC method of providing warning of an impending solar flare.
07 p0899 A73-19941

Global electron density distributions from the Ariel 3 satellite at mid-latitudes during quiet magnetic periods.
07 p0819 A73-20054

Observations of periodic variations in the X-ray intensity of Cygnus X-3.
07 p0872 A73-20240

Distribution of the total ozone content in the atmosphere according to satellite observations.
07 p0820 A73-20346

GARP Global Experiment design with satellite and balloon borne systems for meteorological observation and atmospheric research, discussing sounding data numerical simulation
07 p0820 A73-20442

Uhuru satellite observations of X ray sources, discussing binary sources and identification in visible stars
07 p0872 A73-20525

Correlation of ground-based measurements of structured Pc 1 micropulsations withOGO-V plasmopause observations.
08 p0937 A73-20652

VLF ion cyclotron whistler propagation in upper ionosphere, noting polarization reversal and mode coupling from satellite observation
08 p0937 A73-20653

Auroral particle influx behavior and electric field aligned electron precipitation observation by Ba release and electrostatic probe in rocket and satellite experiments
08 p0957 A73-20662

Solar soft X-ray bursts data recorded by satellite telemetry, considering production by thermal plasma and nonrelativistic electrons with power law energy distribution
08 p0996 A73-20765

Evidence for a common origin of the electrons responsible for the impulsive X-ray and type III radio bursts.
08 p0996 A73-20766

Ultraviolet photometry from the Orbiting Astronomical Observatory. VII alpha squared Canum Venaticorum.
08 p1008 A73-21158

Identification of discontinuities at the magnetosphere boundary
08 p0958 A73-21277

Magnetic storm of March 8-10, 1970 from Cosmos-321 and ground observations. I - Morphology of the disturbance
08 p0959 A73-21290

Galactic cosmic ray particle intensity decrease relationship to low energy proton flux increase based on interplanetary Zond 3 and Venera probes measurements
08 p0999 A73-21326

Primary cosmic rays energy spectrum at .100-1000 TeV from Proton 4 satellite data
08 p0999 A73-21329

Primary cosmic rays alpha particles and protons energy spectra similarity and intensity difference at .05 to 1.6 TeV, using Proton satellites data
08 p0999 A73-21331

Covariance matrices and means of atmospheric Planck function profiles for application to temperature sounding from satellite measurements.
08 p0967 A73-21385

Preliminary results of a spectrophotometric survey of the sky in the ultraviolet with the aid of the TD-1 A satellite
08 p0967 A73-21499

Measurement of short- and longwave radiant fluxes from the Kosmos-320 satellite.
08 p0961 A73-21586

The interstellar reddening law in the ultraviolet deduced from filter photometry obtained by the OAO-2 satellite.
09 p1141 A73-22029

Proton scattering in the region near the earth's bow shock.
09 p1137 A73-22054

Relations between ionospheric electric fields and energetic trapped and precipitating electrons.
09 p1073 A73-22056

Neutral thermosphere temperatures from density scale height measurements.
09 p1074 A73-22063

Nonlinear frequency correction to plasma instability at half harmonics of electron gyrofrequency as observed by OGO 5 near geomagnetic equator outside plasmopause
09 p1075 A73-22069

Simultaneous observations of low energy electron fluxes and the polar red emission at 6300 A.
09 p1075 A73-22137

Global time and space changes of satellite radiances received from the stratosphere and lower mesosphere.
09 p1076 A73-22149

Residual geomagnetic field from the satellite Cosmos 49.
09 p1076 A73-22192

Mars surface ellipticity discrepancy with dynamic value obtained from satellite orbital precession explained by solid state convection in deep interior and Martian evolution
09 p1144 A73-22268

Preliminary results of studies of the Martian atmosphere with the aid of the Mars-2 satellite
09 p1146 A73-22486

Field-aligned currents between 400 and 3000 km in auroral and polar latitudes.
09 p1078 A73-22834

The electron density experiment on-board the Ariel 4 satellite.
09 p1085 A73-22916

Application of some numerical techniques in combining satellite and conventional data in the tropics.
09 p1115 A73-23175

Satellite measurements of the charge composition of solar cosmic rays in the Z = 6 to 26 interval.
10 p1264 A73-23537

Direct measurements of solar-wind fluctuations between 0.0048 and 13.3 Hz.
10 p1264 A73-23539

D-2A /Tournesol/ satellite data processing procedures for technological controls, operation in flight and scientific purposes
10 p1187 A73-23620

Esro 4 performance of abandoned TD-2 experiments for particle measurements over polar regions, describing satellite construction, thermal control, power supply, attitude control and measurement
10 p1285 A73-23748

Investigation of geoeactive corpuscular particles and photoelectrons on board the Cosmos 261 satellite. V - Spectra of ionospheric photoelectrons and migration of the latter from the conjugate ionosphere
10 p1211 A73-23887

Fluxes of electrons with energies above 80 MeV at the equator on the basis of measurements by the Cosmos 490 satellite
10 p1265 A73-23897

Certain data concerning heavy primary nuclei /Z above 33/ obtained outside the earth's magnetosphere
10 p1266 A73-23915

Comparative characteristics of the soft component of solar and galactic cosmic rays on the basis of rocket and stratospheric measurements at Heis Island and Apatite Station
10 p1267 A73-23920

Investigation of charged-particle fluxes at altitudes of 200 to 300 km with the aid of the Saliut orbital station
10 p1267 A73-23930

Development of a global cloud model for simulating earth-viewing space missions.
10 p1244 A73-23979

Satellite observed cloud signatures associated with mature and decaying depressions over high and middle southern latitudes, deriving surface pressure and upper geopotential anomaly patterns
10 p1244 A73-23980

Preliminary interpretation of the polarization measurements performed on 'Intercosmos-4' during three X-ray solar flares.
10 p1268 A73-24142

Secular geomagnetic field variation of the epoch 1965-1970, according to observatory and satellite observations.
10 p1212 A73-24232

The radiation balance of the earth-atmosphere system - Recent results from satellite measurements
10 p1213 A73-24399

The magnetic field in the immediate vicinity of Mars according to Mars 2 and Mars 3 satellite data
10 p1281 A73-24461

Mathematical processing of measurement data in the orbital method of space geodesy
10 p1281 A73-24486

Solar flare particle propagation - Comparison of a new analytic solution with spacecraft measurements.
10 p1269 A73-24727

Anisotropies in the interplanetary intensity of solar protons with energies greater than 0.3 MeV.
10 p1269 A73-24728

Energetic solar proton observations by Explorer 33 and 35 /interplanetary medium/ and Injun 5 /polar caps/, comparing proton fluxes in space and poles
10 p1269 A73-24729

Satellite measurement of variable intensities for geomagnetically trapped protons during magnetic storms, noting ring current source of low-altitude protons
10 p1213 A73-24731

Ogo 6 retarding potential analyzer observation of vertical and longitudinal gradients in ion concentrations below F region peak near magnetic equator
10 p1214 A73-24738

Solar wind flow vector from detection of unshocked wind by plasma detector aboard ATS-5 during 8 March 1970 geomagnetic storm
10 p1270 A73-24741

Interplanetary plasma shock event of 8 March 1970 from Heos 1 data, noting magnetospheric compression and solar wind velocity at geosynchronous orbit
10 p1270 A73-24742

OGO 5 observation of ULF geomagnetic fluctuation at polar cusp boundaries in terms of ionospheric drift wave and Kelvin-Helmholtz instabilities
10 p1214 A73-24744

Ionospherically diffracted monochromatic VHF/UHF plane wave statistics characterization, noting Gaussian and log-normal distributions from ATS-3 satellite data recording
10 p1190 A73-24896

Weather satellite capabilities - Present and future.
11 p1429 A73-25149

Alpha particles in solar cosmic rays over the last 80,000 years.
11 p1412 A73-25375

ISIS-1 satellite observations of the ionosphere at high southern latitudes.
11 p1353 A73-25753

Ariel 3 satellite observations of the ionosphere at high southern latitudes.
11 p1353 A73-25754

Supernova remnant Cas A identification as extended source of soft X rays from grazing incidence X ray telescopes aboard OAO Copernicus
11 p1412 A73-25776

Preliminary mapping of the lunar magnetic field.
11 p1421 A73-25903

Spatial and temporal variations of the Lyman-alpha airglow and related atomic hydrogen distributions.
11 p1356 A73-25909

Radio Astronomy Explorer /RAE/, I - Observations of terrestrial radio noise.
11 p1356 A73-25920

Two-component temperature analysis of OSO-5 X-ray flare data.
11 p1413 A73-25947

Solar X-ray bursts from OSO-7 observations, analyzing spectra obtained from proportional and scintillation counters
11 p1413 A73-25948

Gravity field of Mars from Mariner 9 tracking data.
11 p1425 A73-26138

Determination of the relative position of points on the earth surface with the aid of satellite observations
11 p1357 A73-26294

Study of terrestrial resources by space objects and international law
11 p1454 A73-26295

Sea ice observation by means of satellite.
11 p1358 A73-26346

Simple model for scanning-angle distribution of planetary albedo gamma-rays.
11 p1414 A73-26475

Application of Nimbus 4 THIR 6.7-micron observations to regional and global moisture and wind field analyses.
12 p1520 A73-26812

A two-satellite microwave occultation system for determining pressure altitude references.
12 p1521 A73-26813

Cosmic ray electrons from 0.2 to 8 MeV - Pioneer 8 and 9 measurements of their spectrum, time variations, and interplanetary radial gradient.
12 p1533 A73-26976

Distributions and characteristics of high-latitude field-aligned electron precipitation. 12 p1534 A73-26988

Heos 2 magnetometer observations of magnetosheath high and low energy electron flux during magnetopause boundary crossings in polar regions 12 p1489 A73-27004

Simultaneous recording of solar cosmic rays near Venus and in the earth magnetosphere 12 p1534 A73-27354

Cosmos 321 geomagnetic measurement data for construction of satellite geomagnetic survey and geomagnetic field models 12 p1491 A73-27359

Auroral heating and the composition of the neutral atmosphere. 12 p1492 A73-27602

Space distribution of the intensity of excess radiation at low altitudes. 12 p1535 A73-27637

Longitudinal magnetospheric currents contribution to auroral electrojet from satellite observation data, noting magnetosphere electric field excitation of meridional Pedersen and Hall currents 12 p1493 A73-27650

Worldwide geodetic system construction by using satellites at sufficient altitude, discussing gravity waves avoidance 12 p1493 A73-27691

Negative horizontal gradients of the integral electron content of the ionosphere - A comparison of satellite and ionosonde data 12 p1494 A73-27774

GEOS geostationary satellite experiments for dc magnetic fields, dc/ac electric fields and plasma resonances, thermal plasma, electrons and protons 12 p1499 A73-27775

Galactic and extragalactic radio emission and satellite observations of RF cosmic radiation and noise intensity 12 p1544 A73-27783

Characteristics of electron and high-energy proton flares. 12 p1536 A73-27849

Remote sensing capability development program planning, discussing world participation in ERTS and alternatives 12 p1500 A73-27951

Space geodetic techniques since 1957 covering photography, radar and laser uses in satellite observations with geodetic applications 13 p1671 A73-28006

Earth figure theory and gravimetric measurements using satellite observations and photography 13 p1605 A73-28007

Photographic satellite observations with the Automatic Camera for Astrogeodesy. 13 p1611 A73-28150

Determination of the height of ionospheric irregularities with the holographic method. 13 p1606 A73-28155

Comparison of the coordinates of the pole as obtained by classical astrometry /IPMS, BIH/ and as obtained by Doppler measurements on artificial satellites /Dahlgren polar monitoring service/. 13 p1679 A73-28390

Atmosphere Explorer mission of lower thermosphere and ionosphere physics investigation, discussing orbit selection 13 p1687 A73-28626

Atmosphere Explorer for satellite observation of thermosphere, discussing design goals, spacecraft components and data system 13 p1687 A73-28627

Atmosphere Explorer pressure measurements - Ion gauge and capacitance manometer. 13 p1688 A73-28632

Low-energy electron experiment for Atmosphere Explorer-C and -D. 13 p1689 A73-28642

Second positive system of nitrogen bands in dayglow, according to Kosmos-224 data. 13 p1607 A73-28703

Dayglow nitrogen ion 3914 A emission profiles for average solar activity at 110-240 km heights from Cosmos 224 observations 13 p1607 A73-28704

Equatorial electrojet, according to Kosmos-321 measurements. 13 p1670 A73-28716

Radiation temperatures of the earth's blankets in the microwave and infrared ranges according to experiment data on the Cosmos-384 artificial earth satellite 13 p1609 A73-29154

Investigation of cloud cover parameters from measurements on the Cosmos 384 satellite 13 p1654 A73-29155

Mesoscale cloud systems analysis from meteorological observations and weather satellite data nephanalysis, applying to weather forecasting 13 p1655 A73-29191

Atmospheric effects on ocean surface temperature sensing from the NOAA satellite scanning radiometer. 13 p1610 A73-29195

Computerized simulation of Ionosphere Sounding Satellite topside sounder system techniques for observation of critical frequencies and apparent distance-frequency characteristic relation 13 p1586 A73-29248

Simultaneous determination of chord length and direction by artificial earth satellite geodetic observations in Arctic and Antarctic regions 13 p1610 A73-29320

Determination of the density of protons in the magnetosphere on the basis of observations of Pc-3 type geomagnetic pulsations 13 p1610 A73-29560

Gaussian curvature of smoothed equipotential surfaces from satellite orbit dynamics. 13 p1611 A73-29659

Interkosmos 5 investigation of VLF electromagnetic signals and emissions, discussing onboard instruments to measure particle fluxes 13 p1622 A73-29662

SMC X-1 binary source observation via UCSD OSO-7 X ray telescope, discussing luminosity and optical identification with variable star SK 160 14 p1786 A73-29738

Solar flare ejected protons intensity increase during July 1970 from Pioneer 6 and 8 and Explorer 41 data 14 p1786 A73-29859

Investigation of scattered ultraviolet radiation in the upper Martian atmosphere from the Mars-3 automatic interplanetary station 14 p1796 A73-29866

Observation of a current-driven plasma instability at the outer zone-plasma sheet boundary. 14 p1747 A73-29966

OAO-2 observations of HD 153919 = 2U 1700-37. 14 p1797 A73-30007

White dwarfs, neutron stars and black hole identification by satellite X ray astronomy, discussing gas temperature and mass relation to cluster parameters 14 p1797 A73-30075

Preliminary results of Martian-atmosphere research with the Mars-2 satellite. 14 p1798 A73-30321

The significance of atmospheric measurements for interior models of the major planets. 14 p1799 A73-30532

Spectrophotometric results from the Copernicus satellite. II - Composition of interstellar clouds. 14 p1801 A73-30745

Spectrophotometric results from the Copernicus satellite. V - Abundances of molecules in interstellar clouds. 14 p1802 A73-30748

A uniform belt of diffuse auroral emission seen by the ISIS-2 scanning photometer. 15 p1866 A73-31069

An observation of polar auroral and airglow from the ISIS-II spacecraft. 15 p1866 A73-31071

Diffuse auroral belt observation by Isis-2 scanning auroral photometer verified by analysis of ground based all sky photographs 15 p1866 A73-31074

Isis-2 observations of auroral emissions characteristics in polar region during December 1971 magnetic storm recovery phase 15 p1866 A73-31076

Spectrophotometric results from the Copernicus satellite. VI - Extinction by grains at wavelengths between 1200 and 1000 A. 15 p1936 A73-31561

Some results of ozone observations by satellite on June 17 and 18, 1966 15 p1868 A73-31607

Artificial satellites photographic observations reduction by Turner and colineation methods, considering IBM 360 FORTRAN program application 15 p1843 A73-31648

Equatorial scintillation variation with magnetic storm from ATS 3 VHF telemetry signal recordings, comparing with spread F observation 15 p1870 A73-31763

Equatorial ionospheric anomaly related neutral thermospheric composition variation observation from OGO-6 mass spectroscopic data, noting static diffusion model limitations 15 p1870 A73-31767

Equatorial electrojet characteristics observation during 1967-1970 with POGO satellite-borne magnetometers, noting anomaly characterized by sharp negative V-signature in width and variable amplitude 15 p1870 A73-31768

POGO satellite observed electrojet signature data comparison with daily geomagnetic variation amplitude measurement at equatorial ground station in India 15 p1870 A73-31769

The electrojet field from satellite and surface observations in the Indian equatorial region. 15 p1870 A73-31770

Correlation of 'satellite estimates' of the equatorial electrojet intensity with ground observations at Addis Ababa. 15 p1870 A73-31771

POGO satellite observed electrojet current data comparison with ground measurement at Ibadan, discussing data ratios variation by upper earth mantle conductivity structure 15 p1870 A73-31772

POGO satellite observation of electrojet profiles compared with H variation around measurements, interpreting data by classical band current model 15 p1871 A73-31773

Atmosphere optical thickness determination from satellite and ground measurements of scattered light in solar vertical 15 p1905 A73-31820

Estimate of the probability of observing solar cosmic-ray proton fluxes at the earth orbit 15 p1926 A73-31877

The low-latitude and equatorial outer ionosphere during the magnetic storm of January 2-4, 1964 15 p1871 A73-31881

Relationship of the Pc 3 and 4 geomagnetic pulsation period with the parameters of the interplanetary medium at the earth orbit 15 p1937 A73-31904

The possibility of measuring gravitational redshift by means of earth satellites. 15 p1940 A73-32074

Geodetic control point accurate position determination by Navy navigation Doppler satellite observations with geocenter and teletype tape 15 p1873 A73-32268

Solar cosmic-ray burst of July 7, 1966 and its measurement by Proton-3 satellite. 15 p1927 A73-32611

Latitudinal and time variations of total electron number and its gradients in the ionosphere at high latitudes. 15 p1874 A73-32625

Extra-atmospheric observations of the luminosity of the sky from the Cosmos 51 and Cosmos 213 satellites. I - Method and calibration of the measurements 16 p2011 A73-32706

Extra-atmospheric observations of the luminosity of the sky from the Cosmos 51 and Cosmos 213 satellites. II - Measurement data and their interpretation 16 p2001 A73-32707

Uhuru observed galactic X ray sources, discussing whole-galaxy X ray emission, Sco X-1 type binary sources and emissions in GX263+2 and Small Magellanic Cloud 16 p2049 A73-32728

Observations of cosmic X-ray sources by the MIT instrument on the OSO-7. 16 p2049 A73-32729

Uhuru extragalactic X ray observations including normal galaxies, quasars, giant radio galaxies, Seyferts and galactic clusters 16 p2050 A73-32741

Hard X-ray solar bursts observed from the OSO-6 satellite. 16 p2052 A73-32828

The extreme ultraviolet emissions of solar flares - A comparison between OSO-6 spectroheliograph observations and SFDs. 16 p2053 A73-32959

Spectra of solar flares from 8.5 A to 16 A. 16 p2053 A73-32960

Solar proton, helium, and medium nuclei /Z from 6 to 9/ observed from the IMP-VI satellite. 16 p2054 A73-33280

Improved Tiros Operational Satellite and future near-polar orbiting environmental system, discussing scanning radiometer and vidicon and automatic picture transmission camera remote sensors 16 p2015 A73-33352

Nonlinear filter evaluation for estimating vehicle position and velocity using satellites. 16 p1988 A73-33410

Space observations of the variability of solar irradiance in the near and far ultraviolet. 16 p2062 A73-33428

Properties of the satellite photoelectron sheath derived from photoemission laboratory measurements. 16 p2062 A73-33435

Ion cyclotron waves observed in the polar cusp. 16 p2003 A73-33437

Additional results from an Ogo 6 experiment concerning ionospheric electric and electromagnetic fields in the range 20 Hz to 540 kHz. 16 p2003 A73-33438

Observations of the auroral oval and a westward traveling surge from the Isis 2 satellite and the Alaskan meridian all-sky cameras. 16 p2004 A73-33445

Satellite studies of magnetospheric substorms on August 15, 1968. II - Solar wind and outer magnetosphere. 16 p2004 A73-33450

Satellite studies of magnetospheric substorms on August 15, 1968. IV - Ogo 5 magnetic field observations. 16 p2004 A73-33452

Satellite studies of magnetospheric substorms on August 15, 1968. V - Energetic electrons, spatial boundaries, and wave-particle interactions at Ogo 5.
16 p2056 A73-33453

Satellite studies of magnetospheric substorms on August 15, 1968. VI - Ogo 5 energetic electron observations - Pitch angle distributions in the nighttime magnetosphere.
16 p2056 A73-33454

Satellite studies of magnetospheric substorms on August 15, 1968. VII - Ogo 5 energetic proton observations - Spatial boundaries.
16 p2056 A73-33455

Satellite studies of magnetospheric substorms on August 15, 1968. VIII - Ogo 5 plasma wave observations.
16 p2004 A73-33456

Satellite studies of magnetospheric substorms on August 15, 1968. IX - Phenomenological model for substorms.
16 p2004 A73-33457

Quiet time magnetospheric field depression at 2.3-3.6 earth radii.
16 p2005 A73-33464

The abnormal stratosphere studied with the aid of satellite radiation measurements.
[ALAA PAPER 73-493] 16 p2005 A73-33537

Millimeter wave propagation measurements from an orbiting earth satellite.
16 p1982 A73-33716

Investigation of the chemical composition of the atmosphere of Venus by the automatic station Venus 4.
16 p2066 A73-33799

Atmosphere and ionosphere of Venus on the basis of data obtained by Mariner 5 in the S band during radio occultation
16 p2067 A73-33801

Study of ultraviolet radiation from the Venera interplanetary probe
16 p2056 A73-33803

The magnetic field in the vicinity of Venus
16 p2067 A73-33805

Certain results of a combined treatment of the Venera 4 interplanetary probe and ground-based radio-astronomical and radar measurements
16 p2068 A73-33819

Estimates of water content in the atmosphere of Venus on the basis of radio-astronomical measurements and space probe data
16 p2068 A73-33823

Measurement of cosmic rays and searches for radiation belts near Venus
16 p2057 A73-33829

The plasmasphere during a magnetic recovery period - A combined study of the OGO 4 and OGO 5 satellite data and of whistlers received at the ground
16 p2008 A73-33876

Monitoring earth's resources from space.
17 p2157 A73-34279

Intrinsic ultraviolet colors from OAO-2 Telescope observations for stars on the main sequence.
17 p2225 A73-34290

The Pioneer 9 electric field experiment. III - Radial gradients and storm observations.
17 p2230 A73-34513

Radio emissions from solar flares.
17 p2224 A73-34723

Observations of gamma-ray bursts of cosmic origin.
17 p2224 A73-34770

Space probe observed VLF hiss powers disparity with theoretical prediction for incoherent Cerenkov radiation, considering Landau instability generated wave amplification
17 p2160 A73-34788

Ionospheric scintillation at 4 and 6 GHz.
17 p2122 A73-34869

The control of the terrestrial environment from space: International collaboration, methods and technologies; International Conference on Space, 13th, Rome, Italy, March 22-24, 1973, Proceedings
17 p2160 A73-34926

Satellite monitoring of climate parameters, discussing energy transfer in atmosphere, energy distribution, radiation balance, climatic models
17 p2205 A73-34928

Satellite remote monitoring of earth environment and natural resources by high resolution multispectral scanners for European requirements
17 p2160 A73-34931

Earth resources monitoring from satellites, aircraft and ground stations for fast data acquisition and management
17 p2161 A73-34934

Role of the meteorological satellites of the earth atmosphere observation system for the first global experiment of the 'Global Atmospheric Research Programme'
17 p2205 A73-34935

Satellite imagery of land resources, discussing synoptic views, spatial dependence, closed loop information and sequential sampling
17 p2161 A73-34945

Orbital mapping of the lunar magnetic field.
17 p2235 A73-35739

Climatological studies based on satellite data, including cloud, snow and ice cover, wind measurement, convection currents, temperature fields and earth thermal balance
18 p2331 A73-35914

Properties of cosmic X-ray sources.
18 p2343 A73-35924

Particle entry into the equatorial magnetosphere.
18 p2344 A73-35928

An investigation on the spatial distribution of the quasi-trapped energetic electrons observed on board the satellite 'Shinsei.'
18 p2344 A73-35929

Observation of trapped and solar particles since 2 October 1972.
18 p2344 A73-35931

Satellite geodesy application to earth internal structure and gravity field relationship to geomagnetism, noting magnetic secular variation correspondence with large scale mass motion
18 p2302 A73-35932

Need for and aspects of a cooperative European earth resources program.
18 p2372 A73-35933

Surveyor observations of lunar horizon-glow.
18 p2348 A73-35938

OGO-5 observations of the physical processes occurring in the disturbed polar cusp and the cusp-magnetosheath interface.
18 p2303 A73-35943

Ground and synchronous orbit magnetic observations of magnetospheric and ionospheric wave propagation to model substorm current system variations
18 p2303 A73-35945

Satellite measurements of atmospheric composition in the altitude range 150 to 450 km.
18 p2303 A73-35957

Extreme temperature deviations from the climatological mean in the upper stratosphere - observed by rockets, confirmed by satellites.
18 p2304 A73-35962

Vertical ozone profiles from observations of eclipsing satellites.
18 p2304 A73-35971

Satellite measurements of interstellar gamma radiation, describing spark chamber and optical recording system
18 p2349 A73-35975

Report on the telescope ultraviolet observations from the OAO-2 satellite and associated research at the Smithsonian Astrophysical Observatory.
18 p2349 A73-35996

Investigation of the solar X-ray flare spectra by the 'Intercoms-4' and 'Intercoms-7' satellites.
18 p2345 A73-36015

Construction of D-region electron-density profiles by combined use of ground-based reflection and satellite-based transmission measurements.
18 p2306 A73-36016

Mapping of snow cover in the Swiss Alps from ERTS-1 imagery.
18 p2306 A73-36021

Prospects for physical oceanography from space.
18 p2306 A73-36024

New ways to monitor the mass and areal extent of snowcover.
18 p2307 A73-36025

Applications of the ERTS-1 satellite in remote sensing of water resource data in Canada.
18 p2307 A73-36026

Vertical temperature profiles from satellites - Results from second generation instruments aboard Nimbus-5.
18 p2307 A73-36029

Remote sensing of ocean color as an index of biological and sedimentary activity.
18 p2307 A73-36030

Recent stratospheric temperature measurement compatibility tests at Wallops Island.
18 p2307 A73-36035

High-level circulation studies based on rawinsonde, rocketsonde and satellite observations.
18 p2350 A73-36040

Infrared transmittances for indirect soundings of the atmosphere from satellite-based measurements.
18 p2308 A73-36043

Aerological soundings of the atmosphere from NOAA-2 data for operational systems.
18 p2308 A73-36044

Global temperature distributions from OGO VI 6300 A airglow measurements.
18 p2309 A73-36058

The evolution of location and data collection systems in the United States.
[ALAA PAPER 73-584] 18 p2372 A73-36076

Density of the radiation of the earth/atmosphere system into space
18 p2309 A73-36112

Nature of some optical effects observed on spacecraft at sunrise
18 p2309 A73-36122

Gamma ray and neutron measurements and their relation to the solar flare problem.
18 p2345 A73-36126

Earth satellite measurements as applied to sea ice problems.
18 p2310 A73-36134

Satellite imagery in national resource surveys and vegetation growth monitoring on mine dumps from ERTS-1 data
18 p2311 A73-36151

A photometric study of the counterflow from space.
18 p2351 A73-36182

Solar wind interaction with the earth's magnetic field. I - Magnetosheath.
18 p2346 A73-36270

ULF magnetic fluctuations in the plasma sheet as recorded by the Explorer 34 satellite.
18 p2352 A73-36276

Satellite observations of strong Balmer alpha atmospheric emissions around the magnetic equator.
18 p2346 A73-36284

Satellite measurements of solar X-ray flux and ground observations of sudden ionospheric disturbances.
18 p2347 A73-36389

Teledetection of terrestrial resources by satellites
18 p2373 A73-36390

Gulf Stream eddies - Recent observations in the western Sargasso Sea.
18 p2313 A73-36642

Measurement of the position and spectrum of Hercules X-1 from the OSO-7 satellite.
18 p2356 A73-36982

Book - Advances in satellite meteorology.
18 p2333 A73-37051

Method for analyzing the moisture field by the use of satellite cloud data.
18 p2334 A73-37056

Use of satellite cloud data in moisture field analysis.
18 p2334 A73-37057

Some results of determining cloud top heights from satellite infrared measurements.
18 p2334 A73-37060

Features of the evolution of depressions and their cloud systems over the Pacific Ocean.
18 p2334 A73-37061

Statistical structure of the brightness field of reflected radiation in the 0.6-0.8 micron spectral interval.
18 p2314 A73-37063

Assessment of characteristics of the atmospheric moisture distribution with the aid of satellite measurements.
18 p2334 A73-37064

Interrelationship between developments of synoptic processes and evolution of the integral moisture field according to satellite measurements
18 p2334 A73-37065

Comparison of satellite-measured and radar-observed cloud-top heights.
18 p2334 A73-37066

Utilization of satellite radiation measurements in analyzing the temperature near the ground.
18 p2334 A73-37067

Effect of cloud cover on the variability of outgoing radiation.
18 p2314 A73-37069

Effectiveness of utilizing cloudiness data obtained from satellites in objective analysis of the wind field.
18 p2334 A73-37071

Some characteristics of the vertical structure of the humidity field over the North Atlantic.
18 p2334 A73-37076

Some aspects of the solution of inverse problems of satellite meteorology.
18 p2335 A73-37078

Limits to the spectra of the Perseus and Coma clusters above 7 keV from the OSO-7.
18 p2357 A73-37101

Imp-3 satellite measurement-based investigation of variability of interplanetary magnetic field component normal to plane of ecliptic during passage across sector field boundary
19 p2480 A73-37241

Structural formations in the interplanetary medium
19 p2481 A73-37342

Copernicus satellite observation of eclipsing binary Her X-1 to search for steady soft X ray flux strong enough to heat companion star
19 p2482 A73-37391

Interpretation of the H-alpha atmospheric emissions observed by the D-2A Tournesol satellite around the magnetic equator
19 p2423 A73-37538

Accuracy and coverage of temperature data derived from the IR radiometer on the NOAA 2 satellite.
19 p2424 A73-37665

Russian book on satellite measurement of magnetic fields and plasmas in interplanetary medium, magnetosphere, moon and Venus vicinity and geomagnetic field-solar wind interaction region
19 p2486 A73-37772

Identification of discontinuities at the magnetosphere boundary.
19 p2424 A73-37906

Magnetic storm of March 8-10, 1970, according to ground-based and Kosmos-321 observations.
19 p2424 A73-37919

Generation and decay of a narrow belt of energetic electrons in the earth's magnetosphere.

19 p2476 A73-37934

Satellite and ground-based observations during the onset phase of the 2 November 1969 PCA event.

19 p2426 A73-38016

Localization of sources of two-hop whistlers observed aboard the Interkosmos 3 satellite over Europe.

19 p2404 A73-38021

Magnetic field in the near vicinity of Mars from data of the Mars-2 and Mars-3 satellites.

19 p2486 A73-38127

Density measurements in the equatorial atmosphere by means of the San Marco 3 satellite

19 p2426 A73-38151

Mapping of foF2 by means of topside sounder satellites.

19 p2427 A73-38285

The determination of foF2 and hmF2 from satellite-borne probe data.

19 p2427 A73-38286

The X-ray structure of the Vela X region observed from Uhuru.

19 p2488 A73-38514

Atmospheric temperature and humidity vertical profiles from satellite-borne IR spectral radiance measurements, using linear extrapolation and statistical regression techniques

[AAS PAPER 73-124] 20 p2521 A73-38584

Management looks at the Canadian program of remote sensing, phase I, 1971-1975.

[AAS PAPER 73-129] 20 p2521 A73-38587

Contributions of the EROS Program to the Department of the Interior's resources and management responsibilities.

[AAS PAPER 73-130] 20 p2550 A73-38588

Study of laser remote sensing techniques from space platforms.

[AAS PAPER 73-136] 20 p2521 A73-38591

Ocean currents observation by ship and satellite tracking of free-drifting Lagrangian platforms

[AAS PAPER 73-144] 20 p2550 A73-38593

Oceanographic satellite capabilities, considering sea-air interactions, currents, upwellings, deep sea tides, sea-earth interactions and water mass identification

[AAS PAPER 73-145] 20 p2550 A73-38594

DCS - A global satellite environmental data collection system.

20 p2525 A73-38744

An attitude control system for earth observation spacecraft.

[AIAA PAPER 73-854] 20 p2585 A73-38792

Investigation of geoeactive corpuscles and photoelectrons with the Cosmos 261 satellite. V - Spectra of ionospheric photoelectrons and their transfer from the conjugate ionosphere.

20 p2550 A73-38906

Electron fluxes with energies greater than 80 MeV at the equator based on measurement data from the Cosmos-490 satellite.

20 p2601 A73-38916

Pioneer 8 observations and interpretations of sixteen interplanetary shock waves observed in 1968.

20 p2603 A73-38931

Mariner 9 ultraviolet spectrometer experiment - Mars atomic oxygen 1304-A emission.

20 p2604 A73-38932

Dynamic variations in intensity and energy spectra of electrons in the inner radiation belt.

20 p2601 A73-38934

Whistler-mode hiss at low and medium frequencies in the dayside-cusp ionosphere.

20 p2529 A73-38935

TD 1 A astronomical satellite detection of UV dayglow emissions above F 2 peak in equatorial zone, considering Mg ions resonance scattering to account for emission features

20 p2551 A73-38940

Predawn enhancement of 6300-A emission observed near the plasmapause from the Isis-2 spacecraft.

20 p2551 A73-38945

Initial observations of geomagnetically trapped alpha particles at the equator.

20 p2552 A73-38950

Magnetic storm inflation analysis from Explorer 45 and ground observation data, noting proton penetration into magnetosphere evening quadrant

20 p2552 A73-38951

Energy spectra and pitch angle distributions of storm-time and substorm injected protons.

20 p2552 A73-38953

Proton flux density and differential energy spectra recorded by solid state proton detectors and three-axis fluxgate magnetometer aboard Explorer 45 at plasmapause

20 p2552 A73-38955

Plasma wave observations near the plasmapause with the S3-A satellite.

20 p2552 A73-38956

Explorer 45 search coil magnetometer detection of ELF signals during magnetic storms, noting signal variation with storm phases and satellite magnetospheric position

20 p2552 A73-38957

Particle and field observations from Explorer 45 during the December 1971 magnetic storm period.

20 p2552 A73-38958

GX5-1 X ray source position determination from lunar occultation observations by Copernicus satellite, noting error bounds

20 p2605 A73-39014

Auroral arc mechanism of solar wind intrusion and electron and proton energization and precipitation in magnetosphere from Isis photometric and spectrometric observations

20 p2553 A73-39124

Spatial distribution of outgoing long wave radiation fluxes according to Cosmos-320 satellite data

20 p2555 A73-39188

Satellite detection of melting snow and ice by simultaneous visible and near-IR measurements.

20 p2556 A73-39840

Satellite measurements of microwave and infrared radiobrightness temperature of the earth's cover and clouds.

20 p2556 A73-39844

An experimental model for the automated detection, measurement, and quality control of low-level cloud motion vectors from geosynchronous satellite data.

20 p2533 A73-39853

Structure of dust storms from ITOS-1 T.V. images obtained over Iraq and the Gulf of Persia.

20 p2584 A73-39854

Water quality determinations in the Virgin Islands from ERTS-A data.

20 p2558 A73-39867

Interdisciplinary research on the application of ERTS-1 data to the regional land use planning process.

20 p2563 A73-39910

The usefulness of ERTS-1 and supporting aircraft data for monitoring plant development in rangeland environments.

20 p2563 A73-39911

Rainfall estimation from satellite visible and IR imagery, discussing calibration and accuracy requirements

21 p2730 A73-40093

Influence of a sudden compression of the magnetosphere on outer zone electron fluxes measured at arbitrary pitch-angle.

21 p2682 A73-40161

Beacon Explorer C satellite laser tracking for effects of lunar and solar tides on orbit, noting geogravitational field distortion

21 p2765 A73-40275

Certain parameters of cellular convection according to observations by meteorological earth satellites and from a high mast

21 p2731 A73-40492

Influence of the resolution of television cameras and radiometers on the accuracy of determining the quantity of clouds from satellites

21 p2731 A73-40493

Investigation of primary gamma radiation from the northern polar region of the Galaxy

21 p2756 A73-40578

Fluxes of electrons with energies greater than 10 MeV at heights from 200 to 500 km

21 p2758 A73-40603

Satellite counting of excess radiation measured as ionospheric electron and proton intensity dependent on geomagnetic activity, discussing proton energy spectra and electron albedo

21 p2758 A73-40604

The definition of the geotectonic domains of the Southern African crystalline shield by ERTS 1 imagery and its economic importance.

21 p2685 A73-40810

Earth surveys by remote sensing in Israel.

21 p2685 A73-40816

Post GARP Global Experiment programs, considering tropical vertical wind structure, satellite temperature measurement accuracy increase, data handling for real time and long term prediction

21 p2732 A73-40819

Comparison of Apollo and earth-based observations - Definition of surface units in Mare Serenitatis.

21 p2769 A73-40821

An attempt to explain satellite observations of high latitude VLF hiss in terms of generation by incoherent Cerenkov radiation.

21 p2685 A73-40828

Diurnal density variations measured by the San Marco III satellite in equatorial orbit.

21 p2685 A73-40830

Latitudinal distributions and composition of the radiation on nonclosed drift shells in the altitude range from 200 to 400 km

21 p2686 A73-40908

A study of geoeactive corpuscles and photoelectrons on the Cosmos 261 satellite. VI - Epithelial electrons in the energy range from 30 to 150 eV in the region of the dayside and nightside polar cusps

21 p2686 A73-40909

Extra-atmospheric photoelectric study of the brightness of the earth's atmosphere

21 p2686 A73-40912

Optical properties of the lower atmosphere of Venus /for interpreting measurements of the Venera 8 planetary probe/

21 p2686 A73-40913

Dependence of high-energy electron fluxes at an altitude of 200 to 300 km on threshold rigidity

21 p2686 A73-40917

The aurora oval in the region of influx of electrons into the earth's atmosphere

21 p2686 A73-40919

Penetration of solar cosmic rays into the earth's polar caps

21 p2760 A73-40920

Space research XIII; Proceedings of the Fifteenth Plenary Meeting, Madrid, Spain, May 10-24, 1972. Volumes 1 & 2.

21 p2687 A73-41325

Determination of equations of conditions between harmonics of resonance of the order of 14 starting with observations from the Eole satellite

21 p2781 A73-41327

The use of radio beacons in geophysics and their applications.

21 p2657 A73-41331

Remote sounding of water surface conditions from aboard artificial satellites.

21 p2657 A73-41333

Use of meteorological rocketsonde and satellite radiation data for constant-pressure analyses at levels between 5 and 0.4 mb.

21 p2732 A73-41336

Equatorial thermospheric composition and its variations.

21 p2688 A73-41347

Thermal positive ions in the dayside polar cusp measured on the ISIS 1 satellite.

21 p2690 A73-41368

Field aligned electron anisotropies observed by the ESRO 1 A /Aurora/ satellite.

21 p2691 A73-41370

The detection of 'intermediate' size magnetic anomalies in Cosmos 49 and OGO 2, 4, 6 data.

21 p2691 A73-41374

Observational comparison with a self-consistent model of the geomagnetic tail.

21 p2691 A73-41377

Energetic protons at low L-values of the equatorial magnetosphere.

21 p2761 A73-41379

Ariel 3 evidence of zones of VLF emission at medium invariant latitudes which co-rotate with the earth.

21 p2691 A73-41382

Solar corona observations in white light by OSO 7 and in XUV by Naval Research Laboratory, discussing contributions from other observatories and satellites

21 p2773 A73-41383

First results of the solar hard X-ray spectrometer on board the ESRO TD-1 A satellite.

21 p2761 A73-41386

Enhancements of the photoelectron-excited dayglow during solar flares.

21 p2761 A73-41389

Investigations of meteoritic matter in the vicinity of the earth and the moon from the orbiting station Salyut and the moon satellite Luna 19.

21 p2775 A73-41409

Helicentric Pioneers 8 and 9 hyperbolic cosmic dust data suggesting cosmic dust origin of previously solar effect generated noise

21 p2775 A73-41410

Observations of zodiacal light from the Pioneer 10 Asteroid-Jupiter probe - Preliminary results.

21 p2776 A73-41423

Observations of the highly variable X-ray source GX 339-4.

22 p2905 A73-41767

The combined use of satellite differential Doppler and ground-based measurements for ionospheric studies.

22 p2843 A73-41837

Mariner 5 observations of solar wind shock-like structures including density, velocity, and proton temperature increases, suggesting nonlinear magnetoacoustic waves under steepening process

22 p2901 A73-41902

Magnetotail plasma flow observation with Vela 4A oriented perpendicular to ecliptic plane, considering plasma sheet recovery relation to auroral electrojet poleward shift

22 p2844 A73-41907

An evaluation of experimental errors in electromagnetic wave measurements aboard satellites.

22 p2844 A73-41911

Electron concentrations calculated from the lower hybrid resonance noise band observed by Ogo 3.

22 p2901 A73-41912

Latitude and local time dependence of precipitated low-energy electrons at high latitudes.

22 p2901 A73-41914

Results of solar plasma electron observations on Mars-2 and Mars-3 spacecraft.

22 p2906 A73-41941

Midday recovery of HF absorption during PCA events relationship to satellite observation of solar proton latitudinal variations

22 p2846 A73-41943

Measurement of attenuation of 9.303 MHz waves from ISIS-II through the ionosphere.

22 p2825 A73-42193

Analysis of the results of the geometric satellite world network

22 p2849 A73-42589

Accuracy of the determination of satellite orbits

22 p2910 A73-42641

Sky region mobile barrier concept to predict satellite appearance for telescopic visual observation

22 p2910 A73-42642

A direct comparison of satellite and aircraft infrared /10 to 12 microns/ remote measurements of surface temperature.

22 p2850 A73-42729

Measurements of the energy exchange between earth and space from satellites during the 1960's.

22 p2851 A73-42858

The abundances of galactic cosmic-ray carbon, nitrogen, and oxygen and their astrophysical implications.

22 p2914 A73-43012

Data reduction for annual, diurnal and satellite observation aberrations via rectangular coordinate method, discussing parallax, refraction, instrument eccentricity and computer applications

22 p2915 A73-43034

Simultaneous recording of solar cosmic-rays near Venus and the earth's magnetosphere.

23 p3020 A73-43251

Cosmos 321 geomagnetic measurement data for construction of satellite geomagnetic survey and geomagnetic field models

23 p2971 A73-43259

Russian book - Studies of the natural environment from manned orbital stations.

23 p2971 A73-43330

Spectrophotometric investigations of the earth from manned orbital stations

23 p2979 A73-43333

Venera 8 - Measurements of temperature, pressure and wind velocity on the illuminated side of Venus.

23 p3028 A73-43602

Venera 8 - Measurements of solar illumination through the atmosphere of Venus.

23 p3029 A73-43603

A magnetospheric field model incorporating the OGO 3 and 5 magnetic field observations.

23 p2972 A73-43693

Ionospheric sounding by ATS-3 emitted signal polarization measurement during partial solar eclipse of 10 July 1972, noting electron content decrease and diffusion rate

23 p2972 A73-43697

Use of space techniques for the determination and monitoring of climate parameters and air contaminants

23 p3003 A73-43780

Comet Kohoutek earth orbit properties and rocket and satellite observations, including parent molecule and inner solar system measurements

23 p3034 A73-44222

Provisional climatology of most probable wind for application to low latitude operational weather analysis and forecasting, based on ATS-3 observed low level winds

23 p3004 A73-44262

A comparison of radar-determined cloud height and reflected solar radiance measured from the geosynchronous satellite ATS-3.

23 p3005 A73-44269

On the variation with height of the top brightness of precipitating convective clouds.

23 p3005 A73-44270

Mariner 9 ultraviolet spectrometer experiment - 1971 Mars' dust storm.

24 p3127 A73-44396

Ultraviolet observations of Mars made by the Orbiting Astronomical Observatory.

24 p3128 A73-44397

Investigations of Mars from the Soviet automatic stations Mars 2 and 3.

24 p3128 A73-44431

Periodic variations in geostationary satellite polarisation observations.

24 p3082 A74-4735

Long-term X-ray observations of Scorpius X-1 by OSO-III.

24 p3138 A73-45045

Energy spectra of cosmic gamma-ray bursts.

24 p3125 A73-45053

Heos 1 plasma and magnetic field experiments during bow shock crossings for turbulent bow structure, discussing proton velocity distribution

24 p3125 A73-45111

Satellite measurement of magnetopause location, speed and thickness during satellite immersion within adjacent steep proton flux gradient

24 p3126 A73-45113

High-latitude proton precipitation and light ion density profiles during the magnetic storm initial phase.

24 p3126 A73-45114

Simultaneous observations of auroras from the South Pole Station and of precipitating electrons by Isis 1.

24 p3126 A73-45115

Distribution of atomic oxygen in the upper atmosphere deduced from Ogo 6 airglow observations.

24 p3086 A73-45121

Bow shock position from OGO-5, Explorer 35 and Heos satellites observation, emphasizing shock in tail for low Mach numbers

24 p3086 A73-45136

Triaxial magnetic measurements of field-aligned currents at 800 kilometers in the auroral region - Initial results.

24 p3087 A73-45140

ESRO I/Aurorae/ satellite observations of aurora, magnetosphere-ionosphere interaction at high latitudes and auroral particle flux density

24 p3087 A73-45207

ISIS 2 scanning photometric analysis of E and F region airglow at O I 5577 A, noting height difference of airglow components at midlatitudes and near equator

24 p3088 A73-45214

SATELLITE ORBIT CALCULATION

U ORBIT CALCULATION

SATELLITE ORBITS

NT POLAR ORBITS

NT STATIONARY ORBITS

NT TWENTY-FOUR HOUR ORBITS

Stable longitudes for 12-hr eccentric orbit satellites.

01 p0095 A73-10104

Polar motion from laser tracking of artificial satellites.

01 p0039 A73-10406

Three station interferometric observation of TAC-SAT synchronous communications satellite radio signals for orbit determination, discussing method feasibility for tracking and geodesy applications

01 p0097 A73-10407

Satellite orbit inclination function computation as representative problem in symbolic programming applied to celestial mechanics

01 p0099 A73-10688

Planetary orbits numerical relationships applied to artificial satellite orbits for earth gravity studies, expressing gravitational potential as latitude dependent spherical harmonics series

01 p0040 A73-10875

Some considerations on utilization control of the near earth space in future.

01 p0074 A73-11125

Orbit determination for the scientific satellite in Japan.

01 p0105 A73-11186

Comparison of Kalman filter and stepwise methods for real time orbit determination.

01 p0105 A73-11187

Evolution of a satellite orbit under the influence of light pressure

02 p0211 A73-11777

Optimization of the apogee impulse during the positioning of a geostationary satellite. [ONERA, TP NO. 1218]

02 p0228 A73-11992

Processing of results of observations of the satellite 65-011-04 carried out within the framework of INT-EROS program 1966.

02 p0159 A73-12170

Analysis of the orbit of Cosmos 316 /1969-108 A/.

02 p0225 A73-12824

Lunar librations results of Koziel reevaluation, noting elasticity effects and elastic strain perturbation on satellite

03 p0367 A73-13077

Nearly-optimal single impulsive transfers between coplanar elliptical satellite orbits with identical pericenter altitude

03 p0372 A73-13299

Statistical data processing method for accuracy evaluation of satellite orbit parameters obtained from onboard measurements of two stars angular positions

03 p0379 A73-14554

Optimum elliptic orbit characteristics of planetary artificial satellite based on earth-planet-earth flight

03 p0379 A73-14572

A new method for calculating the preliminary orbit of an artificial satellite with the aid of simultaneous observations

03 p0379 A73-14579

Earth normal gravity field spherical harmonics in terms of Stokes constants from satellite orbit dynamics, comparing with Helmer system

03 p0305 A73-14613

Propagation of errors in orbits computed from density layer models.

04 p0438 A73-14790

Improvement of zonal harmonics by the use of observations of low-inclination satellites Dial, SAS, and Peole.

04 p0438 A73-14795

Gravity anomalies determination from satellite orbit perturbations, using least squares method

04 p0439 A73-14799

Satellite orbits allocation by international conventions to prevent interference with existing vehicles,

noting international cooperation in communication frequencies allocation

04 p0524 A73-15157

A state covariance matrix computation algorithm for satellite orbit determination sequential filtering.

04 p0431 A73-15267

Satellite motion in the equatorial plane of an oblate primary body and apsidal line shift evaluation.

04 p0498 A73-15296

Ocean color measurements utilizing a noon orbit for earth resources satellite applications.

04 p0445 A73-15776

Secular inequalities in the motion of earth satellites.

04 p0503 A73-16020

Subsatellite point coordinates calculation for artificial earth satellites with nearly circular orbits, noting ephemeris application

05 p0613 A73-16203

Analysis of the effect of errors in determining the orbit parameters of a satellite on the accuracy of prediction of its motion

05 p0614 A73-16312

Equations of motion for precession theory of two rotor gyroscopes on earth satellites for orbit plane determination, noting noise spectrum transformation

05 p0628 A73-16407

Satellite motion near the equatorial plane of a slowly rotating planet

05 p0617 A73-16468

Calculus of variations for equations of relative motion of two satellites with unperturbed Kepler orbits of arbitrary eccentricity

05 p0620 A73-17006

Orbit determination by range-only data.

08 p0103 A73-21816

Launch and orbital injection of Intelsat IV satellites.

09 p1152 A73-22699

Satellite resonance with longitude-dependent gravity. III - Inclination changes for close satellites.

09 p1154 A73-22837

Lunar and solar perturbation effects on communication satellite orbits, considering Kozai luni-solar theories

09 p1149 A73-22913

Exact analytical solutions for orbits of bodies with atmospheric drag.

09 p1152 A73-23454

Predicting network for artificial satellite tracking data acquisition and preprocessing and orbit parameters computation

10 p1187 A73-23622

Upper atmosphere analytical density model for satellite motion prediction, allowing for diurnal and semiannual density variations and solar activity and geomagnetic disturbances effects

10 p1211 A73-23883

Configuration control of dual satellite systems in earth orbit, obtaining equations of motion, deployment paths and force functions

10 p1276 A73-24008

Determination of the coordinates of points in a cosmic geodetic grid by the orbital method

10 p1281 A73-24481

Relative motion of near orbiting satellites.

10 p1283 A73-24662

Stability of planar oscillations of a satellite in an elliptic orbit.

10 p1287 A73-24663

Investigation of long-term periodic changes of the orbital elements of artificial earth satellites

10 p1283 A73-24699

Geopause satellite orbit, tracking, environment, gravity and station position properties and applications to earth and oceanographic dynamics studies

11 p1430 A73-25317

Precession, nutation and the choice of reference system for close earth satellite orbits.

11 p1423 A73-26067

On the determination of the long period tidal perturbations in the elements of artificial earth satellites.

11 p1423 A73-26074

An analytical iterative algorithm for the prediction of special satellite orbit points with the Brouwer orbit theory.

11 p1423 A73-26075

Earth satellites and the gravitational potential.

12 p1539 A73-27148

Least squares method for satellite motion parameters determination in orbital plane, using altimeter distance to planet surface measurements

12 p1543 A73-27627

Transcendental equations solution for satellite Kepler orbit determination from coordinates, velocity and time components, using Lambert-Euler relation

12 p1543 A73-27629

Artificial satellite orbit determination from range measurements, applying to orbits around earth and other planets

12 p1543 A73-27722

Determination of the circular orbit of an artificial earth satellite from optical observations at undetermined moments of time

12 p1547 A73-27867

Effect of some external factors on accuracy of observations of active satellites. 13 p1680 A73-28516

AEROS aeronomy satellite successfully completes acquisition phase. 13 p1689 A73-28783

Orbit selection for satellite missions, determining elements of sun-synchronous, recurrent, near-recurrent, polar, synchronous and stationary orbits 13 p1684 A73-29246

Radiation doses during a prolonged orbital space flight about the earth 14 p1721 A73-29867

Satellite oscillation in circular orbit plane, determining gravitational stability in minimum time with least fuel consumption 14 p1803 A73-29868

Motion of a satellite in the equatorial plane of a spheroid. 15 p1929 A73-31107

Basic theory for PROD, a program for computing the development of satellite orbits. 15 p1930 A73-31108

Intermediate orbit of an artificial earth satellite obtained by the averaging method - First order perturbations 15 p1936 A73-31644

Efficient utilization of orbit/frequency for satellite broadcasting. 16 p1979 A73-33401

Nomograms for determining horizontal coordinates of artificial earth satellites 16 p2063 A73-33662

Electron depletion in the wake of ionospheric spacecraft - A comparison between results from Langmuir probes and antennas. 17 p2159 A73-34783

Satellite operation mode coordination with space program mission, considering orbital position and velocity and time at ground station horizon 17 p2160 A73-34932

Key technological challenges of the Earth Resources Technology Satellite program. 17 p2161 A73-34943

Zonal gravity harmonics from long satellite arcs by a seminumeric method. 17 p2233 A73-35269

Quasi-periodic orbits about the translunar libration point. 18 p2352 A73-36420

Orbital design strategy for domestic communication satellite systems. 20 p2527 A73-38761

Upper atmosphere analytical density model for satellite motion prediction, allowing for diurnal and semiannual density variations and solar activity and geomagnetic disturbances effects 20 p2550 A73-38902

Determination of a circular orbit for an earth satellite from optical observations at unknown times. 20 p2608 A73-39241

Experiments to determine satellite orbit geometry in spherically symmetric gravitational field, discussing aging asymmetry in clock paradox 21 p2739 A73-40623

Secular perturbations of the motion of artificial satellites, caused by atmospheric drag 21 p2768 A73-40725

A study of planar deployment control and libration damping of a tethered orbiting interferometer satellite. 21 p2781 A73-40900

Russian book - Accuracy of comet and satellite orbits. 22 p2910 A73-42640

Accuracy of the determination of satellite orbits 22 p2910 A73-42641

Russian book - Studies of spacecraft flight dynamics. 23 p3027 A73-43260

Utilization of tangential trajectories for lowering high-altitude elliptic orbits of artificial satellites of planets 23 p3027 A73-43265

Evaluation of the accuracy of predicting the motion parameters of low-orbit artificial earth satellites 23 p3027 A73-43266

Prediction of satellite motion by a combined method of recurrent relations 23 p3027 A73-43267

Determination of the orbital period of a satellite moving in the earth's gravitational field 23 p3027 A73-43268

Impulse application for optimal correction of angular position of orbital plane line of apsides, expressing axis angle of rotation as linear function 23 p3027 A73-43269

Orbit osculation control algorithm guaranteeing satellite repeated passage over given point of earth surface, deriving functional for satellite thrust control 23 p3027 A73-43271

The global solution of the problem of the critical inclination. 23 p3031 A73-43836

Some useful results on initial node locations for near-equatorial circular satellite orbits. 23 p3031 A73-43837

Gravitational perturbations of equatorial orbits. 23 p3032 A73-43839

Orbit improvement from satellite imaging data obtainable from outer planet missions. 23 p3032 A73-43840

Quadrature solution for the general relativistic motion of a satellite or a planet. 24 p3142 A73-45291

Fast computation of high eccentricity orbits by the stroboscopic method. 24 p3142 A73-45292

SATELLITE ORIENTATION

Normality condition derivation for algorithm of first order solution to ideal resonance problem, applying to critical inclination of oblate planet satellite 01 p0077 A73-10686

Radio sensors for the three-axis attitude fine measurement of geostationary communication satellites 02 p0228 A73-11822

Matrix transformations for spacecraft attitude determination. 02 p0228 A73-11905

Stability criteria for a free dual-spin satellite. 02 p0228 A73-12398

Nonoriented astronomical satellite attitude determination from onboard measurements of geomagnetic field and stellar luminosity 03 p0379 A73-14560

Dynamics of three-axis spacecraft orientation 05 p0628 A73-16405

The attitude measuring system of the AEROS satellite. 05 p0629 A73-16849

Influence of eddy currents on the rotation and orientation of an asymmetric artificial earth's satellite 08 p1014 A73-21547

Attitude control of the AEROS aeronomy satellite during the acquisition phase. 08 p1014 A73-21660

Star sensor/mapper for the Small Astronomy Satellites. 08 p0970 A73-21733

Satellite orientation relative to force center, considering condition for maximum lock strength of resonance rotation 09 p1149 A73-22912

Precision and economy estimates for manual control of spacecraft orientation 10 p1286 A73-23893

Some limiting parameters of an optoelectronic device for determining the orientation of a spacecraft with respect to the sun 14 p1803 A73-29872

Choice of a zero approximation of the angular position of a satellite on a trajectory segment of oriented motion in the case of a dipolar approximation of the geomagnetic field 15 p1942 A73-31237

The problem of choosing a zero approximation of the angular position of an oriented satellite in the case of a nondipolar approximation of the geomagnetic field 15 p1942 A73-31238

Zero order approximation for attitude angle of stabilized satellite at high orbits under solar pressure perturbation, using trigonometric polynomials based on magnetometer data 15 p1943 A73-31241

Determination of the attitude and angular velocities at the end of a phase of active change in angular velocity 15 p1943 A73-31242

Existence of stable relative equilibria of an artificial satellite in a model magnetic field 15 p1872 A73-31956

Digital attitude reference system for three-axis-stabilized earth oriented satellites, using gyrocompasses with solar and horizon sensors 17 p2209 A73-34875

The precession of unsymmetric spin-stabilized satellites. 18 p2361 A73-36878

Techniques for flat-spin recovery of spinning satellites. [AIAA PAPER 73-859] 20 p2614 A73-38797

Development and test of a double gimbalbed momentum wheel stabilization system for communication satellites. [AIAA PAPER 73-906] 20 p2614 A73-38840

Evaluation of precision and economy of systems of manual spacecraft orientation. 20 p2614 A73-38912

Problems of the aerodynamics of satellites with uniaxial orientation 21 p2781 A73-40902

Existence of stable relative equilibria for an artificial satellite in a model magnetic field. 24 p3081 A73-44481

SATELLITE PERTURBATION

Earth satellites in resonance with the moon and the sun as objects of laser ranging - Analytical solution for their motion. 01 p0099 A73-10695

Evolution of a satellite orbit under the influence of light pressure 02 p0211 A73-11777

Synchronous satellite ground track drift analysis for ecological survey application, discussing zonal, tesseral and sectorial harmonics and perturbation compensation 03 p0370 A73-13150

About the motion of a heavy flexible string attached to the satellite in the central field of attraction. 03 p0376 A73-14267

Geostationary artificial satellite orbital parameters calculation, taking into account lunar, solar and light pressure perturbations 03 p0378 A73-14551

Rarefied gas interaction with spacecraft surface, calculating aerodynamic forces and accommodation coefficient for Proton 2 satellite 03 p0383 A73-14574

Geos-C mini arc orbit determination from radar altimeter observations under perturbations from gravitational anomalies 04 p0437 A73-14784

Lunar gravity model obtained by using spherical harmonics with mascon terms. 04 p0495 A73-14811

Comparison of theory with experiment for electron density distribution in the near wake of an ionospheric satellite. 04 p0444 A73-15541

Secular inequalities in the motion of earth satellites. 04 p0503 A73-16020

Spin stabilization of a satellite 05 p0629 A73-16422

Satellite motion near the equatorial plane of a slowly rotating planet 05 p0617 A73-16468

Effects of resonant tesseral gravity coefficients on Viking-type orbits. [AIAA PAPER 73-146] 06 p0748 A73-17648

Evaluation of gravity anomalies directly from satellite observations. 07 p0813 A73-19025

Analytical theory of the motion of the fifth Jupiter satellite 07 p0876 A73-19395

Combined gravitational and solar radiation pressure effects on the semimajor axis of the earth's satellite. 08 p1010 A73-21314

Literary theory of the motion of a satellite in the tesseral-harmonic field of the earth's gravitational potential at small eccentricities 09 p1143 A73-22097

Linear perturbations of the coordinates of satellites in the normal gravitational field of the earth 09 p1143 A73-22099

Application of Gauss' method to the determination of secular radiational perturbations of artificial earth satellites 09 p1143 A73-22100

Satellite resonance with longitude-dependent gravity. III - Inclination changes for close satellites. 09 p1154 A73-22837

Lunar and solar perturbation effects on communication satellite orbits, considering Kozai luni-solar theories 09 p1149 A73-22913

Perturbed satellite motion differential equations, on basis of fixed center problem and perturbing forces with no force function 10 p1274 A73-23721

Perturbation function expansion in series of orbital elements for satellite motion in rotating oblate planet gravitational field with two fixed centers 10 p1282 A73-24493

Precession, nutation and the choice of reference system for close earth satellite orbits. 11 p1423 A73-26067

On the determination of the long period tidal perturbations in the elements of artificial earth satellites. 11 p1423 A73-26074

Small oscillations of gravity gradient satellite in circular near-equatorial orbit, discussing operational efficiency of magnetic damping systems 12 p1549 A73-27648

Stabilization of steady motions of mechanical systems with respect to some of the variables 13 p1660 A73-29076

Nonlinear two-dimensional oscillations of a satellite in an elliptic orbit 14 p1803 A73-29854

Motion of a satellite in the equatorial plane of a spheroid. 15 p1929 A73-31107

Effects of motion of the equatorial plane on the orbital elements of an earth satellite. 15 p1930 A73-31112

Two dimensional nonlinear oscillations around center of mass of vehicle moving along circular orbit

SATELLITE POWER TRANSMISSION [TO EARTH]

- with magnetic damping under gravitational field and external perturbation
15 p1942 A73-31233
- Application of methods of mathematical statistics to study the motion of an artificial earth satellite about its center of mass
15 p1931 A73-31234
- Asymmetrical spun satellite rotation prediction in circular orbit at 700 km in terms of perturbing moment vector function
15 p1931 A73-31235
- Zero order approximation for attitude angle of a stabilized satellite at high orbits under solar pressure perturbation, using trigonometric polynomials based on magnetometer data
15 p1943 A73-31241
- Intermediate orbit of an artificial earth satellite obtained by the averaging method - First order perturbations
15 p1936 A73-31644
- Damping of gravity stabilized satellite small rotary oscillations in circular orbit via stepwise change of moment of inertia
16 p2072 A73-33232
- Differential transformation for satellite injection.
16 p2070 A73-33999
- Stable tumbling motions of a dual-spin satellite subject to gravitational torques.
17 p2237 A73-34177
- Approximate description of the evolution of a synchronous-satellite orbit
18 p2350 A73-36101
- Perturbed satellite motion differential equations derivation on basis of fixed center problem and perturbing forces with no force function, obtaining intermediate orbital elements
18 p2355 A73-36746
- Canonical elements of the translational-rotational motion of a planet satellite
19 p2476 A73-37199
- On stabilization of steady-state motions of mechanical systems with respect to a part of the variables.
19 p2459 A73-37631
- Beacon Explorer C satellite laser tracking for effects of lunar and solar tides on orbit, noting geogravitational field distortion
21 p2765 A73-40275
- Secular perturbations of the motion of artificial satellites, caused by atmospheric drag
21 p2768 A73-40275
- Solar pressure induced librations of spinning axisymmetric satellites.
22 p2910 A73-42633
- Orbit osculation control algorithm guaranteeing satellite repeated passage over given point of earth surface, deriving functional for satellite thrust control
23 p3027 A73-43271
- Some useful results on initial node locations for near-equatorial circular satellite orbits.
23 p3031 A73-43837
- Secular perturbations of third order with respect to oblateness from all zonal harmonics of the gravitational potential of a planet
23 p3037 A73-44253
- Satellite intermediate orbit and secular perturbations due to second zonal harmonics of planetary potential and outer body attraction
23 p3037 A73-44254
- Fast computation of high eccentricity orbits by the stroboscopic method.
24 p3142 A73-45292
- Canonical elements based on polar coordinates in Kustaanheimo-Stiefel space and applications to satellite motion perturbation from oblate bodies
24 p3111 A73-45293
- SATELLITE POWER TRANSMISSION [TO EARTH]**
Feasibility analysis of satellite solar/thermal power generation and transmission to earth, describing Brayton cycle heat engine for initial energy conversion
19 p2391 A73-38404
- SATELLITE RENDEZVOUS**
U ORBITAL RENDEZVOUS
SATELLITE ROTATION
Effects of gravity-gradient torque on the rotational motion of a triaxial satellite in a precessing elliptic orbit.
01 p0099 A73-10685
- Instability of rotation about a centroidal axis of maximum moment of inertia.
01 p0077 A73-10743
- Experimental satellite for attitude control. II - Numerical analysis and a test of a yo-yo de-spinner.
01 p0111 A73-11190
- Communications satellite Symphonie stability during perigee-apogee transfer in terms of liquid filled spinning top nutation
03 p0381 A73-13295
- Equilibrium motions of rigid spinning satellite in circular orbit around central body subject to gravitational torque
03 p0376 A73-14268
- Certain states of rotation of a magnetized spin-stabilized satellite in the geomagnetic field
05 p0627 A73-16291

- The motion and stability of a dual-spin satellite during the momentum wheel spin-up maneuver.
[AIAA PAPER 73-142] 05 p0629 A73-16891
- Spinning satellite with partially filled viscous ring damper, solving equations of motion for nutation-synchronous and spin-synchronous modes
[AIAA PAPER 73-143] 05 p0629 A73-16892
- Analytical design of optimal nutation dampers.
05 p0630 A73-17206
- Influence of eddy currents on the rotation and orientation of an asymmetric artificial earth's satellite
08 p1014 A73-21547
- Satellite orientation relative to force center, considering condition for maximum lock strength of resonance rotation
09 p1149 A73-22912
- The effect of aerodynamic moments on the rotational motion of Proton satellites
12 p1548 A73-26820
- Russian book - Mechanics of controlled motion and problems of cosmic dynamics.
15 p1930 A73-31226
- Asymmetrical spun satellite rotation prediction in circular orbit at 700 km in terms of perturbing moment vector function
15 p1931 A73-31235
- Optimal damping and stochastic control in certain problems of astrodynamics
15 p1931 A73-31236
- Determination of the attitude and angular velocities at the end of a phase of active change in angular velocity
15 p1943 A73-31242
- Satellite rotation period determination from visual photometric observations reduction, noting solar and geomagnetic activity effects
15 p1843 A73-31649
- Damping of gravity stabilized satellite small rotary oscillations in circular orbit via stepwise change of moment of inertia
16 p2072 A73-33232
- Artificial earth satellite brightness attenuation and rotation periods from spectral analyses of photometric curves by mathematical simulation
18 p2315 A73-36142
- Satellite vibration-rotation motions studied via canonical transformations.
18 p2352 A73-36422
- Attitude stability conditions of multiple spin satellites.
18 p2361 A73-36877
- Dynamic passivation of a spinning and tumbling satellite using free-flying teleoperators.
19 p2490 A73-37306
- Inertial force field patterns due to nutational motion of spinning satellites.
19 p2492 A73-37709
- Oscillations of a spinning satellite due to small deflections of its dipole antennae.
21 p2780 A73-40089
- Mathematical model for ISIS satellite attitude and spin rate computerized predictions during electromagnetic torque control operation
21 p2781 A73-40615
- Attitude stability conditions of multiple spin satellites.
22 p2916 A73-42189
- The precession of unsymmetric spin-stabilized satellites.
22 p2916 A73-42190
- Solar pressure induced librations of spinning axisymmetric satellites.
22 p2910 A73-42633
- SATELLITE SOLAR ENERGY CONVERSION**
Electric power generation on earth via satellite solar power station, assessing technologies of energy collection and conversion, microwave transmission and rectification
17 p2110 A73-35313
- Electromagnetic interference caused by a solar array.
18 p2269 A73-36958
- Feasibility analysis of satellite solar/thermal power generation and transmission to earth, describing Brayton cycle heat engine for initial energy conversion
19 p2391 A73-38404
- A method of providing rain margins for 18/30 GHz communications satellites without increasing the solar power requirement.
20 p2524 A73-38731
- SATELLITE SOLAR POWER STATIONS**
Electric power generation on earth via satellite solar power station, assessing technologies of energy collection and conversion, microwave transmission and rectification
17 p2110 A73-35313
- Feasibility analysis of satellite solar/thermal power generation and transmission to earth, describing Brayton cycle heat engine for initial energy conversion
19 p2391 A73-38404
- Feasibility of satellite solar power station technology concepts, discussing cost analysis, energy conversion efficiency, weight, space environment and microwave transmission
20 p2510 A73-39247

SATELLITE TELEVISION

- Optimization study of the satellite broadcasting system for television.
01 p0018 A73-11180
- Required carrier-to-interference ratios for frequency sharing between frequency-modulation television signal and amplitude-modulation vestigial sideband television signal.
01 p0018 A73-11181
- TV satellite system feasibility and design study for Germany, discussing technical and economic aspects
[DGLR PAPER 72-051] 02 p0140 A73-11664
- Feasibility study for direct TV transmission and reception via satellite, discussing technical and economic aspects
[DGLR PAPER 72-050] 02 p0140 A73-11679
- Satellite educational TV systems for underdeveloped countries, discussing installation problems, capital investments requirements and potential benefits
03 p0401 A73-14173
- Some international legal issues on the direct television broadcast satellites.
04 p0523 A73-15149
- Real time programmable data compression system with minicomputers for operation between TV data acquisition ground stations and ATS satellites
04 p0425 A73-15442
- A DPCM codec using edge coding and line replacement.
04 p0422 A73-15443
- Communications technology satellite /CTS/ with transponder and TWT operating into steerable antenna, discussing experiments on TV broadcast, data transmission, FM and transportable terminals
04 p0422 A73-15446
- Surface winds from sun-glitter measurements from a spacecraft.
04 p0474 A73-15777
- ERTS two-inch RBV cameras performance characteristics.
05 p0579 A73-17144
- Mariner 9 television observations of Phobos and Deimos.
06 p0745 A73-17480
- Canadian Anik I synchronous domestic communication satellite for color TV broadcasting or telephony, considering northerners reaction and community beneficiaries
06 p0668 A73-18432
- Satellite-borne TV vidicon design requirements and operational specifications, considering storage, relaxation, resolution, sensitivity, electrostatic focusing and deflection, image magnification and enhancement
07 p0821 A73-18982
- The experimental telecommunication satellite Project Symphonie.
07 p0905 A73-19140
- Scanning electron microscope and energy dispersive X-ray analysis of the surface features of Surveyor III television mirror.
07 p0872 A73-19899
- ERTs return beam vidicon TV cameras and ground based electron beam recording system resolution and distortion characteristics from preflight and in-flight simulation and calibration studies
09 p1082 A73-22385
- Canadian telecommunications satellite system for TV, voice and analog or digital data transmission, describing space segment, satellite control and ground station network
11 p1431 A73-26259
- Problems and possibilities related to transmissions by satellites covering large zones in Africa
11 p1454 A73-26274
- A transmission and receiving system for a direct broadcasting television satellite - Telecommunications, satellite, broadcasting, experimentation, microwaves
12 p1469 A73-27074
- Requirements regarding the position and the attitude of future application satellites
15 p1907 A73-31134
- Digital computer processing for automatic feature classification of ERTS-borne MSS and RBV imagery data, emphasizing interactive man-machine analysis for image enhancement
16 p1985 A73-33366
- German national geostationary TV satellite project, discussing thermal and attitude control, launch and guidance problems, solar power supply and antenna systems
16 p2074 A73-33737
- Ultraviolet proximity focussed converters for use in a satellite SEC-TV system.
17 p2170 A73-35296
- Canadian domestic satellite system applications.
17 p2124 A73-35311
- Regional and international communication satellite systems, discussing frequencies assignment, power supplies, three axis stabilization trends and military, navigation and TV developments
[DGLR PAPER 73-039] 17 p2125 A73-35478

Selection of a direct-transmission television satellite system from the point of view of stringent pointing requirements
[DGLR PAPER 73-047] 17 p2126 A73-35483

Communications systems of television-radio satellites
[DGLR PAPER 73-053] 17 p2126 A73-35487

Radio-TV satellite ground support systems, discussing frequency ranges, satellite orbit, transponder signal amplification and ground reception systems
[DGLR PAPER 73-055] 17 p2126 A73-35488

Computer processing and analysis of TV cloud photographs. 18 p2334 A73-37058

Indian national educational communications program for information dissemination on health, family planning, hygiene and agriculture, discussing satellite TV development project
[AAS PAPER 73-106] 20 p2629 A73-38576

Television sound subcarrier transmission in space communication. 20 p2524 A73-38737

Worldwide TV satellite systems, discussing transmission channels, power limitations, quality objectives, conversion and digital techniques. 20 p2530 A73-39204

Telesat Canada-Anik - Canada's domestic satellite communications system. 24 p3069 A73-45392

SATELLITE TEMPERATURE

A design study of thermal louver system. 01 p0111 A73-11152

Heat pipe and phase changing material (PCM) sounding rocket experiment.
[AIAA PAPER 73-759] 18 p2371 A73-36374

An insight into the features of the OAO-C thermal design.
[ASME PAPER 73-ENAS-4] 19 p2493 A73-37966

Development of a cryogenic heat pipe radiator for a detector cooling system.
[ASME PAPER 73-ENAS-47] 19 p2493 A73-37994

Measurement of the thermo-optical characteristics of satellite thermal control coatings. 22 p2929 A73-41872

SATELLITE TRACKING

Constant-envelope spread spectrum random access satellite communication system, discussing message and multiple access modem, signal acquisition, tracking, ranging, etc. 01 p0018 A73-11178

Orbit determination for the scientific satellite in Japan. 01 p0105 A73-11186

A semiautomatic tracking device for satellites. 02 p0190 A73-12013

Ionospheric and ionospheric refraction errors in satellite tracking over the Indian sub-continent. 02 p0141 A73-12299

Photographic satellite tracking instrument technology and data reduction methods, describing various camera types and for photogrammetric and astrometric position determination. 03 p0274 A73-13252

Artificial earth satellites photographic position determination, discussing instrumental and procedural technologies. 03 p0274 A73-13255

Tropospheric refraction effects on satellite range measurements. 04 p0415 A73-14750

Singularity solutions to critical configurations of geodetic range networks with distributed and in plane ground stations and target satellites. 04 p0436 A73-14777

Geometric accuracy obtainable from simultaneous range measurements to satellites. 04 p0436 A73-14778

Absolute topocentric directions and geograv coordinate system for satellite triangulation, using photographs against star background from different camera sites. 04 p0436 A73-14779

Secor equatorial network evaluation of satellite geodesy program, discussing range data and geocentric coordinate computation and adjustments. 04 p0437 A73-14782

Secor range observations on Geos 1 satellite in Pacific tracking network, determining station coordinates, relative positions and geodetic heights. 04 p0437 A73-14783

Earth gravitational field representation via potential of simple layer in satellite geodesy applied to satellite optical observations and Doppler data. 04 p0438 A73-14789

Refinement of the gravity field by satellite-to-satellite Doppler tracking. 04 p0438 A73-14793

Orbital elements and geopotential coefficients estimation with increased accuracy by satellite-satellite tracking. 04 p0438 A73-14794

Geopotential coefficient error model using Geos 2 tracking data and SAO 1969 standard earth. 04 p0439 A73-14797

Atmospheric correction for the troposphere and stratosphere in radio ranging of satellites. 04 p0439 A73-14808

Geometric properties and basic errors of rotating support devices of the gimbal suspension type. 04 p0447 A73-14848

Method and equipment for localizing satellites by laser range and direction finding.
[ONERA, TP NO. 1149] 04 p0417 A73-15096

An empirically derived lunar gravity field. 04 p0498 A73-15184

Spin and three-axis stabilized geosynchronous tracking and data relay satellite system for telecommunication service to user spacecraft in low earth orbit. 04 p0420 A73-15422

The potential application of space technology to the radio tracking and biotelemetry of unrestrained animals. 05 p0545 A73-17134

Calculation of the satellite tracking accuracy for ground stations with medium-diameter parabolic antennas. 07 p0791 A73-19373

A new VHF-interferometer with three steerable high-gain-antennas for satellite-tracking. 09 p070 A73-23434

Predicting network for artificial satellite tracking data acquisition and preprocessing and orbit parameters computation. 10 p1187 A73-23622

The concentric double spherical reflector as an antenna for simple scanning over a limited angular range. 10 p1187 A73-23739

Electromagnetic window for a trajectory radar. 11 p1327 A73-25280

Geopause satellite orbit, tracking, environment, gravity and station position properties and applications to earth and oceanographic dynamics studies. 11 p1430 A73-25317

Integral equation numerical solution by minimum mean-squared estimator for atmospheric electromagnetic refractivity profile from satellite radio tracking data, noting iterative procedure convergence. 11 p1330 A73-25686

Measuring the positions of satellites with the aid of laser pulses. 13 p1582 A73-28149

ATS-F and Nimbus-E satellites use for range and range rate determination, earth gravity anomaly detection and orbital position determination. 13 p1656 A73-28391

Earth rotation axis motion determination through satellite tracking via laser range observation, estimating orbit computation error sources. 13 p1656 A73-28392

Pole position studied with artificial earth satellites. 13 p1656 A73-28393

Baseline arrangement of radio interferometer array for tracking artificial satellites. 13 p1586 A73-29233

Methods of evaluation of tracking procedures used at the French Guiana Space Center. 14 p1727 A73-30093

Satellite tracking interferometer systems with three steerable directional antennas mounted over azimuth mounts near Lichtenau /German Federal Republic/. 14 p1742 A73-30100

Eole meteorological balloon sounding experiment in Southern Hemisphere, discussing mean circulation, eddy diffusion and data collection and satellite tracking system. 15 p1904 A73-31723

Synchronous communication satellite crosslink antenna design and tracking and acquisition procedures for Ka band frequencies, describing reflectors, paraboloids, and five horn feed system. 16 p1977 A73-32721

FAA air traffic control systems projected improvements, including microwave landing system, aeronautical satellites, electronic voice switching and discrete address radar beacon. 16 p2087 A73-33179

Faraday rotation based total ionospheric electron content information for correction of near real time satellite position determination errors, using spherically stratified ionospheric model. 16 p2035 A73-33414

Detection probability of laser radars for satellite ranging. 18 p2290 A73-36882

Radio interferometer for the range from 136 to 138 MHz in the central German ground station. 19 p2432 A73-38273

Space research XIII; Proceedings of the Fifteenth Plenary Meeting, Madrid, Spain, May 10-24, 1972. Volumes 1 & 2. 21 p2687 A73-41325

Accuracy of photographic artificial earth satellite observations at the observational station in Riga. 22 p2910 A73-42644

Mare Humorum mascon anomaly characteristics from gravity measurements obtained by Doppler tracking of Apollo 15 subsatellite. 23 p3030 A73-43759

Satellite laser ranging instruments operated at Tokyo Astronomical Observatory. 24 p3068 A73-44998

SATELLITE TRACKING AND DATA ACQUISITION NETWORK

U STADAN [SATELLITE TRACKING NETWORK]
SATELLITE TRANSMISSION

Application of random time and frequency multiplexing to a data collection satellite. 01 p0018 A73-11182

Beyond the horizon ionospheric propagation experiment from an equatorial orbiting satellite to a middle latitude station. 03 p0274 A73-12892

Multifrequency radio beacon on polar orbiting satellite for wideband transmission through ionosphere without significant signal distortion. 03 p0275 A73-13627

A technique for synoptic measurement of ionospheric propagation delays by ranging from geostationary satellites to a network of unmanned transponders. 03 p0308 A73-13629

Satellite transmitted impulse response transfer function evaluation by ray tracing technique for ionospheric model with Chapman ionization vertical profile. 03 p0299 A73-13630

On investigation of the electron concentration and inhomogeneous structure of the outer ionosphere by means of coherent radiowaves emitted from artificial earth satellites. 03 p0299 A73-13631

Traveling ionospheric disturbance analysis based on quasi-periodic perturbations in satellite transmitted VHF signal Faraday rotation, obtaining wave-like variations in electron content. 03 p0300 A73-13634

ATS-F satellite borne radio beacon transmitter experiment for obtaining ionospheric electron content, discussing design, in-orbit performance, calibration information dissemination and propagation measurement. 03 p0275 A73-13639

A simple apparatus for signal reception of transit system satellites and principal results. 03 p0308 A73-13649

The influence of atmospheric layer structure on space - Earth links. 03 p0275 A73-13653

Wavelike structure of magnetic field-aligned irregularities detected by phase interferometry. 03 p0300 A73-13696

Noise temperature and signal characteristics of parametric microwave superheterodyne receiver with downconverter for satellite communication, radio and TV transmission. 03 p0277 A73-13986

The role of solar cell technology in the satellite solar power station. 03 p0258 A73-14252

Current and near future data transmission via satellites of the Intelsat network. 03 p0280 A73-14659

Satellite digital communications over domestic and international networks for data, voice and video signal transmission. 04 p0415 A73-14739

A digital echo suppressor for satellite circuits. 04 p0416 A73-14995

Juridical problems connected with European network of telecommunication satellites, discussing satellite direct transmission. 04 p0497 A73-15146

Results of the World Conference of Space Telecommunications, Geneva, 1971. 04 p0523 A73-15150

The ERTS wideband image communication system. 04 p0418 A73-15382

ATS-F COMSAT millimeter wave propagation experiment. 04 p0418 A73-15386

Information transfer satellite system /ITSS/ design for earth resource and meteorological data collection and relay from remote sensing platforms. 04 p0419 A73-15404

Effects of hardlimiting on bandlimited transmissions with conventional and offset QPSK modulation. 04 p0420 A73-15412

Time division multiple access for tactical trunking via satellite. 04 p0420 A73-15424

Environmental data transmission from arctic data buoys via polar orbiting satellite. 04 p0421 A73-15431

A method for reproducing pictures transmitted by meteorological satellites. 04 p0449 A73-15452

Error analysis of ionospheric parameter measurement by satellite transmitted or reflected multiple frequency pulsed radiation signal, using perturbation method. 05 p0547 A73-16051

SATELLITE-BORNE INSTRUMENTS

Mariner 9 Martian surface mapping, describing science instrumentation, orbit characteristics, mapping cycles sequence design and data telecommunications [AIAA PAPER 73-204] 05 p0630 A73-16938

A theoretical and experimental study of non-ducted VLF waves after propagation through the magnetosphere. 05 p0551 A73-17054

The effect of a bandpass nonlinearity on signal detectability. 06 p0664 A73-17713

Satellite solar power station for solar energy conversion and transmission to earth via microwave beam, discussing technology status and weight and cost projections 06 p0750 A73-18027

Satellite S-band telemetry evanescent mode waveguide diplexer design with foreshortened band-pass filters to eliminate I junction and connecting flanges 06 p0678 A73-18741

Satellite data concentration, memorization, transmission and processing, discussing central computer control unit, ground stations peripheral links, magnetic tapes and system reliability 07 p0795 A73-18952

Third generation satellite PCM telemetry data processing with computer control for optimization and supervision, discussing system reliability, automatic control and diagnostic routine 07 p0795 A73-18954

Path diversity for mm-wave earth-to-satellite links. [AD-757967] 07 p0791 A73-19376

TDMA satellite telephonic communication network with preassigned channelled radio carrier, describing four phase demodulator and channel units regrouping 09 p1050 A73-22320

Satellite solar power station systems engineering study, examining basic concept technical and economic feasibility 09 p1154 A73-22814

High data rate hard decision digital IC sequential decoder for earth-orbiting satellite space missions, discussing computational efficiency of modified Fano algorithm 09 p1056 A73-23398

Clock synchronization experiments performed via the ATS-1 and ATS-3 satellites. 10 p1217 A73-23996

Measurement of the integral parameters of the nighttime ionosphere from observations of Intercomos-2 signals 10 p1212 A73-24238

Satellite electric power station for conversion of solar energy to microwaves beamed to earth, discussing structural design, flight control, transportation and technology assessment 10 p1178 A73-24554

ESRO TD-1A satellite signal hibernation in sky-scanning experiments after successful performance during first orbital life, noting tape recorder failure 11 p1431 A73-25750

Project management and installation of the Arvi satellite communication earth station. 11 p1344 A73-26147

Real time quantitative display for visible and IR scanning radiometer in ITOS-D satellite-borne automatic picture transmission system with stations access to computers 12 p1520 A73-26811

The disc antenna - A possible L-band aircraft antenna. 12 p1471 A73-27655

A radiating element giving circularly polarised radiation over a large solid angle. 12 p1471 A73-27656

A planning study for a multi-purpose communications satellite serving northern Canada. 12 p1471 A73-27657

The provision of ground station facilities for an aeronautical satellite system. 12 p1471 A73-27658

Factors affecting the frequency chosen for aircraft to satellite communications. 12 p1472 A73-27667

Message organisation in the ground segment of an aeronautical satellite system. 12 p1472 A73-27668

Transmission characteristics of PSK wave in non-linear system - Application to INTELSAT IV satellite systems. 13 p1586 A73-29234

European geostationary communication satellite system for telephone and TV transmission, discussing stabilization, command and power subsystems, modulation methods, power budgets, satellite configurations, etc 14 p1728 A73-30431

Total electron content of the equatorial ionosphere. 15 p1865 A73-31063

Dispersion of electromagnetic waves on a weak isolated inhomogeneity. 15 p1843 A73-31522

Scintillations of satellite signals and their observation. 15 p1843 A73-31524

Efficient utilization of orbit/frequency for satellite broadcasting. 16 p1979 A73-33401

Helical antenna for satellite transmission. 16 p1980 A73-33686

The R.S.R.S. ground stations for receiving 11.6 GHz transmission from the SIRIO satellite. 16 p1982 A73-33717

Italian SIRIO satellite cross polarization signal measurements aided by ground station antenna system using narrow bandwidth 16 p1983 A73-33725

Some results obtained in ESRO satellite data compression. 17 p2239 A73-34955

Evolution of the satellite telemetry data processing facility at the Goddard Space Flight Center. 17 p2123 A73-35300

Time division multiple access in the INTELSAT system. 17 p2124 A73-35306

Television satellite transmission systems capabilities and technology, discussing Communications Technology Satellite [DGLR PAPER 73-040] 17 p2125 A73-35479

Communications system of the Symbionie satellite and special transmission parameters [DGLR PAPER 73-056] 17 p2126 A73-35489

Ionospheric electron content and its horizontal gradients at high and middle latitudes from radiowave propagation from satellites. 18 p2304 A73-35972

Soviet communications satellite systems 18 p2289 A73-36400

Raindrops in satellite communications. 18 p2289 A73-36515

Measurement of the attenuation of 9.303 MHz waves from ISIS-II through the ionosphere. 18 p2289 A73-36876

A limited steerable dual reflector antenna. 18 p2293 A73-36881

Technological trends in commercial satellite communications. 18 p2290 A73-37034

Data compression techniques as a means of reducing the storage requirements for satellite data - A quantitative comparison. 19 p2405 A73-38196

Measurements of artificial satellite signal Doppler spectrum. 19 p2407 A73-38351

The Satellite Nuclear Power Station - An option for future power generation. 19 p2455 A73-38412

Communication satellites future use in Europe, considering mission requirements, data transmission, specialized TV distribution, cost effectiveness and shuttle/tug launch system [AAS PAPER 73-148] 20 p2521 A73-38596

Design features of an unattended earth terminal for satellite communications. 20 p2522 A73-38716

Small ship antennas for fleet satellite communications. 20 p2523 A73-38727

Adaptive ground implemented phased arrays. 20 p2523 A73-38729

A satellite-switched SDMA/TDMA system for a wideband multibeam satellite. 20 p2524 A73-38730

Multiple-beam satellite repeater tradeoffs applied to a multifunctional system. 20 p2524 A73-38732

GOES system data collection performance estimates. 20 p2525 A73-38743

Multipath channel characterization for Aerosat. 20 p2526 A73-38755

Excitation of the earth-ionosphere waveguide by point dipoles at satellite heights. 20 p2528 A73-38846

Some results and accuracy of satellite measurements of the electron content in the ionosphere 20 p2528 A73-39166

Worldwide TV satellite systems, discussing transmission channels, power limitations, quality objectives, conversion and digital techniques 20 p2530 A73-39204

Calculation of structurally compressed satellite radio lines 20 p2531 A73-39469

The total electron content of the ionosphere and its horizontal gradients, measured on the basis of recordings of satellite signals at scattered points 21 p2686 A73-40910

Seasonal variation of atmospheric composition in the F region as a function of solar activity. 21 p2690 A73-41360

ATS-1 borne Random Access Discrete Address System for multiple access satellite communication, discussing repeater performance concerning CW

signal transmission efficiency, intermodulation and SNR 22 p2825 A73-42187

SATELLITE-BORNE INSTRUMENTS

Monograph - Satellite-borne instrument for the measurement of soft solar X-rays. 01 p0045 A73-10150

A method for calculating atmospheric thicknesses directly from satellite radiation measurements. 01 p0073 A73-10378

Global nitric oxide and gamma emission measurement with Ebert-Fastie scanning spectrometer on-board polar orbiting OGO 4 satellite 01 p0040 A73-10878

Apparatus PG-1 for the study of the radiation characteristics in the neighbourhood of the earth by satellite Intercomos 3. 01 p0051 A73-11021

Satellite-borne HF ionospheric noise meter receiver system with narrow band monolithic crystal filters, comparing with Ariel 3 01 p0026 A73-11175

Constant-envelope spread spectrum random access satellite communication system, discussing message and multiple access modem, signal acquisition, tracking, ranging, etc 01 p0018 A73-11178

Scientific payload of Aeros German aeronomy satellite for atmospheric upper layers investigation, discussing instruments operation and location and measurement technique [DGLR PAPER 72-069] 02 p0190 A73-11656

The plasma diagnostics experiments of the Aeros satellite [DGLR PAPER 72-070] 02 p0166 A73-11669

Weather satellite Meteosat operational features and objectives, describing instrumentation, communication, data acquisition and processing facilities [DGLR PAPER 72-082] 02 p0227 A73-11695

Ionospheric electron and ion temperature profile measurements with satellite- and rocket-borne probes, comparing merits and discrepancies 02 p0163 A73-12303

Ion concentration measurements in the earth's ionosphere at altitudes from 200 to 6000 km 02 p0164 A73-12462

Fabrication of a lightweight circular orbit passive radiative cooler. 03 p0329 A73-13010

Traveling wave tube for satellite applications. 03 p0281 A73-13174

ATS-F satellite borne radio beacon transmitter experiment for obtaining ionospheric electron content, discussing design, in-orbit performance, calibration information dissemination and propagation measurement 03 p0275 A73-13639

Radar and Nimbus 4 infrared measurements of the Oklahoma City tornados, 30 April 1970. 03 p0338 A73-14512

Geopotential /geoid/ representation with spherical harmonics sampling functions for satellite altimeter applications 04 p0438 A73-14792

Orbiting altimeter system feasibility for global scale geoidal mapping via satellite altimetry 04 p0439 A73-14803

Satellite borne Ku-band pulsed radar altimeter for altitude measurement above ocean surface, evaluating random and bias errors due to instrument, propagation and geometry 04 p0446 A73-14805

Earth geodetic mapping with rotating torsional gravity gradiometers onboard spin stabilized satellite in low polar orbit 04 p0446 A73-14806

High-data-rate, spacecraft tape recorders. 04 p0449 A73-15383

Investigations of high-energy charged particles and VLF radiation with the Interkosmos 3 satellite. 05 p0608 A73-16085

ESRO 1A satellite-borne Langmuir probe measurement for anisotropy in ionospheric thermal electron temperature relative to geomagnetic field 05 p0571 A73-17053

Observations of Vela XR-1 by the UCSD X-ray telescope on OSO-7. 05 p0627 A73-17390

Electron-proton spectrometer for the GEOS satellite. 06 p0692 A73-17826

Circuit design, manufacture and testing of static memory for D2 satellite computer, considering test equipment, quality control and fabrication 07 p0796 A73-18958

Mechanical and electrical performance of satellite-borne magnetic tape recording system for computer data storage in radio telemetry 07 p0820 A73-18960

Satellite-borne TV vidicon design requirements and operational specifications, considering storage, relaxation, resolution, sensitivity, electrostatic focusing and deflection, image magnification and enhancement 07 p0821 A73-18982

Critical analysis of the results obtained by SIRS-A in remote sensing of the temperature field over the Mediterranean

17 p2205 A73-34936
The use of satellites for remote sensing of the sea surface

17 p2162 A73-34956
Space application of SEC vidicons - The OSO 7 coronagraph.

17 p2170 A73-35293
Range and range-rate measuring equipments for communication satellites.

17 p2130 A73-35813
Atmospheric density values from radar-determined
low altitude satellite orbit decay and accelerometer

data 18 p2302 A73-35942
Apollo 15 and 16 subsatellite magnetometer mea-

Satellite measurements of atmospheric composition

Low energy electron fluxes and spectra correlation with auroral forms from weather satellite electrostatic

18 p2304 A73-35964
Interstellar absorption lines observed with the orbit-

Analysis of solar flare X-ray radiation with Bragg

18 p2344 A73-36014
Vertical temperature profiles from satellites -

Results from second generation instruments aboard
Nimbus-5. 18 p2307 A73-36029

EROS Program and ERTS-1 satellite applications to geophysical problems. 18 p2307 A73-36032

IMP and Pioneer satellite-borne sensors for cataloging solar particle events, discussing onset time, multiple flare injections, enhancement differentiation and

Intercosmos satellite-borne X ray polarimeter measurements of solar flares

The Harvard experiment on OSO-6 - Instrumentation, calibration, operation, and description of obser-

18 p2357 A73-37108
A digital optimization device for directional

charged particle measurements in space research.
19 p2428 A73-37148
ISIS-II scanning auroral photometer.

ISIS-2 red line photometer for global distribution mapping of atomic oxygen 6300 Å emission in airglow

and auroras, discussing atomic excitation processes in upper atmosphere 19 p2428 A73-37257

Evaluation of pinholes in unbacked metal film filters to be used in rocket- and satellite-borne XUV spectroheliographs.

System for calibrating on-board instruments and for laboratory simulation of low-density plasma flows past models

19 p2417 A73-37351
Satellite retarding potential trap contamination relationship to electron and ion temperatures evaluation.

19 p2429 A73-37373

Use of charged particle beams for low temperature plasma measurement in magnetosphere and interplanetary space.

19 p2429 A73-37381
Localization of sources of two-hop whistlers observed aboard the Interkosmos 3 satellite over Europe.

The fine sun sensor of the astronomical Netherlands satellite.

Atmospheric sounding by satellite-borne remote sensors, discussing radiometric measurements of temperature, composition, and reflected and emitted radi-

[AAS PAPER 73-125] 20 p2550 A73-38585
Intercosmos 2 satellite design, construction, on-

board scientific instrumentation, ionospheric experiments and data processing equipment
20 p2565 A73-38905

Role of gas-surface interactions in the reduction of
Ogo 6 neutral particle mass spectrometer data.
20 p2551 A73-38941

Explorer 45 /S3-A/ symmetrical floating probes for plasmopause dc electric fields, discussing plasma sheaths, noise storms, whistlers, electric field strength

Proton flux density and differential energy spectra recorded by solid state proton detectors and three ori-

fluxgate magnetometer aboard Explorer 45 at
plasma pause 20 p2552 A73-38955

Satellite-borne power amplifier state of art, compar-
ing TWT development to different technological solu-
tions 20 p2538 A73-39772

Satellite borne diffused pulsed laser with scattered
light detection by optical receiver on ground for ap-
plications to wide range geodetic survey 21 p2681 A73-40133

Influence of the resolution of television cameras
and radiometers on the accuracy of determining the
quantity of clouds from satellites 21 p2731 A73-40493

Flux measurements of galactic cosmic-ray albedo
neutrons by the Molnia 1 satellite in 1972 21 p2758 A73-40605

First results of the solar hard X-ray spectrometer on
board the ESRO TD-1 A satellite. 21 p2761 A73-41386

Ultraviolet stellar spectra obtained with the Utrecht
orbiting stellar spectrophotometer S 59 aboard the
ESRO TD-1 A satellite. 21 p2773 A73-41395

Investigations of meteoritic matter in the vicinity of
the earth and the moon from the orbiting station Salyut
and the moon satellite Luna 19. 21 p2775 A73-41409

Remote sounding of atmospheric temperature from
satellites. IV - The selective chopper radiometer for
Nimbus 5. 21 p2706 A73-41601

Preliminary results of Martian altitude determina-
tions with CO₂ bands /2 micron wavelength/ from the
automatic interplanetary space station Mars 3. 22 p2905 A73-41807

Enhancement of 0.24- to 0.96-MeV trapped protons
during the May 25, 1967, magnetic storm 22 p2901 A73-41909

Satellite ultraviolet measurements of nitric oxide
fluorescence with a diffusive transport model. 22 p2845 A73-41925

The determination of surface temperature from
satellite 'window' radiation measurements. 22 p2846 A73-42057

The Netherlands astronomical satellite /ANSI/. 22 p2917 A73-42291

Satellite-borne swept frequency impedance probe
/gyroplasma probe/ for ionospheric plasma parameters
including electron density and ion composition, noting
PCM telemetry system 22 p2917 A73-42571

Monograph - Development and performance of a
solar hard X-ray spectrometer. 22 p2861 A73-42674

French monograph - Preliminary photometric study
in the far ultraviolet of the zodiacal and galactic emis-
sion. 22 p2910 A73-42716

Interpretation of measurement results with ion traps
in a bicomponent medium. 22 p2911 A73-42735

Solar observatories and satellite-borne instruments
for solar coronal structure determination, considering
30 June 1973 eclipse and instrumented Concorde air-
craft use 22 p2916 A73-43117

Cepheus X-4 X ray source observation by X ray
telescope on OSO-7, confirming position by second
telescope aboard 22 p2904 A73-43122

Estimation of atmospheric moisture profiles from
satellite measurements by a combination of linear and
non-linear methods. 23 p3001 A73-43526

Magnetospheric plasma motion during a sudden
commencement. 23 p2972 A73-43689

Nimbus 5 satellite-borne selective chopper radiome-
ter /SCR/ for remote sounding of stratospheric tem-
perature, water vapor and cirrus clouds 23 p2978 A73-43952

Stratospheric temperature measuring instrument
development for Tiros N satellites and ESRO geosta-
tionary meteorological satellite development for cloud
photography 23 p3004 A73-44103

Scientific equipment for studying cosmic rays on
Prognostic satellites. I 24 p3144 A73-44783

Physical characteristics of the set of scientific
devices used to record the cosmic-ray ionizing com-
ponent on 'Prognostic' satellites 24 p3089 A73-44784

A procedure for estimating cloud amount and height
from satellite infrared radiation data. 24 p3084 A73-44925

Simultaneous in situ electron temperature com-
parison of Alouette 2 probe and plasma resonance
data. 24 p3086 A73-45129

Triaxial magnetic measurements of field-aligned
currents at 800 kilometers in the auroral region - Initial
results. 24 p3087 A73-45140

SATELLITE-BORNE PHOTOGRAPHY

Geology, hydrology, land use and transportation net
of Dallas-Fort Worth area from Apollo 6 photographs,
comparing with ground based data 01 p0035 A73-10139

Simultaneous measurements of solar radiation from
aircraft and satellites during BOMEX. 01 p0038 A73-10377

Digital image processing for the earth resources
technology satellite data. 01 p0020 A73-11457

Digital image-processing activities in remote sensing
for earth resources. 01 p0021 A73-11476

A program for plate reduction in the case of satellite
observations with a satellite observation camera 03 p0274 A73-13254

A method for reproducing pictures transmitted by
meteorological satellites. 04 p0449 A73-15452

Satellite data and estimates of precipitation for
hydrologic applications. 04 p0473 A73-15774

Satellite-borne solid state multispectral image
remote sensors with photodiode linear arrays for data
acquisition, noting system performance and reliability
advantages 04 p0451 A73-15781

Multispectral additive color viewer for ERTS satel-
lite photography, discussing colorimetric measure-
ment usefulness and photo processing and image den-
sity control effects on color characteristics 05 p0579 A73-17145

Satellite oceanographic measurements and observa-
tions and required sensors assessment, noting benefits
to marine and coastal interests and to weather
forecasting. 06 p0690 A73-17605

IR satellite photographs in the earth sciences - A
comparison of the IR ranges from 3 to 4 micrometers
and from 10 to 12 micrometers 06 p0691 A73-18438

ERTS program, describing satellite design and imag-
ing and data collection systems for real time or
delayed taped transmission to ground stations 07 p0905 A73-19112

Variation with altitude of the scatter coefficient in
the stratosphere, based on measurements from the
Soyuz-3 spacecraft 07 p0817 A73-19585

Mariner 9 stellar photography and camera param-
eters for point source photometric calibration and
reference for optical navigation 08 p0964 A73-21043

Multispectral imagery data compression for earth
resources satellites, comparing performance of spec-
tral-spatial-delta-interleave and Rice coding al-
gorithms 09 p1055 A73-23391

Dual channel high resolution radiometer of French
synchronous meteorological satellite Meteosat for full
time cloud coverage of earth in visible and IR ranges
11 p1368 A73-26508

Skylab earth terrain camera for high resolution
photography of areas covered by other Earth
Resources Experiment Package sensors to aid in data
interpretation 12 p1500 A73-27958

Photogrammetric solution for precision processing
of E.R.T.S. images. 12 p1501 A73-27964

Earth figure theory and gravimetric measurements
using satellite observations and photography 13 p1605 A73-28007

Photographic experiments during a spacecraft flight
lasting a number of days 13 p1611 A73-28008

Skylab A solar and terrestrial observation and
photography hardware, including solar observatory,
microwave scanner, IR spectrometer and multispec-
tral photographic facility 13 p1612 A73-28276

A high performance large aperture window for
photography from a space platform. 13 p1621 A73-29326

Simulated ERTS data for coastal management. 17 p2157 A73-34285

Dynamic climatology in the light of satellite infor-
mation /1973 Harry Wexler Memorial Lecture/. 17 p2204 A73-34375

A synoptic model for evaluation of vertical tempera-
ture and geopotential profiles from satellite pictures. 17 p2206 A73-34939

Airborne and satellite remote sensing of Anacapa
Island for hydrology and aquatic biology. 17 p2161 A73-34944

ERTS-1 satellite-borne multispectral scanner photo-
graphic mapping of Israel vegetation, hydrology,
geological structure, atmospheric phenomena and
oceanography 17 p2162 A73-34947

Applications of ERTS data to oceanography and the
marine environment. 18 p2302 A73-35935

The cartographic and scientific application of
ERTS-1 imagery in polar regions. 18 p2306 A73-36019

Applications of ERTS imagery to snow and glacier
hydrology. 18 p2306 A73-36022

ERTS-1 MSS imagery - A tool for identifying soil
associations. 18 p2306 A73-36023

Remote sensing with VHRR satellite imagery. 18 p2308 A73-36041

Natural resources research and development in
Lesotho using ERTS imagery. 18 p2308 A73-36045

Mars maps based on Mariner 9 pictures and
photomosaics, with emphasis on southwest quadrant
and south pole topographies 18 p2356 A73-37035

Computer processing and analysis of TV cloud
photographs. 18 p2334 A73-37058

Meteorological satellite TV cloud cover photo-
graphs of cyclogenesis over Mediterranean Sea and
cyclone arrival to European U.S.S.R. and Scandinavi-
an Peninsula 18 p2334 A73-37074

The growth of remote sensing through the Nimbus
and ERTS spacecraft. 19 p2430 A73-37712

Techniques for deriving winds from cloud move-
ment. 20 p2583 A73-38586

Enhancement of Earth Resources Technology
Satellite /ERTS/ and aircraft imagery using at-
mospheric corrections. 20 p2567 A73-39835

Time sensing and analysis of coastal water dynamic
features obtained from aircraft and satellite provided
sequential photographic data 20 p2560 A73-39885

Small scale Gemini photographs of Indian regions
for interpretation of tonal variations, geomorphologic,
geologic and structural features and drainage patterns
20 p2561 A73-39898

ERTS-1 satellite return beam vidicon and multispec-
tral scanner comparative evaluation for image quality,
considering response functions, resolution, measur-
ability, detectability and image motion effects 20 p2563 A73-39909

A study of lineaments from a Zond 5 photograph of
northern Africa. 21 p2687 A73-41332

Multi-stage acquisition of forest information from
space and aircraft imagery and ground sampling. 21 p2687 A73-41334

ERTS-1 satellite-borne multispectral scanner
remote sensor for global pollution monitoring, geologi-
cal and heat balance surveys, and storm and
earthquake caused damage 21 p2692 A73-41520

ERTS-1 satellite-borne TV cameras and multispec-
tral band scanners for remote sensing and data collec-
tion with applications in agriculture, forestry, and
water resources survey 21 p2692 A73-41521

Oceanographic analysis of orbital photographs of
the upper Gulf of California. 21 p2692 A73-41634

Suspended sediment observations from ERTS-1. 22 p2850 A73-42726

An analysis of the earth's resources satellite /ERTS-
1/ data. 22 p2850 A73-42732

Russian book - Studies of the natural environment
from manned orbital stations. 23 p2971 A73-43330

Satellite-borne photography of earth surface cover-
ing environment and flight dynamics effects, space
photogrammetry principles, natural environment
imagery interpretation and natural resource photog-
raphy 23 p2971 A73-43332

The use of Skylab and ERTS data in an integrated
natural resources development programme. 23 p2973 A73-43785

Mars surface evolution from analysis of Mariner 6
and 7 equatorial photographs, discussing internal
dynamic activity 24 p3128 A73-44432

Some characteristics of satellite-observed bands of
persistent cloudiness over the Southern Hemisphere. 24 p3107 A73-45015

Picture of the month - NOAA 2 scanning radiometer
visual and infrared imagery received real-time over a
50,000-mile transmission link. 24 p3085 A73-45020

SATELLITES

NT AEROS SATELLITE
NT ALOUETTE 2 SATELLITE
NT APPLICATIONS TECHNOLOGY SATEL-
LITES
NT ARIEL SATELLITES
NT ARTIFICIAL SATELLITES

- NT ASTRONOMICAL NETHERLANDS SATELLITE
 NT ATS 1
 NT ATS 3
 NT ATS 5
 NT ATS 6
 NT BEACON SATELLITES
 NT COMMUNICATION SATELLITES
 NT COSMOS SATELLITES
 NT COSMOS 137 SATELLITE
 NT COSMOS 381 SATELLITE
 NT DEIMOS
 NT DIADEME SATELLITES
 NT EARTH RESOURCES TECHNOLOGY SATELLITE 1
 NT EARTH RESOURCES TECHNOLOGY SATELLITES
 NT EARTH SATELLITES
 NT ECHO 1 SATELLITE
 NT ECHO 2 SATELLITE
 NT ELEKTRON SATELLITES
 NT ENVIRONMENTAL RESEARCH SATELLITES
 NT EOLE SATELLITES
 NT EROS (SATELLITES)
 NT ESRO 1 SATELLITE
 NT ESRO 2 SATELLITE
 NT EXPLORER SATELLITES
 NT EXPLORER 31 SATELLITE
 NT EXPLORER 35 SATELLITE
 NT EXPLORER 43 SATELLITE
 NT GEODETIC SATELLITES
 NT GEOPHYSICAL SATELLITES
 NT GEOS 1 SATELLITE
 NT GEOS 2 SATELLITE
 NT GEOS-C SATELLITE
 NT GOE SATELLITES
 NT GRAVITY GRADIENT SATELLITES
 NT HELIOS SATELLITES
 NT HEOS A SATELLITE
 NT HEOS B SATELLITE
 NT HEOS SATELLITES
 NT IAPETUS
 NT INTELSAT SATELLITES
 NT INTERCOSMOS SATELLITES
 NT ISIS SATELLITES
 NT ITOS 1
 NT IUE
 NT LUNAR ORBITER
 NT LUNAR SATELLITES
 NT METEOROLOGICAL SATELLITES
 NT METEOSAT SATELLITE
 NT MOLNIYA SATELLITES
 NT MOON
 NT NATURAL SATELLITES
 NT NAVIGATION SATELLITES
 NT NIMBUS SATELLITES
 NT NIMBUS 3 SATELLITE
 NT NIMBUS 4 SATELLITE
 NT NIMBUS 5 SATELLITE
 NT OAO
 NT ORBITAL SPACE STATIONS
 NT ORBITAL WORKSHOPS
 NT OSO
 NT OSO-7
 NT PAGOS SATELLITE
 NT PHOBOS
 NT POGO
 NT PROTON SATELLITES
 NT PROTON 2 SATELLITE
 NT PROTON 3 SATELLITE
 NT PROTON 4 SATELLITE
 NT RADIO ASTRONOMY EXPLORER SATELLITE
 NT RELAY SATELLITES
 NT SAN MARCO SATELLITE
 NT SCIENTIFIC SATELLITES
 NT SIRIO SATELLITE
 NT SKYNET SATELLITES
 NT SMALL ASTRONOMY SATELLITES
 NT SPUTNIK SATELLITES
 NT SYMPHONIE SATELLITES
 NT SYNCHRONOUS METEOROLOGICAL SATELLITE
 NT SYNCHRONOUS SATELLITES
 NT SYCOM SATELLITES
 NT TD-1 SATELLITE
 NT TELSTAR 1 SATELLITE
 NT TIROS M
 NT TIROS SATELLITES
 NT TRANSIT SATELLITES
 NT UHURU SATELLITE
 NT VELA SATELLITES
 NT VENERA SATELLITES
 NT VENERA 4 SATELLITE
 NT VENERA 6 SATELLITE
 NT VENERA 7 SATELLITE
 Research at O.N.E.R.A. on ion thrusters suitable for satellite station-keeping 04 p0505 A73-15719
 SATURATED HYDROCARBONS
 U ALKANES
 SATURATION
 Experimental study of the saturated-vapor pressure of rubidium and cesium 01 p0080 A73-10858
 Predicting performance of heat pipes with partially saturated wicks.
 [ASME PAPER 72-WA/HT-38] 04 p0518 A73-15817
 Discharge current dependence of saturation parameter of a He-Ne gas laser. 08 p0976 A73-21463
 Ion saturation currents to planar Langmuir probes in a collision-dominated flowing plasma. 08 p0993 A73-21597
 An indirect method for measuring equatorial electrojet currents and its relation to nonlinear saturation of type I instabilities. 09 p1075 A73-22070
 High gain gas laser oscillators saturation, verifying with 3.51 micron Xe oscillator having unsaturated single pass intensity gain of ten million 09 p1091 A73-22086
 Current saturation and small-signal characteristics of GaAs field-effect transistors. 10 p1197 A73-24868
 Mathematical description by Gaussian error function for metals diffusive saturation and diffusion constants determination 10 p1236 A73-24952
 Experimental investigation of the pressure of the saturated vapor of rubidium and cesium. 12 p1526 A73-27907
 The determination of the evaporation from a class-A pan by means of empirical evaporation formulas 13 p1653 A73-28746
 On the validity of the gradual channel approximation for junction field effect transistors with drift velocity saturation. 20 p2535 A73-39006
 Saturation effect in RF spectroscopy for transverse optical pumping. 21 p2713 A73-40473
 Plasma decay instability nonlinear saturation spectrum in small spontaneous emission limit for comparable ion and electron temperatures from kinetic equation numerical solution 24 p3118 A73-45460
 SATURN (PLANET)
 NT SATURN RINGS
 The mass and figure of Saturn by photographic astrometry of its satellites. 01 p0096 A73-10316
 Time variations of the ultraviolet absorption in the continuous spectrum of Jupiter and Saturn 01 p0101 A73-10843
 Polarimetric investigations of the giant planets. II - Phase variation of the polarization of selected regions on the Saturn disk 01 p0102 A73-10941
 Radii, albedos, and 20-micron brightness temperatures of Iapetus and Rhea. 01 p0104 A73-11050
 Gravitational fields of Jupiter and Saturn. 01 p0107 A73-11332
 The transmission of mass and angular momentum from a satellite or planetary system to its primary. 02 p0225 A73-12810
 Circular polarization of Saturn. 04 p0499 A73-15368
 Far IR brightness temperature, opacity and emissivity of Jupiter, Venus, Mars and Saturn 05 p0626 A73-17348
 On the origin of the commensurabilities amongst the satellites of Saturn. 06 p0752 A73-18238
 On the analytical study of Saturn's satellites, Enceladus-Dione 08 p1005 A73-20921
 Investigation of molecular absorption in the atmospheres of the giant planets 08 p1007 A73-21064
 Photometric characteristics of Jupiter and Saturn in the 0.48-0.33-micron range. 08 p1012 A73-21578
 Polarimetric observations of the major planets. II - Phase dependence of the polarization for selected areas on the disk of Saturn. 09 p1147 A73-22736
 Saturn magnetospheric model for bounds on surface field strength and trapped particle population 10 p1283 A73-24724
 Survey of the outer planets Jupiter, Saturn, Uranus, Neptune, Pluto, and their satellites. 11 p1417 A73-25315
 Thermal radio emission from Jupiter and Saturn. 11 p1420 A73-25883
 Electrical conductivity of condensed molecular hydrogen in the giant planets. 11 p1420 A73-25885
 Thermodynamic parameters for metallic hydrogen-helium alloy of Saturn and Jupiter interiors, using Monte Carlo chains and dielectric function theory 11 p1420 A73-25888
 Saturn 49.5 and 94.3 cm brightness temperature, considering magnetic field effects, synchrotron emission and atmosphere 11 p1424 A73-26127
 Saturn disk and ring dimensions, discussing photometric parameters, ice as ring constituent and ring models 11 p1425 A73-26139
 Optical properties and structure of the atmosphere of Saturn. II - Latitudinal variations of absorption in the CH₄ 0.62-micron line and the characteristic features of the planet in the near ultraviolet 12 p1546 A73-27862
 Hidalgo orbit near Saturn, discussing resemblance to extinct comet nucleus, nongravitational forces effects and planetary mass determination 14 p1792 A73-29812
 Saturn mass determination from Hidalgo orbit trajectory and variational equation, obtaining probable error from fitted parabola 14 p1792 A73-29813
 The major planets as powerful transformers of cometary orbits. 14 p1794 A73-29834
 The significance of atmospheric measurements for interior models of the major planets. 14 p1799 A73-30532
 Long wave measurements of brightness temperature for thermal structure of major planet atmospheres at great depths, discussing Jupiter and Saturn microwave spectra 14 p1800 A73-30537
 Temporal variation of ultraviolet absorption in continuous spectra of Jupiter and Saturn. 15 p1928 A73-30979
 Observational constraint on the structure of hydrogen planets. 15 p1936 A73-31565
 Horseshoe and Trojan orbits associated with Jupiter and Saturn. 15 p1937 A73-31948
 Upper limit to the 11.4 m flux of Saturn using VLB1. 16 p2061 A73-33221
 Jupiter and Saturn optical observations, discussing atmospheric composition, cloud layers and temperature distribution 16 p2069 A73-33837
 An experiment in photographic equidensitometry of the moon and planets 16 p2070 A73-33848
 Interior of Jupiter and Saturn. 17 p2226 A73-34357
 Carbon isotope abundance ratios in comets and Jupiter atmosphere, discussing hydrogen isotope ratio determination for Saturn and Jupiter atmospheres 17 p2228 A73-34418
 Saturn - A study of the 3 nu sub 3 methane band. 17 p2231 A73-34765
 Determination of the mass of Saturn from the motion of Trojans. 17 p2234 A73-35615
 Scientific considerations for a common Saturn/Uranus atmospheric entry probe. 18 p2350 A73-36080
 Plasma physics phenomena in the outer planet magnetospheres. 18 p2345 A73-36097
 Thermal control subsystem design of a Saturn/Uranus atmospheric entry probe for descent missions to 20 bars. 18 p2360 A73-36384
 Jupiter and Saturn interior structure models based on state equations and transport properties of hydrogen and helium at high pressures and temperatures 18 p2354 A73-36644
 Molecular absorption in the atmospheres of the giant planets. 18 p2355 A73-36865
 Optical properties and structure of Saturn's atmosphere. II - Latitudinal variations of absorption in the 0.62-micron CH₄ band and characteristics of the planet in the near ultraviolet. 20 p2608 A73-39236
 Navigation system design for the Mariner Jupiter/Saturn Mission. 21 p2736 A73-40503
 Narrow band IR vidicon Jupiter and Saturn photography, showing limb darkening and surface details 23 p3032 A73-43942
 Exploring Jupiter, Saturn and their satellites. 23 p3034 A73-44221
 Methane absorption in the atmosphere of Saturn - Rotational temperature and abundance from the 3 nu sub 3 band. 24 p3129 A73-44445
 High-angular-resolution observations of Saturn at 21.1-centimeter wavelength. 24 p3138 A73-45051
 SATURN LAUNCH VEHICLES
 NT SATURN 5 LAUNCH VEHICLES
 Exhaust cloud rise and growth for Apollo Saturn engines. 15 p1906 A73-31920
 Rocket power, Redstone to Saturn V, now Space Shuttle, 20 years of development. 19 p2493 A73-37886
 SATURN PROJECT
 Mariner Jupiter/Saturn 1977 - The mission frame. 02 p0221 A73-12597
 SATURN RINGS
 Saturn rings formation explanation by electromagnetic effects, presenting mathematical model 01 p0097 A73-10551

SATURN 5 LAUNCH VEHICLES

- Thickness of Saturn's rings from observations in 1966. 01 p0107 A73-11325
- On the formation of Saturn's rings. 02 p0225 A73-12805
- Saturn ring dynamics via numerical simulations of jet streams, discussing non-Maxwellian velocity distribution and energy consumption decrease with thickness 03 p0373 A73-13355
- Saturn ring spectral reflectivity at 0.36-1.06 microns, noting maximum at both ends of spectral range for amplitude of opposition effect 11 p1424 A73-26126
- Saturn disk and ring dimensions, discussing photometric parameters, ice as ring constituent and ring models 11 p1425 A73-26139
- Optical scattering properties of Saturn's ring. 11 p1429 A73-26683
- Gaseous ring mechanism of Titan atmosphere, considering atmospheric particle outgassing and recapture under Saturn gravitational field to form torus at Titan orbit 14 p1788 A73-29719
- Temperatures of Saturn's rings. 14 p1797 A73-30010
- Optical thickness of Saturn rings along cross section from intensity of radiation transmitted through rings, considering dark side illumination sources 15 p1939 A73-32008
- Saturn ring thickness according to 1966 observation data of the Pic-du-Midi Observatory 16 p2070 A73-33845
- Observations of the Saturn rings during the earth's passage through the ring plane in 1966 16 p2070 A73-33846
- Some preliminary conclusions from the available observation results of the International Saturn Patrol of 1966 16 p2070 A73-33847
- The occultation of the star SAO 93826 by Saturn's ring 20 p2606 A73-39076
- The Saturn rings in 1969: Morphological and photometric study. I - Photograph acquisition and evaluation 24 p3128 A73-44434
- The Saturn rings in 1969: Morphological and photometric study. II - Deconvolution of the raw photometric curves 24 p3128 A73-44435

SATURN 5 LAUNCH VEHICLES

- The optical temperature of the Apollo 15 exhaust plume. [AD-757298] 03 p0358 A73-13497
- Hybrid computer technique for desensitized optimal design of system with uncertain plant parameters, with application to Saturn 5 Apollo attitude control system design 18 p2291 A73-36426
- Skylab program mission profile, vehicle components, ground station data links, Apollo telescope mount, Saturn V rocket, solar cells and Salyut spacecraft comparison 20 p2615 A73-39150

SAVANNAHS

U GRASSLANDS

SAWTOOTH WAVEFORMS

- Determination of the optimal structure of a unit measuring the effective value of a nonsinusoidal periodic voltage 05 p0560 A73-16330
- Transistor sawtooth voltage generator design for accelerated rise time piecewise linear leading edge, using capacitor charge/discharge acceleration 10 p1196 A73-24604

SCALAR MAGNETIC CHARGE

U MAGNETIC CHARGE DENSITY

SCALARS

- Backscattering of a scalar wave field by an ideally reflecting object situated near the caustic surface 09 p1052 A73-23081
- Zero-mass scalar and electrostatic fields with the central symmetry in the general relativity. 09 p1121 A73-23148
- Scalar sequence spaces theory extension to vectorial sequence spaces based on bounded ensemble concept 10 p1241 A73-23763
- Extendibility over the entire plane and the functional equation of a scalar product of Hecke L-series of two quadratic fields 13 p1648 A73-28344
- Asymptotic behaviour of a scalar in an axisymmetric final period turbulent wake. 20 p2507 A73-39086
- Scalar waves in the mixmaster universe. I - The Helmholtz equation in a fixed background. 21 p2766 A73-40317
- On the choice of second-order difference schemes furnishing shock profiles without oscillation 24 p3110 A73-45217

SCALE [CORROSION]

- Effects of inhibitors PB-5 and of dialkyl-dimethyl ammonium chloride on the corrosion resistance and mechanical strength of structural materials during the cleaning of heat exchangers from scale by the hydrochloric acid method 02 p0174 A73-12537
- The functional form of rate curves for the high-temperature oxidation of dispersion-containing alloys forming Cr₂O₃ scales. 04 p0461 A73-14924
- Composition and structure of rust layers and corrosion rate of chromium steels exposed to a marine atmosphere. 05 p0586 A73-16137
- Effect of oxygen on the scale resistance of titanium-titanium alloys. 06 p0709 A73-18208
- Simulated microscale erosion on the lunar surface by hypervelocity impact, solar wind sputtering, and thermal cycling. 07 p0896 A73-19867
- Concentration profiles through thin oxide scales by ion-probe microanalysis. 09 p1101 A73-22402
- Variation of chemical composition on the surface of cobalt-base alloys by oxidation in air. 15 p1891 A73-32016
- Subscale inclusions formation in solid Fe alloys with small amounts of Mn and other elements, noting inward oxygen thermal diffusion role and metallurgical implications 15 p1891 A73-32171
- High-temperature oxidation of tungsten boride in oxygen and the effect of scale evaporation. 16 p1976 A73-33076
- The role of yttrium in high-temperature oxidation behavior of Ni-Cr-Al alloys. 16 p2025 A73-33077
- Microstructure and phase composition of oxide scale formation on Ti-Al alloys, noting dependence on Al concentration 17 p2188 A73-34557
- The effect of carbon on the sulphidation of Co-Cr alloys. 19 p2443 A73-38250

SCALE [RATIO]

- Component errors of digital frequency meter with nonius estimation of measured quantity smaller digits 02 p0167 A73-11863
- A note on Eulerian-Lagrangian time scale transformation for large-scale atmospheric turbulence. 08 p0985 A73-21424
- Classification, scale sequence, and nomenclature of lunar maps 13 p1672 A73-28117
- Experience in constructing analytical planar phototriangulation grids from 1:40,000 and 1:75,000 scale aerial photographs for the preparation of 1:10,000 scale photographic maps 14 p1753 A73-30416
- The superiority of the pair-comparisons method for scaling visual illusions. 17 p2118 A73-35497
- A meteorological and a geophysical example of the use of the scale autocorrelation coefficient to determine ratios of frequencies present in periodic phenomena. 22 p2883 A73-42542

SCALE EFFECT

- Processing conditions and sample dimensions and shapes effects on Ti alloy creep characteristics at room temperature 01 p0064 A73-10487
- Some experiences in the scaling of the NASA 8-stage transonic axial flow compressor. [SAE PAPER 720711] 02 p0203 A73-12008
- Interplanet variations in scale of crater morphology - Earth, Mars, Moon. 06 p0745 A73-17442
- P-n junction size effect on thermal resistance of reverse biased Si mesa-type diode, considering junction area, mesa height and power dissipation 06 p0674 A73-17795
- Limited cavitation and the related scale effects problem. 06 p0686 A73-18435
- On fracture toughness and its size dependence for steels showing thickness delamination. 06 p0709 A73-18476
- Scale effects on the fatigue and corrosion fatigue of steel 07 p0839 A73-19657
- Euler, Lagrange and time turbulence scales for Prandtl mixing length, relating with velocity and pressure pulsations in steady turbulent gas flow 10 p1204 A73-23474
- Cavitation erosion in geometrically similar nozzles with lead and plastic liners, presenting expressions for erosion rates dependence on scale 10 p1206 A73-24669
- Stress gradient as one of the causes of the scale effect on the brittle fracture of materials. 13 p1703 A73-29614

Processing conditions and sample dimensions and shapes effects on Ti alloy creep characteristics at room temperature 14 p1759 A73-30311

Scale effect in fatigue and in corrosion fatigue of steel. 14 p1760 A73-30322

Euler, Lagrange and time turbulence scales for Prandtl mixing length, relating with velocity and pressure pulsations in steady turbulent gas flow 21 p2678 A73-41322

The scale effect and design method of the regenerative pump with non-radial vanes. 23 p2986 A73-44274

Some scale estimates of the three-dimensional structure of cloud fields from aircraft-based aerial photographs 24 p3107 A73-44962

SCALE HEIGHT

- Ionospheric scale height from the refraction of satellite signals. 04 p0415 A73-14953
- Shallow-solar-zenith-angle control to topside ionospheric parameters. 04 p0445 A73-15636
- Neutral thermosphere temperatures from density scale height measurements. 09 p1074 A73-22063
- On the relation between optical scale height and density scale height in a stellar atmosphere. 10 p1281 A73-24406
- The topside ionosphere at mid-latitudes during local sunrise. 11 p1353 A73-25757
- The effect of a uniform external pressure on the ionospheric boundary of a non-magnetic planet in a steady solar wind. 11 p1421 A73-25925
- Variations of the global values of F₂-layer thickness and the parameters of the neutral atmosphere. 13 p1608 A73-28722
- Primary scattering theory for twilight luminance calculation, considering luminance atmospheric scale height growth in thermosphere and seasonal variation. 16 p2009 A73-33889
- Ionospheric slab thickness relationship to electron density profile shape, plasma and neutral constituents scale heights and electron to ion temperature ratio 22 p2846 A73-41947

SCALE MODELS

- Some problems in the substantiation and application of discrete large-element design schemes for complex zero-moment shells 02 p0230 A73-11716
- Jet interaction in a simplified model of a bistable fluid amplifier. [ASME PAPER 72-WA/FLCS-6] 04 p0409 A73-15863
- Operation modes simulation of single stage gas turbine at subcritical and supercritical gas flow, noting scale model tests 05 p0532 A73-17024
- Application of elastooptical modeling studies in determining optimal shapes for plane structures 06 p0760 A73-17782
- Similarity condition for the lateral contraction coefficient in photoelasticity 06 p0761 A73-17785
- Triangular obstacle caused microwave shadow zone diffraction pattern calculation by ray optics theory, comparing with scale model test results 06 p0666 A73-18201
- Hypersonic flows in large-scale inlet models. 07 p0773 A73-19189
- Icing testing in the large Modane wind-tunnel on full-scale and reduced scale models 07 p0808 A73-20244
- Generalization of J. K. Lunde's method for determining the flow around models in a rectangular-section test tank 08 p0955 A73-21195
- Reduced scale experimental study of propeller propulsion system ignition phases, defining pressure buildup curve shape and ignition limits [ONERA, TP NO. 1182] 09 p1135 A73-22711
- Buffeting pressures on a swept wing in transonic flight - Comparison of model and full scale measurements. [AIAA PAPER 73-311] 11 p1305 A73-25542
- Experimental tests on scale models of conical variable geometry propulsion nozzle with short petals for fighter aircraft, discussing aerodynamic and thrust coefficients 12 p1533 A73-27388
- Acoustic and fluid dynamic tests of multilobed discharge silencers scale models, noting optimum jet noise attenuation configuration 12 p1486 A73-27390
- Structural analysis via thermoplastic scale model testing with resistance strain gages, considering temperature and humidity effects on measurement accuracy and reliability 14 p1750 A73-29701

Experimental data processing system for EU-ROCONTROL scale model semiautomatic digital route control system for operational conditions simulation
15 p1907 A73-31132

Experimental investigation and correlation of the ground impact acceleration characteristics of a full scale capsule and a 1/4 scale model aircraft emergency crew escape capsule system.
[AIAA PAPER 73-480] 15 p1829 A73-31463
German book - Similarity laws and model rules of aerodynamics.
15 p1863 A73-31475

Development of experimental turbine facilities for testing scaled models in air or freon.
17 p2145 A73-34381

Test on fuselage models at reduced sizes.
17 p2107 A73-35443

Preliminary results from dynamic model tests of an air cushion landing system.
19 p2382 A73-37694

Design modeling of external and internal cooling systems for bodies exposed to high temperature gas flow, discussing operation similarity conditions
20 p2628 A73-39419

Scale model development of a high efficiency dual polarized line feed for the Arecibo spherical reflector.
22 p2831 A73-41830

An engineering flight simulation visual display system.
[AIAA PAPER 73-924] 22 p2838 A73-41970

Results of the application of the physical modeling method to a study of the tangential component of the magnetic field of a linear inductor on the surface of a massive ferromagnetic body
22 p2800 A73-42214

Book on engineering dynamics similarity and scaling methods covering blast waves and gas dynamics, transient loads, fluid-structure interaction, soil dynamics, thermal modeling, etc
23 p3039 A73-43460

Analog scale model of radio interferometry depth sounding at centimeter wavelengths, examining glacier layer boundaries
24 p3082 A73-44750

SCALING
Extensive air showers and Feynman scaling above 1000 GeV.
06 p0743 A73-18325

Perceived level calculation methods for aircraft flyover noise scaling, rating jets, turboprops, piston aircraft and helicopters with frequency weighting functions, duration and tone corrections
10 p1175 A73-24391

Multidimensional scaling methods and data visualization [Review]
23 p2949 A73-43578

SCALING LAWS
Simulation of unsteady gas exchange in internal combustion engines
02 p0202 A73-11632

Scaling relations to predict size of submarine generated wake in stratified water flow, measuring velocity and temperature profiles
[AIAA PAPER 73-108] 06 p0644 A73-17644

Scaling invariance hypothesis for local structure of turbulence, using quantum field theory methods
06 p0686 A73-17977

Measurement of cosmic-ray muon charge ratio at sea level between energies of 10 and 1500 GeV.
14 p1787 A73-30455

Scaling laws for outer planet magnetospheres, noting energetic trapped particles radiation belts possibility
14 p1800 A73-30538

German book - Similarity laws and model rules of aerodynamics.
15 p1863 A73-31475

Plasma characteristics with TEA-CO₂ laser and wavelength scaling law.
19 p2468 A73-37520

Power-generation potential of various IMPATT structures from a scaling approximation.
21 p2668 A73-41591

Russian book on scale selection in modeling for analog and digital computers covering similarity theory, error formation, accuracy optimization, etc
22 p2829 A73-41883

Book on engineering dynamics similarity and scaling methods covering blast waves and gas dynamics, transient loads, fluid-structure interaction, soil dynamics, thermal modeling, etc
23 p3039 A73-43460

Production of lunar fragmental material by meteoroid impact.
24 p3129 A73-44447

SCANDIUM
Temperature dependence of the solubility of scandium in solid magnesium
12 p1510 A73-26908

Rare-earth elements, Co, Sc and Hf in the Steens Mountain basalts.
15 p1874 A73-32389

SCANDIUM COMPOUNDS
NT SCANDIUM OXIDES

The nature of the interaction between scandium and aluminum in the aluminum-rich part of the Al-Sc system
21 p2718 A73-40486

SCANDIUM OXIDES

Magnetic permeability dependence on temperature and composition of hexaferrites with various Sc ion contents
09 p1134 A73-22982

SCANNERS

NT FLYING SPOT SCANNERS
NT HORIZON SCANNERS
NT INFRARED SCANNERS
NT OPTICAL SCANNERS

Working prototype image dissector photoelectron beam scanning by crossed electric and magnetic fields to measure beam density distribution in proton synchrotron
01 p0048 A73-10528

Spin-scan imaging devices for various space missions, describing monochromatic and multicolor cameras, IR radiometer, multispectral scanner and imaging photopolarimeter
02 p0170 A73-12339

A dual wavelength ground-based auroral scanner.
03 p0299 A73-12888

Pattern classification in scan-type nondestructive tests.
04 p0447 A73-14928

Low energetic efficiency of semiconductor microwave scanning converters for radio images of fog obscured objects
05 p0556 A73-16072

Scanning and transmission type electron microscopes, discussing operating principles, image quality, resolution and applications
05 p0575 A73-16311

Optimal correlation of sensor data with tracks in surveillance systems.
06 p0682 A73-18822

Defects analysis and the possibilities brought by the scanning electron microscope
07 p0823 A73-19408

Multielement scanning system for acoustic holography application in nondestructive testing, combining multiple mechanical sensors with simultaneous electronic commutation
09 p1080 A73-22297

Microwave landing system /MLS/ with Doppler scanning technique for aircraft guidance precision improvement over standard VHF/UHF ILS, detailing five-year development plan
10 p1246 A73-23652

A mechanized eddy current scanning system for aircraft struts.
10 p1225 A73-24631

Linear open signal scanning system distortion of stationary stochastic signals, examining transfer characteristic improvement by optimal filter
17 p2121 A73-34245

Diffraction pattern scanning display technique using electron detector in microscope final image, discussing gold particle demonstration, lens configuration, illumination angle and sawtooth currents
21 p2700 A73-40466

Linear scan receiver for electronic beam steering of the north-south array of the DKR-1000 radio telescope
21 p2662 A73-40543

SCANNING

NT CONICAL SCANNING
NT FREQUENCY SCANNING
NT PANORAMIC SCANNING
NT RADAR SCANNING

Class of stepped-reflector antennas with improved frequency response.
05 p0547 A73-16159

Acoustic holographic scanning techniques for imaging flaws in thick metal sections.
05 p0574 A73-16284

Properties of magnetic focusing systems for picture tubes
10 p1194 A73-23850

Acoustic wave propagation, scanning and liquid surface techniques in acoustical holography, noting applications in geophysics, oceanography, medicine and nondestructive testing
11 p1371 A73-26542

Cylindrical scan acoustical holographic transmitter/sensor system for ultrasonic under ocean surveillance and NDT applications
13 p1615 A73-28588

Electrostatic and magnetic fields methods comparison for small angle scanning of electron beam, considering particle trajectories, field energy and circuit electrical parameters
14 p1732 A73-29913

A dual-mirror antenna with beam scanning over a ninety-degree sector
14 p1736 A73-30561

Photon counting with a self-scanned diode array.
17 p2169 A73-35283

Mass property control of a synchronous meteorological satellite scanning experiment.
[SAWE PAPER 964] 19 p2492 A73-37882

Large scanning and multibeam reflector antennas for space communications.
20 p2524 A73-38738

On the use of a dual spin vehicle for scanning a celestial body.
[AIAA PAPER 73-910] 20 p2614 A73-38844
A mechanically scanned interferometer-echelle spectrometer for the middle ultraviolet.
21 p2692 A73-39924

A single-plane electronically scanned antenna for airborne radar applications.
21 p2653 A73-40684

Physical design considerations for airborne electronic-scanning antennas.
21 p2654 A73-40685

Experimental verification of the possibility of beam scanning in a variable profile antenna by radial displacement of the primary radiating element
21 p2667 A73-41469

An array technique with grating-lobe suppression for limited-scan applications.
22 p2830 A73-41826

SCANNING DEVICES

U SCANNERS
SCARS [GEOLOGY]
U EROSION

SCAT

U SUPERSONIC COMMERCIAL AIR TRANSPORT

SCATTER PROPAGATION

NT IONOSPHERIC F-SCATTER PROPAGATION

Gaussian channel model for long tropospheric scatter link verification by time varying bandpass impulse response measurements, using Kolmogoroff-Smirnov tests
04 p0418 A73-15392

Investigation of a signal scattered in the lower ionosphere on the basis of a group delay model
05 p0548 A73-16254

Ionospheric attenuation of 3-100 MHz radio waves, interpreting scatter mode propagation mechanism as total reflection from lower ionizational irregularities
07 p0792 A73-19458

Energy characteristics of radio signals scattered by statistically uneven surface, proposing statistical variables substitution
10 p1191 A73-24934

Microwave transhorizon propagation in atmospheric evaporative dust layer by superdiffraction, using Monin-Obukhov similarity theory for computerized prediction
16 p1981 A73-33712

Measurements of wind-induced Doppler shifts at 16 GHz over a long range bistatic scatter link.
16 p1983 A73-33726

Forward scatter propagation measurements /transhorizon and line-of-sight/ applied to specific forms of instabilities in layers.
19 p2406 A73-38247

SCATTERED CLOUDS

U CLOUDS [METEOROLOGY]

SCATTERERS

U SCATTERING

SCATTERING

NT ACOUSTIC SCATTERING
NT ATMOSPHERIC SCATTERING
NT BACKSCATTERING
NT COHERENT SCATTERING
NT COMPTON EFFECT
NT ELASTIC SCATTERING
NT ELECTROMAGNETIC SCATTERING
NT ELECTRON SCATTERING
NT FORWARD SCATTERING
NT INCOHERENT SCATTERING
NT INELASTIC SCATTERING
NT ION SCATTERING
NT IONOSPHERIC F-SCATTER PROPAGATION

NT LIGHT SCATTERING

NT MICROWAVE SCATTERING

NT MIE SCATTERING

NT NEUTRON SCATTERING

NT NUCLEAR SCATTERING

NT PROTON SCATTERING

NT RADAR SCATTERING

NT RAMAN SPECTRA

NT RAYLEIGH SCATTERING

NT RESONANCE SCATTERING

NT REVERBERATION

NT THOMSON SCATTERING

NT TROPOSPHERIC SCATTERING

NT WAVE SCATTERING

NT X RAY SCATTERING

Comparison of scatter under program and random loading and influencing factors.
[DFVLR-SONDDR-259] 03 p0387 A73-13232

On the probabilistic determination of scatter factors using Miner's rule in fatigue life studies.
03 p0388 A73-13237

Investigation of hole scattering in surface inversion channels arising on a cleaved germanium surface
03 p0349 A73-13659

SCATTERING AMPLITUDE

Perturbation theory for field moments in an inhomogeneous medium. 17 p2123 A73-35151

SCATTERING AMPLITUDE

Intermediate energy nucleon-deuteron scattering theory. 14 p1776 A73-29766

Observations of Type I bursts at 169 MHz and coronal scattering. 24 p3140 A73-45182

SCATTERING COEFFICIENTS

Rocket photometric observations of dayglow sky radiation in O green line, noting aerosol scattering coefficient and particle concentration. 02 p0161 A73-12277

Variation with altitude of the scatter coefficient in the stratosphere, based on measurements from the Sotuz-3 spacecraft. 07 p0817 A73-19585

Determination of the concentration and scattering indicatrix of atmospheric dust from primary twilight brightness. 07 p0817 A73-19589

Characteristics of the calculation of radiant transfer in a system of diathermic bodies separated by an absorbing and scattering medium. 07 p0921 A73-20080

A nephelometric method for transparency determination in scattering media. 14 p1771 A73-30463

Investigation of the lunar surface by the method of the scattering of radio waves emitted by lunar satellites. 16 p2064 A73-33773

Tall buildings induced microwave scattering coefficient measurement with helicopter-borne bistatic pulse radar, explaining coefficient dependence on azimuth, elevation and range. 20 p2530 A73-39127

The arrival of solar radiation on variously oriented inclined surfaces. 20 p2555 A73-39818

The effects of scattering and conduction upon radiative transfer in lunar and Mercurian surfaces. 24 p3133 A73-44541

Determination of the parameters of particle density and size distribution functions from measurements of attenuation and backscattering coefficients. 24 p3112 A73-45519

SCATTERING CROSS SECTIONS

Transfer of electronic excitation by atomic collision between highly excited cesium atoms. 01 p0079 A73-10174

Discussion of radiative-transfer methods applied to electromagnetic reflection from turbulent plasma. 01 p0081 A73-10196

Oxygen emission volume rate in auroras due to direct electron impact excitation, obtaining integral cross sections and quenching rates. 01 p0036 A73-10336

The electron diffusion scattering cross section of cesium atoms. 01 p0080 A73-10852

Thickness of Saturn's rings from observations in 1966. 01 p0107 A73-11325

Momentum transfer interaction of a laser-produced plasma with a low-pressure background. [AD-75558] 02 p0197 A73-12062

Diffraction of elastic waves by two coplanar and parallel rigid strips. 02 p0234 A73-12088

Optical properties of the Apollo laser ranging retroreflector arrays. 02 p0141 A73-12250

Ionization calorimeter study of cosmic ray hadrons inelastic collision cross sections and partial K-neutral pion inelasticity factor. 02 p0208 A73-12656

Inelasticity factor dependence on particle energy spectra to explain nucleon flux calculations and Proton satellite data, considering scattering cross sections. 02 p0208 A73-12658

The relation between momentum transfer and capture and total scattering cross sections for ion-dipole collisions. 02 p0195 A73-12842

Electron scattering by molecules with and without vibrational excitation. VI - Elastic scattering by CO at 6-80 eV. 03 p0344 A73-13284

Average monostatic scattering cross section for plane electromagnetic wave incident on ideally conducting convex body, considering wavelength relation to body dimensions. 03 p0278 A73-14072

Close coupled calculations of electron-hydrogen atom scattering using a noniterative integral equation technique. 04 p0477 A73-14818

Backward-elastic proton-deuteron differential cross sections at different energies, describing experimental setup. 05 p0601 A73-17322

Absolute Raman scattering cross-section of molecular hydrogen. 05 p0601 A73-17340

Absolute cross section for producing C-11 from carbon by 270-MeV/nucleon N-14 ions. 06 p0725 A73-17519

Nonequilibrium plasma wave scattering cross section dependence on energy bands shape and field orientation in semiconductors. 06 p0735 A73-17975

Collision matrix elements near a pseudocrossing of potential energy curves. 06 p0726 A73-18249

Scattering of a transverse elastic wave by an elastic sphere in a solid medium. 06 p0737 A73-18351

Differential light scattering cross section derivation for photon interaction with relativistic electrons, comparing with quantum electrodynamical calculation and Thomson scattering experiment. 07 p0851 A73-19516

Collision cross sections for electrons with atmospheric species. 08 p0957 A73-20659

Cross sections for emission of Lyman-alpha radiation in collisions of 1-25 keV protons and hydrogen atoms with constituents of planetary atmospheres. 08 p0957 A73-20660

Spaced radar observation of auroral scattering cross sections, noting radar backscattering intensity peak and echo detection probability relationship to aspect angles. 08 p0957 A73-20661

Diatomic molecules dissociation investigation from effective cross section measurement of slow atomic negative ions formation by molecules collisions with fast ions and atoms. 08 p0990 A73-21694

On the self-shielding coefficient of plates against neutron fluxes. 09 p1117 A73-22018

On the analysis of glory scattering data for the extraction of information on the interatomic potential well. 09 p1122 A73-22072

Inelastic collision of fast charged particles with arbitrary levelled hydrogen-like atoms. 10 p1250 A73-23575

Intermolecular potential energy curve crossing probabilities and associated phases determination for low energy elastic scattering cross section of He cations by Ne, noting rainbow effect. 10 p1250 A73-23670

Electron impact excitation rates calculation for He I and II transitions, comparing measured, theoretical and semiempirical impact cross sections. 10 p1251 A73-24133

A theory of tracking for a dynamic radar scatterer ensemble. 10 p1189 A73-24532

Effect of rapidly rising proton-proton total cross sections on idealized extensive air showers. 11 p1412 A73-25745

Two-position scattering of radio waves by the sea surface at small slip angles. 11 p1331 A73-26154

Theory of sound scattering by turbulence applied to scattering cross section calculation for turbulent jet flow and wind, discussing jet noise reduction. 11 p1349 A73-26496

Radar scatterer ensemble cross section centroid tracking by raster scan observation technique, estimating mean-squared dimensions. 11 p1333 A73-26644

The diffusion cross section for scattering of electrons by cesium atoms. 12 p1526 A73-27902

Stellar opacity and energy transport based on radiation-matter interactions, discussing radiative transfer, absorption and scattering cross sections, quantum mechanical methods, etc. 13 p1682 A73-28987

Detection of oil spills using a 13.3-GHz radar scatterometer. 13 p1610 A73-29196

Scattering by a gyrotropic cylinder coated with another gyrotropic layer. 13 p1586 A73-29232

On the scattering cross section of passive linear arrays. 14 p1735 A73-30229

Asymptotic form for the cross section for the Coulomb interacting rearrangement collisions. 14 p1777 A73-30551

Vibrational excitation of H2 by proton impact. 14 p1777 A73-30957

General properties of electromagnetic scattering by inhomogeneous anisotropic composite obstacles of arbitrary shape. 15 p1844 A73-31930

Extinction and scattering by several types of silicate sphere of radius 0.05-1.0 micron, for the wavelength range 0.21-50 microns. 15 p1939 A73-32012

Low-energy elastic differential scattering of He++ by He. 15 p1916 A73-322908

Excitation of atomic nitrogen by electron impact. 16 p2038 A73-330994

Scattering of electromagnetic radiation from a black hole. 16 p2060 A73-33129

Momentum transfer and total scattering cross sections for ions with polar molecules. 17 p2213 A73-35178

The composite scattering model for radar sea return. 17 p2163 A73-35364

Investigation of scattering of microwaves in a plasma-beam discharge. 17 p2217 A73-35716

Measurements of F2, NO, and ONF Raman cross sections and depolarization ratios for diagnostics in chemical lasers. 18 p2322 A73-36978

Relative Raman cross section of O3 for four Ar+ laser frequencies. 20 p2595 A73-38893

Treatment of molecular reaction equilibria and opacity calculations for cool circumstellar envelopes. 20 p2606 A73-39079

Diffraction of optical radiation by a reflecting disk in a turbulent atmosphere. 20 p2531 A73-39680

Oil spill radar scatterometer detection at 13.3 GHz through backscattering cross sections, discussing ground truth, data correlation and wind velocity. 20 p2560 A73-39892

Fredholm-uniformization computation of elastic scattering amplitudes in the presence of arbitrarily many open channels. 21 p2738 A73-40212

Gravitational Compton effect and graviton photoproduction by electrons. 21 p2742 A73-40351

Proton beam measurement of absolute cross section for neutron knockout reaction on C 12 at pion-nucleon resonance, correcting for muon and electron contamination. 21 p2743 A73-40686

Photon retinue and infra-red divergence problem in quantum electrodynamics. 22 p2889 A73-42426

Electron scattering from diatomic molecules in the first Born approximation. 22 p2889 A73-42446

Measurement of the effective cross section of inelastic interaction between protons and carbon nuclei in the energy range 0.1 TeV to 1.0 TeV, on the Proton-4 space station. 23 p3021 A73-43539

Extinction and scattering cross sections of small planetesimal particles with iron cores and silicate mantles in circumstellar dust of young T Tauri stars. 23 p3030 A73-43748

Reorientation/collision/cross sections for hydrogen intermolecular potentials, taking into account quadrupole-quadrupole interaction effects. 24 p3113 A73-44980

He and Ne cross sections in natural Mg, Al, and Si targets and radionuclide cross sections in natural Si, Ca, Ti, and Fe targets bombarded with 14- to 45-MeV protons. 24 p3125 A73-45103

Electron cooling rates calculation based on measured impact cross sections of molecular oxygen for vibrational and low lying electronic excitation. 24 p3086 A73-45123

Predicted electron transport coefficients and operating characteristics of CO2-N2-He laser mixtures. 24 p3097 A73-45420

SCATTERING FUNCTIONS

On the diffusion function of a stochastic transmission system. 01 p0017 A73-10975

On combined operations method for transfer problems in homogeneous, cylindrical media. 02 p0193 A73-12383

The interaction between ground reflecting power and celestial brightness. 04 p0441 A73-15292

Eigenfunction expansions and scattering theory for perturbed elliptic partial differential equations. 06 p0719 A73-18698

Effects of Compton scattering in a moving gas. 07 p0853 A73-20308

Albedo and illuminance of the surface of a planet with an inhomogeneous, purely scattering atmosphere. 07 p0820 A73-20345

Combined-operations method for diffuse reflection by an isotropic, non-coherent scattering homogeneous sphere. 10 p1271 A73-23484

Optical properties of polydisperse media with different size distributions of particles. 11 p1398 A73-25611

Light scattering functions in the atmospheric ground layer for a range of large scattering angles. 11 p1393 A73-25616

- Compton-scattering effects in a moving gas.
12 p1526 A73-27280
- The connection between the thermodynamics of chemisorption on semiconductor surfaces and surface scattering of carriers.
13 p1668 A73-28454
- Analytical description of the three-dimensional distribution of the scattering of a gyromotor magnetic field
13 p1618 A73-29149
- Comparison of the resolutions of two projective holography methods by comparing their line scattering functions corresponding to holographic images
14 p1753 A73-30376
- Experimental gain and noise parameters of microwave GaAs FET's in the L and S bands.
17 p2136 A73-34972
- Non-coherent scattering in transfer problems in spherical shell media. I - Frequency-independent source function.
17 p2236 A73-35780
- Dispersion model of a single-vortex function of structural scattering of atoms by surfaces
19 p2462 A73-37842
- Calculation of the radiation field in a semiinfinite medium in the presence of isotropic scattering
19 p2460 A73-37850
- Limits of applicability of the Delano model for describing the process of wave scattering by a complex-shaped body
19 p2407 A73-38343
- Performance estimate for coherent QPSK with random intersymbol interference due to time-varying scatter.
20 p2527 A73-38765
- Improved point-matching method with application to scattering from a periodic surface.
22 p2824 A73-41833
- SCATTERING MATRIX**
U S MATRIX THEORY
SCATTEROMETERS
- Oil spill radar scatterometer detection at 13.3 GHz through backscattering cross sections, discussing ground truth, data correlation and wind velocity
20 p2560 A73-39892
- Radio techniques applied to oceanography and earth science - Oceanic wind measurement and overland imaging as examples.
21 p2654 A73-40817
- SELF**
U SELF CONSISTENT FIELDS
SCHEDULES
NT COUNTDOWN
SCHEDULING
NT PREDICTION ANALYSIS TECHNIQUES
- Scheduling algorithms for multiprogramming in a hard-real-time environment.
08 p0941 A73-20961
- Aircraft operations computerized simulation for commercial flight schedules evaluation and optimization, describing operational modeling and programming
10 p1203 A73-23685
- Dynamic scheduling of large digital computer systems using adaptive control and clustering techniques.
14 p1730 A73-30039
- Charters, the new mode - Setting a new course for international air transportation.
16 p2087 A73-33101
- PLANET scheduling algorithms and their effect on availability.
17 p2130 A73-34822
- Simulating the introduction of 747 aircraft into airport operations.
18 p2296 A73-36423
- SCHEMATICS**
U CIRCUIT DIAGRAMS
SCHLIEREN PHOTOGRAPHY
- Linear schlieren photography with concave mirror and variable ultrasonic source for high resolution display of acoustic free field pressure gradient on TV screen
03 p0342 A73-12990
- Turbulent gas mixing measurements using a laser schlieren technique.
03 p0296 A73-14202
- Flame propagation in premixed propane /air or propane/ oxygen vortex rings, describing normal and schlieren photographic techniques
03 p0399 A73-14399
- Visualization of boundary layer flow patterns around protuberances using an optical-surface indicator technique.
07 p0808 A73-19530
- Band position predictions in schlieren visualization of hypersonic entropy wake behind blunt bodies, assuming bow shock geometry
07 p0775 A73-19970
- Plasma self radiation and absorption, schlieren signals and lasing levels recording methods based on dioxide lasers, using Mach-Zehnder IR interferometer
10 p1253 A73-23517
- Reflection plate interferometer with thin glass shearing plate replacing knife edge in Schlieren system, noting optimum operating range and fringe spacing
11 p1365 A73-26238
- The application of holography to sonic boom investigations.
11 p1371 A73-26633
- Entropy layer effects in constant pressure hypersonic boundary layers.
13 p1564 A73-28812
- Experimental studies on high speed performance of two-dimensional turbine cascades.
13 p1566 A73-29019
- Correlation and statistical characteristics of turbulence fronts in the wakes of hypervelocity bodies.
13 p1567 A73-29269
- Flame propagation in a transverse electric field
15 p1957 A73-31869
- Plasma self radiation and absorption, schlieren signals and lasing levels recording methods based on carbon dioxide lasers, using Mach-Zehnder IR interferometer
17 p2217 A73-35197
- Time evolution of pulsating air jets from schlieren photography and velocity measurements, using motor driven piston
17 p2157 A73-35514
- Interaction of a strong shock wave with electromagnetic field.
19 p2464 A73-37157
- Schlieren and computer studies of the interaction of ultrasound with defects.
19 p2461 A73-38201
- A method for the calibration of a quantitative high-speed schlieren procedure involving photographic recording
21 p2694 A73-39955
- Aeroballistic gas flow investigation using holographic device to schlieren system.
21 p2696 A73-39981
- Study of turbulent wakes behind cones in hypersonic flight using Schlieren photograph correlation
21 p2696 A73-39985
- Schlieren-optic and interferometric methods using TEA-CO₂ lasers and thermal liquid crystal IR image converters in the diagnostics of fast processes
21 p2744 A73-39998
- Photographic laboratory studies of explosions.
21 p2706 A73-41553
- SCHMIDT CAMERAS**
- Echelle spectrographs design, applications and performance, discussing modified Czerny-Turner mounting and Schmidt camera arrangements
01 p0046 A73-10510
- Schmidt and Maksutov spectrographic cameras, discussing correcting devices for mirror aberrations
01 p0047 A73-10512
- Conference on the Role of Schmidt Telescopes in Astronomy, Hamburg, West Germany, March 21-23, 1972, Proceedings.
08 p0966 A73-21354
- The role of Schmidt telescopes in the study of galactic structure /Photometric methods/.
08 p1011 A73-21355
- Astrometry with Schmidt telescopes, discussing automated computerized plate scanner and measuring machine for star position and relative motion determination
08 p0966 A73-21356
- Computational solution for positions on whole Schmidt-plates - Report on reduction of coordinates measured on 22 plates of the Bergeford Schmidt telescope.
08 p0966 A73-21357
- Schmidt telescopes application in astrometry, noting image quality uniformity across total field of view
08 p0966 A73-21358
- Astronomical spectroscopy with prism in front of Schmidt correcting plate, considering spectral resolution and light loss characteristics in plate field
08 p0966 A73-21359
- A proposal for a flint objective prism for the ESO Schmidt camera.
08 p0966 A73-21360
- The role of Schmidt telescopes in the study of external galaxies.
08 p1011 A73-21361
- Schmidt telescopes for quasars and blue stars radio astronomy in southern sky survey, considering UV filtering-out for image quality improvement
08 p1011 A73-21362
- Surface colour photometry of galaxies with Schmidt telescopes.
08 p1011 A73-21363
- Schmidt telescopes in stellar photography of Magellanic clouds, galactic center and Scorpio-Centaurus and globular clusters for southern hemisphere Milky Way structure investigation
08 p1011 A73-21364
- Schmidt telescopes for northern and southern hemispheres, discussing optical design with achromatic corrector to achieve high angular resolution and conversion to Cassegrain configuration
08 p0966 A73-21366
- Ten years of research with the 134 cm Schmidt telescope.
08 p0966 A73-21367
- Optical system and performance potential of telescopic high-aperture-ratio Schmidt camera designed for photographic studies of faint extended objects
11 p1361 A73-25230
- SCHOTTKY BARRIER DIODES**
U SCHOTTKY DIODES
SCHOTTKY DIODES
- On a 'memory' effect in N-type silicon Schottky diodes in the presence of metallic impurities
11 p1338 A73-25872
- Efficiencies of Schottky-barrier GaAs and both complementary structures of Si IMPATT diodes.
13 p1595 A73-29579
- High-power high-efficiency operation of Read-type IMPATT-diode oscillators.
14 p1736 A73-30447
- The Schottky-barrier silicon photodetector in perspective with other detection devices in the 200 nm to 1100 nm range.
16 p2013 A73-32885
- Integrated semiconductor storage devices, discussing bipolar transistor, Schottky diode and MOS memories and RAM, ROM and PROM types with circuit compatibility considerations
16 p1991 A73-33960
- Current-voltage characteristic of a real diode with a Schottky barrier, allowing for tunneling through the spatial charge region
18 p2293 A73-36718
- Schottky barrier diode solar cells using dielectric antireflection coatings, discussing Nb, Mo and Cr diode metal characteristics, photovoltaic characteristics and conducting properties
19 p2391 A73-38406
- Millimeter wave solid state technology for 60 GHz communication systems, discussing silicon Schottky diode and varactor mixer/receiver, parametric amplifiers and upconverters
20 p2534 A73-38748
- Intrinsic AM noise in singly tuned IMPATT diode oscillators.
20 p2537 A73-39417
- Superconductor-semiconductor Schottky barrier diode video detector with proper doping and electron tunneling to obtain high degree nonlinearity in I-V characteristics
21 p2662 A73-40463
- The rectifying barrier in gallium arsenide Schottky diodes
23 p2959 A73-43618
- Shot noise of a real Schottky-barrier diode during tunneling through the space charge region
23 p2960 A73-43619
- Influence of the surface level on the differential slope of the semilogarithmic current-voltage characteristic of Schottky diodes
23 p2960 A73-43620
- Influence of the image force and tunnel effect on shot noise in diodes with a Schottky barrier
23 p2960 A73-43715
- SCHOTTKY EFFECT**
U WORK FUNCTIONS
SCHROEDINGER EQUATION
- Reductive perturbation theory application to nonlinear Schrodinger equation for plasma of cold ions and isothermal electrons, investigating ion oscillation mode automodulation
01 p0082 A73-10420
- An equation for the product of semigroups defined by the method of bilinear forms and its application to the Schroedinger equation.
01 p0071 A73-11333
- Second-order abstract and Schroedinger linear differential equations in Beurling spaces
02 p0186 A73-11570
- Semiclassical theory of inelastic collisions. II - Momentum-space formulation.
06 p0726 A73-18262
- Solution to a time-dependent Schrodinger equation in the case of a specific potential
09 p1122 A73-22021
- S matrix method featuring eigenenergy and eigenfunction trials number reduction for rapid numerical determination of bound states of partial-wave-projected Schrodinger equation
10 p1248 A73-23669
- The initial value problem for the free-space Schrodinger equation.
10 p1244 A73-24787
- Asymptotic behavior of the eigenvalues of self-conjugate expansions of the Schroedinger operator in a multidimensional bounded domain
11 p1391 A73-26463
- Laser photons multiple absorption by atoms, determining transition probabilities from Schrodinger equation solution via space translation operation
14 p1776 A73-29698
- On the diffraction of dense electron beams in quantum mechanics.
20 p2595 A73-39766

SCHUMANN-RUNGE BANDS

SCHUMANN-RUNGE BANDS

Lower thermosphere thermal energy and oxygen transport due to photochemical reactions, noting Schumann-Runge band absorption, atomic recombination and collisional deactivation

11 p1358 A73-26706

Radiative transfer considerations for kinetic modeling and sensitivity studies.
[AIAA PAPER 73-505]

16 p2005 A73-33545

Atmospheric attenuation effects on nitric oxide dissociation in mesosphere and stratosphere, noting dissociation profile dependence on absorption of discrete oxygen Schumann-Runge bands

17 p2119 A73-34778

SCHWARTZ METHOD

Schwartz method application to stripline fields and impedance calculations for different cross sections and internal conductor dimensions

03 p0278 A73-14078

Numerical implementation of the Schwarz alternating procedure for elliptic partial differential equations.

14 p1768 A73-29938

SCHWARTZ-CHRISTOFFEL TRANSFORMATION

On a stagnation condition for combining or branching inviscid flows.

20 p2546 A73-39091

SCHWARZSCHILD METRIC

Schwarzschild coordinate system identification with frames of reference within exterior gravitational field of spherical nonrotating star

02 p0211 A73-11896

Equations of motion for steady state spherically symmetric flow of polytropic gases into or out of neutron stars, black holes or Schwarzschild singularities

02 p0223 A73-12729

Computation of Schwarzschild's periodic solutions in the restricted three-body problem.

02 p0226 A73-12838

Astronomical applications of general relativity, considering energy and matter outbursts, black holes and Kerr and Schwarzschild metrics

03 p0374 A73-13895

Schwarzschild interior metric singularity for ideal fluid sphere radius relation to Schwarzschild radius, noting conditions for emitted light red shift

03 p0380 A73-14588

Radiation fields in the Schwarzschild background.

08 p0988 A73-21202

Vector and tensor radiation from Schwarzschild relativistic circular geodesics.

10 p1249 A73-24346

Sidereal periods in a gravitational field characterized by Schwarzschild's internal solution

11 p1416 A73-25237

Motion of fast particles in a spherically-symmetric gravitational field

11 p1416 A73-25239

Painleve metric replacement for Schwarzschild metric in tests of general relativity, considering problem of supermassive celestial body gravitational collapse

15 p1937 A73-31650

Superposition of Schwarzschild solutions and metric of a gravitational dipole

17 p2212 A73-35561

Centrosymmetrical nonstatic pulsating metric development, discussing minipulsar particles, perihelion displacement, gravitational energy, red shift, luminous ray curvature and Schwarzschild metric

20 p2594 A73-39765

Schwarzschild solution indeterminacy as indicator of physical singularity analogous to intrinsically singular vertex of cone in Euclidean space

21 p2741 A73-41630

Transformation between orbital parameters in different coordinate systems of the general relativistic Schwarzschild problem.

22 p2886 A73-41967

Gravitational energy quantization model of noncharged particle based on proposed centrosymmetric metric with nonzero Einstein matter tensor and without Schwarzschild singularity

22 p2887 A73-42430

Global coordinate systems for spherical collapsing and expanding Oppenheimer-Snyder dust cloud behavior after critical Schwarzschild radius attainment

22 p2908 A73-42438

The Laplace and Poisson equations in Schwarzschild's space-time.

23 p3005 A73-43345

Gravitational red shift - A simple quantum field-theoretical consideration in a curved space.

23 p3006 A73-43607

SCIENTIFIC SATELLITES

NT APPLICATIONS TECHNOLOGY SATELLITES

NT ATS 1

NT ATS 3

NT ATS 5

NT ATS 6

NT ENVIRONMENTAL RESEARCH SATELLITES

Japanese sounding rocket and scientific satellite program.

01 p0110 A73-11102

The structure of scientific satellites developed by the University of Tokyo.

01 p0110 A73-11119

Thermal mathematical model development for spacecraft design as exemplified by small scientific satellite, comparing analytical results with test data

01 p0110 A73-11144

Power control unit for the scientific satellite.

01 p0111 A73-11165

Digital attitude sun sensor for ionosphere sounding satellite.

01 p0053 A73-11171

Orbit determination for the scientific satellite in Japan.

01 p0105 A73-11186

Experience obtained so far in connection with the German scientific spacecraft program

[DGLR PAPER 72-052]

02 p0227 A73-11654

Design principles for contamination abatement in scientific satellites.

02 p0136 A73-11991

High performance three axis attitude control system of TD1/A European scientific satellite, describing control circuits, logic, ancillaries and packaging procedure

07 p0904 A73-18968

Sun sensors for D-2B scientific satellite spin axis alignment and attitude stabilization with pointing control accuracy, discussing tests, compensatory tracking and solar simulation

07 p0821 A73-18986

German scientific research satellite Aeros, discussing program planning and management, mission analysis, attitude control, power supplies, test methods, yo-yo despin and ground operations systems

08 p1014 A73-21658

The automatic checkout of the Prospero Satellite.

09 p1070 A73-22917

Data collecting and sequencing equipment for Prospero satellite PCM telemetry system, describing encoders, programming unit and tape recorder for orbital data storage

09 p1051 A73-22918

X4 scientific satellite subsystems development status, discussing solar array, attitude control, data handling, power conditioning and antenna systems

09 p1154 A73-22919

UK5 X ray astronomy satellite, discussing structural design, attitude sensing for pointing control, data handling, attitude control and power supply systems

09 p1155 A73-22920

D-2A /Touresol/ satellite data processing procedures for technological controls, operation in flight and scientific purposes

10 p1187 A73-23620

D-2A satellite experiments for sky mapping and radiation intensity measurement, discussing attitude correction processing

10 p1285 A73-23623

SPACEWARN - An international mechanism for rapid distribution of information on satellites and space probes.

11 p1454 A73-25569

Computerized simulation of Ionosphere Sounding Satellite topside sounder system techniques for observation of critical frequencies and apparent distance-frequency characteristic relation

13 p1586 A73-29248

Preparation on the launch base and setting in operation in the launch area of the D2 A scientific satellite

14 p1804 A73-30108

Scientific and applications satellite launch site facilities, discussing payload preparation

14 p1742 A73-30109

Book on earth satellites covering transmission technology, cost effectiveness and materials development for communication, meteorological, earth resources, navigational, research and military applications

15 p1944 A73-32292

Electric propulsion interactive effects with spacecraft science payloads.

18 p2353 A73-36497

Versatile logic system for use in nuclear experiments on scientific satellites.

19 p2412 A73-37147

Precise attitude control of the Stanford relativity satellite.

19 p2494 A73-38080

SCIENTISTS

Project form of organization adoption for managing innovation, stressing impact of technology on career progression of scientist engineers

17 p2258 A73-35217

SCINTILLATION

Long-lived sectors of enhanced density irregularities in the solar wind.

02 p0205 A73-11911

Scintillation phenomenon due to radio wave propagation through ionospheric and tropospheric regions with irregularities in refractive index

02 p0162 A73-12300

Diurnal and latitudinal variations and frequency dependence of scintillation due to ionospheric irregularities, using rms electron density fluctuation and transverse scale size model

03 p0275 A73-13643

Estimation of the cumulative amplitude probability distribution function of ionospheric scintillations.

[AD-756247]

03 p0275 A73-13644

UHF airborne measurement of equatorial ionospheric scintillation fading.

03 p0275 A73-13647

Some results about the satellite scintillation on 150/400 MHz and the horizontal gradient of the total electron content in the polar ionosphere.

03 p0300 A73-13648

Wavelike structure of magnetic field-aligned irregularities detected by phase interferometry.

03 p0300 A73-13696

Note on solar plasma irregularities and plasma instabilities.

03 p0378 A73-14420

Airborne laser-beam scintillation measurements at high altitudes.

03 p0305 A73-14657

Equatorial scintillation diurnal and seasonal variations and F region electron density irregularities, noting unusual post sunset behavior of Faraday rotation angle

04 p0440 A73-14951

Multipath fading and ionospheric scintillation modes of propagation anomalies measurement to formulate models of propagation media

04 p0422 A73-15440

Estimation of the cumulative amplitude probability distribution function of ionospheric scintillations.

04 p0443 A73-15477

Cosmic-ray scintillations. I - Inside the magnetosphere.

04 p0492 A73-15526

Vertical scintillation propagation from ground characterized by log normal probability distribution, universal spectral function and variance behavior dependent on near ground meteorological conditions

05 p0569 A73-16625

Noise figures, detection probabilities and scintillation energy distributions in second generation image intensifier tubes

06 p0676 A73-18299

The recurrent solar wind streams observed by interplanetary scintillation of 3C 48.

07 p0870 A73-19595

Heat conductivity, plasma instabilities, and radio star scintillations in the solar wind.

08 p0998 A73-21165

Time dependent radio stars scintillation spectra with allowance for interplanetary plasma discontinuities velocity dispersion at small solar distances

10 p1274 A73-23716

Empirical model for F layer electron density irregularities responsible for VHF/UHF amplitude scintillation, considering geomagnetic latitude, local time, season and sunspot effects

10 p1190 A73-24895

Interplanetary scintillations observations from solar wind plasma density fluctuations power spectrum

12 p1533 A73-26980

Experimental determination of two-dimensional spatiotemporal power spectra of stellar light scintillation - Evidence for a multilayer structure of the air turbulence in the upper troposphere.

12 p1521 A73-27120

Analysis of the non-Gaussian spectra of interplanetary scintillations.

12 p1547 A73-27877

Spectra of star and planet scintillation and dependence of their characteristics on meteorological conditions

13 p1683 A73-29097

Calculation of probability of detection with target scintillation.

13 p1586 A73-29219

Pulsar detections at frequencies of 8.4 and 15.1 GHz.

14 p1802 A73-30751

Interplanetary scintillations of cosmic rays.

14 p1788 A73-30752

Calibration of turbulence and visual and photographic scintillation parameters in Pulkovo, Tashkent and Shternberg Institute astrolclimate systems for 50 inch reflector

15 p1934 A73-31425

Scintillations of satellite signals and their observation.

15 p1843 A73-31524

Equatorial scintillation variation with magnetic storm from ATS 3 VHF telemetry signal recordings, comparing with spread F observation

15 p1870 A73-31763

A test for revealing the fine-scale velocity structure of the solar wind

16 p2059 A73-32888

Correlation measurements on the complex amplitude of stellar plane waves perturbed by atmospheric turbulence.

16 p2037 A73-33684

Interplanetary-scintillation observations of 203 sources identified as radio galaxies or quasars. 17 p2225 A73-34289

Ionospheric scintillation at 4 and 6 GHz. 17 p2122 A73-34869

Simplified space/earth signal scintillation parameters as auxiliary reference for measurements concerning ionospheric irregularities. 17 p2162 A73-34949

Slant-path scintillation in the planetary boundary layer. 17 p2185 A73-35417

Analysis of multiwavelength observations of optical scintillation. 17 p2212 A73-35418

Time dependent radio sources scintillation spectra with allowance for interplanetary plasma discontinuities velocity dispersion at small solar distances. 18 p2355 A73-36741

Comparison of vertical profile turbulence structure with stellar observations. 19 p2446 A73-37259

Scintillation measurements for large integrated-path turbulence. 19 p2461 A73-38486

Analysis of VHF/UHF frequency dependence, space, and polarization properties of ionospheric scintillation in the equatorial region. 20 p2525 A73-38741

Analysis of the control circuit of a seeing measurement device. 20 p2565 A73-39069

Power spectrum of small-scale irregularities in the solar wind. 21 p2755 A73-40163

Quasar scintillations at an inhomogeneous interstellar plasma. 21 p2767 A73-40535

Variations of pulsar intensity as a result of scintillations at an inhomogeneous plasma. 21 p2767 A73-40536

Turbulence and scintillations in the interplanetary plasma. 21 p2748 A73-41235

Radio source signal scintillation correlation with high power HF transmitter caused F region electron density fluctuations. 22 p2825 A73-41920

On the relation between the pattern and wind velocities in interplanetary scintillations. 22 p2903 A73-42702

Enhanced scintillation sectors outside the plane of the ecliptic. 23 p3029 A73-43679

SCINTILLATION COUNTERS

Scintillation and anticoincidence Cerenkov counters for recording heavy nonrelativistic single charge particles in cosmic rays at sea level. 02 p0209 A73-12670

Electron photon shower particle flux transition effect on ionization chamber and scintillation counter readings. 02 p0210 A73-12685

Recording and data processing equipment proposed for scintillation measurements. 03 p0308 A73-13646

Molniiya 1 satellite slow neutron monitor with photomultiplier scanned scintillator, noting limiting effect of geomagnetic perturbations. 07 p0823 A73-19428

Lateral distribution of u.h.f. radio emission associated with cosmic ray showers. 09 p1137 A73-22174

Large scintillation counter with a high amplitude resolution. 09 p1085 A73-23003

Energy resolution of scintillation counters employing a light guide. 09 p1085 A73-23004

A charged-particle scintillation spectrometer with large geometric factor. 11 p1364 A73-25965

Amplitude analysis of extensive air shower particle fluxes. 12 p1496 A73-27202

Dependence of the light yield of a plastic scintillator on the energy of protons and electrons. 12 p1496 A73-27206

The BD-9 integral discriminator in the circuit of a scintillation-type fast neutron detector. 12 p1497 A73-27207

Radioactive spallation induced scintillator errors in satellite measurements of diffuse cosmic X ray spectrum, considering astrophysical implications. 12 p1537 A73-27882

Russian book on elementary particle counters covering gas discharge /Geiger-Muller/, scintillation, Cerenkov and semiconductor counters and matter-radiation interactions. 15 p1880 A73-32418

Video instrumentation for radionuclide angiocardiology. 19 p2399 A73-37796

A meson supertelescope using plastic scintillators and the coupling coefficients for it. 21 p2701 A73-40611

Transition effects during the recording of the electron-photon component of extensive air showers. 23 p3023 A73-43558

A device for recording the energy spectrum and fluxes of electrons with energies greater than 100 MeV in cosmic rays. 24 p3124 A73-44782

SCINTILLATION SPECTROMETERS

U SCINTILLATION COUNTERS

U SPECTROMETERS

SCINTILLATORS

U SCINTILLATION COUNTERS

SCINTILLOMETERS

U SCINTILLATION COUNTERS

SCISSION

U CLEAVAGE

SCOPOLAMINE

U HYOSCINE

SCOUT HELICOPTER

U P-531 HELICOPTER

SCR [RECTIFIERS]

U SILICON CONTROLLED RECTIFIERS

SCRAMBLING [COMMUNICATION]

Speech scrambling by the matrixing of amplitude samples. 21 p2657 A73-41206

SCRAMJET ENGINES

U SUPERSONIC COMBUSTION RAMJET ENGINES

SCRAMJETS

U SUPERSONIC COMBUSTION RAMJET ENGINES

SCRAP

Recovery of nonferrous metals from scrap automobiles by magnetic fluid levitation. [AIAA PAPER 73-959] 22 p2878 A73-42531

SCREEN EFFECT

Screen and porous absorbing liner design for damping pressure oscillations in ramjet combustors based on acoustic absorption efficiency and combustion instability calculation. [AIAA PAPER 73-226] 06 p0767 A73-17665

Diffraction of the emission field of a horizontal dipole on a circular hole in a plane screen in the presence of a circular disk coaxial with the hole. 06 p0664 A73-17716

Electron-beam tube with semiconducting laser screen. 06 p0677 A73-18636

Calculated pattern of a vertical antenna with a finite radial-wire ground system. [AD-756789] 07 p0792 A73-19384

Diffraction of a plane wave by a random phase screen. 07 p0793 A73-20056

Calculation of the aerodynamic characteristics of a rectangular wing with tip plates moving at a low subsonic speed in the proximity of a screen. 07 p0775 A73-20094

Simulation of velocity profiles by shaped gauze screen. 08 p0953 A73-20717

Coherent optical processing with spatial frequency diversity speckle and reflection noise reduction, discussing coding by illuminating input transparency through square screen mesh. 08 p0964 A73-21045

Effect of shielding on charge carrier mobility in compensated materials. 09 p1133 A73-22674

Effect of edge reflections on the performance of antenna ground screens. 11 p1329 A73-25673

Solid profile wing motion in ideal incompressible fluid at variable distance from screen in terms of small perturbation theory. 12 p1488 A73-27815

Screen effect on the radiation heat transfer in an area of penetrating radiation. 14 p1816 A73-30013

Dynamic scattering of oscillating charged centers in semiconductors. 19 p2471 A73-38541

Flow through non-uniform gauze screens. 20 p2508 A73-39811

Diffraction of a plane electromagnetic wave by a slit in a thick screen placed between two different media. 22 p2821 A73-41744

SCREENING

Ti alloy coating and surface treatment to prolong fatigue life by eliminating fretting damage, discussing design parameters selection, screening and strength tests and performance evaluation. 11 p1383 A73-25838

SCREENS

The energetic degree of shielding provided by hail-protection screens in the case of certain distribution spectra of hailstone diameters. 11 p1394 A73-26373

SCREW DISLOCATIONS

Behavior of dislocations in niobium under stress. 02 p0179 A73-11576

The effect of shear stress on the screw dislocation core structure in body-centred cubic lattices. 08 p0978 A73-21525

The analysis of dislocation systems by the finite element method. 10 p1290 A73-24298

New mechanism of slowing down screw dislocations in ordered alloys with a bcc lattice. 12 p1508 A73-26837

Dislocation structure in molybdenum single crystals after deformation at 293 and 400 deg K. 13 p1634 A73-28221

A treatise on the stress-fields produced by moving dislocations. Supplementary remarks and applications. 13 p1697 A73-28915

SCRUDDING

U WASHING

SEA ICE

Aircraft measurements of microwave emission from Arctic Sea ice. 02 p0171 A73-12773

Mapping of atmospheric and sea ice parameters with an imaging microwave radiometer from the Nimbus 5 satellite. 06 p0667 A73-18281

Analysis and interpretation of air-borne multifrequency side-looking radar sea ice imagery. 09 p1080 A73-22150

Sea ice observation by means of satellite. 11 p1358 A73-26346

Toros side-looking radar system for sea-ice distribution and geomorphological mapping and agricultural soil studies. 12 p1474 A73-27962

Millimeter wave backscatter measurements for snow, ice and sea ice, discussing penetration into snow and ice. 16 p1983 A73-33728

Microwave signatures of first-year and multiyear sea ice. 17 p2163 A73-35466

Polar albedo changes and its climatic consequences. 18 p2307 A73-36028

Earth satellite measurements as applied to sea ice problems. 18 p2310 A73-36134

Two-dimensional statistic analysis of radar imagery of sea ice. 20 p2556 A73-39843

Satellite measurements of microwave and infrared radiobrightness temperature of the earth's cover and clouds. 20 p2556 A73-39844

Statistical comparison of airborne laser and stereophotogrammetric sea ice profiles. 22 p2850 A73-42731

SEA KNIGHT HELICOPTER

U CH-46 HELICOPTER

SEA ROUGHNESS

Remote sounding of water surface conditions from aboard artificial satellites. 21 p2657 A73-41333

SEA STATES

A noncoherent model for microwave emissions and backscattering from the sea surface. 02 p0164 A73-12362

Asymptotic scheme for a class of partial differential equations. 09 p1112 A73-22477

Microwave radiometric observations of simulated sea surface conditions. 11 p1355 A73-25774

Detection of oil spills using a 13.3-GHz radar scatterometer. 13 p1610 A73-29196

Comments on the determination of the total heat flux from the sea with a two-wavelength radiometer system as developed by McAlister. 13 p1610 A73-29197

Experimental investigation of microwave signal fluctuations for propagation above the sea at low slip angles. 16 p1978 A73-32889

On radar mapping of sea surface. 17 p2123 A73-35153

SEA WATER

Stress corrosion cracking behavior of 18% Ni /300/ maraging steel. 01 p0066 A73-11295

Diffusion coefficients and current velocities in coastal waters by remote sensing techniques. 05 p0572 A73-17141

Struvite precipitation from evaporating sea water with added ammonia, considering importance for prebiotic phosphorylation. 07 p0787 A73-19168

Investigations of the electrochemical processes in titanium alloys as applied to stress-corrosion crack tip state in sea water. 15 p1896 A73-32572

Remote sensing of the ocean. 19 p2405 A73-38240

Remote measurement of subsurface sea water temperature by airborne Raman scattering with cross polarizer in front of light source and detector, noting precision. 20 p2568 A73-39889

SEALANTS

- Oceanic contribution to atmospheric CO budget estimation from Northern Hemisphere water carbon monoxide content, comparing to anthropogenic production 21 p2680 A73-40083
- Shallow lake or sea with large class of bottom topographies, obtaining wind-driven current analytic solution with conformal mapping technique 21 p2686 A73-41015
- Measurements of the dielectric properties of seawater and NaCl solutions at 2.65 GHz. 22 p2849 A73-42549
- Remote measurement of salinity in an estuarine environment. 22 p2850 A73-42730

SEALANTS

U SEALERS

SEALERS

- Technical and safety aspects of maintenance work on commercial aircraft wing fuel tanks, considering wing deformation effects and sealant materials and reapplications 18 p2286 A73-36932

SEALING

- Elastomer compatibility considerations relative to O-ring and sealant selection. 08 p0982 A73-20691 [SAE AIR 786 A]
- Ceramic-to-metal sealing and joining technology assessment, discussing noble filler metal properties, ceramic surface preparation and thermal tests for performance evaluation 09 p1088 A73-22444
- Thin film sealing techniques at temperatures below 300 C for binding Pyrex to various materials, using Au layer as alloy flux 09 p1085 A73-22950
- Development of a new kind of Lallemand camera. 14 p1751 A73-29905

SEALS (STOPPERS)

- NT GASKETS
- NT HERMETIC SEALS
- NT O RING SEALS
- NT PLUGS

- An elastohydrodynamic analysis of the sleeve type high pressure seal. 01 p0055 A73-10224 [ASME PAPER 72-LUB-M]
- Analysis of face deformation effects on gas film seal performance. 01 p0055 A73-10246
- Application of the turbulent eddy diffusivity transport equation to the analysis of turbulent flow in the radial face seal. 03 p0293 A73-13315
- Handbook on mechanical face seals covering applications, operational capabilities, design, environmental control, handling, installation, malfunctions, auxiliary equipment, optical flats, etc 03 p0313 A73-13995

- On the influence of the contact pattern on the sealing capacity and the power loss of hydrodynamic lip seals. [ASLE PREPRINT 72LC-7A-1]

- A hydrodynamic theory of radial-face mechanical seals. 03 p0316 A73-14367
- A compact demountable superleak-tight seal for low temperature experiments. 10 p1223 A73-23698

- Aerospace cryogenic static seals. 11 p1375 A73-26317

- How to select shaft seal materials. 13 p1624 A73-28800 [ASLE PREPRINT 73AM-6E-2]

- Recent developments on noncontacting face seals. [ASLE PREPRINT 73AM-8B-3]

- Influence of hydrodynamics on the performance of radial lip seals. 17 p2179 A73-34995 [ASLE PREPRINT 73AM-9B-2]

- Self-acting and hydrodynamic shaft seals. 17 p2179 A73-34998

- Analytical study of pressure balancing in gas film seals. 17 p2179 A73-34999

- Aeroelastic vibrations in labyrinth seals. 17 p2180 A73-35000

- Mechanical face seal between rotating shaft and surrounding member using stationary and rotating ultraflat radial sealing faces, discussing temperature and chemical considerations 20 p2569 A73-39373

- Dynamic shaft seal types for high speed continuous shaft rotation, considering service life, failure modes and materials selection 22 p2865 A73-41775

- 22 p2865 A73-41776

SEAMS (JOINTS)

- Small-scale explosion seam welding. 10 p1223 A73-23626

SEARCH PROFILES

- The detection of a point source in the presence of nongaussian background noise. 01 p0017 A73-10832

- Application of Liapunov functions for studying the convergence of unconstrained minimization methods 13 p1657 A73-28018

- Accelerating search-variable metric algorithm combination for space shuttle atmospheric flight optimization, comparing with cubic fit-golden section method 13 p1650 A73-28825

- Search properties of some sequential decoding algorithms. 22 p2829 A73-42706

SEARCH RADAR

- Optimal search scanning for electronic surveillance radar based on antenna beam position with highest echo signal for maximum likelihood target acquisition 13 p1581 A73-27999
- On the angular resolution of a search radar with a mechanically rotated antenna. 17 p1215 A73-35369

SEARCHING

NT SEARCH PROFILES

- Search stability and steady motion region characteristics of self oscillatory extremal automatic control system under additive disturbances on controlled object input 05 p0560 A73-16293

- One- and multistage multivariable function max-min problem solution by random search type method through regression curve construction based on statistical test and root determination 06 p0715 A73-17563

- On the convergence of random search algorithms in continuous time with applications to adaptive control. 06 p0671 A73-18623

- Dynamic programming as applied to feature subset selection in a pattern recognition system. 08 p0941 A73-21666

- Comparative analysis of optimal failure search procedures, considering criteria, failure extent, initial data, reliability and compatibility 10 p1226 A73-24696

- Significant elements of an effective search, rescue, and survival system. 10 p1176 A73-24712

- Quadratically convergent algorithms and one-dimensional search schemes. 12 p1517 A73-27118

- Multistep conjugate gradient search methods with memory, describing convergence of iterative procedure for functional minimization 12 p1485 A73-27617

- Eye movements during visual search and memory search. 13 p1579 A73-29125

- On the uniqueness of search directions in variable-metric algorithms. 21 p2726 A73-40837

SEAS

- NT BALTIC SEA
- NT CARIBBEAN SEA
- NT CASPIAN SEA
- NT MEDITERRANEAN SEA
- NT NORTH SEA

SEASONAL VARIATIONS

U ANNUAL VARIATIONS

SEASONS

- NT SUMMER
- NT WINTER

SEAT BELTS

- Single point emergency equipment divestment system for instantaneous parachute harness, lap belt and leg restraint release, describing pyrotechnic actuation system 16 p1966 A73-32666

- Restraint systems /lap belts and shoulder harnesses/ for military, transport and general aviation aircraft, with emphasis on pilot and crew systems [SAE PAPER 730291] 17 p2114 A73-34656

- Severe intraabdominal injuries without abdominal protective rigidity after an air crash - Seat belt injury 20 p2517 A73-39209

SEATS

NT EJECTION SEATS

- Support method and equipment for observer at Cassegrain focus of large telescopes, emphasizing universal chair structural details and operation principles 01 p0029 A73-10545
- The effects of various seat surface inclinations on posture and subjective feeling of comfort 03 p0266 A73-13121

- Aircraft crash injury reduction through seat and restraint design, discussing dummy size considerations, seat belts, aircraft acceleration and injury types [SAE PAPER 730290] 17 p2114 A73-34655

SECTANTS

U TRIGONOMETRIC FUNCTIONS

SECONDARY AIR

U AIR

SECONDARY COSMIC RAYS

- Inelastic nuclear interactions between 200-GeV cosmic ray particles and polyethylene targets, correlating similarity property, momentum spectra and secondary particle pairs 02 p0208 A73-12652

- Secondary cosmic ray shower charged particles and angular distribution asymmetry in center-of-mass system and azimuthal plane related to single fireball formation. 02 p0208 A73-12652

- Russian book - Meteorological effects on cosmic rays. 05 p0608 A73-16122

- Solar and geomagnetic modulation of low-energy secondary cosmic ray electrons. 12 p1533 A73-26977

- Measurement of geomagnetic cutoff rigidities and particle fluxes below geomagnetic cutoff near Palestine, Texas. 12 p1533 A73-26977

- International Conference on Cosmic Rays, 12th, University of Tasmania, Hobart, Tasmania, Australia, August 16-25, 1971, Papers. Volume 7 & Invited and Rapporteur Papers. 16 p2054 A73-33276

- High-transverse-momentum secondaries and rising total cross sections in cosmic-ray interactions. 19 p2476 A73-38229

- Events in a photoemulsion indicating the formations of superheavy fireballs 23 p3021 A73-43538

- Properties of secondary high-energy particles in hadron interactions 23 p3021 A73-43538

SECONDARY EMISSION

- Computed secondary-electron and electric field distributions in an electron-beam-controlled gas-discharge laser. 01 p0058 A73-10130

- Cosmic ray muon component integral multiplicity calculations with allowance for angular distribution of secondary particles in elementary collision event on atmospheric boundary, using computer 02 p2025 A73-12172

- Secondary particles in pion-nucleon and coherent interactions, measuring momentum from multiple Coulomb scattering 02 p0209 A73-12666

- Total electron backscatter and backemission yields from metals bombarded at several angles by 0.4 to 1.4 MeV electrons. 05 p0604 A73-16514

- Miniaturized second generation night vision image intensifier system operation and performance based on secondary photoelectron emission 06 p0694 A73-18300

- A gas cell method for the measurement of secondary electron ejection coefficients for metastable atoms on metal surfaces. 06 p0726 A73-18846

- Secondary electron emission characteristics of lunar surface fines. 07 p0871 A73-19861

- Calculations of the transport of neutrons and secondary gamma rays through concrete for incident neutrons in the energy range 15 to 75 MeV. 08 p0987 A73-21528

- Spatial and temporal ionization growth characteristics in nitrogen at moderate electric field strength, noting dominant secondary emission effect due to cathode bombardment by metastable molecules 09 p1122 A73-22120

- Excitation of long-wave oscillations by a secondary electron stream in a plasma generated by an ion beam 09 p1129 A73-22684

- Secondary particles multiplicity law validity in cosmic ray showers highest energy interactions 09 p1138 A73-23035

- On the secondary production of galactic cosmic ray electrons. 10 p1270 A73-24910

- Ionization vacuum chambers for radiation measurement, discussing secondary emission, Greening theory and dosimeters, electron beam monitors, pulse measurement, energy spectrometers and interface dosimetry applications 11 p1362 A73-25422

- Monoenergetic particle beam instabilities in homogeneous plasma due to secondary emission wave interactions 13 p1664 A73-28289

- Band structure, electron energy distribution and emission efficiency of negative electron affinity secondary emitters and cold cathodes 14 p1732 A73-29912

- Secondary electrons and energy per ion-pair in a thermal gas for electron, proton and X-ray ionization. 16 p2052 A73-32826

- On the abundance of secondary nuclei in cosmic rays. 19 p2475 A73-37572

- Effect of secondary emission of the potential of a metallic body in the electron radiation belts of the earth. 20 p2601 A73-38875

- Effect of longitudinal magnetic field on the performance of a channel electron multiplier. 20 p2565 A73-38884

- Complete hydrogen and helium particle spectra from 30- to 60-MeV proton bombardment of nuclei 02 p0208 A73-12652

with $A = 12$ to 209 and comparison with the intranuclear cascade model. 21 p2744 A73-41019

Chemical analysis of surfaces by mass spectrography with secondary ion emission 21 p2648 A73-41595

Monoeenergetic particle beam bunching instabilities in homogeneous plasma due to secondary emission wave interactions 22 p2890 A73-41813

Low-energy cosmic ray protons from nuclear interactions of cosmic rays with the interstellar medium. 22 p2902 A73-41927

Pion-nucleon interaction structure based on negative pion beam data from Serpukhov accelerator, showing secondary particle energy distribution asymmetry 23 p3021 A73-43537

Inelastic interaction between pions and emulsion nuclei at an energy of 60 GeV 23 p3021 A73-43541

Multichannel secondary electron image intensifier design, using dynode and separate channel transmission 23 p2961 A73-44386

Spectrometer design with particle preacceleration for measuring energy spectra of secondary electrons and photoelectrons with high resolution 24 p3092 A73-45553

SECONDARY FLOW

Secondary flow in the entrance region boundary layers of an expanding square duct. [ASME PAPER 72-WA/FE-34] 04 p0404 A73-15851

Visualization study of flow in axial flow inducer. [ASME PAPER 72-FE-33] 05 p0565 A73-16547

Closed form analytical solution for secondary flow in viscous liquids axisymmetric flow past oblate and prolate ellipsoids 06 p0687 A73-18507

The secondary flow about circular cylinders mounted normal to a flat plate. 08 p0926 A73-21440

Periodic semi-integral solutions of secondary unsteady convective flows in external force field for critical Rayleigh numbers by Liapunov-Schmidt method 10 p1204 A73-23584

Secondary flows - Theory, experiment, and application in turbomachinery aerodynamics. 10 p1171 A73-23860

Calculation of a three-dimensional boundary layer in revolving channels of centrifugal rotors 10 p1173 A73-24672

Interaction of free and forced convection in horizontal tubes in the transition regime. 11 p1448 A73-25153

Viscous incompressible Jeffery-Hamel fluid flow in divergent channel, discussing secondary supercritical flow, winding and vortex formation 11 p1346 A73-25223

Laminar incompressible fluid steady secondary flow in circular cross section curved tube at various Reynolds numbers 11 p1346 A73-25225

Newtonian and non-Newtonian liquids rotating adjacent to a stationary surface. 11 p1346 A73-25369

Noise reduction for subsonic fluid flow over flat plate via interposition of secondary fluid layer at trailing edge 11 p1300 A73-25386

Secondary flow in blade cascades of axial turbomachines and the possibility of reducing its unfavourable effects. 13 p1565 A73-29008

Studies on bounded jets. 13 p1603 A73-29032

The origin of secondary flow in turbulent flow along a corner. 14 p1744 A73-30164

Spiral flows with multiple circulation in channels of simple shape 15 p1861 A73-31284

Secondary loss measurements in a cascade of turbine blades. 17 p2092 A73-34380

Kinetic energy transfer during multiple jet mixing from primary jet array to secondary stream for various velocity ratios 17 p2156 A73-35511

Generalized expressions for secondary vorticity using intrinsic co-ordinates. 18 p2299 A73-36506

Generation of time-periodic secondary convective flows 18 p2301 A73-37006

The investigation on the secondary flow induced by jets. I. 19 p2422 A73-38349

Investigation of secondary flows between coaxial rotating cylinders 21 p2676 A73-40574

A three-dimensional MHD boundary layer in an incompressible fluid 21 p2747 A73-40882

SECONDARY FRONTS

U FRONTS [METEOROLOGY]

SECONDARY HARMONIC GENERATION

U HARMONIC GENERATIONS

SECONDARY INJECTION

A series of evolved shadowgraphs of shock waves induced by secondary injection in a conical supersonic flow. 01 p0003 A73-11128

Dynamic response of an on-off type secondary injection thrust vector control. 01 p0091 A73-11196

Secondary jet interaction with emphasis on outflow and jet location. 03 p0243 A73-13496

Turbulent intensity induced by wakes near secondary air jet inlet to gas turbine engine flame tube 07 p0867 A73-19625

An experimental study of strong injection at axisymmetrical bodies of revolution. 21 p2633 A73-41057

Experiments on the propagation of mixing and combustion injecting hydrogen transversely into hot supersonic streams. 22 p2934 A73-42785

Burn-up of the high temperature products of incomplete combustion in a supersonic flow by a second injection of oxidizer 24 p3156 A73-45076

SECONDARY RADAR

Secondary radar interrogator based on IC technology, discussing video processing and monitoring 15 p1847 A73-32436

Secondary surveillance radar - Current usage and improvements. 19 p2451 A73-37808

Basic principles and the theory of operation of the equipment for the identification-friend or foe (SIF) in military aircraft 21 p2650 A73-40348

Secondary Surveillance Radar application to aircraft identification in upper airspace of Eurocontrol member states, emphasizing code assignment 22 p2884 A73-42322

SECONDARY WAVES

U S WAVES

SECRECTIONS

NT ENDOCRINE SECRETIONS

NT HORMONES

NT INSULIN

NT SWEAT

Russian book - Mutual relationship of water and salt secretion functions in digestive and excretory organs under conditions of high temperature. 21 p2641 A73-41438

SECULAR PERTURBATION

U LONG TERM EFFECTS

SECULAR VARIATIONS

Secular variation of the stratospheric ozone layer over middle Europe during the solar cycles from 1951 to 1972. 04 p0445 A73-15635

Anomaly configuration maps showing westward drift and positions of residual geomagnetic fields and eccentric dipoles during 1885-1965 period 06 p0689 A73-17544

Long-term variations of total and polarized fluxes, absolute energy distribution, and line strength of BL Lacertae and four quasi-stellar sources. 07 p0873 A73-19051

Total solar eclipses of great duration. 07 p0876 A73-19400

Distribution of electrical conductivity in the earth's mantle from data on the secular variations of the geomagnetic field 08 p0959 A73-21295

Analytical description of the geomagnetic field of past epochs and the determination of the magnetic-wave spectrum in the earth's core 08 p0959 A73-21297

Application of Gauss' method to the determination of secular radiational perturbations of artificial earth satellites 09 p1143 A73-22100

Secular geomagnetic field variation of the epoch 1965-1970, according to observatory and satellite observations. 10 p1212 A73-24232

Possibility of determining the secular variation of geomagnetic field components from the distribution of variations of the absolute value of the total vector. 10 p1212 A73-24234

Secular stability. V - The perturbation of chemical abundances. 10 p1280 A73-24404

Solar quiet long-term modulation of cosmic ray intensity diurnal variation explained via interplanetary sector pattern changes 10 p1269 A73-24448

A study of commensurable motion in the asteroid belt. 11 p1417 A73-25264

Lunar rotation secular acceleration and tidal friction related to earth rotational velocity and creep properties 13 p1677 A73-28378

Power spectral analysis of Chandler wobble latitude variations over 70 year period, showing doubtfulness of two-peak resonance pattern in wobble 13 p1678 A73-28381

Earth axis 14 month variation with latitude/Eulerian nutation/as free vibration subject to damping, obtaining nonuniform drift rate from seven year interval observations 13 p1678 A73-28382

Analysis of the Chandler period of polar coordinates calculated by the Orlov method. 13 p1678 A73-28383

On the regularity of fluctuations in annual and secular polar motions. 13 p1678 A73-28385

Secular pole motion vs continental drift effects from geodetic, astronomical and time base observations 13 p1678 A73-28386

Non-periodic latitude variations and the secular motion of the earth's pole. 13 p1678 A73-28387

Washington observatory latitude variations observations compared with earth rotation pole secular variations from International Polar Motion Service data, suggesting seismic influences 13 p1678 A73-28388

Earth pole secular motion analyzed by latitude observations, suggesting northward drift of major continents 13 p1679 A73-28389

The excess secular change in the obliquity of the ecliptic and its relation to the internal motion of the earth. 13 p1679 A73-28401

Earth mantle convection theory, calculating polar secular wandering from inertia product change due to mass transfer 13 p1607 A73-28404

Secular stability of an 8 solar mass star during central helium burning. 13 p1685 A73-29355

Cometary observations and variations in cometary brightness. 14 p1789 A73-29778

Disturbing functions application to secular perturbation calculation for periodic comets with validity for any eccentricity and inclination 14 p1790 A73-29787

Borrelly periodic comet motion, including secular acceleration due to nongravitational forces and orbital elements perturbations by planets from Venus to Pluto 14 p1791 A73-29805

Cometary nucleus evolution dependence on secular brightness decrease relationship to dust particle size distribution, nuclear radius and screened surface area 14 p1792 A73-29817

Meteoritic particles orbits secular evolution under planetary perturbation and Poynting-Robertson effects, considering osculating orbital elements long term variations via simplified model 14 p1795 A73-29842

Deformation of a meteor stream caused by an approach to Jupiter. 14 p1795 A73-29843

On approximate calculation of the principal part of disturbances in an interior bounded three-body problem. 14 p1802 A73-30953

Motion of a satellite in the equatorial plane of a spheroid. 15 p1929 A73-31107

Critique of Poincare technique for construction of global solution of resonance of dynamical system, considering procedure using secular terms and regularizing function 15 p1930 A73-31111

On the stability of the light-variations of RR Lyrae stars. 15 p1933 A73-31308

Horseshoe and Trojan orbits associated with Jupiter and Saturn. 15 p1937 A73-31948

Anomaly configuration maps showing westward drift and positions of residual geomagnetic fields and eccentric dipoles during 1885-1965 period 16 p2002 A73-32768

Complex roots onset in secular stellar spectrum extended to case with shell sources present, determining eigenvalues for different intensity and position parameters 16 p2058 A73-32830

Geomagnetic effects on cosmic ray cut-off daily, seasonal and secular variations, considering north-south symmetry and magnetospheric models 16 p2055 A73-33297

Characteristic features of secular and super-secular cycles of solar activity - The 180-year cyclic variation of solar activity 16 p2056 A73-33657

Analysis of atmosphere circulation and climate fluctuations in different portions of the Northern Hemisphere of the earth 18 p2331 A73-35913

Large-scale variations in the obliquity of Mars. 18 p2348 A73-35921

SEDATIVES

Satellite geodesy application to earth internal structure and gravity field relationship to geomagnetism, noting magnetic secular variation correspondence with large scale mass motion

18 p2302 A73-35932

Approximate description of the evolution of a synchronous-satellite orbit

18 p2350 A73-36101

Planetary elements for 10 000 000 years.

18 p2352 A73-36418

Distribution of electric conductivity in the mantle of the earth, according to data on secular geomagnetic field variations.

19 p2425 A73-37924

Analytical description of the geomagnetic field of past epochs and determination of the spectrum of magnetic waves in the core of the earth.

19 p2425 A73-37926

Determination of equations of conditions between harmonics of resonance of the order of 14 starting with observations from the Eole satellite

21 p2781 A73-41327

Secular geomagnetic variation consequences for steady state inner zone of energetic protons, discussing minimum altitude decrease and mirror point field magnitude increase

21 p2761 A73-41375

Rotation of the earth's magnetic field.

21 p2692 A73-41641

An analytical expression for the secular variation of the geomagnetic field and a comparison of the activity of secular variations with some astronomical phenomena

23 p2973 A73-43793

Global climatological ozone changes in terms of secular, annual and sunspot cycle-related variability

23 p2974 A73-43858

Fourteen-year series of vertical ozone distribution over Arosa, Switzerland, from Umkehr measurements.

23 p2974 A73-43869

Six years of regular ozone soundings over Switzerland.

23 p2974 A73-43870

The influence of solar activity on the stratospheric ozone layer.

23 p2976 A73-43884

Secular perturbations of third order with respect to oblateness from all zonal harmonics of the gravitational potential of a planet

23 p3037 A73-44253

Motion of the inertia pole of the earth over a hundred years

23 p3037 A73-44255

Secular variations in H alpha, H beta and metal line spectra of Be star 88 Hercules from intensity decrease observations, noting envelope hydrogen absorption lines visibility

24 p3140 A73-45187

SEDATIVES

Effects of some antinotion sickness drugs and secobarbital on postural equilibrium functions at sea level and at 12,000 feet/simulated/.

09 p1045 A73-22529

SEDIMENTARY ROCKS

NT CARBONACEOUS ROCKS

NT COAL

NT SANDSTONES

NT SHALES

Sedimentology of clastic rocks returned from the moon by Apollo 15.

01 p0103 A73-11016

The isolation of a series of acyclic isoprenoid alcohols from an ancient sediment - Approaches to a study of the diagenesis and maturation of phytol.

11 p1326 A73-25465

SEDIMENTS

NT MUD

NT SANDS

Bottle green microtektites from Australasian and Ivory Coast deep sea sediments, discussing physical and chemical properties, age and origin

05 p0615 A73-16383

Geochemical significance of perylene occurrence in marine sediments, discussing land organism biogenic pigment precursors and polycyclic aromatic hydrocarbon conversion

10 p1211 A73-24105

Laboratory simulation of organic geochemical processes.

11 p1325 A73-25460

Deep sea drilling core sample analysis methods and results relation to sediment age and fossil fauna and flora

11 p1325 A73-25462

The diagenesis and maturation of phytol - The stereochemistry of 2,6,10,14-tetramethylpentadecane from an ancient sediment.

11 p1326 A73-25466

Acids obtained by oxidation of kerogens of ancient sediments of different geographic origin.

11 p1326 A73-25467

The origin and incorporation of organic molecules in sediments as elucidated by studies of the sedimentary sequence from a residual Pleistocene lake.

11 p1326 A73-25468

Geochemistry of amino acid enantiomers - Gas chromatography of their diastereomeric derivatives.

11 p1326 A73-25469

Amino acid composition significance in sedimentary fossil skeletal protein calcification, discussing diagenetic temperature effects

11 p1326 A73-25470

Trace fossils from the Nama Group, south-west Africa.

12 p1490 A73-27250

Upper Cretaceous Spumellarina from the Great Valley Sequence, California coast ranges.

13 p1605 A73-28023

Late Precambrian microfossils - A new stromatolitic biota from Boothanna, South Australia.

14 p1713 A73-29723

Remote sensing of ocean color as an index of biological and sedimentary activity.

18 p2307 A73-36030

North American microtektites from the Caribbean Sea and their fission track age.

18 p2354 A73-36511

Paleomagnetic excursion recorded in latest Pleistocene deep-sea sediments, Gulf of Mexico.

18 p2313 A73-36513

Distribution and diagenesis of organic compounds in JOIDES sediment from Gulf of Mexico and western Atlantic.

21 p2683 A73-40562

Suspended sediment observations from ERTS-1.

22 p2850 A73-42726

Racemization of amino acids in marine sediments determined by gas chromatography.

23 p2973 A73-43843

SEEDING (INOCULATION)

U INOCULATION

SEEDS

Anomalous lower dynamic pressure in piezometer of pitot tube in liquid flow containing solid particles, using seeds in aqueous solution of calcium chloride

11 p1367 A73-26476

Life processes in ammonia - Anomalous germination behavior of onion seed in ammonia and amines.

11 p1321 A73-26491

Fatty acids of Pinus eliottii tissues.

15 p1841 A73-32199

Cytogenetic analysis of diploid and autotetraploid Crepis capillaris seeds following space travel on the 'Cosmos-368' artificial earth satellite

18 p2271 A73-36117

Results of cytogenetic studies of seeds after their extended orbital flight aboard the Salyut orbital scientific station.

22 p2804 A73-42169

SEENERS

U HOMING DEVICES

SEISMIC WAVES

NT LOVE WAVES

NT MICROSEISMS

NT RAYLEIGH WAVES

Periodicities in seismic response caused by pulsar CP1133.

03 p0367 A73-13056

Possible sidereal period for the seismic lunar activity.

03 p0367 A73-13057

Search for seismic signals from gravitational radiation of pulsar CP1133.

03 p0367 A73-13058

A possible mechanism of the generating of the unusually long lunar seismic oscillations.

03 p0368 A73-13092

On the interaction between tectonic processes of the earth and the moon.

03 p0299 A73-13093

Resonant coupling of ocean Rayleigh waves to atmospheric shock waves from Apollo rockets.

05 p0569 A73-16380

Lunar seismic wave velocity change at 25 km interpreted in terms of fine rock powder undergoing final densification

05 p0622 A73-17181

Moonquakes and lunar tectonism results from the Apollo passive seismic experiment.

07 p0894 A73-19848

Range of earth structure nonuniqueness implied by body wave observations.

10 p1215 A73-24779

Seismic measurement data from Cornish cottage during Concorde sonic boom flight, using moving coil geophones

11 p1306 A73-26292

Compressional wave velocity profile of lunar near-surface and crust derived from seismic refraction data at Apollo 14 and 16 sites

12 p1541 A73-27486

Washington observatory latitude variations observations compared with earth rotation pole secular variations from International Polar Motion Service data, suggesting seismic influences

13 p1678 A73-28388

Lunar structure and dynamics - Results from the Apollo passive seismic experiment.

17 p2236 A73-35744

New seismic data on the state of the deep lunar interior.

17 p2237 A73-35805

Lunar surface fine rock powders seismic measurements in terms of Q factor and acoustic propagation velocity under various temperatures and pressures

20 p2612 A73-39712

Dispersed signal filtering and filtered signal duration relation to filter bandwidth and dispersiveness, isolating fundamental mode of Rayleigh waves from earthquake 650 km deep

21 p2648 A73-39931

SEISMOGRAMS

Application of the ambiguity function to seismic signatures.

06 p0690 A73-18009

SEISMOGRAPHS

NT LUNAR SEISMOGRAPHS

Seismometer compensation for broadband, low-level acceleration measurements.

20 p2563 A73-38773

Linear acceleration insensitive balanced rotor seismic angular motion sensor with optical pickoff system, discussing mathematical model and performance tests

20 p2564 A73-38774

Selected applications of a biaxial tiltmeter in the ground motion environment.

20 p2564 A73-38781

Geophysical effects of Concorde sonic boom.

20 p2509 A73-39624

SEISMOLOGY

NT MOONQUAKES

Cometary collision energy triggering of catastrophic changes in climate, geological period terminations and lava flow initiation, noting tektite-geologic period ages correlation

10 p1275 A73-23823

Seismicity as a guide to global tectonics and earthquake prediction.

11 p1352 A73-25563

The elastic energy and character of quakes in solid stars and planets.

11 p1420 A73-25894

Lunar interior materials seismic compressional velocities, indicating differentiated structure consistent with solidus thermal history

11 p1421 A73-25895

Bullen solid core model for earth and Venus vindicated by free earth oscillations records and detection of PKJKP seismic phase, discussing compressibility effects

11 p1421 A73-25897

On the correlation between earthquake occurrence and disturbances in the path of the rotation pole.

13 p1607 A73-28405

Excitation of the Chandler wobble by large earthquakes.

13 p1607 A73-28407

Apollo 17 seismic profiling - Probing the lunar crust.

16 p2059 A73-32903

Ancient lunar mega-regolith and subsurface structure.

24 p3129 A73-44448

Lunar 25 km discontinuity seismically examined, discussing hypotheses with shock metamorphism lack and annealing of shock induced microcracks

24 p3131 A73-44470

SEISMOMETERS

U SEISMOGRAPHS

SEIZURES

Effect of sleep-wake reversal and sleep deprivation on the circadian rhythm of oxygen toxicity seizure susceptibility.

02 p0135 A73-12561

CNS epinephrine tone, a possible etiology for the threshold in susceptibility to oxygen toxicity seizures.

03 p0263 A73-14156

SELECTION

NT PERSONNEL SELECTION

NT PILOT SELECTION

SELECTIVE DISSEMINATION OF INFORMATION
Computer experiments in selective distribution of hydrometeorological bibliographic information

15 p1904 A73-31611

SELECTIVE FADING

Computer simulation of HF frequency-selective fading and performance of the mode-averaging diversity combiner.

10 p1190 A73-24894

Selective properties and form of a signal transmitted through a statistically nonhomogeneous layer of arbitrary thickness

16 p1978 A73-32896

SELECTIVITY

Influence of selectivity on the observed orbital-parameter distribution of radio meters

01 p0101 A73-10846

Selectivity evaluation for reflection and transmission regenerative amplifiers of complex design

03 p0284 A73-14034

Tunnel diodes in receivers to reduce noise level and improve selectivity, discussing distortions, crosstalk and passband dependence on signal amplitude

10 p1195 A73-24385

Preliminary frequency selection for signal matched filtering.

12 p1469 A73-27268

Effect of selectivity on the observed distribution of orbital parameters for radio meteors.

15 p1928 A73-30982

Electronic integrated HF selective gyrator for TV IF filter development

21 p2661 A73-40230

ELECTORS

Determination of the molecular velocity distribution function in a molecular beam by the method of mechanical selection

02 p0194 A73-11606

Amplitude selector for linear transistorized devices

09 p1064 A73-23006

ELENIDES

NT CADMIUM SELENIDES

NT GALLIUM SELENIDES

NT LEAD SELENIDES

NT ZINC SELENIDES

Linear and nonlinear optical properties of some ternary selenides.

03 p0350 A73-14458

Optical band gap energies and stacking sequences of molybdenum tellurides and tungsten selenides derived from dielectric constant measurements

04 p0482 A73-14868

Saturation and acoustoelectric oscillations of a photocurrent in CdS and CdSe

06 p0737 A73-18218

Electrophysical parameters of TiSbSe_2 thin films

10 p1260 A73-24471

Bi_2Se_3 Hall effect magnetometer for reliable low temperature use.

13 p1612 A73-28368

Mechanism of the lubricating action of sulfides and selenides of refractory metals

14 p1755 A73-30717

X-ray diffraction at high temperatures for a study of thermal expansion of MnSe and MnSe_2

15 p1925 A73-32651

Crystal growth by vapor transport of GeSe , GeSe_2 , and GeTe and transport mechanism and morphology of GeTe .

15 p1842 A73-32652

Electron emission of In_2Se crystals in strong electric fields

17 p2219 A73-35555

ELENIUM

Russian book on spectral composition-dependent photoconductivity in Hg doped amorphous Se films covering effect of quasi-macroscopic centers in semiconductors

02 p0201 A73-12864

The process of reinforcement of lead shields in electroradiography

07 p0822 A73-19330

Energy loss measurements with 60 keV electrons in the case of amorphous and polycrystalline selenium and tellurium and the determination of optical constants

07 p0862 A73-20017

Switching in amorphous selenium.

11 p1407 A73-25147

High-resolution photodetachment study of Se^- ions.

21 p2710 A73-40213

Measurements of the upper and lower level lifetime in He-Se lasers.

22 p2871 A73-43086

ELENIUM COMPOUNDS

NT CADMIUM SELENIDES

NT GALLIUM SELENIDES

NT LEAD SELENIDES

NT SELENIDES

NT ZINC SELENIDES

Inhibition by selenium of the free-radical states of the retina of the eye

24 p3059 A73-44724

ELENOGRAPHY

Eclipse calculations of lunar features.

01 p0095 A73-10294

Ultraviolet photometry of the moon with the telescope experiment on the OAO-II.

01 p0096 A73-10317

Determination of the relative orientation of nine selenodetic catalogs in terms of Eulerian angles.

01 p0107 A73-11326

Catalog of selenographic coordinates for libration-zone and far-side points.

04 p0503 A73-16017

A new unified system for designating objects on the moon.

04 p0504 A73-16030

Accuracy of the moon potential computation based on integral formulae

06 p0751 A73-18151

Apollo 15 panoramic camera with 24 inch focal length for stereophotography of lunar surface, presenting pictures of lunar craters and landing sites

07 p0824 A73-20021

Book - Maps of lunar hemispheres: Giving the views of the lunar globe from six cardinal directions in space.

11 p1429 A73-26742

Classification, scale sequence, and nomenclature of lunar maps

13 p1672 A73-28117

Selenographic coordinates determination of ALSEP 12 and 14 telemetry transmitters via differential interferometric signal reception at two tracking stations, discussing instrument error reduction

20 p2603 A73-38894

The influence of laser ranging on selenodetic control.

21 p2774 A73-41408

SELENOLOGY

NT LUNAR CORE

Preliminary observations of stratified rocks of the Hadley Appennines photographed by the Apollo 15 astronauts

01 p0095 A73-10268

Selenodesy and planetary geodesy progress review, discussing gravitational fields and topography variations, outer planets oblateness and mass determinations, lunar body tides, etc

04 p0496 A73-14813

Model for lateral variations of lunar density minimizing total shear strain energy of moon, noting gravitational potential equal to observed potential at surface

12 p1541 A73-27488

Astronomical, geochemical and geophysical data and constraints for lunar evolution, considering remanent magnetization, electrical conductivity and early evolution model

12 p1541 A73-27491

Russian papers on lunar surface features from ground and spacecraft observations covering Luna 16 samples, geology, morphology, thermal emission, cartography, drilling and soil properties

13 p1672 A73-28113

Lunar interior composition, structure and thermal evolution models to fit surface igneous activity chronology and lithosphere stress history implied by mascons presence

15 p1937 A73-31778

Polarimetric observation of moon and planets via imaging system consisting of slot scanner, telescope, condenser lens, rotating disk analyzer and photomultiplier tube

15 p1876 A73-31960

Solid state convection role in moon from analysis of models with homogeneous initial distribution of radioactive heat sources

17 p2232 A73-35262

Calcium oxide and aluminum oxide constraints removal for lunar interior composition models

17 p2232 A73-35264

Properties of the solar nebula and the origin of the moon.

17 p2235 A73-35742

Lunar structure and dynamics - Results from the Apollo passive seismic experiment.

17 p2236 A73-35744

Moon - 'Ghost' craters formed during Mare filling.

17 p2236 A73-35746

Polarimetric instrument of moon and planets via imaging system consisting of slot scanner, telescope, condenser lens, rotating disk analyzer and photomultiplier tube

24 p3089 A73-44485

SELF ABSORPTION

The self absorption of gyro-synchrotron emission in a magnetic dipole field - Microwave impulsive burst and hard X-ray burst.

03 p0364 A73-14416

SELF ADAPTIVE CONTROL SYSTEMS

Application of frequency-pulse modulation to adaptive automatic control systems

01 p0027 A73-10597

Combinational servosystem with a self-adjusting loop

05 p0561 A73-17250

Synthesis of adaptive systems by Lyapunov's direct method.

06 p0723 A73-17959

Switching time dependence on input signal amplitude in self adaptive servosystem with open and closed control loops

06 p0680 A73-18382

Analytic construction of adaptive systems with stabilization of the dynamic characteristics.

07 p0805 A73-20039

Synthesis of nonsearching self-adjusting systems by the root-locus method. II

07 p0807 A73-20637

Inertialess smoothing of multiplier signals in automatic control system under sinusoidal signal, noting analog simulation of inertialess synchronous detector for self adaptive control

09 p1069 A73-22654

SELF CONSISTENT FIELDS

Improvement of the static and dynamic accuracy of a dual-loop control system for an electric actuating element with a proportional velocity controller

09 p1037 A73-22940

Vehicle coordinate-parametric control problems and some solution methods.

10 p1198 A73-24007

Synthesis of searchless self-adjusting systems based on the root locus method. I.

12 p1484 A73-27460

Nonsearch self-adapting identification systems

12 p1485 A73-27900

Synthesis of searchless selfadjusting systems on the basis of the root-locus method. II.

15 p1854 A73-31691

Relation between the N. M. Krylov-N. N. Bogoliubov averaging method and the method of envelopes in studies of a class of control systems

15 p1854 A73-31801

Searchless self-adjusting identification systems.

18 p2294 A73-36752

Adaptive /learning/ intelligent system design and simulation for control with stochastic goal and environment conditions

20 p2532 A73-38685

Minimum risk classification algorithms in automatic learning system design, applying to learning pulse signal receiver

20 p2532 A73-38686

Dynamics and stability of the algorithm of a digital adaptive system using a prediction technique

20 p2532 A73-38688

An analysis of recent advances in autonomous navigation for near earth applications.

20 p2587 A73-38812

[AIAA PAPER 73-875] Iteration methods for identification of multiple-link controlled plants for self-adaptation purposes

22 p2836 A73-42617

Adaptive measurement of vigilance decrement.

23 p2947 A73-43211

On the connection of the Krylov-Bogolyubov averaging method with the envelop method for investigating one class of control systems.

23 p2965 A73-44330

SELF ALIGNMENT

Camera calibration technique treating inner cone parameters as variables subject to adjustment or recovery in simultaneous analytical stereotriangulation solution

04 p0446 A73-14768

Laser interferometric alignment sensor for the large space telescope /LST/.

08 p0970 A73-21732

Finite difference programs with grid self adjustment for steady or unsteady problems with arbitrary boundaries and without coordinate hierarchy, noting computer time saving

09 p1071 A73-22400

Tilt-table alignment for inertial-platform maintenance without a surveyed site.

15 p1858 A73-31728

A modified interferometer for vibration amplitude measurement.

16 p2013 A73-32878

Problems in the theory and practice of the self-tuning of compensating signals in complex control systems

20 p2541 A73-38994

Experimental study of an autocollimation method for alignment of a variable-profile antenna

21 p2675 A73-41457

SELF CONSISTENT FIELDS

Electric dipole moment of diatomic molecules by configuration interaction. V - Two states of $1/2\Sigma_g^+$ symmetry in CN.

04 p0477 A73-14816

The self-consistent geomagnetic tail under static conditions.

04 p0440 A73-14957

Small perturbations solution for spatially homogeneous expanding gravitating medium, using Vlasov kinetic equation with self consistent Newtonian field

07 p0901 A73-20315

Numerical simulation of small amplitude whistler waves in thermal plasma, describing particle motion under self consistent and external magnet fields via Lorentz equation

10 p1255 A73-24269

Small perturbations solution for spatially homogeneous expanding gravitating medium, using Vlasov kinetic equation with self consistent Newtonian field

12 p1539 A73-27287

Self consistent one dimensional plasma layer model with current layer at center described by Vlasov equation and nonexistent normal magnetic field component

14 p1796 A73-29870

High-frequency current states in small-size superconductors

16 p2044 A73-34066

Self consistent field calculations of CO positive ion dipole moment in ground state

17 p2119 A73-35180

The propagation of an intense electromagnetic wave in a plasma. 19 p2469 A73-38087

Laser threshold behavior analogy with thermodynamic ferromagnetic order-disorder phase transition, using self-consistent field theory 20 p2571 A73-38628

Self-consistent microscopic theory of Rayleigh light scattering by molecular aggregates based on random phase modulation and stochastic theories 21 p2739 A73-40219

Computer model of Ba ion cloud expansion in magnetosphere, taking into account self-consistent electric and magnetic field interactions 22 p2846 A73-41938

Hartree-Fock equation with allowance for the correlation 22 p2889 A73-42647

SELF DEPLOYING SPACE STATIONS

U SELF ERECTING DEVICES

U SPACE STATIONS

SELF ERECTING ANTENNAS

U ANTENNAS

U SELF ERECTING DEVICES

SELF ERECTING DEVICES

A self deployable high attenuation light shade for spaceborne astronomical sensors. 08 p0970 A73-21734

Development of a deployable and selfrigidizing solar cell array for the multikilowatt range. 11 p1310 A73-26002

Transverse deflection of guided projectile tail fins during deployment. 22 p2797 A73-42629

SELF EXCITATION

Optimization of hybrid gas lubricated conical bearings. 01 p0057 A73-10698

The behavior of a self-excited system acted upon by a sequence of random impulses. 04 p0469 A73-14664

Cosmic-ray evolution due to interactions with self-excited plasma waves. 05 p0612 A73-17385

Analysis of self-excited and forced vibrations of a rectangular plate on many supports in supersonic flow. 13 p1700 A73-29392

Truncated general equations and a characteristic equation of a self-excited transistor oscillator 14 p1736 A73-30562

Self-induced effects of radio waves in the vicinity of plasma resonance 15 p1918 A73-31706

Self excited whirl stability limits and frequencies of continuous rotors under gyroscopic, damping and hydrodynamic bearing film forces 16 p2022 A73-34035

Distortions of signal frequency in FM oscillators. 17 p2136 A73-35154

Spontaneous emission and self-excitation of a small volume in a classical, nonlinear active medium 19 p2463 A73-38540

Complex self-excited vibrations of space vehicles during maneuver. 20 p2614 A73-38895

Low voltage self triggering vacuum gap characteristics under dc conditions, comparing with thyatron pulse generator technique 21 p2692 A73-39917

Self excited mixer/detector of Gunn diode oscillator, calculating detection characteristics from combined equivalent circuit and computer simulated analysis 21 p2664 A73-41092

Study of self-excitation conditions in an acoustic oscillator in relation to the type of boundary conditions 22 p2886 A73-41900

Oscillations caused by solid friction. III - In the case of maximum static friction different from kinetic friction without slipping. 23 p2986 A73-44272

SELF FOCUSING

Interaction of opposed beams of electromagnetic waves in a transparent nonlinear medium 01 p0016 A73-10208

Investigation of laser radiation self-focusing by alkali halide single crystals according to data on the damage-focus displacement effect 01 p0061 A73-11443

Self focusing of two dimensional cylindrical waves propagating in inhomogeneous natural duct, noting tropospheric communications and ionospheric and sound propagation applications 02 p0142 A73-12527

Laser beam self focusing possibility in GaAs, considering nonlinear mechanism of intervalley carrier transfer due to applied dc field 04 p0458 A73-14874

CW laser beams steady state thermal self focusing stability, deriving nonlinear absorbing medium geometrical optics ray equation and aberration pattern 06 p0702 A73-18583

External self focusing of converging short duration pulsed light beams, analyzing resultant focal points trebling, nonlinear focus motion and intensity distribution 06 p0702 A73-18590

Investigation of self-focusing of laser radiation with alkali halide single crystals from data concerning the displacement of the focus of damage. 11 p1376 A73-26065

Influence of external self-focusing on the performance of laser amplifiers 11 p1364 A73-26156

Confirmation of an electron avalanche causing laser-induced bulk damage at 1.06 micron. 11 p1377 A73-26227

Angular distribution of induced combinational light scattering in liquid nitrogen 12 p1505 A73-26889

Transient self focusing theory of high power laser pulse for homogeneous isotropic transparent solid dielectric with allowance for electrostriction and thermal effects 13 p1629 A73-29440

Influence of self-focusing on the stability of steady-state laser emission. 13 p1629 A73-29441

Nonlinear mechanisms for self-focusing of microwaves in semiconductors. 14 p1732 A73-29920

Role of laser radiation self-focusing during breakdown in liquid He4 15 p1884 A73-31701

Self-focusing of CO2 laser radiation in resonantly absorbing gases. 17 p2186 A73-35811

Investigation of 'external' self-focusing of ruby laser emission in CdS crystals 18 p2322 A73-36674

Application of image-converter technique in quantum radiophysics and nonlinear optics [Survey paper]. 21 p2709 A73-39940

Semiconductor laser beam self focusing action due to combined effects of linear and nonlinear dielectric constant and absorption coefficients, considering n-InSb sample 21 p2711 A73-40226

GaAs two-photon absorption coefficient obtained from transmission measurements with Q switched Nd-YAG laser, noting thermal self focusing 21 p2713 A73-40459

Self-focusing and self-trapping of light beams in a non-linear medium. 22 p2888 A73-43050

Propagation velocity of picosecond pulse from mode locked Nd-glass laser investigated by optically induced birefringence, self phase modulation and self focused light 23 p2988 A73-44120

SELF INDUCED VIBRATION

NT PANEL FLUTTER

NT SUBSONIC FLUTTER

NT SUPERSONIC FLUTTER

NT TRANSONIC FLUTTER

Electromagnetic self induced vibrations in homogeneous unbounded electron beam moving with time dependent velocity, noting longitudinal and transverse wave generation 02 p0198 A73-12102

Self-excited and forced vibrations of an aeroelastic system subject to a follower force. 04 p0513 A73-15597

German monograph - The calculation of the stability limit of statically operating circular gas bearings, taking into account the effect of the supported mass. 07 p0832 A73-20390

Dynamic stability of cable in incompressible flow at angle of incidence, calculating characteristic lengths and vibration frequencies by singular perturbation theory [AIAA PAPER 73-395] 11 p1440 A73-25524

Self induced vibration of friction bearing mounted rigid rotor, considering oscillation damping or enhancing effect of oil film 16 p1968 A73-33236

Oscillations caused by solid friction. III - In the case of maximum static friction different from kinetic friction without slipping. 23 p2986 A73-44272

SELF LUBRICATING MATERIALS

Self lubricating bearing materials strength, friction, wear, thermal and dimensional stability properties, considering plastic, metal matrix and carbon graphite composites 07 p0842 A73-19555

Bearing materials from graphite fiber composites. 10 p1238 A73-23974

Lubricant film and self lubricating composite materials optimum selection in solid lubricant design, considering performance and cost criteria [ASME PAPER 73-DE-8] 14 p1766 A73-30817

A study on some metal-base self-lubricating composites containing tungsten disulfide. [ASLE PREPRINT 73AM-3C-1] 17 p2196 A73-34986

High speed oscillating tests of lubricating composites. [ASLE PREPRINT 73AM-3C-2] 17 p2179 A73-34986

Antifriction materials employing fibers and liquid metal lubricants 24 p3101 A73-44411

SELF LUBRICATION

The gas liquid interface and the load capacity of helical grooved journal bearings. 03 p0314 A73-14343

Cu and Cu-Sn base self lubricating composites, testing solid lubricants effects on friction coefficient, wear, electrical resistance, hardness, porosity and structure 04 p0454 A73-14949

Friction in ultrahigh vacuum, discussing physicochemical problems, self lubricating materials, advantages and drawbacks, and solid lubricant choices for space applications 07 p0828 A73-18900

Friction and wear of self-lubricating composite materials. 13 p1624 A73-28770

SELF ORGANIZING SYSTEMS

Automaton synthesis and perceptron learning for controlled objects classification according to unknown features, noting adaptive relationships between retinal and associative elements 07 p0786 A73-20047

Adaptation algorithms in multilayer pattern-recognition systems 10 p1192 A73-24502

Self organized biological systems analysis, including deterministic and phenomenological selection theories, molecular level cell instructive properties and self-reproducing hypercycles 15 p1835 A73-31825

Application of self-organizing control to remote piloting of vehicles. 19 p2449 A73-37332

Self organizing behavior of multivariable stochastic extremal control systems with environmental or intrinsic positive feedback under perturbation 20 p2539 A73-38689

Structure of self-organizing automated design systems and the processes of their functioning 20 p2569 A73-39391

SELF OSCILLATION

The five-minute oscillations as nonradial pulsations of the entire sun. 01 p0104 A73-11049

Tunnel-effect and propagation of 5-min oscillations in the solar atmosphere. 01 p0107 A73-11381

Periodic motions elimination in servo driven analog to digital converters on phase plane, noting dependence on autooscillations in relay system with time lag 02 p0148 A73-11862

Beat conditions during synchronization of an oscillator by an external sinusoidal force 02 p0147 A73-12492

Possibility of the occurrence of self-oscillations in a circuit containing a constant source of current and a homogeneous semiconductor specimen with small response times 03 p0349 A73-12907

Hydrodynamics in weak gravitational fields - Plane oscillations of an ideal fluid in a rectangular channel 03 p0294 A73-13606

Autooscillations in the directional hydrodynamic servocontrol with play in the reaction linkage 03 p0252 A73-13771

Quartz self-oscillator short term frequency instability lower limit estimation by calculating Q values and nonlinearity and resonator parameter fluctuation effects 03 p0284 A73-14064

Oscillations of injected carriers in p-type indium antimonide. 04 p0482 A73-14869

Search stability and steady motion region characteristics of self oscillatory extremal automatic control system under additive disturbances on controlled object input 05 p0560 A73-16293

A study of complex auto-oscillations of spacecraft 05 p0628 A73-16404

Three dimensional self oscillating motion study of roll and pitch stabilized vehicle with thrust vector control under resonance, using averaging method 05 p0599 A73-17086

Investigation of auto-oscillations of a continuous medium, occurring at loss of stability of a stationary mode. 07 p0809 A73-19018

The oscillation probability of self-excited multimode oscillators. 08 p0945 A73-20803

Intersynchronization processes in Thomson oscillators with constraints of different nature placed on the amplitudes 08 p0948 A73-21518

Oscillation of the earth's inner core and its relation to the generation of geomagnetic field.
09 p1077 A73-22194

Self excited LC and RC oscillator networks based on FETs, discussing frequency tuning and FM methods
10 p1197 A73-24941

Parametric synchronization of self-oscillators with feedback delay and nonlinear circuit
11 p1337 A73-25429

Dynamics of a two-frequency self-oscillator with 'hard' excitation
11 p1331 A73-26157

Auto-oscillations, stability at the origin, overall stability of nonlinear systems with distributed parameter
13 p1596 A73-28473

German monograph - Rapid excitation of quasi-harmonic oscillations in a class of nonlinear oscillators.
13 p1594 A73-29285

Quasi-periodic oscillations in a nonautonomous oscillator
14 p1728 A73-30268

Periodic conditions in artificial-muscle autopulsators
14 p1721 A73-30289

Mathematical model for shimmy auto-oscillations of aircraft landing gear nose wheel with pneumatic tire under velocity changes
15 p1825 A73-31044

Parachute axisymmetric self excited breathing oscillations dependence on descent velocity, Froude number, canopy/line length ratio, drag and line stiffness
[AIAA PAPER 73-452]
15 p1826 A73-31438

Experimental study of cavitation oscillations in a centrifugal screw pump
15 p1832 A73-31499

Interaction of self-excited vibrations in mechanical vibrational systems
19 p2494 A73-37181

Oscillations in nonlinear feedback systems.
19 p2414 A73-38069

Self-pulsing in laser amplification of broadband noise.
20 p2571 A73-38635

Aeroelastic vibrations in labyrinth seals
20 p2569 A73-39373

Self-resonant LSA oscillator diode of rectangular cross-section.
22 p2832 A73-41895

Self-termination of free oscillations in ruby at low temperatures.
22 p2896 A73-42251

Self-action of electromagnetic wave in plasma under parametric instability.
22 p2895 A73-43022

Backward ionization waves linear evolution to nonlinear saturated state from gaseous plasma self oscillation instability viewpoint, noting electron temperature and density increase
23 p3011 A73-43829

Experimental study of the adiabatic invariant of self-oscillating processes
23 p3006 A73-43850

Solid friction oscillation characteristics of self excited rotational shaft-spring system with sliding contact surfaces
23 p2986 A73-44273

Parametric oscillations in an oscillating circuit utilizing negative resistance.
24 p3075 A73-45479

Self and excited oscillations in a circuit composed of a non-linear element and a delay line.
24 p3075 A73-45487

SELF REGULATING
U AUTOMATIC CONTROL
SELF REPAIRING DEVICES
Reliability of a self-repairing system with scheduled maintenance.
09 p1088 A73-22443

The concept of coverage and its effect on the reliability model of a repairable system.
10 p1226 A73-24871

Influence of control periodicity on the reliability of repairable devices
12 p1502 A73-26760

Probabilistic analysis of a two-unit system with a warm standby and a single repair facility.
17 p2149 A73-35809

SELF SUSTAINED EMISSION
High voltage square pulse oscillator and recording circuit for negative and positive autoelectron emission properties
01 p0024 A73-10795

SELSYNS (TRADEMARK)
U SERVOMOTORS
SEMICIRCULAR CANALS
Semicircular canals as a primary etiological factor in motion sickness.
02 p0135 A73-12560

Equivalence of the action of Coriolis accelerations to that of certain angular accelerations in their effects on the receptors of semicircular canals
12 p1463 A73-27718

Calculation of a Coriolis acceleration acting on semicircular canal receptors of man in rotating systems
15 p1835 A73-31518

Endolymph fluid mechanics in semicircular canals approximated by rigid torus filled with incompressible Newtonian fluid
18 p2281 A73-36430

A non-Newtonian model for fluid flow in the semicircular canals.
18 p2281 A73-36431

Vestibular and spinal control of eye movements.
18 p2272 A73-36440

SEMICONDUCTING FILMS
Semiconductor thin film image amplifiers and converters based on electroluminescent and photoconducting films
01 p0022 A73-10037

Contribution to the theory of the current-voltage characteristic of a contact between a metal and a thin-film semiconductor
01 p0087 A73-10042

Metallographic macro- and microstructural study of semiconductor compounds, discussing single crystal imperfections, polycrystals and semiconducting films
02 p0199 A73-11582

Spectral characteristics and black body radiation sensitivity of submillimeter band radiometer based on n-type epitaxial GaAs films
02 p0147 A73-12496

Russian book on spectral composition-dependent photoconductivity in Hg doped amorphous Se films covering effect of quasi-macroscopic centers in semiconductors
02 p0201 A73-12864

Effect of surface states on surface-wave amplification in a composite structure of CdSe film on LiNbO₃.
05 p0559 A73-17073

Morphological, structural and electrical nonuniformities correlation in epitaxial GaAs films on planes, noting Miller indices effects on morphological and electrical properties
05 p0605 A73-17290

Electron diffraction investigations of the short-range order in GaAs and GaP films
05 p0605 A73-17291

The design of electronic equipment for biotelemetry using microcircuit techniques.
06 p0673 A73-17674

Resistivity of doped polycrystalline silicon films.
06 p0733 A73-17745

Electrical properties of evaporated mercury telluride films.
06 p0734 A73-17815

Influence of vacuum conditions in fabrication on the structure and electrophysical properties of epitaxial silicon films on sapphire
06 p0736 A73-18089

Exciton-phonon interaction in recrystallized CdTe layers
06 p0737 A73-18219

Low-resistance CdTe films exhibiting a constant emf under the action of an ac field
06 p0737 A73-18222

IR and thermal extinction spectra of luminescence and photoconductivity of zinc cadmium sulfide solid solution films doped with Cu and Cl
06 p0738 A73-18643

Preswitching and postswitching phenomena in amorphous semiconducting films.
06 p0739 A73-18800

Reversible high speed high resolution imaging in amorphous semiconductors.
07 p0862 A73-19609

Photocurrent pulse shape in thin organic semiconductor films
07 p0862 A73-20008

Transconductance and distortion of a thin-film transistor
07 p0801 A73-20025

Amorphous chalcogenide Te-As-Si-Ge thin film switch, discussing pressure effect energy accumulation time delay and behavior after voltage removal
09 p1133 A73-21988

The influence of substrate properties on microwave losses in thin films of semiconductors.
09 p1064 A73-23041

The electrical properties of anodically grown silicon dioxide films.
09 p1064 A73-23042

Investigation of the growth surface of GaAs epitaxial films by chemical decoration and small-angle shadowing technique.
10 p1259 A73-23570

Electrophysical properties of BiTeI thin films
10 p1259 A73-24154

Conduction mechanisms in resistive films deposited by the silk-screen process
10 p1259 A73-24412

Electrophysical parameters of TiSbSe₂ thin films
10 p1260 A73-24471

Indirect transitions in thin quantized semiconductor films
11 p1410 A73-26450

Optoelectronic step-up voltage transformer with optical coupling electrical isolation, using light emitting diode and semiconductor film with high photovoltage levels
12 p1496 A73-26964

Cd doped CdTe microwave film detectors sensitivity, frequency response, thermal characteristics and stability
14 p1737 A73-30855

Structure, composition and photoelectrical properties of cadmium sulfide and selenide epitaxial films subjected to heat treatment
14 p1784 A73-30856

Avalanche injection effects in MIS structures and realization of n-channel enhancement type MOS FETS.
15 p1851 A73-32017

Scattering of a nonlocalized exciton on phonons in thin quantized semiconductor films
17 p2218 A73-34118

Electrical properties of single-crystal films of p-type PbTe
17 p2219 A73-35556

A study of the static S-shaped current-voltage characteristics of chalcogenide glass switching devices
18 p2293 A73-36722

Injection and field processes in thin semiconductor films in the current jump region
18 p2341 A73-36723

Application of the four-probe method to the determination of the resistance of thin films deposited on various substrates
19 p2470 A73-37953

RF sputtering of ZnO shear-wave transducers.
21 p2702 A73-40952

A new vapor growth method for GaP using a single flat temperature zone.
24 p3119 A73-44412

SEMICONDUCTOR DEVICES

NT AVALANCHE DIODES
NT FIELD EFFECT TRANSISTORS
NT GALLIUM ARSENIDE LASERS
NT GERMANIUM DIODES
NT JUNCTION DIODES
NT JUNCTION TRANSISTORS
NT LIGHT EMITTING DIODES
NT METAL OXIDE SEMICONDUCTORS
NT MIS [SEMICONDUCTORS]
NT NEURISTORS
NT PARAMETRIC DIODES
NT PHOTODIODES
NT PHOTOTRANSISTORS
NT PHOTOVOLTAINIC CELLS
NT SCHOTTKY DIODES
NT SEMICONDUCTOR LASERS
NT SILICON TRANSISTORS
NT THERMISTORS
NT THYRISTORS
NT TRANSISTOR AMPLIFIERS
NT TRANSISTORS
NT VARACTOR DIODES
NT VARISTORS

Investigation of residual resistance in semiconductor switches used to commutate the measuring circuits of alternating-current bridge networks
01 p0022 A73-10080

A new program for the dc one-dimensional analysis of semiconductor devices.
01 p0023 A73-10576

Excitation of space charge waves in a one-carrier semiconductor with variable doping.
01 p0088 A73-10680

Semiconductor device with current regulated switching from high voltage/low current to low voltage/high current state, noting I-R characteristics
01 p0026 A73-11096

Pulse commutation at microwave bit rates using Gunn domains.
02 p0145 A73-11534

A cryostat for measuring electrical values of semiconductor devices in the temperature range from 77 to 300 K
02 p0165 A73-11550

Standing wave approximation of distributed dual frequency parametric oscillators consisting of semiconductor diodes and transmission line in steady state
02 p0147 A73-12490

Photomultiplier operation pulse control in semiconductor circuit for background cosmic radiation noise error minimization in air shower station
02 p0171 A73-12688

Microelectronic metal-dielectric-semiconductor devices for physical properties of multilayer multiphase systems, noting field effect transistors, integrated circuits and electro-optical elements
03 p0349 A73-13656

Noise characteristics, channel capacities, power requirements and transmission efficiencies of various semiconductor transmitter designs for FM directional radio systems
03 p0284 A73-14125

Causes of defects arising in semiconductor devices encapsulated with plastic
04 p0427 A73-15350

- Low energetic efficiency of semiconductor microwave scanning converters for radio images of fog obscured objects 05 p0556 A73-16072
- Semiconductor photodetection matrices for holographic memory reading 05 p0553 A73-16170
- Semiconductor device degradation by high amplitude current pulses. 05 p0557 A73-16505
- Aging effects on electrical and radiation characteristics of discrete semiconductors. 05 p0557 A73-16510
- Simple mathematical model of shift of threshold voltage induced in an m.o.s. transistor by testing at elevated temperatures. 05 p0560 A73-17324
- Use of ion implantation in the fabrication of semiconductor devices 06 p0672 A73-17449
- Design of modern semiconductor senders for frequency-modulated directional radio systems. I 06 p0663 A73-17585
- Investigation of static and transient current-voltage characteristics of diodes made of nickel-modified silicon 06 p0676 A73-18248
- Resonance characteristics of semiconductor mechanical components. 06 p0676 A73-18344
- Semiconductor-insulator-semiconductor (SIS) tunneling current characteristics, noting negative resistance feature for degenerate p-n diode 06 p0677 A73-18359
- Convolution and correlation by nonlinear interaction in a diode-coupled tapped delay line. 06 p0678 A73-18746
- Preservation of threshold on-regime in amorphous semiconductor threshold switch. 06 p0739 A73-18790
- Amorphous semiconductor devices, materials, operation and technology, noting nonvolatile and optical memories, radiation and noise immune circuits and dry process photographic applications 07 p0861 A73-19150
- Noise performance of gallium-arsenide and indium-phosphide injection-limited diodes. 07 p0798 A73-19158
- Semiconductor radiation detectors fabrication methods, discussing p-n junctions diffusion and ion implantation techniques and surface barrier, dE/dx, chessboard and rod type counters 07 p0822 A73-19172
- On the form and stability of electric-field profiles within a negative differential mobility semiconductor. 07 p0799 A73-19344
- Quality control of semiconductor elements manufactured in low-run series production - Ultrahigh frequency components 07 p0801 A73-19422
- Failure analysis of semiconductor device bonds under on-off operation, noting fatigue testing machine for accelerated life tests 08 p0972 A73-20744
- GaAs Schottky-barrier diodes for ultrahigh-frequency communication systems. 08 p0945 A73-20808
- Book - Introduction to quantum electronics. 08 p0994 A73-20951
- Sensitivity limits for extrinsic and intrinsic infrared detectors. 08 p0967 A73-21422
- Computer simulation of semiconductor devices. 08 p0948 A73-21534
- Semiconductors for microwave frequencies. 08 p0949 A73-21649
- Semiconductor strain transducer 08 p0950 A73-21720
- Possibilities of determining the permissible reverse-bias current and voltage in semiconductor devices by a nondestructive method 09 p1061 A73-21979
- Application circuits for amorphous semiconductor switching devices with thin film active components, discussing electrical characteristics 09 p1061 A73-21990
- Processing the spectra of semiconductor detectors in a semiautomatic system containing data storage elements and a computer 09 p1085 A73-23005
- Book - Transferred electron devices. 09 p1066 A73-23299
- Semiconductor electroluminescent diode displays. 10 p1218 A73-24118
- Piezoresistive semiconductor strain gage optimum applications and practical merits comparison with wire or foil resistance types, considering stability, accuracy and temperature compensation 10 p1195 A73-24571
- Equivalent circuit analysis of noise in bulk semiconductor devices. 10 p1197 A73-24869
- Perturbation theory for multistep acoustoelectric surface-wave amplifier. 11 p1337 A73-25362
- Status of silicon germanium air-vac converter development. 11 p1312 A73-26032
- InSb and Ga-doped Ge bolometers performance tests, discussing detector circuitry and dc, noise and responsivity measurements 11 p1368 A73-26512
- Analysis of an oscillator using a sequence of negative resistance devices 12 p1477 A73-26871
- Chalcogenide glass threshold switch conceptual model based on electronic origin of firing, discussing applications to contactless switches, bistable relays decoupling and display triggering 12 p1478 A73-27042
- Design and performance of deflected-beam electron-bombarded semiconductor amplifiers. 12 p1478 A73-27113
- Book on semiconductor opto-electronics covering solids optical constants, classical and quantum mechanical dispersion theory, absorption processes, magneto-optical and photo-electrical effects, etc 12 p1531 A73-27449
- Analog voltage squaring circuits with series-connected resistors shunted by semiconductor diodes or ladder network, discussing design, construction and operation principles 12 p1481 A73-27591
- Silicon semiconductor resistance strain gage intrinsic thermal noise characteristics at 20 Hz-10 kHz, noting 1/f type as dominant noise component in audio frequency range 13 p1611 A73-28021
- Carrier heating or cooling in semiconductor devices. 13 p1590 A73-28540
- Ion implantation method and diffusion process for microelectronics semiconductor components manufacture 13 p1590 A73-28573
- Analysis of the operation of a diode phase detector with allowance for the diode recovery time 13 p1591 A73-28866
- Charge transfer semiconductor devices operational principles and possible structures with two or three phases, discussing efficiency, regeneration circuitry and noise and dissipation problems 14 p1731 A73-29727
- Description of the measurement design and the measurement principle in the measurement of the chip impedance of coaxially mounted semiconductor diodes in the microwave range 14 p1733 A73-30058
- A wideband radiometer for the four-millimeter band built with semiconductor devices 14 p1735 A73-30272
- Study of excitation conditions for a piezo-semiconductor oscillator by the electron modeling method 14 p1737 A73-30946
- Mathematical description and calculation of the static mode of operation of a microwave power regulator with a semiconductor attenuator. 15 p1849 A73-30993
- The influence of Auger recombination on the forward characteristic of semiconductor power rectifiers at high current densities. 15 p1850 A73-31130
- Two-phase charge-coupled devices with overlapping polysilicon and aluminum gates. 15 p1850 A73-31373
- Russian book on elementary particle counters covering gas discharge (Geiger-Muller), scintillation, Cerenkov and semiconductor counters and matter-radiation interactions 15 p1880 A73-32418
- Epoxy adhesive materials evaluation for microelectronic assemblies of hermetically sealed hybrid circuits with semiconductor chips and thin film substrates 16 p1989 A73-33468
- Prolonged monitoring of experimental equipment with the aid of semiconductor emitters 17 p2133 A73-34152
- Oscillographic equipment for research in the field of semiconductor microwave electronics 17 p2218 A73-34160
- Gamma detectors using mercuric iodide and other heavy metal compounds as semiconductors with charge carriers for current surge in quantum energy resolution 17 p2134 A73-34247
- Convergence of periodic solutions of differential equations for resonance circuits with nonlinear semiconductor capacitance 17 p2144 A73-34585
- Performance and economic advantages offered by a diffused semiconductor strain gage pressure transducer. 17 p2167 A73-34626
- Transient temperature response of semiconductor devices under pulsed power operation. 17 p2135 A73-34728
- Failure analysis used to vindicate JANTX components. 17 p2135 A73-34731
- Review of some mathematical models of non-linear domain dynamics in bulk-effect semiconductors. 17 p2219 A73-35595
- Semiconductor carrier mobility measurements with Hall generator, calculating sample geometry and finite dimension electrical contact effects on error 19 p2430 A73-37770
- Analysis and temperature control of hybrid microcircuits. 19 p2412 A73-37990
- [ASME PAPER 73-ENAS-6] Temperature-humidity acceleration of metal-electrolysis failure in semiconductor devices. 19 p2411 A73-38470
- Long term life tests for thermal shock cycles effects on plastic encapsulated semiconductor device reliability, presenting salt atmosphere testing data for silicon package 19 p2471 A73-38470
- Screening of metallization step coverage on integrated circuits. 19 p2411 A73-38470
- A study of the characteristics of surface charge transfer devices 20 p2534 A73-38830
- Book - Design performance and applications of microwave semiconductor control components. 20 p2535 A73-39130
- Influence of electric field strength on effective carrier mobility in polycrystalline CdSe thin films 20 p2536 A73-39200
- Determination of the parameters A and j/sub 0/ of the loaded portion of the current-voltage characteristic of a photoelectric converter 20 p2510 A73-39450
- Investigation of the gain instability of a semiconductor radiometer 21 p2700 A73-40530
- The theory of the current-voltage characteristic of diodes fabricated out of compensated semiconductors 21 p2663 A73-40790
- Coupled mode analysis for solid travelling-wave amplifiers. 21 p2665 A73-41120
- Noise in solid travelling-wave tubes using coupled mode analysis. 21 p2665 A73-41120
- Russian book on semiconductor radio transmitter design covering power amplifiers, frequency multipliers, oscillators and Gunn effect devices for sub-microwave frequencies 21 p2666 A73-41420
- Prediction methods for the susceptibility of solid state devices to interference and degradation from microwave energy. 22 p2823 A73-41790
- Book - Avalanche-diode microwave oscillators. 22 p2833 A73-42490
- Optimum design of electron beam-semiconductor linear low-pass amplifiers. II - Output capabilities. 23 p2958 A73-43450
- Cellular dynamic memory array with reduced data access time. 23 p2956 A73-44110
- Some results in predicting the states of semiconductor triodes from noise factors on the basis of the statistical theory of pattern recognition 23 p2961 A73-44290
- Two-loop frequency multipliers employing the barrier capacitance of a p-n junction and exhibiting maximum energetic indices 24 p3071 A73-44590
- Switching of semiconductor devices in pulsed voltage regulators 24 p3072 A73-44900
- Series resistance of rectangular and cylindrical semiconductor photocells with linear and circular contacts and thin base, noting dependence on contact strip width 24 p3058 A73-45251
- Efficient numerical solution of the transmission-line equivalent-circuit model of a semiconductor. 24 p3119 A73-45261
- A simple theory of the anomalous Hall effect in semiconductors. 24 p3120 A73-45320
- Diffusion treatment of CdS and ZnO crystals and their applications in microwave acoustics. 24 p3120 A73-45430

SEMICONDUCTOR JUNCTIONS

NT JOSEPHSON JUNCTIONS

NT N-N JUNCTIONS

NT N-P-N JUNCTIONS

NT P-I-N JUNCTIONS

NT P-N JUNCTIONS

NT P-N-P JUNCTIONS

NT P-N-P-N JUNCTIONS

NT SILICON JUNCTIONS

- High-efficiency Ga/1-x/Al/x/As-GaAs solar cells. 01 p0005 A73-10132
- Many-body effects at metal-semiconductor junctions. I - Surface plasmons and the electron-electron screened interaction. 01 p0087 A73-10147

Optical degradation and thermal restoration - New inputs to the mechanism of the photovoltaic effects in Cu₂S-CdS heterojunctions.

03 p0350 A73-14218

Cadmium sulfide/cuprous sulfide solar cell abrupt heterojunction band model description by two quasi-Fermi levels

03 p0350 A73-14219

Radiation produced trapping effects in devices.

05 p0605 A73-16521

Buried channel MOS, double junction and Schottky barrier charge coupled devices, noting higher speeds, charge transfer efficiencies and radiation resistance

05 p0559 A73-16810

Heterojunction injection lasers with high efficiency and low threshold currents, discussing amplification, emission, epitaxial layers, and performance superiority over homostructures

05 p0586 A73-17266

Energy structure, I-V characteristics and optical and photoelectrical properties of heterojunctions between different semiconductor materials, noting interface state effects

06 p0736 A73-18091

Effect of impurity gradient on the time delays and Q-switching in junction lasers.

07 p0836 A73-20189

Influence of the Schottky effect and the peculiarities in the distribution of the applied voltage on the thickness of the depletion layer and the volt-ampere characteristics of a semiconductor with blocking contact.

07 p0802 A73-20191

Response time of metal-insulator-metal tunnel junctions.

08 p0945 A73-20844

The effect of stress on metal semiconductor junctions.

08 p0995 A73-21482

/GaAl/As lasers with a heterostructure for optical confinement and additional heterojunctions for extreme carrier confinement.

09 p1092 A73-22243

The development of SiGe-PbTe segmented thermoelectric couples involving pressure-contacted junctions.

11 p1409 A73-26035

French monograph on metal-semiconductor junction electron tunneling effect covering phonon interaction mechanisms, control and characterization problems

13 p1669 A73-29290

Measurement of semiconductor junction parameters using lock-in amplifiers.

13 p1595 A73-29578

Principles of photovoltaic solar energy conversion.

13 p1573 A73-29591

Influence of the difference in effective masses on the efficiency of heterojunction solar cells.

14 p1713 A73-30000

Thermal noise behavior of a FET as a function of the doping profile of the gate-channel junction

16 p1988 A73-33274

Polarization charge capture dependence of two layer dielectric metal-silicon nitride-silica-silicon semiconductor structures on pulse duration and temperature

16 p1991 A73-34003

Temperature dependence of the parameters of an n-p-i structure with negative resistance

20 p2535 A73-38860

Measurements of refractive index step and of carrier confinement at /AlGa/As-GaAs heterojunctions.

21 p2752 A73-40962

Cw degradation at 300 K of GaAs double-heterostructure junction lasers. I - Emission spectra. II - Electronic gain.

21 p2715 A73-40964

Anisotropy of galvanomagnetic effects in laminarly inhomogeneous semiconductors

23 p3017 A73-44044

Stationary charge transport in metal-semiconductor-metal/MSM/ structures.

24 p3120 A73-45421

SEMICONDUCTOR LASERS

NT GALLIUM ARSENIDE LASERS

Spatial distribution of charge carriers and radiant energy in single and double heterostructure semiconductor lasers, noting technology of potential barriers formation

01 p0059 A73-10715

Two component magnetic pulsed modulator for electroluminescent and laser diodes, using ac source with nonresonance input capacitance charge

01 p0059 A73-10793

Coherence of the radiation of a pulsed single-mode injection semiconductor laser.

01 p0061 A73-11335

Optical communication systems with glass fiber waveguide, using semiconductor lasers and photodiodes as transmitters and receivers respectively

01 p0019 A73-11486

Laser diodes cavity radiative efficiency loss due to sidewall induced internally circulating modes, considering cavity length, width and reflectivity relations

06 p0701 A73-18358

Waveguide resonator structure of an electron-beam-pumped semiconductor laser.

06 p0702 A73-18584

Use of a semiconductor laser diode as a modulator of gas laser radiation.

06 p0702 A73-18592

Electron-beam tube with semiconducting laser screen.

06 p0677 A73-18636

Some characteristics of a miniature pulsed laser with electron excitation.

07 p0836 A73-20136

Direct modulation of double-heterostructure lasers at rates up to 1 Gbit/s.

08 p0975 A73-21120

Semiconductor Laser Conference, Boston, Mass., May 15-17, 1972, Proceedings.

09 p1091 A73-22235

Transverse mode control in semiconductor lasers.

09 p1092 A73-22242

Theory of second-order mode locking in semiconductor lasers.

09 p1092 A73-22244

Time delays and Q switching in homostructure and heterostructure injection lasers.

09 p1092 A73-22246

Semiconductor electron-beam-pumped lasers of the radiating mirror type.

09 p1092 A73-22248

Broad-band laser emission from optically pumped PbS(1-x)Se/x.

[AD-759091] 09 p1092 A73-22249

PbTe-SnTe stripe junction diode lasers, discussing fabrication, electrical properties, and mode characteristics from emission spectra, polarization, mirror illumination and far field pattern measurements

[AD-759093] 09 p1092 A73-22250

A limitation on repetition rate of pulsations of junction lasers due to the repetitively Q-switched mechanism.

09 p1093 A73-22253

Feasibility analysis of MIS sandwich structure for pulsed laser based on calculation for field distribution and TE and TM modes in optical cavity

09 p1093 A73-22254

The directivities and spectral contents of radiation of multi-diode injection lasers.

09 p1097 A73-23049

An analysis of pulsation in coupled-cavity structure semiconductor lasers.

12 p1505 A73-27014

Semiconductor injection lasers, discussing optical transitions threshold effects, radiative recombination, coherent emission, etc

12 p1506 A73-27136

Reconstruction of the images of transparencies with a semiconductor laser.

12 p1498 A73-27512

Stimulated emission of light from solid solutions of tin and lead chalcogenides in the region of 10 microns.

12 p1507 A73-27519

KGP-2 - An electron-beam pumped cadmium sulfide laser.

12 p1507 A73-27520

Output radiation influence on catastrophic and slow degradation process in heterojunction injection lasers, noting service life dependence on current density

12 p1508 A73-27525

Electron kinetics and stationary emission from semiconductor lasers

12 p1508 A73-27983

Quantum oscillations and pump depletion effects in an efficient high-power tunable spin-flip laser.

13 p1626 A73-28216

Semiconductor lasers pumped by pulsed electric discharge in vacuum.

13 p1626 A73-28545

Electrooptical and piezoelectric alignment of a composite resonator in a semiconductor laser

13 p1627 A73-28764

Thermal deformation of an injection laser crystal during the passage of pumping current pulses.

13 p1630 A73-29443

Optoelectronic semiconductor components under the influence of ionizing radiation

14 p1733 A73-30070

Heterojunction laser diode fabrication procedures operation and details, considering peak power levels, wavelengths and operating temperatures for CW and pulsed operations

14 p1736 A73-30575

Direct modulation of a double heterostructure laser at a rate of 2.3 Gbit/s

14 p1758 A73-30700

GaAs and GaAlAs semiconductor injection lasers, discussing system design and applications for ranging, illumination and communication with peak power and repetition rate requirements

16 p2023 A73-32866

Fast random access permanent storage read only optical memory, using light emitting diode matrix addressing, semiconductor laser and holographic lens system

16 p2012 A73-32870

Determination of the diffusivity-mobility ratio in highly degenerate semiconductors at low temperatures from linewidth measurements in junction lasers.

16 p1990 A73-33689

High peak power from /GaAl/As-GaAs double-heterostructure injection lasers.

17 p2183 A73-34202

Theory of the threshold of an injection laser operating at the experimental band tails

17 p2184 A73-34922

Dynamics of the emission of semiconductor lasers whose refractive index depends on the emission intensity

18 p2322 A73-36560

Laser-pumped tunable spin-flip InSb Raman lasers in terms of low field operation, linewidth measurement technique, power output and applications

20 p2571 A73-38623

Influence of semiconductor laser heating on the parameters of the output pulses

21 p2710 A73-40006

Semiconductor laser beam self focusing action due to combined effects of linear and nonlinear dielectric constant and absorption coefficients, considering n-InSb sample

21 p2711 A73-40226

Tunable Pb-Sn-Te junction laser characteristics and fabrication by impurity diffusion for IR CW operation at liquid helium temperatures

21 p2716 A73-40967

A semiconductor-laser communication system using differential pulse position modulation.

21 p2656 A73-41094

Influence of mechanical treatment of the resonator on the parameters of an electron-beam-pumped cadmium sulfide laser.

22 p2869 A73-42259

SEMICONDUCTOR PLASMAS

Satellite dimensional resonances in microwave helicon transmission through semiconductors.

06 p0739 A73-18788

Ionization energy of adhesion levels and heat-generation centers in the microplasma volume in germanium p-n junctions

08 p0995 A73-21274

Periodic instability induced in semiconductor situated in crossed electric and magnetic fields via electron gas heating, deriving expressions for properties of steady nonlinear waves

10 p1261 A73-24764

Pinch effect in a germanium electron-hole plasma.

11 p1409 A73-26189

Electromagnetic wave propagation in p-type Ge and Si semiconductor plasmas, studying dispersion, cyclotron resonance, and kinetic equations

15 p1925 A73-32214

Theory of the oscillations and stability of a semiconductor plasma with a small number of carriers in a strong electric field

16 p2042 A73-33734

Surface wave propagation parallel to applied magnetic field in electron hole plasma, explaining observed resonances in InSb by LF mode

21 p2751 A73-40325

Instability of transverse electromagnetic waves in a drifting electron-hole plasma

21 p2751 A73-40368

Propagation of microwaves in a solid-state plasma

21 p2753 A73-41292

Determination of valence electron plasma frequencies and optical permittivity in single crystals of trisulfide of antimony

22 p2897 A73-42648

Wave propagation through a highly restrained solid-state plasma.

23 p3012 A73-44141

SEMICONDUCTORS [MATERIALS]

NT ACCEPTOR MATERIALS

NT AMORPHOUS SEMICONDUCTORS

NT DONOR MATERIALS

NT METAL OXIDE SEMICONDUCTORS

NT METAL-NITRIDE-OXIDE-SILICON

NT MIS (SEMICONDUCTORS)

NT N-TYPE SEMICONDUCTORS

NT ORGANIC SEMICONDUCTORS

NT P-TYPE SEMICONDUCTORS

NT PHOTOCONDUCTORS

Influence of gamma-radiation on the electrical properties of a real germanium surface

01 p0087 A73-10039

Doped CdSb single crystal production and physical properties for IR detectors and thermocouple use

01 p0087 A73-10040

Light waves interaction in nonlinear medium, noting operational principles and optical properties of parametric optical generators with semiconductors

01 p0059 A73-10717

Investigation of the statistical properties of ultrashort light pulses with the aid of two-photon absorption in semiconductors

01 p0061 A73-11282

Multiphonon transition theory for electron transitions probability between conduction and forbidden bands, noting semiconductor surface states with long relaxation time

01 p0089 A73-11438

Metallographic macro- and microstructural study of semiconductor compounds, discussing single crystal imperfections, polycrystals and semiconductor films

02 p0199 A73-11582

Van Vleck paramagnetism and bonding parameters in semiconductors

02 p0201 A73-11900

GaAs-GaAlAs heterojunction transistor for high frequency operation

02 p0147 A73-12046

Doping additions dissociation effect on impurities distribution in grown semiconductor crystals of melts, calculating atomic and molecular concentration

02 p0201 A73-12356

Possibility of the occurrence of self-oscillations in a circuit containing a constant source of current and a homogeneous semiconductor specimen with small response times

03 p0349 A73-12907

Investigation of the disintegration of semiconductor exposed to laser radiation

03 p0349 A73-13660

Influence of gamma irradiation on the surface properties of metal-dielectric-semiconductor structures

03 p0349 A73-13661

Calculation of the complex conductivity of a monopolar semiconductor with a finite-injection contact

03 p0349 A73-13662

Frequency conversion using the real current-voltage characteristic of a metal-semiconductor contact

03 p0349 A73-13663

Noise measurement in p-n junction surface of Si semiconductor wafer under transverse electric field, noting reverse current contribution

03 p0350 A73-13665

Indirect interaction of nuclear spins through valence band electrons in semiconductors

03 p0350 A73-13754

Effect of illumination on the form of current-voltage characteristics of SbSi in the paraelectric region

03 p0350 A73-13756

Metal ions implantation to produce alloy or semiconductor, discussing transmission electron microscopy use for viewing target material defect clusters

03 p0350 A73-13794

Rayleigh wave propagation at the boundary between a piezoelectric insulator and a semiconductor

03 p0350 A73-14037

Solar cell graded band gap materials, determining I-V characteristics, junction capacitance and photovoltaic spectral response

03 p0254 A73-14207

Linear and nonlinear optical properties of some ternary selenides

03 p0350 A73-14458

Impurity centers effect on I-V characteristics of double injection level semiconductors, noting negative resistance region

04 p0482 A73-14877

Spectral line shape for interband light absorption with excitons formation in incompletely ordered semiconductor, taking into account interaction with random electrostatic field

04 p0483 A73-14879

Metal-semiconductor system phase diagram for temperature dependence of substrate surface epitaxial film thickness during single crystal growth, determining equilibrium saturation time

04 p0483 A73-14880

Magnetic semiconductor materials compositions and magnetoelectric characteristics, discussing magnetic-electric interactions, fabrication techniques and applications for magnetically controllable diodes, temperature sensors, etc

04 p0483 A73-15323

Observation of Kohn-type anomalies in the electron-phonon interaction on the Fermi surface of degenerate semiconductors

04 p0483 A73-15469

Strong electromagnetic waves in semiconductors under conditions of inelastic scattering of current carriers by optical phonons

04 p0484 A73-15568

Charge carrier cooling in nonhomogeneous semiconductors by static electric field, plotting average electron temperature as function of current

04 p0484 A73-15569

Passage of electric current through an illuminated semiconductor under conditions where the anisotropy parameters, the electrical conductivity, and the relaxation time are nonuniform. I

04 p0484 A73-15641

Colloid thruster propellants selection for semiconductor liquids with suitable electrochemical properties via cyclic voltammetry

04 p0485 A73-15724

Non-ohmic transport and phonon amplification in polar semiconductors

04 p0484 A73-16035

Book - Advances in electronics and electron physics. Volume 31.

05 p0558 A73-16601

Influence of nonlinear polarization on the ultrasonic gain factor in piezosemiconductors

05 p0605 A73-16821

Theory of scattering of electrons in a non-degenerate-semiconductor-surface inversion layer by surface-oxide charges

06 p0733 A73-17747

Space-time distribution of excess carriers and their space charge in doped semiconductors

06 p0734 A73-17814

Theory of one-dimensional Mott semiconductors and electronic structure of long molecules with conjugate bonds

06 p0734 A73-17923

Energy absorption inelastic surface mechanisms effect on I-V characteristics profile for bounded semiconductor with negative differential conductivity

06 p0735 A73-17974

Nonequilibrium plasma wave scattering cross section dependence on energy bands shape and field orientation in semiconductors

06 p0735 A73-17975

Kadomtsev-Nedospasov helical instability during a strong pinch effect in an electron-hole plasma

06 p0729 A73-18119

Investigation of X-ray atomic scattering functions taking into consideration the tetrahedral covalent bonds in some semiconductors

06 p0736 A73-18217

Absorption coefficient due to band-band optical transitions in heavily doped semiconductor, obtaining electron and hole quasi-Fermi levels

06 p0738 A73-18586

Anisotropy of piezoelectrical scattering in semiconductors with a wurtzite structure

06 p0738 A73-18648

High reliability semiconductors development, discussing research in Si single crystals growth, epitaxial films, photoengraving, oxidation/passivation and large-scale integration techniques

07 p0829 A73-18919

Charge carriers concentration growth and decay for semiconductor model with independent capture centers, determining capture level activation energy

07 p0861 A73-19328

A semiconductor in a microwave electromagnetic field and in a steady magnetic field

07 p0862 A73-20012

Concentration and mobility of electrons in indium-doped zinc oxide crystals

07 p0862 A73-20016

Aircraft and land vehicle electric generators and motors, noting semiconductors application and cooling systems

07 p0779 A73-20124

Criteria for evaluating semiconductor materials in epipolar technology applications

08 p0994 A73-21079

Iterative method for calculating hot carrier distributions in semiconductors

08 p0994 A73-21221

The bus-probe and multiprobe methods of measuring Hall mobility in semiconductor layers of nonuniform depth

08 p0995 A73-21272

Concentrations of carriers and electric field along an insulating or semiconducting sample: Developments of steady solutions up to the second order Case of weak potentials

08 p0995 A73-21443

Reflection of a microwave signal from a semiconductor plate of finite thickness

08 p0995 A73-21517

Surface photovoltage spectroscopy - A new approach to the study of high-gap semiconductor surfaces

08 p0968 A73-21620

Investigation of the anisotropy of effective masses in the conduction band of semiconductors under uniaxial compression

09 p1132 A73-21959

The continuity and Poisson's equations for semiconductors with many coexisting kinds of multiple energy-level defects

09 p1133 A73-22306

Frequency multiplication due to nonparabolicity of dispersion law in semiconductor structure subbands, noting electromagnetic signal transformation

09 p1133 A73-22665

Effect of shielding on charge carrier mobility in compensated materials

09 p1133 A73-22674

Influence of changes in the contact region on the basic characteristics of a semiconductor in the illuminated mode

09 p1134 A73-22685

A relationship between photoemission-determined valence band gaps in semiconductors and insulators and ionicity parameters

09 p1134 A73-22903

Structure diagram, crystal growth, band structure, physical, optical and photoelectric properties of A/II/B/V/ compounds, emphasizing CdSb-ZnSb solid solutions

10 p1258 A73-23566

Double-injection negative differential resistance in compensated gold-doped germanium

10 p1259 A73-23752

Semiconductor and semi-insulator resistivity measurements using a direct current four point probe apparatus with non-penetrating tips

10 p1194 A73-24158

Positive thermal coefficient of electrical resistance in BaTiO₃ single crystals near the Curie point

10 p1260 A73-24473

High temperature superconductivity in three dimensional systems of metals and nonmetals, discussing electron collectivization in metals, dielectrics, organic compounds, semiconductors and molecular crystals

10 p1261 A73-24692

Characteristics of the vibrational spectrum of laminar As₂S₃ semiconductors

11 p1408 A73-25244

Investigation of the relationship between 'edge' and exciton emission in CdS single crystals

11 p1408 A73-25246

Determination of attachment center parameters in semiconductors from the temperature dependence of the photocurrent

11 p1408 A73-25248

Application of the invariant of a homographic transformation to measure the series resistance of semiconductor elements

11 p1336 A73-25319

Electronic charge densities in semiconductors

11 p1408 A73-25374

On the stability of finite difference schemes in transient semiconductor problems

11 p1408 A73-25438

Photoluminescence of ZnTe during laser stimulation

11 p1376 A73-26145

Influence of a powerful electromagnetic wave on the electrical conductivity of a semiconductor

11 p1409 A73-26165

Resonance between spin and magnetohydrodynamic waves in antiferromagnetic semiconductors and metals

11 p1409 A73-26190

Dissociation of semiconductor compounds under the action of a laser beam

11 p1378 A73-26675

The kinetic reflection coefficient in a formula for the current at a plasma/semiconductor interface in the case of an inelastic mechanism of electron energy relaxation

12 p1527 A73-26928

Electrical conductivity of semiconductor glass crystals on an arsenic and lead selenide base

12 p1531 A73-27195

Influence of the impurity compensation effect on the magnitude of the negative reluctance of alloys of the $\text{In}_2\text{Te}_3/\text{x-Hg}_3\text{Te}_3/1-\text{x}$ system

12 p1532 A73-27940

A transport equation treatment of tunnelling in semiconductors

13 p1668 A73-28218

Cleaved Si and Ge surfaces roughness investigation by low energy electron diffraction, electron microscopy and optical reflection technique

13 p1668 A73-28452

The connection between the thermodynamics of chemisorption on semiconductor surfaces and surface scattering of carriers

13 p1668 A73-28454

Determination of the basic characteristics of an impurity level by Hall effect measurements

13 p1668 A73-28461

Phenomenological analysis of thermostimulated depolarization effects

13 p1668 A73-28463

Low-temperature negative differential microwave conductivity in semiconductors following elastic scattering of electrons

13 p1669 A73-28614

Quantization effects in semiconductor inversion and accumulation layers

13 p1669 A73-29291

Possibility of a superconducting transition in a semiconductor subjected to high-power laser radiation

13 p1629 A73-29439

Propagation of ultrashort light pulses in a semiconductor under two-photon resonance conditions

13 p1630 A73-29445

Parametric excitation of ultrasonic waves in piezoelectric semiconductors

14 p1783 A73-29916

Nonlinear mechanisms for self-focusing of microwaves in semiconductors.

14 p1732 A73-29920

Implication of contact thermalization effect in two-valley semiconductors for the high frequency device performance.

14 p1783 A73-29929

Model of degenerate semiconductor transition to superconducting state in terms of electron interactions with phonons of low-lying spectral branch

14 p1783 A73-30343

Determination of the main details of the band structure of semiconductors from edge absorption data

14 p1783 A73-30366

International Conference on the Physics of Semiconductors, 11th, Warsaw, Poland, July 25-29, 1972, Proceedings. Volumes 1 & 2.

14 p1783 A73-30572

'Anomalous' alteration of the Moessbauer isomer shift of Te125 in defect diamond-like semiconductors

14 p1784 A73-30809

Nuclear gamma resonance spectra of Sn119 and Te125 and the electron structure of ternary diamond-like semiconductors Cu2SnS3, Cu2SnSe3 and Cu2SnTe3

14 p1784 A73-30851

Some problems in measuring the electrical properties of semiconductors

14 p1784 A73-30924

Possibility of using semiconductor photocells as receivers of ultraviolet radiation

14 p1713 A73-30949

Thin dielectric films as protective coatings for metallic mirrors and antireflective coatings for semiconductors and active laser materials

15 p1884 A73-31416

Investigation of the structure of electron bands in In(1-x)Ga(x)As(1-y)P(y) on the basis of luminescence

15 p1923 A73-31716

Interaction of nearly monochromatic LA phonons with excitons in CdS crystals

15 p1924 A73-31718

Studies of galvanomagnetic and thermomagnetic phenomena in selenium and tellurium doped InSb.

15 p1924 A73-32159

Russian book - Electrons and holes in semiconductors: Energy spectrum and dynamics.

15 p1852 A73-32298

Electrical properties of semiconductors with non-spherical radiation damage regions.

16 p2044 A73-33198

Ultrasound absorption coefficient measurement in semiconductor crystal lattices based on acoustoelectrical effect

17 p2218 A73-34159

Assembly for optical studies of semiconductors under pressures up to 10 kbar at 77 K

17 p2145 A73-34175

Polarization plane rotation under magnetic field for IR waves in nonmagnetic semiconductors with cubic crystal lattices, explained by magneto-optical Faraday effect

17 p2219 A73-34342

Book - Compatibility and testing of electronic components.

17 p2134 A73-34573

Cooling associated with minority carriers exclusion effect in semiconductors, discussing influence of electroconductivity and forbidden bandwidth

17 p2219 A73-35160

Resistance anomaly in semiconductor barium and strontium niobates

17 p2219 A73-35554

Determination of ultramicro-impurities in CdS-type semiconductor materials - Determination of copper

17 p2220 A73-35558

Principal component determination in mercury and cadmium tellurides and in solid solutions of them

17 p2220 A73-35559

Electric potential and current distribution in a rectangular sample of anisotropic material with application to the measurement of the principal resistivities by an extension of van der Pauw's method.

17 p2220 A73-35653

Influence of the reflection forces and the tunnel effect on the current-voltage characteristic of a metal-semiconductor contact with a Schottky barrier

18 p2340 A73-36668

Formulation of the basic approximations of the field theory of static current-voltage characteristics of quasi-monopolar semiconductors

18 p2341 A73-36724

Some characteristics of the microplastic deformation of the surface layers of semiconductor crystals at temperatures below and above the thermal brittleness threshold

18 p2341 A73-36805

Injection currents in semiconductors with deep polarizable impurity centers

18 p2341 A73-37046

Influence of extended defects on the electron spectrum of semiconductors

19 p2470 A73-37952

Influence of intervalley scattering on the size effect in the electrical conductivity of semiconductors

19 p2471 A73-37956

Current carriers and electron impurity centers in ferrimagnetic semiconductors - The case of weak interaction

19 p2471 A73-37959

Dynamic scattering of oscillating charged centers in semiconductors

19 p2471 A73-38541

Theory of quantum oscillations of the Nernst-Ettingshausen thermomagnetic coefficient in semiconductors

20 p2599 A73-39397

Substrate effect estimation for space charge limited current in intrinsic materials and planar structures, discussing I-V curves

20 p2543 A73-39593

Semiconducting ground influence on input impedance and radiation resistance of horizontal magnetic dipoles, covering short wave band for various antenna elevations and conductivity levels

21 p2661 A73-40203

Theory of the phase transition in group IV-VI compound semiconductors

21 p2751 A73-40369

Superconductor-semiconductor Schottky barrier diode video detector with proper doping and electron tunneling to obtain high degree nonlinearity in I-V characteristics

21 p2662 A73-40463

Dynamic properties of surface layers in semiconductors

21 p2752 A73-40845

CAD for realization of an impurity distribution in a semiconductor.

21 p2753 A73-41095

Noise of space-charge-limited current in solids is thermal.

21 p2668 A73-41559

Optical and electrical properties of doped semiconductors in a strong electromagnetic field.

22 p2896 A73-42252

Kinetic reflection coefficient at a plasma-semiconductor boundary for inelastic electron energy relaxation.

22 p2891 A73-42262

Illumination aftereffects due to semiconducting ferrite electron and ion motion, discussing dielectric properties and electron hole deficiencies

22 p2833 A73-42514

Generation of electrical current by impact in metallic and semiconductor bodies

23 p3015 A73-43476

Regularities in the behavior of semiconductors and dielectrics in connection with deviation from stoichiometry

23 p2959 A73-43479

Compressive strength and plastic deformation of monocrystal bismuth telluride, polycrystal lead telluride, Cu-Te compounds and Pb-Sn-Te solid solution

23 p3015 A73-43480

Investigation of the statistical properties of ultrashort light pulses by two-photon absorption in semiconductors.

23 p2987 A73-43503

Diffusionless theory of the current-voltage characteristics of a metal/monopolar semiconductor contact in the case of current limiting by an arbitrary space charge

23 p3015 A73-43621

Light absorption coefficient of disordered semiconductor with random field due to charged impurity centers in presence of constant external electric field

23 p3016 A73-43648

Eigenfunction calculation of injected carrier density in doped semiconductor filaments, relating negative eigenvalues to Suhl effect and lifetime dependence to bulk and surface recombination

23 p3016 A73-43674

Role of electron processes in the vaporization mechanism and in the formation of binary semiconductor alloy compositions with ion bonds

23 p3016 A73-43711

Quantum transport theory of high-field conduction in semiconductors.

23 p3016 A73-43775

Theory of donor-acceptor radiative and Auger recombination in simple semiconductors.

23 p3016 A73-43796

Optical orientation in a system of electrons and lattice nuclei within semiconductors - Experiment

23 p3016 A73-44022

Optical orientation in a system of electrons and lattice nuclei within semiconductors - Theory

23 p3017 A73-44023

Linear external electric field approximation for intervalley scattering effects on nondegenerate semiconductor surface electroconductivity

23 p3017 A73-44045

Concentration effect in semiconductors with bipolar conductivity in an alternating external magnetic field

23 p3017 A73-44046

Theory of one-dimensional Mott semiconductors and the electronic structure of long molecules having conjugated bonds.

23 p3018 A73-44323

Optical modulation of X band microwave transmission by acoustoelectric domains in cylindrical CdS single crystal, noting domain conductivity and permittivity changes

23 p3018 A73-44365

Analyses of some potential problems in cylindrical coordinates in connection with four-point probe technique.

23 p3018 A73-44368

Determination of hole and electron traps from capacitance measurements.

24 p3119 A73-44405

Kadomtsev-Nedospasov helical instability in a strong pinch effect in an electron-hole plasma.

24 p3114 A73-44503

Influence of radiation on the current-voltage characteristic of tunnel diodes /Survey/

24 p3072 A73-44926

Possible causes of failures in pulse-switched thyristors

24 p3072 A73-44933

Development and properties of CdP2S4

24 p3119 A73-44951

Electrical and mechanical characteristics of thermocell arms reinforced by metal frames

24 p3058 A73-45252

Detection of phosphorus in heavily diffused silicon by He+/+ backscattering.

24 p3120 A73-45262

Influence of heat treatment on the posistor effect of semiconductive BaTiO3-ceramic.

24 p3120 A73-45367

Ion-implanted nitrogen in gallium arsenide.

24 p3120 A73-45402

Concentration contours in regions with both normal and enhanced diffusion coefficients.

24 p3120 A73-45404

The relation between the diffusivity-mobility ratio and the linewidth of spontaneous emission in degenerate semiconductors at relatively high temperatures.

24 p3120 A73-45488

SEMIEMPIRICAL EQUATIONS

Toward simpler prediction of transonic airfoil lift, drag, and moment.

09 p1028 A73-22434

Runway visual range equation derivation, taking into account background luminance, atmospheric absorption and illumination

15 p1906 A73-32351

SEMI-METALS

U METALLOIDS

SENDERS

U TRANSMITTERS

SENSATIONS

U PERCEPTION

SENSE ORGANS

NT BARORECEPTORS

NT CHEMORECEPTORS

NT COCHLEA

NT CORNEA

NT CORTI ORGAN

NT EAR

NT EARDRUMS

NT EYE [ANATOMY]

NT FOVEA

NT GRAVIRECEPTORS

NT LABYRINTH

NT MECHANORECEPTORS

NT MIDDLE EAR

NT OCULOMOTOR NERVES

NT OTOLITH ORGANS

NT PHOTORECEPTORS

NT PUPILS

NT RETINA

NT SEMICIRCULAR CANALS

NT THERMORECEPTORS

NT VESTIBULES

Orientation: Sensory basis; Proceedings of the Conference, New York, N.Y., February 8-10, 1971.

06 p0653 A73-18030

Book - Sensory coding in the mammalian nervous system.

11 p1317 A73-25799

SENSES

U SENSORY PERCEPTION

SENSIBILITY

U SENSITIVITY

SENSITIVITY

NT IMPACT RESISTANCE

NT LIGHT ADAPTATION

NT NOTCH SENSITIVITY

NT PAIN SENSITIVITY

NT PHOTOSENSITIVITY

NT RADIATION TOLERANCE

Sensitivity of optical autodyne quantum receiver in presence of output noise, using photomultiplier signal model

03 p0319 A73-14076

The design of optimally parameter insensitive control systems.

10 p1199 A73-24030

SENSITIZING

- Single input n-th order linear constant discrete-time adaptive control systems, deriving phase canonical form sensitivity functions by z-transform
11 p1342 A73-26636
- Closed loop formulations of optimal control problems for minimum sensitivity.
17 p2144 A73-34363
- Parametric sensitivity in the problem of control with reference to an incomplete model of the plant
20 p2542 A73-39350
- Sensitivity of an intensity radio interferometer
21 p2705 A73-41471
- Thin film temperature sensor with polymer coating for medical research providing good sensitivity and stability for rapid temperature changes in biochemical reactions
22 p2813 A73-42055
- Sensitivity of optimal control systems with bang-bang control.
22 p2837 A73-43068
- Sensitivity, adaptivity and optimality; Proceedings of the Third Symposium, Ischia, Italy, June 18-23, 1973.
23 p2961 A73-43277
- Standard sensitivity and covariance matrices for statistical estimation of overall performance.
23 p2962 A73-43279
- Reduction of the sensitivity of optimal control systems by using two degrees of freedom.
23 p2962 A73-43285
- SENSITIZING**
Influence of certain wetting agents on the optical sensitization and retention of the photographic properties of a finished layer
21 p2647 A73-40271
- SENSOR-AIRBORNE TERRAIN ANALYSIS**
U SENSORS
U TERRAIN ANALYSIS
- SENSORIMOTOR PERFORMANCE**
NT PSYCHOMOTOR PERFORMANCE
NT PSYCHOSOMATICS
- Correlations between motor learning and visual and arm adaptation under conditions of computer-simulated visual distortion.
03 p0267 A73-13556
- Visual-motor coordination characteristics of parachute jumpers
06 p0657 A73-17750
- Role of visual and articular afferentation in the implementation of motor reactions involving complex coordination and precision
06 p0653 A73-18164
- Structural models of simple sensory motor coordination.
06 p0660 A73-18890
- Disorienting effects of aircraft catapult launchings.
07 p0785 A73-19480
- Changes in the amplitudinal and temporal characteristics of sensorimotor-cortex evoked potentials after deactivation of spinocervical tracts in cats
07 p0781 A73-20004
- Heart activity characteristics in a human operator during a control process
10 p1183 A73-23806
- Features of the spontaneous and evoked neuronal activity of deep brain structures in man during voluntary movements
10 p1181 A73-24517
- Organization of the activity of a group of motor neurons in man during voluntary contraction of a muscle
10 p1182 A73-24599
- Experimental study of emotional stress in operators
11 p1321 A73-25038
- Adjustment of saccade characteristics during head movements.
11 p1319 A73-26222
- Work movement performance of the astronaut in flight.
12 p1465 A73-27645
- Some aversive characteristics of centrifugally generated gravity.
13 p1575 A73-28506
- Motor functions and control of sensorial messages of somatic origin
13 p1576 A73-29174
- Anatomo-functional bases of cerebello-cerebral interrelations
15 p1836 A73-32287
- Intervention of cerebello-cortical and cortico-cerebellar paths in the organization and regulation of movement
15 p1836 A73-32288
- Self-estimates of distractibility as related to performance decrement on a task requiring sustained attention.
15 p1839 A73-32394
- A comparison of visual, auditory, and cutaneous tracking displays when divided attention is required to a cross-adaptive loading task.
15 p1839 A73-32395
- Brain alpha rhythm activity relationship to perceptual and motor performance, correlating with reaction time and computer cycle time analogy
16 p1972 A73-33159

- Information processing in the visual periphery.
17 p2113 A73-34150
- Space-time adaptation of visual position constancy.
17 p2114 A73-34223
- Central programming and peripheral feedback during eye-head coordination in monkeys.
18 p2273 A73-36452
- Interference of 'attend to and learn' tasks with tracking.
19 p2401 A73-38377
- Ultradian rhythms in human telemetered gross motor activity.
20 p2512 A73-39102
- Inversion of lighting regimen alters acrophase relations of circadian rhythms in body temperature, heart rate and movement of pocket mice.
20 p2513 A73-39480
- A study of evoked slow activities in man which follow a voluntary movement and articulated speech
20 p2514 A73-39759
- Experimental analysis of conditions for onset of emotional stress
20 p2516 A73-39800
- Contingent negative variation expectancy waveform relation to human psychic state in response to visual and imperative acoustic stimuli
20 p2516 A73-39804
- Sleep deprivation effects on accuracy and speed of response selection and execution.
21 p2644 A73-40853
- Variations in the motor potential with force exerted during voluntary arm movements in man.
21 p2638 A73-41013
- Automatic apparatus for the study of conditioned reflexes in a monkey seated in the primate chair
21 p2644 A73-41140
- Frequency of anti-collision observing responses by solo pilots as a function of traffic density, ATC traffic warnings, and competing behavior.
21 p2645 A73-41158
- Response delays and the timing of discrete motor responses.
21 p2645 A73-41177
- Russian book - Electrical activity of the human brain in the process of motor action.
21 p2640 A73-41289
- Operator reaction functional readiness manifestation in evoked potential characteristics of stimulus-response situations, obtaining response amplitude distribution
22 p2812 A73-41891
- Human sensorimotor coordination following space flights.
22 p2814 A73-42170
- Human phasic reflex response to parameters of a mechanical stimulus as an index of muscle-spindle sensitivity.
22 p2816 A73-42679
- Neuronal activity of the sensorimotor and visual cortex in rabbits during development of a summation focus in the reticular formation
24 p3058 A73-44550
- Use of the conditioned reflex method to study the motor analyzer during hygienic evaluation of working conditions in the presence of vibrations
24 p3062 A73-44673
- Two components and two stages in search performance - A case study in visual search.
24 p3065 A73-45339
- SENSORS**
Calculation of the coverage factor of a NMR sensor for an externally located sample
09 p1080 A73-22339
- High temperature fatigue sensor based on conductive composite device irreversible resistance increase resulting from cumulative strain damage
09 p1083 A73-22504
- The use of television type sensors in astronomy.
17 p2169 A73-35278
- Digital hardware and computer system for a digital image recorder.
17 p2131 A73-35280
- Television sensors for ultraviolet space astronomy.
17 p2170 A73-35292
- Depth sensing, camera and touch/force sensing systems for autonomous industrial robotics and planetary exploration
19 p2429 A73-37322
- Recent test results - A strapdown IMU utilizing hydrodynamic spin bearing rate sensors and pulse rebalance loops.
20 p2564 A73-38833
- [AIAA PAPER 73-898]
Optimal parameters on fluidic noncontact sensors for drives of exact positioning.
23 p2945 A73-43427
- SENSORY DEPRIVATION**
Modulated light transmission for electrical isolation in a multichannel physiological monitoring system.
07 p0785 A73-19482
- Effect of light deprivation on the metabolic reaction development in retinal ganglion cells
10 p1178 A73-23681
- Effects of prolonged dark adaptation on autokinetic movement.
11 p1324 A73-26322

- Characteristics of the higher nervous activity of monkeys during a postneurotic period
12 p1462 A73-27108
- Sensory versus perceptual isolation - A comparison of their electrophysiological effects.
14 p1722 A73-30517
- SENSORY DISCRIMINATION**
NT BRIGHTNESS DISCRIMINATION
NT TACTILE DISCRIMINATION
NT VISUAL DISCRIMINATION
- The null magnetic field as reference for the study of geomagnetic directional effects in animals and man.
06 p0658 A73-18033
- Cortical potentials evoked by confirming and disconfirming feedback following an auditory discrimination.
09 p1039 A73-21895
- SENSORY FEEDBACK**
Extraretinal feedback and visual localization.
01 p0008 A73-10437
- Stable frequency and synchronicity alterations in the discharges of cortical neuron populations in feedback experiments
01 p0010 A73-11445
- Psychological test for relative contributions of specific and nonspecific components to intersensory transfer between vision and touch
03 p0266 A73-13525
- Correlations between motor learning and visual and arm adaptation under conditions of computer-simulated visual distortion.
03 p0267 A73-13556
- Polarity cue for visual accommodation response of trained subjects to target motion direction change, considering retinal image blur and feedback relation
08 p0932 A73-21569
- Cortical potentials evoked by confirming and disconfirming feedback following an auditory discrimination.
09 p1039 A73-21895
- The operational control of the alpha component in the electroencephalogram by means of auditory feedback
11 p1324 A73-26549
- Forward and backward conditional link formation as physiological mechanism for reinforcement conditioning connection
14 p1718 A73-30568
- Teleoperator system incorporating touch feedback and sequenced automatic control for experimental investigation of human touch sensing relation to manipulative skills
19 p2397 A73-37328
- An electrical model of the inertial and adaptive properties of vision as a self-regulating system with delayed feedback
20 p2517 A73-39004
- A short description of the NAE airborne simulator feel system.
21 p2672 A73-40854
- SENSORY PERCEPTION**
NT AUDITORY PERCEPTION
NT AUTOKINESIS
NT CONSCIOUSNESS
NT CRITICAL FLICKER FUSION
NT EXTRASENSORY PERCEPTION
NT OLFACTORY PERCEPTION
NT PAIN SENSITIVITY
NT PROPRIOCEPTION
NT SPACE PERCEPTION
NT TACTILE DISCRIMINATION
NT TOUCH
NT VERTICAL PERCEPTION
NT VIBRATION PERCEPTION
NT VISUAL DISCRIMINATION
NT VISUAL PERCEPTION
- Human thresholds for perceiving sudden changes in atmospheric pressure.
03 p0260 A73-13554
- Vestibular adaptation in man - Effects of increased acceleration during different phases of adaptation.
04 p0411 A73-15218
- Human perception of humidity under four controlled conditions.
06 p0657 A73-17864
- Orientation: Sensory basis; Proceedings of the Conference, New York, N.Y., February 8-10, 1971.
06 p0653 A73-18030
- Examination of responses evoked in the sensory cortex by thalamic stimulation.
10 p1178 A73-23772
- Perceived level calculation methods for aircraft flyover noise scaling, rating jets, turboprops, piston aircraft and helicopters with frequency weighting functions, duration and tone corrections
10 p1175 A73-24391
- Book - Sensory coding in the mammalian nervous system.
11 p1317 A73-25799
- Equivalence of the action of Coriolis accelerations to that of certain angular accelerations in their effects on the receptors of semicircular canals
12 p1463 A73-27718
- Sensory versus perceptual isolation - A comparison of their electrophysiological effects.
14 p1722 A73-30517

Acquisition of signal concepts under conditions of aversion activation. I - Theoretical part and form interpretation test

16 p1972 A73-33091

Participation of cholinergic mechanisms in negative human emotions

20 p2515 A73-39799

Effects of single exposures of carbon monoxide on sensory and psychomotor response.

21 p2637 A73-40409

Human perception of moderate strength low frequency magnetic fields tested by whole body immersion in large Helmholtz coil field under acoustic isolation

22 p2811 A73-41789

Relation between vibratory sensibility and electric signal of living body.

22 p2816 A73-42680

Determination of performance precision and informativeness of electronic models of the sensory system of man

24 p3064 A73-44911

SENSORY STIMULATION

Changes in the vibratory sensation threshold after exposure to powerful vibration.

01 p0013 A73-10772

Aerodynamic and temporal parameters of olfactory stimulation - Discussion concerning the lowering of the threshold by prenasal injection in man

03 p0262 A73-13787

Skin sensitivity of palms, wrists and forearms to focused ultrasound, noting evoked touch, pulsation, cold, warmth and prick sensations and applications in receptor physiology

05 p0540 A73-16695

Statistical distribution methods for analyzing formation of reflexes conditioned to time intervals between periodic unconditioned stimuli

06 p0653 A73-18166

Human performance measures relationship determination across sense modes under visual, auditory and combined stimulus conditions by controlling for task difficulty on individual basis

06 p0658 A73-18244

Visual evoked responses elicited by rapid stimulation.

06 p0654 A73-18350

German monograph on human information transmission by multidimensional tactile stimuli investigation using method of learned signals identification

07 p0786 A73-20393

Polysensory responses and sensory interaction in pulvinar and related postero-lateral thalamic nuclei in cat.

09 p1040 A73-22696

Useful future action models of instrumental reflexes and voluntary actions based on memory role in engram storage of received stimuli

11 p1314 A73-25199

Adaptation-level and theory of signal detection - An examination and integration of two judgment models for voluntary stimulus generalization.

12 p1464 A73-26749

The role of analyzers of conditional and unconditional stimuli in the functional system of the behavioral conditioned-reflex action

12 p1461 A73-27105

Changes in visual functions after the action of weak vestibular stimuli

12 p1464 A73-27719

Late visual cortical region reactions during the convergence of light stimulation and electrocutaneous stimulation

13 p1576 A73-29073

Alpha wave peak amplitude dependence on blocking pattern after stimulation during habituation-pseudoconditioning, conditioning and extinction

14 p1714 A73-29992

Sustained human skin and muscle vasoconstriction with reduced baroreceptor activity.

15 p1833 A73-31344

Neuronal elements of the orienting response - Microrecordings and stimulation experiments in rabbits.

18 p2272 A73-36444

Determination of the type of higher nervous activity from the aftereffect characteristics of multidimensional stimuli

18 p2277 A73-36577

Reinforcement of unconscious traces of stimuli in the human being during ontogenesis

19 p2393 A73-37251

A study of evoked slow activities in man which follow a voluntary movement and articulated speech

20 p2514 A73-39759

Formation of various functional states in the symmetrical structures of the brain as a function of the intensity of unconditioned excitation

20 p2516 A73-39801

Diminution of uncertainty in the firing of hippocampal units in response to a stimulus

20 p2516 A73-39803

Contingent negative variation expectancy waveform relation to human psychic state in response to visual and imperative acoustic stimuli

20 p2516 A73-39804

SENTENCES

NT WORDS [LANGUAGE]

SEPARATED FLOW

NT BOUNDARY LAYER SEPARATION

Numerical method for describing turbulent, compressible, subsonic separated jet flows.

01 p0035 A73-11467

Higher-order delta wings with flow separation at subsonic leading edges

02 p0127 A73-11581

Separated flow noise.

03 p0291 A73-12975

Breakup and penetration of transverse liquid jets in supersonic air cross flow

[AIAA PAPER 72-1180]

03 p0293 A73-13475

A free-streamline theory for bluff bodies attached to a plane wall.

04 p0403 A73-15160

Basic flow characteristics of a linear aerospoke nozzle segment.

[ASME PAPER 72-WA/AERO-2]

04 p0405 A73-15908

Optimization of drag minimums including effects of flow separation.

[ASME PAPER 72-WA/AERO-1]

04 p0405 A73-15909

Empirical equations for calculating the heat and mass transfer for the special case of separated flow

04 p0520 A73-15941

Multivortex model for bodies of arbitrary cross-sectional shapes.

[AIAA PAPER 73-104]

05 p0529 A73-16864

High Reynolds number steady separated flow past a wedge of negative angle.

06 p0685 A73-17710

Supersonic flow past notch in lateral body surface or in two closely lying coaxial bodies, applying turbulent jet theory to separation zone

07 p0774 A73-19618

A new probe for measurement of velocity and flow direction in separated flows.

08 p0963 A73-20871

Dynamic model of flow separation of plane fluid past body in channel with eddy wake formation

08 p0954 A73-21183

Unsteady aerodynamics of separating and reattaching flow on bodies of revolution.

10 p1173 A73-24816

Transient flows, effects of unsteady surface conditions on stability, and flow separation in buoyancy induced flows.

10 p1208 A73-24817

Unsteady detachment in the three-dimensional laminar regime

10 p1208 A73-24819

Aerodynamical and aeromechanical investigations involving pin-equipped models in hypersonic flow

11 p1300 A73-25441

Aeroelastic dynamic response to shock induced flow separation, analyzing wing buffet components at high Mach number subsonic flow

[AIAA PAPER 73-308]

11 p1300 A73-25539

Supersonic flow around a delta wing, taking into account flow separation at the leading edges

12 p1457 A73-27098

Theoretical investigation on stall flutter of an aerofoil /the case of trailing edge stall/.

13 p1566 A73-29027

Visualization of unsteady flow over oscillating airfoils.

13 p1620 A73-29270

Separated flow past a slender delta wing at incidence.

15 p1821 A73-31121

Unsteady separated free jet flow of an ideal fluid past a wing

15 p1861 A73-31155

Flows past thin blunt bodies with shock layer separation

15 p1822 A73-31291

On the polarographic measurement of the wall gradient of velocity in the upstream stagnation zone or of detachment from the cylinder

15 p1878 A73-32209

Two dimensional wedge flow singularities for free and fixed boundaries at flow separation points, applying to water entry problem

16 p1999 A73-32928

The prevention of separation and flow reversal in the corners of compressor blade cascades.

17 p2094 A73-34448

Analysis of flow separation in an annular expansion - Contraction with inner cylinder rotating.

[ASME PAPER 73-FE-7]

17 p2152 A73-35006

Cryptosteady flow energy separation mechanisms, considering bearing friction and rotor torque effects and rotor nozzle proportion equations

[ASME PAPER 73-FE-24]

17 p2153 A73-35019

Observation and calculation of a steady, laminar separated flow.

17 p2157 A73-35866

Prediction of turbulent separated boundary layers.

[AIAA PAPER 73-663]

18 p2261 A73-36214

Turbulent boundary layer flow separation measurements using holographic interferometry.

[AIAA PAPER 73-664]

18 p2261 A73-36215

Rearward-facing steps in laminar supersonic flows with and without suction.

[AIAA PAPER 73-667]

18 p2261 A73-36218

Steady separated flow over finite flat plate in linearly decelerated free stream, using numerical solution of two dimensional Navier-Stokes equation

20 p2546 A73-39089

Incompressible turbulent boundary layer separation from a curved axisymmetric body.

20 p2548 A73-39525

Numerical integration method for Navier-Stokes equation of time dependent flow past impulsively started circular cylinder, calculating length of separated wake and pressure distribution

21 p2631 A73-40248

The reflexion of an acoustic pulse by a plane vortex sheet.

22 p2842 A73-42348

An approximate model of a separated turbulent flow in an abruptly widening channel

23 p2968 A73-43471

Airfoil theory calculation of bent thin foil lift coefficient and longitudinal moment characteristics at arbitrary flow separation point location

23 p2940 A73-43720

Pressure fluctuations underlying attached and separated supersonic turbulent boundary layers and shock waves.

[AIAA PAPER 73-996]

24 p3053 A73-44831

Nonlinear transient effects of separated unstable flow on vortex generated acoustic waves in cavities

[AIAA PAPER 73-1014]

24 p3078 A73-44846

A method for solving problems involving viscous flows past bodies at large Reynolds numbers

24 p3081 A73-45530

SEPARATORS

NT CLASSIFIERS

NT DUST COLLECTORS

NT FLUID FILTERS

Effects of fuel corrosion inhibitors on filter-separator coalescence.

[SAE PAPER 720862]

05 p0582 A73-16666

Measurement of zincate permeation in a polyethylene battery separator with controlled external hydrodynamic conditions.

11 p1307 A73-24974

Long-life, high energy Ni-Cd aerospace cells.

13 p1572 A73-29585

Sealed nickel zinc cells with nonsintered and supplementary oxygen recombination electrodes and layer structure inorganic separators

13 p1572 A73-29587

SEQUENCING

PLANEX 1 plan executor program for robot system, creating plan for sequence of actions via problem solving program STRIPS

01 p0020 A73-11452

Comparison of digital-signal multiplexing methods by means of sequencing

01 p0021 A73-11485

SEQUENTIAL ANALYSIS

Reliability and failure sequence characteristics of automatic system, using input rarefaction of Markov renewal process

01 p0058 A73-11423

An exact analysis of the Method-One maintainability demonstration plan in MIL-STD-471.

03 p0336 A73-13731

An adaptive Kalman filter using decomposition of the innovations sequence.

04 p0431 A73-15258

Evaluation of the performance of a variance estimation algorithm using order statistics.

04 p0471 A73-15259

Estimation of unmodeled forces on a low-thrust space vehicle.

04 p0504 A73-15272

Performance versus complexity of Viterbi and sequential decoding.

04 p0424 A73-15398

A very high speed hard decision sequential decoder.

04 p0423 A73-15917

Channel equalization in presence of intersymbol interference, comparing sequential statistical, dynamic programming, delay line and minimum mean square error techniques

04 p0425 A73-15419

Radar sequential detector for digital processing of signal masked by noise, determining false alarm and detection probabilities and mean sampling time

04 p0423 A73-15917

Information-loss and risk-increase estimation during observational data reduction in successive estimation problems

05 p0589 A73-16299

Book - Sequential analysis and optimal design.

05 p0590 A73-16352

Spectroheliogram SNR improvement via time averaging of 6103 A core sequence, considering sunspot evolution observed by time lapse technique

05 p0621 A73-17030

Recent advances in low light level field sequential color television.

06 p0694 A73-18298

Sequentially best estimators for linear systems with non-linear noise-free sensors. 06 p0681 A73-18522

Numerical solution of the integral equations for optimal sequential filtering. 06 p0719 A73-18814

Wideband multiphase radio signal processing with given ambiguity function via sequential synthesis 07 p0794 A73-20292

Simulation of sequential decoding with phase-locked demodulation. 07 p0794 A73-20498

Nonlinear system analysis based on Fokker-Planck equation, simplifying solution sequence for steady state or variance of states combination 09 p1111 A73-22114

Digital phase locked loops with sequential loop filters - A case for coarse quantization. 09 p1054 A73-23374

High data rate hard decision digital IC sequential decoder for earth-orbiting satellite space missions, discussing computational efficiency of modified Fano algorithm 09 p1056 A73-23398

External static and dynamic characteristics of input-output sequences of logic elements 12 p1475 A73-26764

Earth polar motion and angular velocity sequential estimation in presence of unmodelled random accelerations, via Gauss-Markov process representation 13 p1679 A73-28397

Numerical solution of the integral equations for optimal sequential filtering. 15 p1844 A73-32039

Investigation of mounting discrete chip components for hybrid microelectronic applications. 16 p1989 A73-33467

Universal operating characteristic curves for sequential probability ratio tests. 16 p2020 A73-33611

Probabilistic analysis of sequential test plans. 16 p1986 A73-33636

Satellite imagery of land resources, discussing synoptic views, spatial dependence, closed loop information and sequential sampling 17 p2161 A73-34945

Sequential analysis algorithm for data channel detection of received signal represented by Poisson sequence of quantum transitions under large SNR 17 p2129 A73-35711

Wideband multiphase radio signal processing with given ambiguity function via sequential synthesis 18 p2290 A73-37129

Determination of the structural features of nonlinear dynamic systems 20 p2540 A73-38709

Two-stage detection of signals in normal noise of unknown intensity. 20 p2529 A73-38922

Optimal statistical solution methods in recognition, data processing, and control problems 20 p2532 A73-38997

Three dimensional transponders array for exact solution to positioning problem, discussing large measurements sequential interrogation effects on accuracy 21 p2734 A73-40034

Clear air turbulence mesoscale history from sequential analysis of rawinsonde stations network observed data 21 p2728 A73-40057

Sequential nondestructive neutron activation analysis for bulk abundance of Fe, Al, Na, Mn, Cr, Sc, Co and Ir in chondrites from chondrites 21 p2647 A73-40563

Search properties of some sequential decoding algorithms. 22 p2829 A73-42706

Sequential determination of inspection epochs for reliability systems with general lifetime distributions. 24 p3093 A73-44576

SEQUENTIAL COMPUTERS

Minicomputer for real time sequential decoding of convolutional code transmission in space communication, discussing system design, performance and metric bias effect 01 p0020 A73-11185

SEQUENTIAL CONTROL

Electronic programming timer with crystal oscillator, IC counters and memory core matrix for event sequence radio control during spacecraft or rocket launchings 01 p0020 A73-11167

Systematic method of designing fluidic-pneumatic control circuits. 02 p0133 A73-12646

A sequenced PWM controlled power conditioning unit for a regulated bus satellite power system. 03 p0252 A73-13930

Extremal control system efficiency enhancement by information storage, noting algorithms for sequential data storage 05 p0560 A73-16298

Data link control procedures for error-free transmission channels, discussing serialization and synchronization techniques and reverse interrupt facilities in sequential machine model 05 p0551 A73-16802

Optimal sequence for introducing elements of large system into operation, using resource allocation cost criterion 09 p1068 A73-22551

Sequential systems fault detection methods based on topological description and Boolean analysis of internal variables, obtaining fanout free equivalent network by tree expansion 10 p1201 A73-24055

Description of random processes with allowance for irregularity of changes in their properties 11 p1340 A73-25008

Sequential pneumatic distribution system /Biselector/ with logic control by leakage obstruction, describing industrial pressure perforated card programmer 11 p1307 A73-25377

Phase discriminator of a nonregular signal. 12 p1480 A73-27270

Decentralized coalition control in data processing systems 15 p1848 A73-31804

Construction of a diagnostic sequence of tests of a combination automaton 15 p1848 A73-31913

Teleoperator system incorporating touch feedback and sequenced automatic control for experimental investigation of human touch sensing relation to manipulative skills 19 p2397 A73-37328

Multiple queueing system of control plants, determining optimal order and initiation moments for minimized total time for all requests 20 p2530 A73-38989

Fluidic logic circuits applications under adverse environmental conditions, considering sequential control devices and rocket engine roll axis numerical control 23 p2941 A73-43394

Application of fluidic shift-register modules for sequential control of pneumatic sequential circuits. 23 p2943 A73-43412

Pneumatic sequential circuits assembly method involving modules with switching elements and shift register, considering control valves and operation modes 23 p2943 A73-43416

Large-scale systems and operations management decentralized coalition control in data processing systems. 23 p2956 A73-44333

SEQUENTIAL DETECTION

U SEQUENTIAL ANALYSIS SERIES [MATHEMATICS]

NT ASYMPTOTIC SERIES

NT FOURIER SERIES

NT PADE APPROXIMATION

NT POWER SERIES

NT PRONY SERIES

NT TAYLOR SERIES

Axissymmetrical planet gravitational field potential expression in spherical function series, noting expansion coefficient decrease in power law for smooth density body 01 p0099 A73-10691

Series expansion of the perturbation function 01 p0102 A73-10948

Classes of limiting distributions for the sums of a random number of independent equally distributed random quantities 01 p0071 A73-11247

On the multi-parameter characteristic perturbation method - Application to nonlinear supersonic nonequilibrium flow over a wedge. 01 p0004 A73-11425

On the prediction of the expansion coefficients in a variational calculation. 04 p0471 A73-15228

A new numerical method for the inversion of the Laplace transform. 04 p0471 A73-15229

Generalized m series in tree enumeration. 06 p0717 A73-18000

On the series solution to the laminar boundary layer with stationary origin on a continuous, moving porous surface. 06 p0687 A73-18055

Matrix exponential series approach to distributed parameter systems. 06 p0719 A73-18803

Geomagnetic field optimal model with expansion of spherical harmonic series by least squares method 08 p0960 A73-21353

Composite approximations to the solutions of the Orr-Sommerfeld equation. 08 p0956 A73-21686

Estimates of the coefficients of a spherical harmonics expansion of the geopotential 09 p1143 A73-22095

Isotropic homogeneous elastic medium internal crack analysis based on Laurent series expansions of

complex potentials consistent with displacements and stress-strain single valuedness 09 p1162 A73-23179

Use of modal solutions in elastic wave propagation problems. 09 p1166 A73-23456

On the duality of sequence spaces with vectorial values 10 p1243 A73-24123

Tensorial expansions for the plastic flow of partially compressible media. 10 p1290 A73-24325

Smithsonian Package for Algebraic and Symbolic Manipulation /SPASM/ computer program with generality and efficiency for Poisson series processing in celestial mechanics 10 p1283 A73-24667

Solution in Dirichlet series to a system of linear partial differential equations 12 p1518 A73-27223

Influence function of a nonheated region and the relationship between the method of superposition and the method of expanding solutions in series of form parameters 12 p1558 A73-27312

Conditions for convergence of spectral decompositions corresponding to self-adjoint expansions of elliptic operators. IV - Negative-type theorems for arbitrary expansion of a general self-adjoint second-order elliptic operator 12 p1518 A73-27726

Extendibility over the entire plane and the functional equation of a scalar product of Hecke L-series of two quadratic fields 13 p1648 A73-28344

Chebyshev polynomial series solution method for highly eccentric perturbed orbits of comets, using modified Hansen method of partial anomalies 14 p1790 A73-29783

Boundary value problems for a first-order differential equation with operator coefficients and for the expansion of this equation in a series of its eigenvalues 15 p1899 A73-31216

Book on perturbation methods covering parameter variation, strained coordinates, averaging, multiple scale and matched and composite asymptotic expansions 15 p1902 A73-32578

Small parameter series convergence evaluation in geometrically nonlinear problems by Cauchy majorants, applying to flat curvilinear beam deflection 16 p2074 A73-32689

Contribution to the theory of biplane wing sections. 17 p2091 A73-34325

Magnitude error bounds for sampled-data frequency response obtained from the truncation of an infinite series. 17 p2145 A73-35640

Homogeneous isotropic body thermoelasticity boundary value problems solved by quadrature series using Green function of Laplace equation, determining circular cylinder stress concentration 18 p2366 A73-36753

Series expansion of the magnetic vector-potential computed for a current carrying ring. 19 p2425 A73-37927

Series representation of the solution of nonlinear partial differential equations and its use in determining the dynamic characteristics of nonlinear plants with distributed parameters 20 p2581 A73-38986

Celestial bodies gravitational potential mathematical representation by Lamé functions via series expansion of Laplace differential equation in ellipsoidal coordinates 20 p2606 A73-39080

Multiplicative rule failure in matched asymptotic expansion solutions for velocity distribution in steady incompressible flow of thin elliptic airfoils 20 p2550 A73-39814

Recursive formulas for the partial fraction expansion of a rational function with multiple poles. 21 p2660 A73-40097

Convergence of perturbation-theory series in the problem of short-wave propagation through a randomly nonhomogeneous medium 21 p2657 A73-41514

On the Volterra series functional evaluation of the response of non-linear discrete-time systems. 22 p2837 A73-43069

Topological modification and bounded length of decomposition series for convergence space 23 p3000 A73-44301

Solution of plane problems of elasticity utilizing partitioning concepts. [ASME PAPER 73-APM-C] 23 p3047 A73-44378

Strong plasma turbulence theory, discussing convergence of perturbation series formed with renormalized particle propagator 24 p3118 A73-45462

SERIES EXPANSION

U SERIES [MATHEMATICS]

SEROTONIN

Brain serotonin content - Physiological regulation by plasma neutral amino acids.

01 p0008 A73-10408

Radiation protective effect of a mixture of ATP, AET, and serotonin on yields of 600-R X-ray-induced chromosome aberrations in the rat.

02 p0134 A73-12187

Hydroxyindole-O-methyl transferases in rat pineal, retina and Harderian gland.

02 p0136 A73-12644

The role of biogenic amines in sleep.

03 p0264 A73-14260

Daily rhythm of biogenetic amine/histamine and serotonin/ contents in human blood during usual and shifted work schedules

06 p0650 A73-17688

Mediator systems and respiratory function during an acute lethal loss of blood

07 p0781 A73-19645

Influence of certain brain structures on the sulfhydryl-group, diphosphopyridine-nucleotide, and serotonin contents of the blood

09 p1040 A73-22856

Organic and species-related differences in the action of certain hydrazine derivatives and of aminoperhydroacridine on the oxidative deamination of serotonin

10 p1183 A73-23679

Neurochemical aspects of the formation of electrographical and behavioral reactions

10 p1184 A73-24327

Serotonin content in various parts of the brain during hibernation and awakening

15 p1834 A73-31390

Serotonin content variations in the fore-brain during hibernation

18 p2276 A73-36567

The inhibiting action of 5-oxytryptophan on thermal regulation during the awakening from hibernation

19 p2393 A73-37252

Regional serotonin content variations in the brain of cats during a prolonged absence of sleep

19 p2393 A73-37394

SERT (ROCKET TESTS)

U SPACE ELECTRIC ROCKET TESTS

SERUMS

Action of a serum protein on muscular contraction.

08 p0930 A73-21200

Effects of oxygen-augmented atmosphere on the immune response.

17 p2115 A73-34743

Serum tryptophan level after carbohydrate ingestion - Selective decline in non-albumin-bound tryptophan coincident with reduction in serum free fatty acids.

21 p2640 A73-41218

Blood group A sub-groups and serum cholesterol.

22 p2811 A73-43107

Apparatus for measuring the colloid osmotic pressure in blood serum

23 p2949 A73-43792

SERVICE LIFE

The generalized gamma distribution and the power distribution as element lifetime distributions

02 p0145 A73-11584

Lifetime of Dural structural elements operating in aggressive media

02 p0180 A73-11794

Generalized and modified parametric methods for extrapolating results of long term high temperature strength tests for service life determination

02 p0181 A73-12205

Study of the nonstationary characteristics of a doubled system with an unreliable servicing device

02 p0188 A73-12588

A versatile silver oxide-zinc battery for synchronous orbit and planetary missions.

02 p0133 A73-12622

Spacecraft lubrication systems design for long mission lifetimes, discussing mechanical design parameters and liquid and solid lubricant characteristics

03 p0330 A73-13012

Machine components dimensioning and testing for fatigue strength, presenting methods for service life determination

03 p0385 A73-13132

Changes in microhardness as a basis of service life estimates for smooth AlCuMg specimens

03 p0321 A73-13135

Vibrational strength of structural members from Woehler lines, calculating service life from S-N diagrams

03 p0385 A73-13138

Evaluating adhesives for joining aluminum.

03 p0334 A73-13271

Solid propellant rocket service life prediction based on propellant grain structural failure analysis, discussing surveillance program rationale for various conditions

03 p0354 A73-13407

Considerations concerning the service life, handling and storage of double base solid propellant rocket motors.

03 p0351 A73-13408

The service life of rocket motors filled with double base propellants.

[AIAA PAPER 72-1109]

03 p0351 A73-13424

One-millipound colloid thruster system development.

[AIAA PAPER 72-1153]

03 p0356 A73-13456

Circuitry for battery cell control and protection from overcharge and over-discharge for long service life operation

03 p0253 A73-13937

Creep life and strain estimation for Nimonic alloy by monitoring cavity density under optical microscope

03 p0326 A73-13965

Aircraft gas turbine mainshaft ball bearings fatigue life estimation via failure distribution

[ASME PAPER 72-LUB-10]

03 p0313 A73-14328

Consideration of a number of factors involved in determining the long-term strength of dies used for the extrusion of hollow sections of aluminum alloys

03 p0318 A73-14651

The additivity of cumulative damage in the test or use environment.

04 p0507 A73-14716

Predictive testing in elevated temperature fatigue and creep - Status and problems.

04 p0453 A73-14853

Predicting the service life of neoprene launch tube liner pads for the Poseidon missile.

04 p0468 A73-14861

Carbon-PtFE fuel cell electrode for hydrogen-KOH-air batteries for operation over long time periods, discussing rolling technique and industrialization possibilities

04 p0407 A73-15114

Active control heat pipe performance for long life battery cooling.

[ASME PAPER 72-WA/HT-43]

04 p0518 A73-15813

Extending the life and recycle capability of earth storable propellant systems.

[SAE PAPER 720837]

05 p0629 A73-16631

Cantilever aircraft tires - More than a break for brakes.

[SAE PAPER 720870]

05 p0534 A73-16652

Non-steady-state thermal analysis of a rolling aircraft tire.

[SAE PAPER 720871]

05 p0535 A73-16667

Quartz light pipe for scanning electron microscope, noting photomultiplier voltage reduction and indefinite service life

05 p0580 A73-17259

Service life estimation of electro-optic devices and degradation kinetics, noting reliability of light transmitters and receivers

07 p0800 A73-19407

Operational reliability of onboard equipment subjected to very long idling periods

07 p0831 A73-19418

Evaluation of the lubricating properties of chemically upgraded MoS₂.

07 p0842 A73-19553

Structural service life from carrying capacity during rupturing stage, noting microstructural properties effect

07 p0917 A73-20504

Durability of foil-type tensometric sensors under varying load conditions

07 p0827 A73-20536

Spacecraft Ni-Cd battery cycle life performance tests, noting cycle life-cycle duration relationship

09 p1034 A73-22755

High energy density long life Ni-Cd battery systems for synchronous satellites, discussing radiation protection, charge and discharge control electronics and temperature control

09 p1034 A73-22756

Nonleaking battery terminals design for polyphenylene oxide plastic cased Ag-Zn battery for synchronous satellite applications, describing life tests under thermal and electrical cycling

09 p1034 A73-22757

Low peak temperatures and hydrodynamic bearings - Key to long life organic Rankine cycle systems.

09 p1034 A73-22770

Summary of gas bearing applications in the field of space electric power systems.

09 p1089 A73-22771

Solid polymer electrolyte fuel cell technology application to space shuttle orbiter requirements, noting 2000 hours maintenance free life and thermal stability

09 p1035 A73-22786

Thermionic fuel unit cell major component materials selection for life and performance improvements, giving out-of-pile and in-pile results

09 p1036 A73-22816

The phosphoric acid fuel cell, a long life power source for the low to medium wattage range.

09 p1037 A73-22821

The load life characteristics of thick-film resistors.

09 p1065 A73-23048

Radio telemetering trends in post-Apollo space programs, emphasizing service lifetimes and orbiting space station data bit generation rate

09 p1053 A73-23362

Long life 100 W triode for ATC and telemetry transponders.

09 p1066 A73-23427

Cryogenic cooling systems technology for spacecraft applications, comparing passive and phase-change coolers and closed cycle refrigerator for capacity and service life

10 p1285 A73-23790

Gas turbine engine turbine blades service life increase by Cr and Al vacuum diffusion metallization, presenting full scale endurance test results

10 p1227 A73-24965

Leakable gases and water vapor loss rates and service life predictions for sealed alkaline cells in vacuum or aerospace environments, using mass transfer equations

[ECS PAPER 32]

11 p1307 A73-24973

Experimental evaluation of the single-cell concept for a lightweight, rechargeable hydrogen-oxygen fuel cell.

11 p1309 A73-25987

Heat pipe thermal control of spacecraft batteries.

11 p1309 A73-25992

Five-year lifetime thirty-watt radioisotope thermoelectric generator for NAVY Transit Navigational Satellite, discussing system design, major components, reliability and performance tests

11 p1397 A73-26041

Consideration of creep probability in a low-alloyed heat-resistant CrMoV steel

11 p1384 A73-26111

Features of the engineering theory for combined estimates of automatic control system reliability and lifetime

12 p1482 A73-26763

Prediction for a park of helicopters of the same type

12 p1561 A73-27077

Justification and calculation of the lifetimes and efficiency of new equipment

12 p1562 A73-27468

Empirical estimation of the service life of injection lasers from short-term tests.

12 p1507 A73-27523

Statistical distribution of the failure of injection lasers.

12 p1508 A73-27524

Fundamentals of the theory of combined reliability and service life estimates for machines and instruments

13 p1624 A73-29134

Hydrolytic reversion of elastomeric potting compounds.

13 p1646 A73-29274

Maximum loads on pulse-discharge light sources producing short flashes.

13 p1629 A73-29437

Long-life, high energy Ni-Cd aerospace cells.

13 p1572 A73-29585

Investigation of some principles in the processes of creep and fracture in heat-resistant materials.

13 p1643 A73-29626

Influence of transient conditions on the overall service life of turbine blades

14 p1785 A73-30676

Service life determination in heat-resistant alloys under unsteady working conditions with allowance for brief overloading

14 p1763 A73-30690

Russian book - Accelerated wear-resistance tests for machine components and machinery.

15 p1881 A73-31582

Concorde aircraft fuel system and component valves design for long term service reliability and ease of maintenance, discussing refueling, fuel jettisoning and feed controls

16 p2046 A73-32923

Some statistical techniques useful in system aging studies.

16 p2020 A73-33603

Equipment life cycle costs dependence on acquisition decision making, discussing stochastic computer simulation of failure times, repairs, inventory replacement and personnel availability

16 p2089 A73-33655

Carbon dioxide laser active element design features for service life extension through regenerating working mixture composition while preserving discharge tube seal tightness

17 p1812 A73-34167

New relationships between stress testing, failure and reliability.

17 p1718 A73-34730

Short- and long-term strength characteristics of particulate-filled cast epoxy resin.

17 p1917 A73-35343

Bayesian estimation of life parameters in the Weibull distribution.

17 p2204 A73-35810

Requirements of an economic approach to maintenance.

18 p2373 A73-37142

DC 10 airframe structure full scale fatigue tests for crack initiation and growth, residual strength and service life

[AIAA PAPER 73-803]

19 p2379 A73-37463

- Structural service life from carrying capacity during rupturing stage, noting microstructural properties effect 19 p2499 A73-37779
- Applications Technology Satellite F aluminum-ammonia heat pipes design, fabrication and life and thermal vacuum testing [ASME PAPER 73-ENAS-46] 19 p2493 A73-37993
- Extending the useful life of radioisotope thermoelectric generators through active power control. 19 p2455 A73-38392
- Analysis of integrated circuit failure modes and failure mechanisms derived from high temperature operating life tests. 19 p2411 A73-38449
- Pulsed RF life of an L-band power transistor. 19 p2411 A73-38460
- High power transistor amplifier thermal design with heat sink convective and radiant cooling for low junction temperature and long service life 19 p2411 A73-38474
- Prediction of long-term heat-pipe performance from accelerated life tests. 21 p2643 A73-40438
- Dynamic shaft seal types for high speed continuous shaft rotation, considering service life, failure modes and materials selection 22 p2865 A73-41776
- German monograph - Lifetime detection in the case of acoustically loaded structures on the basis of the appropriate form of vibration. 22 p2924 A73-42741
- Turbine wheel strength, lifetime and safety margin calculations based on classical elasticity and plasticity theories 23 p3020 A73-44225
- Determination of lifetime characteristics from crack growth kinetics data 24 p3145 A73-44523
- Sequential determination of inspection epochs for reliability systems with general lifetime distributions. 24 p3093 A73-44576
- SERVICE MODULES**
- Apollo command and service module environmental control system - Mission performance and experience. [ASME PAPER 73-ENAS-29] 19 p2493 A73-37984
- SERVICES**
- NT MEDICAL SERVICES
- NT METEOROLOGICAL SERVICES
- SERVO LOOPS**
- U FEEDBACK CONTROL
- U SERVOCONTROL
- SERVOACTUATORS**
- U ACTUATORS
- U SERVOMOTORS
- SERVOCONTROL**
- Stable optico-mechanical Q-factor modulator for a laser resonator 01 p0059 A73-10797
- Special features of the calculation of electromechanical instrument servosystems with velocity feedbacks 02 p0148 A73-11861
- Periodic motions elimination in servo driven analog to digital converters on phase plane, noting dependence on autooscillations in relay system with time lag 02 p0148 A73-11862
- Russian book - The designing of quasi-optimal combined-control servosystems. 02 p0149 A73-12867
- Autooscillations in the directional hydromechanical servocontrol with play in the reaction linkage 03 p0252 A73-13771
- Image quality in telescopes with image motion compensation by secondary mirror control. 03 p0309 A73-14429
- Automated calibration of blood pressure signal conditioners. 04 p0411 A73-14846
- Control of the motion of a solid body with servo couplings 05 p0597 A73-16611
- Active flutter control - An adaptable application to wing/store flutter. [AIAA PAPER 73-194] 05 p0531 A73-16930
- Combinational servosystem with a self-adjusting loop 05 p0561 A73-17250
- Aircraft hydraulic system and servocontrol design and performance, noting system reliability and fluid loss prevention 06 p0649 A73-17995
- Switching time dependence on input signal amplitude in self adaptive servosystem with open and closed control loops 06 p0680 A73-18382
- Time-invariant single input/output controllable and observable tracking servosystem, discussing dynamic trajectory controller and cost functional selection for zero steady state error 06 p0680 A73-18516
- Astrolabe universal balloon gondola for solar and visible stars targeting, describing acquisition functions and attitude control servos design 07 p0776 A73-18940

- French satellites attitude stabilization and control systems, describing electronic sensor and servocontrol circuitry 07 p0904 A73-18967
- Servomanometer designs with two membrane sensing elements for absolute and excess pressure measurements 07 p0827 A73-20542
- Packaged servosystem drives mobile missile launcher. 08 p0929 A73-21844
- Analysis of the mechanical and energetic characteristics in pulse-coded regulation of an asynchronous motor 09 p1037 A73-22939
- Micromovement servocontrollers in closed loop system, using piezoelectric device, ceramic element actuators and rotary switch derived logic control signal 10 p1199 A73-24027
- Conditions for termination of tracking in electronic servo systems 10 p1202 A73-24610
- The effect of servomechanical control and stability systems on the flutter behavior of aircraft [DFVLR-SONDDR-272] 11 p1304 A73-25349
- French book - Hydraulic and electrohydraulic automatic control. Volume 1 - Theory and technique. Volume 2 - Supplementary techniques and technologies 11 p1313 A73-26253
- A servo-controlled axial fatigue machine with strain rate feedback for testing polymers and composites. 11 p1344 A73-26311
- Choosing the transmission ratio of position servomechanism reduction gears 12 p1460 A73-26792
- Discrete wideband FM signals optimal filter synthesis by coupling two nonlinear servosystems 12 p1467 A73-26869
- Frequency-agile coaxial magnetrons. 12 p1477 A73-26925
- Analysis of the distortions of an FM signal in a servo loop with external control 12 p1470 A73-27576
- Testing machine for thermal fatigue with variable constraint ratio. 13 p1611 A73-28195
- Synthesis of a control coupling in a nonlinear servosystem 14 p1738 A73-30287
- Servo-controlled moving stimulus generator for single unit studies in vision. 14 p1722 A73-30401
- Convergence criteria for reverse error coefficient expansion under transient conditions for tracking servo system with open loop transfer function 15 p1854 A73-31735
- Quad redundant fly by wire servocontrol system design and tests in F-8C high speed jet aircraft, using fail/safe hydraulic actuators 16 p1970 A73-33080
- A study of thermal ratcheting using closed-loop, servo-controlled test machines. 18 p2296 A73-36585
- Computerized design for moving-base three man aircraft flight simulator servocontrol, considering disturbance torques, damping ratios, natural frequencies, load acceleration and smoothness 18 p2296 A73-36833
- Electro-mechano-hydraulic servovalve system, calculating dynamic frequency response in vibrating accelerated field under external disturbance 19 p2388 A73-37670
- Design and evaluation of a backhoe model with a master slave control. 19 p2401 A73-38085
- A 'type one' servo explicit model following adaptive scheme. [AIAA PAPER 73-862] 20 p2586 A73-38800
- Pneumatic fluidic operational amplifier application to proportional position servocontrol with hydraulic actuator for high force output, considering working fluid and Reynolds number effects 23 p2941 A73-43397
- SERVO MECHANISMS**
- NT SERVOMOTORS
- Algorithms for phase vector coordinates calculation of servomechanism, using measuring instrument data as starting information 01 p0028 A73-10676
- Estimating the mean time until follow-up cutoff in a nonlinear sampled-data servosystem for irregular arrival of the signal. 04 p0430 A73-15205
- Striding devices for astronautical application areas 04 p0433 A73-15630
- Combinational servosystem with a self-adjusting loop 05 p0561 A73-17250
- Equations of motion for mechanical system with imposed servo couplings, discussing Gauss variational principle applicability for system analysis 07 p0851 A73-19128

- Determination of limits bounding the bifurcational relationship between parameters of two-stage nonlinear servo mechanisms 09 p1033 A73-22653
- Design and evaluation of miniature control surface actuation systems for aeroelastic models. [AIAA PAPER 73-323] 11 p1305 A73-25553
- Ilushin 62 aircraft horizontal stabilizer structural design and control, discussing mounting hardware and electrically driven servomechanism 11 p1305 A73-25795
- Book on fluid power control covering servovalve orifices discharge characteristics, flow forces, hydraulic and pneumatic servomechanisms, fluid logic and sequential circuits 11 p1313 A73-26258
- Incremental servomechanism design and application as substitute for step motor, discussing servomotor properties, mechanical torsional vibration and loading moment effects 12 p1483 A73-27422
- High gain hydromechanical servomechanism with multispurging, mass damping and feedback control, deriving transfer function response, with application to aircraft control surface actuator design 13 p1596 A73-29150
- High speed photoelectric photometer for night sky scanning 15 p1878 A73-32137
- Book - Introduction to servomechanism system design. 17 p2110 A73-35275
- An anthropomorphic master-slave manipulator system. 19 p2397 A73-37316
- Discrete stochastic linear servomechanism with observation costs, deriving optimal control solution with extension to nonlinear systems suggested by dynamic population models 19 p2412 A73-38029
- Comparison of optimized active and passive vibration absorbers. 19 p2435 A73-38084
- Modern control techniques applied to energy conservation flight control systems. 19 p2392 A73-38415
- Problems in the theory and practice of the self-tuning of compensating signals in complex control systems 20 p2541 A73-38994
- An adaptive, time-suboptimal position servomechanism 20 p2511 A73-39664
- The effect of valve area gain on the performance of the hydraulic servomechanism. 20 p2511 A73-39755
- The Large Amplitude Multi-Mode Aerospace Research (LAMAR) Simulator. [AIAA PAPER 73-922] 21 p2673 A73-40870
- Standard sensitivity and covariance matrices for statistical estimation of overall performance. 23 p2962 A73-43279
- Fluidic logic circuit universal block with turbulence amplifiers for control of servomechanisms, comparing with use of conventional fluid logical elements 23 p2943 A73-43414
- The frequency stability and noise of passive Rb standard. 23 p2965 A73-44137
- On the limit-cycle characteristics of a bang-bang servo. 24 p3075 A73-45556
- SERVOMOTORS**
- A linear motion generator for physiological research. 01 p0011 A73-10173
- Photographic equipment for astronomical telescopes, considering mechanical devices for plate translation and rotation, guiding microscope and digitally controlled servomotors with incremental feedback 01 p0049 A73-10541
- Dc servomotor transfer function equalization, noting stability conditions for linear system design 06 p0680 A73-18380
- Electronic six-channel phase shifter 08 p0950 A73-21715
- Analysis of the mechanical and energetic characteristics in pulse-coded regulation of an asynchronous motor 09 p1037 A73-22939
- A positional, asynchronous, thyristor-based, electrical servo actuating element with directional shaping of the phase trajectories 12 p1460 A73-26787
- Choosing the transmission ratio of position servomechanism reduction gears 12 p1460 A73-26792
- Incremental servomechanism design and application as substitute for step motor, discussing servomotor properties, mechanical torsional vibration and loading moment effects 12 p1483 A73-27422

- Synthesis of optimal control with allowance for the real characteristics of the executive mechanism
22 p2835 A73-42363
- Servomechanism design techniques and applications - Aerospace problems.
23 p2945 A73-43450
- Periodic oscillations of a closed hydraulic throttle servomechanism with inertial and positional loads
23 p2945 A73-43739
- SERVOSTATIC CONTROL**
U SERVOCONTROL
- SET THEORY**
NT BOREL SETS
NT EQUIVALENCE
NT THRESHOLD LOGIC
- Canonical expansions of random processes, discussing discrete and continuous set transformations for spectral representation and shaping filters in time domain
01 p0068 A73-10027
- Nonlinear differential equations with logarithmically small perturbations.
01 p0071 A73-11268
- Liapunov stability, boundedness and attraction conditions, using modified quantification theory
04 p0469 A73-14668
- A new method of obtaining Q solutions to extremal problems in certain special classes of analytic functions associated with functions whose real part is positive in a circle
04 p0470 A73-15083
- Existence and conical intersection theorems for extremum conditions of Euclidean space subset function, noting discrete objects optimality conditions
05 p0589 A73-16334
- Instability of the exponential discreteness characteristic of solutions to a system of differential equations, and the asymmetry of the near-reducibility ratio of a system of differential equations with an integral discreteness of solutions
05 p0590 A73-16335
- Air combat roles identification by reachable sets technique, evaluating aircraft/weapon systems potential performance vs given threat
05 p0536 A73-16957
- Existence of analytic solutions of partial differential equations with constant coefficients in an arbitrary number of variables
05 p0591 A73-17246
- Fuzzy multi-stage decision-making, fuzzy state and terminal regulators and their relationship to non-fuzzy quadratic state and terminal regulators.
06 p0681 A73-18523
- Outline of a new approach to the analysis of complex systems and decision processes.
06 p0671 A73-18622
- Boundedness of infinitely extendable solutions to a system of two equations with quadratic right members, and the manifold of Liapunov's characteristic exponents of solutions to this system
06 p0718 A73-18679
- Construction of a set of systems of second-order delayed-argument differential equations having a prescribed integral curve
06 p0718 A73-18687
- Ergodicity criteria of homogeneous Markov chains in a special phase space. I, II
07 p0844 A73-19326
- Adaptive algorithms for reducing a random field to a prescribed set of states with constraints on the elements of the approximating sequences
07 p0796 A73-20079
- An attainable sets approach to optimal control of functional differential equations with function space terminal conditions.
07 p0846 A73-20497
- Dynamic programming as applied to feature subset selection in a pattern recognition system.
08 p0941 A73-21666
- Initial circuit equation transformation into equation of variable states, noting linear and nonlinear circuits in static and dynamic regimes
09 p1068 A73-22452
- Optimal self learning classification of point in set for image recognition systems, using proximity functions
09 p1060 A73-22944
- On the solution of linear inequalities with applications to threshold logic.
10 p1191 A73-23746
- Uniform estimate of the residual term in the multidimensional limiting theorem for homogeneous Markov chains on the basis of a class of all measured convex sets. II
10 p1242 A73-23814
- Allowable set construction of noncrossing branched paths over prescribed length in unidirectional finite multinetworks
10 p1201 A73-24062
- Capacity theory and removable sets for finite energy harmonic functions extended to nonlinear Navier-Stokes equations, using multiple trigonometric series
13 p1648 A73-28539
- Rate of convergence of a class of methods of feasible directions.
13 p1649 A73-28609
- A convergence theory for a class of nonlinear programming problems.
13 p1649 A73-28610
- Duality relationships for a nonlinear version of the generalized Neyman-Pearson problem.
18 p2330 A73-36636
- Riesz representability, sigma-additivity and Daniell-integral properties of measures on uniform spaces
21 p2726 A73-40945
- Compact integral varieties existence in certain meromorphic Pfaff differential equation systems
21 p2726 A73-40946
- Multicriterial optimization problems solution by method of effective sets defined in criterion or variable vector spaces, noting advantages over global criteria and additive value methods
21 p2670 A73-40992
- On quasi-concave and strictly quasi-concave functions on a convex set relative to one of its nonvacant subsets
21 p2727 A73-41023
- Sufficient optimality conditions for control system described by ordinary differential equations in Banach space with Lebesgue measure of material quantity set
22 p2882 A73-42604
- Numerical stability of various summation schemes in a floating-type R subset
23 p2999 A73-44098
- Typical characteristics of dynamic systems nearly all of whose trajectories remain stable under steadily acting disturbances
24 p3109 A73-44424
- SETTLING**
The slow unsteady settling of two fluid spheres along their line of centres.
22 p2840 A73-41742
- SEX GLANDS**
NT GONADS
NT TESTES
- SEXTANTS**
Gyroscopic device for compensating external moments of sextants or binoculars optical axis due to spontaneous hand movements
09 p1084 A73-22673
- SEYFERT GALAXIES**
The infrared variability of a dust model for Seyfert galaxies.
05 p0624 A73-17311
- Quasar optical luminosities compared to Seyfert galaxies and radio-quiet objects showing broad emission lines of permitted transitions and sharp lines of forbidden transitions
13 p1687 A73-29656
- Photometry and some characteristics of spiral Seyfert galaxies beyond the nucleus boundary
15 p1938 A73-31951
- The properties of extragalactic X-ray sources from visible light observations.
16 p2050 A73-32742
- An upper limit to the angular diameter of the nucleus of NGC 4151.
17 p2231 A73-34751
- Intense outburst /S/ of radio radiation detected with the Goldstone-Haystack interferometer.
19 p2485 A73-37624
- Observations of further outbursts in the radio galaxy 3C 120.
19 p2485 A73-37625
- Photometry and some features of Seyfert spiral galaxies beyond the nuclear region.
24 p3131 A73-44476
- A radially streaming proton model for the broad component of hydrogen emission in Seyfert galaxies.
24 p3138 A73-45039
- SHADES**
A self deployable high attenuation light shade for spaceborne astronomical sensors.
08 p0970 A73-21734
- SHADOWGRAPH PHOTOGRAPHY**
NT SCHLIEREN PHOTOGRAPHY
- Low Reynolds number flow past a transverse cylinder at Mach two.
01 p0003 A73-10758
- A series of evolved shadowgraphs of shock waves induced by secondary injection in a conical supersonic flow.
01 p0003 A73-11128
- Shadowgraph photography for electromagnetic excitation of shock waves in normal pressure gas, noting plasma and shock compressed regions in shock tube
04 p0434 A73-15618
- Thermal tagging for laminar and turbulent liquid flow shadowgraph visualization by ND glass laser beam
06 p0696 A73-18573
- Shadowgraph photography for electromagnetic excitation of shock waves in normal pressure gas, noting plasma and shock compressed regions in shock tube
10 p1205 A73-24208
- Thermal tagging for laminar and turbulent liquid flow shadowgraph visualization by Nd glass laser beam
16 p2016 A73-33598
- An introduction to holography by shadow casting.
16 p2016 A73-33950
- Hyperballistics range erosion tests, describing dust, rain and ice simulation, dust and water fixed grid screens and shadowgraph and laser photography
[AIAA PAPER 73-765] 18 p2295 A73-36380
- Flash photography using laser excited fluorescent tracers.
21 p2709 A73-39969
- SHADOWGRAPHS**
U SHADOWGRAPH PHOTOGRAPHY
- SHADOWS**
NT LUNAR SHADOW
NT PENUMBRAS
- Twilight sounding method for earth upper atmosphere investigation, taking into account earth shadow and effective altitude of solar radiation attenuation /shielding/ zone
07 p0818 A73-19591
- Vertical velocity field oscillations in photospheric sunspot umbras interpretation in terms of gravity or acoustic waves traveling along magnetic field lines
08 p1001 A73-20756
- Observations of sunspot umbral velocity oscillations.
08 p1001 A73-20758
- Observations during total lunar eclipse on 6 August, 1971, noting low visibility of lunar features and earth shadow reddish hue
08 p1007 A73-21071
- Sunspot umbral intensity measurements at IR and visual wavelengths, discussing correction methods for earth atmosphere and instrument induced stray light
11 p1422 A73-25937
- Fine bright umbral spot structures from photographic line spectra observation of sunspot, noting magnetic field strength, outflow velocity and photospheric temperature
12 p1545 A73-27834
- Observations during total lunar eclipse on 6 August 1971, noting low visibility of lunar features and earth shadow reddish hue
18 p2356 A73-36872
- Trajectory of a solar-electric propelled vehicle passing through the shadow cone of a celestial body
21 p2779 A73-41556
- SHAFTS [MACHINE ELEMENTS]**
NT TURBOSHAFTS
- Lateral displacement of discontinuous vibrating wire, noting solution application to longitudinal vibrations of discontinuous shafts and torsional vibrations of circular shafts
02 p0237 A73-12612
- Conditional margin of plastic strength for shaft-type elements subjected to torsion at low temperatures
12 p1554 A73-27478
- Automatic machine test equipment and procedures for hydraulic systems, tractor shafts and automobile wheels
13 p1625 A73-29135
- Torsion of a reversible flexible wire shaft
15 p1946 A73-31140
- Choice of the geometrical parameters, R, r, and r₁, of a roller-ring mechanism as a function of maximum load capacity
15 p1832 A73-31277
- Calculation of stress-concentration factors for grooved shafts in bending using the point-matching technique.
15 p1948 A73-31616
- Torsion of a cylindrical shaft having an annular semicircular cutout
17 p2244 A73-34791
- How to select shaft seal materials.
[ASLE PREPRINT 73AM-6E-2] 17 p2196 A73-34990
- Application of simultaneous iteration method to torsional vibration problems.
21 p2783 A73-40289
- Light weight shaft design using minimum principle for nonlinear multipoint boundary value problem
[ASME PAPER 73-DET-10] 22 p2919 A73-42068
- Complex elastoplastic torsion of cylindrical shafts
23 p3045 A73-44184
- SHAKERS**
Free vibrations of elastic systems with discrete dynamic systems attached.
03 p0384 A73-12983
- Vibration test facilities and control techniques for application to industrial products, discussing shakers, signal generation and amplification, and data recording and reduction
07 p0809 A73-20575
- Prediction of IC and LSI performance by specialized vibration/detection test for presence of conductive particles.
08 p0943 A73-20732
- Automated vibration shaker calibration data acquisition and analysis system with minicomputer for working transfer standard voltage monitoring and acceleration level determination
09 p1070 A73-22508
- Multiple shaker resonance testing for structural dynamic characteristics, considering natural frequencies, mode shapes, damping and generalized masses
[AIAA PAPER 73-402] 11 p1440 A73-25531

SHAKING

SHAKING NT DITHERS SHALES

Thermal analysis-mass spectrometer computer system and its application to the evolved gas analysis of Green River shale and lunar soil samples.

08 p0936 A73-20824
A new approach to the isolation of milligram amounts of significant geochemical compounds.

11 p1325 A73-25463
The isolation of a series of acyclic isoprenoid alcohols from an ancient sediment - Approaches to a study of the diagenesis and maturation of phytol.

11 p1326 A73-25465
Acids obtained by oxidation of kerogens of ancient sediments of different geographic origin.

11 p1326 A73-25467
A search for porphyrin biomarkers in Nonesuch Shale and extraterrestrial samples.

11 p1319 A73-26481
17alpha/H/ hopane identified in oil shale of the Green River formation/Eocene/ by carbon-13 NMR.

14 p1746 A73-29734

SHALLOW SHELL EQUATIONS

Approximate solution of equations describing the thermal stressed state of a shallow spherical shell

01 p0113 A73-10017

Study of the stressed state of a shallow spherical shell whose thickness varies along its circumference

01 p0113 A73-10018

Existence of solutions in nonlinear shallow shell theory

01 p0116 A73-10962

Asymptotic method of determining critical buckling loads for strictly convex shallow shells of revolution

01 p0116 A73-10963

Fourier transformation for stress analysis of anisotropic shells under concentrated forces, solving shallow shell equations via MacDonald functions

01 p0118 A73-11408

Construction of a general solution for an elastic anisotropic shallow shell with arbitrary boundary conditions, and some of its applications

02 p0230 A73-11714

Design of a shallow shell with a large rectangular hole

02 p0231 A73-11803

Thin walled shells strength dependence on residual stresses, noting stress analysis of shallow spherical shell with variable residual deformations

02 p0232 A73-11932

Stress-strain state of shallow spherical shell with variable wall thickness under uniformly distributed load, using Vlasov shell theory

02 p0235 A73-12192

Correlation theory for equations of motion of constant thickness shallow shell vibration under random loads

03 p0387 A73-13158

The solvability of integral equations of shell theory

04 p0511 A73-15082

Influence areas for some cross sectional parameters of shallow double-curvature shells

04 p0513 A73-15507

Singular solutions for shallow cylindrical shells. [ASME PAPER 72-WA/APM-27]

04 p0515 A73-15891

Classical and nonlinear buckling analyses of spherical sandwich shells.

05 p0631 A73-16121

Introduction of two solving functions into the equations for nonshallow shells.

05 p0634 A73-16796

Stiffness matrix formulation and eigenvalue analysis for high order shallow shell finite element of rectangular plan

07 p0916 A73-20439

Effect of the curvature of a shallow spherical shell on its vibrations with losses

08 p1018 A73-21449

Stress-strain state of transversely isotropic shells under concentrated loads

08 p1019 A73-21760

Stability of a shallow three-layer shell with a linearly viscoelastic filler

09 p1157 A73-21994

Large deflection analysis of plates and shallow shells using the finite element method.

09 p1158 A73-22396

Remarks on a system of nonlinear equations

09 p1113 A73-22987

Inelastic buckling of shallow spherical shells under external pressure.

09 p1164 A73-23270

Stability of the axisymmetric form of motion of flexible shallow shells

09 p1164 A73-23344

Weight minimization constrained design of rotational shallow spherical shells, comparing simplex and variable metric methods

09 p1165 A73-23446

Difference equations of elastic equilibrium for shells with variable characteristics in polar coordinates

11 p1433 A73-25027

Singular nonaxisymmetric shallow shell equation solutions for concentrated normal and tangential forces and bending and twisting moments

12 p1550 A73-27034

Instability of asymmetric strongly convex thin shallow shells

12 p1553 A73-27414

On the existence of solutions of the nonlinear theory of shallow shells.

12 p1554 A73-27538

Asymptotic method of determining the critical buckling loads of shallow strictly convex shells of revolution.

12 p1554 A73-27539

Shallow conical closed shell stability under axisymmetric loads, using variational difference method

12 p1556 A73-27799

Solvability of the boundary value problem in the theory of shallow shells of revolution and estimation of errors in the approximate solution

12 p1556 A73-27813

Shallow spherical shell dynamic stability under axisymmetric loads, noting small HF vibrations effect on static stability

12 p1556 A73-27814

Branched solution of integro-power equation for nonlinear bending of shallow spherical shells with clamped edge under uniform radial compression load

12 p1556 A73-27816

Perturbation techniques in the analysis of geometrically nonlinear shells.

13 p1694 A73-28251

Finite deflection of a shallow spherical membrane.

13 p1697 A73-28815

General solution of an equation system on plate equilibrium

15 p1945 A73-31033

A variational principle for finite deformations of quasi-shallow shells.

15 p1955 A73-32162

The behaviour with diminishing curvature of strain-based arch finite elements.

16 p2076 A73-32921

A new form of the integral equations of a boundary value problem in the theory of simply supported shallow spherical shells

19 p2495 A73-37198

Large deflection of shallow paraboloid shells.

21 p2782 A73-40005

Resolvent boundary solutions for Vlasov shallow shell equations in terms of force and deflection functions over entire contour

22 p2928 A73-43055

Determination of the stressed state near a curvilinear hole in a transversely isotropic spherical shell

23 p3043 A73-43924

SHALLOW SHELLS

The load carrying capacities of symmetrically loaded shallow shells.

05 p0631 A73-16120

Determination of the initial stress-strain state of a shallow spherical shell under the action of a dynamic load

10 p1290 A73-24310

Conformal mapping technique for stress concentration around elliptical hole in shallow spherical shell under internal pressure

14 p1806 A73-30045

Influence of curvature on the vibrations of an oblate spherical shell with losses.

15 p1945 A73-31013

The dynamic plastic behavior of simply supported spherical shells.

15 p1948 A73-31369

Finite deflections of transversally-isotropic plates and shallow shells

15 p1953 A73-32089

Application of stress functions to dynamic analysis of shallow shells.

16 p2077 A73-32987

Non-linear problems of slender webs and of shallow shells.

16 p2078 A73-33006

Book - Stresses in shells /2nd edition/.

17 p2242 A73-34469

Dynamic buckling of shallow spherical shells. [ASME PAPER 73-APM-A]

17 p2249 A73-35104

Rigid-plastic collapse of compression-bent shallow shells.

20 p2616 A73-39114

Supercritical strains in nonlinear elastic shells

20 p2616 A73-39259

A numerical realization of the Bubnov-Galerkin method using a computer for the solution of nonlinear problems in the theory of shallow shells

20 p2617 A73-39307

Theory of shallow shells with allowance for couple stresses without applying the Kirchhoff-Love hypothesis

20 p2618 A73-39309

Axisymmetrical bending of circular plates and shallow spherical cupolas with allowance for physical and geometrical nonlinearities

20 p2618 A73-39310

Inverse bending problems for two-layer orthotropic shallow shells

20 p2618 A73-39313

Elastoplastic strains and carrying capacity of shallow shells /Review/

21 p2786 A73-40976

Stress-strain state of stiffened shallow shells of rectangular planform

22 p2928 A73-43054

Torsion of a cylindrical shell with a lateral surface containing an elastic circular inclusion

23 p3042 A73-43727

Function space approach to prestressed nonlinear orthotropic shallow shell theory boundary value problems

24 p3149 A73-45006

Thermoelasticity problem of a spherical shell with multiply connected regions

24 p3149 A73-45175

Equilibrium of two elastic shallow shells of revolution which are connected by radial ribs

24 p3152 A73-45355

SHALLOW WATER

Shallow lake or sea with large class of bottom topographies, obtaining wind-driven current analytic solution with conformal mapping technique

21 p2686 A73-41015

SHANKS

U JOINTS (JUNCTIONS)

SHANNON INFORMATION THEORY

U INFORMATION THEORY

SHAPED CHARGES

Numerical study of the problem of explosion of a cylindrical charge of finite length

24 p3076 A73-44654

SHAPES

NT CONVEXITY

NT ELLIPTICITY

NT LINE SHAPE

Structural members optimal shaping in terms of stress concentration, analyzing plane elasticity boundary value problem

01 p0114 A73-10600

On the apparent visual forms of relativistically moving objects.

03 p0343 A73-13294

SHARP LEADING EDGES

Nonlinear characteristics of a slender triangular wing near an interface

02 p0127 A73-11630

Experimental determination of bound vortex lines and flow in the environment of the trailing edge of a slender delta wing

05 p0528 A73-16600

Numerical computation of the hypersonic rarefied flow near the sharp leading edge of a flat plate.

05 p0531 A73-16934

The influence of the accommodation coefficients on the flow variables in the viscous interaction region of a hypersonic slip-flow boundary layer.

07 p0773 A73-19206

Corner pressures and fillet shock locations for symmetrical corners by an approximate method.

07 p0774 A73-19494

Density measurements in high speed arc heated flows.

13 p1622 A73-29640

Influence of weak viscous interaction on the drag of a wing profile

15 p1822 A73-31195

The role of jet stability in edgetone generation. [AIAA PAPER 73-628]

18 p2263 A73-36255

A modulation technique for measuring small disturbances in the upstream flow field of a sharp leading edge in a rarefied hypersonic flow.

19 p2377 A73-37714

SHATTERING

U FRAGMENTATION

SHOCK

Holographic shearing interferometer using two linearly polarized reference light beams with application to refractivity and density gradient measurements in aqueous solutions

24 p3088 A73-44406

SHEAR DISTURBANCES

U S WAVES

SHEAR FATIGUE

U SHEAR STRESS

SHEAR FLOW

Representation of a 1/N power law boundary layer in the sheared flow acoustic transmission problem.

01 p0033 A73-10783

The fourth annual Fairey lecture - The propagation of sound through moving fluids.

01 p0077 A73-10784

Shear waves and perturbations in linearized steady plane flows of a thermally nonconducting compressible ideal fluid

01 p0034 A73-11359

Nondecaying turbulence field production by mean shear in spite of flow viscosity effects

02 p0154 A73-12056

Local transport equations for turbulent shear flow.

02 p0154 A73-12825

Sound propagation in sheared flow in a duct with transverse temperature gradients.

03 p0342 A73-12988

Concentration probability of a passive admixture in turbulent shear flows

03 p0294 A73-13614

Turbulent shear flow structure parameters in conical diffuser, investigating Reynolds number and turbulent kinetic energy effects

03 p0247 A73-14176

Extension of the Miles-Howard theorem to the circular flows of a compressible fluid.

03 p0297 A73-14443

Mean velocity and turbulence intensity profiles of asymptotic sink flow turbulent boundary layers, measuring Reynolds and wall shear stresses

04 p0434 A73-15166

The Reynolds tensor in a homogeneous turbulence associated with a mean shearing flow

04 p0436 A73-15995

Asymptotic solution for vertical propagation of equatorial planetary waves in shear, noting gravity-Rossby and Kelvin waves and wind effects on diurnal tides

05 p0591 A73-16190

Effect of bulk-reacting liners on wave propagation in ducts.

[ALAA PAPER 73-227]

05 p0566 A73-16952

Shear stress distribution from measured nondimensional mean velocity profile measured in plane turbulent mixing layer formed at cascade wind tunnel exit

05 p0567 A73-17106

The correlations of the vortex in a homogeneous turbulence associated with a mean shearing flow

05 p0567 A73-17227

Singular perturbation and turbulent shear flow near walls.

06 p0686 A73-18378

Critical conditions for steady/unsteady laminar shear flow breakdown into HF oscillations, using kinematic wave theory

[AD-758579]

06 p0687 A73-18533

Diffusion on a particle in the shear flow of a viscous fluid - Approximation of the diffusion boundary layer.

07 p0809 A73-19021

Further results concerning the forces on a flat plate in a Couette flow.

08 p0926 A73-21402

On the shearing flow of a fluid, heavy or not, with constant vortex, around a thin profile placed under a free line, in linear theory

08 p0926 A73-21490

Statistical properties of intermittency in large scale turbulent flows, considering boundary layer, shear and convective flows

10 p1205 A73-23855

Book - Turbulence transport modeling.

10 p1206 A73-24350

Parallel magnetic field effect upon plane interface stability between two conducting viscous fluids in uniform relative motion, obtaining neutral shear flow stability curves

11 p1402 A73-25054

On Howard's technique for perturbing neutral solutions of the Taylor-Goldstein equation.

11 p1345 A73-25157

Diffusion of heat from a line source downstream of a turbulence grid.

11 p1453 A73-26399

Hydromagnetic stability of plane heterogeneous shear flow.

12 p1527 A73-27129

Turbulent interface detector using a multiple array of single hot wires.

13 p1619 A73-29252

Turbulence measurements with the split-film anemometer probe.

13 p1619 A73-29253

Turbulent shear research, considering nondimensional data correlation, governing equations solution for parameters, statistical and experimental methods for structure determination

13 p1604 A73-29259

Free parallel shear flow approximation by velocity discontinuity involving Kelvin-Helmholtz waves longer than shear layer thickness

13 p1605 A73-29448

Valve effect of inhomogeneities on anisotropic wave propagation.

14 p1780 A73-30165

The calculation of low-Reynolds-number phenomena with a two-equation model of turbulence.

14 p1746 A73-30606

Gas flow properties in curvilinear turbine ducts, considering pressure gradient, outer flow shear and Coriolis force on boundary layer

14 p1712 A73-30649

Modification of Sygne's criterion for stratified shear flow for spatially growing disturbances.

15 p1862 A73-31334

Influence of a magnetic field on turbulent shear flow

15 p1917 A73-31402

Finite amplitude dynamic motion of viscoelastic materials.

15 p1956 A73-32223

Keraug near-ground wind profiles approximation by Monin-Obuchov universal function, obtaining solutions for turbulent heat flux and shear flow velocity

15 p1906 A73-32343

Approximation for thin boundary layers in the sheared flow duct transmission problem.

16 p2000 A73-33679

Bifurcated small parameter perturbation solutions in boundary layer theory, applying to Falkner-Skan equation and instability in stratified shear flow

16 p2001 A73-33871

A comparison of hydraulic fluid characterizations in two evaluation systems.

[ASLE PREPRINT 73AM-9A-2]

17 p2196 A73-34997

Turbulent flow research, discussing time domain analysis of velocity, displacement and pressure, potential flow models of vortices, and shear flow turbulence

17 p2155 A73-35330

Book - Buoyancy effects in fluids.

17 p2155 A73-35336

Calculation of free turbulent mixing by interaction approach.

[ALAA PAPER 73-649]

18 p2297 A73-36204

Turbulence measurements in interacting wakes.

18 p2301 A73-36698

On energy, group velocity and small damping of sound waves in ducts with shear flow.

18 p2302 A73-37031

Weakly ionized continuum plasma turbulent shear flow and transport properties calculation, noting ratio of Debye shielding length to local integral scale

19 p2463 A73-37153

Compressible fluid dynamic theory, using stress tensors to derive constitutive equations for plane homogeneous and shear flows

19 p2420 A73-37644

Laboratory vortices in rotating, sheared flow.

19 p2420 A73-37664

Stability of stratified shear flows.

19 p2421 A73-38226

Linear viscous stability theory for stably stratified shear flow - A review.

19 p2421 A73-38227

Observed generation of an atmospheric gravity wave by shear instability in the mean flow of the planetary boundary layer.

19 p2448 A73-38229

Some properties of horizontally homogeneous, statistically steady turbulence in a stratified fluid.

19 p2449 A73-38236

Measurements of internal waves and turbulence in two-dimensional stratified shear flows.

19 p2422 A73-38238

Hydrodynamics of stratified fluids - The applicability of linear theory.

19 p2422 A73-38243

Non-parallel flow corrections for the stability of shear flows.

20 p2546 A73-39092

Homogeneous anisotropic to isotropic turbulence convergence based on shear flow component measurements of turbulence energy distribution in axisymmetric flow

20 p2546 A73-39097

Neighboring body effects on bluff body form drag.

20 p2507 A73-39519

Neighboring body effects on bluff body tipping moment.

20 p2507 A73-39520

Finite amplitude dynamic motion of viscoelastic materials.

23 p3038 A73-43273

Numerical study of the unstable modes of a hyperbolic-tangent barotropic shear flow.

23 p3002 A73-43591

Vortex shedding from and base pressure distribution on bluff body measured in shear or uniform flow, calculating Strouhal number

23 p2940 A73-43939

Acoustic propagation in ducts with varying cross sections and sheared mean flow.

[ALAA PAPER 73-1008]

24 p3078 A73-44841

Transmission and far field radiation of sound waves in and from lined ducts containing shear flow.

[ALAA PAPER 73-1013]

24 p3078 A73-44845

Boundary layer on flat plate in shear flow, calculating induced pressure gradients near leading edge and far downstream

24 p3080 A73-45369

SHEAR LAYERS

Shear layer extent caused by slip surface in inviscid flow with shock interactions, noting viscous effect in hypersonic flow

01 p0033 A73-10747

The influence of planetary vorticity gradient and vertical entropy gradient on the stability of an atmospheric shear layer.

04 p0441 A73-15288

Calculation of interacting turbulent shear layers - Duct flow.

[ASME PAPER 72-WA/FE-25]

04 p0435 A73-15849

Heat transfer downstream of attachment of a turbulent supersonic shear layer.

05 p0533 A73-17112

Sound field generated by spatial instabilities interaction on shear layer shed from duct with nozzle lip, discussing excess noise of subsonic jets

06 p0687 A73-18529

Experiments on the nonlinear stages of free-shear-layer transition.

06 p0687 A73-18530

Instability of free shear layers adjacent to a vibrating flame surface.

10 p1296 A73-24804

Prominent vertical shear layers and zonal currents in axisymmetric fluid filled spherical/conical rotating container due to nonlinear interactions in boundary layers

10 p1210 A73-24839

Two dimensional inviscid flow model of shear layer motion and vortex shedding in near wake of bluff-based body, using Schwarz-Christoffel transformation

11 p1300 A73-25155

Sound absorption in lined rectangular ducts with wall shear layers - Convergence of the numerical procedure to the analytical solution.

13 p1658 A73-28061

Observation of Kelvin-Helmholtz billows and their mesoscale environment by radar, instrumented aircraft, and a dense radiosonde network.

13 p1652 A73-28268

The influence of acoustic disturbances on the mechanics in shear layer behind a circular cylinder in air flow.

13 p1563 A73-28530

Free parallel shear flow approximation by velocity discontinuity involving Kelvin-Helmholtz waves longer than shear layer thickness

13 p1605 A73-29448

The stability of a thermally radiating stratified shear layer.

14 p1816 A73-30169

On the free shear layer downstream of a backstep in supersonic flow.

[ASME PAPER 73-FE-3]

17 p2095 A73-35003

Mean flow and turbulence measurements in a Mach 5 shear layer.

17 p2097 A73-35506

Statistical models of turbulent free shear mixing layer structure in incompressible air streams

17 p2156 A73-35507

Turbulent flow fields with two dynamically significant scales.

[ALAA PAPER 73-646]

18 p2297 A73-36201

Turbulent correlation measurements in a two-stream mixing layer.

18 p2298 A73-36311

Laboratory observations of shear-layer instability in a stratified fluid.

19 p2422 A73-38232

Subsonic and supersonic turbulent shear layer aerodynamic noise emission derivation from differential wave equations via Fourier transformation and WKB method

20 p2507 A73-39087

Some investigation on base flow behind cylindrical bodies in incompressible flow.

22 p2797 A73-42997

Shear layer effect on acoustic duct wall impedance for sound propagation in uniform flow in terms of parabolic cylinder functions

22 p2900 A73-43138

Spatial and temporal stability of laminar axisymmetric jet and wake shear layers in viscous and inviscid flow

24 p3079 A73-45308

SHEAR PROPERTIES

NT SHEAR STRENGTH

Experimental determination of shear moduli in a compact bone tissue

03 p0267 A73-13742

Tresca type plastic material shear, considering hypocoelastic yield interrelation to Tresca yields

06 p0763 A73-18457

Torsion of an axisymmetrical anisotropic body with mixed boundary conditions on the edge surface

13 p1698 A73-29086

Torsion of an inhomogeneous body of revolution with variable shear moduli

16 p2074 A73-32682

Influence of the structure of a composite material on its elastic properties

17 p2194 A73-34269

Vibration of layered shells.

18 p2367 A73-37029

Torsion of an axisymmetric anisotropic body with mixed boundary conditions on the side surface.

19 p2498 A73-37636

Fibrous composite materials orthogonal shear properties related to laminate construction, discussing shear load tests, fiber orientation, boron, graphite, aluminum and titanium properties

[SAWE PAPER 993]

19 p2443 A73-37893

Double frequency diffraction grating lateral shear interferometer for lens focusing and heterodyne phase detection

21 p2698 A73-40137

SHEAR STRAIN

SHEAR STRAIN

Application of the Dirac delta function in the calculation of the bending of a rectangular beam with shear strain

03 p0384 A73-13130

Finite element analysis of thick, thin and sandwich plates, considering quadrilateral elements with allowance for transverse shear effect

03 p0390 A73-13344

Shear strains and elastic anisotropy of transversely isotropic cylindrical shell with circular hole under uniform internal pressure, using shallow shell equations

03 p0394 A73-14020

Modified shear-flexible orthotropic plate theory application to simply supported rectangular sandwich plates buckling problem, comparing results with Reissner theory and experimental data

04 p0509 A73-14946

Matrix displacement analysis of shells and plates including transverse shear strain effects

04 p0509 A73-15005

Equations for the oscillations of multilayer shells with allowance for shear deformation and for fiber pressing in the filler

05 p0634 A73-16749

Bending of nonuniform plates with asymmetric thickness variation inclusion of shear deformation

08 p0105 A73-20716

Effect of transverse shear deformation on vibrations of planar structures composed of beam-type elements

08 p0107 A73-21192

Material resistance analogies, relating shear, force and strain factors for bar deformation in tension, compression, torsion and bending

09 p1157 A73-22162

An analysis of plastic instability in pure shear in high strength AISI 4340 steel

09 p1101 A73-22405

Strain boundary conditions and complex representations of joining conditions in the theory of shells with finite shear rigidity

09 p1159 A73-22588

On the vibration of shear deformable curved anisotropic composite plates

11 p1442 A73-25711

Shear correction factors for orthotropic laminates under static load

11 p1442 A73-25713

Shock wave determination of shear velocity at high pressures for understanding of planetary interior behavior with abrupt change in density from seismic interpretation

11 p1355 A73-25898

Finite element theory of plates and shells including transverse shear strain effects

13 p1693 A73-28235

Aspect of cumulative fatigue damage under multiaxial strain cycling

13 p1701 A73-29497

Maxwell kinetic theory of gases with elasticity of shape/modulus of rigidity and obeying Hooke's law, deriving expressions for simple shear and relaxation time

14 p1745 A73-30477

Finite deflections of transversely-isotropic plates and shallow shells

15 p1953 A73-32089

Resolvent equations, in complex form, of the theory of transversely isotropic shells of revolution

16 p2074 A73-32686

Large deformations of cord-reinforced multilayered axisymmetric shells

20 p2621 A73-39542

Free vibration of arches flexible in shear

21 p2782 A73-40002

Mindlin theory extension to transverse shear effects in laminate plates, taking into account continuous stress across thickness and discontinuous shear strain

21 p2784 A73-40432

Material resistance analogies, relating shear, force and strain factors for bar deformation in tension, compression, torsion and bending

22 p2919 A73-42110

On the behavior of a numerical approximation to the rotary inertia and transverse shear plate

[ASME PAPER 73-APMW-7] 22 p2924 A73-42880

Dynamic contact problem for the case of longitudinal shear strain

22 p2927 A73-43051

Three dimensional elasticity solution for layer interaction and shear coupling and deflection effects of laminated anisotropic composite cylinders under bending

24 p3149 A73-45152

SHEAR STRENGTH

High temperature adhesive shear tests at ambient temperature as function of loading rate and bond overlap length

03 p0332 A73-13040

Evaluating adhesives for joining aluminum

03 p0334 A73-13271

Fiber reinforced plastics with adhesive bonded elements, investigating ply number and adhesive pressure effects on shear, bending and impact strengths

07 p0844 A73-20330

Criteria for selecting resin matrices for improved composite strength

10 p1238 A73-23966

The influence of interfacial bonding on the properties of carbon fiber composites

10 p1239 A73-23976

High modulus graphite fiber-epoxy composite shear strength and structural observation by X ray and electron diffraction and surface dark field electron microscopy

10 p1239 A73-23977

Calculation of the shear strength of an axisymmetric joint constructed out of Loctite

10 p1224 A73-24091

Effects of shear damage on the torsional behaviour of carbon fibre reinforced plastics

10 p1240 A73-24280

Interlaminar shear strength of a carbon fibre reinforced composite material under impact conditions

10 p1240 A73-24286

Microscopic, kinetic and microhardness observations of Ti-W metal matrix composite solid state interface reactions, showing enhanced shear resistance

11 p1384 A73-26049

Probability characteristics of the shear modulus of fiberglass-strengthened plastics

13 p1644 A73-27997

Determination of the mechanical characteristics of fiberglass-strengthened plastics in the winding state

13 p1644 A73-27998

The shear strength of thin lubricant films

14 p1754 A73-30050

An improved test for interfacial shear strength

21 p2719 A73-40922

Calculation of shear-sensitive orthotropic shells with residual stresses

21 p2786 A73-40977

Calculation of the physicochemical constants of metals associated with the strength of interatomic bonds

22 p2874 A73-42097

Post-yielding behavior of torsionally loaded composite tubes

23 p3041 A73-43640

Surveyor 3 lunar soil shear strength measurements for range of bulk densities obtained by different packing procedures, calculating void ratios

23 p3031 A73-43761

Upper bounds to in-plane shear strength of unidirectional fiber-reinforced composites

23 p3048 A73-44383

Shear strength of whiskered-fiber reinforced composites

24 p3102 A73-44513

SHEAR STRESS

NT TORSIONAL STRESS

Temperature dependence of the critical shear stress in single crystals of Al-Mg alloys of various concentration at temperatures between 1.6 and 300 K

01 p0064 A73-10488

Curvilinear holes bi-periodic array in isotropic plane, determining hole shape for constant shear stress around contours

02 p0235 A73-12193

Accommodation of the stress field at a grain boundary under heterogeneous shear by initiation of microcracks

02 p0237 A73-12812

Effect of transverse shear on limit load of cylindrical shells

03 p0383 A73-12873

On the influence of acceleration stresses on the yielding of disks of uniform thickness

03 p0384 A73-13118

Conditionally sampled measurements near the outer edge of a turbulent boundary layer

03 p0293 A73-13526

Magnetic field effect on friction shear stress in turbulent slipstreams of conducting fluids, calculating mixing zone width

03 p0346 A73-13609

Axial shear vibrations of cylinders made of a micropolar elastic solid

03 p0393 A73-13781

Shear stresses below asperities in Hertzian contact as measured by photoelasticity

[ASME PAPER 72-LUB-14] 03 p0314 A73-14330

The relative validity of the concepts of coefficient of friction and interface friction shear factor for use in metal deformation studies

[ASLE PREPRINT 72LC-7A-3]

A method for including the effects of transverse shear and rotary inertia on flexural motion of elastic plates

03 p0316 A73-14368

Velocity profiles and wall shear stress of three-dimensional turbulent boundary layers

04 p0510 A73-15074

[ONERA, TP NO. 1134] 04 p0403 A73-15092

Wall shear stress inference from two and three-dimensional turbulent boundary layer velocity profiles

[ASME PAPER 72-WA/FE-4] 04 p0434 A73-15840

Calculation of interacting turbulent shear layers - Duct flow

[ASME PAPER 72-WA/FE-25] 04 p0435 A73-15849

Linear analytical procedure for adhesively bonded flat joints design with minimized shear stress concentration, presenting finite element and automated iterative procedure

[ASME PAPER 72-WA/DE-13] 04 p0514 A73-15874

Plastic behavior of two-layer sandwich structures

[ASME PAPER 72-WA/APM-11] 04 p0516 A73-15901

A simple procedure for experimental determination of the longitudinal shear modulus of unidirectional composites

05 p0588 A73-16119

Asymmetric principal stress bounds in terms of symmetric part of tensor, considering existence conditions and maximum shear and normal stresses

[ASME PAPER 72-APM-QQ] 05 p0633 A73-16535

Thermal stresses in circular plates including the influence of transverse shear

05 p0633 A73-16539

Calculations of turbulent shear stress in supersonic turbulent boundary layer zero and adverse pressure gradient flow

[ALAA PAPER 73-166] 05 p0566 A73-16911

Crack growth and failure of aluminum plate under in-plane shear

[ALAA PAPER 73-253] 05 p0635 A73-16975

Shear stress distribution from measured nondimensional mean velocity profile measured in plane turbulent mixing layer formed at cascade wind tunnel exit

05 p0567 A73-17106

Tresca-type plastic materials in the theory of hypoelasticity. I Mechanical constitutive equations and simple shear deformation

07 p0909 A73-19161

Turbulent flow characteristics of an impinging jet

07 p0810 A73-19569

Effects of shearing force and rotary inertia to dynamical behaviours of thin cylindrical shells subjected to impulsive inner pressures

07 p0915 A73-20286

Stabilization of normal drift modes in an inhomogeneous plasma by a magnetic shear field

07 p0860 A73-20611

Parameters governing load transfer for single reinforcing members

08 p1016 A73-20799

The mixing length derived from Karman's similarity hypothesis

08 p0955 A73-21442

The effect of shear stress on the screw dislocation core structure in body-centred cubic lattices

08 p0978 A73-21525

Stacked membrane elements for plate and shell analysis, noting spurious shear components suppression

09 p1159 A73-22401

Nonlinear elastic behavior of unidirectional composite laminae

10 p1289 A73-24283

In-plane shear stress-strain response of unidirectional composite materials

10 p1240 A73-24285

Investigation of the strong anisotropy and resistance of fiber-strengthened plastics to interlayer shearing and compression normal to the fibers

10 p1240 A73-24353

Creep-rupture strength criterion in the case of interlayer shearing of oriented fiberglass plastics

10 p1240 A73-24355

Shear stresses and displacements of each layer of elastic plate with multiple layers of varying rigidity resting on elastic Winklerian base

11 p1433 A73-25029

Shear decohesion mechanism of fatigue crack propagation in ductile metals under cyclic loads, considering secondary microfracture and creep cavitation effects at elevated temperatures

11 p1381 A73-25814

The effect of fretting corrosion in fatigue crack initiation

11 p1383 A73-25835

Edge buckling of cylindrical shells with low in-plane shear moduli

11 p1445 A73-26392

Tresca-type plastic materials in the theory of hypoelasticity. II Optical constitutive equations and birefringence in simple shear

11 p1447 A73-26649

Shear stress and deformation inclusion in elastic plate bending finite element theory, discussing stiffness matrix improvement for thin shells

11 p1447 A73-26651

Model for lateral variations of lunar density minimizing total shear strain energy of moon, noting gravitational potential equal to observed potential at surface

12 p1541 A73-27488

Compressible boundary layer flow at a three-dimensional stagnation point with intensive suction or injection
12 p1458 A73-27699

Approximate calculation of the incompressible laminar boundary layer on a plate with suction
13 p1600 A73-28446

Application of Papkovitch-Neuber potentials to a crack problem.
13 p1635 A73-28756

Elliptic notch interaction with nearby crack in elastic solid under longitudinal shear, obtaining stress intensity factor
13 p1697 A73-28914

Temperature and rate dependence of the critical shearing stress in magnesium single crystals
13 p1636 A73-29056

Graphite- and boron-epoxy composite curved panels, determining shear buckling stress and post-buckling strength by visual and photographic observations [SESA PAPER 2030A]
13 p1699 A73-29308

The optimum distribution of diagonal stiffeners reinforcing a clamped infinitely long plate buckling under shear.
13 p1700 A73-29386

A theoretical study of fracture and yield conditions derived from hypo-elasticity.
13 p1639 A73-29464

Fatigue analysis considering rotating principal stress axes for aluminum alloy 2024-T351.
13 p1641 A73-29502

Refined method of determining tangential stresses and testing the strength of cylinders subjected to transverse flexure.
13 p1703 A73-29635

The origin of secondary flow in turbulent flow along a corner.
14 p1744 A73-30164

Nonlinear stability of a liquid film adjacent to a superersonic stream.
14 p1711 A73-30166

Critical shear stress temperature dependence in Al-Mg single crystal alloys of various concentrations in the range 1.6-300 K.
14 p1759 A73-30313

Couple-stress effects near an interior hole of an infinite elastic plane subjected to a concentrated force.
14 p1813 A73-30593

The contact problem of two coaxial cylindrical shells.
14 p1813 A73-30663

Influence of ordering in a Ni3Mn alloy on the magnitude of the critical shearing stresses
14 p1764 A73-30859

Brittle fracture of a body with a crack under variable shear load
15 p1945 A73-31040

Use of surface fences to measure wall shear stress in three-dimensional boundary layers.
15 p1874 A73-31118

Reynolds stresses in plane-parallel flows disturbed by Tollmein-Schlichting waves
15 p1861 A73-31193

Effect of Poisson's ratio strains in adherends on stresses of an idealized lap joint.
15 p1948 A73-31620

Considerations on the centres of shear and of twist in the theory of beams.
15 p1954 A73-32111

Pre-macro yielding and the orientation dependence of the 'shear' stress in molybdenum single crystals.
16 p2025 A73-33197

The effect of transverse shear stresses on the yield surface for thin shells.
16 p2082 A73-33905

The dynamic field of a growing plane elliptical shear crack.
16 p2082 A73-33907

Effect of transverse shear on the stability of an orthotropic cylindrical shell with an elastic filler under axial compression
16 p2082 A73-33931

Dynamic stability of an orthotropic cylindrical shell allowing for transversal shear
16 p2083 A73-33937

Experimental evidence of a couple-stress effect.
17 p2241 A73-34200

A steadily moving longitudinal-shear crack with an infinitely narrow plastic zone
17 p2241 A73-34266

Elastic isotropic infinite body with interior tunneling crack under dynamic shear force perpendicular to crack propagation direction, obtaining solution via Mathieu functions
17 p2241 A73-34329

A note on bending-shear interaction in the limit analysis of cylindrical shells
17 p2243 A73-34650

Turbulent mixing in the developing region of coaxial jets.
[ASME PAPER 73-FE-19]
17 p2153 A73-35015

An assessment of three-dimensional turbulent boundary layer prediction methods.
[ASME PAPER 73-FE-25]
17 p2153 A73-35020

Modes and frequencies of transversely isotropic slightly curved Timoshenko beams.
[ASME PAPER 73-APM-27]
17 p2248 A73-35043

Layered composite plate theory with interlaminar transverse shear stress as unknown variables, demonstrating agreement with elasticity solutions
17 p2250 A73-35116

Thin turbulent film analysis with approximation for relationship between flow and wall shear stress and effects of surface roughness and inertia at steps
[ASME PAPER 73-LUBS-17]
17 p2181 A73-35396

Calculation of pressure, shear, and flow in lubricating films for high speed bearings.
[ASME PAPER 73-LUBS-21]
17 p2182 A73-35399

Analysis of nonequilibrium particulate flow.
[ALAA PAPER 73-687]
18 p2298 A73-36238

Computation of hypersonic turbulent boundary layers with heat transfer.
[ALAA PAPER 73-699]
18 p2263 A73-36248

Limiting equilibrium of a circular plate with allowance for the shearing stress
18 p2363 A73-36405

The strength prediction problem of unidirectional fiberglass-reinforced plastics under transverse tension and shear
18 p2326 A73-36409

Two-point correlation model and the redistribution of Reynolds stresses.
18 p2300 A73-36627

Ratio of Reynolds shear stress to turbulence kinetic energy in a boundary layer.
18 p2300 A73-36633

The singularity at boundary layer separation due to mass injection.
18 p2301 A73-36696

Critical shear stress temperature and rate dependence in magnesium single crystals.
18 p2325 A73-36888

Transient stress distribution caused by water-jet impact.
19 p2435 A73-38300

Transonic laminar boundary layers with surface curvature.
19 p2423 A73-38480

A difference-energy method of studying the stability of rectangular plates in shear
20 p2617 A73-39306

Stability criteria for incompressible elastic isotropic materials subject to shearing displacement superimposed on homogeneous elastic deformation, discussing Cauchy stress and shear modulus
20 p2620 A73-39530

Mindlin theory extension to transverse shear effects in laminate plates, taking into account continuous stress across thickness and discontinuous shear strain
21 p2784 A73-40432

The plane elastostatic solution for a symmetrically loaded crack in a strip composite.
21 p2789 A73-41669

Interaction of cracks with rigid inclusions in longitudinal shear deformation. II - Further results.
22 p2920 A73-42134

Turbulent boundary layer velocity distribution skewness and flatness factors over smooth wall compared with rough wall, discussing Reynolds shear stress fluctuations
22 p2842 A73-42231

Introduction of shear deformations into a thin plate displacement formulation.
22 p2923 A73-42559

Generalized initial yield surfaces for unidirectional composites.
[ASME PAPER 73-APMW-24]
22 p2925 A73-42886

The elliptical crack subjected to nonuniform shear loading.
[ASME PAPER 73-APMW-42]
22 p2926 A73-42898

Flow patterns and velocity and shear stress distribution downstream of steady and pulsatile flow models for fluid dynamics of blood vessel branches
22 p2816 A73-43103

Mathematical model of collateral blood vessels caliber changes due to hydrodynamic drag /shear stress/ effects on vascular endothelium
22 p2817 A73-43105

Second order cross stress study of elastic shear deformation, considering rotation invariant Cauchy tensor and Poynting effect
23 p3039 A73-43306

An explanation of anomalously large Reynolds stresses within the convective planetary boundary layer.
23 p3002 A73-43593

Influence of the free edge upon the strength of angle-ply laminates.
23 p3041 A73-43635

Orientation dependent slip in polycrystalline titanium.
23 p2993 A73-44028

Shear crack stress intensity and displacement jump solution for half space under plane strain in form of singular integral equation
24 p3146 A73-44677

Transverse shear extensions to Ilyushin-Shapiro thin shell and plate theory for yield surfaces in rigid-plastic materials
24 p3147 A73-44746

Evaluating structural adhesives under sustained load in a hostile environment.
24 p3093 A73-44767

Generalized shear stress and shearing strain rate variables for thick circular plate, using von Mises yield criterion for limit load analysis
24 p3148 A73-44895

A note on determination of the shear stress-strain response of unidirectional composites.
24 p3149 A73-45150

Load concentration factors for circular holes in composite laminates.
24 p3149 A73-45151

Measurements of the structure of the Reynolds stress in a turbulent boundary layer.
24 p3079 A73-45310

An examination of the edge effect in a cantilever beam.
24 p3152 A73-45371

SHEAR WAVES
U S WAVES

SHEARING STRESS
U SHEAR STRESS

SHEATHS
NT ION SHEATHS
NT PLASMA SHEATHS

SHEET METAL
U METAL SHEETS

SHELL STABILITY
Existence of solutions in nonlinear shallow shell theory
01 p0116 A73-10962

Asymptotic method of determining critical buckling loads for strictly convex shallow shells of revolution
01 p0116 A73-10963

Optimal thickness of a cylindrical shell under external pressure
01 p0116 A73-10964

Dynamic stability of the state of moment stress in a cylindrical shell with allowance for inertia of the sub-critical state
01 p0117 A73-11093

Stability of orthotropic circular cylindrical shells reinforced by annular ribs under external pressure
01 p0118 A73-11409

Spot welded stainless steel cylindrical strip shells supercritical behavior, analyzing equilibrium states dependence on axial loads and buckling forces
01 p0119 A73-11441

Determination of geometrical characteristics in computer solutions of strength problems for shells of complex configuration
02 p0231 A73-11809

Stability of a cylindrical shell under the action of concentrated axial compression loads
02 p0231 A73-11815

Effect of the length on the stability of cylindrical shells compressed by longitudinal local forces
02 p0231 A73-11816

Circular cylindrical shell stability for thermal shock on end face, calculating critical thermal flux
02 p0232 A73-11818

Critical stress in an anisotropic cylindrical shell under nonuniform compression
02 p0233 A73-11938

Experimental investigation of the influence of initial flexures on the stability of smooth conical shells loaded by external pressure
02 p0236 A73-12576

Effect of transverse shear on limit load of cylindrical shells.
03 p0383 A73-12873

Algorithm for stress tensor and stability analysis of glass fiber reinforced plastic shells under hydrostatic pressure
03 p0392 A73-13741

Stability of fiberglass-reinforced cylindrical shell under the action of axial dynamic loads
03 p0392 A73-13746

Dynamic stability of a cylindrical shell in an acoustic medium.
03 p0393 A73-13834

Experiments on shell stability in air-driven shock tubes.
03 p0288 A73-13836

Two types of loss of stability and strength in cylindrical shells
05 p0634 A73-16747

Thin shells stability equations based on Bernoulli normal hypothesis, investigating stresses and deformations for equilibrium state under arbitrary load conditions
06 p0759 A73-17743

Truncated conical shell buckling and stability beyond elastic limit, deriving lower critical loads by orthogonalization method
06 p0760 A73-17781

Study of the stability of nonshallow spherical shells with finite displacements by applying various equations of the theory of shells
07 p0911 A73-19318

The effect of variable temperature on creep collapse of a cylindrical shell under external pressure
07 p0913 A73-20070

SHELL THEORY

Stability of the state of moment stress of a three-layer orthotropic cylindrical shell under uniform and nonuniform external pressure 08 p1018 A73-21374

Stability of a shallow three-layer shell with a linearly viscoelastic filler 09 p1157 A73-21994

Remarks on a system of nonlinear equations 09 p1113 A73-22987

Book - Structural analysis of shells. 09 p1164 A73-23273

Stability of the axisymmetric form of motion of flexible shallow shells 09 p1164 A73-23344

Vertical circular cylindrical shells buckling under axisymmetric compressive stress due to own structural weight, using Timoshenko elastic stability theory 09 p1166 A73-23459

Stability analysis of axially compressed closed circular cylindrical shells with reinforcement rings 10 p1290 A73-24301

Stability of transversely isotropic cylindrical shells in nonuniform subcritical states 10 p1290 A73-24311

Difference equations of elastic equilibrium for shells with variable characteristics in polar coordinates 11 p1433 A73-25027

Strength and weight optimization of strengthened spherical shells under external pressure 11 p1434 A73-25389

Experimental investigation of the stability of shells with holes 11 p1434 A73-25390

Stability of cylindrical shells with filler under axial compression and external pressure 11 p1435 A73-25396

Stability of a shell in the form of a hyperbolic paraboloid subjected to compression along straight generating lines 11 p1435 A73-25397

Stress, stability, and vibration of complex, branched shells of revolution. 11 p1437 A73-25496 [AIAA PAPER 73-360]

Spot welded stainless steel cylindrical shells post-critical loading behavior, analyzing equilibrium states dependence on axial loads and buckling forces 11 p1443 A73-26058

Edge buckling of cylindrical shells with low in-plane shear moduli. 11 p1445 A73-26392

Asymptotic analysis of the equations of oscillations and stability of bodies of revolution in the case of turning points 11 p1445 A73-26459

Experiments on the non-linear dynamic response of shells under blast waves. 11 p1446 A73-26492

Deformation of zero-moment shells subjected to internal pressure under creep conditions 12 p1551 A73-27179

Stability of a cylindrical anisotropic shell under the action of a ring load with allowance for subcritical deflection 12 p1553 A73-27373

Instability of asymmetric strongly convex thin shallow shells 12 p1553 A73-27414

Stability of cylindrical shells of variable thickness during torsion 12 p1553 A73-27462

Stability of a reinforced cylindrical shell during axial compression 12 p1553 A73-27463

Stability of a nonuniformly heated circular shell 12 p1554 A73-27471

Asymptotic method of determining the critical buckling loads of shallow strictly convex shells of revolution. 12 p1554 A73-27539

On optimal thickness of a cylindrical shell loaded by external pressure. 12 p1554 A73-27540

Shallow conical closed shell stability under axisymmetric loads, using variational difference method 12 p1556 A73-27799

One-dimensional zero-moment problem of a thin elastic shell of variable thickness 12 p1556 A73-27800

Shallow spherical shell dynamic stability under axisymmetric loads, noting small HF vibrations effect on static stability 12 p1556 A73-27814

Perturbation techniques in the analysis of geometrically nonlinear shells. 13 p1694 A73-28251

Nonlinear axisymmetric subcritical deformation effect on elastic stability of locally loaded thin circular cylindrical shells under free end compressive load 13 p1698 A73-29089

German monograph - A contribution to the stability calculation and the test of cylindrical shells of glass-fiber reinforced plastics under uniform external pressure. 13 p1646 A73-29280

Stability criteria for rigid plastic cylindrical shells at yield point load as function of deformation rate and geometry changes 14 p1809 A73-30257

Formulation of local stability problems of shells of revolution. 14 p1810 A73-30326

Buckling of circular cylindrical shells under compression. IV - Solutions based on the modified Flugge equations considering prebuckling edge rotations. 14 p1813 A73-30573

The influence of back pressure on the point of instability of axisymmetric shells deformed by fluid pressure. 14 p1813 A73-30662

Supersonic flutter of truncated multilayered orthotropic conical thin shells. 14 p1814 A73-30702

Stability and free oscillations of conjugate conical shells 15 p1944 A73-30972

Limit equilibrium of thin-walled containers composed of joined conical sections 15 p1944 A73-30973

Zero moment equilibrium stress state for multiply connected convex shells with curvilinear holes 15 p1945 A73-31031

Buckling analysis of elastically constrained stiffened conical shells under hydrostatic pressure by the collocation method. 15 p1948 A73-31642

Stability of a stochastically excited nonlinear cylindrical shell. 15 p1949 A73-31654

Stringer stiffened cylindrical shells stability characteristics under axial compression, using Donnell thin-shell and Vlasov thin-walled beam theories 15 p1949 A73-31656

Stability of a spherical shell containing an elastic filler 15 p1950 A73-31828

Influence of preliminary dynamic loading on the load-bearing capacity of cylindrical shells 16 p2075 A73-32693

The finite element method in shell stability analysis. 16 p2075 A73-32789

Stability analysis of shell-like structures by complementary energy. 16 p2078 A73-33000

Effect of transverse shear on the stability of an orthotropic cylindrical shell with an elastic filler under axial compression 16 p2082 A73-33931

Stability of composite-material cylindrical shells under unsteady heating and axial compression 16 p2083 A73-33934

Book - Stresses in shells /2nd edition/. 17 p2242 A73-34469

Meridional geometries for orthotropic shells with bending suppressed for different loading conditions, deriving shell configurations for combined loading via equilibrium equations 17 p2243 A73-34530

Determination of the carrying capacity of axisymmetric shells under piecewise linear plasticity conditions 17 p2244 A73-34738

Stability of a cylindrical shell under dynamic axial load 17 p2244 A73-34739

Shell stability effects of holes from review of published studies, emphasizing cylindrical shells under uniformly distributed compression loads 17 p2244 A73-34789

Stability of truncated conical shells under dynamic external pressure 18 p2363 A73-36413

Stability of cylindrical shells during rapid loadings 18 p2365 A73-36599

Nonlinear axisymmetric subcritical deformation effect on elastic stability of locally loaded thin circular cylindrical shells under free end compressive load 19 p2498 A73-37639

Supercritical strains in nonlinear elastic shells 20 p2616 A73-39259

Calculation of joint shells differing in their material and thickness 20 p2619 A73-39365

Numerical solution of problems of stability of three-layer cylindrical shells 20 p2620 A73-39503

Some mathematically equivalent problems in the statics of shells of revolution 20 p2624 A73-39649

Stability of the state of moment stress of a toroidal shell 20 p2624 A73-39650

Stability of the bending equilibrium of shells beyond the elastic limit 20 p2625 A73-39657

Effect of the yield point of the material on the stability of cylindrical shells under axial compression 20 p2625 A73-39658

Evaluation of various analytical models for buckling and vibration of stiffened shells. 21 p2784 A73-40424

Linearized characteristics method for supersonic flow past vibrating shells. 21 p2632 A73-40426

Elastoplastic strains and carrying capacity of shallow shells /Review/ 21 p2786 A73-40976

Stability of cylindrical shells beyond the elastic limit 21 p2786 A73-40979

Critical pressure and vibration frequencies of cylindrical shells with edges elastically reinforced in the axial direction 21 p2786 A73-40980

Stability of a cylindrical shell of linearly variable thickness beyond the elastic limit 21 p2787 A73-41195

Nondestructive shell-stability estimation by a combined-loading technique. 21 p2708 A73-41266

Plastic collapse of steep conical shells under axial compression. 21 p2789 A73-41684

Free vibrations of fluid-conveying cylindrical shells. [ASME PAPER 73-DET-96] 22 p2919 A73-42075

Buckling of segments of toroidal shells. 22 p2923 A73-42553

Buckling of toroidal shells under hydrostatic pressure. 22 p2923 A73-42560

German monograph - A contribution to the investigation of the stability of pipelines with flowing liquids according to the method of finite elements. 22 p2924 A73-42737

The Morley-Koiter equations for thin-walled circular cylindrical shells. II - Solution for a line loaded cylinder with close-spaced circumferential grooves. [ASME PAPER 73-APMW-23] 22 p2925 A73-42885

Numerical integration of shell equations using the field method. 22 p2925 A73-42888

Critical velocity for collapse of a shell of circular cross section without buckling. [ASME PAPER 73-APMW-31] 22 p2925 A73-42891

Stress-strain state of stiffened shallow shells of rectangular planform 22 p2928 A73-43054

Vibrations of a rotating solid body containing a cavity partially filled with a viscous fluid 22 p2843 A73-43058

Arbitrarily variable thickness cylindrical shell behavior under radial concentrated load calculated using Fourier series, differential equations and matrices 22 p2928 A73-43063

Stability under torsion of a moderately long cylindrical shell with different walls 23 p3042 A73-43738

Buckling of short viscoplastic cylindrical shells subjected to radial impulse. 23 p3045 A73-44080

Experimental evaluation of the load capacity of smooth fiberglass-reinforced plastic shells under external hydrostatic pressure 23 p2998 A73-44191

Critical equilibrium of cylindrical shells made from an ideal rigid-plastic material with different yield points in tension and compression 23 p3047 A73-44280

Nonlinear vibrations of viscoelastic cylinder with elastic shell under harmonic forces, showing steady state equilibrium stability conditions 24 p3145 A73-44530

Dynamic stability of a viscoelastic orthotropic cylindrical shell 24 p3146 A73-44532

Chebyshev solution to elliptical equilibrium equations of elastic reticular cylindrical and toroidal shells under distributed loads, applying to extensible fiber structures/tires/ 24 p3146 A73-44652

Skylab complex stiffened structure shell instability analysis by computer program, discussing convergence of finite difference formulation and eigenvalue calculation 24 p3144 A73-45234

Equilibrium of two elastic shallow shells of revolution which are connected by radial ribs 24 p3152 A73-45355

SHELL THEORY

Basic behavioral characteristics of viscoelastic orthotropic shell prepared from a generalized thermorheologically simple material 01 p0112 A73-10001

Shell designs by the theory of small elastoplastic deformations with allowance for the compressibility of material 01 p0112 A73-10005

Numerical solution to the axisymmetric thermoplasticity problem of a shell of revolution 01 p0112 A73-10007

Thin shell theory for thermal stresses in ogival shell used in nose cone design 01 p0113 A73-10016

Study of the stressed state of a shallow spherical shell whose thickness varies along its circumference 01 p0113 A73-10018

- Free vibration of prestressed cylindrical shells having arbitrary homogeneous boundary conditions. 01 p0114 A73-10730
- Application of shell equations to an unsymmetrically loaded corrugated shell of revolution. 01 p0115 A73-10769
- Existence of solutions in nonlinear shallow shell theory 01 p0116 A73-10962
- Optimal thickness of a cylindrical shell under external pressure 01 p0116 A73-10964
- Finite difference solution to Vekua thin shell equations, using differential and equivalent energetic operators 01 p0116 A73-11076
- A semimomentless theory of asymmetrically structured cylindrical sandwich shells with a rigid compressible filler 01 p0118 A73-11406
- Oscillations of nonshallow cylindrical shells loaded by distributed and concentrated masses 01 p0118 A73-11407
- Construction of a general solution for an elastic anisotropic shallow shell with arbitrary boundary conditions, and some of its applications 02 p0230 A73-11714
- Some problems in the substantiation and application of discrete large-element design schemes for complex zero-moment shells 02 p0230 A73-11716
- Finite difference method for transverse elliptical cross section effect of spiral shell on stress concentration 02 p0231 A73-11802
- Solution of axisymmetrical problems of the interaction between a cylindrical shell and an elastic filler by the finite difference method 02 p0231 A73-11806
- Equilibrium equations in theory of anisotropic shells and plates with arbitrary boundary conditions under external loads, noting thin walled reinforced shells 02 p0231 A73-11807
- Determination of geometrical characteristics in computer solutions of strength problems for shells of complex configuration 02 p0231 A73-11809
- Shell and plate theory covering constitutive and equilibrium equations, Cosserat surfaces and uniqueness theorem 02 p0234 A73-11981
- Prediction of the response of a cylindrical shell to arbitrary or boundary-layer-induced random pressure fields. 02 p0237 A73-12601
- Analytical representation of boundary conditions in the technical theory of shells 03 p0384 A73-13127
- On bending and vibration of reinforced and bireinforced elastic and viscoelastic shells. 03 p0387 A73-13160
- Finite element equations of motion of elastoplastic shell, applying theory to edge clamped circular plate dynamic response 03 p0389 A73-13321
- Curved element for geometrical approximation of thin shell structures, deriving element stiffness equations in terms of nodal displacement degrees of freedom 03 p0389 A73-13325
- On higher-order theory for thermoelastic analysis of heterogeneous orthotropic cylindrical shells. 03 p0389 A73-13327
- A consistent approximation in the linear theory of elastic lattice-type shells. 03 p0393 A73-13780
- Finite difference theory for bending stress concentration in shells of revolution, noting constitutive equation for thermal stress analysis 03 p0393 A73-13793
- Natural frequencies of a hemispherical shell. 03 p0395 A73-14474
- Thick elastic or inelastic shells finite deformation, presenting multicouple theory for stress-strain distribution 04 p0508 A73-14941
- Matrix displacement analysis of shells and plates including transverse shear strain effects. 04 p0509 A73-15005
- On the application of the SHEBA shell element. 04 p0510 A73-15016
- Theoretical formulation of finite-element methods in linear-elastic analysis of general shells. 04 p0510 A73-15026
- The solvability of integral equations of shell theory 04 p0511 A73-15082
- Stressed state of a planarly elliptical, hyperbolic shell 04 p0511 A73-15088
- Analytical investigation of a cylindrical shell embedded in a soft medium. 04 p0511 A73-15172
- Russian book on orthotropic laminated cylindrical shells strength and optimal design covering glass ribbon reinforced zero moment shells and interlayer shear theory 04 p0514 A73-15702
- An approximate rigid-plastic analysis of shell intersections loaded dynamically. [ASME PAPER 72-WA/DE-1] 04 p0515 A73-15876
- Singular solutions for shallow cylindrical shells. [ASME PAPER 72-WA/APM-27] 04 p0515 A73-15891
- The load carrying capacities of symmetrically loaded shallow shells. 05 p0631 A73-16120
- Nonlinear shell theory with finite rotation and stress-function vectors. [ASME PAPER 72-APM-CC] 05 p0633 A73-16533
- On finite symmetrical strain in thin shells of revolution. 05 p0633 A73-16536
- Introduction of two solving functions into the equations for nonshallow shells. 05 p0634 A73-16796
- The influence of the reference geometry on the response of elastic shells. 05 p0637 A73-17236
- Stress analysis of hyperbolic paraboloid membrane shells for applications in architecture 06 p0757 A73-17395
- Lagrange description of equations for finite deflections of incompressible plastic shells, classifying stress-strain relations 06 p0760 A73-17778
- The thermal shock on the shell of revolution-coupled and uncoupled theory. 06 p0763 A73-18452
- Derivation of the linear shell theory from the theory of Cosserat medium. 06 p0763 A73-18454
- Calculus of variations for mathematical model of elastic shell with internal degrees of freedom, noting boundary and discontinuity conditions 06 p0766 A73-18877
- A linear theory of thin elastic shells, based on conservation of a non-normal straight line. 07 p0908 A73-19091
- Study of the stability of nonshallow spherical shells with finite displacements by applying various equations of the theory of shells 07 p0911 A73-19318
- Static-geometric analogy and complex transformation in the theory of three-layer shells with a light-weight filler 07 p0912 A73-19470
- Deformations and stresses in a hollow sphere with spherical transversal isotropy under impulsive pressure. 07 p0913 A73-20116
- Nonlinear multiple-scale solution of a cylindrical shell. 07 p0915 A73-20337
- Stiffness matrix formulation and eigenvalue analysis for high order shallow shell finite element of rectangular plan 07 p0916 A73-20439
- Method of determining the mass removal from heat-shield materials on the basis of strain measurements in loaded shells 08 p1023 A73-21369
- Deformation of a frame coupled to a fiberglass-plastic shell under the action of local loads 08 p1017 A73-21372
- Stress-strain state of transversely isotropic shells under concentrated loads 08 p1019 A73-21760
- Investigation of the deformation of a hollow sphere under an impulsive load on the basis of three-dimensional elasticity theory and shell theory 08 p1019 A73-21761
- Weight optimization for multilayered plates and shells with given load, end conditions and middle surface shape and dimension 08 p1019 A73-21762
- Rigidly plastic shells yield point, deriving yield surface in generalized stress space 09 p1158 A73-22360
- Large deflection analysis of plates and shallow shells using the finite element method. 09 p1158 A73-22396
- Stacked membrane elements for plate and shell analysis, noting spurious shear components suppression 09 p1159 A73-22401
- Strain boundary conditions and complex representations of joining conditions in the theory of shells with finite shear rigidity 09 p1159 A73-22588
- A deficiency in current finite elements for thin shell applications. 09 p1160 A73-22893
- A cylindrical shell with an axial crack under skew-symmetric loading. 09 p1160 A73-22894
- Design of rotating discs of irregular outline. 09 p1161 A73-23051
- Book - Structural analysis of shells. 09 p1164 A73-23273
- Deformation of shells of revolution with attached rings under different local loads, deriving approximate expressions for stressed state 10 p1287 A73-23592
- A comparison of solutions in first approximation shell theory. 10 p1291 A73-24337
- Method of variable directions for solving the equations of an isotropic cylindrical shell 10 p1292 A73-24501
- A method for obtaining stresses and displacements in thick cylindrical shells under arbitrary boundary conditions. [ASME PAPER 72-APM-LLL] 11 p1442 A73-25708
- A corrected assessment of the cylindrical shell finite element of Bogner, Fox and Schmit when applied to arches. 11 p1443 A73-26090
- Transient creep of shells of revolution. 11 p1444 A73-26336
- Bending problem for shell of revolution with finite displacements, axisymmetric loading and nonlinear strain functions 11 p1445 A73-26460
- Estimates for stress derivatives and error in interior equations for shells of variable thickness with applied forces. 11 p1446 A73-26548
- Axisymmetric buckling of rigidly clamped hemispherical shells. 11 p1447 A73-26648
- Second order closed form asymptotic solution to Donnell type nonlinear equations of elastic homogeneous conical shells for displacement and stress resultants 11 p1447 A73-26650
- Soft shell strength analysis for contact and static loads 12 p1554 A73-27470
- On the existence of solutions of the nonlinear theory of shallow shells. 12 p1554 A73-27538
- On optimal thickness of a cylindrical shell loaded by external pressure. 12 p1554 A73-27540
- The Castigliano variational equation and strain continuity relations for a thin shell 12 p1555 A73-27788
- Russian papers on mathematical physics boundary value problems covering electrodynamics, electromagnetic fields in conducting channels and ferromagnetic cylinders, heat transfer, shell theory, etc. 12 p1525 A73-27803
- Solvability of the boundary value problem in the theory of shallow shells of revolution and estimation of errors in the approximate solution 12 p1556 A73-27813
- Criteria for finite element discretization of shells of revolution. 13 p1691 A73-28084
- Finite element theory of plates and shells including transverse shear strain effects. 13 p1693 A73-28235
- Computer programs for analysis of shells of revolution based on numerical integration and finite difference procedures 13 p1693 A73-28236
- The application of a curved, mixed-type shell element. 13 p1693 A73-28237
- Incremental solution of axisymmetric plate and shell finite deformation. 13 p1694 A73-28250
- The mechanical interpretation of high accuracy multipoint difference methods for plates and shells. 13 p1694 A73-28255
- An evaluation of finite difference and finite element techniques for analysis of general shells. 13 p1694 A73-28256
- Finite deflection of a shallow spherical membrane. 13 p1697 A73-28815
- The static-geometric duality and a staggered mesh scheme in the numerical solution of some shell problems. 13 p1699 A73-29373
- Principle of virtual work and equations of shells 14 p1805 A73-29761
- Apparent symmetry of certain thin elastic shells. 14 p1805 A73-29763
- Free vibrations of shells of revolution with variable thickness. 14 p1805 A73-29768
- Numerical time integration methods in shell transient response finite element analysis, considering conditionally stable explicit and unconditionally or conditionally stable implicit schemes 14 p1807 A73-30187
- A comparison of theory and experiments on the dynamic plastic behavior of shells. 14 p1811 A73-30476
- The contact problem of two coaxial cylindrical shells. 14 p1813 A73-30663
- Construction of refined applied theories for a truncated hollow cone of variable thickness 14 p1815 A73-30786

SHELLS [STRUCTURAL FORMS]

- Internal stress-strain boundary layer theory of shells and orthotropic plates with zero stress conditions at upper and lower planes and edge distance dependent attenuation 14 p1815 A73-30815
- Traveling wave solutions of differential equations describing thin elastic shell oscillations due to point source 14 p1815 A73-30951
- Natural oscillations of multilayer shells and plates with fillers 15 p1944 A73-30970
- Projection method in the shell theory and its realization on a computer 15 p1944 A73-30971
- Solution of the fundamental boundary value problems for a closed semiinfinite cylindrical shell 15 p1945 A73-31023
- Derivation of a normal displacement function for the triangular finite element of plates and shells 15 p1945 A73-31032
- The dynamic plastic behavior of simply supported spherical shells. 15 p1948 A73-31369
- Forced motion of cylindrical shells - A comparison of shell theory with elasticity theory. 15 p1949 A73-31651
- Static-geometric analogy and complex transformation in the theory of three-layered shells with light fillers. 15 p1952 A73-32072
- Theory for cylindrical wavy shells via fiberglass-plastic models, noting application to wavy rod torsion problem 15 p1952 A73-32083
- Finite deflections of transversally-isotropic plates and shallow shells 15 p1953 A73-32089
- Theorem concerning possible bendings in zero-moment shell theory 15 p1953 A73-32090
- A variational principle for finite deformations of quasi-shallow shells. 15 p1955 A73-32162
- Calculus of variations for mathematical model of elastic shell with internal degrees of freedom, noting boundary and discontinuity conditions 15 p1956 A73-32402
- Resolvent equations, in complex form, of the theory of transversely isotropic shells of revolution 16 p2074 A73-32686
- Forced vibrations of elastic shells of revolution filled with liquid 16 p2074 A73-32687
- Stress concentration near a cutout on the surface of an orthotropic cylindrical shell 16 p2075 A73-32694
- Nonlinear behavior of shells of revolution under cyclic loading. 16 p2075 A73-32791
- The behaviour with diminishing curvature of strain-based arch finite elements. 16 p2076 A73-32921
- Constraints theory for Cosserat surfaces with applications in thermomechanics and shell theory, investigating equilibrium laws transformation properties and constitutive equations restrictions 16 p2076 A73-32936
- Mixed variational principles based on stationary potential energy concept applied to finite element method in thin shell theory 16 p2077 A73-32986
- Ring finite elements for axisymmetric and non axisymmetric thin shell analysis. 16 p2077 A73-32989
- Galerkin variational method combination with least squares error distribution technique for application in plate and shell theory 16 p2077 A73-32992
- Nonlinear shell theory, obtaining differential equilibrium equations and boundary conditions from three dimensional variational energy expression by kinematic hypothesis and Ritz method 16 p2078 A73-32996
- The application of finite elements to the large deflection geometrically non-linear behaviour of cylindrical shells. 16 p2078 A73-32998
- Incremental variational method for the large displacement analysis of shells with geometric imperfections. 16 p2078 A73-32999
- Stability analysis of shell-like structures by complementary energy. 16 p2078 A73-33000
- Curved rotational shell elements by the constraint method. 16 p2078 A73-33002
- Asymptotic integration method solution for three dimensional equations of geometrically nonlinear theory for thin shells and plates 16 p2080 A73-33243
- Torsional vibrations of shells of revolution of variable thickness. 16 p2081 A73-33682
- The effect of transverse shear stresses on the yield surface for thin shells. 16 p2082 A73-33905
- Thin shell elastoplastic deformation theory development for small strains, using Hooke's law to analyze hardening, stress and unloading 16 p2084 A73-34033
- Lagrangian formulation of sandwich shell theory. 17 p2242 A73-34526
- Finite element analysis of inflatable shells. 17 p2242 A73-34528
- Strongly curved finite element for shell analysis. 17 p2242 A73-34529
- Some properties of dynamic equation integrals from the theory of shells 17 p2244 A73-34736
- Forced plane strain motion of cylindrical shells - A comparison of shell theory with elasticity theory. 17 p2247 A73-35034
- [ASME PAPER 73-APM-9] On the buckling of cylinders in axial compression. 17 p2250 A73-35113
- [ASME PAPER 72-APM-BBB] On an accurate theory for circular cylindrical shells. 17 p2250 A73-35114
- [ASME PAPER 73-APM-E] Dynamically-induced large deformations of multilayer, variable thickness shells. 18 p2362 A73-36317
- Book - Theory and design of shells on the basis of asymptotic analysis: A unifying approach to the variety of thick and thin elastic shell theories and problems. 18 p2367 A73-36967
- Approximate method for solving a boundary value problem in the theory of zero-moment elastic spherical shells 18 p2367 A73-36988
- A new form of the integral equations of a boundary value problem in the theory of simply supported shallow spherical shells 19 p2495 A73-37198
- Membrane statics of parachute-like shells. 19 p2496 A73-37480
- Nonlinear parametric vibrations of closed cylindrical shells 19 p2499 A73-37764
- Some new results for the vibrations of circular cylinders. 19 p2500 A73-38107
- A numerical realization of the Bubnov-Galerkin method using a computer for the solution of nonlinear problems in the theory of shallow shells 20 p2617 A73-39307
- Theory of shallow shells with allowance for couple stresses without applying the Kirchhoff-Love hypothesis 20 p2618 A73-39309
- Certain approximations in the solution of shell and plate bending problems with allowance for physical and geometrical nonlinearity 20 p2618 A73-39311
- Improved relations in the dynamics of moderately thick shells and plates under the action of massive moving loads 20 p2618 A73-39316
- Symmetrical three-layer shells with a light-weight elastic filler 20 p2618 A73-39328
- Some mathematically equivalent problems in the statics of shells of revolution 20 p2624 A73-39649
- Study of elastoplastic deformations in a two-layer shell under dynamic loads 20 p2625 A73-39653
- Calculation of shear-sensitive orthotropic shells with residual stresses 21 p2786 A73-40977
- Deformation of shells with a circular axis and variable cross-section parameters 21 p2786 A73-40978
- Discretized solution of junction problems in shells. 22 p2917 A73-41740
- Finite element analysis of rotating shells. 22 p2919 A73-42074
- [ASME PAPER 73-DET-94] The calculation of open circular cylindrical shells with the aid of partial discretization 22 p2922 A73-42528
- Contact pressure problem solution for circular cylindrical shell resting on circular Winklerian bases under external load in terms of Fourier expansion 22 p2928 A73-43053
- Resolvent boundary solutions for Vlasov shallow shell equations in terms of force and deflection functions over entire contour 22 p2928 A73-43055
- Sandwich shells nonlinear theory with stress-strain relations in tensor notation, using Hamilton principle for equations of motion and boundary conditions 23 p3044 A73-44078
- Numerical calculation of simply supported cylindrical shells of arbitrary cross section 23 p3046 A73-44192
- Traveling wave solutions of differential equations describing thin elastic shell oscillations due to point source 23 p3047 A73-44327
- Power series solution to Volterra equations in nonlinear viscoelastic dynamic plate and shell theory with application to flexible cylindrical shell vibrations under periodic loads 24 p3145 A73-44518
- Equations of linear elastic theory of thin shells based on model of anisotropic Cosserat surface 24 p3147 A73-44744
- Function space approach to prestressed nonlinear orthotropic shallow shell theory boundary value problems 24 p3149 A73-45006
- Convergence of finite difference transient response computations for thin shells. 24 p3150 A73-45228
- On the problem of flexure of anisotropic cylindrical shells. 24 p3151 A73-45302

SHELLS [STRUCTURAL FORMS]

- NT ANISOTROPIC SHELLS
- NT CIRCULAR SHELLS
- NT CONICAL SHELLS
- NT CORRUGATED SHELLS
- NT CYLINDRICAL SHELLS
- NT DOMES [STRUCTURAL FORMS]
- NT ELASTIC SHELLS
- NT HEMISPHERICAL SHELLS
- NT LIQUID FILLED SHELLS
- NT METAL SHELLS
- NT ORTHOTROPIC SHELLS
- NT PERFORATED SHELLS
- NT RADOMES
- NT REINFORCED SHELLS
- NT SHALLOW SHELLS
- NT SPHERICAL CAPS
- NT SPHERICAL SHELLS
- NT THIN WALLED SHELLS
- NT TOROIDAL SHELLS
- Transient response of inelastic shells of revolution. 03 p0392 A73-13686

Thick elastic or inelastic shells finite deformation, presenting multicouple theory for stress-strain distribution 04 p0508 A73-14941

Explosive forming for axisymmetric dished shells without clamped blank around edge, discussing design parameters, formability limits and optimization techniques [SME PAPER MF 72-237] 06 p0698 A73-18095

Multiparameter optimal design of plates and shells. 07 p0912 A73-19367

Finite-element analysis of shells of revolution by two doubly curved quadrilateral elements. 07 p0912 A73-19368

The application of nodal stress concepts to the bending of plates and shells. 08 p1019 A73-21691

Application of double trigonometric series to the calculation of shell plates of variable thickness 11 p1446 A73-26600

Dynamics of structural systems subjected to moving loads. II - Half-spaces, plates, and shells under the action of moving loads 20 p2617 A73-39304

Spaced annular ring shell-to-shell and shell-to-tube view factors for finite difference radiative heat transfer solutions 22 p2923 A73-42564

SHIELDING

- NT ELECTROMAGNETIC SHIELDING
- NT ELECTROSTATIC SHIELDING
- NT HEAT SHIELDING
- NT MAGNETIC SHIELDING
- NT RADIATION SHIELDING
- NT RADIO FREQUENCY SHIELDING
- NT REENTRY SHIELDING
- NT SOLAR RADIATION SHIELDING
- NT SPACECRAFT SHIELDING
- The energetic degree of shielding provided by ball-protection screens in the case of certain distribution spectra of hailstone diameters 11 p1394 A73-26373

SHIFT REGISTERS

- Moving-target-indicator recursive radar filter using bucket-brigade circuits. 09 p1065 A73-23096
- Two-phase charge-coupled devices with overlapping polysilicon and aluminum gates. 15 p1850 A73-31373
- Bucket-brigade shift-register operation-exact correlation between experimental data and a computer model. 16 p1988 A73-33397
- Bipolar LSI building blocks for digital filtering applications. 17 p2138 A73-35228
- A study of the characteristics of surface charge transfer devices 20 p2534 A73-38854
- Application of fluidic shift-register modules for sequential control of pneumatic sequential circuits. 23 p2943 A73-43412

Pneumatic sequential circuits assembly method involving modules with switching elements and shift register, considering control valves and operation modes
23 p2943 A73-43416

Information dependent frequency control of an automatic typewriter.
23 p2944 A73-43423

SHIPS

U COMPENSATORS

SHIP PROPULSION

U MARINE PROPULSION

SHIPS

NT AIRCRAFT CARRIERS

NT CARGO SHIPS

NT NUCLEAR POWERED SHIPS

NT SATELLITE COMMUNICATIONS SHIPS

NT SUBMARINES

NT TANKER SHIPS

Fire suppression for shipboard machinery spaces - Extinguishing and inerting with Halon 1301.

[WSCIPAPER 72-33] 05 p0639 A73-16682

Modulation and speech processing techniques for a maritime-satellite service.
12 p1472 A73-27662

A maritime communications concept using spaceborne phased arrays.
12 p1472 A73-27665

Satellite communication channels assignment to ships and aircraft, considering automated digital calling method for ship-to-shore communication
12 p1472 A73-27670

A simple stabilized antenna platform for maritime satellite communications.
12 p1481 A73-27673

Technical factors determining the choice of frequency bands for the links between satellite and coast stations of a maritime communications satellite service.
12 p1473 A73-27674

The operational requirements for a maritime satellite communication service.
12 p1473 A73-27676

Engineering economic considerations for a maritime-satellite service.
12 p1473 A73-27677

An overview of fatigue and fracture for design and certification of advanced high performance ships.
17 p2246 A73-34881

Hybrid-inertial navigation with range updates in a relative grid.
20 p2587 A73-38810

Fluidic linear nozzle-flapper valve accelerometer for ship motion sensing, describing circuit configuration and performance tests
23 p2981 A73-43428

SHIVERING

NT DITHERS

SHOCK ABSORBERS

Review of theories and experimental results pertaining to the dynamic behavior of porous bodies
07 p0912 A73-19905

Method of variation of parameters starting with linear damped vibration solution as its generating solution.
09 p1121 A73-23324

Damping of an aerial photo camera with the aid of polymeric materials
10 p1219 A73-24478

Shock absorbing-vibration insulating viscoelastic systems design under singular influence function assumption, determining ranges of parameters change
12 p1516 A73-27177

Kneeling landing gear - The C5 variable geometry development.
13 p1568 A73-28158

Parachute webbing designs for opening shock energy absorption and force limitation, discussing drop tower and ballistic piston test results for various designs
16 p2018 A73-33066

Isolation of mechanical vibration, impact, and noise; Proceedings of the Colloquium, Cincinnati, Ohio, September 9-12, 1973.
22 p2926 A73-42920

Modeling methods for shock isolation systems for fragile equipment protection from HF effects generated by high loading rates and/or random multifrequency input displacement signatures
22 p2927 A73-42925

Biodynamic applications regarding isolation of humans from shock and vibration.
22 p2816 A73-42926

SHOCK DIFFUSERS

U DIFFUSERS

U SHOCK WAVE ATTENUATION

SHOCK DISCONTINUITY

Classification, orientational characteristics, and some examples of rotational discontinuities in the solar wind
08 p0998 A73-21278

Statistical phenomena during shock wave formation
08 p0955 A73-21447

Global solutions to a class of nonlinear hyperbolic systems of equations.
13 p1647 A73-28024

Investigation of high-temperature gas flow around axisymmetric bodies in the presence of several discontinuity surfaces
13 p1708 A73-29404

Statistical effects in the generation of shock waves.
15 p1860 A73-31011

The transonic aerofoil problem with embedded shocks.
15 p1821 A73-31122

Discontinuity of the vortex on a shock in thermodynamic variables
17 p2154 A73-35047

A new shock capturing numerical method with applications to some simple supersonic flow fields.
17 p2096 A73-35144

Classification, characteristics of orientation, and some examples of rotational discontinuities in the solar wind.
19 p2476 A73-37907

Thermodynamic conditions of conservation of irrotational or oligotropic motions across a shock wave
21 p2677 A73-40948

Transformation of a symmetric wave-type process of deformation into an asymmetric process in a plate during the development of a shock wave
22 p2927 A73-42930

SHOCK FRONTS

Sonic boom avoidance by flight path maneuvers, investigating shock front development in curved flight
02 p0130 A73-11856

Thermodynamics and shocks in nonelastic mediums
04 p0520 A73-15994

Radiation effects on state of gas behind strong shock wave, representing power density of non-relativistic fully ionized hydrogen plasma
07 p0920 A73-19508

Supersonic flow past large-angle pointed cones
07 p0775 A73-19981

Instability of shock waves in inhomogeneous gases.
07 p0812 A73-20445

Solar cosmic rays propagation between shock front and solar flare hot plasma, examining fine structure from Explorer 34 and Venera 6 data
08 p0999 A73-21328

Small perturbations analysis of hydrodynamic relations of shock front propagation in inhomogeneous medium
09 p1070 A73-21888

Investigation of the motion of the medium near the point of contact of shock waves in linear and nonlinear formulations
09 p1070 A73-21921

Simultaneous diffusion of photons and particles in a semiinfinite space. II - Concentration of excited atoms before a shock wavefront
09 p1123 A73-23069

One dimensional supersonic shock front location by sonic circle involute point by point plotting, using geometric considerations
09 p1030 A73-23467

Isolated reactive and nonreactive Mach stem structure in exothermic systems under conditions encountered behind detonation waves front
10 p1294 A73-23553

Ionization front propagation velocity as function of microwave power density, showing dependence on precursor electron density profiles
10 p1251 A73-24257

Interplanetary plasma shock event of 8 March 1970 from Heos 1 data, noting magnetospheric compression and solar wind velocity at geosynchronous orbit
10 p1270 A73-24742

Variational equations of unsteady near-similar perfect gas flow at strong shock front in terms of mass, energy and momentum in perturbed region
12 p1487 A73-27408

Ray method for solving dynamic problems in viscoelastoplastic media
12 p1553 A73-27415

Interplanetary shock fronts thickness, calculating magnetosonic Mach number and Larmor radius
15 p1942 A73-32620

Spectrophotometric determination of the rate of dissociation of nitrogen trifluoride behind shock waves.
16 p1977 A73-34017

Hydrodynamic equilibrium structure of plane shock waves in arbitrary liquid or gas at large distance behind shock front
16 p2001 A73-34059

Small perturbations analysis of hydrodynamic relations of shock front propagation in inhomogeneous medium
17 p2150 A73-34311

Uniqueness requirements for calculated jump conditions across embedded shock waves based on relaxation methods, comparing to time dependent finite difference calculation
17 p2154 A73-35130

Simulation of driven flare-associated disturbances in the solar wind.
18 p2346 A73-36263

Rarefied collisionless plasma turbulence and dissipation process due to instability, examining magnetic field effects on shock wave front nature
19 p2464 A73-37154

Evidence for confinement of low-energy cosmic rays ahead of interplanetary shock waves.
21 p2763 A73-41504

Shock wave structure analysis via averaging over nonsinusoidal functions, discussing shock front length in cubic nonlinear medium, adiabatic invariants and harmonic functions
21 p2749 A73-41518

Mariner 5 observations of solar wind shock-like structures including density, velocity, and proton temperature increases, suggesting nonlinear magnetoacoustic waves under steepening process
22 p2901 A73-41902

German monograph - Investigation of relaxation effects behind secondary shock fronts in shock-wave heated and partially ionized argon plasmas.
22 p2895 A73-42850

A simple thermodynamic method of estimating the shock compression temperature of a condensed medium
24 p3155 A73-44709

Similarity of flows arising during reflection of weak shock waves from a rigid wall and from a free surface.
24 p3076 A73-44713

Propagation of shock waves in anisotropic composite plates.
24 p3149 A73-45149

SHOCK HEATING

Oblique shock waves heating of high beta plasma ions, suggesting Landau damping of wave energy
02 p0197 A73-12059

Iron and stony-iron meteorites kamacite hardness and shock histories, hypothesizing preterrestrial collisions between asteroid sized objects
05 p0615 A73-16377

Population inversion by mixing in a shock tube flow.
05 p0600 A73-16556

Study of exothermic processes in shock ignited gases by the use of laser shear interferometry.
05 p0640 A73-16920

Shock impingement caused by boundary layer separation ahead of blunt fins.
05 p0532 A73-16961

[ATAIA PAPER 73-236] Shockwave-boundary layer interference heating analysis.
05 p0532 A73-16962

[ATAIA PAPER 73-237] Ionization-relaxation time measurements upon krypton and xenon in a shock-wave heated plasma
06 p0728 A73-17912

Shock tube investigation of bromine dissociation rates in the presence of carbon dioxide.
06 p0661 A73-18123

Determination of thermal conductivity of gases by shock-tube studies.
07 p0918 A73-19187

Characteristics of the unsteady shock-induced laminar boundary layer on a flat plate.
07 p0810 A73-19505

Radiation and shock effects on Apollo 14 and 15 breccias substructure history, reporting optical microscope observations of solar flares and cosmic ray tracks
07 p0896 A73-19872

Flowfield calculations for some supersonic sections with ducted heat addition.
09 p1028 A73-23089

X ray background emission and behavior of infalling intergalactic gas into Galaxy resulting from shock wave generation and heating in accretion process
10 p1264 A73-23495

Induction flowmeter theory in a T-tube of circular section.
10 p1220 A73-24619

Gasdynamic laser with a high water vapor content.
12 p1507 A73-27510

Meteoritic vs lunar origin of Luna 20 lunar soil samples metal particles and metallic inclusions discussing meteoritic microstructural obliteration due to shock reheating of crust
13 p1675 A73-28315

Generation of acoustic waves during the passage of a shock wave through a heated gaseous element.
13 p1705 A73-28494

Variation of parameters in a shock-heated argon plasma flow.
13 p1665 A73-28624

Mode factor and stress concentration parameter for sudden heating of solid cylinders and disks, noting thermal stability criterion with allowance for statistical strength
13 p1703 A73-29611

Investigation of the heating of a plasma ion component by a collisionless shock wave.
14 p1780 A73-30336

Artificial viscosity related to shocks for studying anomalous wall heating and solution behavior at interface by substituting Rankine-Hugoniot equation
14 p1775 A73-30908

Heat transfer behind a shock wave in a two-phase gasdynamic flow
15 p1862 A73-31294

Recent developments in strong shock wave research.
19 p2415 A73-37155

SHOCK LAYERS

- Gasdynamic processes in obtaining inversion in shock tubes 21 p2677 A73-40696
- Short duration temperature measurements by infrared emission-absorption. 22 p2853 A73-41990
- Investigation of the electron concentration behind strong shock waves 22 p2893 A73-42385
- A single-pulse shock-tube study of the reaction between nitrous oxide and carbon monoxide. 22 p2933 A73-42757
- German monograph - Investigation of relaxation effects behind secondary shock fronts in shock-wave heated and partially ionized argon plasmas. 22 p2895 A73-42850
- Experimental study of shocked-plasma flows with a double search-coil conductivity probe. 24 p3113 A73-44402
- Further aspects of weak shock theory applied to the solar chromosphere. 24 p3135 A73-44630
- A simple thermodynamic method of estimating the shock compression temperature of a condensed medium 24 p3155 A73-44709
- Magnetically induced electrothermal instability in unseeded partially ionized shock heated argon plasma 24 p3117 A73-45454

SHOCK LAYERS

- Hypersonic, viscous shock layer with chemical nonequilibrium for spherically blunt cones. 01 p0002 A73-10746
- Shock layer measurements of decomposition reactions of water cluster ions. 01 p0014 A73-10900
- Calculation of supersonic viscous gas flow past blunt bodies at large Reynolds numbers 05 p0527 A73-16448
- Viscous shock layer flow in the windward plane of cones at angle of attack. 05 p0530 A73-16886
- Closed form solutions for dust density and temperature distributions in shock layer of hypersonic wedge flow 05 p0533 A73-17115
- On the solution of the Navier-Stokes equations for a spherically symmetric expanding flow. 06 p0684 A73-17707
- Radiant heat flux distribution on the surface of a sphere in hypersonic flow of an inviscid radiating gas 10 p1171 A73-23581
- Electron temperature profile in stagnation region flow of blunt bodies with consideration of ionization recombination in shock layer 10 p1296 A73-24256
- Numerical computation for entropy layer on blunt nosed cone in terms of shock layer fraction for given free stream and Mach number 11 p1299 A73-25113
- Asymptotic solution of shock-layer equations in the vicinity of the stagnation point of a sphere in the case of strong blowing 11 p1304 A73-26442
- The thin shock layer in the hypersonic flow problem 15 p1821 A73-31194
- Flows past thin blunt bodies with shock layer separation 15 p1822 A73-31291
- An improved separability approximation for line radiative transport in nonhomogeneous media. 15 p1959 A73-32391
- Hypersonic merged stagnation shock layers. 18 p2260 A73-36197
- [AIAA PAPER 73-639] Engineering approximations for radiating nonequilibrium shock layers. 18 p2297 A73-36224
- [AIAA PAPER 73-673] Ablation and radiation coupled viscous hypersonic shock layers. 18 p2264 A73-36315
- Planetary atmospheric entry vehicles shock layer energy transport with nongray radiation, using optical thick-thin approximation for radiative transfer in temperature distribution calculation 18 p2369 A73-36334
- [AIAA PAPER 73-715] Composition of the earth's atmosphere by shock-layer radiometry during the PAET entry probe experiment. 18 p2313 A73-36797
- Nonequilibrium effects on shock-layer radiometry during earth entry. 18 p2338 A73-36798
- Certain patterns of heat transfer in a hypersonic shock layer in the presence of mass entrainment 18 p2266 A73-37014
- Measurements of hydrogen-helium radiation at shock-layer temperatures appropriate for Jupiter entry. 22 p2938 A73-42993
- Flows past exponential bodies in the presence of strong compression in the shock layer 24 p3055 A73-45534

SHOCK LOADS

NT BLAST LOADS

Electro-optical fiducial system for shock wave interferometry relating impact time to free surface motion 05 p0580 A73-17261

Electron microscopy of some experimentally shocked counterparts of lunar minerals. 07 p0885 A73-19750

Methods and application of system identification in shock and vibration. 07 p0916 A73-20429

Shock and vibration disturbance identification based on structural system response, discussing linear programming, curve fitting, constraints, objective functions and applications 07 p0916 A73-20430

Dynamic yield, compressional, and elastic parameters for several lightweight intermetallic compounds. 09 p1099 A73-21926

Dielectric breakdown of shock-loaded PZT 65/35. 09 p1132 A73-21927

Brittle fracture tests of Ti-Cr steels with/without nitrogen hardened layer under shock impact loads 09 p1107 A73-23199

Procedure for recording stresses by dielectric sensors in the case of impulsive loads 10 p1219 A73-23367

Shock induced phase change in single crystal orthoclase at 115 kb, noting high pressure phase with hollandite-structure properties 11 p1352 A73-25586

Stony-iron meteorite shock histories, determining crystallographic character of kamacite in samples via back reflection X ray diffraction technique 11 p1419 A73-25780

Influence of impact deformation on the strengthening and aging kinetics of austenitic steel 4Kh12N8G8MFB 12 p1510 A73-26901

Forced vibration solution and wind tunnel investigation of shallow cylindrical shells under moving pulsating pressure discontinuities, noting compression shock effects 13 p1703 A73-29602

Deformation and transformation of rock-forming minerals by natural and experimental shock processes. I - Behavior of minerals under shock compression. 14 p1750 A73-30958

Computerized stress analysis of shock load induced circular elastic membrane interaction with fluid stream via method of characteristics related to aerodynamic decelerator design 15 p1948 A73-31429

Phase and structural changes in titanium under impulsive loads 15 p1894 A73-32523

Vibration and shock stresses in the case of ballistic rockets. II - Measurement, evaluation, simulation 16 p2072 A73-33388

Vibration and shock stresses in the case of ballistic rockets. III - Evaluation of the results and comparison with the specifications available 16 p2073 A73-33389

Reaction of a cylindrical shell to periodic shock waves propagating in its interior 17 p2243 A73-34735

Shock unloading phenomena in fiber-reinforced composites. 17 p2247 A73-34916

Dynamic mechanical loading of solid material resulting in stress levels with impulse process described by fluid flow equations with application to shock compression of mechanical mixtures 17 p2193 A73-35541

Shock and compression by TEA-CO₂-laser pulses drastically enhanced by liquid layers spread on surfaces of solids. 19 p2438 A73-38024

Optimal control of stochastic systems with random shocks and discontinuous trajectories, using functional minimization 20 p2582 A73-39388

Dynamic fracture criteria for a polycarbonate. 21 p2723 A73-40956

Effect of explosive impact on hardening and kinetics of aging of austenitic steel 4Kh12N8G8MFB. 21 p2720 A73-41034

Quartz transformation to stishovite in shock loaded quartz-copper mixture, discussing relationship to short range order phase 22 p2848 A73-42497

Method of determining the susceptibility of metals to brittle fracture under shock loads 23 p2965 A73-43470

Transformation of meteorite material in experiments on explosively produced shock compression at pressures of 500 and 1000 kbar 24 p3137 A73-44710

Thin plate in two dimensional supersonic flow, deriving vibration amplitude response to shock pressure load by numerical analysis with Laplace transform 24 p3055 A73-45432

SHOCK MEASURING INSTRUMENTS

Laser interferometer for measuring high velocities of any reflecting surface. 02 p0171 A73-12818

Piezoelectric transducers for the study of short-duration mechanical loads 04 p0448 A73-15374

Load amplifiers for vibration and shock measurements 07 p0808 A73-19009

Measurements of the structure of an ionizing shock wave in a hydrogen-helium mixture. 07 p0813 A73-20475

Instrument Society of America, Annual Conference, 27th, New York, N.Y., October 9-12, 1972, Proceedings, Part 2. 09 p1082 A73-22501

Q switched ruby laser optical diagnostic system for plasma shock waves and plasmoid observation, noting schlieren photographs of exploding wire experiments 14 p1782 A73-30925

Method of observing processes in the interior of explosives 21 p2695 A73-39966

SHOCK RESISTANCE

NT IMPACT RESISTANCE

Analysis of the resistance of reed contacts to shock and vibration impacts 05 p0559 A73-17237

Sheet, tecto-, ortho- and chain silicates crystal lattice breakdown under shock from ballistic range experiments, using Debye-Scherrer method for X ray diffraction studies 10 p1277 A73-24078

Coating development of Martin Marietta's reusable surface insulation /MAR-SI/ for Space Shuttle applications. 16 p2071 A73-33059

Improvement of thermal shock resistance by surface prestressing. 22 p2921 A73-42462

SHOCK SENSITIVITY

U SHOCK RESISTANCE

SHOCK SIMULATORS

Calibration of Sandia Laboratories' 19-foot diameter explosively driven blast simulator. 16 p1994 A73-33136

Vibration test techniques used to simulate transients and match shock spectra. 20 p2544 A73-39268

SHOCK SPECTRA

Spectral shift between components of homogeneous /radiation or shock/ line, using ring laser spatial and frequency burnout effects 10 p1228 A73-24464

Structural shock response spectrum analysis for maximum dynamic loads and damage potential determination 16 p2014 A73-33135

The use and evaluation of shock spectra in the dynamic analysis of structures. 17 p2248 A73-35041

[ASME PAPER 73-APM-22] Spectral shift between components of homogeneous /radiation or shock/ line, using ring laser spatial and frequency burnout effects 19 p2438 A73-38136

Vibration test techniques used to simulate transients and match shock spectra. 20 p2544 A73-39268

Shock spectrum analysis and structural design. 20 p2617 A73-39270

SHOCK TESTS

Vibration and shock qualification testing of an airborne early warning radar. 16 p1987 A73-33137

Multihundred watt radioisotope thermoelectric generator full scale thermal performance, vibration, shock, acoustic, acceleration and magnetic field tests 19 p2456 A73-38421

Quartz transformation to stishovite in shock loaded quartz-copper mixture, discussing relationship to short range order phase 22 p2848 A73-42497

SHOCK TUBES

NT MAGNETIC ANNULAR SHOCK TUBES

NT SHOCK TUNNELS

Compressible boundary layer formation on shock tube walls after bursting of diaphragm separating gases at different pressures 03 p0293 A73-13527

A phenomenological study of the steady-state current sheet speed in a magnetically driven shock tube. 03 p0288 A73-13809

Experiments on shell stability in air-driven shock tubes. 03 p0288 A73-13836

Shock-tube study of vibrational energy transfers in the CO₂-N₂ and the CO₂-CO systems. 03 p0345 A73-14442

Shadowgraph photography for electromagnetic excitation of shock waves in normal pressure gas, noting plasma and shock compressed regions in shock tube 04 p0434 A73-15618

Appraisal of UTIAS implosion-driven hypervelocity launchers and shock tubes. 05 p0562 A73-16180 [AD-753252]

Experimental studies of a Ludwig tube high Reynolds number transonic tunnel. [AIAA PAPER 73-212] 06 p0645 A73-17661

Amplification factor of light in a CO₂ + N₂ + He mixture expanding in a supersonic jet. 06 p0723 A73-17964

Temperature dependence of diatomic gases thermal conductivity coefficient from shock tube tests, noting molecular gases above dissociation temperature. 06 p0687 A73-18561

Use of oblique shock waves in high-temperature shock-tube studies. 06 p0683 A73-18793

Dissociative recombination at elevated temperatures. III - O₂+/- dominated afterglows. 07 p0852 A73-19148

Cone shaped arc discharge driver chamber for high energy shock tube, presenting performance characteristics test data. 07 p0808 A73-19969

Gas-phase ignition model for some solid fuels in a shock tube. 07 p0865 A73-19989

Study of the ignition reaction in an oxygen-hydrogen mixture at relatively high pressures and low temperatures in the shock tube. 07 p0920 A73-19993

Gas dynamic characteristics of the helium two stage shock tube for MHD power generation experiments. 07 p0808 A73-20117

Slow combustion of n-pentane in single pulse chemical shock tube, discussing yields of oxygenated products. 07 p0788 A73-20356

Compression wave interaction induced shock wave formation in shock tube, studying unsteady gas flow near opening diaphragm. 08 p0955 A73-21520

Parallel plate electromagnetic shock tube, investigating drive current, gas pressure and electrode material effects on electrode ablation and current sheet velocity. 08 p0953 A73-21632

Optimal use of double pin ionization gauges for shock wave detection. 09 p1080 A73-22106

Dense air plasma compression and heating by TNT explosive charge, noting shock tube flow patterns. 10 p1203 A73-23515

Shadowgraph photography for electromagnetic excitation of shock waves in normal pressure gas, noting plasma and shock compressed regions in shock tube. 10 p1205 A73-24208

Shock tubes with cryogenically cooled test section for experimental investigation of pressure and temperature pulse effects on cryogenic materials. 10 p1203 A73-24267

Time decay of weak shock waves in shock tubes based on energy rate of change balance with energy dissipation at walls and at shock front. 10 p1206 A73-24389

Microwave cavity measurements of electron densities in a shock tube. 10 p1220 A73-24620

On some aspects of unsteady boundary layers induced by shock waves. 10 p1209 A73-24832

Nonlinear problem of a shock-tube interaction-region boundary layer. 11 p1348 A73-26391

Experiments on the non-linear dynamic response of shells under blast waves. 11 p1446 A73-26492

Shock attenuation in a shock tube due to boundary layer. 12 p1486 A73-27174

Investigation of high-temperature gas flow around axisymmetric bodies in the presence of several discontinuity surfaces. 13 p1708 A73-29404

MHD acceleration in the unsteady expansion of a shock tube driver. 15 p1917 A73-31376

The shock wind tunnel of the Institute of Aerodynamics and Gasdynamics of Stuttgart University. 15 p1858 A73-32042

Calibration of Sandia Laboratories' 19-foot diameter explosively driven blast simulator. 16 p1994 A73-33136

Shock-tube measurements of soot oxidation rates. 16 p2085 A73-33344

The pressure-shock simulation of the Ernst-Mach-Institute in the test location Wintersweiler. 16 p1998 A73-33395

Temperature dependence of diatomic gases thermal conductivity coefficient from shock tube tests, noting molecular gases above dissociation temperature. 16 p2086 A73-33586

Spectrophotometric determination of the rate of dissociation of nitrogen trifluoride behind shock waves. 16 p1977 A73-34017

Dissociation of carbon dioxide behind reflected shock waves. 17 p2119 A73-35173

Dense air plasma compression and heating by TNT explosive charge, noting shock tube flow patterns. 17 p2147 A73-35195

Book - Experimental methods of hypersonics. 17 p2097 A73-35338

Shock tube study of the effect of unsymmetric dimethyl hydrazine on the ignition characteristics of hydrogen-air mixtures. 18 p2372 A73-37098

High enthalpy supersonic ionized gas flow in shock tube experiment, investigating pinch effect on flow acceleration and setup performance. 19 p2415 A73-37168

Plasma accelerators in gas dynamics, discussing ion propulsion systems, high velocity wind tunnels with electric arc heating and electromagnetic shock tubes. 19 p2466 A73-37354

A shock tube study on condensation kinetics. 21 p2792 A73-41143

Design of a piston-driven shock tube. 21 p2675 A73-41552

Shock tube kinetics of NO decomposition in mixtures with Ar, measuring ground state atomic oxygen formation rate by resonance absorption spectrophotometry. 22 p2818 A73-42766

Study of the processes in a gasdynamic laser in a large-diameter shock tube. 24 p3095 A73-44701

Total shock-tube working time in the investigation of the discharge through holes in the end face. 24 p3076 A73-44755

Opening time of brittle shock-tube diaphragms for dense fluids. 24 p3075 A73-44820

SHOCK TUNNELS

Numerical study of the interaction of a shock-wave caused, supersonic, ionized-argon flow with electric and magnetic fields, using the method of characteristics. 15 p1918 A73-31571

SHOCK WAVE ATTENUATION

Time decay of weak shock waves in shock tubes based on energy rate of change balance with energy dissipation at walls and at shock front. 10 p1206 A73-24389

Shock attenuation in a shock tube due to boundary layer. 12 p1486 A73-27174

Oblique shock wave generation and quenching in curved supersonic diffusers at Mach 1.6, noting dependence on boundary layer properties. 13 p1566 A73-29021

Shock wave large particle model of ion density discontinuity decay in nonisothermal plasma, assuming high electron temperature and Boltzmann distribution. 13 p1667 A73-29171

Test gas properties behind a decelerating shock wave in a shock tube. 16 p2000 A73-33319

Shock attenuation dependence on gas specific heat ratio and wall divergence angle and area ratio of expansion section attached to shock tube. 23 p2969 A73-43930

SHOCK WAVE CONTROL

Supercritical shock free transonic profiles for transport aircraft wings of large and medium aspect ratio, discussing straight and yawed wing tests [DGLR PAPER 72-130] 03 p0248 A73-14383

SHOCK WAVE GENERATORS

NT MAGNETIC ANNULAR SHOCK TUBES

NT SHOCK TUBES

NT SHOCK TUNNELS

Shock wave generation for industrial applications in graphite to diamond conversion and incompatible materials bonding. 07 p0850 A73-19048

A magnetic thyristor pulse generator with shock-wave generation in the transmission line. 08 p0949 A73-21712

X ray background emission and behavior of infalling intergalactic gas into Galaxy resulting from shock wave generation and heating in accretion process. 10 p1264 A73-23495

Procedure for recording stresses by dielectric sensors in the case of impulsive loads. 10 p1219 A73-24367

Plasma research in space and in the laboratory. 12 p1526 A73-26849

Cauchy problem solution for motion of piston generating shock wave after fast impact under influence of one dimensional gas flow. 15 p1822 A73-31289

The pressure-shock simulation of the Ernst-Mach-Institute in the test location Wintersweiler. 16 p1998 A73-33395

Gravitational and electromagnetic shock waves. 17 p2212 A73-35048

Shock wave generation by moving distributed non-diffusive force, solving initial value problem for single fluid model to obtain supersonic force field velocity. 18 p2299 A73-36323

High temperature relativistic plasmas, calculating post-shock properties for steady hydromagnetic shock wave production. 19 p2464 A73-37156

Streaming plasma interaction with variable longitudinal magnetic fields. 19 p2465 A73-37171

SHOCK WAVE INTERACTION

Reflexion and diffraction of shocks interacted by yawed wedges. 01 p0002 A73-10272

Shear layer extent caused by slip surface in inviscid flow with shock interactions, noting viscous effect in hypersonic flow. 01 p0033 A73-10747

Oblique shock wave interaction with approach boundary layer at combustor entrance in supersonic scramjet engines, observing wall pressure distribution [AIAA PAPER 72-1181] 03 p0357 A73-13476

Polar streamline directions at the triple point of Mach interaction of shock waves. 03 p0244 A73-13566

Resonant coupling of ocean Rayleigh waves to atmospheric shock waves from Apollo rockets. [AD-755609] 05 p0569 A73-16380

Turbulence measurements in a compressible boundary layer subjected to a shock-wave-induced adverse pressure gradient. 05 p0566 A73-16912

Unsteady flow generated by shock-turbulent boundary layer interactions. [AIAA PAPER 73-168] 05 p0566 A73-16913

Initial conditions for the hypersonic shock/boundary layer interaction problem. 05 p0532 A73-16935

Shock wave-turbulent boundary layer interactions in rectangular channels. II - The influence of sidewall boundary layers on incipient separation and scale of the interaction. [AIAA PAPER 73-234] 05 p0566 A73-16959

Shock impingement caused by boundary layer separation ahead of blunt fins. [AIAA PAPER 73-236] 05 p0532 A73-16961

Shockwave-boundary layer interference heating analysis. [AIAA PAPER 73-237] 05 p0532 A73-16962

Aerothermodynamic aspects of shock-interference patterns for shuttle configurations during entry. [AIAA PAPER 73-238] 05 p0532 A73-16963

Shock wave-boundary layer interactions in laminar transonic flow. [AIAA PAPER 73-239] 05 p0532 A73-16964

Weak normal shock wave interactions with materials, investigating incident pressure ratio, thickness, perforation diameter, close area and flow resistance effects on acoustic reflectance [AIAA PAPER 73-244] 05 p0598 A73-16968

Shock tube investigation of bromine dissociation rates in the presence of carbon dioxide. 06 p0661 A73-18123

One-dimensional electrodynamic flow with shock waves in the case of a small parameter of the electrohydraulic interaction. 06 p0733 A73-18883

A new integral-variational method for calculation of relaxation regions behind shock and detonation waves. 07 p0809 A73-19050

The effect of higher alkanes on the ignition of methane-oxygen-argon mixtures in shock waves. [AD-756982] 07 p0918 A73-19389

Characteristics of the unsteady shock-induced laminar boundary layer on a flat plate. 07 p0810 A73-19505

Atomic oxygen formation times obtained from measurements of electron density profiles behind shock waves in air. 07 p0853 A73-19510

Atomization of cryogenic liquid droplets by shock waves. 07 p0811 A73-19656

Oblique shock-sound interaction at a freestream Mach number of about 20 in helium. 07 p0775 A73-19984

MHD shock wave decay in oblique magnetic field, considering shock and rarefaction waves interaction. 07 p0858 A73-20071

German monograph - Unsteady processes of the interaction between shock-produced plasma flows and magnetic fields - A theoretical investigation. 07 p0859 A73-20384

Reflection from the earth's surface of shock waves generated by falling meteorites. 08 p0958 A73-21065

Shock waves and flares by meteors. 08 p1010 A73-21317

Proton scattering in the region near the earth's bow shock. 09 p1137 A73-22054

Shock wave compression of iron-silicate garnet. 09 p1076 A73-22146

Solar plasma electron density and temperature measurement by Mars 2 and Mars 3 orbiter-borne retarding potential analyzers, considering solar wind shock front interaction role. 09 p1126 A73-22263

Ion velocity temperature observation at Mars surface boundary, suggesting solar plasma interaction with outer atmosphere from ion flux disturbance ahead of shock wave

09 p1126 A73-22264

Intrinsic coordinate method of characteristics application to supersonic steady two dimensional nonisentropic inviscid flow, noting shock wave interaction [ONERA, TP NO. 1186]

09 p1072 A73-22714

Simultaneous diffusion of photons and particles in a semiinfinite space. II - Concentration of excited atoms before a shock wavefront

09 p1123 A73-23069

Allowance for diffraction occurring in the interaction between a weak shock wave and a plate

10 p1206 A73-24488

On some aspects of unsteady boundary layers induced by shock waves.

10 p1209 A73-24832

Aeroelastic dynamic response to shock induced flow separation, analyzing wing buffet components at high Mach number subsonic flow [AIAA PAPER 73-308]

11 p1300 A73-25539

A simple model of normal shock wave and turbulent boundary-layer interaction.

11 p1347 A73-25710

Shock wave determination of shear velocity at high pressures for understanding of planetary interior behavior with abrupt change in density from seismic interpretation

11 p1355 A73-25898

Initial conditions for the hypersonic-shock/boundary-layer interaction problem.

11 p1303 A73-26384

Approximate calculation of flow parameters during interaction of supersonic jets

11 p1304 A73-26443

The task of constructing transition functions in problems involving interaction of weak shock waves with cylindrical and spherical surfaces

12 p1486 A73-27241

Condensation of cesium from an incident shock wave in cesium vapors

12 p1528 A73-27323

Type IV bursts on August 4 and 7, 1972

12 p1535 A73-27784

Generation of acoustic waves during the passage of a shock wave through a heated gaseous element.

13 p1705 A73-28494

An approximate method for calculating the interaction between shock wave and turbulent boundary layer.

13 p1602 A73-29018

Breakdown of a drop of cryogenic liquid by shock waves.

14 p1745 A73-30322

Unsteady shock wave interaction with plane hypersonic flow about a blunt body investigated by second order difference method

15 p1862 A73-31326

One-dimensional electro-gasdynamics flow with shock waves and a small electrohydraulic interaction parameter.

15 p1921 A73-32408

Study of the similarity solution in three dimensional compressible laminar boundary layer.

17 p2157 A73-35862

Flow field measurements in an asymmetric axial corner at $M = 12.5$.

18 p2297 A73-36227

Interference heating due to shock wave impingement on laminar boundary layers.

18 p2368 A73-36229

Reynolds number effects on the shock wave - Turbulent boundary layer interaction at transonic speeds. [AIAA PAPER 73-661]

18 p2298 A73-36262

Reflection of meteorite generated shock waves from the earth's surface.

18 p2313 A73-36866

Interaction of a strong shock wave with electromagnetic field.

19 p2464 A73-37157

Theoretical and experimental research on the electromagnetic acceleration of shock-induced flow in argon.

19 p2419 A73-37174

Structural formations in the interplanetary medium

19 p2481 A73-37342

Working of titanium by high energy due to detonation of an explosive charge

19 p2433 A73-37836

Characteristic overpressure of a supersonic transport of given length in a homogeneous atmosphere.

19 p2377 A73-38006

Some transient MHD-flows with finite magnetic Reynolds numbers.

19 p2470 A73-38319

On the interaction of shocks and simple waves of the same family. II.

20 p2545 A73-39011

Recording of diffraction patterns by X-ray pulses of materials subjected to a shock wave compression

21 p2695 A73-39967

Improvement to Klineberg's method for the calculation of viscous-inviscid interactions in supersonic flow.

21 p2632 A73-40429

Plume boundary jump of an underexpanded jet exhausting counter to a freestream.

21 p2790 A73-40433

Cosmic ray intensity variation observation during August 2-8, 1972, suggesting complex interactions with interplanetary shock waves and magnetic field and magnetosphere

21 p2757 A73-40590

A kinetic description of the interaction between cosmic rays and shock waves

21 p2758 A73-40596

Interaction of a shock wave with blunt bodies in supersonic flow

21 p2633 A73-41222

Noise caused by supersonic jet shock waves as function of jet pressure ratio, determining spectral characteristics

22 p2795 A73-41702

Reflection of a shock wave from a thermally accommodating wall - Molecular simulation.

22 p2842 A73-42234

Diffraction and reflection of shocks from corners.

22 p2843 A73-42567

Elementary reaction rates from post-induction-period profiles in shock-initiated combustion.

22 p2933 A73-42755

High-temperature oxidation of hydrogen by nitrous oxide in shock waves.

22 p2933 A73-42756

Influence of aerodynamic field on shock-induced combustion of hydrogen and ethylene in supersonic flow.

22 p2934 A73-42786

Fuel tank wall response to hydraulic ram during the shock phase.

22 p2843 A73-43114

Density and velocity fluctuations in young nebulas of Orion type

23 p3035 A73-44232

Free surface profile of wedge-shaped cavity in metal during collapse due to incident shock wave with decreasing pressure behind shock front

24 p3093 A73-44711

Similarity of flows arising during reflection of weak shock waves from a rigid wall and from a free surface

24 p3076 A73-44713

Solid fuels combustion stability and shock wave induced detonations propagation stability in aerosols investigation based on one dimensional turbulence, using multistage mathematical models

24 p3157 A73-45383

Analysis of the self-ignition of fuel droplets behind a reflected shock wave

24 p3121 A73-45390

Optimization of compression constants for cumulated plane shock waves in a closed tube.

24 p3117 A73-45428

SHOCK WAVE LUMINESCENCE

Nature of the emission of UV Ceti-type stars

01 p0100 A73-10708

A shock tube determination of the CN ground state dissociation energy and the CN violet electronic transition moment.

08 p0989 A73-20789

SHOCK WAVE PROFILES

Corner pressures and fillet shock locations for symmetrical corners by an approximate method.

07 p0774 A73-19494

Band position predictions in schlieren visualization of hypersonic entropy wake behind blunt bodies, assuming bow shock geometry

07 p0775 A73-19970

Measurements of the structure of an ionizing shock wave in a hydrogen-helium mixture.

07 p0813 A73-20475

Diagram of the shock wave processes in the unsteady interaction between a jet and an obstacle

08 p0927 A73-21607

The structure of the shock wave in the vicinity of the shock tube sidewall.

10 p1209 A73-24824

Nonequilibrium radiative and inelastic collisional transitions structuring of ionizing shock waves in He and Ar

11 p1449 A73-25253

Collisional transverse MHD shock wave structure within magnetic field inducing anisotropic plasma transport properties, using singular perturbation approach

11 p1403 A73-25254

On the origin of oscillations appearing in shock profiles calculated by difference methods

11 p1390 A73-25868

The configuration of interplanetary shock waves produced by strong chromospheric flares /according to space sonde measurements/

12 p1536 A73-27859

Earth nonuniform bow shock oblique structure and pulsation, obtaining statistical occurrences from three dimensional distribution of interplanetary field directions for solar wind sector

14 p1749 A73-29983

Vibrational relaxation effects in weak shock waves in air and the structure of sonic bangs.

14 p1711 A73-30171

Shock waves, jump relations, and structure.

15 p1864 A73-31939

Time dependent one dimensional Navier-Stokes differential equations solved via difference scheme determining reflected shock wave structure and wall pressure

16 p1999 A73-33229

Hydrodynamic equilibrium structure of plane shock waves in arbitrary liquid or gas at large distance behind shock front

16 p2001 A73-34039

Shock wave structure in elastoplastic media

17 p2211 A73-34144

Shock wave pattern visualization and static pressure distribution in supersonic diffusers for mixed flow supersonic compressors, using closed Freon loop test rig [ASME PAPER 73-FE-35]

17 p2095 A73-35021

Solar wind interaction with the earth's magnetic field. III - On the earth's bow shock structure.

18 p2346 A73-36272

Dielectric impulse pressure recorders consisting of organic glass, cellulose-ether film and muscovite mica: investigating shock wave profiles and electrode voltage amplitude

18 p2317 A73-36768

Structure of almost collisionless shocks in a magnetoplasma and the ion-acoustic instability.

19 p2464 A73-37155

Shock waves within the two fluid model in the presence of the magnetic field.

19 p2464 A73-37160

On steady wave profiles in solids.

19 p2461 A73-38262

Effects of dispersion on steady state electromagnetic shock profiles.

20 p2595 A73-38864

Structural determination of electric field conditions in ionizing shock waves.

20 p2596 A73-38964

Boltzmann equation with Gross-Krook type model: for investigation of steady plane shock wave structure in fully ionized gas

20 p2596 A73-38968

Configuration of interplanetary shock waves from powerful chromospheric flares /from space probe measurements/.

20 p2602 A73-39233

Shock wave structure in liquid/gas bubble medium from theoretical two-phase model and experimental piezoelectric pressure profile measurements

20 p2547 A73-39283

Stability of waves and shock structure in generalised thermoelasticity at low temperatures.

20 p2624 A73-39564

Shock wave structure analysis via averaging over nonsinusoidal functions, discussing shock front length in cubic nonlinear medium, adiabatic invariants and harmonic functions

21 p2749 A73-41518

Structure of ionizing shock waves with radiative energy loss.

22 p2841 A73-42200

Methods for calculating nonlinear flows with attached shock waves over conical wings.

22 p2796 A73-42562

Finite difference and truncation method comparison for supersonic conical flow equations solution, obtaining flow field and shock wave shape

22 p2796 A73-42574

Correlation of hypersonic zero-lift drag data.

22 p2797 A73-42635

Collisionless shock wave propagation parallel to magnetic field for large plasma/magnetic pressure ratio, discussing shock structure in developing turbulence

22 p2851 A73-42932

Nonlinear gas vibrations maintained in a closed tube by a heat source

23 p2968 A73-43719

Numerical study of the problem of explosion of a cylindrical charge of finite length

24 p3076 A73-44654

Hypersonic flow about a spatial body with an attached shock wave

24 p3054 A73-45172

On the choice of second-order difference schemes furnishing shock profiles without oscillation

24 p3110 A73-45217

MHD partial differential equations solution via hyperbolic system indicating shock wave structure existence satisfying Rankine-Hugoniot relation and entropy condition

24 p3116 A73-45222

Kinetic models and the problem of shock-wave structure

24 p3081 A73-45537

SHOCK WAVE PROPAGATION

Incidence of a plane electromagnetic wave on a moving shock wave in an ionized gas
01 p0016 A73-10205

Slightly oblique shock waves in a collisionless magnetized plasma.
01 p0082 A73-10421

Shock waves existence and behavior in elastic non-conductors, investigating Hugoniot stress-strain curve properties
01 p0033 A73-10778

Remarks on the paper by J. M. Nicholls and B. F. James, 'The location of the ground focus line produced by a transonically accelerating aircraft.'
01 p0005 A73-10786

MHD detonation waves properties and propagation velocities within relativistic theory, discussing shock equations nontrivial solution existence and uniqueness
01 p0085 A73-11260

Propagation through the solar corona of the shock waves responsible for type II radio bursts.
01 p0093 A73-11314

Self-similar flows with increasing energy. II - Isothermal flow.
02 p0238 A73-12091

The propagation of non-uniform slow shock waves.
02 p0198 A73-12092

The scattering characteristics of a sonic boom at the passage through a turbulent layer
03 p0290 A73-12967

Stress shock waves effect on polycrystalline metals grain structure, discussing strain rate critical value zones
03 p0386 A73-13147

Initially uniform gas expansion into ambient atmosphere and subsequent flow into perfect vacuum, noting infinite-strength shock separation from gas-vacuum interface
03 p0294 A73-13532

Equations of motion in electrohydrodynamics of multiphase one dimensional flow, noting shock wave propagation and attenuation
03 p0346 A73-13611

The thickness of perpendicular collisionless shocks in a hot plasma.
04 p0479 A73-15191

Theoretical structure and spectrum of a shock wave in the interstellar medium - The Cygnus Loop.
04 p0499 A73-15359

A closed-form solution of the propagation problem of an unloading shock wave in a bilinear elastic body.
04 p0513 A73-15595

Solution of some boundary-value problems in the theory of potential flows of a gas and the propagation of weak shock waves.
05 p0565 A73-16790

Gudunov-method computation of the flow field associated with a sonic-boom focus.
[AIAA PAPER 73-240] 05 p0536 A73-16965

Numerical simulation of high Mach number supercritical magnetosonic collisionless shock wave propagation perpendicular to magnetic field, considering cause of anomalous ion heating
05 p0604 A73-17365

Distortion of near-sonic shocks by layers with weak thermal fluctuations.
05 p0537 A73-17374

Study of the adiabatic curve of an ionizing shock wave in an inclined magnetic field
06 p0727 A73-17460

Speed of propagation of shock waves responsible for geomagnetic storms and Forbush decreases
06 p0689 A73-17548

An investigation of shock strengthening in a conical convergent channel.
06 p0684 A73-17706

Experiments of magnetohydrodynamic conversion with ionization out of equilibrium
06 p0730 A73-18541

Method of solution of certain boundary value problems for nonlinear hyperbolic equations and propagation of weak shock waves
07 p0809 A73-19015

Similarity solution for equations of nonplanar relativistic flow from point energy source, applying to spherical shock propagation and cosmic ray generation
07 p0810 A73-19506

Initial free-surface motion of an impulsively loaded half-space.
07 p0810 A73-19509

Investigation of the burnup process structure under spin conditions
07 p0923 A73-20424

Instability of shock waves in inhomogeneous gases.
07 p0812 A73-20445

The structure of a weak shock wave in a gas/liquid medium
08 p0954 A73-21129

Statistical phenomena during shock wave formation
08 p0955 A73-21447

Penetration of a solid into a half-space of compressible liquid in the presence of a magnetic field
08 p0994 A73-21724

Small perturbations analysis of hydrodynamic relations of shock front propagation in inhomogeneous medium
09 p1070 A73-21888

Self-similar cylindrical magnetogasdynamic and ionizing shock waves.
10 p1204 A73-23564

Forbush decreases and their relation to solar activity and the parameters of the interplanetary medium
10 p1267 A73-23921

Low energy solar proton events intensity increase near time of magnetic storm sudden commencement and Forbush decrease, using propagation shock wave model
10 p1268 A73-24146

Determination of the velocity of shock waves in the interplanetary medium.
10 p1279 A73-24236

The structure of the shock wave in the vicinity of the shock tube sidewall.
10 p1209 A73-24824

Quasi-linear partial differential equations of non-linear pulse shock wave propagation in two- and three-dimensional steady transonic gas flow near critical point
11 p1302 A73-25854

Shock wave formation in an elastic half-space during one-dimensional nonlinear transient wave processes generated by a continuous force
11 p1445 A73-26456

Molecule formation. I - In normal H I clouds. II - In interstellar shock waves.
12 p1547 A73-27973

Instability of hydromagnetic perpendicular shocks in inhomogeneous fluids.
13 p1601 A73-28775

Shock wave produced in a solid by means of supersonic thermal sources.
13 p1700 A73-29390

Plasma radiation from collisionless MHD shock waves and the high-frequency waves in the upstream solar wind.
14 p1786 A73-29978

Shock wave propagation in atmospheres with spatially inhomogeneous density and temperature fields, using ideal polytropic gas model
14 p1750 A73-30654

Ion Mach number of ion shock embedded in collisional shock wave propagating in electron proton gas plasma
14 p1777 A73-30660

An accurate method for solving some theoretical problems of spatial supersonic gas flows
14 p1712 A73-30826

Transition of a shock wave into a sound wave.
15 p1912 A73-31010

Statistical effects in the generation of shock waves.
15 p1860 A73-31011

Observation of stable, high Mach number collisionless electrostatic shocks.
15 p1916 A73-31079

Interacting continuum theory concerning steady shock wave in composite materials, discussing energy interaction terms error correction effects on Hugoniot relations
15 p1949 A73-31685

Automatic measurement of intervals of shock wave transit across a base section
15 p1876 A73-31862

Perturbation solution for shock waves in a dissipative lattice.
15 p1913 A73-31937

Structure of a weak shock wave in a gas-liquid medium.
15 p1864 A73-32064

Propagation velocity of shock waves causing geomagnetic storms and Forbush decreases.
16 p2002 A73-32772

On the possibility of turbulent thickening of weak shock waves.
16 p1967 A73-32794

Pulsed interferometric holography of laser-produced air breakdown.
16 p2014 A73-33175

One dimensional shock waves in heat conducting materials with memory. III - Evolutionary behaviour.
16 p2081 A73-33747

Small perturbations analysis of hydrodynamic relations of shock front propagation in inhomogeneous medium
17 p2150 A73-34311

Acceleration wave propagation in a nonlinear viscoelastic solid.
[ASME PAPER 73-APM-2] 17 p2247 A73-35028

Close connexion between flare-generated coronal and interplanetary shock waves.
17 p2232 A73-35147

Solution by characteristics at fixed time interval of the equations of one dimensional unsteady flow.
18 p2300 A73-36608

Supersonic boom structure studies, discussing shock wave propagation during flight trajectory and amplification due to overpressure wave focusing
18 p2268 A73-36907

SHOCK WAVE PROFILES

A density scale for the interplanetary medium from observations of a type II solar radio burst out to 1 astronomical unit.
18 p2348 A73-37113

Cold collisionless plasma flow along magnetic field, deriving quasi-shock wave characteristics from Vlasov-Maxwell equations
19 p2463 A73-37152

Recent developments in strong shock wave research.
19 p2415 A73-37155

Experiments of shock waves in a fully ionized plasma flow.
19 p2464 A73-37159

Interplanetary shock waves and cosmic rays.
19 p2476 A73-37759

Propagation of mechanical waves in the solar atmosphere
20 p2606 A73-39078

Unsteady shock waves in a rarefied plasma
20 p2597 A73-39277

High-speed photographic observation of the propagation of a shockwave in a branched-tunnel system
21 p2676 A73-39983

High-speed camera study of the shock wave propagation.
21 p2697 A73-39993

Self-similar flows behind shock waves in a gravitational field
21 p2676 A73-40190

Streamline curvature and velocity gradient behind curved shocks.
21 p2632 A73-40441

Investigation of shock waves responsible for Forbush decreases
21 p2757 A73-40595

Self-similar flows with increasing energy. III - Radiation-driven shock wave.
21 p2793 A73-41673

German monograph - Model of a parallel shock wave with turbulent dissipation in a hot plasma.
22 p2895 A73-42718

Collisionless shock wave propagation parallel to magnetic field for large plasma/magnetic pressure ratio, discussing shock structure in developing turbulence
22 p2851 A73-42932

Effects of translational disequilibrium on the structure of a shock wave in an ionized monatomic gas
22 p2895 A73-43045

Plane shock wave propagation, reflection and transmission in subsonic flow regime through T-junctions, predicting pressure variation upstream and downstream for comparison with experiment
23 p2967 A73-43295

Precise method for solving certain problems of the theory of three-dimensional supersonic gas flows.
23 p2939 A73-43582

Elastic semispace motion under the action of a shock wave in a magnetic field
23 p3006 A73-43919

Compacting of metallic powders by plane high-explosive charges. I
24 p3092 A73-44414

Investigation of some theoretical point-explosion problems by the difference method
24 p3076 A73-44656

Calculation of a supersonic gas flow about the atmosphere of a spherical body
24 p3053 A73-44658

Damping of a plane shock wave during high-velocity impact
24 p3076 A73-44712

Total shock-tube working time in the investigation of the discharge through holes in the end face
24 p3076 A73-44755

Cold gas noncentral point explosion generated shock wave propagation in interplanetary medium, discussing shock front geometry, earth orbit parameters and gas dynamics
24 p3137 A73-44781

Inlet geometry and axial Mach number effects on fan noise propagation.
[AIAA PAPER 73-1022] 24 p3122 A73-44854

Far field effects of weak spatially periodic inhomogeneities.
[AIAA PAPER 73-1036] 24 p3109 A73-44864

Propagation of shock waves in anisotropic composite plates.
24 p3149 A73-45149

Neutron emission from laser produced plasmas and collisionless electrostatic shock waves.
24 p3116 A73-45242

Recent results in nonlinear viscoelastic wave propagation.
24 p3151 A73-45305

Far-field analysis of nonlinear shock waves in a lattice.
24 p3112 A73-45412

Transformation of shock compression into isentropic compression in a nonhomogeneous body.
24 p3117 A73-45429

SHOCK WAVES

- Shock wave propagation in colliding elastic bars under axial end-on impact, deriving closed form solution for curvilinear stress-strain characteristics
24 p3112 A73-45430
- Book - Solid-state mechanics 3.
24 p3153 A73-45495
- Longitudinal and transverse shock and acceleration waves propagation and decay in anisotropic and isotropic elastic bodies based on theory of singular surfaces
24 p3153 A73-45498
- Determination of the impulses and moments imparted by shock waves to bodies of revolution
24 p3055 A73-45542

SHOCK WAVES

- NT DETONATION WAVES
NT MACH CONES
NT NORMAL SHOCK WAVES
NT OBLIQUE SHOCK WAVES
NT RIEMANN WAVES
NT SONIC BOOMS
- Some numerical experiments with Dafermos's method for nonlinear hyperbolic equations.
01 p0069 A73-10071
- Shock wave reflections along the axis in a steady axisymmetric flow
[ONERA, TP NO. 1128] 01 p0001 A73-10237
- Explosive shock hardening effects on roller steel fatigue strength, surface hardness and wear resistance
01 p0056 A73-10493
- The origin of chains of type I bursts
01 p0092 A73-10938
- A series of evolved shadowgraphs of shock waves induced by secondary injection in a conical supersonic flow.
01 p0003 A73-11128
- Numerical model and computational results for earth bow shock structure, discussing linear dispersion relation for magnetized plasma with counterstreaming ion beams
02 p0155 A73-11728
- Pioneer 6 crossing of earth bow shock on 16 December 1965 reexamined and reinterpreted by magnetic field measurement combination with plasma data
02 p0155 A73-11729
- Russian book on physics of explosive hardening and welding covering high velocity inelastic collisions, shock wave generation, strengthening mechanisms of metals, etc
02 p0173 A73-11892
- Statistical mechanics of the Burgers model of turbulence.
02 p0153 A73-12039
- Experimental study of the luminous front produced by a coaxial plasma accelerator.
02 p0197 A73-12060
- The pressure on flat and anhedral delta wings with attached shock waves.
02 p0128 A73-12501
- Hypersonic and supersonic flow over caret wings at off-design conditions with attached bow shock at leading edges
02 p0128 A73-12502
- Constitutive equation for shock waves under dynamic load in prismatic bar axially prestressed to plastic range
03 p0383 A73-12903
- Shock wave and isentropic compression/expansion in plasma with anomalous thermodynamic properties due to strong particle interactions, discussing phase transitions types
03 p0346 A73-13190
- Numerical model of transient behavior of radiation dominated shock calculated for neutron star core of imploding supernovae
03 p0372 A73-13354
- Determination of the flow past a cylinder and a sphere in the presence of an incident shock wave
03 p0294 A73-13615
- Pressure distribution and shock wave intensity variations in supersonic flow past two plane wings forming dihedral angle
03 p0245 A73-13623
- Acoustic and shock waves interaction in axisymmetric gas flow through variable section channel, calculating flow characteristics variations via isentropic theory of steady flow
03 p0295 A73-13673
- Compression shock formation in arbitrary medium described by first order quasi-linear partial differential equations, considering strongly radiating and emission dominated gases
03 p0400 A73-14629
- Shock waves in spiral arms and star formation.
04 p0496 A73-14970
- One-dimensional shock waves in heat conducting materials with memory. II.
04 p0511 A73-15225
- Shadowgraph photography for electromagnetic excitation of shock waves in normal pressure gas, noting plasma and shock compressed regions in shock tube
04 p0434 A73-15618
- Pyrotechnic shock synthesis using nonstationary broad band noise.
[ASME PAPER 72-WA/APM-19]

- 04 p0516 A73-15897
- Study on ionizing shock waves in argon. I - Precursor phenomena.
04 p0436 A73-15974
- Study on ionizing shock waves in argon. II - Ionization relaxation.
04 p0436 A73-15975
- On the numerical solution of two-dimensional, laminar compressible flows with imbedded shock waves.
05 p0564 A73-16545
- [ASME PAPER 72-FE-7] Experimental relations determining the position of shock waves in a jet impinging against an obstacle perpendicular to the jet axis
05 p0528 A73-16769
- Calculation of shock wave relaxation zones including dissipative transport phenomena.
05 p0567 A73-17114
- Calculation of stagnation-point pressure during shock-wave incidence on a body moving at supersonic velocity
06 p0643 A73-17459
- Evolutionary aspects of shock waves in the Chew, Goldberg, and Low approximation
06 p0727 A73-17471
- Temporal and spatial changes in cosmic ray intensity increases preceding Forbush decreases
06 p0742 A73-17531
- A universal method of calculation of the state of a real gas behind primary and reflected shock waves.
06 p0684 A73-17700
- Visible light flash emission due to strong shock wave of laser spark, investigating strong external magnetic field effect and time variation of luminous intensity
06 p0700 A73-17966
- Applications of shock expansion theory to the flow over non-conical delta wings.
06 p0645 A73-18512
- Pulsed X-ray photography of a shock wave in cesium vapor using two X-ray tubes
06 p0731 A73-18554
- Temperature of an emitting cone in a supersonic flow of transparent gas
06 p0646 A73-18570
- Electrohydrodynamic shock wave evolution in steady gas flow with positive space charge in electric field
06 p0733 A73-18881
- One dimensional steady electrohydrodynamic duct flow with shock waves for continuous and discontinuous electric fields
06 p0733 A73-18882
- Scorpius X-1 representation via old-nova model consisting of standing shock and X ray source formed by mass accretion at white dwarf surface
07 p0874 A73-19063
- German monograph on collective dissipation processes in collisionless shock waves in high ion temperature plasma, using laser beam scattering technique
07 p0837 A73-20387
- Effect of ionization nonequilibrium on the shock wave in the stagnation region
07 p0776 A73-20616
- Population II variable stars shock waves detection via Balmer lines emission and metal line doubling, discussing model for numerical calculations of radiating shock structures
07 p0903 A73-20631
- Effect of diffusion on the growth and decay of acceleration waves in gases.
08 p0955 A73-21189
- Shock wave formation in a statistically inhomogeneous gas
08 p0955 A73-21450
- Compression wave interaction induced shock wave formation in shock tube, studying unsteady gas flow near opening diaphragm
08 p0955 A73-21520
- Self-similar hypersonic flows of an inviscid gas
08 p0927 A73-21545
- Central shock position in supersonic jet impinging on wall, noting flow velocity dependence on pressure
08 p0927 A73-21605
- Investigation of the applicability of some statistical models to the shock-wave structure problem
08 p0956 A73-21606
- Shock deformation of K-state in Ni-Cr alloys.
08 p0979 A73-21626
- Stellar formation and cloud collision energy dissipations as energy sources for self gravitating shock waves maintenance in Galactic spiral theory
09 p1141 A73-22008
- Chromospheric flares and shock waves in interplanetary space
09 p1137 A73-22540
- Thermal wave generation and transformation into shock waves due to energy release in stellar interior, considering nova outburst
09 p1146 A73-22547
- Origin of chains of type I solar radio bursts.
09 p1138 A73-22733
- Investigation of the electrical explosion of conductors by holographic methods
10 p1248 A73-23507

- Circumstellar envelope model and shock wave calculations for type II supernovae with radiation transport via diffusion, predicting Rayleigh-Taylor instability
10 p1273 A73-23544
- Self consistent computerized solutions to acoustic wave propagation and shock wave transformation with energy dissipation for solar and stellar chromosphere models
10 p1274 A73-23717
- The use of electret films as time-of-arrival detectors for shock and detonation waves.
10 p1218 A73-24122
- Collisionless plasma compression shock waves thermodynamics, noting entropy variations along shock adiabat under plasma heating in magnetic field
10 p1254 A73-24171
- Shadowgraph photography for electromagnetic excitation of shock waves in normal pressure gas, noting plasma and shock compressed regions in shock tube
10 p1205 A73-24208
- Transient compressional wave propagation in a two-layered circular rod with imperfect bonding.
10 p1291 A73-24390
- Temperature at the surface of a heat-conducting liquid behind a shock wave in the presence of mass transfer and chemical reactions in the boundary layer
10 p1296 A73-24679
- Pressure shocks in thermally and electrically conducting viscous gas, discussing growth equation and radiation effects
11 p1403 A73-25164
- Experimental study of shock-wave reflection from a thermally accommodating wall.
11 p1449 A73-25252
- Experimental determination of the ionization rate behind a strong shock wave in air
11 p1304 A73-26444
- An analytical solution to the problem of hypersonic gas flow past a slender wing
12 p1457 A73-27078
- Measurements of free stream velocity and ionization relaxation behind a shock in xenon.
12 p1527 A73-27172
- Study on ionizing shock waves in argon. III - Thermodynamic properties of the plasma.
12 p1527 A73-27173
- Propagation of a nonlinear wave in a weakly turbulent plasma.
13 p1665 A73-28676
- Solar wind proton temperature anomalies relation to interplanetary shock waves, considering solar flare induced material ejection and magnetic bottle formation
14 p1786 A73-29952
- Greenstadt binary index criterion for laminar and pulsating bow shock crossings separation in terms of angle, solar wind velocity and Galilean invariance
14 p1748 A73-29979
- Spherical concentric shock wave excitation in elastic medium by hypersonic thermal wave in terms of displacements, particle velocity and stresses
14 p1817 A73-30252
- Explosive shock hardening effects on roller steel fatigue strength, surface hardness and wear resistance
14 p1755 A73-30318
- Artificial viscosity related to shocks for studying anomalous wall heating and solution behavior at interface by substituting Rankine-Hugoniot equation
14 p1775 A73-30908
- Q switched ruby laser optical diagnostic system for plasma shock waves and plasmoid observation, noting schlieren photographs of exploding wire experiments
14 p1782 A73-30922
- Shock-wave generation in a randomly inhomogeneous gas.
15 p1860 A73-31014
- Upper and lower stability limits criterion for plane shock waves, based on Hugoniot curve positive slope
15 p1860 A73-31090
- The transonic aerofoil problem with embedded shocks.
15 p1821 A73-31122
- Influence of weak viscous interaction on the drag of a wing profile
15 p1822 A73-31195
- Unified geometric and analytical treatment of magnetogasdynamic shocks. I - General solutions and theorems.
15 p1917 A73-31339
- A pseudo shock theory of pressure depression in externally pressurized circular thrust gas bearings.
15 p1882 A73-31699
- Calculation of the parameters of a chemically reacting gas behind an incident and reflected shock wave
15 p1840 A73-31855
- Condition of the medium before the flame front during the initial phase of a combustion process
15 p1957 A73-31867
- Permeable elastic piston models of shock wave formation before flame front during inflammable gas mixture combustion in channels
15 p1957 A73-31868

Stability analysis procedure for shock wave in steady compressible fluid flow, obtaining equations of motion
15 p1864 A73-32113

Structure of the current front of an electron-acoustic wave in a plasma
15 p1920 A73-32301

Kinetics of physicochemical processes in a shock wave in mercury vapors. II - The relaxation zone: Region of initial ionization
15 p1916 A73-32314

Electrohydrodynamic shock wave evolution in steady gas flow with positive space charge in electric field
15 p1921 A73-32406

One dimensional steady electrohydrodynamic duct flow with shock waves for continuous and discontinuous electric fields
15 p1921 A73-32407

Time and space variations of cosmic-ray intensity increases prior to Forbush decreases.
16 p2052 A73-32755

The radiative properties of high density argon plasma in explosively driven shock waves.
16 p2040 A73-32907

Pulse X-ray photography of a shock wave in cesium vapor using two X-ray tubes.
16 p2042 A73-33579

Temperature of a radiating cone in a supersonic flow of transparent gas.
16 p1964 A73-33595

Book - Gasdynamic theory of detonation.
17 p2253 A73-34297

Shock waves in gas flows in close binary dwarf star systems
17 p2226 A73-34366

An initial value method for the study of shock-induced laminar compressible boundary layers.
17 p2152 A73-35004

Uniqueness requirements for calculated jump conditions across embedded shock waves based on relaxation methods, comparing to time dependent finite difference calculation
17 p2154 A73-35130

Dissociation of carbon dioxide behind reflected shock waves.
17 p2119 A73-35173

Holographic investigation of electrical explosions of conductors.
17 p2212 A73-35187

Jet aircraft noise research, emphasizing pure jet mixing noise, shock wave associated noise, and tail-pipe noise produced in engine or nozzle exit plane
17 p2096 A73-35332

Transonic inviscid flows over lifting airfoils with embedded shock wave using method of integral relations.
[AIAA PAPER 73-658]
18 p2261 A73-36212

On the higher approximations of the supersonic projectile theory.
[AIAA PAPER 73-669]
18 p2262 A73-36220

Solar wind heat transport in the vicinity of the earth's bow shock.
18 p2346 A73-36269

Review of current sonic boom studies.
18 p2267 A73-36393

Self consistent computerized solutions to acoustic wave propagation and shock wave transformation with energy dissipation for solar and stellar chromosphere models
18 p2355 A73-36742

Nonlinear acoustics of a radiating gas. II - Weak shock waves
18 p2337 A73-36989

Solution of the problem of the flow past a V-shaped wing with a strong shock wave at the leading edge
18 p2265 A73-37011

Similarity parameters and approximate relations for the axisymmetric supersonic flow past an ellipsoid
18 p2266 A73-37019

Quasi-steady plasma wind tunnel for Alfvén wave measurements of MHD flow involving shock waves and wakes, using Langmuir probes
19 p2465 A73-37172

A note on Beltrami and complex-lamellar flows behind a three-dimensional curved gasdynamic shock wave.
19 p2420 A73-37753

Galactic shocks as consequence of large amplitude nonlinear density waves in interstellar gas perturbed via steady forcing by spiral gravitational fields
19 p2488 A73-38511

Pioneer 8 observations and interpretations of sixteen interplanetary shock waves observed in 1968.
20 p2603 A73-38931

Structural determination of electric field conditions in ionizing shock waves.
20 p2596 A73-38965

Hydrogen plasma compression producing collisionless shock waves, measuring turbulence intensity as function of cut-off angle and anisotropy
20 p2596 A73-38966

Non-turbulent electric fields in soliton and shock-like structures in magnetized plasmas.
20 p2596 A73-38967

Book - Hyperbolic systems of conservation laws and the mathematical theory of shock waves.
20 p2581 A73-39140

Electron plasma wave shocks in a collisionless plasma.
20 p2598 A73-39301

A new method of solving one-dimensional unsteady flow equations and its application to shock wave stability in sonic inlets.
20 p2548 A73-39522

Study of shock wave and turbulent boundary layer interaction using the energy integral equation.
20 p2548 A73-39524

Thermodynamic formation of negative/rarefaction/shock waves in single-phase viscous fluids by approximate continuum model
21 p2790 A73-40251

HF and DF molecules vibrational relaxation investigation by recording IR radiation behind incident shock wave at 1500-5000 K
21 p2743 A73-40360

Supersonic gas flow pattern at blunt body of revolution with attached shock wave
21 p2632 A73-40400

Calculations of state functions behind ionizing shock-waves in potassium and caesium vapour.
21 p2745 A73-40474

Certain characteristics of the August 1972 solar flares which generated cosmic radiation, plasma clouds, and interplanetary shock waves
21 p2757 A73-40587

Shock oscillation associated with Hartmann resonance tubes excited by underexpanded sonic jets, using schlieren streak photography
21 p2677 A73-40616

Propagation of steady shock waves in non-linear thermoviscoelastic solids.
21 p2724 A73-41548

Acoustic turbulence generation of shock waves in compressed gas or plasma excited by random potential forces based on energy transfer along spectrum
22 p2840 A73-41809

Magnetogasdynamic shock polar - Exact solution in aligned fields.
22 p2893 A73-42393

Studies of the relaxation of internal energy of molecular hydrogen.
22 p2898 A73-42762

Precise measurements of diatomic dissociation rates in shock waves.
22 p2818 A73-42765

Breakup of liquid drops due to convective flow in shocked sprays.
22 p2937 A73-42819

Interferometric measurement of thermodynamic variables of rare gas plasmas produced by shock waves
22 p2896 A73-43168

Generation of electrical current by impact in metallic and semiconductor bodies
23 p3015 A73-43476

Weakly-shocked flows of the solar wind plasma through atmospheres of comets and planets.
23 p3024 A73-43682

Unsteady transonic flows with shock waves in two-dimensional channels.
23 p2969 A73-43938

Thermodynamic treatment of plastic media with application to viscoplastic materials, elastoplastic deformation and entropy jump across weak shock waves
23 p3043 A73-43969

Structure of the current front of an electron-acoustic wave in a plasma.
24 p3114 A73-44609

A high resolution study in time, position, intensity, and frequency of the radio event of January 14, 1971.
24 p3136 A73-44643

A divergent difference scheme for calculation of steady supersonic flows with complex structures
24 p3053 A73-44651

Piecewise-one-dimensional models of supersonic combustion and pseudoshock in a channel
24 p3154 A73-44702

Pressure fluctuations underlying attached and separated supersonic turbulent boundary layers and shock waves.
[AIAA PAPER 73-996]
24 p3053 A73-44831

Bow shock position from OGO-5, Explorer 35 and Heos satellites observation, emphasizing shock in tail for low Mach numbers
24 p3086 A73-45136

Investigation of the diffraction of strong shock waves on convex corners
24 p3081 A73-45536

Flow field over pointed wedges in isoelectric flow of thermally and calorically perfect gases with nonuniform incident supersonic flow, noting attached shock formation
24 p3056 A73-45547

SHOOTING STAR AIRCRAFT
U T-33 AIRCRAFT
SHORT CIRCUITS
Statistical analysis applied to solar cell shorting caused by reverse bias voltage stress.
03 p0255 A73-14223

A new uncomplicated method for the simultaneous determination of various parameters in explosive welding
06 p0698 A73-18446

Influence of wave currents on the windings of electrical equipment during short circuiting
09 p1037 A73-22942

Matrix, pyramid and rectangular decoder reliability and operational probability during short circuit/cut-off failures
14 p1736 A73-30566

Solid tantalum capacitor failure modes, discussing slug impurities, dielectric imperfections, short circuits, scintillation shorts, anodizing, soldering, screening methods and cost reduction
19 p2410 A73-38443

Substrates with end effect in shorted slot, measuring normalized inductive reactance dependence on thickness to wavelength ratio
23 p2954 A73-44068

SHORT HAUL AIRCRAFT

NT MERCURE AIRCRAFT
Low noise STOL aircraft as solution for short haul transportation, discussing German, British and Swedish industrial development efforts
01 p0004 A73-10468

Short haul twin jet passenger aircraft Iak-40 for small airfields, noting flight characteristics and cost analysis
03 p0249 A73-13070

Book - The local service airline experiment.
05 p0534 A73-16360

European regional airports planning for short haul point-to-point air transport and international airports congestion alleviation
05 p0562 A73-16565

Washington Airlines - The short haul /STOL/ experiment.
[AIAA PAPER 73-26]
06 p0771 A73-17615

Research on future short-haul aircraft at the NASA Langley Research Center.
[AIAA PAPER 73-27]
06 p0647 A73-17616

VTOL aircraft and short-haul transportation.
06 p0648 A73-18150

Short haul air travel with Intermodal Automated Transfer system for integrating ground transportation to allow passenger to stay in seat from origin to destination
10 p1174 A73-23653

Status of short haul air transportation.
13 p1570 A73-29108

Progress report on Tel Aviv offshore airport project.
15 p1857 A73-31544

VFW 614 twin-jet short haul aircraft, discussing layout, auxiliary power supply system for ground handling independence, surface movements maneuverability and low noise characteristics
15 p1830 A73-32365

STOL operational impact on ATC system support, considering short haul metropolitan and rural transportation modes, landing/takeoff facilities and all-weather operational reliability
15 p1831 A73-32547

Pressurized fuselage design studies for short haul transport aircraft, discussing sandwich structures and bonding techniques for Al and Ti alloy construction materials
16 p2018 A73-33069

Short haul aircraft design and marketing, examining competing modes, noise factors, airport traffic density patterns and aircraft types dependence on utilization
16 p2088 A73-33184

Rotary wing aircraft ecological advantages in logging, off shore oil exploration and short haul passenger transport for airport size reduction
16 p2088 A73-33185

Independently targeted short haul individual rotorcraft for air taxi service, considering traffic control system, market possibilities, environmental impact and projected utilization
16 p2088 A73-33186

STOL short haul system development, discussing airport congestion, operational costs and environmental considerations
16 p1968 A73-33192

Short haul V/STOL air transportation social and economic aspects in comparison with ground transportation modes, emphasizing convenience and frequency of service
16 p2088 A73-33193

Development of the A300B wide-body twin.
[SAE PAPER 730353]
17 p2102 A73-34701

Aircraft installation requirements and considerations for variable pitch fan engines.
[AIAA PAPER 73-807]
19 p2379 A73-37465

On-board navigation and landing systems for local airlines in the USSR
19 p2452 A73-37819

Europeplane QSTOL economical solution to noise and congestion problem in short and medium haul transport
22 p2798 A73-41862

SHORT TAKEOFF AIRCRAFT
NT DHC 5 AIRCRAFT

Low noise STOL aircraft as solution for short haul transportation, discussing German, British and Swedish industrial development efforts

01 p0004 A73-10468

Effect of aircraft reliability regulations on takeoff and landing performance of QSTOL aircraft

02 p0130 A73-11658

STOL aircraft technology, operation and markets in view of future European air traffic development, discussing various lift devices, noise aspects and economic factors

02 p0130 A73-11662

STOL aircraft with mechanical high-lift systems in comparison to STOL aircraft with wings having blown flaps

02 p0130 A73-11665

The technical evolution of air transport in the seventies - European contribution to this evolution

02 p0238 A73-11702

Rigid airships as versatile and ecologically clear STOL aircraft, discussing computerized structural analysis, nuclear propulsion and radar guidance systems

02 p0131 A73-12596

Hydraulic system on de Havilland Twin Otter STOL aircraft for flaps, wheel brakes and nose wheel steering, noting power supply mounting

03 p0252 A73-13350

Variable pitch fan experimental design for quiet STOL propulsion, testing blade designs for aerodynamic and acoustic performance

03 p0359 A73-14147

Flap noise measurements for STOL configurations using external upper surface blowing

04 p0487 A73-14922

Interactive real time simulation for scheduling and monitoring of STOL aircraft in the terminal area

05 p0535 A73-16909

A statistical analysis of pilot control during a simulation of STOL landing approaches

05 p0536 A73-16922

Washington Airlines - The short haul /STOL/ experiment

06 p0771 A73-17615

Arrested landing studies for STOL aircraft

06 p0647 A73-17627

Technical and economical analysis of various QSTOL concepts

06 p0647 A73-17675

Multiple purpose STOL aircraft for passenger or cargo transport, discussing design features, performance and market prospects

06 p0648 A73-17999

The capacity of a single-runway S.T.O.L./R.T.O.L. airport

07 p0849 A73-19352

A flight control system for STOL aircraft

07 p0777 A73-20171

Acoustic results obtained with upper-surface-blowing lift-augmentation systems

07 p0776 A73-20458

Mass air transportation development in Sweden, discussing flight scheduling, fare structure and quiet STOL aircraft introduction in 1980s

07 p0778 A73-20618

Benefit-cost analysis of delay reduction with STOL

08 p1025 A73-21000

Arava STOL turboprop passenger aircraft flutter flight test program, describing measurement instrumentation and data recording system

09 p1031 A73-22185

STOL Seminar, St. Louis, Mo., March 24, 1978, Record

09 p1032 A73-22524

Automotive approach systems certification and short distance takeoff and landing trajectory by cinetheodolites, digital optical, airborne and inertial/radiosonde equipment

10 p1246 A73-23656

Comparison of conventional flight control systems with a modern integrated flight control system

10 p1175 A73-23762

A comparative study of augmentor wing, ejector nozzle and power jet flap low noise STOL concepts

11 p1300 A73-25385

Display system for monitoring automatically controlled STOL landing glide paths, discussing computer controlled simulation

11 p1362 A73-25440

Parametric studies of the wing flutter behavior of a STOL transport

11 p1304 A73-25523

Variations in the sound field of a STOL aircraft as a function of wing-flap deflection

11 p1306 A73-26592

Status of short haul air transportation

13 p1570 A73-29108

Simulated flight tests of a digitally autopiloted STOL-craft on a curved approach with scanning microwave guidance

13 p1657 A73-29413

STOL aircraft flight and landing area considerations

15 p1856 A73-31389

French civil aviation inexpensive C band landing system with ILS angular coding and simplified on-board equipment for STOL and Alpine airports

15 p1910 A73-32467

AIL-CO-SCAN landing system for STOL and heliports, combining localizer and glide control functions in 20 by 20 deg approach window

15 p1910 A73-32470

STOL operational impact on ATC system support, considering short haul metropolitan and rural transportation modes, landing/takeoff facilities and all-weather operational reliability

15 p1831 A73-32547

Critical study of the effects of gusts on an aircraft

16 p1961 A73-32808

Wind tunnel gust simulation for STOL aircraft behavior during low velocity flight in turbulent atmosphere near ground

16 p1962 A73-32813

Aspects of investigating STOL noise using large-scale wind-tunnel models

16 p1994 A73-33170

Canadian air transportation survey, outlining history of other modes, transportation investment trends, modal traffic distribution, STOL applications, airline social services and marketing

16 p2087 A73-33177

STOL jet aircraft with variable pitch fan, discussing engine handling, noise reduction and efficiency

16 p2046 A73-33189

STOL short haul system development, discussing airport congestion, operational costs and environmental considerations

16 p1968 A73-33192

VTOL and STOL projects flight simulation trials for autostabilization, head-up displays and flight controls effectiveness in handling qualities improvement and pilot workload reduction

16 p1996 A73-33209

Considerations concerning the design of an electronic landing display for STOL aircraft

17 p2146 A73-34478

Flight control problems during STOL landing approaches, considering navigation aids, pilot work load and flight safety

17 p2207 A73-34483

Noise reduction of STOL aircraft during landing approach and takeoff via thrust reduction and steepest descent flight paths

17 p2100 A73-34488

Ground visual aids for civil STOL aircraft steep gradient approach and blind landing, discussing flight trials and simulator experiments

17 p2208 A73-34489

Terminal and flight control navigation guidance systems for restricted and short takeoff and landing aircraft air traffic and approach techniques

17 p2100 A73-34490

Flight mechanics problems associated with landing approaches using direct lift control, as exemplified by the HFB 320 Hansa aircraft

17 p2100 A73-34496

STOL light aircraft wing with circulation control through blowing around trailing edge, boundary layer control through suction, leading edge modification and increase in chord length

17 p2094 A73-34682

Airtransit - The Canadian demonstration interurban STOL service

17 p2103 A73-34704

STOL aircraft choice for air transportation in low passenger density areas, discussing market characteristics in U.S. and tradeoffs between airline operation and airfield costs

17 p2209 A73-34705

Civil STOL aircraft engine thrust reverser and fast selection control system designs for high performance, low specific weight and acoustic compatibility requirements

17 p2222 A73-34706

The Air Force/Boeing advanced medium STOL transport prototype

17 p2103 A73-34710

Technical basis for the STOL characteristics of the McDonnell Douglas/USAF YC-15 prototype airplane

17 p2103 A73-34711

Fundamental aspects of noise reduction from powered-lift devices

17 p2103 A73-34715

Status of current development activity related to STOL propulsion noise reduction

17 p2222 A73-34716

The C-401, a STOL transport for many applications

17 p2107 A73-35666

DHC-7 four engine turboprop transport aircraft, emphasizing quietness and STOL capability

18 p2266 A73-36067

Structural design and technology developments for SST and STOL aircraft, discussing computerized and damage tolerant design, composite materials and cost reducing manufacturing techniques

18 p2362 A73-36167

On the role of the radiation directivity in noise reduction for STOL aircraft

19 p2378 A73-37277

Direct side force control for STOL crosswind landings

19 p2379 A73-37467

Air cushion landing systems for STOL transport aircraft, investigating structural and power requirements on ground and in-flight handling, mission capability, operational life, weight and cost

19 p2381 A73-37682

ACLS trade study for application to STOL tactical aircraft

19 p2381 A73-37683

Air cushion landing system applications and operational considerations

19 p2381 A73-37688

ACLS equipped vehicles in inter-city transportation

19 p2381 A73-37686

The aircraft modification phase of the joint U.S./Canadian ACLS program

19 p2382 A73-37689

STOL pilot functional requirements on air transportation system in terms of airport design, aircraft, ATC, route selection, navigation and communications

19 p2450 A73-37730

Simulated flight tests of a digitally autopiloted STOL-craft on a curved approach with scanning microwave guidance

19 p2386 A73-38049

Flight director design for a STOL aircraft

20 p2508 A73-38649

Overall sound pressure levels of STOL thrust reverse noise as function of jet velocity at touchdown

20 p2600 A73-38650

STOL passenger aircraft ride smoothing control system based on vertical and lateral acceleration limits for design flight condition of 7 fps rms gust velocity

20 p2509 A73-38821

Direct side-force control for STOL transport aircraft

20 p2588 A73-38823

European QSTOL economical solution to noise and congestion problem in short and medium haul transport

22 p2798 A73-41862

Short takeoff and landing /STOL/ aircraft technology developments for high density air transport, discussing lift system, handling, airfoil design, acoustics and operating economics

23 p2940 A73-43520

Program plan to develop airworthiness standards for STOL aircraft

24 p3056 A73-44994

SHORT WAVE RADIATION

NT DECIMETER WAVES

NT MICROWAVES

NT MILLIMETER WAVES

NT SUBMILLIMETER WAVES

Upward short wave radiation polarization characteristics observation by airborne polarimeter over grey sand desert, dense altocumulus liquid drops and cumulonimbus clouds and seas

02 p0169 A73-12269

Calculation of averaged values for short- and long-wave fluxes and influxes in a real atmosphere

05 p0593 A73-16243

Pulse and monochromatic short wave signals phase/amplitude autocorrelation functions and probability distributions during oblique incidence reflection from ionosphere

05 p0550 A73-16776

Short-wave spectral radiant heat influx in the atmosphere

08 p0984 A73-21133

Measurements of absorbed short-wave energy in a tropical atmosphere

08 p0958 A73-21267

Measurement of short- and longwave radiant fluxes from the Kosmos-320 satellite

08 p0961 A73-21586

Some results of investigations programmed according to the complex atmospheric energetics experiment /1970-1972/

09 p1115 A73-22989

A null-reading method of measuring the complex reflection coefficient in the short-wave end of the millimeter band

14 p1728 A73-30271

Short wave radiation flux calculation method for cloudless and cloudy atmospheres, computing geographic distribution of daily absorbed solar radiation

15 p1905 A73-31787

Certain methodological aspects of measurements of the average short-wave radiation fluxes in the presence of cloudiness

15 p1905 A73-31790

Spatial structure of the short-wave radiation field in stratocumulus and cumulus clouds

15 p1905 A73-31795

Light scattering intermolecular and Raman spectra in liquid and solid hydrogen, showing short wave collective excitations in relation to phonon processes

23 p3007 A73-44171

The thermospheric heating function. III - The function describing the heating of the thermosphere by short-wave solar radiation during a period of high solar activity

24 p3084 A73-44800

SHORT WAVE RADIO TRANSMISSION

The influence of chordal paths on signals propagating to the near antipode of an HF radio transmitter.

01 p0015 A73-10182

Probability of short-wave signal transmission over a medium-range path

05 p0548 A73-16263

Role of the sporadic E layer in short radio wave propagation at frequencies exceeding the maximum usable frequencies of the F2 layer

05 p0548 A73-16264

Computerized short- and long term ionospheric propagation forecasting for HF communications, frequency scheduling and broadcasting circuits

09 p1048 A73-21983

High-frequency radio-wave propagation through plane-stratified ionospheric models.

09 p1077 A73-22430

Properties of plane asymmetric plasma waveguides as applied to short-wave propagation along inhomogeneities of the topside ionosphere.

10 p1188 A73-24216

Long-periodicity fading of short-wave signals

12 p1473 A73-27759

An automatic reflectometer for the upper shortwave range

13 p1590 A73-28569

Noise immunity evaluation for noncoherent demodulators or FSK and PSK signals in short wave channels, using minimum a priori information on additive noise properties

13 p1592 A73-28899

Ionospheric tilts and long-range short-wave communications.

15 p1843 A73-31525

Short-wave skip distance for various models of the ionosphere

15 p1843 A73-31575

Theory of short radio wave propagation over very great distances

15 p1844 A73-31888

Reliability of diversity reception by antennas with different polarizations.

16 p1991 A73-33984

Measurements of artificial satellite signal Doppler spectrum.

19 p2407 A73-38351

Investigation of the fine-structure inhomogeneities of the Es layer at oblique radio wave incidence

20 p2554 A73-39163

Correlation of random phases spaced over oscillation frequencies

20 p2531 A73-39457

Semiconducting ground influence on input impedance and radiation resistance of horizontal magnetic dipoles, covering short wave band for various antenna elevations and conductivity levels

21 p2661 A73-40203

Convergence of perturbation-theory series in the problem of short-wave propagation through a randomly nonhomogeneous medium

21 p2657 A73-41514

Short wave radio signal fadeout due to ionospheric disturbances, obtaining experimental equation on magnitude relationship with solar zenith angle and operating frequency

22 p2825 A73-42194

Short-wave propagation in a randomly inhomogeneous medium with an arbitrary law of permittivity fluctuations

22 p2826 A73-42335

Short-wave propagation along several paths during auroral storm periods

24 p3067 A73-44796

HOT NOISE

The noise of microwave Schottky diodes at 70 MHz

06 p0673 A73-17579

Shot noise in a Schottky barrier diode in the presence of surface electronic states at the contact

06 p0675 A73-18077

Shot noise in diodes with a Schottky barrier in the case of a disturbed carrier distribution function

06 p0676 A73-18090

Electrical fluctuations in ideal forward-biased nondegenerate diodes.

12 p1480 A73-27272

Theory of shot noise depression in a modified diode

14 p1737 A73-30943

Quantum mechanics /semiclassical/ theory investigation of shot and thermal noise effects on laser behavior, deriving Fokker-Planck equations for field probability distribution

21 p2711 A73-40215

Noise in solid travelling-wave tubes using coupled-mode analysis.

21 p2665 A73-41122

Shot noise of a real Schottky-barrier diode during tunneling through the space charge region

23 p2960 A73-43619

Influence of the image force and tunnel effect on shot noise in diodes with a Schottky barrier

23 p2960 A73-43715

SHRINKAGE

Magnesium oxide crystal dislocation loop shrinkage rate measurement, suggesting oxygen ion diffusion as rate controlling process for dislocation climb

13 p1634 A73-28257

SHROUDED BODIES

U SHROUDS

SHROUDED PROPELLERS

Application of external aerodynamic diffusion to reduce shrouded propeller noise.

05 p0528 A73-16623

Computer aided shrouded propeller design.

[AIAA PAPER 73-54] 06 p0644 A73-17630

Shrouded Q-FAN propulsor for light aircraft, discussing propulsion system performance, weight, noise and cost trends

[SAE PAPER 730323] 17 p2221 A73-34680

SHROUDED TURBINES

Experiments on a shrouded, parallel disk system with rotation and coolant throughflow.

[AD-759594] 08 p1023 A73-21256

Static tests of the working-channel cascade of a tangential turbine

09 p1028 A73-22571

Influence of an intermediate stiffener on the vibration frequency spectrum of a cantilever plate

10 p1291 A73-24357

SHROUDS

Effect of shroud eccentricity on suppression of flow induced vibrations.

13 p1690 A73-28059

Experimental evaluation of a roll control system for a shrouded cone.

17 p2239 A73-35500

A contact problem for a transversely isotropic cylindrical shell of finite length

18 p2363 A73-36404

Blade tip clearance loss between centrifugal impellers and shrouds during two dimensional viscous laminar flow, discussing energy dissipation and pressure and temperature distribution

19 p2474 A73-38417

SHUNTS

U BYPASSES

U CIRCUITS

SHUTTERS

Coanda effect physical explanation and applications to free jet and partially bounded jet, analyzing surface shutter characteristics

13 p1601 A73-28913

High speed camera with locked mode laser activated Kerr cell shutter to obtain picoseconds exposure duration

21 p2709 A73-39945

SHUTTLE BOOSTERS

U SPACE SHUTTLE BOOSTERS

SHUTTLE ORBITERS

U SPACE SHUTTLE ORBITERS

SI

U INTERNATIONAL SYSTEM OF UNITS

SIBERIA

Blocking anticyclones over Siberia in the cold half-year period and the possibility of forecasting them

12 p1521 A73-27745

SIC [COEFFICIENT]

U STRUCTURAL INFLUENCE COEFFICIENTS

SICKNESSES

NT ALTITUDE SICKNESS

NT DECOMPRESSION SICKNESS

SID [IONOSPHERIC DISTURBANCES]

U SUDDEN IONOSPHERIC DISTURBANCES

SIDE-LOOKING RADAR

NT RADAR IMAGERY

Side-look radar provides a new tool for topographic and geological surveys.

02 p0140 A73-11850

Imaging radar techniques for remote sensing applications.

03 p0278 A73-14486

Receiving antenna polarization parameters selection in side-looking synthetic aperture radars

04 p0423 A73-15914

Applications of the discriminant function in automatic pattern recognition of side-looking radar imagery.

05 p0553 A73-16289

Synthetic aperture SLAR systems and their application for regional resources analysis.

05 p0578 A73-17133

The use of a simulator in a synthetic aperture radar data processing tradeoff study.

05 p0554 A73-17149

Radar techniques for planetary mapping with orbiting vehicle.

06 p0664 A73-18011

Coherent optical processing and display techniques for microwave imagery generation from synthetic aperture radar system data, discussing hologram and side-looking radar

06 p0667 A73-18279

Radar imagery and supporting aerial photography tests for topographic mapping capabilities and metric quality of side-looking stereo radar system

06 p0667 A73-18283

Similarities and differences in the interpretation of air photos and SLAR imagery.

06 p0693 A73-18284

Clustering phenomena in side-looking radar /SLR/ microtexture.

06 p0667 A73-18285

Analysis and interpretation of air-borne multifrequency side-looking radar sea ice imagery.

09 p1080 A73-22150

Wave front reconstruction principle application to side-looking radar, diffused holograms, holographic interferometry and computer storage

11 p1369 A73-26527

Toros side-looking radar system for sea-ice distribution and geomorphological mapping and agricultural soil studies

12 p1474 A73-27962

Mapping of mangrove and perpendicular-oriented shell reefs in southeastern Panama with side-looking radar.

13 p1606 A73-28170

Side-looking pulse Doppler radar data presuming prior to correlation to obtain desired resolution performance with minimal digital storage

13 p1585 A73-29203

Mapping with coherent-radiation focused synthetic-aperture side-looking radar.

16 p2015 A73-33357

Controlled-quality images from synthetic-aperture radar data.

16 p2015 A73-33358

Holography, radar data and interpreter performance.

17 p2165 A73-34286

SIDEBANDS

The sideband instability of electrostatic waves in an inhomogeneous medium.

07 p0858 A73-19667

Noise in single-frequency oscillators and amplifiers.

10 p1196 A73-24864

Ionospheric echoes due to sidelobe and harmonic radiation from Isis topside sounder transmitters, discussing effects of satellite spread and ion sheath distortions

14 p1752 A73-29974

Effect of upper sideband impedance on a lower sideband up-converter.

17 p2123 A73-34971

SIDELobe REDUCTION

Low-side lobe paraboloidal antenna with microwave absorber.

01 p0018 A73-11054

Target angular characteristics of direction finding antenna in sidelobe region for wideband signals, using single coordinate measurement and amplitude scanning

02 p0146 A73-12023

Sidelobe reduction for linear arrays with elements sampled from equally spaced arrays, using Fourier coefficients of sampling functions

03 p0274 A73-12998

Linear array antenna radiation pattern synthesis for minimum sidelobe level outside of given intervals, calculating current distribution

03 p0278 A73-14060

Array factor of statistically thinned antenna arrays with an increased element-interspace minimum

06 p0674 A73-17810

A statistical estimate of the achievable sidelobe level in phased array antennas with nonlinear initial phase distribution.

07 p0801 A73-20130

High volume wideband PSK system design for minimal sidelobe, calculating signal number relationship to maximum sidelobe level of cross correlation and autocorrelation

10 p1187 A73-23733

Design of multiple-edge blenders for large horn reflector antennas.

11 p1337 A73-25653

Directivities of planar arrays with triangular arrangement of elements.

11 p1333 A73-26699

Surface elastic wave microwave bandpass filter for miniaturized frequency synthesizer in satellite communications systems, noting insertion loss and sidelobe reduction

12 p1484 A73-27573

Optimum mismatched filters for sidelobe suppression.

13 p1593 A73-29209

The application of Gegenbauer polynomials to antenna array synthesis.

14 p1725 A73-29747

Comparison between the peak sidelobe of the random array and algorithmically designed aperiodic arrays.

14 p1734 A73-30217

The effect of weighting upon signal-to-noise ratio in pulse bursts.

21 p2649 A73-40327

SIDLOBES

- Effects of modulation nonlinearity on the range response of FM radars. 21 p2650 A73-40341
- Digitally scanned planar phased arrays, deriving optimum phase perturbation function for quantization and reflection lobe dispersion in terms of aperture distribution amplitude 21 p2652 A73-40667
- Basic theoretical aspects of spherical phased arrays. 21 p2653 A73-40678
- An array technique with grating-lobe suppression for limited-scan applications. 22 p2830 A73-41826
- Nonlinear optimization reduces the sidelobes of Yagi antenna. 22 p2831 A73-41847
- Synthesis of antennas with minimum mean sidelobe level of the radiation pattern. 24 p3068 A73-44939

SIDELOBES

- Indeterminacy functions side maxima for phase manipulated signals with low sidelobe levels in autocorrelation functions, noting Doppler frequency shift effect 04 p0423 A73-15925
- Dependence of sidelobe level on random phase error in a linear array antenna. 17 p2129 A73-35697

SIDEREAL TIME

- Sidereal periods in a gravitational field characterized by Schwarzschild's internal solution 11 p1416 A73-25237
- Application of long-baseline radio interferometers to astrometric tasks 21 p2701 A73-40726

SIDERITE METEORITES

IRON METEORITES

SIDERITES

- Siderophile and volatile elements in Luna 20 fine soil and breccia samples from radiochemical neutron activation analysis, noting comparing with Apollo 16 results 13 p1676 A73-28325

SIDELIP

- Theory of the motion of a rigid model of an aircraft with a vertical landing-gear strut on a runway 01 p0005 A73-10917
- Indicating instrument for angle of attack and sideslip on subsonic flight vehicles via static pressure sensing, noting wind tunnel tests 02 p0166 A73-11724
- Rubber friction effect on vehicle tire force-slip and braking behavior in terms of peripheral and sideslip components and structural and operational parameters 03 p0251 A73-13242
- Wake vorticity of side-slipping slender thin wings at transonic speeds, deriving integral equation for vortex strength based on Prandtl-Glauert rule [DGLR PAPER 72-127] 03 p0247 A73-14376
- Lifting-surface theory for a wing oscillating in yaw and sideslip with an angle of attack. 13 p1564 A73-28802
- Application of direct side force control to commercial transport. [AIAA PAPER 73-886] 20 p2588 A73-38822
- Direct side-force control for STOL transport aircraft. [AIAA PAPER 73-887] 20 p2588 A73-38823

SIDEWASH

U BACKWASH

SIGHT

U VISUAL PERCEPTION

SIGNAL ANALYSIS

- Hilbert transform for single and narrow band signal analysis with 90 deg spectral component phase shift in frequency region 01 p0015 A73-10076
- Study of the ac small-signal dynamic characteristic of p-i-n silicon diodes 01 p0024 A73-10921
- Large-signal calculations on IMPATT oscillators with voltage waveforms giving close-to-optimum efficiency. 01 p0026 A73-11297
- Digital filters applicable to electroencephalographic pattern recognition. 01 p0013 A73-11464
- Instabilities and small-signal response of double injection structures with deep traps. 02 p0146 A73-12042
- Stroboscope-like frequency spectrum examination of short impulses. 03 p0308 A73-13570
- Optimal matched Wiener discrete filters investigated with operator-matrix concepts, considering signal decorrelation 03 p0278 A73-14030
- Application of frequency discrimination technique to the analysis of electroencephalographic signals. 04 p0411 A73-15052
- Visual field image analysis via investigation of receptor-furnished signal analysis by network of neuron-like structures 04 p0413 A73-15789

A model for the automatic classification of signals with applications for the automatic language recognition 06 p0663 A73-17591

Time and frequency functional analysis of speech for quantitative information parameters determination and signal recognition, considering German phoneme system two-formant signal structure 06 p0663 A73-17592

Autocorrelation function synthesis from arbitrary function on finite interval for case of random signals 08 p0951 A73-21102

Microwave oscillation in germanium avalanche diodes. I, II. 08 p0947 A73-21461

Correlation techniques in the analysis of transient processes. 08 p0988 A73-21466

Noiselike FM signals shaping by numerical periodic pseudoeven sequences, analyzing FSK signals 09 p1049 A73-22049

Classification of weak signals on a non-Gaussian noise background 09 p1051 A73-22557

Reconstruction of analog signals and choice of sampling rates in telemetry. 09 p1058 A73-23421

Best approximation in digital filtering 10 p1242 A73-23764

Analysis and synthesis of automatic control systems with controlled converters. 10 p1198 A73-24019

Calculation of the characteristics of nonlinear elements in first-order circuits for given signal conversion conditions 10 p1196 A73-24603

Current saturation and small-signal characteristics of GaAs field-effect transistors. 10 p1197 A73-24868

Two dimensional signals Fourier transformations, discussing digital techniques application to linear and optical systems 11 p1397 A73-24993

Effect of time-quantization errors on the accuracy in periodogram analysis of random processes 11 p1360 A73-25015

Computerized large signal model of IMPATT diode, calculating output power and admittance as function of frequency and amplitude 11 p1336 A73-25320

A spectral analysis method for single radio signals 11 p1331 A73-26101

Dynamic AGC correction for angle signal variations in monopulse radar receivers with reference signal, analyzing signal statistics 12 p1469 A73-27163

Investigation of the phase variation of a NWC signal /22.3 kHz/ along a transequatorial path 12 p1469 A73-27339

Analytical representation of complex signals by expansion in Fourier, Kotelnikov, and Taylor series 12 p1471 A73-27584

Small-signal analysis of punch-through injection microwave devices. 13 p1590 A73-28541

Analysis of correlation functions of space-time wideband signals received by linear antennas. 13 p1591 A73-28657

Representation of real narrowband signals with the use of nonuniformly displaced base functions with positive coefficients. 13 p1583 A73-28668

Correlation and indeterminate functions of signals with discrete frequency-time structure, noting linear frequency modulation of signal element 13 p1583 A73-28669

Calculation of the amplitude of pulse signals at the output of linear filters in optical communications systems. 13 p1583 A73-28671

Linear and nonlinear first order closed loop tracking radar systems, predicting noise performance by Gaussian signal amplitude fluctuation modeling 13 p1585 A73-29206

Computer simulations of large-signal oscillation behavior of avalanche diodes. 13 p1594 A73-29235

Spectral analysis of the signal from the Laser Doppler Velocimeter - Turbulent flows. 14 p1752 A73-29919

Extraterrestrial messenger probe recognition from inhabited planet via message involving home constellation binary coded signals 14 p1796 A73-29946

Spectral analysis of optical pulse signals in application to the problem of synchronizing PCM laser communications lines 14 p1729 A73-30556

Evaluation of composite failures through fracture signal analysis. 15 p1879 A73-32250

The explanation and investigation of biological rhythms. 16 p1972 A73-33155

Small-signal modelling and characterization of microwave transistors. 16 p1990 A73-33683

Gunn diode parameters from a small signal analysis. 17 p2142 A73-35635

The value of data processing in the analysis of visual evoked potentials 18 p2279 A73-36911

An investigation of the combined amplification of monochromatic and noise signals in a TWT. 20 p2529 A73-38940

Optimization and data analysis of the Frascati gravitational-wave detector. 20 p2565 A73-39013

Transformation of random signals by circuits containing a majoritarian element 20 p2542 A73-39040

Calculation of the current of a nonlinear element with inertia in the presence of a biharmonic input 20 p2537 A73-39450

Dispersed signal filtering and filtered signal duration relation to filter bandwidth and dispersiveness, isolating fundamental mode of Rayleigh waves from earthquake 650 km deep 21 p2648 A73-39930

The total electron content of the ionosphere and its horizontal gradients, measured on the basis of recordings of satellite signals at scattered points 21 p2686 A73-40910

Sensitivity of an intensity radio interferometer 21 p2705 A73-41470

Antenna coupling induced intersystem electromagnetic interference prediction, discussing tradeoffs between analysis level, input information, measurements, cost results and user requirements 22 p2822 A73-41790

Signal and noise in the human oculomotor system. 22 p2810 A73-42964

Study of phase changes of the NWC signal /22.3 kHz/ on a transequatorial path. 23 p2952 A73-43237

Signal theory problems of discrete signal representation decomposition and characterization by Walsh and orthogonal functions, noting voiced speech analysis 23 p2952 A73-43309

Level transgressions and extremal values of continuous stochastic signals 23 p2952 A73-43310

Signal analysis using stochastic-ergodic principles, discussing PCM correlation procedures, analog-digital signal conversion and measurement methods 23 p2983 A73-44140

Calculation of the spectrum of a sinusoidal signal modulated by phase displacement with one, two, or three states for any values of phase jumps 24 p3068 A73-44972

A mathematical model of real signal spectra 24 p3068 A73-45005

SIGNAL ANALYZERS

Equipment for determining the amplitude-frequency characteristics of nonlinear elements in the range of low and extra-low frequencies 01 p0023 A73-10679

Russian book on machine-based determination of random process characteristics covering correlation, moment functions, spectral features, probability functions, etc 02 p0149 A73-12866

Shaping of the one-dimensional distribution and correlation function of a reference signal when checking statistical analyzers 11 p1360 A73-25022

Signal conditioning, separation and parameter measurement in modular digital Elinat analysis system for airborne, shipboard or ground based reconnaissance applications 17 p2137 A73-35207

The geometrical factor of large aperture hemispherical electrostatic analyzers. 20 p2564 A73-38877

Photoelastic investigation of dynamic stress conditions involving rapidly varying principal stress directions 21 p2695 A73-39965

SIGNAL DETECTION

NT CORRELATION DETECTION

Observers detecting a signal in two multiple observation tasks. 01 p0011 A73-10350

Effects of signal duration and masker duration on detectability under diotic and dichotic listening conditions. 01 p0008 A73-10436

The detection of a point source in the presence of nongaussian background noise. 01 p0017 A73-10832

Signal search networks for enlargement of locking bandwidth of tracking filters in automatic control systems, examining transistorized signal search and acquisition circuits 02 p0145 A73-11793

Earth based and spaceborne stellar interferometer with optical balanced mixer system for coherent de-

tection, discussing principles, construction, SNR and sensitivity

Partially coherent detection of binary FSK system with adaptive receiver, determining optimum and sub-optimum estimators of channel parameters for phase and bit synchronization

Cell averaging constant-false-alarm-rate radar receiver with noise estimated from logarithmic detector output, determining performance in Gaussian noise by Monte Carlo simulation

Standard deviation of thresholding time during detection of pulse perturbed by Gaussian noise

Neumann-Pearson-optimal signal detection procedure invariant with respect to amplitude and random noise intensity

Signal detection in ruby element quantum paramagnetic amplifier operating at liquid nitrogen temperature

Optimum detection and signal design for channels with non- but near-Gaussian additive noise.

Complex detection - A waveform preserving technique for single-sideband demodulation.

Differentially encoded multiple phase shift keyed signals transmission and detection, analyzing digital communication system performance

Phase and frequency tracking accuracy in direct-detection optical-communication systems.

Detection of multichannel FSK signals using chirp dispersion method.

Comparison of coherent and noncoherent detection of phase continuous binary FM signals.

Acquisition time evaluation at different input SNR values for pseudonoise signal demodulation, noting common bandwidth detection system advantage

A model of signal detection for the instrument landing system.

A method for reproducing pictures transmitted by meteorological satellites.

Experimental results on absolute phonon detection sensitivity of superconducting tunneling junctions.

Large ruby laser radar for remote detection and recording of atmospheric scattering data, describing tracking mount, optics, electronic signal processing and display features

Almost-coherent detection of phase-shift-keyed signals using an injection-locked oscillator.

Single photon detection and timing - Experiments and techniques.

Digital transmission performance on fading dispersive diversity channels.

The effect of a bandpass nonlinearity on signal detectability.

Optimal and suboptimal systems for detecting fluctuating optical radar pulses.

Numerical solution of the integral equations for optimal sequential filtering.

Detection of signals using receivers with processing of moduli.

Detection of a two-frequency signal buried in noise of unknown power.

Majority logic detection scheme of differentially phase-modulated waves.

Characteristics of the adaptive optimal detection of Gaussian signals on a pulse-noise background in receivers with a logarithmic amplifier

Optimization of detection systems for quasi-classical optical signals

Atmospheric turbulence effects on laser beam transmitted signals, considering filtering and detection based on doubly stochastic Poisson process

Optimal binary quantum signal detection in two dimensional Hilbert space by a priori probability vector projection method, using randomized decision strategy

Doppler signal detection with negative-resistance diode oscillators.

Algorithm for optimal radio signals detection under narrow band anisotropic noise, noting two channel space diversity receiver system

Noise immunity in detection of pseudorandom FSK signals with allowance for synchronization errors, noting reception fidelity dependence on signal to noise ratio

Coherent and noncoherent signal burst detection in background noise of unknown intensity, using maximum likelihood estimates

Classification of weak signals on a non-Gaussian noise background

Phase locked bit synchronization design tradeoffs between acquisition and noise performance, considering frequency tolerance of decision-directed loop with nonreturn-to-zero input

Missile and spacecraft radio telemetry data acquisition site polarization diversity signal combiner transient response requirements, comparing bench test with flight test data

Phase locked loop and coherent detection performance prediction, considering desirable phase detector characteristics in terms of SNR and noise spectral density

The detection and resolution of incoherent objects by an aberrated optical system in the presence of background noise.

Group performance in a visual signal-detection task.

Adaptation-level and theory of signal detection - An examination and integration of two judgment models for voluntary stimulus generalization.

Effectiveness of analog storage in the detection of signals on a background of noise and strong random pulsed interference

Dual magnetometer systems with cross correlation signal enhancement to overcome intrinsic sensor ambient noise and spacecraft magnetic field fluctuation effects on single detection performance

Unified approach to the performance analysis of linear modulation systems with coherent detection.

Range-gated moving target indicator with digital filters.

Visual temporal integration for threshold, signal detectability, and reaction time measures.

Analysis of various ultrasonic holographic imaging methods for medical diagnosis.

Theoretical and experimental investigations of a phase-coordinate second-order receiver.

Detection of Doppler signals by a receiver which incorporates a counter of the number of excursions of additive noise.

Probability of error in selecting the information signal and the synchronization signal by frequency multiplication

Psychoacoustic theory of signal detectability based on mathematical input-output mapping model and memory role in human auditory system

Vector correlation theory and neural mechanisms of binaural signal detection in human auditory system

Binaural signal detection - Equalization and cancellation theory.

Manipulating the response criterion in visual monitoring.

Tapped delay line filter for optimal single pulse detection in band-limited PCM/NRZ system in presence of Gaussian noise

Pulsar detections at frequencies of 8.4 and 15.1 GHz.

Evaluation of the performance of a signal detection system by counting the overshoots of an internal threshold

An asymptotically optimal rank detection algorithm for a signal in noise of unknown distribution

Decision-directed detector for overlapping PCM/NRZ signals.

Maximum likelihood M-ary detection theory application to incoherent optical system model based on photodetectors governed by Laguerre counting statistics, deriving error probability

A nomographic comparison of coherent and non-coherent detection statistics.

Effect of bandlimiting on the noncoherent detection of Amplitude-Shift Keying /ASK/ signals.

Sequential analysis algorithm for data channel detection of received signal represented by Poisson sequence of quantum transitions under large SNR

Effectiveness of certain easily realizable rank algorithms for detections of signals against a background of noise.

Analysis of optimal recognition of space-time signals.

Main trends of development of avalanche photodiodes as high-speed photodetectors /Review/

Kalman filter for rapid detection and adaptive estimation of state and covariance, deriving Bayes decision rule and algorithm for spacecraft tracking

Recursive ideal observer detection of known M-ary signals in multiplicative and additive Gaussian noise.

Methods of adaptation in problems involving non-parametric detection and resolution of signals

Signal/noise ratio in optical radar systems.

Detection of weak signals in narrowband noises.

Two-stage detection of signals in normal noise of unknown intensity.

Nonbiased rule for detection of radar signals in noise of unknown power.

Optimal Markov sequence signal detection in correlated FM random electronic countermeasure background noise

Optimal detection of binary signals with an arbitrary distribution of state durations at the output of a binary symmetrical Markov channel

Mutual coherence function of a finite optical beam and application to coherent detection.

Pulse-position modulation based on energy detection.

Optimum detection of an optical image on a photoelectric surface.

The effect of staggered PRF's on MTI signal detection.

Phase-tracking performance of direct-detection optical receivers.

Optical communication system performance with tracking error induced signal fading.

Sensitivity of an intensity radio interferometer

Detection of radio emission from V1016 Cygni.

Matched-filter detection of mode-locked laser signals.

Resolution of point sources of light as analyzed by quantum detection theory.

Autocorrelation functions for meteorological scatterer velocity measurements in Doppler spectrum from linear, quadratic and logarithmic radar signal detectors

A search for narrow band 21-cm wavelength signals from ten nearby stars.

Project Cyclops investigation of extraterrestrial civilization signal detection, discussing microwave apparatus, frequency bands, antenna arrays and research implementation proposals

Heterodyne detection of Arcturus at 10.6 microns.

Output signal-to-noise ratios in frequency measurement system using correlation detector.

Designing limiter/detectors for ECM receivers.

The use of tolerance detectors for data protection in the case of FM data transfer 04 p0415 A73-14773

Mathematical model for multipath transmission in aircraft and spacecraft communications, presenting Bayes detector for binary PSK 04 p0422 A73-15462

Stochastic signal reflection by passive element, synthesizing optimal echo-signal detector for space diversity reception 05 p0550 A73-16777

Radio astronomy receiver with digital integrator for weak radio source detection, noting minimum detectable field density 05 p0552 A73-17166

Security system signal detector with time delay and prediction filters and optimal noise suppression, noting detection time dependence on cost effectiveness 06 p0679 A73-17806

Sensitivity of Josephson junctions in video detection of microwave and millimeter-wave radiation. 06 p0677 A73-18371

Response of edge- and face-electroded pyroelectric detectors to infrared laser signals. 06 p0704 A73-18798

Measuring the off-duty factor of chaotic pulsed interference on a Gaussian noise background 09 p1050 A73-22338

A single channel command detector for deep space missions. 09 p1057 A73-23417

Intersymbol interference in binary communication systems with single-pole band-limiting filters. 10 p1186 A73-23498

Nonparametric signal detectors in the case of dependent sampled magnitudes 12 p1467 A73-26868

Photoresistor synchronous detector circuits with rectangular light pulse switching elements for capacitive and resistive loads 13 p1592 A73-28900

Noise rejection estimation for sinusoidal signal detectors which use information on zero-crossing moments 15 p1842 A73-31251

Signal interference and improvement of signal-to-noise ratios in a half-wave linear detector. 15 p1843 A73-31729

Optical method for submillimeter band phase measurements by probing spatially separated compared fields and summing two signals at detector 17 p1210 A73-34155

Quadratic antenna systems and noise excited antennas. 17 p1218 A73-35682

ML receiver for binary signals with intersymbol interference in Gaussian noise. 20 p2524 A73-38733

Nonparametric properties of detectors optimized for Gaussian interference of unknown intensity. 20 p2529 A73-38923

Transient processes in FM discriminators 20 p2537 A73-39458

Signal to noise ratios of inertial detector of mixture of stationary, normal, random and harmonic voltages, varying RC circuit time constants 20 p2537 A73-39459

Superconductor-semiconductor Schottky barrier diode video detector with proper doping and electron tunneling to obtain high degree nonlinearity in I-V characteristics 21 p2662 A73-40463

Self excited mixer/detector of Gunn diode oscillator, calculating detection characteristics from combined equivalent circuit and computer simulated analysis 21 p2664 A73-41092

Properties of a light-modified-breakdown detector in GaAs. 22 p2864 A73-43164

The design, fabrication, and evaluation of a silicon junction field-effect photodetector. 23 p2981 A73-43453

Analysis of the detection characteristics of frequency discriminators with nonminimum-phase loops 24 p3071 A73-44597

SIGNAL DISCRIMINATORS

U SIGNAL DETECTORS

SIGNAL DISTORTION

Towards faithful radio transmission of very wide bandwidth signals. 01 p0015 A73-10176

Multifrequency radio beacon on polar orbiting satellite for wideband transmission through ionosphere without significant signal distortion 03 p0275 A73-13627

Complex detection - A waveform preserving technique for single-sideband demodulation. 04 p0415 A73-14989

Reconstitution of signals deformed by a fast AGC application to plasma resonances. 04 p0417 A73-15297

FM Gaussian electromagnetic pulse distortion during reflection from ionospheric model with linear electron density profile and constant collision frequency 04 p0422 A73-15479

Modulating /multiplicative/ noise effects on output signal characteristics of receiver designed for optimal reception against background of Gaussian noise 04 p0423 A73-15915

Correction of the dynamic distortions of signals resulting from measurement information compression 05 p0577 A73-16986

Undistorted short sounding pulse reception at exit from ionosphere obtained by signal carrier frequency modulation 06 p0663 A73-17537

Deformation of the power spectrum of a random function during frequency translation 06 p0664 A73-17807

A 2-cycle algorithm for source coding with a fidelity criterion. 06 p0671 A73-18142

Distortion of electromagnetic pulses undergoing total internal reflection from a moving dielectric half-space. 06 p0666 A73-18200

Circuit model for characterizing the nearly linear behavior of avalanche diodes in amplifier circuits. [AD-757849] 06 p0677 A73-18738

A study on accumulation of waveform distortions in PCM hybrid transmission. 07 p0791 A73-19369

Improvement of frequency characteristics of digital filters. 08 p0945 A73-20801

Doppler effect intermodulation distortion derivation by perturbation method for loudspeaker modeled with pulsating sphere, considering boundary condition and nonlinear effect in wave propagation 08 p0987 A73-21123

Pressure-induced optical distortion in laser windows. 09 p1090 A73-21937

Theory of incoherent-scatter measurements using compressed pulses. 09 p1050 A73-22429

The accuracy of an approximate representation of the correlation functions of complex signals distorted in the linear stages of a radio channel 09 p1051 A73-22461

Record/reproduce process induced phase distortion in magnetic tape recorders as function of record head gap length 09 p1087 A73-23368

Microwave system with direct, AM, FM and pulse propagation techniques for swept-frequency group delay measurement, discussing error sources and various distortions 10 p1193 A73-23610

Modulation distortions during fading in frequency-modulated multichannel radio communication 10 p1187 A73-23740

Influence of signal amplitude changes in systems with phase and frequency modulation 10 p1189 A73-24377

Spacecraft transmitted TV picture geometrical distortion in terms of root-mean-square errors, considering applications to ESSA-7, Surveyor-7 and Mariner 4 data samples 10 p1219 A73-24485

Comparison of observed and predicted phase-front distortion in line-of-sight microwave signals. 11 p1330 A73-25687

Circular aperture antenna with quadratic phase distortions, deriving near and far field patterns in terms of linear combinations of Bessel and Lommel functions 12 p1479 A73-27233

Experimental investigation of the AM-FM distortions of a signal passing through a linear filter 12 p1481 A73-27589

Aerial radar photograph restitution for photogrammetric application, discussing geometric qualities and methods and instruments for partial removal of distortion 12 p1502 A73-27972

A comparison of holographic versus lens type acoustic image systems by computer simulation. 13 p1616 A73-28595

Combination and crosstalk distortions in microwave parametric systems. 13 p1583 A73-28665

Reduction of nonlinear distortions in a two-port network exhibiting a small nonlinearity 13 p1592 A73-28894

Influence of the nonlinearity of the phase characteristic of the RF signal path in an FM receiver on the signal distortions 13 p1584 A73-28897

On the propagation of electromagnetic waves through a time-varying dielectric layer. 14 p1726 A73-29932

Ionospheric and pulse compression induced distortions in chirped Gaussian electromagnetic pulses 14 p1728 A73-30232

Distortions of UHF pulse signals propagating along the earth at distances below the radio horizon 14 p1729 A73-30559

Computation of nonlinear distortions of a wideband amplifier in the vicinity of the overload point 14 p1737 A73-30896

Nonlinear distortions of series-connected two-port networks 15 p1850 A73-31253

Sporadic E layer pulsed ultrashort oblique wave sounding, analyzing reflected signal distortion 15 p1872 A73-31866

Undistorted short sounding pulse reception at exit from ionosphere obtained by signal carrier frequency modulation 16 p1978 A73-32766

Radio direction finder of increased accuracy with a moving antenna. 16 p1991 A73-33976

Linear open signal scanning system distortion of stationary stochastic signals, examining transfer characteristic improvement by optimal filter 17 p2121 A73-34246

Distortions of signal frequency in FM oscillators. 17 p2136 A73-35154

Digital flight control systems data sampling rate selection effects on intersample ripple, spectral folding and distortion and system bandwidth 17 p2138 A73-35224

The problem of applying information theory to efficient image transmission. 17 p2124 A73-35302

Frequency distortions of signals in frequency-modulated oscillators with a delayed feedback. 17 p2130 A73-35714

FET for AM large signal processing and regulations without distortion in resonant circuits, discussing characteristics and harmonic analysis 19 p2409 A73-37433

FM distortion of a TV signal and subcarriers due to bandpass filtering and additive Gaussian noise. 20 p2523 A73-38722

The domain analysis of intersymbol interference effects on phase shift keyed /PSK/ and quadrature phase shift keyed /QPSK/ communication systems. 20 p2524 A73-38734

Analysis and design of single-cycle stages in MOS transistors with allowance for nonlinear distortions 20 p2535 A73-38857

Amplitude stability and distortion in thermistor-controlled oscillators. 20 p2535 A73-39131

Approximation of the characteristics of two-port networks with a complex nonlinearity 20 p2537 A73-39464

Evaluation of phase distortions in the magnetic recording of signals with a high-frequency magnetic bias 20 p2531 A73-39468

IR scanner for aerial stereoscopic photography, discussing use of computer controlled orthophoto printer for image distortion reduction by rectification 20 p2566 A73-39671

Determination of optimal regimes of a common-emitter transistor cascade which ensure minimal distortions 21 p2659 A73-40012

Equipment for measuring cross-modulation distortions in high-frequency power transistors 21 p2660 A73-40014

Image restoration filter with preprocessing to minimize distortion due to truncation errors and edge effects 21 p2697 A73-40131

Baseband modeling and distortion equalization of the DeLange FM oscillator by functional methods. 21 p2662 A73-40337

Frequency-dependent parasitic modulation component effects on null distortion in spectrometer and temperature measurement accuracy 21 p2700 A73-40546

Holographic image nonlinear distortion analysis based on photographic film material characteristic curve representation by Taylor series 22 p2861 A73-42410

Applications of digital frequency warping to unequal bandwidth and Vernier spectrum analysis. 23 p2952 A73-43312

Cepstrum signal processing with complex algorithm involving Fourier transforms and logarithm for multipath interference distortion reduction in single sideband or multiplexed transmission channels 23 p2953 A73-43321

Aspects of field-effect transistor applications in amplifier stages with feedback 24 p3072 A73-44936

SIGNAL ENCODING

Coding technique to record computer generated binary hologram on numerically controlled CRT with resolution cell of two beam spots 01 p0019 A73-11235

Differentially encoded multiple phase shift keyed signals transmission and detection, analyzing digital communication system performance 04 p0415 A73-14991

High-data-rate, spacecraft tape recorders. 04 p0449 A73-15383

Manned spacecraft digital TV system channel error correcting encoder and decoder performance test data including bit error rate versus SNR and decoding depth 04 p0419 A73-15400

Real time digital spacecraft TV with data compression/error correction test system, evaluating source encoding algorithm performance from processed picture quality
04 p0449 A73-15409

Source encoding with fixed word length and synchronous bit rate.
04 p0425 A73-15420

Digital link for bidirectional communication between manned spacecraft and ground terminal by synchronous communication relay satellite, noting coding parameters effects on error rate
04 p0421 A73-15426

Carrier-frequency photography - Principle and application of lattice-coded image tracing
06 p0692 A73-17754

A 2-cycle algorithm for source coding with a fidelity criterion.
06 p0671 A73-18142

Compact digital coding of electrocardiographic data.
06 p0660 A73-18815

Coherent optical processing with spatial frequency diversity speckle and reflection noise reduction, discussing coding by illuminating input transparency through square screen mesh
08 p0964 A73-21045

Constant factor delta modulator with adaptive voltage feedback to error point in coder for SNR improvement and hunting characteristic removal
09 p1065 A73-23100

Delta modulation and differential PCM systems performance comparison at high sampling rates for color video signal coding
09 p1055 A73-23389

Multispectral imagery data compression for earth resources satellites, comparing performance of spectral-spatial-delta-interleave and Rice coding algorithms
09 p1055 A73-23391

Adaptive algorithm with error control for line by line encoder for image transmission, noting reconstructed image quality improvement
09 p1055 A73-23392

Effects of multipath fading on low data-rate space communications.
09 p1058 A73-23422

Comparing bandwidth requirements for digital baseband signals.
09 p1058 A73-23423

A combined coding and modulation approach for communication over dispersive channels.
10 p1186 A73-23496

Block quantizers for encoding pictures at low bit rates, noting maximum nonstationary error signal incurred at block edges
10 p1186 A73-23497

Problems involving efficient transmission of informative parameters in the adaptive discretization of an analog signal
13 p1583 A73-28852

Code division multiplexing system for multiple signal binary transmission in branched glass fiber optical communication network
14 p1729 A73-30696

A rotation angle-to-digital code photoelectric converter
15 p1877 A73-32133

Compression of weather charts by the segmented Lynch-Davison code.
16 p1983 A73-33744

Analysis of the correlation properties of certain PSK signal systems
17 p2121 A73-34586

Huffman binary codes for pulse compression radar, evaluating ambiguity or cross correlation by computer program for replicas formation performance
17 p2131 A73-35221

Applications of error-correcting codes to TDMA satellite communications.
20 p2526 A73-38751

Color holographic technique through wave front coding of colored object, discussing He-Ne, He-Cd and argon laser irradiation, coding masks and image reconstruction
21 p2697 A73-40128

ASCII code applications to alphanumeric display terminals.
21 p2655 A73-40835

Digital communication channel with noisy errors, discussing statistical analysis of binary burst sequences for coding design
21 p2655 A73-41090

Error detection and synchronization with pseudoternary codes for data transmission.
22 p2827 A73-42464

SIGNAL FADEOUT
U SIGNAL FADING
SIGNAL FADING
NT SELECTIVE FADING
Investigation of fading radio echoes from meteor trails. I
01 p0016 A73-10201

Theory of the signal suppression effect in an M-type TWT amplifier with preliminary modulation of the electron beam
01 p0025 A73-10983

Vertical ionospheric sounding station observation for spread F layer effect on scattered signal fading, using oscillograph display and camera
02 p0142 A73-12498

UHF airborne measurement of equatorial ionospheric scintillation fading.
03 p0275 A73-13647

Characteristics of large scale ionospheric irregularities.
03 p0300 A73-13652

Rain attenuation of vertically and horizontally polarized signals of 18 GHz communication system
04 p0419 A73-15395

Ground reflection multipath effects on airborne communications.
04 p0422 A73-15439

Multipath fading and ionospheric scintillation modes of propagation anomalies measurement to formulate models of propagation media
04 p0422 A73-15440

Estimation of the cumulative amplitude probability distribution function of ionospheric scintillations.
04 p0443 A73-15477

Diurnal variation of the effective earth's radius factor k_f over India and its influence on microwave propagation.
04 p0423 A73-15928

Digital transmission performance on fading dispersive diversity channels.
06 p0664 A73-17711

Adaptive reception in a channel with slow total fading.
07 p0794 A73-20132

Noise immunity of diversity reception with threshold switching of antennas
07 p0802 A73-20291

Some characteristics of the ionospheric irregularities over the magnetic equator derived from spaced fading records.
08 p0957 A73-20656

Statistics of laser beam fade induced by pointing jitter.
08 p0975 A73-21058

Selectively faded nondiversity and space diversity narrowband microwave radio channels.
08 p0939 A73-21086

A special purpose computer for the study of fading signals.
08 p0939 A73-21139

Midlatitude signal fading during sunrise and sunset transitions, noting amplitude ratio independence of propagation direction in earth-ionosphere waveguide
09 p1049 A73-22131

Cross correlation functions skewness of fading records, noting dispersion correlation with ionospheric irregularities horizontal drift
09 p1076 A73-22143

Effects of multipath fading on low data-rate space communications.
09 p1058 A73-23422

Modulation distortions during fading in frequency-modulated multichannel radio communication
10 p1187 A73-23740

Use of semiconductor lasers in compact communication systems.
12 p1470 A73-27521

Arbeitsgemeinschaft Ionosphäre, URSI, and Nachrichtentechnische Gesellschaft, General Session, Kleinheubach, West Germany, October 9-14, 1972, Reports
12 p1493 A73-27750

Long-periodicity fading of short-wave signals
12 p1473 A73-27759

Scintillations of satellite signals and their observation.
15 p1843 A73-31524

Signal fading and topside electron density profile observation over VHF transequatorial path between Europe and Southern Africa, noting great circle F transmission role
15 p1844 A73-31766

Microwave guidance system for aircraft landing, discussing civil and military requirements, position measurement capability, shadowing in propagation, and ground reflection induced signal fading
15 p1910 A73-32468

Experimental investigation of microwave signal fluctuations for propagation above the sea at low slip angles
16 p1978 A73-32889

Propagation of radio waves at frequencies above 10 GHz; Proceedings of the Conference, London, England, April 10-13, 1973.
16 p1980 A73-33701

Rain attenuation and fade duration statistics for design of satellite-based communication system, predicting outage for 16 GHz path diversity system
16 p1981 A73-33706

Methods for investigating the effects of multipath fading on 2-phase digital radio systems.
16 p1981 A73-33708

The respective influences of multi-path configurations and precipitation rates for frequencies lying between 10 GHz and 30 GHz.
16 p1981 A73-33710

Fading correlation on terminal point and spaced microwave paths, discussing switched path diversity to overcome rain attenuation effects
16 p1983 A73-33732

Noise immunity of diversity reception with antenna threshold switching.
18 p2290 A73-37128

Diversity combining of UHF signals under rapid fading conditions.
20 p2523 A73-38724

Analysis of ground tests of a microwave, earth-occultation, pressure-reference-level system.
21 p2729 A73-40065

Performance degradation plots for comparison of signal fading and intersymbol interference effects in two-component specular multipath digital microwave communication channel
21 p2649 A73-40336

One dimensional computer simulation model of spaced-receiver drift experiment with radio fading produced by reflections from perfectly reflecting ionosphere
21 p2684 A73-40783

Optical communication system performance with tracking error induced signal fading.
21 p2657 A73-41171

Fading characteristics and drift and anisotropy parameters of the ground diffraction pattern of the radio waves reflected from the equatorial ionosphere during spread F conditions.
22 p2825 A73-41929

Short wave radio signal fadeout due to ionospheric disturbances, obtaining experimental equation on magnitude relationship with solar zenith angle and operating frequency
22 p2825 A73-42194

Measurement methods for sudden ionospheric disturbances caused by solar flares, discussing short wave fading, sudden phase anomaly and sudden enhancement of atmospherics techniques
22 p2904 A73-43036

Determination of the vertical parameters of wavelike ionospheric disturbances
24 p3083 A73-44797

Determination of the difference in group paths by the method of frequency-diversity reception
24 p3068 A73-44810

SIGNAL FLOW GRAPHS
Design of active filter sections performing biquadratic transfer functions on the basis of a branched operational-amplifier configuration
07 p0796 A73-18895

Signal flow graph methods for four and three degree of freedom linear conservative mechanical vibration systems solution, noting Chan-Mai method superiority
11 p1434 A73-25193

Dynamic analyses of hybrid bio/mechanical networks with feedback characterization.
16 p1975 A73-33161

Book - Graph theory in modern engineering: Computer aided design, control, optimization, reliability analysis.
17 p2132 A73-35600

Structural methods of multichannel systems synthesis with the aid of the graph theory
22 p2836 A73-42602

SIGNAL GENERATORS
NT FREQUENCY SYNTHESIZERS
NT FUNCTION GENERATORS
Optical sweep generator using single frequency He-Ne lasers with Michelson interferometer for mode selection to provide smooth tuning throughout Doppler width
03 p0319 A73-14065

A system for the precise calibration of air navigation receivers.
03 p0310 A73-14501

A signal simulator for testing laser-Doppler fluid-flow velocimeter systems.
05 p0562 A73-16442

Vibration test facilities and control techniques for application to industrial products, discussing shakers, signal generation and amplification, and data recording and reduction
07 p0809 A73-20575

A magnetically controlled tube generator of very-low-frequency sinusoidal oscillations
09 p1063 A73-22337

Digital quartz pressure transducer for FM signal output to interface with digital computer and telemetry, noting insensitivity to temperature and vibration interference effects
09 p1082 A73-22503

Error analysis of a generator with a uniform probability distribution of instantaneous values
11 p1331 A73-26100

Short term frequency stability and single sideband phase noise measurements on signal generators, considering frequency deviation and amplitude modulation produced by noise
13 p1582 A73-28570

Book - Topics in intersystem electromagnetic compatibility.
14 p1729 A73-30596

- The application of digital techniques to a VOR signal generator. 16 p1979 A73-33405
- Two-phase radio-frequency generators employing phase-lock AFC 17 p2135 A73-34590
- An automatic sweep generator for a strobed oscilloscope 21 p2664 A73-41098
- Bispectrum synthesizer by using multiple Poisson processes. 23 p2965 A73-44089
- Generation of complex phase-shift-keyed signals by the optical correlation method 24 p3067 A73-44595

SIGNAL MEASUREMENT

- Measurement of phase fluctuation dispersion for narrow-band signals 01 p0015 A73-10077
- Signal amplitude ratios measurement in automatic control applications by digital differential logometer, using time-pulse dividing circuits 01 p0022 A73-10082
- Application of the algorithm of a median for accuracy and reliability improvement in data processing 01 p0020 A73-10678
- Microwave dual frequency propagation experiment using the Mariner Venus Mercury probe. 03 p0275 A73-13628
- Gaussian channel model for long tropospheric scatter link verification by time varying bandpass impulse response measurements, using Kolmogoroff-Smirnoff tests 04 p0418 A73-15392
- Method for calculating the delay in a time-service photoelectric phase apparatus. 04 p0451 A73-16019
- Nonlinear conversion of a measured value aimed at reducing the influence of dependent errors 05 p0577 A73-16985
- Correction of the dynamic distortions of signals resulting from measurement information compression 05 p0577 A73-16986
- Point plot recording instrument for instantaneous signal values measurement, discussing dynamic characteristics of constant plotting rate devices 06 p0693 A73-18168
- Most convenient intervals of amplitude quantization in direction finding 08 p0939 A73-21394
- Calculation of the coverage factor of a NMR sensor for an externally located sample 09 p1080 A73-22339
- An optimal algorithm for measuring the dispersion of a random process in the case of separate allowance for the influence of external and internal additive noise 09 p1051 A73-22462
- Radiometer measurements of atmospheric attenuation at 19 and 37 GHz along sun-earth paths. 09 p1052 A73-22957
- Microwave system with direct, AM, FM and pulse propagation techniques for swept-frequency group delay measurement, discussing error sources and various distortions 10 p1193 A73-23610
- Relaxation time measurements by an electronic method. 10 p1217 A73-23998
- Digital microwave receiver with passive discriminator for precise and instantaneous pulsed RF signal frequency measurement 10 p1188 A73-24168
- Electrical interference/noise/ effects on measurements of high accuracy low-level differential data signals, discussing noise reduction, capacitive coupling problem and design principles 10 p1189 A73-24570
- Methods of representation and machine analysis of random fields and processes; All-Union Symposium, 5th, Vilnius, Lithuanian SSR, May 1972, Transactions. Sections 1, 2, 3 & 4 11 p1339 A73-25001
- Optimal control methods for combined signal processing, using complex filtration-compensation system principles and mean square measurement error criteria 11 p1340 A73-25003
- Measurement of certain one-dimensional characteristics describing the evolution of the two-dimensional probability density of random processes when changing the interval between readings 11 p1340 A73-25004
- Determination of the statistical characteristics of signals parametrically affecting a dynamic plant 11 p1340 A73-25006
- Application of the characteristics of singular points to the determination of the period of quantization in time 11 p1340 A73-25009
- Effect of time-quantization errors on the accuracy in periodogram analysis of random processes 11 p1360 A73-25015

- Use of simple test signals in experimental investigations of devices for measuring the one-dimensional probability characteristics of random signals 11 p1360 A73-25019
- Accuracy of statistical measurements of random field characteristics in interferometric systems 11 p1360 A73-25020
- Statistical synthesis of digital parameter-measuring equipment and analysis of its efficiency 11 p1360 A73-25021
- Errors in the determination of random process characteristics with the aid of measuring converters with randomly varying parameters 11 p1341 A73-25024
- Comparison of observed and predicted phase-front distortion in line-of-sight microwave signals. 11 p1380 A73-25687
- Precise measurement of reflection coefficients by means of tuned microwave reflectometers. 12 p1478 A73-27047
- Characteristics of amplitude discriminators built with transistors operating in the avalanche mode 12 p1479 A73-27209
- Phase discriminator of a nonregular signal. 12 p1480 A73-27270
- Measurements of wave normal direction of whistler mode signals in the ionosphere by means of the rocket-Doppler technique. 12 p1492 A73-27610
- Modified X band microwave calorimeter design for precision power and attenuation measurements in GHz and MHz ranges 12 p1498 A73-27752
- Stochastic-ergodic electronic U-functionmeter for signal electrical characteristics measurement, discussing design, operational features and applications 12 p1499 A73-27874
- Short term frequency stability and single sideband phase noise measurements on signal generators, considering frequency deviation and amplitude modulation produced by noise 13 p1582 A73-28570
- Faraday effect of incoherently scattered radar signals. 13 p1583 A73-28712
- Measurement of an energy-independent parameter of a radio signal in the presence of high-level additive and modulating interference. 13 p1583 A73-28729
- Investigation of an analog memory for the computational-measurement complex of an electrodynamic model 13 p1588 A73-29420
- Narrowband time domain reflectometer uses pulse modulated Gunn-oscillator to measure small reflections in 6 and 7.5 GHz band waveguides. 14 p1733 A73-30057
- Measurement equipment for the PCM transmission system KPK 30/32 14 p1736 A73-30373
- Scintillations of satellite signals and their observation. 15 p1843 A73-31524
- Central digital measuring and data logging systems for electrical and nonelectrical analog signal conversion, display and recording 15 p1849 A73-32204
- Signal bandwidth consideration for electromagnetic compatibility specifications, comparing broad and narrow band measurements performance by computerized simulation 16 p1979 A73-33169
- The R.S.R.S. ground stations for receiving 11.6 GHz transmission from the SIRIO satellite. 16 p1982 A73-33717
- Microwave radiometer measurement at 17 GHz to investigate atmospheric attenuation and radio noise and interference sources for optimal satellite communication systems design 16 p1982 A73-33718
- Earth-space slant path radio attenuation measurements above 10 GHz over four year period, noting caution in use of long term statistics 16 p1982 A73-33721
- Italian SIRIO satellite cross polarization signal measurements aided by ground station antenna system using narrow bandwidth 16 p1983 A73-33725
- Optical method for submillimeter band phase measurements by probing spatially separated compared fields and summing two signals at detector 17 p2120 A73-34155
- Laser pulse shape measurement by successive oscillographing of pulse front areas and concurrent signal amplitude variation 17 p2183 A73-34168
- Simplified space/earth signal scintillation parameters as auxiliary reference for measurements concerning ionospheric irregularities. 17 p2162 A73-34949
- Accurate measurement of antenna gain and polarization at reduced distances by an extrapolation technique. 17 p2127 A73-35676

- A practical method for measuring the complex polarization ratio of arbitrary antennas. 17 p2127 A73-35677
- The measurement of large antennas with cosmic radio sources. 17 p2127 A73-35680
- A comparison of time- and frequency-domain measurement techniques in antenna theory. 17 p2129 A73-35702
- Experimental results of radio wave absorption measurements in Southwest Europe. 18 p2288 A73-35940
- Trans-horizon propagation techniques for examining disturbances in stratified tropospheric layers. 19 p2405 A73-38221
- Measurements of artificial satellite signal Doppler spectrum. 19 p2407 A73-38351
- The most advantageous amplitude quantization intervals for direction finding. 19 p2407 A73-38352
- Some results and accuracy of satellite measurements of the electron content in the ionosphere 20 p2554 A73-39166
- Study of a correlator using two auxiliary noise sources 20 p2532 A73-39203
- Holographic method of recording temporal characteristics of optical signals. 21 p2695 A73-39958
- Equipment for measuring cross-modulation distortions in high-frequency power transistors 21 p2660 A73-40014
- Geoelectric passive Doppler receiver precision capabilities and accuracy experience, noting portability, commercial availability, error sources enumerated and quantified 21 p2705 A73-41329
- Antenna coupling induced intersystem electromagnetic interference prediction, discussing tradeoffs between analysis level, input information, measurements, cost results and user requirements 22 p2822 A73-41795
- Radio receiver intermodulation characteristics description by generic model, discussing frequency/distance separation criteria to avoid interference, signal measurement procedure and application to equipment standards 22 p2823 A73-41801
- Antenna radiation pattern measurement using time-to-frequency transformation/TFT/ techniques. 22 p2831 A73-41842
- Angle and Doppler measurements of the quasi-coherent and incoherent components of microwave transhorizon signals. 22 p2824 A73-41859
- Measurement of attenuation of 9.303 MHz waves from ISIS-II through the ionosphere. 22 p2825 A73-42193
- Root-mean-square signal amplitude variation measurements of LF radio emission from extensive air showers by whip antenna 22 p2827 A73-42486
- Use of cancellation techniques in the measurement of atmospheric crosspolarisation. 23 p2955 A73-44111
- Signal analysis using stochastic-ergodic principles, discussing PCM correlation procedures, analog-digital signal conversion and measurement methods 23 p2983 A73-44149
- A phase discriminator with feedbacks 24 p3071 A73-44545
- Correlometry of ergodic nonstationary random processes 24 p3074 A73-45095

SIGNAL MIXING

- Phase and amplitude balance - Key to image rejection mixers. 02 p0148 A73-12571
- Single band optical mixer heterodyne spectrum analyzer for laser radiation image spectrum suppression 03 p0319 A73-14083
- Convolution and correlation by nonlinear interaction in a diode-coupled tapped delay line. 06 p0678 A73-18746
- Difference frequency generation using non-linear interaction between a modulated electron beam and a collisionless plasma. 06 p0733 A73-18839
- Analog-computer studies on microwave mixing in superconducting weak links. 07 p0863 A73-20103
- Mixing properties of germanium thermoelectric indicators of SHF radiation with 'hot' charge carriers 09 p1063 A73-22456
- Double balanced microwave mixer circuit with local oscillator input and IF outputs for achieving low noise and image rejection 14 p1737 A73-30622
- Josephson junction mixing of monochromatic sources at two microwave frequencies, noting output power dependence on dc bias 18 p2340 A73-36624

- Difference frequency generation by optical mixing of two dye lasers in proustite. 19 p2438 A73-38165
- UHF airborne antenna diversity combiner for signal reception using correlation technique for phase variation removal to improve SNR and gain 20 p2523 A73-38725
- SIGNAL NOISE**
- U SIGNAL TO NOISE RATIOS**
- SIGNAL PROCESSING**
- Signal interpolation errors in adaptive-discretization systems 01 p0015 A73-10029
- Spatial-temporal processing of thermal radio signals from emitters moving in the near zone of an interferometer 01 p0017 A73-10213
- White noise signal correction for nonlinear nonstationary systems, using orthonormalized functionals 01 p0027 A73-10593
- Multichannel differential coincidence circuit in the nanosecond range 01 p0024 A73-10792
- Two-beam TWT /electron-wave TWT/ under large input-signal conditions - Effects of parameters 01 p0025 A73-10985
- Analysis of a dual-signal balanced TWT amplifier 01 p0025 A73-10988
- System design, breadboard construction and tests of slope reversal video processor based on tapped delay line estimation with timing discriminator 02 p0167 A73-11957
- Elastic surface waves - Many new applications. 02 p0193 A73-12598
- Laser anemometry developments review covering reference-beam, fringe and single-beam modes optical arrangements, signal processing systems and light scattering particles 03 p0308 A73-13535
- Multiple overlapping signal decomposition in noisy environment by inverse filtering, considering tradeoff between resolution and output SNR, and optimum pulse duration 03 p0277 A73-13908
- Pontryagin maximum principle application to optimal linear filtration for multivariable systems with signal processing 03 p0286 A73-14082
- Pulse pair estimation of Doppler spectrum parameters. 03 p0279 A73-14527
- New developments in EEG signal processing. 04 p0411 A73-15279
- Reconstitution of signals deformed by a fast AGC application to plasma resonances. 04 p0417 A73-15297
- Optimal processing of the backscatter signal in determining the structure of atmospheric inhomogeneities. 04 p0417 A73-15325
- Special features of recording 'pure' phase /binary/ acoustic holograms 04 p0450 A73-15619
- Radar sequential detector for digital processing of signal masked by noise, determining false alarm and detection probabilities and mean sampling time 04 p0423 A73-15917
- Indeterminacy functions side maxima for phase manipulated signals with low sidelobe levels in autocorrelation functions, noting Doppler frequency shift effect 04 p0423 A73-15925
- Parametric amplification of a UHF signal by plasma-beam interaction in the presence of a magnetic field of finite amplitude 04 p0424 A73-15996
- Spatial-temporal coherent processing technique application to thermal radio emission random signal reception, deriving ambiguity function 05 p0547 A73-16057
- Description and utilization of the TMS 4062 dynamic memory 05 p0553 A73-16171
- Equipment for observation of fast fluctuations in the solar radio emission flux 05 p0573 A73-16269
- Theory and practice of the signal processor in surveillance radars 05 p0550 A73-16473
- Nonlinear conversion of a measured value aimed at reducing the influence of dependent errors 05 p0577 A73-16985
- Low cost electronic method of delaying speech signals based on adaptive delta modulators 05 p0552 A73-17375
- The GaAs traveling-wave amplifier as a new kind of microwave transistor. 06 p0673 A73-17788
- Optimal sampling and quantization rates for analog signal by mean-square-error estimates and information content quantitative measure, describing probabilistic properties estimation 06 p0664 A73-17854
- Mean square error automatic equalizer for synchronous data transmission by gradient projection method for parameter optimization in discrete frequency domain, noting algorithm convergence 06 p0665 A73-18141
- Coherent and non-coherent optical processing of analog signals. 06 p0667 A73-18313
- Radar engineering developments, discussing microwave and optical systems, plan position indicators, antennas, displays, receivers, transmitters, solid state IC devices and signal processing 06 p0668 A73-18440
- Optical device for three dimensional multiplication of input signal recorded on photographic film, noting pattern recognition and optical communication applications 07 p0823 A73-19909
- A relationship between the antenna synthesis for a given radiation pattern and the statistical synthesis of systems for spatial signal processing. 07 p0801 A73-20129
- Detection of signals using receivers with processing of moduli. 07 p0794 A73-20133
- Wideband multiphase radio signal processing with given ambiguity function via sequential synthesis 07 p0794 A73-20292
- Information processing in the visual system. 07 p0786 A73-20374
- On stochastic approximation and the hierarchy of adaptive array algorithms. 07 p0846 A73-20585
- Microwave baritt /barrier-injection-transit-time/ diodes large signal performance, noting phase delay between injected and total current densities 08 p0945 A73-21074
- Fourier transformation of two-dimensional signals. I 09 p0119 A73-21899
- Transient analysis of phase-locked tracking systems in the presence of noise. 09 p1066 A73-22113
- Equivalence of systems that follow a stochastic principle of computation 09 p1059 A73-22554
- Inertial smoothing of multiplier signals in automatic control system under sinusoidal signal, noting analog simulation of inertialless synchronous detector for self adaptive control 09 p1069 A73-22654
- Frequency multiplication due to nonparabolicity of dispersion law in semiconductor structure subbands, noting electromagnetic signal transformation 09 p1133 A73-22665
- Group delay equalization in waveguide communications systems for signal regeneration with tapered meander transmission line 09 p1053 A73-23110
- Matched filters for extracting synchronization in signaling, nonreturn-to-zero and split phase PCM systems, using finite-time-duration trigonometric pulse synthesis 09 p1056 A73-23402
- The complex digital filter and its applications in digital signal processing. 09 p1058 A73-23425
- Signal synthesis based on desired autocorrelation function for pulse shaping applications in radar and communications, discussing nonlinear equations solution by decomposition into source polynomials 10 p1187 A73-23730
- High volume wideband PSK system design for minimal sidelobe, calculating signal number relationship to maximum sidelobe level of cross correlation and autocorrelation 10 p1187 A73-23733
- Wide view field laser target designation seeker system with photodetector for multiple returns discrimination, discussing sensor breadboard model, signal processing and design feasibility 10 p1216 A73-23788
- Signal processing in a randomly time varying system. 10 p1197 A73-23800
- Nonlinear /binary/ transformation effects on acoustic hologram spatial signal amplitude noting multiple images and reconstructed image distortion 10 p1218 A73-24209
- Optimal reconstruction of a stationary random process from discrete readings 10 p1202 A73-24611
- Quantization circuit for radio astronomical signals conversion into binary code and bit blocks recording on magnetic tape via Razdan-3 computer 10 p1220 A73-24698
- Optimal control methods for combined signal processing, using complex filtration-compensation system principles and mean square measurement error criteria 11 p1340 A73-25003
- Random analog signal quantization and reconstruction from discrete sample values by optimal filtration according to statistical criteria 11 p1341 A73-25013
- Image processing using acoustic surface waves. 11 p1334 A73-25358
- Normalization of stochastic system analog of linear determinate system with combined normal distribution of input/output signal, noting theorems for random variable distributions 11 p1341 A73-25632
- Sampling circuit for HF repetitive waveforms reproduction on standard x-y recorder, noting SNR improvement by signal averaging 11 p1366 A73-26304
- Human visual evoked response signal decomposition by complex demodulation in terms of after-discharge time, envelope and frequency parameters 11 p1324 A73-26497
- Utilization of thermal phenomena in the construction of signal-energy converters for coupling automatic control devices belonging to different categories of the State Instrument System 12 p1459 A73-26765
- Hybrid type discrete jet-membrane relay system technology and design for discrete signals transformations 12 p1460 A73-26770
- Discrete wideband FM signals optimal filter synthesis by coupling two nonlinear servosystems 12 p1467 A73-26869
- Signal accumulation efficiency for single-site coherent pulse radar moving over earth surface, using Taraschin approximation of signal/ground clutter ratio for monopulse radars 12 p1467 A73-26944
- An optimal electrooptical method of signal processing in coherent pulse reception 12 p1468 A73-26947
- Signal processing in the Air Traffic Control Radar Beacon System. 12 p1469 A73-27165
- Amplitude analysis of extensive air shower particle fluxes 12 p1496 A73-27202
- Preliminary frequency selection for signal matched filtering. 12 p1469 A73-27268
- Signal processing device with parametric interaction between opposite acoustic waves passing through delay line considering real time convolution and time inversion capabilities 12 p1470 A73-27569
- Application of acoustic surface-wave technology to spread spectrum communications. 12 p1470 A73-27570
- An electrooptical method for storage of weak linear-FM signals 12 p1470 A73-27577
- Modulation and speech processing techniques for a maritime-satellite service. 12 p1472 A73-27662
- Continuous analog signals optimal discretization involving selected quantization steps and sampling rates 13 p1595 A73-28017
- Comparison of different methods of reconstitution of a signal furnished under a sampled form 13 p1582 A73-28475
- Null level of a field-effect-transistor modulator of small constant-voltage signals 13 p1592 A73-28873
- Thermal IR radiation receiver with ferroelectric capacitor for amplification and transformation of signals from RF oscillator 13 p1618 A73-29133
- Radar technology applied to air traffic control. 14 p1725 A73-29895
- Application of acoustic surface-wave technology to spread spectrum communications. 14 p1733 A73-29934
- Algorithm for statistical error detection in digital control computers 14 p1730 A73-30038
- Automatic methods for smoothing and separation of characteristic points in an electrocardiographic signal 14 p1721 A73-30387
- Opto-acoustic signal processors extend radar and communication system capabilities. 14 p1729 A73-30675
- A high-accuracy digital star tracker for advanced planetary missions. 15 p1907 A73-31356
- Russian book - Radiation receivers of automatic electron optics devices. 15 p1875 A73-31588
- Relation between the N. M. Krylov-N. N. Bogoliubov averaging method and the method of envelopes in studies of a class of control systems 15 p1854 A73-31801
- Papers on digital signal processing covering digital filters, fast Fourier transform, finite word length effects, algorithms, and design and programming considerations 15 p1855 A73-32425
- A VOR sensor of advanced design - The Bendix RVA-33A. 15 p1909 A73-32454

French monograph - Contribution to the study of systems with periodically variable parameters in time, intended for the continuous amplification of signals of weak amplitude.

15 p1847 A73-32588

Signal conditioning, separation and parameter measurement in modular digital Elint analysis system for airborne, shipboard or ground based reconnaissance applications

17 p2137 A73-35207

Information transfer system of digital avionics system, examining signal reduction by baseband time division multiplexing and video distribution systems

17 p2138 A73-35230

Digital step transform for airborne radar linear FM signal pulse compression, reducing data memory requirements

17 p2123 A73-35237

High performance surface wave bandpass filters for signal processing applications.

17 p2140 A73-35320

Coherent optical processing of linear phased array radar signals.

17 p2132 A73-35649

Effect of modulating /multiplicative/ interference on signal processing in a system consisting of a phased array antenna and a receiver.

17 p2129 A73-35710

Optimal processing of signals in systems with multiple elements /channels/ of reception.

17 p2130 A73-35723

Analysis of the operation of devices for normalizing random signals

18 p2293 A73-36851

The scope for electron-optical devices for the optimal processing of composite signals in communications systems.

18 p2290 A73-37127

Wideband multiphase radio signal processing with given ambiguity function via sequential synthesis

18 p2290 A73-37129

FET for AM large signal processing and regulation without distortion in resonant circuits, discussing characteristics and harmonic analysis

19 p2409 A73-37433

DONAR - A computer processing system to extend ultrasonic pulse-echo testing.

19 p2407 A73-37448

Normalization of stochastic system analog of linear determinate system with combined normal distribution of input/output signal, noting theorems for random variable distributions

19 p2414 A73-38143

Probability of error in binary communication systems with causal band-limiting filters. I - Non-return-to-zero signal. II - Split-phase signal.

19 p2415 A73-38384

Parallel resonator with a resistance and a frequency dependent negative resistance realized with a single operational amplifier.

19 p2411 A73-38536

Correctness of the solution of signal filtration and reconstruction problems by an analog computer

20 p2522 A73-38702

Quantum signal superposition in radio communication, discussing Glauber convolution formula limitations and minimum three signal rule

20 p2529 A73-38924

Signal filtering using hard-limited digital processing. II - Performance with a single target in a coloured-noise background.

20 p2530 A73-39126

Spectra of signals with functional phase modulation in digital frequency synthesizers

20 p2537 A73-39461

Evaluation of the noise immunity of pulse systems for continuous message transmission allowing for quantization and interpolation errors. II

20 p2531 A73-39462

Reproduction of a useful signal by linear feedback systems

20 p2543 A73-39506

Acoustic surface wave thin film guides for nonlinear signal processing, discussing relative advantages over nonguided arrangements, and application to transverse wave front imaging

20 p2531 A73-39596

Horizontal aircraft maneuver strategy for maximum miss distance and minimum course deviation, examining filtering techniques, collision avoidance system and signal error analysis

21 p2734 A73-40032

Acoustic surface wave energy detection via combination of MOSFET array and ZnO overlay piezoelectric transducer, deriving signal processing technique

21 p2660 A73-40100

A radio signal shaping device with large signal attenuation in the intervals between signals

21 p2661 A73-40174

Bounds estimation for normalized second spectral moment of random radar signal process in terms of measured quantities statistics without weighting

21 p2650 A73-40343

Russian book on radar signal synthesis optimization problems covering proximity criterion, ambiguity and autocorrelation functions and FM and PSK signals

21 p2650 A73-40419

Signal extraction from channel with noise- and signal-like interferences, analyzing clipping effect on SNR in time averaging processor

21 p2650 A73-40452

Optical processing of radar signals

21 p2651 A73-40515

Russian monograph on linear signal system models covering steady state, variance and transducers of continuous and discrete signals and random and nonstationary estimates

21 p2669 A73-40798

AM radio receiver diode resonance circuit design for large signal processing, considering FET pinch-off voltage effects and correct circuit parameter selection

21 p2664 A73-41089

A method of optimization of algorithms for secondary processing of radio signals

21 p2656 A73-41129

Linear signal processing by acoustic surface-wave transversal filters.

21 p2705 A73-41426

Sampling phase rotator for removal of Doppler shift in a lunar radar.

21 p2658 A73-41590

Russian book on radio telemetry systems analysis and theory covering analog and digital data, signal processing, algebraic and trigonometric polynomials and discrete representations

22 p2824 A73-41879

Optimum processing for delay-vector estimation in passive signal arrays.

22 p2825 A73-42198

Laguerre transform of a continuous signal - Application to the study of the asymptotic regime of a Kalman filter

22 p2832 A73-42352

The application of standardized control and interface circuits to three dc to dc power converters.

22 p2802 A73-42918

Signal processing; Specialists' Conference, Erlangen, West Germany, April 4-6, 1973, Reports

23 p2952 A73-43308

Signal theory problems of discrete signal representation decomposition and characterization by Walsh and orthogonal functions, noting voiced speech analysis

23 p2952 A73-43309

Interpolation using finite duration impulse response digital filters.

23 p2952 A73-43313

Design and structure of a flexible recursive digital filter

23 p2957 A73-43315

Signal processing in medical technology

23 p2948 A73-43317

Cepstrum signal processing with complex algorithm involving Fourier transforms and logarithm for multipath interference distortion reduction in single sideband or multiplexed transmission channels

23 p2953 A73-43321

Radio astronomy interferometer receiver IF control for centimeter wave polarized signal processing and parabolic antenna instrumentation

23 p2980 A73-43377

Certain problems of frequency settling in ideal filters

23 p2959 A73-43514

Ultrasonic holography free from phase turbulence - Construction of the device and experimental results.

23 p2983 A73-44087

On the connection of the Krylov-Bogolyubov averaging method with the envelop method for investigating one class of control systems.

23 p2965 A73-44330

Meteorological Doppler radar for measurements of particle velocity and horizontal winds inside convective storms, discussing signal processing and multiple radar method

24 p3107 A73-44687

Adaptive array based on feedback concept for interference rejection, discussing processing of modulated signal with CW reference system

24 p3067 A73-44737

Signal conditioning electronics for a laser vector velocimeter.

24 p3090 A73-44819

German book on digital systems for signal processing covering discrete linear systems characteristics and design, fast Fourier transformation, digital filters, multiplexing, etc

24 p3074 A73-45000

Limitation of m.t.i. improvement factor due to oscillator instability.

24 p3069 A73-45259

SIGNAL RECEPTION

NT SYMBOLS

NT TELEVISION RECEPTION

Ground reflection effects upon radiated and received signals as viewed via image theory.

01 p0015 A73-10181

Maximum likelihood estimate of carrier frequency and arrival direction of radio signals in background noise for large aperture antennas

03 p0278 A73-14081

Cosmos 381 onboard ionospheric station signals received from magnetically conjugate region by ground wideband antennas

03 p0280 A73-14576

Receiving characteristics of antennas in the case of coherent and incoherent radiation

04 p0427 A73-14775

Performance of correlation receivers in the presence of impulse noise.

04 p0419 A73-15404

Modulating /multiplicative/ noise effects on output signal characteristics of receiver designed for optimum reception against background of Gaussian noise

04 p0423 A73-15915

Spatial-temporal coherent processing technique application to thermal radio emission random signals reception, deriving ambiguity function

05 p0547 A73-16057

PM signal cross-correlated receiver output SNR in presence of random misalignments with respect to carrier frequency and signal arrival time

05 p0547 A73-16058

Laser communication lines in atmospheric ground layer, comparing SNR for direct-reception and superheterodyne video systems

05 p0585 A73-16787

Height-gain experimental data for groundwave propagation. I - Homogeneous paths.

07 p0791 A73-19377

Height-gain experimental data for groundwave propagation. II - Heterogeneous paths.

07 p0791 A73-19378

Adaptive reception in a channel with slow total fading.

07 p0794 A73-20132

Noise immunity of autocorrelated reception of singly phase-shift-keyed signals

07 p0794 A73-20298

Determination of the apparatus constant during multifrequency measurements of radio-wave absorption by the A1 method

08 p0939 A73-21303

Noise immunity in the reception of binary radio signals on a correlated-noise background

08 p0939 A73-21553

Optical communications links with EDM digital data channels, examining signal optimal reception and noise stability

09 p1048 A73-22043

Digital FM signal receiver with postdetector integration, determining error probability as function of input SNR and noise stability

09 p1049 A73-22044

Delay-lock discriminator to measure spatial delay time of noiselike signal received by two spaced antennas

09 p1049 A73-22048

Demonstration of the transmission and reception of modulated oscillations with a helium-neon laser beam

09 p1097 A73-23328

Digital coherent demodulator techniques for moderate data rate PSK signal reception in real time, describing synchronous bandpass sampling receiver with IF signal A/D conversion

09 p1053 A73-23371

L orthogonal signaling scheme transmission bandwidth tradeoff with error probability performance of associated receiver used for data detection

09 p1054 A73-23383

The effect of carrier phase and timing on a single-sideband data signal.

10 p1187 A73-23500

Investigation of the mutual ambiguity function of a wideband signal with complex angle modulation

10 p1187 A73-23731

Zero-steering antenna system for receiving a signal close to the direction of strong interference.

11 p1332 A73-26284

Pulsar decametric radiation reception hindrance by SNR deterioration caused by bandwidth decrease and background radiation, discussing signal processing methods

11 p1426 A73-26474

Evaluation of the efficiency of the polarization selection method in suppressing fluctuating polarization noise

12 p1468 A73-26946

Long duration radio signals reception on noise background, recording signal/noise mixture on photographic film

12 p1470 A73-27578

Precision of amplitude-comparison direction finding by phased array antennas

12 p1470 A73-27579

Application of adaptive arrays to suppress strong jammers in the presence of weak signals.

13 p1593 A73-29215

Receiving characteristics of antennas in an isotropic compressible plasma.

13 p1594 A73-29230

Post-occultation reception of lunar ship America radio transmission. 14 p1725 A73-29733

Finding the approximate angular probability density function of wave arrival by using a directional antenna. 14 p1727 A73-30210

Noise immunity of the optimal noncoherent reception of an FM signal in the presence of fluctuations in the synchronization channel 14 p1729 A73-30558

Book - Topics in intersystem electromagnetic compatibility. 14 p1729 A73-30596

Optimal reception of digital signals on an additive noise background 15 p1843 A73-31493

Ionospheric tilts and long-range short-wave communications. 15 p1843 A73-31525

Investigation of the signal-to-noise ratio of ionospheric reflection by the method of coherent reception 15 p1844 A73-31890

The influence of the sea evaporation duct on the phase of the received field on a line-of-sight path. 16 p1981 A73-33713

Phase modulated data transmission with partial pilot signals, interpolating reference demodulation signals at receiving end by maximum cross correlation 16 p1984 A73-33978

Error probability of binary optical communications in turbulent atmosphere - Experimental results. 16 p1984 A73-33995

Quasi-optimal signal reception in asynchronous addressing communication systems with a time-frequency matrix 17 p2121 A73-34587

Transient response in a receiving system with AGC under the influence of fluctuating signals 17 p2121 A73-34591

Linear antenna directivity loss for fluctuating signal reception, noting effects of signal to noise ratio and antenna length 17 p2129 A73-35709

Optimal processing of signals in systems with multiple elements/channels/of reception. 17 p2130 A73-35723

Noise immunity of autocorrelation reception of single PSK signals. 18 p2291 A73-37135

Determination of the instrument constant in multifrequency measurements of radio wave absorption by the A1 method. 19 p2404 A73-37932

Optimization in the design of a 12 GHz low cost ground receiving system for broadcast satellites. 20 p2527 A73-38762

The effect of carrier recovery and bit timing errors in the coherent reception of 2 and 4 phase PSK signals. 20 p2527 A73-38766

Method for the computation of radio paths up to 4000 km long 20 p2530 A73-39180

Sensitivity and resolution of panoramic analyzers 20 p2537 A73-39455

Correlation of random phases spaced over oscillation frequencies 20 p2531 A73-39457

The estimate feedback equalizer - A suboptimum nonlinear receiver. 21 p2656 A73-41165

Phase-locked loop operation in the presence of impulsive and Gaussian noise. 21 p2656 A73-41166

A digital system for receiving binary phase-coded signals 23 p2952 A73-43319

Adaptive maximum-likelihood receiver for synchronous data signals 23 p2957 A73-43320

Radio astronomical problems due to pulsar radiation dispersal by frequency dependent propagation velocity in interstellar medium, discussing signal reception and data recording techniques 23 p2953 A73-43368

Noise immunity of quasi-optimal noncoherent reception during resynchronization with respect to time and frequency 24 p3067 A73-44590

SIGNAL REFLECTION

A modernized technique for ionospheric drifts with spectral analysis. 02 p0161 A73-12286

Correlation of noisy radiation reflected from a statistically uneven surface. 03 p0344 A73-14039

Lunar surface SEP transmitter-receiver ground wave experiment, discussing electronic equipment, multifrequency antennas and signal variation 04 p0428 A73-15391

Ground reflection multipath effects on airborne communications. 04 p0422 A73-15439

Doppler spectral width of radar signal reflected from sea surface as function of illuminated region dimensions, waviness scale and emission factors 04 p0423 A73-15913

Error analysis of ionospheric parameter measurement by satellite transmitted or reflected multiple frequency pulsed radiation signal, using perturbation method 05 p0547 A73-16051

Investigation of a signal scattered in the lower ionosphere on the basis of a group delay model 05 p0548 A73-16254

Pulse and monochromatic short wave signals phase/amplitude autocorrelation functions and probability distributions during oblique incidence reflection from ionosphere 05 p0550 A73-16776

Stochastic signal reflection by passive element, synthesizing optimal echo-signal detector for space diversity reception 05 p0550 A73-16777

Ionospheric radio signal reflection fields verified via quantitative statistical reliability criterion 07 p0815 A73-19434

Differential phase experiment on signal reflections from D region, noting systematic error in phase jitter calculation with pulse nonoverlap explanation 07 p0820 A73-20067

Reflection of a microwave signal from a semiconductor plate of finite thickness 08 p0995 A73-21517

Signal reflection height seasonal variations effect on radio waves absorption estimation from vertical ionospheric sounding 10 p1188 A73-24242

Some results of ionospheric measurements based on observations of geophysical rocket signals from spaced points and observations of signals reflected by space objects 11 p1350 A73-25077

Reduction of ILS errors caused by building reflections. 11 p1330 A73-25784

Problem of the reflection of pulse signals from a moving mirror 11 p1332 A73-26167

Ionospheric tilts and long-range short-wave communications. 15 p1843 A73-31525

Investigation of the signal-to-noise ratio of ionospheric reflection by the method of coherent reception 15 p1844 A73-31890

Turbulent scattering phenomenological model for D region partial coherent reflection experiments with measurement noise, presenting amplitude and phase statistics 15 p1845 A73-32230

Phase-difference distributions in a D-region partial-reflection experiment. 15 p1845 A73-32231

D region partial reflection mechanism model based on multiple reflector concept, presenting electron density vertical distribution 15 p1845 A73-32233

The multipath challenge for the microwave landing system. 15 p1912 A73-32503

The MADGE system - Operational results and stretch potential. 15 p1912 A73-32505

Influence of a reflected signal on the operation of a laser 16 p1978 A73-32892

Computer analysis of reflected signals obtained during radar sounding of Venus 16 p2067 A73-33807

Possibilities for improving conventional ILS systems 17 p2207 A73-34479

Drift measurement with spectral analysis during period of chemical releases into the ionosphere. 18 p2314 A73-35955

Velocity of the reflection points reveals structure and motions in the ionosphere. 18 p2305 A73-36000

Tromso (Norway) Auroral Observatory partial reflection experiment, considering data processing techniques, height resolution, phase detection, antenna arrays and D region drift measurements 18 p2315 A73-36009

VLF pulse ionosounder measurements of the reflection properties of the lower ionosphere. 18 p2305 A73-36010

Construction of D-region electron-density profiles by combined use of ground-based reflection and satellite-based transmission measurements. 18 p2306 A73-36016

Influence of the reflection forces and the tunnel effect on the current-voltage characteristic of a metal-semiconductor contact with a Schottky barrier 18 p2340 A73-36668

Correction procedure for outdoor noise measurements. 19 p2458 A73-37285

Polarization of signals which are reflected from a group of independently fluctuating targets. 20 p2529 A73-38927

Statistics of a pulse signal reflected from an inhomogeneous ionosphere 20 p2530 A73-39157

Russian book on statistical properties of ionosphere reflected signals covering statistical modeling, random processes, perturbation method and wave reflection problems 21 p2657 A73-41284

Theoretical and experimental investigations of the coefficients of reflection from plant foliages at small slip angles 22 p2847 A73-42332

SIGNAL STABILIZATION

Investigation of nonstationary processes in the ionosphere and space with quantum frequency standards. 10 p1211 A73-24214

Stabilization of relaxation oscillators based on devices with an S-type current-voltage characteristic. 10 p1197 A73-24933

Noise in cavity-stabilized microwave oscillators. 13 p1595 A73-29294

Microwave signal source amplitude stabilization, analyzing circuit with doubly balanced electronically regulated attenuator with p-i-n diodes 14 p1733 A73-30055

Si transistor amplifier design for power gain stability against temperature variations, considering emitter and collector base voltage as stability parameters 16 p1988 A73-33399

Total power filter spectrometer for radio astronomy, featuring local oscillators with commutation for removing output instabilities to reduce instrument errors 21 p2703 A73-41149

SIGNAL TO NOISE RATIOS

The quasi-linear intensity interferometer. 01 p0045 A73-10184

Instrumental considerations in high dispersion requirements of stellar spectroscopy and interstellar absorption and emission line studies, emphasizing spectral resolution and SNR optima determination 01 p0046 A73-10503

Required carrier-to-interference ratios for frequency sharing between frequency-modulation television signal and amplitude-modulation vestigial sideband television signal. 01 p0018 A73-11181

Output signal-to-noise ratios in frequency measurement system using correlation detector. 01 p0018 A73-11183

Optimization of input-signal levels during amplification in a TWT 01 p0026 A73-11266

Computer based data processing system with display for improving ultrasonic pulse echo NDT test equipment resolution and SNR 02 p0173 A73-11983

Lunar laser ranging system for experimental data acquisition, discussing preliminary design, SNR, photodetection method and data processing 02 p0141 A73-12245

Earth based and spaceborne stellar interferometer with optical balanced mixer system for coherent detection, discussing principles, construction, SNR and sensitivity 02 p0170 A73-12341

FM threshold performance of the frequency demodulator with feedback. 03 p0276 A73-13903

Multiple overlapping signal decomposition in noisy environment by inverse filtering, considering tradeoff between resolution and output SNR, and optimum pulse duration 03 p0277 A73-13908

Cell averaging constant-false-alarm-rate radar receiver with noise estimated from logarithmic detector output, determining performance in Gaussian noise by Monte Carlo simulation 03 p0277 A73-13910

Equivalence of the likelihood ratio processor, the maximum signal-to-noise ratio filter, and the Wiener filter. 03 p0282 A73-13917

Noise temperature and signal characteristics of parametric microwave superheterodyne receiver with downconverter for satellite communication, radio and TV transmission 03 p0277 A73-13986

Neumann-Pearson-optimal signal detection procedure invariant with respect to amplitude and random noise intensity 03 p0278 A73-14073

Mathematical expectation of angularly modulated signal in unsteady linear random noise, using Marchenko formula 03 p0278 A73-14074

Variance estimate of random process second order moment by nonlinear correlator in presence of additive amplitude and phase modulated and normal noise processes 03 p0278 A73-14075

Optimum detection and signal design for channels with nonc but near-Gaussian additive noise.

04 p0415 A73-14988

The performance of a noncoherent FSK receiver preceded by a bandpass limiter.

04 p0416 A73-14992

Optimal processing of the backscatter signal in determining the structure of atmospheric inhomogeneities.

04 p0417 A73-15325

Quadrature amplitude-shift key satellite communication feasibility based on SNR and transmitter power efficiency comparison with multiphase-shift key system

04 p0420 A73-15411

Acquisition time evaluation at different input SNR values for pseudonoise signal demodulation, noting common bandwidth detection system advantage

04 p0421 A73-15427

Equivalent, filter realization and threshold CNR determination for optimum design of extended range phase locked loop

04 p0421 A73-15436

Transient phenomena in a phase-locked loop with a noisy reference.

04 p0421 A73-15437

Narrow band linear filter output SNR relationship to orthogonal radiating elements system directional gain and radiation patterns

05 p0555 A73-16056

PM signal cross-correlated receiver output SNR in presence of random misalignments with respect to carrier frequency and signal arrival time

05 p0547 A73-16058

Almost-coherent detection of phase-shift-keyed signals using an injection-locked oscillator.

05 p0549 A73-16368

Laser communication lines in atmospheric ground layer, comparing SNR for direct-reception and superheterodyne video systems

05 p0585 A73-16787

Spectroheliogram SNR improvement via time averaging of 6103 A core sequence, considering sunspot evolution observed by time lapse technique

05 p0621 A73-17030

Intermodulation noise and system analysis in SSB-PM multiple access system.

05 p0552 A73-17169

Some applications of interferometry in coherent light

05 p0586 A73-17321

Examples for signal-noise improvement with the aid of polarity correlation analysis in the biological sector

06 p0656 A73-17593

Digitalized or sampled data FM demodulator recursive algorithm synthesis and SNR performance comparison with optimum analog and conventional limiter discriminator demodulators

06 p0664 A73-17712

The probability density function for the output of a cross-correlator with bandpass inputs.

06 p0665 A73-18139

Atmospheric conditions effects on line-of-sight microwave PCM data transmission system performance, comparing predicted error probability vs predetection SNR with measurement

06 p0665 A73-18187

Noise figures, detection probabilities and scintillation energy distributions in second generation image intensifier tubes

06 p0676 A73-18299

Modulated laser beam photographic recorder/reproducer system bandwidth and SNR tradeoff alternatives consideration for high dynamic range performance, suggesting FM recording technique superiority

06 p0701 A73-18309

High resolution infrared spectrometer with multiplex advantage.

06 p0695 A73-18318

Optimal and suboptimal systems for detecting fluctuating optical radar pulses.

06 p0668 A73-18393

HF radio signal reception behavior near maximum usable frequency during evening and at midnight, noting SNR

07 p0792 A73-19456

Low noise VHF preamplifier design for backscatter radar, presenting circuit diagram

07 p0801 A73-19536

The performance of a satellite-borne infrared target acquisition system.

07 p0824 A73-19946

Noise considerations in space communication antennas.

07 p0794 A73-20228

Synthesis of a system with a Pi-shaped amplitude-frequency characteristic and a 'zero' equivalent phase-frequency characteristic

07 p0794 A73-20293

Matching of capacitive sensors to low-noise amplifiers based on field effect transistors

07 p0802 A73-20296

The effect of a nonlinearity upon signals in the presence of noise.

07 p0795 A73-20499

Differentiators and integrators with RC circuits for piezoelectric transducer signals, noting instrument errors and SNR

07 p0827 A73-20534

An analysis of an arbitrary n-element adaptive array.

07 p0795 A73-20583

Preemphasis for an S-band constant bandwidth FM/FM system.

08 p0939 A73-21085

Noise immunity in the reception of binary radio signals on a correlated-noise background

08 p0939 A73-21553

Theoretical performance figures for low light level TV cameras.

08 p0972 A73-21757

Digital FM signal receiver with postdetector integration, determining error probability as function of input SNR and noise stability

09 p1049 A73-22044

Kalman filtering theory application to optimal causal demodulator for pulse amplitude modulated signals in white Gaussian noise

09 p1067 A73-22116

Investigation of the detectability of defects in the ultrasonic testing of joints obtained by friction welding.

09 p1088 A73-22299

Time jitter in line regenerators with pattern dependent pulse waveforms.

09 p1062 A73-22301

Noise immunity in detection of pseudorandom PSK signals with allowance for synchronization errors, noting reception fidelity dependence on signal to noise ratio

09 p1050 A73-22455

An optimal algorithm for measuring the dispersion of a random process in the case of separate allowance for the influence of external and internal additive noise

09 p1051 A73-22462

Optimum holographic recording of complex light fields generated by diffusive objects in presence of point sources, maximizing SNR or distortion-free diffraction level

09 p1084 A73-22880

Constant factor delta modulator with adaptive voltage feedback to error point in coder for SNR improvement and hunting characteristic removal

09 p1065 A73-23100

Acquisition detectability parameter (output SNR) for unrestricted random access through ideal hard-limiter in multiple access communication systems

09 p1053 A73-23365

Effects of tape flutter on notch noise loading test performance of predetection recording of a frequency modulated carrier.

09 p1087 A73-23367

Digital phase locked loop for FM demodulation in real time, computing SNR for frequency offsets and sinusoidal modulation

09 p1054 A73-23373

Video signals differential pulse code modulation, improving SNR by quantizing characteristics modification via nonlinear coder

09 p1054 A73-23375

Hybrid coding/decoding scheme for deep space probes data transmission, estimating bit error probability for given SNR

09 p1054 A73-23376

Amplitude-phase-keying with M-ary alphabets - A technique for bandwidth reduction.

09 p1054 A73-23385

Phase locked bit synchronization design tradeoffs between acquisition and noise performance, considering frequency tolerance of decision-directed loop with nonreturn-to-zero input

09 p1056 A73-23403

Digitally implemented clock acquisition loops for low SNR data signals.

09 p1056 A73-23405

Concatenated coding for deep space interplanetary communication with low data rate and SNR, comparing performance of three binary codes

09 p1058 A73-23424

Tracking performance of a phase locked loop with a linear phase detector.

09 p1058 A73-23432

Phase locked loop and coherent detection performance prediction, considering desirable phase detector characteristics in terms of SNR and noise spectral density

09 p1058 A73-23433

Improvement of photomultiplier performance in astronomical applications.

10 p1215 A73-23483

Intersymbol interference in binary communication systems with single-pole band-limiting filters.

10 p1186 A73-23498

Statistical analysis and computer simulation of laser Doppler velocimeter systems.

10 p1217 A73-23997

Noise in single-frequency oscillators and amplifiers.

10 p1196 A73-24864

Noise immunity of quasi-coherent reception of phase-shift keyed signals with respect to additive fluctuation noise.

10 p1191 A73-24938

Suboptimal input signal synthesis for linear control system identification based on output SNR maximization, bandwidth matching and pseudorandom binary noise nature

11 p1327 A73-25197

Zero-steering antenna system for receiving a signal close to the direction of strong interference.

11 p1332 A73-26284

Sampling circuit for HF repetitive waveforms reproduction on standard x-y recorder, noting SNR improvement by signal averaging

11 p1366 A73-26304

Amorphous thin films of rare earth transition metal alloys for magneto-optic applications, noting SNR in thermomagnetically written film

11 p1409 A73-26325

Pulsar decametric radiation reception hindrance by SNR deterioration caused by bandwidth decrease and background radiation, discussing signal processing methods

11 p1426 A73-26474

Investigation of the permissible power level of FM radio interference at the input of the frequency converter in an FM-signal receiver

12 p1477 A73-26873

Signal accumulation efficiency for single-site coherent pulse radar moving over earth surface, using Tarasnik approximation of signal/ground clutter ratio for monopulse radars

12 p1467 A73-26944

Evaluation of the efficiency of the polarization selection method in suppressing fluctuating polarization noise

12 p1468 A73-26946

Video-signal improvement using comb filtering techniques.

12 p1468 A73-27012

Preliminary frequency selection for signal matched filtering.

12 p1469 A73-27268

Analysis of the information capacity of optical matched filters.

12 p1498 A73-27516

Long duration radio signals reception on noise background, recording signal/noise mixture on photographic film

12 p1470 A73-27578

Theoretical and experimental investigations of a phase-coordinate second-order receiver.

13 p1591 A73-28658

Measurement of an energy-independent parameter of a radio signal in the presence of high-level additive and modulating interference.

13 p1583 A73-28729

SNR improvement by negative feedback and deterioration by positive feedback in amplifiers, discussing input circuit thermal noise

13 p1591 A73-28735

Noise immunity evaluation for noncoherent demodulators or FSK and PSK signals in short wave channels, using minimum a priori information on additive noise properties

13 p1592 A73-28899

Radar system with spatial (antenna pattern) and temporal (Doppler filter) responses adaptively controlled for optimum SNR and detection performance

13 p1586 A73-29213

Establishment of hologram memory system with capacity as high as 10,000,000 bits.

13 p1588 A73-29236

Aeronautical communication technology for civil ATC system development through 1990s, discussing SNR design and need for radio channel models

14 p1725 A73-29890

Multibeam satellite Effective Isotropic Radiative Power (EIRP) for aeronautical communications, discussing carrier-to-noise density increase and communication load per channel decrease

14 p1726 A73-29900

Optimal antenna array signal to noise ratio gain comparison with conventional array for narrow band signal environment

14 p1735 A73-30222

Manipulating the response criterion in visual monitoring.

14 p1722 A73-30499

Noise immunity of the optimal noncoherent reception of an FM signal in the presence of fluctuations in the synchronization channel

14 p1729 A73-30558

Tapped delay line filter for optimal single pulse detection in band-limited PCM/NRZ system in presence of Gaussian noise

14 p1729 A73-30698

Effect of nonlinearity in a coherent pulse integrator on signal-to-noise gain.

15 p1842 A73-30988

Accurate flux densities at 8.87 GHz of 195 radio sources. 15 p1933 A73-31379

The influence of pulsed noise on the performance of incoherent digital communications systems. 15 p1843 A73-31567

Signal interference and improvement of signal-to-noise ratios in a half-wave linear detector. 15 p1843 A73-31729

An analysis of helicopter rotor modulation interference. 15 p1843 A73-31731

Decision-directed detector for overlapping PCM/NRZ signals. 15 p1843 A73-31732

Output signal-to-noise ratio for a random-access repeater link with an ideal hard limiter. 15 p1844 A73-31733

Investigation of the signal-to-noise ratio of ionospheric reflection by the method of coherent reception. 15 p1844 A73-31890

Mutual coupling in the signal-to-noise ratio optimization of antenna arrays. 16 p1979 A73-33168

Single-loop delay line integrator SNR enhancement properties in additive zero mean correlated noise channels for finite signal observation times. 16 p1979 A73-33406

Optimization of input signal levels in TWT amplifiers. 17 p2134 A73-34319

Effects of cochannel interference and Gaussian noise in M-ary PSK systems. 17 p2122 A73-34871

Application of data compression techniques to spacecraft imaging systems. 17 p2122 A73-34910

Optical communication channel optimization with binary signals preamplified in optical parametric amplifier, noting amplifier gain and SNR. 17 p2123 A73-35155

The signal-to-noise ratio of a photodetector with a virtual cathode. 17 p2168 A73-35172

The effect of system blocking in an intensifier disector scanner. 17 p2169 A73-35284

A rapid-scanning image intensifier spectrometer for astronomy. 17 p2169 A73-35286

The effects of cycle slips and phase jitter on the probability of bit error in suppressed carrier phase-shift keyed communications. 17 p2126 A73-35628

Linear antenna directivity loss for fluctuating signal reception, noting effects of signal to noise ratio and antenna length. 17 p2129 A73-35709

Sequential analysis algorithm for data channel detection of received signal represented by Poisson sequence of quantum transitions under large SNR. 17 p2129 A73-35711

Linear filtering of random signals according to the criterion of maximum signal-to-noise ratio. 17 p2145 A73-35719

Effectiveness of certain easily realizable rank algorithms for detections of signals against a background of noise. 17 p2130 A73-35720

Optimal processing of signals in systems with multiple elements/channels/of reception. 17 p2130 A73-35723

Incoherent radar target extraction in clutter of unknown level by recursive integration for signal and threshold. 18 p2290 A73-37089

Synthesis of a system of pi-shaped amplitude-frequency and 'zero' equivalent phase-frequency characteristics. 18 p2291 A73-37130

Matching of capacitive pickups to low-noise junction-gate field-effect transistor amplifiers. 18 p2294 A73-37133

Digital filter tasks and applications, discussing recursive and transversal filters, waveforms, SNR, truncation errors and complex filtering. 19 p2414 A73-38301

Probability of error in binary communication systems with causal band-limiting filters. I - Non-return-to-zero signal. II - Split-phase signal. 19 p2415 A73-38384

Signal set design for bandwidth constrained multiple phase amplitude shift keyed /MPASK/ communication system, considering minimum error probability for given energy/noise ratio. 20 p2522 A73-38717

UHF airborne antenna diversity combiner for signal reception using correlation technique for phase variation removal to improve SNR and gain. 20 p2523 A73-38725

PPM pulse waveform synthesis with SNR performance improvement while retaining bandwidth-mean-square error properties inherent in wideband modulation system. 20 p2524 A73-38736

Television sound subcarrier transmission in space communication. 20 p2524 A73-38737

GOES system data collection performance estimates. 20 p2525 A73-38743

Performance estimate for coherent QPSK with random intersymbol interference due to time-varying scatter. 20 p2527 A73-38765

Signal/noise ratio in optical radar systems. 20 p2528 A73-38849

The sensitivity of optoelectronic scanning systems with out-of-phase connection of the radiation detector elements. 20 p2564 A73-38850

Detection of weak signals in narrowband noises. 20 p2529 A73-38921

Nonparametric properties of detectors optimized for Gaussian interference of unknown intensity. 20 p2529 A73-38923

Optimization and data analysis of the Frascati gravitational-wave detector. 20 p2565 A73-39013

Application of the method of equivalent nonlinear systems to noise rejection analysis in FM tracking receivers. 20 p2537 A73-39451

Signal to noise ratios of inertial detector of mixture of stationary, normal, random and harmonic voltages, varying RC circuit time constants. 20 p2537 A73-39459

Optical heterodyne radiometry of the solar surface. 20 p2611 A73-39591

Interference filter laser Raman spectrometry of gases and volatile liquids, discussing instrument sensitivity and response linearity, signal to noise ratios, and bandwidths. 21 p2698 A73-40140

The effect of weighting upon signal-to-noise ratio in pulse bursts. 21 p2649 A73-40327

Probability of error in a bandlimited quadriphase communication system. 21 p2649 A73-40334

Degradation of probability of error due to IF filtering. 21 p2649 A73-40335

Signal extraction from channel with noise- and signal-like interferences, analyzing clipping effect on SNR in time averaging processor. 21 p2650 A73-40452

Considerations about the atmospheric background and the technique of differential modulation in infrared astronomy. 21 p2740 A73-40690

The estimate feedback equalizer - A suboptimum nonlinear receiver. 21 p2656 A73-41165

Combined effects of intersymbol, interchannel, and co-channel interferences in M-ary CPSK systems. 21 p2656 A73-41167

Lunar laser telemetry technological developments, discussing light beam generation and detection, SNR and ranging accuracy improvements, and receiver-optics diameter reduction. 21 p2774 A73-41407

Lyot birefringent filter contrast element thickness effects on SNR performance and transmission loss. 21 p2706 A73-41505

Electromagnetic interference and compatibility control in aircraft communication, discussing RF current, voltage, impedance and SNR measurement techniques. 22 p2821 A73-41692

Laser Doppler velocity measuring system parameters and SNR analysis, comparing photomultiplier, p-i-n and avalanche photodiode detectors for performance. 22 p2825 A73-42298

A study of the physics and non-linear effects in photomultipliers. 22 p2860 A73-42302

Signal/noise ratio in the recording of human nerve-action potentials. 22 p2814 A73-42372

The comparison of sensitivities of atmospheric echo-sounders. 22 p2862 A73-42727

Matched-filter detection of mode-locked laser signals. 22 p2872 A73-43152

Spectral-line analysis of very-long-baseline interferometric data. 23 p2980 A73-43357

A digital correlation spectrometer employing multiple-level quantization. 23 p2981 A73-43378

Evaluation of the correctness of Gaussian approximation in noise immunity theory. 23 p2954 A73-43519

Noise and stable operation conditions in associative memory devices. 23 p2956 A73-43580

Crosstalk interference and regenerative amplifier noise effects on PCM signal transmission over twin- and four-conductor lines. 23 p2954 A73-43784

Optimum mean-square decision feedback equalization. 23 p2964 A73-43988

Maximum SNR performance calculation for heterodyne laser detection system with parameters optimization under assumed total cost. 24 p3096 A73-44875

Receiving antenna optimum polarization determination by mapping on Poincare sphere for maximum ratio of signal to summed external interference and internal noise. 24 p3068 A73-44943

Reducing the level of additive noise in the output signal of a laser velocimeter. 24 p3096 A73-44958

SIGNAL TRANSMISSION

NT AUTOMATIC PICTURE TRANSMISSION

NT BIOTELEMETRY

NT DATA TRANSMISSION

NT DOUBLE SIDEBAND TRANSMISSION

NT IONOSPHERIC F-SCATTER PROPAGATION

NT IONOSPHERIC PROPAGATION

NT MANDELSTAM REPRESENTATION

NT MESSAGES

NT MICROWAVE ATTENUATION

NT MICROWAVE TRANSMISSION

NT MULTIPATH TRANSMISSION

NT PCM TELEMETRY

NT PULSE FREQUENCY MODULATION TELEMETRY

NT RADAR TRANSMISSION

NT RADIO TELEMETRY

NT RADIO TRANSMISSION

NT SATELLITE TRANSMISSION

NT SHORT WAVE RADIO TRANSMISSION

NT SINGLE SIDEBAND TRANSMISSION

NT TELEMETRY

NT TELEVISION TRANSMISSION

NT TRANSEQUATORIAL PROPAGATION

On the diffusion function of a stochastic transmission system. 01 p0017 A73-10975

Synchronous multiplexing of digital signals using a combination of time- and code-division multiplexing /t.d.m. and c.d.m./. 02 p0140 A73-11588

Satellite digital communications over domestic and international networks for data, voice and video signal transmission. 04 p0415 A73-14739

Differentially encoded multiple phase shift keyed signals transmission and detection, analyzing digital communication system performance. 04 p0416 A73-14991

OMEGA time transmissions and receiver design. 04 p0416 A73-15063

State and integral equations formulations for signal design problem of channels with known time dispersion and additive white Gaussian noise. 04 p0419 A73-15405

Optimal equalization of discrete signals passed through a random channel. 04 p0420 A73-15418

Discrete frequency modulated signals with frequency shifted identical-envelope pulses, discussing transmission, construction and correlation functions. 05 p0550 A73-16778

Bandpass error free wideband PCM communications system response to pulse signal. 06 p0668 A73-18391

Height-gain experimental data for groundwave propagation. II - Heterogeneous paths. 07 p0791 A73-19378

Some problems of statistical estimation of a signal source in a dispersive medium. 07 p0792 A73-19912

Fluctuations in the level and phase of a field in a waveguide with a random boundary. 07 p0793 A73-19916

German monograph on human information transmission by multidimensional tactile stimuli investigation using method of learned signals identification. 07 p0786 A73-20393

Frequency-dependent transmission properties of coupled strip lines in a laminar dielectric. 08 p0945 A73-21072

Passage of useful and noise signals through a nonlinear circuit containing a p-n junction capacitance. 08 p0946 A73-21111

Oscillator synchronization by FM signal for constant central frequency-sideband phase difference operation. 08 p0946 A73-21112

Optimal search strategy to investigate probability of habitable systems with civilization transmitting detectable signals. 08 p1013 A73-21645

Atmospheric turbulence effects on laser beam transmitted signals, considering filtering and detection based on doubly stochastic Poisson process
09 p1067 A73-22229

I. orthogonal signaling scheme transmission bandwidth tradeoff with error probability performance of associated receiver used for data detection
09 p1054 A73-23383

Bending waves dispersion properties in rod applied to acoustic LF dispersion delay line design, analyzing signal distortion and attenuation during propagation
10 p1291 A73-24366

Linear codes and transverse equalization for limiting the effects of intersymbolic interference in the transmission of digital signals
10 p1189 A73-24416

Optimum bandlimited signal synthesis with pulse compression for transionospheric propagation along vertical path, considering statistical effects of total ionospheric electron content variations
11 p1330 A73-25689

Super-Alfven displacement of hydromagnetic pulses in the earth's radiation belt
12 p1491 A73-27349

Satellite design considerations.
12 p1549 A73-27659

Relative transit time measurements of high-frequency signals using an FM-CW technique
12 p1474 A73-27763

German monograph on signal transmission and radiation distribution in optical waveguide consisting of glass fibers with refractive index gradient and optically dense envelope
13 p1628 A73-29282

Book - Topics in intersystem electromagnetic compatibility.
14 p1729 A73-30596

Selective properties and form of a signal transmitted through a statistically nonhomogeneous layer of arbitrary thickness
16 p1978 A73-32896

Isolation and sampling of random signals transmitted by several hot-wire anemometers
16 p2017 A73-34016

VLF and Omega signal air navigation at 3 to 30 kHz supplementing VOR-DME and Loran-A navigation frequencies, considering transmission techniques
17 p2209 A73-34614

Effect of upper sideband impedance on a lower sideband up-converter.
17 p2123 A73-34971

A simple yet theoretically based time domain model for fluid transmission line systems.
[ASME PAPER 73-FE-27] 17 p2153 A73-35021

French book - Theory of communication: Signals, noises, and modulations.
17 p2123 A73-35149

Passage of pulses through an inhomogeneous plasma medium
19 p2406 A73-38329

Multimode glass fiber as transmission medium for digital signals.
20 p2521 A73-38659

Signal set design for bandwidth constrained multiple phase amplitude shift keyed /MPASK/ communication system, considering minimum error probability for given energy/noise ratio
20 p2522 A73-38717

Evaluation of the noise immunity of pulse systems for continuous message transmission allowing for quantization and interpolation errors. II
20 p2531 A73-39462

Calculation of processes taking place in digital automatic control systems with finite switch-closing times
20 p2543 A73-39477

New developments regarding wide-band communication with waveguide, glass fiber, and superconductivity
21 p2655 A73-41072

Russian book on airport cable communication lines, discussing design construction, signal transmission theory and structural and electrical characteristics
21 p2675 A73-41283

Modulation of spectrum and amplitude of VLF signal in the magnetosphere.
21 p2657 A73-41381

Intervire coupling noise and cable resonance equations for fast rise time signal switching at resonant frequencies
22 p2823 A73-41800

Russian monograph on signal transmission channel identification systems in statistical communication theory covering mathematical models, design principles, radio electronic systems, etc
22 p2827 A73-42600

Super-Alfven displacement of hydromagnetic pulses in the radiation belt of the earth.
23 p2970 A73-43246

Digital fluidic systems application to binary signal transmission via system with fluid transmission lines and switching element-based transmitters and receivers
23 p2944 A73-43417

Theoretical and experimental investigation of fluidic signal and noise filters with application to DC and AC fluidic systems.
23 p2944 A73-43418

Signal transmission in analog fluidic systems mainly with respect to noise influence.
23 p2944 A73-43421

Influence of a random transport-velocity component on the space-time correlations of signal fluctuations
23 p2954 A73-43647

Crosstalk interference and regenerative amplifier noise effects on PCM signal transmission over twin- and four-conductor lines
23 p2954 A73-43784

Choice of the duration of an elementary signal in the presence of fluctuations in the synchronization channel
24 p3067 A73-44605

SIGNATURE ANALYSIS

Application of the ambiguity function to seismic signatures.
06 p0690 A73-18009

Noise control modification to HH-43B helicopter for 50 percent reduction in forward flight octave band sound pressure level signature
11 p1304 A73-25383

Laboratory simulation of development of superbooms by atmospheric turbulence.
13 p1568 A73-28495

TVAC - A television area correlator tracking system.
17 p2171 A73-35381

Microwave signatures of first-year and multiyear sea ice.
17 p2163 A73-35466

SIGNATURES

NT MAGNETIC SIGNATURES

NT RADAR SIGNATURES

NT SPECTRAL SIGNATURES

SIGNS (SYMBOLS)

U SYMBOLS

SIGNS AND SYMPTOMS

NT ASPHYXIA

NT BRADYCARDIA

Usefulness of vectorcardiography combined with His bundle recordings and cardiac pacing in evaluation of the preexcitation /Wolff-Parkinson-White/ syndrome.
02 p0138 A73-12445

Semicircular canals as a primary etiological factor in motion sickness.
02 p0135 A73-12560

Pathology of angina pectoris.
05 p0542 A73-12726

Clinical diagnosis of angina pectoris, implicating obstructive disease of coronary arteries and effects of paroxysmal events on heart rate and blood pressure
05 p0542 A73-12727

Correlation of electrocardiographic studies and arteriographic findings with angina pectoris.
05 p0546 A73-12729

Familial syndrome of midsystolic click and late systolic murmur.
11 p1317 A73-25697

Phonocardiogram and apex cardiogram in systolic click-late systolic murmur syndrome.
11 p1317 A73-25698

Prophylaxis and treatment of the motion sickness syndrome
13 p1580 A73-29410

Drug therapy for treatment of cardiogenic shock syndrome following myocardial infarction, discussing sympathomimetics, alpha-adrenergic blocks and combinations
18 p2276 A73-36546

Changes in respiration accompanying a diencephalic vegetative-vascular syndrome under the action of a hypoxic mixture
21 p2636 A73-40280

Transient S-T elevation detected by 24-hour ECG monitoring during normal daily activity.
23 p2946 A73-43492

SIKHOTE-ALIN METEORITE

New data on the cosmic history of the Sikhote-Alin meteorite
10 p1281 A73-24462

Some characteristics of the surface scattering of the Sikhote-Alin meteorite shower
19 p2480 A73-37240

New data on the cosmic history of the Sikhote-Alin meteorite.
19 p2486 A73-38128

SIKORSKY AIRCRAFT

NT H-53 HELICOPTER

NT H-56 HELICOPTER

NT S-61 HELICOPTER

Sikorsky CH-53D helicopter main rotor head design, considering spherical elastomeric bearing, microstructural analysis, flight and ground fatigue tests and forging techniques
[AHS PREPRINT 713] 17 p2104 A73-35059

SIKORSKY MILITARY HELICOPTERS

U SIKORSKY AIRCRAFT

SIKORSKY S-61 HELICOPTER

U S-61 HELICOPTER

SIKORSKY S-65 HELICOPTER

U H-53 HELICOPTER

SILANES

The chemistry of urethane adhesives incorporating silane coupling agents.
03 p0332 A73-130377

SILENCERS

Acoustic and fluid dynamic tests of multibore discharge silencers scale models, noting optimum jet noise attenuation configuration
12 p1486 A73-27390

SILICA

U SILICON DIOXIDE

SILICA GLASS

Development of internal damage in silicate glasses and polymers under the action of laser radiation
02 p0184 A73-11616

Evaluation of cerium stabilised microsheet coverslips for higher solar cell outputs.
03 p0256 A73-14229

Effect of alkali-earth oxides on the optical and EPR spectra of irradiated alkali silicate glass
05 p0589 A73-17296

Metallic mounds produced by reduction of material of simulated lunar composition and implications on the origin of metallic mounds on lunar glasses.
07 p0884 A73-19738

Spun on arsenosilica films as sources for shallow arsenic diffusions with high surface concentration.
08 p0995 A73-21478

Investigation of the structure of sodium silicate glass containing oxides of multivalent metals by nuclear spectroscopy methods
09 p1110 A73-22980

Chemistry and surface morphology of soil particles from Luna 20 LRL sample 22003.
13 p1674 A73-28308

High precision photoelastic and ultrasonic techniques for determining absolute and differential thermal expansion of titania-silica glasses.
17 p2171 A73-35410

Chromium-ytterbium energy transfer in silicate glass.
21 p2752 A73-40963

High temperature creep of lithium zinc silicate glass-ceramics. I - General behaviour and creep mechanisms. II - Compression creep and recovery.
23 p2997 A73-44030

SILICATES

NT ALUMINUM SILICATES

NT ANDESITE

NT ARAGONITE

NT ENSTATITE

NT FELDSPARS

NT FORSTERITE

NT GARNETS

NT KAOLINITE

NT PYROPHYLLITE

NT PYROXENES

NT SODIUM SILICATES

NT TALC

NT YTTRIUM-ALUMINUM GARNET

NT YTTRIUM-IRON GARNET

Infrared excesses in supergiant stars - Evidence for silicates.
02 p0225 A73-12827

Petrographic features and petrologic significance of melt inclusions in Apollo 14 and 15 rocks.
07 p0880 A73-19694

Deformation of silicates in some Fra Mauro breccias.
07 p0883 A73-19734

Sheet, tecto-, ortho- and chain silicates crystal lattice breakdown under shock from ballistic range experiments, using Debye-Scherrer method for X ray diffraction studies
10 p1277 A73-24078

Mixed valencies and site occupancies of iron in silicate minerals from Moessbauer spectroscopy.
11 p1324 A73-25142

Iron silicate disproportionation by ruby laser and static heating in resistance furnace, discussing X ray diffraction patterns
11 p1409 A73-25901

Partitioning of potassium between silicates and sulphide melts - Experiments relevant to the earth's core.
11 p1355 A73-25902

Extinction and scattering by several types of silicate sphere of radius 0.05-1.0 micron, for the wavelength range 0.21-50 microns.
15 p1939 A73-32012

Silicates and water identification in interstellar grains, considering possibility of iron and carbon components
17 p2227 A73-34410

Planetary accretion from grains in intersecting solar orbits, investigating velocity impact behavior of silicate particles
17 p2228 A73-34423

Characteristics of tracks of ions of 14 less than or equal to Z less than or equal to 36 in common rock silicates.
21 p2682 A73-40242

Distribution of Ni, Ga, Ge and Ir between metal and silicate portions of H-group chondrites.

21 p2771 A73-41009

Formation of lunar carbide from lunar iron silicates.

21 p2780 A73-41643

Phase relations and diagram investigation for zirconium silicate-titanium dioxide system by quenching method, obtaining solid solution formation conditions and lattice constants

23 p2998 A73-44131

SILICIDES

NT DISILICIDES

Structure and electrical characteristics of epitaxial palladium silicide contacts on single crystal silicon and diffused P-N diodes.

02 p0147 A73-12045

Si and silicon carbide effects on silicided graphite thermal and electrical conductivities

06 p0714 A73-18558

Thermodynamic characteristics of molybdenum silicides in the temperature interval between 400 and 1200 K

06 p0710 A73-18560

Morphology and spontaneous crystallization conditions of silicides of the transition metals from solutions in metallic melts

09 p1104 A73-22976

Creep and long-term strength of molybdenum with a boron silicide coating in vacuum at temperatures from 1000 to 1400 C

12 p1512 A73-27257

Physicochemical properties of metal silicides under vacuum at high temperatures, assessing suitability as antineutron materials on Mo grids in high power vacuum electron tubes

15 p1898 A73-31842

Effect of some activators on the molybdenum and niobium siliciding process

15 p1892 A73-32247

Si and silicon carbide effects on silicided graphite thermal and electrical conductivities

16 p2030 A73-33584

Thermodynamic properties of molybdenum silicides in the temperature range 400-1200 K.

16 p2026 A73-33585

Effect of interphase boundaries on the kinetics of molybdenum silicizing

18 p2318 A73-35881

Effect of impurities on the temperature of the superconducting transition in W3Si type compounds

20 p2600 A73-39731

Study of the electronic structure of iron, cobalt, and nickel monosilicides by X-ray photoelectron spectroscopy and X-ray spectroscopy

20 p2578 A73-39734

Thermal and electrical properties of superconducting vanadium silicide tapes, plotting transition temperature vs heat treatment time and temperature and critical current vs current density

24 p3119 A73-44411

SILICON

NT SILICON ISOTOPES

A study of the spectrum-variable silicon Ap star 56 Ari.

01 p0106 A73-11305

EPR in alpha-particle bombarded silicon single crystals

02 p0201 A73-12171

Economic analysis of silicon solar cells production noting cost reduction from feasibility studies of edge defined film fed crystal growth in ribbon form

03 p0258 A73-14251

The edge-defined, film-fed growth (EFG) of silicon single crystal ribbon for solar cell applications.

03 p0258 A73-14254

The reactions of titanium and silicon with Al2O3-CaO-CaF2 slags in the ESR process.

04 p0455 A73-15744

Silicon X band oscillation TRAPATT diodes with high power efficiency, presenting electric field variation with distance

05 p0559 A73-16809

Third side of the Lampert triangle - Evidence of traps-filled-limit single-carrier injection.

05 p0605 A73-17349

Resistivity of doped polycrystalline silicon films.

06 p0733 A73-17745

Si and silicon carbide effects on silicided graphite thermal and electrical conductivities

06 p0714 A73-18558

Optical constants measurement for far IR materials of crystalline quartz, sapphire, Ge and Si at room temperature and 1.5 K

08 p0994 A73-21049

Investigations on "doping stacking fault" pyramids.

08 p0995 A73-21479

Properties of silicon implanted with boron ions through thermal silicon dioxide.

09 p1064 A73-23040

The effect of an interfacial layer on minority carrier injection in forward-biased silicon Schottky diodes.

09 p1135 A73-23044

A non-LTE study of silicon line formation in early-type main-sequence atmospheres.

10 p1272 A73-23532

Effect of compressive stress on silicon bipolar devices.

11 p1410 A73-26422

Investigation of radiation defects in silicon and germanium single crystals irradiated by 50-MeV electrons

11 p1410 A73-26449

Use of high cooling rates to obtain aluminum alloys with special properties

13 p1623 A73-28110

Cleaved Si and Ge surfaces roughness investigation by low energy electron diffraction, electron microscopy and optical reflection technique

13 p1668 A73-28452

A comparison of silicon and gallium arsenide large signal IMPATT diode behaviour between 10 and 100 GHz.

15 p1850 A73-31131

Two-phase charge-coupled devices with overlapping polysilicon and aluminum gates.

15 p1850 A73-31373

Low-frequency noise characteristics of commercial silicon and gallium arsenide IMPATT diodes.

15 p1851 A73-32188

Electromagnetic wave propagation in p-type Ge and Si semiconductor plasmas, studying dispersion, cyclotron resonance, and kinetic equations

15 p1925 A73-32214

Changes of the Balmer-series lines of hydrogen in the spectrum of the spectrally variable silicon Ap star CU Vir

16 p2057 A73-32711

Si and silicon carbide effects on silicided graphite thermal and electrical conductivities

16 p2030 A73-33584

Surface diffusion and migration on dispersed silicon and basalt during weak heating in a vacuum

16 p1977 A73-33757

The solar abundance of silicon.

19 p2483 A73-37570

Photoelectric plasma arc measurements of Si I oscillator line intensities in 2500-8000 A range, relating with transition probabilities

20 p2595 A73-39590

Combined Auger electron spectroscopy and electron impact desorption studies of silicon surfaces.

20 p2595 A73-39665

Noise of space-charge-limited current in solids is thermal.

21 p2668 A73-41559

Microdefects in dislocation-free silicon crystals.

22 p2896 A73-42276

German monograph - Doping profiles of boron-implanted silicon layers.

22 p2897 A73-42717

German monograph - The back-scattering method as a procedure for the determination of the radiation damage profile in silicon doped by ion implantation.

22 p2897 A73-42852

Interface properties of oxidized germanium-doped silicon.

23 p3016 A73-43778

Si and Ge doping characteristics and energy levels in vapor phase epitaxially grown GaAs from sample photoluminescence spectra

23 p3018 A73-44370

Detection of phosphorus in heavily diffused silicon by He⁺/backscattering.

24 p3120 A73-45262

SILICON ALLOYS

Temperature dependence of magnetic susceptibility in nickel-film-coated iron-silicon alloy specimens

01 p0062 A73-10254

Cast Al-Si alloy strengthening by Mg, Be, Ti, Cu, Cd, Zr and B alloying, refining and modifying techniques

03 p0324 A73-13512

Structural and phase transformations in silicon steels during heat treatment

06 p0707 A73-18035

Matthiessen's rule and the electric resistance of solid solutions of silicon in iron at high temperatures

09 p1104 A73-22602

Room temperature electrical properties and dopant precipitation for SiGe thermoelectric alloys.

09 p1134 A73-22758

Silicon-germanium technology program of the Jet Propulsion Laboratory.

09 p1117 A73-22759

Vaporization and compatibility of SiGe radioisotope thermoelectric generators.

09 p1117 A73-22761

SiGe alloys thermoelectric properties long term time and temperature dependent behavior, using diffusion limited dopant precipitation model

09 p1136 A73-22762

Radioisotope thermoelectric generator SiGe thermopile power degradation and operating temperature changes, discussing performance prediction model

09 p1117 A73-22763

The calculated long-term performance characteristics of a typical silicon-germanium RTG.

11 p1312 A73-26030

New mechanism of slowing down screw dislocations in ordered alloys with a bcc lattice

12 p1508 A73-26837

SILICON CONTROLLED RECTIFIERS

Integral emittance of silicon alloyed with iron, cobalt, and nickel in the temperature range from 900 to 1750 C

12 p1513 A73-27309

Dynamic strain ageing in some titanium-silicon alloys.

13 p1634 A73-28184

Liquid Ni-Si alloy short range order structure analyzed by X ray scattering, revealing Ni atoms position relation to Si atoms

14 p1764 A73-30870

The behavior of xenon when used as a fill-gas in a silicon germanium radioisotope thermoelectric generator.

19 p2455 A73-38388

High temperature material interactions of thermoelectric systems using silicon germanium.

19 p2455 A73-38390

Analytical model for long term performance prediction of multihundred watt radioisotope thermoelectric generator with Si-Ge alloy as thermoelectric material, noting degradation mechanisms

19 p2390 A73-38391

Amorphous alloy resistance thermometer development.

22 p2856 A73-42015

Formation of the overheating structure in cast AL9 and VAL5 Silumin alloys

24 p3098 A73-44473

Influence of small beryllium, titanium, and zirconium additions on the structure and properties of Al9 alloy

24 p3098 A73-44571

SILICON CARBIDES

Preparations and properties of boron and silicon carbide filaments

03 p0334 A73-13588

Boron filament reinforced Al and Ti matrices manufactured by pressure-sintering method, investigating filament external silicon carbide effects on mechanical properties

11 p1379 A73-25402

Silicon carbide whisker reinforced Al composite production by powder metallurgy, discussing mechanical strength and extrusion process for fiber orientation

11 p1373 A73-25414

Possibility of silicon carbide recrystallization in the process of reactive sintering

12 p1503 A73-27555

Phenomenon of negative differential resistance in silicon carbide crystals

14 p1783 A73-30384

Compatibility of silicon carbide fiber with a tungsten base and a titanium matrix

15 p1888 A73-31595

Room temperature creep of Borsic-aluminum composites.

17 p2189 A73-34644

Borsic/Ti-Al composite properties, fracture modes and fabrication, discussing tensile strength and temperature dependence of longitudinal strength

17 p2192 A73-35532

Study of the deformation structure in alpha-SiC single crystals

24 p3099 A73-44741

SILICON COMPOUNDS

NT ALUMINUM SILICATES

NT ANDESITE

NT ARAGONITE

NT DISILICIDES

NT ENSTATITE

NT FELDSPARS

NT FORSTERITE

NT GARNETS

NT KAOLINITE

NT ORGANIC SILICON COMPOUNDS

NT PYROPHYLLITE

NT PYROXENES

NT QUARTZ

NT SILANES

NT SILICATES

NT SILICIDES

NT SILICON CARBIDES

NT SILICON DIOXIDE

NT SILICON NITRIDES

NT SILICON OXIDES

NT SODIUM SILICATES

NT TALC

NT YTTRIUM-ALUMINUM GARNET

NT YTTRIUM-IRON GARNET

The development of SiGe-PbTe segmented thermoelectric couples involving pressure-contacted junctions.

11 p1409 A73-26035

SILICON CONTROLLED RECTIFIERS

Procedure for automatic statistical processing of experimental data in determining the rated current-voltage characteristic of TD-320 thyristors

03 p0285 A73-14325

Book - Introduction to semiconductor devices: Diodes, bipolar transistors, JFETs, IGFETs, SCRs and integrated circuits.

12 p1478 A73-27050

SILICON DIOXIDE

High energy ignition systems using silicon controlled rectifiers. 12 p1533 A73-27931

SILICON DIOXIDE
NT QUARTZ
NT STISHOVITE

Influence of low-temperature heat treatment on the electrical and recombinational properties of silicon-silicon dioxide systems 06 p0736 A73-18085

Effect of additives on ablation of phenolic-silica composites. 07 p0842 A73-19486

Properties of silicon implanted with boron ions through thermal silicon dioxide. 09 p1064 A73-23040

The electrical properties of anodically grown silicon dioxide films. 09 p1064 A73-23042

Avalanche injection effects in MIS structures and realization of n-channel enhancement type MOS FETS. 15 p1851 A73-32017

Surface ablation of silica-reinforced composites. 18 p2368 A73-36316

Thin film capacitor with anodic tantalum oxide overlaid with silicon dioxide deposited by RF sputtering, noting reliability under various voltage, temperature and humidity conditions 21 p2663 A73-40771

Three layer semiconductor dielectric interface model of structural and electrical properties of silicon-silicon dioxide system involving amorphous regions 23 p3015 A73-43614

SILICON FILMS

Effect of structural factors on the surface properties of single crystal silicon films 01 p0087 A73-10038

Alloying profile measurer for epitaxial films 01 p0050 A73-10799

N-type Si MNOS random access memory devices for data storage without applied voltage, noting threshold shifts vs writing pulse width for various oxide thicknesses 05 p0553 A73-16166

Influence of vacuum conditions in fabrication on the structure and electrophysical properties of epitaxial silicon films on sapphire 06 p0736 A73-18089

Investigation of static and transient current-voltage characteristics of diodes made of nickel-modified silicon 06 p0676 A73-18248

Miniature pressure transducers with a silicon diaphragm. 09 p1084 A73-22692

SILICON ISOTOPES

Oxygen and silicon isotope ratios of the Luna 20 soil. 13 p1677 A73-28337

SILICON JUNCTIONS

Heterojunction photocell, sensitive in the near infrared. 01 p0051 A73-10834

Study of the ac small-signal dynamic characteristic of p-n silicon diodes 01 p0024 A73-10921

Noise measurement in p-n junction surface of Si semiconductor wafer under transverse electric field, noting reverse current contribution 03 p0350 A73-13665

Design and practical aspects of maximum efficiency silicon solar cells for satellite applications. 03 p0254 A73-14205

An experimental investigation into the feasibility of higher efficiency silicon solar cells. 03 p0254 A73-14206

Diffusion, recombination and combined models demonstrating shunting and second current conduction effects on forward I-V characteristics for dark and illuminated Si solar cells 03 p0254 A73-14211

Breakdown phenomena in reverse biased silicon solar cells. 03 p0256 A73-14234

Li and Si p-n solar cells performance comparison for simulated earth orbit environment by real time irradiation with Sr 90 beta particles 03 p0257 A73-14243

Progress in the development of radiation-resistant aluminum-doped silicon solar cells. 03 p0258 A73-14248

The effect of boron concentration on radiation damage in silicon solar cells. 03 p0258 A73-14249

Radiation sensitivity of silicon imaging sensors on missions to the outer planets. 05 p0557 A73-16512

Beta irradiation of silicon junction devices - Effects on diffusion length. 05 p0537 A73-16522

Solar cells with Si Schottky function diode, discussing fabrication and barrier metal and thickness effects on output power and energy conversion efficiency 05 p0538 A73-16816

P-n junction size effect on thermal resistance of reverse biased Si mesa-type diode, considering junction area, mesa height and power dissipation 06 p0674 A73-17795

Measurements of the photomultiplication factor of silicon avalanche photodiodes. 06 p0674 A73-17796

Solid-phase epitaxial growth of Si mesas from Al metallization. 06 p0738 A73-18650

Si varactor diode series resistance resonance measurements in UHF band, noting approximate invariance with frequency 06 p0678 A73-18842

Fine structure in the optical-absorption edge of silicon. 07 p0863 A73-20175

Low-frequency current oscillations in high-resistivity, Au-doped silicon junctions with two Schottky contacts. 07 p0864 A73-20190

Silicon planar diodes produced by the ion implantation process 08 p0946 A73-21080

Characterization of p-n junctions under the influence of a time varying mechanical strain. 08 p0951 A73-21481

Solid-state devices and components for mm-wave receiver-transmitter systems. 09 p1064 A73-22498

Complementary MOS/silicon-on-sapphire LSI technology developments, assessing impact of incorporated Al and Si gates applications on high speed and low power capabilities 10 p1259 A73-23791

Numerical analysis of the properties of an avalanche diode in the avalanche multiplication range 11 p1337 A73-25321

AC impedance of silicon solar cells. 11 p1310 A73-26000

Use of Sirtl etch for silicon-slice evaluation. 12 p1530 A73-27044

Small-signal analysis of punch-through injection microwave devices. 13 p1590 A73-28541

Thermal noise measurements on space-charge-limited hole current in silicon. 13 p1668 A73-28542

Quantization effects in semiconductor inversion and accumulation layers. 13 p1669 A73-29291

Efficiencies of Schottky-barrier GaAs and both complementary structures of Si IMPATT diodes. 13 p1595 A73-29579

The impact of silicon technology on near-infrared and low-light-level imaging. 16 p2012 A73-32867

Binary capacitors made with p-channel MOS Si gate technology, discussing threshold voltage effects, structural characteristics, bootstrapping and artificial voltage enhancement 16 p1991 A73-33962

Complementary MOS/silicon on sapphire LSI technology for high speed digital multiplier and correlator logical building blocks design, fabrication and subsystem array implementations 17 p2140 A73-35318

The electrical properties of phosphorus doped silicon layers obtained by ion implantation through a passivating oxide. 17 p2220 A73-35654

Low-frequency 1/f noise in MOSFET's. 19 p2409 A73-37581

Application of the semiconductor p-n junction to measurements of rapidly varying pressures. 19 p2432 A73-38308

Millimeter wave solid state technology for 60 GHz communication systems, discussing silicon Schottky diode and varactor mixer/receiver, parametric amplifiers and upconverters 20 p2534 A73-38748

Silicon-on-sapphire thin film junction diodes, investigating second breakdown onset delay time and minimum energy dependence on high resistivity side heating 20 p2536 A73-39415

Ion implanted megohm silicon monolithic IC resistors with buried n-guard layer protection against slice-to-slice variations of fixed surface charge 20 p2537 A73-39416

Analytic theory for silicon double-sided n+/n-p-p/+ TRAPATT-diode structures. 20 p2538 A73-39594

Storage tube with silicon target captures very fast transients. 21 p2661 A73-40228

Determination of the bulk carrier lifetime in the low-doped region of a silicon power diode, by the method of open circuit voltage decay. 21 p2665 A73-41123

Effective recombination levels in N- and P-type silicon irradiated by 4.5 MeV electrons. 21 p2753 A73-41558

Electron and hole ionization rates in epitaxial silicon at high electric fields. 21 p2668 A73-41561

Low noise Si multijunction IMPATT diode measurements for large signal FM X band oscillator performance 21 p2668 A73-41588

The design, fabrication, and evaluation of a silicon junction field-effect photodetector. 23 p2981 A73-43453

Three layer semiconductor dielectric interface model of structural and electrical properties of silicon-silicon dioxide system involving amorphous regions 23 p3015 A73-43614

SILICON NITRIDES

Passivation of gallium arsenide with silicon nitride. 07 p0864 A73-20571

Degradation of MNOS memory transistor characteristics and failure mechanism model. 08 p0944 A73-20741

Silicon nitride materials for gas turbine components. [ASME PAPER 73-GT-47] 16 p2048 A73-33508

Threshold voltage stability improvement of p- and n-channel SNOS FET by annealing silicon nitride in oxygen or steam prior to gate deposition 19 p2471 A73-38451

Properties of anodic oxide films formed in the anodization of silicon nitride. [ECS PAPER 81] 21 p2702 A73-40844

SILICON OXIDES

NT QUARTZ

NT SILICON DIOXIDE

Electron beam technique for evaporating titanium and silicon oxides antireflection coatings on solar cells, noting humidity and thermal resistances and UV radiation darkening 03 p0256 A73-14228

Interpretation of K X-ray emission spectra and chemical bonding in oxides of Mg, Al and Si using quantitative molecular orbital theory. 10 p1211 A73-24107

The electrical properties of phosphorus doped silicon layers obtained by ion implantation through a passivating oxide. 17 p2220 A73-35654

Threshold voltage stability improvement of p- and n-channel SNOS FET by annealing silicon nitride in oxygen or steam prior to gate deposition 19 p2471 A73-38451

Observations of silicon monoxide in cool stars at 4.05 microns. 22 p2905 A73-41768

SILICON POLYMERS

NT METHYL POLYSILOXANE

NT SILICONES

NT SILOXANES

SILICON RADIATION DETECTORS

Apparatus PG-1 for the study of the radiation characteristics in the neighbourhood of the earth by satellite Intercomos 3. 01 p0051 A73-11021

Features of voltage-capacitance relationships in Si/Li/p-i-n detectors 06 p0675 A73-18080

Characteristics of infrared photodetectors produced by radiation doping. 09 p1079 A73-21934

A monolithic pair of dielectrically isolated high-sensitivity photodiodes operating in the visible spectrum. 16 p2012 A73-32854

The Schottky-barrier silicon photodetector in perspective with other detection devices in the 200 nm to 1100 nm range. 16 p2013 A73-32885

A low noise, very low power charge sensitive amplifier for space applications. 17 p2134 A73-34272

Photoeffect applications in MDS systems with a nonstationary depletion layer in ionizing radiation detectors 18 p2316 A73-36716

SILICON SOLAR CELLS

U SOLAR CELLS

SILICON TRANSISTORS

On the measurement of the specific 'emitter efficiency factor in bipolar transistors.' 02 p0147 A73-12043

Thermal design and tests of transcathode solid state power thyristor, rectifier and transistor devices, using heat pipe-silicon wafer construction 03 p0283 A73-13940

Arsenic emitter silicon bipolar transistor and gallium arsenide FET transistor devices for low noise microwave amplification to 10 GHz 04 p0426 A73-14731

Investigation of the influence of the emitter current on the collector junction capacitance of transistors 07 p0799 A73-19399

Mathematical models for failure rates of electronic components, considering tantalum condensers, Zener diodes and n-p-n Si transistors 07 p0830 A73-19413

Co-60 source gamma irradiation of Mo-Au doped p-type Si MOS transistors, noting threshold voltage increase and current carrier mobility decrease
07 p0862 A73-19541

The low temperature strain sensitivity of MOS transistors.
08 p0948 A73-21476

Ion-implanted bipolar transistor carrier concentration profiles.
10 p1194 A73-24155

The analytically determined response of silicon detectors to a polyenergetic neutron beam.
11 p1365 A73-26210

Analysis of the thermal stability of high- and low-power silicon planar transistors in the dynamic regime
12 p1478 A73-26949

Analog transducers based on monocrystalline silicon semiconductor piezoresistivity properties, describing various piezo-FET circuits
14 p1751 A73-29728

Anomalous low-frequency noise in MOS transistors at low temperatures.
14 p1731 A73-29749

Si transistor amplifier design for power gain stability against temperature variations, considering emitter and collector base voltage as stability parameters
16 p1988 A73-33399

Charge carrier mobility distribution along the channel of an MDS field transistor
18 p2293 A73-36720

Capacitance of a field-effect MDS transistor gate
18 p2293 A73-36721

Selection of conditions for the fabrication of planar n-p-n silicon transistors with the application of the ion-beam alloying method
20 p2535 A73-38858

Computer-aided two-dimensional analysis of bipolar transistors.
20 p2536 A73-39410

A two-dimensional numerical analysis of a silicon n-p-n transistor.
20 p2536 A73-39413

Theory and operation of space-charge-limited transistors with transverse injection.
22 p2833 A73-42598

New device techniques for microwave bipolar power transistors.
22 p2833 A73-42692

V groove MOS transistor fabrication by preferential silicon etching and masking process with noncritical alignment tolerances
23 p2960 A73-44115

Microwave transistor oscillators design based on Si overlay transistors and microstrip transmission lines as passive elements, obtaining negative resistance between collector-base terminals
23 p2961 A73-44144

SILICONE RUBBER
Material evaluation under direct rocket exhaust impingement.
[ALAA PAPER 72-1167] 03 p0287 A73-13465

Heat conductivity of system composed of a silicone-gel elastomer and a powdered mineral filler
05 p0589 A73-16771

Thermochemical properties of a silicone elastomeric ablator.
[ALAA PAPER 73-741] 18 p2326 A73-36358

SILICONES
NT METHYL POLYSILOXANE
NT SILOXANES
Performance tests for steel-steel lubrication capability of dimethyl silicone oils and greases modified by soluble, heat-stable extreme pressure and antiwear additives
03 p0329 A73-13011

Thermally conducting alumina and boron nitride filled silicone and polysulfide elastomer sheet materials for electrical insulation and heat sink applications
03 p0331 A73-13028

Additives for heat transfer reduction in the propellant combinations N2O4-MMH and N2O4-A-50.
[ALAA PAPER 72-1132] 03 p0352 A73-13439

New high performance silicone greases and their applications.
07 p0842 A73-19557

Nonhydrocarbon liquid lubricants based on phosphate and neopentyl esters, perfluoroalkyl and polyphenyl ethers, silicone and perfluorotriazines, discussing performance testing techniques
07 p0843 A73-19559

Silicone oil lubricants technology for steel-steel lubrication over wide temperature and load ranges
07 p0843 A73-19560

Spacecraft thermal control coatings development, discussing zinc orthotitanate/silicone properties as solar reflector
[ASME PAPER 73-ENAS-7] 19 p2389 A73-37969

Long term life tests for thermal shock cycles effects on plastic encapsulated semiconductor device reliability, presenting salt atmosphere testing data for silicone package
19 p2471 A73-38454

SILICONIZING
Inhibition of stress corrosion cracking of AISI 4340 steel in 10% potassium nitrate solution at 100 C.
01 p0061 A73-10138

Si addition effect on Ni-Cr alloy calorized layer depth, microhardness, phase structure, chemical composition and scaling resistance
10 p1227 A73-24960

Thermodynamic equilibrium calculation and demonstration of Mo siliciding by circulation method in hydrogen-free gaseous medium containing silicon chlorides
10 p1227 A73-24961

Boridosilicide and boridoaluminide diffusion coatings on iron and steel, investigating formation kinetics structure and properties
10 p1227 A73-24963

Effect of interphase boundaries on the kinetics of molybdenum siliconizing
18 p2318 A73-35881

SILOXANES
Hydrolysis of a disiloxane/ester fluid in a simulated hydraulic system at 275 F.
[ASLE PREPRINT 72LC-6C-1] 03 p0335 A73-14365

Influence of temperature on the behavior of the rheological properties of plastic carbon-black systems
24 p3101 A73-44471

SILTS
U SEDIMENTS
SILVER
Disilicides solubility in silver and tin melts, discussing ternary phase formation
02 p0181 A73-12367

A reliable all-silver front contact for silicon solar cells.
03 p0256 A73-14230

Electrical contacts to ion cleaned n-type gallium arsenide.
07 p0797 A73-19136

Microwave energy absorbing elements based on Pd/Ag
17 p2141 A73-35549

High energy density silver-hydrogen cells for space and terrestrial applications.
19 p2391 A73-38403

SILVER ALLOYS
Internal oxidation of silver-beryllium and silver-lithium alloys.
08 p0977 A73-21022

Development and investigation of fine-grain metal ceramic contacts of silver/graphite and silver/nickel/graphite composition for low-voltage device applications
10 p1225 A73-24320

Constitution and phase relationships in copper-silver-aluminum ternary system.
11 p1385 A73-26566

Thermodynamic analysis of the distribution of silver in the Cu-Cu2S system in the presence of Ni3S2 and FeS
17 p2188 A73-34556

Metastable phases produced by laser melt quenching.
22 p2878 A73-42576

SILVER BROMIDES
Silver halogenide bichromatic gelatin chemical and photographic properties, noting decelerating development effect
21 p2647 A73-40266

Stability of silver bromide dispersions in the presence of gelatin and other surface-active substances
21 p2647 A73-40267

SILVER CHLORIDES
Solid state AgCl detectors for nuclear tracks with on- and off-response at choice - Applications to life sciences.
22 p2814 A73-42179

SILVER COMPOUNDS
NT SILVER BROMIDES
NT SILVER CHLORIDES
NT SILVER HALIDES
NT SILVER IODIDES
Nonlinear optical susceptibility measurements for zinc silver indium sulfide quaternary compounds, noting agreement with bond charge theory
09 p1120 A73-22090

Some properties of synthesized stephanite (Ag5SbS4) specimens
17 p2219 A73-35551

SILVER HALIDES
NT SILVER BROMIDES
NT SILVER CHLORIDES
NT SILVER IODIDES
Investigation of the dependence of the quality of a reconstructed holographic image on the parameters of the photoemulsion layer. I - Diffraction efficiency of the hologram
14 p1753 A73-30370

SILVER IODIDES
Silver powder anode, perylene-iodide cathode and ionically conductive solid cyanide-iodide electrolyte battery construction and performance tests
[ECS PAPER 12] 21 p2635 A73-40841

Thermoelectric effects and power calculation of solid electrolyte silver-silver iodide-silver thermocell as function of impurity ion concentration and temperature
21 p2636 A73-40842

SILVER OXIDE ZINC BATTERIES
U SILVER ZINC BATTERIES
Recent research results in the field of hermetically sealed miniature silver-zinc storage batteries.
02 p0133 A73-12513

A versatile silver oxide-zinc battery for synchronous orbit and planetary missions.
02 p0133 A73-12622

Nonleaking battery terminals design for polyphenylene oxide plastic cased Ag-Zn battery for synchronous satellite applications, describing life tests under thermal and electrical cycling
09 p1034 A73-22757

Measurement of zincate permeation in a polyethylene battery separator with controlled external hydrodynamic conditions.
11 p1307 A73-24974

Design criteria and candidate electrical power systems for a reusable Space Shuttle booster.
11 p1311 A73-26016

Power supply requirements during the AEROS acquisition phase.
13 p1689 A73-28784

Sealed silver oxide zinc cells for orbiting and planetary missions.
13 p1572 A73-29586

SIMICOR (IMAGE CORRELATOR)
U IMAGE CORRELATORS
SIMILARITIES
U ANALOGIES
SIMILARITY NUMBERS
The three-dimensional turbulent boundary layer - Theoretical and experimental analysis
16 p1961 A73-32810

Similarity parameters and approximate relations for the axisymmetric supersonic flow past an ellipsoid
18 p2266 A73-37019

SIMILARITY THEOREM
NT LAGRANGE SIMILARITY HYPOTHESIS
Similarity theory of planetary atmosphere circulations applied to solar atmosphere in terms of radius and rotational Mach number
01 p0106 A73-11316

Mathematical models for elastic solid bodies via similarity theory, noting rheological simulation for thermal stress analysis
03 p0386 A73-13146

Similarity solution for the curved two-dimensional jet.
[ASME PAPER 72-APM-JJ] 05 p0564 A73-16527

Similarity condition for the lateral contraction coefficient in photoelasticity
06 p0761 A73-17785

Similarity solution for equations of nonplanar relativistic flow from point energy source, applying to spherical shock propagation and cosmic ray generation
07 p0810 A73-19506

The mixing length derived from Karman's similarity hypothesis.
08 p0955 A73-21442

Similarity solutions of unsteady, compressible plane and axisymmetric laminar boundary layer equations.
10 p1208 A73-24807

Heat conduction nonlinear boundary value problems approximate solution via Westphal similarity theorem, considering inhomogeneous media with temperature dependent heat transfer coefficients
11 p1451 A73-25742

Application of similarity theory to the calculation of certain characteristics of an electrical explosion of wires
12 p1523 A73-26937

Turbulent surface layer shear convection analysis, using similarity model based on weak interaction between vertical motion and mechanical turbulence
13 p1655 A73-29340

Similarity properties of shockless axisymmetric flows with heat addition, considering convergent base and divergent duct flows
13 p1567 A73-29449

Power law recompression of fully developed centered gas expansion, obtaining flow distribution via closed form integral solution based on similarity theory
16 p2000 A73-33317

Half plane stress boundary value problems in elastodynamics, obtaining similarity solutions in terms of analytic functions via integral transforms
16 p2082 A73-33903

Similarity in the flow of a magnetized plasma around a plate and cylinder
17 p2215 A73-34260

Correspondence laws of diabatic and adiabatic gas flows referring to similarity between pressure, temperature, sound velocity and Mach numbers
18 p2299 A73-36488

The structure of internal intermittency in turbulent flows at large Reynolds number - Experiments on scale similarity.
20 p2546 A73-39090

Similarity relations derived for unsteady powder burning with light irradiation or occurrence in semiclosed volume
21 p2791 A73-40700

SIMILITUDE LAW

Application of similitude theory to exploding wire experiments. 22 p2886 A73-42271

Book on engineering dynamics similitude and scaling methods covering blast waves and gas dynamics, transient loads, fluid-structure interaction, soil dynamics, thermal modeling, etc 23 p3039 A73-43460

SIMILITUDE LAW

Simulation of unsteady gas exchange in internal combustion engines 02 p0202 A73-11632

Similarity relationship for wing-like bodies at high Mach numbers. [AIAA PAPER 73-203] 05 p0532 A73-16937

Locally similar solutions of equations of a turbulent boundary layer on a circular cone 08 p0925 A73-20646

Heat transfer law for free convection in cylindrical and spherical interlayers 11 p1450 A73-25726

German book - Similarity laws and model rules of aerodynamics. 15 p1863 A73-31475

Design modeling of external and internal cooling systems for bodies exposed to high temperature gas flow, discussing operation similarity conditions 20 p2628 A73-39419

A natural frequency analogy between spherically curved panels and flat plates. 21 p2785 A73-40754

SIMULATED ALTITUDE

Cardiopulmonary responses of male and female swine to simulated high altitude. 24 p3060 A73-45058

SIMULATION

NT ACOUSTIC SIMULATION
NT ALTITUDE SIMULATION
NT ANALOG SIMULATION
NT ATMOSPHERIC ENTRY SIMULATION
NT COMPUTERIZED SIMULATION
NT CONTROL SIMULATION
NT DIGITAL SIMULATION
NT ENVIRONMENT SIMULATION
NT EXHAUST FLOW SIMULATION
NT FLIGHT SIMULATION
NT LANDING SIMULATION
NT RHEOELECTRICAL SIMULATION
NT SPACE ENVIRONMENT SIMULATION
NT THERMAL SIMULATION
NT WEIGHTLESSNESS SIMULATION

Randrop impact erosion damage on ceramic radome materials, discussing Rayleigh wave mathematical model comparison with sled test data, and laboratory simulation 11 p1336 A73-25306

Electric coil systems for magnetic field simulation, discussing field size and characteristics and coil configurations 16 p1997 A73-33383

Teleoperator monoscopic television system and stereoscopic TV system with Fresnel display, using static simulations to investigate camera locations and depth alignment [AIAA PAPER 73-920] 21 p2673 A73-40868

SIMULATOR TRAINING

U TRAINING SIMULATORS
SIMULATORS

NT COCKPIT SIMULATORS
NT CONTROL SIMULATION
NT ENVIRONMENT SIMULATORS
NT FLIGHT SIMULATORS
NT LUNAR GRAVITY SIMULATOR
NT SHOCK SIMULATORS
NT SOLAR SIMULATORS
NT SPACE SIMULATORS
NT TARGET SIMULATORS
NT TRAINING SIMULATORS
NT VIBRATION SIMULATORS

A high-performance test facility for laboratory simulation of the Large Space Telescope orbiting vehicle in a single-degree-of-freedom mode of rotation. [AIAA PAPER 73-884] 20 p2544 A73-38820

A new flush mounted antenna element for phased array application. 21 p2663 A73-40662

Sensor data display simulator for airborne target acquisition with improved sensors, using TV scanning of film based imagery [AIAA PAPER 73-921] 21 p2673 A73-40869

SIMULTANEOUS EQUATIONS

Power series method for accurate solution of eigenvalue problems and simultaneous equations representing static, dynamic and stability responses to structural design parameter changes 07 p0906 A73-19027

FORTAN IV program and recursive matrix partitioning algorithm for solution of photogrammetric simultaneous equations, noting computation time 09 p1059 A73-22382

Positive solutions of infinite equation and inequality systems and Lagrange multipliers for infinite differentiable optimization problems 10 p1243 A73-24163

Partitioning techniques for solving large systems of equations in structural analysis. 11 p1442 A73-25844

Radiant heat transfer on circular-finned cylinders. 14 p1817 A73-30574

Sturm comparison and separation theorems for linear, second order, self-adjoint, ordinary, differential equations and for first order systems. 15 p1902 A73-32377

Computer oriented algorithms for solving systems of simultaneous nonlinear algebraic equations. 17 p2199 A73-34107

Simplex method for linear programming for computerized design global optimization problems involving large numbers of equations and variables 19 p2407 A73-37406

SIMULTANEOUS IMAGE CORRELATOR U IMAGE CORRELATORS

SINE U TRIGONOMETRIC FUNCTIONS

SINE WAVES

Statistical properties of two sine waves in Gaussian noise. 09 p1120 A73-22115

A magnetically controlled tube generator of very-low-frequency sinusoidal oscillations 09 p1120 A73-22115

Conditions for stability of incompressible elastic material obtained from small-amplitude plane sinusoidal waves superposed on finitely deformed state of material 13 p1696 A73-28753

Noise rejection estimation for sinusoidal signal detectors which use information on zero-crossing moments 15 p1842 A73-31251

The relation of tests with electrodynamic vibrators to the Woehler testing technique 16 p2037 A73-33379

The application of digital techniques to a VOR signal generator. 16 p1979 A73-33405

Propagation of acoustic waves in a fluid flowing through a cylindrical duct 21 p2677 A73-40944

Analysis of the accuracy of a system for controlling vibration tests with sinusoidal excitation 21 p2674 A73-40996

Time-average holography of objects vibrating sinusoidally and moving with constant acceleration. 22 p2863 A73-43092

SINGLE CRYSTALS

NT WHISKERS [SINGLE CRYSTALS]

Effect of structural factors on the surface properties of single crystal silicon films 01 p0087 A73-10038

Doped CdSb single crystal production and physical properties for IR detectors and thermocouple use 01 p0088 A73-10040

Dislocation damping in ultrasound-irradiated molybdenum single crystals 01 p0061 A73-10251

Role of the crystalline structure and orientation of single crystals in the formation of the external friction process 01 p0062 A73-10259

Influence of the polarization of phonons on the thermal conductivity of single crystals of indium phosphide between 300 and 800 K 01 p0087 A73-10430

Some optical properties of CaMoO₄ single crystals 01 p0088 A73-10626

Influence of light on the electron work function of GaAs single crystals at low temperatures 01 p0088 A73-10631

Investigation of the emission of donor-acceptor pairs and of their phonon echoes in CdS single crystals 01 p0088 A73-10634

Microhardness anisotropy of hardened and aged Be single crystal as function of purity 01 p0067 A73-11353

Investigation of laser radiation self-focusing by alkali halide single crystals according to data on the damage-focus displacement effect 01 p0061 A73-11443

The thermally activated deformation of niobium-molybdenum and niobium-rhenium alloy single crystals. 02 p0179 A73-11574

Metallographic macro- and microstructural study of semiconductor compounds, discussing single crystal imperfections, polycrystals and semiconducting films 02 p0199 A73-11582

EPR in alpha-particle bombarded silicon single crystals 02 p0201 A73-12171

Stresses governing the high-temperature creep rate in single crystals with a bcc lattice 03 p0326 A73-13971

Substructural changes during high-temperature creep deformation of aluminum single crystals 03 p0327 A73-13978

An analysis of thermally-induced plane waves in elastic-plastic single crystals. 03 p0394 A73-13980

The edge-defined, film-fed growth (EFG) of silicon single crystal ribbon for solar cell applications. 03 p0258 A73-14254

A fourth-order nonlinear equation of state - Application to the determination of the elastic moduli of single-crystal and polycrystalline solids 03 p0350 A73-14601

Metal-semiconductor system phase diagram for temperature dependence of substrate surface epitaxial film thickness during single crystal growth, determining equilibrium saturation time 04 p0483 A73-14880

Electron beam float zone melting and vacuum degassing of niobium single crystals. 04 p0456 A73-15762

Anomalous slip in high-purity niobium single crystals deformed at 77 K in tension. 04 p0467 A73-15931

Charge density distribution in Be single crystals from X ray structure amplitudes for lowest angle Bragg reflections, comparing with Hartree-Fock and free electron plane wave models 04 p0467 A73-15932

Calculation of X-ray elastic constants on the basis of single crystal coefficients of metals with a hexagonal structure 05 p0588 A73-17244

A method for performing high precision lattice parameter change measurements on quenched aluminum. 05 p0580 A73-17257

Galvanomagnetic effects measured in p-type bismuth selenide single crystal within magnetic field for Hall and conductivity mobilities, determining temperature dependences 06 p0733 A73-17741

Resistivity of doped polycrystalline silicon films. 06 p0733 A73-17745

Influence of annealing at near melting point temperatures on the substructure of aluminum single crystals 06 p0707 A73-18036

Creep in molybdenum single crystals at 0.57 of the melting temperature 06 p0708 A73-18047

Structural changes in molybdenum single crystals during high temperature creep 06 p0708 A73-18048

Bismuth germanate and silicate single crystals refractive index and electro-optic coefficient measurement 06 p0737 A73-18367

Laser-radiation-induced damage to the surface of lithium niobate and tantalate single crystals. 06 p0738 A73-18591

The orientation dependence of deformation mode and structure in stoichiometric NiAl single crystals deformed by high temperature steady-state creep. 06 p0712 A73-18758

Crystal field spectra of lunar pyroxenes. 07 p0881 A73-19709

Optical properties of Nd³⁺/ in lanthanum oxyfluoride single crystals 07 p0837 A73-20205

The anisotropy of carrier lifetime in graphite. 08 p0982 A73-21220

Uniaxial magnetic anisotropy of single-crystal permalloy films 09 p1132 A73-21958

Work function measurements by the field emission retarding potential method. 09 p1133 A73-22196

Certain properties of an electron plasma in a strong electromagnetic field 09 p1130 A73-22704

Amplitude-dependent anelasticity in aluminum and copper single crystals 10 p1231 A73-23693

Contribution to the study of the elasticity of monocrystalline aluminum under very low stresses 10 p1231 A73-23771

Temperature dependence of kinetic properties of photoconductivity produced by carrier redistribution across attachment centers, discussing results with Ag and Al doped ZnS single crystals 10 p1260 A73-24468

Positive thermal coefficient of electrical resistance in BaTiO₃ single crystals near the Curie point 10 p1260 A73-24473

Temperature-induced changes of the electron-vibration spectrum of LaAlO₃-Cr³⁺/ crystals 10 p1260 A73-24578

Drift mobilities of holes and electrons in naphthalene single crystals. 11 p1407 A73-24988

Effect of impurities and X-ray irradiation on the motion of pores in ionic crystals under the action of an external electric field 11 p1401 A73-25242

Investigation of the relationship between 'edge' and exciton emission in CdS single crystals 11 p1408 A73-25246

Shock induced phase change in single crystal orthoclase at 115 kb, noting high pressure phase with hollandite-structure properties 11 p1352 A73-25586

Investigation of self-focusing of laser radiation with alkali halide single crystals from data concerning the displacement of the focus of damage. 11 p1376 A73-26065

Parallel spin-wave pumping in yttrium garnet single crystals. 11 p1409 A73-26188

Coherent production of electron-positron pairs and bremsstrahlung on a corundum crystal. 11 p1410 A73-26447

Amplitude-dependent anelasticity in aluminum and copper single crystals. II - Studies in amplitude range III during and after plastic deformation. 11 p1385 A73-26567

Gliding, twin formation and fracture of iron-single crystals at 78 K and at 4 K. 11 p1386 A73-26571

Influence of plastic deformation on the electrical resistance of molybdenum single crystals. 12 p1512 A73-27260

Mechanical properties of strip molybdenum with a polygonized single-crystal structure. 12 p1513 A73-27265

Drift mobility of holes and electrons in perdeuterated anthracene single crystals. 12 p1531 A73-27688

Surface effects on trapping and recombination processes in BiI₃ single crystals. 12 p1531 A73-27938

Effect of impurities on the substructure and dislocation formation in metal crystals grown from melts. 13 p1631 A73-28103

Effect of the degree of purity on the dislocation structure of tungsten single crystals. 13 p1631 A73-28104

Study of the structure and properties of oriented tungsten single crystals. 13 p1631 A73-28105

Investigation of structure and imperfections in molybdenum single crystals grown by electron-beam zone refining techniques. 13 p1631 A73-28106

Application of similarity criteria in calculations of a mobile magnetic field to be used for growth stimulation in single crystals of metals. 13 p1667 A73-28108

Petrology of fine-grained rock fragments and petrologic implications of single crystal from the Luna 20 soil. 13 p1674 A73-28307

Factors controlling the corrosion behavior of titanium and titanium-nickel alloys in saline solutions. [NACE PAPER 64] 13 p1637 A73-29311

Transgranular stress corrosion cracking of austenitic stainless steels - A single crystal study. 13 p1642 A73-29520

NMR measurements of the speed of vortices in flux flow in a type II superconductor. 14 p1783 A73-30433

Diffusion creep by dislocation climb in beryllium and Be-Cu single crystals. 14 p1761 A73-30633

A data display device for switching and logic elements constructed from single-crystal ferromagnetic materials. 14 p1731 A73-30941

Investigation of phase transitions in BaTiO₃. 15 p1923 A73-31204

Preparation of CdS single crystals with a radiation-stable sensitivity to ionizing emissions. 15 p1923 A73-31208

Temperature dependence of the single-crystal elastic constants of Co-rich Co-Fe alloys. 15 p1890 A73-31926

Effect of specimen thickness on the fracture surface energy of 100 axis tungsten single crystals. 15 p1891 A73-32022

Single crystal mechanical and electrophysical properties in refractory compounds, including temperature effects, microhardness, resistivity, heat transfer, deformation and Hall effect. 15 p1898 A73-32241

Russian book on single crystals of high melting and rare metals and alloys covering structure, interatomic bonds, growth, plastic deformation, heat treatment, etc. 15 p1893 A73-32297

Single crystals for optical applications - Problem of index homogeneity of double niobates Ba_x/Sr_{1-x}/Nb₂O₆ and Ba₂Nb₅O₁₅. 16 p2043 A73-32862

Pre-macro yielding and the orientation dependence of the 'shear' stress in molybdenum single crystals. 16 p2025 A73-33197

Thermal properties of rhenium single crystals at high temperatures. 16 p2026 A73-33581

Dependence of laser-induced breakdown field strength on pulse duration. 17 p2183 A73-34201

Temperature dependence of low-temperature strength in aluminum single crystals. 17 p2189 A73-34581

Optical and luminescent properties of CdBr₂-Sn and CdCl₂-Sn single crystals. 17 p2219 A73-35553

Electron emission of In₂Se crystals in strong electric fields. 17 p2219 A73-35555

Electrical properties of single-crystal films of p-type PbTe. 17 p2219 A73-35556

Determination of ultramicro-impurities in CdS-type semiconductor materials - Determination of copper. 17 p2220 A73-35558

Parameters of fast recombination centers in CdS single crystals and the effect of the parameters on photosensitivity. 18 p2340 A73-36669

Infrared absorption and local symmetry of negative ClO₄ and ReO₄ impurity ions in KI and CsI crystals. 18 p2340 A73-36673

Influence of plastic strain on the paramagnetic susceptibility of molybdenum single crystals. 18 p2324 A73-36802

A study of electrical conductivity inhomogeneities in CdS single crystals. 18 p2341 A73-36963

Study of the behavior of metallic single crystals - Application to the tension of the fcc single crystal. 19 p2495 A73-37425

Grain refinement by titanium in the unidirectionally solidified aluminum alloys. 19 p2442 A73-37949

Changes in the microhardness of lithium fluoride crystals subjected to cyclic elastic compression. 19 p2470 A73-37954

Luminescence of CdS single crystals doped with various donors and acceptors. 19 p2471 A73-37955

Effect of the surface condition on the reflection and luminescence spectra of CdS crystals. 19 p2471 A73-37961

The preparation and anisotropic hardness of tantalum single crystals with principal orientations. 20 p2575 A73-38637

Injection-modulation devices as elements of integrated circuits. 20 p2534 A73-38855

Two-photon absorption in cadmium sulfide selenide single crystals employing pulsed ruby laser, discussing optical pumping, absorption anisotropy, ray refraction and luminous intensity. 20 p2573 A73-39682

Kinetics of recovery of luminescence properties of gallium arsenide single crystals irradiated with high-energy electrons. 20 p2574 A73-39697

Structural changes during plastic deformation and annealing of tungsten single crystals. 20 p2579 A73-39738

Faulty structure in niobium single crystals deformed by rolling at 77 K. 20 p2579 A73-39743

NiO and CoO single crystal thermal conductivities, reporting specific heat and electrical resistivity near magnetic transition. 20 p2600 A73-39826

Emission spectra of ZnS.Cu single crystals. 21 p2751 A73-40311

Influence of electrically active impurities on the mobility of individual dislocations in germanium. 21 p2751 A73-40370

Large mercuric iodide single crystals application to high resolution X ray detectors, discussing fabrication by coating platelet face with thin Aquadag film and mounting upon carbon substrate. 21 p2699 A73-40465

Raman spectrum of PbZrO₃. 21 p2752 A73-40894

A detailed investigation of slip line pattern and sub-surface dislocation structure of molybdenum single crystals. 21 p2722 A73-41566

Combined LEED, Auger electron and flash desorption spectroscopy of metals on single crystal surfaces. 21 p2706 A73-41596

The yield stress of Ni₃Al, W/. 22 p2880 A73-43075

Investigation of the substructure in molybdenum single crystals deformed by compression. 23 p2991 A73-43712

Two-phonon absorption in SbSI single crystals. 23 p3016 A73-43713

Microstrain gage for plastic deformation measurements of crystalline solids in compression, obtaining stress-strain diagrams for Ta single crystals. 23 p2986 A73-44036

Wettability and interfacial tension of magnesium single crystals by molten magnesium oxide-aluminum trioxide-silicon dioxide glasses, discussing contact angle relationship to temperature. 23 p2998 A73-44132

The hardness of titanium-diboride single crystal grown from metal bath. 23 p2994 A73-44154

Optical modulation of X band microwave transmission by acoustoelectric domains in semiconducting CdS single crystal, noting domain conductivity and permittivity changes. 23 p3018 A73-44365

Biaxial potassium niobate single crystal nonlinear optical coefficients determination by Marker fringe pattern method, using CW Nd doped yttrium-aluminum garnet laser. 23 p3018 A73-44369

Temperature dependence of dc electroconductivity of CdSe single crystals and compressed micron particle size powders, noting pressure and annealing effects on powder conductivity. 23 p3018 A73-44372

Some experiments on a voltage-induced optical waveguide in LiNbO₃. 23 p3019 A73-44374

Study of the deformation structure in alpha-SiC single crystals. 24 p3099 A73-44741

Certain properties of synthetic diamond crystals of various habits. 24 p3104 A73-44970

Aircraft gas turbine engines with single crystal blades to avoid conventional casting grain boundary weakness and premature damage. 24 p3094 A73-45155

Diffusion treatment of CdS and ZnO crystals and their applications in micro-wave acoustics. 24 p3120 A73-45433

Fatigue hardening in niobium single crystals. 24 p3101 A73-45474

SINGLE SIDEBAND DEMODULATION

U SINGLE SIDEBAND TRANSMISSION

SINGLE SIDEBAND MODULATION

U SINGLE SIDEBAND TRANSMISSION

SINGLE SIDEBAND RECEIVERS

U SINGLE SIDEBAND TRANSMISSION

SINGLE SIDEBAND TRANSMISSION

Complex detection - A waveform preserving technique for single-sideband demodulation. 04 p0415 A73-14989

Channel filters with longitudinally coupled flexural mode resonators. 04 p0427 A73-15320

Intermodulation noise and system analysis in SSB-PM multiple access system. 05 p0552 A73-17169

Weaver modulator with digital filter for single sideband transmission in radio communication and telemetry, discussing FORTRAN simulation for cost, computation time and accuracy. 10 p1186 A73-23499

The effect of carrier phase and timing on a single-sideband data signal. 10 p1187 A73-23500

Direct conversion s.s.b. receivers - A comparison of possible circuit configurations for speech communication. 12 p1467 A73-26800

Digital single sideband mixing circuit for sum or difference frequency conversion in phase quadrature, using exclusive-or logic gates. 13 p1593 A73-29117

Carrier-phase tracking-loop computer simulation and performance evaluation in high-speed SSB data transmission. 23 p2953 A73-43322

SINGLE STAGE ROCKET VEHICLES

NT AGENA ROCKET VEHICLES

NT BLACK KNIGHT ROCKET VEHICLE

NT VIKING ROCKET VEHICLE

High pressure dual fuel chemical LOX/hydrocarbon rocket vehicle concepts for reusable one stage to orbit shuttles. 16 p2072 A73-33085

Propulsion system optimisation for a single-stage constant-thrust relativistic rocket. 18 p2361 A73-37037

SINGLE-PHASE FLOW

Exact solutions of some problems of the Stefan type. 20 p2627 A73-39335

Thermodynamic formation of negative rarefaction/shock waves in single-phase viscous fluids by approximate continuum model. 21 p2790 A73-40251

SINGULAR INTEGRAL EQUATIONS

Lame equations for stress concentration in half plane with extracted elastic inclusion, solving via Fourier integrals reduced to singular integral equation. 07 p0910 A73-19301

Mixed boundary value problems in solid contact and crack mechanics, discussing numerical solution of singular integral equations with simple and generalized Cauchy kernels. 09 p1162 A73-23184

Remark on the behavior of an approximated process related to singular integrals near the terminals of an integration segment. 11 p1391 A73-26077

Equivalence of one type of a Riemann boundary value problem for a system of a pairs of functions relative to a complete singular integral equation with a Cauchy kernel. 12 p1518 A73-27730

A direct integral equation method for the potential flow about arbitrary bodies. 13 p1563 A73-28083

Semiinfinite and finite crack motion models comparison without loading restrictions, considering finite length dislocation pile up role and singular integral equation use 15 p1946 A73-31106

Contribution to the theory of mixed-type equations whose order degenerates along the line describing the changes in the type 15 p1900 A73-32080

General linear boundary value problem with measurable coefficients for numerous analytical functions of class E sub p 15 p1900 A73-32092

Optimal algorithms for numerical solutions of singular integral equations 15 p1900 A73-32096

Solution to a three-dimensional mixed boundary value problem in the theory of elasticity 15 p1953 A73-32102

System of arbitrarily oriented cracks in elastic bodies 17 p2240 A73-34144

Solution of the mixed boundary value problem of plane elasticity theory with the aid of singular integral equations 21 p2785 A73-40931

Local and global theorems of existence and uniqueness for solutions to nonlinear singular integral equations on a denumerable set of contours 22 p2882 A73-42472

An integral equation approach to the semi-infinite strip problem. [ASME PAPER 73-APMW-5] 22 p2924 A73-42878

Singular integral equations with a Carleman shift in the case of discrete coefficients and investigation of the Noetherian character of a class of linear operators with involution 24 p3105 A73-44425

Singular approximation in the calculation of the elastic properties of reinforced systems 24 p3145 A73-44514

Singular eigenfunction solution of the monoenergetic neutron transport equation for finite radially reflected critical cylinders. 24 p3109 A73-44700

A layered composite with a broken laminate. 24 p3151 A73-45301

Approximate calculation of the cavitation flow past low-aspect-ratio wings 24 p3055 A73-45540

SINGULARITY [MATHEMATICS]

Planar three body problem singularities due to binary collisions, regularizing equations of motion by Levi-Civita coordinate transformation 01 p0099 A73-10692

Study of a mixed problem for a third-order nonlinear differential equation with degeneration or singularity 01 p0070 A73-10920

Deformation and stress analysis in continuum mechanics problems of solid bodies near singular points, noting applicability of linear theory of elasticity 01 p0118 A73-11404

Method of calculating vortex-free flow around hydrodynamic cascades composed of arbitrary profiles 02 p0128 A73-11788

A Liapounov function for an autonomous second-order ordinary differential equation. 02 p0186 A73-11974

Second order trajectory optimization tests in terms of Kelley-Contensou extremals and conjugate points, applying to astrodynamical singular arc 02 p0187 A73-11996

Equations of motion for steady state spherically symmetric flow of polytropic gases into or out of neutron stars, black holes or Schwarzschild singularities 02 p0223 A73-12729

Polar streamline directions at the triple point of Mach interaction of shock waves. 03 p0244 A73-13566

Study of the asymptotic behavior of axial perturbation velocities in the vicinity of singularities 03 p0245 A73-13770

Dynamic singularity in the continuum theory of dislocations 03 p0343 A73-13775

Singular solutions of the plane distortion problem of micropolar elasticity. 03 p0392 A73-13776

Schwarzschild interior metric singularity for ideal fluid sphere radius relation to Schwarzschild radius, noting conditions for emitted light red shift 03 p0380 A73-14588

On the application of the SHEBA shell element. 04 p0510 A73-15016

Asymptotic waves and Cauchy problem with singular data for a system of linear equations with a double characteristic 04 p0471 A73-15245

Aerodynamic influence coefficient method using singularity splines. [AIAA PAPER 73-123] 06 p0644 A73-17645

The properties of a solution of the equations of motion of a mechanical system subject to irregular/singular perturbations. 06 p0722 A73-17755

Influence of scalar and vector fields on the nature of a cosmological singularity 06 p0751 A73-18101

On the analysis of scattering and antenna problems using the singularity expansion technique. 06 p0665 A73-18184

Calculation of the transonic flow around an airfoil, taking account of the exact law of compressibility. 09 p1027 A73-22210

Application of a singular perturbation method to the study of beginning cavitation 09 p1071 A73-22215

On the convergence of the finite element method for problems with singularity. 09 p1160 A73-22891

Stress field singularities due to cracks in isotropic elastic bodies, assuming Hookes law stress-strain relationship in integral equation representations 09 p1162 A73-23182

Applications of the finite element method to the calculations of stress intensity factors. 09 p1162 A73-23185

Parallel perturbation solution for ideal resonance problem characterized by one degree of freedom Hamiltonian system, considering singularities at separatrix 10 p1283 A73-24666

Gravitational collapse with a physical singularity on an isotropic hypersurface 10 p1283 A73-24751

Evolution of universe filled with cold baryons at cosmological singularity from Friedmann solution and equation of state for cold baryons 10 p1284 A73-24753

Equivalent formulations of quasilinear Dirichlet problem driven by positive sources, examining limiting and similarity singular solutions and uniqueness properties 10 p1250 A73-24785

Singularities and collisions in linear many body problem of Newtonian gravitational systems, noting moment of inertia role 10 p1284 A73-24788

Application of the characteristics of singular points to the determination of the period of quantization in time 11 p1340 A73-25009

Field of attraction of a singularity of a nonlinear recurrence of the second order - Method of determination of the boundary 11 p1389 A73-25137

Potential flow past axisymmetric ring wing profiles via singularity method, applying source and vortex distributions to curved thick profiles [DFVLR-SONDDR-271] 11 p1300 A73-25348

Higher order numerical solution of the integral equation for the two-dimensional Neumann problem. 11 p1300 A73-25434

Critique of theory on monotonic entropy of black hole as linear function of area, considering gravitational energy and compression to singularity 11 p1418 A73-25650

Edge condition of a perfectly conducting wedge with its exterior region divided by a resistive sheet. 11 p1329 A73-25676

Construction of a general cosmological solution of the Einstein equation with a time singularity. 11 p1425 A73-26178

Singular nonaxisymmetric shallow shell equation solutions for concentrated normal and tangential forces and bending and twisting moments 12 p1550 A73-27034

Singular perturbation analysis of a certain Volterra integral equation. 13 p1648 A73-28412

Propagation of a brittle crack at constant and accelerating speeds. 13 p1635 A73-28755

Stress-singularities due to uniformly distributed loads along straight boundaries. 13 p1696 A73-28757

Quantum and relativity theories compatibility based on hypothesis of matter tensor delta structure and Plancks constant for action singularity 14 p1775 A73-30425

Singularity and matter creation in cosmological models. 14 p1800 A73-30599

Poisson formula analogs for a class of higher-order elliptic-type differential equations with a singular line in the case of a half-space 15 p1898 A73-31020

Nonplanar wings in nonplanar ground effect. 15 p1824 A73-31744

Bulk viscosity effects in imperfect fluid Friedmann cosmology, considering implications for singularity problem 15 p1939 A73-32011

A numerical technique for determining the effect of singularities in finite difference solutions illustrated by application to plane elastic problems. 15 p1951 A73-32031

A periodic solution of a singular differential system with a retarded argument - Construction and approximate calculation 15 p1900 A73-32163

Local structure of space-time singularity and gravitational collapse. 15 p1940 A73-32177

Singularities of solutions to linear, second order, analytic elliptic equations in two independent variables. II - The piecewise regular boundary. 15 p1901 A73-32374

Active networks state equations with singular A matrix, considering algebraic method of reduction to equivalent set of equations with nonsingular A matrix. 16 p1992 A73-32912

Calculation of compressible subsonic flow in cascades with varying blade height. [ASME PAPER 73-GT-59] 16 p1964 A73-33514

The dynamic field of a growing plane elliptical shear crack. 16 p2082 A73-33907

Asymptotic expansions for product integration. 17 p2200 A73-34213

Use of the Singularity Expansion Method in electromagnetic transient scattering problems. 17 p2124 A73-35360

The singularity at boundary layer separation due to mass injection. 18 p2301 A73-36696

On the use of singular perturbation methods in the solution of variational problems. 19 p2386 A73-38038

Stress singularities associated with a crack inclined to a bi-material interface. 20 p2620 A73-39531

Oscillating spherically symmetric charge-matter fluid for avoidance of singularities in gravitational collapse models 21 p2766 A73-40316

A method of treating boundary singularities in time-dependent problems. 21 p2726 A73-40997

Cosmological singularity structures, taking into account initial singularity inevitability, uniform models, mixmaster model quantal limitations and physical processes 21 p2772 A73-41249

Schwarzschild solution indeterminacy as indicator of physical singularity analogous to intrinsically singular vertex of cone in Euclidean space 21 p2741 A73-41630

The use of singularity programming in finite-difference and finite-element computations of temperature. 22 p2930 A73-42287

Dynamic programming application to extremal fields topological singularity in optimal control theory for flight vehicle with state variables satisfying initial conditions and ordinary differential equations 22 p2917 A73-43030

Study of the existence of compact laminar for certain complex analytical laminated structures 23 p2999 A73-44097

Effect of scalar and vector fields on the nature of the cosmological singularity. 24 p3132 A73-44493

SINKS

NT HEAT SINKS
U STRUCTURAL BASINS
SINKS (GEOLOGY)

U STRUCTURAL BASINS
SINTERED ALUMINUM POWDER

Use of high cooling rates to obtain aluminum alloys with special properties 13 p1623 A73-28110

SINTERING

The early stages of the mechanism of sintering. 01 p0062 A73-10277

Potential titanium airframe applications. 01 p0063 A73-10285

Sinterability of stainless steel powders. 01 p0065 A73-10813

Corrosion behavior of sintered stainless steels. 01 p0065 A73-10815

Sintered chromium-nickel steel of high tungsten content. 01 p0065 A73-10816

Hot extrusion and properties of rods from sintered molybdenum and tungsten blanks. 01 p0065 A73-10817

Effect of high isostatic pressures on the compressibility and sinterability of tungsten powders. 01 p0065 A73-10819

Preparation and sintering of tungsten-rhenium alloy powders. 01 p0065 A73-10820

A sintered Nb-Ti-Zr alloy. 01 p0065 A73-10822

Activated sintering of ThO₂ and ThO₂-Y₂O₃ with NiO. 01 p0066 A73-11014

Porosity measurement of porous bronze, nichrome and steel sintered specimens by fluid displacement technique 02 p0178 A73-11540

- Sintering of nonstoichiometric nickel monoxide
02 p0179 A73-11546
- High resolution marker transport sintering study.
02 p0175 A73-12771
- Consolidation of tungsten and molybdenum powders.
03 p0322 A73-13262
- Mechanical properties of pressed and sintered titanium powder.
03 p0322 A73-13264
- Studies of the elastic properties of molybdenum
04 p0464 A73-15372
- A process for delubrication, presintering, sintering, and rapid cooling in a vacuum induction furnace.
04 p0455 A73-15751
- Investigation in the sintering of Y2O3 powders in the temperature range 1000 to 1400 C.
04 p0457 A73-15987
- Viscosity investigation of sintered fiberglass in the region of softening and annealing temperatures
06 p0715 A73-18657
- Experimental study of the effective thermal conductivity of liquid saturated sintered fiber metal wicks.
06 p0770 A73-18836
- Beryllium for nonstructural and structural applications in aerospace systems, considering high dimensional stability, mechanical and thermodynamic properties, and metal sintering techniques for production
07 p0828 A73-18904
- Investigation of the sintering process and physicomachanical properties of products prepared from spherical bronze pellets
10 p1225 A73-24319
- Boron filament reinforced Al and Ti matrices manufactured by pressure-sintering method, investigating filament external silicon carbide effects on mechanical properties
11 p1379 A73-25402
- Possibility of silicon carbide recrystallization in the process of reactive sintering
12 p1503 A73-27555
- Sintering of refractory titanium carbide with varied bound nitrogen content, discussing crystal dislocation effects on initial stage compaction intensification in nonstoichiometric specimens
12 p1503 A73-27556
- Investigation of the sintering of binary alloys with limited solubility in the solid state. I - Concentration dependence of shrinkage during sintering of two-component systems with a eutectic type of phase diagram
12 p1503 A73-27558
- The role of micropores in the fracture of forged sintered steel.
13 p1639 A73-29468
- Powder metallurgical preparation (sintering) of conventional maraging steel and similar alloys with Ni and/or Mo replacement by Mn and Ti, considering age hardening characteristics
14 p1765 A73-30936
- Some laws of chromium oxide-chromium cermet sintering
15 p1892 A73-32240
- Effect of treatment factors on the properties of friction materials. II - Effect of sintering conditions on the structure and friction and wear properties of friction materials
15 p1892 A73-32244
- High pressure-sintering preparation of barium ferrites, discussing temperature and compression effects on density and magnetic properties
16 p2044 A73-32947
- Experimental studies and applications of vanadium oxides.
16 p2044 A73-33471
- Sintering and hot pressing of Fra Mauro composition glass and the lithification of lunar breccias.
16 p2070 A73-33875
- Influence of a solid-phase nickel coating on the sintering kinetics of tungsten wire
18 p2320 A73-36858
- Capillarity induced stresses effects on dislocations generation during early stage sintering, predicting plastic flow via modified Hirth method of surface nucleation
20 p2576 A73-39221
- Molybdenum sintering and the molybdenum-oxygen-carbon system.
21 p2722 A73-41585
- Deformation and microfracture characteristics of two-phase tungsten-composite materials sintered with the liquid phase
22 p2872 A73-41948
- Precipitation and magnetic hardening in sintered WC-Co composite materials.
23 p2997 A73-43776
- Kinetics of shrinkage during the sintering of porous glass/metal composites
24 p3092 A73-44415
- Temperature range for centrifugal thermal diffusion sintering in Cr-Ni powder coatings, relating upper and lower bounds to heating rate
24 p3092 A73-44419
- SINUSES
NT PARANASAL SINUSES
- Sinus venosus atrial septal defect - Analysis of fifty cases.
07 p0784 A73-20368
- Pathophysiological and clinical aspects of aeroinfluenza and frontal sinus nematoma formation due to barometric pressure changes from pilot case history studies
09 p1039 A73-22538
- Slow and fast heart rates and syncope and dizzy attacks as manifestations of sick sinus syndrome, discussing ventricular artificial pacemaker as therapy
11 p1319 A73-26289
- Cerebral tolerance to asphyxial hypoxia in the dog.
22 p2805 A73-42202
- SINUSOIDS
U SINE WAVES
SIRIO SATELLITE
The R.S.R.S. ground stations for receiving 11.6 GHz transmission from the SIRIO satellite.
16 p1982 A73-33717
- SITES
NT LANDING SITES
NT LAUNCHING PADS
NT LAUNCHING SITES
NT LUNAR LANDING SITES
Trends in offshore airports.
[ASCE PREPRINT 1273]
Fast pulse VHF background noise measurements in site selection for radio detection of cosmic ray air showers
01 p0030 A73-10824
22 p2813 A73-42073
16 p1984 A73-33924
- SITTING POSITION
The effects of various seat surface inclinations on posture and subjective feeling of comfort
03 p0266 A73-13121
Normal pulmonary pressure-flow relationship during exercise in the sitting position.
03 p0266 A73-13124
A model to predict the mechanical impedance of the sitting primate during sinusoidal vibration.
[ASME PAPER 73-DET-78]
22 p2813 A73-42073
- SIZE [DIMENSIONS]
Scale factors of adsorptive reduction in the strength of metals in the presence of melts
06 p0711 A73-18667
- SIZE DETERMINATION
NT PRECIPITATION PARTICLE MEASUREMENT
Lunar occultation of stars to determine moon diameter and orbital elements, noting time measurement difficulties due to scintillation effects
01 p0102 A73-10994
Radii, albedos, and 20-micron brightness temperatures of Iapetus and Rhea.
01 p0104 A73-11050
An electrostatic cloud droplet probe.
01 p0052 A73-11058
Measurement of particle size, number density, and velocity using a laser interferometer.
01 p0053 A73-11226
Determining the size of defects in standardizing sensitivity using a spherical reflector.
02 p0169 A73-12149
Design study for long-lived compact 750 kW industrial gas turbine, discussing optimal aerodynamic proportioning and size determination
[ONERA, TP NO. 1174]
02 p0204 A73-12791
Machine components dimensioning and testing for fatigue strength, presenting methods for service life determination
03 p0385 A73-13132
Prediction of the critical diameter of composite propellants.
[AIAA PAPER 72-1117]
03 p0351 A73-13432
Optimal sizing of modular bus bars for rectangular solar cell arrays as function of power/weight ratio
03 p0255 A73-14225
Pulse Doppler radar observations of hailstone maximum diameters as function of time
03 p0337 A73-14506
The angular diameter of X Cancri.
04 p0500 A73-15518
Measurements of diameters of galaxies on the Palomar Observatory Sky Survey.
05 p0613 A73-16211
The use of a gas laser for sizing single particles of airborne dust.
05 p0584 A73-16444
Mars diameter optical measurements by earth based refractor telescopes with birefringent double image micrometer
06 p0747 A73-17489
Defect size determination by ultrasonic scanning with a relative threshold
09 p1088 A73-22220
New optical measurements of planetary diameters.
IV - Size of the North polar cap of Mars.
09 p1145 A73-22273
Photometric analysis of earth photographs from Zond space station, determining earth sidereal magnitude
10 p1281 A73-24477
- Numerical procedure for determining optimal member sizes of aircraft structural components with weight minimization and flutter speed lower bound
[AIAA PAPER 73-391]
11 p1439 A73-25520
Size determination of a perfectly conducting sphere from the extrema of Mie scattering intensities.
11 p1329 A73-25679
Solar system planets and satellites fundamental properties, considering observational uncertainty in masses and dimensions
11 p1419 A73-25878
A survey of dynamical data for the major planets and satellites.
11 p1420 A73-25880
The angular diameter of upsilon Capricorni and an occultation of SAO 118655.
12 p1540 A73-27427
Nonuniform heat transfer coefficient effect on double-pipe heat exchanger analysis with effectiveness method, discussing exchanger sizing
12 p1559 A73-27693
Cometary nuclei size determination methods based on model of surface ice regions with mineral crust spots, analyzing brightness decrease
14 p1792 A73-29818
Determination of the radius of a cometary nucleus from photometric data
15 p1928 A73-31024
New techniques for determining sizes of satellites and asteroids.
15 p1940 A73-32075
The infrared spectrum and angular size of Eta Carinae.
15 p1940 A73-32197
Censored sample size selection for life tests.
[AD-758315]
16 p2033 A73-33630
New determinations of the diameters of planets and satellites
16 p2066 A73-33792
Radio astronomical, radar and interplanetary probe measurements of Venus rotation, dimensions, atmosphere and magnetic field
16 p2066 A73-33798
Revision of initial size, mass and angular momentum of the solar nebula and the problem of its origin.
17 p2229 A73-34431
An upper limit to the angular diameter of the nucleus of NGC 4151.
17 p2231 A73-34751
Some considerations about the upper and the lower limits of the planetary dimensions.
19 p2486 A73-38152
Method of measuring the size of defects without using calibrating standards and adjusting the sensitivity of ultrasonic defectoscopes.
19 p2432 A73-38358
Imaging system pointing precisions, deriving ground target size relationships to spread function and modulation transfer function respectively
20 p2567 A73-39672
Airborne remote sensing of cloud particle size and shapes via IR polarimeter, obtaining polarization vs phase angle curve for thick tropical cirrus clouds
20 p2567 A73-39859
Measurement of change in a cross section and position of small particles by diffraction techniques.
21 p2695 A73-39959
A non-contacting length comparator with 10 nanometer precision.
21 p2704 A73-41257
Shakhbazian I compact galactic cluster, discussing red shift, angular size, galactic type, velocity dispersion, mass/light ratio and photographic plates
22 p2909 A73-42586
High resolution image formation through the turbulent atmosphere.
22 p2863 A73-43097
Interferometric measurements of apparent stellar diameters
22 p2863 A73-43102
Ultrasonic determination of shape and size of hidden defects in solids.
23 p2984 A73-43298
High angular resolution very long baseline interferometry for emission spectra and angular size determination and structure mapping of galactic and extragalactic radio sources
23 p2980 A73-43355
Determination of radii of satellites and asteroids from radiometry and photometry.
24 p3130 A73-44453
- SIZE PERCEPTION
U SPACE PERCEPTION
SIZE SEPARATION
Endogenic craters count and measurement for Hyginus Rille floor, establishing size distributions by Lunar Orbiter 5 photographs processing
07 p0900 A73-20278
- SIZING [SEPARATION]
U SIZE SEPARATION
SKELETON
U MUSCULOSKELETAL SYSTEM

SKEWNESS

SKEWNESS

Low order spatial modes principal resonance region of in-plane loaded skew stiffened plate, obtaining equation of motion by Hamilton principle
[ASME PAPER 72-WA/APM-32]

04 p0515 A73-15887

Natural frequencies and vibration modes determination for skew plates with different edge conditions involving support and clamping based on Ritz variational method

07 p0909 A73-19094

Vibration of simply supported-clamped skew plates at large amplitudes.

13 p1690 A73-28057

Postbuckling behavior of orthotropic skew plates.

13 p1697 A73-28813

Large amplitude flexural vibration of simply supported skew plates.

21 p2784 A73-40423

SKID LANDINGS

Aquaplaning prevention during take-off and landing, discussing friction loss factors, aircraft tires and runway surface treatment by antiskid overlays and grooving

11 p1343 A73-25209

SKIN [ANATOMY]

NT EPIDERMIS

NT EPITHELIUM

Fingerprint patterns incidence relation in congenital vitium cordis patients, using Henry dactyloscopic classification

01 p0009 A73-11080

Skin sensitivity of palms, wrists and forearms to focused ultrasound, noting evoked touch, pulsation, cold, warmth and prick sensations and applications in receptor physiology

05 p0540 A73-16695

UV-induced lipid peroxidation in human epidermis, dermis, and hypodermis in vitro

09 p1038 A73-21873

Influence of histamine on cutaneous capillary circulation and on the oxygen tension of subcutaneous cellular tissue in various age periods

10 p1178 A73-23676

An experimental basis for carcinogenic effects of ultraviolet radiation.

11 p1320 A73-26485

Bactericide activity of the integument of man at different times of the day

12 p1463 A73-27716

Investigation of the influence of biologically active substances on the permeability of the skin

15 p1838 A73-31174

A new method for determining the degree of oxygenation of hemoglobin spectra in the case of inhomogeneous light paths, explained in an analysis of spectra of the human skin

20 p2517 A73-39145

Laser hazards and safety performance standards, discussing ocular and skin damage and exposure limits and operational regulation

20 p2517 A73-39205

Torsional elasticity of human skin in vivo.

21 p2642 A73-41625

SKIN [STRUCTURAL MEMBER]

Alternating-pressure measurements involving mushroom-nozzle flows with regard to dynamic stresses in the case of the skin structures of reusable carrier rockets

[DGLR PAPER 72-076]

02 p0128 A73-11686

Attempts at using fiberglass cloth as skin for aircraft

02 p0185 A73-12450

Stretch formed corrugated Rene 41 panel development for space shuttle booster nose section hot area skin, discussing tooling and formation techniques

[SAE PAPER 720873]

05 p0582 A73-16670

The status of engineering knowledge concerning the damping of built-up structures.

07 p0909 A73-19099

Behavior of a wing panel under transient conditions in a gas flow

17 p2091 A73-34139

Heavy lift helicopter rotor blade design including airfoils, fiberglass skin, titanium spar, fail-safety and aerodynamic and structural features

[AHS PREPRINT 710]

17 p2104 A73-35056

High frequency vibration of aircraft structures.

17 p2250 A73-35329

Structural adhesive bonding of titanium - Superior surface preparation techniques.

24 p3093 A73-44765

SKIN FRICTION

NT AERODYNAMIC DRAG

NT FRICTION DRAG

NT VISCIOUS DRAG

Two-dimensional boundary layers in a free stream which oscillates without reversing.

01 p0032 A73-10446

Skin friction on porous surfaces calculated by a simple integral method.

01 p0057 A73-10726

Calculation of compressible turbulent boundary layers with roughness and heat transfer.

03 p0296 A73-14179

Viscous compressible flow near right angle corner of two flat plates, presenting streamwise and secondary flow velocities and skin friction coefficient distribution

06 p0687 A73-18532

Perturbation about one dimensional parabolic flow field in three dimensional boundary layer separation, obtaining skin friction from linear equation eigen-solutions

[AD-755557]

07 p0774 A73-19502

Two-dimensional turbulent jets at a porous wall.

07 p0811 A73-19613

Reference temperature method for predicting turbulent compressible skin-friction coefficient.

08 p0925 A73-20722

Skin friction and heat flux in the impingement region of a low speed air jet upon a normal flat plate.

08 p0925 A73-20941

Unsteady boundary layer flows at general three-dimensional stagnation points.

08 p0954 A73-21008

Heat transfer through the unsteady laminar boundary layer on a semi-infinite flat plate. I - Theoretical considerations. II - Experimental results from an oscillating plate.

08 p1024 A73-21635

Parabolic flow over a flat plate with wave disturbance in the main stream.

09 p1071 A73-21950

Prototype skin friction measuring instrument for short period or continuous operation at high temperature, considering alternative feasible systems design and experimental data

10 p1217 A73-24013

Calculation of turbulent skin friction on a rotating disk.

11 p1348 A73-26387

Prediction of heat transfer for turbulent boundary layer with pressure gradient.

11 p1453 A73-26393

A note on the effect of Hall currents on hydromagnetic flow near an accelerated plate.

13 p1664 A73-28617

A new approach to the problem of predicting the performance of centrifugal compressors.

13 p1565 A73-29012

Effects of free stream velocity profile on turbulent boundary layer, with some reference to the effects of free stream turbulence.

13 p1602 A73-29013

Use of surface fences to measure wall shear stress in three-dimensional boundary layers.

15 p1874 A73-31118

Analysis of turbulent skin friction in thick axisymmetric boundary layers.

15 p1863 A73-31658

Magnetohydrodynamic boundary layer control with suction or injection.

15 p1864 A73-31931

Leading edge effects on displacement thickness and skin friction variations of unsteady boundary layer on flat plate under impulsive motion in viscous fluid

16 p1962 A73-32927

Calculation of turbulent heat transfer and skin friction.

17 p2150 A73-34196

Lubricating properties of micropolar fluids in composite and step slider bearings, obtaining analytic expressions for load carrying capacity and skin friction

24 p3092 A73-44409

SKIN FRICTION DRAG

U FRICTION DRAG

SKIN RESISTANCE

Integral equation for electromagnetic field in diffuse boundary plasma, noting anomalous skin effect

11 p1405 A73-26184

Theory of the anomalous skin effect in a plasma with a diffuse boundary

16 p2043 A73-34060

Acclimatization to severe dry heat by brief exposures to humid heat.

03 p0267 A73-13700

Thermoregulatory behavior of man during rest and exercise.

10 p1178 A73-23572

Cerebral temperature oscillations and vascular responses in man

10 p1179 A73-23805

Quantitative influence of CO₂ inhalation on thermal sweating in man.

11 p1314 A73-25331

Hypothalamus, septum and ventrobasal thalamus nuclei single neuron responses to skin thermal stimulation, indicating afferent connections between cerebrum thermoregulatory center and peripheral thermoreceptors

11 p1317 A73-26086

Human thermoregulatory system examination under thermodynamic equilibrium based on conductive and convective metastable heat transfer from skin to environment

[ASME PAPER 73-AUT-J]

13 p1577 A73-29414

Differential thermal sensitivity in the human skin.

14 p1720 A73-30912

Calculation of temperature distribution in the human body.

15 p1839 A73-31999

The effects of core temperature elevation and thermal sensation on performance.

15 p1839 A73-32396

Control of forearm skin blood flow during periods of steadily increasing skin temperature.

18 p2278 A73-36657

Human calorimeter with a new type of gradient layer.

18 p2282 A73-36662

Thermographic evaluation of relative heat loss areas of man during cold water immersion.

18 p2283 A73-36781

Tolerance to immersion in cold water

18 p2280 A73-36943

Effect of skin wetting on finger cooling and freezing.

20 p2518 A73-39779

Heat conduction in blackened skin accompanying pulsatile heating with a xenon flash lamp.

20 p2519 A73-39791

A comparison of predicted skin temperatures with thermographic measurements.

22 p2813 A73-42053

Spectral emissivity of skin and pericardium.

23 p2950 A73-44213

Radiation heat transmission from human underlying and surface skin effect on epidermal temperature gradient

23 p2950 A73-44217

SKIN TEMPERATURE [NON-BIOLOGICAL]
Preliminary study for the design of a satellite thermal control heat pipe.

07 p0918 A73-18913

A theoretical analysis of the recovery factor for high-speed turbulent flow.

15 p1865 A73-32280

SKULL

NT CRANIUM

NT INTRACRANIAL CAVITY

Simple simulated human head for checking echoencephalographic equipment.

22 p2815 A73-42672

SKY

NT NIGHT SKY

SKY BRIGHTNESS

Meteor shower and cosmic dust effects on twilight sky brightness from mountain top and balloon observations

02 p0215 A73-12261

On the application of satellite data on cloud brightness to the study of tropical wave disturbances.

02 p0190 A73-12790

The interaction between ground reflecting power and celestial brightness

04 p0441 A73-15292

Cosmological models based on 18th and early 19th century physics for sky darkness resulting from universe expansion, speculating upon Olbers paradox resolution

05 p0614 A73-16308

ATS-3 observed cloud brightness field related to a meso-to-synoptic scale rainfall pattern.

06 p0720 A73-17867

Brightness temperatures in the southern sky at 408 MHz.

07 p0876 A73-19357

A photometric model of the zodiacal light.

07 p0876 A73-19359

Fraunhofer line depth in daytime airglow

07 p0817 A73-19471

Optical sounding methods for the upper atmosphere and the earth's dust cloud

07 p0817 A73-19584

Analysis of light polarization variations in a twilight sky in terms of upper atmosphere effects

07 p0817 A73-19588

Determination of the concentration and scattering indicatrix of atmospheric dust from primary twilight brightness

07 p0817 A73-19589

Polarization measurement of clear sky light and comparison with theoretical data

07 p0818 A73-19590

Photoelectric measurement of twilight sky brightness distribution for separation of primary brightness component, noting possibility of secondary component due to dust

07 p0818 A73-19593

Night sky background radiation measurement by far IR radiometer carried on rocket launched from Hawaii

07 p0825 A73-20187

Preliminary results of a spectrophotometric survey of the sky in the ultraviolet with the aid of the TD-1 A satellite

08 p0967 A73-21499

The relation of brightness phase functions to the optical thickness of the atmosphere.

08 p0986 A73-21585

Distribution of diffuse solar radiation over regions of the sky for various regions of the spectrum in the absence of cloudiness

09 p1138 A73-22994

Computer program for extraterrestrial physics barium ion cloud project determining daily release launch window for sky target experiments
[AIAA PAPER 73-297] 09 p1116 A73-23216

New limit on small-scale irregularities of 'blackbody' radiation. 10 p1272 A73-23543

Imaging photopolarimeter for measuring orthogonal, sky glow and gegenschein brightness and polarization in sky mapping mode 11 p1415 A73-25177

Daytime sky brightness from atmospheric transmittance, noting single and multiple scattering calculations 11 p1352 A73-25603

Brightness and polarization of the sky in the solar almucantar in the near infrared region of the spectrum 11 p1353 A73-25604

Correlation between the absolute brightness characteristic of day sky and the optical thickness of the atmosphere 11 p1353 A73-25605

Optical characteristics of bright day sky in the visual region of the spectrum and the atmospheric aerosol 11 p1353 A73-25606

Sky brightness in solar aureole region relationship to solar radiation single scattering on atmospheric aerosol particles 11 p1353 A73-25607

Daytime cloudless sky glow, atmospheric transmittance, neutral polarization and aerosol optical characteristics in solar almucantar and vertical 11 p1353 A73-25608

Possibility of polarimetric monitoring of the optical stability of the atmosphere 11 p1392 A73-25609

Polarization of the cloudless daytime sky in the 1.25- to 2.42-micron range 11 p1353 A73-25645

Polarographic observations of the solar corona at the total eclipse on March 7, 1970 in Mexico. 11 p1425 A73-26264

B system calculation of night airglow stellar component from cataloged photometric scales, obtaining night sky brightness 12 p1546 A73-27857

Photographic experiments during a spacecraft flight lasting a number of days 13 p1611 A73-28008

Light scattering by atmospheric aerosols. 13 p1653 A73-28517

Theory of a photometer/actinometer/ measuring the brightness of a fixed annular zone of sky around the sun. 13 p1613 A73-28519

Altitudinal variations of the brightness indicatrices and angular characteristics of polarization levels in daytime skies in the 1.27-micron oxygen emission band 13 p1609 A73-29157

Starry sky energetic simulator design, analyzing comparative brightness of stars 13 p1598 A73-29321

Cloud-free line-of-sight calculations. 15 p1903 A73-31317

Depth of the Fraunhofer lines in the spectrum of the daytime sky. 15 p1873 A73-32061

Extra-atmospheric observations of the luminosity of the sky from the Cosmos 51 and Cosmos 213 satellites. I - Method and calibration of the measurements 16 p2011 A73-32706

Extra-atmospheric observations of the luminosity of the sky from the Cosmos 51 and Cosmos 213 satellites. II - Measurement data and their interpretation 16 p2001 A73-32707

Sky brightness observation of post-dusk effect in Spanish Sierra Nevada for relationship to predawn enhancement, noting insufficient evidence for quantitative analysis 16 p2008 A73-33880

Relation between turbulence in a clear sky and the evolution of the baric field 17 p2204 A73-34543

Preliminary results obtained with astrophotometer installed on Lunokhod II. 18 p2315 A73-35992

Spatial frequencies of clear sky radiance in the range 4.5 to 5.2 microns 18 p2314 A73-36899

On the Zeeman photometer observing upper atmospheric winds in the daytime. 19 p2429 A73-37377

Estimation of the absorptive capacity of atmospheric haze from the brightness of clouds 20 p2583 A73-39183

Application of G. V. Rozenberg's asymptotic formulas in the interpretation of cloud brightness measurements 20 p2584 A73-39189

B system calculation of night airglow stellar component from cataloged photometric scales, obtaining night sky brightness 20 p2608 A73-39231

Extra-atmospheric photoelectric study of the brightness of the earth's atmosphere 21 p2686 A73-40912

Mic scattering computation of cosmic dust flux in upper atmosphere from twilight luminance increase during meteor showers 21 p2775 A73-41418

Russian book - Scattered daytime sky light. 21 p2691 A73-41439

Rocket observations of electron precipitation in a westward-traveling surge. 22 p2902 A73-41915

Stanford radio telescope array with five paraboloid antennas for fast image forming interferometry, using earth rotation synthesis to produce sky continuous radiation brightness map 23 p2957 A73-43359

SKY RADIATION

NT AIRGLOW

NT DAYGLOW

NT GEOCORONAL EMISSIONS

NT NIGHTGLOW

NT TWILIGHT GLOW

The detection of a point source in the presence of nongaussian background noise. 01 p0017 A73-10832

Verification of an approximation method for calculating multiple scattering of sky radiation. 01 p0074 A73-11236

Generation of vibrationally excited O₂ and nonthermal infrared emission in the upper atmosphere 08 p0959 A73-21289

D-2A satellite experiments for sky mapping and radiation intensity measurement, discussing attitude correction processing 10 p1285 A73-23623

Determination of emission spectra of the sky in the infrared between 45 and 500 micrometer using an interferometer aboard an airplane 10 p1210 A73-23749

Production of vibrationally excited O₂ and nonthermal infrared emission in the upper atmosphere. 19 p2424 A73-37918

Scanning the sky with the aid of the RATAN-600 radio telescope 21 p2776 A73-41464

Polarization - A key to an airborne optical system for the detection of oil on water. 23 p2979 A73-43225

Inference of total ozone from photometric measurements of sky radiation. 23 p2973 A73-43856

Ozone related spectral measurements of total solar radiation. 23 p2975 A73-43882

Angstrom pyroheliometer scale correction for ratio of incident circumsolar radiation to electric current heating power derived from nonuniform painted surface strip illumination 23 p3025 A73-43985

SKY WAVES

NT WHISTLERS

Type variation of solar sudden field anomaly (SFA) on 164 kHz as an indicator of seasonal structure changes in the D-region. 09 p1076 A73-22141

Ionospherically propagated backscatter from Pacific Ocean via swept frequency continuous wave recordings, noting sky wave polarization rotation modulation of received signal 15 p1845 A73-32228

On the relative response and absolute gain toward the zenith of HF field-expedient antennas - measured with an ionospheric sounder. 17 p2129 A73-35698

Methods of measurements and some results of lower ionosphere by using VLF and LF radio waves. 18 p2302 A73-35926

Measurements of ionospheric reflectivity from 6 to 35 kHz. 18 p2289 A73-36286

SKYHAWK AIRCRAFT

U A-4 AIRCRAFT

SKYHOOK BALLOONS

Skyhook plastic balloons for transporting scientific instruments to high altitudes for long durations 11 p1306 A73-26348

SKYLAB PROGRAM

Skylab instrumentation and solar observation objectives in coordinated program of correlative ground based, rocketborne and other spaceborne observations 02 p0169 A73-12337

Skylab orbital laboratory design, experiment programs and planned missions schedule, considering rescue measures, life support system and attitude control 03 p0383 A73-14171

Skylab experiments in life sciences, solar physics, earth observations, astrophysics, engineering and technology 03 p0376 A73-14172

Solar Array System for the Skylab Orbital Workshop. 03 p0257 A73-14238

Automatic digital image processing for remote sensing with ERTS, Skylab and NASA survey aircraft, considering image registration, projective transformation and ground truth information 03 p0309 A73-14487

Average return pulse form and bias for the S193 radar altimeter on Skylab as a function of wave conditions. 04 p0446 A73-14804

Computer application for management of Skylab launch operations. 04 p0424 A73-14905

NASA space program value to humanity, discussing Skylab solar and earth observations and communications satellites 05 p0613 A73-16181

Computer and interactive graphics as applied to mission analysis. 05 p0554 A73-16870

An experimental investigation of attitude control systems for astronaut maneuvering units. 05 p0563 A73-16973

Skylab experiment for measuring color indices of extended sources and of spectral types O, B and A hot stars at various galactic latitudes 07 p0822 A73-18989

Atlas S183 spectrophotometer for Skylab orbital laboratory UV observations, discussing electrical, optical and mechanical interface problems 07 p0822 A73-19007

Skylab project mission objectives in long duration spaceflight, describing crew training under simulated space environment conditions, foods, clothing, waste disposal, physical exercise, etc 09 p1152 A73-22188

The earth resources experiment package on Skylab and proposed resource investigations. 09 p1082 A73-22389

An approach to performance assessment and management of a large solar array/battery power system. 09 p1035 A73-22775

Spinning Skylab space station dynamics, investigating motion stability from simplified models with flexible appendages by digital simulation 10 p1286 A73-24003

Observing programs in solar physics during the 1973 ATM Skylab program. 10 p1278 A73-24126

The American space program for the future. 12 p1560 A73-27062

Microbiological testing of Skylab foods. 12 p1464 A73-27075

Skylab earth terrain camera for high resolution photography of areas covered by other Earth Resources Experiment Package sensors to aid in data interpretation 12 p1500 A73-27958

Skylab A solar and terrestrial observation and photography hardware, including solar observatory, microwave scanner, IR spectrometer and multispectral photographic facility 13 p1612 A73-28276

Skylab experiments through airlock studying earth atmosphere, particles, background sky light, solar spectra, nebulae, stars and galaxies 13 p1617 A73-28945

Apollo, Skylab and shuttle programs, discussing crews, tasks, national economic benefits and earth resources experiments effects 15 p1941 A73-32544

Skylab astronaut vestibular function experiment in orbital flight, discussing motion sickness susceptibility, stimulation thresholds and space perception measurements 17 p2115 A73-34741

Electric corona assessment of Skylab spacecraft high voltage electrical/electronic equipment and instruments, considering operating temperature and environment contaminants effects 17 p2109 A73-35256

Skylab design technology assessment based on past manned spacecraft subsystems, noting advances in mission duration, spacecraft size and living accommodation comfort features 18 p2358 A73-36082

Skylab experience with Apollo docking/latching loads. 18 p2358 A73-36091

Skylab Mission Simulator Facility software, describing electric power systems, solar measurements, display panels, earth resource sensors and spacecraft environmental control 18 p2296 A73-36832

Soaps, detergents and surfactants dermatological hazards in personal hygiene use by spacecrews during long term space flight/Skylab/ [ASME PAPER 73-ENAS-26] 19 p2400 A73-37981

Skylab medical experiments altitude test crew observations. 19 p2400 A73-37985

Trash management during Skylab and long duration missions with compactors, autoclaves, biocides and isotope powered water recovery/waste management systems [ASME PAPER 73-ENAS-31] 19 p2401 A73-37986

- Skylab Medical Experiments Altitude Test /SMEAT/ facility design and operation. [ASME PAPER 73-ENAS-44] 19 p2401 A73-37991
Skylab medical experiments altitude test /SMEAT/ chamber atmosphere trace contaminants analysis, describing sample acquisition techniques and instrumentation [ASME PAPER 73-ENAS-45] 19 p2395 A73-37992
Skylab ATM solar array performance characteristics prediction via mathematical model, discussing I-V characteristics, test data computer programming and polynomial curves 19 p2391 A73-38407
Automatic control of the Skylab Astronaut Maneuvering Research Vehicle. [ALAA PAPER 73-857] 20 p2586 A73-38795
Skylab program mission profile, vehicle components, ground station data links, Apollo telescope mount, Saturn V rocket, solar cells and Salyut spacecraft comparison 20 p2615 A73-39150
Skylab flight schedule emphasizing Command Service, Module, discussing meteoroid shield deployment difficulties and rescue team development of solar heat shield 21 p2767 A73-40415
Skylab 1 medical experiments concerning astronaut physiological responses and work capability as affected by exposure to space flight environment 21 p2778 A73-41519
The use of Skylab and ERTS data in an integrated natural resources development programme. 23 p2973 A73-43785
Skylab 26 day rescue mission diary, describing docking, communications, extravehicular activity, repair work, medical checkouts, physical exercises, solar array problems, etc 23 p3038 A73-43992
X-ray observations of characteristic structures and time variations from the solar corona - Preliminary results from Skylab. 24 p3139 A73-45057
Skylab complex stiffened structure shell instability analysis by computer program, discussing convergence of finite difference formulation and eigenvalue calculation 24 p3144 A73-45234

SKYLARK

U SKYLARK ROCKET VEHICLE
SKYLARK ROCKET VEHICLE

- Skylark rocket measurement of earth atmosphere and ionosphere, examining payload capacity, camera image quality, cost, use of smaller rockets and practical applications 17 p2239 A73-34953
Test flight and configuration of Skylark based SL 1081 earth resources rocket prototype with two photographic cameras and earth albedo sensors 20 p2615 A73-39874

SKYNET SATELLITES

- The effect of direct solar radiation on the attitude of the SKYNET spacecraft. 11 p1431 A73-26261
Skynet satellite communication service for small dish antenna equipped mobile ground stations, emphasizing necessity of rapid central control response to configuration and propagation condition changes 12 p1471 A73-27660

SLABS

- The solution of Maxwell's equation for inhomogeneous dielectric slabs. 06 p0699 A73-17809
Transmission of electromagnetic waves through a conducting slab. IV - A simple multiple-reflection method. 07 p0852 A73-20172
Hemispherical reflectivity and transmissivity of an absorbing, isotropically scattering slab with a reflecting boundary. 08 p1025 A73-21643
Equivalence relationships between diffuse radiation fields for finite slabs bounded by a perfect specular reflector and a perfect absorber. 09 p1121 A73-23072
Book - Optical waveguides. 09 p1066 A73-23274
Approximate calculation of thermoclastic stresses in an arbitrarily heated slab 11 p1434 A73-25393
Reflection and transmission of radio waves at a dielectric slab with variable permittivity. 11 p1329 A73-25675
Local form of the radiation condition - Application to curved dielectric structures. 24 p3069 A73-45257

SLANT PERCEPTION

U SPACE PERCEPTION

SLATS

U LEADING EDGE SLATS

SLEDS

NT ROCKET PROPELLED SLEDS

SLEEP

- Structural change in the paradoxical phase of sleep due to the stimulation of the reticular formation and hypothalamus on a background of deep slow sleep 01 p0009 A73-11081
Sleep and the maturing nervous system; Proceedings of the Symposium on the Maturation of Brain Mechanisms Related to Sleep Behavior, Boiling Springs, Pa., June 21-24, 1970. 03 p0263 A73-14255
Differential housing/isolation vs aggregation/ as factor in postnatal development of mouse brain cell specificity and metabolism, noting relation to sleep behavior 03 p0264 A73-14259
The role of biogenic amines in sleep. 03 p0264 A73-14260
Developmental changes in neurochemistry during the maturation of sleep behavior. 03 p0264 A73-14261
Maturation of neurobiochemical systems related to the ontogeny of sleep behavior. 03 p0264 A73-14262
Development of wakefulness-sleep cycles and associated EEG patterns in mammals. 03 p0264 A73-14263
Patterns of reflex excitability during the ontogenesis of sleep and wakefulness. 03 p0264 A73-14264
Rapid eye movement state beneficial effects on memory refuted in favor of delta wave slumber, emphasizing stage 4 sleep 06 p0653 A73-18225
The effects of Dalmane /flurazepam hydrochloride/ on human EEG characteristics. 08 p0931 A73-21464
Non-Gaussian properties of the EEG during sleep. 08 p0931 A73-21465
Alpha-delta sleep as replacement for delta sleep in various psychiatric patients with chronic fatigue and depression 09 p1045 A73-22694
Rapid eye movement analyzer. 09 p1045 A73-22697
Investigation of the sleep and wakefulness rhythms in the crewmembers of Soiuz-3 through Soiuz-9 spacecraft prior to, during, and after space flight 10 p1182 A73-24697
Nature and significance of periodic electrical activity variations in the neocortex and the hippocampus during the paradoxical phase of sleep 11 p1317 A73-26083
Influence of synchronized sleep upon spontaneous and induced discharges of single units in visual system. 11 p1319 A73-26223
On the functional significance of subcortical single unit activity during sleep. 14 p1714 A73-29993
A vecto-oculographic approach to fast sleep eye movements in man. 14 p1715 A73-29994
Accommodation of the eye during sleep and anesthesia. 14 p1716 A73-30391
Memory fixation during sleep, discussing EEG, EOG, EMG and ECG recordings for differences between light and paradoxal sleep 15 p1835 A73-31749
Sleep behaviour as a biorhythm. 16 p1972 A73-33158
Investigation of the possibility of human adaptation to a 16-hour day 17 p2114 A73-34238
Sonic booms and sleep - Affect change as a function of age. 18 p2282 A73-36780
Further sleep problems in airline pilots on worldwide schedules. 18 p2283 A73-36792
Changes in some behavioral reactions and in the bioelectric activity of the brain in cats during the development of sleep under polarization of individual brain structures 19 p2393 A73-37393
Ultradian rhythms in human telemetered gross motor activity. 20 p2512 A73-39102
Variations of heart rate during sleep as a function of the sleep cycle. 20 p2514 A73-39762
Similarities and differences concerning the sleep of two baboons, Papio hamadryas and Papio papio 20 p2514 A73-39764
The nature and significance of the dynamics of electrical activity in the neocortex and hippocampus during the paradoxical phase of sleep 24 p3059 A73-44718
Application of factor analysis to the encephalographic characterization of sleep 24 p3062 A73-44722

SLEEP DEPRIVATION

- Effect of sleep-wake reversal and sleep deprivation on the circadian rhythm of oxygen toxicity seizure susceptibility. 02 p0135 A73-12561
Wakefulness and sleep states in developing organism, discussing REM sleep deprivation effects on behavior, brain excitability, pharmacology and biochemistry 03 p0265 A73-14265
Effects of 24-hour sleep deprivation on rate of decrement in a 10-minute auditory reaction time task. 04 p0411 A73-15220
Behavioural awakening and subjective reactions to indoor sonic booms. 04 p0412 A73-15592
Effects of aircraft noise on human sleep. 06 p0659 A73-18546
Lone woman pilot sleep patterns and sleep disruptions on global flight across time zones 17 p2115 A73-34745
Gaze-positioning eye movement perturbations during somnolence states 18 p2280 A73-36950
Regional serotonin content variations in the brain of cats during a prolonged absence of sleep 19 p2393 A73-37394
Sleep loss in air cabin crew. 20 p2517 A73-39109
Sleep deprivation effects on accuracy and speed of response selection and execution. 21 p2644 A73-40853
Effects of repeated simulated sonic booms of 1.0 PSF on the sleep behavior of young and old subjects. 21 p2644 A73-41151
Spiral aftereffect durations following awakening from REM sleep and non-REM sleep. 21 p2639 A73-41179

SLENDER BODIES

NT SLENDER CONES

- Approximate method based on quasi-one dimensional theory for calculation of transonic wave propagation in slender nozzles 01 p0034 A73-11368
Buoyancy distribution of slender axisymmetric bodies of higher order in the case of compressible subsonic flow [DGLR PAPER 72-067] 02 p0127 A73-11681
Influence of the boundaries of wind-tunnel flow on the flow past a small-aspect-ratio wing 02 p0128 A73-11707
Far field steady inviscid flow behavior of hyper-sonic blunt axisymmetric slender body, obtaining unsteady two dimensional solution with cylindrical symmetry 03 p0242 A73-13310
Experimental investigation of a turbulent boundary layer on a highly elongated body of revolution in a supersonic flow 03 p0245 A73-13669
Experimental investigation of the base pressure on slender circular cylinders 03 p0245 A73-13674
On the effective moduli of composite materials - Slender rigid inclusions at dilute concentrations. 05 p0630 A73-16099
Experimental and theoretical investigations regarding the unsteady aerodynamic derivatives of the longitudinal motion in the case of slender flight bodies at moderate velocity [DFVLR-SONDDR-206] 05 p0528 A73-16757
Matched asymptotic expansions method application to slender cylindrical beams, calculating displacement far field by Navier-Stokes elasticity equation 07 p0913 A73-20075
Calculation of forces on stores in the vicinity of aircraft. 09 p1028 A73-22433
Aerodynamic forces and moments estimation for slender bodies of circular and noncircular cross section without and with lifting surfaces at 0-90 degree angles of attack 09 p1030 A73-23468
Liquid film cooling on hypersonic slender bodies. 10 p1172 A73-24540
Acoustically induced vibrations of slender rods in a cylindrical duct with parallel flow. 11 p1432 A73-24983
Fish like slender body propulsion and flow theory, discussing fin surface-body thickness interaction, vortex sheets, trailing edges and lifting force 11 p1301 A73-25852
The force acting from the direction of a flow of liquid on a thin curved body of circular cross section 11 p1348 A73-26427
Variational method for a generalized class of functionals and its application to aeromechanics problems 11 p1304 A73-26438
Nonlinear effects in steady supersonic dissipative gasdynamics. II - Three-dimensional axisymmetric flow. 14 p1711 A73-30167

- The nature of viscous flow around the forward stagnation point in the presence of strong injection of a gas through the surface of a slender pointed body
15 p1821 A73-31043
- The thin shock layer in the hypersonic flow problem
15 p1821 A73-31194
- The turbulent boundary layer on a long thin filament
15 p1822 A73-31197
- Optimum shapes of slender axisymmetric missile bodies with minimum ballistic factor, using calculus of variations
16 p2071 A73-32904
- Analytic and numerical investigations of boundary layer flows about slender axisymmetrical bodies
16 p1962 A73-33248
- Bow shock waves and flow field preceding pointed slender bodies subject to supersonic flow, analyzing wave distance from body and frozen flow characteristics
16 p1962 A73-33249
- Method for the interpretation of surface pressure measurements under rarefied hypersonic conditions.
16 p1963 A73-33316
- Correlation of the mass flow rate in the laminar boundary layer on a sphere-cone.
17 p2091 A73-34195
- Axisymmetrical turbulent boundary layer along a slender cylinder.
17 p2150 A73-34400
- Relaxation solutions for inviscid axisymmetric transonic flow over blunt or pointed bodies.
17 p2095 A73-35128
- Support wire disturbances in near viscous wakes of slender supersonic bodies.
18 p2295 A73-36155
- Prediction of the lift and moment on a slender cylinder-segment wing-body combination.
19 p2377 A73-38007
- Analysis of the effects of a probe in the transonic region of a nozzle.
22 p2796 A73-42568
- Aircraft aerodynamics problems covering slender body theory, atmospheric turbulence and boundary layers, wind tunnel contractions, radiator blocks, vortex induced oscillations, etc
24 p3053 A73-44690
- ### SLENDER CONES
- Three-degree-of-freedom motions of a slender asymmetric cone in a hypersonic wind tunnel.
03 p0287 A73-13494
- Measured axial and normal force coefficients for 9-deg cones in rarefied, hypersonic flow.
05 p0531 A73-16902
- Transition effects on slender vehicle stability and trim characteristics.
06 p0756 A73-17646
- Dynamic viscous pressure interaction on a cone.
10 p1173 A73-24821
- Wind tunnel study of flows generated by slender cones in subcritical Reynolds number regime, examining vortex shedding and drag
10 p1174 A73-24845
- Viscous flow over a cone at moderate incidence. I - Hypersonic tip region.
11 p1300 A73-25114
- Laminar film condensation on the inside of slender, rotating truncated cones.
15 p1958 A73-32279
- Foreign gas injection at windwardmost meridians of yawed sharp cones.
18 p2264 A73-36379
- A theoretical and experimental study of sound attenuation in an annular duct.
24 p3077 A73-44838
- ### SLENDER WINGS
- Nonlinear characteristics of a slender triangular wing near an interface
02 p0127 A73-11630
- Wake vorticity of side-slipping slender thin wings at transonic speeds, deriving integral equation for vortex strength based on Prandtl-Glauert rule
03 p0247 A73-14376
- Experimental determination of bound vortex lines and flow in the environment of the trailing edge of a slender delta wing
05 p0528 A73-16600
- German monograph - The steady and unsteady aerodynamic coefficients for the rolling motion of slender wings.
07 p0774 A73-19578
- A correction to 'lifting-line theory as a singular perturbation problem.'
07 p0775 A73-19964
- Slender delta-wings for future supersonic passenger planes
09 p1027 A73-21992
- An analytical solution to the problem of hypersonic gas flow past a slender wing
12 p1457 A73-27078
- Three dimensional turbulent boundary layers prediction methods and flow measurements, considering swept and slender wings
14 p1744 A73-30173
- Separated flow past a slender delta wing at incidence.
15 p1821 A73-31121
- Some effects of camber on swept-back wings.
17 p2094 A73-34661
- Designing a slender-wing-type cantilever plate under conditions of unsteady creep
23 p3042 A73-43728
- Hypersonic flow about a spatial body with an attached shock wave
24 p3054 A73-45172
- ### SLEWING
- Two concepts for the reduction of payload attitude slewing times.
09 p1155 A73-23209
- ### SLICKS
- #### U OIL SLICKS
- #### SLIDES
- #### U CHUTES
- ### SLIDING CONTACT
- Elastohydrodynamic lubrication in rolling and sliding contacts.
03 p0315 A73-14351
- Investigations into film failure /transition point/ of lubricated concentrated contacts.
05 p0580 A73-16103
- Boundary lubrication and wear of slow moving sliding concentrated hardened steel contacts as function of geometry, load, speed, lubricant and oxygen content
05 p0580 A73-16104
- Thermal collapse theory of hydrodynamic oil lubrication films failure for slider bearing, noting frictional forces role
05 p0580 A73-16105
- Solid-solid interface temperature rise during sliding from model with surface topography statistics, frictional conditions, surface hardness and thermal parameters
07 p0832 A73-20483
- Some observations of the relationship between film thickness and load in high Hertz pressure sliding elastohydrodynamic contacts.
19 p2433 A73-37450
- ### SLIDING FRICTION
- Elastohydrodynamic lubrication in rolling and sliding contacts.
01 p0055 A73-10222
- An autoradiographic investigation of material transfer and wear during high speed/low load sliding.
01 p0056 A73-10438
- Elemental analysis of a friction and wear surface during sliding using Auger spectroscopy.
01 p0057 A73-11277
- Steel/pig iron friction pair natural vibrations due to starting force and sliding friction force difference, noting starting force dependence on loading rate
01 p0058 A73-11403
- An estimate of the decrease in friction during vibrations of normal direction
01 p0058 A73-11437
- Problem of the influence of an instantaneous change in normal pressure on the magnitude of contact friction force
02 p0172 A73-11796
- Vibratory loads effect on metal microstructure under sliding friction, noting rheological criteria for fretting corrosion wear resistance
02 p0180 A73-11934
- The friction of boron carbide in controlled atmospheres.
03 p0315 A73-14340
- Transitions in the friction coefficients, the wear rates, and the compositions of the wear debris produced in the unlubricated sliding of chromium steels.
03 p0316 A73-14369
- Evaluation of materials for sliding at 600F-1800F in air.
03 p0317 A73-14371
- Solid-state sliding friction and wear in the case of iron, cobalt, copper, silver, magnesium, and aluminum, kept in an oxygen-nitrogen mixture at pressures from 760 torr to 0.2 microrr
05 p0581 A73-16107
- Early diagnosis of machine damage on the basis of the determination of rubbed-off materials in highly stressed lubricating oils - Employment of spectrographic methods for the analysis of the oil
05 p0582 A73-16998
- Manifestation of the adsorption-induced loss of strength in metals under conditions of selective transfer in boundary friction.
06 p0698 A73-18637
- A review of thermoelectrohydrodynamic lubrication in rolling and sliding contacts.
07 p0831 A73-20223
- Friction and wear of graphite fiber composites.
07 p0833 A73-20500
- Sliding friction welding of nonferrous Cu, wrought Al alloy and Ti, resting rubbing speed and axial pressure effects on equilibrium condition transition
08 p0973 A73-21238
- Features of the influence of the ambient medium on the friction of plastics against metal during intermittent travel
09 p1089 A73-22855
- Polytetrafluoroethylene friction and wear properties as function of heat treatment, speed and temperature, attributing high wear rate to slippage in banded fine structure
10 p1224 A73-24164
- Friction reduction by perpendicular oscillation.
11 p1374 A73-26064
- The reason for noncorrespondence of the values of the static and kinematic coefficients of sliding friction
12 p1502 A73-27445
- 'Glazes' produced on nickel-base alloys during high temperature wear.
12 p1513 A73-27598
- Friction and wear of self-lubricating composite materials.
13 p1624 A73-28776
- Investigation of fatigue effects in thinnest surface layers of metals with boundary friction
14 p1815 A73-30838
- German monograph on frictional fatigue failure covering microcrack initiation due to shear induced vibrational stresses
15 p1956 A73-32587
- German monograph - Model wear investigations concerning the effect of the intermediate medium on the sliding characteristics in the case of a contact between different materials.
15 p1883 A73-32593
- Region of existence of frictional noise and experimental verifications
16 p2036 A73-33215
- Friction induced surface activity of some simple organic chlorides and hydrocarbons with iron.
[ASLE PREPRINT 73AM-8A-1]
- Static-kinetic dichotomy in friction theory, examining atmospheric contaminants effects on surfaces, theoretical basis of static friction postulation and sliding velocity effect on theory
17 p2179 A73-34991
- Experimental investigation of the antifriction properties of Teflon-base materials at low temperatures
21 p2724 A73-41197
- The nature of the high microhardness of surfaces strain-hardened by friction
23 p2984 A73-43467
- Oscillations caused by solid friction. III - In the case of maximum static friction different from kinetic friction without slipping.
23 p2986 A73-44272
- Solid friction shaft characteristics of self excited rotational shaft-spring system with sliding contact surfaces
23 p2986 A73-44273
- Influence of cooling on surface dispersion during the friction process
24 p3092 A73-44417
- ### SLIP
- Constitutive analysis of elastic-plastic crystals at arbitrary strain.
03 p0394 A73-13983
- The influence of anisotropy and crystalline slip on relaxation at a crack tip.
06 p0709 A73-18331
- Acoustic emission measurements during plastic deformation of metals.
22 p2919 A73-41975
- ### SLIP BANDS
- #### U EDGE DISLOCATIONS
- ### SLIP FLOW
- Shear layer extent caused by slip surface in inviscid flow with shock interactions, noting viscous effect in hypersonic flow
01 p0033 A73-10747
- The influence of the accommodation coefficients on the flow variables in the viscous interaction region of a hypersonic slip-flow boundary layer.
07 p0773 A73-19206
- Kinetic theory of suction flow, discussing slip coefficient determination for perturbation boundary conditions in Chapman-Enskog-Hilbert method and pressure gradient effects
07 p0812 A73-20474
- Slip parameter for electrogasdynamic generators with unsteady flow.
09 p1037 A73-22825
- Radiative slip between two adjacent absorbing-emitting gases and its application to air pollution.
11 p1353 A73-25722
- Slow motions of bodies in gas mixtures
15 p1861 A73-31198
- Hypersonic merged stagnation shock layers.
[AIAA PAPER 73-639]
- Evaluation of slip factor of centrifugal impellers.
22 p2796 A73-42625
- Moment equation solutions for plane nonisothermal Poiseuille gas flow slip rate and temperature and pressure gradients in terms of molecular models
24 p3081 A73-45541
- ### SLIPSTREAMS
- #### NT PROPELLER SLIPSTREAMS

SLITS

Calculation of an axisymmetric supersonic gas jet injected in a supersonic slipstream past a given body with heat supply 02 p0129 A73-12583

Vortex sheath formalism based on coupled integral equations for rectangular wing-slipstream aerodynamic interference 03 p0244 A73-13562

Magnetic field effect on friction shear stress in turbulent slipstreams of conducting fluids, calculating mixing zone width 03 p0346 A73-13609

Three-dimensional interaction of jets propagating in a supersonic slipstream 06 p0643 A73-17458

Application of the energy equation for turbulence in the theory of jet flows 15 p1862 A73-31288

Influence of viscosity on the flow of an under-expanded jet propagating in a supersonic slipstream 15 p1822 A73-31299

Effect of a slipstream on the acoustic radiation of ultrasonic annular jets 24 p3055 A73-45358

SLITS

Luminosity and efficiency of spectrographs with a slit 01 p0046 A73-10508

Diffraction of a two-dimensional electromagnetic field by an ideally conducting plane with a boundless rectilinear slit 04 p0423 A73-15608

Diffraction of a two-dimensional electromagnetic field on an ideally conducting plane with an infinite straight slit 10 p1188 A73-24198

SLOPES

NT GLIDE PATHS

Analysis of voltage steps with a time resolution of 12 picoseconds 08 p0962 A73-20833

An analytical and numerical study of the Martian planetary boundary layer over slopes 08 p1011 A73-21381

High resolution radar observation of Martian surface topography and scattering properties, noting dielectric constant and rms surface slope variations 09 p1144 A73-22261

Permanent frost formation on steep north-facing Mars surface slopes above 25 deg north latitude, considering explanation by insolation and surface albedo 09 p1145 A73-22274

Slope angle determination with respect to photograph surface from visible horizon line configuration 16 p2017 A73-34049

SLOSHING

U LIQUID SLOSHING

SLOT ANTENNAS

Transverse resonance solutions for a long slot leaky wave antenna 01 p0023 A73-10187

X band microstripline slot antenna measurement for input impedance and radiation pattern dependence on slot-to-reflector spacing, applying to array design 02 p0141 A73-12100

Radiation from an axial slot antenna coated with a homogeneous material 06 p0665 A73-18138

Effect of dielectric loading on the radiation power of an axial slot antenna 08 p0938 A73-20837

Two mode rectangular waveguide longitudinal and transverse narrow half wave slots properties, discussing measurement apparatus and techniques and radiation patterns 11 p1328 A73-25661

Near-field analysis by the plane-wave spectrum approach 11 p1329 A73-25674

Flush mountable elliptically polarized low silhouette blade antenna for aircraft, describing polarization and radiation characteristics 12 p1478 A73-27043

Shaping of antenna radiation patterns by passive radiating slots 12 p1479 A73-27230

Circular aperture antenna with quadratic phase distortions, deriving near and far field patterns in terms of linear combinations of Bessel and Lommel functions 12 p1479 A73-27233

A radiating element giving circularly polarized radiation over a large solid angle 12 p1471 A73-27656

Radiating slot antenna immittance reactive term due to energy storage in feeding waveguide, discussing resonance characteristics 15 p1849 A73-31097

Equivalent conductivity of a longitudinal slot on the broad wall of a uniformly curved rectangular waveguide 21 p2648 A73-40199

Tilted, off-center, matched slots on the broad wall of a uniformly curved rectangular waveguide 21 p2648 A73-40200

Numerical solution of edge effects of external coupling between elements in linear phased array of slots covered by dielectric slab, using scattering matrix 21 p2651 A73-40654

Realized gain function for a cylindrical array of open-ended waveguides 21 p2653 A73-40677

Circularly polarized linear waveguide array 22 p2831 A73-41843

Impedance properties of a longitudinal slot antenna in the broad face of a rectangular waveguide 22 p2831 A73-41845

Radiating near-field power density and directivity reduction of tapered circular apertures 22 p2829 A73-43181

SLOTS

Linearized solutions to supersonic laminar boundary layer structure near flat plate with slot injection, using triple deck separation theory 08 p0956 A73-21524

Axisymmetric deformation of an elastic layer containing coaxial circular slots 09 p1158 A73-22359

Application of paired integral equations to the problem of the torsion of an elastic space weakened by a conical slot of finite dimensions 13 p1698 A73-29090

Mass transfer effects on turbulent heating in the vicinity of slots 18 p2371 A73-36381

On the stability of the conduction regime of natural convection in a vertical slot 19 p2505 A73-38476

Film effectiveness and heat transfer coefficient downstream of a metered injection slot 20 p2625 A73-38570

Conformal arrays on surfaces with rotational symmetry 21 p2653 A73-40676

Yagi type antenna array of vertical monopoles with optimized slot reradiation to modify foreground reflection for performance improvement 22 p2832 A73-42295

Substrates with end effect in shorted slot, measuring normalized inductive reactance dependence on thickness to wavelength ratio 23 p2954 A73-44068

Slot microwave transmission line with thick metal coating on dielectric substrate, calculating phase constant variation with frequency, slot width and coating thickness 23 p2954 A73-44069

SLOTTED ANTENNAS

U SLOT ANTENNAS

SLOTTED WIND TUNNELS

Flow of a gas in a flat channel at a diminishing flow rate 05 p0533 A73-17090

SLOW NEUTRONS

U THERMAL NEUTRONS

SLV (SOFT LANDING VEHICLES)

U SOFT LANDING SPACECRAFT

SMALL ASTRONOMY SATELLITES

Star sensor/mapper for the Small Astronomy Satellites 08 p0970 A73-21733

A self deployable high attenuation light shade for spaceborne astronomical sensors 08 p0970 A73-21734

SMALL PERTURBATION FLOW

Scattering of sound by an aerofoil of finite span in a compressible stream 02 p0129 A73-12609

Some laws of the propagation of discrete-tone perturbations in a free supersonic jet 03 p0245 A73-13668

Three dimensional ideal incompressible fluid flows under small velocity perturbation, using Euler equations linearized with respect to steady flow 03 p0296 A73-14048

Nonlinear instability of two dimensional unbounded incompressible viscous fluid flows under periodic small perturbation 03 p0296 A73-14049

Small disturbance theory of rotating subsonic and transonic cascades 03 p0246 A73-14136

Incompressible plane flow subject to infinitely small vibrations, expressing complex potential as Abelian integral [ONERA, TP NO. 1191] 04 p0472 A73-15993

Equations of motion for two dimensional steady conducting gas flow in transverse magnetic field, deriving flow equations for transcritical region via small perturbation theory 05 p0602 A73-16585

Small perturbation stability of two dimensional incompressible viscous fluid flow with periodic velocity function, reduced to undulating surface boundary layer problem 06 p0684 A73-17452

A correction to 'lifting-line theory as a singular perturbation problem.' 07 p0775 A73-19964

Special relativity theory for steady irrotational ideal gas flow, noting subsonic, supersonic and transonic flow calculations based on small perturbation theory 08 p0926 A73-21128

Numerical study of the stability of a supersonic laminar boundary layer 09 p1028 A73-22624

On the stability of plane Couette flow to infinitesimal disturbances 11 p1346 A73-25158

Finite core model of self induced motions and stability of filament vortex rings in inviscid fluid under small sinusoidal perturbation 11 p1348 A73-26202

Acoustic field produced in a gas by arbitrary disturbances on a moving plate 14 p1775 A73-30834

Harmonic vibrations of inclined plate in separated free surface flow of ideal fluid in terms of weak perturbation flow theory 15 p1946 A73-31157

Special relativity theory for steady irrotational ideal gas flow, noting subsonic, supersonic and transonic flow calculations based on small perturbation theory 15 p1864 A73-32060

Hydromagnetic stability of parallel flow of an ideal heterogeneous fluid 16 p2043 A73-33872

Small perturbations analysis of hydrodynamic relations of shock front propagation in inhomogeneous medium 17 p2150 A73-34311

Theory of supersonic laminar non-adiabatic boundary layer flow past small rearward-facing steps including viscous-inviscid interaction 18 p2261 A73-36219

A modulation technique for measuring small disturbances in the upstream flow field of a sharp leading edge in a rarefied hypersonic flow 19 p2377 A73-37714

Stability of stratified shear flows 19 p2421 A73-38226

Some features of the propagation of a discrete tone perturbation in a free supersonic jet 21 p2633 A73-41318

The dynamic behavior of articulated pipes conveying fluid with periodic flow rate 22 p2925 A73-42892

Stability of a plane boundary layer with allowance for nonparallelism 23 p2968 A73-43472

Sound field created in a gas by arbitrary perturbations on a moving plate 23 p3006 A73-43584

The effect of walls on the lifting force of a solid-foil wing 23 p2940 A73-43722

Hypersonic flow about a spatial body with an attached shock wave 24 p3054 A73-45172

SMALLPOX

Air-transport, a main cause of smallpox epidemics today 18 p2283 A73-36791

SMELL

U OLFACTORY PERCEPTION

SMOKE

Smoke and fire propagation in compartment spaces. [WSCI PAPER 72-32] 05 p0639 A73-16683

Evaluation of the smoke and flammability characteristics of polymer systems 12 p1515 A73-27143

SMOKE ABATEMENT

Solid propellant rocket motors exhaust smoke minimization, discussing smoke formation mechanism and optical properties relationship to propellant characteristics [AIAA PAPER 72-1192] 03 p0352 A73-13482

Reducing the smoke hazard in small transformer failures 03 p0252 A73-13572

SMOKE TRAILS

Observations of atmospheric effects on the transport and decay of trailing vortex wakes. [AIAA PAPER 73-110] 05 p0529 A73-16869

Experimental determination of small scale transport mechanisms in the stratosphere. [AIAA PAPER 73-496] 16 p2010 A73-34044

Smoke visualization of three-dimensional flow patterns in a nominally two-dimensional wake 19 p2375 A73-37423

SMOOTHING

NT DATA SMOOTHING

SMS

U SYNCHRONOUS

SATELLITE

SNAKING

U LATERAL OSCILLATION

SNAP

NT SNAP 19

NT SNAP 27

NT SNAP 29

Thermoelectric generators long term tests, discussing SNAP 11, 19 and 27, TEM-10 and

SiGe/PbTe cascaded generator performance characteristics
09 p1136 A73-22760

SNAP 19
SNAP 19 thermoelectric generator long term performance tests, attributing output degradation to sublimation and hot junction bond loss due to internal gas cover depletion
09 p1118 A73-22765
SNAP 19/Pioneer radioisotope thermoelectric generator program status report, stressing Jupiter first mission converters performance prediction
09 p1118 A73-22800
Testing of the improved SNAP 19-primary power for advanced space missions.
09 p1038 A73-23285
The SNAP-19 radioisotopic thermoelectric generator experiment - Flight performance on the Nimbus III observatory.
11 p1396 A73-26037
The long term performance characteristics of a SNAP-19 generator operating under vacuum conditions.
11 p1396 A73-26038
Preliminary testing of a SNAP-19 TAGS RTG in support of the Pioneer F and G missions.
11 p1396 A73-26039
Design and testing of a 150 watt SNAP 19 high performance generator.
[IECEC PAPER 739090]
19 p2458 A73-38437

SNAP 27
SNAP-27/ALSEP power subsystem used in the Apollo program.
11 p1312 A73-26021

SNAP 29
Low altitude orbit feasibility study of integrated SNAP 29/Agna satellite configuration, comparing with solar cell power system
11 p1396 A73-26040

SNATCHING
U SPACECRAFT RECOVERY
SNELLS LAW
Reflection and transmission of plane waves at a boundary between two conducting media.
21 p2655 A73-41047

SNOW
Backscatter from snow and ice surfaces at near incident angles.
01 p0016 A73-10191

SNOW COVER
The albedo of snow in relation to the sun position.
01 p0038 A73-10392
Spectroscopic sounding of cloud; snow and ice covers from below /earth surface/ and above /space or planet/
04 p0473 A73-15570
Millimeter wave backscatter measurements for snow, ice and sea ice, discussing penetration into snow and ice
16 p1983 A73-33728
Climatological studies based on satellite data, including cloud, snow and ice cover, wind measurement, convection currents, temperature fields and earth thermal balance
18 p2331 A73-35914
Mapping of snow cover in the Swiss Alps from ERTS-1 imagery.
18 p2306 A73-36021
Applications of ERTS imagery to snow and glacier hydrology.
18 p2306 A73-36022
New ways to monitor the mass and areal extent of snow cover.
18 p2307 A73-36025
Problems related to high-performance flight in the Arctic regions
18 p2287 A73-36953
Satellite detection of melting snow and ice by simultaneous visible and near-IR measurements.
20 p2556 A73-39840
High resolution measurements of snowpack stratigraphy using a short pulse radar.
20 p2556 A73-39842
The effect of snow on antenna radiation patterns - A presentation of results.
22 p2831 A73-41850

SNOW PACKS
U SNOW
SNOWFLOW EFFECT
U PLASMA DYNAMICS
SOAKING
Mechanical behavior of plastically deformed polycrystalline metal subjected to hydrostatic pressure soaking.
13 p1634 A73-28196

SOAPS
Soaps, detergents and surfactants dermatological hazards in personal hygiene use by spacecrews during long term space flight /Skylab/
[ASME PAPER 73-ENAS-26]
19 p2400 A73-37981

SOARING
Glider soaring flight energy budget analysis, discussing rate of climb indicator error compensation
08 p0968 A73-21656

Electronic developments for performance gliding.
III
16 p2014 A73-33023

SOCIAL FACTORS
Future NASA communication satellite technology applications in meeting national education, health care, culture and data transfer needs, considering ATS F and CTS spacecraft
02 p0143 A73-12846
The influence of background noise on disturbance due aircraft.
03 p0249 A73-12979
Differential housing /isolation vs aggregation/ as factor in postnatal development of mouse brain cell specificity and metabolism, noting relation to sleep behavior
03 p0264 A73-14259
Social, economic and political factors associated with earth resources observation and information analyses.
05 p0642 A73-17137
Economically viable and socially acceptable second-generation SST, discussing technological developments for range/payload, airport noise and sonic boom improvements
[AIAA PAPER 73-15]
06 p0646 A73-17608
Astronauts diurnal life cycle inversion during space flight missions, considering social factors and work-rest cycle effects
12 p1463 A73-27715
Offshore airport planning, discussing selection economics from cost effective alternatives based on usage projection, community benefits and intrinsic and social costs
15 p1856 A73-31531
Offshore airport planning in Osaka-Bay, Japan - New Kansai International Airport.
15 p1857 A73-31542
Canadian government planning for second land based or offshore jet airport in Toronto area, considering environmental and community factors
15 p1858 A73-31545
Aircraft noise abatement technological and social aspects, considering aircraft design, airport noise pattern minimization and population removal
15 p1831 A73-32560
Toronto airport relocation project, summarizing provincial government planning and decision making process, site choice and community resistance to airport
16 p1995 A73-33181
Short haul V/STOL air transportation social and economic aspects in comparison with ground transportation modes, emphasizing convenience and frequency of service
16 p2088 A73-33193
Some economic aspects of aviation safety.
16 p2089 A73-33648
Social acceptability of heliports particularly from the standpoint of noise.
17 p2146 A73-34441
Book - Satellite broadcasting.
17 p2121 A73-34473
The effect of social-emotional environmental stress on the functional state of the neocortical structures of rhesus monkeys
19 p2394 A73-37755
Myocardial infarction susceptibility correlated with psychosocial factors in life change measurement studies
22 p2809 A73-42833

SOCIAL ISOLATION
Histopathological and histochemical studies of one year isolation and six months immobilization effects on rhesus monkeys internal organs and tissues
18 p2270 A73-35983

SOCIOLOGY
NT SOCIAL FACTORS
Apollo project management techniques transfer to socio-economic programs, discussing systems oriented approach to city planning, mass transportation, pollution control, public hygiene, etc
09 p1167 A73-21898

SODIUM
NT LIQUID SODIUM
NT SODIUM ISOTOPES
NT SODIUM VAPOR
NT SODIUM 22
NT SODIUM 24
Renal vascular response to saline infusion from radioactive Xe washout and sodium excretion concentration data
01 p0008 A73-10170
Daytime laser radar measurements of the atmospheric sodium layer.
02 p0157 A73-11875
Tunable dye laser radar observation for Na layer nocturnal vertical distribution, suggesting meteor shower effect on layer content increase
04 p0444 A73-15543
Upper atmospheric dust particle temperature and related Na atom abundance seasonal variation based on energy budget and Na sublimation rate considerations
05 p0571 A73-17061

Increase of Na twilight emission after the earth's crossing of the orbital planes of Comets Halley and Encke.
07 p0899 A73-20063

Inert-gas transport in liquid metals during boiling experiments.
08 p1023 A73-21263

Diurnal variation of nightglow Na emission, noting linear intensity variation with time, oscillatory and anticovariation characteristics
13 p1610 A73-29337

Predawn enhancement of 6300 A forbidden OI nightglow emission from observations at Abastumani
15 p1867 A73-31263

Vertical distribution and temperature profile of the night time atmospheric sodium layer obtained by laser backscatter.
16 p2009 A73-33890

A comparison of two methods of analysis for the twilight sodium airglow data.
16 p2009 A73-33891

Enhancement of upper atmospheric sodium from sporadic dust influxes.
16 p2010 A73-33917

Diurnal, annual and solar cycle variations of hydroxyl and sodium nightglow intensities in the Europe-Africa sector.
17 p2160 A73-34785

FFTF probe-type eddy-current flowmeter - Wet versus dry performance evaluation in sodium.
21 p2738 A73-40768

Effect of hypothermia on renal sodium reabsorption.
21 p2641 A73-41623

Comet Bennett neutral sodium atom and dust particle distribution across head and tail measured by photometry of Na emission radial profile
24 p3133 A73-44560

SODIUM CARBONATES
Use of sodium hydrocarbonate for medication and prophylaxis of motion sickness
08 p0933 A73-20990

SODIUM CHLORIDES
A salt-inhibited cytochrome c reductase obtained from the moderately halophilic bacterium, *Micrococcus halodenitrificans*.
03 p0261 A73-13598
High temperature behavior of superalloys exposed to sodium chloride. I - Mechanical properties. II - Corrosion.
06 p0713 A73-18766
Inhibition of corrosion fatigue in 7075 aluminum alloys.
07 p0840 A73-20351
Lattice model calculation of elastic and thermodynamic properties at high pressure and temperature.
11 p1399 A73-25900
Kramers-Kronig analysis of relative reflectance spectra measured at an oblique angle.
11 p1400 A73-26421
Preparation and investigation of EuS thin films
11 p1410 A73-26672
Sodium chloride electrolyte data at high temperatures and pressures.
16 p1971 A73-33532
Dependence of laser-induced breakdown field strength on pulse duration.
17 p2183 A73-34201
Effect of iron and salt on prodigiosin synthesis in *Serratia marcescens*.
17 p2112 A73-34399
The hydrogen evolution reaction on Ti-6Al-4V in acidic solutions of NaCl-HCl.
19 p2402 A73-37585
Effect of prior adaptation to cold on the development of experimental hypertonia
21 p2636 A73-40209
Russian book - Mutual relationship of water and salt secretion functions in digestive and excretory organs under conditions of high temperature.
21 p2641 A73-41438
Measurements of the dielectric properties of seawater and NaCl solutions at 2.65 GHz.
22 p2849 A73-42549

SODIUM COMPOUNDS
NT SODIUM CARBONATES
NT SODIUM CHLORIDES
NT SODIUM HYDROXIDES
NT SODIUM IODIDES
NT SODIUM SILICATES
NT TALC
Phenomenological theory of antiferroelectricity and ferroelectricity applied to NaNbO3 and the system KNaO3-NaNbO3.
06 p0737 A73-18354
Nickel-base alloys hot corrosion mechanism due to sodium sulfate induced accelerated or catastrophic oxidation as result of protective oxide scale dissolution
06 p0712 A73-18763
Na2SO4-induced attack of Ni-20Cr-2TiO2.
15 p1896 A73-32575
The relationship between relative oxide ion content of Na2SO4, the presence of liquid metal oxides and sulfidation attack.
20 p2575 A73-39022

SODIUM COOLING

SODIUM COOLING

Nb heat pipe design with Na coolant for high temperature operation, discussing slopes effect on transmitted power
20 p2628 A73-39418

SODIUM D-LINE

U D LINES

SODIUM HYDROXIDES

Two modes of interaction of NaOH and SO₂ in gases from fuel-lean H₂-air flames.
22 p2820 A73-42802

SODIUM IODIDES

A target design for irradiation of NaI at high beam current.
07 p0853 A73-20469

SODIUM ISOTOPES

NT SODIUM 22

NT SODIUM 24

Temperature dependence of the Na-23 quadrupole coupling constants in Rochelle salt.
11 p1409 A73-25875

SODIUM SILICATES

NT TALC

Investigation of the structure of sodium silicate glass containing oxides of multivalent metals by nuclear spectroscopy methods
09 p1110 A73-22980

SODIUM VAPOR

Photometer for detection of sodium day airglow.
19 p2428 A73-37261

SODIUM 22

Al-26 and Na-22 measurements on Luna 16 samples by non-destructive gamma-gamma coincidence spectrometry.
21 p2774 A73-41405

SODIUM 24

Sodium Na-24 and potassium K-42 availability for sweat production after intravenous injection and their handling by sweat glands.
19 p2395 A73-37757

SOFT LANDING

A control system for soft landings on the lunar surface
05 p0595 A73-16424

Stochastically optimal terminal control system synthesis for loss function dependence on finite phase coordinates of dynamic system, considering soft landing of flight vehicle
07 p0805 A73-20037

SOFT LANDING SPACECRAFT

NT APOLLO SPACECRAFT

NT LUNAR MODULE

NT SURVEYOR LUNAR PROBES

NT SURVEYOR 3 LUNAR PROBE

Dynamic stress analysis during inflation of disk-gap-band Viking 75 parachute for Mars soft landing
[AIAA PAPER 73-444]
15 p1825 A73-31430

SOFT RECOVERY

U SOFT LANDING

SOFTENING

Alloy hardening and softening in binary molybdenum alloys as related to electron concentration.
03 p0323 A73-13300

Viscosity investigation of sintered fiberglass in the region of softening and annealing temperatures
06 p0715 A73-18657

Cu annealability tests for assessing suitability for applications requiring low softening temperature, discussing recrystallization behavior and softness measures
11 p1379 A73-25130

Hardening and softening of aluminum alloys under an applied load at 135 to 150 C
15 p1889 A73-31808

Temperature dependent softening effect due to state transition and electronic drag coefficient for dislocations in pure two band superconductors
18 p2341 A73-36768

Investigation of the softening processes in molybdenum and its alloys under conditions of creep
23 p2995 A73-44281

SOFTWARE [COMPUTERS]

U COMPUTER PROGRAMS

U COMPUTER SYSTEMS PROGRAMS

SOIL MAPPING

Toros side-looking radar system for sea-ice distribution and geomorphological mapping and agricultural soil studies
12 p1474 A73-27962

Remote sensing applications in agriculture and forestry including land inventories, soil classification and water resources detection
17 p2162 A73-34948

ERTS-1 MSS imagery - A tool for identifying soil associations.
18 p2306 A73-36023

The reliability of the interpretation of soils from aerial photographs in highway planning practice.
20 p2558 A73-39872

Experimental design to produce visible-reflective IR ratio image from ERTS data for geological mapping of iron compounds
20 p2561 A73-39899

SOIL MECHANICS

Luna 16 direct measurements for soil mechanical properties, determining bulk density, failure characteristics, compressibility and shear and bearing strength
02 p0213 A73-12232

Lunar soil bearing strength, shear and cohesion properties in natural state along Lunokhod 1 self propelled vehicle route
02 p0213 A73-12233

Southeastern Conference on Theoretical and Applied Mechanics, 6th, University of South Florida, Tampa, Fla., March 23, 24, 1972, Proceedings.
03 p0388 A73-13301

Microphysical, microchemical, and adhesive properties of lunar material. III - Gas interaction with lunar material.
07 p0892 A73-19832

Mechanical properties of lunar soil - Density, porosity, cohesion, and angle of internal friction.
07 p0898 A73-19902

Lunar soil porosity and its variation as estimated from footprints and boulder tracks.
07 p0898 A73-19903

German book - Soil mechanics of retaining structures, roads, and runways.
11 p1344 A73-26255

Power series solution of quasi-linear parabolic heat conduction equation for temperature wave propagation in soil
12 p1560 A73-27807

Lunar soil models for equipment environmental testing, using vibrationally compacted volcanic granular materials
13 p1606 A73-28119

Propagation of thermoelastic waves in an undefined isotropic soil
16 p2081 A73-33369

Mechanical erasure of particle tracks - A tool for lunar microstratigraphic chronology.
20 p2612 A73-39713

Magnetic investigations of lunar soil delivered by AIS Luna 16.
21 p2773 A73-41399

Surveyor 3 lunar soil shear strength measurements for range of bulk densities obtained by different packing procedures, calculating void ratios
23 p3031 A73-43761

SOIL MOISTURE

On the measuring of soil moisture by microwave radiometric techniques.
17 p2170 A73-35363

Progress report on aircraft gamma-ray surveys for soil-moisture detection at a NOAA test site near Phoenix, Arizona.
20 p2558 A73-39871

Polar region soil moisture content remote sensing based on electromagnetic backscattering and depolarization by ice and terrain, considering radar, microwave and IR sensors
21 p2654 A73-40814

SOIL SCIENCE

Russian book - Fundamentals of lunar soil science: Physicomechanical properties of lunar soils.
02 p0211 A73-11893

Viking lander-borne gas chromatograph mass spectrometer for Martian atmosphere sampling and soil analyses
02 p0168 A73-12000

Resistance of soil microorganisms to starvation.
02 p0136 A73-12627

Triaxial plastic compression soil theory generalization to three dimensional complex stress fields, discussing yield surface for granular materials
03 p0390 A73-13332

Remote sensing of the near-surface moisture profile of specular soils with multi-frequency microwave radiometry.
04 p0446 A73-15782

Apollo 14 soils - Size distribution and particle types.
07 p0884 A73-19740

Survival of Arthrobacter crystallopoietes during prolonged periods of extreme desiccation.
07 p0782 A73-20026

Lunar highland soils and breccias chemistry representation by model for mixing during intense cratering period, discussing chemical composition
12 p1466 A73-27493

Responses of indigenous microorganisms to soil incubation as viewed by transmission electron microscopy of cell thin sections.
14 p1714 A73-29724

Survival of soil bacteria during prolonged desiccation.
14 p1720 A73-30959

Development of soil on the lunar surface.
15 p1941 A73-32226

Apollo 17 lunar soil magnetic characteristics, covering ilmenite basalts mineralogy and petrology, electrical properties, orange and green glasses origin, and trace elements
16 p2061 A73-33171

Lunar surface light reflection phase function, discussing topsoil atomization and brightness distribution over lunar disk
16 p2063 A73-33755

Progress in remote optical analysis of lunar surface composition.
17 p2119 A73-35747

Preliminary measurements of spherules of the Pontina Plain and of micrometeorites of Apollo 12 and related impact studies.
21 p2775 A73-41412

Soil microbiological tests to evaluate Antarctica Mars environment model for quarantine standards
22 p2803 A73-42162

SOILS

NT LUNAR DUST

NT LUNAR SOIL

NT MUD

NT PERMAFROST

NT SANDS

SOLAR ACTIVITY

NT FACULAE

NT SOLAR FLARES

NT SOLAR PROMINENCES

NT SOLAR STORMS

NT SPICULES

NT SUNSPOTS

Ionospheric propagation indexes prediction based on computer filtered values obtained during solar activity cycles ascending and descending parts
01 p0017 A73-10416

Solar active regions analysis on far UV spectroheliograms obtained by OSO 4 satellite, investigating transition zone structure
01 p0098 A73-10560

Wolf number solar activity and planetary tidal force correlation during 1770-1970, noting 11-year cycle relation
01 p0101 A73-10848

Evidence for an ultra-long cycle of solar activity /Research note/.
01 p0108 A73-11397

Enhanced N2 vibrational temperatures in the thermosphere.
03 p0298 A73-12881

Solar active region growth in terms of magnetic flux emergence in shape of new arch filament system
03 p0367 A73-12946

Solar X-ray source unassociated with sunspots.
03 p0363 A73-13955

The magnetic structure of arch filament systems.
03 p0378 A73-14415

Evolution of coronal helmets during the ascending phase of solar cycle 20.
03 p0378 A73-14419

Heliographic and spectroscopic observations of solar southern hemisphere active region during August 1971 cycle, noting photospheric changes, sunspots and flares
03 p0379 A73-14581

Solar activity observations and predictions, Proceedings of the Conference, Huntsville, Ala., November 16-18, 1970.
04 p0490 A73-14827

Magnetic fields in solar active regions.
04 p0490 A73-14828

Forecast facilities for solar events and activity and sudden ionospheric disturbances, noting forecast centers activity, resources and techniques
04 p0491 A73-14840

Identification and adjustment of psychological factors to improve solar patrol observing.
04 p0411 A73-14841

Investigation of the chromosphere in the D3 helium line at the eclipse of September 22, 1968.
04 p0503 A73-16014

Interdependence of the basic elements of the 22-year solar activity cycle
05 p0609 A73-16205

Relations between the elements of a 22-year solar activity cycle
05 p0609 A73-16206

Solar X-ray emission in July 1964 and in November-December 1965 according to data from the 'Elektron-4' satellite and the 'Venera-2' station
05 p0610 A73-17017

On the dynamo action of the global convection in the solar convection zone.
05 p0627 A73-17387

Further study of the theta component of the interplanetary magnetic field.
07 p0875 A73-19230

Photoelectron precipitation induced dissociation of atmospheric nitrogen molecules during moderate solar activity
07 p0816 A73-19459

Earth electrical conductivity radial distribution effect on solar quiet day geomagnetic field variations
07 p0816 A73-19466

Funnel prominences evolution and relation to solar active regions from H alpha filter observations
08 p0999 A73-21311

Solar cosmic ray heavy nuclei acceleration independence from solar activity phenomena, based on Elektron 4 satellite observation

08 p0999 A73-21332

Summary of daily observational results of solar phenomena, cosmic ray, geomagnetic variation, ionosphere, radio wave propagation and airglow during October 1969 through December 1971.

08 p0961 A73-21393

Catalog of geomagnetic activity indices for the years 1841-1864 and 1870

09 p1077 A73-22543

Cosmic-ray anisotropy during the disturbed period from Oct. 25 to Nov. 10, 1968

10 p1267 A73-23919

On the random nature of the eruption of magnetic flux at the solar surface.

11 p1422 A73-25939

Detailed correlation of type III radio bursts with H alpha activity. I - Active region of 22 May 1970

11 p1413 A73-25950

Day-to-day variability of the quiet-day solar-diurnal variations and the orientation of the interplanetary magnetic field

12 p1540 A73-27358

Annual solar activity changes due to interstellar matter capture by sun, noting uneven sunspots distribution

12 p1535 A73-27770

Geomagnetic storm families, direction of the interplanetary magnetic field, and solar activity.

13 p1608 A73-28718

Variation of the cosmic-ray gradient during the solar activity cycle.

13 p1670 A73-28721

Emerging flux regions /EFR/ spatial distribution on sun, discussing absence of preferential longitudes, latitudinal preference and time distribution behavior

14 p1787 A73-30648

Wolf number solar activity and planetary tidal force correlation during 1770-1970, noting 11-year cycle relation

15 p1928 A73-30984

The extreme-ultraviolet spectrum of a solar active region.

15 p1936 A73-31560

Yearly and trimonthly variations in solar activity and cosmic-ray intensity

15 p1926 A73-31879

Velocity field in the active regions of the sun

16 p2057 A73-32702

High pass filter and power spectral analysis of periodicity in solar activity time series, applying statistical tests to sunspot and flare indices

16 p2060 A73-32955

Millisecond time scale atmospheric light pulses associated with solar and magnetospheric activity.

16 p2004 A73-33447

Characteristic features of secular and super-secular cycles of solar activity - The 180-year cyclic variation of solar activity

16 p2056 A73-33657

Book - Space physics and space astronomy.

17 p2230 A73-34575

Solar magnetic field spatial structure in relation to solar activity phenomena, discussing measurements based on Zeeman effect in absorption line spectra formation

20 p2605 A73-39059

Circular polarized emission from solar active regions at millimeter wavelengths.

20 p2601 A73-39070

Sunspot activity, flare observation, electromagnetic and magnetic disturbances, auroral activity and solar radio bursts in March and April 1973

21 p2767 A73-40567

Observations of the X-ray emission of solar active regions on 28 November 1970 and 20 August 1971.

21 p2761 A73-41387

MHD frequency wavelength relation to five-minute period oscillation in solar magnetically active regions

21 p2777 A73-41483

Multidirectional scanning of active regions with a slit-jaw spectrograph and a solar chromatograph. I - Description of the method and some preliminary results for the flare event of August 4th 1972.

21 p2777 A73-41491

On the source of the slowly varying component at centimeter and millimeter wavelengths.

21 p2778 A73-41496

Analysis and synthesis of coronal and interplanetary energetic particle, plasma, and magnetic field observations over three solar rotations.

22 p2901 A73-41901

Some statistical characteristics of active regions with the yellow coronal line.

22 p2915 A73-43037

Day-to-day variability of quiet-day solar daily variations and the direction of the interplanetary magnetic field.

23 p3027 A73-43258

Solar activity forecasting, considering flare site identification from active center microscopic magnetic components, and particle acceleration observations

23 p3021 A73-43370

An analytical expression for the secular variation of the geomagnetic field and a comparison of the activity of secular variations with some astronomical phenomena

23 p2973 A73-43793

Revision of the probability laws of sunspot variations.

24 p3137 A73-44648

Space-time limits of stable oscillations of solar surface active zones spanning multiple solar rotations, noting correlation coefficients for north and south hemispheres

24 p3138 A73-45013

SOLAR ACTIVITY EFFECTS

Airglow 6300 A emission predawn enhancement amplitude variation with geomagnetic and solar activity

01 p0037 A73-10347

Solar events and their effects on the earth surface in August, 1972

01 p0097 A73-10469

Ion composition dependent recombination coefficient loss rate changes in D region during solar flares, using electron density and X ray flux measurements

01 p0042 A73-10903

Solar-activity effects and zonal wind in the stratosphere and lower mesosphere

01 p0043 A73-10945

Changes of lower ionosphere electron concentrations with solar activity.

02 p0159 A73-12029

Effect of solar activity delays on the processes in solar-terrestrial space.

02 p0212 A73-12185

E and F regions ion composition measurement with rockets, noting nitric oxide variation with molecular/oxygen cations ratios at different solar activity phases

02 p0206 A73-12305

Solar cosmic ray bursts in November-December 1970 according to data from Venus 7 space probe and Lunokhod 1 station.

02 p0206 A73-12321

Sunspot number relationship to planetary tides on sun, considering earth-Venus conjunctions and opposition

02 p0219 A73-12436

Correlation between the brightness of comets and solar wind fluctuations

02 p0208 A73-12471

Lyman-alpha emission of comet Bennett 1969i and the determination of the solar wind flux

02 p0208 A73-12472

Conjugate ducted echoes observed on Alouette II ionograms.

02 p0143 A73-12624

Geomagnetic indexes Kp, ap, AE and Dst computation, interpretation, reliability and use in statistical studies of solar-terrestrial interactions

03 p0301 A73-13708

EUV emitting plasma structure of solar quiet and active atmospheres, noting extreme departures from LTE

03 p0363 A73-13952

Solar activity and the variations of the geomagnetic K sub p-index. I.

03 p0378 A73-14422

Solar activity effects on geomagnetic variations from spacecraft particle measurements, showing statistical correlations between solar wind, flares and magnetic storms

04 p0491 A73-14838

Solar flare effects in ionosphere, discussing long term variability, sudden ionospheric disturbances, PCA and magnetic storms

04 p0491 A73-14839

Prediction of proton flares and Forbush effects.

04 p0491 A73-14843

Decametre-wave radiation from Jupiter and solar activity.

04 p0491 A73-14956

The residual cosmic ray modulation at the 1954 solar minimum.

04 p0492 A73-14968

Monopole aspects of solar magnetic field at sunspot cycle maximum and minimum, considering different explanations

04 p0496 A73-14972

An effect of the solar wind on the earth's rotation

04 p0498 A73-15282

Solar cycle control of the ionospheric E-region.

04 p0441 A73-15291

Modulation of low-energy galactic cosmic rays over solar maximum /cycle 20/.

04 p0493 A73-15549

Solar core stability via model including plain parallel stratified fluid layer with energy generation, noting ice age correlation with mixing phases during evolution

04 p0501 A73-15623

Secular variation of the stratospheric ozone layer over middle Europe during the solar cycles from 1951 to 1972.

04 p0445 A73-15635

Characteristics of interplanetary electron irregularities according to observations in 1967-1969.

04 p0503 A73-16015

Geomagnetic storm effects in the nighttime E layer during increasing and maximal solar activities

05 p0568 A73-16215

Russian papers on solar radiation effects on ionospheric propagation covering proton flares, thermal fluxes, lunisolar tides, radio propagation and cosmic radio emission

05 p0568 A73-16251

Electron density increase in the F region after proton bursts

05 p0609 A73-16257

Solar activity effects on tree growth, farm crop yield, fish availability and human sickness trends, discussing indirect effects via meteorological factors

05 p0622 A73-17171

Contribution of hard solar X-ray radiation to D-region ionization.

05 p0611 A73-17172

Diurnal amplitude variations of equatorial electrojet intensity as functions of solar activity, using 1958 South American observatory data

06 p0690 A73-17556

Solar outer atmospheric eruption from photographic recording by OSO 7 spacecraft borne coronagraph, noting ejected gas and plasma clouds caused by flare

06 p0753 A73-18374

Energy dependent time lag in the long-term modulation of cosmic rays.

07 p0869 A73-19252

Sporadic E relation to ionized particle redistribution in E layer during solar eclipse

07 p0815 A73-19256

Long term atmospheric pressure fluctuations in relationship to solar activity over Northern Hemisphere, confirming 22 year cycle

07 p0816 A73-19448

Solar flare intensity estimation based on measurements for Ar 37 radioactivities and depth dependence of tritium in Apollo 11 and 12 lunar rock samples

07 p0889 A73-19794

Interlaboratory comparison for solar flare track density data on feldspars in individual sections of lunar rock 14310, noting depth dependence and irradiation history

07 p0896 A73-19878

Record-breaking cosmic ray storm stemming from solar activity in August 1972.

08 p0996 A73-20664

Lunar eclipse brightness dependence on eleven year sunspot activity cycle

08 p1007 A73-21068

Ion composition and photochemistry of the E region

08 p0958 A73-21282

Diurnal temperature variations in the thermosphere with solar activity

08 p0959 A73-21288

Solar modulation of cosmic ray intensity in stratosphere, examining relationship to sunspots group number and heliographic latitudes over 11 year period

08 p0999 A73-21339

Galactic cosmic ray modulation region evaluation from meteoroid orbit, velocity and radioactive dating data

08 p1000 A73-21342

Solar active regions effects on galactic cosmic ray distribution and interplanetary magnetic field structure

08 p1000 A73-21344

Diurnal, sporadic and yearly variations in cosmic ray flux based on neutron component data, noting relation to solar activity cycles

08 p1000 A73-21345

Study on the solar activity dependence of the E-region peak electron density and some atmospheric parameters.

08 p0961 A73-21652

Study on the electron density profile in the F1 region.

08 p0961 A73-21653

Evening/forenoon asymmetry in the 27-day oscillation of the low-latitude magnetic field.

09 p1076 A73-22140

Type variation of solar sudden field anomaly /SFA/ on 164 kHz as an indicator of seasonal structure changes in the D-region.

09 p1076 A73-22141

Variation of atmospheric radio noise level with sunspot number.

09 p1051 A73-22493

Effects of solar activity on zonal winds in the stratosphere and lower mesosphere.

09 p1078 A73-22740

Distribution of radiation doses in the earth's radiation belts during years of maximum solar activity

10 p1264 A73-23889

Cosmic ray, solar activity, supernova outbursts and geomagnetic field effects on atmospheric C-14 concentration

10 p1266 A73-23911

Relationship between the 27-day cosmic-ray variations and various solar-activity indices during the period from 1957 to 1970

10 p1266 A73-23918

Forbush decreases and their relation to solar activity and the parameters of the interplanetary medium
10 p1267 A73-23921

Frequency spectrum of cosmic ray intensity and solar activity variations
10 p1267 A73-23924

Ionospheric magnetic disturbances during March 1970 related to solar flare corpuscular and proton fluxes, generating ring current and PCA absorption
10 p1211 A73-24218

Solar quiet long-term modulation of cosmic ray intensity diurnal variation explained via interplanetary sector pattern changes
10 p1269 A73-24448

Solar modulation of the galactic cosmic rays - Implications of the Compton-Getting coefficient.
10 p1269 A73-24726

Ionospheric radio wave absorption coefficient correlation with solar activity Wolf number in IGY, IGC and IQSY
11 p1327 A73-25083

Time dependent geophysical effects associated with chromospheric and coronal flares, tabulating for 1957-1961
11 p1411 A73-25099

Solar activity variation of XUV emission segregation into quiet sun and active region components via correlations of sunspots with observed fluxes and intensities
11 p1415 A73-25173

Observations on the time and frequency structure of solar decimeter radio bursts.
11 p1413 A73-25951

A rigorous cosmic-ray transport equation with no restrictions on particle energy.
11 p1414 A73-26609

Solar and geomagnetic modulation of low-energy secondary cosmic ray electrons.
12 p1533 A73-26977

Solar radiation effects on terrestrial electromagnetic environment, considering interplanetary space, earth internal structure, geomagnetism, upper atmosphere, dynamo action, energetic particles and magnetospheric storms
12 p1538 A73-27053

Complex studies of the disturbance of March 8, 1970 from observations in the midnight sector
12 p1490 A73-27342

Magnetosphere boundary location relationship to geomagnetic activity level and solar activity cycle during 1963-68 based on theoretical model
12 p1491 A73-27348

Solar magnetic sector structure - Relation to circulation of the earth's atmosphere.
12 p1491 A73-27441

Midlatitudinal standard ionospheric profile to construct F-region noon electron density profiles and thermal response to solar activity changes
12 p1493 A73-27761

Solar-terrestrial relations in the retrospective world interval from July 26 to August 14, 1972.
12 p1535 A73-27766

The first results of balloon measurements during the solar proton events in the period from August 2 to August 10, 1972
12 p1535 A73-27777

Dynamics and localization of surges in the chromosphere.
12 p1545 A73-27846

Photometric investigation of the atmospheric activity of Jupiter during 1962-1969
13 p1673 A73-28297

On the relation between the rotation of the earth and solar activity.
13 p1680 A73-28408

Statistical analysis of Forbush decreases and of cosmic-ray intensity increases preceding them.
13 p1670 A73-28701

Second positive system of nitrogen bands in dayglow, according to Kosmos-224 data.
13 p1607 A73-28703

Variations of the global values of F2-layer thickness and the parameters of the neutral atmosphere.
13 p1608 A73-28722

Rocket-borne scientific experiment program Sun-Atmosphere 1971, using meteorological rockets for meteor trail, atmospheric and ionospheric observations during geomagnetic disturbances
13 p1609 A73-29188

Discontinuous change in earth's spin rate following great solar storm of August 1972.
14 p1800 A73-30602

Anisotropy parameters of the ionospheric irregularities at Thumba during high solar activity period.
14 p1750 A73-30905

Predawn enhancement of 6300 Å forbidden OI nightglow emission from observations at Abastumani
15 p1867 A73-31263

On the origin of SC-storms with respect to forecasting geomagnetic activity.
15 p1868 A73-31520

Geomagnetically calm intervals and their forecasts.
15 p1868 A73-31521

Some statistical characteristics of atmospheric ozone measurements
15 p1868 A73-31612

Solar and lunar effects on neutral atmospheric tidal winds and induced electrostatic and geomagnetic fields effects on low latitude F2 and sporadic E layers
15 p1868 A73-31751

Equatorial Esq disappearance relationship to daily magnetic Sr variation inverted latitudinal profiles during magnetic quiet periods, considering counter electrojet current belt hypothesis
15 p1869 A73-31757

Semi-annual variation in the true height of the F2-peak in low latitudes /at Puerto Rico/.
15 p1869 A73-31762

Solar surface and atmosphere activity due to magnetic field production, transport and dissipation, discussing flares, sunspots, corona, dynamo, plasma turbulence and prominences
15 p1937 A73-31848

Concorde-borne astronomical observation for Fraunhofer corona IR and photospheric and chromospheric radiations in lunar shadow during 30 June 1973 solar eclipse
15 p1940 A73-32184

Correlation between the brightness of comets and fluctuations of the solar wind.
15 p1927 A73-32622

Lyman-alpha radiation from comet Bennet 1969i.
15 p1927 A73-32623

Diurnal amplitude variations of equatorial electrojet intensity as functions of solar activity, using 1958 South American observatory data
16 p2002 A73-32780

Solar activity centers configuration and accelerated particle storage and release in coronal regions for all solar events
16 p2055 A73-33292

Transient solar modulation of cosmic rays.
16 p2055 A73-33294

Steady-state solar modulation of cosmic rays.
16 p2055 A73-33296

Calculated cosmic ray neutron monitor response to solar modulation of galactic cosmic rays.
16 p2056 A73-33444

Stability levels of the reflectivity of lunar surface details
16 p2063 A73-33761

Equatorial spread F layer height nocturnal variations due to magnetic disturbances during solar activity cycles
16 p2008 A73-33878

Atmospheric composition changes and the F2-layer seasonal anomaly.
16 p2010 A73-33915

A search for periodic variations in geomagnetic activity and their solar cycle dependence.
17 p2157 A73-34073

A new test for solar modulation theory - The 1972 May-July low-energy galactic cosmic-ray proton and helium spectra.
17 p2224 A73-34769

Solar energy cycle and its relation to geomagnetic activity.
17 p2236 A73-35777

Comparison of electron density profiles in the lower ionosphere at Equator and midlatitudes.
18 p2305 A73-36007

Electron temperature profile and its solar activity dependence in the middle latitude region.
18 p2308 A73-36047

An analysis of the solar-activity effects in the upper atmosphere.
18 p2309 A73-36060

Characteristics of the influence of the solar wind on cosmic-ray intensity during 1969
18 p2345 A73-36108

Periodic variations of the cosmic radiation. III - The 27-day variation.
18 p2345 A73-36180

Simulation of driven flare-associated disturbances in the solar wind.
18 p2346 A73-36263

Lunar eclipse brightness dependence on eleven year sunspot activity cycle
18 p2355 A73-36869

SID effects as observed in intensities of LF radio waves.
18 p2290 A73-36879

Interplanetary shock waves and cosmic rays.
19 p2476 A73-37759

Ion composition and photochemistry of the E-region.
19 p2424 A73-37911

Variations in the temperature of the thermosphere in the course of the day and with solar activity.
19 p2424 A73-37917

The effect of solar activity on temperatures in the equatorial mesosphere.
19 p2426 A73-38015

Radiation dose distribution in the earth's radiation belts during year of maximum solar activity.
20 p2601 A73-38908

Dynamics of ionization inhomogeneities in the ionosphere
20 p2553 A73-39152

Structure of vortical motion systems in the ionosphere that generate Sq variations of the geomagnetic field
20 p2553 A73-39153

Altitude distribution of the drift velocity and direction of ionosphere inhomogeneities over Ashkhabad in years of maximum and minimum solar activity
20 p2554 A73-39162

Latitudinal distribution change in the conditions for F1 layer occurrence from the solar-activity maximum to minimum
20 p2554 A73-39170

Correlational relations between F2 critical frequency deviations and the solar activity cycle according to a number of high-latitude stations
20 p2555 A73-39176

Method of studying magnetic-ionospheric disturbances and solar flare effects on long-upset periods.
20 p2555 A73-39767

Neutral air wind influences deduced from solar cycle changes in the F2 region equatorial anomaly.
21 p2679 A73-39932

New evidence for effects of variable solar corpuscular emission on the weather.
21 p2755 A73-40073

Russian book - Certain problems concerning solar-terrestrial links and physics of the atmosphere.
21 p2730 A73-40102

Differences between geomagnetic storms with gradual and sudden commencements
21 p2681 A73-40103

Investigation of solar activity and its association with cosmic ray variations
21 p2755 A73-40113

Criticism of Gribbin and Plagemann findings on universal time observations as evidence of day length and earth rotation rate changes due to 1972 solar storm
21 p2766 A73-40375

Certain characteristics of the August 1972 solar flares which generated cosmic radiation, plasma clouds, and interplanetary shock waves
21 p2757 A73-40587

Ground level cosmic ray variations in August 1972, relating intensities and Forbush decreases with solar flares and shock wave parameters
21 p2757 A73-40591

The 11-year cycle of cosmic ray intensity in the stratosphere and its dependence on solar activity
21 p2758 A73-40597

Differences in the correlations of 27-day and 11-year cosmic ray variations with solar activity parameters
21 p2758 A73-40598

Investigation of isotropic and anisotropic effects of cosmic rays during October through November 1968
21 p2758 A73-40600

Diurnal, semidiurnal, and the eight-hour components of cosmic-ray anisotropy
21 p2758 A73-40601

Exospheric and thermospheric structure variations with solar activity, diurnal variation, geomagnetic activity, seasonal-latitudinal variations of He, H and density waves
21 p2683 A73-40630

Characteristic features of the solar diurnal variation according to data obtained by magnetic observatories in Kazakhstan
21 p2686 A73-40846

Evidence of features in atmospheric spectra at around 8 per cm of probable solar origin.
21 p2687 A73-41079

Seasonal variation of atmospheric composition in the F region as a function of solar activity.
21 p2690 A73-41360

Tropospheric and stratospheric response to solar influence during geomagnetic disturbances.
21 p2690 A73-41364

Solar-interplanetary disturbances during 5-18 June 1969 /The PFF interval/IASY/.
21 p2773 A73-41385

Umbral flashes and running penumbral waves relation to overstable hydromagnetic oscillation in sunspots, noting depth dependence and electrical conductivity variation effects
21 p2777 A73-41487

Optical solar flare kinematic model, relating chromosphere response to downward propagating supersonic disturbance
21 p2762 A73-41490

Photometric studies of atmospheric activity of Jupiter during 1962-1969.
21 p2779 A73-41541

Solar cycle control in the 27-day variation of geomagnetic activity.
22 p2846 A73-41945

A modified composite wave technique for OMEGA.
22 p2884 A73-42325

- Some statistical characteristics of sudden ionospheric disturbances, and the distribution of geoeactive chromospheric flares over the solar disk
22 p2847 A73-42326
- Increased influx of stratospheric air into the lower troposphere after solar H alpha and X ray flares.
22 p2848 A73-42538
- Polar magnetic storm temporal properties and distribution patterns, discussing solar activity, annual and twenty-seven day variations and sudden commencement
22 p2851 A73-42749
- Resistive diffusion of force-free magnetic fields in a passive medium. II - A nonlinear analysis of the one-dimensional case.
22 p2914 A73-43009
- Measurement methods for sudden ionospheric disturbances caused by solar flares, discussing short wave fading, sudden phase anomaly and sudden enhancement of atmospheric techniques
22 p2904 A73-43036
- Magnetosphere boundary location relationship to geomagnetic activity level and solar activity cycle during 1963-68 based on theoretical model
23 p2970 A73-43245
- The solar coronal green line as an index of cosmic ray modulation.
23 p3024 A73-43683
- Statistical analysis for autocorrelation and cross correlation coefficients of mean annual total atmospheric ozone and relative sunspot number as solar activity indicator
23 p2976 A73-43883
- The influence of solar activity on the stratospheric ozone layer.
23 p2976 A73-43884
- Appleton seasonal anomaly in E region maximum electron density investigated by critical frequency data statistical analysis, showing solar activity effects
23 p2979 A73-44006
- A study of solar radio emission in the light of Sengupta's model of coronal active regions.
24 p3123 A73-44637
- Sunspot cycle effects on solar and lunar tide-produced diurnal and seasonal variations in equatorial electrojet
24 p3124 A73-44730
- Diurnal ion composition variations in E region under quiet and perturbed solar conditions, using continuity equations for positive ions and electroneutrality equations
24 p3083 A73-44793
- The thermospheric heating function. III - The function describing the heating of the thermosphere by short-wave solar radiation during a period of high solar activity
24 p3084 A73-44800
- Positive nitrogen ions in midlatitude atmosphere, discussing concentration dependence on height, solar zenith angle and activity level
24 p3084 A73-44801
- Energetic dissociative recombination oxygen atom production and exospheric redistribution for high/low solar conditions in terms of ballistic trajectories and neutral density models
24 p3086 A73-45131
- Solar activity cycles effects on physical and biological processes in helioterrestrial domain, discussing crops, tree growth, diseases and fishing
24 p3088 A73-45364
- ## NOLAR ARRAYS
- NASA technology program for auxiliary and primary electric propulsion systems, noting flight tests and solar arrays
[AIAA PAPER 72-1127] 03 p0355 A73-13437
- Stress analysis and design of silicon solar cell arrays and related material properties.
03 p0255 A73-14224
- Optimal sizing of modular bus bars for rectangular solar cell arrays as function of power/weight ratio
03 p0255 A73-14225
- Evaluation and reduction on the electromagnetic fields associated with a solar array.
03 p0256 A73-14233
- Performance test of flexible rolled-up solar array (FRUSA) via telemetered data from accelerometers, strain gauges and temperature sensors, noting feasibility for spacecraft power supply
03 p0256 A73-14236
- Solar array and supporting technologies development, discussing manufacturing, handling, design qualification tests in space environment and comparison between fold-up and roll-up types
03 p0257 A73-14237
- Solar Array System for the Skylab Orbital Workshop.
03 p0257 A73-14238
- Flexible circular solar array for power to weight ratio increase at satellite outer surface, noting central supported structure superiority
03 p0257 A73-14239
- Cost goals for silicon solar arrays for large scale terrestrial applications.
03 p0258 A73-14250
- Russian book - Power systems of spacecraft.
04 p0408 A73-15704
- Attitude dynamics of a three-axis stabilized satellite with a large flexible solar array.
06 p0757 A73-18379
- Passive solar array orientation devices for terrestrial application.
09 p1033 A73-22440
- An approach to performance assessment and management of a large solar array/battery power system.
09 p1035 A73-22775
- Large solar array photovoltaic power systems for manned orbital space stations, discussing technology evaluation and design feasibility studies
09 p1153 A73-22780
- Electrical Power Subsystem definition for shuttle launched modular space station.
09 p1153 A73-22781
- Configuration survey of lightweight solar array power systems for future missions.
09 p1153 A73-22782
- A solar array and battery electrical power subsystem for the shuttle-launched modular space station.
09 p1153 A73-22783
- Space station solar array-energy storage-power control and distribution system based on regenerative fuel cell integrated with life support system
09 p1153 A73-22784
- Intelsat 4 power subsystem with solar panels, Ni-Cd batteries, controller and relays for bus paralleling, discussing spacecraft and system configurations and performance
09 p1154 A73-22788
- The flexible solar array - A spacecraft electrical power source technology option.
09 p1154 A73-22790
- Computer simulation concept for a large solar array/battery power system.
09 p1060 A73-22803
- Design and development of a lightweight flexible solar array compatible with mass production techniques.
09 p1036 A73-22813
- Near-equatorial synchronous orbit Satellite Solar Power Station system with photovoltaic cell arrays energy conversion into microwave power for transmission to earth
10 p1285 A73-23601
- Structural failures in light weight solar cell arrays under thermal cycling.
11 p1310 A73-25999
- AC impedance of silicon solar cells.
11 p1310 A73-26000
- Concept for a high voltage solar array with integral power conditioning.
11 p1310 A73-26001
- Development of a deployable and selfrigidizing solar cell array for the multikilowatt range.
11 p1310 A73-26002
- Solar array concept for a portable retractable oriented power system.
11 p1310 A73-26007
- A 25 kW solar array/battery design for an earth orbiting space station.
11 p1311 A73-26010
- Space shuttle orbiter power system requirements and design tradeoffs, comparing fuel cells, solar array/battery and radioisotope Brayton cycle and cryogenic fueled turboalternators
11 p1312 A73-26017
- Design and performance of the TACSAT power subsystem.
11 p1312 A73-26020
- Power system for a 4.1 kilowatt synchronous satellite.
11 p1312 A73-26023
- Low altitude orbit feasibility study of integrated SNAP 29/Agena satellite configuration, comparing with solar cell power system
11 p1396 A73-26040
- Solar array cost reductions.
13 p1573 A73-29592
- Large area silicon solar array development.
13 p1573 A73-29593
- Solar energy conversion development relative to Department of Defense space power requirements.
13 p1573 A73-29595
- An appreciation of the design of carbon fibre rigid solar panels for spacecraft.
17 p2238 A73-34812
- Some major terrestrial applications of solar energy.
17 p2110 A73-35312
- Electromagnetic interference caused by a solar array.
18 p2269 A73-36958
- Solar arrays for the next generation of communication satellites.
18 p2269 A73-37036
- Skylab ATM solar array performance characteristics prediction via mathematical model, discussing I-V characteristics, test data computer programming and polynomial curves
19 p2391 A73-38407
- Development of a lightweight body-mounted solar cell array with a high power to weight ratio.
19 p2391 A73-38408
- Low cost modular power systems for multi mission earth observations.
19 p2494 A73-38435
- Attitude control of a large flexible spacecraft using three-axis mass expulsion control.
20 p2588 A73-38829
- [AIAA PAPER 73-893] British X4 spacecraft mechanical design configuration with honeycomb sandwich panels, on yo-yo principle based despun system and flexible solar array
20 p2615 A73-39774
- Coupled bending-twisting vibrations of a single boom flexible solar array and spacecraft.
21 p2781 A73-40619
- Development of a hybrid microelectronics solid state relay for 2500 volts isolation and -120 C to 80 C thermal cycling range.
22 p2835 A73-42914
- ## SOLAR ATMOSPHERE
- ### NT SOLAR GRANULATION
- The five-minute oscillations as nonradial pulsations of the entire sun.
01 p0104 A73-11049
- Similarity theory of planetary atmosphere circulations applied to solar atmosphere in terms of radius and rotational Mach number
01 p0106 A73-11316
- Solar outer layer models of convective zone, photosphere, chromosphere, corona and solar wind, using electron density dependence
01 p0107 A73-11379
- Tunnel-effect and propagation of 5-min oscillations in the solar atmosphere.
01 p0107 A73-11381
- Trapped gravity waves velocity oscillations in solar plages under magnetic field, comparing with Bilderberg continuum atmosphere
01 p0108 A73-11386
- A search of a connection between the polarization of Decam-type III bursts and magnetic fields in different heights of the solar atmosphere.
01 p0093 A73-11392
- Ground based solar astronomy potential for obtaining photographs with factor of two in resolution and time series, discussing optical performance of vacuum solar telescope
02 p0216 A73-12329
- Alfven wave induced bulk velocity amplitudes in lower solar atmosphere, discussing relationship between energy flux, bulk velocity, wavelengths and scale height
03 p0360 A73-12944
- Hydrodynamics of the convective zone of the sun
03 p0373 A73-13608
- Differential rotation in the solar atmosphere inferred from optical, radio, and interplanetary data.
03 p0377 A73-14404
- Neutral Mg line at 4571 A in solar atmosphere, computing line profiles from Harvard-Smithsonian Reference Atmosphere and Bilderberg Continuum Atmosphere
03 p0377 A73-14405
- Solar atmosphere inhomogeneities from observations, discussing theoretical analysis via two dimensional model atmosphere
03 p0377 A73-14406
- Umbral spectra absorption line feature observation by photoelectric spectroscopy, suggesting Ti abundance in solar atmosphere
03 p0378 A73-14423
- Effects of uncertainties in damping and microturbulence on theoretical deductions from solar equivalent widths.
04 p0500 A73-15491
- Double layer formation in homogeneous plasma with constant current, considering occurrence in ionosphere and solar atmosphere
05 p0601 A73-16146
- Some studies on the solar microwave bursts in relation to the slowly varying component.
05 p0621 A73-17038
- Influence of ionization losses on the conditions of cosmic ray generation on the sun
06 p0742 A73-17530
- Fokker-Planck equation for solar atmosphere modulation of galactic proton and electron flux at earth, including convection, diffusion and adiabatic deceleration effects
07 p0870 A73-19576
- Nonlinear Boussinesq convective model for large scale solar circulations.
08 p1001 A73-20751
- Solar two-component atmospheric model for prediction of Ca II emission arches in spectrogram of strong lines near limb from kinetic equilibrium calculation
08 p1001 A73-20753
- On the radio optical depth of the layer where the temperature equals the brightness temperature.
08 p1002 A73-20761
- Isotopic composition of helium in solar corpuscular fluxes
10 p1266 A73-23912

SOLAR AUXILIARY POWER UNITS

Model solar atmosphere with quiet component involving supergranular velocity field in corona-chromosphere transition layer and vertical magnetic field
10 p1279 A73-24140

Observations and theoretical reconstruction of the green flash.
11 p1351 A73-25168

Sky brightness in solar aureole region relationship to solar radiation single scattering on atmospheric aerosol particles
11 p1353 A73-25607

Daytime cloudless sky glow, atmospheric transmittance, neutral polarization and aerosol optical characteristics in solar altimetric and vertical
11 p1353 A73-25608

Heating effects due to radiative energy loss from acoustic waves in solar atmosphere, estimating temperature difference between radiative equilibrium and empirical model
11 p1421 A73-25931

The role of convection in stellar atmospheres. I - Observable effects of convection in the solar atmosphere.
11 p1427 A73-26611

An investigation of the structure of coronal active regions.
12 p1545 A73-27847

Solar photosphere turbulent velocity relation to optical depth and deviation from LTE based on Goldberg-Unno method
13 p1683 A73-29093

Interplanetary gas dynamics, discussing solar atmospheric structure, plasma kinetics, continuous flows, collective particle behavior, hydrodynamic coronal and free expansions
15 p1939 A73-31975

Cosmic abundance of boron.
15 p1942 A73-32648

The large-scale velocity field, the magnetic fields, and the brightness of the solar atmosphere
16 p2057 A73-32701

Effect of ionization losses on cosmic-ray generation conditions on the sun.
16 p2052 A73-32754

On some transient H-alpha features associated with metric type III bursts.
16 p2053 A73-32963

Noble gas isotopes abundances for solar wind and outer convective zone of sun, emphasizing isotopic abundance of deuterium
17 p2228 A73-34416

Observation of the absolute intensity and the center-to-limb variations of the sun in the vacuum ultraviolet region.
19 p2482 A73-37376

On the energetics and momentum balance of pole-equator temperature differences in the sun.
19 p2485 A73-37620

On the nature and origin of the solar five-minute oscillations.
20 p2606 A73-39071

H alpha line contrast profiles evaluation from solar chromosphere supergranulation observations, obtaining chromospheric fine structure characteristics
20 p2606 A73-39072

Propagation of mechanical waves in the solar atmosphere
20 p2606 A73-39078

Meridional flow and the validity of the two-dimensional approximation in stellar-wind modeling.
20 p2602 A73-39430

Solar atmosphere origin for submicrometer cosmic dust in ionosphere and noctilucent clouds, noting anomalously high atomic weight
21 p2775 A73-41416

The formation of Mg I 4571 A in the solar atmosphere. III - The Holweger solar model /Research note/.
21 p2777 A73-41480

Solar spicule morphology, observing diameter, height, expansion and threshold intensity with H alpha filtergrams
21 p2777 A73-41484

Possible mechanism of surge formation in the solar atmosphere.
21 p2777 A73-41493

Further observations of the structure of the chromosphere-corona transition region from limb and disk intensities.
21 p2779 A73-41537

Structure of the solar chromosphere. I - Basic computations and summary of the results.
22 p2905 A73-41762

Absolute oscillator strengths in neutral chromium and the solar chromium abundance.
22 p2905 A73-41764

Coupling between thermal conduction and radiative transfer in a moving atmosphere.
22 p2907 A73-42305

The inversion of the mean and spatially resolved sodium D2 line profiles from the sun.
22 p2908 A73-42311

Vertically nonpropagating magnetoatmospheric waves investigation based on local dispersion relations

governing magnetoacoustic and magnetogravitational wave propagation with emphasis on solar atmosphere conditions
22 p2914 A73-43010

Radiative damping of trapped gravity waves in the solar atmosphere.
24 p3135 A73-44629

Further aspects of weak shock theory applied to the solar chromosphere.
24 p3135 A73-44630

Statistical analysis of transient brightenings in solar chromosphere /Ellerman bombs/ from H alpha filtergrams, obtaining histograms for durations near disk center and limb
24 p3136 A73-44641

The latitudinal motion of sunspots and solar meridional circulations.
24 p3136 A73-44647

Height distribution and directionality of 2-12 A X-ray flare emission in the solar atmosphere.
24 p3124 A73-45046

Flare triggering by coherent oscillations.
24 p3124 A73-45048

SOLAR AUXILIARY POWER UNITS
An approach to performance assessment and management of a large solar array/battery power system.
09 p1035 A73-22775

The flexible solar array - A spacecraft electrical power source technology option.
09 p1154 A73-22790

SOLAR AZIMUTH U AZIMUTH U SOLAR POSITION SOLAR CELLS

High-efficiency Ga/1-x/Al/x/As-GaAs solar cells.
01 p0005 A73-10132

Three point check method of solar panel characteristics for satellite.
01 p0006 A73-11162

Effects of chemical impurities, oxygen and dopant, on the gamma and neutron damage of silicon solar cells.
01 p0006 A73-11163

The accurate prediction of radiation environment and solar cell degradation.
01 p0006 A73-11164

Power control unit for the scientific satellite.
01 p0111 A73-11165

Solar cell generator design for Helios solar probe, considering thermal stresses at sun proximity and sufficient power generating capacity at orbital apogee [DGLR PAPER 72-091]
02 p0131 A73-11663

Secondary ionisation and its possible bearing on the performance of a solar cell.
02 p0132 A73-12048

Photovoltaic Specialists Conference, 9th, Silver Spring, Md., May 2-4, 1972, Record.
03 p0254 A73-14203

Tables summarizing Si solar cell fabrication parameters, complex design evolution and performance achievement
03 p0254 A73-14204

Design and practical aspects of maximum efficiency silicon solar cells for satellite applications.
03 p0254 A73-14205

An experimental investigation into the feasibility of higher efficiency silicon solar cells.
03 p0254 A73-14206

Solar cell graded band gap materials, determining I-V characteristics, junction capacitance and photovoltaic spectral response
03 p0254 A73-14207

Vertical multijunction solar cells light generated current spectral response and I-V characteristics derivation from minority carrier diffusion equations
03 p0254 A73-14208

Silicon solar cell design, describing handbook organization and derivation of design curves and data tables
03 p0254 A73-14209

Laser energy conversion into electrical energy with photovoltaic cells, noting Si and GaAs cells power efficiencies improvement compared to operation in sunlight
03 p0254 A73-14210

Diffusion, recombination and combined models demonstrating shunting and second current conduction effects on forward I-V characteristics for dark and illuminated Si solar cells
03 p0254 A73-14211

Silicon violet solar cell energy conversion efficiency improvement through extended spectral response and increased fill factor
03 p0254 A73-14212

Minority carrier lifetime and diffusion constant as function of impurity concentration in double junction vertical solar cell, determining power efficiency
03 p0254 A73-14213

The effect of surface recombination velocity on the performance of vertical multi-junction solar cell.
03 p0255 A73-14214

Accelerated tests for long term stability of CdS solar cells, noting stoichiometry, wavelength, doping and residual atmosphere effects on cell performance
03 p0255 A73-14215

High efficiency Cu2S-CdS-solar cells with improved thermal stability.
03 p0255 A73-14216

Cadmium sulfide/cuprous sulfide solar cell abrupt heterojunction band model description by two quasi-Fermi levels
03 p0350 A73-14219

New results on the development of a thin-film p-CdTe-n-CdS heterojunction solar cell.
03 p0255 A73-14220

Thin film CdS solar cell stability improvement by etching, noting cuprous sulfide oxidation effects on degradation from short term tests at high temperature
03 p0255 A73-14221

Investigations of the inhomogeneity of polycrystalline Cu₂S/S-CdS solar cells.
03 p0255 A73-14222

Statistical analysis applied to solar cell shorting caused by reverse bias voltage stress.
03 p0255 A73-14223

Stress analysis and design of silicon solar cell arrays and related material properties.
03 p0255 A73-14224

Solar cell optical properties effects on electrical and thermal performance and cost savings in panel design optimization
03 p0255 A73-14226

RF sputtered integral covers of glass coating for thermal protection of Si solar cells, noting intrinsic stress, adhesion, transparency and radiation damage resistance
03 p0256 A73-14227

Electron beam technique for evaporating titanium and silicon oxides antireflection coatings on solar cells, noting humidity and thermal resistances and UV radiation darkening
03 p0256 A73-14228

Evaluation of cerium stabilised microsheet coverslips for higher solar cell outputs.
03 p0256 A73-14229

A reliable all-silver front contact for silicon solar cells.
03 p0256 A73-14230

Photovoltaic and I-V characteristics of integral diode solar cells as function of temperature and radiation exposure
03 p0256 A73-14231

Metal stripline connector technology to fabricate flexible silicon solar cell arrays, noting cost reduction
03 p0256 A73-14232

Breakdown phenomena in reverse biased silicon solar cells.
03 p0256 A73-14234

Solar cells and generator technology for the Helios sun probe.
03 p0256 A73-14235

Summary of results of JPL lithium-doped solar cell development program.
03 p0257 A73-14240

Voltage and power relationships in lithium-containing solar cells.
03 p0257 A73-14241

Fabrication criteria, mission design factors and I-V characteristics of Li solar cells
03 p0257 A73-14242

Li and Si p-n solar cells performance comparison for simulated earth orbit environment by real time irradiation with Sr 90 beta particles
03 p0257 A73-14243

ATS-5 solar cell experiment after 699 days in synchronous orbit.
03 p0257 A73-14244

Irradiation of solar cell candidates for the ATS-F solar cell flight experiment.
03 p0257 A73-14245

Electron irradiated float-zone Si solar cell I-V performance degradation due to photon irradiation, noting base region minority carrier lifetime role
03 p0257 A73-14246

Further observed degradation on the LES-6 synchronous solar cell experiment.
03 p0258 A73-14247

Progress in the development of radiation-resistant aluminum-doped silicon solar cells.
03 p0258 A73-14248

The effect of boron concentration on radiation damage in silicon solar cells.
03 p0258 A73-14249

Cost goals for silicon solar arrays for large scale terrestrial applications.
03 p0258 A73-14250

Economic analysis of silicon solar cells production noting cost reduction from feasibility studies of edge defined film fed crystal growth in ribbon form
03 p0258 A73-14251

The role of solar cell technology in the satellite solar power station.
03 p0258 A73-14252

The edge-defined, film-fed growth /EF/G/ of silicon single crystal ribbon for solar cell applications.
03 p0258 A73-14254

Effects of 10-150 keV proton bombardment on silicon solar cells.

04 p0406 A73-14984

Speed-torque characteristics of a solar cell motor.

04 p0406 A73-15068

Solar cells with Si Schottky function diode, discussing fabrication and barrier metal and thickness effects on output power and energy conversion efficiency

05 p0538 A73-16816

Thermally stable heterocyclic ladder polymer films preparation techniques in manufacture of solar cells with CdS or CdTe thin films for space applications

07 p0841 A73-18903

Preliminary study for the design of a satellite thermal control heat pipe.

07 p0918 A73-18913

Diffusion equation for current carriers in solar cell with inhomogeneous internal electric field, determining photoelectric current in p-n junction

07 p0778 A73-19299

Effects of boron density on radiation resistance of copper-contaminated n/p type silicon solar cells.

08 p0928 A73-21114

A system for the evaluation of solar cell samples.

09 p1033 A73-22438

Calculation of series and shunt resistances on the basis of the current-voltage characteristics of a solar cell

09 p1033 A73-22720

Intelsat 3 power system design and orbital performance, discussing solar arrays, cell bypass, output, conversion efficiency, regulation, reliability and testing

09 p1153 A73-22787

Solar cell interconnections with different weld types, discussing semiautomatic and automatic ultrasonic processes, solder thickness control and quality inspection methods and criteria

09 p1035 A73-22807

Solar cell fatigue life prediction by statistical analysis and extrapolation for determining failure probability curve as function of stress and time

09 p1036 A73-22808

Fatigue life prediction and design optimization for solar cell interconnectors based on elastoplastic material stress distribution calculation by finite element methods

09 p1036 A73-22809

The determination and treatment of temperature coefficients of silicon solar cells for interplanetary spacecraft application.

09 p1036 A73-22810

Silicon solar cells radiation damage from orbital flight and electron and proton irradiation laboratory test data, discussing radiation hardening by Li doping

09 p1036 A73-22811

Large area wraparound contact silicon solar cell, application and development.

09 p1036 A73-22812

Solar cell battery operational performance test equipment and computerized simulation programs for post-1975 satellite and space station systems integration and design

11 p1309 A73-25986

Structural failures in light weight solar cell arrays under thermal cycling.

11 p1310 A73-25999

AC impedance of silicon solar cells.

11 p1310 A73-26000

Development of a deployable and selfrigidizing solar cell array for the multi-kilowatt range.

11 p1310 A73-26002

Solar cell dark I-V characteristics and their applications.

11 p1310 A73-26003

Temperature reducing solar cell arrangements for spin stabilized planetary and solar probes, analyzing thermal performance

11 p1313 A73-26668

Power Sources Symposium, 25th, Atlantic City, N.J., May 23-25, 1972, Proceedings.

13 p1572 A73-29581

Historical development of solar cells.

13 p1573 A73-29590

Principles of photovoltaic solar energy conversion.

13 p1573 A73-29591

Research plans for solar power in space.

13 p1573 A73-29594

Influence of the difference in effective masses on the efficiency of heterojunction solar cells.

14 p1713 A73-30000

CdTe thin film fabrication by direct synthesis of vacuum evaporated Cd and Te, noting solar cell efficiency increase after storage in room temperature excicator

14 p1713 A73-30475

Possibility of using semiconductor photocells as receivers of ultraviolet radiation

14 p1713 A73-30949

Space radiation environment effects on Intelsat 4 design, emphasizing trapped electrons and protons influences on solar cell shielding requirements

17 p2108 A73-34864

Communication satellites attitude control methods, considering conventional attitude gyros, control moment gyroscopes, reaction wheels and optimal solar cell utilization

17 p2239 A73-35476

Dynamic behavior of satellites with large-area solar cell panels

17 p2239 A73-35485

Attitude control, rotational and positioning mechanisms for orientation of mechanically despun antennas and solar arrays in communication satellites

17 p2126 A73-35486

Schottky barrier diode solar cells using dielectric antireflection coatings, discussing Nb, Mo and Cr diode metal characteristics, photovoltaic characteristics and conducting properties

19 p2391 A73-38406

A new electric field effect in silicon solar cells.

24 p3058 A73-45426

SOLAR CHROMOSPHERE

U CHROMOSPHERE

U SOLAR ATMOSPHERE

SOLAR COLLECTORS

Linear solar collector conversion efficiency over wide operating temperature range via model consisting of long pipe with energy injection at points along length

[ASME PAPER 72-WA/SOL-7] 04 p0408 A73-15802

The Solar Collector Thermal Power System - Its potential and development status.

09 p1035 A73-22792

Brayton cycle solar dynamic turboalternator space electric power system technology developments during 1962-1972, considering power efficiency, components reliability and future missions

11 p1309 A73-25982

Analysis of the parameters of solar-heat power sources with energy storage units

17 p2108 A73-34283

An analysis of linear focused collectors for solar power.

19 p2391 A73-38409

A method for studying the radiant flux distribution in the circumfocal area of a concentrator with the aid of an asymptotic calorimeter

24 p3058 A73-45253

SOLAR CONSTANT

Lens projection system for a solar simulator providing irradiance of 100 solar constants.

08 p0952 A73-21042

New radiometric techniques and solar constant measurements.

08 p0966 A73-21270

Russian book - The solar constant and the energy distribution in the solar spectrum.

21 p2769 A73-40804

SOLAR CONVERTERS

U SOLAR GENERATORS

SOLAR CORONA

Radio emission from traveling disturbances in solar corona, considering contributions of interplanetary observations, plasma theory and ground observations

01 p0091 A73-10058

Solar coronal plasma cyclotron radiation, taking into account temperature effects

01 p0096 A73-10309

The origin of chains of type I bursts

01 p0092 A73-10938

Polarization of the inner corona during the solar eclipse of March 7, 1970

01 p0102 A73-10939

Propagation through the solar corona of the shock waves responsible for type II radio bursts.

01 p0093 A73-11314

Solar outer layer models of convective zone, photosphere, chromosphere, corona and solar wind, using electron density dependence

01 p0107 A73-11379

Temperature structure and conductive flux in the chromosphere-corona transition region.

01 p0107 A73-11380

The results of coronal investigation at the September 22, 1968 solar eclipse.

01 p0108 A73-11383

Faint H alpha emissions in solar corona prominences photographed through coronagraph and Lyot filter

01 p0108 A73-11388

Particle motions in coronal streamers and type III radio bursts.

01 p0093 A73-11393

Maxima in coronal intensity during 1966-1970 period of solar cycle, discussing north-south asymmetry correlation with sunspot activity

01 p0108 A73-11395

Evidence for two maxima of activity in the 20th solar cycle.

01 p0108 A73-11396

Filters for solar corona polarization observations, deriving equations for arbitrary settings to obtain data reduction with simplified polarization direction calculation

02 p0170 A73-12370

Type 3 bursts exciter duration and decay time constant from time profiles analysis in decimeter range, explaining coronal temperature

03 p0361 A73-13213

The coronal X-spectrum - Problems and prospects.

03 p0363 A73-13954

Mapping the solar corona in X-ray lines of O VII and Ne IX.

03 p0375 A73-13956

Differential rotation in the solar atmosphere inferred from optical, radio, and interplanetary data.

03 p0377 A73-14404

Radio evidence of twisted bi-polar magnetic fields in the solar corona.

03 p0378 A73-14417

Solar corona X-ray emission from O VII and Ne IX ions by rocket-borne Bragg spectrometers observations, determining electron temperature from resonance lines intensity

03 p0364 A73-14418

Evolution of coronal helmets during the ascending phase of solar cycle 20.

03 p0378 A73-14419

Time dependent hydrodynamic models of solar wind, considering coronal electron density and temperature distribution and magnetic field

04 p0491 A73-14835

Solar corona properties and nuclear reactions in flares from August 1972 OSO 7 observation, noting hard X ray bursts from electron streams

04 p0502 A73-15971

Stability of a model current sheet with finite transverse field and finite flow velocity.

05 p0568 A73-16141

Nonspherically symmetric polytrope model of azimuthally dependent solar wind in sun equatorial plane, considering coronal temperature, density and radial magnetic component

05 p0609 A73-16143

Coronal abundance of elements and a model of the quiet sun from radio observations.

05 p0621 A73-17034

Coronal holes during 12 November 1966 eclipse, comparing distribution to calculated current-free coronal magnetic field

05 p0621 A73-17035

On emission lines of hydrogen, helium and ionized calcium seen on a coronal spectrogram of the March 7, 1970 eclipse.

05 p0621 A73-17036

Equatorial coronal arches and geomagnetic disturbance.

05 p0621 A73-17037

Book - Coronal expansion and solar wind.

06 p0742 A73-17671

Electron density distribution in a coronal condensation

07 p0902 A73-20321

Threadlike solar coronal streamer observation at 20 July 1963 eclipse, noting electron density from photometric analysis

08 p1002 A73-20763

On the long-term behaviour of the circular polarization from coronal condensation radio emission at 4.3 cm wavelength.

08 p0997 A73-20769

Nonthermal turbulent heating in the solar envelope.

08 p1003 A73-20887

The heating of the solar corona. I - Observation of ion energies in the transition zone.

08 p1005 A73-20919

Solar nebula Lu 176-Hf 176 pair and Zr abundance determinations, using chondrite fraction and s-process model

08 p1006 A73-20937

Temperature variations in coronal regions in the proximity of a prominence

08 p1007 A73-21067

Polarization of the total coronal emission during the solar eclipse of March 7, 1970

08 p1007 A73-21070

X-ray emission of coronal condensations during the eclipse on 20 May 1966 and its connection with optical and radio observations.

08 p0998 A73-21310

Polarimeter-photometer to study solar corona or disk over wide photon arrival rate range, measuring magnitude of polarization effects

08 p0971 A73-21746

Dissipation of hydromagnetic waves with application to the outer solar corona. I - Collisionless protons and collisional electrons. II - Transition from collisional to collisionless electrons.

09 p1142 A73-22038

Origin of chains of type I solar radio bursts.

09 p1138 A73-22733

Polarization of the inner corona at the total eclipse of March 7, 1970.

09 p1147 A73-22734

Problem of the time dependence of the polarization level of Type III solar radio bursts.

10 p1264 A73-23719

Solar cosmic ray heavy nucleus abundances relation to oxygen nuclei in solar corona and photosphere

10 p1265 A73-23898

Solar rotation as determined from OSO-4 EUV spectroheliograms. 10 p1278 A73-24127

Energy balance in the chromosphere-corona transition region. 10 p1279 A73-24138

A model for the polar transition layer and corona for November 1967. 10 p1279 A73-24139

Coronal polar plume observed electron density dependence on assumed density distribution normal to axis, analyzing errors in measurements 10 p1279 A73-24141

Lifetime of solar flare particles in coronal structure regions. 10 p1268 A73-24144

Simultaneous determination of the electron temperature and density in the chromospheric-coronal transition region of the sun. 10 p1281 A73-24409

Time dependent geophysical effects associated with chromospheric and coronal flares, tabulating for 1957-1961 11 p1411 A73-25099

The 1969 solar occultation of the Crab Nebula pulsar. 11 p1417 A73-25583

Coupling coefficients for resonant interaction between three waves with well-defined phases in cold magnetized plasma, applying to solar corona 11 p1405 A73-25917

Thermal instability of coronal neutral sheets and the formation of quiescent prominences. 11 p1422 A73-25940

The solar wind and the temperature-density structure of the solar corona. 11 p1413 A73-25954

Photometric and polarimetric analysis of the coronal streamers observed at the March 7, 1970 Mexican eclipse. 11 p1425 A73-26263

Polarigraphic observations of the solar corona at the total eclipse on March 7, 1970 in Mexico. 11 p1425 A73-26264

Dissipation of hydromagnetic waves with application to the outer solar corona. III - Transition from collisional to collisionless protons. 11 p1428 A73-26619

Polarization measurements in the green coronal line. 11 p1428 A73-26623

Polarization of the emission from the solar corona in the 5303 Å line 12 p1538 A73-26859

Solar corona electron densities and temperatures as function of distance from solar center during 22 September 1968 eclipse 12 p1538 A73-26860

Solar corona streamers polarization, intensity and electron density and temperature during 22 September 1968 total eclipse 12 p1533 A73-26861

Electron-density distribution in a coronal condensation. 12 p1540 A73-27293

On the variation of the coronal lambda-5303 intensity relative to the interplanetary and solar magnetic sector structure, and to geomagnetic activity. 12 p1542 A73-27615

Solar prominences during period between sunspot minimum and maximum, investigating secondary polar zone coronal activity phase shift relationship to main zone anomaly 12 p1545 A73-27837

Some comments on the low intensity H alpha emission observed by J.-L. Leroy in the solar corona. 12 p1545 A73-27838

EUV and radio observation of energy flux from corona into chromosphere, considering coronal holes as source of high energy streams of solar wind 12 p1545 A73-27839

Improved three-dimensional mapping of the electron density distribution of the solar corona. 12 p1536 A73-27843

On the Aller's admixture radiation effect during the compression process in the solar corona and generation of coronal formations. 12 p1536 A73-27844

Solar corona anomalous polarization degree and E vector vibration direction, interpreting discrepancy from Thomson scattering prediction by scattered electron velocity effects 12 p1545 A73-27845

An investigation of the structure of coronal active regions. 12 p1545 A73-27847

Flare-produced coronal MHD-fast-mode wavefronts and Moreton's wave phenomenon. 12 p1536 A73-27848

Results of observations of coronal condensation in photographic rays during the solar eclipse of Sept. 22, 1968 13 p1673 A73-28299

Theory of a photometer/actinometer/ measuring the brightness of a fixed annular zone of sky around the sun. 13 p1613 A73-28519

Conditions of Cr IX and Fe XI luminescence in the corona 13 p1683 A73-29094

Observation of linear polarization of the Crab nebula during an occultation by the solar corona. 13 p1586 A73-29247

Excitation of the Fe XIII spectrum in the solar corona. 13 p1684 A73-29353

Fe XVII emission from the solar corona. 13 p1685 A73-29356

Photometric analysis of monochromatic photographs of the solar corona taken in the green line /5303 Å/ and the red line /6374 Å/. 13 p1685 A73-29363

Coronal densities and temperatures derived from monochromatic images in the red and green lines. 13 p1685 A73-29364

On the origin of SC-storms with respect to forecasting geomagnetic activity. 15 p1868 A73-31520

Geomagnetically calm intervals and their forecasts. 15 p1868 A73-31521

Interplanetary gas dynamics, discussing solar atmospheric structure, plasma kinetics, continuous flows, collective particle behavior, hydrodynamic coronal and free expansions 15 p1939 A73-31975

The color deficiency of the solar halo of 22 deg radius 15 p1873 A73-32358

Model of the chromosphere and the transition layer between the chromosphere and solar corona 16 p2057 A73-32703

Observations of the inner F and K coronas below 2220-Å wavelength. 16 p2060 A73-32954

Non-existence of linear polarization in type III solar bursts at 80 MHz. 16 p2053 A73-32962

Radioheliograph observations of high-energy phenomena in the solar corona. 16 p2061 A73-33284

Solar activity centers configuration and accelerated particle storage and release in coronal regions for all solar events 16 p2055 A73-33292

Solar cycle and coronal heating theories implications for cycle variations phase coincidence, discussing sunspots, coronal green lines, etc 17 p2224 A73-34510

Close connexion between flare-generated coronal and interplanetary shock waves. 17 p2232 A73-35147

A multi-channel coronal spectrophotometer. 17 p2170 A73-35291

Space application of SEC vidicons - The OSO 7 coronagraph. 17 p2170 A73-35293

Electron temperature and emission measure variations in the solar corona. 18 p2350 A73-36062

Nature of some optical effects observed on spacecraft at sunrise 18 p2309 A73-36122

Coronal propagation of low-energy solar protons. 18 p2347 A73-36290

Time dependence of the polarization of type III solar radio bursts. 18 p2347 A73-36744

Temperature variations of coronal regions near a solar prominence. 18 p2355 A73-36868

Polarization of the resultant emission of the corona during the solar eclipse of March 7, 1970. 18 p2355 A73-36871

Models of the chromospheric-coronal transition layer and lower corona derived from extreme-ultraviolet observations. 18 p2357 A73-37107

Four-stage planetesimal accretion from solar nebula describing dust particle condensation, disk formation, gas drag, orbital decay and particle collisions 19 p2489 A73-38524

Solar cosmic ray heavy nucleus abundances relation to oxygen nuclei in solar corona and photosphere 20 p2601 A73-38917

Relation between coronal 5303-Å intensity, recurrent geomagnetic storms, and solar sector structure. 20 p2553 A73-38960

Solar eclipse of July 10, 1972 - Comparison of photographic-photometry and K-coronometer measurement data 20 p2611 A73-39589

Solar wind velocity investigation based on solar corona and interplanetary plasma data, analyzing possible acceleration mechanisms 21 p2755 A73-40533

Evaluation of the magnitude of the magnetic field in the solar corona from measurements of the linear polarization of solar radio bursts 21 p2755 A73-40538

Method and results of observations of the occultation of the source 3C144 by the solar corona with the DKR-1000 FIAN cross-array radio telescope 21 p2767 A73-40545

A possible mechanism for acceleration of eruptive prominences 21 p2759 A73-40720

Solar corona observations in white light by OSO 7 and in XUV by Naval Research Laboratory, discussing contributions from other observatories and satellites 21 p2773 A73-41387

Observations of the X-ray emission of solar active regions on 28 November 1970 and 20 August 1971. 21 p2761 A73-41387

Particle emitting flares and the large-scale distribution of solar magnetic fields and green corona. 21 p2762 A73-41390

Observational results on coronal condensation in photographic light during the September 22, 1968 solar eclipse. 21 p2779 A73-41543

Analysis and synthesis of coronal and interplanetary energetic particle, plasma, and magnetic field observations over three solar rotations. 22 p2901 A73-41901

Solar corona plasma temperature estimation from ground observations based on ionization theory, line width, radio and radar measurements and hydrostatic equilibrium assumption 22 p2906 A73-42067

Pitfalls of configuration interaction - Transition probabilities in Fe XIII. 22 p2908 A73-42312

Spectral characteristics of solar corona measured by visual, rocket and satellite observation, discussing K and F coronal regions, eclipse phenomena and analysis techniques 22 p2910 A73-42650

French eclipse studies. 22 p2911 A73-42870

Airborne studies of the African eclipse. 22 p2911 A73-42871

Some statistical characteristics of active regions with the yellow coronal line. 22 p2915 A73-43037

Solar observatories and satellite-borne instruments for solar coronal structure determination, considering 30 June 1973 eclipse and instrumented Concorde aircraft use 22 p2916 A73-43117

The solar coronal green line as an index of cosmic ray modulation. 23 p3024 A73-43683

Origination of Type-IV decimetric bursts in the solar corona 23 p3036 A73-44248

Solar coronal Fe XIII 10747 Å emission line resonance polarization observations during 12 November 1966 eclipse, discussing magnetic field effects 24 p3135 A73-44633

Proton collisional excitation in the ground configuration of Fe/+12/. 24 p3123 A73-44634

Solar Fe 13 coronal lines relative intensity calculation as function of electron density from cross sections for collisional excitation by protons 24 p3136 A73-44635

Observation of a possible neutral sheet in the corona. 24 p3136 A73-44636

A study of solar radio emission in the light of Sengupta's model of coronal active regions. 24 p3123 A73-44637

Spatial relationship between 5303-Å and H alpha components of a loop prominence system. 24 p3123 A73-44640

A theory of the origin of the split pair burst emission from the solar corona. 24 p3123 A73-44646

Changes in the distribution of density and radio scattering in the solar corona in 1971. 24 p3138 A73-45049

X-ray observations of characteristic structures and time variations from the solar corona - Preliminary results from Skylab. 24 p3139 A73-45057

Observations of Type I bursts at 169 MHz and coronal scattering. 24 p3140 A73-45182

Solar coronal radio spectra emitted by synchrotron process, computing radio wave suppression due to isotropic and anisotropic plasma 24 p3118 A73-45484

SOLAR CORPUSCULAR RADIATION

NT SOLAR ELECTRONS

NT SOLAR PROTONS

Solar neutrino detection methods, capture cross sections, model construction and results 01 p0091 A73-10053

Particle motions in coronal streamers and type III radio bursts. 01 p0093 A73-11393

Effect of a neutrino-photon interaction on the solar-neutrino flux. 02 p0205 A73-12165

Satellite-borne radio telescope observation of traveling solar radio bursts for energetic solar particle

- propagation in interplanetary space, discussing wind density and magnetic field 02 p0208 A73-12419
- Solar corpuscular irradiation induced latent and etched nuclear particle tracks in lunar dust grains, presenting electron microscopic studies of Apollo 11/12 lunar soil samples 03 p0361 A73-13099
- Low energy solar nuclear particle irradiation of lunar and meteoritic breccias. 03 p0361 A73-13100
- The abundances of solar accelerated nuclei from carbon to iron. 03 p0362 A73-13719
- Preferential particle arrival at polar caps during solar events, noting north pole flux increase from ESRO 1 measurements 03 p0362 A73-13861
- Observation of solar particle fluxes over extended solar longitudes. 03 p0365 A73-14421
- Solar radio emission measurement and interpretation, discussing source mapping, coronal density, magnetic field and flare and particle events predictions 04 p0496 A73-14830
- Solar electrons and alpha particles during polar-cap absorption events. 04 p0493 A73-15558
- Pitch angle distribution of solar flare particles in interplanetary space. 07 p0869 A73-19228
- Time dependence of cosmic ray intensity during the anisotropic phase of solar flares 08 p0998 A73-21279
- Solar neutrino problem - No low energy He-3 + He-3 resonance. 08 p1000 A73-21530
- Solar neutrino flux prediction discrepancies with observation, considering cosmic ray background and flaws in calculation of capture rate 09 p1136 A73-21995
- Realization of a zero-force magnetic field configuration in the case of axisymmetric magnetohydrodynamic flows 09 p1146 A73-22541
- Solar particle measurements interpretation for closed vs open magnetospheric model determination, considering electron-proton polar cap differences, magnetotail flux asymmetries, etc 09 p1149 A73-22951
- Measurements of the iron-group abundance in energetic solar particles. 10 p1264 A73-23538
- All-Union Conference on the Physics of Cosmic Rays, Tiflis, Georgian SSR, October 18-21, 1971, Proceedings 10 p1265 A73-23901
- Particle scattering in interplanetary space and the properties of solar corpuscular streams 10 p1265 A73-23902
- Eruptive, loop shaped prominences and rapid irreversible bursts relation to high energy particle concentrations 10 p1265 A73-23905
- Isotopic composition of helium in solar corpuscular fluxes 10 p1266 A73-23912
- Lifetime of solar flare particles in coronal storage regions. 10 p1268 A73-24144
- Direct observations of low-energy solar electrons associated with a Type III solar radio burst. 10 p1268 A73-24145
- Possibility of estimating the flux of energetic particles in the ionospheric D-region at sunrise and during the daytime. 10 p1212 A73-24219
- Solar flare particle propagation - Comparison of a new analytic solution with spacecraft measurements. 10 p1269 A73-24727
- Solar He abundance from neutrino flux, He lines intensity in prominences and chromosphere spectra, solar cosmic rays and solar wind He/H ratio 10 p1284 A73-24780
- Energetic solar particles and their relation to optical flares. 11 p1413 A73-25952
- Estimation of an upper limit for the solar neutron emission during large flares. 11 p1413 A73-25953
- Charge states and energy-dependent composition of solar-flare particles. 11 p1413 A73-26207
- Solar neutrino flux, discussing effects of temperature oscillations on neutrino and photon luminosities 15 p1926 A73-31358
- Determination of a probable interval for the mean transit time of geomagnetic-storm /SSC/ solar particles 15 p1926 A73-31647
- Solar neutrino flux deficiency explanation based on solar core nuclear reactions theory with consequences for luminosity and earth climate 15 p1937 A73-31849
- Charge and energy spectra of particles with E from 0.2 to 30 MeV/nuc in the January 23, 1971 solar flare. 16 p2054 A73-33281
- Solar activity centers configuration and accelerated particle storage and release in coronal regions for all solar events 16 p2055 A73-33292
- Solar neutrino deficiency related to solar core periodic expansion, considering Martian river-like channel formation and Praesepe cluster distribution through main sequence 17 p2229 A73-34434
- IMP and Pioneer satellite-borne sensors for cataloging solar particle events, discussing onset time, multiple flare injections, enhancement differentiation and contamination problems 18 p2345 A73-36061
- Time dependence of cosmic-ray intensity at the anisotropic stage of solar flares. 19 p2476 A73-37908
- Solar neutrinos. IV - Effect of radiative opacities on calculated neutrino fluxes. 20 p2602 A73-39427
- Nonspherically symmetric thermal instabilities implied by discrepancy between theory and observation for solar neutrino problem, noting absence in solar numerical model 20 p2608 A73-39429
- New evidence for effects of variable solar corpuscular emission on the weather. 21 p2755 A73-40073
- Isotopes of helium and hydrogen in solar corpuscular fluxes 21 p2757 A73-40593
- Particle emitting flares and the large-scale distribution of solar magnetic fields and green corona. 21 p2762 A73-41390
- Solar atmosphere origin for submicrometer cosmic dust in ionosphere and noctilucent clouds, noting anomalously high atomic weight 21 p2775 A73-41416
- Solar neutrino fluxes on earth from solar model and analytical approach, discussing neutrino capture rate contributions 21 p2764 A73-41539
- Solar U burst radio source spectrographic and polarization observations, using Waldmeier corona model for particle exciter in magnetic field 23 p0306 A73-44247
- SOLAR COSMIC RAYS**
- Absorbing boundary propagation model for solar cosmic rays energy spectrum kink time behavior, using Gleeson-Ng theory 02 p0205 A73-11753
- Solar cosmic ray bursts in November-December 1970 according to data from Venus 7 space probe and Lunokhod 1 station. 02 p0206 A73-12321
- Solar cosmic ray burst on July 7, 1966 and its measurement on the Proton-3 artificial earth satellite 02 p0208 A73-12461
- Characteristics of quiet as well as enhanced diurnal anisotropy of cosmic radiation. 03 p0360 A73-12876
- Bombardment of the polar-cap ionosphere by solar cosmic rays. 03 p0301 A73-13710
- Propagation of solar cosmic rays in the solar wind. 04 p0491 A73-14837
- Enrichment of heavy nuclei in the 17 April 1972 solar flare. 05 p0609 A73-16571
- Evidence for a two-component injection of cosmic rays from the solar flare of 1969, March 30. 05 p0610 A73-17046
- Evidence for the existence of adiabatic energy loss in interplanetary space from observations of the decay of the February 25-March 2, 1969 series of solar cosmic ray events. 05 p0611 A73-17048
- Influence of ionization losses on the conditions of cosmic ray generation on the sun 06 p0742 A73-17530
- Possibility of detecting weak solar cosmic ray fluxes by ground-based radio engineering methods 06 p0742 A73-17532
- Solar cosmic rays spectrum and geomagnetic cut-off rigidity determination from ion production rates in lower ionosphere 07 p0870 A73-19427
- Solar energetic particles and wide-band continuum storms from metric to hectometric frequencies. 07 p0870 A73-19663
- Radionuclides in lunar rocks from solar and galactic cosmic ray bombardment, examining long and short-lived isotopes activity 07 p0889 A73-19793
- Record-breaking cosmic ray storm stemming from solar activity in August 1972. 08 p0996 A73-20664
- The time-latitude distribution of solar flares accompanied by type IV radio bursts during the period 1956 to 1969. 08 p0997 A73-20770
- Solar cosmic ray sectorial anisotropy pattern observation, suggesting theoretical propagation model to distinguish between rival candidates for parent flare 08 p0997 A73-20772
- Time dependence of cosmic ray intensity during the anisotropic phase of solar flares 08 p0998 A73-21279
- Characteristics of cosmic ray variations near the solar equator plane 08 p0998 A73-21299
- Solar cosmic rays propagation between shock front and solar flare hot plasma, examining fine structure from Explorer 34 and Venera 6 data 08 p0999 A73-21328
- Solar cosmic ray heavy nuclei acceleration independence from solar activity phenomena, based on Elektron 4 satellite observation 08 p0999 A73-21332
- Solar cosmic ray flare recording in stratosphere in Murmansk and Antarctic regions during February-April 1969 08 p1000 A73-21347
- Solar cosmic ray flare of 11-18 April 1969, investigating effect on polar cap absorption in lower ionosphere 08 p1000 A73-21348
- Short-term nonperiodic variations in the intensity of the neutron component of cosmic rays during a period of transition from a quiet to an active sun 09 p1137 A73-22019
- Satellite measurements of the charge composition of solar cosmic rays in the Z = 6 to 26 interval. 10 p1264 A73-23537
- Measurements of the iron-group abundance in energetic solar particles. 10 p1264 A73-23538
- Solar cosmic ray heavy nucleus abundances relation to oxygen nuclei in solar corona and photosphere 10 p1265 A73-23898
- Particle scattering in interplanetary space and the properties of solar corpuscular streams 10 p1265 A73-23902
- Solar cosmic ray diffusion, convection, accumulation and acceleration as function of interplanetary medium perturbation and flare coordinates 10 p1266 A73-23909
- Comparative characteristics of the soft component of solar and galactic cosmic rays on the basis of rocket and stratospheric measurements at Heis Island and Apatite Station 10 p1267 A73-23920
- Low energy solar proton events intensity increase near time of magnetic storm sudden commencement and Forbush decrease, using propagation shock wave model 10 p1268 A73-24146
- Solar cosmic ray anisotropy 27-day variations during IGY from global network stations neutron component data 10 p1268 A73-24237
- Alpha particles in solar cosmic rays over the last 80,000 years. 11 p1412 A73-25375
- Additional evidence for the existence of a very high energy solar particle component. 11 p1413 A73-26473
- A rigorous cosmic-ray transport equation with no restrictions on particle energy. 11 p1414 A73-26609
- Selection of a propagation model for computing the solar-proton injection spectrum 12 p1534 A73-27333
- Simultaneous recording of solar cosmic rays near Venus and in the earth magnetosphere 12 p1534 A73-27354
- The results of measurements of the intensity of cosmic rays by the automatic station "Venera-7". 12 p1535 A73-27638
- Rocket measurements of particle flux during the April 1969 solar cosmic ray event. 12 p1535 A73-27651
- Cometary nuclei chemical composition and molecular structure, suggesting radial-forming organic molecules synthesis by solar and galactic cosmic radiation 14 p1723 A73-29816
- On the generation of high-energy particles in solar flares. 15 p1925 A73-31068
- Estimate of the probability of observing solar cosmic-ray proton fluxes at the earth orbit 15 p1926 A73-31877
- The direct and inverse problems of cosmic-ray propagation in interplanetary space 15 p1926 A73-31878
- Solar cosmic-ray burst of July 7, 1966 and its measurement by Proton-3 satellite. 15 p1927 A73-32611
- Effect of ionization losses on cosmic-ray generation conditions on the sun. 16 p2052 A73-32754
- Possibility of detecting weak solar-cosmic-ray fluxes by ground-based radio methods. 16 p2052 A73-32756

SOLAR CYCLES

Time dependent diffusion equation for solar flare cosmic ray propagation through interplanetary space, specifying continuous emission curve shape and period 16 p2053 A73-32966

Radioheliograph observations of high-energy phenomena in the solar corona. 16 p2061 A73-33284

Solar electrons, Galactic electron radiation modulation and spectrum of high energy cosmic ray electrons 16 p2055 A73-33293

Solar flare cosmic rays at and beyond the modulation boundary. 16 p2056 A73-33458

Solar cosmic ray alpha particles and protons flux measurement after events in 1967-1969 for 1-10 MeV particles 18 p2347 A73-36289

Energetic neutrons leaking from the top of the atmosphere. 19 p2474 A73-37299

Investigation of cosmic radiation about the moon aboard the Luna 10, 11, and 12 artificial lunar satellites 19 p2474 A73-37344

Low-energy protons of solar origin and interplanetary medium studies 19 p2474 A73-37345

Time dependence of cosmic-ray intensity at the anisotropic stage of solar flares. 19 p2476 A73-37908

Characteristics of cosmic-ray variations near the solar equatorial plane. 19 p2476 A73-37928

Solar cosmic ray heavy nucleus abundances relation to oxygen nuclei in solar corona and photosphere 20 p2601 A73-38917

Study of cosmic rays by the Prognostic satellites 21 p2756 A73-40577

Certain characteristics of the August 1972 solar flares which generated cosmic radiation, plasma clouds, and interplanetary shock waves 21 p2757 A73-40587

High flux cosmic ray variations following solar chromospheric flares in August 1972 from stratospheric balloon measurements 21 p2757 A73-40589

Solar proton measurements during August 1972 cosmic ray and magnetic field events caused by chromospheric flares associated with sunspots on east limb 21 p2757 A73-40592

Isotopes of helium and hydrogen in solar corpuscular fluxes 21 p2757 A73-40593

Investigation of shock waves responsible for Forbush decreases 21 p2757 A73-40595

Certain features of the 27-day variations in cosmic-ray anisotropy 21 p2758 A73-40599

Structural and dynamic features of solar cosmic-ray penetration into polar regions 21 p2758 A73-40606

Penetration of solar cosmic rays into the earth's polar caps 21 p2760 A73-40920

Quiet-time solar neutron flux upper limit from OGO-6 neutron detector, evaluating solar cosmic ray acceleration, nuclear reaction and energy region 21 p2763 A73-41498

Energy losses of solar cosmic rays in interplanetary space. 21 p2763 A73-41503

Selection of a propagation model for calculating the injection spectrum of solar protons. 23 p3020 A73-43231

Simultaneous recording of solar cosmic-rays near Venus and the earth's magnetosphere. 23 p3020 A73-43251

North-south asymmetry of the interplanetary magnetic field 23 p3025 A73-44250

SOLAR CYCLES

NT SUNSPOT CYCLE

Observations of galactic cosmic-ray intensity at heliocentric radial distances of from 1.0 to 2.0 astronomical units. 01 p0093 A73-11044

Maxima in coronal intensity during 1966-1970 period of solar cycle, discussing north-south asymmetry correlation with sunspot activity 01 p0108 A73-11395

Evidence for two maxima of activity in the 20th solar cycle. 01 p0108 A73-11396

Evidence for an ultra-long cycle of solar activity /Research note/. 01 p0108 A73-11397

Evolution of coronal helmets during the ascending phase of solar cycle 20. 03 p0378 A73-14419

Solar cyclic intensity variation of excess radiation with respect to galactic radiation background at low altitudes from satellite data analysis 03 p0365 A73-14575

Heliographic and spectroscopic observations of solar southern hemisphere active region during August 1971 cycle, noting photospheric changes, sunspots and flares 03 p0379 A73-14581

Secular variation of the stratospheric ozone layer over middle Europe during the solar cycles from 1951 to 1972. 04 p0445 A73-15635

Heliographic latitude distribution of pronounced prominences in both hemispheres of the sun during the eighteenth and nineteenth 11-year solar activity cycles 05 p0609 A73-16204

Large-scale photospheric magnetic field - The diffusion of active region fields. 05 p0620 A73-17028

Harmonic analysis of solar wind geometry and geomagnetic activity levels during even and odd cycles based on cosmic ray intensity variations for 1900-1969 period 07 p0870 A73-19451

The time-latitude distribution of solar flares accompanied by type IV radio bursts during the period 1956 to 1969. 08 p0997 A73-20770

Solar modulation of cosmic ray intensity in stratosphere, examining relationship to sunspots group number and heliographic latitudes over 11 year period 08 p0999 A73-21339

Diurnal, sporadic and yearly variations in cosmic ray flux based on neutron component data, noting relation to solar activity cycles 08 p1000 A73-21345

Diurnal, seasonal and solar cycle changes in southern midlatitude ionosphere electron content from June 1965-August 1971 11 p1359 A73-26712

Variation of the cosmic-ray gradient during the solar activity cycle. 13 p1670 A73-28721

Spatial distribution of H alpha emission in the earth's upper atmosphere, the variations of the emission during a solar cycle, and the dependence of the emission on geomagnetic perturbations 15 p1867 A73-31262

High pass filter and power spectral analysis of periodicity in solar activity time series, applying statistical tests to sunspot and flare indices 16 p2060 A73-32955

Steady-state solar modulation of cosmic rays. 16 p2055 A73-33296

Characteristic features of secular and super-secular cycles of solar activity - The 180-year cyclic variation of solar activity 16 p2056 A73-33657

Difference between even and odd 11-year solar activity cycles 16 p2056 A73-33658

Equatorial spread F layer height nocturnal variations due to magnetic disturbances during solar activity cycles 16 p2008 A73-33878

Solar cycle and coronal heating theories implications for cycle variations phase coincidence, discussing sunspots, coronal green lines, etc 17 p2224 A73-34510

Fine structure in the sunspot spectrum - 2 to 70 years. 17 p2230 A73-34514

Diurnal, annual and solar cycle variations of hydroxyl and sodium nightglow intensities in the Europe-Africa sector. 17 p2160 A73-34785

Solar energy cycle and its relation to geomagnetic activity. 17 p2236 A73-35777

Stratifications in the F region of the ionosphere 20 p2554 A73-39174

Position of the equatorial boundary of the anomalous ionization occurrence region in relation to the planet's magnetic activity during the solar activity cycle 20 p2554 A73-39175

Seasonal and solar cycle dependence of the position of the cusp region of the magnetosphere. 20 p2555 A73-39828

Neutral air wind influences deduced from solar cycle changes in the F2 region equatorial anomaly. 21 p2679 A73-39932

Investigation of solar activity and its association with cosmic ray variations 21 p2755 A73-40113

The 11-year cycle of cosmic ray intensity in the stratosphere and its dependence on solar activity 21 p2758 A73-40597

Differences in the correlations of 27-day and 11-year cosmic ray variations with solar activity parameters 21 p2758 A73-40598

Diurnal, semidiurnal, and the eight-hour components of cosmic-ray anisotropy 21 p2758 A73-40601

Estimate of the spectrum of cosmic-ray variations in the high-energy range on the basis of subterranean observations 21 p2758 A73-40602

Solar cycle control in the 27-day variation of geomagnetic activity. 22 p2846 A73-41945

SOLAR DISK

U SUN

SOLAR ECLIPSES

Changes of electron density with zenith angle, with the sunspot cycle, and during eclipses. 01 p0043 A73-10907

Highlights of the COSPAR Symposium on the solar eclipse of 7 March 1970. 01 p0101 A73-10911

Polarization of the inner corona during the solar eclipse of March 7, 1970 01 p0102 A73-10933

The results of coronal investigation at the September 22, 1968 solar eclipse. 01 p0108 A73-11383

Atmospheric gravity waves to be expected from the solar eclipse of June 30, 1973. 02 p0159 A73-12223

Investigation of the chromosphere in the D3 helium line at the eclipse of September 22, 1968. 04 p0503 A73-16014

Vertical motion of the lower ionosphere during a solar eclipse 05 p0569 A73-16262

Coronal holes during 12 November 1966 eclipse, comparing distribution to calculated current-free coronal magnetic field 05 p0621 A73-17035

On emission lines of hydrogen, helium and ionized calcium seen on a coronal spectrogram of the March 7, 1970 eclipse. 05 p0621 A73-17036

Correlations between X-rays and UV ionizing radiation in the E region from data obtained during the solar eclipse of 25 February 1971 06 p0742 A73-17534

Sporadic E relation to ionized particle redistribution in E layer during solar eclipse 07 p0815 A73-19256

Total solar eclipses of great duration. 07 p0876 A73-19400

Threadlike solar coronal streamer observation at 20 July 1963 eclipse, noting electron density from photometric analysis 08 p1002 A73-20763

Polarization of the total coronal emission during the solar eclipse of March 7, 1970 08 p1007 A73-21070

X-ray emission of coronal condensations during the eclipse on 20 May 1966 and its connection with optical and radio observations. 08 p0998 A73-21310

Polarization of the inner corona at the total eclipse of March 7, 1970. 09 p1147 A73-22734

Supersonic generation of atmospheric gravity waves, via atmospheric cooling by moon shadows during lunar eclipses, noting analogy to terminator action 10 p1211 A73-23825

Effect of the May 20, 1966 solar eclipse in the ionosphere on the basis of observations at Rostov on the Don and at Adler 11 p1351 A73-25100

Rocket-borne high spatial resolution solar L alpha photographs during 10 July 1972 eclipse, describing instrumentation and photographic details 11 p1422 A73-25935

Photometric and polarimetric analysis of the coronal streamers observed at the March 7, 1970 Mexican eclipse. 11 p1425 A73-26263

Polarigraphic observations of the solar corona at the total eclipse on March 7, 1970 in Mexico. 11 p1425 A73-26264

Light velocity from Io eclipse times observation by Picard and Roemer, noting rms deviation with present value 11 p1429 A73-26685

Solar corona electron densities and temperatures as function of distance from solar center during 22 September 1968 eclipse 12 p1538 A73-26860

Solar corona streamers polarization, intensity and electron density and temperature during 22 September 1968 total eclipse 12 p1533 A73-26861

Solar and lunar eclipses, orbits and perturbations prediction from Saros /recurring time periods/ 12 p1540 A73-27481

Further evidence for a complex limb structure in the solar radial brightness distribution at mm wavelengths. 12 p1545 A73-27841

Results of observations of coronal condensation in photographic rays during the solar eclipse of Sept. 22, 1968 13 p1673 A73-28299

Conditions of Cr IX and Fe XI luminescence in the corona 13 p1683 A73-29094

Stratospheric cooling and perturbation of the meridional flow during the solar eclipse of 7 March 1970. 14 p1771 A73-30765

Concorde-borne astronomical observation for Fraunhofer corona IR and photospheric and chromospheric radiations in lunar shadow during 30 June 1973 solar eclipse

15 p1940 A73-32184

Structure of a noise-storm source according to observations of the eclipse of September 22, 1968 at the 1.37-m wavelength

16 p2057 A73-32704

Correlations between X-rays and ionizing ultraviolet radiation in the E-region, according to data from the solar eclipse of February 25, 1971.

16 p2052 A73-32758

D region electron and ion density profiles, recombination coefficient and electron detachment rate changes during solar eclipse

18 p2310 A73-36127

Predicted acoustic gravity wave enhancement during the solar eclipse of June 30, 1973.

18 p2352 A73-36301

Polarization of the resultant emission of the corona during the solar eclipse of March 7, 1970.

18 p2355 A73-36871

Solar eclipse of July 10, 1972 - Comparison of photographic-photometry and K-coronometer measurement data

20 p2611 A73-39589

Solar eclipse of 10 July 1972 observed by visual and photographic method from aircraft, taking into account coronal structure

21 p2767 A73-40565

Observational results on coronal condensation in photographic light during the September 22, 1968 solar eclipse.

21 p2779 A73-41543

Atmospheric gravity wave observations after the solar eclipse of June 30, 1973.

22 p2847 A73-42487

Spectral characteristics of solar corona measured by visual, rocket and satellite observation, discussing K and F coronal regions, eclipse phenomena and analysis techniques

22 p2910 A73-42650

French eclipse studies.

22 p2911 A73-42870

Airborne studies of the African eclipse.

22 p2911 A73-42871

Solar observatories and satellite-borne instruments for solar coronal structure determination, considering 30 June 1973 eclipse and instrumented Concorde aircraft use

22 p2916 A73-43117

Ionospheric sounding by ATS-3 emitted signal polarization measurement during partial solar eclipse of 10 July 1972, noting electron content decrease and diffusion rate

23 p2972 A73-43697

Solar coronal Fe XIII 10747 A emission line resonance polarization observations during 12 November 1966 eclipse, discussing magnetic field effects

24 p3135 A73-44633

Observation of a possible neutral sheet in the corona.

24 p3136 A73-44636

SOLAR ELECTRIC PROPULSION

Solar electric propulsion for payloads earth orbit injection, discussing communication satellites and space shuttle/tug system applications

[AIAA PAPER 73-1126] 04 p0486 A73-14912

Estimation of unmodeled forces on a low-thrust space vehicle.

04 p0504 A73-15272

Constrained low thrust guidance algorithms for three axis and spin stabilized constant power solar electric propelled spacecraft on fixed time rendezvous missions

[AIAA PAPER 73-173] 05 p0595 A73-16917

Earth-based orbit determination for solar electric spacecraft with application to a Comet Encke rendezvous.

[AIAA PAPER 73-174] 06 p0748 A73-17651

Solar electric space mission risk analysis, describing computerized multistage failure process simulation procedure with application to Encke comet rendezvous mission

[AIAA PAPER 73-208] 06 p0748 A73-17660

The feasibility of geostationary emplacement of satellites by solar electric tug.

11 p1431 A73-26260

Influence of the thrust interruption during passage through the shadow cone of a celestial body on the trajectory of a space vehicle using solar electric propulsion - First-approximation calculation

12 p1540 A73-27393

Solar electric propulsion comet and asteroid rendezvous missions, examining asteroid perihelion data base, optimum mission length, flight time and exploration vehicle power levels

[AIAA PAPER 73-597] 18 p2350 A73-36081

Electric propulsion interactive effects with spacecraft science payloads.

[AIAA PAPER 73-559] 18 p2353 A73-36497

SOLAR ELECTRONS

Solar electrons, Galactic electron radiation modulation and spectrum of high energy cosmic ray electrons

16 p2055 A73-33293

SOLAR ENERGY

Synchronous satellite solar power station for solar energy conversion to microwaves for transmission to earth discussing technical, economic and social aspects

[ASME PAPER 72-WA/SOL-6] 04 p0408 A73-15801

Satellite solar power station for solar energy conversion and transmission to earth via microwave beam, discussing technology status and weight and cost projections

06 p0750 A73-18027

Electrical and isotope power from space for terrestrial use.

06 p0750 A73-18028

Measurements of solar energy reflected by the earth and atmosphere from meteorological satellites.

08 p0958 A73-21268

Spacecraft dynamic solar electric power/thermal control system with cold liquid flow and regenerator cooling for energy conversion efficiency and weight characteristics improvements

09 p1153 A73-22785

Satellite solar power station for solar energy conversion into electricity and transmission to ground receiving stations via microwave beams

09 p1035 A73-22791

Satellite electric power station for conversion of solar energy to microwaves beamed to earth, discussing structural design, flight control, transportation and technology assessment

10 p1178 A73-24554

Principles of photovoltaic solar energy conversion.

13 p1573 A73-29591

Solar energy conversion development relative to Department of Defense space power requirements.

13 p1573 A73-29595

The utilization of solar energy to help meet our nation's energy needs.

15 p1832 A73-32193

Analysis of the parameters of solar-heat power sources with energy storage units

17 p2108 A73-34283

Some major terrestrial applications of solar energy.

17 p2110 A73-35312

Solar energy conversion into thermal, chemical or electric energy, discussing high efficiency collector design with thin film for absorber and glass envelope improvement

[AIAA PAPER 73-710] 18 p2269 A73-36331

Effect of aerosols on the transfer of solar energy through realistic model atmospheres. I - Non-absorbing aerosols.

18 p2333 A73-36704

Intersociety Energy Conversion Engineering Conference, 8th, University of Pennsylvania, Philadelphia, Pa., August 13-16, 1973, Proceedings and Addendum.

19 p2390 A73-38386

A solar engine using the thermal expansion of metals.

19 p2392 A73-38473

Variations in the M/3000/F2 coefficient as a function of the solar energy entering the earth's atmosphere

20 p2555 A73-39179

SOLAR ENERGY ABSORBERS

Solar energy conversion into thermal, chemical or electric energy, discussing high efficiency collector design with thin film for absorber and glass envelope improvement

[AIAA PAPER 73-710] 18 p2269 A73-36331

Optical stability of coatings exposed to four years space environment on OSO-III.

[AIAA PAPER 73-734] 18 p2336 A73-36351

SOLAR FACULAE

U FACULAE

SOLAR FLARES

Flare spectrum in region accessible to ground based optical solar spectrographs, considering Balmer line broadening, electron density, optical thickness, LTE, electron temperature, etc

01 p0091 A73-10052

Some peculiarities of the development of the magnetic storm on March, 5-10, 1970.

01 p0036 A73-10342

Ion composition dependent recombination coefficient loss rate changes in D region during solar flares, using electron density and X ray flux measurements

01 p0042 A73-10903

Energy balance in the current sheath of a solar flare and the acceleration of cosmic rays by plasma waves

01 p0092 A73-10936

Nonthermal X-radiation and electric currents in solar flares

01 p0092 A73-10937

Heating of plasma by high-energy electrons, and nonthermal X-ray emission in solar flares.

01 p0093 A73-11313

H alpha subflare associated X-ray burst of 10 October 1970 observed by balloon-borne scintillator and OGO 5 and SOLRAD 9 satellites

01 p0093 A73-11389

Pitch-angle distributions of polarized hard X-radiation from solar flares, assuming electron-proton bremsstrahlung mechanism

01 p0093 A73-11390

Electron production rates and density profiles in D region during solar flares, presenting ionization vertical distribution model

02 p0206 A73-12304

Solar cosmic ray bursts in November-December 1970 according to data from Venus 7 space probe and Lunokhod 1 station.

02 p0206 A73-12321

Solar white light flares induced neutron and gamma ray emission, discussing acceleration mechanism through high energy proton bombardment induced photospheric heating

02 p0206 A73-12322

Fe ions optical transition lines in solar flares soft X ray spectra, noting continuum emission near 8A

03 p0367 A73-12945

The abundances of solar accelerated nuclei from carbon to iron.

03 p0362 A73-13719

Two stage analytical model for mechanism of heavy nuclei acceleration in solar flares, considering ion Fermi acceleration to higher energies

03 p0362 A73-13720

Auroral flux enhancements due to solar proton injection at medium energies during flares from ESR0 2 satellite measurements

03 p0362 A73-13859

Laboratory-produced radiation related to the solar flare emission.

[AD-758606] 03 p0364 A73-13957

X ray spectra of solar flares at 0.4-250 keV, emphasizing soft X ray spectra and emission line and continuum features interpolation

03 p0364 A73-13958

Production of different non-thermal electron groups in small solar flares.

03 p0364 A73-13959

The transient highly excited solar flare plasma.

03 p0364 A73-13960

Analysis of some aspects of 25 chromospheric events. I - Reduction of the optical data. II - Discussion on the optical data.

03 p0364 A73-14414

Observation of solar particle fluxes over extended solar longitudes.

03 p0365 A73-14421

Cosmic radio wave anomalous absorption height dependence on zenith distance in midlatitude ionosphere during solar flare emission from polarization study

03 p0365 A73-14561

Solar radio emission measurement and interpretation, discussing source mapping, coronal density, magnetic field and flare and particle events predictions

04 p0496 A73-14830

Extreme ultraviolet observations of solar flares.

04 p0490 A73-14831

X-ray line emission associated with solar flares.

04 p0490 A73-14832

Solar flare development particle acceleration phase model, noting association with white light emission, hard X-rays and PCA

04 p0490 A73-14833

Magnetic models of solar flares.

04 p0490 A73-14834

Solar flare effects in ionosphere, discussing long term variability, sudden ionospheric disturbances, PCA and magnetic storms

04 p0491 A73-14839

Solar flares recognition from H-alpha centered birefringent filtered photographs, determining statistical pattern of filament movements

04 p0491 A73-14842

Prediction of proton flares and Forbush effects.

04 p0491 A73-14843

Quantitative short-term prediction of proton and nonproton flares.

04 p0491 A73-14844

Dielectronic satellite spectra for highly-charged helium-like ion lines.

04 p0500 A73-15490

Solar corona properties and nuclear reactions in flares from August 1972 OSO 7 observation, noting hard X ray bursts from electron streams

04 p0502 A73-15971

New results of solar X-ray flare studied

05 p0609 A73-16372

Enrichment of heavy nuclei in the 17 April 1972 solar flare.

05 p0609 A73-16571

X-radiation /E greater than 10 keV/, H-alpha and microwave emission during the impulsive phase of solar flares.

05 p0610 A73-17041

Search for weak white-light flares by time-wise photographic cancellation.

05 p0610 A73-17042

SOLAR FLARES

Solar flares EUV observations by OSO 5 three band grating spectrophotometer, discussing flare intensity time dependence with superimposed impulsive bursts
05 p0610 A73-17044

The directivity and polarisation of thick target X-ray bremsstrahlung from solar flares.
05 p0610 A73-17045

Evidence for a two-component injection of cosmic rays from the solar flare of 1969, March 30.
05 p0610 A73-17046

Type 3 radio bursts correlation with solar flares and electron events from OGO 5, IMP 5 and Explorer 35 observations
05 p0610 A73-17047

Solar flare activity during August 1972, discussing sunspots filter- and spectrograms, proton emissions and geomagnetic disturbances
05 p0622 A73-17095

Speed of propagation of shock waves responsible for geomagnetic storms and Forbush decreases
06 p0689 A73-17548

Solar outer atmospheric eruption from photographic recording by OSO 7 spacecraft borne coronagraph, noting ejected gas and plasma clouds caused by flare
06 p0753 A73-18374

Solar flare frequency and associated physical phenomena diversity, discussing earth atmosphere protective effects and impact on Concorde flights
07 p0784 A73-19210

Pitch angle distribution of solar flare particles in interplanetary space.
07 p0869 A73-19228

Solar proton flare prediction, examining diurnal rotation of axis connecting two stable spots and change in horizontal gradient of spots magnetic field
07 p0870 A73-19449

Solar energetic particles and wide-band continuum storms from metric to hectometric frequencies.
07 p0870 A73-19663

Solar flare intensity estimation based on measurements for Ar 37 radioactivities and depth dependence of tritium in Apollo 11 and 12 lunar rock samples
07 p0889 A73-19794

Lunar craters and exposure ages derived from crater statistics and solar flare tracks.
07 p0896 A73-19869

Radiation effects in soils from five lunar missions.
07 p0896 A73-19875

Solar flare and galactic cosmic ray studies of Apollo 14 and 15 samples.
07 p0871 A73-19876

The ABC method of providing warning of an impending solar flare.
07 p0899 A73-19941

Ion acceleration in the current sheath of a solar flare
07 p0872 A73-20320

Solar gamma ray lines observed during the solar activity of August 2 to August 11, 1972.
08 p0996 A73-20665

Detection of relativistic solar particles before the H alpha maximum of a solar flare.
08 p0996 A73-20666

Flares, magnetic configurations, and magnetic energy release.
08 p0996 A73-20764

Polarization structure of a solar flare region at 9.5 mm wavelength.
08 p0997 A73-20767

The time-latitude distribution of solar flares accompanied by type IV radio bursts during the period 1956 to 1969.
08 p0997 A73-20770

On the S- and B-components of solar radio and X-emission and their relationships to energetic solar events.
08 p0997 A73-20771

Solar cosmic ray sectorial anisotropy pattern observation, suggesting theoretical propagation model to distinguish between rival candidates for parent flare
08 p0997 A73-20772

Time dependence of cosmic ray intensity during the anisotropic phase of solar flares
08 p0998 A73-21279

Solar cosmic rays propagation between shock front and solar flare hot plasma, examining fine structure from Explorer 34 and Venera 6 data
08 p0999 A73-21328

Solar cosmic ray flare recording in stratosphere in Murmansk and Antarctic regions during February-April 1969
08 p1000 A73-21347

Solar cosmic ray flare of 11-18 April 1969, investigating effect on polar cap absorption in lower ionosphere
08 p1000 A73-21348

Nucleon and electromagnetic cosmic particle generation, energy spectrum and diffusion during solar flares
08 p1000 A73-21349

Oppositely directed magnetic fields reconnection rate role in solar flares and small scale turbulent field reduction in photosphere
09 p1142 A73-22037

The extreme-ultraviolet spectrum of Fe XV in a solar flare.
09 p1137 A73-22039

Chromospheric flares and shock waves in interplanetary space
09 p1137 A73-22540

Energy balance in the current sheet of a solar flare, and the acceleration of cosmic rays by plasma waves.
09 p1138 A73-22731

Nonthermal X rays and electric currents in solar flares.
09 p1138 A73-22732

Solar cosmic ray diffusion, convection, accumulation and acceleration as function of interplanetary medium perturbation and flare coordinates
10 p1266 A73-23909

Forbush decreases and their relation to solar activity and the parameters of the interplanetary medium
10 p1267 A73-23921

Preliminary interpretation of the polarization measurements performed on 'Intercoms-4' during three X-ray solar flares.
10 p1268 A73-24142

A simulation of the directivity effect to be expected in hard X-ray flares.
10 p1268 A73-24143

Lifetime of solar flare particles in coronal storage regions.
10 p1268 A73-24144

Ionospheric magnetic disturbances during March 1970 related to solar flare corpuscular and proton fluxes, generating ring current and PCA absorption
10 p1211 A73-24218

Solar flare particle propagation - Comparison of a new analytic solution with spacecraft measurements.
10 p1269 A73-24277

Directivity of high-energy X-ray emission during flares.
10 p1270 A73-24774

Time dependent geophysical effects associated with chromospheric and coronal flares, tabulating for 1957-1961
11 p1411 A73-25099

Determination of the temperature in a solar X-ray flare.
11 p1412 A73-25755

Some studies on the association of solar optical flares and microwave bursts with sudden ionospheric disturbances.
11 p1354 A73-25769

Hourly and daily variations of H values for sunspot minimum, showing uncorrelated night time level departures and range implications for solar flares
11 p1355 A73-25772

Harmonic structure of flare related type 5 burst, suggesting plasma wave emission
11 p1412 A73-25856

D-region recombination coefficients and the short wavelength X-ray flux during a solar flare.
11 p1356 A73-25914

Solar surges magnetic properties analysis from high resolution H alpha filtergrams, matching surge trajectories by computed magnetic lines of force
11 p1412 A73-25941

Solar flares association with emerging flux regions /EFR/ near sunspots, noting correlation between area and brightness changes
11 p1412 A73-25942

Time variations in the X-ray emission of solar active regions.
11 p1412 A73-25944

Thick target X-ray bremsstrahlung from partially ionised targets in solar flares.
11 p1412 A73-25945

Two-component temperature analysis of OSO-5 X-ray flare data.
11 p1413 A73-25947

Superthermal plasma nodules and their relation to solar flares.
11 p1413 A73-25949

Energetic solar particles and their relation to optical flares.
11 p1413 A73-25952

Estimation of an upper limit for the solar neutron emission during large flares.
11 p1413 A73-25953

Charge states and energy-dependent composition of solar-flare particles.
11 p1413 A73-26207

Magnetic field effect on plage, prominence and sunspot flares, considering radio, UV and X-ray emission
11 p1413 A73-26208

Additional evidence for the existence of a very high energy solar particle component.
11 p1413 A73-26473

Geomagnetic latitude variation of cosmic radiation rates measured onboard Concorde SST prototypes, investigating solar flares
11 p1324 A73-26588

Hydrogen and helium isotopes differential energy spectra during solar flare particle acceleration related to nuclear interaction processes
11 p1414 A73-26610

Resistive diffusion of force-free magnetic fields in a passive medium.
11 p1428 A73-26620

Daily variation of geomagnetic field at the Indian stations under the electrojet during the period of the July 1966 proton flare.
12 p1534 A73-26999

Ion acceleration in the current layer of a solar flare
12 p1534 A73-27299

Intensive chromospheric flares and rotation discontinuities in the solar wind
12 p1534 A73-27359

Rocket measurements of particle flux during the April 1969 solar cosmic ray event.
12 p1535 A73-27659

Flare-produced coronal MHD-fast-mode wavefronts and Moreton's wave phenomenon.
12 p1536 A73-27659

Characteristics of electron and high-energy proton flares.
12 p1536 A73-27889

Beginning, maximum and ending times uncertainty and maximum areas of H alpha flares, stressing international coordination in solar patrol service
12 p1536 A73-27889

The configuration of interplanetary shock waves produced by strong chromospheric flares (according to space sonde measurements/
12 p1536 A73-27889

Solar flare heavy ion damage in Luna 20 soil samples producing angular amorphous micron-sized grains via accumulated radiation damage
13 p1676 A73-28359

Solar flare ejected protons intensity increase during July 1970 from Pioneer 6 and 8 and Explorer 41 data.
14 p1786 A73-29839

Solar wind proton temperature anomalies relation to interplanetary shock waves, considering solar flare induced material ejection and magnetic bottle formation
14 p1786 A73-29939

On the origin of SC-storms with respect to forecasting geomagnetic activity.
15 p1868 A73-31529

The correlation between 10.7-cm /2800 MHz/ solar radio emission and chromospheric flares
15 p1926 A73-31669

Determination of a probable interval for the mean transit time of geomagnetic-storm /SSC/ solar particles
15 p1926 A73-31669

Solar surface and atmosphere activity due to magnetic field production, transport and dissipation: discussing flares, sunspots, corona, dynamo, plasma turbulence and prominences
15 p1937 A73-31849

Metallic lines in the solar flare of July 12, 1961 and properties of the corresponding emission regions
15 p1938 A73-31919

Propagation velocity of shock waves causing geomagnetic storms and Forbush decreases.
16 p2002 A73-32779

Spectral analysis of sunspot flares.
16 p2052 A73-32959

Non-thermal ionization and recombination processes during solar flares.
16 p2052 A73-32959

The extreme ultraviolet emissions of solar flares - comparison between OSO-6 spectroheliograph observations and SFDs.
16 p2053 A73-32959

Spectra of solar flares from 8.5 A to 16 A.
16 p2053 A73-32959

The solar albedo of hard X-ray flares.
16 p2053 A73-32959

Time dependent diffusion equation for solar flare cosmic ray propagation through interplanetary space specifying continuous emission curve shape and period
16 p2053 A73-32959

Development of moving type IV solar radio bursts and relation to expanding magnetic bottles from flare regions.
16 p2054 A73-33009

High resolution radio observation of sun at 3.71 and 11.1 cm with three-element interferometer, noting flare near east limb
16 p2060 A73-33009

Solar proton, helium, and medium nuclei /Z from 1 to 9/ observed from the IMP-VI satellite.
16 p2054 A73-33289

Charge and energy spectra of particles with E from 0.2 to 30 MeV/nuc in the January 25, 1971 solar flare.
16 p2054 A73-33289

Solar flare cosmic rays at and beyond the modulation boundary.
16 p2056 A73-33449

Radio emissions from solar flares.
17 p2224 A73-34729

Directional diffusion coefficients of solar proton inside and outside the bow shock.
17 p2224 A73-34789

Close connexion between flare-generated coronal and interplanetary shock waves.
17 p2232 A73-35149

Forecasting of proton flares.
18 p2344 A73-35919

19-20 May 1969, an example of type III emission during the impulsive phase of flares. 18 p2344 A73-36013

Analysis of solar flare X-ray radiation with Bragg spectrometers. 18 p2344 A73-36014

Investigation of the solar X-ray flare spectra by the 'Intercosmos-4' and 'Intercosmos-7' satellites. 18 p2345 A73-36015

Electron temperature and emission measure variations in the solar corona. 18 p2350 A73-36062

Gamma ray and neutron measurements and their relation to the solar flare problem. 18 p2345 A73-36126

Intercosmos satellite-borne X ray polarimeter measurements of solar flares 18 p2345 A73-36144

Simulation of driven flare-associated disturbances in the solar wind. 18 p2346 A73-36263

Coronal propagation of low-energy solar protons. 18 p2347 A73-36290

A density scale for the interplanetary medium from observations of a type II solar radio burst out to 1 astronomical unit. 18 p2348 A73-37113

Model experiment on solar flares and the neutral sheet. III. 19 p2475 A73-37383

Kinematic theory of magnetic field reconnection rate for analysis of turbulent flows in solar photosphere, flare phenomena and galaxy 19 p2467 A73-37439

Time dependence of cosmic-ray intensity at the anisotropic stage of solar flares. 19 p2476 A73-37908

Lines of Fe XVII and Fe XVIII during a solar flare. 19 p2476 A73-38170

Configuration of interplanetary shock waves from powerful chromospheric flares /from space probe measurements/. 20 p2602 A73-39233

Magnetic fields of the sun and stars 20 p2609 A73-39569

Method of studying magnetic-ionospheric disturbances and solar flare effects on long-upset periods. 20 p2555 A73-39767

Evidence for solar flare rare gases in the Khor Temiki aurbite. 21 p2764 A73-40231

Sunspot activity, flare observation, electromagnetic and magnetic disturbances, auroral activity and solar radio bursts in March and April 1973 21 p2767 A73-40567

Propagation of protons injected near 1 AU in a medium with a constant transport length 21 p2756 A73-40583

Certain characteristics of the August 1972 solar flares which generated cosmic radiation, plasma clouds, and interplanetary shock waves 21 p2757 A73-40587

The Forbush effect in the nuclear component of primary cosmic rays in August 1972 21 p2757 A73-40588

High flux cosmic ray variations following solar chromospheric flares in August 1972 from stratospheric balloon measurements 21 p2757 A73-40589

Ground level cosmic ray variations in August 1972, relating intensities and Forbush decreases with solar flares and shock wave parameters 21 p2757 A73-40591

Solar proton measurements during August 1972 cosmic ray and magnetic field events caused by chromospheric flares associated with sunspots on east limb 21 p2757 A73-40592

Investigation of shock waves responsible for Forbush decreases 21 p2757 A73-40595

Heliographic latitudinal zonality of periodic sunspot and flare distributions during 1957-1964 and 1923-1962 21 p2759 A73-40722

Analysis of the solar X-ray spectrum of 20 August 1971. 21 p2760 A73-40826

Nonthermal electromagnetic and thermal X ray sources of accelerated electrons during solar flares 21 p2761 A73-41384

Solar-interplanetary disturbances during 5-18 June 1969 /The PFP interval/IASY/. 21 p2773 A73-41385

Enhancements of the photoelectron-excited dayglow during solar flares. 21 p2761 A73-41389

Particle emitting flares and the large-scale distribution of solar magnetic fields and green corona. 21 p2762 A73-41390

Solar flare forecasting method developed and applied at Crimean observatory, using magnetic instability model for active regions 21 p2762 A73-41391

Solar flare prediction objective baseline calculation, applying regression analysis to sunspot, magnetic field, calcium plage and radio brightness temperature data 21 p2762 A73-41392

Optical solar flare kinematic model, relating chromosphere response to downward propagating super-sonic disturbance 21 p2762 A73-41490

Solar limb flare observations on 11 August 1972, examining temporal relationships of flash, spray, surge and loop phase 21 p2762 A73-41492

Chromospheric hydrogen and helium spectral lines investigation in solar flares determining plasma and ionization temperatures, energy spectra and electron density 22 p2903 A73-42066

Some statistical characteristics of sudden ionospheric disturbances, and the distribution of geoeactive chromospheric flares over the solar disk 22 p2847 A73-42326

Monograph - Development and performance of a solar hard X-ray spectrometer. 22 p2861 A73-42674

Resistive diffusion of force-free magnetic fields in a passive medium. II - A nonlinear analysis of the one-dimensional case. 22 p2914 A73-43009

Measurement methods for sudden ionospheric disturbances caused by solar flares, discussing short wave fading, sudden phase anomaly and sudden enhancement of atmospherics techniques 22 p2904 A73-43036

Saha's equation under deviation from thermodynamic equilibrium. 22 p2915 A73-43040

Powerful chromospheric flares and rotational discontinuities in the solar wind. 23 p3020 A73-43228

The effect of nonstationarity in the chemical composition of plasma flows from the sun. 23 p3027 A73-43252

Solar activity forecasting, considering flare site identification from active center microscopic magnetic components, and particle acceleration observations 23 p3021 A73-43370

Metal lines in the solar flare of July 12, 1961, and the properties of the emission region. 24 p3132 A73-44482

Photometric study of a diffuse reinforcement observed in the zodiacal light at a distance of 100 solar radii from the sun 24 p3134 A73-44566

Height distribution and directionality of 2-12 A X-ray flare emission in the solar atmosphere. 24 p3124 A73-45046

X-ray flare plasma temperature - A comment on a paper by Deshpande and Tandon. 24 p3124 A73-45047

Flare triggering by coherent oscillations. 24 p3124 A73-45048

SOLAR FLUX

Theory and design of economical net solar flux radiometer adaptable to conventional short wave radiosonde system, discussing prototype instrument tests and modifications 01 p0045 A73-10386

Temperature structure and conductive flux in the chromosphere-corona transition region. 01 p0107 A73-11380

Measurements of flux fluctuation in solar radio emission at a wavelength of 3 cm 05 p0573 A73-16270

Global mean thermosphere temperature profiles as function of solar EUV flux, considering neutral gas heating and ionospheric electron temperature 07 p0869 A73-19246

Solar energy outside the earth's atmosphere. 08 p1010 A73-21265

Solar Lyman alpha changes and related hydrogen density distribution at the earth's exobase /1969-1970/. 10 p1269 A73-24736

On the variation of the coronal lambda-5303 intensity relative to the interplanetary and solar magnetic sector structure, and to geomagnetic activity. 12 p1542 A73-27615

A procedure for studying the statistical structure of solar radiation fluxes at the ground under clouded conditions 15 p1905 A73-31792

Solar radiation fluxes at the earth's surface in the presence of cumulus clouds 15 p1905 A73-31794

Radiative transfer considerations for kinetic modeling and sensitivity studies. 16 p2005 A73-33545

[AIAA PAPER 73-505] Spherical harmonics approximation for radiative transfer in polluted atmospheres. 18 p2313 A73-36365

[AIAA PAPER 73-749] Low solar neutrino flux explained by evolution model emphasizing internal rotation effects on solar structure 19 p2488 A73-38519

High flux cosmic ray variations following solar chromospheric flares in August 1972 from stratospheric balloon measurements 21 p2757 A73-40589

Incompatibility of solar EUV fluxes and incoherent scatter measurements at Arecibo. 22 p2902 A73-41923

Aeronomic consequences of solar flux variations between 2000 and 1325 angstroms. 22 p2902 A73-41931

On the backscatter of solar He II, 304 A radiation from interplanetary He/+. 23 p3024 A73-43695

SOLAR FLUX DENSITY

NT SOLAR CONSTANT

Correlation between the brightness of comets and solar wind fluctuations 02 p0208 A73-12471

Lyman-alpha emission of comet Bennett 1969i and the determination of the solar wind flux 02 p0208 A73-12472

Solar UV Lyman alpha radiation intensity measurements, using Vertikal-1 rocket-borne photometer and photoelectron analyzer 03 p0379 A73-14565

He 3 burning border complication of mixing in solar core for solar luminosity variations resulting from central temperature decrease 05 p0611 A73-17187

Effects of sudden mixing in the solar core on solar neutrinos and ice ages. 05 p0623 A73-17188

Zonal and seasonal peculiarities in the influx of diffuse solar radiation 07 p0848 A73-20625

Solar particle measurements interpretation for closed vs open magnetospheric model determination, considering electron-proton polar cap differences, magnetotail flux asymmetries, etc 09 p1149 A73-22951

Extreme ultraviolet line intensities from the sun. 11 p1425 A73-26201

Simultaneous recording of solar cosmic rays near Venus and in the earth magnetosphere 12 p1534 A73-27354

Experimental investigations of solar radiation fluxes in the lower troposphere in the presence of St and Sc clouds 15 p1905 A73-31788

Solar neutrino flux deficiency explanation based on solar core nuclear reactions theory with consequences for luminosity and earth climate 15 p1937 A73-31849

Correlation between the brightness of comets and fluctuations of the solar wind. 15 p1927 A73-32622

Lyman-alpha radiation from comet Bennet 1969i. 15 p1927 A73-32623

Space observations of the variability of solar irradiance in the near and far ultraviolet. 16 p2062 A73-33428

The arrival of solar radiation on variously oriented inclined surfaces 20 p2555 A73-39818

Russian book - The solar constant and the energy distribution in the solar spectrum. 21 p2769 A73-40804

On the spectrum of the S- and B-components of solar radio emission at dm-wavelengths. 22 p2915 A73-43038

Simultaneous recording of solar cosmic-rays near Venus and the earth's magnetosphere. 23 p3020 A73-43251

Venera 8 - Measurements of solar illumination through the atmosphere of Venus. 23 p3029 A73-43603

Track density gradient and light noble gas isotope analysis of lunar breccia, postulating higher solar flux densities during early brecciation history 23 p2950 A73-43766

SOLAR GENERATORS

NT SOLAR AUXILIARY POWER UNITS

NT SOLAR CELLS

The role of solar cell technology in the satellite solar power station. 03 p0258 A73-14252

Technological evolution of solar generators for terrestrial applications and sounding balloons, discussing environment caused problems and solutions, energy cost estimate and future prospects 03 p0258 A73-14253

Satellite solar power station for solar energy conversion and transmission to earth via microwave beam, discussing technology status and weight and cost projections 06 p0750 A73-18027

Solar generator technology on the Symphonie satellite. 07 p0778 A73-18976

Solar cell generator technology development based on German AEROS satellite project and work on roll-up structure, discussing module concepts and test results 09 p1033 A73-22439

SOLAR GRANULATION

Satellite solar power station for solar energy conversion into electricity and transmission to ground receiving stations via microwave beams

09 p1035 A73-22791

Satellite solar power station systems engineering study, examining basic concept technical and economic feasibility

09 p1154 A73-22814

Solar/battery space station power plants combined with nuclear configurations, discussing rectified alternator current, direct energy transfer, and high voltage dc sources

11 p1311 A73-26008

Unmanned interplanetary spacecraft power systems with nickel-cadmium batteries, solar panels or radioisotope thermoelectric generators

11 p1312 A73-26022

The feasibility of a satellite solar power station.

16 p1970 A73-32718

An analysis of linear focused collectors for solar power.

19 p2391 A73-38409

SOLAR GRANULATION

A possible new interpretation of power spectra of solar-granulation brightness fluctuations.

04 p0499 A73-15367

Sunspot temperature increase stimulation of supergranule motion leading to spot decay and magnetic field diurnal fluctuation development

04 p0503 A73-16012

A mechanism for the exploding granule phenomenon.

[AD-759887] Methods of studying solar granulation fields in the presence of atmospheric disturbances

07 p0876 A73-19396

On the size of the structure elements in the solar chromosphere.

08 p1001 A73-20754

The cooling of a sunspot. I - A Carnot cycle and the hydromagnetic interactions. II - Convection zone models and the magnetic power supply.

10 p1279 A73-24137

Model solar atmosphere with quiet component involving supergranular velocity field in corona-chromosphere transition layer and vertical magnetic field

10 p1279 A73-24140

Photospheric convective network as a determining factor in sunspot and group development and stabilization.

11 p1426 A73-26574

Effect of instability of earth's atmosphere on results of solar granulation observations.

13 p1680 A73-28515

H alpha line contrast profiles evaluation from solar chromosphere supergranulation observations, obtaining chromospheric fine structure characteristics

20 p2606 A73-39072

First observations of the granulation at 1.65 microns, center to limb variation of the contrast.

21 p2776 A73-41476

Solar photospheric granulation plate statistical properties, establishing two dimensional autocorrelation function and power spectrum as function of wave number

21 p2776 A73-41477

Studies of granular velocities. III - The influence of finite spectral and spatial resolution upon the measurement of granular Doppler shifts.

21 p2776 A73-41478

Spectroscopic investigation of the chromosphere. III - H-alpha line profile from the interior of supergranular cells.

21 p2777 A73-41485

Density variation and radiative exchange effects on convective instability of plane-parallel polytropic atmosphere heated from below with application to solar granulation

24 p3135 A73-44628

SOLAR GRAVITATION

Precision measurement of the sun's gravitational field by means of the twin probe method.

02 p0218 A73-12414

The deflection of light at the sun and the change of its velocity and wavelength

02 p0225 A73-12809

Error sources in numerical integration of spacecraft equations of motion in solar and planetary gravitational fields, suggesting methods for improving accuracy

03 p0379 A73-14553

Effects of the sun and the moon on a near-equatorial synchronous satellite.

08 p1011 A73-21430

Motion of fast particles in a spherically-symmetric gravitational field

11 p1416 A73-25239

A measurement of the gravitational deflection of radio waves by the sun during 1972 October.

13 p1673 A73-28281

Relation between the tidal-force momentum and atmospheric depressions

13 p1609 A73-28862

Forward precession motion of the moon caused by attraction to the earth and the sun

15 p1939 A73-31966

Temperature difference between pole and equator of the sun.

21 p2776 A73-41479

Radial and vertical force balance in primitive solar nebula, describing techniques for gravitational potential and gas opacity computation for energy transport

24 p3127 A73-44392

Translational-precessional motion of the moon in the gravitational field of the earth and sun.

24 p3132 A73-44491

Sunspot cycle effects on solar and lunar tide-produced diurnal and seasonal variations in equatorial electrojet

24 p3124 A73-44730

SOLAR HEAT FLOW

U HEAT FLUX

U SOLAR FLUX

SOLAR HEATING

Annual and sub-annual effects of EUV heating. I - Harmonic analysis. II Comparison with density variations.

02 p0158 A73-11914

Solar white light flares induced neutron and gamma ray emission, discussing acceleration mechanism through high energy proton bombardment induced photospheric heating

02 p0206 A73-12322

Mercury thermal stress and strain fields of elastic deformation from solar heating variations due to resonance rotation

02 p0223 A73-12721

Infrared radiative heating and cooling in the Venusian mesosphere. I - Global mean radiative equilibrium.

05 p0613 A73-16197

Numerical solution for the composition of a thermosphere in the presence of a steady subsolar-to-antisolar circulation with application to Venus.

05 p0613 A73-16198

The absence of flares in 3835 A and the heating of the chromosphere.

05 p0610 A73-17040

The heating of the solar corona. I - Observation of ion energies in the transition zone.

08 p1005 A73-20919

Mars polar regions layered deposits annual solar insolation variations due to eccentricity

13 p1687 A73-29674

Solar cycle and coronal heating theories implications for cycle variations phase coincidence, discussing sunspots, coronal green lines, etc

17 p2224 A73-34510

Semiannual effect in thermosphere due to solar heat input associated with subsolar point migration and auroral heating by magnetic storms

18 p2312 A73-36300

Longitudinal displacements of the secondary mirror of a parabolic antenna

21 p2672 A73-40550

Comet Kohoutek development predictions for various orbital locations, discussing brightness changes, tail production, nucleus ice melting by solar heating at perihelion, etc

23 p3033 A73-43956

SOLAR INSTRUMENTS

NT SPECTROHELIOGRAPHS

Theory and design of economical net solar flux radiometer adaptable to conventional short wave radioisotope system, discussing prototype instrument tests and modifications

01 p0045 A73-10386

Solar IR imaging techniques for providing high resolution data with short exposure time

02 p0169 A73-12333

Skylab instrumentation and solar observation objectives in coordinated program of correlative ground based, rocketborne and other spaceborne observations

02 p0169 A73-12337

Spaceborne high resolution solar telescopes optical systems, discussing construction, alignment and thermal control problems

02 p0169 A73-12338

Adaptation of the electronic camera to the coronagraph

02 p0170 A73-12544

Equipment for observation of fast fluctuations in the solar radio emission flux

05 p0573 A73-16269

Electronic imaging systems with TV vidicon competition with film photography for spaceborne solar astronomy, comparing resolution, sensitivity and SNR

08 p0971 A73-21749

Solar chromatograph for monochromatic image production with variable bandwidth and simple shift to visible spectrum, discussing design and applications

11 p1365 A73-26235

Skylab A solar and terrestrial observation and photography hardware, including solar observatory, microwave scanner, IR spectrometer and multispectral photographic facility

13 p1612 A73-28276

Some limiting parameters of an optoelectronic device for determining the orientation of a spacecraft with respect to the sun

14 p1803 A73-29808

Equipment for recording and computer input of solar magnetograph data

15 p1878 A73-32111

Atmospheric turbulence vs residual surface inaccuracy refracting and reflecting telescopic image degradation for solar observations

16 p2014 A73-32424

Atmospheric attenuation measurements via microwave radiometer yielding excess attenuation statistics for communications systems planners

16 p1982 A73-33737

Real time digital videomagnetograph at Aerospace San Fernando Solar Observatory.

17 p2168 A73-34949

A multi-channel coronal spectrophotometer.

17 p2170 A73-35222

IMP and Pioneer satellite-borne sensors for cataloging solar particle events, discussing onset time, multiple flare injections, enhancement differentiation and contamination problems

18 p2345 A73-36060

An 8-mm interferometer for solar radio astronomy at Bordeaux, France.

23 p2980 A73-43331

Millimeter wave radio telescope with high resolution for obtaining heliograph, discussing fast rotation synthesis and array redundancy design features

23 p2958 A73-43331

SOLAR LIMB

The spectra of near-vertical structures on the solar disk.

08 p1001 A73-20771

Centimeter radiation associated with the solar limb prominence of 8 February 1972.

08 p0996 A73-20771

Further observations of the solar limb spectrum in the region 550-2000 A.

10 p1278 A73-24111

Properties of solar halos in the limb zone and at the terminator of Mars.

12 p1540 A73-27222

Solar limb Ca I Fraunhofer line polarization ray computation, considering radiation field anisotropy effects and depolarizing collisions in wings

12 p1544 A73-27811

Further evidence for a complex limb structure in the solar radial brightness distribution at mm wavelengths

12 p1545 A73-27811

Solar limb brightening at the 8-mm wavelength

16 p2057 A73-32777

Solar limb flare observations on 11 August 1972, examining temporal relationships of flash, spray, surge and loop phase

21 p2762 A73-41444

Airborne studies of the African eclipse.

22 p2911 A73-42811

SOLAR MAGNETIC FIELD

The origin of chains of type I bursts

01 p0092 A73-10933

Relative polarization of type III solar radio bursts 23.5 and 30 MHz.

01 p0093 A73-11333

Trapped gravity waves velocity oscillations in solar plages under magnetic field, comparing with Beerberg continuum atmosphere

01 p0108 A73-11333

A search of a connection between the polarization of Decam-type III bursts and magnetic fields in different heights of the solar atmosphere.

01 p0093 A73-11333

Solar active region growth in terms of magnetic flux emergence in shape of new arch filament system

03 p0367 A73-12911

The magnetic structure of arch filament systems.

03 p0378 A73-14411

Radio evidence of twisted bi-polar magnetic fields in the solar corona.

03 p0378 A73-14411

Magnetic fields in solar active regions.

04 p0490 A73-14811

Magnetograph instrumentation and measurement presenting solar magnetic field fine structure observations

04 p0496 A73-14811

Magnetic models of solar flares.

04 p0490 A73-14811

Monopole aspects of solar magnetic field at sunspot cycle maximum and minimum, considering different explanations

04 p0496 A73-14911

Sunspot temperature increase stimulation of supergranule motion leading to spot decay and magnetic field diurnal fluctuation development

04 p0503 A73-16011

Large-scale photospheric magnetic field - The distribution of active region fields.

05 p0620 A73-17011

Coronal holes during 12 November 1966 eclipses comparing distribution to calculated current-free coronal magnetic field

05 p0621 A73-17011

- The magnetic configuration of the November 18, 1968 loop prominence system. 05 p0621 A73-17043
- Magnetic fields and the vibrational motions of the solar photosphere 07 p0901 A73-20319
- Flares, magnetic configurations, and magnetic energy release. 08 p0996 A73-20764
- The energy spectrum of small-scale solar magnetic fields. 08 p1003 A73-20888
- Observations of the variation of temperature with latitude in the upper solar photosphere. II - Magnetic-field comparison, implications for solar-oblateness measurements, and harmonic analysis. 08 p1009 A73-21166
- Photomultiplier pairs arrays operation as solar magnetograph detector using fiber optics, comparing to photographic methods 08 p0970 A73-21737
- Two dimensional photon counting - A design based on the Aerospace-NASA videomagnetograph. 08 p0972 A73-21756
- Oppositely directed magnetic fields reconnection rate role in solar flares and small scale turbulent field reduction in photosphere 09 p1142 A73-22037
- Realization of a zero-force magnetic field configuration in the case of axisymmetric magnetohydrodynamic flows 09 p1146 A73-22541
- Origin of chains of type I solar radio bursts. 09 p1138 A73-22733
- Measurements of the magnetic field vector of a sunspot. 10 p1275 A73-23827
- On the small-scale structure of solar magnetic fields. 10 p1279 A73-24135
- The cooling of a sunspot. I - A Carnot cycle and the hydromagnetic interactions. II - Convection zone models and the magnetic power supply. 10 p1279 A73-24137
- Model solar atmosphere with quiet component involving supergranular velocity field in corona-chromosphere transition layer and vertical magnetic field. 10 p1279 A73-24140
- Thermal instability of coronal neutral sheets and the formation of quiescent prominences. 11 p1422 A73-25940
- Time variations in the X-ray emission of solar active regions. 11 p1412 A73-25944
- The solar wind and the temperature-density structure of the solar corona. 11 p1413 A73-25954
- Magnetic field effect on plage, prominence and sunspot flares, considering radio, UV and X ray emission. 11 p1413 A73-26208
- Photospheric convective network as a determining factor in sunspot and group development and stabilization. 11 p1426 A73-26574
- Magnetic fields and oscillatory motion in the solar photosphere. 12 p1540 A73-27291
- Solar magnetic sector structure - Relation to circulation of the earth's atmosphere. 12 p1491 A73-27441
- On the variation of the coronal lambda-5303 intensity relative to the interplanetary and solar magnetic sector structure, and to geomagnetic activity. 12 p1542 A73-27615
- Type IV bursts on August 4 and 7, 1972. 12 p1535 A73-27784
- Fine bright umbral spot structures from photographic line spectra observation of sunspot, noting magnetic field strength, outflow velocity and photospheric temperature. 12 p1545 A73-27834
- On the Aller's admixture radiation effect during the compression process in the solar corona and generation of coronal formations. 12 p1536 A73-27844
- Solar radio burst of 7 August 1972, discussing peak flux density, magnetic field intensity, energy distribution and polarization degree. 12 p1536 A73-27850
- Observation of linear polarization of the Crab nebula during an occultation by the solar corona. 13 p1586 A73-29247
- Permanent magnetization of lunar deep interior due to formation as gas sphere in solar magnetic field. 13 p1687 A73-29673
- Correspondence of solar field sector direction and polar cap geomagnetic field changes for 1965. 14 p1747 A73-29960
- Book - Vistas in astronomy. Volume 13. 15 p1932 A73-31302
- The general magnetic field on the sun and its changes with time. 15 p1932 A73-31304
- Recurrent magnetic storms in relation to the structure of solar and interplanetary magnetic fields. 15 p1868 A73-31384
- Equipment for recording and computer input of solar magnetograph data. 15 p1878 A73-32139
- The large-scale velocity field, the magnetic fields, and the brightness of the solar atmosphere. 16 p2057 A73-32701
- Restrictions on radial magnetic field and flow solutions for the solar wind. 16 p2053 A73-32967
- Development of moving type IV solar radio bursts and relation to expanding magnetic bottles from flare regions. 16 p2054 A73-33096
- Solar convective motions and associated magnetic fields, discussing photospheric cellular and chromospheric vertical motions, fibril structures, sunspot magnetic properties and faculae. 16 p2061 A73-33283
- Relation between coronal 5303-A intensity, recurrent geomagnetic storms, and solar sector structure. 20 p2553 A73-38960
- Solar magnetic field spatial structure in relation to solar activity phenomena, discussing measurements based on Zeeman effect in absorption line spectra formation. 20 p2605 A73-39059
- Magnetic fields of the sun and stars. 20 p2609 A73-39569
- Solar atmosphere and ionosphere phenomena in terms of conducting gas motion at magnetic field neutral points. 21 p2681 A73-40106
- Evaluation of the magnitude of the magnetic field in the solar corona from measurements of the linear polarization of solar radio bursts. 21 p2755 A73-40538
- Preferential acceleration of heavy nuclei on the sun. 21 p2756 A73-40582
- Particle emitting flares and the large-scale distribution of solar magnetic fields and green corona. 21 p2762 A73-41390
- MHD frequency wavelength relation to five-minute period oscillation in solar magnetically active regions. 21 p2777 A73-41483
- Possible mechanism of surge formation in the solar atmosphere. 21 p2777 A73-41493
- Representation method for force free magnetic field class, including current free fields and applications to solar fields. 21 p2779 A73-41536
- Analysis and synthesis of coronal and interplanetary energetic particle, plasma, and magnetic field observations over three solar rotations. 22 p2901 A73-41901
- Solar magnetic fields and their influence on the earth. 22 p2906 A73-41959
- The generation and dissipation of solar and galactic magnetic fields. 22 p2911 A73-42934
- Some statistical characteristics of active regions with the yellow coronal line. 22 p2915 A73-43037
- Strong magnetic fields occurrence in sunspot penumbras dark filaments related to hypothesis of penumbral convection rolls existence. 23 p3026 A73-43224
- Dependence of some noise-storm characteristics on the solar activity cycle. 23 p3036 A73-44249
- Observation of a possible neutral sheet in the corona. 24 p3136 A73-44636
- The topological association of H alpha structures and magnetic fields. 24 p3136 A73-44639
- Why Syrovatskii's mechanism of dynamic dissipation of magnetic fields does not work. 24 p3136 A73-44642
- A high resolution study in time, position, intensity, and frequency of the radio event of January 14, 1971. 24 p3136 A73-44643
- Interpretation of distinct type IVmA- and IVmubursts on the basis of micro-instabilities and of resonant nonlinear interaction of waves. 24 p3123 A73-44645
- SOLAR NEBULA**
U SOLAR CORONA
SOLAR NOISE
U SOLAR RADIO EMISSION
SOLAR OBLATENESS
Observations of the variation of temperature with latitude in the upper solar photosphere. II - Magnetic-field comparison, implications for solar-oblateness measurements, and harmonic analysis. 08 p1009 A73-21166
- Numerical computation of photosphere temperature-associated equatorial brightening in red and green bands used in solar oblateness measurements [AD-758969] 09 p1142 A73-22040
- Equator-pole temperature difference and the solar oblateness /Research note/. 12 p1544 A73-27831
- Photospheric faculae and the solar oblateness - A reply to 'Faculae and the solar oblateness' by R. H. Dicke. 19 p2488 A73-38520
- SOLAR OBSERVATORIES**
NT OSO
NT OSO-7
On the dependence of quietness and sharpness of solar image on local and large scale atmospheric circulation. 01 p0098 A73-10561
- High angular resolution solar observation from balloon borne instruments. 02 p0169 A73-12334
- Preliminary results of the third flight of the Soviet stratospheric solar observatory. 02 p0216 A73-12335
- Skylab instrumentation and solar observation objectives in coordinated program of correlative ground based, rocketborne and other spaceborne observations. 02 p0169 A73-12337
- Forecast facilities for solar events and activity and sudden ionospheric disturbances, noting forecast centers activity, resources and techniques. 04 p0491 A73-14840
- Identification and adjustment of psychological factors to improve solar patrol observing. 04 p0411 A73-14841
- Correction of solar observations for stray light by numerical integration, with application to Mercury's drop. 05 p0621 A73-17032
- Observing programs in solar physics during the 1973 ATM Skylab program. 10 p1278 A73-24126
- Solar observatories and satellite-borne instruments for solar coronal structure determination, considering 30 June 1973 eclipse and instrumented Concorde aircraft use. 22 p2916 A73-43117
- An 8-mm interferometer for solar radio astronomy at Bordeaux, France. 23 p2980 A73-43365
- The solar radio patrol network of the USAF and its application. 23 p2958 A73-43371
- SOLAR ORBITS**
NT APHELIONS
NT PERIHELIONS
Planetary orbits numerical relationships applied to artificial satellite orbits for earth gravity studies, expressing gravitational potential as latitude dependent spherical harmonics series. 01 p0040 A73-10875
- Characteristics of the quiet solar wind beyond the earth's orbit. 01 p0092 A73-11042
- Physical processes responsible for Bode law, noting sufficiency of point mass perturbations for existing distributions of satellite and planetary orbits. 02 p0211 A73-11874
- Brady trans-Plutonian planet existence rejection from dynamical considerations, noting disruption of coplanar configuration in outer solar system. 02 p0226 A73-12833
- Computation of Schwarzschild's periodic solutions in the restricted three-body problem. 02 p0226 A73-12838
- Trans-Plutonian planet calculations by Brady, discussing Halley, Olbert and Pons-Brook comet trajectories and perturbations and planet parameters. 03 p0370 A73-13199
- Motion stability of librational points in gravitational field of rotating triaxial ellipsoid, applying to planets of solar system. 03 p0376 A73-14266
- Trajectory analysis for swingby technique using Jovian gravitational field for leaving plane of ecliptic along heliocentric orbit and for solar flyby at specified distance. 03 p0378 A73-14552
- Stability of the solar system - Evidence from the asteroids. 04 p0497 A73-15179
- Resonances and encounters in the inner solar system. 04 p0500 A73-15519
- Normal matrix equations for major planet orbital element corrections from optical observations, testing by numerical experiment for Mercury. 09 p1143 A73-22096
- Metallic dust particles in quasi circular solar orbit, discussing evolution, thermal evaporation, atomization and size. 10 p1274 A73-23720
- Note on Brady's hypothetical trans-Plutonian planet. 10 p1275 A73-23847
- Position and velocity components for Jupiter VIII-XII. 11 p1429 A73-26684
- Resonances and librations of some Apollo and Amor asteroids with the Earth. 11 p1429 A73-26688

SOLAR PHYSICS

Structure and evolution of the asteroid belt.
12 p1540 A73-27296

The origin of Jupiter's family of comets.
13 p1672 A73-28037

Numerical integration of orbits for evolution of different configurations, discussing Titius-Bode law and stability limits of planetoid and hypothetical planet orbits
13 p1686 A73-29366

Evolution of cometary orbits on a cosmogenic time scale.
14 p1789 A73-29777

Comet orbit and ephemeris calculations with reference to position and magnitude to facilitate reobservation with long focus telescopes
14 p1789 A73-29782

On the application of Hansen's method of partial anomalies to the calculation of perturbations in cometary motions.
14 p1790 A73-29784

Standardization of the calculation of nearly parabolic cometary orbits.
14 p1790 A73-29795

Osculating orbital elements and nongravitational parameters for non-Newtonian orbit of periodic comet Borrelly
14 p1791 A73-29804

Hidalgo orbit near Saturn, discussing resemblance to extinct comet nucleus, nongravitational forces effects and planetary mass determination
14 p1792 A73-29812

Saturn mass determination from Hidalgo orbit trajectory and variational equation, obtaining probable error from fitted parabola
14 p1792 A73-29813

Splitting and sudden outbursts of comets as indicators of nongravitational effects.
14 p1793 A73-29819

New estimates of cometary disintegration times and the implications for diffusion theory.
14 p1794 A73-29829

Evolution of short-period cometary orbits due to close approaches to Jupiter.
14 p1794 A73-29832

The major planets as powerful transformers of cometary orbits.
14 p1794 A73-29834

Theoretical cometary radiants and the structure of meteor streams.
14 p1795 A73-29845

Isochronous derivatives of certain spacecraft-trajectory parameters
14 p1796 A73-29857

Book on Cartesian vortex theory of planetary motions covering celestial mechanics theories of Galileo, Kepler, Descartes, Leibniz and Newton
15 p1960 A73-32422

The effect of multiple encounters on short-period comet orbits.
17 p2226 A73-34291

Planetary accretion from grains in intersecting solar orbits, investigating velocity impact behavior of silicate particles
17 p2228 A73-34423

Monte Carlo model of cometary evolution based on hypothetical perturbed orbit calculations, with emphasis on short-period comets
17 p2228 A73-34426

Large-scale variations in the obliquity of Mars.
18 p2348 A73-35921

Planetary elements for 10 000 000 years.
18 p2352 A73-36418

Metallic dust particles in quasi-circular solar orbit, discussing evolution, thermal evaporation, atomization and size
18 p2355 A73-36745

New statistical laws governing the system of long-period comets
19 p2480 A73-37235

Scientific exploration with an out-of-ecliptic spacecraft.
19 p2485 A73-37760

A study of commensurable motion in the asteroid belt.
20 p2606 A73-39075

Minor planets and related objects. XIII - Long-term orbital evolution of /1685/ Toro.
20 p2607 A73-39123

Evolution of the orbits and radiants of meteor swarms of the Jupiter family
21 p2768 A73-40724

Planetary flybys resulting in heliocentric orbits normal to the ecliptic with fixed perihelia.
22 p2909 A73-42628

Determination of nongravitational forces in the motion of comets. I - Analysis of observation errors
22 p2910 A73-42643

Development of an H₂O atmosphere around Comet Kohoutek /1973/ and its possible detection.
23 p3033 A73-43955

Comet Kohoutek development predictions for various orbital locations, discussing brightness changes, tail production, nucleus ice melting by solar heating at perihelion, etc
23 p3033 A73-43956

Comet Kohoutek earth orbit properties and rocket and satellite observations, including parent molecule and inner solar system measurements
23 p3034 A73-44222

Influence of nongravitational effects on the evolution of dust particles moving along elliptic orbits around the sun
23 p3036 A73-44251

SOLAR PHYSICS

Absorption line shape computerized functional analysis in solar physics, deriving $H/\lambda, v$ function from Faddeyeva-Terentev probability
01 p0107 A73-11377

Neutrino archaeology - The simulation of double beta-decay by solar neutrinos.
03 p0344 A73-13293

Time dependent hydrodynamic models of solar wind, considering coronal electron density and temperature distribution and magnetic field
04 p0491 A73-14835

Interaction contributions to the solar proton-proton reaction.
05 p0612 A73-17339

Magnetic field effects on effective thermal conductivity of partially ionized plasmas, indicating neutral component role in solar magnetoplasma heat transport
08 p1001 A73-20755

Criticism of solar core mixing hypothesis of solar neutrino problem, discussing implications for semiconvection theory
08 p1012 A73-21532

Observing programs in solar physics during the 1973 ATM Skylab program.
10 p1278 A73-24126

The sun rotation and the Brans-Dicke cosmology.
14 p1798 A73-30140

A proposed correction to the solar abundances of carbon and oxygen utilizing new and accurate theoretical forbidden transition probabilities.
16 p2060 A73-32952

Internal structure of the convective shell of the sun
19 p2481 A73-37343

Astronomische Gesellschaft, Scientific Meeting, Vienna, Austria, September 18-23, 1972, Reports
20 p2605 A73-39056

Solar neutrinos. IV - Effect of radiative opacities on calculated neutrino fluxes.
20 p2602 A73-39427

Stability of the sun against spherical thermal perturbations.
20 p2608 A73-39428

Inhomogeneous structure of plasma near sun due to drift, slipping and anisotropic temperature distribution instabilities, noting association with radio astronomy observed fine structure
21 p2767 A73-40537

Preferential acceleration of heavy nuclei on the sun
21 p2756 A73-40582

A possible mechanism for acceleration of eruptive prominences
21 p2759 A73-40720

Space research XIII; Proceedings of the Fifteenth Plenary Meeting, Madrid, Spain, May 10-24, 1972. Volumes 1 & 2.
21 p2687 A73-41325

Nonthermal electromagnetic and thermal X ray sources of accelerated electrons during solar flares
21 p2761 A73-41384

Solar flare forecasting method developed and applied at Crimean observatory, using magnetic instability model for active regions
21 p2762 A73-41391

Statistical model for phase relations derived from observations of photospheric oscillations, criticizing horizontal propagation theory for phase propagation
21 p2777 A73-41482

Solar structure and evolution, calculating neutrino emission for Pleistocene glacial age caused by solar luminosity reduction
21 p2764 A73-41613

Solar activity forecasting, considering flare site identification from active center microscopic magnetic components, and particle acceleration observations
23 p3021 A73-43370

SOLAR PLASMA (RADIATION)

U SOLAR WIND

SOLAR POSITION

The albedo of snow in relation to the sun position.
01 p0038 A73-10392

Possible dependence of the differential shifts of Fraunhofer telluric lines on the solar zenith distance
01 p0106 A73-11241

Shallow-solar-zenith-angle control to topside ionospheric parameters.
04 p0445 A73-15636

A graph-analytical method for precalculation of the moments of solar transition through the field of view of electrooptical systems
05 p0575 A73-16313

Possible dependence of differential shifts of telluric Fraunhofer lines on zenith distance of the sun.
10 p1279 A73-24177

Brightness and polarization of the sky in the solar almucantar in the near infrared region of the spectrum
11 p1353 A73-25604

Distance to the subsolar point of the magnetospheric boundary for various magnetic activity indices
15 p1932 A73-31262

Atmosphere optical thickness determination from satellite and ground measurements of scattered light in solar vertical
15 p1905 A73-31822

On the motion of the tropical red arc north boundary.
16 p2008 A73-33882

Relationship between anomalous radio absorption and the solar zenith angle during periods of sudden ionospheric disturbances
19 p2406 A73-38322

Functional relation between the F₂-layer ionization state in daylight time and the zenith angle of the sun
20 p2555 A73-39172

Total ozone measurements in cloudy weather.
23 p2973 A73-43822

Stellar vortex formation in solar apex region in terms of retrograde motion and solar orbit characteristics
23 p3036 A73-44242

Thunderstorm excited cavity resonances between earth and ionosphere measured by solenoidal coil antenna, finding diurnal frequency variations related to solar and geomagnetic effects
24 p3088 A73-45222

SOLAR POWER GENERATION

U SOLAR GENERATORS

SOLAR POWER SOURCES

U SOLAR GENERATORS

SOLAR PROBES

Scientific mission and German and U.S. plans/design for Helios cooperative solar probe stressing advanced technology requirements
01 p0110 A73-11102

The development of the heat control system of the Helios solar probe
02 p0227 A73-11659

[DGLR PAPER 72-102] Helios solar probe structural adapter design for linking to booster rocket end stage, investigating orthotropic cylindrical shell carrying capacity
02 p0227 A73-11688

[DGLR PAPER 72-101] The onboard data processing system of the Helios probe
02 p0228 A73-11700

[DGLR PAPER 72-092] German-American cooperative solar probe project Helios, discussing design features, mission objectives and project development status
02 p0228 A73-11700

[DGLR PAPER 72-104] Solar cells and generator technology for the Helios solar probe.
03 p0256 A73-14222

Recent development results on the HELIOS S-band command receiver.
09 p1057 A73-23412

A single channel command detector for deep space missions.
09 p1057 A73-23412

A telecommunications link model for deep space. With applications to the HELIOS probe.
09 p1058 A73-23412

Temperature reducing solar cell arrangements for spin stabilized planetary and solar probes, analyzing thermal performance
11 p1313 A73-26662

German command station for Helios solar probe, discussing antenna design, transmitter parameters, back-up operation and compatibility with deep space network
13 p1598 A73-29272

[DFVLR-SONDDR-263] Precession damping of solar probes by radiatively forces.
21 p2737 A73-40726

SOLAR PROMINENCES

Radio spectrum analysis of loop prominence development, temperature and H atom density on May 13, 1971, noting consistency with Jefferies-Orrall model
01 p0108 A73-11382

Faint H alpha emissions in solar coronal prominences photographed through coronagraph and Lyot filter
01 p0108 A73-11382

Heliographic latitude distribution of pronounced prominences in both hemispheres of the sun during the eighteenth and nineteenth 11-year solar activity cycles
05 p0609 A73-16200

The magnetic configuration of the November 11, 1968 loop prominence system.
05 p0621 A73-17042

Extreme-ultraviolet emission from solar prominences.
05 p0612 A73-17332

Periodicities in the longitude distribution of sunspots.
08 p1001 A73-20742

Centimeter radiation associated with the solar limb prominence of 8 February 1972.
08 p0996 A73-20742

Temperature variations in coronal regions in the proximity of a prominence
08 p1007 A73-21062

Funnel prominences evolution and relation to solar active regions from H alpha filter observations
08 p0999 A73-21311

Eruptive, loop shaped prominences and rapid irreversible bursts relation to high energy particle concentrations
10 p1265 A73-23905

Thermal instability of coronal neutral sheets and the formation of quiescent prominences.
11 p1422 A73-25940

Solar corona streamers polarization, intensity and electron density and temperature during 22 September 1968 total eclipse
12 p1533 A73-26861

Isophotes comparison of quiescent and quasi-quiescent solar prominences in D3 and H alpha lines, noting structural similarity from narrow band filter observation
12 p1545 A73-27836

Solar prominences during period between sunspot minimum and maximum, investigating secondary polar zone coronal activity phase shift relationship to main zone anomaly
12 p1545 A73-27837

Some comments on the low intensity H alpha emission observed by J.-L. Leroy in the solar corona.
12 p1545 A73-27838

Dynamics and localization of surges in the chromosphere.
12 p1545 A73-27846

Spectrophotometry of prominences in the decay-preceding phase
13 p1670 A73-29095

Cavity-like instability observed in quiescent prominence from H alpha slit-yaw pictures shown with Ca ion 8542 A spectra
13 p1670 A73-29371

Temperature variations of coronal regions near a solar prominence.
18 p2355 A73-36868

A possible mechanism for acceleration of eruptive prominences
21 p2759 A73-40720

Spatial relationship between 5303-A and H alpha components of a loop prominence system.
24 p3123 A73-44640

SOLAR PROPULSION
NT **SOLAR ELECTRIC PROPULSION**
Trajectory of a solar-electric propelled vehicle passing through the shadow cone of a celestial body
21 p2779 A73-41556

SOLAR PROTONS
Spectral behaviour and proton effects of the type IV broad-band continua.
01 p0093 A73-11394

Flux and energy spectra of solar protons observed aboard the ESRO 2 satellite in 1968-1969.
02 p0206 A73-12316

Solar cosmic ray bursts in November-December 1970 according to data from Venus 7 space probe and Lunokhod 1 station.
02 p0206 A73-12321

North/south asymmetric entry of solar protons during the November 18, 1968 event.
03 p0360 A73-12878

Magnetospheric field fluctuations and the penetration of solar protons to low geomagnetic latitude.
03 p0360 A73-12891

Mechanisms for the injection of protons into the magnetosphere.
03 p0362 A73-13858

Auroral flux enhancements due to solar proton injection at medium energies during flares from ESRO 2 satellite measurements
03 p0362 A73-13859

Interplanetary anisotropy measurements of energetic solar proton entry into geomagnetic tail by ESRO 2 satellite
03 p0362 A73-13860

Prediction of proton flares and Forbush effects.
04 p0491 A73-14843

Quantitative short-term prediction of proton and nonproton flares.
04 p0491 A73-14844

Solar proton intensity structures in the magnetosphere during interplanetary anisotropies.
04 p0492 A73-14962

A solar-wind model including proton thermal anisotropy.
04 p0492 A73-15365

12.5-minute periodicity in solar proton fluxes at balloon altitude and in magnetic micropulsations.
04 p0492 A73-15527

Anisotropy of low-energy solar protons at the boundary of the magnetotail.
04 p0493 A73-15544

Electron density increase in the F region after proton bursts
05 p0609 A73-16257

Evidence for a two-component injection of cosmic rays from the solar flare of 1969, March 30.
05 p0610 A73-17046

ELF signal generation by solar protons observed via tape recording of north-south horizontal geomagnetic field variations in 3-75 Hz resonance range
05 p0571 A73-17064

Solar flare activity during August 1972, discussing sunspots filter- and spectrograms, proton emissions and geomagnetic disturbances
05 p0622 A73-17095

Directional measurements of the solar wind by the ESRO HEOS 1 probe, S 58-73
06 p0749 A73-17863

Propagation anisotropies of solar flare protons and electrons at low energies in interplanetary space.
07 p0869 A73-19227

Strong pitch angle diffusion and magnetospheric solar protons.
07 p0869 A73-19229

Solar proton flare prediction, examining diurnal rotation of axis connecting two stable spots and change in horizontal gradient of spots magnetic field
07 p0870 A73-19449

Solar energetic particles and wide-band continuum storms from metric to hectometric frequencies.
07 p0870 A73-19663

Numerical studies of the transport of solar protons in interplanetary space.
07 p0870 A73-19664

Np-237, U-236, and other actinides on the moon.
07 p0888 A73-19785

Ion acceleration in the current sheath of a solar flare
07 p0872 A73-20320

Detection of relativistic solar particles before the H alpha maximum of a solar flare.
08 p0996 A73-20666

Penetration of solar protons into the geomagnetic tail
08 p0998 A73-21276

Solar protons propagation from instantaneous injection source and inhomogeneities interaction description by mean free path and scattering angle specification
08 p0999 A73-21327

Nonadiabatic particle motion in the magnetosphere.
09 p1073 A73-22052

Low-energy solar protons in the pseudo-trapping region of the magnetosphere.
09 p1137 A73-22053

Observation of the entrance of solar protons in the magnetosphere at very high latitudes
10 p1211 A73-23769

Cosmic ray bursts in 1970-1971 according to measurements in the stratosphere
10 p1266 A73-23916

Solar proton energy spectra recorded in stratosphere during two solar cycles, approximating generation spectra by power law
10 p1266 A73-23917

Low energy solar proton events intensity increase near time of magnetic storm sudden commencement and Forbush decrease, using propagation shock wave model
10 p1268 A73-24146

First order approximation of collisionless protons expansion in quiet solar wind
10 p1269 A73-24651

Anisotropies in the interplanetary intensity of solar protons with energies greater than 0.3 MeV.
10 p1269 A73-24728

[AD-759099]
Energetic solar proton observations by Explorer 33 and 35 /interplanetary medium/ and Injun 5 /polar caps/, comparing proton fluxes in space and poles
10 p1269 A73-24729

Estimation of an upper limit for the solar neutron emission during large flares.
11 p1413 A73-25953

A charged-particle scintillation spectrometer with large geometric factor.
11 p1364 A73-25965

Daily variation of geomagnetic field at the Indian stations under the electrojet during the period of the July 1966 proton flare.
12 p1534 A73-26998

Ion acceleration in the current layer of a solar flare.
12 p1534 A73-27292

Selection of a propagation model for computing the solar-proton injection spectrum
12 p1534 A73-27333

Millimeter wave burst mean duration relation to PCA event intensity derived from relationship between impulsive single frequency microwave bursts and solar proton events
12 p1543 A73-27616

The first results of balloon measurements during the solar proton events in the period from August 2 to August 10, 1972
12 p1535 A73-27777

Characteristics of electron and high-energy proton flares.
12 p1536 A73-27849

Solar flare ejected protons intensity increase during July 1970 from Pioneer 6 and 8 and Explorer 41 data
14 p1786 A73-29859

On the generation of high-energy particles in solar flares.
15 p1925 A73-31068

Estimate of the probability of observing solar cosmic-ray proton fluxes at the earth orbit
15 p1926 A73-31877

French monograph - Interpretation of particle measurements carried out aboard rocket probes during the solar event of Jan. 28 1967.
15 p1927 A73-32586

Solar proton, helium, and medium nuclei /Z from 6 to 9/ observed from the IMP-VI satellite.
16 p2054 A73-33280

Directional diffusion coefficients of solar protons inside and outside the bow shock.
17 p2224 A73-34781

Experimental results on combined ultraviolet-proton excitation of moon rock luminescence.
17 p2233 A73-35273

Observations of the entry of solar protons into the magnetosphere by use of riometers.
18 p2344 A73-35930

Observation of trapped and solar particles since 2 October 1972.
18 p2344 A73-35931

Forecasting of proton flares.
18 p2344 A73-35974

Solar cosmic ray alpha particles and protons flux measurement after events in 1967-1969 for 1-10 MeV particles
18 p2347 A73-36289

Coronal propagation of low-energy solar protons.
18 p2347 A73-36290

Validity of CGL equations in solar wind problems.
18 p2347 A73-36291

Solar proton and galactic background radiation measurements project Cold Flare at SST cruising altitudes, using high altitude radiation instrument system /HARIS/
18 p2347 A73-36905

Energetic neutrons leaking from the top of the atmosphere.
19 p2474 A73-37299

Low-energy protons of solar origin and interplanetary medium studies
19 p2474 A73-37345

Penetration of solar protons into the geomagnetic tail.
19 p2476 A73-37905

Interplanetary gas. XVIII - Models and the mean free path of protons at 1 astronomical unit.
19 p2489 A73-38523

Propagation of protons injected near 1 AU in a medium with a constant transport length
21 p2756 A73-40583

Determination and interpretation of solar proton spectra at the earth and in the source
21 p2756 A73-40584

Solar proton measurements during August 1972 cosmic ray and magnetic field events caused by chromospheric flares associated with sunspots on east limb
21 p2757 A73-40592

Structural and dynamic features of solar cosmic-ray penetration into polar regions
21 p2758 A73-40606

Limit of the region of low-energy solar proton irruption into the polar ionosphere
21 p2758 A73-40607

Penetration of solar cosmic rays into the earth's polar caps
21 p2760 A73-40920

Uneven illumination of the polar caps by solar protons - Comparison of different particle entry models.
22 p2901 A73-41906

Midday recovery of HF absorption during PCA events relationship to satellite observation of solar proton latitudinal variations
22 p2846 A73-41943

Selection of a propagation model for calculating the injection spectrum of solar protons.
23 p3020 A73-43231

Higher order Compton-Getting anisotropies in particle population distribution function of low energy solar protons in interplanetary space
23 p3024 A73-43698

Solar wind proton thermal anisotropy association with moments of proton velocity distribution and dependence on temperature decrease
24 p3125 A73-45105

Role of the neutral sheet in the illumination of polar caps by solar protons.
24 p3086 A73-45132

SOLAR RADIATION

NT **SOLAR CORPUSCULAR RADIATION**
NT **SOLAR COSMIC RAYS**
NT **SOLAR ELECTRONS**
NT **SOLAR PROTONS**
NT **SOLAR RADIO BURSTS**
NT **SOLAR RADIO EMISSION**
NT **SOLAR WIND**
NT **SOLAR X-RAYS**
NT **SUNLIGHT**
NT **TYPE 2 BURSTS**
NT **TYPE 3 BURSTS**
NT **TYPE 4 BURSTS**
NT **TYPE 5 BURSTS**

- Inexpensive solar radiation measuring instruments comparison to standard solarimeter for mean and weekly errors
01 p0044 A73-10146
- Influence of haze layers upon remotely-sensed surface properties.
01 p0037 A73-10360
- Extraterrestrial solar flux attenuation and photodissociation cross sections effects on errors in photochemical kinetic model calculations
01 p0014 A73-10369
- Simultaneous measurements of solar radiation from aircraft and satellites during BOMEX.
01 p0038 A73-10377
- The effect of solar radiation reflected from the surfaces on airborne and surface measurements in the thermal infrared.
01 p0038 A73-10385
- Ionization sources of the ionospheric D and E regions.
01 p0041 A73-10886
- Highlights of the COSPAR Symposium on the solar eclipse of 7 March 1970.
01 p0101 A73-10911
- Prediction of strength of a polymer body with allowance for solar radiation
01 p0068 A73-11078
- Faint H alpha emissions in solar corona prominences photographed through coronagraph and Lyot filter
01 p0108 A73-11388
- Annual and sub-annual effects of EUV heating. I. - Harmonic analysis. II Comparison with density variations.
02 p0158 A73-11914
- Backscatter of solar resonance radiation. II.
02 p0205 A73-11917
- Molecular oxygen densities in atmosphere near 100 km from solar hydrogen Lyman alpha absorption measurements by Intercoms 4 satellite and Vertical 1 rocket
02 p0160 A73-12275
- Solar white light flares induced neutron and gamma ray emission, discussing acceleration mechanism through high energy proton bombardment induced photospheric heating
02 p0206 A73-12322
- Seasonal and monthly global atmosphere radiative profiles of thermal and solar heating due to ozone and cooling due to carbon dioxide
02 p0165 A73-12780
- On the formation of Saturn's rings.
02 p0225 A73-12805
- EUV emitting plasma structure of solar quiet and active atmospheres, noting extreme departures from LTE
03 p0363 A73-13952
- Solar UV Lyman alpha radiation intensity measurements, using Vertikal-1 rocket-borne photometer and photoelectron analyzer
03 p0379 A73-14565
- Solar cyclic intensity variation of excess radiation with respect to galactic radiation background at low altitudes from satellite data analysis
03 p0365 A73-14575
- Intensity and polarization of the solar light scattered by an isolated volume of interplanetary matter
03 p0380 A73-14611
- Vela 4 Lyman-alpha observations - Evidence for an aspherical hydrogen geocorona at 18 earth radii.
04 p0492 A73-15528
- Calculation of averaged values for short- and long-wave fluxes and influxes in a real atmosphere
05 p0593 A73-16243
- Solar luminance via light nuclei fusion into heavier nuclei with temperature gradient maintenance by gravity, relating to H-R diagram of different star clusters
05 p0614 A73-16302
- Uncertainties in determining the effective UV radiation at various altitudes.
[AIAA PAPER 73-102]
05 p0570 A73-16862
- Solar flares EUV observations by OSO 5 three band grating spectrophotometer, discussing flare intensity time dependence with superimposed impulsive bursts
05 p0610 A73-17044
- Annual fluctuation in atmospheric transmission of normal incidence solar radiation
05 p0611 A73-17183
- Solar radiation absorptivity control by metal film coatings, relating thermal control coatings for heat shielding
07 p0778 A73-19300
- Reflection and absorption of solar radiant energy by cloud layers.
07 p0820 A73-20344
- Solar gamma ray lines observed during the solar activity of August 2 to August 11, 1972.
08 p0996 A73-20665
- The Iarkovskii-Radzievskii effect and the evolution of condensations in a meteor stream
08 p1007 A73-21066
- Polarization of the total coronal emission during the solar eclipse of March 7, 1970
08 p1007 A73-21070
- Measurements of absorbed short-wave energy in a tropical atmosphere.
08 p0958 A73-21267
- Effects of changes in the atmosphere on solar insolation.
08 p0958 A73-21269
- Combined gravitational and solar radiation pressure effects on the semimajor axis of the earth's satellite.
08 p1010 A73-21314
- Interstellar gas role in cosmic ray yearly variations determined from solar short wave radiation induced gas ionization
08 p0999 A73-21338
- Nucleon and electromagnetic component generation, energy spectrum and diffusion during solar flares
08 p1000 A73-21349
- Direct measurement of water vapor absorption of solar radiation in the free atmosphere.
08 p0985 A73-21389
- Evidence for polarised radiation from the sun in the far infrared.
08 p1000 A73-21419
- Measurement of short- and longwave radiant fluxes from the Kosmos-320 satellite.
08 p0961 A73-21586
- Intensities and half-widths of lines in the A and B bands of the red atmospheric system of O2 bands
09 p1077 A73-22664
- Solar oscillatory phenomenon at 9.6 mm with atmospheric absorption effects minimized, discussing power spectra
09 p1149 A73-22962
- Distribution of diffuse solar radiation over regions of the sky for various regions of the spectrum in the absence of cloudiness
09 p1138 A73-22994
- Formation of neutron star spots and its connection with pulsars. II - Close similarities between radiation from the sun and pulsars.
10 p1275 A73-23829
- Apollo 14 lunar fines thermal radiation properties as function of bulk density, illumination angle and wavelength, calculating solar albedo and total emittance
10 p1277 A73-24080
- Solar radiation climate correlation with long term sunshine records, comparing radiation measurements with predictions based on regression equations for Brisbane area
10 p1269 A73-24450
- Broad band solar EUV absorption in the earth's upper atmosphere.
10 p1214 A73-24747
- Measurement of the absorption of solar ultraviolet radiation with the aid of a photoelectron analyzer
11 p1350 A73-25080
- Recombination coefficient, heat flux, ionization balance and photoelectron kinetic energy from ionospheric electron temperature and density profiles and solar UV absorption data
11 p1350 A73-25081
- Observations and theoretical reconstruction of the green flash.
11 p1351 A73-25168
- Solar activity variation of XUV emission segregation into quiet sun and active region components via correlations of sunspots with observed fluxes and intensities
11 p1415 A73-25173
- Aeros meteorological research satellite for F region aeronomic parameters and solar UV radiation measurements, discussing performance since launch
11 p1430 A73-25442
- Sky brightness in solar aureole region relationship to solar radiation single scattering on atmospheric aerosol particles
11 p1353 A73-25607
- On the solar Lyman alpha control of the ionospheric absorption at 2775 kHz.
11 p1412 A73-25770
- Ultra-violet argon dayglow lines in the atmosphere of Mercury.
11 p1421 A73-25916
- Extreme ultraviolet line intensities from the sun.
11 p1425 A73-26201
- The effect of direct solar radiation on the attitude of the SKYNET spacecraft.
11 p1431 A73-26261
- Transfer of solar irradiance through cirrus cloud layers.
11 p1357 A73-26345
- Investigations of atmospheric extinction using direct solar radiation measurements made with a multiple wavelength radiometer.
12 p1520 A73-26810
- Solar corona anomalous polarization degree and E vector vibration direction, interpreting discrepancy from Thomson scattering prediction by scattered electron velocity effects
12 p1545 A73-27845
- Book - Atmospheric optics. Volume 2.
13 p1680 A73-28513
- The cloud bright spot.
13 p1619 A73-29238
- New estimates of cometary disintegration times and the implications for diffusion theory.
14 p1794 A73-29829
- Solar Lyman alpha radiation scattering analysis to determine neutral hydrogen atom distribution in upper atmosphere
14 p1747 A73-29865
- Some limiting parameters of an optoelectronic device for determining the orientation of a spacecraft with respect to the sun
14 p1803 A73-29872
- The annual radiation balance of the earth-atmosphere system during 1969-70 from Nimbus 3 measurements.
14 p1750 A73-30762
- The effect of unmodulated sunlight on the integral voltage sensitivity of some radiation detectors.
14 p1754 A73-30954
- Short wave radiation flux calculation method for cloudless and cloudy atmospheres, computing geographic distribution of daily absorbed solar radiation
15 p1905 A73-31787
- Solar radiation fluxes at the earth's surface in the presence of cumulus clouds
15 p1905 A73-31794
- Transmission of solar radiation by stratified cloudiness as a function of the statistical characteristics of its structure
15 p1905 A73-31796
- Photometric device for an ISP-28 spectrograph in optical atmospheric studies
15 p1875 A73-31822
- Solar radiation pressure on Mariner 9 Mars orbiter from mathematical model of illuminance and reflectivity characteristics
16 p2052 A73-32906
- Manifestations and causes of atmospheric optical phenomena related to solar light dispersion and diffraction by particles, noting halos, polar auroras and mirages
16 p2002 A73-32949
- A biased model for calculating the evolution in solar absorptance.
16 p2060 A73-33128
- Trace gases, aerosols, and solar radiation in the stratosphere - Explored and unexplored problem areas.
[AIAA PAPER 73-509]
16 p2006 A73-33547
- The characteristics of the solar ultraviolet radiation at Arosa.
[AIAA PAPER 73-523]
16 p2056 A73-33558
- On the temperature of the Jovian thermosphere.
17 p2232 A73-34860
- Solar Lyman alpha control of the A3 ionospheric absorption on 2775 kHz.
18 p2288 A73-35948
- Photo-absorption of the upper atmosphere in the middle ultraviolet region.
18 p2308 A73-36050
- Nature of some optical effects observed on spacecraft at sunrise
18 p2309 A73-36122
- Neutron flux and energy spectra measurements in space related to theoretical predictions, discussing neutron leakage flux, solar neutron observations and radiation detector configurations
18 p2347 A73-36645
- Yarkovskii-Radzievskii effect and the evolution of meteor swarms.
18 p2355 A73-36867
- Polarization of the resultant emission of the corona during the solar eclipse of March 7, 1970.
18 p2355 A73-36871
- Extraterrestrial ultraviolet radiation and the parameter of the HI medium near the sun
20 p2601 A73-39074
- Solar brightness temperature measurement relative to lunar brightness temperature, noting agreement with HSRA model
20 p2610 A73-39582
- The arrival of solar radiation on variously oriented inclined surfaces
20 p2555 A73-39818
- Ocular hazard from viewing the sun unprotected and through various windows and filters.
21 p2698 A73-40143
- Neutral interstellar hydrogen and extraterrestrial Lyman alpha radiation.
21 p2773 A73-41396
- Solar pressure induced librations of spinning axisymmetric satellites.
22 p2910 A73-42633
- Instrumentation for remote sensing solar radiation from light aircraft.
22 p2864 A73-43161
- Angstrom pyroheliometer scale correction for ratio of incident circumsolar radiation to electric current heating power derived from nonuniform painted surface strip illumination
23 p3025 A73-43985
- Looking at the solar system in the far-ultraviolet.
23 p3034 A73-44220

Rocket-borne spectrometer measurement of solar UV flux for thermospheric vertical distribution of molecular oxygen 24 p3135 A73-44632

Thunderstorm excited cavity resonances between earth and ionosphere measured by solenoidal coil antenna, finding diurnal frequency variations related to solar and geomagnetic effects 24 p3088 A73-45211

SOLAR RADIATION OBSERVATION
U SOLAR RADIATION
SOLAR RADIATION SHIELDING
Prevention of damage to the science instruments of Mariner-Mars '71 spacecraft due to accidental viewing of the sun during sun-acquisition following exit from earth shadow. 24 p0696 A73-18829

SOLAR RADIO BURSTS
NT TYPE 2 BURSTS
NT TYPE 3 BURSTS
NT TYPE 4 BURSTS
NT TYPE 5 BURSTS
Radio emission from traveling disturbances in solar corona, considering contributions of interplanetary observations, plasma theory and ground observations 01 p0091 A73-10058
Monograph - A multi-channel solar radio spectrograph. 01 p0044 A73-10149
The origin of chains of type I bursts 01 p0092 A73-10938
Satellite-borne radio telescope observation of traveling solar radio bursts for energetic solar particle propagation in interplanetary space, discussing wind density and magnetic field 02 p0208 A73-12419
Free-free absorption of gyro-synchrotron radiation in solar microwave bursts. 04 p0492 A73-15366
Some studies on the solar microwave bursts in relation to the slowly varying component. 05 p0621 A73-17038
Meter-wavelength observations of the solar radio burst storm of August 17-22, 1968. 08 p0997 A73-20768
Origin of chains of type I solar radio bursts. 09 p1138 A73-22733
Spatial distributions of intensity and polarization over the source of microwave impulsive bursts. 10 p1275 A73-23828
Some studies on the association of solar optical flares and microwave bursts with sudden ionospheric disturbances. 11 p1354 A73-25769
Solar microwave burst radiation spectrum, explaining burst intensity decreasing phase by gyromagnetic absorption model 11 p1413 A73-25946
Detailed correlation of type III radio bursts with H alpha activity. I - Active region of 22 May 1970. 11 p1413 A73-25950
Observations on the time and frequency structure of solar decameter radio bursts. 11 p1413 A73-25951
Millimeter wave burst mean duration relation to PCA event intensity derived from relationship between impulsive single frequency microwave bursts and solar proton events 12 p1543 A73-27616
Type IV bursts on August 4 and 7, 1972 12 p1535 A73-27784
Solar radio bursts of 4 and 7 August 1972, deducing positron synchrotron process effects on radio spectrum from gamma ray measurements 12 p1535 A73-27785
Solar radio burst of 7 August 1972, discussing peak flux density, magnetic field intensity, energy distribution and polarization degree 12 p1536 A73-27850
High resolution space-time structure and centre-limb distribution of solar type I sources observed at 169 MHz. 13 p1671 A73-28032
Structure of a noise-storm source according to observations of the eclipse of September 22, 1968 at the 1.37-m wavelength 16 p2057 A73-32704
Radioheliograph observations of high-energy phenomena in the solar corona. 16 p2061 A73-33284
Evaluation of the magnitude of the magnetic field in the solar corona from measurements of the linear polarization of solar radio bursts 21 p2755 A73-40538
Solar U burst radio source spectrographic and polarization observations, using Waldmeier corona model for particle exciter in magnetic field 23 p3036 A73-42427
A high resolution study in time, position, intensity, and frequency of the radio event of January 14, 1971. 24 p3136 A73-44643
On the observation of linear polarization of solar microwave bursts. 24 p3136 A73-44644

A theory of the origin of the split pair burst emission from the solar corona. 24 p3123 A73-44646
Observations of Type I bursts at 169 MHz and coronal scattering. 24 p3140 A73-45182

SOLAR RADIO EMISSION
NT SOLAR RADIO BURSTS
NT TYPE 2 BURSTS
NT TYPE 3 BURSTS
NT TYPE 4 BURSTS
NT TYPE 5 BURSTS
On quasi-periodic components with periods from 30 to 60 min of amplitude fluctuations of X-band solar radio emission. 01 p0108 A73-11382
Solar radio emission measurement and interpretation, discussing source mapping, coronal density, magnetic field and flare and particle events predictions 04 p0496 A73-14830
Equipment for observation of fast fluctuations in the solar radio emission flux 05 p0573 A73-16269
Measurements of flux fluctuation in solar radio emission at a wavelength of 3 cm 05 p0573 A73-16270
Evidence for a two-component injection of cosmic rays from the solar flare of 1969, March 30. 05 p0610 A73-17046
Brightness distribution of the sun at 8.6 mm wavelength. 07 p0877 A73-19596
On the radio optical depth of the layer where the temperature equals the brightness temperature. 08 p1002 A73-20761
On the long-term behaviour of the circular polarization from coronal condensation radio emission at 4.3 cm wavelength. 08 p0997 A73-20769
On the S- and B-components of solar radio and X-emission and their relationships to energetic solar events. 08 p0997 A73-20771
Radiometer measurements of atmospheric attenuation at 19 and 37 GHz along sun-earth paths. 09 p1052 A73-22957
Culgoora /Australia/ solar radio observatory site, facilities, instrumentation and research activities 10 p1203 A73-24150
The radio diameter of the sun from interferometer measurements at 9 mm wavelength. 10 p1284 A73-24773
Polarization interferometer for 2800 MHz solar noise studies with a 0.5-min fan beam. 11 p1422 A73-25943
Quiet sun millimeter wave emission and brightness temperature, discussing observational difficulties arising from fog, cloud and rain attenuation 12 p1543 A73-27725
Solar microwave emission height determination from latitude shift, noting precision comparable with observation based on rate of motion in longitude 12 p1536 A73-27842
The correlation between 10.7-cm /2800 MHz/ solar radio emission and chromospheric flares 15 p1926 A73-31646
The possible nature of the fine structure of sporadic radio emission from the sun and other cosmic sources having a high density of electromagnetic radiation 15 p1926 A73-31876
Solar limb brightening at the 8-mm wavelength 16 p2057 A73-32705
Studies of the solar chromosphere from millimetre and sub-millimetre observations. I - Isophotometric mapping. 16 p2060 A73-32953
Absolute calibration of solar radio flux density in the microwave region. 16 p1993 A73-32968
High resolution radio observation of sun at 3.71 and 11.1 cm with three-element interferometer, noting flare near east limb 16 p2060 A73-33097
Radio emission from the moon and sun at the 2.25-mm wavelength and from Jupiter at the 2.1-mm wavelength 16 p2064 A73-33768
Radio emissions from solar flares. 17 p2224 A73-34723
Methods of measurements and some results of lower ionosphere by using VLF and LF radio waves. 18 p2302 A73-35926
A study of the time lag of the 27-day variation in the thermospheric density. 18 p2303 A73-35961
Search for solar recombination lines in the frequency range 110-115 GHz. 19 p2488 A73-38521
Circular polarized emission from solar active regions at millimeter wavelengths. 20 p2601 A73-39070
Solar radio frequency radiation characteristics, considering flare stars, pulsars, X ray sources, Antares

types, novae, red supergiants and stars with gas and dust envelopes 20 p2613 A73-39749
Observation of solar submillimeter-band emission at sea level with the aid of a Fourier spectrometer 21 p2760 A73-40731
Correlation and spectral analysis of daily solar radio flux. 21 p2762 A73-41494
Polarization inversions in the radio emission at 237 MHz of McMath zone 11482 /Research note/. 21 p2657 A73-41495
On the source of the slowly varying component at centimeter and millimeter wavelengths. 21 p2778 A73-41496
On the spectrum of the S- and B-components of solar radio emission at dm-wavelengths. 22 p2915 A73-43038
Computer controlled steerable array of multiple conical log spiral antennas for solar and discrete radio source studies 23 p2965 A73-43363
The solar radio patrol network of the USAF and its application. 23 p2958 A73-43371
Dependence of some noise-storm characteristics on the solar activity cycle 23 p3036 A73-44249
A study of solar radio emission in the light of Sengupta's model of coronal active regions. 24 p3123 A73-44637
The thermospheric heating function. III - The function describing the heating of the thermosphere by short-wave solar radiation during a period of high solar activity 24 p3084 A73-44800
Solar coronal radio spectra emitted by synchrotron process, computing radio wave suppression due to isotropic and anisotropic plasma 24 p3118 A73-45484

SOLAR RADIO WAVES
U SOLAR RADIO EMISSION
SOLAR ROTATION
Similarity theory of planetary atmosphere circulations applied to solar atmosphere in terms of radius and rotational Mach number 01 p0106 A73-11316
Photospheric height gradient and solar rotation measurements for Fraunhofer lines by magnetograph, considering telluric lines effect 01 p0107 A73-11376
Interplanetary gas. XVII - An astrometric determination of solar-wind velocities from orientations of ionic comet tails. 03 p0361 A73-12947
Hydrodynamics of the convective zone of the sun 03 p0373 A73-13608
On the sun's differential rotation and pole-equator temperature difference. 03 p0377 A73-14402
Solar rotation as measured in EUV chromospheric and coronal lines. 03 p0377 A73-14403
[AD-759854] Differential rotation in the solar atmosphere inferred from optical, radio, and interplanetary data. 03 p0377 A73-14404
On the dynamo action of the global convection in the solar convection zone. 05 p0627 A73-17387
Solar rotation as determined from OSO-4 EUV spectroheliograms. 10 p1278 A73-24127
Geomagnetic disturbance recurrence interval correlation with long term sunspots rotation period 12 p1494 A73-27771
Societa Astronomica Italiana, Meeting, 15th and Workshop on Rotation as a Phenomenon and Evolutionary Factor in the Universe, Universita degli Studi, Bologna, Italy, October 8, 9, 1971, Proceedings 14 p1797 A73-30138
Solar rotation angular velocity variation with heliographic latitude, depth and time, considering superficial circulation as cause of angular momentum transport 14 p1797 A73-30139
The sun rotation and the Brans-Dicke cosmology. 14 p1798 A73-30140
Space observations of the variability of solar irradiance in the near and far ultraviolet. 16 p2062 A73-33428
Low solar neutrino flux explained by evolution model emphasizing internal rotation effects on solar structure 19 p2488 A73-38519
Certain features of the 27-day variations in cosmic-ray anisotropy 21 p2758 A73-40599
Temperature difference between pole and equator of the sun. 21 p2776 A73-41479
Comparison of the sectorial structure of the interplanetary magnetic field and the occurrence of SC and SI events. 22 p2908 A73-42447

Space-time limits of stable oscillations of solar surface active zones spanning multiple solar rotations, noting correlation coefficients for north and south hemispheres

24 p3138 A73-45013

SOLAR SAILS

Derivation of an approximate solution to the equation of geocentric motion of a space vehicle with a solar sail

19 p2492 A73-37849

SOLAR SENSORS

Sun, earth and star attitude sensors for spacecraft, describing design, analysis and hardware aspects in terms of critical parameters

01 p0053 A73-11170

Digital attitude sun sensor for ionosphere sounding satellite.

01 p0053 A73-11171

Spacecraft control hardware for use with digital processors.

04 p0424 A73-14737

An amplitude-type position sensor for an optical sun-tracking system

06 p0692 A73-17766

Optical instrumentation for satellite attitude control, solar direction and earth magnetic field sensors, thermal detection, star tracking and Lunokhod I laser reflector

07 p0821 A73-18979

Solar, stellar and IR sensors, discussing structural, optical and electronic design features, operational requirements and performance specifications

07 p0821 A73-18984

Sun sensors for D-2B scientific satellite spin axis alignment and attitude stabilization with pointing control accuracy, discussing tests, compensatory tracking and solar simulation

07 p0821 A73-18986

Passive solar array orientation devices for terrestrial application.

09 p1033 A73-22440

The fine solar sensor of the Astronomical Netherlands Satellite.

16 p2012 A73-32852

An integrated-circuit solar aspect sensor for spacecraft use.

16 p2013 A73-32884

Digital attitude reference system for three-axis-stabilized earth oriented satellites, using gyrocompasses with solar and horizon sensors

17 p2209 A73-34875

The fine sun sensor of the astronomical Netherlands satellite.

19 p2431 A73-38100

Application of silicon photoelectric converters in solar orientation sensors

20 p2510 A73-39449

Airborne IR spectrometer with solar sensor for stratospheric minor molecular constituents vertical distribution, indicating spectral resolution for vibrational-rotational absorption bands

22 p2847 A73-42221

Fluidic bolometer type sensor for reaction wheel control to maintain spacecraft and rocket vehicle attitude relative to sun, discussing design, simulation and tests

23 p3038 A73-43395

SOLAR SIMULATORS

Design and performance of solar simulator with water cooled Xe lamp, calculating irradiance distribution by ray tracing method

01 p0030 A73-11149

The Toulouse centre's space environment simulator - 'The sun.'

07 p0807 A73-19002

The space environment simulation chamber of the Toulouse space center

07 p0808 A73-20245

Lens projection system for a solar simulator providing irradiance of 100 solar constants.

08 p0952 A73-21042

Determination of the temperature of a sample undergoing pulsed irradiation by sunlight

15 p1896 A73-30997

Ocular hazard from viewing the sun unprotected and through various windows and filters.

21 p2698 A73-40143

SOLAR SPECTRA

Flare spectrum in region accessible to ground based optical solar spectrographs, considering Balmer line broadening, electron density, optical thickness, LTE, electron temperature, etc

01 p0091 A73-10052

Optical, far UV and radio spectra observations and results for solar spicules, considering morphology, spectroscopic properties and dynamic models

01 p0094 A73-10055

Nonthermal X-radiation and electric currents in solar flares

01 p0092 A73-10937

Possible dependence of the differential shifts of Fraunhofer telluric lines on the solar zenith distance

01 p0106 A73-11241

Photospheric height gradient and solar rotation measurements for Fraunhofer lines by magnetograph, considering telluric lines effect

01 p0107 A73-11376

The empirical determination of line source functions, beta-L-values, and the microturbulent and convective velocity components as functions of depth in the photosphere-chromosphere transition region.

01 p0107 A73-11378

Photospheric network properties and transition to sunspot of solar bright points in 3840 A and H alpha, comparing with Ellerman bomb

01 p0108 A73-11384

Physical properties of solar chromospheric plages. I - Line profiles of the CaII H, K, and infrared triplet lines.

01 p0108 A73-11385

Spectral behaviour and proton effects of the type IV broad-band continua.

01 p0093 A73-11394

Solar UV spectra with high angular resolution from rocket observations, obtaining center to limb intensity variations

02 p0207 A73-12325

High angular resolution observations from rockets - Solar XUV observations.

02 p0216 A73-12336

Statistics on the solar spectrum suitable for the study of the blanketing effect in stars of spectral types F, G and K.

03 p0373 A73-13360

The spectrum of FeH - Laboratory and solar identification.

03 p0374 A73-13718

The coronal X-spectrum - Problems and prospects.

03 p0363 A73-13954

Solar rotation as measured in EUV chromospheric and coronal lines.

[AD-759854]

03 p0377 A73-14403

Neutral Mg line at 4571 A in solar atmosphere, computing line profiles from Harvard-Smithsonian Reference Atmosphere and Bilderberg Continuum Atmosphere

03 p0377 A73-14405

The interpretation of absorption-line shifts in the solar spectrum.

03 p0377 A73-14407

Observations of the intensity of the penumbra of sunspots.

03 p0377 A73-14409

Depth profiles of Fe I 5250 A line for three sunspot models, noting line-to-continuous absorption ratio relation to emergent intensity location

03 p0377 A73-14410

On the minimum intensity of the Na D2-5890 A line in sunspot umbra /Research note/.

03 p0377 A73-14411

Solar spectra line intensities in band 201 of visible and near IR regions, noting water vapor bands presence in sunspot spectra

03 p0377 A73-14412

Moustaches in solar H alpha filtergrams and spectra, studying relations to photospheric and chromospheric phenomena

03 p0378 A73-14413

Umbral spectra absorption line feature observation by photoelectric spectroscopy, suggesting Ti abundance in solar atmosphere

03 p0378 A73-14423

Heliographic and spectroscopic observations of solar southern hemisphere active region during August 1971 cycle, noting photospheric changes, sunspots and flares

03 p0379 A73-14581

X-ray line emission associated with solar flares.

04 p0490 A73-14832

Dielectronic satellite spectra for highly-charged helium-like ion lines.

04 p0500 A73-15490

Effects of uncertainties in damping and microturbulence on theoretical deductions from solar equivalent widths.

04 p0500 A73-15491

Investigation of the chromosphere in the D3 helium line at the eclipse of September 22, 1968.

04 p0503 A73-16014

Behavior of carbon monoxide in the upper photosphere.

04 p0504 A73-16027

New results of solar X-ray flare studied

05 p0609 A73-16372

Solar Rb isotopic ratio from Rb I resonance lines at 7800 and 7947 A in photospheric spectrum

05 p0620 A73-17026

A search for the solar Sr-87 content and the solar Rb/Sr ratio.

05 p0620 A73-17027

Spectroheliogram SNR improvement via time averaging of 6103 A core sequence, considering sunspot evolution observed by time lapse technique

05 p0621 A73-17030

Equator-pole differences in the solar chromosphere from Lyman-continuum data.

05 p0621 A73-17033

On emission lines of hydrogen, helium and ionized calcium seen on a coronal spectrogram of the March 7, 1970 eclipse.

05 p0621 A73-17036

The absence of flares in 3835 A and the heating of the chromosphere.

05 p0610 A73-17040

Extreme-ultraviolet emission from solar prominences.

05 p0612 A73-17337

Analysis of the extreme-ultraviolet quiet solar spectrum.

05 p0625 A73-17338

The damping of the NaD lines in the solar spectrum by atomic hydrogen.

06 p0753 A73-18239

Solar cosmic rays spectrum and geomagnetic cut-off rigidity determination from ion production rates in lower ionosphere

07 p0870 A73-19427

Solar gamma ray lines observed during the solar activity of August 2 to August 11, 1972.

08 p0996 A73-20665

The spectra of near-vertical structures on the solar disk.

08 p1001 A73-20752

Observations of sunspot umbral velocity oscillations.

08 p1001 A73-20758

Measurements of the solar spectrum between 30 and 128 A.

[AD-757958]

08 p1002 A73-20760

Magnesium II doublet profiles of chromospheric inhomogeneities at the center of the solar disk.

08 p1004 A73-20908

The heating of the solar corona. I - Observation of ion energies in the transition zone.

08 p1005 A73-20919

The extreme-ultraviolet spectrum of Fe XV in a solar flare.

09 p1137 A73-22039

Nonthermal X rays and electric currents in solar flares.

09 p1138 A73-22732

Intermediate-coupling line strengths in the iron spectrum and the solar abundance of iron.

10 p1272 A73-23540

Quasi-periodic /wave/ motions in the solar photosphere. I - Preliminary results

10 p1274 A73-23718

Further observations of the solar limb spectrum in the region 550-2000 A.

10 p1278 A73-24128

High resolution spectroscopic analysis for photospheric Eu II lines with spectrum synthesis techniques, determining solar isotopic composition and abundance

10 p1278 A73-24129

Solar Mn abundance derivation based on center-limb absorption line profiles, taking into account hyperfine structure broadening

10 p1278 A73-24130

Cross correlation coefficients for H, K and H beta lines of solar spectrum related to observed peculiarities from microphotometer intensity traces

[AD-759889]

10 p1278 A73-24131

Suggested interpretation of the correlations in intensity fluctuations in the lines Ca II H and K, magnesium b, and hydrogen H beta /Research note/.

10 p1278 A73-24132

A subtractive double pass spectrograph for solar observations.

10 p1218 A73-24149

Possible dependence of differential shifts of telluric Fraunhofer lines on zenith distance of the sun.

10 p1279 A73-24177

Solar Lyman alpha changes and related hydrogen density distribution at the earth's exobase /1969-1970/.

10 p1269 A73-24736

Solar Fraunhofer spectral lines having simple Zeeman triplet splitting with large Lande g-factors tabulated, noting missing lines in identification

11 p1421 A73-25932

The absorption spectrum of atmospheric water vapor in the vicinity of the He 10830 A triplet.

11 p1421 A73-25933

Solar disk emission lines in Ca II H and K line wings from high resolution spectral observations

11 p1422 A73-25934

Sunspot umbral intensity measurements at IR and visual wavelengths, discussing correction methods for earth atmosphere and instrument induced stray light

11 p1422 A73-25937

Polarization measurements in the green coronal line.

11 p1428 A73-26623

Polarization of the emission from the solar corona in the 5303 A line

12 p1538 A73-26859

Solar limb Ca I Fraunhofer line polarization rate computation, considering radiation field anisotropy effects and depolarizing collisions in wings

12 p1544 A73-27826

Fraunhofer line data reduction and wavelengths identification in solar UV spectra recorded during flight of Skylark rocket SL 601

12 p1544 A73-27827

Solar surface photospheric oscillation spatiotemporal power spectrum observation, considering long-period oscillation correlation with chromospheric flare 12 p1544 A73-27828

Spectral investigation of the chromosphere. II. 12 p1544 A73-27829

Temporal intensity fluctuation measurements in K line wing near solar disk center, noting power spectrum peaks and brightness relationship to Fe I line displacement 12 p1544 A73-27830

Solar pole-equator temperature distribution in high photosphere layers from Mg spectral line observations 12 p1544 A73-27832

Fine bright umbral spot structures from photographic line spectra observation of sunspot, noting magnetic field strength, outflow velocity and photospheric temperature 12 p1545 A73-27834

Emission core widths of K Ca II line in umbra and penumbra of sunspots near solar disk center, noting relationship to stellar luminosity 12 p1545 A73-27835

Isophotes comparison of quiescent and quasi-quiescent solar prominences in D3 and H alpha lines, noting structural similarity from narrow band filter observation 12 p1545 A73-27836

A recalibration of the quiet sun millimeter spectrum based on the moon as an absolute radiometric standard. 12 p1545 A73-27840

Dynamics and localization of surges in the chromosphere. 12 p1545 A73-27846

Large sunspot high dispersion line spectrum at 6610-6770 Å, noting umbral/photospheric contrast and drift curves across limb from photographic recording 12 p1547 A73-27925

Theory of a photometer/actinometer/ measuring the brightness of a fixed annular zone of sky around the sun. 13 p1613 A73-28519

Influence of a traveling acoustic wave on spectral line profiles. II - Asymmetry of weak Fraunhofer lines 13 p1683 A73-29092

Spectrophotometry of prominences in the decay-preceding phase 13 p1670 A73-29095

Excitation of the Fe XIII spectrum in the solar corona. 13 p1684 A73-29353

Fe XVII emission from the solar corona. 13 p1685 A73-29356

New observations of Fe XVII in the solar X-ray spectrum. 13 p1685 A73-29357

Photometric analysis of monochromatic photographs of the solar corona taken in the green line [5303 Å] and the red line [6374 Å]. 13 p1685 A73-29363

Coronal densities and temperatures derived from monochromatic images in the red and green lines. 13 p1685 A73-29364

Cavity-like instability observed in quiescent prominence from H alpha slit-yaw pictures shown with Ca ion 8542 Å spectra 13 p1670 A73-29371

An analysis of the solar extreme-ultraviolet spectrum between 50 and 300 Å. 14 p1801 A73-30742

The extreme-ultraviolet spectrum of a solar active region. 15 p1936 A73-31560

Rocket flight observations of solar UV chromosphere at 1190-1320 Å, considering spectral and angular resolutions 15 p1936 A73-31564

Metallic lines in the solar flare of July 12, 1961 and properties of the corresponding emission regions 15 p1938 A73-31957

Determination of damping constants and turbulent speed in the solar photosphere by the Voigt method 15 p1938 A73-31958

Visible solar disk contrasts in radiation controlled line, noting role of lateral differences in local shapes of line absorption profile 16 p2059 A73-32951

A proposed correction to the solar abundances of carbon and oxygen utilizing new and accurate theoretical forbidden transition probabilities. 16 p2060 A73-32952

Studies of the solar chromosphere from millimetre and sub-millimetre observations. I - Isophotometric mapping. 16 p2060 A73-32953

Observations of the inner F and K coronas below 2220-Å wavelength. 16 p2060 A73-32954

Spectral analysis of sunspot flares. 16 p2052 A73-32957

Spectra of solar flares from 8.5 Å to 16 Å. 16 p2053 A73-32960

Properties of the satellite photoelectron sheath derived from photoemission laboratory measurements. 16 p2062 A73-33435

Some results of lunar surface luminescence studies at the Kharkov Astronomical Observatory 16 p2063 A73-33762

Fine structure in the sunspot spectrum - 2 to 70 years. 17 p2230 A73-34514

Solar absorption in the CO fundamental region. 17 p2231 A73-34761

Forecasting of proton flares. 18 p2344 A73-35974

Gamma ray and neutron measurements and their relation to the solar flare problem. 18 p2345 A73-36126

Quasiperiodic/wavelike/ motions in the solar photosphere. I - Preliminary results. 18 p2355 A73-36743

Models of the chromospheric-coronal transition layer and lower corona derived from extreme-ultraviolet observations. 18 p2357 A73-37107

Observation of the absolute intensity and the centre-to-limb variations of the sun in the vacuum ultraviolet region. 19 p2482 A73-37376

Arizona-NASA Atlas of the Infrared Solar Spectrum. X. 19 p2483 A73-37576

Lines of Fe XVII and Fe XVIII during a solar flare. 19 p2476 A73-38170

Search for solar recombination lines in the frequency range 110-115 GHz. 19 p2488 A73-38521

Relation between coronal 5303-Å intensity, recurrent geomagnetic storms, and solar sector structure. 20 p2553 A73-38960

Optical heterodyne radiometry of the solar surface. 20 p2611 A73-39591

Determination and interpretation of solar proton spectra at the earth and in the source 21 p2756 A73-40584

Russian book - The solar constant and the energy distribution in the solar spectrum. 21 p2769 A73-40804

Observations of the X-ray emission of solar active regions on 28 November 1970 and 20 August 1971. 21 p2761 A73-41387

First observations of the granulation at 1.65 microns, center to limb variation of the contrast. 21 p2776 A73-41476

Studies of granular velocities. III - The influence of finite spectral and spatial resolution upon the measurement of granular Doppler shifts. 21 p2776 A73-41478

Microturbulence and the effect of departures from LTE on photospheric iron lines. 21 p2777 A73-41481

Solar spicule morphology, observing diameter, height, expansion and threshold intensity with H alpha filtergrams 21 p2777 A73-41484

Relative sunspot number periodicities determination, using power spectral analysis 21 p2777 A73-41489

Correlation and spectral analysis of daily solar radio flux. 21 p2762 A73-41494

Carbon, CN, CH, MgH, NH and OH line behavior in solar photospheric spectra 21 p2778 A73-41528

Further observations of the structure of the chromosphere-corona transition region from limb and disk intensities. 21 p2779 A73-41537

Structure of the solar chromosphere. I - Basic computations and summary of the results. 22 p2905 A73-41762

Aeronomical consequences of solar flux variations between 2000 and 1325 angstroms. 22 p2902 A73-41931

The inversion of the mean and spatially resolved sodium D2 line profiles from the sun. 22 p2908 A73-42311

Pitfalls of configuration interaction - Transition probabilities in Fe XIII. 22 p2908 A73-42312

A high-resolution Fourier-transform infrared spectrometer. 22 p2861 A73-42587

Spectral characteristics of solar corona measured by visual, rocket and satellite observation, discussing K and F coronal regions, eclipse phenomena and analysis techniques 22 p2910 A73-42650

Airborne studies of the African eclipse. 22 p2911 A73-42871

Ionised molecules in BCA photospheric model. 22 p2915 A73-43039

Vertical phase variation and mechanical flux in the solar 5-minute oscillation. 22 p2916 A73-43124

High resolution analysis of the sun's radiation received at the ground from 9 to 11.6 microns. 23 p3003 A73-43888

Background concentrations of photochemically active trace constituents in the stratosphere and upper troposphere. 23 p2976 A73-43889

Atmospheric water vapor concentration in upper stratosphere above tropopause from balloon observations of solar IR absorption spectra 23 p2976 A73-43890

Electron temperature of regions of the formation of recombinational continua on the sun - Temperature of the carbon emission regions 23 p3036 A73-44246

Origination of Type-IV decimetric bursts in the solar corona 23 p3036 A73-44248

Temperature and oxygen abundance determination in the sun from the oxygen lines 23 p3037 A73-44257

Metal lines in the solar flare of July 12, 1961, and the properties of the emission region. 24 p3132 A73-44482

Damping constants and turbulence velocities in the solar photosphere determined by the Voigt method. 24 p3132 A73-44483

Neutral Fe line profiles for low-lying transitions measured from solar disk center to limb by double pass spectrometer, considering limb darkening effect 24 p3135 A73-44626

Solar abundance of Th and Pb based on photospheric line spectrum analysis for comparison with chondritic composition data 24 p3135 A73-44627

SOLAR SPECTROMETERS

Monograph - A multi-channel solar radio spectrograph. 01 p0044 A73-10149

Fourier spectrometer design for high resolution solar optical spectra, emphasizing short scan time 01 p0049 A73-10534

A solar radio spectrograph with high time resolution. 05 p0621 A73-17039

Radio spectrographs operating at wavelengths between 0.3 and 3 m 08 p0969 A73-21714

A subtractive double pass spectrograph for solar observations. 10 p1218 A73-24149

High resolution rocket EUV solar spectrograph. 11 p1360 A73-25059

Use of the Fabry-Perot etalon to study absorption spectra of the atmosphere 11 p1363 A73-25613

Far infrared broad band interferometry. 11 p1369 A73-26518

A broadband antenna and multiplexer system in the decimeter-wave range for solar radio astronomy 12 p1481 A73-27782

Analysis of solar flare X-ray radiation with Bragg spectrometers. 18 p2344 A73-36014

First results of the solar hard X-ray spectrometer on board the ESRO TD-1 A satellite. 21 p2761 A73-41386

Spectroscopic investigation of the chromosphere. III - H-alpha line profile from the interior of supergranular cells. 21 p2777 A73-41485

Multidirectional scanning of active regions with a slit-jaw spectrograph and a solar chromatograph. I - Description of the method and some preliminary results for the flare event of August 4th 1972. 21 p2777 A73-41491

Crystal spectrometry of active regions on the sun. 21 p2706 A73-41602

Monograph - Development and performance of a solar hard X-ray spectrometer. 22 p2861 A73-42674

Ozone related spectral measurements of total solar radiation. 23 p2975 A73-43882

SOLAR STORMS

Radio evidence of twisted bi-polar magnetic fields in the solar corona. 03 p0378 A73-14417

Record-breaking cosmic ray storm stemming from solar activity in August 1972. 08 p0996 A73-20664

Meter-wavelength observations of the solar radio burst storm of August 17-22, 1968. 08 p0997 A73-20768

Complex studies of the disturbance of March 8, 1970 from observations in the midnight sector 12 p1490 A73-27342

Discontinuous change in earth's spin rate following great solar storm of August 1972. 14 p1800 A73-30602

Structure of a noise-storm source according to observations of the eclipse of September 22, 1968 at the 1.37-m wavelength 16 p2057 A73-32704

Criticism of Gribbin and Plagemann findings on universal time observations as evidence of day length and earth rotation rate changes due to 1972 solar storm
21 p2766 A73-40375

SOLAR STREAMS U SOLAR CORPUSCULAR RADIATION SOLAR SYSTEM

Gravitational constant anisotropy effects on planets with orbits close to ecliptic in solar system two body problem
01 p0099 A73-10689

Lunar motion numerical analysis, discussing flaws due to inadequate solar system model and arithmetic-algebraic procedural deficiencies
01 p0099 A73-10694

Solar system origin and variable gravitational constant theory from earth history viewpoint
01 p0101 A73-10874

Solar system origin and evolution theory, describing planets and satellites condensation from embryo grains captured in particle streams
01 p0109 A73-11481

Evidence for objects of lunar mass in the early solar system and for capture as a general process for the origin of satellites.
02 p0217 A73-12394

Lunar surface cratering history from Apollo rock age data, implying earth-moon and solar system evolution mechanism
02 p0217 A73-12406

The meteoroid influx and the maintenance of the solar system dust cloud.
03 p0365 A73-12889

Moon and solar system origin in view of chemical evidence and Apollo lunar rock RB-87/SR-87 ages and remelting conditions
03 p0370 A73-13111

Solar-planetary system mechanical parameters determination based on astronomical unit, discussing conversion into terrestrial units via radar distance measurements
03 p0376 A73-14174

The internal structure of planetary bodies.
04 p0495 A73-14772

Stability of the solar system - Evidence from the asteroids.
04 p0497 A73-15179

Gravitation theory - Empirical status from solar system experiments.
04 p0498 A73-15249

Resonances and encounters in the inner solar system.
04 p0500 A73-15519

Orbital eccentricity of Mercury and the origin of the moon.
04 p0501 A73-15625

Russian monograph on relativistic celestial mechanics covering celestial and solar system bodies motion, Riemann geometry, tensor analysis, N body problem and cosmology
04 p0502 A73-15969

Book - Evolution of the protoplanetary cloud and formation of the earth and the planets.
05 p0615 A73-16356

Natural remanent magnetizations of carbonaceous chondrites and the magnetic field in the early solar system.
05 p0619 A73-16839

Solar system planets spin rate change and core growth, discussing Mars geology and earth evolution
06 p0749 A73-18006

Inner planets of the solar system - A comparative study.
06 p0749 A73-18007

Exploring the origin of the solar system by space missions to asteroids.
06 p0750 A73-18025

In-depth exploration of the solar system and its utilization for the benefit of Earth.
06 p0751 A73-18029

Solar system other planets suitability for terrestrial organisms, noting life forms possible existence on Venus, Mars and Jupiter
06 p0654 A73-18349

Book - The Titius-Bode Law of planetary distances: Its history and theory.
06 p0753 A73-18403

Potential atmospheric composition of smaller bodies in the solar system and some aspects of planetary evolution.
07 p0875 A73-19249

Trigonometric series for earth rotation velocity around solar system center of mass
07 p0902 A73-20325

Definitive orbit of the comet 1937 V Finsler.
08 p1012 A73-21580

On the accretion mechanism for the formation of a protoplanetary disc.
09 p1143 A73-22110

Planetary atmospheres
09 p1152 A73-23471

Solar system planets and satellites fundamental properties, considering observational uncertainty in masses and dimensions
11 p1419 A73-25878

Critique of Anderson hypothesis of moon origin by condensation of material off median plane of initial solar nebula
11 p1428 A73-26664

Bode law rationalization based on Dole computer-generated planetary system with constant spacing ratio generated by random number sequence and accretion process closeness constraints
11 p1428 A73-26665

Vortex motions of cosmic matter as cosmological evolution mechanism, considering galactic and solar system kinetics
13 p1681 A73-28780

Lunar origin and composition relationship to solar system evolution, discussing various theories and evidence from Apollo flights
13 p1687 A73-29665

A library of standard programmes for constructing numerical theories for studying the motion and evolution of the orbits of the minor bodies of the solar system.
14 p1790 A73-29789

Comets and cometesimals formation from icy material during solar system evolution from collapsing dust and gas cloud
14 p1794 A73-29835

On the origin of comets and their importance for the cosmogony of the solar system.
14 p1794 A73-29836

The origin and evolution of the comets and other small bodies in the solar system.
14 p1794 A73-29837

Comets origin in interstellar space or solar system evaluated with reference to comet streaming from perihelions statistical analysis, assuming Oort cloud accretion
14 p1794 A73-29838

A strategy for investigation of the outer solar system - Outer planets, their satellites, and particles and fields at great distances from the sun.
14 p1799 A73-30526

Outer planet formation from gaseous solar nebula with absence of magnetic effects, discussing gravitational instabilities, gas capture onto planetary core and model construction
14 p1799 A73-30528

Outer solar system planetary and subplanetary objects magnetic field existence, discussing internal dynamo fields, externally driven dynamos and fossil fields
14 p1800 A73-30540

Outer solar system, including planetary atmospheres, natural satellites, solar wind, interstellar cosmic rays and spacecraft missions
14 p1800 A73-30616

Solar system evolution and planets configuration regularity and geometrical shape considerations in terms of tidal dissipation, stray body collision and close approach
15 p1937 A73-31776

Numerical experiments by Monte Carlo method to examine comet orbits evolution within solar system, noting Trojan, horseshoe and Jupiter-Saturn midrange orbits
15 p1938 A73-31949

Solar system elemental abundance from chondritic meteorites, solar atmosphere and neighborhood stars, considering Galactic and universal compositions
16 p2061 A73-33285

Planetary cosmogony theory review emphasizing cold evolution through dust-gas protoplanetary cloud nucleosynthesis, discussing iron fractionation, organic compounds and planetary thermal history
16 p2066 A73-33793

The origin of the solar system; Symposium, Nice, France, April 3-7, 1972, Proceedings
17 p2226 A73-34401

Solar system origin models in terms of cataclysmic theories, solar nebula concept, planetary accumulation, protoplanets, etc
17 p2226 A73-34402

Magnetohydrodynamics, hydrodynamics and dynamics of solar system model as contracting rotating cloud, discussing effects of turbulence
17 p2226 A73-34403

Presentation of the models.
17 p2227 A73-34404

Numerical model construction for primitive solar nebula and physical accumulation processes within collapsing interstellar gas cloud
17 p2227 A73-34405

Some remarks on solar nebula type theories of the origin of the solar system.
17 p2227 A73-34406

Small grain aggregates created by equalized grain orbits on Kepler trajectories, with low collisional frequency in early state of solar system planetary evolution
17 p2227 A73-34407

Protoplanetary gas-dust cloud evolution and planetary formation, investigating earth initial state
17 p2227 A73-34408

Collapse calculations and their implications for the formation of the solar system.
17 p2227 A73-34411

Mass and angular momentum distribution in primitive solar nebula during rotation and contraction hydrodynamics of collapse
17 p2227 A73-34412

Accretion processes to account for chemical differences among chondrites formed in cooling solar nebula
17 p2227 A73-34414

Evidence for objects of lunar mass in the early solar system and for capture as a general process for the origin of satellites.
17 p2228 A73-34415

Planetary accretion from grains in intersecting solar orbits, investigating velocity impact behavior of silicate particles
17 p2228 A73-34423

Stellar wind radiation damage in cosmic dust grains - Implications for the history of early accretion in the solar nebula.
17 p2228 A73-34424

Bode's law and the preference for near-commensurability among pairs of orbital periods in the solar system.
17 p2229 A73-34429

Revision of initial size, mass and angular momentum of the solar nebula and the problem of its origin.
17 p2229 A73-34431

Mass transport rate in solar nebula model due to turbulence induced by convection
17 p2229 A73-34432

Cosmic ray bombardment of meteorites allowing solar system age estimation from spallation product concentration and subatomic particle track distribution
17 p2232 A73-34975

Properties of the solar nebula and the origin of the moon.
17 p2235 A73-35742

Structure and evolutionary history of the solar system. III.
17 p2236 A73-35784

Cometary exploration - A case for Encke.
18 p2353 A73-36501

[AIAA PAPER 73-596]
Book - General astrophysics with elements of geophysics.
18 p2356 A73-36968

Russian papers on populated cosmos covering space exploration impact on human civilization, extraterrestrial life, space medicine and biology, solar system, space law, etc
19 p2393 A73-37398

Reports of fourth Lunar Science Conference covering lunar rock chemical composition assessment as information source on early solar system, lunar early geologic history, etc
19 p2487 A73-38293

Four-stage planetesimal accretion from solar nebula describing dust particle condensation, disk formation, gas drag, orbital decay and particle collisions
19 p2489 A73-38524

Statistical dynamics formulation of motion equations for particle system in gravitational interaction with neither gas law nor hydromagnetic effects, applying to solar system evolution
21 p2766 A73-40313

Computerized simultaneous numerical integration of motion equations for solar system, star cluster and galaxies, considering radar observations of moon, Mercury, Venus, Mars and Icarus
21 p2772 A73-41241

Mass and position limits for an hypothetical tenth planet of the solar system.
22 p2907 A73-42209

Micrometeorite and cosmic dust studied for solar system and universe origin and evolution and for medium range weather forecasting, discussing cosmic matter infall to earth
22 p2913 A73-42988

Galactic nucleosynthesis time interval from birth to solar system formation /Galactic age/ from radioactive decay nuclear yield ratios
22 p2916 A73-43049

Lunar and planetary chemical composition dependence on condensation temperature in solar nebula
23 p3030 A73-43760

The observational evidence for mass distribution in the meteoritic complex.
23 p3031 A73-43770

Comet Kohoutek earth orbit properties and rocket and satellite observations, including parent molecule and inner solar system measurements
23 p3034 A73-44222

Planetary formation processes in primitive solar nebula analyzed from collapse phase for accumulation time
24 p3127 A73-44393

On the process of accretion in the formation of the planets and comets.
24 p3128 A73-44400

Early solar system deuterium abundance based on nebular chemical equilibrium, comparing with Jupiter atmosphere and meteorite data
24 p3131 A73-44468

Solar system cosmochemistry concerning element abundances, structure and composition of comets, planets, moon, exospheric dust and meteoroids, protosolar magnetic field, nucleosynthesis and cosmic rays
24 p3134 A73-44569

Chondrites - Initial strontium-87/strontium-86 ratios and the early history of the solar system.
24 p3137 A73-44688

Relativistic gravity in the solar system, III - Experimental disproof of a class of linear theories of gravitation.
24 p3138 A73-45034

Curium-248 in the early solar system.
24 p3143 A73-45348

SOLAR TEMPERATURE

Temperature structure and conductive flux in the chromosphere-corona transition region.
01 p0107 A73-11380

Radio spectrum analysis of loop prominence development, temperature and H atom density on May 13, 1971, noting consistency with Jefferies-Orrall model
01 p0108 A73-11387

Type 3 bursts exciter duration and decay time constant from time profiles analysis in decameter range, explaining coronal temperature
03 p0361 A73-13213

On the sun's differential rotation and pole-equator temperature difference.
03 p0377 A73-14402

Sunspot temperature increase stimulation of super-granule motion leading to spot decay and magnetic field diurnal fluctuation development
04 p0503 A73-16012

Nonspherically symmetric polytrope model of azimuthally dependent solar wind in sun equatorial plane, considering coronal temperature, density and radial magnetic component
05 p0609 A73-16143

He 3 burning burst complication of mixing in solar core for solar luminosity variations resulting from central temperature decrease
05 p0611 A73-17187

Effects of sudden mixing in the solar core on solar neutrinos and ice ages.
05 p0623 A73-17188

Temperature variations in coronal regions in the proximity of a prominence
08 p1007 A73-21067

Numerical computation of photosphere temperature-associated equatorial brightening in red and green bands used in solar oblateness measurements [AD-758969]
09 p1142 A73-22040

Ultraviolet ion chamber measurements of the solar minimum brightness temperature.
10 p1279 A73-24136

Determination of the temperature in a solar X-ray flare.
11 p1412 A73-25755

Heating effects due to radiative energy loss from acoustic waves in solar atmosphere, estimating temperature difference between radiative equilibrium and empirical model
11 p1421 A73-25931

The solar wind and the temperature-density structure of the solar corona.
11 p1413 A73-25954

Equator-pole temperature difference and the solar oblateness /Research note/.
12 p1544 A73-27831

Solar pole-equator temperature distribution in high photosphere layers from Mg spectral line observations
12 p1544 A73-27832

An investigation of the structure of coronal active regions.
12 p1545 A73-27847

Solar rotational and vibrational temperature based on turbulent velocity determined from CN molecular line profiles half widths
12 p1547 A73-27870

Solar neutrino flux, discussing effects of temperature oscillations on neutrino and photon luminosities
15 p1926 A73-31358

Electron temperature and emission measure variations in the solar corona.
18 p2350 A73-36062

Temperature variations of coronal regions near a solar prominence.
18 p2355 A73-36868

Solar rotational and vibrational temperature based on turbulent velocity determined from CN molecular line profiles half widths
20 p2608 A73-39244

Determination of the temperature behavior in a photospheric facula through the solution of an integral equation by the gradient-random search method
21 p2759 A73-40721

Temperature difference between pole and equator of the sun.
21 p2776 A73-41479

Electron temperature of regions of the formation of recombinational continua on the sun - Temperature of the carbon emission regions
23 p3036 A73-44246

Temperature and oxygen abundance determination in the sun from the oxygen lines
23 p3037 A73-44257

X-ray flare plasma temperature - A comment on a paper by Deshpande and Tandon.
24 p3124 A73-45047

SOLAR VELOCITY

Secular parallaxes of stars and the speed of the sun according to absolute intrinsic motions of 14,600 stars with respect to galaxies
15 p1938 A73-31962

Secular parallaxes and space velocity of the sun from absolute proper motions of 14,600 stars relative to galaxies.
24 p3132 A73-44487

SOLAR WIND

NT SOLAR WIND VELOCITY

Some peculiarities of the development of the magnetic storm on March, 5-10, 1970.
01 p0036 A73-10342

Characteristics of the quiet solar wind beyond the earth's orbit.
01 p0092 A73-11042

Natural oscillations of type-I comet tails.
01 p0107 A73-11331

Solar outer layer models of convective zone, photosphere, chromosphere, corona and solar wind, using electron density dependence
01 p0107 A73-11379

Upper limits on the lunar atmosphere determined from solar-wind measurements.
02 p0211 A73-11727

Magnetopause motions at lunar distance determined from the Explorer 35 plasma experiment.
02 p0155 A73-11730

Earth atmosphere He isotopes abundance based on calculation of ionization rates and solar wind interaction during geomagnetic dipole reversal
02 p0156 A73-11741

Number density estimation for neutral hydrogen hot component required for solar wind heating to satisfy observed proton temperature relationship to wind velocity
02 p0205 A73-11745

On the plasma sheet contribution to the force balance requirements in the geomagnetic tail.
02 p0156 A73-11746

Solar wind observations on the lunar surface with the Apollo-12 ALSEP.
02 p0205 A73-11903

Long-lived sectors of enhanced density irregularities in the solar wind.
02 p0205 A73-11911

Correlation between the brightness of comets and solar wind fluctuations
02 p0208 A73-12471

Lyman-alpha emission of comet Bennett 1969i and the determination of the solar wind flux
02 p0208 A73-12472

Geomagnetic field variations caused by changes in the quiet-time solar wind pressure.
03 p0298 A73-12885

Physical mechanisms of magnetospheric processes, discussing matter and energy exchange between solar wind and magnetosphere, substorms, interaction with ionosphere, etc
03 p0302 A73-13853

Solar wind interaction with geomagnetic field, discussing magnetosphere polar cusp region and geomagnetic tail neutral sheet structure
03 p0302 A73-13871

Atmospheric model for substorm triggering mechanism, plasma sheath behavior and substorm recovery, noting solar wind interaction with magnetosphere
03 p0304 A73-13886

Note on solar plasma irregularities and plasma instabilities.
03 p0378 A73-14420

Hypersonic solar wind flow interactions with comet emitted gas forming tails, discussing contact surface with stagnation point and bow shock front
04 p0494 A73-14758

Time dependent hydrodynamic models of solar wind, considering coronal electron density and temperature distribution and magnetic field
04 p0491 A73-14835

Propagation of solar cosmic rays in the solar wind.
04 p0491 A73-14837

Solar activity effects on geomagnetic variations from spacecraft particle measurements, showing statistical correlations between solar wind, flares and magnetic storms
04 p0491 A73-14838

Electrodynamic sailing - Beating into the solar wind.
04 p0487 A73-15073

An effect of the solar wind on the earth's rotation
04 p0498 A73-15282

Magnetosphere configuration models based on open and closed field line hypotheses, discussing solar wind-magnetosphere interactions, magnetotail, substorm growth, flux transport, etc
04 p0441 A73-15327

Solar wind plasma entry into earth magnetosphere, reviewing major uncertainties in light of current observational knowledge
04 p0442 A73-15330

Auroral and magnetospheric phenomena caused by solar wind particles entry and energization via magnetosheath into magnetosphere and upper atmosphere
04 p0492 A73-15331

Magnetospheric convection, discussing ionospheric twin vortex pattern, reconnection model for solar wind induced generation, plasmasphere response and magnetotail dynamics
04 p0442 A73-15337

A solar-wind model including proton thermal anisotropy.
04 p0492 A73-15365

Fluctuations in geomagnetic wake region at 500 earth radii connected with magnetotail Kelvin-Helmholtz instability, using plasma cylinder model
04 p0445 A73-15556

Observation of the region of interaction between the solar-wind plasma and Mars.
05 p0608 A73-16095

Nonspherically symmetric polytrope model of azimuthally dependent solar wind in sun equatorial plane, considering coronal temperature, density and radial magnetic component
05 p0609 A73-16143

Dayside magnetopause distance calculation at subsolar point for various solar wind parameters, allowing for southward interplanetary field component diffusion
05 p0610 A73-17008

Solar wind magnetic field and particle concentration disturbances near moon, noting electric field effect on ion motion
05 p0620 A73-17009

Demarcation layer between magnetosphere central portion and geomagnetic tail as layer of least resistance to incident solar plasma
05 p0610 A73-17010

Electrostatic ion cyclotron waves in an anisotropic plasma.
05 p0611 A73-17305

Earth magnetosphere essential processes, discussing outermost atmosphere, solar wind theory and sector structure, models, plasmapause, polar cusps, tail theory and ionospheric currents
06 p0688 A73-17502

Dependence of the position of the magnetopause on the orientation of the interplanetary magnetic field
06 p0690 A73-17560

Book - Coronal expansion and solar wind.
06 p0742 A73-17671

Directional measurements of the solar wind by the ESRO HEOS 1 probe, S 58-73
06 p0749 A73-17863

Biogenic elemental distribution and isotopic abundance in lunar samples, discussing heavy isotopes enrichment by solar wind irradiation, meteorite impacts and hydrogen stripping
06 p0654 A73-18417

Solar wind, meteoritic, and cometary carbon sources for moon, discussing lunar atmospheric steady state carbon component sustained by meteoritic and cometary carbon vaporization
06 p0754 A73-18427

Activities in space research at the Max-Planck-Institut fuer extraterrestrische Physik, Garching bei Muenchen /G.F.R./.
07 p0868 A73-19173

On the relation between solar wind structure and solar wind rotational and tangential discontinuities.
07 p0869 A73-19231

Interaction of singly charged interstellar helium ions with the solar wind.
07 p0870 A73-19253

Minimum magnetic field energy of two dimensional magnetosphere with neutral sheet for arbitrary dipole inclination to solar wind as function of potential difference on boundary points
07 p0816 A73-19443

Harmonic analysis of solar wind geometry and geomagnetic activity levels during even and odd cycles based on cosmic ray intensity variations for 1900-1969 period
07 p0870 A73-19451

Trapped solar wind noble gases in Apollo 12 lunar fines 12001 and Apollo 11 breccia 10046.
07 p0871 A73-19800

Classification and source of lunar soils; clastic rocks; and individual mineral, rock, and glass fragments from Apollo 12 and 14 samples as determined by the concentration gradients of the helium, neon, and argon isotopes.
07 p0889 A73-19804

Lunar magnetic field measurements with Apollo 15 subsatellite, discussing surface remanent magnetization, solar wind interactions and limb shocks
07 p0892 A73-19833

Surface magnetometer experiments - Internal lunar properties and lunar field interactions with the solar plasma.
07 p0892 A73-19834

Electrostatic turbulence at colliding plasma streams as the source of ion heating in the solar wind.

08 p0997 A73-20886

Nonthermal turbulent heating in the solar envelope.

08 p1003 A73-20887

Landau damping of type III solar radiobursts.

08 p0997 A73-20902

Magnetic irregularities in interplanetary space and geomagnetic activity.

08 p1007 A73-21004

Turbulent heating of colliding streams in the solar wind.

08 p0998 A73-21164

Heat conductivity, plasma instabilities, and radio star scintillations in the solar wind.

08 p0998 A73-21165

Classification, orientational characteristics, and some examples of rotational discontinuities in the solar wind

08 p0998 A73-21278

Pulsed magnetic system /terrella/ for model of earth radiation belts and geomagnetic field-solar wind interaction

08 p0960 A73-21309

Solar and magnetic fields characteristics relative to 11 year cosmic ray modulation in interplanetary space

08 p0999 A73-21340

Nonstationary and asymmetric cosmic ray modulation theory, discussing moving boundary problem and solar wind model with spherical singularity

08 p0999 A73-21341

Diffusion and stochastic variations of galactic cosmic rays in solar wind

08 p1000 A73-21346

Solar plasma electron density and temperature measurement by Mars 2 and Mars 3 orbiter-borne retardation potential analyzers, considering solar wind shock front interaction role

09 p1126 A73-22263

Ion velocity temperature observation at Mars surface boundary, suggesting solar plasma interaction with outer atmosphere from ion flux disturbance ahead of shock wave

09 p1126 A73-22264

Two dimensional model of solar wind passage past magnetosphere, assuming hot plasma current sheath in geomagnetic tail

09 p1077 A73-22485

Interaction of the interplanetary medium with the earth's magnetosphere

09 p1146 A73-22542

Contributions to the kinematics of type I tails of comets.

10 p1271 A73-23477

Direct measurements of solar-wind fluctuations between 0.0048 and 13.3 Hz.

10 p1264 A73-23539

Influence of pressure anisotropy on the fluctuations of the magnetospheric tail

10 p1276 A73-23884

Particle scattering in interplanetary space and the properties of solar corpuscular streams

10 p1265 A73-23902

Solar wind effect on azimuthal and radial galactic cosmic ray currents, noting Forbush decreases relation to current structures

10 p1265 A73-23907

The asymptotic behavior of the supersonic solutions of the two-fluid solar wind equations.

10 p1268 A73-24147

Determination of the velocity of shock waves in the interplanetary medium.

10 p1279 A73-24236

First order approximation of collisionless protons expansion in quiet solar wind

10 p1269 A73-24651

Solar wind He nuclei kinetic temperature, considering resonant heating and proton temperature

10 p1269 A73-24723

Solar wind flow vector from detection of unshocked wind by plasma detector aboard ATS-5 during 8 March 1970 geomagnetic storm

10 p1270 A73-24741

Solar He abundance from neutrino flux. He lines intensity in prominences and chromosphere spectra, solar cosmic rays and solar wind He/H ratio

10 p1284 A73-24780

Kinetic equations describing thermalization of anisotropic solar wind plasma via linear and nonlinear wave-particle interaction

10 p1270 A73-24912

Ionospheric currents induced by solar wind interaction with planetary atmospheres.

11 p1412 A73-25921

Rotational discontinuities in an anisotropic plasma. II.

11 p1405 A73-25922

Precise calculation of the magnetosphere surface for a tilted dipole.

11 p1421 A73-25923

The effect of a uniform external pressure on the ionospheric boundary of a non-magnetic planet in a steady solar wind.

11 p1421 A73-25925

The solar wind and the temperature-density structure of the solar corona.

11 p1413 A73-25954

Plasma research in space and in the laboratory.

12 p1526 A73-26849

High speed corotating plasma streams in solar wind from time dependent radial MHD flow model

12 p1533 A73-26979

Interplanetary scintillations observations from solar wind plasma density fluctuations power spectrum

12 p1533 A73-26980

Conjugate asymmetries in sudden commencement absorption and the sudden commencement absorption event of February 28, 1969.

12 p1534 A73-26982

Solar wind-lunar limb interaction from viscous MHD approach including continuum fluids, kinetic plasma and magnetic boundary layer

12 p1534 A73-27003

Intensive chromospheric flares and rotational discontinuities in the solar wind

12 p1534 A73-27330

Modulation of galactic cosmic rays by a solar wind asymmetric with respect to the heliostatitude

12 p1534 A73-27332

The mean free path in the transition region beyond the boundary of the magnetosphere

12 p1528 A73-27355

Solar magnetic sector structure - Relation to circulation of the earth's atmosphere.

12 p1491 A73-27441

Photoelectrons and solar wind/lunar limb interaction.

12 p1534 A73-27495

Nonlinear helical waves formation due to Kelvin-Helmholtz instability in type I comet tail modeled as plasma cylinder immersed in solar wind

12 p1542 A73-27609

EUV and radio observation of energy flux from corona into chromosphere, considering coronal holes as source of high energy streams of solar wind

12 p1545 A73-27839

The configuration of interplanetary shock waves produced by strong chromospheric flares /according to space sonde measurements/

12 p1536 A73-27859

Variations of solar-wind parameters, magnetic activity, and the electron tail of the magnetosphere and of the outer radiation zone.

13 p1608 A73-28714

Variation of the cosmic-ray gradient during the solar activity cycle.

13 p1670 A73-28721

Solar wind proton temperature anomalies relation to interplanetary shock waves, considering solar flare induced material ejection and magnetic bottle formation

14 p1786 A73-29952

Solar wind interpenetrating ion streams from Imp 6 electrostatic analyzer measurements, considering origin due to interplanetary high velocity filaments merging into rarefied plasma regions

14 p1786 A73-29954

Induced lunar magnetosphere and solar wind formed downstream cylindrical cavity for interplanetary magnetic fields arbitrary orientation, assuming lunar core and shell electrical conductivity model

14 p1796 A73-29962

Plasma radiation from collisionless MHD shock waves and the high-frequency waves in the upstream solar wind.

14 p1786 A73-29978

Earth nonuniform bow shock oblique structure and pulsation, obtaining statistical occurrences from three dimensional distribution of interplanetary field directions for solar wind sector

14 p1749 A73-29983

Alfven waves in a two-fluid model of the solar wind.

14 p1787 A73-30005

Asymptotic behavior of a kinetic model of the solar wind

14 p1787 A73-30424

Outer solar system planetary and subplanetary objects magnetic field existence, discussing internal dynamo fields, externally driven dynamos and fossil fields

14 p1800 A73-30540

Solar wind properties near and beyond Jupiter orbit, considering steady state wind extrapolation to large distances, cosmic ray modulation and interactions with planetary bodies

14 p1787 A73-30541

Interaction of the interstellar medium with the solar wind.

14 p1787 A73-30543

Outer solar system, including planetary atmospheres, natural satellites, solar wind, interstellar cosmic rays and spacecraft missions

14 p1800 A73-30616

Stability of solar wind against electromagnetic streaming instability.

14 p1788 A73-30743

Pi 2 micropulsations occurrence time, morphology change with magnetic activity and source meridian shift from solar wind variations effects

15 p1866 A73-31072

Mars 3 solar wind probe of upper Mars atmosphere, showing plasma interaction with ionosphere measured by energy spectra

15 p1930 A73-31150

Interaction of solar wind with interstellar neutral gas at the heliospheric boundary.

15 p1926 A73-31380

Kinetic models of the solar and polar winds.

15 p1926 A73-31847

The direct and inverse problems of cosmic-ray propagation in interplanetary space

15 p1926 A73-31878

Interaction of the geomagnetic field with the antiparallel solar-wind field

15 p1926 A73-31891

Interaction between the interstellar medium and solar wind plasma.

15 p1927 A73-32001

Solar wind flow in interplanetary space, discussing comets, cometary tail, interplanetary magnetic field and Alfvén waves characteristics

15 p1940 A73-32183

Correlation between the brightness of comets and fluctuations of the solar wind.

15 p1927 A73-32622

Lyman-alpha radiation from comet Bennet 1969.

15 p1927 A73-32623

Dependence of the position of the magnetopause on the orientation of the interplanetary magnetic field.

16 p2002 A73-32784

The prevalence of second harmonic radiation in type III bursts observed at kilometric wavelengths.

16 p2053 A73-32964

Solar wind density model from km-wave type III bursts.

16 p2053 A73-32965

Restrictions on radial magnetic field and flow solutions for the solar wind.

16 p2053 A73-32967

Transient solar modulation of cosmic rays.

16 p2055 A73-33294

Satellite studies of magnetospheric substorms on August 15, 1968. II - Solar wind and outer magnetosphere.

16 p2004 A73-33450

Single-fluid model of the distant solar wind.

16 p2056 A73-33459

Traveling regions of high solar wind density observed in early August 1972.

16 p2056 A73-33460

On the role of fluctuations in the interplanetary magnetic field on heat conduction in the solar wind.

16 p2056 A73-33461

On the extent of the Martian ionosphere.

16 p2062 A73-33462

Explorer 35 lunar studies, discussing orbit characteristics, circumlunar magnetic field, surface electromagnetic properties and solar wind model

16 p2065 A73-33782

Noble gas isotopes abundances for solar wind and outer convective zone of sun, emphasizing isotopic abundance of deuterium

17 p2228 A73-34416

The propagation of Alfvén waves and their directional anisotropy in the solar wind.

17 p2223 A73-34501

Wave-trains in the solar wind. I - General theory and its application to an ideal, isotropic, one-fluid plasma.

17 p2224 A73-34505

The Pioneer 9 electric field experiment. III - Radial gradients and storm observations.

17 p2230 A73-34513

Two fluid models for solar wind heating under boundary conditions, considering enhanced energy transfer between electrons and protons in kinetic theory calculations

17 p2224 A73-34515

Radial variation of magnetic fluctuations and the cosmic-ray diffusion tensor in the solar wind.

17 p2224 A73-34762

Isotopic composition of solar wind xenon in carbonaceous chondrites, discussing evolution of meteoritic matter

17 p2233 A73-35266

Darkening of silicate rock powders by solar wind sputtering.

17 p2235 A73-35740

Russian monograph on polar auroras and magnetospheric geomagnetic disturbances from rocket, balloon and ground station soundings covering magnetic storms, solar wind and geoelectric fields

18 p2302 A73-35873

Observations of the entry of solar protons into the magnetosphere by use of riometers.

18 p2344 A73-35930

Characteristics of the influence of the solar wind on cosmic-ray intensity during 1969

18 p2345 A73-36108

Some characteristics of charged particle flux studies using traps and analyzers. II - Modulation trap utilization for investigating the solar wind

18 p2345 A73-36113

On solar wind interaction with the earth's magnetosphere.

18 p2346 A73-36184

Simulation of driven flare-associated disturbances in the solar wind. 18 p2346 A73-36263

Alfven waves in the solar wind - Wave pressure, Poynting flux, and angular momentum. 18 p2346 A73-36264

Photoelectron layer above sunlit lunar surface due to solar photon flux, using models neglecting solar wind electron flux 18 p2351 A73-36267

Solar wind heat transport in the vicinity of the earth's bow shock. 18 p2346 A73-36269

Solar wind interaction with the earth's magnetic field. I - Magnetosheath. 18 p2346 A73-36270

Solar wind interaction with the earth's magnetic field. II - Magnetohydrodynamic bow shock. 18 p2346 A73-36271

Solar wind interaction with the earth's magnetic field. III - On the earth's bow shock structure. 18 p2346 A73-36272

Solar wind-Mercury atmosphere interaction - Determination of the planet's atmospheric density. 18 p2352 A73-36294

Plasma columnar content measurement between earth and Mariner 9 at small solar elongations by phase-group velocity difference technique 19 p2479 A73-37224

Magnetic measurements in laboratory model tests of solar wind-geomagnetic field interactions 19 p2481 A73-37338

Solar wind-geomagnetic field interaction simulation by plasma flow and magnetic dipole, proving collisionless dissipation presence 19 p2481 A73-37339

Structural formations in the interplanetary medium 19 p2481 A73-37342

Oscillations of the earth's magnetic tail 19 p2482 A73-37349

Plasma acceleration techniques in space studies, discussing simulation experiments, solar wind-geomagnetic field interaction and astronomical models 19 p2482 A73-37355

Classification, characteristics of orientation, and some examples of rotational discontinuities in the solar wind. 19 p2476 A73-37907

Effect of pressure anisotropy on oscillations of magnetotail. 20 p2603 A73-38903

Lunar thermal ionosphere acceleration and detection within lunar electric field for electric potential of moon in solar wind or magnetosheath 20 p2604 A73-38933

Auroral arc mechanism of solar wind intrusion and electron and proton energization and precipitation in magnetosphere from Isis photometric and spectrometric observations 20 p2553 A73-39124

Configuration of interplanetary shock waves from powerful chromospheric flares /from space probe measurements/. 20 p2602 A73-39233

Interplanetary gas. XIX - Observational evidence for a meridional solar-wind flow diverging from the plane of the solar equator. 20 p2602 A73-39431

Distribution of gases within Apollo 15 samples - Implications for the incorporation of gases within solid bodies of the solar system. 20 p2612 A73-39715

Seasonal and solar cycle dependence of the position of the cusp region of the magnetosphere. 20 p2555 A73-39828

Numerical calculation for polar ionospheric current under realistic electric field and conductivity distributions, considering solar wind effect on charged particles in magnetosphere 21 p2681 A73-40155

Power spectrum of small-scale irregularities in the solar wind. 21 p2755 A73-40163

Resonant nuclear measurement of hydrogen concentration vs depth in Apollo 11, 15 and 16 lunar soil fragments and platinum foil exposed to solar event 21 p2765 A73-40237

Helios probe design for solar wind acceleration mechanism, magnetic and electric fields, interplanetary dust and cosmic radiation 21 p2780 A73-40449

Study of cosmic rays by the Prognos satellites 21 p2756 A73-40577

Isotopes of helium and hydrogen in solar corpuscular fluxes 21 p2757 A73-40593

Nonlinear and nonstationary effects in the solar wind 21 p2757 A73-40594

Trapped solar wind noble gases and exposure age of Luna 16 lunar fines. 21 p2770 A73-41001

Observations of electron fluxes and related variations of ionospheric plasma parameters in the south polar cusp. 21 p2690 A73-41369

Surface and orbital magnetic results from Apollo 15. 21 p2691 A73-41398

Non-thermal solar wind heating by supra-thermal ions. 21 p2763 A73-41499

Solar wind interaction with Comet Bennett near for momentum flux change-ion tail kink correlations 21 p2763 A73-41501

Solar wind properties at the earth as predicted by the two-fluid model. 21 p2763 A73-41502

Magnetohydrodynamic waves in the solar wind plasma 21 p2763 A73-41506

Induced magnetosphere of the moon. II - Experimental results from Apollo 12 and Explorer 35. 22 p2906 A73-41905

Effects on the geomagnetic tail at 60 earth radii of the geomagnetic storm of April 9, 1971. 22 p2844 A73-41908

Effects of electrostatic instabilities on planetary and interstellar ions in the solar wind. 22 p2902 A73-41940

Results of solar plasma electron observations on Mars-2 and Mars-3 spacecraft. 22 p2906 A73-41941

Solar magnetic fields and their influence on the earth. 22 p2906 A73-41959

Comparison of the sectorial structure of the interplanetary magnetic field and the occurrence of SC and SI events. 22 p2908 A73-42447

Interaction of the solar wind with the outer planets. 22 p2903 A73-42937

Interactions of plasmas with magnetic field boundaries. 22 p2851 A73-42977

Jupiter and terrestrial upper atmospheres comparison, discussing solar wind interactions with planetary magnetic fields, Jovian Van Allen belt and cold plasma distribution 22 p2913 A73-42985

Powerful chromospheric flares and rotational discontinuities in the solar wind. 23 p3020 A73-43228

Modulation of galactic cosmic-rays by solar wind which is unsymmetric in solar latitude. 23 p3020 A73-43230

The effect of nonstationarity in the chemical composition of plasma flows from the sun. 23 p3027 A73-43252

Mean free path in the transition region beyond the boundary of the magnetosphere. 23 p3008 A73-43253

Small amplitude Alfven waves propagation in solar wind under interplanetary magnetic field, relating wave and wind velocity 23 p3029 A73-43612

Weakly-shocked flows of the solar wind plasma through atmospheres of comets and planets. 23 p3024 A73-43682

Magnetospheric plasma motion during a sudden commencement. 23 p2972 A73-43689

Rare gas diffusion studies in individual lunar soil particles and in artificially implanted glasses. 23 p3031 A73-43769

Looking at the solar system in the far-ultraviolet. 23 p3034 A73-44220

North-south asymmetry of the interplanetary magnetic field 23 p3025 A73-44250

Large-scale inhomogeneities in the sector structure of the solar wind 24 p3124 A73-44779

Interaction between flows with different velocities in the solar wind 24 p3124 A73-44780

Solar wind fluctuations mapping procedure applied to Explorer 35 wind data for solar wind structure to Mars orbit 24 p3125 A73-45104

Solar wind proton thermal anisotropy association with moments of proton velocity distribution and dependence on temperature decrease 24 p3125 A73-45105

Lunar electromagnetic scattering. I - Propagation parallel to the diamagnetic cavity axis. 24 p3139 A73-45109

Solar wind and magnetosheath electron temperature measurements by triaxial electron analyzer onboard Ogo-5, presenting data for bow shock 24 p3125 A73-45112

Heat current and anisotropy-driven instabilities in connection with the solar wind. 24 p3126 A73-45126

Solar wind interaction modes with lunar magnetic fields, discussing moon surface charging, magnetic field compression and wind deflection 24 p3126 A73-45127

Power spectra of solar wind parameters at 20 solar radii derived from Mariner 5 data. 24 p3126 A73-45133

Resonance scattering from interstellar and interplanetary helium. 24 p3140 A73-45188

Collisionless magnetospheric-solar wind plasmas interactions, noting boundary stability and tail instability 24 p3127 A73-45213

SOLAR WIND VELOCITY

Interplanetary gas. XVII - An astrometric determination of solar-wind velocities from orientations of ion comet tails. 03 p0361 A73-12947

In situ prediction techniques for solar wind velocity at earth based on probability theory, statistical correlation coefficients and autocorrelation analysis 04 p0491 A73-14836

Solar wind rotational and tangential velocity discontinuities in anisotropic media, discussing Ivanov, Burlage and Hudson data 06 p0742 A73-17528

Excitation of natural oscillations in the earth's magnetic tail 06 p0748 A73-17540

The recurrent solar wind streams observed by interplanetary scintillation of 3C 48. 07 p0870 A73-19595

Numerical studies of the transport of solar protons in interplanetary space. 07 p0870 A73-19664

Characteristics of cosmic ray variations near the solar equatorial plane 08 p0998 A73-21299

Physical conditions in the magnetosphere and interplanetary space during the excitation of pc 1 geomagnetic pulsations 08 p0960 A73-21306

Anisotropies in the interplanetary intensity of solar protons with energies greater than 0.3 MeV. [AD-759099] 10 p1269 A73-24728

Interplanetary plasma shock event of 8 March 1970 from Heos 1 data, noting magnetospheric compression and solar wind velocity at geosynchronous orbit 10 p1270 A73-24742

The effect of the earth's bow shock and magnetosheath on the interaction of a discontinuity in the solar wind with the magnetosphere. 11 p1357 A73-25924

Solar wind velocity and proton temperature time dependent relations, considering interplanetary medium nonlinear unsteady processes effects 14 p1786 A73-29955

Solar wind velocity fluctuations with heliocentric distance beyond one AU via nonlinear fluid dynamic equations numerical solution, considering interplanetary plasma turbulence effects 14 p1786 A73-29956

Interplanetary medium rotational discontinuities polarization, vorticity transport and angular momentum properties, implying solar wind velocity jump from magnetic field transverse perturbation 14 p1796 A73-29961

Greenstadt binary index criterion for laminar and pulsating bow shock crossings separation in terms of angle, solar wind velocity and Galilean invariance 14 p1748 A73-29979

Test for detection of fine structure of the solar wind velocity. 15 p1927 A73-32015

Excitation of natural oscillations of the geomagnetic tail. 16 p2058 A73-32764

A test for revealing the fine-scale velocity structure of the solar wind 16 p2059 A73-32888

Observation and analysis of abrupt changes in the interplanetary plasma velocity and magnetic field. 18 p2351 A73-36265

Validity of CGL equations in solar wind problems. 18 p2347 A73-36291

Characteristics of cosmic-ray variations near the solar equatorial plane. 19 p2476 A73-37928

Physical conditions in the magnetosphere and in interplanetary space during excitation of type Pcl geomagnetic pulsations. 19 p2425 A73-37935

Effect of the solar wind on geomagnetic activity 19 p2476 A73-38154

Interplanetary gas. XVIII - Models and the mean free path of protons at 1 astronomical unit. 19 p2489 A73-38523

Solar wind velocity investigation based on solar corona and interplanetary plasma data, analyzing possible acceleration mechanisms 21 p2755 A73-40533

Nonlinear and nonstationary effects in the solar wind 21 p2757 A73-40594

Solar wind alpha particle abundance variations as function of wind velocity from HEOS-1, Vela 3-A and 3-B observations 21 p2763 A73-41500

Analysis and synthesis of coronal and interplanetary energetic particle, plasma, and magnetic field observations over three solar rotations. 22 p2901 A73-41901

Mariner 5 observations of solar wind shock-like structures including density, velocity, and proton temperature increases, suggesting nonlinear magnetoacoustic waves under steepening process 22 p2901 A73-41902

On the relation between the pattern and wind velocities in interplanetary scintillations. 22 p2903 A73-42702

Enhanced scintillation sectors outside the plane of the ecliptic. 23 p3029 A73-43679

Plasma fine velocity structure and dynamics from diffraction pattern of interplanetary radio sources scintillation 24 p3132 A73-44484

Vela 3 proton data analysis for compressions and rarefactions effects on solar wind density, temperature and velocity behavior 24 p3125 A73-45106

SOLAR X-RAYS

Monograph - Satellite-borne instrument for the measurement of soft solar X-rays. 01 p0045 A73-10150

Two X-ray bursts /1 August 1967 and 30 January 1968/ and some associated VLF disturbances. 01 p0091 A73-10556

Estimation of nitric oxide concentration in the lower E region from rocket and satellite measurements of electron densities and X-ray fluxes. 01 p0041 A73-10882

Nonthermal X-radiation and electric currents in solar flares 01 p0092 A73-10937

Heating of plasma by high-energy electrons, and nonthermal X-ray emission in solar flares. 01 p0093 A73-11313

H alpha subflare associated X-ray burst of 10 October 1970 observed by balloon-borne scintillator and OGO 5 and SOI-RAD 9 satellites 01 p0093 A73-11389

Pitch-angle distributions of polarized hard X-radiation from solar flares, assuming electron-proton bremsstrahlung mechanism 01 p0093 A73-11390

The role of energetic electrons in the correlation of meter and decimeter type III bursts with 4 keV X-ray emission. 01 p0093 A73-11391

Fe ions optical transition lines in solar flares soft X-ray spectra, noting continuum emission near 8 Å 03 p0367 A73-12945

The coronal X-spectrum - Problems and prospects. 03 p0363 A73-13954

Solar X-ray source unassociated with sunspots. 03 p0363 A73-13955

X ray spectra of solar flares at 0.4-250 keV, emphasizing soft X ray spectra and emission line and continuum features interpolation 03 p0364 A73-13958

The transient highly excited solar flare plasma. 03 p0364 A73-13960

Advances in solar and cosmic X-ray astronomy - A survey of experimental techniques and observational results. 03 p0364 A73-14167

The self absorption of gyro-synchrotron emission in a magnetic dipole field - Microwave impulsive burst and hard X-ray burst. 03 p0364 A73-14416

Solar corona X-ray emission from O VII and Ne IX ions by rocket-borne Bragg spectrometers observations, determining electron temperature from resonance lines intensity 03 p0364 A73-14418

X-ray line emission associated with solar flares. 04 p0490 A73-14832

Solar flare development particle acceleration phase model, noting association with white light emission, hard X-rays and PCA 04 p0490 A73-14833

Dielectronic satellite spectra for highly-charged helium-like ion lines. 04 p0500 A73-15490

Solar corona properties and nuclear reactions in flares from August 1972 OSO 7 observation, noting hard X ray bursts from electron streams 04 p0502 A73-15971

New results of solar X-ray flare studied 05 p0609 A73-16372

Solar X-ray emission in July 1964 and in November-December 1965 according to data from the 'Elektron-4' satellite and the 'Venera-2' station 05 p0610 A73-17017

X-radiation /E greater than 10 keV/, H-alpha and microwave emission during the impulsive phase of solar flares. 05 p0610 A73-17041

The directivity and polarisation of thick target X-ray bremsstrahlung from solar flares. 05 p0610 A73-17045

Contribution of hard solar X-ray radiation to D-region ionization. 05 p0611 A73-17172

Correlations between X-rays and UV ionizing radiation in the E region from data obtained during the solar eclipse of 25 February 1971 06 p0742 A73-17534

Solar soft X-ray bursts data recorded by satellite telemetry, considering production by thermal plasma and nonrelativistic electrons with power law energy distribution 08 p0996 A73-20765

Evidence for a common origin of the electrons responsible for the impulsive X-ray and type III radio bursts. 08 p0996 A73-20766

On the S- and B-components of solar radio and X-emission and their relationships to energetic solar events. 08 p0997 A73-20771

X-ray emission of coronal condensations during the eclipse on 20 May 1966 and its connection with optical and radio observations. 08 p0998 A73-21310

Nonthermal X rays and electric currents in solar flares. 09 p1138 A73-22732

Preliminary interpretation of the polarization measurements performed on 'Intercoms-4' during three X-ray solar flares. 10 p1268 A73-24142

A simulation of the directivity effect to be expected in hard X-ray flares. 10 p1268 A73-24143

Directivity of high-energy X-ray emission during flares. 10 p1270 A73-24774

Determination of the temperature in a solar X-ray flare. 11 p1412 A73-25755

Solar 1.9 Å X ray spectral line effects on SOLRAD satellite-borne photometer sensitivity and lower ionospheric ion production rate 11 p1354 A73-25771

D-region recombination coefficients and the short wavelength X-ray flux during a solar flare. 11 p1356 A73-25914

Time variations in the X-ray emission of solar active regions. 11 p1412 A73-25944

Thick target X-ray bremsstrahlung from partially ionized targets in solar flares. 11 p1412 A73-25945

Two-component temperature analysis of OSO-5 X-ray flare data. 11 p1413 A73-25947

Solar X-ray bursts from OSO-7 observations, analyzing spectra obtained from proportional and scintillation counters 11 p1413 A73-25948

Superthermal plasma nodules and their relation to solar flares. 11 p1413 A73-25949

An investigation of the structure of coronal active regions. 12 p1545 A73-27847

Characteristics of electron and high-energy proton flares. 12 p1536 A73-27849

Effective recombination coefficient in the ionospheric D-region. 13 p1608 A73-28711

New observations of Fe XVII in the solar X-ray spectrum. 13 p1685 A73-29357

Correlations between X-rays and ionizing ultraviolet radiation in the E-region, according to data from the solar eclipse of February 25, 1971. 16 p2052 A73-32758

Hard X-ray solar bursts observed from the OSO-6 satellite. 16 p2052 A73-32828

Non-thermal ionization and recombination processes during solar flares. 16 p2052 A73-32958

Spectra of solar flares from 8.5 Å to 16 Å. 16 p2053 A73-32960

The solar albedo of hard X-ray flares. 16 p2053 A73-32961

19-20 May 1969, an example of type III emission during the impulsive phase of flares. 18 p2344 A73-36013

Analysis of solar flare X-ray radiation with Bragg spectrometers. 18 p2344 A73-36014

Investigation of the solar X-ray flare spectra by the 'Intercoms-4' and 'Intercoms-7' satellites. 18 p2345 A73-36015

Intercoms satellite-borne X ray polarimeter measurements of solar flares 18 p2345 A73-36144

Satellite measurements of solar X-ray flux and ground observations of sudden ionospheric disturbances. 18 p2347 A73-36389

Analysis of the solar X-ray spectrum of 20 August 1971. 21 p2760 A73-40826

Nonthermal electromagnetic and thermal X ray sources of accelerated electrons during solar flares 21 p2761 A73-41384

Observations of the X-ray emission of solar active regions on 28 November 1970 and 20 August 1971. 21 p2761 A73-41387

The impulsive increase in the intensity of solar X-rays. 21 p2761 A73-41388

Crystal spectrometry of active regions on the sun. 21 p2706 A73-41602

Monograph - Development and performance of a solar hard X-ray spectrometer. 22 p2861 A73-42674

Height distribution and directionality of 2-12 Å X-ray flare emission in the solar atmosphere. 24 p3124 A73-45046

X-ray flare plasma temperature - A comment on a paper by Deshpande and Tandon. 24 p3124 A73-45047

X-ray observations of characteristic structures and time variations from the solar corona - Preliminary results from Skylab. 24 p3139 A73-45057

SOLDERED JOINTS

An investigation of fatigue life performance in lap-type solder joints. 04 p0452 A73-14852

A metallurgical approach to cracked solder joints. 11 p1375 A73-26355

Torque and thermal cycling as methods of testing reliability of reflow-soldered chip-to-substrate joints. 19 p2436 A73-38445

Soldering technique using reaction flux for metal deposition, obtaining strong joints of Al with other metals 23 p2985 A73-43999

Some considerations on solder flow-up into plated-through holes. 23 p2986 A73-44002

SOLDERING

Printed circuit and electronic component solderability tests subsequent to adverse environment exposure, comparing electroplated materials with pressure leveled solder and Cu and Be coatings 03 p0333 A73-13046

Attempt at estimating the parameters of soldering processes 04 p0454 A73-15349

Surface preparation, protective coatings, materials selection and equipment used in soldering, discussing quality control 12 p1504 A73-27990

Structure of powdered solders with a Ni-Cr-Si-Fe-B-C/Mo/ base 15 p1892 A73-32245

Soldering technique using reaction flux for metal deposition, obtaining strong joints of Al with other metals 23 p2985 A73-43999

Soldering and brazing of advanced metal-matrix structures. 23 p2986 A73-44003

SOLDERS

Solar cell interconnections with different weld types, discussing semiautomatic and automatic ultrasonic processes, solder thickness control and quality inspection methods and criteria 09 p1035 A73-22807

Exploratory study of a fluxless aluminum brazing process for beryllium. 11 p1375 A73-26359

Selection of brazing solders according to technical requirements and economy 16 p2026 A73-33350

SOLENOIDS

Electromagnetic systems of noise-immunized nuclear-precession sensors 06 p0692 A73-17562

Experience in developing and using laboratory superconducting solenoids with fields up to 119 kOe 10 p1177 A73-23936

Electromagnetic systems of noiseproof nuclear precession sensors. 16 p2011 A73-32786

50 kG gas cooled superconducting solenoid operated at 13 K. 21 p2702 A73-41103

SOLID ARGON

U SOLIDIFIED GASES

SOLID LUBRICANTS

High temperature solid lubrication technology developments, discussing bonded films, plastic and metal bonded composites and temperature ranges 03 p0330 A73-13013

The assessment of recently developed lubricants for rolling elements.

[ASLE PREPRINT 72LC-4C-2]

Development of solid lubricant compact bearings for the supersonic transport. [ASLE PREPRINT 72LC-7C-1] 03 p0316 A73-14361

Lubricating characteristics of polyimide bonded graphite fluoride and polyimide thin films. [ASLE PREPRINT 72LC-7C-3] 03 p0316 A73-14370

Metallic additions effect on wear and friction behavior of lead monoxide, lead silicate and calcium fluoride solid lubricants coatings for high temperature operations [ASLE PREPRINT 72LC-7C-5] 03 p0317 A73-14372

Antifriction bearing with lubricated rubber and metal laminations for wear elimination in limited rotation applications, discussing design guidelines and advantages 03 p0317 A73-14374

Cu and Cu-Sn base self lubricating composites, testing solid lubricants effects on friction coefficient, wear, electrical resistance, hardness, porosity and structure 03 p0317 A73-14424

Frictional behaviour of molybdenum disulphide in high vacuum. 04 p0454 A73-14996

Electron microscopic investigation of lubricating mechanism of dry and oil-suspended molybdenum disulfide powder, discussing physical and chemical properties effects 04 p0454 A73-14997

Friction in ultrahigh vacuum, discussing physicochemical problems, self lubricating material advantages and drawbacks, and solid lubricant choice for space applications 05 p0589 A73-17067

Review of recent advances in bonded solid film lubrication at high temperatures. 07 p0828 A73-18906

Evaluation of the lubricating properties of chemically upgraded MoS₂. 07 p0842 A73-19552

Aircraft components solid film lubrication problems, discussing surface pretreatment, contamination susceptibility, corrosion prevention and aerosol applicability 07 p0842 A73-19553

Moisture absorption characteristics of solid lubricant coatings 07 p0842 A73-19554

Metal cladding lubricants tests with powdered lead, copper, zinc, iron, silver and bearing alloys fillers for friction and wear reduction 10 p1239 A73-24247

Accelerated testing of solid film lubricants. 10 p1239 A73-24249

Effect of solid lubricants on the physicochemical and friction properties of materials 10 p1225 A73-24635

Friction and wear of self-lubricating composite materials. 10 p1225 A73-24686

Mechanism of the lubricating action of sulfides and selenides of refractory metals 13 p1624 A73-28776

Lubricant film and self lubricating composite materials optimum selection in solid lubricant design, considering performance and cost criteria [ASME PAPER 73-DE-8] 14 p1766 A73-30817

High temperature solid lubricants lubricating and environmental stability characteristics, discussing ball and journal bearings wear test results [ASME PAPER 73-DE-9] 14 p1767 A73-30818

Static, dynamic and fatigue load influence on solid lubricant compact bearings. [ASLE PREPRINT 73AM-1A-1] 17 p2178 A73-34976

A study on some metal-base self-lubricating composites containing tungsten disulfide. [ASLE PREPRINT 73AM-3C-1] 17 p2196 A73-34986

High speed oscillating tests of lubricating composites. [ASLE PREPRINT 73AM-3C-2] 17 p2179 A73-34987

Structure of sputtered molybdenum disulfide films at various substrate temperatures. [ASLE PREPRINT 73AM-3C-3] 17 p2196 A73-34988

Solid film lubricant corrosion study employing salt spray test with sulfur dioxide and synthetic sea water, examining molybdenum disulfide, antimony trioxide and graphite films [ASLE PREPRINT 73AM-3C-4] 17 p2196 A73-34989

German monograph - The tribology of solid lubricants of the type of the alkaline-earth hydroxides in the system Fe-Me/OH₂. 22 p2881 A73-42846

Antifriction materials employing fibers and liquid-metal lubricants 24 p3101 A73-44413

Influence of temperature on the behavior of the rheological properties of plastic carbon-black systems 24 p3101 A73-44471

SOLID NITROGEN
Empirical intermolecular potentials for N₂ and CO₂ from crystal data. 15 p1915 A73-31272

SOLID PHASES
Solid-solid phase transitions determined by differential scanning calorimetry. 01 p0014 A73-11062

Interdendritic structures of a directionally solidified cobalt-base alloy. 02 p0184 A73-12770

Solid phase stretch forming of thermoplastic polypropylene at temperatures below crystalline melting point 03 p0332 A73-13034

Ni, Si and Mn alloying effect on structural transformations, phase composition and mechanical properties of cast Cr-Ni steels 03 p0327 A73-14002

Influence of the composition and structure on the mechanical properties of ultraplasic alloys of the Al-Zn system 04 p0464 A73-15497

Characteristics of secondary phases in heat-resisting alloys. 04 p0465 A73-15580

Structure and composition of certain Laves phases and identification of chi phases in Fe-Mn-Ti alloys 06 p0708 A73-18100

Solid-phase epitaxial growth of Si mesas from Al metallization. 06 p0738 A73-18650

Plagioclase and Ba-K phases from Apollo samples 12063 and 14310. 07 p0881 A73-19714

Phase composition of Nb-1% Zr-C and Nb-2% Hf-C alloys 09 p1108 A73-23237

Peritectic solid phase transformations in cast homogenized Al-Cu-Li-Mn-Cd alloy, noting Li strengthening effect 10 p1236 A73-24927

Zr additions effect on quenched and aged Al-Mg-Li alloy having phases in equilibrium with solid solution 10 p1236 A73-24928

Diffusion layer structure and phase composition during quenched and annealed steel saturation by Cr at high heating rates 10 p1236 A73-24962

Metal matrix composites microstructural alignment by solid state transformation process involving eutectoid decomposition and cellular precipitation 12 p1513 A73-27682

Experimental and thermodynamic study of the equilibria between ferrite, austenite and intermediate phases in the Fe-Mo, Fe-W, and Fe-Mo-W systems. 13 p1633 A73-28136

Nb-Al alloys sigma phase superconductivity characteristics, investigating critical temperature, composition and heat treatment relations 14 p1759 A73-30236

Dependence of some physicochemical properties of plasma-deposited aluminum oxide on sputtering conditions 15 p1881 A73-31211

Study of a niobium-aluminum-silicon system. I - Partial isothermal sections at 1500 and 1300 deg C, and the behavior of the Fe/Si, Al/2 phase 15 p1890 A73-31991

A physical basis for solid-solution strengthening and phase stability in alloys of titanium. 15 p1892 A73-32272

Certain mechanisms of the solid-phase interaction arising during the formation and operation of high-temperature coatings 18 p2322 A73-35877

Effect of interphase boundaries on the kinetics of molybdenum siliconizing 18 p2318 A73-35881

Influence of a solid-phase nickel coating on the sintering kinetics of tungsten wire 18 p2320 A73-36858

Grain growth in commercial alpha and alpha + beta/Ti alloys. 18 p2326 A73-37143

Structure and phase composition of welded joints of zirconium alloy with 2.5% Nb 19 p2439 A73-37266

Effect of iron on the phase composition and mechanism of plastic deformation of titanium 20 p2579 A73-39737

The homogeneity regions of superconducting phases in the molybdenum-platinum system 21 p2717 A73-40320

Binary and ternary Laves phases in systems composed of zirconium and transition metals of the V through VII groups of the periodic system 21 p2718 A73-40848

The influence of phase size on the creep of lamellar and particulate Al-CuAl₂ eutectic composites. 21 p2719 A73-40896

Two phase alloy internal oxidation kinetics, deriving mathematical model with linear law for penetration velocity fluctuations 21 p2719 A73-40898

A study of the real structure of titanium mononitride in its homogeneity region 21 p2721 A73-41225

Diffusion parameters of oxygen in alpha and beta titanium modifications 22 p2874 A73-42098

Specific structural features of the binary phase diagrams of some transition metals in a region containing Laves phases 22 p2877 A73-42453

SOLID PROPELLANT IGNITION
Ignition system development for end-burning solid propellant rocket motor, describing tubular, orifice and perforated type igniter configurations experiments [AIAA PAPER 72-1137] 03 p0355 A73-13444

Physical and chemical properties of solid propellant igniter materials, determining averaged heat of reaction and burning rate values 03 p0352 A73-13485

The starting transient of solid-propellant rocket motors with high internal gas velocities. 04 p0486 A73-14909

Hot particle igniter for end-burning solid propellant rocket motors, noting ignition capability at 219 K and 110,000 ft simulated altitude 04 p0485 A73-14919

Propellant grain surface contamination effect on ignition transient characteristics of solid rocket motor. [AIAA PAPER 72-1198] 04 p0487 A73-14920

German book - Solid rocket propulsion systems II: Theory and technology. 06 p0740 A73-18074

Gas-phase ignition model for some solid fuels in a shock tube 07 p0865 A73-19989

An asymptotic analysis of radiant and hypergolic heterogeneous ignition of solid propellants. 07 p0866 A73-20364

Reduced scale experimental study of prepropul propulsion system ignition phases, defining pressure buildup curve shape and ignition limits [ONERA, TP NO. 1182] 09 p1135 A73-22711

Loading configurations with large combustion surface and reduced thickness for solid propellant rocket ignition [ONERA, TP NO. 1211] 10 p1262 A73-23658

Restart transients of hybrid rocket engines. 11 p1411 A73-26669

Thermal limit of heterogeneous ignition 19 p2503 A73-37512

Concentration and combination limits of heterogeneous ignition 21 p2791 A73-40704

Ignition and flame spreading over a solid fuel - Non-similar theory for a hot oxidizing boundary layer. 22 p2936 A73-42809

Dynamic effects on ignitability limits of solid propellants subjected to radiative heating. 22 p2899 A73-42813

SOLID PROPELLANT ROCKET ENGINES
Development of a small end-burning type motor by using pellet impregnated propellant. 01 p0090 A73-11108

Stability boundaries of solid rocket motors. 01 p0091 A73-11116

Lambda-4S solid propellant four-stage sounding rocket and scientific satellite launcher, describing design, operational and performance features 01 p0091 A73-11157

M-4 S four-stage solid propellant rocket launch vehicle for scientific satellites, detailing design and performance characteristics 01 p0111 A73-11158

Thrust modulation of solid propellant rocket motors [ONERA, TP NO. 1155] 02 p0203 A73-11990

Research on combustion instability and application to solid propellant rocket motors. II. [AIAA PAPER 72-1049] 03 p0353 A73-13380

Review of nozzle damping in solid rocket instabilities. [AIAA PAPER 72-1050] 03 p0353 A73-13381

Solid propellant combustion instability suppression devices [AIAA PAPER 72-1051] 03 p0353 A73-13382

Survey of ONERA and SNPE work on combustion instability in solid propellant rockets. [AIAA PAPER 72-1052] 03 p0353 A73-13383

Solid propellant rocket service life prediction based on propellant grain structural failure analysis, discussing surveillance program rationale for various conditions [AIAA PAPER 72-1085] 03 p0354 A73-13407

Considerations concerning the service life, handling and storage of double base solid propellant rocket motors. [AIAA PAPER 72-1086] 03 p0351 A73-13408

Thrust reversal systems for solid propellant rocket motors last stage separation from payloads, examining pressure decay under isothermal and adiabatic assumptions [AIAA PAPER 72-1110] 03 p0355 A73-13425

Solar escape achievement by solid propulsion augmentation system and design independent of multiplanetary swingby, analyzing cost effectiveness of different programs
[AIAA PAPER 72-1163] 03 p0382 A73-13464

Radiation base heating from solid propellant launch vehicle exhaust plumes.
[AIAA PAPER 72-1168] 03 p0397 A73-13466

Titan III convective base heating from solid rocket motor exhaust plumes.
[AIAA PAPER 72-1169] 03 p0382 A73-13467

Solid propellant rocket motors exhaust smoke minimization, discussing smoke formation mechanism and optical properties relationship to propellant characteristics
[AIAA PAPER 72-1192] 03 p0352 A73-13482

Fluidic ignition system with two-component aerodynamic resonance heating/pneumatic match/and hand pump for solid propellant sounding rocket engine
[AIAA PAPER 72-1197] 03 p0252 A73-13486

The starting transient of solid-propellant rocket motors with high internal gas velocities.
[AIAA PAPER 72-1119] 04 p0486 A73-14909

Propellant grain surface contamination effect on ignition transient characteristics of solid rocket motor
[AIAA PAPER 72-1198] 04 p0487 A73-14920

Russian book - Strength of viscoelastic materials relative to solid-propellant rocket-motor charges.
04 p0517 A73-15967

Solid rocket motors for the Space Shuttle booster.
[SAE PAPER 720804] 05 p0607 A73-16648

An experimental investigation of some heat transfer characteristics on an orbiter/HO-tank/SRM Space Shuttle configurations, freestream Mach number equal to 8.0.
[AIAA PAPER 73-92] 05 p0640 A73-16856

Subliming solid propellant microthruster for satellite stabilization, discussing operational principles and design features
07 p0866 A73-18927

Solid propellant rocket engines - Design and development of components in refractory and stratified materials.
07 p0867 A73-18992

Astrobac F sounding rocket system design and development, describing advanced propulsion technology test program and results
[AIAA PAPER 73-300] 09 p1156 A73-23219

U.S. double-base solid propellant tactical rockets of the 1940-1955 era.
[AIAA PAPER 73-274] 09 p1135 A73-23248

Russian book - Fundamentals of the theory of operational processes in solid-propellant rocket systems.
10 p1262 A73-23948

Improved corrosion protection for solid rocket propulsion systems.
13 p1645 A73-29273

Russian book - Solid-fuel ballistic rockets.
14 p1804 A73-30356

Cost effective space shuttle solid rocket booster recovery parachute system planning, discussing model drop and structural load testings
[AIAA PAPER 73-441] 15 p1825 A73-31427

Russian book - Physical principles of rocket weaponry.
15 p1944 A73-32419

Space-flight qualification of solid-propellant units in the example of the cold-gas generator for the booster rocket Europa I/II
16 p2047 A73-33394

Solid propellant rocket burning rate optimization at constant thrust by imbedded inert heat conducting fibers, analyzing flight performance
18 p2342 A73-36064

Space shuttle solid rocket boosters ocean recovery, discussing mission requirements, parachute configurations, tradeoff studies and model testing
[AIAA PAPER 73-602] 18 p2358 A73-36084

Space shuttle solid rocket boosters mission and systems requirements, considering thrust vector control and staging/separation, electrical and recovery systems
[AIAA PAPER 73-606] 18 p2358 A73-36086

Impingement of small, very high pressure solid rocket motor plumes upon nearby surfaces.
[AIAA PAPER 73-730] 18 p2342 A73-36347

Space Shuttle solid rocket stage recovery, retrieval, and refurbishment.
19 p2492 A73-37599

Kennedy Space Center Space Shuttle facilities.
19 p2417 A73-37601

Space Shuttle development, qualification, acceptance and horizontal/vertical flight tests for Orbiter, solid rocket motor and drop tank element subsystems
19 p2492 A73-37602

On the ultrasonic inspection of separation in solid propellant rocket motors.
20 p2568 A73-38646

Russian book - Solid-propellant rocket engines.
22 p2900 A73-41880

Induced plasticization - An inner bore surface treatment technique for solid-propellant rocket motors.
22 p2897 A73-42626

SOLID PROPELLANTS

NT CASE BONDED PROPELLANTS

NT COMPOSITE PROPELLANTS

NT DOUBLE BASE ROCKET PROPELLANTS

NT PLASTIC PROPELLANTS

NT SOLID ROCKET PROPELLANTS

Recent developments in testing unstable burning characteristics of solid propellants.

01 p0089 A73-11115

On some relation between the mechanical properties and the bond strength of elastomer to solid inclusion in solid propellant.

01 p0090 A73-11117

Photoelastic stress analysis of solid propellant grains.

01 p0090 A73-11118

The determination of moisture in propellant charge powders and solid propellants

02 p0202 A73-11565

Measuring combustion response by a forced oscillation method.

[AIAA PAPER 72-1054] 03 p0397 A73-13385

Failure detection in solid propellants.

[AIAA PAPER 72-1087] 04 p0485 A73-14906

Propellants and combustion. I - Role of binder in solid propellant combustion.

[AIAA PAPER 72-1121] 04 p0485 A73-14910

A novel high area ratio T-burner for characterizing metalized propellants.

[AIAA PAPER 73-219] 05 p0563 A73-16949

Acoustic amplification during solid propellant combustion.

07 p0865 A73-19390

Combustion catalysis model of a single-component fuel/as applied to ammonium perchlorate/

07 p0865 A73-19391

Solid propellant ballistic properties from pressure changes due to combustion, considering transient effects

13 p1669 A73-28997

Strain measurements in the solid propellant of a large booster structural test vehicle.

13 p1669 A73-29304

Simulation of the compounding in a single base propellant (SBP) process.

17 p2220 A73-34819

Viscoelastic fracture of solid propellant pressurization condition.

[SESA PAPER 2114A] 17 p2220 A73-35449

Stability of a conical burning surface during solid fuel combustion in a semiclosed volume

20 p2627 A73-39290

Quasi-steady gas-phase flame theory in unsteady burning of a homogeneous solid propellant.

21 p2790 A73-40430

Combustion of a solid fuel in a gaseous oxidizer flow

21 p2754 A73-40701

A method for calculating the burning rates of solid fuels in a turbulent gaseous oxidizer flow at Le unequal to unity

23 p3049 A73-43729

SOLID ROCKET BINDERS

Catalytic effects of copper chromite and iron oxide on AP-HTPB binder sandwich combustion to 3200 psia by cinerphotomacrography

[AIAA PAPER 72-1120] 03 p0352 A73-13434

SOLID ROCKET PROPELLANTS

NT DOUBLE BASE ROCKET PROPELLANTS

Characterization of the mixed oxides of lithium and aluminum.

01 p0089 A73-11113

The T-burner test method for determining the combustion response of solid propellants.

[AIAA PAPER 72-1053] 03 p0353 A73-13384

Failure criterion for a propellant of a spherical solid rocket motor.

[AIAA PAPER 72-1088] 03 p0351 A73-13409

Determination of solid-propellant transient regression rates using a microwave Doppler shift technique.

[AIAA PAPER 72-1118] 03 p0351 A73-13433

Pressure exponent of controllable solid rocket propellants.

[AIAA PAPER 72-1135] 03 p0352 A73-13442

Continuing development of the short-pulsed ablative space propulsion system.

[AIAA PAPER 72-1154] 03 p0356 A73-13457

The influence of combustor parameters on the combustion of particle-laden fuels in ducted flows.

[AIAA PAPER 73-177] 05 p0640 A73-16919

Computing pressure cure viscoelastic effects in solid propellants.

05 p0606 A73-17208

Interaction of sound and flow in T-burners - Experiments compared with theory.

[AIAA PAPER 73-220] 06 p0741 A73-17662

German book - Solid rocket propulsion systems II: Theory and technology.

06 p0740 A73-18074

Reduced scale experimental study of propergol propulsion system ignition phases, defining pressure buildup curve shape and ignition limits

[ONERA, TP NO. 1182] 09 p1135 A73-22711

U.S. double-base solid propellant tactical rockets of the 1940-1955 era.

[AIAA PAPER 73-274] 09 p1135 A73-23248

The influence of diameter on the burning velocity of strands of solid propellant.

10 p1261 A73-23560

Perchlorate degradation of ethyl oleate in solid propellants.

10 p1262 A73-23758

Heterogeneity effect on L instability of solid rocket propellant combustion, using sideways sandwich model

11 p1450 A73-25373

Homogeneous and composite solid propellants, discussing rocket motor performance, energetics, smokeless exhaust, energy-weight relations and cost

14 p1784 A73-30135

Linear nonstationary effects - A source of information on the kinetics of reactions on the surface of a solid fuel

14 p1818 A73-30873

Effects of composition on acceleration induced burning-rate augmentation.

15 p1925 A73-31661

Experimental study of the condensed phase in the combustion products of metallized solid propellants

16 p2086 A73-33965

Contribution to the theory of high-frequency pulsations caused by instability of the combustion process in a solid-propellant rocket engine

21 p2753 A73-40391

Effect of secondary oxidizer supply through a porous solid fuel on the hybrid combustion process

23 p3019 A73-43783

Solid propellants with a pulsating burning rate

24 p3121 A73-45200

Mechanism of erosive burning of solid rocket propellants.

24 p3121 A73-45385

SOLID ROTATION

U ROTATING BODIES

SOLID SOLUTIONS

High temperature effects on near order transformations in TiC-WC solid solutions during heat treatment and cooling, using X ray diffraction scattering measurements

01 p0064 A73-10615

Singularities of the temperature dependences of the heat conduction coefficients of solid solutions of the niobium-zirconium system.

01 p0066 A73-11338

Cast Nb alloys ductility enhancement by heat treatment, discussing solid solution decay kinetics and carbides composition of Nb-Mo-Zr-C system

01 p0066 A73-11344

Influence of the degree of decomposition of a solid solution of zirconium in aluminum on the recrystallization temperature of an aluminum-zinc-magnesium-zirconium system alloy

03 p0327 A73-13972

Dislocation dynamics in niobium-oxygen solid solutions.

04 p0462 A73-15303

Solubility of zirconium and niobium in solid-state copper

04 p0464 A73-15495

Some factors affecting high-temperature strength of matrix in heat resisting alloys.

04 p0464 A73-15577

Intercrystalline structures effect on precipitation reactions in supersaturated solid solutions, noting Widmanstatten structure growth in U alloy

04 p0467 A73-15953

Phase transformations in Al-rich Al-W alloys rapidly quenched from the melt.

04 p0468 A73-15983

Some optical properties of solid solutions in the 2GaAs-ZnSAs₂ section

05 p0605 A73-16612

Investigation of precipitation morphology in Cu-Ti alloys

06 p0707 A73-18037

Cr effect on N solubility increase during Fe alloy nitriding, noting temperature effect on nitrides precipitation

06 p0697 A73-18054

Heat conductivity and the Lorentz number of tungsten-rhenium alloys within the solid-solution limits from 0 to 27% Re at temperatures between 1200 and 3000 K

06 p0710 A73-18556

Thoria stability in TD-NiCr at high temperatures in the presence of chromium in solution.

06 p0713 A73-18771

Solubility of oxygen in ZrC.

07 p0838 A73-19199

On the influence of grain size and vacancy annihilation on the Portevin-Le Chatelier-effect

08 p0977 A73-21021

Strengthening mechanisms in ferritic creep resistant steels.

08 p0982 A73-21797

The solubility of hydrogen in rhodium, ruthenium, iridium and nickel.

09 p1047 A73-21981

Alloying elements effects on voids nucleation in irradiated Al alloys, tabulating defect concentration

09 p1101 A73-22175

Matthiessen's rule and the electric resistance of solid solutions of silicon in iron at high temperatures 09 p1104 A73-22602

Confirmation of electronic paramagnetic resonance of the existence of an ordered phase in the zirconium-calcium system 09 p1135 A73-23031

High temperature creep in nickel and its alloys 09 p1108 A73-23229

Mechanical behavior of solid solutions of centered cubic symmetry obtained by limited addition of titanium to the iron 10 p1231 A73-23770

Work function of the principal faces of single crystals of rhenium solutions in molybdenum 10 p1231 A73-23818

Formation of continuous solid solutions of intermetallic compounds 10 p1260 A73-24512

Change in the superconducting properties of vanadium after the introduction of tantalum impurity atoms 10 p1261 A73-24761

Determination of alpha plus gamma/gamma phase boundaries in Fe-Cr-Ni, Fe-Cr-Co, and Fe-Cr-Mn systems 11 p1384 A73-26108

Temperature dependence of the activity and solubility of carbon in pure nickel 11 p1384 A73-26110

Ion distribution in the crystal structure of complex spinel phases of the Mn-Fe-Ti-O system 11 p1386 A73-26674

Relaxation stability of iron and nickel alloys at high temperatures 12 p1509 A73-26898

Interaction of molybdenum with elements of the iron group and carbon 12 p1510 A73-26903

Temperature dependence of the solubility of scandium in solid magnesium 12 p1510 A73-26908

Precipitation and its hardening effect in Ni-rich NiTi. 12 p1511 A73-27057

Stimulated emission of light from solid solutions of tin and lead chalcogenides in the region of 10 microns. 12 p1507 A73-27519

Determination of the boundaries of single-phase edge regions in the Mo-Cu-Ni system in solid state 12 p1513 A73-27559

Equilibrium of vanadium carbide with an alpha or gamma solid solution in the iron-rich Fe-Cr-V-C system at temperatures from 700 to 1150 C and at a carbon concentration of 0.30% 12 p1513 A73-27684

Possibility of atom displacements in solids under the action of laser light pulses 13 p1626 A73-28003

Crystallization of nickel-based alloys and indium-lithium system alloys at ultrahigh cooling rates 13 p1632 A73-28112

Ternary nickel-vanadium-oxygen compound and solid solutions formation by vacuum calcination of vanadium and nickel oxides mixtures 13 p1634 A73-28203

Determination of the boundaries of fluorite-type Y2O3 solid solutions in HfO2 13 p1645 A73-28292

NiO-CoO solid solutions defect structure from high temperature measurements of integrated Bragg peak intensities 13 p1645 A73-28934

Surface solid solutions and chemical compounds formation due to gas sorption by titanium and barium 13 p1663 A73-28968

Solubility of nitrogen and hydrogen in cobalt and cobalt alloys - A review. 13 p1637 A73-29245

Strengthening and fracture of Ta, Nb, Mo and W binary solid solutions with short range order. 13 p1638 A73-29452

Dynamic and static strain aging in Al-Mg solid solution alloys. 13 p1639 A73-29458

Development of austenitic heat-resistant steel containing a high concentration of nitrogen. 13 p1642 A73-29516

Crystallostructural investigation of the eutectoid decomposition of copper-beryllium alloys - Ordering accompanied by formation of Cu2Be metastable solid solution 14 p1760 A73-30587

Characteristics of the decomposition of an interstitial-impurities solid solution in molybdenum during recrystallization 14 p1760 A73-30589

Solid solution strengthening of high purity niobium alloys. 14 p1761 A73-30631

Solute aluminum strengthening and strain aging in Ti-Al alloys at 78-810 K 14 p1761 A73-30639

Superconductivity and electron structures of a solid solution of titanium in niobium 14 p1784 A73-30811

Investigation of interdiffusion in the nickel-tungsten and palladium-tungsten systems 14 p1764 A73-30864

Application of a cluster component technique in the interpretation of concentration dependences of the properties of binary metal alloys and anion-substituted spinel solid solutions 15 p1923 A73-31205

Subscale inclusions formation in solid Fe alloys with small amounts of Mn and other elements, noting inward oxygen thermal diffusion role and metallurgical implications 15 p1891 A73-32171

Transition metal alloys solid solutions, discussing thermodynamics, interatomic interactions, Debye temperatures, free energy, entropy, magnetic effects and incomplete d shells 15 p1892 A73-32213

A physical basis for solid-solution strengthening and phase stability in alloys of titanium. 15 p1892 A73-32272

Al addition effect on strength of Ti via short range order, considering strengthening by alpha stabilizing solutes 15 p1893 A73-32273

Critical survey of studies of the equilibrium phase diagram of the Ti-W system 15 p1893 A73-32513

Effect of ordering on the properties of oxygen solid solutions in titanium 15 p1893 A73-32516

Structure and decay characteristics of unstable beta-solid solutions of the Ti-V system 15 p1893 A73-32519

Passive alpha structure Ti base alloys with Al, Mn, Sn, Nb, Cr or Mo, investigating dissolution characteristics by chronoamperometric measurement using sulfuric acid 15 p1895 A73-32568

Thermal conductivity and Lorenz number of tungsten-rhenium alloys in the solid-solution region (0-27% Re/ at temperatures of 1200-3000 K. 16 p2026 A73-33582

Principal component determination in mercury and cadmium tellurides and in solid solutions of them 17 p2220 A73-35559

Thermodynamics of b.c.c. solid solutions of hydrogen in niobium, vanadium and tantalum. 17 p2193 A73-35623

X ray diffraction analysis of Mo-Ta and Mo-C solid solutions, relating transition and nontransition metal electronic structures and stacking fault energy 18 p2325 A73-36808

Some electron structure characteristics of W-Re solid solutions 18 p2325 A73-36809

Limit of the two-phase region of Mo/Ni, Cu/ and Cu/Ni, Mo/ solid solutions in the Mo-Cu-Ni system 18 p2325 A73-36859

Selection of the composition for the matrix of a composite material, which will not dissolve the reinforcing fibers 18 p2328 A73-36860

Titanium carbide nitride and zirconium niobium carbide solid solutions electromotive forces, examining temperature-concentration dependencies, carbide and carbonitride conductivity mechanisms, resistivity and Hall effect 18 p2325 A73-36964

The influence of primary precipitates on the tensile strength of unidirectionally solidified /Fe, Cr/-/Cr, Fe/7C3 in-situ grown composites containing 30 wt % Cr. 19 p2442 A73-38088

Continuous decomposition of gamma solid solution in iron-nickel-titanium alloys 20 p2579 A73-39736

Lattice constants vs compositions of body centered tetragonal solid solutions of mixed rare earth dicarbides according to Vegard law 21 p2751 A73-40322

Ta-Nb-Re system phase diagram plotted by physicochemical analysis methods, establishing region of existence of ternary solid solutions and temperature dependence 21 p2718 A73-40488

Relaxation resistance of alloys based on iron and nickel at high temperatures. 21 p2720 A73-41031

Electrical conductivity and superconductivity of vanadium, niobium, and chromium solid solutions 22 p2873 A73-41963

Study of the structure and properties of alloys of the V-Al, Cr-Al and V-Cr-Al systems in the region of solid solution bcc ordering 22 p2873 A73-42088

Interaction of interstitial impurities with iron-subgroup metals in as-cast molybdenum-based dilute solid solutions 22 p2873 A73-42090

Decay of the solid beta-solution in beta alloys of titanium and zirconium during tempering 22 p2874 A73-42092

Nature of the strain-hardening of titanium beta solid solutions 22 p2874 A73-42096

Structure of the phase diagrams of the ternary systems /Mo, W/ - /Ti, Zr, Hf, V, Nb, Ta/ - C 22 p2877 A73-42455

Thermodynamics of transition metal-hydrogen solid solutions. 22 p2880 A73-43076

Mo content influence on heat resistant Ni base alloys corrosion and oxidation resistance and gamma-prime phase solution temperature and amount 23 p2989 A73-43435

Phase relations and diagram investigation for zirconium silicate-titanium dioxide system by quenching method, obtaining solid solution formation conditions and lattice constants 23 p2998 A73-44131

Steady-state creep characteristics of an Fe alloy containing 3.5 at.% Mo. 23 p2994 A73-44153

Surface solid solutions and chemical compounds formation due to gas sorption by titanium and barium 23 p3008 A73-44320

Optical characteristics of phononless lines 24 p3109 A73-44427

Stability of the gamma-prime Co3Ti compound in simple and complex cobalt alloys. 24 p3099 A73-45075

Investigation of the kinetics of the redistribution of alloying elements between the alpha solid solution and cementite in cobalt and nickel steels 24 p3100 A73-45362

SOLID STATE

Pulsed laser irradiation effects on solid deuterium slab, deriving two-temperature electron-ion model 15 p1884 A73-31660

Effect of the superplasticity of titanium and its alloys, and the use of this phenomenon for welding in a solid state 22 p2866 A73-42093

SOLID STATE DEVICES

NT AVALANCHE DIODES

NT FIELD EFFECT TRANSISTORS

NT GALLIUM ARSENIDE LASERS

NT GERMANIUM DIODES

NT JUNCTION DIODES

NT JUNCTION TRANSISTORS

NT METAL OXIDE SEMICONDUCTORS

NT MIS (SEMICONDUCTORS)

NT NEURISTORS

NT PARAMETRIC DIODES

NT PHOTODIODES

NT PHOTOTRANSISTORS

NT PHOTOVOLTAIC CELLS

NT RUBY LASERS

NT SEMICONDUCTOR DEVICES

NT SEMICONDUCTOR LASERS

NT SILICON TRANSISTORS

NT SOLID STATE LASERS

NT THERMISTORS

NT THERYSTORS

NT TRANSISTOR AMPLIFIERS

NT TRANSISTORS

NT VARACTOR DIODES

NT VARISTORS

NT YAG LASERS

The effect of the surface electric charge on the gain of a solid-state traveling-wave amplifier 01 p0023 A73-10429

Linear rapid frequency settling time solid state voltage controlled oscillators /VCO/ for electronic countermeasure and B-scan tracking radar applications 01 p0024 A73-10723

Prototype solid state radio sounder with digitization concept of multipulse integration for LF sounding of lower ionosphere, noting performance 01 p0043 A73-10909

Resolution of a solid-state image amplifier 03 p0282 A73-13664

Improvements in solid state radiographic converter screens. 05 p0574 A73-16280

On some noise properties of high frequency solid-state oscillators. 06 p0673 A73-17714

Optimum R.F.-power transport in Nd-limited gallium-arsenide travelling-wave amplifiers. 07 p0798 A73-19159

Solid state microwave electronics technology review covering parametric amplifier, maser, tunnel and avalanche diodes, transistors, and transmission, filtering and passive signal processing techniques 08 p0942 A73-20701

Radar systems development under solid state electronics advances impact, discussing silicon ICs, HF transistors, hybrid microwave circuits, parametric amplifiers and p-i-n diodes applications 08 p0949 A73-21650

Microstrip solid state power amplifiers with transistors and varactors for spaceborne applications in L and S band ranges 09 p1066 A73-23428

Operating conditions of a triggered pulse generator with a limiter diode 10 p1195 A73-24380

Development of cavities for microwave solid state sources. 11 p1338 A73-26150

Multiple target CW FM Doppler radar with solid state devices and CRT indicator, noting range resolution advantage over pulse radar 12 p1469 A73-27164

A new statistical design method for thinned solid-state phased arrays. 13 p1594 A73-29231

NEREM 72; Northeast Electronics Research and Engineering Meeting, Boston, Mass., October 30-November 3, 1972, Record. Part 1 - Technical Papers. 16 p1886 A73-32717

The impact of silicon technology on near-infra-red and low-light-level imaging. 16 p2012 A73-32867

Solid-state transmitter for VHF/UHF space telemetry. 16 p1979 A73-33104

Annual National Relay Conference, 21st, Oklahoma State University, Stillwater, Okla., May 1, 2, 1973, Proceedings. 17 p2132 A73-34088

A user-oriented guide to the design and application of solid state relays. 17 p2132 A73-34089

High reliability solid state force sensors for flight control systems. 17 p2165 A73-34603

A solid state bonding and packaging technique for integrated sensor transducers. 17 p2166 A73-34618

Expanded built-in-test for advanced electrical systems for aircraft. 17 p2109 A73-35248

The cause and effects of dc offset voltage in solid state ac power controllers. 17 p2109 A73-35255

Book - Solid state electronic circuits: For engineering technology. 18 p2292 A73-35899

Ground stations in Intelsat 4 communication satellite radio relay system, discussing all-solid-state equipment design, carrier frequency assignment and antenna installation 20 p2523 A73-38723

Papers on adaptive electronic devices, circuits and systems covering logic nets, solid state and ferroelectric devices and memory devices and artificial intelligence 20 p2535 A73-39135

Design, performance, and cost considerations for solid-state arrays. 21 p2662 A73-40648

Silver powder anode, perylene-iodide cathode and ionically conductive solid cyanide-iodide electrolyte battery construction and performance tests [ECS PAPER 12] 21 p2635 A73-40841

Solid state AgCl detectors for nuclear tracks with on- and off-response at choice - Applications to life sciences. 22 p2814 A73-42179

Radio astronomical traveling wave maser with ruby or doped rutile single crystals, superconducting magnet, cryogenic equipment and low noise temperature 23 p2953 A73-43375

Theory for the steady-state operation of a thin-film regenerative optron 23 p2959 A73-43617

An automated Dobson spectrophotometer. 23 p2982 A73-43855

SOLID STATE LASERS

NT GALLIUM ARSENIDE LASERS

NT RUBY LASERS

Nd glass and ruby lasers in mode locking operation for picosecond light pulses emission, noting pulse duration measurement 01 p0059 A73-10713

Stable optico-mechanical Q-factor modulator for a laser resonator 01 p0059 A73-10797

Investigation of the statistical properties of ultrashort light pulses with the aid of two-photon absorption in semiconductors 01 p0061 A73-11282

Gas and solid state lasers amplitude and phase fluctuations calculated from Langevin equations, noting spectral line width and ring laser wave coupling 01 p0061 A73-11355

Polycrystalline organic compounds effect on second harmonic generation of neodymium laser, noting relation between nonlinear susceptibility and intramolecular charge transport 02 p0176 A73-12097

Astronomical observatory lunar ranging system with high radiance neodymium-glass laser and transmitting telescope, noting tracking accuracy 02 p0151 A73-12246

Spectroscopic properties of ruby and neodymium lasers under the action of a Co-60 gamma ray 02 p0176 A73-12355

Investigation of the disintegration of semiconductors exposed to laser radiation 03 p0349 A73-13660

Direct measurement of pulse broadening in the second harmonic of mode-locked Nd-glass laser. 05 p0585 A73-17221

Mode locking picosecond pulse Nd glass laser design for reliable and reproducible operation as function of pump power, mirror alignment and saturable absorber 06 p0700 A73-18293

Second-harmonic conversion of laser radiation generated under free-oscillation conditions. 06 p0702 A73-18594

High-power Y3Al5O12:Nd3+/ laser with an explosion-type lamp. 06 p0703 A73-18597

Large-aperture Nd-glass laser amplifier for high-peak-power application. 06 p0704 A73-18791

Pulsed laser produced holograms with iron doped lithium niobate, noting application in high capacity information storage 08 p0964 A73-21051

The powering and synchronization of a solid-state laser operating at a repetition rate of several Hertz 08 p0976 A73-21716

Quasi-stationary emission from ruby and neodymium-glass lasers 08 p0976 A73-21718

Laser optical double resonance and efficient infrared quantum counter upconversion in LaCl3:Pr3+/ and LaF3:Pr3+/ 09 p1090 A73-21936

A new approach to picosecond laser pulse analysis shaping and coding. 09 p1090 A73-22077

Peak-mode operation and self-Q-switching in a solid state laser 09 p1094 A73-22487

A picosecond single-pulse laser 09 p1095 A73-22661

Resonant multiphoton ionization of a cesium atomic beam by a tunable-wavelength Q-switched neodymium-glass laser. 09 p1098 A73-23472

Immersion liquids for a homogeneous optically mixed laser 10 p1227 A73-23768

Lasing characteristics of neodymium glasses at the 0.92-micron wavelength 10 p1260 A73-24581

Neodymium-glass laser with tunable pulse width 11 p1376 A73-25433

Stability of the monochromatic mode of emission in a multimode solid-state laser 11 p1376 A73-25631

Mechanism of passive negative feedback in the cavity of a solid-state laser 12 p1504 A73-26884

Influence of the spectral characteristics of liquid filters on the thermal regime and efficiency of a neodymium-glass laser 12 p1505 A73-26891

Improving the angular divergence of the emission from a neodymium-glass laser with a high pulse energy level 12 p1505 A73-26963

Single-frequency neodymium-glass lasers under nonspiking free-oscillation and Q-switched conditions. 12 p1506 A73-27502

Investigation of a pulsed laser utilizing an exploding-film Q switch. 12 p1507 A73-27504

Influence of a nonlinear lens on the stability of steady-state laser emission. 12 p1507 A73-27506

Influence of the inversion inhomogeneity on the transverse structure of oscillations in solid-state lasers. 12 p1507 A73-27518

Investigation of the delay of stimulated emission from a CaF2:Dy2+/ laser relative to pumping pulses. 13 p1629 A73-29431

Detection of transient absorption in YAG laser crystals using combined laser. 14 p1756 A73-29930

Quantum irreversible statistical thermodynamics with allowance for occurrence of many temperatures based on principle of isentropic motion, applying to laser action 14 p1756 A73-30150

Lunar range measurements with a high-radiance frequency-doubled neodymium-glass laser system. 14 p1756 A73-30152

Spectral width of stationary emission from a laser with a spectrally inhomogeneous solid active element 14 p1757 A73-30266

Spike operation and self Q-switching in a solid-state laser. 14 p1757 A73-30323

Gas absorption lines detection based on multiple light passage through absorbing medium during generation process, noting radiation spectra of neodymium glass laser 14 p1757 A73-30331

A controlled single-pulse neodymium-glass laser 14 p1757 A73-30369

Concentration dependence of the lasing parameters of a laser based on CaF2:Dy2+ crystals 15 p1884 A73-31221

Emission characteristics of a tube-shaped laser oscillator. 15 p1885 A73-31940

Unsteady processes in multimode lasers with a nonuniformly widening line of lasing 15 p1886 A73-32329

Phase correlations of longitudinal modes in a laser under free emission conditions 15 p1886 A73-32336

A review of near-infra-red optically pumped solid state lasers. 16 p2023 A73-32856

Spatial correlation functions of the field and intensity of laser radiation 16 p2024 A73-34053

Electrooptical Q-switching /EQQS/ in solid-state laser resonators 17 p2184 A73-34917

Laser energy absorption by plasma for controlled thermonuclear fusion, comparing uses of electrically pumped gas, chemical and solid state lasers 17 p2185 A73-35379

Investigation of the characteristics of a mode-locked Nd:glass laser with the aid of a picosecond streak camera. 17 p2186 A73-35796

Russian book on solid state pulsed laser design and construction covering optical, electronic and cooling elements, amplifiers, energy storage, illuminators and semiconductor instruments 18 p2321 A73-35875

Control of laser-pulse shape with the aid of an organic dye switch 18 p2322 A73-36558

Stability of the output oscillation amplitude in a linear laser amplifier 18 p2322 A73-36665

Theory of two-channel laser action in spectrally inhomogeneous media. I - Noncorrelated frequencies 19 p2437 A73-37958

Improving the angular divergence of a neodymium-glass laser beam having a high radiation energy per pulse. 19 p2438 A73-38146

Stability of the monochromatic generation mode in multimode solid-state lasers. 19 p2438 A73-38147

A frequency-tunable mode-locked CW Nd:glass laser. 19 p2438 A73-38276

Methods for alignment of lasers with unstable resonators. 20 p2573 A73-39686

Generation of fifth picosecond laser harmonic. 20 p2574 A73-39700

Probability balance equations for energy level population analysis of ultrashort pulse solid state laser generation and amplification 21 p2712 A73-40309

Electron temperature and ionization state in laser produced plasmas. 21 p2745 A73-40470

Characteristics of a laser using a grid as the resonator output mirror 21 p2713 A73-40528

Cw degradation at 300 K of GaAs double-heterostructure junction lasers. I - Emission spectra. II - Electronic gain. 21 p2715 A73-40964

Surface wave radiation pattern determination for solid state lasers, taking into account dielectric interface presence 21 p2716 A73-41113

Generation of high-power light pulses at wavelengths 1.06 and 0.53 microns and their application in plasma heating. II - Neodymium-glass laser with a second-harmonic converter. 22 p2869 A73-42248

German monograph - Materials removal in the case of the drilling of holes with the aid of solid-state lasers. 22 p2866 A73-42699

Stimulation of two-valent rare earth ion luminescence in CaF2 crystals by ruby and neodymium lasers 22 p2870 A73-42725

Maximum inversion measurement above threshold as function of pump power for Nd glass laser operating in transverse mode 22 p2871 A73-43081

Investigation of the statistical properties of ultrashort light pulses by two-photon absorption in semiconductors. 23 p2987 A73-43503

Study of the parameters of three-dimensional holographic gratings in LiNbO3 crystals 23 p2987 A73-43717

Theoretical possibilities for the creation of a gamma laser /gazer/ using nuclear transitions 23 p2988 A73-44092

Stimulated gamma emission in long-lived nuclear isomers, proposing gamma lasers based on Mossbauer line broadening effect 23 p2988 A73-44093

Nd-doped Yttralox ceramic lasing performance and interrelationship between ceramic processing, microstructure and optical quality of sintered product
24 p3097 A73-45414

SOLID STATE PHYSICS

Propagation of submillimeter-band electromagnetic waves in the drifting plasma of a solid
01 p0017 A73-10976

Laser related Bell Laboratories research on light scattering, solid state physics, nonlinear optics, materials science, quantum electronics and ultrashort light pulses
01 p0060 A73-11214

Book - Solid-state mechanics 2.
02 p0233 A73-11976

Lunar thermal convection via solid state creep processes, discussing departure from hydrostatic equilibrium figure
03 p0369 A73-13105

Relative importance of forces of interaction which create, the grains of a very thin metallic film, the radiation of thermodynamic equilibrium on the one hand, and zero oscillations of the field on the other hand
03 p0349 A73-13605

Influence of carrier drift on the propagation of electromagnetic wave in a solid-state plasma.
04 p0480 A73-15473

Thermal noise calculation of single-carrier space-charge-limited current in a non-insulating solid.
12 p1530 A73-27029

Book on semiconductor opto-electronics covering solids optical constants, classical and quantum mechanical dispersion theory, absorption processes, magneto-optical and photo-electrical effects, etc
12 p1531 A73-27449

Russian book on quantum radio physics, Volume 1 covering photons and nonlinear media, matter-radiation interaction, electromagnetic fields, relaxation, emission, solid state physics, etc
12 p1508 A73-27924

Book - The physics and circuit properties of transistors.
15 p1850 A73-31574

SOLID SURFACES

NT CRYSTAL SURFACES

Book on surface ionization covering atomic and molecular ionization during thermal desorption from high melting point solid surfaces
03 p0345 A73-13996

Ion microprobe analyzers for solid surfaces high resolution mass spectrometric chemical analysis, using focused ion beam sputtering technique
07 p0822 A73-19171

Diffusion theory for adsorption and desorption of gas atoms at surfaces.
09 p1047 A73-22073

The solid-vacuum interface; Proceedings of the Second International Symposium on Surface Physics, Technische Hogeschool Twente, Enschede, Netherlands, June 21-23, 1972.
11 p1325 A73-25201

Electric field interaction with polar molecules at varying density diffusing through solid body surface, deriving dispersion law for density and potential fluctuations
12 p1526 A73-27939

Gas molecule-solid surface interactions, considering rainbow scattering, roughness at molecular scale, potential well and statistical analysis procedures
13 p1663 A73-28912

Dislocation-type mechanism of the influence of solid surface films on the deformation and fracture of metals
18 p2319 A73-35891

Two field continuum model of magnetic sheath adjacent to absorbing solid surfaces, using Bohm criterion and MHD boundary layer equation approximation
19 p2464 A73-37162

Dispersion model of a single-vortex function of structural scattering of atoms by surfaces
19 p2462 A73-37842

Formation of a periodic wave structure on the dry surface of a solid by TEA-CO₂-laser pulses.
19 p2438 A73-38025

The ignition of solid materials in oxygen by electrical sparks.
19 p2504 A73-38275

A general expression for the rate of evaporation of a layer of liquid on a solid body.
19 p2505 A73-38483

No-slip boundary condition origin for viscous incompressible Newtonian fluid flow over family of models for rough wall
20 p2549 A73-39810

Mechanical, chemical and physical characteristics of glass and ceramics with respect to adhesion, friction and wear behavior
21 p2707 A73-40633

Law of micro-liquid-layer formation between a growing bubble and a solid surface with a special reference to nucleate boiling.
21 p2792 A73-41144

Study of surface by spectrometry of slow electrons
21 p2706 A73-41598

Analysis of the effects of a probe in the transonic region of a nozzle.
22 p2796 A73-42568

Solid friction oscillation characteristics of self excited rotational shaft-spring system with sliding contact surfaces
23 p2986 A73-44273

SOLID SUSPENSIONS

Solid propellant rocket motors exhaust smoke minimization, discussing smoke formation mechanism and optical properties relationship to propellant characteristics
[AIAA PAPER 72-1192] 03 p0352 A73-13482

Supersonic flow of a gas with solid particles about a wedge
08 p0926 A73-21404

Investigation of iron content of lubricating oil using a ferrograph and an emission spectrometer.
10 p1218 A73-24165

SOLID-SOLID INTERFACES

Many-body effects at metal-semiconductor junctions. I - Surface plasmons and the electron-electron screened interaction.
01 p0087 A73-10147

Measurement of transient heat-transfer coefficients in the contact between solid materials
01 p0120 A73-10413

Influence of fiber/matrix interfaces on the plasticity and strength of fiber-reinforced composites
02 p0184 A73-11623

Performance tests for steel-steel lubrication capability of dimethyl silicone oils and greases modified by soluble, heat-stable extreme pressure and antiwear additives
03 p0329 A73-13011

Stressed state of adhesively bonded plane interfaces in composite systems, applying two dimensional Vocke theory
03 p0311 A73-13129

On the unbonded contact between a beam and a semi-infinite plate.
03 p0389 A73-13324

Rayleigh wave propagation at the boundary between a piezoelectric insulator and a semiconductor.
03 p0350 A73-14037

The solid-solid interface in thermal phonon radiation.
04 p0483 A73-15468

One-dimensional periodic superconducting weak-link systems.
04 p0484 A73-16040

Investigation of surface states in the MOS system by gate controlled diode structure.
05 p0559 A73-17170

Energy structure, I-V characteristics and optical and photoelectrical properties of heterojunctions between different semiconductor materials, noting interface state effects
06 p0736 A73-18091

Collocated interfacial stress intensity factors for finite bi-material plates.
06 p0763 A73-18477

Two dimensional indentation of elastic half space by rigid punch under slowly applied normal load for case with finite friction between surfaces
06 p0765 A73-18508

Extension of an interface flaw under the influence of transient waves.
07 p0908 A73-19080

Device for studying the effect of ultrasonic oscillations on contact interaction in high vacuum
07 p0822 A73-19295

The behaviour of an edge dislocation in non-homogeneous anisotropic body with cracks.
07 p0915 A73-20285

Solid-solid interface temperature rise during sliding from model with surface topography statistics, frictional conditions, surface hardness and thermal parameters
07 p0832 A73-20483

[ASME PAPER 72-LUB-34] 07 p0832 A73-20483

Contact problem with one governing parameter in elasticity theory
08 p1017 A73-21099

A theoretical study of the effect of the interface on composite toughness.
10 p1288 A73-23955

The influence of interfacial bonding on the properties of carbon fiber composites.
10 p1239 A73-23976

Thermoelastic boundary value problem for heat conduction in elastic bodies with linear and three dimensional inserts
10 p1290 A73-24305

Circular cylindrical tube lap joints elastic strain relations based on plane contact problem reduction to Prandtl type equation in finite-span wing theory
10 p1225 A73-24363

Transient compressional wave propagation in a two-layered circular rod with imperfect bonding.
10 p1291 A73-24390

Solid body contact interaction devices at high temperatures in vacuum, gas and air for evaluation of sur-

face coatings, adhesion, diffusion, mechanical properties, etc
10 p1222 A73-24966

CdS-metal contact at higher curating densities.
11 p1407 A73-24984

The effect of deformations in the measurement of the force and the couple of friction
11 p1374 A73-25871

Reactivity and interface characteristics of titanium-alumina composites.
11 p1384 A73-26043

Microscopic, kinetic and microhardness observations of Ti-W metal matrix composite solid state interface reactions, showing enhanced shear resistance
11 p1384 A73-26049

Composite solid with two contacting or bonded half planes of different elastic moduli, considering interplane force transmission from stress distribution calculation
11 p1443 A73-26277

Property control in reinforced plastics through interface tailoring.
11 p1389 A73-26296

'Glazes' produced on nickel-base alloys during high temperature wear.
12 p1513 A73-27598

The effect of brittle interfacial compounds on deformation and fracture of molybdenum-aluminum fiber composites.
13 p1636 A73-28794

French monograph on metal-semiconductor junction electron tunneling effect covering phonon interaction mechanisms, control and characterization problems
13 p1669 A73-29290

Couple-stresses effects in vicinity of interface for infinite elastic plane with a rigid inclusion.
13 p1702 A73-29533

Bonding characterization in reinforced composites.
13 p1702 A73-29536

Interfiber failure of unidirectional composite material.
13 p1702 A73-29538

On fatigue damage and debonding of glass fiber reinforced plastics.
13 p1647 A73-29546

Steady state solution for moving point force on solid-solid interface for supersonic load velocities, using DeHoop modification of Cagniard technique
14 p1812 A73-30493

Solution of three-dimensional contact problems in elasticity theory
14 p1775 A73-30831

Stress distribution due to a Griffith crack at the interface of an elastic half plane and a rigid foundation.
14 p1815 A73-30917

Dependence of the closeness of two contacting bodies on the load under a high contour-applied pressure with a plastic contact
15 p1880 A73-31143

The ultrasonic pulse-echo technique as applied to adhesion testing.
15 p1882 A73-31673

Mechanism of breakdown in the interface region of glass reinforced polyester by artificial weathering.
15 p1898 A73-31838

An invariant treatment of interfacial discontinuities in elastic composites.
15 p1954 A73-32121

Current-voltage characteristic of a metal-dielectric contact with allowance for thermionic and field emission of electrons
16 p1972 A73-34010

Solving some contact problems by electrical model.
17 p2244 A73-34795

Thermal contact conductance of porous metallic materials in a vacuum environment.
18 p2323 A73-36363

[AIAA PAPER 73-747] 18 p2323 A73-36363

A contact problem for a transversely isotropic cylindrical shell of finite length
18 p2363 A73-36404

Contact problem for infinite elastic isotropic plane weakened by rectilinear cut with free, slipping and adhesive segments and uniformly distributed load at infinity
18 p2363 A73-36415

A theory of adhesion at a bimetallic interface - Overlap effects.
18 p2287 A73-37032

Calculation of a system of two infinite beams on an elastic base
19 p2495 A73-37190

Contact problem of the elastic interaction between a plate and an elliptic insert
19 p2499 A73-37762

Thermoelasticity of coupled bodies in the case of stress-dependent heat transfer
20 p2618 A73-39327

Investigation of the transition zone structure in composite materials under cyclic loads
20 p2580 A73-39379

Problem of an elastic semiinfinite cover plate fastened to a linearly deformable base
20 p2624 A73-39646

- Two-dimensional contact problem for a prestressed elastic body 20 p2625 A73-39652
- Instability of the interface between colliding metal surfaces 21 p2707 A73-40706
- RF sputtering of ZnO shear-wave transducers. 21 p2702 A73-40952
- Surface wave radiation pattern determination for solid state lasers, taking into account dielectric interface presence 21 p2716 A73-41113
- Continuous distributions of dislocations in bonded half spaces. 21 p2742 A73-41666
- The stress field near a Griffith crack at the interface of two bonded dissimilar elastic half-planes. 21 p2789 A73-41672
- Thermoelastic dilatational deformation in two perfectly bonded orthotropic half-planes, showing linear relations between elastic and homogeneous field 21 p2789 A73-41674
- Local deformations arising in the contact between a cylindrical shell and a solid 22 p2921 A73-42281
- Elastic-plastic wave reflection and refraction obtained by method of singular surfaces, discussing interface and plastic deformation effects [ASME PAPER 73-APMW-38] 22 p2926 A73-42895
- Contact pressure problem solution for circular cylindrical shell resting on circular Winklerian bases under external load in terms of Fourier expansion 22 p2928 A73-43053
- Solution of spatial contact problems of the theory of elasticity. 23 p3040 A73-43585
- Three layer semiconductor dielectric interface model of structural and electrical properties of silicon-dioxide system involving amorphous regions 23 p3015 A73-43614
- Interface properties of oxidized germanium-doped silicon. 23 p3016 A73-43778
- A method for solving ill-posed integral equations of the first kind. 23 p2999 A73-43803
- Transmission of anti-plane shear waves past an interface crack in dissimilar media. 23 p3043 A73-43815
- Probabilistic molecular contact rupture strength at solid-solid adhesive joint interface 24 p3092 A73-44516
- Plastic relaxation of a shear crack near a planar interface. 24 p3152 A73-45403
- ### SOLIDIFICATION
- Nucleation during solidification and melting of metals and alloys 02 p0181 A73-12363
- Effect of vacuum solidification on the porosity of wound fiberglass-reinforced plastics 02 p0174 A73-12577
- The solidification sequence in an 18-8 stainless steel, investigated by directional solidification. 02 p0184 A73-12769
- Successive solidification origin of central peaks and terrace ring wall in lunar crater formations filled with melt after impacts, using freezing water experiments 03 p0369 A73-13094
- Microstructure alignment in Ni-In system eutectic alloys due to directional solidification 04 p0463 A73-15312
- Solidification pressure effect on hydrogen in Al ingots, noting blister formation correlation to pressure 05 p0587 A73-16579
- Dendritic solidification of Cu-Ni alloys. I - Initial growth of dendrite structure. 06 p0712 A73-18756
- Dendritic solidification of Cu-Ni alloys. II - The influence of initial dendrite growth temperature on microsegregation. 06 p0712 A73-18757
- Superrefractory Ni-based alloys mechanical properties enhancement through unidirectional solidification, considering grain boundary structure 07 p0838 A73-19116
- Distinct subsolidus cooling histories of Apollo 14 basalts. 07 p0881 A73-19707
- On the influence of grain size and vacancy annihilation on the Portevin-Le Chatelier-effect 08 p0977 A73-21021
- Mechanical behaviour of unidirectionally solidified composites. [ONERA, TP NO. 1147] 08 p0983 A73-21676
- Thermophysical effects of solidification on dendritic structure and mechanical properties of cast stainless and low alloy carbon steels for different crystallization rates 09 p1107 A73-23198
- Advances in directional solidification spur usage in turbine airfoil shapes. 09 p1089 A73-23293
- Equipment for casting directionally solidified parts. 09 p1089 A73-23294
- Ultrasonic treatment of alloy MA2-1 during solidification. 10 p1236 A73-24930
- Directionally solidified eutectic high temperature alloys. 11 p1379 A73-25404
- Unidirectional solidification formed interdendritic eutectic composition related to solidification variables, discussing Al-Cu and Al-Cu-Ni systems 13 p1632 A73-28131
- Directionally solidified eutectic alloy composites for high temperature turbine blade and vane applications, considering morphology, crystallography and thermal stability properties 13 p1635 A73-28778
- Grain refinement in aluminium-zirconium and aluminium-titanium alloys by metastable phases. 19 p2440 A73-37444
- Grain refinement by titanium in the unidirectionally solidified aluminium alloys. 19 p2442 A73-37949
- Observations on the directional solidification of cobalt-base alloys strengthened by carbide fibres. 19 p2443 A73-38249
- Observations of solid/liquid interfaces in dilute binary and ternary Al-rich alloys. 21 p2721 A73-41120
- Experimental aspects of the mechanical behavior of fiber composites produced by oriented solidification [ONERA, TP NO. 1205] 22 p2876 A73-42215
- The copper-boron eutectic - Unidirectionally solidified. 23 p2993 A73-44035
- ### SOLIDIFIED GASES
- #### NT SOLID NITROGEN
- Application of the method of Bhatnagar-Gross-Krook-Morse to the Knudsen layer of a polyatomic gas which is solidified or in equilibrium - Expression of discontinuities of wall temperatures 09 p1072 A73-23033
- Ground state energy of solid molecular hydrogen at high pressure. 11 p1401 A73-25891
- Preliminary data on the optical properties of solid ammonia and scattering parameters for ammonia cloud particles. 17 p2211 A73-34858
- Data acquisition technique for Fabry-Perot spectroscopy, noting application to Brillouin spectra recording of solid Ne 17 p2171 A73-35403
- Far infrared and Raman spectra of gaseous carbon suboxide and the potential function for the low frequency bending mode. 21 p2740 A73-40935
- High field NMR thermometry below 1 K using HD. 22 p2856 A73-42024
- Light scattering intermolecular and Raman spectra in liquid and solid hydrogen, showing short wave collective excitations in relation to phonon processes 23 p3007 A73-44171
- ### SOLIDS
- #### NT SOLIDIFIED GASES
- Dynamics of angular motions of a solid body carrying a rotating rotor, with allowance for energy dissipation 01 p0075 A73-10087
- Wave motion in an elastic solid due to a nonuniformly moving line load. 01 p0114 A73-10301
- Equations of the time-dependent strength of solid bodies 01 p0114 A73-10479
- Research performed on the thermomechanics of deformable solids at the Ukrainian Academy of Sciences 01 p0114 A73-10569
- Ultrasonic studies of the nonlinear properties of solids. 01 p0057 A73-11003
- Deformation and stress analysis in continuum mechanics problems of solid bodies near singular points, noting applicability of linear theory of elasticity 01 p0118 A73-11404
- Polychromatic X-ray diffraction - A rapid and versatile technique for the study of solids under high pressure and high temperature. 01 p0054 A73-11482
- Solid deformable body mean stress determination by statistical summation of stress squares on faces of parallelepiped rotated within Euler angle limits 02 p0235 A73-12207
- Control of the motion of a solid body with servo couplings 05 p0597 A73-16611
- Ion microprobe mass analyzer for solid materials science research, discussing instrument potential and limitations 05 p0576 A73-16675
- Surface effects in solid bodies undergoing deformation and fracture 06 p0734 A73-17922
- Contribution to the classical theory of solids with statistical structural characteristics 06 p0762 A73-17994
- Scattering of a transverse elastic wave by an elastic sphere in a solid medium. 06 p0737 A73-18351
- Extremum principles on time independent elastoplastic solids nonisothermal deformation properties based on yield function dependence on temperature 06 p0763 A73-18456
- Variational methods in solid media linear theory of elasticity, discussing Rayleigh-Ritz method application to linear static, harmonic response and linearized stability problems 06 p0765 A73-18724
- Numerical integration over Brillouin zone for solids spectral properties calculation, considering crystal optical spectra, phonon effects, IR absorption, electron emission and magnetic susceptibilities 07 p0861 A73-19266
- Integral method for nonlinear transient heat transfer in a semi-infinite solid. 07 p0919 A73-19493
- Crystal defect model of crack propagation in three dimensional solid, assuming nonlinear dependence of Young modulus on strain with term for time lag 08 p1017 A73-21025
- Book - Vibration of solids and structures under moving loads. 09 p1159 A73-22526
- Influence of absorption on the optical properties of solids - Propagation of uniform, plane, heterogeneous electromagnetic waves in isotropic and homogeneous mediums 09 p1121 A73-22963
- Finite-element method applied to heat conduction in solids with nonlinear boundary conditions. 10 p1295 A73-23778
- Book - Thermal radiative properties: Nonmetallic solids. 11 p1387 A73-25275
- EM induction in a semi-infinite solid, impulsively moving in a uniform magnetic field. 11 p1397 A73-25371
- Interdisciplinary computer analyses of three-dimensional solids defined by polyhedral surfaces. [AIAA PAPER 73-354] 11 p1437 A73-25491
- Applications of solid mechanics; Proceedings of the Symposium, University of Waterloo, Waterloo, Ontario, Canada, June 26, 27, 1972. 11 p1442 A73-25842
- Saint Venant principle for plane deformation of anisotropic elastic solid extended to analysis of fiber reinforced transversely isotropic composites 11 p1444 A73-26280
- Energy flux into extending crack in elastic solid calculated in terms of stress intensity factor for plane and antiplane strain problems 11 p1444 A73-26281
- Displacement boundary value problem of linearized elastodynamics with superimposed small and large deformations in homogeneous anisotropic elastic solid, proving solution uniqueness theorem 11 p1444 A73-26282
- Photon conductivity analysis for homogeneous isotropic solid body based on convective-radiant transfer equations, determining molten quartz thermal conductivity and diffusivity 12 p1516 A73-27311
- Ideal plasticity theory for solid bodies of isotropic materials with different yield points in extension and compression 12 p1553 A73-27374
- Thermally activated low temperature creep of solids at constant load, considering creep curve stages and plastic deformation mechanism 13 p1635 A73-28263
- Solid fracture theories based on brittle region toughness parameter and absorbed specific fracture work factor above ductile-brittle transition respectively 13 p1640 A73-29479
- Statistical criteria of ultimate strength and plasticity of materials in the complex stress state. 13 p1703 A73-29620
- Book on solids structure effects on materials strength characteristics covering interatomic binding forces, elastic properties, crystal defects, work hardening, heat treatment, temperature effects, etc 14 p1759 A73-29948
- Equations for the time-dependent strength of a solid. 14 p1810 A73-30304
- Some considerations regarding the dynamics problem for an elastic space and the use of its solution 15 p1956 A73-32545
- Relativistic elasticity theory for solids based on Cattaneo definitions for Riemann metric, considering hyper- and hypoelastic media 16 p2036 A73-33108
- Atomic modeling of internal friction in solids, considering paraelastic point defects relaxation time 16 p2037 A73-33227

Discrete /microscopic, atomic/, continuous /macroscopic, phenomenological/ and quasi-continuous models of elastic solids, exemplifying elastic crystals linear model

Steady state diffraction of stress waves by semi-infinite running crack in elastic solid under dynamic loading, obtaining solution based on Wiener Hopf technique

Book - Nonlinear viscoelastic solids.

Dynamic mechanical loading of solid material resulting in stress levels with impulse process described by fluid flow equations with application to shock compression of mechanical mixtures

Book - Acoustic fields and waves in solids. Volumes 1 & 2.

A numerical method for creep deformation of solids.

A unified theory of thermoviscoplasticity of crystalline solids.

On steady wave profiles in solids.

Theory of resonant light scattering processes in solids.

High-speed photography of laser damage in solids.

Sound propagation in gases, liquids and solids, discussing effects of nonlinear terms in wave and state equations and boundary conditions on solution

Propagation of steady shock waves in non-linear thermoviscoelastic solids.

Unified plastic yield criterion for ductile solids.

Indentation of the semi-infinite elastic solid by a hot sphere.

Ultrasonic determination of shape and size of hidden defects in solids.

Slow growth of cracks in a rate sensitive Tresca solid.

Oscillations caused by solid friction. III - In the case of maximum static friction different from kinetic friction without slipping.

Surface phenomena in solids during the course of their deformation and failure.

Static theory of plane micropolar strain for homogeneous orthotropic elastic solids, deriving existence and uniqueness theorems and reducing boundary value problems to Fredholm equations

SOLIDS FLOW

Three dimensional dynamic characteristics of solid particles suspended by polluted air flow in a turbine stage.

Solid particle transport effect on structure and axial speed characteristics of two phase submerged turbulent jet

An explanation of transient lunar phenomena from studies of static and fluidized lunar dust layers.

Continuum mechanics analysis of solid particle suspension flow of viscous gas, noting demixed region near wall

SOLIDUS

Lunar rocks petrogenesis, determining liquidus and solidus temperatures and crystalline phases sequence in lunar samples and synthesized oxides and silicates

Apollo 14 - Subsolidus reduction and compositional variations of spinels.

Comparison of a suggested polynomial method with the method of F. M. Perelman in the calculation of the solidus surface of the W-Ta-Mo-Nb system

SOLSTICES

Morphology and interpretation of magnetospheric plasma waves at conjugate points during December solstice.

SOLUBILITY

Disilicides solubility in silver and tin melts, discussing ternary phase formation

Activity of carbon and solubility of carbides in the fcc Fe-Mo-C, Fe-Cr-C, and Fe-V-C alloys.

Effects of alloying elements on the solubility of hydrogen in beta titanium.

The diffusivity and solubility of oxygen in liquid tin and solid silver and the diffusivity of oxygen in solid nickel.

Solubility of zirconium and niobium in solid-state copper

Solubility of oxygen in ZrC.

The solubility of hydrogen in rhodium, ruthenium, iridium and nickel.

Thermodynamic properties of the nickel-tungsten system as determined from its hydrogen solubility

Temperature dependence of the activity and solubility of carbon in pure nickel

Interaction of molybdenum with elements of the iron group and carbon

Mo-Nb-Ta alloys phase and composition-hardness diagrams for 20-1100 C, establishing mutual solubility of system components

Rhenium solubility determination for deformed and annealed Re-Al alloy at 500 and 600 C by microstructural analysis and hardness and electrical resistance measurements

Temperature dependence of the solubility of scandium in solid magnesium

Distribution coefficients and solubility curves of certain rare-earth elements in GaAs

Cast and annealed chromium-yttrium and chromium-lanthanum alloys peak solubility from metallographic, durometric and differential thermal analyses

Investigation of the sintering of binary alloys with limited solubility in the solid state. I - Concentration dependence of shrinkage during sintering of two-component systems with a eutectic type of phase diagram

Solubility of vanadium and tungsten in alpha and gamma phases in the Fe-V and Fe-W binary systems

Contribution to the study of the behavior of liquid cobaltous oxide in an oxidizing atmosphere

Solubilities of noble gases in magnetite - Implications for planetary gases in meteorites.

Solubility of nitrogen and hydrogen in cobalt and cobalt alloys - A review.

Composition and temperature effects on hydrogen solubility in Ni-Al liquid alloys

Gas solubility in hydraulic liquids from measurements of air in mineral oils, noting oil molecular weight effect

Influence of Co, Ni, Mo, and W on the solubility of Fe16N2 in alpha-iron.

SOLUTES

Solute rejection by porous glass membranes. II - Pore size distributions and membrane permeabilities.

SOLUTIONS

NT AQUEOUS SOLUTIONS
NT DETONABLE GAS MIXTURES
NT GAS MIXTURES
NT NUCLEAR EMULSIONS
NT PHOTOGRAPHIC EMULSIONS
NT SOLID SOLUTIONS

Experimental investigation of thermal and induced molecular scattering of light in solutions within a wide spectral range

Direct measurement of the fluorescence energy yield of a rhodamine 6G solution with the aid of an Ar+ laser

Relationship between the equilibrium vapor pressure of the solvent and the surface activity in dilute solutions of inactive and surface-active materials

Influence of certain hydroxyl- and nitrogen-containing low-molecular-weight substances on the structural viscosity of cellulose acetate solutions

SOLVENT EXTRACTION

Quantitative evaluation of superficial organic contaminants, soluble in halogenated solvents, discussing sampled surface solvent extraction method and subsequent IR absorption spectrographic analysis

SOLVENTS

Solvent effects on enzymes - Implications for extraterrestrial life.

Effect of prepregging solvent on high-temperature stability of KERIMID 601 composites.

Relationship between the equilibrium vapor pressure of the solvent and the surface activity in dilute solutions of inactive and surface-active materials

SOMMERFELD APPROXIMATION

Analysis of wire antennas in the presence of a conducting half-space. II - The horizontal antenna in free space.

Composite approximations to the solutions of the Orr-Sommerfeld equation.

SOMME

The University of Oklahoma acoustic radar.

Acoustic sounding of meteorological phenomena in the planetary boundary layer.

Ship positioning by sonar group and ultrasonic transponder beacons with tracking station axis direction definition capability

Radar and sodar probing of waves and turbulence in statically stable clear-air layers.

Capabilities of radar, sodar and lidar for measuring the structure and motion of the stably stratified atmosphere.

SOMDES

NT DROPSONDES
NT IONOSONDES
NT PETREL SOUNDING ROCKET
NT RADIOSONDES
NT RAWINSONDES

On the self-shielding coefficient of plates against neutron fluxes.

Structure variations in the winter polar atmosphere.

SONIC ANEMOMETERS

A comparison of turbulence measurements by different instruments - Tsingyansk field experiment 1970.

Three-component sonic anemometer for wind speed measurement, calculating transfer functions for effect of line averaging and path separation on spectral response

SONIC BOOMS

Optimum configurations for bangless sonic booms.

Remarks on the paper by J. M. Nicholls and B. F. James, 'The location of the ground focus line produced by a transonically accelerating aircraft.'

Conical solutions for diffraction of plane pulse wave by three dimensional trihedron corner via boundary conditions reduction to eigenvalue problem, presenting sonic boom example

Sonic boom avoidance by flight path maneuvers, investigating shock front development in curved flight

The scattering characteristics of a sonic boom at the passage through a turbulent layer

Sonic boom induced underwater pressure oscillations, noting strong attenuation with depth

SST aircraft wing design for sonic boom avoidance and noise reduction in airport vicinity, describing aerodynamic characteristics from wind tunnel and flying model tests

Behavioural awakening and subjective reactions to indoor sonic booms.

Thermodynamic considerations for the design of a sonic-boom reducing powerplant.

Gudunov-method computation of the flow field associated with a sonic-boom focus.

The acoustic response of rooms with open windows to airborne sounds.

The transmission of sonic boom signals into rooms through open windows.

Distortion of near-sonic shocks by layers with weak thermal fluctuations.

Sonic boom reduction through aircraft design and operation.

[AIAA PAPER 73-241]

SONIC FLOW

- Effects of aircraft noise on human sleep. 06 p0659 A73-18546
- One dimensional supersonic shock front location by sonic circle involute point by point plotting, using geometric considerations 09 p1030 A73-23467
- Seismic measurement data from Cornish cottage during Concorde sonic boom flight, using moving coil geophones 11 p1306 A73-26292
- The application of holography to sonic boom investigations. 11 p1371 A73-26633
- Laboratory simulation of development of weak booms by atmospheric turbulence. 13 p1568 A73-28495
- Vibrational relaxation effects in weak shock waves in air and the structure of sonic bangs. 14 p1711 A73-30174
- On the possibility of turbulent thickening of weak shock waves. 16 p1967 A73-32794
- Concorde aircraft design, testing and projected environmental impact, discussing flight tests, sonic booms, atmospheric pollution, ATC problems and fueling 16 p1968 A73-33182
- Ground and air transportation noise propagation and effects, including aircraft engines, airfoils, sonic booms, auto traffic, railroads, subways, seismic noise and vibration 17 p2100 A73-34460
- Human response to transportation noise and vibration. 17 p2117 A73-35328
- Review of current sonic boom studies. 18 p2267 A73-36393
- Sonic booms and sleep - Affect change as a function of age. 18 p2282 A73-36780
- Supersonic boom structure studies, discussing shock wave propagation during flight trajectory and amplification due to overpressure wave focusing. 18 p2268 A73-36907
- Cardiovascular reactions of a healthy man exposed to sonic booms 18 p2284 A73-36909
- Effect of sonic boom on hearing and vestibular equilibrium 18 p2284 A73-36910
- The design or operation of aircraft to minimize their sonic boom. [AIAA PAPER 73-817] 19 p2380 A73-37470
- Nonlinear response of plates subjected to inplane and lateral pressure pulses. 20 p2622 A73-39547
- Geophysical effects of Concorde sonic boom. 20 p2509 A73-39624
- Effects of repeated simulated sonic booms of 1.0 PSF on the sleep behavior of young and old subjects. 21 p2644 A73-41151
- Sonic bang investigations associated with the Concorde's test flying. 21 p2635 A73-41174
- A study to determine the feasibility of a low sonic boom supersonic transport. [AIAA PAPER 73-1035] 24 p3056 A73-44863
- Acoustic velocity and sound propagation differences in incompressible and compressible fluids related to Mach cone formation and sonic boom effects. 24 p3054 A73-45269
- SONIC FLOW**
- U TRANSONIC FLOW**
- SONIC NOZZLES**
- Results of an experimental program for the development of sonic inlets for turbofan engines. [AIAA PAPER 73-222] 06 p0645 A73-17664
- Calculation of the relaxed one-dimensional flow of a gas in a convergent-divergent sonic nozzle 11 p1348 A73-25869
- Two-dimensional calculation of revolution of the relaxed flow of a gas in a convergent-divergent sonic nozzle 13 p1563 A73-28563
- Low-density jets behind a sonic nozzle at large pressure gradients 17 p2150 A73-34263
- Noise reducing choked /sonic/ inlet design for V/STOL jet aircraft, discussing aerodynamic theoretical and experimental studies 19 p2375 A73-37295
- Level populations in plasmas - RF discharges and sonic channel. 22 p2895 A73-42994
- SONIC SPEED**
- U ACOUSTIC VELOCITY**
- SONIC WAVEGUIDES**
- U ACOUSTIC DELAY LINES**
- SONOGRAMS**
- Magnetospheric electric field under quiet conditions on the basis of ground-based observations of whistlers 15 p1872 A73-31903
- SONOHOLOGRAPHY**
- U ACOUSTICAL HOLOGRAPHY**

SOOT

- Soot particles oxidation by oxygen diffusion in laminar hydrocarbon flames, deriving kinetic expression from observed time dependent particle concentration variations 03 p0399 A73-14395
- Effect of fuel composition on particulate emissions from gas turbine engines. 06 p0740 A73-17733
- Soot oxidation kinetics at combustion temperatures. 12 p1557 A73-26844
- Shock-tube measurements of soot oxidation rates. 16 p2085 A73-33344
- Soot formation by combustion of an atomized liquid fuel. 22 p2936 A73-42800
- Burner dimension and flame size effects on relative contributions of luminous soot and nonluminous molecular band radiations from combustion fires 23 p3048 A73-43329

SORBENTS

- NT ABSORBENTS**
- Investigation of the disinfecting properties of sorbents which are used in a spacecraft life support system 17 p2114 A73-34240

SORPTION

- NT ADSORPTION**
- NT CHEMISORPTION**
- Effectiveness of the application of tightly bonded sulfo-cation exchange resins in water recycling by the sorption method 06 p0656 A73-17677
- Investigation of gas sorption and desorption in polymer materials in the process of gaseous sterilization of such materials 06 p0656 A73-17681
- Surface solid solutions and chemical compounds formation due to gas sorption by titanium and barium 13 p1663 A73-28968
- Lunar specific surface adsorption-desorption processes discussing near-surface atmospheric diurnal variations, nitrogen temperature, sorption capacity, gas concentration from regolith structure 21 p2774 A73-41402
- Surface solid solutions and chemical compounds formation due to gas sorption by titanium and barium 23 p3008 A73-44320

SORTIE CAN

U SPACELAB

SORTIE LAB

U SPACELAB

SORTING

U CLASSIFYING

SOUND

U ACOUSTICS

SOUND ABSORPTION

U SOUND TRANSMISSION

SOUND BARRIER

U ACOUSTIC VELOCITY

SOUND DETECTORS

U SOUND TRANSDUCERS

SOUND FIELDS

- Acoustic field of an infinite annular cylindrical transducer partially coated with an acoustically soft material 01 p0077 A73-10927
- Computation of the sound energy radiated from turbulent flows [DGLR PAPER 72-074] 02 p0153 A73-11699
- Sound field for noise extinction via controlled interference, stressing sonic generators installation near noise sources 03 p0341 A73-12962
- A problem of coupling between the vibration of a thin plate and an acoustic field in a fluid 03 p0383 A73-12982
- Linear schlieren photography with concave mirror and variable ultrasonic source for high resolution display of acoustic free field pressure gradient on TV screen 03 p0342 A73-12990
- Reproduction of sound propagation in the standard atmosphere 03 p0342 A73-12993
- Space-modulated side radiation from an ultrasonic beam in a solid. 03 p0344 A73-14042
- Numerical determination of the sound field and the characteristic frequencies in a circular enclosure by the discretization method 04 p0476 A73-15375
- The acoustic response of rooms with open windows to airborne sounds. 05 p0537 A73-17369
- Sound field generated by spatial instabilities interaction on shear layer shed from duct with nozzle lip, discussing excess noise of subsonic jets 06 p0687 A73-18529
- Spatial crosscorrelation in anisotropic sound fields. 08 p0987 A73-21125
- A method of calculating heat and mass transfer between liquid droplets and a gaseous phase in an acoustic wave field 08 p1022 A73-21196

Acoustic emission of a body moving along a circle near a sphere

- 08 p0988 A73-214458
- On the near- and far-field radiation patterns generated by the non-linear interaction of two separated and non-planar monochromatic sources. 08 p0988 A73-214698
- Sound field of an infinite circular cylindrical transducer partially coated with an acoustically compliant layer. 10 p1249 A73-24187
- Effect of an ultrasonic field on the behavior of a vapor bubble in liquid hydrogen. 10 p1249 A73-24189
- Interaction between a sound field and natural convection on a horizontal cylinder. 10 p1296 A73-24840
- Noise radiated from a turbulent boundary layer. 11 p1344 A73-24979
- Holographic interferograms for demonstration of an acoustic field near supersonic air, nitrogen and helium jets, noting generated Mach wave convection velocity. 11 p1346 A73-25382
- Aerodynamic noise field associated with pressure distributions generated by local protuberance on a launch vehicle during atmospheric flight. 11 p1300 A73-25384
- Variations in the sound field of a STOL aircraft as a function of wing-flap deflection 11 p1306 A73-26592
- A two-dimensional mathematical model for an acoustically soft parabolic cylinder reflector. 13 p1597 A73-28493
- The influence of acoustic disturbances on the mechanics in shear layer behind a circular cylinder in air flow. 13 p1563 A73-28530
- Radiation from line vortex filaments exhausting from a two-dimensional semi-infinite duct. 14 p1744 A73-30168
- Binaural acoustic field sampling, head movement and echo effect in auditory localization of sound sources position, distance and orientation 14 p1715 A73-30282
- Natural convection in a sound field giving large streaming Reynolds numbers. 14 p1817 A73-30613
- Acoustic field produced in a gas by arbitrary disturbances on a moving plate 14 p1775 A73-30834
- Sound radiation from a body moving in a circle near a sphere. 15 p1912 A73-31009
- The use of the terms nearfield and farfield in ultrasonic non-destructive testing 15 p1882 A73-32052
- Ultrasonic probes sound fields from thermal effects via IR camera or liquid crystals, sound pressure via Pohlmann image converter and light modulation via schlieren method 15 p1882 A73-32055
- A note on the use of the finite difference method for predicting steady state sound fields. 16 p2036 A73-33217
- Acoustic energy flow in lined ducts containing uniform or 'plug' flow. 16 p2038 A73-33945
- The problem of electron-pair tunneling in a sound field in superconductors 16 p2045 A73-34069
- Diffraction of acoustic waves on plates interconnected at right angles 17 p2211 A73-34140
- Fundamentals of aerodynamic sound theory and flow duct acoustics. 17 p2155 A73-35331
- Book - Acoustic fields and waves in solids. Volumes 1 & 2. 17 p2213 A73-35597
- On the effect of swirling motion of sources of subsonic jet noise. 21 p2676 A73-40286
- Burning gunpowder interaction with an acoustic field in the presence of balanced chemical reactions behind the flame 21 p2791 A73-40699
- Quantitative analysis of sonic fields during their visualization by holographic methods 22 p2852 A73-41899
- Refraction, convection, and diffusion flame effects in combustion-generated noise. 22 p2934 A73-42780
- Sound field created in a gas by arbitrary perturbations on a moving plate. 23 p3006 A73-43584
- Sound interaction with a helical flow contained in an annular duct with radial gradients of flow, density and temperature. [AIAA PAPER 73-1010] 24 p3078 A73-44842
- Sound generation by wake cutting. [AIAA PAPER 73-1019] 24 p3054 A73-44851
- Emission of sound from a rectangular plate vibrating under the action of pressure pulsations in a turbulent boundary layer 24 p3109 A73-44899

Influence of a discrete component of acoustic vibration on flow in a supersonic jet with a nondesign ratio of active to passive pressure 24 p3055 A73-45538

SOUND GENERATORS

Effect of streamwise vortices on wake properties associated with sound generation. 01 p0001 A73-10045

Ultrasonic waves generation by plasma of activated flame, presenting sound pressure and light emission graphs 01 p0086 A73-11272

Sound generation at an elastic plate acting as an obstruction in a turbulent free jet [DGLR PAPER 72-085] 02 p0152 A73-11667

Sound field for noise extinction via controlled interference, stressing sonic generators installation near noise sources 03 p0341 A73-12962

Reproduction of sound propagation in the standard atmosphere 03 p0342 A73-12993

Aerodynamic sound generation, discussing Lighthill theory, multipole sonic sources, wave equation, power and turbulence models and sound radiating flows 03 p0242 A73-13167

Effect of wake-wake interactions on the generation of noise in axial-flow turbomachinery. 03 p0246 A73-14129

Programmable, digital, rapidly frequency-shift-keyed, high-frequency generators for driving acoustooptical light deflectors 05 p0586 A73-17239

Acoustic emission of a body moving along a circle near a sphere 08 p0988 A73-21445

Unconventional methods of generating, detecting and coupling of ultrasound in non-destructive testing 09 p1088 A73-22218

Synthesis of helicopter rotor tips for less noise. 11 p1299 A73-24981

Generation of acoustic waves during the passage of a shock wave through a heated gaseous element. 13 p1705 A73-28494

Laboratory simulation of development of superbooms by atmospheric turbulence. 13 p1568 A73-28495

Generation and detection of sound by distributed piezoelectric sources. 13 p1661 A73-29289

Sound radiation from a body moving in a circle near a sphere. 15 p1912 A73-31009

Acoustic generation and propagation in annular ducts of axial flow fans, discussing techniques for in-duct fan noise modal distribution measurement 16 p1999 A73-32846

The role of jet stability in edgetone generation. [AIAA PAPER 73-628] 18 p2263 A73-36255

A closed-loop automatic control system for high-intensity acoustic test systems. 18 p2296 A73-36712

Combustion noise prediction techniques for small gas turbine engines. 19 p2473 A73-37296

Intensity modulated laser with expansion and contraction of absorbing medium for thermoacoustic broadside array with highly directional acoustic propagation 20 p2572 A73-39052

Some kinematic considerations of tone generation in axial turbomachinery. 22 p2899 A73-41710

Sound generation by open supersonic rotors. 22 p2795 A73-41712

Study of self-excitation conditions in an acoustic oscillator in relation to the type of boundary conditions 22 p2886 A73-41900

Measurements of the distribution of sound source intensities in turbulent jets. [AIAA PAPER 73-989] 24 p3053 A73-44826

The momentum potential field description of fluctuating fluid motion as a basis for a unified theory of internally generated sound. [AIAA PAPER 73-1000] 24 p3077 A73-44835

Sound generation by wake cutting. [AIAA PAPER 73-1019] 24 p3054 A73-44851

SOUND HOLOGRAPHY

U ACOUSTICAL HOLOGRAPHY

SOUND INTENSITY

Loudness enhancement following contralateral stimulation. 01 p0013 A73-10827

Contribution to the study of noise measured by a microphone placed in a gaseous flow 03 p0290 A73-12973

Some modeling problems of loudness transformations by the auditory system 04 p0413 A73-15790

Optimal and preferred listening levels for speech in aircraft acoustical environments. 11 p1304 A73-25387

Equivalent continuous sound level determination from instantaneous sonic intensity measurement during representative time period, describing electron measuring device and circuitry 11 p1367 A73-26416

Pure-tone equal-loudness contours for standard tones of different frequencies. 21 p2645 A73-41176

Analysis of the changes in glial cell numbers in the auditory cortex during the application of acoustic stimuli of various intensities 22 p2807 A73-42653

Experimental substantiation of the optimal method for scaling the duration of acoustic stimuli 22 p2814 A73-42654

Inferior colliculus neuron responses to an amplitude-modulated signal with varying intensity levels 24 p3061 A73-45248

SOUND LOCALIZATION

Electrophysiological investigation of noise rejection in an auditory system receiving sound from a localized source 09 p1040 A73-22580

Problem of localization in the median plane - Effect of pinnae cavity occlusion. 11 p1321 A73-24976

German monograph - Investigations regarding auditory depth perception and the problem of in-head localization of acoustic events. 13 p1577 A73-29278

Binaural acoustic field sampling, head movement and echo effect in auditory localization of sound sources position, distance and orientation 14 p1715 A73-30282

Estimate of integrative cerebral activity using an orientation response example 22 p2807 A73-42651

SOUND MEASUREMENT

U ACOUSTIC MEASUREMENTS

SOUND PERCEPTION

U AUDITORY PERCEPTION

SOUND PRESSURE

Experimental investigation of stresses in plates acted on by acoustic loads. 02 p0235 A73-12135

Measurements of pressure and velocity fluctuations in turbulent pipe flow 03 p0290 A73-12963

Linear schlieren photography with concave mirror and variable ultrasonic source for high resolution display of acoustic free field pressure gradient on TV screen 03 p0342 A73-12990

Study of the influence of the volumetric mass of a jet on acoustic sound emission 03 p0359 A73-14143

Sound pressure level spectra measurements for four- and three-engine jet transport during concrete and grassy surface runway and flyover [SAE AIR 1216] 08 p0927 A73-20693

Possibility of improving the erosive activity of a cavitation bubble by the combined effect of continuous and pulsed sound 08 p0955 A73-21448

Noise radiated from a turbulent boundary layer. 11 p1344 A73-24979

Noise control modification to HH-43B helicopter for 50 percent reduction in forward flight octave band sound pressure level signature 11 p1304 A73-25383

Asymptotic pressure calculation of plane acoustic wave diffraction by infinitely long isotropic solid elastic circular cylinder in viscous liquid medium 13 p1583 A73-28863

Piezoelectric sound pressure sensor for damping measurement of structural element coatings under intense acoustic loads 13 p1618 A73-29060

Possibility of enhancing the erosive activity of a cavitation void under the simultaneous action of continuous and pulsed sound. 15 p1860 A73-31012

Ultrasonic probes sound fields from thermal effects via IR camera or liquid crystals, sound pressure via Pohlmann image converter and light modulation via schlieren method 15 p1882 A73-32055

An impedance tube for precision measurement of acoustic impedance and insertion loss at high sound pressure levels. 16 p2013 A73-32916

Determination of maximum ground noise during a rocket launch - Discussion and simple prediction method. 16 p2072 A73-33142

Procedure for the simulation of sonic fields, particularly for fatigue tests 16 p1997 A73-33384

Spectral moving frame representation of jet noise by far field acoustic pressure autocorrelation and density function 16 p2000 A73-33681

Diffraction of acoustic waves on plates interconnected at right angles 17 p2211 A73-34140

Piezoelectric sound pressure sensor for damping measurement of structural element coatings under intense acoustic loads 18 p2317 A73-36892

The acoustic impedance of perforates at medium and high sound pressure levels. 18 p2337 A73-37030

Application of the coherence function to acoustic noise measurements. 19 p2458 A73-37284

Overall sound pressure levels of STOL, thrust reverse noise as function of jet velocity at touchdown 20 p2600 A73-38650

The design and construction of an anechoic chamber lined with panels and intended for investigation of aerodynamic noise 21 p2674 A73-40942

Experiments on radiatively driven harmonic acoustic waves in a confined gas. 22 p2930 A73-42236

Helicopter noise experiments in an urban environment. 22 p2800 A73-42944

A model for the pressure excitation spectrum and acoustic impedance of sound absorbers in the presence of grazing flow. 24 p3077 A73-44830

The momentum potential field description of fluctuating fluid motion as a basis for a unified theory of internally generated sound. 24 p3077 A73-44835

The effects of modulated blade spacing on static rotor acoustics and performance. [AIAA PAPER 73-1020] 24 p3121 A73-44852

SOUND PROPAGATION

NT VOICE

Nonlinear magnetic sound in a gravitational field 01 p0016 A73-10202

The fourth annual Fairley lecture - The propagation of sound through moving fluids. 01 p0077 A73-10784

Book - Sound, structures, and their interaction. 02 p0192 A73-11880

Self focusing of two dimensional cylindrical waves propagating in inhomogeneous natural duct, noting tropospheric communications and ionospheric and sound propagation applications 02 p0142 A73-12527

Sound propagation in a combustion can with axial temperature and density gradients. 02 p0238 A73-12608

A problem of coupling between the vibration of a thin plate and an acoustic field in a fluid 03 p0383 A73-12982

Sound propagation in sheared flow in a duct with transverse temperature gradients. 03 p0342 A73-12988

Some laws of the propagation of discrete-tone perturbations in a free supersonic jet 03 p0245 A73-13668

Acoustic-Doppler-radar scattering equation and general solution. 03 p0276 A73-13830

Mathematical treatment of long wave sound propagation in curved ducts and junctions, obtaining principal mode from linearized equation of motion solved for eigenvalues 03 p0343 A73-13832

Space-modulated side radiation from an ultrasonic beam in a solid. 03 p0344 A73-14042

Attenuation of spiral modes in a circular and annular lined duct. 04 p0487 A73-15591

Computing meteorological effects on aircraft noise. 05 p0536 A73-17121

High-frequency sound waves to eliminate a horizon in the mixmaster universe. 06 p0724 A73-18550

Images and sound rays in the numerical calculation of echograms 09 p1121 A73-23104

Sound directivity pattern radiated from small airfoils. 11 p1345 A73-24980

Cavity-backed panel resonance. 13 p1690 A73-28062

Reference wave elimination in acoustic holographic experiments via boundary surface of medium having sound wave propagation used as hologram 13 p1616 A73-28687

The attenuation of ultrasonic waves in cylindrical work pieces with central bore-hole 15 p1882 A73-32053

Multiple scattering of sound by turbulence and other inhomogeneities. 15 p1865 A73-32151

Ray models for sound propagation and attenuation in ducts, in the absence of mean flow. 15 p1865 A73-32153

Nonlinear acoustics of inviscid fluid in duct with varying cross section, obtaining propagation velocity potential as power series for reduction to Neumann problem 15 p1865 A73-32154

SOUND TRANSDUCERS

- The propagation and attenuation of sound in lined ducts containing uniform or 'plug' flow.
16 p1970 A73-33944
- Some aspects of 'sound' attenuation in lined ducts containing inviscid mean flows with boundary layers.
16 p2049 A73-33946
- Ground and air transportation noise propagation and effects, including aircraft engines, airfoils, sonic booms, auto traffic, railroads, subways, seismic noise and vibration
17 p2100 A73-34460
- Harmonic and impulsive acoustic source-produced sound propagation across vortex sheet separating two subsonic fluids, investigating instability waves
17 p2151 A73-34825
- Sound measurements within and in the radiated field of an annular duct with flow.
18 p2302 A73-37028
- On energy, group velocity and small damping of sound waves in ducts with shear flow.
18 p2302 A73-37031
- Sound propagation in gases, liquids and solids, discussing effects of nonlinear terms in wave and state equations and boundary conditions on solution
21 p2739 A73-40621
- Some features of the propagation of a discrete tone perturbation in a free supersonic jet.
21 p2633 A73-41318
- Some kinematic considerations of tone generation in axial turbomachinery.
22 p2899 A73-41710
- Attenuation of spiral modes in a circular and annular lined duct.
22 p2839 A73-41714
- Sound propagation in rotating vortex flow downstream from delta wing in wind tunnel, discussing acoustic ray refraction by flow
22 p2839 A73-41715
- Shear layer effect on acoustic duct wall impedance for sound propagation in uniform flow in terms of parabolic cylinder functions
22 p2900 A73-41318
- Response of panels to turbulence-induced, surface-pressure fluctuations and resulting acoustic radiation to the flow field.
24 p3077 A73-44828
- Unsteady aerodynamic loads on slender cones at free-stream Mach numbers from 0 to 22.
24 p3053 A73-44833
- Acoustic propagation in ducts with varying cross sections and sheared mean flow.
24 p3078 A73-44841
- Theoretical studies of sound emission from aircraft ducts.
24 p3078 A73-44844
- Velocity of hypersonic waves in liquid oxygen.
24 p3110 A73-44984
- Acoustic velocity and sound propagation differences in incompressible and compressible fluids related to Mach cone formation and sonic boom effects
24 p3054 A73-45269
- SOUND TRANSDUCERS**
NT ELECTROACOUSTIC TRANSDUCERS
NT LOUDSPEAKERS
NT MICROPHONES
- Piezoelectric matrices for reception of acoustic images and holograms
01 p0051 A73-10930
- Unconventional methods of generating, detecting and coupling of ultrasound in non-destructive testing
09 p1088 A73-22218
- Piezoelectric matrices for the reception of acoustic images and holograms.
10 p1218 A73-24190
- Improvements in surface-acoustic-wave pulse-compression filters.
13 p1595 A73-28048
- Flat circular acoustic transducer for pressure spectrum analysis, deriving flow noise response correction factor in terms of polynomial coefficients and frequency-dependent constants
13 p1613 A73-28492
- Generation and detection of sound by distributed piezoelectric sources.
13 p1661 A73-29289
- The design and applications of highly dispersive acoustic surface-wave filters.
14 p1732 A73-29933
- Long range fluidic acoustic sensors cross air currents and temperature gradient effects on operational characteristics and resolution, and prototype design for industrial applications
20 p2511 A73-39753
- SOUND TRANSMISSION**
Representation of a $1/N$ power law boundary layer in the sheared flow acoustic transmission problem.
01 p0033 A73-10783
- Effect of gas-surface interaction on the transmission of sound through a collisionless gas.
01 p0077 A73-10972
- The transmission of sound in an acoustically treated rectangular duct with boundary layer.
04 p0476 A73-15586

- The transmission of sonic boom signals into rooms through open windows.
05 p0537 A73-17370
- Conservation of energy in random media, with application to the theory of sound absorption by an inhomogeneous flexible plate.
07 p0851 A73-19153
- A mathematical analysis concerning the edge effect of sound absorbing materials.
08 p0987 A73-21124
- A single number rating for effective noise reduction.
11 p1397 A73-25000
- Cavity-backed panel resonance.
13 p1690 A73-28062
- The optimization of modal sound attenuation in ducts, in the absence of mean flow.
15 p1865 A73-32152
- Acoustic radiation from the end of a two-dimensional duct - Effects of uniform flow and duct lining.
16 p1999 A73-32914
- Approximation for thin boundary layers in the sheared flow duct transmission problem.
16 p2000 A73-33679
- Shear waves in infinitely extended double walls with coupling rods of circular cross section. I - Shear waves in the infinitely extended disk
17 p2241 A73-34246
- Transmission of upstream sound through a subsonic jet.
18 p2259 A73-36175
- [AIAA PAPER 73-630] Extraneous modes in sound absorbent ducts.
19 p2459 A73-37294
- The effect of stiffeners on the sound radiation and the transmission loss of metal walls
19 p2460 A73-38181
- A high resolution pulse transmission technique for determining ultrasonic velocities.
20 p2564 A73-38881
- Experimental correlation techniques for the characterization of vibration transmission paths.
20 p2617 A73-39267
- Noise reduction by enclosures to block airborne and structure-borne acoustic paths, developing models for insertion loss in different frequency ranges
22 p2888 A73-42924
- Computational methods for studying acoustic propagation in nonuniform waveguides.
24 p3078 A73-44839
- [AIAA PAPER 73-1006] Transmission and far field radiation of sound waves in and from lined ducts containing shear flow.
24 p3078 A73-44845
- SOUND VELOCITY**
U ACOUSTIC VELOCITY
SOUND WAVES
NT AERODYNAMIC NOISE
NT AIRCRAFT NOISE
NT ELECTROACOUSTIC WAVES
NT ENGINE NOISE
NT ION ACOUSTIC WAVES
NT JET AIRCRAFT NOISE
NT LAMB WAVES
NT NOISE [SOUND]
NT ROCKET ENGINE NOISE
NT SONIC BOOMS
NT THERMAL NOISE
- Response of the ionosphere to the spectrum of acoustic-ionic waves emitted by a localized impulse source in space - Application to suddenly arising geomagnetic storms
01 p0035 A73-10327
- Amplitude modulation of electromagnetic waves by acoustic waves in a dispersive plasma - Modified theory.
01 p0083 A73-10455
- Acoustic field of an infinite annular cylindrical transducer partially coated with an acoustically soft material
01 p0077 A73-10927
- Reflection coefficients for acoustic waves interacting with stratified media.
01 p0078 A73-11097
- Energy transfer between interacting electromagnetic waves propagating in half space media, applying to acoustic surface wave excitation by electromagnetic converter
02 p0140 A73-11568
- Computation of the sound energy radiated from turbulent flows
02 p0153 A73-11699
- [DGLR PAPER 72-074] Book - Sound, structures, and their interaction.
02 p0192 A73-11880
- Book - Radiation and scattering of waves.
02 p0192 A73-11882
- Nonrelativistic collisionless plasma ion acoustic waves modulation by hf electromagnetic oscillation, calculating wave complex frequency
02 p0197 A73-12069
- [AD-753362] Mesoscale traveling ionospheric disturbances in electron density interpretation in terms of acoustic gravity waves
02 p0162 A73-12295
- An analysis of the acoustic power radiated by a point dipole source into a rectangular reverberation chamber.
02 p0194 A73-12603

- The investigation of the effect of acoustic oscillations on the combustion process of gaseous fuel
03 p0396 A73-12955
- Inlet sound power of axial compressors.
03 p0241 A73-12956
- Noise from free jets and airfoils in jets.
03 p0290 A73-12969
- Discrete tone radiation arising from a supersonic jet flowing into an unlimited gaseous medium and into a cylindrical ejector.
03 p0290 A73-12970
- Structural and aerodynamic characteristics changes in turbulent propane-butane and air jets interacting with sound
03 p0290 A73-12971
- An investigation of the near wake properties which lead to the generation of vortex shedding sound from airfoils.
03 p0242 A73-12976
- Partial optical coherence theory based Greenspan modification for calculation of sound power radiation from statistically vibrating flat surfaces
03 p0384 A73-12991
- Perturbation technique for approximation of sound radiation from controlled boundary layer on thin plate, deriving random stationary functions in terms of Fourier integral
03 p0291 A73-12992
- Chromospheric heating of very hot stars by radiation driven sound waves.
03 p0371 A73-13222
- Some laws of the propagation of discrete-tone perturbations in a free supersonic jet
03 p0245 A73-13668
- Acoustic and shock waves interaction in axisymmetric gas flow through variable section channel, calculating flow characteristics variations via isentropic theory of steady flow
03 p0295 A73-13673
- Frequency spectra of acoustic emissions generated by deforming metals and ceramics.
04 p0448 A73-15122
- Geometric dispersion of acoustic waves by a fibrous composite.
05 p0597 A73-16114
- Acoustic holographic scanning techniques for imaging flaws in thick metal sections.
05 p0574 A73-16284
- Display of HF acoustic holograms utilizing liquid crystals.
05 p0574 A73-16285
- Thin wing induced undulating viscous wake and far field acoustic wave through interaction with turbulent cylindrical jet, using dipole force field model
05 p0532 A73-16950
- [AIAA PAPER 73-223] Use of a paraboloidal layer to study gas-wall interaction
06 p0685 A73-17772
- Measurements of the acoustical parameters of rock powders and the Gold-Soter lunar model.
07 p0894 A73-19850
- Acoustic radiation from two concentric cylindrical shells.
07 p0851 A73-19958
- Stroboscopic investigation of the effect of standing acoustic waves on turbulent flames
07 p0920 A73-19992
- IR radiometers for free jets sound emission mechanism probing, describing optical and electronic equipment
07 p0825 A73-20164
- [ONERA, TP NO. 1212] Use of a surface-acoustic-wave delay line to provide pseudocoherence in a clutter-reference pulse doppler radar.
08 p0939 A73-21113
- Statistical phenomena during shock wave formation
08 p0955 A73-21447
- Shock wave formation in a statistically inhomogeneous gas
08 p0955 A73-21450
- Acoustic radiation from plates excited by flow noise.
08 p0988 A73-21470
- Theory of a generalized Helmholtz resonator.
08 p0952 A73-21471
- Acoustic emission for monitoring fatigue crack growth.
09 p1083 A73-22511
- Mathematical model for nonlinear interactions between HF waves and LF acoustic waves applied to electromagnetic wave stability in plasmas and dielectrics
09 p1128 A73-22614
- Chromospheric heating of very hot stars by radiation driven sound waves. II.
09 p1148 A73-22868
- Deformation of a spherical shell under the action of an unsteady spherical hydroacoustic wave
09 p1165 A73-23354
- Acoustic emission studies of large advanced composite rocket motor cases.
10 p1288 A73-23967
- Stimulated emission of acoustic power as analog to lasers and masers, noting nonpreservation of phase between incident and stimulated pressure
10 p1249 A73-24388

- Image processing using acoustic surface waves.
11 p1334 A73-25358
- Perturbation theory for multistrip acoustoelectric surface-wave amplifier.
11 p1337 A73-25362
- Perturbation theory for the surface-wave multistrip coupler.
11 p1337 A73-25363
- Heating effects due to radiative energy loss from acoustic waves in solar atmosphere, estimating temperature difference between radiative equilibrium and empirical model
11 p1421 A73-25931
- A source of nonlinear distortions in acoustic emission
11 p1399 A73-26093
- Geometric interpretation of conditions for resonant wave interactions valid under nondispersive conditions, noting relevance for acoustic waves in crystals and slowness vectors
11 p1400 A73-26278
- Measuring projection weld strength by acoustic emission.
12 p1502 A73-27038
- Book - An introduction to acoustical holography.
12 p1496 A73-27052
- VHF and microwave surface acoustic wave band-pass filter design with impulse model for frequency response and interdigital transducer input admittance calculation
12 p1484 A73-27563
- Thermospheric neutral gas dynamics, discussing acoustic, gravity, tidal and planetary waves disturbance spectrum, propagation characteristics, latitude structure and energy sources
12 p1493 A73-27756
- Improvements in surface-acoustic-wave pulse-compression filters.
13 p1595 A73-28048
- Effects of wall admittance changes on duct transmission and radiation of sound.
13 p1658 A73-28060
- A unified analysis of fan stator noise.
13 p1563 A73-28500
- Acoustic hologram irradiation with sound waves to yield image as acoustic intensity pattern, noting parallels in optical holography
13 p1615 A73-28587
- The effects of scanning position and motion errors on hologram resolution.
13 p1615 A73-28590
- Ray optics model analysis for spherical aberration effects on acoustic hologram resolution in image reconstruction, discussing computer generated correction for quality improvement
13 p1615 A73-28591
- Phase and amplitude only scanned acoustical holograms, noting Fraunhofer diffraction region reconstructed images
13 p1615 A73-28592
- Acoustic imaging by Bragg diffraction using point sources and spherical optics
13 p1616 A73-28594
- A comparison of holographic versus lens type acoustic image systems by computer simulation.
13 p1616 A73-28595
- Asymptotic pressure calculation of plane acoustic wave diffraction by infinitely long isotropic solid elastic circular cylinder in viscous liquid medium
13 p1583 A73-28863
- Influence of a traveling acoustic wave on spectral line profiles. II - Asymmetry of weak Fraunhofer lines
13 p1683 A73-29092
- A Fabry-Perot acoustic surface vibration detector-application to acoustic holography.
13 p1622 A73-29422
- Internal fracture and acoustic emission of fiberglass reinforced plastics.
13 p1647 A73-29544
- Application of acoustic surface-wave technology to spread spectrum communications.
14 p1733 A73-29934
- Acoustic-gravity modes and large-scale traveling ionospheric disturbances of a realistic, dissipative atmosphere.
14 p1748 A73-29977
- Investigation of rough surfaces by a method based on the scattering of coherent light by the sound reflected from such surfaces
14 p1753 A73-30583
- Transition of a shock wave into a sound wave.
15 p1912 A73-31010
- Statistical effects in the generation of shock waves.
15 p1860 A73-31011
- Shock-wave generation in a randomly inhomogeneous gas.
15 p1860 A73-31014
- Detection of gravitational waves by the method of light scattering by elastic oscillations
15 p1913 A73-31321
- Evaluation of composite failures through fracture signal analysis.
15 p1879 A73-32250
- Russian book - Asymptotic theory of diffraction of electromagnetic waves by finite structures.
15 p1845 A73-32294
- Cosmic ray pulses conduction to interstellar gas by magnetic field, describing effects on sound vibration
17 p2223 A73-34369
- A perturbation method for low-frequency fluid-structure interaction problems.
[ASME PAPER 72-APM-WWW] 17 p2248 A73-35102
- Application of surface acoustic wave devices to radar.
17 p2140 A73-35319
- Flexural vibration frequencies of right circular cylindrical tensor gravitational wave detectors in regime with sound wavelength comparable to diameter
17 p2176 A73-35763
- Predicted acoustic gravity wave enhancement during the solar eclipse of June 30, 1973.
18 p2352 A73-36301
- Diffraction of an acoustic wave at a moving plate
18 p2265 A73-37012
- Oblique reflection of a plane acoustic wave from a burning surface
19 p2503 A73-37513
- Acoustical radiation reaction by conservation of energy and Dirac prescription methods and derivation of acoustic index of refraction for system of soft spheres
20 p2592 A73-39049
- Dispersion curve computation for elastic acoustic waves propagation in /001/-cut cubic free anisotropic plate, noting relationship with slowness curves for bulk waves
20 p2616 A73-39050
- Aerodynamic sound and the low-wavenumber wall-pressure spectrum of nearly incompressible boundary-layer turbulence.
20 p2545 A73-39053
- Second harmonic amplitude modulation of an electromagnetic wave by an acoustic wave in a dispersive plasma.
20 p2597 A73-39199
- Infrasound from convective storms - Examining the evidence.
21 p2679 A73-40070
- Propagation velocities and amplitudes of thermoacoustical waves in thermo-plastic materials.
21 p2789 A73-40088
- Acoustic surface wave energy detection via combination of MOSFET array and ZnO overlay piezoelectric transducer, deriving signal processing technique
21 p2660 A73-40100
- Vortex sheet model of directional acoustic wave radiation near nozzle exit from supersonic helium jet shear layer instability
21 p2677 A73-40617
- Peak subsonic noise level reduction by jet refraction, showing directivity patterns as function of jet velocities and temperature ratios
21 p2754 A73-40753
- On the radiation from an aerodynamic acoustic dipole source
21 p2633 A73-40943
- Propagation of acoustic waves in a fluid flowing through a cylindrical duct
21 p2677 A73-40944
- Surface acoustic wave devices and applications. II - Pulse compression systems.
21 p2703 A73-41137
- Some features of the propagation of a discrete tone perturbation in a free supersonic jet.
21 p2633 A73-41318
- Interaction of sound with jets.
22 p2795 A73-41704
- Acoustic turbulence generation of shock waves in compressed gas or plasma excited by random potential forces based on energy transfer along spectrum
22 p2840 A73-41809
- On the derivation of Zone I spectra for a pulsed finite-amplitude source operating in a nonviscous nondispersive fluid medium.
22 p2885 A73-41819
- Sonic wave excitation by optical radiation, considering electrostriction effect and radiation absorption with subsequent intensity inhomogeneity-caused pressure gradients
22 p2868 A73-41898
- Radiatively driven harmonic acoustic waves in vibrational equilibrium in closed cylindrical tube, deriving pressure response, radiative absorption coefficient and spectral detail
22 p2930 A73-42235
- Experiments on radiatively driven harmonic acoustic waves in a confined gas.
22 p2930 A73-42236
- The reflexion of an acoustic pulse by a plane vortex sheet.
22 p2842 A73-42348
- Monograph - Generation of acoustic waves in piezoelectric devices.
22 p2861 A73-42700
- KRSS - A new high-performance acousto-optical material
22 p2897 A73-43100
- Resonance conditions for nonlinear interaction of acoustic gravity waves with viscous damping taken into account
22 p2828 A73-43178
- Current instability of atmospheric gravitational waves
24 p3083 A73-44786
- Nonlinear transient effects of separated unstable flow on vortex generated acoustic waves in cavities [AIAA PAPER 73-1014]
24 p3078 A73-44846
- SOUND-SOUND INTERACTIONS**
On the near- and far-field radiation patterns generated by the non-linear interaction of two separate and non-planar monochromatic sources.
08 p0988 A73-21469
- SOUNDERS**
U SOUNDING
SOUNDING
NT BALLOON SOUNDING
NT IONOSPHERIC SOUNDING
NT ROCKET SOUNDING
Spectroscopic sounding of cloud; snow and ice covers from below /earth surface/ and above /space or planet/
04 p0473 A73-15570
- The comparison of sensitivities of atmospheric echo-sounders.
22 p2862 A73-42727
- SOUNDING ROCKETS**
NT AEROBEE ROCKET VEHICLE
NT ASTROBEE ROCKET VEHICLES
NT LAMBDA ROCKET VEHICLES
NT PETREL SOUNDING ROCKET
NT SKYLARK ROCKET VEHICLE
Japanese sounding rocket and scientific satellite program.
01 p0110 A73-11102
- Lambda-4S solid propellant four-stage sounding rocket and scientific satellite launcher, describing design, operational and performance features
01 p0091 A73-11157
- Fluidic ignition system with two-component aerodynamic resonance heating /pneumatic match/ and hand pump for solid propellant sounding rocket engine
03 p0252 A73-13486
- Gun launched sounding rockets and sabot projectiles for low cost meteorological and geophysical data acquisition, considering cost advantages
06 p0756 A73-18020
- Cassiopee triaxial gyroscopic aiming device for sounding rocket attitude control, using stellar and inertial sensors and jet micropulsation
07 p0866 A73-18924
- Sounding rocket payload recovery systems [ONERA, TP NO. 1153]
08 p1014 A73-21681
- Use of open-structure channel electron multipliers in sounding rocket experiments.
01 p080 A73-22105
- A method for calculating aerodynamic heating on sounding rocket tangent ogive noses.
09 p1167 A73-23202
- Study of the influence of asymmetries on the flight behaviour of a sounding rocket.
09 p1155 A73-23203
- Sounding rocket vehicles aerolelastic structural analysis, calculating structural flexibility, dynamic pressure and angle of attack effects on aerodynamic stability
09 p1155 A73-23204
- Computerized method for designing plate type sounding rocket fins.
09 p1155 A73-23205
- Prediction of pressure fluctuation in sounding rockets and manifolded recovery systems.
09 p1155 A73-23206
- ARIES, the Minuteman I second stage as a controlled sound rocket.
09 p1155 A73-23207
- [AIAA PAPER 73-287]
STRAP IV - High accuracy, low drift attitude control system.
09 p1116 A73-23208
- An attitude control system for a stellar X-ray source mapping payload.
09 p1116 A73-23210
- [AIAA PAPER 73-291]
A digital attitude control system for orientation of rocket launched scientific payloads.
09 p1116 A73-23211
- [AIAA PAPER 73-292]
Dispersion of the direction of the angular momentum vector of sounding rocket payloads due to atmosphere exit and certain vehicle activities.
09 p1116 A73-23212
- [AIAA PAPER 73-293]
Recovery of sounding rocket payloads by center-of-gravity position control.
09 p1155 A73-23213
- [AIAA PAPER 73-294]
Low level wind measurement error as it affects sounding rocket dispersion.
09 p1116 A73-23215
- [AIAA PAPER 73-296]
Six degree of freedom guided sounding rocket flight simulations and trajectory program, discussing financial and technical feasibility
09 p1117 A73-23218
- [AIAA PAPER 73-299]
Astrobee F sounding rocket system design and development, describing advanced propulsion technology test program and results
09 p1156 A73-23219
- [AIAA PAPER 73-300]
Recoverable sounding rocket payload field refurbishment for data acquisition with time and monetary savings, noting micrometeorite collection experiments [AIAA PAPER 73-301]
09 p1156 A73-23220

- Rocket motor, Dart vehicle, booster and launcher design and instruments and payload description for Super Loki meteorological rocket systems
[AIAA PAPER 73-303] 09 p1156 A73-23222
- High resolution accelerometer for sounding rocket, describing calibration methods
[ONERA, TP NO. 1215] 10 p1219 A73-24398
- Rocket-borne scientific experiment program Sun-Atmosphere 1971, using meteorological rockets for meteor trail, atmospheric and ionospheric observations during geomagnetic disturbances
13 p1609 A73-29188
- DFVLR Mobile Rocket Base use of foreign ranges to launch sounding rockets
14 p1741 A73-30084
- Sounding rocket range facilities at Erange /Sweden/ for auroral studies, discussing telemetry support for simultaneous launchings
14 p1741 A73-30085
- Sounding rocket payload recovery systems
14 p1804 A73-30088
- The problem of launching bases in the meteorological rocket network.
14 p1743 A73-30116
- The application of Kalman filtering to the attitude determination of spinning space vehicles.
15 p1371 A73-32219
- Possibility of utilizing the ERIDAN rocket probe as an experimental vehicle
16 p2071 A73-32817
- Pyrotechnic explosive power devices and systems for aerospace applications.
16 p2045 A73-33106
- Airborne mechanical system for sounding rocket experiments.
16 p2072 A73-33119
- Heat pipe and phase changing material /PCM/ sounding rocket experiment.
[AIAA PAPER 73-759] 18 p2371 A73-36374
- A simple graphical solution for rocket wake boundaries.
23 p2939 A73-43680
- SOURCES**
Some remarks on the behaviour of surface source distributions near the edge of a body.
08 p0926 A73-21437
- SOUTH AFRICA**
The definition of the geotectonic domains of the Southern African crystalline shield by ERTS 1 imagery and its economic importance.
21 p2685 A73-40810
- SOUTH AMERICA**
Proton whistlers in the ionospheric F-region over the South American equatorial area.
18 p2304 A73-35970
- Expected results of hydrologic and geologic studies using ERTS imagery of the Atacama Desert, Altiplano, and Puna de Atacama, South America /Southwest Bolivia, Northwest Argentina, and Northern Chile/.
20 p2563 A73-39914
- SOUTH DAKOTA**
Organizational design for South Dakota state government to apply remote sensing technology to resources research and management, emphasizing hardware and information dissemination
20 p2629 A73-39831
- Utilizing remote sensing data for land use decisions for Indian lands in South Dakota.
20 p2557 A73-39850
- SOUTHEAST ASIA**
Southeast Asia weather during southwest monsoon in summer, discussing relation to westward moving equatorial waves from wind, pressure and cloudiness synoptic pattern analysis
12 p1520 A73-26805
- SOUTHERN HEMISPHERE**
ANTARCTIC REGIONS
Russian book on atmospheric circulation covering temperature distribution, tropospheric and stratospheric winds, jet streams and Southern Hemisphere meteorological features
04 p0474 A73-15961
- A synoptic climatology of satellite observed cloud vortices over the Southern Hemisphere.
07 p0846 A73-19039
- Schmidt telescopes in stellar photography of Magellanic clouds, galactic center and Scorpio-Centaurus and globular clusters for southern hemisphere Milky Way structure investigation
08 p1011 A73-21364
- The mean upper-air flow in Southern Hemisphere temperate latitudes determined from several years of GHOST balloon flights at 200 and 100 mb.
08 p0960 A73-21376
- Differences in auroral intensity at conjugate points.
09 p1074 A73-22059
- Satellite observed cloud signatures associated with mature and decaying depressions over high and middle southern latitudes, deriving surface pressure and upper geopotential anomaly patterns
10 p1244 A73-23980
- Southern Hemisphere troposphere atmospheric carbon dioxide monitoring program based on aircraft air sampling, discussing vertical profile data
11 p1358 A73-26472

Eole meteorological balloon sounding experiment in Southern Hemisphere, discussing mean circulation, eddy diffusion and data collection and satellite tracking system
15 p1904 A73-31723

Differences in circulation of the upper atmosphere in low latitudes of the southern and northern hemispheres.
18 p2310 A73-36138

Southern Hemisphere earth rotational synthesis radio telescope array with paraboloids arranged as compound grating interferometer for astronomical radio sources mapping
23 p2958 A73-43361

Aerosol ice nuclei concentration measurements in remote regions of Southern Hemisphere near Australia by shipborne membrane filters, noting land or stratospheric sources
23 p3002 A73-43598

Some characteristics of satellite-observed bands of persistent cloudiness over the Southern Hemisphere.
24 p3107 A73-45015

SOVEREIGNTY

Spaceflight and the problem of vertical limit of state sovereignty.
04 p0524 A73-15153

German book on national airspace protection against foreign aircraft intrusion in peacetime covering sovereign rights according to international law, conventions and treaties
11 p1454 A73-26257

Earth studies from space and their legal problems
19 p2506 A73-38267

SOYUZ SPACECRAFT

Measurements of the isotopic composition of particle fluxes carried out on spacecrafts Soyuz, Zond 8 and Luna 16.
02 p0206 A73-12317

Soyuz 9 spectrophotometry of earth surface features, comparing manned spacecraft-obtained and conventional spectrographs
03 p0304 A73-14564

Apollo-Soyuz docking project for flight testing systems compatibility for safe and reliable crew transfer, discussing program objectives, technical requirements and solutions
09 p1152 A73-22187

Some results of spectrophotometric studies of natural formations from the manned spacecraft 'Soyuz-9'.
20 p2558 A73-39858

Visual observations of the earth and of the circumterrestrial space environment from manned orbital stations
23 p2971 A73-43331

SPACE BASES

Co-60 kernel modular power and reentry system design for space station and base, noting fuel and launch cost savings over Pu-238 systems
11 p1310 A73-25998

Reactor-thermoelectric power systems for NASA Space Station/Space Base.
11 p1395 A73-26012

A modular Space Station/Base electrical power system - Requirements and design study.
11 p1311 A73-26015

Preliminary design of reactor power systems for the manned space base.
11 p1395 A73-26018

In-core 100 kW thermionic power system design to meet manned spacecraft shielding requirements, discussing waste heat removal and integration with space base
11 p1395 A73-26026

Nuclear thermionic power plants in the 50-300 kW range.
11 p1396 A73-26027

Determination of the motion and rotation parameters of an asteroid by the measurement of distances to a space station situated on the asteroid surface
14 p1796 A73-29858

SPACE BIOLOGY

U EXO BIOLOGY

SPACE BUSES

U FERRY SPACECRAFT

SPACE CAPSULES

NT ESCAPE CAPSULES

SPACE CHARGE

Determination of the complete set of physical parameters of Schottky-barrier diodes
01 p0022 A73-10041

Excitation of space charge waves in a one-carrier semiconductor with variable doping.
01 p0088 A73-10680

Relativistic dispersion equation for a circular waveguide with a rotating tubular electron beam, allowing for the effect of the space charge
01 p0017 A73-10982

Limited space charge accumulation oscillations in gallium arsenide
02 p0199 A73-11530

Instabilities and small-signal response of double injection structures with deep traps.
02 p0146 A73-12042

On the measurement of the specific 'emitter efficiency factor in bipolar transistors'.
02 p0147 A73-12043

Purity evaluation of n type GaAs LSA diodes from low-field temperature-dependent mobility.
05 p0556 A73-16454

Electronic transport in insulating films.
05 p0604 A73-16505

GaAs Gunn diode LSA operation mode in multiole circuit to extend high frequency limit
05 p0558 A73-16749

Rocket sounding for space charge distribution and electric field strength in stratosphere and mesosphere noting vertical distribution of atmospheric conductivity
05 p0570 A73-17010

Space-time distribution of excess carriers and the space charge in doped semiconductors.
06 p0734 A73-17811

Electrohydrodynamic shock wave evolution in steady gas flow with positive space charge in electric field
06 p0733 A73-18868

Concentrations of carriers and electric field along an insulating or semiconducting sample: Development of steady solutions up to the second order Case of weak potentials
08 p0995 A73-21444

Thermal free electron constant approximation in space charge current theory, considering I-V characteristics and ionized donor concentrations at injection levels
08 p0951 A73-21484

Transient photocurrent pulse shapes and transition times in insulators with uniform and exponential trapped space charge in excitation layer or insulator surface
09 p1119 A73-21944

On the interaction of the electromagnetic field with electron beams in resistive wall waveguides
09 p1062 A73-22324

Photoconductor-metal contact at higher densities.
11 p1407 A73-24988

Overlength modes of transferred-electron oscillators.
11 p1337 A73-25359

Metal surfaces structure, chemical segregation, electronic properties, space charge and electrode behavior
11 p1381 A73-25809

Analysis of the static modes of a magnetron with allowance for electron-velocity scatter
11 p1332 A73-26163

Thermal noise calculation of single-carrier space-charge-limited current in a non-insulating solid.
12 p1530 A73-27029

Thermal noise measurements on space-charge-limited hole current in silicon.
13 p1668 A73-28542

Allowance for the influence of the space charge in the kinematic theory of microwave devices
15 p1850 A73-31491

Third-order treatment of combined effects of space charge and external fields on cylindrical ion and electron beams.
15 p1915 A73-31933

Electrohydrodynamic shock wave evolution in steady gas flow with positive space charge in electric field
15 p1921 A73-32406

Diffusive motion of initially ellipsoidal plasma irregularities or ion clouds in upper atmosphere, considering space charge electric field effects
17 p2160 A73-34787

Current-voltage characteristic of a real diode with a Schottky barrier, allowing for tunneling through the spatial charge region
18 p2293 A73-36718

Formulation of the basic approximations of the field theory of static current-voltage characteristics of quasi-monopolar semiconductors
18 p2341 A73-36724

A study of the effect of the emitter current on the barrier capacitance of a transistor collector junction. II
20 p2536 A73-39395

Substrate effect estimation for space charge limited current in intrinsic materials and planar structures, discussing I-V curves
20 p2543 A73-39593

Noise of space-charge-limited current in solids is thermal.
21 p2668 A73-41559

Theory and operation of space-charge-limited transistors with transverse injection.
22 p2833 A73-42598

Photoelectric methods of determining the electrical characteristics of MDS systems
23 p3006 A73-43616

Shot noise of a real Schottky-barrier diode during tunneling through the space charge region
23 p2960 A73-43619

Diffusionless theory of the current-voltage characteristics of a metal/monopolar semiconductor contact in the case of current limiting by an arbitrary space charge
23 p3015 A73-43621

A computational study of the diffusion of meteor trains using a self-consistent model for the space-charge electric field. 23 p3029 A73-43684

Interpretation of distinct type IVm-A- and IVm-bursts on the basis of micro-instabilities and of resonant nonlinear interaction of waves. 24 p3123 A73-44645

Redistribution of charged particles and self-distortion of high-amplitude electromagnetic waves in a plasma. 24 p3117 A73-45413

SPACE COMMUNICATION

NT INTERPLANETARY COMMUNICATION

NT LUNAR COMMUNICATION

NT SPACECRAFT COMMUNICATION

International telecommunication law with respect to space laboratories /space vehicles, orbital stations or lunar bases/, discussing protection for communication satellites 04 p0521 A73-15128

Results of the World Conference of Space Telecommunications, Geneva, 1971 04 p0523 A73-15150

Millimeter wave propagation measurement for attenuation probability statistics by ATS-5 satellite, considering impact on space communication system design 04 p0418 A73-15387

Auto and cross correlation functions of combined binary pseudorandom sequences in digital space communication systems 04 p0423 A73-15916

U.S.S.R. sponsored international space communication system, discussing technological, organizational and legal aspects 07 p0923 A73-19202

Noise considerations in space communication antennas. 07 p0794 A73-20228

Concatenated and hybrid coding system performance and implementation complexity for moderate speed deep space communication 09 p1056 A73-23401

Improvements in deep-space tracking by use of third-order loops. 09 p1056 A73-23406

A single channel command detector for deep space missions. 09 p1057 A73-23417

A telecommunications link model for deep space - With applications to the HELIOS probe. 09 p1058 A73-23419

Effects of multipath fading on low data-rate space communications. 09 p1058 A73-23422

Book - The law of outer space. 10 p1297 A73-23944

Frequency response of helix and coupled cavity traveling wave tubes and amplifiers power output, discussing electronic countermeasures and space communications 11 p1339 A73-26692

Source altitude for experiments to simulate space-to-earth laser propagation. 14 p1756 A73-30151

Solid-state transmitter for VHF/UHF space telemetry. 16 p1979 A73-33104

Millimeter wave propagation measurements from an orbiting earth satellite. 16 p1982 A73-33716

Problems connected with an employment of carbon dioxide lasers in space communications systems 18 p2290 A73-37087

Large scanning and multibeam reflector antennas for space communications. 20 p2524 A73-38738

Book - Twelfth report by the International Telecommunication Union on telecommunication and the peaceful uses of outer space. 20 p2607 A73-39151

SPACE DEBRIS

Impact gages for detecting meteoroid and other orbital debris impacts on space vehicles. 17 p2238 A73-34606

SPACE DENSITY

Multiple subuniverses concept for wide mean space density variations in closed universe, considering radio and optical observation possibility 10 p1275 A73-23822

SPACE DIVERSITY

U RECEPTION DIVERSITY

SPACE ELECTRIC ROCKET TESTS

NASA technology program for auxiliary and primary electric propulsion systems, noting flight tests and solar arrays [AIAA PAPER 72-1127] 03 p0355 A73-13437

SPACE ENVIRONMENT

U AEROSPACE ENVIRONMENTS

SPACE ENVIRONMENT SIMULATION

NT WEIGHTLESSNESS SIMULATION

Simulation program for satellite operation status prediction in space environment. 01 p0110 A73-11146

Space simulation chamber tests of thermal louver model for spacecraft temperature control 01 p0110 A73-11150

Test of horizon sensor for the ionosphere sounding satellite. 01 p0053 A73-11172

Lunokhod 1 vehicle terrestrial mobility tests, simulating lunar gravity, soil and traction on scale and mockup models 02 p0151 A73-12234

Fabrication of a lightweight circular orbit passive radiative cooler. 03 p0329 A73-13010

Space simulation experiments on reaction control system thruster plumes. [AIAA PAPER 72-1071] 03 p0354 A73-13398

Li and Si p-n solar cells performance comparison for simulated earth orbit environment by real time irradiation with Sr 90 beta particles 03 p0257 A73-14243

Irradiation of solar cell candidates for the ATS-F solar cell flight experiment. 03 p0257 A73-14245

The space environment simulation chamber of Toulouse. 07 p0807 A73-19000

The Toulouse centre's space environment simulator - "The Sun." 07 p0807 A73-19002

Simulated microscale erosion on the lunar surface by hypervelocity impact, solar wind sputtering, and thermal cycling. 07 p0896 A73-19867

Skylab project mission objectives in long duration spaceflight, describing crew training under simulated space environment conditions, foods, clothing, waste disposal, physical exercise, etc 09 p1152 A73-22188

The determination and treatment of temperature coefficients of silicon solar cells for interplanetary spacecraft application. 09 p1036 A73-22810

Cryogenic applications for environment simulation. 11 p1344 A73-25580

A nongravitational effect in the simulation of cometary phenomena. 14 p1793 A73-29824

Source altitude for experiments to simulate space-to-earth laser propagation. 14 p1756 A73-30151

Viking 75 lander deceleration system qualification flight tests at expected Mars conditions, discussing design requirements and full scale vehicle simulation in earth atmosphere [AIAA PAPER 73-457] 15 p1827 A73-31443

Magnetogasdynamic compression of a coaxial plasma accelerator flow for micrometeoroid simulation. 15 p1919 A73-31932

Aeros satellite simulated environmental testing for thermal behavior under space vacuum, temperature and solar radiation conditions, comparing results with mathematical model calculations 16 p1997 A73-33392

Satellite systems space environmental simulation tests, discussing thermal models design, temperature field and error calculations by computerized data processing 16 p1998 A73-33393

Radiative property degradation of water impinging on thermally-controlled surfaces under space conditions. [AIAA PAPER 73-733] 18 p2336 A73-36350

Skylab Medical Experiments Altitude Test /SMEAT/ facility design and operation. [ASME PAPER 73-ENAS-44] 19 p2401 A73-37991

Skylab medical experiments altitude test /SMEAT/ chamber atmosphere trace contaminants analysis, describing sample acquisition techniques and instrumentation [ASME PAPER 73-ENAS-45] 19 p2395 A73-37992

Effect of simulated lunar impact on the survival of bacterial spores. 20 p2513 A73-39485

Developments in the analysis of planetary quarantine requirements. 22 p2803 A73-42159

SPACE ENVIRONMENTAL LUBRICATION

U SPACECRAFT LUBRICATION

SPACE ERECTABLE STRUCTURES

NT BEACON SATELLITES

Metallized fiberglass antenna meshes for spacecraft deployable reflectors, discussing low mass/area, long term stability and performance characteristics and degradation tests 03 p0333 A73-13045

Space deployed expandable structures, discussing vehicular and environmental constraint effects on design, large structure requirements, and applications 07 p0828 A73-18905

Reliability estimate of a Space Deployable Antenna. 16 p1989 A73-33620

SPACE EXPLORATION

NT VIKING MARS PROGRAM

Missions for the systematic unmanned exploration of Mars. 01 p0105 A73-11160

Helios A and B interplanetary exploration objectives, considering solar plasma, high energy particles and interplanetary dust characteristics [DGLR PAPER 72-068] 02 p0227 A73-11688

Jupiter exploration current status, discussing orbital and physical data, mass, density, rotation, atmosphere, band structure, red spot, radio emission, magnetic field, internal structure, etc 02 p0212 A73-11948

Heos 2 satellite instrumentation and space exploration objectives, considering earth and interplanetary magnetic fields, electron and proton energies, solar radiation and wind, cosmic dust and micrometeoroids 02 p0228 A73-11949

Space experience and ethics impact on world development, considering knowledge advancement, regional applications, economy stimulation, environment improvement and international cooperation 02 p0239 A73-11998

Space research XII; Proceedings of the Fourteenth Plenary Meeting, Seattle, Wash., June 18-July 2, 1971. Volumes 1 & 2. 02 p0212 A73-12226

The international magnetospheric study 1975-1977 - Scientific fundamentals and objectives. 02 p0164 A73-12313

Mars exploration by spacecraft, discussing erosional processes, atmospheric pressure and composition, heat absorption and radiation and polar caps formation 02 p0221 A73-12575

Polish space research and prospects, discussing Intercosmos and Intersputnik participation and studies in space physics, communications, meteorology, geodesy, biology, radiology and medicine 04 p0521 A73-15021

Earth environment pollution protection in space exploration, noting international law principles application 04 p0522 A73-15140

Space exploration and celestial bodies natural resources exploitation legislation proposals evaluation 04 p0523 A73-15152

NASA space research costs balanced with scientific and technological achievements in relation to space law 04 p0524 A73-15156

The benefits of space exploration related to the Space Shuttle. 05 p0568 A73-16184

Space exploration and the origin of life. 06 p0651 A73-17930

Picture information acquisition, storage and transmission characteristics of film and vidicon systems for photographic reconnaissance of planets 06 p0750 A73-18010

Planetary exploration with electrically propelled vehicles. 06 p0750 A73-18021

In-depth exploration of the solar system and its utilization for the benefit of Earth. 06 p0751 A73-18029

Mariner Mars 1971 project historical background, and Mariner 9 orbiter mission science objects and planning for Mars surface observations and measurements 09 p1144 A73-22265

Mars dust storm observations at time of great oppositions, suggesting local time and space meteorological conditions and feedback processes favoring global dust spread 09 p1144 A73-22269

The American space program for the future. 12 p1560 A73-27062

Space shuttle missions relationship to post-Apollo, European and joint European-U.S. space exploration programs 13 p1690 A73-29387

Soviet-French cooperation in space exploration 14 p1818 A73-30250

A strategy for investigation of the outer solar system - Outer planets, their satellites, and particles and fields at great distances from the sun. 14 p1799 A73-30526

Mission building blocks for outer solar system exploration. 14 p1805 A73-30527

Imaging as primary exploration tool for outer planets and satellites, considering flyby and orbital imaging for planetary atmospheres 14 p1800 A73-30536

Extraatmospheric space utilization and exploration concepts, discussing international agreements and space law 14 p1819 A73-30899

Terrestrial quarantine considerations for unmanned sample return missions. 18 p2349 A73-35977

Cometary exploration - A case for Encke. [AIAA PAPER 73-596] 18 p2353 A73-36501

SPACE FLIGHT

- Remotely manned systems: Exploration and operation in space; Proceedings of the First National Conference, California Institute of Technology, Pasadena, Calif., September 13-15, 1972. 19 p2415 A73-37301
- Depth sensing, camera and touch/force sensing systems for autonomous industrial robotics and planetary exploration 19 p2429 A73-37322
- Russian papers on populated cosmos covering space exploration impact on human civilization, extraterrestrial life, space medicine and biology, solar system, space law, etc 19 p2393 A73-37398
- Scientific exploration with an out-of-ecliptic spacecraft. 19 p2485 A73-37760
- Russian book on Soviet news agency space exploration articles for 1971 covering Soyuz, Salyut, Molniya, Luna, Meteor and Lunokhod programs, agricultural satellites and lunar exploration 19 p2486 A73-37771
- Space-related research in mycology concurrent with the first decade of manned space exploration. 20 p2513 A73-39478
- Long range post-Apollo space exploration goals, considering earth orbital station, moon base, manned Mars landing and interstellar flights 23 p3038 A73-43990
- ## SPACE FLIGHT
- NT APOLLO FLIGHTS
NT APOLLO 11 FLIGHT
NT APOLLO 12 FLIGHT
NT APOLLO 14 FLIGHT
NT APOLLO 15 FLIGHT
NT APOLLO 16 FLIGHT
NT APOLLO 17 FLIGHT
NT HYPERBOLIC REENTRY
NT HYPERSONIC REENTRY
NT INTERPLANETARY FLIGHT
NT INTERSTELLAR TRAVEL
NT MANNED REENTRY
NT MANNED SPACE FLIGHT
NT RETURN TO EARTH SPACE FLIGHT
NT SPACECRAFT REENTRY
NT VIKING MARS PROGRAM
- Spaceflight and the problem of vertical limit of state sovereignty. 04 p0524 A73-15153
- The Mariner Venus Mercury flight data subsystem. 04 p0425 A73-15423
- Russian book - Biomedical problems of space flights: Index of domestic and foreign literature. 04 p0410 A73-16034
- Russian book on celestial and space flight mechanics covering trajectory and orbit evolution problems, resonance effects, relative motion dynamics and mathematical treatment 09 p1146 A73-22350
- Russian book - Pioneers rocket engineering: Selected works 1929-1945/. 15 p1943 A73-31576
- Vehicle and ground support in space shuttle sortie and delivery-retrieval mission profiles 19 p2491 A73-37594
- ## SPACE FLIGHT FEEDING
- U.S. manned space flight food system development experience assessment, covering Mercury, Gemini, Apollo and manned orbiting laboratory programs 03 p0269 A73-14168
- Microbiological testing of Skylab foods. 12 p1464 A73-27075
- Apollo diet evaluation - A comparison of biological and analytical methods including bioisolation of mice and gamma radiation of diet. 20 p2517 A73-39103
- Nutrition systems for pressure suits. 20 p2517 A73-39105
- ## SPACE FLIGHT STRESS
- Effect of a 5-day space flight on cardiodynamics during physical work of moderate intensity 02 p0138 A73-12467
- Prolonged control of cardiac bioelectrical activity in man in ground experiments and during spaceflight 06 p0657 A73-17694
- Emotional stresses during a space flight 07 p0785 A73-19297
- Vertical posture control after Sojuz 6, 7 and 8 flights and 120-day hypokinesia 08 p0933 A73-20985
- Findings on American astronauts bearing on the issue of artificial gravity for future manned space vehicles. 09 p1045 A73-22531
- Investigation of the sleep and wakefulness rhythms in the crewmembers of Sojuz-3 through Sojuz-9 spacecraft prior to, during, and after space flight 10 p1182 A73-24697
- Physiological response to exercise after space flight - Apollo 7 to Apollo 11. 11 p1314 A73-25326
- Work movement performance of the astronaut in flight. 12 p1465 A73-27645

- Peripheral blood composition changes in cosmonauts during 18- and 24-day space flights 12 p1463 A73-27710
- International literature survey of microbiological space research for 1930-1970, discussing high altitude balloon, rocket and satellite experiments, weightlessness effects, mutagenesis, etc 15 p1838 A73-31501
- Asymmetry of otolith responses in fish 15 p1834 A73-31507
- Effect of a 5-day space flight on the cardiac dynamics during moderately severe physical work. 15 p1840 A73-32617
- Effects of the hypodynamics and other factors of a spaceflight on the excretion of 17-oxy corticosteroids and aldosterone 17 p2111 A73-34233
- Skylab astronaut vestibular function experiment in orbital flight, discussing motion sickness susceptibility, stimulation thresholds and space perception measurements 17 p2115 A73-34741
- Physiological effects of acceleration and weightlessness during space flight, discussing cardiovascular system, renal function, respiration, blood volume, metabolism, work capacity, etc [AFOSR-72-2451TR] 17 p2113 A73-35856
- A monkey metabolism pod for space-flight weightlessness studies. 18 p2270 A73-35963
- Effect of dynamic factors of space flights on green alga *Chlorella vulgaris*. 18 p2270 A73-36098
- Prolonged space flight and hypokinesia. 18 p2278 A73-36789
- Effect of certain flight factors on crew efficiency 21 p2643 A73-40350
- Interaction between radiation effects, gravity and other environmental factors in *Tribolium confusum*. 21 p2643 A73-40808
- Skylab 1 medical experiments concerning astronaut physiological responses and work capability as affected by exposure to space flight environment 21 p2778 A73-41519
- Effects of space flight factors on the heredity of higher and lower plants. 22 p2804 A73-42168
- Human sensorimotor coordination following space flights. 22 p2814 A73-42170
- Free fall effects on differential growth and radiation sensitivity of higher plants in space flight and ground based clinostat experiments 22 p2804 A73-42172
- Space flight factors effects on *Drosophila* development in terms of dominant, autosomal and sex-linked recessive lethals frequency, noting gametogenesis stage sensitivity 22 p2804 A73-42173
- Apollo 16 flight program for investigating physiological effects of prolonged weightlessness on central nervous system, vestibular, neuromuscular and cardiovascular functions, metabolism, radiation sensitivity and body weight 22 p2814 A73-42176
- ## SPACE FLIGHT TRAINING
- Skylab project mission objectives in long duration spaceflight, describing crew training under simulated space environment conditions, foods, clothing, waste disposal, physical exercise, etc 09 p1152 A73-22188
- ## SPACE GLIDERS
- ## U LIFTING REENTRY VEHICLES
- ## SPACE LABORATORIES
- NT MANNED ORBITAL LABORATORIES
NT MANNED ORBITAL RESEARCH LABORATORIES
- International telecommunication law with respect to space laboratories /space vehicles, orbital stations or lunar bases/, discussing protection for communication satellites 04 p0521 A73-15128
- Terrestrial law adaption to lunar surface or orbital space laboratories requirements 04 p0521 A73-15130
- The legal status of Orbital Laboratories as the next step to the development of the collaboration between the cosmic powers on earth. 04 p0522 A73-15131
- Legal aspects of laboratories on the moon. 04 p0522 A73-15132
- Lunar laboratories space law aspects, emphasizing need for prohibition of military activities and right of international community to information 04 p0522 A73-15133
- Research and applications modules /RAM/ program for manned space research satellites transportation and support, discussing mission requirements and design concepts [AIAA PAPER 73-72] 06 p0755 A73-17637
- Langley Research Center shuttle-compatible spaceborne advanced technology laboratory concept with sortie flight operation mode [AIAA PAPER 73-611] 18 p2358 A73-36089

- Space Shuttle in space lab operations, propulsion stage retrieval/delivery, satellite servicing, passenger transportation and short duration orbital missions 19 p2492 A73-37603
- Cloud microphysics spaceborne laboratory experimentation under zero-gravity conditions, discussing salt nuclei distribution mechanism due to spray breakup as task for Apollo-Soyuz program [AAS PAPER 73-135] 20 p2583 A73-38590
- ## SPACE LAW
- Liability under international law for damages caused by space objects 01 p0124 A73-10567
- Colloquium on the Law of Outer Space, 14th, Brussels, Belgium, September 20-25, 1971, Proceedings. 04 p0521 A73-15126
- Space Treaty legislative provisions for freedom of movement of orbital and lunar laboratories 04 p0521 A73-15127
- International telecommunication law with respect to space laboratories /space vehicles, orbital stations or lunar bases/, discussing protection for communication satellites 04 p0521 A73-15128
- Terrestrial law adaption to lunar surface or orbital space laboratories requirements 04 p0521 A73-15130
- The legal status of Orbital Laboratories as the next step to the development of the collaboration between the cosmic powers on earth. 04 p0522 A73-15131
- Legal aspects of laboratories on the moon. 04 p0522 A73-15132
- Lunar laboratories space law aspects, emphasizing need for prohibition of military activities and right of international community to information 04 p0522 A73-15133
- NASA's space station and the need for quantifiable components of a responsive legal regime. 04 p0522 A73-15134
- Soviet Union-proposed draft International Treaty governing lunar exploration and use 04 p0522 A73-15135
- Legal problems for the protection of the earth's environment. 04 p0522 A73-15136
- Space law provisions concerning terrestrial and celestial bodies environmental contamination, advocating establishment of international code of conduct and control authority 04 p0522 A73-15138
- International law for earth environment protection against pollution by activities in outer space, noting International Court of Justice Advisory Opinion procedure 04 p0522 A73-15141
- Legal problems relating to the evaluation, conservation and development of earth resources by means of space objects. 04 p0523 A73-15144
- Legal regulation of investigation of natural environment from outer space. 04 p0523 A73-15145
- Space exploration and celestial bodies natural resources exploitation legislation proposals evaluation 04 p0523 A73-15152
- Spaceflight and the problem of vertical limit of state sovereignty. 04 p0524 A73-15153
- The future of international space cooperation in treaty-making. 04 p0524 A73-15154
- The influence of space law on the development of public international law 04 p0524 A73-15155
- NASA space research costs balanced with scientific and technological achievements in relation to space law 04 p0524 A73-15156
- International law principles application to space liability codification, noting United Nations role in Draft Convention on space liability 04 p0524 A73-15159
- The legal position of earth orbiting stations 07 p0923 A73-19201
- Book - The law of outer space. 10 p1297 A73-23944
- Legal definition of space objects for international space law purposes regarding damage liabilities 14 p1818 A73-30292
- UN accomplishments in space law, discussing ESRO and ELDO application satellites and international agreements 14 p1819 A73-30898
- Extraatmospheric space utilization and exploration concepts, discussing international agreements and space law 14 p1819 A73-30899
- Russian papers on populated cosmos covering space exploration impact on human civilization, extraterrestrial life, space medicine and biology, solar system, space law, etc 19 p2393 A73-37398
- Earth studies from space and their legal problems 19 p2506 A73-38267

Book - The law of international spaces.
19 p2506 A73-38365

SPACE MAINTENANCE
On-orbit checkout and repair as a factor in economic spacecraft design and operation.
12 p1549 A73-27439
Lower payload costs through refurbishment and module replacement.
14 p1803 A73-29944
A reliability, cost and risk analysis of establishing and maintaining a space communications satellite network.
[AIAA PAPER 73-582] 18 p2288 A73-36074
Experimental evaluation of remote manipulator systems.
19 p2416 A73-37305
Space Shuttle in space lab operations, propulsion stage retrieval/delivery, satellite servicing, passenger transportation and short duration orbital missions
19 p2492 A73-37603
Possibility of using the Space Tug for the recovery and maintenance of satellites
21 p2782 A73-41554

SPACE MANUFACTURING
Extraterrestrial propellant resupply for advanced manned missions.
02 p0221 A73-12599
A business man views commercial ventures in space.
[AIAA PAPER 73-78] 06 p0771 A73-17640

SPACE MECHANICS
NT ASTRODYNAMICS
NT CELESTIAL MECHANICS
NT KEPLER LAWS
NT ORBITAL MECHANICS

SPACE MISSIONS
Interstellar flight and intelligence in the Universe.
03 p0370 A73-13198
Skylab orbital laboratory design, experiment programs and planned missions schedule, considering rescue measures, life support system and attitude control
03 p0383 A73-14171
Spacecraft low thrust propulsion systems applications to earth orbital and planetary missions, discussing payload capabilities vs flight time
[AIAA PAPER 72-1125] 04 p0486 A73-14911
A computerized technique for mission profile design analysis.
[AIAA PAPER 73-114] 05 p0629 A73-16872
Space shuttle orbiter applications to manned high energy missions from low earth orbit, considering refueling requirements, aerobraking and overall mission capability
[AIAA PAPER 73-206] 05 p0630 A73-16939
Reusable space tug system study for space shuttle payload delivery, retrieval and support capability augmentation, discussing mission requirements, costs and program scheduling
[AIAA PAPER 73-74] 06 p0756 A73-17639
Solar electric space mission risk analysis, describing computerized multistage failure process simulation procedure with application to Encke comet rendezvous mission
[AIAA PAPER 73-208] 06 p0748 A73-17660
Psychological and psychophysiological factors of human performance in manned space missions, considering environmental effects of space flight and man-machine system
06 p0650 A73-17775
Conference on Planetology and Space Mission Planning, 3rd, New York, N.Y., October 28-30, 1970, Proceedings.
06 p0749 A73-18001
Earth orbital, lunar, and planetary missions of the space tug.
06 p0750 A73-18019
Exploring the origin of the solar system by space missions to asteroids.
06 p0750 A73-18025
Space transportation systems and payload concepts for proposed space missions, discussing available and projected technology and environmental, economic and political aspects
06 p0757 A73-18096
Mariner Mars 1971 project historical background, and Mariner 9 orbiter mission science objects and planning for Mars surface observations and measurements
09 p1144 A73-22265
Mission building blocks for outer solar system exploration.
14 p1805 A73-30527
Interaction of the interstellar medium with the solar wind.
14 p1787 A73-30543
Cometary Science Working Group, Meeting, Williams Bay, Wis., June 9-11, 1971, Proceedings.
15 p1941 A73-32413
Skylab design technology assessment based on past manned spacecraft subsystems, noting advances in mission duration, spacecraft size and living accommodation comfort features
[AIAA PAPER 73-598] 18 p2358 A73-36082

Representative Space Shuttle missions and their impact on shuttle design.
[AIAA PAPER 73-608] 18 p2358 A73-36087
Design considerations for space mission wash water processing by reverse osmosis.
[ASME PAPER 73-ENAS-3] 19 p2493 A73-37965
Laundering in space - A summary of recent developments.
[ASME PAPER 73-ENAS-43] 19 p2401 A73-37990

SPACE NAVIGATION
NT INTERPLANETARY NAVIGATION
Autonomous satellite navigation from strapdown landmark measurements.
04 p0474 A73-15266
An autonomous navigation technology system.
04 p0474 A73-15274
Atomic nuclei physical properties for space navigation system gyroscopes, noting nuclear magnetic resonance and nuclei polarization
06 p0692 A73-17774
Russian book - Optoelectronic devices in spacecraft.
07 p0825 A73-20379
Mariner 9 stellar photography and camera parameters for point source photometric calibration and reference for optical navigation
08 p0964 A73-21043
Analytical estimates of the accuracy of spacecraft autonomous navigation based on measurements of flight altitude and zenith-distance inertial-space reference point.
12 p1523 A73-27647
Altitude damping of space-stable inertial navigation systems.
16 p2034 A73-33403
Stardrift - A navigational system for relativistic interstellar flight.
17 p2210 A73-35659
Russian book - Methods and systems of spacecraft navigation, guidance and control.
18 p2335 A73-35867
Sensor concept and algorithms for a completely strapdown autonomous navigation approach.
19 p2452 A73-38057
An analysis of recent advances in autonomous navigation for near earth applications.
[AIAA PAPER 73-875] 20 p2587 A73-38812
Navigation of the Titan IIIC space launch vehicle using the Carousel VB IMU.
[AIAA PAPER 73-905] 20 p2589 A73-38839
The impact of space navigation on the spherical gas bearing gyro.
21 p2697 A73-40025
Calculations of the limb radiance of Venus in the 600 to 700 per cm region and their application to spacecraft navigation.
21 p2767 A73-40693
Optimal navigation function for spacecraft orbit defined by initial conditions and acting force constants, determining matrix minimizing variance estimate
23 p3005 A73-43270

SPACE PERCEPTION
NT AUTOKINESIS
Some differences among figural aftereffects, apparent motion, and paracontrast.
01 p0011 A73-10435
Influence of border and background on perception of straightness.
02 p0137 A73-12081
Orientation illusion and masking in central and peripheral vision.
03 p0266 A73-12999
Verbal estimates of perceived time of flashing lights interval, relating to lights separation distance
03 p0260 A73-13552
Correlations between motor learning and visual and arm adaptation under conditions of computer-simulated visual distortion.
03 p0267 A73-13556
Tests for binocular rivalry of light contours for detection of randomness in disappearance patterns
03 p0261 A73-13557
A relationship between the detection of size, rate, orientation and direction in the human visual system.
03 p0261 A73-13758
Stereoscopic depth magnitude in viewing background-contrasted superimposed half-fields, noting relation to binocular disparity detection
03 p0261 A73-13762
Influence of a visual frame and vertical-horizontal illusion of shape and size perception.
04 p0411 A73-15219
Mathematical models for distance perception of earth surface features observed from ascending vehicle, considering convergence, accommodation and monocular parallax mechanisms
04 p0413 A73-15785
Angular velocity magnitude conversion into visually perceived apparent velocity, using psychophysical mathematical model based on axisymmetric annular visual field perception
04 p0413 A73-15796

Visibility, resolution and spatial acuities in terms of target-background contrast, diffraction, luminance, stimuli wavelength and anatomical variations effects on retinal images
05 p0542 A73-16477
Monocular and binocular clues interaction in depth perception and spatial orientation, discussing stereopsis testing
05 p0542 A73-16483
Ophthalmological assessment of visual functional impairment due to glare, stimulus motion and aging changes
05 p0540 A73-16485
Space-time relations - The effects of variations in stimulus and interstimulus interval duration on perceived visual extent.
05 p0545 A73-17199
A new illusion - The underestimation of distance during pursuit eye movements.
06 p0656 A73-17575
Sensory, learned, and cognitive mechanisms of size perception.
06 p0657 A73-18031
Tilt discrimination and motion aftereffect independence of flicker rate of stroboscopically illuminated contours visual stimuli
06 p0660 A73-18624
Disorienting effects of aircraft catapult launchings.
07 p0785 A73-19480
Observations on perceived changes in aircraft attitude attending head movements made in a 2-g bank and turn.
07 p0785 A73-19485
Psychophysical areal summation and stimulus contour and threshold visibility effects on size selective adaptation in human vision for single- and multichannel models
08 p0931 A73-21563
Human retina-patterned ideal perceiving machine to calculate visual acuities for spatial arrangement in line figures
08 p0932 A73-21564
Polarity cue for visual accommodation response of trained subjects to target motion direction change, considering retinal image blur and feedback relation
08 p0932 A73-21569
Visibility of an afterimage alone and in the presence of one or two additional afterimages.
09 p1039 A73-21894
Visual discrimination of motion - Stimulus relationships at threshold and the question of luminance-time reciprocity.
09 p1044 A73-21897
Spatial analysis in monkeys of various ages after extirpation of the parietal areas of the cerebral cortex
10 p1180 A73-24329
Independence of the recognition of an object's orientation and position in the field of vision
10 p1180 A73-24331
Differential effects of central versus peripheral vision on egocentric and exocentric motion perception.
11 p1318 A73-26221
Possible stimulus hypothesis and visual space perception.
11 p1324 A73-26321
Foveal contrast sensitivity edge effect dependence on test stimulus size, form and duration
11 p1321 A73-26716
Tachistoscopically measured independent image size and visual field recognition capacities of human eye
12 p1462 A73-27109
Visual perception of motion in depth - Application of a vector model to three-dot motion patterns.
13 p1577 A73-28091
Implications of measurement of eye fixations for a psychophysics of form perception.
13 p1577 A73-28092
Apparent motion of stimuli presented stroboscopically during pursuit movement of the eye.
13 p1577 A73-28093
Constancy and illusion of apparent direction of rotary motion in depth - Tests of a theory.
13 p1577 A73-28094
Absolute motion parallax and the specific distance tendency.
13 p1578 A73-28096
Scalar perceptions with binocular cues of distance.
13 p1578 A73-28176
Properties of human visual orientation detectors - A new approach using patterned afterimages.
13 p1579 A73-29124
German monograph - Investigations regarding auditory depth perception and the problem of in-head localization of acoustic events.
13 p1577 A73-29278
The Mach-Dvorak phenomenon and binocular fusion of moving stimuli.
14 p1717 A73-30392
Space-time adaptation of visual position constancy.
17 p2114 A73-34223
Stereoscopic depth aftereffects with random-dot patterns.
17 p2115 A73-34841

Temporal factors of movements in visual aftereffects 17 p2115 A73-34843

Movement perception during voluntary saccadic eye movements. 17 p2112 A73-34845

Book - The psychology of visual perception. 17 p2117 A73-35474

Distance perception and the ambiguity of visual stimulation - A theoretical note. 17 p2117 A73-35492

Influence of stimulus symmetry on visual scanning patterns. 17 p2118 A73-35494

On the perception of a class of bilaterally symmetric forms. 17 p2118 A73-35495

On the rate of acquisition of visual information about space, time, and intensity. 17 p2118 A73-35496

Cerebral control of eye movements and motion perception; Proceedings of the Symposium, Freiburg im Breisgau, West Germany, July 20-22, 1971. 18 p2271 A73-36432

Comparative physiology of movement-detecting neuronal systems in lower vertebrates (anura and urodela). 18 p2273 A73-36454

Ambivalent optokinetic stimulation and motion detection. 18 p2273 A73-36458

Visual-vestibular interaction and motion perception. 18 p2273 A73-36460

Scanning movements in space perception in terms of convergence role during cue conflict and cue isolation experiments 18 p2274 A73-36462

Visual perception of direction and voluntary saccadic eye movements. 18 p2274 A73-36463

Real-time, three-dimensional, visual scene generation with computer related images. 18 p2291 A73-36831

Problems related to high-performance flight in the Arctic regions 18 p2287 A73-36953

Spatial determinants of the aftereffect of seen motion. 19 p2394 A73-37415

Orientation specificity and response variability of cells in the striate cortex. 19 p2394 A73-37421

Invariance of visual receptive-field size and visual acuity with viewing distance. 19 p2396 A73-38484

A Lie algebra of visual piloting 20 p2590 A73-39038

Aircraft pilot spatial disorientation and illusory perceptual break-off sensations during flight associated with minor vestibular asymmetry 20 p2512 A73-39111

Sudden incapacitation in flight - 1 Jan. 1966-30 Nov. 1971. 20 p2512 A73-39112

Disparity detectors in human depth perception - Evidence for directional selectivity. 21 p2637 A73-40413

A descriptive model of multi-sensor human spatial orientation with applications to visually induced sensations of motion. [AIAA PAPER 73-915] 21 p2644 A73-40863

Human motion perception in motion drive logic design for flight simulation discussing feedback control, angular velocity and degrees of freedom [AIAA PAPER 73-931] 21 p2674 A73-40878

Compensating for distortion in viewing pictures obliquely. 21 p2639 A73-41178

A comparison of the Ponzo illusion with a textual analogue. 21 p2639 A73-41180

Sufficient conditions for the discrimination of motion. 21 p2639 A73-41181

Reaction times for focal and nonfocal/peripheral processing of simultaneously presented color and form stimuli 21 p2639 A73-41182

Effect of eye movements on backward masking and perceived location. 21 p2639 A73-41184

Visually perceived motion in depth resulting from proximal changes. I, II. 21 p2640 A73-41186

Comparison of tilt and displacement adaptation in visual perception, establishing qualitative differences by interocular transformation magnitude and exposure time methods 21 p2640 A73-41188

Effect of lateral body tilts and visual frames on perception of the apparent vertical. 22 p2811 A73-41736

Visual perception of relative object dimension during monocular and binocular rod equalization experi-

ment in various visual field restriction conditions, recording eye movements and focusing characteristics 22 p2812 A73-41890

Optimal input rates for tilt adaptation. 22 p2814 A73-42500

Stimulus specificity in the human visual system. 22 p2810 A73-42960

Mathematical model for physical space transformation into subjective field metric for monocular vision 24 p3064 A73-44906

Optical electronic model of local detectors of the visual analyzer 24 p3064 A73-44912

Visual evoked potentials to changes in the motion of a patterned field. 24 p3061 A73-45167

Comparison of visual evoked potentials to stationary and to moving patterns. 24 p3061 A73-45168

SPACE PHOTOGRAPHY

U SPACEBORNE PHOTOGRAPHY

SPACE POWER REACTORS

NT SPACE POWER UNIT REACTORS
Atmospheric entry and impact behavior of modular disk shaped radioactive isotope heat source for space nuclear power 19 p2454 A73-38387

SPACE POWER UNIT REACTORS

Zirconium hydride space power reactor design and fabrication technology evaluation, emphasizing requirements for coupling with power conversion and applications for thermoelectric power generation 09 p1118 A73-22801

Application of heat pipes to unmanned space power systems. 11 p1452 A73-25994

Reactor-thermoelectric power systems for NASA Space Station/Space Base. 11 p1395 A73-26012

Low temperature-reactor Brayton cycle for Space Station/Base application. 11 p1311 A73-26013

66 kWe ZrH reactor-organic Rankine power systems for large manned orbiting space systems. 11 p1311 A73-26014

Preliminary design of reactor power systems for the manned space base. 11 p1395 A73-26018

Unmanned reactor-thermoelectric systems for applications in the 1970's. 11 p1395 A73-26024

Nuclear thermionic power plants in the 50-300 kWe range. 11 p1396 A73-26027

The Satellite Nuclear Power Station - An option for future power generation. 19 p2455 A73-38412

SPACE PROBES

NT JUPITER PROBES

NT LUNAR PROBES

NT LUNIK LUNAR PROBES

NT LUNIK 9 LUNAR PROBE

NT LUNIK 13 LUNAR PROBE

NT LUNIK 16 LUNAR PROBE

NT LUNIK 17 LUNAR PROBE

NT LUNIK 20 LUNAR PROBE

NT MARINER SPACE PROBES

NT MARINER SPACECRAFT

NT MARINER VENUS-MERCURY 1973

NT MARINER 3 SPACE PROBE

NT MARINER 5 SPACE PROBE

NT MARINER 9 SPACE PROBE

NT MARS PROBES

NT MARS 2 SPACECRAFT

NT PIONEER SPACE PROBES

NT PIONEER 6 SPACE PROBE

NT PIONEER 8 SPACE PROBE

NT PIONEER 9 SPACE PROBE

NT PIONEER 10 SPACE PROBE

NT SOLAR PROBES

NT SURVEYOR LUNAR PROBES

NT SURVEYOR 3 LUNAR PROBE

NT VENERA SATELLITES

NT VENERA 4 SATELLITE

NT VENERA 6 SATELLITE

NT VENERA 7 SATELLITE

NT VENUS PROBES

NT VIKING MARS PROGRAM

Thermal analysis and its verification test of a small probe for space use. 01 p0052 A73-11147

Precision measurement of the sun's gravitational field by means of the twin probe method. 02 p0218 A73-12414

Design of a space probe for the experimental investigation of Einstein's theory of gravitation 03 p0381 A73-13296

Ground control facilities and organization of Helios space probe mission and flight operations system based on U.S.-German cooperation 03 p0381 A73-13297

Extraterrestrial messenger probe recognition from inhabited planet via message involving home constellation binary coded signals 14 p1796 A73-29946

Low energy galactic cosmic ray exploration via space mission to Jupiter and Saturn, considering nuclear abundances and galactic evolution theories 14 p1787 A73-30524

Propulsion system optimization for interstellar probes. 15 p1943 A73-32217

Scientific considerations for a common Saturn/Uranus atmospheric entry probe. [AIAA PAPER 73-594] 18 p2350 A73-36046

Planetary Atmosphere Experiments Test vehicle reentry into earth atmosphere for flight experience discussing onboard instrumentation 24 p3088 A73-44404

SPACE PROGRAMS

NT APOLLO PROJECT

NT EUROPEAN SPACE PROGRAMS

NT FRENCH SPACE PROGRAMS

NT JUPITER PROJECT

NT LUNAR PROGRAMS

NT U.S.S.R. SPACE PROGRAM

Japanese sounding rocket and scientific satellite program. 01 p0110 A73-111029

Japanese space program progress, current state and future objectives, giving tables of rockets and satellites with mission objectives and design/performance specifications 03 p0401 A73-13846

NASA's space station and the need for quantifiable components of a responsive legal regime. 04 p0522 A73-15134

Earth environment damage potential of space program side effects, discussing environmental protection from international responsibility viewpoint 04 p0522 A73-15142

The evaluation, conservation, and international development of terrestrial resources from outer space 04 p0523 A73-15143

The growing role of standards in the national and international coordination of space programs. 04 p0524 A73-15381

The attitude of the public towards the Space Programme - Its assessment and its influence as a guiding policy factor. 11 p1454 A73-26275

The American space program for the future. 12 p1560 A73-27062

Space cost effectiveness through space shuttle orbiter programs based on payload recovery and reuse in routine round trip operations 14 p1803 A73-29941

Launching bases; International Conference, Kourou, French Guiana, November 22-28, 1972. Proceedings 14 p1741 A73-30076

Sounding rocket and satellite launcher facilities at Kagoshima Space Center, considering physical plant for assembling, launching, tracking and data acquisition 14 p1741 A73-30079

Satellite operation mode coordination with space program mission, considering orbital position and velocity and time at ground station horizon 17 p2160 A73-34932

A fundamental methodology for planning and management of research and development programmes. 17 p2258 A73-35836

Impact of the space tug concept on space program economics. 19 p2490 A73-37192

Canadian space programs in communications, navigation and atmospheric science, considering telephony, data transmission, TV broadcasting and remote sensing [AAS PAPER 73-118] 20 p2584 A73-38580

Aerosol program for civil aviation needs established by Seventh Air Navigation Conference of ICAO, discussing airborne equipments specification development [AAS PAPER 73-120] 20 p2520 A73-38581

Aeronautics and astronautic history, developments and impact upon civilization, noting Canada role in space age, Apollo program and U.S.S.R. programs 21 p2793 A73-41086

Space research XIII; Proceedings of the Fifteenth Plenary Meeting, Madrid, Spain, May 10-24, 1972. Volumes 1 & 2. 21 p2687 A73-41325

SPACE RADIATION

U EXTRATERRESTRIAL RADIATION

SPACE RADIATORS

U SPACECRAFT RADIATORS

SPACE RENDEZVOUS

NT ORBITAL RENDEZVOUS

Unmanned rendezvous applications for space rescue. 01 p0105 A73-11156

Simulation of rendezvous of a man in deep space. 03 p0288 A73-13569

- Iterative technique for the calculation of double-impulse spacecraft rendezvous maneuvers. 05 p0627 A73-16092
- Optimization of multiple target electric propulsion maneuvers. 06 p0748 A73-17658
- AIAP PAPER 73-205] 06 p0748 A73-17658
- Solar electric space mission risk analysis, describing computerized multistage failure process simulation procedure with application to Encke comet rendezvous mission. 06 p0748 A73-17660
- AIAP PAPER 73-208] 06 p0748 A73-17660
- Solar electric propulsion comet and asteroid rendezvous missions, examining asteroid perihelion at base, optimum mission length, flight time and exploration vehicle power levels. 18 p2350 A73-36081
- AIAP PAPER 73-597] 18 p2350 A73-36081
- Viking type spacecraft rendezvous with the Martian moons. 19 p2482 A73-37401
- Spacecraft rendezvous in orbit, discussing unchaining, transfer maneuver, target location, approach phase, docking and mechanical coupling. 19 p2487 A73-38302
- Study of a method of exponential control of a spacecraft rendezvous. 21 p2781 A73-40905
- SPACE RENDEZVOUS MANEUVERS**
- SPACE RENDEZVOUS**
- SPACECRAFT MANEUVERS**
- SPACE SCIENCES**
- AEROSPACE SCIENCES**
- SPACE SHUTTLE BOOSTERS**
- A study of the plume impingement environment experienced by the booster during the space shuttle nominal staging maneuver. 03 p0273 A73-13468
- AIAP PAPER 72-1171] 03 p0273 A73-13468
- Solid rocket motors for the Space Shuttle booster. SAE PAPER 720804] 05 p0607 A73-16648
- Stretch formed corrugated Rene 41 panel development for space shuttle booster nose section hot area kin, discussing tooling and formation techniques. SAE PAPER 720873] 05 p0582 A73-16670
- Application of the control configured vehicle concept to a Space Shuttle configuration. 05 p0629 A73-16905
- AIAP PAPER 73-158] 05 p0629 A73-16905
- Convective heating on delta-wing Space-Shuttle boosters including interference effects. 05 p0533 A73-17202
- A fracture control program for the reusable Space shuttle booster. 06 p0764 A73-18493
- Space shuttle phase B program, discussing orbiter and booster configurational studies, ground simulation, propulsion systems, structure, avionics, environment control and life support systems, etc. 09 p1152 A73-22189
- Design criteria and candidate electrical power systems for a reusable Space Shuttle booster. 11 p1311 A73-26016
- Space shuttle solid rocket boosters ocean recovery, discussing mission requirements, parachute configurations, tradeoff studies and model testing. 18 p2358 A73-36084
- AIAP PAPER 73-602] 18 p2358 A73-36084
- Space shuttle solid rocket boosters mission and systems requirements, considering thrust vector control and staging/separation, electrical and recovery systems. 18 p2358 A73-36086
- AIAP PAPER 73-606] 18 p2358 A73-36086
- Rocket power, Redstone to Saturn V, now Space Shuttle, 20 years of development. 19 p2493 A73-37886
- SAE PAPER 971] 19 p2493 A73-37886
- SPACE SHUTTLE ORBITERS**
- Light weight graphite-polyimide composite oneycomb core and sandwich panel design, fabrication and tests for shuttle orbiter thermal protection system. 03 p0333 A73-13051
- Calculation of metric coefficients for streamline coordinates. 03 p0247 A73-14196
- Some design aspects of Space Shuttle orbiters. 05 p0627 A73-16178
- Hydraulic and flight control system for Space Shuttle Orbiter. 05 p0537 A73-16630
- SAE PAPER 720838] 05 p0537 A73-16630
- Storable fueled power system for Space Shuttle. 05 p0537 A73-16632
- SAE PAPER 720836] 05 p0537 A73-16632
- Maintainability of the Space Shuttle Orbiter main engine. 05 p0606 A73-16642
- SAE PAPER 720808] 05 p0606 A73-16642
- Space Shuttle Orbiter main engine design. 05 p0607 A73-16644
- SAE PAPER 720807] 05 p0607 A73-16644
- Maneuvering engines for Space Shuttle Orbiter. 05 p0607 A73-16646
- SAE PAPER 720806] 05 p0607 A73-16646
- Airbreathing engines for Space Shuttle. 05 p0607 A73-16647
- SAE PAPER 720805] 05 p0607 A73-16647
- Aerothermodynamics of the Space Shuttle reaction control system. 05 p0629 A73-16857
- AIAP PAPER 73-93] 05 p0629 A73-16857
- Space shuttle orbiter applications to manned high energy missions from low earth orbit, considering refueling requirements, aerobraking and overall mission capability. 05 p0630 A73-16939
- AIAP PAPER 73-206] 05 p0630 A73-16939
- Weight sensitivity of a space shuttle orbiter to thermal structural combined loads design criteria. 05 p0635 A73-16979
- [AIAP PAPER 73-257] 05 p0635 A73-16979
- Thermal performance evaluation of REI panel gaps for Space Shuttle Orbiter. 09 p0919 A73-19487
- Space shuttle phase B program, discussing orbiter and booster configurational studies, ground simulation, propulsion systems, structure, avionics, environment control and life support systems, etc. 09 p1152 A73-22189
- Space shuttle orbiter electrical power system requirements and constraints, considering hydrogen/oxygen fuel cell for compact energy storage and turbine driven generators. 09 p1153 A73-22776
- Auxiliary power units and their application to the space shuttle. 09 p1153 A73-22778
- Solid polymer electrolyte fuel cell technology application to space shuttle orbiter requirements, noting 2000 hours maintenance free life and thermal stability. 09 p1035 A73-22786
- Shuttle Orbiter fuel cell power system simulation, describing data management, programming and computational control. 09 p1060 A73-22804
- Space shuttle orbiter power system requirements and design tradeoffs, comparing fuel cells, solar array/battery and radioisotope Brayton cycle and cryogenic fueled turboalternators. 11 p1312 A73-26017
- Space cost effectiveness through space shuttle orbiter programs based on payload recovery and reuse in routine round trip operations. 14 p1803 A73-29941
- Space shuttle orbiter system planning and operational modes, considering propulsion into orbit, automated observatories, sortie workshop and European cooperation. 14 p1803 A73-29943
- Graphite-epoxy composite door landing gear assembly for space shuttle orbiter, discussing design, analysis, fabrication and structural testing. 16 p2029 A73-33058
- Coating development of Martin Marietta's reusable surface insulation /MAR-SI/ for Space Shuttle applications. 16 p2071 A73-33059
- Low-cost fabrication and installation of ablative heat shields for the space shuttle orbiter. 16 p2072 A73-33060
- Reusable space shuttle orbiter design evolution during 1972-1973, discussing payloads, vertical launching capability and advanced materials technology. 16 p2072 A73-33063
- Impact of space shuttle orbiter reentry on mesospheric NOx. 16 p2007 A73-33559
- [AIAP PAPER 73-525] 16 p2007 A73-33559
- Space shuttle orbiter and subsystem design, discussing crew cabin, payload accommodations, flight characteristics and aerothermodynamics. 18 p2358 A73-36085
- [AIAP PAPER 73-604] 18 p2358 A73-36085
- A concept for Space Shuttle payload ground operations. 18 p2359 A73-36093
- [AIAP PAPER 73-615] 18 p2359 A73-36093
- Four Space Shuttle wing leading edge concepts. 18 p2359 A73-36355
- [AIAP PAPER 73-738] 18 p2359 A73-36355
- Initial development of an ablative leading edge for the Space Shuttle orbiter. 18 p2369 A73-36356
- [AIAP PAPER 73-739] 18 p2369 A73-36356
- Aspects of the finite element method as applied to aero-space structures. 18 p2365 A73-36725
- [ISD-138] 18 p2365 A73-36725
- Mach number and Reynolds number effect on orbiter/tank interference heating. 19 p2491 A73-37403
- Kennedy Space Center Space Shuttle facilities. 19 p2417 A73-37601
- H2-O2 auxiliary power unit for Space Shuttle vehicles - A progress report. 19 p2392 A73-38436
- [IECEC PAPER 739028] 19 p2392 A73-38436
- Space shuttle orbiter abort guidance for premature or abnormal termination of mission due to system or human failure, discussing predictive algorithm. 21 p2735 A73-40045
- Thermal characterization of reusable external insulation for the space shuttle. 22 p2931 A73-42403
- [ECTP PAPER B2-8] 22 p2931 A73-42403
- SPACE SHUTTLES**
- Stage separation of parallel-staged shuttle vehicles - A capability assessment. 01 p0109 A73-10105
- Atmospheric reentry optimal lateral guidance for low lift/drag ratio space shuttle vehicle, presenting formulation as optimal stochastic control problem. 01 p0074 A73-10106
- [AIAP PAPER 71-914] 01 p0074 A73-10106
- Space stations and shuttle vehicles design and placement in earth orbit, reviewing life support, energy production and data transmission systems. 01 p0096 A73-10300
- Space shuttle abort - Downrange basing and cross-range capability requirements. 02 p0228 A73-12371
- Chemical and nuclear space tugs in the earth orbital shuttle mission. 02 p0216 A73-12372
- Computerized operational simulation for space shuttle program in terms of flight units, launch rate, success probabilities and costs. 03 p0381 A73-13298
- Cryogenic liquid O2/H2 reaction control systems for Space Shuttle. 03 p0382 A73-13458
- [AIAP PAPER 72-1155] 03 p0382 A73-13458
- Advanced technology for Space Shuttle Auxiliary Propellant Valves. 03 p0356 A73-13459
- [AIAP PAPER 72-1157] 03 p0356 A73-13459
- Hydrogen-oxygen Space Shuttle ACS thruster technology review. 03 p0356 A73-13460
- [AIAP PAPER 72-1158] 03 p0356 A73-13460
- Application of an improved transpiration cooling concept to space shuttle type vehicles. 03 p0397 A73-13492
- Computer application for management of Skylab launch operations. 04 p0424 A73-14905
- [AIAP PAPER 72-1083] 04 p0424 A73-14905
- Hydrogen oxygen propulsion component design and hot firing tests for space shuttle auxiliary systems and upper stage applications. 04 p0486 A73-14918
- [AIAP PAPER 72-1156] 04 p0486 A73-14918
- Computerized ground support acceptance checkout systems for space shuttle program, discussing capabilities, future goal and unified test equipment. 04 p0432 A73-15458
- Space shuttle cost effectiveness studies from viewpoint of combined civil and military payloads and simplified systems design. 05 p0613 A73-16182
- Space shuttle missions and configurations, discussing payload, external tank, solid rocket engines, orbiter vehicle and alternate delivery system costs. 05 p0627 A73-16183
- The benefits of space exploration related to the Space Shuttle. 05 p0568 A73-16184
- Extending the life and recycle capability of earth storable propellant systems. 05 p0629 A73-16631
- [SAE PAPER 720837] 05 p0629 A73-16631
- Turbomachinery design for Space Shuttle auxiliary power systems. 05 p0537 A73-16633
- [SAE PAPER 720835] 05 p0537 A73-16633
- Design and analysis of an APU monopropellant gas generator. 05 p0537 A73-16635
- [SAE PAPER 720834] 05 p0537 A73-16635
- Propulsion systems for orbital maneuvering stages. 05 p0607 A73-16656
- [SAE PAPER 720843] 05 p0607 A73-16656
- Space shuttle bipropellant reaction control system /RCS/ engine design, characteristics and tests, emphasizing reusability and minimum servicing. 05 p0607 A73-16668
- [SAE PAPER 720839] 05 p0607 A73-16668
- An experimental investigation of some heat transfer characteristics on an orbiter/HO-tank/SRM Space Shuttle configurations, freestream Mach number equal to 8.0. 05 p0640 A73-16856
- [AIAP PAPER 73-92] 05 p0640 A73-16856
- Experimental investigation of hypersonic buzz on a high cross-range shuttle configuration. 05 p0531 A73-16904
- [AIAP PAPER 73-157] 05 p0531 A73-16904
- Aerothermodynamic aspects of shock-interference patterns for shuttle configurations during entry. 05 p0532 A73-16963
- [AIAP PAPER 73-238] 05 p0532 A73-16963
- Zero-g propellant gauging. 06 p0755 A73-17573
- Space shuttle technology, discussing configurational aerothermodynamics, aeroelastic effects on vehicle dynamics and structural design and materials. 06 p0755 A73-17619
- [AIAP PAPER 73-31] 06 p0755 A73-17619
- Space shuttle flight operations ground support systems for trajectory control and systems/mission management, discussing payloads data acquisition and transmission to user. 06 p0755 A73-17620
- [AIAP PAPER 73-36] 06 p0755 A73-17620
- Aerothermodynamics R and D for space shuttle configurational design, discussing program organization and wind tunnel testing to generate design technology base. 06 p0755 A73-17632
- [AIAP PAPER 73-59] 06 p0755 A73-17632
- Technology applied to the Space Shuttle Main Engine. 06 p0741 A73-17633
- [AIAP PAPER 73-60] 06 p0741 A73-17633
- Reusable space tug system study for space shuttle payload delivery, retrieval and support capability augmentation, discussing mission requirements, costs and program scheduling. 06 p0756 A73-17639
- [AIAP PAPER 73-74] 06 p0756 A73-17639
- Space shuttle cost effectiveness from earth orbital mission analysis, discussing potential performance and shuttle derived high energy transportation system. 06 p0756 A73-18017
- Revolutionary implications of the space shuttle. 06 p0756 A73-18018
- Space shuttle air breathing gas turbine engine design, modification, weight and test requirements associated with launch, space residence and reentry. 07 p0906 A73-20463
- Open cycle hydrogen-oxygen turbine driven generator system for space shuttle auxiliary power supply,

discussing components, control mode and performance potential

09 p1153 A73-22779

Space propulsion future assessment, discussing space shuttle and tug, NERVA project and electric and photon propulsion

10 p1262 A73-23611

Space shuttle ascent-flyback trajectory optimization with in-flight inequality constraints based on accelerated gradient parameters determination including attitude control angles

10 p1276 A73-24002

Evaluation of columbium alloy thermal protection systems for space shuttle.

[AIAA PAPER 73-378]

11 p1380 A73-25508

Synthesis of shuttle vehicle damping using substructure test results.

[AIAA PAPER 73-400]

11 p1430 A73-25529

Space shuttle aerodynamic interference and elastic response to atmospheric turbulence during ascent flight, including propellant sloshing, gust and automatic control system effects

[AIAA PAPER 73-310]

11 p1430 A73-25541

Stabilizing the elastic modes of the Space Shuttle vehicle during launch.

[AIAA PAPER 73-319]

11 p1430 A73-25550

Thermal and mechanical properties of zirconia cloth, felt and braid for heat shielding of reusable space shuttle

12 p1548 A73-27379

Refurbishable spacecraft - Modules and components for the Shuttle era.

12 p1549 A73-27437

Shuttle payloads - Saving dollars by offsetting risks.

12 p1549 A73-27438

On-orbit checkout and repair as a factor in economical spacecraft design and operation.

12 p1549 A73-27439

Accelerating search-variable metric algorithm combination for space shuttle atmospheric flight optimization, comparing with cubic fit-golden section method

13 p1650 A73-28825

Space shuttle missions relationship to post-Apollo, European and joint European-U.S. space exploration programs

13 p1690 A73-29387

Sortie lab experiment management, integration and operational techniques, discussing airborne science/shuttle experiment system simulation /AS-SESS/ program

14 p1803 A73-29942

Lower payload costs through refurbishment and module replacement.

14 p1803 A73-29944

Design considerations for shuttle information management.

14 p1818 A73-29945

Cost effective space shuttle solid rocket booster recovery parachute system planning, discussing model drop and structural load testings

[AIAA PAPER 73-441]

15 p1825 A73-31427

Apollo, Skylab and shuttle programs, discussing crews, tasks, national economic benefits and earth resources experiments effects

15 p1941 A73-32544

Space shuttle lightweight thermal protective insulation materials lab erosion resistance determination at 200-400 MPH and various angles of attack, using rotating arm test apparatus

16 p2071 A73-33030

Oxidation resistant carbon-carbon composite for Space Shuttle application.

16 p2028 A73-33043

High pressure dual fuel chemical LOX/hydrocarbon rocket vehicle concepts for reusable one stage to orbit shuttles

16 p2072 A73-33085

Economic tradeoff study of design criteria cost effectiveness, applying to reusable nuclear shuttle /RNS/ engine concepts

16 p2035 A73-33650

Evolution of the Space Shuttle. I.

16 p2074 A73-34024

X-reference frame bilateral control for the Shuttle Attached Manipulator System.

17 p2180 A73-35317

Evolution of the Space Shuttle. II.

17 p2240 A73-35660

The Space Shuttle and its utilization.

18 p2357 A73-35936

Space shuttle implementation prognosis, discussing spacecraft configurations, international cooperation, research possibilities in TR telescoping, space physics laboratories and exobiology

18 p2348 A73-35937

A reliability, cost and risk analysis of establishing and maintaining a space communications satellite network.

[AIAA PAPER 73-582]

18 p2288 A73-36074

The impact of launch vehicle reliability on the financial risks associated with multiple payload space functions.

[AIAA PAPER 73-591]

18 p2358 A73-36079

Computerized processing system with real time control, data analysis and display capabilities for space shuttle checkout, servicing, launching and landing to reduce cost

18 p2295 A73-36083

[AIAA PAPER 73-601]

Representative Space Shuttle missions and their impact on shuttle design.

18 p2358 A73-36087

Reusable space tug system and missions for space shuttle operations with 1980s planned payloads, discussing interfaces and configuration alternatives

18 p2358 A73-36088

Langley Research Center shuttle-compatible spaceborne advanced technology laboratory concept with sortie flight operation mode

18 p2358 A73-36089

[AIAA PAPER 73-611]

Vehicle management and mission planning in support of shuttle operations.

18 p2358 A73-36090

Effect of nose geometry on the aerothermodynamic environment of shuttle entry configurations.

18 p2260 A73-36196

Evaluation of aerodynamic heating uncertainties for Space Shuttle.

18 p2359 A73-36354

IR spectral measurements of reusable surface insulations via radiative four flux model

18 p2370 A73-36361

Baseplate heat pipe system for waste heat dispersion and temperature control of TWT microwaves amplifier in space shuttle communication equipment, discussing design and performance

18 p2370 A73-36371

[AIAA PAPER 73-755]

Computation of launch vehicle system requirements using hybrid computer.

18 p2360 A73-36838

Shuttle-Attached Manipulator System requirements.

19 p2491 A73-37307

Shuttle Payload Accommodation System teleoperator.

19 p2491 A73-37308

Preliminary design and simulations of a Shuttle-Attached Manipulator System.

19 p2491 A73-37309

Simulation concepts for a full-sized Shuttle manipulator system.

19 p2416 A73-37310

Space Shuttle Program; Proceedings of the Short Course, Boulder, Colo., October 6, 7, 1972.

19 p2491 A73-37591

Space shuttle program, discussing master planning schedule, vehicle design, payloads and initial flight tests

19 p2491 A73-37592

Space shuttle payload definition, design and planning, using computers for scheduling and costing

19 p2491 A73-37593

Vehicle and ground support in space shuttle sortie and delivery-retrieval mission profiles

19 p2491 A73-37594

Space Shuttle Orbiter aerodynamics, discussing wing/body matching, lateral/directional stability, control and reaction systems

19 p2491 A73-37595

Space Shuttle Orbiter radiative, ablative and insulative thermal protection system design, performance and reliability

19 p2492 A73-37596

Space shuttle liquid propellant reusable rocket engine design, discussing regenerative cooling, fuel pump, oxidizer turbopumps and electronic control systems

19 p2492 A73-37597

Space shuttle external tank, discussing Orbiter engine, propellant conditioning, solid rocket boosters structural support, environment effects and safe disposals

19 p2492 A73-37598

Space Shuttle solid rocket stage recovery, retrieval, and refurbishment.

19 p2492 A73-37599

Compatibility and satisfactory performance of individual Space Shuttle elements, discussing development/flight cost tradeoff, booster thrust vector and optimal control

19 p2492 A73-37600

Space Shuttle development, qualification, acceptance and horizontal/vertical flight tests for Orbiter, solid rocket motor and drop tank element subsystems

19 p2492 A73-37602

Space Shuttle in space lab operations, propulsion stage retrieval/delivery, satellite servicing, passenger transportation and short duration orbital missions

19 p2492 A73-37603

Space Shuttle Orbiter Environmental Control and Life Support System for atmosphere revitalization, crew life support, thermal conditioning and airlock support

19 p2400 A73-37979

[ASME PAPER 73-ENAS-23]

Zero-gravity and ground testing of a waste collection subsystem for the Space Shuttle.

19 p2401 A73-37989

[ASME PAPER 73-ENAS-42]

Standardized space shuttle launched multipurpose spacecraft design using nuclear electric power systems with radioisotope thermoelectric generators and Brayton cycle alternators

19 p2455 A73-38390

Application of digital computer APU modeling techniques to control system design.

19 p2392 A73-38411

Nuclear safety considerations for the design of a shuttle launched 500 to 2000 watt isotope Brayton power system.

19 p2457 A73-38434

Redundant independent guidance, navigation and control system application to space shuttle, estimating channel output divergence due to sensor bias and scale factor errors

21 p2735 A73-40004

Space shuttle ascent guidance, using quadratic performance index and reference trajectory kinematics to obtain optimal time-varying feedback control gain

21 p2735 A73-40004

Space shuttle program budget difficulties, discussing consequences of cost increase or program suspension

21 p2793 A73-40234

Space shuttle design program with Mark I and II stages, considering thermal protection weight analysis for minimum maintenance and turnaround time

21 p2780 A73-40410

Large space vehicles - Platforms for second generation in-situ wake observations.

21 p2781 A73-40901

Example of dynamic interference effects between two oscillating vehicles.

22 p2917 A73-42634

Two stage recoverable space shuttle structural design, discussing configurations, costs and orbiters and booster materials and thermal protection systems

23 p3038 A73-43780

SPACE SIMULATORS

Vibration, radiation and thermal vacuum test procedures and facilities for evaluating spacecraft reliability during launching and in space environment

07 p0807 A73-18995

The space environment simulation chamber of Toulouse.

07 p0807 A73-19000

The large space simulation chamber of Toulouse and its evacuations pumps

07 p0808 A73-19000

The space environment simulation chamber of the Toulouse space center

07 p0808 A73-20240

A distribution of molecular flow in the interior of a cylindrical space-simulation chamber with spherical gas source

11 p1343 A73-25111

SPACE STATIONS

NT ORBITAL SPACE STATIONS

NT ORBITAL WORKSHOPS

NT ORBITING LUNAR STATIONS

NT SALYUT SPACE STATION

Invariant poles feedback control of flexible highly variable spacecraft.

03 p0285 A73-13522

The role of solar cell technology in the satellite solar power station.

03 p0258 A73-14252

NASA space program value to humanity, discussing Skylab solar and earth observations and communications satellites

05 p0613 A73-16181

International space station program for global resources and ecological monitoring and management, reviewing US Skylab and Space Shuttle and USSR Soyuz projects

06 p0757 A73-18026

The earth resources experiment package on Skylab and proposed resource investigations.

09 p1082 A73-22389

Electrical Power Subsystem definition for shuttle launched modular space station.

09 p1153 A73-22781

Configuration survey of lightweight solar array power systems for future missions.

09 p1153 A73-22782

Large area wraparound contact silicon solar cell, application and development.

09 p1036 A73-22812

Radio telemetering trends in post-Apollo space programs, emphasizing service lifetimes and orbiting space station data bit generation rate

09 p1053 A73-23362

Spinning Skylab space station dynamics, investigating motion stability from simplified models with flexible appendages by digital simulation

10 p1286 A73-24003

Simulation capability for dynamics of rotating counterweight space stations.

11 p1343 A73-25551

Co-60 kernel modular power and reentry system design for space station and base, noting fuel and launch cost savings over Pu-238 systems

11 p1310 A73-25998

Solar/battery space station power plants combined with nuclear configurations, discussing rectified alternator current, direct energy transfer, and high voltage dc sources 11 p1311 A73-26008

Low temperature-reactor Brayton cycle for Space Station/Base application. 11 p1311 A73-26013

A modular Space Station/Base electrical power system - Requirements and design study. 11 p1311 A73-26015

Wideband multidrop asynchronous TDM/FDM multichannel data distribution system for space station application, discussing analog and digital buses design 17 p2124 A73-35308

A regenerative fuel cell system for modular space station integrated electrical power. 19 p2390 A73-38402

Large space vehicles - Platforms for second generation in-situ wake observations. 21 p2781 A73-40901

SPACE STORAGE

Optimum design of space storable gas/liquid coaxial injectors. [AIAA PAPER 72-1076] 03 p0354 A73-13400

SPACE SUITS

Light weight impact protective helmet shell materials and designs, noting E- or S-glass and polyimide resin for oxygen rich space station/shuttle applications 16 p2027 A73-32677

Mercury, Gemini and Apollo space suits, discussing glove development, boot design, portable life support equipment and extravehicular mobility 16 p1976 A73-34025

SPACE SURVEILLANCE [SPACEBORNE]

Synchronous satellite systems for civilian air, ship and land vehicle traffic control, communication, navigation and surveillance, discussing technology requirements for continental and oceanic systems [AIAA PAPER 73-583] 18 p2288 A73-36075

Earth satellite measurements as applied to sea ice problems. 18 p2310 A73-36134

SPACE SYSTEMS ENGINEERING

U AEROSPACE ENGINEERING

SPACE TRANSPORTATION

Performance potential of the colloid core reactor concept in near-earth applications. [AIAA PAPER 72-1065] 03 p0340 A73-13394

Space shuttle cost effectiveness from earth orbital mission analysis, discussing potential performance and shuttle derived high energy transportation system 06 p0756 A73-18017

Space transportation systems and payload concepts or proposed space missions, discussing available and projected technology and environmental, economic and political aspects 06 p0757 A73-18096

Refurbishable spacecraft - Modules and components for the Shuttle era. 12 p1549 A73-27437

Space shuttle implementation prognosis, discussing spacecraft configurations, international cooperation, research possibilities in TR telescoping, space physics laboratories and exobiology 18 p2348 A73-35937

Cost reductions in transportation to geosynchronous and lunar orbits by a swing station. 19 p2490 A73-37193

The transportation of highly active nuclear waste products to the sun 20 p2590 A73-39148

SPACE TUGS

Chemical and nuclear space tugs in the earth orbital shuttle mission. 02 p0216 A73-12372

High performance reactorless nuclear propulsion of reusable orbital space tug by laser rocket engine [AIAA PAPER 72-1095] 03 p0341 A73-13415

Propulsion systems for orbital maneuvering stages. [SAE PAPER 720843] 05 p0607 A73-16656

Reusable space tug system study for space shuttle payload delivery, retrieval and support capability augmentation, discussing mission requirements, costs and program scheduling [AIAA PAPER 73-74] 06 p0756 A73-17639

Earth orbital, lunar, and planetary missions of the space tug. 06 p0750 A73-18019

Performance of recoverable single and multiple Space Tugs for missions beyond earth escape. 07 p0906 A73-20471

Space propulsion future assessment, discussing space shuttle and tug, NERVA project and electric and photon propulsion 10 p1262 A73-23611

The feasibility of geostationary emplacement of satellites by solar electric tug. 11 p1431 A73-26260

European space tug conception evolution, discussing docking system 12 p1549 A73-27382

Refurbishable spacecraft - Modules and components for the Shuttle era. 12 p1549 A73-27437

The Space Shuttle and its utilization.

The impact of launch vehicle reliability on the financial risks associated with multiple payload space functions. [AIAA PAPER 73-591] 18 p2357 A73-35936

Reusable space tug system and missions for space shuttle operations with 1980s planned payloads, discussing interfaces and configuration alternatives [AIAA PAPER 73-609] 18 p2358 A73-36079

Some considerations for Space Tug launch site support operations. [AIAA PAPER 73-620] 18 p2360 A73-36502

Impact of the space tug concept on space program economics. 19 p2490 A73-37192

Earth-orbit mission considerations and Space Tug requirements. 19 p2490 A73-37302

Possibility of using the Space Tug for the recovery and maintenance of satellites 21 p2782 A73-41554

SPACE VEHICLE CHECKOUT PROGRAM

Computerized ground support acceptance checkout systems for space shuttle program, discussing capabilities, future goal and unified test equipment 04 p0432 A73-15458

The automatic checkout of the Prospero Satellite. 09 p1070 A73-22917

Space missile test center development for checkout, launch and data processing for space boosters, intermediate and intercontinental range ballistic missiles and supersonic aircraft 16 p1993 A73-33087

SPACE VEHICLE CONTROL

U SPACECRAFT CONTROL

SPACE-TIME CONTINUUM

U RELATIVITY

SPACE-TIME FUNCTIONS

Curves of spatial isocorrelations and space-time isocorrelations relative to longitudinal velocity fluctuations in a smooth circular duct 01 p0031 A73-10418

Classical mechanics and field theory derivation based on material points motion in space, discussing space-time metric, electromagnetic and gravitational fields and quantum mechanics 01 p0076 A73-10599

On space-time, reference frames and the structure of relativity groups. 01 p0079 A73-11255

Space-time finite element method for determining dynamic response of continuous media, using Hamilton principle for nodal displacements variations 03 p0389 A73-13320

Correlation of noisy radiation reflected from a statistically uneven surface. 03 p0344 A73-14039

Stress equations solutions existence near Minkowskian solution for asymptotic behavior, demonstrating flat space-time stability [AD-756017] 03 p0344 A73-14604

Experimental test for Mach-Einstein doctrine concerning particle inertial mass variation due to tension or space-time curvature created by interlocking gravitational field 04 p0476 A73-15524

The universe as a black hole. 04 p0501 A73-15624

How to measure the earth's velocity with respect to absolute space. 05 p0615 A73-16363

Matrix transformation in hyperplanes method for successive solution of boundary value problems of multidimensional differential equations, using space-time functions 06 p0715 A73-17718

Electrodynamics of anisotropic media with space and time dispersion. 06 p0723 A73-17787

The variational derivative of degenerate Lagrange densities. 06 p0718 A73-18504

Time /T-field/ solutions to Einstein equations of test particles and light rays in nonstatic spherically symmetric gravitational field 06 p0724 A73-18646

Space-time transformation for equation of relative motion of two bodies on gravitating matter background of Einstein-de Sitter universe 06 p0724 A73-18689

Black hole polar flattening and equatorial circumference lengthening as function of angular momentum, considering effects of highly curved space-time 07 p0899 A73-20176

Preliminary quasar model based on the Yilmaz exponential metric. 07 p0899 A73-20178

Black hole creation via partial gravitational collapse of matter ejected by explosion within asymptotically Friedmannian space-time 07 p0900 A73-20182

Measurements and graphs of turbulence autocorrelations in space and time. 09 p1071 A73-22332

Relativistic MHD formulation in terms of non-holonomic tetrad field for rotating plasma coupled to frozen-in magnetic field, noting Alfvén waves propagation velocity 09 p1131 A73-22921

Tensor theory of perturbations in atmospheric dynamics 09 p1115 A73-23150

Conformal invariance of the equations of motion in curved spaces. 10 p1241 A73-23637

Gravitational waves - A progress report. 10 p1280 A73-24324

Anisotropic and isotropic descriptions of physical process speeds in special relativity theory space-time metric 10 p1250 A73-24944

Some considerations on the continuous space-time spectral analysis of atmospheric disturbances. 11 p1394 A73-25723

Construction of a general cosmological solution of the Einstein equation with a time singularity. 11 p1425 A73-26178

Observational constraints imposed by Brans-Dicke cosmologies. 11 p1426 A73-26413

Combined electromagnetic and gravitational field equations derivation with explicit interaction term and tensors for curved space-times unrestrained in Einstein-Maxwell equations framework 11 p1401 A73-26658

Space time cross spectral method to resolve transient disturbances into quasi-standing wave oscillations, giving formulas for node and antinode location 12 p1521 A73-26814

A characteristic initial value problem in general relativity in the case of a perfect fluid with axial symmetry. 13 p1658 A73-28199

Continuous-discrete and probability-deterministic theory of space-time and matter, considering resolution of antagonism between relativity and quantum theories 13 p1658 A73-28373

Analysis of correlation functions of space-time wideband signals received by linear antennas. 13 p1591 A73-28657

Kerr metric properties and astrophysical implications, presenting perfect fluid boundaries family in weak field approximation and photon orbits behavior in equatorial plane 14 p1798 A73-30143

First derivative discontinuities of space-time metric tensor in Einstein equations solution for nonisotropic and isotropic hypersurfaces, proving coordinate system existence for continuity 14 p1774 A73-30328

Kinematic invariants and their relation to chronometric invariants in Einstein's theory of gravitation 15 p1913 A73-31246

Painleve metric replacement for Schwarzschild metric in tests of general relativity, considering problem of supermassive celestial body gravitational collapse 15 p1937 A73-31650

Local structure of space-time singularity and gravitational collapse. 15 p1940 A73-32177

Einstein-Maxwell fields in conformal space, studying field equations, reducible electromagnetic field in space-time and constraints on metric tensor by Rainich conditions 17 p2212 A73-35560

Nonconformally plane relativistic recurrent-curvature spaces 17 p2212 A73-35567

Quantum theory of the spinor field in the two-dimensional space-time of de Sitter 17 p2213 A73-35571

Analysis of optimal recognition of space-time signals. 17 p2130 A73-35721

Book on large scale structure of space-time covering gravity roles, differential geometry, general relativity, gravitational collapse, black holes, spatially homogeneous cosmological models, etc 18 p2336 A73-35901

Centrosymmetrical nonstatic pulsating metric development, discussing minimupuls particles, perihelion displacement, gravitational energy, red shift, luminous ray curvature and Schwarzschild metric 20 p2594 A73-39765

Autocorrelation and space-time correlations for probe separations aligned with mean flow to test Pielke-Panofsky hypothesis, comparing laboratory tests to atmospheric turbulence 21 p2733 A73-41575

Schwarzschild solution indeterminacy as indicator of physical singularity analogous to intrinsically singular vertex of cone in Euclidean space 21 p2741 A73-41630

Gravitational waves in a space-time of any dimension. 22 p2885 A73-41773

SPACE-TIME METRIC

General relativistic gravitation theories based space-time curvature tests near sun from interplanetary probe motion analysis using probe-borne laser light transmission

[ONERA, TP NO. 1210] 22 p2907 A73-42216

Gravitational energy quantization model of noncharged particle based on proposed centrosymmetric metric with nonzero Einstein matter tensor and without Schwarzschild singularity

22 p2887 A73-42430

Centrosymmetric metric generator of field models of particles, discussing Einstein tensor components representation

22 p2887 A73-42431

Matter representation in general theory of relativity in terms of sourceless metric tensor and Einstein matter tensor, examining Mach principle status

22 p2887 A73-42435

General relativistic time analysis leading to scalar Hamiltonian formalism for particle mass based on Riemannian metric, considering Hamilton-Jacobi equation in particle dynamics

22 p2888 A73-43048

The Laplace and Poisson equations in Schwarzschild's space-time.

23 p3005 A73-43345

Unaccelerated-returning-twin paradox in flat space-time.

23 p3006 A73-43608

SPACE-TIME METRIC

U SPACE-TIME FUNCTIONS

SPACEBORNE ASTRONOMY

Secondary electron conduction /SEC/ vidicon television system for space astronomy, discussing data reduction requirements, costs and quasar spectrum observation

01 p0048 A73-10530

Space astronomy-developments in the sixties to scientific achievements in the seventies.

01 p0112 A73-11203

Skylab instrumentation and solar observation objectives in coordinated program of correlative ground based, rocketborne and other spaceborne observations

02 p0169 A73-12337

The Large Space Telescope program.

03 p0382 A73-13550

L. Alpha photometry of Comet Bennett.

04 p0494 A73-14757

High energy astronomy research in space, discussing HEAO A and B, UV astronomy, X ray astronomy, gamma rays, cosmic rays, hot stars, stellar energy sources and elementary particles

06 p0743 A73-18016

Astrolabe universal balloon gondola for solar and visible stars targeting, describing acquisition functions and attitude control servos design

07 p0776 A73-18940

Observing from space with the Orbiting Astronomical Observatory.

08 p1015 A73-21727

Electronic imaging systems with TV vidicon competition with film photography for spaceborne solar astronomy, comparing resolution, sensitivity and SNR

08 p0971 A73-21749

Cooling systems for spaceborne infrared experiments.

11 p1453 A73-26515

A SISAM interferometer and a simple Michelson-interferometer with spherical mirrors for space application.

11 p1369 A73-26519

Optical space astronomy and goals of the large space telescope.

12 p1497 A73-27436

Variable star observations from outside the earth's atmosphere - Review and prospects.

15 p1935 A73-31488

OAO-2 observations of Beta Lyrae and a provisional interpretation.

15 p1935 A73-31489

Traveling regions of high solar wind density observed in early August 1972.

16 p2056 A73-33460

Television sensors for ultraviolet space astronomy.

17 p2170 A73-35292

Imaging techniques in spaceborne X ray astronomy, discussing ray focusing, data processing and observational requirements of single photon detection and high time resolution

17 p2170 A73-35294

Properties of cosmic X-ray sources.

18 p2343 A73-35924

Interstellar absorption lines observed with the orbiting spectrophotometer S59.

18 p2349 A73-35993

A photometric study of the counterflow from space.

18 p2351 A73-36182

The X-ray structure of the Vela X region observed from Uhuru.

19 p2488 A73-38514

Investigation of primary gamma radiation from the northern polar region of the Galaxy

21 p2756 A73-40578

Cepheus X-4 X ray source observation by X ray telescope on OSO-7, confirming position by second telescope aboard

22 p2904 A73-43122

Apollo 16 far-ultraviolet camera/spectrograph - Instrument and operations.

22 p2864 A73-43165

X-ray observations of characteristic structures and time variations from the solar corona - Preliminary results from Skylab.

24 p3139 A73-45057

Observations of Cyg X-1 and Cyg X-3 above 7 keV from OSO-7.

24 p3144 A73-45494

SPACEBORNE PHOTOGRAPHY

NT SATELLITE-BORNE PHOTOGRAPHY

Colour separation and electronic analysis of Gemini V and Apollo spacecraft photography.

01 p0045 A73-10275

Meteorological and atmospheric physics observations by Soyuz manned spacecraft, analyzing spectrophotometry, photography and visual observation data of twilight, night and day horizons

02 p0160 A73-12265

Small view field high resolution all-reflective optical image scanner capable of straight line production for space applications

02 p0170 A73-12374

The prediction of resolving power of air and space photographic systems.

02 p0171 A73-12567

Photoelectric measurement of satellite camera shutter opening time delay and photographic plate motion synchronization, calculating root-mean-square error in observation time

03 p0307 A73-13253

The use of orbital photography for earth-resources satellite mission planning.

03 p0301 A73-13843

Electro-optical multiband cameras for spaceborne remote sensing, discussing optical multiplexing, return beam vidicon, intensifier vidicon storage tube, image spectrophotometer and dissector

04 p0450 A73-15770

Satellite pictures as aids for the determination of the structure of upper-level cyclones

05 p0593 A73-16347

Investigation of color detail, color analysis and false-color representation in satellite photographs.

05 p0578 A73-17136

Planets geometric figure via visible site photography from spacecraft, noting coordinate transformation for conical projection surface

06 p0751 A73-18152

Solar outer atmospheric eruption from photographic recording by OSO 7 spacecraft borne coronagraph, noting ejected gas and plasma clouds caused by flare

06 p0753 A73-18374

Mars surface volcano and canyon features from Mariner 9 photographs and geological map, suggesting internal heating, water erosion, atmospheric evolution and life problem solution

06 p0754 A73-18672

Apollo 17 spacecraft telemetered IR scanner remote sensing data, reduction, discussing use of interpolating and smoothing splines for restored image resolution improvement

06 p0696 A73-18807

Mariner spacecraft photographed Mars surface volcanic mountains and water in polar caps, suggesting recurring rainfall and rivers during successive interglacial periods

07 p0875 A73-19166

Lunar surface properties as determined from earthshine and near-terminator photography.

07 p0897 A73-19892

Real time display, processing and image-data products production system for supporting Mariner 9 TV experiment, discussing computer algorithms

09 p1080 A73-22266

Influence of atmospheric haze on the color of the underlying surface observed from a manned spacecraft

09 p1077 A73-22484

Determination of the transfer function of a planet atmosphere by spectrophotometry of the planet surface from space

09 p1077 A73-22488

Application of a narrow-angle television camera for determining the rotation elements of the moon.

09 p1084 A73-22739

Photometric analysis of earth photographs from Zond space station, determining earth sidereal magnitude

10 p1281 A73-24477

The facsimile camera - Its potential as a planetary lander imaging system.

12 p1495 A73-26875

Determination of the polarization transfer function in space-based spectrophotometric observations of natural formations on a planetary surface

12 p1488 A73-26965

Mariner Mars 1971 photogrammetry, discussing spacecraft scan platform mounted TV camera calibration procedure for interior orientation parameters and opto-mechanical orthogonality

12 p1500 A73-27953

Spaceborne imaging sensors planimetric resolution characteristics, describing Apollo, Mariner, ERTS, Jupiter Pioneer, Skylab and Viking imaging systems

12 p1500 A73-27957

Instruments and techniques for cartographic processing of space photographs.

12 p1500 A73-27959

Apollo 15 photogrammetric measurements of lunar figure, describing system characteristics and analytical triangulation techniques

12 p1501 A73-27967

Space geodetic techniques since 1957 covering photography, radar and laser uses in satellite observations with geodetic applications

13 p1671 A73-28006

Identification of certain details on photographs of Mars obtained from Mariner 4 and on the ground

16 p2069 A73-33834

Craters on photographs of the Mars surface taken by the Mariner 4 probe in 1965

16 p2069 A73-33835

Application of data compression techniques to spacecraft imaging systems.

17 p2122 A73-34910

Satellite imagery of land resources, discussing synoptic views, spatial dependence, closed loop information and sequential sampling

17 p2161 A73-34945

Exploration of Mars by Mariner 9 - Television sensors and image processing.

17 p2170 A73-35298

Automatic analysis of cloud cover by infrared photography of the earth from meteor satellites.

18 p2334 A73-37068

An overview of geological results from Mariner 9.

19 p2477 A73-37200

Martian volcanic and tectonic features from Mariner 9 photography, comparing evolutionary phases with lunar and terrestrial morphology

19 p2477 A73-37203

Mars troughs from Mariner 9 pictures, interpreting evolutionary origin in terms of surface and core processes

19 p2477 A73-37204

Mariner 9 evidence for wind erosion in the equatorial and mid-latitude regions of Mars.

19 p2477 A73-37209

Variable features on Mars. II - Mariner 9 global results.

19 p2478 A73-37212

Mariner 9 observations of the surface of Mars in the north polar region.

19 p2478 A73-37213

Mars atmosphere during the Mariner 9 Extended Mission - Television results.

19 p2478 A73-37218

Martian surface primary and secondary triangulation networks based on multiphotograph stereophotogrammetry and rectified photographs by Mariner 9, discussing control nets and points

19 p2479 A73-37227

Photogrammetric evaluation of Mariner 9 photography.

19 p2479 A73-37229

Cartographic products from the Mariner 9 mission.

19 p2480 A73-37231

Verification of performance of the Mariner 9 television cameras.

19 p2428 A73-37258

Airborne and spaceborne microwave imaging techniques for earth surface surveys, discussing resolution capabilities and applications for side-looking radar, microwave radiometers and scatterometers [AAS PAPER 73-111]

20 p2533 A73-38577

Atmospheric radiative transfer model for correction of Apollo photographic remote imagery data degradation due to radiation scattering

20 p2559 A73-39881

Assessment of applications of space-borne remote sensing to hydrology and water resources - An overview.

21 p2686 A73-40832

SPACEBORNE TELESCOPES

NT LARGE SPACE TELESCOPE

Space astronomy-developments in the sixties to scientific achievements in the seventies.

01 p0112 A73-11203

Spaceborne high resolution solar telescopes optical systems, discussing construction, alignment and thermal control problems

02 p0169 A73-12338

The Large Space Telescope program.

03 p0382 A73-13550

Alpha Lyra and beta Cen spectrograms from Merse- nsen system telescope aboard Salyut space station, demonstrating viability of space observatories

03 p0375 A73-13953

General analysis of aplanatic Cassegrain, Gregorian, and Schwarzschild telescopes.

03 p0309 A73-14426

Image quality in telescopes with image motion compensation by secondary mirror control.

03 p0309 A73-14429

High-resolution imagery of Uranus obtained by Stratoscope II.

05 p0627 A73-17388

Observing from space with the Orbiting Astronomical Observatory.

08 p0105 A73-21727

Offset guiding through large space telescopes.

08 p0970 A73-21731

A study of optical image sensors for the large space telescope.

08 p0971 A73-21742

Balloon-borne UV stellar spectrometer telescope pointing and stabilization, discussing in-house feasibility studies by small scale test payload experiments

08 p0971 A73-21750

Optimization studies in the support design for the Large Space Telescope.

11 p1437 A73-25488

Optical space astronomy and goals of the large space telescope.

12 p1497 A73-27436

The detector system of the International Ultraviolet Explorer satellite.

17 p2170 A73-35295

Large orbiting telescopes fine guidance system for ultrahigh pointing stability based on disturbance accommodation standard deviation optimal controller design

20 p2588 A73-38818

SPACECRAFT ANTENNAS

Graphite-epoxy composite properties, fabrication and tests for light weight low distortion spacecraft antenna reflector applications

03 p0331 A73-13023

Metallized fiberglass antenna meshes for spacecraft deployable reflectors, discussing low mass/area, long term stability and performance characteristics and degradation tests

03 p0333 A73-13045

Noise considerations in space communication antennas.

07 p0794 A73-20228

Antennas have it tough - when forced to ride on spacecraft.

07 p0803 A73-20491

Design and fabrication of a flight antenna for a planetary spacecraft.

16 p2018 A73-33057

Reliability estimate of a Space Deployable Antenna.

16 p1989 A73-33620

Attitude control, rotational and positioning mechanisms for orientation of mechanically despun antennas and solar arrays in communication satellites

17 p2126 A73-35486

Phased array antennas for applications on spacecraft.

21 p2662 A73-40647

SPACECRAFT CABIN ATMOSPHERES

Thermal analysis of combustion of fabric in oxygen-enriched atmospheres.

[ASME PAPER 72-WA/HT-22] Microflora of a sealed cabin with human subjects in a 3-day experiment with reduced temperature and high relative humidity

06 p0657 A73-17697

SPACECRAFT CABINS

Evaluation of hazard presented by gas-off products from polymeric materials intended for use in space cabins.

18 p2286 A73-36931

SPACECRAFT COMMUNICATION

Constant-envelope spread spectrum random access satellite communication system, discussing message and multiple access modem, signal acquisition, tracking, ranging, etc

01 p0018 A73-11178

Unified S-band ground system design and management for Apollo program, deep space and manned space flight network tracking and communications requirements

01 p0030 A73-11184

Microwave dual frequency propagation experiment using the Mariner Venus Mercury probe.

03 p0275 A73-13628

A review of microwave parametric amplifiers with particular reference to satellite communications and radio astronomy.

03 p0284 A73-13999

Ionospheric scale height from the refraction of satellite signals.

04 p0415 A73-14952

Synthesis of an optimal receiver structure for amplitude modulated pseudo-noise signals.

04 p0415 A73-14982

Quadrature amplitude-shift key satellite communication feasibility based on SNR and transmitter power efficiency comparison with multiphase-shift key system

04 p0420 A73-15411

Time division multiple access for tactical trunking via satellite.

04 p0420 A73-15424

Digital link for bidirectional communication between manned spacecraft and ground terminal by synchronous communication relay satellite, noting coding parameters effects on error rate

04 p0421 A73-15426

Radio set design requirements for communication link between meteorological sensor platforms and spacecraft in Geostationary Operational Environmental Satellite System

04 p0421 A73-15432

Mathematical model for multipath transmission in aircraft and spacecraft communications, presenting Bayes detector for binary PSK

04 p0422 A73-15462

Pulsed electric thrusters theoretical and experimental radiation intensities and spectra, estimating interference with onboard satellite communication systems [AIAA PAPER 73-263]

05 p0608 A73-16984

Modeling and evaluating the performance of high data rate digital satellite communication systems with limiters.

06 p0669 A73-18830

Design and performance of VHF telemetry transmitter and remote controlled radio receiver for Eole satellite, noting production technology and block diagram

07 p0790 A73-18961

Design and performance of UHF transmitter and receiver system for two way links between Eole satellite and constant ceiling balloons

07 p0790 A73-18962

Antenna design for Eole satellite radio communications with balloons, noting wave polarization and sea reflection effects

07 p0797 A73-18963

Symphonic satellite radio link equipment design and performance, noting transmission characteristics and frequency response of repeater

07 p0821 A73-18965

8-phase and 16-phase high speed PSK modems for PCM-TDMA satellite communication.

07 p0791 A73-19370

TDMA system and full scale test programs for Symphonic satellite telecommunication with ground

09 p1049 A73-22316

Decimicrometer band laser operated communication system to link earth observation satellites with geosynchronous satellites, discussing key technologies

09 p1055 A73-23393

A new type of PSK anti-ambiguity system for satellite applications.

09 p1156 A73-23431

A computer method of optimal redundancy allocation in satellite communication system.

10 p1188 A73-23753

Surface elastic wave microwave bandpass filter for miniaturized frequency synthesizer in satellite communications systems, noting insertion loss and sidelobe reduction

12 p1484 A73-27573

The provision of ground station facilities for an aeronautical satellite system.

12 p1471 A73-27658

A maritime communications concept using spaceborne phased arrays.

12 p1472 A73-27665

Satellite communication channels assignment to ships and aircraft, considering automated digital calling method for ship-to-shore communication

12 p1472 A73-27670

Satellite communication systems for long haul air transport operations, discussing political, operational/technical and economic problems

12 p1472 A73-27671

A simple stabilized antenna platform for maritime satellite communications.

12 p1481 A73-27673

The operational requirements for a maritime satellite communication service.

12 p1473 A73-27676

Engineering economic considerations for a maritime-satellite service.

12 p1473 A73-27677

AEROS satellite launching from Western Test Range, describing time sequence of satellite and rocket countdowns and communication system activities coordinated by project management

13 p1689 A73-28781

NASA computer generated 136/400-MHz radio sky maps covering whole celestial sphere for earth-based receiver noise temperature determination in satellite communication

13 p1585 A73-29115

Post-occultation reception of lunar ship America radio transmission.

14 p1725 A73-29733

Aircraft-satellite multipath communication characteristics, considering surface scatter, ionospheric scintillation and refraction and tropospheric refraction and scatter

14 p1725 A73-29891

Effect of multipath on ranging error for an airplane-satellite link.

14 p1725 A73-29892

SPACECRAFT CONFIGURATIONS

The use of specialized antenna technology for air traffic control and communications.

14 p1732 A73-29894

Satellite-aircraft multipath and ranging experiment results at L band.

14 p1726 A73-29898

Multibeam satellite Effective Isotropic Radiative Power (EIRP) for aeronautical communications, discussing carrier-to-noise density increase and communication load per channel decrease

14 p1726 A73-29900

Book - The politics and technology of satellite communications.

14 p1818 A73-29949

The contribution of the German Telecommand Station to the overall command safety in the Helios project.

14 p1727 A73-30101

An analysis of helicopter rotor modulation interference.

15 p1843 A73-31731

Objectives and employment of the integration and system test equipment for Aeros

15 p1943 A73-32180

Aircraft onboard data link and Aerosat equipment integration, considering antenna, duplexer, amplifier and receiver systems

15 p1846 A73-32428

The characteristics of millimeter wavelength satellite-to-ground space diversity links.

16 p1981 A73-33707

On rainfall and space diversity for millimeter-wave earth-satellite communications systems.

18 p2289 A73-36709

Multiple-beam spherical-reflector antenna systems for satellite communications.

20 p2525 A73-38739

A digital communications system for manned spacecraft applications.

20 p2527 A73-38763

Thermal design and analysis aspects of advanced communication spacecraft.

20 p2531 A73-39773

SPACECRAFT COMPONENTS

NT COMMAND MODULES

NT SERVICE MODULES

NT SPACECRAFT CABINS

NT SPACECRAFT MODULES

Test chamber for on board moving parts in ultrahigh vacuum.

01 p0030 A73-11148

Aeros satellite component tests for design and manufacturing error detection and failure prevention, using structural, thermal and electrical integration models

03 p0288 A73-13918

Electro-gilding of coverings and light alloy component parts for satellites D2 and EOLE.

07 p0829 A73-18911

French Concerto program for component reliability and quality assurance in manufacturing and procurement controls for Symphonic satellite

07 p0790 A73-18975

Satellite systems space environmental simulation tests, discussing thermal models design, temperature field and error calculations by computerized data processing

16 p1998 A73-33393

Improved technology for multiwatt radioisotope heater units.

18 p2336 A73-36681

Compatibility and satisfactory performance of individual Space Shuttle elements, discussing development/flight cost tradeoff, booster thrust vector and optimal control

19 p2492 A73-37600

Dual spin gas bearing reaction wheel for spacecraft fine pointing applications requiring long component life, describing manufacturing methods, safety factors and testing

[AIAA PAPER 73-907]

20 p2568 A73-38841

Fabrication methods for beryllium spacecraft components.

20 p2615 A73-39775

SPACECRAFT CONFIGURATIONS

NT APOLLO TELESCOPE MOUNT

NT SATELLITE CONFIGURATIONS

Stage separation of parallel-staged shuttle vehicles - A capability assessment.

01 p0109 A73-10105

Space shuttle missions and configurations, discussing payload, external tank, solid rocket engines, orbiter vehicle and alternate delivery system costs

05 p0627 A73-16183

Aerothermodynamic aspects of shock-interference patterns for shuttle configurations during entry.

[AIAA PAPER 73-238]

05 p0532 A73-16963

Convective heating on delta-wing Space-Shuttle boosters including interference effects.

05 p0533 A73-17202

Stabilization concepts for a spherical planetary entry probe configuration.

[AIAA PAPER 73-184]

06 p0756 A73-17653

Space shuttle phase B program, discussing orbiter and booster configurational studies, ground simulation, propulsion systems, structure, avionics, environment control and life support systems, etc
09 p1152 A73-22189

Intelsat 4 power subsystem with solar panels, Ni-Cd batteries, controller and relays for bus paralleling, discussing spacecraft and system configurations and performance
09 p1154 A73-22788

Configuration control of dual satellite systems in earth orbit, obtaining equations of motion, deployment paths and force functions
10 p1276 A73-24008

A contribution to the calculation of aerodynamic force and moment coefficients of spacecraft
12 p1457 A73-26819

Experimental study of a high lift re-entry vehicle configuration.
13 p1564 A73-28822

Space shuttle implementation prognosis, discussing spacecraft configurations, international cooperation, research possibilities in TR telescopes, space physics laboratories and exobiology
18 p2348 A73-35937

Reusable space tug system and missions for space shuttle operations with 1980s planned payloads, discussing interfaces and configuration alternatives [AIAA PAPER 73-609]
18 p2358 A73-36088

British X4 spacecraft mechanical design configuration with honeycomb sandwich panels, on yo-yo principle based despin system and flexible solar array
20 p2615 A73-39774

SPACECRAFT CONSTRUCTION MATERIALS

Material and structural studies of metal and polymer matrix composites.
02 p0182 A73-12621

Materials and processes for thermal control surfaces.
03 p0329 A73-13009

Glass reinforced structural components for the synchronous meteorological satellite.
03 p0331 A73-13030

Unmanned spacecraft adhesives and adhesive bonding applications in solar panels, mirrors, circuit boards, antennas, platforms, lunar capsules and reentry heat shields
03 p0333 A73-13049

Light weight graphite-polyimide composite honeycomb core and sandwich panel design, fabrication and tests for shuttle orbiter thermal protection system
03 p0333 A73-13051

Thermal conductance of gasket materials for spacecraft joints.
[AIAA PAPER 73-119]
05 p0640 A73-16875

Space shuttle technology, discussing configurational aerothermodynamics, aeroleastic effects on vehicle dynamics and structural design and materials [AIAA PAPER 73-31]
06 p0755 A73-17619

Beryllium for nonstructural and structural applications in aerospace systems, considering high dimensional stability, mechanical and thermodynamic properties, and metal sintering techniques for production
07 p0828 A73-18904

Highly-rigid sandwich structures for interstages.
07 p0906 A73-18994

The thermal conductivity of a number of alloys at elevated temperatures.
[ECTP PAPER B1-4]
14 p1760 A73-30435

New horizons in materials and processing; Proceedings of the Eighteenth National Symposium and Exhibition, Los Angeles, Calif., April 3-5, 1973.
16 p2027 A73-33026

Oxidation resistant carbon-carbon composite for Space Shuttle application.
16 p2028 A73-33043

Brazed honeycomb structure design, fabrication and aerospace applications covering brazing methods, filler metal selection, nondestructive testing, sandwich designs, aircraft and spacecraft structures, etc
17 p2177 A73-34100

High modulus filament wound vessels for cryogenic containers in spacecraft.
17 p2238 A73-34807

The potential application of carbon fibres to spacecraft.
17 p2238 A73-34811

Fabrication methods for beryllium spacecraft components.
20 p2615 A73-39775

SPACECRAFT CONTAMINATION

Design principles for contamination abatement in scientific satellites.
02 p0136 A73-11991

Comparative evaluations of outgassing results between the vacuum thermogravimetric method and the SRI method.
03 p0330 A73-13019

Outgassing and contamination properties of prospective Apollo Telescope Mount materials.
03 p0330 A73-13020

Space simulation experiments on reaction control system thruster plumes.
[AIAA PAPER 72-1071]
03 p0354 A73-13398

Action of Freon-114B2 on the activity of lactate-dehydrogenase iso-enzymes
06 p0650 A73-17696

Removal of hydrocarbon contaminant film from spacecraft optical surfaces using a radiofrequency-excited oxygen plasma.
08 p0989 A73-21835

Estimating the number of terrestrial organisms on the moon.
11 p1320 A73-26488

Gas flow analysis during thermal vacuum test of a spacecraft.
16 p1994 A73-33150

Monitoring for microbial flora contamination on spacecraft surface, discussing cultural techniques and sampling methods for microorganisms detection and sterilization
16 p1976 A73-33698

Ten years of development of the Planetary Quarantine Program of the United States.
18 p2281 A73-35966

IMP and Pioneer satellite-borne sensors for cataloging solar particle events, discussing onset time, multiple flare injections, enhancement differentiation and contamination problems
18 p2345 A73-36061

The significance of outer planet satellite quarantine constraints on aim-point selection.
[AIAA PAPER 73-553]
18 p2359 A73-36096

Spacecraft microbial burden reduction due to atmospheric entry heating - Jupiter.
18 p2281 A73-36100

Adsorption of spacecraft contaminants on Bosch carbon.
[ASME PAPER 73-ENAS-15]
19 p2399 A73-37972

Spacecraft environmental optical contamination problems associated with thermal control surface outgassing.
[ASME PAPER 73-ENAS-32]
19 p2395 A73-37987

Microbial contamination of water - Traditional and space-age problems and approaches.
[ASME PAPER 73-ENAS-33]
19 p2395 A73-37988

Space-related research in mycology concurrent with the first decade of manned space exploration.
20 p2513 A73-39478

Vacuum effects on materials and environment contamination - Screening method and results obtained at CNES
22 p2880 A73-41873

Safety margins in the implementation of planetary quarantine requirements.
22 p2803 A73-42161

SPACECRAFT CONTROL

NT SATELLITE ATTITUDE CONTROL

NT SATELLITE CONTROL

Some considerations on utilization control of the near earth space in future.
01 p0074 A73-11125

Discrete control algorithms for spaceborne terminal systems.
01 p0075 A73-11194

Dynamical interaction in biaxial control systems.
01 p0075 A73-11198

Development of pulsed hydrogen/oxygen attitude-control engines
[DGLR PAPER 72-077]
02 p0202 A73-11689

Ground control facilities and organization of Helios space probe mission and flight operations system based on U.S.-German cooperation
03 p0381 A73-13297

Invariant poles feedback control of flexible highly variable spacecraft.
03 p0285 A73-13522

Design of a digital adaptive control system for reentry vehicles.
03 p0286 A73-14482

Pontryagin maximum principle for optimal terminal velocity control of automatic space probe descent in Mars atmosphere
03 p0383 A73-14556

Oscillations of spacecraft with on-off attitude control under constant perturbation moment, calculating energy expenditures for desired orientation maintenance
03 p0383 A73-14559

Spacecraft optimal control after transfer from hyperbolic trajectory to planetary orbit by atmospheric drag, minimizing engine thrust
03 p0340 A73-14570

Spacecraft digital attitude control.
04 p0504 A73-14736

Spacecraft control hardware for use with digital processors.
04 p0424 A73-14737

Demonstration of digital three axis spacecraft control.
04 p0432 A73-14738

Reorientation of a spacecraft
04 p0504 A73-14885

Prediction in control of re-entry into the atmosphere.
05 p0627 A73-16076

Synthesis of a nonlinear control law for the motion of a space vehicle in the earth's atmosphere.
05 p0627 A73-16077

Russian book - Control of moving objects.
05 p0628 A73-16404

Dynamics of three-axis spacecraft orientation
05 p0628 A73-16404

Dynamics of an astronaut's movement on a tethal towards a spacecraft and a spacecraft control concept based on the variable-structure systems theory
05 p0628 A73-16404

Methods of optimization of a spacecraft angular position control program
05 p0594 A73-16404

Problems of the synthesis of spacecraft onboard data computation units
05 p0553 A73-16404

Statistical synthesis of optimal pulsed control systems for spacecraft while taking into account system structural constraints
05 p0595 A73-16413

Optimal control of extraatmospheric spacecraft maneuverability by variable structure system with logic circuits
05 p0628 A73-16423

A control system for soft landings on the lunar surface
05 p0595 A73-16423

Spacecraft motion control as stochastic dynamic problem formulated according to single criterion for deterministic programmed and stochastic perturbed motions
05 p0629 A73-16423

Hydraulic and flight control system for Space Shuttle Orbiter.
[SAE PAPER 720838]
05 p0537 A73-16634

Aerothermodynamics of the Space Shuttle reaction control system.
[AIAA PAPER 73-93]
05 p0629 A73-16857

Application of the control configured vehicle concept to a Space Shuttle configuration.
[AIAA PAPER 73-158]
05 p0629 A73-16902

Optimal control of a combined propulsion system of a rotating spacecraft
05 p0630 A73-17003

Quality /probability/ evaluation of human operator/ergatic processes controlling spacecraft during rendezvous and docking with orbital station
06 p0657 A73-17689

Aerodynamic entry vehicle autopilots.
06 p0721 A73-18511

Diamant launcher tilting system.
07 p0905 A73-18997

Operational set up of Europa II launch vehicle control units.
07 p0808 A73-19007

The conjugate gradient method and its application to aerospace vehicle guidance and control. I - Basic results in the conjugate gradient method.
08 p0951 A73-21428

The conjugate gradient method and its application to aerospace vehicle guidance and control. II - Mars entry guidance and control.
08 p0986 A73-21428

Second order digital phase locked loop for Viking Orbiter 1975 command system, using filtered sequence of phase error polarity to correct system clocks
09 p1053 A73-23372

The German telecommand ground station for HELIOS - A new concept.
09 p1070 A73-23418

Phase double plane as a method to study the dynamics of a spacecraft with limited constructional rigidity.
10 p1286 A73-24006

Vehicle coordinate-parametric control problems and some solution methods.
10 p1198 A73-24007

Principles of spacecraft telemetry data management.
11 p1333 A73-25351

Correction of a spacecraft with a static corrective thruster chamber
11 p1431 A73-26465

Optimization of the parameters of heterogeneous multipurpose controlled systems using standard elements.
12 p1484 A73-27456

An algorithm for controlling the descent of a spacecraft from an artificial earth satellite orbit.
12 p1543 A73-27631

Work movement performance of the astronaut in flight.
12 p1465 A73-27645

Spacecraft single-turn reorientation optimization with respect to fuel expenditure depending on maneuver duration and reaction control torque constraints
14 p1803 A73-29852

Time optimal propulsion system parameters for thrust vector control during spacecraft maneuver performance
14 p1772 A73-29855

Design considerations for shuttle information management.
14 p1818 A73-29945

The contribution of the German Telecommand Station to the overall command safety in the Helios project.

14 p1727 A73-30101

Utilization of PCM telemetry for the control of the Europa III launcher

14 p1804 A73-30111

Russian book on aircraft, rocket and spacecraft control systems design methods covering ground and on-board systems synthesis, performance estimates, system effectiveness, etc

14 p1773 A73-30353

Optimal damping and stochastic control in certain problems of astrodynamics

15 p1931 A73-31236

Application of the theory of Markov processes in state estimation of dynamic systems and in control of flight-vehicle oscillations

15 p1942 A73-31239

Russian book - Radio devices for flight vehicle control systems.

15 p1908 A73-32421

Russian book - Methods and systems of spacecraft navigation, guidance and control.

18 p2335 A73-35867

Computerized processing system with real time control, data analysis and display capabilities for space shuttle checkout, servicing, launching and landing to reduce cost

[AIAA PAPER 73-601]

18 p2295 A73-36083

Titan/Centaur launch vehicle for high payload escape missions and large synchronous orbit spacecraft, describing propulsion, control/guidance and telemetry systems

[AIAA PAPER 73-617]

18 p2359 A73-36094

Study of the frequency impulse system of spacecraft orientation control

18 p2359 A73-36102

Application of the dynamic filtration method to spacecraft orientation control problems

18 p2359 A73-36104

Some problems of orientation accuracy for a gyroscopic orbit with nonlinear control laws

18 p2335 A73-36118

Computer simulation for time optimal or energy optimal attitude control of spin-stabilized spacecraft.

18 p2360 A73-36837

Digital control system development for the Delta launch vehicle.

[AIAA PAPER 73-847]

20 p2613 A73-38786

Three-axis attitude control system air-bearing tests with flexible dynamics.

[AIAA PAPER 73-866]

20 p2543 A73-38804

A nonlinear programming algorithm for the automated design and optimization of flexible space vehicle autopilots.

[AIAA PAPER 73-892]

20 p2588 A73-38828

Attitude control of a large flexible spacecraft using three-axis mass expulsion control.

[AIAA PAPER 73-893]

20 p2588 A73-38829

Design of a digital controller for spinning flexible spacecraft.

[AIAA PAPER 73-894]

20 p2589 A73-38830

Optimal motions of a spacecraft relative to its center of mass

21 p2781 A73-40903

Study of a method of exponential control of a spacecraft rendezvous

21 p2781 A73-40905

SPACECRAFT DESIGN

NT SATELLITE DESIGN

Stage separation of parallel-staged shuttle vehicles - A capability assessment.

01 p0109 A73-10105

Space stations and shuttle vehicles design and placement in earth orbit, reviewing life support, energy production and data transmission systems

01 p0096 A73-10300

Thermal mathematical model development for spacecraft design as exemplified by small scientific satellite, comparing analytical results with test data

01 p0110 A73-11144

Thermal requirements considerations for all components and systems in initial design phase of spacecraft to obviate need for full scale tests

01 p0110 A73-11145

The Delta launch vehicle for scientific and applications satellites.

01 p0111 A73-11159

German-American cooperative solar probe project Helios, discussing design features, mission objectives and project development status

[DGLR PAPER 72-104]

02 p0228 A73-11706

Rocket payload designs simulated by Monte Carlo method for aerodynamic properties during D region composition measurements

02 p0156 A73-11740

Book - Fundamentals of spacecraft thermal design.

02 p0237 A73-11885

Russian book on physico-technological basis of space research covering near earth and interplanetary environmental factors and effects on spacecraft designs and materials

02 p0211 A73-11886

Structural weight analysis of single stage and multistage spacecraft for given payload and initial vehicle weight, considering optimization problem

02 p0229 A73-12469

Application of an improved transpiration cooling concept to space shuttle type vehicles.

03 p0397 A73-13492

Some design aspects of Space Shuttle orbiters.

05 p0627 A73-16178

Turbomachinery design for Space Shuttle auxiliary power systems.

[SAE PAPER 720835]

05 p0537 A73-16633

Venus atmosphere engineering models for use in spacecraft design and mission planning from Mariner 5 and Venera spacecraft and earth based measurements

[AIAA PAPER 73-130]

05 p0619 A73-16883

Aerothermodynamics R and D for space shuttle configurational design, discussing program organization and wind tunnel testing to generate design technology base

[AIAA PAPER 73-59]

06 p0755 A73-17632

Research and applications modules (RAM) program for manned space research satellites transportation and support, discussing mission requirements and design concepts

[AIAA PAPER 73-72]

06 p0755 A73-17637

Design of low-cost, refurbishable spacecraft for use with the Shuttle.

[AIAA PAPER 73-73]

06 p0756 A73-17638

Grand Tour missions to the outer solar system with Saturn /Intermedie 20/.

06 p0750 A73-18024

Space deployed expandable structures, discussing vehicular and environmental constraint effects on design, large structure requirements, and applications

07 p0828 A73-18905

ERTS program, describing satellite design and imaging and data collection systems for real time or delayed taped transmission to ground stations

07 p0905 A73-19112

Pioneer Jupiter spacecraft magnetic field control with periodically updated magnetic model for tradeoffs in subsystem moments within allowed magnetic budget

[IEEE PAPER 41, 4]

07 p0905 A73-19364

Short guide to Titan III launch vehicles.

08 p1014 A73-20800

Modular space station operation as general purpose laboratory with attached or free flying R and D modules for specific projects

09 p1152 A73-22325

Electrical power subsystem for the Synchronous Meteorological Satellite (SMS).

09 p1154 A73-22789

Spacecraft nuclear power source optimization, considering radioisotope and reactor heat sources, cryogenic cooler cycle types and spacecraft design

09 p1118 A73-22799

Computerized design of an outer planets spacecraft structure to survive the meteoroid environment.

[AIAA PAPER 73-349]

11 p1430 A73-25487

Automating the design process - Progress, problems, prospects, potential.

[AIAA PAPER 73-410]

11 p1373 A73-25538

Radioisotope heater design and optimization for manned spacecraft thermal control and life support systems and various mission times

11 p1310 A73-25996

On-orbit checkout and repair as a factor in economical spacecraft design and operation.

12 p1549 A73-27439

Structural weight optimization of single stage and multistage spacecraft for given payload and initial vehicle weight

15 p1944 A73-32619

Reusable space shuttle orbiter design evolution during 1972-1973, discussing payloads, vertical launching capability and advanced materials technology

16 p2072 A73-33063

Evolution of the Space Shuttle. I.

16 p2074 A73-34024

An appreciation of the design of carbon fibre rigid solar panels for spacecraft.

17 p2238 A73-34812

Systems engineering at the Jet Propulsion Laboratory.

17 p2258 A73-35574

Evolution of the Space Shuttle. II.

17 p2240 A73-35660

Skylab design technology assessment based on past manned spacecraft subsystems, noting advances in mission duration, spacecraft size and living accommodation comfort features

[AIAA PAPER 73-598]

18 p2358 A73-36082

Space shuttle orbiter and subsystem design, discussing crew cabin, payload accommodations, flight characteristics and aerothermodynamics

[AIAA PAPER 73-604]

18 p2358 A73-36085

Representative Space Shuttle missions and their impact on shuttle design.

[AIAA PAPER 73-608]

18 p2358 A73-36087

Temperature control of the Mariner class spacecraft - A seven mission summary.

[AIAA PAPER 73-769]

18 p2360 A73-36383

Thermal control and structures approach for fluorinated propulsion.

[AIAA PAPER 73-772]

18 p2360 A73-36386

Aspects of the finite element method as applied to aero-space structures.

[ISD-138]

18 p2365 A73-36725

Europa III heat shields - Aerothermodynamic analysis and design.

18 p2361 A73-36954

Free flying teleoperator spacecraft systems for automated satellites retrieval, cargo transfer and orbital operations support

19 p2490 A73-37303

Preliminary design and simulations of a Shuttle-Attached Manipulator System.

19 p2491 A73-37309

Design for teaching aerospace engineering at Texas A & M University.

[AIAA PAPER 73-786]

19 p2505 A73-37456

Space shuttle program, discussing master planning schedule, vehicle design, payloads and initial flight tests

19 p2491 A73-37593

Space shuttle payload definition, design and planning, using computers for scheduling and costing

19 p2492 A73-37599

Space Shuttle solid rocket stage recovery, retrieval, and refurbishment.

19 p2492 A73-37599

An insight into the features of the OAO-C thermal design.

[ASME PAPER 73-ENAS-4]

19 p2493 A73-37966

Standardized space shuttle launched multipurpose spacecraft design using nuclear electric power systems with radioisotope thermoelectric generators or Brayton cycle alternators

19 p2455 A73-38393

Multi-mission nuclear electric propulsion stage design.

19 p2457 A73-38433

Thermal design and analysis aspects of advanced communication spacecraft.

20 p2531 A73-39773

Space shuttle design program with Mark I and II stages, considering thermal protection weight analysis for minimum maintenance and turnaround time

21 p2780 A73-40416

A failure tolerant power subsystem for outer planet spacecraft.

22 p2801 A73-42902

Two stage recoverable space shuttle structural design, discussing configurations, costs and orbiter and booster materials and thermal protection systems

23 p3038 A73-43786

SPACECRAFT DOCKING

Quality /processability/ evaluation of human operator ergatic processes controlling spacecraft during rendezvous and docking with orbital station

06 p0657 A73-17686

Apollo-Soyuz docking project for flight testing systems compatibility for safe and reliable crew transfer, discussing program objectives, technical requirements and solutions

09 p1152 A73-22187

European space tug conception evolution, discussing docking system

12 p1549 A73-27382

Skylab experience with Apollo docking/latching loads.

[AIAA PAPER 73-613]

18 p2358 A73-36091

System requirements for a free-flying teleoperator to despin the ATS-V.

19 p2490 A73-37304

Shuttle-Attached Manipulator System requirements.

19 p2491 A73-37307

Shuttle Payload Accommodation System teleoperator.

19 p2491 A73-37308

Description of the docking module ECS for the Apollo-Soyuz Test Project.

[ASME PAPER 73-ENAS-21]

19 p2493 A73-37977

Spacecraft rendezvous in orbit, discussing launching, transfer maneuver, target location, approach phase, docking and mechanical coupling

19 p2487 A73-38302

SPACECRAFT ELECTRONIC EQUIPMENT

NT AIRBORNE/SPACEBORNE COMPUTERS

Experimental satellite for attitude control. V - Attitude control electronics.

01 p0112 A73-11192

The radiation environments of outer-planet missions.

05 p0617 A73-16511

French spacecraft electronic components reliability program, considering failure characteristics, operating limits, environmental conditions and confidence level

07 p0797 A73-18915

Satellite electronic equipment reliability and quality control at preproject, project, fabrication and mission levels, noting electric welding quality specification

07 p0904 A73-18974

Russian book - Optoelectronic devices in spacecraft.

07 p0825 A73-20379

SPACECRAFT ENVIRONMENTS

Thermal/electrical design of spaceborne microelectronic components. 13 p1588 A73-28046

Electric corona assessment of Skylab spacecraft high voltage electrical/electronic equipment and instruments, considering operating temperature and environment contaminants effects 17 p2109 A73-35256

Optical data storage and data processing, and holography in aerospace and electronic instrumentation. 17 p2131 A73-35382

Aircraft and spacecraft radio navigation systems, discussing Doppler, inertial and VHF omnirange techniques, Apollo spacecraft guidance systems, TACAN, Harrier and Swedish SAAB37 aircraft navigation 21 p2736 A73-40514

Decentralized power processing for large-scale systems. 22 p2801 A73-42905

SPACECRAFT ENVIRONMENTS

A derivation of thermal mathematical model with measured nodal temperatures. 01 p0123 A73-11142

Sensitivity analysis method application to spacecraft thermal environment control system design, determining mathematical model input parameters uncertainty effects on temperature determination 01 p0123 A73-11143

The operational condition of heat pipes. 01 p0111 A73-11153

Collisionless plasma flow over a conducting sphere. 02 p0158 A73-11919

Vacuum thermogravimetric analysis system for determination of continuous weight change and total condensable materials. 03 p0330 A73-13018

The Ranque-Hilsch vortex tube and its application to spacecraft environmental control systems. 03 p0287 A73-13313

A study of the plume impingement environment experienced by the booster during the space shuttle nominal staging maneuver. 03 p0273 A73-13468
[ALAA PAPER 72-1171]
Further observed degradation on the LES-6 synchronous solar cell experiment. 03 p0258 A73-14247

Developments in space medicine. 06 p0649 A73-17569

Lumped parameter network modeling for spacecraft surface thermal environment analysis, discussing computer program and application to Skylab ATM 07 p0919 A73-19496

Results and prospects of microbiological studies in outer space. 11 p1320 A73-26487

Safety and survival in manned space laboratory, discussing experimental and environment hazard elimination 16 p2071 A73-32673

A biased model for calculating the evolution in solar absorptance. 16 p2060 A73-33128

Aeros satellite simulated environmental testing for thermal behavior under space vacuum, temperature and solar radiation conditions, comparing results with mathematical model calculations 16 p1997 A73-33392

Satellite systems space environmental simulation tests, discussing thermal models design, temperature field and error calculations by computerized data processing 16 p1998 A73-33393

Investigation of the disinfecting properties of sorbents which are used in a spacecraft life support system 17 p2114 A73-34240

Cytogenetic analysis of diploid and autotetraploid Crepis capillaris seeds following space travel on the 'Cosmos-368' artificial earth satellite 18 p2271 A73-36117

Apollo 14 and Apollo 16 heavy-particle dosimetry experiments. 19 p2396 A73-37150

Advanced methods of recovery for space life support systems. 19 p2398 A73-37711

Reverse osmosis for wash water recovery in space vehicles. 19 p2399 A73-37971

Skylab medical experiments altitude test crew observations. 19 p2400 A73-37985

Axial grooved heat pipes - Cryogenic through ambient. 19 p2434 A73-37995

Design and test of a self-controlled heat pipe radiator. 19 p2435 A73-37996

Effects of space flight factors on the heredity of higher and lower plants. 22 p2804 A73-42168

Results of cytogenetic studies of seeds after their extended orbital flight aboard the Salyut orbital scientific station. 22 p2804 A73-42169

Estimation of the biological danger of the very high energy component of space radiation. 22 p2805 A73-42180

Apollo 16 Biostack experiment for biological effects of cosmic ray heavy primaries on cell and tissue development and mutations of bacilli, Artemia and plant seeds 22 p2805 A73-42185

A variation of the Davis-Smith method for in-flight determination of spacecraft magnetic fields. 24 p3139 A73-45107

SPACECRAFT GUIDANCE

NT SATELLITE GUIDANCE

Atmospheric reentry optimal lateral guidance for low lift/drag ratio space shuttle vehicle, presenting formulation as optimal stochastic control problem [ALAA PAPER 71-914] 01 p0074 A73-10106

Guidance of spacecraft controlled by low-thrust rocket engines and evolving in the plane of the initial trajectory 02 p0227 A73-11580

Aircraft and spacecraft guidance and remote and automatic control of moving objects, using calculus of variations for systems synthesis 05 p0560 A73-16402

Constrained low thrust guidance algorithms for three axis and spin stabilized constant power solar electric propelled spacecraft on fixed time rendezvous missions 05 p0595 A73-16917

[ALAA PAPER 73-173]
Soft constraint trajectory optimization formulation as real time optimal feedback guidance method for multiburn orbital maneuvers 05 p0596 A73-16972

[ALAA PAPER 73-249]
Study of accuracy requirements for autonomous trajectory measurements providing conditions for entering planetary atmospheres 05 p0619 A73-17001

Space /rocket/ launch vehicle computer guidance and targeting equations, discussing Q, Delta, explicit, linear tangent, optimal, numerical integration and parameter optimization techniques 06 p0721 A73-18824

The conjugate gradient method and its application to aerospace vehicle guidance and control. I - Basic results in the conjugate gradient method. 08 p0951 A73-21428

Six degree of freedom guided sounding rocket flight simulations and trajectory program, discussing financial and technical feasibility 09 p1117 A73-23218

[ALAA PAPER 73-299]
Radio-guidance algorithms applied to the control of spacecrafts descending in the earth's atmosphere 10 p1247 A73-23880

Optimal entry algorithm and multiimpulse correction times for spacecraft guidance trajectory of minimum fuel consumption 10 p1247 A73-23881

High-reliability strapdown platforms using two-degree-of-freedom gyros. 13 p1657 A73-29214

Russian book - Methods and systems of spacecraft navigation, guidance and control. 18 p2335 A73-35867

Titan/Centaur launch vehicle for high payload escape missions and large synchronous orbit spacecraft, describing propulsion, control/guidance and telemetry systems 18 p2359 A73-36094

[ALAA PAPER 73-617]
Algorithms for radio guidance with application to control of landing of spacecraft in the earth's atmosphere. 20 p2590 A73-38899

Optimal entry algorithm and multiimpulse correction times for spacecraft guidance trajectory at minimum fuel consumption 20 p2590 A73-38900

Redundant independent guidance, navigation and control system application to space shuttle, estimating channel output divergence due to sensor bias and scale factor errors 21 p2735 A73-40043

Space shuttle orbiter abort guidance for premature or abnormal termination of mission due to system or human failure, discussing predictive algorithm 21 p2735 A73-40045

Navigation system design for the Mariner Jupiter/Saturn Mission. 21 p2737 A73-40906

[ALAA PAPER 73-838]
A linear method of autonomous space navigation and guidance 21 p2737 A73-40906

Mathematical model of spacecraft onboard digital guidance computer under data acquisition conditions, using imbedded Markov chains 23 p2955 A73-43261

SPACECRAFT INSTRUMENTS

NT LASER ALTIMETERS

NT SATELLITE INSTRUMENTS

NT SPACECRAFT POSITION INDICATORS

Sun, earth and star attitude sensors for spacecraft, describing design, analysis and hardware aspects in terms of critical parameters 01 p0053 A73-11170

Spacecraft-borne IR optical remote sensor for detection, identification and distribution measurement of asteroid and meteoroid particles 01 p0105 A73-11205

On the calibration system of the amplifying tract of spherical ion trappers. 02 p0169 A73-12186

Spin-scan imaging devices for various space missions, describing monochromatic and multicolor cameras, IR radiometer, multispectral scanner and imaging photopolarimeter 02 p0170 A73-12339

Effects of proton irradiation on several spacecraft science components. 05 p0596 A73-16513

Spaceborne IR systems cryogenic cooling, considering passive radiators and open or closed cycle cryogenic fluid systems 06 p0683 A73-18315

The selection and design of electro-optical instruments for outer planet exploration. 06 p0695 A73-18320

Prevention of damage to the science instruments of Mariner-Mars '71 spacecraft due to accidental viewing of the sun during sun-acquisition following exit from earth shadow. 06 p0696 A73-18829

Spacecraft-borne optical components and systems design and operational requirements, considering thin film filters and mirrors, detectors, diffraction gratings and materials 07 p0821 A73-18978

Atlas S183 spectrophotometer for Skylab orbital laboratory UV observations, discussing electrical, optical and mechanical interface problems 07 p0822 A73-19007

Crew station lighting - Commercial aircraft. [SAE ARP 1161] 08 p0925 A73-20692

Apollo alpha particle spectrometer design, operation, calibration, packaging and flight results 11 p1363 A73-25957

A SISAM interferometer and a simple Michelson-interferometer with spherical mirrors for space application. 11 p1369 A73-26519

Dual magnetometer systems with cross correlation signal enhancement to overcome intrinsic sensor ambient noise and spacecraft magnetic field fluctuation effects on single detection performance 12 p1468 A73-27002

Note on analysis of cryogenic suspensions for space vehicles. 12 p1524 A73-27633

Pioneer 10 spacecraft spin-scan imaging photopolarimetric optical system for Jupiter mapping 15 p1880 A73-32385

Apollo 15 and 16 lunar orbital X and gamma ray spectrometer for lunar surface composition and radioisotopes surveys, detailing experimental results 16 p2015 A73-33353

Electric corona assessment of Skylab spacecraft high voltage electrical/electronic equipment and instruments, considering operating temperature and environment contaminants effects 17 p2109 A73-35256

Radon emanation from the moon - Spatial and temporal variability. 18 p2349 A73-36033

Verification of performance of the Mariner 9 television cameras. 19 p2428 A73-37258

Data collection platforms, ground receiving and processing equipment for environmental study and management 20 p2520 A73-38583

[AAS PAPER 73-122]
Comments on paper by N. F. Ness, K. W. Behannon, R. P. Lepping, and K. H. Schatten, 'Use of two magnetometers for magnetic field measurements on a spacecraft.' 20 p2615 A73-38963

Spacecraft attitude gyro reference system and readout accuracy, discussing strapdown guidance, electrical suspension, instrument errors, spin and damping coils and degrees of freedom 21 p2733 A73-40026

Mariner Mars 1969 infrared spectrometer - Gas delivery system and Joule-Thomson cryostat. 21 p2702 A73-41101

Russian book on gyroscope theory covering maritime, aircraft, rocket and spacecraft applications, instrument error, differential equations of motion, rotor precession and degrees of freedom 21 p2705 A73-41437

Comparison of temperature sensors for space instrumentation. 22 p2859 A73-42064

Fluidic bolometer type sensor for reaction wheel control to maintain spacecraft and rocket vehicle attitude relative to sun, discussing design, simulation and tests 23 p3038 A73-43395

SPACECRAFT LANDING

NT LUNAR LANDING
NT MARS LANDING
NT PLANETARY LANDING
Sighting methods during flights from the moon to the earth
18 p2351 A73-36107

SPACECRAFT LAUNCHING

Computerized operational simulation for space shuttle program in terms of flight units, launch rate, success probabilities and costs
03 p0381 A73-13298

The optical temperature of the Apollo 15 exhaust plume.
[AD-757298] 03 p0358 A73-13497

Computer application for management of Skylab launch operations.
[AIAA PAPER 72-1083] 04 p0424 A73-14905

European space conference, discussing space program priorities relative to applications or research satellites, communication satellites, launch vehicles and facilities and participation in post-Apollo program
04 p0523 A73-15151

L 17 satellite booster development from Emeraude stage, discussing gas generator, Valois thruster engine and assembly tests, combustion instability and launching results
07 p0905 A73-18990

The utilization of detonating fuses on launchers.
07 p0865 A73-18996

Pitch amplitude stabilization in a spacecraft carrier body
09 p1155 A73-23107

SPACEWARN - An international mechanism for rapid distribution of information on satellites and space probes.
11 p1454 A73-25569

AEROS satellite launching from Western Test Range, describing time sequence of satellite and rocket countdowns and communication system activities coordinated by project management
13 p1689 A73-28781

Present and future plans for the development of Sriharikota satellite launching range.
14 p1741 A73-30081

Definition, philosophy, and development of safety interventions in flight at the Guiana Space Center
14 p1804 A73-30096

Manufacturing, integration and launching phases of Diamant B launcher inspection, discussing automatic control and testing bench structure and safety
14 p1742 A73-30104

Satellite payloads preparation and launching methods in European space programs, evaluating firing range apparatus and firing range/satellite interfaces
14 p1804 A73-30106

Scientific and applications satellite launch site facilities, discussing payload preparation
14 p1742 A73-30109

Space missile test center development for checkout, launch and data processing for space boosters, intermediate and intercontinental range ballistic missiles and supersonic aircraft
16 p1993 A73-33087

Differential transformation for satellite injection.
16 p2070 A73-33999

Computerized processing system with real time control, data analysis and display capabilities for space shuttle checkout, servicing, launching and landing to reduce cost
[AIAA PAPER 73-601] 18 p2295 A73-36083

Computation of launch vehicle system requirements using hybrid computer.
18 p2360 A73-36838

Shuttle-Attached Manipulator System requirements.
19 p2491 A73-37307

Kennedy Space Center Space Shuttle facilities.
19 p2417 A73-37601

Spacecraft rendezvous in orbit, discussing launching, transfer maneuver, target location, approach phase, docking and mechanical coupling
19 p2487 A73-38302

Standardized space shuttle launched multipurpose spacecraft design using nuclear electric power systems with radioisotope thermoelectric generators or Brayton cycle alternators
19 p2455 A73-38393

Trajectory of a solar-electric propelled vehicle passing through the shadow cone of a celestial body
21 p2779 A73-41556

SPACECRAFT LUBRICATION

Spacecraft lubrication systems design for long mission lifetimes, discussing mechanical design parameters and liquid and solid lubricant characteristics
03 p0330 A73-13012

The evaporation of various lubricant fluids in vacuum.
[ASLE PREPRINT 72LC-6C-2] 03 p0335 A73-14366

SPACECRAFT MANEUVERS

NT MANEUVERABLE REENTRY BODIES
Optimal energetic characteristics of the parallel guidance method in satellite rendezvous
02 p0219 A73-12456

Iterative technique for the calculation of double-impulse spacecraft rendezvous maneuvers.
05 p0627 A73-16092

Control of a maneuver involving rotation of the plane of a circular satellite orbit while ensuring passage through a prescribed point
05 p0595 A73-16426

Optimal correction of a planetary-approach trajectory for transfer to an artificial-satellite orbit
05 p0616 A73-16428

Maneuvering engines for Space Shuttle Orbiter.
[SAE PAPER 720806] 05 p0607 A73-16646

Propulsion systems for orbital maneuvering stages.
[SAE PAPER 720843] 05 p0607 A73-16656

Maneuvering a tumbling dual-spin spacecraft - The recovery of OSO-7.
[AIAA PAPER 73-248] 05 p0630 A73-16971

Soft constraint trajectory optimization formulation as real time optimal feedback guidance method for multiburn orbital maneuvers
[AIAA PAPER 73-249] 05 p0596 A73-16972

Russian book - Mechanics of optimal spatial motion of flight vehicles in the atmosphere.
07 p0777 A73-20380

Complex natural vibrations of space vehicles performing a maneuver
10 p1285 A73-23876

Investigation of the dynamics of a rotation scheme of a spacecraft composed of two units
10 p1286 A73-23877

Quasi time-optimal spacecraft reorientation maneuvers using single gimbal control moment gyros /SG CMG's/.
12 p1548 A73-27153

Optimal descent maneuver with a limited-thrust engine for entry at a prescribed angle into the atmosphere of a planet
13 p1689 A73-29139

Spacecraft single-turn reorientation optimization with respect to fuel expenditure depending on maneuver duration and reaction control torque constraints
14 p1803 A73-29852

Time optimal propulsion system parameters for thrust vector control during spacecraft maneuver performance
14 p1772 A73-29855

Energy optimal four impulse transfer maneuver with return between two moving points in circular coplanar orbits under transit time and stay duration constraints
15 p1931 A73-31230

Spacecraft reorientation by successive rotations about nonorthogonal axes, deriving classical Euler angles as special case of general solution
15 p1908 A73-31662

Optimum energetic characteristics of the parallel-guidance method of bringing satellites into proximity.
15 p1941 A73-32606

Realization of a geostationary orbit by means of an electromagnetic propulsion system /quasi-steady MPD/
17 p2239 A73-34954

Rapid estimation and detection of impulse inputs under continuity constraints for space vehicles.
17 p2144 A73-35375

The path independence of orbit inclination momentum.
17 p2234 A73-35661

Complex self-excited vibrations of space vehicles during maneuver.
20 p2614 A73-38895

Dynamics of a twisting mode for a two-section space vehicle.
20 p2614 A73-38896

Determination of disturbances acting on a space vehicle from the liquid-disposal nozzle
21 p2781 A73-41199

Synthesis of programmed extensive control of a spatial turning maneuver
23 p3005 A73-43718

SPACECRAFT MODELS

Design and construction of a reverberation chamber for high-intensity acoustic testing.
16 p1998 A73-33677

Experimental evaluation of a roll control system for a shrouded cone.
17 p2239 A73-35500

Angle of attack tests for graphite ablation models simulating spacecraft reentry using arc heating, showing temperature and pressure effects, model size and flow field characteristics
[AIAA PAPER 73-736] 18 p2295 A73-36353

System for calibrating on-board instruments and for laboratory simulation of low-density plasma flows past models
19 p2417 A73-37351

SPACECRAFT MODULES

NT LUNAR MODULE
Earth resources exploration with a sortie laboratory within the framework of the Post-Apollo Program /PAP/
[DGLR PAPER 72-080] 02 p0227 A73-11677

Research and applications modules /RAM/ program for manned space research satellites transportation

and support, discussing mission requirements and design concepts
[AIAA PAPER 73-72] 06 p0755 A73-17637

Design of low-cost, refurbishable spacecraft for use with the Shuttle.
[AIAA PAPER 73-73] 06 p0756 A73-17638

Modular space station operation as general purpose laboratory with attached or free flying R and D modules for specific projects
09 p1152 A73-22325

Electrical Power Subsystem definition for shuttle launched modular space station.
09 p1153 A73-22781

A solar array and battery electrical power subsystem for the shuttle-launched modular space station.
09 p1153 A73-22783

A modular Space Station/Base electrical power system - Requirements and design study.
11 p1311 A73-26015

Lower payload costs through refurbishment and module replacement.
14 p1803 A73-29944

SPACECRAFT MOTION

Dynamical interaction in biaxial control systems.
01 p0075 A73-11198

Oscillations of spacecraft with on-off attitude control under constant perturbation moment, calculating energy expenditures for desired orientation maintenance
03 p0383 A73-14559

Pulsed motion of gravity gradient vehicle in central gravity field, presenting expressions of optimized attitude control
03 p0383 A73-14573

Spacecraft oscillatory motion as function of attitude control impulse magnitude
05 p0627 A73-16080

Analysis of the effect of errors in determining the orbit parameters of a satellite on the accuracy of prediction of its motion
05 p0614 A73-16312

Motion of a body of variable mass in a many-body gravitational field near collision
05 p0615 A73-16326

A quasi-inertial attitude mode for orbiting spacecraft.
05 p0630 A73-17203

Investigation of the dynamics of a rotation scheme of a spacecraft composed of two units
10 p1286 A73-23877

Phase double plane as a method to study the dynamics of a spacecraft with limited constructional rigidity.
10 p1286 A73-24006

Unsteady three-dimensional motion of a flight vehicle during hypersonic reentry in the atmosphere
10 p1286 A73-24304

Correction of a spacecraft with a static corrective thruster chamber
11 p1431 A73-26465

Nutation dampers vs precession dampers for asymmetric spinning spacecraft.
11 p1432 A73-26670

Parameter estimation for a specular-diffusion reflection model from the motion of 'Proton' series satellites about their centers of mass
14 p1803 A73-29851

Spatial oscillations of a vehicle with a nonlinear stabilization system during reentry
14 p1803 A73-29853

Nonlinear two-dimensional oscillations of a satellite in an elliptic orbit
14 p1803 A73-29854

Russian book - Mechanics of controlled motion and problems of cosmic dynamics.
15 p1930 A73-31226

Dynamics of a twisting mode for a two-section space vehicle.
20 p2614 A73-38896

Coupled bending-twisting vibrations of a single boom flexible solar array and spacecraft.
21 p2781 A73-40619

Optimal motions of a spacecraft relative to its center of mass
21 p2781 A73-40903

Interference parameters in the problem of estimating the accuracy of prediction of spacecraft motion
21 p2781 A73-40904

Perturbation of ion density by a body moving through the ionosphere.
23 p3008 A73-43254

SPACECRAFT ORBITAL ASSEMBLY

U ORBITAL ASSEMBLY
SPACECRAFT ORBITS

NT INTERPLANETARY TRANSFER ORBITS
NT POLAR ORBITS
NT SATELLITE ORBITS
NT STATIONARY ORBITS
NT TRANSFER ORBITS
NT TROJAN ORBITS
NT TWENTY-FOUR HOUR ORBITS

Gravity thrust Jupiter orbiter trajectories generated by encountering the Galilean satellites.
01 p0095 A73-10103

SPACECRAFT PERFORMANCE

Space stations and shuttle vehicles design and placement in earth orbit, reviewing life support, energy production and data transmission systems
01 p0096 A73-10300

Guidance of spacecraft controlled by low-thrust rocket engines and evolving in the plane of the initial trajectory
02 p0227 A73-11580

Data processing method for optimal prediction of spacecraft orbital elements, using dynamic and quadratic programming
03 p0379 A73-14555

Analysis of the orbit of Cosmos 268 rocket /1969-20B/.
04 p0496 A73-14964

Air density at heights near 200 km from the orbit of 1969-20B.
04 p0440 A73-14965

Analytical approach to orbit determination in the presence of model errors.
[AIAA PAPER 73-170]
05 p0619 A73-16915

The effect of direct solar radiation on the attitude of the SKYNET spacecraft.
11 p1431 A73-26261

Differential coefficient computation for spacecraft orbital velocity component variations in case of universal elements utilization for orbit improvement problems
12 p1538 A73-26864

Spacecraft local vertical estimation and error limits in meridional and equatorial planes based on terrestrial IR radiation measuring instruments
12 p1543 A73-27630

Dynamic characteristics, stability and steady state accuracy for orbital gyroscope with digital control, noting bit density requirements of onboard computer
12 p1523 A73-27632

Scientific exploration with an out-of-ecliptic spacecraft.
19 p2485 A73-37760

Spacecraft rendezvous in orbit, discussing launching, transfer maneuver, target location, approach phase, docking and mechanical coupling
19 p2487 A73-38302

The design of a two wheel momentum bias system for the attitude control of spacecraft in low altitude orbits.
[AIAA PAPER 73-855]
20 p2585 A73-38793

Optimal navigation function for spacecraft orbit defined by initial conditions and acting force constants, determining matrix minimizing variance estimate
23 p3005 A73-43270

SPACECRAFT PERFORMANCE

Simulation program for satellite operation status prediction in space environment.
01 p0110 A73-11146

A computerized technique for mission profile design analysis.
[AIAA PAPER 73-114]
05 p0629 A73-16872

Prospero satellite orbital/operational performance and control, describing ground-satellite telemetry and data processing operations
07 p0905 A73-19142

Short guide to Titan III launch vehicles.
08 p1014 A73-20800

Apollo 16 lunar mission results, discussing lunar geology, spacecraft operational procedures and hardware
09 p1152 A73-22186

Aeros meteorological research satellite for F region aeronomic parameters and solar UV radiation measurements, discussing performance since launch
11 p1430 A73-25442

ESRO TD-1A satellite signal hibernation in sky-scanning experiments after successful performance during first orbital life, noting tape recorder failure
11 p1431 A73-25750

AEROS research satellite acquisition phase performance, considering injection, attitude determination and control, trajectory measurement and correction, nutation reduction, solar alignment, etc
13 p1689 A73-28782

Technology requirements for ballistic mode Mercury orbiter mission, discussing performance potential with Venus gravity assist and conventional spacecraft propulsion techniques
[AIAA PAPER 73-581]
18 p2350 A73-36073

Apollo Lunar Module environmental control system - Mission performance and experience.
[ASME PAPER 73-ENAS-28]
19 p2400 A73-37983

SPACECRAFT POSITION INDICATORS

Matrix transformations for spacecraft attitude determination.
02 p0228 A73-11905

Selection of the measurement frequency in the determination of satellite orientation
05 p0630 A73-17007

The selection of measurable parameters in the determination of the trajectory of a space vehicle.
12 p1543 A73-27626

Spacecraft local vertical estimation and error limits in meridional and equatorial planes based on terrestrial IR radiation measuring instruments
12 p1543 A73-27630

An integrated-circuit solar aspect sensor for spacecraft use.
16 p2013 A73-32884

SPACECRAFT POWER SUPPLIES

Power control unit for the scientific satellite.
01 p0111 A73-11165

Electrical power source for spacecraft reentry trajectory control system, thermal protection and radio communication based on reentry vehicle external surfaces utilization as generator electrodes.
01 p0111 A73-11174

Experimental satellite for attitude control. V - Attitude control electronics.
01 p0112 A73-11192

Solar cell generator design for Helios solar probe, considering thermal stresses at sun proximity and sufficient power generating capacity at orbital apogee [DGLR PAPER 72-091]
02 p0131 A73-11663

A versatile silver oxide-zinc battery for synchronous orbit and planetary missions.
02 p0133 A73-12622

Design point characteristics of a 500 - 2500 watt isotope-Brayton power system.
[AIAA PAPER 72-1059]
03 p0252 A73-13388

Nuclear rocket engine reactor utilization as energy center for propulsion, attitude control, refrigeration and scientific experiments, emphasizing dual mode electrical power generation
[AIAA PAPER 72-1091]
03 p0340 A73-13412

A sequenced PWM controlled power conditioning unit for a regulated bus satellite power system.
03 p0252 A73-13930

Electric power processing, distribution and control for advanced aerospace vehicles.
03 p0253 A73-13947

Performance test of flexible rolled-up solar array /FRUSA/ via telemetered data from accelerometers, strain gages and temperature sensors, noting feasibility for spacecraft power supply
03 p0256 A73-14236

Flexible circular solar array for power to weight ratio increase at satellite outer surface, noting central supported structure superiority
03 p0257 A73-14239

Analog signal to discrete time interval converter /ASDTIC/ feedback control for high performance aerospace power supply conditioning
[AIAA PAPER 72-1057]
04 p0486 A73-14901

Advanced aerospace power distribution and control techniques.
04 p0408 A73-15389

The liquid metal slip ring experiment for the Communications Technology Satellite.
04 p0408 A73-15449

Russian book - Power systems of spacecraft.
04 p0408 A73-15704

Storable fueled power system for Space Shuttle.
[SAE PAPER 720836]
05 p0537 A73-16632

German book - New energy systems for space flight.
06 p0741 A73-17668

Solar generator technology on the Symbionic satellite.
07 p0778 A73-18976

Physical and thermal constraints on batteries of electrochemical power supply systems onboard satellites, sounding and booster rockets and balloons
07 p0778 A73-18977

Isotope Brayton space power systems and their technology.
07 p0850 A73-20467

Characteristics, design and performance of power sources in auxiliary systems for spacecraft applications, noting long term standby under environmental conditions
[SAE AIR 744 A]
08 p0928 A73-20690

Solar cell generator technology development based on German AEROS satellite project and work on roll-up structure, discussing module concepts and test results
09 p1033 A73-22439

Communications, despin control, electrical power, telemetry and command, positioning and orientation subsystems of Intelsat 4 satellite
09 p1152 A73-22698

A nickel-hydrogen secondary cell for synchronous orbit application.
09 p1033 A73-22753

Spacecraft Ni-Cd battery cycle life performance tests, noting cycle life-cycle duration relationship
09 p1034 A73-22755

High energy density long life Ni-Cd battery systems for synchronous satellites, discussing radiation protection, charge and discharge control electronics and temperature control
09 p1034 A73-22756

Silicon-germanium technology program of the Jet Propulsion Laboratory.
09 p1117 A73-22759

Radioisotope thermoelectric converter for Navy TRANSIT navigational satellite 5 year power supply, describing design and performance test data
09 p1034 A73-22767

Summary of gas bearing applications in the field of space electric power systems.
09 p1089 A73-22771

Fuel cell for Apollo command and service module power supply, discussing voltage-power requirements and operating temperature control
09 p1035 A73-22774

An approach to performance assessment and management of a large solar array/battery power system.
09 p1035 A73-22775

Space shuttle orbiter electrical power system requirements and constraints, considering hydrogen/oxygen fuel cell for compact energy storage and turbine driven generators
09 p1153 A73-22776

Hydrogen-oxygen fuel cell as reliable electric power supply for space shuttle mission requirements, assessing technological developments
09 p1035 A73-22777

Auxiliary power units and their application to the space shuttle.
09 p1153 A73-22778

Open cycle hydrogen-oxygen turbine driven generator system for space shuttle auxiliary power supply, discussing components, control mode and performance potential
09 p1153 A73-22779

Large solar array photovoltaic power systems for manned orbital space stations, discussing technology evaluation and design feasibility studies
09 p1153 A73-22780

Electrical Power Subsystem definition for shuttle launched modular space station.
09 p1153 A73-22781

Configuration survey of lightweight solar array power systems for future missions.
09 p1153 A73-22782

A solar array and battery electrical power subsystem for the shuttle-launched modular space station.
09 p1153 A73-22783

Space station solar array-energy storage-power control and distribution system based on regenerative fuel cell integrated with life support system
09 p1153 A73-22784

Spacecraft dynamic solar electric power/thermal control system with cold liquid flow and regenerator cooling for energy conversion efficiency and weight characteristics improvements
09 p1153 A73-22785

Intelsat 3 power system design and orbital performance, discussing solar arrays, cell bypass, output, conversion efficiency, regulation, reliability and testing
09 p1153 A73-22787

Intelsat 4 power subsystem with solar panels, Ni-Cd batteries, controller and relays for bus paralleling, discussing spacecraft and system configurations and performance
09 p1154 A73-22788

Electrical power subsystem for the Synchronous Meteorological Satellite /SMS/.
09 p1154 A73-22789

The flexible solar array - A spacecraft electrical power source technology option.
09 p1154 A73-22790

The Solar Collector Thermal Power System - Its potential and development status.
09 p1035 A73-22792

Concepts for application of 500- to 2500-W Brayton power systems for shuttle-launched missions.
09 p1154 A73-22794

Radioisotope thermoelectric generators for Nimbus 3 weather satellite, Pioneer 10 Jupiter probe and SNAP 27 powered ALSEP station missions, summarizing operational experience
09 p1154 A73-22795

Navy transit RTG safety and test integration from users viewpoint.
09 p1118 A73-22796

The modeling and design optimization of a space-oriented thermoelectric power supply.
09 p1118 A73-22797

Thermionic reactor power systems design for spacecraft auxiliary power supply and electrical propulsion, discussing performance and design guidelines for various applications
09 p1118 A73-22798

Spacecraft nuclear power source optimization, considering radioisotope and reactor heat sources, cryogenic cooler cycle types and spacecraft design
09 p1118 A73-22799

Viking Orbiter power subsystem performance prediction computer program simulating solar array, battery charge controls, zener diodes and power conditioning equipment characteristics and interactions
09 p1060 A73-22802

Shuttle Orbiter fuel cell power system simulation, describing data management, programming and computational control
09 p1060 A73-22804

Modularised power conditioning units for high power satellite applications.
09 p1035 A73-22806

The determination and treatment of temperature coefficients of silicon solar cells for interplanetary spacecraft application.

09 p1036 A73-22810

UK5 X ray astronomy satellite, discussing structural design, attitude sensing for pointing control, data handling, attitude control and power supply systems

09 p1155 A73-22920

Recent technology advances in the NASA-Lewis Research Center Brayton program.

09 p1037 A73-23249

Five year lifetime space radioisotope thermoelectric generator with lead telluride panels and plutonium 238 dioxide heat source, analyzing reliability, design and performance

09 p1038 A73-23284

Operational safety experience and advances of space nuclear power systems fueled with Pu-238, discussing modular heat sources

09 p1119 A73-23287

The optimization of nuclear reactor energy supply installations with turbogenerators

11 p1395 A73-25352

Review of liquid-metal magnetohydrodynamic spacecraft energy conversion cycles.

11 p1308 A73-25977

Brayton cycle solar dynamic turboalternator space electric power system technology developments during 1962-1972, considering power efficiency, components reliability and future missions

11 p1309 A73-25982

An electrochemical cell equivalent circuit for storage battery/power system calculations by digital computer.

11 p1309 A73-25985

Solar cell battery operational performance test equipment and computerized simulation programs for post-1975 satellite and space station systems integration and design

11 p1309 A73-25986

Experimental evaluation of the single-cell concept for a lightweight, rechargeable hydrogen-oxygen fuel cell.

11 p1309 A73-25987

Heat pipe thermal control of spacecraft batteries.

11 p1309 A73-25992

Study of fuel cell thermal control systems for advanced missions.

11 p1309 A73-25993

Co-60 kernel modular power and reentry system design for space station and base, noting fuel and launch cost savings over Pu-238 systems

11 p1310 A73-25998

Concept for a high voltage solar array with integral power conditioning.

11 p1310 A73-26001

Development of a deployable and selfrigidizing solar cell array for the multikilowatt range.

11 p1310 A73-26002

Alkali metal purification and handling for advanced space power systems.

11 p1310 A73-26004

A 6 kW organic Rankine power conversion system for space applications.

11 p1310 A73-26006

Solar/battery space station power plants combined with nuclear configurations, discussing rectified alternator current, direct energy transfer, and high voltage dc sources

11 p1311 A73-26008

An integrated system for space station power, life support, and propulsion.

11 p1311 A73-26009

A 25 kW solar array/battery design for an earth-orbiting space station.

11 p1311 A73-26010

ZrH space power reactors design, discussing long life fuel elements, high temperature hard vacuum irradiation environment control drive components and shield fabrication

11 p1395 A73-26011

A modular Space Station/Base electrical power system - Requirements and design study.

11 p1311 A73-26015

Design criteria and candidate electrical power systems for a reusable Space Shuttle booster.

11 p1311 A73-26016

Space shuttle orbiter power system requirements and design tradeoffs, comparing fuel cells, solar array/battery and radioisotope Brayton cycle and cryogenic fueled turboalternators

11 p1312 A73-26017

An isotope heat source integrated with a 7 kW/e/ to 25 kW/e/ Brayton cycle space power supply.

11 p1312 A73-26019

Design and performance of the TACSAT power subsystem.

11 p1312 A73-26020

Unmanned interplanetary spacecraft power systems with nickel-cadmium batteries, solar panels or radioisotope thermoelectric generators

11 p1312 A73-26022

Power system for a 4.1 kilowatt synchronous satellite.

11 p1312 A73-26023

In-core 100 kW thermionic power system design to meet manned spacecraft shielding requirements, discussing waste heat removal and integration with space base

11 p1395 A73-26026

Multi-Hundred Watt converter design considerations.

11 p1396 A73-26029

TRANSIT radioisotope thermoelectric generator technology, discussing structural design, thermal efficiency, performance prediction, panel configurations and life test data

11 p1312 A73-26034

Performance of the thermoelectric converter for the zirconium hydride reactor thermoelectric space power supply.

11 p1396 A73-26036

The SNAP-19 radioisotopic thermoelectric generator experiment - Flight performance on the Nimbus III observatory.

11 p1396 A73-26037

Preliminary testing of a SNAP-19 TAGS RTG in support of the Pioneer F and G missions.

11 p1396 A73-26039

Low altitude orbit feasibility study of integrated SNAP 29/Agenda satellite configuration, comparing with solar cell power system

11 p1396 A73-26040

Five-year lifetime thirty-watt radioisotope thermoelectric generator for NAVY Transit Navigational Satellite, discussing system design, major components, reliability and performance tests

11 p1397 A73-26041

Solar independent power source with radioisotope thermoelectric generator for Grand Tour missions, discussing radiation and thermal interfaces

11 p1313 A73-26042

Power supply requirements during the AEROS acquisition phase.

13 p1689 A73-28784

OA0 2 satellite nickel-cadmium batteries with auxiliary electrodes for overcharge control, discussing operation and degradation mechanism

13 p1572 A73-29583

Nickel-cadmium cells for low earth orbit applications.

13 p1572 A73-29584

Sealed silver oxide zinc cells for orbiting and planetary missions.

13 p1572 A73-29586

Historical development of solar cells.

13 p1573 A73-29590

Solar array cost reductions.

13 p1573 A73-29592

Large area silicon solar array development.

13 p1573 A73-29593

Research plans for solar power in space.

13 p1573 A73-29594

Solar energy conversion development relative to Department of Defense space power requirements.

13 p1573 A73-29595

Long-life light weight reliable fuel cell development for long term space missions power supplies, describing system components and construction materials

13 p1573 A73-29596

Theoretical and practical design aspects on spacecraft propellant and pressurant loading systems.

14 p1742 A73-30107

Book on aerospace propulsion covering nozzle, combustors and diffusers flow, space power generation, electrothermal engines, chemical rockets and central force fields

14 p1785 A73-30361

Regional and international communication satellite systems, discussing frequencies assignment, power supplies, three axis stabilization trends and military, navigation and TV developments

17 p2125 A73-35478

[DGLR PAPER 73-039]

A regenerative fuel cell system for modular space station integrated electrical power.

19 p2390 A73-38402

The multi-hundred watt RTG - Technology background and flight systems program.

19 p2456 A73-38418

The MHW heat source - An advance in radioisotope heat source technology for space applications.

19 p2456 A73-38420

Multihundred watt radioactive isotope heat source assembly for multiple space missions, discussing aerodynamic heating, shield ablation and thermal stress performance during reentry

19 p2456 A73-38426

Design of a nuclear isotope heat source assembly for a spaceborne mini-Brayton power module.

19 p2457 A73-38431

Low cost modular power systems for multi mission earth observations.

19 p2494 A73-38435

H2-O2 auxiliary power unit for Space Shuttle vehicles - A progress report. [IECEC PAPER 73-9028]

19 p2392 A73-38436

Fuel capsule vent system development for the Viking radioisotope thermoelectric generator.

21 p2737 A73-40766

Power Electronics Specialists Conference, California Institute of Technology, Pasadena, Calif., June 11-13, 1973, Record.

22 p2801 A73-42901

A failure tolerant power subsystem for outer planet spacecraft.

22 p2801 A73-42902

Power subsystem for Skylab radiometer/scatterometer/altimeter experiment.

22 p2801 A73-42903

Flight performance of the ERTS-1 spacecraft power system.

22 p2801 A73-42904

High-efficiency converter and battery charger for an RTG power source.

22 p2801 A73-42906

Bilateral power conditioner with common filters and transistor control circuits for battery charge and discharge functions onboard near earth orbit spacecraft

22 p2802 A73-42916

SPACECRAFT PRELAUNCH TESTS

U SPACE VEHICLE CHECKOUT PROGRAM

SPACECRAFT PROPULSION

NT ELECTROMAGNETIC PROPULSION

NT ELECTROSTATIC PROPULSION

NT ION PROPULSION

NT PHOTONIC PROPULSION

NT PLASMA PROPULSION

NT SOLAR PROPULSION

Unmanned planetary spacecraft chemical rocket propulsion.

01 p0090 A73-10102

Synerjet composite rocket-air breathing propulsion system for reusable spacecraft mission profile optimization, discussing multimode operation and performance capabilities

01 p0112 A73-11300

Development and qualification results of the monergolic propulsion system for the aeronomy satellite Aeras

02 p0228 A73-11696

Technology assessment of nuclear rocket engines based on solid core reactors for space propulsion

02 p0191 A73-11995

Extraterrestrial propellant resupply for advanced manned missions.

02 p0221 A73-12599

Prospects for rocket propulsion with laser-induced fusion microexplosions.

03 p0353 A73-13392

Development of a radioisotope-fueled thruster for satellite propulsion.

03 p0354 A73-13395

Unmanned outer planets and round trip mission nuclear rocket engine design for carrying payload into orbit by single earth orbital shuttle

03 p0340 A73-13411

Dual mode applications of nuclear rocket engine for spacecraft propulsion and electrical power generation, considering payloads and missions competitiveness with nonuclear system

03 p0341 A73-13413

Optimization of ion propulsion for north-south stationkeeping of communications satellites.

03 p0356 A73-13454

Solar escape achievement by solid propulsion augmentation system and design independent of multiplanetary swingby, analyzing cost effectiveness of different programs

03 p0382 A73-13464

Engine concepts for space applications.

03 p0360 A73-14475

Spacecraft low thrust propulsion systems applications to earth orbital and planetary missions, discussing payload capabilities vs flight time

04 p0486 A73-14911

Solar electric propulsion for payloads earth orbit injection, discussing communication satellites and space shuttle/tug system applications

04 p0486 A73-14912

Experimental evolution of an earth-storable bimodal rocket engine.

04 p0486 A73-14913

An operational satellite propulsion system providing for vernier velocity, high and low level attitude control and spin trim.

04 p0486 A73-14916

Hydrogen oxygen propulsion component design and hot firing tests for space shuttle auxiliary systems and upper stage applications

04 p0486 A73-14918

[AIAA PAPER 72-1156]

Electrodynamic sailing - Beating into the solar wind.

04 p0487 A73-15073

Estimation of unmodeled forces on a low-thrust space vehicle.

04 p0504 A73-15272

The RIT engine family. - From microthruster to main propulsion units.

04 p0488 A73-15716

Electrostatic ion thrusters of the DFVLR Braunschweig for primary propulsion.

04 p0488 A73-15717

SPACECRAFT RADIATORS

Quasi-steady MPD thruster research at Rome University. 04 p0489 A73-15730

Contribution to the analysis and conception of satellite stabilization systems based on ion propulsion 04 p0505 A73-15737

ESKA ion thrusters - Development and application for geocentric missions. 04 p0489 A73-15739

Hydrogen resistojets for primary propulsion of communications satellites. 04 p0489 A73-15741

Optimal control problems of spacecraft mass minimization and nuclear power engine operation under uncontrollable perturbations due to errors and external field interactions 05 p0596 A73-16414

Maintainability of the Space Shuttle Orbiter main engine. [SAE PAPER 720808] 05 p0606 A73-16642

Space Shuttle Orbiter main engine design. [SAE PAPER 720807] 05 p0607 A73-16644

Maneuvering engines for Space Shuttle Orbiter. [SAE PAPER 720806] 05 p0607 A73-16646

Propulsion systems for orbital maneuvering stages. [SAE PAPER 720843] 05 p0607 A73-16656

Optimal control of a combined propulsion system of a rotating spacecraft 05 p0630 A73-17003

Comparison of advanced propulsion concepts for deep space exploration. 05 p0608 A73-17201

Planetary exploration with electrically propelled vehicles. 06 p0750 A73-18021

Nuclear pulse propulsion system for interplanetary space flight, describing operational principles and design concepts 06 p0722 A73-18022

Book - French space technology. Volumes 1 and 2. 07 p0904 A73-18901

Propulsion system for space applications, based on the catalytic decomposition of hydrazine 07 p0866 A73-18929

Monopropellant and bipropellant thruster systems with afterburning for geostationary satellite orbital control, evaluating performance and reliability based on calculation and test data 07 p0866 A73-18930

Space propulsion future assessment, discussing space shuttle and tug, NERVA project and electric and photon propulsion 10 p1262 A73-23611

Magnetic intake limitations on interstellar ramjets. 10 p1262 A73-24539

Reaction equilibrium and energy balance in thermonuclear fusion propulsion for interstellar space flight, discussing nuclear fuel and ion temperature effects 10 p1262 A73-24544

An integrated system for space station power, life support, and propulsion. 11 p1311 A73-26009

Thermionic reactor systems for electric propulsion. 11 p1395 A73-26025

The feasibility of geostationary emplacement of satellites by solar electric tug. 11 p1431 A73-26260

Certain considerations concerning a magnetoplasma-dynamic flux in the one-dimensional hypothesis 12 p1527 A73-27061

Time optimal propulsion system parameters for thrust vector control during spacecraft maneuver performance 14 p1772 A73-29855

Space shuttle orbiter system planning and operational modes, considering propulsion into orbit, automated observatories, sortie workshop and European cooperation 14 p1803 A73-29943

Book on aerospace propulsion covering nozzle, combustors and diffusers flow, space power generation, electrothermal engines, chemical rockets and central force fields 14 p1785 A73-30361

Battery-powered electric propulsion for north-south stationkeeping. 17 p2222 A73-34872

Superrelativistic interstellar flight or cracks in the light barrier. 17 p2234 A73-35658

Evolution of the Space Shuttle. II. 17 p2240 A73-35660

Technology requirements for ballistic mode Mercury orbiter mission, discussing performance potential with Venus gravity assist and conventional spacecraft propulsion techniques [AIAA PAPER 73-581] 18 p2350 A73-36073

Space Shuttle in space lab operations, propulsion stage retrieval/delivery, satellite servicing, passenger transportation and short duration orbital missions 19 p2492 A73-37603

Test stand for the propulsion systems of the 'Symphonie' communications satellite in vacuum 19 p2419 A73-38271

Multi-mission nuclear electric propulsion stage design. 19 p2457 A73-38433

Development costs for a nuclear electric propulsion stage. 19 p2458 A73-38434

German book on rocket propulsion theory covering orbital mechanics, equations of motion, performance parameters and nuclear, electric and chemical propulsion types 22 p2909 A73-42493

SPACECRAFT RADIATORS

Space simulation chamber tests of thermal lower model for spacecraft temperature control 01 p0110 A73-11150

Russian book on space flight radiative heat transfer problems covering spacecraft thermal conditions, solar and planetary heat flux, radiant cooling and vacuum tests 09 p1166 A73-22348

Development of a cryogenic heat pipe radiator for a detector cooling system. [ASME PAPER 73-ENAS-47] 19 p2493 A73-37994

SPACECRAFT RECOVERY

Sounding rocket payload recovery systems [ONERA, TP NO. 1153] 08 p1014 A73-21681

Recovery objectives - Review of the most interesting aspects of problems related to this technique 14 p1804 A73-30087

Diver lockout submarine Shelf Diver evaluation for missile recovery use, noting design and navigation systems 14 p1742 A73-30089

Free flying teleoperator spacecraft systems for automated satellites retrieval, cargo transfer and orbital operations support 19 p2490 A73-37303

Shuttle-Attached Manipulator System requirements. 19 p2491 A73-37307

Space Shuttle solid rocket stage recovery, retrieval, and refurbishment. 19 p2492 A73-37599

Kennedy Space Center Space Shuttle facilities. 19 p2417 A73-37601

Possibility of using the Space Tug for the recovery and maintenance of satellites 21 p2782 A73-41554

SPACECRAFT REENTRY

Minimization of spacecraft maximum acceleration in atmosphere after reentry, applying results to reentry trajectory optimization and associated optimal control problems 02 p0219 A73-12457

Prediction in control of re-entry into the atmosphere. 05 p0627 A73-16076

Synthesis of a nonlinear control law for the motion of a space vehicle in the earth's atmosphere. 05 p0627 A73-16077

Analytical estimate of the landing range of a spacecraft for hyperbolic return-flight paths. 05 p0627 A73-16078

Investigation of the range interval of the landing phase for hyperbolic velocities of re-entry into the earth's atmosphere. 05 p0627 A73-16079

Tibero rocket launched Electre nose cones reentry impact safety optimization policy based on probabilistic viewpoint [ONERA, TP NO. 1152] 08 p1014 A73-21679

Radio-guidance algorithms applied to the control of spacecrafts descending in the earth's atmosphere 10 p1247 A73-23880

Optimal entry algorithm and multipulse correction times for spacecraft guidance trajectory of minimum fuel consumption 10 p1247 A73-23881

Co-60 kernel modular power and reentry system design for space station and base, noting fuel and launch cost savings over Pu-238 systems 11 p1310 A73-25998

An algorithm for controlling the descent of a spacecraft from an artificial earth satellite orbit. 12 p1543 A73-27631

Electre nose cones reentry impact safety policy, discussing launcher trajectory, cost and performance indices and ascent optimization 14 p1804 A73-30097

Minimization of spacecraft maximum acceleration in atmosphere after reentry, applying results to reentry trajectory optimization and associated optimal control problems 15 p1941 A73-32607

Algorithms for radio guidance with application to control of landing of spacecraft in the earth's atmosphere. 20 p2590 A73-38899

Optimal entry algorithm and multipulse correction times for spacecraft guidance trajectory at minimum fuel consumption 20 p2590 A73-38900

SPACECRAFT RELIABILITY

Apollo program predictive testing for man machine and environmental capabilities in terms of engineering, qualification, manufacturing, maintenance and training aspects 04 p0453 A73-14863

Transoceanic telephony via communication satellites, discussing satellite reliability and placement in synchronous orbit 06 p0663 A73-17577

Satellite electronic equipment reliability and quality control at preproject, project, fabrication and mission levels, noting electric welding quality specification 07 p0904 A73-18974

Vibration, radiation and thermal vacuum test procedures and facilities for evaluating spacecraft reliability during launching and in space environment 07 p0807 A73-18999

Figure of merit for fault-tolerant space computers. 10 p1192 A73-24870

Evaluation of columbium alloy thermal protection systems for space shuttle. [AIAA PAPER 73-378] 11 p1380 A73-25508

Design considerations for shuttle information management. 14 p1818 A73-29945

Analyses of flight model spacecraft performance during thermal-vacuum tests. 16 p2072 A73-33149

Testing of spacecraft in long-term storage. 16 p2073 A73-33615

Data sample analysis of anomalous in-flight behavior incidents for spacecraft reliability covering incident causes and occurrence time, effects on mission and corrective actions 16 p2073 A73-33625

The impact of launch vehicle reliability on the financial risks associated with multiple payload space functions. [AIAA PAPER 73-591] 18 p2358 A73-36079

Thermoelectric device application to spacecraft thermal control. [AIAA PAPER 73-722] 18 p2369 A73-36339

Availability, maintenance and cost of communication satellite systems. 20 p2613 A73-38768

Book - The role of testing in achieving aerospace systems effectiveness. 21 p2675 A73-41201

ing, qualification, manufacturing, maintenance and training aspects

Transoceanic telephony via communication satellites, discussing satellite reliability and placement in synchronous orbit

Satellite electronic equipment reliability and quality control at preproject, project, fabrication and mission levels, noting electric welding quality specification

Vibration, radiation and thermal vacuum test procedures and facilities for evaluating spacecraft reliability during launching and in space environment

Figure of merit for fault-tolerant space computers.

Evaluation of columbium alloy thermal protection systems for space shuttle.

Design considerations for shuttle information management.

Analyses of flight model spacecraft performance during thermal-vacuum tests.

Testing of spacecraft in long-term storage.

Data sample analysis of anomalous in-flight behavior incidents for spacecraft reliability covering incident causes and occurrence time, effects on mission and corrective actions

The impact of launch vehicle reliability on the financial risks associated with multiple payload space functions.

Thermoelectric device application to spacecraft thermal control.

Availability, maintenance and cost of communication satellite systems.

Book - The role of testing in achieving aerospace systems effectiveness.

SPACECRAFT RENDEZVOUS

U SPACE RENDEZVOUS

SPACECRAFT SENSORS

U SPACECRAFT INSTRUMENTS

SPACECRAFT SHIELDING

Materials and processes for thermal control surfaces. 03 p0329 A73-13009

Investigation of heatproof materials under unsteady operating conditions 11 p1450 A73-25730

In-core 100 kW thermionic power system design to meet manned spacecraft shielding requirements, discussing waste heat removal and integration with space base 11 p1395 A73-26026

Radiation doses during a prolonged orbital space flight about the earth 14 p1721 A73-29867

Impact gages for detecting meteoroid and other orbital debris impacts on space vehicles. 17 p2238 A73-34606

Spacecraft thermal control coatings development, discussing zinc orthotitanate/silicone properties as solar reflector [ASME PAPER 73-ENAS-7] 19 p2389 A73-37969

Effect of secondary emission of the potential of a metallic body in the electron radiation belts of the earth. 20 p2601 A73-38875

Skylab flight schedule emphasizing Command Service, Module, discussing meteoroid shield deployment difficulties and rescue team development of solar heat shield 21 p2767 A73-40415

SPACECRAFT STABILITY

Automatic impulse frequency stabilization of space vehicle rotation angle with respect to inertial coordinates by Liapunov discrete method 01 p0110 A73-10595

Orientation accuracy of the Symphonie communication antennas [DGLR PAPER 72-063] 02 p0140 A73-11684

Flexible satellite with three axisymmetrical bodies spinning at different rates about common axis of symmetry, deriving stability conditions based on Sturm theorem 02 p0228 A73-11997

Stability criteria for a free dual-spin satellite. 02 p0228 A73-12398

Multistep three-parameter algorithm for spacecraft stabilization on an atmospheric reentry trajectory 02 p0229 A73-12451

Communications satellite Symphonie stability during perigee-apogee transfer in terms of liquid filled spinning top nutation 03 p0381 A73-13295

On the stability of dual-spin bodies with unbalancing mass. 03 p0381 A73-13364

Constant and variable amplitude limit cycles in dual-spin spacecraft. 03 p0382 A73-13493

Analysis of the unbalances in spin-stabilized satellites 03 p0382 A73-13725

About the motion of a heavy flexible string attached to the satellite in the central field of attraction. 03 p0376 A73-14267

Gravitational stabilization systems parameters determination for minimum amplitude of satellite eccentric vibrations 03 p0383 A73-14557

Optimal efficiency of satellite passive nutation damper, noting system moment of inertia and flywheel axis relationship and viscous friction coefficient 03 p0383 A73-14558

Description of power conditioning systems intended for satellite stabilization thrusters 04 p0489 A73-15732

Contribution to the analysis and conception of satellite stabilization systems based on ion propulsion 04 p0505 A73-15737

A study of complex auto-oscillations of spacecraft 05 p0628 A73-16404

Dynamics of three-axis spacecraft orientation 05 p0628 A73-16405

Theory of a single-rotor gyro orbit of a satellite stabilized with respect to roll angle 05 p0628 A73-16408

Some problems of the optimal angular stabilization of an artificial earth satellite 05 p0628 A73-16413

Optimal control of extraatmospheric spacecraft motion stability by variable structure system with logic circuits 05 p0628 A73-16421

Spin stabilization of a satellite 05 p0629 A73-16422

Periodic attitude control of a slowly spinning spacecraft. [AIAA PAPER 73-246] 05 p0596 A73-16970

Application of a mathematical filter in the design of a spacecraft inertial stabilization system without a platform 05 p0630 A73-17005

Principle of operations and characteristics of electric propulsion devices - Application to satellite stabilization. I 05 p0608 A73-17193

An optimization technique for the transient response of passively stable satellites. 06 p0755 A73-17566

French Monograph - Contribution to the study of the stabilization of gyroscopic satellites - Conception and development of an active nutation damper. 06 p0757 A73-18097

Attitude dynamics of a three-axis stabilized satellite with a large flexible solar array. 06 p0757 A73-18379

Pneumatic torque generator subsystem of French D2 satellite, discussing engineering technical difficulties. 07 p0778 A73-18925

Geostationary satellites stabilization by microthrusters based on solid sublimation or hydrazine monopropellant, describing propulsion system development 07 p0866 A73-18926

French technology assessment on satellite stabilization by ion propulsion, stressing geostationary satellites orbit correction 07 p0904 A73-18934

Diademe satellite passive magnetic stabilization system, describing magnet and damper design 07 p0904 A73-18935

Eole satellite gravity gradient stabilized pointing control system, discussing implementation by eddy current, inertia and magnetic hysteresis devices 07 p0904 A73-18936

Magnetic articulation damping for gravity gradient satellite stabilization, using digital simulation 07 p0904 A73-18937

Work carried out by Societe Bertin under contract to CNES in the field of fluidic control 07 p0904 A73-18938

French satellites attitude stabilization and control systems, describing electronic sensor and servocontrol circuitry 07 p0904 A73-18967

The double gimbaled 'DRALLRAD' and its possible use for three-axis-stabilization of application satellites. 07 p0849 A73-19143

Operational principle and characteristics of electric propulsion systems. II - Application to satellite stabilization 07 p0906 A73-20247

Satellites elastic structures equations of state for stability and attitude control systems analysis, deriv-

ing translational and rotational momentum equations for moving coordinate systems 08 p1014 A73-20779

Axisymmetric hydroelastic sloshing in a circular cylindrical container. 08 p0956 A73-21690

Complex natural vibrations of space vehicles performing a maneuver 10 p1285 A73-23876

Spinning Skylab space station dynamics, investigating motion stability from simplified models with flexible appendages by digital simulation 10 p1286 A73-24003

Liapunov stability analysis and attitude response of a passively stabilized space system. 10 p1286 A73-24541

Liapunov stability analysis of spinning flexible spacecraft. 11 p1431 A73-26378

Small oscillations of gravity gradient satellite in circular near-equatorial orbit, discussing operational efficiency of magnetic damping systems 12 p1549 A73-27648

Stabilization of steady motions of mechanical systems with respect to some of the variables 13 p1660 A73-29076

European telephony traffic and Eurovision TV program exchanges via three-axis stabilized communications satellite with fold out solar panel arrays 14 p1724 A73-29715

Equilibrium configurations and attitude stability criteria for articulated satellite idealized as point-connected rigid two gyrostatt problem 14 p1802 A73-29757

Spatial oscillations of a vehicle with a nonlinear stabilization system during reentry 14 p1803 A73-29853

Satellite oscillation in circular orbit plane, determining gravitational stability in minimum time with least fuel consumption 14 p1803 A73-29868

Effects of flexibility on a momentum-stabilized communication-satellite attitude-control system. 15 p1942 A73-31099

Application of methods of mathematical statistics to study the motion of an artificial earth satellite about its center of mass 15 p1931 A73-31234

Existence of stable relative equilibria of an artificial satellite in a model magnetic field 15 p1872 A73-31956

The application of Kalman filtering to the attitude determination of spinning space vehicles. 15 p1944 A73-32219

Three-parameter multistep algorithms for stabilization of a spacecraft on the descent trajectory through the atmosphere. 15 p1944 A73-32601

Damping of gravity stabilized satellite small rotary oscillations in circular orbit via stepwise change of moment of inertia 16 p2072 A73-33232

Study of the frequency impulse system of spacecraft orientation control 18 p2359 A73-36102

Algorithm construction for the stabilization of a deformable spacecraft using an onboard digital computer 18 p2359 A73-36105

Precession rate matching for a space station in orbit about an oblate planet. 18 p2351 A73-36153

Dual and triple spin-stabilized deformable spacecraft attitude stability, comparing results based on Sturm theorem with Liapunov analysis 18 p2359 A73-36306

Attitude stability conditions of multiple spin satellites. 18 p2361 A73-36877

The precession of unsymmetric spin-stabilized satellites. 18 p2361 A73-36878

On stabilization of steady-state motions of mechanical systems with respect to a part of the variables. 19 p2459 A73-37631

Inertial symmetrization of large spin-stabilized spacecraft. [SAWE PAPER 965] 19 p2493 A73-37883

Assessment of fine stabilization problems for the LST. [AIAA PAPER 73-881] 20 p2587 A73-38817

Large orbiting telescopes fine guidance system for ultrahigh pointing stability based on disturbance accommodation standard deviation optimal controller design [AIAA PAPER 73-882] 20 p2588 A73-38818

Achieving ultrahigh accuracy with a body pointing CMG/RW control system. [AIAA PAPER 73-883] 20 p2588 A73-38819

Complex self-excited vibrations of space vehicles during maneuver. 20 p2614 A73-38895

Investigation of a stabilization system with a relay angular sensor 20 p2593 A73-39321

Determination of disturbances acting on a space vehicle from the liquid-disposal nozzle 21 p2781 A73-41199

Attitude stability conditions of multiple spin satellites. 22 p2916 A73-42189

Existence of stable relative equilibria for an artificial satellite in a model magnetic field. 24 p3081 A73-44481

SPACECRAFT STERILIZATION

Spacecraft decontamination and sterilization by formaldehyde, beta-propiolactone, ethylene oxide, radiation and dry heat, noting effects on polymers 14 p1721 A73-30137

Viking lander capsule decelerator system candidate materials evaluation, discussing in-situ testing for high density packing and heat sterilization effects on strength [AIAA PAPER 73-447] 15 p1881 A73-31433

Sterilization technology in the United States space program. 16 p1976 A73-33697

Monitoring for microbial flora contamination on spacecraft surface, discussing cultural techniques and sampling methods for microorganisms detection and sterilization 16 p1976 A73-33698

Ten years of development of the Planetary Quarantine Program of the United States. 18 p2281 A73-35966

Developments in the analysis of planetary quarantine requirements. 22 p2803 A73-42159

Spacecraft polyurethane foam jacket sterilization by gas method, discussing ethylene oxide and methyl bromide sorption and desorption 22 p2803 A73-42160

SPACECRAFT STRUCTURES

The structure of scientific satellites developed by the University of Tokyo. 01 p0110 A73-11119

Composite materials technology for aircraft and spacecraft structures, discussing various fiber-matrix combinations mechanical properties and production volume/price relations 05 p0589 A73-16759

A fracture control program for the reusable Space Shuttle booster. 06 p0764 A73-18493

French D2A satellite construction, describing AG5 sheet covering and gold coating fabrication methods 07 p0829 A73-18912

Highly-rigid sandwich structures for interstages. 07 p0906 A73-18994

Reinforced plastics role in construction and shielding of Diamant B satellite booster main components 07 p0905 A73-18995

Satellites elastic structures equations of state for stability and attitude control systems analysis, deriving translational and rotational momentum equations for moving coordinate systems 08 p1014 A73-20779

High modulus composites versus beryllium for achieving stiffness in spacecraft structural applications. [AIAA PAPER 73-384] 11 p1430 A73-25513

Impact tests for aid in data interpretation of measured meteor particles impact on spacecraft structures, noting transducer response dependence on impact angle 12 p1554 A73-27643

Al alloys, steels and superalloys properties improvements for aerospace vehicles structural applications, discussing diffusion bonding and isothermal forging techniques 13 p1633 A73-28180

Fiber composite materials properties, technological assessment and future development and application for aerospace flight structures, considering manufacturing cost, tailorability and stiffness requirements 13 p1699 A73-29346

Reinforced plastics under ablative conditions for thermal insulation and structural applications. 17 p2195 A73-34805

Aspects of the finite element method as applied to aero-space structures. [ISD-138] 18 p2365 A73-36725

SPACECRAFT TELEVISION

NT DIGITAL SPACECRAFT TELEVISION

NT SATELLITE TELEVISION

Mars atmosphere observation from Mariner 9 TV pictures, discussing global and local dust storms, condensate clouds, albedo and polar cover 06 p0745 A73-17479

Apollo 15 and 16 ground-commanded television assembly. 07 p0823 A73-19375

Spacecraft transmitted TV picture geometrical distortion in terms of root-mean-square errors, considering applications to ESSA-7, Surveyor-7 and Mariner 4 data samples 10 p1219 A73-24485

Mars topographic and geologic mapping with Mariner 9 TV pictures, ground based radar and IR pressure techniques 16 p2015 A73-33354

SPACECRAFT TRACKING

Exploration of Mars by Mariner 9 - Television sensors and image processing. 17 p2170 A73-35298

Mariner 9 television observations of Phobos and Deimos. II. 19 p2479 A73-37222

Spacecraft television image comparison between earth and Mars surface features and geology, discussing mountain chains, deserts and tectonic mapping techniques 20 p2613 A73-39897

SPACECRAFT TRACKING

NT SATELLITE TRACKING

Unified S-band ground system design and management for Apollo program, deep space and manned space flight network tracking and communications requirements 01 p0030 A73-11184

On-line parameter estimation of nonlinear dynamic system with unknown impulsive inputs by Kalman filter with application to maneuvering spacecraft tracking 04 p0431 A73-15270

Design of communication systems using short-constraint-length convolutional codes. 04 p0419 A73-15396

Improvements in deep-space tracking by use of third-order loops. 09 p1056 A73-23406

Atmospheric temperature measurement with X and K band radiometers, discussing meteorological conditions variation effects on microwave propagation and comparison with spacecraft tracking data 16 p1983 A73-33730

Evolution of the satellite telemetry data processing facility at the Goddard Space Flight Center. 17 p2123 A73-35300

Kalman filter for rapid detection and adaptive estimation of state and covariance, deriving Bayes decision rule and algorithm for spacecraft tracking 19 p2410 A73-38030

SPACECRAFT TRAJECTORIES

NT EARTH-MARS TRAJECTORIES

NT EARTH-MOON TRAJECTORIES

NT EARTH-VENUS TRAJECTORIES

NT INTERPLANETARY TRAJECTORIES

NT LUNAR TRAJECTORIES

NT MOON-EARTH TRAJECTORIES

A Chebyshev minimax technique oriented to aerospace trajectory optimization problems. 01 p0100 A73-10729

Systematics of earth-to-moon trajectories. I 01 p0102 A73-10995

Multistep three-parameter algorithm for spacecraft stabilization on an atmospheric reentry trajectory 02 p0229 A73-12451

Prediction in control of re-entry into the atmosphere. 05 p0627 A73-16076

Earth-based orbit determination for solar electric spacecraft with application to a Comet Encke rendezvous. [AIAA PAPER 73-174] 06 p0748 A73-17651

Launch and orbital injection of Intelsat IV satellites. 09 p1152 A73-22699

Real-time analysis and ground command control to achieve accurate vehicle and payload event functions. [AIAA PAPER 73-298] 09 p1117 A73-23217

Six degree of freedom guided sounding rocket flight simulations and trajectory program, discussing financial and technical feasibility [AIAA PAPER 73-299] 09 p1117 A73-23218

Some problems of optimal control of space-vehicle trajectories in the Martian atmosphere 10 p1247 A73-23878

Distribution of radiation doses in the earth's radiation belts during years of maximum solar activity 10 p1264 A73-23889

Russian book on earth satellite, lunar, interplanetary and reentry trajectory analysis and optimal control covering motions under low thrust, aerodynamic heating and ablation 10 p1286 A73-23949

Electromagnetic window for a trajectory radar 11 p1327 A73-25280

Satellite ascent transfer trajectories equations of motion numerical integration, replacing time parameter by regularizing independent variable for gravitational singularity elimination [DFVLR-SONDDR-283] 12 p1537 A73-26822

Influence of the thrust interruption during passage through the shadow cone of a celestial body on the trajectory of a space vehicle using solar electric propulsion - First approximation calculation 12 p1540 A73-27393

The selection of measurable parameters in the determination of the trajectory of a space vehicle. 12 p1543 A73-27626

Nonlinear problems in analyzing the observability of the trajectories of spacecraft motion according to measurement data. 12 p1543 A73-27628

Three-parameter multistep algorithms for stabilization of a spacecraft on the descent trajectory through the atmosphere. 15 p1944 A73-32601

Planetary quarantine constraints for outer planet satellite encounter missions, determining spacecraft impact probability in terms of trajectory analysis and navigation error numerical integration 18 p2349 A73-35976

The significance of outer planet satellite quarantine constraints on aim-point selection. 18 p2359 A73-36096

Derivation of an approximate solution to the equation of geocentric motion of a space vehicle with a solar sail 19 p2492 A73-37849

Some problems in the optimal control of spacecraft trajectories in the Martian atmosphere. 20 p2589 A73-38897

Radiation dose distribution in the earth's radiation belts during year of maximum solar activity. 20 p2601 A73-38908

Pioneer 10 flyby trajectory relationship to analogy between earth and Jupiter bow shocks with emphasis on oblique shock structure 22 p2906 A73-41942

Russian book - Studies of spacecraft flight dynamics. 23 p3027 A73-43260

Orbit improvement from satellite imaging data obtainable from outer planet missions. 23 p3032 A73-43840

SPACELAB

Earth resources exploration with a sortie laboratory within the framework of the Post-Apollo Program /PAP/ [DGLR PAPER 72-080] 02 p0227 A73-11677

Sortie module/pallet scientific European space program based on system performing orbital zero-g or earth/celestial bodies observation platforms functions. 12 p1549 A73-27381

Sortie lab experiment management, integration and operational techniques, discussing airborne science/shuttle experiment system simulation /AS-SESS/ program 14 p1803 A73-29942

Langley Research Center shuttle-compatible spaceborne advanced technology laboratory concept with sortie flight operation mode [AIAA PAPER 73-611] 18 p2358 A73-36089

SPACING

NT AIRCRAFT APPROACH SPACING

Multipole sine-cosine azimuth patterns for wide aperture Adcock direction finders, determining spacing and radiation errors and array pickup factor 02 p0142 A73-12529

The effects of modulated blade spacing on static rotor acoustics and performance. [AIAA PAPER 73-1020] 24 p3121 A73-44852

SPALLATION

Spallation production of He-3, Ne-21, and Ar-38 from target elements in the Bruderheim chondrite. 10 p1277 A73-24103

Laser-induced shock effects in Plexiglas and 6061-T6 aluminum. 15 p1956 A73-32259

SPARK CHAMBERS

Spark calorimeter calibration by particle accelerator induced high energy pions, noting neutral and charged particles track detectors high geometric resolution 02 p0171 A73-12686

Analysis procedure of gamma ray astronomy spark chamber data. 07 p0828 A73-20644

Investigation of rigid gamma rays in the atmosphere with the aid of a telescope with an acoustic spark chamber 10 p1267 A73-23923

Development of spark chambers for use in measurements of the charge spectrum of high energy cosmic rays. 11 p1363 A73-25961

High spatial resolution wire spark chamber system using electromagnetic delay line readout. 11 p1363 A73-25962

Acoustical spark chamber in a telescope designed for investigations of primary cosmic gamma radiation 21 p2701 A73-40612

A study of elementary acts of interaction between hadrons with energies of about 10 TeV 23 p3021 A73-43533

Intercoms 6 cosmic ray shower experiment using emulsion stack, spark chamber and scintillation counter to measure particle energy, angular distribution and production multiplicity 23 p2981 A73-43540

Spark calorimetry investigation of trident and extensive air showers muon component generated high energy penetrating particles at large zenith angles 23 p3024 A73-43565

Large wire spark chambers with an information output and storage system 23 p2982 A73-43570

SPARK DISCHARGES

U ELECTRIC SPARKS

SPARK GAPS

Importance of arc gap control in vacuum consumable arc remelting of superalloys. 04 p0454 A73-15743

Digital electrode breakdown potential controller for spark source mass spectrometer automation, using radio frequency pulse amplitude sensing 11 p1367 A73-26315

Commutation of spark gaps with the aid of a pulsed gas laser emitting in the ultraviolet range 12 p1506 A73-27211

Temporal characteristics of spark gaps with discharge initiation by a laser flare 12 p1506 A73-27212

High energy ignition systems using silicon controlled rectifiers. 12 p1533 A73-27931

Ultrafast spark gaps for electro-optical device control, discussing trigger system design and performance in terms of delay, jitter and internal voltage time response 16 p2013 A73-32874

Ruby laser light spark ion-electron currents in gap between copper plates under electric field 18 p3222 A73-37047

Low voltage self triggering vacuum gap characteristics under dc conditions, comparing with thyatron pulse generator technique 21 p2692 A73-39917

SPARK IGNITION

Unflanged electrode spark ignition tests for minimum energy to trigger gas mixtures explosion, using spark energy relation for outward propagating quasi-spherical flame 03 p0399 A73-14400

A testing procedure for flame arrestors for marine spark ignition engines. [WSCF PAPER 72-34] 05 p0563 A73-16681

One dimensional model for spark ignition Wankel engine combustion, presenting unsteady turbulent flame propagation equations 09 p1136 A73-22824

Book - Engine emissions: Pollutant formation and measurement. 19 p2474 A73-38321

The ignition of hydrocarbon-air mixtures with laser radiation 22 p2938 A73-43190

SPARK MACHINING

Errors due to electrode-instrument wear during the electric-erosion treatment of cavities 15 p1881 A73-31146

SPARK SHADOWGRAPH PHOTOGRAPHY

U SHADOWGRAPH PHOTOGRAPHY

SPARKS

NT ELECTRIC SPARKS

Balanced heat transfer type calorimeter designed and tested for spark energy measurement, comparing performance to conventional calorimeters of transient heat transfer type 07 p0922 A73-20365

Investigation of the absorption of laser radiation in a laser spark in air 15 p1885 A73-32313

Absorption of laser radiation in a laser spark in air. 24 p3095 A73-44621

SPATIAL DEPENDENCIES

The adjustment of a spatial terrestrial net according to the method of satellite geodesy 03 p0299 A73-13257

Ionospheric plasma flow past a semi-infinite cylinder. 04 p0440 A73-14967

Turbulent space-time correlation measurements in a plane two-stream mixing layer at velocity ratio 0.3. [AIAA PAPER 73-225] 05 p0566 A73-16951

Conservation of quasiparticles in weakly turbulent plasmas. 06 p0730 A73-18273

Diffuser box for holography spatial and temporal coherence requirements relaxation, explaining speckling and SNR reduction by time and frequency domain analysis 08 p0963 A73-21035

Analysis and space-time reconstitution of the circumferential component of instantaneous velocity in immediate proximity to the wall of a cylinder 08 p0926 A73-21496

Spatial-temporal structure of emission from a ruby laser irradiated by gamma rays 11 p1378 A73-26523

Temporal and spatial features in detecting one- and two-dimensional constraints in complementary visual displays. 13 p1578 A73-28095

Spatially dependent electron relaxation near a thermionic emitting electrode. 14 p1713 A73-30473

Satellite imagery of land resources, discussing synoptic views, spatial dependence, closed loop information and sequential sampling 17 p2161 A73-34945

Statistical characteristics of the temperature field near the ground for Europe. 18 p2334 A73-37070

Spatial characteristics of chromatic induction - The segregation of lateral effects from straylight artefacts. 19 p2394 A73-37419

Asteroidal dust population model coinciding with spatial density demonstrating distribution below astrodynamical mass limit and larger time for distribution function extrapolation
21 p2776 A73-41422

Human recognition of dynamic pattern changes in numerical series displayed on spatiotemporal panels, discussing learning times and reactions to pattern disruptions
22 p2812 A73-41887

Enhanced scintillation sectors outside the plane of the ecliptic.
23 p3029 A73-43679

Space-time limits of stable oscillations of solar surface active zones spanning multiple solar rotations, noting correlation coefficients for north and south hemispheres
24 p3138 A73-45013

Space-time autocorrelation and cross correlation coefficients for transverse turbulent velocity fluctuations in pipe flow
24 p3080 A73-45451

SPATIAL DISTRIBUTION
NT STAR DISTRIBUTION

Diurnal latitudinal composition variations in light ion trough from OGO mass spectrometric observations, noting magnetic storm effects
02 p0157 A73-11904

Cosmic dust distribution measurement by satellites, relating accuracy to sensor calibration conditions and region characteristics
02 p0215 A73-12258

The zodiacal light as seen from the Pioneer F/G and Helios probes.
02 p0215 A73-12263

Extensive air showers radio emission polarization, spatial distribution and electric field strength, noting geomagnetic mechanism effect
02 p0209 A73-12672

Statistical analysis of galaxy counts in small red shift quasar fields, comparing to number of galaxies around randomly chosen point
03 p0370 A73-13194

Some results about the satellite scintillation on 150/400 MHz and the horizontal gradient of the total electron content in the polar ionosphere.
03 p0300 A73-13648

Wavelike structure of magnetic field-aligned irregularities detected by phase interferometry.
03 p0300 A73-13696

German monograph - Effect of spatial partial coherence on the measurement of optical transfer functions.
03 p0343 A73-13813

German monograph - Spatial oscillations of light in the refraction and image field of rough objects.
03 p0319 A73-13817

A theory on the latitude and local time distribution of precipitating electrons during a sudden commencement.
03 p0304 A73-13885

Spatial plasma echoes of ion acoustic waves in low pressure He and Ne discharges in anode direction
03 p0348 A73-14622

Longitudinal variation of the equatorial anomaly.
04 p0440 A73-14960

Observed anisotropy in the distribution of radio sources.
04 p0499 A73-15352

Surface distribution of interacting and normal galaxies near the galactic north pole
05 p0613 A73-16212

Spatial variations in F2 layer critical frequencies
05 p0568 A73-16258

A neutral hydrogen survey of the galaxy M 33. I.
05 p0618 A73-16740

Investigation of the process of the explosive disintegration and simultaneous collision of n gravitating material points
05 p0619 A73-16844

A matrix Green's formula and optimal control of linear distributed-parameter systems.
06 p0679 A73-17564

Total number and mass of Pultusk meteorite shower fragments, using spatial distribution rule
06 p0748 A73-17838

Spatial distributions of plasma density in a high-frequency discharge with a superimposed static magnetic field.
07 p0856 A73-19518

Periodicities in the longitude distribution of sunspots.
08 p1001 A73-20759

A neutral hydrogen survey of the galaxy M33. II - Distribution and kinematics of the neutral hydrogen.
08 p1005 A73-20913

Spatial-temporal distribution of E/sf formations associated with visible forms of polar aurorae
08 p0958 A73-21283

Calculation of the moments of the electron spatial distribution function without allowance for ionization losses
08 p1000 A73-21514

Measurement of spatial plasma-density distributions with the aid of an open barrel-shaped resonant cavity
09 p1124 A73-21879

Holographic method of controlling the spatial-angular characteristics of laser emission
09 p1090 A73-21951

Galactic absorbing material effects on quasar apparent distribution, noting brightness decrease with red shift
09 p1147 A73-22572

Electron intensities over auroral arcs from rocket flight, noting electron phase-space density increase with northward progress
09 p1078 A73-22833

The structure of the Crab Nebula. II - The spatial distribution of the relativistic electrons.
09 p1151 A73-23290

Visual display of the spatial distribution of colloidal particle beams.
09 p1136 A73-23448

Spatial distributions of intensity and polarization over the source of microwave impulsive bursts.
10 p1275 A73-23828

Spatial variations of cosmic rays on the basis of data for the radioactivity of meteorites with known orbits
10 p1266 A73-23910

Reply to criticism of local fluctuation interpretation of radio source counts deviation from Euclidean distribution
10 p1280 A73-24273

An up-to-date picture of galactic spiral features based on young open star clusters.
10 p1281 A73-24410

An optimal control problem for a class of distributed parameter systems.
10 p1202 A73-24549

Spatial amplitude distribution of vibrating ribbon two dimensional wake mean, periodic and random velocity components measured in uniform flow by hot-wire anemometry
10 p1173 A73-24828

Luminosity functions for K giant stars derived from the two-micron sky survey.
11 p1414 A73-25066

The spatial distribution of the 11.7 micron radiation of NGC 7027.
11 p1415 A73-25071

Spatial correlation of the critical frequencies of the F2 layer on the basis of data from stationary mid-latitude stations
11 p1351 A73-25091

The diurnal and semidiurnal barometric oscillations, global distribution and annual variation.
11 p1351 A73-25167

Composite distribution function for absolute magnitudes of uniformly distributed galaxies
11 p1416 A73-25238

The spatial correlation method and a time-varying flexible structure.
11 p1440 A73-25535

[AIAA PAPER 73-406] Spatial distribution of elements in tektites and comparable materials by charged particle activation analysis.
11 p1418 A73-25584

Ariel 3 satellite observations of the ionosphere at high southern latitudes.
11 p1353 A73-25754

Explosive disintegration and simultaneous collision of n material gravitating points.
11 p1423 A73-26054

Influence of field inhomogeneity on the intrinsic spectral linewidth of a laser
11 p1332 A73-26166

Solar surface photospheric oscillation spatiotemporal power spectrum observation, considering long-period oscillation correlation with chromospheric flare
12 p1544 A73-27828

The large-scale distribution of low-velocity hydrogen gas at high galactic latitudes.
13 p1671 A73-28028

High Galactic latitude intermediate-negative velocity neutral hydrogen properties, noting large complexes and systematic velocity pattern
13 p1671 A73-28029

Confined optical and radio source image reconstruction from spatial frequency components of source not passed by imaging system
13 p1671 A73-28030

Andromeda galaxy absorbing material distribution obtained with population I cepheids in Baade four variable star fields
13 p1671 A73-28031

High resolution space-time structure and centre-limb distribution of solar type I sources observed at 169 MHz.
13 p1671 A73-28032

Abundance and lateral distribution of muons in inclined showers.
13 p1670 A73-28371

Holographic recording of three-dimensional ensembles of rapidly moving particles
13 p1616 A73-28767

Properties of human visual orientation detectors - A new approach using patterned afterimages.
13 p1579 A73-29124

Analytical description of the three-dimensional distribution of the scattering of a gyromotor magnetic field
13 p1618 A73-29149

Spatial separation of 3914- and 3160-A emissions of nitrogen in an aurora.
14 p1749 A73-29987

Human average evoked potential distribution over scalp to associate cortical electrical activity with voluntary movement, reacting to EMG activity
14 p1714 A73-29990

Point-spread functions, line-spread functions, and edge-response functions associated with MTFs of the form negative exp(-n-th power of the ratio of spatial frequency to the MTF frequency constant).
14 p1768 A73-30158

Spatial distribution of stars in the Orion constellation region
14 p1799 A73-30385

Emerging flux regions /EFR/ spatial distribution on sun, discussing absence of preferential longitudes, latitudinal preference and time distribution behavior
14 p1787 A73-30648

The number-intensity distribution of X-ray sources observed by Uhuru.
14 p1788 A73-30733

Electron-microscopic investigation of the spatial distribution parameters of second-phase precipitation in aging nickel-base alloys
14 p1764 A73-30862

Spatial distribution of H alpha emission in the earth's upper atmosphere, the variations of the emission during a solar cycle, and the dependence of the emission on geomagnetic perturbations
15 p1867 A73-31262

The perturbation of alternating geomagnetic fields by discontinuities with high conductivity contrasts.
15 p1871 A73-31780

Spatial structure of the short-wave radiation field in stratocumulus and cumulus clouds
15 p1905 A73-31795

Experimental investigation of the plasma focus in erosion-source plasma accelerators. I
15 p1921 A73-32325

Axial distribution for a hot electron plasma.
16 p2041 A73-33325

Thermospheric wind effects on the distribution of helium and argon in the earth's upper atmosphere.
16 p2004 A73-33441

Evidence for the existence of galactic superclusters near the galactic North Pole
16 p2063 A73-33661

Spatially growing wave trails of an inviscid fluid discontinuity.
16 p2001 A73-33868

The latitudinal variation of the electron concentration in the topside ionosphere in winter.
16 p2010 A73-33913

Spatial correlation functions of the field and intensity of laser radiation
16 p2024 A73-34053

Measurement of plasma density distribution using an open barrel-shaped cavity.
17 p2215 A73-34303

Convection dominated electrons in auroral zone, discussing plasma sheet as magnetospheric electron source, convection electron spatial distribution and convection-precipitation coupling
17 p2223 A73-34358

Interstellar matter observations, discussing densest stages spatial distribution near solar system and dense clouds
17 p2227 A73-34409

A generalization of the equations governing the evolution of a particle distribution in a random force field.
17 p2213 A73-34449

Evidence for non-linear response processes in the human visual system from measurements on the thresholds of spatial beat frequencies.
17 p2112 A73-34839

The visual cortex as a spatial frequency analyser.
17 p2112 A73-34840

A three-dimensional picture of the development of instability during the interaction of a modulated electron beam with a plasma.
17 p2216 A73-35170

Spatial information coding in the human visual system - Psychophysical data.
17 p2116 A73-35240

A discussion of the distribution of interstellar matter close to the sun.
17 p2234 A73-35619

An investigation on the spatial distribution of the quasi-trapped energetic electrons observed on board the satellite 'Shinsei.'
18 p2344 A73-35929

Latitudinal and temporal variability of temperature in the lower thermosphere.
18 p2304 A73-35991

Spatial extent of the winter anomaly in absorption.
18 p2305 A73-36003

Second phase particle redistribution in dispersion-hardened alloys by directed particle diffusion via chemical potential control
18 p2325 A73-36807

Latitudinal distribution of a debris mantle on the Martian surface. 19 p2477 A73-37208

Some characteristics of the surface scattering of the Sikhote-Alin meteorite shower 19 p2480 A73-37240

Structure of the Perseids radiants in 1971 19 p2481 A73-37243

Spatial frequency channels in human vision and the threshold for adaptation. 19 p2394 A73-37416

Feature recognition method in small scale structure analyses of neutral hydrogen emissions, applying to surveys at negative intermediate galactic latitudes 19 p2483 A73-37562

Nonuniform model construction for dense intergalactic medium with gravitational binding of all galactic groups and clusters by ionized gas 19 p2484 A73-37608

Space-time distribution of Es formations associated with visible auroral forms. 19 p2424 A73-37912

Spatial distributions of H₂ desorbed from Fe, Pt, Cu, Nb, and stainless steel surfaces. 19 p2402 A73-37951

Theory of resonant light scattering processes in solids. 20 p2570 A73-38612

Increasing the storage density of holographic recording by spatial frequency multiplexing. 20 p2563 A73-38670

Application of mathematical methods for the description of the planetary distribution of ionosphere parameters 20 p2554 A73-39169

Spatial distribution of outgoing long wave radiation fluxes according to Cosmos-320 satellite data 20 p2555 A73-39188

A Green Bank sky survey in search of radio sources at 1400 MHz. IV - Anisotropy and counts of radio sources. 20 p2610 A73-39574

The Synthesis Radio Telescope at Westerbork - Methods of polarization measurement. 20 p2566 A73-39581

Spatially locked laser mode formation of coherent wave fields with improved angular divergence by degenerate oscillation superposition in laser resonator 20 p2573 A73-39681

Wave absorption by a plasma with a nonmonotonic longitudinal distribution of the concentration 21 p2746 A73-40524

Hole-type confocal active optical cavity resonator loss distribution, discussing Fresnel zone oscillation type intensity within resonator and diffraction at cavity 21 p2714 A73-40559

Upper atmospheric models dealing with diurnal variation and latitudinal density dependence to derive time and space dependencies 21 p2683 A73-40631

Distribution density of small lunar craters - Models and actual distribution 21 p2770 A73-40915

Large scale heat transfer in turbulent boundary layer at heated flat plate in incompressible viscous fluid, discussing temperature fluctuation spatial correlation as function of wall law and flow core 21 p2678 A73-41062

Interstellar extinction, relation to spatial dust distribution, light scattering by grains, diffuse absorption lines and polarization 21 p2772 A73-41247

Studies of granular velocities. III - The influence of finite spectral and spatial resolution upon the measurement of granular Doppler shifts. 21 p2776 A73-41478

The east-west asymmetry in the number of spot-groups in relation to their classification. 21 p2777 A73-41488

Space-variant system analysis of image motion. 21 p2706 A73-41609

Uneven illumination of the polar caps by solar protons - Comparison of different particle entry models. 22 p2901 A73-41906

Midday recovery of HF absorption during PCA events relationship to satellite observation of solar proton latitudinal variations 22 p2846 A73-41943

Comparison of calculated characteristics of extensive atmospheric showers with experimental results at various altitudes 22 p2903 A73-42733

A reexamination of the mean H I density along the Hubble sequence. 22 p2913 A73-43003

Variations in the distribution and physical properties of Perseid meteors. 22 p2914 A73-43015

Parameter behavior in mass distribution analysis of overdense Geminid trail radio echoes 22 p2915 A73-43041

The assembly edge effect and the spatial distribution of extensive air shower particles in an assembly with widely spaced detectors 23 p3022 A73-43547

Spatial electron distribution in extensive air showers at energies of one thousand to one billion TeV 23 p3022 A73-43552

The structure of the spatio-angular distribution function of electron-photon shower particles near the axis 23 p3023 A73-43556

Some characteristics of the muon component of extensive air showers at mountain level 23 p3023 A73-43562

The production and distribution of nitrogen oxides in the lower stratosphere. 23 p2977 A73-43897

Asteroid belt observation, spatial distribution and mission planning, considering IR, spectrophotometric, interferometric, polarization and Doppler measurement techniques 23 p3034 A73-43991

Distribution of interstellar hydroxyl in the Cyg X region 23 p3035 A73-44231

Approximate formula for completeness estimation of radio source distributions in spherical zones in terms of distance to system central source 23 p3037 A73-44358

Measurements of the distribution of sound source intensities in turbulent jets. 24 p3053 A73-44826

[ALAA PAPER 73-989] Radon transform application in holographic interferometry for reconstructing two and three dimensional spatial distribution of refractivity in object 24 p3091 A73-44944

Numerical experiments on the steady-state meridional structure and ozone distribution in the stratosphere. 24 p3085 A73-45017

Solar wind fluctuations mapping procedure applied to Explorer 35 wind data for solar wind structure to Mars orbit 24 p3125 A73-45104

Determination of the voltage distribution in the interelectrode space of a grid probe immersed in a Maxwellian plasma 24 p3116 A73-45328

Smoothing and filtering of apparent surface distribution of galaxies. 24 p3143 A73-45363

SPATIAL FILTERING

Talbot shearing interferometer based on Fourier imaging behind grating illuminated by plane monochromatic wave with spatial filtering, obtaining radial and lateral derivatives 01 p0053 A73-11227

Coherent intensity spatial filtering applied to inspection of photolithography masks for LSI. 06 p0694 A73-18288

A relationship between the antenna synthesis for a given radiation pattern and the statistical synthesis of systems for spatial signal processing. 07 p0801 A73-20129

Coherent optical processing with spatial frequency diversity speckle and reflection noise reduction, discussing coding by illuminating input transparency through square screen mesh 08 p0964 A73-21045

Millimeter wave imagery of complex three dimensional target by diffuse reflection with spatial filtering, discussing range, resolution and view field capabilities 10 p1188 A73-23798

Analysis of the information capacity of optical matched filters. 12 p1498 A73-27516

Spatial filtering considerations in Bragg diffraction imaging. 13 p1615 A73-28593

Developments in the optical spatial filtering of superposed, crossed gratings. 13 p1620 A73-29302

Spatially filtered helium-neon laser link operation parallel to IR radiometer for real time atmospheric propagation monitoring over short path 13 p1661 A73-29328

Photosensor aperture shaping to reduce aliasing in optical-mechanical line-scan imaging systems. 14 p1753 A73-30161

Optimal receiver design for discrete information in the presence of non-Gaussian noise 16 p1990 A73-33669

Pattern recognition techniques suggested from psychological correlates of a model of the human visual system. 17 p2116 A73-35241

Restoration of degraded images by composite gratings in a coherent optical processor. 17 p2173 A73-35435

Single step detection of blurred images in a coherent optical processor. 17 p2173 A73-35436

Optical processing of radar signals 21 p2651 A73-40515

Investigation of complex and hypercomplex receptive fields of visual cortex of the cat as spatial frequency filters. 22 p2810 A73-42958

Kinoform production method combining pen-drum plotter with low pass spatial filter converting binary transmittance of precursory mask 22 p2862 A73-43088

Spatial resolution of an incoherent-to-coherent converter using bismuth germanium oxide. 22 p2863 A73-43098

SPATIAL ISOTROPY

U ISOTROPY

U SPATIAL DISTRIBUTION

SPATIAL ORIENTATION

U ATTITUDE (INCLINATION)

SPECIES DIFFUSION

Certain characteristics of the initial phase of the nitriding process 01 p0055 A73-10255

Diffusive boronizing of molybdenum and niobium in boron carbide powder 02 p0178 A73-11544

Uniform junction microwave transistor fabrication by automatically controlled diffusion technique, using low temperature phosphosilicate glass films on silicon wafers 02 p0147 A73-12164

Soot particles oxidation by oxygen diffusion in laminar hydrocarbon flames, deriving kinetic expression from observed time dependent particle concentration variations 03 p0399 A73-14395

Chromium diffusion in Ni-20 wt pct Cr-3 vol pct Y2O3 and Co-21 wt pct Cr-3 vol pct Y2O3. 04 p0463 A73-15317

Study of the diffusion of carbon in structural steel plates clad with stainless steels 04 p0467 A73-15951

Dynamics of moisture diffusion through a partially liquid filled porous matrix. 06 p0649 A73-18259

Method of plasticity enhancement in aluminum and nickel-aluminum diffusion coatings on medium-carbon steel 06 p0711 A73-18665

The concentration-dependent diffusion of chromium in nickel oxide. 06 p0712 A73-18760

Diffusion of hydrogen in titanium alloys due to composition, temperature, and stress gradients. 06 p0712 A73-18764

Successive diffusion in a ternary system of the iron-metal-carbon type 07 p0841 A73-20520

A review of the diffusion path concept and its application to the high-temperature oxidation of binary alloys. 08 p0978 A73-21414

Spun on arsenosilica films as sources for shallow arsenic diffusions with high surface concentration. 08 p0995 A73-21478

Unidirectional filament reinforced metal matrix composites compositional changes due to temperature induced interatomic diffusion, using diffusion equation finite difference solutions superposition technique 09 p1101 A73-22404

Loading mode effects on high strength steel hydrogen embrittlement, considering stress tensor invariants and interstitial diffusion relationships 09 p1102 A73-22414

Ni diffusion in Nb at 988 to 1246 C, using residual activity technique with Ni-63 as tracer 09 p1103 A73-22436

Investigation of carbon- and manganese-diffusion processes in the metal-ceramic steel G13M 09 p1103 A73-22466

Vaporization and compatibility of SiGe radioisotope thermoelectric generators. 09 p1117 A73-22761

SiGe alloys thermoelectric properties long term time and temperature dependent behavior, using diffusion limited dopant precipitation model 09 p1136 A73-22762

Interaction of graphite with titanium and zirconium 09 p1105 A73-22977

Application of the Moessbauer effect to the study of the mechanism of iron diffusion in beta-titanium 09 p1108 A73-23240

Influence of the combined effect of plastic deformation and high temperatures on the diffusion mobility of carbon 09 p1108 A73-23241

Annealing of effects arising during ion-bombardment alloying of metals at energies up to 10 keV 10 p1223 A73-23817

An observation of vacancy sources during substitutional diffusion in thoriated nickel alloys. 10 p1234 A73-24433

Elements distribution in ternary alloy system during simultaneous saturation and burning-out of two components and successive diffusion into third 10 p1236 A73-24953

Cr diffusion into Ni-Cr alloys in presence of aluminized layer, noting increased diffusive mobility
10 p1226 A73-24959

Influence of the intercrystalline structure on the diffusion of zinc in the symmetrical joints of bending of aluminum
11 p1379 A73-25324

Influence of the chrome content and the interstitial impurities content /carbon and nitrogen/ on the volumetric and intergranular diffusion of iron 59° in iron-chrome alloys with from 0 to 15 per cent chrome - Relations with alpha to alpha plus gamma reversible transformations
12 p1514 A73-27985

Investigation of interdiffusion in the nickel-tungsten and palladium-tungsten systems
14 p1764 A73-30864

Diffusion-controlled processes in the homogeneity region of zirconium carbide
15 p1881 A73-31593

Saturation of Kh18N10T steel by molybdenum from the vapor phase
15 p1889 A73-31807

Tracer diffusion of Ni-63 in Fe-17 wt pct Cr-12 wt pct Ni.
17 p2189 A73-34641

Effect of interphase boundaries on the kinetics of molybdenum siliconizing
18 p2318 A73-35881

Investigation of the transition zone structure in composite materials under cyclic loads
20 p2580 A73-39379

Interdiffusion in the titanium-zirconium system
22 p2874 A73-42099

The influence of carbon on the interdiffusion of Mo and Ni.
22 p2878 A73-42579

Atomic diffusion mechanisms in multiphase and multicomponent alloys covering relaxation, crystal lattice atom exchange and motion along dislocation lines and to neighboring vacancies
23 p2989 A73-43439

Concentration curves and phase diagram plotted for Nb-Zr system diffusion layers during annealing at 700 to 1700 C
23 p2991 A73-43649

Hemoglobin species diffusion effect on oxygen transport in moving and stationary flat films of hemoglobin solution
23 p2949 A73-43993

Impurity diffusion of iron in molybdenum.
23 p2994 A73-44157

Saturation of steel Kh18N10T with molybdenum from the vapor phase.
24 p3100 A73-45270

SPECIFIC HEAT

The specific isochoric heat capacity of pure fluids on the dew curve and the boiling curve
03 p0400 A73-14633

The effect of gravity on the thermal and caloric measurements for pure fluid substances at the critical point
03 p0400 A73-14634

Magnetic-field-induced one-dimensional behavior in the specific-heat transition in dirty bulk superconductors.
05 p0605 A73-16569

Enthalpy and heat capacity of boron carbide in the temperature range 273-2600 K.
06 p0714 A73-17415

Heat capacity of the TV-10 tantalum-tungsten alloy at low temperatures
06 p0708 A73-18051

Enthalpy and heat capacity of graphite in the temperature interval between 273 and 3650 K.
06 p0714 A73-18557

Thermodynamic characteristics of molybdenum silicides in the temperature interval between 400 and 1200 K
06 p0710 A73-18560

Enthalpy and specific heat of the orthophosphates of lanthanum, neodymium, and yttrium at high temperatures
06 p0738 A73-18654

Enthalpy and specific heat of tantalum carbide in the range 273-3600 K.
08 p0977 A73-20865

Dependence of the base pressure on the ratio of specific heats at supersonic velocities
09 p1027 A73-21917

Ablation of large meteor particles
09 p1147 A73-22573

Change in the superconducting properties of vanadium after the introduction of tantalum impurity atoms
10 p1261 A73-24761

Acoustical method for determining thermal diffusivity and relative difference in molar heat capacities of tantalum and vanadium.
11 p1448 A73-25127

Investigation of the enthalpy and heat capacity of niobium carbide based materials at high temperatures
12 p1513 A73-27310

Determination of the temperature dependence of the Debye-Waller factor for thin gold films by electron diffraction observations
12 p1532 A73-27944

A method for calculating the low temperature surface specific heat of a crystal lattice.
13 p1704 A73-28214

Investigation at the Moscow University of the thermal characteristics of material
13 p1704 A73-28426

High-speed /subsecond/ simultaneous measurement of specific heat, electrical resistivity, and hemispherical total emittance of Ta-10/wt.%W alloy in the range 1500 to 3200 K.
[ECTP PAPER D2-4] 14 p1760 A73-30437

Specific heat of alloys of the niobium-titanium system near the superconducting transition temperature
15 p1886 A73-31184

High temperature specific heats of iron-rich iron-titanium alloys between 600 and 1150 K.
15 p1891 A73-31994

Electronic specific heat of nickel-base alloys containing small amounts of transition metals
[ONERA, TP NO. 1250] 15 p1924 A73-32210

Bottom pressure and specific-heat ratio at supersonic velocities.
15 p1825 A73-32643

Variation with temperature of free enthalpy of formation of certain carbides
15 p1898 A73-32644

Enthalpy and specific heat of graphite in the temperature range 273-3650 K.
16 p2030 A73-33583

Thermodynamic properties of molybdenum silicides in the temperature range 400-1200 K.
16 p2026 A73-33585

Air/water mist spray coolant for high gas temperature and pressure environment at gas turbine inlet
17 p2221 A73-34388

Simultaneous measurement of specific heat, electrical resistivity, and hemispherical total emittance of niobium-1 /wt. %/ zirconium alloy in the range 1500 to 2700 K by a transient /subsecond/ technique.
17 p2187 A73-34499

Differential calorimetry technique with heat link placement between samples for maintaining near equilibrium state to achieve accuracy in specific heat ratio measurement
17 p2175 A73-35753

Low temperature specific heat of neodymium magnesium nitrate.
18 p2341 A73-36977

Differential method for determining specific heat
20 p2627 A73-39299

NiO and CoO single crystal thermal conductivities, reporting specific heat and electrical resistivity near magnetic transition
20 p2600 A73-39826

Ehrenfest equations for thermostatic equilibrium in classical body second order phase changes using caloric equations of state, relating specific heat discontinuities and equilibrium manifold
22 p2885 A73-41737

Application of precise heat-capacity data to the analysis of the temperature intervals of the International Practical Temperature Scale of 1968 in the region of 90 K.
22 p2852 A73-41977

High temperature thermophysical properties of tungsten.
[ECTP PAPER D1-5] 22 p2876 A73-42405

Measurement of the heat capacity of graphite in the range 1500 to 3000 K by a pulse heating method.
22 p2881 A73-42510

Shock attenuation dependence on gas specific heat ratio and wall divergence angle and area ratio of expansion section attached to shock tube
23 p2969 A73-43930

Temperature field boundary value problem with variable heat transfer coefficients and specific heat, using Laplace transformation and variation methods
24 p3156 A73-45083

SPECIFIC IMPULSE

Mission performance of a 360 mw nuclear rocket engine.
[AIAA PAPER 72-1064] 03 p0381 A73-13393

Development of a radioisotope-fueled thruster for satellite propulsion.
[AIAA PAPER 72-1066] 03 p0354 A73-13395

Experimental evaluation of a 600 lbf spacecraft rocket engine.
[AIAA PAPER 72-1129] 04 p0486 A73-14914

Theoretical and experimental study of the performance of quasi-steady MPD thrusters
10 p1262 A73-24499

EUROPA III - Description of the work performed during the preparatory phase and characteristics of the booster
12 p1548 A73-27377

Propulsion by absorption of laser radiation.
[AIAA PAPER 73-624] 18 p2342 A73-36172

Some characteristics of two-phase nozzle flows
18 p2265 A73-37005

SPECIFICATIONS

NT AIRCRAFT SPECIFICATIONS
NT EQUIPMENT SPECIFICATIONS

Syntax specification system for computerized handwritten pattern grammar generation with user style description for concurrent inputting and analysis at high recognition speed
06 p0671 A73-18535

Elastomer compatibility considerations relative to O-ring and sealant selection.
[SAE AIR 786 A] 08 p0982 A73-20691

SPECIMENS

Influence of small local deviations in specimen diameter on conventional strain at maximum load in tensile test
11 p1380 A73-25448

Effects of specimen geometry on the strength of composite materials.
23 p2996 A73-43633

SPECTRA

NT ABSORPTION SPECTRA
NT ATOMIC SPECTRA
NT BALMER SERIES
NT CONTINUOUS SPECTRA
NT D LINES
NT ELECTROMAGNETIC SPECTRA
NT ELECTRONIC SPECTRA
NT EMISSION SPECTRA
NT ENERGY SPECTRA
NT FRAUNHOFER LINES
NT H ALPHA LINE
NT H BETA LINE
NT H GAMMA LINE
NT H LINES
NT HERZBERG BANDS
NT INFRARED SPECTRA
NT K LINES
NT LINE SPECTRA
NT LYMAN SPECTRA
NT MASS SPECTRA
NT MICROWAVE SPECTRA
NT MOLECULAR SPECTRA
NT NEUTRON SPECTRA
NT NOISE SPECTRA
NT OXYGEN SPECTRA
NT PASCHEN SERIES
NT PLASMA SPECTRA
NT POWER SPECTRA
NT RADIATION SPECTRA
NT RADIO SPECTRA
NT RAMAN SPECTRA
NT RYDBERG SERIES
NT SCHUMANN-RUNGE BANDS
NT SHOCK SPECTRA
NT SOLAR SPECTRA
NT SPECTRAL BANDS
NT STELLAR SPECTRA
NT TELLURIC LINES
NT UVB SPECTRA
NT ULTRAVIOLET SPECTRA
NT VIBRATIONAL SPECTRA

SPECTRAL ABSORPTION

U ABSORPTION SPECTRA
U SPECTRUM ANALYSIS

SPECTRAL BANDS

NT ABSORPTION SPECTRA
NT FRAUNHOFER LINES
NT HERZBERG BANDS
NT SCHUMANN-RUNGE BANDS
NT TELLURIC LINES

Atmospheric windows in different spectral bands due to various gases, comparing continuum and line absorption spectra properties
01 p0037 A73-10364

Vibration-rotation bands of NH in the spectrum of alpha Orionis.
01 p0104 A73-11041

Energy flux intensity in IR bands of selectively radiating molecular gas nonisothermal layer from radiative transfer equation and mathematical model
03 p0396 A73-13183

Solar spectra line intensities in band 201 of visible and near IR regions, noting water vapor bands presence in sunspot spectra
03 p0377 A73-14412

Spectral line shape for interband light absorption with excitons formation in incompletely ordered semiconductor, taking into account interaction with random electrostatic field
04 p0483 A73-14879

Luminous flames thermal radiation total emissivity analysis, considering water vapor, carbon dioxide and soot particles overlapping spectral bands
[WSCI PAPER 72-41] 05 p0638 A73-16677

Optimum spectral band of an infrared detection system for use against forest background radiation.
08 p0662 A73-20811

Intensity variation across Uranus disk during limb darkening-brightening cycles observations to test cloud absence theory, predicting limb brightening in methane bands
08 p1003 A73-20889

Jupiter upper atmosphere temperature inversion to explain brightness temperature variation in 7.9 micron methane band, observing limb brightening
08 p1004 A73-20900

Investigation of long-chain molecule dynamics in condensed state by the IR-spectroscopy and Rayleigh-scattering methods
09 p1122 A73-21956

Spectral properties of laser crystal materials, noting deactivation energy storage in nonuniformly widened luminescence band
09 p1095 A73-22671

Algorithm for spectrum decomposition during continuous man-computer interaction, noting Gaussian distribution of spectral bands and linear approximation for background
09 p1046 A73-22971

Broad band solar EUV absorption in the earth's upper atmosphere.
10 p1214 A73-24747

Second positive system of nitrogen bands in daylight, according to Kosmos-224 data.
13 p1607 A73-28703

Sulfur dioxide infrared-active vibration-rotation combination spectral band, examining quantum numbers, infrared absorption, centrifugal distortion effects and dipole moments
19 p2402 A73-37896

Hydroxyl emission band high resolution spectra in airglow, examining doublet state ratio and rotational temperatures, vibration-rotation levels, temperature sensitivity and Boltzmann equilibrium
20 p2551 A73-38946

Line intensities of CO₂ in the 2.0 micron region.
22 p2890 A73-42708

Effect of line or band shape on the radiative flux of an isothermal spherical layer.
22 p2938 A73-42990

Airglow hydroxyl emission IR spectral bands intensity measurements with allowance for atmospheric extinction, deriving vibrational level excitation rates from spontaneous emission transition probabilities
23 p2972 A73-43690

The C-classification of the spectra of carbon stars.
24 p3138 A73-44997

Spectral data for the nu sub 2 bands of ammonia with applications to radiative transfer in the atmosphere of Jupiter.
24 p3142 A73-45324

SPECTRAL CORRELATION

Russian book on machine-based determination of random process characteristics covering correlation, moment functions, spectral features, probability functions, etc
02 p0149 A73-12866

SPECTRAL EMISSION

Spectrographic observation of quasi-periodic pc 1 micropulsation emission after geomagnetic storm associated with geotail plasma bunching in night time magnetosphere
02 p0158 A73-11918

X ray spectra of solar flares at 0.4-250 keV, emphasizing soft X ray spectra and emission line and continuum features interpolation
03 p0364 A73-13958

Molecular clouds in the galactic center region - Carbon monoxide observations at 2.6 millimeters.
04 p0499 A73-15357

On emission lines of hydrogen, helium and ionized calcium seen on a coronal spectrogram of the March 7, 1970 eclipse.
05 p0621 A73-17036

Spectral emission of natural and artificially induced thermoluminescence in Apollo 14 lunar sample 14163.147.
07 p0897 A73-19884

Nitric oxide densities during sunrise derived from overhead emission measurement as function of altitude
09 p1074 A73-22065

Spectral self modulation and pulsation instabilities of single mode injection GaAs laser with tunable composite cavity
09 p1093 A73-22258

Equation of motion derived for laser resonator with frequency dispersion effect on emission kinetics and spectral features, analyzing unsteady /transient/ processes
09 p1094 A73-22596

Chemical composition of the interstellar gas - X-ray determinations.
10 p1263 A73-23480

Possibility of smoothly tuning the emission frequency of a mixed-dye laser
10 p1228 A73-24582

Optical orientation of metastable He-3 atoms and its influence on the electron density and on the emission of helium atoms in a plasma
10 p1257 A73-24755

Influence of elastic collisions on the intensity of natural oscillations in a He-Ne laser
11 p1376 A73-25432

Relationship between macroinhomogeneity of the field and the kinetics of free regular emission from a ruby laser
11 p1376 A73-26140

Determination of van der Waals broadening of Fe I emission lines induced by neutral He
13 p1685 A73-29360

Balmer-line emission from auroral protons.
17 p2213 A73-34766

The emittance of blackbody cavities.
22 p2930 A73-41981

Theory and technique for surface temperature determinations by measuring the radiance temperatures and the absorptance ratio for two wavelengths.
22 p2853 A73-41986

Spectral emissivity of skin and pericardium.
23 p2950 A73-44213

Polarization variations in the emission of some M-type supergiants
23 p3037 A73-44357

Influence of photodecomposition on the emission of a lamp-pumped dye laser
24 p3098 A73-45518

SPECTRAL ENERGY DISTRIBUTION

Spectral classification through seven-colour photometry.
01 p0095 A73-10295

Energy distribution in the near infrared from nuclei of galaxies. I - M31, M32, NGC 3115, NGC 4151, NGC 4406.
01 p0098 A73-10552

Observational data on galaxies with UV continuum, listing objects with emission lines, s-sd classification and quasar spectral energy distribution
01 p0099 A73-10701

Light scattering from an inhomogeneous fluid.
01 p0077 A73-10971

Recent results of the Goddard rocket program for observing stars.
02 p0215 A73-12324

Mathematical model for spectral distribution function of brain waves, noting analogy with RC oscillator
02 p0135 A73-12557

Performance characteristics of a helical TEA CO₂ laser.
02 p0177 A73-12745

Spectral density curves for intensity fluctuations of stimulated emission from low and IR frequency gas lasers as function of thermal oscillation, mode interference and beat effects
03 p0319 A73-14087

I Zw 1727+50 energy distribution relationship to lacertid spectra, noting featureless optical spectrum, flat or inverted radio spectrum and fast irregular variations
03 p0380 A73-14636

NGC 2992 and the blue stellar object Weedman No. 2.
04 p0502 A73-15690

Pulsed random process energy spectra methods for spectral distribution of signal power in multichannel AM, FM and PM PCM systems with time division multiplexing
04 p0423 A73-15918

Spectroscopic study of the nebula NGC 7635 and the star BD +60.2522 deg.
04 p0503 A73-16005

Zonal spectrophotometric standards - Energy distribution in the spectra of 109 stars in absolute units
05 p0617 A73-16465

Form of the spectrum of radar signals due to precipitation
05 p0552 A73-17356

The distribution of redshifts of quasi-stellar objects and related emission-line objects.
05 p0626 A73-17376

Signal level fluctuations line spectra energy characteristics comparison for oblique and oblique-backscatter sounding, noting changes in harmonics intensity and period
07 p0792 A73-19438

Energy distribution in the spectra of some binaries in a wide spectral range /3300-7300 A and 0.88-1.53 microns/
07 p0901 A73-20318

Structure of lunar maria from their albedo data
07 p0902 A73-20323

Variations in spectral-energy distributions and absorption-line strengths among elliptical galaxies.
08 p1002 A73-20878

Spectral energy distribution and IR radiation source size of M8 star cluster, determining stellar dust temperature
08 p1003 A73-20893

Solar energy outside the earth's atmosphere.
08 p1010 A73-21265

New radiometric techniques and solar constant measurements.
08 p0966 A73-21270

Classical theory of spectral distribution of isolated nonlinear oscillations at combined frequencies
09 p1119 A73-21953

A discussion of the new variations observed in the nucleus of the Seyfert galaxy NGC 5316.
09 p1140 A73-22004

Some results of investigations programmed according to the complex atmospheric energetics experiment /1970-1972/
09 p1115 A73-22989

Carbon stars molecular band strength variations in two-micron spectral region due to thermal emission from circumstellar dust shell
09 p1149 A73-23129

Pulsed gamma ray emission at 5-25 MeV from Crab Nebula pulsar, noting time-averaged energy flux with consideration for telescope efficiency
10 p1272 A73-23535

Spectral energy distribution, photometric gradients and Balmer discontinuities for eclipsing binary RZ Scutum from spectrograms with low dispersion in H-gamma line
10 p1273 A73-23707

Determination of the instrumental profile of the DFS-13 diffraction spectrograph
11 p1363 A73-25615

Influence of the shape of radiators on the energy resolution of Cerenkov shower spectrometers
12 p1496 A73-27205

Spectral energy distribution in several binaries at 3300-7300 A and 0.88-1.53 micron wavelengths.
12 p1540 A73-27290

Albedo distribution in lunar maria.
12 p1540 A73-27295

Emission field structure during transverse mode synchronization in a laser
13 p1626 A73-28005

Dependence of the integrated background light on cosmology, galactic spectra, and galactic evolution.
13 p1671 A73-28035

Maxwell equations for lasing modes of bounded region in laser beam with finite spectral width in form of Fourier integrals
14 p1757 A73-30461

The shape of the spectrum of radar echoes from precipitation.
15 p1842 A73-31006

Spectral-energy dispersal in digital communication-satellite systems.
15 p1842 A73-31096

Proportional counter energy deposition spectral quality prediction from experimental data, using folding procedure to produce composite energy absorption distributions for biological materials
15 p1839 A73-31549

Classical calculation of intensity distribution in the oscillatory-rotational spectra of diatomic molecules
15 p1916 A73-32338

Multicolor photometry of five SBC galaxies: NGC 925, NGC 1073, NGC 3359, NGC 4088, and NGC 7741
16 p2058 A73-32713

Spectral intensity of thermal radiation in a medium for frequencies in the neighbourhood of an absorption line.
16 p2038 A73-34028

Far-infrared observations of galactic nuclei.
17 p2232 A73-34771

Thermal blooming of pulsed laser radiation.
17 p2184 A73-34898

Investigation of the solar X-ray flare spectra by the 'Intercosmos-4' and 'Intercosmos-7' satellites.
18 p2345 A73-36015

Spectral energy distribution, spectrophotometric gradients and Balmer discontinuities for eclipsing binary RZ Scuti from spectrograms with low dispersion in H gamma line
18 p2354 A73-36732

Frequency spectra of strong fluctuations of laser radiation in a turbulent atmosphere
19 p2406 A73-38337

Intensity limitation and energy spreading in an optical field under transient thermal defocusing conditions.
20 p2574 A73-39689

Self-switching in single-heterojunction injection lasers.
20 p2574 A73-39690

Emission spectrum of a Q-switched ruby laser and its dependence on the density of the bleachable filter
21 p2711 A73-40304

Russian book - The solar constant and the energy distribution in the solar spectrum.
21 p2769 A73-40804

Galactic positronium annihilation gamma ray spectrum with 476 keV photon peak, indicating possible origin in supernova explosive nucleosynthesis of positrons
21 p2770 A73-40941

Energy distribution in stellar spectra of various spectral types and luminosities
22 p2906 A73-41974

Analysis of the ultraviolet spectrum of A-type stars observed by the OAO II satellite.
22 p2907 A73-42301

Cerenkov-effect based standard radiation source designed for the calibration of space experiments - Spectral energy distribution measurement
22 p2860 A73-42307

The H II region G333.6-0.2, a very powerful 1-20 micron source.
23 p3028 A73-43527

- Spectrophotometric gradients, temperatures and continuous spectra energy distribution of star SS Cyg, showing dependence on flare development
23 p0306 A73-44245
- Type I and II supernovae spectra, identifying different lines and obtaining energy distributions
24 p3138 A73-45043
- SPECTRAL LINE WIDTH**
Measuring the spread function of infrared spectrometers by means of gas lasers.
01 p0060 A73-10838
- Absorption line profile and equivalent line width derivation for planetary atmosphere with low and high optical thicknesses, assuming arbitrary scattering coefficients
01 p0106 A73-11321
- Gas and solid state lasers amplitude and phase fluctuations calculated from Langevin equations, noting spectral line width and ring laser wave coupling
01 p0061 A73-11355
- Hydrogen reactions and detection by line broadening in beta transformed Ti-Al-V alloy, using X ray diffraction analysis
02 p0183 A73-12759
- Absorption line width method for stellar population of galaxies NGC 1052, 2655, 2903 and 4569 nuclei
03 p0371 A73-13221
- Foreign gas collision broadening effects on 15 micron carbon dioxide bands radiation absorption lines
03 p0345 A73-13697
- Spectroscopic investigation of turbulent plasma parameters.
03 p0347 A73-14095
- Calculation of pressure-broadened linewidths of SO₂ and NO₂.
04 p0414 A73-14815
- Electron spin resonance of manganese ions in frozen methanol solution.
04 p0414 A73-15025
- Effects of uncertainties in damping and microturbulence on theoretical deductions from solar equivalent widths.
04 p0500 A73-15491
- Phononless lines shift and broadening during electron phonon interaction in lanthanum trifluoride-Nd crystal, obtaining temperature dependence of non-radiative transition probability
04 p0484 A73-15566
- Doppler spectral width of radar signal reflected from sea surface as function of illuminated region dimensions, waviness scale and emission factors
04 p0423 A73-15913
- Behavior of carbon monoxide in the upper photosphere.
04 p0504 A73-16027
- Kappa Cassiopeia H, He and O absorption spectra line widths from spectrophotometric analysis
05 p0613 A73-16207
- Microwave method of investigating the quality of ruby boules.
06 p0734 A73-17813
- Absorption-line profiles in the quasi-stellar object PHL 957.
06 p0751 A73-18125
- Emission spectrum of a polyhedral-resonator laser pumped by long pulses.
06 p0702 A73-18580
- On the differing molecular line widths in dense interstellar clouds.
07 p0874 A73-19072
- Turbulent transport measurements with a laser Doppler velocimeter.
07 p0826 A73-20462
- One-dimensional line radiative transfer.
08 p1021 A73-20792
- Line broadening of Lyman alpha wings due to protons calculated via positive molecular hydrogen ion wave functions
08 p0997 A73-20892
- Spatial spectroscopic diagnostic of planetary nebulae. III - Numerical investigation of local absolute monochromatic energies and local absolute energies in spherically symmetric models.
08 p1010 A73-21313
- Stark effect and line broadening in three-dimensional stochastic fields.
09 p1125 A73-21939
- E resonance line broadening due to superhyperfine interactions in ruby, noting angular dependence of mosaic structure mechanism
09 p1132 A73-21954
- Lamb dip measurements on low pressure CO laser vibrational-rotational lines, determining line widths, velocity-changing collision rate and saturation intensities with curve fitting
09 p1090 A73-22078 [AD-758943]
- Spectral behavior and linewidth of /GaAl/As-GaAs double-heterostructure lasers at room temperature with stripe geometry configuration.
09 p1093 A73-22252
- Intensities and half-widths of lines in the A and B bands of the red atmospheric system of O2 bands
09 p1077 A73-22664
- Spectral properties of laser crystal materials, noting deactivation energy storage in nonuniformly widened luminescence band
09 p1095 A73-22671
- Doppler broadening of OI 1304 A multiplet in dissociative excitation of CO₂ and O₂.
10 p1251 A73-24243
- Spectral shift between components of homogeneous /radiation or shock/ line, using ring laser spatial and frequency burnout effects
10 p1228 A73-24464
- Paramagnetic resonance line broadening in ferrite garnets with small additions of rare-earth elements
10 p1261 A73-24703
- Line source functions with variable Doppler width and noncoherent scattering.
11 p1415 A73-25135
- Influence of field inhomogeneity on the intrinsic spectral linewidth of a laser
11 p1332 A73-26166
- Influence of laser field polarization on nonlinear interference effects.
11 p1377 A73-26180
- Luminescence line width in ruby crystals of a laser resonator
12 p1505 A73-26892
- Atoms and molecules in astrophysics; Proceedings of the Twelfth Session of the Scottish Universities Summer School in Physics, University of Stirling, Stirling, Scotland, August 1971.
12 p1538 A73-26920
- Laser dynamic theory with uniformly broadened and Doppler spectral lines based on nonlinear interactions between harmonic oscillations
12 p1506 A73-27139
- Single-frequency neodymium-glass lasers under nonspiking free-oscillation and Q-switched conditions.
12 p1506 A73-27502
- Emission core widths of K Ca II line in umbra and penumbra of sunspots near solar disk center, noting relationship to stellar luminosity
12 p1545 A73-27835
- Solar rotational and vibrational temperature based on turbulent velocity determined from CN molecular line profiles half widths
12 p1547 A73-27870
- Large sunspot high dispersion line spectrum at 6610-6770 A, noting umbral/photospheric contrast and drift curves across limb from photographic recording
12 p1547 A73-27925
- Luminescence quenching and zero-phonon line broadening associated with defect interactions in diamond.
13 p1667 A73-28212
- Formation of spectral lines in planetary atmospheres. V - Collision narrowed profiles of quadrupole lines in hydrogen atmospheres.
13 p1680 A73-28456
- Formation of spectral lines and study of growth curves in a semiinfinite scattering atmosphere
13 p1680 A73-28458
- Spectrophotometry of prominences in the decay-preceding phase
13 p1670 A73-29095
- German monograph - Determination of the OH-concentration distribution in a axisymmetric methane/oxygen flame.
13 p1708 A73-29279
- Determination of van der Waals broadening of Fe I emission lines induced by neutral He
13 p1685 A73-29360
- Spectral width of stationary emission from a laser with a spectrally inhomogeneous solid active element
14 p1757 A73-30266
- Quantum theory of a high energy gas laser
14 p1757 A73-30363
- Stark broadening of high-principal-quantum-number α -alpha lines of hydrogen.
14 p1777 A73-30552
- Some aspects of the exchange-interaction and dipole-dipole broadening of the individual hyperfine components of the EPR spectrum
14 p1775 A73-30580
- Spectrophotometric results from the Copernicus satellite. IV - Molecular hydrogen in interstellar space.
14 p1802 A73-30747
- The spectrum variable α Centauri (HD 125 823).
15 p1935 A73-31485
- Method for measuring the collision-induced broadening of spectral lines
15 p1884 A73-31702
- Determination of atmospheric water-vapor densities from measurements of the 6943.8-A absorption line strength.
15 p1845 A73-32227
- Theory of satellite structures on spectral-line profiles.
15 p1915 A73-32289
- An improved separability approximation for line radiative transport in nonhomogeneous media.
15 p1959 A73-32391
- The equivalent widths of Mg II lines near 2800 A in the spectra of 31 stars.
16 p2059 A73-32838
- Stark broadening and shift of singly ionized aluminum lines.
16 p2040 A73-32845
- Tunable-laser derivative spectroscopy on spectral lines with combined Doppler and collision broadening.
16 p2039 A73-33741
- Equivalent widths of the oxygen A-band absorption lines at different pressures
16 p2039 A73-33815
- Spectral line absorption measurement using optical cavities.
17 p2184 A73-34913
- Single mode operation of flashlamp pumped dye laser achieved after emission spectrum line narrowing by interference filter and successive quartz Fabry-Perot etalons
17 p2185 A73-35769
- Spectral shift between components of homogeneous /radiation or shock/ line, using ring laser spatial and frequency burnout effects
19 p2438 A73-38136
- Detuned single mode laser detailed balance and line width factor in threshold region expressed by Fokker-Planck equation and nonhermitian eigenvalue
20 p2571 A73-38622
- Laser-pumped tunable spin-flip InSb Raman lasers in terms of low field operation, linewidth measurement technique, power output and applications
20 p2571 A73-38623
- Light shift and light broadening in the Rb-87 maser.
20 p2572 A73-38861
- Line widths of CaII K2 and H-alpha and the chromospheres of late stars
20 p2606 A73-39073
- Solar rotational and vibrational temperature based on turbulent velocity determined from CN molecular line profiles half widths
20 p2608 A73-39244
- Ruby laser with a wide emission spectrum.
20 p2574 A73-39696
- Lasing mode generation during normal competition in channels with common upper level, assuming line broadening and atomic diffusion
21 p2712 A73-40307
- Theory of Stark broadening of hydrogen spectral lines in a plasma
21 p2745 A73-40365
- Observations of ultraviolet stellar spectra by the Utrecht Orbiting Stellar Spectrophotometer S59.
21 p2769 A73-40811
- Analysis of the solar X-ray spectrum of 20 August 1971.
21 p2760 A73-40826
- Modulation of spectrum and amplitude of VLF signal in the magnetosphere.
21 p2657 A73-41381
- Stellar chromospheric velocity fields and the width luminosity relations.
21 p2779 A73-41540
- Light spectral width and constant frequency shift during spontaneous diffusion in ideal gas for fixed photon wave
22 p2885 A73-41721
- Solar corona plasma temperature estimation from ground observations based on ionization theory, line width, radio and radar measurements and hydrostatic equilibrium assumption
22 p2906 A73-42067
- Frequency-locking band of a traveling-wave laser.
22 p2869 A73-42255
- Measurement of the natural linewidth of a traveling wave neon-helium laser in the 0.63-micron range
22 p2870 A73-42411
- The temperature dependence of the half widths of some self- and foreign-gas-broadened lines of methane.
22 p2821 A73-42989
- The influence of electron plasma formation on superbroadening in light filaments.
22 p2871 A73-43077
- Pulsed laser saturation spectroscopy - Observation of power broadening by optical nutations.
22 p2871 A73-43082
- Wolf-Rayet stars continuous and line spectral features interpretation by model involving wide emission lines due to Doppler effect in rapidly expanding envelope
23 p3026 A73-43201
- Line identifications, elemental abundances, and equivalent widths for 21 sharp-lined cool peculiar A stars and two comparison standards.
23 p3028 A73-43491
- Theory of wide-band laser radiation in a spectrally-inhomogeneous medium
23 p2987 A73-43708
- Some electric and spectroscopic properties of the radiofrequency plasma in a steady magnetic field.
23 p3012 A73-43831
- EPR-line splitting in irradiated ruby containing impurities
23 p3017 A73-44039
- Theoretical possibilities for the creation of a gamma laser /gazer/ using nuclear transitions
23 p2988 A73-44092

Stimulated gamma emission in long-lived nuclear isomers, proposing gamma lasers based on Mossbauer line broadening effect

23 p2988 A73-44093

On the level of H₂ quadrupole absorption in the Jovian atmosphere.

24 p3129 A73-44443

Formation of spectral lines in planetary atmosphere. IV - Theoretical evidence for structure of the Jovian clouds from spectroscopic observations of methane and hydrogen quadrupole lines.

24 p3129 A73-44449

Methane absorption in the Jovian atmosphere. I - The Lorentz half-width in the 3nu/sub 3/ band at 1.1 micron.

24 p3132 A73-44537

Rotational line overlap in CO₂ laser transitions.

24 p3096 A73-44872

Strengths and air-broadened widths of H₂O lines in the 2950 to 3400 cm region.

24 p3066 A73-45322

The relation between the diffusivity-mobility ratio and the linewidth of spontaneous emission in degenerate semiconductors at relatively high temperatures.

24 p3120 A73-45488

SPECTRAL LINES

U LINE SPECTRA

SPECTRAL NOISE

U WHITE NOISE

SPECTRAL RECONNAISSANCE

Remote measurement of salinity in an estuarine environment.

22 p2850 A73-42730

An analysis of the earth's resources satellite /ERTS-1/ data.

22 p2850 A73-42732

SPECTRAL REFLECTANCE

Mercury - Surface composition from the reflection spectrum.

02 p0218 A73-12420

Spectral transmittance of cryodeposits on a transmitting substrate.

[AIAA PAPER 73-149] 05 p0598 A73-16897

Diffraction effects encountered in the measurement of bidirectional reflectance from square pyramids.

[AIAA PAPER 73-150] 05 p0598 A73-16898

Surface roughness effects on bidirectional reflectance.

[AIAA PAPER 73-152] 05 p0598 A73-16900

Mercury - Interpretation of optical observations.

06 p0743 A73-17430

Electronic spectra of pyroxenes and interpretation of telescopic spectral reflectivity curves of the moon.

07 p0897 A73-19885

Ground based radar measurement of Martian topography, surface temperature and thermal properties by microwave and IR radiometry and spectral reflectivity observation

09 p1144 A73-22259

Reflectance and internal structure of leaves from several crops during a growing season.

11 p1352 A73-25566

Saturn ring spectral reflectivity at 0.36-1.06 microns, noting maximum at both ends of spectral range for amplitude of opposition effect

11 p1424 A73-26126

The spectral albedo of water clouds in the 1-6 micron band.

11 p1357 A73-26195

Kramers-Kronig analysis of relative reflectance spectra measured at an oblique angle.

11 p1400 A73-26421

Asteroidal spectral reflectivity measurement with data reduction for various curve types, noting correlations with UVB color, orbital and physical property parameters and albedo

11 p1429 A73-26686

Graphs for the design of laser mirrors at normal incidence.

13 p1627 A73-28598

Broadband ultraviolet reflectance filters for space applications.

15 p1914 A73-32381

Optical effects of cryodeposits on low scatter mirrors.

[AIAA PAPER 73-732] 18 p2336 A73-36349

Apparent reflectance from a semi-infinite absorbing-scattering medium.

[AIAA PAPER 73-753] 18 p2337 A73-36369

Spectral albedos of the Galilean satellites.

19 p2483 A73-37578

Minor planets and related objects. X - Spectrophotometric study of the composition of /1685/ Toro.

20 p2607 A73-39120

Minor planets and related objects. XI - 0.4-0.8 micron spectrophotometry of /1685/ Toro.

20 p2607 A73-39121

Some results of spectrophotometric studies of natural formations from the manned spacecraft 'Soyuz-9.'

20 p2558 A73-39858

Multispectral reflectance scanning of crop image signatures during April-July growing season, examin-

ing time dependent image changes, discrimination tests and crop types

20 p2561 A73-39900

Crop identification by microwave remote sensing obtained spectral response data from fields with corn, sorghum, soybeans and alfalfa

20 p2562 A73-39902

Remote mapping of standing crop biomass for estimation of the productivity of the shortgrass prairie, Pawnee National Grasslands, Colorado.

20 p2562 A73-39907

Application of the 'differential reflectometer' to materials research in corrosion, ordering and alloying.

21 p2719 A73-40897

Absorption spectra of lunar sections from different lunar areas.

21 p2774 A73-41406

Spectrophotometric study of products formed in the course of superficial oxidation of titanium and TA6V alloy

21 p2722 A73-41587

Low albedo lunar areas, discussing spectral reflectivity, radar backscatter characteristics and Apollo 17 landing site

22 p2909 A73-42495

The wall condition of the specific density of a radiation field

22 p2888 A73-43046

Evaluation of a high accuracy reflectometer for specular materials.

22 p2864 A73-43160

Properties of laser mirrors at non-normal incidence.

22 p2872 A73-43186

Planetary surface reflectivity and topography mapping by ground based radar with emphasis on observational methods

23 p2953 A73-43353

Diffusion in thin film couples of platinum-gold.

23 p3015 A73-43528

Spectral reflectivity of Humorum basin region, comparing to Apollo 11 site and Mare Serenitatis

24 p3129 A73-44436

Comparisons of meteorite and asteroid spectral reflectivities.

24 p3132 A73-44538

Photometric and polarimetric properties of the Bruderheim chondritic meteorite.

24 p3133 A73-44557

Octave bandwidth microwave spectral response.

24 p3068 A73-44996

SPECTRAL RESOLUTION

Design features and observational feasibility of high resolution Michelson interferometer for use in visible spectral range at coude focus of astronomical telescope

01 p0049 A73-10533

Diffraction limited astronomical telescope resolution retrieval by speckle interferometer, noting information extraction via Fourier analysis

01 p0049 A73-10536

Michelson interferometer on Mariner 9 space probe for thermal emission spectrum measurement, discussing spectral resolution, external vibration problem and instrument performance

01 p0054 A73-11228

Solar UV spectra with high angular resolution from rocket observations, obtaining center to limb intensity variations

02 p0207 A73-12325

Optical design of an imaging spectral radiometer for earth resources applications.

04 p0451 A73-15780

A solar radio spectrograph with high time resolution.

05 p0621 A73-17039

High resolution Mossbauer spectrometer design and applications, describing electromechanical Doppler shifter, control electronics and data storage

07 p0822 A73-19170

Numerical integration over Brillouin zone for solids spectral properties calculation, considering crystal optical spectra, phonon effects, IR absorption, electron emission and magnetic susceptibilities

07 p0861 A73-19266

Astronomical spectroscopy with prism in front of Schmidt correcting plate, considering spectral resolution and light loss characteristics in plate field

08 p0966 A73-21359

Digicon multichannel image tube photoelectron counter for astronomical spectroscopy, discussing design information density and accuracy, noise and quantum efficiency

08 p0971 A73-21747

Balloon-borne telescope-UV spectrometer for stellar spectrophotometric measurement with high spectral resolution, discussing system design and operation, image motion compensation and data acquisition

08 p0971 A73-21751

High-resolution study of anomalous dispersion in the ruby R lines.

09 p1090 A73-21940

A subtractive double pass spectrograph for solar observations.

10 p1218 A73-24149

Influence of the shape of radiators on the energy resolution of Cerenkov shower spectrometers

12 p1496 A73-27205

Worldwide variations in atmospheric transmission. I - Baseline results from Smithsonian observations.

15 p1904 A73-31724

Device for spectral line interspace measurements

15 p1878 A73-32145

High-resolution atmospheric-transmission measurement using a laser heterodyne radiometer.

15 p1886 A73-32378

Airborne passive IR line scanner, noting spectral resolution and thermal sensitivity for land and water surfaces energy

17 p2174 A73-35577

Sensitivity and resolution of panoramic analyzers

20 p2537 A73-39455

Optical heterodyne radiometry of the solar surface.

20 p2611 A73-39591

Remotely sensed multispectral scanner data collection over agricultural area, discussing spatial resolution modification for crops and unresolved objects classification

20 p2559 A73-39882

CIE interlaboratory comparison of measurements of photocell spectral sensitivity.

21 p2698 A73-40141

Monte-Carlo-method based calculation of the linearity and resolving power of a Cerenkov spectrometer for purposes of gamma astronomy

21 p2701 A73-40613

Line identifications in the near ultraviolet spectrum of the peculiar A star epsilon Ursae Majoris.

21 p2769 A73-40829

Studies of granular velocities. III - The influence of finite spectral and spatial resolution upon the measurement of granular Doppler shifts.

21 p2776 A73-41478

The inversion of the mean and spatially resolved sodium D2 line profiles from the sun.

22 p2908 A73-42311

A high-resolution Fourier-transform infrared spectrometer.

22 p2861 A73-42587

Spectrum sensitive high amplification solar blind UV sensor for flame surveillance in jet engine environments at 1000 F, using miniature Geiger-Mueller tube

22 p2861 A73-42694

Line intensities of CO₂ in the 2.0 micron region.

22 p2890 A73-42708

Design and performance of light-intensification night vision telescopes

23 p2979 A73-43220

Performances and physical limitations of image intensifiers

23 p2979 A73-43221

Spectral-line analysis of very-long-baseline interferometric data.

23 p2980 A73-43357

Electrooptical radio spectrograph design for high resolution in time and frequency based on photographic film recording density and coherent optical processing data rate

23 p2980 A73-43374

SPECTRAL SIGNATURES

Carbon dioxide laser output signature calculation as function of cavity length based on homogeneously broadened line with dispersion

03 p0320 A73-14455

Spectral signature variability model based on multispectral band scanner data and clustering experiments, discussing data processing algorithms

05 p0555 A73-17151

Luminescence signatures induced by lasers with enhanced specificity for remote active sensing.

05 p0585 A73-17157

Multispectral scanner data analysis by application of spectral radiance signature extension techniques based on preprocessing to reduce atmospheric and scanner look angle effects

20 p2559 A73-39880

Ultrasonic spectroscopy for NDT of composite material tube, noting role of frequency signature and pulse spreading in flaw detection

23 p2984 A73-43641

SPECTRAL THEORY

On the mapping associated with the complex representation of functions and processes.

11 p1333 A73-26645

Laser emission spectral theory, calculating cross relaxation in three and four level systems, monochromatic radiation effects on matter and laser action in inhomogeneous media

17 p2184 A73-34923

SPECTROGRAMS

Soyuz 9 spectrophotometry of earth surface features, comparing manned spacecraft-obtained and conventional spectrograms

03 p3004 A73-14564

Absolute intensity of the H-alpha line in the nebulae NGC 2068 and S-57

05 p0617 A73-16464

Solar flare activity during August 1972, discussing sunspots filter- and spectrograms, proton emissions and geomagnetic disturbances
05 p0622 A73-17095

Spectral energy distribution, photometric gradients and Balmer discontinuities for eclipsing binary RZ Scutum from spectrograms with low dispersion in H-gamma line
10 p1273 A73-23707

Computerized stellar spectrum processing using semiautomatic diagram-code converters, least squares method and reference spectral lines
15 p1878 A73-32141

Device for spectral line interspace measurements
15 p1878 A73-32145

Spectral energy distribution, spectrophotometric gradients and Balmer discontinuities for eclipsing binary RZ Scuti from spectrograms with low dispersion in H gamma line
18 p2354 A73-36732

SPECTROGRAPHS

Radio spectrograms operating at wavelengths between 0.3 and 3 m
08 p0969 A73-21714

Polar coupling coefficients and generalization of the spectrographic method for studying cosmic-ray variations of magnetospheric and interplanetary origin
10 p1267 A73-23927

Analysis of the variations of cosmic rays of magnetospheric and interplanetary origins according to spectrographic data
10 p1267 A73-23928

Determination of the instrumental profile of the DFS-13 diffraction spectrograph
11 p1363 A73-25615

Photometric device for an ISP-28 spectrograph in optical atmospheric studies
15 p1875 A73-31822

Experimental use of self-scanned photodiode arrays in astronomy.
17 p2169 A73-35287

Radiospectrographs for the RATAN-600 radio telescope
21 p2705 A73-41461

SPECTROHELIOGRAPHS

Solar active regions analysis on far UV spectroheliograms obtained by OSO 4 satellite, investigating transition zone structure
01 p0098 A73-10560

High angular resolution observations from rockets - Solar XUV observations.
02 p0216 A73-12336

Heliographic and spectroscopic observations of solar southern hemisphere active region during August 1971 cycle, noting photospheric changes, sunspots and flares
03 p0379 A73-14581

Heliographic latitude distribution of pronounced prominences in both hemispheres of the sun during the eighteenth and nineteenth 11-year solar activity cycles
05 p0609 A73-16204

Spectroheliogram SNR improvement via time averaging of 6103 A core sequence, considering sunspot evolution observed by time lapse technique
05 p0621 A73-17030

Quasi-periodic /wave/ motions in the solar photosphere. I - Preliminary results
10 p1274 A73-23718

Solar rotation as determined from OSO-4 EUV spectroheliograms.
10 p1278 A73-24127

A subtractive double pass spectrograph for solar observations.
10 p1218 A73-24149

Rocket-borne high spatial resolution solar L alpha photographs during 10 July 1972 eclipse, describing instrumentation and photographic details
11 p1422 A73-25935

Studies of the solar chromosphere from millimetre and sub-millimetre observations. I - Isophotometric mapping.
16 p2060 A73-32953

The extreme ultraviolet emissions of solar flares - A comparison between OSO-6 spectroheliograph observations and SFDs.
16 p2053 A73-32959

Radio emissions from solar flares.
17 p2224 A73-34723

Evaluation of pinholes in unbacked metal film filters to be used in rocket- and satellite-borne XUV spectroheliographs.
19 p2429 A73-37262

Heliographic latitudinal zonality of periodic sunspot and flare distributions during 1957-1964 and 1923-1962
21 p2759 A73-40722

Multifrequency meter wave Culgoora radioheliograph design, picture format and operation, using automatic switching and track-scan computer
23 p2958 A73-43372

Millimeter wave radio telescope with high resolution for obtaining heliograph, discussing fast rotational synthesis and array redundancy design features
23 p2958 A73-43373

SPECTROHELIOSCOPES

U SPECTROHELIOGRAPHS

SPECTROMETERS

NT FABRY-PEROT SPECTROMETERS

NT INFRARED SPECTROMETERS

NT MASS SPECTROMETERS

NT SOLAR SPECTROMETERS

NT SPECTROHELIOGRAPHS

NT TIME OF FLIGHT SPECTROMETERS

NT ULTRAVIOLET SPECTROMETERS

Intermediate dispersion spectrograph instrument design for Cassegrain focus of Anglo-Australian telescope, discussing optical and mechanical layouts and remote control
01 p0046 A73-10509

Echelle spectrographs design, applications and performance, discussing modified Czerny-Turner mounting and Schmidt camera arrangements
01 p0046 A73-10510

Prototype design of echelle grating spectrographs for Anglo-Australian 3.8 meter telescope Cassegrain focus, presenting main parameters
01 p0047 A73-10511

A new Cassegrain grating spectrograph. I - Optical design.
01 p0047 A73-10513

A new Cassegrain grating spectrograph. II - Mechanical design and operation.
01 p0047 A73-10514

Grating mosaic for use in conjunction with coude focus of 3.6 meter reflecting telescope, discussing optical and optomechanical implementation methods
01 p0047 A73-10521

Spectrographic equipment of the coude focus of the 3.60-meter telescope - Feasibility study of a universal spectrograph
01 p0048 A73-10522

Blank pupil arrangement of coude spectrograph with echelette for 1.52 meter reflector, describing dispersions obtained, receivers used and electronic camera adaptation
01 p0048 A73-10523

Design study of the coude spectrographs for the 2.2-m telescopes of the MPI for astronomy.
01 p0048 A73-10524

The coude spectrograph and echelle scanner of the 2.7 m telescope at McDonald Observatory.
01 p0048 A73-10525

Fast spectrograph and image slicers for avoidance of light transmission loss caused by central obscuration in astronomical telescope and image intensifier tubes
01 p0048 A73-10526

Electronographic image receptor advantages in spectrography, noting linearity, efficiency and detection threshold and receiver noise absence
01 p0049 A73-10540

The image tube nebular spectrograph of the Asiago Observatory.
01 p0050 A73-10543

A combined magnetic circular dichroism and electron paramagnetic resonance spectrometer.
02 p0167 A73-11951

A versatile Moessbauer spectrometer and its applications in structural mechanics.
03 p0305 A73-12875

A digitally controlled scanning device for a high resolution spectrograph.
05 p0576 A73-16439

Investigation of the gamma-emission of lunar soil delivered by the automatic station Luna 16
05 p0620 A73-17020

Electron-proton spectrometer for the GEOS satellite.
06 p0692 A73-17826

High resolution Mossbauer spectrometer design and applications, describing electromechanical Doppler shifter, control electronics and data storage
07 p0822 A73-19170

An image intensifier spectrometer for remote sensing applications.
07 p0824 A73-19943

Brightness balancing spectrograph method for flame temperature measurement of liquid fuel drop
07 p0826 A73-20423

Photoelectron detection ability increase of image dissector by buffer intensifier tube, noting application for photon counting spectroscopy
08 p0971 A73-21745

Cerenkov shower spectrometer with a conical radiator made of TF-5 glass
09 p1085 A73-23002

Emission spectrographic analysis of used aero engine oil - A tool of maintenance.
09 p1136 A73-23242

The Elbrus cosmic ray spectrograph
10 p1203 A73-23926

Apollo alpha particle spectrometer design, operation, calibration, packaging and flight results
11 p1363 A73-25957

A charged-particle scintillation spectrometer with large geometric factor.
11 p1364 A73-25965

Calibrations of the airglow photometers and spectrometers.
11 p1365 A73-26237

Retarding field electron spectrometer for low kinetic energy electron analysis, discussing design, construction and performance in terms of resolution, sensitivity, luminosity and SNR
11 p1366 A73-26301

Microwave spectrometer with internal dc glow discharge for transient paramagnetic molecules observation, discussing design features and operating parameters effects on spectrum
11 p1366 A73-26303

Influence of the shape of radiators on the energy resolution of Cerenkov shower spectrometers
12 p1496 A73-27205

Quantitative analysis of specific gases by means of a microwave cavity spectrometer.
13 p1612 A73-28224

The photoelectron-spectrometer experiment on Atmosphere Explorer.
13 p1689 A73-28641

High temperature-microwave spectrometer for Zeeman-effect measurements involving diamagnetic molecules
14 p1753 A73-30235

A spectrometric setup for magnetic-tape recording of spectra
15 p1878 A73-32140

NMR spectrometer magnetic field strength-HF field frequency ratio instability spectral density in presence of spin stabilizers
16 p2011 A73-32824

Experimental study of a new geometry for a microwave molecular-beam spectrometer
16 p2038 A73-33173

Apollo 15 and 16 lunar orbital X and gamma ray spectrometer for lunar surface composition and radioisotopes surveys, detailing experimental results
16 p2015 A73-33353

Parameters and energy resolution of the KP303 field effect transistors at low temperatures
17 p1233 A73-34162

The KP303 field transistor in a soft gamma radiation spectrometer
17 p1233 A73-34163

Laser spectrometer for combination scattering, recording polarized spectra with thermoelectrically cooled photomultiplier by photon count
17 p1264 A73-34164

Astronomical optics, including two mirror systems, aspherical plates, lens type field correctors, spectrograph cameras, focal reducers and optical adjustments
17 p1271 A73-35407

Cylindrical X ray source with Al K-alpha radiation production for spherical photoelectron spectrometer, discussing radiation intensity with minimum bremsstrahlung
17 p1276 A73-35765

High resolution nondispersive electron energy analyzer for electron spectroscopy for chemical analysis, using spherical mirror and grid retarding potential field as filters
17 p2176 A73-35770

Radon emanation from the moon - Spatial and temporal variability.
18 p2349 A73-36033

Non-critical Rayleigh scattering from pure liquids.
20 p2570 A73-38618

Ultraminiature X-ray fluorescence spectrometer for in-situ geochemical analysis on Mars.
21 p2765 A73-40241

Lunar orbital gamma ray measurements from Apollo 15 and Apollo 16.
21 p2762 A73-41397

A digital correlation spectrometer employing multiple-level quantization.
23 p2981 A73-43378

Spectrometer design with particle preacceleration for measuring energy spectra of secondary electrons and photoelectrons with high resolution
24 p3092 A73-45553

SPECTROMETRY

U SPECTROMETERS

SPECTROPHOTOGRAPHY

Schmidt and Maksutov spectrographic cameras, discussing correcting devices for mirror aberrations
01 p0047 A73-10512

A subtractive double pass spectrograph for solar observations.
10 p1218 A73-24149

SPECTROPHOTOMETERS

NT INFRARED SPECTROPHOTOMETERS

NT ULTRAVIOLET SPECTROPHOTOMETERS

Two beam optical recording instrument for atmospheric IR transmissivity, discussing spectrophotometers with changeable NaCl, KBr and LiF prisms
04 p0450 A73-15575

Spectrophotofluorometers for returned lunar samples and geological materials organic analyses, discussing optical component performance and calibration to avoid instrumental artifacts effect on spectra
06 p0662 A73-18415

An automated two-channel scanning spectrophotometer system.
08 p0970 A73-21740

- Recorder adapter operational circuit design for continuous logarithmic readout recording of atomic absorption double beam spectrophotometers
11 p1367 A73-26313
- A microspectrophotometer that records the first derivative of the absorption spectrum
12 p1496 A73-26957
- Spectrophotometry of individual regions of Venus
16 p2068 A73-33814
- Single beam spectrophotometer for transmittance measurement constructed from off-axis parabolic mirrors and plane grating monochromator, considering systematic errors
17 p2172 A73-35426
- Use of a stable polarization modulator in a scanning spectrophotometer and ellipsometer.
17 p2175 A73-35751
- A photometric system for automatic recording of optical absorption spectra
21 p2700 A73-40561
- Spectrophotometer design for total ozone measurement for Dobson instrument replacement, describing spectrograph, reads, electronic control, photon counter, readout system and accuracy
23 p2982 A73-43852
- An automated Dobson spectrophotometer.
23 p2982 A73-43855
- Description of a photometer suitable for measuring twilight ozone content variations from a stratospheric balloon gondola
23 p2982 A73-43875
- ### SPECTROPHOTOMETRY
- #### NT STELLAR SPECTROPHOTOMETRY
- Design of an extremely sensitive flame-photometer for analyses in the picogram range using a lock-in amplifier
01 p0051 A73-10925
- Meteorological and atmospheric physics observations by Soyuz manned spacecraft, analyzing spectrophotometry, photography and visual observation data of twilight, night and day horizons
02 p0160 A73-12265
- Airborne photometric measurements of auroral emissions, indicating soft zone and superimposed energetic electron precipitation
03 p0363 A73-13870
- Soyuz 9 spectrophotometry of earth surface features, comparing manned spacecraft-obtained and conventional spectrographs
03 p0304 A73-14564
- Absolute intensity of the H-alpha line in the nebulae NGC 2068 and S-57
05 p0617 A73-16464
- Zonal spectrophotometric standards - Energy distribution in the spectra of 109 stars in absolute units
05 p0617 A73-16465
- Spectrophotometric determination of vanadium with 4-(2-pyridylazo)resorcinol by extraction of tetraphenylphosphonium and arsonium salts.
06 p0661 A73-18269
- Some results of spectrophotometry of the methane absorption band /7250 A/ on the Jovian disk
08 p1007 A73-21063
- Spectrophotometry of Ton 524a, b.
08 p1009 A73-21170
- Bennett comet head spectrophotometry over 352-612 millimicrons, identifying CN, CH, C2 and Na emission features
08 p1010 A73-21315
- Preliminary results of a spectrophotometric survey of the sky in the ultraviolet with the aid of the TD-1 A satellite
08 p0967 A73-21499
- Optical properties of Apollo 12 moon samples.
09 p1144 A73-22191
- Influence of atmospheric haze on the color of the underlying surface observed from a manned spacecraft
09 p1077 A73-22484
- Determination of the transfer function of a planet atmosphere by spectrophotometry of the planet surface from space
09 p1077 A73-22488
- The photometric determination of aluminium in steel after separation on a cation-exchanger
11 p1380 A73-25447
- Determination of the polarization transfer function in space-based spectrophotometric observations of natural formations on a planetary surface
12 p1488 A73-26965
- Stable auroral red arc equatorial edge observation with photometer during recovery phase of magnetic storm on 18 December 1971 in Southern Africa
12 p1492 A73-27611
- Spectrophotometry of prominences in the decay-preceding phase
13 p1670 A73-29095
- Spectrophotometric results from the Copernicus satellite. VI - Extinction by grains at wavelengths between 1200 and 1000 A.
15 p1936 A73-31561
- Study of a niobium-aluminum-silicon system. II - Analysis of ternary niobium-aluminum-silicon alloys by atom absorption spectrophotometry
15 p1890 A73-31992
- Spectrophotometric setup with a detector for individual photon count
17 p2164 A73-34165
- The use of television type sensors in astronomy.
17 p2169 A73-35278
- Spectrophotometry of the 7250-A methane absorption band over the disk of Jupiter.
18 p2355 A73-36864
- Some results of spectrophotometric studies of natural formations from the manned spacecraft 'Soyuz-9'.
20 p2558 A73-39858
- Russian book - Spectrophotometry of niobium and tantalum.
21 p2648 A73-40803
- Spectrophotometric study of products formed in the course of superficial oxidation of titanium and TA6V alloy
21 p2722 A73-41587
- A comparison of the sensitivity of atomic-fluorescent and atomic-absorption flame photometry
22 p2862 A73-42720
- Russian book - Studies of the natural environment from manned orbital stations.
23 p2971 A73-43330
- Spectrophotometric investigations of the earth from manned orbital stations
23 p2979 A73-43333
- Inference of total ozone from photometric measurements of sky radiation.
23 p2973 A73-43856
- Total ozone increase over North America during the 1960's.
23 p2973 A73-43857
- ### SPECTRORADIOMETERS
- Optical design of an imaging spectral radiometer for earth resources applications.
04 p0451 A73-15780
- ERTS-1 satellite-borne high resolution multispectral radiometer scanner, discussing optical surface performance during exposure to direct and reflected sunlight
13 p1621 A73-29331
- Field spectroradiometer system to measure incident and reflected radiation intensity, discussing optical equipment, detectors, electronics and reference blackbodies
15 p1876 A73-31979
- VUV radiometry with hydrogen arcs. I - Principle of the method and comparisons with blackbody calibrations from 1650 A to 3600 A.
17 p2212 A73-35425
- Composition of the earth's atmosphere by shock-layer radiometry during the PAET entry probe experiment.
18 p2313 A73-36797
- Nonequilibrium effects on shock-layer radiometry during earth entry.
18 p2338 A73-36798
- Investigation of the gain instability of a semiconductor radiometer
21 p2700 A73-40539
- Frequency-dependent parasitic modulation component effects on null distortion in spectrometer and temperature measurement accuracy
21 p2700 A73-40541
- Radiospectrographs for the RATAN-600 radio telescope
21 p2705 A73-41461
- Radiometric calibration of a multi-spectral aerial camera.
22 p2862 A73-42824
- ### SPECTROSCOPES
- #### U SPECTROMETERS
- #### SPECTROSCOPIC ANALYSIS
- Computer programs for realistic calculation of atmospheric absorption spectra, discussing spectroscopic data critical survey, procedures, coefficient generation and data presentation
01 p0037 A73-10368
- Thermogravimetric-quadrupole mass-spectrometric analysis of geochemical samples.
01 p0015 A73-11251
- Elemental analysis of a friction and wear surface during sliding using Auger spectroscopy.
01 p0057 A73-11277
- Mossbauer spectroscopic analysis of Sea of Fertility regolith core samples, noting olivine content increase with depth
02 p0214 A73-12242
- Spectral characteristics in visible and UV regions of laser plasma-air interaction, using focused beams on metal targets at atmospheric pressure and vacuum
02 p0176 A73-12351
- Spectroscopic properties of ruby and neodymium lasers under the action of a Co-60 gamma ray
02 p0176 A73-12355
- Spectroscopic study and molecular structure of 1,1-dimethylhydrazine-mono-borane.
02 p0139 A73-12628
- Laser applications to spectroscopic analysis, Raman, maximum resolution and excited state spectroscopies, and spectral instruments manufacture
02 p0177 A73-12725
- Optimization of spectral intervals for remote sensing of atmospheric temperature profiles.
02 p0171 A73-12774
- Mars oxygen photoelectric spectral and aeronautical study, noting water vapor and carbon dioxide photolytic effects
02 p0224 A73-12787
- Use of LEED, Auger emission spectroscopy and field ion microscopy in microstructural studies.
02 p0171 A73-12843
- Laser anemometry in an unseeded supersonic wind tunnel by means of photon correlation spectroscopy of backscattered light.
02 p0172 A73-12860
- Spectroscopic investigation of turbulent plasma parameters.
03 p0347 A73-14095
- Properties of photons determined by interferometric spectroscopy.
04 p0475 A73-15046
- Spectroscopic sounding of cloud; snow and ice covers from below /earth surface/ and above /space or planet/
04 p0473 A73-15570
- High altitude remote spectroscopy of the ocean.
04 p0451 A73-15779
- Early diagnosis of machine damage on the basis of the determination of rubbed-off materials in highly stressed lubricating oils - Employment of spectrographic methods for the analysis of the oil
05 p0582 A73-16998
- Twin spectrograph measurements at 2520-3375 A of metal trace elements in biological sample solutions
06 p0657 A73-17692
- Spectrophotofluorometers for returned lunar samples and geological materials organic analyses, discussing optical component performance and calibration to avoid instrumental artifacts effect on spectra
06 p0662 A73-18415
- Neutron flux anisotropy from plasma focus measured by gamma spectroscopy of activated Ag target, discussing axial concentration
07 p0857 A73-19529
- Moessbauer spectroscopy of lunar regolith returned by the automatic station Luna 16.
07 p0879 A73-19683
- Russian book - Spectroscopy of laser crystals with ionic structure.
07 p0836 A73-20201
- Certain problems of spectroscopy of laser crystals with ionic structure
07 p0836 A73-20202
- Electron-spectroscopic investigations of two modifications of the alloy steel Kh18N10T
09 p1104 A73-22690
- Investigation of the structure of sodium silicate glass containing oxides of multivalent metals by nuclear spectroscopy methods
09 p1110 A73-22980
- Moessbauer spectroscopic studies of iron-doped rutile.
10 p1258 A73-23567
- Spectroscopic study of the vibrational-energy dissipation of the I2 molecule excited by a He-Ne laser
10 p1228 A73-24577
- Mixed valencies and site occupancies of iron in silicate minerals from Moessbauer spectroscopy.
11 p1324 A73-25142
- Multibeam holographic spectroscopy
12 p1497 A73-27453
- Properties of iron impurity in aluminium matrix studied by Moessbauer spectroscopy.
13 p1634 A73-28220
- Preliminary data on lunar soil collected by the Luna 20 unmanned spacecraft.
13 p1674 A73-28302
- Lunar differentiation model based on chemical data from Luna 20 soil and Apollo 16 core samples analysis by combined semimicro atomic absorption spectrophotometric and colorimetric method
13 p1676 A73-28326
- Estimates of possible detection limits for combustion intermediates and products with line-center absorption and derivative spectroscopy using tunable lasers.
13 p1618 A73-28996
- Spectroscopic observations of subsonic and sonic vapor flow inside an open-ended heat pipe.
15 p1958 A73-31936
- Study of a niobium-aluminum-silicon system. II - Analysis of ternary niobium-aluminum-silicon alloys by atom absorption spectrophotometry
15 p1890 A73-31992
- Spectroscopic laser methods of automatic gas analysis based on Raman backscattering, resonance fluorescence or absorption measurements for atmospheric pollutant and exhaust gas detection
16 p2023 A73-32876
- Tunable-laser derivative spectroscopy on spectral lines with combined Doppler and collision broadening.
16 p2039 A73-33741
- Time dependent studies of the aurora. II - Spectroscopic morphology.
18 p2311 A73-36185

Spectroscopic investigations of the combustion zone of flame jets of compacted systems
19 p2402 A73-37508

Oxidation of titanium between 25 C and 400 C.
19 p2442 A73-37950

Al foil surface properties from electron spectroscopic analysis, determining oxide film thickness, annealing effects and oxidation dependence on surface hydrocarbon deposits
19 p2442 A73-38171

Free atom and molecule energy levels studied by electron scattering spectroscopy, discussing energy losses, monochromated electron beams, particle resonance and electric fields
20 p2520 A73-39635

The application of high-speed photography and spectrography for investigations of erosive pulsed plasma streams.
21 p2744 A73-39999

Spectral discharge plasma emission analysis with controlled electrical synchronization of laser vaporized microsamples of steel and wolframite
21 p2711 A73-40302

Spectral determination of rare-earth components in Seignette-ceramic and piezoceramic materials
21 p2752 A73-40555

Spectroscopic studies of supersonic heterogeneous flows with a combustible condensed phase
21 p2754 A73-40702

Gamma-spectrometric analysis of lunar samples from Luna 16.
21 p2774 A73-41404

Al-26 and Na-22 measurements on Luna 16 samples by non-destructive gamma-gamma coincidence spectrometry.
21 p2774 A73-41405

Study of surface by spectrometry of slow electrons
21 p2706 A73-41598

Multiple-beam holographic spectroscopy.
22 p2852 A73-41812

The spectral comparison method for temperature measurement in two-phase flames.
22 p2853 A73-41987

Effect of radiometric errors on accuracy of temperature-profile measurement by the spectral-scanning method.
22 p2853 A73-41988

Spectroscopic measurement of upper atmospheric temperature.
22 p2846 A73-42062

Pulsed laser saturation spectroscopy - Observation of power broadening by optical nutations.
22 p2871 A73-43082

Spectral-line analysis of very-long-baseline interferometric data.
23 p2980 A73-43357

Ultrasonic spectroscopy for NDT of composite material tube, noting role of frequency signature and pulse spreading in flaw detection
23 p2984 A73-43641

Spectroscopic measurements of plasma temperatures and density at X type magnetic neutral points, suggesting ion acoustic instability role in turbulent conductivity
24 p3118 A73-45461

PETROSCOPIC TELESCOPES

NT STRATOSCOPE TELESCOPES

A new Cassegrain grating spectrograph. I - Optical design.
01 p0047 A73-10513

Spectroscopic telescope diffraction gratings, discussing fabrication methods and performance characteristics of echelle and Coude gratings
01 p0047 A73-10518

Design study of the coude spectrographs for the 2.2-m telescopes of the MPI for astronomy.
01 p0048 A73-10524

Spectrophotometric results from the Copernicus satellite. I - Instrumentation and performance.
14 p1754 A73-30744

A high-resolution photoelectric spectrophotometer at the coude focus of a 2.6-m telescope
16 p2011 A73-32714

Monte-Carlo-method based calculation of the linearity and resolving power of a Cerenkov spectrometer for purposes of gamma astronomy
21 p2701 A73-40613

PETROSCOPY

NT ABSORPTION SPECTROSCOPY

NT ASTRONOMICAL SPECTROSCOPY

NT AUORAL SPECTROSCOPY

NT GAS SPECTROSCOPY

NT INFRARED SPECTROSCOPY

NT MAGNETIC SPECTROSCOPY

NT MASS SPECTROSCOPY

NT MOLECULAR SPECTROSCOPY

NT NUCLEAR RADIATION SPECTROSCOPY

NT OPTICAL EMISSION SPECTROSCOPY

NT RADIO SPECTROSCOPY

NT RAMAN SPECTROSCOPY

NT SPECTROPHOTOGRAPHY

NT SPECTROPHOTOMETRY

NT SPECTROSCOPIC ANALYSIS

NT STELLAR SPECTROPHOTOMETRY

NT ULTRAVIOLET SPECTROSCOPY

NT VACUUM SPECTROSCOPY

NT X RAY SPECTROSCOPY

Surface photovoltage spectroscopy - A new approach to the study of high-gap semiconductor surfaces.
08 p0968 A73-21620

A probe system for spectrometric determination of temperature and concentration distributions in combustion gases.
13 p1612 A73-28432

Auger spectroscopy usefulness demonstration by determination of impurity segregation in localized regions, reviewing grain boundary segregation role in metal properties deterioration
15 p1892 A73-32248

Spectroscopic measurement of material samples refractive index at submillimeter wavelengths
17 p2120 A73-34157

Book - Progress in high temperature physics and chemistry. Volume 5.
17 p2255 A73-35592

Materials testing via ultrasonic spectroscopy developed from pulse-echo technique, discussing application to metal grain size determination and carbon fiber composite quality control
21 p2707 A73-41136

Combined LEED, Auger electron and flash desorption spectroscopy of metals on single crystal surfaces.
21 p2706 A73-41596

Plasma temperature measurement by a spectroscopic technique with continuous automatic recording
24 p3115 A73-44757

SPECTRUM ANALYSIS

Canonical expansions of random processes, discussing discrete and continuous set transformations for spectral representation and shaping filters in time domain
01 p0068 A73-10027

Hilbert transform for single and narrow band signal analysis with 90 deg spectral component phase shift in frequency region
01 p0015 A73-10076

The spectral density technique for the determination of eddy fluxes.
01 p0072 A73-10145

A two-component model of the annual line in the spectrum of the geomagnetic field.
01 p0036 A73-10331

Measurement of the complex index of refraction of atmospheric aerosols using optical spectral analysis techniques.
01 p0045 A73-10375

A computer-controlled digital spectrum scanner for La Silla.
01 p0047 A73-10515

The spectrum of the compact galaxy IIZw43.
01 p0098 A73-10557

Accuracy of the determination of the spectral density of a vibrational process with the aid of a spectrum analyzer
01 p0077 A73-10677

Nature of galaxies with an ultraviolet continuum. I - Basic spectral and color characteristics
01 p0099 A73-10702

Hydrogen lines in the spectrum of the Markarian 6 galaxy during its activity period
01 p0100 A73-10703

A study of the spectrum-variable silicon Ap star 56 Ari.
01 p0106 A73-11305

Radio spectrum analysis of loop prominence development, temperature and H atom density on May 13, 1971, noting consistency with Jefferies-Orrall model
01 p0108 A73-11387

Latitudinal characteristics search in Pc 4 and Pc 5 micropulsations events via generalized three dimensional spectral analysis
02 p0156 A73-11737

Possibility of using a laser flame as a source of light in the isotope spectral method
02 p0176 A73-12094

Possibilities of using organic compound lasers in spectral analysis
02 p0176 A73-12095

A modernized technique for ionospheric drifts with spectral analysis.
02 p0161 A73-12286

Study of energy spectra of primary cosmic rays at very high energies on the proton series of satellites.
02 p0207 A73-12328

Mercury - Surface composition from the reflection spectrum.
02 p0218 A73-12420

Midlatitude excess radiation energy density relation to primary cosmic ray background from spectrum measurement data
02 p0208 A73-12460

A 1.1 micron spectrogram of the central coma of Comet Bennett /1969 i/.
02 p0226 A73-12832

Cross spectral analysis for auroral pulsations coherency in spatially separated patches, noting TV image recording of frequency and energy spectra
03 p0298 A73-12879

SPECTRUM ANALYSIS

Light scattering from systems with chemical oscillations and dissipative structures.
03 p0273 A73-13285

A balloon-borne observation of the X-ray source Cygnus XR-1.
03 p0361 A73-13367

Stroboscope-like frequency spectrum examination of short impulses.
03 p0308 A73-13570

MWC 349 - A new radio star.
03 p0374 A73-13849

Radially conducting cone wave spectrum calculation for noncophasal excitation, noting circularly polarized TEM and elliptically polarized TM wave amplitudes
03 p0278 A73-14058

Single band optical mixer heterodyne spectrum analyzer for laser radiation image spectrum suppression
03 p0319 A73-14083

Uncertainties in coherent measurement of the mean frequency and variance of the Doppler spectrum from meteorological echoes.
03 p0279 A73-14525

Pulse pair estimation of Doppler spectrum parameters.
03 p0279 A73-14527

Observation and spectral analysis of instantaneous signals of velocity fluctuation in the laminar boundary layer
03 p0297 A73-14602

I Zw 1727+50 energy distribution relationship to lacertid spectra, noting featureless optical spectrum, flat or inverted radio spectrum and fast irregular variations
03 p0380 A73-14636

Comets Tago-Sato-Kosaka and Bennett spectra twilight observation by 200 inch reflector, considering Comet d'Arrest for in situ study by instrumented space probe
04 p0495 A73-14761

Cometary heads observations indicating precursor decay lengths from 100-10,000 km, considering visible and UV molecular and atomic emissions
04 p0495 A73-14764

Investigation of certain characteristics of induced Raman scattering produced in a plane-parallel ruby-laser resonator
04 p0458 A73-14882

Status and prospects of EEG spectral analysis.
04 p0411 A73-15278

A study of simple chromatogram - Compression algorithm efficiency.
04 p0449 A73-15445

One dimensional analysis of saturation spectral lines for energy transfer in plasma waves interaction, noting Landau damping effect on parametric instability
04 p0482 A73-15650

Spectral analysis of the vibrations of mechanical systems with continuous mass which have a finite number of attached concentrated masses
04 p0476 A73-15659

Correlation analysis of the continuum radio emission of noise storms.
04 p0504 A73-16028

Oxygen 1S production efficiency of photons at 812-1216 A measured by O I 5577 A green line detection during carbon dioxide photodissociation
05 p0546 A73-16049

Observations of low-energy protons with the Molniya 1 satellite in July-August, 1970.
05 p0608 A73-16084

Ionospheric propagation effects on riometer recorded cosmic radio emission spectra, noting temporal and frequency spectra dependence on ionospheric plasma turbulence scale
05 p0573 A73-16266

Luminous flames thermal radiation total emissivity analysis, considering water vapor, carbon dioxide and soot particles overlapping spectral bands [WSCJ PAPER 72-41]
05 p0638 A73-16677

Measurement of vibration characteristics by impact testing.
05 p0637 A73-17233

Methods and techniques in spectral analysis of random-vibration data
05 p0637 A73-17271

X-ray spectral investigation of some vanadium compounds with a Cr3Si structure
05 p0588 A73-17295

Effect of alkali-earth oxides on the optical and EPR spectra of irradiated alkali silicate glass
05 p0589 A73-17296

Absolute Raman scattering cross-section of molecular hydrogen.
05 p0601 A73-17340

Venus high resolution spectra for carbon dioxide abundance variations, discussing CO, HF and HCl composition
06 p0744 A73-17435

Characteristics of spectra of pi2-type geomagnetic pulsations along the meridional profile
06 p0689 A73-17543

The charge transfer spectrum of /LiNa+/.
06 p0726 A73-18250

SPECTRUM ANALYSIS

Spectrophotometric determination of vanadium with 4/2-pyridylazo/resorcinol by extraction of tetraphenylphosphonium and arsonium salts. 06 p0661 A73-18269

The radio continuum of the Large Magellanic Cloud. IV - Spectra of sources. 06 p0754 A73-18632

X-ray spectral studies of manganese-aluminum binary alloy systems 06 p0710 A73-18644

Luminosity classification of stars earlier than O9. 07 p0875 A73-19120

Reflection spectra of lunar dust grains with amorphous coatings. 07 p0876 A73-19583

Scattered twilight light variations at 5500 to 6600-A wavelengths according to spectral observations in 1962 through 1968 at Abastumani 07 p0817 A73-19587

Extremely compact galaxy CGCG 1439 + 5344. 07 p0877 A73-19601

Nuclear magnetic resonance properties of lunar samples. 07 p0893 A73-19846

Electrical conductivity and Moessbauer study of Apollo lunar samples. 07 p0898 A73-19896

Laser microspectral analyzer operation in Q switched mode, discussing microplasma generation under inert gas at variable pressure 07 p0836 A73-20162

Search for 3C 191 ionization potential-red shift correlations to other quasar absorption lines 07 p0900 A73-20237

Repeated cascade structure and kinetic description for homogeneous turbulence spectrum, considering coupled hierarchies origin from transfer function and eddy viscosity development 07 p0812 A73-20472

On the S- and B-components of solar radio and X-emission and their relationships to energetic solar events. 08 p0997 A73-20771

An application of the Michelson interferometer to nonthermalized spectral features in the night airglow. 08 p0963 A73-20870

Magnesium II doublet profiles of chromospheric inhomogeneities at the center of the solar disk. 08 p1004 A73-20908

Revised chemical abundances of four population-II A-type stars. 08 p1006 A73-20932

Spectrophotometry of Ton 524a, b. 08 p1009 A73-21170

Some statistical characteristics of the spectra of polar magnetic substorms 08 p0959 A73-21293

Special features of the dynamic spectrum of Pi2 type pulsations 08 p0960 A73-21307

Non-Gaussian properties of the EEG during sleep. 08 p0931 A73-21465

Image tube spectra of planetary nebulae for relative line intensities and radial velocities, considering nebulae properties 09 p1141 A73-22015

Objective prism spectrum surveys for H alpha emission of stars in Chamaleon T association, listing emission line stars 09 p1142 A73-22033

Fine structure of Pc 1 pulsations. I - Experimental evidence. 09 p1074 A73-22068

A new approach to picosecond laser pulse analysis shaping and coding. 09 p1090 A73-22077

Balloon flight observations of Uhuru sources for spectral characteristics, noting hard X ray band sources 09 p1137 A73-22173

Residual geomagnetic field from the satellite Cosmos 49. 09 p1076 A73-22192

Influence of combinational coupling on the spectral and statistical properties of multimode fluctuations in a traveling-wave laser 09 p1094 A73-22599

On the use of running means in the power spectrum analysis of ionospheric data. 09 p1078 A73-22831

Algorithm for spectrum decomposition during continuous man-computer interaction, noting Gaussian distribution of spectral bands and linear approximation for background 09 p1046 A73-22971

Processing the spectra of semiconductor detectors in a semi-automatic system containing data storage elements and a computer 09 p1085 A73-23005

The structure of the Crab Nebula. II - The spatial distribution of the relativistic electrons. 09 p1151 A73-23290

On the calibration of flux densities and the determination of spectra at radio frequencies. 10 p1272 A73-23527

Some aspects of measuring the differential cosmic-ray spectrum. 10 p1268 A73-24213

Dispersion equation and spectrum conversions for slow wave excitation and propagation in plane waveguide with homogeneous isotropic impedance 10 p1190 A73-24601

Estimate of the spectral density of a stationary random process by an indirect method 11 p1341 A73-25017

Spectral observations of southern planetary nebulae. I. 11 p1415 A73-25070

Photometric characteristics and structure of nebulae NGC 6914a, IC 5076, and Ced 201 11 p1416 A73-25228

C-13 nuclear magnetic resonance in organic geochemistry. 11 p1325 A73-25461

Near-field analysis by the plane-wave spectrum approach. 11 p1329 A73-25674

Some considerations on the continuous space-time spectral analysis of atmospheric disturbances. 11 p1394 A73-25723

Solar X-ray bursts from OSO-7 observations, analyzing spectra obtained from proportional and scintillation counters 11 p1413 A73-25948

A spectral analysis method for single radio signals 11 p1331 A73-26101

On the estimation of the directional spectrum of surface gravity waves from a programmed aircraft altimeter. 11 p1358 A73-26347

Kramers-Kronig analysis of relative reflectance spectra measured at an oblique angle. 11 p1400 A73-26421

Simplified photoionization analysis of quasar emission spectra. 11 p1427 A73-26616

Interferometric studies of interstellar CH₄/ molecules. 11 p1427 A73-26617

The spectrum and variability of Hercules X-1 observed by OSO-7. 11 p1428 A73-26626

Digitally scanned spectral convolution by computerized filtering for noise spectra quality improvement with instrument signature removal 11 p1334 A73-26679

Harmonically unrelated spectral components of Pi 2 micropulsations generated by oscillations in magnetospheric tail cavities 11 p1359 A73-26711

Temperature dependence of the Moessbauer spectra of iron-cobalt-vanadium alloys 12 p1509 A73-26839

Automatic classification of G5-K5 stars by means of 166 A/mm objective prism spectra /4000-4550 A/. 12 p1538 A73-26858

A microspectrophotometer that records the first derivative of the absorption spectrum 12 p1496 A73-26957

Ring cavity for analyzing the spectral composition of CO₂-laser radiation 12 p1506 A73-27217

Facility to determine spectra of light scattered at free plasma electrons during single laser pulse, obtaining electron component profiles with high speed streak camera 12 p1506 A73-27301

Anisotropic piezoelectric heterogeneous acoustic surface waveguides of arbitrary cross section computing mode spectrum by efficient and accurate numerical techniques 12 p1480 A73-27568

A uniqueness theorem for the solution of the inverse problem of spectral analysis in the case of a differential equation with periodic boundary conditions 12 p1518 A73-27727

Analysis of the non-Gaussian spectra of interplanetary scintillations. 12 p1547 A73-27877

Spectral analysis of a physical system which can be represented by a stationary linear active electronic network 13 p1589 A73-28474

Harmonic spectral analysis of nystagmus waveform frequency content for clinical vestibular examination via digital computer 13 p1579 A73-28502

Representation of real narrowband signals with the use of nonuniformly displaced base functions with positive coefficients. 13 p1583 A73-28668

Some results of an analysis of stable geomagnetic Pc4 pulsations at a network of stations. 13 p1608 A73-28719

Wavevector/frequency spectrum of turbulent-boundary-layer pressure. 13 p1604 A73-29262

Angle-of-arrival difference spectrum of a simple interferometer in turbulent air. 13 p1621 A73-29330

Spectral analysis of the signal from the Laser Doppler Velocimeter - Turbulent flows. 14 p1752 A73-29919

Redshift-magnitude bands, quasi-stellar sources, and systems of redshift. 14 p1797 A73-30004

Transition probabilities of neutral and singly ionized germanium. 14 p1783 A73-30243

Measurements of the electronic recombination coefficient in a helium plasma jet. 14 p1780 A73-30245

Absorption spectrum analysis of free Cu, Ca, Na, Zn, Ni and Cr atom concentration in acetylene air flame zones 14 p1817 A73-30458

Spectral analysis of optical pulse signals in application to the problem of synchronizing PCM laser communications lines 14 p1729 A73-30556

The cosmic gamma-ray spectrum between 0.3 and 27 MeV measured on Apollo 15. 14 p1788 A73-30731

Nuclear gamma resonance spectra of Sn119 and Te125 and the electron structure of ternary diamond-like semiconductors Cu₂SnS₃, Cu₂SnSe₃ and Cu₂SnTe₃ 14 p1784 A73-30851

Heart rate variability analysis for ergonomics purposes, discussing interpolations, algorithms and physiological effects and spectral analysis methods 14 p1720 A73-30882

Varactor frequency multipliers of the parallel type. I - Spectrum analysis of the voltage on a partially open-circuited varactor. 15 p1849 A73-30991

Investigations of Pi2 micropulsations. I - Frequency spectra and polarisation. II - Relevance of observations to generation theories. 15 p1866 A73-31064

Spectral investigations of 6300 A forbidden OI twilight emission at Abastumani 15 p1867 A73-31264

Stellar atmospheric conditions taking into account A5 and early stars, considering spectral characteristics, absorption spectra and spectrum prediction 15 p1932 A73-31305

Spectral investigations of UV Ceti-type flare stars and search for new variables of this type carried out at Crimea. 15 p1934 A73-31479

Pulsar fluctuation spectra and the generalized drifting-subpulse phenomenon. 15 p1936 A73-31558

Effect of dispersy on spectral analysis data for alloyed powders 15 p1888 A73-31597

Some statistical characteristics of atmospheric ozone measurements 15 p1868 A73-31612

Comparison of methods for calculating long-wave radiation fields 15 p1904 A73-31785

Software design and implementation for real time power spectral analysis on IBM-1130 8K-core computer, discussing coherence and cross spectra estimation and arithmetic errors 15 p1848 A73-32032

Intensity of thermal fluctuations of plasma flute instabilities in open confinement systems in the presence of a feedback system 15 p1920 A73-32307

Upper level populations in optically excited cesium vapor 15 p1914 A73-32337

The dynamics of the Andromeda Nebula. 15 p1941 A73-32400

Midlatitude excess radiation energy density relation to primary cosmic ray background from spectrum measurement data 15 p1927 A73-32610

Quantitative analysis of the spectrum of beta Lyr. I - Variation of certain hydrogen and helium emission lines 16 p2057 A73-32710

Extragalactic diffuse X ray background above 30 keV, discussing spectral breaks and bumps at various energies 16 p2051 A73-32749

Properties of geomagnetic Pi2 pulsation spectra along a meridional profile. 16 p2001 A73-32767

Spectral analysis of sunspot flares. 16 p2052 A73-32957

Structural shock response spectrum analysis for maximum dynamic loads and damage potential determination 16 p2014 A73-33135

Solar electrons, Galactic electron radiation modulation and spectrum of high energy cosmic ray electrons 16 p2055 A73-33293

Evaluation of machinery characteristics through on-line vibration spectrum monitoring. [ASME PAPER 73-GT-68] 16 p2048 A73-33520

- Scanning IR spectrometer combination with optical telescope for 0.8-2.2 microns reflected IR light measurement during full moon phases in lunar surface composition determination 16 p2064 A73-33763
- Infrared radiation of the moon at 3.5 to 3.9 microns 16 p2064 A73-33764
- Spectral studies of the atmospheres of Mars and Venus 16 p2067 A73-33812
- Spectrophotometry of individual regions of Venus 16 p2068 A73-33814
- Application of frequency analysis to ultrasonic non-destructive testing 16 p2016 A73-34014
- A search for periodic variations in geomagnetic activity and their solar cycle dependence. 17 p2157 A73-34073
- Measurement of the spectrum of a helical TEA CO₂ laser. 17 p2183 A73-34208
- Intrinsic ultraviolet colors from OAO-2 Telescope observations for stars on the main sequence. 17 p2225 A73-34290
- Saturn - A study of the 3 nu sub 3 methane band. 17 p2231 A73-34765
- The effects of the observational system and the method of interpolation on the computation of spectra. 17 p2201 A73-34852
- Automatic analysis and classification of electroencephalograms 17 p2116 A73-34966
- The use and evaluation of shock spectra in the dynamic analysis of structures. 17 p2248 A73-35041
- [ASME PAPER 73-APM-22] U.S. Army helicopter vibration data for OH-6A, OH-58A, UH-1H and CH-54B models obtained from triaxial accelerometer locations, presenting spectral and statistical analyses 17 p2106 A73-35086
- [AHS PREPRINT 763] Application of surface acoustic wave devices to radar. 17 p2140 A73-35319
- Development of data analysis in sound and vibration. 17 p2131 A73-35335
- Aqueous ammonium sulfate aerosol optical properties via attenuated total reflectance /ATR/ spectroscopy 17 p2171 A73-35402
- CO laser emission lines attenuation measurements in atmosphere, attributing inconsistencies in previous experiments to model 17 p2185 A73-35405
- Faraday depolarization of radio galaxies and quasars with simple spectra. 17 p2234 A73-35621
- Decomposition of pulse-type data by cepstrum techniques. 17 p2127 A73-35635
- Spectral characteristics of the scatter field from a rotating impedance cylinder in uniform motion. 17 p2129 A73-35707
- Drift measurement with spectral analysis during period of chemical releases into the ionosphere. 18 p2314 A73-35955
- Velocity of the reflection points reveals structure and motions in the ionosphere. 18 p2305 A73-36000
- Artificial earth satellite brightness attenuation and rotation periods from spectral analyses of photometric curves by mathematical simulation 18 p2315 A73-36142
- Fluorescence excitation and photoelectron spectra of CO₂ induced by vacuum ultraviolet radiation between 185 and 716 angstroms. 18 p2346 A73-36266
- Some applications of spectral analysis in ultrasonic testing. 18 p2316 A73-36485
- Objective analysis method tested via comparison to known function at radiosonde observation stations, considering description of spectral analyses of wind field kinetic energy 18 p2332 A73-36702
- Laboratory for the automatic treatment of analog signals 18 p2297 A73-37086
- X-ray spectrum of the entire Cygnus Loop. 18 p2357 A73-37103
- 8-13-micron spectra of NGC 7027, BD +30.3639 deg, and NGC 6572. 18 p2357 A73-37104
- Spectrum analysis of tropical cloudiness. II. 19 p2446 A73-37430
- Infrared spectrum of the Orion Nebula between 55 and 200 microns. 19 p2484 A73-37614
- The absorption spectrum of Rb I between 350 and 810 A. 19 p2462 A73-37623
- Use of spectral characteristics for the determination of the parameters of a corrector for thermal pickups 19 p2430 A73-37844
- Some statistical characteristics of the spectra of polar magnetic substorms. 19 p2425 A73-37922
- Characteristics of the dynamic spectrum of Pi2 type pulsations. 19 p2425 A73-37936
- Measurements of artificial satellite signal Doppler spectrum. 19 p2407 A73-38351
- Spectral analysis and a synthesis of linear systems with variable and random parameters in finite time intervals 20 p2540 A73-38704
- Hydroxyl emission band high resolution spectra in airglow, examining doublet state ratio and rotational temperatures, vibration-rotation levels, temperature sensitivity and Boltzmann equilibrium 20 p2551 A73-38946
- Approximate methods for the mathematical description and analysis of processes controlling the spectral characteristics of random vector signals 20 p2542 A73-39047
- A new method for determining the degree of oxygenation of hemoglobin spectra in the case of inhomogeneous light paths, explained in an analysis of spectra of the human skin 20 p2517 A73-39145
- Shock spectrum analysis and structural design. 20 p2617 A73-39270
- Optical heterodyne radiometry of the solar surface. 20 p2611 A73-39591
- Photoelectron energy spectra for atomic and molecular binding energies, examining spectrum signatures, angular distribution, autoionization, rare gases, carbon monoxide and cyanocobalamin 20 p2520 A73-39634
- Muon production in large air showers, determining mean origin height via magnetic spectrography, distance from shower core, geomagnetic deflection and trajectory angles 20 p2603 A73-39707
- Cosmic ray muon zenith angle distribution during horizontal air showers, discussing kaon and pion decay, spectrum characteristics, bremsstrahlung effects and flux upper limits 20 p2603 A73-39708
- Relationship between sea wave parameters and the spectra of aerial photography and radar imagery of sea surface. 20 p2531 A73-39891
- Remote mapping of standing crop biomass for estimation of the productivity of the shortgrass prairie, Pawnee National Grasslands, Colorado. 20 p2562 A73-39907
- Infrasound from convective storms - Examining the evidence. 21 p2679 A73-40070
- CO atmospheric vertical distribution from balloon-borne IR grating spectrometer observations, noting concentration decrease with altitude 21 p2680 A73-40078
- Harmonic frequency content analysis from fluxgate magnetometer recorded Pi 2 pulsation spectral waveform, noting agreement with earth current spectrum 21 p2681 A73-40154
- Investigation of the spectral properties of sensitized polyvinylcinnamate 21 p2646 A73-40256
- A fast IR spectral transform imager. 21 p2699 A73-40273
- Bounds estimation for normalized second spectral moment of random radar signal process in terms of measured quantities statistics without weighting 21 p2650 A73-40343
- Q switched carbon dioxide laser pulse forms and spectrum, covering mirror and prism configurations, sodium chloride plate irradiation, laser wavelengths and pressure effects 21 p2714 A73-40572
- Estimate of the spectrum of cosmic-ray variations in the high-energy range on the basis of subterranean observations 21 p2758 A73-40602
- Chromium-rare-earth energy transfer in YAlO₃. 21 p2752 A73-40957
- Clinical applications of spectral analysis and extraction of features from electroencephalograms with slow waves in adult patients. 21 p2638 A73-41011
- Complete hydrogen and helium particle spectra from 30- to 60-MeV proton bombardment of nuclei with A = 12 to 209 and comparison with the intranuclear cascade model. 21 p2744 A73-41019
- Materials testing via ultrasonic spectroscopy developed from pulse-echo technique, discussing application to metal grain size determination and carbon fiber composite quality control 21 p2707 A73-41136
- MK spectral classification system validity, discussing standards for O4-G2 spectral range and limits in visual spectral classification 21 p2771 A73-41236
- Relative sunspot number periodicities determination, using power spectral analysis 21 p2777 A73-41489
- Correlation and spectral analysis of daily solar radio flux. 21 p2762 A73-41494
- Carbon, CN, CH, MgH, NH and OH line behavior in solar photospheric spectra 21 p2778 A73-41528
- Effect of Gaunt factors on analysis of X-ray spectra - Viability of a thermal intergalactic medium in the Coma cluster. 22 p2900 A73-41753
- Titan narrow band observations at 8-13 microns, noting temperature inversion and spectroscopically active component 22 p2905 A73-41770
- Scattering of electromagnetic waves from rough oscillating surfaces using spectral Fourier method. 22 p2824 A73-41855
- Solar cycle control in the 27-day variation of geomagnetic activity. 22 p2846 A73-41945
- The inference of temperature from the infrared spectra of planets. 22 p2906 A73-42065
- Experiment involving the application of the LMA-1 laser microanalyzer to the investigation of metallic materials 22 p2868 A73-42100
- Wave spectrum analysis of electron beam-plasma longitudinal electrostatic fluctuations, finding triplet wave line shape and intensity and dispersion relations 22 p2891 A73-42240
- Spectral structure of tropospheric vertical temperature profiles over Cape Kennedy, Florida. 22 p2849 A73-42544
- Spectral characteristics of solar corona measured by visual, rocket and satellite observation, discussing K and F coronal regions, eclipse phenomena and analytical techniques 22 p2910 A73-42650
- Aircraft flyover noise - Spectral analysis of sounds and sound intensity fluctuations. 22 p2800 A73-42946
- Variations in the distribution and physical properties of Perseid meteors. 22 p2914 A73-43015
- Energy level transitions in Ca XVII and Ti XIX UV spectra, basing identifications on extrapolation method 22 p2914 A73-43016
- On the spectrum of the S- and B-components of solar radio emission at dm-wavelengths. 22 p2915 A73-43038
- Fireball spectral data reduction for self absorption, Fe abundance, excitation temperatures, relaxation time and optical thickness effects 22 p2915 A73-43043
- Laser cross-beam intensity-correlation spectrum for a turbulent flow. 22 p2872 A73-43158
- Spectral theory and convolution systems of diagonal and nondiagonal discrete transformation filters on Abelian groups, comparing with computational simulations 23 p2957 A73-43311
- Applications of digital frequency warping to unequal bandwidth and Vernier spectrum analysis. 23 p2952 A73-43312
- Digital filter bank with integrated FFT computer 23 p2956 A73-43326
- Kinetics of chemical high-pressure lasers 23 p2987 A73-43716
- Spectral analysis of traveling planetary scale waves - Vertical structure in middle latitudes of Northern Hemisphere. 23 p2978 A73-43982
- Simciz 59 /Sharpless 104/ nebula radial and expansion velocity indicating type I supernova origin, discussing spectral and interferometric measurements and relativistic electron energy and density 23 p3035 A73-44233
- Spectral reflectivity of Humorom basin region, comparing to Apollo 11 site and Mare Serenitatis 24 p3129 A73-44436
- Terrestrial rock optical constants, finding refractive index and reflectivity for andesite, basalt, basaltic glass, obsidian and obsidian glass through spectrophotometric analysis 24 p3081 A73-44558
- Thermal flute perturbations in an open plasma device with feedback. 24 p3114 A73-44615
- Spectral analysis of frequency noise of oscillators by the Hadamard variance 24 p3073 A73-44974
- A mathematical model of real signal spectra 24 p3068 A73-45005
- An expanded theoretical interpretation of the Venus 1.05-micron CO₂ line and the Venus 0.8226-micron H₂O line. 24 p3139 A73-45052

Turbulent motions in an artificial plasma inhomogeneity released in the ionosphere.
24 p3088 A73-45238

Photographic observation of type I supernovae at Asiago Observatory, discussing analysis of B and V light curves and spectra
24 p3143 A73-45437

Observations of Cyg X-1 and Cyg X-3 above 7 keV from OSO-7.
24 p3144 A73-45494

Dependence of electrical erosion on the interatomic bond strength in binary titanium alloys
24 p3101 A73-45514

Use of the fractional-distillation effect to increase the sensitivity of spectral analysis of metallic titanium
24 p3066 A73-45515

Determination of the size distribution function of erythrocytes by the spectral transparency method
24 p3065 A73-45521

SPECULAR REFLECTION

Holographic inspection of shapes of unpolished surfaces.
01 p0051 A73-10835

The destruction of reflecting dielectric coatings by laser radiation.
01 p0059 A73-10836

Optical measurements of lunar albedo, angular illumination, diffuse and specular reflectance and scattering coefficients on Mare Focunditatis regolith powder of various sizes
02 p0213 A73-12238

Remote sensing of the near-surface moisture profile of specular soils with multi-frequency microwave radiometry.
04 p0446 A73-15782

Surface roughness effects on bidirectional reflectance.
[AIAA PAPER 73-152]
05 p0598 A73-16900

Surface absorption coefficient of electromagnetic wave incident on plasma boundary, considering particle specular reflection and density-frequency relation
06 p0732 A73-18642

Analysis of He-Ne laser surface reflections from an off-axis parabolic mirror.
08 p0974 A73-21032

Block defocused spherical Fabry-Perot interferometer.
08 p0964 A73-21038

Specular reflection of heat radiation from an arbitrary reflector surface to an arbitrary receiver surface.
08 p1022 A73-21254

Heat flux contours on a plane for parallel radiation specularly reflected from a cone, a hemisphere and a paraboloid.
08 p1022 A73-21255

Equivalence relationships between diffuse radiation fields for finite slabs bounded by a perfect specular reflector and a perfect absorber.
09 p1121 A73-23072

Images and sound rays in the numerical calculation of echograms
09 p1121 A73-23104

Cauchy problem solution stability for non-homogeneous heat conduction equation with two space variables, allowing specular reflection on rectilinear boundary
12 p1560 A73-27809

Forward and specular scattering from a rough surface - Theory and experiment.
13 p1659 A73-28490

Parameter estimation for a specular-diffusion reflection model from the motion of 'Proton' series satellites about their centers of mass
14 p1803 A73-29851

Thermal expansion coefficient measurements of specularly reflecting samples.
15 p1877 A73-31981

View function in generalized curvilinear coordinates for specular reflection of radiation from a curved surface.
17 p2256 A73-35849

Path-length distributions of photons diffusely reflected from a semi-infinite atmosphere.
18 p2314 A73-37110

Comparison of the Beckmann model with bidirectional reflectance measurements.
[ASME PAPER 73-HT-11]
20 p2563 A73-38567

Diffraction of optical radiation by a reflecting disk in a turbulent atmosphere.
20 p2531 A73-39680

Diffuse parasitics gain thresholds of laser modes for rectangular geometries, discussing radiation field and boundary conditions
21 p2710 A73-40145

Reflection of conductivity electrons from an atomically pure (110) face of a tungsten crystal
21 p2751 A73-40367

Infrared reflection characteristics of lunar mare regolith.
21 p2774 A73-41400

Pulse scattering from a sphere coated with an inhomogeneous sheath.
22 p2824 A73-41852

Reflection function for an isotropically scattering finite medium.
22 p2887 A73-42565

Real laser cavity with nonideal reflecting mirrors, showing Q factor increase relation to mode order for plane monochromatic linearly polarized waves
23 p2987 A73-43650

SPEECH

NT ARTICULATION

NT PHONEMES

NT WORDS [LANGUAGE]

EEG alterations by short time stress due to delayed speech feedback during reading, noting alpha and beta wave changes
03 p0265 A73-14473

Cerebral localization of speech, discussing cortical lesions, aphasia and mental activity correlation theories
08 p0931 A73-21425

Formation of conditioned responses to symbolic stimulations in healthy individuals of different age
15 p1833 A73-31158

Speech scrambling by the matrixing of amplitude samples.
21 p2657 A73-41206

SPEECH DISCRIMINATION

U SPEECH RECOGNITION

SPEECH RECOGNITION

A model for the automatic classification of signals with applications for the automatic language recognition
06 p0663 A73-17591

Time and frequency functional analysis of speech for quantitative information parameters determination and signal recognition, considering German phoneme system two-formant signal structure
06 p0663 A73-17592

Optimal and preferred listening levels for speech in aircraft acoustical environments.
11 p1304 A73-25387

Intelligibility improvement of analog communication systems using an amplitude control technique.
14 p1726 A73-29901

Book - Foundations of modern auditory theory. Volume 2.
14 p1715 A73-30276

Acoustic model and linguistic, syntactic, lexical and semantic factors in speech perception and production process
14 p1721 A73-30277

Impairment to hearing from exposure to noise.
16 p1973 A73-33676

Corti organ lesion effects on signal perception in patients with noise induced hearing loss, correlating speech discrimination with age and sound level
19 p2396 A73-38182

SPEED

U VELOCITY

SPEED BRAKES

U BRAKES [FOR ARRESTING MOTION]

SPEED CONTROL

An all-regime optimal speed control for a single-shaft jet engine
06 p0741 A73-17721

The influence of recording speed on apexcardiographic timing - A multi-observer study of precision and performance utilizing randomized tracings in multiple subjects.
07 p0785 A73-19932

Fluidic sensing of rotational speed using spur gears.
08 p0928 A73-21829

Parallel operation of two Brynton-cycle alternators with parasitic speed controllers.
09 p1035 A73-22773

Improvement of the static and dynamic accuracy of a dual-loop control system for an electric actuating element with a proportional velocity controller
09 p1037 A73-22940

Synchronous motors as speed control system actuators, using static converters for instantaneous voltage or current amplitude and frequency control
10 p1177 A73-24026

Speed control for an air motor using fluidic techniques.
[ASME PAPER 73-DE-35]
14 p1713 A73-30824

Variable speed single- and multi-quadrant drives using thyristor electronic regulating unit with static converter motor and frequency changers
16 p1971 A73-33961

Ram air turbine with hydraulic pitch change servo regulated speed as emergency power source for aircraft control in event of main engine failure
24 p3058 A73-45475

SPEED INDICATORS

NT ANEMOMETERS

NT HOT-FILM ANEMOMETERS

NT HOT-WIRE ANEMOMETERS

NT SONIC ANEMOMETERS

NT TACHOMETERS

Determination of the location of a moving object with the aid of navigation systems using information on the cruising speed of the object
02 p0190 A73-11779

Laser velocity meters - A comparative study.
05 p0580 A73-17265

Turbulent transport measurements with a laser Doppler velocimeter.
07 p0826 A73-204626

Influence of the nonidentity of the antennas of a Doppler speed meter on the accuracy of its operation
10 p1195 A73-243866

Vertical aircraft flight control and navigation instrumentation avionics developments, emphasizing inertial-lead Vertical Speed Indicator design and command and advisory information displays
13 p1621 A73-2934

Maintenance of pitot-static systems of transport aircraft.
[SAE AIR 975]
16 p2014 A73-330144

SPEED REGULATION

U SPEED CONTROL

SPEED REGULATORS

Basic principles of variable speed drives.
17 p2182 A73-35472

SPEEDOMETERS

U SPEED INDICATORS

SPERMATOCYTES

U GAMETOCYTES

SPERMATOGENESIS

Regulation of testis function in golden hamsters - A circadian clock measures photoperiodic time.
02 p0134 A73-12422

Morphological changes in the testicles of dogs exposed to chronic and combined gamma-radiation
08 p0929 A73-20981

SPHALERITE

U ZINCLENDE

SPHERES

NT CELESTIAL SPHERE

NT POINCARÉ SPHERES

NT ROTATING SPHERES

On the integration of Einstein's equation for energy density inside a perfect fluid sphere.
01 p0076 A73-10250

Universal dimensionless formulas for physical property and trajectory computation in cosmic spherical media, applying to Kepler orbits, particle motions and radio wave paths
01 p0103 A73-11019

Effective solutions to the third and fourth boundary value problems of a sphere in the theory of elasticity
01 p0116 A73-11077

Linear MHD equations for inviscid medium under external forces, discussing magnetoacoustic wave generation by radially pulsating cylinder and sphere
02 p0196 A73-11605

Heat transfer from a sphere with injection in a slow moving flow
02 p0152 A73-11611

Relativistic spheres of hadron gas with zero baryon number constructed from Hagedorn hadronic equation of state, considering sphere stability properties
03 p0370 A73-13211

Incompressible viscous fluid creep flow past deforming sphere for small Reynolds numbers, considering cases of different Strouhal numbers
03 p0244 A73-13529

Oscillation effects upon film boiling from a sphere.
03 p0398 A73-13548

Determination of the flow past a cylinder and a sphere in the presence of an incident shock wave
03 p0294 A73-13615

Ball lightning events appearing with cloud to ground lightning discharge, discussing possible explanations
05 p0594 A73-16399

Structure of turbulent wakes of hypersonic spheres as inferred with ion probes.
05 p0527 A73-16568

Initial and boundary value problems for melting propagation from solid cylinder axis and sphere center, assuming pure conductive heat transfer
05 p0638 A73-16595

Radiation characteristics of waveguide-excited dielectric spheres with matched sphere-air boundary.
08 p0947 A73-21121

Natural vibrations of laminated orthotropic spheres.
09 p1160 A73-22890

Radiant heat flux distribution on the surface of a sphere in hypersonic flow of an inviscid radiating gas
10 p1171 A73-23581

Temperature fluctuations in the turbulent wake behind an optically heated sphere.
10 p1296 A73-24251

Solid sphere meandering trajectory in viscous liquid filled cylinder, postulating oscillating molecular surface tension layer at interface
10 p1206 A73-24701

Size determination of a perfectly conducting sphere from the extrema of Mie scattering intensities.
11 p1329 A73-25679

Inverse scattering method application to plane wave incident on perfectly conducting sphere, comparing results to simulation experiments
11 p1329 A73-25680

One dimensional temperature equalization process in planar plate, infinitely long cylinder and sphere for range of Biot and Fourier numbers, estimating approximate solution error
11 p1452 A73-26372

Asymptotic solution of shock-layer equations in the vicinity of the stagnation point of a sphere in the case of strong blowing

11 p1304 A73-26442

Displacement and finite-strain fields in a sphere subjected to large deformations.

11 p1447 A73-26647

Derivation of shape change equations for asymmetrically heated ablating reentry vehicles.

13 p1706 A73-28750

Sphere packings constructed from BCH and Justesen codes.

13 p1584 A73-28919

Alpha-omega dynamo problem of electrically conducting sphere magnetic field, obtaining eigenvalues from variational principle with free decay modes as trial functions

13 p1685 A73-29365

On the motion of small spheres in gases. III - Drag and heat transfer.

13 p1567 A73-29425

Low Hartmann number MHD flow of weakly conducting viscous fluid past nonconducting sphere within aligned uniform magnetic field

14 p1781 A73-30655

Motion of a sphere in a conducting fluid under the action of crossed electric and magnetic fields

15 p1917 A73-31405

Three layer concentric sphere microwave filter resonators, considering eigenvalue equation for arbitrary conductivity and complex permittivity and permeability effects on resonant frequencies and Q factors

16 p1987 A73-33092

Scaled illustration of unit sphere geometry with navigation applications.

17 p2209 A73-34874

On the torsional oscillations of a sphere placed at the axis of a rotating viscous incompressible fluid.

19 p2419 A73-37422

Incompressible potential flow past sphere parallel to contact plane tangent as model to determine critical velocity for dissipation onset in superfluid liquid He II

19 p2421 A73-37853

Stress field in a sphere subjected to large deformations.

19 p2500 A73-38111

Random loading on a spherical pressure vessel of Hooke-Norton material.

19 p2501 A73-38252

Bounded spherical body wave diffraction field represented by diverging wave series expansion, examining Rayleigh hypothesis, Butrov algebraic solution and converging waves

19 p2406 A73-38339

Van der Waals energy calculation from electromagnetism mode quantum energy in spheres and cylinders, considering finite boundary conditions, Green function techniques, and periodic lattices

20 p2538 A73-39706

Calculation of the radiative characteristics of polydisperse concentric spheres

20 p2531 A73-39728

The slow unsteady settling of two fluid spheres along their line of centres.

22 p2840 A73-41742

Pulse scattering from a sphere coated with an inhomogeneous sheath.

22 p2824 A73-41852

Indentation of the semi-infinite elastic solid by a hot sphere.

22 p2929 A73-43174

Forced convective heat transfer from isothermal sphere in steady incompressible flow at low Reynolds and various Prandtl numbers, obtaining mean Nusselt number

23 p3049 A73-43934

Electromagnetic resonances and Q-factors of lossy dielectric spheres.

23 p2960 A73-44067

SPHERICAL ANTENNAS

The concentric double spherical reflector as an antenna for simple scanning over a limited angular range

10 p1187 A73-23739

Arched and spherical antenna arrays synthesis for given vectorial radiation patterns by numerical solution via algorithm using eigenfunctions

12 p1479 A73-27229

Multiple-beam spherical-reflector antenna systems for satellite communications.

20 p2525 A73-38739

Implementation of fixed multiple beam spherical antenna systems and measured test results.

20 p2525 A73-38740

Basic theoretical aspects of spherical phased arrays.

21 p2653 A73-40678

SPHERICAL CAPS

Surface tractions, heat fluxes and body forces required for deformation of flat perforated thermoelastic circular plate into pierced spherical cap

06 p0759 A73-17757

Axissymmetric buckling of uniformly loaded spherical caps undergoing plastic deformation.

07 p0913 A73-19971

Bielayev's point in poroelastic bodies in contact.

08 p1016 A73-20829

Flow characteristics of spherically capped gas bubbles buoyancy induced motion in liquids, discussing Reynolds and Froude number effects

10 p1205 A73-23854

A photoelastic and finite-element investigation of a nonsymmetrical plug-hatch configuration.

10 p1293 A73-24721

Isogrid as integral stiffened waffle with triangular pattern to allow simple graphical solution for optimizing spherical caps or cylinders under various buckling loads

[AIAA PAPER 73-365] 11 p1438 A73-25500

Radar cross section measurements for right circular cones with spherically blunted noses, presenting as functions of diameter/wavelength ratio and aspect angle

11 p1330 A73-25682

Spherical harmonic representation of the gravitational potential of a point mass, a spherical cap, and a spherical rectangle.

13 p1681 A73-28846

Note on forced vibration of a non-homogeneous cone with spherical caps.

14 p1814 A73-30708

SPHERICAL HARMONICS

Axissymmetrical planet gravitational field potential expression in spherical function series, noting expansion coefficient decrease in power law for smooth density body

01 p0099 A73-10691

Planetary orbits numerical relationships applied to artificial satellite orbits for earth gravity studies, expressing gravitational potential as latitude dependent spherical harmonics series

01 p0040 A73-10875

Estimation of gravity field harmonics in the presence of spin-axis direction error using radio tracking data.

02 p0164 A73-12373

Earth normal gravity field spherical harmonics in terms of Stokes constants from satellite orbit dynamics, comparing with Helmert system

03 p0305 A73-14613

Isostatic reduction potential of earth mass distribution for spherical harmonic solutions of satellite determined gravity anomalies

04 p0437 A73-14788

Interior point mass earth potential model for satellite geodesy, considering geoid heights, gravity anomalies and spherical harmonics

04 p0438 A73-14791

Geopotential /geoid/ representation with spherical harmonics sampling functions for satellite altimeter applications

04 p0438 A73-14792

Lunar gravity model obtained by using spherical harmonics with mascon terms.

04 p0495 A73-14811

An empirically derived lunar gravity field.

04 p0498 A73-15184

Time variation of the geomagnetic main field /on the basis of spherical harmonics analyses of geomagnetic world charts for the period from 1880 to 1960/

04 p0440 A73-15281

Spherical analysis of the geomagnetic field during the epoch of 1965 from ground data up to $n = 23$. I

06 p0689 A73-17545

Geomagnetic field optimal model with expansion of spherical harmonic series by least squares method

08 p0960 A73-21353

Estimates of the coefficients of a spherical harmonics expansion of the geopotential

09 p1143 A73-22095

Alternative algorithmic scheme for spherical harmonics series summation, noting high speed and precision loss at high resolution in comparison with conventional methods

10 p1246 A73-23993

Spherical analyses of the main geomagnetic field in 1550-1800.

10 p1212 A73-24235

Lunar gravity derived from long-period satellite motion - A proposed method.

10 p1283 A73-24664

Relationship between the coefficients of spherical and ellipsoidal expansion of the gravity force in the case of the biaxial earth ellipsoid

11 p1352 A73-25431

Spherical harmonic analysis of the geomagnetic field during the epoch 1965.0 up to $n = 23$ from ground data. II - Results

12 p1491 A73-27353

Earth main magnetic field description by cartography and analytic methods based on dipole or spherical harmonic series representations

13 p1608 A73-28713

Spherical harmonic representation of the gravitational potential of a point mass, a spherical cap, and a spherical rectangle.

13 p1681 A73-28846

Gaussian curvature of smoothed equipotential surfaces from satellite orbit dynamics.

13 p1611 A73-29659

Geoid equatorial section approximation by zonal spherical harmonics using axially-symmetric features

15 p1940 A73-32050

Spherical analysis of the geomagnetic field of the 1965 epoch to $n = 23$ from ground-based data. I.

16 p2002 A73-32769

Approximation of the geometric figure of the moon by using spherical functions

17 p2230 A73-34596

Spherical harmonics approximation for radiative transfer in polluted atmospheres.

[AIAA PAPER 73-749] 18 p2313 A73-36365

Thermospheric density diurnal and seasonal variations from cosmos drag data, discussing amplitude, density distribution, coefficients of expansion, summer solstice spherical functions

21 p2689 A73-41351

Spherical harmonic analysis of the geomagnetic field for the 1965 epoch up to $n = 23$ according to ground-based data. II - Results.

23 p2971 A73-43250

Spherical harmonic analysis of geomagnetic and gravitational field correlation, showing longitudinal shift in magnetic field pattern over six epochs

24 p3084 A73-44812

SPHERICAL SHELLS

NT SPHERICAL CAPS

Approximate solution of equations describing the thermal stressed state of a shallow spherical shell

01 p0113 A73-10017

Study of the stressed state of a shallow spherical shell whose thickness varies along its circumference

01 p0113 A73-10018

Load carrying capacity of ceramic spherical shells under external pressure

01 p0114 A73-10481

Asymptotic method of determining critical buckling loads for strictly convex shallow shells of revolution

01 p0116 A73-10963

Backward Monte Carlo calculations of the polarization characteristics of the radiation emerging from spherical-shell atmospheres.

01 p0078 A73-11233

Magnetohydrodynamic flow around a hollow sphere

01 p0085 A73-11259

Thermoelastic equilibrium of a doubly connected spherical shell

02 p0231 A73-11804

Thin walled shells strength dependence on residual stresses, noting stress analysis of shallow spherical shell with variable residual deformations

02 p0232 A73-11932

Stress-strain state of shallow spherical shell with variable wall thickness under uniformly distributed load, using Vlasov shell theory

02 p0235 A73-12192

Calculation of thermal stresses in spherical storage vessels.

02 p0236 A73-12215

Large amplitude oscillations of a hollow spherical dielectric.

02 p0236 A73-12518

The state of ionization in nova shells.

02 p0222 A73-12706

Numerical simulation of initial value problem of axisymmetric equatorially trapped oscillation modes of constant density viscous fluid in rotating spherical shell

03 p0384 A73-13064

Vibrational frequency density analysis of thin spherical and cylindrical shells of revolution, using asymptotic integration method

03 p0394 A73-14051

Natural vibration frequency spectra of circular cylindrical and spherical shells of revolution, using Bessel function

03 p0395 A73-14052

Inelastic spherical shells elastic-plastic buckling, presenting numerical procedure for critical loads and stresses

04 p0508 A73-14942

Plastic deformations and crack propagation in cylindrical and spherical shells under uniform pressure, calculating stress intensity factor

04 p0512 A73-15239

An approximate rigid-plastic analysis of shell intersections loaded dynamically.

[ASME PAPER 72-WA/DE-1] 04 p0515 A73-15876

Classical and nonlinear buckling analyses of spherical sandwich shells.

05 p0631 A73-16121

Variable thickness orthotropic shell of revolution with bending suppressed.

05 p0633 A73-16537

Time variable stress-strain state of viscoelastoplastic hollow sphere under internal pressure, using piecewise linear differential law

05 p0635 A73-17080

Stabilization concepts for a spherical planetary entry probe configuration.

[AIAA PAPER 73-184] 06 p0756 A73-17653

Low Reynolds number flow past a porous spherical shell.

06 p0687 A73-18506

The concept of snap-buckling illustrated by a simple model. 07 p0909 A73-19163

Study of the stability of nonshallow spherical shells with finite displacements by applying various equations of the theory of shells 07 p0911 A73-19318

Deformation of an elastic spherical shell with random initial imperfections 07 p0911 A73-19319

Deformations and stresses in a hollow sphere with spherical transversal isotropy under impulsive pressure. 07 p0913 A73-20116

Steady-state heat conduction in slabs, cylindrical and spherical shells with non-uniform heat generation. 07 p0921 A73-20181

Effect of the curvature of a shallow spherical shell on its vibrations with losses 08 p1018 A73-21449

Investigation of the deformation of a hollow sphere under an impulsive load on the basis of three-dimensional elasticity theory and shell theory 08 p1019 A73-21761

Probabilistic model for the resolvent kernel in diffusion problems in spherical-shell media. 09 p1121 A73-23071

An evaluation of finite element methods for the computation of elastic stress intensity factors. [ASME PAPER 72-PVP-19] 09 p1163 A73-23267

Inelastic buckling of shallow spherical shells under external pressure. [ASME PAPER 72-PVP-6] 09 p1164 A73-23270

An approximate rigid-plastic analysis of shell intersections loaded dynamically. [ASME PAPER 72-WA/DE-1] 09 p1164 A73-23272

Stability of the axisymmetric form of motion of flexible shallow shells 09 p1164 A73-23344

Deformation of a spherical shell under the action of an unsteady spherical hydroacoustic wave 09 p1165 A73-23354

Weight minimization constrained design of rotational shallow spherical shells, comparing simplex and variable metric methods 09 p1165 A73-23446

Determination of the initial stress-strain state of a shallow spherical shell under the action of a dynamic load 10 p1290 A73-24310

On hydromagnetic Rossby waves excited by travelling forcing effects. 11 p1403 A73-25154

Strength and weight optimization of strengthened spherical shells under external pressure 11 p1434 A73-25389

Heat transfer law for free convection in cylindrical and spherical interlayers 11 p1450 A73-25726

Deformation of zero-moment shells subjected to internal pressure under creep conditions 12 p1551 A73-27179

Investigation of the stress-strain state of spherical shells with an eccentric hole on the basis of the three-dimensional theory of elasticity by the finite element method 12 p1552 A73-27262

Deformation of a nonshallow spherical shell under local loads 12 p1553 A73-27469

Soft shell strength analysis for contact and static loads 12 p1554 A73-27470

Stability of a nonuniformly heated circular shell 12 p1554 A73-27471

Asymptotic method of determining the critical buckling loads of shallow strictly convex shells of revolution. 12 p1554 A73-27539

Shallow spherical shell dynamic stability under axisymmetric loads, noting small HF vibrations effect on static stability 12 p1556 A73-27814

Branched solution of integro-power equation for nonlinear bending of shallow spherical shells with clamped edge under uniform radial compression load 12 p1556 A73-27816

Large amplitude vibrations of certain deformable bodies. I - Discs, membranes and rings. 12 p1556 A73-27929

Vibration analysis of thick-walled hollow spheres and cylinders, determining periodic response and fundamental frequency as function of wave reflection number and dimensions 13 p1695 A73-28489

Finite deflection of a shallow spherical membrane. 13 p1697 A73-28815

Axisymmetric inertial oscillations of a fluid in a rotating spherical shell. 13 p1601 A73-28916

Investigation of the elastoplastic state of a spherical shell with a unreinforced circular hole 13 p1698 A73-29061

Analytical solution to problems of eddy current distribution in a thin plate and a conducting spherical shell 14 p1774 A73-30029

Conformal mapping technique for stress concentration around elliptical hole in shallow spherical shell under internal pressure 14 p1806 A73-30045

Load-bearing capacity of ceramic spherical shells under external pressure. 14 p1810 A73-30306

A comparison of theory and experiments on the dynamic plastic behavior of shells. 14 p1811 A73-30476

Maximum stress calculation for I beam and thin walled sphere redundant structures under stationary creep by perturbation method 14 p1811 A73-30487

Influence of curvature on the vibrations of an oblate spherical shell with losses. 15 p1945 A73-31013

The dynamic plastic behavior of simply supported spherical shells. 15 p1948 A73-31369

Stability of a spherical shell containing an elastic filler 15 p1950 A73-31828

Transition theory application to creep deformation, considering spherical shells 15 p1954 A73-32117

Free vibration of an inflated oblate spheroidal shell. 15 p1955 A73-32155

Dynamic buckling of shallow spherical shells. [ASME PAPER 73-APM-A] 17 p2249 A73-35104

Non-coherent scattering in transfer problems in spherical shell media. I - Frequency-independent source function. 17 p2236 A73-35780

Non-coherent scattering in transfer problems in spherical shell media. II - Frequency-dependent source function. 17 p2237 A73-35789

Shells of revolution belonging to a spherical class subjected to local loads at the pole 18 p2362 A73-36402

Study of elastoplastic state of a spherical shell with round unsupported apertures. 18 p2366 A73-36893

Approximate method for solving a boundary value problem in the theory of zero-moment elastic spherical shells 18 p2367 A73-36988

Axisymmetric deformation of soft spherical shells 18 p2367 A73-37139

A new form of the integral equations of a boundary value problem in the theory of simply supported shallow spherical shells 19 p2495 A73-37198

Rigid-plastic collapse of compression-bent shallow shells. 20 p2616 A73-39114

Creep relaxation approximations and exact solutions, discussing rectangular beam pure bending, spherical shell internal pressure loading and thin circular tube bending 20 p2616 A73-39115

Supercritical strains in nonlinear elastic shells 20 p2616 A73-39259

Modal technique to obtain forced axisymmetric response of elastic spherical shells from free vibration response relations, taking into account transverse shear and rotational inertia 20 p2621 A73-39541

Numerical solution of the radiative transfer equation in spherical shells. 21 p2727 A73-41000

A note on the finite elastic inflation of a thin spherical shell. 21 p2789 A73-41688

Experiments on free vibration of shells of revolution. 23 p3039 A73-43384

Determination of the stressed state near a curvilinear hole in a transversely isotropic spherical shell 23 p3043 A73-43924

Thermoelasticity problem of a spherical shell with multiply connected regions 24 p3149 A73-45175

SPHERICAL TANKS

Thermal stresses in a spherical vessel filled with liquefied gas 07 p0917 A73-20507

Stressed state of multilayer spherical vessels, cylindrical tubes and circular disks consisting of a linear viscoelastic material 13 p1690 A73-27994

Thermal stresses in spherical reservoirs while filling with liquefied gas. 19 p2499 A73-37782

SPHERICAL WAVES

Spherical wave propagation in a viscoplastic medium. 03 p0393 A73-13788

Diffraction of waves generated by a magnetic-dipole current system on a variable-radius sphere 05 p0550 A73-16397

Outer-scale effects in turbulence-degraded light-beam spectra. 05 p0597 A73-16498

Boundary value problems of elastic wave diffraction by spherical cavities, using vector equation of motion solutions 05 p0636 A73-17091

The development of magnetohydrodynamic flow due to the passage of an electric current past a sphere immersed in a fluid. 06 p0728 A73-17705

On the solution of the Navier-Stokes equations for a spherically symmetric expanding flow. 06 p0684 A73-17707

Eigenvalues of a class of spherical wave functions. 06 p0665 A73-18177

A new approach to the problem of wave fluctuations in localized smoothly varying turbulence. 06 p0665 A73-18183

Electromagnetic scattering from a radially moving spherical discontinuity. 06 p0669 A73-18785

Deformation of a spherical shell under the action of an unsteady spherical hydroacoustic wave 09 p1165 A73-23354

Study of the Rayleigh zone of circular radiating apertures 11 p1328 A73-25283

Time-dependent electromagnetic field scattering and diffraction by half plane during illumination by impulsive plane cylindrical or spherical wave 11 p1330 A73-25683

Source altitude for experiments to simulate space-to-earth laser propagation. 14 p1756 A73-30151

Implicit predictor-corrector difference scheme for boundary value problem solution in propagation of spherical and cylindrical N waves /asymptotic pulse forms/ 14 p1745 A73-30175

Concentric, uniform elastic spherical wave excited by thermal explosion of the envelope. 14 p1816 A73-30251

Spherical concentric shock wave excitation in elastic medium by hypersonic thermal wave in terms of displacements, particle velocity and stresses 14 p1817 A73-30252

Scattering of a spherical wave by spherical inhomogeneity with arbitrary refractive index distribution along the radius. 17 p2123 A73-35163

Nearly spherical constant-power detonation waves as driven by focused radiation. [ALAA PAPER 73-674] 18 p2322 A73-36225

Self-similar flows behind shock waves in a gravitational field 21 p2676 A73-40190

SPHEROIDS

NT OBLATE SPHEROIDS

NT PROLATE SPHEROIDS

Magnetic spheroid mass determination with microbalance and internal cavity observation by X ray photography, noting meteor showers as extraterrestrial source 05 p0621 A73-17055

Motion equation solutions for three flattened spheroids with coincident equatorial symmetry planes in Lagrange form by Duboshin transforms 10 p1274 A73-23722

Motion equation solutions for three flattened spheroids with coincident equatorial symmetry planes in Lagrange form by Duboshin transforms 18 p2355 A73-36747

SPHERULES

Cosmic black glassy spherules composition, mineralogy and physical properties compared to lunar fines, considering possible common origin 02 p0214 A73-12254

Petrochemistry and chemical features of lunar glassy spherules. 03 p0273 A73-13089

Dynamical model for evolution of melted spherical drop of homogeneous glassy material to explain observed glassy spherules in lunar dust 03 p0368 A73-13090

Surface features on glass spherules from the Luna 16 sample. 04 p0498 A73-15187

Order c-square bulk stress derivation for force-free spherical particles suspension in Newtonian ambient fluid with uniform viscosity, noting error bounds 06 p0722 A73-17701

Temperature-dependent magnetic properties of individual glass spherules, Apollo 11, 12, and 14 lunar samples. 07 p0893 A73-19844

Optical properties of lunar glass spherules from Apollo 14 fines. 07 p0898 A73-19893

Green spherules from Apollo 15 - Inferences about their origin from inert gas measurements. 12 p1541 A73-27490

- Lunar and terrestrial impact crater spherules.
17 p2236 A73-35749
Apollo 17 'orange soil' and meteorite impact on liquid lava.
19 p2482 A73-37390
Preliminary measurements of spherules of the Pontina Plain and of micrometeorites of Apollo 12 and related impact studies.
21 p2775 A73-41412
- PHYSGIOGRAPHY**
Method for measuring the contractions of small hearts in organ culture.
08 p0933 A73-21218
- PICULES**
Optical, far UV and radio spectra observations and results for solar spicules, considering morphology, spectroscopic properties and dynamic models
01 p0094 A73-10055
Solar spicule morphology, observing diameter, height, expansion and threshold intensity with H alpha filtergrams
21 p2777 A73-41484
- PIKE ANTENNAS**
U MONOPOLE ANTENNAS
PIKE NOZZLES
Basic flow characteristics of a linear aerospike nozzle segment.
[ASME PAPER 72-WA/AERO-2]
04 p0405 A73-15908
- PIKE POTENTIALS**
Peripheral electromyography spike and ventral root unit discharge intervals during tonic vibration reflex of cat soleus motoneuron
01 p0008 A73-10410
Reaction time method using EEG monitored paroxysm controlled auditory stimuli for responsiveness /consciousness/ evaluation of spike wave burst onset during epileptic seizures
09 p1040 A73-22695
Rise time of the spike potential in fast and slowly contracting muscle of man.
10 p1181 A73-24500
Short-term latent reactions of the lateral geniculate body neurons in the rat to electrical stimulation of the optical tract
10 p1182 A73-24595
Conditional computer analysis of the onset-to-onset duration of spikes from the electromyographic interference pattern of extraocular muscles.
22 p2802 A73-41731
Computer acquisition of multiunit nerve-spikes signals.
22 p2815 A73-42671
- SPIKES**
Aerodynamical and aeromechanical investigations involving pin-equipped models in hypersonic flow
11 p1300 A73-25441
Analysis of spikes in occultation curves - A critique of Brinkmann's method.
24 p3129 A73-44444
- SPINNING**
Pulsed Nd-YAG laser output spiking for control of materials machining parameters
24 p3098 A73-45552
- SPIN**
NT ELECTRON CAPTURE
NT ELECTRON SPIN
NT METAL SPINNING
NT NUCLEAR SPIN
NT PARTICLE SPIN
NT SPIN-ORBIT INTERACTIONS
Nonlinear hydrodynamic and hydromagnetic spin-up driven by Ekman-Hartmann boundary layers.
11 p1403 A73-25156
- SPIN DYNAMICS**
Stability of a spinning body containing an elastic membrane via Liapunov's direct method.
01 p0077 A73-10728
Flexible satellite with three axisymmetrical bodies spinning at different rates about common axis of symmetry, deriving stability conditions based on Sturm theorem
02 p0228 A73-11997
Estimation of gravity field harmonics in the presence of spin-axis direction error using radio tracking data.
02 p0164 A73-12373
Astronomical evidence concerning non-gravitational forces in the earth-moon system.
02 p0217 A73-12385
Three-roll flow turning.
06 p0697 A73-17827
Spinning test bodies motion in metric fields, applying to spinning stars in orbit around black holes
06 p0749 A73-17869
Solar system planets spin rate change and core growth, discussing Mars geology and earth evolution
06 p0749 A73-18006
Free vibration analysis of spinning structural systems.
07 p0907 A73-19032
An improved method for calculating the spin torque in a fully lubricated ball-race contact.
07 p0833 A73-20485
- Simulation capability for dynamics of rotating counterweight space stations.
[AIAA PAPER 73-320]
11 p1343 A73-25551
Stability of transverse waves in a spinning membrane disk.
[ASME PAPER 72-APM-MM]
11 p1441 A73-25706
A mechanism for ablation-induced spin-up.
11 p1431 A73-26402
Nutation dampers vs precession dampers for asymmetric spinning spacecraft.
11 p1432 A73-26670
The mechanism of gyroscopic tracking. I.
[ASME PAPER 72-MECH-32]
15 p1883 A73-32284
The mechanism of gyroscopic tracking. II.
[ASME PAPER 72-MECH-33]
15 p1883 A73-32285
Periodic solutions of singularly perturbed equations arising from gyroscopic systems.
16 p2032 A73-33310
General aviation aircraft stall/spin prevention device for limiting tail power near wing stall angle of attack
[SAE PAPER 730333]
17 p2102 A73-34686
Strapdown electrostatic gyroscope spin axis precession drift rate calibration, using virtual work technique for modeling bearing torques on rotor
17 p2137 A73-35210
A nonlinear oscillator analog of rigid body dynamics.
18 p2337 A73-36416
Dynamic passivation of a spinning and tumbling satellite using free-flying teleoperators.
19 p2490 A73-37306
Earth rotation measurements relative to reference frames and changes and mechanisms of axis orientation and spin rate
20 p2553 A73-39125
Mathematical modeling of spinning elastic bodies for modal analysis.
21 p2784 A73-40421
- SPIN EXCHANGE**
Some aspects of the exchange-interaction and dipole-dipole broadening of the individual hyperfine components of the EPR spectrum
14 p1775 A73-30580
- SPIN FORGING**
U METAL SPINNING
SPIN REDUCTION
Experimental satellite for attitude control. II - Numerical analysis and a test of a yo-yo de-spinner.
01 p0111 A73-11190
Yo-yo system despin mechanism for the Aeros aeronomy satellite.
03 p0382 A73-13919
An amplitude-steered, electronically despun antenna for the synchronous meteorological satellite.
04 p0428 A73-15453
Spinning satellite with partially filled viscous ring damper, solving equations of motion for nutation-synchronous and spin-synchronous modes
[AIAA PAPER 73-143]
05 p0629 A73-16892
Dispersion of the direction of the angular momentum vector of sounding rocket payloads due to atmosphere exit and certain vehicle activities.
09 p1116 A73-23212
Asymmetrical spun satellite rotation prediction in circular orbit at 700 km in terms of perturbing moment vector function
15 p1931 A73-31235
Optimal damping and stochastic control in certain problems of astrodynamics
15 p1931 A73-31236
Failure modes and accelerated life test methods for despun antenna bearings.
[ASLE PREPRINT 73AM-1A-4]
17 p2178 A73-34979
Attitude control, rotational and positioning mechanisms for orientation of mechanically despun antennas and solar arrays in communication satellites
[DGLR PAPER 73-050]
17 p2126 A73-35486
System requirements for a free-flying teleoperator to despin the ATS-V.
19 p2490 A73-37304
British X4 spacecraft mechanical design configuration with honeycomb sandwich panels, on yo-yo principle based despin system and flexible solar array
20 p2615 A73-39774
- SPIN RESONANCE**
Resonance between spin and magnetohydrodynamic waves in antiferromagnetic semiconductors and metals.
11 p1409 A73-26190
Quantum interference effects due to singlet-spin pairing in superconductors, considering normal metal, electron correlations, single particle excitations, thermodynamic properties and ideal superconductors
21 p2752 A73-40642
- SPIN STABILIZATION**
Test of horizon sensor for the ionosphere sounding satellite.
01 p0053 A73-11172
Experimental satellite for attitude control. IV - Nutational damping of a spinning satellite.
01 p0112 A73-11191
- Satellite attitude control estimators and observers, discussing applications to reaction wheel, spinning attitude and drag-free satellite translation control systems
01 p0075 A73-11193
The attitude-measuring and attitude-control system of the satellite Aeros and its employment in the acquisition phase
[DGLR PAPER 72-062]
02 p0227 A73-11653
Flexible satellite with three axisymmetrical bodies spinning at different rates about common axis of symmetry, deriving stability conditions based on Sturm theorem
02 p0228 A73-11997
Stability criteria for a free dual-spin satellite.
02 p0228 A73-12398
Communications satellite Symphonie stability during perigee-apogee transfer in terms of liquid filled spinning top nutation
03 p0381 A73-13295
Analysis of the unbalances in spin-stabilized satellites
03 p0382 A73-13725
Equilibrium motions of rigid spinning satellite in circular orbit around central body subject to gravitational torque
03 p0376 A73-14268
An operational satellite propulsion system providing for vernier velocity, high and low level attitude control and spin trim.
[AIAA PAPER 72-1130]
04 p0486 A73-14916
Spin and three-axis stabilized geosynchronous tracking and data relay satellite system for telecommunication service to user spacecraft in low earth orbit
04 p0420 A73-15422
Certain states of rotation of a magnetized spin-stabilized satellite in the geomagnetic field
05 p0627 A73-16291
Spin stabilization of a satellite
05 p0629 A73-16422
The motion and stability of a dual-spin satellite during the momentum wheel spin-up maneuver.
[AIAA PAPER 73-142]
05 p0629 A73-16891
Periodic attitude control of a slowly spinning spacecraft.
[AIAA PAPER 73-246]
05 p0596 A73-16970
French Monograph - Contribution to the study of the stabilization of gyroscopic satellites - Conception and development of an active nutation damper.
06 p0757 A73-18097
A simple method for precise attitude determination of a spinning spacecraft.
06 p0722 A73-18827
Sun sensors for D-2B scientific satellite spin axis alignment and attitude stabilization with pointing control accuracy, discussing tests, compensatory tracking and solar simulation
07 p0821 A73-18986
The double gimbaled 'DRALLRAD' and its possible use for three-axis-stabilization of application satellites.
07 p0849 A73-19143
Attitude control of the AEROS aeronomy satellite during the acquisition phase.
08 p1014 A73-21660
Spinning Skylab space station dynamics, investigating motion stability from simplified models with flexible appendages by digital simulation
10 p1286 A73-24003
The effect of direct solar radiation on the attitude of the SKYNET spacecraft.
11 p1431 A73-26261
Liapunov stability analysis of spinning flexible spacecraft.
11 p1431 A73-26378
Temperature reducing solar cell arrangements for spin stabilized planetary and solar probes, analyzing thermal performance
11 p1313 A73-26668
AEROS aeronomy satellite successfully completes acquisition phase.
13 p1689 A73-28783
The use of a spinning dissipator for attitude stabilization of earth-orbiting satellites.
13 p1690 A73-29216
Spin stability of torque-free elastic dissipative systems with finite number of degrees of freedom, deriving Liapunov function via energy considerations
15 p1943 A73-31663
The application of Kalman filtering to the attitude determination of spinning space vehicles.
15 p1944 A73-32219
NMR spectrometer magnetic field strength-HF field frequency ratio instability spectral density in presence of spin stabilizers
16 p2011 A73-32824
Time and fuel consumption optimal nutation damping and attitude-angular velocity control of spin-stabilized flight vehicles
16 p2072 A73-33234
Regional and international communication satellite systems, discussing frequencies assignment, power supplies, three axis stabilization trends and military, navigation and TV developments
[DGLR PAPER 73-039]
17 p2125 A73-35478

SPIN TESTS

- Dual and triple spin-stabilized deformable spacecraft attitude stability, comparing results based on Sturm theorem with Liapunov analysis 18 p2359 A73-36306
- Computer simulation for time optimal or energy optimal attitude control of spin-stabilized spacecraft. 18 p2360 A73-36837
- Attitude stability conditions of multiple spin satellites. 18 p2361 A73-36877
- The precession of unsymmetric spin-stabilized satellites. 18 p2361 A73-36878
- Spinning HEOS-A2 satellite active deconing with pulse sequence from attitude reorientation system, discussing optimal control pulse number and timing 18 p2361 A73-36957
- Inertial force field patterns due to nutational motion of spinning satellites. 19 p2492 A73-37709
- Inertial symmetrization of large spin-stabilized spacecraft. 19 p2493 A73-37883
- [SAWE PAPER 965] A method of providing rain margins for 18/30 GHz communications satellites without increasing the solar power requirement. 20 p2524 A73-38731
- Attitude measurement and control system of the aeronomy satellite AEROS. [ALAA PAPER 73-856] 20 p2585 A73-38794
- Techniques for flat-spin recovery of spinning satellites. [ALAA PAPER 73-859] 20 p2614 A73-38797
- Energy-sink analysis for asymmetric dual-spin spacecraft. [ALAA PAPER 73-909] 20 p2614 A73-38843
- Investigation of a stabilization system with a relay angular sensor 20 p2593 A73-39321
- Oscillatory motions of an axisymmetric spin-stabilized solid body 20 p2593 A73-39495
- Oscillations of a spinning satellite due to small deflections of its dipole antennae. 21 p2780 A73-40089
- Precession damping of solar probes by reradiative forces. 21 p2737 A73-40767
- Possibility of using the Space Tug for the recovery and maintenance of satellites 21 p2782 A73-41554
- Attitude stability conditions of multiple spin satellites. 22 p2916 A73-42189
- The precession of unsymmetric spin-stabilized satellites. 22 p2916 A73-42190
- Russian book on satellite attitude stabilization systems design covering gravity gradients, linear and nonlinear control laws, spin stabilization, high torque control moment gyros, etc 23 p3038 A73-43335
- Ionospheric electric field measurements with a spin stabilized detector. 24 p3090 A73-44818
- SPIN TESTS**
- Stall/spin studies relating to light general-aviation aircraft. [SAE PAPER 730320] 17 p2102 A73-34678
- SPIN-LATTICE RELAXATION**
- Spin relaxation times in ferromagnetic materials with magnetic anisotropy, discussing temperature effects and energy considerations 09 p1134 A73-22686
- UV radiation effects on gamma irradiated Cr ions spin lattice relaxation rate in ruby and on resonant phonon scattering 13 p1668 A73-28219
- CW NMR millidegree thermometer using oscillator to detect resonance, noting Curie law, magnetogyric ratio, spin-lattice relaxation time and low electrical conductivity 13 p1618 A73-29072
- Optical orientation in a system of electrons and lattice nuclei within semiconductors - Experiment 23 p3016 A73-44022
- Optical orientation in a system of electrons and lattice nuclei within semiconductors - Theory 23 p3017 A73-44023
- SPIN-ORBIT INTERACTIONS**
- NT ELECTRON CAPTURE**
- The exciton energy spectrum in diamond and spherulitic type crystals 09 p1134 A73-22683
- Spin contamination in unrestricted Hartree-Fock calculations. 22 p2889 A73-42442
- Curve crossing theory for N molecule-O atom reactions in terms of spin-orbit coupling, considering nitrous oxide unimolecular decomposition and molecular N vibrational relaxation 24 p3113 A73-44979
- SPINAL CORD**
- Changes in ventilatory patterns after ablation of various respiratory feedback mechanisms. 01 p0007 A73-10162

- Topochemical differences in RNA content in spinal cord motoneurons during hypoxia and hypokinesia 02 p0135 A73-12558
- Response of motoneurons of the spinal cord to gamma radiation - A cytochemical study. 03 p0262 A73-13808
- Correlation between the voltage-time curves of H- and M-responses of a human muscle during various functional states of the spinal center 03 p0262 A73-13819
- Maturing neuronal subsystems - The dendrites of spinal motoneurons. 03 p0264 A73-14257
- Electrophysiological investigation of supraspinal motor control systems evolution through Cyclostomata-Primate series, noting preservation of reticulomotor neuron projection characteristics 07 p0781 A73-20001
- Cortico- and rubrofugal activation of interneurons forming propriospinal paths in the dorsolateral funiculus of the cat spinal cord 07 p0781 A73-20002
- Functional organization of the mechanisms of presynaptic inhibition evoked by stimulation of cutaneous afferents 07 p0781 A73-20003
- Changes in the amplitudinal and temporal characteristics of sensorimotor-cortex evoked potentials after deactivation of spinocervical tracts in cats 07 p0781 A73-20004
- Ontogenic cerebrospinal reflex activity studies, covering spinal cord morphology, reflex arches, inhibition, intracranial responses and post-tetanic potentiation 07 p0784 A73-20366
- Synaptic activation of thoracic spinal cord interneurons through reticulo-spinal pathways 09 p1039 A73-22576
- Structural characteristics of connections between medial efferent systems and spinal cord neurons 09 p1040 A73-22577
- Cortico-pyramidal and cortico-extrapyramidal synaptic effects on lumbar motor neurons in monkeys 09 p1040 A73-22578
- Investigation of evoked activity in the ventral horn of lumbar segments during the interaction of efferent extrapyramidal and cortical stimuli 09 p1040 A73-22579
- Organization of spontaneous muscular activity in man 09 p1040 A73-22863
- Features of supraspinal control of the reflex paths of the spinal cord during walking 10 p1178 A73-23677
- Electrophysiological study of the topographic organization of Deiters' lateral vestibular nucleus 10 p1181 A73-24515
- Reflex excitability of spinal motor neurons in man under high atmospheric pressure 10 p1182 A73-24525
- Influence of increased air atmosphere pressure on the excitability of the neuro-motor apparatus in man 14 p1719 A73-30845
- Mathematical analysis of the operation of regulatory mechanisms of the spinal cord 20 p2517 A73-39005
- Effect of chronic pyramid insufficiency on the function of spinal centers of shin and foot muscles in man 22 p2807 A73-42658
- Spinal cord heating effects on frog thermoregulatory behavior in aqueous thermal gradient, noting preference for colder ambient temperature 23 p2947 A73-43994
- Spinal and spino-bulbo-spinal neuron mechanisms of somatic and visceromotor reflex transfer in the thoracic spinal cord 24 p3061 A73-45249
- SPINDLES**
- A frequency response analysis of fusimotor-driven muscle spindles. 09 p1041 A73-22934
- SPINE**
- Aerodynamic pumping-caused spinal fractures in two pilots during high speed flight 02 p0137 A73-12154
- A method of determining spinal alignment and level of vertebral fracture during static evaluation of ejection seats. 16 p1967 A73-32676
- A distributed parameter model of the inertially loaded human spine. 18 p2281 A73-36429
- Vestibular and spinal control of eye movements. 18 p2272 A73-36440
- The role of the elastic properties of brain and spine cavities in hyperemia compensation 18 p2276 A73-36572
- Motor unit reactions of man to spinal and supraspinal inhibitory stimuli 19 p2395 A73-37943
- Effect of the electrical stimulation of the sensorimotor cortex on the potentials of dorsal roots and on the depolarization of primary spinal afferents 22 p2807 A73-42652

- Radiological assessment of the vertebral column from the point of view of aviation medicine 22 p2817 A73-43131
- SPINEL**
- Stability relations of ilmenite and ulvospinel in the Fe-Ti-O system and application of these data to lunar mineral assemblages. 02 p0220 A73-12482
- Spinel troctolite and anorthosite in Apollo 16 samples. 05 p0615 A73-16323
- An experimental investigation of the significance of zirconium partitioning in lunar ilmenite and ulvospinel. 05 p0619 A73-16838
- Apollo 14 - Subsolidus reduction and compositional variations of spinels. 07 p0880 A73-19697
- The magnesium spinel-bearing rocks from the Fra Mauro formation. 07 p0883 A73-19733
- Ion distribution in the crystal structure of complex spinel phases of the Mn-Fe-Ti-O system 11 p1386 A73-26674
- Luna 20 - Mineral chemistry of spinel, pleonaste, chromite, ulvospinel, ilmenite and rutile. 13 p1675 A73-28316
- Application of a cluster component technique in the interpretation of concentration dependences of the properties of binary metal alloys and anion-substituted spinel solid solutions 15 p1923 A73-31205
- Effect of aluminum-containing components on phase alloying in periclase ceramic materials 24 p3104 A73-44953
- SPINNING [METALLURGY]**
- U METAL SPINNING**
- SPINOR GROUPS**
- Spinorial solution associated to a radially symmetric radiation field in general relativity. 01 p0079 A73-11257
- Construction of the spinor field equations in cosmological space 08 p1010 A73-21271
- Bireductive spaces, Jordanian algebras, and spinor representations of non-Euclidean and quasi-non-Euclidean motions 17 p2212 A73-35566
- Geometric interpretation of spinor representations for groups of motions in quasi-elliptic 5-spaces 17 p2213 A73-35568
- Quantum theory of the spinor field in the two-dimensional space-time of de Sitter 17 p2213 A73-35571
- SPIRAL ANTENNAS**
- NT LOG SPIRAL ANTENNAS**
- Comparing ECM antennas - Horns vs spirals. 02 p0147 A73-12568
- Radiation from a continuous semi-circular arc antenna array. 02 p0148 A73-12852
- Dispersion characteristics of multiloop cylindrical spiral antennas with opposite winding 12 p1480 A73-27237
- Spiral top-loaded antenna (STLA) characteristics and design procedure derivation via self consistent field method, noting VLF applications 14 p1734 A73-30204
- SPIRAL GALAXIES**
- NT MILKY WAY GALAXY**
- Spiral structure and kinematics of the galaxy from a study of the H II regions - Fabry-Perot interference methods applied to ionized hydrogen. 01 p0096 A73-10297
- Structure and dynamics of barred spiral galaxies, in particular of the Magellanic type. 01 p0096 A73-10298
- Direction of winding in spiral galaxies. 01 p0106 A73-11317
- An asymmetrically rotating fluid disc with applications. [AD-751727] 02 p0217 A73-12393
- The radio emission of NGC 4258 and the possible origin of spiral structure. 02 p0221 A73-12701
- 21-cm neutral hydrogen line study of early type galaxies. 02 p0222 A73-12716
- The spiral arm structure on the southwestern border of M31. 02 p0227 A73-12840
- A radio map of the spiral galaxy Maffei 2 at 1415 MHz. 03 p0370 A73-13210
- The relative merits of galactic density functions - An orbit computational viewpoint. 03 p0373 A73-13363
- A method of solution of Vlasov's equation - Application to a nonlinear overall theory of the galactic rotation and of the galactic spiral structure 03 p0380 A73-14608
- Shock waves in spiral arms and star formation. 04 p0496 A73-14970
- The compact central region of the galaxy NGC 1614. 04 p0499 A73-15356

Stochastic wave model of spiral galaxy rotation based on weak interaction, obtaining frequency spectrum integrals for Milky Way Galaxy
05 p0616 A73-16454

Open spiral density wave propagation and distortion due to differential rotation in Lindblad resonance region
05 p0616 A73-16455

A neutral hydrogen survey of the galaxy M 33. I.
05 p0618 A73-16740

Positional evidence of Virgo X ray source correspondence with spiral galaxy IC 3576, noting optical and radio data incompatibility
05 p0626 A73-17346

Tidal gravity models of interacting pair formation of galactic bridges and tails in terms of orbit geometry, outer shapes and forced spiral waves
05 p0626 A73-17378

Star formation and evolution in spiral galaxies.
07 p0873 A73-19055

Radiation-driven efflux and circulation of dust in spiral galaxies.
07 p0875 A73-19345

Photometric plane and spherical characteristics of spiral galaxies from statistical analysis of SQ, S and Irr morphological profiles
07 p0901 A73-20314

Spiral arm structure as standing wave, of magnetically controlled star creation, considering various hydromagnetic models, dust and H I distributions
08 p1002 A73-20879

A neutral hydrogen survey of the galaxy M33. II - Distribution and kinematics of the neutral hydrogen.
08 p1005 A73-20913

Aperture synthesis study of neutral hydrogen in the galaxies NGC 6946 and IC 342.
08 p1005 A73-20914

High velocity clouds as part of Galactic spiral arms, obtaining spiral structure maps from observations of Galactic plane
08 p1005 A73-20918

The distribution of the mass-to-luminosity ratio of spiral and irregular galaxies.
08 p1006 A73-20930

The role of Schmidt telescopes in the study of external galaxies.
08 p1011 A73-21361

H beta emitting diffuse nebulae as reflection nebulae illuminated by galactic light, based on photometric observation of H alpha emitting external spiral galaxies
08 p1013 A73-21809

Stellar formation and cloud collision energy dissipations as energy sources for self gravitating shock waves maintenance in Galactic spiral theory
09 p1141 A73-22008

Cloud-cloud collision destruction of interstellar clouds in inter-spiral arm regions, discussing observational tests
09 p1141 A73-22028

Observations of the outer spiral structure of the Milky Way and its relation to the high velocity clouds.
09 p1151 A73-23292

Optical and near-infrared observations of the near-by spiral galaxy Maffei 2.
10 p1272 A73-23528

An up-to-date picture of galactic spiral features based on young open star clusters.
10 p1281 A73-24410

Continuum radio emission from NGC 4656/7 and NGC 891 at 408 MHz.
11 p1415 A73-25170

Infrared and radio observations of the nucleus of NGC 253.
11 p1428 A73-26625

Photometric plane and spherical characteristics of spiral galaxies from statistical analysis of SQ, S and Irr morphological profiles
12 p1539 A73-27286

A high resolution neutral hydrogen study of the galaxy M 51.
13 p1671 A73-28033

Identification and radio spectra of bright galaxies in the second Bologna Catalogue of radio sources and their radio luminosity function.
13 p1671 A73-28034

A survey of elliptical galaxies at 6 cm.
13 p1685 A73-29361

A forcing mechanism for spiral density waves in galaxies.
13 p1686 A73-29372

The process of galaxy formation according to the universal turbulence hypothesis.
14 p1798 A73-30142

The particle resonance in spiral galaxies - Nonlinear effects.
14 p1801 A73-30727

Patterns of waves in galactic disks.
14 p1801 A73-30728

Ionization of the intercloud medium and the central disk regions of spiral galaxies.
14 p1801 A73-30729

On the kinematical and spatial coincidence of optical and radio spiral arms in our galaxy.
15 p1929 A73-31055

Photometry and some characteristics of spiral Seyfert galaxies beyond the nucleus boundary
15 p1938 A73-31951

The dynamics of the Andromeda Nebula.
15 p1941 A73-32400

Multicolor photometry of five SBC galaxies: NGC 925, NGC 1073, NGC 3359, NGC 4088, and NGC 7741
16 p2058 A73-32713

Theories of galactic spiral structure comparisons with observations.
16 p2062 A73-33575

Radio maps of sources around spiral galaxies and associated peculiar companion galaxies
19 p2487 A73-38509

Galactic shocks as consequence of large amplitude nonlinear density waves in interstellar gas perturbed via steady forcing by spiral gravitational fields
19 p2488 A73-38511

Optical and radio observations of NGC 4258 anomalous arms indicating eruptive processes in galactic nucleus as possible source of spiral structure
20 p2605 A73-39057

A search for 21-centimeter absorption in quasars and other sources near to spiral galaxies.
20 p2609 A73-39437

Comparison of rotation curves of different galaxy types /Research note/.
20 p2611 A73-39592

Galactic spiral arm structure mapping by 21 cm data taken at different latitudes, discussing high velocity hydrogen clouds distribution
21 p2778 A73-41533

Relaxation time in disk galaxy simulations.
22 p2904 A73-41754

An attempt to interpret the mean properties of the velocity field of young stars in terms of Lin's theory of spiral waves.
22 p2908 A73-42310

The angular momentum of spiral galaxies. I - Methods of rotation-curve analysis. II - Detailed models and correlations for 17 galaxies.
22 p2913 A73-43002

Neutral hydrogen spectral line observation for Milky Way Galaxy mapping, discussing role of spiral structure density wave theory in interpretation
23 p3028 A73-43348

Structural characteristics of galaxies caused by screening of the Newtonian gravitational potential
23 p3029 A73-43646

The problem of the apparent-flattening characteristic of spiral galaxies
23 p3035 A73-44234

Photometry and some features of Seyfert spiral galaxies beyond the nuclear region.
24 p3131 A73-44476

Physical conditions in nuclei of spiral galaxies. I - Study of galaxies with a nuclear radio-component.
24 p3141 A73-45192

SPIRAL WRAPPING
Spiral wrap - A technique for fabricating thick-wall carbon composites.
01 p0057 A73-11294

SPIRALES
Finite difference method for transverse elliptical cross section effect of spiral shell on stress concentration
02 p0231 A73-11802

SPIROMETERS
A system for continuous measurement of gas exchange and respiratory functions.
01 p0011 A73-10172

Single breath nitrogen washout method for measurement of functional residual capacity.
11 p1315 A73-25332

Validation of open-circuit method for the determination of oxygen consumption.
17 p2117 A73-35462

Respiratory nitrogen elimination - A potential source of error in closed-circuit spirometry.
20 p2512 A73-39113

SPLASH POINTS
U RECOVERY ZONES
U WATER LANDING
SPLINE FUNCTIONS
Power spectral density estimation by spline smoothing in the frequency domain.
04 p0471 A73-15254

Interpolation methods in aeroelastic analysis, comparing wing structural influence coefficients derived by surface splines and interpolation-in-the-small techniques with static test data
05 p0637 A73-17215

Aerodynamic influence coefficient method using singularity splines.
06 p0644 A73-17645

[AIAA PAPER 73-123]
A method for solving moving boundary problems in heat flow using cubic splines or polynomials.
06 p0768 A73-17979

Solution of a boundary problem for a second-order delayed-argument differential equation by the spline-function method
06 p0719 A73-18688

Apollo 17 spacecraft telemetered IR scanner remote sensing data, reduction, discussing use of interpolating

and smoothing splines for restored image resolution improvement
06 p0696 A73-18807

Spline function interpolation in interactive hemodynamic simulation.
06 p0660 A73-18889

Subgrid resolution achievement by spline fitting during flow and force field sources conversion from Lagrangian distribution onto Eulerian grid and interpolation
10 p1248 A73-23603

Spline approximation to the solution of the Volterra integral equation of the second kind.
10 p1241 A73-23642

Higher-order numerical differentiation of experimental information.
10 p1244 A73-24719

Linear system modeling via optimal finite dimensional approximation based on Sard generalized spline, giving error bounds
11 p1391 A73-26580

Spline representation by finite functions
12 p1518 A73-27238

The mathematical foundations of the finite element method with applications to partial differential equations; Proceedings of the Symposium, University of Maryland, Baltimore, Md., June 26-30, 1972.
12 p1519 A73-27921

Generalized smoothing spline functions for operators.
13 p1649 A73-28604

A direct method approximation to the linear parabolic regulator problem over multivariate spline bases.
13 p1649 A73-28605

Spline interpolation techniques for approximation of boundary value problem solutions, relating approximation error norm to interpolation error norm from variational formulation
17 p2203 A73-35607

Solution of a boundary-value problem for a second-order differential equation with a lagging argument by the method of spline functions - A scheme of increased accuracy
20 p2582 A73-39472

SPLINES
Curve fitting by application of splines under tension, discussing polynomial interpolation drawbacks and linear system solution for unknown second derivatives
24 p3070 A73-45090

SPLITS [GEOLOGY]
U GEOLOGICAL FAULTS
SPLITTING
Splitting and sudden outbursts of comets as indicators of nongravitational effects.
14 p1793 A73-29819

SPOILERS
A linearized potential flow theory for airfoils with spoilers.
11 p1301 A73-25853

Flight tests of approach path angles and airspeed effects on landing of spoiler equipped light aircraft
13 p1569 A73-28830

Study of flow around an airfoil with a spoiler at Mach numbers ranging from 0.5 to 2.3
21 p2634 A73-41584

SPONGES [MATERIALS]
Sponge rubber absorption coefficient of sound and acoustic impedance measurements to test porous material sound absorption theories
14 p1767 A73-30894

SPONTANEOUS COMBUSTION
Chain interaction and heat release near the lower limit for self-ignition of hydrogen with oxygen
12 p1465 A73-26967

Hydroxyl radical mechanism for autoignition inhibition of alkane fuels for antiknock additives at various concentrations
13 p1707 A73-29000

SPONTANEOUS EMISSION
Spontaneous active medium emission effect on amplification characteristics of linear and nonlinear traveling wave IR gas laser amplifier
01 p0060 A73-11084

Kinetics of the deactivation of the vibrations of highly excited oscillators in an inert gas medium with allowance for spontaneous emission
02 p0194 A73-11607

Nonlinear interaction between a spontaneous radiation field and the active media of high-gain gas laser amplifiers
02 p0177 A73-12489

Variation of spontaneous emission with current in GaAs homostructure and double-heterostructure injection lasers.
09 p1091 A73-22236

Spontaneous emission and stimulated recombination of p-n-a double heterojunction /AlGaAs-GaAs laser diodes above and below threshold currents
09 p1093 A73-22256

Spontaneous Cerenkov emission of longitudinal waves produced by single particle and cylindrical elec-

iron beam moving inside magnetosphere along magnetic field 10 p1269 A73-24722

Theory of spontaneous and stimulated electroluminescence of ZnS-Mn layers 10 p1261 A73-24766

Spontaneous-emission feedback in a three-level quantum system - A case of conflict between semiclassical and quantum theories of radiation. 13 p1659 A73-28375

Group theory generalization of Dicke quantum theory for spontaneous coherent radiation of multilevel molecules, noting angular distribution of photon echo effects 14 p1757 A73-30332

Spontaneous emission and self-excitation of a small volume in a classical, nonlinear active medium 19 p2463 A73-38540

Survey of the present status of neoclassical radiation theory. 20 p2590 A73-38604

Nonlinear radiation reaction field effects on operator self-field and oscillating dipole, taking into account one-atom spontaneous emission and superradiance theories 20 p2590 A73-38607

Master equations in the theory of incoherent and coherent spontaneous emission. 20 p2570 A73-38608

A quantum treatment of spontaneous emission without photons. 20 p2594 A73-38611

Amplified spontaneous emission comparison with laser stimulated emission during He-Ne transitions, noting threshold condition relation to population inversion density 20 p2570 A73-38619

Collective spontaneous emission of polyatomic systems 23 p2988 A73-44010

Plasma decay instability nonlinear saturation spectrum in small spontaneous emission limit for comparable ion and electron temperatures from kinetic equation numerical solution 24 p3118 A73-45460

The relation between the diffusivity-mobility ratio and the linewidth of spontaneous emission in degenerate semiconductors at relatively high temperatures. 24 p3120 A73-45488

SPONTANEOUS IGNITION TEMPERATURE

U IGNITION TEMPERATURE

U SPONTANEOUS COMBUSTION

SPORADIC E LAYER

Simultaneous measurements of height wind profiles and electron concentration for verifying theory of sporadic E layer formation in midlatitudes under wind shear action 02 p0163 A73-12306

Electron density and wind structure observations in lower ionosphere by rocket, noting sporadic E layer due to wind shear 02 p0163 A73-12307

Sporadic E cloud focusing of radio waves as interpretation of observed short duration bursts accompanied by rapid phase variation 03 p0280 A73-14592

Constant height sporadic E velocities and heights at night explained via instabilities generated from recombination and photoionization rate variations induced by gravity wave perturbations 03 p0305 A73-14596

Altitude variations of the sporadic E layer at geographical mid-latitudes 05 p0568 A73-16217

Role of the sporadic E layer in short radio wave propagation at frequencies exceeding the maximum usable frequencies of the F2 layer 05 p0548 A73-16264

Midlatitude sporadic E layer vertical electron and ion distributions from rocket experimental wind velocity profile, assuming molecular and metallic ions in ionosphere 06 p0742 A73-17535

Three dimensional summer time sporadic E layer structure and electron concentration during 1966-1969 by ionospheric space diversity sounding 06 p0689 A73-17553

Sporadic E relation to ionized particle redistribution in E layer during solar eclipse 07 p0815 A73-19256

Auroral sporadic E layer diurnal distribution correlation to charged particle integral flux diurnal variations observed by satellite in winter, noting Kp index effect 07 p0816 A73-19455

Ionograms for slant sporadic E layer under continuous sunlight inside polar cap, noting occurrence probability and auroral activity 07 p0819 A73-20065

Equatorial electrojet currents effect on sporadic E layer near magnetic equator, noting cross field irregularities 07 p0819 A73-20066

Magnesium and associated ionospheric processes in Es-layer formation. 08 p0957 A73-20655

Equatorial sporadic E and cross-field instability. 08 p0958 A73-21150

Spatial-temporal distribution of E/s formations associated with visible forms of polar aurorae 08 p0958 A73-21283

The gradient instability in Gaussian sporadic E-layers. 09 p1075 A73-22133

Experimental observations of the amplitudes of Es and F-region reflections and their comparison with the thin-layer model for Es. 09 p1076 A73-22138

Ionogram traces production by mode coupling process in thin sporadic E layers, using calculated reflection and transmission coefficients for radio waves incidence 09 p1076 A73-22139

Mode coupling importance in midlatitude nonblanketing sporadic E layers from observations of ordinary and extraordinary blanketing frequencies 09 p1076 A73-22142

Some effects of the equatorial ionosphere on terrestrial HF radiocommunication. 09 p1051 A73-22500

Nighttime electron density in the E region at auroral latitudes in sunspot maximum. 09 p1078 A73-22747

Es-q layer at Huancayo during the March 1970 geomagnetic storm. 09 p1078 A73-22836

Sporadic ionization of the ionospheric E-region at high latitudes as a function of magnetic activity. 10 p1212 A73-24221

Upper sporadic E layer downward velocity, considering corkscrew mechanism, ionization following gravity wave particular phase and velocity decrease 10 p1215 A73-24750

Field-aligned ionospheric E-region irregularities and sporadic E. 10 p1191 A73-24897

Relationship of the sporadic E layer parameters with the absorption of radio waves in the ionosphere 11 p1350 A73-25085

Disturbances observation in E-F region and sporadic E layer by vertical ionospheric sounding during IQSY 11 p1351 A73-25098

Effect of the May 20, 1966 solar eclipse in the ionosphere on the basis of observations at Rostov on the Don and at Adler 11 p1351 A73-25100

Metal ions role in sporadic E layer formation in terms of magnesium ions profile redistribution by vertical gradient in neutral particle wind 13 p1608 A73-28723

Formation of blanketing sporadic E-layers at the magnetic equator due to horizontal wind shears. 15 p1866 A73-31070

Equatorial sporadic E layer during geomagnetic storms. 15 p1871 A73-31836

Sporadic E random electron concentration due to wind shift spectral composition, determining empirical autocorrelation functions for frequency parameters 15 p1871 A73-31885

Sporadic E layer pulsed ultrashort oblique wave sounding, analyzing reflected signal distortion 15 p1872 A73-31886

Comparison of true and effective altitudes of the sporadic E layer 15 p1872 A73-31899

The effect of polar magnetic sub-storms on the equatorial sporadic E. 15 p1874 A73-32596

Midlatitude sporadic E layer vertical electron and ion distributions from rocket experimental wind velocity profile, assuming molecular and metallic ions in ionosphere 16 p2052 A73-32759

Three dimensional summer time sporadic E layer structure and electron concentration during 1966-1969 by ionospheric space diversity sounding 16 p2002 A73-32777

Some characteristics of the ionospheric irregularities associated with Esq layers. 16 p2004 A73-33443

Sudden disappearance of Es-q and the reversal of the equatorial electric fields. 16 p2008 A73-33879

Empirical formula suitability for analysis of ionosonde data on blanketing sporadic E, noting time variation effects of limiting frequency and layer intensities 17 p2159 A73-34776

Downward transport of nighttime Es layers into the lower E-region at Arecibo. 18 p2302 A73-35941

Evidence of frontal structures in nonblanketing sporadic-E layers. 18 p2304 A73-35990

The sporadic E layer and the variation of the geomagnetic field 18 p2313 A73-36650

Space-time distribution of Es formations associated with visible auroral forms. 19 p2424 A73-37912

Skylark rocket magnetometer measurement of sporadic E layer magnetic fields, testing wind shear theory of ionization redistribution at midlatitudes 19 p2426 A73-38022

Fine-scale inhomogeneities of the mid-latitude sporadic E layer 19 p2427 A73-38332

Spread E occurrence relationship to blanketing frequency from cross field plasma instability mechanism 20 p2552 A73-38949

Investigation of the fine-structure inhomogeneities of the Es layer at oblique radio wave incidence 20 p2554 A73-39163

Wind component exchange and the rapid vertical movement of a sporadic E layer. 22 p2845 A73-41922

Rocket-borne magnetometer measurement of magnetic field changes associated with electron density fluctuations and wind structure, testing wind shear theory of sporadic E formation 23 p3024 A73-43701

Experimental test of the wind-shear theory: A reply - Rocket-borne magnetometers do measure B. 23 p3024 A73-43702

Layering of the neutral metals of meteoric origin in the lower ionosphere. 24 p3066 A73-44733

Formation of the sporadic E layer and the nighttime E region of the ionosphere at midlatitudes 24 p3083 A73-44794

Nighttime sporadic E layer measurements and integrated content measurements at Arecibo Observatory, using Barker coded incoherent scatter radar pulses 24 p3087 A73-45142

SPORADIC METEOROIDS

Mineralogical density of sporadic meteoric bodies 13 p1673 A73-28298

Method of detecting meteor streams and associations 19 p2480 A73-37236

Mineralogical density of sporadic meteoric bodies. 21 p2779 A73-41542

SPOT WELDS

Electron microanalysis of backfilled hot cracks in Inconel 600. 01 p0067 A73-11373

Bibliography on Resistance Welding, 1950-1971. 01 p0058 A73-11374

Spot welded stainless steel cylindrical strip shells: supercritical behavior, analyzing equilibrium states, dependence on axial loads and buckling forces 01 p0119 A73-11441

Some fatigue properties of welded high temperature alloys. 08 p0978 A73-21241

Influence of welding parameters on the strength properties of spot welds of MST1X steel with protective coatings 11 p1374 A73-26293

Development of a data-processing installation for the automatic quality control of spot-welding joints 16 p2019 A73-33222

Spot weld adhesive bonding procedures, examining process and quality control, tooling, curing, surface preparation, adhesive types and corrugated panel application 24 p3093 A73-44769

Unsteady combustion of a confined spray. [AICHE PREPRINT 23] 20 p2626 A73-39250

Time variation in the reaction-zone structure of two-phase spray detonations. 22 p2936 A73-42811

Liquid fuel spray burning characteristics in stabilizer disk wake of luminous hollow cone pressure jet flame, using spark photographic technique 22 p2937 A73-42818

Calculation of heat and mass transfer in devices employing spray nozzles 06 p0769 A73-18130

A gasdynamic test stand and its use in studying sprayer nozzles for spraying metallic solutions. I 24 p3075 A73-44742

SPRAYED COATINGS

Ni-Cr-thoria alloy surface oxidation induced by sprayed coating of sodium sulfate for gas turbine blade hot corrosion investigation

04 p0468 A73-15316

Some aspects of the metallurgy and wear resistance of surface coatings.

05 p0580 A73-16102

Cermet-oxide plasma jet spray coating of metal surfaces, determining thermal performance characteristics by calorimetric measurements

06 p0714 A73-18448

Effectiveness of using the energy of a plasma jet in powder coating deposition

10 p1226 A73-24689

Investigation of the preparation of high-temperature strain gauges based on heat-resistant oxides

11 p1362 A73-25455

Part manufacturing with plasma arc torch by extending plasma spray coating technology to mandrel design and machining with consideration for base materials

13 p1624 A73-28907

Dependence of some physicochemical properties of plasma-deposited aluminum oxide on sputtering conditions

15 p1881 A73-31211

Enhancement of the electrical strength of deposited aluminum oxide coatings by electrophoretically filling the pores

15 p1881 A73-31212

Effect of base material on the formation of thin plasma coatings

15 p1881 A73-31590

The technology of plasma arc spraying.

16 p2017 A73-32698

Plasma sprayed coatings

18 p2318 A73-35882

Detonation propelled metal particle sprayed coatings adhesion strength relation to particle kinetic energy

18 p2318 A73-35884

Ferrite thick film deposition by arc plasma spraying, discussing apparatus, process and film properties after annealing

19 p2435 A73-38096

Investigation of the effective heat conductivity of plasma-sprayed alumina coatings subject to radiative heating in the temperature range from 100 to 900 C

21 p2792 A73-41220

International Metal Spraying Conference, 7th, London, England, September 10-14, 1973, Proceedings.

22 p2879 A73-42591

Investigations into the mechanism of exothermically reacting nickel-aluminum spraying materials.

22 p2879 A73-42595

Low temperature thermionic cathode.

22 p2834 A73-42695

Mechanical properties of glass fiber reinforced plastic laminate formed by spraying unsaturated polyester resin on fiber rovings

24 p3094 A73-44890

SPRAYED PROTECTIVE COATINGS

U PROTECTIVE COATINGS

U SPRAYED COATINGS

SPRAYING

NT ARC SPRAYING

NT FLAME SPRAYING

NT METAL SPRAYING

NT PLASMA SPRAYING

The rapid cooling of a hot gas discharge by liquid sprays.

22 p2929 A73-41743

SPREAD F

Vertical ionospheric sounding station observation for spread F layer effect on scattered signal fading, using oscillograph display and camera

02 p0142 A73-12498

Moment equations of temperature and high latitude spread F instability in presence of north-south electric field, relating to maximum Pedersen current and barium cloud deformation

07 p0814 A73-19243

Equatorial spread F formation convective electric fields generation by neutral winds and conductivity caused by metallic ion concentrations

14 p1749 A73-29988

Equatorial scintillation variation with magnetic storm from ATS 3 VHF telemetry signal recordings, comparing with spread F observation

15 p1870 A73-31763

Large scale equatorial spread F irregularities motion velocity observation in Africa, interpreting quasi-periodic structures in west-east extension by atmospheric gravity waves

15 p1870 A73-31764

Equatorial spread F layer height nocturnal variations due to magnetic disturbances during solar activity cycles

16 p2008 A73-33878

Midlatitude spread F relationship to F region trough formation, considering multiple reflections emanating from steep ionization contours

21 p2684 A73-40784

A current mechanism for the formation of inhomogeneities resulting in the ionospheric spread F region at high latitudes

21 p2692 A73-41508

Fading characteristics and drift and anisotropy parameters of the ground diffraction pattern of the radio waves reflected from the equatorial ionosphere during spread F conditions.

22 p2825 A73-41929

Low latitude whistler activity during geomagnetic storms related to spread F conditions and magnetospheric and ionospheric electron density

23 p2972 A73-43696

SPREAD REFLECTION

U DIFFUSE RADIATION

U REFLECTION

SPRINGS [ELASTIC]

Dynamic calculation of the stretching of a spring with allowance for redistribution of mass along its length

02 p0230 A73-11720

Approximate conditions to account for spring mass redistribution with kinetic energy conversion into strain energy over small critical time interval

02 p0230 A73-11795

Similar normal mode vibrations in certain conservative systems with two degrees-of-freedom.

02 p0193 A73-12515

Response of a system of cascaded nonlinear springs

02 p0193 A73-12521

Data acquisition, processing and retrieval in information system for product design and development, noting storage system for spring material data

03 p0400 A73-13238

Mechanical properties of heat and corrosion resistant nonmagnetic Ni-Cr-Nr spring alloys with W addition tested in aggressive and nitric acid base media

06 p0709 A73-18211

Free vibration of multi-degree-of-freedom nonlinear systems.

07 p0909 A73-19164

Forced vibration of a class of non-linear two-degree-of-freedom oscillators.

07 p0851 A73-19165

Dynamic behaviour of thin cylindrical shells collided with dampers.

08 p1019 A73-21527

Irradiation creep in some austenitic stainless steels, nimonic PE16 alloy and nickel.

08 p0982 A73-21794

Ag- or Cu-based fiber reinforced composite materials for springs in electrical contact devices, investigating mechanical strength and contact and wear resistances

11 p1387 A73-25410

Vibrations of an Euler beam with a system of discrete masses, springs, and dashpots.

11 p1442 A73-25788

Stability of the steady motions of a gyroscope with spring limiters on a revolving platform in a Newtonian central force field

11 p1364 A73-26095

Ritz method extension to mechanics problems by introducing artificial spring parameters at boundary and using Legendre functions as coordinate functions

12 p1555 A73-27740

Application of holographic interferometry to predict long time torsional relaxation.

13 p1620 A73-29301

High performance vibration isolated tables.

20 p2544 A73-39266

A new weighting function for solving nonlinear oscillation problems.

24 p3148 A73-44893

Periodic solutions of a spring-pendulum system.

24 p3111 A73-45294

SPUR [REACTORS]

U SPACE POWER UNIT REACTORS

SPUTNIK SATELLITES

Book - The politics and technology of satellite communications.

14 p1818 A73-29949

SPUTTERING

RF sputtered integral covers of glass coating for thermal protection of Si solar cells, noting intrinsic stress, adhesion, transparency and radiation damage resistance

03 p0256 A73-14227

Preparation and corrosion properties of a tantalum sputtered thick film.

04 p0456 A73-15759

Low-temperature epitaxy of Ge films by sputter deposition.

06 p0739 A73-18777

Solid material ion source discharge chamber with cathode sputtering-introduced metal vapor, based on conventional ion source with electrons oscillating in magnetic field

08 p0993 A73-21515

Ion gun sputter cleaning of thin film metal substrate for in situ corrosion studies by UHV transmission electron microscopy

08 p0990 A73-21616

Dependence of some physicochemical properties of plasma-deposited aluminum oxide on sputtering conditions

15 p1881 A73-31211

Structure of sputtered molybdenum disulfide films at various substrate temperatures. [ASLE PREPRINT 73AM-3C-3]

17 p2196 A73-34988

Thin film capacitor with anodic tantalum oxide overlaid with silicon dioxide deposited by RF sputtering, noting reliability under various voltage, temperature and humidity conditions

21 p2663 A73-40771

RF sputtering of ZnO shear-wave transducers.

21 p2702 A73-40952

SQUARE WAVES

Multiple soliton excitation by ion acoustic square pulse wave in double plasma device in frame of Korteweg-de Vries equation

04 p0477 A73-14771

Selection of the parameters of a rectangular-pulse generator with quartz-crystal controlled frequency

12 p1481 A73-27587

Shaping circuit for complex RF pulse consisting of simultaneous equilength square pulses with different frequencies, discussing carrier frequencies selection

13 p1583 A73-28730

A generator of rectangular voltage pulses with 50 kV amplitude

17 p2120 A73-34153

A radio signal shaping device with large signal attenuation in the intervals between signals

21 p2661 A73-40174

A square-wave generator with digital frequency setting

21 p2662 A73-40346

ST VENANT FLEXURE PROBLEM

U SAINT VENANT PRINCIPLE

STABILITY

NT ACOUSTIC INSTABILITY

NT AERODYNAMIC STABILITY

NT AIRCRAFT STABILITY

NT ATTITUDE STABILITY

NT BOUNDARY LAYER STABILITY

NT COMBUSTION STABILITY

NT CONTROL STABILITY

NT DIMENSIONAL STABILITY

NT DIRECTIONAL STABILITY

NT DYNAMIC STABILITY

NT FLAME STABILITY

NT FLOW STABILITY

NT FREQUENCY STABILITY

NT GYROSCOPIC STABILITY

NT HOVERING STABILITY

NT LONGITUDINAL STABILITY

NT MAGNETOHYDRODYNAMIC STABILITY

NT MAGNETOSPHERIC INSTABILITY

NT MOTION STABILITY

NT ROTARY STABILITY

NT SHELL STABILITY

NT SPACECRAFT STABILITY

NT STATIC STABILITY

NT STORAGE STABILITY

NT STRUCTURAL STABILITY

NT SURFACE STABILITY

NT SYSTEMS STABILITY

NT THERMAL STABILITY

Uniqueness and stability of positive periodic solutions of differential equations with a delayed argument

02 p0187 A73-12357

Stress equations solutions existence near Minkowskian solution for asymptotic behavior, demonstrating flat space-time stability

03 p0344 A73-14604

Stability of the Bubnov-Galerkin method for unstable operator equations with variable coefficients

04 p0470 A73-15085

STABILITY AUGMENTATION

U FEEDBACK CONTROL

U STABILIZATION

STABILITY DERIVATIVES

NT PITCHING MOMENTS

NT ROLLING MOMENTS

NT YAWING MOMENTS

Experimental and theoretical investigations regarding the unsteady aerodynamical derivatives of the longitudinal motion in the case of slender flight bodies at moderate velocity

05 p0528 A73-16757

Unsteady transonic flow analysis for low aspect ratio, pointed wings.

05 p0530 A73-16878

A four-level technique for estimation of tactical missile aerodynamic parameters.

07 p0777 A73-20592

A four-level technique for estimation of tactical missile aerodynamic parameters.

10 p1172 A73-24538

Dynamic viscous pressure interaction on a cone.

10 p1173 A73-24821

The effect of aerodynamic moments on the rotational motion of Proton satellites

12 p1548 A73-26820

STABILITY TESTS

Parameter estimation for a specular-diffusion reflection model from the motion of 'Proton' series satellites about their centers of mass
14 p1803 A73-29851

Identification of YT-2B stability and control derivatives via the maximum likelihood method.
19 p2386 A73-38043

STABILITY TESTS

NT FLIGHT STABILITY TESTS

NT WIND TUNNEL STABILITY TESTS

Accelerated tests for long term stability of CdS solar cells, noting stoichiometry, wavelength, doping and residual atmosphere effects on cell performance
03 p0255 A73-14215

Thin film CdS solar cell stability improvement by etching, noting cuprous sulfide oxidation effects on degradation from short term tests at high temperature
03 p0255 A73-14221

Experiments on the stability of various water-lubricated fixed geometry hydrodynamic journal bearings at zero load.
[ASME PAPER 72-LUB-46] 03 p0315 A73-14350

German monograph - A contribution to the stability calculation and the test of cylindrical shells of glass-fiber reinforced plastics under uniform external pressure.
13 p1646 A73-29280

Investigation of reactionless mode stability characteristics of a stiff inplane hingeless rotor system.
[AHS PREPRINT 734] 17 p2105 A73-35070

STABILIZATION

NT SIGNAL STABILIZATION

NT SPIN STABILIZATION

Wiener-Kolmogoroff optimal filtration theory for synthesis of linear stabilization systems under steady random external perturbations, noting control optimality conditions
01 p0028 A73-10670

Calculation of a photoelectric system for stabilizing the optical axis of an instrument
05 p0575 A73-16316

Stabilization of the austenitic phase of iron-nickel base alloys by cumulative thermal cycling
11 p1379 A73-25323

UPSTARS - A single escape subsystem providing stabilization, retardation, and separation.
16 p1966 A73-32668

ESCAPAC IE stabilized ejection seat for Navy S-3A and Air Force A-9A aircraft, describing propulsion, stabilization, separation and lateral divergence subsystems
16 p1966 A73-32669

Remote feedback stabilization of ion acoustic type instability in plasma with LF density modulation, noting Van der Pol approach agreement and crossed field diffusion decrease
16 p2041 A73-33327

Separate surfaces for automatic flight controls.
[SAE PAPER 730304] 17 p2101 A73-34665

Control requirements for sling-load stabilization in heavy lift helicopters.
20 p2509 A73-39406

STABILIZED PLATFORMS

Precession equations of a triaxial power-driven gyrostabilizer
02 p0167 A73-11775

Stability criteria for a free dual-spin satellite.
02 p0228 A73-12398

Errors in measuring the angles of rotation of an object with a triaxial gyrostabilized platform with allowance for its drift
09 p1115 A73-22343

Stability of the steady motions of a gyroscopic with spring limiters on a revolving platform in a Newtonian central force field
11 p1364 A73-26095

Stable-member mounted instrument environment simulation model development.
11 p1395 A73-26638

A simple stabilized antenna platform for maritime satellite communications.
12 p1481 A73-27673

High-reliability strapdown platforms using two-degree-of-freedom gyros.
13 p1657 A73-29214

Kalman filter design considerations for space-stable inertial navigation systems.
13 p1657 A73-29220

Three-axis attitude control system air-bearing tests with flexible dynamics.
[AIAA PAPER 73-866] 20 p2543 A73-38804

Extremal search method errors in determining azimuthal position of gyrostabilized platform relative to meridian plane, comparing with gyrocompasses
24 p3109 A73-45022

STABILIZERS

Reducing the thermal bending of a gravity-gradient stabilizer with the aid of a protective covering
10 p1286 A73-23894

Reduction of thermal deflection of gravitational stabilizer using shielding cover.
20 p2614 A73-38913

Flight simulation requirement in artificial stabilizer design for VTOL aircraft flight control system, noting agreement with flight tests
22 p2838 A73-41751

STABILIZERS [AGENTS]

The service life of rocket motors filled with double base propellants.
[AIAA PAPER 72-1109] 03 p0351 A73-13424

Measuring apparatus for residual effective stabilizer content in single and double base propellants by passing nitrogen dioxide through ground sample
09 p1135 A73-22300

Effects of some carbide stabilizing elements on creep-rupture strength and microstructural changes of 18-10 austenitic steel.
14 p1761 A73-30627

Stability of silver bromide dispersions in the presence of gelatin and other surface-active substances
21 p2647 A73-40267

STABILIZERS [FLUID DYNAMICS]

Iliushin 62 aircraft horizontal stabilizer structural design and control, discussing mounting hardware and electrically driven servomechanism
11 p1305 A73-25795

STABLE OSCILLATIONS

Analysis of limit cycles in a two-transistor saturation-core parallel inverter.
03 p0252 A73-13929

Stationary nonlinear ion acoustic oscillations in dense weakly ionized current carrying plasma, considering wave propagation velocity and instability process
06 p0728 A73-17971

Resonator parameters effect on stability characteristics of ultrashort pulse produced by ruby laser, using mirror and thin reflector
10 p1227 A73-24070

Ultrastable atomic and molecular oscillators and their applications to navigation
19 p2429 A73-37384

Analysis of limit cycles in a two-transistor saturation-core parallel inverter.
21 p2662 A73-40339

Rayleigh-Taylor problem of thermal instability of density-stratified layer of incompressible fluid heated from above, considering oscillatory and nonoscillatory modes stability
23 p3048 A73-43346

Temperature field and motion oscillations in water-methanol and water-isopropanol Benard cells, taking into account thermal diffusion
23 p3049 A73-43936

Space-time limits of stable oscillations of solar surface active zones spanning multiple solar rotations, noting correlation coefficients for north and south hemispheres
24 p3138 A73-45013

STACKING FAULT ENERGY

Creep characteristics and substructure disorientation in metals with an fcc lattice
06 p0706 A73-17904

Investigation of the structural changes in austenite during martensitic transformation in steels with high stacking-fault energy
07 p0841 A73-20521

The effect of creep strain on stacking-fault precipitation in Nb-stabilized 20/25 austenitic stainless steels.
08 p0981 A73-21787

High temperature creep in nickel and its alloys
09 p1108 A73-23229

Fatigue crack initiation and propagation in low stacking fault energy austenite steel related to plastic deformation induced gamma alpha transformation and martensite failure
13 p1640 A73-29481

Stacking fault energy in iron-nickel and iron-nickel-chromium alloys
14 p1764 A73-30869

The effect of stacking-fault energy on the stress-strain curve of dispersion-hardened Ni-Co alloys.
15 p1887 A73-31351

Special features of high-temperature creep in metals with an fcc lattice
17 p2188 A73-34563

Low temperature tensile tests for strength and plasticity of pure bcc, hcp and fcc polycrystalline metals, indicating stacking fault energy role
18 p2324 A73-36804

X ray diffraction analysis of Mo-Ta and Mo-C solid solutions, relating transition and nontransition metal electronic structures and stacking fault energy
18 p2325 A73-36808

The effect of stacking fault energy on the plastic deformation of polycrystalline Ni-Co alloys.
22 p2879 A73-43074

Plastic deformation of Co-Ni-Cr and Co-Ni-Cr-Mo alloys
24 p3101 A73-45525

STACKING FAULTS

U CRYSTAL DEFECTS

STACKS

Pseudoelastic design method for bottle-crate stack instability performance prediction through failure by creep buckling, assessing effectiveness by comparison with measurements
12 p1514 A73-26874

STADAN [SATELLITE TRACKING NETWORK]

The ground operations system for the AEROS research satellite.
08 p0953 A73-21644

STAGE SEPARATION

Stage separation of parallel-staged shuttle vehicles - A capability assessment.
01 p0109 A73-10103

Rocket stages separation distance measurement by monitoring gamma ray flux variation, noting separation mechanisms and retromotor performances
01 p0052 A73-11164

Thrust reversal systems for solid propellant rocket motors last stage separation from payloads, examining pressure decay under isothermal and adiabatic assumptions
03 p0355 A73-13422

A study of the plume impingement environment experienced by the booster during the space shuttle nominal staging maneuver.
[AIAA PAPER 72-1171] 03 p0273 A73-13468

The utilization of detonating fuses on launchers.
07 p0865 A73-18996

Satellite-equipment compartment separation system.
07 p0905 A73-18997

Space-flight qualification of solid-propellant units in the example of the cold-gas generator for the booster rocket Europa I/II
16 p2047 A73-33394

Design, capability, and cost of a Versatile Upper Stage /VUS/ family of vehicles.
[AIAA PAPER 73-589] 18 p2357 A73-36078

Diversity combining of UHF signals under rapid fading conditions.
20 p2523 A73-38724

Example of dynamic interference effects between two oscillating vehicles.
22 p2917 A73-42634

STAGGERING

Distribution of equivalent attenuations and generalized detunings in a stagger single-tuned IF amplifier with critical staggering.
10 p1197 A73-24934

Spread of transistor parameters as a factor in the design of IF amplifiers with pairs of staggered stages.
10 p1197 A73-24933

STAGING [ROCKETS]

U STAGE SEPARATION

STAGNATION

U STAGNATION POINT

STAGNATION FLOW

On unsteady forced flow against a rotating disk.
06 p0643 A73-17394

Mass-transfer effects on higher-order boundary layer solutions - The leading edge of a swept cylinder.
06 p0688 A73-18833

On laminar free convection stagnation heat transfer from an isothermal cylinder with internal sources/sinks.
07 p0918 A73-19101

Spatial stability of stagnation water boundary layers with heat transfer.
07 p0919 A73-19503

Characteristics of unsteady interaction between a supersonic jet and an infinite obstacle
08 p0927 A73-21604

Electron temperature profile in stagnation region of flow of blunt bodies with consideration of ionization recombination in shock layer
10 p1296 A73-24256

Two dimensional opposing incompressible viscous fluid jets impingement, investigating stagnation surface stability characteristics
13 p1603 A73-29036

Local potential variational method for analytic approximation of stagnation in plane flow, discussing generalized entropy method for accuracy improvement
15 p1957 A73-31665

Ion current at the forward stagnation region of an electrically conducting body.
15 p1918 A73-31669

On the polarographic measurement of the wall gradient of velocity in the upstream stagnation zone of detachment from the cylinder
15 p1878 A73-32205

Nonlinear stability of cylindrical vortex enclosing a central jet of light or dense fluid.
24 p3080 A73-45452

STAGNATION POINT

Radiative and convective heating during Venus entry.
01 p0003 A73-10757

Forced convection droplet evaporation with finite vaporization kinetics and liquid heat transfer.
01 p0122 A73-10803

Effects of forced flow, noncondensables, and variable properties on film condensation of pure and binary vapors at the forward stagnation point of a horizontal cylinder.

01 p0122 A73-10806

Convective heat transfer coefficients at stagnation point of blunt body immersed in flames of fuel gases combustion with pure oxygen

01 p0122 A73-10807

Boundary-layer development at a two-dimensional rear stagnation point.

03 p0294 A73-13536

Radiative and convective heat transfer occurring in the hypersonic flow past a blunt body

03 p0244 A73-13617

On the deviation of the flame from the stagnation point in opposed-jet diffusion flames.

03 p0399 A73-14388

Hypersonic solar wind flow interactions with comet emitted gas forming tails, discussing contact surface with stagnation point and bow shock front

04 p0494 A73-14758

Stagnation-point free-convection film boiling on a hemisphere.

05 p0638 A73-16353

Calculation of stagnation-point pressure during shock-wave incidence on a body moving at supersonic velocity

06 p0643 A73-17459

Heat transfer in a periodic boundary layer near a two-dimensional stagnation point.

06 p0769 A73-18526

An iterative procedure for the oscillatory laminar boundary layer.

07 p0809 A73-19035

Further results on the stagnation point boundary layer with hydrogen injection.

07 p0921 A73-20358

Effect of ionization nonequilibrium on the shock wave in the stagnation region

07 p0776 A73-20616

Unsteady boundary layer flows at general three-dimensional stagnation points.

08 p0954 A73-21008

Experimental investigation of heat transfer using facilities for testing heatproof materials

08 p1022 A73-21094

Flow near the stagnation point of a body which undergoes a sudden change in a steady stream.

[ASME PAPER 72-APM-UU] 11 p1347 A73-25701

Asymptotic solution of shock-layer equations in the vicinity of the stagnation point of a sphere in the case of strong blowing

11 p1304 A73-26442

Stagnation conditions in systems with Coulomb friction

11 p1400 A73-26451

Effect of surface catalytic activity on stagnation heat-transfer rates.

13 p1706 A73-28804

The nature of viscous flow around the forward stagnation point in the presence of strong injection of a gas through the surface of a slender pointed body

15 p1821 A73-31043

Hypersonic merged stagnation shock layers.

[AIAA PAPER 73-639] 18 p2260 A73-36197

Viscous effects in massively-ablating planetary entry body flow fields.

[AIAA PAPER 73-716] 18 p2264 A73-36335

Convective heating in dust-laden hypersonic flows.

[AIAA PAPER 73-761] 18 p2371 A73-36376

On a stagnation condition for combining or branching inviscid flows.

20 p2546 A73-39091

Aerodynamic forces on a triangular cylinder.

21 p2782 A73-40003

Unsteady stagnation point heat transfer due to unsteady free stream temperature.

22 p2931 A73-42290

Numerical analysis of magnetic field lines of force reconnection along transition layers or at flow stagnation point of incompressible conducting viscous fluid

22 p2894 A73-42396

Flowing gas mixture ignition at heated blunt body stagnation point, examining Van't Hoff criterion

23 p3048 A73-43328

Nonstationary mass transfer during the longitudinal flow of a nonlinearly viscous fluid past a flat plate and the forward stagnation point

23 p2967 A73-43440

Gaseous fuel combustion in water flow by introducing fuel-oxygen mixture in stagnation region behind body for flame stabilization

24 p3158 A73-45386

The incompressible boundary layer of higher order at the axisymmetrical stagnation point in the case of strong suction or blowing

24 p3056 A73-45545

FAGNATION PRESSURE

A high pressure gas-dynamic laser powered by a slow compression heater

[ONERA, TP NO. 1184] 09 p1096 A73-22712

Flowing through moving cascades of lifting lines with fluctuating lift.

10 p1171 A73-23697

STAGNATION REGION

U STAGNATION POINT

STAGNATION TEMPERATURE

An aerodynamic test facility with free molecular flow and high stagnation temperature

20 p2545 A73-39615

Determination of vibrational and translational temperatures in gas-dynamic lasers.

24 p3095 A73-44588

STAINLESS STEELS

NT AUSTENITIC STAINLESS STEELS

NT FERRITIC STAINLESS STEELS

NT MARTENSITIC STAINLESS STEELS

Investigation of creep in Kh18Ni10T steel at varying temperatures

01 p0066 A73-11094

Fatigue crack propagation in stainless steel weldments at high temperature.

01 p0067 A73-11372

Demonstration of the inhibiting action of certain mineral iodides on the stress corrosion of type 18-10 low-carbon stainless steel

02 p0178 A73-11524

Mechanism of transformation of a low-carbon 18-10 stainless steel by reaction in liquid tin

02 p0178 A73-11525

Ultrasonic measurements of cold-work percentages in Type 316 stainless steel.

02 p0173 A73-11987

Surface preparation and pit propagation in stainless steels.

03 p0325 A73-13726

Aluminum-stainless steel and Ni-Mo composites prepared by dynamic hot pressing, determining bond strength between fibers and reinforced metal matrix

03 p0328 A73-14013

Hold-time effects on the elevated temperature fatigue-crack propagation of type 304 stainless steel.

03 p0328 A73-14448

The effect of frequency upon the fatigue-crack growth of Type 304 stainless steel at 1000 F.

04 p0459 A73-14689

Pseudo-subgrain-boundaries in stainless steel.

04 p0461 A73-14872

Cr heat vacuum decarburization equipment for stainless steel vacuum melting, noting cost analysis, vacuum pumping curve and desulfurization

04 p0455 A73-15745

Study of the diffusion of carbon in structural steel plates clad with stainless steels

04 p0467 A73-15951

Nitriding by ion bombardment of 18-10 stainless steels

04 p0457 A73-15954

Material variability as measured by low temperature electrical resistivity.

05 p0588 A73-17287

Heat exchange between gas and air cooled porous metal plate prepared from stainless steel powder under induction and resistance heating

06 p0768 A73-18129

Magnetostriiction of stainless steels in relation to heat treatment.

06 p0709 A73-18212

Postirradiation mechanical properties of Types 304 and 304 + 0.15% titanium stainless steel.

06 p0710 A73-18545

Study of pitting corrosion and stress corrosion in stainless steels with the aid of alloys of very high purity

07 p0838 A73-19114

Fine grained weld structures.

07 p0832 A73-20273

Characterization of passivation films formed at the surface of stainless steels in magnesium chloride solutions

08 p0976 A73-20650

The temperature dependence of steady state creep in 20% Cr, 25% Ni, Nb stabilized stainless steel.

08 p0981 A73-21785

Dispersion-strengthened ferritic alloys for high-temperature application.

08 p0982 A73-21798

On the influence of deformation rate on intergranular crack propagation in Type 304 stainless steel.

09 p1100 A73-22000

Electric charges on stainless steel surfaces - The effects of hydrogen, charged particles, illumination, and electric fields on the work function.

09 p1133 A73-22195

Study and realization of special parts for aerospace construction by brazing in a fluorided reducing atmosphere

09 p1088 A73-22202

Effect of thermomechanical processing on fatigue crack propagation.

09 p1102 A73-22415

Effects of hold time on low-cycle fatigue behavior of AISI Type 304 stainless steel at 593 C.

09 p1102 A73-22417

Thermophysical effects of solidification on dendritic structure and mechanical properties of cast stainless and low alloy carbon steels for different crystallization rates

09 p1107 A73-23198

Quantitative characterization of the substructure of AISI 316 stainless steel resulting from creep.

10 p1234 A73-24436

The effect of carbon and titanium on the hot workability of 25Cr-6Ni stainless steels.

10 p1235 A73-24440

Temperature change induced material properties variations effects on impact stresses in graphite and stainless steels, considering impact velocity

10 p1220 A73-24575

Carbon and stainless steels chemical composition effects on diffusion layer structure and fatigue strength after diffusive boriding

10 p1236 A73-24954

Vacuum contactless metallization of carbon steels, stainless steels and nickel alloys, considering Si, Cr and Al coatings

10 p1227 A73-24964

On the nature of films over corrosion pits in stainless steel.

11 p1378 A73-24975

Study on the superposition of intergranular corrosion and pitting corrosion by fatigue cracking of stainless steels.

11 p1383 A73-25831

Neutron irradiation effects on room and high temperature fatigue behavior of stainless steel, noting fatigue life enhancement at low temperature and strains

11 p1383 A73-25832

Alpha phase lattice constant curves and composition effects of Cr-Ni-Co-Mo steels on microstress rate reduction during age hardening

12 p1509 A73-26840

Tensile behaviors of high Cr-low Ni two-phase stainless steels at room and low temperatures.

12 p1511 A73-27056

The influence of the thermal properties of the heating-surface on the heat-transfer of bubble boiling

12 p1539 A73-27698

A comparative study of the thermal diffusivities of stainless steel, hafnium, and Zircaloy.

[ECTP PAPER C-6] 13 p1630 A73-28051

Transverse creep and stress-rupture of Borsic-aluminum composites and Borsic-aluminum composites containing stainless steel and titanium.

13 p1633 A73-28143

Measurement of interfacial free energies and associated temperature coefficients in 304 stainless steel.

13 p1634 A73-28259

Recent developments in precipitation hardenable stainless steels.

13 p1637 A73-29271

Compatible coatings for corrosion resistant aerospace fasteners.

[NACE PAPER 116] 13 p1638 A73-29316

Production of a niobium-stainless steel bimetal by explosion welding

14 p1755 A73-30386

Automated machining and surface finishing of heat resistant stainless steel nozzles for wind tunnel applications

15 p1855 A73-31200

Intergranular corrosion in iron and nickel base alloys.

15 p1888 A73-31739

Plane stress fracture testing using center-cracked panels.

15 p1951 A73-31987

Cold forming stainless steels and other specialty grades.

15 p1883 A73-32168

High strain rate tensile properties of AISI type 304 stainless steel.

18 p2323 A73-36619

Adsorption of hydrogen, carbon monoxide, and oxygen on vacuum degassed stainless steel 304 at 20 C.

19 p2402 A73-37194

Post-buckling behavior of cold-formed thin-walled stainless steel beams.

19 p2496 A73-37481

Spatial distributions of H₂ desorbed from Fe, Pt, Cu, Nb, and stainless steel surfaces.

19 p2402 A73-37951

The thermal and electrical conductivities of porous copper and stainless steel to elevated temperatures.

[ASME PAPER 73-HT-47] 20 p2575 A73-38572

Anisotropy of the mechanical properties of aluminum hardened by a stainless steel grid

20 p2578 A73-39382

Substructure of type 316 stainless steel deformed in slow tension at temperatures between 21 and 816 C.

20 p2578 A73-39491

Mechanical properties of AFC77 stainless steel bolts.

21 p2721 A73-41085

Brazeability of Ni-Cr heat resistant cermets on stainless steel.

23 p2986 A73-44005

Hydrogen-induced transformation and embrittlement in 18-8 stainless steel.

23 p2994 A73-44158

STAIRSTEPS

STAIRSTEPS

Exercise testing for evaluation of cardiac performance. 03 p0259 A73-13538

Practical exercise test for physical fitness and cardiac performance. 03 p0259 A73-13540

STALL

U BOUNDARY LAYER SEPARATION

STAMPING

Stress analysis for two stamps impression into linearly deformable base, solving integral stress equation by orthogonal polynomials method 01 p0118 A73-11411

Contact problem with one governing parameter in elasticity theory 08 p1017 A73-21099

Stability of sheet metal drawn by a rigid stamp to cylindrical and conical shapes 12 p1503 A73-27476

Solution of three-dimensional contact problems in elasticity theory 14 p1775 A73-30831

Dynamic contact problem for the case of longitudinal shear strain 22 p2927 A73-43051

Solution of spatial contact problems of the theory of elasticity. 23 p3040 A73-43585

STANDARD ATMOSPHERES

U REFERENCE ATMOSPHERES

STANDARD DEVIATION

Standard deviation of thresholding time during detection of pulse perturbed by Gaussian noise 03 p0277 A73-13912

Relaxation time measurements by an electronic method. 10 p1217 A73-23998

The effect of limiting upon the mean cross section of log-normal radar clutter. 13 p1586 A73-29224

CIE interlaboratory comparison of measurements of photocell spectral sensitivity. 21 p2698 A73-40141

Wind speed variability /standard deviation difference/ over 16.25 km distance between observation sites compared to generalized models for varying conditions of cyclonic activity 23 p3004 A73-44267

STANDARDIZATION

Contributions to the standardization of control systems for satellites and peak payloads 02 p0228 A73-11705

New norms and standardization trends for dosimetry and protection against radiation 11 p1322 A73-25311

Coordinate systems standardization in stress analysis, considering vector orientation definitions 11 p1444 A73-26374

Industrial material management, considering department requirements, identification effort, costs and benefit, numbering and standardization systems, and uniform commodity description problem 13 p1624 A73-28788

Computerized approach for aerospace electronic components standardization for procurement cost, logistics and warehousing problems reduction and reliability improvement 17 p2140 A73-35260

Book - Twelfth report by the International Telecommunication Union on telecommunication and the peaceful uses of outer space. 20 p2607 A73-39151

Overview of Department of Defense Electromagnetic Radiation Hazards Standardization Program. 22 p2822 A73-41790

Land-air-sea intermodal cargo container movement procedures and equipment design standardization to meet air transportability requirements [ASME PAPER 73-ICT-30] 23 p2965 A73-43493

STANDARDS

NT FREQUENCY STANDARDS

NT REFERENCE ATMOSPHERES

Intermediate resistance standards for low resistivity resistance thermometer calibration, discussing accuracy requirements and error analysis 02 p0167 A73-11866

A criterion for establishing the principal dimensions of /metallic/ standard measures of volume 03 p0306 A73-12897

A new variant of the Knudsen vacuumeter as a measurement standard for low pressures 03 p0306 A73-12898

An exact analysis of the Method-One maintainability demonstration plan in MIL-STD-471. 03 p0336 A73-13731

The growing role of standards in the national and international coordination of space programs. 04 p0524 A73-15381

The USAF aircraft structural integrity program /ASIP/. [AIAA PAPER 73-18] 06 p0759 A73-17611

Minimum performance standards - Airborne distance measuring equipment /DME/ operating

within the radio-frequency range of 960-1215 megahertz. 07 p0849 A73-19575

Calibration procedure for instruments to measure the delta ferrite content of austenitic stainless steel weld metal. 07 p0832 A73-20272

Crew station lighting - Commercial aircraft. [SAE ARP 1161] 08 p0925 A73-20692
Flight research to develop airworthiness standards for civil aircraft. 09 p1031 A73-22184

Remarks on the ISO international standards relating to "Terms and Symbols for Flight Dynamics" 10 p1174 A73-23657

Standardization, loading methods and environments for stress corrosion cracking tests, noting prevention of crevice, galvanic and hydrogen embrittlement effects 10 p1232 A73-23871

Photoemission diode standards with high sensitivity, time stability and response uniformity for accurate measurement of monochromatic UV light, discussing design and construction 11 p1365 A73-26234

Problems and design of black-body references. 11 p1401 A73-26514

The moon as a proposed radiometric standard for microwave and infrared observations of extended sources. 11 p1426 A73-26545

A recalibration of the quiet sun millimeter spectrum based on the moon as an absolute radiometric standard. 12 p1545 A73-27840

Airport layout and planning standards, considering dimensions, height restrictions, noise exposure, land use compatibility, and long term community and aeronautical requirements 13 p1598 A73-29347

Arc plasmas as radiation standards in the vacuum ultraviolet. 16 p2036 A73-32942

Identification and coding of fluid and electrical piping system functions. [SAE AIR 1273] 16 p1970 A73-33019

Standard indoor method of collection and presentation of the bare turboshaft engine noise data for use in helicopter installations. [SAE ARP 1279] 16 p2046 A73-33020

MIL-STD-810 uniform test methods for determining military equipment environmental resistance, discussing inadequacies, misapplications and planned revision for improvement 16 p2087 A73-33144

Military specifications provisions regarding load transfer. 17 p2133 A73-34093

International Civil Aviation standards concerning rights and duties of appointed observers at inquiry by state of aircraft accident occurrence 19 p2505 A73-37737

High reliability manufacturing technology for COS/MOS IC devices, discussing failure mechanisms and MIL-STD-883 and MIL-M-38510 tests for quality control 20 p2534 A73-38656

Technical progress on new vibration and acoustic tests for proposed MIL-STD-810C, 'environmental test methods.' 21 p2674 A73-41200

Electromagnetic radiation hazard test facility, instrumentation, and weapon system susceptibility evaluation for providing environment protection and military standards 22 p2822 A73-41791

Platinum resistance thermometer as standard instrument for interpolation on International Practical Temperature Scale, discussing design development, operational characteristics and errors 22 p2855 A73-42010

Revision of the standard reference data for thermocouples. 22 p2857 A73-42032

STANDING WAVE RATIOS

Standing wave approximation of distributed dual frequency parametric oscillators consisting of semiconductor diodes and transmission line in steady state 02 p0147 A73-12490

Statistical analysis of microwave transmission line coefficients, discussing line losses, inhomogeneity distribution, input voltage standing wave ratios and rms deviations 21 p2648 A73-40204

STANDING WAVES

Nonlinear monochromatic Langmuir standing waves in a plasma 04 p0478 A73-15033

Stationary waves properties dependence on weak skin effect in distributed tunnel diode type of nonlinear active transmission lines 04 p0429 A73-15911

Calculation of input-voltage standing-wave ratio for a reflector antenna. 05 p0547 A73-16161

Frequency and time description of mode locked laser system, discussing active and passive phase locking of longitudinal standing wave modes in laser cavity 05 p0583 A73-16337

Scorpius X-1 representation via old-nova model consisting of standing shock and X ray source formed by mass accretion at white dwarf surface 07 p0874 A73-19051

Stroboscopic investigation of the effect of standing acoustic waves on turbulent flames 07 p0920 A73-19595

Spiral arm structure as standing wave, of magnetically controlled star creation, considering various hydromagnetic models, dust and H I distributions 08 p1002 A73-20873

Electron plasma oscillation due to beam plasma interaction with standing wave formation between electrodes, observing temporal growth rate during beam modulation removal 08 p0992 A73-21001

Measurement of the current distribution at the surface of a doublet immersed in an isotropic hot plasma. 09 p1131 A73-23073

A quality criterion test for tubes intended for measurement of acoustic absorption and impedance coefficients 09 p1121 A73-23101

Freezing-in phenomenon and acoustical streaming in standing ultrasonic waves 11 p1400 A73-26299

Space-time cross spectral method to resolve transient disturbances into quasi-standing wave oscillations, giving formulas for node and antinode locations 12 p1521 A73-26818

High power microwave nanosecond pulse generation with waveguide standing wave resonator, noting power gain and pulse shape 13 p1583 A73-28673

Narrow nonlinear resonances of excited molecular densities in a standing wave of light 14 p1775 A73-30801

Radio anechoic chamber reflectivity level evaluation, comparing antenna pattern method and free space voltage standing wave ratio technique 17 p1218 A73-35648

Concentrated vortex nonlinear oscillations: discussing vortex ring and helical vortex filament stability, mode shape and frequency changes and standing and traveling wave solutions 18 p2301 A73-37001

A periodicity phenomenon occurring instantly when a standing ultrasonic wave is switched off 21 p2738 A73-39948

Wave equation solutions for free plane standing wave fields formation in unbounded elastic media 21 p2740 A73-40759

STANDS

U SUPPORTS

STANNATES

Some anionic tetrahalo/2,4-pentanedionato/stannate(IV) complexes. 06 p0661 A73-18273

STANNIDES

NT NIOBIUM STANNIDES

STANTON NUMBER

Radiative-convective heat transfer in flows of heated air past a flat plate. 21 p2791 A73-41051

STAPHYLOCOCCUS

Cinematographic study of the development of surface colonies of Staphylococcus aureus in solid agar. 08 p0933 A73-21833

STAR CLUSTERS

NT PRAESEPE STAR CLUSTERS

NT VIRGO STAR CLUSTER

Southern open star clusters. I - UB-V-H band photometry of 15 clusters between Galactic longitude 231 and 256 deg. 01 p0096 A73-10311

An investigation of four southern open clusters. 01 p0096 A73-10321

Three color photometric study of open cluster NGC 1647, obtaining distance, B-V and U-B excesses and age 01 p0098 A73-10521

Characteristic phase mixing time for spherically symmetric systems with different stellar mean velocity at each individual integral phase space surface 01 p0100 A73-10711

Velocity variation of a star as a purely discontinuous random process. III Stars with different masses in an open cluster 01 p0100 A73-10711

Physical reality of apparent carbon star group in Ariga from radial velocity measurements, spectral classification and VR photometry observations 01 p0104 A73-11031

Single gaseous object and stellar cluster models of quasars and galactic nuclei stability, noting neutron and collapsing star lifetimes

01 p0106 A73-11302

Mean absolute magnitudes and color indices of the red-giant concentrations in the color-magnitude diagrams of open clusters.

01 p0106 A73-11319

Radial density distribution and luminosity functions for stars in alpha Persei cluster

01 p0106 A73-11320

The structure of the close vicinity of the sun - Investigations concerning star troops, star families, and star streams

02 p0212 A73-12017

The dynamical evolution of a stellar cluster with initial subclustering.

02 p0222 A73-12709

Separate star groups in Sco OB 1 association coinciding with previously established gaseous subgroups

02 p0222 A73-12711

Star formation in the galaxy.

02 p0224 A73-12744

Statistical fractions of variable A and F stars, considering main sequence stars, giants, subgiants and open clusters NGC 2548, Praesepe and Coma

02 p0226 A73-12834

Investigations regarding the structure of young star clusters and the evolutionary phases of their members. II - NGC 6530. III - NGC 6611

02 p0226 A73-12835

A search for He-weak stars in very young clusters.

03 p0372 A73-13227

A numerical experiment in the accretion problem.

04 p0503 A73-16004

Luminosity function of the star cluster M 67

05 p0613 A73-16208

Solar luminance via light nuclei fusion into heavier nuclei with temperature gradient maintenance by gravity, relating to H-R diagram of different star clusters

05 p0614 A73-16302

The determination of distance, absorption, probable physical members and age for the open clusters Haffner 8, Haffner 6, Basel 11 and NGC 2374.

05 p0618 A73-16743

The old open cluster NGC 6819.

05 p0618 A73-16744

Occultation of the Pleiades by the moon on March 19, 1972

06 p0753 A73-18375

Evolution of scattered star clusters due to dissipation

07 p0901 A73-20316

Spectral energy distribution and IR radiation source size of M8 star cluster, determining stellar dust temperature

08 p1003 A73-20893

The history of star formation and the colors of late-type galaxies.

08 p1008 A73-21155

Schmidt telescopes in stellar photography of Magellanic clouds, galactic center and Scorpio-Centaurus and globular clusters for southern hemisphere Milky Way structure investigation

08 p1011 A73-21364

Objective prism spectrum surveys for H alpha emission of stars in Chamaeleon T association, listing emission line stars

09 p1142 A73-22033

Infra-red observations of young stars. I - Stars in young clusters. II - T Tauri stars and the Orion population. III - Nebulous emission-line stars

09 p1143 A73-22112

Fluid dynamical method for computing spherical star cluster evolution based on Fourier transformation of Liouville-Boltzmann equation

10 p1273 A73-23612

A star-cluster model with axial symmetry and star composition of uniform mass

10 p1274 A73-23715

Relative proper motions of faint stars in the Pleiades.

10 p1279 A73-24166

An up-to-date picture of galactic spiral features based on young open star clusters.

10 p1281 A73-24410

Search for neutral hydrogen in the galactic cluster NGC 2287.

11 p1415 A73-25119

Model of a stationary stellar cluster with a high binding energy.

11 p1425 A73-26176

Metal content in the atmospheres of red giants which are members of dispersed star clusters and dynamical groups

12 p1537 A73-26853

Interstellar light absorption and distribution of stars about the star cluster NGC 6834

12 p1537 A73-26854

Interstellar light absorption and distribution of stars about the star cluster NGC 7654

12 p1537 A73-26855

Investigation of star orbits in stellar clusters with allowance for the disturbing force of the galaxy

12 p1538 A73-26863

Evolution of open star clusters through dissipation.

12 p1539 A73-27288

Iris photometer electronic control system, presenting NGC 1778 cluster stars photoelectric UBv magnitudes

12 p1498 A73-27723

Stellar evolutionary stages of near-main sequence stars and clusters, discussing mass-luminosity and mass-radius relations

13 p1682 A73-28978

White dwarfs, neutron stars and black hole identification by satellite X ray astronomy, discussing gas temperature and mass relation to cluster parameters

14 p1797 A73-30075

Young open star clusters. II - Their nature and their significance for galaxy research

14 p1798 A73-30274

A new age indicator for Galactic clusters.

14 p1799 A73-30449

A photometric study of the integrated light of clusters in the Magellanic Clouds and the Fornax dwarf galaxy.

14 p1801 A73-30726

Russian papers on young stellar complexes and astrophysics covering physical nature and activity of nonstationary stars, stellar evolution, T-associations and earth atmosphere optical instability

15 p1934 A73-31418

O-B stars in young star clusters associated with nebulae

15 p1934 A73-31420

Relationship between T-associations and the interstellar medium in the northern region of the Monoceros complex

15 p1934 A73-31421

Flare star implications for stellar evolution, noting observational data relating to stars in associations and clusters

15 p1934 A73-31478

Motion of fourteen stars in the Orion nebula cluster.

15 p1936 A73-31555

On the use of UBv photometric diagrams for inferring the existence of an open star cluster.

16 p2058 A73-32833

Structure of the nucleus of the open cluster NGC 1245

16 p2063 A73-33660

Resonance damping of oscillations in a model of a spherical stellar cluster

17 p2226 A73-34367

Model for axisymmetric clusters of stars with uniform mass.

18 p2355 A73-36740

Quasar and galactic nuclei energy source models, considering supermassive rotating magnetoplasma body, black hole and compact star cluster with flares and collisions

20 p2609 A73-39570

Computerized simultaneous numerical integration of motion equations for solar system, star cluster and galaxies, considering radar observations of moon, Mercury, Venus, Mars and Icarus

21 p2772 A73-41241

The stability of gravitating systems with a quadratic potential. II - The stability of models of spherically symmetric and axisymmetric clusters with elliptic orbits of particles

23 p3035 A73-44236

Telescopic observation of Pleiades I flare stars, determining stellar magnitudes and flare brightness

23 p3037 A73-44352

Photometry of selected flare stars in the Pleiades

23 p3037 A73-44354

UBV spectral and photographic observations of blue objects around M 92 globular cluster

23 p3037 A73-44355

STAR DISTRIBUTION

Electronographic photometry of very weak stars of extragalactic origin with shift towards red, discussing accuracy limitation causes

01 p0049 A73-10538

Study of variable stars in two stellar fields in the Lacerta and Lyra constellations

01 p0098 A73-10558

Radial density distribution and luminosity functions for stars in alpha Persei cluster

01 p0106 A73-11320

Search for a visible counterpart of the September 2, 1972 radio outburst in Cygnus.

02 p0204 A73-11562

Stellar sources UV photography from sounding rocket, obtaining mean interstellar absorption, stars magnitudes and distribution and UBv spectrum

02 p0216 A73-12326

The spiral arm structure on the southwestern border of M31

02 p0227 A73-12840

Absorption line width method for stellar population of galaxies NGC 1052, 2655, 2903 and 4569 nuclei

03 p0371 A73-13221

Time and latitude observations of star groups with photographic zenith tube, including random, layer distortion and coordinate errors

03 p0307 A73-13249

Shock waves in spiral arms and star formation.

04 p0496 A73-14970

UBV photometry of the metal-rich globular cluster NGC 6171.

04 p0500 A73-15487

Bright red giants in the globular clusters M3, M5, and M13.

04 p0503 A73-16006

Structure of the Cepheid instability strip in the small Magellanic Cloud.

04 p0503 A73-16007

Astronomical catalogs for galactic superclusters existence including north galactic pole region, noting distance differentiation for structural singularities isolation

05 p0613 A73-16213

Integral equations suitability and solution instability of stellar system models, referring to globular cluster densities and mass distribution equations

05 p0616 A73-16452

Diffuse radiation of a two-layer galaxy with carbon-silicate particles

05 p0617 A73-16460

The luminosity function and density distribution of disk population stars.

07 p0876 A73-19358

Axial ratio and position angle of the major axis of the globular cluster M 92

07 p0901 A73-20317

Observational aspects of RR Lyrae and W Virginis stars - Some conundrums of stellar populations and galactic distribution.

07 p0903 A73-20629

Three-colour photometry in a field in the direction of the galactic anticentre near M 35.

08 p1005 A73-20923

Nonaxisymmetric kinematics in galaxies with axisymmetric mass distributions.

08 p1008 A73-21154

The role of Schmidt telescopes in the study of galactic structure /Photometric methods/.

08 p1011 A73-21355

Galactic structure at high galactic latitudes.

08 p1011 A73-21365

Frequency of star eliminations in the meridian catalogues constitutive of the Melchior-Dejaiffe ILS stars catalogue.

09 p1141 A73-22011

Statistical significance of some optical evidence for the bending of the galactic plane.

10 p1271 A73-23492

Luminosity functions for K giant stars derived from the two-micron sky survey.

11 p1414 A73-25066

A finding list of faint UV-bright stars in the galactic plane.

11 p1414 A73-25067

Stellar system gravitational field structure in terms of system-media attraction /regular force/ and force due to random distribution of stars /irregular force/

11 p1416 A73-25236

Model of a stationary stellar cluster with a high binding energy.

11 p1425 A73-26176

Interstellar light absorption and distribution of stars about the star cluster NGC 6834

12 p1537 A73-26854

Interstellar light absorption and distribution of stars about the star cluster NGC 7654

12 p1537 A73-26855

Tables of relative positions of stars in trapezium-type multiple star systems based on photographic observation data

12 p1537 A73-26857

Axial ratio and position angle of the major axis for the globular cluster M92.

12 p1539 A73-27289

Andromeda galaxy absorbing material distribution obtained with population I cepheids in Baade four variable star fields

13 p1671 A73-28031

Numerical experiments on the stability of spherical stellar systems.

13 p1685 A73-29359

Spatial distribution of stars in the Orion constellation region

14 p1799 A73-30385

Patterns of waves in galactic disks.

14 p1801 A73-30728

Selection of stars for observations from the lunar surface by the method of equal altitudes

15 p1938 A73-31963

On the use of UBv photometric diagrams for inferring the existence of an open star cluster.

16 p2058 A73-32833

Theories of galactic spiral structure comparisons with observations.

16 p2062 A73-33575

Structure of the nucleus of the open cluster NGC 1245

16 p2063 A73-33660

STAR FIELDS

- Distances of 26 stars of the stellar ring 58.
20 p2610 A73-39576
- Observations of neutral hydrogen near the galactic center. II - The nuclear disc.
20 p2610 A73-39578
- Classification and distribution of WR stars and an interpretation of the WN sequence.
23 p3025 A73-43193
- Pulsar properties covering galactic distribution, pulse periodicity computed from arrival time measurements, models, emission mechanisms, total intensity pulse shapes, etc
23 p3028 A73-43351
- Statistical correlation between pulsar and supernova remnant distribution along galactic longitudes, noting difference due to relative motions
23 p3037 A73-44359
- Galactic structure in the direction of Cepheus
24 p3140 A73-45191

STAR FIELDS

U STAR DISTRIBUTION

STAR TRACKERS

- Sun, earth and star attitude sensors for spacecraft, describing design, analysis and hardware aspects in terms of critical parameters
01 p0053 A73-11170
- Measuring rocket attitude by starlight.
05 p0594 A73-16300
- An amplitude-type position sensor for an optical sun-tracking system
06 p0692 A73-17766
- Cassiopea triaxial gyroscopic aiming device for sounding rocket attitude control, using stellar and inertial sensors and jet micropulsion
07 p0866 A73-18924
- Optical instrumentation for satellite attitude control, solar direction and earth magnetic field sensors, thermal detection, star tracking and Lunokhod 1 laser reflector
07 p0821 A73-18979
- Solar, stellar and IR sensors, discussing structural, optical and electronic design features, operational requirements and performance specifications
07 p0821 A73-18984
- Offset guiding through large space telescopes.
08 p0970 A73-21731
- Star sensor/mapper for the Small Astronomy Satellites.
08 p0970 A73-21733
- Image integration and display system for guiding on stars beyond the visual detection limit.
08 p0987 A73-21748
- Balloon-borne UV stellar spectrometer telescope pointing and stabilization, discussing in-house feasibility studies by small scale test payload experiments
08 p0971 A73-21750
- Automatic electronic pendulum astrolabe featuring altitude and azimuth tracking mechanisms, azimuth setter and 180 degree turning mechanism
13 p1612 A73-28394
- Methods of evaluation of tracking procedures used at the French Guiana Space Center
14 p1727 A73-30093
- A high-accuracy digital star tracker for advanced planetary missions.
15 p1907 A73-31356

STAR TRACKING

U STAR TRACKERS

STARCHES

- Starch hydrolysis in man - An intraluminal process not requiring membrane digestion.
20 p2519 A73-39789

STARK EFFECT

- Application of the Stark effect to the determination of the fields in the region of microwave/plasma interaction
04 p0423 A73-15611
- Line broadening of Lyman alpha wings due to protons calculated via positive molecular hydrogen ion wave functions
08 p0997 A73-20892
- Stark effect and line broadening in three-dimensional stochastic fields.
09 p1125 A73-21939
- H emission line shape of plasma radiation under anisotropic electric microfields, calculating field distribution function, dispersion and frequency
10 p1254 A73-24191
- Determination of field strength in a microwave-plasma interaction by means of the Stark effect.
10 p1254 A73-24201
- Stark broadening of high-principal-quantum-number n-alpha lines of hydrogen.
14 p1777 A73-30552
- Stark broadening and shift of singly ionized aluminum lines.
16 p2040 A73-32845
- Theory of optical polarization measurements of the turbulence spectrum in a plasma
17 p2216 A73-34627
- Theory of Stark broadening of hydrogen spectral lines in a plasma
21 p2745 A73-40365

Stark broadening of high quantum number delta n = 1 transitions of carbon V and VI in a laser-produced plasma.
21 p2745 A73-40471

Dipole moment of water from Stark measurements of H₂O, HDO, and D₂O.
24 p3113 A73-44978

Calculation of the Lyman-alpha asymmetry in a dense, partially-ionized hydrogen plasma.
24 p3116 A73-45323

STARLIFTER AIRCRAFT

U C-141 AIRCRAFT

STARS

- NT A STARS
NT B STARS
NT BINARY STARS
NT BLACK HOLES [ASTRONOMY]
NT CEPHEID VARIABLES
NT COMPANION STARS
NT DWARF STARS
NT EARLY STARS
NT ECLIPSING BINARY STARS
NT EXTARs
NT GIANT STARS
NT HERCULES NOVA
NT HOT STARS
NT INFRARED STARS
NT LATE STARS
NT M STARS
NT MAGNETIC STARS
NT MAIN SEQUENCE STARS
NT NEUTRON STARS
NT NOVAE
NT O STARS
NT PRAESEPE STAR CLUSTERS
NT PROTOSTARS
NT PULSARS
NT RADIO STARS
NT REFERENCE STARS
NT STELLAR GRAVITATION
NT SUBDWARF STARS
NT SUN
NT SUPERGIANT STARS
NT SUPERNOVAE
NT T TAURI STARS
NT VARIABLE STARS
NT WHITE DWARF STARS
- High resolution image formation through the turbulent atmosphere.
22 p2863 A73-43097

STARTERS

- NT ENGINE STARTERS
A study of startup regimes of high-temperature heat pipes.
21 p2792 A73-41060
- Analysis of starting circuits for a class of hard oscillators - Two-transistor saturable-core parallel inverters.
22 p2834 A73-42909

STARTING

- Supersonic annular blade cascades starting conditions, presenting static pressure and Mach number distributions
13 p1565 A73-28837

STATE EQUATIONS

U EQUATIONS OF STATE

STATE ESTIMATION

U ORBITAL POSITION ESTIMATION

STATE VECTORS

- Acceleration waves in anisotropic thermoelastic materials with internal state variables.
01 p0118 A73-11367
- Non-interacting control of non-linear multivariable systems.
01 p0028 A73-11517
- Linearized Kalman filtering for turbopump rotating assembly inertial and bearing parameter identification and state estimation, noting state-space model feasibility
03 p0313 A73-13904
- Book on control engineering covering dynamic system state representation, finite and infinite dimensional optimization, dynamic programming, stochastic estimation, applications, etc
03 p0285 A73-13987
- An adaptive Kalman filter using decomposition of the innovations sequence.
04 p0431 A73-15258
- Estimation of the statistical parameters of the Kalman-Bucy filter.
04 p0431 A73-15261
- A higher measurement space filter for passive tracking.
04 p0431 A73-15262
- Optimum quantization and parallel algorithms for nonlinear state estimation.
04 p0472 A73-15276
- Pseudo state measurements applied to recursive nonlinear filtering.
04 p0431 A73-15277
- Existence theorems for multidimensional control systems with lower-dimensional controls.
05 p0561 A73-16489

Finite-dimensional approximations of state-controlled continuous optimal control problems.
05 p0561 A73-16489

Estimation of the state vector of a plant minimizing a distance in metric space when using discrete sampling
05 p0561 A73-17272

Dynamic system optimal control problems with higher order state variable inequality constraints, obtaining solutions with boundary arcs and isolated points
06 p0680 A73-18272

Optimal control of a class of linear multivariable systems with integral quadratic energy constraint.
06 p0681 A73-18273

Sequentially best estimators for linear systems with non-linear noise-free sensors.
06 p0681 A73-18274

Fuzzy multi-stage decision-making, fuzzy state as terminal regulators and their relationship to non-linear quadratic state and terminal regulators.
06 p0681 A73-18275

State estimation of nonlinear system by applying stochastic approximation method.
06 p0681 A73-18276

Properties of linear time-invariant multivariable systems subject to arbitrary output and state feedback.
06 p0682 A73-18277

Frequency domain synthesis algorithm for linear multivariable system via state variable feedback combined with input dynamics compensation, applying decoupling and model matching
06 p0682 A73-18278

An algorithm for the assignment of closed-loop poles using output feedback in large linear multivariable systems.
06 p0672 A73-18279

The determination of state-space representations for linear multivariable systems.
07 p0804 A73-19171

Reduced-order observers for linear discrete-time systems.
07 p0805 A73-20171

Scalar and block decoupling of time varying and invariant linear multivariable control systems discussing sufficiency conditions, state estimation and order reduction possibility
08 p0950 A73-21060

Constitutive equation for electronic circuits with topologically dependent variables, noting numerical analysis of equations of state for nonlinear circuits.
08 p0951 A73-21061

Nonlinear system analysis based on Fokker-Planck equation, simplifying solution sequence for steady state or variance of states combination
09 p1111 A73-22171

Realization of two-dimensional state space digital filters.
09 p1068 A73-22172

Initial circuit equation transformation into equations of variable states, noting linear and nonlinear circuits in static and dynamic regimes
09 p1068 A73-22173

State-of-art review in identification, state estimation and decision processes for time variant systems discussing parametric, nonparametric, static and dynamic models
10 p1197 A73-23471

Optimal filtering for systems described by linear partial differential equations.
10 p1200 A73-24192

Estimation theory and system state and parameter identification, developing algorithms for optimum linear sequential and nonlinear filters
10 p1200 A73-24193

Order determination and parameter identification of time-invariant state variable models.
10 p1201 A73-24194

On optimization of control systems according to vector-valued performance criteria.
10 p1201 A73-24195

Linear multivariable control systems - A survey.
10 p1201 A73-24196

Coherent state systems for groups of motions; Hermitian bounded homogeneous regions in terms of Bergman kernels
10 p1249 A73-24197

A theory of tracking for a dynamic radar scatterer ensemble.
10 p1189 A73-24198

Necessary and sufficient conditions for differentiable nonscalar-valued functions to attain extrema.
10 p1243 A73-24199

Real time digital computer algorithm for linear and nonlinear electronic circuit modeling in state variable form for static and dynamic regimes
10 p1196 A73-24200

Description of random processes with allowance for irregularity of changes in their properties
11 p1340 A73-25171

Nonlinear dynamic feedback control system with variable observers reconstruction error convergence and digital simulation for performance
11 p1390 A73-25172

Beta estimation accuracy for reentry vehicles using a priori target information with 6-component state vectors to reduce computation time

Control system equations of motion construction based on program manifold, determining multidimensional piecewise continuous controller vectors under assigned inequalities

Nonlinear problems in analyzing the observability of the trajectories of spacecraft motion according to measurement data.

Estimation of the state vector of a linear plant by the method of distance minimization in metric space on the basis of continuous measurement of plant inputs and outputs

State space approach to mixed boundary value problems.

Minimum time response control problem of moving point in state space, determining piecewise-continuous vector function for optimal system transfer to coordinate reference point

Application of the theory of Markov processes in state estimation of dynamic systems and in control of flight-vehicle oscillations

Integral action in the optimal control of linear systems with some inaccessible state variables.

Optimal control theory for systems with inequality restrictions on control and state variables and time delay, using maximum principle and variational techniques

An adaptive estimation algorithm for time-varying bit synchronizers.

State space attitude control synthesis for a satellite with flexible appendages.

Linear and nonlinear filtering techniques for estimating the state of reentry vehicles from optical tracking data.

A constraining hyperplane technique for state variable constrained optimal control techniques.

Second-order optimality conditions for the Bolza problem with variable endpoints and separated end conditions.

Feedback controller design for multivariable systems by linear programming.

Derivation of aggregation matrices for simplified models of linear dynamic systems and their applications for optimal control.

A projection operator algorithm for optimal control problems with unspecified initial state values.

Nonlinear control systems analysis, discussing phase space method, Taylor-Cauchy transform, Volterra functions, Liapunov stability, Popov-Kalman-Yakubovich theorems and limit cycle oscillations

Information processes in control systems, discussing stability, state reproduction, invariance, entropy balance and statistical physics analogies

Methods for calculating and enhancing the efficiency of automatic systems

French monograph - On the representation of linear dynamic systems with distributed parameters and its application to the study of intrinsic properties of these systems.

Liapunov-like theorems of quantitative stability information on trajectory bounds in state space subset form

The state space and transfer function approaches in practical linear multivariable systems design.

A computer program SNR-2 for solving an optimal control problem with state constraints.

Closed loop linear control system synthesis possibility under condition of incomplete information on state vector with application to aircraft longitudinal motion

Certain problems of the correctness of the minimum-impulse linear optimal control problem. I - Dependence of the optimal control on the initial state and parameters

Weak invariance conditions and synthesis algorithms for control systems with discontinuities on hypersurfaces in phase space

STATIC DEFORMATION

Static-geometric analogy and complex transformation in the theory of three-layer shells with a light-weight filler

A comparison of the effects of explosive forming and static deformation on the mechanical properties of pressure vessel steels.

Finite static deformations of elastic solids at constant temperature, discussing couples for different deformations

Finite element static structural analysis for small elastoplastic strains and geometric nonlinearities, considering total Lagrangian and incremental moving coordinate formulations

Extremum principles in the dynamics of rigid-plastic bodies and mathematical programming.

Analysis of the static deformations of flexible extensible gas-filled shells

Static-geometric analogy and complex transformation in the theory of three-layered shells with light fillers

Static and dynamic finite deformations of cables using rate equations.

STATIC ELECTRICITY

Charge carrier cooling in nonhomogeneous semiconductors by static electric field, plotting average electron temperature as function of current

Role of static electricity in the incidents recorded during the F11 firing

Investigation of the antistatic properties of lacquer coatings based on quaternary polyniopyridine salts

Tuned loop antenna for radio observation of electrostatic spark and corona discharges generated during oil tanker cleaning operations

STATIC FIRING

The geometry and physical properties of exhaust clouds generated during the static firing of large rocket engines.

STATIC FRICTION

Pulsating vertical load effect on friction force magnitude between two horizontal solid surfaces during initial phase of static to kinetic friction transition

The reason for noncorrespondence of the values of the static and kinematic coefficients of sliding friction

Static-kinetic dichotomy in friction theory, examining atmospheric contaminants effects on surfaces, theoretical basis of static friction postulation and sliding velocity effect on theory

STATIC INVERTERS

A time-optimal response inverter.

Sequence amplitude modulated inverters.

STATIC LOADS

Application of the method of forces to the statics of composite systems

Two coordinate oscillograph recording device with automatic reversing for stress-strain tests under static and cyclic loads

The relationship between design allowables and load induced micromechanical damage in composite materials.

Method of repeatedly determining the fracture roughness with one specimen.

Design criteria for structural elements subjected to stationary random loads.

Short-term longitudinal dynamic stability of rods with allowance for clamping methods and for previous transverse deflection

Subcritical crack growth of TRIP steels in air under static loads.

Quasi-static load acting on a rotating shaft in the presence of creep

Characteristics and properties of WED-05 tensometers

Variable-load endurance criteria for steels under conditions of uniaxial and biaxial static tension

Comparison of the fracture strength K_{1s} of aluminum /AK4-IT1, V95T1, and D16T/ and titanium /VT8 and VT9/ alloys under static and cyclic loads.

Stresses and displacements in reinforced orthotropic panels under static loads, obtaining differential equations solution as numerically derived transfer matrices

Temperature dependence of conditions for static, quasi-static and fatigue failure of titanium alloys

Design stability of composite samples with a soft interlayer in static tension

Investigation of the fracture of carbon-graphite materials in a complex stress-strain state

Discrete creep of AMg6 aluminum alloy subjected to repeated static loading

Subcritical crack growth measurement during static loading of precracked Ti alloys in salt water, discussing arrested crack propagation at different stress intensities

Mathematical programming optimization procedure applicable to minimum weight structural design, considering static stress and displacement constraints under alternative loading conditions

Shear correction factors for orthotropic laminates under static load.

Environmental stress cracking of epoxy adhesives.

Influence of elastic deformations on the lasing-threshold characteristics of a ruby laser

Corrosion fatigue due to static and cyclic stress, noting electrochemical adsorption theory

Soft shell strength analysis for contact and static loads

Book - Introductory structural analysis with matrix methods.

Relative magnitudes of stresses caused by static and dynamic launch vehicle loads.

Relationship between the strain curves of a material subjected to static and to cyclic loads

Effect of deep annular grooves on the strength of some metals under static tension and torsion

Quantitative classification criterion for corrosion causes in metal under static and cyclic loads, examining failure mechanism

Some plastic deformation laws for titanium under static and alternating loads

Influence of preliminary dynamic loading on the load-bearing capacity of cylindrical shells

The supporting effect of bending specimens under static load in the temperature range from 400 to 500 C

Statistics calculation method for natural frequencies and mode shapes of vibration for structures under external static loads

Static, dynamic and fatigue load influence on solid lubricant compact bearings.

Relation of strain curves of material in static and cyclical loading.

On the flexural vibration frequencies of statically loaded beams.

Series analysis of cylindrical shells - New look at an old problem.

Criteria relating to the fatigue life of steels subjected to alternating loads under conditions of uniaxial and biaxial static strain.

Vibration analysis of laminated plates and shells by a hybrid stress element.

Gas saturated surface layer effect on Ti alloy resistance to static cyclic tensile loads, noting increased fatigue strength after etching

Pressure distributions in manifolds with return ducts.

Pressure distributions in manifolds with return ducts.

Pressure distributions in manifolds with return ducts.

Pressure distributions in manifolds with return ducts.

Pressure distributions in manifolds with return ducts.

Pressure distributions in manifolds with return ducts.

Pressure distributions in manifolds with return ducts.

Pressure distributions in manifolds with return ducts.

STATIC STABILITY

- Indicating instrument for angle of attack and sideslip on subsonic flight vehicles via static pressure sensing, noting wind tunnel tests 02 p0166 A73-11724
- Some details of the pressure and velocity fields near the nozzle of a round turbulent jet. 03 p0293 A73-13311
- The load carrying capacities of symmetrically loaded shallow shells. 05 p0631 A73-16120
- Pressure gage performance tests for air turbine through flow static pressure measurement 07 p0824 A73-20100
- Diffuser static pressure recovery coefficient for varying turbulence intensity at inlet, considering performance correlation with geometrical and/or velocity profile parameters 12 p1488 A73-27930
- Study of the effects of geometrical parameters on the characteristics of air jet flow by some optical methods. 13 p1618 A73-29039
- Interaction position and static pressure measurements of two opposing plane turbulent wall jets in still air in terms of frozen flow 15 p1863 A73-31342
- Maintenance of pitot-static systems of transport aircraft. [SAE AIR 975] 16 p2014 A73-33014
- The determination of the static pressure and relative velocity distribution in a two-dimensional radially bladed rotor. 17 p2093 A73-34396
- Shock wave pattern visualization and static pressure distribution in supersonic diffusers for mixed flow supersonic compressors, using closed Freon loop test rig [ASME PAPER 73-FE-35] 17 p2095 A73-35026
- An experimental-analytical method to study steady spray combustion. 17 p2255 A73-35499
- Mean flow and turbulence measurements in a Mach 5 shear layer. 17 p2097 A73-35506
- Specie number density, pitot pressure, and flow visualization in the near field of two supersonic nozzle banks used for chemical laser systems. [AIAA PAPER 73-642] 18 p2322 A73-36200
- Some investigation on base flow behind cylindrical bodies in incompressible flow. 22 p2797 A73-42997
- Experimental investigation of a turbulent boundary layer on a triangular plate with a wedge 23 p2939 A73-43473
- Approximate method for calculating the turbulent boundary layer in front of a recess 23 p2968 A73-43732
- ## STATIC STABILITY
- ### NT DIMENSIONAL STABILITY
- ### NT SHELL STABILITY
- ### NT STRUCTURAL STABILITY
- Thermoelastic equilibrium of a doubly connected spherical shell 02 p0231 A73-11804
- Three-dimensional problem of the deformation instability of incompressible layered materials in the case of highly elastic strains 02 p0235 A73-12191
- Reduction of a three-dimensional quasi-static problem of thermoelasticity for plates to a two-dimensional problem by a symbolic method and by the method of passing to the limit 02 p0235 A73-12194
- Elastic and plastic deformations of circular ring with initial machining produced stresses distributed across thickness, calculating critical load for static stability 02 p0236 A73-12581
- From theory to practical use of air cushions for transport of heavy loads in the factory 05 p0535 A73-16753
- Three dimensional static and dynamic stability equations of viscoelastoplastic deformation under axial compression 05 p0635 A73-17078
- On the torsional static stability and response of open section tubes subjected to thermal radiation loading. 07 p0908 A73-19086
- Static stability and drag studies for bodies of revolution in supersonic flow. [AIAA PAPER 73-295] 09 p1156 A73-23214
- Elastic circular ring stability under uniformly distributed equal radial concentrated forces 10 p1287 A73-23594
- An analytical estimate of the effect of mobility of a small internal mass on oscillations of a body during deceleration in the atmosphere 10 p1286 A73-24451
- External static and dynamic characteristics of input-output sequences of logic elements 12 p1475 A73-26764
- Static and dynamic stability of simply supported imperfect beam resting on nonlinear elastic foundation under axial load 12 p1550 A73-27033

- Russian book - Design of structural elements with the use of electronic digital computers. 12 p1556 A73-27923
- Equilibrium equations for static computations of symmetrical plates with large number of rods, point supports or holes 14 p1815 A73-30814
- Control-configured general aviation aircraft. [SAE PAPER 730303] 17 p2101 A73-34664
- Compatibility of maneuver load control and relaxed static stability. [AIAA PAPER 73-791] 19 p2379 A73-37458
- Analytical estimate of the effect of the motion of a small internal mass on the oscillation of a body decelerating in the atmosphere. 19 p2494 A73-38131
- The lower atmosphere in hydrostatically stable conditions. 19 p2449 A73-38245
- Some mathematically equivalent problems in the statics of shells of revolution 20 p2624 A73-39649
- German monograph - Theoretical and experimental investigation of digital hydraulic positioning devices. 22 p2801 A73-42848
- Application of the finite difference method to the elastic stability problem 24 p3152 A73-45357

STATIC TESTS

- ### NT STATIC FIRING
- High temperature gas turbine engines rotor blades cooling, deriving generalized dimensionless relations for heat transfer data extension from static tests to operational conditions 05 p0607 A73-16797
- Complete identification of some non-linear closed-loop systems. 06 p0681 A73-18525
- Static and dynamic behavior of welded aluminum beams. 07 p0839 A73-20270
- Static tests of the working-channel cascade of a tangential turbine 09 p1028 A73-22571
- Evaluation of static test methods for determining the fundamental mechanical properties of fiberglass-reinforced plastics 10 p1237 A73-23663
- Phenomenological approach to low-cycle fatigue fracture of a typical aircraft full scale component static test. [AIAA PAPER 73-324] 11 p1305 A73-25554
- Wing spar static and fatigue tests and S-N curve for lifetime measurement of root sections of small trainer and passenger aircraft 15 p1955 A73-32190
- Two dimensional static, dynamic and three dimensional photoelasticity measurement techniques for stress intensity, factors determination in boundary value problems of fracture mechanics 17 p2252 A73-35673
- The STAN /R/ 'S' Integral Weight and Balance System for the C-130 aircraft. [SAWE PAPER 985] 19 p2385 A73-37889
- Two wavelength variable sensitivity interferometry, extending static technique to real time dynamic testing 21 p2698 A73-40138
- The influence of flaw density and flaw size distribution on the static and dynamic fatigue behaviour of graphite. 23 p2998 A73-44037
- Static and fatigue strength of the KhN40MDTiU/EP 543/ alloy after various hardening treatments 24 p3098 A73-44475
- Correlation between the static and fatigue strength of reinforced plastics 24 p3102 A73-44509
- ### STATIC THRUST
- Wind tunnel test for Dolphin airship model static thrust measurements, discussing thrust direction torque moment coefficients and propeller rotation 21 p2635 A73-41648

STATICS

- ### NT ELECTROSTATICS
- ### NT HYDROSTATICS
- ### NT MAGNETOHYDROSTATICS
- Application of the method of forces to the statics of composite systems 02 p0229 A73-11639
- Geometrically nonlinear static and dynamic analysis of shells of revolution. 13 p1693 A73-28239
- The asynchronous formulation of relativistic statics and thermodynamics. 22 p2931 A73-42436
- ### STATIONARY FRONTS
- ### U FRONTS [METEOROLOGY]
- ### STATIONARY ORBITS
- Optimization of the apogee impulse during the positioning of a geostationary satellite. [ONERA, TP NO. 1218] 02 p0228 A73-11992
- Field dynamics equilibrium equation for particle rotational motion in gravitational field of central body, noting energy spectra of stationary orbits 03 p0374 A73-13751

Transfer from a standby to a stationary orbit using electric propulsion 04 p0505 A73-157404

An optimal orbit control system for a stationary artificial earth satellite 05 p0616 A73-164272

Polydynamic equilibrium equation for steady particle motion along stationary orbits in central body attraction field, comparing with Schroedinger wave equation 13 p1657 A73-28060

First order perturbation theory for geostationary satellites orbit calculation, taking into account earth oblateness, equator ellipticity and solar and lunar gravitational effects 15 p1930 A73-31111

Requirements regarding the position and the attitude of future application satellites 15 p1907 A73-31134

Realization of a geostationary orbit by means of an electromagnetic propulsion system /quasi-steady MPD/ 17 p2239 A73-34954

Aeronautical and maritime traffic control by stationary orbit navigation satellites, discussing frequency ranges, aircraft distance control, antenna array and multiple data access 17 p1215 A73-35477

Approximate description of the evolution of a synchronous-satellite orbit 18 p2350 A73-36101

Geostationary injection dispersions and thrusting error elimination by apogee motor firing attitude optimization 21 p2780 A73-40614

Station acquisition fuel minimization for third stage apogee motor impulse compensation of geostationary transfer orbit dispersions 21 p2781 A73-40618

STATIONKEEPING

- High and low thrust systems for primary and auxiliary spacecraft propulsion, noting electron bombardment electrostatic thruster for north-south station-keeping [AIAA PAPER 72-1123] 03 p0355 A73-13435
- Optimization of ion propulsion for north-south stationkeeping of communications satellites. [AIAA PAPER 72-1150] 03 p0356 A73-13454
- Effect of the guidance reserve of the Europa II third stage on the consumption of propellants for stationing 04 p0504 A73-15294
- Integration of an ion engine on the Communications Technology Satellite. 04 p0487 A73-15448
- Development of electrical propulsion in the Federal Republic of Germany. 04 p0487 A73-15713
- Cs ion bombardment engines for communication satellites stationkeeping and attitude control, noting mission life and test facilities 04 p0488 A73-15718
- Research at O.N.E.R.A. on ion thrusters suitable for satellite station-keeping 04 p0505 A73-15719
- Orbit transfer, -corrections, and attitude control of a lightweight direct broadcasting satellite for Europe. 04 p0505 A73-15738
- An optimal orbit control system for a stationary artificial earth satellite 05 p0616 A73-16427
- Ammonia resistojet development for satellite stabilization and position control with 5-year service life, discussing dissociation catalysis research and high efficiency heat exchanger design 07 p0867 A73-18932
- Electric propulsion systems for satellite station-keeping, discussing developments in colloid thrusters and diagnostic equipment for performance measurement 07 p0867 A73-19222
- Optimum strategy for the correction of orbit-injection errors of arbitrary orientation. 09 p1151 A73-23451
- Battery-powered electric propulsion for north-south stationkeeping. 17 p2222 A73-34872
- Utilization of electric propulsion systems in communications satellites [DGLR PAPER 73-048] 17 p1216 A73-35844
- Station acquisition fuel minimization for third stage apogee motor impulse compensation of geostationary transfer orbit dispersions 21 p2781 A73-40618
- ## STATIONS
- ### NT GLOBAL TRACKING NETWORK
- ### NT GROUND STATIONS
- ### NT ORBITAL SPACE STATIONS
- ### NT ORBITAL WORKSHOPS
- ### NT ORBITING LUNAR STATIONS
- ### NT SALYUT SPACE STATION
- ### NT SPACE STATIONS
- ### NT STADAN [SATELLITE TRACKING NETWORK]
- ### NT TRACKING STATIONS
- ### NT WEATHER STATIONS

STATISTICAL ANALYSIS

NT AMPLITUDE DISTRIBUTION ANALYSIS
 NT BIVARIATE ANALYSIS
 NT CORRELATION COEFFICIENTS
 NT FACTOR ANALYSIS
 NT KOLMOGOROFF-SMIRNOFF TEST
 NT MAXWELL-BOLTZMANN DENSITY FUNCTION
 NT MULTIVARIATE STATISTICAL ANALYSIS
 NT NONPARAMETRIC STATISTICS
 NT NORMAL DENSITY FUNCTIONS
 NT POISSON DENSITY FUNCTIONS
 NT PROBABILITY DENSITY FUNCTIONS
 NT PROBABILITY DISTRIBUTION FUNCTIONS
 NT RANK TESTS
 NT RAYLEIGH DISTRIBUTION
 NT REGRESSION ANALYSIS
 NT REGRESSION COEFFICIENTS
 NT SEQUENTIAL ANALYSIS
 NT STANDARD DEVIATION
 NT STATISTICAL CORRELATION
 NT STATISTICAL DECISION THEORY
 NT STATISTICAL TESTS
 NT VARIANCE [STATISTICS]
 NT WEIBULL DENSITY FUNCTIONS
 Book - Introduction to mathematical techniques in pattern recognition.
 01 p0019 A73-10050
 Steady creep bending in a beam with random material parameters.
 01 p0113 A73-10198
 Mathematical and statistical modeling of wall flow turbulence, considering experimental velocity and temperature measuring techniques
 01 p0031 A73-10292
 A note on the angular dispersion of a fluid line element in isotropic turbulence.
 01 p0032 A73-10443
 Sensitivity analysis method application to spacecraft thermal environment control system design, determining mathematical model input parameters uncertainty effects on temperature determination
 01 p0123 A73-11143
 Statistical characteristics for duralumin sheets mechanical properties, fatigue life and crack growth
 01 p0117 A73-11298
 Statistical method of determining the load or stress distribution from the failure characteristics of mechanical systems
 01 p0118 A73-11370
 The structure of the close vicinity of the sun - Investigations concerning star troops, star families, and star streams
 02 p0212 A73-12017
 Statistical method of calculating scattering matrix elements and parameter deviations of SHF octupole networks /square bridge, hybrid ring or directional junction/
 02 p0146 A73-12025
 Experimental estimation of the deformation criterion of long-term /creep/ strength.
 02 p0180 A73-12130
 Cloud characteristics in problems of radiation energetics in the earth's atmosphere.
 02 p0159 A73-12146
 Numerical analysis of spontaneous electric activity of the brain - Study of the statistical properties of the power density spectra
 02 p0138 A73-12160
 Solid deformable body mean stress determination by statistical summation of stress squares on faces of parallelepiped rotated within Euler angle limits
 02 p0235 A73-12207
 Statistical properties of traveling ionospheric disturbances in F region from phase height and angle of arrival data
 02 p0162 A73-12296
 Analysis of fundamental flight parameters and properties of aerobatic aircraft in a statistical framework
 02 p0131 A73-12448
 Statistical analysis of the sound-level distribution of aircraft noise as a function of time. II
 02 p0131 A73-12449
 Iteration method for statistical treatment of measurements when information on measurement error characteristics is incomplete
 02 p0219 A73-12455
 Statistical fractions of variable A and F stars, considering main sequence stars, giants, subgiants and open clusters NGC 2548, Praesepe and Coma
 02 p0226 A73-12834
 The statistical evaluation of the measurement of viscosity of a non-Newtonian liquid.
 03 p0306 A73-12899
 Statistical analysis of atmospheric sudden changes in VLF bands, suggesting lower ionosphere ionization increase due to meteors incidence
 03 p0299 A73-12948
 New method for the statistical evaluation of constant stress amplitude fatigue-test results.
 03 p0387 A73-13229

Estimating the median fatigue limit for very small up-and-down quantal response tests and for S-N data with runouts.
 03 p0387 A73-13230

A reliability approach to the fatigue of structures.
 03 p0387 A73-13234

Statistics on the solar spectrum suitable for the study of the blanketing effect in stars of spectral types F, G and K.
 03 p0373 A73-13360

Failure criterion for a propellant of a spherical solid rocket motor.
 [AIAA PAPER 72-1088] 03 p0351 A73-13409

Aircraft engine inlets total pressure fluctuations and distortion factors, presenting extreme-value statistical method for maximum distortion level probability estimate
 [AIAA PAPER 72-1100] 03 p0354 A73-13419

Statistical characteristics of antenna gain threshold as function of link trajectory during radiation pattern shift with respect to fixed orientation
 03 p0278 A73-14061

Mathematical expectation of angularly modulated signal in unsteady linear random noise, using Marchenko formula
 03 p0278 A73-14074

Vector summation dial for analysis of time-nonstationary cyclic biological data, applying to peak time change detection and random walks
 03 p0263 A73-14120

Statistical analysis applied to solar cell shorting caused by reverse bias voltage stress.
 03 p0255 A73-14223

Statistical considerations for structural reliability analysis.
 04 p0507 A73-14707

Recent studies towards the development of procedures for design of brittle materials.
 04 p0508 A73-14725

Discussion of the Colloquium on Structural Reliability.
 04 p0468 A73-14727

Statistical linearization of nonlinear single-mass mechanical system for given distribution function of random disturbances, noting amplitude frequency distribution
 04 p0475 A73-14977

Accelerated method of estimating the growth rate of fatigue cracks.
 04 p0514 A73-15671

Mean field equations for dynamic response of homogeneous linearly elastic solids, obtaining formulation for ensemble averaged displacement and stress fields of composite
 [ASME PAPER 72-WA/APM-28] 04 p0515 A73-15890

Statistical transfer theory in non-homogeneous turbulence.
 04 p0520 A73-15937

1968 solar spot observations and statistics
 04 p0502 A73-15950

Lower ionosphere at medium latitudes during geomagnetic disturbances.
 05 p0568 A73-16214

Physicostatistical investigations of the general atmospheric circulation
 05 p0592 A73-16231

Approximate analytical solutions of the diffusion equation for Jacchia's statistical models of the upper atmosphere
 05 p0570 A73-17014

Automatic analysis and classification methods based on statistical characteristics of aerial photometric and TV photographs, noting contour related interval distribution
 05 p0579 A73-17143

Aerial imagery data statistical processing, discussing probability density and autocorrelation functions and power spectra for automatic pattern recognition
 06 p0695 A73-18322

Optimal conditions for indirect probing of the atmosphere
 06 p0721 A73-18732

Microinhomogeneous plane with a circular hole in tension
 07 p0911 A73-19320

Statistical diagnostics and information synthesis relating to the reliability and maintenance of an equipment
 07 p0830 A73-19414

Lunar soil porosity and its variation as estimated from footprints and boulder tracks.
 07 p0898 A73-19903

Some problems of statistical estimation of a signal source in a dispersive medium
 07 p0792 A73-19912

Diffraction of a plane wave by a random phase screen.
 07 p0793 A73-20056

Fourier transformations and statistical analysis for spectral content of geomagnetic micropulsations, noting polarization sense preference
 07 p0819 A73-20064

A statistical estimate of the achievable sidelobe level in phased array antennas with nonlinear initial phase distribution.
 07 p0801 A73-20130

Theory and application of the optimal linear approximation of linear processes
 08 p0983 A73-20645

A statistical model for electromigration induced failure in thin film conductors.
 08 p0944 A73-20745

The distribution of the mass-to-luminosity ratio of spiral and irregular galaxies.
 08 p1006 A73-20930

Statistical expectation application to risk density functions and fee/incentive-element relationships for contract incentive structuring, considering C-5A procurement
 08 p1025 A73-20958

Statistics of laser beam fade induced by pointing jitter.
 08 p0975 A73-21058

Statistical approach to the prediction of M.O.S.-device performance.
 08 p0946 A73-21116

Determination of the statistical characteristics of temperature fluctuation in pool boiling.
 08 p1022 A73-21252

Pyranometer calibration by substandard and working instrument comparison on X-Y recorder, using computerized statistical analysis
 08 p0966 A73-21264

Some statistical characteristics of the spectra of polar magnetic substorms
 08 p0959 A73-21293

Shock wave formation in a statistically inhomogeneous gas
 08 p0955 A73-21450

Blocking situations lasting less than five days over the Euro-Atlantic region in the 20-year period from 1951 through 1970
 08 p0986 A73-21486

Description of hydrodynamics in the theory of gravitation on the basis of covariant statistical equations
 08 p0989 A73-21522

Renal lithiasis among civil operating aircrew
 08 p0931 A73-21536

Probabilistic analysis of the statistical accuracy of a transistor blocking generator with a common emitter
 08 p0949 A73-21590

Investigation of the applicability of some statistical models to the shock-wave structure problem
 08 p0956 A73-21606

Application of statistics to results in gamma ray astronomy.
 08 p1012 A73-21644

Mean vector and covariance matrix estimation for training class sample statistics updating in pattern recognition, applying to crops or any category of objects
 08 p0984 A73-21668

Frequency of star eliminations in the meridian catalogues constitutive of the Melchior-Dejaiffe ILS stars catalogue.
 09 p1141 A73-22011

Statistical analysis of continuous neutron component intensity measurements in cosmic rays
 09 p1137 A73-22020

Statistical properties of two sine waves in Gaussian noise.
 09 p1120 A73-22115

Use of model output statistics for predicting ceiling height.
 09 p1114 A73-22125

Optimal control problems under conditions of a priori indeterminateness
 09 p1069 A73-22566

Quasi-monochromatic radiation pulse reflection from rough surfaces, analyzing echoes statistical properties
 09 p1120 A73-22575

Influence of combinational coupling on the spectral and statistical properties of multimode fluctuations in a traveling-wave laser
 09 p1094 A73-22599

Best linear unbiased estimator of the parameter of the Rayleigh distribution. I - Small sample theory for censored order statistics.
 09 p1112 A73-22645

Equivalent number method of optimal interval selection for meteorological observations with independent statistical samplings
 09 p1114 A73-22853

Block diagram of transistorized phase instability meter for statistical analysis of one dimensional density distributions, noting two series connected identical delay lines
 09 p1064 A73-23008

Weibull distribution government of dispersion of destructive temperature gradients characteristic of fireproof ceramic materials heat resistance
 09 p1110 A73-23061

The evolution of interstellar clouds. II - Hydrodynamic treatment of the phase change. III - Cloud collisions and statistical theory.

10 p1272 A73-23531

Strong irradiance fluctuations in turbulent air - Plane waves.

10 p1248 A73-23837

Statistical properties of intermittency in large scale turbulent flows, considering boundary layer, shear and convective flows

10 p1205 A73-23855

Statistical analysis and computer simulation of laser Doppler velocimeter systems.

10 p1217 A73-23997

Improved Hanle effect measurement technique for fast ions.

10 p1251 A73-24117

Book - Turbulence transport modeling.

10 p1206 A73-24350

Statistical analysis of multiple absorption spectra in QSO.

10 p1284 A73-24905

Determination of the proper integration level of the unified functional units of a complex of statistical-measurement methods

11 p1340 A73-25002

Description of random processes with allowance for irregularity of changes in their properties

11 p1340 A73-25008

Random analog signal quantization and reconstruction from discrete sample values by optimal filtration according to statistical criteria

11 p1341 A73-25013

Problem of forming classes of input processes in the study of errors in devices for statistical measurements

11 p1359 A73-25014

Effect of measuring-device error on the accuracy of the determination of the mathematical expectation and dispersion of a stationary random process

11 p1360 A73-25016

Accuracy of statistical measurements of random field characteristics in interferometric systems

11 p1360 A73-25020

Statistical synthesis of digital parameter-measuring equipment and analysis of its efficiency

11 p1360 A73-25021

Shaping of the one-dimensional distribution and correlation function of a reference signal when checking statistical analyzers

11 p1360 A73-25022

Statistical characteristics of E and F regions maximum electron density and ionization height, discussing electron content in vertical unit column in upper and lower ionosphere

11 p1351 A73-25092

Structure statistical identification method based on experimental measurements of natural frequencies and mode shapes to modify finite element model structural parameters

11 p1436 A73-25479

A statistical theory for failure of brittle materials under combined stresses.

11 p1439 A73-25511

Statistical model of meteor streams. III - Stream search among 19303 radio meteors.

11 p1425 A73-26135

Strapdown inertial system alignment using statistical filters - A simplified formulation.

11 p1395 A73-26377

Additional evidence for the existence of a very high energy solar particle component.

11 p1413 A73-26473

Dynamic AGC correction for angle signal variations in monopulse radar receivers with reference signal, analyzing signal statistics

12 p1469 A73-27163

Statistical characteristics of the mechanical constants of glass-fiber-reinforced plastics

12 p1516 A73-27184

Asymptotic behavior of some statistical estimates. II - Limit theorems for a-posteriori density and Bayesian estimates

12 p1517 A73-27188

Calculation of the statistical characteristics of a long waveguide line in a two-wave model

12 p1469 A73-27189

An analysis of the effectiveness of ways of increasing the accuracy of a treatment

12 p1503 A73-27467

The use of sampling quantiles for the compression of telemetric transmission and the statistical handling of medical information.

12 p1465 A73-27646

Statistical description of the wind field in the upper troposphere and lower stratosphere with allowance for the scale of motion

12 p1521 A73-27741

Russian thunderstorms mean annual duration chart and calculation nomograms

12 p1522 A73-27746

Light scattering from independent particles - Non-gaussian correction to the clipped intensity correlation function.

13 p1658 A73-28208

Statistical analysis of Forbush decreases and of cosmic-ray intensity increases preceding them.

13 p1670 A73-28701

Gas molecule-solid surface interactions, considering rainbow scattering, roughness at molecular scale, potential well and statistical analysis procedures

13 p1663 A73-28912

A new statistical design method for thinned solid-state phased arrays.

13 p1594 A73-29231

Absolute magnitude of stars of the RR Lyrae type

13 p1686 A73-29370

Automatic evaluation of strain gage data reliability by comparison with a preset parameter and determination of a statistical yield strength.

13 p1622 A73-29549

Statistical criteria of ultimate strength and plasticity of materials in the complex stress state.

13 p1703 A73-29620

Comet motion and hyperbolic orbital statistics, discussing secular accelerations, decelerations and nongravitational effects

14 p1794 A73-29830

Comets origin in interstellar space or solar system evaluated with reference to comet streaming from perihelions statistical analysis, assuming Oort cloud accretion

14 p1794 A73-29838

Meteor streams and comet orbital statistics from radar observations during 1967-1968

14 p1795 A73-29847

Statistics of photoelectric sensor readings during propagation of light in a turbulent medium

14 p1753 A73-30270

Statistical computation of compatibility of tropospheric and satellite communication lines.

15 p1842 A73-30986

Fundamental statistical characteristics of a modified phase AFC (PAFC) system.

15 p1842 A73-30989

Hydroxyl emission intensity and rotational and vibrational temperatures, discussing statistical properties of geomagnetic storm effects and diurnal, seasonal and latitudinal variations

15 p1867 A73-31260

Collision induced dissociation - A statistical theory.

15 p1915 A73-31275

Fluctuations of light fluxes propagating in a scattering medium

15 p1903 A73-31323

Certain methodological aspects of measurements of the average short-wave radiation fluxes in the presence of cloudiness

15 p1905 A73-31790

Solar radiation fluxes at the earth's surface in the presence of cumulus clouds

15 p1905 A73-31794

Transmission of solar radiation by stratified cloudiness as a function of the statistical characteristics of its structure

15 p1905 A73-31796

Theory of turbulence with a vortex-type anisotropy

15 p1864 A73-32084

Turbulent scattering phenomenological model for D region partial coherent reflection experiments with measurement noise, presenting amplitude and phase statistics

15 p1845 A73-32230

Iterative method for the statistical processing of measurements with incomplete information on the measurement error characteristics.

15 p1902 A73-32605

Compact X ray source models from statistical analysis of Uhuru catalog sources with respect to luminosities, lifetimes and stellar populations

16 p2050 A73-32737

British Airline Pilots Association and RAF Institute of Aviation Medicine questionnaire results on training simulator effectiveness, analyzing auditory and visual aids

16 p1996 A73-33213

Problems and methods of simulating the environment; Annual Meeting, Karlsruhe, West Germany, September 27-29, 1972, Reports

16 p1997 A73-33376

Interpretation of the results of simulation tests, taking into account scatter effects

16 p2019 A73-33378

A nomographic comparison of coherent and non-coherent detection statistics.

16 p1980 A73-33415

Some statistical techniques useful in system aging studies.

16 p2020 A73-33603

Analysis of early failures in unequal size samples.

16 p2020 A73-33622

Statistical and probabilistic MTBF models for parts, sockets and systems reliability

16 p2020 A73-33628

A statistical analysis of product reliability due to random vibration.

16 p2020 A73-33637

Rain attenuation and fade duration statistics for design of satellite-based communication system, predicting outage for 16 GHz path diversity system

16 p1981 A73-33706

Atmospheric attenuation measurements via solar microwave radiometer yielding excess attenuation statistics for communications systems planners

16 p1982 A73-33722

Microwave propagation in atmosphere with oblate spheroidal raindrops, discussing linear and circular cross-polarization effectiveness statistical analysis with allowance for raindrop orientation

16 p1983 A73-33724

Radio aurora occurrence data from statistical data on radio echo occurrence, comparing radio zone to optical auroral belts

16 p2009 A73-33892

A statistical method for evaluating structural reliability and minimum structural creep life at elevated temperature.

16 p2084 A73-33974

Allowance for the influence of temperature in statistical estimates of the strength of metals in the brittle condition

17 p2186 A73-34328

Poisson frequency distribution of flare stars in Pleiades, including statistical analysis of photographic amplitudes

17 p2226 A73-34364

Statistics calculation method for natural frequencies and mode shapes of vibration for structures under external static loads

17 p2242 A73-34527

Two-variable asymptotic solution to unsteady three-dimensional turbulent flow equations describing small scale deformation, determining hot spot or macromolecular size statistical behavior

17 p2201 A73-34800

The effects of the observational system and the method of interpolation on the computation of spectra.

17 p2201 A73-34852

U.S. Army helicopter vibration data for OH-6A, OH-58A, UH-1H and CH-54B models obtained from triaxial accelerometer locations, presenting spectral and statistical analyses

17 p2106 A73-35086

Statistical models of turbulent free shear mixing layer structure in incompressible air streams

17 p2156 A73-35507

Analysis of optimal recognition of space-time signals.

17 p2130 A73-35721

Statistical theory of weakly interacting perturbations and low amplitude turbulence in fluids, considering diffusion, dispersive and acoustic wave characteristics and plasma instabilities

18 p2299 A73-36504

Explicit solution for the photocount statistics with application to atmospheric turbulence.

18 p2337 A73-36625

Determination of statistics of turbulence in clear air

18 p2332 A73-36687

Aircraft accident statistics for passenger fatalities, worldwide jet hull losses and estimated costs to suggest proposals for approach, landing and takeoff accident reduction

18 p2268 A73-36846

Use of satellite cloud data in moisture field analysis.

18 p2334 A73-37057

Statistical characteristics of the temperature field near the ground for Europe.

18 p2334 A73-37070

Statistical models for rounding-off error studies in linear algebraic problems

18 p2292 A73-37144

New statistical laws governing the system of long-period comets

19 p2480 A73-37235

Turbulent Couette flow statistical theory, applying stochastic analysis to Navier-Stokes equation

19 p2421 A73-37855

Some statistical characteristics of the spectra of polar magnetic substorms.

19 p2425 A73-37922

Periodic analysis of arrival times in delayed cosmic-ray coincidences.

19 p2476 A73-38086

Time delay statistics of photoelectric emissions - An experimental test of classical radiation theory.

20 p2570 A73-38606

Master equations in the theory of incoherent and coherent spontaneous emission.

20 p2570 A73-38608

Non-Gaussian statistics of superradiant radiation from saturated xenon 3.5-micron laser amplifier.

20 p2570 A73-38620

Determination of an optimal dynamic system according to complex statistical criteria in the presence of constraints

20 p2539 A73-38680

Correctness, regularization, and the maximum complexity principle in the statistical dynamics of automatic control systems

20 p2540 A73-38699

Uses of image recognition methods without teaching, in product quality control and lost observation estimations

20 p2568 A73-38712

Prediction of the outcomes of myocardial infarction from formulas derived by the dynamic programming method

20 p2516 A73-39000

Statistical characteristics of the diurnal drift velocity variations in the F2 layer

20 p2554 A73-39160

Corporate aircraft accident analysis to reduce accident rate, examining seasonal and diurnal statistics, aircraft types, runway conditions, crew factors and maintenance defects

20 p2509 A73-39219

Statistically optimal sampled data terminal guidance algorithm for complex probabilistic multipurpose control system, using linearized equations

20 p2590 A73-39344

Statistical characteristics of the fatigue strength of heat-resistant 1Kh18N9T steel under steady and programmed loading conditions at high temperatures

20 p2577 A73-39355

Development of a program basis for statistical data processing on an analog-digital complex

20 p2532 A73-39392

Two-dimensional statistic analysis of radar imagery of sea ice.

20 p2556 A73-39843

Dispersed signal filtering and filtered signal duration relation to filter bandwidth and dispersiveness, isolating fundamental mode of Rayleigh waves from earthquake 650 km deep

21 p2648 A73-39931

Fog dispersal technique evaluation for cost effectiveness by statistical method, taking into account time dependent probability of natural visibility improvement

21 p2729 A73-40066

Application of linear programming in the statistical theory of antennas

21 p2661 A73-40201

Statistical analysis of microwave transmission line coefficients, discussing line losses, inhomogeneity distribution, input voltage standing wave ratios and rms deviations

21 p2648 A73-40204

Russian book - The stochastic structure of cloud and radiation fields.

21 p2730 A73-40243

Bounds estimation for normalized second spectral moment of random radar signal process in terms of measured quantities statistics without weighting

21 p2650 A73-40343

Demodulated Doppler signal analyzed for uniform steady flow, noting non-Gaussian phase fluctuations statistics

21 p2699 A73-40454

Russian book - Introduction to the statistical dynamics of systems with possible disturbances.

21 p2669 A73-40775

A study of the statistical patterns of visual perception of a black and white raster image

21 p2644 A73-40861

Digital communication channel with noisy errors, discussing statistical analysis of binary burst sequences for coding design

21 p2655 A73-41090

Russian book on statistical properties of ionosphere reflected signals covering statistical modeling, random processes, perturbation method and wave reflection problems

21 p2657 A73-41284

Russian book - Economic efficiency and planning of air freight transportation.

21 p2793 A73-41294

Structure of the neutral atmosphere between 150 and 500 km.

21 p2689 A73-41352

Influence of the polarity of the interplanetary magnetic field on magnetic activity at high latitudes.

21 p2773 A73-41378

Russian book on probabilistic computer simulation and statistical processing techniques covering linear algebra and partial differential equations, Markov chains, random numbers, automata, and analog modeling

21 p2659 A73-41432

Solar photospheric granulation plate statistical properties, establishing two dimensional autocorrelation function and power spectrum as function of wave number

21 p2776 A73-41477

Prediction and measurement of the proportionality constant in statistical energy analysis of structures.

22 p2918 A73-41821

Ability of a human operator to estimate the probability characteristics of alternative stimuli

22 p2813 A73-41893

Analysis of the results of the geometric satellite world network

22 p2849 A73-42589

Russian monograph on signal transmission channel identification systems in statistical communication theory covering mathematical models, design principles, radio electronic systems, etc

22 p2827 A73-42600

Objective method for classification of multicellular activity patterns of neuron population in the cerebrum of man

22 p2807 A73-42656

Statistical treatment of evoked cerebral potentials during experiments on a Dnepr-1 computer

22 p2814 A73-42657

Experimental determination of the turbulent Prandtl number near a smooth wall

22 p2937 A73-42952

Prevalence of hyperlipoproteinaemias in a random sample of men and in patients with ischaemic heart disease.

22 p2811 A73-42975

Some statistical characteristics of active regions with the yellow coronal line.

22 p2915 A73-43037

Laser cross-beam intensity-correlation spectrum for a turbulent flow.

22 p2872 A73-43158

Standard sensitivity and covariance matrices for statistical estimation of overall performance.

23 p2962 A73-43279

Statistical analysis of two dimensional turbulence, noting probability characteristics ergodicity with respect to class of two dimensional characteristic functions with converging mean squares

23 p2968 A73-43475

Statistical analysis for autocorrelation and cross correlation coefficients of mean annual total atmospheric ozone and relative sunspot number as solar activity indicator

23 p2976 A73-43883

Gilbert burst noise model for statistical analysis of nonindependent errors in digital data transmission systems, noting performance and utility in communication theory

23 p2954 A73-43986

Investigation on the optimum tightening force of bolted joint in torque control method.

23 p2986 A73-44140

Statistical properties of radio sources at centimeter wavelengths in a range of terminally weak flux densities

23 p3034 A73-44229

Simultaneous statistical treatment of the readings of a directional gyroscope and a magnetic compass

24 p3089 A73-45457

Statistical analysis of transient brightenings in solar chromosphere /Ellieman bombs/ from H alpha filtergrams, obtaining histograms for durations near disk center and limb

24 p3136 A73-44641

Transient vibration processes during diamond grinding and their statistical evaluation

24 p3094 A73-44971

Solar activity cycles effects on physical and biological processes in helioterrestrial domain, discussing crops, tree growth, diseases and fishing

24 p3088 A73-45364

STATISTICAL COMMUNICATION THEORY

U COMMUNICATION THEORY

STATISTICAL CORRELATION

Correlation and structure functions for pulse propagation in a turbulent atmosphere.

01 p0016 A73-10195

Annoyance reactions from aircraft noise exposure.

01 p0005 A73-10781

Statistical evaluation of strength of metals at brittle fracture.

02 p0235 A73-12133

Approach for obtaining prognostic relations on the basis of meteorological data

02 p0189 A73-12369

Statistical studies in stellar rotation. II - A method of analyzing rotational coupling in double stars and an introduction to its applications.

03 p0366 A73-12938

Correlation analysis as applied to the observation of fluctuations of laser light diffracted on an ultrasonic wave in an inhomogeneous medium.

03 p0318 A73-12994

Statistical data processing method for accuracy evaluation of satellite orbit parameters obtained from onboard measurements of two stars angular positions

03 p0379 A73-14554

Solar activity effects on geomagnetic variations from spacecraft particle measurements, showing statistical correlations between solar wind, flares and magnetic storms

04 p0491 A73-14838

Digital image registration by correlation techniques.

04 p0449 A73-15413

Allowance for the correlation of factors in the method of priorities for electrical system optimization

05 p0560 A73-16272

He-Ne laser beam intrinsic third order intensity statistical correlation function measurement by digital technique for comparison with calculations

06 p0699 A73-17520

STATISTICAL DECISION THEORY

Examples for signal-noise improvement with the aid of polarity correlation analysis in the biological sector

06 p0656 A73-17593

Statistical correlation between human mental activity and EEG beta rhythm wave energy and frequency characteristics

06 p0653 A73-18159

Statistical correlations of maximum oxygen consumption, body weight and endurance /work/ performance in exercise-oxygen studies

06 p0659 A73-18472

Correlation of ground-based measurements of structured Pc 1 micropulsations withOGO-V plasmopause observations.

08 p0937 A73-20652

Correlation techniques in the analysis of transient processes.

08 p0988 A73-21466

The accuracy of an approximate representation of the correlation functions of complex signals distorted in the linear stages of a radio channel

09 p1051 A73-22461

Correlation analysis of the accuracy of the machining of micromachine components

09 p1088 A73-22660

Solar radiation climate correlation with long term sunshine records, comparing radiation measurements with predictions based on regression equations for Brisbane area

10 p1269 A73-24450

A probabilistic model of an optical-field and the statistical properties of a videosegment from a vidicon target

11 p1360 A73-25025

Correlation analysis of systems with stochastic inertialess elements.

12 p1484 A73-27458

Geomagnetic disturbance recurrence interval correlation with long term sunspots rotation period

12 p1494 A73-27771

Correlation of random noise levels in short-wave radio channels

13 p1584 A73-28888

Spatial correlation functions of velocity and temperature components in the atmospheric boundary layer

13 p1654 A73-29153

Correlation and statistical characteristics of turbulence fronts in the wakes of hypervelocity bodies.

13 p1567 A73-29269

Correlation of reported gravitational radiation events with terrestrial phenomena.

14 p1749 A73-30554

Application of methods of mathematical statistics to study the motion of an artificial earth satellite about its center of mass

15 p1931 A73-31234

Statistical properties of precipitation patterns.

15 p1903 A73-31316

Some statistical characteristics of atmospheric ozone measurements

15 p1868 A73-31612

A procedure for studying the statistical structure of solar radiation fluxes at the ground under clouded conditions

15 p1905 A73-31792

Single-loop delay line integrator SNR enhancement properties in additive zero mean correlated noise channels for finite signal observation times

16 p1979 A73-33406

Difference between even and odd 11-year solar activity cycles

16 p2056 A73-33658

Probability distributions and correlations in a turbulent boundary layer.

18 p2300 A73-36626

Some aspects of the solution of inverse problems of satellite meteorology.

18 p2335 A73-37078

Third- and higher-order intensity correlations in laser light.

20 p2571 A73-38630

Study of a correlator using two auxiliary noise sources

20 p2532 A73-39203

Statistical characteristics of the vertical ozone distribution in mid-latitudes.

23 p2975 A73-43874

Statistical correlation between pulsar and supernova remnant distribution along galactic longitudes, noting difference due to relative motions

23 p3037 A73-44359

Spherical harmonic analysis of geomagnetic and gravitational field correlation, showing longitudinal shift in magnetic field pattern over six epochs

24 p3084 A73-44812

STATISTICAL DECISION THEORY

Fuzzy multi-stage decision-making, fuzzy state and terminal regulators and their relationship to non-fuzzy quadratic state and terminal regulators.

06 p0681 A73-18523

Detection of a two-frequency signal buried in noise of unknown power.

07 p0794 A73-20144

Linear decision rule for probabilistic signal estimation in image recognition problems with sampling 09 p1060 A73-22556

Theory of optimal AGC system synthesis. 17 p2134 A73-34318

Nonbiased rule for detection of radar signals in noise of unknown power. 20 p2529 A73-38928

A probabilistic algorithm for grouped handling of arguments with sequential discrimination of input features 21 p2658 A73-40994

Noise blurred image recognition probability characteristics from experimental investigation, showing difference from statistical decision theory data 24 p3062 A73-44667

STATISTICAL DISTRIBUTIONS NT PROBABILITY DISTRIBUTION FUNCTIONS

NT RAYLEIGH DISTRIBUTION
A systematic approach to the problem of crossings by a random process. 01 p0070 A73-10577

The generalized gamma distribution and the power distribution as element lifetime distributions 02 p0145 A73-11584

Gamma time-dependency in Blaxter's compartmental model. 02 p0187 A73-12550

Blue objects in the vicinity of M31. I - Discovery probability of newly found blue objects 02 p0226 A73-12837

Application of the Monte Carlo technique to fatigue-failure analysis under random loading. 03 p0388 A73-13236

Hot worked Al alloy machine elements mechanical properties scattering, discussing quality control procedures 03 p0327 A73-14004

Statistical stress concentration effects in composites. 04 p0468 A73-14718

Random antenna array design for narrow beam radiation and blind angle avoidance, determining mutual coupling effect on performance 04 p0416 A73-15059

Surface distribution of interacting and normal galaxies near the galactic north pole 05 p0613 A73-16212

Buckling of a long, axially compressed, thin cylindrical shell with random initial imperfections. [ASME PAPER 72-APM-MMM] 05 p0632 A73-16532

Array factor of statistically thinned antenna arrays with an increased element-interphase minimum 06 p0674 A73-17810

Statistical distribution methods for analyzing formation of reflexes conditioned to time intervals between periodic unconditioned stimuli 06 p0653 A73-18166

Energy spectra of mixed discrete random processes in statistical multiplexing systems with pulse position, delta and pulse code modulation 06 p0668 A73-18390

Numerical experiments on probability distribution of random force in stellar gravitational systems, noting agreement with Chandrasekhar and von Neumann theory 08 p1003 A73-20884

Bayesian prior distributions for multi-component systems. 09 p1111 A73-22374

Engineering significance of statistical and temperature-induced fracture mechanics toughness variations on fracture-safe assurance. [ASME PAPER 72-PVP-15] 09 p1163 A73-23265

Statistical characteristics of phase variable states and phase operators in optical quantum fields by intrinsic state factorization method 10 p1228 A73-24151

Statistical laws governing the wind velocity distribution in the atmospheric boundary layer 10 p1246 A73-24373

Statistical velocity and temperature characteristics of turbulent electron beams in crossed HF electric and magnetic fields, comparing with Brillouin flow 10 p1258 A73-24880

Ionospherically diffracted monochromatic VHF/UHF plane wave statistics characterization, noting Gaussian and log-normal distributions from ATS-3 satellite data recording 10 p1190 A73-24896

Energy characteristics of radio signals scattered by statistically uneven surface, proposing statistical variables substitution 10 p1191 A73-24934

Determination of the statistical characteristics of signals parametrically affecting a dynamic plant 11 p1340 A73-25006

Radar angels cross section statistical distribution model based on radar measurement and direct ornithological data on bird populations density 11 p1332 A73-26630

Measurements of distributed targets with the random signal radar. 11 p1332 A73-26632

Probability of detecting aircraft targets. 11 p1333 A73-26634

Asymmetric positively skewed distributions family for precipitation data analysis, using two-sample non-parametric test 12 p1520 A73-26804

Effective 'radius of operation' of a system for measuring ionospheric drifts 12 p1490 A73-27341

Statistical distribution of the failure of injection lasers. 12 p1508 A73-27524

Statistical distribution of albedo over the lunar disk 12 p1546 A73-27863

Turbulent diffusion downstream of a linear source in a plane parietal jet 13 p1599 A73-28070

On the robustness of properties characterizing the normal distribution. 13 p1650 A73-28797

A reliability analysis of fatigue limits based on large sample quantal response data. 13 p1702 A73-29548

Comparison between the peak sidelobe of the random array and algorithmically designed aperiodic arrays. 14 p1734 A73-30217

Shock-wave generation in a randomly inhomogeneous gas. 15 p1860 A73-31014

Exponential distributions of protons according to adiabatic invariants in the outer radiation belt 15 p1926 A73-31898

Integral transform theory for derivation of compound binomial beta, uniform, and gamma distributions with applications to series-parallel systems reliability determination in manufacturing 16 p2020 A73-33604

Evidence for the existence of galactic superclusters near the galactic North Pole 16 p2063 A73-33661

Statistical brightness distributions for photometric planetary image improvement, considering telescope resolution, diaphragm diffraction and atmospheric turbulence 16 p2069 A73-33832

Book - Statistical design and analysis of engineering experiments. 17 p2200 A73-34456

Stress distribution near a circular hole on a plane consisting of a stochastically inhomogeneous material 17 p2244 A73-34798

The asymptotic dispersion characteristics of the best unbiased linear estimate obtained by the uniform division of the observation interval for the unknown mathematical expectation of a stationary random process 18 p2329 A73-36162

On the identifiability of finite mixtures of Laguerre distributions. 18 p2330 A73-36984

Statistical structure of the brightness field of reflected radiation in the 0.6-0.8 micron spectral interval. 18 p2314 A73-37063

Method of detecting meteor streams and associations 19 p2480 A73-37236

Comparison and synthesis of the characteristics of long- and short-duration blocking systems over the Euroatlantic region 19 p2447 A73-38124

Statistical uniformity of hydrological data from series of river drainage pattern observations 19 p2446 A73-38546

Complex stochastic control system identification by distribution and moments characteristics in form of Gaussian densities, perturbation polynomials and scedastic functions 20 p2540 A73-38708

General remarks concerning theories dealing with scattering and diffraction in random media. 20 p2528 A73-38845

Statistical analysis of the influence of various factors on the quality of photolithographic operations in the production of integrated circuits 20 p2534 A73-38851

Two-stage detection of signals in normal noise of unknown intensity. 20 p2529 A73-38922

Statistical distribution of the albedo over the lunar disk. 20 p2608 A73-39237

Effect of a statistically uneven underlying surface on the radiation characteristics of a phased antenna array 20 p2537 A73-39453

Statistical effects in the transient response of a He-Ne laser with a given initial photon distribution 21 p2714 A73-40568

Surface and bulk laser-damage statistics and the identification of intrinsic breakdown processes. 21 p2714 A73-40758

Convergence of perturbation-theory series in the problem of short-wave propagation through a randomly nonhomogeneous medium 21 p2657 A73-41514

Statistical velocity and temperature characteristics of turbulent electron beams in crossed HF electric and magnetic fields, comparing with Brillouin flow 21 p2749 A73-41658

Effective 'radius of action' of a device for measuring ionospheric drifts. 23 p2970 A73-43234

STATISTICAL MECHANICS

Statistical mechanics of the Burgers model of turbulence. 02 p0153 A73-12030

The mass spectrum of interstellar clouds and the assumption of total coalescence. 04 p0500 A73-15489

Contribution to the classical theory of solids with statistical structural characteristics 06 p0762 A73-17994

Statistical mechanics and virial functions for equation of state of dense gas with spherical nonpolar molecules, calculating compressibility factor for methane and Ar 06 p0726 A73-18555

Thermodynamic probability and statistical interpretations of entropy, with particular attention to information theory, negentropy and Boltzmann-Gibbs theory 08 p1022 A73-21234

Method of integral equations in the statistical theory of fluids 09 p1121 A73-22724

Quantum statistical mechanics of dense partially ionized hydrogen. 11 p1405 A73-25886

Book - Statistical mechanics, kinetic theory, and stochastic processes. 14 p1774 A73-29947

Quantum irreversible statistical thermodynamics with allowance for occurrence of many temperatures based on principle of isentropic motion, applying to laser action 14 p1756 A73-30150

Book on statistical mechanics, covering thermodynamics, canonical ensembles, quantum statistics, simple gases, ensemble theory, phase transitions, cluster expansions and interacting systems 14 p1775 A73-30360

Central limiting theorem in the 'noncommutative' probability theory 15 p1899 A73-31215

Statistical mechanics and virial functions for equation of state of dense gas with spherical nonpolar molecules, calculating compressibility factor for methane and Ar 16 p2039 A73-33580

Book - Principles of plasma physics. 17 p2216 A73-34467

The applications of relativistic kinetic theory to cosmological models - Some observational consequences. 17 p2234 A73-35616

Statistical continuum mechanics and constitutive theories governing microfluid behavior, noting relations with aid of tables 20 p2547 A73-39343

The equations of fast-process hydrodynamics 21 p2676 A73-40205

Statistical dynamics formulation of motion equations for particle system in gravitational interaction with neither gas law nor hydromagnetic effects, applying to solar system evolution 21 p2766 A73-40313

Russian book - Statistical physics and quantum field theory. 21 p2741 A73-41296

Quasi-averages for Green functions construction in solving quantum statistical mechanics problems with degenerate equilibrium states 21 p2741 A73-41297

Nonequilibrium statistical operators and quasi-means in the theory of irreversible processes 21 p2741 A73-41298

Statistical model for phase relations derived from observations of photospheric oscillations, criticizing horizontal propagation theory for phase propagation 21 p2777 A73-41482

Israel Conference on Theoretical and Applied Mechanics, 20th, Tel Aviv, Israel, April 18, 1973, Proceedings. 23 p3038 A73-43302

Statistical theory of solid heterogeneous materials, discussing constant elastic bounds, fiber reinforced cell model, thermal expansion and stress-strain relations 23 p3038 A73-43303

Method of integral equations in statistical theory of liquids. 23 p3007 A73-44324

Physical particle description of moderately dense gases. II - Equilibrium properties. 24 p3111 A73-45397

STATISTICAL MOMENTS

U DISTRIBUTION MOMENTS

STATISTICAL PROBABILITY

U PROBABILITY THEORY

STATISTICAL TESTS

NT KOLMOGOROFF-SMIRNOFF TEST

NT RANK TESTS

Information criterion for optimal planning of reliability control tests, maximizing average effect

Correlation analysis of the continuum radio emission of noise storms.

E layer ionization diurnal exponent independence of seasons and station latitude ascertained by statistical tests

One- and multistage multivariable function max-min problem solution by random search type method through regression curve construction based on statistical test and root determination

Estimation of reliability in storage - Optimal test procedure

Ionospheric radio signal reflection fields verified via quantitative statistical reliability criterion

Limits of suitability of pseudorandom signals for statistical tests

Use of simple test signals in experimental investigations of devices for measuring the one-dimensional probability characteristics of random signals

Asymmetric positively skewed distributions family for precipitation data analysis, using two-sample non-parametric test

Traffic analysis by statistical tests for batch mode operated digital computer network design, considering user habits, and interarrival, waiting and partition times

A semicoherent detection and Doppler estimation statistic.

High pass filter and power spectral analysis of periodicity in solar activity time series, applying statistical tests to sunspot and flare indices

Specifying maintainability-demonstration-test parameters.

Accuracy of type K thermocouple wire below 500 F - A statistical analysis.

The superiority of the pair-comparisons method for scaling visual illusions.

Some problems in the analysis and synthesis of statistically optimal constrained control

Possibilities of calculating the spectral albedo of Venus in the near infrared

Solar flare prediction objective baseline calculation, applying regression analysis to sunspot, magnetic field, calcium plage and radio brightness temperature data

STATISTICAL WEATHER FORECASTING

Approach for obtaining prognostic relations on the basis of meteorological data

Attempt at the application of the theory for linear extrapolation of probabilistic processes in long-range temperature forecasts

Investigation of planetary high-altitude frontal zones with the aid of natural orthogonal functions

The use of model output statistics /MOS/ in objective weather forecasting.

Influence of coherence of sampling on the accuracy of linear statistical forecasting and on the optimal predictor dimension

Tropical cyclone track statistical forecasting comparing methods based on synoptic, empirical and combined data

Statistical aspects of lower atmospheric disturbances delineated from conventional and satellite data over the tropical Pacific.

A 4-year experiment in long-range weather forecasting, using circulation analogues.

Statistical model of gust factor relation to lake and terrain surface roughness and height from wind velocity measurement data

On the existence of extended range predictability.

German book - Long-term weather forecaster: Fundamentals of a new experiment with monthly predictions.

A basis for four-dimensional /continuous/ processing of meteorological observation data, using a dynamic statistical approach

An aid for the prediction of the nighttime minimum temperature

Vector partition of probability /Brier/ score providing reliability and resolution measures of weather forecasts

Very short range local area weather forecasting using measurements from geosynchronous meteorological satellites.

Long term weather forecasting techniques, criteria and implementation, discussing statistical weather analysis, cloud types, air masses, sunspot activity, precipitation and pressure systems

A scheme for synoptic-hydrodynamic-statistical weather forecasting for 3 to 10 days

Statistical analysis of satellite-observed trade wind cloud clusters in the western North Pacific.

Provisional climatology of most probable wind for application to low latitude operational weather analysis and forecasting, based on ATS-3 observed low level winds

Climatic means finite time average estimation standard error calculation by stochastic model with application to long range forecasting

STATISTICS

Some exact statistics of two-dimensional viscous flow with random forcing.

Worst inputs and a bound on the highest peak statistics of a class of non-linear systems.

Design and test of a small, high-pressure ratio, axial compressor with tandem and swept stators.

Subsonic centrifugal compressor efficient operating range extension by collector and diffuser blade cascade separation, presenting performance test results

A unified analysis of fan stator noise.

Supersonic annular blade cascades starting conditions, presenting static pressure and Mach number distributions

The use of a finite difference technique to predict cascade, stator, and rotor deviation angles and optimum angles of attack.

Transonic flow through a turbine stator treated as an axisymmetric problem.

Application of harmonic analysis to the calculation of stators with variable blade pitch

Calculation of the flow of a viscous compressible fluid past a parabolic obstacle

Free and forced convection from fine hot wires.

Viscous steady Couette flow between two parallel flat walls with particle injection, obtaining velocity and temperature distribution

Magnetohydrodynamic flow around a hollow sphere

Shear waves and perturbations in linearized steady plane flows of a thermally nonconducting compressible ideal fluid

Confined laminar jet mixing in a circular channel with arbitrary entrance velocity distribution.

An explicit difference method for steady supersonic flow

On the uniqueness of solutions of the Falkner-Skan equation.

Microplanar model of blood steady flow through rigid circular tubes, presenting equations solutions and velocity profiles

Applying quasilinearization to the steady laminar flow between two parallel porous plates.

Application of a pseudo-viscous method to the calculation of the steady supersonic flow past a waisted body.

Steady flow of neutrally buoyant flat-faced rigid cylindrical capsules along pipeline under hydraulic pressure gradient effect, noting toroidal vortices

Steady transverse plane magnetogasdynamics flows.

On similarity solution of an unsteady laminar boundary layer along a flat plate.

The steady-state flow quality of an open return wind tunnel model.

Study of the laminar free convection wake above an isothermal vertical plate.

Navier-Stokes equation solutions for steady laminar viscous flow of incompressible fluid with mixed no-slip and no-shear conditions

Numerical solution of a boundary value problem for the Navier-Stokes equations

Negative Magnus forces in the critical Reynolds number regime.

High Reynolds number steady separated flow past a wedge of negative angle.

Steady rectilinear universal motions of a Navier-Stokes fluid.

Discharge of a capillary fluid from under a rectilinear shield

Pressure surfaces and flow lines geometry of three dimensional parallel steady flow, noting geodesics formation on surfaces of constant pressure

Critical conditions for steady/unsteady laminar shear flow breakdown into HF oscillations, using kinematic wave theory

One dimensional steady electrohydrodynamic duct flow with shock waves for continuous and discontinuous electric fields

Stability of clamped rectangular plates in uniform subsonic flow.

Steady almost parallel flows linear stability, using multiple scales method for perturbation waves analysis

Flow of a conductive fluid through a cylindrical duct with periodic deformations in the presence of an azimuthal magnetic field

Two dimensional steady nonrotational flow of perfect compressible fluid around symmetric convex profile, reducing to variational inequality in hodograph plane

Comparison of four simple models of steady flow combustion of pyrolyzed methane and air.

Propane-oxygen pilot flame ignition of steady flowing Al powder stream in oxygen

On the steady flow of a non-equilibrium ionized gas around sharp corners in the presence of a crossed magnetic field.

Special relativity theory for steady irrotational ideal gas flow, noting subsonic, supersonic and transonic flow calculations based on small perturbation theory

Three dimensional steady flow of incompressible viscous fluid near thin wing trailing edge, using Stewartson-Williams triple layer method

Steady nonviscous nonheat-conducting plane flow of compressible fluid, calculating entropy, speed and pressure under assumption of variable pressure along streamlines

Two approximate methods for describing the steady motions of an incompressible viscous fluid with a free boundary

Two phase channel flow behavior from three dimensional phase diagram for one dimensional steady flow of ideal gas carrying solid particles

Intrinsic coordinate method of characteristics application to supersonic steady two dimensional nonisentropic inviscid flow, noting shock wave interaction

STEADY STATE

Accuracy studies of the numerical method of characteristics for axisymmetric, steady supersonic flows.

10 p1171 A73-23602

Numerical study of the flow of a viscous incompressible fluid around a circular cylinder

10 p1171 A73-23766

Instability, transition, and turbulence in buoyancy-induced flows.

10 p1205 A73-23859

Velocity field determination for limitless steady boundary layer on circular cylinder and swirling flow produced by generalized vortex

10 p1210 A73-24843

One parameter family of axisymmetric vortex rings propagating steadily through unbounded ideal fluid at rest at infinity

11 p1345 A73-25051

Laminar incompressible fluid steady secondary flow in circular cross section curved tube at various Reynolds numbers

11 p1346 A73-25225

Steady plane flow of viscous fluid in symmetrical channels with curved walls, considering approximate series for stream function

11 p1347 A73-25646

Second-order solutions for steady magnetohydrodynamic channel flow with anisotropic conductivity.

11 p1404 A73-25746

Two-dimensional steady magneto-fluid-dynamic flows with orthogonal magnetic and velocity field distributions.

12 p1527 A73-27020

Flows with wakes about a zero-incidence symmetric profile

13 p1599 A73-28069

On the numerical treatment of the Navier-Stokes equations for an incompressible fluid.

13 p1599 A73-28090

Steady universal motions of a Navier-Stokes fluid - The case when the velocity magnitude is constant on a Lamb surface.

13 p1599 A73-28285

Two dimensional incompressible steady potential electrohydrodynamic flows past flat dielectric plate, using quasi one dimensional and boundary layer approximation

13 p1664 A73-28442

Flow of viscous fluid at small Reynolds numbers past a porous body.

13 p1601 A73-28625

Two dimensional steady subsonic flow through airfoil cascades, predicting turbomachine performance from boundary layer calculation for comparison with experiments

13 p1565 A73-29005

Existence of a corner-type steady flow for an ideal fluid with a free surface

13 p1605 A73-29554

Book - A course in continuum mechanics. Volume 3 - Fluids, gases and the generation of thrust.

14 p1745 A73-30594

Chandrasekhar equations for axisymmetric MHD flows generalized for steady and unsteady flows

14 p1781 A73-30701

The local role of the limit line in the well-posedness of steady state problems in gas dynamics. I - Problems involving one space dimension.

15 p1862 A73-31328

Linearized theory of finite conductivity steady ideal MGD flow past thin wedge in aligned magnetic field, using Fourier integral transform

15 p1917 A73-31338

Special relativity theory for steady irrotational ideal gas flow, noting subsonic, supersonic and transonic flow calculations based on small perturbation theory

15 p1864 A73-32060

Boundary layer separation in a steady plane-parallel incompressible fluid flow

15 p1864 A73-32110

Stability analysis procedure for shock wave in steady compressible fluid flow, obtaining equations of motion

15 p1864 A73-32113

Steady induced capillary-gravitational finite-amplitude waves on the surface of a finite-depth liquid

15 p1865 A73-32116

Electrical network analogy application to thermal energy steady diffusion within Knudsen gas filled enclosure, discussing free molecule limit and transition regime

15 p1959 A73-32283

One dimensional steady electrohydrodynamic duct flow with shock waves for continuous and discontinuous electric fields

15 p1921 A73-32407

Stationary isothermal gas flow subject to self gravitation, finding subsonic regime oscillatory solutions for plane parallel, spherical and rotational symmetric cases

16 p2058 A73-32832

The computation of the flow in the gap between two concentrically rotating spherical surfaces

16 p2000 A73-33255

Viscous flow in radial turbomachine blade passages.

17 p2093 A73-34389

Method for calculating the steady irrotational isentropic flow in a two-dimensional supercritical turbine cascade.

17 p2093 A73-34390

Study of a stationary flow of rigidly plastic material by the numerical finite element method

17 p2244 A73-34796

Turbulent viscosities for swirling flow in a stationary annulus.

[ASME PAPER 73-FE-16] 17 p2152 A73-35013

Cryptosteady flow energy separation mechanisms, considering bearing friction and rotor torque effects and rotor nozzle proportion equations

[ASME PAPER 73-FE-24] 17 p2153 A73-35019

PoPli vortices stability for two dimensional inviscid irrotational steady flow past circular cylinder

17 p2154 A73-35117

Numerical calculation of the three dimensional transonic flow over a yawed wing.

17 p2096 A73-35129

Relaxation factors for supercritical flows.

17 p2154 A73-35131

Finite difference solution of Prandtl boundary layer equations for steady incompressible laminar and turbulent boundary layer flows

17 p2154 A73-35136

Near continuum impact of an underexpanded jet plume on a wall.

17 p2096 A73-35137

Boundary condition calculation procedures for inviscid supersonic flow fields.

17 p2155 A73-35143

A new shock capturing numerical method with applications to some simple supersonic flow fields.

17 p2096 A73-35144

Numerical studies of viscous, incompressible flow through an orifice for arbitrary Reynolds number.

17 p2157 A73-35602

Observation and calculation of a steady, laminar separated flow.

17 p2157 A73-35866

Geometry of relaxing gas flows.

18 p2299 A73-36330

On Burgers' model equations for turbulence.

18 p2299 A73-36507

Magnetohydrodynamic steady aligned flow past an oblique flat plate at a high Reynolds number.

18 p2300 A73-36664

Rheology of steady turbulent flows of an incompressible fluid

18 p2301 A73-37001

Experimental investigations on arc-heated steady plasma flow.

19 p2415 A73-37169

Mises variables in problems with a free boundary for the Navier-Stokes equations

19 p2419 A73-37245

Thin steady two dimensional potential flow with free and/or rigid boundaries in presence of gravity, determining outer and inner expansions characteristics

20 p2546 A73-39085

Steady separated flow over finite flat plate in linearly decelerated free stream, using numerical solution of two dimensional Navier-Stokes equation

20 p2546 A73-39089

Vibration of tubes containing flowing fluid.

[MERL-TN-72-2] 20 p2616 A73-39147

Stationary water flow stability through 90-deg bend with rectangular cross section, noting preserved laminar structure of flow along convex wall

20 p2549 A73-39565

Laminar steady state flow resistor design featuring temperature independence achieved with flattened core capillary tube

20 p2511 A73-39754

Vertical plate steady flow thermal diffusion chamber for cloud condensation nucleus counter, featuring long available growth time for operation below 0.2 percent supersaturation

21 p2697 A73-40059

Two types of instability of steady convective motion caused by internal heat sources

21 p2789 A73-40192

Exact steady-state analogy of transient gas compression by coalescing waves.

21 p2790 A73-40439

Demodulated Doppler signal analyzed for uniform steady flow, noting non-Gaussian phase fluctuations statistics

21 p2699 A73-40454

Linearized models of two dimensional steady air flow around mountain obstacle for constant temperature gradients and invariant velocity

21 p2731 A73-40741

Spatial stability of incompressible two-dimensional Gaussian wake in steady viscous flow.

22 p2796 A73-42243

Vapor flow in cylindrical heat pipes.

[ASME PAPER 73-HT-P] 22 p2931 A73-42289

Unsteady stagnation point heat transfer due to unsteady free stream temperature.

22 p2931 A73-42290

A note on the drag due to steady flow of a conducting fluid past a disk at high Hartmann number.

22 p2894 A73-42475

Helium bubble survey of an opening parachute flowfield.

22 p2798 A73-43112

Forced convective heat transfer from isothermal sphere in steady incompressible flow at low Reynolds and various Prandtl numbers, obtaining mean Nusselt number

23 p3049 A73-43934

Study of the steady flow of an incompressible viscous fluid around a cylinder in rotation

24 p3079 A73-45219

STEADY STATE

Steady state conditions for maximal and minimal energy transfer between any load form and any system displacement shape, examining coincidence and resonance

02 p0194 A73-12604

The steady state performance of an externally pressurized gas lubricated porous thrust bearing with a uniform film.

03 p0311 A73-13203

A phenomenological study of the steady-state current sheet speed in a magnetically driven shock tube.

03 p0288 A73-13809

Theory of steady-state burning of porous propellants by means of a gas-penetrative mechanism.

[AIAA PAPER 73-211] 06 p0767 A73-17663

On the controllability conditions for systems with distributed delays in state and control.

06 p0716 A73-17852

Globally equivalent representations for reciprocal stationary nonlinear systems in equilibrium or steady state conditions, considering electric circuits and thermodynamic system examples

06 p0716 A73-17993

Melehy thermodynamics hypotheses based on average electron energy for examination of equilibrium and steady state conditions in semiconductor p-n junctions

06 p0770 A73-18840

Noisy data filtering of linear steady state control problems based on nearest neighbor interaction, discussing dimensionality reduction model for saving computer time

06 p0682 A73-18868

Steady state slow stellar velocity solution for accretion stream beyond neutral point, estimating cutoff range for braking force of gas cloud

07 p0898 A73-19936

Nearest neighbor approximation for Kalman-Bucy filtering noisy data generated by multidimensional processes via dimensionality reduction for linear steady state problems

07 p0805 A73-20579

Simultaneous diffusion of photons and particles in a semiinfinite space. II - Concentration of excited atoms before a shock wavefront

09 p1123 A73-23069

A structural model of random processes and its invariant properties

11 p1340 A73-25007

Rational methods for controlling multistable elements on the basis of an analysis of the preferential domains of steady states

12 p1482 A73-26774

Influence of a nonlinear lens on the stability of steady-state laser emission.

12 p1507 A73-27506

Influence of self-focusing on the stability of steady-state laser emission.

13 p1629 A73-29441

Solar wind properties near and beyond Jupiter orbit, considering steady state wind extrapolation to large distances, cosmic ray modulation and interactions with planetary bodies

14 p1787 A73-30541

Mathematical description and calculation of the static mode of operation of a microwave power regulator with a semiconductor attenuator.

15 p1849 A73-30993

Investigation of the steady-state temperature field in a composite cathode of a plasmatron

15 p1917 A73-31192

Steady motions of three nonpoint bodies moving freely in space with centers of inertia describing uniform circle

16 p2059 A73-32908

Steady state arc discharge physical properties, discussing boundary geometry of plasma column, and stabilities in gas flow and high current and vacuum conditions

16 p2040 A73-32939

Steady-state solar modulation of cosmic rays.

16 p2055 A73-33296

Analyticity of the plane steady state solutions of the Navier-Stokes equation.

17 p2150 A73-34324

A comparative study of two basic approaches to extremum control.

19 p2413 A73-38037

On steady wave profiles in solids.

19 p2461 A73-38262

Effects of dispersion on steady state electromagnetic shock profiles. 20 p2595 A73-38864

The local role of the limit line in the well-posed of steady state problems in gas dynamics. II - Two dimensional plane flow. 20 p2549 A73-39562

Exact steady-state analogy of transient gas compression by coalescing waves. 21 p2790 A73-40439

Steady-state heat transfer between fluids divided by a thin wall 21 p2792 A73-41224

Steady-state solutions for relativistically strong electromagnetic waves in plasmas. 22 p2891 A73-42238

The steady-state and transient performance of some large-scale vortex diodes. 23 p2942 A73-43407

Certain problems of frequency settling in ideal filters 23 p2959 A73-43514

STEADY STATE CREEP

Steady creep bending in a beam with random material parameters. 01 p0113 A73-10198

Grain growth in alloyed molybdenum under conditions of creep 01 p0063 A73-10486

Disordered precipitation effect on steady state creep rate of gamma prime Ni-Al-Ti single crystals 03 p0326 A73-13963

High temperature steady state creep determination in Al by dip test technique interpreted in terms of slip and recovery activation energy due to effective and internal stress 04 p0467 A73-15933

The orientation dependence of deformation mode and structure in stoichiometric NiAl single crystals deformed by high temperature steady-state creep. 06 p0712 A73-18758

A creep bending analysis of plates by the finite element method. 07 p0908 A73-19093

Inequalities for torsion rigidity of a prismatic rod with steady creep 07 p0912 A73-19323

The influence of prior fatigue deformation on creep behaviour. 08 p0979 A73-21672

Mechanisms of transient and steady state creep in a gamma-prime hardened austenitic steel. 08 p0980 A73-21778

Dislocation distributions during creep and recovery of a 20% Cr-35% Ni steel at 700 deg C. 08 p0981 A73-21784

The temperature dependence of steady state creep in 20% Cr, 25% Ni, Nb stabilized stainless steel. 08 p0981 A73-21785

The effect of niobium content on the steady-state creep of stabilized 20/25 austenitic stainless steels. 08 p0981 A73-21786

Creep associated with hot pressing titanium carbide powders 10 p1224 A73-24315

Application of the extended Newton method to the creep analysis of shells of revolution. 11 p1432 A73-24998

Deformation bounds for a creeping structure approaching rupture. 11 p1447 A73-26654

Nickel base alloys high temperature steady creep rate and stress relations 12 p1512 A73-27256

Transverse creep and stress-rupture of Borsic-aluminum composites and Borsic-aluminum composites containing stainless steel and titanium. 13 p1633 A73-28143

Grain growth during creep of alloyed molybdenum. 14 p1759 A73-30311

Maximum stress calculation for I beam and thin walled sphere redundant structures under stationary creep by perturbation method 14 p1811 A73-30487

Steady-state creep of a thin-walled tube in the general case of applied forces 21 p2787 A73-41194

Steady-state creep characteristics of an Fe alloy containing 3.5 at.% Mo. 23 p2994 A73-44153

Changes in surface structure during high-temperature creep flow. 23 p2994 A73-44159

Discontinuous flow in steady-state creep of Al-Mg alloys at high temperatures. 23 p2995 A73-44162

STEADY STATE FLOW

U EQUILIBRIUM FLOW

STEAM

Second virial coefficients for polar molecules in steam based on PVT data, using Stockmayer potential for curve fitting at 100-1000 C 02 p0238 A73-12643

STEAM FLOW

Influence of geometrical parameters on the energetic separation of superheated water vapor in a conical vortex tube 02 p0153 A73-11789

STEAM GENERATORS

U BOILERS

STEAM TURBINES

Possibilities of rationalizing the design of flow-through turbomachine components 03 p0353 A73-13239

A method of analytical error identification in the inspection of the working profiles of blades 16 p2019 A73-33300

Gas turbine vibration limits - A fundamental view. [ASME PAPER 73-GT-48] 16 p2048 A73-33509

Conference on Heat and Fluid Flow in Steam and Gas Turbine Plant, University of Warwick, Coventry, England, April 3-5, 1973, Proceedings. 17 p2092 A73-34376

Development of experimental turbine facilities for testing scaled models in air or freon. 17 p2145 A73-34381

STEARATES

Oxystearate-based multipurpose lithium lubricants 07 p0843 A73-20013

STEATITE

U TALC

STEEL STRUCTURES

A certain case of stress-concentration analysis by an elastooptical method 01 p0114 A73-10574

Internal friction and heat release in engineering and tool steels in the presence of intense ultrasonic oscillations 01 p0065 A73-10926

Experimental investigation of the behavior of cylindrical shells under dynamic loads 02 p0229 A73-11626

Ni-Cr-Ti steel aircraft structural element fatigue life calculation based on failure mechanism involving crack propagation 03 p0394 A73-14011

Postirradiation notch ductility and fracture strength of pressure vessel steel plate by Charpy V tests 04 p0460 A73-14702

Relationship between material fracture toughness using fracture mechanics and transition temperature tests. 04 p0506 A73-14703

Study of the diffusion of carbon in structural steel plates clad with stainless steels 04 p0467 A73-15951

Pressure vessel proof test variables and flaw growth. 05 p0581 A73-16129

Dynamic response of a vertical cantilever structure in the natural wind. 07 p0823 A73-19565

Resistance to brittle fracture of high-strength steel. 09 p1106 A73-23161

Resistance of high strength structural steel to environmental stress corrosion cracking. 10 p1232 A73-23875

High speed welding of sheet steel with a CO2 laser. 11 p1375 A73-26351

Strength characteristics of layers obtained by spark-alloying steels with high-melting metals 12 p1512 A73-27264

Steel structures analysis based on cubic interpolating functions with parameters of nodal displacements, discussing method extension to natural vibration 14 p1809 A73-30199

Inelastic buckling of columns - The effect of imperfections. 16 p2084 A73-33975

Young elastic modulus determination in steel and alloy disks by contact method 17 p2177 A73-34338

Vibration and noise damping of steel structures by prebonded laminates or viscoelastic layer additions, discussing steel sheets 21 p2717 A73-40236

STEELS

NT AUSTENITIC STAINLESS STEELS

NT CARBON STEELS

NT CHROMIUM STEELS

NT FERRITIC STAINLESS STEELS

NT HIGH STRENGTH STEELS

NT MARAGING STEELS

NT MARTENSITIC STAINLESS STEELS

NT NICKEL STEELS

NT STAINLESS STEELS

Inhibition of stress corrosion cracking of AISI 4340 steel in 10% potassium nitrate solution at 100 C. 01 p0061 A73-10138

Inter- and transcrystallite breakdown of steels and alloys under the action of various media [A review] 01 p0062 A73-10258

Structural changes in Kh18N9T steel during explosion welding 01 p0055 A73-10262

Physical nature of the processes of formation of the set of mechanical properties of quench-hardened alloyed structural steel during tempering 01 p0055 A73-10263

Unalloyed and alloyed steels hardening by pulse heating methods, noting hardness and ductility characteristics due to fine-grained structure 01 p0056 A73-10307

Explosive shock hardening effects on roller steel fatigue strength, surface hardness and wear resistance 01 p0056 A73-10493

Development and present state of the non-destructive testing of semi-finished products 01 p0056 A73-10587

Effect of various surface-active media on the changes taking place in the strength of U8 steel in the high-strength state. 01 p0066 A73-11337

Correlations between the properties of some heat-resistant alloys 02 p0180 A73-11627

Fatigue strength and stress-rupture strength of KhN77TiU and KhN70VMTiU steels with a protective coating 02 p0180 A73-11628

Automatic two-coordinate compensator for resistance-measurement studies of steels and special alloys 02 p0167 A73-11867

Effect of the quality of electrolytic chromium plating on the endurance of steel 02 p0173 A73-11926

Effect of diamond smoothing on the surface finish and fatigue strength of E1961 steel. 02 p0174 A73-12141

Isotropy postulate verification for strain vectors measurement in annealed steel tubular specimens, showing coincidence of tension-internal pressure and tension-torsion test values 02 p0235 A73-12206

The influence of stress concentrators on the properties of steel in cryogenic technology. 02 p0181 A73-12213

Analysis of electrolytes for electrochemical polishing of steel with cationic application 02 p0174 A73-12536

Boron segregation at austenite grain boundary and matrix sites in steel by autoradiography 02 p0183 A73-12761

Minimum deformation forging of prealloyed steel powder for weapon components, discussing mechanical properties, processing and cost analysis 03 p0322 A73-13265

Warm forging of steels for increased precision and mechanical properties. 03 p0323 A73-13269

A new criterion for predicting rolling-element fatigue lives of through-hardened steels. [ASME PAPER 72-LUB-32] 03 p0328 A73-14342

Elevated temperature toughness and a dimensionless parameter involving the zero-ductility temperature. 04 p0459 A73-14670

Extensive study of low fatigue crack growth rates in A533 and A508 steels. 04 p0459 A73-14686

Fatigue crack propagation growth rates under a wide variation of Delta K for an ASTM A517 Grade F T-1 steel. 04 p0459 A73-14687

Fatigue crack propagation of D6ac steel in air and distilled water. 04 p0459 A73-14688

Rice path independent J integral fracture strength criterion estimation as function of crack size and elastoplastically adjusted load point displacement for Ni-Cr-Mo-V steel 04 p0506 A73-14696

The dependence of the lower yield strength in iron and steel on grain size and temperature. 04 p0463 A73-15308

Plastic anisotropy of low-carbon, low-manganese steels containing niobium. 04 p0463 A73-15309

Boundary lubrication and wear of slow moving sliding concentrated hardened steel contacts as function of geometry, load, speed, lubricant and oxygen content 05 p0580 A73-16104

Product quality concept definition in terms of use requirements, characteristic properties reproducibility/quality control/and cost, discussing steel metallurgy and fabrication methods 05 p0582 A73-16999

Titanium nitrides effect on austenite grains formation by high temperature fusion, considering electric arc and vacuum melting of structural steels 06 p0706 A73-17883

Weldability, corrosion resistance and heat resistance increase in Nb alloyed steels, noting aging temperature effects and microstructure 06 p0706 A73-17886

Influence of rare-earth metals on the grain growth process during recrystallization of heat-resistant steels 06 p0706 A73-17887

Stacking faults effect on martensitic phase formation during steel hardening based on X ray diffraction analysis and Paterson theory 06 p0735 A73-18034

Structural and phase transformations in silicon steels during heat treatment 06 p0707 A73-18035

On fracture toughness and its size dependence for steels showing thickness delamination. 06 p0709 A73-18476

Subcritical crack growth of TRIP steels in air under static loads. 06 p0710 A73-18485

Electrostatic field effects on the fatigue of steel in vacuum 06 p0711 A73-18661

Method for increasing the fatigue strength of hardened steels 06 p0711 A73-18666

Saturation of 1Kh18N9T steel with beryllium and corrosion resistance of the coating in a lithium melt 06 p0711 A73-18669

A new relationship between pre-strain and yield stress drop due to Bauschinger effect. 06 p0713 A73-18772

Scale effects on the fatigue and corrosion fatigue of steel 07 p0839 A73-19657

Creep tests and fracture mechanics for high temperature properties of steels and alloys under static load, noting discrepancies for brittle materials 07 p0840 A73-20510

Creep strength in steel and high temperature alloys; Meeting, Sheffield, England, September 20-22, 1972, Preprints. 08 p0980 A73-21776

Steel and Ni-based alloys structural stability during long term high temperature creep, noting matrix structure dependence on initial dislocation and interparticle spacing 08 p0980 A73-21780

Investigation of the failure characteristics of electrically heated samples of heat-resistant steels and alloys in a high-pressure oxidizing flow 09 p1069 A73-21980

Variable-load endurance criteria for steels under conditions of uniaxial and biaxial static tension 09 p1100 A73-22152

Twinning deformation of mild steel at low temperatures as function of stress-strain state 09 p1100 A73-22154

Temperature dependent chemisorption effects on hydrogen embrittlement of steel, showing strength-ductility correlation 09 p1100 A73-22158

Investigation of carbon- and manganese-diffusion processes in the metal-ceramic steel G13M 09 p1103 A73-22466

Electron-spectroscopic investigations of two modifications of the alloy steel Kh18N10T 09 p1104 A73-22690

Third elements effect on electrical erosion of steels noting influence of atmospheric composition 09 p1104 A73-22967

Investigation of the effect of surface finish and method of surface treatment on the endurance of the steels Kh18N10T and Kh16N6 and of alloy AMG6 at normal and low temperatures. 09 p1106 A73-23163

Fatigue crack growth under C.O.D. cycling. 09 p1163 A73-23252

Engineering significance of statistical and temperature-induced fracture mechanics toughness variations on fracture-safe assurance. [ASME PAPER 72-PVP-15] 09 p1163 A73-23265

Study of the wear resistance of nitrided electrolytic chromium coatings on certain alloy steels 10 p1223 A73-24065

A comparison of the effects of explosive forming and static deformation on the mechanical properties of pressure vessel steels. 10 p1225 A73-24426

Influence of pressure on VT14 alloy wear and friction against 30KhGSA steel 10 p1226 A73-24797

Alloy steels supercooled austenite nitriding in ammonia flow, examining diffusion layers by X ray analysis and hardness tests 10 p1236 A73-24956

Diffusion layer structure and phase composition during quenched and annealed steel saturation by Cr at high heating rates 10 p1236 A73-24962

Boridosilicide and boridoaluminide diffusion coatings on iron and steel, investigating formation kinetics structure and properties 10 p1227 A73-24963

Cyclic stress, strain, and energy variations under cumulative damage tests in low-cycle fatigue. 11 p1379 A73-25132

The effect of strain rate on the characteristic value of the linear-elastic fracture mechanics determined on large and small specimens 11 p1380 A73-25446

The photometric determination of aluminium in steel after separation on a cation-exchanger 11 p1380 A73-25447

Corrosion fatigue crack propagation behavior in steels above/below stress intensity threshold within framework of linear elastic fracture mechanics 11 p1382 A73-25821

Influence of welding parameters on the strength properties of spot welds of MST1X steel with protective coatings 11 p1374 A73-26293

Chromium coated steels corrosion fatigue in normal conditions, aggressive media and high temperature environments 11 p1386 A73-26733

Influence of gas carburizing on the structure and properties of electrolytically deposited chromium 11 p1375 A73-26734

Influence of fretting on the endurance of 40KhNMA steel with various thermochemical processing 11 p1386 A73-26735

Cumulative creep formulas for construction steels at stepwise increasing temperatures 12 p1510 A73-26900

Kinetic strain criteria of cyclic failure at high temperatures 12 p1552 A73-27252

The changes in structural and mechanical properties of construction materials under loads 12 p1513 A73-27500

Precipitation processes in Nb microalloyed converter steel 12 p1514 A73-27685

Plasticity and fracture of structural metals in complex stress state at low temperatures. 13 p1639 A73-29462

The role of micropores in the fracture of forged sintered steel. 13 p1639 A73-29468

A method for the calculation of the fatigue life of unnotched and notched specimens loaded with alternating stresses. 13 p1641 A73-29501

Present situation of Japanese research on the long-time creep and creep rupture properties of steels. 13 p1642 A73-29513

The relation between tensile bond strength and crystalline properties of the adhesive on the steel-nylon 12-steel system. 13 p1642 A73-29531

Deformation criteria of failure under simple and composite stresses. 13 p1703 A73-29621

Explosive shock hardening effects on roller steel fatigue strength, surface hardness and wear resistance 14 p1755 A73-30318

Scale effect in fatigue and in corrosion fatigue of steel. 14 p1760 A73-30324

Investigation of fatigue and brittle failure patterns in 15G2AFDps steel at low temperatures 14 p1762 A73-30678

Application of fiber optics to the observation of fatigue crack development 14 p1754 A73-30691

Effect of cooling /to -269 C/ on failure in Kh18N10T and Kh16N6 steels under impact bending 14 p1763 A73-30692

Saturation of Kh18N10T steel by molybdenum from the vapor phase 15 p1889 A73-31807

Superplasticity of the Kh18N10T steel 15 p1890 A73-31816

Comparison of R-curves determined from different specimen types. 15 p1951 A73-31988

A method of programmed fatigue tests with short-time overloads. 17 p2165 A73-34277

Method of recording the deformation diagram in thermal-fatigue tests. 17 p2165 A73-34278

The supporting effect of bending specimens under static load in the temperature range from 400 to 500 C. 17 p2187 A73-34521

Relationship between K_{1c}/ and plane-strain tensile ductility and microscopic mode of fracture. 17 p2190 A73-34876

A numerical and experimental investigation of the use of J-integral. 17 p2246 A73-34880

Continuous monitoring of fatigue crack growth by acoustic emission techniques. [TR-DE-73-2] 17 p2148 A73-35445

Evaluation of finite-plasticity theories for torsion-tension members made of Tresca materials. [SESA PAPER 2109] 17 p2251 A73-35447

Fatigue strength of materials under a two-frequency load [Review/ 18 p2366 A73-36754

Theory of hardening applicability to the description of deformation law singleness under various conditions of uniaxial tension 18 p2366 A73-36759

Effect of prestress levels on the long term strength of 1Kh18N9T steel at elevated temperatures 18 p2323 A73-36761

Residual stress relaxation stability in 13Kh12NVM-FA steel 18 p2323 A73-36763

Influence of the structural state of the surface layers on the resistance to crack propagation of steel products 18 p2366 A73-36819

Influence of stresses on the nature of the distribution of dislocations in Kh18N10T steel at a temperature of 650 C 18 p2325 A73-36820

Studies of the renewal of stress relaxation on a high-grade steel wire subjected to stress corrosion after being treated for total elimination of relaxation 19 p2497 A73-37553

Some studies of the influence of localized and gross plasticity on the monotonic and cyclic concentration factors. 19 p2497 A73-37589

Creep tests and fracture mechanics for high temperature properties of steels and alloys under static load, noting discrepancies for brittle materials 19 p2440 A73-37785

Statistical characteristics of the fatigue strength of heat-resistant 1Kh18N9T steel under steady and programmed loading conditions at high temperatures 20 p2577 A73-39355

Work hardening of copper, nickel, and alloy H31 by compression and explosion 21 p2707 A73-40705

Cumulative creep formulas for construction steels at stepwise increasing temperatures 21 p2720 A73-41033

Influence of hydrogen, alcohols, and moisture on the ultimate strength and electrical resistance of tungsten and steel wire samples 21 p2721 A73-41227

Possibility of predicting the residual stress pattern in boronized steels 21 p2721 A73-41229

Influence of thermal cutting and its quality on the fatigue strength of steel. 21 p2722 A73-41253

The interaction of creep and fatigue for a rotor steel /The William M. Murray Lecture, 1972/. 21 p2722 A73-41264

Criteria relating to the fatigue life of steels subjected to alternating loads under conditions of uniaxial and biaxial static strain. 22 p2874 A73-42102

Temperature dependent chemisorption effects on hydrogen embrittlement of steel, showing strength-ductility correlation 22 p2874 A73-42106

Fatigue-crack growth under variable-amplitude loading in ASTM A514-B steel. 22 p2875 A73-42140

Effect of a loading sequence on threshold stress intensity determination. 22 p2875 A73-42141

Fatigue and corrosion-fatigue crack growth of 4340 steel at various yield strengths. 22 p2875 A73-42142

German monograph on cyclic stress-strain curves and fracture strength of steels with various compositions covering plastic strain energy, S-N diagrams and test equipment 22 p2879 A73-42739

Book - Advances in corrosion science and technology. Volume 3. 23 p2990 A73-43455

Corrosion and deposition of steels and nickel-base alloys in liquid sodium. 23 p2990 A73-43456

Development of methods for long-term prediction of heat-resistance characteristics 24 p3099 A73-44768

Saturation of steel Kh18N10T with molybdenum from the vapor phase. 24 p3100 A73-45270

Superplasticity of steel Kh18N10T. 24 p3100 A73-45279

STEEP GRADIENT AIRCRAFT
U VISTOL AIRCRAFT
STEEPEST ASCENT METHOD
U STEEPEST DESCENT METHOD
STEEPEST DESCENT METHOD

A computational method for optimal structural design. I - Piecewise uniform structures. 03 p0390 A73-13337

Numerical calculation of cumulative probability from the moment-generating function. 05 p0591 A73-16815

Iterative least-squares synthesis of nonuniformly spaced linear arrays. 06 p0666 A73-18194

Identification of multivalued nonlinearities in a class of noisy time invariant dynamic systems. 06 p0681 A73-18811

On parameter identification for distributed systems using Galerkin's criterion. 07 p0804 A73-19130

The modeling and design optimization of a space-oriented thermoelectric power supply.
09 p1118 A73-22797

Book - Iterative methods for nonlinear optimization problems.
10 p1242 A73-23947

An optimal control approach to terminal area air traffic control.
11 p1394 A73-25786

Aircraft flight simulator with coordinated adaptive filter derived from continuous steepest descent method
18 p2295 A73-36836

Use of weighting functions in conjugate gradient methods
18 p2295 A73-37079

Polynomial approximations of the characteristics of low-sensitivity filters
21 p2666 A73-41315

STEERABLE ANTENNAS

A fixed reflector, steerable beam, earth station antenna.
04 p0428 A73-15415

The 15 m Cracow radiotelescope. I - Technical description and observational possibilities.
08 p0952 A73-20850

A new VHF-interferometer with three steerable high-gain-antennas for satellite-tracking.
09 p1070 A73-23434

A simple stabilized antenna platform for maritime satellite communications.
12 p1481 A73-27673

Galactic radio emission at 38 MHz using steerable reflector telescope with defined beam and small side lobes
13 p1673 A73-28278

Satellite tracking interferometer systems with three steerable directional antennas mounted over azimuth mounts near Lichtenau /German Federal Republic/
14 p1742 A73-30100

Radio direction finder of increased accuracy with a moving antenna.
16 p1991 A73-33976

On the angular resolution of a search radar with a mechanically rotated antenna.
17 p2125 A73-35369

A limited steerable dual reflector antenna.
18 p2293 A73-36881

VM 256 - Experimental system of a 3-D radar installation
18 p2335 A73-37040

Adaptive ground implemented phased arrays.
20 p2523 A73-38729

Beam steering system of the north-south array of the DKR-1000 FIAN radio telescope
21 p2662 A73-40542

Linear scan receiver for electronic beam steering of the north-south array of the DKR-1000 radio telescope
21 p2662 A73-40543

Phased array antennas for applications on spacecraft.
21 p2662 A73-40647

Design, performance, and cost considerations for solid-state arrays.
21 p2662 A73-40648

A survey of the simulator technique for designing a radiating element in a phased-array antenna.
21 p2652 A73-40657

Planar phased array beam steering methods, emphasizing electronic driver and logic circuit sharing between phase shifters for cost reduction
21 p2652 A73-40666

Time scanned array radar with time delay or phase gradient for electronic beam steering control by signal
21 p2652 A73-40669

High resolution beam steering phased array radar antenna design by subarray techniques, using time delay circuit for cost effective driver control simplification
21 p2653 A73-40672

Dual beam antenna - A unique waveguide phased array with independently steered beams.
21 p2653 A73-40683

An array technique with grating-lobe suppression for limited-scan applications.
22 p2830 A73-41826

Computer controlled steerable array of multiple conical log spiral antennas for solar and discrete radio source studies
23 p2965 A73-43363

Computer controlled steerable radio telescope construction and performance for decimeter and centimeter wavelength observations
23 p2958 A73-43367

STEFAN-BOLTZMANN LAW

Axisymmetric Stefan problem with boundary conditions of the third kind
08 p1022 A73-21100

STELLAR ATMOSPHERES

NT CHROMOSPHERE

NT SOLAR ATMOSPHERE

Element abundances in O- and early B-stars.
01 p0096 A73-10296

Homogeneous gas sphere model light scattering for different energy source distributions in planetary and stellar atmospheres
01 p0100 A73-10704

Possibility of accelerating the matter of hot stars by absorption in spectral lines
01 p0100 A73-10706

Nature of the emission of UV Ceti-type stars
01 p0100 A73-10708

Trapping of condensed plasma loops and arcs in cosmic atmospheres.
01 p0103 A73-11020

The consequences of grains in the atmospheres of late-type stars. I - Intrinsic polarization, infrared excesses, and emission lines.
01 p0103 A73-11035

Two quantum induced photon-plasmon transition probability for hydrogen atom in processes of nebulas and stellar chromospheres
01 p0080 A73-11308

Book - Radiation transport in spectral lines.
02 p0194 A73-11876

Self consistent model of closed field lines of pulsar magnetosphere valid for oblique rotators and unipolar inductors
02 p0216 A73-12382

He 4, C 12, O 16, Ne 20, Mg 24, Si 28 and Fe 56 abundance computed as function of time for neutron star atmospheres with strong magnetic fields
02 p0223 A73-12728

Average magnetic field strength relationships with angular velocity and stellar activity cycle period, using Leighton solar cycle model with differential rotation and cyclonic turbulence
02 p0224 A73-12741

Analyses of light-ion spectra in stellar atmospheres. I - Magnesium II in B and O stars.
03 p0366 A73-12934

A search for density and pressure inversions in high-temperature, low-gravity model atmospheres.
03 p0366 A73-12935

Microturbulence in atmospheres of F, G, K, type stars. I - Curve of growth analysis of G, K, type subgiants.
03 p0370 A73-13196

Radial velocity and microturbulence dependence on excitation potential and time in A type supergiants atmosphere, deriving chemical composition
03 p0371 A73-13215

Blanketed model atmospheres for cool hydrogen-rich white dwarfs.
03 p0371 A73-13225

Pulsar magnetosphere evolution, discussing electron and positive ion supply at surface, plasma flow and Crab Nebula characteristics
07 p0900 A73-20276

Atmospheric abundances in the carbon star HD 156074.
08 p1006 A73-20935

The metallic-line star 15 UMa and the F 5 V star 5 And.
09 p1141 A73-22013

Comparison of telescope magnitudes with model-atmosphere predictions for A, F, and G supergiants.
09 p1142 A73-22030

Cooling effects of CO IR opacity in stellar atmospheres of dwarfs and supergiants, considering application to sun and grain formation in cooler stars
09 p1142 A73-22031

On ultraviolet absorption by molecular hydrogen in stellar atmospheres.
09 p1148 A73-22867

Opacity probability distribution functions for application to non-grey late-type stars model atmospheres.
09 p1149 A73-23131

A non-LTE study of silicon line formation in early-type main-sequence atmospheres.
10 p1272 A73-23532

Stellar model chromospheres. I - On the temperature minima of F, G, and K stars.
10 p1272 A73-23533

Photospheric and circumstellar H-alpha line profiles in M-supergiant spectra
10 p1273 A73-23706

On the relation between optical scale height and density scale height in a stellar atmosphere.
10 p1281 A73-24406

Spectrophotometric investigation of the star alpha-2 CVn. II
11 p1416 A73-25232

Molecular abundances in stellar atmospheres. II.
11 p1417 A73-25265

Electric conductivity in the atmosphere of early-type stars.
11 p1427 A73-26575

Velocity gradients and microturbulence in Cepheids.
11 p1427 A73-26607

Equations derived for magnetic field line configuration and plasma flow about rotating object having axisymmetric field with emphasis on pulsar magnetosphere
11 p1427 A73-26614

Metal content in the atmospheres of red giants which are members of dispersed star clusters and dynamical groups
12 p1537 A73-26853

LTE and hydrogen and ionized He lines approximations for model atmosphere computations of hot early stars, discussing UV line blanketing
13 p1686 A73-29367

About the influence of a magnetic field on the model atmosphere of a magnetic star.
13 p1687 A73-29657

Hydrostatic, flux constant and LTE stellar atmospheric models at 3800 and 3500 K for Betelgeuse
14 p1801 A73-30737

Thermal convective instability in uniformly rotating magnetized isothermal stellar atmosphere with constant Alfvén speed, discussing heat loss mechanism dependence on temperature
15 p1929 A73-31060

Stellar atmospheric conditions taking into account A5 and early stars, considering spectral characteristics, absorption spectra and spectrum prediction
15 p1932 A73-31305

Bands of the light molecules in Mira variables.
15 p1932 A73-31307

Radiation absorption in stellar atmospheres due to photoionization in magnetic field, discussing frequency relation to propagation direction and Larmor frequency
15 p1872 A73-31955

X-ray and radio emission from stellar coronae.
16 p2052 A73-32827

A model-atmosphere abundance analysis of the B9 V star nu Capricorni.
17 p2231 A73-34758

Late B6 stars line spectra, atmospheric electron density, microturbulence velocity, excitation temperature, flux envelopes and energy distributions
17 p2233 A73-35612

Curvature effects in extended stellar atmospheres - Pure absorption.
17 p2237 A73-35788

Profiles of the photospheric and circumstellar H alpha line in the spectra of type M supergiants.
18 p2354 A73-36731

The spectrum of eta canis majoris, B5 Ia.
18 p2355 A73-36779

CN red system line opacity codes for late star model atmosphere calculation
19 p2488 A73-38513

Russian book - Stellar atmospheres and interplanetary plasma.
21 p2671 A73-40531

Permissible hydrodynamic and hydrostatic stellar atmosphere models described by system of equations dependent on initial level conditions
21 p2767 A73-40532

Possibility of radiative acceleration of the gas in stellar atmospheres
21 p2767 A73-40534

Variations of pulsar intensity as a result of scintillations at an inhomogeneous plasma
21 p2767 A73-40536

Possibility of radiative acceleration of the gas in stellar atmospheres
21 p2767 A73-40554

Effect of the absorbers upon the thermal structure of a LTE atmosphere, hydrogen and helium.
22 p2908 A73-42309

Spectral variabilities of magnetic peculiar A stars associated with atmospheric chemical composition anomalies, using inclined rotator model
22 p2908 A73-42345

Light curve for eclipsing binary systems with an extensive atmosphere.
22 p2916 A73-43044

The Wolf-Rayet stars - The general problems of extended atmospheres and non-classical atmospheric models.
23 p3025 A73-43192

Classification and distribution of WR stars and an interpretation of the WN sequence.
23 p3025 A73-43193

WC and WR binary stars spectra differences attributed to variations in effects of companion on principal star atmosphere
23 p3026 A73-43203

Interaction of the X-ray source radiation with the atmosphere of the normal star in close binary systems.
23 p3030 A73-43750

Curvature effects in extended stellar atmospheres - Absorption and scattering.
23 p3030 A73-43751

Chromosphere models for cool stars of various spectral types, calculating temperature-density dependence for sun, giant and dwarf stars
23 p3036 A73-44243

Radiation absorption in stellar atmospheres due to photoionization in magnetic field, discussing frequency relation to propagation direction and Larmor frequency
24 p3081 A73-44480

Interstellar reddening calculation with respect to U-B/V-B diagram for hot and main sequence stars as

STELLAR DOPPLER SHIFT

function of luminosity based on model stellar atmospheres 24 p3138 A73-45012

STELLAR DOPPLER SHIFT

U DOPPLER EFFECT

U EXTRATERRESTRIAL RADIATION

STELLAR ENVELOPES

Nonthermal turbulent heating in the solar envelope. 08 p1003 A73-20887

Magnetic field in the plasmasphere of a compact star. 08 p1007 A73-21001

Observations of circumstellar circular polarization in four more infrared stars. 08 p1013 A73-21813

Elongated shells around novae and concentration near orbital planes resulting from perpetual matter losses, considering close dwarf binaries and recurrent novae 09 p1145 A73-22288

Evolution of a white dwarf during accretion of hydrogen-rich matter. II 09 p1145 A73-22291

Radio halos around old pulsars - Ghost supernova remnants. 09 p1148 A73-22871

Carbon stars molecular band strength variations in two-micron spectral region due to thermal emission from circumstellar dust shell 09 p1149 A73-23129

The interpretation of continuum and line absorption and radiation by circumstellar dust. 09 p1150 A73-23132

Rotating neutron star gas cocoon heating by LF radiation absorption, noting X ray emission 10 p1263 A73-23481

Circumstellar envelope model and shock wave calculations for type II supernovae with radiation transport via diffusion, predicting Rayleigh-Taylor instability 10 p1273 A73-23546

On the nature of X Persei - Evidence from the 1957 outburst. 10 p1275 A73-23845

Dust emission nebulae around Orion O and B stars. 11 p1427 A73-26606

Chemical composition of stars in globular clusters and the morphological characteristics of their horizontal branches 12 p1546 A73-27852

Stellar maser output observations application to analysis of mass loss rate or physical conditions in circumstellar shell 15 p1934 A73-31477

Chemical composition of the classical Cepheids in the Galaxy and the Magellanic Clouds. 18 p2354 A73-36730

Observations of carbon monoxide at 4.7 microns in IRC + 10216, VY Canis Majoris, and NML Cygni. 19 p2484 A73-37612

Treatment of molecular reaction equilibria and opacity calculations for cool circumstellar envelopes 20 p2606 A73-39079

Chemical composition of globular-cluster stars and the form of the horizontal branch. 20 p2608 A73-39226

Shell nebulae and Wolf-Rayet stars - Observations of NGC 2359 21 p2768 A73-40714

Variations in the abundance of chemical elements in the classical Cepheids of the Galaxy 21 p2768 A73-40718

Static stellar envelopes at radiative equilibrium for power law dependence of opacity on temperature and density 22 p2911 A73-42935

The common convective envelope model for W Ursae Majoris systems and the analysis of their light curves. 22 p2912 A73-42939

STELLAR EVOLUTION

Stellar structure and angular momentum evolution of rotating stars, describing interaction in terms of redistribution processes of momentum 01 p0094 A73-10054

Supernova remnants descriptions, distance and hydrodynamic evolution, considering galactic nonthermal radio sources, radio maps, and X ray and radio polarization 01 p0094 A73-10057

Dynamic and thermodynamic effects addition to basic Boussinesq convection for convection in stars, discussing rotation, magnetic fields, radiative transfer and state equation 01 p0094 A73-10061

Pulsar structure theory with respect to rotating neutron star hypothesis, discussing evolutionary elements 01 p0095 A73-10065

Evolutionary models for helium white dwarves with uniformly accreting hydrogen shell, noting thermally unstable laminar energy source formation in shell lower layers 01 p0100 A73-10709

Evolutionary sequences for massive stars with various initial chemical compositions, studying semiconvection effects on core helium burning star distribution in H-R diagram 01 p0104 A73-11037

Single gaseous object and stellar cluster models of quasars and galactic nuclei stability, noting neutron and collapsing star lifetimes 01 p0106 A73-11302

Unsteady accretion of optically thick gas cloud on neutron star as hydrodynamic phenomenon due to supernova explosions or collision with ordinary star 01 p0106 A73-11303

Mean absolute magnitudes and color indices of the red-giant concentrations in the color-magnitude diagrams of open clusters. 01 p0106 A73-11319

The evolution of galaxies - A heretical view. 02 p0211 A73-11592

Nonstellar origin of Jupiter from tidal instability considerations, discussing binary star formation 02 p0216 A73-12377

Binary stars tidal evolution theory, deriving energy and momentum equations for arbitrary internal structures 02 p0218 A73-12411

Hydrodynamic model calculations for supermassive stars. II - The collapse and explosion of a nonrotating 520,000 solar-mass star. 02 p0222 A73-12713

Star formation in the galaxy. 02 p0224 A73-12744

Massive stars evolution in hydrogen and helium burning phases, taking into account mass loss from light pressure in optically thick media 02 p0224 A73-12801

Self-accretion of matter, red subluminescent stars and early evolution of low-mass stars. 02 p0225 A73-12808

Investigations regarding the structure of young star clusters and the evolutionary phases of their members. II - NGC 6530. III - NGC 6611 02 p0226 A73-12835

Condensation and protostar expansion hypotheses of stellar and galactic evolution in view of discoveries of quasars, central bodies and stellar associations 03 p0365 A73-12902

Gaseous star as first limit to nebular matter gravitational collapse, considering equilibrium, neutron stars, black holes, forbidden lines and ionized hydrogen clouds 03 p0365 A73-12913

Thermal instability of the hydrogen-burning shell in nondegenerate stars. 03 p0366 A73-12937

Rapid changes in the new shell star HR 6000. 03 p0366 A73-12941

Chromospheric heating of very hot stars by radiation driven sound waves. 03 p0371 A73-13222

Giant envelopes structure triple solutions yielding bottom pressure-radius curves, discussing stellar evolution, Cepheid variables and secular instability 03 p0371 A73-13226

Molecular clouds and stellar origin in interstellar space 03 p0376 A73-14175

Shock waves in spiral arms and star formation. 04 p0496 A73-14970

M giant atmospheric molecular evolution, discussing carbon/oxygen ratios, s-process overabundances and relationships between M, S and C stars 04 p0496 A73-14971

Cooling and evolution of a supernova remnant. 04 p0499 A73-15360

Thermal pulses in helium shell-burning stars. 04 p0499 A73-15364

Contact binaries - Opacity and rotation. 04 p0500 A73-15488

The mass spectrum of interstellar clouds and the assumption of total coalescence. 04 p0500 A73-15489

The abundances of the elements in the oldest disk stars. 04 p0500 A73-15514

Solar core stability via model including plain parallel stratified fluid layer with energy generation, noting ice age correlation with mixing phases during evolution 04 p0501 A73-15623

Pulsars and the evolution of supernova remnants. 04 p0501 A73-15686

Self similar procedure derived for gas inflow to solid surface in constant gravitational field, applying to initial phase of neutron star matter accretion 04 p0503 A73-16003

A numerical experiment in the accretion problem. 04 p0503 A73-16004

Luminosity function of the star cluster M 67 05 p0613 A73-16208

Crab Nebula evolution from 1054 supernova to neutron star and nebula expansion, discussing pulsar properties 05 p0614 A73-16304

Stellar evolution, explosion and mass ejection, considering Crab Nebula filaments and supernovae Cygnus and Vela X remnants 05 p0618 A73-16825

Linear series and of stellar models. I - Thermal stability of stars. 05 p0621 A73-17069

Gravitational field effects on processes near stars and galaxies in late evolution phases, describing particle motion and light propagation near rotating sources 05 p0623 A73-17197

Theoretical evolution of a hydrogen-helium star of 3 solar-mass units from the pre-main sequence to the core helium-exhaustion phase. 05 p0625 A73-17319

Comments on a PLC relationship for Cepheids and on the comparison between pulsation and evolution masses for Cepheids. 05 p0625 A73-17334

Pulsars as rotating magnetic neutron stars created during catastrophic collapses of old stars, discussing radiation mechanism 06 p0750 A73-18012

Multiple and intrinsic variable stars, considering pulsars, binary systems, Cepheids, stellar structure and evolution 06 p0750 A73-18014

Gravitational contraction and energy dissipation and compensation in stellar nuclear reactions, noting He thermonuclear reactions and nucleosynthesis 06 p0751 A73-18158

Mass transfer during evolution of close binaries within zero velocity surfaces related to nova outbursts and Wolf-Rayet star composition 06 p0753 A73-18246

Star formation and evolution in spiral galaxies. 07 p0873 A73-19055

Advanced evolution of massive stars. III - Hydrostatic carbon-burning nucleosynthesis and energy generation. 07 p0874 A73-19062

Luminosity classification of stars earlier than O9. 07 p0875 A73-19120

Star formation from interstellar clouds gravitational collapse, discussing protostars evolution based on model calculations 07 p0878 A73-19675

Steady state slow stellar velocity solution for accretion stream beyond neutral point, estimating cutoff range for braking force of gas cloud 07 p0898 A73-19936

Pulsar magnetosphere evolution, discussing electron and positive ion supply at surface, plasma flow and Crab Nebula characteristics 07 p0900 A73-20276

Evolution of scattered star clusters due to dissipation 07 p0901 A73-20316

Time variation of metal abundance in galaxies - Super-metal-rich stage. 07 p0902 A73-20446

The evolution of population II stars; Proceedings of the Conference, State University of New York, Stony Brook, N.Y., December 3, 4, 1970. 07 p0903 A73-20626

He core burning and shell hydrogen burning in horizontal and posthorizontal branch stars 07 p0903 A73-20627

Evolution of single stars. VII - Evolution of massive stars. 08 p1002 A73-20848

Evolution from the main sequence to the helium flash for population II stars. 08 p1005 A73-20915

The history of star formation and the colors of late-type galaxies. 08 p1008 A73-21155

Stellar evolution at high mass based on the Ledoux criterion for convection. 08 p1008 A73-21159

Nucleocosmochronology and stellar nucleosynthesis models for Galaxy origin and solar system formation 08 p1010 A73-21231

Mass transfer in close binaries. III - Gaseous rings in algol-like binaries. 08 p1010 A73-21312

Galactic dust region molecular cloud effects on cloud chemical evolution, star and planetary formation and life development on planets 09 p1140 A73-21975

A numerical model of the structure and evolution of young supernova remnants. 09 p1143 A73-22111

Infra-red observations of young stars. I - Stars in young clusters. II - T Tauri stars and the Orion population. III - Nebulous emission-line stars. 09 p1143 A73-22112

Evolution of a white dwarf during accretion of hydrogen-rich matter. II 09 p1145 A73-22291

Analytical expressions for the parameters of rotating stars 09 p1145 A73-22292

Thermal wave generation and transformation into shock waves due to energy release in stellar interior, considering nova outburst 09 p1146 A73-22547

Thermal conductivity approximation for gasdynamic equations describing stellar gravitational collapse, calculating neutrino and antineutrino energy and momentum transport processes 09 p1147 A73-22701

Close binaries and their significance in the theory of evolution of stars 09 p1151 A73-23332

Star magnetic field origin in dynamo action associated with nuclear energy generation in stellar evolution, discussing effects on flares, chromosphere and coronal activities 10 p1271 A73-23489

Fluid dynamical method for computing spherical star cluster evolution based on Fourier transformation of Liouville-Boltzmann equation 10 p1273 A73-23612

Ejection of supernova shells by magnetic pumping 10 p1273 A73-23701

Thermal instability caused primary interstellar dust cloud fragmentation and resulting star formation according to Peebles-Dicke hypothesis for cosmological origin of globular clusters 10 p1274 A73-23713

Formation of stars in a rotating cloud with magnetic field. 10 p1275 A73-23830

Secular stability. V - The perturbation of chemical abundances. 10 p1280 A73-24404

The manifold of galaxies - Galaxies with known dynamical parameters. 10 p1281 A73-24407

Dense stellar systems dynamics, considering gravitation relaxation, star evaporation, antiequpartition, growth of dense galactic cores, stellar coalescence, disruption and formation 11 p1414 A73-25065

Probabilistic fragmentation model for collapsing interstellar cloud, predicting stellar mass spectrum 11 p1415 A73-25171

Kinetic equations for gravitating point rotating system model of stellar systems evolution phases, taking into account dissipation-produced motions 11 p1416 A73-25235

Stellar evolutionary calculation for Jupiter, considering gravitational contraction 11 p1420 A73-25892

Evolution of stars with suppressed core convection. 11 p1427 A73-26608

Evolution of open star clusters through dissipation. 12 p1539 A73-27288

Metal-poor stars. IV - The evolution of red giants. 12 p1540 A73-27328

Hydrogen ignition in flat rotating disk phase of stellar formation, determining central conditions from total mass and adiabatic constant 12 p1542 A73-27575

Late stage nonrotating star evolution, discussing red giant models, planetary nebulae, degenerate carbon cores, supernova explosions and pulsars 12 p1543 A73-27748

Relativistic astrophysics. III - Gravitational collapse, singularities, and black holes 12 p1543 A73-27749

Interstellar molecules and radio spectroscopy in the cm- and mm-wave range 12 p1544 A73-27779

Chemical composition of stars in globular clusters and the morphological characteristics of their horizontal branches 12 p1546 A73-27852

Condensation of stars and magnetic field formation in protogalaxies 12 p1547 A73-27868

Nuclear reactions in carbon stars. 13 p1672 A73-28038

URCA process and the evolution of carbon stellar core. 13 p1673 A73-28173

Dynamical contraction of rotating gaseous spheroids. 13 p1680 A73-28774

Interstellar cloud collapse into protostellar objects and star formation, discussing young stellar objects observation 13 p1681 A73-28946

Papers on stellar evolution from main sequence to white dwarf stage covering pulsars, supernovae luminosity, neutron stars, nucleosynthesis, etc 13 p1681 A73-28976

Stellar structure and evolution models in conformity with observational luminosity, mass and size from H-R diagram 13 p1682 A73-28977

Stellar evolutionary stages of near-main sequence stars and clusters, discussing mass-luminosity and mass-radius relations 13 p1682 A73-28978

Massive main sequence stars structure and evolution within core hydrogen burning models, giving mathematical relation and conditions for convective instability 13 p1682 A73-28979

Stellar evolution as succession of quasi-equilibrium states, investigating dynamic stability via hydrodynamic and state equations 13 p1682 A73-28980

Novae physical processes during subdwarf-explosive variable-subdwarf evolution, describing spectroscopic indications for various luminous stages vs time 13 p1682 A73-28984

Stellar evolution lifetime shortening due to thermal instability of nuclear energy generation shell, discussing relaxation oscillations and S-process nucleosynthesis 13 p1683 A73-28990

Theory of the thermal explosion in the hydrogen shell of a white dwarf 13 p1683 A73-29091

Secular stability of an 8 solar mass star during central helium burning. 13 p1685 A73-29355

Pulsational instability of a star of 0.5 solar mass during core hydrogen burning. 13 p1685 A73-29362

The effect of interstellar medium parameters on the accretion by neutron stars. 13 p1687 A73-29658

Magnetic stars formation from interstellar matter in presence of interstellar magnetic field, considering critical mass based on Chandrasekhar-Fermi virial theorem 14 p1799 A73-30426

Contact binary star evolution, discussing adiabatic convection zone entropy, mass flow and relative frequency 15 p1928 A73-31054

Stellar nuclear hydrogen burning shell thermal stability to radial perturbations, discussing growth rate, energy generation and temperature increases 15 p1929 A73-31058

The adiabatic stability of stars containing magnetic fields. I. 15 p1933 A73-31395

Russian papers on young stellar complexes and astrometric covering physical nature and activity of nonstationary stars, stellar evolution, T-associations and earth atmosphere optical instability 15 p1934 A73-31418

IR objects in Orion Nebula, discussing temperature range and pre T Tauri evolutionary stage 15 p1934 A73-31419

O-B stars in young star clusters associated with nebulae 15 p1934 A73-31420

Flare star implications for stellar evolution, noting observational data relating to stars in associations and clusters 15 p1934 A73-31478

The effect of binary motion on period changes in RR Lyrae stars. 15 p1935 A73-31486

Eruptive binary stars evolutionary origin, outburst mechanisms and effects on Galactic evolution 15 p1935 A73-31487

Thermal instability of the helium-burning shell in massive stars. 15 p1936 A73-31557

Complex roots onset in secular stellar spectrum extended to case with shell sources present, determining eigenvalues for different intensity and position parameters 16 p2058 A73-32830

Central gravitational field of stars and evolution to red giants. 16 p2058 A73-32837

Hydrodynamic model calculations of Population I chemical composition massive objects, discussing evolution termination by violent thermonuclear explosions 16 p2059 A73-32840

Presentation of the models. 17 p2227 A73-34404

Some remarks on solar nebula type theories of the origin of the solar system. 17 p2227 A73-34406

Collapse calculations and their implications for the formation of the solar system. 17 p2227 A73-34411

Mass and angular momentum distribution in primitive solar nebula during rotation and contraction hydrodynamics of collapse 17 p2227 A73-34412

Disk formation by collapsing rotating gas cloud, considering free turbulence and intermittency effects on gravitational instability 17 p2227 A73-34413

Revision of initial size, mass and angular momentum of the solar nebula and the problem of its origin. 17 p2229 A73-34431

Mass transport rate in solar nebula model due to turbulence induced by convection 17 p2229 A73-34432

IR and molecular radio emissions from interstellar clouds representing formation stage of normal stars, discussing dust screening effects 17 p2229 A73-34433

Evolutionary considerations involving the internal density concentration parameter of binary stars. 17 p2237 A73-35786

Ejection of supernova envelopes by magnetic pumping. 18 p2354 A73-36726

Thermal instability caused primary interstellar dust cloud fragmentation and resulting star formation according to Peebles-Dicke hypothesis for cosmological origin of globular clusters 18 p2355 A73-36738

Viscous effects in rapidly rotating stars with application to white-dwarf models. I, II. 18 p2357 A73-37106

Structure of helium burning regions in stars - Dependence on molecular weight and burning rates. 19 p2483 A73-37560

Observations of galactic supernova remnants at 1.7 and 2.7 GHz. 19 p2483 A73-37566

Evolutionary track calculation for 1.8 solar mass close binary systems, noting luminosity transfer to secondary from primary 19 p2483 A73-37569

Stellar kinetic energy gain in spherical systems by transient external gravitational perturbations, computing dynamic models for compressive shocks 19 p2484 A73-37616

Low solar neutrino flux explained by evolution model emphasizing internal rotation effects on solar structure 19 p2488 A73-38519

Planetary nebula evolution model to explain FG Sagittae luminosity changes due to thermal pulse in He burning shell 19 p2489 A73-38530

Magnetic stars origin from gravitational collapse of ionized hydrogen clouds, discussing implications of interstellar magnetic fields and critical mass according to Chandrasekhar-Fermi virial theorem 20 p2605 A73-39058

Book - Introduction to the physics of stellar interiors. 20 p2607 A73-39144

Chemical composition of globular-cluster stars and the form of the horizontal branch. 20 p2608 A73-39226

Star contraction and magnetic-field generation in protogalaxies. 20 p2608 A73-39242

Stability of the sun against spherical thermal perturbations. 20 p2608 A73-39428

The peculiar A stars and the origin of the heaviest chemical elements. 20 p2611 A73-39623

Black hole formation conditions in terms of critical masses, spherical symmetry and asymmetrical star collapse 21 p2765 A73-40233

Numerical model for cold gaseous planets (Jupiter, Saturn, Uranus, Neptune) as remnants of star formation attempts, taking into account density fluctuations in collapse region 21 p2766 A73-40374

Possibility of radiative acceleration of the gas in stellar atmospheres 21 p2767 A73-40534

Evolution of supermassive stars with a strong magnetic field 21 p2767 A73-40711

Stellar masses on the asymptotic branch of red giants in globular clusters 21 p2768 A73-40719

Stellar explosive nucleosynthesis foundations in nuclear experiments and numerical schemes for solutions in limits of strong and weak coupling of abundances by nuclear reactions 21 p2771 A73-41238

Carbon star classification problems in effective temperatures, luminosities and radii, considering mass measurement, surface gravity, chemical composition, model atmospheres, stellar evolution, etc 21 p2772 A73-41240

Solar structure and evolution, calculating neutrino emission for Pleistocene glacial age caused by solar luminosity reduction 21 p2764 A73-41613

Gravitational radiation in the scalar-tensor gravitation theory. 22 p2885 A73-41718

Origin of cosmic rays, atomic nuclei, and pulsars in explosions of massive stars. 22 p2905 A73-41765

The role of rotation in close binary systems of high mass. 22 p2909 A73-42584

Neutrino losses effects on 4-8 solar mass stars leading to collapse of degenerate carbon-oxygen cores, discussing type II supernovae and pulsar formation 22 p2914 A73-43008

STELLAR FIELDS

Wolf-Rayet and high temperature stars; Proceedings of the Symposium, Buenos Aires, Argentina, August 9-14, 1971.

23 p3025 A73-43191

Wolf-Rayet stars luminosity to mass ratios, internal structure, mass loss to companion or interstellar space and spectral peculiarities related to evolutionary status

23 p3026 A73-43200

Wolf-Rayet binary stars detection and use in WR stellar mass, evolutionary status and luminosity estimation, noting atmospheric stratification relationship to temperature

23 p3026 A73-43202

Summary of problems and conclusions on the nature and physical structure of Wolf-Rayet stars.

23 p3026 A73-43204

Radial and vertical force balance in primitive solar nebula, describing techniques for gravitational potential and gas opacity computation for energy transport

24 p3127 A73-44392

STELLAR FIELDS

U STAR DISTRIBUTION

STELLAR GRAVITATION

Theory for the stability of a star with a toroidal magnetic field.

01 p0106 A73-11312

Schwarzschild coordinate system identification with frames of reference within exterior gravitational field of spherical nonrotating star

02 p0211 A73-11896

Stellar system gravitational field structure in terms of system-media attraction /regular force/ and force due to random distribution of stars /irregular force/

11 p1416 A73-25236

Duplicity and its consequences among variable stars in general.

15 p1935 A73-31484

Central gravitational field of stars and evolution to red giants.

16 p2058 A73-32837

Galactic shocks as consequence of large amplitude nonlinear density waves in interstellar gas perturbed via steady forcing by spiral gravitational fields

19 p2488 A73-38511

A numerical integration scheme for the N-body gravitational problem.

20 p2604 A73-38973

Intermediate-band photometry of RR Lyrae stars. II - Colors of RR Lyrae and ultrashort-period variables.

22 p2906 A73-41962

The stability of gravitating systems with a quadratic potential. II - The stability of models of spherically symmetric and axisymmetric clusters with elliptic orbits of particles

23 p3035 A73-44236

STELLAR INERTIAL NAVIGATION

U CELESTIAL NAVIGATION

U INERTIAL NAVIGATION

STELLAR LUMINOSITY

Spectral classification through seven-colour photometry.

01 p0095 A73-10295

Photoelectric light-curves of TW Cas.

01 p0098 A73-10555

White dwarfs gravitational red shifts, radial velocities and mass-radius relationships, considering colors and luminosities

01 p0104 A73-11036

The classification of intrinsic variable stars. II - The red variables of S and related types.

01 p0104 A73-11038

Mean absolute magnitudes and color indices of the red-giant concentrations in the color-magnitude diagrams of open clusters.

01 p0106 A73-11319

Radial density distribution and luminosity functions for stars in alpha Persei cluster

01 p0106 A73-11320

Stellar sources UV photography from sounding rocket, obtaining mean interstellar absorption, stars magnitudes and distribution and UVB spectrum

02 p0216 A73-12326

Mass-luminosity relation for eclipsing and visual binary stars, analyzing observational data by least squares method

02 p0218 A73-12409

RR Lyrae star mean absolute magnitude determination via maximum likelihood method after elimination of stars with high velocity or errors in proper motion

02 p0222 A73-12707

Self-accretion of matter, red subdwarf stars and early evolution of low-mass stars.

02 p0225 A73-12808

Polarization of light by circumstellar material.

02 p0226 A73-12828

Light variation and extinction of the variable WW Vulpeculae

02 p0226 A73-12836

Rapid changes in the new shell star HR 6000.

03 p0366 A73-12941

Microturbulence in atmospheres of F, G, K, type stars. I - Curve of growth analysis of G, K, type subgiants.

03 p0370 A73-13196

Surface gravities, Doppler broadening velocities, effective temperatures and metal abundances of K giants from narrow band photometry

03 p0371 A73-13224

Luminosity and mass functions for low main-sequence stars.

03 p0373 A73-13359

Importance of high time resolution in flare star observations.

03 p0373 A73-13373

Catalog of angular diameters, absolute magnitudes, spectroscopic parallaxes and linear diameters for 2301 stars, discussing accuracy and frequency distributions of log functions

03 p0375 A73-13948

Nonoriented astronomical satellite attitude determination from onboard measurements of geomagnetic field and stellar luminosity

03 p0379 A73-14560

On the Napier method for the photometric reflection effect in close binary stars.

03 p0379 A73-14583

Atmospheric microthermal turbulence vertical distribution from balloon flights compared with stellar scintillation data, predicting irradiance spectra from turbulence and wind velocity measurement

03 p0305 A73-14656

UBV photometry of the metal-rich globular cluster NGC 6171.

04 p0500 A73-15487

Contact binaries - Opacity and rotation.

04 p0500 A73-15488

The period and light curve of HZ Herculis.

04 p0501 A73-15683

Bright red giants in the globular clusters M3, M5, and M13.

04 p0503 A73-16006

Interaction of stars with local dust formations.

04 p0503 A73-16008

Stratification of the emission in the envelope of the eclipsing-binary Wolf-Rayet star V444 Cygni.

04 p0503 A73-16009

Solutions of the light curves of eclipsing binaries by the generalized method of least squares.

04 p0503 A73-16010

Luminosity function of the star cluster M 67

05 p0613 A73-16208

Some relations between the photometric characteristics of the brightness curves and color indexes of Cepheid variables in the system U,B,V, II

05 p0613 A73-16209

On the location of pulsational blue edges and estimates of the luminosity and helium content of RR Lyrae stars.

05 p0625 A73-17335

Skylab experiment for measuring color indices of extended sources and of spectral types O, B and A hot stars at various galactic latitudes

07 p0822 A73-18989

Luminosity classification of stars earlier than O9.

07 p0875 A73-19120

The luminosity function and density distribution of disk population stars.

07 p0876 A73-19358

Light variations of high luminosity O and B stars in the Large Magellanic Cloud.

07 p0877 A73-19597

Isotropic X ray and optical emissions from supernovae and pulsars, deriving pulsar synchrotron emission evolution formulas

07 p0900 A73-20304

Spectrophotometric observation of He-rich subdwarf peculiar O-type star CPD-31 1701, noting spectrum dominance by extremely stark-broadened He lines

08 p1003 A73-20894

He red giants models with degenerate C-O cores, He burning shell sources and He-rich envelopes, noting stellar luminosity

08 p1004 A73-20903

Equatorial coordinates and photographic magnitudes for new carbon stars in Northern Milky Way, noting classification by spectral discontinuity

08 p1005 A73-20916

Least squares method for eclipsing binary stars minimum epoch, noting application to artificial and observed light curves

08 p1006 A73-20928

The distribution of the mass-to-luminosity ratio of spiral and irregular galaxies.

08 p1006 A73-20930

Neutral hydrogen in Markarian galaxies.

08 p1006 A73-20933

Galactic structure at high galactic latitudes.

08 p1011 A73-21365

Activity in flare stars of the solar neighborhood.

08 p1013 A73-21773

Luminous blue variables in M 31 and 33, discussing light curves, color index and luminosity

09 p1141 A73-22014

Photoelectric observation of variable star V725 Sagittarii for significant magnitude and period changes since 1935

09 p1146 A73-22449

Periodic components in the flux-density variation of the radio source VRO 42.22.01 /BL Lacertae/.

09 p1147 A73-22728

Precision spectropolarimetry of starlight - Development of a wide-band version of the Dollfus polarization modulator.

09 p1084 A73-22866

The interpretation of continuum and line absorption and radiation by circumstellar dust.

09 p1150 A73-23132

Luminosity and frequency spectrum of radiation from spherically symmetric steady state accretion of interstellar gas onto nonrotating black hole at rest

10 p1272 A73-23534

20-micron fluxes of bright stellar standards.

10 p1282 A73-24639

Luminosity functions for K giant stars derived from the two-micron sky survey.

11 p1414 A73-25066

Near infra-red magnitudes of 248 early-type emission-line stars and related objects.

11 p1415 A73-25172

Two-color electrophotometry of RW in the Northern Crown

11 p1416 A73-25233

Photoelectric observations of the close binary system SZ Camelopardalis.

11 p1425 A73-26266

The light variation and orbital elements of VV Bootis.

11 p1429 A73-26680

Photometric characteristics of the star AC Herculis

12 p1537 A73-26851

Two-color electrophotometric observations of the BD Dra variable

12 p1537 A73-26852

Interstellar light absorption and distribution of stars about the star cluster NGC 6834

12 p1537 A73-26854

Interstellar light absorption and distribution of stars about the star cluster NGC 7654

12 p1537 A73-26855

Isotropic X ray and optical emissions from supernovae and pulsars, deriving pulsar synchrotron emission evolution formulas

12 p1539 A73-27276

Iris photometer electronic control system, presenting NGC 1778 cluster stars photoelectric UBV magnitudes

12 p1498 A73-27723

Radiation pressure effects on close binary mass loss and luminosity in terms of Roche potential, using contact surface model

12 p1537 A73-27881

On a correlation between the magnitude and the radial velocity of hot stars.

13 p1672 A73-28036

Photoelectric light curve of the Algol system TW Andromedae and the interpretation of its distortions by the effects of hot spots.

13 p1672 A73-28040

Galactic continuum loops and the diameter-surface brightness relation for supernova remnants.

13 p1672 A73-28041

Papers on stellar evolution from main sequence to white dwarf stage covering pulsars, supernovae luminosity, neutron stars, nucleosynthesis, etc

13 p1681 A73-28976

Cepheid variables model characteristics, determining luminosity, radial velocity and radius time dependent variations

13 p1682 A73-28981

Novae physical processes during subdwarf-explosive variable-subdwarf evolution, describing spectroscopic indications for various luminous stages vs time

13 p1682 A73-28984

Starry sky energetic simulator design, analyzing comparative brightness of stars

13 p1598 A73-29321

Absolute magnitude of stars of the RR Lyrae type

13 p1686 A73-29370

The effect of interstellar medium parameters on the accretion by neutron stars.

13 p1687 A73-29658

Black holes in binary systems, discussing radiation spectrum, disk formation, optical luminosity, X rays, UV regions and temperature distribution

15 p1928 A73-31051

A problem in distance-determination for Mira variables with an appendix on OB-star distances.

15 p1932 A73-31306

On the stability of the light-variations of RR Lyrae stars.

15 p1933 A73-31308

Solar nearby star velocity field variation model for Oort constants derivation with application to faint stars motion analysis and galactic center distance calculation

15 p1933 A73-31397

Photoelectric photometric investigation of brightness behavior of Orion nebula variable stars

15 p1934 A73-31422

Spectral investigations of UV Ceti-type flare stars and search for new variables of this type carried out at Crimea. 15 p1934 A73-31479

Techniques and results of observations of rapid and ultrarapid variable stars. 15 p1935 A73-31481

High-frequency stellar oscillations - The Cerro Tololo search for luminosity-variable white dwarfs. 15 p1935 A73-31482

Period determination method for variable stars using interpolation in light curves, noting applicability to light curves with few branches 15 p1936 A73-31645

Solar neutrino flux deficiency explanation based on solar core nuclear reactions theory with consequences for luminosity and earth climate 15 p1937 A73-31849

Selection of stars for observations from the lunar surface by the method of equal altitudes 15 p1938 A73-31963

Sco X-1 noncorrelation of radio with optical or X ray intensities, noting paucity of simultaneous observations of other X ray sources 16 p2050 A73-32732

Compact X ray source models from statistical analysis of Uhuru catalog sources with respect to luminosities, lifetimes and stellar populations 16 p2050 A73-32737

Nature of the light variation of the peculiar A-star HD 221568. 16 p2058 A73-32836

Photometric investigation of star magnitude and color index data in Palomar Atlas and Washington Star Catalog, obtaining calibration curves and average error calculations 16 p2063 A73-33659

Structure of the nucleus of the open cluster NGC 1245 16 p2063 A73-33660

Optical appearance of binary X-ray sources. 17 p2232 A73-35146

The spectrum of eta canis majoris, B5 Ia. 18 p2355 A73-36779

Cygnids and Taurids - Two classes of infrared objects. 18 p2357 A73-37111

Comparison of vertical profile turbulence structure with stellar observations. 19 p2446 A73-37259

Evolutionary track calculation for 1.8 solar mass close binary systems, noting luminosity transfer to secondary from primary 19 p2483 A73-37569

Planetary nebula evolution model to explain FG Sagittae luminosity changes due to thermal pulse in He burning shell 19 p2489 A73-38530

Polarization of stellar light between the two Magellanic clouds 20 p2606 A73-39063

The eclipsing contact binary VW Cephei. 20 p2610 A73-39577

Carbon star classification problems in effective temperatures, luminosities and radii, considering mass measurement, surface gravity, chemical composition, model atmospheres, stellar evolution, etc. 21 p2772 A73-41240

Stellar chromospheric velocity fields and the width luminosity relations. 21 p2779 A73-41540

Solar structure and evolution, calculating neutrino emission for Pleistocene glacial age caused by solar luminosity reduction 21 p2764 A73-41613

Intermediate-band photometry of RR Lyrae stars. II - Colors of RR Lyrae and ultrashort-period variables. 22 p2906 A73-41962

Energy distribution in stellar spectra of various spectral types and luminosities 22 p2906 A73-41974

Luminosity and velocity distribution of high-luminosity stars near the sun. II - The young disk giants. 22 p2909 A73-42585

Static stellar envelopes at radiative equilibrium for power law dependence of opacity on temperature and density 22 p2911 A73-42935

The common convective envelope model for W Ursae Majoris systems and the analysis of their light curves. 22 p2912 A73-42939

Frequency distribution functions of pulsars, supernovae and sunspot groups relationship to age and lifetime, considering stellar mass and initial luminosity 22 p2915 A73-43033

Classification and distribution of WR stars and an interpretation of the WN sequence. 23 p3025 A73-43193

P Cygtype O and B supergiant stars relationship to Wolf-Rayet stars in terms of spectra, absolute magnitudes, mass and variability 23 p3026 A73-43198

Wolf-Rayet stars luminosity to mass ratios, internal structure, mass loss to companion or interstellar space and spectral peculiarities related to evolutionary status 23 p3026 A73-43200

Wolf-Rayet binary stars detection and use in WR stellar mass, evolutionary status and luminosity estimation, noting atmospheric stratification relationship to temperature 23 p3026 A73-43202

Telescopic observation of Pleiades I flare stars, determining stellar magnitudes and flare brightness 23 p3037 A73-44352

Selection of stars for observation from the lunar surface by the method of equal altitudes. 24 p3132 A73-44488

The C-classification of the spectra of carbon stars. 24 p3138 A73-44997

Interstellar reddening calculation with respect to U-B/V-B diagram for hot and main sequence stars as function of luminosity based on model stellar atmospheres 24 p3138 A73-45012

Calibration of luminosity criteria for G and K giants by means of trigonometric parallaxes. 24 p3140 A73-45181

STELLAR MAGNETIC FIELDS

NT SOLAR MAGNETIC FIELD

Trapping of condensed plasma loops and arcs in cosmic atmospheres. 01 p0103 A73-11020

Theory for the stability of a star with a toroidal magnetic field. 01 p0106 A73-11312

Self consistent model of closed field lines of pulsar magnetosphere valid for oblique rotators and unipolar inductors 02 p0216 A73-12382

Average magnetic field strength relationships with angular velocity and stellar activity cycle period, using Leighton solar cycle model with differential rotation and cyclonic turbulence 02 p0224 A73-12741

Thermal conductivity and hot magnetic poles of pulsars. 03 p0374 A73-13796

Influence of a random magnetic field on the properties of stellar absorption lines. 04 p0503 A73-16011

The generation of the highest cosmic ray energies. 07 p0872 A73-20193

The hydromagnetic oscillations and stability of self-gravitating masses. III - Magnetic polytropes. 08 p1005 A73-20917

Magnetic field in the plasmasphere of a compact star. 08 p1007 A73-21001

Plasma effects and the acceleration of charged particles in pulsar fields. 09 p1141 A73-22016

Ultrarelativistic plasma momentum loss perpendicular to pulsar magnetic field, considering synchrotron compression of electrons leading to emission mechanisms 09 p1144 A73-22172

Stability of a rotating inhomogeneous star 09 p1145 A73-22293

Ultrarelativistic pulsar plasmas with one dimensional distribution functions in strong magnetic fields, considering dispersion ratios of plasma waves along magnetic lines 09 p1145 A73-22294

Star magnetic field origin in dynamo action associated with nuclear energy generation in stellar evolution, discussing effects on flares, chromosphere and coronal activities 10 p1271 A73-23489

Synchrotron emission amplification by magnetic field in cosmic sources from analysis of relativistic electron system, noting pulsars and UV Ceti stars 10 p1264 A73-23708

Formation of stars in a rotating cloud with magnetic field. 10 p1275 A73-23830

Turbulent plasma dynamo mechanisms of magnetic field origin in astrophysics, noting Steenbeck and Parker theories 10 p1285 A73-24942

Pair annihilation into neutrinos in strong magnetic fields. 11 p1402 A73-26414

Equations derived for magnetic field line configuration and plasma flow about rotating object having axisymmetric field with emphasis on pulsar magnetosphere 11 p1427 A73-26614

Pulsar magnetospheres, braking index, polar caps, and period-pulse-width distribution. 11 p1428 A73-26618

Stellar magnetism origin via fossil, battery and dynamo theories, discussing two fluid plasma model and turbulence 13 p1683 A73-28992

Cosmic ray properties and origin, discussing pulsars and superstrong magnetic fields existence effects 14 p1787 A73-30233

Magnetic stars formation from interstellar matter in presence of interstellar magnetic field, considering critical mass based on Chandrasekhar-Fermi virial theorem 14 p1799 A73-30426

Thermal convective instability in uniformly rotating magnetized isothermal stellar atmosphere with constant Alfvén speed, discussing heat loss mechanism dependence on temperature 15 p1929 A73-31060

The adiabatic stability of stars containing magnetic fields. I. 15 p1933 A73-31395

Model for X-ray sources based on magnetic field twisting. 15 p1927 A73-32047

Crab Nebula pulsar electromagnetic radiation emission model based on high energy electron circular motion around magnetic field lines 15 p1942 A73-32649

Magnetic moment generation in pulsars based on baryon model with superconducting proton fluid and normal electron field 17 p2226 A73-34365

Synchrotron radiation stimulated amplification by magnetic field in cosmic sources from analysis of relativistic electron system, noting pulsars and UV Ceti stars 18 p2347 A73-36733

Zeeman effect in the X-ray star candidates HD 77581 and theta super 2 Orionis. 19 p2482 A73-37399

Pulsar model magnetosphere for uniformly rotating infinitely conducting magnetized neutron star with aligned magnetic field 19 p2488 A73-38515

Magnetic fields of the sun and stars 20 p2609 A73-39569

Spectrographic observations of the peculiar Be star with infrared excess HD 45677. 20 p2611 A73-39586

Quantized magnetic bremsstrahlung from white dwarfs surface layer as possible source of Galactic center infrared radiation 20 p2611 A73-39709

Evolution of supermassive stars with a strong magnetic field 21 p2767 A73-40711

Radio binaries observation, noting black hole, large magnetic field or thermal bremsstrahlung as possible origin of strong X-ray radiation 21 p2770 A73-40940

Equilibrium structure of polytropes with toroidal magnetic fields. 22 p2912 A73-42941

Radiation transfer equations for atomic spectra lines in stellar magnetic field, allowing for nonequilibrium population of atomic ground state and excited atom-particle collisions 23 p3036 A73-44242

STELLAR MASS

NT STELLAR GRAVITATION

Velocity variation of a star as a purely discontinuous random process. III Stars with different masses in an open cluster 01 p0100 A73-10711

White dwarfs gravitational red shifts, radial velocities and mass-radius relationships, considering colors and luminosities 01 p0104 A73-11036

Evolutionary sequences for massive stars with various initial chemical compositions, studying semiconvection effects on core helium burning star distribution in H-R diagram 01 p0104 A73-11037

The mass and angular momentum losses from spinars. 02 p0217 A73-12384

Mass-luminosity relation for eclipsing and visual binary stars, analyzing observational data by least squares method 02 p0218 A73-12409

Solar neighborhood dynamically determined mass discrepancy with observed stars and interstellar matter, proposing low mass invisible stars existence 02 p0218 A73-12413

Hydrodynamic model calculations for supermassive stars. II - The collapse and explosion of a nonrotating 520,000 solar-mass star. 02 p0222 A73-12713

Thermal instability of the hydrogen-burning shell in nondegenerate stars. 03 p0366 A73-12937

Mass flow and period changes of contact binaries. 03 p0370 A73-13212

Luminosity and mass functions for low main-sequence stars. 03 p0373 A73-13359

Stability criteria for equal mass triple star systems, considering direct or retrograde revolution and outer periastron distance to inner semimajor axis ratio 03 p0376 A73-14271

Orbital period variations of eclipsing binary TW Draconis caused by third body effect, apsidal motion and matter exchange 03 p0379 A73-14582

On the maximum value of the mass of a star.
04 p0500 A73-15525

Subnuclear density state equation for minimum mass and binding energy of neutron star converting into white dwarf
04 p0502 A73-15978

A numerical experiment in the accretion problem.
04 p0503 A73-16004

Comments on a PLC relationship for Cepheids and on the comparison between pulsation and evolution masses for Cepheids.
05 p0625 A73-17334

Determination of properties of old stars in general relativity by a variational method.
07 p0874 A73-19065

Evolution of single stars. VII - Evolution of massive stars.
08 p1002 A73-20848

Spectroscopic observations of the optical candidate for Cygnus X-1.
08 p1004 A73-20896

Stellar evolution at high mass based on the Ledoux criterion for convection.
08 p1008 A73-21159

Mass differentiation of X ray sources based on Roche model, identifying pulsating sources with neutron stars and black holes as nonpulsating sources
08 p1013 A73-21810

A star-cluster model with axial symmetry and star composition of uniform mass
10 p1274 A73-23715

Probabilistic fragmentation model for collapsing interstellar cloud, predicting stellar mass spectrum
11 p1415 A73-25171

Radiation pressure effects on close binary mass loss and luminosity in terms of Roche potential, using contact surface model
12 p1537 A73-27881

URCA process and the evolution of carbon stellar core.
13 p1673 A73-28173

Massive main sequence stars structure and evolution within core hydrogen burning models, giving mathematical relation and conditions for convective instability
13 p1682 A73-28979

White dwarfs model based on zero temperature Fermi gas theory, determining mass-radius relation and limit mass
13 p1682 A73-28982

Secular stability of an 8 solar mass star during central helium burning.
13 p1685 A73-29355

Differentially rotating neutron star models calculation for given state equation, examining mass increase relationship to rotational rigidity relaxation via Ostriker-Tassoul instability criterion
15 p1929 A73-31093

Variable star observations from outside the earth's atmosphere - Review and prospects.
15 p1935 A73-31488

Thermal instability of the helium-burning shell in massive stars.
15 p1936 A73-31557

Perturbation technique investigation of nonlinear pulsations of vibrationally unstable main sequence stars between 70-170 solar masses
17 p2225 A73-34288

Revision of initial size, mass and angular momentum of the solar nebula and the problem of its origin.
17 p2229 A73-34431

Model for axisymmetric clusters of stars with uniform mass.
18 p2355 A73-36740

Evolutionary track calculation for 1.8 solar mass close binary systems, noting luminosity transfer to secondary from primary
19 p2483 A73-37569

Mass-luminosity relations for unevolved stars in high mass eclipsing binaries and low mass visual binary systems for hydrogen and metal abundances of Population I stars
20 p2609 A73-39439

Black hole formation conditions in terms of critical masses, spherical symmetry and asymmetrical star collapse
21 p2765 A73-40233

Evolution of supermassive stars with a strong magnetic field
21 p2767 A73-40711

Stellar masses on the asymptotic branch of red giants in globular clusters
21 p2768 A73-40719

Relaxation time in disk galaxy simulations.
22 p2904 A73-41754

The stability of rotating supermassive stars.
22 p2907 A73-42304

Frequency distribution functions of pulsars, supernovae and sunspot groups relationship to age and lifetime, considering stellar mass and initial luminosity
22 p2915 A73-43033

P Cyg type O and B supergiant stars relationship to Wolf-Rayet stars in terms of spectra, absolute magnitudes, mass and variability
23 p3026 A73-43198

Wolf-Rayet binary stars detection and use in WR stellar mass, evolutionary status and luminosity estimation, noting atmospheric stratification relationship to temperature
23 p3026 A73-43202

STELLAR MASS EJECTION

Cool giant star-ejected high velocity dust grains interaction with interstellar clouds, discussing solid state defect accumulation, sputtering and grain and cloud heating
01 p0098 A73-10582

Trapping of condensed plasma loops and arcs in cosmic atmospheres.
01 p0103 A73-11020

Stellar gas injection into nucleus of radio galaxy NGC 4486, estimating energy release during gas accretion
01 p0106 A73-11301

Massive stars evolution in hydrogen and helium burning phases, taking into account mass loss from light pressure in optically thick media
02 p0224 A73-12801

On the stationary mass outflow from stars. I - The computational method and the results for a 1 solar mass star.
03 p0370 A73-13195

The location and size of the hot spot in cataclysmic variable stars.
04 p0499 A73-15486

Stellar evolution, explosion and mass ejection, considering Crab Nebula filaments and supernovae Cygnus and Vela X remnants
05 p0618 A73-16825

Stellar winds and mass loss of a rotating star.
05 p0624 A73-17312

Solar outer atmospheric eruption from photographic recording by OSO 7 spacecraft borne coronagraph, noting ejected gas and plasma clouds caused by flare
06 p0753 A73-18374

Evidence for ejection of radio sources from supernova remnants.
07 p0873 A73-19056

2.8 cm radio emission from alpha Orionis, HBV 475 and MWC 349.
07 p0899 A73-20120

Hydrodynamic calculations for novae origin and mass ejection from luminous red giants, considering planetary nebulae and plausible models
07 p0903 A73-20628

Elongated shells around novae and concentration near orbital planes resulting from perpetual matter losses, considering close dwarf binaries and recurrent novae
09 p1145 A73-22288

Supernova explosions in close binary systems
09 p1145 A73-22289

Ejection of supernova shells by magnetic pumping
10 p1273 A73-23701

Chemical composition of stars in globular clusters and the morphological characteristics of their horizontal branches
12 p1546 A73-27852

A nongravitational effect in the simulation of cometary phenomena.
14 p1793 A73-29824

Stellar maser output observations application to analysis of mass loss rate or physical conditions in circumstellar shell
15 p1934 A73-31477

Ejection of supernova envelopes by magnetic pumping.
18 p2354 A73-36726

Chemical composition of globular-cluster stars and the form of the horizontal branch.
20 p2608 A73-39226

Possibility of radiative acceleration of the gas in stellar atmospheres
21 p2767 A73-40534

Static stellar envelopes at radiative equilibrium for power law dependence of opacity on temperature and density
22 p2911 A73-42935

Wolf-Rayet stars luminosity to mass ratios, internal structure, mass loss to companion or interstellar space and spectral peculiarities related to evolutionary status
23 p3026 A73-43200

High rotational velocity correlation with metal abundance interpreted by coronal mass loss rate in metal-poor stars
24 p3140 A73-45184

Single component wind model for stellar rotation dependent mass loss from hot corona with application to T Tauri star observations
24 p3140 A73-45186

STELLAR MOTIONS

NT STELLAR ROTATION

Stellar positions and proper motions representation of fundamental reference system, improving and extending to faint objects and radio sources
01 p0094 A73-10056

Photoelectric determination of radial velocities.
01 p0047 A73-10517

The accuracy of measurements of star transits
01 p0098 A73-10553

Stellar proper motion effects on precession and galactic rotation constants determination, considering star velocity fields in solar neighborhood
01 p0098 A73-10583

Characteristic phase mixing time for spherical systems with different stellar mean velocity at each individual integral phase space surface
01 p0100 A73-10716

Velocity variation of a star as a purely discontinuous random process. III Stars with different masses in an open cluster
01 p0100 A73-10711

An approximate form of the third integral in the Galaxy.
01 p0103 A73-11017

A solution to the problem of the third integral of motion. I.
01 p0106 A73-11318

The dynamical evolution of triple star systems - A numerical study.
02 p0221 A73-12702

The dynamical evolution of a stellar cluster with initial subclustering.
02 p0222 A73-12709

Separate star groups in Sco OB 1 association coinciding with previously established gaseous subgroups
02 p0222 A73-12711

A numerical hydrodynamic study of coalescence in head-on collisions of identical stars.
02 p0223 A73-12727

Measurement of radial velocities with coude spectrograph of the 152-cm telescope of the Haute Provence Observatory
03 p0371 A73-13223

Orbital period variations of eclipsing binary TW Draconis caused by third body effect, apsidal motion and matter exchange
03 p0379 A73-14582

Determination of the coefficient of displacement of the line connecting the apsides in stellar models and comparison of it with observations
03 p0379 A73-14584

Epicyclic motion of stars at different regions of the galaxy.
03 p0379 A73-14586

Nonlinear stability analysis of nonhomogeneous self-gravitating unstable equilibrium stellar systems, using numerical techniques and water bag configurations
05 p0624 A73-17317

Velocity dispersions in galaxies. II - The ellipticals NGC 1889, 3115, 4473, and 4494.
07 p0873 A73-19054

Steady state slow stellar velocity solution for accretion stream beyond neutral point, estimating cutoff range for braking force of gas cloud
07 p0898 A73-19936

On the third integral of motion in stellar dynamics. I.
08 p1002 A73-20849

Numerical experiments on probability distribution of random force in stellar gravitational systems, noting agreement with Chandrasekhar and von Neumann theory
08 p1003 A73-20884

Galactic differential rotation derived from the radial velocities of some population I objects.
08 p1005 A73-20912

Three body problem of stellar system subjected to isoenergetic variations, evaluating escape and ejection parameters
08 p1005 A73-20920

Nonaxisymmetric kinematics in galaxies with axisymmetric mass distributions.
08 p1008 A73-21154

Astrometry with Schmidt telescopes, discussing automated computerized plate scanner and measuring machine for star position and relative motion determination
08 p0966 A73-21356

Close binary systems orbital elements perturbations due to stellar material viscosity effects on dynamical tide lag
10 p1271 A73-23478

An exact solution for a collisionless flat galactic model.
10 p1275 A73-23826

Relative proper motions of faint stars in the Pleiades.
10 p1279 A73-24166

Additional observations of supergiants and foreground stars in the direction of the Large Magellanic Cloud.
10 p1279 A73-24167

Dense stellar systems dynamics, considering gravitation relaxation, star evaporation, antiequijartition, growth of dense galactic cores, stellar coalescence, disruption and formation
11 p1414 A73-25065

Kinetic equations for gravitating point rotating system model of stellar systems evolution phases, taking into account dissipation-produced motions
11 p1416 A73-25235

Investigation of star orbits in stellar clusters with allowance for the disturbing force of the galaxy
12 p1538 A73-26863

- Numerical experiments on the stability of spherical stellar systems. 13 p1685 A73-29359
- Astronomical model for Oort comet cloud destruction rate during stellar passage, noting cumulative dispersion mechanism and half life estimates 14 p1793 A73-29826
- The particle resonance in spiral galaxies - Nonlinear effects. 14 p1801 A73-30727
- Stellar resonant motion in axisymmetric galactic potential, deriving invariant energy mappings from Hamiltonian system of differential equations 14 p1770 A73-30772
- On the kinematical and spatial coincidence of optical and radio spiral arms in our galaxy. 15 p1929 A73-31055
- Solar nearby star velocity field variation model for Oort constants derivation with application to faint stars motion analysis and galactic center distance calculation 15 p1933 A73-31397
- Motion of fourteen stars in the Orion nebula cluster. 15 p1936 A73-31555
- Determination of the absolute intrinsic motions of stars with respect to galaxies in area 32 of a special Kapteyn map 15 p1938 A73-31961
- Secular parallaxes of stars and the speed of the sun according to absolute intrinsic motions of 14,600 stars with respect to galaxies 15 p1938 A73-31962
- Circumzenithal instrument for latitude and longitude determination and star transits observation, through almucentar 16 p2017 A73-34048
- Fundamental data for contact binaries - RZ Comae Berenices, RZ Tauri, and AW Ursae Majoris. 17 p2231 A73-34759
- Overall existence of a solution of the Cauchy problem for the system of equations with Liouville-Newton partial derivatives 17 p2201 A73-35045
- A technique for measuring small displacements in digital spectra. 17 p2170 A73-35297
- Stardrift - A navigational system for relativistic interstellar flight. 17 p2210 A73-35659
- On the possibility of determining stellar radial velocities to 0.01 km per sec. 22 p2907 A73-42207
- Properties of galactic orbits and motion integrals of high-velocity stars. II - Periodic and nonperiodic orbits in the 2nd Schmidt potential 22 p2907 A73-42303
- An attempt to interpret the mean properties of the velocity field of young stars in terms of Lin's theory of spiral waves. 22 p2908 A73-42310
- Luminosity and velocity distribution of high-luminosity stars near the sun. II - The young disk giants. 22 p2909 A73-42585
- Globular cluster mass determination from analysis of field stars proper motions 23 p3035 A73-44237
- Galactic rotation of the centroids of various objects 23 p3035 A73-44239
- Stellar vortex formation in solar apex region in terms of retrograde motion and solar orbit characteristics 23 p3036 A73-44240
- Study of the kinematics of O and B spectral type stars 23 p3036 A73-44241
- Statistical correlation between pulsar and supernova remnant distribution along galactic longitudes, noting difference due to relative motions 23 p3037 A73-44359
- Determination of absolute stellar proper motions relative to galaxies in selected area 32 of the special Kapteyn plan. 24 p3132 A73-44486
- Secular parallaxes and space velocity of the sun from absolute proper motions of 14,600 stars relative to galaxies. 24 p3132 A73-44487
- Barnard star proper motion and planetary system orbital analysis, indicating massive planet companions in inclined orbits 24 p3133 A73-44556
- ## STELLAR OCCULTATION
- Lunar occultation of stars to determine moon diameter and orbital elements, noting time measurement difficulties due to scintillation effects 01 p0102 A73-10994
- The role of occultations in the improvement of the lunar ephemeris. 03 p0369 A73-13107
- Jupiter atmosphere density fluctuations as cause of time symmetric light flash occurrence during Beta Scorpii occultation 04 p0496 A73-14926
- The angular diameter of X Cancri. 04 p0500 A73-15518
- Jovian atmosphere upper layers high temperature evidenced during star Beta Scorpio occultation by Jupiter 06 p0745 A73-17475
- Occultation of the Pleiades by the moon on March 19, 1972 06 p0753 A73-18375
- The beta Scorpii occultation by Jupiter. I - The Jovian diameter. 08 p1006 A73-20934
- Gravitational constant constancy from 1663-1972 earth rotation and 1943-1972 stellar occultations by moon, discussing various time scales used 09 p1079 A73-22948
- The 1969 solar occultation of the Crab Nebula pulsar. 11 p1417 A73-25583
- Stellar occultation measurements of molecular oxygen in the lower thermosphere. 11 p1356 A73-25911
- Evidence for the binary nature of 2U 1700-37. 11 p1428 A73-26628
- The angular diameter of upsilon Capricorni and an occultation of SAO 118655. 12 p1540 A73-27427
- On the results of observations of occultations of stars by the moon according to the double image principle 13 p1686 A73-29559
- The occultation of the star SAO 93826 by Saturn's ring 20 p2606 A73-39076
- Occultation of beta Scorpio by Jupiter on May 13, 1971. 21 p2779 A73-41544
- An atmosphere on Ganymede from its occultation of SAO 186800 on 7 June 1972. 23 p3027 A73-43337
- Photographic observations of the occultation of Beta Scorpii by Jupiter. 23 p3033 A73-43944
- Analysis of spikes in occultation curves - A critique of Brinkmann's method. 24 p3129 A73-44444
- ## STELLAR RADIATION
- ### NT STELLAR WINDS
- Electronographic image tubes for stellar field photometry. 01 p0049 A73-10539
- Possibility of accelerating the matter of hot stars by absorption in spectral lines 01 p0100 A73-10706
- Diffusion of radiation in a stellar shell expanding at a constant rate 01 p0100 A73-10707
- UV Cet-type variable star quiet state and flare spectra, discussing flare mechanism relation to magnetic effects and star evolutionary position 01 p0102 A73-10970
- Unsteady accretion of optically thick gas cloud on neutron star as hydrodynamic phenomenon due to supernova explosions or collision with ordinary star 01 p0106 A73-11303
- Short-term pulsar intensity variation in the frequency range 70-115 MHz. I - Correlation measurements. 01 p0106 A73-11306
- Nuclear energy sources in superdense celestial bodies. 01 p0106 A73-11311
- Infrared excesses in supergiant stars - Evidence for silicates. 02 p0225 A73-12827
- Circumstellar infrared emission. 02 p0226 A73-12829
- A polarimetric method of measuring radial velocities. 02 p0171 A73-12830
- Interstellar OH lambda doublet radiation observations at 5 cm from six galactic sources and IR star, observing various transitions 03 p0366 A73-12930
- Ultraviolet and X-ray spectroscopy of astrophysical and laboratory plasmas; Proceedings of the Third Symposium, Utrecht, Netherlands, August 24-26, 1971. 03 p0363 A73-13951
- On the circular polarization of Sco X-1 and the adjacent sky. 04 p0501 A73-15634
- Infrared measurements of R. Coronae Borealis through its 1972 March-June minimum. 05 p0627 A73-17391
- Star sensor of spin stabilized Uhuru satellite for detection and location of stellar X ray sources with accuracies of one arc-minute 06 p0695 A73-18323
- VV 281-427, variable stars in a Cepheus-Lacerta field of the Milky Way. 07 p0874 A73-19117
- Preliminary observations of variable polarization in epsilon Aurigae. 07 p0875 A73-19118
- Time dependent hydrodynamics of meridional circulation in rotating star radiative zone, confirming Eddington-Sweet velocity formulation 07 p0877 A73-19599
- Uhuru satellite observations of X ray sources, discussing binary sources and identification in visible stars 07 p0872 A73-20525
- Cyclic variations of the Be star beta-one Monocerotis. 08 p1006 A73-20924
- Infrared circular polarization of NML Cygni and VY Canis Majoris. 08 p1009 A73-21172
- Stability of a rotating inhomogeneous star 09 p1145 A73-22293
- Observation of mesospheric ozone at low latitudes. 09 p1079 A73-22841
- A finding list of faint UV-bright stars in the galactic plane. 11 p1414 A73-25067
- Luminescence of isolated dark clouds caused by the integral field of stellar galactic radiation 11 p1416 A73-25234
- IR sources at 1-5 microns, discussing Betelgeuse, R Doradus, dying stars, new stars and galaxies 11 p1422 A73-25974
- Experimental determination of two-dimensional spatiotemporal power spectra of stellar light scintillation - Evidence for a multilayer structure of the air turbulence in the upper troposphere. 12 p1521 A73-27120
- B system calculation of night airglow stellar component from cataloged photometric scales, obtaining night sky brightness 12 p1546 A73-27857
- The heating of interstellar clouds by vibrationally excited molecular hydrogen. 13 p1673 A73-28279
- Scintillation and vibration of stars and structure of a turbulent atmosphere. 13 p1680 A73-28514
- Distribution law of light-ray direction fluctuations in telescopes 13 p1618 A73-29098
- High-speed UVB photometry of Scorpius X-1 flares. 14 p1801 A73-30646
- Positron-annihilation radiation from neutron stars. 14 p1788 A73-30738
- New directions and new frontiers in variable star research; Colloquium on Variable Stars, 5th, Bamberg, West Germany, August 31-September 3, 1971, Proceedings. 15 p1934 A73-31476
- Stellar maser output observations application to analysis of mass loss rate or physical conditions in circumstellar shell 15 p1934 A73-31477
- Duplicity and its consequences among variable stars in general. 15 p1935 A73-31484
- Model for X-ray sources based on magnetic field twisting. 15 p1927 A73-32047
- X-ray and radio emission from stellar coronae. 16 p2052 A73-32827
- The ultraviolet flux envelopes of main-sequence B stars. 17 p2234 A73-35613
- On the ionization of the intercloud medium by ultraviolet stars. 19 p2484 A73-37611
- The optical polarization of the Crab Nebula pulsar. I - A relativistic vector model. 19 p2488 A73-38517
- Ground based photometry of planets, stars and galactic nebulae at 34 microns 19 p2489 A73-38529
- Analysis of the control circuit of a seeing measurement device 20 p2565 A73-39069
- A catalog of data on optically visible H II regions. 20 p2607 A73-39084
- B system calculation of night airglow stellar component from cataloged photometric scales, obtaining night sky brightness 20 p2608 A73-39231
- X ray source Hercules X-1 observation from Uhuru satellite, relating regular dips in intensity to orbital phase 20 p2602 A73-39440
- Possibility of radiative acceleration of the gas in stellar atmospheres 21 p2767 A73-40534
- A system for the photographic recording of pulsar pulses 21 p2700 A73-40552
- Nova and supernova stars as sources of relativistic particles 21 p2756 A73-40580
- Stellar chromospheric velocity fields and the width luminosity relations. 21 p2779 A73-41540

German monograph - Polarization measurements in galactic latitudes b less than -45° .
22 p2910 A73-42698
Interaction of the X-ray source radiation with the atmosphere of the normal star in close binary systems.
23 p0300 A73-43750
Stellar radiation Thomson scattering by free electrons compared to atomic processes as mechanism for H II regions continuous emission
23 p0300 A73-43756
A search for narrow band 21-cm wavelength signals from ten nearby stars.
24 p1133 A73-44552
Are the recently observed soft gamma-ray bursts from stellar superflares.
24 p1124 A73-44989
Gravitational radiation emission by star tidally deformed by black hole, computing energy loss rate
24 p1138 A73-45037
A double image chopping polarimeter.
24 p0911 A73-45185
Nature of the peculiar emission object V1016 Cygni.
24 p1143 A73-45490
Heterodyne detection of Arcturus at 10.6 microns.
24 p1143 A73-45493

STELLAR REFRACTION

U ATMOSPHERIC REFRACTION

U STELLAR RADIATION

STELLAR ROTATION

NT SOLAR ROTATION

Stellar structure and angular momentum evolution of rotating stars, describing interaction in terms of redistribution processes of momentum
01 p0094 A73-10054
Pulsar structure theory with respect to rotating neutron star hypothesis, discussing evolutionary elements
01 p0095 A73-10065
The effect of the Coriolis force on the stability of rotating magnetic stars.
01 p0103 A73-11034
Theory for the stability of a star with a toroidal magnetic field.
01 p0106 A73-11312
The mass and angular momentum losses from spinars.
02 p0217 A73-12384
The nature of radio emission from pulsars.
02 p0218 A73-12407
Uniformly rotating stars with hydrogen- and metallic-line blanketed model atmospheres.
02 p0222 A73-12712
Average magnetic field strength relationships with angular velocity and stellar activity cycle period, using Leighton solar cycle model with differential rotation and cyclonic turbulence
02 p0224 A73-12741
Statistical studies in stellar rotation. II - A method of analyzing rotational coupling in double stars and an introduction to its applications.
03 p0366 A73-12938
Astronomical model for variable RR Lyrae stars pulsation, noting rotation effect on oscillation period
03 p0379 A73-14585
Contact binaries - Opacity and rotation.
04 p0500 A73-15488
Differential rotation of polytropic stellar models from structural equations, disproving Porfiriev theory
04 p0504 A73-16025
Stellar winds and mass loss of a rotating star.
05 p0624 A73-17312
Mass formula for Kerr black holes.
06 p0747 A73-17521
Spinning test bodies motion in metric fields, applying to spinning stars in orbit around black holes
06 p0749 A73-17869
Pulsars as rotating magnetic neutron stars created during catastrophic collapses of old stars, discussing radiation mechanism
06 p0750 A73-18012
Time dependent hydrodynamics of meridional circulation in rotating star radiative zone, confirming Eddington-Sweet velocity formulation
07 p0877 A73-19599
Photometric investigations of magnetic stars.
08 p1006 A73-20925
Heating of astrophysical plasma due to rotation.
08 p1007 A73-20957
Magnetic field in the plasmasphere of a compact star.
08 p1007 A73-21001
Stellar survey at 2000-4100 A via balloon-borne observations, discussing intensity distributions and earth atmospheric ozone layer density
09 p1140 A73-22006
Electromagnetic field configuration about aligned rotating magnetic star from relativistic model of rotating magnetosphere
09 p1142 A73-22034
Radial pulsations of a white dwarf in the case of nonuniform rotation
09 p1145 A73-22290
Analytical expressions for the parameters of rotating stars
09 p1145 A73-22292

Stability of a rotating inhomogeneous star
09 p1145 A73-22293
Rotating neutron star gas cocoon heating by LF radiation absorption, noting X ray emission
10 p1263 A73-23481
Partial differential post-Newtonian equations numerically solved for stellar models with polytropic pressure-density relation for uniform rotation
10 p1271 A73-23490
Formation of stars in a rotating cloud with magnetic field.
10 p1275 A73-23830
Influence of interaction on the stability and pulsations of rotating neutron stars
10 p1283 A73-24704
Wave amplification during the reflection from a rotating 'black hole'
10 p1283 A73-24752
The elastic energy and character of quakes in solid stars and planets.
11 p1420 A73-25894
Criticism of Galactic cosmic ray production model with rotating magnetic white dwarfs, noting contrary evidence in magnetic field observations and decay theories
12 p1539 A73-27149
Integral parameters and pulsation frequencies for equilibrium configurations of rotating neutron stars, expanding energy characteristics into series of relativistic members
12 p1546 A73-27854
Wave model of Galaxy spiral structure, assuming subsystem mass distribution and old star rotating bar mechanism
12 p1547 A73-27879
The role of the Coriolis force on the stability of rotating magnetic stars and the origin of convective motions.
12 p1547 A73-27883
Rotation effects in stellar and quasi-stellar relativistic objects models required for pulsars and quasars explanation, discussing gravitation theories
14 p1798 A73-30141
Rotating neutron star matter and model properties with emphasis on pulsar observations, discussing equations of state, transport processes and relativistic effects
14 p1798 A73-30234
Primordial cosmic ray abundance from rotating magnetic A stars with accelerating ionized interstellar gas particles
15 p1925 A73-31059
Differentially rotating neutron star models calculation for given state equation, examining mass increase relationship to rotational rigidity relaxation via Ostriker-Tassoul instability criterion
15 p1929 A73-31093
HZ Hercules periodically pulsating variable star in binary system detected by Uhuru satellite, detailing X ray emission, rotation pattern and mass exchange mechanism
16 p2059 A73-32948
Quasiradial pulsation of rotating white dwarfs and neutron stars in general relativity.
18 p2354 A73-36736
Viscous effects in rapidly rotating stars with application to white-dwarf models. I, II.
18 p2357 A73-37106
Thermal instabilities and energy relations in convective shells of slowly rotating stars
19 p2481 A73-37346
Pulsar model magnetosphere for uniformly rotating infinitely conducting magnetized neutron star with aligned magnetic field
19 p2488 A73-38515
Optical polarization of the Crab Nebula pulsar. II - Observational results and fits by the relativistic vector model.
19 p2488 A73-38518
Integral parameters and pulsation frequencies for equilibrium configurations of rotating neutron stars, expanding energy characteristics into series of relativistic members
20 p2608 A73-39228
A model for compact X-ray sources - Accretion by rotating magnetic stars.
20 p2602 A73-39443
Magnetized and nonmagnetized rotating neutron star reactions to applied torques for pulsar slowdown, discussing magnetosphere and wind zone
21 p2778 A73-41529
The stability of rotating supermassive stars.
22 p2907 A73-42304
Spectral variabilities of magnetic peculiar A stars associated with atmospheric chemical composition anomalies, using inclined rotator model
22 p2908 A73-42345
The role of rotation in close binary systems of high mass.
22 p2909 A73-42584
High rotational velocity correlation with metal abundance interpreted by coronal mass loss rate in metal-poor stars
24 p3140 A73-45184

Single component wind model for stellar rotational dependent mass loss from hot corona with application to T Tauri star observations
24 p3140 A73-45184

STELLAR SPECTRA

NT SOLAR SPECTRA

Preliminary report on the infrared spectrum of Nova Serpentis 1970.
01 p0095 A73-10282
Spectral classification through seven-color photometry.
01 p0095 A73-10282
Element abundances in O- and early B-stars.
01 p0096 A73-10252
An investigation of four southern open clusters.
01 p0096 A73-10313
Stellar spectroscopy with holographic gratings.
01 p0047 A73-10525
UV Cet-type variable star quiet state and flare spectra, discussing flare mechanism relation to magnetic effects and star evolutionary position
01 p0102 A73-10979
Eta Aquilae star molecular abundances of CO, C₂, carbon, OH, NH and CH with respect to dissociation equilibrium and light curve correspondence
01 p0103 A73-11029
The consequences of grains in the atmospheres of late-type stars. I - Intrinsic polarization, infrared excesses, and emission lines.
01 p0103 A73-11039
The classification of intrinsic variable stars. II - The red variables of S and related types.
01 p0104 A73-11039
Physical reality of apparent carbon star group in Auriga from radial velocity measurements, spectral classification and VR photometry observations
01 p0104 A73-11039
Vibration-rotation bands of NH in the spectrum of alpha Orionis.
01 p0104 A73-11044
A study of the spectrum-variable silicon A par star 56 Ari.
01 p0106 A73-11300
Recent results of the Goddard rocket program for observing stars.
02 p0215 A73-12324
LTE fine analysis of omicron-tw C Ma line profiles showing chemical composition near Iota Her
02 p0221 A73-12703
Long wavelength spectrometry and photometry of M, S and C-stars.
02 p0222 A73-12708
Uniformly rotating stars with hydrogen- and metallic-line blanketed model atmospheres.
02 p0222 A73-12712
Search for OH-IR stars with emission concentrated in main lines, considering water vapor line emission absorption band in near IR
02 p0222 A73-12717
Remarks on the comparison of the Sanduleak and Fehrenbach-Dufort catalogs of stars belonging to the Large Magellanic Cloud
02 p0223 A73-12718
Continuous near-infrared spectrum of two Be stars HD 50138 and HD 51585
02 p0224 A73-12735
Spectra of several Be stars between 7000 and 9600 A.
02 p0224 A73-12736
New ultraviolet line identifications for early-type stars.
02 p0226 A73-12831
Analyses of light-ion spectra in stellar atmospheres. I - Magnesium II in B and O stars.
03 p0366 A73-12934
Rocket-ultraviolet spectra of eight stars in Ophiuchus and Scorpius.
03 p0366 A73-12947
Rocket-ultraviolet spectra of six stars in Perseus.
03 p0366 A73-12943
Microturbulence in atmospheres of F, G, K, type stars. I - Curve of growth analysis of G, K, type subgiants.
03 p0370 A73-13196
On the extended van Wijk sequence in the Large Magellanic Cloud.
03 p0371 A73-13217
Two new He I lines in the spectra of B-type supergiants.
03 p0371 A73-13218
On the 4686-A He II line intensity in H II regions and the cosmic ray flux.
03 p0361 A73-13222
A search for He-weak stars in very young clusters.
03 p0372 A73-13227
Statistics on the solar spectrum suitable for the study of the blanketing effect in stars of spectral types F, G and K.
03 p0373 A73-13366
Observations of carbon monoxide in cool stars at 4.6 microns.
03 p0374 A73-13711
GX 17 + 2 X ray source optical counterpart identification, noting interstellar absorption role in magnitude estimation
03 p0374 A73-13792

- MWC 349 - A new radio star. 03 p0374 A73-13849
- A-type supergiants - A list of line intensities and radial velocity measurements. 03 p0375 A73-13950
- Alpha Lyra and beta Cen spectrograms from Merse-
n system telescope aboard Salyut space station,
demonstrating viability of space observatories 03 p0375 A73-13953
- Atmospheric microthermal turbulence vertical dis-
tribution from balloon flights compared with stellar
scintillation data, predicting irradiance spectra from
turbulence and wind velocity measurement 03 p0305 A73-14656
- Secondary component minimum deepening in UV
light curve of Beta Lyr eclipsing binary star, suggest-
ing black hole model 04 p0501 A73-15637
- Spectroscopic observations of HZ Herculis. 04 p0501 A73-15684
- Frequency correlation measurement of pulsar spec-
tral fine structure due to radio emission scattering by
interstellar plasma 04 p0503 A73-16002
- Spectroscopic study of the nebula NGC 7635 and the
star BD +60.2522 deg. 04 p0503 A73-16005
- Stratification of the emission in the envelope of the
eclipsing-binary Wolf-Rayet star V444 Cygni. 04 p0503 A73-16009
- Influence of a random magnetic field on the proper-
ties of stellar absorption lines. 04 p0503 A73-16011
- Kappa Cassiopeia H, He and O absorption spectra
line widths from spectrophotometric analysis 05 p0613 A73-16207
- Zonal spectrophotometric standards - Energy dis-
tribution in the spectra of 109 stars in absolute units 05 p0617 A73-16465
- Rapid variations of Psi Per shell star H beta line, in-
dicating shell and stellar atmosphere activity 05 p0617 A73-16466
- O stars line spectra from high dispersion photo-
graphic spectrograms at 3059-6683 Å, tabulating ab-
sorption and emission lines identifications, equivalent
widths and profiles 05 p0618 A73-16742
- The determination of distance, absorption, probable
physical members and age for the open clusters
Haffner 8, Haffner 6, Basel 11 and NGC 2374. 05 p0618 A73-16743
- Ultraviolet photometry from the Orbiting As-
tronomical Observatory. VI - Magnesium II 2800 Å
emission in cool stars. 05 p0625 A73-17336
- Spectroscopic observations of HZ Herculis and a
model for Hercules X-1. 05 p0625 A73-17344
- A study of the unidentified interstellar diffuse fea-
tures. 05 p0626 A73-17379
- Spectroscopic studies of O-type stars. III - The ef-
fective-temperature scale. 07 p0873 A73-19060
- Interstellar molecular hydrogen observed in the ul-
traviolet spectrum of delta Scorpii. 07 p0874 A73-19071
- HD 215441 and 53 Camelopardalis - Intrinsic
polarization of H-beta and the continuum. 07 p0874 A73-19075
- Luminosity classification of stars earlier than O9. 07 p0875 A73-19120
- Violet shift of the H alpha absorption line of the
hydrogen-depleted star HD 30353 07 p0877 A73-19598
- Spectrum of a dust-embedded Wolf-Rayet star in
Cygnus OB2. 07 p0900 A73-20241
- Energy distribution in the spectra of some binaries
in a wide spectral range /3300-7300 Å and 0.88-1.53
microns/ 07 p0901 A73-20318
- Observational aspects of RR Lyrae and W Virginis
stars - Some conundrums of stellar populations and
galactic distribution. 07 p0903 A73-20629
- Population II variable stars shock waves detection
via Balmer lines emission and metal line doubling,
discussing model for numerical calculations of radiat-
ing shock structures 07 p0903 A73-20631
- Linear series of stellar models. II - Pure carbon
stars. 08 p1002 A73-20847
- Stellar and interstellar K lines - Gamma Pegasi and
iota Herculis. 08 p1003 A73-20882
- Spectrophotometric observation of He-rich sublu-
minous subdwarf peculiar O-type star CPD-31 1701,
noting spectrum dominance by extremely stark-
broadened He lines 08 p1003 A73-20894
- Spectroscopic observations of the Cygnus X-1 opti-
cal candidate. 08 p1003 A73-20895
- Equatorial coordinates and photographic mag-
nitudes for new carbon stars in Northern Milky Way,
noting classification by spectral discontinuity 08 p1005 A73-20916
- The spectral classification of the beta Cephei stars
and their location in the theoretical Hertzsprung-Rus-
sell Diagram. 08 p1006 A73-20927
- Interferometer observations of W 3/OH/ at 2.695
GHz and 8.085 GHz. 08 p1006 A73-20929
- Spectral variations of 53 Cam /AX Cam/. 08 p1006 A73-20931
- Revised chemical abundances of four population-II
A-type stars. 08 p1006 A73-20932
- Atmospheric abundances in the carbon star HD
156074. 08 p1006 A73-20935
- On the metal abundance of RR Lyrae stars in the
globular cluster M22. 08 p1009 A73-21169
- Problem of the selective mechanism for the excita-
tion of the C III 5696-Å line in the spectra of certain
stars. I 08 p1012 A73-21549
- Properties and nature of shell stars. III - Periodic
radial-velocity changes of 4 Herculis. 09 p1140 A73-22003
- The metallic-line star 15 UMa and the F 5 V star 5
And. 09 p1141 A73-22013
- Objective prism spectrum surveys for H alpha emis-
sion of stars in Chamaleon T association, listing emis-
sion line stars 09 p1142 A73-22033
- White dwarf flares UVB energy spectra, assuming
mechanism of nonthermal bremsstrahlung due to fast
electrons 09 p1146 A73-22296
- The infrared and microwave spectra of stars; In-
ternational Colloquium on Astrophysics, 17th, Universite
de Liege, Liege, Belgium, June 28-30, 1971,
Proceedings 09 p1149 A73-23126
- Molecular absorption spectra of S-type stars in the
one-micron region. 09 p1123 A73-23130
- Balloon observations of galactic and extragalactic
objects at 100 microns. 09 p1150 A73-23134
- Photospheric and circumstellar H-alpha line profiles
in M-supergiant spectra 10 p1273 A73-23706
- Time dependent radio stars scintillation spectra with
allowance for interplanetary plasma discontinuities
velocity dispersion at small solar distances 10 p1274 A73-23716
- Infrared observations of southern RV Tauri stars. 10 p1275 A73-23844
- Relative proper motions of faint stars in the
Pleiades. 10 p1279 A73-24166
- The thermal radiation spectra of supermassive stars
and X-ray sources. 10 p1270 A73-24902
- Fabry-Perot interferometer with etalon for studying
gas movements and planetary nebulae in Large Maga-
lanic Cloud by spectral analysis from pressure
scanning 11 p1361 A73-25176
- Linear polarization and spectrum of PSR0833-45
and the effects of scattering. 11 p1419 A73-25748
- Photoelectric observations of the close binary
system SZ Camelopardalis. 11 p1425 A73-26266
- Interferometric studies of interstellar CH/+/
molecules. 11 p1427 A73-26617
- Spectral types and UVB photometry of G-K giants
at the North Galactic Pole. 11 p1429 A73-26678
- The eclipsing binary system RU Ursae Minoris. 11 p1429 A73-26681
- Two-color electrophotometric observations of the
BD Dra variable 12 p1537 A73-26852
- Interstellar light absorption and distribution of stars
about the star cluster NGC 6834 12 p1537 A73-26854
- Interstellar light absorption and distribution of stars
about the star cluster NGC 7654 12 p1537 A73-26855
- Automatic classification of G5-K5 stars by means of
166 Å/mm objective prism spectra /4000-4550 Å/. 12 p1538 A73-26858
- Spectral energy distribution in several binaries at
3300-7300 Å and 0.88-1.53 micron wavelengths. 12 p1540 A73-27290
- Nebular stage of Nova Delphini 1967. I 13 p1672 A73-28039
- Blue OB stars detection by flicker comparison, as-
tronomical photography and two color diagrams,
discussing classification as quasars and white dwarfs 13 p1673 A73-28148
- Spectra of star and planet scintillation and depen-
dence of their characteristics on meteorological condi-
tions 13 p1683 A73-29097
- Spatial distribution of stars in the Orion constella-
tion region 14 p1799 A73-30385
- Landstreet null line list revision and null lines tabu-
lation to identify spectra of magnetic Ap star at-
mospheres 14 p1801 A73-30647
- Stellar atmospheric conditions taking into account
A5 and early stars, considering spectral charac-
teristics, absorption spectra and spectrum prediction 15 p1932 A73-31305
- Bands of the light molecules in Mira variables. 15 p1932 A73-31307
- Spectral investigations of UV Ceti-type flare stars
and search for new variables of this type carried out at
Crimea. 15 p1934 A73-31479
- The red dwarf stars of the UV Ceti-type in the
neighbourhood of the sun. 15 p1935 A73-31480
- The spectrum variable a Centauri /HD 125 823/. 15 p1935 A73-31485
- Motion of fourteen stars in the Orion nebula cluster. 15 p1936 A73-31555
- Mariner 9 ultraviolet spectrometer experiment - In-
terstellar absorption at Lyman alpha in OB stars. 15 p1936 A73-31556
- Radial velocity, light and colour curves of RZ Cep,
an RR Lyrae star. 15 p1937 A73-31700
- A spectrometric setup for magnetic-tape recording
of spectra 15 p1878 A73-32140
- Computerized stellar spectrogram processing using
semiautomatic diagram-code converters, least squares
method and reference spectral lines 15 p1878 A73-32141
- The infrared spectrum and angular size of Eta
Carinae. 15 p1940 A73-32197
- Spectrographic investigation of the flare star YZ
CMi in January 1969 16 p2057 A73-32709
- Quantitative analysis of the spectrum of beta Lyr. I -
Variation of certain hydrogen and helium emission
lines 16 p2057 A73-32710
- Changes of the Balmer-series lines of hydrogen in
the spectrum of the spectrally variable silicon Ap star
CU Vir 16 p2057 A73-32711
- Complex roots onset in secular stellar spectrum ex-
tended to case with shell sources present, determining
eigenvalues for different intensity and position
parameters 16 p2058 A73-32830
- The equivalent widths of Mg II lines near 2800 Å in
the spectra of 31 stars. 16 p2059 A73-32838
- The radial velocity variations of HD 125823 a Cent-
auri. 16 p2059 A73-32843
- Photometric investigation of star magnitude and
color index data in Palomar Atlas and Washington Star
Catalog, obtaining calibration curves and average
error calculations 16 p2063 A73-33659
- Late B6 stars line spectra, atmospheric electron
density, microturbulence velocity, excitation tempera-
ture, flux envelopes and energy distributions 17 p2233 A73-35612
- Profiles of the photospheric and circumstellar H
alpha line in the spectra of type M supergiants. 18 p2354 A73-36731
- The spectrum of eta canis majoris, B5 Ia. 18 p2355 A73-36779
- Early type stellar line spectra, discussing LTE,
hydrogen and helium lines, spectral element abundance
and O and B stars 18 p2356 A73-36875
- The He I lambda 5876 line in O-star spectra. 18 p2356 A73-36973
- On the nature of the infrared point source in the
Orion Nebula. 18 p2356 A73-36975
- Measurement of the position and spectrum of Her-
cules X-1 from the OSO-7 satellite. 18 p2356 A73-36982
- Studies of beta Coronae Borealis. I - Identification
of the Actinides. 18 p2357 A73-37105
- Cygnids and Taurids - Two classes of infrared ob-
jects. 18 p2357 A73-37111
- Hard X-ray spectrum of Hercules X-1. 19 p2475 A73-37388

Multicolor observations of stars in the vicinity of the Orion Nebula.

19 p2484 A73-37613

Profiles of emission lines in Be stars. II - Interpretation of the long-period V/R variation.

19 p2484 A73-37615

Bragg spectroscopy of Scorpius X-1 in search of the Fe XXV emission lines.

19 p2485 A73-37627

CN red system line opacity codes for late star model atmosphere calculation

19 p2488 A73-38513

Line widths of CaII K2 and H-alpha and the chromospheres of late stars

20 p2606 A73-39073

Radial velocity fluctuations of the Ap star HD 224801

20 p2607 A73-39083

X-ray spectrum of Cassiopeia A - Evidence for iron line emission.

20 p2603 A73-39446

Distances of 26 stars of the stellar ring 58.

20 p2610 A73-39576

Spectrographic observations of the peculiar Be star with infrared excess HD 45677.

20 p2611 A73-39586

Shell nebulae and Wolf-Rayet stars - Observations of NGC 2359

21 p2768 A73-40714

Investigation of the planetary nebula NGC 1360 and its nucleus

21 p2768 A73-40715

Narrow-band photoelectric observations of the Wolf-Rayet type eclipsing binary star V444 Cyg in the continuum /4244 - 7512A/

21 p2768 A73-40717

Observations of ultraviolet stellar spectra by the Utrecht Orbiting Stellar Spectrophotometer S59.

21 p2769 A73-40811

The near ultraviolet spectrum of early type stars obtained with S 59.

21 p2769 A73-40825

MK spectral classification system validity, discussing standards for O4-G2 spectral range and limits in visual spectral classification

21 p2771 A73-41236

Carbon star classification problems in effective temperatures, luminosities and radii, considering mass measurement, surface gravity, chemical composition, model atmospheres, stellar evolution, etc

21 p2772 A73-41240

The effects of departures from LTE in stellar spectra.

21 p2772 A73-41243

Measurements of neutral-hydrogen absorption in the spectra of eight pulsars.

21 p2779 A73-41538

Energy distribution in stellar spectra of various spectral types and luminosities

22 p2906 A73-41974

Accurate wavelengths of stellar and telluric absorption lines near lambda 7000 A.

22 p2907 A73-42208

Analysis of the ultraviolet spectrum of A-type stars observed by the OAO II satellite.

22 p2907 A73-42301

Observations in linearly polarized light of the intensity of the diffuse 6180 A absorption band in 49 O, B, and A stars.

22 p2908 A73-42308

Linear polarization in the Orion Nebula.

22 p2908 A73-42313

Spectral variabilities of magnetic peculiar A stars associated with atmospheric chemical composition anomalies, using inclined rotator model

22 p2908 A73-42345

French monograph - Preparation of a space experiment intended for high resolution study of the far ultraviolet spectrum of the star gamma Gemin.

22 p2910 A73-42714

Wolf-Rayet and high temperature stars; Proceedings of the Symposium, Buenos Aires, Argentina, August 9-14, 1971.

23 p3025 A73-43191

Classification and distribution of WR stars and an interpretation of the WN sequence.

23 p3025 A73-43193

Wolf-Rayet stars UV spectra from OAO-2 satellite-borne spectrometer measurements, considering radio spectra of W stars with symmetrical nebulae from ground based observations

23 p3025 A73-43194

Line identification and profiles in emission spectra of Wolf-Rayet stars from microphotometer tracings at high dispersion, noting effects of companion stars

23 p3026 A73-43196

O, Of, Oe and Wolf-Rayet star comparison in terms of emission and absorption line spectra, noting relationship to evolutionary status on H-R diagram

23 p3026 A73-43197

P Cyg type O and B supergiant stars relationship to Wolf-Rayet stars in terms of spectra, absolute magnitudes, mass and variability

23 p3026 A73-43198

Planetary nebulae nuclei emission line spectral features similarity to spectra of Population I Wolf-Rayet and O-type stars

23 p3026 A73-43199

Wolf-Rayet stars continuous and line spectral features interpretation by model involving wide emission lines due to Doppler effect in rapidly expanding envelope

23 p3026 A73-43201

WC and WR binary stars spectra differences attributed to variations in effects of companion on principal star atmosphere

23 p3026 A73-43203

Summary of problems and conclusions on the nature and physical structure of Wolf-Rayet stars.

23 p3026 A73-43204

Line identifications, elemental abundances, and equivalent widths for 21 sharp-lined cool peculiar A stars and two comparison standards.

23 p3028 A73-43491

Radiation transfer equations for atomic spectra lines in stellar magnetic field, allowing for nonequilibrium population of atomic ground state and excited atom-particle collisions

23 p3036 A73-44242

Chromosphere models for cool stars of various spectral types, calculating temperature-density dependence for sun, giant and dwarf stars

23 p3036 A73-44243

Investigation of anomalously fast stars of early spectral class. III - Search for the He-3 isotope

23 p3036 A73-44244

Spectrophotometry of i Hercules

23 p3037 A73-44356

Polarization variations in the emission of some M-type supergiants

23 p3037 A73-44357

The C-classification of the spectra of carbon stars.

24 p3138 A73-44997

Type I and II supernovae spectra, identifying different lines and obtaining energy distributions

24 p3138 A73-45043

Secular variations in H alpha, H beta and metal line spectra of Be star 88 Hercules from intensity decrease observations, noting envelope hydrogen absorption lines visibility

24 p3140 A73-45187

Photographic observation of type I supernovae at Asiago Observatory, discussing analysis of B and V light curves and spectra

24 p3143 A73-45437

Observations of Cyg X-1 and Cyg X-3 above 7 keV from OSO-7.

24 p3144 A73-45494

STELLAR SPECTROPHOTOMETRY

Southern open star clusters. I - UV-B/H beta photometry of 15 clusters between Galactic longitudes 231 and 256 deg.

01 p0096 A73-10318

Photoelectric determination of radial velocities.

01 p0047 A73-10517

On-line digital recording of stellar spectrum with photoelectron-counting spectrophotometer, noting discrimination against spurious signals from noise and pulse height distribution measurements

01 p0048 A73-10531

Photoelectric light-curves of TW Cas.

01 p0098 A73-10555

Photometry and spectroscopy of red variables in Omega Centauri.

01 p0098 A73-10584

Photometry of supernova 1972 in NGC 5253.

01 p0104 A73-11046

Investigations regarding the structure of young star clusters and the evolutionary phases of their members. II - NGC 6530. III - NGC 6611

02 p0226 A73-12835

Light variation and extinction of the variable WW Vulpeculae

02 p0226 A73-12836

Rapid changes in the new shell star HR 6000.

03 p0366 A73-12941

Rocket-ultraviolet spectra of six stars in Perseus.

03 p0366 A73-12943

Kappa Cassiopeia H, He and O absorption spectra line widths from spectrophotometric analysis

05 p0613 A73-16207

Some relations between the photometric characteristics of the brightness curves and color indexes of Cepheid variables in the system U.B.V. II

05 p0613 A73-16209

The old open cluster NGC 6819.

05 p0618 A73-16744

Ultraviolet photometry from the orbiting astronomical observatory. IV - Photometry of late-type stars.

05 p0626 A73-17381

Stellar UV observations with spectrophotometer onboard ESRO TD-1A satellite in retrograde near polar orbit

07 p0875 A73-19259

Light variations of high luminosity O and B stars in the Large Magellanic Cloud.

07 p0877 A73-19597

A proposal for a flint objective prism for the ESO Schmidt camera.

08 p0966 A73-21360

Observing from space with the Orbiting Astronomical Observatory.

08 p1015 A73-21722

Balloon-borne telescope-UV spectrometer for stellar spectrophotometric measurement with high spectral resolution, discussing system design and operation, image motion compensation and data acquisition.

08 p0971 A73-21727

Aberrations, astigmatism and coma control for large UV stellar spectrograph design by grating shape and ruling space modification

08 p0972 A73-21728

Stellar survey at 2000-4100 A via balloon-borne observations, discussing intensity distributions and earth atmospheric ozone layer density

09 p1140 A73-22000

Cosmic absorption of stellar light in the belt of a local system

09 p1148 A73-22861

Stellar spectrometry by Fourier transformation from 2 to 5 micron

09 p1150 A73-23142

Close binaries and their significance in the theory of evolution of stars

09 p1151 A73-23332

Interstellar Na I, K I, Ca II, and CH/+/- line profiles toward zeta Ophiuchi.

10 p1273 A73-23549

Spectral energy distribution, photometric gradients and Balmer discontinuities for eclipsing binary RZ Scutum from spectrograms with low dispersion in H-gamma line

10 p1273 A73-23707

Photometric and spectroscopic observations of eclipsing binary object BM Orionis interpreted in terms of thin disk model with collapsed star/black hole

10 p1284 A73-24906

The extinction curve for Cygnus OB2 no. 12.

11 p1414 A73-25068

Differential UVB photometry of beta Lyrae. III.

11 p1415 A73-25072

Spectrophotometric investigation of the star alpha-2 CVn. II

11 p1416 A73-25233

Spectrophotometry of the supernova in NGC 5253 from 0.33 to 2.2 microns.

11 p1427 A73-26613

Opticomechanical system of an automatic stellar electrophotometer

12 p1495 A73-26863

Photoelectric light curve of the Algol system TW Andromedae and the interpretation of its distortions by the effects of hot spots.

13 p1672 A73-28040

Photometry of field horizontal-branch stars.

13 p1682 A73-28986

Spectrophotometric results from the Copernicus satellite. I - Instrumentation and performance.

14 p1754 A73-30744

Spectrophotometric results from the Copernicus satellite. II - Composition of interstellar clouds.

14 p1801 A73-30743

Optical study of BL Lacertae. II - Brightness variation from March 1969 to January 1971

15 p1928 A73-31052

Scanner observations of hot helium-carbon stars.

15 p1932 A73-31263

O-B stars in young star clusters associated with nebulae

15 p1934 A73-31403

OAO-2 observations of Beta Lyrae and a provisional interpretation.

15 p1935 A73-31488

Low cost two-beam multimode nebular/stellar photometer design, construction and use on extended and discrete objects emitting 3700-9000 A radiation

15 p1877 A73-32007

Spectrographic investigation of the flare star YZ CMi in January 1969

16 p2057 A73-32709

A high-resolution photoelectric spectrophotometer at the coude focus of a 2.6-m telescope

16 p2011 A73-32714

Galactic X-ray polarimetry and high-resolution X-ray spectroscopy.

16 p2058 A73-32736

On the use of UVB photometric diagrams for inferring the existence of an open star cluster.

16 p2058 A73-32833

A multi-channel coronal spectrophotometer.

17 p2170 A73-35291

Interstellar absorption lines observed with the orbiting spectrophotometer S59.

18 p2349 A73-35993

Report on the telescope ultraviolet observations from the OAO-2 satellite and associated research at the Smithsonian Astrophysical Observatory.

18 p2349 A73-35996

Spectral energy distribution, spectrophotometric gradients and Balmer discontinuities for eclipsing bi-

nary RZ Scuti from spectrograms with low dispersion in H gamma line 18 p2354 A73-36732

Multicolor observations of stars in the vicinity of the Orion Nebula. 19 p2484 A73-37613

Distances of 26 stars of the stellar ring 58. 20 p2610 A73-39576

Observations of ultraviolet stellar spectra by the Utrecht Orbiting Stellar Spectrophotometer S59. 21 p2769 A73-40811

Line identifications in the near ultraviolet spectrum of the peculiar A star epsilon Ursae Majoris. 21 p2769 A73-40829

Ultraviolet stellar spectra obtained with the Utrecht orbiting stellar spectrophotometer S 59 aboard the ESRO TD-1 A satellite. 21 p2773 A73-41395

Intermediate-band photometry of RR Lyrae stars. II - Colors of RR Lyrae and ultrashort-period variables. 22 p2906 A73-41962

Photometry of southern globular clusters. I - Bright stars in omega Centauri. II - Bright stars in NGC 6752. 22 p2907 A73-42206

Observation of the star gamma-Cassiopeia of the Be spectral type by Fourier spectrometry from 1 to 2.5 micron 22 p2908 A73-42354

Russian book on eclipsing binary stars covering limb darkening law, photometric eclipsing phases, computer applications and models 22 p2911 A73-42747

Interferometric measurements of apparent stellar diameters 22 p2863 A73-43102

Spectrophotometric gradients, temperatures and continuous spectra energy distribution of star SS Cyg, showing dependence on flare development 23 p3036 A73-44245

Telescopic observation of Pleiades I flare stars, determining stellar magnitudes and flare brightness 23 p3037 A73-44352

Photometric study of new variable stars in NGC 2264 23 p3037 A73-44353

Photometry of selected flare stars in the Pleiades 23 p3037 A73-44354

UBV spectral and photographic observations of blue objects around M 92 globular cluster 23 p3037 A73-44355

Spectrophotometry of i Hercules 23 p3037 A73-44356

Calibration of luminosity criteria for G and K giants by means of trigonometric parallaxes. 24 p3140 A73-45181

Galactic structure in the direction of Cepheus 24 p3140 A73-45191

The 35-day cycle of HZ Herculis. 24 p3143 A73-45491

STELLAR STRUCTURE

Pulsar structure theory with respect to rotating neutron star hypothesis, discussing evolutionary elements 01 p0095 A73-10065

Binary stars tidal evolution theory, deriving energy and momentum equations for arbitrary internal structures 02 p0218 A73-12411

Classical hard-sphere gas in spherical box with coupling between local thermodynamics and gravitation, noting stellar core-halo structure from equilibrium state calculations 03 p0366 A73-12936

Numerical model of transient behavior of radiation dominated shock calculated for neutron star core of imploding supernovae 03 p0372 A73-13354

Thermal conductivity and hot magnetic poles of pulsars. 03 p0374 A73-13796

Cooling and evolution of a supernova remnant. 04 p0499 A73-15360

Beta Persei decimetric-centimetric radio emission variations, relating observational data to discontinuous structural adjustment model based on starquakes hypothesis 05 p0627 A73-17392

Multiple and intrinsic variable stars, considering pulsars, binary systems, Cepheids, stellar structure and evolution 06 p0750 A73-18014

He red giants models with degenerate C-O cores, He burning shell sources and He-rich envelopes, noting stellar luminosity 08 p1004 A73-20903

Criticism of solar core mixing hypothesis of solar neutrino problem, discussing implications for semiconvection theory 08 p1012 A73-21532

Dwarf binary component convective shell behavior under gravitational field periodic tidal action, noting conditions for thermal instability 08 p1012 A73-21548

A new cosmological model - Formation of organic molecules, planets, and comets. 09 p1151 A73-23147

Chemical composition of classical Cepheids in the Galaxy and Magellanic Clouds 10 p1273 A73-23705

Formula approximating Fermi-Dirac integrals for electron gas density, pressure and internal energy, discussing pressure ionization effect on equation of state in stellar interiors 11 p1417 A73-25261

Evolution of stars with suppressed core convection. 11 p1427 A73-26608

Stellar structure and evolution models in conformity with observational luminosity, mass and size from H-R diagram 13 p1682 A73-28977

Massive main sequence stars structure and evolution within core hydrogen burning models, giving mathematical relation and conditions for convective instability 13 p1682 A73-28979

Neutron stars physical model, deriving mass-density-energy relationships for degenerate electron gas 13 p1682 A73-28985

Stellar opacity and energy transport based on radiation-matter interactions, discussing radiative transfer, absorption and scattering cross sections, quantum mechanical methods, etc 13 p1682 A73-28987

Radiative transport in stars, considering radiation field, transfer equation and radiative heat equation 13 p1683 A73-28988

Thermonuclear reactions and nucleosynthesis in stellar interiors, initial big bang, supermassive objects and supernovae explosions 13 p1663 A73-28989

Relativistic stars and gravitational waves - An account for non-relativists. 13 p1683 A73-28991

Theory of the thermal explosion in the hydrogen shell of a white dwarf 13 p1683 A73-29091

Stellar structure deviation from neutron star models, deriving equations for relativistic models with deviation from Einstein principle of equivalence 13 p1686 A73-29655

On convection and gravitational layering in Jupiter and in stars of low mass. 14 p1797 A73-30009

Relativistic stellar stability - An empirical approach. 14 p1801 A73-30740

Stellar nuclear hydrogen burning shell thermal stability to radial perturbations, discussing growth rate, energy generation and temperature increases 15 p1929 A73-31058

Thermal instability of the helium-burning shell in massive stars. 15 p1936 A73-31557

Neutron matter solidification in neutron star cores, discussing energy minimization through strongly interacting baryon system via arrangement into lattice structure 16 p2061 A73-33220

Evolutionary considerations involving the internal density concentration parameter of binary stars. 17 p2237 A73-35786

Book - Physics of stellar interiors. 18 p2356 A73-36965

Book - General astrophysics with elements of geophysics. 18 p2356 A73-36968

Internal structure of the convective shell of the sun 19 p2481 A73-37343

Thermal instabilities and energy relations in convective shells of slowly rotating stars 19 p2481 A73-37346

Structure of helium burning regions in stars - Dependence on molecular weight and burning rates. 19 p2483 A73-37560

The effect of hot white dwarfs on the interstellar medium. II - The changes in its structure with height above the galactic plane and some consequences of the finite lifetimes and velocities of the white dwarfs. 19 p2483 A73-37561

Observations of galactic supernova remnants at 1.7 and 2.7 GHz. 19 p2483 A73-37566

Low solar neutrino flux explained by evolution model emphasizing internal rotation effects on solar structure 19 p2488 A73-38519

Book - Introduction to the physics of stellar interiors. 20 p2607 A73-39144

Linear convective modes and the energy transport in stellar convection zones. 22 p2905 A73-41761

On turbulent stress and the structure of young convective stars. 22 p2908 A73-42306

The Wolf-Rayet stars - The general problems of extended atmospheres and non-classical atmospheric models. 23 p3025 A73-43192

Wolf-Rayet stars luminosity to mass ratios, internal structure, mass loss to companion or interstellar space and spectral peculiarities related to evolutionary status 23 p3026 A73-43200

Summary of problems and conclusions on the nature and physical structure of Wolf-Rayet stars. 23 p3026 A73-43204

Configurations of hot white dwarfs with nuclear energy sources 23 p3025 A73-44360

Multiple solutions of the equations of stellar structure. II - E model sequences. 24 p3140 A73-45179

STELLAR TEMPERATURE

Spectroscopic studies of O-type stars. III - The effective-temperature scale. 07 p0873 A73-19060

The angular diameter of upsilon Capricorni and an occultation of SAO 118655. 12 p1540 A73-27427

Radio emission from pulsars and surface temperature of neutron stars. 13 p1681 A73-28925

White dwarfs model based on zero temperature Fermi gas theory, determining mass-radius relation and limit mass 13 p1682 A73-28982

IR objects in Orion Nebula, discussing temperature range and pre T Tauri evolutionary stage 15 p1934 A73-31419

Line blanketing theory tested via G-I index, discussing underestimation of extreme subdwarf effective temperatures 16 p2058 A73-32834

Planetary nebula evolution model to explain FG Sagittae luminosity changes due to thermal pulse in He burning shell 19 p2489 A73-38530

Investigation of the planetary nebula NGC 1360 and its nucleus 21 p2768 A73-40715

Intermediate-band photometry of RR Lyrae stars. II - Colors of RR Lyrae and ultrashort-period variables. 22 p2906 A73-41962

Wolf-Rayet stars effective temperature estimation from UVB photometry of surrounding ring nebulae with optically thick H II region excited by stellar Lyman radiation 23 p3025 A73-43195

Chromosphere models for cool stars of various spectral types, calculating temperature-density dependence for sun, giant and dwarf stars 23 p3036 A73-44243

Spectrophotometric gradients, temperatures and continuous spectra energy distribution of star SS Cyg, showing dependence on flare development 23 p3036 A73-44245

STELLAR WINDS

Polytropic subsonic stellar winds with magnetic fields. 03 p0361 A73-13368

Stellar winds and mass loss of a rotating star. 05 p0624 A73-17312

Optically thin stellar winds in early-type stars. 07 p0873 A73-19061

Heating of astrophysical plasma due to rotation. 08 p1007 A73-20957

Neutron-star accretion in a stellar wind - Model for a pulsed X-ray source. 08 p0997 A73-21160

Stellar wind radiation damage in cosmic dust grains - Implications for the history of early accretion in the solar nebula. 17 p2228 A73-34424

Optical appearance of binary X-ray sources. 17 p2322 A73-35146

Meridional flow and the validity of the two-dimensional approximation in stellar-wind modeling. 20 p2602 A73-39430

Interaction of the X-ray source radiation with the atmosphere of the normal star in close binary systems. 23 p3030 A73-43750

Density and velocity fluctuations in young nebulas of Orion type 23 p3035 A73-44232

STELLARATORS

Floating potential and diffusion coefficients of viscosity damping of convective cells in stellarator for confined He, Ar and Xe plasmas 01 p0083 A73-10462

Purification of hydrogen plasmoids by the magnetic field in an injector-diverter. 02 p0198 A73-12113

Racetrack configuration design of Uragan stellarator for plasma diagnostics and heating, noting shear and rotational angle of magnetic system 04 p0432 A73-15038

Low pressure plasma equilibrium in helicon device with stellarator confinement system, calculating plasma pressure from MHD equations 04 p0479 A73-15039

Methods of plasma injection into closed magnetic confinement systems 04 p0479 A73-15041

STEP FAULTS

Density and electric field oscillations of plasma in stellarator, considering magnetic field strength effect, stabilization by ionic collisions and energy pumping mechanism 06 p0728 A73-17968

Measurement of plasma density in a torsatron by a multimode resonator technique 07 p0855 A73-19283

Method for experimental determination of the magnetic well depth in stellarator-type systems 07 p0855 A73-19285

Multimode cavity measurements of plasma density in a torsatron. 13 p1665 A73-28683

Experimental determination of magnetic well depth in stellarators. 13 p1665 A73-28685

Investigation of the feasibility of the injection of electrons into heliotron-type closed magnetic mirror configurations 13 p1666 A73-28957

Perturbation of the magnetic configuration of a stellarator by a longitudinal current in the plasma. 21 p2750 A73-41678

Ion temperature in the case of ohmic heating of the plasma in the 'Uragan' stellarator 22 p2893 A73-42382

Electron injection through the diverter in a heliotron. 23 p3013 A73-44309

STEP FAULTS

U GEOLOGICAL FAULTS

STEP FUNCTIONS

Analysis of non-linear systems defined by their response to arbitrary disturbances. 01 p0028 A73-11456

Applications of the theory of impulsive parametric excitation and new treatments of general parametric excitation problems. [ASME PAPER 72-WA/APM-6] 04 p0476 A73-15903

Calculation of the asymptotic behaviour of the TDR step response related to the asymptotic behaviour of dielectrics in the frequency domain. 07 p0797 A73-19107

Weak convergence of stepwise random processes 09 p1112 A73-22886

The task of constructing transition functions in problems involving interaction of weak shock waves with cylindrical and spherical surfaces 12 p1486 A73-27241

A note on the period of oscillation of non-linear systems. 19 p2460 A73-38108

Discrete reproduction of a random parameter change process in standard automation equipment elements 20 p2543 A73-39393

Problem of synthesizing a control system in the case of a plant involving random jerky forces 23 p2963 A73-43577

STEPS

Rearward-facing steps in laminar supersonic flows with and without suction. [AIAA PAPER 73-667] 18 p2261 A73-36218

STEREOCHEMISTRY

Stereo-enriched poly-alpha-amino acids - Synthesis under postulated prebiotic conditions. 06 p0661 A73-17940

Syntheses and conformational studies of polyacidic amino acids containing optical active side chains. 06 p0661 A73-17942

Resolution by gas-liquid chromatography of diastereomers of five nonprotein amino acids known to occur in the Murchison meteorite. 06 p0662 A73-18468

Sterically controlled syntheses of optically active organic compounds. XV - Syntheses of optically active aspartic acid through beta-lactam. 07 p0787 A73-19204

Mass spectrometry in structural and stereochemical problems. CCXVII - Electron impact promoted fragmentation of O-methyl oximes of some alpha, beta-unsaturated ketones and methyl substituted cyclohexanones. 10 p1186 A73-23550

Gas-liquid chromatographic resolution of several protein amino acid enantiomers on a packed column. 10 p1186 A73-24658

Optical resolution of DL-aspartic acid in the presence of optically active amino acid and copper (II) ion. 11 p1324 A73-25146

The isolation of a series of acyclic isoprenoid alcohols from an ancient sediment - Approaches to a study of the diagenesis and maturation of phytol. 11 p1326 A73-25465

The diagenesis and maturation of phytol - The stereochemistry of 2,6,10,14-tetramethylpentadecane from an ancient sediment. 11 p1326 A73-25466

Criteria for distinguishing biogenic and abiogenic amino acids - Preliminary considerations. 11 p1319 A73-26480

Sterically controlled syntheses of optically active organic compounds. XVI - Temperature dependence of hydrogenolytic asymmetric transamination. 12 p1467 A73-27974

On the asymmetric adsorption of phenylalanine enantiomers by kaolin. 24 p3066 A73-44772

STEREOGRAPHY

U STEREOPHOTOGRAPHY

STEREOPHOTOGRAPHY

Lunar topography - Global determination by radar. 03 p0378 A73-14445

Topographic earth observations using radar techniques with a single flight. 04 p0419 A73-15403

Daytime and nighttime stereophotogrammetric photography of moving object using stroboscopic effect, noting pulsed light sources for fast moving near objects 05 p0575 A73-16314

Radar imagery and supporting aerial photography tests for topographic mapping capabilities and metric quality of side-looking stereo radar system 06 p0667 A73-18283

Apollo 15 panoramic camera with 24 inch focal length for stereophotography of lunar surface, presenting pictures of lunar craters and landing sites. 07 p0824 A73-20021

Stereophotogrammetric compilation of large scale topographic chart using convergent panoramic photos obtained with Apollo 15 spacecraft 07 p0824 A73-20022

Drobyshev stereograph corrector operation for aerial photographs processing with transformed beam of stereoprojector 07 p0824 A73-20043

Lunar control densification with panoramic space photography. 08 p0968 A73-21702

Close range photogrammetry of objects moving at high speed. 09 p1081 A73-22377

Graphical method of profiling and contouring microcraters on lunar rocks from stereomicrograph pair obtained by scanning electron microscope 09 p1081 A73-22378

Reduction of lunar panoramic photography on the analytical stereoplotter. 09 p1081 A73-22379

Moire topography for full size living human body contour stereophotographic pictures with high contrast, discussing instrument construction, performance and accuracy 11 p1365 A73-26239

Remote sensor dynamic imageries produced by stereo systems, discussing line-by-line and section-by-section orientation methods and triple channel recording scheme 12 p1500 A73-27956

Signal color effects on stereoplotter measurements in aerial mapping of built-up areas 12 p1501 A73-27968

Use of a computer to design surveys made by the stereotopographic method 13 p1621 A73-29416

Experience in constructing analytical planar phototriangulation grids from 1:40,000 and 1:75,000 scale aerial photographs for the preparation of 1:10,000 scale photographic maps 14 p1753 A73-30416

Experiment in stereophotogrammetric processing of aerial photographs with decenterations on an STD-2 stereometer 14 p1753 A73-30417

An introduction to holography by shadow casting. 16 p2016 A73-33950

IR line scanners using stereoscopic techniques for aerial remote sensing of topography, discussing pivoting mechanism, scanner cameras and scan planes 17 p2168 A73-34957

Photogrammetric evaluation of Mariner 9 photography. 19 p2479 A73-37229

Digital processing of stereoscopic image pairs. 19 p2432 A73-38534

Photogrammetry in Apollo lunar roving vehicle conducted geometry and geology exploration, using horizontal stereophotography with special gnomon for sun-line and vertical control 20 p2611 A73-39669

IR scanner for aerial stereoscopic photography, discussing use of computer controlled orthophoto printer for image distortion reduction by rectification 20 p2566 A73-39671

Statistical comparison of airborne laser and stereophotogrammetric sea ice profiles. 22 p2850 A73-42731

An improved single flight technique for radar stereo. 23 p2953 A73-43449

STEREOSCOPIC PHOTOGRAPHY

U STEREOPHOTOGRAPHY

STEREOSCOPIC VISION

Stereoscopic depth magnitude in viewing background-contrasted superimposed half-fields, noting relation to binocular disparity detection 03 p0261 A73-13762

The stereoscopic frame of reference in asymmetric convergence of the eyes - Response to 'point' stimulation of the retina. 05 p0573 A73-16149

Monocular and binocular clues interaction in depth perception and spatial orientation, discussing stereopsis testing 05 p0542 A73-16483

The role of colour perception and 'pattern' recognition in stereopsis. 07 p0783 A73-20266

Scalar perceptions with binocular cues of distance. 13 p1578 A73-28176

Stereoscopic depth aftereffects with random-dot patterns. 17 p2115 A73-34841

Stereoscopic vision - Cortical limitations and a disparity scaling effect. 18 p2269 A73-35922

STEREOSCOPY

NT STEREOPHOTOGRAPHY

High-speed stereoscopic investigation of paths of luminous objects 08 p0969 A73-21719

STEREOTELEVISION

Mars surface exploration by self-guided stereo TV equipped roving vehicle (robot), describing computerized object and scene ranging and recognition 19 p2429 A73-37321

STERILIZATION

NT CHEMICAL STERILIZATION

NT SPACECRAFT STERILIZATION

Investigation of gas sorption and desorption in polymer materials in the process of gaseous sterilization of such materials 06 p0656 A73-17681

Industrial sterilization; Proceedings of the International Symposium, Amsterdam, Netherlands, September 1972. 16 p1975 A73-33691

Microorganism heat sterilization process design and control based on logarithmic thermal destruction and Bigelow temperature coefficient models, determining lethality by statistical procedure 16 p1976 A73-33695

Lunar sample quarantine procedures - Interaction with non-quarantine experiments. 18 p2281 A73-35978

Development of sulfonated polyphenylene oxide membranes for the reverse osmosis purification of wash water at sterilization temperatures (165 F). [ASME PAPER 73-ENAS-16] 19 p2399 A73-37973

STERILIZATION EFFECTS

NT CHEMICAL EFFECTS

NT CORROSION

NT DECONTAMINATION

NT DEGRADATION

NT THERMAL DEGRADATION

Biological indicators and the effectiveness of sterilization procedures. 16 p1976 A73-33692

The effects of radiation sterilization on plastics. 16 p2030 A73-33693

Formaldehyde gas as a sterilant. 16 p1976 A73-33694

The synergistic inactivation of biological systems by thermoradiation. 16 p1976 A73-33696

STERNS

U AFTERBODIES

STERIODS

NT ACTINOMYCIN

NT ALDOSTERONE

NT CHOLESTEROL

NT CORTICOSTEROIDS

NT CORTISONE

NT PENICILLIN

Tripuranol inhibition of sterol biosynthesis in *Chlorella emersonii*. 02 p0139 A73-12547

Adaptive hormone action and nonspecific adaptive function of steroid hormones, discussing stress resistance mechanisms of steroids pharmacologically classified as syntoxic and catatonic 09 p1045 A73-22536

The origin and incorporation of organic molecules in sediments as elucidated by studies of the sedimentary sequence from a residual Pleistocene lake. 11 p1326 A73-25468

Total lipid and sterol components of *Rhizopus arrhizus* - Identification and metabolism. 16 p1973 A73-33900

Gas chromatography-mass spectrometry study of sterols from *Pinus eliotii* tissues. 24 p3065 A73-44698

Sterols of the fungi - Distribution and biosynthesis. 24 p3059 A73-44699

- STETHOSCOPES**
Stethoscope- or phonocardiograph-detectable systole-associated left atrial sound in terms of activity recording, sound genesis, hemodynamic correlations and clinical applications
11 p1317 A73-25696
- STIELTJES INTEGRAL**
Operational algorithms for probabilistic digital integrators for Stieltjes integral and nonhypertranscendental functions
09 p1060 A73-22555
High-speed universal digital integrators with multistage increments as elements of automatic control systems
12 p1475 A73-26781
- STIFF STRUCTURES**
U RIGID STRUCTURES
STIFFENING
General instability of cylinders with inclined stiffeners under axial compression.
05 p0633 A73-16541
Imperfection-sensitivity of a wide integrally stiffened panel under compression.
07 p0908 A73-19087
Parameters governing load transfer for single reinforcing members.
08 p1016 A73-20799
Influence of an intermediate stiffener on the vibration frequency spectrum of a cantilever plate
10 p1291 A73-24357
Isogrid as integral stiffened waffle with triangular pattern to allow simple graphical solution for optimizing spherical caps or cylinders under various buckling loads
[AIAA PAPER 73-365] 11 p1438 A73-25500
Elastic stability of biaxially loaded longitudinally stiffened composite structures.
[AIAA PAPER 73-367] 11 p1438 A73-25502
The optimum distribution of diagonal stiffeners reinforcing a clamped infinitely long plate buckling under shear.
13 p1700 A73-29386
Elastic deformation of thin walled U-bars lateral stiffeners under torsion, eccentric tension and bending loads, determining vaulting stiffness by finite element method
15 p1950 A73-31906
The residual strength characteristics of stiffened panels containing fatigue cracks.
17 p2246 A73-34888
Further experimental studies on buckling of integrally ring-stiffened cylindrical shells under axial compression.
17 p2250 A73-35441
The effect of stiffeners on the sound radiation and the transmission loss of metal walls
19 p2460 A73-38181
Boron-stiffened longerons on the B-1.
[SME PAPER EM 73-719] 19 p2436 A73-38499
Weight reduction in stiffened panels with specified initial buckling load in uniform longitudinal compression by stiffeners utilization
21 p2787 A73-41190
Fatigue behavior of stiffened flat panels
21 p2788 A73-41555
- STIFFNESS**
On the general solution of externally pressurized gas journal bearings.
[ASME PAPER 72-LUB-Q] 01 p0055 A73-10218
Grillages of maximum strength and maximum stiffness.
01 p0115 A73-10767
Curved element for geometrical approximation of thin shell structures, deriving element stiffness equations in terms of nodal displacement degrees of freedom
03 p0389 A73-13325
A strain energy basis for studies of element stiffness matrices.
03 p0395 A73-14184
Finite elements for axisymmetric solids under arbitrary loadings with nodes on origin.
03 p0395 A73-14192
On the re-inforcement of thermoplastics by imperfectly aligned discontinuous fibres.
04 p0469 A73-15986
Effective stiffness of randomly oriented fibre composites.
05 p0631 A73-16116
Comparison between sparse stiffness matrix and sub-structure methods.
07 p0907 A73-19031
Automated generation and condensation of large mass- and rigidity-matrices
07 p0909 A73-19175
Stiffness matrix formulation and eigenvalue analysis for high order shallow shell finite element of rectangular plan
07 p0916 A73-20439
Stiffness matrix for a beam with an axial force.
08 p1015 A73-20725
Elastic stiffness properties and structural designs of fiber composite materials, including laminate and plate problems
09 p1110 A73-22516
- Shear stresses and displacements of each layer of elastic plate with multiple layers of varying rigidity resting on elastic Winklerian base
11 p1433 A73-25029
High modulus composites versus beryllium for achieving stiffness in spacecraft structural applications.
[AIAA PAPER 73-384] 11 p1430 A73-25513
Eigenvalue problem and stiffness optimization procedure for incremental flutter analysis, describing method use in computer graphics mode
[AIAA PAPER 73-392] 11 p1439 A73-25521
Optimization of aircraft structures with multiple stiffness requirements.
11 p1444 A73-26298
Influence of a small bending stiffness on the lateral vibrations of a clamped rectangular membrane
[DFVLR-SONDDR-226] 11 p1445 A73-26425
Shear stress and deformation inclusion in elastic plate bending finite element theory, discussing stiffness matrix improvement for thin shells
11 p1447 A73-26651
Formulation of time variant stiffness matrices due to changing joint properties.
12 p1555 A73-27737
Discrete flexural analyses of rectangular plates of abruptly varying stiffnesses.
12 p1556 A73-27926
Effective use of the incremental stiffness matrices in nonlinear geometric analysis.
13 p1694 A73-28252
Investigation of some principles in the processes of creep and fracture in heat-resistant materials.
13 p1643 A73-29626
Determination of stiffness and critical loads of a circular plate from a simple bending test.
18 p2362 A73-36327
The elastic properties of carbon fibres and their composites.
18 p2329 A73-37095
Limiting zero and infinite edge beam stiffness effect on natural vibrational frequencies of reinforced annular plates
20 p2622 A73-39548
Resiliently mounted objects holographic system sensitivity threshold control by proper selection of support stiffness and vibration damping
21 p2698 A73-40132
- STIFFNESS MATRIX**
Numerical difficulties and accuracy losses avoidance methods for ill conditioned stiffness matrices encountered in complex structural analyses
05 p0636 A73-17113
Computational efficiency of equilibrium models in eigenvalue analysis.
13 p1694 A73-28248
An algorithm for numerical integration in triangular domains.
14 p1806 A73-30047
Quadrature errors effect on finite element method solutions accuracy, considering stiffness matrix numerical stability
14 p1806 A73-30179
Stress hybrid model extension to stiffness matrix of element with discontinuous stress distribution, considering transverse shear strains in laminated plate layers
14 p1807 A73-30181
Matrix method analysis of stiffened plates free vibrations, deriving governing equation in stiffness matrix form by combining plane stress theory and lateral vibration equation
14 p1807 A73-30186
Mass and stiffness matrices reduction in determining linearly elastic structure natural modes and frequencies with computational accuracy improvement
15 p1949 A73-31672
Locally modified and unmodified structures eigenvalues and eigenvectors solutions, considering computational accuracy improvement and application to dynamic stiffness matrix equation
15 p1951 A73-32035
Blocking procedure for large scale structural analysis in conjunction with plane truss using stiffness matrix method, considering computer subroutines in finite element method
16 p1985 A73-32793
A survey of finite element methods in continuum mechanics.
16 p2036 A73-32988
Ring finite elements for axisymmetric and non axisymmetric thin shell analysis.
16 p2077 A73-32989
Application of the finite element method to cases requiring the combination of elements possessing different numbers of degrees of freedom.
16 p2077 A73-32991
The application of finite elements to the large deflection geometrically non-linear behaviour of cylindrical shells.
16 p2078 A73-32998
Matrix displacement solution to elastica problems of beams and frames.
16 p2082 A73-33906
- Optimum finite element idealization characterization based on displacement formulation, system potential energy true minimum, stiffness matrix gradients and geometry considerations
16 p2082 A73-33909
Instability analysis using the incremental stiffness matrices.
17 p2245 A73-34838
Stiffness matrix displacement analysis via curved elements for plane stress and thin plate bending problems
17 p2252 A73-35606
Bounds on the spectral and maximum norms of the finite element stiffness, flexibility and mass matrices.
19 p2500 A73-38110
Finite element program for flight structure analysis.
22 p2917 A73-41739
Finite element analysis of rotating shells.
[ASME PAPER 73-DET-94] 22 p2919 A73-42074
On the computation of natural modes of an unsupported vibrating structure by simultaneous iteration.
23 p3042 A73-43801
Structural design optimization by iterative analysis using proper stiffness matrix with applications to sandwich plate and frame problems
24 p3150 A73-45236
- STIMULANT**
NT CENTRAL NERVOUS SYSTEM STIMULANTS
NT NOREPINEPHRINE
STIMULATED EMISSION
Spectral composition of thermal and stimulated light scattering in the wing of the Rayleigh line
02 p0194 A73-11945
Stimulated molecular light scattering in gases
02 p0195 A73-11946
Saturation of stimulated ruby laser radiation under the action of CO-60 gamma rays
02 p0176 A73-12353
Spectrum of stimulated radiation in a flat-mirror resonator.
02 p0177 A73-12695
Spectral density curves for intensity fluctuations of stimulated emission from low and IR frequency gas lasers as function of thermal oscillation, mode interference and beat effects
03 p0319 A73-14087
Effect of H2 pressure on pulsed H2 + F2 laser - Experiment and theory.
05 p0583 A73-16043
Four-field parametric frequency selection in stimulated emission lines from nonlinear mirror, noting reflection coefficient
05 p0584 A73-16554
Angular distribution of first Stokes component for stimulated combinational Raman scattering investigated under various excitation conditions
06 p0700 A73-17965
Stimulated Compton scattering of laser radiation by electron plasma, determining electrons diffusion coefficient and velocity distribution function
06 p0700 A73-17970
Plasma heating, emission spectrum distortion and light pressure effects under stimulated Compton scattering, noting upper bound of cosmic maser brightness temperature
06 p0729 A73-18110
Rayleigh scattering influence on stimulated Raman effect, determining occurrence conditions for absolute instability due to feedback
06 p0702 A73-18593
Effect of impurity gradient on the time delays and Q-switching in junction lasers.
07 p0836 A73-20189
German monograph - Observation of stimulated Raman-anti-Stokes radiation of higher order and its significance for the starting phase of plasma generation by laser.
07 p0837 A73-20383
Room temperature pulsed n-type GaAs cleaved platelet lasers bulk optically pumped near band gap by tunable parametric oscillator, noting emission peak at threshold
[AD-758950] 09 p1092 A73-22240
Time behavior of the internal Q switching in GaAs lasers under electron-beam excitation.
09 p1092 A73-22245
Behavior of threshold current and polarization of stimulated emission of GaAs injection lasers under uniaxial stress.
09 p1092 A73-22247
Spontaneous emission and stimulated recombination of p-n-n double heterojunction (AlGaAs-GaAs laser diodes above and below threshold currents
09 p1093 A73-22256
A photochemical method of determining the optical pumping energy absorbed by rhodamine dyes under conditions corresponding to stimulated emission of radiation
09 p1095 A73-22668
A search for stimulated emission of radiation from superconducting tunnel junctions.
09 p1135 A73-23341

Stimulated emission of acoustic power as analog to lasers and masers, noting nonpreservation of phase between incident and stimulated pressure
10 p1249 A73-24388

Theory of spontaneous and stimulated electroluminescence of ZnS-Mn layers
10 p1261 A73-24766

Stimulated emission due to the interaction between a relativistic high-current beam and a plasma
11 p1403 A73-25241

Possible utilization of a vapor, formed by the action of a high-power electron beam on a target, as an active medium for stimulated emission of light.
12 p1507 A73-27517

Investigation of the delay of stimulated emission from a $\text{CaF}_2:\text{Dy}^{2+}$ laser relative to pumping pulses.
13 p1629 A73-29431

Influence of self-focusing on the stability of steady-state laser emission.
13 p1629 A73-29441

Observations of stimulated anti-Stokes radiation in barium vapour.
14 p1776 A73-29697

Cooperative mechanisms during laser excitation of luminescence in Yb-Tb and Yb-Eu ion activated glass.
15 p1884 A73-31713

Perfectly stirred reactor - New concept for a CW chemical laser.
17 p2184 A73-34911

Amplified spontaneous emission comparison with laser stimulated emission during He-Ne transitions, noting threshold condition relation to population inversion density
20 p2570 A73-38619

Stimulated linear acceleration radiation - A pulsar radio emission mechanism.
20 p2602 A73-39444

Stimulated Raman scattering in sulfur hexafluoride.
20 p2574 A73-39688

Asymptotic nature of threshold conditions and multimode laser emission.
20 p2574 A73-39691

Switching of the resonator Q factor by stimulated Mandel'shtam-Brillouin scattering.
20 p2574 A73-39703

Amplification of stimulated Raman scattering of light in various nonlinear amplifier pumping circuits
21 p2711 A73-40306

The mechanism responsible for shortening of the stimulated Mandelstam-Brillouin scattering-light-pulse duration and for generation of nanosecond-duration pulses
21 p2739 A73-40355

Effect of saturation on light amplification in stimulated Mandelstam-Brillouin scattering
21 p2739 A73-40359

Stimulated emission in multiple-photon-pumped xenon and argon excimers.
21 p2713 A73-40456

Stimulated entropy /temperature/ scattering and its effect on stimulated Mandel'shtam-Brillouin scattering.
22 p2868 A73-41720

Radiation field frequency dependent source function for two level atom, noting different stimulated emission and absorption line profiles
22 p2907 A73-42205

Stimulated gamma emission in long-lived nuclear isomers, proposing gamma lasers based on Mossbauer line broadening effect
23 p2988 A73-44093

Plasma heating, emission spectrum distortion and light pressure effects under stimulated Compton scattering, noting upper bound of cosmic maser brightness temperature
24 p3114 A73-44499

STIMULATED EMISSION DEVICES

NT ARGON LASERS
NT CARBON DIOXIDE LASERS
NT CARBON MONOXIDE LASERS
NT CHEMICAL LASERS
NT GALLIUM ARSENIDE LASERS
NT GAS LASERS
NT GAS MASERS
NT HCN LASERS
NT HELIUM-NEON LASERS
NT INFRARED LASERS
NT INJECTION LASERS
NT LASERS
NT LIQUID LASERS
NT MASERS
NT ORGANIC LASERS
NT PULSED LASERS
NT Q SWITCHED LASERS
NT RAMAN LASERS
NT RING LASERS
NT RUBY LASERS
NT SEMICONDUCTOR LASERS
NT SOLID STATE LASERS
NT TRAVELING WAVE MASERS

The macroscopic high-frequency quantum generator and detector of the gravitational radiation.
08 p0987 A73-21017

Quantum oscillators employing the luminescence of self-localized excitons in condensed inert gases
15 p1885 A73-31714

STIMULATION

NT AUDITORY STIMULI
NT SENSORY STIMULATION

STIRLING CYCLE

Miniature Stirling cycle refrigerators to cool IR detectors, discussing refrigerators with rhombic drive, thermal coupling to detector, triple expansion and Vuilleumier cycle
13 p1707 A73-29066

STIRRING

Stirring factors in combustion chambers - A finite-element model of mixing along an 'information flow path.'
22 p2934 A73-42784

STISHOVITE

Quartz transformation to stishovite in shock loaded quartz-copper mixture, discussing relationship to short range order phase
22 p2848 A73-42497

STOCHASTIC PROCESSES

NT MARKOV CHAINS
NT MARKOV PROCESSES
NT RANDOM PROCESSES
NT RANDOM WALK

Analysis of certain nonstationary processes by using Wiener functionals
01 p0026 A73-10026

Almost sure exponential bounds for stochastic operator systems, with applications to randomly sampled control.
01 p0027 A73-10426

Stochastic behaviour of a complex system with standby redundancy.
01 p0023 A73-10649

On the diffusion function of a stochastic transmission system
01 p0017 A73-10975

On the almost-sure sample stability of systems with randomly time-varying delays.
03 p0285 A73-13898

Book on control engineering covering dynamic system state representation, finite and infinite dimensional optimization, dynamic programming, stochastic estimation, applications, etc
03 p0285 A73-13987

Nonlinear stochastic optimal control theory application to guidance policies determination of nonmaneuvering target interception or rendezvous and goal-tending game
03 p0286 A73-14478

Limit analysis of structures with stochastic strength variations.
04 p0510 A73-15027

Partial differential equations with random coefficients and boundary conditions for stochastic processes in plasma, using parabolic equations for distribution function
04 p0479 A73-15037

Power spectral density estimation by spline smoothing in the frequency domain.
04 p0471 A73-15254

System identification using approximate nonlinear filters.
04 p0430 A73-15257

Functional analysis approach of the partial differential equation arising from non-linear filtering theory.
04 p0472 A73-15263

On the stability of linear stochastic differential equations.
[ASME PAPER 72-WA/APM-16]
04 p0472 A73-15898

Sinusoidal signal and stationary quasi-white Gaussian noise mixture effects on stochastic phase locked AFC system operation, noting phase error probability density function
05 p0547 A73-16060

Warm cloud droplet growth analysis based on stochastic coalescence equation model in terms of probability function and time evolution
05 p0592 A73-16194

Spacecraft motion control as stochastic dynamic problem formulated according to single criterion for deterministic programmed and stochastic perturbed motions
05 p0629 A73-16425

Stochastic wave model of spiral galaxy rotation based on weak interaction, obtaining frequency spectrum integrals for Milky Way Galaxy
05 p0616 A73-16454

Stochastic signal reflection by passive element, synthesizing optimal echo-signal detector for space diversity reception
05 p0550 A73-16777

Computer adaptive optimization system for problems with nonlinear criteria function and constraints, noting algorithms of deterministic and stochastic categories
05 p0555 A73-17284

Stochastic kinetic theory of strong wave-plasma interaction. I - Kinetic equations.
05 p0603 A73-17323

A stochastic model of creep in the heat-resistant low-alloy CrMoV steel
06 p0705 A73-17846

Nonsearch algorithms for parametric synthesis of stochastic automatic control systems
06 p0680 A73-18381

On weak convergence of empirical processes for random number of independent stochastic vectors.
06 p0718 A73-18520

State estimation of nonlinear system by applying stochastic approximation method.
06 p0681 A73-18813

Some preliminary notions towards improved stochastic controller synthesis via transformed indices of performance.
06 p0681 A73-18813

Adaptive control of linear stochastic systems.
07 p0804 A73-19132

Stochastic model application to divergence of horse pig lineage from common ancestor in terms of hemoglobin and fibrinopeptides alpha and beta chains
07 p0780 A73-19218

Stochastic linear system observer eigenvalue optimal placement with respect to quadratic error criterion for adaptation to digital computation and applicability to higher order system
07 p0849 A73-19966

Stochastically optimal terminal control system synthesis for loss function dependence on finite phase coordinates of dynamic system, considering soft landing of flight vehicle
07 p0805 A73-20037

Optimal control of stochastic systems with continuous and discontinuous random disturbances, obtaining problem solution conditions for linear system via dynamic programming
07 p0805 A73-20038

One dimensional elastoplastic system optimal design by stochastic programming, determining limiting stresses and random load distribution
07 p0914 A73-20151

Air-terminal queues under time-dependent conditions.
07 p0850 A73-20375

Nearest neighbor approximation for Kalman-Bucy filtering noisy data generated by multidimensional processes via dimensionality reduction for linear steady state problems
07 p0805 A73-20579

Reduced-order observers for linear discrete-time systems.
07 p0805 A73-20581

On stochastic approximation and the hierarchy of adaptive array algorithms.
07 p0846 A73-20585

The estimation of order and parameters in a process of stochastic differential equations with uncertain observations.
07 p0846 A73-20594

A discrete separation principle with a stochastic terminal constraint.
07 p0806 A73-20599

On the adaptive control of linear systems using the open-loop-feedback-optimal approach.
07 p0806 A73-20602

Wiener and Kalman-Bucy filters design with error covariance bound for performance divergence prevention under stochastic processes with unknown signal and noise densities
07 p0806 A73-20603

Theory and application of the optimal linear approximation of linear processes
08 p0983 A73-20645

The oscillation probability of self-excited multimode oscillators.
08 p0945 A73-20803

A dynamic model of some multistage aspects of research and development portfolios.
08 p1025 A73-20972

An analytical method for the filtering error evaluation of sub-optimal filters in a noisy non-linear dynamic system.
08 p0950 A73-21091

Distributed parameter system a priori stochastic optimal control, deriving canonical differential equations from dynamic programming formulation for insight into feedback control problem
08 p0950 A73-21093

Diffusion and stochastic variations of galactic cosmic rays in solar wind
08 p1000 A73-21346

Book - Stochastic differential equations.
08 p0984 A73-21833

Atmospheric turbulence effects on laser beam transmitted signals, considering filtering and detection based on doubly stochastic Poisson process
09 p1067 A73-22229

Equivalence of systems that follow a stochastic principle of computation
09 p1059 A73-22554

Optimal observation laws for certain controlled motions
09 p1069 A73-22565

- Asymptotic behavior of the distribution of the solution of a stochastic differential equation with coefficients depending on the entire history of the process
09 p1112 A73-22844
- Randomized solutions in stochastic-programming problems
09 p1112 A73-22845
- Conversion of the wave spectrum in a medium with smooth spatial-temporal fluctuations
09 p1052 A73-23082
- Wiener and Kalman filters theory for stochastic processes in communication, demonstrating optimum demodulator derivation by Kalman-Bucy theory application to double sideband amplitude modulation
09 p1065 A73-23112
- First order phase locked loop statistical transient behavior in presence of noise from differential equation numerical solution, noting correlation with computer simulation
09 p1056 A73-23404
- On-board registration and redundancy reduction method for quasi-stationary Poisson processes.
09 p1058 A73-23420
- A probabilistic approach to a differential-difference equation arising in analytic number theory.
10 p1241 A73-23643
- Function generation technique based on variables stochastic representation and clocked random pulses in data processing operations, noting application to closed loop control systems
10 p1242 A73-24016
- Linear stochastic, multivariable, optimal control, realization and time-varying systems theory developments covering external and internal representations and variance computation problems
10 p1200 A73-24045
- Optimal filtering for systems described by linear partial differential equations.
10 p1200 A73-24050
- Estimation of noise covariance matrices for a linear time-varying stochastic process.
10 p1201 A73-24053
- Problems of accuracy in the representation of values by stochastic sequences
10 p1202 A73-24418
- Wide-sense adaptive dual control for nonlinear stochastic systems.
10 p1202 A73-24533
- An actively adaptive control for linear systems with random parameters via the dual control approach.
10 p1202 A73-24534
- Sufficiently informative functions and the minimax feedback control of uncertain dynamic systems.
10 p1202 A73-24535
- Optimal stochastic linear systems with exponential performance criteria and their relation to deterministic differential games.
10 p1202 A73-24536
- Solution of the stochastic control problem in unbounded domains.
10 p1203 A73-24705
- Memory included linear stochastic system optimum control over finite time, using Liapunov-Krasovskii functionals
11 p1398 A73-25618
- Synthesis, with the aid of Liapunov functions, of optimal and suboptimal discrete systems for controlling determinate and stochastic plants
11 p1341 A73-25619
- Normalization of stochastic system analog of linear determinate system with combined normal distribution of input/output signal, noting theorems for random variable distributions
11 p1341 A73-25632
- The principle of complexity and the method of regularization in stochastic problems of optimal automatic control system synthesis
11 p1341 A73-25634
- Efficiency estimates of methods for analyzing the precision of nonlinear control systems
11 p1342 A73-26094
- Loading time to failure and creep rupture strength from interatomic stochastic bond fracture
11 p1448 A73-26739
- Several estimates in the theory of stochastic integrals
12 p1517 A73-27186
- Convergence of distributions of point complexes in Z /super m / to Poisson processes
12 p1523 A73-27191
- Stochastic equations of nonlinear filtering of random processes
12 p1518 A73-27222
- Correlation analysis of systems with stochastic inertial elements.
12 p1484 A73-27458
- Analysis of the stochastic stability of pulsed control systems in the frequency domain
12 p1485 A73-27622
- Optimal control with probabilistic quadratic performance criterion and constraints, using stochastic principle for reduction to time derivative maximization problem
12 p1485 A73-27897
- Stability of stochastic dynamical systems; Proceedings of the International Symposium, University of Warwick, Coventry, England, July 10-14, 1972.
12 p1519 A73-27920
- Raman scattering from phonon bath using quantum mechanical model with random and stochastic Stokes and anti-Stokes coupled modes in light fields
13 p1658 A73-28209
- Numerical study of the stochasticity of dynamical systems with more than two degrees of freedom.
13 p1648 A73-28425
- Other stability criteria for distributed and Gaussian stochastic systems with diagonal nonlinearity
13 p1596 A73-28564
- The stochastic and deterministic aspects of the 'classical' approach to problems of quantum mechanics.
13 p1661 A73-29388
- Fatigue crack propagation as successive stochastic processes and fatigue fracture toughness.
13 p1701 A73-29490
- Zero sum differential game theory for two players, discussing strategies, stochastic versions and saddle value and points existence
13 p1651 A73-29650
- A first-harmonic method for nonlinear distributed-parameter systems subjected to deterministic or stochastic loads
14 p1738 A73-29707
- Book - Statistical mechanics, kinetic theory, and stochastic processes.
14 p1774 A73-29947
- Ion acoustic wave scattering effects on stochastic ion heating in turbulent plasma
14 p1780 A73-30340
- Statistical displacement characteristics of random multiphase composite elastic structures in terms of stochastic Green functions and Neumann series
14 p1811 A73-30482
- Nonlinear feedback systems and weakly stationary stochastic processes.
14 p1739 A73-30503
- Cone-bounded nonlinearities and mean-square bounds - Estimation upper bound.
14 p1769 A73-30505
- Frequency-domain criteria for stability of a class of nonlinear stochastic systems.
14 p1739 A73-30506
- Mathematical models and identification of bilinear systems.
14 p1740 A73-30782
- Application of the Poisson stochastic process for collision relaxation calculations in a nonequilibrium
15 p1915 A73-30968
- Stability of a stochastically excited nonlinear cylindrical shell.
15 p1949 A73-31654
- Stochastic heating of a plasma during development of a Langmuir turbulence instability
15 p1918 A73-31705
- Optimal stochastic guidance laws for tactical missiles.
15 p1908 A73-31917
- Stochastic integrals of cylindrical Brownian movements on Hilbert space
15 p1900 A73-32207
- Differential equations with free boundaries in stochastic control problems
16 p2031 A73-32822
- Solutions of a class of random differential equations.
16 p2032 A73-33308
- The relation of tests with electrodynamic vibrators to the Woehler testing technique
16 p2037 A73-33379
- Equipment life cycle costs dependence on acquisition decision making, discussing stochastic computer simulation of failure times, repairs, inventory replacement and personnel availability
16 p2089 A73-33655
- Propagation of frequency-modulated pulses in a randomly stratified plasma.
17 p2214 A73-34095
- Linear open signal scanning system distortion of stationary stochastic signals, examining transfer characteristic improvement by optimal filter
17 p2121 A73-34245
- Optimal observer techniques for linear discrete time systems.
17 p2144 A73-34361
- A projection model for Bayesian estimation of distributed functions.
17 p2202 A73-35373
- Unsupervised learning of the optimal linear signal estimator in the presence of unknown multiplicative, additive, and message generating noise.
17 p2144 A73-35374
- Optimal control with probabilistic quadratic performance criterion and constraints, using stochastic principle for reduction to time derivative maximization problem
18 p2294 A73-36602
- Application of the Ornstein-Uhlenbeck stochastic process to the study of dynamic systems in an environment of stochastic disturbances.
18 p2330 A73-36829
- Optimal feedback control and Kalman filter design via an interactive computing and visual display system.
18 p2295 A73-36839
- A stochastic model of the galactic magnetic field.
18 p2356 A73-36974
- Discrete stochastic linear servomechanism with observation costs, deriving optimal control solution with extension to nonlinear systems suggested by dynamic population models
19 p2412 A73-38029
- A sensitivity approach to the decoupling of linear systems with parameter disturbances.
19 p2412 A73-38034
- Performance of LQG control systems using optimal k-step-ahead control laws.
19 p2413 A73-38062
- A computational algorithm for design of regulators for linear jump parameter systems.
19 p2408 A73-38066
- Normalization of stochastic system analog of linear determinate system with combined normal distribution of input/output signal, noting theorems for random variable distributions
19 p2414 A73-38143
- Synthesis of optimal automatic control systems by use of the complexity principle and of the regularization method.
19 p2414 A73-38145
- Construction of improving variations during the optimization of determinate and stochastic systems
20 p2539 A73-38677
- Synthesis problems of adaptive systems for processing information and accepting solutions
20 p2531 A73-38684
- Adaptive /learning/ intelligent system design and simulation for control with stochastic goal and environment conditions
20 p2532 A73-38685
- Self organizing behavior of multivariable stochastic extremal control systems with environmental or intrinsic positive feedback under perturbation
20 p2539 A73-38689
- Stochastic process control with a regulated control interval duration
20 p2540 A73-38701
- Complex stochastic control system identification by distribution and moments characteristics in form of Gaussian densities, perturbation polynomials and seastatic functions
20 p2540 A73-38708
- Certain methods of determining the dynamic characteristics of stochastic objects
20 p2540 A73-38710
- Design and analysis of a practical on-line filter to process gyrocompass data.
20 p2564 A73-38782
- [AIAA PAPER 73-841] Management of the treatment of illnesses as a problem of modern control theory
20 p2518 A73-39348
- Optimal control of stochastic systems with random shocks and discontinuous trajectories, using functional minimization
20 p2582 A73-39388
- Excitation of parametric vibrations in stochastic systems with two degrees of freedom
20 p2594 A73-39641
- Plant canopy models for simulating composite scene spectroradiance in the 0.4 to 1.05 micrometer region.
20 p2562 A73-39906
- Self consistent microscopic theory of Rayleigh light scattering by molecular aggregates based on random phase modulation and stochastic theories
21 p2739 A73-40219
- Russian book - The stochastic structure of cloud and radiation fields.
21 p2730 A73-40243
- Passive stochastic feedback stability. I - A general theory. II - Applications.
21 p2669 A73-40450
- Application of stochastic programming methods for solving certain optimization problems of multiple-link plants without memory
22 p2836 A73-42612
- Monograph - Fatigue and stochastic loadings.
22 p2923 A73-42673
- German monograph - Principles concerning proofs regarding optimality conditions in the case of time-dependent processes.
22 p2888 A73-42853
- Radar altimeter signal propagation delay estimation, calculating and plotting noise fluctuation characteristics as function of aircraft ground speed, altitude and other parameters
22 p2828 A73-43067
- Synthesis of two-level controller for a class of linear plants in an unknown environment.
23 p2963 A73-43289
- Level transgressions and extremal values of continuous stochastic signals
23 p2952 A73-43310

- Fluidic circuits application to stochastic computer with analog to digital converter and logic gates for arithmetic operations 23 p2944 A73-43419
- Comparative studies of model reference adaptive control systems. 23 p2963 A73-43817
- On the adaptive control of linear systems using the open-loop-feedback-optimal approach. 23 p2964 A73-43824
- Optimal stopping time for stochastic games corresponding to diffusion process, obtaining saddle point characterization via elliptical variational inequality solution 23 p2999 A73-44083
- Bispectrum synthesizer by using multiple Poisson processes. 23 p2965 A73-44089
- An existence and uniqueness theorem for the solution of a stochastic integrodifferential equation 23 p2999 A73-44101
- Signal analysis using stochastic-ergodic principles, discussing PCM correlation procedures, analog-digital signal conversion and measurement methods 23 p2983 A73-44149
- Representation of functions of Markov processes as solutions of stochastic equations. 23 p3000 A73-44207
- Synthesis of cascaded multiple-loop feedback systems with large plant parameter ignorance. 24 p3073 A73-44584
- Application of stochastic differential equations in description of automatic control plants 24 p3074 A73-45098
- A criterion for a free choice of decisions involving continuous control systems 24 p3074 A73-45100
- STOICHIOMETRY**
- Vibrational and chemical nonequilibrium in a stoichiometric turbojet engine using kerosene-type fuel. [ALAA PAPER 72-1208] 03 p0273 A73-13491
- Stoichiometric gas turbines - Development problems. 03 p0359 A73-14146
- Accelerated tests for long term stability of CdS solar cells, noting stoichiometry, wavelength, doping and residual atmosphere effects on cell performance 03 p0255 A73-14215
- Fuel-rich and stoichiometric carbon monoxide-nitrous oxide premixed laminar flames with varying water contents, determining flame temperature by line reversal method 03 p0399 A73-14396
- On supposedly five-co-ordinate titanium (IV) complexes - The crystal and molecular structure of $\text{Cl}_3\text{Ti}/\text{CSH}_7\text{O}_2$. 06 p0661 A73-18266
- Titanium monoxide system cation self-diffusion coefficients, and quenched-in vacancy concentrations as function of stoichiometry, tabulating Arrhenius parameters 13 p1633 A73-28145
- Reaction $\text{H} + \text{C}_2\text{H}_4$ - Investigation into the effects of pressure, stoichiometry, and the nature of the third body species. 13 p1581 A73-29426
- Regularities in the behavior of semiconductors and dielectrics in connection with deviation from stoichiometry 23 p2959 A73-43479
- STOKES FLOW**
- The stability of oscillatory Stokes layers. 03 p0291 A73-13065
- A model for eddy conductivity and turbulent Prandtl number. [ASME PAPER 72-WA/HT-13] 04 p0434 A73-15834
- The applicability of Stokes expansions to reversed flow. 05 p0565 A73-16606
- Numerical solution of the Navier-Stokes equations by the finite element method. 07 p0810 A73-19501
- Differential solutions of the biharmonic Poisson and first order Stokes equations. 08 p0983 A73-21203
- The Stokes problems for a suspension of particles. 08 p0955 A73-21426
- Nonlinear streaming effects associated with viscous incompressible fluid near oscillating cylinder, considering theory based on outer-inner expansion technique with Stokes drift correction 20 p2546 A73-39088
- STOKES LAW**
- Light scattering in coherent systems for Stokes and anti-Stokes impurity centers in terms of classical and quantum mechanical theories 13 p1660 A73-28770
- STOKES LAW [FLUID MECHANICS]**
- Liquid droplet drag in vapor flow as function of drop vaporization rate, using Stokes formula 11 p1451 A73-25736
- On unsteady Stokes, Ekman and Rayleigh layers in a rotating fluid. 17 p2150 A73-34322

- Bilinear hydrodynamics and the Stokes-Einstein law. 21 p2676 A73-40218
- The slow unsteady settling of two fluid spheres along their line of centres. 22 p2840 A73-41742
- STOKES THEOREM [VECTOR CALCULUS]**
- An explicit form of the Mie phase matrix for multiple scattering calculations in the I, Q, U and V representation. 11 p1390 A73-25718
- Nonholonomic generalization of the Stokes theorem 19 p2462 A73-38542
- STOL AIRCRAFT**
- U SHORT TAKEOFF AIRCRAFT
- STONES [ROCKS]**
- U ROCKS
- STONY METEORITES**
- NT ACHONDrites
- NT BRUDERHEIM METEORITE
- NT CARBONACEOUS METEORITES
- NT CHONDrites
- NT ORGUEIL METEORITE
- NT TEKITTES
- NT TUNGUSK METEORITE
- The Angra dos Reis /stone/ mineral assemblage and the Genesis of stony meteorites. 03 p0374 A73-13797
- Iron and stony-iron meteorites kamacite hardness and shock histories, hypothesizing preterrestrial collisions between asteroid sized objects 05 p0615 A73-16377
- Stony meteorite discovery at Ness County, Kansas, noting three separate falls and composition and mineralogical differences from Kansada, Franklinville and Wellmanville meteorites 09 p1138 A73-21851
- Seminole meteorite external form chondrite composition and structure, noting brecciation and chondrules 09 p1139 A73-21854
- The Oro Grande, New Mexico, chondrite and its lithic inclusion. 09 p1139 A73-21858
- Ransom /Kansas/ stony meteorites discovery location map, describing megascopic appearance, petrology and chemical group 09 p1139 A73-21859
- The chemical composition of the Haveroe meteorite and the genesis of the ureilites. 09 p1140 A73-21864
- Tillaberi /Niger/ stony meteorite elements abundance and radioactivity determination by gamma ray spectrometry 09 p1149 A73-23032
- Certain peculiarities in the distribution of mercury in meteorites. 10 p1278 A73-24106
- Temperature gradients and atmospheric ablation rates for the Barwell meteorite. 11 p1419 A73-25779
- Stony-iron meteorite shock histories, determining crystallographic character of kamacite in samples via back reflection X ray diffraction technique 11 p1419 A73-25780
- Aluminum-26 in meteorites. VII - Ureilites, their unique radiation history. 17 p2237 A73-35803
- Nuclide production rates in stone meteorites and lunar samples by galactic cosmic radiation. 20 p2612 A73-39716
- The Mighei meteorite. 24 p3137 A73-44950
- STOPPING**
- NT THRUST TERMINATION
- STOPPING POWER**
- The stopping power of atomic matter for relativistic ions, mesons, electrons and positrons. 07 p0852 A73-19036
- Charged stopping pions from nuclear-electromagnetic cascades in rock, calculating number and energy spectra by Monte Carlo method 13 p1671 A73-29667
- STORABLE PROPELLANTS**
- NT AIRCRAFT FUELS
- Mono- and multipropellant, storable and cryogenic, liquid rocket propulsion engines developments including gas generators and engines [ALAA PAPER 72-1104] 03 p0355 A73-13422
- Experimental evolution of an earth-storable bimodal rocket engine. [ALAA PAPER 72-1128] 04 p0486 A73-14913
- STORAGE**
- Testing of spacecraft in long-term storage. 16 p2073 A73-33615
- STORAGE BATTERIES**
- NT NICKEL CADMIUM BATTERIES
- NT NICKEL ZINC BATTERIES
- NT SILVER ZINC BATTERIES
- A nickel-hydrogen secondary cell for synchronous orbit application. 09 p1033 A73-22753

- Autonomous composite power system with electrochemical generator, ion exchange membrane and storage battery 11 p1308 A73-25640
- An electrochemical cell equivalent circuit for storage battery/power system calculations by digital computer. 11 p1309 A73-25640
- STORAGE RINGS [PARTICLE ACCELERATORS]**
- A computational study of the non-linear stage of development of radiation instability in relativistic electron rings. 09 p1131 A73-22750
- STORAGE STABILITY**
- Estimation of reliability in storage - Optimal test procedure 07 p0830 A73-19490
- A megard plastic film dosimeter. 23 p2949 A73-44207
- STORAGE TANKS**
- Influence of the flexibility of the walls on the oscillations of the liquid masses of storage tanks 12 p1487 A73-27390
- Cape Kennedy Space Center ground support equipment welding machines and techniques, emphasizing propellant storage tanks and mobile launcher transporters 16 p1995 A73-33100
- STORMS**
- NT CYCLOGENESIS
- NT CYCLONES
- NT HURRICANES
- NT IONOSPHERIC STORMS
- NT MAGNETIC STORMS
- NT NOISE STORMS
- NT POLAR SUBSTORMS
- NT RAINSTORMS
- NT SOLAR STORMS
- NT STORMS [METEOROLOGY]
- NT SUDDEN IONOSPHERIC DISTURBANCES
- NT THUNDERSTORMS
- NT TORNADOES
- NT TROPICAL STORMS
- NT TYPHOONS
- Meteorological Doppler radar for measurements of particle velocity and horizontal winds inside convective storms, discussing signal processing and multiple radar method 24 p3107 A73-44600
- STORMS [METEOROLOGY]**
- NT HURRICANES
- NT POLAR SUBSTORMS
- NT RAINSTORMS
- NT THUNDERSTORMS
- NT TORNADOES
- NT TROPICAL STORMS
- NT TYPHOONS
- Measurement of wind gradients in convective storms by Doppler radar. [AD-751716] 03 p0278 A73-14530
- Storm cell models from digital radar data. 03 p0338 A73-14530
- Convective storm updraft shape calculation based on horizontal momentum changes in rising air, noting effects of mixing and aerodynamic drag 05 p0592 A73-16100
- Time lapse stereo photogrammetry of ring vortex type circulation in cumulonimbus cloud tops of high bearing storms 07 p0847 A73-19000
- Mars dust storm observations at time of great oppositions, suggesting local time and space meteorological conditions and feedback processes favoring global dust spread 09 p1144 A73-22220
- Wind profile measurements in proximity of moderate storm. 13 p1651 A73-28220
- Digitized weather radar data models of intense storm cells with 1-2 km resolution and 10 dBZ reflectivity 16 p1983 A73-33770
- Pulsed-Doppler velocity isotach displays of storm winds in real time. 18 p2333 A73-36770
- Structure of dust storms from ITOS-I T.V. images obtained over Iraq and the Gulf of Persia. 20 p2584 A73-39800
- Infrasound from convective storms - Examining the evidence. 21 p2679 A73-40000
- Point discharge current measurements in trees at metal points during storms, discussing implications for structure of electrified clouds 21 p2684 A73-40070
- Mapping of North Atlantic winds by HF radar scatter interpretation. 22 p2882 A73-41800
- Stormy weather vertical air motion velocity calculation for use in synoptic field and atmospheric energy budget evaluations 23 p3003 A73-43900
- STOSS-AND-LEE TOPOGRAPHY**
- U GLACIAL DRIFT

STRAIGHT WINGS

U RECTANGULAR WINGS

STRAIN AGING

U PRECIPITATION HARDENING

STRAIN DISTRIBUTION

U STRESS CONCENTRATION

STRAIN ENERGY METHODS

The fracture energy of carbon-fibre reinforced glass.

01 p0068 A73-11500

Approximate conditions to account for spring mass redistribution with kinetic energy conversion into strain energy over small critical time interval.

02 p0230 A73-11795

Application of the basic concepts of structural-energetic theory to the problem of physical fatigue limit.

02 p0235 A73-12131

A strain energy basis for studies of element stiffness matrices.

03 p0395 A73-14184

Inflation-extension and eversion of a tube of incompressible isotropic elastic material.

04 p0512 A73-15234

Lateral rigidity of longitudinally stiffened plates.

05 p0633 A73-16543

Wave propagation in a micro-isotropic, micro-elastic solid.

06 p0762 A73-17990

Stress intensity factors and singularity power and strain energy release rate near localized cracks and inclusions in composite materials

06 p0764 A73-18489

Uniqueness of non-linear elastic equilibrium for prescribed boundary displacements and sufficiently small strains.

06 p0719 A73-18700

A special theory of crack propagation.

09 p1161 A73-23177

A comparison of solutions in first approximation shell theory.

10 p1291 A73-24337

Russian book on linear truss systems potential strain energy and displacements covering matrix and graph-analytic methods, influence functions, simple and complex strains, etc

11 p1442 A73-25775

Energy flux into extending crack in elastic solid calculated in terms of stress intensity factor for plane and antiplane strain problems

11 p1444 A73-26281

Estimates for stress derivatives and error in interior equations for shells of variable thickness with applied forces.

11 p1446 A73-26548

Model for lateral variations of lunar density minimizing total shear strain energy of moon, noting gravitational potential equal to observed potential at surface

12 p1541 A73-27488

Criteria for finite element discretization of shells of revolution.

13 p1691 A73-28084

Limit of linear viscoelastic behavior - An energy criterion.

13 p1700 A73-29465

Inelastic strain and hysteresis energy criteria for fatigue fracture of metals.

13 p1641 A73-29499

Evaluation of dissipation and damage in metals submitted to dynamic loading.

13 p1701 A73-29505

Finite deformation behavior of elastomers - Dependence of strain energy density on degree of crosslinking for SBR.

13 p1646 A73-29527

Finite element method investigation of branch and secondary crack formation and multiple fracture, solving sequences of boundary value problems and strain energy release rates

14 p1808 A73-30195

Minimum potential and complementary energy rate principle formulation for finite plastic deformation, applying to cylindrical shell under uniformly distributed internal load

14 p1809 A73-30258

A numerical and experimental investigation of the use of J-integral.

17 p2246 A73-34880

Classical fracture mechanics concepts, considering Griffith theory and modifications for ductile materials and strain energy density field

17 p2246 A73-34883

Approximate method for determining the natural frequencies of flexible rectangular plates

18 p2363 A73-36408

Stress field in a sphere subjected to large deformations.

19 p2500 A73-38111

Some further results of J-integral analysis and estimates.

22 p2920 A73-42144

A comparison of the J-integral fracture criterion with the equivalent energy concept.

22 p2920 A73-42145

J-integral and equivalent energy method parameter relationship from elastic and inelastic stress concentration factors for notches and cracks

22 p2920 A73-42146

Experimental verification of lower bound K sub Ic values utilizing the equivalent energy concept.

22 p2875 A73-42147

Combined radial-axial large amplitude oscillations of hyperelastic cylindrical tubes.

22 p2923 A73-42637

Piecewise linear law of the relation between stresses and strains for large deformations

23 p3043 A73-43920

Numerical analysis of pre- and post-critical response of elastic continua at finite strains.

24 p3150 A73-45227

Optimization of fiber reinforced composite structures.

24 p3151 A73-45304

STRAIN FATIGUE

U FATIGUE [MATERIALS]

STRAIN GAGE ACCELEROMETERS

Characteristics of beam- and membrane-type strain-gage sensors of linear acceleration

07 p0826 A73-20529

STRAIN GAGE BALANCES

Six-channel strain-gauge system for dynamic measurements

07 p0827 A73-20539

Fabrication of high precision strain gauge dynamometers and balances at the O.N.E.R.A. Modane Centre.
[ONERA, TP NO. 1196]

22 p2839 A73-42217

STRAIN GAGES

Performance test of flexible rolled-up solar array /FRUSA/ via telemetered data from accelerometers, strain gages and temperature sensors, noting feasibility for spacecraft power supply

03 p0256 A73-14236

Error effects in dynamic force measurements performed on materials testing pulsators

04 p0450 A73-15475

Understanding and applying strain gages. II - Carriers, adhesives, and coatings.

06 p0696 A73-18675

The measurement of thermal strain using self-temperature compensated strain gages.

07 p0823 A73-19567

Transverse sensitivity effect on measurement errors and rig calibrating of strain gages

07 p0823 A73-19568

Self-compensating strain measurement in rotating disks subjected to elastic and plastic deformation

07 p0826 A73-20516

Strain gauge for measuring longitudinal and transverse strains

07 p0826 A73-20518

A modified sensor of linear accelerations, velocities, and displacements over a path of 0 to 1500 mm

07 p0826 A73-20527

Durability of foil-type tensometric sensors under varying load conditions

07 p0827 A73-20536

Calibration of resistance strain gages

07 p0827 A73-20538

Strain-gauge sensor of flow velocity and fluid discharge

07 p0828 A73-20544

A dynamic polariscope for stress wave analysis.

08 p0962 A73-20668

Semiconductor strain transducer

08 p0950 A73-21720

Instrument Society of America, Annual Conference, 27th, New York, N.Y., October 9-12, 1972, Proceedings. Part 2.

09 p1082 A73-22501

Stress miscalculation due to resistance strain gage errors, deriving expressions for stress-strain error relationships

09 p1083 A73-22505

Prefabricated strain gage bridge instrumentation for flight testing under time and environment installation restrictions, including tail vibration, wing load and tail boom tests

09 p1083 A73-22506

Strain gage measurement errors under long term installation conditions, considering drift, temperature and moisture effects, connection wires impedance and selector switch contact resistance

10 p1219 A73-24568

Piezoresistive semiconductor strain gage optimum applications and practical merits comparison with wire or foil resistance types, considering stability, accuracy and temperature compensation

10 p1195 A73-24571

A note on the arrangement of strain gages and the sensitivity of strain measurement.

10 p1219 A73-24572

Equipment for highly accurate and repeatable strain gage factor determination.

10 p1220 A73-24574

Russian papers on thermal stresses investigation in machine and structural elements covering stress simu-

lation and strain gage methods for model and full scale structures

11 p1435 A73-25451

Strain gages and photoelastic coating methods of thermal stress determination for model and full scale tests

11 p1435 A73-25452

Investigation of the preparation of high-temperature strain gages based on heat-resistant oxides

11 p1362 A73-25455

Thermal characteristics of constantan, Ni-Cr-Fe, Ni-Mo, Ce-Al-Fe and Ni-Cr alloy filaments for high temperature strain gages

11 p1362 A73-25456

Methods and means of studying the characteristics of heat-resistant strain gages by means of devices heated by electric current

11 p1362 A73-25457

Implantable transducer for in vivo measurement of bone strain.

12 p1464 A73-27443

Silicon semiconductor resistance strain gage intrinsic thermal noise characteristics at 20 Hz-10 kHz, noting 1/f type as dominant noise component in audio frequency range

13 p1611 A73-28021

Strain gage measurements of elastoplastic deformations under biaxial and triaxial stresses with application to cylindrical steel container

13 p1617 A73-28843

Tensometric strain gage evaluation of stress analysis methods for hollow cylindrical shells under uniform internal pressure

13 p1698 A73-29057

Automatic evaluation of strain gage data reliability by comparison with a preset parameter and determination of a statistical yield strength.

13 p1622 A73-29549

Electrical model for calculation of resistance strain gage errors due to grid-grid and grid-body shunt currents

13 p1622 A73-29617

Structural analysis via thermoplastic scale model testing with resistance strain gages, considering temperature and humidity effects on measurement accuracy and reliability

14 p1750 A73-29701

Design and development of Manganin and other wire sensors together with a resistance strain gage transducer for use at pressures up to 200 000 lbf/sq in /1.38 GN/sq m/.

14 p1750 A73-29702

Radio telemetry for strain measurements in turbines.

14 p1752 A73-30064

High reliability solid state force sensors for flight control systems.

17 p2165 A73-34603

Use of cellulose crystallite structures with solid state strain gages for humidity and moisture measurement.

17 p2166 A73-34621

Strain gage circuit with exponential pulsed power supply for data recovery in presence of high amplitude electrical noise

17 p2167 A73-34625

Performance and economic advantages offered by a diffused semiconductor strain gage pressure transducer.

17 p2167 A73-34626

The application of strip strain gages for measuring residual surface stresses in beryllium.

17 p2191 A73-35438

Airborne flight-test strain gage instrumentation from installation, calibration and data recording and reduction standpoint, discussing ground and airborne minicomputer use

17 p2148 A73-35442

YF-12 aircraft flight loads measurement program with strain gage bridges in fuselage, fuel tanks, control surfaces and left wing

17 p2107 A73-35444

Interferometric surface strain measurement with optical strain gage using laser-generated interference pattern with linear fringe motion-intensity relation

17 p2173 A73-35453

The use of a high modulus inclusion gage in nonlinear viscoelastic materials.

17 p2173 A73-35457

Factors affecting the results of strain gage measurements performed by electrical resistance strain gages

18 p2316 A73-36473

Tensometric strain gage evaluation of stress analysis methods for hollow cylindrical shells under uniform internal pressure

18 p2366 A73-36889

Autocompensatory strain measurement of rotating disks subjected to elastic and plastic deformation.

19 p2430 A73-37792

Strain gauge for measurement of axial and transverse strains.

19 p2430 A73-37794

- Fluidic strain gages based on detection of flow resistance or pressure drop changes due to elongation, comparing various type gage factors
20 p2564 A73-38873
- Effects of misalignment on the pre-macroyield region of the uniaxial stress-strain curve.
20 p2576 A73-39030
- Detuning of Wheatstone-bridge circuit during the measurement with wire strain gages - Influence and elimination of undesired effects on detuning
20 p2566 A73-39630
- An improved method of triggering oscilloscopes for dynamic-strain measurements.
21 p2704 A73-41267
- Russian book - High-temperature strain gauges based on heat-resistant oxides.
21 p2704 A73-41286
- Microstrain gage for plastic deformation measurements of crystalline solids in compression, obtaining stress-strain diagrams for Ta single crystals
23 p2986 A73-44036
- Errors produced by the influence of unsteady heating in strain measurement by wire-type resistance strain gages
23 p2983 A73-44292
- Digital microstress gauge for magneto-thermal gas transport studies.
24 p3089 A73-44815
- ### STRAIN HARDENING
- The Bauschinger effect in annealed and irradiated titanium
01 p0064 A73-10495
- Unit for fatigue testing with a pulsating load at a specified force and deflection.
01 p0054 A73-11299
- Cr, Ti, Ce, V and Nb carbide-forming additives effects on crystal dislocations growth and movement during strain hardening of Mn rich steel
01 p0066 A73-11345
- Surfaces of constant rate of energy dissipation and deformation velocity for arbitrary thin walled shell under steady creep with given strain hardening
02 p0233 A73-11937
- The creep of materials being weakly strengthened in nonsteady temperature and force conditions.
02 p0180 A73-12138
- Fatigue induced microstructural changes in metals and alloys, considering crystal lattice defects, crack formation and propagation, dislocations and strengthening effects
03 p0321 A73-13133
- Impulsive loading of rectangular plates with finite plastic deformations.
03 p0389 A73-13322
- Microstructural changes that drilling and reaming can cause in the bore holes in DTD 5014 /RR58 extrusions/.
03 p0325 A73-13573
- Mechanical properties of base and coating metals for explosive plating, noting heat treatment for strain hardening prevention
03 p0312 A73-13584
- Some factors affecting high-temperature strength of matrix in heat resisting alloys.
04 p0464 A73-15577
- Upper yield point removal in pure Ta by reversed cyclic stressing at room temperature, indicating cumulative mobile dislocation multiplication
05 p0586 A73-16136
- Partial yielding of cylindrical pressure vessel with elastic modulus and yield function as arbitrary functions of radial coordinate, assuming elastoplastic strain hardening material
06 p0761 A73-17895
- Stress-strain diagrams and strain hardening curves, proposing unified representation plane
07 p0913 A73-20089
- The effect of grain size on the fatigue of an Al-Mg alloy.
07 p0839 A73-20114
- Theoretical and experimental prediction for pulsating creep failure.
07 p0917 A73-20489
- Influence of the type of the stress-strain state on strain-hardening of materials
09 p1157 A73-22155
- Austenitic alloys internal friction and strain aging under quenching, cold working and electron irradiation, considering carbon vacancies stress induced reorientation effects
09 p1101 A73-22407
- Ti based beta alloy strain hardening and failure characteristics, emphasizing initial deformation phase and microdefect onset and development
09 p1105 A73-23064
- Plane stress rupture criterion for age hardening materials during plastic deformation, calculating resistance to shear and torsion of solid and hollow round bars
09 p1106 A73-23157
- Stability of structure and mechanical properties of molybdenum under prolonged influence of temperature and stress.
09 p1106 A73-23160

- Causes of embrittlement in the 11Kh18M steel
09 p1107 A73-23195
- Elastoplastic deformation and hardening function of perforated plates under in-plane tensile loads
09 p1164 A73-23346
- Increasing the fatigue strength of metals by optimizing the thermal regime during strain hardening
10 p1226 A73-24799
- Impact response of curved box beam-columns with large global and local deformations.
11 p1440 A73-25530
- The soft surface effect in plastic deformation and fatigue of metals and alloys.
11 p1381 A73-25808
- An empirical analysis of titanium stress-strain curves.
13 p1632 A73-28133
- Strain hardening and instability in biaxially stretched sheets.
13 p1623 A73-28139
- Nimonic and Mg alloys creep behavior interpretation by constitutive law, discussing recovery activation and strain hardening from microstructural behavior
13 p1642 A73-29515
- Serrated flow in quenched duralumin alloy.
14 p1758 A73-29745
- Bauschinger effect in annealed and irradiated titanium.
14 p1759 A73-30320
- The Portevin-Le Chatelier effect in the case of alloys of copper with aluminum, gallium, germanium, arsenic, and indium
14 p1760 A73-30443
- Strengthening of chromium-nickel steels with unstable austenite
15 p1889 A73-31809
- Transient thermal stresses in a disc of linearly strain-hardening material.
17 p2243 A73-34547
- High strength steel strain hardening residual stresses, discussing rolling treatment, complex strengthening, fatigue strength, asymmetric stress cycles and torsional stress
18 p2323 A73-36762
- Effect of temperature on the effectiveness of hardening components made of heat-resistant alloys
19 p2439 A73-37268
- Effects of interstitial content and grain size on the strength of titanium at low temperatures.
19 p2440 A73-37542
- A model of strain hardening during high-temperature creep.
19 p2442 A73-38168
- Anisotropic nature of strain hardening during unsteady creep of alloy AK4-1 subject to combined tension and torsion
20 p2577 A73-39288
- Round bars of an anisotropically hardening material in torsion
20 p2619 A73-39356
- Strain-hardening anisotropy and original anisotropy in creep
20 p2580 A73-39364
- Dislocation structure of Ni3Fe and Ni3FeCr alloys in various stages of strain hardening
20 p2579 A73-39742
- Nature of the strain-hardening of titanium beta solid solutions
22 p2874 A73-42096
- Effect of stressed state on strain hardening.
22 p2919 A73-42104
- Unified plastic yield criterion for ductile solids.
22 p2923 A73-42555
- Influence of structural changes arising during the hardening process on element lifetime
23 p2984 A73-43438
- The nature of the high microhardness of surfaces strain-hardened by friction
23 p2984 A73-43467
- Metal fatigue phases investigation including strain hardening under cyclic loads and microcrack nucleation due to dislocation formation under hydrostatic pressure
23 p2993 A73-43966
- Classical viscoplasticity and Mandel plasticity theories comparison with emphasis on strain hardening, acceleration wave propagation and plastic and elastic deformations
23 p3043 A73-43968
- Evolution of the stress state and hardening for certain materials with positive hardening
23 p3044 A73-43975
- Potential theory-based relationships between plastic deformation and strain hardening properties of elastoviscoplastic and elastoplastic media, considering specific entropy and free energy contributions
23 p3045 A73-44099
- On the age-hardening of Fe-Pt-Mn ternary alloys.
23 p2994 A73-44139
- Influence of electrolytic polishing on the stress-concentration sensitivity of some alloys in fatigue
23 p2995 A73-44283

- An elastoplastic strain-hardening material - Quasi-static evolution of the stress distribution
24 p3147 A73-44770
- Hardening and softening of aluminum alloys under load at 135-150 C.
24 p3100 A73-45755
- Strengthening of Cr-Ni steels with unstable austenite.
24 p3100 A73-45752
- Structural analysis for idealized nonlinear material behavior.
24 p3152 A73-45336
- ### STRAIN RATE
- An analysis of the breaking elongation in high velocity impact of the power law hardening materials.
01 p0117 A73-11111
- Remotely sensing strain-rate meter based on Doppler shift of laser light.
02 p0168 A73-11900
- Effect of strain-rate and temperature on the resistance to torsional deformation of several aluminum alloys.
03 p0384 A73-13110
- Stress shock waves effect on polycrystalline metal grain structure, discussing strain rate critical value zones
03 p0386 A73-13116
- Impulsive loading of rectangular plates with finite plastic deformations.
03 p0389 A73-13322
- Optimal temperature and strain rate for deformation in superplastic state for alpha-beta Ti alloy
04 p0464 A73-15440
- Viscoplasticity theory based on strain rate vector perpendicularity to quasi-static yield surface, comparing results to Perzyna theory
07 p0907 A73-19000
- The critical rate of tensile stress application and its significance for characterizing the behavior of materials under impact loads
07 p0838 A73-19220
- Creep strength of low alloy ferritic steels at high strain rates as function of grain boundary structure and matrix deformation
08 p0979 A73-21600
- Rheological equation for expansion rate effects on stress-strain relation of polyester binders hardened thermochemically and by gamma radiation
08 p1019 A73-21700
- On dynamic plasticity. I
08 p1020 A73-21800
- Plastic strain rates within discrete crack tip zones and running brittle cracks in mild steel plates, identifying twinning as main deformation mode
09 p1163 A73-23200
- Upper bounds to plastic strains in shake-down structures subjected to cyclic loads.
11 p1434 A73-25200
- The effect of strain rate on the characteristic values of the linear-elastic fracture mechanics determined on large and small specimens
11 p1380 A73-25400
- Prediction of inelastic high temperature material behavior by strain-rate approach.
11 p1450 A73-25500
- [AIAA PAPER 73-386]
Udimet 700 creep behavior under cyclic tensile stresses at 925 C from hodograph of monotonic stress-strain relations, taking into account strain rate effects [AIAA PAPER 73-387]
11 p1439 A73-25510
- A servo-controlled axial fatigue machine with strain rate feedback for testing polymers and composites.
11 p1344 A73-26300
- Dynamic strain ageing in some titanium-silicon alloys.
13 p1634 A73-28100
- Mechanical properties of 6061 Al-Mg-Si alloy after very rapid heating.
13 p1636 A73-28790
- The effect of strain rate and heat developed during deformation on the stress-strain curve of plastics. [SESA PAPER 2088A]
13 p1646 A73-29300
- Pure Al compression tests for strain rate effects on strength in wide temperature range, using split Hopkinson bar apparatus and Instron testing machine
13 p1639 A73-29400
- Deformation mechanism and strength of metals under impulsive loading.
13 p1639 A73-29400
- The effect of wave form and cyclic frequency on the fatigue life of aluminium alloys.
13 p1640 A73-29490
- Effect of temperature and strain rate on the high temperature, low cycle fatigue behaviour of a 17Cr-10Ni-2Mo stainless steel.
13 p1708 A73-29500
- Interfiber failure of unidirectional composite material.
13 p1702 A73-29530
- Dependence of the variation of the electronic dislocation drag force in a superconducting transition of the stress, temperature, and velocity.
14 p1783 A73-30300

Energy methods in plasticity theory extension to creep mechanics with respect to stress-strain rate tensors relationships 14 p1811 A73-30478

Some effects of prestraining nickel at various rates on its subsequent tensile properties. 14 p1761 A73-30637

Kinetics of changes in deformability of a heat-resistant nickel-base alloy 14 p1764 A73-30861

Aluminum structure effects on thermal activation parameters of plastic deformation, proposing strain rate control mechanism 14 p1764 A73-30867

Characteristics of dynamic hot pressing with high deformation rates 15 p1881 A73-31589

Unconventional processes for faster extrusion of aluminum hard alloys 16 p2021 A73-33951

Mechanical properties, microstructure and failure characteristics of binary alloys of Al-Mg system determined under different tensile stress rates and temperatures 17 p2187 A73-34339

Stress relaxation measurements for strain rate sensitivity of dispersion hardened thoriated Ni alloys as function of applied stress concentration 17 p2190 A73-34647

Role of stress in the stress corrosion cracking of a Mg-Al alloy. 17 p2191 A73-35100

Mechanical and optical characterization of an anelastic polymer at large strain rates and large strains. [SESA PAPER 2198A] 17 p2198 A73-35458

Influence of interstitials on the behavior in tension of niobium between 20 and 1000 C 17 p2193 A73-35624

High strain rate tensile properties of AISI type 304 stainless steel. 18 p2323 A73-36619

[ASME PAPER 73-MAT-D] 18 p2323 A73-36619

Influence of temperature and strain rate on the load-elongation curve and plastic properties of molybdenum 18 p2324 A73-36801

The effect of very short time-at-temperature on the yield stress of 6061-T651 aluminum. 19 p2440 A73-37590

The compression yield behaviour of polymethyl methacrylate over a wide range of temperatures and strain-rates. 19 p2444 A73-38097

The problem of wave propagation in physically nonlinear rods of finite length 20 p2618 A73-39315

Experimental investigation of changes in the fracture toughness of aluminum alloys 20 p2577 A73-39359

Effect of the degree of plastic deformation on the structure and mechanical properties of low-alloy molybdenum 20 p2579 A73-39741

A method for measuring $K_{sub Ic}$ at very high strain rates. 22 p2866 A73-42148

Induced plasticization - An inner bore surface treatment technique for solid-propellant rocket motors. 22 p2897 A73-42626

Static and dynamic finite deformations of cables using rate equations. 23 p3042 A73-43804

Creep rate relationship in terms of stress and strain rate for anisotropic metal based on single crystal theory, applying to pressurized thin cylinder 23 p3045 A73-44167

Generalized shear stress and shearing strain rate variables for thick circular plate, using von Mises yield criterion for limit load analysis 24 p3148 A73-44895

STRAIN SOFTENING

U PLASTIC DEFORMATION

STRAPDOWN INERTIAL GUIDANCE

Autonomous satellite navigation from strapdown landmark measurements. 04 p0474 A73-15266

An autonomous navigation technology system. 04 p0474 A73-15274

Strapdown inertial system alignment using statistical filters - A simplified formulation. 11 p1395 A73-26377

Constant-Q pulsed feedback electronics for strapped-down gyro systems. 11 p1342 A73-26635

Microprogrammed digital filters for strapdown guidance application. 12 p1483 A73-27168

High-reliability strapdown platforms using two-degree-of-freedom gyros. 13 p1657 A73-29214

Strapdown electrostatic gyroscope spin axis precession drift rate calibration, using virtual work technique for modeling bearing torques on rotor 17 p2137 A73-35210

Strapdown air navigation with dry inertial instruments and high speed general purpose digital computer predicting system performance by position error analysis 17 p2210 A73-35211

Strap-down inertial guidance systems study. 18 p2335 A73-36955

Strapped down inertial navigation systems. 19 p2452 A73-37876

Airborne IRP alignment using acceleration and angular rate matching. 19 p2386 A73-38048

Sensor concept and algorithms for a completely strapdown autonomous navigation approach. 19 p2452 A73-38057

System error analysis and algorithms for a strap-down navigation system. 19 p2452 A73-38058

Competitive evaluation of failure detection algorithms for strapdown redundant inertial instruments. 20 p2585 A73-38791

[AIAA PAPER 73-853] 20 p2585 A73-38791

Recent test results - A strapdown IMU utilizing hydrodynamic spin bearing rate sensors and pulse rebalance loops. 20 p2564 A73-38833

[AIAA PAPER 73-898] 20 p2564 A73-38833

Attitude determination for a strapdown inertial system using the Euler axis/angle and quaternion parameters. 20 p2589 A73-38834

[AIAA PAPER 73-900] 20 p2589 A73-38834

Strapdown inertial navigation with high speed digital computer, discussing attitude propagation algorithms and life cycle system cost advantages 21 p2734 A73-40036

Low cost strapdown inertial navigator with miniature electrostatically suspended gyros, discussing system performance goal in terms of position, velocity and attitude errors 21 p2734 A73-40037

Failure detection and isolation techniques for gimbaled and strapdown inertial systems examining redundant system reliability relationship to MTBF [AIAA PAPER 73-852] 22 p2884 A73-41969

STRATA

NT SUBSTRATES

Preliminary observations of stratified rocks of the Hadley Appennines photographed by the Apollo 15 astronauts 01 p0095 A73-10268

Radio wave propagation in stratified media with nonuniform boundaries and varying electromagnetic parameters - Full wave analysis. 07 p0791 A73-19261

Magnetic and gravitational potential anomalies due to uneven nonuniform material layers, using Fourier transforms 13 p1607 A73-28623

Radiation transfer in a multilayer plane-parallel system with nonisotropic scattering 24 p3154 A73-44659

STRATEGY

Influence of observing strategies and stimulus variables on watchkeeping performances. 01 p0012 A73-10771

Decomposition strategies for one on one aerial dog-fight game models with reinforcement learning [AIAA PAPER 73-233] 05 p0536 A73-16958

Objective trees as technological forecasting technique in structuring program options for selected strategies, considering R and D, marketing and other functional business programs 08 p1026 A73-21699

Zero sum differential game theory for two players, discussing strategies, stochastic versions and saddle value and points existence 13 p1651 A73-29650

A strategy for investigation of the outer solar system - Outer planets, their satellites, and particles and fields at great distances from the sun. 14 p1799 A73-30526

Effects of prestimulus cuing and target load variability on maintenance of response strategies in a visual search task. 19 p2402 A73-38378

Optimum minimax strategy in pursuit game with observation of evading player phase vector at fixed times 21 p2724 A73-40180

Dynamic programming method for constructing stable bridges based on mixed strategies in differential games of rendezvous-evasion 21 p2669 A73-40856

STRATHS

U VALLEYS

STRATIFICATION

NT ATMOSPHERIC STRATIFICATION

Arbitrary source emitted electromagnetic radiation in anisotropic stratified media, evaluating transverse and scattered fields and plane wave response 07 p0791 A73-19382

Response to critiques of paper on earth core paradox consisting of stratification inhibition on outer core fluid circulation needed for dynamo theory of geomagnetic field generation 09 p1077 A73-22193

Electromagnetic propagation in bianisotropic stratified media, obtaining Maxwell and constitutive equations in operator form 09 p1049 A73-22312

Natural oscillations of density-stratified ideal incompressible liquid in rectangular vessel, solving oscillation equation for various density distributions 11 p1349 A73-26441

Solutions of boundary value problems of multilayer analogs of geoelectrics and hydrology. 15 p1872 A73-32040

Russian book on wave propagation in stratified media covering elastic and electromagnetic fields, waveguides, whispering galleries, diffraction rays, caustic surfaces, etc 21 p2741 A73-41279

STRATIFIED FLOW

Stability of rotating stratified flow produced by tangential injection of high pressure gas into closed cylindrical vessel filled with gas of different density 01 p0033 A73-10752

Reflection coefficients for acoustic waves interacting with stratified media. 01 p0078 A73-11097

Sturm-Liouville solution of unsteady stratified two dimensional Couette flow equations of motion 03 p0292 A73-13304

Oscillatory point force generated motion in inviscid incompressible rotating stratified fluid, obtaining closed form solutions via Fourier transforms 03 p0296 A73-14313

Extension of the Miles-Howard theorem to the circular flows of a compressible fluid. 03 p0297 A73-14443

Finite difference technique for numerical calculation of two dimensional stratified incompressible fluid flows 04 p0433 A73-15162

Scaling relations to predict size of submarine generated wake in stratified water flow, measuring velocity and temperature profiles [AIAA PAPER 73-108] 06 p0644 A73-17644

Upwelling of a stratified fluid in a rotating annulus - Steady state. I - Linear theory. 06 p0684 A73-17702

Small amplitude viscous similarity solution for vertical two dimensional internal wave production by circular cylinder resonant oscillation in incompressible stratified fluid 06 p0646 A73-18527

Oscillation of axisymmetric bodies in a stratified fluid. 10 p1205 A73-23625

The motion of a viscous, stratified fluid subjected to forced oscillations. 10 p1210 A73-24844

An investigation of internal gravity waves generated by a buoyantly rising fluid in a stratified medium. 11 p1351 A73-25152

The observed relation between the Kolmogorov and von Karman constants in the surface boundary layer. 11 p1393 A73-25694

Hydrodynamic stability of density-stratified spiral flows. 11 p1348 A73-26388

Similarity theory of diffusion and the observed vertical spread in the diabatic surface layer. 13 p1655 A73-29339

The stability of a thermally radiating stratified shear layer. 14 p1816 A73-30169

Modification of Sygne's criterion for stratified shear flow for spatially growing disturbances. 15 p1862 A73-31334

Unbounded nondiffusive high Reynolds number stratified flow with lee waves over vertical barrier investigated for Froude number range on basis of Oseen-Boussinesq approximation 15 p1863 A73-31341

Laminar stratified flow of a conducting medium in ring channels in the event of great MHD-interaction parameters 15 p1918 A73-31409

Korteweg-de Vries equation solution for long nonlinear wave amplification and decay in rotating and stratified fluids with application to shallow water waves 16 p1998 A73-32795

Stratified Taylor column model for topography effect on slow rotating baroclinic flow, considering Jupiter Red Spot and oceanic observations 16 p1998 A73-32797

Bifurcated small parameter perturbation solutions in boundary layer theory, applying to Falkner-Skan equation and instability in stratified shear flow 16 p2001 A73-33871

Book - Buoyancy effects in fluids. 17 p2155 A73-35336

Stability of stratified shear flows. 19 p2421 A73-38226

Linear viscous stability theory for stably stratified shear flow - A review. 19 p2421 A73-38227

- Instabilities in buoyancy-driven boundary-layer flows in a stably stratified medium.
19 p2422 A73-38231
- Laboratory observations of shear-layer instability in a stratified fluid.
19 p2422 A73-38232
- Turbulence in stably stratified fluids - A review of laboratory experiments.
19 p2449 A73-38234
- Thermal structure and stability study of internal and Kelvin-Helmholtz waves in low Reynolds number flows by sampling and stratified wind tunnel methods.
19 p2422 A73-38235
- Some properties of horizontally homogeneous, statistically steady turbulence in a stratified fluid.
19 p2449 A73-38236
- Interactions between internal gravity waves and their traumatic effect on a continuous stratification.
19 p2422 A73-38237
- Measurements of internal waves and turbulence in two-dimensional stratified shear flows.
19 p2422 A73-38238
- Hydrodynamics of stratified fluids - The applicability of linear theory.
19 p2422 A73-38243
- The formation and breakdown of Kelvin-Helmholtz billows.
19 p2422 A73-38244
- Motion of a two-component stratified gas-liquid flow in a horizontal pipe.
21 p2677 A73-40989
- Gravity-shear waves in jet flow near tropopause with arbitrary temperature-wind stratification.
23 p3001 A73-43462
- The linear spin-up of a strongly stratified fluid of small Prandtl number.
24 p3079 A73-45312

STRATIFIED LAYERS

U STRATA

STRATIGRAPHY

- A crustal-upper-mantle model for the Colorado plateau based on observations of crystalline rock fragments in the Moses Rock dike.
05 p0569 A73-16381
- A technique for extracting Radiolaria from radiolarian cherts.
11 p1324 A73-25141
- Proposed stratigraphic controls on the composition of crude oils reservoirs in the Green River formation, Uinta Basin, Utah.
11 p1352 A73-25471
- Possible stratotype sequences for the basal Paleozoic in North America.
15 p1865 A73-31025
- Apollo 16 neutron stratigraphy.
18 p2354 A73-36514
- Thermal track fading factor in Georgia tektite stratigraphy and fission track ages, noting agreement with K/Ar ages.
20 p2612 A73-39717

STRATOCUMULUS CLOUDS

- Some characteristics of stratiform St-Sc clouds in various synoptic situations.
13 p1654 A73-28885
- Experimental investigations of solar radiation fluxes in the lower troposphere in the presence of St and Sc clouds.
15 p1905 A73-31788
- Spatial structure of the short-wave radiation field in stratocumulus and cumulus clouds.
15 p1905 A73-31795
- Long wave radiation flux, water content and temperature measurements in stratus and cumulostratus clouds by aircraft radiometry.
21 p2731 A73-40496

STRATOFORTRESS AIRCRAFT

U B-52 AIRCRAFT

STRATOPAUSE

- Evidence for high-frequency synoptic disturbances near the stratopause.
19 p2447 A73-37663

STRATOSCOPE TELESCOPES

- High angular resolution solar observation from balloon borne instruments.
02 p0169 A73-12334

- High-resolution imagery of Uranus obtained by Stratoscope II.
05 p0627 A73-17388

STRATOSCOPE 1 TELESCOPE

U STRATOSCOPE TELESCOPES

STRATOSCOPE 2 TELESCOPE

U STRATOSCOPE TELESCOPES

STRATOSPHERE

- Hemispheric synoptic analysis of upper stratospheric warming for energy transformations in troposphere and lower and middle stratosphere.
01 p0072 A73-10141
- An inversion technique developed to determine characteristics of mic scatterers differing in index of refraction interspersed in the stratosphere.
01 p0037 A73-10353
- Inference of stratospheric temperature structure from limb radiance profiles.
01 p0072 A73-10356

- Return of normal stratospheric turbidity and a new short dust event during October 1971.
01 p0038 A73-10374

- Solar-activity effects and zonal wind in the stratosphere and lower mesosphere.
01 p0043 A73-10945

- Aeronomic chemistry of the stratosphere.
02 p0158 A73-11910

- Nitrogen hydride as a possible stratospheric constituent.
02 p0159 A73-12225

- Atmospheric stratification stability at heights of 30-90 km from grenade test determined wind and temperature data, presenting Richardson number latitudinal and seasonal distribution.
02 p0160 A73-12273

- Distribution of nitric acid vapor in the stratosphere as determined from infrared atmospheric emission data.
02 p0189 A73-12786

- Rocket sounding and grenade experiments for stratosphere-mesosphere interaction, showing simultaneous winter temperature changes of opposite sign.
02 p0165 A73-12789

- Climatic impact assessment for high-flying aircraft fleets.
04 p0436 A73-14672

- Atmospheric correction for the troposphere and stratosphere in radio ranging of satellites.
04 p0439 A73-14808

- Stratospheric nitrogen dioxide from infrared absorption spectra.
04 p0445 A73-15626

- Secular variation of the stratospheric ozone layer over middle Europe during the solar cycles from 1951 to 1972.
04 p0445 A73-15635

- Adiabatic inviscid quasi-geostrophic planetary scale perturbations forced by stratospheric disturbance, obtaining vertical propagation from layered models representation for zonal wind.
05 p0591 A73-16189

- Interrelation between processes occurring along a vertical, and the forecasting of stratospheric wind.
05 p0592 A73-16232

- Relationship of atmospheric processes in the troposphere and stratosphere.
05 p0593 A73-16233

- Diurnal variability of temperature and of isobaric surface heights in the troposphere and lower stratosphere.
05 p0593 A73-16241

- Radio-wave absorption in the lower ionosphere and stratospheric effects.
05 p0569 A73-16265

- Equatorial stratosphere quasi-biennial oscillation variations from temperatures and zonal winds measured at Canton Island, Ascension Island and Balboa (Canal Zone).
05 p0594 A73-16573

- Direct determination of the thickness of stratospheric layers from single-channel satellite radiance measurements.
05 p0569 A73-16574

- Turbojet exhaust reactions in stratospheric flight. [AIAA PAPER 73-99]
05 p0608 A73-16859

- Rocket sounding for space charge distribution and electric field strength in stratosphere and mesosphere, noting vertical distribution of atmospheric conductivity.
05 p0570 A73-17013

- Planetary-scale fluctuations of pressure in the E-layer, f-min, and pressure in the stratosphere.
05 p0571 A73-17057

- The thermal structure within the stratospheres of Venus and Mars.
06 p0747 A73-17493

- Meteorological rocket observations of amplitudes and phases of zonal wind quasi-biennial oscillations at 25-60 km during 1962-1969.
07 p0846 A73-19040

- Variation with altitude of the scatter coefficient in the stratosphere, based on measurements from the Soiuz-3 spacecraft.
07 p0817 A73-19585

- Mid-latitude winter anomalies in radio absorption and stratospheric temperature distribution - Observations concerning the influence of auroral and magnetic activity.
07 p0819 A73-20058

- Fine structure of the temperature stratification in the troposphere and stratosphere.
07 p0848 A73-20348

- Stratospheric aerosol measurements with implications for global climate. [AD-759856]
08 p0984 A73-21041

- Solar modulation of cosmic ray intensity in stratosphere, examining relationship to sunspots group number and heliographic latitudes over 11 year period.
08 p0999 A73-21339

- Solar cosmic ray flare recording in stratosphere in Murmansk and Antarctic regions during February-April 1969.
08 p1000 A73-21347

- Monograph - The quasi-biennial oscillation in the stratosphere.
08 p0986 A73-21848

- Effects of solar activity on zonal winds in the stratosphere and lower mesosphere.
09 p1078 A73-22000

- Measurements of some hydrogen-oxygen-nitrogen compounds in the stratosphere from Concord 002.
09 p1079 A73-22800

- Models of the extremal arctic winter atmosphere at heights between 20 and 80 km.
09 p1115 A73-22900

- A comparative study of the wind structure in the stratosphere at Sonmiani vis-a-vis CIRA 1965.
10 p1244 A73-23600

- Direct measurements of the electrical conductivity and relaxation time of ionized air in the stratosphere and mesosphere.
10 p1211 A73-23800

- Solar proton energy spectra recorded in stratosphere during two solar cycles, approximating generation spectra by power law.
10 p1266 A73-23900

- Bremsstrahlung X-rays in the stratosphere and a solar activity on January 21 and February 3, 1969.
10 p1268 A73-24200

- Macroscale interaction between the atmosphere and oceans and the role of the latter in the formation of anomalous circulation in the stratosphere.
10 p1246 A73-24300

- Stratospheric aerosol layer detection.
11 p1355 A73-25700

- Mountain waves and CAT encountered by the X-15 in the stratosphere.
11 p1394 A73-25700

- Stratospheric aerosol properties and their effects on infrared radiation.
11 p1357 A73-26300

- U.S., UK and French research programs on conditions encountered by civil aviation and supersonic transports in stratosphere.
11 p1455 A73-26500

- Statistical description of the wind field in the upper troposphere and lower stratosphere with allowance for the scale of motion.
12 p1521 A73-27700

- Stratospheric geopotential pressure field numerical prediction based on quasi-geostrophic atmospheric model, considering stratospheric heating period.
12 p1521 A73-27700

- Ozone variation in the lower stratosphere and mechanism.
13 p1611 A73-29600

- Ground-based measurement of millimeter wavelength emission by upper stratospheric O2.
14 p1751 A73-29700

- Distribution of water vapor in the stratosphere as determined from balloon measurements of atmospheric emission spectra in the 24- to 29-micron region.
14 p1749 A73-30100

- Stratospheric cooling and perturbation of the meridional flow during the solar eclipse of 7 March 1970.
14 p1771 A73-30700

- General circulation of the tropical lower stratosphere.
15 p1906 A73-31800

- Upper stratosphere and lower mesosphere vertical mixing implications of methane observations at 50 km: assuming modelability by eddy transport.
15 p1873 A73-32200

- Map series for description of annual temperature wave in lower stratosphere in Northern Hemisphere establishing easterly circulation on south side of Aleutian high.
15 p1873 A73-32200

- Gravity wave magnitudes and horizontal and vertical scales measured and applied to eddy diffusion coefficients in upper stratosphere.
16 p2005 A73-33500

- Stratospheric mixing estimated from high altitude turbulence measurements. [AIAA PAPER 73-497]
16 p2005 A73-33500

- Monthly mean values of eddy diffusion coefficients in the lower stratosphere.
16 p2005 A73-33500

- A simple technique to estimate large-scale eddy coefficients in the stratosphere. [AIAA PAPER 73-499]
16 p2005 A73-33500

- Atmospheric modelling and the chemical data problem. [AIAA PAPER 73-500]
16 p1977 A73-33500

- Recent measurements of stratospheric reactions in flash photolysis resonance fluorescence. [AIAA PAPER 73-502]
16 p2005 A73-33500

- The extinction coefficients of NO2 between 195 nm and 410 nm. [AIAA PAPER 73-503]
16 p2005 A73-33500

- Trace gases, aerosols, and solar radiation in the stratosphere - Explored and unexplored problems.
16 p2006 A73-33500

- Distributions and associations of some of the chemical elements found in the stratosphere. [AIAA PAPER 73-514]
16 p2006 A73-33500

- Vertical profiles of molecular H₂ and CH₄ in the stratosphere.
[ALAA PAPER 73-518] 16 p2006 A73-33555
- Lidar measurements of the variability of stratospheric particulates.
[ALAA PAPER 73-520] 16 p2007 A73-33556
- Global balloon monitoring program of stratospheric dust, ozone, water vapor, temperature and aerosol determination in northern and southern hemispheres
[ALAA PAPER 73-521] 16 p2007 A73-33557
- Coordinated measurements of atmospheric parameters at stratospheric levels.
[ALAA PAPER 73-526] 16 p2007 A73-33560
- Photochemical, radiative and dynamic modeling of the stratosphere.
[ALAA PAPER 73-527] 16 p2007 A73-33561
- A three-dimensional stratospheric point-source tracer experiment and its implications for dispersion of effluent from a fleet of supersonic aircraft.
[ALAA PAPER 73-528] 16 p2007 A73-33562
- Numerical atmospheric circulation model of SST effects on stratospheric ozone distribution
[ALAA PAPER 73-529] 16 p2007 A73-33563
- Stratospheric contamination experiments with a one-dimensional atmospheric model.
[ALAA PAPER 73-531] 16 p2007 A73-33564
- Aircraft exhaust plume dispersion and flight corridor concentration profiles in stratosphere as function of flight frequency and scale dependent diffusion
[ALAA PAPER 73-532] 16 p2046 A73-33565
- Subsonic jet aircraft contribution to NO_x in the stratospheric ozone layer - 1968 to 1990.
[ALAA PAPER 73-534] 16 p2046 A73-33566
- A model for studying the effects of injecting contaminants into the stratosphere and mesosphere.
[ALAA PAPER 73-539] 16 p2008 A73-33569
- Aerochemistry of combustion products in the stratosphere.
[ALAA PAPER 73-540] 16 p1977 A73-33570
- A two-dimensional theoretical model for stratospheric ozone density distributions in the meridional plane.
[ALAA PAPER 73-541] 16 p2008 A73-33571
- The production of nitric oxide in the stratosphere by oxidation of nitrous oxide.
16 p2008 A73-33885
- Relationship between stratospheric warming and ionospheric absorption.
16 p2009 A73-33887
- Experimental determination of small scale transport mechanisms in the stratosphere.
[ALAA PAPER 73-496] 16 p2010 A73-34044
- An initial estimate of aircraft emissions in the stratosphere in 1990.
[ALAA PAPER 73-508] 16 p2011 A73-34046
- On the possible effect of NO_x injection in the stratosphere due to past atmospheric nuclear weapons tests.
[ALAA PAPER 73-538] 16 p2011 A73-34047
- The permissible scale of spatial averaging of geopotential values in the stratosphere when the impact of wind on the flight of a supersonic aircraft is taken into account
17 p2100 A73-34546
- Nitric oxide detection in stratosphere from characteristic absorption line spectrum via airborne IR spectrometer, obtaining molecular concentration
[ONERA, TP NO. 1256] 17 p2159 A73-34552
- Mesospheric and stratospheric nitrogen oxides behavior from model with nitric oxide photodissociation and nitric acid formation
17 p2119 A73-34779
- The effects of water vapor and oxides of nitrogen on the ozone and temperature structure of the stratosphere.
17 p2160 A73-34857
- Relative efficiencies of filters and impactors for collecting stratospheric particulate matter.
17 p2167 A73-34863
- Application of temperature soundings by the Nimbus 3 satellite to the analysis of the hemispheric-scale stratospheric environment
17 p2206 A73-34937
- Basic characteristics of the temperature distribution and air currents in the free atmosphere of the earth
18 p2332 A73-35915
- Operational radiance maps of the stratosphere, with preliminary details of a major stratospheric warming.
18 p2303 A73-35950
- The use of VLF propagation measurements for studies of the magnetosphere and meteorological influences on the lower ionosphere.
18 p2303 A73-35953
- Extreme temperature deviations from the climatological mean in the upper stratosphere - observed by rockets, confirmed by satellites.
18 p2304 A73-35962
- Recent stratospheric temperature measurement compatibility tests at Wallops Island.
18 p2307 A73-36035
- Midwinter mesospheric cooling during stratospheric warming, discussing circulation, stratosphere-mesosphere interactions and summertime temperature values at midwinter mesopause
18 p2308 A73-36037
- A prediction of the phenomena that take place during so called 'sudden warmings.'
18 p2308 A73-36038
- The stratospheric-mesospheric circulation over the North Pacific Ocean.
18 p2308 A73-36039
- High-level circulation studies based on rawinsonde, rocketsonde and satellite observations.
18 p2350 A73-36040
- Influence of longitudinal variations on the structure of temperature, pressure and wind fields in the stratosphere and mesosphere of the Northern Hemisphere.
18 p2310 A73-36139
- SST environment impact aspects in areas of fuel and oxygen consumption, noise, sonic boom, stratospheric pollution and climate modification
18 p2268 A73-36906
- Photochemistry of the ozone in the stratosphere
18 p2287 A73-36938
- Observation of stratospheric nitric oxide by infrared absorption spectrometry from a balloon
19 p2423 A73-37533
- A comparison of geostrophic and rocket winds at stratospheric levels, measured from a small network of rocket sounding stations.
19 p2424 A73-37604
- Dynamic coupling of the stratosphere with the troposphere and sudden stratospheric warmings.
19 p2449 A73-38288
- Direct measurements of the electrical conductivity and relaxation time of ionized air in the stratosphere and mesosphere.
20 p2551 A73-38909
- Stratospheric temperature profiles from limb radiance measurement by Aerobee rocket, comparing with rocket sounding and radiosonde data
21 p2729 A73-40064
- Balloon-borne measurement of stratospheric methane as function of altitude absorption spectroscopy, obtaining mixing ratios
21 p2680 A73-40076
- Tropospheric and stratospheric vertical profiles of methane concentration via air sampling and gas chromatography, noting temporal and spatial variations
21 p2680 A73-40077
- Photochemical model with vertical transport for CO and hydrocarbons profiles in stratosphere and mesosphere, discussing boundary conditions and water vapor
21 p2681 A73-40086
- The 11-year cycle of cosmic ray intensity in the stratosphere and its dependence on solar activity
21 p2758 A73-40597
- COSPAR mean international reference atmosphere for 25-500 km region, considering 25-75, 75-120 and regions above 120 km
21 p2683 A73-40627
- Atmospheric structure and its variations in the region from 25 to 120 km.
21 p2683 A73-40628
- Nitrogen oxides, nuclear weapon testing, Concorde and stratospheric ozone.
21 p2686 A73-41076
- Evidence of features in atmospheric spectra at around 8 per cm of probable solar origin.
21 p2687 A73-41079
- Use of meteorological rocketsonde and satellite radiation data for constant-pressure analyses at levels between 5 and 0.4 mb.
21 p2732 A73-41336
- The stratospheric circulation over Middle Atlantic latitudes in the 1966-1971 period.
21 p2687 A73-41339
- Results of simultaneous wind measurements in the stratosphere, mesosphere and low thermosphere.
21 p2732 A73-41340
- Ionospheric research by rocket, satellite and ground based methods, discussing ion and neutral chemistry, stratospheric-ionospheric coupling, ionospheric thermal structure, etc
21 p2689 A73-41358
- Tropospheric and stratospheric response to solar influence during geomagnetic disturbances.
21 p2690 A73-41364
- Ablation debris and primary micrometeoroids in the stratosphere.
21 p2775 A73-41419
- Lidar measurements for the exploration of the atmosphere
22 p2823 A73-41825
- Airborne IR spectrometer with solar sensor for stratospheric minor molecular constituents vertical distribution, indicating spectral resolution for vibrational-rotational absorption bands
[ONERA, TP NO. 1216] 22 p2847 A73-42221
- The effect of atmospheric and physiological conditions on the homogeneity of observations of noctilucent clouds
22 p2847 A73-42448
- Ozone composition and nitric oxide injection upper and lower limits for stratosphere by nuclear bomb tests, comparing to estimated SST contribution
22 p2848 A73-42534
- Increased influx of stratospheric air into the lower troposphere after solar H alpha and X ray flares.
22 p2848 A73-42538
- Transition probability matrix method for calculating residence times of moving particles in region of space, determining stratosphere residence time against exit to tropopause
22 p2849 A73-42543
- Structure of global geopotential fields in view of the quasi-two-year cyclicity in the equatorial stratosphere
23 p3001 A73-43463
- A theoretical investigation of tropospheric ozone and stratospheric-tropospheric exchange processes.
23 p2974 A73-43861
- Radiosonde ground station ozone concentration measurements as stratospheric motions Lagrangian tracer, noting sonde data inadequacy and alternative measurement possibilities
23 p2975 A73-43873
- Variations in the stratospheric ozone field inferred from Nimbus satellite observations.
23 p2975 A73-43878
- The mean ozone distribution from several series of rocket soundings to 52 km at latitudes from 58 deg S to 64 deg N.
23 p2975 A73-43880
- The influence of solar activity on the stratospheric ozone layer.
23 p2976 A73-43884
- Stratospheric methane and nitrogen dioxide from infrared spectra.
23 p2976 A73-43887
- Atmospheric water vapor concentration in upper stratosphere above tropopause from balloon observations of solar IR absorption spectra
23 p2976 A73-43890
- The concentration of molecular H₂ and CH₄ in the stratosphere.
23 p2976 A73-43891
- Recent developments in photochemistry of atmospheric ozone.
23 p2951 A73-43892
- A discussion of the chemistry of some minor constituents in the stratosphere and troposphere.
23 p2951 A73-43893
- On the vertical distribution of carbon monoxide and methane in the stratosphere.
23 p2976 A73-43894
- OH radical concentration in the stratosphere.
23 p2976 A73-43895
- On the behavior of nitrogen oxides in the stratosphere.
23 p2976 A73-43896
- The production and distribution of nitrogen oxides in the lower stratosphere.
23 p2977 A73-43897
- On the theoretical model for vertical ozone density distributions in the mesosphere and upper stratosphere.
23 p2977 A73-43898
- Nitrogen oxides role in global stratospheric ozone balance demonstrated by observed instantaneous photochemical rates comparison with Chapman ozone formation theory
23 p2952 A73-43900
- Ozone and temperature change in the winter stratosphere.
23 p2977 A73-43901
- The effects of water vapour and oxides of nitrogen on ozone and temperature structure of the stratosphere.
23 p2977 A73-43902
- Atmospheric ozone and the movement of the air in the stratosphere.
23 p2977 A73-43903
- Influence of the vertical motion field on ozone concentration in the stratosphere.
23 p2977 A73-43904
- Relation between the intensity of the stratospheric circumpolar vortex and the accumulation of ozone in the winter hemisphere.
23 p2977 A73-43905
- Ozone variation in the lower stratosphere and its mechanism.
23 p2977 A73-43908
- Application of general circulation models to the study of stratospheric ozone.
23 p2978 A73-43909
- Nimbus 5 satellite-borne selective chopper radiometer (SCR) for remote sounding of stratospheric temperature, water vapor and cirrus clouds
23 p2978 A73-43952
- IR absorption spectrometry to determine vertical distribution of nitric oxide abundance in stratosphere
23 p2978 A73-43959
- Relationship between midstratospheric temperatures and tropospheric synoptic features.
24 p3107 A73-45014
- Numerical experiments on the steady-state meridional structure and ozone distribution in the stratosphere.
24 p3085 A73-45017

STRATOSPHERE RADIATION

STRATOSPHERE RADIATION

Stratospheric cosmic ray short period variations at 30 km by spectral density method

08 p1000 A73-21351

High resolution spectra of the stratosphere between 30 and 200/cm.

08 p0961 A73-21533

Global time and space changes of satellite radiances received from the stratosphere and lower mesosphere.

09 p1076 A73-22149

Cosmic ray bursts in 1970-1971 according to measurements in the stratosphere

10 p1266 A73-23916

Comparative characteristics of the soft component of solar and galactic cosmic rays on the basis of rocket and stratospheric measurements at Heis Island and Apatite Station

10 p1267 A73-23920

The abnormal stratosphere suitable for measuring of satellite radiation measurements.

[AIAA PAPER 73-493]

16 p2005 A73-33537

Remote sensing of stratospheric gases using submillimeter radiation.

20 p2557 A73-39856

Description of a photometer suitable for measuring twilight ozone content variations from a stratospheric balloon gondola

23 p2982 A73-43875

STRATUS CLOUDS

An experimental investigation of the nature of changes in the intensity of precipitations from stratiform and cumuliiform clouds

12 p1522 A73-27747

Study of droplet size distribution in a two-phase stratiform cloud - A numerical experiment

13 p1653 A73-28877

Stratiform cloud electrical characteristic changes under solid carbon dioxide seeding in aircraft experiments

13 p1654 A73-28884

Some characteristics of stratiform St-Sc clouds in various synoptic situations

13 p1654 A73-28885

Experimental investigations of solar radiation fluxes in the lower troposphere in the presence of St and Sc clouds

15 p1905 A73-31788

Numerical model of a two-phase stratiform cloud taking its microstructure into account

20 p2583 A73-39185

Long wave radiation flux, water content and temperature measurements in stratus and cumulostratus clouds by aircraft radiometry

21 p2731 A73-40496

STREAM FUNCTIONS [FLUIDS]

Streaming two dimensional Oseen MHD flow of conducting fluid past semiinfinite needle within aligned field

01 p0031 A73-10305

Empirical formulae for the universal functions M sub m/mu and N/mu in the resistance law for a barotropic and diabatic planetary boundary layer.

04 p0473 A73-15696

Parabolic flow over a flat plate with wave disturbance in the main stream.

09 p1071 A73-21950

A numerical-analytical method of calculating stream flow of a heavy liquid around curvilinear obstacles

10 p1205 A73-23585

Interaction between a sound field and natural convection on a horizontal cylinder.

10 p1296 A73-24846

Newton method for calculation of viscous flow around circular cylinder with Fourier series truncation for stream function and vorticity, evaluating numerical error

11 p1345 A73-25115

A numerical solution of the Navier-Stokes equations using the finite element technique.

11 p1345 A73-25116

Steady plane flow of viscous fluid in symmetrical channels with curved walls, considering approximate series for stream function

11 p1347 A73-25646

Flow near the stagnation point of a body which undergoes a sudden change in a steady stream. [ASME PAPER 72-APM-UU]

11 p1347 A73-25701

Gas jet flow at high subsonic velocities, determining stream function, contraction coefficient, convergence at critical velocity and pressure above obstacle

11 p1302 A73-26215

Conjugating a Chaplygin operator with a differential operator in gasdynamics

13 p1563 A73-28443

Book - Computational fluid dynamics.

14 p1745 A73-30359

Some computation-steeple in fluid mechanics.

14 p1745 A73-30412

Approximate solution of a stream problem of subsonic gasdynamics

15 p1821 A73-31152

Theory of mountain lee waves for an arbitrary-profile elevation

15 p1905 A73-31818

Stochastic wind field effects on baroclinic wave disturbances vertical propagation through turbulent atmosphere, obtaining stream function and dispersion equation

15 p1907 A73-32356

Prediction of flow outlet angle in blade rows with conical stream surfaces.

[ASME PAPER 73-GT-32]

16 p2048 A73-33502

Inviscid flow through a cascade of thick, cambered airfoils. II - Compressible flow.

[ASME PAPER 73-GT-85]

16 p1964 A73-33528

Nonlinear streaming effects associated with viscous incompressible fluid near oscillating cylinder, considering theory based on outer-inner expansion technique with Stokes drift correction

20 p2546 A73-39088

Navier-Stokes equation formulation in parabolic coordinates for flow in trailing vortex, obtaining asymptotic expansions for stream function and angular momentum

23 p2939 A73-43205

Zonally symmetric global general circulation models with and without the hydrologic cycle.

23 p2978 A73-43981

Approximate calculation of dividing streamline of heterogeneous coaxial supersonic jets.

23 p2940 A73-44127

STREAMLINE FLOW

U LAMINAR FLOW

STREAMLINED BODIES

NT FAIRINGS

Unsteady wakes of bluff and streamlined bodies with screens behind them.

10 p1173 A73-24823

Using the singularity method in studies of potential flow about bulbous streamline bodies

14 p1712 A73-30706

STREAMLINING

Streamline curvature and velocity gradient behind curved shocks.

21 p2632 A73-40441

STREAMS

NT GAS STREAMS

Oblique electromagnetic wave propagation with respect to double stream in plasma, calculating unstable wave oscillation frequency and growth rate dependence on stream direction

08 p0993 A73-21633

STRENGTH

Russian book on orthotropic laminated cylindrical shells strength and optimal design covering glass ribbon reinforced zero moment shells and interlayer shear theory

04 p0514 A73-15702

STRENGTH OF MATERIALS

U MECHANICAL PROPERTIES

STRESS [PHYSIOLOGY]

NT ACCELERATION STRESSES [PHYSIOLOGY]

NT CENTRIFUGING STRESS

Formalization of certain functional aspects of the external respiration system

01 p0012 A73-10657

Cardiac dysrhythmias associated with exercise stress testing.

03 p0260 A73-13544

Prediction tests for pulmonary elasticity model of expansion stresses in lung region restricted by obstructed airways

03 p0262 A73-14114

Organ and body mass changes in restrained and fasted domestic fowl.

04 p0409 A73-14975

Elevated ST segments with exercise in ventricular aneurysm.

04 p0410 A73-15643

Changes in whole body force transmission of dogs exposed repeatedly to vibration. [ASME PAPER 72-WA/BHF-11]

04 p0410 A73-15878

Uses and limitations of stress testing in the evaluation of ischemic heart disease.

05 p0552 A73-17278

Evaluation of the state of the cardiovascular system from polycardiographic test data

06 p0650 A73-17749

The biodynamic aspects of low altitude, high speed flight.

06 p0659 A73-18471

Role of adrenalin and alpha-receptor deactivation in reactions of hemopoietic organs to stress

07 p0781 A73-19644

The contractile function of the myocardium in two types of cardiac adaptation to a chronic load.

07 p0781 A73-19931

Human tendon stress recovery after load removal as function of time, sex, age and side differences

07 p0782 A73-20033

Catecholamine exchange in the hormonal and mediator links of the sympathoadrenal system under stress

07 p0784 A73-20367

Inability of the submaximal treadmill stress test to predict the location of coronary disease.

08 p0932 A73-21802

Thirty-month follow-up of maximal treadmill stress test and double Master's test in normal subjects.

08 p0932 A73-21802

Intravascular platelet aggregation in the heart induced by stress.

08 p0933 A73-21802

Adaptive hormone action and nonspecific adaptation function of steroid hormones, discussing stress resistance mechanisms of steroids pharmacologically classified as syntoxic and catatonic

09 p1045 A73-22515

Coronary flow and left ventricular function during environmental stress.

09 p1047 A73-23938

Isometric effects on treadmill exercise response of healthy young men.

10 p1179 A73-23808

Human forearm-muscle blood supply regimes after 'static' exercise with increasing stress

10 p1181 A73-24515

Comparison of the metabolic effects of centrifugation and heat stress in man.

11 p1315 A73-25312

Ergonomic endurance limits, physiological strain, and fatigue assessment in video coding information task performance as function of work shift time length

11 p1323 A73-25666

High temperature tolerance enhancement in rats by thermal training and medicinal preparations

12 p1462 A73-27767

Vestibular stresses effects on systemic and cerebral hemodynamics, considering human acceleration adaptation and compensation mechanisms

12 p1463 A73-27777

Motor, thermal and sensory factors in heart rate variation A methodology for indirect estimation of intermittent muscular work and environmental heat loads.

14 p1720 A73-30888

Functional condition of skeletal muscles in rats under lasting movement constraints (up to 120 days)

15 p1834 A73-31553

A standard psychophysiological preparation for the study of environmental stress.

16 p1975 A73-33131

Annual Scientific Meeting, Las Vegas, Nev., May 10, 1973, Preprints.

16 p1973 A73-33404

Cobalt compound administration effects on hypoxia stress control, testing polycythemic response and cobalt retention in rats

17 p2115 A73-34715

Localizing factors in arteriosclerosis.

18 p2275 A73-36515

Tolerance to heat following cold stress.

18 p2283 A73-36789

Use of the single-breath method of estimating cardiac output during exercise-stress testing.

18 p2283 A73-36789

Behavioral stress response RE - Passenger briefing and emergency warning systems on commercial airlines.

18 p2285 A73-36915

Serial correlation of physiological time series and significance for a stress analysis

19 p2401 A73-38115

Circadian rhythms of free radical state concentrations in the organs of mice.

20 p2512 A73-39101

Physiological and operational state of a group of aeroplane pilots under the conditions of stressing tracking tests.

21 p2645 A73-41115

Influence of preliminary adaptation to the main environmental factors on the ATP level and phosphorylation potential in the myocardium during severe heart strain

21 p2640 A73-41275

The relationship between left ventricular ejection time and stroke volume during passive cardiovascular stress.

21 p2641 A73-41566

The energetic metabolism and some reactions of the cardiovascular system during multichannel electrical stimulation and voluntary stressing of muscles

24 p3059 A73-44653

Influence of physical stress on the state of human higher nervous activity under conditions of underwater labor

24 p3059 A73-44653

STRESS [PSYCHOLOGY]

Noise effects on the critical tracking performance of the human operator.

01 p0010 A73-10101

Variations of evoked potentials during various mental stress situations

03 p0268 A73-13823

Telemetric transmission of ergonomic and time study data to describe work load of radar controllers.

03 p0272 A73-14306

EEG alterations by short time stress due to delayed speech feedback during reading, noting alpha and beta wave changes

03 p0265 A73-14473

Personal life changes and health stresses in contrast to accident proneness as factors in pilot error
05 p0545 A73-16732

Physiological tests for hypothalamus regions stimulation effects on coronary circulation, noting hypoxia and emotional stress effects
06 p0650 A73-17770

German monograph - Work-physiological investigations for the objectivization of the tracking behavior, the mental load, and its psychopharmacological modifiability.
07 p0786 A73-20388

German monograph - The objectivization of the effect of load and stress on an information-reception process of man with the aid of acoustically evoked potentials.
07 p0786 A73-20389

Central nervous system stresses effects estimation, discussing ocular positioning movements functional significance and psychological processes
08 p0935 A73-21542

Psychic stress detection and measurement, discussing psychological test methods and physiological correlates
10 p1183 A73-23684

Electromyographic alterations in articular muscles during emotional shifts
10 p1180 A73-24328

Experimental study of emotional stress in operators
11 p1321 A73-25038

Utilization of human voice for estimation of man's emotional stress and state of attention.
11 p1322 A73-25329

Emotional stimulation traces in the spectra of EEG and cutaneo-galvanic reaction of man under normal conditions and in the case of memory impairment
12 p1461 A73-27106

Changes in blood-flow distribution during acute emotional stress in dogs.
13 p1576 A73-28533

Emotional overstress effects on the indices of the blood coagulation system in monkeys
14 p1719 A73-30846

Heart rate variability and the measurement of mental load; Proceedings of the Symposium, London, England, October 1971.
14 p1720 A73-30876

Psychological factors influencing the relationship between cardiac arrhythmia and mental load.
14 p1720 A73-30877

Heart rate variability and work-load measurement.
14 p1720 A73-30879

Mental load and the measurement of heart rate variability.
14 p1720 A73-30881

Behavioral stress response related to passenger briefings and emergency warning systems on commercial airlines.
16 p1965 A73-32660

Self destructive behavior of aircraft pilot due to stress accumulation, discussing man machine relationship, coping mechanisms, competence and invulnerability myth
17 p2115 A73-34746

Initial results of a psychophysiological study of certified parachutists
18 p2284 A73-36917

Study of Indian naval aircrew experiences and psychic factors in disorientation.
18 p2285 A73-36919

The mechanisms of the occurrence of emotional stress in man.
18 p2279 A73-36920

Physiological shifts in the human organism under increased neuropsychic stresses
19 p2393 A73-37392

Flight deck management and pilot operation priorities in high pressure and emergency situations, using integrated aircraft-environment mental model
19 p2384 A73-37731

The effect of social-emotional environmental stress on the functional state of the neocortical structures of rhesus monkeys
19 p2394 A73-37755

Quantitative evoked-potential analyses for the neurophysiological characterization of faulty learning processes in the experimental arterial hypertension-pathogenesis
19 p2394 A73-37756

Amplitude variations of acoustically evoked potentials as a function of signal information and fatigue due to stress
19 p2396 A73-38161

Experimental analysis of conditions for onset of emotional stress
20 p2516 A73-39800

Stress and strain in student helicopter pilots.
21 p2644 A73-41155

Cognitions and 'placebos' in behavioral research on ambient noise.
22 p2816 A73-42950

Effect of adaptation to altitude hypoxia on the behavior of animals in a conflict situation
24 p3058 A73-44549

STRESS ANALYSIS

NT PHOTOGRAPHIC MEASUREMENT
NT SCHWARTZ METHOD
NT X RAY STRESS ANALYSIS

Axisymmetric thermoelasticity problem for an infinite body weakened by two parallel circular cracks
01 p0113 A73-10014

Study of the stressed state of a shallow spherical shell whose thickness varies along its circumference
01 p0113 A73-10018

A continuum analysis of a two-dimensional mechanical model of the lung parenchyma.
01 p0010 A73-10168

Steady creep bending in a beam with random material parameters.
01 p0113 A73-10198

Wave motion in an elastic solid due to a nonuniformly moving line load.
01 p0114 A73-10301

A certain case of stress-concentration analysis by an elastoptical method
01 p0114 A73-10574

Plane stress analysis of an annular disk with distorted inner hole.
01 p0115 A73-10754

Stress separation in the photoelastic study of centrifugal stresses.
01 p0116 A73-11013

Stress determination below thin elastic stiffeners partially braced to finite boundary of elastic half space
01 p0117 A73-11091

The deformations and stresses in floating ice plates.
01 p0118 A73-11366

Deformation and stress analysis in continuum mechanics problems of solid bodies near singular points, noting applicability of linear theory of elasticity
01 p0118 A73-11404

Fourier transformation for stress analysis of anisotropic shells under concentrated forces, solving shallow shell equations via MacDonald functions
01 p0118 A73-11408

Stress analysis for two stamps impression into linearly deformable base, solving integral stress equation by orthogonal polynomials method
01 p0118 A73-11411

Topologic group theory for stress analysis of nonlinearly elastic body under complex load, representing loads set by Lie group
01 p0119 A73-11428

Assessment of the stressed state of a material from the strain nomogram
02 p0229 A73-11618

Stress analysis and dynamic investigation of turbine blades from constrained torsion theory, calculating free torsional vibration frequencies
02 p0229 A73-11621

Designing of shells with a zero Gaussian curvature under an edge load applied to a portion of the shell contour
02 p0230 A73-11717

Stress analysis of cantilever thin walled cylindrical shell with concentrated force on free reinforcement ring, noting members rigidity relationship to internal stress concentration
02 p0230 A73-11718

Investigation of the first forming phase of transverse corrugations
02 p0172 A73-11722

Stressed state of an anisotropic plate with a finite number of curvilinear holes
02 p0230 A73-11783

Curvilinear coordinates for deformation tensor and stress analysis of structures, using finite element method
02 p0231 A73-11812

Thin walled shells strength dependence on residual stresses, noting stress analysis of shallow spherical shell with variable residual deformations
02 p0232 A73-11932

Impact and contact stress analysis in multilayer media.
02 p0234 A73-12072

Analysis of unbalanced angle-ply rectangular plates.
02 p0234 A73-12073

Plastic limit behavior and failure of filament reinforced materials.
02 p0234 A73-12074

Plastic material turbine blades adaptability under nonsteady start-stop thermal and mechanical stress cycle conditions, noting residual stress effects
02 p0235 A73-12129

Relation between plasticity characteristics and geometrical dimensions of cylindrical specimens under tension.
02 p0235 A73-12140

Solid deformable body mean stress determination by statistical summation of stress squares on faces of parallelepiped rotated within Euler angle limits
02 p0235 A73-12207

Effect of the thickness on the stressed state of rotating disks
03 p0384 A73-13128

STRESS ANALYSIS

Dynamic plastic tensile stress analysis based on equation of motion, kinematic equation and material law with conditions regarding disturbance propagation velocity
03 p0385 A73-13142

Mathematical models for elastic solid bodies via similarity theory, noting rheoelectrical simulation for thermal stress analysis
03 p0386 A73-13146

Tensor analysis for micropolar elastic body deformation and stresses, solving differential equations of thermoelasticity
03 p0386 A73-13153

The calculation of supporting planar-surface structures with the aid of the characteristic functions of correlated simplified basic problems
03 p0386 A73-13154

Mechanical properties and stress analysis of elastoplastic body, noting yield conditions and Bauschinger effect
03 p0386 A73-13155

Photoelastic methods of studying dynamic stress problems
03 p0306 A73-13163

New method for the statistical evaluation of constant stress amplitude fatigue-test results.
03 p0387 A73-13229

Regression models for the effect of stress ratio on fatigue crack growth rate.
03 p0387 A73-13231

Computers and the analysis of pressure vessels.
03 p0391 A73-13678

Thermal stress analysis of reentry vehicle nosetips at angle of attack.
03 p0392 A73-13688

Edge dislocation in an infinite anisotropic elastic medium under consideration of the core conditions.
03 p0392 A73-13774

Plane strain limit analysis of plastic material described by piecewise analytic nonlinear yield condition and associated flow rule
03 p0393 A73-13778

Creep rupture under multi-axial states of stress.
03 p0327 A73-13981

Shear strains and elastic anisotropy of transversely isotropic cylindrical shell with circular hole under uniform internal pressure, using shallow shell equations
03 p0394 A73-14020

Stress analysis of thick walled hollow viscoelastic circular cylinder enclosed in elastic shell and subjected to nonlinear creep conditions, noting temperature effects
03 p0394 A73-14021

A strain energy basis for studies of element stiffness matrices.
03 p0395 A73-14184

Torsion of certain prismatic bars.
03 p0395 A73-14198

Stress analysis and design of silicon solar cell arrays and related material properties.
03 p0255 A73-14224

Determination of critical stresses for elements of cylindrical shells in the plastic state
03 p0396 A73-14619

Dimensionless results for plane stress creep behavior of thin disks with central rigid inserts under combined loading
03 p0396 A73-14644

National Symposium on Fracture Mechanics, 5th, University of Illinois, Urbana, Ill., August 31-September 2, 1971, Proceedings. Part 1 - Stress analysis and growth of cracks.
04 p0505 A73-14676

A study of local stresses near surface flaws in bending fields.
04 p0505 A73-14678

Some crack tip finite elements for plane elasticity.
04 p0506 A73-14683

Fatigue crack growth data for various materials deduced from the fatigue lives of precracked plates.
04 p0506 A73-14684

Elastoplastic slip line analysis of specimen geometry effects on J fracture strength criterion for medium strength steel center cracked panel and bend bar
04 p0506 A73-14695

Anisotropic structures reliability in terms of design safety factor, analyzing composite rocket motor cases under plane stress
04 p0452 A73-14723

Accelerated life testing of component reliability in aerospace systems, discussing stress tests, Arrhenius model and time transformation method
04 p0453 A73-14854

Extended validity of single segment stepwise integration schemes for solution of two-point boundary value problems.
04 p0510 A73-15015

Torsion of prismatic bars made of various materials
04 p0510 A73-15077

Stressed state of a planarly elliptical, hyperbolic shell
04 p0511 A73-15088

Note on the thermal stresses in an elastic semi-circular disc due to an internal source of heat, the curved boundary being exposed to radiation while the straight insulated boundary is in contact with a smooth rigid surface.

04 p0511 A73-15173

Upper bound tensile strength analysis of reinforced composite materials in terms of matrix/particle bond strength, void formation and geometrical factors [ASME PAPER 72-WA/PROD-7]

04 p0469 A73-15805

On the forced vibration of a rectangular plate.

[ASME PAPER 72-WA/DE-20] 04 p0514 A73-15838

A finite element based procedure for simulating the transient response and failure of a two-dimensional continuum with nonlinear material characteristics.

[ASME PAPER 72-WA/DE-4] 04 p0515 A73-15875

Analysis of transverse cracks in an orthotropic strip with edge stiffeners.

[ASME PAPER 72-WA/APM-4] 04 p0516 A73-15904

Stress analysis of thick laminated composite and sandwich plates.

05 p0631 A73-16110

Application of general Boussinesq-Galerkin forms of the Navier equation solution to a plane problem

05 p0632 A73-16328

On the similarity conditions in the photorheological method of stress analysis.

05 p0632 A73-16430

Elastic-plastic analysis of stresses near fastener holes.

[AIAA PAPER 73-252] 05 p0635 A73-16974

Methods of birefringence-parameter determination in tension studies by photoelasticity techniques

05 p0635 A73-17077

Stress analysis of hyperbolic paraboloid membrane shells for applications in architecture

06 p0757 A73-17395

Calculation of general surface-supporting structures with the aid of dynamic relaxation

06 p0758 A73-17516

Stress principle relationship to mechanical power additivity, presenting topological, measure theory and functional analysis theorems

06 p0760 A73-17762

Application of elastooptical modeling studies in determining optimal shapes for plane structures

06 p0760 A73-17782

Stress analysis for homogeneous elastic disk under continuous and concentrated load distribution

06 p0760 A73-17783

Crack problem of transversely isotropic strip.

06 p0762 A73-17986

Stress analysis of sharply notched plates and measurement of notch tip blunting.

06 p0764 A73-18487

Plate stretching and plane strain and plate bending.

06 p0765 A73-18723

Viscoplasticity theory based on strain rate vector perpendicularity to quasi-static yield surface, comparing results to Perzyna theory

07 p0907 A73-19078

Weight minimization of axisymmetric clamped plates subject to constraints.

07 p0908 A73-19092

Integral representations for a nonhomogeneous region in couple stress theory of elasticity.

07 p0909 A73-19105

Analysis of the thermal stress-strain state and cooling effectiveness of some turbine-blade designs

07 p0868 A73-20085

Deformations and stresses in a hollow sphere with spherical transversal isotropy under impulsive pressure.

07 p0913 A73-20116

Postbuckling analysis of rectangular orthotropic plates.

08 p1015 A73-20673

Stress concentration in rotating orthotropic elliptic disks solution via Chen-Hsu modification of stress function for bounded plates

08 p1017 A73-20943

The movement of Volterra disclinations and the associated mechanical forces.

08 p0995 A73-21627

Multi-axial and reversing stress effects in dislocation creep - A mechanical equation of states.

08 p0980 A73-21781

Material resistance analogies, relating shear, force and strain factors for bar deformation in tension, compression, torsion and bending

09 p1157 A73-22162

Determination of stresses during pure elastoplastic bending and torsion

09 p1157 A73-22163

Inversion of Prony series characterization for viscoelastic stress analysis.

09 p1158 A73-22393

Stress miscalculation due to resistance strain gauge errors, deriving expressions for stress-strain error relationships

09 p1083 A73-22505

Stresses and displacements in reinforced orthotropic panels under static loads, obtaining differential

equations solution as numerically derived transfer matrices

09 p1161 A73-23091

The effect of a transverse shear acting on the edge of a circular cutout in a simply supported circular cylindrical shell.

09 p1161 A73-23092

Determination of tensile stresses in wide flat samples

09 p1165 A73-23359

Hybrid stress finite element models for elastic continuum, discussing variational principle and macroscopic equilibrium

09 p1166 A73-23457

Elasto-plastic stress analysis of prismatic bar under combined bending and torsion.

10 p1289 A73-24160

Interdisciplinary computer analyses of three-dimensional solids defined by polyhedral surfaces.

[AIAA PAPER 73-354] 11 p1437 A73-25491

Stress, stability, and vibration of complex, branched shells of revolution.

[AIAA PAPER 73-360] 11 p1437 A73-25496

Linear elastic finite element stress analysis of lap and tapered adhesive joint bonding of composite to metal substrate

[AIAA PAPER 73-371] 11 p1438 A73-25505

Crippling allowances for elevated temperature and creep environments.

[AIAA PAPER 73-388] 11 p1439 A73-25517

A method for obtaining stresses and displacements in thick cylindrical shells under arbitrary boundary conditions.

[ASME PAPER 72-APM-LLL] 11 p1442 A73-25708

Applications of solid mechanics; Proceedings of the Symposium, University of Waterloo, Waterloo, Ontario, Canada, June 26, 27, 1972.

11 p1442 A73-25842

Topologic group theory for stress analysis of non-linearly elastic body under complex load, representing loads set by Lie group

11 p1443 A73-26057

Fretting fatigue strength of several materials combinations.

11 p1385 A73-26335

Coordinate systems standardization in stress analysis, considering vector orientation definitions

11 p1444 A73-26374

Bending stresses and strains in anisotropic semi-infinite plates with arbitrary edge and surface loadings.

11 p1445 A73-26404

Gradient decomposition and kinematic constitutive equations for elastoplastic material behavior under large strains

11 p1445 A73-26410

Two component system reliability model, taking into account stress effects under failure normal distribution assumption

11 p1448 A73-26730

Fatigue resistant design with fiber reinforced plastics (FRP), discussing stress analysis, failure criteria, material anisotropy, multiaxial stress conditions and cumulative damage

12 p1515 A73-26880

Contribution to the theory of the finite element method applied to the overall stress analysis of a fuselage

12 p1551 A73-27084

Determination of the stressed state of a circular cylindrical shell with stepwise variation in wall thickness along the generatrix under the action of a local load

12 p1552 A73-27261

Investigation of the stress-strain state of spherical shells with an eccentric hole on the basis of the three-dimensional theory of elasticity by the finite element method

12 p1552 A73-27262

Constant cross section composite circular rod, deriving torsional stress behavior near division line intersection with rod contour from closed solution

12 p1552 A73-27368

Soft shell strength analysis for contact and static loads

12 p1554 A73-27470

Book - Introductory structural analysis with matrix methods.

12 p1554 A73-27548

Finite element theory of plates and shells including transverse shear strain effects.

13 p1693 A73-28235

Three dimensional elastic stress analysis by finite element method within reasonable computer costs, noting problem simplification

13 p1693 A73-28240

Effective use of the incremental stiffness matrices in nonlinear geometric analysis.

13 p1694 A73-28252

Analysis of centrifugal stresses in anisotropic viscoelastic cylinder.

13 p1697 A73-28810

Tensometric strain gauge evaluation of stress analysis methods for hollow cylindrical shells under uniform internal pressure

13 p1698 A73-29057

Stresses in adhesive bonds of thin cylindrical shells

13 p1698 A73-29040

Analytical elasticity methods for airfield pavement structural stress-strain, failure and reliability performance evaluation

13 p1598 A73-29101

German monograph on calculation of thermal expansion transformation stresses in long circular cylinders covering austenite-martensite transformation, thermal expansion and viscous bodies

13 p1699 A73-29202

Three-dimensional scattered-light stress analyses of discontinuous fiber reinforced composites.

[SESA PAPER 2033] 13 p1699 A73-29303

Three-dimensional photoelastic tests of thin shell pressure vessels.

13 p1699 A73-29303

Parametric finite element stress analysis of multiple crack propagation in nonhomogeneous nonisotropic materials, using Griffith criterion

13 p1701 A73-29470

Fatigue damage by a stress below the endurance limit.

13 p1641 A73-29490

Fatigue analysis considering rotating principal stress axes for aluminum alloy 2024-T351.

13 p1641 A73-29500

Thermal stress analysis of metals with temperature dependent mechanical properties.

13 p1701 A73-29500

Stress differentiation procedure for stress-strain technique studies in dynamic photoelasticity, giving expressions for elastic modulus and Poisson ratio

13 p1703 A73-29613

Statistical criteria of ultimate strength and plasticity of materials in the complex stress state.

13 p1703 A73-29620

Investigation of the strength of construction materials for different ratios of the main stresses.

13 p1703 A73-29622

Refined method of determining tangential stresses and testing the strength of cylinders subjected to transverse flexure.

13 p1703 A73-29635

Calculation and design of highly stressed fiberglass-reinforced plastic components

13 p1703 A73-29653

Principle of virtual work and equations of shells

14 p1805 A73-29761

Frame structures dynamic analysis, comparing force method derived from stress and velocities variational principles with displacement method derived from Hamilton principle

14 p1807 A73-30188

Stress determination approximation in structural mechanics problems by linear first order differential equations reduction to linear algebraic equations

14 p1810 A73-30378

Stress convexity domains for rigid perfectly plastic continuum, using directional derivative and distance function

14 p1811 A73-30483

Maximum stress calculation for I beam and thin walled sphere redundant structures under stationary creep by perturbation method

14 p1811 A73-30487

Finite bending of incompressible hyperelastic plastic strip, analyzing stress and stored energy function

14 p1812 A73-30496

A method for studying the stressed state during torsion of hollow prismatic beams

14 p1815 A73-30790

Stress and fracture analysis of adhesive joints.

[ASME PAPER 73-DE-21] 14 p1755 A73-30822

Saint Venant principle investigation for plane problem of linear elastostatics for anisotropic media by energy method, calculating exponential stress decay constant lower bound

15 p1946 A73-31102

Muskhelishvili elastodynamic theorem concerning natural stress-free state extension to three dimensional theory of inhomogeneous anisotropic elastic bodies

15 p1946 A73-31105

Fredholm integral equation singularity method solution for calculating stresses and elastic displacements in bodies of revolution of arbitrary shape under torsional loads

15 p1947 A73-31327

Computerized stress analysis of shock load induced circular elastic membrane interaction with fluid stream via method of characteristics related to aerodynamic decelerator design

[AIAA PAPER 73-443] 15 p1948 A73-31429

Dynamic stress analysis during inflation of disk-gap-band Viking 75 parachute for Mars soft landing

[AIAA PAPER 73-444] 15 p1825 A73-31430

Nonlinear tension and buckling stress behavior of angle ply unidirectional laminated composites

15 p1949 A73-31683

Finite element methods in continuum mechanics.

15 p1950 A73-31973

Solution to a three-dimensional mixed boundary value problem in the theory of elasticity

15 p1953 A73-32102

Strain analysis of composites by moire methods.
15 p1956 A73-32269

A stress-strain relation for homogeneous and isotropic continua
16 p2035 A73-32934

Determination of the displacement for a membrane stretched over a constant-curvature surface
16 p2076 A73-32935

Convolutional variational principles for stress distribution in anisotropic plates of linear viscoelastic material
16 p2077 A73-32981

Plane stress fields in isotropic disks due to singular and distributed loads, obtaining Fredholm integral equation solution via cubic spline function
16 p2079 A73-33238

Matrix theory algorithms for static stresses and elastic deformations in truss structures, deriving equilibrium equations in terms of forces, deformations and node displacements
16 p2080 A73-33258

Stress calculation for plates and beams via finite element method, improving accuracy by smoothing stress and strain distributions at element boundaries
16 p2080 A73-33262

Physiological factors and optical parameters as bases of vegetation discrimination and stress analysis.
16 p2003 A73-33355

Half plane stress boundary value problems in elastodynamics, obtaining similarity solutions in terms of analytic functions via integral transforms
16 p2082 A73-33903

An assumed stress hybrid finite element model for linear elastodynamic analysis.
17 p2241 A73-34189

Constrained continuous media mechanics, discussing basic assumptions, integrable and nonintegrable constraints and motion
17 p2241 A73-34321

Book - Stresses in shells /2nd edition/.
17 p2242 A73-34469

Lagrangian formulation of sandwich shell theory.
17 p2242 A73-34526

New relationships between stress testing, failure and reliability.
17 p2178 A73-34730

Elastic equilibrium of an ellipsoid under the action of concentrated loads
17 p2244 A73-34790

Stress analysis of composite materials with strong fibers in weak matrix, obtaining tensile stress boundary layer equations via elasticity theory and perturbation methods
17 p2249 A73-35110

On the stress analysis of creeping structures subject to variable loading.
[ASME PAPER 72-APM-TTT] 17 p2250 A73-35115

Diffractography versus holography - A stress analyst's comparison.
17 p2173 A73-35440

Test on fuselage models at reduced sizes.
17 p2107 A73-35443

Micromechanic stresses in photoelastic composite coupons.
[SESA PAPER 2175A] 17 p2251 A73-35456

Stiffness matrix displacement analysis via curved elements for plane stress and thin plate bending problems
17 p2252 A73-35606

Book - Stress analysis of polymers.
17 p2253 A73-35861

Stresses in molybdenum coatings obtained by thermal decomposition of Mo/CO/6
18 p2319 A73-35892

A method for determining the stressed state of anisotropic plates with a nonsymmetrically reinforced edge
18 p2363 A73-36407

Applications of finite element stress analysis and stress-strain properties in determining notch fatigue specimen deformation and life.
18 p2364 A73-36591

Engineering analysis of the inelastic stress response of a structural metal under variable cyclic strains.
18 p2364 A73-36594

Yielding and failure of metals in a complex state of stresses
18 p2366 A73-36756

Tensometric strain gage evaluation of stress analysis methods for hollow cylindrical shells under uniform internal pressure
18 p2366 A73-36889

Stresses in bonded joints of thin cylindrical shells.
18 p2366 A73-36895

Two dimensional steady and transient thermal stress analysis in rectangular solid with varying surface temperature, noting thermoelastic problems solution by analog method
19 p2498 A73-37668

German book - Practical photoelasticity /3rd revised and enlarged edition/.
20 p2566 A73-39273

Calculation of joint shells differing in their material and thickness
20 p2619 A73-39365

Midwestern Mechanics Conference, 13th, University of Pittsburgh, Pittsburgh, Pa., August 13-15, 1973, Proceedings.
20 p2620 A73-39513

Stability criteria for incompressible elastic isotropic materials subject to shearing displacement superimposed on homogeneous elastic deformation, discussing Cauchy stress and shear modulus
20 p2620 A73-39530

Stress singularities associated with a crack inclined to a bi-material interface.
20 p2620 A73-39531

On stress-concentration analysis of laminated composite plates.
20 p2622 A73-39551

The vibrations of non-circular cylindrical shells with initial stresses.
21 p2783 A73-40288

Boundary residual methods limitation on elasticity problem solution accuracy, considering torsional stress analysis of square and hexagonal cylinders with circular hollow cores
21 p2784 A73-40431

Stress and temperature analysis for surface cooling or heating of laser window materials.
21 p2716 A73-40966

Critical load analysis of strip /beam/ with arched crack under compressive stress and bending moments
21 p2786 A73-40985

Thermal stress calculation for elastic half strip in nonuniform temperature field by functions in terms of Castigliano variational principle
21 p2786 A73-40986

Polish book - Theory of coupled stresses.
21 p2787 A73-41219

Plane strain and generalized plane stress problems for fibre-reinforced materials.
21 p2788 A73-41546

Measurement accuracy achievable in photographed isochromatic pictures
21 p2706 A73-41605

Material resistance analogies, relating shear, force and strain factors for bar deformation in tension, compression, torsion and bending
22 p2919 A73-42110

Determination of the stresses for pure elastic-plastic flexure and torsion.
22 p2919 A73-42111

Accelerating the convergence of elastic-plastic stress analysis.
22 p2922 A73-42481

On the integral equations of three-dimensional multiple inclusion problems.
22 p2924 A73-42682

Experimental determination of the transient uniaxial stress in a bar by dynamic photoplasticity.
[ASME PAPER 73-APMW-37] 22 p2926 A73-42894

Stress-strain state of stiffened shallow shells of rectangular planform
22 p2928 A73-43054

The yield stress of Ni3Al, W/.
22 p2880 A73-43075

Matrix methods application to stress in elastic structures, examining Mohr circles, design implications and orthogonality anisotropy
22 p2929 A73-43173

Book - Elasticity.
23 p3039 A73-43434

Determination of the deflections and stresses in a small-aspect-ratio wing by the displacement method
23 p3041 A73-43723

Research and development of aerospace adhesive bonded systems and concepts.
24 p3093 A73-44763

Three-dimensional axisymmetric problem of a normal load concentrated on an elastic free-underface plate of constant thickness - Expression for the stresses in the vicinity of the load
24 p3149 A73-45218

Mixed finite-difference scheme for analysis of simply supported thick plates.
24 p3150 A73-45226

On the hybrid stress finite element model for incremental analysis of large deflection problems.
24 p3151 A73-45303

Computational assessment of the numerical influence of the cutting step size and evaluation equation on the precision of experimental and analytical residual-stress determinations
24 p3153 A73-45446

Continuity equation and equations of motion for ideal plastic body based on von Mises yield condition, considering stress discontinuity and boundary value problems
24 p3153 A73-45499

STRESS CALCULATIONS
U STRESS ANALYSIS
STRESS CONCENTRATION

Approximate solution of equations describing the thermal stressed state of a shallow spherical shell
01 p0113 A73-10017

Thermal diffusion theory for deformations of thin isotropic shells and plates subjected to nonuniform temperature and stress concentration fields
01 p0113 A73-10019

Unsteady temperature and stress distribution in variable thickness disk under convective heat transfer with ambient medium, using approximation method
01 p0113 A73-10021

Effect of heat propagation rates on the temperature field and stresses in thin plates
01 p0113 A73-10022

Temperature fields and stresses in bodies of simple geometry when the ambient medium temperature is unsteady
01 p0113 A73-10023

Mathematical model for the buildup of imperfections in plastic isotropic materials
01 p0114 A73-10476

Stress concentration at circular holes in a cylindrical shell of moderate thickness
01 p0114 A73-10480

Crack formation in orthogonally reinforced fiberglass plastics
01 p0067 A73-10482

Physical fatigue limit of hardened steels
01 p0063 A73-10485

A certain case of stress-concentration analysis by an elastooptical method
01 p0114 A73-10574

Structural members optimal shaping in terms of stress concentration, analyzing plane elasticity boundary value problem
01 p0114 A73-10600

Application of shell equations to an unsymmetrically loaded corrugated shell of revolution.
01 p0115 A73-10769

Two dimensional elasticity theory for radial crack effects on tensile stress concentration in circular elastic isotropic plate
01 p0117 A73-11092

Dynamic stability of the state of moment stress in a cylindrical shell with allowance for inertia of the subcritical state
01 p0117 A73-11093

Stress concentration in disk with radial slot and with outer boundary subject to arbitrary continuous load, using plane elasticity theory
01 p0117 A73-11095

Photoelastic stress analysis of solid propellant grains.
01 p0090 A73-11118

Elastic-plastic analysis on the structural elements with different values of stress concentration factor.
01 p0117 A73-11122

Ti-V and Ti-Nb alloys mechanical strength and stress concentration resistance at low temperatures
01 p0067 A73-11348

Reynolds stresses and turbulent kinetic energy production in wall jets on flat and concave walls
01 p0034 A73-11357

Statistical method of determining the load or stress distribution from the failure characteristics of mechanical systems
01 p0118 A73-11370

Oscillations of nonshallow cylindrical shells loaded by distributed and concentrated masses
01 p0118 A73-11407

Temperature fields and stresses during local tempering of helical welds of a cylindrical shell
01 p0118 A73-11413

Determination of the strains and displacements for a rectangular shaped viscoelastic body
02 p0229 A73-11578

Determination of the theoretical stress-concentration factors in composite systems in bending
02 p0229 A73-11638

Stress analysis of cantilever thin walled cylindrical shell with concentrated force on free reinforcement ring, noting members rigidity relationship to internal stress concentration
02 p0230 A73-11718

Stressed state of an isotropic half-plane with a finite number of circular holes situated along the boundary
02 p0230 A73-11782

Stressed state of an anisotropic plate with a finite number of curvilinear holes
02 p0230 A73-11783

Finite difference method for transverse elliptical cross section effect of spiral shell on stress concentration
02 p0231 A73-11802

Design of a shallow shell with a large rectangular hole
02 p0231 A73-11803

Stress distribution in elastic shell of revolution under axisymmetrical loads, noting thickness distribution for uniform stress in critical edge loading zone
02 p0231 A73-11805

Russian book on temperature and stress distributions in thin plates covering unsteady heat transfer and thermoelasticity of isotropic and anisotropic plates
02 p0232 A73-11891

Determination of elastic stresses at notches and corners by integral equations.
02 p0234 A73-12075

On two coplanar cracks in an infinite transversely isotropic medium.
02 p0234 A73-12087

STRESS CONCENTRATION

Application of the basic concepts of structural-energetic theory to the problem of physical fatigue limit.
02 p0235 A73-12131

Statistical evaluation of strength of metals at brittle fracture.
02 p0235 A73-12133

Study of the effect of small elastoplastic deformations on the load-bearing capacity of specimens with stress concentrators under repeated variable loading.
I.
02 p0235 A73-12202

Study of the effect of small elastoplastic deformations on the load-bearing capacity of specimens with stress concentrators under repeated variable loading.
II.
02 p0181 A73-12203

Engineering method of calculating the parameter of fracture toughness.
02 p0235 A73-12210

The influence of stress concentrators on the properties of steel in cryogenic technology.
02 p0181 A73-12213

Calculation of thermal stresses in spherical storage vessels.
02 p0236 A73-12215

Elastic and plastic deformations of circular ring with initial machining produced stresses distributed across thickness, calculating critical load for static stability.
02 p0236 A73-12581

Stress concentration near a circular hole reinforced with a wide ring in the case of a nonlinear law of elasticity
02 p0236 A73-12584

Stress concentration in a plane weakened by two different circular holes in the presence of small elastoplastic strains
02 p0237 A73-12585

Fracture mechanics equations for crack propagation braking by elliptic and circular holes at crack tip, noting stress concentration
02 p0237 A73-12586

Elastoplastic stressed state of cylindrical shells weakened by a circular hole
02 p0237 A73-12590

Mercury thermal stress and strain fields of elastic deformation from solar heating variations due to resonance rotation
02 p0223 A73-12721

Accommodation of the stress field at a grain boundary under heterogeneous shear by initiation of microcracks.
02 p0237 A73-12812

Vibrations of circular cylindrical shells subjected to nonuniform initial stress.
03 p0384 A73-12984

Stressed state of adhesively bonded plane interfaces in composite systems, applying two dimensional Vocke theory
03 p0311 A73-13129

Nonlinear stress properties in vicinity of crack tip, taking into account finite crack width effect by parabolic model
03 p0385 A73-13131

Calculation of the stress distribution in rotating disks in the case of unsteady creep with the aid of a digital computer
03 p0385 A73-13140

Effect of residual or characteristic stresses on the deformation of plates
03 p0385 A73-13143

Temperature, velocity, and stress distribution in thermo-viscoplastic boundary layers
03 p0386 A73-13145

A procedure for the determination of hysteresis losses at a point of a body in the case of variable stresses
03 p0306 A73-13149

Nonclassical flow theory for continuum mechanics with asymmetrical stress concentration, noting rheological problems in laminar high polymers flow, hydrodynamic instability and turbulent flow
03 p0291 A73-13152

Stress field and deformed shapes of liquid filled axisymmetric sessile neo-Hookean membrane during submergence to various depths
03 p0292 A73-13303

On the unbonded contact between a beam and a semi-infinite plate.
03 p0389 A73-13324

Thermal stresses due to a moving heat source in a circular disk.
03 p0389 A73-13328

Triaxial plastic compression soil theory generalization to three dimensional complex stress fields, discussing yield surface for granular materials
03 p0390 A73-13332

Stress redistribution model for anisotropic fiber reinforced laminates with internal cracks, assuming preferred directions to bonding planes and fiber orientation
03 p0334 A73-13333

Finite difference theory for bending stress concentration in shells of revolution, noting constitutive equation for thermal stress analysis
03 p0393 A73-13793

Creep life and strain estimation for Nimonic alloy by monitoring cavity density under optical microscope
03 p0326 A73-13965

Stresses governing the high-temperature creep rate in single crystals with a bcc lattice
03 p0326 A73-13971

The fracture mechanics of slit-like cracks in anisotropic elastic media.
03 p0394 A73-13979

Disks with inclined face, investigating effects of joint between hub and disk face on stress-strain state in elastic deformation range
03 p0394 A73-14012

Radially symmetrical thermoelastic disturbances in generalised dynamical theory of thermoelasticity.
03 p0395 A73-14311

Stress intensity factor for an elliptical crack approaching the surface of a plate in bending.
04 p0505 A73-14677

Stress intensity factors for surface cracks in bending.
04 p0505 A73-14679

Stress intensity factors for internally pressurized thick-wall cylinders.
04 p0505 A73-14680

Crack shapes and stress intensity factors for edge-cracked specimens.
04 p0506 A73-14681

Elliptical, annular, through, part-through and irregularly shaped crack front curvature effect on stress intensity factor calibration
04 p0506 A73-14682

Rayleigh waves for continuous monitoring of a propagating crack front.
04 p0452 A73-14691

Colloquium on Structural Reliability notes on 'Fatigue Lecture.'
04 p0507 A73-14706

Statistical stress concentration effects in composites.
04 p0468 A73-14718

Thick elastic or inelastic shells finite deformation, presenting multicouple theory for stress-strain distribution
04 p0508 A73-14941

The force on a crack deviating from its original plane.
04 p0509 A73-14950

Analytical investigation of a cylindrical shell embedded in a soft medium.
04 p0511 A73-15172

Safety factor calculation procedure for perfectly plastic body under given plane stress based on complex variable functions
04 p0511 A73-15175

Fourier transformations and Wiener-Hopf equations for stress intensity factor of crack propagation in linearly elastic homogeneous isotropic strip
04 p0512 A73-15238

Plastic deformations and crack propagation in cylindrical and spherical shells under uniform pressure, calculating stress intensity factor
04 p0512 A73-15239

Stress intensity factor for axially stressed thin polymethyl methacrylate plate with cracks, noting fracture angle prediction
04 p0512 A73-15240

Linear analytical procedure for adhesively bonded flat joints design with minimized shear stress concentration, presenting finite element and automated iterative procedure
[ASME PAPER 72-WA/DE-13] 04 p0514 A73-15874

Mean field equations for dynamic response of homogeneous linearly elastic solids, obtaining formulation for ensemble averaged displacement and stress fields of composite
[ASME PAPER 72-WA/APM-28] 04 p0515 A73-15890

Stresses in laminated composites containing a broken layer.
[ASME PAPER 72-WA/APM-14] 04 p0516 A73-15899

Russian book - Strength of viscoelastic materials relative to solid-propellant rocket-motor charges.
04 p0517 A73-15967

Fretting-fatigue mechanisms and the effect of direction of fretting motion on fatigue strength.
05 p0581 A73-16128

On the determination of the centers of twist and of shear for cylindrical shell beams.
[ASME PAPER 72-APM-XX] 05 p0633 A73-16534

Asymmetric principal stress bounds in terms of symmetric part of tensor, considering existence conditions and maximum shear and normal stresses
[ASME PAPER 72-APM-QQQ] 05 p0633 A73-16535

On finite symmetrical strain in thin shells of revolution.
05 p0633 A73-16536

Thermal stresses in circular plates including the influence of transverse shear.
05 p0633 A73-16539

Stress-strain state of a spheroidal inclusion/measuring device/ embedded in a thermoelastic medium
05 p0633 A73-16616

Crack tip stress field variation via elastic pulses for crack path alteration and subsequent fracturing process termination, using photoelastic analysis
05 p0634 A73-16797

Calculations of turbulent shear stress in supersonic turbulent boundary layer zero and adverse pressure gradient flow.
[AIAA PAPER 73-166] 05 p0566 A73-16900

A numerical solution of an elastoplastic thick-walled tube subjected to thermal loading.
[AIAA PAPER 73-256] 05 p0635 A73-16977

Sandwich beams of unsymmetrical structure.
06 p0759 A73-17696

Order c-square bulk stress derivation for force-free spherical particles suspension in Newtonian ambient fluid with uniform viscosity, noting error bounds
06 p0722 A73-17700

The axisymmetric Boussinesq problem in the micropolar theory of elasticity.
06 p0760 A73-17765

The stress intensity factor of an edge crack in a finite elastic disc.
06 p0762 A73-17983

Edge crack in a strip of an elastic solid.
06 p0762 A73-17990

Stress distribution on astronomical telescope mirror outer surface, calculating deflection and relief load
06 p0693 A73-18157

A couple-stresses elastic solution of an infinite tension plate bounded by an elliptical hole.
06 p0717 A73-18173

Collocated interfacial stress intensity factors for finite bi-material plates.
06 p0763 A73-18477

An experimental investigation into the mechanics of deep semielliptical surface cracks in mode I loading.
06 p0763 A73-18478

Influence of local variations of yield strength on plastic zones at crack tips.
06 p0709 A73-18480

Method of analysis and prediction for variable amplitude fatigue crack growth.
06 p0709 A73-18482

Subcritical crack growth of TRIP steels in air under static loads.
06 p0710 A73-18485

An assessment of factors influencing data obtained by the photoelastic stress freezing technique for stress fields near crack tips.
06 p0764 A73-18488

Stress intensity factors and singularity power and strain energy release rate near localized cracks and inclusions in composite materials
06 p0764 A73-18489

Dynamic stress intensity factor for an unbounded plate having collinear cracks.
[AD-758426] 06 p0764 A73-18492

The influence of stress intensity and microstructure on fatigue crack propagation in ferritic materials.
06 p0710 A73-18498

Diffusion of hydrogen in titanium alloys due to composition, temperature, and stress gradients.
06 p0712 A73-18764

Transient stresses induced by heating a plane boundary.
07 p0907 A73-19077

Extension of an interface flaw under the influence of transient waves.
07 p0908 A73-19080

Stress-induced rotation of polarization directions of elastic waves in slightly anisotropic materials.
07 p0908 A73-19083

A note on the Cherepanov calculation of viscoelastic fracture.
07 p0908 A73-19090

Notch induced stress concentrations at elastic rectangular core/inclusion/ in extended rectangular plate with rigidly supported edges, using finite element method
07 p0910 A73-19196

Comparative considerations concerning parametric stress concentration studies involving finite elements and complex stress functions
07 p0910 A73-19208

Lame equations for stress concentration in half plane with extracted elastic inclusion, solving via Fourier integrals reduced to singular integral equation
07 p0910 A73-19301

Solution of a contact problem for an infinite elastic cylinder with two contact areas by the method of triple integral equations
07 p0910 A73-19307

Investigation of the stressed state of a rod with a cut under elastoplastic torsion
07 p0911 A73-19308

Extremal stresses in the first basic two-dimensional problem of elasticity theory for a half-plane
07 p0911 A73-19310

Infinite triangular wedge, with a notch at its bisectrix, under the action of concentrated forces applied to the edges of the notch
07 p0911 A73-19312

Two dynamic contact problems for a half-plane with elastic cover pieces
07 p0911 A73-19314

Transmission of the load from an annular cover piece to a plane with a circular hole
07 p0911 A73-19321

Stress intensity factors for nozzle corner cracks.
07 p0912 A73-19564

The influence of fretting and geometric stress concentrations on the fatigue strength of clamped joints.
07 p0912 A73-19572

Nonlinear effect of initial stress on crack propagation between similar and dissimilar orthotropic media.
07 p0915 A73-20334

Probability theory for vibrational strength of turbomachine parts, calculating statistical maximum stress for given stress distribution conditions
07 p0917 A73-20502

The stress intensity factor of an edge crack in a finite rotating elastic disc.
07 p0918 A73-20566

Equilibrium method for stress concentration around hole in plate under tension, comparing with Kolosov-Muskhelishvili potential method
08 p0105 A73-20699

Parameters governing load transfer for single reinforcing members.
08 p0106 A73-20799

Bielayev's point in poroelastic bodies in contact.
08 p0106 A73-20829

Stress concentration in rotating orthotropic elliptic disks solution via Chen-Hsu modification of stress function for bounded plates
08 p0107 A73-20943

Optical stress rosette based on caustics for stress distribution and differences measurement in perforated plate, using gas laser light for interferometry
08 p0964 A73-21047

The effect of stress on metal semiconductor junctions.
08 p0995 A73-21482

Effects of thermal loading on foil and sheet composites with constituents of differing thermal expansivities.
[ASME PAPER 72-MAT-E] 08 p0979 A73-21572

Cr-Ni carbon steel testing for stress and temperature dependencies of secondary creep rate, noting grain boundary diffusion controlled mechanism
08 p0980 A73-21674

A problem for a half-plane with a finite vertical cut
08 p0109 A73-21722

Steady temperature fields and stresses in a half-space heated by a linear inductive source
08 p0109 A73-21759

Stress-strain state of transversely isotropic shells under concentrated loads
08 p0109 A73-21760

Stress-strain state of a piecewise homogeneous plane with thin-walled elastic inclusions of finite length
08 p0109 A73-21765

Stressed state of an isotropic elliptical plate weakened by elliptical holes
08 p0120 A73-21767

Experimental investigation of the failure mechanism of fiber-reinforced composites subjected to uniaxial tension.
09 p1156 A73-21874

Sectioning method for residual stress measurement in structural members, describing test procedure, specimen preparation, tools and measuring devices and working conditions
09 p1156 A73-21875

Theoretical calculation of the compressibility of porous media.
09 p1157 A73-22144

Deformation and rupture of molybdenum under conditions of creep
09 p1100 A73-22161

Stress concentration and groove design as factors in crack failure of low power single stage gas turbine rotor disk, using optical polarization technique
09 p1157 A73-22166

Finite element stress field solution of the problem of Saint Venant torsion.
09 p1158 A73-22390

A comparison of first and second order axially symmetric finite elements.
09 p1158 A73-22399

Fatigue life prediction and design optimization for solar cell interconnectors based on elastoplastic material stress distribution calculation by finite element methods
09 p1036 A73-22809

Muskhelishvili boundary value problem of plate bending and point deformation for round and annular plates under uniform loads
09 p1159 A73-22854

Effects of circular holes on the fatigue resistance of AMg6BM aluminum-alloy sheet in symmetrical bending.
09 p1105 A73-23053

Calculation of the stress concentration produced by an internal pressure in the region where a cylindrical shell is connected to a branch pipe.
09 p1161 A73-23058

Asymptotic approximation to crack problems with emphasis on stress intensity factor, discussing interpolation procedure based on simplified problem form
09 p1162 A73-23180

Stress field singularities due to cracks in isotropic elastic bodies, assuming Hooke's law stress-strain relationship in integral equation representations
09 p1162 A73-23182

Applications of the finite element method to the calculations of stress intensity factors.
09 p1162 A73-23185

Linear elastic and general yielding fracture mechanics compatibility, investigating crack opening displacement relationship to stress intensity factor
09 p1109 A73-23263

An evaluation of finite element methods for the computation of elastic stress intensity factors.
[ASME PAPER 72-PVP-19] 09 p1163 A73-23267

Stress state around an elliptic hole in a conical shell under tension.
[ASME PAPER 72-PVP-11] 09 p1163 A73-23269

Action of a concentrated force on an elastic ring pressed into a circular hole in an isotropic plate
09 p1165 A73-23357

Some results of a study of the interaction between Rayleigh pulses and edge cracks
10 p1287 A73-23591

Deformation of shells of revolution with attached rings under different local loads, deriving approximate expressions for stressed state
10 p1287 A73-23592

Elastoplastic deformation and stresses in clamped multilayer cylinders
10 p1287 A73-23593

Analysis of load distribution in multiple-row bolt joints
10 p1222 A73-23595

Contribution to the study of the elasticity of monocrystalline aluminum under very low stresses
10 p1231 A73-23771

A theoretical study of the effect of the interface on composite toughness.
10 p1288 A73-23955

Stress differences in the moon as an evidence for a cold moon.
10 p1277 A73-24084

Note on an approximate method for computing consistent conjugate stresses in elastic finite elements.
10 p1290 A73-24293

Stresses in a partly yielded notched bar - An assessment of three alternative programs.
10 p1290 A73-24294

The analysis of dislocation systems by the finite element method.
10 p1290 A73-24298

Polymer chain model with internal rotations for elastic body stress-strain state, internal work, elastic energy and equations of motion
10 p1240 A73-24307

Investigation of the fracture of carbon-graphite materials in a complex stress-strain state
10 p1240 A73-24360

Investigation of the load-carrying capacity of rotating disks by the method of optically sensitive coatings
10 p1291 A73-24364

Subcritical crack growth measurement during static loading of precracked Ti alloys in salt water, discussing arrested crack propagation at different stress intensities
10 p1234 A73-24429

Al alloy stress intensity range estimation from surface fatigue striation incidence and modulus of elasticity, noting relationship to crack growth closure in fractography
10 p1235 A73-24447

Nonlinear problem for a plane continuous medium in Euler coordinates
10 p1292 A73-24489

Calculation of the steady thermal and stress boundary conditions in the Phebus 2 reactor
10 p1248 A73-24495

Temperature change induced material properties variations effects on impact stresses in graphite and stainless steels, considering impact velocity
10 p1220 A73-24575

Elastic deformation of an orthotropic semi-infinite plate with straight boundary asymmetric with respect to the elastic axes of the material under uniform partial loading.
10 p1293 A73-24922

New arrangement for testing materials in the volume stressed state and at elevated temperatures /Exchange of experience/.
10 p1222 A73-24947

Stress distribution in a half-plane with a hole strengthened by an elastic insert
11 p1432 A73-25026

Reissner's edge effect in three-layer plates with filler
11 p1433 A73-25030

Stress concentration in an anisotropic plate with an insert in pure bending
11 p1433 A73-25031

Plane strain dynamics on magneto-thermoviscoelastic materials, noting conductivity, heat sources, potential and rotation
11 p1433 A73-25163

Stress-strain state of a thermoelastic spheroidal insert in a thermal viscoelastic medium
11 p1434 A73-25388

Experimental verification of the applicability of small elastoplastic deformation theory to the calculation of rotating disks
11 p1434 A73-25392

Polynomial solutions to the plane problem of electroelasticity theory
11 p1434 A73-25394

Stability of a shell in the form of a hyperbolic paraboloid subjected to compression along straight generating lines
11 p1435 A73-25397

The effect of strain rate on the characteristic value of the linear-elastic fracture mechanics determined on large and small specimens
11 p1380 A73-25446

Concentration of thermal stresses at joints between heterogeneous materials
11 p1435 A73-25458

Fatigue crack delay and arrest due to single peak tensile overloads.
[AIAA PAPER 73-325] 11 p1441 A73-25555

Stress redistribution and rupture due to creep in a uniformly stretched thin plate containing a circular hole.
[ASME PAPER 72-APM-KKK] 11 p1442 A73-25709

Metal fatigue crack nucleation behavior and dislocation microstructures, including slip band and extrusion-intrusion pairs
11 p1380 A73-25804

Brittle cleavage crack propagation in crystals in terms of bonds acting between pairs of atoms, considering stress distribution around crack tip
11 p1409 A73-25812

Stress and displacement fields around growing corrosion fatigue crack, discussing intensity factor, plastic zones, cyclic loading and fluid pressure effects
11 p1381 A73-25813

Application of some aspects of low-cycle fatigue research in structural design.
11 p1443 A73-25846

Crack growth rate due to steels and Ti and Ni alloys electrochemical dissolution, noting tensile stress intensity factor
11 p1385 A73-26173

Composite solid with two contacting or bonded half planes of different elastic moduli, considering interplane force transmission from stress distribution calculation
11 p1443 A73-26277

Energy flux into extending crack in elastic solid calculated in terms of stress intensity factor for plane and antiplane strain problems
11 p1444 A73-26281

Optical fiber breaking stress distributions obtained by a cantilever method.
11 p1344 A73-26312

Effect of compressive stress on silicon bipolar devices.
11 p1410 A73-26422

Method of initial functions for the plane problem of a linearly orthotropic body in the theory of elasticity
11 p1445 A73-26457

Antiplane deformation near a cut in a hardening elastoplastic material
11 p1445 A73-26458

Estimates for stress derivatives and error in interior equations for shells of variable thickness with applied forces.
11 p1446 A73-26548

Bi-harmonic solutions of problems for elastoplastic bodies in the presence of nonuniformity of the stress field
11 p1446 A73-26598

Application of double trigonometric series to the calculation of shell plates of variable thickness
11 p1446 A73-26600

Displacement and finite-strain fields in a sphere subjected to large deformations.
11 p1447 A73-26647

Nonsingular control, determining optimum shape of straight bar under stress and inertial moment restrictions
12 p1482 A73-26793

The determination of Mode I stress-intensity factors by holographic interferometry.
12 p1550 A73-27021

Design of zero-moment axisymmetric tanks made of a reinforced hereditary-elastic material
12 p1551 A73-27181

Stresses in bonded joints of circular cylindrical shells and panels
12 p1551 A73-27182

Bending-produced cracks, stresses and fracture of rectangular cross section beam from brittle body homogeneous model
12 p1552 A73-27255

Nickel base alloys high temperature steady creep rate and stress relations 12 p1512 A73-27256

Investigation of the stress-strain state of spherical shells with an eccentric hole on the basis of the three-dimensional theory of elasticity by the finite element method 12 p1552 A73-27262

Strength characteristics of layers obtained by spark-alloying steels with high-melting metals 12 p1512 A73-27264

Ray method for solving dynamic problems in viscoelastic media 12 p1553 A73-27415

Stability of a nonuniformly heated circular shell 12 p1554 A73-27471

The Castigliano variational equation and strain continuity relations for a thin shell 12 p1555 A73-27788

Bending of a circular nonlinearly-elastic plate by a concentrated force 12 p1555 A73-27794

One-dimensional zero-moment problem of a thin elastic shell of variable thickness 12 p1556 A73-27800

Brittle failure of infinite plate with circular hole and radial cracks under two perpendicular uniformly distributed tensile loads 12 p1556 A73-27802

Stressed state of multilayer spherical vessels, cylindrical tubes and circular disks consisting of a linear viscoelastic material 13 p1690 A73-27994

Integrated force method for discrete structural analysis, discussing analogy with continuous problem Beltrami-Michell formulation and applications to pin and rigid connected frames 13 p1691 A73-28082

Criteria for finite element discretization of shells of revolution. 13 p1691 A73-28084

Strain hardening and instability in biaxially stretched sheets. 13 p1623 A73-28139

Analysis of stress intensity factor for surface-flawed tension plate. 13 p1692 A73-28231

A hypothesis of non-propagating fatigue crack. 13 p1635 A73-28644

Propagation of a brittle crack at constant and accelerating speeds. 13 p1635 A73-28755

Application of Papkovitch-Neuber potentials to a crack problem. 13 p1635 A73-28756

Stress-singularities due to uniformly distributed loads along straight boundaries. 13 p1696 A73-28757

Crack propagation in an elastic solid subjected to general loading. III - Stress wave loading. 13 p1696 A73-28792

Symmetrical crack branching in polymethyl methacrylate plates, using method of caustics for stress intensity factor evaluation 13 p1645 A73-28842

Elliptic notch interaction with nearby crack in elastic solid under longitudinal shear, obtaining stress intensity factor 13 p1697 A73-28914

A treatise on the stress-fields produced by moving dislocations Supplementary remarks and applications. 13 p1697 A73-28915

Determination of the nominal strength characteristics of fiberglass-strengthened plastics in the stress-concentration zones 13 p1645 A73-29051

Methods of simulating the thermal and stressed state at the edges of gas turbine blades 13 p1698 A73-29054

Investigation of the elastoplastic state of a spherical shell with a unreinforced circular hole 13 p1698 A73-29061

Equilibrium of an anisotropic plate reinforced by an isotropic circular ring 13 p1698 A73-29131

Titanium flow curves in octahedral coordinates for various conditions of deformation 13 p1636 A73-29132

Application of fracture mechanics to the analysis of statically indeterminate structures. 13 p1700 A73-29466

Effects of specimen geometry and loading conditions on the crack tip plastic zone. 13 p1701 A73-29474

Finite element method application to elastoplastic analysis of cracked metal plates, discussing plate thickness effects on plastic zone growth and stress distributions along crack tip 13 p1701 A73-29476

X-ray investigation of fatigue-crack growth - On critical strain for fracture at the crack tip. 13 p1625 A73-29482

Further consideration of crack propagation by oscillating crystal X-ray microbeam diffraction technique. 13 p1625 A73-29483

A study of fatigue crack propagation in high strength aluminum alloys at high stresses. 13 p1640 A73-29488

Life prediction of metals subjected to high temperature fatigue. 13 p1708 A73-29503

Minimum creep lives of structural metallic materials at elevated temperatures. 13 p1701 A73-29514

Couple-stresses effects in vicinity of interface for infinite elastic plane with a rigid inclusion. 13 p1702 A73-29533

Mathematical theory of elasticity for stress concentration in homogeneous isotropic perfectly elastic composites with spherical inclusions, noting grain boundary stresses 13 p1702 A73-29535

Mode factor and stress concentration parameter for sudden heating of solid cylinders and disks, noting thermal stability criterion with allowance for statistical strength 13 p1703 A73-29611

Stress gradient as one of the causes of the scale effect on the brittle fracture of materials. 13 p1703 A73-29614

Stress distribution about defects such as rigid sharp-angled inclusions. 13 p1703 A73-29619

Effect on the stresses around a crack due to the presence of circular inclusion. 14 p1806 A73-30042

Conformal mapping technique for stress concentration around elliptical hole in shallow spherical shell under internal pressure 14 p1806 A73-30045

Stress hybrid model extension to stiffness matrix of element with discontinuous stress distribution, considering transverse shear strains in laminated plate layers 14 p1807 A73-30181

Stress formulation of the 'second' axially symmetric problem of micropolar theory of elasticity. 14 p1809 A73-30253

A mathematical model of damage accumulation in plastic isotropic materials. 14 p1810 A73-30301

Stress concentrations close to circular holes in a cylindrical shell of medium thickness. 14 p1810 A73-30305

Crack formation in orthogonally reinforced glass-fiber ware. 14 p1765 A73-30307

Physical fatigue limit of hardened steels. 14 p1759 A73-30310

Thermal stress in an anisotropic elastic half-space. 14 p1810 A73-30407

Some basic solutions in strain gradient elasticity theory of an arbitrary order. 14 p1812 A73-30546

Couple-stress effects near an interior hole of an infinite elastic plane subjected to a concentrated force. 14 p1813 A73-30593

Three-dimensional stress-strain state of turbine blades 14 p1813 A73-30677

Stress concentration determination near a small hole on a plate in three-dimensional representation 14 p1813 A73-30682

Influence of stress concentrations on the mechanical properties of cast molybdenum with protective coatings 14 p1763 A73-30688

Influence on the stress-strain state of the way a concentrated force is applied to the tip of a crack in a plate 14 p1814 A73-30718

Construction of refined applied theories for a truncated hollow cone of variable thickness 14 p1815 A73-30815

Internal stress-strain boundary layer theory of shells and orthotropic plates with zero stress conditions at upper and lower planes and edge distance dependent attenuation 14 p1772 A73-30904

Engineering structures design, discussing stress and strain distributions, mechanical defects, symmetric loading and fracture models [ASME PAPER 73-DE-19] 14 p1815 A73-30820

Fracture strength of fiber reinforced plastics, investigating crack propagation susceptibility, stress concentration and fracture mechanics [ASME PAPER 73-DE-20] 14 p1767 A73-30821

The wind profile very close to the ground. 14 p1772 A73-30904

Stress distribution due to a Griffith crack at the interface of an elastic half plane and a rigid foundation. 14 p1815 A73-30917

Two coplanar cracks in an infinitely long elastic strip bonded to semi-infinite elastic planes. 14 p1815 A73-30918

Static problem of elastic body with stresses at boundary, solving incompatible difference equations by explicit iteration methods 15 p1945 A73-31026

Propagation of elastic Lamb waves in an initially stressed body 15 p1945 A73-31030

Zero moment equilibrium stress state for multiply connected convex shells with curvilinear holes 15 p1945 A73-31031

Solution of axisymmetrical thermoelasticity problems for an infinite region with several spherical cavities 15 p1945 A73-31036

Dynamic stress concentration at an elliptic hole due to plane SH-waves 15 p1947 A73-31331

Effect of a crack in an infinite plane containing a circular hole under uniform normal pressure. 15 p1947 A73-31333

The effect of couple-stresses on the stress concentration around an elliptic hole. 15 p1947 A73-31335

The effects of couple-stresses on thermal stress distributions in multiply-connected domains. 15 p1947 A73-31362

Effect of openings on stresses in rigid pavements. 15 p1856 A73-31387

Russian book - Strength of turbine wheels. 15 p1948 A73-31578

Strains and stress-concentration factors in plates under out-of-phase biaxial cyclic loads. 15 p1948 A73-31614

A simple model of uniaxial creep recovery and stress relaxation based on residual-stress redistribution. 15 p1948 A73-31615

Calculation of stress-concentration factors for grooved shafts in bending using the point-matching technique. 15 p1948 A73-31616

Effect of Poisson's ratio strains in adherends on stresses of an idealized lap joint. 15 p1948 A73-31620

Stresses in a pressurized ribbed cylindrical shell with a reinforced hole. 15 p1948 A73-31621

Critical stress intensity factors applied to glass reinforced polyester resin. 15 p1897 A73-31676

Brittle fracture and crack propagation prediction in unidirectionally fiber reinforced composites via Sc theory, comparing with stress intensity factor K_{IC} concept 15 p1949 A73-31681

Nature of stresses in the internal vicinity of the edge of the joint surface in a compound body loaded under conditions of the plane problem of the theory of elasticity 15 p1950 A73-31827

Thin Al alloy sheet plane stress testing with zero K gradient specimen based on tapered double cantilever beam modification, considering fracture toughness and crack propagation 15 p1950 A73-31985

A note on the use of a simple technique for failure prediction using resistance curves. 15 p1951 A73-31989

Determination of stress intensity factors in cracked plates by the finite element method. 15 p1951 A73-32034

Accuracy of the finite element analysis for the elastic plate with a circular hole. 15 p1951 A73-32036

Bonded structural connections analysis by finite element method, presenting stress distribution in adhesive 15 p1952 A73-32038

Self similar dynamic problems for elastic plane and half-plane with/without propagating crack, assuming application of instantaneous perturbation source or uniform stress field 15 p1952 A73-32078

Two component glass fiber reinforced plastic model describing stress-strain state via elastic properties analysis, internal energy production and Hooke's Law application 15 p1952 A73-32085

The stress field near a system of four symmetrically situated line cracks of equal length. 15 p1953 A73-32093

Stress distribution near holes 15 p1953 A73-32097

Structural components shape optimization for stress concentration reduction, solving complex boundary value problem via conformal transformation to curvilinear coordinates 15 p1954 A73-32108

Influence of structure and of stress concentration on the mechanical properties of Ti-Ta-Mo system alloys 15 p1894 A73-32533

Axisymmetrical and antisymmetrical stresses and deformations in shells of revolution with a meridional cutout 16 p2074 A73-32683

Deformation of a multilayer shell of revolution under nonisothermal loading 16 p2074 A73-32684

Stress concentration in plates with holes for large curvatures at the points of inflection 16 p2074 A73-32688

Stress concentration near a cutout on the surface of an orthotropic cylindrical shell 16 p2075 A73-32694

Composite material design criteria, discussing fatigue, stress concentration, safety factors, scaling effects and load characteristics 16 p1967 A73-33028

Plane stress fields in isotropic disks due to singular and distributed loads, obtaining Fredholm integral equation solution via cubic spline function 16 p2079 A73-33238

Viscoelastic body stress-strain state under quasi-static loads, obtaining boundary value problem solution via finite element method 16 p2080 A73-33244

A designer's approach to the fatigue failure mechanism. 16 p2081 A73-33644

Stresses in plastics reinforced by anisotropic fibers in the presence of transversal normal loads 16 p2030 A73-33928

Equilibrium conditions for multilayer anisotropic viscoelastic plates in a complex stressed state 16 p2083 A73-33933

Stress concentration on an ellipsoidal inhomogeneity in an anisotropic elastic medium 17 p2240 A73-34142

Torsion and extension of a cylinder with an outer annular cut 17 p2240 A73-34143

System of arbitrarily oriented cracks in elastic bodies 17 p2240 A73-34144

Stresses in a symmetrically-laminar plate weakened by a central crack 17 p2240 A73-34145

Experimental evidence of a couple-stress effect. 17 p2241 A73-34200

Influence of the structure of a composite material on its elastic properties 17 p2194 A73-34269

Book - Diffraction of elastic waves and dynamic stress concentrations. 17 p2242 A73-34468

Creep and recovery of polycarbonate. 17 p2194 A73-34525

Characteristics of deformation texture development in austenitic steel in a plane stressed state 17 p2188 A73-34564

Stress relaxation measurements for strain rate sensitivity of dispersion hardened thoriated Ni alloys as function of applied stress concentration 17 p2190 A73-34647

Some properties of dynamic equation integrals from the theory of shells 17 p2244 A73-34736

Determination of the carrying capacity of axisymmetric shells under piecewise linear plasticity conditions 17 p2244 A73-34738

Elastic semiinfinite cylindrical shell stress-strain state after axial impact against static rigid plane, obtaining solutions for small time values 17 p2244 A73-34740

Elastic equilibrium of an ellipsoid under the action of concentrated loads 17 p2244 A73-34790

Torsion of a cylindrical shaft having an annular semicircular cutout 17 p2244 A73-34791

Approximate method based on the application of hydrodynamic analogy 17 p2244 A73-34794

Stress distribution near a circular hole on a plane consisting of a stochastically inhomogeneous material 17 p2244 A73-34798

Relationship between K_{Ic} and plane-strain tensile ductility and microscopic mode of fracture. 17 p2190 A73-34876

Forced plane strain motion of cylindrical shells - A comparison of shell theory with elasticity theory. [ASME PAPER 73-APM-9] 17 p2247 A73-35034

Propagation of stress gradient through an inclusion. II. [ASME PAPER 73-APM-16] 17 p2247 A73-35039

Effect of orthotropy on singular stresses for a finite crack. [ASME PAPER 72-APM-VVV] 17 p2249 A73-35109

On the opening of a finite crack normal to an interface. 17 p2250 A73-35122

Alleviation of stress concentration with analogue reinforcement. [SESA PAPER 2102] 17 p2250 A73-35446

A new non-destructive method for three-dimensional photoelasticity. [SESA PAPER 2143A] 17 p2182 A73-35451

Effects of material and stacking sequence on behavior of composite plates with holes 17 p2198 A73-35452

[SESA PAPER 2157A] 17 p2198 A73-35452

On the fracture of high-strength metals in the stress fields of various stress-concentration factors. [SESA PAPER 2163A] 17 p2191 A73-35454

Dynamic mechanical loading of solid material resulting in stress levels with impulse process described by fluid flow equations with application to shock compression of mechanical mixtures 17 p2193 A73-35541

Two dimensional static, dynamic and three dimensional photoelasticity measurement techniques for stress intensity, factors determination in boundary value problems of fracture mechanics 17 p2252 A73-35673

On one-dimensional large-displacement finite-strain beam theory. 17 p2252 A73-35828

Book - Advanced experimental techniques in the mechanics of materials. 17 p2176 A73-35834

Stresses in an anisotropic half-space. 18 p2362 A73-36319

Method of orthogonal projections for three-dimensional problems of elasticity theory 18 p2362 A73-36401

Shells of revolution belonging to a spherical class subjected to local loads at the pole 18 p2362 A73-36402

Geometrically nonlinear axisymmetric deformation of toroidal shells 18 p2362 A73-36403

Stress concentration determination under biaxial tension in a plate weakened by a randomly-shaped hole 18 p2363 A73-36414

On stress concentration factors in orthotropic glass-fiber reinforced plastics. 18 p2327 A73-36474

The median problem of the theory of elastic mobility with polar effects of spectral type. 18 p2364 A73-36492

A relaxation method for solving nonlinear stress equilibrium problems. 18 p2365 A73-36611

Stress distribution in a bonded anisotropic lap joint. [ASME PAPER 73-MAT-M] 18 p2365 A73-36618

Effect of prestress levels on the long term strength of 1Kh18N9T steel at elevated temperatures 18 p2323 A73-36761

Influence of stresses on the nature of the distribution of dislocations in Kh18N10T steel at a temperature of 650 C 18 p2325 A73-36820

Determination of rated strength characteristics of fiberglass in zones of stress concentration. 18 p2328 A73-36883

Methods of modeling thermal and stressed states in the edges of gas turbine blades. 18 p2366 A73-36886

Study of elastoplastic state of a spherical shell with round unsupported apertures. 18 p2366 A73-36893

Solid refractory metal and nonmetal alloys for machine structural components under dynamic and steady cumulative stresses 18 p2326 A73-37000

Stress concentration in tubes with a hole of star-shaped profile 19 p2494 A73-37185

Limiting equilibrium of a plate weakened by two arbitrarily oriented cracks 19 p2494 A73-37186

The method of virtual powers in mechanics of continuous media. I - Theory of the second gradient 19 p2495 A73-37424

Membrane statics of parachute-like shells. 19 p2496 A73-37480

Stresses and strains in a rotating disk 19 p2497 A73-37555

Some studies of the influence of localized and gross plasticity on the monotonic and cyclic concentration factors. 19 p2497 A73-37589

The effect of very short time-at-temperature on the yield stress of 6061-T651 aluminum. 19 p2440 A73-37590

A version of the couple stress theory of elasticity for a one-dimensional continuous medium with inhomogeneous periodic structure. 19 p2498 A73-37635

Contact problem of the elastic interaction between a plate and an elliptic insert 19 p2499 A73-37762

Boundary layer concept /attenuating stress-strain state with homogeneous boundary conditions/ incorporation into internal stress-strain state theory for orthotropic rectangular elastic plates 19 p2499 A73-37763

Probability theory for vibrational strength of turbomachine parts, calculating statistical maximum stress for given stress distribution conditions 19 p2499 A73-37777

Effect of rivet spacing on crippling loads of joined aluminium angles. 19 p2499 A73-38009

Stress field in a sphere subjected to large deformations. 19 p2500 A73-38111

Influence of non-singular stress terms and specimen geometry on small-scale yielding at crack tips in elastic-plastic materials. 19 p2501 A73-38264

System for determining the critical range of stress-intensity factor necessary for fatigue-crack propagation. 19 p2501 A73-38297

Transient stress distribution caused by water-jet impact. 19 p2435 A73-38300

The state of stress produced in a quadrant shaped plate by concentrated forces acting in its plane. 19 p2501 A73-38305

The effect of stress amplitude below the fatigue limit on cumulative fatigue lives in perforated round specimens. 19 p2501 A73-38344

Partitioning of stress between fiber and matrix during tensile deformation of the Al-Al3Ni eutectic composite. 20 p2576 A73-39024

Moisture effect on Ni steel fatigue crack propagation under low stresses 20 p2617 A73-39291

Theory of shallow shells with allowance for couple stresses without applying the Kirchhoff-Love hypothesis 20 p2618 A73-39309

Thermoelectricity of coupled bodies in the case of stress-dependent heat transfer 20 p2618 A73-39327

Group properties of the equations of strain theory of thermoplasticity 20 p2618 A73-39329

Stress-concentration at a hole with periodic irregularities 20 p2619 A73-39334

Coefficients of stress intensity near rigid acute-angled inclusions 20 p2619 A73-39370

Study of the effect of stress concentration on the variation of stability characteristics in graphite 20 p2580 A73-39383

Experimental study of the stressed state of an elastic beam undergoing transverse impact 20 p2620 A73-39385

Some three-dimensional boundary value problems for an elastic medium bounded by cylindrical surfaces 20 p2620 A73-39508

Buckling analysis of deformation and stress distribution in axially compressed longitudinally stiffened cylindrical shells, considering prebuckling deformation effects 20 p2621 A73-39539

On stress-concentration analysis of laminated composite plates. 20 p2622 A73-39551

Fatigue life under random loading with varying mean stress and rms value. 20 p2622 A73-39553

Finite difference technique for elastic-plastic buckling of edge-loaded rectangular plates, finding bifurcation stresses via Hill and Prandtl-Reuss expressions 20 p2623 A73-39560

Yield criterion in plane stress state for description of second order effect relating to axial strain accumulation in cyclic torsion 20 p2624 A73-39568

General two-dimensional problem in the theory of ideal plasticity of anisotropic materials 20 p2624 A73-39643

Determination of the stress strain state of closed cylindrical shells and infinite plates with cracks 20 p2624 A73-39645

Stability of the state of moment stress of a toroidal shell 20 p2624 A73-39650

Photoelastic investigation of dynamic stress conditions involving rapidly varying principal stress directions 21 p2695 A73-39965

Uniqueness of solutions and some approximate methods of solving problems in linear viscoelasticity 21 p2782 A73-40186

Ellipsoidal crack and needle in an anisotropic elastic medium 21 p2783 A73-40187

Some results of fuselage calculations on a digital computer by the finite-element method 21 p2783 A73-40387

Frame of a cylindrical shell under the action of a concentrated radial force 21 p2783 A73-40388

Experimental error equation of stress intensity factor for fracture toughness and crack growth rate testing 21 p2785 A73-40635

Stress distribution in thin circular plate with equiaxed cruciform crack, obtaining stress intensity factor and crack energy by numerical solution of Fredholm equation 21 p2785 A73-40932

Effect of orthotropy on singular stresses produced near a crack tip by incident SH-waves.

21 p2786 A73-40933

Elastoplastic stressed state of a long thick-walled cylinder subjected to the action of a magnetic field

21 p2786 A73-40981

Plane crack problems for ideal fibre-reinforced materials.

21 p2787 A73-41014

Possibility of predicting the residual stress pattern in boronized steels

21 p2721 A73-41229

Temperature and stress fields in a cylindrical shell subjected to induction heat treatment

21 p2787 A73-41233

The plane elastostatic solution for a symmetrically loaded crack in a strip composite.

21 p2789 A73-41669

The stress field near a Griffith crack at the interface of two bonded dissimilar elastic half-planes.

21 p2789 A73-41672

Discretized solution of junction problems in shells.

22 p2917 A73-41740

Improvement of damping capacity of structural members by introduced stress concentration.

[ASME PAPER 73-DET-76] 22 p2919 A73-42072

The deformation and fracture of molybdenum under creep conditions.

22 p2874 A73-42109

Stress concentration and groove design as factors in crack failure of low power single stage gas turbine rotor disk, using optical polarization technique

22 p2920 A73-42114

Some observations on fracture under combined loading.

22 p2920 A73-42133

Local stresses near deep surface flaws under cylindrical bending fields.

22 p2880 A73-42135

Prior to failure extension of flaws in a rate sensitive Tresca solid.

22 p2880 A73-42136

Threshold for fatigue crack propagation and the effects of load ratio and frequency.

22 p2875 A73-42137

Fatigue-crack growth under variable-amplitude loading in ASTM A514-B steel.

22 p2875 A73-42140

Effect of a loading sequence on threshold stress intensity determination.

22 p2875 A73-42141

J-integral and equivalent energy method parameter relationship from elastic and inelastic stress concentration factors for notches and cracks

22 p2920 A73-42146

A method for measuring $K_{sub\ 1c}$ at very high strain rates.

22 p2866 A73-42148

Influence of stress intensity level during fatigue precracking on results of plane-strain fracture toughness tests.

22 p2876 A73-42149

Influence of sheet thickness upon the fracture resistance of structural aluminum alloys.

22 p2876 A73-42150

Plane-stress fracture toughness and fatigue-crack propagation of aluminum alloy wide panels.

22 p2876 A73-42151

Structure of polymers and fatigue crack propagation.

22 p2880 A73-42152

Effects of strain gradients on the gross strain crack tolerance of A 533-B steel.

22 p2876 A73-42153

Applications of the compliance concept in fracture mechanics.

22 p2920 A73-42154

Failure stress levels of flaws in pressurized cylinders.

22 p2921 A73-42156

The hydrodynamic analogy and its application to a two-dimensional problem in elasticity theory

22 p2921 A73-42282

Effect of a Griffith crack on the distribution of stress in a semi-infinite two-dimensional medium.

22 p2922 A73-42470

Stress distribution around an elliptic hole in an infinite micropolar elastic plate.

22 p2924 A73-42684

Nature and significance of alterations in myocardial compliance.

22 p2808 A73-42689

The effect of plasticity and crack blunting on the stress distribution in orthotropic composite materials.

[ASME PAPER 73-APMW-2] 22 p2924 A73-42876

The load transfer problem in shafts coupled through a sleeve.

[ASME PAPER 73-APMW-3] 22 p2867 A73-42877

An integral equation approach to the semi-infinite strip problem.

[ASME PAPER 73-APMW-5] 22 p2924 A73-42878

Thermal response of a viscoelastic rod under cyclic loading.

[ASME PAPER 73-APMW-39] 22 p2926 A73-42896

The elliptical crack subjected to nonuniform shear loading.

[ASME PAPER 73-APMW-42] 22 p2926 A73-42898

Equilibrium of an elastic paraboloid of revolution under a concentrated load applied to its apex

22 p2927 A73-43052

Stability of nonlinearly elastic plates in the presence of random initial stresses

22 p2928 A73-43060

Indentation of the semi-infinite elastic solid by a hot sphere.

22 p2929 A73-43174

Normalized stresses around an elliptic hole in a finite plate of linear material subjected to large uniform in-plane loading.

23 p3039 A73-43386

Stress-strain state of disk with internal rectilinear cracks under load, solving Fredholm equations

23 p3039 A73-43468

Method for estimating fracture strength of specially orthotropic composite laminates.

23 p3040 A73-43630

Free-edge effects in the characterization of composite materials.

23 p3040 A73-43632

Cylindrical shell design with a frame-connected bottom and a system of concentrated forces applied to the bottom

23 p3042 A73-43726

A method for solving ill-posed integral equations of the first kind.

23 p2999 A73-43803

Analysis of stress intensity factors for the tension of a centrally cracked strip with stiffened edges.

23 p2992 A73-43812

Piecewise linear law of the relation between stresses and strains for large deformations

23 p3043 A73-43920

Determination of the stressed state near a curvilinear hole in a transversely isotropic spherical shell

23 p3043 A73-43924

Order of magnitude of the differences between theory and experiment in viscoplasticity under varying stress and temperature

23 p3044 A73-43971

Evolution of the stress state and hardening for certain materials with positive hardening

23 p3044 A73-43975

Finite element analysis on L-L type vibration energy concentrator/divider considering its design.

23 p2961 A73-44138

Papkovich-Neiber solution for stress-strain state of initially isotropic mixture of two elastic bodies

23 p3007 A73-44183

Saint Venant continuity equation for identical formulation of Lamé equations and elasticity theory problem of stress-strain state in bodies of revolution

23 p3045 A73-44185

Investigation of the stress-strain state at a strengthened hole in an orthotropic cylindrical shell

23 p3046 A73-44193

Determination of the temperature fields and thermal stresses in a bimetallic layer subjected to induction heating

23 p3046 A73-44194

Solution of boundary value problems in thermoviscoelasticity with allowance for mass forces exhibiting a potential

23 p3046 A73-44196

Determination of the strained state of a thick elastoplastic plate with an elliptical hole

23 p3046 A73-44201

On Papkovitch-Fadle solutions of crack problems relating to an elastic strip.

23 p3046 A73-44227

Evaluation of the sensitivity of materials to stress concentrations in cyclic loading

23 p3047 A73-44279

Influence of electrolytic polishing on the stress-concentration sensitivity of some alloys in fatigue

23 p2995 A73-44283

Improved turbine blade attachment profiles with shoulder locks

23 p2986 A73-44291

Fatigue failure predictions for plates with holes and edge notches.

23 p3047 A73-44350

Boundary layer equations of magnetohydrodynamics with moment stresses

23 p3015 A73-44385

The strength of unidirectionally reinforced plastics subjected to tension at an angle to the direction of reinforcement

24 p3102 A73-44511

Determination of the magnitude and distribution of initial stresses in fiberglass-reinforced plastics. I

24 p3103 A73-44527

Mixed boundary value problem solution for stress-strain state of anisotropic elastic cylinder and layer under joint torsion, using Fourier and Hankel transforms

24 p3146 A73-44676

Shear crack stress intensity and displacement jump solution for half space under plane strain in form of singular integral equation

24 p3146 A73-44677

An elastoplastic strain-hardening material - Quasi-static evolution of the stress distribution

24 p3147 A73-44748

The static axisymmetric problem of the micropolar theory of elasticity and thermoelasticity

24 p3148 A73-44913

Plastic plate bending under concentrated forces defining stress and strain principles at yield limit

24 p3148 A73-44919

Possible causes of failures in pulse-switched thyristors

24 p3072 A73-44937

Effect of the characteristics of diamond grinding on the stressed state and strength of hard alloy VK6

24 p3094 A73-44968

Semicircular plate uniformly loaded over diameter and with concentrated force at arc top, determining stress distribution by complex variable and conformal mapping

24 p3148 A73-45001

Load concentration factors for circular holes in composite laminates.

24 p3149 A73-45151

Bending of transversely isotropic plates with a reinforced edge

24 p3149 A73-45174

Thermoelasticity problem of a spherical shell with multiply connected regions

24 p3149 A73-45175

Stress concentration in infinite strip with periodically spaced circular holes under uniformly distributed bending loads

24 p3149 A73-45176

Influence of initial deflections on the work of a rectangular plate subject to bending in its plane

24 p3150 A73-45244

A layered composite with a broken laminate.

24 p3151 A73-45301

Measurements of the structure of the Reynolds stress in a turbulent boundary layer.

24 p3079 A73-45310

An examination of the edge effect in a cantilever beam.

24 p3152 A73-45371

Effects of stress on metal-oxide-semiconductor structures.

24 p3120 A73-45415

STRESS CORROSION

NT STRESS CORROSION CRACKING

The effect of oxide thickness on the hot salt stress corrosion susceptibility of Ti-6Al-4V.

01 p0061 A73-10137

Inhibition of stress corrosion cracking of AISI 4340 steel in 10% potassium nitrate solution at 100 C.

01 p0061 A73-10138

Inter- and transcrystallite breakdown of steels and alloys under the action of various media/A review/

01 p0062 A73-10258

Stress corrosion cracking behavior of 18% Ni/300/ maraging steel.

01 p0066 A73-11295

Demonstration of the inhibiting action of certain mineral iodides on the stress corrosion of type 18-10 low-carbon stainless steel

02 p0178 A73-11524

Polyamide compounds stress corrosion properties and chemical resistance in different test fluids, discussing fluid effect on flaw development rate

02 p0184 A73-11583

Performance of an inhibitor-protector of steel against corrosion-fatigue failure at elevated temperatures and pressures.

02 p0182 A73-12700

Stress history effect on incubation time for stress corrosion crack growth in AISI 4340 steel.

02 p0183 A73-12763

Book - Corrosion and corrosion control: An introduction to corrosion science and engineering /2nd edition/.

03 p0321 A73-13125

Effects of hot-salt stress corrosion on titanium alloys.

03 p0323 A73-13268

Cracking and corrosion of plastic materials under stress

03 p0334 A73-13592

High strength alloys hydrogen embrittlement mechanisms and effects and preventive measures, considering steel decarburization, stress corrosion cracking, hydride sheath formation and failure modes

03 p0328 A73-14425

Fracture mechanics consideration of hydrogen sulfide cracking in high strength steels.

04 p0459 A73-14692

Study by autoradiography at high resolution power of the role of hydrogen in the mechanism of cracking of TA6V titanium alloy in salt water

04 p0461 A73-15097

Influence of microstructure on the mechanical properties and stress corrosion susceptibility of 7075 aluminum alloy. 04 p0463 A73-15314

Fractographic aspects of the stress corrosion cracking of titanium in a methanol/HCl mixture. 06 p0705 A73-17800

A comparison of hydrogen embrittlement and stress corrosion cracking in high-strength steels. 06 p0709 A73-18479

Probability of stress-corrosion fracture under random loading. 06 p0763 A73-18483

Study of pitting corrosion and stress corrosion in stainless steels with the aid of alloys of very high purity. 07 p0838 A73-19114

On relationship between stress corrosion resistance and grain shape of extruded Al-Zn-Mg alloys with heavy section. 08 p0977 A73-21140

Atmospheric corrosion fatigue tests for environmental conditions and superimposed stress wave effects on Cr-Mo steel fatigue life under rotating bending. 10 p1235 A73-24917

Corrosive aspects of the fatigue of rubber. 11 p1388 A73-25841

Corrosion fatigue due to static and cyclic stress, noting electrochemical adsorption theory. 11 p1386 A73-26737

Effect of microstructure and environment on stress corrosion of 7075 aluminum alloy. [NACE PAPER 97] 13 p1637 A73-29312

Compatible coatings for corrosion resistant aerospace fasteners. [NACE PAPER 116] 13 p1638 A73-29316

Scale effect in fatigue and in corrosion fatigue of steel. 14 p1760 A73-30324

Quantitative classification criterion for corrosion causes in metal under static and cyclic loads, examining failure mechanism. 14 p1763 A73-30712

Study of multiple surface compound precipitation during passivation of D6AC-steel. 15 p1895 A73-32566

Acoustic emission instrumentation and application for plastic deformation, flaw detection monitoring of fatigue crack growth, stress corrosion and hydrogen embrittlement. 17 p2175 A73-35670

Influence of cold work on the stress corrosion susceptibility of Ti-13V-11Cr-3Al. 17 p2194 A73-35675

Studies of the renewal of stress relaxation on a high-grade steel wire subjected to stress corrosion after being treated for total elimination of relaxation. 19 p2497 A73-37553

The influence of heat treatment on the stress-corrosion susceptibility of a ternary Al-5.3 pct Zn-2.5 pct Mg alloy. 20 p2576 A73-39031

Influence of structural changes arising during the hardening process on element lifetime. 23 p2984 A73-43438

The stress corrosion of titanium materials - The present status of research. 23 p2992 A73-43910

STRESS CORROSION CRACKING

Book - Advances in corrosion science and technology. Volume 2. 06 p0704 A73-17506

Stress-corrosion cracking of high-strength aluminum alloys. 06 p0704 A73-17509

Lattice dilatation and hydrogen embrittlement cracking. 07 p0840 A73-20353

Effect of addition of Bi on stress-corrosion cracking of Al-Mg alloy. 09 p1102 A73-22421

Stress corrosion cracking of commercial Al-Mg alloys and its prevention. 09 p1102 A73-22422

Mechanisms of stress corrosion cracking of titanium-aluminum alloys in methanol-HCl solutions. 09 p1106 A73-23166

Galvanic interaction between active and passive titanium. 09 p1106 A73-23167

An electrochemical testing method for stress corrosion cracking by separating crack anode from cathode. 09 p1106 A73-23168

Improved fracture resistance of 7075 through thermomechanical processing. 09 p1109 A73-23257

Stress corrosion cracking of metals - A state of the art; Proceedings of the Symposium, Detroit, Mich., October 18, 1971. 10 p1231 A73-23867

Stress corrosion cracking characteristics and test data interpretation, considering pitting, brittle frac-

ture, crack propagation, chemical environment and smooth and cracked specimens. 10 p1232 A73-23868

Stress corrosion cracking of a high strength steel. 10 p1232 A73-23869

Stress corrosion cracking behavior of nickel and nickel alloys. 10 p1232 A73-23870

Standardization, loading methods and environments for stress corrosion cracking tests, noting prevention of crevice, galvanic and hydrogen embrittlement effects. 10 p1232 A73-23871

The resistance of wrought high strength aluminum alloys to stress corrosion cracking. 10 p1232 A73-23872

Overview of corrosion cracking of titanium alloys. 10 p1232 A73-23873

Stress corrosion crack protection from coatings on high strength H-11 steel aerospace bolts. 10 p1232 A73-23874

Resistance of high strength structural steel to environmental stress corrosion cracking. 10 p1232 A73-23875

Corrosion fatigue: Chemistry, mechanics and microstructure; Proceedings of the International Conference, University of Connecticut, Storrs, Conn., June 14-18, 1971. 11 p1380 A73-25801

Corrosion fatigue considerations in engineering materials selection and design, discussing alleviation and control. 11 p1442 A73-25802

Aerospace component failure due to corrosion fatigue in aluminum wing attachment spar, helicopter rotor blade, landing gear cylinder and engine bearings. 11 p1380 A73-25803

Metal surfaces corrosion fatigue due to environmentally induced localized attack, discussing protective film growth, crack propagation hydrogen interaction and stresses. 11 p1381 A73-25811

Stress and displacement fields around growing corrosion fatigue crack, discussing intensity factor, plastic zones, cyclic loading and fluid pressure effects. 11 p1381 A73-25813

Corrosion fatigue and stress corrosion crack growth in high strength aluminum alloys, magnesium alloys, and titanium alloys exposed to aqueous solutions. 11 p1381 A73-25815

Environment enhanced corrosion fatigue crack growth and fracture mechanics, discussing inspection intervals to maintain structural integrity. 11 p1382 A73-25819

On the superposition model for environmentally-assisted fatigue crack propagation. 11 p1382 A73-25820

Corrosion fatigue crack propagation behavior in steels above/below stress intensity threshold within framework of linear elastic fracture mechanics. 11 p1382 A73-25821

Effect of cyclic stress form on corrosion fatigue crack propagation below K_{Isc} in a high yield strength steel. 11 p1382 A73-25822

Effects of stress wave form and cycle frequency on low cycle corrosion fatigue. 11 p1382 A73-25823

Stress corrosion cracking and corrosion fatigue for hydraulic aluminum pressure cylinders used for landing gear, stabilizers and aircraft systems. 11 p1383 A73-25827

Environmental stress cracking of epoxy adhesives. 11 p1388 A73-25840

Crack growth rate due to steels and Ti and Ni alloys electrochemical dissolution, noting tensile stress intensity factor. 11 p1385 A73-26173

Effect of high dislocation density on stress corrosion cracking and hydrogen embrittlement of type 304L stainless steel. 11 p1385 A73-26174

Cracking of Ti-6Al-4V in methanol solutions containing sulfates. 11 p1385 A73-26175

On the relationship between grainboundary corrosion and stress corrosion cracking of Al-Zn-Mg alloys. 12 p1511 A73-27059

Dissolution of Ti-6Al-4V at cathodic potentials in 5N HCl. 12 p1512 A73-27249

Study of the mechanical-metalurgical characteristics of martensitic steels in a corrosive medium. 12 p1514 A73-27686

Stress-corrosion cracking of Ti-8Al-1Mo-1V in aqueous environments. I - The kinetics of subcritical crack propagation. II - Plastic zones, crack morphology, and fractography. 13 p1632 A73-28135

Transgranular stress corrosion cracking of austenitic stainless steels - A single crystal study. 13 p1642 A73-29520

An X-ray study of the stress corrosion of austenitic stainless steels. 13 p1625 A73-29521

Study on stress corrosion cracking of austenitic stainless steel under pulsating load. 13 p1642 A73-29523

Ferritic martensitic stainless steels stress corrosion cracking, emphasizing heat treatment and environment conditions effects on corrosion resistance. 15 p1891 A73-32170

The passivation behaviour of the Ti-6Al-4V alloy. 15 p1895 A73-32567

Notched austenitic stainless steel stress corrosion cracking tests in boiling magnesium chloride solutions, obtaining relationship between maximum stress and strain rate in graph. 15 p1895 A73-32569

Study on stress corrosion cracking of austenitic stainless steel under pulsating load. 15 p1895 A73-32570

Corrosion-fatigue crack growth in high-strength aluminum alloys with and without susceptibility to stress-corrosion cracking. 15 p1895 A73-32571

Investigations of the electrochemical processes in titanium alloys as applied to stress-corrosion crack tip state in sea water. 15 p1896 A73-32572

Stress corrosion cracking of titanium alloys in hydrogen chloride. 15 p1896 A73-32573

Effect of thermomechanical treatment on the stress corrosion cracking of metastable beta III titanium. 15 p1896 A73-32574

Scanning electron microscopic observation of fracture surfaces of austenitic stainless steels in stress corrosion cracking. 16 p2025 A73-33021

Anodic oxidation and stress corrosion cracking /SCC/ of titanium alloys. I - Factors affecting SCC and their influence on the anodic behavior of alloy Ti-6Al-6V-2.5Sn. 17 p2187 A73-34524

An electrochemical model for hot-salt stress-corrosion of titanium alloys. 17 p2189 A73-34643

Hydrogen embrittlement and stress corrosion cracking in Ti-Al binary alloys. 17 p2191 A73-35099

Role of stress in the stress corrosion cracking of a Mg-Al alloy. 17 p2191 A73-35100

A test procedure to evaluate the relative susceptibility of materials to stress corrosion cracking. 17 p2191 A73-35125

Environment-assisted fracture in engineering alloys. II - Cyclic loading and future work. [ASME PAPER 73-MAT-S] 18 p2365 A73-36614

Fatigue and corrosion-fatigue crack propagation in intermediate-strength aluminum alloys. [ASME PAPER 73-MAT-N] 18 p2323 A73-36615

Fractography of stress corrosion in Ti-8Al tested in fatigue. 18 p2326 A73-36972

A simple method for studying slow crack growth. 19 p2497 A73-37588

Effects of small amounts of additional elements on directionality of stress corrosion resistance of the Al-Zn-Mg alloys. 19 p2442 A73-37948

Influence of preloading on the sustained load cracking behavior of maraging steels in hydrogen. 21 p2719 A73-40924

Fractography of stress corrosion cracks in aluminum alloy 7075. 21 p2720 A73-40925

Effect of a loading sequence on threshold stress intensity determination. 22 p2875 A73-42141

Fatigue and corrosion-fatigue crack growth of 4340 steel at various yield strengths. 22 p2875 A73-42142

Book - Advances in corrosion science and technology. Volume 3. 23 p2990 A73-43455

Titanium alloys mechanical, electrochemical and metallurgical parameters effects on stress corrosion cracking, discussing crack growth kinetics, failure features and component hazard minimization. 23 p2990 A73-43457

STRESS CYCLES

Facility for investigating low-cycle fatigue of alloys at cryogenic temperatures. 01 p0029 A73-10491

Plastic material turbine blades adaptability under nonsteady start-stop thermal and mechanical stress cycle conditions, noting residual stress effects. 02 p0235 A73-12129

Study of the effect of small elastoplastic deformations on the load-bearing capacity of specimens with stress concentrators under repeated variable loading. II. 02 p0181 A73-12203

Characteristics of the fatigue curve of plastics. 02 p0185 A73-12699

Cumulative fatigue damage tests of Al alloy, evaluating Miner cycle/stress ratio. 03 p0325 A73-13571

Low-cycle fatigue behavior of quenched and tempered UNI 38NiCrMo4 steel 04 p0462 A73-15300

Low cycle fatigue tests of medium strength Al alloys, showing agreement with Manson-Halford fatigue life-strain relation 05 p0586 A73-16135

Upper yield point removal in pure Ta by reversed cyclic stressing at room temperature, indicating cumulative mobile dislocation multiplication 05 p0586 A73-16136

The probability of fracture as parameter of crack propagation under cyclic stress 05 p0635 A73-17065

Determination of constants in the equation for the fatigue-crack propagation rate with allowance for properties of the plastic zone 06 p0761 A73-17847

Theoretical and experimental prediction for pulsating creep failure. 07 p0917 A73-20489

Low cycle torsion fatigue, determining empirical relationship between strain amplitude and fatigue life 08 p0977 A73-21020

Characterization of p-n junctions under the influence of a time varying mechanical strain 08 p0951 A73-21481

Multi-axial and reversing stress effects in dislocation creep - A mechanical equation of states. 08 p0981 A73-21788

Stress varied creep of 20Cr-25Ni-Nb stabilised austenitic stainless steel. 08 p0980 A73-21781

Influence of the frequency of the tension-compression cycle on the fatigue life of D16T alloy 09 p1100 A73-22153

A strain criterion for failure of materials subjected to stress and temperature cycles 09 p1159 A73-22570

A generalization of equations of the outline of a hysteresis loop for the case of an asymmetrical cycle. 09 p1161 A73-23152

Plasticity and failure of heat-resistant materials at a low number of cycles of simultaneous fluctuations of temperature and load. 09 p1105 A73-23154

Refractory materials cyclic elastoplastic tests under shear with holding creep, showing relationship between creep rate and recurrent static deformation 09 p1161 A73-23155

Influence of temperature on the damping characteristics of heat resistant EP452 and EL696 steels in a uniform stress-strain state produced by tension and compression 10 p1233 A73-24358

Cyclic stress, strain, and energy variations under cumulative damage tests in low-cycle fatigue. 11 p1379 A73-25132

Udimet 700 creep behavior under cyclic tensile stresses at 925 C from hodograph of monotonic stress-strain relations, taking into account strain rate effects [AIAA PAPER 73-387] 11 p1439 A73-25516

The influence of environment and the surface layer on crack propagation and cyclic behavior. 11 p1380 A73-25807

Effect of cyclic stress form on corrosion fatigue crack propagation below K_{Isc} in a high yield strength steel. 11 p1382 A73-25822

Effects of stress wave form and cycle frequency on low cycle corrosion fatigue. 11 p1382 A73-25823

Frequency and environmental interactions in the fatigue of aluminum alloys. 11 p1382 A73-25824

Application of some aspects of low-cycle fatigue research in structural design. 11 p1443 A73-25846

Field-ion microscopic study of the high-speed deformation of tungsten 12 p1509 A73-26838

Monotonic and cyclic prestrain influence on alpha-Ti fatigue life, suggesting twin/grain boundary dislocation interactions 13 p1640 A73-29486

Crack initiation and propagation in notched plates subjected to cyclic inelastic strains. 13 p1701 A73-29489

The effect of wave form and cyclic frequency on the fatigue life of aluminum alloys. 13 p1640 A73-29491

Random and program fatigue tests of Cr-Mo steel specimen with V-grooved notch. 13 p1641 A73-29494

Aspect of cumulative fatigue damage under multi-axial strain cycling. 13 p1701 A73-29497

A method for the calculation of the fatigue life of unnotched and notched specimens loaded with alternating stresses. 13 p1641 A73-29501

A static-to-dynamic transition in creep of metallic materials under cyclic stress conditions as caused by an interaction of creep and creep recovery. 13 p1642 A73-29512

Low carbon steel S-N diagram for stresses ranging to fatigue limit, noting cyclic creep, macroplastic cyclic stress and fatigue failure 13 p1703 A73-29603

The effects of out-of-phase biaxial-strain cycling on low-cycle fatigue. 14 p1806 A73-29774

A unit for investigating the low-cycle fatigue of alloys at cryogenic temperatures. 14 p1743 A73-30316

Service life determination in heat-resistant alloys under unsteady working conditions with allowance for brief overloading 14 p1763 A73-30690

The metallurgical implications of welding processes. 16 p2021 A73-33863

Heat treated polyacrylonitrile filament produced carbon fiber strengthened after fatigue testing, noting maximum strengthening effect after 1000 load cycles 17 p2194 A73-34635

Polymers fatigue life under cyclic deformation, discussing stress-strain and failure behavior as function of reversed stress cycle frequency 18 p2328 A73-36587

High strength steel strain hardening residual stresses, discussing rolling treatment, complex strengthening, fatigue strength, asymmetric stress cycles and torsional stress 18 p2323 A73-36762

Some studies of the influence of localized and gross plasticity on the monotonic and cyclic concentration factors. 19 p2497 A73-37589

Quantitative estimation of the fatigue crack propagation under varying load conditions. 19 p2501 A73-38346

A finite element approach to the critical cyclic stress required to propagate a crack. 20 p2615 A73-38639

High-frequency fatigue tests at low temperatures 20 p2619 A73-39363

Fatigue life under random loading with varying mean stress and rms value. 20 p2622 A73-39553

The interaction of creep and fatigue for a rotor steel /The William M. Murray Lecture, 1972/. 21 p2722 A73-41264

Effect of the frequency of cyclic tension-compression on the fatigue limit of alloy D16T. 22 p2874 A73-42103

Fatigue failure analysis of low carbon steel endurance under cyclic loading with time dependent viscoelastic effects, using Hooke's-Trouton laws 23 p3040 A73-43469

Fatigue crack growth detection by acoustic emission monitoring in correlation with stress intensity for high cycle fatigue Al alloy 23 p2992 A73-43814

Acoustic emission from low-cycle high-stress-intensity fatigue. 23 p2992 A73-43816

The effect of the intermediate principal stress on triaxial fatigue of 7075-T6 aluminum alloy. 23 p3047 A73-44351

STRESS DISTRIBUTION

U STRESS CONCENTRATION

STRESS FUNCTIONS

Stress function for estimating mutual effects of strain and temperature fields in dynamic coupled thermoelasticity problem for thin circular plates. 01 p0113 A73-10094

Bending of a uniformly loaded clamped sector plate. 01 p0116 A73-11006

Elasticity theory contact problem for rectangle under compression loads, using Airy stress function for reduced linear algebraic equations system 01 p0117 A73-11090

Effect of transverse shear on limit load of cylindrical shells. 03 p0383 A73-12873

Singular solutions of the plane distortion problem of micropolar elasticity. 03 p0392 A73-13776

Stress equations solutions existence near Minkowskian solution for asymptotic behavior, demonstrating flat space-time stability [AD-756017] 03 p0344 A73-14604

On the modified Westergaard equations for certain plane crack problems. 04 p0512 A73-15236

Singular solutions for shallow cylindrical shells. [ASME PAPER 72-WA/APM-27] 04 p0515 A73-15891

Galerkin stress functions for non-local theories of elasticity. 05 p0631 A73-16123

Nonlinear shell theory with finite rotation and stress-function vectors. [ASME PAPER 72-APM-CC] 05 p0633 A73-16533

Comparative considerations concerning parametric stress concentration studies involving finite elements and complex stress functions 07 p0910 A73-19208

Stress functions for the 'second' plane problem of micropolar elasticity. 07 p0914 A73-20198

On the generalization of stress function procedures for dynamic analysis of plates. 09 p1158 A73-22399

Remarks on a system of nonlinear equations 09 p1113 A73-22967

Small perturbation approximations of plane biaxial tensile deformation of semilinear elastic medium without cavity, using Piola-Kirchhoff stress functions 09 p1164 A73-23347

An elastic ribbon under the action of a nonuniform load 09 p1165 A73-23348

Thin reinforcing coatings effect on mechanical behavior of homogeneous isotropic prismatic bars under torsion, obtaining stress-strain expressions 09 p1165 A73-23358

Post-buckling behaviour of rectangular orthotropic plates. 10 p1288 A73-23699

Finite element method for structural analysis, discussing theory for isoparametric stress quadrilateral plate bending elements with curved boundaries 11 p1435 A73-25437

Bending problem for shell of revolution with finite displacements, axisymmetric loading and nonlinear strain functions 11 p1445 A73-26460

On moderately large deflection of multiply connected plates. 12 p1557 A73-27933

On the uniqueness of solutions of stress equations of motion of the Beltrami-Michell type. 14 p1809 A73-30254

Rate-type constitutive equations for plateau predictions in dynamic plasticity for stress, strain and particle velocity functions 14 p1812 A73-30492

Thermal stresses and couple-stresses in square cylinder with a circular hole. 14 p1815 A73-30919

Metric tensor properties of physical space with deformable continuum in terms of kinetic stress function, approximating Einstein constant 15 p1945 A73-31041

Kinetic stress functions and the geometry of space in a deformed continuum 15 p1953 A73-32099

Torsion of an inhomogeneous body of revolution with variable shear moduli 16 p2074 A73-32682

Application of stress functions to dynamic analysis of shallow shells. 16 p2077 A73-32987

Chernin type second order equation for complex stress function for elastic shells of revolution under lateral load and tilting moment 16 p2084 A73-34034

Two and three dimensional elasticity theory of linear fracture mechanics covering stress functions, finite element method and crack behavior in solids 17 p2252 A73-35669

Elastic stresses in rotating orthotropic discs of variable thickness. 19 p2496 A73-37436

On a formulation of the bending of elastic plates. 19 p2500 A73-38112

Determination of kinetic stress functions in elastodynamic problems of plates 20 p2617 A73-39262

Construction of a stress tensor according to Papkovitch-Filonenko-Borodich method 20 p2618 A73-39324

Second-approximation boundary layer equations in Prandtl-Mises variables 20 p2549 A73-39610

Generalized shear stress and shearing strain rate variables for thick circular plate, using von Mises yield criterion for limit load analysis 24 p3148 A73-44895

Constitutive equations, creep laws, stress functions, variational principles and differential operators in dynamic and static linear viscoelasticity theory 24 p3153 A73-45496

STRESS MEASUREMENT

NT X RAY STRESS MEASUREMENT

Utilization of polarized ultrasound in stress investigations 02 p0166 A73-11645

Isotropy postulate verification for strain vectors measurement in annealed steel tubular specimens, showing coincidence of tension-internal pressure and tension-torsion test values 02 p0235 A73-12206

Dynamic errors in force measuring transducers, simulating unsteady processes by analog model with varying step function input signals 02 p0170 A73-12540

Displacement and stress determination in the case of the profile-planar viscoelastic disk 03 p0385 A73-13141

Comparison and analysis of residual stress measuring techniques and the effect of post-weld heat treatment on residual stresses in Inconel 600, Inconel X-750 and Rene 41 weldments. 03 p0313 A73-13596

Shear stresses below asperities in Hertzian contact as measured by photoelasticity.
[ASME PAPER 72-LUB-14] 03 p0314 A73-14330

Error effects in dynamic force measurements performed on materials testing pulsators
04 p0450 A73-15475

Stress-strain state of a spheroidal inclusion/measuring device/embedded in a thermoelastic medium
05 p0633 A73-16616

Strain gauge for measuring longitudinal and transverse strains
07 p0826 A73-20518

Measurement of dynamic mechanical quantities; Scientific-Engineering Conference, 3rd, Warsaw, Poland, October 26-28, 1972, Summaries
07 p0826 A73-20526

Characteristics and properties of WED-05 tensometers
07 p0827 A73-20537

Optical stress rosette based on caustics for stress distribution and differences measurement in perforated plate, using gas laser light for interferometry
08 p0964 A73-21047

Method of determining the mass removal from heat-shield materials on the basis of strain measurements in loaded shells
08 p1023 A73-21369

Sectioning method for residual stress measurement in structural members, describing test procedure, specimen preparation, tools and measuring devices and working conditions
09 p1156 A73-21875

Stress distortion coefficient of uniaxial tension/compression/ of elastic isotropic medium with flattened ellipsoidal sensor from sensor stress recording
09 p1159 A73-22590

Tensile creep modulus, creep lateral contraction ratio and torsional creep measurements on small non-rigid specimens.
10 p1218 A73-24120

Procedure for recording stresses by dielectric sensors in the case of impulsive loads
10 p1219 A73-24367

A note on the arrangement of strain gauges and the sensitivity of strain measurement.
10 p1219 A73-24572

Investigation of stress state at fatigue crack tip by means of X-ray microbeam.
10 p1293 A73-24918

Strain gages and photoelastic coating methods of thermal stress determination for model and full scale tests
11 p1435 A73-25452

Investigation of thermoelastic stresses by means of 'freezing' involving the realization of a prescribed temperature gradient
11 p1435 A73-25454

Dual-beam polariscope and framing camera for dynamic photoelasticity.
12 p1496 A73-27025

Strain gage measurements of elastoplastic deformations under biaxial and triaxial stresses with application to cylindrical steel container
13 p1617 A73-28843

Strain measurements in the solid propellant of a large booster structural test vehicle.
13 p1669 A73-29304

Biaxial tensile test facility for three dimensional characterization of nonlinear viscoelastic materials based on variable ratio principal strains in plane stress
13 p1598 A73-29309

Automatic evaluation of strain gage data reliability by comparison with a preset parameter and determination of a statistical yield strength.
13 p1622 A73-29549

A sandwich-transducer technique for measurement of internal dynamic stress.
14 p1751 A73-29773

Radio telemetry for strain measurements in turbines.
14 p1752 A73-30064

Stress measurement on cloth of inflated solid circular parachute model, noting sensor interference with canopy shape and stress pattern
[AIAA PAPER 73-445] 15 p1825 A73-31431

Residual stress measurement and analysis using ultrasonic techniques.
15 p1879 A73-32249

Investigation of thermal deformations by methods of holographic interferometry
17 p2164 A73-34172

Nickel-titanium memory material stress measurement methods, energy absorption capacity and cyclic response, discussing nickel foil surface temperature sensing devices
17 p2166 A73-34616

Acoustic emission coincidence detector for monitoring high residual stress areas in symmetrical pressure vessels.
17 p2166 A73-34620

On the limitations of interferometric methods in three-dimensional photoelasticity.
[SESA PAPER 2165] 17 p2251 A73-35455

The use of a high modulus inclusion gauge in nonlinear viscoelastic materials.
[SESA PAPER 2187A] 17 p2173 A73-35457

Determination of slope and strain contours by double-exposure shearing interferometry.
[SESA PAPER 2215A] 17 p2174 A73-35459

Compliance measurement for determination of crack extension force, specimen dimensions and elastic constants in linear fracture mechanics, discussing instrumentation, precautions and data reduction
17 p2252 A73-35671

Factors affecting the results of strain gauge measurements performed by electrical resistance strain gauges
18 p2316 A73-36473

Studies of fiberglass plastic under tensile load with the aid of transparency measurements
18 p2327 A73-36476

Strain analysis of a disk subjected to diametral compression by means of holographic interferometry.
19 p2429 A73-37264

Autocompensatory strain measurement of rotating disks subjected to elastic and plastic deformation.
19 p2430 A73-37792

Strain gauge for measurement of axial and transverse strains.
19 p2430 A73-37794

Measurement of residual stresses in a cylinder. III - On the effect of eccentricity of holes bored out in Sachs method.
19 p2501 A73-38345

Process control stress test of MOS IC circuit susceptibility to charge spreading with channel formation
19 p2436 A73-38452

Study of the photoviscoelasticity method
20 p2619 A73-39331

Residual-stress measurement using surface displacements around an indentation.
21 p2704 A73-41265

Effects of strain gradients on the gross strain crack tolerance of A 533-B steel.
22 p2876 A73-42153

Some results of the application of the nondestructive ultrasonic method to the measurement of residual stresses
23 p2996 A73-44289

Errors produced by the influence of unsteady heating in strain measurement by wire-type resistance strain gages
23 p2983 A73-44292

Digital microstress gauge for magneto-thermal gas transport studies.
24 p3089 A73-44815

STRESS PROPAGATION

Bending stresses propagating from the clamped support of an impulsively loaded beam.
01 p0115 A73-10753

Propagation of elastic waves in a cylindrical bar subject to a moving load on its lateral surface.
03 p0343 A73-13833

Impact loading on structures with random properties.
04 p0510 A73-15028

On the uniqueness of singular solutions to boundary-initial value problems in linear elastodynamics.
04 p0512 A73-15226

A dynamic polariscope for stress wave analysis.
08 p0962 A73-20668

Thin panels stresses diffusion analysis, comparing Bleich, variational, Conway finite difference and finite element methods
09 p1159 A73-22717

The propagation of waves from a cylindrical cavity.
10 p1289 A73-24282

Axially symmetric transient wave propagation in elastic rods with nonuniform section.
11 p1447 A73-26652

Extension of the hodograph method for the one-dimensional elastic-plastic wave propagation.
13 p1696 A73-28646

Acceleration wave propagation in a nonlinear viscoelastic solid.
[ASME PAPER 73-APM-2] 17 p2247 A73-35028

Propagation of stress gradient through an inclusion. I.
[ASME PAPER 73-APM-15] 17 p2247 A73-35038

Propagation of stress gradient through an inclusion. II.
[ASME PAPER 73-APM-16] 17 p2247 A73-35039

Continuum theory for elastic laminates in terms of effective stiffness, deriving displacement and stress interface boundary conditions with illustrative wave propagation examples
[ASME PAPER 72-WA/APM-13] 17 p2249 A73-35112

On steady wave profiles in solids.
19 p2461 A73-38262

Propagation of stress wave with plastic deformation in metal obeying the constitutive equation of the Johnston-Gilman type.
20 p2615 A73-38888

The problem of wave propagation in physically nonlinear rods of finite length
20 p2618 A73-39315

Impact generated elastic strain low amplitude pulses propagating in filamentary composite rods, using Fourier transform technique and viscoelastic relation
20 p2623 A73-39557

A mixture theory of the response of a laminated plate to impulsive loads.
21 p2783 A73-40291

Velocity of a stress wave superimposed on the initial plastic stress state of a rod.
21 p2784 A73-40436

The stress pulses propagated as a result of the rapid growth of brittle fracture.
23 p3042 A73-43805

Transmission of anti-plane shear waves past an interface crack in dissimilar media.
23 p3043 A73-43815

Variational principles in dynamic thermoviscoelasticity.
24 p3151 A73-45306

Shock wave propagation in colliding elastic bars under axial end-on impact, deriving closed form solution for curvilinear stress-strain characteristics
24 p3112 A73-45430

STRESS RATIO

Fatigue crack propagation growth rates under a wide variation of Delta K for an ASTM A517 Grade F (T-1) steel.
04 p0459 A73-14687

Optimal experimental measurements of anisotropic failure tensors.
05 p0631 A73-16113

Strain ratio data for commercial Al alloys in various temper conditions as drawability criterion for sheet press performance, discussing single tensile test method
14 p1762 A73-30643

Threshold for fatigue crack propagation and the effects of load ratio and frequency.
22 p2875 A73-42137

STRESS RELAXATION

Temperature fields and stresses during local tempering of helical welds of a cylindrical shell
01 p0118 A73-11413

Influence of repeated loads on the resistance to relaxation of a heat-resistant nickel-chromium alloy
02 p0180 A73-11624

The influence of oxygen concentration on the internal stress and dislocation arrangements in alpha titanium.
02 p0184 A73-12768

Biaxial stress relaxation in glassy polymers - Polymethylmethacrylate.
02 p0186 A73-12811

Studies in stress-relaxation and distensibility characteristics of small skin veins in vivo by a combined photoelectric-photographic and plethysmographic technique.
05 p0541 A73-17098

Load-time dependent relaxation of residual stresses.
05 p0636 A73-17214

Evaluation of multiaxial theories for room-temperature plasticity and elevated-temperature creep and relaxation of several metals.
06 p0759 A73-17599

Effect of recovery on recrystallization of aluminum 99.85
06 p0705 A73-17849

Cyclic loads for decrease in relaxation softening of heat resistant Ni-Cr alloys, noting working temperature effects
06 p0706 A73-17885

The influence of scatter on some simple variable-stress creep predictions.
08 p0106 A73-20798

A recovery creep model based on dislocation distributions.
08 p0980 A73-21777

Stress varied creep of 20Cr-25Ni-Nb stabilized austenitic stainless steel.
08 p0981 A73-21788

Inversion of Prony series characterization for viscoelastic stress analysis.
09 p1158 A73-22393

High temperature creep resistance enhancement by stress relaxation or removal of unstable surface layers, increasing activation energy for different alloys
09 p1101 A73-22403

Plastic strain and zero stress concepts as specific properties of materials with long range memory, formulating functional plasticity and moving dislocations theory
10 p1289 A73-24159

Prediction of inelastic high temperature materials behavior by strain-rate approach.
11 p1450 A73-25515

[AIAA PAPER 73-386] Solution of the problem of plane deformation for a tube consisting of a physically nonlinear quadratic viscoelastic material
13 p1690 A73-27995

- Dynamic strain ageing in some titanium-silicon alloys. 13 p1634 A73-28184
- Relaxation spectra of niobium irradiated at low temperature. 13 p1638 A73-29455
- A molecular theory of elastomer deformation and rupture. 13 p1646 A73-29528
- A simple model of uniaxial creep recovery and stress relaxation based on residual-stress redistribution. 15 p1948 A73-31615
- Stress relaxation measurements for strain rate sensitivity of dispersion hardened thoriated Ni alloys as function of applied stress concentration. 17 p2190 A73-36447
- A relaxation method for solving nonlinear stress equilibrium problems. 18 p2365 A73-36611
- Residual stress relaxation stability in 13Kh12NVM-FA steel. 18 p2323 A73-36763
- Effect of temperature on the effectiveness of hardening components made of heat-resistant alloys. 19 p2439 A73-37268
- Studies of the renewal of stress relaxation on a high-grade steel wire subjected to stress corrosion after being treated for total elimination of relaxation. 19 p2497 A73-37553
- Study of the phenomenon of stress relaxation of flow in the case of titanium. 19 p2442 A73-37840
- The motion of a brittle crack. 19 p2444 A73-38263
- Creep relaxation approximations and exact solutions, discussing rectangular beam pure bending, spherical shell internal pressure loading and thin circular tube bending. 20 p2616 A73-39115
- Il'yushin linear theory for defect accumulation generalized for endurance limit of materials under noncyclic loads, examining time to failure under creep and relaxation conditions. 20 p2624 A73-39644
- Stress relaxation and mechanical equation of state in austenitic stainless steels. 22 p2878 A73-42578
- Influence of initial transients on stress relaxation and creep measurements on visco-elastic materials. 22 p2868 A73-43172
- Laws governing the behavior of the electrical resistance during process of inelastic-strain relaxation. 23 p3040 A73-43574
- Fabrication techniques for Ti alloys in aerospace applications, discussing hot forming, electron beam and diffusion welding under vacuum and stress relaxation annealing. 23 p2985 A73-43911
- Constitutive equations of elastoplastic and elastoviscoplastic bodies based on thermodynamic state, considering deformation velocity and stress relaxation. 23 p3043 A73-43967

STRESS RELIEVING

- How deformation affects the mechanical properties of aluminum forgings. 03 p0322 A73-13266
- Mutual compensation of the unloading-force errors in the axial- and lateral-unloading systems of an astronomical mirror. 05 p0575 A73-16317
- Stress distribution on astronomical telescope mirror outer surface, calculating deflection and relief load. 06 p0693 A73-18157
- Body centered cubic transition metal stage 3 electrical resistivity recovery mechanism from experiment on recrystallized and stress-relieved plastically deformed Nb wire. 07 p0839 A73-20112
- Optimal conditions for residual stress reduction in a cylindrical shell by local annealing. 14 p1814 A73-30721
- Influence of relief annealing on the mechanical properties of high-strength hydrogenized steel. 21 p2721 A73-41228

STRESS RUPTURE STRENGTH
U CREEP RUPTURE STRENGTH
STRESS TENSORS

- Hydrodynamics and heat transfer in a fluid with an asymmetrical stress tensor. 03 p0398 A73-13722
- Algorithm for stress tensor and stability analysis of glass fiber reinforced plastic shells under hydrostatic pressure. 03 p0392 A73-13741
- Potential methods in the linear couple-stress theory of elasticity. 04 p0514 A73-15676
- The Reynolds tensor in a homogeneous turbulence associated with a mean shearing flow. 04 p0436 A73-15995
- Optimal experimental measurements of anisotropic failure tensors. 05 p0631 A73-16113

- Relativistic stress tensor in general relativity theory. 05 p0597 A73-16469
- Asymmetric principal stress bounds in terms of symmetric part of tensor, considering existence conditions and maximum shear and normal stresses [ASME PAPER 72-APM-QQ]. 05 p0633 A73-16535
- Electrodynamics of anisotropic media with space and time dispersion. 06 p0723 A73-17787
- A finite element tensor approach to plate buckling and postbuckling. 07 p0907 A73-19028
- A linear theory of thin elastic shells, based on conservation of a non-normal straight line. 07 p0908 A73-19091
- Swirl injector driven air flow in cylindrical tube, measuring flow velocity and turbulent stress tensor components. 08 p0956 A73-21601
- Elastic potentials application to second axisymmetric problem solution in micropolar elasticity, considering moments loaded semiinfinite elastic body deformation and stress tensor components. 09 p1157 A73-22170
- Loading mode effects on high strength steel hydrogen embrittlement, considering stress tensor invariants and interstitial diffusion relationships. 09 p1102 A73-22414
- Lie operators admitted by Lamé equations in three dimensional dynamic elasticity theory for arbitrary particle velocity and displacement and linear stress-strain tensor relation. 09 p1159 A73-22585
- Yield criteria derivation for laminated media with isotropic and anisotropic layers based on strength constants characterization as tensors. 10 p1289 A73-24277
- Tensorial expansions for the plastic flow of partially compressible media. 10 p1290 A73-24325
- A survey of the mean turbulent field closure models. 13 p1601 A73-28801
- A uniqueness theorem for a system of stress equations of motion in linear elasticity. 14 p1809 A73-30255
- Existence of generalized tensorial fields in linear axisymmetric elastodynamics. 14 p1809 A73-30256
- Energy methods in plasticity theory extension to creep mechanics with respect to stress-strain rate tensors relationships. 14 p1811 A73-30478
- Yield conditions for plastic deformation of anisotropic bodies, using stress tensor invariants and Tresca form. 14 p1811 A73-30480
- Asymptotic solutions for shells with general boundary curves. 14 p1812 A73-30523
- Nonlinear differential equation solutions for prismatic body elastic equilibria in terms of deformation and stress tensor relations by small parameter method. 15 p1945 A73-31042
- Theory of conjugate projections in finite element analysis. 17 p2201 A73-34828
- On an anomaly of the theory of beams with directors. 19 p2497 A73-37527
- Compressible fluid dynamic theory, using stress tensors to derive constitutive equations for plane homogeneous and shear flows. 19 p2420 A73-37644
- Construction of a stress tensor according to Papkovitch-Filonenko-Borodich method. 20 p2618 A73-39324
- Material indifference - A principle or a convenience. 20 p2619 A73-39337
- Continuum thermodynamics-based formulation of mixture theory using Boolean algebra with emphasis on partial stress tensors, considering force, moment and energy balance equations. 22 p2885 A73-41771
- Second order cross stress study of elastic shear deformation, considering rotation invariant Cauchy tensor and Poynting effect. 23 p3039 A73-43306
- Mean Reynolds stress tensor model for analytical prediction of turbulence structure of density-stratified atmospheric boundary layer. 23 p3002 A73-43592
- Role of constraining forces for ultrarelativistic particle motion as a source of gravitational radiation. 23 p3006 A73-43606
- Plane boundary layer equations for viscous incompressible fluid with asymmetric stress tensor produced by moment stresses and mass moments. 23 p2968 A73-43922
- Geometry, kinematics and dynamics of dislocations in non-linear continuum mechanics. 23 p3045 A73-44082

STRESS WAVES

- Reflection of plane stress waves in an elastoplastic medium with a variable yield limit. 01 p0114 A73-10570
- Laser-induced stress-wave and impulse augmentation. 02 p0177 A73-12746
- Stress shock waves effect on polycrystalline metals grain structure, discussing strain rate critical value zones. 03 p0386 A73-13147
- Acoustic emission source location using single and multiple transducer arrays. 04 p0448 A73-15121
- A closed-form solution of the propagation problem of an unloading shock wave in a bilinear elastic body. 04 p0513 A73-15595
- Thermally induced stress waves in an elastic layer. [ASME PAPER 72-WA/APM-22]. 04 p0516 A73-15894
- Far field solution for stress wave attenuation and dispersion in composite materials, noting pulse shape. 05 p0633 A73-16540
- Stress wave propagation in a laminated plate under impulsive loads. 07 p0908 A73-19089
- The Kaiser effect in stress wave emission testing of carbon fibre composites. 07 p0843 A73-20185
- Propagation of monochromatic waves in an initially stressed infinite micropolar elastic plate. 09 p1160 A73-23024
- A numerical method for the analysis of longitudinal elastic-plastic stress wave propagation. 10 p1290 A73-24297
- Cylindrical metal projectile impact induced elastoplastic deformation, determining dynamic yield point by computer simulation of Taylor stress wave propagation model. 10 p1292 A73-24529
- An upper bound solution for rectangular plate in plane stress compression. 10 p1292 A73-24640
- Nonlinear transient stress-waves in cylindrical and conical shells. 11 p1432 A73-24978
- Incremental deformations in orthotropic laminated plates under initial stress. [ASME PAPER 72-APM-VV]. 11 p1441 A73-25707
- Stress waves in finite longitudinally layered shells. 11 p1442 A73-25712
- Effects of stress wave form and cycle frequency on low cycle corrosion fatigue. 11 p1382 A73-25823
- Crack propagation in an elastic solid subjected to general loading. III - Stress wave loading. 13 p1696 A73-28792
- Method of recording elastoplastic stress waves in solids with a dielectric sensor. 13 p1618 A73-29059
- Coupled thermoplasticity model of two stress-strain regions characterized by nonevolutionary plastic flow equations and simple wave collapse, with and without thermal conductivity. 13 p1698 A73-29087
- Extension of Mandel inequalities to plastic acceleration wave velocities in a finitely deformed medium. 13 p1703 A73-29553
- Steady state diffraction of stress waves by semi-infinite running crack in elastic solid under dynamic loading, obtaining solution based on Wiener Hopf technique. 16 p2082 A73-33910
- Anisotropic laminated fiber composite plates under short duration impact line forces, calculating one dimensional transient stress and displacement waves by fast Fourier transform. [ASME PAPER 73-APM-L]. 17 p2249 A73-35108
- A biaxial split Hopkinson bar for simultaneous torsion and compression. 17 p2149 A73-35754
- A method of recording elastoplastic stress waves in solids by means of a dielectric pickup. 18 p2317 A73-36891
- Coupled thermoplasticity model of two stress-strain regions characterized by nonevolutionary plastic flow equations and simple wave collapse, with and without thermal conductivity. 19 p2498 A73-37637
- Book - Stress wave propagation in solids: An introduction. 19 p2502 A73-38363
- Propagation of stress wave with plastic deformation in metal obeying the constitutive equation of the Johnston-Gilman type. 20 p2615 A73-38888
- Front-end collision of a partially liquid-filled cylindrical shell with a solid body. 20 p2616 A73-39261
- The problem of wave propagation in physically nonlinear rods of finite length. 20 p2618 A73-39315

Repetitive recording of stress waves in a photoelastic material using a multi-pulsed laser and an inexpensive streak camera.

Spallation and fracture resulting from reflected and intersecting stress waves.

Finite plasticity theory in acoustic tensor calculation for elastic, viscoplastic and plastic wave propagation

Weak longitudinal waves in a nonlinear viscoelastic medium

Electronic logic device for crack arresting pentrite microcharge pulse initiation, including crack and stress wave propagation measurements

Stress wave calculations in composite plates using the fast Fourier transform.

Recent results in nonlinear viscoelastic wave propagation.

STRESS-STRAIN DIAGRAMS

Combined heating and irradiation effects on body elastoplastic stress-strain state, deriving thermoradiative plasticity equations

Singular integral equations analysis of elasticity theory boundary value problem to determine axisymmetric thermoelastic stress-strain state of half space with cylindrical cavity

Upper bounds to the load for the plane strain working of anisotropic metals.

Solution of stresses and strains for laminated monoclinic cylinders.

Re-interpretation of some simple tension and bulge test data for anisotropic metals.

Shock waves existence and behavior in elastic non-conductors, investigating Hugoniot stress-strain curve properties

Assessment of the stressed state of a material from the strain nomogram

Determination of the theoretical stress-concentration factors in composite systems in bending

Two coordinate oscillograph recording device with automatic reversing for stress-strain tests under static and cyclic loads

Use of ultrasonic emission in nondestructive inspection.

Stress-strain state of shallow spherical shell with variable wall thickness under uniformly distributed load, using Vlasov shell theory

The relation between creep at room temperature and the characteristics of the stress-strain diagram in the case of metallic materials

Effect of strain-rate and temperature on the resistance to torsional deformation of several aluminum alloys.

Displacement and stress determination in the case of the profile-planar viscoelastic disk

Stress-strain diagrams for stability of structures under plastic bending, noting differential equations for rigidity characteristics

Yield and plastic flow theory for porous metal powder compacts and preforms, discussing stress-strain and deformation-densification relations

Experiments on shell stability in air-driven shock tubes.

Tubular materials plane stress-strain test facility for combined axial load and internal pressure effects

Techniques for smooth specimen simulation of the fatigue behavior of notched members.

Local stress-strain response of notched members to predict fatigue life of stress relieved and as-received weldments with internal cavities

Dynamic response of nonlinear media at large strains.

An inelastic stress-strain law for elevated temperature and slowly time varying loads.

Precipitation hardening effect on Co-Ni-Ti-Al alloys stress-strain, grain size and strain resistance behavior in micro- and macrodeformation yield point region

Elastic-plastic deformation in edge-notched tension specimens under plane stress conditions.

On the re-inforcement of thermoplastics by imperfectly aligned discontinuous fibres.

A simple procedure for experimental determination of the longitudinal shear modulus of unidirectional composites.

Finite element model use for deducing errors magnitude in stress-strain properties obtained from laboratory compression test results

Predicting failures with conducting-polymer fatigue-damage indicators.

Lagrange description of equations for finite deflections of incompressible plastic shells, classifying stress-strain relations

Structural design with allowance for shakedown in the case of temperature-dependent elastic constants

A new relationship between pre-strain and yield stress drop due to Bauschinger effect.

Approximate method of studying the symmetrical deformation of orthotropic bodies

Stress-strain diagrams and strain hardening curves, proposing unified representation plane

Piecewise linear approximation of thin walled rib and diaphragm reinforced conical beams under thermal field and axial loads, using limit stress-strain diagrams

Some further comments on Stage III recovery in Group VA body-centered cubic transition metals.

The yield point phenomenon in a Be-Al composite.

A visco-plasto-elastic expression for stress-strain diagram of fiber reinforced plastics subjected to repeated low frequency loads.

A new method of measurement to determine the stress-strain relation in a bending fatigue specimen.

Investigation of the plastic state of disks by the hardness measurement method

Estimation of the fatigue characteristics of D16T and AVT1 aluminum alloys from the breaking stress

Stress-strain state of transversely isotropic shells under concentrated loads

Rheological equation for expansion rate effects on stress-strain relation of polyester binders hardened thermochemically and by gamma radiation

Secondary terms of thin multilayer plate equations, involving edge and stress-strain state fluctuation effects on boundary condition formulation

Some empirical relationships between creep strain, stress, time and temperature in 1Cr-Mo-V rotor forgings.

Twinning deformation of mild steel at low temperatures as function of stress-strain state

Influence of the type of the stress-strain state on strain-hardening of materials

Investigation of the strength and deformability of thin composite materials used as magnetic recording media. II - Strength and deformability at low temperatures

Low-temperature impact bending with recording of the stress-strain diagrams

Experiment on the mechanical anisotropy of titanium, zirconium, and Zircaloy-2 rolled sheets.

Yield and fracture of D16T alloy at low temperatures in the presence of a complex stress pattern.

Consideration of the hysteresis behavior of a solid medium in a complex stress state under the conditions of simple cyclic loading.

Conical shell inversion - An approximate energy analysis.

Inelastic buckling of shallow spherical shells under external pressure.

Stress-strain relations for materials with different tension, compression yield strengths.

Effect of fiber-matrix adhesion on the properties of short fiber reinforced ABS.

Fiberglass reinforced plastics dynamic models, discussing stress-strain relationship, Poisson ratio and fatigue

Criteria for selecting resin matrices for improved composite strength.

A yield-surface corner lowers the buckling stress of an elastic-plastic plate under compression.

Nonlinear elastic behavior of unidirectional composite laminate.

In-plane shear stress-strain response of unidirectional composite materials.

Determination of the initial stress-strain state of a shallow spherical shell under the action of a dynamic load

Stress-strain state in the filler of a three-layer strip under local loading

Application of a digital computer in the processing and presentation of tensile test results.

On the identification of the unknown functions in Brucker's work-hardening relation for plastic deformation of crystalline materials.

Cyclic stress, strain, and energy variations under cumulative damage tests in low-cycle fatigue.

Influence of small local deviations in specimen diameter on conventional strain at maximum load in tensile test

Prediction of inelastic high temperature materials behavior by strain-rate approach.

An elastic-plastic buckling solution using the incremental theory.

Theoretical and experimental investigation of the nonlinear behavior of angleplyed boron/aluminum composites.

Estimates for stress derivatives and error in interior equations for shells of variable thickness with applied forces.

Deformation bounds for a creeping structure approaching rupture.

Tensile behaviors of high Cr-low Ni two-phase stainless steels at room and low temperatures.

Calculation of the stress-strain state of a toroidal shell with holes

Influence of deformation history on the yield locus and stress-strain behavior of aluminum and copper.

An empirical analysis of titanium stress-strain curves.

A theory of an elastic-plastic continuum with special emphasis to artificial graphite.

Elastic and creep limits of heteroplastic micrograin metallic/duralumin materials in terms of stress-strain curve, sliding plane and stress hardening and relaxation

Elastostatic invariance in the composite plane.

Relationship between the strain curves of a material subjected to static and to cyclic loads

The effect of strain rate and heat developed during deformation on the stress-strain curve of plastics.

Plasticity and fracture of structural metals in complex stress state at low temperatures.

Deformation mechanism and strength of metals under impulsive loading.

Conditions for rational arrangement of reinforcing fibres in materials and structures.

Stress-strain state of thin circular perforated Cu plate under uniform tensile load, showing applicability of small elastoplastic finite deformation theory

Epoxy-thiocol binder viscoelastic deformation under short and long term loads, noting stress-strain linearity limit

Strain curves of titanium alloys VT-6S and VT-14 in the temperature range 20-400 C.

Three-dimensional stress-strain state of turbine blades 14 p1813 A73-30677

Rotating turbine disks ultimate strength relation to stress-strain state, material mechanical properties and plastic deformation 14 p1814 A73-30684

The effect of stacking-fault energy on the stress-strain curve of dispersion-hardened Ni-Co alloys. 15 p1887 A73-31351

Cast thermosetting epoxy resin linear elastic stress-strain characteristics under tension, compression, torsional and bending loads 15 p1897 A73-31619

Notched austenitic stainless steel stress corrosion cracking tests in boiling magnesium chloride solutions, obtaining relationship between maximum stress and strain rate in graph 15 p1895 A73-32569

A stress-strain relation for homogeneous and isotropic continua 16 p2035 A73-32934

Characteristic matrix method for automatic recognition and extraction of rigid body modes from inconsistent to natural force-deformation relationship of stress and strain elements 16 p2077 A73-32990

Discrete approximations of elastic-plastic bodies by variational methods. 16 p2078 A73-32994

Inelastic buckling of columns - The effect of imperfections. 16 p2084 A73-33975

Evaluation of finite-plasticity theories for torsion-tension members made of Tresca materials. [SESA PAPER 2109] 17 p2251 A73-35447

Ni-Fe-Cr alloy and austenitic stainless steel cyclic stress-strain behavior at 70-1400 F 18 p2323 A73-36586

Polymers fatigue life under cyclic deformation, discussing stress-strain and failure behavior as function of reversed stress cycle frequency 18 p2328 A73-36587

Applications of finite element stress analysis and stress-strain properties in determining notch fatigue specimen deformation and life. 18 p2364 A73-36591

Influence of temperature and strain rate on the load-elongation curve and plastic properties of molybdenum 18 p2324 A73-36801

Relation of strain curves of material in static and cyclical loading. 18 p2366 A73-36887

Some studies of the influence of localized and gross plasticity on the monotonic and cyclic concentration factors. 19 p2497 A73-37589

Plastic state of disks studied from hardness measurements. 19 p2499 A73-37789

Evaluation of the fatigue properties of aluminum alloys D16T and AVT1 on the basis of limit stresses. 19 p2440 A73-37790

On the relationship of stress crazing and yielding of polymethyl methacrylate. 20 p2579 A73-38641

Effects of misalignment on the pre-macroyield region of the uniaxial stress-strain curve. 20 p2576 A73-39030

Isotropic elastic material fracture and yield criteria in terms of frame-indifferent relation between stress and strain increments 20 p2623 A73-39563

The elastic layer with a cylindrical hole subjected to a nonuniform axisymmetric radial displacement. 20 p2624 A73-39566

Effect of stressed state on strain hardening. 22 p2919 A73-42104

Recording strain diagrams in low-temperature impact bending tests. 22 p2874 A73-42105

Some further results of J-integral analysis and estimates. 22 p2920 A73-42144

Experimental verification of lower bound K sub Ic values utilizing the equivalent energy concept. 22 p2875 A73-42147

Comparison of some penalty function based optimization procedures for the synthesis of a planar truss. 22 p2922 A73-42478

Testing set-up for cyclic torsion with tension on a small number of loading cycles. 22 p2861 A73-42530

German monograph on cyclic stress-strain curves and fracture strength of steels with various compositions covering plastic strain energy, S-N diagrams and test equipment 22 p2879 A73-42739

Statistical theory of solid heterogeneous materials, discussing constant elastic bounds, fiber reinforced cell model, thermal expansion and stress-strain relations 23 p3038 A73-43303

Method of determining the susceptibility of metals to brittle fracture under shock loads 23 p2965 A73-43470

Influence of the free edge upon the strength of angle-ply laminates. 23 p3041 A73-43635

Post-yielding behavior of torsionally loaded composite tubes. 23 p3041 A73-43640

Plastic deformation and anisotropy of sapphire crystals via nonbasal plane slip under bending, obtaining stress-strain curves and flow stresses temperature dependence 23 p2997 A73-43772

Piecewise linear law of the relation between stresses and strains for large deformations 23 p3043 A73-43920

Microstrain gage for plastic deformation measurements of crystalline solids in compression, obtaining stress-strain diagrams for Ta single crystals 23 p2986 A73-44036

Sandwich shells nonlinear theory with stress-strain relations in tensor notation, using Hamilton principle for equations of motion and boundary conditions 23 p3044 A73-44078

Influence of high hydrostatic pressure on the flow stress of 18-8 stainless steel. 23 p2994 A73-44161

Nonlinear stress-strain hysteresis equation of cyclic straining for vibrating imperfectly elastic systems, using Masing principle 23 p3047 A73-44276

Testing of composite materials with the aid of annular samples 23 p2998 A73-44295

Fracture criteria for a unidirectional glass fiber/plastic material under planar short-term and long-term stress 24 p3103 A73-44884

The Portevin-Le Chatelier effect in compression tests of polycrystalline aluminum 24 p3148 A73-44914

Theoretical post-yielding behavior of composite laminates. II - Inelastic macromechanics. 24 p3104 A73-45145

Convergence of finite difference transient response computations for thin shells. 24 p3150 A73-45228

Shock wave propagation in colliding elastic bars under axial end-on impact, deriving closed form solution for curvilinear stress-strain characteristics 24 p3112 A73-45430

Reduced equilibrium equations solution for plane deformations of isotropic incompressible elastic media, using stress-strain relations 24 p3153 A73-45549

STRESS-STRAIN DISTRIBUTION U STRESS CONCENTRATION STRESS-STRAIN RELATIONSHIPS U STRESS-STRAIN DIAGRAMS STRESS-STRAIN-TIME RELATIONS

Stress history effect on incubation time for stress corrosion crack growth in AISI 4340 steel. 02 p0183 A73-12763

Nonlinear physical stress-strain relation for reticular polymers and fiberglass plastics under conditions of microcreep and elastic aftereffect 04 p0468 A73-15508

Time variable stress-strain state of viscoelastoplastic hollow sphere under internal pressure, using piecewise linear differential law 05 p0635 A73-17080

Parametrization of low-temperature deformation characteristics in single crystals of molybdenum. 09 p1099 A73-21928

Heat resistant alloys stress-rupture strength tests for operating temperatures based on equivalent high temperatures damageability 09 p1106 A73-23156

Limit of linear viscoelastic behavior - An energy criterion. 13 p1700 A73-29465

Finite deformation behavior of elastomers - Dependence of strain energy density on degree of crosslinking for SBR. 13 p1646 A73-29527

Investigation of the thermal fatigue of type Kh18NiOT steel under complex stress distributions. 13 p1643 A73-29623

Flow stress of metals and its application in metal forming analyses. [ASME PAPER 73-PROD-4] 16 p2019 A73-33534

Nonlinear dynamic problem concerning a cylinder with a slowly changing internal boundary 16 p2082 A73-33932

Prediction of the deformation properties of polymer materials 17 p2194 A73-34268

Fatigue life of structural components under random loading 17 p2242 A73-34520

Cyclic stress-strain behavior - Analysis, experimentation, and failure prediction; Proceedings of the Symposium, Bal Harbour, Fla., December 7, 8, 1971. 18 p2364 A73-36584

Calculation of shear-sensitive orthotropic shells with residual stresses 21 p2786 A73-40977

A note on determination of the shear stress-strain response of unidirectional composites. 24 p3149 A73-45150

STRESSED-SKIN STRUCTURES

Optimization and design of the rear fuselage of the A 300 B aircraft structure. 10 p1288 A73-23790

Optimum design of stressed skin structures using a sequence of linear programs method. [AIAA PAPER 73-342] 11 p1436 A73-25481

Creep analysis of a thin-walled wing on the basis of the plate analogy 12 p1551 A73-27081

Titanium Stressskin panel fabrication and assembly - discussing forming, cutting, thermal processing, welding and applications [SME PAPER MF 73-158] 19 p2437 A73-38502

Acoustic fatigue resistance of aircraft structures at elevated temperatures. [AIAA PAPER 73-994] 24 p3056 A73-44829

STRESSES

NT AXIAL STRESS

NT COMBINED STRESS

NT CRITICAL LOADING

NT RESIDUAL STRESS

NT SHEAR STRESS

NT TENSILE STRESS

NT THERMAL STRESSES

NT TORSIONAL STRESS

NT TRIAXIAL STRESSES

NT VIBRATIONAL STRESS

STRETCH FORMING

Solid phase stretch forming of thermoplastic polypropylene at temperatures below crystalline melting point 03 p0332 A73-13034

Stretch formed corrugated Rene 41 panel development for space shuttle booster nose section hot area skin, discussing tooling and formation techniques [SAE PAPER 720873] 05 p0582 A73-16670

STRETCHING

Dynamic calculation of the stretching of a spring with allowance for redistribution of mass along its length 02 p0230 A73-11720

On the unity of the constant strain/constant moment finite element methods. 13 p1691 A73-28075

STRIATION

Deformation and striation of plasma clouds in the ionosphere. I, II. 09 p1074 A73-22062

STRINGERS

Integrodifferential equation for three dimensional contact problem of elastic half space strengthened by elastic stringer, solving by Fourier series 06 p0766 A73-18876

Some contact problems for an infinite plate strengthened by elastic cover pieces 07 p0910 A73-19305

Singular integrodifferential and linear integral equations for load transfer from stringer to wedge under concentrated force and for stringer-coupled wedge shaped regions 07 p0910 A73-19306

Two dynamic contact problems for a half-plane with elastic cover pieces 07 p0911 A73-19314

Vibration and flutter of cylindrical shells including the effects of stringer stiffening. [AIAA PAPER 73-312] 11 p1441 A73-25543

Stringer stiffened cylindrical shells stability characteristics under axial compression, using Donnell thin-shell and Vlasov thin-walled beam theories 15 p1949 A73-31656

Integrodifferential equation for three dimensional contact problem of elastic half space strengthened by elastic stringer, using Fourier series 15 p1956 A73-32401

Analysis of stress intensity factors for the tension of a centrally cracked strip with stiffened edges. 23 p2992 A73-43812

STRINGS

Randomly separated ends scattering effect on linear and nonlinear coherent oscillations of elastic string by perturbation technique 06 p0723 A73-17900

Recursive solution for steady forced vibration modes of tensed string under concentrated harmonic forces 09 p1120 A73-22583

Corresponding function solutions of discrete mechanics problems based on difference polynomials, applying to Lagrange problem of string natural vibrations for distributed point masses 16 p2035 A73-32680

Estimation of the effect of the internal properties of the material on the characteristics of string sensors 22 p2860 A73-42370

STRIP

Geometrical theory to approximate HF electromagnetic wave diffraction from moving conducting strip under incident field 01 p0016 A73-10192

Unsteady thermal stress in an infinite strip with mixed boundary conditions 01 p0115 A73-10916

Fourier transformations and Wiener-Hopf equations for stress intensity factor of crack propagation in linearly elastic homogeneous isotropic strip 04 p0512 A73-15238

The linear thermoelastic problem of uniform heat flow disturbed by a two-dimensional crack in a strip. 06 p0762 A73-17985

Edge crack in a strip of an elastic solid. 06 p0762 A73-17991

Stress-strain state in the filler of a three-layer strip under local loading 10 p1291 A73-24354

Two coplanar cracks in an infinitely long elastic strip bonded to semi-infinite elastic planes. 14 p1815 A73-30918

Mixed boundary value problem solution for strip under elastic deformation due to external loads based on reduction to system of integrodifferential equations 15 p1952 A73-32088

An integral equation approach to the semi-infinite strip problem. [ASME PAPER 73-APMW-5] 22 p2924 A73-42878

Oblique radiation of ultrasound by an electromagnetic-acoustical method. 24 p3109 A73-44697

STRIP TRANSMISSION LINES

Transverse resonance solutions for a long slot leaky wave antenna. 01 p0023 A73-10187

Application of the variational method in the analysis of a limiter based on a symmetrical strip line 01 p0026 A73-11264

Design and fabrication of helix-like strip meander line delay equalizer in printed circuit technology, noting group delay and insertion loss frequency responses 02 p0145 A73-11823

X band microstripline slot antenna measurement for input impedance and radiation pattern dependence on slot-to-reflector spacing, applying to array design 02 p0141 A73-12100

Standing wave approximation of distributed dual frequency parametric oscillators consisting of semiconductor diodes and transmission line in steady state 02 p0147 A73-12490

Schwartz method application to stripline fields and impedance calculations for different cross sections and internal conductor dimensions 03 p0278 A73-14078

Eigenvalues and eigenfunctions of electric and magnetic waves of shielded strip transmission line, calculating electromagnetic field in cylindrical waveguide 04 p0417 A73-15089

MIS and Schottky barrier microstrip devices consisting of microstrip transmission line fabricated on semiconductor substrate, causing capacitance dependence on electric field 05 p0559 A73-16818

Distributed base resistance effect on stripline geometry transistor input characteristic, using equivalent circuit with pseudo-junction having high saturation current 06 p0677 A73-18396

Microstrip transmission line microwave IC, discussing electrical characteristics, dielectric and conductor materials, photo-etching processes, connection fabrication and circuit encapsulation 08 p0942 A73-20702

Microwave integrated circuits on a ferrite substrate. 08 p0942 A73-20704

Frequency-dependent transmission properties of coupled strip lines in a laminar dielectric 08 p0945 A73-21072

Effect of engineering-design factors on the parameters of microstrip transmission lines 08 p0951 A73-21109

Transmission zeros in microstrip discontinuities, considering structure effective width for TEM and higher modes 09 p1049 A73-22315

Microwave bandpass filters formed by shunt and series stubs with quarter wave matching strip lines, noting advantage of equal lengths 09 p1063 A73-22463

Fundamental and parasitic modes of a shielded microstrip transmission line 09 p1052 A73-23085

Microstrip bandpass filters with reduced radiation effects. 09 p1065 A73-23098

Experimental investigation of the effective permittivity and of the resonator Q of slot lines on ceramic substrates in the frequency range from 1 to 18 GHz 10 p1194 A73-23994

Microwave electronic packaging with integrated multifunction assemblies, considering stripline choice for transmission line 11 p1338 A73-26113

Wave devices built with ferromagnetic and electrically conducting film strips 12 p1460 A73-26772

Investigation of the synchronization of Gunn diode oscillators having a stripline resonance system 12 p1480 A73-27448

Surface acoustic wave multistrip components and their applications. 12 p1484 A73-27567

Determination of parameter tolerances for microstrip transmission lines 12 p1470 A73-27580

Coupled asymmetrical microstrip transmission lines odd and even mode wave impedances as functions of conductor strip width and spacing 12 p1481 A73-27582

Resonant RLC tank circuit design with coupled stripline segments, using lumped and distributed parameter system synthesis theory 13 p1592 A73-28895

Influence of tolerances on printed directional-coupler circuit parameters 15 p1850 A73-31498

Russian book - Design and calculation of microwave stripline elements. 15 p1852 A73-32295

Determination of the geometrical dimensions of a bandpass filter for a microwave hybrid integrated circuit 17 p2134 A73-34584

Design of second-order phase circuits constructed with TEM-line segments 17 p2144 A73-34592

Application of distributed p-n and p-i-n structures in the development of integrated circuits for electrically controlled SHF devices 20 p2535 A73-38856

Surface strip coplanar waveguide characteristic impedance measurement as function of aspect ratio and substrate thickness 20 p2538 A73-39595

Microstrip junction circulators with fixed ferrite disks, achieving broadband impedance matching between center conductor and transmission line by transformer on alumina substrate 20 p2538 A73-39668

Physical modeling of active microcircuits for the SHF range 21 p2668 A73-40020

Russian book on wideband microwave oscillatory systems covering stepwise and smoothly irregular stripline and coaxial line resonators for radio receivers, multipliers, etc 22 p2832 A73-41881

Two dimensional microstrip transmission line with step discontinuities, predicting microwave filtering behavior by broadband equivalent circuit for comparison with experiment 22 p2835 A73-42465

Hybrid numerical solution to electromagnetic wave scattering and diffraction with application to microstrip transmission lines, echelette gratings and dielectric step discontinuities in waveguides 22 p2828 A73-42844

Damping in a strip waveguide with a central conductor composed of two equipotential strips 23 p2959 A73-43517

Slot microwave transmission line with thick metal coating on dielectric substrate, calculating phase constant variation with frequency, slot width and coating thickness 23 p2954 A73-44069

TEM-TE coupled transmission line model for microstrip, calculating frequency-dependent wave dispersion curves for comparison with experiment 23 p2964 A73-44073

Microwave transistor oscillators design based on Si overlay transistors and microstrip transmission lines as passive elements, obtaining negative resistance between collector-base terminals 23 p2961 A73-44144

Electronically tunable microwave bandpass filters 24 p3071 A73-44606

Extension of Kirchhoff's theory to coupled strip lines - Application to the calculation of band line couplers 24 p3068 A73-44975

Parameter evaluation method for lossy strip transmission lines, assuming microwave propagation in waveguide system with dielectric between two conducting plates 24 p3074 A73-45007

STROBOSCOPES

Stroboscope-like frequency spectrum examination of short impulses. 03 p0308 A73-13570

Daytime and nighttime stereophotogrammetric photography of moving object using stroboscopic effect, noting pulsed light sources for fast moving near objects 05 p0575 A73-16314

A triple-exposure technique to reduce recording time in stroboscopic holographic interferometry. 05 p0576 A73-16557

Tilt discrimination and motion aftereffect independence of flicker rate of stroboscopically illuminated contours visual stimuli 06 p0660 A73-18624

Stroboscopic investigation of the effect of standing acoustic waves on turbulent flames 07 p0920 A73-19992

Visualization of pulsed ultrasound using stroboscopic photoelasticity. 08 p0973 A73-21078

Apparent motion of stimuli presented stroboscopically during pursuit movement of the eye. 13 p1577 A73-28093

Solid state Digital Slip Sync Strobe/Camera Control System design for powered wind tunnel helicopter models testing 17 p2101 A73-34622

A direct approach to reduce recording time in stroboscopic holographic interferometry. 19 p2429 A73-37541

An automatic sweep generator for a strobed oscilloscope 21 p2664 A73-41098

Photographic laboratory studies of explosions. 21 p2706 A73-41553

STRONTIUM

NT STRONTIUM ISOTOPES

NT STRONTIUM 90

Lunar highlands soil analysis from Luna 20 and Apollo 16 samples, estimating lunar crust differentiation process age from Rb-Sr concentrations 05 p0618 A73-16833

Violet and UV laser transitions in Ca II and Sr II resulting from impact radiation recombination of doubly charged metal ions 21 p2712 A73-40358

STRONTIUM COMPOUNDS

NT STRONTIUM FLUORIDES

Molecular beam study on BaO and SrO formation for clarifying interaction of metal-vapors with upper atmosphere oxygen. 07 p0818 A73-19668

Optical centers of Nd³⁺/+ in calcium and strontium fluorophosphate crystals 07 p0836 A73-20204

Resistance anomaly in semiconductor barium and strontium niobates 17 p2219 A73-35554

STRONTIUM FLUORIDES

Spectroscopy of optical centers of Nd³⁺/+ in CaF₂ and SrF₂ crystals 07 p0836 A73-20203

Investigation of the lasing and luminescent properties of fluorite and strontium fluoride crystals containing bivalent dysprosium impurities 07 p0837 A73-20207

STRONTIUM ISOTOPES

NT STRONTIUM 90

Rb-87/Sr-87 'ages' of the soil and rock fragments brought back from the lunar mountains by the automatic probe Luna 20/Apollonius crater region/ 05 p0546 A73-16830

Genetic significance of chemical, isotopic, and petrographic features of some peralkaline salic rocks from the island of Pantelleria. 05 p0570 A73-16842

A search for the solar Sr-87 content and the solar Rb/Sr ratio. 05 p0620 A73-17027

Rb-Sr ages and initial strontium in basalts from Apollo 15. 08 p0936 A73-20839

Lunar Rb-Sr age correction according to stable isotope tracer (spike) recalibration, using stoichiometric salts 10 p1278 A73-24112

Rb-87 - Sr-87 age of fragments and soils from the lunar Sea of Fertility. 21 p2770 A73-41005

Chondrites - Initial strontium-87/strontium-86 ratios and the early history of the solar system. 24 p3137 A73-44688

STRONTIUM 90

Direct nuclear-to-electric power conversion based on Sr 90 electron emission and collection system, noting spacecraft applications 09 p1119 A73-22828

Comparison of strontium-90 and plutonium-238 milliwatt thermoelectric generators. 09 p1037 A73-23277

STROUHAL NUMBER

Strouhal number and flat plate oscillation in an air stream. 21 p2782 A73-40125

Vortex shedding from and base pressure distribution on bluff body measured in shear or uniform flow, calculating Strouhal number 23 p2940 A73-43939

Study of the field of fluctuating pressures at the surface of a circular cylinder 24 p3079 A73-45220

STRUCTURAL ANALYSIS

NT BERNSTEIN ENERGY PRINCIPLE

NT DYNAMIC STRUCTURAL ANALYSIS

NT ENERGY METHODS

NT EQUILIBRIUM METHODS

NT FLUTTER ANALYSIS

NT MATRIX METHODS

NT STRAIN ENERGY METHODS

Load carrying capacity of ceramic spherical shells under external pressure

01 p0114 A73-10481

A certain case of stress-concentration analysis by an elastostatic method

01 p0114 A73-10574

Elastic-plastic analysis on the structural elements with different values of stress concentration factor.

01 p0117 A73-11122

Lifetime of Dural structural elements operating in aggressive media

02 p0180 A73-11794

Curvilinear coordinates for deformation tensor and stress analysis of structures, using finite element method

02 p0231 A73-11812

Elastic deformation of lightweight mirrors.

02 p0236 A73-12375

Digital simulation of random processes and its applications.

02 p0144 A73-12607

Material and structural studies of metal and polymer matrix composites.

02 p0182 A73-12621

Elasto-plastic analysis of three-dimensional structures using the isoparametric element.

03 p0383 A73-12874

A reliability approach to the fatigue of structures.

03 p0387 A73-13234

Southeastern Conference on Theoretical and Applied Mechanics, 6th, University of South Florida, Tampa, Fla., March 23, 24, 1972, Proceedings.

03 p0388 A73-13301

Finite element analysis of thick, thin and sandwich plates, considering quadrilateral elements with allowance for transverse shear effect

03 p0390 A73-13344

Computers and the analysis of pressure vessels.

03 p0391 A73-13678

Computer method for analysis of multistory structures.

03 p0391 A73-13683

The analysis of nonlinear three dimensional frames.

03 p0391 A73-13684

Computation and solution procedures for nonlinear analysis by combined finite element-finite difference methods.

03 p0391 A73-13685

A theoretical and numerical comparison of elastic nonlinear finite element methods.

03 p0392 A73-13689

Computerized multiple level substructuring analysis.

03 p0392 A73-13690

Selective reinforcement of wing structure for flutter prevention.

03 p0392 A73-13705

Application of finite-element methods to lubrication - An engineering approach.

[ASME PAPER 72-LUB-N] 03 p0315 A73-14353

Minimum potential principles application to elastic-plastic analysis of nonhardening materials, using quadratic programming

04 p0509 A73-14948

Limit analysis of structures with stochastic strength variations.

04 p0510 A73-15027

Use of Green's function in the study of the natural oscillations of two-dimensional structures

04 p0511 A73-15087

Structural comparison of articulated plane kinematic chains (PKC) with the aid of graph theory

04 p0476 A73-15656

Russian book - Strength of viscoelastic materials relative to solid-propellant rocket-motor charges.

04 p0517 A73-15967

Classical and nonlinear buckling analyses of spherical sandwich shells.

05 p0631 A73-16121

Finite element limit analysis using linear programming.

05 p0631 A73-16124

Book - Non-linear structures: Matrix methods of analysis and design by computers.

05 p0632 A73-16358

Effect of additive damping on transfer function characteristics of structures.

[SAE PAPER 720811] 05 p0634 A73-16641

Modal damping predictions using substructure test-

[SAE PAPER 720810] 05 p0634 A73-16643

The determination of free-body responses of a structure from constrained test data.

[AIAA PAPER 73-191] 05 p0635 A73-16928

Finite element analysis of the post-buckling behavior of structures.

[AIAA PAPER 73-255] 05 p0635 A73-16977

Methods of birefringence-parameter determination in tension studies by photoelasticity techniques

05 p0635 A73-17077

Numerical difficulties and accuracy losses avoidance methods for ill conditioned stiffness matrices encountered in complex structural analyses

05 p0636 A73-17113

Load-time dependent relaxation of residual stresses.

05 p0636 A73-17214

Limit analysis of plates with piecewise linear yield surface.

06 p0758 A73-17398

Analysis of noncircular cylindrical shells.

06 p0758 A73-17446

Indirect structural analysis by finite element method.

06 p0758 A73-17447

Geometric nonlinearity effects on rigid joint deformation of three dimensional skeletal structures, including roofing, cable and shallow dome systems

06 p0762 A73-18342

Derivation of the linear shell theory from the theory of Cosserat medium.

06 p0763 A73-18454

Workshop on the Application of Variational Methods to the Calculation of Structures, Senlis, Oise, France, June 19-21, 1972, Proceedings. Numbers 1, 2, 3, 4 & 5

06 p0765 A73-18721

Differential operators transformation into integral functions by Green function and distributions theory methods in structural analysis

06 p0719 A73-18727

Comparison between sparse stiffness matrix and sub-structure methods.

07 p0907 A73-19031

A theoretical and experimental investigation of torsional-flexural buckling in thin-walled prismatic members.

07 p0912 A73-19366

Finite-element analysis of shells of revolution by two doubly curved quadrilateral elements.

07 p0912 A73-19368

Stress functions for the 'second' plane problem of micropolar elasticity.

07 p0914 A73-20198

Computerized static and dynamic structural analysis, discussing modeling, programs, input preparation, solution algorithms, numerical errors, output interpretation and applications

07 p0914 A73-20209

Numerical analysis of anisotropic rotational shells subjected to nonsymmetric loads.

07 p0914 A73-20210

Finite element analysis of buckling and post-buckling behaviors of arches with geometric imperfections.

07 p0914 A73-20211

Some results of finite element applications in finite elasticity.

07 p0914 A73-20213

Approximations for large deflection of a cantilever beam.

07 p0915 A73-20339

Structural service life from carrying capacity during rupturing stage, noting microstructural properties effect

07 p0917 A73-20504

Large deflexion, geometrically non-linear finite element analysis of circular arches.

08 p1015 A73-20670

Elastoplastic analysis by matrix displacement or finite element method, presenting various direct and iterative solution techniques

08 p1016 A73-20776

Corner supported equilateral triangular plates.

08 p1016 A73-20827

Thermoelastic bending theory based on structural analysis of multilayer reinforced shells and plates

08 p1017 A73-21373

On one-dimensional finite-strain beam theory - The plane problem.

08 p1018 A73-21405

Anisotropic membrane shells with, if necessary, uniform strength

08 p1018 A73-21407

Stressed state of an isotropic elliptical plate weakened by elliptical holes

08 p1020 A73-21767

Bending of an orthotropic prismatic beam by a transverse force in a geometrically nonlinear formulation

08 p1020 A73-21769

Book - Aircraft structures for engineering students.

08 p1020 A73-21839

Ultrasonic structure analyzer for nondestructive inspection of fine grained metallic materials

09 p1080 A73-22298

Stacked membrane elements for plate and shell analysis, noting spurious shear components suppression

09 p1159 A73-22401

Using fracture mechanics with aluminum alloy structures.

09 p1103 A73-22494

Computerized two dimensional boundary value problem solutions for bounded multiply connected structural regions with periodic inclusions, using three step R-functions and Rvachev method

09 p1120 A73-22586

Design of rotating discs of irregular outline.

09 p1161 A73-230515

Experimental study of the damping of bending vibrations in supported square plates with coatings.

09 p1161 A73-231535

Alternating method with combined analytical and numerical calculations for two dimensional edge and three dimensional surface crack problems

09 p1162 A73-231815

Sounding rocket vehicles aeroelastic structural analysis, calculating structural flexibility, dynamic pressure and angle of attack effects on aerodynamic stability

09 p1155 A73-232004

[AIAA PAPER 73-284] Book - Structural analysis of shells.

09 p1164 A73-23271

Finite element analysis of curved structures discussing shape functions generation method for convergence determination

09 p1165 A73-234304

Numerical solution of some boundary value problems for an isotropic cylindrical shell

10 p1288 A73-240664

On the normality and accuracy of simulated random processes.

10 p1292 A73-243955

A photoelastic and finite-element investigation of a nonsymmetrical plug-hatch configuration.

10 p1293 A73-247211

Some finite extremum principles in piecewise linear elasto-plasticity.

11 p1434 A73-252155

Finite element method for structural analysis, discussing theory for isoparametric stress quadrilateral plate bending elements with curved boundaries

11 p1435 A73-254377

Russian papers on thermal stresses investigation in machine and structural elements covering stress simulation and strain gage methods for model and full scale structures

11 p1435 A73-254511

Taylor series algorithms for computerized structural design and reanalysis of modified structures, applying to aircraft fuselage midsection

11 p1436 A73-25478

Applications of solid mechanics; Proceedings of the Symposium, University of Waterloo, Waterloo, Ontario, Canada, June 26, 27, 1972.

11 p1442 A73-25842

Partitioning techniques for solving large systems of equations in structural analysis.

11 p1442 A73-25844

Approximate dependences for the vibration frequencies of smooth cylindrical shells and for ones with concentrated inclusions

12 p1555 A73-27789

Integrated force method for discrete structural analysis, discussing analogy with continuous problem Beltrami-Michell formulation and applications to pin and rigid connected frames

13 p1691 A73-28082

High speed computing of elastic structures; Proceedings of the Symposium, Universite de Liege, Liege, Belgium, August 23-28, 1970. Volumes 1 & 2.

13 p1692 A73-28226

The convergence theorems and their role in the theory of structures.

13 p1692 A73-28227

Analysis of finite deformations of elastic solids by the finite element method.

13 p1692 A73-28229

Finite element method analysis of thin shells, discussing reference surface geometry and membrane and bending theory

13 p1693 A73-28234

Triangular elements descriptive of sandwich panels for finite element analysis of symmetric panels, comparing numerical solutions to experimental data and analytical results

13 p1693 A73-28238

Automatic mesh generation in two and three dimensional inter-connected domains.

13 p1693 A73-28242

Automatic system for kinematic analysis /ASKA/ computer programs for structural finite element solution, discussing design concepts, element types, user interface and computation time

13 p1693 A73-28243

Response time in the application of interactive graphics in structural analysis.

13 p1693 A73-28244

Computer graphics applied to production structural analysis.

13 p1693 A73-28245

An evaluation of finite difference and finite element techniques for analysis of general shells.

13 p1694 A73-28256

Plane strain slip line theory for anisotropic rigid/plastic materials.

13 p1697 A73-28793

Effect of out-of-planeness of membrane quadrilateral finite elements.

13 p1697 A73-28818

Advanced elastic postbuckling analysis by a perturbation procedure.

13 p1697 A73-28826

- A variant of the moment theory of elasticity for a one-dimensional continuous medium with a non-homogeneous periodic structure 13 p1698 A73-29085
- Analytical elasticity methods for airfield pavement structural stress-strain, failure and reliability performance evaluation 13 p1598 A73-29106
- Application of fracture mechanics to the analysis of statically indeterminate structure. 13 p1700 A73-29466
- Structural analysis via thermoplastic scale model testing with resistance strain gages, considering temperature and humidity effects on measurement accuracy and reliability 14 p1750 A73-29701
- Ritz method application to structural eigenvalue problems, considering plate buckling in box beams 14 p1805 A73-29741
- Advances in computational methods in structural mechanics and design; Proceedings of the Second U.S.-Japan Seminar, Berkeley, Calif., August 1972. 14 p1806 A73-30176
- Finite element models for continuum structural analysis, considering variational principles, element base functions and general purpose computer program 14 p1807 A73-30183
- Finite element static structural analysis for small elastoplastic strains and geometric nonlinearities, considering total Lagrangian and incremental moving coordinate formulations 14 p1807 A73-30189
- Incremental formulation for problems with geometric and material nonlinearities. 14 p1808 A73-30190
- Nonlinear thermal elastoplastic structural analysis, using principle of virtual work in finite element method 14 p1808 A73-30192
- Incremental solution procedures for finite element nonlinear structural analysis, considering combined material and geometric nonlinearities 14 p1808 A73-30193
- Perturbation method in the analysis of geometrically nonlinear and stability problems. 14 p1808 A73-30196
- Finite element analysis programs for general applications, considering state of art 14 p1808 A73-30197
- NASTRAN digital computer program for static and dynamic structural analysis by finite element method, including nonlinear static and dynamic response 14 p1808 A73-30198
- Steel structures analysis based on cubic interpolating functions with parameters of nodal displacements, discussing method extension to natural vibration 14 p1809 A73-30199
- Finite element analysis of sweptback wing structures based on beam theory, presenting low aspect ratio models 14 p1809 A73-30201
- Load-bearing capacity of ceramic spherical shells under external pressure. 14 p1810 A73-30306
- Stress determination approximation in structural mechanics problems by linear first order differential equations reduction to linear algebraic equations 14 p1810 A73-30378
- Structural requirements for decoupling, disturbance insensitivity and parametric insensitivity, considering synthesis procedures for multivariable dynamic regulators 14 p1739 A73-30779
- Equilibrium equations for static computations of symmetrical plates with large number of rods, point supports or holes 14 p1815 A73-30814
- Designs of statically undeterminable elastoplastic systems under complex loads 15 p1946 A73-31141
- Mass and stiffness matrices reduction in determining linearly elastic structure natural modes and frequencies with computational accuracy improvement 15 p1949 A73-31672
- Locally modified and unmodified structures eigenvalues and eigenvectors solutions, considering computational accuracy improvement and application to dynamic stiffness matrix equation 15 p1951 A73-32035
- Bonded structural connections analysis by finite element method, presenting stress distribution in adhesive 15 p1952 A73-32038
- Structural components shape optimization for stress concentration reduction, solving complex boundary value problem via conformal transformation to curvilinear coordinates 15 p1954 A73-32108
- An approach to the analysis of boundary value problems in the theory of functions and two-dimensional problems in the theory of elasticity 15 p1954 A73-32124
- Blocking procedure for large scale structural analysis in conjunction with plane truss using stiffness matrix method, considering computer subroutines in finite element method 16 p1985 A73-32793
- Variational methods applied to nonconservative stability problems of elastic continua. 16 p2078 A73-32995
- Mathematical programming methods in structural analysis. 16 p2078 A73-33001
- Classical and natural conduction and deformation modes concepts for axisymmetric variational problems. 16 p2079 A73-33007
- Modified finite difference procedures for structural mechanics, discussing interior and boundary discretization errors and accuracy improvement 16 p2079 A73-33012
- Matrix analysis of multilayered and sandwich shells by the finite element method 16 p2083 A73-33968
- Lagrangian formulation of sandwich shell theory. 17 p2242 A73-34526
- Estimation of the response of a mechanical structure to arbitrary excitation 17 p2243 A73-34649
- Theory of conjugate projections in finite element analysis. 17 p2201 A73-34828
- Linear structure theory from analysis of structural mechanical models, proposing three dimensional model for behavior of granular materials 17 p2245 A73-34832
- Isoparametric element forms in finite element analysis. 17 p2245 A73-34834
- Finite element method application to solution of structural dynamics problems, considering equations of motion and vibration mode shapes 17 p2245 A73-34836
- The integration of NASTRAN into helicopter airframe design/analysis. [AHS PREPRINT 780] 17 p2106 A73-35093
- The application of interactive graphics to the numerical methods used in structural analysis. 17 p2250 A73-35314
- Book - Computer methods in structural analysis. 17 p2251 A73-35473
- NASA airframe structures program, discussing automated analysis and design, advanced composites, supersonic and hypersonic vehicles technology, active controls, aircraft loads and aeroelasticity prediction methods 18 p2362 A73-36168
- National Symposium on Computerized Structural Analysis and Design, George Washington University, Washington, D.C., March 27-29, 1972, Proceedings. 19 p2496 A73-37476
- Applications of a symbolic algebra manipulation language for composite structures analysis 19 p2496 A73-37482
- A version of the couple stress theory of elasticity for a one-dimensional continuous medium with inhomogeneous periodic structure. 19 p2498 A73-37635
- Structural service life from carrying capacity during rupturing stage, noting microstructural properties effect 19 p2499 A73-37779
- Some aspects of the approximation of functions of many variables, and effective direct methods for solving problems in elasticity theory 20 p2618 A73-39326
- Mixed finite-difference scheme for a class of linear and nonlinear structural mechanics problems. 20 p2621 A73-39544
- Probabilistic and deterministic solutions of random vibration response problems. 21 p2783 A73-40294
- The problem of structural analysis of a wave gear 21 p2708 A73-41198
- Finite element program for flight structure analysis. 22 p2917 A73-41739
- Applications of the compliance concept in fracture mechanics. 22 p2920 A73-42154
- Study of the existence of compact laminar for certain complex analytical laminated structures 23 p2999 A73-44097
- Computerized structural analysis by finite element method, discussing round-off and truncation errors with emphasis on inherited error effects minimization 24 p3150 A73-45233
- Structural analysis for idealized nonlinear material behavior. 24 p3152 A73-45316
- STRUCTURAL BASINS**
Some observations on the cenozoic volcano-tectonic evolution of the Great Basin, western United States. 05 p0570 A73-16841
- Comparison of Martian and lunar multiringed circular basins. 19 p2477 A73-37206
- STRUCTURAL BEAMS**
U BEAMS (SUPPORTS)
- STRUCTURAL DESIGN**
NT PRESSURE VESSEL DESIGN
Shell designs by the theory of small elastoplastic deformations with allowance for the compressibility of material 01 p0112 A73-10005
- Dynamic programming and a max-min problem in the theory of structures. 01 p0019 A73-10199
- Support method and equipment for observer at Cassegrain focus of large telescopes, emphasizing universal chair structural details and operation principles 01 p0029 A73-10545
- A note on optimality conditions for trusses with a zero minimum cross-section. 01 p0115 A73-10766
- Grillages of maximum strength and maximum stiffness. 01 p0115 A73-10767
- Some exact solutions in the design of technically orthotropic axisymmetric plates. 01 p0118 A73-11365
- Application of the method of forces to the statics of composite systems 02 p0229 A73-11639
- Technological and structural design ensuring optimum clearance and aerodynamic coupling of moving units /wing-aileron or aileron-trim tab/ 02 p0129 A73-11648
- Helios solar probe structural adapter design for linking to booster rocket end stage, investigating orthotropic cylindrical shell carrying capacity [DGLR PAPER 72-101] 02 p0227 A73-11685
- Design of a shallow shell with a large rectangular hole 02 p0231 A73-11803
- Calculus of variations and finite difference method for equilibrium equations in axisymmetric plastic shell design 02 p0232 A73-11821
- Book on functional pavements design covering support condition, quality control and construction tolerance, environmental and landing gear effects, mathematical models, etc 02 p0150 A73-11879
- Structural design via finite element method, noting object discretization, displacement forms and nonlinear problems of deformable body mechanics 02 p0233 A73-11936
- Structural and thermal design and fabrication of Lunokhod retroreflecting panel mounted on lunar surface for earth-moon distance determination by laser telemetry 02 p0176 A73-12251
- Design, development, fabrication and qualification load testing of high modulus graphite-epoxy reflector support truss for ATS F and G 03 p0330 A73-13021
- Hypersonic flight vehicles aerodynamic heating, structural design and materials and propulsion problems, discussing research work and facilities 03 p0242 A73-13055
- On optimal design of prestressed elastic structures. 03 p0384 A73-13119
- A computational method for optimal structural design. I - Piecewise uniform structures. 03 p0390 A73-13337
- Monte Carlo solution of structural dynamics. 03 p0391 A73-13681
- Speed brake in carbon fibre composite construction. 03 p0393 A73-13920
- The design and development of fracture resistant structures. 04 p0507 A73-14712
- The relationship between design allowables and load induced micromechanical damage in composite materials. 04 p0508 A73-14719
- Toward reliable composites - An examination of design methodology. 04 p0508 A73-14720
- Structural reliability definition and determination in terms of survival probability concept, discussing analytical errors effect on design and applications to aerospace vehicles 04 p0508 A73-14724
- Minimum weight design of plastic and elastic grillages and fiber reinforced plates of given strength or stiffness, presenting optimal solutions for various boundary conditions 04 p0509 A73-15011
- Constrained optimal design of columns against buckling. 04 p0510 A73-15029
- Minimum-weight plastic design of continuous beams subjected to one single movable load. 04 p0510 A73-15030
- Monograph on structural element and structures reliability covering structural design, failure analysis and reinforced element collapse under moment and force loads 04 p0472 A73-15694
- Design criteria for structural elements subjected to stationary random loads. [ASME PAPER 72-WA/DE-19] 04 p0514 A73-15837

Book - Non-linear structures: Matrix methods of analysis and design by computers. 05 p0632 A73-16358

Weight sensitivity of a space shuttle orbiter to thermal structural combined loads design criteria. [AIAA PAPER 73-257] 05 p0635 A73-16979

Probabilistic minimum weight limit design of one dimensional pin jointed structures with random continuous variables, using stochastic programming 06 p0757 A73-17397

The effects of various parameters on an aeroelastic optimization problem. 06 p0758 A73-17565

NASA airframes structures program, discussing automated design, composites, supersonic and hypersonic technologies, control systems, load and aeroelasticity prediction and integrity concepts [AIAA PAPER 73-17] 06 p0759 A73-17610

Structural design of future commercial transports. [AIAA PAPER 73-20] 06 p0759 A73-17613

Structural design with allowance for shakedown in the case of temperature-dependent elastic constants 06 p0760 A73-17780

Constrained optimal design of circular plates against buckling. 06 p0762 A73-18338

Limit design in the absence of a given layout - A finite element, zero-one programming approach. 06 p0762 A73-18340

A unified formulation of the theory of optimal plastic design with convex cost function. 06 p0763 A73-18343

Space deployed expandable structures, discussing vehicular and environmental constraint effects on design, large structure requirements, and applications 07 p0828 A73-18905

Highly-rigid sandwich structures for interstages. 07 p0906 A73-18994

Power series method for accurate solution of eigenvalue problems and simultaneous equations representing static, dynamic and stability responses to structural design parameter changes 07 p0906 A73-19027

Multiparameter optimal design of plates and shells. 07 p0912 A73-19367

Thin walled beam composed indeterminate elastic framed structures minimum weight design, obtaining solutions by nonlinear programming algorithm 07 p0912 A73-19951

Piecewise linear approximation of thin walled rib and diaphragm reinforced conical beams under thermal field and axial loads, using limit stress-strain diagrams 07 p0913 A73-20096

Approximate solutions to some static and dynamic optimal structural design problems. 07 p0915 A73-20341

Optimization in construction of the Jaguar and other military aircraft. 08 p0928 A73-20947

Optimized design - Characteristic vibration shapes and resonators. 08 p1017 A73-21191

Elastic stiffness properties and structural designs of fiber composite materials, including laminate and plate problems 09 p1110 A73-22516

Fatigue life prediction and design optimization for solar cell interconnectors based on elastoplastic material stress distribution calculation by finite element methods 09 p1036 A73-22809

Weight minimization constrained design of rotational shallow spherical shells, comparing simplex and variable metric methods 09 p1165 A73-23446

Polyester fiber/glass fiber composite sandwich structural design, considering thickness loss during abrasion test, physical properties and flexural strength 10 p1237 A73-23954

Fiber reinforced composite design and application within performance and cost parameters, considering composite structure cost reduction and functional redesign increase 10 p1238 A73-23968

Structural design for weight or volume minimization in deformable body under combined loads, comparing structures with different boundary configurations 10 p1226 A73-24791

Structural design errors resulting from conventional treatment of distribution law for local radial and torque loads 11 p1433 A73-25028

Design of lowest-cost prestressed combined metallic systems 11 p1371 A73-25035

Aircraft design philosophies and structural integrity considerations for reliability without major NDT and maintenance, proposing research program for future computerized design 11 p1433 A73-25128

Design and manufacture of structure components made of fiber-reinforced materials 11 p1373 A73-25417

Automated structural synthesis using a reduced number of design coordinates. 11 p1436 A73-25476 [AIAA PAPER 73-336]

A unified approach to the problem of optimization in the design of structures. 11 p1436 A73-25477 [AIAA PAPER 73-337]

Structure statistical identification method based on experimental measurements of natural frequencies and mode shapes to modify finite element model structural parameters [AIAA PAPER 73-339] 11 p1436 A73-25479

Mathematical programming optimization procedure applicable to minimum weight structural design, considering static stress and displacement constraints under alternative loading conditions [AIAA PAPER 73-341] 11 p1436 A73-25480

Optimum design of stressed skin structures using a sequence of linear programs method. 11 p1436 A73-25481 [AIAA PAPER 73-342]

Linear programming and gradient search algorithms for minimum weight design of finite element structures, applying to bar truss problems [AIAA PAPER 73-343] 11 p1436 A73-25482

Mathematical programming techniques of dimensionless index solutions for optimal structural design by iterative search on computer, applying to beam column steel structures [AIAA PAPER 73-344] 11 p1436 A73-25483

Computer programs for structural design optimization, discussing automated structural optimization program [ASOP], component display analysis and stiffened panel programs [AIAA PAPER 73-345] 11 p1436 A73-25484

Synthesis of compression panels having non-uniform stiffener sections. 11 p1437 A73-25485 [AIAA PAPER 73-347]

A synthesis procedure for mechanically fastened joints in advanced composite materials. 11 p1437 A73-25486 [AIAA PAPER 73-348]

Computerized design of an outer planets spacecraft structure to survive the meteoroid environment. 11 p1430 A73-25487 [AIAA PAPER 73-349]

Optimization studies in the support design for the Large Space Telescope. 11 p1437 A73-25488 [AIAA PAPER 73-350]

Computer design of antenna reflectors. 11 p1437 A73-25489 [AIAA PAPER 73-351]

Application of computer-aided aircraft design in a multidisciplinary environment. 11 p1304 A73-25490 [AIAA PAPER 73-353]

High modulus composites versus beryllium for achieving stiffness in spacecraft structural applications. 11 p1430 A73-25513 [AIAA PAPER 73-384]

Numerical procedure for determining optimal member sizes of aircraft structural components with weight minimization and flutter speed lower bound [AIAA PAPER 73-391] 11 p1439 A73-25520

Automating the design process - Progress, problems, prospects, potential. 11 p1373 A73-25538 [AIAA PAPER 73-410]

Iliushin 62 aircraft horizontal stabilizer structural design and control, discussing mounting hardware and electrically driven servomechanism 11 p1305 A73-25795

Corrosion fatigue considerations in engineering materials selection and design, discussing alleviation and control 11 p1442 A73-25802

Application of some aspects of low-cycle fatigue research in structural design. 11 p1443 A73-25846

Statistical method for fiber-reinforced plate design optimization for important boundary conditions, noting topographies associated with piecewise linear specific cost functions 11 p1443 A73-26092

Optimization of aircraft structures with multiple stiffness requirements. 11 p1444 A73-26298

Minimum-mass design of multielement structures under a frequency constraint. 11 p1444 A73-26380

Wave devices built with ferromagnetic and electrically conducting film strips 12 p1460 A73-26772

Computer technology aided machine design automation and structural synthesis by coded information table formulation and conversion, discussing algorithm construction 12 p1502 A73-26784

Pseudoelastic design method for bottle-crest stack instability performance prediction through failure by creep buckling, assessing effectiveness by comparison with measurements 12 p1514 A73-26876

Glass fiber reinforced polyester laminates mechanical properties evaluation for structural design, considering failure criteria in terms of fiber debonding and resin and gel coat cracking 12 p1515 A73-26877

Light motorized glider-type aircraft design, development and flight testing, discussing aerodynamic configuration, structural design and performance characteristics 12 p1459 A73-27732

Optimum design of composite shells subject to natural frequency constraints. 12 p1554 A73-27734

Design optimization of prestressed concrete spans for high speed ground transportation. 12 p1554 A73-27735

Design of an infinite beam with an elastic base in a nonclassical formulation 12 p1555 A73-27796

Russian book - Design of structural elements with the use of electronic digital computers. 12 p1556 A73-27923

Lift and drag at off-design Mach numbers of conically cambered wings with subsonic leading edges and supersonic trailing edge 12 p1458 A73-27927

Computer graphics applied to production structural analysis. 13 p1693 A73-28245

Application of Pontryagin's maximum principle for minimum weight design of rigid-plastic circular plates. 13 p1696 A73-28754

Influence of the variation of cascade geometry on the performance in axial flow machinery. 13 p1565 A73-29007

Calculation and design of highly stressed fiberglass-reinforced plastic components 13 p1703 A73-29653

The optimization of the supporting structures of parabolic antennas 14 p1740 A73-29742

On the optimal design of statically indeterminate elastic structures subjected to multiple loading systems and multiple constraints. 14 p1805 A73-29760

Advances in computational methods in structural mechanics and design; Proceedings of the Second U.S.-Japan Seminar, Berkeley, Calif., August 1972. 14 p1806 A73-30176

Engineering structures design, discussing stress and strain distributions, mechanical defects, symmetric loading and fracture models [ASME PAPER 73-DE-19] 14 p1815 A73-30820

Fracture mechanics approach to fatigue analysis in design. [ASME PAPER 73-DE-22] 14 p1763 A73-30823

Use of the surface of influence of the clamping couple on a circular plate for design calculation under an asymmetrical load 15 p1944 A73-30974

Choice of the geometrical parameters, R, r, and ρ , of a roller-ring mechanism as a function of maximum load capacity 15 p1832 A73-31277

Parameters of rational airfield pavement design system. [ASCE PREPRINT 1700] 15 p1855 A73-31386

Russian book - Strength of turbine wheels. 15 p1948 A73-31578

Design of stiffened cylinders to resist axial compression. 15 p1950 A73-31921

Automatic nodal point renumbering algorithm for interconnectivity matrix bandwidth reduction in computer aided structural analysis and design 15 p1848 A73-32029

A method for complex design of axial-flow compressor stages at the mean streamline 15 p1925 A73-32203

Optimal structural design of elastic rotating disks by dynamic programming 16 p2079 A73-33009

Glass fabric structures, properties and designs of reinforced polyester and epoxy laminates for aerospace applications 16 p2030 A73-33064

Pressurized fuselage design studies for short haul transport aircraft, discussing sandwich structures and bonding techniques for Al and Ti alloy construction materials 16 p2018 A73-33069

A designer's approach to the fatigue failure mechanism. 16 p2081 A73-33644

Dual extremum principles relating to optimum beam design. 16 p2081 A73-33748

Mechanical faster types, design considerations and economic factors, detailing nut and bolt joint assembly design, static and dynamic loads and production engineering 16 p2021 A73-33862

Iterative finite element method for minimum weight structural design with respect to buckling constraints applied to beam and orthogonal frame design 16 p2082 A73-33908

Brazed honeycomb structure design, fabrication and aerospace applications covering brazing methods, filler metal selection, nondestructive testing, sandwich designs, aircraft and spacecraft structures, etc 17 p2177 A73-34100

Book - Optimum structural design: Theory and applications. 17 p2242 A73-34350

Development of airframe design technology for crashworthiness. 17 p2101 A73-34677 [SAE PAPER 730319]

Interdisciplinary communications problems of metal physicists, fracture mechanists, structural designers and reliability analysts for fatigue crack generation and growth 17 p2246 A73-34886

Exploratory development of composite missile fuselages. 17 p2181 A73-35354

Commercial transport aircraft structural design and technology advances, discussing materials and fabrication processes with respect to costs, durability and reliability 18 p2266 A73-36166

Structural design and technology developments for SST and STOL aircraft, discussing computerized and damage tolerant design, composite materials and cost reducing manufacturing techniques 18 p2362 A73-36167

NASA airframe structures program, discussing automated analysis and design, advanced composites, supersonic and hypersonic vehicles technology, active controls, aircraft loads and aeroelasticity prediction methods 18 p2362 A73-36168

Optimal plastic design for partially preassigned strength distribution. 18 p2365 A73-36638

Book - Theory and design of shells on the basis of asymptotic analysis: A unifying approach to the variety of thick and thin elastic shell theories and problems. 18 p2367 A73-36967

Straightforward design of a three-layer cylindrical shell 19 p2494 A73-37183

Design for teaching aerospace engineering at Texas A & M University. 19 p2505 A73-37456 [AIAA PAPER 73-786]

National Symposium on Computerized Structural Analysis and Design, George Washington University, Washington, D.C., March 27-29, 1972, Proceedings. 19 p2496 A73-37476

Algorithm for optimal material selection by seeking tradeoff between conflicting multifunctional structural design objectives 19 p2496 A73-37477

Structural optimization by methods of feasible directions. 19 p2496 A73-37478

Matrix formulation of reliability analysis and reliability-based design. 19 p2496 A73-37479

Automated structural design and analysis of advanced composite wing models. 19 p2497 A73-37486

Applications Technology Satellite F aluminum-ammonia heat pipes design, fabrication and life and thermal vacuum testing [ASME PAPER 73-ENAS-46] 19 p2493 A73-37993

Monograph on optimal structure design by linear programming and calculus of variations covering pin jointed frameworks, beams, circular sandwich plates, Michell continua, etc 19 p2502 A73-38364

Composite fabrication and structural design for commercial aircraft, discussing graphite post installation and testing and pultrusion and autoclave molding processes [SME PAPER EM 73-717] 19 p2436 A73-38497

Shock spectrum analysis and structural design. 20 p2617 A73-39270

Sandwich plates minimum volume design for elliptic, triangular and annular structures, discussing Mises criterion and bending coordinates 20 p2623 A73-39559

Optimum design of three-layer shells 20 p2625 A73-39655

Powder geometry and structural design of the high volumetric efficiency tantalum electrolytic capacitor. 21 p2663 A73-40770

Optimum tapering design of vibrating cantilever beams, considering geometrically similar and rectangular cross sections and degenerated end mass case 21 p2785 A73-40839

Optimal design of linearly elastic vibrating structural members for minimized total mass and maximized fundamental frequency respectively, noting solution existence dependence on boundary conditions 21 p2785 A73-40840

Risk analysis and reliability based design for probabilistic approach implementation for safety and performance of structures and structural components 21 p2788 A73-41650

An analytical method of designing long turbine blades 22 p2918 A73-41960

Fracture mechanics technology for optimum pressure vessel design. 22 p2920 A73-42155

Prestressing force and tendon configuration optimization for indeterminate structure with prescribed cross sectional dimensions, using linear programming and design variable transformation 22 p2922 A73-42476

Comparison of some penalty function based optimization procedures for the synthesis of a planar truss. 22 p2922 A73-42478

Analytic treatment of minimum weight design of cantilevers. 22 p2925 A73-42889 [ASME PAPER 73-APMW-29]

Matrix methods application to stress in elastic structures, examining Mohr circles, design implications and orthogonality anisotropy 22 p2929 A73-43173

A new approach to optimal design of elastic structures. 23 p3042 A73-43798

Environmental effects on fracture resistant and biaxial fatigue design of aircraft structures. 23 p3042 A73-43811

Experimental investigations regarding optimally designed three-layer wound glass fiber/plastic tubes under internal pressure 24 p3147 A73-44882

Optimum design of lattice structures in creep conditions with consideration of the Kempner-Hoff theory of buckling. 24 p3148 A73-45002

Bellman dynamic programming principle for elastic-perfectly plastic beam structure design optimization with respect to cross-sections, span lengths and weight 24 p3148 A73-45003

On response of initially stressed structures to random excitations. 24 p3150 A73-45229

Representation of the computer-aided design process by a network of decision tables. 24 p3070 A73-45230

Algorithmic and computational aspects of the use of optimization methods in engineering design. 24 p3070 A73-45235

Structural design optimization by iterative analysis using proper stiffness matrix with applications to sandwich plate and frame problems 24 p3150 A73-45236

STRUCTURAL DESIGN CRITERIA

Optimality criteria for structural design of statically determinate or indeterminate truss with prescribed compliance and cross sectional area 03 p0391 A73-13679

Composite material design criteria, discussing fatigue, stress concentration, safety factors, scaling effects and load characteristics 16 p1967 A73-33028

STRUCTURAL DYNAMICS

U DYNAMIC STRUCTURAL ANALYSIS

STRUCTURAL ENGINEERING

A certain case of stress-concentration analysis by an elastooptical method 01 p0114 A73-10574

Application of the method of forces to the statics of composite systems 02 p0229 A73-11639

Solution to the bending problem and to the plane problem of an anisotropic rectangular plate with arbitrary boundary conditions and the application of the solution to composite structure designs 02 p0230 A73-11715

Some problems in the substantiation and application of discrete large-element design schemes for complex zero-moment shells 02 p0230 A73-11716

Designing of shells with a zero Gaussian curvature under an edge load applied to a portion of the shell contour 02 p0230 A73-11717

Rigidly plastic cylindrical shell design for axial-load and lateral-pressure combinations with allowance for large deflections 02 p0231 A73-11808

Determination of geometrical characteristics in computer solutions of strength problems for shells of complex configuration 02 p0231 A73-11809

The calculation of supporting planar-surface structures with the aid of the characteristic functions of correlated simplified basic problems 03 p0386 A73-13154

Structure-property relationships for composites. 03 p0334 A73-13587

Finite element method for calculating temperature distributions in complex structures, taking into account heat transfer by radiation, conduction and convection 03 p0400 A73-14632

Aircraft structural engineers prospects in commercial aircraft design, discussing markets, technology escalation and cost effective structural development [AIAA PAPER 73-19] 06 p0759 A73-17612

First-excursion probability in non-stationary random vibration. 13 p1691 A73-28064

Engineering structures design, discussing stress and strain distributions, mechanical defects, symmetric loading and fracture models [ASME PAPER 73-DE-19] 14 p1815 A73-30820

International Conference on Variational Methods in Engineering, University of Southampton, Southampton, England, September 25-29, 1972, Proceedings. Sessions 1-4, 6-12. 16 p2076 A73-32976

Russian book on structural mechanics of tapered thin walled conical bodies and wings in aviation and rocket technology 21 p2788 A73-41281

Book - Dynamics in engineering structures. 22 p2922 A73-42491

Modeling methods for shock isolation systems for fragile equipment protection from HF effects generated by high loading rates and/or random multifrequency input displacement signatures 22 p2927 A73-42925

STRUCTURAL FAILURE

Mathematical model for the buildup of imperfections in plastic isotropic materials 01 p0114 A73-10476

Structural hardening calculation procedures and thermal strength problems. 02 p0235 A73-12201

Lunar aseismicity interpretation in terms of warm moon based on lunar-therm placement in stable sliding field of rock failure 02 p0219 A73-12437

In-flight structural failures involving general aviation aircraft. 02 p0131 A73-12566

Failure mechanisms in transversely loaded boron-aluminum. 02 p0184 A73-12861

Solid propellant rocket service life prediction based on propellant grain structural failure analysis, discussing surveillance program rationale for various conditions 03 p0354 A73-13407

Ni-Cr-Ti steel aircraft structural element fatigue life calculation based on failure mechanism involving crack propagation 03 p0394 A73-14011

Thermal shock produced edge effect in thermoelectric heated cylinder analyzing brittle material heat resistance and failure 03 p0394 A73-14019

Verification of structural integrity of pressure vessels by acoustic emission and periodic proof testing. 04 p0453 A73-14859

Accelerated method of estimating the growth rate of fatigue cracks. 04 p0514 A73-15671

Monograph on structural element and structures reliability covering structural design, failure analysis and reinforced element collapse under moment and force loads 04 p0472 A73-15694

Nonstationary envelope process and first excursion probability. 06 p0762 A73-18341

FORTAN sequence with economical computer storage requirement for matrix method application to rigid plastic collapse analysis of frame, considering bounded variable problem 07 p0907 A73-19034

Approximate analysis of containment/deflection ring responses to engine rotor fragment impact. 07 p0910 A73-19188

Russian book - Heat resistance of welded joints. 07 p0831 A73-20230

Stress concentration and groove design as factors in crack failure of low power single stage gas turbine rotor disk, using optical polarization technique 09 p1157 A73-22166

An apparatus for testing components in a high temperature supersonic gas stream containing abrasive particles. 09 p1070 A73-23065

Temperature dependence of conditions for static, quasi-static and fatigue failure of titanium alloys 09 p1107 A73-23193

Cantilever cylindrical shells of rigid-plastic material, determining collapse loads under external pressure combined with end moment by numerical solution to limit analysis [ASME PAPER 72-PVP-B] 09 p1164 A73-23271

Probable collapse mechanisms in indefinite plates on an elastoplastic continuum. 11 p1434 A73-25217

Preliminary design of aircraft structures to meet structural integrity requirements. 11 p1439 A73-25506

Crippling allowables for elevated temperature and creep environments. [AIAA PAPER 73-388] 11 p1439 A73-25517

STRUCTURAL FATIGUE

Aerospace component failure due to corrosion fatigue in aluminum wing attachment spar, helicopter rotor blade, landing gear cylinder and engine bearings 11 p1380 A73-25803

Environment enhanced corrosion fatigue crack growth and fracture mechanics, discussing inspection intervals to maintain structural integrity 11 p1382 A73-25819

Application of some aspects of low-cycle fatigue research in structural design. 11 p1443 A73-25846

Structural failures in light weight solar cell arrays under thermal cycling. 11 p1310 A73-25999

Temperature, testing rate and substrate choice effects on characteristic energy required to produce separation and failure of adhesively bonded pieces 11 p1443 A73-26203

Coarse grain Al alloys strength characteristics, crack resistance and specific energy of failure due to brittle fracture 11 p1386 A73-26736

Influence of the shape of inclusions on the initial stage of failure of two-component composite materials 11 p1389 A73-26738

Loading time to failure and creep rupture strength from interatomic stochastic bond fracture 11 p1448 A73-26739

Method of studying the fatigue damage of metals with automatic data processing on a computer 13 p1597 A73-29053

Behavior of random micro-structural systems. 13 p1701 A73-29530

The employment of special methods of the matrix-eigenvalue theory in the calculation of the resistance to buckling according to Vianello 14 p1805 A73-29740

A mathematical model of damage accumulation in plastic isotropic materials. 14 p1810 A73-30301

Failure under thermal loads of cylindrical bodies consisting of brittle materials 14 p1813 A73-30683

Critical rpm of a radial-flow turbine wheel of the closed type 14 p1814 A73-30685

Effect of cooling /to -269 C/ on failure in Kh18N10T and Kh16N6 steels under impact bending 14 p1763 A73-30692

Mechanical deformation and failure of metals under the action of a 0.01-sec laser light pulse 14 p1758 A73-30714

Brittle fracture of a body with a crack under variable shear load 15 p1945 A73-31040

A note on the use of a simple technique for failure prediction using resistance curves. 15 p1951 A73-31989

Time required for the destruction of a nonuniformly heated wall 15 p1953 A73-32098

Light aircraft vertical gust induced structural failures, analyzing 1960-71 accident reports for injuries biomechanics and environmental conditions 16 p1967 A73-32678

Lightweight coatings for protecting boron filament and graphite fiber reinforced plastic composites from structural damage by lightning 16 p2028 A73-33033

Forecasting failures with acoustic emission. 16 p2022 A73-33992

Experimental evaluation of the strength of elements of thin-walled pressure vessels during severe cooling 17 p2177 A73-34331

Analysis of sudden death tests of bearing endurance. [ASLE PREPRINT 73AM-3B-2] 17 p2179 A73-34984

On the opening of a finite crack normal to an interface. 17 p2250 A73-35122

Method of investigating fatigue damage of metals with automatic information processing by computer. 18 p2297 A73-36885

Fracture toughness, ductility and cleavage mechanisms of crack extension in structural materials 19 p2502 A73-38550

Strength of fibrous composite materials. 19 p2502 A73-38551

Rigid-plastic collapse of compression-bent shallow shells. 20 p2616 A73-39114

Multiplicative rule failure in matched asymptotic expansion solutions for velocity distribution in steady incompressible flow of thin elliptic airfoils 20 p2550 A73-39814

Water damage in polyester/glass laminates. II - Microscopic evidence. 21 p2723 A73-40921

Stress concentration and groove design as factors in crack failure of low power single stage gas turbine rotor disk, using optical polarization technique 22 p2920 A73-42114

Characterization of composites for the purpose of reliability evaluation. 23 p3040 A73-43627

Deformation and failure of boron-epoxy plate with circular hole. 23 p3040 A73-43631

Limit loads of circular plates under combined loading. [ASME PAPER 73-APM-G] 23 p3047 A73-44379

Upper bounds to in-plane shear strength of unidirectional fiber-reinforced composites. 23 p3048 A73-44383

Evaluating structural adhesives under sustained load in a hostile environment. 24 p3093 A73-44767

STRUCTURAL FATIGUE

U FATIGUE [MATERIALS]

STRUCTURAL FOUNDATIONS

U FOUNDATIONS

STRUCTURAL INFLUENCE COEFFICIENTS
Interpolation methods in aeroelastic analysis, comparing wing structural influence coefficients derived by surface splines and interpolation-in-the-small techniques with static test data 05 p0637 A73-17215

Influence coefficients for end-loaded conical frustums. 07 p0913 A73-19983

Computerized method for designing plate type sounding rocket fins. 09 p1155 A73-23205

[AIAA PAPER 73-285]
Application of Krylov's method to the solution of the frequency equation describing the weak vibrations of a truss structure 10 p1288 A73-23624

Applications of the compliance concept in fracture mechanics. 22 p2920 A73-42154

STRUCTURAL MATERIALS

U CONSTRUCTION MATERIALS

STRUCTURAL MEMBERS

NT ANISOTROPIC PLATES
NT ANNULAR PLATES
NT BEAMS [SUPPORTS]
NT BOX BEAMS
NT CANTILEVER BEAMS
NT CANTILEVER PLATES
NT CIRCULAR PLATES
NT COLUMNS [SUPPORTS]
NT CORRUGATED PLATES
NT CURVED BEAMS
NT ELASTIC PLATES
NT FLAT PLATES
NT GIRDS
NT I BEAMS
NT LONGERONS
NT MEMBRANE STRUCTURES
NT ORTHOTROPIC PLATES
NT PERFORATED PLATES
NT PLATES [STRUCTURAL MEMBERS]
NT POROUS PLATES
NT RECTANGULAR BEAMS
NT REINFORCED PLATES
NT SADDLES [SUPPORTS]
NT SKIN [STRUCTURAL MEMBER]
NT STRINGERS
NT STRUTS
NT TRUSSES
NT WING PANELS

Structural members optimal shaping in terms of stress concentration, analyzing plane elasticity boundary value problem 01 p0114 A73-10600

Vibrational strength of structural members from Woehler lines, calculating service life from S-N diagrams 03 p0385 A73-13138

Transverse oscillations produced by dynamic loads in structural elements of parabolic arc shape 04 p0513 A73-15506

Complex resilient-base structure designs incorporating the reaction to an external load 05 p0636 A73-17083

Application of elastooptical modeling studies in determining optimal shapes for plane structures 06 p0760 A73-17782

Sectioning method for residual stress measurement in structural members, describing test procedure, specimen preparation, tools and measuring devices and working conditions 09 p1156 A73-21875

Light weight beaded and tubular structural panels for heat shielded aerodynamic surfaces [AIAA PAPER 73-370] 11 p1438 A73-25504

Test assembly for structural component members under different climatic conditions 14 p1743 A73-30689

Shear waves in infinitely extended double walls with coupling rods of circular cross section. I - Shear waves in the infinitely extended disk 17 p2241 A73-34246

Estimation of corrosion damage levels in thin-walled structural elements by the punching method 18 p2320 A73-36825

New multiple-support radially-symmetric design of the parabolic-reflector suspension for a radio telescope 21 p2672 A73-40547

STRUCTURAL PROPERTIES [GEOLOGY]

EROS Program and ERTS-1 satellite applications (a) geophysical problems. 18 p2307 A73-36032

STRUCTURAL RELIABILITY

Colloquium on Structural Reliability: The Impact of Advanced Materials on Engineering Design, Carnegie Mellon University, Pittsburgh, Pa., October 9-12, 1972, Proceedings. 04 p0507 A73-14700

Colloquium on Structural Reliability notes on 'Fatigue Lecture.' 04 p0507 A73-14700

Statistical considerations for structural reliability analysis. 04 p0507 A73-14700

Tutorial lecture notes for experimental modelling in testing. 04 p0452 A73-14711

The design and development of fracture resistant structures. 04 p0507 A73-14712

Reliability analysis methods for metallic structures. 04 p0452 A73-14714

Evaluation of a reliability analysis method for fatigue life of aircraft structures. 04 p0452 A73-14715

The additivity of cumulative damage in the test on use environment. 04 p0507 A73-14716

Kinetic model considering cumulative fatigue damage interaction with chance overload on component or structure under probabilistic service load, discussing crack growth in composites 04 p0508 A73-14717

Toward reliable composites - An examination of design methodology. 04 p0508 A73-14720

Anisotropic structures reliability in terms of design safety factor, analyzing composite rocket motor cases under plane stress 04 p0452 A73-14723

Structural reliability definition and determination in terms of survival probability concept, discussing analytical errors effect on design and applications to aerospace vehicles 04 p0508 A73-14724

Discussion of the Colloquium on Structural Reliability. 04 p0468 A73-14727

Limit analysis of structures with stochastic strength variations. 04 p0510 A73-15027

Structural reliability under cumulative fatigue damage and chance overload interaction, postulating kinetic fracture model based on probabilistic service load histories 04 p0512 A73-15243

Monograph on structural element and structures reliability covering structural design, failure analysis and reinforced element collapse under moment and force loads 04 p0472 A73-15694

Synthesis of optimal control problems with allowance for a prescribed reliability 05 p0561 A73-16416

The USAF aircraft structural integrity program [ASIP]. [AIAA PAPER 73-18] 06 p0759 A73-17611

Probability of stress-corrosion fracture under random loading. 06 p0763 A73-18483

A fracture control program for the reusable Space Shuttle booster. 06 p0764 A73-18493

Fail-safe aircraft composite structures, achieving crack arrestment by integral buffer strips in primary load carrying laminates 06 p0764 A73-18494

Fatigue life of aircraft structures 07 p0914 A73-20246

Engineering significance of statistical and temperature-induced fracture mechanics toughness variations on fracture-safe assurance. [ASME PAPER 72-PVP-15] 09 p1163 A73-23265

Thick walled multilayer wideband radomes for supporting high hydrostatic pressures and protecting weakly directional submarine antennas with circular polarization 11 p1336 A73-25305

Preliminary design of aircraft structures to meet structural integrity requirements. [AIAA PAPER 73-374] 11 p1439 A73-25506

Wing spar static and fatigue tests and S-N curve for lifetime measurement of root sections of small trainer and passenger aircraft 15 p1955 A73-32190

Factors affecting the survivability of stressed bonds in adverse environments. 16 p2017 A73-33055

Surface integrity - A new requirement for improving reliability of aerospace hardware.

A designer's approach to the fatigue failure mechanism.

A statistical method for evaluating structural reliability and minimum structural creep life at elevated temperature.

B-1 technology applications to advanced transport design.

[SAE PAPER 730348]
An overview of fatigue and fracture for design and certification of advanced high performance ships.

Performance, structural reliability and fatigue life of glass fiber-epoxy twin beam helicopter rotor blades [AHS PREPRINT 782]

USAF aircraft structural integrity requirements, discussing safety and durability concepts for designing, evaluating and substantiating future systems

General methods of determining the limiting load in brute-force reliability tests

Functional reliability of structures.

Some considerations on solder flow-up into plated-through holes.

Toward reliable composites - An examination of design methodology.

16 p2018 A73-33067
16 p2081 A73-33644
16 p2084 A73-33974
17 p2102 A73-34696
17 p2246 A73-34881
17 p2106 A73-35095
18 p2267 A73-36169
18 p2321 A73-37023
19 p2501 A73-38279
23 p2986 A73-44002
24 p3094 A73-45144

STRUCTURAL RIGIDITY

U STRUCTURAL STABILITY

STRUCTURAL STABILITY

NT SHELL STABILITY

Axisymmetric buckling and stability of annular sandwich panel under radially varying in-plane stresses

Long-wave approximation in problems of stability loss by impact

Development of dynamic modes of the loss of stability in elastic systems during intense loading over a finite interval of time

Rectangular plate stability under compression by uniformly distributed loads applied to two opposite simply supported edges with mixed boundary conditions at other edges

Numerical solution to the problem of the elastoplastic stability of doubly connected plates with curvilinear boundaries

Stability characteristics of thin elastic plate with time varying temperature under transversal magnetic field, calculating buckling probability

Stress-strain diagrams for stability of structures under plastic bending, noting differential equations for rigidity characteristics

The stability theory of elastic bodies and the theory of thermal stresses of piecewise anisotropic bodies

Matrix analysis of local instability in plates, stiffened panels and columns.

Bounds for eigenvalues in some vibration and stability problems.

Stability of an idealized circular three-layer plate beyond the elastic limit

Beams subjected to follower force within the span.

Stability of a transversely isotropic solid under large elastic deformation.

Characteristics of the ingot crystallization process under conditions of melting in vacuum furnaces with a consumable electrode, and the stability of the cast structure in alloys of the Nb-Ti system

Stability of thick circular plates subjected to compressive loads and finite strains

Stability of a thin-wing model with one and two degrees of freedom

The application of Newton's method to the problem of elastic stability.

[ASME PAPER 72-APM-P]
General instability of cylinders with inclined stiffeners under axial compression.

Aeroelastic instabilities of hingeless helicopter blades.

[AIAA PAPER 73-193]

Finite element analysis of the post-buckling behavior of structures.

[AIAA PAPER 73-255] Effect of external-load nonconservativeness on the stability of an idealized elastoplastic rod

Some finite element solutions for plate bending problems by simplified hybrid displacement method.

Buckling of a circular sandwich plate beyond the elastic limit

Book - On elastic stability under nonconservative loads.

Tensor-linear approach to the stability problem of nonlinearly elastic isotropic plates

Directionally solidified NiAl-Cr and NiAl-Mo eutectic composites microstructural stability as function of time and temperature

Power series method for accurate solution of eigenvalue problems and simultaneous equations representing static, dynamic and stability responses to structural design parameter changes

Initial postbuckling behavior of optimally designed columns and plates.

On the torsional static stability and response of open section tubes subjected to thermal radiation loading.

Damping configurations that have a stabilizing influence on nonconservative systems.

A theoretical and experimental investigation of torsional-flexural buckling in thin-walled prismatic members.

A computerized flutter solution procedure.

Thin elastic plate stability characteristic values control through elemental boundary forces variation, applying von Karman nonlinear differential equations system eigenvalue problem

Buckling load of shallow circular vaults, investigating boundary conditions, load intensity and interconnecting beam flexibility and spacing effects

Effect of major axis curvature on I-beam stability.

Stiffness matrix for a beam with an axial force.

Lateral buckling of cantilevered I beam columns.

Lateral vibration and stability relationship of elastically restrained skew plates.

Large deflections and stability of a long cylindrical panel prepared from an orthotropic fiberglass plastic under the action of piecewise-uniform loading

The influence of orthotropy on the stability of some multi-plate structures in compression.

Calculation of the stability of rectangular plates in an air flow by the finite-element method

Stability of a ferromagnetic plate within a gas flow in the presence of a magnetic field

Neutron bombardment radiative effects on thin metal plate stability, considering compressive force, lattice defects and critical flux relations

Steel and Ni-based alloys structural stability during long term high temperature creep, noting matrix structure dependence on initial dislocation and interparticle spacing

Stability of structure and mechanical properties of molybdenum under prolonged influence of temperature and stress.

Elastic circular ring stability under uniformly distributed equal radial concentrated forces

Application of the finite element method to the study of the stability of plane structures

Design stability of composite samples with a soft interlayer in static tension

The analytical treatment of the nonlinear aeroelastic galloping problem

[DFVLR-SONDDR-289]
On the role of the adjoint problem in dissipative, nonconservative problems of elastic stability.

Upper bounds to plastic strains in shake-down of structures subjected to cyclic loads.

11 p1432 A73-24997
11 p1434 A73-25214
11 p1434 A73-25216

STRUCTURAL STABILITY

Elastic stability of biaxially loaded longitudinally stiffened composite structures.

[AIAA PAPER 73-367] The stability of simply supported rectangular surfaces in uniform subsonic flow.

[ASME PAPER 72-APM-ZZ] Transient characteristics of simple systems to modulated random noise.

[ASME PAPER 72-APM-FFF] Russian book on airplane and helicopter design and stability covering selection of wing /rotor/ configuration and power plant, subsystem design, strength, reliability, lifetime, etc

Pseudoelastic design method for bottle-crate stack instability performance prediction through failure by creep buckling, assessing effectiveness by comparison with measurements

Flattening and creep stability loss of nonlinear viscoelastic ring under external pressure

Stability of rectangular plates under mixed boundary conditions

Stability of sheet metal drawn by a rigid stamp to cylindrical and conical shapes

Finite element matrix formulation of post-buckling stability and imperfection sensitivity.

German book - Elastostatics and elastokinetics in matrix notation: The procedure of transmission matrices.

Austenitic stainless steels at cryogenic temperatures. I - Structural stability and magnetic properties.

Application of a variational method to dissipative, non-conservative problems of elastic stability.

The employment of special methods of the matrix-eigenvalue theory in the calculation of the resistance to buckling according to Vianello

Progress in nonlinear finite element analysis using asymptotic solution techniques.

A survey of recent results in differential equations.

Critical load determination for nonsymmetrical stability losses of ring shaped plates clamped against bending

Stability of metal-based composite materials

Design of stiffened cylinders to resist axial compression.

First fundamental problem of the theory of elasticity for a bi-periodic system of cuts

Elastic buckling instability of rotating rods and plates due to compressive stress under critical speed

Variational methods applied to nonconservative stability problems of elastic continua.

Acoustic fatigue in ceramic materials, analyzing strength degradation as function of microstructure, structural integrity and properties

Circular elastic membrane stability against wrinkling under radial peripheral tension and transverse pressure loading, considering solutions via Foepl-Hencky theory

Lateral instability of thin-walled beams - Considerations regarding methods of experimental investigation

Interpretation of the results of simulation tests, taking into account scatter effects

Equilibrium conditions for multilayer anisotropic viscoelastic plates in a complex stressed state

Monotonically convergent approximate solutions for finite element eigenvalues in structural vibration and stability problems, assessing accuracies

Instability analysis using the incremental stiffness matrices.

Out-of-plane vibration and stability of curved tubes conveying fluid.

[ASME PAPER 72-WA/APM-36]
Stability of the general plane membrane adjacent to a supersonic airstream.

[ASME PAPER 72-APM-UUU] Limiting equilibrium of a plate weakened by two arbitrarily oriented cracks

Elastic bodies nonlinear thermomechanical stability under conditions of loaded equilibrium configuration, using Liapunov type energy-like functionals
20 p2615 A73-39010

Unique relations between equilibrium and Galimov-Novozhilov stability equations of geometrically nonlinear elasticity theory based on Hooke's law
20 p2617 A73-39305

A difference-energy method of studying the stability of rectangular plates in shear
20 p2617 A73-39306

Experimental investigation of the stability of oblique conical panels under the action of uniform external pressure
20 p2617 A73-39308

Large deflections and stability of a long shallow orthotropic cylindrical panel under the action of a local load
20 p2618 A73-39312

Stability and postbuckling behavior of hyperelastic bodies at finite strain by the finite element method.
20 p2620 A73-39529

Stability criteria for incompressible elastic isotropic materials subject to shearing displacement superimposed on homogeneous elastic deformation, discussing Cauchy stress and shear modulus
20 p2620 A73-39530

Column instability under nonconservative forces, with internal and external damping - Finite element using adjoint variational principles.
20 p2621 A73-39540

Calculation of three-layer minimum-weight panels as a problem of mathematical programming
20 p2625 A73-39651

Nonsymmetric buckling of cylinders with axisymmetric thermal discontinuities.
21 p2784 A73-40425

Influence of the geometrical configuration of a structure on its carrying capacity
21 p2786 A73-40982

Influence of nonuniform heating on the stability of plates beyond the elastic limit
21 p2786 A73-40983

Application of R-functions to a calculation of the dynamic stability of plates with a complex planform geometry
21 p2786 A73-40984

Determination of the limiting equilibrium of a brittle body weakened by a system of cracks whose form on a plane approaches a circular form
22 p2921 A73-42284

An exact method for the study of the dynamic stability of supporting structures acted upon by periodic impulses.
22 p2927 A73-43031

Stability of nonlinearly elastic plates in the presence of random initial stresses
22 p2928 A73-43060

Parametric instability of clamped-clamped and clamped-simply supported columns under periodic axial load.
22 p2929 A73-43137

Non-linear creep buckling with random temperature variations.
23 p3045 A73-44166

Creep buckling stability for deformable rod with initial deflection, determining perturbed and unperturbed motion of random and deterministic components
23 p3046 A73-44188

The use of glass-fiber-reinforced plastics for containers which are subjected to external pressure
24 p3147 A73-44881

Optimum design of lattice structures in creep conditions with consideration of the Kempner-Hoff theory of buckling.
24 p3148 A73-45002

A method for qualitatively studying the oscillations and stability of systems with distributed parameters
24 p3111 A73-45354

STRUCTURAL STRAIN

The challenge to unify treatment of high-temperature fatigue - A partisan proposal based on strainrange partitioning.
07 p0917 A73-20461

Curved finite elements by the method of initial strains.
08 p1016 A73-20727

Plane strain plastic yielding due to bending of end-loaded cantilevers containing circular, triangular or diamond-shaped holes.
11 p1443 A73-26091

Deformation of a nonshallow spherical shell under local loads
12 p1553 A73-27469

Deformation criteria of failure under simple and composite stresses.
13 p1703 A73-29621

Investigation of some physicochemical and X-ray structural changes in a superconducting wire prepared from 60T alloy, as a function of the strain level and duration of annealing in vacuum
15 p1887 A73-31187

The behaviour with diminishing curvature of strain-based arch finite elements.
16 p2076 A73-32921

Strain accumulation and rupture during creep under variable uniaxial tensile loading.
19 p2495 A73-37434

Resonance methods for the dynamic study of deformable structures
19 p2497 A73-37556

Large deflection of shallow paraboloid shells.
21 p2782 A73-40005

Transverse displacements of the radiating element of the parabolic antenna of a mobile radio telescope
21 p2672 A73-40548

Longitudinal displacements of the secondary mirror of a parabolic antenna
21 p2672 A73-40550

Elastoplastic strains and carrying capacity of shallow shells/Review/
21 p2786 A73-40976

STRUCTURAL VIBRATION

NT BENDING VIBRATION

NT BREATHING VIBRATION

NT FLUTTER

NT LINEAR VIBRATION

NT PANEL FLUTTER

NT SELF INDUCED VIBRATION

NT SUBSONIC FLUTTER

NT SUPERSONIC FLUTTER

NT TORSIONAL VIBRATION

NT TRANSONIC FLUTTER

Calculation and measurement of the aerodynamic forces on an oscillating airfoil profile with and without stall
01 p0002 A73-10240

[ONERA, TP NO. 1132]
Simulation of the flow past turbomachine blades in the study of plane-cascade vibrations
01 p0029 A73-10494

Optimization of hybrid gas lubricated conical bearings.
01 p0057 A73-10698

A linearized analysis for frictionally damped systems.
01 p0090 A73-10782

Dynamic edge effect in rods - Formulation of shortened problems
01 p0118 A73-11405

Reaction of a damped system to the simultaneous action of an isolated semisinusoidal impact pulse and of vibrational oscillations
01 p0054 A73-11418

An estimate of the decrease in friction during vibrations of normal direction
01 p0058 A73-11437

Incompressible elastic circular cylinders quasi-equilibrated motions analysis, obtaining free and forced oscillations periods
02 p0191 A73-11573

Free three-dimensional vibration processing of gas-turbine engine blades
02 p0172 A73-11723

Study of the oscillations of plates, shells and combined systems by the basis vector method with difference discretization
02 p0232 A73-11817

Non-linear vibration of rotating cantilever blades treated by the Ritz averaging process.
02 p0232 A73-11859

Book - Sound, structures, and their interaction.
02 p0192 A73-11880

Oscillations of open cylindrical shells of variable curvature
02 p0233 A73-11941

Behavior of certain turbine-blade materials under asymmetric loading.
02 p0180 A73-12128

Prediction of the response of a cylindrical shell to arbitrary or boundary-layer-induced random pressure fields.
02 p0237 A73-12601

Vibration of a square plate symmetrically supported at four points.
02 p0237 A73-12605

On the evaluation of tri-diagonal secular determinants.
02 p0188 A73-12606

Lateral displacement of discontinuous vibrating wire, noting solution application to longitudinal vibrations of discontinuous shafts and torsional vibrations of circular shafts
02 p0237 A73-12612

A versatile Moessbauer spectrometer and its applications in structural mechanics.
03 p0305 A73-12875

A problem of coupling between the vibration of a thin plate and an acoustic field in a fluid
03 p0383 A73-12982

Free vibrations of elastic systems with discrete dynamic systems attached.
03 p0384 A73-12983

Vibrations of circular cylindrical shells subjected to nonuniform initial stress.
03 p0384 A73-12984

An accurate approximate formula for assessing the vibration frequency of structures axially loaded.
03 p0384 A73-13116

Correlation theory for equations of motion of constant thickness shallow shell vibration under random loads
03 p0387 A73-13116

On bending and vibration of reinforced and birch forced elastic and viscoelastic shells.
03 p0387 A73-13116

Beam vibration frequencies tables handbook preparation technique
03 p0388 A73-13139

Parametric vibration of simply supported rectangular plate and cylindrical shell under random excitation using Markov process theory and Fokker-Planck equation
03 p0388 A73-13376

Nonlinear responses for a circular plate subjected to a dynamic ring load.
03 p0388 A73-13376

A finite element analogue of the modified Rayleigh-Ritz method for vibration problems.
03 p0390 A73-13376

Bounds for eigenvalues in some vibration and stability problems.
03 p0390 A73-13376

Convergence of consistently derived Timoshenko beam finite elements.
03 p0390 A73-13376

Resonant frequencies of free vibrating plate via finite difference method, noting difference equation for plate equilibrium
03 p0391 A73-13376

Vibration and buckling of a rectangular plate with an internal support.
03 p0391 A73-13376

Axial shear vibrations of cylinders made of micropolar elastic solid.
03 p0393 A73-13781

The modal density for flexural vibration of thin plates and bars.
03 p0393 A73-13833

Vibrational frequency density analysis of thin spherical and cylindrical shells of revolution, using asymptotic integration method
03 p0394 A73-14055

Gravitational stabilization systems parameters determination for minimum amplitude of satellite eccentric vibrations
03 p0383 A73-14555

Oscillations of spacecraft with on-off attitude control under constant perturbation moment, calculating energy expenditures for desired orientation maintenance
03 p0383 A73-14555

Topological analysis of mechanical vibrating linear systems by the method of structural numbers
03 p0396 A73-14599

Beam transverse vibration with nonlinear-spring supported free end and concentrated mass, determining free vibration frequencies
04 p0508 A73-14944

Influence of the nonlinear thermomechanical effect on the thermal stability of rubber-metallic couplings of vibration machines
04 p0509 A73-14988

Determination of the natural oscillation frequency of three-layer circular cylindrical shells by a numerical method
04 p0510 A73-15087

Application of the method of summary representations to problems of cylindrical shell oscillations
04 p0511 A73-15087

Use of Green's function in the study of the natural oscillations of two-dimensional structures
04 p0511 A73-15087

Symmetrical bending for the general case of oscillating beams under transverse loads
04 p0511 A73-15174

Law governing the oscillations of a circular cylindrical shell of finite length containing a liquid with a variable level
04 p0434 A73-15505

Free vibration of cantilever circular cylindrical shells - A comparative study.
04 p0513 A73-15588

Flow induced vibration of cantilever mounted flat plates in an enclosed passage An experimental investigation.
04 p0513 A73-15590

Spectral analysis of the vibrations of mechanical systems with continuous mass which have a finite number of attached concentrated masses
04 p0476 A73-15653

On the forced vibration of a rectangular plate. [ASME PAPER 72-WA/DE-20]
04 p0514 A73-15833

Vortex induced vibration of circular cylindrical structures. [ASME PAPER 72-WA/FE-39]
04 p0404 A73-15855

Low order spatial modes principal resonance region of in-plane loaded skew stiffened plate, obtaining equation of motion by Hamilton principle [ASME PAPER 72-WA/APM-32]
04 p0515 A73-15888

The vibration of cantilever beams of fiber reinforced material.
05 p0631 A73-16111

- A study of complex auto-oscillations of spacecraft
05 p0628 A73-16404
- Digital vibration control systems for structural design dynamic testing and evaluation, discussing state of art and trends toward multichannel and multi-axis control
[SAE PAPER 720820] 05 p0553 A73-16628
- Study of modeling of substructure damping matrices.
[SAE PAPER 720813] 05 p0634 A73-16645
- Equations for the oscillations of multilayer shells with allowance for shear deformation and for fiber pressing in the filler
05 p0634 A73-16749
- Use of associated matrices in deriving frequency equations for rods with variable rigidities and masses
05 p0636 A73-17082
- Influence of a moving load on the vibrational characteristics of plates
05 p0636 A73-17093
- Vibration of thermally stressed plates with various boundary conditions.
05 p0636 A73-17101
- Finite element analysis of nonlinear vibration of beam columns.
05 p0636 A73-17118
- Vibrations of circular cylinders of a perfectly conducting elastic material.
05 p0637 A73-17298
- Constant curvature beam finite elements for in-plane vibration.
05 p0637 A73-17371
- Comparison of eigenvalues and characteristic vibration modes of circular ring bars, circular ring disks, and circular ring fibers
06 p0758 A73-17584
- Thermal shock induced transverse vibrations in rectangular plate with combined simple and clamped edge supports, deriving infinite series solutions
06 p0761 A73-17896
- Transversal vibrations of the thin shell of revolution produced by the thermal shock.
06 p0763 A73-18453
- Dynamic stress intensity factor for an unbounded plate having collinear cracks.
[AD-758426] 06 p0764 A73-18492
- Vibration theory optimization problems for rectilinear rods, noting Lagrange multipliers continuity in linear hyperbolic equations
06 p0766 A73-18886
- Acquisition and processing system of vibration measurements
07 p0807 A73-19001
- Natural frequencies and vibration modes determination for skew plates with different edge conditions involving support and clamping based on Ritz variational method
07 p0909 A73-19094
- Steady state vibrational frequencies of grid stiffened rectangular plates with monolithic connection at node points for simply supported case
07 p0909 A73-19095
- Kron algorithm for complex eigenvalue problems of damped vibrating mechanical systems, using Newton method
07 p0909 A73-19098
- The status of engineering knowledge concerning the damping of built-up structures.
07 p0909 A73-19099
- The use of straight beam finite elements for analysis of vibrations of curved beams.
07 p0909 A73-19100
- Torsion of a viscoelastic prismatic rod under the action of a vibrational load
07 p0911 A73-19315
- Lateral vibration and stability relationship of elastically restrained circular plates.
07 p0913 A73-19967
- Vibration of cylindrically orthotropic circular plates.
07 p0913 A73-19968
- Nonlinear vibrations of rectangular plates with cutouts.
07 p0913 A73-19978
- Longitudinal vibration analysis of partially-filled ellipsoidal tanks.
07 p0914 A73-20215
- System identification of vibrating structures: Mathematical models from test data; Proceedings of the Winter Annual Meeting, New York, N.Y., November 26-30, 1972.
07 p0915 A73-20426
- Methods and application of system identification in shock and vibration.
07 p0916 A73-20429
- Shock and vibration disturbance identification based on structural system response, discussing linear programming, curve fitting, constraints, objective functions and applications
07 p0916 A73-20430
- Response of nonlinear beam to random excitation.
07 p0916 A73-20436
- Designing turbomachine blades for forced vibrations under various excitation conditions
07 p0917 A73-20503
- Electrodynamic exciter power amplifier with pulse width modulation and Schmitt trigger output stage for structural vibration tests
07 p0803 A73-20535
- Synthesis of two discrete vibratory systems using eigenvalue modification.
08 p1015 A73-20726
- Free vibrations of an infinite strip of variable thickness.
08 p1016 A73-20940
- Lateral vibration and stability relationship of elastically restrained skew plates.
08 p1017 A73-20944
- Criteria for self loosening of fasteners under vibration. II.
08 p0972 A73-20948
- Dispersion of axially symmetric waves in empty and fluid-filled cylindrical shells.
08 p0987 A73-21075
- Effect of transverse shear deformation on vibrations of planar structures composed of beam-type elements.
08 p1017 A73-21192
- Beams and membranes nonlinear vibrations via modified perturbation method based on Linstedt-Poincare technique
08 p1018 A73-21406
- Improved finite elements for vibration analysis of tapered beams.
08 p1018 A73-21439
- Effect of the curvature of a shallow spherical shell on its vibrations with losses
08 p1018 A73-21449
- Some delinearization problems in the dynamics of complex vibrational systems
08 p0989 A73-21768
- Vibration measurement by vibrating-plate holograms.
09 p1079 A73-21997
- Influence of the nonlinear compliance of rolling contact bearings on the vibrations of a balanced shaft
09 p1088 A73-22479
- Book - Vibration of solids and structures under moving loads.
09 p1159 A73-22526
- Generator of rectilinear vibrations for the study of structures at low frequency
[ONERA, TP NO. 1185] 09 p1084 A73-22713
- Optimal beam frequencies by the finite element displacement method.
09 p1160 A73-22898
- A generalization of equations of the outline of a hysteresis loop for the case of an asymmetrical cycle.
09 p1161 A73-23152
- Three layered sandwich rings damped vibrations under time-harmonic radial concentrated load, comparing experimental and theoretical mechanical impedance data
09 p1165 A73-23440
- High-damping measurements and a preliminary evaluation of an equation for constrained-layer damping.
09 p1166 A73-23458
- Application of Krylov's method to the solution of the frequency equation describing the weak vibrations of a truss structure
10 p1288 A73-23624
- Bending and vibration of multilayer sandwich beams and plates.
10 p1289 A73-24290
- Solution of quadratic matrix equations for free vibration analysis of structures.
10 p1290 A73-24299
- Influence of an intermediate stiffener on the vibration frequency spectrum of a cantilever plate
10 p1291 A73-24357
- Vibration analysis of clamped, rectangular plates of generalized orthotropy.
10 p1291 A73-24387
- Axisymmetric vibrations of circular plates with stepped thickness.
10 p1291 A73-24394
- Application of a variational difference method to the calculation of forced vibrations of shells of revolution
10 p1292 A73-24487
- Three-dimensional problem of the vibrations of a circular plate with initial stresses
10 p1292 A73-24506
- Vibrations of segmented shells.
10 p1293 A73-24720
- Acoustically induced vibrations of slender rods in a cylindrical duct with parallel flow.
11 p1432 A73-24983
- The analytical treatment of the nonlinear aeroelastic galloping problem
[DFVLR-SONDDR-289] 11 p1432 A73-24997
- Thermoelastic response of a cylinder in the generalized dynamical theory of thermoelasticity.
11 p1433 A73-25161
- Formulation of Pontryagin's maximality principle in a problem of structural mechanics.
11 p1434 A73-25185
- Small parameter method, with the parameter proportional to the friction forces, in the case of forced vibrations of complex trusses
11 p1435 A73-25395
- Stress, stability, and vibration of complex, branched shells of revolution.
[AIAA PAPER 73-360] 11 p1437 A73-25496
- Computer generated displays of structures in vibration.
[AIAA PAPER 73-362] 11 p1334 A73-25498
- Buckling and vibration of unsymmetrically laminated cross-ply rectangular plates.
[AIAA PAPER 73-368] 11 p1438 A73-25503
- Gradient optimization of structural weight for specified flutter speed.
[AIAA PAPER 73-390] 11 p1439 A73-25519
- A dynamic transformation method for modal synthesis.
[AIAA PAPER 73-396] 11 p1440 A73-25525
- A finite element method for nonaxisymmetric vibrations of pressurized shells of revolution partially filled with liquid.
[AIAA PAPER 73-399] 11 p1440 A73-25528
- Synthesis of shuttle vehicle damping using substructure test results.
[AIAA PAPER 73-400] 11 p1430 A73-25529
- Multiple shaker resonance testing for structural dynamic characteristics, considering natural frequencies, mode shapes, damping and generalized masses
[AIAA PAPER 73-402] 11 p1440 A73-25531
- The spatial correlation method and a time-varying flexible structure.
[AIAA PAPER 73-406] 11 p1440 A73-25535
- Vibration and flutter of cylindrical shells including the effects of stringer stiffening.
[AIAA PAPER 73-312] 11 p1441 A73-25543
- Stabilizing the elastic modes of the Space Shuttle vehicle during launch.
[AIAA PAPER 73-319] 11 p1430 A73-25550
- European contribution to structural response to noise.
[AIAA PAPER 73-332] 11 p1305 A73-25561
- Vibrations of an Euler beam with a system of discrete masses, springs, and dashpots.
11 p1442 A73-25788
- Friction reduction by perpendicular oscillation.
11 p1374 A73-26064
- Minimum-mass design of multiclement structures under a frequency constraint.
11 p1444 A73-26380
- Clamped orthotropic skew plates under uniformly distributed transverse load, considering nonlinear analysis based on numerical technique of dynamic relaxation involving critically damped vibration
11 p1444 A73-26381
- Galerkin finite element method for vibration problems.
11 p1445 A73-26389
- Influence of a small bending stiffness on the lateral vibrations of a clamped rectangular membrane
[DFVLR-SONDDR-226] 11 p1445 A73-26425
- Effect on shell dynamics of a shell mass distributed within a shell surface area
11 p1446 A73-26461
- Oscillations of a shell partially filled with a liquid and containing sources of the liquid
11 p1446 A73-26462
- Hamilton variational principle for deriving equations of motion for small elastic displacements of thin circular rings, noting twist equation occurrence
11 p1446 A73-26493
- Rayleigh-Ritz method for natural frequencies of transversely vibrating polar orthotropic annular perforated plates, proposing coordinate transformations for asymmetric mode solutions
11 p1446 A73-26495
- In-flight flutter testing methods for determining aircraft structure natural frequencies and vibration damping ratios with air flow
[ONERA, TP NO. 1224] 11 p1306 A73-26593
- Multilocal difference method for free vibration analysis of closed and open orthotropic noncircular cylindrical shells with supported curved edges
12 p1551 A73-27035
- Condition monitoring - A new technology for aircraft engine maintenance
12 p1486 A73-27389
- Magnetoelastic vibration of electrically conducting thin shells and plates in steady magnetic field from asymptotic integration of electrodynamics equations
12 p1553 A73-27413
- Solid body on elastic supports as model for helicopter stability and nonlinear oscillations analysis
12 p1459 A73-27791
- Influence of rotational inertia on the frequency spectrum of the natural vibrations of a cylindrical shell
12 p1556 A73-27801
- Free vibration of cantilever beam with/without tip mass and with nonlinear material properties, using perturbation and finite element techniques
12 p1556 A73-27928
- Large amplitude vibrations of certain deformable bodies. I - Discs, membranes and rings.
12 p1556 A73-27929

Vibrations of a system with memory, non-linear elasticity, friction and relaxation.

13 p1690 A73-28055

Natural frequencies of a beam considering support characteristics.

13 p1691 A73-28065

German book - Elastostatics and elastokinetics in matrix notation: The procedure of transmission matrices.

13 p1695 A73-28300

Axisymmetric vibrations of circular plates of linearly varying thickness.

13 p1695 A73-28415

Nonlinear transverse vibrations of beams with properties that vary along the length.

13 p1695 A73-28488

Vibration analysis of thick-walled hollow spheres and cylinders, determining periodic response and fundamental frequency as function of wave reflection number and dimensions

13 p1695 A73-28489

Elastic structures nonlinear free vibrations theory based on Hamilton principle and perturbation method, applying to beams and rectangular plates

13 p1696 A73-28751

Visualization of unsteady flow over oscillating airfoils.

13 p1620 A73-29270

Line and rectangular plane finite element models for accurate and efficient dynamic vibration frequency analysis of frames and shear walls respectively

13 p1700 A73-29377

High frequency model U-20P fatigue testing unit with program control of the specimen vibration amplitude.

13 p1599 A73-29637

Holographic visualization of large amplitude vibration using reference beam phase modulation.

13 p1622 A73-29642

Free vibrations of shells of revolution with variable thickness.

14 p1805 A73-29768

Large amplitude vibrations of certain deformable bodies. II Plates and shells.

14 p1806 A73-30041

Radio telemetry for strain measurements in turbines.

14 p1752 A73-30064

Deleterious vibrations development in support structure of launch pad during initial firing of launch vehicle, noting frequency spectrum dependence on soil characteristics and structural design

14 p1742 A73-30105

Stability and convergence of finite element methods for elastic structures vibration analysis, stressing application to mixed boundary value problems

14 p1807 A73-30185

Steel structures analysis based on cubic interpolating functions with parameters of nodal displacements, discussing method extension to natural vibration

14 p1809 A73-30199

Providing a model of flow round a turbine blade when investigating the vibration of flat blading.

14 p1743 A73-30319

Russian book on elastic structures vibration in aircraft covering integral equations for beams, damping principles and transcendental equations for flexural and torsional vibrations natural frequencies

14 p1810 A73-30354

Optimal shapes of simply supported vibrating elastic beams for maximum fundamental frequency under axial compressive load

14 p1812 A73-30494

Book - Optimal control theory for the damping of vibrations of simple elastic systems.

14 p1813 A73-30674

Traveling wave solutions of differential equations describing thin elastic shell oscillations due to point source

14 p1815 A73-30951

Natural oscillations of multilayer shells and plates with fillers

15 p1944 A73-30970

Nonlinear vibrations of rectangular plates.

15 p1944 A73-31060

Influence of curvature on the vibrations of an oblate spherical shell with losses.

15 p1945 A73-31013

Harmonic vibrations of inclined plate in separated free surface flow of ideal fluid in terms of weak perturbation flow theory

15 p1946 A73-31157

On dynamic response of prestressed cylindrical shells - Green's tensor technique.

15 p1947 A73-31367

Effect of nonlinear compliance in rolling motion bearings on the vibrations of a balanced shaft.

15 p1883 A73-32066

Free vibration of an inflated oblate spheroidal shell.

15 p1955 A73-32155

On the vibrations of a rotor with rotating inequality and with variable rotating speed.

15 p1883 A73-32216

Vibration theory optimization problems for rectilinear rods, noting Lagrange multipliers continuity in linear hyperbolic equations.

15 p1956 A73-32411

Natural vibrations of variable-thickness shells of revolution with apparent additional masses

16 p2074 A73-32685

Ring finite elements for axisymmetric and non axisymmetric thin shell analysis.

16 p2077 A73-32989

Dynamic analysis procedure to locate vibration sources without simulated service tests, mapping structural surfaces at all frequencies via transfer function or mechanical impedance analysis

16 p2019 A73-33098

Structural shock response spectrum analysis for maximum dynamic loads and damage potential determination

16 p2014 A73-33135

Transverse vibrations of variable rectangular cross section rod, reducing fourth order differential equation to second order via Kirchhoff relation

16 p2080 A73-33259

Flexural vibrations of clamped orthotropic plates.

16 p2081 A73-33680

Monotonically convergent approximate solutions for finite element eigenvalues in structural vibration and stability problems, assessing accuracies

16 p2083 A73-33949

Determination of the eigenmodes of a structure by vibration tests with nonadjusted excitation

16 p2074 A73-33967

Free vibrations of multilayered composite plates.

17 p2241 A73-34192

The influence of pitch and twist on blade vibrations.

17 p2099 A73-34440

Statistics calculation method for natural frequencies and mode shapes of vibration for structures under external static loads

17 p2242 A73-34527

Some properties of dynamic equation integrals from the theory of shells

17 p2244 A73-34736

Finite element method application to solution of structural dynamics problems, considering equations of motion and vibration mode shapes

17 p2245 A73-34836

Vibration analysis of finite element systems.

17 p2245 A73-34837

A perturbation method for low-frequency fluid-structure interaction problems.

[ASME PAPER 72-APM-WWW] 17 p2248 A73-35102

High frequency vibration of aircraft structures.

17 p2250 A73-35329

Applications of the speckle pattern techniques to the visualization of modulation transfer functions and quantitative study of vibrations of mechanical structures.

17 p2173 A73-35433

Vibration analysis of plates by real-time stroboscopic holography.

[SESA PAPER 2111] 17 p2173 A73-35448

Oscillations of a system with two degrees of freedom during resonance

17 p2213 A73-35591

Mass condensation and simultaneous iteration for vibration problems.

17 p2252 A73-35605

Book - Dynamics and vibration of structures.

17 p2252 A73-35833

Book - Vibration of linear mechanical systems.

18 p2361 A73-35900

Alteration of a static vibration result by rigidizing some degrees of freedom

18 p2361 A73-36066

SkyLab experience with Apollo docking/latching loads.

[AIAA PAPER 73-613] 18 p2358 A73-36091

Vibration of layered shells.

18 p2367 A73-37029

Forecast of mode variation subsequent to structure modifications

18 p2367 A73-37083

On the flexural vibration frequencies of statically loaded beams.

18 p2367 A73-37091

Influence of the structure of the material of a three-layered cylindrical shell on the natural frequencies

19 p2494 A73-37184

Measurements of surface pressure on an elliptic airfoil oscillating in uniform flow.

19 p2375 A73-37374

Computer based analyses of the response of box type structures to random pressures.

19 p2497 A73-37485

Resonance methods for the dynamic study of deformable structures

19 p2497 A73-37556

Nonlinear parametric vibrations of closed cylindrical shells

19 p2499 A73-37764

Calculating the fundamental oscillations in turboengine blades with different types of excitation.

19 p2499 A73-37778

Some new results for the vibrations of circular cylinders.

19 p2500 A73-38101

The vibrations of a circular plate with uniformly distributed load around the outer periphery.

19 p2502 A73-38344

Virtual motion principle implication for structural damping differential equations for cases of homogeneous, inhomogeneous and aerodynamic flutter for various degrees of freedom

20 p2616 A73-39099

Simulation of complex excitation of structures in random vibration by one-point excitation.

20 p2617 A73-39264

Investigation of the free vibrations of sectorial plates and conical panels by a theoretical-experimental method

20 p2618 A73-39311

Limiting zero and infinite edge beam stiffness effects on natural vibrational frequencies of reinforced annular plates

20 p2622 A73-39544

Free and forced nonlinear oscillations of anisotropic orthotropic annular plate with free inner boundary and fixed immovable outer boundary

20 p2623 A73-39564

The vibrations of non-circular cylindrical shells with initial stresses.

21 p2783 A73-40288

Square plate symmetrically supported at four diagonal points, evaluating fundamental vibration frequency with accuracy by finite element method

21 p2783 A73-40293

A natural frequency analogy between spherically curved panels and flat plates.

21 p2785 A73-40754

Optimal design of linearly elastic vibrating structural members for minimized total mass and maximized fundamental frequency respectively, noting solution existence dependence on boundary conditions

21 p2785 A73-40844

Russian book on R-function method for solving boundary value problems of bending and vibration of thin plates with complex configurations

21 p2787 A73-41250

Identification and simulation of antenna dynamics.

21 p2667 A73-41522

Dynamic behaviour of orthotropic plates using finite difference technique.

22 p2917 A73-41710

Effect of support flexibility on the fundamental frequency of vibrating beams.

22 p2918 A73-41966

Improvement of damping capacity of structural members by introduced stress concentration.

[ASME PAPER 73-DET-76] 22 p2919 A73-42072

Cylindrical circular shell vibrational frequencies, examining free surface or solid plane influence on shell natural vibrations in incompressible fluids

22 p2920 A73-42130

Bilateral estimates of the critical parameters of elastic systems experiencing flutter

22 p2921 A73-42280

Vibration of beams with overhangs.

22 p2923 A73-42564

Vibration analysis of laminated plates and shells by a hybrid stress element.

22 p2923 A73-42564

Forced motion of lumped mass systems including the effect of axial force.

22 p2923 A73-42630

Example of dynamic interference effects between two oscillating vehicles.

22 p2917 A73-42634

Combined radial-axial large amplitude oscillations of hyperelastic cylindrical tubes.

22 p2923 A73-42637

Complex structural dynamic response reduction, discussing methods for mathematical models establishment and application to thin cylindrical shell

22 p2926 A73-42921

Isolation of machinery vibration from nonrigid structures using multiple antivibration mountings.

22 p2927 A73-42923

Dynamic contact problem for the case of longitudinal shear strain

22 p2927 A73-43051

Vibrations of a rotating solid body containing a cavity partially filled with a viscous fluid

22 p2843 A73-43058

High frequency vibrations and waves in laminated orthotropic plates.

22 p2928 A73-43135

Probability displacement and modal cross spectral density parameters of two span beam random vibrations under white noise

23 p3039 A73-43304

Application of harmonic analysis to the calculation of stators with variable blade pitch

23 p3019 A73-43734

Vibrations of turbojet-engine components containing structural dampers of the type of sandwich rods

23 p3020 A73-43735

- On the computation of natural modes of an unsupported vibrating structure by simultaneous iteration. 23 p3042 A73-43801
- In-plane vibration of continuous curved beams. 23 p3045 A73-44165
- Nonlinear stress-strain hysteresis equation of cyclic straining for vibrating imperfectly elastic systems, using Masing principle 23 p3047 A73-44276
- Traveling wave solutions of differential equations describing thin elastic shell oscillations due to point source 23 p3047 A73-44327
- Nonlinear parametric vibrations of cylindrical shells prepared from composite materials 24 p3145 A73-44517
- Response of panels to turbulence-induced, surface-pressure fluctuations and resulting acoustic radiation to the flow field. [AIAA PAPER 73-993] 24 p3077 A73-44828
- Emission of sound from a rectangular plate vibrating under the action of pressure pulsations in a turbulent boundary layer 24 p3109 A73-44899
- Vibration of rectangular plates with mixed boundary conditions. 24 p3151 A73-45268
- Boundaries of natural frequency variations during the longitudinal oscillations of rods 24 p3152 A73-45360
- STRUCTURAL WEIGHT**
- Structural weight analysis of single stage and multistage spacecraft for given payload and initial vehicle weight, considering optimization problem 02 p0229 A73-12469
- A computational method for optimal structural design. I - Piecewise uniform structures. 03 p0390 A73-13337
- Flexible circular solar array for power to weight ratio increase at satellite outer surface, noting central supported structure superiority 03 p0257 A73-14239
- Minimum weight rectangular beam grillages and reinforced plates of given strength or stiffness, presenting solutions for various boundary conditions 04 p0508 A73-14937
- Minimum weight design of plastic and elastic grillages and fiber reinforced plates of given strength or stiffness, presenting optimal solutions for various boundary conditions 04 p0509 A73-15011
- Minimum-weight plastic design of continuous beams subjected to one single moveable load. 04 p0510 A73-15030
- On the weight optimization problem for supersonic rectangular flat panels with specified flutter speed. 04 p0511 A73-15170
- Weight sensitivity of a space shuttle orbiter to thermal structural combined loads design criteria. [AIAA PAPER 73-257] 05 p0635 A73-16979
- Probabilistic minimum weight limit design of one dimensional pin jointed structures with random continuous variables, using stochastic programming 06 p0757 A73-17397
- A unified formulation of the theory of optimal plastic design with convex cost function. 06 p0763 A73-18343
- Weight minimization of axisymmetric clamped plates subject to constraints. 07 p0908 A73-19092
- Thin walled beam composed indeterminate elastic framed structures minimum weight design, obtaining solutions by nonlinear programming algorithm 07 p0912 A73-19951
- The minimum weight structural configuration of pin-jointed truss cantilevers of given external shape. 08 p1015 A73-20671
- Weight optimization for multilayered plates and shells with given load, end conditions and middle surface shape and dimension 08 p1019 A73-21762
- Configuration survey of lightweight solar array power systems for future missions. 09 p1153 A73-22782
- Weight minimization constrained design of rotational shallow spherical shells, comparing simplex and variable metric methods 09 p1165 A73-23446
- Vertical circular cylindrical shells buckling under axisymmetric compressive stress due to own structural weight, using Timoshenko elastic stability theory 09 p1166 A73-23459
- Structural design for weight or volume minimization in deformable body under combined loads, comparing structures with different boundary configurations 10 p1226 A73-24791
- Strength and weight optimization of strengthened spherical shells under external pressure 11 p1434 A73-25389
- Mathematical programming optimization procedure applicable to minimum weight structural design, considering static stress and displacement constraints under alternative loading conditions [AIAA PAPER 73-341] 11 p1436 A73-25480
- Linear programming and gradient search algorithms for minimum weight design of finite element structures, applying to bar truss problems [AIAA PAPER 73-343] 11 p1436 A73-25482
- Synthesis of compression panels having non-uniform stiffener sections. 11 p1437 A73-25485
- A synthesis procedure for mechanically fastened joints in advanced composite materials. [AIAA PAPER 73-348] 11 p1437 A73-25486
- Light weight beaded and tubular structural panels for heat shielded aerodynamic surfaces [AIAA PAPER 73-370] 11 p1438 A73-25504
- Aeroelastic structural weight optimization under strength and flutter constraints, using finite element and displacement methods to describe equations of motion in matrix form [AIAA PAPER 73-389] 11 p1439 A73-25518
- Gradient optimization of structural weight for specified flutter speed. [AIAA PAPER 73-390] 11 p1439 A73-25519
- Numerical procedure for determining optimal member sizes of aircraft structural components with weight minimization and flutter speed lower bound [AIAA PAPER 73-391] 11 p1439 A73-25520
- Experimental evaluation of the single-cell concept for a lightweight, rechargeable hydrogen-oxygen fuel cell. 11 p1309 A73-25987
- Structural failures in light weight solar cell arrays under thermal cycling. 11 p1310 A73-25999
- Minimum-mass design of multiclement structures under a frequency constraint. 11 p1444 A73-26380
- A new method for the study of the phenomenon of dynamic instability of thin-walled bars used in the construction of aeroplanes, ships and bridges. 12 p1551 A73-27063
- Determination of the required thickness of thermal insulation casings and evaluation of the weight-based effectiveness of materials 12 p1558 A73-27092
- Selection of optimal parameters for unidirectionally compressed three-layer plates 12 p1555 A73-27795
- Application of Pontryagin's maximum principle for minimum weight design of rigid-plastic circular plates. 13 p1696 A73-28754
- Light-weight Al isogrid panel design with triangular reinforcement elements for aerospace structural applications, discussing load response characteristics, fabrication and cost reduction 13 p1624 A73-28906
- On the optimal design of statically indeterminate elastic structures subjected to multiple loading systems and multiple constraints. 14 p1805 A73-29760
- Optimal forms of the thin-walled closed cross-section of a beam subjected to bending 15 p1947 A73-31365
- Mortar design for parachute ejection and deployment into airstream to decelerate spacecraft and aircraft pilot escape modules, estimating hardware weight and reaction load [AIAA PAPER 73-459] 15 p1827 A73-31445
- Design of stiffened cylinders to resist axial compression. 15 p1950 A73-31921
- Structural weight optimization of single stage and multistage spacecraft for given payload and initial vehicle weight 15 p1944 A73-32619
- Dual extremum principles relating to optimum beam design. 16 p2081 A73-33748
- Iterative finite element method for minimum weight structural design with respect to buckling constraints applied to beam and orthogonal frame design 16 p2082 A73-33908
- Rigid lightweight honeycomb core radome development from materials and processes standpoint, discussing cost reduction and fabrication [SAE PAPER 730310] 17 p2177 A73-34670
- Cost/weight tradeoff ratios for fiber reinforced plastic aircraft structural components [SAE PAPER 730338] 17 p2257 A73-34689
- A parametric weights study of a composite material prop/rotor blade. [SAWE PAPER 950] 19 p2385 A73-37878
- The weight/performance interface - An argument for weight control. [SAWE PAPER 967] 19 p2385 A73-37884
- Cost estimating techniques for airframe weight-cost interface study for military aircraft design [SAWE PAPER 969] 19 p2385 A73-37885
- Design and development of lightweight wheel braking equipment. [SAWE PAPER 995] 19 p2434 A73-37894
- "The hub of the wheel" - A project designer's view of weight. [SAWE PAPER 996] 19 p2386 A73-37895
- Structural composites on future fighter aircraft. [AIAA PAPER 73-806] 19 p2388 A73-38371
- Development of a lightweight body-mounted solar cell array with a high power to weight ratio. 19 p2391 A73-38408
- Designing equal-life minimum-weight truss structures 20 p2619 A73-39357
- Sandwich plates minimum volume design for elliptic, triangular and annular structures, discussing Mises criterion and bending coordinates 20 p2623 A73-39559
- Calculation of three-layer minimum-weight panels as a problem of mathematical programming 20 p2625 A73-39651
- Optimum design of three-layer shells 20 p2625 A73-39653
- Influence of the effectiveness of jet vanes on the characteristics of VTOL aircraft 21 p2634 A73-40401
- Weight reduction in stiffened panels with specified initial buckling load in uniform longitudinal compression by stiffeners utilization 21 p2787 A73-41190
- Light weight shaft design using minimum principle for nonlinear multipoint boundary value problem [ASME PAPER 73-DET-10] 22 p2919 A73-42068
- Analytic treatment of minimum weight design of cantilevers. [ASME PAPER 73-APMW-29] 22 p2925 A73-42889
- STRUTS**
- Flexural vibrations of a cantilever strut mounted on a rotating disk 10 p1290 A73-24308
- A mechanized eddy current scanning system for aircraft struts. 10 p1225 A73-24631
- STUDS (STRUCTURAL MEMBERS)**
- Stud welding on 5083 aluminum and 9% Ni steel for cryogenic use. 11 p1375 A73-26352
- STURM-LIOUVILLE OPERATOR**
- U STURM-LIOUVILLE THEORY**
- STURM-LIOUVILLE THEORY**
- Asymptotic properties of eigenvalues in the Sturm-Liouville problem of a class of equations with random coefficients 01 p0070 A73-10099
- Uniqueness of a solution to an inverse problem in the case of a second order equation with continuous boundary conditions: Regularized sums of a portion of eigenvalues - Factorization of the characteristic determinant 01 p0071 A73-11440
- Sturm-Liouville solution of unsteady stratified two dimensional Couette flow equations of motion 03 p0292 A73-13304
- Spectrum of the self-adjoint extensions of a minimal operator generated by the Sturm-Liouville equation with an operator potential 04 p0470 A73-14931
- Sturm-Liouville problem monotone proper function zeros lower and upper bounds evaluation using Barta inequality and Schwartz iteration 09 p1113 A73-23026
- Estimating the eigenvalues of Sturm-Liouville problems by approximating the differential equation. 13 p1649 A73-28606
- Dual and triple spin-stabilized deformable spacecraft attitude stability, comparing results based on Sturm theorem with Liapunov analysis 18 p2359 A73-36306
- An iterative solution to the second order eigenvalue equation with periodic boundary conditions. 18 p2330 A73-36609
- STYRENES**
- NT POLYSTYRENE**
- Photo-decarbonylation of beta-styryl isocyanates. 12 p1466 A73-27225
- SUBARCTIC REGIONS**
- Three-dimensional polarization characteristics of high-latitude Pc 5 geomagnetic micropulsations. 02 p0156 A73-11738
- Models of extreme arctic and subarctic winter atmospheres between 20 and 90 km. 02 p0160 A73-12274
- SUBCARRIER WAVES**
- U CARRIER WAVES**
- SUBCIRCUITS**
- U CIRCUITS**
- SUBCONTRACTS**
- Aircraft structural components in-house or subcontracted fabrication, discussing technical performance, economic and manpower aspects 10 p1297 A73-23521
- SUBCOOLING**
- U SUPERCOOLING**
- SUBCRITICAL FLOW**
- The prediction of airfoil pressure distributions for subcritical viscous flow and for supercritical inviscid flow. 03 p0247 A73-14378
- Operation modes simulation of single stage gas turbine at subcritical and supercritical gas flow, noting scale model tests 05 p0532 A73-17024

SUBDWARF STARS

Wind tunnel study of flows generated by slender cones in subcritical Reynolds number regime, examining vortex shedding and drag

10 p1174 A73-24845

Effect of shroud eccentricity on suppression of flow induced vibrations.

13 p1690 A73-28059

Subcritical and supercritical compressible shock-free flows in blade cascades

16 p1962 A73-32812

SUBDWARF STARS

Spectrophotometric observation of He-rich subluminescent subdwarf peculiar O-type star CPD-31 1701, noting spectrum dominance by extremely stark-broadened He lines

08 p1003 A73-20894

Novae physical processes during subdwarf-explosive variable-subdwarf evolution, describing spectroscopic indications for various luminous stages vs time

13 p1682 A73-28984

Line blanketing theory tested via G-I index, discussing underestimation of extreme subdwarf effective temperatures

16 p2058 A73-32834

SUBGRAVITY

U REDUCED GRAVITY

SUBGROUPS

Infinite groups with constraints on subgroups, discussing Chernikov theorems, minimality requirements, laminary finite groups and Abelian subgroups

01 p0070 A73-11075

SUBHARMONIC GENERATORS

Generation and stability of subharmonic and modulated subharmonic oscillations in nonlinear systems.

01 p0076 A73-10303

Subharmonic generation and its implications in Gunn effect devices.

04 p0427 A73-15055

Cascade phase-lock loops for the generation of harmonic and subharmonic components.

04 p0421 A73-15433

Parametric subharmonic oscillators - Static behaviour.

04 p0429 A73-15929

Microwave oscillator subharmonic phase locking, discussing nonlinear capacitance and linear frequency-dependent parameter and broadband tuning characteristics comparison with fundamental injection locking

06 p0677 A73-18739

Subharmonic resonance of order 1/2 with an asymmetrical restoring force.

10 p1292 A73-24649

Two coupled nonlinear oscillators driven by sinusoidal input, calculating fractional harmonic frequency pairs relationship to driving and resonance frequencies

13 p1659 A73-28487

Impulse analysis of subharmonic oscillations in control systems with thyristor converters.

22 p2835 A73-42299

Experimental study of the adiabatic invariant of self-oscillating processes

23 p3006 A73-43850

SUBLATTICES

U LATTICES [MATHEMATICS]

U SUBGROUPS

SUBLAYERS

U SUBSTRATES

SUBLIMATION

Access to uncombined titanium through an inhibiting film in sublimation pumping of deuterium.

02 p0194 A73-12844

Mass transfer technique for investigation of heat transfer by jet-impingement systems.

03 p0400 A73-14642

Carbon and graphite sublimation in inert gas flow at 2800-3000 K, determining rate dependence on temperature under kinetic and diffusive conditions

06 p0713 A73-17411

Solid-gas mass transfer in the case of laminar free convection

06 p0768 A73-17919

Vaporization and compatibility of SiGe radioisotope thermoelectric generators.

09 p1117 A73-22761

Vacuum sublimation of ammonium perchlorate.

12 p1466 A73-27127

Icy cometary nuclei laboratory simulation by sublimation of dust particle containing ice and frozen electrolyte mixtures in high vacuum at low temperature

14 p1793 A73-29823

SUBLIMINAL STIMULI

Limulus photoreceptor response to single photon stimulation, discussing flash intensity, dim lights, discrete waves and subliminal responses

09 p1042 A73-23308

Increment thresholds for multiple identical flashes in the peripheral retina.

23 p2946 A73-43343

SUBMARINES

Scaling relations to predict size of submarine generated wake in stratified water flow, measuring velocity and temperature profiles

06 p0644 A73-17644

Diver lockout submarine Shelf Diver evaluation for missile recovery use, noting design and navigation systems

14 p1742 A73-30089

Nuclear submarine atmospheric constituent monitoring, covering mass spectrometers, IR carbon monoxide sensors, system development, requirements testing and spacecraft applications

[ASME PAPER 73-ENAS-9] 19 p2399 A73-37970

SUBMERGED BODIES

NT DIVING [UNDERWATER]

Stress field and deformed shapes of liquid filled axisymmetric sessile neo-Hookean membrane during submergence to various depths

03 p0292 A73-13303

Role of mineralocorticoids in the natriuresis of water immersion in man.

09 p1040 A73-22676

Linear axisymmetric self similar solution for blunt nosed rigid cone immersed into ideal compressible fluid at subsonic velocity, computing wetted surface radius increase

12 p1487 A73-27410

Vertical submersion of a floating cylindrical solid

15 p1861 A73-31283

A perturbation method for low-frequency fluid-structure interaction problems.

[ASME PAPER 72-APM-WWW] 17 p2248 A73-35102

SUBMERGING

Integral method of calculating a semibounded laminar jet

02 p0153 A73-11784

Effects of immersion with the head above water on tissue nitrogen elimination in man.

02 p0135 A73-12563

Respiration mechanics during weightlessness simulation in an immersion medium

08 p0929 A73-20986

Exfoliation corrosion testing of 7178 and 7075 aluminum alloys.

15 p1889 A73-31742

Roentgenographic study of relative heart motion during vibration in water-immersed cats.

16 p1973 A73-34039

SUBMILLIMETER WAVES

Propagation of submillimeter-band electromagnetic waves in the drifting plasma of a solid

01 p0017 A73-10976

Spectral characteristics and black body radiation sensitivity of submillimeter band radiometer based on n-type epitaxial GaAs films

02 p0147 A73-12496

Electromagnetic measurement at submillimeter wavelengths for solids and liquids absorption and refraction and atmospheric gases and plasmas emission based on Fourier transform spectrometry

03 p0310 A73-14496

Domain-wall related, natural, submillimeter-wave resonance in orthoferrites

06 p0736 A73-18114

Problem of the influence of absorption on the amplitude fluctuations of submillimeter radio waves in the atmosphere

07 p0793 A73-19922

Millimeter and submillimeter wave detection and mixing with superconducting weak links.

07 p0863 A73-20102

Josephson junction millimeter microwave source and homodyne detector.

07 p0863 A73-20104

Submillimeter radio telescope employing an n-InSb detector

07 p0825 A73-20311

Theoretical possibilities for determining the moisture content of the atmosphere through the thermal radio emission in the submillimeter range.

07 p0848 A73-20347

Submillimeter-band gas laser pumped by a CO₂ laser.

08 p0976 A73-21654

Production of a coherent submillimetric radiation by a heterodyne method

09 p1097 A73-23030

Open resonator operating at 337-micron wavelength.

09 p1097 A73-23094

Equivalent circuits of diodes in millimeter and submillimeter wave frequencies.

10 p1193 A73-23667

Modulation of infrared and sub-mm waves with crossed forward-biased junction diodes.

10 p1194 A73-24171

Water vapor lines controlled atmospheric absorption spectrum in 220 GHz window region, discussing approximate calculation for submillimeter lines residual effect

11 p1330 A73-25688

A balloon-borne helium-cooled interferometer for investigation of the isotropic submillimetre background.

11 p1368 A73-26506

Submillimeter radio telescope with an n-InSb detector.

12 p1497 A73-27283

Further measurements of the submillimeter background at balloon altitude.

13 p1606 A73-28188

Radio emission of the moon at millimeter and submillimeter wavelengths

16 p2064 A73-33766

Optical method for submillimeter band phase measurements by probing spatially separated comparison fields and summing two signals at detector

17 p2120 A73-34123

Spectroscopic measurement of material sample refractive index at submillimeter wavelengths

17 p2120 A73-34151

Visualization of the amplitude-phase structure of electromagnetic fields in the millimeter and submillimeter ranges

17 p2121 A73-34191

Gas discharge plasma diagnostics based on polarization rotation of submillimeter laser radiation

20 p2598 A73-39625

Observation of solar submillimeter-band emission at sea level with the aid of a Fourier spectrometer

21 p2760 A73-40719

Submillimeter wave spectroscopy with a vacuum Fabry-Perot interferometer

22 p2852 A73-41788

Measurement of the atmospheric brightness temperature at submillimeter wavelengths

22 p2847 A73-42330

Modified H guide for millimeter and submillimeter wavelengths.

23 p2960 A73-44070

Prospects for studying mechanisms responsible for the nonthermal effects of millimeter- and submillimeter-band electromagnetic radiation on biologically active compounds

23 p2949 A73-44090

Cyclotron resonance breakdown with submillimeter lasers.

24 p3095 A73-44588

SUBORBITAL FLIGHT

Use of magnetometers and asymmetric antenna patterns for attitude determination.

05 p0596 A73-17205

SUBREFLECTORS

Shaping of subreflectors in Cassegrainian antennas for maximum aperture efficiency.

14 p1734 A73-30200

Frequency-selective surfaces for multiple-frequency antennas Design data plus experimental results.

14 p1737 A73-30623

SUBROUTINES

FORTRAN subroutine for X-Y plotting and display of two dimensional alphanumeric finite element mesh on line printer

03 p0280 A73-13344

A computational technique for the efficient handling of large matrices.

19 p2445 A73-38191

Efficient subroutines for the solution of general elliptic and parabolic partial differential equations.

24 p3106 A73-45099

SUBSETS [MATHEMATICS]

U SET THEORY

SUBSONIC AIRCRAFT

Indicating instrument for angle of attack and sideslip on subsonic flight vehicles via static pressure sensing, noting wind tunnel tests

02 p0166 A73-11723

Subsonic aircraft noise - A solution by the wider application of today's new engines.

03 p0249 A73-13065

Subsonic commercial transport aircraft reduces noise and increased cruise Mach number effects on nacelle design in terms of inlet, fan, cowl and nozzle

03 p0358 A73-13461

Sound field generated by spatial instabilities interaction on shear layer shed from duct with nozzle lip, discussing excess noise of subsonic jets

06 p0687 A73-18521

Slender delta-wings for future subsonic passenger planes

09 p1027 A73-21993

Aircraft design parameters optimization based on criterion function representing overall deviation from specifications with application to subsonic passenger aircraft

12 p1458 A73-27059

Book - Methods for estimating drag polars of subsonic airplanes.

16 p1963 A73-33442

Book - Methods for estimating stability and control derivatives of conventional subsonic airplanes.

16 p1969 A73-33442

On the unsteady supersonic cascade with a subsonic leading edge - An exact first order theory. II.

16 p1964 A73-33449

Subsonic jet aircraft contribution to NOx in the stratospheric ozone layer - 1968 to 1990.

16 p2046 A73-33561

A finite-element method for calculating aerodynamic coefficients of a subsonic airplane.

18 p2265 A73-36359

Subsonic aircraft turbojet engines, discussing the aerodynamic cycles, entry temperature increase, propulsive efficiency and economy improvements and ecological requirements

18 p2343 A73-36995

SUBSONIC FLOW

Subsonic plasma motion in continuous laser light.
01 p0084 A73-10472

Numerical solution of one-dimensional non-steady flow with supersonic and subsonic flows and heat transfer.
01 p0003 A73-10765

Numerical method for describing turbulent, compressible, subsonic separated jet flows.
01 p0035 A73-11467

Buoyancy distribution of slender axisymmetric bodies of higher order in the case of compressible subsonic flow
[DGLR PAPER 72-067] 02 p0127 A73-11681

Further studies of the aeroacoustics of jets perturbed by screens.
02 p0154 A73-12200

Characteristics of pressure fluctuations in the subsonic free jet
03 p0290 A73-12966

Separated flow noise.
03 p0291 A73-12975

The optimisation of sound attenuation in lined ducts containing uniform, axial, subsonic, mean flow.
03 p0291 A73-12987

Polytropic subsonic stellar winds with magnetic fields.
03 p0361 A73-13368

Effects of transverse ribs on pressure recovery in two-dimensional subsonic diffusers.
[AIAA PAPER 72-1141] 03 p0243 A73-13447

Computer methods for simulation of multidimensional, nonlinear, subsonic, incompressible flow.
[ASME PAPER 72-HT-61] 03 p0294 A73-13546

Acoustic power spectrum of a subsonic jet.
03 p0295 A73-14040

Inverse Laval problem of three dimensional subsonic and supersonic flows in nozzles and ducts of variable cross section in terms of asymptotic series
03 p0246 A73-14046

An improved kernal function formulation for unsteady subsonic flow.
05 p0567 A73-17122

Calculation of subsonic and transonic flow at the stern of bodies of revolution
06 p0643 A73-17468

High subsonic flow past airfoils at 2 deg angle of attack, describing relaxation method for hyperbolic Euler equations conversion to parabolic form
06 p0645 A73-17738

Boundary value problem for subsonic gas flow, proving existence theorem for gas dynamics problem solution
06 p0645 A73-18069

Pressure, temperature, current density and potential difference fluctuations in subsonic flow of combustion products plasma, noting steadiness, ergodicity and distribution functions
06 p0732 A73-18616

Variational mixed boundary value problems of subsonic gas flows for plane parallel symmetric Laval nozzle and transonic wedge, using singular integral equation
06 p0646 A73-18888

Penetration of retrorocket exhausts into subsonic counterflows.
07 p0773 A73-19491

Stability of clamped rectangular plates in uniform subsonic flow.
07 p0913 A73-19982

Unsteady thin-airfoil theory for subsonic flow.
08 p0925 A73-20718

A subsonic diffuser with moving walls for boundary-layer control.
08 p0953 A73-20723

Prediction of aeroelastic instabilities in turbines
09 p1135 A73-22204

Solution of the direct problem of mixed subsonic and supersonic gas flow in a nozzle of finite length
09 p1072 A73-22480

Rayleigh-Ritz solution of boundary value problem for plane compressible subsonic flow past aerofoil noting convergence
09 p1028 A73-22954

Experimental study of the heat transfer in the separation zones in front of cylindrical projections
10 p1294 A73-23587

Compressible magnetorelative flow character in subsonic, supersonic and transonic regions, obtaining pressure coefficient, free stream Mach number and eleven speed interrelationships
10 p1210 A73-24921

Plane subsonic jet free boundaries flapping measurements from oppositely placed hot-wire probes
11 p1346 A73-25251

Noise reduction for subsonic fluid flow over flat plate via interposition of secondary fluid layer at trailing edge
11 p1300 A73-25386

Aeroelastic dynamic response to shock induced flow separation, analyzing wing buffet components at high Mach number subsonic flow
[AIAA PAPER 73-308] 11 p1300 A73-25539

Unsteady subsonic compressible flow around finite thickness wings.
[AIAA PAPER 73-313] 11 p1301 A73-25544

Numerical method for predicting unsteady aerodynamic loadings caused by control surface motions in subsonic flow.
[AIAA PAPER 73-315] 11 p1301 A73-25546

The stability of simply supported rectangular surfaces in uniform subsonic flow.
[ASME PAPER 72-APM-22] 11 p1441 A73-25702

Noise intensity in the field of subsonic turbulent jets
11 p1347 A73-25738

Gas jet flow at high subsonic velocities, determining stream function, contraction coefficient, convergence at critical velocity and pressure above obstacle
11 p1302 A73-26215

Study of disturbance reflection from the subsonic section of a Laval nozzle
11 p1411 A73-26437

Linear axisymmetric self similar solution for blunt nosed rigid cone immersed into ideal compressible fluid at subsonic velocity, computing wetted surface radius increase
12 p1487 A73-27410

Downwash-velocity potential method for oscillating surfaces.
13 p1564 A73-28803

Control by pressure drop of the radial distribution of the Mach number behind a subsonic annular cascade
[ONERA, TP NO. 1220] 13 p1565 A73-28838

Calculation of the unsteady subsonic aerodynamic pressures on compressor blades
[ONERA, TP NO. 1221] 13 p1565 A73-28839

Two dimensional steady subsonic flow through airfoil cascades, predicting turbomachine performance from boundary layer calculation for comparison with experiments
13 p1565 A73-29005

Reduction of noise generated by flow of fluid over plate.
14 p1746 A73-30915

Calculation of a subsonic radiating gas flow by an adjustment method
15 p1821 A73-30969

Approximate solution of a stream problem of subsonic gasdynamics
15 p1821 A73-31152

An approximate method for the calculation of the velocities induced by a wing oscillating in subsonic flow
15 p1824 A73-31905

Spectroscopic observations of subsonic and sonic vapor flow inside an open-ended heat pipe.
15 p1958 A73-31936

Design and performance characteristics of a small subsonic flow HF chemical laser.
15 p1885 A73-31978

Solution of the direct problem on mixed subsonic and supersonic flow of a gas in a nozzle of finite length.
15 p1824 A73-32067

Variational mixed boundary value problems of subsonic gas flows for plane parallel symmetric Laval nozzle and transonic wedge, using singular integral equation
15 p1824 A73-32412

On the unsteady supersonic cascade with a subsonic leading edge - An exact first order theory.
[ASME PAPER 73-GT-15] 16 p1963 A73-33492

Calculation of compressible subsonic flow in cascades with varying blade height.
[ASME PAPER 73-GT-59] 16 p1964 A73-33514

Acoustic instability of a bounded weakly ionized plasma
17 p2214 A73-34135

Theoretical and experimental work on losses in 2-D turbine cascades with supersonic outlet flow.
17 p2092 A73-34377

General solution to the subsonic through-flow problem in a turbomachine including losses.
17 p2092 A73-34385

Effect of axial velocity variation on the subsonic flow through a compressor cascade.
17 p2094 A73-34397

Harmonic and impulsive acoustic source-produced sound propagation across vortex sheet separating two subsonic fluids, investigating instability waves
17 p2151 A73-34825

Analytical study of pressure balancing in gas film seals.
17 p2180 A73-35000

Further data on the pressure recovery performance of straight-channel, plane-divergence diffusers at high subsonic Mach numbers.
[ASME PAPER 73-FE-5] 17 p2152 A73-35005

Transmission of upstream sound through a subsonic jet.
[AIAA PAPER 73-630] 18 p2259 A73-36175

Forces acting on conical diffusers and their relation to integral performance parameters.
[AIAA PAPER 73-686] 18 p2262 A73-36237

Graphite oxidation at low temperature in subsonic air.
[AIAA PAPER 73-735] 18 p2326 A73-36352

Investigation of the flow in regions of turbulent boundary layer separation in front of a subsonic jet blown from a circular nozzle
18 p2265 A73-37003

New contributions to the iterative method for aerodynamic calculations of wings in subsonic flows
19 p2376 A73-37545

Subsonic and supersonic turbulent shear layer aerodynamic noise emission derivation from differential wave equations via Fourier transformation and WKBJ method
20 p2507 A73-39087

On the effect of swirling motion of sources of subsonic jet noise.
21 p2676 A73-40286

Small-scale suppressor of the aerodynamic noise of a subsonic gas jet
21 p2754 A73-40404

Simplified aerodynamic theory of oscillating thin surfaces in subsonic flow.
21 p2632 A73-40427

Closed-form lift and moment for Osborne's unsteady thin-airfoil theory.
21 p2632 A73-40442

Pressure distribution and boundary layer separation measurement on circular cylinder at critical subsonic velocities for various Reynolds and Mach numbers
21 p2632 A73-40476

Peak subsonic noise level reduction by jet refraction, showing directivity patterns as function of jet velocities and temperature ratios
21 p2754 A73-40753

A parallel algorithm for high subsonic compressible flow over a circular cylinder.
21 p2727 A73-41474

The panel method for the calculation of the pressure distribution on missiles in the subsonic range
22 p2797 A73-43028

Nozzle design for subsonic flow in axisymmetric contractions based on potential flow theory and visual observation, obtaining velocity distribution along wall
22 p2798 A73-43029

On the application of a new version of lifting surface theory to nonslender and kinked wings.
23 p2939 A73-43210

Some effects of pipe flow generated entry conditions on the performance of straight walled conical diffusers with high sub-sonic entry Mach number.
23 p2939 A73-43294

Plane shock wave propagation, reflection and transmission in subsonic flow regime through T-junctions, predicting pressure variation upstream and downstream for comparison with experiment
23 p2967 A73-43295

A study of the interaction between two compressible fluid flows in a flat channel at low Mach numbers
23 p2968 A73-43731

Acoustic wave propagation in axisymmetric swirling subsonic jet flow, obtaining directivity patterns for spinning and nonspinning modes from wave equation numerical integration
[AIAA PAPER 73-1004] 24 p3077 A73-44837

A new device for measuring local acoustic power output of subsonic jets.
[AIAA PAPER 73-1042] 24 p3090 A73-44866

SUBSONIC FLUTTER

Acoustic resonance during the vibrations of a plate cascade in subsonic gas flow
03 p0294 A73-13619

Flutter technology in the United Kingdom - A survey.
[AIAA PAPER 73-330] 11 p1441 A73-25559

Control law synthesis and sensor design for active flutter suppression.
[AIAA PAPER 73-832] 21 p2784 A73-40502

SUBSONIC SPEED

Criteria concerning the adaptation of the rear components of a propulsion system to the subsonic and transonic altitude flight
[DGLR PAPER 72-065] 02 p0128 A73-11690

Power spectrum due to point source convection at uniform subsonic speed along round jet flow axis
03 p0246 A73-13841

The influence of a strake on the flow field of a delta wing/lambd 0.2/ at near-sonic velocities
[DGLR PAPER 72-125] 03 p0248 A73-14385

Fighter aircraft maneuverability improvement at high subsonic speeds by slotted and unslotted leading- and trailing-edge flaps on delta wing
[DGLR PAPER 72-126] 03 p0248 A73-14386

Flight and wind tunnel investigation of the effects of Reynolds number on installed boattail drag at subsonic speeds.
[AIAA PAPER 73-139] 05 p0530 A73-16888

Calculation of the aerodynamic characteristics of a rectangular wing with tip plates moving at a low subsonic speed in the proximity of a screen
07 p0775 A73-20094

Experimental results in the case of the Nonweiler wave-rider in the subsonic, transonic, and supersonic range
16 p1963 A73-33265

Noise source distribution in subsonic jets.
19 p2472 A73-37290

SUBSONIC WIND TUNNELS

- Subsonic jet noise measurements on model jet rig in anechoic chamber, discussing correlation and prediction 19 p2473 A73-38106
- Progress in source noise suppression of subsonic tip speed fans. [AIAA PAPER 73-1032] 24 p3122 A73-44861
- ## SUBSONIC WIND TUNNELS
- Powered model wind tunnel investigation to determine performance trends with nacelle location. [AIAA PAPER 72-1114] 03 p0243 A73-13429
- Subsonic wind tunnel tests for laminar boundary layer investigation in low level turbulence flow, noting turbulence measurement with hot-wire anemometers 03 p0308 A73-13666
- Application of certain generalized data from wind-tunnel tests with plane subsonic compressor cascades to the calculation of the characteristic flow regimes in supersonic cascades 12 p1458 A73-27480
- Subsonic free jet wind tunnel turbulence damping in settling chamber via screen, yielding uniform velocity profile and low turbulence level in nozzle exit 16 p1996 A73-33266
- Subsonic wind tunnel tests for laminar boundary layer investigation in low level turbulence flow, noting turbulence measurement with hot-wire anemometers 21 p2704 A73-41316
- Electric analogy method for subsonic wind tunnel contraction cone design providing uniform velocity distribution in test section, obtaining pressure distribution in cone boundary 22 p2797 A73-43000
- Approximate method for calculating the turbulent boundary layer in front of a recess 23 p2968 A73-43732
- ## SUBSTRATES
- The effect of substrate temperature on the structure of titanium carbide deposited by activated reactive evaporation. 04 p0456 A73-15757
- Radiation damage effects in microwave dielectric substrate materials. 05 p0557 A73-16507
- On the establishment of a diffusion barrier between a boron fiber and its tungsten substrate 05 p0589 A73-17049
- Influence of the substrate and the structure of the metal film on the nature of the annealing treatment of defects formed in the film by proton bombardment 07 p0864 A73-20524
- Microwave integrated circuits on a ferrite substrate. 08 p0942 A73-20704
- The influence of substrate properties on microwave losses in thin films of semiconductors. 09 p1064 A73-23041
- A quick accurate method to measure the dielectric constant of microwave integrated-circuit substrates. 10 p1197 A73-24866
- Design of temperature-controlled substrates for hybrid microcircuits. 13 p1588 A73-28044
- Effect of base material on the formation of thin plasma coatings 15 p1881 A73-31590
- Book - Handbook of adhesive bonding. 17 p2180 A73-35337
- Substrate effect estimation for space charge limited current in intrinsic materials and planar structures, discussing I-V curves 20 p2543 A73-39593
- Influence of chemical composition on the structure and mechanical properties of polycarbonate films and the possibility of using them as a substrate for moving-picture films 21 p2646 A73-40259
- The relation between the internal thermal resistance of transistors and the method of alloying 23 p2960 A73-43677
- Substrates with end effect in shorted slot, measuring normalized inductive reactance dependence on thickness to wavelength ratio 23 p2954 A73-44068
- ## SUBSTRUCTURES
- Comparison between sparse stiffness matrix and sub-structure methods. 07 p0907 A73-19031
- The optimization of the supporting structures of parabolic antennas 14 p1740 A73-29742
- Finite element method round-off errors relation to fundamental equations conditioning, considering round-off errors effect on precision of method of sub-structures 14 p1806 A73-30180
- ## SUBTRACTORS
- ## U ADDING CIRCUITS
- ## SUBTROPICAL REGIONS
- ## U TEMPERATE REGIONS
- ## U TROPICAL REGIONS
- ## SUCROSE
- Plasma insulin and carbohydrate metabolism after sucrose ingestion during rest and prolonged aerobic exercise. 21 p2641 A73-41622

SUCTION

- Hydrodynamic stability of boundary layers with surface suction. 01 p0033 A73-10749
- Variational analysis of high mass transfer rates from spherical particles - Boundary-layer injection suction considerations at low particle Reynolds numbers and high Peclet numbers. 01 p0122 A73-10802
- Suction force suppression during takeoff, landing and transition of VTOL turbojet via wing turning wing about axis parallel to earth plane 02 p0129 A73-11631
- Similarity solution of boundary layer flow due to uniform streaming past infinite flat plate with uniform suction at plate surface 03 p0292 A73-13306
- Hypersonic rarefied flow past an insulated flat plate with suction/injection. 04 p0520 A73-15939
- Flow of a viscous incompressible fluid between a fixed porous disk and a rotating nonporous disk, with radial discharge 07 p0811 A73-20069
- Kinetic theory of suction flow, discussing slip coefficient determination for perturbation boundary conditions in Chapman-Enskog-Hilbert method and pressure gradient effects 07 p0812 A73-20474
- Steady turbulent boundary layer of compressible perfect gas on heat insulated surface with suction and longitudinal pressure gradient 08 p0954 A73-21177
- Turbulent incompressible boundary layer on porous heat insulated plate with uniform suction, calculating ratio of friction drag coefficients 08 p0954 A73-21178
- Boundary layers calculation for nonporous surface extended to porous with suction by replacing velocity distribution with longitudinal pressure gradient 08 p0954 A73-21179
- Heat transfer for turbulent flow with suction in a porous tube. 08 p1024 A73-21637
- Development of unsteady boundary layers under variable suction. 10 p1209 A73-24831
- On MHD flow along an infinite flat wall with constant suction. 11 p1405 A73-25975
- Approximate calculation of the incompressible laminar boundary layer on a plate with suction 13 p1600 A73-28446
- Application of small perturbation method in calculations of turbulent boundary layers on a curvilinear surface with suction 13 p1600 A73-28447
- Heat transfer by fluctuating flow of an elastico-viscous liquid past an infinite plate with time varying suction. 14 p1816 A73-29999
- Free convection effects on the oscillatory flow past an infinite, vertical, porous plate with constant suction. I, II. 14 p1816 A73-30049
- Magnetohydrodynamic boundary layer control with suction or injection. 15 p1864 A73-31931
- The solutions of the boundary layer equations in the case of extremely intensive blowing or suction 16 p1963 A73-33250
- Three dimensional turbulent boundary layer of yawed wing suction surface in uniform flow, examining cross flow profile, velocity distribution and weighting functions 16 p1963 A73-33267
- Vortex-lift prediction for complex wing planforms. 17 p2094 A73-34438
- Laminar boundary layers along an infinite flat plate with oblique suction. 19 p2420 A73-37646
- Turbofan suction noise level measurements, discussing octave noise analysis, angular velocity distributions, discharge coefficient, takeoff and landing operations 19 p2473 A73-37816
- On the effects of uniform high suction on the rotationally symmetric flow of a conducting liquid near a stationary disc in the presence of a transverse magnetic field. 19 p2469 A73-38186
- Investigation of nozzles with cryogenic suction of the boundary layer 21 p2678 A73-41221
- On unsteady flow of an elastico-viscous fluid past an infinite plate with variable suction. 22 p2840 A73-41747
- Approximate calculation of the optimal suction of a compressible gas on a thermally insulated surface at Prandtl numbers other than unity 22 p2795 A73-42118
- Experimental investigation of the filtration characteristics of porous materials used in boundary-layer control systems 22 p2841 A73-42119

- Influence of suction on the supercavitation flow behind a body in a porous tube 22 p2841 A73-42122
- Flow of a viscous gas at a slot with strong suction 22 p2796 A73-42222
- Heat transfer from an enclosed rotating disk with uniform suction and injection. 22 p2938 A73-42922
- Asymptotic suction boundary layer profile past porous plane surface, obtaining upper and lower bounds on energy stability limit 23 p2969 A73-44382
- ## SUD AVIATION AIRCRAFT
- ## NT CONCORDE AIRCRAFT
- ## SUDDEN ENHANCEMENT OF ATMOSPHERICS
- Measurement methods for sudden ionospheric disturbances caused by solar flares, discussing shock wave fading, sudden phase anomaly and sudden enhancement of atmospherics techniques 22 p2904 A73-43062
- ## SUDDEN IONOSPHERIC DISTURBANCES
- Solar flare effects in ionosphere, discussing long term variability, sudden ionospheric disturbances PCA and magnetic storms 04 p0491 A73-14833
- Forecast facilities for solar events and activity and sudden ionospheric disturbances, noting forecast centers activity, resources and techniques 04 p0491 A73-14844
- The ionospheric effects of geomagnetic sudden commencements as measured with an HF Doppler sounder at Hawaii. 05 p0571 A73-17061
- The influence of negative-ion changes in the D-region during sudden ionospheric disturbances. 09 p1075 A73-22122
- Chromospheric flares and shock waves in interplanetary space 09 p1137 A73-22544
- Some studies on the association of solar optical flares and microwave bursts with sudden ionospheric disturbances. 11 p1354 A73-25766
- D-region recombination coefficients and the shock wavelength X-ray flux during a solar flare. 11 p1356 A73-25911
- Conjugate asymmetries in sudden commencement absorption and the sudden commencement absorption event of February 28, 1969. 12 p1534 A73-26909
- Effective recombination coefficient in the ionospheric D-region. 13 p1608 A73-28717
- The extreme ultraviolet emissions of solar flares - comparison between OSO-6 spectroheliograph observations and SFDs. 16 p2053 A73-32959
- Results of simultaneous in-situ-observations in Spain of electron concentration, neutral wind and pressure in the D-region in different seasons and during an SID-event and their relevance to the winter anomalous state of the atmosphere. 18 p2305 A73-36000
- Satellite measurements of solar X-ray flux around observations of sudden ionospheric disturbances. 18 p2347 A73-36383
- SID effects as observed in intensities of LF radio waves. 18 p2290 A73-36873
- Relationship between anomalous radio absorption and the solar zenith angle during periods of sudden ionospheric disturbances 19 p2406 A73-38323
- Solar-interplanetary disturbances during 5-18 June 1969 /The PFP interval/LASY/. 21 p2773 A73-41383
- Sudden ionospheric disturbance effects on LF radio pulse train amplitude during reception from Loran-transmitters, comparing with VLF sudden phase anomaly 22 p2825 A73-42118
- Some statistical characteristics of sudden ionospheric disturbances, and the distribution of geomagnetic chromospheric flares over the solar disk 22 p2847 A73-42323
- Measurement methods for sudden ionospheric disturbances caused by solar flares, discussing shock wave fading, sudden phase anomaly and sudden enhancement of atmospherics techniques 22 p2904 A73-43062
- ## SUDDEN STORM COMMENCEMENTS
- Low energy solar proton events intensity increases near time of magnetic storm sudden commencement and Forbush decrease, using propagation shock wave model 10 p1268 A73-24141
- Results of an investigation of the ionospheric effect of a sudden commencement of a magnetic storm 11 p1351 A73-25093
- A study of ionospheric absorption in conjugate regions produced by storm sudden commencements and sudden impulses in the geomagnetic field. 12 p1489 A73-26993

- Observation and first evaluation of geomagnetic pulsations near the polar aurora zone in connection with the occurrence of si's and ssc's
12 p1494 A73-27778
- On the origin of SC-storms with respect to forecast-
ing geomagnetic activity.
15 p1868 A73-31520
- Determination of a probable interval for the mean
transit time of geomagnetic-storm /SSC/ solar particles
15 p1926 A73-31647
- Energy and momentum theorems in magnetospheric
processes.
15 p1871 A73-31846
- Intensity variations of low-energy protons and electrons in the outer magnetosphere at the sudden onset of a magnetic storm
18 p2309 A73-36109
- Radio aurora, storm sudden commencements, and hydromagnetic waves.
18 p2313 A73-36646
- Differences between geomagnetic storms with gradual and sudden commencements
21 p2681 A73-40103
- Effects on the geomagnetic tail at 60 earth radii of the geomagnetic storm of April 9, 1971.
22 p2844 A73-41908
- Sudden commencement and sudden impulse absorption events at high latitudes.
22 p2845 A73-41928
- Azimuthal drift and precipitation of electrons into the South Atlantic geomagnetic anomaly during an SC magnetic storm.
22 p2846 A73-41946
- Comparison of the sectorial structure of the interplanetary magnetic field and the occurrence of SC and SI events.
22 p2908 A73-42447
- Polar magnetic storm temporal properties and distribution patterns, discussing solar activity, annual and twenty-seven day variations and sudden commencement
22 p2851 A73-42749
- Magnetospheric plasma motion during a sudden commencement.
23 p2972 A73-43689
- UGARS**
NT DEXTRANS
NT GLUCOSE
NT INOSITOLS
NT SUCROSE
Branched-chain carbohydrate structures resulting from formaldehyde condensation.
15 p1842 A73-32550
- UHL EFFECT**
Eigenfunction calculation of injected carrier density in doped semiconductor filaments, relating negative eigenvalues to Suhl effect and lifetime dependence to bulk and surface recombination
23 p3016 A73-43674
- UITS**
NT PRESSURE SUITS
NT SPACE SUITS
ULFATES
NT AMMONIUM SULFATES
An atomic absorption method for cation measurements in Kjeldahl digests of biological materials.
02 p0139 A73-12424
- Ni-Cr-thoria alloy surface oxidation induced by sprayed coating of sodium sulfate for gas turbine blade hot corrosion investigation
04 p0468 A73-15316
- Cracking of Ti-6Al-4V in methanol solutions containing sulfates.
11 p1385 A73-26175
- Na2SO4-induced attack of Ni-20Cr-2ThO2.
15 p1896 A73-32575
- Relative efficiencies of filters and impactors for collecting stratospheric particulate matter.
17 p2167 A73-34863
- The relationship between relative oxide ion content of Na2SO4, the presence of liquid metal oxides and sulfidation attack.
20 p2575 A73-39022
- Coherent X ray emission from plasma generated by laser irradiation of copper sulfate doped thin gelatin layer
21 p2710 A73-40126
- ULFIDES**
NT CADMIUM SULFIDES
NT CARBON DISULFIDE
NT COPPER SULFIDES
NT DISULFIDES
NT HYDROGEN SULFIDE
NT INDIUM SULFIDES
NT INORGANIC SULFIDES
NT LEAD SULFIDES
NT MOLYBDENUM DISULFIDES
NT MOLYBDENUM SULFIDES
NT POLYSULFIDES
NT PYRITES
NT TROILITE
NT WURTZITE
NT ZINC SULFIDES
NT ZINCBLLENDE
- Magnetic transitions observed in sulfide minerals at elevated pressures and their geophysical significance.
06 p0691 A73-18576
- Partitioning of potassium between silicates and sulphide melts - Experiments relevant to the earth's core.
11 p1355 A73-25902
- Mechanism of the lubricating action of sulfides and selenides of refractory metals
14 p1755 A73-30717
- The effect of carbon on the sulphidation of Co-Cr alloys.
19 p2443 A73-38250
- SULFONES**
Thermoplastic temperature range extended up to 260 C by polysulphones.
18 p2326 A73-36068
- SULFUR**
Refinement of primary silicon crystals in a hypereutectic Al-20% Si alloy by sulphur addition.
02 p0179 A73-11597
- Sulphur concentrations and isotope ratios in lunar samples.
07 p0887 A73-19775
- Ionospheric production and loss processes of atomic sulfur ions, considering dissociative ionization sources
12 p1489 A73-26999
- AC polarographic determination of sulfur in molybdenum-rhenium alloy.
17 p2118 A73-34276
- Molybdenum-oxygen-sulfur fuel cell anode catalysts capable of oxidizing low cost fuels in acid electrolytes
19 p2390 A73-38401
- SULFUR CHLORIDES**
Influence of thionyl chloride on the lasing characteristics of the liquid phosphor POC13-SnCl4-Nd3+/12 p1506 A73-27197
- SULFUR COMPOUNDS**
NT AMMONIUM SULFATES
NT CADMIUM SULFIDES
NT CARBON DISULFIDE
NT COPPER SULFIDES
NT DISULFIDES
NT HYDROGEN SULFIDE
NT INDIUM SULFIDES
NT INORGANIC SULFIDES
NT LEAD SULFIDES
NT MOLYBDENUM DISULFIDES
NT MOLYBDENUM SULFIDES
NT POLYSULFIDES
NT PYRITES
NT SULFATES
NT SULFIDES
NT SULFONES
NT SULFUR CHLORIDES
NT SULFUR FLUORIDES
NT SULFUR OXIDES
NT SULFURIC ACID
NT TROILITE
NT WURTZITE
NT ZINC SULFIDES
NT ZINCBLLENDE
- Influence of certain brain structures on the sulphydryl-group, diphosphopyridine-nucleotide, and serotonin contents of the blood
09 p1040 A73-22856
- Preparation and investigation of EuS thin films
11 p1410 A73-26672
- Detection of interstellar thiophomaldehyde.
15 p1933 A73-31378
- Corrosiveness of naturally occurring sulfur compounds and organic peroxides in aviation turbine fuels toward Cu and Ag, detailing maximum tolerable ratios
20 p2600 A73-39637
- SULFUR FLUORIDES**
Practical protective atmospheres for molten magnesium.
03 p0323 A73-13267
- Laser induced infrared fluorescence - Thermal heating, mass diffusion, and collisional relaxation in SF6.
03 p0318 A73-13281
- Pressure of radiation due to the absorption of resonant light
03 p0318 A73-13604
- CO2 laser radiation absorption in SF6-air boundary layers.
05 p0585 A73-16983
- [AIAA PAPER 73-262]
Effect of H2O, SF6 and CCl3F additions on the electron concentration in highly heated air
15 p1840 A73-31852
- Stimulated Raman scattering in sulfur hexafluoride.
20 p2574 A73-39688
- Sulfur hexafluoride pyrolysis and subsequent oxidation in mixtures with oxygen atoms and molecules, measuring decomposition rate at high temperature in shock tube experiment
22 p2818 A73-42767
- SULFUR OXIDES**
Kinetics of the sulphur dioxide catalyzed recombination of radicals in hydrogen flames.
03 p0352 A73-14393
- Calculation of pressure-broadened linewidths of SO2 and NO2.
04 p0414 A73-14815
- Excitation mechanism of the far-infrared sulfur dioxide molecular laser.
09 p1090 A73-21938
- [AD-760378]
Observation of Raman scattering by SO2 in a generating plant stack plume.
13 p1607 A73-28547
- Sulfur dioxide infrared-active vibration-rotation combination spectral band, examining quantum numbers, infrared absorption, centrifugal distortion effects and dipole moments
19 p2402 A73-37896
- Two modes of interaction of NaOH and SO2 in gases from fuel-lean H2-air flames.
22 p2820 A73-42802
- SULFURIC ACID**
Effect of temperature and polarization rate on the electrochemical behavior of titanium alloys in a sulfuric medium
02 p0178 A73-11523
- Bipolar noble-metal free electrodes for fuel cells with acid electrolytes.
04 p0407 A73-15113
- Sulfuric acid in the Venus clouds.
19 p2483 A73-37579
- Sulfuric acid solution composition to account for Venus cloud temperature, stratosphere dryness and IR spectrum
24 p3129 A73-44441
- The relation of surface condition after pretreatment to bondability of aluminum alloys.
24 p3093 A73-44764
- SUM RULES**
Conditions for localization of Cesaro's rectangular means and of Abel's method means in the limited summing of a multiple trigonometric Fourier series in the Liouville classes
01 p0071 A73-11439
- X ray K absorption spectra shifts /Bergad additivity rule deviations/ in Fe-Cr, Fe-V, Fe-Ni and Fe-Co systems due to lattice characteristics and electron structure changes
06 p0707 A73-18039
- SUMMER**
The altitude of the scattering layer near the mesopause over the summer poles.
14 p1750 A73-30768
- Northern summer tropical upper tropospheric large scale flow dynamics, energy exchange diagram and limited area numerical weather prediction problems
24 p3108 A73-45094
- SUN**
NT SOLAR OBLATENESS
The five-minute oscillations as nonradial pulsations of the entire sun.
01 p0104 A73-11049
- Solar core stability via model including plain parallel stratified fluid layer with energy generation, noting ice age correlation with mixing phases during evolution
04 p0501 A73-15623
- Four body problem reduction to three body problem via perturbation region, noting Moon-Earth-Sun system
05 p0623 A73-17198
- Revision of initial size, mass and angular momentum of the solar nebula and the problem of its origin.
17 p2229 A73-34431
- The solar abundance of silicon.
19 p2483 A73-37570
- The transportation of highly active nuclear waste products to the sun
20 p2590 A73-39148
- SUN SENSORS**
U SOLAR SENSORS
SUNLIGHT
Polarization of near-infrared sunlight reflected by terrestrial clouds.
01 p0073 A73-10363
- Sunlight scattering by dust along lunar horizon at sunset, presenting atmospheric model for dust cloud production
07 p0895 A73-19862
- Ionograms for slant sporadic E layer under continuous sunlight inside polar cap, noting occurrence probability and auroral activity
07 p0819 A73-20065
- Solar radiation climate correlation with long term sunshine records, comparing radiation measurements with predictions based on regression equations for Brisbane area
10 p1269 A73-24450
- An analytic formula for heating due to ozone absorption.
14 p1750 A73-30767
- Surveyor observations of lunar horizon-glow.
18 p2348 A73-35938
- Pioneer 10 space probe measurement of interplanetary particulates and aggregates via reflected and scattered sunlight, with emphasis on distribution in asteroid belt
18 p2350 A73-36095
- [AIAA PAPER 73-546]
Russian book - Scattered daytime sky light.
21 p2691 A73-41439
- SUNRISE**
Geomagnetic control over evolution of F2-layer at sunrise.
02 p0159 A73-12183

SUNSET

- Electron concentration variation in E layer after sunrise, noting critical frequency deviations from Chapman law 05 p0568 A73-16216
 - Sunrise changes in concentrations of minor neutral constituents in the mesosphere. 07 p0819 A73-20062
 - Nitric oxide densities during sunrise derived from overhead emission measurement as function of altitude 09 p1074 A73-22065
 - Midlatitude signal fading during sunrise and sunset transitions, noting amplitude ratio independence of propagation direction in earth-ionosphere waveguide 09 p1049 A73-22131
 - Possibility of estimating the flux of energetic particles in the ionospheric D-region at sunrise and during the daytime. 10 p1212 A73-24219
 - Nature of some optical effects observed on spacecraft at sunrise 18 p2909 A73-36122
- ## SUNSET
- Midlatitude signal fading during sunrise and sunset transitions, noting amplitude ratio independence of propagation direction in earth-ionosphere waveguide 09 p1049 A73-22131
 - Observations and theoretical reconstruction of the green flash. 11 p1351 A73-25168
 - Mesospheric and lower thermospheric ozone concentration measurement at sunset via occultation technique from rocket payloads 17 p2159 A73-34780
 - Rocket measurements of electron density and electron temperature at sunset. 18 p2311 A73-36148
 - Postsunset oxygen emission observation by radiometer on rocket launched at Natal, Brazil, observing 10-km thick emission layer. 22 p2848 A73-42536
 - The behaviour of the upper ionosphere over North America at sunset. 24 p3087 A73-45203
- ## SUNSPOT CYCLE
- Wolf number solar activity and planetary tidal force correlation during 1770-1970, noting 11-year cycle relation 01 p0101 A73-10848
 - Changes of electron density with zenith angle, with the sunspot cycle, and during eclipses. 01 p0043 A73-10907
 - Winter anomaly in ionospheric absorption of radio waves on 1.725 MHz during sunspot minimum. 01 p0043 A73-10910
 - Evidence for an ultra-long cycle of solar activity /Research note/. 01 p0108 A73-11397
 - Monopole aspects of solar magnetic field at sunspot cycle maximum and minimum, considering different explanations 04 p0496 A73-14972
 - Solar cycle control of the ionospheric E-region. 04 p0441 A73-15291
 - Interdependence of the basic elements of the 22-year solar activity cycle 05 p0609 A73-16205
 - Relations between the elements of a 22-year solar activity cycle 05 p0609 A73-16206
 - Lunar and solar geomagnetic tides in declination at Alibag. 07 p0819 A73-20055
 - Lunar eclipse brightness dependence on eleven year sunspot activity cycle 08 p1007 A73-21068
 - Geomagnetic disturbance recurrence interval correlation with long term sunspots rotation period 12 p1494 A73-27771
 - Solar prominences during period between sunspot minimum and maximum, investigating secondary polar zone coronal activity phase shift relationship to main zone anomaly 12 p1545 A73-27837
 - Seasonal and sunspot cycle variations of F region electron temperatures and protonospheric heat fluxes. 14 p1749 A73-29986
 - Wolf number solar activity and planetary tidal force correlation during 1770-1970, noting 11-year cycle relation 15 p1928 A73-30984
 - On the annual variation of solar faculae. 16 p2053 A73-33073
 - Lunar eclipse brightness dependence on eleven year sunspot activity cycle 18 p2355 A73-36869
 - Relative sunspot number periodicities determination, using power spectral analysis 21 p2777 A73-41489
 - Correlation and spectral analysis of daily solar radio flux. 21 p2762 A73-41494
 - Global climatological ozone changes in terms of secular, annual and sunspot cycle-related variability 23 p2974 A73-43858

- Dependence of some noise-storm characteristics on the solar activity cycle 23 p3036 A73-44249
 - Revision of the probability laws of sunspot variations. 24 p3137 A73-44648
 - Sunspot cycle effects on solar and lunar tide-produced diurnal and seasonal variations in equatorial electrojet 24 p3124 A73-44730
- ## SUNSPOTS
- Solar events and their effects on the earth surface in August, 1972 01 p0097 A73-10469
 - Relative polarization of type III solar radio bursts at 23.5 and 30 MHz. 01 p0093 A73-11315
 - Photospheric network properties and transition to sunspot of solar bright points in 3840 A and H alpha, comparing with Ellerman bomb 01 p0108 A73-11384
 - Physical properties of solar chromospheric plages. I - Line profiles of the CaII H, K, and infrared triplet lines. 01 p0108 A73-11385
 - Maxima in coronal intensity during 1966-1970 period of solar cycle, discussing north-south asymmetry correlation with sunspot activity 01 p0108 A73-11395
 - Evidence for two maxima of activity in the 20th solar cycle. 01 p0108 A73-11396
 - Preliminary results of the third flight of the Soviet stratospheric solar observatory. 02 p0216 A73-12335
 - Sunspot number relationship to planetary tides on sun, considering earth-Venus conjunctions and opposition 02 p0219 A73-12436
 - Current sheet model for sunspot structure, considering ohmic dissipation as decay mechanism 03 p0377 A73-14408
 - Observations of the intensity of the penumbra of sunspots. 03 p0377 A73-14409
 - Depth profiles of Fe I 5250 A line for three sunspot models, noting line-to-continuous absorption ratio relation to emergent intensity location 03 p0377 A73-14410
 - On the minimum intensity of the Na D2-5890 A line in sunspot umbra /Research note/. 03 p0377 A73-14411
 - Solar spectra line intensities in band 201 of visible and near IR regions, noting water vapor bands presence in sunspot spectra 03 p0377 A73-14412
 - Prediction of proton flares and Forbush effects. 04 p0491 A73-14843
 - 1968 solar spot observations and statistics 04 p0502 A73-15950
 - Sunspot temperature increase stimulation of supergranule motion leading to spot decay and magnetic field diurnal fluctuation development 04 p0503 A73-16012
 - Spectroheliogram SNR improvement via time averaging of 6103 A core sequence, considering sunspot evolution observed by time lapse technique 05 p0621 A73-17030
 - Sunspot fine structure from photographs taken on U.S.S.R. Stratospheric Solar Station, noting high Rayleigh resolution of small elements 05 p0621 A73-17031
 - Solar flare activity during August 1972, discussing sunspots filter- and spectrograms, proton emissions and geomagnetic disturbances 05 p0622 A73-17095
 - Running waves in quiet sunspots with well developed penumbras, noting intensity fluctuation in H alpha centerline or wing 05 p0626 A73-17347
 - Solar proton flare prediction, examining diurnal rotation of axis connecting two stable spots and change in horizontal gradient of spots magnetic field 07 p0870 A73-19449
 - Vertical velocity field oscillations in photospheric sunspot umbras interpretation in terms of gravity or acoustic waves traveling along magnetic field lines 08 p1001 A73-20756
 - H alpha observations of vertical velocity distribution periodic oscillations in sunspot, noting transverse waves formation and propagation to penumbral boundary 08 p1001 A73-20757
 - Observations of sunspot umbral velocity oscillations. 08 p1001 A73-20758
 - Periodicities in the longitude distribution of sunspots. 08 p1001 A73-20759
 - Solar modulation of cosmic ray intensity in stratosphere, examining relationship to sunspots group number and heliographic latitudes over 11 year period 08 p0999 A73-21339

- Short-term nonperiodic variations in the intensity of the neutron component of cosmic rays during a period of transition from a quiet to an active sun 09 p1137 A73-22019
- Variation of atmospheric radio noise level with sunspot number. 09 p1051 A73-22494
- Measurements of the magnetic field vector of a sunspot. 10 p1275 A73-23827
- Formation of neutron star spots and its connections with pulsars. II - Close similarities between radiations from the sun and pulsars. 10 p1275 A73-23828
- The cooling of a sunspot. I - A Carnot cycle and the hydromagnetic interactions. II - Convection zones models and the magnetic power supply. 10 p1279 A73-24137
- Solar activity variation of XUV emission segregation into quiet sun and active region components via correlations of sunspots with observed fluxes and intensities 11 p1415 A73-251734
- Hourly and daily variations of H values for sunspot minimum, showing uncorrelated night time level departures and range implications for solar flares 11 p1355 A73-25772
- Asymmetric intensities of Zeeman components of electronic transitions of diatomic molecular spectra in sunspots, considering CN red lines 11 p1422 A73-25936
- Sunspot umbral intensity measurements at IR and visual wavelengths, discussing correction methods for earth atmosphere and instrument induced stray light 11 p1422 A73-25937
- Sunspots moving magnetic features analysis from longitudinal magnetograms time series and H alpha filtergrams 11 p1422 A73-25938
- Solar surges magnetic properties analysis from high resolution H alpha filtergrams, matching surge trajectories by computed magnetic lines of force 11 p1422 A73-25941
- Solar flares association with emerging flux regions /EFR/ near sunspots, noting correlation between areas and brightness changes 11 p1412 A73-25942
- Photospheric convective network as a determining factor in sunspot and group development and stabilization. 11 p1426 A73-26571
- Annual solar activity changes due to interstellar matter capture by sun, noting uneven sunspots distribution 12 p1535 A73-27770
- Sunspot observations by means of a vidicon camera. I. 12 p1545 A73-27833
- Fine bright umbral spot structures from photographic line spectra observation of sunspot, noting magnetic field strength, outflow velocity and photospheric temperature 12 p1545 A73-27834
- Emission core widths of K Ca II line in umbra and penumbra of sunspots near solar disk center, noting relationship to stellar luminosity 12 p1545 A73-27835
- Large sunspot high dispersion line spectrum at 6610-6770 A, noting umbral/photospheric contrast and drift curves across limb from photographic recording 12 p1547 A73-27925
- Photometric and spectral observations of Churyumov-Gerasimenko short period comet 1969 IV by fast telescopes, correlating nuclear magnitude with sunspot area 14 p1789 A73-29781
- Emerging flux regions /EFR/ spatial distribution on sun, discussing absence of preferential longitudes, latitudinal preference and time distribution behavior 14 p1787 A73-30648
- Geomagnetically calm intervals and their forecasts. 15 p1868 A73-31521
- Some statistical characteristics of atmospheric ozone measurements 15 p1868 A73-31612
- Solar surface and atmosphere activity due to magnetic field production, transport and dissipation, discussing flares, sunspots, corona, dynamo, plasma turbulence and prominences 15 p1937 A73-31848
- Morphological and kinematic study of the fine structures of a sunspot 16 p2052 A73-32956
- Spectral analysis of sunspot flares. 16 p2052 A73-32957
- Solar convective motions and associated magnetic fields, discussing photospheric cellular and chromospheric vertical motions, fibril structures, sunspot magnetic properties and faculae 16 p2061 A73-33283
- Difference between even and odd 11-year solar activity cycles 16 p2056 A73-33658

Solar cycle and coronal heating theories implications for cycle variations phase coincidence, discussing sunspots, coronal green lines, etc
17 p2224 A73-34510

Fine structure in the sunspot spectrum - 2 to 70 years.
17 p2230 A73-34514

Forecasting of proton flares.
18 p2344 A73-35974

Investigation of solar activity and its association with cosmic ray variations
21 p2755 A73-40113

Sunspot activity, flare observation, electromagnetic and magnetic disturbances, auroral activity and solar radio bursts in March and April 1973
21 p2767 A73-40567

Solar proton measurements during August 1972 cosmic ray and magnetic field events caused by chromospheric flares associated with sunspots on east limb
21 p2757 A73-40592

Heliographic latitudinal zonality of periodic sunspot and flare distributions during 1957-1964 and 1923-1962
21 p2759 A73-40722

First observations of the granulation at 1.65 microns, center to limb variation of the contrast.
21 p2776 A73-41476

On the possibility of constructing a radiative sunspot model in magnetohydrostatic equilibrium.
21 p2777 A73-41486

Umbral flashes and running penumbral waves relation to overstable hydromagnetic oscillation in sunspots, noting depth dependence and electrical conductivity variation effects
21 p2777 A73-41487

The east-west asymmetry in the number of spot-groups in relation to their classification.
21 p2777 A73-41488

Frequency distribution functions of pulsars, supernovae and sunspot groups relationship to age and lifetime, considering stellar mass and initial luminosity
22 p2915 A73-43033

Strong magnetic fields occurrence in sunspot penumbras dark filaments related to hypothesis of penumbral convection rolls existence
23 p3026 A73-43224

Statistical analysis for autocorrelation and cross correlation coefficients of mean annual total atmospheric ozone and relative sunspot number as solar activity indicator
23 p2976 A73-43883

On the generation of umbral flashes and running penumbral waves.
24 p3136 A73-44638

Why Syrovatskii's mechanism of dynamic dissipation of magnetic fields does not work.
24 p3136 A73-44642

The latitudinal motion of sunspots and solar meridional circulations.
24 p3136 A73-44647

UPERALLOYS
U HEAT RESISTANT ALLOYS
UPERCAVITATING FLOW
Supercavitating pumps for cryogenic liquids.
05 p0582 A73-17286

Unsteady separated free jet flow of an ideal fluid past a wing
15 p1861 A73-31155

UPERCAVITATION
U SUPERCAVITATING FLOW
UPERCARGERS
Design and development of a small highly loaded, two-stage, transonic axial compressor.
[SAE PAPER 720712]
02 p0203 A73-12009

Piston engine turbocharging system based on split low and high pressure exhaust gas discharge porting, discussing different turbine staging arrangements
10 p1263 A73-24925

UPERCARGING
U SUPERCARGERS
UPERCARGING MAGNETS
Superconducting magnetic systems reliability engineering and design, noting combined conductors for uncontrolled transition prevention in normal state under subcritical currents
01 p0005 A73-10616

Feasibility model of airborne ac synchronous generator with rotating superconducting field winding, comparing predicted performance, size and weight with conventional technology
02 p0131 A73-11827

Rotating electrical machine superconducting field winding design requirements in terms of size, magnetic energy storage, power level, rotation speed and pole number
02 p0132 A73-11828

Flooded rotor, direct current acyclic motor, with superconducting field winding.
02 p0132 A73-11829

Magnetic energy storage and transfer from coil into resistive load with superconducting switch, discussing voltage and circuit conditions for full normalization
02 p0200 A73-11830

Model coil test results for a pulsed superconducting magnet energy storage system.
02 p0132 A73-11831

Three-phase-synchronous alternator with a superconducting field winding.
02 p0132 A73-11832

Superconducting magnet ac generators development, emphasizing conversion efficiency, manufacturing, relative costs, machine geometry and interwinding coupling factor effects
02 p0132 A73-11833

Synchronous electric generators with superconducting field windings, discussing fundamental characteristics, operating modes, refrigeration and cryogenic equipment and applications
02 p0132 A73-11834

Superconducting magnet for a Ku-band maser.
02 p0200 A73-11835

Design and model tests for a 5 Tesla superconducting saddle magnet.
02 p0132 A73-11837

A 12-coil superconducting 'bumpy torus' magnet facility for plasma research.
02 p0150 A73-11839

Change in critical current of superconducting NbTi by neutron irradiation.
02 p0200 A73-11842

Engineering problems in the design of controlled thermonuclear reactors.
[AIAA PAPER 73-259]
05 p0596 A73-16980

High resolution automatic magnetometer using a superconducting magnet Application to high field susceptibility measurements.
[IEEE PAPER 48,2]
07 p0823 A73-19365

Large-scale applications of superconducting coils.
07 p0863 A73-20107

Design considerations for high-current-density superconducting saddle magnets for MHD.
07 p0852 A73-20405

Performance of a 12-coil superconducting 'bumpy torus' magnet facility.
07 p0809 A73-20460

Experience in developing and using laboratory superconducting solenoids with fields up to 119 kOe
10 p1177 A73-23936

Optimal, elliptic and circular windings for superconducting nonferrous magnetic MHD generators, comparing cross sections
10 p1178 A73-24594

A Lallemand electronic camera focused by a superconducting magnetic coil.
14 p1751 A73-29904

Applications of superconductivity.
17 p2218 A73-34111

Features of a high voltage airborne superconducting generator.
17 p2109 A73-35254

Radio astronomical traveling wave maser with ruby or doped rutile single crystals, superconducting magnet, cryogenic equipment and low noise temperature
23 p2953 A73-43375

SUPERCONDUCTIVITY

Differing roles of electron scattering processes in the thermodynamics of metals in the normal and superconducting states
01 p0088 A73-10613

Singularities of the temperature dependences of the heat conduction coefficients of solid solutions of the niobium-zirconium system.
01 p0066 A73-11338

Applied Superconductivity Conference, 5th, Annapolis, Md., May 1-3, 1972, Proceedings.
02 p0200 A73-11826

Investigation of cryogenic stability and reliability of operation of Nb3Sn coils in helium gas environment.
02 p0200 A73-11838

Superconducting Mo-Re alloy thin film prepared by sputtering and deposition onto sapphire substrate, measuring transition temperature, critical current and magnetic field characteristics
02 p0200 A73-11841

Ti-Al-V alloys as differential measurement method for metallurgical processing and microstructure effects on superconducting critical temperature and magnetic permeability/susceptibility
02 p0200 A73-11843

Operating characteristics of cylindrical thin film weak link circuits used as the sensing element in ultrasensitive magnetometer systems.
02 p0200 A73-11845

Superconducting time variant filter tracking test for RF signal amplitude modulation, using photodiode electric perturbation in semiconductor cavity resonant frequency
02 p0146 A73-11847

Weakly superconducting, thin-film structures as radiation detectors.
02 p0167 A73-11849

Effect of alternating current on the steady-state characteristics of a Josephson junction.
03 p0344 A73-14097

Superconducting tunnel junctions as phonon sources and detectors.
04 p0428 A73-15466

Experimental results on absolute phonon detection sensitivity of superconducting tunneling junctions.
04 p0483 A73-15467

Superconductivity theory and applications, considering cryogenic problems low-loss and magnetic properties and Josephson junction effect on low power technology
04 p0484 A73-15958

One-dimensional periodic superconducting weak-link systems.
04 p0484 A73-16040

Parametric regeneration in Josephson superconducting point contacts for combination frequency signal amplification and conversion in microwave application
05 p0556 A73-16073

Book - Superconductive tunnelling and applications.
05 p0556 A73-16357

Stabilization of superconducting beryllium by addition of aluminum.
05 p0605 A73-16794

Influence of fluctuations on the electromagnetic properties of the Josephson tunnel junction.
06 p0733 A73-17425

Conversion of electromagnetic into acoustic energy via indium films.
06 p0734 A73-17834

Josephson tunneling devices - A new technology with potential for high-performance computers.
06 p0735 A73-18066

Field-ion microscopic investigation of the microstructure of deformable superconducting niobium-based alloys
06 p0736 A73-18115

Wave attenuation in superconducting elliptical waveguides
07 p0793 A73-19924

Attainment of a low-noise high-power and highly stable Gunn oscillator by coupling to a superconducting cavity.
07 p0801 A73-20109

Magnetometers using superconducting galvanometers.
07 p0826 A73-20406

Aircraft power supply alternators with superconductive field windings, calculating specific weights and performance characteristics
07 p0779 A73-20408

Effect of paramagnetic impurities on Josephson currents through junctions with normal-metal barriers.
07 p0864 A73-20574

Study of the geometrical resonances of superconducting tunnel junctions.
08 p0994 A73-21207

Influence of nickel on the superconductivity parameters of Nb3Al + Ni
09 p1098 A73-21845

High temperature superconductivity in three dimensional systems of metals and nonmetals, discussing electron collectivization in metals, dielectrics, organic compounds, semiconductors and molecular crystals
10 p1261 A73-24692

Change in the superconducting properties of vanadium after the introduction of tantalum impurity atoms
10 p1261 A73-24761

Synthesis of superconducting suspensions with a maximum lifting force
11 p1372 A73-25049

Critical transition temperatures and magnetic moment measurements of superconducting state of binary Be alloys
11 p1409 A73-25630

High field superconductivity in alkali metal intercalates of MoS2.
11 p1410 A73-26745

Phase diagrams, microstructure and superconducting properties of thermally diffused Nb-Sn system
12 p1508 A73-26835

Lossless electric energy transmission via superconductivity above 20 K, noting intense magnetic field generation
12 p1531 A73-27689

Fluctuating shift in the transition temperature of thin superconducting films
12 p1532 A73-27984

Superconductivity of cadmium-magnesium alloys.
13 p1668 A73-28223

Possibility of a superconducting transition in a semiconductor subjected to high-power laser radiation.
13 p1629 A73-29439

Properties and structure of Ti-Nb-base superconducting alloys
13 p1643 A73-29644

Nb-Al alloys sigma phase superconductivity characteristics, investigating critical temperature, composition and heat treatment relations
14 p1759 A73-30236

Dependence of the variation of the electronic dislocation drag force in a superconducting transition on the stress, temperature, and velocity.
14 p1783 A73-30341

Model of degenerate semiconductor transition to superconducting state in terms of electron interactions with phonons of low-lying spectral branch
14 p1783 A73-30343

German monograph - The effect of germanium additions on the superconducting characteristics and the transition processes in technical titanium-niobium alloys.
14 p1762 A73-30666

Radio-frequency size effect in a normal metal layer adjacent to a superconducting phase
14 p1784 A73-30810

Superconductivity and electron structures of a solid solution of titanium in niobium
14 p1784 A73-30811

Russian book - Superconducting alloys and compounds.
15 p1922 A73-31176

Attempted prediction of the superconducting transition temperature for some metallic compounds with the aid of a computer
15 p1922 A73-31177

Electron characteristics of sprayed vanadium-gallium alloys
15 p1922 A73-31178

Moessbauer effect in Nb₃Sn as a function of heat treatment
15 p1922 A73-31180

Investigation of the oxygen content in superconducting vanadium- and niobium-base compounds
15 p1922 A73-31181

Structure and superconducting properties of alloys of the vanadium-tantalum system
15 p1923 A73-31183

Specific heat of alloys of the niobium-titanium system near the superconducting transition temperature
15 p1886 A73-31184

Influence of heat treatment on the critical currents in binary alloys of niobium with zirconium and titanium
15 p1887 A73-31185

Temperature dependence of the electrical resistance of superconducting Ti-Nb and Ti-Nb-Zr alloys subjected to working by hydrostatic pressure
15 p1887 A73-31186

Investigation of some physicochemical and X-ray structural changes in a superconducting wire prepared from 60T alloy, as a function of the strain level and duration of annealing in vacuum
15 p1887 A73-31187

Changes in the superconducting transition temperature of alloys of variable composition, as exemplified by the niobium-tantalum system
15 p1887 A73-31189

Temperature effects in quadrupole interaction in NbHf alloys
15 p1923 A73-31710

Effects of high omnidirectional pressures and residual stresses on the superconductivity of alloys of the V₃Si_{1-x}Gex system
16 p2027 A73-34062

Trends in physics; General Conference, 2nd, Wiesbaden, West Germany, October 3-6, 1972, Lectures.
17 p2256 A73-34109

Properties of a superconducting point contact connected to a resonator.
17 p2220 A73-35725

Superconducting fluctuations in complexes of tetracyanoquinodimethane and structural imperfections.
19 p2482 A73-37387

Papers on materials science covering optical and spectroscopic surface analyses, neutron effects, amorphous semiconductors, high temperature superconductivity, etc
19 p2502 A73-38547

Superconducting Josephson junction power flow relations dependence on harmonically or subharmonically phase locked autonomous frequency
20 p2536 A73-39411

Measurement of superheating and supercooling fields of superconducting thin films.
20 p2599 A73-39724

Energy spectrum of transition metals in the superconducting state
20 p2600 A73-39727

Superconductivity and electronic structure of ultrahigh-purity niobium. I - Synthesis of ultrahigh-purity niobium
20 p2600 A73-39732

Superconductivity of films made from aluminum oxide and niobium mixtures
20 p2579 A73-39744

The homogeneity regions of superconducting phases in the molybdenum-platinum system
21 p2717 A73-40320

One dimensional model of electron-phonon system exhibiting Peierls instability for tetrahydrofulvalinium tetracyanoquinodimethane conductivity, considering high temperature superconductivity achievement via Peierls instability suppression
21 p2751 A73-40508

Quantum interference effects due to singlet-spin pairing in superconductors, considering normal metal, electron correlations, single particle excitations, thermodynamic properties and ideal superconductors
21 p2752 A73-40642

Properties and structure of superconducting Ti-Nb alloys.
21 p2720 A73-41037

New developments regarding wide-band communication with waveguide, glass fiber, and superconductivity
21 p2655 A73-41072

Effect of high pressure on the superconducting transition temperature of Pd-H.
21 p2753 A73-41126

Electrical conductivity and superconductivity of vanadium, niobium, and chromium solid solutions
22 p2873 A73-41963

Superconductivity of copper containing small amounts of niobium.
23 p3017 A73-44033

Short-term frequency stability of an L band oscillator with a superconducting cavity.
23 p2961 A73-44117

Josephson junction I-V characteristics and measurements of phase modulated quasi-particle current in superconducting weak links, taking into account thermal noise
23 p3018 A73-44174

Solvable pair potential for the Bogoliubov-de Gennes equations of space-dependent superconductivity.
23 p3018 A73-44275

Josephson junction principles for superconducting metals at cryogenic temperatures, considering ultrasensitive electronic measuring instruments and computer components
24 p3073 A73-45224

Metallic hydrogen concept and experimental investigations, considering high temperature superconductivity and role in outer planets structure
24 p3110 A73-45225

SUPERCONDUCTORS

Twisted, multifilament Nb₃Sn superconductive ribbon.
01 p0087 A73-10245

Controlled low-resistance shunt method for determining the volt-ampere characteristics of composite superconductors
01 p0088 A73-10617

Investigation of the tunnel characteristics of deposited superconducting Nb₃Sn films
01 p0089 A73-11290

Superconductor/exiton-dielectric phase transition in a semimetal
01 p0089 A73-11292

Influence of the thickness of a copper coating on the critical current of a superconducting wire made from niobium-based alloys
01 p0089 A73-11435

Glass reinforced epoxy structure for a lightweight superconducting dipole magnet.
02 p0232 A73-11836

Superconducting-normal phase boundary as function of applied magnetic field and transition temperature in Nb-Ga alloys
02 p0200 A73-11840

AC studies of a superconducting Nb-52 at. % Ti alloy.
02 p0200 A73-11844

The superconductor maser - A calculation of the gain from the two-level model and the BCS theory, and some new experimental results.
02 p0175 A73-11848

Materials properties data tables on composition, preparation, temperature and field strength parameters of superconducting compounds in Ni alloys
02 p0201 A73-11878

Direct observation of the magnetic microstructure in niobium-based superconducting alloys subject to deformation
02 p0201 A73-12554

Influence of the pinning forces for flux lines on the critical current density in magnetic fields of up to 10 Tesla in superconducting titanium-niobium alloys
03 p0328 A73-14654

Fermions spin polarization reversal for HF high intensity gravitational waves generation and detection, suggesting superconducting metals for waves receiver
04 p0476 A73-15633

Magnetic-field-induced one-dimensional behavior in the specific-heat transition in dirty bulk superconductors.
05 p0605 A73-16569

Low temperature tests for magnetic field and temperature effects on differential resistance of lead alloy superconductors, calculating viscous friction coefficient
06 p0736 A73-18116

Effect of hydrostatic extrusion on the composition and properties of Nb₃Sn compounds.
06 p0736 A73-18213

Tunneling observation of bound states in a normal metal-superconductor sandwich.
07 p0862 A73-19606

Low-frequency applications of superconducting quantum interference devices.
07 p0863 A73-20107

Millimeter and submillimeter wave detection and mixing with superconducting weak links.
07 p0863 A73-20108

Analog-computer studies on microwave mixing in superconducting weak links.
07 p0863 A73-20109

Comparative studies of noise limitations in superconducting thin-film radiation detectors.
07 p0863 A73-20110

Superconductors HF properties and losses measurement and separation techniques, discussing applications to filters, oscillators, mixers, transmission lines, and radiation detection
07 p0863 A73-20111

Technology assessment of superconductivity application to windings of electric machinery
07 p0863 A73-20112

The a.c. losses of non-ideal type II superconductors under parallel configurations of electric currents and magnetic fields.
07 p0864 A73-20403

Power frequency losses in superconductors.
07 p0864 A73-20404

Superconducting a.c. machines - An approach to development.
07 p0779 A73-20407

Magnetic field dependence of the surface resistance of pure and impure superconducting aluminum at photon energies near the energy gap.
07 p0864 A73-20573

Dynamic behavior of Josephson tunnel junctions in the subnanosecond range.
09 p1132 A73-21944

A search for stimulated emission of radiation from superconducting tunnel junctions.
09 p1135 A73-23344

Metallurgical investigations of phase equilibria in the titanium-niobium-germanium ternary system
10 p1231 A73-23693

Direct observation of magnetic microstructure in deformed niobium-based superconducting alloys.
10 p1259 A73-24188

Tunnel and Gunn diode oscillators coupled to superconducting cavity as S and X band frequency standards
10 p1195 A73-24399

Three phase alternators with two/four poles superconducting inductors and with outer/inner induction winding, determining magnetic field radial distribution
10 p1177 A73-24411

Characteristics of viscous vortex flows in superconducting alloys near the critical temperature
10 p1261 A73-24768

Critical current value for a superconductor niobium alloy wire as a function of its copper coating thickness
11 p1409 A73-26066

Electrodynamics analysis of superconducting vortex interaction with cylindrical cavities (pinning), calculating critical currents in type II superconductors in external magnetic field
11 p1409 A73-26199

Investigation with an electron microscope of the structure of wires prepared from the 60T superconducting alloy
12 p1509 A73-26844

Breakdown of the superheated Meissner state and spontaneous vortex nucleation in type II superconductors.
13 p1669 A73-29188

Equilibrium equations for vortex lines with allowance for interaction with boundary of ideal superconductor, calculating extremum values of magnetic field
14 p1774 A73-30344

NMR measurements of the speed of vortices in flux flow in a type II superconductor.
14 p1783 A73-30438

Resistance of superconductors near the critical field Hc2
14 p1784 A73-30811

Structure and properties of alloys of the V₃Si-V₃Ga-V₃Al system
15 p1922 A73-31177

Properties of the superconducting alloy 35BT
15 p1887 A73-31118

Structure and properties of alloys of the V₃Si-V₃Ga-V₃Ge system
15 p1923 A73-31119

High-frequency current states in small-size superconductors
16 p2044 A73-34066

Fluctuation theory of the two-dimensional mixed state of superconductors of the first kind
16 p2044 A73-34067

The problem of electron-pair tunneling in a sound field in superconductors
16 p2045 A73-34068

Polarization operator of a superconducting electron gas - The Kohn anomalies and charge screening in superconductors
18 p2337 A73-36666

Internal low-frequency friction in niobium in a normal and superconducting state 18 p2323 A73-36676

Superconductivity of beryllides of some transition metals 18 p2340 A73-36678

Temperature dependent softening effect due to state transition and electronic drag coefficient for dislocations in pure two band superconductors 18 p2341 A73-36768

Superconducting properties of alloys of the vanadium-niobium-chromium system 18 p2325 A73-36898

Ultrahigh-speed quenching of niobium and vanadium 19 p2439 A73-37250

Theory of cryogenic suspensions for navigational devices 20 p2566 A73-39353

Effect of impurities on the temperature of the superconducting transition in W3Si type compounds 20 p2600 A73-39731

Magnetic properties of layered superconductors with a weak layer interaction 21 p2751 A73-40371

Superconductor-semiconductor Schottky barrier diode video detector with proper doping and electron tunneling to obtain high degree nonlinearity in I-V characteristics 21 p2662 A73-40463

50 kG gas cooled superconducting solenoid operated at 13 K. 21 p2702 A73-41103

Pure two band superconductor theory, discussing thermodynamic and electromagnetic properties, London group, mixed state, critical field and weak field penetration 21 p2753 A73-41299

Thermal conductivity of superconducting layer in intermediate state with Andreev electron excitation trajectories in magnetic field, using Green function and impurity distribution technique 22 p2896 A73-41728

Liquid helium temperature range thermometry using superconducting tunnel junction devices with temperature dependent I-V characteristics 22 p2856 A73-42018

Propagating thermal waves in force-cooled superconducting devices. 22 p2938 A73-42953

Investigation of tunnel characteristics of sputtered superconducting Nb3Sn films. 23 p3015 A73-43511

The superconductor-excitonic dielectric phase transition in a semimetal. 23 p3015 A73-43513

Magnetic susceptibility of a degenerate electron gas - Interaction of nuclear magnetic moments in normal metals and superconductors 23 p3016 A73-43709

Conductivity of Type II superconductors near the transition temperature 23 p3016 A73-44019

Thermal and electrical properties of superconducting vanadium silicide tapes, plotting transition temperature vs heat treatment time and temperature and critical current vs current density 24 p3119 A73-44411

The damping of electromagnetic waves in smooth, superconductive waveguides. 24 p3068 A73-44945

SUPERCOOLING

Numerical simulation of precipitation development in supercooled cumuli. I, II. 05 p0594 A73-16572

Dendritic solidification of Cu-Ni alloys. I - Initial growth of dendrite structure. 06 p0712 A73-18756

Ogo 6 measurements of supercooled plasma in the equatorial exosphere. 09 p1074 A73-22066

Alloy steels supercooled austenite nitriding in ammonia flow, examining diffusion layers by X ray analysis and hardness tests 10 p1236 A73-24956

A technique for measuring relative threshold nucleation temperatures for active nucleation catalysts. 12 p1521 A73-26816

Hailstones icicle lobe formation growth in wind tunnel, using supercooled or frozen hydrometeors 12 p1521 A73-26817

Spectroscopy of the vapors of weakly volatile compounds, supercooled in a supersonic flow 16 p2038 A73-34054

Development of a high capacity variable conductance heat pipe. 18 p2369 A73-36345

[AIAA PAPER 73-728] Measurement of superheating and supercooling fields of superconducting thin films. 20 p2599 A73-39724

High speed cinematographic study of mass flow rate of pressurized subcooled liquid nitrogen inward

choked flow through radial gap at various stagnation pressures 21 p2740 A73-40634

SUPERCritical FLOW

Forced flow, single-phase helium cooling systems. 01 p0123 A73-11099

The prediction of airfoil pressure distributions for subcritical viscous flow and for supercritical inviscid flow. 03 p0247 A73-14378

Analog-analytic construction of supercritical flows past profiles [DGLR PAPER 72-129] 03 p0248 A73-14384

Calculation of supercritical flow past airfoils by the Murman-Krupp difference method [DGLR PAPER 72-128] 03 p0248 A73-14387

Forced convective heat transfer to supercritical water flowing in tubes. 04 p0520 A73-15945

Operation modes simulation of single stage gas turbine at subcritical and supercritical gas flow, noting scale model tests 05 p0532 A73-17024

Viscous incompressible Jeffery-Hamel fluid flow in divergent channel, discussing secondary supercritical flow, winding and vortex formation 11 p1346 A73-25223

Large particle method for calculation of transonic supercritical vortex flow fields around flat and axisymmetric bodies 11 p1302 A73-26330

Wavelength and cell size determination of steady supercritical Taylor vortex flow for long rotating cylinders with radius, viscosity and end boundary variations 16 p1998 A73-32798

Subcritical and supercritical compressible shock-free flows in blade cascades 16 p1962 A73-32812

Relaxation factors for supercritical flows. 17 p1254 A73-35131

Development and effects of super-critical Taylor-vortex flow in a lightly-loaded journal bearing. [ASME PAPER 73-LUBS-4] 17 p1281 A73-35390

Applicability of difference methods for solving Navier-Stokes equations at large Reynolds numbers 24 p3076 A73-44426

SUPERCritical PRESSURES

Spot welded stainless steel cylindrical strip shells supercritical behavior, analyzing equilibrium states dependence on axial loads and buckling forces 01 p0119 A73-11441

Experimental investigation of worsened heat-transfer conditions with the turbulent flow of carbon dioxide at supercritical pressure. 06 p0766 A73-17410

Thermo-acoustic oscillations in forced convection heat transfer to supercritical pressure water. 08 p1022 A73-21253

Certain results of an experimental study of local heat transfer under supercritical pressure in a unilaterally heated rectangular channel 10 p1293 A73-23510

Temperature conditions at the wall of an annular channel with internal heating at supercritical pressures. 12 p1560 A73-27910

German monograph on laser and schlieren photographic investigation of supersonic free jet flow from nozzle at supercritical pressure ratio into free atmosphere 13 p1567 A73-29286

Results of an experimental investigation of local heat transfer at supercritical pressure in a rectangular channel heated from one side. 17 p2255 A73-35190

An approach to the determination of conditions impairing heat transfer under supercritical pressure 20 p2628 A73-39614

SUPERCritical WINGS

Transonic profile theory - Critical comparison of various procedures 03 p0247 A73-14377

Supercritical shock free transonic profiles for transport aircraft wings of large and medium aspect ratio, discussing straight and yawed wing tests [DGLR PAPER 72-130] 03 p0248 A73-14383

Transonic flow past lifting wings. 13 p1564 A73-28824

A synthesis of transonic, 2-D airfoil technology. [AIAA PAPER 73-792] 19 p2375 A73-37459

SUPERFLUID FLOW

U SUPERFLUIDITY

SUPERFLUIDITY Pulsar glitches and the metastability of the superfluid core. 02 p0211 A73-11895

Effect of counterflows of normal and superfluidic fluid on the second-sound velocity in helium II 02 p0154 A73-12543

Critical flows in open vertical ducts filled with superfluid helium under pressure 05 p0599 A73-17230

Discontinuity conditions for two fluid model of liquid helium 2 from total energy and superfluid linear momentum balance and entropy production inequality postulations 07 p0850 A73-19106

The nuclear resonance in a hypothetical superfluid phase of helium three 08 p0989 A73-21491

Liquid He 3 superfluidity near absolute zero, noting two solid and four liquid phases within millidegrees 14 p1775 A73-30617

Helium superleak metastable persistent current quantum states use to provide nondecaying angular momentum for gyroscopic element 15 p1876 A73-31942

Measurement of relaxation time during acceleration of rotation of vessels containing helium II, and superfluidity in pulsars 16 p2038 A73-34065

Superfluidity of the Fermi component in a Fermi-Bose gas and in He3-He4 solutions 16 p2038 A73-34067

Incompressible potential flow past sphere parallel to contact plane tangent as model to determine critical velocity for dissipation onset in superfluid liquid He II 19 p2421 A73-37853

Energy spectra of localized elementary excitations for dilute solutions of He 3 atoms in superfluid He 4 using Feynman type wave function, considering Raman scattering 23 p3007 A73-44173

SUPERGIANT STARS

Vibration-rotation bands of NH in the spectrum of alpha Orionis. 01 p0104 A73-11041

LTE fine analysis of omicron-tw C Ma line profiles, showing chemical composition near iota Her 02 p0221 A73-12705

Remarks on the comparison of the Sanduleak and Fehrenbach-Duflo catalogs of stars belonging to the Large Magellanic Cloud 02 p0223 A73-12718

Infrared excesses in supergiant stars - Evidence for silicates. 02 p0225 A73-12827

A search for density and pressure inversions in high-temperature, low-gravity model atmospheres. 03 p0366 A73-12935

Radial velocity and microturbulence dependence on excitation potential and time in A type supergiants atmosphere, deriving chemical composition 03 p0371 A73-13215

Two new He I lines in the spectra of B-type supergiants. 03 p0371 A73-13218

A-type supergiants - A list of line intensities and radial velocity measurements. 03 p0375 A73-13950

Small Magellanic cloud large depth along line of sight shown from supergiant stars and cepheids observation 03 p0380 A73-14610

Supergiant stars with very strong hydrogen lines in the Great Cloud of Magellan 04 p0502 A73-15998

Evolution of single stars. VII - Evolution of massive stars. 08 p1002 A73-20848

Spectra of the Becklin-Neugebauer point source and the Kleinmann-Low nebula from 2.8 to 13.5 microns. 08 p1008 A73-21157

Comparison of telescope magnitudes with model-atmosphere predictions for A, F, and G supergiants. 09 p1142 A73-22030

Cooling effects of CO IR opacity in stellar atmospheres of dwarfs and supergiants, considering application to sun and grain formation in cooler stars 09 p1142 A73-22031

Photospheric and circumstellar H-alpha line profiles in M-supergiant spectra 10 p1273 A73-23706

Additional observations of supergiants and foreground stars in the direction of the Large Magellanic Cloud. 10 p1279 A73-24167

The thermal radiation spectra of supermassive stars and X-ray sources. 10 p1270 A73-24902

UBV photometry of 32 Cygni during the 1971 eclipse. 11 p1426 A73-26268

Hydrostatic, flux constant and LTE stellar atmospheric models at 3800 and 3500 K for Betelgeuse 14 p1801 A73-30737

Hydrodynamic model calculations of Population I chemical composition massive objects, discussing evolution termination by violent thermonuclear explosions 16 p2059 A73-32840

Profiles of the photospheric and circumstellar H alpha line in the spectra of type M supergiants. 18 p2354 A73-36731

The spectrum of eta canis majoris, B5 Ia. 18 p2355 A73-36779

SUPERHARMONICS

- The stability of rotating supermassive stars.
22 p2907 A73-42304
- P Cygtype O and B supergiant stars relationship to Wolf-Rayet stars in terms of spectra, absolute magnitudes, mass and variability
23 p3026 A73-43198
- Polarization variations in the emission of some M-type supergiants
23 p3037 A73-44357
- SUPERHARMONICS**
Ultraharmonic motion of a viscously damped nonlinear beam.
13 p1697 A73-28809
- Superharmonic resonance in piecewise-linear system - Effect of damping and stability problem.
19 p2459 A73-37669
- Second harmonic amplitude modulation of an electromagnetic wave by an acoustic wave in a dispersive plasma.
20 p2597 A73-39199

SUPERHEATING

- Influence of geometrical parameters on the energetic separation of superheated water vapor in a conical vortex tube
02 p0153 A73-11789
- Determination of the statistical characteristics of temperature fluctuation in pool boiling.
08 p1022 A73-21252
- Experimental investigation of the viscosity of cesium vapors
10 p1253 A73-23506
- Breakdown of the superheated Meissner state and spontaneous vortex nucleation in type II superconductors.
13 p1669 A73-29183
- Experimental investigation of the viscosity of cesium vapor.
17 p2217 A73-35186
- Measurement of superheating and supercooling fields of superconducting thin films.
20 p2599 A73-39724

SUPERHETERODYNE RECEIVERS

- A simple apparatus for signal reception of transit system satellites and principal results.
03 p0308 A73-13649
- Noise temperature and signal characteristics of parametric microwave superheterodyne receiver with downconverter for satellite communication, radio and TV transmission
03 p0277 A73-13986
- Reciprocity theorem for antenna directivity pattern measurement of optical superheterodyne receiver for carbon dioxide laser radiation
03 p0284 A73-14084
- Laser communication lines in atmospheric ground layer, comparing SNR for direct-reception and superheterodyne video systems
05 p0585 A73-16787
- Direct conversion s.s.b. receivers - A comparison of possible circuit configurations for speech communication.
12 p1467 A73-26800
- An ILS sensor for fail operative autoland systems - The Bendix RIA-32A.
15 p1880 A73-32461
- The use of selective RC amplifiers in the RF amplifier of a superheterodyne receiver.
16 p1991 A73-33982

SUPERHIGH FREQUENCIES

- Design and modeling of periodic magnetic systems for SHF devices. I, II
01 p0025 A73-10981
- Noise factor and power formula for cooled SHF broadband frequency converters with semiconductor mixer diode
01 p0026 A73-11265
- On quasi-periodic components with periods from 30 to 60 min of amplitude fluctuations of X-band solar radio emission.
01 p0108 A73-11382
- Centimeter waves radio sources survey, tabulating position coordinates, 5 GHz flux densities, spectral index and optical identification
07 p0876 A73-19353
- Mixing properties of germanium thermoelectric indicators of SHF radiation with 'hot' charge carriers
09 p1063 A73-22456
- Wide-band varactor-tuned X-band Gunn oscillators in full-height waveguide cavity.
10 p1197 A73-24865
- Two-position scattering of radio waves by the sea surface at small slip angles
11 p1331 A73-26154
- Influence of a SHF field on the inhomogeneities of a nonequilibrium plasma from a low-pressure gas discharge
12 p1528 A73-27304
- Centimeter wave propagation beyond horizon, considering terrestrial surface curvature and mountain effects on deflection and atmospheric refractivity inhomogeneity caused scattering
12 p1473 A73-27754

- Anomalous absorption of superhigh-frequency waves in a plasma at frequencies close to the upper hybrid frequency
15 p1846 A73-32323
- Kinetic instability of a plasma located in an SHF field
15 p1921 A73-32332
- Lunar radio emission in the 1.25- to 2.5-cm band
16 p2064 A73-33767
- Investigation of the dielectric properties of terrestrial rocks at super-high frequencies for the purpose of improving accuracy for the composition of lunar material
16 p2064 A73-33771
- Noise factor and power formula for cooled SHF broadband frequency converters with semiconductor mixer diode
17 p2134 A73-34317
- Radiation efficiency of an X-band waveguide antenna.
17 p2127 A73-35637
- Ion implanted X-band IMPATT/TRAPATT back-to-back diodes.
19 p2408 A73-37146
- S band radio occultation measurements of the atmosphere and topography of Mars with Mariner 9 - Extended mission coverage of polar and intermediate latitudes.
19 p2479 A73-37225
- Application of distributed p-n and p-i-n structures in the development of integrated circuits for electrically controlled SHF devices
20 p2535 A73-38856
- Physical modeling of active microcircuits for the SHF range
21 p2668 A73-40020
- Raman scattering of SHF radiation in a bounded plasma of a solid
21 p2657 A73-41509
- Theory of power rectification and harmonic generation processes at super-high frequencies
22 p2800 A73-42213
- Approximate nonlinear theory of orotron as SHF hybrid-type monotron oscillator, calculating output power and efficiency as function of tube electrical parameters and geometry
22 p2826 A73-42338
- SUPERIMPOSITION [MATHEMATICS]**
U SUPERPOSITION [MATHEMATICS]
SUPERNOVAE
Supernova remnants descriptions, distance and hydrodynamic evolution, considering galactic nonthermal radio sources, radio maps, and X ray and radio polarization
01 p0094 A73-10057
- Autocorrelation function of the 'rapid' brightness variations of the 3C 273 quasar
01 p0101 A73-10932
- Observations of soft X-rays - Two supernova remnants in the constellation Lupus and the diffuse background.
01 p0103 A73-11031
- Photometry of supernova 1972 in NGC 5253.
01 p0104 A73-11046
- Unsteady accretion of optically thick gas cloud on neutron star as hydrodynamic phenomenon due to supernova explosions or collision with ordinary star
01 p0106 A73-11303
- Investigation of the faint nebula identified with radio source HB-21.
01 p0106 A73-11304
- Observational evidence relating to a recent theory on the origin of the universal X-ray background /Research note/.
02 p0207 A73-12395
- The absorption by the interstellar medium of 80 MHz radio emission from galactic supernova remnants.
03 p0372 A73-13346
- Numerical model of transient behavior of radiation dominated shock calculated for neutron star core of imploding supernovae
03 p0372 A73-13354
- Pulsar associated with the supernova remnant IC 443.
03 p0374 A73-13848
- Theoretical structure and spectrum of a shock wave in the interstellar medium - The Cygnus Loop.
04 p0499 A73-15359
- Cooling and evolution of a supernova remnant.
04 p0499 A73-15360
- An evolutionary thermal model for the Cygnus Loop.
04 p0499 A73-15361
- Pulsars and the evolution of supernova remnants.
04 p0501 A73-15866
- Crab Nebula evolution from 1054 supernova to neutron star and nebula expansion, discussing pulsar properties
05 p0614 A73-16304
- Stellar evolution, explosion and mass ejection, considering Crab Nebula filaments and supernovae Cygnus and Vela X remnants
05 p0618 A73-16825

- A soft X-ray survey of the galactic plane from Cygnus to Norma.
05 p0612 A73-173899
- Evidence for ejection of radio sources from supernova remnants.
07 p0873 A73-190564
- Recent supernova in NGC 5253 and the supernova rate.
07 p0900 A73-202381
- Isotropic X ray and optical emissions from supernovae and pulsars, deriving pulsar synchrotron emission evolution formulas
07 p0900 A73-20304
- Gamma-ray lines from an expanding supernova shell.
08 p1008 A73-21162
- The X-ray surface brightness of the Cygnus Loop.
08 p1013 A73-21811
- A numerical model of the structure and evolution of young supernova remnants.
09 p1143 A73-22111
- Supernova explosions in close binary systems
09 p1145 A73-22289
- Radio halos around old pulsars - Ghost supernova remnants.
09 p1148 A73-22871
- Charged particle thermonuclear reactions in nucleosynthesis.
10 p1271 A73-23479
- Circumstellar envelope model and shock wave calculations for type II supernovae with radiation transport via diffusion, predicting Rayleigh-Taylor instability
10 p1273 A73-23546
- Short-term temporal studies of the X-ray emission from Cassiopeia A, Tycho, and Scorpius X-1.
10 p1264 A73-23547
- Observation of structure in the X-ray spectrum of Puppis A.
10 p1264 A73-23548
- Ejection of supernova shells by magnetic pumping
10 p1273 A73-23701
- Cosmic ray, solar activity, supernova outbursts and geomagnetic field effects on atmospheric C-14 concentration
10 p1266 A73-23911
- Remarks on the soft X-ray emission from the galactic radio spurs.
10 p1270 A73-24904
- Supernova remnant Cas A identification as extended source of soft X rays from grazing incidence X ray telescopes aboard OAO Copernicus
11 p1412 A73-25776
- Spectrophotometry of the supernova in NGC 5253 from 0.33 to 2.2 microns.
11 p1427 A73-26613
- Isotropic X ray and optical emissions from supernovae and pulsars, deriving pulsar synchrotron emission evolution formulas
12 p1539 A73-27276
- General relativistic effects detection experiments for supernova and collapsed objects, noting gravitational radiation transfer of energy equal to entire energy generation during thermonuclear evolution
12 p1542 A73-27550
- Convection and diffusion transport equation of galactic cosmic ray electrons with energy loss and absorption allowance for supernova compressed halo models
12 p1535 A73-27635
- Late stage nonrotating star evolution, discussing red giant models, planetary nebulae, degenerate carbon cores, supernova explosions and pulsars
12 p1543 A73-27748
- Supernova outbursts and the formation of relativistic objects. I
12 p1546 A73-27853
- Galactic continuum loops and the diameter-surface brightness relation for supernova remnants.
13 p1672 A73-28041
- Galactic loops as supernova remnants in the local galactic magnetic field.
13 p1672 A73-28042
- Papers on stellar evolution from main sequence to white dwarf stage covering pulsars, supernovae luminosity, neutron stars, nucleosynthesis, etc
13 p1681 A73-28976
- Thermonuclear reactions and nucleosynthesis in stellar interiors, initial big bang, supermassive objects and supernovae explosions
13 p1663 A73-28989
- Time-dependent models of the interstellar gas.
14 p1802 A73-30960
- Interstellar gas excitation due to supernova explosions using time dependent model based on statistical correlation of gas neutral density, ionization and temperature parameters
15 p1928 A73-31053
- Low energy X-ray map of Puppis A supernova remnant.
15 p1933 A73-31353
- Cosmic abundance of boron.
15 p1942 A73-32648

Supernovae remnant X radiation observations, discussing Crab Nebula, Cas A, SN 1572, Cygnus Loop, Vela X and Puppis A and possibilities from Uhuru catalog
16 p2050 A73-32735

Variable radio emission from the extragalactic supernova 1970g in M101.
16 p2060 A73-33094

Continuum radio emission from the vicinity of pulsars.
16 p2061 A73-33219

Observations of soft X-rays - Upper limits on the flux from SN 1972E and measurements of the diffuse background in Centaurus.
17 p2224 A73-34754

Ejection of supernova envelopes by magnetic pumping.
18 p2354 A73-36726

X-ray spectrum of the entire Cygnus Loop.
18 p2357 A73-37103

Observations of galactic supernova remnants at 1.7 and 2.7 GHz.
19 p2483 A73-37566

The X-ray structure of the Vela X region observed from Uhuru.
19 p2488 A73-38514

Supernova outbursts and the formation of relativistic objects. I.
20 p2608 A73-39227

X-ray spectrum of Cassiopeia A - Evidence for iron line emission.
20 p2603 A73-39446

Nova and supernova stars as sources of relativistic particles
21 p2756 A73-40580

Effects of nuclear reactions with fast protons in a supernova shell and the origin of cosmic rays
21 p2756 A73-40581

A numerical study of the explosion of a supernova into the interstellar magnetic field.
22 p2914 A73-43007

Neutrino losses effects on 4-8 solar mass stars leading to collapse of degenerate carbon-oxygen cores, discussing type II supernovae and pulsar formation
22 p2914 A73-43008

Frequency distribution functions of pulsars, supernovae and sunspot groups relationship to age and lifetime, considering stellar mass and initial luminosity
22 p2915 A73-43033

Galactic nuclei, pulsars and supernovae as sources of primary cosmic rays from ground based and satellite observations, relating chemical composition to origin
22 p2904 A73-43116

Ion-grain collision cooling rate for hot gas above million K, discussing applications to supernova explosions, Seyfert nuclei and intergalactic matter within galactic clusters
22 p2916 A73-43121

An optical Atlas of galactic supernova remnants.
23 p3028 A73-43448

Galactic and extragalactic gamma ray bursts contribution to diffuse cosmic X ray flux, noting superposition of supernovae outbursts
23 p3025 A73-43957

Simeiz 59 /Sharpless 104/ nebula radial and expansion velocity indicating type I supernova origin, discussing spectral and interferometric measurements and relativistic electron energy and density
23 p3035 A73-44233

Statistical correlation between pulsar and supernova remnant distribution along galactic longitudes, noting difference due to relative motions
23 p3037 A73-44359

Electron transitions in interstellar dust 4430 A line, indicating ferric oxide /alpha-hematite/ in type I supernovae
24 p3138 A73-44990

Type I and II supernovae spectra, identifying different lines and obtaining energy distributions
24 p3138 A73-45043

Photographic observation of type I supernovae at Asiago Observatory, discussing analysis of B and V light curves and spectra
24 p3143 A73-45437

SUPEROXIDES
U INORGANIC PEROXIDES
SUPERPLASTICITY
Effect of the superplasticity of titanium and its alloys, and the use of this phenomenon for welding in a solid state
22 p2866 A73-42093

Superplasticity and residual tensile properties of a microduplex copper-nickel-zinc alloy.
22 p2879 A73-42582

SUPERPOSITION [MATHEMATICS]
On the superposition model for environmentally-assisted fatigue crack propagation.
11 p1382 A73-25820

Influence function of a nonheated region and the relationship between the method of superposition and the method of expanding solutions in series of form parameters
12 p1558 A73-27312

Quasi-conformal mapping theory of two- and multidimensional regions, considering superposition, hyperbolic and mixed systems and Chebyshev problem
13 p1647 A73-28339

Implicit separation of variables (via superposition principle/ and explicit and implicit traveling wave methods of solving nonlinear partial differential equations
13 p1648 A73-28437

Superposition method for potential distribution in plane tetraed field with unipotential and bipotential grids, noting electro-optical effect in cylindrical lenses
13 p1591 A73-28667

Superposition of Schwarzschild solutions and metric of a gravitational dipole
17 p2212 A73-35561

Quantum signal superposition in radio communication, discussing Glauber convolution formula limitations and minimum three signal rule
20 p2529 A73-38924

SUPERSATURATION
A study of droplet spectra in fogs.
19 p2447 A73-37660

Vertical plate steady flow thermal diffusion chamber for cloud condensation nucleus counter, featuring long available growth time for operation below 0.2 percent supersaturation
21 p2697 A73-40059

Experimental investigation of transient supersaturations in a thermal diffusion chamber.
23 p3004 A73-44259

SUPERSONIC AIRCRAFT
NT B-70 AIRCRAFT
NT CONCORDE AIRCRAFT
NT F-4 AIRCRAFT
NT F-8 AIRCRAFT
NT F-14 AIRCRAFT
NT F-15 AIRCRAFT
NT F-111 AIRCRAFT
NT JAGUAR AIRCRAFT
NT SUPERSONIC COMMERCIAL AIR TRANSPORT
NT SUPERSONIC TRANSPORTS
A note on the use of airborne 30-millimetre radar at long ranges.
04 p0423 A73-15699

Long-range energy-state maneuvers for minimum time to specified terminal conditions.
05 p0536 A73-16954

Control and stability analysis of supersonic aircraft jet engines with afterburner for improved low altitude operation
06 p0741 A73-17722

Vapor pressure of supersonic aircraft fuels
07 p0865 A73-20014

Experimental method for analyzing the unsteady flow in a transonic aircraft compressor
09 p1028 A73-22715

Stiletto air-launched supersonic aerial target design, development and capabilities, describing configuration, propulsion and control systems and operational envelope
09 p1032 A73-23121

Critique of paper on supersonic aircraft configuration with zero wave drag, discussing tubular outer structure and convergent-divergent inner duct
11 p1305 A73-25798

Influence of air oxygen concentration on the thermochemical stability of jet fuels
15 p1925 A73-31833

Design considerations for supersonic V/STOL aircraft.
16 p1969 A73-33517

Conceptual study of high performance V/STOL fighters.
16 p1969 A73-33518

The design or operation of aircraft to minimize their sonic boom.
19 p2380 A73-37470

The development of the F-12 series aircraft manual and automatic flight control system.
19 p2380 A73-37474

SUPERSONIC AIRFOILS
Flowfield calculations for some supersonic sections with ducted heat addition.
09 p1028 A73-23089

The transonic aerofoil problem with embedded shocks.
15 p1821 A73-31122

SUPERSONIC BOUNDARY LAYERS
Correlation function for prediction of surface roughness induced supersonic boundary layer transition on blunt bodies, taking into account compressibility and centrifugal force effects
01 p0002 A73-10742

Measurements on separated supersonic boundary layer flows after an expansion corner.
01 p0003 A73-11135

Role of the anelastic behavior of the ablation material on cross-hatching.
03 p0398 A73-14189

Numerical analysis of eddy viscosity models in supersonic turbulent boundary layers.
05 p0566 A73-16910

Calculations of turbulent shear stress in supersonic turbulent boundary layer zero and adverse pressure gradient flow.
05 p0566 A73-16911

Heat transfer downstream of attachment of a turbulent supersonic shear layer.
05 p0533 A73-17112

Supersonic boundary layer on a permeable surface
05 p0534 A73-17268

Method of approximate calculation of the laminar boundary layer outside of vibrational equilibrium
08 p1023 A73-21259

Linearized solutions to supersonic laminar boundary layer structure near flat plate with slot injection, using triple deck separation theory
08 p0956 A73-21524

Numerical study of the stability of a supersonic laminar boundary layer
09 p1028 A73-22624

Incipient separation pressure rise for a Mach 3.8 turbulent boundary layer.
13 p1601 A73-28827

Plate-injection into a separated supersonic boundary layer.
14 p1711 A73-30172

Weak disturbances upstream propagation in supersonic boundary layer, deriving homogeneous boundary value problem for complex amplitude function
16 p2000 A73-33263

Generalized random forces in time domain for rectangular panels under subsonic and supersonic boundary layer turbulence, investigating probabilistic nature by Monte Carlo method
17 p2241 A73-34182

Supersonic, turbulent boundary layer separation measurements at Reynolds number of 10,000,000 to 100,000,000.
18 p2261 A73-36216

Separation of a supersonic turbulent boundary layer at moderate to high Reynolds numbers.
18 p2261 A73-36217

Theory of supersonic laminar non-adiabatic boundary layer flow past small rearward-facing steps including viscous-inviscid interaction.
18 p2261 A73-36219

Supersonic turbulent boundary-layer flows with tangential slot injection.
18 p2262 A73-36245

Recent progress in boundary layer research.
19 p2419 A73-37451

Viscous flow over a cone at moderate incidence. II - Supersonic boundary layer.
20 p2507 A73-39093

Porous cooling in a supersonic turbulent boundary layer
20 p2628 A73-39609

Flow measurements over compression corner in supersonic separated laminar boundary layers with hot-wire probes
21 p2631 A73-40247

Branching solutions for supersonic interacting boundary layers.
21 p2632 A73-40440

Aerodynamic interference of pitot tubes in a turbulent boundary layer at supersonic speeds.
22 p2796 A73-42552

A numerical study of separating supersonic laminar boundary layers.
23 p2969 A73-44376

Pressure fluctuations underlying attached and separated supersonic turbulent boundary layers and shock waves.
24 p3053 A73-44831

Measurement of turbulence transport properties in a supersonic boundary-layer flow using laser velocimeter and hot-wire anemometer techniques.
24 p3090 A73-44869

SUPERSONIC COMBUSTION
Supersonic mixing and combustion of confined coaxial hydrogen-air streams.
03 p0397 A73-13473

Studies leading to the realization of supersonic combustion in propulsion applications.
03 p0398 A73-14141

Extension of combustion in the supersonic flow downstream of a pilot flame stabilized with the help of a Mach configuration
06 p0769 A73-18539

Mixing controlled supersonic combustion for air breathing engine equipped hypersonic aircraft, discussing chemical and fluid dynamic interaction effects
10 p1295 A73-23862

Supersonic combustion aid for liquid and gaseous fuels.
17 p2253 A73-34191

Calculation and measurement of MHD generator boundary layer velocity profiles.
19 p2470 A73-38315

Experiments on the propagation of mixing and combustion injecting hydrogen transversely into hot supersonic streams.
22 p2934 A73-42785

Influence of aerodynamic field on shock-induced combustion of hydrogen and ethylene in supersonic flow. 22 p2934 A73-42786

Piecewise-one-dimensional models of supersonic combustion and pseudoshock in a channel. 24 p3154 A73-44702

A laser Doppler velocimeter for studying fast gas-dynamic flows. 24 p3089 A73-44714

Burn-up of the high temperature products of incomplete combustion in a supersonic flow by a second injection of oxidizer. 24 p3156 A73-45076

SUPERSONIC COMBUSTION RAMJET ENGINES

Supersonic mixing and combustion of confined coaxial hydrogen-air streams. [AIAA PAPER 72-1178] 03 p0397 A73-13473

Oblique shock wave interaction with approach boundary layer at combustor entrance in supersonic scramjet engines, observing wall pressure distribution. [AIAA PAPER 72-1181] 03 p0357 A73-13476

Hydrocarbon fuels diffusion flame ignition characteristics in hypersonic ramjet engines, testing additives effect for thermal self-ignition improvement. 03 p0398 A73-14132

Performance optimization for supersonic ramjet - Theoretical and experimental studies [ONERA, TP NO. 1106] 03 p0359 A73-14144

Inlet-combustor interface problems in scramjet engines. 03 p0360 A73-14153

Design analysis of plane asymmetric nozzles with a supersonic velocity at the inlet. 08 p0927 A73-21608

Problems of mixing and supersonic combustion of hydrogen in a hypersonic ramjet [ONERA, TP NO. 973] 08 p1025 A73-21684

Potentials and problems of hydrogen fueled supersonic and hypersonic aircraft. 09 p1032 A73-22830

Mean flow data analysis of supersonic combustion ramjet turbulent jet mixing at high free stream Mach number. 16 p2000 A73-33268

Correlation of hypersonic zero-lift drag data. 22 p2797 A73-42635

SUPERSONIC COMBUSTION RAMJET MISSILE

U RAMJET MISSILES

U SUPERSONIC COMBUSTION RAMJET ENGINES

SUPERSONIC COMMERCIAL AIR TRANSPORT

The technical evolution of air transport in the seventies - European contribution to this evolution. 02 p0238 A73-11702

Supersonic transportation inauguration by Concorde, discussing technological, economic and environmental aspects. [AIAA PAPER 73-16] 06 p0646 A73-17609

Second generation supersonic transport, discussing fuel costs, changing markets, travel patterns, electronic displays and sound suppressor development [SAE PAPER 730349] 17 p2102 A73-34697

SUPERSONIC COMPRESSORS

Behaviour of boundary layers on plane or annular fixed or mobile supersonic blade cascades [ONERA, TP NO. 1110] 01 p0001 A73-10232

Study of the waves configuration in an axial-flow supersonic compressor [ONERA, TP NO. 1104] 03 p0246 A73-14135

Supersonic compressor performance for gas turbine engines, discussing cascade, single stage compressor rigs and experimental engine test results. 03 p0360 A73-14152

Application of certain generalized data from wind-tunnel tests with plane subsonic compressor cascades to the calculation of the characteristic flow regimes in supersonic cascades. 12 p1458 A73-27480

A contribution to the theoretical and experimental examination of the flow through plane supersonic deceleration cascades and supersonic compressor rotors. [ASME PAPER 73-GT-17] 16 p2047 A73-33494

Interface effects between a moving supersonic blade cascade and a downstream diffuser cascade. [ASME PAPER 73-GT-23] 16 p1964 A73-33497

Shock wave pattern visualization and static pressure distribution in supersonic diffusers for mixed flow supersonic compressors, using closed Freon loop test rig [ASME PAPER 73-FE-35] 17 p2095 A73-35026

High performance supersonic axial and centrifugal compressors theoretical and experimental research, assessing and forecasting technological developments. 18 p2343 A73-36992

SUPERSONIC DIFFUSERS

Mach numbers up to 30 obtained in a continuous operating wind tunnel. 05 p0533 A73-17194

Oblique shock wave generation and quenching in curved supersonic diffusers at Mach 1.6, noting dependence on boundary layer properties. 13 p1566 A73-29021

Shock wave pattern visualization and static pressure distribution in supersonic diffusers for mixed flow supersonic compressors, using closed Freon loop test rig [ASME PAPER 73-FE-35] 17 p2095 A73-35026

SUPERSONIC FLIGHT

Optimum configurations for bangless sonic booms. 01 p0031 A73-10302

Evaluation of turbulent heating predictions with flight data. 05 p0532 A73-16943

Exhaust plume prediction model for a low-altitude supersonic missile. [AIAA PAPER 72-1170] 06 p0741 A73-18399

Nonstationary load distribution on an arbitrary-planform wing in supersonic motion. 08 p0927 A73-21725

Calculation of the temperature distribution within an ogival radome in supersonic flight. 11 p1336 A73-25302

Aircraft turbine engine exhaust emissions under simulated high altitude, supersonic free-stream flight conditions. [AIAA PAPER 73-507] 17 p2223 A73-35625

Supersonic boom structure studies, discussing shock wave propagation during flight trajectory and amplification due to overpressure wave focusing. 18 p2268 A73-36907

Flight testing the F-12 series aircraft. 19 p2380 A73-37475

Airframe/propulsion system interactions - An important factor in supersonic aircraft flight control. [AIAA PAPER 73-831] 21 p2634 A73-40501

Sonic bang investigations associated with the Concorde's test flying. 21 p2635 A73-41174

Monograph - Quasi homogeneous approximations for the calculation of wings with curved subsonic leading edges flying at supersonic speeds. 22 p2797 A73-42675

SUPERSONIC FLOW

Equivalent solid obstacle for gas injection into a supersonic stream. 01 p0002 A73-10734

Numerical solution of one-dimensional non-steady flow with supersonic and subsonic flows and heat transfer. 01 p0003 A73-10765

Use of a mirror shearing interferometer for gas dynamics research. 01 p0050 A73-10830

A series of evolved shadowgraphs of shock waves induced by secondary injection in a conical supersonic flow. 01 p0003 A73-11128

Experimental investigation of the supersonic two-dimensional flow past a sail at small angles of attack. 01 p0004 A73-11371

On the multi-parameter characteristic perturbation method - Application to nonlinear supersonic nonequilibrium flow over a wedge. 01 p0004 A73-11425

Higher-order delta wings with flow separation at subsonic leading edges. 02 p0127 A73-11581

An explicit difference method for steady supersonic flow [DGLR PAPER 72-066] 02 p0127 A73-11670

The influence of the Mach number on fuselages and profiles with optimized wave resistance in the case of supersonic flow [DGLR PAPER 72-108] 02 p0128 A73-11691

Ethanol condensation by homogeneous nucleation and growth of liquid droplets in steady state supersonic nozzle flow of ethanol-air and ethanol-nitrogen mixtures. 02 p0153 A73-12051

The pressure on flat and anhedral delta wings with attached shock waves. 02 p0128 A73-12501

Hypersonic and supersonic flow over caret wings at off-design conditions with attached bow shock at leading edges. 02 p0128 A73-12502

An investigation into the flow around a family of elliptically nosed cylinders at zero incidence at free-stream Mach numbers of 2.5 and 4. 02 p0129 A73-12507

Model development of supersonic trough wind with shocks. 03 p0298 A73-12887

The oscillations of supersonic gas flows. 03 p0289 A73-12953

Application of a pseudo-viscous method to the calculation of the steady supersonic flow past a waisted body. 03 p0242 A73-13335

Breakup and penetration of transverse liquid jets in supersonic air cross flow [AIAA PAPER 72-1180] 03 p0293 A73-13475

Combustion of stabilized ethylene within a supersonic flow by a Mach configuration. 03 p0352 A73-13578

Calculation of the supersonic region of three-dimensional nonequilibrium air flow past bodies. 03 p0245 A73-13618

Pressure distribution and shock wave intensity variations in supersonic flow past two plane wings forming dihedral angle. 03 p0245 A73-136232

Experimental investigation of a turbulent boundary layer on a highly elongated body of revolution in a supersonic flow. 03 p0245 A73-136694

Experimental investigation of the base pressure on slender circular cylinders. 03 p0245 A73-13674

Flutter of flat rectangular sandwich type panels in supersonic, coplanar gas flow, with arbitrary direction. 03 p0392 A73-137684

Equilibrium equation for weightless flexible two-dimensional sail in inviscid supersonic airstream, noting centred isentropic compression. 03 p0246 A73-137895

Inverse Laval problem of three dimensional subsonic and supersonic flows in nozzles and ducts of variable cross section in terms of asymptotic series. 03 p0246 A73-14046

Flow conditions at inlet and exit of a flat plate cascade at supersonic velocities. 03 p0246 A73-141399

Aerodynamic noise and boundary-layer transition measurements in supersonic test facilities. 03 p0296 A73-14191

Theoretical and experimental pressure distribution in supersonic domain for an inherently compensated circular thrust bearing. [ASME PAPER 72-LUB-43] 03 p0315 A73-143499

Supersonic electrical-discharge copper vapor laser. 04 p0457 A73-14746

The aerodynamic characteristics of the thin delta wing fitted with a conical body in supersonic flow. 04 p0404 A73-15167

Tangential slot injection of carbon dioxide and helium into a supersonic air stream. [ASME PAPER 72-WA/FE-37] 04 p0435 A73-15854

Laser Doppler velocity measurements in a supersonic flow without artificial seeding. 05 p0576 A73-16361

Calculation of supersonic viscous gas flow past blunt bodies at large Reynolds numbers. 05 p0527 A73-16448

Density changes in a laser cavity including wall reflections and kinetics of energy release. [AIAA PAPER 73-141] 05 p0585 A73-16890

Unsteady flow generated by shock-turbulent boundary layer interactions. [AIAA PAPER 73-168] 05 p0566 A73-16913

Optimal profiles of a nozzle for axisymmetric supersonic discharge of a Lighthill dissociating gas. 05 p0534 A73-17270

Numerical solution to kinetic equations of rarefied supersonic steady gas flow normal to plate by method of characteristics. 06 p0643 A73-17461

Stabilization concepts for a spherical planetary entry probe configuration. [AIAA PAPER 73-184] 06 p0756 A73-17653

Measurements of base pressure upon a plate and a wedge in the 2.8 to 6.8 Mach number range [DFVLR-SONDDR-256] 06 p0645 A73-17740

Applications of shock expansion theory to the flow over non-conical delta wings. 06 p0645 A73-18512

Extension of combustion in the supersonic flow downstream of a pilot flame stabilized with the help of a Mach configuration. 06 p0769 A73-18539

Transition of the boundary layer on a cone in a supersonic flow. 06 p0646 A73-18540

Experiments of magnetohydrodynamic conversion with ionization out of equilibrium. 06 p0730 A73-18541

Supersonic flow past notch in lateral body surface or in two closely lying coaxial bodies, applying turbulent jet theory to separation zone. 07 p0774 A73-19618

Experimental and theoretical study of supersonic viscous flow over a yawed circular cone. 07 p0775 A73-19957

Supersonic flow past large-angle pointed cones. 07 p0775 A73-19981

Turbulent boundary layer separation in supersonic air flow around flat rectangular plate, calculating flow geometry and pressure distribution. 07 p0775 A73-20082

Parameter calculations for a supersonic axisymmetric flow near its expansion center. 07 p0775 A73-20093

Aerodynamic characteristics of thin asymmetric wing profiles in supersonic flow. 07 p0776 A73-20487

Experimental determination of the vibrational temperature of a supersonic gas flow. 08 p1021 A73-20854

Supersonic flow of a gas with solid particles about a wedge. 08 p0926 A73-21404

Calculation of the stability of rectangular plates in an air flow by the finite-element method
08 p1018 A73-21512

Design analysis of plane asymmetric nozzles with a supersonic velocity at the inlet
08 p0927 A73-21608

Dependence of the base pressure on the ratio of specific heats at supersonic velocities
09 p1027 A73-21917

Solution of the direct problem of mixed subsonic and supersonic gas flow in a nozzle of finite length
09 p1072 A73-22480

Supersonic flow of a viscous gas about a spherically blunt cooled object
09 p1028 A73-22620

Intrinsic coordinate method of characteristics application to supersonic steady two dimensional nonisentropic inviscid flow, noting shock wave interaction [ONERA, TP NO. 1186]
09 p1072 A73-22714

Static stability and drag studies for bodies of revolution in supersonic flow.
09 p1156 A73-23214

[AIAA PAPER 73-295]
Laminar boundary layer on a cone near a plane of symmetry.
09 p1029 A73-23442

One dimensional supersonic shock front location by sonic circle involute point by point plotting, using geometric considerations
09 p1030 A73-23467

Accuracy studies of the numerical method of characteristics for axisymmetric, steady supersonic flows.
10 p1171 A73-23602

Perturbation method for linearizing equations of supersonic flow over conical bodies, obtaining potential velocity and entropy solutions
10 p1171 A73-23615

Hot-wire measurements of gas mixture concentrations in a supersonic flow.
10 p1220 A73-24637

Compressible magnetorelative flow character in subsonic, supersonic and transonic regions, obtaining pressure coefficient, free stream Mach number and Alfvén speed interrelationships
10 p1210 A73-24921

Nonstationary flow downwash behind a delta wing during supersonic motion
11 p1299 A73-25046

Development and applications of supersonic unsteady consistent aerodynamics for interfering parallel wings.
[AIAA PAPER 73-317]
11 p1301 A73-25548

Influence of total temperature on transition in supersonic flow.
11 p1303 A73-26400

Supersonic gas flow past the leeward side of a conical wing
11 p1304 A73-26439

Investigation of the flutter of cylindrical panels in a supersonic gas flow
12 p1550 A73-26954

Supersonic flow around a delta wing, taking into account flow separation at the leading edges
12 p1457 A73-27098

Wind tunnel interference on oscillating airfoils in low supersonic flow.
13 p1563 A73-28166

Base pressures in flow expansions by hydraulic analogy.
13 p1564 A73-28811

Base drag calculations in supersonic turbulent axisymmetric flows.
13 p1564 A73-28835

Supersonic annular blade cascades starting conditions, presenting static pressure and Mach number distributions
[ONERA, TP NO. 1219]
13 p1565 A73-28837

Relaxation processes in electrically excited discharge pumped gasdynamic lasers with supersonic gas mixture flow
13 p1627 A73-28967

A study of switching process and design parameters of supersonic fluidic amplifiers.
13 p1571 A73-29042

Analysis of self-excited and forced vibrations of a rectangular plate on many supports in supersonic flow.
13 p1700 A73-29392

Nonlinear stability of a liquid film adjacent to a supersonic stream.
14 p1711 A73-30166

Nonlinear effects in steady supersonic dissipative gasdynamics. II - Three-dimensional axisymmetric flow.
14 p1711 A73-30167

Some relations for the ultrasonic region of flow of a real gas in the presence of heat transfer.
14 p1817 A73-30603

An accurate method for solving some theoretical problems of spatial supersonic gas flows
14 p1712 A73-30826

Influence of viscosity on the flow of an underexpanded jet propagating in a supersonic slipstream
15 p1822 A73-31299

Linear problem for delta and V-shaped wings
15 p1823 A73-31301

Supersonic flow along a wavy wall in a channel
15 p1823 A73-31332

Numerical study of the interaction of a shock-wave caused, supersonic, ionized-argon flow with electric and magnetic fields, using the method of characteristics
15 p1918 A73-31571

A pseudo shock theory of pressure depression in externally pressurized circular thrust gas bearings.
15 p1882 A73-31699

Interaction between an ionized metal vapor flow and a body at Mach numbers equal to or larger than unity
15 p1919 A73-31863

Solution of the direct problem on mixed subsonic and supersonic flow of a gas in a nozzle of finite length.
15 p1824 A73-32067

German monograph - The flow around wings of arbitrary planform in the case of supersonic flow - A computational method.
15 p1824 A73-32581

Bottom pressure and specific-heat ratio at supersonic velocities.
15 p1825 A73-32643

Bow shock waves and flow field preceding pointed slender bodies subject to supersonic flow, analyzing wave distance from body and frozen flow characteristics
16 p1962 A73-33249

On the unsteady supersonic cascade with a subsonic leading edge - An exact first order theory.
[ASME PAPER 73-GT-15]
16 p1963 A73-33492

On the unsteady supersonic cascade with a subsonic leading edge - An exact first order theory. II.
[ASME PAPER 73-GT-16]
16 p1964 A73-33493

A contribution to the theoretical and experimental examination of the flow through plane supersonic deceleration cascades and supersonic compressor rotors.
[ASME PAPER 73-GT-17]
16 p2047 A73-33494

Spectroscopy of the vapors of weakly volatile compounds, supercooled in a supersonic flow
16 p2038 A73-34054

Mathematical formulation of viscous-inviscid interaction problems in supersonic flow.
17 p2091 A73-34178

Successive approximations for calculating supersonic flow past wings with subsonic leading edges
17 p2091 A73-34347

Theoretical and experimental work on losses in 2-D turbine cascades with supersonic outlet flow.
17 p2092 A73-34377

Characteristics of the heat exchange in the region of injection into a supersonic high-temperature flow
17 p2254 A73-34772

The instability due to acoustic radiation striking a vortex sheet on a supersonic stream.
17 p2151 A73-34824

The analysis of nonequilibrium, chemically reacting, supersonic flow in three dimensions using a bicharacteristics method.
17 p2151 A73-34891

On the free shear layer downstream of a backstep in supersonic flow.
[ASME PAPER 73-FE-3]
17 p2095 A73-35003

Stability of the general plane membrane adjacent to a supersonic airstream.
[ASME PAPER 72-APM-UUU]
17 p2248 A73-35103

Supersonic and hypersonic two-dimensional laminar flow over a compression corner.
17 p2096 A73-35134

Boundary condition calculation procedures for inviscid supersonic flow fields.
17 p2155 A73-35143

A new shock capturing numerical method with applications to some simple supersonic flow fields.
17 p2096 A73-35144

Supersonic flow around concave and convex blunt bodies.
17 p2097 A73-35865

Computation of three dimensional flows about aircraft configurations.
18 p2259 A73-36158

Theoretical investigation of the CO supersonic electric discharge laser.
[AIAA PAPER 73-623]
18 p2321 A73-36171

Calculation of the flow on a cone at high angle of attack.
[AIAA PAPER 73-636]
18 p2260 A73-36195

Rearward-facing steps in laminar supersonic flows with and without suction.
18 p2261 A73-36218

[AIAA PAPER 73-667]
On the higher approximations of the supersonic projectile theory.
18 p2262 A73-36220

[AIAA PAPER 73-669]
A kernel function method for computing steady and oscillatory supersonic aerodynamics with interference.
[AIAA PAPER 73-670]
18 p2262 A73-36221

Numerical solution for the inviscid supersonic flow in the corner formed by two intersecting wedges.
[AIAA PAPER 73-675]
18 p2262 A73-36226

Foreign gas injection at windward-most meridians of yawed sharp cones.
[AIAA PAPER 73-764]
18 p2264 A73-36379

Solution of the problem of the flow past a V-shaped wing with a strong shock wave at the leading edge
18 p2265 A73-37011

Similarity parameters and approximate relations for the axisymmetric supersonic flow past an ellipsoid
18 p2266 A73-37019

High enthalpy supersonic ionized gas flow in shock tube experiment, investigating pinch effect on flow acceleration and setup performance
19 p2415 A73-37168

Streaming plasma interaction with variable longitudinal magnetic fields.
19 p2465 A73-37171

Supersonic-hypersonic motion past a permeable cone at zero angle of attack
19 p2376 A73-37544

Supersonic conical flow past delta and tapered structures, considering angle of attack, leading edges, flow separation, negative slope concept and pressure distribution
19 p2376 A73-37546

Determination of a combustion wave in a conical supersonic flow
19 p2503 A73-37551

Effect of yaw on supersonic and hypersonic flow over delta wings.
19 p2377 A73-38008

Investigation of the flutter of cylindrical panels in a supersonic gas flow.
19 p2500 A73-38139

Subsonic and supersonic turbulent shear layer aerodynamic noise emission derivation from differential wave equations via Fourier transformation and WKBJ method
20 p2507 A73-39087

Construction of a minimum-wave-drag profile in inhomogeneous supersonic flow
21 p2631 A73-40184

Self-similar flows behind shock waves in a gravitational field
21 p2676 A73-40190

Analysis of gas flow in multinozzle jets
21 p2631 A73-40393

Supersonic gas flow pattern at blunt body of revolution with attached shock wave
21 p2632 A73-40400

Linearized characteristics method for supersonic flow past vibrating shells.
21 p2632 A73-40426

Improvement to Klineberg's method for the calculation of viscous-inviscid interactions in supersonic flow.
21 p2632 A73-40429

Exact steady-state analogy of transient gas compression by coalescing waves.
21 p2790 A73-40439

Effect of supersonic gas flows on the structure and heat resistance of metal alloys
21 p2717 A73-40481

Spectroscopic studies of supersonic heterogeneous flows with a combustible condensed phase
21 p2754 A73-40702

Application of R-functions to a calculation of the dynamic stability of plates with a complex planform geometry
21 p2786 A73-40984

Interaction of a shock wave with blunt bodies in supersonic flow
21 p2633 A73-41222

Methods for calculating nonlinear flows with attached shock waves over conical wings.
22 p2796 A73-42562

Finite difference and truncation method comparison for supersonic conical flow equations solution, obtaining flow field and shock wave shape
22 p2796 A73-42574

The unsteady aerodynamics of a finite supersonic cascade with subsonic axial flow.
[ASME PAPER 73-APMW-6]
22 p2797 A73-42879

Precise method for solving certain problems of the theory of three-dimensional supersonic gas flows.
23 p2939 A73-43582

Relaxation processes in electrically excited discharge pumped gasdynamic lasers with supersonic gas mixture flow
23 p2989 A73-44319

Determination of vibrational and translational temperatures in gas-dynamic lasers.
24 p3095 A73-44588

A divergent difference scheme for calculation of steady supersonic flows with complex structures
24 p3053 A73-44651

Calculation of supersonic flow around blunt bodies using complete and simplified Navier-Stokes equations
24 p3053 A73-44657

Calculation of a supersonic gas flow about the atmosphere of a spherical body
24 p3053 A73-44658

The calculation of flow in nozzles using a time-marching technique based on the method of characteristics.
24 p3079 A73-44894

Supersonic laminar flow over wedge or backward-facing step for large Reynolds number and small base

or step height, predicting pressure distribution at reattachment 24 p3055 A73-45314

This plate in two dimensional supersonic flow, deriving vibration amplitude response to shock pressure load by numerical analysis with Laplace transform 24 p3055 A73-45432

Determination of the impulses and moments imparted by shock waves to bodies of revolution 24 p3055 A73-45542

Flow field over pointed wedges in isoelectric flow of thermally and calorically perfect gases with nonuniform incident supersonic flow, noting attached shock formation 24 p3056 A73-45547

U SUPERSONIC INLETS

SUPERSONIC FLUTTER
Aerodynamic generalized forces for supersonic shell flutter. 01 p0003 A73-10751

On the weight optimization problem for supersonic rectangular flat panels with specified flutter speed. 04 p0511 A73-15170

Self-excited and forced vibrations of an aeroelastic system subject to a follower force. 04 p0513 A73-15597

Flutter technology in the United Kingdom - A survey. [AIAA PAPER 73-330] 11 p1441 A73-25559

Supersonic flutter of truncated multilayered orthotropic conical thin shells. 14 p1814 A73-30702

On the weight minimization of supersonic, axisymmetric circular cylindrical shells of finite length. 14 p1814 A73-30709

Cylindrically curved panels flutter characteristics in supersonic flow parallel to generators, investigating in-plane boundary conditions and panel geometry effects 15 p1949 A73-31652

First-order frequency effects in supersonic panel flutter of finite cylindrical shells. [ASME PAPER 73-APM-K] 17 p2249 A73-35106

Aeroelastic vibrations in labyrinth seals. 20 p2569 A73-39373

SUPERSONIC HEAT TRANSFER

Temperature of an emitting cone in a supersonic flow of transparent gas 06 p0646 A73-18570

Approximate method for calculating heat transfer to yawed cylinders in laminar flow. 08 p1025 A73-21818

Temperature of a radiating cone in a supersonic flow of transparent gas. 16 p1964 A73-33595

SUPERSONIC INLETS

Boundary layer bleed system design for supersonic inlets, discussing bleed hole geometry effects on boundary layer velocity profile and inlet efficiency [AIAA PAPER 72-1138] 03 p0243 A73-13445

Viscous interaction in integrated supersonic intakes. 03 p0246 A73-14149

Survey of some current aerodynamic problems pertaining to supersonic air intakes [ONERA, TP NO. 1102] 03 p0247 A73-14150

Inlet-combustor interface problems in scramjet engines. 03 p0360 A73-14153

Inlet system design procedures and wind tunnel facility modifications allowing for verification on large scale models at Mach 4.5 15 p1824 A73-31743

French monograph - Contribution to the experimental study of a boundary layer trap in a supersonic air inlet. 22 p2797 A73-42740

SUPERSONIC JET FLOW

Numerical calculation of supersonic opposing jet directed upstream against supersonic main stream by the use of time-dependent finite-difference method. 01 p0003 A73-11130

Calculation of an axisymmetric supersonic gas jet injected in a supersonic slipstream past a given body with heat supply 02 p0129 A73-12583

Supersonic jet noise suppression using coaxial flow interaction. 03 p0241 A73-12964

Discrete tone radiation arising from a supersonic jet flowing into an unlimited gaseous medium and into a cylindrical ejector. 03 p0290 A73-12970

Performance and noise generation studies of supersonic air ejectors. 03 p0290 A73-12972

Supersonic mixing and combustion of a hydrogen jet in a coaxial high-temperature test gas. [AIAA PAPER 72-1179] 03 p0397 A73-13474

Some laws of the propagation of discrete-tone perturbations in a free supersonic jet 03 p0245 A73-13668

Experimental relations determining the position of shock waves in a jet impinging against an obstacle perpendicular to the jet axis 05 p0528 A73-16769

Analytical and experimental supersonic jet noise research. [AIAA PAPER 73-188] 05 p0531 A73-16926

Three-dimensional interaction of jets propagating in a supersonic slipstream 06 p0643 A73-17458

Amplification factor of light in a CO₂ + N₂ + He mixture expanding in a supersonic jet. 06 p0723 A73-17964

Experimental investigation of two-dimensional, supersonic flow impingement on a normal surface. 08 p0925 A73-20720

Central shock position in supersonic jet impinging on wall, noting flow velocity dependence on pressure. 08 p0927 A73-21605

Characteristics of unsteady interaction between a supersonic jet and an infinite obstacle 08 p0927 A73-21609

Nozzle-target system geometry and gas dynamics parameters effect on supersonic underexpanded jets interaction with walls, noting frequency response and pressure oscillations 08 p0927 A73-21610

Flow of a supersonic nitrogen jet and of a low-density nitrogen-hydrogen mixture around a blunt body 10 p1171 A73-23582

Holographic interferograms for demonstration of acoustic field near supersonic air, nitrogen and helium jets, noting generated Mach wave convection velocity 11 p1346 A73-25382

Approximate calculation of flow parameters during interaction of supersonic jets 11 p1304 A73-26443

Diffusion of a hypersonic flow by a supersonic gas jet in the case of a free-molecular mode of interaction 11 p1304 A73-26446

Convective heat transfer in the region of interaction between a supersonic overexpanded jet and an oblique obstacle 12 p1458 A73-27324

Laboratory simulation of development of superbooms by atmospheric turbulence. 13 p1568 A73-28495

Diffusion processes in the mixing zone of a low-density supersonic jet 13 p1567 A73-29170

German monograph on laser and schlieren photographic investigation of supersonic free jet flow from nozzle at supercritical pressure ratio into free atmosphere 13 p1567 A73-29286

HF laser flow visualization with an infrared television system. 15 p1874 A73-31357

Drop size distribution resulting from liquid jet injection across a supersonic stream. 15 p1863 A73-31659

Jet boundary and a free surface behind a body of revolution in the presence of a longitudinal pressure gradient 17 p2094 A73-34774

Experimental studies of chemically reactive F + H₂ flow in supersonic free jet mixing layers. [AIAA PAPER 73-640] 18 p2321 A73-36198

An investigation of supersonic swirling jets. 19 p2376 A73-37488

The magnetic channeling of a supersonic axisymmetric plasma jet. 19 p2470 A73-38318

Vortex sheet model of directional acoustic wave radiation near nozzle exit from supersonic helium jet shear layer instability 21 p2677 A73-40617

Some features of the propagation of a discrete tone perturbation in a free supersonic jet. 21 p2633 A73-41318

Noise caused by supersonic jet shock waves as function of jet pressure ratio, determining spectral characteristics 22 p2795 A73-41702

Experimental study on optimization parameters of a supersonic jet ejector thrust augmentor. 22 p2798 A73-43113

Turbulence generation by supersonic nozzle gas flow interaction with plasmas, discussing high current electric arc in axis 22 p2895 A73-43166

Approximate calculation of dividing streamline of heterogeneous coaxial supersonic jets. 23 p2940 A73-44127

Supersonic jet noise generated by large scale disturbances. [AIAA PAPER 73-992] 24 p3077 A73-44827

Subsonic and supersonic jets and supersonic suppressor characteristics. [AIAA PAPER 73-999] 24 p3077 A73-44834

Effect of a slipstream on the acoustic radiation of ultrasonic annular jets 24 p3055 A73-45358

Influence of a discrete component of acoustic vibration on flow in a supersonic jet with a nondesign ratio of active to passive pressure 24 p3055 A73-45358

SUPERSONIC NOZZLES

Theoretical consideration on the supersonic axisymmetrical nozzle. 01 p0003 A73-11131

Computation of the axisymmetrical free expansion of a nonequilibrium hydrogen plasma 02 p0196 A73-11604

Supersonic nozzle design for prescribed flight trajectory and variable gas flow parameters, solving variational problem of optimal contour for given Mach number 03 p0244 A73-13616

The behavior of vapors of soluble binary systems during expansion in supersonic nozzles - Droplet coalescence in a potential vortex flow 10 p1205 A73-24162

The shape of a supersonic three-dimensional nozzle with a maximum thrust 11 p1302 A73-26334

Sonic line for a coaxial axisymmetric nozzle. 11 p1303 A73-26403

Ballistic burning rate in sonic gas flow in supersonic conical nozzles as function of flow velocity and combustion chamber pressure 13 p1706 A73-28972

Determination of the shape of a plane supersonic nozzle 15 p1822 A73-31196

Gas dynamic lasers - A state-of-the-art survey. 16 p2022 A73-32726

Supersonic mixing nozzle for gas-dynamic lasers. 17 p1813 A73-34205

Theoretical and experimental analysis of the design and off-design performance of supersonic turbine nozzles. 17 p2093 A73-34387

Inlet state limitations and flow characteristics equations for supersonic ejector jet mixing duct 17 p2156 A73-35504

Two dimensional Mach 5 supersonic nozzle configurations with hot nitrogen expansion for mixing carbon dioxide gasdynamic laser, calculating and measuring gain distribution [AIAA PAPER 73-622] 18 p2321 A73-36170

An investigation of velocity flowfields in chemical laser nozzles. [AIAA PAPER 73-641] 18 p2322 A73-36199

Specie number density, pitot pressure, and flow visualization in the near field of two supersonic nozzle banks used for chemical laser systems. [AIAA PAPER 73-642] 18 p2322 A73-36200

Structure of the base flow in a four-nozzle cluster rocket engine 21 p2754 A73-40392

Investigation of nozzles with cryogenic suction of the boundary layer 21 p2678 A73-41221

Analysis of the effects of a probe in the transonic region of a nozzle. 22 p2796 A73-42568

Solution of the variational problem of designing the contour of a two-mode nozzle 24 p3055 A73-45533

SUPERSONIC PRESSURE DISTRIBUTION

U PRESSURE DISTRIBUTION

U SUPERSONIC FLOW

SUPERSONIC SPEEDS

Calculation of stagnation-point pressure during shock-wave incidence on a body moving at supersonic velocity 06 p0643 A73-17459

Supersonic-hypersonic motion around a porous circular cone 07 p0776 A73-20615

Supersonic generation of atmospheric gravity waves, via atmospheric cooling by moon shadows during lunar eclipses, noting analogy to terminator action 10 p1211 A73-23825

Effects of sweepback angle and unit Reynolds number on boundary layer transition at supersonic velocities 13 p1567 A73-29172

Shock wave produced in a solid by means of supersonic thermal sources. 13 p1700 A73-29390

Steady state solution for moving point force on solid-solid interface for supersonic load velocities, using DeHoop modification of Cagniard technique. 14 p1812 A73-30493

Experimental results in the case of the Nonweiler wave-rider in the subsonic, transonic, and supersonic range 16 p1963 A73-33265

Mean flow data analysis of supersonic combustion ramjet turbulent jet mixing at high free stream Mach number 16 p2000 A73-33268

Investigation of the expansion side of a delta wing at supersonic speed. 18 p2263 A73-36312

Shock wave generation by moving distributed non-diffusive force, solving initial value problem for single fluid model to obtain supersonic force field velocity
18 p2299 A73-36323

Sound generation by open supersonic rotors.
22 p2795 A73-41712

SUPERSONIC STRIKE AIRCRAFT
U ATTACK AIRCRAFT
U SUPERSONIC AIRCRAFT
SUPERSONIC TEST APPARATUS

An apparatus for testing components in a high temperature supersonic gas stream containing abrasive particles.
09 p1070 A73-23065

SUPERSONIC TRANSPORTS
NT CONCORDE AIRCRAFT
NT SUPERSONIC COMMERCIAL AIR TRANSPORT

Meteorological effects on SST operations during various flight phases, considering ATC and communications aspects
01 p0074 A73-10348

Nongray atmospheric model to assess radiative effects of water vapor and carbon dioxide layer injected into lower stratosphere by SST and HST exhaust gases
01 p0038 A73-10388

SST related ozone photochemical reactions and metastable oxygen system below 100 km, discussing oxygen dissociation and recombination, photolysis, UV absorption, etc
01 p0042 A73-10898

Nuclear explosions released nitric oxide effect on atmospheric ozone concentration compared with potential effect from SST flights
01 p0043 A73-11068

United States SST electrical power system evaluation.
[AIAA PAPER 72-1055] 03 p0252 A73-13386

Aerodynamic interference between jet propulsion system and airframe for supersonic transport with wing-mounted nacelles, noting wing performance role in lift effectiveness
[AIAA PAPER 72-1113] 03 p0243 A73-13428

Development of solid lubricant compact bearings for the supersonic transport.
[ASLE PREPRINT 72LC-7C-1] 03 p0316 A73-14370

Supercritical shock free transonic profiles for transport aircraft wings of large and medium aspect ratio, discussing straight and yawed wing tests
[DGLR PAPER 72-130] 03 p0248 A73-14383

Climatic impact assessment for high-flying aircraft fleets.
04 p0436 A73-14672

SST aircraft wing design for sonic boom avoidance and noise reduction in airport vicinity, describing aerodynamic characteristics from wind tunnel and flying model tests
04 p0405 A73-14673

The concept of an SST Oceanic Computer Clearance System.
05 p0595 A73-16621

Long range air transportation technical and economic future prospects, discussing passenger and cargo developments, noise reduction and SST technology
[AIAA PAPER 73-14] 06 p0646 A73-17607

Economically viable and socially acceptable second-generation SST, discussing technological developments for range/payload, airport noise and sonic boom improvements
[AIAA PAPER 73-15] 06 p0646 A73-17608

Sonic boom reduction through aircraft design and operation.
[AIAA PAPER 73-241] 06 p0647 A73-17666

Predicting light flashes due to alpha-particle flux on SST planes.
07 p0777 A73-20157

U.S., UK and French research programs on conditions encountered by civil aviation and supersonic transports in stratosphere
11 p1455 A73-26594

World air traffic patterns projected to 1988, including present traffic features, supersonic transport utilization, ground transport alternatives, air freight and aircraft types
16 p2088 A73-33180

Numerical atmospheric circulation model of SST effects on stratospheric ozone distribution
[AIAA PAPER 73-529] 16 p2007 A73-33563

Preliminary estimates of the fate of SST exhaust materials using a coupled diffusion/chemistry model.
[AIAA PAPER 73-535] 16 p2046 A73-33567

The permissible scale of spatial averaging of geopotential values in the stratosphere when the impact of wind on the flight of a supersonic aircraft is taken into account
17 p2100 A73-34546

B-1 technology applications to advanced transport design.
[SAE PAPER 730348] 17 p2102 A73-34696

Flight-critical fail-operative and endurance tests for SST electrical power system
17 p2109 A73-35252

Structural design and technology developments for SST and STOL aircraft, discussing computerized and damage tolerant design, composite materials and cost reducing manufacturing techniques
18 p2362 A73-36167

Solar proton and galactic background radiation measurements project Cold Flare at SST cruising altitudes, using high altitude radiation instrument system /HARIS/
18 p2347 A73-36905

SST environment impact aspects in areas of fuel and oxygen consumption, noise, sonic boom, stratospheric pollution and climate modification
18 p2268 A73-36906

Study of performances in a warm environment in case of air conditioning breakdown on a supersonic transport
18 p2286 A73-36947

Characteristic overpressure of a supersonic transport of given length in a homogeneous atmosphere.
19 p2377 A73-38006

Air traffic control in the EUROCONTROL area.
22 p2884 A73-42321

Ozone composition and nitric oxide injection upper and lower limits for stratosphere by nuclear bomb tests, comparing to estimated SST contribution
22 p2848 A73-42534

A study to determine the feasibility of a low sonic boom supersonic transport.
[AIAA PAPER 73-1035] 24 p3056 A73-44863

SUPERSONIC TURBINES
Navy development of low-cost supersonic turbojet engines.
[SAE PAPER 730362] 17 p2222 A73-34708

Unsteady aerodynamic forces in transonic turbomachines
18 p2266 A73-37084

SUPERSONIC WAKES
Low Reynolds number flow past a transverse cylinder at Mach two.
01 p0003 A73-10758

Annular truncated plug nozzle flowfield and base pressure characteristics.
[AIAA PAPER 73-137] 05 p0530 A73-16887

Supersonic laminar wakes past wedge, determining pressure distribution, velocity profiles and stream line patterns in recirculation region
16 p1962 A73-32905

Support wire disturbances in near viscous wakes of slender supersonic bodies.
18 p2295 A73-36155

Inviscid supersonic far wake flow past pointed bodies using the method of integral relations.
[AIAA PAPER 73-671] 18 p2262 A73-36222

A simple graphical solution for rocket wake boundaries.
23 p2939 A73-43680

SUPERSONIC WIND TUNNELS
Laser anemometry in an unseeded supersonic wind tunnel by means of photon correlation spectroscopy of backscattered light.
02 p0172 A73-12860

Method for increasing wind tunnel Mach number for large-scale inlet testing.
[AIAA PAPER 72-1096] 03 p0287 A73-13416

Supersonic blowdown wind tunnel modification for transonic airfoil profile aerodynamic characteristics measurement, discussing design criteria and operational range
[DGLR PAPER 72-133] 03 p0288 A73-14380

Improved flexible supersonic wind-tunnel nozzle operated by a single jack.
07 p0808 A73-19972

Some heat transfer measurements in compressible turbulent boundary layers.
10 p1296 A73-24648

Influence of total temperature on transition in supersonic flow.
11 p1303 A73-26400

Diagnostic simulation of a pneumatically controlled blowdown wind tunnel.
11 p1344 A73-26546

The shock wind tunnel of the Institute of Aerodynamics and Gasdynamics of Stuttgart University
15 p1858 A73-32042

Development of experimental turbine facilities for testing scaled models in air or freon.
17 p2145 A73-34381

Turbulent boundary layer flow separation measurements using holographic interferometry.
[AIAA PAPER 73-664] 18 p2261 A73-36215

Experimental investigation of a turbulent boundary layer on a triangular plate with a wedge
23 p2939 A73-43473

SUPINE POSITION
Effects of tilting on pulmonary capillary blood flow in normal man.
20 p2519 A73-39786

Functional state of the auditory analyzer under conditions of prolonged clinostatic hypokinesia
23 p2946 A73-43789

SUPPORT INTERFERENCE
Interferometric measurements of the vibrostability of a holographic stand
01 p0050 A73-10798

Stability of a gyroscope on a vibrating base under resonance conditions
08 p0972 A73-21763

Dynamic error of solid body-elastic rod pendulum system hinged on vibrating suspension point in terms of tensile rigidity finiteness
11 p1399 A73-26096

Support wire disturbances in near viscous wakes of slender supersonic bodies.
18 p2295 A73-36155

SUPPORT SYSTEMS
NT GROUND OPERATIONAL SUPPORT SYSTEM
NT GROUND SUPPORT SYSTEMS
NT PORTABLE LIFE SUPPORT SYSTEMS

Earth orbital, lunar, and planetary missions of the space tug.
06 p0750 A73-18019

Automatic support systems for advanced maintainability; Symposium, Philadelphia, Pa., November 13-15, 1972, Record.
08 p0951 A73-20676

Deleterious vibrations development in support structure of launch pad during initial firing of launch vehicle, noting frequency spectrum dependence on soil characteristics and structural design
14 p1742 A73-30105

SUPPORTS
NT SADDLES [SUPPORTS]
Book on functional pavements design covering support condition, quality control and construction tolerance, environmental and landing gear effects, mathematical models, etc
02 p0150 A73-11879

Newly developed bolometer mounts for the short millimeter wave region.
03 p0310 A73-14500

Load and support configurations associated with aspherical diopter of revolution with variable thickness profile generating diopters deformed by elasticity
08 p0967 A73-21492

Nelson Tyler helicopter camera mount for aerial reconnaissance photography providing camera balance and motion stability under combat flight conditions
10 p1222 A73-24949

Effect of support flexibility on the fundamental frequency of vibrating beams.
22 p2918 A73-41966

SUPPRESSORS
NT ECHO SUPPRESSORS
Inhibitory interaction in the retina of Limulus.
09 p1043 A73-23311

SURFACE CHEMISTRY
U SURFACE REACTIONS
SURFACE COATINGS
U COATING
SURFACE COOLING

Calculation of thermal stresses in spherical storage vessels.
02 p0236 A73-12215

Analysis of sublimation-cooled coated mirrors in convective and radiative environments.
05 p0641 A73-17108

Variable-property turbulent flow in a horizontal smooth tube during uniform heating and constant surface-temperature cooling.
10 p1295 A73-23779

The temperature field and thermal stresses in a symmetrical system of three infinite plates
10 p1293 A73-24795

Transient cooling of a solid cylinder by combined convection and radiation at its surface.
13 p1704 A73-28086

Application of the optimal linearization method to the heat transfer problem.
14 p1817 A73-30605

The significance of the climate factor air velocity in environmental simulation
16 p1997 A73-33381

Shape of porous cooled region for surface heat flux and temperature both specified.
19 p2505 A73-38482

Stress and temperature analysis for surface cooling or heating of laser window materials.
21 p2716 A73-40966

Nonisothermal surface cooling for arbitrary temperature distribution and Prandtl number approaching zero, solving thermal boundary layer equations by series expansion
21 p2792 A73-41323

Influence of cooling on surface dispersion during the friction process
24 p3092 A73-44417

SURFACE CRACKS
The influence of X-ray parameters on crack detection capability.
[NA-72-779] 02 p0173 A73-11985

Fatigue scoring - A new form of lubricant failure.
[ASLE PREPRINT 72LC-3B-1] 03 p0316 A73-14356

A study of local stresses near surface flaws in bending fields.
04 p0505 A73-14678

SURFACE DEFECTS

- Stress intensity factors for surface cracks in bending. 04 p0505 A73-14679
- An experimental investigation into the mechanics of deep semielliptical surface cracks in mode I loading. 06 p0763 A73-18478
- Fractographic investigation of the resistance to fracture of aluminum and titanium alloys. 07 p0840 A73-20505
- Surface fatigue crack morphology comparison to bulk crack developments, considering surface grains constraints by adjoining grains. 09 p1103 A73-22441
- Book - Methods of analysis and solutions of crack problems: Recent developments in fracture mechanics; Theory and methods of solving crack problems. 09 p1161 A73-23176
- Alternating method with combined analytical and numerical calculations for two dimensional edge and three dimensional surface crack problems. 09 p1162 A73-23181
- Surface crack slow growth onset investigation with near tip strain as ductile fracture criterion, measuring fracture strength. 09 p1109 A73-23264
- Analysis of stress intensity factor for surface-flawed tension plate. 13 p1692 A73-28231
- An X-ray study of hydrogen induced phenomena affecting mechanical behaviours of austenitic stainless steels. 13 p1625 A73-29522
- Lattice theory of fracture and crack creep. 15 p1890 A73-31927
- Strongly active surfactant effects on metal surface fracture characteristics under various loading conditions. 15 p1952 A73-32071
- Effect of orthotropy on singular stresses for a finite crack. [ASME PAPER 72-APM-VVV] 17 p2249 A73-35109
- Fractographic investigation of the ductility of fracture in aluminum and titanium alloys. 19 p2440 A73-37780
- On the relationship of stress crazing and yielding of polymethyl methacrylate. 20 p2579 A73-38641
- Water damage in polyester/glass laminates. II - Microscopic evidence. 21 p2723 A73-40921
- Magnetic rubber inspection to extend NDT capabilities for locating cracks and defects on or near magnetic material surface. 21 p2708 A73-41324
- The plane elastostatic solution for a symmetrically loaded crack in a strip composite. 21 p2789 A73-41669
- Effects of strain gradients on the gross strain crack tolerance of A 533-B steel. 22 p2876 A73-42153
- The elliptical crack subjected to nonuniform shear loading. [ASME PAPER 73-APMW-42] 22 p2926 A73-42898
- Fracture of thin sections containing surface cracks. 23 p2992 A73-43807
- Fracture analysis of surface- and through-cracked sheets and plates. 23 p3042 A73-43813
- Mechanism of surface microcracking of matrix in glass-reinforced polyester by artificial weathering. 23 p2997 A73-44034
- Hydrogen-induced transformation and embrittlement in 18-8 stainless steel. 23 p2994 A73-44158

SURFACE DEFECTS

- Influence of gamma-radiation on the electrical properties of a real germanium surface. 01 p0087 A73-10039
- Investigation of the sensitivity of a duct sensor to discontinuities in alternating fields of square-pulse or sinusoidal shape - Detectability of surface defects on nonmagnetic and ferromagnetic specimens. I. 08 p0967 A73-21587
- Effect of surface damage on the strength of Al2O3 ceramics with compressive surface stresses. [ACS PAPER 37-BN-71P] 08 p0983 A73-21843
- Method of calculating yield for LSI arrays considering radial distribution of defects on wafers. 10 p1193 A73-23668
- Experimental study of the diffusion of electrons of conduction by superficial defects of thin gold films. 13 p1668 A73-28453
- Initial plastic deformations due to surface defects, deriving corresponding elastic distortions and velocity fields of medium from equilibrium equations. 14 p1812 A73-30544
- Book - Advanced experimental techniques in the mechanics of materials. 17 p2176 A73-35834
- Aircraft hydraulic tubing permissible defects in Cr-Ni-Mn, Al and Ti tubes and return lines, noting wall thickness, chafing, denting, weld seam cracks and impulse tests [SAE SP-378] 19 p2434 A73-37866

- Defects in high quality aircraft tubing and inspection methods. 19 p2434 A73-37867
- Influence of extended defects on the electron spectrum of semiconductors. 19 p2470 A73-37952
- Schlieren and computer studies of the interaction of ultrasound with defects. 19 p2461 A73-38201
- Local stresses near deep surface flaws under cylindrical bending fields. 22 p2880 A73-42135
- A technique for placing known defects in weldments. 23 p2986 A73-44170
- Some results in predicting the states of semiconductor triodes from noise factors on the basis of the statistical theory of pattern recognition. 23 p2961 A73-44297

SURFACE DIFFUSION

- Molybdenum disulfide in oils and greases under boundary conditions. [ASME PAPER 72-LUB-37] 03 p0335 A73-14345
- Intermetallics formation and diffusion of contacting Al-Au thin films dependence on temperature, thickness ratio and contact time. 06 p0706 A73-17903
- Structure of the borated layer after diffusion saturation with other elements. 06 p0707 A73-18040
- Structure and properties of nickel-phosphorus coatings in relation to annealing temperature and time. 06 p0698 A73-18214
- Transition of oxide film on a molybdenum surface from a two-dimensional structure to a three-dimensional structure. 06 p0738 A73-18617
- The mechanism of surface mass transfer in the thin-film Ge-Al system. 06 p0738 A73-18651
- The experimental determination of wall-fluid mass transfer coefficients using plasticized polymer surface coatings. 08 p1023 A73-21261
- Diffusion theory for adsorption and desorption of gas atoms at surfaces. 09 p1047 A73-22073
- Mathematical description by Gaussian error function for metals diffusive saturation and diffusion constants determination. 10 p1236 A73-24952
- Carbon and stainless steels chemical composition effects on diffusion layer structure and fatigue strength after diffusive boring. 10 p1236 A73-24954
- Austenitic stainless steels diffusion layer formation and structure by gaseous carburization with FeAl-ammonium chloride powder mixture, describing elements redistribution. 10 p1226 A73-24958
- Boridosilicide and boridoaluminide diffusion coatings on iron and steel, investigating formation kinetics structure and properties. 10 p1227 A73-24963
- Effect of carbon on the growth of boride layers. 11 p1374 A73-26109
- Investigation of adhesional and diffusional interaction of instrumental materials with titanium alloys. 12 p1502 A73-27466
- Electric field interaction with polar molecules at varying density diffusing through solid body surface, deriving dispersion law for density and potential fluctuations. 12 p1526 A73-27939
- Experimental evaluation of the role of surface reactions in studies of hydrogen penetration through titanium, nickel and copper. 13 p1630 A73-28009
- Investigation of diffused titanium coatings on refractory metals. 13 p1630 A73-28015
- The extension of self-registered gate and doped-oxide diffusion technology to the fabrication of complementary MOS transistors. 13 p1595 A73-29576
- Saturation of Kh18Ni10T steel by molybdenum from the vapor phase. 15 p1889 A73-31807
- Fused salt techniques for metal diffusion coatings with beryllium, boron, silicon, aluminum, titanium and chromium. 16 p2017 A73-32697
- Surface diffusion and migration on dispersed silicon and basalt during weak heating in a vacuum. 16 p1977 A73-33757
- Certain mechanisms of the solid-phase interaction arising during the formation and operation of high-temperature coatings. 18 p2322 A73-35877
- Application of activators in contact diffusion saturation processes in metals and powders. 18 p2318 A73-35878
- Effect of atom self-diffusion on evaporation processes and porosity development in solid bodies during electron-beam treatment. 18 p2320 A73-36900

- Diffusion of hydrogen and deuterium in Ta, Nb, and V. 20 p2576 A73-39134
- Investigation of the transition zone structure in composite materials under cyclic loads. 20 p2580 A73-39379
- Titanium oxide film dissolution indication by tempering colors and weld tensile strength dependence on film thickness and temperature. 21 p2717 A73-40486
- The influence of carbon on the interdiffusion of Mo and Ni. 22 p2878 A73-42579
- German monograph - Doping profiles of boron-implanted silicon layers. 22 p2897 A73-42717
- Saturation of steel Kh18Ni10T with molybdenum from the vapor phase. 24 p3100 A73-45270

SURFACE DISTORTION

- Analysis of face deformation effects on gas film seal performance. 01 p0055 A73-10246
- Surface damage under fretting fatigue as function of applied normal load and clamping pressure. 11 p1383 A73-25836
- Atmospheric turbulence vs residual surface inaccuracy refracting and reflecting telescopic image degradation for solar observations. 16 p2014 A73-32969
- Nondestructive optical contour mapping for non-contact testing of reflecting surface deformations from interference pattern due to monochromatic illumination of grating. 17 p2172 A73-35419
- Interference between a wing and a surface of velocity discontinuity. 19 p2376 A73-37490
- Errors arising in the RATAN-600 radio telescope due to temperature effects. 21 p2675 A73-41453
- Surface buckling of a laminated medium. 24 p3145 A73-44525

SURFACE ENERGY

- Effect of various surface-active media on the changes taking place in the strength of U8 steel in the high-strength state. 01 p0066 A73-11337
- Improvements in the transverse properties of composites. I - Fracture surface energy and mechanism of transverse fracture in glass fibre composites. 04 p0469 A73-15984
- Surface effects in solid bodies undergoing deformation and fracture. 06 p0734 A73-17922
- Manifestation of the adsorption-induced loss of strength in metals under conditions of selective transfer in boundary friction. 06 p0698 A73-18637
- Assembly for measurement of free surface energy, contact angles, and melt densities by a lying drop technique. 09 p1085 A73-23017
- Effect of specimen thickness on the fracture surface energy of 100 axis tungsten single crystals. 15 p1891 A73-32022
- Airborne passive IR line scanner, noting spectral resolution and thermal sensitivity for land and water surfaces energy. 17 p2174 A73-35577
- Influence of the surface level on the differential slope of the semilogarithmic current-voltage characteristic of Schottky diodes. 23 p2960 A73-43620
- Surface phenomena in solids during the course of their deformation and failure. 23 p3018 A73-44322

SURFACE EROSION

U EROSION

SURFACE FINISHING

- Effect of diamond smoothing on the surface finish and fatigue strength of EI961 steel. 02 p0174 A73-12141
- Applying surface integrity principles in jet engine production. 03 p0312 A73-13272
- Surface preparation and pit propagation in stainless steels. 03 p0325 A73-13726
- Beryllium parts machining and surface finishing techniques for maximum fracture strength and fatigue life. 05 p0587 A73-16754
- Surface preparation and heating and control processes in diffusion brazing and welding, illustrating with turboreactor construction. 06 p0698 A73-18695
- Surface work hardening as a means of increasing the resistance of machine parts to low cycle fatigue. 09 p1089 A73-23162
- Investigation of the effect of surface finish and method of surface treatment on the endurance of the steels Kh18Ni10T and Kh16N6 and of alloy AMG6 at normal and low temperatures. 09 p1106 A73-23163

The dependence of piezo-electric accelerometer response on method of attachments. 12 p1496 A73-26974

Surface preparation, protective coatings, materials selection and equipment used in soldering, discussing quality control 12 p1504 A73-27990

Automated machining and surface finishing of heat resistant stainless steel nozzles for wind tunnel applications 15 p1855 A73-31200

Durability of bonded titanium joints increased by new process treatments. 16 p2017 A73-33052

Surface treatments of titanium and its alloys 19 p2441 A73-37828

The influence of fabrication and structure processes on the result of control by ultrasonics of semifinished products of titanium alloys 19 p2441 A73-37830

Surface conditioning of titanium alloy tubing. [SAE SP-378] 19 p2434 A73-37872

Aerospace applications of heat resistant alloy diffusion welding techniques, describing mechanical properties, metal bonding, surface cleaning, vacuum levels, temperature effects and microstructure 20 p2569 A73-39246

Influence of mechanical treatment of the resonator on the parameters of an electron-beam-pumped cadmium sulfide laser. 22 p2869 A73-42259

Induced plasticization - An inner bore surface treatment technique for solid-propellant rocket motors. 22 p2897 A73-42626

Bulk and surface damage mechanisms of laser crystalline and nonlinear optical materials and thin films, noting plasma thresholds and surface polishing 23 p2989 A73-44210

Influence of heat treatment and surface quality on the endurance of E1961 steel 23 p2995 A73-44288

Structural adhesive bonding of titanium - Superior surface preparation techniques. 24 p3093 A73-44765

SURFACE GEOMETRY

Specular reflection of heat radiation from an arbitrary reflector surface to an arbitrary receiver surface. 08 p1022 A73-21254

Heat flux contours on a plane for parallel radiation specularly reflected from a cone, a hemisphere and a paraboloid. 08 p1022 A73-21255

The stationary-phase method for a double integral with an arbitrarily located stationary point 09 p1048 A73-21918

Mars surface ellipticity discrepancy with dynamic value obtained from satellite orbital precession explained by solid state convection in deep interior and Martian evolution 09 p1144 A73-22268

Microwave small signal bipolar transistor evolution, design and applications, noting cost effectiveness and surface geometry control 09 p1064 A73-22499

Internal equation numerical solution for excitation of multilayer arbitrary shape dielectric body of revolution, considering radome curvature effects on antenna radiation pattern 09 p1052 A73-23084

Bistatic-radar estimation of surface-slope probability distributions with applications to the moon. 10 p1190 A73-24892

Precise calculation of the magnetosphere surface for a tilted dipole. 11 p1421 A73-25923

A new conception of modeling the process of heat transfer on a surface with artificial roughnesses and microfins 12 p1557 A73-26798

A method for the calculation of the aerodynamic coefficients of a body of any form. 12 p1457 A73-27067

Numerical Master Geometry computer programs for smooth surface shape mathematical representation, manipulation, definition and interrogation in design and production 13 p1623 A73-28053

The evolution and application of lofting techniques at Hawker Siddeley Aviation. 13 p1623 A73-28054

Scattering from a periodic corrugated surface - Semi-infinite alternately filled plates. 13 p1659 A73-28484

Arrangement of integral surfaces in weakly-non-linear systems of differential equations 13 p1650 A73-29137

Modeling irregular surfaces. 13 p1619 A73-29242

On the stability of natural convection boundary layer flow over horizontal and slightly inclined surfaces. 14 p1817 A73-30608

Flux density for ray propagation in discrete index media expressed in terms of the intrinsic geometry of the deflecting surface. 15 p1913 A73-31135

Free surface shape of MHD flow due to constant mass source expansion into uniform magnetic field as function of time 16 p2041 A73-33329

Acceleration waves in simple elastic materials. 16 p2081 A73-33746

Three-dimensional nosetip shape changes in hypersonic flow. I - Illustration of a mathematical model-characteristic method. [AIAA PAPER 73-762] 18 p2264 A73-36377

The optimisation of wing design. 19 p2495 A73-37408

Geometric deformation of spherical dielectric lens antennas 19 p2409 A73-37715

Transonic laminar boundary layers with surface curvature. 19 p2423 A73-38480

The geometrical factor of large aperture hemispherical electrostatic analyzers. 20 p2564 A73-38877

Method for determining the unsteady thermal field of piecewise homogeneous plates of complex shape 20 p2627 A73-39256

Transformation symmetry of x-space coordinates of geometric transors, tensors and M-objects with constant length dimensionality 20 p2594 A73-39729

Geometrical characteristics of flat-faced bodies of revolution. 22 p2842 A73-42425

The use of analytic surfaces for the design of centrifugal impellers by computer graphics. 22 p2900 A73-42477

Reattachment of a separated boundary layer to a convex surface. 22 p2843 A73-42554

The Minkowski problem generalized for ovaloids 23 p2999 A73-43613

Use of the fractional-distillation effect to increase the sensitivity of spectral analysis of metallic titanium 24 p3066 A73-45515

SURFACE INTERACTIONS

U SURFACE REACTIONS

SURFACE IONIZATION

Book on surface ionization covering atomic and molecular ionization during thermal desorption from high melting point solid surfaces 03 p0345 A73-13996

Certain results of flight tests of a model ion thruster employing contact ionization of cesium on tungsten 10 p1262 A73-23892

Nickel single crystal target ionization by high voltage electron beam bombardment, using time of flight mass spectroscopic analysis 13 p1663 A73-28666

Mechanism of damage of the surface of a transparent dielectric during illumination with short light pulses. 13 p1629 A73-29429

Work function and surface ionization currents in statite ceramics from nickel electrode and thermocouple measurements, plotting temperature dependent Paschen curves 16 p2031 A73-34011

Some results of flight tests of an ion-engine model using surface ionization of cesium on tungsten. 20 p2600 A73-38911

SURFACE LAYERS

NT MONOMOLECULAR FILMS

Application of the basic concepts of structural-energetic theory to the problem of physical fatigue limit. 02 p0235 A73-12131

Complex phenomena in metal surface layers after high velocity impact loading in Ar atmosphere 02 p0182 A73-12698

The growth process of oxide layers during the initial oxidation of a 80Ni-20Cr alloy. 03 p0321 A73-12917

Metal-semiconductor system phase diagram for temperature dependence of substrate surface epitaxial film thickness during single crystal growth, determining equilibrium saturation time 04 p0483 A73-14880

Water frost absorptions in IR reflectivities of Jupiter Galilean satellites, discussing surface cover distributions and underlying material reflectivity 04 p0497 A73-15070

Theory of scattering of electrons in a non-degenerate-semiconductor-surface inversion layer by surface-oxide charges. 06 p0733 A73-17747

Use of a paraboloidal layer to study gas-wall interaction 06 p0685 A73-17772

Technology and properties of epitaxial GaAs layer grown from liquid phase, considering GaAs solubility in Ga 06 p0734 A73-17798

Investigation of molybdenum after exposure to single-charge helium atom radiation 06 p0707 A73-17909

Surface layer grain boundary corrosion damage of Ti alloys during vacuum annealing, reducing rupture strength, vibration resistance and bending fatigue limit 06 p0698 A73-18205

Adsorption conditions and vapor molecule balance in wall layer at liquid boiling initiation, noting heat flux dependence on underheating effect, pressure and velocity 06 p0769 A73-18564

Transition of oxide film on a molybdenum surface from a two-dimensional structure to a three-dimensional structure. 06 p0738 A73-18617

Kinetics of electrostatic image formation during exposure of electrophotographic layers 07 p0823 A73-19331

Difference between the principal element concentrations on the surface and in the volume of lunar regolith particles 07 p0876 A73-19474

Initial free-surface motion of an impulsively loaded half-space. 07 p0810 A73-19509

Occurrence of oriented structures under the action of a laser beam in metals 07 p0839 A73-19658

Study of the surface layer of drift currents in the laboratory 08 p0985 A73-21455

Experimental investigation of the failure mechanism of fiber-reinforced composites subjected to uniaxial tension. 09 p1156 A73-21874

High temperature creep resistance enhancement by stress relaxation or removal of unstable surface layers, increasing activation energy for different alloys 09 p1101 A73-22403

Comparison of the efficiency of photocells with stepwise and exponential distributions of the impurities in the doped layer 09 p1033 A73-22721

Structural features of surface layers in molybdenum alloy sheets 09 p1106 A73-23188

Effects of metal grain size on friction and wear characteristics 10 p1223 A73-24067

Character and magnitude determination of residual stresses in surface layers of rolling bodies 10 p1289 A73-24068

Difference of the plastic deformation of the surface and internal layers of polycrystalline iron under fatigue loading. 10 p1233 A73-24183

Lunar permafrost - Dielectric identification. 10 p1282 A73-24629

Solid sphere meandering trajectory in viscous liquid filled cylinder, postulating oscillating molecular surface tension layer at interface 10 p1206 A73-24701

Alloy steels supercooled austenite nitriding in ammonia flow, examining diffusion layers by X ray analysis and hardness tests 10 p1236 A73-24956

Cr diffusion into Ni-Cr alloys in presence of aluminumized layer, noting increased diffusive mobility 10 p1226 A73-24959

Si addition effect on Ni-Cr alloy carburized layer depth, microhardness, phase structure, chemical composition and scaling resistance 10 p1227 A73-24960

Diffusion layer structure and phase composition during quenched and annealed steel saturation by Cr at high heating rates 10 p1236 A73-24962

Wear-resistant surfaces through electrical spark hardening 11 p1371 A73-24992

The influence of environment and the surface layer on crack propagation and cyclic behavior. 11 p1380 A73-25807

Effect of carbon on the growth of body layers 11 p1374 A73-26109

Study of the variations of the microhardness of the surface layer hardened by ball rolling in relation to the heating temperature 12 p1502 A73-26799

Dissolution of Ti-6Al-4V at cathodic potentials in 5N HCl. 12 p1512 A73-27249

Strength characteristics of layers obtained by spark-alloying steels with high-melting metals 12 p1512 A73-27264

Plastically deformed Fe-Si and Al alloys surface layer crystal dislocation density and plastic flow onset determination as function of depth 13 p1635 A73-28264

Optical studies of the inhomogeneities of metallic layers deposited in vacuum 13 p1660 A73-28761

Quantization effects in semiconductor inversion and accumulation layers.

13 p1669 A73-29291

On nongravitational effects in two classes of models for cometary nuclei.

14 p1793 A73-29820

Static electromagnetic field structure in elastic homogeneous medium for sources distributed by simple and double layers in terms of scalar and vector potentials

14 p1774 A73-30030

Formation of oriented structures by action of a laser beam on metals.

14 p1760 A73-30325

Behavior of the electrode potential of a metal under conditions of fretting corrosion

14 p1763 A73-30711

Investigation of fatigue effects in thinnest surface layers of metals with boundary friction

14 p1815 A73-30838

Investigation of friction and wear mechanisms in a friction coupling with a small overlapping coefficient

15 p1882 A73-31599

Gas saturated surface layer effect on Ti alloy resistance to static cyclic tensile loads, noting increased fatigue strength after etching

15 p1890 A73-31815

Adsorption conditions and vapor molecule balance in wall layer at liquid boiling initiation noting heat flux dependence on underheating effect, pressure and velocity

16 p2086 A73-33589

Determination of the heat flux from the lunar interior for a nonhomogeneous structure of the lunar surface layer

16 p2065 A73-33783

Planet Mars atmospheric physics covering optical parameters, brightness distributions, pressure, aerosol, chemical composition, photometric and surface layer properties and topography

16 p2069 A73-33830

Contraction of an elastic layer by girder slabs

17 p2240 A73-34148

Protective coating-metal adhesion dependence on chemical bonds, double electric layers at interface and thermoelectric stresses

18 p2319 A73-35893

Some characteristics of the microplastic deformation of the surface layers of semiconductor crystals at temperatures below and above the thermal brittleness threshold

18 p2341 A73-36805

Influence of the structural state of the surface layers on the resistance to crack propagation of steel products

18 p2366 A73-36819

Latitudinal distribution of a debris mantle on the Martian surface.

19 p2477 A73-37208

Martian south polar region pitted and etched terrain features, interpreting surface layered blanketing material as due to wind action

19 p2478 A73-37215

Nature and origin of layered deposits of the Martian polar regions.

19 p2478 A73-37216

Martian polar stacked laminae interpreted in terms of conditions for carbon dioxide liquefaction, considering atmosphere history

19 p2478 A73-37217

Optical properties of the Mercury surface layer

19 p2480 A73-37233

Fine structure of rolled annealed tungsten sheet, discussing subsurface layer recrystallization and deformation effects based on radiographic examinations

19 p2440 A73-37443

Russian book on cosmogenic nuclear reactions in meteorites and asteroid and lunar surface layers covering vertical /depth/ distributions of isotopes and nuclear-active particles

19 p2486 A73-37775

Earth surface turbulent boundary layer analysis, considering similarity theory limitation, flux profiles, velocity, temperature and humidity spectra, energy budgets, local isotropy, etc

19 p2427 A73-38212

Turbulence spectra, length scales and structure parameters in the stable surface layer.

19 p2448 A73-38216

Edge dislocation in an anisotropic material with a surface layer.

20 p2593 A73-39342

Ion implanted megohm silicon monolithic IC resistors with buried n-guard layer protection against slice-to-slice variations of fixed surface charge

20 p2537 A73-39416

Certain features of sensitive layers containing bifunctional polymers /fixatives/ on a blank film

21 p2646 A73-40257

Dynamic properties of surface layers in semiconductors

21 p2752 A73-40845

Results of radar experiments performed on automatic stations Luna 16 and Luna 17.

21 p2774 A73-41401

Thermal conductivity of superconducting layer in intermediate state with Andreev electron excitation trajectories in magnetic field, using Green function and impurity distribution technique

22 p2896 A73-41728

Improvement of thermal shock resistance by surface prestressing.

22 p2921 A73-42462

Expected gamma ray emission spectra from the lunar surface as a function of chemical composition.

22 p2903 A73-42494

Surface ozone in the arctic atmosphere.

23 p2974 A73-43866

Ozone concentration studies and ozone flux measurements near the ground at Poona.

23 p2974 A73-43868

Whisker junctions between growth structures on CdS layers.

23 p2997 A73-44027

Transverse elastic wave propagation in CdS crystal wafer coated on both sides with AgBr, titanium oxide, Si or polystyrene

23 p3017 A73-44038

Gas saturated surface layer effect on Ti alloy resistance to static cyclic tensile loads, noting increased fatigue strength after etching

24 p3100 A73-45278

SURFACE NAVIGATION

Comparison of medium-distance navigation systems. II

02 p0191 A73-12014

Omega navigation system.

04 p0474 A73-15061

Communication satellite application to shipping company operations for cost benefits and alleviation of distress alerting, search and rescue, and heavy weather damage problems

06 p0755 A73-17625

Retroflecting satellite with laser range finder for Martian roving vehicle navigation, discussing error analysis and minimization by measurement geometry choice through nonlinear programming

10 p1247 A73-24005

Satellite systems for mobile communications and surveillance; Proceedings of the International Conference, London, England, March 13-15, 1973.

12 p1471 A73-27652

Landmark navigational and topographical mapping techniques for planetary surface exploration using unmanned vehicles and earth based computers

17 p2210 A73-35383

Aeronautical and maritime traffic control by stationary orbit navigation satellites, discussing frequency ranges, aircraft distance control, antenna arrays and multiple data access

17 p2125 A73-35477

A study of remote guidance and control for planetary surface vehicles.

19 p2403 A73-37313

Satellites for maritime applications.

19 p2494 A73-38099

Digital processing of stereoscopic image pairs.

19 p2432 A73-38534

Aeronautical/maritime satellite borne two-way L-band transponder weight and power limitation effects on channel capacity

20 p2531 A73-39771

SURFACE PROPERTIES

NT ADHESION

NT COEFFICIENT OF FRICTION

NT INTERFACIAL TENSION

NT SKIN TEMPERATURE [NON-BIOLOGICAL]

NT SPECTRAL REFLECTANCE

NT SURFACE CRACKS

NT SURFACE DEFECTS

NT SURFACE ENERGY

NT SURFACE ROUGHNESS

NT SURFACE STABILITY

NT SURFACE TEMPERATURE

NT WALL TEMPERATURE

Effect of structural factors on the surface properties of single crystal silicon films

01 p0087 A73-10038

Many-body effects at metal-semiconductor junctions. I - Surface plasmons and the electron-electron screened interaction.

01 p0087 A73-10147

Influence of haze layers upon remotely-sensed surface properties.

01 p0037 A73-10360

The effect of the surface electric charge on the gain of a solid-state traveling-wave amplifier

01 p0023 A73-10429

The mechanism of the metallic adhesion bond.

01 p0087 A73-10473

Explosive shock hardening effects on roller steel fatigue strength, surface hardness and wear resistance

01 p0056 A73-10493

Bidimensional and surface effects in a coplanar-contact Gunn diode

02 p0144 A73-11533

Surface properties improvement of Al products by metal coatings, noting corrosion prevention, anodic coatings, enameling and brazing

03 p0312 A73-13588

Investigation of hole scattering in surface inversion channels arising on a cleaved germanium surface

03 p0349 A73-13656

Influence of gamma irradiation on the surface properties of metal-dielectric-semiconductor structures

03 p0349 A73-13661

Role of the anelastic behavior of the ablation material on cross-hatching.

03 p0398 A73-14189

The effect of surface recombination velocity on the performance of vertical multi-junction solar cell.

03 p0255 A73-14214

Propellant grain surface contamination effect on ignition transient characteristics of solid rocket motor [AIAA PAPER 72-1198]

04 p0487 A73-14920

Surface features on glass spherules from the Luna 16 sample.

04 p0498 A73-15187

Exact frequency dependent complex admittance of the MOS diode including surface states, Shockley-Read-Hall /SRH/ impurity effects, and low temperature dopant impurity response.

04 p0427 A73-15347

Engineering support activities for the Apollo 17 Surface Electrical Properties Experiment.

04 p0428 A73-15390

Stationary waves properties dependence on weak skin effect in distributed tunnel diode type of nonlinear active transmission lines

04 p0429 A73-15911

Energy absorption inelastic surface mechanisms effect on I-V characteristics profile for bounded semiconductor with negative differential conductivity

06 p0735 A73-17974

Control of the electrical properties of a surface with the aid of adsorption of molecules /Stability of surface parameters and slow relaxation/

06 p0735 A73-18083

Photodiode structure performance dependence on surface properties in static and kinetic operations, noting surface recombination and photoelectric relaxation

06 p0676 A73-18086

Yield surface equation derivation for plastically prestrained anisotropic material from simple tension and compression tests

06 p0763 A73-18455

Metal surface active properties effects on fracture characteristics and deformation and failure conditions

07 p0912 A73-19472

Some surface characteristics and gas interactions of Apollo 14 fines and rock fragments.

07 p0891 A73-19831

Lunar surface properties as determined from earthshine and near-terminator photography.

07 p0897 A73-19892

On the unequal accuracy of radio range finder measurements in the reflection of radio waves from an underlying surface.

07 p0793 A73-20041

Lost-model method of precision casting - Its possibilities, limitations and present trends

07 p0831 A73-20160

The casting of titanium and its alloys by the lost-model method

07 p0831 A73-20161

Magnetic field dependence of the surface resistance of pure and impure superconducting aluminum at photon energies near the energy gap.

07 p0864 A73-20573

Radiation between finite surfaces with variable radiative characteristics.

08 p1021 A73-20794

Ground based radar measurement of Martian topography, surface temperature and thermal properties by microwave and IR radiometry and spectral reflectivity observation

09 p1144 A73-22259

Radar measurement of altitude profiles and reflected power for Martian topography and surface properties, noting heavy cratering

09 p1144 A73-22260

Investigation of the growth surface of GaAs epitaxial films by chemical decoration and small-angle shadowing technique.

10 p1259 A73-23570

Metallic and nonmetallic surface investigation by scanning electron microscopy, discussing operational features and applications to wear, fracture and corrosion studies

11 p1361 A73-25107

Microwave radiometric observations of simulated sea surface conditions.

11 p1355 A73-25774

Metal surfaces structure, chemical segregation, electronic properties, space charge and electrode behavior

11 p1381 A73-25809

Galilean satellites surface thermal properties from radiometry of 20-micron band during eclipses of Jupiter

11 p1424 A73-26132

Ten-micron eclipse observations of Io, Europa, and Ganymede.

11 p1424 A73-26133

Coated laser windows characterized by strong surface absorption, calculating absorptivity, transmittance and reflectivity under assumption of insignificant interference effects within substrate

11 p1377 A73-26243

Study of the variations of the microhardness of the surface layer hardened by ball rolling in relation to the heating temperature

12 p1502 A73-26799

An analytical model for the prediction of liquid rocket plume contamination effects on sensitive surfaces.

[AIAA PAPER 72-1172]

12 p1532 A73-27099

Influence of the physical properties of metal melts on the spheroidization of droplets in the process of their crystallization

12 p1503 A73-27551

Results of lunar surface investigations based on its intrinsic radiation

13 p1672 A73-28116

A method for calculating the low temperature surface specific heat of a crystal lattice.

13 p1704 A73-28214

Book on fretting corrosion covering contacting surface theory, damage characteristics, wear variables effect, fatigue, adhesion and electrochemical properties, etc

13 p1643 A73-29575

Wolter-Schwarzschild telescopes for X-ray astronomy.

14 p1752 A73-30159

Explosive shock hardening effects on roller steel fatigue strength, surface hardness and wear resistance

14 p1755 A73-30318

Application of a scanning electron microscope in powder investigations

15 p1892 A73-32239

Surface morphology after pretreatment in relation with bondability of aluminium alloys.

16 p2018 A73-33056

Surface integrity - A new requirement for improving reliability of aerospace hardware.

16 p2018 A73-33067

A method of analytical error identification in the inspection of the working profiles of blades

16 p2019 A73-33300

Effectiveness and heat transfer with full-coverage film cooling.

[ASME PAPER 73-GT-18]

16 p2086 A73-33495

The Apollo 17 Surface Electrical Properties Experiment antenna performance.

17 p2171 A73-35370

The application of strip strain gages for measuring residual surface stresses in beryllium.

[UCRL-74078]

17 p2191 A73-35438

Surface oscillations of a magneto-active plasma.

17 p2217 A73-35522

IR spectral measurements of reusable surface insulations via radiative four flux model

18 p2370 A73-36361

Modeling the effect of air and oil upon the thermal resistance of a sphere-flat contact.

[AIAA PAPER 73-746]

18 p2370 A73-36362

Surface properties of carbon and graphite fibers

18 p2327 A73-36465

Al foil surface properties from electron spectroscopic analysis, determining oxide film thickness, annealing effects and oxidation dependence on surface hydrocarbon deposits

19 p2442 A73-38171

Papers on materials science covering optical and spectroscopic surface analyses, neutron effects, amorphous semiconductors, high temperature superconductivity, etc

19 p2502 A73-38547

Minor planets and related objects. XII - Radar observations of /1685/ Toro.

20 p2607 A73-39122

Investigation of a thermomechanical surface during unloading according to the theory of thermoplasticity

20 p2617 A73-39264

Experimental investigation of the integral hemispherical emissivity of refractory metals and alloys.

20 p2593 A73-39426

Combined Auger electron spectroscopy and electron impact desorption studies of silicon surfaces.

20 p2595 A73-39665

Magnetic field effects on slab surface plasmons in the local limit.

20 p2599 A73-39720

Automatic surface mapping via holographic system, describing Q switched ruby laser holograms, image disector, computer video signal analysis and scan signals

21 p2699 A73-40150

Surface and bulk laser-damage statistics and the identification of intrinsic breakdown processes.

21 p2714 A73-40758

Measurement of the doping level distribution in the surface region of a semiconductor

21 p2753 A73-41097

Lunar specific surface adsorption-desorption processes discussing near-surface atmospheric diurnal variations, nitrogen temperature, sorption capacity, gas concentration from regolith structure

21 p2774 A73-41402

The existence of a minimal surface with a free boundary of a given length

22 p2885 A73-41774

Improved point-matching method with application to scattering from a periodic surface.

22 p2824 A73-41833

Electromagnetic inverse boundary conditions determination of profile and material surface characteristics of conducting circular cylindrical shape scatterer

22 p2824 A73-41834

Reflection function for an isotropically scattering finite medium.

22 p2887 A73-42565

Heavy elements in surface materials - Determination by alpha particle scattering.

23 p2981 A73-43529

Linear external electric field approximation for intervalley scattering effects on nondegenerate semiconductor surface electroconductivity

23 p3017 A73-44045

The relation of surface condition after pretreatment to bondability of aluminum alloys.

24 p3093 A73-44764

Structure of lanthanum-hexaboride-coated rhenium filaments.

24 p3105 A73-45401

SURFACE REACTIONS

On turbulent flows with fast chemical reactions. II - The distribution of reactants and products near a reacting surface.

[AD-753565]

01 p0032 A73-10638

Effects of transverse diffusion and transverse stored charge in alloy transistor base.

01 p0023 A73-10681

Effect of gas-surface interaction on the transmission of sound through a collisionless gas.

01 p0077 A73-10972

Elemental analysis of a friction and wear surface during sliding using Auger spectroscopy.

01 p0057 A73-11277

Isotherm data for physical adsorption of Ar on pyrex surface at low pressure, noting correlation in terms of Dubinin-Radushkevich equation

04 p0456 A73-15765

Some problems of gas-solid surface interaction.

05 p0638 A73-16177

Mean free path of molecules from a surface in rarefied flow with application to correlating drag data.

[AIAA PAPER 73-198]

05 p0531 A73-16933

Laser-induced fast thermal desorption from solid surfaces

06 p0699 A73-17914

Surface effects in solid bodies undergoing deformation and fracture

06 p0734 A73-17922

Quantitative evaluation of superficial organic contaminants, soluble in halogenated solvents, discussing sampled surface solvent extraction method and subsequent IR absorption spectrographic analysis

06 p0660 A73-18547

Durability and fracture mechanics of polymethylmethacrylate under the action of liquid, surface-active media

06 p0715 A73-18670

Interaction of TEA-CO₂-laser pulses with metals enhanced by liquid layers.

07 p0836 A73-20195

Phase transition effects at the collecting droplet surface on the capture coefficient magnitude

07 p0922 A73-20418

High-energy electron-beam deposition onto a hot graphite surface.

08 p0990 A73-21210

Spectroscopic investigation of the interaction of oxides with a metallic surface. III - Systems Al₂O₃-Me/Al, Cu, Ti, Khl8N9T steel, Ni, Co, Mo, W, Si/

09 p1103 A73-22470

Relationship between adsorption processes on the cathode surface and processes in the region near the electrode in a high-current plasma discharge

09 p1127 A73-22608

Gasdynamic and thermal processes during giant laser pulse impingement on target material, considering heat wave propagation at supersonic and subsonic velocities

09 p1127 A73-22610

Surface and body vaporization mechanisms during intense energy flux interaction with substance, relating flux density to mean depth of surface-to-bulk vaporization shift

09 p1095 A73-22611

Estimate of the influence of thermal diffusion on the surface burnout rate in a nonhomogeneous turbulent boundary layer

09 p1167 A73-22618

The solid-vacuum interface; Proceedings of the Second International Symposium on Surface Physics,

Technische Hogeschool Twente, Enschede, Netherlands, June 21-23, 1972.

11 p1325 A73-25201

Transition metal borides ESCA spectra observation for metal-boron bonding energy based on spectral sensitivity to surface oxidation, discussing relevant features

11 p1325 A73-25202

Ruby and Nd-YAG pulsed laser induced surface damage probability comparison at 1.06 and 0.69 micron wavelengths by breakdown starting time distribution measurement

11 p1377 A73-26226

The task of constructing transition functions in problems involving interaction of weak shock waves with cylindrical and spherical surfaces

12 p1486 A73-27241

Experimental evaluation of the role of surface reactions in studies of hydrogen penetration through titanium, nickel and copper

13 p1630 A73-28009

Effect of surface catalytic activity on stagnation heat-transfer rates.

13 p1706 A73-28804

Growth rate calculation for hygroscopic condensation nuclei in the presence and absence of a monolayer of a surface-active substance

13 p1654 A73-28880

Gas molecule-solid surface interactions, considering rainbow scattering, roughness at molecular scale, potential well and statistical analysis procedures

13 p1663 A73-28912

Surface solid solutions and chemical compounds formation due to gas sorption by titanium and barium

13 p1663 A73-28968

Surface materials ablation cooling for thermal protection during reentry, discussing chemical reactions, plastics pyrolysis and propulsion chemistry

14 p1724 A73-30133

Layered and aggregate product displacement reaction kinetics in solid state /metal-metal oxide/ couples for metal matrix composites at 1000 C from thermodynamic and diffusion data

14 p1783 A73-30634

Linear nonstationary effects - A source of information on the kinetics of reactions on the surface of a solid fuel

14 p1818 A73-30873

The reaction of a titanium alloy with hydrogen gas at low temperatures.

15 p1890 A73-31993

Strongly active surfactant effects on metal surface fracture characteristics under various loading conditions

15 p1952 A73-32071

Study of multiple surface compound precipitation during passivation of D6AC-steel.

15 p1895 A73-32566

High-energy pulsed CO₂-laser-target interactions in air.

17 p2184 A73-34914

Friction induced surface activity of some simple organic chlorides and hydrocarbons with iron.

[ASLE PREPRINT 73AM-8A-1]

17 p2179 A73-34991

A new technique for Auger analysis of surface species subject to electron-induced desorption.

17 p2175 A73-35757

Phase formation investigation in the Mo-Al and W-Al systems when the Mo and W surfaces are saturated with aluminum by diffusion from a vapor phase in a vacuum

18 p2318 A73-35879

Study of the conditions defining the passivating action of surface-active substances on hygroscopic condensation nuclei

18 p2332 A73-35918

The role of physicochemical processes in surface wear under rolling friction in low-molecular hydrocarbon media

18 p2343 A73-36821

Role of gas-surface interactions in the reduction of Ogo 6 neutral particle mass spectrometer data.

20 p2551 A73-38941

Existence and uniqueness conditions for solid surface vaporization products dispersion into vacuum formulated for equations of motion of ideal gas under variable energy release

20 p2573 A73-39282

Relationship between the equilibrium vapor pressure of the solvent and the surface activity in dilute solutions of inactive and surface-active materials

21 p2646 A73-40122

Stability of silver bromide dispersions in the presence of gelatin and other surface-active substances

21 p2647 A73-40267

Burnout of a graphite surface during the blowing of an inert gas through it

21 p2790 A73-40698

Study of surface by spectrometry of slow electrons

21 p2706 A73-41598

Scattering and transmission functions of radiation by finite atmospheres with reflecting surfaces.

23 p3030 A73-43755

Surface solid solutions and chemical compounds formation due to gas sorption by titanium and barium 23 p3008 A73-44320

Surface phenomena in solids during the course of their deformation and failure. 23 p3018 A73-44322

Intensity of charged particle recombination on the surface of certain borides of high-melting-point metals in a weakly ionized hydrogen plasma 24 p3098 A73-44418

Specific surface changes in tungsten and molybdenum oxides during reduction processes 24 p3099 A73-44738

Laser supported gaseous detonation wave propagation above solid surface, calculating momentum transfer as functions of laser energy, pulse duration, and beam and target areas 24 p3097 A73-45455

SURFACE ROUGHNESS

Holographic inspection of shapes of unpolished surfaces. 01 p0051 A73-10835

Surface roughness of turbine blades machined by circular milling 02 p0174 A73-12579

Calculation of compressible turbulent boundary layers with roughness and heat transfer. 03 p0296 A73-14179

Moon and Venus relief from backscattering diagrams based on radar echoes, calculating root-mean-square angles of surface inclination 03 p0379 A73-14568

Determination of the average duration of a machining process on automatic production lines 05 p0582 A73-16997

Radar brightness mapping of Venus surface, noting roughness of terrain from polarization studies and signal processing for extraction of echo power 06 p0744 A73-17440

Isostasy and relief of the Earth, the Moon and Mars 07 p0878 A73-19661

Scanning electron microscope for heat transfer surface characterization, noting Inconel surface roughness change in convective heat transfer experiment 08 p1025 A73-21642

Energy characteristics of radio signals scattered by statistically uneven surface, proposing statistical variables substitution 10 p1191 A73-24934

Aquaplaning prevention during take-off and landing, discussing friction loss factors, aircraft tires and runway surface treatment by antiskid overlays and grooving 11 p1343 A73-25209

Cleaved Si and Ge surfaces roughness investigation by low energy electron diffraction, electron microscopy and optical reflection technique 13 p1668 A73-28452

Investigation of the influence of compressibility and the pressure gradient on the value of the permissible Reynolds number of roughness 13 p1567 A73-29406

Rayleigh-fast Fourier transformation techniques for electromagnetic scattering over rough sinusoidal surface, comparing numerical validity with perturbation, physical optics and integral equation methods 14 p1728 A73-30230

Investigation of rough surfaces by a method based on the scattering of coherent light by the sound reflected from such surfaces 14 p1753 A73-30583

Dependence of the closeness of two contacting bodies on the load under a high contour-applied pressure with a plastic contact 15 p1880 A73-31143

Radar observations of Venus at 3.8 cm 16 p2067 A73-33806

A method for computing roughwall heat transfer rates on reentry nosetips. [AIAA PAPER 73-763] 18 p2264 A73-36378

Optical wave measurement technique and experimental comparison with conventional wave height probes. 19 p2458 A73-37263

Some consequences of introducing the geometrical-dynamic characteristic ratio in studies of the heat transfer to surfaces with artificial roughnesses or to microwaving surfaces 19 p2504 A73-37655

Formation of a periodic wave structure on the dry surface of a solid by TEA-CO₂-laser pulses. 19 p2438 A73-38025

Comparison of the Beckmann model with bidirectional reflectance measurements. [ASME PAPER 73-HT-11] 20 p2563 A73-38567

SURFACE ROUGHNESS EFFECTS

Backscatter from snow and ice surfaces at near incident angles. 01 p0016 A73-10191

Relations among stability parameters in the surface layer. 01 p0073 A73-10497

Correlation function for prediction of surface roughness induced supersonic boundary layer transition on blunt bodies, taking into account compressibility and centrifugal force effects 01 p0002 A73-10742

Radiation heat transfer in isothermal adjoint plate system with directionally emitting and nondiffuse reflecting surfaces, considering surface roughness effects 01 p0123 A73-11140

Influence of roughness on the process of interaction between a rarefied gas and the surface of a solid 02 p0194 A73-11608

Relation of the diffuse reflectance remission function to the fundamental optical parameters. 02 p0193 A73-12350

Turbulent pressure fluctuations on smooth and rough walls. 03 p0289 A73-12960

German monograph - Spatial oscillations of light in the refraction and image field of rough objects. 03 p0319 A73-13817

Influence of distributed grit-type roughness on the spectrum of wall pressure fluctuations of turbulent flow in a tube. 03 p0295 A73-14038

Correlation of noisy radiation reflected from a statistically uneven surface. 03 p0344 A73-14039

Shear stresses below asperities in Hertzian contact as measured by photoelasticity. 03 p0314 A73-14330

Average return pulse form and bias for the S193 radar altimeter on Skylab as a function of wave conditions. 04 p0446 A73-14804

Study of the effect of surface roughness on the laminar boundary layer transition in a turbulent boundary layer 04 p0404 A73-15653

Wind profile models for atmospheric turbulent boundary layers over smooth and rough surfaces, using Heisenberg energy transfer theory and von Karman constant 04 p0473 A73-15695

Relative importance of terms in the turbulent-energy and momentum equations as applied to the problem of a surface roughness change. 05 p0591 A73-16191

Angular distribution of radiation reflected from roughened brass - Experiment and analysis. [AIAA PAPER 73-151] 05 p0598 A73-16899

Surface roughness effects on bidirectional reflectance. [AIAA PAPER 73-152] 05 p0598 A73-16900

Emission of metals under the action of non-relativistic electrons 06 p0725 A73-18102

Backscattering of electromagnetic waves from a rough surface model. 06 p0664 A73-18134

Space wave field produced by a vertical electric dipole above a perfectly conducting sinusoidal ocean surface. 06 p0665 A73-18181

Effects of surface roughness and form factor on rolling contact fatigue. 07 p0831 A73-20119

A generalized correlation of roughness density effects on the turbulent boundary layer. 08 p0953 A73-20724

Cylinder surface roughness and transverse curvature effects on turbulent boundary layer in incompressible and compressible flows, deriving formula for skin friction coefficient 08 p0956 A73-21603

Influence of various surface roughness on the natural convection. 08 p1024 A73-21639

Quasi-monochromatic radiation pulse reflection from rough surfaces, analyzing echoes statistical properties 09 p1120 A73-22575

Error analysis of approximate formula for transform of rarefied gas particle reflection from homogeneous anisotropic random surface 09 p1123 A73-22615

Velocity distribution in tubes of circular cross section 09 p1072 A73-22846

Investigation of the effect of surface finish and method of surface treatment on the endurance of the steels Kh18Ni10T and Kh16Ni6 and of alloy AMG6 at normal and low temperatures. 09 p1106 A73-23163

An experimental study of turbulent flow in pipes with artificial wall roughness 10 p1206 A73-24460

Field scattered by rough surface generated by stationary random process, constructing two dimensional density from given marginals and correlation coefficient 11 p1328 A73-25656

Kirchhoff and small perturbation methods identity in composite model calculation for rough surface electromagnetic scattering of circularly polarized wave by perfectly conducting body 11 p1329 A73-25678

Some considerations on the atmospheric internal boundary layer over the ground surface. 11 p1394 A73-25725

A new conception of modeling the process of heat transfer on a surface with artificial roughnesses and microfins 12 p1557 A73-26798

Forward and specular scattering from a rough surface - Theory and experiment. 13 p1659 A73-28490

The thick turbulent boundary layers on rotating cylinders in axial flow. 13 p1602 A73-29016

Amplitude modulation effects of the Doppler return at low altitudes. 13 p1586 A73-29223

Turbulent velocity and pressure fields in boundary-layer flows over rough surfaces. 13 p1604 A73-29264

Energy relations for turbulent flow in rough pipes. 13 p1604 A73-29265

Statistical model of gust factor relation to lake and terrain surface roughness and height from wind velocity measurement data 13 p1655 A73-29341

Some results of a theoretical study of radio emission polarization on a rough moon 16 p2064 A73-33770

Asymptotic development method for the determination of the field reflected by a random surface 16 p1984 A73-33966

A survey and comparison of methods for predicting the profile loss of turbine blades. 17 p2093 A73-34391

Experimental study of turbulent boundary layer along a flat plate with linear increase of roughness height. 17 p2151 A73-34537

Thin turbulent film analysis with approximation for relationship between flow and wall shear stress and effects of surface roughness and inertia at steps [ASME PAPER 73-LUBS-17] 17 p2181 A73-35396

Remote sensing using microwave radiometry. 17 p2174 A73-35639

Experimental study of turbulent flow in pipes with artificially roughened walls. 19 p2421 A73-38130

The boundary layer above 30 m. III. 19 p2448 A73-38214

Effect of a statistically uneven underlying surface on the radiation characteristics of a phased antenna array 20 p2537 A73-39453

No-slip boundary condition origin for viscous incompressible Newtonian fluid flow over family of models for rough wall 20 p2549 A73-39810

Influence of thermal cutting and its quality on the fatigue strength of steel. 21 p2722 A73-41253

Drag due to regular arrays of roughness elements of varying geometry. 21 p2633 A73-41569

Scattering of electromagnetic waves from rough oscillating surfaces using spectral Fourier method. 22 p2824 A73-41855

Experimental investigations of the effects of polymer additions on the kinematic characteristics of a plane turbulent flow in a tube with variable wall roughness 22 p2841 A73-42121

Turbulent boundary layer velocity distribution skewness and flatness factors over smooth wall compared with rough wall, discussing Reynolds shear stress fluctuations 22 p2842 A73-42231

On an integral equation governing the reflection of electromagnetic waves by a random surface 22 p2888 A73-42948

The effect of change of polarisation of the illuminating beam on the microstructure of speckles produced by a random diffuser. 22 p2871 A73-43095

Lagrangian analysis of multiple scatter in acoustic and electromagnetic reflexion. 24 p3111 A73-45394

SURFACE STABILITY

Concerning the stability of the triple-phase boundary in gas-diffusion electrodes of fuel cells. 21 p2636 A73-41320

Determination of the equilibrium state of a capillary liquid in a vessel 24 p3080 A73-45526

SURFACE TEMPERATURE

NT SKIN TEMPERATURE [NON-BIOLOGICAL]

NT WALL TEMPERATURE

Measurement of surface temperatures by means of an infrared camera - Application in non-destructive testing 01 p0050 A73-10590

An experimental investigation of the downstream effects of upstream boundary-layer injection. 01 p0002 A73-10732

Nonstationary interaction of thermal radiation with surfaces of pure metals 01 p0124 A73-11434

Equations of motion for nonuniformly heated gas past hot bodies, noting gas heating between two parallel flat surfaces with different temperatures 02 p0152 A73-11612

Instrument errors of film type thermocouple pyrometers for surface temperature measurement, discussing effects of shunting and junction geometry 02 p0166 A73-11636

Pyrometer for measurement of surface temperature distribution on a rotating turbine blade. 02 p0171 A73-12617

Kinetic heating in structures with a nonuniform surface temperature 03 p0398 A73-13723

The effect of substrate temperature on the structure of titanium carbide deposited by activated reactive evaporation. 04 p0456 A73-15757

Cloudiness as a global climatic feedback mechanism - The effects on the radiation balance and surface temperature of variations in cloudiness. 05 p0591 A73-16187

Calculation of the thermal fluxes and the temperatures of the surfaces of a plate with heat transfer between fluids flowing around the plate. 06 p0766 A73-17408

Lunar fines thermal diffusivity measurement, calculating lunar surface temperature distribution [AIAA PAPER 73-40] 06 p0767 A73-17622

Infrared scanning radiometer for temperature mapping of the lunar surface on the Apollo 17 flight. 06 p0695 A73-18319

Experiments on objectively predicting some atmospheric and oceanic variables for the winter of 1971-72. [AD-758469] 06 p0720 A73-18702

Integral method for nonlinear transient heat transfer in a semi-infinite solid. 07 p0919 A73-19493

Thermal behavior of a plasma-heated tungsten probe in the presence of tungsten vapor. [ECS PAPER 88] 07 p0788 A73-20447

Solid-solid interface temperature rise during sliding from model with surface topography statistics, frictional conditions, surface hardness and thermal parameters [ASME PAPER 72-LUB-34] 07 p0832 A73-20483

Thermal state of a porous plate cooled by intense blowing under conditions of radiative-convective heating 08 p1021 A73-20993

Permanent frost formation on steep north-facing Mars surface slopes above 25 deg north latitude, considering explanation by insolation and surface albedo 09 p1145 A73-22274

An axisymmetrical nonstationary heat-conduction problem for a system of two cylinders contacting at the end faces 09 p1166 A73-22363

Assessment of temperature rise suppression by edge losses during irradiation. 09 p1045 A73-22533

Numerical study of the stability of a supersonic laminar boundary layer 09 p1028 A73-22624

Finite-element method applied to heat conduction in solids with nonlinear boundary conditions. 10 p1295 A73-23778

Temperature at the surface of a heat-conducting liquid behind a shock wave in the presence of mass transfer and chemical reactions in the boundary layer 10 p1296 A73-24679

Preliminary results of measurements of the infrared temperature of the Mars surface by the Mars 3 interplanetary spacecraft 11 p1418 A73-25629

Influence of heating-surface orientation in a gravitational field on the nucleate boiling crisis of liquid 11 p1450 A73-25729

Nonstationary interaction of thermal radiation with surfaces of pure metals. 11 p1452 A73-26061

Soot oxidation kinetics at combustion temperatures. 12 p1557 A73-26844

Nonlinear problems for a system of two heat-radiating gray bodies separated by a diathermic medium 12 p1560 A73-27810

Modified separable kernel method for heat conduction with a nonlinear boundary condition. 13 p1706 A73-28819

Radio emission from pulsars and surface temperature of neutron stars. 13 p1681 A73-28925

Surface temperature measurement of regressing polymethyl methacrylate slabs burning in oxygen-nitrogen mixtures, discussing chemical mechanism for condensed phase depolymerization 13 p1707 A73-28994

Atmospheric effects on ocean surface temperature sensing from the NOAA satellite scanning radiometer. 13 p1610 A73-29195

Fog frequency and characteristics at the site of the proposed New York offshore airport, as compared with those at J. F. Kennedy International Airport - A preliminary report. 15 p1903 A73-31546

Some effects of variable surface temperature on heat transfer to a partially porous flat plate. [ASME PAPER 73-GT-4] 16 p2086 A73-33482

Determination of the density of the surface covering of the moon from given surface temperatures during eclipse and lunar-night periods 16 p2063 A73-33754

Infrared sensing of the surface temperature of certain lakes of Northern Italy 17 p2206 A73-34942

Radiometric measurements of temperature of the ocean surface - Improvement brought by use of a polarizing radiometer 17 p2161 A73-34946

Gulf Stream eddies - Recent observations in the western Sargasso Sea. 18 p2313 A73-36642

Some problems associated with wind drag and infrared images of the sea surface. 18 p2313 A73-36643

An upper limit on the 4.9-micron flux from Titan. 18 p2357 A73-37112

Some effects of surface anomalies in a global general circulation model. 19 p2446 A73-37539

Outermost low surface brightness regions of interacting galaxies in Stephan Quintet from interference filter, hydrogen spectra and long exposure direct photograph observations 19 p2484 A73-37609

Two dimensional steady and transient thermal stress analysis in rectangular solid with varying surface temperature, noting thermoelastic problems solution by analog method 19 p2498 A73-37668

Preliminary results of infrared temperature measurements of the surface of Mars by the Mars-3 automatic interplanetary station. 19 p2486 A73-38141

IR quasi-synoptic global sensing of ocean surface temperature, covering IR theory, airborne radiation thermometry and single band satellite data analysis techniques [AAS PAPER 73-146] 20 p2550 A73-38595

Salinity surveys using an airborne microwave radiometer. 20 p2558 A73-39865

Thermal structure of the sand desert from the data of IR acrophotography. 20 p2558 A73-39869

Small surface plate calorimeter for convection and radiation heat transfer measurements from heated body in air 21 p2692 A73-39920

Improvements brought to the measurement of the ocean surface temperature by utilization of a polarizing infrared radiometer 21 p2698 A73-40142

Evaporation of a water drop 21 p2791 A73-40745

Climatic change on Mars. 21 p2773 A73-41301

Fluctuating flow and heat transfer from a vertical surface. 21 p2792 A73-41524

Temperature measurements with an infrared television system. 22 p2853 A73-41984

Theory and technique for surface temperature determinations by measuring the radiance temperatures and the absorptance ratio for two wavelengths. 22 p2853 A73-41986

The determination of surface temperature from satellite 'window' radiation measurements. 22 p2846 A73-42057

Remote sensing of atmospheric and surface temperatures with microwaves. 22 p2825 A73-42060

A direct comparison of satellite and aircraft infrared /10 to 12 microns/ remote measurements of surface temperature. 22 p2850 A73-42729

Linear pyrolysis of various polymers under combustion conditions. 22 p2898 A73-42807

High pressure burning rates of liquid alcohol and hydrocarbon fuels with droplet simulation by porous spheres, deriving surface temperature, pressure distribution and critical burning conditions 22 p2937 A73-42817

Direct methods for solving inverse linear problems of thermal conductivity 23 p3048 A73-43444

An investigation of the numerical properties of the surface heat-balance equation. 23 p3004 A73-44265

SURFACE WAVES

General atmospheric circulation driven by polar and diurnal surface temperature variations. 24 p3131 A73-44463

Radiation pyrometric probe /homogeneous thermally insulated rod/ for measuring body surface thermal loads and heat transfer coefficients 24 p3089 A73-44758

Numerical solution of a nonlinear inverse heat-conduction problem 24 p3156 A73-45084

SURFACE TENSION

U INTERFACIAL TENSION

SURFACE TO AIR MISSILES

NT CHAPARRAL MISSILE

NT TALOS MISSILE

Microelectronic technologies for SAM-D system, discussing thick film hybrid circuits and microstrip applications 02 p0148 A73-12594

Command and control for a missile air defense system. I - SAM-D communications. 04 p0417 A73-15377

Command and control for a missile air defense system. II - Implementation of system requirements. 04 p0418 A73-15378

SAM-D system for field army forces to provide air defense against advanced tactical aircraft, discussing equipment, performance, cost reduction and combat readiness [AIAA PAPER 73-65] 06 p0755 A73-17634

Probabilistic Monte Carlo computerized simulation of surface to air missile systems reaction time from aircraft attack in non-jamming environment and over flat terrain 16 p1985 A73-33418

SAM-D guidance system simulator for design verification, preflight checkout and performance demonstration based on real time digital communication between missile computer and simulator hybrid computer [AIAA PAPER 73-877] 20 p2587 A73-38814

Optimal SAM defense system - An application of optimal control concept to operations research. 23 p2964 A73-43823

SURFACE TO SURFACE MISSILES

NT INTERCONTINENTAL BALLISTIC MISSILES

NT MINUTEMAN ICBM

NT POLARIS MISSILES

NT POSEIDON MISSILES

SURFACE TREATMENT

U SURFACE FINISHING

SURFACE VEHICLES

NT AIRCRAFT CARRIERS

NT AUTOMOBILES

NT CARGO SHIPS

NT LUNAR ROVING VEHICLES

NT LUNAR SURFACE VEHICLES

NT NUCLEAR POWERED SHIPS

NT ROCKET PROPELLED SLEDS

NT ROVING VEHICLES

NT SATELLITE COMMUNICATIONS SHIPS

NT TANK TRUCKS

NT TANKER SHIPS

NT TRACTORS

NT WALKING MACHINES

Advanced transport systems for airports. 05 p0562 A73-16566

The development of light tracked vehicles for lunar and planetary exploration 08 p0952 A73-20781

Terrain-vehicle dynamic interaction studies of a mobility concept (ELMS) for planetary surface exploration. [AIAA PAPER 73-407] 11 p1343 A73-25536

Interaction of an air-cushioned vehicle with an elastic guideway. 17 p2098 A73-34181

Ground and air transportation noise propagation and effects, including aircraft engines, airfoils, sonic booms, auto traffic, railroads, subways, seismic noise and vibration 17 p2100 A73-34460

AIRTRANS - Intra-airport transportation system. [SAE PAPER 730384] 17 p2146 A73-34721

Remote control of planetary surface vehicles. 17 p2148 A73-35316

Landmark navigational and topographical mapping techniques for planetary surface exploration using unmanned vehicles and earth based computers 17 p2210 A73-35383

The possible future of air transport and the airports 17 p2148 A73-35665

Book - The aerodynamics of high speed ground transportation. 17 p2097 A73-35854

Science aspects of a remotely controlled Mars surface roving vehicle. 19 p2416 A73-37311

Mars surface exploration by self-guided stereo TV equipped roving vehicle /robot/, describing computerized object and scene ranging and recognition 19 p2429 A73-37321

SURFACE WAVES

NT BAROCLINIC WAVES

NT CAPILLARY WAVES
NT ELECTROMAGNETIC SURFACE WAVES
NT GRAVITY WAVES

Nonlinear waves on interface of two incompressible inviscid fluids of different densities and arbitrary surface tension analyzed by multiple scales method

01 p0032 A73-10445

Generation and detection of helical surface waves at cylindrical bodies by means of contactless electrodynamic transducers

01 p0051 A73-10974

Transition radiation from a plasma boundary.

01 p0085 A73-11063

Tunnel-effect and propagation of 5-min oscillations in the solar atmosphere.

01 p0107 A73-11381

Energy transfer between interacting electromagnetic waves propagating in half space media, applying to acoustic surface wave excitation by electromagnetic converter

02 p0140 A73-11568

Kinetic theory of surface waves in a cylindrical plasma waveguide.

02 p0198 A73-12106

Propagation of surface waves along a plane boundary between two magnetoactive plasmas.

02 p0198 A73-12107

Elastic surface waves - Many new applications.

02 p0193 A73-12598

Time-periodic fluid surface wave radiation and scattering by partially immersed objects in short wave asymptotic limit of nondimensional wavelength approaching zero

03 p0397 A73-13533

Rayleigh waves for continuous monitoring of a propagating crack front.

04 p0452 A73-14691

Effect of surface states on surface-wave amplification in a composite structure of CdSe film on LiNbO₃.

05 p0559 A73-17073

Frequency spectra of the inner and outer structures of wind waves at different stages of wave development

05 p0594 A73-17359

Boundary conditions for penetration of an electromagnetic wave into a plasma.

06 p0727 A73-17418

Emission of metals under the action of non-relativistic electrons

06 p0725 A73-18102

A specific feature of surface waves at the boundary of inhomogeneous plasma.

06 p0730 A73-18466

Instability of surface ion-acoustic waves of finite amplitude

07 p0855 A73-19291

Surface wave characteristics of circular cylindrical corrugated and uniform dielectric rod excited in E sub 0-mode.

07 p0792 A73-19545

A wide-band low-shape-factor amplifier module using an acoustic surface-wave bandpass filter.

07 p0804 A73-20557

Use of a surface-acoustic-wave delay line to provide pseudocoherence in a clutter-reference pulse doppler radar.

08 p0939 A73-21113

Intermittence effects in the equilibrium range of developing wind waves

08 p0986 A73-21458

Quasi-static ion acoustic surface wave propagation along warm plasma layer-dielectric boundary

08 p0993 A73-21460

Parametric excitation of surface waves in a non-homogeneous magnetized plasma

09 p1124 A73-21892

Surface oscillations of a weakly ionized plasma in a magnetic field

09 p1124 A73-21901

Propagation of backward surface wave along an annular plasma guide with azimuthal electron density variation.

09 p1125 A73-21930

Two approximate methods for describing the steady motions of an incompressible viscous fluid with a free boundary

09 p1072 A73-22619

Propagation of surface waves and instability wave growth in an ion beam-plasma system.

09 p1131 A73-22906

Thickness dependence of effective coupling factors of ZnO thin-film surface-wave transducers.

09 p1086 A73-23097

Fatigue crack initiation and propagation in part through crack metal specimens under cyclic loading, discussing plasticity effects and surface wave interaction

09 p1163 A73-23253

Book - Optical waveguides.

09 p1066 A73-23274

Microsonics /acoustic surface waves/ technology developments covering materials, heteroepitaxial systems, propagation, electron phonon interaction, acoustic amplifiers and waveguides, electromechanical transducers and signal processing

10 p1223 A73-23782

Small amplitude surface and plate waves propagation in incompressible biaxially stressed elastic media, obtaining dispersion equation for various phase velocities

11 p1434 A73-25166

Image processing using acoustic surface waves.

11 p1334 A73-25358

Perturbation theory for multistrip acoustoelectric surface-wave amplifier.

11 p1337 A73-25362

Perturbation theory for the surface-wave multistrip coupler.

11 p1337 A73-25363

Waves produced by a source of harmonic oscillations located in a cylindrical layer of liquid

11 p1349 A73-26468

Laddertron oscillator /klystron/ cavity dispersion characteristics via electrodynamic analysis of dispersion equation for surface wave operation and coupled modes

12 p1477 A73-26948

The task of constructing transition functions in problems involving interaction of weak shock waves with cylindrical and spherical surfaces

12 p1486 A73-27241

Directional antenna formed by a system of two wires lying along the generatrices of a profiled impedance cylinder.

12 p1480 A73-27269

The design and applications of highly dispersive acoustic surface-wave filters.

12 p1484 A73-27564

The use of surface-elastic-wave reflection gratings in large time-bandwidth pulse-compression filters.

12 p1480 A73-27566

Surface acoustic wave multistrip components and their applications.

12 p1484 A73-27567

Anisotropic piezoelectric heterogeneous acoustic surface waveguides of arbitrary cross section computing mode spectrum by efficient and accurate numerical techniques

12 p1480 A73-27568

Surface elastic wave microwave bandpass filter for miniaturized frequency synthesizer in satellite communications systems, noting insertion loss and sidelobe reduction

12 p1484 A73-27573

A programmable surface acoustic wave matched filter for phase-coded spread spectrum waveforms.

12 p1484 A73-27574

Improvements in surface-acoustic-wave pulse-compression filters.

13 p1595 A73-28048

Propagation of electrohydrodynamic surface waves in a conducting fluid.

13 p1663 A73-28160

Optical interferometry for ultrasonic surface wave detection, using two coherent light beams focusing for recording standing wave ratio, attenuation, transmission and harmonic content

13 p1613 A73-28497

Theory for errors, resolution, and separation of unknown variables in inverse problems, with application to the mantle and the crust in Southern Africa and Scandinavia.

13 p1607 A73-28621

Instability of ion-acoustic surface waves of finite amplitude.

13 p1665 A73-28691

Theory of surface wave dispersion in an inhomogeneous plasma situated in a strong HF field

13 p1667 A73-29161

A Fabry-Perot acoustic surface vibration detector-application to acoustic holography.

13 p1622 A73-29422

Wave propagation in the ion sheath of an antenna immersed in a plasma

14 p1731 A73-29730

Book - Computer fluid dynamics: Recent advances.

14 p1744 A73-29743

The design and applications of highly dispersive acoustic surface-wave filters.

14 p1732 A73-29933

Application of acoustic surface-wave technology to spread spectrum communications.

14 p1733 A73-29934

Ranging and data transmission using digital encoded FM-'chirp' surface acoustic wave filters.

14 p1733 A73-29935

Electromagnetic wave radiation and reflection at guiding structure discontinuity, calculating TE mode surface wave by boundary perturbation technique

14 p1727 A73-30214

Bluestein-Gulyaev shear surface waves in piezoelectric-dielectric-perfect conductor layered system, applying theoretical results to lithium iodate crystals

14 p1783 A73-30259

Structure-dependent transfer parameters of interdigital transducers for surface waves.

14 p1754 A73-30895

Electromagnetic emission during surface wave excitation by a relativistic electron beam in a plasma

15 p1921 A73-32321

Surface oscillations of a weakly ionized plasma in a magnetic field.

15 p1921 A73-32626

The effect of plasma resonance on the propagation of surface waves along plasma-vacuum channel.

16 p2043 A73-34023

Parametric excitation of surface waves in an inhomogeneous magnetized plasma.

17 p2215 A73-34315

Application of surface acoustic wave devices to radar.

17 p2140 A73-35319

High performance surface wave bandpass filters for signal processing applications.

17 p2140 A73-35320

Parametric excitation of surface waves in an inhomogeneous magnetized plasma

18 p2339 A73-36556

Absorption and transformation of electrostatic surface waves in the transition layer of a magneto-active plasma.

19 p2467 A73-37438

Visualization of surface elastic waves on structural materials.

19 p2432 A73-37449

Magnetodynamic and magnetostatic surface waves in a ferrite layered structure

19 p2470 A73-37724

Reconstruction of surface-wave fields in liquids with the aid of holographic methods

19 p2431 A73-38158

Electromagnetic wave propagation in inhomogeneous multilayered structures of arbitrarily varying thickness - Generalized field transforms.

19 p2461 A73-38379

Building a dynamic test complex near an inertial test facility and general test pad considerations.

[AIAA PAPER 73-827]

20 p2543 A73-38772

Instability of electromagnetic surface waves supported by a bounded plasma stream.

20 p2595 A73-38891

An integral-equation approach to dispersion relations for guided elastic surface waves.

20 p2592 A73-39048

The theory of parametric excitation of electrostatic surface waves in a plasma layer

20 p2597 A73-39194

Acoustic surface wave thin film guides for nonlinear signal processing, discussing relative advantages over nonguided arrangements, and application to transverse wave front imaging

20 p2531 A73-39596

Acoustic surface wave energy detection via combination of MOSFET array and ZnO overlay piezoelectric transducer, deriving signal processing technique

21 p2660 A73-40100

Linear wave motion analysis of viscous incompressible fluid of infinite depth at small and large times by asymptotic quadrature method

21 p2676 A73-40207

Surface wave propagation parallel to applied magnetic field in electron hole plasma, explaining observed resonances in InSb by LF mode

21 p2751 A73-40325

Nonlinear ion surface oscillations in a semibounded current-carrying plasma

21 p2745 A73-40361

Surface-wave effects and blindness in phased-array antennas.

21 p2651 A73-40653

Surface acoustic wave devices and applications. II - Pulse compression systems.

21 p2703 A73-41137

Linear signal processing by acoustic surface-wave transversal filters.

21 p2705 A73-41426

On the surface-to-bulk mode conversion of Rayleigh waves.

21 p2705 A73-41429

Microwave acoustic surface wave devices design tradeoffs, considering propagation losses, air loading, beam steering and diffraction, and transducer effects in curves and data

22 p2833 A73-42399

Monograph - Generation of acoustic waves in piezoelectric devices.

22 p2861 A73-42700

Amplification of magnetostatic surface waves in the YIG-Ge hybrid system.

24 p3120 A73-45431

SURFACES

Variational principle application to nonself adjoint lifting surface integral equation from finite element viewpoint, considering two dimensional flat plate

05 p0529 A73-16852

Compactness criterion for the formation of averaged trapped surfaces in gravitational collapse.

17 p2234 A73-35734

SURFACTANTS

Physicochemical parameters associated with surfactants, investigating effects on hydrocarbon fuels coalescence

05 p0582 A73-16674

Suppression of evaporation of hydrocarbon liquids and fuels by aqueous films.
[WSCI PAPER 72-27] 05 p0639 A73-16687

Strongly active surfactant effects on metal surface fracture characteristics under various loading conditions
15 p1952 A73-32071

Soaps, detergents and surfactants dermatological hazards in personal hygiene use by spacecrews during long term space flight [Skylab]
[ASME PAPER 73-ENAS-26] 19 p2400 A73-37981

Relationship between the equilibrium vapor pressure of the solvent and the surface activity in dilute solutions of inactive and surface-active materials
21 p2646 A73-40122

Blood plasma contamination of the lung alveolar surfactant obtained by various sampling techniques.
21 p2642 A73-41637

SURGEONS
NT FLIGHT SURGEONS

SURGERY
NT LABYRINTHECTOMY
Carpentier reconstructive valvuloplasty technique of mitral valve insertion from viewpoint of pilots return to flying duties
02 p0138 A73-12157

Coronary heart disease; Proceedings of the Second International Symposium, Frankfurt am Main, West Germany, June 1972.
22 p2809 A73-42856

SURGES
Cherenkov and transient radiation of uniformly moving charge in random inhomogeneous medium.
02 p0193 A73-12381

Possible mechanism of surge formation in the solar atmosphere.
21 p2777 A73-41493

SURGICAL INSTRUMENTS
Development of neurosurgical instrumentation and procedures for emergency use in null and low-gravity environments - A speculative approach.
11 p1323 A73-25342

SURVEILLANCE
NT SPACE SURVEILLANCE [SPACEBORNE]
A new filter for optimal tracking in dense multi-target environments.
03 p0286 A73-14477

Modeling of aircraft position errors with independent surveillance.
[AIAA PAPER 73-162] 05 p0595 A73-16908

Satellite systems for mobile communications and surveillance; Proceedings of the International Conference, London, England, March 13-15, 1973.
12 p1471 A73-27652

Improvements in Airport Surface Traffic Control surveillance.
14 p1740 A73-29887

Passive low light level television for military and civilian ground surveillance under poor visibility conditions
17 p2168 A73-34906

ASTRO-DABS communication system with hybrid satellite and terrestrial discrete address beacon system for accurate aerial surveillance and navigation with reliable data link
20 p2527 A73-38759

SURVEILLANCE RADAR
Theory and practice of the signal processor in surveillance radars
05 p0550 A73-16473

Surveillance radar cosecant reflectors electromagnetic energy emission distribution, discussing design and directional characteristics
05 p0550 A73-16474

Optimal correlation of sensor data with tracks in surveillance systems.
06 p0682 A73-18822

Most convenient intervals of amplitude quantization in direction finding
08 p0939 A73-21394

Weather radar surveillance data short term distribution to airline users through weather message switching center, describing data coding, teletype network and data plotting operations
10 p1189 A73-24550

Optimal search scanning for electronic surveillance radar based on antenna beam position with highest echo signal for maximum likelihood target acquisition
13 p1581 A73-27999

The development of the ATC radar beacon system - Past, present, and future.
14 p1725 A73-29881

Military ATC systems and equipment in U.S. National Aviation System, discussing operations, organizational and facility interfaces, communications, navigation, and surveillance radar requirements
14 p1773 A73-29889

Multiple access technique for future communication, surveillance and navigation subsystems to meet ATC demands, considering satellite surveillance radar system
14 p1725 A73-29893

Radar technology applied to air traffic control.
14 p1725 A73-29895

Automatic runway and aircraft approach path surveillance system /CORAIL/ consisting of Doppler radar, signal extractor and data processing, alarm, display and control equipment
14 p1773 A73-30444

Bringing data processing to projects and tests of large antennas
15 p1846 A73-32430

The Corail radar - Automatic equipment for runway surveillance
15 p1846 A73-32431

Secondary surveillance radar - Current usage and improvements.
19 p2451 A73-37808

The most advantageous amplitude quantization intervals for direction finding.
19 p2407 A73-38352

Low cost airport surveillance and Localized Cable Radar with runway or taxiway vehicle guidance capability for ground traffic control, using solid state equipment
21 p2736 A73-40051

BMD requirements for phased array radars.
21 p2651 A73-40644

Russian book - Digital methods and systems in radar technology.
21 p2657 A73-41433

Secondary Surveillance Radar application to aircraft identification in upper airspace of Eurocontrol member states, emphasizing code assignment
22 p2884 A73-42322

SURVEYOR LUNAR PROBES
NT SURVEYOR 3 LUNAR PROBE
Comparison of the analytical results from the Surveyor, Apollo, and Luna missions.
04 p0498 A73-15185

Preparation of high-level alpha-particle sources for the Surveyor Alpha Scattering Experiment.
16 p2035 A73-32975

Surveyor observations of lunar horizon-glow.
18 p2348 A73-35938

SURVEYOR 3 LUNAR PROBE
Micrometeoroid particle flux impacting on lunar surface measured by observation of Surveyor 3 glass surfaces craters
02 p0214 A73-12256

Meteoroid activity on the lunar surface from the Surveyor 3 sample examination.
02 p0214 A73-12257

Scanning electron microscope and energy dispersive X-ray analysis of the surface features of Surveyor III television mirror.
07 p0872 A73-19899

On-surface and laboratory size measurements of fine lunar particles.
07 p0900 A73-20184

Emission measurement of Surveyor 3 spacecraft aluminum support tubing returned from moon by Apollo 12, noting lunar environment effects from control sample data
24 p3139 A73-45110

SURVEYS
NT GEODETTIC SURVEYS
NT GEOLOGICAL SURVEYS
American Society of Photogrammetry and American Congress of Surveying and Mapping, Fall Convention, Columbus, Ohio, October 11-14, 1972, Proceedings.
08 p0968 A73-21701

British Airline Pilots Association and RAF Institute of Aviation Medicine questionnaire results on training simulator effectiveness, analyzing auditory and visual aids
16 p1996 A73-33213

SURVIVAL
Survival probability of a system with a Poisson flow of losses in life-sustaining elements
01 p0028 A73-11422

Ballistic-tolerant helicopter flight control components from plastic composite materials.
10 p1237 A73-23964

Helium-cold induced hypothermia in the white rat.
12 p1461 A73-26975

On the improvement in survivability for avionics equipment.
12 p1478 A73-27158

Survival of soil bacteria during prolonged desiccation.
14 p1720 A73-30959

Sea survival after ejection and parachute descent, describing hand operated canopy connector release to free pilot from entanglement or dragging
16 p1974 A73-32665

Tolerance to immersion in cold water
18 p2280 A73-36943

SURVIVAL EQUIPMENT
Human threats to air safety; Proceedings of the Twenty-fifth Annual International Air Safety Seminar, Washington, D.C., October 16-18, 1972.
10 p1176 A73-24707

Post-crash survival planning and procedures, discussing passenger instructions and control, crew training and rescue signalling devices
10 p1176 A73-24711

Significant elements of an effective search, rescue, and survival system.
10 p1176 A73-24712

Survival and Flight Equipment Association, Annual Symposium, 10th, Phoenix, Ariz., October 2-5, 1972, Proceedings.
16 p1965 A73-32653

U-2 and SR-71 aircrews physiological training for high altitude and supersonic flight hazards, discussing pressure suits, ejection seats, parachutes and survival and life support equipment
16 p1974 A73-32657

Multiple occupant flotation devices for commercial transport aircraft survivors sea ditching, discussing slide/raft design improvement for high density loading
16 p1974 A73-32658

DC-10 aircraft slide/raft system for emergency personnel evacuation, discussing certification test program for performance, reliability, seaworthiness and compliance with regulations
16 p1965 A73-32659

Certification program for the DC-10 slide/raft.
17 p2108 A73-35807

SUSCEPTIBILITY [MAGNETISM]
U MAGNETIC PERMEABILITY
SUSPENDING [HANGING]
NT MAGNETIC SUSPENSION
Azimuthal pointing control system for balloon observations of celestial bodies, analyzing suspension rope twisting method
01 p0075 A73-11207

Effect of suspension-line viscous damping on parachute opening load amplification.
07 p0777 A73-14945

Synthesis of superconducting suspensions with a maximum lifting force
11 p1372 A73-25049

Dynamic error of solid body-elastic rod pendulum system hinged on vibrating suspension point in terms of tensile rigidity finiteness
11 p1399 A73-26096

Drift moments produced by rotor nonsphericity in a suspension system with an axially-symmetric field
11 p1367 A73-26453

Oscillations of a mathematical pendulum of variable length during rectilinear motion of the suspension point
11 p1401 A73-26466

Swing wing - Modifications in variable geometry configuration concepts.
13 p1568 A73-28157

Influence of the orthogonal axes of the suspension of an electrostatic gyroscope at zero rotor potential
13 p1618 A73-29148

Force-strain characteristics of dacron parachute suspension-line cord under dynamic loading conditions.
[AIAA PAPER 73-446] 15 p1825 A73-31432

High performance vibration isolated tables.
20 p2544 A73-39266

Control requirements for sling-load stabilization in heavy lift helicopters.
20 p2509 A73-39406

New multiple-support radially-symmetric design of the parabolic-reflector suspension for a radio telescope
21 p2672 A73-40547

Effect of the elastic deformation of a gimbal suspension on the nutation oscillation frequency of a gyroscope
22 p2860 A73-42359

Combinational parametric resonance in a gyro-pendulum mounted on a mobile base
22 p2860 A73-42367

An electrostatic suspension method for determining photoionization energies of solids.
23 p3015 A73-43447

SUSPENDING [MIXING]
Electron microscopic investigation of lubricating mechanism of dry and oil-suspended molybdenum disulfide powder, discussing physical and chemical properties effects
05 p0589 A73-17067

Order c-square bulk stress derivation for force-free spherical particles suspension in Newtonian ambient fluid with uniform viscosity, noting error bounds
06 p0722 A73-17701

Nonequilibrium transport process calculation by theoretical microscopic model for interaction between ionized gas and solid particles in suspension, noting free electron concentration change
09 p1130 A73-22826

Emulsion and suspension effective viscosity dependence on dispersed phase volume concentration and particle interactions in two phase flows
13 p1580 A73-28465

Heat transfer to flowing gas-solid mixtures.
17 p2254 A73-34353

Continuum mechanics analysis of solid particle suspension flow of viscous gas, noting demixed region near wall
17 p2156 A73-35508

SUSPENSION SYSTEMS [VEHICLES]

Lunokhod 1 vehicle chassis design and mobility characteristics in Mare Imbrium, discussing wheels, suspension, movement control, traction, cohesion and lunar surface maneuverability

02 p0151 A73-12235

Nonlinear modeling and dynamic simulation of vehicle air cushion suspensions.
[ASME PAPER 72-WA/AUT-5] 04 p0406 A73-15883
The development of light tracked vehicles for lunar and planetary exploration

08 p0952 A73-20781

SUSPENSIONS

The Stokes problems for a suspension of particles.

08 p0955 A73-21426

Motion of a magnetizable fluid in the lubrication film of a cylindrical bearing

10 p1225 A73-24586

Flow of a dust suspension over an ellipsoid of revolution.

17 p2091 A73-34348

Flows with and without suspensions in channels with curvilinear segments

22 p2842 A73-42229

Theoretical studies and experimental verifications of thermal and electrical conductivity, molecular diffusivity and viscosity of a partially ionized suspension in an electric field.

22 p2894 A73-42512

SWALLOWING

Phasic discharge activity and localization of sheep medullary neurons in relation to swallowing reflex after superior laryngeal nerve stimulation

03 p0262 A73-13786

SWAMPS

U MARSHLANDS

WWEAT

Perspiration secretion distribution over human body based on extended Kerslake cylinder model, comparing with predicted 4 hr sweat rate

03 p0259 A73-13122

Quantitative influence of CO₂ inhalation on thermal sweating in man.

11 p1314 A73-25331

Transductal fluxes of Na, K, and water in the human eccrine sweat gland.

15 p1836 A73-31923

Sodium Na-24 and potassium K-42 availability for sweat production after intravenous injection and their handling by sweat glands.

19 p2395 A73-37757

Responses of men and women to two-hour walks in desert heat.

20 p2518 A73-39784

Desoxyribonucleases in sweat gland secretion of man

24 p3059 A73-44674

SWEAT COOLING

Application of an improved transpiration cooling concept to space shuttle type vehicles.

03 p0397 A73-13492

Compact gas transpiration cooling system for thermal protection of hypersonic flight leading edges, discussing computer program

11 p1452 A73-26212

Transpiration nosetip coolant flow control.

[AIAA PAPER 73-767] 18 p2371 A73-36382

On some further applications of the variational formulation based on local potential to the solution of diffusion equation. I - Temperature distribution in a transpiration cooled half-space with variable thermal properties. II - Heat conduction in an ablating solid with variable thermal properties.

22 p2931 A73-42468

Stability criteria for two phase transpiration, cooling system with equilibrium phase transition inside porous wall

24 p3156 A73-45079

SWEATING

U PERSPIRATION

SWEDEN

The Marsta micro-meteorological field project - Profile measurement system and some preliminary data.

21 p2732 A73-41567

SWEEP ANGLE

NT LEADING EDGE SWEEP

SWEPT CIRCUITS

Ultrafast streaking camera for picosecond laser diagnostics.

21 p2694 A73-39948

SWEPT EFFECT

Jupiter's radiation belts and the sweeping effect of its satellites.

16 p2062 A73-33429

SWEPT FREQUENCY

Optical sweep generator using single frequency He-Ne lasers with Michelson interferometer for mode selection to provide smooth tuning throughout Doppler width

03 p0319 A73-14065

Microwave system with direct, AM, FM and pulse propagation techniques for swept-frequency group

delay measurement, discussing error sources and various distortions

10 p1193 A73-23610

Heterodyne detection of frequency sweeping in the output of transverse-excitation CO₂ lasers.

13 p1628 A73-29186

Ionospherically propagated backscatter from Pacific Ocean via swept frequency continuous wave recordings, noting sky wave polarization rotation modulation of received signal

15 p1845 A73-32228

An automatic sweep generator for a strobed oscilloscope

21 p2664 A73-41098

Satellite-borne swept frequency impedance probe/gyroplasma probe for ionospheric plasma parameters including electron density and ion composition, noting PCM telemetry system

22 p2917 A73-42571

SWEEPBACK

NT LEADING EDGE SWEEP

SWEPT FORWARD WINGS

NT TRAPEZOIDAL WINGS

SWEPT WINGS

NT ARROW WINGS

NT DELTA WINGS

NT SWEEPBACK WINGS

NT TRAPEZOIDAL WINGS

Theoretical investigation of transition phenomena in the boundary layer on an infinite swept wing

[DGLR PAPER 72-124] 03 p0248 A73-14379

Supercritical shock free transonic profiles for transport aircraft wings of large and medium aspect ratio, discussing straight and yawed wing tests

[DGLR PAPER 72-130] 03 p0248 A73-14383

Buffeting pressures on a swept wing in transonic flight - Comparison of model and full scale measurements.

[AIAA PAPER 73-311] 11 p1305 A73-25542

Three dimensional turbulent boundary layers prediction methods and flow measurements, considering swept and slender wings

14 p1744 A73-30173

A conceptual study of leading-edge-vortex enhancement by blowing.

[AIAA PAPER 73-656] 18 p2261 A73-36210

Analytical investigation of compressibility and three-dimensionality on the unsteady response of an airfoil in a fluctuating flow field.

[AIAA PAPER 73-683] 18 p2262 A73-36234

Solution of the problem of the flow past a V-shaped wing with a strong shock wave at the leading edge

18 p2265 A73-37011

The aerodynamic development of the wing of the A 300B.

21 p2633 A73-41192

SWEEPBACK TAIL SURFACES

Turbulent heat transfer to a fin leading edge - Flight test results.

11 p1303 A73-26405

SWEEPBACK WINGS

NT ARROW WINGS

NT DELTA WINGS

NT TRAPEZOIDAL WINGS

Experimental study of a high lift re-entry vehicle configuration.

13 p1564 A73-28822

Effects of sweepback angle and unit Reynolds number on boundary layer transition at supersonic velocities

13 p1567 A73-29172

Finite element analysis of sweepback wing structures based on beam theory, presenting low aspect ratio models

14 p1809 A73-30201

Theoretical and experimental study of a swept-back wing at low velocity over a wide range of angles of attack

16 p1962 A73-32814

Some effects of camber on swept-back wings.

[SAE PAPER 730298] 17 p2094 A73-34661

SWIMMING

Oxygen uptake, heart rate and pulmonary ventilation during swimming for different speeds and styles, comparing to running and cycling data

01 p0008 A73-10171

Analysis of swimming motions.

11 p1322 A73-25184

SWINGBY TECHNIQUE

Trajectory analysis for swingby technique using Jovian gravitational field for leaving plane of ecliptic along heliocentric orbit and for solar flyby at specified distance

03 p0378 A73-14552

Computational aspects of multilevel trajectory optimization.

07 p0903 A73-20589

Navigation system design for the Mariner Jupiter/Saturn Mission.

[AIAA PAPER 73-838] 21 p2736 A73-40503

Planetary flybys resulting in heliocentric orbits normal to the ecliptic with fixed perihelia.

22 p2909 A73-42628

Three body problem triple close approaches without escape mechanism, discussing method to control numerical integrations accuracy

24 p3141 A73-45281

SWIRLING

Swirling jet of gases mixture into vacuum.

03 p0289 A73-12908

Combustion effectiveness in high speed swirling flow tested in chamber with premixed air-kerosene mixture injected tangentially in annular channel [ONERA, TP NO. 1076]

04 p0517 A73-15098

Turbulent flow characteristics of swirling jets with opposite rotation, discussing lateral spreading into potential ambient fluid

[ASME PAPER 72-WA/FE-17] 04 p0435 A73-15844

The swirling turbulent jet.

[ASME PAPER 72-FE-18] 05 p0564 A73-16544

Swirl injector driven air flow in cylindrical tube, measuring flow velocity and turbulent stress tensor components

08 p0956 A73-21601

Species separation in swirling expansion jet of gases mixture.

08 p0956 A73-21774

Velocity field determination for limitless steady boundary layer on circular cylinder and swirling flow produced by generalized vortex

10 p1210 A73-24843

Flow measurement in the presence of strong swirl using a laser Doppler anemometer.

10 p1221 A73-24857

Linear stability to axisymmetric perturbations of compressible nonaxisymmetric swirling flow, noting Richardson number role

13 p1605 A73-29374

Swirl decay in circular pipe air flow in terms of angular and axial momenta, dimensionless parameter and velocity profiles

16 p1999 A73-32825

Turbulent viscosities for swirling flow in a stationary annulus.

[ASME PAPER 73-FE-16] 17 p1512 A73-35013

Finite difference theory predictions for turbulent boundary layer swirling flames, discussing flow simulation, turbulence models and flame size, shape and stability characteristics

18 p2367 A73-36206

Swirling flows in streamtubes of variable cross section.

18 p2298 A73-36314

An investigation of supersonic swirling jets.

19 p2376 A73-37488

On the effect of swirling motion of sources of subsonic jet noise.

21 p2676 A73-40286

Effect of combustion upon precessing vortex cores generated by swirl combustors.

22 p2934 A73-42781

Combustion in high speed swirling flow in gas turbine combustion chamber, discussing flame stability, pressure measurements and chamber configuration

22 p2935 A73-42790

Swirling flow effect on jet noise suppression based on acoustic field and engine thrust measurements with and without stationary swirl vanes in exhaust nozzle [AIAA PAPER 73-1003]

24 p3077 A73-44836

Acoustic wave propagation in axisymmetric swirling subsonic jet flow, obtaining directivity patterns for spinning and nonspinning modes from wave equation numerical integration

24 p3077 A73-44837

Sound interaction with a helical flow contained in an annular duct with radial gradients of flow, density and temperature.

24 p3078 A73-44842

SWIRLING WAKES

U TURBULENT WAKES

SWITCHES

NT CAPACITANCE SWITCHES

NT ELECTRIC RELAYS

NT ELECTRIC SWITCHES

NT FLUID SWITCHING ELEMENTS

NT SWITCHING CIRCUITS

NT THERMOSTATS

Reliability of sealed reed switches/SRS/

07 p0801 A73-19423

SWITCHING

NT BEAM SWITCHING

NT MAGNETIC SWITCHING

NT MICROWAVE SWITCHING

On the origin of strongly conducting states in thin insulator films.

06 p0734 A73-17812

Preswitching and postswitching phenomena in amorphous semiconducting films.

06 p0739 A73-18800

Switching in amorphous selenium.

11 p1407 A73-25147

The satellite system as an integrated telecommunications switching center.

12 p1468 A73-27011

Switching effect in amorphous semiconductors at discontinuous changes in the heat transfer from the sample.

14 p1783 A73-30434

- Conditioned reflex switching effects in higher nervous system reactions as function of experimental stimuli background conditions /arousal, diurnal rhythms, test conditions, physiological condition/ 14 p1718 A73-30567
- Transmission of nerve pulses at the switching locations of the brain 16 p1973 A73-33424
- Off state I-V characteristics and thermal switching phenomena for tellurium selenium germanide chalcogenide glass semiconductors, assuming internal heat generation 24 p3119 A73-44407
- SWITCHING CIRCUITS**
- NT FLUID SWITCHING ELEMENTS**
- Investigation of residual resistance in semiconductor switches used to commutate the measuring circuits of alternating-current bridge networks 01 p0022 A73-10080
- Quick-response automatic range switch for electronic potentiometers 01 p0045 A73-10257
- Coaxial gas discharge tubes for pulsed lasers 01 p0059 A73-10796
- Semiconductor device with current regulated switching from high voltage/low current to low voltage/high current state, noting I-R characteristics 01 p0026 A73-11096
- Russian book on nanosecond multiphase multivibrators covering transistorized single- and dual-stage amplifiers and wave shaping circuits for digital control and computer logic applications 02 p0146 A73-11887
- Investigation of the dynamics of a pulsed phase-lock automatic frequency control system 02 p0142 A73-12493
- Analysis of dynamic-excitation conditions for electroluminescent panels 03 p0282 A73-13658
- Pre-threshold conductance and polarization effects in amorphous semiconductor switches. 04 p0427 A73-15343
- Message switching for multiplexing data of computer users with interactive access onto common facilities, evaluating traffic induced time delay performance 04 p0425 A73-15428
- Switch transistor control using an intensity transformer 04 p0489 A73-15736
- Jet interaction in a simplified model of a bistable fluid amplifier. [ASME PAPER 72-WA/FLCS-6] 04 p0409 A73-15863
- P-n-p-n junction thyristor turnoff process under reverse anode voltage at high injection level, examining current voltage curve and switching time constant. 05 p0556 A73-16068
- Metal-dielectric-semiconductor junction transistor HF response analysis by digital computer, deriving switching time as function of impurity concentration and electrode voltage 05 p0556 A73-16069
- Datran TDM switching system with stored program controller and IC components providing reliability, flexibility and high channel capacity in data transmission 05 p0551 A73-16804
- Short pulse laser based on versatile 60 kV fast switching circuit, noting application as pump source for organic dye molecule solutions 05 p0586 A73-17252
- Choice of thermal parameters for a photoelectric switch operating with a capacitive load 06 p0676 A73-18087
- The pulse-controlled photoelectric switch as an element in automatic control circuits and in computer equipment 06 p0676 A73-18088
- Time difference measuring instrument for asynchronous and synchronized positive pulses in automatic control system, noting pulse generator and switching, trigger and logic circuits 06 p0677 A73-18384
- Preservation of threshold on-regime in amorphous semiconductor threshold switch. 06 p0739 A73-18790
- A switching circuit for a low voltage, medium current dc power supply. 06 p0649 A73-18847
- Noise immunity of diversity reception with threshold switching of antennas 07 p0802 A73-20291
- P-I-N switching diodes in phase-shifters for electronically scanned aerial arrays. 08 p0943 A73-20712
- Investigation of a high-level power switch based on p-i-n diodes 08 p0948 A73-21560
- Amorphous semiconductors for switching, memory, and imaging applications. 09 p1132 A73-21984
- Electronic conduction and switching in chalcogenide glasses. 09 p1133 A73-21985
- Reversible thermal breakdown as a switching mechanism in chalcogenide glasses. 09 p1133 A73-21986
- Switching and memory effects in amorphous chalcogenide thin films. 09 p1133 A73-21987
- Amorphous chalcogenide Te-As-Si-Ge thin film switch, discussing pressure effect energy accumulation time delay and behavior after voltage removal 09 p1133 A73-21988
- Application circuits for amorphous semiconductor switching devices with thin film active components, discussing electrical characteristics 09 p1061 A73-21990
- Design curves for PIN diode transmitter receiver switch based on lumped circuit filter suited to high frequency bands 09 p1063 A73-22496
- Cutpoint cellular switching array synthesis by combined cascade simplification rule, noting algorithm efficiency increase 09 p1065 A73-23101
- Satellite-borne programmable communications distribution subsystem, controlling microwave switch matrix by ground command via onboard memory for traffic flow data 09 p1053 A73-23364
- A nanovolt-level MOSFET reversing switch for low temperature applications. 11 p1367 A73-26310
- Questionnaire approach for technical diagnostics problem formulation covering hardware failure analysis coding, combinational switching device synthesis and optimal program construction 12 p1482 A73-26752
- Diagnosis of switching devices in the case where faults are represented by tests of individual elements 12 p1476 A73-26756
- An electronic relay constructed according to the principle of amplifiers with a controlled amplitude characteristic 12 p1477 A73-26791
- Chalcogenide glass threshold switch conceptual model based on electronic origin of firing, discussing applications to contactless switches, bistable relays decoupling and display triggering 12 p1478 A73-27042
- Analysis of commutator inverters with allowance for capacitive coupling to an ac amplifier 13 p1591 A73-28854
- Influence of the parasitic capacitance of a field effect transistor and of the input capacitance of the amplifier on the null shift of a modulator 13 p1591 A73-28856
- Null level of a field-effect-transistor modulator of small constant-voltage signals 13 p1592 A73-28873
- Effect of the input capacitance of an ac amplifier on the performance of key modulators 13 p1592 A73-28874
- Photoresistor synchronous detector circuits with rectangular light pulse switching elements for capacitive and resistive loads 13 p1592 A73-28900
- Dynamic losses in a transistorized switch operating on an active-capacitance load 13 p1593 A73-28944
- Suppressing spurious signals in saturated switching systems. 13 p1595 A73-29394
- An electronically-switched microwave radiometer. 13 p1622 A73-29423
- A data display device for switching and logic elements constructed from single-crystal ferromagnetic materials 14 p1731 A73-30941
- Ferrite component for waveguide commutator used as microwave switching element and modulator, noting application in navigation instruments and avionics 15 p1849 A73-30995
- Multidigit switching circuit synthesis for functionally complete redundant systems with incomplete splicing correlation 15 p1853 A73-31038
- An analog computer study of a thyristor inverter with opposite-parallel diodes under load switched-on between input throttles 15 p1851 A73-31697
- Charge-storage diodes with an internal field in the base 15 p1851 A73-31774
- Repetitively switched circuit analysis via matrix formalism and eigenvalue techniques with application to dc-dc converter 16 p1992 A73-33409
- Broad X band multichannel waveguide matrix for high speed switching from one input to one of four outputs at high power levels 16 p1990 A73-33897
- A user-oriented guide to the design and application of solid state relays. 17 p2132 A73-34089
- Demand-assignment multiple-access control techniques. 17 p2144 A73-35304
- B-1 aircraft electrical multiplex system. 17 p2110 A73-35309
- Pulse modulation of Gunn-effect oscillator. 17 p2142 A73-35652
- A study of the static S-shaped current-voltage characteristics of chalcogenide glass switching devices 18 p2293 A73-36722
- Noise immunity of diversity reception with antenna threshold switching. 18 p2290 A73-37128
- Electromagnetic core storage and switching elements design for Setun threshold ternary logic computer 19 p2408 A73-38562
- Low power laser-triggered switching at voltages greater than 500 kV. 20 p2572 A73-38883
- Book - Design performance and applications of microwave semiconductor control components. 20 p2535 A73-39136
- Digitally switched phase shifter operating at metric wavelengths 21 p2662 A73-40544
- Mechanically and electronically switched circular symmetric phased arrays with hybrid matrix phase shifter and lens switch combinations, assessing design and performance characteristics 21 p2672 A73-40675
- Use of switching circuits as redundant multiplier elements in canonic digital networks. 21 p2658 A73-41209
- Semiconductor rectifiers and thyristor devices, discussing transistor switching, Zener diode, controlled and light activated p-n-p-n diodes 21 p2668 A73-41619
- Prediction methods for the susceptibility of solid state devices to interference and degradation from microwave energy. 22 p2823 A73-41796
- Interwire coupling noise and cable resonance equations for fast rise time signal switching at resonant frequencies 22 p2823 A73-41800
- Triple Modular Redundancy Single Single voter-switch with majority voting of three parallel data channels or converters, estimating reliability for short and long missions 22 p2825 A73-42294
- Dynamic properties of transistor current switches 22 p2833 A73-42369
- Theory and operation of space-charge-limited transistors with transverse injection. 22 p2833 A73-42598
- Rapid-switching, broadband 1:4 WG switch matrix. II. 22 p2834 A73-42874
- Power Electronics Specialists Conference, California Institute of Technology, Pasadena, Calif., June 11-13, 1973, Record. 22 p2801 A73-42901
- High voltage waveform generation at low power levels by circuit techniques and system configurations involving parallel series chains of light triggered bilateral switches 22 p2834 A73-42907
- Requirements of switching devices in dc-to-dc converters. 22 p2801 A73-42908
- System oscillations from negative input resistance at power input port of switching-mode regulator, amplifier, dc/dc converter, or dc/ac inverter. 22 p2802 A73-42911
- Logic-controlled solid-state switchgear for 270 volt dc. 22 p2802 A73-42915
- The application of standardized control and interface circuits to three dc to dc power converters. 22 p2802 A73-42918
- A symmetry correcting pulse-width modulator for power conditioning applications. 22 p2802 A73-42919
- Pneumatic sequential circuits assembly method involving modules with switching elements and shift register, considering control valves and operation modes 23 p2943 A73-43416
- Bayes theorem for probabilistic analysis of logic circuits applied to reliability estimation of switching circuits 23 p2965 A73-44107
- Switching of semiconductor devices in pulsed voltage regulators 24 p3072 A73-44938
- AC starter generator featuring variable-to-constant frequency conversion by cycloconverters as switching device for use with aircraft engines 24 p3057 A73-45154
- Tunnel diode equivalent circuit analysis based on empirical expressions for composite T-V characteristics, predicting series resistance effect on switching time 24 p3073 A73-45485
- SWITCHING ELEMENTS**
- U SWITCHING CIRCUITS**
- SWITCHING FUNCTIONS**
- U BOOLEAN FUNCTIONS**

U SWITCHING
SWITCHING THEORY

Switching time dependence on input signal amplitude in self adaptive servosystem with open and closed control loops

06 p0680 A73-18382

A doped highly compensated crystal semiconductor as a model of amorphous semiconductors.

16 p2044 A73-33196

Stochastic differential equation solutions for Markov processes with diffuse switching, including limit theorem on convergence

20 p2582 A73-39386

SWITZERLAND

NT ALPS MOUNTAINS [EUROPE]

SYLLABLES

NT MESSAGES

SYMBOLIC PROGRAMMING

NT COMPUTER PROGRAMMING

Electronic computer design and programming for solving high order linear equations, using matrix determinants and graph trees in letter symbols

01 p0019 A73-10033

Satellite orbit inclination function computation as representative problem in symbolic programming applied to celestial mechanics

01 p0099 A73-10688

Automatic optimization of Symbolic Algol programs. I - General principles.

07 p0796 A73-19269

Applications of symbolic computing methods to the dynamic analysis of large systems.

10 p1192 A73-24029

Command language for supervisory control of remote manipulation.

19 p2403 A73-37329

Applications of a symbolic algebra manipulation language for composite structures analysis.

19 p2496 A73-37482

SYMBOLS

NT MESSAGES

Symbol ring as alphabetic element in information processing technique, defining address substitution operation

02 p0143 A73-11642

Double cross-validation of video cartographic symbol location performance.

05 p0543 A73-16719

Fluidics terminology and vocabulary development and practical use, describing control functions and symbols

11 p1307 A73-25378

Integrated image and symbolic display hierarchy with increasing horizontal and vertical information content for superposition as helicopter aid in approach and precision hovering

17 p2168 A73-35065

[AHS PREPRINT 724]
Symbol set for multigenerated digital transmission featuring highly redundant timing for low frequency phase noise suppression

21 p2656 A73-41110

SYMMETRICAL BODIES

NT AXISYMMETRIC BODIES

NT BODIES OF REVOLUTION

NT CELESTIAL SPHERE

NT CONICAL BODIES

NT CYLINDRICAL BODIES

NT ELLIPSOIDS

NT FAIRINGS

NT LENTICULAR BODIES

NT PARABOLIC BODIES

NT POINCARÉ SPHERES

NT ROTATING CYLINDERS

NT ROTATING SPHERES

NT SLENDER CONES

NT SPHERES

NT STREAMLINED BODIES

NT TORUSES

Equilibrium equations for static computations of symmetrical plates with large number of rods, point supports or holes

14 p1815 A73-30814

SYMMETRY

Collisionless magnetoactive plasma nonlinear responses tensors symmetry properties, stressing Onsager relations generalization

01 p0083 A73-10454

A new method for studying the symmetry reduction of a system by means of a perturbation

11 p1326 A73-25867

Symmetries of differential equations - The hypergeometric and Euler-Darboux equations.

13 p1648 A73-28538

Transformation symmetry of x-space coordinates of geometric tensors, tensors and M-objects with constant length dimensionality

20 p2594 A73-39729

SYMPATHETIC NERVOUS SYSTEM

Role of the sympathico-adrenal system during a period of rest and in adaptation to muscular activity

01 p0007 A73-10157

Effects of endotoxin on monoamine metabolism in the rat.

01 p0009 A73-11100

Studies of blood gas analysis at abnormal environment.

01 p0013 A73-11210

Catecholamine exchange in the hormonal and mediator links of the sympathoadrenal system under stress

07 p0784 A73-20367

Role of the sympathetic nervous system in supporting cardiac function in essential arterial hypertension.

08 p0930 A73-21015

The pharmacology of practolol - A cardioselective beta adrenergic blocking drug.

09 p1044 A73-21850

Changes in hemodynamics and efferent sympathetic pulsation during pressor cardiovascular reflexes under conditions of acute hypoxic hypoxia

09 p1039 A73-22365

Heart activity characteristics in a human operator during a control process

10 p1183 A73-23806

Vertebrate cardiac innervation via parasympathetic and sympathetic nervous system, considering synaptic transmission, nerve endings, stimulation and electrical effects

11 p1316 A73-25597

Autoradiographic study of protein synthesis in perikaryons and of nitrogen migration into the axons of hypertrophic sympathetic neurons

13 p1574 A73-28296

Influence of ribonuclease on changes in the membrane potential of muscle fibers evoked by stimulation of the sympathetic nerve

15 p1833 A73-31166

Effect of sympatholytic on metabolism in resting and working muscles in relation to the degree of their adaptation to intensified activity

18 p2276 A73-36571

The role of the sympathetic section of the vegetative nervous system in the training of the organism for the influence of statokinetic irritants.

18 p2279 A73-36903

Control of pineal indole biosynthesis by changes in sympathetic tone caused by factors other than environmental lighting.

19 p2393 A73-37300

Protein synthesis in the neurons and glial cells of the stellate ganglia of rats during the adaptation to the effects of high altitude hypoxia

19 p2393 A73-37396

Alterations of cardiac sympathetic neurotransmitter activity in congestive heart failure.

22 p2808 A73-42690

Neurogenic and local regulation of resistance and capacitance blood vessels, noting sympathetic nervous system influence on musculocutaneous and splanchnic regions

23 p2947 A73-43927

Changes in indices of the carbohydrate and fat metabolism, the state of the sympathoadrenal system, and oxidative processes under varying-intensity cold effects

24 p3059 A73-44671

SYMPATHOMIMETICS

U ADRENERGICS

SYMPHONIE SATELLITES

The telecommunication payload of the satellite

02 p0140 A73-11678

Orientation accuracy of the Symphonie communication antennas

02 p0140 A73-11684

Communications satellite Symphonie stability during perigee-apogee transfer in terms of liquid filled spinning top nutation

03 p0381 A73-13295

Effect of the guidance reserve of the Europa II third stage on the consumption of propellants for stationing

04 p0504 A73-15294

Symphonie satellite radio link equipment design and performance, noting transmission characteristics and frequency response of repeater

07 p0821 A73-18965

French Concerto program for component reliability and quality assurance in manufacturing and procurement controls for Symphonie satellite

07 p0790 A73-18975

Solar generator technology on the Symphonie satellite.

07 p0778 A73-18976

Thermopile IR static horizon sensor for Symphonie satellite three axis attitude stabilization in geostationary orbit

07 p0821 A73-18985

The experimental telecommunication satellite Project Symphonie.

07 p0905 A73-19140

TDMA system and full scale test programs for Symphonie satellite telecommunication with ground

09 p1049 A73-22316

Symphonie satellite communication equipment payload, discussing mission requirements, receiving and transmitting antennas, transponder and ground testing methods and arrangements

11 p1417 A73-25356

This film thermopile for Symphonie geostationary satellite attitude determination based on absorbed energy transformation into heat, discussing design and applications

16 p1988 A73-33274

Mission, project profile, and description of the

Symphonie satellite

[DGLR PAPER 73-043]

17 p2126 A73-35480

Communications system of the Symphonie satellite and special transmission parameters

[DGLR PAPER 73-056]

17 p2126 A73-35480

Test stand for the propulsion systems of the 'Symphonie' communications satellite in vacuum

19 p2419 A73-38277

The telecommunication payload of the satellite

Symphonie

21 p2655 A73-41081

SYMPTOMOLOGY

Motion sickness symptomatology and performance decrements occasioned by hurricane penetrations into C-121, C-130 and P-3 Navy aircraft.

03 p0269 A73-141668

Slow and fast heart rates and syncope and dizzy attacks as manifestations of sick sinus syndrome, discussing ventricular artificial pacemaker as therapy

11 p1319 A73-262898

SYMPTOMS

U SIGNS AND SYMPTOMS

SYNAPSES

Polysynaptic pathways role in tonic vibration and monosynaptic reflexes due to muscle vibratory or nerve electric stimulation, respectively, discussing tetanization effects

01 p0008 A73-10409

Current views on the mechanism of the quantum-induced liberation of a mediator from the motor nerve endings of a skeletal muscle

01 p0009 A73-11023

Morphological, physiological and pharmacological investigations of rat cerebellar cortex synaptic structure and function maturation and neurotransmitter receptivity development

03 p0264 A73-14256

Conditioned reflex learning and phenamine-stimulated functional activation of cerebral synaptic protein synthesizing and energy generating apparatus

05 p0541 A73-17177

Synapse localization study by electron microscopy of primary afferent tissues in cochlear nuclei of the brain stem

07 p0781 A73-19650

Functional organization of the mechanisms of presynaptic inhibition evoked by stimulation of cutaneous afferents

07 p0781 A73-20003

Synaptic activation of thoracic spinal cord interneurons through reticulo-spinal pathways

09 p1039 A73-22576

Cortico-pyramidal and cortico-extrapyramidal synaptic effects on lumbar motor neurons in monkeys

09 p1040 A73-22578

Vertebrate cardiac innervation via parasympathetic and sympathetic nervous system, considering synaptic transmission, nerve endings, stimulation and electrical effects

11 p1316 A73-25597

Loss of information during central summation of local postsynaptic potentials

14 p1719 A73-30825

Transmission of nerve pulses at the switching locations of the brain

16 p1973 A73-33424

Investigation of the distribution of synaptic inputs on an analog model of the motoneurons

19 p2399 A73-37942

Russian book on structural and functional plasticity of interneuron synapses during readjustment to chemical and physical damage covering degenerative and regenerative changes

21 p2640 A73-41280

Structurally functional properties of the dendrites of central neurons

23 p2947 A73-43926

SYNCHRONISM

NT BIT SYNCHRONIZATION

NT FREQUENCY SYNCHRONIZATION

Parameter calculation and design of synchronization circuit for firing pumping lamp of laser with modulator employing total internal reflection prism for Q switching

01 p0059 A73-10831

Clock comparisons by short wave, ULF and VLF signals, Loran C and Omega methods, onboard aircraft atomic clocks and TV synchronizing pulses

03 p0307 A73-13246

Photoelectric measurement of satellite camera shutter opening time delay and photographic plate motion synchronization, calculating root-mean-square error in observation time

03 p0307 A73-13253

Circadian rhythm asynchrony in man during hypokineses.

03 p0263 A73-14121

- Accurate time and frequency comparisons based on TV frame pulses 06 p0692 A73-17587
- The powering and synchronization of a solid-state laser operating at a repetition rate of several Hertz 08 p0976 A73-21716
- Synchronization theory for digital data transmission with random changes in channel characteristics 09 p1049 A73-22045
- Transient analysis of phase-locked tracking systems in the presence of noise. 09 p1066 A73-22113
- Self-synchronization of mechanical vibrators in the event of random disturbances 09 p1120 A73-22356
- Noise immunity in detection of pseudorandom PSK signals with allowance for synchronization errors, noting reception fidelity dependence on signal to noise ratio 09 p1050 A73-22455
- Unified time recording for aerial photographic surveys, using exact time synchronized control signal sequences in recording camera shutter release 09 p1084 A73-22672
- Production of a coherent submillimetric radiation by a heterodyne method 09 p1097 A73-23030
- Matched filters for extracting synchronization in signaling, nonreturn-to-zero and split phase PCM systems, using finite-time-duration trigonometric pulse synthesis 09 p1056 A73-23402
- Sagnac effect on clock synchronization of two clocks moving under equal equatorial westward and eastward velocities 11 p1398 A73-25860
- Emission field structure during transverse mode synchronization in a laser 13 p1626 A73-28005
- Electromagnetic induction microsystems with synchronization. III - Distribution of magnetic characteristics in complex linear and nonlinear regions. IV - Modeling of nonstationary electromechanical processes 16 p1992 A73-33668
- Dynamic electron bunching theory applied to moving solid particles and liquid droplets, describing synchronization mechanism for mechanical particles in oscillating gas 20 p2598 A73-39494
- Automatic accurate full-range synchronization of light strobe with shutter opening of fast-framing camera. 21 p2697 A73-39997
- Possible scientific utilization of long laser bases 21 p2716 A73-41328
- An electronically synchronized drum-type film camera 21 p2706 A73-41580
- Error detection and synchronization with pseudoternary codes for data transmission. 22 p2827 A73-42464
- SYNCHRONIZED OSCILLATORS**
- Microwave Gunn diode oscillators applications, noting use as Doppler radar and synchronized oscillators. 02 p0144 A73-11532
- Beat conditions during synchronization of an oscillator by an external sinusoidal force 02 p0147 A73-12492
- Oscillator synchronization by FM signal for constant central frequency-sideband phase difference operation 08 p0946 A73-21112
- Intersynchronization processes in Thomson oscillators with constraints of different nature placed on the amplitudes 08 p0948 A73-21518
- Parametric synchronization of self-oscillators with feedback delay and nonlinear circuit 11 p1337 A73-25429
- Investigation of the synchronization of Gunn diode oscillators having a stripline resonance system 12 p1480 A73-27448
- Voltage-locked diode oscillators. II - The effect of harmonics on the locking range. 14 p1734 A73-30074
- Tunnel diode oscillator synchronization by external harmonic force with frequency close to generator natural frequency, discussing loading effects 14 p1728 A73-30267
- Quasi-periodic oscillations in a nonautonomous oscillator 14 p1728 A73-30268
- Mutual synchronization of oscillators which are coupled by a segment of a long line. 17 p2143 A73-35715
- Synchronization of the frequency of tunnel-diode, IMPATT-diode, and Gunn-device oscillators 20 p2537 A73-39460
- SYNCHRONIZERS**
- Effects of a synchronizer phase-shift on circadian rhythms in response of mice to ethanol or quabain. 20 p2513 A73-39481
- Ultrahigh-speed high-frequency motion picture camera type W.K.2 21 p2693 A73-39939
- SYNCHRONOUS COMMUNICATION SATELLITES**
- U SYNCOM SATELLITES**
- SYNCHRONOUS DETECTORS**
- U CORRELATORS**
- SYNCHRONOUS METEOROLOGICAL SATELLITE**
- Glass reinforced structural components for the synchronous meteorological satellite. 03 p0331 A73-13030
- Synchronous meteorological satellite (SMS) system responsibilities of NASA and Commerce Department, discussing program objectives, payload, spacecraft subsystems and ground systems 04 p0504 A73-15451
- An amplitude-steered, electronically despun antenna for the synchronous meteorological satellite. 04 p0428 A73-15453
- A novel VHF turnstile antenna for the SMS satellite. 04 p0428 A73-15456
- Electrical power subsystem for the Synchronous Meteorological Satellite (SMS). 09 p1154 A73-22789
- Mass property control of a synchronous meteorological satellite scanning experiment. [SAWE PAPER 964] 19 p2492 A73-37882
- SYNCHRONOUS MOTORS**
- Investigation of the output characteristic and errors of a reversible, contactless, dc tachometric generator designed on the basis of a synchronous machine 09 p1033 A73-22342
- Synchronous motors as speed control system actuators, using static converters for instantaneous voltage or current amplitude and frequency control 10 p1177 A73-24026
- Effect of the gyromotor torque on the dynamics of a gyroscope 24 p3091 A73-45021
- SYNCHRONOUS SATELLITES**
- NT AEROS SATELLITE**
- NT GOE SATELLITES**
- NT SIRIO SATELLITE**
- NT SYNCHRONOUS METEOROLOGICAL SATELLITE**
- NT SYNCOM SATELLITES**
- Three station interferometric observation of TAC-SAT synchronous communications satellite radio signals for orbit determination, discussing method feasibility for tracking and geodesy applications 01 p0097 A73-10407
- Control of electron bombardment ion engine for stationary satellite. 01 p0090 A73-11110
- The telecommunication payload of the satellite Symphonie [DGLR PAPER 72-089] 02 p0140 A73-11678
- Radio sensors for the three-axis attitude fine measurement of geostationary communication satellites 02 p0228 A73-11822
- Optimization of the apogee impulse during the positioning of a geostationary satellite. 02 p0228 A73-11992
- Very long baseline interferometry observations of radio emissions from geostationary satellites. 02 p0215 A73-12270
- Synchronous satellite ground track drift analysis for ecological survey application, discussing zonal, tesseral and sectorial harmonics and perturbation compensation 03 p0370 A73-13150
- A technique for synoptic measurement of ionospheric propagation delays by ranging from geostationary satellites to a network of unmanned transponders. 03 p0308 A73-13629
- ATS-5 solar cell experiment after 699 days in synchronous orbit. 03 p0257 A73-14244
- Geostationary artificial satellite orbital parameters calculation, taking into account lunar, solar and light pressure perturbations 03 p0378 A73-14551
- Spin and three-axis stabilized geosynchronous tracking and data relay satellite system for telecommunication service to user spacecraft in low earth orbit 04 p0420 A73-15422
- Geophysical data transmission from automatic stations in the antarctic via earth synchronous satellites. 04 p0421 A73-15430
- Synchronous satellite solar power station for solar energy conversion to microwaves for transmission to earth discussing technical, economic and social aspects [ASME PAPER 72-WA/SOL-6] 04 p0408 A73-15801
- Transoceanic telephony via communication satellites, discussing satellite reliability and placement in synchronous orbit 06 p0663 A73-17577
- Electron-proton spectrometer for the GEOS satellite. 06 p0692 A73-17826
- Canadian Anik I synchronous domestic communication satellite for color TV broadcasting or telephony, considering northerners reaction and community beneficiaries 06 p0668 A73-18432
- Geostationary satellites stabilization by microthrusters based on solid sublimation or hydrazine monopropellant, describing propulsion system development 07 p0866 A73-18926
- Monopropellant and bipropellant thruster systems with afterburning for geostationary satellite orbital control, evaluating performance and reliability based on calculation and test data 07 p0866 A73-18930
- Management and cost of European-U.S. Aerosat program based on geostationary satellites for air/ground voice and data messages relay and aircraft position determination 07 p0905 A73-19174
- Effects of the sun and the moon on a near-equatorial synchronous satellite. 08 p1011 A73-21430
- Near-equatorial synchronous orbit Satellite Solar Power Station system with photovoltaic cell arrays energy conversion into microwave power for transmission to earth 10 p1285 A73-23601
- Power system for a 4.1 kilowatt synchronous satellite. 11 p1312 A73-26023
- The feasibility of geostationary emplacement of satellites by solar electric tug. 11 p1431 A73-26260
- Dual channel high resolution radiometer of French synchronous meteorological satellite Meteosat for full time cloud coverage of earth in visible and IR ranges 11 p1368 A73-26508
- Meteosat geosynchronous satellite for European meteorological space program, discussing picture taking, data broadcasting and rebroadcasting, central control station and peripheral terminals 12 p1549 A73-27380
- GEOS geostationary satellite experiments for dc magnetic fields, dc/ac electric fields and plasma resonances, thermal plasma, electrons and protons 12 p1499 A73-27775
- Meteosat - Project of a European geostationary meteorological satellite - Status: 9/15/1972 13 p1689 A73-28743
- Orbit selection for satellite missions, determining elements of sun-synchronous, recurrent, near-recurrent, polar, synchronous and stationary orbits 13 p1684 A73-29246
- Scaled silver oxide zinc cells for orbiting and planetary missions. 13 p1572 A73-29586
- European geostationary communication satellite system for telephone and TV transmission, discussing stabilization, command and power subsystems, modulation methods, power budgets, satellite configurations, etc 14 p1728 A73-30431
- First order perturbation theory for geostationary satellites orbit calculation, taking into account earth oblateness, equator ellipticity and solar and lunar gravitational effects 15 p1930 A73-31114
- Requirements regarding the position and the attitude of future application satellites 15 p1907 A73-31134
- Gravity-gradient stabilization of synchronous orbiting satellites - Additional considerations of attitude stability. 15 p1944 A73-32218
- Procedures and ground methods associated with the exploitation of a system of aeronautical satellites 15 p1911 A73-32488
- Synchronous communication satellite crosslink antenna design and tracking and acquisition procedures for Ka band frequencies, describing reflectors, paraboloids, and five horn feed system 16 p1977 A73-32721
- German national geostationary TV satellite project, discussing thermal and attitude control, launch and guidance problems, solar power supply and antenna systems 16 p2074 A73-33737
- Estimation and correction of electric thruster misalignment effects on a geostationary satellite. 17 p2238 A73-34866
- Synchronous satellite systems for civilian air, ship and land vehicle traffic control, communication, navigation and surveillance, discussing technology requirements for continental and oceanic systems [AIAA PAPER 73-583] 18 p2288 A73-36075
- Approximate description of the evolution of a synchronous-satellite orbit 18 p2350 A73-36101
- Cost reductions in transportation to geosynchronous and lunar orbits by a swing station. 19 p2490 A73-37193

Geostationary meteorological satellite network development for static and cinematographic image transmission based on international cooperation
22 p2884 A73-43118

SYNCHROTRON NOISE

U ELECTROMAGNETIC NOISE
U SYNCHROTRON RADIATION
SYNCHROTRON RADIATION

The nature of the first Cygnus X-3 radio outburst.
02 p0204 A73-11551
Radio outbursts observation in X ray source Cyg X-3, showing relativistic electrons sporadic injection dominance of synchrotron radio emission characteristics
02 p0210 A73-11564

FLux density and linear polarization measurements of radio outburst from Cygnus X-3, suggesting synchrotron radiation from expanding cloud of relativistic particles
02 p0205 A73-11871

Cygnus X-3 radio outburst as consequence of synchrotron radiation due to expanding relativistic plasma ejection, considering polarization, flux densities and spectral index
02 p0211 A73-11872

The nature of radio emission from pulsars.
02 p0218 A73-12407

Linear synchrotron instability theory results via quantum method with Einstein coefficients, obtaining synchrotron radiation growth rate in relativistic electrons with anisotropic momentum distribution
02 p0223 A73-12726

Circular polarization of synchrotron radiation in the presence of hydromagnetic waves.
02 p0224 A73-12739

The self absorption of gyro-synchrotron emission in a magnetic dipole field - Microwave impulsive burst and hard X-ray burst.
03 p0364 A73-14416

Free-free absorption of gyro-synchrotron radiation in solar microwave bursts.
04 p0492 A73-15366

Mechanisms of optical, X-ray and gamma-radiation from Crab pulsar.
05 p0611 A73-17314

Rotating black holes - Locally nonrotating frames, energy extraction, and scalar synchrotron radiation.
05 p0625 A73-17331

Frequency dependent synchrotron emission polarization variation in cosmic radio source models, allowing for cold plasma and relativistic distribution nonuniformities
07 p0872 A73-20307

Radio sources with variable circular polarization, noting synchrotron radiation theory applicability
08 p1006 A73-20936

Synchrotron emission, adiabatic invariant, and gradient drift of particles in a linearly inhomogeneous magnetic field
09 p1132 A73-23079

A synchrotron radiation model of the infrared radiation from the nucleus of NGC 1068.
09 p1150 A73-23144

The structure of the Crab Nebula. III - The radio filamentary radiation.
09 p1151 A73-23291

Relativistic electron bremsstrahlung suppression in isotropic plasma, noting analogy to synchrotron radiation
10 p1252 A73-23476

Galactic background spectrum at 230-2600 kHz from IMP-6 radio astronomy, discussing ambient plasma effects on synchrotron emission in galactic models
10 p1272 A73-23529

Synchrotron emission amplification by magnetic field in cosmic sources from analysis of relativistic electron system, noting pulsars and UV Ceti stars
10 p1264 A73-23708

Spatial distributions of intensity and polarization over the source of microwave impulsive bursts.
10 p1275 A73-23828

Polarization of synchrotron radiation from relativistic Schwarzschild circular geodesics.
10 p1252 A73-24347

The circular polarization of sources of synchrotron radiation.
10 p1270 A73-24901

Particle injection in the Cygnus X-3 radio outburst.
11 p1419 A73-25859

Frequency dependent synchrotron emission polarization variation in cosmic radio source models, allowing for cold plasma and relativistic electron distribution nonuniformities
12 p1534 A73-27279

Solar radio bursts of 4 and 7 August 1972, deducing positron synchrotron process effects on radio spectrum from gamma ray measurements
12 p1535 A73-27785

Ignition condition in Tokamak experiments and role of neutral injection heating.
14 p1777 A73-29684

Existence conditions for magnetoactive plasma longitudinal waves with phase velocity near light velocity,
14 p1780 A73-30337

investigating increments during synchrotron instability due to relativistic particles
14 p1780 A73-30337

Possible role of faster-than-light radiation under pulsar conditions
17 p2226 A73-34370

A comparison between Compton-synchrotron and Compton black-body emission in radio sources.
17 p2237 A73-35785

Synchrotron radiation stimulated amplification by magnetic field in cosmic sources from analysis of relativistic electron system, noting pulsars and UV Ceti stars
18 p2347 A73-36733

Synchrotron radiation sources with relativistic particles moving at small pitch angles in magnetic field, discussing emission properties and degrees of polarization
19 p2484 A73-37617

Synchrotron model limitations for optical pulsars and compact extragalactic objects, considering NP 0532, PKS 2134+004, OQ 208 and NGC 1068
19 p2485 A73-37618

Radiative corrections and soft-photon emission in magnetic bremsstrahlung.
20 p2602 A73-39445

Clusters of galaxies - A possible source of background emission in the X-ray band
21 p2759 A73-40709

Basic method for realization of temperature scale at 10,000 K by photometric comparison between vacuum-UV-blackbody radiation of a plasma and synchrotron radiation.
22 p2852 A73-41978

Solar coronal radio spectra emitted by synchrotron process, computing radio wave suppression due to isotropic and anisotropic plasma
24 p3118 A73-45484

SYNCHROTRONS

NT STORAGE RINGS [PARTICLE ACCELERATORS]

SYNCHRONAL VALLEYS

U VALLEYS

SYNCOM SATELLITES

Considerations on transfer into geostationary orbit using ion propulsion - Application to the Europa III booster
04 p0505 A73-15742

Development and test of a double gimballed momentum wheel stabilization system for communication satellites.
[ALAA PAPER 73-906]
20 p2614 A73-38840

SYNCOPE

NT BLACKOUT [PHYSIOLOGY]

Slow and fast heart rates and syncope and dizzy attacks as manifestations of sick sinus syndrome, discussing ventricular artificial pacemaker as therapy
11 p1319 A73-26289

SYNDROMES

U SIGNS AND SYMPTOMS

SYNOPTIC MEASUREMENT

The radiation budget of the earth-atmosphere system as measured from the Nimbus 3 satellite /1969-1970/
02 p0160 A73-12266

A technique for synoptic measurement of ionospheric propagation delays by ranging from geostationary satellites to a network of unmanned transponders.
03 p0308 A73-13629

Project VEMNO - North Sea-Baltic measuring network.
13 p1608 A73-28787

Simulated ERTS data for coastal management.
17 p1257 A73-34285

Satellite imagery of land resources, discussing synoptic views, spatial dependence, closed loop information and sequential sampling
17 p2161 A73-34945

Remote sensing with VHRR satellite imagery.
18 p2308 A73-36041

Synoptic survey for the neutral line in the magnetotail during the substorm expansion phase.
18 p2352 A73-36275

Synoptic survey of geomagnetic field neutral line formation in magnetotail during magnetic substorms noting nighttime magnetosphere reconnection and associated plasma sheet behavior
22 p2849 A73-42573

SYNOPTIC METEOROLOGY

Hemispheric synoptic analysis of upper stratospheric warming for energy transformations in troposphere and lower and middle stratosphere
01 p0072 A73-10141

Atmospheric moisture and wind field synoptic analysis based on Nimbus 4 temperature-humidity IR radiometer /THIR/ measurements
01 p0073 A73-10379

Life cycle of brief CAT episodes determined by mesoscale analysis.
03 p0338 A73-14533

A study of tropospheric radar propagation characteristics during an unusual spell of persistent dust haze
05 p0593 A73-16238

followed by thunderstorm over Delhi during May 1966.
03 p0280 A73-145478

Synoptic conditions of wave formation above convection streets.
04 p0473 A73-148208

Physicostatistical investigations of the general atmospheric circulation
05 p0592 A73-16237

Typification of circulation processes in the atmosphere over the Northern Hemisphere and the possibility for its objectivization with the aid of numerical characteristics
05 p0593 A73-16238

Utilization of meteorological data from earth satellites in the analysis of global weather maps and in studies of planetary atmospheric circulation
05 p0593 A73-16246

A synoptic climatology of satellite observed cloud vortices over the Southern Hemisphere.
07 p0846 A73-19039

Weather forecasting with the aid of satellite data.
[ALAA PAPER 73-21]
07 p0848 A73-19582

Quasi two dimensional turbulence model of energy spectra and potential enstrophy transfer in synoptic large scale quasi-horizontal atmospheric motions
07 p0820 A73-20342

Earth surface and background wind effects on mesoscale and large scale meteorological processes in free stably stratified atmosphere
07 p0848 A73-20343

GARP Global Experiment design with satellite and balloon borne systems for meteorological observation and atmospheric research, discussing sounding data numerical simulation
07 p0820 A73-20442

Planetary boundary layer flow of a stable atmosphere over the globe.
08 p0960 A73-21380

Blocking situations lasting less than five days over the Euro-Atlantic region in the 20-year period from 1951 through 1970
08 p0986 A73-21486

Jupiter surface maps from synoptic observations with refracting telescope, considering white cloud formations and atmosphere motions
08 p1012 A73-21584

Global time and space changes of satellite radiances received from the stratosphere and lower mesosphere.
09 p1076 A73-22149

A synoptic investigation of anomalous warmth in the mid and upper troposphere during February 1964.
10 p1244 A73-23978

Southeast Asia weather during southwest monsoon in summer, discussing relation to westward moving equatorial waves from wind, pressure and cloudiness synoptic pattern analysis
12 p1520 A73-26805

Subsynoptic rainbands within precipitation ahead of surface warm front, discussing midtropospheric large-scale dynamic ascent interaction with upper boundary potential instability
13 p1651 A73-28265

Mechanisms influencing the distribution of precipitation within baroclinic disturbances.
13 p1652 A73-28266

Observation of Kelvin-Helmholtz billows and their mesoscale environment by radar, instrumented aircraft, and a dense radiosonde network.
13 p1652 A73-28268

Vorticity equation advection, divergence and curl terms effects on vorticity changes over isobaric surfaces and on weather and cyclonic development in synoptic meteorology
13 p1653 A73-28745

Some characteristics of stratiform St-Sc clouds in various synoptic situations
13 p1654 A73-28885

Weather forecasting in the recent past, at the present time, and in the near future
13 p1655 A73-29189

Ground wind component calculations from synoptic parameters
13 p1655 A73-29190

A first experiment in constructing a weather forecast for a month by the synoptic method on a computer
13 p1655 A73-29193

Structure of the lower 300-meter atmospheric layer during the passage of a cold front
13 p1655 A73-29194

Cloud-free line-of-sight calculations.
15 p1903 A73-31317

A system of four geosynchronous satellites for global observations
15 p1903 A73-31605

An aid for the prediction of the nighttime minimum temperature
15 p1906 A73-32352

A synoptic model for evaluation of vertical temperature and geopotential profiles from satellite pictures.
17 p2206 A73-34939

The Budrio station of the meteoric radar system of the CNR for the systematic study of the upper atmosphere 17 p2147 A73-34959

Development of methods of forecasting meteorological conditions for aviation 18 p2331 A73-35912

New ways to monitor the mass and areal extent of snowcover. 18 p2307 A73-36025

Book - Advances in satellite meteorology. 18 p2333 A73-37051

Interrelationship between developments of synoptic processes and evolution of the integral moisture field according to satellite measurements. 18 p2334 A73-37065

Some aspects of the solution of inverse problems of satellite meteorology. 18 p2335 A73-37078

The dynamical effects of real Mars orography upon the large-scale air flow and some meteorological phenomena of Mars. 19 p2482 A73-37429

The large-scale displacement of subtropical jet stream over Western Europe in winter. 19 p2446 A73-37431

Some effects of surface anomalies in a global general circulation model. 19 p2446 A73-37539

Evidence for high-frequency synoptic disturbances near the stratopause. 19 p2447 A73-37663

Selection of analogs to composite kinematic charts of natural synoptic periods 19 p2449 A73-38545

On the strategy of combining coarse and fine grid meshes in numerical weather prediction. 21 p2728 A73-40055

Clear air turbulence mesoscale history from sequential analysis of rawinsonde stations network observed data 21 p2728 A73-40057

A scheme for synoptic-hydrodynamic-statistical weather forecasting for 3 to 10 days 21 p2730 A73-40491

Book - Atmospheric circulation systems and climates. 21 p2732 A73-41440

Stormy weather vertical air motion velocity calculation for use in synoptic field and atmospheric energy budget evaluations 23 p3003 A73-43996

Upper tropospheric disturbances of the equatorial atmosphere and their influence on rainfall near the equator. 23 p3004 A73-44104

Relationship between midstratospheric temperatures and tropospheric synoptic features. 24 p3107 A73-45014

National Center for Atmospheric Research collected synoptic meteorological data from earth surface, upper air and satellite observations for handling on computers 24 p3075 A73-45087

SYNTAX

NT WORDS [LANGUAGE]

Syntax specification system for computerized hand-drawn pattern grammar generation with user style description for concurrent inputting and analysis at high recognition speed 06 p0671 A73-18535

SYNTHETIC ARRAYS

Receiving antenna polarization parameters selection in side-looking synthetic aperture radars 04 p0423 A73-15914

Airborne synthetic aperture /hologram/ radar maximum ambiguity range extension by using additional receive-only antenna ahead of transmit-receive unit 05 p0577 A73-16817

Coherent optical processing and display techniques for microwave imagery generation from synthetic aperture radar system data, discussing hologram and side-looking radar 06 p0667 A73-18279

Influence of phase fluctuations of the received radiation on the performance of a synthetic antenna 11 p1331 A73-26158

Controlled-quality images from synthetic-aperture radar data. 16 p2015 A73-33358

Circular synthetic radar with interferometer elements mounted at ends of horizontal boom rotating about vertical mast, predicting echo response to point and multiple targets 21 p2650 A73-40342

SYNTHETIC FIBERS

NT DACRON [TRADEMARK]

NT GLASS FIBERS

NT NYLON [TRADEMARK]

NT RAYON

SYNTHETIC RESINS

NT ACRYLIC RESINS

NT ADDITION RESINS

NT EPOXY RESINS

NT NYLON [TRADEMARK]

NT PHENOLIC RESINS

NT POLYAMIDE RESINS

NT POLYESTER RESINS

NT POLYETHER RESINS

NT POLYMETHYL METHACRYLATE

NT THERMOPLASTIC RESINS

NT THERMOSETTING RESINS

Natural and synthetic thermally stable polymers, discussing pyrolysis, structure-property relationships and bond strengths 14 p1724 A73-30132

SYNTHETIC RUBBERS

NT BUNA [TRADEMARK]

NT CHLOROPRENE RESINS

NT ELASTOMERS

NT THIOPLASTICS

NT VITON RUBBER [TRADEMARK]

Finite deformation behavior of elastomers - Dependence of strain energy density on degree of crosslinking for SBR. 13 p1646 A73-29527

SYSTEM EFFECTIVENESS

An overview - Advantages of imaging techniques for nondestructive testing. 05 p0573 A73-16277

Ancillary information effects on photointerpretation performance under four imagery system operation modes, noting identification accuracy independence on information variables 06 p0658 A73-18245

Relationship between conventional-control-theory figures of merit and quadratic performance index in optimal control theory for a single-input/single-output system. 06 p0680 A73-18445

Some preliminary notions towards improved stochastic controller synthesis via transformed indices of performance. 06 p0681 A73-18817

Distributed ATC with traffic information in cockpit, noting potential for cost and risk reduction and capacity increase based on system performance evaluation 07 p0850 A73-20600

Performance control in government R&D projects - The measurable effects of performing required management and engineering techniques. 08 p1025 A73-20971

Television rate laser scanner with anisotropic Bragg device of paratellurite as acousto-optic horizontal deflector, noting operation efficiency and limiting resolution 08 p0975 A73-21142

Electronic imaging systems with TV vidicon competition with film photography for spaceborne solar astronomy, comparing resolution, sensitivity and SNR 08 p0971 A73-21749

The role of the test pilot in evaluating auto landing systems. II. 09 p1115 A73-22183

Computer protection mechanisms design principles for operating system and hardware architecture implementation, considering access matrix storage, efficiency and subject and object selection 09 p1059 A73-22223

Optimization of system reliability using a parametric approach. 09 p1112 A73-22646

Intelsat 4 power subsystem with solar panels, Ni-Cd batteries, controller and relays for bus paralleling, discussing spacecraft and system configurations and performance 09 p1154 A73-22788

A telecommunications link model for deep space - With applications to the HELIOS probe. 09 p1058 A73-23419

PCM and DPCM digital modulators design and performance comparison for sampling rate effects on quantizing noise, noting tradeoffs between cost and system efficiency 09 p1059 A73-23435

Canadian domestic ANIK communication satellite with all-microwave 12-channel repeater, discussing system components, antenna design and performance parameters 09 p1059 A73-23437

A combined coding and modulation approach for communication over dispersive channels. 10 p1186 A73-23496

Weaver modulator with digital filter for single sideband transmission in radio communication and telemetry, discussing FORTRAN simulation for cost, computation time and accuracy 10 p1186 A73-23499

Multichannel wideband FM communication systems, discussing method for channel density increase with reduced linearity requirement and enhanced noise immunity 10 p1187 A73-23732

Internally modulating and multiplexing mode locked Nd-YAG laser techniques for one gigabit optical communication, noting system efficiency improvement over conventional approaches 10 p1227 A73-23783

Trajectory optimization for the nonlinear combined estimation and control problem. 10 p1200 A73-24044

Significant elements of an effective search, rescue, and survival system. 10 p1176 A73-24712

Two quadratic cost functionals equivalence conditions derivation in terms of system parameters and weighting matrices for optimal control law generation 11 p1341 A73-25196

Solar cell battery operational performance test equipment and computerized simulation programs for post-1975 satellite and space station systems integration and design 11 p1309 A73-25986

Evaluation of the efficiency of automatic control and observation systems on the basis of mathematical models of potential and real automatic systems 12 p1482 A73-26762

A simulation model for a memory organization for a multiprocessor. 12 p1475 A73-27155

Data aided phase locked loops for phase estimation improvement in coherent demodulator to obtain loop acquisition characteristics design flexibility 12 p1483 A73-27157

Improvements in the use of FAA resources for system performance assurance. 12 p1561 A73-27364

Replacement of a system of aeronautical satellites. 12 p1549 A73-27678

Method for synthesizing built-in control circuits of automatic systems with memory 12 p1476 A73-27899

Naval air weaponry logistics support, discussing criteria for management effectiveness evaluation 13 p1709 A73-29573

Multiple access technique for future communication, surveillance and navigation subsystems to meet ATC demands, considering satellite surveillance radar system 14 p1725 A73-29893

Cone-bounded nonlinearities and mean-square bounds - Estimation upper bound. 14 p1769 A73-30505

British Airline Pilots Association and RAF Institute of Aviation Medicine questionnaire results on training simulator effectiveness, analyzing auditory and visual aids 16 p1996 A73-33213

Efficient utilization of orbit/frequency for satellite broadcasting. 16 p1979 A73-33401

Simulation of a multiple element test environment. 16 p1985 A73-33417

The role of testing in achieving aerospace systems effectiveness. 16 p2020 A73-33605

AEGIS Operational Readiness Test System - Design for system effectiveness. 16 p2073 A73-33609

Economic models for satellite system effectiveness. 16 p2073 A73-33618

System effectiveness and the one error per man per day expectation. 16 p2020 A73-33647

ECM systems with TWT dual moding to provide distinct CW and pulsed microwave power levels, evaluating performance beyond octave in bandwidth 16 p1990 A73-33849

Wideband monopulse radio direction finding measurement improvement, using receiver with log video IF amplifier, multiplexing filters and detectors to provide signal normalization 16 p1990 A73-33850

Simulation of a surface traffic control system for John F. Kennedy International Airport. 17 p2147 A73-34818

Key technological challenges of the Earth Resources Technology Satellite program. 17 p2161 A73-34943

Digital fly by wire flight control system with airborne digital processor for increased aircraft survivability, determining redundancy level to satisfy system performance 17 p2138 A73-35222

TDM data bus and interface design for digital avionics system, considering standard remote terminal in terms of system parameters, operation and cost effectiveness 17 p2139 A73-35233

The University College London image photon counting system - Performance and observing configuration. 17 p2169 A73-35279

Time division multiple access in the INTEL SAT system. 17 p2124 A73-35306

Pseudo random modulation - An effective means of enhancing PSK signal transmission in a diffuse multipath environment. 17 p2125 A73-35376

Spacecraft systems design trade-offs for the Earth Resources Technology Satellite. 17 p2239 A73-35631

Solar energy conversion into thermal, chemical or electric energy, discussing high efficiency collector

design with thin film for absorber and glass envelope improvement
[AIAA PAPER 73-710] 18 p2269 A73-36331
B-52 aircraft-borne short range attack missile weapon system air conditioner thermal performance fulfillment with Freon refrigerant and air distribution in heat exchangers
[AIAA PAPER 73-723] 18 p2269 A73-36340
Method of synthesizing built-in monitoring arrangements for automata with memory.

18 p2291 A73-36751
Computer models for air traffic control system simulation.

18 p2335 A73-36843
Some preliminary correlations between control modes of manipulator systems and their performance indices.

19 p2416 A73-37315
Remote viewing system with TV cameras to duplicate human visual field and acuity functions, featuring operator command and data link bandwidth minimization

19 p2416 A73-37319
Performance improvement in remote manipulation with time delay by means of a learning system.

19 p2417 A73-37331
U.S. instrument landing system performance improvements, considering terrain and weather effects, installation requirements, airport limitations, accuracy, reliability and maintainability

19 p2450 A73-37805
A digital simulation facility for air traffic control experimentation.

19 p2451 A73-37809
Computer program for aircraft navigation error synthesis with evaluation of component error distribution on traffic control system effectiveness to provide cost effective guidance

19 p2452 A73-37875
Strapped down inertial navigation systems.

19 p2452 A73-37876
A comparative study of two basic approaches to extremum control.

19 p2413 A73-38037
Performance of LQG control systems using optimal k-step-ahead control laws.

19 p2413 A73-38062
A new approach to the 'inverse problem of optimal control theory' by use of a generalized performance index /GPI/.

19 p2414 A73-38063
Control configuration optimization of linear engineering systems.

19 p2414 A73-38082
Electrolytic hydrogen fuel production with solid polymer electrolyte technology.

19 p2391 A73-38413
Multilayer foil insulated Si-Ge thermoelectric converters with multihundred watt power capacity, presenting thermal performance stability under vacuum operating conditions

19 p2392 A73-38423
Methods for calculating and enhancing the efficiency of automatic systems

20 p2540 A73-38705
The domain analysis of intersymbol interference effects on phase shift keyed /PSK/ and quadrature phase shift keyed /QPSK/ communication systems.

20 p2524 A73-38734
PPM pulse waveform synthesis with SNR performance improvement while retaining bandwidth-mean-square error properties inherent in wideband modulation system

20 p2524 A73-38736
Adaptive multibeam concepts for traffic management satellite systems.

20 p2525 A73-38746
Effect of nonlinear channel characteristics on QPSK system performance.

20 p2526 A73-38752
Variable data rate multimode quadriphase modem for PSK or QPSK operation in digital communication links, noting optimum overall system performance

20 p2527 A73-38764
A rational basis for determining the EMC capability of a system.

20 p2528 A73-38770
Intrasystem electromagnetic compatibility analysis program.

20 p2528 A73-38771
Study of control system effectiveness in alleviating vortex wake upsets.

20 p2507 A73-38776
[AIAA PAPER 73-833]
Ships inertial navigation system automated degradation detection and isolation, specifying decision error probabilities as function of degradation magnitude and observation time

20 p2585 A73-38788
[AIAA PAPER 73-849]
An attitude control system for earth observation spacecraft.

20 p2585 A73-38792
[AIAA PAPER 73-854]
Questionnaire survey covering development, qualification, acceptance and flight test roles in

achieving aerospace vehicles systems effectiveness /reliability, maintainability and safety/
20 p2544 A73-39248

Midair collision avoidance strategies for ATC improvement, discussing relative effectiveness of structural airspace, airborne and ground-based systems based on US statistics

21 p2733 A73-40030
Low cost strapdown inertial navigator with miniature electrostatically suspended gyros, discussing system performance goal in terms of position, velocity and attitude errors

21 p2734 A73-40037
ILS capability improvements on localizer and glide-slope antenna arrays and monitors, considering effects of reflecting objects on or near aerodrome and terrain

21 p2736 A73-40049
Optical communication system performance with tracking error induced signal fading.

21 p2657 A73-41171
Book - The role of testing in achieving aerospace systems effectiveness.

21 p2675 A73-41201
Manned and unmanned aerospace launch vehicle liquid and solid rocket propulsion system effectiveness survey questionnaire response data concerning various tests

21 p2781 A73-41202
NASA program manned and unmanned spacecraft system effectiveness survey questionnaire response data concerning various tests

21 p2781 A73-41203
US Department of Defense aircraft system effectiveness tests survey questionnaire response data from component, subsystem and system suppliers

21 p2635 A73-41204
Commercial aircraft system effectiveness survey questionnaire response data concerning various tests in manufacturing and operational environments

21 p2635 A73-41205
A rational basis for determining the EMC capability of a system.

22 p2823 A73-41802
Application of stochastic programming methods for solving certain optimization problems of multiple-link plants without memory

22 p2836 A73-42612
Standard sensitivity and covariance matrices for statistical estimation of overall performance.

23 p2962 A73-43279
Management of Air Force test and evaluation activities.

23 p3050 A73-44055
Performance efficiency of systems employing information from radio-electronic means of observation

24 p3071 A73-44599
Maximum SNR performance calculation for heterodyne laser detection system with parameters optimization under assumed total cost

24 p3096 A73-44875

SYSTEM FAILURES

Analytical method for diagnostic and checkout testing of logic element faults in complex combinational circuits

01 p0026 A73-10035
Statistical method of determining the load or stress distribution from the failure characteristics of mechanical systems

01 p0118 A73-11370
A method for computing complex system reliability.

03 p0336 A73-13733
Reliability optimization of a series-parallel system.

03 p0336 A73-13735
Effects of test capability on system reliability and availability.

03 p0313 A73-13736
Statistical analysis applied to solar cell shorting caused by reverse bias voltage stress.

03 p0255 A73-14223
Control efficiency of finite automaton with automatic control, considering system failures and independent and unequally probable transitions

05 p0553 A73-16273
Extending the life and recycle capability of earth storable propellant systems.

05 p0629 A73-16631
[SAE PAPER 720837]
Bayesian prior distributions for multi-component systems.

09 p1111 A73-22374
Reliability of a self-repairing system with scheduled maintenance.

09 p1088 A73-22443
The average duration of the failed state in the interval between adjacent tests of a periodically verified standby radio system with z-multiple redundancy

09 p1051 A73-22464
Conditions for termination of tracking in electronic servo systems

10 p1202 A73-24610
Comparative analysis of optimal failure search procedures, considering criteria, failure extent, initial data, reliability and compatibility

10 p1226 A73-24696

Two component system reliability model, taking into account stress effects under failure normal distribution assumption

11 p1448 A73-26757
On the improvement in survivability for avionics equipment.

12 p1478 A73-27190
Mean time of the failure-free operation of a redundant system with allowance for monitoring of operational efficiency

12 p1504 A73-27618
Random failure process similarity in redundancy schemes for systems with binary elements, noting statistical modeling on specialized Monte Carlo machines

12 p1485 A73-27626
Calculation of redundant equipment recovery time when only failures of entire systems are detected by inspection

14 p1754 A73-30036
Matrix, pyramid and rectangular decoder reliability and operational probability during short circuit/cut-off failures

14 p1736 A73-30566
Prediction of failures and efficiency characteristics of a system

14 p1740 A73-30799
Expected value and variance of failure time in redundant systems.

15 p1901 A73-32264
Hydrofluidic component and system reliability.

16 p1971 A73-33478
Gas turbine vibration limits - A fundamental view.

16 p2048 A73-33509
[ASME PAPER 73-GT-48]
Failure data evaluation, determining wear out, degradations, environments causing system failures, repairs, maintenance and sub par performers

16 p2021 A73-33649
Operational behaviour of a complex system with two out of M failed components.

16 p2022 A73-34030
Complex system reliability with general repair time distributions under preemptive repeat repair discipline.

16 p2022 A73-34031
Probabilistic analysis of a two-unit system with a warm standby and a single repair facility.

17 p1249 A73-35809
Competitive evaluation of failure detection algorithms for strapdown redundant inertial instruments.

20 p2585 A73-38791
[AIAA PAPER 73-853]
The selection of test frequencies for system fault diagnosis.

20 p2586 A73-38802
[AIAA PAPER 73-864]
Electric powered commercial jet aircraft emergency power supplies, discussing attitude gyros, Ni-Cd batteries, voltmeters, equipment running times, static inverters and transmitters

20 p2510 A73-39213
Equivalence of redundant systems with respect to time to failure.

22 p2867 A73-42970

SYSTEM LIFE

U RELIABILITY

SYSTEMIZATION

U SYSTEMS ENGINEERING

SYSTEMS ANALYSIS

Validity of averaging methods for certain systems with periodic solutions.

01 p0070 A73-10273
Abstract theory of systems - Current state and development trends

01 p0027 A73-10664
A linearized analysis for frictionally damped systems.

01 p0090 A73-10782
Mathematical models, systems analysis and synthesis in control theory of large scale systems, illustrating on agriculture center planning

01 p0078 A73-11070
Analysis of an altitude control system of a low flying vehicle.

01 p0075 A73-11195
Analysis of non-linear systems defined by their response to arbitrary disturbances.

01 p0028 A73-11456
Transient curve construction for analysis and synthesis of automatic control systems with asymmetrical nonlinearities, comparing with harmonic linearization

02 p0149 A73-12342
Study of the nonstationary characteristics of a doubled system with an unreliable servicing device

02 p0188 A73-12588
Inherent limitations in digital incremental oscillator-analyser systems for mechanical vibration testing.

02 p0171 A73-12610
Rocket nozzle design and analysis techniques, considering requirements for high energy propellants, multiple pulse operation and long duration high temperature exposure

03 p0358 A73-13480
[AIAA PAPER 72-1190]

- A Bayes analysis of availability for a system consisting of several independent subsystems. 03 p0336 A73-13732
- Book on linear optimal control theory covering systems analysis, state reconstruction, stochastic nature and feedback control 03 p0286 A73-13992
- Behavior of the periodic surface for a periodically perturbed autonomous system and periodic solutions. 04 p0469 A73-14665
- Failure diagnostics in mathematical simulators of automatic control systems. 04 p0430 A73-15209
- System time domain simulation computer aided analysis program for communication systems, presenting mathematical and functional models 04 p0425 A73-15459
- Contribution to the analysis and conception of satellite stabilization systems based on ion propulsion 04 p0505 A73-15737
- The concept of an SST Oceanic Computer Clearance System. 05 p0595 A73-16621
- On the decomposition of a dynamical system into non-interacting subsystems. 05 p0591 A73-16824
- A critique of remote sensing evaluation techniques. 05 p0571 A73-17129
- Supervised and unsupervised category identification and classification systems consistency with ERTS satellites high rate multispectral data requirements 05 p0572 A73-17142
- The maximum principle in the identification of distributed-parameter systems 05 p0562 A73-17283
- On the dynamics of randomly excited nonlinear systems. 06 p0715 A73-17393
- SAM-D system for field army forces to provide air defense against advanced tactical aircraft, discussing equipment, performance, cost reduction and combat readiness [AIAA PAPER 73-65] 06 p0755 A73-17634
- Technical and economical analysis of various QSTOL concepts [DGLR PAPER 72-055] 06 p0647 A73-17675
- Decoupling in a class of nonlinear systems by state variable feedback. [ASME PAPER 72-AUT-V] 06 p0679 A73-17725
- Globally equivalent representations for reciprocal stationary nonlinear systems in equilibrium or steady state conditions, considering electric circuits and thermodynamic system examples 06 p0716 A73-17993
- A program for the analysis and design of general dynamic mechanical systems. [AD-75496] 06 p0671 A73-18063
- Outline of a new approach to the analysis of complex systems and decision processes. 06 p0671 A73-18622
- Hawaii International Conference on System Sciences, 6th, University of Hawaii, Honolulu, Hawaii, January 9-11, 1973, Proceedings. [AD-75756] 06 p0681 A73-18801
- Matrix exponential series approach to distributed parameter systems. 06 p0719 A73-18803
- An identification of time varying linear system without a priori information on variation of system parameters. 06 p0681 A73-18812
- Properties of linear time-invariant multivariable systems subject to arbitrary output and state feedback. 06 p0682 A73-18865
- Equations of motion for mechanical system with imposed servo couplings, discussing Gauss variational principle applicability for system analysis 07 p0851 A73-19128
- On parameter identification for distributed systems using Galerkin's criterion. 07 p0804 A73-19130
- The role of basic research in the total R&D process. 07 p0923 A73-19185
- Monograph - System analysis of the air-ground transportation interface problem at Bangkok International Airport. 07 p0808 A73-20382
- System identification of vibrating structures: Mathematical models from test data; Proceedings of the Winter Annual Meeting, New York, N.Y., November 26-30, 1972. 07 p0915 A73-20426
- Engineering systems structure and parameter identification using transfer function, learning model and nonlinear filtering 07 p0796 A73-20427
- Dynamic system model identification computational considerations, discussing equation error methods based on regression analysis, maximum likelihood estimates and gradient dependent algorithms for optimization 07 p0845 A73-20428
- Methods and application of system identification in shock and vibration. 07 p0916 A73-20429
- Identification of large structures using data from ambient and low level excitations. 07 p0916 A73-20431
- The state of the art of system identification of aerospace structures. 07 p0916 A73-20432
- Topologies for neutral functional differential equations. 07 p0845 A73-20493
- Optimal estimation of operator-valued stochastic processes and applications to distributed parameter systems. 07 p0805 A73-20580
- Frequency response of a dynamic system with statistical damping. 08 p0950 A73-20715
- Derivatives of eigenvalues and eigenvectors in non-self-adjoint systems. 08 p0983 A73-20728
- Systems analysis applied to a hybrid computer simulation of a missile reentering the atmosphere. 08 p0941 A73-20825
- Comparative study of methods of analysis of nonlinear systems subjected to random input 08 p0938 A73-20969
- Scalar and block decoupling of time varying and invariant linear multivariable control systems, discussing sufficiency conditions, state estimation and order reduction possibility 08 p0950 A73-21089
- Nonlinear system analysis based on Fokker-Planck equation, simplifying solution sequence for steady state or variance of states combination 09 p1111 A73-22114
- Computer assisted instruction for commercial programmer and systems analyst education and training, discussing government use, pretest importance and future developments 09 p1168 A73-22222
- Annual Allerton Conference on Circuit and System Theory, 10th, Monticello, Ill., October 4-6, 1972, Proceedings. 09 p1067 A73-22226
- Mathematical properties of and optimization methods for bandlimited function systems, discussing applications to engineering problems 09 p1051 A73-22491
- A reliability and comparative analysis of two standby system configurations. 09 p1112 A73-22643
- Operational methods for analysis of discontinuous systems with multiple lumped parameter attachments and concentrated forces, obtaining steady state closed form solutions 09 p1159 A73-22648
- Concatenated and hybrid coding system performance and implementation complexity for moderate speed deep space communication 09 p1056 A73-23401
- Intelsat communication satellites global network analysis, investigating technical factors affecting design options 09 p1059 A73-23436
- State-of-art review in identification, state estimation and decision processes for time variant systems, discussing parametric, nonparametric, static and dynamic models 10 p1197 A73-23635
- Manned vehicle systems analysis techniques application to manual approach-to-landing phase of aircraft flight, developing analytical control model 10 p1247 A73-24011
- Analysis and synthesis of automatic control systems with controlled converters. 10 p1198 A73-24019
- Applications of symbolic computing methods to the dynamic analysis of large systems. 10 p1192 A73-24029
- On the application of the method of decoupling of motions to the analysis and synthesis of nonlinear systems. 10 p1199 A73-24031
- Model reduction of multivariable control systems by means of matrix continued fractions. 10 p1200 A73-24046
- The methods of time-variable systems analysis based on new trends in theory of these systems. 10 p1200 A73-24047
- Estimation theory and system state and parameter identification, developing algorithms for optimum linear sequential and nonlinear filters 10 p1200 A73-24051
- A structural model of random processes and its invariant properties 11 p1340 A73-25007
- Efficiency estimates of methods for analyzing the precision of nonlinear control systems 11 p1342 A73-26094
- Regional airport systems study for San Francisco bay area, discussing commercial and general aviation future needs, environmental and economic aspects and alternative options 11 p1454 A73-26125
- Time-related behavior of causal, anticausal, memoryless and crosscausal nonlinear control systems modeled as operator on group-valued function space 11 p1391 A73-26366
- Stagnation conditions in systems with Coulomb friction 11 p1400 A73-26451
- Rational methods for controlling multistable elements on the basis of an analysis of the preferential domains of steady states 12 p1482 A73-26774
- Automatic control system components optimization for minimal cost, demonstrating algorithm efficiency for servosystem 12 p1482 A73-26775
- Principle of virtual work in the dynamics of systems having variable mass solids for constitutive elements 12 p1523 A73-27102
- Asilomar Conference on Circuits and Systems, 6th, Pacific Grove, Calif., November 15-17, 1972, Conference Record. 12 p1483 A73-27151
- Italian contributions to present aerospace activities; Conference, 2nd, Turin, Italy, June 9, 10, 1972, Proceedings 12 p1548 A73-27376
- Aerospace systems evaluation and optimization via systems analysis, discussing capability, dependability and availability and cost 12 p1561 A73-27384
- Correlation analysis of systems with stochastic inertial elements. 12 p1484 A73-27458
- Stability of coupled systems of nonlinear differential delayed-argument equations 12 p1525 A73-27947
- Numerical study of the stochasticity of dynamical systems with more than two degrees of freedom. 13 p1648 A73-28425
- Airport planning trends and engineering, discussing systems analysis, pavement design, modular terminal facilities, costs and economic efficiency 13 p1598 A73-29111
- Controllability of discrete bilinear systems with bounded control. 14 p1739 A73-30510
- Modelling and identification theory - A flight control application. 14 p1739 A73-30777
- Some results on the abstract realization theory of multilinear systems. 14 p1740 A73-30781
- Algebraic Lie structure theory of bilinear systems in terms of controllability, observability and equivalent realization 14 p1771 A73-30783
- Control systems synthesis via digital computer techniques, describing numerical optimization procedure and analog simulation method 14 p1730 A73-30921
- Multi-parameter sensitivity analysis of linear dynamic systems through the second method of Liapunov. 15 p1854 A73-31632
- Multivariable linear passive systems 15 p1900 A73-32087
- French monograph - Contribution to the study of systems with periodically variable parameters in time, intended for the continuous amplification of signals of weak amplitude. 15 p1847 A73-32588
- Digital simulation of physical systems using CSMP. 16 p1985 A73-33129
- Integral transform theory for derivation of compound binomial beta, uniform, and gamma distributions with applications to series-parallel systems reliability determination in manufacturing 16 p2020 A73-33604
- Book - Methods of nonlinear analysis. Volume 2. 17 p2200 A73-34453
- Book - Statistical design and analysis of engineering experiments. 17 p2200 A73-34456
- The application of system analysis techniques for the solution of complex helicopter crew station design problems. [AHS PREPRINT 723] 17 p2105 A73-35064
- Monte Carlo simulation on CRT display for training and learning system reliability and early decision effects on life cycle cost effectiveness 17 p2140 A73-35261
- Systems engineering at the Jet Propulsion Laboratory. 17 p2258 A73-35574
- Book - Graph theory in modern engineering: Computer aided design, control, optimization, reliability analysis. 17 p2132 A73-35600
- System error analysis and algorithms for a strap-down navigation system. 19 p2452 A73-38058

SYSTEMS COMPATIBILITY

The properties of bond graph junction structure matrices. 19 p2460 A73-38083

Probabilistic automata minimization for system states reduction by deterministic matrix method 19 p2408 A73-38564

Nonlinear control systems analysis, discussing phase space method, Taylor-Cauchy transform, Volterra functions, Liapunov stability, Popov-Kalman-Yakubovich theorems and limit cycle oscillations 20 p2592 A73-38691

Approximate methods for analysis and synthesis of nonlinear systems 20 p2592 A73-38692

Intrasystem electromagnetic compatibility analysis program. 20 p2528 A73-38771

Information content subsetting of highly correlated error sources. [AIAA PAPER 73-867] 20 p2586 A73-38805

Russian book - Applied mathematics and cybernetics. 20 p2541 A73-38977

Multiple queueing system of control plants, determining optimal order and initiation moments for minimized total time for all requests 20 p2530 A73-38989

Resource exchange and allocation /a generalized thermodynamic approach/. II 20 p2629 A73-39351

Quasi-dynamic system with eliminable generalized coordinates to define pseudo-degrees of freedom, identifying characteristics 20 p2594 A73-39537

A survey of satellite-based systems for navigation, position surveillance, traffic control and collision avoidance. 21 p2736 A73-40052

BMD requirements for phased array radars. 21 p2651 A73-40644

Russian book - Introduction to the statistical dynamics of systems with possible disturbances. 21 p2669 A73-40775

Russian book on accuracy of automatic systems using digital computers as control devices covering analysis and synthesis, stochastic inputs, system errors and operator methods 21 p2658 A73-41282

Specific problems of the dynamics of composite systems 21 p2788 A73-41603

Russian book on radio telemetry systems analysis and theory covering analog and digital data, signal processing, algebraic and trigonometric polynomials and discrete representations 22 p2824 A73-41879

Analysis of a damped, non-linear, non-autonomous system. 22 p2887 A73-42621

Development of pilot-in-the-loop analysis. [AIAA PAPER 72-898] 22 p2817 A73-43110

Performance criteria selection for complex system parameter optimization based on minimum deviation from extremal values 23 p2963 A73-43737

Automorphism groups of W algebras operating in Hilbert space with application to noncommutative dynamic systems analysis and ergodic theory 23 p2999 A73-44102

Frequency methods for simulation, analysis and identification of multiply-connected dynamic systems with delay 24 p3074 A73-45097

SYSTEMS COMPATIBILITY

A standard format for mathematical models of fluid power systems. 02 p0132 A73-12001

Verification of a comprehensive thrust chamber compatibility model for liquid rocket engines. [AIAA PAPER 72-1078] 03 p0354 A73-13401

Technology for man 72; Proceedings of the Sixteenth Annual Meeting, Los Angeles, Calif., October 17-19, 1972. 05 p0542 A73-16701

Feedback control system transfer function matrix synthesis, determining design specifications for required compensation filters from compatibility conditions 10 p1200 A73-24049

Recent materials compatibility studies in refractory metal-alkali metal systems for space power applications. 11 p1310 A73-26005

German command station for Helios solar probe, discussing antenna design, transmitter parameters, back-up operation and compatibility with deep space network [DFVLR-SONDDR-263] 13 p1598 A73-29275

Bit synchronized discrete address radar beacon system with ground based U.S. civil interrogator complex for compatibility with ATC and aircraft operator services 14 p1772 A73-29882

Payload/launcher radio compatibility, discussing RF link parameters choice, terminal devices quality and test schedule 14 p1742 A73-30113

Aircraft noise consideration for environmental compatibility, airport development, short haul and supersonic air transport and legislation and regulation problems [AIAA PAPER 73-795] 19 p2387 A73-38368

A rational basis for determining the EMC capability of a system. 22 p2823 A73-41802

SYSTEMS DESIGN

U SYSTEMS ENGINEERING

SYSTEMS ENGINEERING

NT COMPUTER SYSTEMS DESIGN

Minicomputer based CAMAC modular system for astronomical telescope instrumentation, discussing hardware and software interfaces, squad scaler, photoelectric photometer, Michelson interferometer and multichannel spectrometers 01 p0019 A73-10547

Programming and correcting control effects for prescribed interrelationship between variable states of dynamic control, noting system synthesis for programmed motion 01 p0027 A73-10667

Synthesis of a magnetoelastic control medium for stabilization of hydrodynamic flows 01 p0084 A73-10669

Wiener-Kolmogoroff optimal filtration theory for synthesis of linear stabilization systems under steady random external perturbations, noting control optimality conditions 01 p0028 A73-10670

A complex approach to flight vehicle control system designs 01 p0074 A73-10673

Synthesis of a multidimensional automatic optimization system with constraints 01 p0028 A73-10674

Automatic search system synthesis for linear programming, using gradient method and logic operations for system optimization 01 p0028 A73-10675

Algorithms for phase vector coordinates calculation of servomechanism, using measuring instrument data as starting information 01 p0028 A73-10676

Future optical communication systems problems, potentialities and development prospects, considering bandwidth, laser modulation, directionality, fiber transmission, reception, detection, power and efficiency 01 p0018 A73-11066

Sensitivity analysis method application to spacecraft thermal environment control system design, determining mathematical model input parameters uncertainty effects on temperature determination 01 p0123 A73-11143

Thermal requirements considerations for all components and systems in initial design phase of spacecraft to obviate need for full scale tests 01 p0110 A73-11145

Optimization study of the satellite broadcasting system for television. 01 p0018 A73-11180

Experimental satellite for attitude control. I - System design. 01 p0111 A73-11188

The optimum allocation of redundancy - An application of mathematical programming to system design. 01 p0071 A73-11199

Bell Laboratories optical communications research and development on lasers, transmission media, principles, methods and components for systems 01 p0060 A73-11212

Measuring equipment for multipoint data acquisition and recording, noting modular design of party-line system with programmed data processing 01 p0054 A73-11398

The system approach to the design of engineering systems from the standpoint of reliability and efficiency 02 p0145 A73-11547

TV satellite system feasibility and design study for Germany, discussing technical and economic aspects [DGLR PAPER 72-051] 02 p0140 A73-11664

Design and model tests for a 5 Tesla superconducting saddle magnet. 02 p0132 A73-11837

Aircraft fault isolation based on pattern of cockpit indications - A human factors approach. 02 p0136 A73-11857

System design, broadband construction and tests of slope reversal video processor based on tapped delay line estimation with timing discriminator 02 p0167 A73-11957

Lunar laser ranging system for experimental data acquisition, discussing preliminary design, SNR, photodetection method and data processing 02 p0141 A73-12245

Design point characteristics of a 500 - 2500 watt isotope-Brayton power system. 03 p0252 A73-13388

[AIAA PAPER 72-1059] A receiver design for the ATS-F radio beacon experiment. 03 p0275 A73-13600

Application of geometric decoupling theory to synthesis of aircraft lateral control systems. 03 p0250 A73-13702

Multichannel communication system in adaptive system with automatic channel selection based on random parameter extremum criterion for maximum usage time of extremal channel 03 p0278 A73-14000

Silicon solar cell design, describing handbook organization and derivation of design curves and data tables 03 p0254 A73-14200

Annual Allerton Conference on Circuit and System Theory, 9th, Monticello, Ill., October 6-8, 1971. Proceedings. 03 p0286 A73-14476

An improved design technique for parameter adaptive control systems. 03 p0286 A73-14480

Computer-mediated human communications in an air traffic control environment A preliminary design. 03 p0340 A73-14658

Signal relay systems using large space arrays. 04 p0415 A73-14990

Quadrature amplitude-shift key satellite communication feasibility based on SNR and transmitter power efficiency comparison with multiphase-shift key system 04 p0420 A73-15411

Radio set design requirements for communications link between meteorological sensor platforms and spacecraft in Geostationary Operational Environmental Satellite System 04 p0421 A73-15432

System design, hardware and software of RF interference measurement experiment regarding microwave frequency optimal sharing between ATS-F satellite and terrestrial relay telecommunication 04 p0422 A73-15460

Design and realization of microthruster temperature control subsystems - Optimization through refinement of a mathematical model 04 p0489 A73-15735

Prototype data processing system design for automatic correlation of earth resources image data collected from remote sensors and grating vehicle platform forms 04 p0426 A73-15776

Nonlinear heat transfer systems design optimization based on physical properties cost functionals, presenting geometric programming method [ASME PAPER 72-WA/HT-15] 04 p0519 A73-15833

Analog simulation and design of single- and multiple input/output model reference adaptive systems, using hyperstability concept [ASME PAPER 72-WA/AUT-13] 04 p0432 A73-15881

Allowance for the correlation of factors in the method of priorities for electrical system optimization. 05 p0560 A73-16272

Synthesis of an optimal discrete control system in the presence of control delay 05 p0560 A73-16295

Book - Management of engineering design. 05 p0642 A73-16351

Aircraft and spacecraft guidance and remote automatic control of moving objects, using calculus of variations for systems synthesis 05 p0560 A73-16402

Synthesis of optimal control problems with allowance for a prescribed reliability 05 p0561 A73-16416

Statistical synthesis of optimal pulsed control systems for spacecraft while taking into account system structural constraints 05 p0595 A73-16419

Communication satellite technology development, discussing INTELSAT and Russian Orbita systems, spectrum and orbit utilization, modulation, multiplexing, electron devices, radiation environment and power generation 05 p0550 A73-16604

Computerized ATC automation program, considering system management, hardware, software and test facilities problems 05 p0595 A73-16619

Hydraulic and flight control system for Space Shuttle Orbiter. [SAE PAPER 720838] 05 p0537 A73-16630

The use of bivariate distributions in achieving anthropometric compatibility in equipment design. I, II. 05 p0543 A73-16702

Work requirements test program for operator proficiency in tasks analogous to aircraft piloting under difficulty variation, deriving workload capability limits 05 p0544 A73-16722

Computer communication networks with programmable concentrators for combining multiple terminals, discussing structure, message handling and transmission, routing and reliability
05 p0551 A73-16805

Computerized airlines reservations systems with real time conversational interactive characteristics, discussing initial design, simulation, measurement, stability, reliability and data processing techniques
05 p0551 A73-16806

Optimal flight control system design for aircraft with large flight envelopes, using optimal control theory with limited measurement feedback
[AIAA PAPER 73-159] 05 p0535 A73-16906

Factor of fuel pyrolysis in injector design.
05 p0606 A73-17109

Synthetic aperture SLAR systems and their application for regional resources analysis.
05 p0578 A73-17133

Method for planning systems with prescribed design reliability
06 p0670 A73-17857

Synthesis of statistically optimal multiloop control systems containing essentially nonlinear elements.
06 p0679 A73-17955

Automation of reliability evaluation procedures through CARE - The computer-aided reliability estimation program.
06 p0670 A73-18058

A cellular processor for task assignments in polymorphic, multiprocessor computers.
06 p0671 A73-18061

Annual Electro-Optical Systems Design Conference, 4th, New York, N.Y., September 12-14, 1972, Proceedings of the Technical Program.
06 p0693 A73-18276

Modulated laser system application categories in tabular and pictorial summaries, considering ranging, reconnaissance, tracking, guidance, weapons, navigation, data processing, display and controlled fusion
06 p0700 A73-18292

Electro-optical laser beam deflector with lithium niobate for low resolution and high speed operation, discussing system design, construction and tests
06 p0700 A73-18296

Dc servomotor transfer function equalization, noting stability conditions for linear system design
06 p0680 A73-18380

Least square approach for system reliability optimization.
06 p0681 A73-18524

Hawaii International Conference on System Sciences, 6th, University of Hawaii, Honolulu, Hawaii, January 9-11, 1973, Proceedings.
AD-757566 06 p0681 A73-18801

Suboptimal guidance for attitude angle constrained flight trajectories.
06 p0721 A73-18825

Descriptions and plans in an interactive robot simulation system.
06 p0672 A73-18891

Preliminary study for the design of a satellite thermal control heat pipe.
07 p0918 A73-18913

Spacecraft-borne optical components and systems design and operational requirements, considering thin film filters and mirrors, detectors, diffraction gratings and materials
07 p0821 A73-18978

Two-level computer system with main and display processors as scale working model for semiautomatic digital ATC en route control
07 p0796 A73-19183

High-frequency converter for power supply applications.
[IEEE PAPER 17,3] 07 p0779 A73-19363

Pioneer Jupiter spacecraft magnetic field control with periodically updated magnetic model for tradeoffs in subsystem moments within allowed magnetic budget
[IEEE PAPER 41,4] 07 p0905 A73-19364

Lubricants thermophysical properties effects on gas turbine engine design, considering thermal stability, vapor pressure, autoignition, load capacity and bearing life
07 p0843 A73-19563

Economical system design for remote data acquisition.
07 p0824 A73-19948

Stochastically optimal terminal control system synthesis for loss function dependence on finite phase coordinates of dynamic system, considering soft landing of flight vehicle
07 p0805 A73-20037

One dimensional elastoplastic system optimal design by stochastic programming, determining limiting stresses and random load distribution
07 p0914 A73-20151

System modeling and optimal design of a Mars-roving vehicle.
07 p0906 A73-20593

An approximate method for the synthesis of optimal control of distributed systems.
07 p0806 A73-20596

System considerations for a large astronomical space telescope.
08 p0969 A73-21728

The use of image quality criteria in designing a diffraction limited large space telescope.
08 p0969 A73-21730

Laser interferometric alignment sensor for the large space telescope /LST/.
08 p0970 A73-21732

Some design aspects of a multiple-mirror telescope.
08 p0970 A73-21739

Simultaneous design of 24 inch telescope and computer control system, discussing interface and software development
08 p0942 A73-21754

An algorithmically and physically oriented design approach. I - Problems analysis
09 p1087 A73-21900

Computer systems configurations for design and engineering, considering graphic and conversational capability and cost and time reduction
09 p1168 A73-21949

Fighter aircraft survivable flight control system design and flight test philosophy, present status and trends, considering fly-by-wire and power-by-wire systems
09 p1030 A73-22177

Maintenance and repair planning and control of complex series-parallel and hierarchical branched systems with discrete sampling of operational status
09 p1064 A73-22553

Design and development of a lightweight flexible solar array compatible with mass production techniques.
09 p1036 A73-22813

Satellite solar power station systems engineering study, examining basic concept technical and economic feasibility
09 p1154 A73-22814

Rocket motor, Dart vehicle, booster and launcher design and instruments and payload description for Super Loki meteorological rocket systems
[AIAA PAPER 73-303] 09 p1156 A73-23222

Development of an actinium fueled thermionic converter.
09 p1038 A73-23282

Equipment for casting directionally solidified parts.
09 p1089 A73-23294

Communication system for digital image processing services over Advanced Research Project Agency computer network, describing hardware facilities and software capacity
09 p1061 A73-23390

Phase locked bit synchronization design tradeoffs between acquisition and noise performance, considering frequency tolerance of decision-directed loop with nonreturn-to-zero input
09 p1056 A73-23403

Microprogrammable processors applied to telemetry processing systems.
09 p1057 A73-23411

Design philosophy and operation of hardware and data flow of TELFILE real time multiprogrammed telemetry system, discussing support of Minuteman III Weapons Systems
09 p1057 A73-23415

Microwave landing system /MLS/ with Doppler scanning technique for aircraft guidance precision improvement over standard VHF/UHF ILS, detailing five-year development plan
10 p1246 A73-23652

Short haul air travel with Intermodal Automated Transfer system for integrating ground transportation to allow passenger to stay in seat from origin to destination
10 p1174 A73-23653

High volume wideband PSK system design for minimal sidelobe, calculating signal number relationship to maximum sidelobe level of cross correlation and autocorrelation
10 p1187 A73-23733

Fluidic system design based on miniaturized modular high power fluidic logic elements, discussing applications in production process control
10 p1177 A73-23761

Pulsed GaAs illuminators for night-vision systems.
10 p1216 A73-23785

Visible and infrared sensor arrays for imaging systems.
10 p1216 A73-23787

Wide view field laser target designation seeker system with photodetector for multiple returns discrimination, discussing sensor broadband model, signal processing and design feasibility
10 p1216 A73-23788

Holographic read-only memory with high speed and density optical storage on low-cost changeable media, discussing feasibility model design, construction and test
10 p1216 A73-23796

International Federation of Automatic Control, World Congress, 5th, Paris, France, June 12-17, 1972, Proceedings. Part 2 - Transportation, aeronautics and space, ship automation, and control components. Part

3 - Ecology and systems engineering; Large scale, sensitivity, optimization and adaptation theory. Part 4 - Education, feedback, regulators, linear and nonlinear systems; Identification, differential games, discrete and stochastic systems.
10 p1198 A73-24001

Mariner Mars 1971 orbiter spacecraft with sun-Canopus orientation as references, discussing mission objectives, trajectory characteristics, orbital operations, scientific instruments and system design
10 p1276 A73-24004

Vehicle coordinate-parametric control problems and some solution methods.
10 p1198 A73-24007

Realization of digital differential analyser on the basis of multifunction memory units.
10 p1198 A73-24018

A hybrid motor - A high-speed and accuracy final actuator/automatic control element/.
10 p1177 A73-24025

The design of optimally parameter insensitive control systems.
10 p1199 A73-24030

On the application of the method of decoupling of motions to the analysis and synthesis of nonlinear systems.
10 p1199 A73-24031

Optimization methods in control systems design, discussing nonlinear and linear programming, variational and maximum principles, dynamic programming and game and graph theories
10 p1242 A73-24032

Feedback control system transfer function matrix synthesis, determining design specifications for required compensation filters from compatibility conditions
10 p1200 A73-24049

Extension of the principle of variable structure systems to the case where the slip hypersurface is nonlinear - Application to suboptimal control
11 p1341 A73-25574

An integrated system for space station power, life support, and propulsion.
11 p1311 A73-26009

A 25 kW solar array/battery design for an earth-orbiting space station.
11 p1311 A73-26010

Synthesis of time-optimal control for linear systems and the minimal-time Lyapunoff function.
11 p1342 A73-26225

Questionnaire approach for technical diagnostics problem formulation covering hardware failure analysis coding, combinational switching device synthesis and optimal program construction
12 p1482 A73-26752

Hybrid type discrete jet-membrane relay system technology and design for discrete signals transformations
12 p1460 A73-26770

Some methods of assuring the stability of certain classes of nonlinear systems by the intentional use of an additional nonlinearity.
12 p1517 A73-27156

Traffic analysis by statistical tests for batch mode operated digital computer network design, considering user habits, and interarrival, waiting and partition times
12 p1475 A73-27159

Signal processing in the Air Traffic Control Radar Beacon System.
12 p1469 A73-27165

Shock absorbing-vibration insulating viscoelastic systems design under singular influence function assumption, determining ranges of parameters change
12 p1516 A73-27177

Data acquisition process to plan and engineer air traffic system, considering design aspects and piecemeal evolution
12 p1522 A73-27362

Status of funded improvements to the National Aviation System and planned improvements not yet funded.
12 p1561 A73-27363

National aviation system improvement via cost effectiveness, considering FAA facilities and equipment program, ATC automation and terminal aids
12 p1522 A73-27365

Synthesis of searchless self-adjusting systems based on the root locus method. I.
12 p1484 A73-27460

A confidence estimate of the reliability of a system from the results of tests of its components
12 p1503 A73-27618

Mobile satellite communication systems constraints imposed by international institution disagreements on management, procurement and operation, considering US and European conflicts on Aerosat project
12 p1471 A73-27653

A planning study for a multi-purpose communications satellite serving northern Canada.
12 p1471 A73-27657

Message organisation in the ground segment of an aeronautical satellite system.
12 p1472 A73-27668

Calculation of single phase pressure drop in heat exchangers considering the change of fluid properties along the flow path.

12 p1559 A73-27694

Digital computer aided control systems design, discussing components dynamic behavior mathematical modeling and control processes simulation

12 p1476 A73-27872

Russian book - Design of structural elements with the use of electronic digital computers.

12 p1556 A73-27923

Remote sensor dynamic images produced by stereo systems, discussing line-by-line and section-by-section orientation methods and triple channel recording scheme

12 p1500 A73-27956

Thermal/electrical design of spaceborne microelectronic components.

13 p1588 A73-28046

Helicopter automatic flight control system design, testing and development, noting stability and control augmentation and attitude retention units

13 p1656 A73-28903

Long-life light weight reliable fuel cell development for long term space missions power supplies, describing system components and construction materials

13 p1573 A73-29596

Oceanic ATC by application of aeronautical satellite technology, discussing system design requirements, performance evaluation and international program

14 p1773 A73-29888

Determination of some characteristics of random processes describing the operation of transient action systems with allowance for reliability

14 p1730 A73-30037

Theoretical and practical design aspects on spacecraft propellant and pressurant loading systems.

14 p1742 A73-30107

Russian book on aircraft, rocket and spacecraft control systems design methods covering ground and on-board systems synthesis, performance estimates, system effectiveness, etc

14 p1773 A73-30353

Application of human engineering principles and techniques in the design of electronic production equipment.

14 p1722 A73-30497

A minimization algorithm for the design of linear multivariable systems.

14 p1769 A73-30504

Structural requirements for decoupling, disturbance insensitivity and parametric insensitivity, considering synthesis procedures for multivariable dynamic regulators

14 p1739 A73-30779

A high-accuracy digital star tracker for advanced planetary missions.

15 p1907 A73-31356

Viking 75 Mars lander spacecraft mortar system design and environmental requirements, stressing manufacturing and qualification tests and parachute ejection

[AIAA PAPER 73-458]

15 p1827 A73-31444

Parachutes computer aided design and performance analysis system development and operation, presenting information storage and retrieval tasks mechanics

[AIAA PAPER 73-484]

15 p1829 A73-31466

Book - Interorganizational decision making.

15 p1960 A73-31577

Inlet system design procedures and wind tunnel facility modifications allowing for verification on large scale models at Mach 4.5

15 p1824 A73-31743

Self-reconfiguring computer complexes for A.T.C. Systems.

15 p1849 A73-32439

French VOR system with single type equipment for operation on site at performance levels to meet ICAO standards, emphasizing antenna design

15 p1909 A73-32453

Aircraft flight control head-up display system design, equipment installation particulars, performance tests and merits evaluation

15 p1831 A73-32508

Book - MOS integrated circuits: Theory, fabrication, design and systems applications of MOS LSI.

15 p1852 A73-32579

GaAs and GaAlAs semiconductor injection lasers, discussing system design and applications for rangefinding, illumination and communication with peak power and repetition rate requirements

16 p2023 A73-32866

Specific Behavior Objective approach to airline flight simulation, featuring duplicate training elimination and education time reduction

16 p1995 A73-33202

Simulation in the design of automated air traffic control functions.

16 p2035 A73-33419

Time dependent stress-strength models for non-electrical and electrical systems. I.

16 p2020 A73-33621

Statistical and probabilistic MTBF models for parts, sockets and systems reliability

16 p2020 A73-33628

System engineering aspects of the man-machine interface.

16 p1975 A73-33645

Single and dual path propagation at 18 GHz with application to the design of digital radio relay systems.

16 p1981 A73-33703

Atmospheric attenuation measurements via solar microwave radiometer yielding excess attenuation statistics for communications systems planners

16 p1982 A73-33722

Crossed field amplifier selection for application to pulsed radar transmitters, considering system operation effects, power supply regulation and droop limitation method

16 p1991 A73-33899

Man machine systems for flight safety, studying accidents, human factors in system design and implementation of personnel

17 p2113 A73-34078

Theory of optimal AGC system synthesis.

17 p2134 A73-34318

Aircraft microwave landing system development, including conventional system history and short-comings, program objectives and implementation schedule for ATC

17 p2208 A73-34611

Turbo and jet powered general aviation aircraft-borne weather/radar memory radar system with digital processing technique to eliminate direct view storage tube

[SAE PAPER 730316]

17 p2122 A73-34674

Integrated Propulsion Control System program.

[SAE PAPER 730359]

17 p2222 A73-34707

Prototype TDMA system design for Intelsat 4 satellite, discussing separate synchronization and data bursts transmission feature for service quality and reliability improvement

17 p2122 A73-34967

A simple yet theoretically based time domain model for fluid transmission line systems.

[ASME PAPER 73-FE-27]

17 p2153 A73-35021

A frequency response approach to flying qualities criteria and flight control system design.

[AHS PREPRINT 740]

17 p2105 A73-35073

Information transfer system of digital avionics system, examining signal reduction by baseband time division multiplexing and video distribution systems

17 p2138 A73-35230

Intrasystem electromagnetic compatibility analysis program.

17 p2131 A73-35251

Optimal modular redundancy over a set of configurations for attaining specified system availability and reliability requirements.

17 p2139 A73-35257

Time Division Multiple Access for the defense satellite communications system.

17 p2124 A73-35307

Book - Systems concepts: Lectures on contemporary approaches to systems.

17 p2258 A73-35572

The engineering of large-scale systems.

17 p2258 A73-35573

Systems engineering at the Jet Propulsion Laboratory.

17 p2258 A73-35574

A simulation study for the design of an air terminal building.

17 p2149 A73-35826

The evolution of location and data collection systems in the United States.

[AIAA PAPER 73-584]

18 p2372 A73-36076

Space shuttle solid rocket boosters mission and systems requirements, considering thrust vector control and staging/separation, electrical and recovery systems

[AIAA PAPER 73-606]

18 p2358 A73-36086

Book on mechanical reliability from engineering standpoint covering statistical probability, performance quality, systems design and manufacturer and user roles

18 p2321 A73-36970

Man-machine interface for controllers and end effectors.

19 p2397 A73-37325

Plasma accelerators design, discussing physical principles, acceleration techniques, plasma conductivity and optimization

19 p2466 A73-37353

U.S. instrument landing system performance improvements, considering terrain and weather effects, installation requirements, airport limitations, accuracy, reliability and maintainability

19 p2450 A73-37805

Simplification of navigation and flight control systems without compromising integrity.

19 p2452 A73-37826

Apollo Lunar Module environmental control system - Mission performance and experience.

[ASME PAPER 73-ENAS-28]

19 p2400 A73-37983

Design of decoupled multivariable control systems.

19 p2412 A73-38032

Modern control techniques applied to energy conservation flight control systems.

19 p2392 A73-38415

Design concepts for an earth resources data management system.

[AAS PAPER 73-151]

Minimum risk classification algorithms in automatic learning system design, applying to learning pulse signal receiver

20 p2521 A73-38599

International Conference on Communications, Seattle, Wash., June 11-13, 1973, Conference Record Volumes 1 & 2.

20 p2532 A73-38640

Future communication satellite technology improvement, market expansion and cost effectiveness considering foreign domestic, and international light-to-medium and high density systems

20 p2522 A73-38712

Design features of an unattended earth terminal for satellite communications.

20 p2522 A73-38712

TDMA system design for small satellite terminals.

20 p2528 A73-38767

Structure of self-organizing automated design systems and the processes of their functioning

20 p2569 A73-39398

Computer program using successive system reduction on basis of calculation of reliability of pure parallel and series arrangements

20 p2533 A73-39632

Microwave Landing System with air-derived sampled data and scanning narrow beam antennas for signal-in-space generation, discussing design requirements and performance test

21 p2735 A73-40046

Large telescope design, discussing optical telescopes efficiency as function of aperture, exposure time auxiliary instrumental parameters

21 p2703 A73-41245

Russian book on reliability optimization in complex automatic control system information transfer and processing covering performance criteria, noise immunity, error sources and types, etc

21 p2670 A73-41293

The RATAN-600 radio telescope

21 p2675 A73-41441

Design and analysis of an energy absorbing restraint system for light aircraft crash-impact.

[ASME PAPER 73-DET-111]

22 p2799 A73-42080

Russian monograph on signal transmission channel identification systems in statistical communications theory covering mathematical models, design principles, radio electronic systems, etc

22 p2827 A73-42600

Structural methods of multichannel systems synthesis with the aid of the graph theory

22 p2836 A73-42602

Computer-aided design of airport system plans.

[ASCE PREPRINT 2058]

22 p2839 A73-42867

Modeling methods for shock isolation systems for fragile equipment protection from HF effects generated by high loading rates and/or random multi-frequency input displacement signatures

22 p2927 A73-42920

The state space and transfer function approaches in practical linear multivariable systems design.

23 p2962 A73-43281

Synthesis of feedback systems with large plant ignorance for prescribed time domain tolerances.

23 p2962 A73-43282

Russian book on satellite attitude stabilization systems design covering gravity gradients, linear and nonlinear control laws, spin stabilization, high torque control moment gyros, etc

23 p3038 A73-43335

Systems engineering approach to pneumatic hybrid automatic/manual control system with fluid logical elements and reduced air consumption

23 p2943 A73-43413

The design of digital fluidic components and systems - A review.

23 p2945 A73-43433

Nonlinear regulator theory and an inverse optimal control problem.

23 p2963 A73-43820

Model reference adaptive control system design using Kalman-Yacubovich lemma in connection with Lure problem

23 p2964 A73-43827

Management and control of flight test programs of the Naval Air Systems Command.

23 p3050 A73-44056

Europa 2 Inertial Guidance System technology assessment covering design features, sensor, computer and interface units, first launch failure causes and need for improvements

24 p3108 A73-44694

Nonminimum-phase difficulties in multivariable control-system design.

24 p3074 A73-45258

SYSTEMS FOR NUCLEAR AUXILIARY POWER

U SNAP

SYSTEMS MANAGEMENT

Principles of organization and logistical support for systems of automating scientific investigations

04 p0424 A73-14823

- Computerized ATC automation program, considering system management, hardware, software and test facilities problems 05 p0595 A73-16619
- Space shuttle flight operations ground support systems for trajectory control and systems/mission management, discussing payloads data acquisition and transmission to user [AIAA PAPER 73-36] 06 p0755 A73-17620
- Bolt experiment processing network for data pretreatment, system management aid and accuracy study and feasibility demonstration of fast response time operational system 10 p1187 A73-23619
- Requirements of an economic approach to maintenance. 18 p2373 A73-37142
- Air traffic controller responsibilities and performance evaluation criteria development, discussing manager/monitor functions, field evaluation tests and training criteria 19 p2402 A73-38472
- Time, space, and energy management in the airways traffic control medium. 22 p2884 A73-42324
- The capabilities of government test facilities at the Air Force Systems Command. 23 p2966 A73-44065
- ## SYSTEMS STABILITY
- Equations of motion integral properties-based construction of Liapunov functions used to derive sufficient conditions for perturbed nonlinear system solution stability 01 p0075 A73-10090
- R-function numerical analysis method for motion stability criteria, developing algorithms for Liapunov function construction and controller design for conservative control system stability 01 p0076 A73-10096
- Reignition characteristics of low current a.c. TIG welding arcs. 01 p0055 A73-10115
- Generation and stability of subharmonic and modulated subharmonic oscillations in nonlinear systems. 01 p0076 A73-10303
- Stability of large-scale systems under structural perturbations. 01 p0070 A73-10322
- Iteration accuracy effect on optimal discrete control system synthesis and stability, applying to Zubov damping problem 01 p0027 A73-10591
- Instability nature in Gunn diode type system with negative differential conductivity, presenting expressions for oscillation threshold and gain 01 p0088 A73-10629
- Liapunov function for complex system motion stability analysis, noting stability criteria for subsystems satisfying Routh-Hurwitz conditions 01 p0076 A73-10668
- Optimal stabilization of nonlinear control systems for given region of initial perturbations, reducing optimal synthesis to moments problem 01 p0077 A73-10671
- Existence and stability of the secondary periodic solution figuring in Navier-Stokes type evolution problems [ONERA, TP NO. 1172] 01 p0033 A73-10780
- Stabilization of the relative equilibrium and steady motion of a mechanical system by partial dissipation forces 01 p0077 A73-10953
- Gyrostabilized systems stability analysis with allowance for elasticity, internal friction and electric circuits transient processes, examining steady motion under parametric disturbances 01 p0051 A73-10965
- Analysis of an altitude control system of a low flying vehicle. 01 p0075 A73-11195
- Control theory analysis of equilibrium state asymptotic stability of system with dry friction, applying to power driven gyrostabilizer 01 p0054 A73-11402
- Effects of controller dynamics on the stability of a class of optimal control systems. 01 p0028 A73-11518
- A linear approach to the analysis of a force control system incorporating a hydraulic pressure-ratio valve. 02 p0132 A73-12002
- Construction of Lyapunov functions for nonstationary systems containing memoryless nonlinearities. 02 p0193 A73-12123
- Construction of solutions and the application of the joining method to the solution of the Liapunov stability problem for a system of linear homogeneous differential equations with pi-periodic coefficients 02 p0193 A73-12189
- A new circle criterion for the stability of nonlinear control system. 02 p0149 A73-12346
- Amplitude-frequency and stability characteristics of parametric amplification by triple-frequency interaction in nonlinear nonautonomous system 02 p0147 A73-12491
- A method for phenomenological analysis of ecological data. 02 p0188 A73-12629
- Intergalactic ionized hydrogen in nearby groups of galaxies. 02 p0225 A73-12803
- Relativistic spheres of hadron gas with zero baryon number constructed from Hagedorn hadronic equation of state, considering sphere stability properties 03 p0370 A73-13211
- A graphical test for checking the stability of a linear time-invariant feedback system. 03 p0285 A73-13519
- Autooscillations in the directional hydro-mechanical servocontrol with play in the reaction linkage 03 p0252 A73-13771
- On the stability of steady-state response of certain nonlinear dynamic systems subjected to harmonic excitations. 03 p0393 A73-13792
- On the almost-sure sample stability of systems with randomly time-varying delays. 03 p0285 A73-13898
- Stability criteria for equal mass triple star systems, considering direct or retrograde revolution and outer periastron distance to inner semimajor axis ratio 03 p0376 A73-14271
- Large scale systems with linear and nonlinear subsystems and coupling connections, investigating connective stability under perturbations due to subsystem on-off participation 03 p0337 A73-14484
- Liapunov stability, boundedness and attraction conditions, using modified quantification theory 04 p0469 A73-14668
- Subharmonic generation and its implications in Gunn effect devices. 04 p0427 A73-15055
- Application of stochastic stability theory to model-reference systems. 04 p0430 A73-15215
- Stability of Richtmyer type difference schemes in any finite number of space variables and their comparison with multistep Strang schemes. 04 p0471 A73-15233
- Stability analysis of Riccati covariance equations of Kalman filter. 04 p0472 A73-15273
- Determination of root locus for nonlinear multi-variable system. 04 p0472 A73-15879
- [ASME PAPER 72-WA/AUT-21] 04 p0472 A73-15879
- On the stability of linear stochastic differential equations. 04 p0472 A73-15898
- [ASME PAPER 72-WA/APM-16] 04 p0472 A73-15898
- Applications of the theory of impulsive parametric excitation and new treatments of general parametric excitation problems. 04 p0476 A73-15903
- [ASME PAPER 72-WA/APM-6] 04 p0476 A73-15903
- Fredholm operator theory application to linear feedback system input-output stability in terms of origin encirclement counting in complex plane 05 p0561 A73-16488
- Invariance principle extended to bounded uncertain time-varying systems, deriving asymptotic Liapunov stability criteria with application to quaranteed cost control problems 05 p0590 A73-16492
- Linear time-invariant feedback systems with multiple inputs and outputs, deriving necessary and sufficient conditions for stable closed loop impulse response 05 p0561 A73-16493
- Couplings effect on Liapunov stability estimation of higher order linear nonstationary systems, using aggregation method 05 p0599 A73-17084
- Large-signal noise, frequency conversion, and parametric instabilities in IMPATT diode networks. 06 p0679 A73-17789
- Global asymptotic stability of two classes of control systems with pulse duration and pulse frequency modulations. 06 p0680 A73-17957
- Dc servomotor transfer function equalization, noting stability conditions for linear system design 06 p0680 A73-18380
- Describing functions, circle criteria and multiple-loop feedback systems. 06 p0680 A73-18444
- Periodic oscillations in feedback systems with combined pulse modulation. 06 p0680 A73-18518
- Absolute stability of nonlinear systems with a constraint on the derivative - Some extensions. 06 p0682 A73-18820
- Matrices, polynomials, and linear time-invariant systems. 06 p0719 A73-18863
- Absolute stability of nonlinear control systems with nonstationary nonlinearities and tachometric feedback 07 p0805 A73-20046
- Stability behavior of adapting and untrained random logic nets, enabling intelligent interaction with environment 07 p0786 A73-20400
- Analysis of the stability and periodic motions of nonlinear automatic pulsed systems by the root-locus curve method 07 p0806 A73-20636
- Stability of incompletely damped mechanical systems 08 p0104 A73-20780
- Mathematical model selection rules for stability studies of linear mechanical or passive electrical network systems with arbitrary degrees of freedom 08 p0987 A73-20787
- An instability theorem for certain nonlinear hyperbolic equations 08 p0984 A73-21488
- Frequency criteria for the absolute stability and instability of pulse-width modulated control systems 08 p0951 A73-21544
- Parametric instability of an electron beam modulated by an external electrostatic field 09 p1123 A73-21878
- Global asymptotic stability estimation for large scale systems of interconnected exponentially stable subsystems, using aggregated comparison and Liapunov function description 09 p1120 A73-22227
- On the control of linear systems using two level periodic output feedback. 09 p1067 A73-22231
- Periodic regime stability of two channel relay system as function of main channels identicalness and cross coupling symmetry, using Tsypkin method 09 p1063 A73-22340
- Construction of quality diagrams for transient processes in nonlinear systems 09 p1068 A73-22558
- Mathematical model of equilibrium and steady state stability of pulse frequency modulation feedback systems of second kind with time delay filters 09 p1069 A73-22723
- Liapunov vector functions in stability analysis of nonlinear dynamic distributed parameter, interconnected and multivariable systems 09 p1121 A73-22998
- A first-approximation theory of discrete nonautonomous stabilization systems 10 p1248 A73-23745
- Stabilization of linear dynamical systems with output feedback. 10 p1199 A73-24037
- Stability theory of dynamic large scale system under structural perturbations based on comparison principle and vector Liapunov functions 10 p1248 A73-24039
- The evaluation of the domain of attraction of nonlinear control systems with hybrid computing systems. 10 p1192 A73-24040
- New criteria for bounded-input-bounded-output and asymptotic stability of nonlinear systems. 10 p1199 A73-24041
- Study of recurrence relationships and their applications by the Laboratoire d'Automatique et de ses Applications Spatiales. 10 p1200 A73-24042
- The methods of time-variable systems analysis based on new trends in theory of these systems. 10 p1200 A73-24047
- Optimal stochastic linear systems with exponential performance criteria and their relation to deterministic differential games. 10 p1202 A73-24536
- Dispersion equation of parametric longitudinal LF instability of electromagnetic wave propagation in bounded electron beam in metallic waveguide 10 p1257 A73-24876
- Russian book on military application oriented automatic control systems design covering amplifiers, servo elements, stability, performance, optimization, and nonlinear and sampled data systems 10 p1203 A73-24972
- Converse theorems for Liapunov stability and boundedness of nonlinear discrete-time systems described by difference equations 11 p1389 A73-25186
- Nonlinear delay-differential control systems described by periodic functional differential equations with small real parameter, investigating asymptotic stability in Liapunov sense 11 p1390 A73-25190
- On the stability of amplifiers with amplitude modulation and overall contrareaction 11 p1341 A73-25575
- Transient characteristics of simple systems to modulated random noise. 11 p1398 A73-25703
- [ASME PAPER 72-APM-FFF] 11 p1398 A73-25703
- Equilibrium stability of liquid filled body with closed internal cavity partially filled with ideal homogeneous incompressible fluid under gravitation 11 p1401 A73-26470

Some methods of assuring the stability of certain classes of nonlinear systems by the intentional use of an additional nonlinearity.

12 p1517 A73-27156

Stability of nonlinear systems with a transformed argument

12 p1524 A73-27416

On the stabilization of relative equilibrium and steady-state motion of a mechanical system by partial dissipation forces.

12 p1524 A73-27529

Gyrostabilized systems stability analysis with allowance for elasticity, internal friction and electric circuits transient processes, examining steady motion under parametric disturbances

12 p1498 A73-27541

Analysis of the stochastic stability of pulsed control systems in the frequency domain

12 p1485 A73-27622

Integral manifold concept for stability analysis of nonlinear system oscillations, plotting resonance curve for quasi-linear autonomous system

12 p1525 A73-27792

Stability of gravitating systems with a quadratic potential. I - Methods of investigating the stability of systems with a limited phase volume: Vibration spectrum of the Maclaurin stellar disk

12 p1546 A73-27856

Nonsearch self-adapting identification systems

12 p1485 A73-27900

Stability of stochastic dynamical systems; Proceedings of the International Symposium, University of Warwick, Coventry, England, July 10-14, 1972.

12 p1519 A73-27920

Verification of the 'potential' work capacity of dynamic systems by a frequency-time technique

12 p1485 A73-27946

Stability of coupled systems of nonlinear differential delayed-argument equations

12 p1525 A73-27947

Auto-oscillations, stability at the origin, overall stability of nonlinear systems with distributed parameter

13 p1596 A73-28473

Other stability criteria for distributed and Gaussian stochastic systems with diagonal nonlinearity

13 p1596 A73-28564

Instability of equilibrium figures consisting of several isolated components rotating jointly

13 p1684 A73-29141

Determination of the absolute-stability domain of nonlinear time-lag systems

13 p1596 A73-29143

The sensitivity of nominally time-optimal control systems to parameter variation.

13 p1597 A73-29567

A first-harmonic method for nonlinear distributed-parameter systems subjected to deterministic or stochastic loads

14 p1738 A73-29707

Stability considerations for a Volterra integral equation with discontinuous nonlinearity.

14 p1769 A73-30403

A criterion for the bounded-input, bounded-output stability of time-varying nonlinear systems.

14 p1738 A73-30404

Nonlinear feedback systems and weakly stationary stochastic processes.

14 p1739 A73-30503

Frequency-domain criteria for stability of a class of nonlinear stochastic systems.

14 p1739 A73-30506

Necessary and sufficient conditions for stability for n-input, n-output convolution feedback systems with a finite number of unstable poles.

14 p1739 A73-30509

The infinite time quadratic cost problem for certain classes of infinite dimensional control systems.

14 p1770 A73-30758

Mathematical model of equilibrium and steady state stability of pulse frequency modulation feedback systems of second kind with time delay filters

14 p1740 A73-30956

The adiabatic stability of stars containing magnetic fields. I.

15 p1933 A73-31395

Performance/stability of midair recovery system with tandem parachute configuration, discussing gliding and nongliding systems

[AIAA PAPER 73-461]

15 p1827 A73-31447

Multi-parameter sensitivity analysis of linear dynamic systems through the second method of Liapunov.

15 p1854 A73-31632

Analysis of stability and periodic motions in nonlinear sampled-data systems by the root locus method.

15 p1854 A73-31690

Biological order, structure and instabilities in terms of irreversible thermodynamic processes, entropy, dissipative structures, randomness, abiogenesis, hierarchic organization, chemical reactions and molecular biology

15 p1835 A73-31824

Partial stability of mechanical systems, analyzing perturbed motion in vector form, using Liapunov functions

15 p1914 A73-32114

Hadamard theorem on wave propagation existence in elastic body with infinitesimal stability condition proved by linear elliptical partial differential equations systems theory techniques

15 p1914 A73-32120

The geometrical stability of non-linear normal modes in two degree of freedom systems.

15 p1955 A73-32167

Rayleigh-Ritz coefficient application in variational principle calculations of instability and flutter load of nonconservative systems

16 p2031 A73-32980

Altitude damping of space-stable inertial navigation systems.

16 p2034 A73-33403

Determining the stability of nonlinear systems.

16 p2033 A73-33699

Minimization of quadratic functionals in the presence of quadratic constraints and the necessity of a frequency condition in the quadratic criterion of absolute stability for nonlinear control systems

16 p2034 A73-34071

Russian book - Lectures on the theory of stability of the solutions of systems with an aftereffect.

17 p2211 A73-34224

Parametric instability of an electron beam modulated by an external electrostatic field.

17 p2215 A73-34302

Optimal observer techniques for linear discrete time systems.

17 p2144 A73-34361

Liapunov direct method extended to stability of nonlinear parabolic systems, noting application to Burgers equation

17 p2200 A73-34398

Stability of motion in a controlled system consisting of two elastically butted bodies one of which has cavities partially filled with a liquid

17 p2243 A73-34733

A procedure for investigating the Liapunov stability of nonautonomous linear second-order systems.

[ASME PAPER 73-APM-31]

17 p2201 A73-35044

Critical flow speed divergence in aeroelastic systems stability loss, discussing static analysis using partial differential equation

17 p2250 A73-35119

Book - Introduction to servomechanism system design.

17 p2110 A73-35275

Limit cycle stability determination for nonlinear system with single loop feedback, using describing function method and z transform

17 p2202 A73-35517

Frequency-time domain stability criterion for nonlinear negative feedback system with linear transfer function, using Zame positive operator theory

17 p2203 A73-35731

On stability of large-scale systems under structural perturbations.

17 p2213 A73-35827

Searchless self-adjusting identification systems.

18 p2294 A73-36752

Solving M. A. Aizerman's first problem of absolute stability of nonlinear systems on the basis of the general theory of root trajectories

18 p2337 A73-37025

Generalized Galerkin method for approximate solution of eigenvalue self-adjoint boundary value problems in stability analysis of mechanical distributed parameter systems

19 p2458 A73-37189

Qualitative analysis of the behavior of weakly coupled oscillators near the equilibrium position

19 p2458 A73-37191

Stabilization of multivariable systems with constant-gain output feedback.

19 p2413 A73-38046

On the stabilization of aided track pointing systems.

19 p2404 A73-38070

Instability of feedback systems containing several time-varying nonlinear amplifiers.

19 p2414 A73-38078

Nonlinear time-varying differential system stability and asymptotic stability study using equivalent inner product method, discussing global and regional stability

19 p2445 A73-38255

Threshold voltage stability improvement of p- and n-channel SNOS FET by annealing silicon nitride in oxygen or steam prior to gate deposition

19 p2471 A73-38451

Bifurcations and certain qualitative characteristics of a phase-locked automatic frequency control system with a second-order filter

20 p2535 A73-38979

Root trajectories method for stability analysis of two channel automatic control systems with antisymmetric and symmetric cross couplings

20 p2541 A73-38980

Investigation of the stability of solutions to a quasi-stationary system of linear differential equations with quasi-periodic coefficients

20 p2581 A73-38989

A general quadratic criterion for absolute stability of nonlinear automatic control systems and its application to sampled-data systems with pulse-width modulation

20 p2541 A73-38989

Russian book - Complex control systems.

20 p2541 A73-39030

Investigation of the transient process quality of automatic control systems with variable parameters using the method of the biased characteristic equation

20 p2541 A73-39030

Stability and dissipativity of control systems containing unsteady nonlinearities

20 p2542 A73-39040

Approximate methods for the mathematical description and analysis of processes controlling the spectral characteristics of random vector signals

20 p2542 A73-39040

Stability of gravitating systems with a quadrat potential. I - Systems bounded in phase space - Oscillation spectrum for a Maclaurin stellar disk.

20 p2608 A73-39233

Three-dimensional problem of the stability of fibers in a matrix in the presence of highly elastic strains

20 p2581 A73-39644

Dynamic systems stability under influence of white noise-Gaussian random processes, discussing optimal control, Markov processes, linear equations and vector fields

20 p2583 A73-39764

Bifurcation and stability of steady motions of complex mechanical systems

21 p2738 A73-40174

The stability of steady motions of systems with quasi-cyclic coordinates and the stability of mechanical equilibrium under the action of a magnetic field

21 p2738 A73-40177

Passive stochastic feedback stability. I - A general theory. II - Applications.

21 p2669 A73-40450

Conditions of existence of steady representations for discrete linear systems given in terms of unsteady representations

21 p2669 A73-40450

Investigation of the gain instability of a semiconductor radiometer

21 p2700 A73-40533

Dispersion equation of parametric longitudinal instability of electromagnetic wave propagation in a bounded electron beam in metallic waveguide

21 p2744 A73-41653

Transient response simulation model for stability analysis of flexible high speed rotor-bearing systems dynamics, examining nonlinear effects

[ASME PAPER 73-DET-102]

22 p2865 A73-42075

Bilateral estimates of the critical parameters of elastic systems experiencing flutter

22 p2921 A73-42288

Russian book - Theory and methods for constructing multiple-link control systems.

22 p2835 A73-42600

Liapunov vector functions for solving stability problems of complex multidimensional dynamic control systems with nonlinear interactions and delay

22 p2887 A73-42600

Root locus analysis of stability of a class of nonlinear systems.

22 p2837 A73-42624

Linearized stability analysis and design of a flyback dc-dc boost regulator.

22 p2801 A73-42910

System oscillations from negative input resistances at power input port of switching-mode regulator, amplifier, dc/dc converter, or dc/ac inverter.

22 p2802 A73-42911

Dynamic behaviour and z-transform stability analysis of dc/dc regulators with a non linear P.W.M. control loop.

22 p2837 A73-42912

Liapunov-like theorems of quantitative stability information on trajectory bounds in state space subset form

22 p2888 A73-43020

Stability circle criteria extended to signal power gain mean-square criteria for nonlinear feedback distributed parameter system defined by transfer function

22 p2837 A73-43066

Optimal feedback control solution existence and uniqueness conditions for asymptotic stability, discussing relationships with Pontryagin equations and linear regulator problem with quadratic cost functionals

22 p2837 A73-43070

On stability of large-scale systems under structural perturbations.

23 p2963 A73-43290

Radio telescope array of interferometers formed by fixed and movable antennas operating on rotational

- aperture synthesis for radiation observation, emphasizing electronic system stability
23 p2957 A73-43360
- An adaptive observer for single-input single-output linear systems.
23 p2963 A73-43818
- Linear time variant multivariable decentralized system stabilization by feedback control laws with dynamic compensation
23 p2964 A73-43821
- L2-stability and L2-instability of linear time-invariant distributed feedback systems perturbed by a small delay in the loop.
23 p2964 A73-43822
- Discrete time composite system stability with non-periodic sampling in terms of vector Liapunov functions and real symmetric matrix test
23 p2964 A73-43826
- A new method of analyzing the stability of nonlinear dynamic systems.
23 p3006 A73-44084
- System stability analysis technique for nonlinear oscillation via Van der Pol and Duffing equations, noting ease of approximating higher harmonics
23 p3007 A73-44085
- Exponential stability theorems of multivalued difference equations for discrete dynamical systems
23 p3000 A73-44206
- Stabilization of unstable plants through automatic search
24 p3074 A73-44662
- Stability criteria for two phase transpiration, cooling system with equilibrium phase transition inside porous wall
24 p3156 A73-45079
- A method for qualitatively studying the oscillations and stability of systems with distributed parameters
24 p3111 A73-45354
- Equilibrium of two elastic shallow shells of revolution which are connected by radial ribs
24 p3152 A73-45355
- Liapunov functions application to stability analysis of dynamic systems and elastic bodies, considering eigenfunction method, maximum principle and energy criterion
24 p3153 A73-45497
- Aggregation scheme solution for uniform asymptotic stability of large dimensionality system, using L-problem moment theory
24 p3112 A73-45505
- YSTOLE**
Systolic time intervals in constrictive pericarditis and severe primary myocardial disease.
06 p0649 A73-17596
- Geometry of left ventricular contraction in the systolic click syndrome - Characterization of a segmental myocardial abnormality.
06 p0655 A73-18870
- A comparison between the effects of dynamic and isometric exercise as evaluated by the systolic time intervals in normal men.
07 p0784 A73-20369
- Effect of electrostimulation on hemodynamic shifts during prolonged hypokinesia
10 p1180 A73-23940
- Stethoscope- or phonocardiograph-detectable systole-associated left atrial sound in terms of activity recording, sound genesis, hemodynamic correlations and clinical applications
11 p1317 A73-25696
- Familial syndrome of midsystolic click and late systolic murmur.
11 p1317 A73-25697
- Phonocardiogram and apex cardiogram in systolic click-late systolic murmur syndrome.
11 p1317 A73-25698
- Effects of posture on exercise performance - Measurement by systolic time intervals.
19 p2396 A73-38260
- YSTOLIC PRESSURE**
Structural conditions in the hypertrophied and failing heart.
22 p2807 A73-42685
- T**
- T TAURI STARS**
Review of results in infrared space astronomy.
11 p1426 A73-26502
- Russian papers on young stellar complexes and astrophysics covering physical nature and activity of nonstationary stars, stellar evolution, T-associations and earth atmosphere optical instability
15 p1934 A73-31418
- IR objects in Orion Nebula, discussing temperature range and pre T Tauri evolutionary stage
15 p1934 A73-31419
- Extinction and scattering cross sections of small planetesimal particles with iron cores and silicate mantles in circumstellar dust of young T Tauri stars
23 p3030 A73-43748
- Single component wind model for stellar rotation dependent mass loss from hot corona with application to T Tauri star observations
24 p3140 A73-45186
- T-33 AIRCRAFT**
A description of the NAE T-33 turbulence research aircraft, instrumentation and data analysis.
11 p1306 A73-26269
- An in-flight investigation of the influence of flying qualities on precision weapons delivery.
19 p2378 A73-37453
- Fixed base simulation of variable stability T-33 handling qualities, considering pilot performance in pitch tracking during atmospheric turbulence
19 p2386 A73-38072
- T-39 AIRCRAFT**
Cirrus-contrail cloud spectra studies with the Sabreliner.
17 p2206 A73-35579
- TABLES [DATA]**
NT CONVERSION TABLES
NT INTERFERENCE FACTOR TABLE
NT MATHEMATICAL TABLES
- Observations at 750, 1400, and 2700 MHz of radio sources in the Vermilion River Observatory survey.
01 p0096 A73-10312
- Photoelectric light-curves of TW Cas.
01 p0098 A73-10555
- Numerical Laplace transform inversion of a function arising in viscoelasticity.
01 p0119 A73-11469
- Materials properties data tables on composition, preparation, temperature and field strength parameters of superconducting compounds in Ni alloys
02 p0201 A73-11878
- Densities of compressed liquid methane, and the equation of state.
02 p0238 A73-12630
- Re-calculation of efficiency factors for radiation pressure.
02 p0225 A73-12804
- New ultraviolet line identifications for early-type stars.
02 p0226 A73-12831
- Narrow band and broadband light curves for Algol eclipsing binary from differential photometry, calculating reflection effect
03 p0366 A73-12940
- Lunar axis inclination to ecliptic axis as function of time, tabulating variations during 1971
03 p0367 A73-13078
- Beam vibration frequencies tables handbook preparation technique
03 p0388 A73-13317
- Japanese space program progress, current state and future objectives, giving tables of rockets and satellites with mission objectives and design/performance specifications
03 p0401 A73-13846
- Tables summarizing Si solar cell fabrication parameters, complex design evolution and performance achievement
03 p0254 A73-14204
- Thermophysical properties of methane.
04 p0517 A73-15050
- Observations of extragalactic variable sources at 2.8 and 4.5 cm wavelength.
04 p0500 A73-15515
- 1968 solar spot observations and statistics
04 p0502 A73-15950
- Material variability as measured by low temperature electrical resistivity.
05 p0588 A73-17287
- Book - Electronic properties of composite materials.
06 p0714 A73-17872
- Interstellar elemental abundance table from carbonaceous chondrites and solar abundances, considering solar Fe composition
06 p0752 A73-18232
- Photometric orbit and apsidal motion of DR Vulpeculae.
07 p0875 A73-19119
- Total solar eclipses of great duration.
07 p0876 A73-19400
- Observations of radio sources with an interferometer of 24-km baseline. II - The angular structures at 151 and 408 MHz of 46 unidentified radio sources from the revised 3C catalogue.
07 p0899 A73-19938
- Observations of radio sources with an interferometer of 24-km baseline. III - The angular structures at 408 and 1423 MHz of 44 relatively intense radio sources.
07 p0899 A73-19939
- Elastomer compatibility considerations relative to O-ring and sealant selection.
08 p0982 A73-20691
- [SAE AIR 786 A]
Periodicities in the longitude distribution of sunspots.
08 p1001 A73-20759
- Observations of Jupiter with Danjon astrolabes in 1965, 1966, and 1967.
08 p1005 A73-20911
- Summary of daily observational results of solar phenomena, cosmic ray, geomagnetic variation, ionosphere, radio wave propagation and airglow during October 1969 through December 1971.
08 p0961 A73-21393
- Forms of carbon in the new Haveru ureilite of Finland.
09 p1140 A73-21863
- Catalog of geomagnetic activity indices for the years 1841-1864 and 1870
09 p1077 A73-22543
- An abundance analysis of the delta Scuti variable delta Delphini.
10 p1275 A73-23831
- Book - Thermal radiative properties: Nonmetallic solids.
11 p1387 A73-25275
- Contribution to the study and perfecting of materials for radomes in the field of refractory ceramics
11 p1387 A73-25289
- Impedance comparisons for the asymmetrically driven thin cylindrical antenna.
11 p1329 A73-25663
- Solar Fraunhofer spectral lines having simple Zeeman triplet splitting with large Lande g-factors tabulated, noting missing lines in identification
11 p1421 A73-25932
- Photographs of comet Bennett 1969 i.
11 p1426 A73-26267
- Graphs, tables and discussion to aid in the design and evaluation of an acceptance sampling procedure based on cumulative sums.
13 p1709 A73-29297
- Orbital classification for short period comets based on minimum approach distances to respective planets
14 p1794 A73-29833
- Surface photometry of galaxies - Comparison of the luminosity profiles and photometric parameters of southern galaxies measured at Cordoba and Mount Stromlo.
14 p1801 A73-30644
- Landstreet null line list revision and null lines tabulation to identify spectra of magnetic Ap star atmospheres
14 p1801 A73-30647
- Monochromatic phase curves and albedos for the lunar disk.
15 p1932 A73-31271
- Culgoora-1 list of radio source measurements at 80 MHz.
15 p1940 A73-32182
- Book - Equilibrium compositions and thermodynamic properties of mixed plasmas. III - Argon-hydrogen plasmas at .01 to 1000 atmospheres between 2,000 and 35,000 K.
16 p2042 A73-33420
- Microcomputer programs for data reduction and quality control chart work, using Olivetti P-101, HP 9100-B and Wang 700-A calculators
16 p1986 A73-33642
- The meteor showers epsilon-Lyrids, alpha-Coronids, and phi-Draconids in 1969.
18 p2355 A73-36870
- DC-10 Twin design, discussing balance characteristics, loading limits and sample forms
19 p2386 A73-37891
- Tables and graphs for characteristics and pulse profiles of pulsars discovered in low Galactic latitude radio telescope survey
20 p2605 A73-39017
- Results of the 1959 to 1965 six-year series of latitude observations in Blagoveshchensk
21 p2772 A73-41269
- Astronomical constants and cataloging from 1964 International Astronomical Union, discussing inadequacies and different specific reference systems
21 p2780 A73-41612
- Photometry of southern globular clusters. I - Bright stars in omega Centauri. II - Bright stars in NGC 6752.
22 p2907 A73-42206
- Book - Dynamics in engineering structures.
22 p2922 A73-42491
- Zonal wind semiannual variations at 20-65 km, noting wave maximum amplitude and maximum location
22 p2883 A73-42550
- Absorption of vlf and elf waves in whistler mode - Sunrise and sunset effects.
22 p2849 A73-42622
- Book - Thermal radiative properties: Coatings.
22 p2937 A73-42857
- Liquid-vapour equilibria research on systems of interest in cryogenics - A survey.
24 p3155 A73-44821
- The unstable eclipsing giant system RZ Cancri.
24 p3143 A73-45438
- TABS [CONTROL SURFACES]**
Technological and structural design ensuring optimum clearance and aerodynamic coupling of moving units /wing-aileron or aileron-trim tab/
02 p0129 A73-11648
- TABULATING**
U TABULATION PROCESSES

TABULATION PROCESSES

TABULATION PROCESSES

Weather forecasts in tabulated and worded form by computer interpretation of forecast charts.
12 p1520 A73-26806

TACAN

Extension of a portable tactical instrument approach and landing system.
03 p0340 A73-13574

Doppler TACAN navigation system for helicopters obtaining data through computer display method
10 p1247 A73-24475

TACAN based SETAC and L band DME based DLS approach and landing systems for military aircraft, discussing time division multiplexing and antenna array
[DGLR PAPER 73-019] 17 p2208 A73-34493

Low cost data processor and display for ICN1, DME/TACAN, LORAN or range/range difference radar navigation systems in aerospace applications
17 p2210 A73-35213

TACHISTOSCOPES

Tachistoscopically measured independent image size and visual field recognition capacities of human eye
12 p1462 A73-27109

TACHOMETERS

Absolute stability of nonlinear control systems with nonstationary nonlinearities and tachometric feedback
07 p0805 A73-20046

System for in-flight recording of the rotational speed of the turbine of a jet engine
07 p0828 A73-20546

Heated Fleisch pneumotachometer - A calibration procedure.
08 p0935 A73-21509

Investigation of the output characteristic and errors of a reversible, contactless, dc tachometric generator designed on the basis of a synchronous machine
09 p1033 A73-22342

TACHYCARDIA

Controlled tachycardia through voluntary change in exercise regime, investigating relation between heart rate and blood circulation
10 p1185 A73-24521

Emotionally induced increases in heart rate and plasma catecholamine and free fatty acids, noting relation to coronary heart disease
22 p2809 A73-42837

TACTICAL AIR NAVIGATION

U TACAN

TACTICS

Army studies cost effectiveness of communications satellites.
03 p0274 A73-13075

Electronic warfare tactics against remotely piloted unmanned aircraft used for reconnaissance or weapons delivery, considering onboard countermeasures
04 p0418 A73-15379

Pursuit/evasion game problem with two pursuers to one evader, discussing coalition tactic based on open loop and closed loop conjugate points difference
[AIAA PAPER 73-230] 05 p0536 A73-16955

TACTILE DISCRIMINATION

Skin sensitivity of palms, wrists and forearms to focused ultrasound, noting evoked touch, pulsation, cold, warmth and prick sensations and applications in receptor physiology
05 p0540 A73-16695

German monograph on human information transmission by multidimensional tactile stimuli investigation using method of learned signals identification
07 p0786 A73-20393

Interindividual differences in homomodal and heteromodal scaling of auditory and vibrotactile stimulation intensity and duration, using magnitude estimation method
12 p1464 A73-26750

Visual perception dominance over touch related to threshold changes, analyzing nervous system reliance on sense with lower threshold
23 p2946 A73-43847

TACTILE SENSATION

U TOUCH

TAGGING

U MARKING

TAIL ASSEMBLIES

Aerodynamic design parameters effects on static performance of short ducted fans for helicopter tail rotor applications, comparing theoretical analysis and experimental results
[AHS PREPRINT 701] 17 p2104 A73-35052

Helicopter tail rotor teeter hinge with Teflon conical journal bearing allowing axial and radial preload in-service adjustment, discussing oscillatory loads and temperature effects
[AHS PREPRINT 762] 17 p2180 A73-35085

Tail rotor performance in presence of main rotor, ground, and winds.
[AHS PREPRINT 764] 17 p2106 A73-35087

An advanced composite tailboom for the AH-1G helicopter.
[AHS PREPRINT 785] 17 p2107 A73-35098

Transverse deflection of guided projectile tail fins during deployment.
22 p2797 A73-42629

Increasing the critical rotational speed of the tail rotor drive shaft in SM-1 and SM-2 helicopters
24 p3057 A73-45195

TAIL MOUNTINGS

U TAIL ASSEMBLIES

TAIL SURFACES

NT SWEPTBACK TAIL SURFACES
Calculation of the characteristics of tail fins in the vortical field of a wing
16 p1962 A73-32819

The effect of ice formation on the stability and maneuverability characteristics of aircraft
19 p2387 A73-38117

TAILLESS AIRCRAFT

Aeroelastic effects on flying wing aircraft aerodynamic stability characteristics, using elementary beam-rod differential equations and aerodynamic strip theory
[AIAA PAPER 73-397] 11 p1305 A73-25326

Response-optimum control of the angular and torsional oscillations of an elastic flying wing.
12 p1549 A73-27459

TAILORING

U DESIGN

TAILS [ASSEMBLIES]

U TAIL ASSEMBLIES

TAKEOFF

NT VERTICAL TAKEOFF

Schematic design of an automatic device for correcting aircraft takeoff and landing modes of flight
02 p0190 A73-11801

TAKEOFF RUNS

Effect of aircraft reliability regulations on takeoff and landing performance of QSTOL aircraft
[DGLR PAPER 72-056] 02 p0130 A73-11658

Airport runway lights system location and use for aircraft takeoff operations and visual indication of landing approach angle
14 p1743 A73-30242

Safety in the accident prone flight phases of takeoff, approach and landing.
17 p2098 A73-34085

Noise reduction of STOL aircraft during landing approach and takeoff via thrust reduction and steepest descent flight paths
[MBB-UH-06-73] 17 p2100 A73-34488

The Navy SETOLS program and its potential applications to Navy aircraft.
19 p2381 A73-37680

Runway sideline aircraft noise measurements on takeoff and approach for enforcing community noise levels based on FAA aircraft type certification, noting associated problems
22 p2800 A73-42945

Pulsated over-heated water rocket /POHWARO/ thrust augmentation system for combat aircraft takeoff runs from short runways under severe weather conditions
24 p3057 A73-45391

TAKEOFF SYSTEMS

U AIRCRAFT LAUNCHING DEVICES

TALC

Work function and surface ionization currents in steatite ceramics from nickel electrode and thermocouple measurements, plotting temperature dependent Paschen curves
16 p2031 A73-34011

TALKING

NT WORDS [LANGUAGE]

TALOS MISSILE

Drone recovery surface impact and midair techniques involving parachutes and/or hot-air balloons, considering TALOS/Low Altitude Supersonic Target recovery capability
[AIAA PAPER 73-465] 15 p1827 A73-31451

TANDEM ROTOR HELICOPTERS

NT CH-46 HELICOPTER

NT CH-47 HELICOPTER

TANK GEOMETRY

Small steady free oscillations of liquid in rigid tanks, considering HF modes
03 p0296 A73-14047

Design of zero-moment axisymmetric tanks made of a reinforced hereditary-elastic material
12 p1551 A73-27181

TANK TRUCKS

The liquefied ergol supply-trailers for DIAMANT B and EUROPA II launchers.
07 p0807 A73-18948

New developments in aircraft refuelling vehicles.
22 p2838 A73-41861

TANKER SHIPS

Floating superport.

Tuned loop antenna for radio observation of electrostatic spark and corona discharges generated during oil tanker cleaning operations
19 p2418 A73-37748

23 p2945 A73-43960

TANKS [CONTAINERS]

NT CYLINDRICAL TANKS

NT FUEL TANKS

NT PROPELLANT TANKS

NT SPHERICAL TANKS

NT STORAGE TANKS

NT WING TANKS

Free oscillations of a double layer in a turning rectangular basin of constant depth
19 p2419 A73-37530

Synthesis of optimal control of the longitudinal motion of an elastic tank containing liquid
22 p2843 A73-43039

TANTALUM

The thermal and electrical conductivities of tantalum at high temperatures.
03 p0322 A73-13191

Phase structure of vacuum deposited thin Ta films and molecular beam composition obtained by mass spectroscopy
04 p0484 A73-15669

Preparation and corrosion properties of a tantalum sputtered thick film.
04 p0456 A73-15792

Upper yield point removal in pure Ta by reverse cyclic stressing at room temperature, indicating cumulative mobile dislocation multiplication
05 p0586 A73-16130

Proton irradiation at 30 K and isochronal annealing of reactively sputtered Ta thin-film resistors.
06 p0737 A73-18352

Tantalum thin film capacitors fabrication procedures for hybrid ICs, presenting temperature and frequency responses and I-V characteristics of test samples
07 p0801 A73-19532

Tantalum-glass cermet thin-film resistors.
08 p0945 A73-20806

Apparatus for measuring spectral emissivity of metals.
08 p0962 A73-20866

The oxidation of tantalum and niobium in the temperature range 400-600 C.
08 p0978 A73-21410

Comparative investigations regarding the determination of nitrogen in tantalum
08 p0978 A73-21410

Mechanical behaviour of molybdenum and tantalum under high pressures at elevated temperatures.
09 p1105 A73-23018

Thermionic constants and electron reflection from Ta/100 by the Shelton retarding field method.
10 p2159 A73-23695

Acoustical method for determining thermal diffusivity and relative difference in molar heat capacities of tantalum and vanadium.
11 p1448 A73-25122

Study of gas-solid chemical interactions by the molecular beam technique. V - Reactions of oxygen and carbon monoxide with polycrystalline tantalum strips
15 p1841 A73-31970

Phenomena of precipitation observed in carburized tantalum in the vapor phase
15 p1896 A73-32645

Strength and plasticity of tantalum in rapid tests
17 p2188 A73-34561

Thermodynamics of b.c.c. solid solutions of hydrogen in niobium, vanadium and tantalum.
17 p2193 A73-35623

Solid tantalum capacitor failure modes, discussing slug impurities, dielectric imperfections, short circuits, scintillation shorts, anodizing, soldering, screening methods and cost reduction
19 p2410 A73-38440

The preparation and anisotropic hardness of tantalum single crystals with principal orientations.
20 p2575 A73-38637

Effects of hydrogen on tantalum by the cathodic charging.
20 p2575 A73-38638

Elastic properties of tantalum over the temperature range 4-300 K.
20 p2575 A73-38866

Powder geometry and structural design of the high-volumetric efficiency tantalum electrolytic capacitor.
21 p2663 A73-40770

Russian book - Spectrophotometry of niobium and tantalum.
21 p2648 A73-40803

Oxygen interaction with tantalum and niobium at high temperatures
21 p2722 A73-41594

Kinetics of gas absorption by refractory metals in dissociated environments - The nitrogen/tantalum system.
22 p2879 A73-42583

TANTALUM ALLOYS

Structural studies of Laves intermetallic phase precipitation in Fe-Ta alloys by microscopic, X ray diffraction and electron probe techniques
02 p0182 A73-12754

Thermal properties of tantalum-tungsten alloys at high temperatures.
03 p0322 A73-13192

Alloying effects on Ta binary alloy tensile strength brittleness and yield point at low temperatures
04 p0466 A73-15669

Heat capacity of the TV-10 tantalum-tungsten alloy at low temperatures
06 p0708 A73-18051

W-Ta alloys prepared by electron beam melting, testing Ta content effects on oxidation resistance and hardness at high temperatures 09 p1103 A73-22424

Study of the W-Ta-Re phase diagram by the diffusion layer method 09 p1108 A73-23236

Mo-Nb-Ta alloys phase and composition-hardness diagrams for 20-1100 C, establishing mutual solubility of system components 12 p1510 A73-26905

Partial and integral molar thermodynamic properties of solid Ta-W alloys at 1050-1300 K, discussing negative deviations from ideality 13 p1632 A73-28126

High-speed /subsecond/ simultaneous measurement of specific heat, electrical resistivity, and hemispherical total emittance of Ta-10wt.%W alloy in the range 1500 to 3200 K. [ECTP PAPER D2-4] 14 p1760 A73-30437

Structure and superconducting properties of alloys of the vanadium-tantalum system 15 p1923 A73-31183

Changes in the superconducting transition temperature of alloys of variable composition, as exemplified by the niobium-tantalum system 15 p1887 A73-31189

Influence of structure and of stress concentration on the mechanical properties of Ti-Ta-Mo system alloys 15 p1894 A73-32533

Phase equilibria in the metal-rich side of the Ta-N system. 16 p2025 A73-33110

Ti-Ta-V-Mo system phase diagram in Ti corner region for 600-900 C, investigating solubility, electrical resistivity and hardness 17 p2189 A73-34570

Structure and mechanical properties of internally oxidized Ta-8 pct W-2 pct Hf (T-111) alloy. 20 p2576 A73-39025

An arrangement for carrying out metal creep and stress-rupture strength tests under high vacuum conditions 20 p2545 A73-39384

The effect of vanadium, niobium, and tantalum on the electrical resistance of nickel 20 p2578 A73-39396

Ta-Nb-Re system phase diagram plotted by physicochemical analysis methods, establishing region of existence of ternary solid solutions and temperature dependence 21 p2718 A73-40488

Measured drift of irradiated and unirradiated W3%Re/W25%Re thermocouples at a nominal 2000 K. 22 p2858 A73-42046

TANTALUM CARBIDES

Enthalpy and specific heat of tantalum carbide in the range 273-3600 K. 08 p0977 A73-20865

Recrystallization of electron-beam-melted tungsten with tantalum and zirconium carbide additions 09 p1106 A73-23189

Ditantalum carbide thermodynamic stability determination from measurement of carbon monoxide pressure in equilibrium with ditantalum carbide-tantalum oxide-tantalum mixture at 1470-1620 C 13 p1632 A73-28128

Ostwald ripening of transition-metal carbides in liquid nickel and cobalt 14 p1760 A73-30441

A study on graphite-base high-temperature composite materials. II Graphite-tantalum composite materials. 19 p2443 A73-37375

Structures and properties of cobalt base-TaC eutectic alloys. 20 p2575 A73-39020

Carbide reinforcement in two directionally solidified alloyed nickel eutectic alloys. 20 p2576 A73-39028

Investigations regarding structure, preparation, and hardness properties in the system Ta-Hf-C-N 22 p2873 A73-41949

TANTALUM COMPOUNDS

NT TANTALUM CARBIDES

NT TANTALUM NITRIDES

NT TANTALUM OXIDES

Chemical stability of tantalum germanide powders in air and aggressive media, including acids, fluorine ions and perhydrol 09 p1133 A73-22465

Optical damage and internal fields in pyroelectrics. 10 p1260 A73-24531

Crystalline structure of the TaCoB and NbCoB2 compounds 12 p1512 A73-27244

TANTALUM NITRIDES

Phase equilibria in the metal-rich side of the Ta-N system. 16 p2025 A73-33110

Bonding degradation in the tantalum nitride-chromium-gold metallization system. 19 p2435 A73-38440

TANTALUM OXIDES

The growth of dielectric aluminum and tantalum oxide layers 08 p0977 A73-21023

Thin film capacitor with anodic tantalum oxide overlaid with silicon dioxide deposited by RF sputtering, noting reliability under various voltage, temperature and humidity conditions 21 p2663 A73-40771

TAPE MERGING

U DATA PROCESSING

U MAGNETIC TAPES

TAPE RECORDERS

Recording and data processing equipment proposed for scintillation measurements. 03 p0308 A73-13646

High-data-rate, spacecraft tape recorders. 04 p0449 A73-15383

Reliable, high performance magnetic tape recorder/reproducer for third generation telemetry data computer processing lines, noting human error possibility reduction 07 p0795 A73-18955

Mechanical and electrical performance of satellite-borne magnetic tape recording system for computer data storage in radio telemetry 07 p0820 A73-18960

Russian book on multichannel magnetic tape recorders in civil aviation ATC for speech communication monitoring and preservation covering design and operation principles 09 p1086 A73-23245

Ultrawideband longitudinal magnetic tape recording of 120 MHz biased LF/HF signal frequencies, describing high velocity tape transport and recording heads design 09 p1087 A73-23366

Effects of tape flutter on notch noise loading test performance of predetection recording of a frequency modulated carrier. 09 p1087 A73-23367

Record/reproduce process induced phase distortion in magnetic tape recorders as function of record head gap length 09 p1087 A73-23368

Effect of flutter on theoretical bit error rates for digital recording systems. 09 p1087 A73-23369

Magnetic tape recorder parameters effect on PCM telemetry bit error rate, discussing contribution factors and test methods 09 p1087 A73-23370

ESRO TD-1A satellite signal hibernation in sky-scanning experiments after successful performance during first orbital life, noting tape recorder failure 11 p1431 A73-25750

Tape recorder instrumentation for structural dynamic load test data analysis, discussing cable crosstalk, lead length and electrical noise effects in crack propagation measurements 14 p1751 A73-29775

A punched tape recorder for observation data 15 p1878 A73-32142

Antenna array facility with small digital computer and multichannel tape recorder for real time simulation of radiation source movement through view field 17 p2149 A73-35755

Environment effects on tape recorder design for in-flight data collection in military aircraft 19 p2431 A73-38197

Airborne multimode radar digital data system using high transfer rate magnetic tape recording, discussing 8 track tape storage capacity, coding and logic circuits 19 p2431 A73-38198

Modular airborne video tape recording systems using wideband frequencies, describing wideband channels, power supply, transport unit, servo module and bit storage rates 19 p2431 A73-38199

National Radio Astronomy Observatory interferometer system with rotating head video tape recording and computerized sampled data processing equipment for use with radio telescope 23 p2980 A73-43358

TAPER

U TAPERING

TAPERED WINGS

U SWEEP WINGS

TAPERING

On the optimum design of tapered waveguide transitions. 17 p2136 A73-34970

Optimum tapering design of vibrating cantilever beams, considering geometrically similar and rectangular cross sections and degenerated end mass case 21 p2785 A73-40839

Tapered corrugated waveguide low-pass filters. 21 p2666 A73-41427

Plastic collapse of steep conical shells under axial compression. 21 p2789 A73-41684

In-plane free vibrations of tapered oval rings, determining normal modes and resonant frequencies from differential force and moment equilibrium equations 22 p2918 A73-41818

TAPES

Edgewise tape wound reinforced plastic ablative components for rocket motors to provide balance between optimum char strength, heat flow and insulation characteristics 17 p2195 A73-34809

TARE [DATA REDUCTION]

U DATA REDUCTION

TARGET ACQUISITION

Target detection during picture transmission through a TV system 02 p0166 A73-11682

[DGLR PAPER 72-099]

Target angular characteristics of direction finding antenna in sidelobe region for wideband signals, using single coordinate measurement and amplitude scanning 02 p0146 A73-12023

Bistatic-radar detection of high-altitude clear-air-atmospheric targets. 02 p0142 A73-12526

Detection probability in the case of laser distance measurements involving moving targets 03 p0274 A73-13256

Pursuit-evasion reconnaissance game with evader reconnoitering target from close distance with guaranteed safe escape from pursuer 03 p0336 A73-13523

A new filter for optimal tracking in dense multitarget environments. 03 p0286 A73-14477

Nonlinear stochastic optimal control theory application to guidance policies determination of nonmaneuvering target interception or rendezvous and goal-tending game 03 p0286 A73-14478

Optimal nonlinear estimator algorithms for tracking in face of incorrect sensor returns in multitarget environments, using posteriori probability selective measurements 04 p0431 A73-15260

Observer target acquisition performance dependence on target position within restricted visual field 05 p0543 A73-16711

Human factors analysis of forward looking infrared /FLIR/ imagery in air-to-ground target detection/recognition. 05 p0550 A73-16712

Visual time compression. II - Detecting moving targets in dense radar ground clutter. [AD-753746] 05 p0550 A73-16715

Complex images application of target isolation algorithms based on brightness distributions, discussing allocation of target classification parameters 06 p0694 A73-18289

Optimal correlation of sensor data with tracks in surveillance systems. 06 p0682 A73-18822

Space /rocket/ launch vehicle computer guidance and targeting equations, discussing Q, Delta, explicit, linear tangent, optimal, numerical integration and parameter optimization techniques 06 p0721 A73-18824

Cassiopee triaxial gyroscopic aiming device for sounding rocket attitude control, using stellar and inertial sensors and jet micropulsion 07 p0866 A73-18924

Astrolabe universal balloon gondola for solar and visible stars targeting, describing acquisition functions and attitude control servos design 07 p0776 A73-18940

The performance of a satellite-borne infrared target acquisition system. 07 p0824 A73-19946

Comparison of theoretical and simulated performance of optimal and suboptimal filters in a dense multitarget environment. 07 p0806 A73-20604

Extremal targeting in a nonlinear rendezvous game 09 p1112 A73-22476

Computer program for extraterrestrial physics barium ion cloud project determining daily release launch window for sky target experiments [AIAA PAPER 73-297] 09 p1116 A73-23216

Open-loop tracking of moving targets with an Aerobee sounding rocket. [AIAA PAPER 73-302] 09 p1117 A73-23221

Target-detection performance as a function of noise intensity and task difficulty. 11 p1323 A73-26320

Optimal search scanning for electronic surveillance radar based on antenna beam position with highest echo signal for maximum likelihood target acquisition 13 p1581 A73-27999

Calculation of probability of detection with target scintillation. 13 p1586 A73-29219

Accuracy of target angular coordinate estimates by the maximum likelihood method on a correlated noise background 14 p1729 A73-30557

Synthesis and analysis of tracking systems with optimal acquisition. 15 p1854 A73-31727

TARGET DRONE AIRCRAFT

Incoherent radar target extraction in clutter of unknown level by recursive integration for signal and threshold. 18 p2290 A73-37089

Operational principles and testing of a digital radar target extractor 19 p2404 A73-37584

Imaging system pointing precisions, deriving ground target size relationships to spread function and modulation transfer function respectively 20 p2567 A73-39672

Maneuvering target motion modeling with binary random variable in state equation, obtaining optimal tracking solution as weighted combination of two Kalman filter estimates 21 p2649 A73-40331

Linear fire control predictor with non-Gaussian inputs, calculating on-target probability lower bounds for verification by digital simulation 21 p2649 A73-40332

Sensor data display simulator for airborne target acquisition with improved sensors, using TV scanning of film based imagery [AIAA PAPER 73-921] 21 p2673 A73-40869

TARGET DRONE AIRCRAFT

NT JINDIVIK TARGET AIRCRAFT

TARGET RECOGNITION

Human factors analysis of forward looking infrared (FLIR) imagery in air-to-ground target detection/recognition. 05 p0550 A73-16712

High resolution radar target recognition, discussing effects of transfer curves of radar signal strength vs display luminance on operator performance 05 p0550 A73-16716

Probability estimate for visual target detection in terms of luminance threshold and target size and duration 06 p0658 A73-18242

IR tracking system for automatic target acquisition, discussing analyzer operation principles, closed loop characteristics, spectral field and equipment specifications 07 p0789 A73-18945

Autokinetic movement as a function of the implied movement of target shape. 07 p0785 A73-19549

Optimum spectral band of an infrared detection system for use against forest background radiation. 08 p0962 A73-20811

Wide view field laser target designation seeker system with photodetector for multiple returns discrimination, discussing sensor broadband model, signal processing and design feasibility 10 p2126 A73-23788

Millimeter wave imagery of complex three dimensional target by diffuse reflection with spatial filtering, discussing range, resolution and view field capabilities. 10 p1188 A73-23798

Complex target resolution with the random signal radar. 10 p1189 A73-24560

Backward masking and enhancement of multisegmented visual targets. 11 p1321 A73-25133

Field of view and target uncertainty in visual search and inspection. 11 p1322 A73-25181

Probability of detecting aircraft targets. 11 p1333 A73-26634

Beta estimation accuracy for reentry vehicles using a priori target information with 6-component state vectors to reduce computation time 12 p1548 A73-27131

Relationship between pointing precision, spread functions and modulation transfer functions. 12 p1501 A73-27969

Automatic radar terminal system (ARTS) for high density ATC centers, noting improved target identification and alphanumeric data display 15 p1907 A73-31133

Searching for many targets - An analysis of speed and accuracy. 17 p2118 A73-35498

Stationary target identification with radar beam for comet nucleus within coma, noting echo spatial extent and Doppler bandwidth effects on data processing 17 p2174 A73-35634

Basic principles and the theory of operation of the equipment for the identification-friend or foe (SIF) in military aircraft 21 p2650 A73-40348

Use of a digital computer for studying velocity judgements of radar targets. 23 p2948 A73-43213

Performance efficiency of systems employing information from radio-electronic means of observation 24 p3071 A73-44599

Performance prediction in a single-operator simulated surveillance system. 24 p3063 A73-44775

Information seeking with multiple sources of conflicting and unreliable information. 24 p3063 A73-44778

TARGET SIMULATORS

The Large Amplitude Multi-Mode Aerospace Research (LAMAR) Simulator. [AIAA PAPER 73-922] 21 p2673 A73-40870

TARGETS

NT JINDIVIK TARGET AIRCRAFT

NT PARTICLE ACCELERATOR TARGETS

NT RADAR TARGETS

Aerial targets for weapon systems performance testing, discussing converted aircraft, pilotless drones and towed targets 09 p1168 A73-23120

Stiletto air-launched supersonic aerial target design, development and capabilities, describing configuration, propulsion and control systems and operational envelope 09 p1032 A73-23121

Turana drone system design and development for Australian naval guns and guided weapons exercises, describing construction and operational details 09 p1032 A73-23122

High-energy pulsed CO2-laser-target interactions in air. 17 p2184 A73-34914

TASK COMPLEXITY

Intellectual ability and performance on a non-verbal problem-solving task. 03 p0260 A73-13553

Work requirements test program for operator proficiency in tasks analogous to aircraft piloting under difficulty variation, deriving workload capability limits 05 p0544 A73-16722

Human performance measures relationship determination across sense modes under visual, auditory and combined stimulus conditions by controlling for task difficulty on individual basis 06 p0658 A73-18244

Target-detection performance as a function of noise intensity and task difficulty. 11 p1323 A73-26320

Towards an objective assessment of cockpit workload. I - Physiological variables during different flight phases. 14 p1718 A73-30515

Psychological factors influencing the relationship between cardiac arrhythmia and mental load. 14 p1720 A73-30877

Heart rate variability and work-load measurement. 14 p1720 A73-30879

Influence of stimulus symmetry on visual scanning patterns. 17 p2118 A73-35494

Interference of 'attend to and learn' tasks with tracking. 19 p2401 A73-38377

Interactive effects of intense noise and low-level vibration on tracking performance and response time. 21 p2644 A73-41153

Frequency of anti-collision observing responses by solo pilots as a function of traffic density, ATC traffic warnings, and competing behavior. 21 p2645 A73-41158

Adaptive measurement of vigilance decrement. 23 p2947 A73-43211

TASK SEQUENCERS

U CONTROL EQUIPMENT

U SEQUENTIAL CONTROL

TASKS

NT AUDITORY TASKS

NT VISUAL TASKS

TAURID METEORIODS

Metal ion density measurement in sporadic E layer during beta Taurids shower by rocket-borne mass spectrometry, noting origin in cosmic debris ablation 13 p1673 A73-28277

TAURUS CONSTELLATION

A model of the Crab Nebula derived from dual-frequency radio measurements. 05 p0622 A73-17075

TAXIING

Further developments in surface effect takeoff and landing systems concepts - A multicell system. [CASI PAPER 76/11B] 17 p2099 A73-34294

TAXONOMY

Ribosomal RNA base composition and molecular evolution in plants and animals of various taxonomic groups 07 p0780 A73-19220

TAYLOR INSTABILITY

Taylor vortices nonoscillation theory for outward decrease of circulation square, investigating system eigenvalues [AD-754480] 01 p0033 A73-10779

Initially spherical water drops deformation under external flow for wide range of Weber and Bond numbers, investigating drag coefficient and Taylor instability 02 p0153 A73-12037

Infinite Prandtl number fluids with constraint characterized by Taylor number heated from below, choosing boundary conditions for laminar convection 03 p0293 A73-13329

Effects of spanwise rotation on the structure of two-dimensional fully developed turbulent channel flow. 06 p0685 A73-17708

Optimal stabilization of the Rayleigh-Taylor instability in the multiarm fluid pendulum. 09 p1119 A73-21900

On Howard's technique for perturbing neutral solutions of the Taylor-Goldstein equation. 11 p1345 A73-25100

Stratified Taylor column model for topography effect on slow rotating baroclinic flow, considering Jupiter Red Spot and oceanic observations 16 p1998 A73-32700

Wavelength and cell size determination of steady supercritical Taylor vortex flow for long rotating cylinders with radius, viscosity and end boundary variations 16 p1998 A73-32700

The Taylor vortex regime in the flow between concentric rotating cylinders. [ASME PAPER 73-LUBS-8] 17 p2181 A73-35100

Taylor vortex occurrences between rotating electric cylinders 20 p2547 A73-39000

Electrohydrodynamic Rayleigh-Taylor instability of a plane circular interface. 21 p2749 A73-41600

Rayleigh-Taylor instability in octyl alcohol-water interface, observing bubble and spike formation with flattening and curling of spike due to Kelvin-Helmholtz instability 22 p2842 A73-42220

Rayleigh-Taylor problem of thermal instability of density-stratified layer of incompressible fluid heated from above, considering oscillatory and nonoscillatory modes stability 23 p3048 A73-43340

TAYLOR SERIES

Determination of the mean square errors of functions of variables in uniquely determinate geometric constructions 04 p0443 A73-15518

A series expansion of a magnetic vector-potential calculated for a ring with a current 08 p0959 A73-21290

Taylor series algorithms for computerized structural design and reanalysis of modified structures, applying to aircraft fuselage midsection [AIAA PAPER 73-338] 11 p1436 A73-25470

Analytical representation of complex signals by expansion in Fourier, Kotelnikov, and Taylor series 12 p1471 A73-27500

A numerical method of integration by means of Taylor-Steffensen series and its possible use in the study of the motions of comets and minor planets. 14 p1790 A73-29780

Matrix calculus operations and Taylor expansions. 14 p1769 A73-30410

Noise loading analysis of a memoryless nonlinear system characterized by a Taylor series of finite order. 21 p2656 A73-41140

A method of solving a slightly disturbed mixed problem for a hyperbolic equation with a small delay of the argument 22 p2881 A73-42270

Holographic image nonlinear distortion analysis based on photographic film material characteristic curve representation by Taylor series 22 p2861 A73-42410

Solving linear boundary value problems by approximating the coefficients. 22 p2882 A73-42510

Multistep-multistage-multiderivative methods for ordinary differential equations. 24 p3106 A73-45330

A tenth order solution in explicit form to the 'restricted' three-body problem. 24 p3143 A73-45430

TAYLOR THEOREM

U TAYLOR SERIES

TD SATELLITES

NT TD-1 SATELLITE

TD-1 SATELLITE

Development of propellant loading systems and checkout systems for the TD-1A and AEROS satellite projects 11 p1430 A73-25350

ESRO TD-1A satellite signal hibernation in sky scanning experiments after successful performance during first orbital life, noting tape recorder failure 11 p1431 A73-25750

TEA LASERS

U CARBON DIOXIDE LASERS

Fast linear detection system for TE CO2 lasers. 24 p3096 A73-44920

TEACHING

U EDUCATION

TEACHING MACHINES

Computer-assisted instruction in pilot training and certification. 05 p0544 A73-16724

A hybrid analog computer for schooling in control technology 07 p0796 A73-20300

Computer assisted instruction for commercial programmer and systems analyst education and training, discussing government use, pretest importance and future developments 09 p1168 A73-22220

TEAMS

The prediction of team monitoring performance under conditions of varied team size and decision rules.

05 p0543 A73-16710

TECHNIQUES

U METHODOLOGY

TECHNOLOGICAL FORECASTING

Future optical communication systems problems, potentialities and development prospects, considering bandwidth, laser modulation, directionality, fiber transmission, reception, detection, power and efficiency

01 p0018 A73-11066

The laser's impact on crystal technology.

01 p0088 A73-11067

Cost goals for silicon solar arrays for large scale terrestrial applications.

03 p0258 A73-14250

Technological evolution of solar generators for terrestrial applications and sounding balloons, discussing environment caused problems and solutions, energy cost estimate and future prospects

03 p0258 A73-14253

Long range air transportation technical and economic future prospects, discussing passenger and cargo developments, noise reduction and SST technology

[AIAA PAPER 73-14]

06 p0646 A73-17607

Josephson tunneling devices - A new technology with potential for high-performance computers.

06 p0735 A73-18066

Lubricating grease technological development trends, discussing petroleum oils, esters, silicones, others and fluorocarbons base types and different thickeners

07 p0842 A73-19556

Applications technology satellite data handling processing and interpretation for future earth survey, communications and meteorological satellite operational programs

08 p1014 A73-21593

Objective trees as technological forecasting technique in structuring program options for selected strategies, considering R and D, marketing and other functional business programs

08 p1026 A73-21699

Computer assisted instruction for commercial programmer and systems analyst education and training, discussing government use, pretest importance and future developments

09 p1168 A73-22222

Civil transport aircraft future design trends, discussing subsonic, supersonic, hypersonic and V/STOL aircraft, engine design, fuels and noise reduction

10 p1174 A73-23682

Commercial air transportation projections, discussing mass transportation, international fare structure and exchange of rights, security and technology

10 p1298 A73-24646

Integrated microoptical circuit technology with lenses, prisms, reflectors, mixers, detectors, gratings, filters, lasers, amplifiers and modulators fabricated around waveguides, assessing advantages and potentials

11 p1399 A73-26117

Fiber composite materials properties, technological assessment and future development and application for aerospace flight structures, considering manufacturing cost, tailorability and stiffness requirements

13 p1699 A73-29346

Operation of current navigation aids and future prospects.

14 p1773 A73-29883

Aeronautical communication technology for civil ATC system development through 1990s, discussing SNR design and need for radio channel models

14 p1725 A73-29890

Multiple access technique for future communication, surveillance and navigation subsystems to meet ATC demands, considering satellite surveillance radar system

14 p1725 A73-29893

A technological development scenario for offshore jetports.

15 p1857 A73-31534

Microwave power transistors - The present and the future.

15 p1852 A73-32275

Instrument-panel electronic display system

15 p1831 A73-32510

The impact of silicon technology on near-infrared and low-light-level imaging.

16 p2012 A73-32867

Future technical developments and efficiency of helicopters and their derivatives

17 p2098 A73-34252

VTOL and helicopter design considerations, including nonsymmetrical rotor flow characteristics, rotor types, airspeed capacities, compound helicopters, tilt wing and tilt rotor aircraft

17 p2099 A73-34259

Key factors in developing a future wide-bodied twin-jet transport.

[SAE PAPER 730354]

17 p2103 A73-34702

Future trends in computer hardware.

17 p2131 A73-35127

Technological forecasting for microcomputer architecture and fabrication on LSI chip, considering cost effectiveness, pins number, packing density, power and speed factors

17 p2131 A73-35226

High performance supersonic axial and centrifugal compressors theoretical and experimental research, assessing and forecasting technological developments

18 p2343 A73-36992

Financing the new generation of airports.

19 p2506 A73-37745

Future communication satellite technology improvement, market expansion and cost effectiveness, considering foreign domestic, and international light-to-medium and high density systems

20 p2522 A73-38715

The ARINC plan for implementing air/ground DATALINK.

20 p2527 A73-38758

Future technology and economy of jet-supported VTOL transport aircraft

21 p2793 A73-40448

Philosophical approaches of technological forecasting and assessment, discussing Dialectical and Singerian inquiring /information/ systems for ill structured problems

23 p3051 A73-44218

Technological change measurement methodology for cost and production estimates with application to aircraft turbine engine development

23 p3020 A73-44219

Research Aviation Facility collected aircraft data processing, merging and enhancement problems, software development and future resource requirements

24 p3070 A73-45088

TECHNOLOGIES

NT BIOTECHNOLOGY

NT MARINE TECHNOLOGY

NT MILITARY TECHNOLOGY

NT REACTOR TECHNOLOGY

TECHNOLOGY ASSESSMENT

The laser's impact on crystal technology.

01 p0088 A73-11067

Secondary low thrust propulsion systems technology requirements and parameters, covering electrothermal, radioisotope and ion bombardment thrusters

01 p0090 A73-11109

Thin film and thick metal film technology comparison and production cost analysis, emphasizing thin film resistors application in hybrid circuits

01 p0026 A73-11399

A comparison of analog and digital techniques for pattern recognition.

01 p0021 A73-11478

Feasibility study for direct TV transmission and reception via satellite, discussing technical and economic aspects

[DGLR PAPER 72-050]

02 p0140 A73-11679

Earth resources remote survey methods capability assessment, considering radar and passive microwave imaging, IR and multispectral scanning and photographic and absorption spectrometric methods

[DGLR PAPER 72-072]

02 p0155 A73-11703

Feasibility model of airborne ac synchronous generator with rotating superconducting field winding, comparing predicted performance, size and weight with conventional technology

02 p0131 A73-11827

Josephson tunnel junction fabrication technology evaluation in terms of electrode materials, native oxide and artificial barriers, noting factors affecting stability and I-V characteristics

02 p0200 A73-11846

Technology assessment of nuclear rocket engines based on solid core reactors for space propulsion

02 p0191 A73-11995

Microelectronic technology development and applications in transistor-transistor logic, medical devices, computers and thick film hybrid assemblies

02 p0148 A73-12593

General purpose autoclave processable polyimide laminating resin selection, evaluating molding process techniques

03 p0329 A73-13004

High temperature solid lubrication technology developments, discussing bonded films, plastic and metal bonded composites and temperature ranges

03 p0330 A73-13013

Advances in glass fiber fabrics for plastic reinforcement.

03 p0330 A73-13014

Artificial earth satellites photographic position determination, discussing instrumental and procedural techniques

03 p0274 A73-13255

United States SST electrical power system evaluation.

[AIAA PAPER 72-1055]

03 p0252 A73-13386

Engine technology for large subsonic nuclear powered aircraft.

[AIAA PAPER 72-1062]

03 p0353 A73-13391

Dual mode applications of nuclear rocket engine for spacecraft propulsion and electrical power generation, considering payloads and missions competitiveness with nondual system

[AIAA PAPER 72-1092]

03 p0341 A73-13413

Mono- and multipropellant, storable and cryogenic, liquid rocket propulsion engines developments including gas generators and engines

[AIAA PAPER 72-1104]

03 p0355 A73-13422

Resistojet and plasma propulsion system technology.

[AIAA PAPER 72-1124]

03 p0355 A73-13436

Prospects offered by high performance composites with a metallic matrix

03 p0325 A73-13589

Assessment and operational implications for ATC capital investment decision making by relative capacity estimating process using analytical models

03 p0280 A73-13801

Japanese space program progress, current state and future objectives, giving tables of rockets and satellites with mission objectives and design/performance specifications

03 p0401 A73-13846

The development of high performance annular combustion chambers at SNECMA

03 p0360 A73-14151

Book - Advances in space science and technology. Volume 11.

03 p0376 A73-14166

Advances in solar and cosmic X-ray astronomy - A survey of experimental techniques and observational results.

03 p0364 A73-14167

U.S. manned space flight food system development experience assessment, covering Mercury, Gemini, Apollo and manned orbiting laboratory programs

03 p0269 A73-14168

Tables summarizing Si solar cell fabrication parameters, complex design evolution and performance achievement

03 p0254 A73-14204

Metal stripline connector technology to fabricate flexible silicon solar cell arrays, noting cost reduction

03 p0256 A73-14232

Solar array and supporting technologies development, discussing manufacturing, handling, design qualification tests in space environment and comparison between fold-up and roll-up types

03 p0257 A73-14237

Fabrication criteria, mission design factors and I-V characteristics of Li solar cells

03 p0257 A73-14242

Technological evolution of solar generators for terrestrial applications and sounding balloons, discussing environment caused problems and solutions, energy cost estimate and future prospects

03 p0258 A73-14253

Book - Holography: State of the art review 1971-72.

03 p0309 A73-14440

Recent studies towards the development of procedures for design of brittle materials.

04 p0508 A73-14725

Materials processing technology for LSI electronics, considering wafers, doping, diffusion, ion implantation, photomasking and film deposition

04 p0426 A73-14743

Comet research assessment for 1970-1972, discussing coma and nucleus, icy conglomerate and sandbank models

04 p0495 A73-14765

NDT applications of acoustic or stress wave, ultrasonic spectroscopy, imaging, critical angle reflectivity and holography

04 p0447 A73-14927

Air Force weapon system procurement needs, considering industry technological capabilities, nonlinear estimation in cruise navigation and nonlinear systems design, test and implementation

04 p0430 A73-15252

The liquid metal slip ring experiment for the Communications Technology Satellite.

04 p0408 A73-15449

Earth resources sensing technology - 24-channel multispectral sensor system development.

04 p0449 A73-15463

Superconductivity theory and applications, considering cryogenic problems low-loss and magnetic properties and Josephson junction effect on low power technology

04 p0484 A73-15958

The benefits of space exploration related to the Space Shuttle.

05 p0568 A73-16184

An overview - Advantages of imaging techniques for nondestructive testing.

05 p0573 A73-16277

Holographic interferometry techniques and applications, discussing gas and ruby lasers in imaging, measurements and NDT of materials and mechanical components

05 p0574 A73-16286

TECHNOLOGY ASSESSMENT

Communication satellite technology development, discussing INTELSAT and Russian Orbita systems, spectrum and orbit utilization, modulation, multiplexing, electron devices, radiation environment and power generation

05 p0550 A73-16604

Computerized ATC automation program, considering system management, hardware, software and test facilities problems

05 p0595 A73-16619

Small turboshaft aircraft engine historical evolution and current state of art, discussing performance, cost, weight, reliability and maintainability interrelationships

[SAE PAPER 720830]

05 p0606 A73-16626

NASA lift fan V/STOL transport technology status.

[SAE PAPER 720856]

05 p0535 A73-16663

Assessment of ISS topside sounder system by computer simulation.

05 p0579 A73-17168

Technology and operation of Olympus engine cycle on Concorde aircraft, discussing chemical and noise pollution and economic factors

05 p0536 A73-17190

Recent progress in the field of aircraft noise technology

05 p0537 A73-17272

High performance cryogenic multilayer thermal insulation with plastic films coated by vapor deposited metal, discussing heat transfer mechanism for comparison with microsphere insulation

05 p0642 A73-17285

Book - Advances in corrosion science and technology. Volume 2.

06 p0704 A73-17506

Aerodynamic technology developments including advanced transonic airfoils, low-drag/high-lift systems and stability augmentation for transport aircraft performance, economics and noise improvements

[AIAA PAPER 73-9]

06 p0644 A73-17604

Economically viable and socially acceptable second-generation SST, discussing technological developments for range/payload, airport noise and sonic boom improvements

[AIAA PAPER 73-15]

06 p0646 A73-17608

Space shuttle technology, discussing configurational aerothermodynamics, aeroelastic effects on vehicle dynamics and structural design and materials

[AIAA PAPER 73-31]

06 p0755 A73-17619

Air breathing hypersonic aircraft technology developments in propulsion systems and structures with emphasis on use of hydrogen fuel

[AIAA PAPER 73-58]

06 p0647 A73-17631

Intrinsic models for computer storage allocation program locality concept, comparing performance in terms of working set size and missing page probability by experiments

06 p0670 A73-18060

Book - The superalloys.

06 p0708 A73-18073

Space transportation systems and payload concepts for proposed space missions, discussing available and projected technology and environmental, economic and political aspects

06 p0757 A73-18096

Computer output microfilm system technology assessment, discussing two dimensional acousto-optic laser scanner to write on dry process film

06 p0700 A73-18294

High speed wideband laser scanning technology for extremely small focal points

06 p0701 A73-18307

Radar engineering developments, discussing microwave and optical systems, plan position indicators, antennas, displays, receivers, transmitters, solid state IC devices and signal processing

06 p0668 A73-18440

The HR 300 ultrafast photomultiplier with a microchannel plate

06 p0678 A73-18852

Operation, fabrication and structural features of pulsed/CW microwave p-i-n diodes, presenting diode impedance and resistance as function of conduction current

07 p0797 A73-18898

Book - French space technology. Volumes 1 and 2.

07 p0904 A73-18901

High reliability technology assessment for metal film resistors production, discussing qualification tests

07 p0829 A73-18921

French technology assessment on satellite stabilization by ion propulsion, stressing geostationary satellites orbit correction

07 p0904 A73-18934

Fluidic circuits fabrication and design technology for rocket guidance and attitude control

07 p0778 A73-18939

One degree of freedom fluid suspension gyros, direct drive gimbal motors and microelectronic control assemblies review, noting miniature inertial platforms availability

07 p0820 A73-18941

Tracking radar equipment evolution in connection with French space program development, describing reliability technology

07 p0807 A73-18943

Solar generator technology on the Symphonie satellite.

07 p0778 A73-18976

Amorphous semiconductor devices, materials, operation and technology, noting nonvolatile and optical memories, radiation and noise immune circuits and dry process photographic applications

07 p0861 A73-19150

Nonhydrocarbon liquid lubricants based on phosphate and neopentyl esters, perfluoroalkyl and polyphenyl ethers, silicone and perfluorotriazines, discussing performance testing techniques

07 p0843 A73-19559

Silicone oil lubricants technology for steel-steel lubrication over wide temperature and load ranges

07 p0843 A73-19560

Superconductors HF properties and losses measurement and separation techniques, discussing applications to filters, oscillators, mixers, transmission lines and radiation detection

07 p0863 A73-20106

Technology assessment of superconductivity application to windings of electric machinery

07 p0863 A73-20108

TF-34 turbofan engines for S-3A and AX aircraft respectively, discussing technological development, and components and characteristic features

07 p0868 A73-20350

Technology advancement effects on military and commercial transport aircraft development and production costs, considering airframes, engines and avionics

07 p0924 A73-20394

State of the art and survey of learning control applications.

07 p0806 A73-20590

Distributed ATC with traffic information in cockpit, noting potential for cost and risk reduction and capacity increase based on system performance evaluation

07 p0850 A73-20600

Microwave lumped passive and active circuit components properties assessment, considering inductor, capacitor, resistor, gyrator, tunnel diode amplifier, varactor Gunn oscillator, and parametric amplifier

08 p0942 A73-20703

Evaluation of the wavefront aberration in holography.

08 p0963 A73-21013

Radiography and ultrasonic tests for weldment and flaw inspection, discussing choice based on economic, technical and application considerations

08 p0952 A73-21076

Wear resistant coatings deposition by spark discharge alloying of machine part surfaces, examining surface hardening process and assessing state of art

08 p0946 A73-21083

Microwave and millimeter wave receiver noise performance state of art and acoustic measurement methods, discussing traveling wave maser, parametric and transistor amplifiers and tunnel diodes

08 p0940 A73-21625

Integrated circuits fabrication and technology development, discussing digital and analog circuit capabilities, cost reduction and diffusion techniques

08 p0949 A73-21647

Interdigitated power junction transistor technology assessment for power gain, bandwidth and frequency performance, noting packaging effect and thin film module advantage

08 p0949 A73-21648

Radar systems development under solid state electronics advances impact, discussing silicon ICs, HF transistors, hybrid microwave circuits, parametric amplifiers and p-i-n diodes applications

08 p0949 A73-21650

Technology and operation of Olympus engine cycle on Concorde aircraft, discussing chemical and noise pollution and economic factors

08 p0996 A73-21687

Book - MOS/LSI design and application.

08 p0950 A73-21840

Fighter aircraft survivable flight control system design and flight test philosophy, present status and trends, considering fly-by-wire and power-by-wire systems

09 p1030 A73-22177

Hydrodynamics, hydroelasticity, technology and automatic control of H 890 hydrofoil craft

09 p1031 A73-22209

State of the art in the techniques of digital phase modulation

09 p1050 A73-22317

Solar cell generator technology development based on German AEROS satellite project and work on roll-up structure, discussing module concepts and test results

09 p1033 A73-22439

Ceramic-to-metal sealing and joining technology assessment, discussing noble filler metal properties, ceramic surface preparation and thermal tests for performance evaluation

09 p1088 A73-22444

Hydrogen-oxygen fuel cell as reliable electric power supply for space shuttle mission requirements, assessing technological developments

09 p1035 A73-22777

Auxiliary power units and their application to the space shuttle.

09 p1153 A73-22778

Isotope Brayton electric power system for the 500 to 2500 watt range.

09 p1118 A73-22793

Zirconium hydride space power reactor design and fabrication technology evaluation, emphasizing requirements for coupling with power conversion and applications for thermoelectric power generation

09 p1118 A73-22801

Satellite solar power station systems engineering study, examining basic concept technical and economic feasibility

09 p1154 A73-22814

AEC/NASA thermionic reactor program with emphasis on technology utilization, comparing with French, German and Soviet programs

09 p1036 A73-22815

Thermionic fuel unit cell major component materials selection for life and performance improvements, giving out-of-pile and in-pile results

09 p1036 A73-22816

Thermionic fuel elements for in-core reactor power plant space applications, summarizing operating and environmental requirements and technology development

09 p1036 A73-22819

An out-of-core version of a six-cell heat-pipe heated thermionic converter array.

09 p1036 A73-22820

Laser energy transfer - An analytic survey of high power applications.

09 p1096 A73-22822

Photoresist technology for passive ICs production with optical waveguides, describing vaporization deposition and processing for glass films

09 p1086 A73-23075

Research and application problems in fracture of materials and structures in the United States Air Force.

09 p1163 A73-23261

French scientific space research progress assessment, noting ionospheric rocket sounding, plasma wave propagation study and absorption technique for upper atmosphere millimetric radiation measurement

09 p1168 A73-23275

Radio telemetering trends in post-Apollo space programs, emphasizing service lifetimes and orbiting space station data bit generation rate

09 p1053 A73-23362

PCM and DPCM digital modulators design and performance comparison for sampling rate effects on quantizing noise, noting tradeoffs between cost and system efficiency

09 p1059 A73-23435

Temperature measurement and control technology review, discussing analog and digital systems, contact, resistance and radiation thermometers, special temperature sensors and measurement systems

10 p1216 A73-23634

Radio navigation review, discussing Decca, Loran, Omega, VOR/DME, satellite, inertial, integrated, area, approach and landing, collision avoidance and space navigation systems

10 p1246 A73-23636

Microsonics/acoustic surface waves/technology developments covering materials, heteroepitaxial systems, propagation, electron phonon interaction, acoustic amplifiers and waveguides, electromechanical transducers and signal processing

10 p1223 A73-23782

Cryogenic cooling systems technology for spacecraft applications, comparing passive and phase-change coolers and closed cycle refrigerator for capacity and service life

10 p1285 A73-23790

Complementary MOS/silicon-on-sapphire LSI technology developments, assessing impact of incorporated Al and Si gates applications on high speed and low power capabilities

10 p1259 A73-23791

Wideband high-speed high-resolution analog to digital converters technology developments, discussing voltage addressable read-only memory concept and related data sampling

10 p1177 A73-23792

Digital simulation methodology for LSI computer design and technology assessment to assure competitive cost, schedule and implementation cycles in manufacturing

10 p1191 A73-23793

Multicolor documentation type information holographic storage, recording, indexing, registration and reconstruction technology assessment and application, emphasizing displays and automatic test equipment systems

10 p1216 A73-23797

Fast and reliable automatic digital control components and transducers for data processing, display

10 p1216 A73-23797

and storage, assessing technology development trends and preference over analog devices

10 p1199 A73-24028

Linear stochastic, multivariable, optimal control, realization and time-varying systems theory developments covering external and internal representations and variance computation problems

10 p1200 A73-24045

Aircraft noise reduction technology and certification standards, reviewing federal laws and regulations

10 p1175 A73-24553

Commercial communications satellite technology trends, stressing wideband capabilities, flexibility, multiple access and channel capacity increase

10 p1189 A73-24561

Research and technology assessment of high power short wavelength molecular lasers, emphasizing carbon dioxide laser efficiency

10 p1229 A73-24654

State of art of flowmetering, discussing acceptability factors, weirs, laser Doppler velocity method, ultrasonic type, pressure difference technique and turbine and electromagnetic devices

10 p1221 A73-24862

Aircraft design philosophies and structural integrity considerations for reliability without major NDT and maintenance, proposing research program for future computerized design

11 p1433 A73-25128

International Conference on Electromagnetic Windows, 2nd, Ecole Nationale Supérieure de Techniques Avancées, Paris, France, September 8-10, 1971, Proceedings. Volume 1, 2 & 3

11 p1334 A73-25276

The state of technology of ceramic radomes, their use and possibilities for the future.

11 p1335 A73-25286

Military aircraft radome design technology developments in Sweden, discussing use of glass fiber reinforced plastics, manufacturing method, computerized optimization and measurement techniques

11 p1335 A73-25300

Aircraft and missile radomes technology in France, discussing materials, antenna radiation pattern calculation, computer programming for transmission and angular aberrations, and raindrop erosion tests

11 p1336 A73-25301

Radome material technology in UK, summarizing permittivity, loss tangent, internal phase difference, attenuation, aberration, cross polarization and pattern distortion measurements and environmental tests

11 p1336 A73-25308

Personnel radiation protection technology and criteria review, discussing dosimeter specifications and automatic data processing

11 p1322 A73-25314

Possibilities regarding the development and the employment of fiber-reinforced composites in comparison with conventional materials

11 p1454 A73-25419

Flutter technology in the United Kingdom - A survey.

11 p1441 A73-25559

Organic coating technology review, discussing binders, pigments and various processing techniques

11 p1388 A73-25848

Laser beam welding technology review, discussing technical and economic aspects of pulse and CW techniques

11 p1374 A73-25850

Energy 70; Proceedings of the Fifth Intersociety Energy Conversion Engineering Conference, Las Vegas, Nev., September 21-25, 1970. Volumes 1 & 2.

11 p1308 A73-25976

Brayton cycle solar dynamic turboalternator space electric power system technology developments during 1962-1972, considering power efficiency, components reliability and future missions

11 p1309 A73-25982

Concept for a high voltage solar array with integral power conditioning.

11 p1310 A73-26001

Status of silicon germanium air-vac converter development.

11 p1312 A73-26032

Preliminary testing of a SNAP-19 TAGS RTG in support of the Pioneer F and G missions.

11 p1396 A73-26039

Microwave electronic packaging with integrated multifunction assemblies, considering stripline choice for transmission line

11 p1338 A73-26113

Integrated microoptical circuit technology with lenses, prisms, reflectors, mixers, detectors, gratings, filters, lasers, amplifiers and modulators fabricated around waveguides, assessing advantages and potential

11 p1399 A73-26117

A brief survey of monopulse techniques.

11 p1331 A73-26148

French book - Hydraulic and electrohydraulic automatic control. Volume 1 - Theory and technique. Volume 2 - Supplementary techniques and technologies

11 p1313 A73-26253

Eddy current testing - The present situation, results, new developments.

11 p1374 A73-26300

Infrared detectors - Survey of the present state of the art.

11 p1368 A73-26509

Holographic optical memory superiority over conventional localized computer storage devices, considering capacity, access time, immunity to local imperfections, and crosstalk problem

11 p1370 A73-26538

Hologram interferometry adaptation to industrial conditions for dimensions, deformation, vibration and refractivity measurements, noting advantages over ordinary interferometry

11 p1370 A73-26540

High power microwave tubes design trends, considering output capacity and quality, bandwidth, gain, linearity, low noise and intermodulation performance factors

11 p1339 A73-26691

Hybrid type discrete jet-membrane relay system technology and design for discrete signals transformations

12 p1460 A73-26770

Oscillatory operational amplifiers for control systems and computer technology

12 p1477 A73-26773

Automation considerations in technological methods for microcircuit fabrication, emphasizing electron-ion technology

12 p1477 A73-26783

A planning study for a multi-purpose communications satellite serving northern Canada.

12 p1471 A73-27657

Electron-beam welding of small components

12 p1504 A73-27989

Review of microwave-integrated-circuit technology.

13 p1588 A73-28043

Microwave transmitter tubes for surface-based and airborne radar applications, considering ATC, output power, stability, spectrum, size, weight, reliability, maintainability and cost requirements

13 p1590 A73-28532

Circuit technology of a temperature-measurement transmitter for biotelemetry applications

13 p1579 A73-28575

Status of short haul air transportation.

13 p1570 A73-29108

Chemical laser research survey covering device performance, reaction kinetics, theoretical modeling for population inversion and bibliography

13 p1628 A73-29112

Glass fiber for optical communication with existing light source and detector devices, assessing materials and fabrication technology for capacity, attenuation and environmental requirements

13 p1585 A73-29114

Fiber composite materials properties, technological assessment and future development and application for aerospace flight structures, considering manufacturing cost, tailorability and stiffness requirements

13 p1699 A73-29346

General aviation aircraft technology developments based on military and transport aircraft design, considering cost, complexity and reliability

13 p1570 A73-29348

Thick film multilayer IC for electro-optical applications, discussing package techniques, sealing materials, ultrathick printing cold cathode panel and liquid crystal displays

13 p1669 A73-29395

Solar array cost reductions.

13 p1573 A73-29592

Research plans for solar power in space.

13 p1573 A73-29594

Frequency synthesizer technology review, discussing direct frequency synthesis and frequency analysis /phase lock/ techniques

14 p1732 A73-29874

Overview - The role of communication systems in air traffic management.

14 p1725 A73-29876

Historical development of the Air Traffic Control System.

14 p1772 A73-29877

U.S. civil and military air-ground communications development history and expectations, considering information exchange, radar beacon transponders, digital communication and data links

14 p1725 A73-29880

The development of the ATC radar beacon system - Past, present, and future.

14 p1725 A73-29881

Operation of current navigation aids and future prospects.

14 p1773 A73-29883

Computer and digital techniques in ATC automation technology, considering functional organizations, terminal facilities and system capabilities to meet future needs

14 p1730 A73-29886

Finite element analysis programs for general applications, considering state of art

14 p1808 A73-30197

Air navigation evolution and current state of art, discussing MF four axis and nondirectional beacons, VOR, DECCA, DME, TACAN, VOR-Doppler, terminal and landing systems

14 p1773 A73-30445

The impact of satellites on military communications.

14 p1729 A73-30874

Drone recovery surface impact and midair techniques involving parachutes and/or hot-air balloons, considering TALOS/Low Altitude Supersonic Target recovery capability

[AIAA PAPER 73-465]

15 p1827 A73-31451

International Conference on Offshore Airport Technology, 1st, Bethesda, Md., April 29-May 2, 1973, Proceedings. Volume 1.

15 p1856 A73-31526

Heavy marine structure engineering in offshore airport planning, discussing construction types and conditions, environmental factors, materials, methods and equipment

15 p1856 A73-31533

Netherlands international airport planning and site selection, discussing cost/benefit analysis experience from large coastal and offshore projects

15 p1959 A73-31535

Denmark offshore airport projects progress reports covering historical background, present status, political efforts, legislation, market retention, access problem and technical design considerations

15 p1960 A73-31537

Offshore airport planning in Osaka-Bay, Japan - New Kansai International Airport.

15 p1857 A73-31542

Jet noise suppression technology progress review, discussing Lighthill theory of aerodynamic noise, machinery noise and quiet aircraft future

15 p1830 A73-32186

The utilization of solar energy to help meet our nation's energy needs.

15 p1832 A73-32193

Power plants, cost estimates, freighter missions, commercial feasibility and technology for nuclear air cushion vehicles

15 p1912 A73-32194

Microwave power transistors - The present and the future.

15 p1852 A73-32275

Pulse coded scanning beam microwave landing system technology assessment for civil aviation application, describing ground equipment and procedures

15 p1910 A73-32469

Air traffic control technology progress review and future forecast, noting microelectronics and automation need in civil avionics

15 p1960 A73-32479

Aircraft flight control head-up display system design, equipment installation particulars, performance tests and merits evaluation

15 p1831 A73-32508

Instrument-panel electronic display system

15 p1831 A73-32510

All-weather landing technology and economics, considering ground and airborne equipment and benefits and costs

15 p1859 A73-32553

Aircraft noise abatement technological and social aspects, considering aircraft design, airport noise pattern minimization and population removal

15 p1831 A73-32560

High power chemical laser technology.

16 p2022 A73-32724

European Electro-Optics Markets and Technology Conference, 1st, Geneva, Switzerland, September 13-15, 1972, Proceedings.

16 p2022 A73-32851

Current status of Nd:YAG lasers.

16 p2022 A73-32855

Reusable space shuttle orbiter design evolution during 1972-1973, discussing payloads, vertical launching capability and advanced materials technology

16 p2072 A73-33063

Titanium casting technology applications to aircraft structures, considering flap tracks, brake torque tubes and arrestor hook mounting brackets

16 p2018 A73-33071

MIL-STD-810 uniform test methods for determining military equipment environmental resistance, discussing inadequacies, misapplications and planned revision for improvement

16 p2087 A73-33144

Gamma ray astronomical state-of-art, discussing cosmic gamma ray sources observation and diffuse radiation measurement

16 p2055 A73-33290

EHF radio wave limitations and potentialities for high speed data communications systems, considering applications in urban short range relays

16 p1981 A73-33705

Mathematical lunar cartography based on networks of reference points and absolute elevation heights, considering progress since Luna orbiters launchings in 1959

16 p2064 A73-33774

State of the art of GaAs IMPATT diodes.

16 p1990 A73-33896

TECHNOLOGY TRANSFER

Binary capacitors made with p-channel MOS Si gate technology, discussing threshold voltage effects, structural characteristics, bootstrapping and artificial voltage enhancement

16 p1991 A73-33962

German book - Fire protection technology in aviation. Volume 1 - Foundations of aviation and fire-protection technology.

17 p2098 A73-34124

Market trends and technical progress in small gas turbine engines for general aviation and executive aircraft and helicopters

17 p2256 A73-34447

Organization, administration and technological aspects of ERTS system on international scale

17 p2162 A73-34952

Project form of organization adoption for managing innovation, stressing impact of technology on career progression of scientist engineers

17 p2258 A73-35217

Thin configuration flat digital CRT display with electron beam control improvement for military avionics applications, discussing performance advantages and ownership cost

17 p2139 A73-35235

Electric power generation on earth via satellite solar power station, assessing technologies of energy collection and conversion, microwave transmission and rectification

17 p2110 A73-35313

Performance and advantages of FET's as microwave solid state amplifiers.

17 p2141 A73-35322

Apollo program review on resources and technologies utilization, considering budget, radiation and meteoroid hazards, lunar surface, flight design and reliability and Saturn 5 testing

17 p2239 A73-35575

Book - Solid state electronic circuits: For engineering technology.

18 p2292 A73-35899

The preparatory phase of the German Earth Resources program.

18 p2372 A73-35934

Skylab design technology assessment based on past manned spacecraft subsystems, noting advances in mission duration, spacecraft size and living accommodation comfort features

[AIAA PAPER 73-598] 18 p2358 A73-36082

Commercial transport aircraft structural design and technology advances, discussing materials and fabrication processes with respect to costs, durability and reliability

18 p2266 A73-36166

Structural design and technology developments for SST and STOL aircraft, discussing computerized and damage tolerant design, composite materials and cost reducing manufacturing techniques

18 p2362 A73-36167

Solar energy conversion into thermal, chemical or electric energy, discussing high efficiency collector design with thin film for absorber and glass envelope improvement

[AIAA PAPER 73-710] 18 p2269 A73-36331

Book - MOS integrated circuit design.

18 p2294 A73-36966

High performance supersonic axial and centrifugal compressors theoretical and experimental research, assessing and forecasting technological developments

18 p2343 A73-36992

Technological trends in commercial satellite communications.

18 p2290 A73-37034

Satellite telecommunications systems

18 p2290 A73-37050

Some preliminary correlations between control modes of manipulator systems and their performance indices.

19 p2416 A73-37315

An anthropomorphic master-slave manipulator system.

19 p2397 A73-37316

Man-machine interface for controllers and end effectors.

19 p2397 A73-37325

Technological survey of machine intelligence for real time autonomous manipulation with computer recognition sensory feedback and programmed task control to eliminate human operator

19 p2417 A73-37330

A survey study of teleoperators, robotics, and remote systems technology.

19 p2417 A73-37335

The Federal Aviation Administration program to improve terminal area traffic control.

19 p2450 A73-37803

Area navigation technology for air transportation in USA, discussing present systems and projections as related to airline and FAA activities

19 p2451 A73-37807

Strapped down inertial navigation systems.

19 p2452 A73-37876

Boron epoxy, polyimide and aluminum composite materials for cost effective high performance aircraft

and turbine engine structures, assessing development and application status

19 p2443 A73-37892

[SAWE PAPER 992] Autonomous satellite navigation - An historical summary and current status.

19 p2452 A73-38056

Structural composites on future fighter aircraft.

19 p2388 A73-38371

Electrolytic hydrogen fuel production with solid polymer electrolyte technology.

19 p2391 A73-38413

The multi-hundred watt RTG - Technology background and flight systems program.

19 p2456 A73-38418

The MHW heat source - An advance in radioisotope heat source technology for space applications.

19 p2456 A73-38420

Multi-mission nuclear electric propulsion stage design.

19 p2457 A73-38433

The present state of the microwave filter art.

19 p2415 A73-38533

Microwave integrated circuit technology.

19 p2411 A73-38535

Fundamentals of COS/MOS integrated circuits.

20 p2534 A73-38655

International Conference on Communications, Seattle, Wash., June 11-13, 1973, Conference Record. Volumes 1 & 2.

20 p2522 A73-38713

Intrasystem electromagnetic compatibility analysis program.

20 p2528 A73-38771

Satellite-borne power amplifier state of art, comparing TWT development to different technological solutions

20 p2538 A73-39772

Fabrication methods for beryllium spacecraft components.

20 p2615 A73-39775

Morphological indices of digital microelectronic structures

21 p2660 A73-40016

Microwave IC devices covering circulators, directional couplers, frequency multipliers, phase shifters, power amplifiers and reference oscillators, discussing technological development and applications

21 p2668 A73-40019

ILS capability improvements on localizer and glide-slope antenna arrays and monitors, considering effects of reflecting objects on or near aerodrome and terrain

21 p2736 A73-40049

Optical diffraction grating design and production, discussing application of interferometry and electronics to ruling engine control

21 p2698 A73-40136

Phased array antennas in ground based remote sensor system, assessing technologies of AN/FPS-85, HAPDAR and AP/TPN-19 radar systems

21 p2672 A73-40645

Development programs status report on airborne planar, conformal and distributed aperture phased array antennas for use in radar and communication systems

21 p2662 A73-40646

Phased array element types comparison, discussing dipole and open-ended waveguide radiator designs with emphasis on driving point impedance accuracy and active element pattern

21 p2663 A73-40649

Wide-angle impedance matching of phased-array antennas - A survey of theory and practice.

21 p2652 A73-40659

Phased array antenna feed systems developments, discussing relative merits, problems and design choices for air surveillance radar applications in microwave region

21 p2672 A73-40664

Mechanically and electronically switched circular symmetric phased arrays with hybrid matrix phase shifter and lens switch combinations, assessing design and performance characteristics

21 p2672 A73-40675

Assessment of applications of space-borne remote sensing to hydrology and water resources - An overview.

21 p2686 A73-40832

Experiences with an augmented human intellect system - Computer mediated communication.

21 p2654 A73-40833

New developments regarding wide-band communication with waveguide, glass fiber, and superconductivity

21 p2655 A73-41072

Advances in the theory and technology of horn antennas and reflector antennas

21 p2664 A73-41073

ILS technology assessment, considering landing glide path determination, interference due to multipath propagation and ground effects, and operating frequency range problem

21 p2737 A73-41075

Lunar laser telemetry technological developments, discussing light beam generation and detection, SNR

and ranging accuracy improvements, and receiver-optics diameter reduction

21 p2774 A73-41407

A look at Soviet ATC and nav facilities and avionics.

21 p2737 A73-41522

Research carried out by the Aviation Institute on electric welding in protective atmospheres

21 p2708 A73-41578

Overview of Department of Defense Electromagnetic Radiation Hazards Standardization Program.

22 p2822 A73-41790

Germanium resistance thermometers for cryogenic temperature precision measurement, discussing design technology, resistance-temperature characteristics types, installation and measurement methods

22 p2854 A73-41999

Platinum resistance thermometer as standard instrument for interpolation on International Practical Temperature Scale, discussing design development, operational characteristics and errors

22 p2855 A73-42010

Application of electron beam welding to aircraft turbine engine parts.

22 p2866 A73-42196

Laser Doppler velocity measuring system parameters and SNR analysis, comparing photomultiplier, p-i-n and avalanche photodiode detectors for performance

22 p2825 A73-42298

A survey of model reference adaptive techniques /Theory and applications/.

23 p2962 A73-43278

The design, fabrication, and evaluation of a silicon junction field-effect photodetector.

23 p2981 A73-43453

USA government and industry efforts on aircraft midair collision avoidance systems technology advancement, comparing cost effectiveness between airborne and ground based options

23 p3005 A73-43495

Public air transportation service needs for nonurban areas, considering low traffic density problem, operational requirements and future trend

23 p3050 A73-43498

Management of Air Force test and evaluation activities.

23 p3050 A73-44055

Philosophical approaches of technological forecasting and assessment, discussing Dialectical and Singieran inquiring /information/ systems for ill structured problems

23 p3051 A73-44218

Recent advances in thrust vector control for tactical missiles.

24 p3144 A73-44693

Europa 2 Inertial Guidance System technology assessment covering design features, sensor, computer and interface units, first launch failure causes and need for improvements

24 p3108 A73-44694

The role of computers in the development of numerical weather prediction.

24 p3108 A73-45085

TECHNOLOGY TRANSFER

Effective development, documentation, and distribution of computer programs.

03 p0392 A73-13691

Technology transfer from aerospace to public sector, discussing JPL experience, problem definition, funding, user concerns and interpersonal communications

04 p0521 A73-14729

NASA's Technology Utilization Program.

04 p0521 A73-14730

Space technology transfer to community and industry; Proceedings of the Eighteenth Annual Meeting and Tenth Goddard Memorial Symposium, Washington, D.C., March 13, 14, 1972.

06 p0771 A73-17673

Apollo project management techniques transfer to socio-economic programs, discussing systems oriented approach to city planning, mass transportation, pollution control, public hygiene, etc

09 p1167 A73-21898

Technology transfer in New York City - The NASA/NYC Applications Project.

22 p2938 A73-42532

TECHNOLOGY UTILIZATION

Future optical communication systems problems, potentialities and development prospects, considering bandwidth, laser modulation, directionality, fiber transmission, reception, detection, power and efficiency

01 p0018 A73-11066

Bell Laboratories laser optics development and technology applications, discussing CW lasers, light deflectors, holography, optical memories, pattern generator, remote blackboard and micrographics

01 p0060 A73-11213

Applied Superconductivity Conference, 5th, Annapolis, Md., May 1-3, 1972, Proceedings.

02 p0200 A73-11826

- Synchronous electric generators with superconducting field windings, discussing fundamental characteristics, operating modes, refrigeration and cryogenic equipment and applications
02 p0132 A73-11834
- Space experience and ethics impact on world development, considering knowledge advancement, regional applications, economy stimulation, environment improvement and international cooperation
02 p0239 A73-11998
- Laser applications to spectroscopic analysis, Raman, maximum resolution and excited state spectroscopies, and spectral instruments manufacture
02 p0177 A73-12725
- Future NASA communication satellite technology applications in meeting national education, health care, culture and data transfer needs, considering ATS F and CTS spacecraft
02 p0143 A73-12846
- Fundamentals of metrology involving quality and quantity description of reality, emphasizing interrelationship between measurement results in science and technology branches
03 p0305 A73-12895
- Non-metallic materials selection, processing and environmental behavior; Proceedings of the Fourth National Technical Conference and Exhibition, Palo Alto, Calif., October 17-19, 1972.
03 p0328 A73-13001
- Development and evaluation of graphite and boron polyimide composites.
03 p0329 A73-13003
- Rocket nozzles fabrication technology, discussing construction materials and manufacturing processes [AIAA PAPER 72-1191]
03 p0358 A73-13481
- Urban-change detection systems - Remote-sensing inputs.
03 p0301 A73-13845
- Book on modal control theory and applications covering continuous and discrete time lumped parameter linear dynamic systems controllability and observability characteristics
03 p0285 A73-13989
- Book on passive IR sensing devices design and use in industrial and manufacturing problems solution covering detector types, display devices and reliability analysis
03 p0283 A73-13994
- Application of pattern recognition techniques to digitized radar data.
03 p0279 A73-14517
- Strength analyses for design with composite materials using metals technology.
04 p0507 A73-14713
- NASA's Technology Utilization Program.
04 p0521 A73-14730
- Airborne associative parallel array digital computer built with MOS LSI technology for size and weight reduction, discussing design and applications
04 p0424 A73-15065
- NASA space research costs balanced with scientific and technological achievements in relation to space law
04 p0524 A73-15156
- Optical computer technology based on Fourier transform optics and holography, discussing speed and parallel processing capabilities, image deblurring, and applications
04 p0426 A73-15957
- Superconductivity theory and applications, considering cryogenic problems low-loss and magnetic properties and Josephson junction effect on low power technology
04 p0484 A73-15958
- NASA space program value to humanity, discussing Skylab solar and earth observations and communications satellites
05 p0613 A73-16181
- Book - Superconductive tunnelling and applications.
05 p0556 A73-16357
- Data processing remote terminals for real time on-line computer communication systems, discussing design, characteristics and applications
05 p0551 A73-16801
- Considerations and techniques for incorporating remotely sensed imagery into the land resource management process.
05 p0642 A73-17127
- Remote sensing applications in urban and regional planning in the Los Angeles metropolis - Problems and accomplishments.
05 p0642 A73-17132
- The potential application of space technology to the radio tracking and biotelemetry of unrestrained animals.
05 p0545 A73-17134
- Hazardous gas detection system for analysis of gases escaping during cryogenic loading in Apollo-Saturn launch tests, discussing utilization for environment pollution detection
05 p0578 A73-17135
- Communication satellite application to shipping company operations for cost benefits and alleviation of distress alerting, search and rescue, and heavy weather damage problems
[AIAA PAPER 73-47] 06 p0755 A73-17625
- Military contributions to civil aviation.
[AIAA PAPER 73-67] 06 p0647 A73-17635
- A business man views commercial ventures in space.
[AIAA PAPER 73-78] 06 p0771 A73-17640
- Fuel cells for improved electrical power supply.
[AIAA PAPER 73-82] 06 p0649 A73-17641
- The design of electronic equipment for biotelemetry using microcircuit techniques.
06 p0673 A73-17674
- Modulated laser system application categories in tabular and pictorial summaries, considering ranging, reconnaissance, tracking, guidance, weapons, navigation, data processing, display and controlled fusion
06 p0700 A73-18292
- High bandwidth and resolution laser scanners and recorders for imagery transmission, discussing component constraints and integrated optics utilization in modulator and scanner development
06 p0701 A73-18310
- Some applications of a tube with proximity focusing in ultrahigh-speed motion-picture photography
06 p0696 A73-18858
- Fluidic circuits fabrication and design technology for rocket guidance and attitude control
07 p0778 A73-18939
- Superconductors HF properties and losses measurement and separation techniques, discussing applications to filters, oscillators, mixers, transmission lines and radiation detection
07 p0863 A73-20106
- Large-scale applications of superconducting coils.
07 p0863 A73-20107
- State of the art and survey of learning control applications.
07 p0806 A73-20590
- Criteria for evaluating semiconductor materials in eplanar technology applications
08 p0994 A73-21079
- Applications technology satellite data handling processing and interpretation for future earth survey, communications and meteorological satellite operational programs
08 p1014 A73-21593
- Integrated circuits fabrication and technology development, discussing digital and analog circuit capabilities, cost reduction and diffusion techniques
08 p0949 A73-21647
- Radar systems development under solid state electronics advances impact, discussing silicon ICs, HF transistors, hybrid microwave circuits, parametric amplifiers and p-n diodes applications
08 p0949 A73-21650
- Book - MOS/LSI design and application.
08 p0950 A73-21840
- Radioisotope thermoelectric generators for Nimbus 3 weather satellite, Pioneer 10 Jupiter probe and SNAP 27 powered ALSEP station missions, summarizing operational experience
09 p1154 A73-22795
- AEC/NASA thermionic reactor program with emphasis on technology utilization, comparing with French, German and Soviet programs
09 p1036 A73-22815
- Laser energy transfer - An analytic survey of high power applications.
09 p1096 A73-22822
- Block coding for digital computer error detection and correction, considering applications for arithmetic operations, storage media and permanent hardware failure recognition
09 p1061 A73-23400
- Book - RCA advanced technology.
10 p1216 A73-23781
- Complementary MOS/silicon-on-sapphire LSI technology developments, assessing impact of incorporated Al and Si gates applications on high speed and low power capabilities
10 p1259 A73-23791
- Multicolor documentation type information holographic storage, recording, indexing, registration and reconstruction technology assessment and application, emphasizing displays and automatic test equipment systems
10 p1216 A73-23797
- Metal foil panels for radiant heating, describing historical development, design, fabrication methods and applications
10 p1177 A73-24175
- Jet deviation fluidic analog amplifiers, noting industrial application to pressure, flow rate and dimensional measurements
11 p1308 A73-25379
- Vacuum technology at low temperatures; Proceedings of the Symposium, Denver, Colo., August 31, 1970.
11 p1398 A73-25578
- Cryogenic applications for environment simulation.
11 p1344 A73-25580
- Book - Ultrasonics: The low- and high-intensity applications.
11 p1366 A73-26273
- Airport noise control and minimization for community and airline industry interests by technology application and legal-political approaches
11 p1455 A73-26350
- Photochromic glass as reversible optical recording storage medium, discussing image resolution, configuration improvements, merits and applications in holography, random access memory and displays
11 p1370 A73-26537
- Computer technology aided machine design automation and structural synthesis by coded information table formulation and conversion, discussing algorithm construction
12 p1502 A73-26784
- Application of acoustic surface-wave technology to spread spectrum communications.
12 p1470 A73-27570
- Potential applications of acoustic matched filters to air-traffic control systems.
12 p1522 A73-27572
- The use of satellites for aircraft communications and air traffic control.
12 p1472 A73-27666
- Improved uniform-field electrode profiles for TEA laser and high-voltage applications.
13 p1626 A73-28366
- ERAF - Proposal for a European Earth Resources Aircraft.
13 p1569 A73-28786
- Impact body or medium damage prediction and modification technology, discussing test facilities and applications
13 p1699 A73-29310
- The use of the electronic computer for the urgent publication of astronomical material.
14 p1730 A73-29791
- The laser - A unique tool for /for the time being/ unique applications
15 p1884 A73-31325
- Secondary radar interrogator based on IC technology, discussing video processing and monitoring
15 p1847 A73-32436
- Technologies applicable to the development of an onboard L-band transmitter
15 p1852 A73-32481
- NEREM 72; Northeast Electronics Research and Engineering Meeting, Boston, Mass., October 30-November 3, 1972, Record. Part 1 - Technical Papers.
16 p1986 A73-32717
- The application of aerospace technology to patient monitoring.
16 p1975 A73-32804
- European Electro-Optics Markets and Technology Conference, 1st, Geneva, Switzerland, September 13-15, 1972, Proceedings.
16 p2022 A73-32851
- Carbon dioxide laser technological advances and applications including frequency stability systems, remote sensing, air pollution detection, optical heterodyning and pumping
16 p2023 A73-32860
- Titanium casting technology applications to aircraft structures, considering flap tracks, brake torque tubes and arrestor hook mounting brackets
16 p2018 A73-33071
- Technology developments effect on jet aircraft design, discussing flight controls, engine noise suppression, supercritical aerodynamics and composite structures
16 p1968 A73-33188
- Applications of superconductivity.
17 p2218 A73-34111
- Thermosiphon technology advances covering open and closed single-phase natural convection and mixed convection systems, two phase systems and turbine blade cooling
17 p2254 A73-34352
- Applications of advanced aerodynamic technology to light aircraft.
[SAE PAPER 730318] 17 p2101 A73-34676
- B-1 technology applications to advanced transport design.
[SAE PAPER 730348] 17 p2102 A73-34696
- Custom LSI technology utilization in low volume avionic systems, discussing handcrafted chip design, full wafer, array logic and MOS cell approaches and costs
17 p2138 A73-35227
- Apollo program review on resources and technologies utilization, considering budget, radiation and meteoroid hazards, lunar surface, flight design and reliability and Saturn 5 testing
17 p2239 A73-35575
- Applications in aerospace construction and fallout of ONERA thermochemical techniques
[ONERA, TP NO. 1246] 18 p2320 A73-36688
- Cost reductions in transportation to geosynchronous and lunar orbits by a swing station.
19 p2490 A73-37193
- New York offshore airport feasibility study.
[FAA-RD-73-45] 19 p2418 A73-37750
- Space technology utilization for firefighters breathing equipment development, discussing design and field testing program
[ASME PAPER 73-ENAS-24] 19 p2400 A73-37980

TECTONIC MOVEMENT

Management looks at the Canadian program of remote sensing, phase I, 1971-1975. 20 p2521 A73-38587 [AAS PAPER 73-129]

Space science terrestrial applications in biomedical data exchange and telediagnosis, propellant technology, life support atmospheres without fire hazard, industrial mixers and nozzle materials. 20 p2629 A73-38589 [AAS PAPER 73-133]

COS-MOS applications to clock and watch, automotive, aerospace and military, industrial and consumer markets. 20 p2533 A73-38654

Feasibility of satellite solar power station technology concepts, discussing cost analysis, energy conversion efficiency, weight, space environment and microwave transmission. 20 p2510 A73-39247

Organizational design for South Dakota state government to apply remote sensing technology to resources research and management, emphasizing hardware and information dissemination. 20 p2629 A73-39831

Circuit variants and applications of series regulated transistor amplifiers, considering trigger circuit, bistable switch, power amplifier, tape recorder monitoring amplifier, etc. 21 p2659 A73-40011

Microwave IC devices covering circulators, directional couplers, frequency multipliers, phase shifters, power amplifiers and reference oscillators, discussing technological development and applications. 21 p2668 A73-40019

Satellite borne diffused pulsed laser with scattered light detection by optical receiver on ground for applications to wide range geodetic survey. 21 p2681 A73-40133

Atomic time and frequency standards. 21 p2700 A73-40513

Russian book - The laser gyroscope. 21 p2704 A73-41295

Possible scientific utilization of long laser bases. 21 p2716 A73-41328

Vacuum Technology Workshop, Versailles, France, May 30-June 3, 1972, Proceedings. 22 p2886 A73-41867

Technology transfer in New York City - The NASA/NYC Applications Project. 22 p2938 A73-42532

A technology tool for urban applications - The remotely piloted blimp. 22 p2799 A73-42533

A survey of model reference adaptive techniques /Theory and applications/. 23 p2962 A73-43278

Very-long-baseline interferometry techniques applied to problems of geodesy, geophysics, planetary science, astronomy, and general relativity. 23 p2980 A73-43354

Cranfield Fluidics Conference, 5th, University of Uppsala, Uppsala, Sweden, June 13-16, 1972, Proceedings. Volumes 1 & 2. 23 p2941 A73-43390

Hydrazine and methanol fuel cells comparison with hydrogen-air cells in terms of fuel costs and conversion efficiency, considering electric generators and automotive applications. 24 p3057 A73-45025

TECTONIC MOVEMENT

U TECTONICS

TECTONICS

On the interaction between tectonic processes of the earth and the moon. 03 p0299 A73-13093

Some observations on the cenozoic volcano-tectonic evolution of the Great Basin, western United States. 05 p0570 A73-16841

Geographic distribution of anomalies of residual geomagnetic field derived from eccentric dipole and observed field comparing with thermal flux fields and geotectonic features. 06 p0689 A73-17546

Seismicity as a guide to global tectonics and earthquake prediction. 11 p1352 A73-25563

Crustal movements in tectonic areas. 11 p1352 A73-25564

Polar wandering and the earth's dynamical evolution cycle. 13 p1679 A73-28403

Potentialities of lunar laser ranging for measuring tectonic motions. 15 p1873 A73-32201

Geographic distribution of anomalies of residual geomagnetic field derived from eccentric dipole and observed field, comparing with thermal flux fields and geotectonic features. 16 p2002 A73-32770

Worldwide sea level pulsations and inter-pulsations relation to elevation and subsidence of oceanic ridge systems, discussing sea floor spreading hypotheses. 17 p2164 A73-35858

Martian volcanic and tectonic features from Mariner 9 photography, comparing evolutionary phases with lunar and terrestrial morphology. 19 p2477 A73-37203

The definition of the geotectonic domains of the Southern African crystalline shield by ERTS 1 imagery and its economic importance. 21 p2685 A73-40810

A study of lineaments from a Zond 5 photograph of northern Africa. 21 p2687 A73-41332

Mars surface evolution from analysis of Mariner 6 and 7 equatorial photographs, discussing internal dynamic activity. 24 p3128 A73-44432

TEFLON [TRADEMARK]

An experimental method for determining the characteristics of ablative materials. 12 p1557 A73-27068

Helicopter tail rotor teeter hinge with Teflon conical journal bearing allowing axial and radial preload insensitive adjustment, discussing oscillatory loads and temperature effects. 17 p2180 A73-35085

[AHS PREPRINT 762] A reliable Teflon cell with many electrical leads for pressures up to 40 kilobars. 17 p2175 A73-35761

Experimental investigation of the antifriction properties of Teflon-base materials at low temperatures. 21 p2724 A73-41197

TEKTITES

Major, minor and trace elements, specific gravities and refraction indices of Ivory Coast tektites, comparing composition to Bosumtwi crater glasses and Apollo lunar materials. 01 p0109 A73-11475

Chlorine, bromine, iodine, and uranium in tektites, obsidians, and impact glasses. 02 p0223 A73-12720

Bottle green microtektites from Australasian and Ivory Coast deep sea sediments, discussing physical and chemical properties, age and origin. 05 p0615 A73-16383

Spatial distribution of elements in tektites and comparable materials by charged particle activation analysis. 11 p1418 A73-25584

Applications of activation analysis to geochemical, meteoritic and lunar studies. 11 p1326 A73-25800

Indium abundances in cosmo, meteorites, tektites, rock-forming and ore minerals and igneous rocks, considering behavior in magmatogenic processes and rock weathering and alteration. 12 p1490 A73-27125

Tektite ablation calculation taking into account transient effects, internal radiation, melting and nonequilibrium vaporization of glass and drag effect of flanges. 17 p2233 A73-35272

North American microtektites from the Caribbean Sea and their fission track age. 18 p2354 A73-36511

Thermal track fading factor in Georgia tektite stratigraphy and fission track ages, noting agreement with K/Ar ages. 20 p2612 A73-39717

Urey hypothesis for tektites origin via earth-comet collisions dependence on cometary structure, considering solid nucleus vs meteoric particle swarms. 23 p3033 A73-43953

TELECHIRICS

U REMOTE HANDLING

TELECOMMUNICATION

NT AIRCRAFT COMMUNICATION

NT AUTOMATIC PICTURE TRANSMISSION

NT BIOTELEMETRY

NT BROADCASTING

NT CLOSED CIRCUIT TELEVISION

NT COLOR TELEVISION

NT DATA LINKS

NT DEFENSE COMMUNICATIONS SATELLITE SYSTEM

NT DIGITAL SPACECRAFT TELEVISION

NT EDUCATIONAL TELEVISION

NT FACSIMILE COMMUNICATION

NT GROUND-AIR-GROUND COMMUNICATIONS

NT INTERPLANETARY COMMUNICATION

NT LUNAR COMMUNICATION

NT MULTICHANNEL COMMUNICATION

NT OPTICAL COMMUNICATION

NT PULSE COMMUNICATION

NT PULSE FREQUENCY MODULATION TELEMETRY

NT RADIO COMMUNICATION

NT RADIO RELAY SYSTEMS

NT RADIO TELEGRAPHY

NT RADIO TELEMETRY

NT RADIOTELEPHONES

NT SATELLITE TELEVISION

NT SPACE COMMUNICATION

NT SPACECRAFT ANTENNAS

NT SPACECRAFT COMMUNICATION

NT SPACECRAFT TELEVISION

NT STEREOTELEVISION

NT TELEMETRY

NT TELEPHONY

NT TRANSOCEANIC COMMUNICATION

NT VIDEO COMMUNICATION

NT VOICE COMMUNICATION

NT VOICE DATA PROCESSING

NT WIDEBAND COMMUNICATION

Theory of multistep coding and its application to multiphase-modulation communication systems. 01 p0018 A73-11072

Constant-envelope spread spectrum random access satellite communication system, discussing message and multiple access modem, signal acquisition, tracking, ranging, etc. 01 p0018 A73-11177

Optimal fixed message block size for computer communications. 01 p0019 A73-11454

The telecommunication payload of the satellite Symphonie [DGLR PAPER 72-089] 02 p0140 A73-11678

System time domain simulation computer aided analysis program for communication systems, representing mathematical and functional models. 04 p0425 A73-15459

Communications Satellites and the international communications industry. 07 p0923 A73-19139

Computerized short- and long term ionospheric propagation forecasting for HF communications, frequency scheduling and broadcasting circuits. 09 p1048 A73-21983

Canadian telecommunications satellite system for TV, voice and analog or digital data transmission, describing space segment, satellite control and ground station network. 11 p1431 A73-26259

Optimal data sampling in communication channels system, discussing algorithms for data transmission and control. 13 p1587 A73-28870

Optical fibre guide measurements with short coherent light pulses. 14 p1756 A73-30056

Study in curvature of long distance wave guides - The case of helicoidal guides. I 15 p1842 A73-31360

Quasi-optimal signal reception in asynchronous addressing communication systems with a time-frequency matrix. 17 p2121 A73-34587

Control of multiplexed communications channels. 17 p2144 A73-35310

Satellite telecommunications systems. 18 p2290 A73-37050

Canadian space programs in communications, navigation and atmospheric science, considering telephony, data transmission, TV broadcasting and remote sensing [AAS PAPER 73-118] 20 p2584 A73-38580

International Conference on Communications, Seattle, Wash., June 11-13, 1973, Conference Record. Volumes 1 & 2. 20 p2522 A73-38713

The telecommunication payload of the satellite Symphonie. 21 p2655 A73-41081

Russian book on airport cable communication lines, discussing design construction, signal transmission theory and structural and electrical characteristics. 21 p2675 A73-41283

Use of a response surface to optimize digital telecommunication systems. 23 p2948 A73-43214

TELEGRAPH SYSTEMS

An automatic system for broadcasting weather data to international civil aviation. 17 p2122 A73-34962

TELEGRAPHY

U TELEGRAPH SYSTEMS

TELEMETERS

U TELEMETRY

TELEMETRY

NT BIOTELEMETRY

NT PCM TELEMETRY

NT PULSE FREQUENCY MODULATION TELEMETRY

NT RADIO TELEMETRY

The onboard data processing system of the Helios probe [DGLR PAPER 72-092] 02 p0228 A73-11700

The laser telemetry station of the Pic-du-Midi Observatory and the acquisition of the French retroreflectors of Luna 17. 02 p0151 A73-12247

Structural and thermal design and fabrication of Lunokhod retroreflecting panel mounted on lunar surface for earth-moon distance determination by laser telemetry. 02 p0176 A73-12251

Performance test of flexible rolled-up solar array /FRUSA/ via telemetered data from accelerometers, strain gages and temperature sensors, noting feasibility for spacecraft power supply. 03 p0256 A73-14236

NTC '72; National Telecommunications Conference, Houston, Tex., December 4-6, 1972, Record. 04 p0417 A73-15376

The growing role of standards in the national and international coordination of space programs. 04 p0524 A73-15381

Pseudorandom noise for telemetry error rate measurement applications and limitations. 04 p0449 A73-15457

Telemetry with modulated beams short range high resolution systems. 05 p0576 A73-16343

French telemetry processing center, discussing data acquisition and reduction systems and application software 05 p0552 A73-17299

French Guiana space center facilities for missile tracking, telemetry, data processing and transmission of command instructions, discussing PCM, PAM and PDM links equipment 07 p0807 A73-18942

Reliable, high performance magnetic tape recorder/reproducer for third generation telemetry data computer processing lines, noting human error possibility reduction 07 p0795 A73-18955

Computer for automatic equipment monitoring, operation control and breakdown diagnosis in telemetry data processing, discussing management routines and reliability 07 p0795 A73-18956

Satellite-borne vidicon camera and associated control and telemetry electronics for imagery and dimensional parameters of sparks generated by gamma radiation 07 p0822 A73-18987

Prospero satellite orbital/operational performance and control, describing ground-satellite telemetry and data processing operations 07 p0905 A73-19142

Recent studies of the magnetospheric electric field missions above the electron gyrofrequency. 07 p0815 A73-19254

Communications, despin control, electrical power, telemetry and command, positioning and orientation subsystems of Intelsat 4 satellite 09 p1152 A73-22698

International Telemetering Conference, Los Angeles, Calif., October 10-12, 1972, Proceedings. 09 p1053 A73-23361

Bandwidth as measure of dimensions added to signal space per unit time in digital transmission power spectral density computation, presenting comparison for telemetry signals 09 p1054 A73-23384

Impact of solar calibration on telemetry system testing and checkout. 09 p1057 A73-23407

Application of Range Commanders Council Document 118-71 test methods to range management - SAMTEC. 09 p1057 A73-23409

Data quality assurance in a shipboard computer-controlled telemetry system. 09 p1057 A73-23410

Microprogrammable processors applied to telemetry processing systems. 09 p1057 A73-23411

A mobile tone range/RDF system for telemetry tracking of sounding rockets. 09 p1057 A73-23412

Design philosophy and operation of hardware and data flow of TELFILE real time multiprogrammed telemetry system, discussing support of Minuteman III Weapons Systems 09 p1057 A73-23415

The preprocessing of French laser observations from the ISAGEX program 10 p1187 A73-23621

Principles of spacecraft telemetry data management. 11 p1333 A73-25351

Analysis of the first laser echoes obtained on the reflector of Luna 21 13 p1686 A73-29561

ELDO equatorial launching base for Europa 2 vehicle, discussing launch site and telemetry facilities and logistics management/organizational aspects 14 p1741 A73-30077

PCM multiplexing system for incorporation into telemetry systems of large ballistic missiles or spacecraft launch vehicles 14 p1727 A73-30110

Objectives and employment of the integration and system test equipment for Aeros 15 p1943 A73-32180

Extra-atmospheric observations of the luminosity of the sky from the Cosmos 51 and Cosmos 213 satellites. II - Measurement data and their interpretation 16 p2001 A73-32707

Lunar laser telemetry technological developments, discussing light beam generation and detection, SNR and ranging accuracy improvements, and receiver-optics diameter reduction 21 p2774 A73-41407

TELEMETRY AUTO REDUCTION SYSTEM

U DATA REDUCTION

U TELEMETRY

TELEOPERATORS

Operation of spacecraft in orbit with the aid of remote-controlled manipulators - A joint project of ERNA, KYBERTRONIC, KLERA [DGLR PAPER 72-098] 02 p0136 A73-11659

Teleoperators - Manual/automatic system requirements. 17 p2180 A73-35315

X-reference frame bilateral control for the Shuttle Attached Manipulator System. 17 p2180 A73-35317

Earth-orbit mission considerations and Space Tug requirements. 19 p2490 A73-37302

Free flying teleoperator spacecraft systems for automated satellites retrieval, cargo transfer and orbital operations support 19 p2490 A73-37303

System requirements for a free-flying teleoperator to despin the ATS-V. 19 p2490 A73-37304

Dynamic passivation of a spinning and tumbling satellite using free-flying teleoperators. 19 p2490 A73-37306

Shuttle Payload Accommodation System teleoperator. 19 p2491 A73-37308

The multi-moded remote manipulator system. 19 p2416 A73-37314

Some preliminary correlations between control modes of manipulator systems and their performance indices. 19 p2416 A73-37315

An anthropomorphic master-slave manipulator system. 19 p2397 A73-37316

Developments in Canada related to remotely manned systems. 19 p2416 A73-37317

Illumination and television considerations in teleoperator systems. 19 p2416 A73-37318

Remote viewing system with TV cameras to duplicate human visual field and acuity functions, featuring operator command and data link bandwidth minimization 19 p2416 A73-37319

The oculometer in remote viewing systems. 19 p2397 A73-37320

Man-machine interface for controllers and end effectors. 19 p2397 A73-37325

Terminal pointer hand controller and other recent teleoperator controller concepts - Technology summary and application to earth orbital missions. 19 p2397 A73-37326

Evaluation of human operator visual performance capability for teleoperator missions 19 p2397 A73-37327

Teleoperator system incorporating touch feedback and sequenced automatic control for experimental investigation of human touch sensing relation to manipulative skills 19 p2397 A73-37328

Command language for supervisory control of remote manipulation. 19 p2403 A73-37329

Performance improvement in remote manipulation with time delay by means of a learning system. 19 p2417 A73-37331

A survey study of teleoperators, robotics, and remote systems technology. 19 p2417 A73-37335

Design and evaluation of a backhoe model with a master slave control. 19 p2401 A73-38085

Teleoperator monoscopic television system and stereoscopic TV system with Fresnel display, using static simulations to investigate camera locations and depth alignment [ALAA PAPER 73-920] 21 p2673 A73-40868

TELEPHONES

NT RADIOTELEPHONES

TELEPHONY

The transmission of low frequency medical data using delta modulation techniques. 04 p0412 A73-15408

High capacity, dual antenna earth station. 04 p0432 A73-15416

Transoceanic telephony via communication satellites, discussing satellite reliability and placement in synchronous orbit 06 p0663 A73-17577

The experimental telecommunication satellite Project Symphonie. 07 p0905 A73-19140

German monograph - Synchronization of digital telephone networks by means of phase averaging with parameter transfer. 07 p0794 A73-20386

High capacity digital concentrator of telephone circuits for a TDMA station /CELTIC/ 09 p1050 A73-22319

TDMA satellite telephonic communication network with preassigned channeled radio carrier, describing four phase demodulator and channel units regrouping 09 p1050 A73-22320

A method for smoothing level fluctuations caused by echoes in the case of FM directional radio links 11 p1328 A73-25344

Modulation and speech processing techniques for a maritime-satellite service. 12 p1472 A73-27662

European telephony traffic and Eurovision TV program exchanges via three-axis stabilized communications satellite with fold out solar panel arrays 14 p1724 A73-29715

Interference into angle-modulated systems carrying multichannel telephony signals. 16 p1983 A73-33742

Canadian domestic satellite system applications. 17 p2124 A73-35311

Telephone line echo reduction by adaptive filter compensation, using statistical speech-white noise relations 23 p2952 A73-43318

TELESCOPES

NT APOLLO TELESCOPE MOUNT

NT ASTRONOMICAL TELESCOPES

NT CELESCOPES

NT HELIOMETERS

NT LARGE SPACE TELESCOPE

NT PARTICLE TELESCOPES

NT PYROHELIOMETERS

NT RADIO TELESCOPES

NT REFLECTING TELESCOPES

NT REFRACTING TELESCOPES

NT SCHMIDT CAMERAS

NT SPACEBORNE TELESCOPES

NT SPECTROSCOPIC TELESCOPES

NT STRATOSCOPE TELESCOPES

NT X RAY TELESCOPES

Design and performance of light-intensification night vision telescopes 23 p2979 A73-43220

TELETYPEWRITER SYSTEMS

Ground communications networks for aeronautical operations. 14 p1740 A73-29885

TELETYPEWRITERS

A flexible automatic typewriting system using three tape readers. 23 p2944 A73-43422

TELEVISION CAMERAS

Possibility of determining the lunar rotation elements with a narrow-angle television camera 01 p0051 A73-10944

The data-handling problem with television recording of spectra. 02 p0170 A73-12340

An electronic multiband camera film viewer. 04 p0450 A73-15771

ERTS two-inch RBV cameras performance characteristics. 05 p0579 A73-17144

Cost effectiveness and observation speed of small astronomical telescopes array with TV detection systems 06 p0693 A73-18240

Recent advances in low light level field sequential color television. 06 p0694 A73-18298

Apollo 15 and 16 ground-commanded television assembly. 07 p0823 A73-19375

Scanning electron microscope and energy dispersive X-ray analysis of the surface features of Surveyor III television mirror. 07 p0872 A73-19899

Implementation of the 1975 Mars Viking Lander cameras. 08 p0970 A73-21741

Electronic imaging systems with TV vidicon competition with film photography for spaceborne solar astronomy, comparing resolution, sensitivity and SNR 08 p0971 A73-21749

Theoretical performance figures for low light level TV cameras. 08 p0972 A73-21757

ERTs return beam vidicon TV cameras and ground based electron beam recording system resolution and distortion characteristics from preflight and in-flight simulation and calibration studies 09 p1082 A73-22385

Application of a narrow-angle television camera for determining the rotation elements of the moon. 09 p1084 A73-22739

Pulsed GaAs illuminators for night-vision systems. 10 p1216 A73-23785

Sunspot observations by means of a vidicon camera. I. 12 p1545 A73-27833

Mariner Mars 1971 photogrammetry, discussing spacecraft scan platform mounted TV camera calibration

TELEVISION EQUIPMENT

- tion procedure for interior orientation parameters and opto-mechanical orthogonality 12 p1500 A73-27953
- A proximity focused ultraviolet-sensitive SEC camera tube. 14 p1732 A73-29910
- Pick-up storage tube having an electronic shutter, automatic exposure control, wobbling correction, and slow scanning. 14 p1751 A73-29911
- Capabilities and limitations of infrared imaging systems. 17 p2167 A73-34902
- Infrared sensing of the surface temperature of certain lakes of Northern Italy 17 p2206 A73-34942
- The University College London image photon counting system - Performance and observing configuration. 17 p2169 A73-35279
- Digital pulse counting astronomical spectrograph system with TV camera tube, image intensifier and minicomputer for camera scan control and video data processing 17 p2169 A73-35282
- The detector system of the International Ultraviolet Explorer satellite. 17 p2170 A73-35295
- Verification of performance of the Mariner 9 television cameras. 19 p2428 A73-37258
- Remote viewing system with TV cameras to duplicate human visual field and acuity functions, featuring operator command and data link bandwidth minimization 19 p2416 A73-37319
- Influence of the resolution of television cameras and radiometers on the accuracy of determining the quantity of clouds from satellites 21 p2731 A73-40493
- An optimized video output from a wide angle optical probe. [AIAA PAPER 73-918] 21 p2673 A73-40866
- A compound wide angle color visual display system and a high resolution, high sensitivity close circuit color television camera developed for wide angle color visual systems. [AIAA PAPER 73-925] 21 p2702 A73-40872
- ERTS-1 satellite-borne TV cameras and multispectral band scanners for remote sensing and data collection with applications in agriculture, forestry, and water resources survey 21 p2692 A73-41521
- ## TELEVISION EQUIPMENT
- NT IMAGE DISSECTOR TUBES
- NT TELEVISION CAMERAS
- NT TELEVISION RECEIVERS
- A visual stimulator employing a T.V. raster display. 14 p1722 A73-30400
- Characteristics of the U.B.C. television systems. 17 p2169 A73-35288
- Unidirectional small active antenna. 20 p2525 A73-38742
- Electronic integrated HF selective gyrator for TV IF filter development 21 p2661 A73-40230
- Television guidance for astronomical telescopes 23 p2984 A73-44362
- ## TELEVISION RECEIVERS
- Video-signal improvement using comb filtering techniques. 12 p1468 A73-27012
- A transmission and receiving system for a direct broadcasting television satellite - Telecommunications, satellite, broadcasting, experimentation, microwaves 12 p1469 A73-27074
- ## TELEVISION RECEPTION
- Target detection during picture transmission through a TV system [DGLR PAPER 72-099] 02 p0166 A73-11682
- Some developments in semi-direct broadcast satellites and community receiving systems. [AAS PAPER 73-155] 20 p2521 A73-38599
- ## TELEVISION SYSTEMS
- NT CLOSED CIRCUIT TELEVISION
- NT COLOR TELEVISION
- NT DIGITAL SPACECRAFT TELEVISION
- NT EDUCATIONAL TELEVISION
- NT SATELLITE TELEVISION
- NT SPACECRAFT TELEVISION
- NT STEREOTELEVISION
- Secondary electron conduction /SEC/ vidicon television system for space astronomy, discussing data reduction requirements, costs and quasar spectrum observation 01 p0048 A73-10530
- Flight test of narrow band television system. 01 p0052 A73-11169
- A study of frequency sharing between satellite and terrestrial broadcasting systems. 01 p0018 A73-11179
- Computerized multichannel alphanumeric TV system for ATC operational information display, 22 p2845 A73-41936

- describing data acquisition, processor and software peripherals and video display subsystem 02 p0165 A73-11594
- TV satellite system feasibility and design study for Germany, discussing technical and economic aspects [DGLR PAPER 72-051] 02 p0140 A73-11664
- Feasibility study for direct TV transmission and reception via satellite, discussing technical and economic aspects [DGLR PAPER 72-050] 02 p0140 A73-11679
- Television/computer dimensional analysis interface with special application to left ventricular cineangiograms. 06 p0657 A73-17860
- Charged coupled IC image sensors based on MOS capacitors for low light level TV, considering operation, performance and production technologies 06 p0676 A73-18301
- Launching base telelimiter apparatus with image superposition on TV screen for controlling missile or rocket from going beyond security limits during initial flight 07 p0789 A73-18950
- Television rate laser raster scanner, discussing deflectors, beam-shaping and image-forming optics, electronic system and scanning beam frequency response 08 p0975 A73-21141
- Television rate laser scanner with anisotropic Bragg device of paratellurite as acousto-optic horizontal deflector, noting operation efficiency and limiting resolution 08 p0975 A73-21142
- Storage and transmission of sequences of moving images 08 p0941 A73-21559
- Image integration and display system for guiding on stars beyond the visual detection limit. 08 p0987 A73-21748
- TV vidicon image converter with arbitrary scanning format and computer-compatible output signals, using power spectrum redistribution functions 09 p1060 A73-22945
- European telephony traffic and Eurovision TV program exchanges via three-axis stabilized communications satellite with fold out solar panel arrays 14 p1724 A73-29715
- HF laser flow visualization with an infrared television system. 15 p1874 A73-31357
- Television in the control system of an optical telescope 15 p1877 A73-32135
- Optical model of a holographic television system 15 p1879 A73-32331
- Application of the visualization of radar information in television 15 p1911 A73-32484
- Passive low light level television for military and civilian ground surveillance under poor visibility conditions 17 p2168 A73-34906
- Astronomical observations with television-type sensors; Proceedings of the Symposium, University of British Columbia, Vancouver, Canada, May 15-17, 1973. 17 p2168 A73-35276
- The use of television type sensors in astronomy. 17 p2169 A73-35278
- Television sensors for ultraviolet space astronomy. 17 p2170 A73-35292
- TVAC - A television area correlator tracking system. 17 p2171 A73-35381
- Illumination and television considerations in teleoperator systems. 19 p2416 A73-37318
- The oculometer in remote viewing systems. 19 p2397 A73-37320
- Spacecraft television image comparison between earth and Mars surface features and geology, discussing mountain chains, deserts and tectonic mapping techniques 20 p2613 A73-39897
- Teleoperator monoscopic television system and stereoscopic TV system with Fresnel display, using static simulations to investigate camera locations and depth alignment [AIAA PAPER 73-920] 21 p2673 A73-40868
- Sensor data display simulator for airborne target acquisition with improved sensors, using TV scanning of film based imagery [AIAA PAPER 73-921] 21 p2673 A73-40869
- Electrofluorography for human body layer single-plane sections synchronization, using X ray tomography and TV imaging followed by roentgenogram electronic summation 21 p2645 A73-41216
- High resolution television imaging of barium cloud release in magnetosphere, discussing cloud shape development, striation patterns, core behavior and diffusion characteristics 22 p2845 A73-41936

- Temperature measurements with an infrared television system. 22 p2853 A73-41984
- ## TELEVISION TRANSMISSION
- Clock comparisons by short wave, ULF and VLF signals, Loran C and Omega methods, onboard aircraft atomic clocks and TV synchronizing pulses 03 p0307 A73-13264
- Satellite educational TV systems for undeveloped countries, discussing installation problems, capital investments requirements and potential benefits 03 p0401 A73-14137
- Manned spacecraft digital TV system channel error correcting encoder and decoder performance test data including bit error rate versus SNR and decoding depth 04 p0419 A73-15400
- A DPCM codec using edge coding and line replacement. 04 p0422 A73-15443
- Accurate time and frequency comparisons based on TV frame pulses 06 p0692 A73-17587
- Multichannel television coupling modulation experiments using a CO2 laser. 07 p0833 A73-19195
- Subjective comparisons of analog and digital TV transmission system, considering spectral occupancy and picture quality 09 p1055 A73-23387
- Spacecraft transmitted TV picture geometrical distortion in terms of root-mean-square errors, considering applications to ESSA-7, Surveyor-7 and Mariner 4 data samples 10 p1219 A73-24485
- A transmission and receiving system for a direct broadcasting television satellite - Telecommunications, satellite, broadcasting, experimentation, microwaves 12 p1469 A73-27074
- Methods for the comparison and the propagation of time scales 12 p1498 A73-27751
- Problems involving efficient transmission of informative parameters in the adaptive discretization of an analog signal 13 p1583 A73-28852
- Communications aspects of broadcast TV satellites. 14 p1725 A73-29716
- German national geostationary TV satellite project, discussing thermal and attitude control, launch and guidance problems, solar power supply and antenna systems 16 p2074 A73-33737
- Television satellite transmission systems capabilities and technology, discussing Communications Technology Satellite [DGLR PAPER 73-040] 17 p2125 A73-35479
- Selection of a direct-transmission television satellite system from the point of view of stringent pointing requirements [DGLR PAPER 73-047] 17 p2126 A73-35483
- Canadian space programs in communications, navigation and atmospheric science, considering telephony, data transmission, TV broadcasting and remote sensing [AAS PAPER 73-118] 20 p2584 A73-38580
- FM distortion of a TV signal and subcarriers due to bandpass filtering and additive Gaussian noise. 20 p2523 A73-38722
- Television sound subcarrier transmission in space communication. 20 p2524 A73-38737
- Worldwide TV satellite systems, discussing transmission channels, power limitations, quality objectives, conversion and digital techniques 20 p2530 A73-39204
- Precision comparison of time and frequency by means of TV signals. 22 p2859 A73-42191
- Telesat Canada-Anik - Canada's domestic satellite communications system 24 p3069 A73-45392
- ## TELEVISION THEORY
- U GYRATORS
- U NETWORK ANALYSIS
- U NETWORK SYNTHESIS
- ## TELLURIC CURRENT MICROPULSATIONS
- U MICROPULSATIONS
- U TELLURIC CURRENTS
- ## TELLURIC CURRENTS
- DR ring current belt formation due to electron and proton gradient drift in inhomogeneous geomagnetic field, calculating charged particles trajectories 07 p0816 A73-19446
- Earth electrical conductivity radial distribution effect on solar quiet day geomagnetic field variations 07 p0816 A73-19466
- Worldwide distribution of geomagnetic tides. 19 p2425 A73-38104
- Russian book - Certain problems concerning solar-terrestrial links and physics of the atmosphere. 21 p2730 A73-40102

SUBJECT INDEX

Statistical analysis of daily, monthly, annual and seasonal activity of earth currents field, presenting tables of storms and disturbances

21 p2681 A73-40107

The relation between cosmic ray intensity variations and effects due to the electromagnetic complex

21 p2755 A73-40110

TELLURIC FIELDS

U ELECTRIC FIELDS

U TELLURIC CURRENTS

TELLURIC LINES

Possible dependence of the differential shifts of Fraunhofer telluric lines on the solar zenith distance

01 p0106 A73-11241

Photospheric height gradient and solar rotation measurements for Fraunhofer lines by magnetograph, considering telluric lines effect

01 p0107 A73-11376

Observations of sunspot umbral velocity oscillations.

08 p1001 A73-20758

Possible dependence of differential shifts of telluric Fraunhofer lines on zenith distance of the sun.

10 p1279 A73-24177

Seasonal variations in the telluric lines of oxygen and water vapor

11 p1392 A73-25614

Rotational spectral lines of water vapor dimers in the upper troposphere

13 p1609 A73-29152

Accurate wavelengths of stellar and telluric absorption lines near lambda 7000 A.

22 p2907 A73-42208

High resolution analysis of the sun's radiation received at the ground from 9 to 11.6 microns.

23 p3003 A73-43888

TELLURIDES

NT BISMUTH TELLURIDES

NT CADMIUM TELLURIDES

NT INDIUM TELLURIDES

NT LEAD TELLURIDES

NT MERCURY TELLURIDES

NT TIN TELLURIDES

NT ZINC TELLURIDES

Optical band gap energies and stacking sequences of molybdenum tellurides and tungsten selenides derived from dielectric constant measurements

04 p0482 A73-14868

Knudsen measurements of the decomposition and the heat of formation of manganese ditelluride.

09 p1048 A73-22442

Determination of the parameters of r-type recombination centers in germanium-doped GaTe single crystals

11 p1410 A73-26587

Crystal growth by vapor transport of GeSe, GeSe₂, and GeTe and transport mechanism and morphology of GeTe.

15 p1842 A73-32652

TELLURIUM

NT TELLURIUM ISOTOPES

Nonlinear polarization coefficients of proustite and tellurium.

06 p0738 A73-18596

Energy loss measurements with 60 keV electrons in the case of amorphous and polycrystalline selenium and tellurium and the determination of optical constants

07 p0862 A73-20017

TELLURIUM ALLOYS

Effect of oxygen on the structure and properties of Bi₂Te₃-based alloys

15 p1923 A73-31209

TELLURIUM COMPOUNDS

NT BISMUTH TELLURIDES

NT CADMIUM TELLURIDES

NT INDIUM TELLURIDES

NT LEAD TELLURIDES

NT MERCURY TELLURIDES

NT TELLURIDES

NT TIN TELLURIDES

NT ZINC TELLURIDES

Phase equilibrium in the TeO₂-V₂O₅ system

05 p0589 A73-17173

TELLURIUM ISOTOPES

'Anomalous' alteration of the Moessbauer isomer shift of Te₁₂₅ in defect diamond-like semiconductors

14 p1784 A73-30809

TELLURIUM 119

U TELLURIUM ISOTOPES

TELSTAR SATELLITES

NT TELSTAR 1 SATELLITE

TELSTAR 1 SATELLITE

The precession of unsymmetric spin-stabilized satellites.

22 p2916 A73-42190

TEMPER [METALLURGY]

The tempering of low carbon steels containing tungsten.

02 p0183 A73-12760

Temper embrittlement response and toughness of a rare earth treated Ni-Cr-Mo steel.

02 p0183 A73-12762

Hardening by tempering of Fe-Ni-Mo and Fe-Ni-Co-Mo martensites

12 p1514 A73-27987

Some physicochemical characteristics of failure in tempered high strength steels

17 p2189 A73-34580

TEMPERATE REGIONS

Observations of ionospheric electron content at medium latitude geomagnetically conjugate stations.

04 p0440 A73-14955

Moment equations of temperature and high latitude spread F instability in presence of north-south electric field, relating to maximum Pedersen current and barium cloud deformation

07 p0814 A73-19243

The mean upper-air flow in Southern Hemisphere temperate latitudes determined from several years of GHOST balloon flights at 200 and 100 mb.

08 p0960 A73-21376

Effect of geomagnetic activity on occurrence of whistler atmospherics.

09 p1077 A73-22373

Transmission loss at high frequencies on 3260 km temperate-latitude path.

09 p1052 A73-22958

Cosmic ray storm effect on midlatitude and polar neutron monitors, noting comparison with underground mu-meson telescopic observations at high rigidities

12 p1534 A73-27001

Recent observations of Jupiter's North North Temperate Belt Current B.

23 p3033 A73-43949

TEMPERATURE

NT AMBIENT TEMPERATURE

NT ATMOSPHERIC TEMPERATURE

NT AURORAL TEMPERATURE

NT BODY TEMPERATURE

NT BRIGHTNESS TEMPERATURE

NT COMBUSTION TEMPERATURE

NT CRITICAL TEMPERATURE

NT CURIE TEMPERATURE

NT FLAME TEMPERATURE

NT FLASH POINT

NT GAS TEMPERATURE

NT HIGH TEMPERATURE

NT IGNITION TEMPERATURE

NT ION TEMPERATURE

NT IONOSPHERIC TEMPERATURE

NT LOW TEMPERATURE

NT LUNAR TEMPERATURE

NT NOISE TEMPERATURE

NT OPERATING TEMPERATURE

NT PLANETARY TEMPERATURE

NT PLASMA TEMPERATURE

NT ROOM TEMPERATURE

NT SATELLITE TEMPERATURE

NT SKIN TEMPERATURE [BIOLOGY]

NT SKIN TEMPERATURE [NON-BIOLOGICAL]

NT SOLAR TEMPERATURE

NT STAGNATION TEMPERATURE

NT STELLAR TEMPERATURE

NT SURFACE TEMPERATURE

NT TRANSITION TEMPERATURE

NT WALL TEMPERATURE

NT WATER TEMPERATURE

TEMPERATURE COMPENSATION

Thermoanemometer with automatically stabilized temperature of its sensitive element and output signal linearization

02 p0170 A73-12344

An electronic method of temperature compensation in hydrostatic pressure transducers with semiconductor p-n junctions.

03 p0308 A73-13784

Low weight thermostat for temperature compensation of Sharpe quartz gravimeters

03 p0311 A73-14614

The measurement of thermal strain using self-temperature compensated strain gauges.

07 p0823 A73-19567

Self-compensating strain measurement in rotating disks subjected to elastic and plastic deformation

07 p0826 A73-20516

Heated Fleisch pneumotachometer - A calibration procedure.

08 p0935 A73-21509

Accuracy of interferometric plasma investigations involving heating of the optical elements

09 p1131 A73-22883

An IC piezoresistive pressure sensor for biomedical instrumentation.

10 p1183 A73-23649

Piezoresistive semiconductor strain gage optimum applications and practical merits comparison with wire or foil resistance types, considering stability, accuracy and temperature compensation

10 p1195 A73-24571

Methods and means of studying the characteristics of heat-resistant strain gauges by means of devices heated by electric current

11 p1362 A73-25457

TEMPERATURE CONTROL

Analytical fit of the transfer function of a logarithmic electrometer and correction for ambient temperature variations.

11 p1367 A73-26306

The problem of temperature in vacuum metrology.

11 p1371 A73-26552

Si transistor amplifier design for power gain stability against temperature variations, considering emitter and collector base voltage as stability parameters

16 p1988 A73-33399

Autocompensatory strain measurement of rotating disks subjected to elastic and plastic deformation.

19 p2430 A73-37792

A method for thermal stabilization of the parameters of devices with ferrite cores

22 p2833 A73-42371

Temperature compensation in a thermoanemometer

24 p3089 A73-44548

TEMPERATURE CONTROL

Sensitivity analysis method application to spacecraft thermal environment control system design, determining mathematical model input parameters uncertainty effects on temperature determination

01 p0123 A73-11143

Space simulation chamber tests of thermal louver model for spacecraft temperature control

01 p0110 A73-11150

A design study of thermal louver system.

01 p0111 A73-11152

The operational condition of heat pipes.

01 p0111 A73-11153

A cryostat for measuring electrical values of semiconductor devices in the temperature range from 77 to 300 K

02 p0165 A73-11550

The development of the heat control system of the Helios solar probe

02 p0227 A73-11652

[DGLR PAPER 72-102] Book - Fundamentals of spacecraft thermal design.

02 p0237 A73-11885

Electron beam heating test arrangement for high temperature testing of refractory materials in vacuum, describing temperature control systems

02 p0150 A73-12220

The Ranque-Hilsch vortex tube and its application to spacecraft environmental control systems.

03 p0287 A73-13313

Single automatic potentiometer based maximum-minimum temperature control unit, noting elimination of dual temperature regulators

03 p0309 A73-14026

Design and realization of microthruster temperature control subsystems - Optimization through refinement of a mathematical model

04 p0489 A73-15735

Active control heat pipe performance for long life battery cooling.

[ASME PAPER 72-WA/HT-43] 04 p0518 A73-15813

The application of heat pipe techniques to electronic component cooling.

[ASME PAPER 72-WA/HT-42] 04 p0518 A73-15814

Survey of heat transfer techniques applied to electronic equipment.

[ASME PAPER 72-WA/HT-39] 04 p0518 A73-15816

Microwelding equipment with automatic wire breaking and ball melting blocks and electronically controlled wire feeding, noting heating plate with thyristor temperature control

06 p0683 A73-18433

Preliminary study for the design of a satellite thermal control heat pipe.

07 p0918 A73-18913

Some methodological questions concerning the simulation of turbine blade operation on gasdynamic stands

07 p0809 A73-20509

Spacecraft dynamic solar electric power/thermal control system with cold liquid flow and regenerator cooling for energy conversion efficiency and weight characteristics improvements

09 p1153 A73-22785

Temperature measurement and control technology review, discussing analog and digital systems, contact, resistance and radiation thermometers, special temperature sensors and measurement systems

10 p1216 A73-23634

Immersion liquids for a homogeneous optically mixed laser

10 p1227 A73-23768

Electronic equipment thermal management for energy dissipation rejection, summarizing heat pipe, phase-change heat transfer and high pressure gas convection techniques

10 p1295 A73-23789

Plasma sprayed boron fiber reinforced titanium oxide and Al matrix composites, discussing temperature control for particle size and SiC coating effects on strength

11 p1388 A73-25413

Experimental operation of constant temperature heat pipes.

11 p1451 A73-25989

TEMPERATURE DIFFERENCES

Heat pipe thermal control of spacecraft batteries.
11 p1309 A73-25992

Study of fuel cell thermal control systems for advanced missions.
11 p1309 A73-25993

Radioisotope heater design and optimization for manned spacecraft thermal control and life support systems and various mission times
11 p1310 A73-25996

Cryostats with and without radiation passage through window into vacuum space in balloon-borne far IR instruments requiring cooling to liquid He temperature
11 p1453 A73-26516

Temperature reducing solar cell arrangements for spin stabilized planetary and solar probes, analyzing thermal performance
11 p1313 A73-26668

Design of temperature-controlled substrates for hybrid microcircuits.
13 p1588 A73-28044

Long term temperature control and calibration system for creep testing facility temperature drift monitoring and correction
13 p1597 A73-28841

Thermodynamic optimization of current leads into low temperature regions.
13 p1707 A73-29067

Concorde air conditioning, discussing system modifications for production aircraft concerning interconnection of engine air bleeds of adjacent port and starboard groups
14 p1713 A73-30933

A simple, single-frequency He-Ne laser for practical uses.
15 p1885 A73-32018

Simultaneous control of temperature and humidity in a confined space. III Feedback control synthesis via optimal control theory.
15 p1855 A73-32549

Simultaneous control of temperature and humidity in a confined space. I - Mathematical modeling of the dynamic behavior of temperature and humidity in a confined space.
15 p1959 A73-32597

Simultaneous control of temperature and humidity in a confined space. II - Feedback control synthesis via classical control theory.
15 p1855 A73-32598

Experimental heat transfer investigations on modules mounting hybrid packages.
17 p2135 A73-34729

Electron beam current fluctuation reduction by placing hot filament into Wheatstone bridge arm for temperature regulation in power supply for electron guns
17 p2176 A73-35776

Thermal control of the large space telescope /LST/.
[AIAA PAPER 73-720] 18 p2359 A73-36338

Thermoelectric device application to spacecraft thermal control.
[AIAA PAPER 73-722] 18 p2369 A73-36339

B-52 aircraft-borne short range attack missile weapon system air conditioner thermal performance fulfillment with Freon refrigerant and air distribution in heat exchangers
[AIAA PAPER 73-723] 18 p2269 A73-36340

Thermal contact conductance of porous metallic materials in a vacuum environment.
[AIAA PAPER 73-747] 18 p2323 A73-36363

Baseplate heat pipe system for waste heat dispersion and temperature control of TWT microwaves amplifier in space shuttle communication equipment, discussing design and performance
[AIAA PAPER 73-755] 18 p2370 A73-36371

Thermal control flight experiment onboard ATS-F to evaluate feedback controlled variable conductance heat pipe performance in space environment
[AIAA PAPER 73-757] 18 p2370 A73-36372

Heat pipe and phase changing material /PCM/ sounding rocket experiment.
[AIAA PAPER 73-759] 18 p2371 A73-36374

Temperature control of the Mariner class spacecraft - A seven mission summary.
[AIAA PAPER 73-769] 18 p2360 A73-36383

Thermal control subsystem design of a Saturn/Uranus atmospheric entry probe for descent missions to 20 bars.
[AIAA PAPER 73-770] 18 p2360 A73-36384

Thermal control and structures approach for fluorinated propulsion.
[AIAA PAPER 73-772] 18 p2360 A73-36386

Mathematical modeling for ATS-F spacecraft louvers and heat pipes thermal control heat rejection capacity, noting correlation with solar environment simulation data
[AIAA PAPER 73-773] 18 p2360 A73-36387

On some problems of the method of simulating the working conditions of turbine blades on gas-dynamic benches.
19 p2418 A73-37784

An insight into the features of the OAO-C thermal design.
[ASME PAPER 73-ENAS-4] 19 p2493 A73-37966

Analysis and temperature control of hybrid microcircuits.
[ASME PAPER 73-ENAS-6] 19 p2412 A73-37968

Spacecraft thermal control coatings development, discussing zinc orthotitanate/silicone properties as solar reflector
[ASME PAPER 73-ENAS-7] 19 p2389 A73-37969

Reverse osmosis for recovering and recycling water in Space Station Prototype Environmental Thermal Control/Life Support System Integrated Water and Waste Management
[ASME PAPER 73-ENAS-22] 19 p2400 A73-37978

Apollo command and service module environmental control system - Mission performance and experience.
[ASME PAPER 73-ENAS-29] 19 p2493 A73-37984

Development of a cryogenic heat pipe radiator for a detector cooling system.
[ASME PAPER 73-ENAS-47] 19 p2493 A73-37994

Axial grooved heat pipes - Cryogenic through ambient.
[ASME PAPER 73-ENAS-48] 19 p2434 A73-37995

Design and test of a self-controlled heat pipe radiator.
[ASME PAPER 73-ENAS-49] 19 p2435 A73-37996

A cryogenic heat pipe for satellite sensor cooling.
[ASME PAPER 73-ENAS-50] 19 p2494 A73-37997

Thermal design and analysis aspects of advanced communication spacecraft.
20 p2531 A73-39773

Possibilities of improving the characteristics of operational amplifiers by using thermostated input cascades
21 p2660 A73-40023

Symposium on Temperature, 5th, Washington, D.C., June 21-24, 1971, Proceedings. Part 1 - Basic methods. Scales and fixed points. Radiation. Part 2 - Resistance, electronic and magnetic thermometry. Controls and calibration. Bridges. Part 3 - Thermocouples. Biology and medicine. Geophysics and space.
22 p2852 A73-41976

Temperature measurement, monitoring, and control on a Michelson interferometer for ambient-temperature emission spectroscopy.
22 p2856 A73-42025

Heat pipe applications utilizing, high thermal conductivity, small temperature variations, heat flux transformation and temperature sensitivity for heat transportation and distribution and temperature control
22 p2931 A73-42292

TEMPERATURE DIFFERENCES

U TEMPERATURE GRADIENTS

TEMPERATURE DISTRIBUTION

Orthogonal function approximation of uniform thickness plate temperature distribution, using reduced two dimensional unsteady heat conduction equations
01 p0119 A73-10010

Solution of the thermoelasticity problem for half-spaces with boundary conditions divided by circular lines
01 p0113 A73-10013

Thermal diffusion theory for deformations of thin isotropic shells and plates subjected to nonuniform temperature and stress concentration fields
01 p0113 A73-10019

Unsteady temperature and stress distribution in variable thickness disk under convective heat transfer with ambient medium, using approximation method
01 p0113 A73-10021

Effect of heat propagation rates on the temperature field and stresses in thin plates
01 p0113 A73-10022

Temperature fields and stresses in bodies of simple geometry when the ambient medium temperature is unsteady
01 p0113 A73-10023

Stress function for estimating mutual effects of strain and temperature fields in dynamic coupled thermoelasticity problem for thin circular plates
01 p0113 A73-10094

Electrical conductivity and total radiant power of air plasma.
01 p0081 A73-10121

Transient variation of martian ground-atmosphere thermal boundary layer structure.
01 p0097 A73-10400

Thermal convection in a horizontal fluid layer with uniform volumetric energy sources.
01 p0120 A73-10442

An investigation of high-wavenumber temperature and velocity spectra in air.
01 p0039 A73-10448

Pipe array design for thermoelectric air conditioners, noting temperature distribution in half-cell and heat conductor junction
01 p0006 A73-10618

Thermal bending of moderately thick rectangular plate.
01 p0115 A73-10739

Comparison of solutions to the inverse unsteady heat conduction problem by the successive interval method and by the Sparrow, Hadji Sheikh and Lundgren method
01 p0123 A73-10862

Velocity, temperature and component concentration distributions in laminar boundary layer at blown surface for binary mixture flow
01 p0034 A73-10957

Temperature field and heat transfer equation of unsteady conducting fluid motion on porous plate within magnetic field, allowing for Joule dissipation
01 p0085 A73-11079

Thermal analysis and its verification test of a small probe for space use.
01 p0052 A73-11147

Computer programs for radiative heat transfer and thermal equilibrium equations, noting transient temperature distribution measurement of two stage radiant cooler
01 p0111 A73-11151

Temperature fields and stresses during local tempering of helical welds of a cylindrical shell
01 p0118 A73-11413

Nonstationary interaction of thermal radiation with surfaces of pure metals
01 p0124 A73-11434

Determination of a time-dependent thermal stress on a finite cylinder
[DGLR PAPER 72-112] 02 p0230 A73-11671

Russian book on temperature and stress distributions in thin plates covering unsteady heat transfer and thermoelasticity of isotropic and anisotropic plates
02 p0232 A73-11891

Temperature, velocity, and stress distribution in thermo-viscoplastic boundary layers
03 p0386 A73-13145

Incompressible flow characteristics and temperature transverse behavior in completely turbulent wall boundary layer
03 p0292 A73-13172

Cs vapors thermal conductivity at various temperatures and pressures, using low emissivity Ni cylinders
03 p0396 A73-13181

Isothermal vertical plate turbulent thermal boundary layer during free convection, noting temperature pulsations dispersion
03 p0396 A73-13184

Hydrodynamics and heat transfer in a fluid with an asymmetrical stress tensor
03 p0398 A73-13722

Kinetic heating in structures with a nonuniform surface temperature
03 p0398 A73-13723

German monograph - Axisymmetric free jets and free-jet flames and a numerical procedure for calculating them.
03 p0398 A73-13810

German monograph - Propagation of ion acoustic waves in a weakly ionized plasma.
03 p0398 A73-13814

Jovian spectrum at 8-13 microns from 60 inch IR telescope, discussing surface brightness of central disk and brightness temperature spectrum
03 p0374 A73-13850

Basic relationships in turbulent lubrication and their extension to include thermal effects.
[ASME PAPER 72-LUB-16] 03 p0314 A73-14332

Inlet shear heating in elastohydrodynamic lubrication.
[ASME PAPER 72-LUB-21] 03 p0314 A73-14336

Finite element method for calculating temperature distributions in complex structures, taking into account heat transfer by radiation, conduction and convection
03 p0400 A73-14632

Temperature distribution in a plasma filament in the presence of turbulent heat conduction
04 p0482 A73-15621

Temperature and heat flux distributions in incompressible turbulent equilibrium boundary layers.
04 p0520 A73-15942

Unsteady-state conjugated heat transfer between a semi-infinite surface and incoming flow of a compressible fluid. I - Reduction to the integral relation. II - Determination of a temperature field and analysis of results.
04 p0520 A73-15944

Temperature distribution in non-Newtonian MHD channel flow by shear stress integral evaluation, investigating power law and Prandtl-Eyring fluids
04 p0520 A73-15947

Russian book on atmospheric circulation covering temperature distribution, tropospheric and stratospheric winds, jet streams and Southern Hemisphere meteorological features
04 p0474 A73-15961

Sinusoidal thermal wave propagation in horizontal fluid layer with small Prandtl number, deriving induced mean flow from nonlinear equation solution by perturbation approach
05 p0591 A73-16188

Heat transfer in static packed beds - Effects of radiation on temperature distribution.
05 p0638 A73-16219

Relationship of atmospheric processes in the troposphere and stratosphere
05 p0593 A73-16233

Lunar interior temperature and surface heat flux distribution from numerical calculations for convec-

tion cells within self gravitating fluid sphere, comparing with magnetic induction results

05 p0615 A73-16376

The influence of spatial temperature distribution and measuring configuration on line-reversal temperature.

05 p0602 A73-16563

Gas temperature, carbon monoxide and nitric oxide axial and radial distribution in J-33 combustor, presenting combustion process model based on measurements

[WSCI PAPER 72-22]

05 p0639 A73-16690

Temperature distribution at a thermally insulated crack in a plate for various boundary conditions

05 p0640 A73-16774

Stationary temperature field of a disk under conditions of convective heat transfer on its surface

05 p0640 A73-16775

Nonsteady heat conduction of multilayer cylindrical and conical shells in periodic radiation flux, calculating temperature distribution

05 p0640 A73-16798

Closed form solutions for dust density and temperature distributions in shock layer of hypersonic wedge flow

05 p0533 A73-17115

A temperature extrapolation method for hollow cylinders.

05 p0641 A73-17119

Solution of the general heat-transfer problem for flow past cylindrical bodies by the Tolubinskii integral method.

06 p0766 A73-17407

Calculation of the temperature field of the heated zone of a complex shape consisting of a chassis with parts mounted on it.

06 p0766 A73-17412

The thermal structure within the stratospheres of Venus and Mars.

06 p0747 A73-17493

Geographic distribution of anomalies of residual geomagnetic field derived from eccentric dipole and observed field comparing with thermal flux fields and geotectonic features

06 p0689 A73-17546

Lunar fines thermal diffusivity measurement, calculating lunar surface temperature distribution

[AIAA PAPER 73-40]

06 p0767 A73-17622

New procedure for measuring the radial temperature distribution in inhomogeneous and unsteady plasma columns with considerable self-absorption

06 p0728 A73-17913

Two-dimensional temperature fields in straight rectangular fins

06 p0768 A73-17921

Approximate analytical solution of an asymmetrical problem of unsteady heat conduction with nonlinear boundary conditions

06 p0768 A73-18128

Temperature of a duct flow under conditions of unsteady-state heat transfer

06 p0769 A73-18131

Infrared scanning radiometer for temperature mapping of the lunar surface on the Apollo 17 flight.

06 p0695 A73-18319

The thermal shock on the shell of revolution-coupled and uncoupled theory.

06 p0763 A73-18452

Heat transfer in a periodic boundary layer near a two-dimensional stagnation point.

06 p0769 A73-18526

Description of the transfer of heat by natural convection in a horizontal porous layer with the help of a solid-fluid transfer coefficient

06 p0769 A73-18538

Integral equations for temperature distribution in radiative and conductive heat transfer in semitransparent medium, noting temperature oscillation propagation

06 p0769 A73-18565

Influence of the distortion of the temperature field at the point of thermocouple fixation on measurements of the heat conduction coefficient by the steady-state method of radial thermal flux

06 p0770 A73-18566

Nonlinear aspects of cooling of a strongly anisotropic optical element of a laser.

06 p0702 A73-18579

Numerical model for three dimensional air parcels trajectories computation from operational wind forecasts, deriving atmospheric moisture, dew and temperature distributions predictions

06 p0720 A73-18705

Quantitative temperature data from Direct-Readout Infrared (DRIR) pictures.

[AD-759891]

06 p0696 A73-18711

Experimental study of the effective thermal conductivity of liquid saturated sintered fiber metal wicks.

06 p0770 A73-18836

Temperature field structure in strongly heated buoyant thermals.

07 p0919 A73-19504

German monograph - Free convection of air in a horizontal circular gap in the case of temperature- and pressure-dependent density.

07 p0920 A73-19579

Transonic nozzle flow with a parabolic temperature distribution.

07 p0811 A73-19985

Mid-latitude winter anomalies in radio absorption and stratospheric temperature distribution - Observations concerning the influence of auroral and magnetic activity.

07 p0819 A73-20058

Calculation of temperature fields in cooled gas-turbine blades on a digital computer

07 p0868 A73-20099

Establishment of thermal equilibrium in a liquid near the critical point.

08 p1021 A73-20857

Solution of the asymmetric steady-state heat conduction problem for a two-layer hollow cylinder of finite length

08 p1021 A73-20995

Application of the solution to an inverse heat conduction problem to the calculation of the heat transfer coefficient from experimentally measured temperatures at internal point of the body

08 p1021 A73-20996

Cyclically symmetrical heat conduction problems for perforated plates and shells in the presence of heat transfer

08 p1021 A73-20997

Visualization of thermal fields in saturated porous media by the Christiansen effect.

08 p0963 A73-21030

Temperature variations in coronal regions in the proximity of a prominence

08 p1007 A73-21067

Application of the regularization principle to the construction of approximate solutions to inverse heat-conduction problems

08 p1022 A73-21097

Temperature distribution in a wedge-shaped prism

08 p1022 A73-21098

Observations of the variation of temperature with latitude in the upper solar photosphere. II - Magnetic-field comparison, implications for solar-oblateness measurements, and harmonic analysis.

08 p1009 A73-21166

Determination of the statistical characteristics of temperature fluctuation in pool boiling.

08 p1022 A73-21252

Diurnal temperature variations in the thermosphere with solar activity

08 p0959 A73-21288

Steady temperature fields and stresses in a half-space heated by a linear inductive source

08 p1019 A73-21759

Change of vibrational temperature due to laser action in CO₂ lasers.

09 p1089 A73-21933

The thermal future of the universe.

09 p1143 A73-22109

Temperature distribution in gas flow about a linear source of heat variable periodically in function of time.

09 p1166 A73-22169

Possibility of holographic observation of the interference of independent weakly degenerate fields

09 p1084 A73-22670

Heat transfer in horizontal annular air gaps at small Grashof numbers

09 p1167 A73-23108

Temperature range of maximum aging of Mo-Re-C alloys after quenching and tempering, noting carbon solubility effects due to Re content

09 p1106 A73-23187

Thermoelectricity in tungsten at low temperatures.

09 p1135 A73-23335

Temperature distribution in a plasma with turbulent thermal conductivity.

10 p1255 A73-24211

Temperature fluctuations in the turbulent wake behind an optically heated sphere.

10 p1296 A73-24251

Hot-wire anemometer probe operation in constant current in continuous high-temperature hypersonic turbulent boundary layer, computing velocity and temperature fluctuations

10 p1205 A73-24254

Calculation of the steady thermal and stress boundary conditions in the Phoebus 2 reactor

10 p1248 A73-24495

The temperature field and thermal stresses in a symmetrical system of three infinite plates

10 p1293 A73-24795

Increasing the fatigue strength of metals by optimizing the thermal regime during strain hardening

10 p1226 A73-24799

A note on the structure of thermal convection in a slightly slanted slot.

10 p1297 A73-24969

Calculation of the temperature distribution within an ogival radome in supersonic flight

11 p1336 A73-25302

Mechanical simulation of thermoelastic stresses on the basis of a given temperature field

11 p1435 A73-25453

A study of convective elements in the atmospheric surface layer.

11 p1393 A73-25692

The solar wind and the temperature-density structure of the solar corona.

11 p1413 A73-25954

Nonstationary interaction of thermal radiation with surfaces of pure metals.

11 p1452 A73-26061

Automation of thermal design calculations for electrical machines

11 p1313 A73-26115

The variation of temperature with latitude in the lower thermosphere /80-100 km/.

11 p1357 A73-26194

Implicit difference method of temperature determination in problems of radiative gasdynamics

11 p1348 A73-26329

One dimensional temperature equalization process in planar plate, infinitely long cylinder and sphere for range of Biot and Fourier numbers, estimating approximate solution error

11 p1452 A73-26372

Transient temperature distribution of an anisotropic half space.

11 p1453 A73-26401

Temperature-waves in connection with drift type instabilities in a Q-plasma.

11 p1406 A73-26558

Determination of the coefficient alpha real in convection in air with allowance for the Jacq effect

12 p1557 A73-26797

Temperature field in front of or behind gas turbine with additive white noise, deriving optimal filter for dynamic programming technique in random fields analysis

12 p1483 A73-27080

Thermal limitations of CW and pulsed silicon TRAPATT diodes.

12 p1478 A73-27110

Temperature field calculation for certain elements located in microwave channels

12 p1558 A73-27247

Velocity, temperature and component concentration distributions in laminar boundary layer at blown surface for binary mixture flow

12 p1487 A73-27533

Application of the method of power series to derive solutions for one-dimensional problems of thermophysically nonhomogeneous media

12 p1560 A73-27808

Nonlinear problems for a system of two heat-radiating gray bodies separated by a diathermic medium

12 p1560 A73-27810

Solar pole-equator temperature distribution in high photosphere layers from Mg spectral line observations

12 p1544 A73-27832

Comparison of the solutions found for the inverse transient heat-conduction problem by the method of successive intervals and the method of Sparrow, Haji-Sheikh, and Lundgren.

12 p1560 A73-27911

Turbulent diffusion downstream of a linear source in a plane parietal jet

13 p1599 A73-28070

Thermo-acoustical waves in linear thermo-elastic materials.

13 p1691 A73-28088

Temperature conditions of aluminum alloy crystallization at cooling rates of 10,000 to 1,000,000 deg/sec

13 p1632 A73-28111

MHD free convective flow in a vertical channel.

13 p1663 A73-28164

The transient temperature distribution in a slab subjected to radiative and convective heating calculated by variational method.

13 p1704 A73-28429

Nongray radiative transfer and simultaneous turbulent diffusion in layer of molecular gas enclosed by parallel black walls, presenting temperature profiles

13 p1705 A73-28433

Composite materials transient thermal boundary conditions analytical derivation from initial and time dependent internal temperature distribution or gradient

13 p1705 A73-28436

Unsteady temperature condition of a conductor with a nonlinear source of heat

13 p1705 A73-28466

Some specific features of the near-ground temperature field mesostructure and air humidity and their influence on convective processes

13 p1654 A73-28886

Shock wave produced in a solid by means of supersonic thermal sources.

13 p1700 A73-29390

Test equipment for thermal stability determination of brittle refractory material, noting data processing procedure and formulas for temperature distribution and thermal stress

13 p1599 A73-29629

Temperature fields in a hollow cylinder in presence of heat source under the boundary conditions of the second kind.

13 p1708 A73-29666

Screen effect on the radiation heat transfer in an area of penetrating radiation

14 p1816 A73-30013

Temperature distribution and ionization characteristics of sodium and rubidium chlorides, silicon dioxide and atomized carbon jets generated by plasmatron

14 p1781 A73-30464

The thermal analysis of a belt type radiator by the method of matched asymptotic expansions.

14 p1817 A73-30609

Shock wave propagation in atmospheres with spatially inhomogeneous density and temperature fields, using ideal polytropic gas model

14 p1750 A73-30654

Influence of the diathermancy of an arc-shaped crack on the thermoelastic state of the area about the crack

14 p1814 A73-30720

Optimal conditions for residual stress reduction in a cylindrical shell by local annealing

14 p1814 A73-30721

Spatial problem of thermoelasticity of a body with an insulated external circular crack

14 p1814 A73-30725

Thermal stresses and couple-stresses in square cylinder with a circular hole.

14 p1815 A73-30919

Black holes in binary systems, discussing radiation spectrum, disk formation, optical luminosity, X rays, UV regions and temperature distribution

15 p1928 A73-31051

Investigation of the steady-state temperature field in a composite cathode of a plasmatron

15 p1917 A73-31192

Motion of a magnetized fluid between parallel plates

15 p1918 A73-31408

Transient forced convection heat transfer from an isothermal flat plate.

15 p1957 A73-31664

Techniques and equipment for thermal nondestructive quality control of products and materials.

15 p1882 A73-31692

Method for boundary condition selection in the heat transfer problem with phase transition

15 p1958 A73-31872

Calculation of temperature distribution in the human body.

15 p1839 A73-31999

Natural convective heat transfer between vertical parallel plates - One plate with a uniform heat flux and the other thermally insulated.

15 p1958 A73-32057

Density and temperature distributions in hypersonic sphere wakes.

15 p1824 A73-32150

Map series for description of annual temperature wave in lower stratosphere in Northern Hemisphere, establishing easterly circulation on south side of Aleutian high

15 p1873 A73-32254

An improved separability approximation for line radiative transport in nonhomogeneous media.

15 p1959 A73-32391

Book - The general circulation of the tropical atmosphere and interactions with extratropical latitudes. Volume I.

15 p1907 A73-32423

Geographic distribution of anomalies of residual geomagnetic field derived from eccentric dipole and observed field, comparing with thermal flux fields and geotectonic features

16 p2002 A73-32770

Development of model atmospheres for aerothermodynamic calculations.

16 p2034 A73-33138

Isotropic bonded thermoelastic laminar bodies calculations for thermal flux and temperature fields, using linear quasi-static thermal elasticity equations

16 p2080 A73-33242

On the observability and stability of the temperature distribution in a composite heat conductor.

16 p2034 A73-33311

Calculation of temperature distribution in multistage axial gas turbine rotor assemblies when blades are uncooled.

[ASME PAPER 73-GT-8]

16 p2047 A73-33486

Integral equations for temperature distribution in radiative and conductive heat transfer in semitransparent medium, noting temperature oscillation propagation

16 p2086 A73-33590

Effect of temperature field distortions caused by embedded thermocouples on the measurement of the thermal conductivity coefficient by the steady radial heat flux method.

16 p2086 A73-33591

Transistor design and thermal stability.

17 p2133 A73-34218

Transient thermal stresses in a disc of linearly strain-hardening material.

17 p2243 A73-34547

Transient temperature response of semiconductor devices under pulsed power operation.

17 p2135 A73-34728

Radiative heat transfer with no temperature jump at interface of media

17 p2254 A73-34773

Two-variable asymptotic solution to unsteady three dimensional turbulent flow equations describing small scale deformation, determining hot spot or macromolecular size statistical behavior

17 p2201 A73-34800

Basic characteristics of the temperature distribution and air currents in the free atmosphere of the earth

18 p2332 A73-35915

Electron temperature profile and its solar activity dependence in the middle latitude region.

18 p2308 A73-36047

Rocket sounding of upper atmosphere vertical wind profiles, shear, temperature distribution and diffusion coefficient for model atmosphere calculation

18 p2309 A73-36057

Global temperature distributions fromOGO VI 6300 A airglow measurements.

18 p2309 A73-36058

Radiative equilibrium of a gray medium in a rectangular enclosure.

18 p2371 A73-36800

Temperature variations of coronal regions near a solar prominence.

18 p2355 A73-36868

Europa III heat shields - Aerothermodynamic analysis and design.

18 p2361 A73-36954

Statistical characteristics of the temperature field near the ground for Europe.

18 p2334 A73-37070

Calculation of geopotential fields at various atmospheric levels from data on the overall cloudiness and temperature.

18 p2314 A73-37072

Laminar boundary layers along an infinite flat plate with oblique suction.

19 p2420 A73-37646

Variations in the temperature of the thermosphere in the course of the day and with solar activity.

19 p2424 A73-37917

Satellite radiances and clear air turbulence probabilities.

19 p2448 A73-38218

Distribution of a monochromatic electromagnetic field and of temperature in a plane conductor with temperature dependent conductivity

19 p2471 A73-38340

Dynamic thermal properties of IMPATT diodes.

19 p2411 A73-38459

Heat transfer in the case of turbulent and laminar trickle films

19 p2505 A73-38477

Study of a compact counterflow heat-exchanger with mercury at small Peclet numbers.

[ASME PAPER 73-HT-54]

20 p2626 A73-38575

A calculation of the equilibrium temperature distributions in multiple-emitter microwave transistors.

20 p2535 A73-38926

Structural characteristic of the temperature field in the boundary layer of the atmosphere

20 p2555 A73-39182

Temperature field calculation for a plate of a complex shape with systems of double-periodic holes, inclusions, and energy sources

20 p2627 A73-39255

Method for determining the unsteady thermal field of piecewise homogeneous plates of complex shape

20 p2627 A73-39256

Method of studying thermal fatigue from the parameters of the hysteresis loop in temperature-force coordinates

20 p2619 A73-39362

Thermal conductivity of mercury vapors

20 p2595 A73-39607

Method for determining the heat conductivity coefficient of high-temperature materials during unsteady heating

20 p2629 A73-39616

Design and performance characteristics of the Vertical Temperature Profile Radiometer /VTPR/ for atmospheric temperature soundings.

20 p2567 A73-39852

Jovian ionospheric and magnetospheric ionization and temperature distributions from solutions of momentum and chemical equations for electrons, ions and neutrals, and heat transport equation

21 p2764 A73-40165

Asymmetric heat transfer in turbulent flow through a plane slot

21 p2790 A73-40398

Temperature distribution measurement for air about hot object by double exposure interferometry, using beam from He-Ne laser

21 p2701 A73-40625

Determination of the temperature behavior in a photospheric facula through the solution of an integrodifferential equation by the gradient-random search method

21 p2759 A73-40722

Thermal response of microwave transistors under pulsed power operation.

21 p2663 A73-40744

Measuring the boundary layer temperature distributions using ablating specimens in an air plasma flow.

21 p2791 A73-41052

A study of startup regimes of high-temperature heat pipes.

21 p2792 A73-41060

Regularization of solutions of inverse problems of heat conduction.

21 p2792 A73-41064

Integration of a nonlinear partial differential mixed boundary value problem

21 p2792 A73-41065

Temperature and stress fields in a cylindrical shell subjected to induction heat treatment

21 p2787 A73-41233

Nonisothermal surface cooling for arbitrary temperature distribution and Prandtl number approaching zero, solving thermal boundary layer equations by series expansion

21 p2792 A73-41323

Temperature difference between pole and equator of the sun.

21 p2776 A73-41479

Acceleration waves in ideal fluid mixtures with several temperatures.

22 p2929 A73-41772

Measurement of temperature distribution over metal objects using single-wire thermocouples.

22 p2858 A73-42048

A comparison of predicted skin temperatures with thermographic measurements.

22 p2813 A73-42053

Flow of a viscous gas at a slot with strong suction

22 p2796 A73-42283

Transient heat conduction in laminated composites. [ASME PAPER 73-HT-R]

22 p2930 A73-42286

The use of singularity programming in finite-difference and finite-element computations of temperature.

[ASME PAPER 73-HT-K]

22 p2930 A73-42287

Coupling between thermal conduction and radiative transfer in a moving atmosphere.

22 p2907 A73-42305

The inversion of the mean and spatially resolved sodium D2 line profiles from the sun.

22 p2908 A73-42311

A coupled thermo-elastic problem of a half-space under the action of a thermal shock on the bounding surface.

22 p2922 A73-42467

On some further applications of the variational formulation based on local potential to the solution of diffusion equation. I - Temperature distribution in a transpiration cooled half-space with variable thermal properties. II - Heat conduction in an ablating solid with variable thermal properties.

22 p2931 A73-42468

Thermal stresses due to an internal source of heat in a solid elastic hemisphere with radiating curved surface and the plane base resting on a smooth rigid insulating plane surface.

22 p2932 A73-42469

The calculation of open circular cylindrical shells with the aid of partial discretization

22 p2922 A73-42528

Aerodynamic and thermal structures of the laminar boundary layer over a flat plate with a diffusion flame.

22 p2933 A73-42774

Analytical modeling of a spherical combustor including recirculation.

22 p2934 A73-42783

Temperatures in low-pressure magnesium-vapor diffusion flames.

22 p2899 A73-42820

Thermodynamics of transition metal-hydrogen solid solutions.

22 p2880 A73-43076

Viscous laminar Hartmann flow of electrically conducting liquid between parallel walls in transverse magnetic field, assessing thermal radiation effects and temperature distribution

23 p3008 A73-43207

A model of heat transfer in a biological tissue perfused by blood of arbitrary temperature.

23 p2948 A73-43292

Investigation of temperature pulsations accompanying the heating of a laminar sample by alternating and pulsating currents

23 p3048 A73-43446

The structure and dynamics of horizontal roll vortices in the planetary boundary layer.

23 p3002 A73-43594

Effect of the circumferential nonuniformity of a temperature field in front of a turbine on the vibrational stresses in the turbine blades

23 p3020 A73-43740

- Interstellar grain temperature fluctuations due to interstellar radiation field, discussing H atom recombination problem 23 p0329 A73-43747
- The effects of water vapour and oxides of nitrogen on ozone and temperature structure of the stratosphere. 23 p2977 A73-43902
- Temperature field and motion oscillations in water-methanol and water-isopropanol Benard cells, taking into account thermal diffusion 23 p3049 A73-43936
- A correlation between colors of Jovian clouds and their 5-micron temperatures. 23 p3033 A73-43948
- Determination of heat flow shape factors for hollow, regular polygonal prisms. 23 p3049 A73-44164
- Determination of the temperature fields and thermal stresses in a bimetallic layer subjected to induction heating 23 p3046 A73-44194
- Determination of the temperature fields of turbine disks and blades, using irradiated diamond indicators 23 p2987 A73-44294
- A numerical method for determining the temperature structure of planetary atmospheres. 24 p3130 A73-44456
- A numerical study of three-dimensional diurnal variations within the thermosphere. 24 p3082 A73-44731
- The method of forces for thermoviscoelastic rod systems 24 p3148 A73-44918
- Influence of emitter current concentration effects on the temperature distribution in power transistors 24 p3072 A73-44930
- Temperature field boundary value problem with variable heat transfer coefficients and specific heat, using Laplace transformation and variation methods 24 p3156 A73-45083
- Determination of the temperature field in a perforated plate with convective heat transfer 24 p3157 A73-45171
- Thermoelasticity problem of a spherical shell with multiply connected regions 24 p3149 A73-45175
- Calculation of the thermal field of an inhomogeneous plate of complex composition with energy sources 24 p3157 A73-45361
- TEMPERATURE EFFECTS**
- Combined heating and irradiation effects on body elastoplastic stress-strain state, deriving thermoradiative plasticity equations 01 p0112 A73-10004
- Dynamic and thermodynamic effects addition to basic Boussinesq convection for convection in stars, discussing rotation, magnetic fields, radiative transfer and state equation 01 p0094 A73-10061
- Transport phenomena in turbulent plasma with electromagnetic waves. 01 p0081 A73-10117
- Effect of controlled elevation of body temperature on human tolerance to +Gz acceleration. 01 p0007 A73-10159
- Utility of heat stress indices and effect of humidity and temperature on single physiologic strains. 01 p0007 A73-10163 [AD-751735]
- Temperature dependence of magnetic susceptibility in nickel-film-coated iron-silicon alloy specimens 01 p0062 A73-10254
- Formation of carbides in 3% chromium steel after additional alloying 01 p0062 A73-10265
- Solar coronal plasma cyclotron radiation, taking into account temperature effects 01 p0096 A73-10309
- Intensity variation of CN bands with temperature in active nitrogen methylene chloride chemiluminescent reaction. 01 p0014 A73-10333
- Atmospheric radiative transfer by carbon dioxide. 01 p0037 A73-10366
- Nongray theory for temperature wave propagation without turbulent or convective motions, discussing diurnal waves simulation for planetary atmospheres. 01 p0039 A73-10396
- Grain growth in alloyed molybdenum under conditions of creep 01 p0063 A73-10486
- Processing conditions and sample dimensions and shapes effects on Ti alloy creep characteristics at room temperature 01 p0064 A73-10487
- Temperature dependence of the critical shear stress in single crystals of Al-Mg alloys of various concentration at temperatures between 1.6 and 300 K 01 p0064 A73-10488
- French monograph - Experimental study of the thermal conductivity of rare gases and helium-argon mixtures as functions of temperature and pressure. 01 p0120 A73-10604
- Some optical properties of CaMoO₄ single crystals 01 p0088 A73-10626
- Thermal bending of moderately thick rectangular plate. 01 p0115 A73-10739
- Vibrational relaxation in CO₂ with selected collision partners. I - H₂O and D₂O. 01 p0080 A73-10775
- Heat transfer as function of temperature on small horizontal wires in water and organic liquids noting application for heater low gravity behavior prediction 01 p0122 A73-10801
- Investigation of creep in Kh18N10T steel at varying temperatures 01 p0066 A73-11094
- Interaction of thermal radiation with laminar free convection from a heated vertical plate. 01 p0123 A73-11141
- Thermal requirements considerations for all components and systems in initial design phase of spacecraft to obviate need for full scale tests 01 p0110 A73-11145
- Three point check method of solar panel characteristics for satellite. 01 p0006 A73-11162
- Balloon polyethylene film materials orthotropic mechanical properties, considering temperature effects on brittle fracture by transverse tension 01 p0005 A73-11206
- Helical gas lenses for guiding optical beam over long distances, calculating irradiance patterns for various propagation mode numbers and temperatures 01 p0053 A73-11218
- Thermochromic cuprous mercuric iodide for IR recording applications, observing phase transition hysteresis from reflectance-vs-temperature, specific heat and sensitivity measurements 01 p0054 A73-11230
- Stimulated Brillouin scattering for hypersound speed measurement as function of temperature in polystyrene, observing pulsed laser induced damage 01 p0068 A73-11232
- Thermal effect of optical radiation on water drops of small size 01 p0074 A73-11244
- Noise factor and power formula for cooled SHF broadband frequency converters with semiconductor mixer diode 01 p0026 A73-11265
- Electron spin resonance of ultraviolet radiation induced defects in ZnO thermal control coating pigment. 01 p0088 A73-11276
- Construction materials selection for thermal dimensional stability in critically sensitive precision instruments and mechanical components, considering economic factors 01 p0066 A73-11293
- Singularities of the temperature dependences of the heat conduction coefficients of solid solutions of the niobium-zirconium system. 01 p0066 A73-11338
- Cold shortness of W and related refractory metals, noting oxide phases and impurities effects on mechanical properties temperature dependence 01 p0066 A73-11341
- Structured changes and phase transformations of welded joints of Al alloy with Cu addition during welding thermal cycles 01 p0067 A73-11352
- Some variational principles pertaining to non-stationary heat conduction and coupled thermoelasticity. 01 p0118 A73-11369
- Infrared maps of Jupiter. 01 p0109 A73-11490
- Effect of temperature and polarization rate on the electrochemical behavior of titanium alloys in a sulfuric medium 02 p0178 A73-11523
- Influence of high-temperature annealing on the rupture characteristics of zirconium carbide 02 p0178 A73-11541
- The thermally activated deformation of niobium-molybdenum and niobium-rhenium alloy single crystals. 02 p0179 A73-11574
- Dielectric properties of cholesteric liquid crystals. 02 p0199 A73-11577
- Hall mobility measurements on iron rich nickel ferrites from room temperature to 600 C. 02 p0199 A73-11725
- Number density estimation for neutral hydrogen hot component required for solar wind heating to satisfy observed proton temperature relationship to wind velocity 02 p0205 A73-11745
- Pressure and temperature effects on carbon dioxide extinction coefficients, tabulating absorption cross sections 02 p0191 A73-11758
- Superconducting-normal phase boundary as function of applied magnetic field and transition temperature in Nb-Ga alloys 02 p0200 A73-11840
- Spectral composition of thermal and stimulated light scattering in the wing of the Rayleigh line 02 p0194 A73-11945
- Conductivity of 2024-T42 aluminum sheet solution heat treated at various temperatures. 02 p0168 A73-11986
- Behavior of certain turbine-blade materials under asymmetric loading. 02 p0180 A73-12128
- Low-temperature mechanical properties of the alloys AT3 and AT6. 02 p0180 A73-12136
- The creep of materials being weakly strengthened in nonsteady temperature and force conditions. 02 p0180 A73-12138
- Apparatus for testing reinforced plastics during nonuniform heating, with due allowance for the gas permeability of the material. 02 p0150 A73-12143
- The influence of test temperature on the fatigue strength of Zhs6K alloy. 02 p0181 A73-12204
- The mass and angular momentum losses from spinars. 02 p0217 A73-12384
- Rate coefficient calculation for near resonant charge transfer reaction between oxygen cations and hydrogen atoms as function of temperature at thermal energies 02 p0217 A73-12391
- Ni-Cd battery thermal runaways caused by self sustaining temperature increases, discussing operational and maintenance procedures for avoidance or correction 03 p0251 A73-12906
- Effects of alloying elements on elevated-temperature mechanical strength of high Cr, Ni-base heat resistant alloy. 03 p0321 A73-12921
- Acoustical studies of rotational relaxation in gases. 03 p0342 A73-12986
- Lunar gabbroic rock internal origin hypothesis support by petrologic data, giving temperature interval of crystallization from dry silicate melt 03 p0369 A73-13095
- Trapped electrons decay to ground state via nonthermal process in lunar samples during thermoluminescence emission at lunar day temperatures, proposing quantitative model 03 p0369 A73-13101
- Possible thermal history of the moon. 03 p0369 A73-13106
- Effect of strain-rate and temperature on the resistance to torsional deformation of several aluminum alloys. 03 p0384 A73-13117
- High melting point transition metals carbides, nitrides, borides, silicides and oxides thermal conductivity as function of characteristic temperature 03 p0322 A73-13191
- Hydrostatic journal bearings design review covering pad coefficients, flow control, optimization, dynamic behavior, thermal effects, turbulence and tolerances 03 p0311 A73-13207
- Evaluating adhesives for joining aluminum. 03 p0334 A73-13271
- Combustion theory of hybrid rocket propellant-oxidizer combinations based on heat transfer limited model, discussing chemical kinetics and temperature effects on regression rate [AIAA PAPER 72-1143] 03 p0397 A73-13449
- Gas turbine engine exhaust emissions measurement data scatter, investigating temperature and humidity effects and emission variations in tailpipe plane [AIAA PAPER 72-1199] 03 p0358 A73-13487
- Computerized radial turbine blades thickness identification, considering temperature distribution and effects and mathematical model parameters for constraints 03 p0312 A73-13565
- Atmospheric wind and temperature inhomogeneity induced sound wave refraction effects on acoustic sounder measurements, noting scattering volume displacement and Doppler shift 03 p0276 A73-13831
- An analysis of thermally-induced plane waves in elastic-plastic single crystals. 03 p0394 A73-13980
- Monograph on hydrodynamics of nonisothermal laminar duct flows of real fluids with temperature dependent properties 03 p0295 A73-13998
- Stress analysis of thick walled hollow viscoelastic circular cylinder enclosed in elastic shell and subjected to nonlinear creep conditions, noting temperature effects 03 p0394 A73-14021
- Third harmonic generation in Ge induced by conduction nonlinearity during bulk heating of charge carriers by microwave fields 03 p0350 A73-14077
- Cummingtonite temperature dependent Mg and ferric ions order-disorder, estimating crystallization temperatures 03 p0375 A73-14104

TEMPERATURE EFFECTS

Optical degradation and thermal restoration - New inputs to the mechanism of the photovoltaic effects in Cu₂S-CdS heterojunctions.

03 p0350 A73-14218

Photovoltaic and I-V characteristics of integral diode solar cells as function of temperature and radiation exposure

03 p0256 A73-14231

Thermohydrodynamic phenomena in fluid film lubrication.

[ASME PAPER 72-LUB-25] 03 p0314 A73-14338

The influence of temperature on the wear of carbon fiber reinforced resins.

[ASLE PREPRINT 72LC-5B-3]

03 p0335 A73-14363

Hold-time effects on the elevated temperature fatigue-crack propagation of type 304 stainless steel.

03 p0328 A73-14448

Acoustic properties of fluid mixtures for ultrasonic delay lines, noting temperature and composition effects on water-glycol mixture parameters

03 p0280 A73-14620

Elevated temperature toughness and a dimensionless parameter involving the zero-ductility temperature.

04 p0459 A73-14670

Extensive study of low fatigue crack growth rates in A533 and A508 steels.

04 p0459 A73-14686

Investigation of the phonon drag effect in n-GaAs.

04 p0482 A73-14866

Temperature dependence of impurity resistivity in dilute Al-based Ti, V, Fe, Cu, Zn alloys between 78 and 930 K.

04 p0461 A73-14875

Hot particle igniter for end-burning solid propellant rocket motors, noting ignition capability at 219 K and 110,000 ft simulated altitude

[AIAA PAPER 72-1196]

04 p0485 A73-14919

M.O.S.F.E.T. temperature-drift performance limitations.

04 p0427 A73-14983

Fracture criteria in quasi-viscoelastic analysis of crack initiation and propagation in polymethyl methacrylate, noting thermal effects on stress intensity factor

04 p0512 A73-15237

Effect of a temperature gradient on bubble growth in tungsten.

04 p0463 A73-15307

The dependence of the lower yield strength in iron and steel on grain size and temperature.

04 p0463 A73-15308

Exact frequency dependent complex admittance of the MOS diode including surface states, Shockley-Read-Hall /SRH/ impurity effects, and low temperature dopant impurity response.

04 p0427 A73-15347

An evolutionary thermal model for the Cygnus Loop.

04 p0499 A73-15361

Optimal temperature and strain rate for deformation in superplastic state for alpha-beta Ti alloy

04 p0464 A73-15498

Temperature dependence of the elastic micro- and macro-stiffness of dispersion hardenable Co-Ni-Ti and Co-Ni-Ti-Al alloys. II

04 p0465 A73-15640

The effect of substrate temperature on the structure of titanium carbide deposited by activated reactive evaporation.

04 p0456 A73-15757

Thermophysical properties of thermally insulating materials in the cryogenic temperature region.

04 p0520 A73-15938

Temperature effects on intragranular sigma phase precipitation in low carbon superrefractory alloys

04 p0467 A73-15956

Sunspot temperature increase stimulation of supergranule motion leading to spot decay and magnetic field diurnal fluctuation development

04 p0503 A73-16012

Behavior of carbon monoxide in the upper photosphere.

04 p0504 A73-16027

Time-temperature safety thresholds for human epidermal injury related to materials thermal properties

05 p0637 A73-16138

Cloudiness as a global climatic feedback mechanism - The effects on the radiation balance and surface temperature of variations in cloudiness.

05 p0591 A73-16187

Low body temperature effects on learned behavior retention under hibernation conditions in squirrels

05 p0539 A73-16324

An estimate of radiative emission from an isothermal xenon plasma at temperatures up to 50,000 K.

05 p0602 A73-16561

Non-steady-state thermal analysis of a rolling aircraft tire.

[SAE PAPER 720871]

05 p0535 A73-16667

Layout of a thermodynamical theory of the life time scattering in materials testing

05 p0635 A73-17066

Electrical properties of nickel-low-doped n-type gallium arsenide Schottky-barrier diodes.

05 p0559 A73-17072

Dislocation-point defect interactions in fatigued pure aluminum

05 p0588 A73-17231

Soft X-ray spectra of the Cygnus Loop and Cygnus X-2 in the energy range of 0.16-6.7 keV.

05 p0612 A73-17332

Fusion plasma confined by nonpenetrating uniform magnetic field, calculating temperature and density effects on energy balance instabilities from particle conservation equations

05 p0604 A73-17366

Diffusion welding of beryllium. II - The role of the microalloying elements.

06 p0704 A73-17597

Evaluation of multiaxial theories for room-temperature plasticity and elevated-temperature creep and relaxation of several metals.

06 p0759 A73-17599

Galvanomagnetic effects measured in p-type bismuth selenide single crystal within magnetic field for Hall and conductivity mobilities, determining temperature dependences

06 p0733 A73-17741

Structural design with allowance for shakedown in the case of temperature-dependent elastic constants

06 p0760 A73-17780

Electrical properties of evaporated mercury telluride films.

06 p0734 A73-17815

Temperature-dependent hyperfine interactions in Fe₂B.

06 p0734 A73-17833

Conversion of electromagnetic into acoustic energy via indium films.

06 p0734 A73-17834

Thermal effects experienced by meteoritic particles during atmospheric flight and upon earth surface impact

06 p0749 A73-17839

Human perception of humidity under four controlled conditions.

06 p0657 A73-17864

Thermal-influence region properties in a maraging steel as a function of welding heat cycles

06 p0697 A73-17880

Embrittlement of N18K8M3Ti maraging steel after prolonged cooling from high temperatures

06 p0706 A73-17882

Creep characteristics and substructure disorientation in metals with an fcc lattice

06 p0706 A73-17904

Temperature and concentration effects on heterodiffusion coefficient of diffusion welded Mo-W alloy rods

06 p0707 A73-17907

Investigation of the temperature dependence of hardening characteristics in an aging nimonic alloy

06 p0707 A73-17908

Cr effect on N solubility increase during Fe alloy nitriding, noting temperature effect on nitrides precipitation

06 p0697 A73-18054

Mathematical model for electric current in granulated media, establishing temperature dependence of tunneling conductivity for tunnel junction with metallic inclusions in oxide layer

06 p0736 A73-18117

Heat conductivity dependence on temperature for amorphous and crystalline materials, noting integrodifferential equation for conductive heat transfer and Fourier law

06 p0769 A73-18132

Aerial photograph distortion due to sealed compartment temperature and pressure effects in terms of internal refraction

06 p0693 A73-18156

Thermal effects of urbanization and industrialization in the boundary layer A numerical study.

06 p0720 A73-18330

Five temperature model of pumping and output power pulse shape predictions for carbon dioxide-nitrogen-helium TEA lasers

06 p0701 A73-18362

Temperature dependent small signal operation of junction transistors at low supply voltage

06 p0677 A73-18395

On fracture toughness and its size dependence for steels showing thickness delamination.

06 p0709 A73-18476

Temperature dependence of diatomic gases thermal conductivity coefficient from shock tube tests, noting molecular gases above dissociation temperature

06 p0687 A73-18561

CW laser beams steady state thermal self focusing stability, deriving nonlinear absorbing medium geometrical optics ray equation and aberration pattern

06 p0702 A73-18583

Influence of condensation temperature on microstructure and tensile properties of titanium sheet produced by high-rate physical vapor deposition process.

06 p0711 A73-18752

Dendritic solidification of Cu-Ni alloys. II - The influence of initial dendrite growth temperature on microsegregation.

06 p0712 A73-18757

Thoria stability in TD-NiCr at high temperatures in the presence of chromium in solution.

06 p0713 A73-18771

Light emitting diode pumped Nd-YAG laser analysis for pumping rate and output dependence on temperature, using circular and transverse intensity distribution

06 p0704 A73-18787

Some effects of temperature on material properties and device reliability.

07 p0797 A73-19134

Dissociative recombination at elevated temperatures. IV - N₂⁺/dominated afterglows.

07 p0853 A73-19149

Determination of thermal conductivity of gases by shock-tube studies.

07 p0918 A73-19187

Temperature and loading rate effects on yield stress and specific fracture work in tempered carbon steel from notch tests, correlating with linear fracture mechanics

07 p0838 A73-19215

Temperature effects on transistor input and output static characteristics, proposing thermal stabilization by collector circuit resistance decrease and heat dissipation increase

07 p0798 A73-19294

Nonuniformly heated anisotropic rods with variable elastic parameters

07 p0911 A73-19317

Investigation of the temperature dependence of the anisotropy parameter K in n-Si and n-Ge by using magneto-plasma waves

07 p0861 A73-19327

Contribution to the study of the effect of molybdenum on the ageing kinetics of maraging steels.

07 p0838 A73-19499

Optimization of the rheological properties of striazine derivatives.

07 p0787 A73-19561

Synthetic hydrocarbon lubricants performance characteristics under extreme temperature service conditions, considering viscosity, antiwear, oxidation stability, demulsibility and corrosion protection properties

07 p0843 A73-19562

Measurement of the temperature dependence of the vibrational relaxation rate of HF and the effect of SF₆, N₂, and F₂ as diluents.

07 p0853 A73-19628

The effect of temperature on the mitotic activity of human peripheral blood lymphocytes in a culture

07 p0781 A73-19649

Temperature-dependent magnetic properties of individual glass spherules, Apollo 11, 12, and 14 lunar samples.

07 p0893 A73-19844

Thermal expansion of Apollo lunar samples and Fairfax diabase.

07 p0895 A73-19855

Apollo 14 returned lunar rock fine thermal conductivity measurement as function of temperature under vacuum conditions, using least squares curve fitting method

07 p0895 A73-19856

Viscous flow behavior of lunar compositions 14259 and 14310.

07 p0895 A73-19857

Application of the fourth-order anharmonic theory to the prediction of equations of state at high compressions and temperatures.

07 p0851 A73-19925

Concentration and mobility of electrons in indium-doped zinc oxide crystals

07 p0862 A73-20016

The effect of variable temperature on creep collapse of a cylindrical shell under external pressure

07 p0913 A73-20070

Influence of the thermal effect of the gas on the motion of an electric arc in a transverse magnetic field

07 p0858 A73-20081

Numerical method of transient heat conduction with temperature dependent thermal properties.

07 p0921 A73-20118

Nature of localized states in amorphous semiconductors - A study by electron spin resonance.

07 p0863 A73-20174

A method for evaluating the circuit reliability of electronic equipment

07 p0802 A73-20299

Temperature dependent pitting corrosion tests of Mo containing austenitic stainless steels

07 p0840 A73-20354

Prediction of the low-temperature stability of type 304 stainless steel from a room temperature deformation test.

07 p0840 A73-20414

Experimental study of water drop evaporation in a heated air flow

07 p0922 A73-20416

- Evaporation rate and temperature of liquid drops calculated for low and high temperature aerosols
07 p0922 A73-20417
- Residual conductivity in unannealed amorphous germanium.
07 p0864 A73-20455
- Influence of liquid lubricant properties on their performance.
07 p0844 A73-20464
- Design and performance of multichannel current ink jet recording instruments with galvanometers, noting mercury lamp light source, sensitivity and temperature effects
07 p0828 A73-20547
- Thermodynamic properties of gases dissolved in electrolyte solutions.
07 p0789 A73-20642
- Measurement of the dielectric constant of polyvinyl chloride at very low frequencies, and influence of the superposition of a continuous voltage
08 p0942 A73-20648
- Microwave filters with single crystal YIG sample as ferrimagnetic resonators, determining magnetic field and temperature effects on resonator cut-off frequency
08 p0942 A73-20705
- Electrical components heat dissipation via thermal radiation, determining nonlinear temperature dependence from Stefan-Boltzmann law
08 p1020 A73-20775
- Thermonuclear reactor model with core surrounded by dense cold plasma, noting temperature profile effects on fusion and energy release locations
08 p0991 A73-20818
- Single-phonon contribution to the hopping conductivity of amorphous solids.
08 p0994 A73-20955
- Study of the geometrical resonances of superconducting tunnel junctions.
08 p0994 A73-21207
- Thermal hereditary constitutive law for linear viscoelastic materials time response in transient temperature environment
08 p1018 A73-21409
- Superalloys oxidation behavior under long term exposure to high temperatures for suitability as Co-60 heat sources encapsulation materials
08 p0978 A73-21415
- The oxidation of tantalum and niobium in the temperature range 400-600 C.
08 p0978 A73-21416
- The low temperature strain sensitivity of MOS transistors.
08 p0948 A73-21476
- Certain resonance properties of nickel-cadmium ferrites
08 p0995 A73-21513
- Stress rupture behavior of a dispersion strengthened superalloy.
[ASME PAPER 72-MAT-G] 08 p0978 A73-21570
- Influence of high ambient temperatures on the performance and some physiological parameters in a tracking problem and an optical vigilance problem
08 p0935 A73-21575
- Investigation of a single spraying site of a colloid thruster.
08 p0996 A73-21599
- Dislocation glide controlled by linear elastic obstacles - A thermodynamic analysis.
08 p1019 A73-21628
- On the solution of the nonlinear heat conduction equations by numerical methods.
08 p1024 A73-21636
- Cr-Ni carbon steel testing for stress and temperature dependencies of secondary creep rate, noting grain boundary diffusion controlled mechanism
08 p0980 A73-21674
- Some empirical relationships between creep strain, stress, time and temperature in 1Cr-Mo-V rotor forgings.
08 p0981 A73-21783
- The temperature dependence of steady state creep in 20% Cr, 25% Ni, Nb stabilized stainless steel.
08 p0981 A73-21785
- The effect of niobium content on the steady-state creep of stabilized 20/25 austenitic stainless steels.
08 p0981 A73-21786
- Influence of composition and heat treatments on the structure and mechanical characteristics of martensitic stainless steels derived from the 16 percent chrome and 4 percent nickel type
09 p1098 A73-21924
- Grain-boundary internal friction of copper-nickel alloys
09 p1099 A73-21965
- Reversible thermal breakdown as a switching mechanism in chalcogenide glasses.
09 p1133 A73-21986
- Cooling effects of CO IR opacity in stellar atmospheres of dwarfs and supergiants, considering application to sun and grain formation in cooler stars
09 p1142 A73-22031
- Temperature dependent chemisorption effects on hydrogen embrittlement of steel, showing strength-ductility correlation
09 p1100 A73-22158
- Stress corrosion cracking of commercial Al-Mg alloys and its prevention.
09 p1102 A73-22422
- Recrystallization in Ti-15 Mo base beta titanium alloys.
09 p1103 A73-22423
- Ni diffusion in Nb at 988 to 1246 C, using residual activity technique with Ni-63 as tracer
09 p1103 A73-22436
- Numerical study of the stability of a supersonic laminar boundary layer
09 p1028 A73-22624
- Certain physical properties of Nd-Sb system alloys and their correlation with the phase diagram
09 p1134 A73-22679
- Concentrational dependence of resistivity in solid disordered binary alloys of nontransition metals
09 p1104 A73-22687
- Magnetic permeability dependence on temperature and composition of hexaferrites with various Sc ion contents
09 p1134 A73-22982
- Study of average and turbulent characteristics of boundary layers stratified in temperature - Comparison with the corresponding characteristics in low layers of the atmosphere
09 p1072 A73-23028
- Thermal limitation for CW output power of a Gunn diode.
09 p1064 A73-23043
- Drift of the breakdown voltage in highly doped planar junctions.
09 p1064 A73-23047
- The load life characteristics of thick-film resistors.
09 p1065 A73-23048
- Effect of test temperature on energy of fracture of graphite.
09 p1110 A73-23062
- The thermal expansion coefficients of some glass-reinforced plastics and their components at low and high temperatures.
09 p1111 A73-23063
- Influence of material properties on dynamic fracture toughness of steels.
09 p1109 A73-23259
- Engineering significance of statistical and temperature-induced fracture mechanics toughness variations on fracture-safe assurance.
[ASME PAPER 72-PVP-15] 09 p1163 A73-23265
- Temperature dependent combined hardening theory within plasticity formulations for finite element analysis of aerospace vehicle engines under plastic strain and cyclic fatigue
09 p1166 A73-23463
- Temperature dependent thermal conductivity coefficient and electron and phonon components for group IV-VI transition metal diborides at 2300 K, using Wiedemann-Frantz law
10 p1236 A73-23518
- Temperature dependent heat conductivity, Lorentz number and electrical resistivity of high melting Ti, Zr, Nb, Cr, Mo and W carbides and borides at 300-1200 K
10 p1230 A73-23519
- The Knudsen layer in a flow with two-temperature relaxation
10 p1250 A73-23580
- Experimental determination of the temperature and pressure dependence of the absolute viscosity of mineral oils
10 p1237 A73-23661
- Effects of Ni and Fe addition on various properties in heat-resisting aluminum casting alloys.
10 p1231 A73-23675
- Influence of the degree of deformation and annealing temperature on the recovery of 99.999% pure nickel after plastic deformation at -196 C and 25 C, respectively
10 p1231 A73-23690
- Metallic dust particles in quasi circular solar orbit, discussing evolution, thermal evaporation, atomization and size
10 p1274 A73-23720
- Mechanical behavior of solid solutions of centered cubic symmetry obtained by limited addition of titanium to the iron
10 p1231 A73-23770
- Thermosensitive interoreceptors and their interaction with thermosensitive structures of the hypothalamus
10 p1179 A73-23803
- Epoxy resins thermal mechanical properties, considering difference between toughness and flexibility in terms of temperature and loading rate insensitivities
10 p1237 A73-23952
- Analysis, test, and comparison of composite material laminates configured for isotropic low thermal expansion.
10 p1237 A73-23960
- The effect of long-time thermal exposure on the mechanical properties of graphite/polyimide composites.
10 p1238 A73-23970
- Effect of heating water droplets by optical radiation.
10 p1246 A73-24181
- Temperature dependence of the accommodation coefficient of liquid-helium film.
10 p1249 A73-24341
- Influence of temperature on the damping characteristics of heat resistant EP452 and E1696 steels in a uniform stress-strain state produced by tension and compression
10 p1233 A73-24358
- Damping properties of VT3-1, VT-9, and VT-18 titanium alloys of various microstructure
10 p1233 A73-24359
- Grain-boundary corrosion of type 304 stainless steel by cesium oxides.
10 p1234 A73-24427
- Quantitative characterization of the substructure of AISI 316 stainless steel resulting from creep.
10 p1234 A73-24436
- Fine precipitate within coarse gamma-prime particles in cast Ni-base superalloy during elevated temperature exposure
10 p1235 A73-24446
- Temperature dependence of kinetic properties of photoconductivity produced by carrier redistribution across attachment centers, discussing results with Ag and Al doped ZnS single crystals
10 p1260 A73-24468
- Positive thermal coefficient of electrical resistance in BaTiO₃ single crystals near the Curie point
10 p1260 A73-24473
- Strain gage measurement errors under long term installation conditions, considering drift, temperature and moisture effects, connection wires impedance and selector switch contact resistance
10 p1219 A73-24568
- Temperature change induced material properties variations effects on impact stresses in graphite and stainless steels, considering impact velocity
10 p1220 A73-24575
- Temperature-induced changes of the electron-vibration spectrum of LaAlO₃-Cr³⁺/Cr³⁺ crystals
10 p1260 A73-24578
- Change in the superconducting properties of vanadium after the introduction of tantalum impurity atoms
10 p1261 A73-24761
- Thermal oscillations of hexaboride atoms of some metals
10 p1261 A73-24777
- Possibilities and some results of studying the ionosphere by the method of 'incoherent' scattering of radio waves
11 p1350 A73-25088
- The stability of a layer of binary gas mixture heated below.
11 p1449 A73-25222
- Determination of attachment center parameters in semiconductors from the temperature dependence of the photocurrent
11 p1408 A73-25248
- Radome insertion phase delay errors due to element impedance, frequency uncertainty, power instability and heat effects
11 p1327 A73-25278
- Measurement of the critical crack displacement with the help of double-notched specimens
11 p1434 A73-25325
- The joining of fiber-reinforced composite-material components with similar or different components
11 p1373 A73-25418
- Proposed stratigraphic controls on the composition of crude oils reservoir in the Green River formation, Uinta Basin, Utah.
11 p1352 A73-25471
- Heat conduction nonlinear boundary value problems approximate solution via Westphal similarity theorem, considering inhomogeneous media with temperature dependent heat transfer coefficients
11 p1451 A73-25742
- Oxygen and temperature effects on Ni base superalloys fatigue fracture, discussing trans- and intergranular crack propagation and initiation in single and polycrystals and surface coatings
11 p1382 A73-25818
- Neutron irradiation effects on room and high temperature fatigue behavior of stainless steel, noting fatigue life enhancement at low temperature and strains
11 p1383 A73-25832
- On the design of air-cooled radial turbine blades.
11 p1410 A73-25843
- Temperature dependence of the Na-23 quadrupole coupling constants in Rochelle salt.
11 p1409 A73-25875
- Thermochemical calculation for high temperature and pressure formation of interstellar molecules in compact H II regions, considering prestellar and late stellar atmospheres
11 p1423 A73-26105

TEMPERATURE EFFECTS

Temperature dependence of the activity and solubility of carbon in pure nickel

11 p1384 A73-26110

Apollo 12 fines vacuum thermal conductivity as function of temperature for different densities, comparing to terrestrial basalt under vacuum and pressure

11 p1425 A73-26137

The fracture toughness of beryllium.

11 p1384 A73-26168

S-200 grade beryllium fracture toughness properties.

11 p1384 A73-26170

Ultrasonic measurement of elastic moduli in slender specimens using extensional and torsional wave pulses.

11 p1365 A73-26171

Heat treatment effects on the mechanical properties in Ti-6Al-6V-2Sn.

11 p1385 A73-26172

Temperature, testing rate and substrate choice effects on characteristic energy required to produce separation and failure of adhesively bonded pieces

11 p1443 A73-26203

Ultrasonic investigation of the nematic-isotropic phase transition in MBBA.

11 p1409 A73-26213

Gaussian light beam transmitted intensity derivation for thermal lensing in solids by vector Kirchhoff approach, obtaining time dependent shift in diffraction focus

11 p1377 A73-26228

A method of measuring thermal conductivity in the presence of extraneous heat currents and the thermal conductivity of brass at low temperatures.

11 p1367 A73-26307

Effects of upstream wall temperatures on hypersonic tunnel wall boundary-layer profile measurements.

11 p1344 A73-26395

Influence of total temperature on transition in supersonic flow.

11 p1303 A73-26400

Emissions from and within an Allison J-33 combustor. II. The effect of inlet air temperature.

11 p1411 A73-26423

Relaxation processes in metastable beta titanium alloys.

11 p1385 A73-26498

NASA use of liquid and gaseous oxygen under extreme pressure, temperature and flow rate conditions, discussing safety requirements in terms of structural and chemical compatibility

11 p1410 A73-26525

The problem of temperature in vacuum metrology. II

11 p1371 A73-26552

Temperature and concentration dependence of the electrical resistivity of solid alloys in the magnesium-cadmium system

11 p1386 A73-26570

Some physicochemical properties of compounds formed by oxides of rare-earth elements and barium

11 p1410 A73-26673

Utilization of thermal phenomena in the construction of signal-energy converters for coupling automatic control devices belonging to different categories of the State Instrument System

12 p1459 A73-26765

Study of the variations of the microhardness of the surface layer hardened by ball rolling in relation to the heating temperature

12 p1502 A73-26799

Order-disorder alpha and gamma phase transformations as function of temperature in Co-Fe-V alloy by dilatometric, magnetostuctural, neutron diffraction and X ray analyses

12 p1508 A73-26834

Temperature dependence of the Moessbauer spectra of iron-cobalt-vanadium alloys

12 p1509 A73-26839

Temperature dependence of the hardness and estimation of the creep of the Rh-18% Re alloy

12 p1509 A73-26899

Cumulative creep formulas for construction steels at stepwise increasing temperatures

12 p1510 A73-26900

Temperature dependence of the solubility of scandium in solid magnesium

12 p1510 A73-26908

Optimal electrical conductivity and mechanical properties of Cu-Mg-Fe-Si-Zr and Be-B containing heat resistant Al alloys, comparing to Cu at room and elevated temperatures

12 p1511 A73-26918

Temperature sensitivity of cfrp honey-comb structures under holographic adt.

12 p1496 A73-27036

Tensile behaviors of high Cr-low Ni two-phase stainless steels at room and low temperatures.

12 p1511 A73-27056

Effect of prestraining on the brittleness of molybdenum.

12 p1511 A73-27058

An experimental method for determining the characteristics of ablative materials

12 p1557 A73-27068

Gunn microwave oscillators electron temperature dependent noise in absence of 1/f type, considering thermal or Johnson noise augmented by carriers hopping

12 p1478 A73-27111

Development of acoustic and overheat instabilities in a plasma with molecular impurities

12 p1528 A73-27303

The limits and the nature of the onset of influence of thermogravitational forces on turbulent flow and heat transfer in vertical tubes

12 p1487 A73-27313

Alloy creep due to temperature and tensile stress in absence of hardening

12 p1513 A73-27479

Lunar surface thermal response from IR atlas charts of eclipsed moon, noting thermal enhancements in maria

12 p1541 A73-27483

A determination of the intensity of the ancient lunar magnetic field.

12 p1542 A73-27494

Continuous-wave laser with a vortex-stabilized lamp.

12 p1506 A73-27503

Stimulated emission of light from solid solutions of tin and lead chalcogenides in the region of 10 microns.

12 p1507 A73-27519

Highly disperse Fe powder electrodeposition on cathode, examining electrolyte concentration, acidity, current density and bath temperature effects on current efficiency for optimal deposition conditions

12 p1503 A73-27552

Possibility of silicon carbide recrystallization in the process of reactive sintering

12 p1503 A73-27555

The strength differential of steel and Ti alloys as influenced by test temperature and microstructure.

12 p1513 A73-27681

Equilibrium of vanadium carbide with an alpha or gamma solid solution in the iron-rich Fe-Cr-V-C system at temperatures from 700 to 1150 C and at a carbon concentration of 0.30%

12 p1513 A73-27684

Drift mobility of holes and electrons in perdeuterated anthracene single crystals.

12 p1531 A73-27688

Investigation of the influence of temperature and velocity fields on the quality of an astronomical image

12 p1546 A73-27864

Method of calculating the temperature dependence of the integral intensity of light absorption by local vibrations in crystals

12 p1525 A73-27937

Determination of the temperature dependence of the Debye-Waller factor for thin gold films by electron diffraction observations

12 p1532 A73-27944

Sterically controlled syntheses of optically active organic compounds. XVI - Temperature dependence of hydrogenolytic asymmetric transamination.

12 p1467 A73-27974

Investigation of the ferroniobium oxidation process

13 p1630 A73-28010

Quasi-ternary Mo-TiC-ZrC system

13 p1630 A73-28014

Thermal expansion of tungsten from 293 to 1800 K. [ECTP PAPER E-1]

13 p1631 A73-28052

Ti-Al-Sn alloy microstructure effects on low temperature creep, discussing creep stresses, activation energy and yield stress

13 p1632 A73-28127

Vapor-phase deposition of elementary boron at substrate temperatures in the range from 1100 to 1400 C

13 p1645 A73-28181

Contribution to the study of the behavior of liquid cobaltous oxide in an oxidizing atmosphere

13 p1634 A73-28204

Properties of iron impurity in aluminium matrix studied by Mossbauer spectroscopy.

13 p1634 A73-28220

A high resolution dynamic technique of thermoelectric power measurements.

13 p1612 A73-28370

Determination of the basic characteristics of an impurity level by Hall effect measurements

13 p1668 A73-28461

Phenomenological analysis of thermostimulated depolarization effects

13 p1668 A73-28463

Mechanical properties of 6061 Al-Mg-Si alloy after very rapid heating.

13 p1636 A73-28795

Perfect thermal cycles family definition for heat supply and extraction as function of temperature

13 p1706 A73-28911

Temperature dependence of the cross section of O+ ion desorption by electrons from an oxygen layer adsorbed on a tungsten surface

13 p1663 A73-28969

Temperature and rate dependence of the critical shearing stress in magnesium single crystals

13 p1636 A73-29056

Thin ferrosilicon intermediate cylindrical layer tensile strength, microhardness and yield point determination at 20-1000 C

13 p1624 A73-29064

Vanadium galliumide tape preparation and critical temperature and current as function of heat treatment temperature and applied magnetic field, considering pancake current capacity

13 p1669 A73-29069

Injection phase locked microwave oscillator for FM amplifier, calculating frequency drift caused gain limitation in terms of diode and circuit properties temperature effects

13 p1593 A73-29116

Recent developments in precipitation hardenable stainless steels.

13 p1637 A73-29271

Relaxation spectra of niobium irradiated at low temperature.

13 p1638 A73-29455

Pure Al compression tests for strain rate effects on strength in wide temperature range, using split Hopkinson bar apparatus and Instron testing machine

13 p1639 A73-29461

Effect of temperature and strain rate on the high temperature, low cycle fatigue behaviour of a 17Cr-10Ni-2Mo stainless steel.

13 p1708 A73-29504

Influence of temperature on the initial yield of notch strength.

13 p1641 A73-29511

The effect of elevated temperature upon the fatigue-crack propagation behavior of two austenitic stainless steels.

13 p1642 A73-29525

Nylon copolymers dynamical mechanical properties temperature dependence, discussing alpha peak shifts, polyamides relaxation and ordered structure

13 p1646 A73-29526

Nickel-cadmium cells for low earth orbit applications.

13 p1572 A73-29584

Bending vibration test of glass-textolites, noting temperature effect on vibration damping properties

13 p1647 A73-29607

Strain curves of titanium alloys VT-6S and VT-14 in the temperature range 20-400 C.

13 p1643 A73-29612

Creep and fracture in OT-4 titanium alloy at temperatures from 400 to 550 C.

13 p1643 A73-29627

Conditions of brittle strength of weld joints at different temperatures and applied loading rates.

13 p1626 A73-29628

Ignition condition in Tokamak experiments and role of neutral injection heating.

14 p1777 A73-29684

Thermal diffusivity measuring technique for hazardous materials.

14 p1752 A73-29914

Nonlinear heat flow in anisotropic media with property variations and nonlinear heat generation.

14 p1816 A73-29915

Nonlinear mechanisms for self-focusing of microwaves in semiconductors.

14 p1732 A73-29920

Temperature effects on liquid drop evaporation in an air flow

14 p1816 A73-30015

The shear strength of thin lubricant films.

14 p1754 A73-30050

High pressure, radiation, high temperature and vacuum chemistries, discussing planetary matter, solar and cosmic radiation effects, plasma temperatures, solar winds and molecular populations

14 p1723 A73-30127

Diffusion of plasma density and temperature perturbations in a magnetic field

14 p1749 A73-30264

Grain growth during creep of alloyed molybdenum.

14 p1759 A73-30311

Processing conditions and sample dimensions and shapes effects on Ti alloy creep characteristics at room temperature

14 p1759 A73-30312

Critical shear stress temperature dependence in Al-Mg single crystal alloys of various concentrations in the range 1.6-300 K.

14 p1759 A73-30313

Dependence of the variation of the electronic dislocation drag force in a superconducting transition on the stress, temperature, and velocity.

14 p1783 A73-30341

Measurement of the temperature coefficient of the refractive index of infrared materials with the aid of a carbon dioxide laser

14 p1757 A73-30371

Low-temperature internal friction in boron fibers

14 p1766 A73-30380

High-speed /subsecond/ simultaneous measurement of specific heat, electrical resistivity, and hemispherical total emittance of Ta-10/wt.%W alloy in the range 1500 to 3200 K.

[ECTP PAPER D2-4]

14 p1760 A73-30437

Temperature-dependent design parameters of RAPATT diodes. 14 p1736 A73-30446

Influence of recovery and recrystallization on the Young's modulus and its temperature dependence in Fe-Ni-C alloys 14 p1760 A73-30586

Stability of the thermomechanical hardening effect in 60N20 nickel steel 14 p1760 A73-30590

Some relations for high pressure flows with and without heat transfer. 14 p1817 A73-30604

Constant line sources of heat in infinite media, whose thermal resistivities are linear functions of the temperature. 14 p1817 A73-30610

Solute aluminum strengthening and strain aging in Al alloys at 78-810 K 14 p1761 A73-30639

Steel reinforcement fiber arrangement and volume content influence on aluminum composites strength and fatigue resistance at room and elevated temperatures 14 p1766 A73-30710

Mechanism of the lubricating action of sulfides and phosphides of refractory metals 14 p1755 A73-30717

Influence of annealing temperature on the changes in the chemical and phase compositions of the intercrystalline boundaries of weakly-alloyed molybdenum 14 p1764 A73-30865

Effect of rare earth metal additions on the recrystallization of nickel 14 p1765 A73-30887

Influence of heating on the intensity and energy of photoelectrons in deformed aluminum 14 p1765 A73-30889

Carbonyl nickel recrystallization characteristics from hardness-temperature graphs and X ray analyses 14 p1765 A73-30891

The effect of temperature perturbations on ion-acoustic and drift waves in a weakly collisional plasma. 15 p1916 A73-31087

Effect of body temperature on ventilatory transients at start and end of exercise in man. 15 p1832 A73-31127

Deflection of a thin, nonlinearly heated, rectangular strip 15 p1946 A73-31142

Temperature dependence of the electrical resistance of superconducting Ti-Nb and Ti-Nb-Zr alloys subjected to working by hydrostatic pressure 15 p1887 A73-31186

Effect of lasting high temperatures on the mechanical properties and microstructure of bonded glass mat with an aluminophosphate binder 15 p1896 A73-31213

Thermal conductivity of carbon fibers 15 p1896 A73-31214

Hydroxyl emission intensity and rotational and vibrational temperatures, discussing statistical properties of geomagnetic storm effects and diurnal, seasonal and latitudinal variations 15 p1867 A73-31260

The effect of stacking-fault energy on the stress-strain curve of dispersion-hardened Ni-Co alloys. 15 p1887 A73-31351

Solar neutrino flux, discussing effects of temperature oscillations on neutrino and photon luminosities 15 p1926 A73-31358

The effects of couple-stresses on thermal stress distributions in multiply-connected domains. 15 p1947 A73-31362

Yielding in unidirectional composites under external loads and temperature changes. 15 p1949 A73-31679

Transport phenomena in a fully ionized ultrarelativistic plasma 15 p1919 A73-31709

Temperature effects in quadrupole interaction in NbHf alloys 15 p1923 A73-31710

Mono- and polycrystalline barium titanate structural and physical properties, discussing thermally induced structural changes effects on polarization, permittivity and loss tangent 15 p1924 A73-31775

Hardening and softening of aluminum alloys under an applied load at 135 to 150 C. 15 p1889 A73-31808

Response of thermally controlled, vibrating piezoelectric quartz to the deposition of multiple metal layers 15 p1924 A73-31843

Temperature dependence of the single-crystal elastic constants of Co-rich Co-Fe alloys. 15 p1890 A73-31926

The reaction of a titanium alloy with hydrogen gas at low temperatures. 15 p1890 A73-31993

High temperature specific heats of iron-rich iron-titanium alloys between 600 and 1150 K. 15 p1891 A73-31994

Temperature dependent nuclear mass and its application to astrophysical problems. 15 p1939 A73-32013

Field-dependent carrier transport in non-crystalline semiconductors. 15 p1924 A73-32021

Ultrasonic probes sound fields from thermal effects via IR camera or liquid crystals, sound pressure via Pohlmann image converter and light modulation via schlieren method 15 p1882 A73-32055

Multiple scattering of sound by turbulence and other inhomogeneities. 15 p1865 A73-32151

Determination of atmospheric water-vapor densities from measurements of the 6943.8-A absorption line strength. 15 p1845 A73-32227

Electrophysical properties of TiC-Nb, TiC-Ta, TiC-Mo, and TiC-W cermets 15 p1892 A73-32242

Influence of heating rate on the phase composition of the VT3-1 alloy 15 p1894 A73-32525

Effect of temperature on titanium plasticity 15 p1894 A73-32527

Oxidation of OT4 and OT4-1 alloys in the process of prolonged heating in air at temperatures from 200 to 400 deg 15 p1894 A73-32539

Variation with temperature of free enthalpy of formation of certain carbides 15 p1898 A73-32644

A stress-strain relation for homogeneous and isotropic continua 16 p2035 A73-32934

High pressure-sintering preparation of barium ferrites, discussing temperature and compression effects on density and magnetic properties 16 p2044 A73-32947

Heat treatment effects upon the properties of PAN base carbon fibers. 16 p2028 A73-33040

Comparative testing and evaluation of conformal coating materials and processes. 16 p2018 A73-33062

Thermal creep of rarefied gas in a circular tube. 16 p2039 A73-33328

Critical behaviour in chemically reacting systems. I - Difficulties with the Semenov theory. II - An exactly soluble model. 16 p1976 A73-33342

Climate simulation via environmental test chambers examining mechanical, thermal and pressure effects to determine functional component suitability 16 p1997 A73-33382

The consideration of environmental effects in the development of environment-resistant systems 16 p2019 A73-33385

Experimental studies and applications of vanadium oxides. 16 p2044 A73-33471

Some effects of variable surface temperature on heat transfer to a partially porous flat plate. [ASME PAPER 73-GT-4] 16 p2086 A73-33482

Newkirk effect - Thermally induced dynamic instability of high-speed rotors. [ASME PAPER 73-GT-26] 16 p2047 A73-33499

Sodium chloride electrolyte data at high temperatures and pressures. [ASME PAPER 73-PROD-1] 16 p1971 A73-33532

Thermal properties of rhenium single crystals at high temperatures. 16 p2026 A73-33581

Temperature dependence of diatomic gases thermal conductivity coefficient from shock tube tests, noting molecular gases above dissociation temperature 16 p2086 A73-33586

The role of temperature in the environmental acceptance testing of electronic equipment. 16 p1989 A73-33606

Industrial sterilization; Proceedings of the International Symposium, Amsterdam, Netherlands, September 1972. 16 p1975 A73-33691

Microorganism heat sterilization process design and control based on logarithmic thermal destruction and Bigelow temperature coefficient models, determining lethality by statistical procedure 16 p1976 A73-33695

Atmospheric temperature measurement with X and K band radiometers, discussing meteorological conditions variation effects on microwave propagation and comparison with spacecraft tracking data 16 p1983 A73-33730

Unconventional processes for faster extrusion of aluminum hard alloys 16 p2021 A73-33951

The kinetics of the dissolution of oxygen in niobium at low oxygen pressures and high temperatures 16 p2026 A73-33955

Characteristics change of Gunn diodes with uniaxial stress and temperature. 16 p1991 A73-33996

Temperature dependent crystallization and density of Fe-Mn-C alloys with niobium at 1200-1500 C from gamma ray measurements 16 p2027 A73-34012

Thermal conductivity and temperature dependence of energy gaps in niobium samples containing large amounts of impurity atoms 16 p2027 A73-34061

Coupled thermally induced vibrations of beams. 17 p2241 A73-34190

Effect of donor density and temperature on the performance of stabilized transferred-electron devices. 17 p2134 A73-34220

Temperature conditions and blood supply of the brain in animals 17 p2111 A73-34229

Prediction of the deformation properties of polymer materials 17 p2194 A73-34268

Effect of temperature and composition of gas mixture on population inversion in pulsed CO2 laser. 17 p2183 A73-34295

Noise factor and power formula for cooled SHF broadband frequency converters with semiconductor mixer diode 17 p2134 A73-34317

Damping properties of turbine blade materials at operational temperatures 17 p2221 A73-34327

Allowance for the influence of temperature in statistical estimates of the strength of metals in the brittle condition 17 p2186 A73-34328

Mechanism of the micrononhomogeneous deformation of metals throughout a wide interval of temperature 17 p2186 A73-34330

Experimental evaluation of the strength of elements of thin-walled pressure vessels during severe cooling 17 p2177 A73-34331

Young modulus of elasticity measurement in alloys of Fe with Cr, W and Mo, examining concentration dependence at 20 to 500 C 17 p2187 A73-34334

Mechanical properties, microstructure and failure characteristics of binary alloys of Al-Mg system determined under different tensile stress rates and temperatures 17 p2187 A73-34339

Experimental determination of thermal conductivity of nitrogen in the temperature range 100-2200 C. 17 p2254 A73-34372

Effect of 'bulk' heat transfers in aircraft gas turbines on compressor surge margins. 17 p2221 A73-34382

The effect of heat transfer on boundary layer stability in axial flow compressors. 17 p2093 A73-34394

Simultaneous measurement of specific heat, electrical resistivity, and hemispherical total emittance of niobium-1 wt. % zirconium alloy in the range 1500 to 2700 K by a transient/subsecond technique. 17 p2187 A73-34499

The supporting effect of bending specimens under static load in the temperature range from 400 to 500 C. 17 p2187 A73-34521

Effects of cold plastic deformation and aging temperature on the mechanical properties of dispersively hardening Cr-Ni-Co-Mo steel 17 p2188 A73-34559

Inter-crystalline failure in recrystallized low-alloyed molybdenum alloys 17 p2189 A73-34577

Accuracy of type K thermocouple wire below 500 F - A statistical analysis. 17 p2167 A73-34624

High strength Ni-Cr-Mo steel plane-strain fracture toughness measured with circumferentially cracked-notched round bars, discussing heat treatment and test temperature effects 17 p2190 A73-34890

Temperature effects on modulation sensitivity and vibrational spectra in Gunn diode oscillators, suggesting frequency stability improvement method 17 p2136 A73-35162

Temperature dependence of thermionic emission current density of Pt additive powdered zirconium carbide deposit on diode cathode working surface 17 p2109 A73-35171

Temperature dependent thermal conductivity coefficient and electron and phonon components for group IV-VI transition metal diborides at 2300 K, using Wiedemann-Frantz law 17 p2196 A73-35198

Temperature dependent heat conductivity, Lorentz number and electrical resistivity of high melting Ti, Zr, Nb, Cr, Mo and W carbides and borides at 300-1200 K. 17 p2191 A73-35199

Elasticity of water-saturated rocks as a function of temperature and pressure. 17 p2163 A73-35271

Microwave amplifier design with discrete variable components, testing power output and efficiency, bandwidth, and temperature, vacuum and vibration effects on performance

17 p2141 A73-35324

Parametric test results of a swirl-can combustor.

17 p2222 A73-35471

Resistance anomaly in semiconductor barium and strontium niobates

17 p2219 A73-35554

Airborne passive IR line scanner, noting spectral resolution and thermal sensitivity for land and water surfaces energy

17 p2174 A73-35577

Influence of interstitials in the behavior in tension of niobium between 20 and 1000 C

17 p2193 A73-35624

Organic compounds chemical analysis with cold trap to allow materials evaporation according to vapor pressure characteristics for replacing gas chromatograph

17 p2175 A73-35760

Burnett cell design and fabrication for error reduction in high precision P-V-T data generation without volume or mass measurements

17 p2182 A73-35772

Mechanical properties of weld, base metal and coated columbium FS85.

17 p2182 A73-35842

Transient temperatures in a plate from a Gaussian distribution of normal heat flux and current flow with application to the free arc discharge.

17 p2255 A73-35843

Survival and mutability of *Chlorella* under various orientation in the earth's gravitational field.

18 p2270 A73-35997

Investigation of the solar X-ray flare spectra by the 'Intercosmos-4' and 'Intercosmos-7' satellites.

18 p2345 A73-36015

Thermal control of the large space telescope /LST/. [AIAA PAPER 73-720]

18 p2359 A73-36338

Ni-Fe-Cr alloy and austenitic stainless steel cyclic stress-strain behavior at 70-1400 F

18 p2323 A73-36586

Kerr response of nematic liquids.

18 p2340 A73-36620

Metallic dust particles in quasi-circular solar orbit, discussing evolution, thermal evaporation, atomization and size

18 p2355 A73-36745

Prediction of the heat-resistance characteristics of high melting materials

18 p2323 A73-36757

Evaluation of the carrying capacity of reinforced plastics subjected to nonuniform heating

18 p2328 A73-36760

Residual stress relaxation stability in 13Kh12NVM-FA steel

18 p2323 A73-36763

Characteristics of the temperature dependence of the microhardness of a highly heat resistant dispersion-hardened nickel alloy

18 p2324 A73-36765

Effect of temperature on true energy dissipation in heat resistant E1893 nickel alloy

18 p2324 A73-36766

Temperature dependence of the yield point in grain-oriented beryllium

18 p2324 A73-36773

Microwave equipment reliability design for aerospace environment applications, considering vibration, shock, humidity and temperature effects and frequency stability

18 p2293 A73-36778

Influence of temperature and strain rate on the load-elongation curve and plastic properties of molybdenum

18 p2324 A73-36801

Certain law controlling the temperature dependence of the microdeformation of Fe-Cu-Ti, W, and W-Re bcc alloys

18 p2324 A73-36803

Some characteristics of the microplastic deformation of the surface layers of semiconductor crystals at temperatures below and above the thermal brittleness threshold

18 p2341 A73-36805

Friction of hard alloys in vacuum at low temperatures

18 p2320 A73-36861

Critical shear stress temperature and rate dependence in magnesium single crystals.

18 p2325 A73-36888

Thin ferrosilicon intermediate cylindrical layer tensile strength, microhardness and yield point determination at 20-1000 C

18 p2320 A73-36896

Ambient temperature rise effects on pilot performance in a flight simulator

18 p2287 A73-36948

Turbine engine research activity evolution, considering entry temperature increase, pollution sources nonstationary aerodynamics and aeroelasticity in compressors, and noise problem

18 p2343 A73-36991

Chemisorption of CO on tungsten /100/- Combined flash desorption and electron stimulated desorption study. II.

18 p2287 A73-37033

Quasi-stationary theory of hydrocarbon droplet ignition. II - Ignition limits of cold and hot droplets

18 p2372 A73-37117

Method of estimating the circuit reliability of electronic devices.

18 p2294 A73-37136

Mo-W alloys mechanical characteristics dependence on temperature and W content

19 p2439 A73-37265

Effect of temperature on the effectiveness of hardening components made of heat-resistant alloys

19 p2439 A73-37268

Finite element elastic-plastic-creep analysis of two-dimensional continuum with temperature dependent material properties.

19 p2496 A73-37483

On the correction of anemometric measurements in air flows of slowly varying temperature

19 p2429 A73-37529

Attempt at an interpretation of thermal reversals in the spontaneous polarization of ferroelectric microdomains

19 p2470 A73-37537

Studies of the renewal of stress relaxation on a high-grade steel wire subjected to stress corrosion after being treated for total elimination of relaxation

19 p2497 A73-37553

Leidenfrost temperature - Its correlation for liquid metals, cryogenics, hydrocarbons, and water.

19 p2504 A73-37641

Minimum principles and some theorems on the elastoplastic equilibrium of bodies subjected to nonstationary physical and thermal effects

19 p2499 A73-37765

Short-term creep of OT4 alloy.

19 p2440 A73-37786

Some details concerning plastic deformation mechanism of commercial titanium between -100 and 400 C

19 p2441 A73-37839

Oxidation of titanium between 25 C and 400 C.

19 p2442 A73-37950

Influence of thermal effects and particle capture by plasma waves on the dispersion characteristics of nonlinear waves

19 p2469 A73-37960

Analysis and temperature control of hybrid microcircuits.

19 p2412 A73-37968

[ASME PAPER 73-ENAS-6] Effect of heat input on properties of Inconel filler metal 82 weld deposits.

19 p2435 A73-38002

The effect of elevated temperatures on the mechanical properties of B-Al composites.

19 p2442 A73-38095

The compression yield behaviour of polymethyl methacrylate over a wide range of temperatures and strain-rates.

19 p2444 A73-38097

Constitutive equations for isotropic and anisotropic perfectly plastic materials derived from Clausius-Duhem inequality, considering thermal influences, plastic flow, entropy and elastic deformation

19 p2501 A73-38283

Transit satellite-borne radioisotope thermoelectric generators launch aboard Scout missile into circular polar orbit, obtaining electrical and thermal data

19 p2494 A73-38394

Temperature-humidity acceleration of metal-electrolysis failure in semiconductor devices.

19 p2411 A73-38450

Dynamic thermal properties of IMPATT diodes.

19 p2411 A73-38459

The thermal and electrical conductivities of porous copper and stainless steel to elevated temperatures. [ASME PAPER 73-HT-47]

20 p2575 A73-38572

Yield surfaces of metals at elevated temperatures.

20 p2615 A73-38640

Temperature dependence of adhesive fracture of epoxy resin.

20 p2580 A73-38642

Temperature dependence of the parameters of an n-p-i structure with negative resistance

20 p2535 A73-38860

Elastic properties of tantalum over the temperature range 4-300 K.

20 p2575 A73-38886

Operational temperature and frequency effects on radial driving point mechanical impedance of damped thin walled ring with mass segments attached by viscoelastic material

20 p2616 A73-39051

Effects of temperature and velocity fields on the quality of astronomical images.

20 p2608 A73-39238

Methods for identification of thermodynamically similar substances

20 p2593 A73-39296

Statistical characteristics of the fatigue strength of heat-resistant 1Kh18N9T steel under steady and programmed loading conditions at high temperatures

20 p2577 A73-39355

Influence of small oxygen and nitrogen additions on the nature of the temperature dependence of the mechanical properties of niobium

20 p2577 A73-39360

Anisotropy of low-temperature plasticity and the tendency of deformed molybdenum toward exfoliation

20 p2578 A73-39377

Heat transfer through free convection of air between vertical plates, obtaining Nusselt and Grashof numbers, and temperature and pressure effects

20 p2628 A73-39474

Silicon-on-sapphire thin film junction diodes, investigating second breakdown onset delay time and minimum energy dependence on high resistivity side heating

20 p2536 A73-39414

Substructure of type 316 stainless steel deformed in slow tension at temperatures between 21 and 816 C.

20 p2578 A73-39495

Generation of vacancies in tungsten by rapid-rate deformation at elevated temperature.

20 p2578 A73-39495

Cavitation and boiling bubble growth, collapse and damage effects, discussing liquid jet formation temperature effects, glycerol, ethanol and water solutions and bubble geometry

20 p2548 A73-39516

Overheat instability in a flow of electrically conducting incompressible medium under conditions of an internal boundary value problem

20 p2598 A73-39605

Convection in a liquid heated from below in a closed cavity with temperature-dependent viscosity

20 p2628 A73-39612

Detuning of Wheatstone-bridge circuit during their measurement with wire strain gages - Influence and elimination of undesired effects on detuning

20 p2566 A73-39630

Thermal track fading factor in Georgia tektites stratigraphy and fission track ages, noting agreement with K/Ar ages

20 p2612 A73-39717

Laminar steady state flow resistor design featuring temperature independence achieved with flattened capillary tube

20 p2511 A73-39750

Influence of semiconductor laser heating on the parameters of the output pulses

21 p2710 A73-40000

Two types of instability of steady convective motion caused by internal heat sources

21 p2789 A73-40192

Investigation of the crystallization of polyethylene terephthalate

21 p2647 A73-40260

Influence of a mixture of plasticizers, exhibiting a different mechanism of action, on the deformation of cellulose triacetate over a wide range of temperatures

21 p2647 A73-40260

Effect of chemically activated elements on the properties of electron-beam-melted nickel

21 p2718 A73-40482

Ta-Nb-Re system phase diagram plotted by physico-chemical analysis methods, establishing region of existence of ternary solid solutions and temperature dependence

21 p2718 A73-40488

Phase diagram thermal sections and concentration corner of Mo-Zr-B system by microstructure, X ray and electron microscope analysis

21 p2718 A73-40490

Investigation of the gain instability of a semiconductor radiometer

21 p2700 A73-40539

Effect of austenitization temperature on the properties of Kh5Ni2M3Ti steel

21 p2718 A73-40738

Temperature dependence for dissociative recombination of NO⁺/+ in E- and F-region models.

21 p2684 A73-40787

Cathodoluminescence of ruby /0.05 wt %/ at high temperatures

21 p2752 A73-40797

High temperature creep in magnesium strengthened by magnesia particles.

21 p2719 A73-40899

Stress and temperature analysis for surface cooling or heating of laser window materials.

21 p2716 A73-40966

Temperature dependence of hardness and creep of alloy Rh 18Re.

21 p2720 A73-41032

Cumulative creep formulas for construction steels at stepwise increasing temperatures

21 p2720 A73-41033

Some experiments on the influence of surface treatment on the Kapitza conductance between copper and He4 at temperatures from 1.2 to 2.0 K.

21 p2741 A73-41105

AC conductivities of amorphous Ge-As-Te and Ge-As-Se systems.

21 p2753 A73-41119

Calculation of the heat resistance of metals at variable temperatures 21 p2721 A73-41230

An investigation of pulsed GTA welding variables. 21 p2708 A73-41254

Errors arising in the RATAN-600 radio telescope due to temperature effects 21 p2675 A73-41453

Noise of space-charge-limited current in solids is thermal. 21 p2668 A73-41559

High temperature jet noise dependence on velocity and temperature, discussing Lighthill source term, Reynolds stresses, entropy fluctuations and velocity critical threshold 22 p2795 A73-41703

Mechanical face seal between rotating shaft and surrounding member using stationary and rotating ultraflatal radial sealing faces, discussing temperature and chemical considerations 22 p2865 A73-41775

Effect of technological and metallurgical treatment on the properties of electrosag-welded joints in heat resistant steels 22 p2872 A73-41780

The creep characteristics of the heat-resistant ferritic steels X 20 CrMoV 12 1 and X 18 CrMoNi V Nb 12 1 and their welded connections 22 p2852 A73-41870

Influence of the wall temperatures of gauges on the measurement of limit pressures 22 p2873 A73-41968

Cadmium embrittlement of high strength, low alloy steels at elevated temperatures. 22 p2930 A73-41979

Vapour pressures of liquid oxygen and nitrogen. 22 p2854 A73-41996

A survey of thermometric characteristics of recently produced Allen-Bradley/Ohmrite resistors. 22 p2854 A73-41996

Mixed particle sizes in fast carbon thermometry. 22 p2854 A73-41997

Thermistors as cryogenic thermometers. 22 p2854 A73-41998

Germanium resistance thermometers for cryogenic temperature precision measurement, discussing design technology, resistance-temperature characteristics types, installation and measurement methods 22 p2854 A73-41999

Platinum resistance thermometry up to the gold point. 22 p2855 A73-42006

Low temperature thermometry in high magnetic fields. 22 p2856 A73-42017

Equivalent circuit modeling of insulator shunting errors in high temperature sheathed thermocouples. 22 p2858 A73-42045

Temperature dependent chemisorption effects on hydrogen embrittlement of steel, showing strength-ductility correlation 22 p2874 A73-42106

A study of the physics and non-linear effects in photomultipliers. 22 p2860 A73-42302

Anomalous behaviour during interdiffusion in the system Nb-Mo. 22 p2876 A73-42340

Thermal conductivity of low density carbon. [ECTP PAPER C-5] 22 p2881 A73-42404

Dissociation of diatomic molecules. I. 22 p2889 A73-42443

Correction to calculation of temperature rise in connection with gravitational energy release accompanying rapid core formation from undifferentiated earth 22 p2848 A73-42499

The temperature dependence of viscosity and thermal conductivity of dilute noble gases at moderate and high temperatures. 22 p2932 A73-42504

A new determination of the second virial coefficient of carbon dioxide at temperatures between 0 and 150 C, and an evaluation of its reliability. 22 p2932 A73-42507

Low temperature thermionic cathode. 22 p2834 A73-42695

Pyrolysis and oxidation of polymers at high heating rates. 22 p2936 A73-42806

Generalized initial yield surfaces for unidirectional composites. [ASME PAPER 73-APMW-24] 22 p2925 A73-42886

Thermal response of a viscoelastic rod under cyclic loading. [ASME PAPER 73-APMW-39] 22 p2926 A73-42896

Convergent stable three-time level implicit numerical model for phase change problems, evaluating temperature dependent coefficients of parabolic equations at intermediate level 22 p2937 A73-42951

The temperature dependence of the half widths of some self- and foreign-gas-broadened lines of methane. 22 p2821 A73-42989

Large amplitude electromagnetic waves in hot relativistic plasmas. 22 p2895 A73-43024

Low power He-Ne laser beam intensity modulation in thermal medium, applying to temperature fluctuation detection in transparent materials 22 p2872 A73-43154

The effect of variable environment temperature on heat transfer in extended surfaces. 23 p3048 A73-43296

Emissions from and within an Allison J-33 combustor. II - The effect of inlet air temperature. 23 p3019 A73-43327

Corrosion and deposition of steels and nickel-base alloys in liquid sodium. 23 p2990 A73-43456

Microplasticizing mechanism of hydrogen embrittlement due to stress activated chemisorption, noting association with temperature dependent hydrogen-metal atomic interaction 23 p3039 A73-43465

Thermal convection in a large rotating fluid annulus - Some effects of varying the aspect ratio. 23 p3002 A73-43597

Thermodynamic properties and phase composition of the In-Ni system 23 p2991 A73-43706

Plastic deformation and anisotropy of sapphire crystals via nonbasal plane slip under bending, obtaining stress-strain curves and flow stresses temperature dependence 23 p2997 A73-43772

The plastic deformation of NiAl single crystals between 300 K and 1050 K. I - Experimental evidence on the role of kinking and uniform deformation in crystals compressed along the 001 direction. II - The mechanism of kinking and uniform deformation. 23 p2991 A73-43773

Postannealing isothermal decomposition products of Al-Mn alloys studied by transmission electron microscopy, revealing trigonal and hexagonal lattice diffraction patterns 23 p2993 A73-43916

Order of magnitude of the differences between theory and experiment in viscoplasticity under varying stress and temperature 23 p3044 A73-43971

The influence of testing temperature and thermal history on the intergranular embrittlement and penetration of aluminium by liquid gallium. 23 p2993 A73-44026

Effects of axisymmetric loads on inflated non-linear membranes. 23 p3045 A73-44081

Preparation of lanthanum sulfides using carbon disulfide as a sulfurizing agent and the change of these sulfides on heating in air. 23 p3018 A73-44130

Impurity diffusion of iron in molybdenum. 23 p2994 A73-44157

Non-linear creep buckling with random temperature variations. 23 p3045 A73-44166

Errors produced by the influence of unsteady heating in strain measurement by wire-type resistance strain gages 23 p2983 A73-44292

Temperature dependence of the cross section for electron-induced O⁺ desorption from tungsten. 23 p3008 A73-44321

Temperature dependence of dc electroconductivity of CdSe single crystals and compressed micron particle size powders, noting pressure and annealing effects on powder conductivity 23 p3018 A73-44372

Ac electroconductivity of polycrystalline Co-Fe ferrite as function of temperature, composition and frequency at 1 kHz-200 MHz 23 p3119 A73-44403

Off state I-V characteristics and thermal switching phenomena for tellurium selenium germanide chalco-genide glass semiconductors, assuming internal heat generation 23 p3119 A73-44407

Temperature range for centrifugal thermal diffusion sintering in Cr-Ni powder coatings, relating upper and lower bounds to heating rate 24 p3092 A73-44419

Influence of temperature on the behavior of the rheological properties of plastic carbon-black systems 24 p3101 A73-44471

Formation of the overheating structure in cast AL9 and VAL5 Silumin alloys 24 p3098 A73-44473

Dislocation locking by interstitial oxygen atoms and the temperature dependence of the yield point in niobium 24 p3099 A73-44574

Electronic simulation and analog computer studies of the influence of temperature on the process of nerve impulse shaping 24 p3062 A73-44725

Silicon Zener diodes used as temperature sensors 24 p3090 A73-44937

Line of symmetry for the classical equation of state. 24 p3110 A73-44987

A numerical, thermo-mechanical model for the welding and subsequent loading of a fabricated structure. 24 p3150 A73-45231

Influence of heat treatment on the posistor effect of semiconductive BaTiO₃-ceramic. 24 p3120 A73-45367

Hot plasma in contact with cold wall, calculating dynamic behavior in magnetic field from numerical solution of one-fluid two-temperature equations 24 p3117 A73-45456

TEMPERATURE FIELDS

U TEMPERATURE DISTRIBUTION

TEMPERATURE GRADIENTS

Theory of Kapitza's jump in temperature at the interface between a solid body and liquid helium 01 p0079 A73-11281

Trace elements profiles, notably Hg, from a preliminary study of the Apollo 15 deep-drill core. 02 p0220 A73-12477

Sound propagation in a combustion can with axial temperature and density gradients. 02 p0238 A73-12608

Sound propagation in sheared flow in a duct with transverse temperature gradients. 03 p0342 A73-12988

Thermal gradients in the outer lunar layers. 03 p0369 A73-13104

On the sun's differential rotation and pole-equator temperature difference. 03 p0377 A73-14402

Effect of a temperature gradient on bubble growth in tungsten. 04 p0463 A73-15307

Solar luminance via light nuclei fusion into heavier nuclei with temperature gradient maintenance by gravity, relating to H-R diagram of different star clusters 05 p0614 A73-16302

Solutions of thermal boundary layer equations when temperature gradient at the moving flat plate in parabolic flow is prescribed. 06 p0769 A73-18251

Diffusion of hydrogen in titanium alloys due to composition, temperature, and stress gradients. 06 p0712 A73-18764

Transverse hydromagnetic plane waves in the presence of a temperature gradient. 07 p0856 A73-19339

Nonlinear thermal convection in electrically conducting Boussinesq fluid subject to temperature gradient and magnetic field, calculating flow stability limit by energy method 07 p0920 A73-19513

Weibull distribution government of dispersion of destructive temperature gradients characteristic of fireproof ceramic materials heat resistance 09 p1110 A73-23061

Explicit and implicit weather forecast expressions based on differential hydrodynamics equation relating horizontal and vertical wind velocity, geopotential and temperature gradients 10 p1244 A73-23813

Global numerical atmospheric circulation model predictive sensitivity to equator-to-pole temperature gradient changes, applying variance analysis technique to Mintz-Arakawa model 10 p1245 A73-23983

Investigation of the thermoelastic stresses by means of 'freezing' involving the realization of a prescribed temperature gradient 11 p1435 A73-25454

Temperature gradients and atmospheric ablation rates for the Barwell meteorite. 11 p1419 A73-25779

Convection near critical Rayleigh numbers in the case of an almost vertical temperature gradient 11 p1453 A73-26435

Influence of a transverse electron-temperature gradient on the plasma flow in an axisymmetric magnetic field 12 p1528 A73-27305

Heat flow from earth core to mantle, discussing geomagnetic field generation by adiabatic MHD circulation of outer core and core-mantle interfacial temperature gradients 12 p1492 A73-27482

Equator-pole temperature difference and the solar oblateness /Research note/. 12 p1544 A73-27831

On thermal convection between non-uniformly heated planes. 13 p1705 A73-28430

Measurements of temperature fluctuations behind a linear heat source placed in a turbulent boundary layer 17 p2254 A73-34550

Generation of time-periodic secondary convective flows 18 p2301 A73-37006

Unsteady thermal boundary-layer on an infinite yawed wedge whose temperature gradient is prescribed. 19 p2377 A73-37575

Structure of cumulus clouds during various development phases 20 p2583 A73-39186

An approach to the determination of conditions impairing heat transfer under supercritical pressure 20 p2628 A73-39614

Long range fluidic acoustic sensors cross air currents and temperature gradient effects on operational characteristics and resolution, and prototype design for industrial applications 20 p2511 A73-39753

A periodicity phenomenon occurring instantly when a standing ultrasonic wave is switched off 21 p2738 A73-39982

Objective cross-section analyses by Hermite polynomial interpolation on isentropic surfaces. 21 p2728 A73-40054

Nonsymmetric buckling of cylinders with axisymmetric thermal discontinuities. 21 p2784 A73-40425

Temperature gradient in gaseous nebulae 21 p2768 A73-40716

Rotating cylinder model for plasma gradient-temperature instability in gravitational field, showing heat convection due to Coriolis-caused particle drift 21 p2769 A73-40730

Large scale heat transfer in turbulent boundary layer at heated flat plate in incompressible viscous fluid, discussing temperature fluctuation spatial correlation as function of wall law and flow core 21 p2678 A73-41062

Precision measurements of temperature differences with thermistors by a simple technique. 22 p2855 A73-42014

Design considerations and applications of gradient layer calorimeters for use in biological heat production measurement. 22 p2813 A73-42054

Limb scanning as a method for measuring the temperature structure of a planetary atmosphere. 22 p2883 A73-42058

Extrapolation algorithm for inverse thermal conductivity problem solution of body heat flux and temperature gradients, using successive approximations 23 p3048 A73-43445

Theory of the Kapitza temperature discontinuity at a solid body-liquid helium boundary. 23 p3006 A73-43502

Radiation heat transmission from human underlying and surface skin effect on epidermal temperature gradient 23 p2950 A73-44217

Relationship between midstratospheric temperatures and tropospheric synoptic features. 24 p3107 A73-45014

TEMPERATURE INDICATORS

U INDICATING INSTRUMENTS
U TEMPERATURE MEASURING INSTRUMENTS

TEMPERATURE INSTRUMENTS
U TEMPERATURE MEASURING INSTRUMENTS

TEMPERATURE INVERSIONS

NT CENTRIFUGING STRESS
NT INTERFACIAL TENSION
NT STRUCTURAL STRAIN

Measurement of small-scale turbulence and thermal stability in the lower atmosphere by radar. 03 p0279 A73-14536

Jupiter upper atmosphere temperature inversion to explain brightness temperature variation in 7.9 micron methane band, observing limb brightening 08 p1004 A73-20900

Determination of the astronomical refraction near the horizon at different times of the year 13 p1683 A73-29096

Formation of optical discontinuities in the atmospheric inversion layer 15 p1903 A73-31424

Mountain range effects on tropopause turbulence with mountain waves, examining tropopause layer inversions, vertical wind vectors, temperature distribution and buffeting intensity 17 p2204 A73-34542

Fine scale structure and mixing within inversion capping convective boundary layer, proposing atmospheric model for sensible downward heat transfer 19 p2448 A73-38215

Titan narrow band observations at 8-13 microns, noting temperature inversion and spectroscopically active component 22 p2905 A73-41770

The temperature and ammonia profiles in the Jovian atmosphere from inversion of the Jovian emission spectrum. 22 p2915 A73-43017

Mathematical model for temperature inversion rise velocity under penetrative free surface convection based on unstable atmospheric boundary layer environment 23 p3002 A73-43595

Cloud destabilization due to long wave radiative cooling resulting from IR radiative heat transfer in cloudy atmosphere, considering temperature inversion effects and cyclogenesis mechanism 24 p3108 A73-45016

TEMPERATURE MEASUREMENT

Density and temperature measurement in laminar boundary layer and free jet of hypersonic nozzles by electron beam probe. 01 p0045 A73-10239

Mathematical and statistical modeling of wall flow turbulence, considering experimental velocity and temperature measuring techniques 01 p0031 A73-10292

The effects of aerosols on the outgoing terrestrial radiation. 01 p0072 A73-10357

Measurement of surface temperatures by means of an infrared camera - Application in non-destructive testing 01 p0050 A73-10590

Atmospheric tidal measurements at 50 km from a constant-altitude balloon. 01 p0043 A73-11061

A derivation of thermal mathematical model with measured nodal temperatures. 01 p0123 A73-11142

Computer programs for radiative heat transfer and thermal equilibrium equations, noting transient temperature distribution measurement of two stage radiant cooler 01 p0111 A73-11151

Thermophysical properties of arc-cast tungsten using the TPRC multi-property apparatus/direct heating method/. 01 p0067 A73-11483

Instrument errors of film type thermocouple pyrometers for surface temperature measurement, discussing effects of shunting and junction geometry 02 p0166 A73-11636

Thermocouple circuits for measurement of unsteady temperatures in gases by the two-thermoreceiver method and an analysis of thermocouple circuit errors 02 p0166 A73-11710

Pyrometer for measurement of surface temperature distribution on a rotating turbine blade. 02 p0171 A73-12617

Direct temperature measurements for rotating annulus experiments, showing symmetric baroclinic instability and Richardson number for baroclinic wave 02 p0189 A73-12788

Gas-temperature measurement in pulsed H2O laser discharges. 02 p0178 A73-12814

Pyrometric obturation devices effect on sample temperature level during high temperature tests with radiant heating 03 p0306 A73-13189

The optical temperature of the Apollo 15 exhaust plume. 03 p0358 A73-13497

Muscle, skin and esophageal temperature measurement during transient and steady state phases of negative work exercise on bicycle ergometer 03 p0262 A73-14112

Telemetric measurement of local blood flow by heat conduction probes. 03 p0270 A73-14282

An implantable radiotelemetric measuring device for simultaneous long term measurements of body temperature and turnover of rabbit serum albumin/I-125 in unrestrained rabbits. 03 p0271 A73-14301

Measurement of temperature by recording the absolute line intensity with apparent increase of plasma optical thickness. 03 p0348 A73-14439

Radar and Nimbus 4 infrared measurements of the Oklahoma City tornadoes, 30 April 1970. 03 p0338 A73-14512

Measurements of temperatures of vibrationally excited N2. 04 p0477 A73-14819

Properties of photons determined by interferometric spectroscopy. 04 p0475 A73-15046

The solid-solid interface in thermal phonon radiation. 04 p0483 A73-15468

The measurement of atmospheric turbulence from a captive balloon. 04 p0473 A73-15698

Error minimization methods for Planck law remote measurements of single and two color temperature, considering multiple wavelengths 04 p0445 A73-15773

Measurement of longitudinal and normal velocity fluctuations by sensing the temperature downstream of a hot wire. 05 p0576 A73-16438

Gas flow temperature determination in the presence of radiation heat exchange between the heat sensor and some surrounding structures 05 p0578 A73-16996

Cholesteric liquid crystals thermophysical properties application in aerospace sciences and engineering, noting temperature measurement and nondestructive tests 06 p0733 A73-17767

New procedure for measuring the radial temperature distribution in inhomogeneous and unsteady plasma columns with considerable self-absorption 06 p0728 A73-17912

Limiting factors of plasma temperature measurement by spectral line reversal method 07 p0859 A73-20152

Brightness balancing spectrograph method for flame temperature measurement of liquid fuel drop 07 p0826 A73-20422

Rotational temperature measurements in nitrogen as hypersonic flow using an electron beam technique [ONERA, TP NO. 1206] 07 p0853 A73-20609

Temperature determination of rare gas plasmas seeded with alkali, considering oscillator forces of the excited states in He plasma 08 p0990 A73-20642

A method for the determination of temperatures in rolling tires 08 p0962 A73-20745

Experimental determination of the vibrational temperature of a supersonic gas flow. 08 p1021 A73-20854

Measurement of the temperature of an optically thick luminous gas layer in the upper atmosphere by the homodyne detection method 08 p0960 A73-21304

Modulation Langmuir probe and incoherent scatter radar measurements of ionospheric electron temperature. 09 p1075 A73-22128

Assessment of temperature rise suppression by edges losses during irradiation. 09 p1045 A73-22533

Electron beam refined niobium melting temperature determination from black body brightness change 10 p1230 A73-23508

Use of lasers for local measurement of velocity components, species densities, and temperatures. 10 p1217 A73-23852

Ultraviolet ion chamber measurements of the solar minimum brightness temperature. 10 p1279 A73-24136

Measurement of vibrational temperature of CO and N2 using the He/2 3S/ Penning ionization technique. 10 p1218 A73-24246

Measurement of a set of thermal properties of metals at high temperatures by the periodic-heating method 11 p1379 A73-25424

Thermal reference system with linear temperature profile down fin axis for thermography, using scanning IR camera as image detector 11 p1366 A73-26305

High temperature density measuring apparatus using the photon attenuation technique. 11 p1367 A73-26309

Determination of the temperature of a methane-fluorine diffusion flame by means of the vibration-rotation spectrum of the HF molecule 11 p1453 A73-26586

Drosonde for continuous temperature measurement during descent through lower atmospheric level discussing receiving unit and data conversion unit 12 p1495 A73-26815

A technique for measuring relative threshold nucleation temperatures for active nucleation catalysts. 12 p1521 A73-26816

A system for instantaneous measurement of flame temperature 12 p1557 A73-27071

Some effects of cooling and heating areas of the head and neck on body temperature measurement at the ear. 13 p1575 A73-28504

Circuit technology of a temperature-measurement transmitter for biotelemetric applications 13 p1579 A73-28575

Near-satellite neutral gas temperature determination from measurement of molecular nitrogen velocity distribution 13 p1687 A73-28630

Use of inertial heat sensors for measuring the rate of temperature variation 13 p1617 A73-28865

Translational temperature and atomic velocity distribution functions in rarefied binary gas jets by electron beam excited Doppler line measurement 13 p1618 A73-29163

Measurement of electron temperature in the ionosphere by the high-frequency probe method 14 p1746 A73-29861

Ionospheric electron density and temperature measurement by cylindrical Langmuir probes onboard Intercosmos 2 satellite 14 p1746 A73-29862

High-speed/subsecond/simultaneous measurement of specific heat, electrical resistivity, and hemispherical total emittance of Ta-10wt.%W alloy in the range 1500 to 3200 K. [ECTP PAPER D2-4] 14 p1760 A73-30437

High speed pyrometry for high temperature measurement of thermophysical properties, presenting experiment computer program outline [ECTP PAPER 12-3] 14 p1753 A73-30438

Long wave measurements of brightness temperature for thermal structure of major planet atmospheres at great depths, discussing Jupiter and Saturn microwave spectra 14 p1800 A73-30537

The dimensioning of resistance thermometers with an output parameter which is proportional to the temperature 14 p1754 A73-30922

Determination of the temperature of a sample undergoing pulsed irradiation by sunlight 15 p1896 A73-30997

Millstone Hill Thomson scatter results for 1966 and 1967. 15 p1866 A73-31067

A simplified method of calculating thermomodulation curves 15 p1837 A73-31168

Temperature and velocity profiles measurement in hybrid rocket engine combustion, using optical method based on Na line reversal technique 15 p1957 A73-31636

A combinational method of calculating the average velocity and the mean-mass temperature of a gas flow from the phase diagram of the substance 15 p1957 A73-31865

Temperature determination in a gas flow with the aid of two thermocouples 15 p1876 A73-31870

Probe design for orbit-limited current collection. 16 p2041 A73-33320

Errors in ion and electron temperature measurements due to grid plane potential nonuniformities in retarding potential analyzers. 16 p2016 A73-33436

Dynamic gas temperature measurements in a gas turbine transition duct exit. [ASME PAPER 73-GT-7] 16 p2047 A73-33485

Atmospheric temperature measurement with X and K band radiometers, discussing meteorological conditions variation effects on microwave propagation and comparison with spacecraft tracking data 16 p1983 A73-33730

Comparison of the solutions obtained by Tikhonov's and Sparrow's methods for the inverse unsteady-heat-conductivity problem 17 p2253 A73-34134

Multichannel quick-response photoelectric micropyrometer 17 p2164 A73-34173

Measurements of temperature fluctuations behind a linear heat source placed in a turbulent boundary layer 17 p2254 A73-34550

A performance data acquisition and analysis system for turbine engine component testing. 17 p2146 A73-34610

Rotational temperature measurement of gases using laser Raman scattering techniques. 17 p2166 A73-34623

An evaluation of ionospheric probe performance. I - Evidence of contamination and clean-up of probe surfaces. II - The influence of vehicle wake effects on electron density and temperature measurements. 17 p2160 A73-34786

Fast differential thermal analysis. 17 p2119 A73-34799

Application of temperature soundings by the Nimbus 3 satellite to the analysis of the hemispheric-scale stratospheric environment 17 p2206 A73-34937

Radiometric measurements of temperature of the ocean surface - Improvement brought by use of a polarizing radiometer 17 p2161 A73-34946

Electron beam refined niobium melting temperature determination from black body brightness change 17 p2191 A73-35188

Remote measurement of atmospheric temperatures by Raman lidar. 17 p2163 A73-35467

Book - Progress in high temperature physics and chemistry. Volume 5. 17 p2255 A73-35592

Remote sensing of chlorophyll and temperature in marine and fresh waters. 17 p2164 A73-35664

Recent stratospheric temperature measurement compatibility tests at Wallops Island. 18 p2307 A73-36035

Differential temperature measurements in engine fluids. 18 p2315 A73-36071

Neutral wind velocities calculated from temperature measurements during a magnetic storm and the observed ionospheric effects. 18 p2311 A73-36150

A high-speed /subsecond/ system for accurate thermophysical measurements at high temperatures. [ALAA PAPER 73-743] 18 p2316 A73-36359

Diurnal and annual temperature variations in the 30-60 km region as indicated by statistical analysis of rocksonde temperature data. 19 p2424 A73-37662

Use of spectral characteristics for the determination of the parameters of a corrector for thermal pickups 19 p2430 A73-37844

Measurement of the temperature of an optically dense layer of luminous gas in the upper atmosphere by the homodyne detection method. 19 p2425 A73-37933

IR quasi-synoptic global sensing of ocean surface temperature, covering IR theory, airborne radiation thermometry and single band satellite data analysis techniques [AAS PAPER 73-146] 20 p2550 A73-38595

Design and performance characteristics of the Vertical Temperature Profile Radiometer (VTPR) for atmospheric temperature soundings. 20 p2567 A73-39852

Thermal structure of the sand desert from the data of IR aerophotography. 20 p2558 A73-39869

Isothermal mapping of temperature patterns from thermal discharges in Italian coastal waters. 20 p2560 A73-39888

Remote measurement of subsurface sea water temperature by airborne Raman scattering with cross polarizer in front of light source and detector, noting precision 20 p2568 A73-39889

Self balancing ac resistance bridge design with digital readout for low temperature carbon resistance thermometers 21 p2659 A73-39921

Improvements brought to the measurement of the ocean surface temperature by utilization of a polarizing infrared radiometer 21 p2698 A73-40142

Frequency-dependent parasitic modulation component effects on null distortion in spectrometer and temperature measurement accuracy 21 p2700 A73-40541

Temperature distribution measurement for air about hot object by double exposure interferometry, using beam from He-Ne laser 21 p2701 A73-40625

Opto-thermal gas concentration detector operation by measuring temperature variations caused by chopped laser beam in sample cell, using pyroelectric material as temperature sensor 21 p2701 A73-40691

Measuring the boundary layer temperature distributions using ablating specimens in an air plasma flow. 21 p2791 A73-41052

Thermometric applications of ferrite permeability dependence on temperature, describing thermometer for magnetically levitated substrate 21 p2702 A73-41108

Internal gravity waves and turbulence in simultaneous upper atmosphere temperature and wind measurements. 21 p2732 A73-41342

Measurements of thermospheric temperatures by incoherent scatter radar. 21 p2688 A73-41346

The determination of ionospheric charged particle temperatures from in situ measurements. 21 p2690 A73-41362

Measurement of the thermo-optical characteristics of satellite thermal control coatings 22 p2929 A73-41872

Diurnal and semidiurnal nitrogen density and temperature variations from thermosphere probe measurements. 22 p2845 A73-41926

Symposium on Temperature, 5th, Washington, D.C., June 21-24, 1971, Proceedings. Part 1 - Basic methods. Scales and fixed points. Radiation. Part 2 - Resistance, electronic and magnetic thermometry. Controls and calibration. Bridges. Part 3 - Thermocouples. Biology and medicine. Geophysics and space. 22 p2852 A73-41976

Calorimetric measurement of thermodynamic temperatures above 0 C using total blackbody radiation. 22 p2853 A73-41980

Theory and measurement of emissivity properties for radiation thermometry applications. 22 p2886 A73-41982

Temperature measurements with an infrared television system. 22 p2853 A73-41984

Development of an infrared scanning system for the empirical evaluation of aerodynamic heating. 22 p2853 A73-41985

Theory and technique for surface temperature determinations by measuring the radiance temperatures and the absorptance ratio for two wavelengths. 22 p2853 A73-41986

The spectral comparison method for temperature measurement in two-phase flames. 22 p2853 A73-41987

Effect of radiometric errors on accuracy of temperature-profile measurement by the spectral-scanning method. 22 p2853 A73-41988

Measuring transient high temperatures by optical pyrometry. 22 p2853 A73-41989

Short duration temperature measurements by infrared emission-absorption. 22 p2853 A73-41990

Use of edge-tone resonators as gas temperature sensing devices. 22 p2853 A73-41991

Ultrasonic pulse techniques based on acoustic velocity for inert gas thermometry, discussing electroacoustic transducer response time, temperature sensitivity and momentary contact coupling technique 22 p2854 A73-41994

A device for the on-line measurement of nitrogen rotational temperature in low density flows. 22 p2854 A73-41995

A survey of thermometric characteristics of recently produced Allen-Bradley/Ohmite resistors. 22 p2854 A73-41996

Mixed particle sizes in fast carbon thermometry. 22 p2854 A73-41997

Germanium resistance thermometers for cryogenic temperature precision measurement, discussing design technology, resistance-temperature characteristics types, installation and measurement methods 22 p2854 A73-41999

Platinum resistance thermometry up to the gold point. 22 p2855 A73-42006

The high temperature stability of platinum resistance thermometers. 22 p2855 A73-42008

Platinum resistance thermometer as standard instrument for interpolation on International Practical Temperature Scale, discussing design development, operational characteristics and errors 22 p2855 A73-42010

Calibration of platinum resistance thermometers. 22 p2855 A73-42011

Apparatus and methods for the precise determination of Boltzmann temperature. 22 p2856 A73-42021

Nuclear magnetic resonance thermometry. 22 p2856 A73-42022

Instrumentation errors in nuclear resonance thermometry. 22 p2856 A73-42023

Temperature measurement, monitoring, and control on a Michelson interferometer for ambient-temperature emission spectroscopy. 22 p2856 A73-42025

Methods for cryogenic thermocouple thermometry. 22 p2857 A73-42029

Long-term drift of some noble and refractory-metal thermocouples at 1600 K in air, argon, and vacuum. 22 p2857 A73-42033

Catalytic activity in platinum group temperature sensors, discussing elimination by noncatalytic coatings 22 p2857 A73-42034

The effects of catalysis in measuring the temperature of incompletely-burned gases with noble-metal thermocouples. 22 p2857 A73-42035

A new conceptual model for components in measurement/control systems - Practical application to thermocouples. 22 p2859 A73-42050

Limb scanning as a method for measuring the temperature structure of a planetary atmosphere. 22 p2883 A73-42058

Atmospheric temperature measurement using balloons and rockets. 22 p2883 A73-42061

Spectroscopic measurement of upper atmospheric temperature. 22 p2846 A73-42062

Temperature measurements in the thermosphere and ionosphere. 22 p2847 A73-42063

Measurement of the atmospheric brightness temperature at submillimeter wavelengths 22 p2847 A73-42330

European Conference on Thermophysical Properties, 3rd, Turin, Italy, June 20-23, 1972, Proceedings. 22 p2876 A73-42401

Optimal utilization of redundant information in thermal radiation in thermophysical measurements. [ECTP PAPER 11-2] 22 p2931 A73-42408

Applications of liquid crystals to information display, fault detection, and medical thermography. 22 p2897 A73-42524

Evaluating the performance of shell-and-tube heat-exchangers. 23 p3048 A73-43299

Pulse method for determining heat-transfer coefficients of coatings 24 p3155 A73-44756

- A procedure for estimating cloud amount and height from satellite infrared radiation data.
24 p3084 A73-44925
- Solar wind and magnetosheath electron temperature measurements by triaxial electron analyzer onboard Ogo-5, presenting data for bow shock
24 p3125 A73-45112
- Study of the spatial development of oxidation and combustion reactions by means of image photoelectric receivers, and of a thermometric method
24 p3091 A73-45398
- ### TEMPERATURE MEASURING INSTRUMENTS
- NT OPTICAL PYROMETERS
NT PNEUMATIC PROBES
NT PYROMETERS
NT RADIATION PYROMETERS
NT RESISTANCE THERMOMETERS
NT TEMPERATURE PROBES
NT THERMOCOUPLE PYROMETERS
NT THERMOMETERS
- Linear response transistorized FM temperature measuring transducer with thermistor, noting low distortion and digital display convenience
01 p0044 A73-10032
- Analytical study of the sensitivity of a sensor for studying pulsations of the heat-transfer coefficient in a boiling high-temperature layer
01 p0051 A73-10864
- Ceramic film indicator for determining and recording of temperatures on space vehicle heat shield.
01 p0052 A73-11168
- The application of Langmuir probes to the measurement of very low electron temperatures.
02 p0158 A73-11912
- Investigation of the vapor pressure of cesium by the boiling-point method.
06 p0722 A73-17404
- The VDTA-3 apparatus for high-temperature differential thermal analysis
06 p0693 A73-18043
- Pyroelectric IR detector materials thermal and electric properties, discussing applications in thermographs, focal plane reticle scanners, linear array thermal imaging, radiometers and laser detectors
06 p0694 A73-18317
- Hot wire probe applications to radiation, fluid flow, vacuum and temperature measurements, deriving mathematical expressions for physical laws
08 p0962 A73-20750
- A new method for thermographic investigation of high-speed crystallization processes in high-melting-point metals
09 p1103 A73-22483
- Instrument Society of America, Annual Conference, 27th, New York, N.Y., October 9-12, 1972, Proceedings. Part 2.
09 p1082 A73-22501
- A temperature interferometer using laser holography.
09 p1083 A73-22510
- Temperature measuring devices based on operational amplifier circuits, considering design and applications
09 p1085 A73-22924
- Temperature measurement and control technology review, discussing analog and digital systems, contact, resistance and radiation thermometers, special temperature sensors and measurement systems
10 p1216 A73-23634
- Fast response coaxial miniature thermocouples for rapid temperature change measurements in droplets, turbulence and bubbles
12 p1499 A73-27875
- IR thermographic scanners and viewers operational principles, equipment performance specifications and thermal radiation distribution
13 p1611 A73-28020
- Digital temperature-measuring device for medical applications
13 p1578 A73-28338
- Concorde engine monitoring instrumentation, discussing start cycle, temperature sensors and indicators and nozzle position indicators
14 p1754 A73-30931
- New method of thermographic investigation of rapid processes of crystallization of refractory metals.
15 p1891 A73-32070
- Thermographic evaluation of relative heat loss areas of man during cold water immersion.
18 p2283 A73-36781
- The effect of comparison source reflectance on gas temperature measurement by Kurlbaum's method and line reversal methods.
21 p2692 A73-39916
- Remote sounding of atmospheric temperature from satellites. IV - The selective chopper radiometer for Nimbus 5.
21 p2706 A73-41601
- Precision measurements of temperature differences with thermistors by a simple technique.
22 p2855 A73-42014
- Apparatus and methods for the precise determination of Boltzmann temperature.
22 p2856 A73-42021

- Error accumulation in thermocouple thermometry.
22 p2859 A73-42052
- A comparison of predicted skin temperatures with thermographic measurements.
22 p2813 A73-42053
- Technical and economic problems in use of military passive night vision systems including image intensifiers, IR detectors and thermographic imaging devices
23 p2979 A73-43219
- Image formation by light intensification and thermographic imagery compared from energy viewpoint, considering effect of parasitic light sources in visual field
23 p2979 A73-43223
- Determination of the temperature fields of turbine disks and blades, using irradiated diamond indicators
23 p2987 A73-44294
- Direct-display plasma density and temperature meter by the use of Langmuir probe.
23 p3015 A73-44367
- Plasma temperature measurement by a spectroscopic technique with continuous automatic recording
24 p3115 A73-44757
- ### TEMPERATURE PHOTOMETERS
- U PHOTOMETERS
U TEMPERATURE MEASURING INSTRUMENTS
- ### TEMPERATURE PROBES
- NT PNEUMATIC PROBES
- Contact methods of measuring temperatures in low-temperature plasma jets from stationary sources
15 p1876 A73-31871
- Aircraft engine fuel and oil differential temperature measurement via platinum probes, specifying sensor sensitivity, calibration, circuit operation and data reduction
17 p2165 A73-34607
- Development of a thermistor type temperature probe for use at low absolute pressures.
22 p2856 A73-42016
- Catalytic activity in platinum group temperature sensors, discussing elimination by noncatalytic coatings
22 p2857 A73-42034
- Radiation pyrometric probe /homogeneous thermally insulated rod/ for measuring body surface thermal loads and heat transfer coefficients
24 p3089 A73-44758
- ### TEMPERATURE PROFILES
- Atmospheric temperature profile determination by limb radiance inversion radiometer, discussing radiative transfer, instrument parameters and inversion process effects on retrievable information content
01 p0072 A73-10354
- Numerical simulation of radiative-conductive heat transfer in the Martian atmosphere-polar cap utilizing Mariner 9 Iris data.
01 p0097 A73-10401
- Radiometric techniques for observing the atmosphere from aircraft.
01 p0073 A73-10404
- Mixed convection over a heated horizontal plane.
01 p0120 A73-10440
- The role of impurity particles in the combustion of double-base propellants.
01 p0089 A73-10639
- Commencement of routine meteorological rocket observation at Ryori, Japan.
02 p0188 A73-12271
- Atmospheric stratification stability at heights of 30-90 km from grenade test determined wind and temperature data, presenting Richardson number latitudinal and seasonal distribution
02 p0160 A73-12273
- Ionospheric electron and ion temperature profile measurements with satellite- and rocket-borne probes, comparing merits and discrepancies
02 p0163 A73-12303
- Rocket sounding of ionospheric electron density and temperature profiles during moderate auroral event, noting field-aligned motion of irregularities in F region
02 p0163 A73-12309
- The possibilities of determining the temperature profile in the Venusian atmosphere from the thermal radio emission of the planet
02 p0219 A73-12463
- Vertical resolution of temperature profiles obtained from remote radiation measurements.
02 p0165 A73-12778
- Lunar magnetic field measurements, electrical conductivity calculations and thermal profile inferences.
03 p0369 A73-13103
- Development of a process utilizing heated rolls for hot rolling metals.
04 p0454 A73-15001
- Combustion chamber temperature profiles analytical derivation from simultaneous radiative and turbulent diffusion heat transfer of turbulent flame front [ASME PAPER 72-WA/HT-27]
04 p0519 A73-15827
- Temperature fluctuations in the ionospheric F region
05 p0568 A73-16256

- Computation of upper tropospheric reference heights from winds for use with vertical temperature profile observations.
05 p0569 A73-16579
- Cool flame oxidation studies of acyclic and cyclic hydrocarbons.
05 p0606 A73-16691
- A new integral-variational method for calculation of relaxation regions behind shock and detonation waves
07 p0809 A73-19056
- Global mean thermosphere temperature profiles as a function of solar EUV flux, considering neutral gas heating and ionospheric electron temperature
07 p0869 A73-19246
- Predicting the critical boundary temperature of multidimensional explosives.
07 p0918 A73-19386
- A mathematical model of the opposed-jet diffusion flame - Effect of an electric field on concentration and temperature profiles.
07 p0918 A73-19388
- Correlation of microthermal turbulence data with meteorological soundings in the troposphere.
08 p0985 A73-21382
- Covariance matrices and means of atmospheric Planck function profiles for application to temperature sounding from satellite measurements.
08 p0967 A73-21385
- A special form of Galerkin's method applied to heat transfer in plane Couette-Poiseuille flows.
08 p1023 A73-21412
- The vertical thermal structure of the Martian atmosphere - Modification by motions.
09 p1145 A73-22271
- Buoyancy effects in a turbulent boundary layer.
09 p1071 A73-22330
- Temperature and humidity spectra in the atmospheric surface layer.
11 p1393 A73-25693
- Thermal reference system with linear temperature profile down fin axis for thermography, using scanning IR camera as image detector
11 p1366 A73-26305
- Solution of linear equations in remote sensing and picture reconstruction.
14 p1767 A73-29767
- Radiative heat transfer through semitransparent solid plane layer, measuring temperature profile and heat flux for comparison with rectangular multiband model calculation
15 p1958 A73-32276
- The possibilities of determining the temperature profile in Venus' atmosphere from the planet's thermal radio emission.
15 p1942 A73-32613
- The thermal regime and convective motions in the lower layers of the Venusian atmosphere
16 p2068 A73-33825
- Vertical distribution and temperature profile of the night time atmospheric sodium layer obtained by laser backscatter.
16 p2009 A73-33890
- The design, construction and calibration of an infrared temperature profile radiometer (ITPR) for Nimbus E.
17 p2238 A73-34602
- Extreme temperature deviations from the climatological mean in the upper stratosphere - observed by rockets, confirmed by satellites.
18 p2304 A73-35962
- Vertical temperature profiles from satellites - Results from second generation instruments aboard Nimbus-5.
18 p2307 A73-36029
- Aerological soundings of the atmosphere from NOAA-2 data for operational systems.
18 p2308 A73-36044
- Thermal modeling of a plate with coupled heat transfer modes.
18 p2370 A73-36364
- [AIAA PAPER 73-748]
Atmospheric vorticity effects on hexagonal convection cells formation, considering temperature profiles nonlinearity, turbulent viscosity and perturbation scale
18 p2333 A73-37052
- Variability of eigenvectors and eigenvalues of correlation matrices for vertical temperature profiles.
18 p2334 A73-37062
- Accuracy and coverage of temperature data derived from the IR radiometer on the NOAA 2 satellite.
19 p2424 A73-37665
- Vertical profiles of small-scale temperature structure in the atmosphere.
19 p2448 A73-38209
- Atmospheric temperature and humidity vertical profiles from satellite-borne IR spectral radiance measurements, using linear extrapolation and statistical regression techniques
20 p2521 A73-38584
- [AAS PAPER 73-124]
Stratospheric temperature profiles from limb radiance measurement by Aerobee rocket, comparing with rocket sounding and radioonde data
21 p2729 A73-40064

Effect of radiometric errors on accuracy of temperature-profile measurement by the spectral-scanning method.

22 p2853 A73-41988

Inversion techniques for remote sensing of atmospheric temperature profiles.

22 p2883 A73-42056

Spectral structure of tropospheric vertical temperature profiles over Cape Kennedy, Florida.

22 p2849 A73-42544

Kinetics of nitric oxide formation in premixed laminar flames.

22 p2820 A73-42792

Experimental determination of the turbulent Prandtl number near a smooth wall

22 p2937 A73-42952

Heat transfer from an enclosed rotating disk with uniform suction and injection.

22 p2938 A73-42998

The temperature and ammonia profiles in the Jovian atmosphere from inversion of the Jovian emission spectrum.

22 p2915 A73-43017

Eddy heat/momentum diffusivity ratio dependence on Richardson number relationship between Deacon numbers of wind and temperature profiles in Antarctic surface layer

23 p3003 A73-43983

Effect of modified thermal conductivity on the temperature distribution in the protonosphere.

24 p3082 A73-44727

TEMPERATURE SCALES

Lunar breccias lithification and metamorphism model construction from experimental and analytical data, discussing scale of lunar metamorphic temperatures

02 p0220 A73-12476

Spectroscopic studies of O-type stars. III - The effective-temperature scale.

07 p0873 A73-19060

Application of precise heat-capacity data to the analysis of the temperature intervals of the International Practical Temperature Scale of 1968 in the region of 90 K.

22 p2852 A73-41977

Basic method for realization of temperature scale at 0,000 K by photometric comparison between vacuum-UV-blackbody radiation of a plasma and synchrotron radiation.

22 p2852 A73-41978

Platinum resistance thermometry below 13.81 K.

22 p2854 A73-42002

Revision of the standard reference data for thermocouples.

22 p2857 A73-42032

The melting point of molybdenum as a secondary fixed point on the International Practical Temperature Scale.

22 p2877 A73-42407

ECTP PAPER G-5]

TEMPERATURE SENSORS

NT THERMISTORS

Analytical study of the sensitivity of a sensor for studying pulsations of the heat-transfer coefficient in a boiling high-temperature layer

01 p0051 A73-10864

Application of electrical modeling in the analysis of the dynamic properties of temperature sensors

02 p0166 A73-11637

Quasi-steady heat transfer equation for frequency response of wedge shaped hot film sensors for flow temperature, velocity and turbulence measurement

02 p0166 A73-11711

Optimization of spectral intervals for remote sensing of atmospheric temperature profiles.

02 p0171 A73-12774

Gas flow temperature determination in the presence of radiation heat exchange between the heat sensor and some surrounding structures

05 p0578 A73-16996

Transient functions to estimate thermal inertia of gas temperature sensors with film resistance thermometer mounted on wedge shape insulating base

09 p1081 A73-22346

Airborne atmospheric temperature measurements correction for sensor response lag, deriving numerical scheme based on sensing systems wind tunnel calibration

10 p1217 A73-23991

Low noise temperature measurement converter with electrical oscillation frequency output, presenting computer calculations of sensor components

13 p1617 A73-28860

Use of inertial heat sensors for measuring the rate of temperature variation

13 p1617 A73-28865

Fluidic control modules with temperature sensor and thrust reverser pneumatic actuator for aerospace system applications, investigating reliability test data

16 p1971 A73-33477

Nickel-titanium memory material stress measurement methods, energy absorption capacity and cyclic response, discussing nickel foil surface temperature sensing devices

17 p2166 A73-34616

Heat detector signal transients during time constant fluctuations in terms of mathematical expectation of ambient temperature

18 p2317 A73-36857

Use of spectral characteristics for the determination of the parameters of a corrector for thermal pickups

19 p2430 A73-37844

Use of edge-tone resonators as gas temperature sensing devices.

22 p2853 A73-41991

The development of the quartz resonator as a digital temperature sensor with a precision of .0001.

22 p2854 A73-41992

Ultrasonic thermometry using resonance techniques.

22 p2854 A73-41993

Stability of 25 ohm platinum thermometer up to 1100 C.

22 p2855 A73-42007

Unique platinum resistance temperature sensors for lunar heat flow measurements.

22 p2855 A73-42013

Some designs using sheathed thermocouple wire for jet engine applications.

22 p2858 A73-42042

Trends of design in gas turbine temperature sensing equipment.

22 p2858 A73-42043

Thin film temperature sensor with polymer coating for medical research providing good sensitivity and stability for rapid temperature changes in biochemical reactions

22 p2813 A73-42055

Comparison of temperature sensors for space instrumentation.

22 p2859 A73-42064

A two-layer slab method for measuring thermal diffusivity of polymer by irradiated light heat-wave. I. II - Transient response of temperature sensor attached to a polymer substrate. III - Quantitative evaluation of the effect of edge losses in a parallelepiped.

23 p3049 A73-44363

Silicon Zener diodes used as temperature sensors

24 p3090 A73-44937

TEMPERATURE TRANSDUCERS

U TEMPERATURE MEASURING INSTRUMENTS

U TEMPERATURE SENSORS

TEMPERING

Physical nature of the processes of formation of the set of mechanical properties of quench-hardened alloyed structural steel during tempering

01 p0055 A73-10263

Internal friction study of intercrystalline phosphorus adsorption during temper brittleness development in iron alloys

01 p0064 A73-10608

Temperature fields and stresses during local tempering of helical welds of a cylindrical shell

01 p0118 A73-11413

Low-cycle fatigue behavior of quenched and tempered UNI 38NiCrMo4 steel

04 p0462 A73-15300

Molybdenum and nickel alloying effect on time and temperature range of reversible temper brittleness of chromium steels

09 p1107 A73-23200

Characteristics of martensite decomposition during the tempering of rhenium steels

12 p1509 A73-26894

Formation of carbides during tempering of complexly alloyed chromium steel

18 p2324 A73-36770

Principal aspects of thermal treatments of the alloy Ti-11, 5 Mo-6, Zr-4, 5 Sn /Beta III/

19 p2441 A73-37833

Effect of structural and mechanical factors on the nature of cold shortness curves for steels

20 p2578 A73-39378

Titanium oxide film dissolution indication by tempering colors and weld tensile strength dependence on film thickness and temperature

21 p2717 A73-40480

Decomposition of martensite during tempering of rhenium steels.

21 p2720 A73-41027

Decay of the solid beta-solution in beta alloys of titanium and zirconium during tempering

22 p2874 A73-42092

TENDONS

Human tendon stress recovery after load removal as function of time, sex, age and side differences

07 p0782 A73-20033

Organization of spontaneous muscular activity in man

09 p1040 A73-22863

Reflex reaction of antagonist muscles during an evoked tendon reflex

10 p1182 A73-24598

Prestressing force and tendon configuration optimization for indeterminate structure with prescribed cross sectional dimensions, using linear programming and design variable transformation

22 p2922 A73-42476

TENSILE DEFORMATION

Human phasic reflex response to parameters of a mechanical stimulus as an index of muscle-spindle sensitivity.

22 p2816 A73-42679

TENSILE CREEP

Frame photography for temporary creep in cylindrical Al alloy specimen necks under tensile loads, calculating creep diagrams

05 p0634 A73-16748

Four-section equipment for studying creep and long-term strength in deep cooling conditions.

09 p1086 A73-23067

Combined tension-torsion creep of polyethylene with abrupt changes of stress.

15 p1897 A73-31613

Interpretation of tensile and compressive creep behaviour of two nickel alloys.

15 p1888 A73-31618

Damped lateral vibration in an axially creeping beam with random material parameters.

16 p2082 A73-33902

Creep and recovery of polycarbonate.

17 p2194 A73-34525

The anisotropy of creep behaviour in oriented thermoplastics.

17 p2196 A73-35342

Tensile creep in short fibre reinforced thermoplastics.

17 p2197 A73-35344

High temperature creep in magnesium strengthened by magnesia particles.

21 p2719 A73-40899

The creep of sapphire filament with orientations close to the c-axis.

23 p2997 A73-44029

Steady-state creep characteristics of an Fe alloy containing 3.5 at.% Mo.

23 p2994 A73-44153

Fiberglass reinforced plastic laminate creep rate for ultrasonic vibrational and static tensile loads, showing nonlinear viscoelasticity and stress amplitude effects

24 p3102 A73-44504

TENSILE DEFORMATION

Fracture resistance curve calculation from fracturing diagram, noting crack propagation in thin plate under tensile deformation

02 p0232 A73-11930

Relation between plasticity characteristics and geometrical dimensions of cylindrical specimens under tension.

02 p0235 A73-12140

Loading-rate dependence of the deformation mechanism in a Zn-22% Al superplastic alloy

03 p0326 A73-13970

Anomalous slip in high-purity niobium single crystals deformed at 77 K in tension.

04 p0467 A73-15931

Load-time dependent relaxation of residual stresses.

05 p0636 A73-17214

Deformation by Piobert-Lueders bands observed on composites of oriented solidification

06 p0708 A73-18099

The influence of anisotropy and crystalline slip on relaxation at a crack tip.

06 p0709 A73-18331

Influence of the dose of neutron irradiation on the anelastic behavior of an aluminum deformed at 80 K

06 p0710 A73-18542

Welding airframe structures in titanium alloys using tensile loading as a means of overcoming distortion.

08 p0973 A73-21240

A theory for the mechanical properties of metal-matrix composites at ultimate loading.

10 p1235 A73-24443

Improvement on moire technique for in-plane deformation measurements.

11 p1365 A73-26241

Change in the dislocation structure during fatigue of nickel prestrained by tension

11 p1386 A73-26732

Austenitic steel dislocation density, X ray interference width and hardness changes due to intensified crystal fragmentation from biaxial elongation under tension

12 p1512 A73-27246

Dynamic tensile deformation of viscoplastic filament without bending rigidity, displacement constraints and cross sectional area variations

12 p1552 A73-27300

The role of annealing twins in the primary recrystallization of nickel 270 work hardened in tension

12 p1514 A73-27988

Dislocation structure in molybdenum single crystals after deformation at 293 and 400 deg K.

13 p1634 A73-28221

Mechanical behavior of WC-Co composite alloys.

13 p1643 A73-29545

Thoria particle dispersion TD-nickel creep and tensile deformation at elevated temperature dependence on grain size and L/D ratio

14 p1761 A73-30635

A theoretical model for the elevated temperature deformation of dispersion hardened metals.

14 p1761 A73-30636

- Nickel niobide tested along crystal growth direction for twinning mode of intermetallic phase in tensile deformation, projecting crystallographic structure upon crystal plane 14 p1762 A73-30640
- Effect of tensile deformation in the austenite range on transformation kinetics of a high-strength low-alloy /HSLA/ steel. 14 p1762 A73-30641
- Orthotropic characteristics of glass-fibre-epoxy laminates under plane stress. 15 p1897 A73-31698
- Enhanced strain aging of niobium by cyclic deformation. 15 p1890 A73-31990
- Behaviour of aluminium during the passage of large-amplitude plastic waves. 15 p1891 A73-32164
- Mechanical properties, microstructure and failure characteristics of binary alloys of Al-Mg system determined under different tensile stress rates and temperatures 17 p2187 A73-34339
- Tensile fracture of boron-epoxy composites with ordered filament packing geometry. 17 p2198 A73-35535
- Deformation and fracture mechanisms in aluminium reinforced by high strength steel ribbons. 17 p2192 A73-35539
- Noncumulative fracture mode of unidirectional boron filament-aluminum matrix composite under axial tension, measuring critical filament stress 17 p2193 A73-35542
- Influence of interstitials on the behavior in tension of niobium between 20 and 1000 C. 17 p2193 A73-35624
- Theory of hardening applicability to the description of deformation law singleness under various conditions of uniaxial tension 18 p2366 A73-36759
- Influence of temperature and strain rate on the load-elongation curve and plastic properties of molybdenum 18 p2324 A73-36801
- Stresses and strains in a rotating disk 19 p2497 A73-37555
- Microstructural characteristics of the TA6V alloy as a function of thermomechanical treatments in alpha plus beta - Effects on the mechanical characteristics in tension 19 p2441 A73-37831
- Tensile deformation and fracture in high-strength Al-Zn-Mg alloys. 20 p2575 A73-39019
- Partitioning of stress between fiber and matrix during tensile deformation of the Al-Al₃Ni eutectic composite. 20 p2576 A73-39024
- Diagrams of cumulative damage during tension of polycrystalline metals 20 p2577 A73-39371
- Effect of gas diffusion on creep behavior of polycarbonate. 20 p2580 A73-39403
- Substructure of type 316 stainless steel deformed in slow tension at temperatures between 21 and 816 C. 20 p2578 A73-39491
- Influence of the geometrical configuration of a structure on its carrying capacity 21 p2786 A73-40982
- Discontinuous flow in steady-state creep of Al-Mg alloys at high temperatures. 23 p2995 A73-44162
- Mathematical model for fracture strength of material undergoing molecular orientation during tensile strain, accounting for anomalous polymer characteristics 24 p3144 A73-44508
- An elastic-plastic analysis of a bar under repeated axial loading. 24 p3151 A73-45307
- TENSILE PROPERTIES**
- Fracture characteristics of some aluminum alloy sheets in Charpy impact test at super-low temperatures. 02 p0179 A73-11595
- The effects of matrix and interface modification on local fractures of carbon fibers in epoxy. 03 p0335 A73-13982
- Tensile properties of PRD-49 fiber in epoxy matrix. 05 p0588 A73-16118
- Postirradiation mechanical properties of Types 304 and 304 + 0.15% titanium stainless steel. 06 p0710 A73-18545
- Influence of condensation temperature on microstructure and tensile properties of titanium sheet produced by high-rate physical vapor deposition process. 06 p0711 A73-18752
- Tensile, fracture toughness and crack growth properties of a roll-extruded HP 9Ni-4Co-25C steel alloy. 09 p1109 A73-23260

Tensile creep modulus, creep lateral contraction ratio and torsional creep measurements on small non-rigid specimens. 10 p1218 A73-24120

The fracture toughness of beryllium. 11 p1384 A73-26168

S-200 grade beryllium fracture toughness properties. 11 p1384 A73-26170

Tensile properties of high strength Al-Zn-Mg and Al-Zn-Mg-Cu alloy products processed by T-AHA type final thermomechanical treatments 13 p1633 A73-28141

A study of the effects of prestrain on the tensile properties of filamentary composites. 13 p1699 A73-29198

[ASME PAPER 72-MAT-K] Solidification structure and tensile properties of 2014 aluminum alloy welds. 14 p1755 A73-30149

Some effects of prestraining nickel at various rates on its subsequent tensile properties. 14 p1761 A73-30637

Structure, strength, and fracture of electrodeposited nickel and Ni-Co alloys. 16 p2025 A73-33113

Relationship between K_{1c} and plane-strain tensile ductility and microscopic mode of fracture. 17 p2190 A73-34876

Prior-to-failure extension of flaws under monotonic and pulsating loadings. 17 p2246 A73-34884

Filament orientation effect on Al and Ti matrix composite tensile properties, using boron, boron and silicon carbide fibers 17 p2192 A73-35533

Deformation and fracture mechanisms in aluminium reinforced by high strength steel ribbons. 17 p2192 A73-35539

Mechanical properties of weld, base metal and coated columbium FS85. 17 p2182 A73-35842

High strain rate tensile properties of AISI type 304 stainless steel. 18 p2323 A73-36619

[ASME PAPER 73-MAT-D] How composition affects properties of a ferritic stainless steel. 21 p2721 A73-41084

Superplasticity and residual tensile properties of a microduplex copper-nickel-zinc alloy. 22 p2879 A73-42582

TENSILE STRENGTH

Plastic limit behavior and failure of filament reinforced materials. 02 p0234 A73-12074

Glass laminates and high strength oriented fiberglass reinforced plastics failure mechanism in tension and bending, noting equalizing effect through proper cohesion characteristics between layers 02 p0185 A73-12134

The influence of test temperature on the fatigue strength of Zs6K alloy. 02 p0181 A73-12204

The effect of tin on the strength and plasticity of titanium at low temperatures. 02 p0181 A73-12212

Randomly oriented glass fiber reinforced epoxy composites tensile strength properties as function of fiber volume fraction 02 p0185 A73-12427

Tensile strength dependence on temperature and interstitial oxygen and nitrogen concentration in powdered Nb, noting microhardness and yield point 03 p0326 A73-13968

Elevated temperature toughness and a dimensionless parameter involving the zero-ductility temperature. 04 p0459 A73-14670

Empirical strength criteria for anisotropic and isotropic composite materials with unequal tensile and compressive strength 04 p0508 A73-14860

The mechanisms of growth of gamma prime particles and tensile yield in Udimet 520. 04 p0464 A73-15578

Method for fractographic investigation of high-tensile aluminum alloys. 04 p0466 A73-15674

Upper bound tensile strength analysis of reinforced composite materials in terms of matrix/particle bond strength, void formation and geometrical factors [ASME PAPER 72-WA/PROD-7] 04 p0469 A73-15805

Upper bound predictions of composite tensile strength as function of transitions from homogeneous to nonhomogeneous deformation [ASME PAPER 72-WA/PROD-8] 04 p0469 A73-15806

B-Al matrix composites environmental properties, costs and development for aerospace systems, considering corrosion, erosion and thermal cycling effects on tensile strength 04 p0467 A73-15934

Layout of a thermodynamical theory of the life time scattering in materials testing 05 p0635 A73-17066

Experimental analysis of the low-temperature strength of notched bars 06 p0705 A73-17779

Composition affects tensile strength of welded aluminium-magnesium alloy. 06 p0709 A73-18385

Fracture due to damage from projectile impact. 06 p0763 A73-18484

Cu-Ni-Zu alloys high ambient temperature tensile and fatigue strengths due to recrystallization and precipitation produced fine grain microstructure, describing annealing and cold working process 06 p0711 A73-18751

S-N fatigue curve analysis from ultimate tensile strength to cyclic elastic limit below fatigue limit, discussing load cycle zones and discontinuities 07 p0910 A73-19214

Damping properties of 1Kh13 and 2Kh13 high-chromium steels in a uniform stress-strain state in tension and compression at room and high temperatures 07 p0841 A73-20513

Dependence on the cobalt content of the strength of a WC-Co cutting alloy in tension 09 p1159 A73-22473

Stress-strain relations for materials with different tension, compression yield strengths. 09 p1166 A73-23452

Fiber reinforced metal matrix composites mixing rule, determining tensile strength, deformation energy and flow curve 10 p1231 A73-23694

Criteria for selecting resin matrices for improved composite strength. 10 p1238 A73-23966

Design stability of composite samples with a soft interlayer in static tension 10 p1291 A73-24352

Study of the effectiveness of various thermomechanical methods of hardening alpha + beta titanium alloys 10 p1234 A73-24425

Reinforcement of magnesium with boron and tantalum filaments. 10 p1234 A73-24437

Experimental observations of tensile fracture in unidirectional boron filament reinforced aluminum sheet. 10 p1235 A73-24439

Mechanical properties of weld, base metal and coated columbium alloy Cb 752. 11 p1375 A73-26356

Influence of proton irradiation in vacuum on the properties of polymer films 11 p1389 A73-26740

Tensile behaviors of high Cr-low Ni two-phase stainless steels at room and low temperatures. 12 p1511 A73-27056

Large elastic flexural and elongation strains in a portion of tube prepared from a material with different resistance to tensile and compressive strains 12 p1552 A73-27369

Thin ferrosilicon intermediate cylindrical layer tensile strength, microhardness and yield point determination at 20-1000 C 13 p1624 A73-29064

Forged or homogenized aged maraging steels, discussing microstructure, tensile strength and fracture toughness dependence on precipitates morphology 13 p1637 A73-29243

Strength and ductility of two-phase iron alloy composed of austenite and martensite. 13 p1638 A73-29453

Mechanical behavior of high-strength beta-titanium alloys. 13 p1638 A73-29456

Statistical definition of fatigue behavior of strength of low alloy steels. 13 p1641 A73-29492

The relation between tensile bond strength and crystalline properties of the adhesive on the steel-nylon 12-steel system. 13 p1642 A73-29531

Metal-filament-reinforced materials and their mechanical behaviour. 13 p1642 A73-29537

The strength of welded joints in high strength stainless steels at cryogenic temperatures. 13 p1625 A73-29615

Investigation of the strength of construction materials for different ratios of the main stresses. 13 p1703 A73-29622

Investigation of some principles in the processes of creep and fracture in heat-resistant materials. 13 p1643 A73-29626

Random yield limit of stochastically non-homogeneous elements in tension. 14 p1811 A73-30489

Radiation-induced strengthening and embrittlement in aluminum. 14 p1761 A73-30628

Macromechanic model of notch size effects on tensile fracture strength in angle ply laminated composites 15 p1897 A73-31680

Tensile and compressive strength tensor prediction for anisotropic boron-epoxy composites from off axis tests

15 p1897 A73-31682

Influence of vanadium, niobium, carbon, and silicon on the properties of low-pearlite steel

15 p1889 A73-31810

Gas saturated surface layer effect on Ti alloy resistance to static cyclic tensile loads, noting increased fatigue strength after etching

15 p1890 A73-31815

Properties of HSLA steels, with and without molybdenum.

15 p1891 A73-32169

Temperature dependence of low-temperature strength in aluminum single crystals

17 p2189 A73-34581

Short- and long-term strength characteristics of particulate-filled cast epoxy resin.

17 p2197 A73-35343

Ultimate tensile properties and composite structure of flow-molded short fiber composites.

17 p2197 A73-35352

Generalized equation for tensile strength of metal matrix composites from upper bound analysis of simplified model with holes, inclusions and environmental pressure

17 p2251 A73-35528

Borsic/Ti-Al-V composite properties, fracture modes and fabrication, discussing tensile strength and temperature dependence of longitudinal strength

17 p2192 A73-35532

Adhesion effect on the tensile properties of fibre reinforced composite materials.

18 p2328 A73-36683

Thin ferrosilicon intermediate cylindrical layer tensile strength, microhardness and yield point determination at 20-1000 C

18 p2320 A73-36896

The damping properties of high-chrome steels 1Kh13 and 2Kh13 in a homogeneous stress state of tension-compression under the conditions of normal and elevated temperatures.

19 p2440 A73-37788

The influence of primary precipitates on the tensile strength of unidirectionally solidified /Fe, Cr/-/Cr, Fe/7C3 in-situ grown composites containing 30 wt % Cr.

19 p2442 A73-38088

A bonding-wire failure mode in plastic encapsulated integrated circuits.

19 p2410 A73-38442

Structures and properties of cobalt base-TaC eutectic alloys.

20 p2575 A73-39020

The effect of heat treatment on the tensile strength and hardness of a quenched ternary zirconium-base alloy /Zr-0.5 wt. % Nb-1 wt. % Cr/.

21 p2717 A73-40319

The tensile strength of pultruded carbon fibre/epoxy resin composite.

21 p2723 A73-40923

Mechanical properties of AFC77 stainless steel bolts.

21 p2721 A73-41085

Effects of specimen geometry on the strength of composite materials.

23 p2996 A73-43633

Influence of the free edge upon the strength of angle-ply laminates.

23 p3041 A73-43635

Graphite fiber tensile property evaluation, discussing single filament method and improved dry bundle test including electrical resistivity measurement and stress-strain curve analysis

23 p2996 A73-43644

High strength filaments for cables and lines, discussing bundle theory and comparing dielectric and tensile properties for glass, graphite and organic fibers

23 p2997 A73-43645

Fracture of thin sections containing surface cracks.

23 p2992 A73-43807

The copper-boron eutectic - Unidirectionally solidified.

23 p2993 A73-44035

Deformation behaviour and deviation from the simple rule of mixture for the ultimate tensile strength in the cold rolled fibre-reinforced composites.

23 p2998 A73-44151

Correlation between the static and fatigue strength of reinforced plastics

24 p3102 A73-44509

The strength of unidirectionally reinforced plastics subjected to tension at an angle to the direction of reinforcement

24 p3102 A73-44511

Ten years' experience of UMCo-type alloys in a special steel foundry.

24 p3099 A73-45074

Effect of vanadium, niobium, and silicon on the properties of low-pearlite steel.

24 p3100 A73-45273

Gas saturated surface layer effect on Ti alloy resistance to static cyclic tensile loads, noting increased fatigue strength after etching

24 p3100 A73-45278

TENSILE STRESS

Crack formation in orthogonally reinforced fiberglass plastics

01 p0067 A73-10482

Dislocation density in Mo single crystals subject to uniaxial tensile stress or sphere-produced indentation, evaluating plastic strain level

01 p0063 A73-10484

Facility for investigating low-cycle fatigue of alloys at cryogenic temperatures

01 p0029 A73-10491

Mosaic-angle and dislocation-density variations in polycrystalline aluminum alloys under tension

01 p0064 A73-10609

Re-interpretation of some simple tension and bulge test data for anisotropic metals.

01 p0065 A73-10764

Two dimensional elasticity theory for radial crack effects on tensile stress concentration in circular elastic isotropic plate

01 p0117 A73-11092

Fracture strength of helical-wound composite cylinders.

01 p0117 A73-11121

Behavior of dislocations in niobium under stress.

02 p0179 A73-11576

Certain regularities in the influence of preliminary loading by alternating tensile stress on the long-term strength of Kh18N10T steel

02 p0180 A73-11928

The creep of materials being weakly strengthened in nonsteady temperature and force conditions.

02 p0180 A73-12138

Isotropy postulate verification for strain vectors measurement in annealed steel tubular specimens, showing coincidence of tension-internal pressure and tension-torsion test values

02 p0235 A73-12206

Dynamic plastic tensile stress analysis based on equation of motion, kinematic equation and material law with conditions regarding disturbance propagation velocity

03 p0385 A73-13142

Effect of residual or characteristic stresses on the deformation of plates

03 p0385 A73-13143

Analysis of transverse cracks in an orthotropic strip with edge stiffeners.

[ASME PAPER 72-WA/APM-4] 04 p0516 A73-15904

A time hardening transient creep solution for steadily loaded uniaxial tension panels containing circular and elliptical holes under conditions of plane stress.

06 p0761 A73-17820

A couple-stresses elastic solution of an infinite tension plate bounded by an elliptical hole.

06 p0717 A73-18173

Growth of part-through thickness fatigue cracks in sheet polymethylmethacrylate.

06 p0714 A73-18481

Tensile and compressive prestressing effects on notched steel cantilever beam specimens low cycle fatigue life

06 p0764 A73-18490

Direct observation of tensile and fatigue cracks.

06 p0710 A73-18495

On the buckling of thin tensioned sheets with cracks and slots.

06 p0764 A73-18497

Dioptric powers of transparent plates in a plane state of tension

06 p0765 A73-18697

The critical rate of tensile stress application and its significance for characterizing the behavior of materials under impact loads

07 p0838 A73-19213

Microinhomogeneous plane with a circular hole in tension

07 p0911 A73-19320

Equilibrium method for stress concentration around hole in plate under tension, comparing with Kolosov-Muskhelishvili potential method

08 p0105 A73-20699

Mechanism by which hot cracks form during welding aluminium and its alloys.

08 p0977 A73-21236

Influence of the frequency of the tension-compression cycle on the fatigue life of D16T alloy

09 p1100 A73-22153

Stress distortion coefficient of uniaxial tension /compression/ of elastic isotropic medium with flattened ellipsoidal sensor from sensor stress recording

09 p1159 A73-22590

A special theory of crack propagation.

09 p1161 A73-23177

Stress state around an elliptic hole in a conical shell under tension.

[ASME PAPER 72-PVP-11] 09 p1163 A73-23269

Elastoplastic deformation and hardening function of perforated plates under in-plane tensile loads

09 p1164 A73-23346

Brittle fracture of orthogonally reinforced glass-fiber plastics during tension

09 p1111 A73-23349

Determination of tensile stresses in wide flat samples

09 p1165 A73-23359

Fatigue crack delay and arrest due to single peak tensile overloads.

[AIAA PAPER 73-325] 11 p1441 A73-25555

Crack growth rate due to steels and Ti and Ni alloys electrochemical dissolution, noting tensile stress intensity factor

11 p1385 A73-26173

Crack propagation in some aluminum alloys with tensile stresses

12 p1511 A73-26916

Damping properties of a composite material with monodirectional continual fibers

12 p1516 A73-27258

Ideal plasticity theory for solid bodies of isotropic materials with different yield points in extension and compression

12 p1553 A73-27374

Alloy creep due to temperature and tensile stress in absence of hardening

12 p1513 A73-27479

Brittle failure of infinite plate with circular hole and radial cracks under two perpendicular uniformly distributed tensile loads

12 p1556 A73-27802

Initial-boundary value problems of nonlinear extensible beam equation as mathematical model for transverse deflections of beam with hinged or clamped ends

13 p1695 A73-28438

Interaction of elasto-plastic cracks subjected to a uniform tensile stress in an infinite or a semi-infinite plate.

13 p1701 A73-29471

An X-ray study of the stress corrosion of austenitic stainless steels.

13 p1625 A73-29521

Al alloy rupturing analysis in complex stress state, noting sublimation and self diffusion values of activation energy in torsional to tensile state transition

13 p1643 A73-29624

Crack formation in orthogonally reinforced glass-fiber ware.

14 p1765 A73-30307

Assessment of the degree of plastic deformation in a crater with ball imprint.

14 p1810 A73-30309

A unit for investigating the low-cycle fatigue of alloys at cryogenic temperatures.

14 p1743 A73-30316

Three-dimensional stress-strain state of turbine blades

14 p1813 A73-30677

Effect of deep annular grooves on the strength of some metals under static tension and torsion

14 p1763 A73-30693

Study of the elastoplastic stressed state and plastic zones of a plate with a circular hole under tension

14 p1815 A73-30794

Force-strain characteristics of dacron parachute suspension-line cord under dynamic loading conditions.

[AIAA PAPER 73-446] 15 p1825 A73-31432

Nonlinear tension and buckling stress behavior of angle ply unidirectional laminated composites

15 p1949 A73-31683

Hardening and softening of aluminum alloys under an applied load at 135 to 150 C

15 p1889 A73-31808

Infinite elastically isotropic solid under external tensile stress, deriving condition for complete fracture from wedge crack

15 p1951 A73-32023

The transition from thin plate to membrane in the case of a plate under uniform tension.

15 p1953 A73-32094

Saint Venant problem for a continuously inhomogeneous anisotropic beam

15 p1953 A73-32103

Displacements and elastoplastic deformations at a crack edge under tension

15 p1954 A73-32105

Russian book - Plane bending and tension of curvilinear thin-walled beams.

15 p1956 A73-32296

Optimal design of layered structures under dynamic loading.

16 p2075 A73-32790

Circular elastic membrane stability against wrinkling under radial peripheral tension and transverse pressure loading, considering solutions via Foepl-Hencky theory

16 p2080 A73-33246

Hot fatigue strength during fluctuating axial tension of PER 7 and IN 100 superalloys

16 p2026 A73-33971

Torsion and extension of a cylinder with an outer annular cut

17 p2240 A73-34143

Stresses in a symmetrically-laminar plate weakened by a central crack

17 p2240 A73-34145

Strength and plasticity of tantalum in rapid tests

17 p2188 A73-34561

Stress analysis of composite materials with strong fibers in weak matrix, obtaining tensile stress bound-

- ry layer equations via elasticity theory and perturbation methods
[ASME PAPER 72-APM-TTT] 17 p2249 A73-35110
- Solid cadmium cracking of titanium alloys.
17 p2191 A73-35123
- Creep, self heating and failure of thermoplastics under pulsating tensile stress.
17 p2197 A73-35346
- Evaluation of finite-plasticity theories for torsion-tension members made of Tresca materials.
[SESA PAPER 2109] 17 p2251 A73-35447
- Effects of material and stacking sequence on behavior of composite plates with holes.
[SESA PAPER 2157A] 17 p2198 A73-35452
- Brass matrix composites tensile strain characteristics and fracture mode dependence on fiber volume fraction and properties
17 p2192 A73-35531
- Stress concentration determination under biaxial tension in a plate weakened by a randomly-shaped hole
18 p2363 A73-36414
- Studies of fiberglass plastic under tensile load with the aid of transparency measurements
18 p2327 A73-36476
- Study of the behavior of metallic single crystals - Application to the tension of the fcc single crystal
19 p2495 A73-37425
- Strain accumulation and rupture during creep under variable uniaxial tensile loading.
19 p2495 A73-37434
- Influence of cycle ratio on the elastic modulus of glassfiber reinforced plastics subjected to repeated tensile load.
20 p2580 A73-38644
- Two-dimensional contact problem for a prestressed elastic body
20 p2625 A73-39652
- Spallation and fracture resulting from reflected and intersecting stress waves.
21 p2782 A73-39989
- Residual-stress measurement using surface displacements around an indentation.
21 p2704 A73-41265
- Effect of the frequency of cyclic tension-compression on the fatigue limit of alloy D16T.
22 p2874 A73-42103
- Prior to failure extension of flaws in a rate sensitive Tresca solid.
22 p2880 A73-42136
- Overload effects on subcritical crack growth in austenitic manganese steel.
22 p2875 A73-42138
- A method for measuring $K_{sub Ic}$ at very high strain rates.
22 p2866 A73-42148
- Estimation of the effect of the internal properties of the material on the characteristics of string sensors
22 p2860 A73-42370
- Analysis of stress intensity factors for the tension of a centrally cracked strip with stiffened edges.
23 p2992 A73-43812
- Fracture analysis of surface- and through-cracked sheets and plates.
23 p3042 A73-43813
- Prediction of failure processes in fiberglass-reinforced plastics by a seismographic method. II - Features of damage buildup in woven fiberglass-reinforced plastics in uniaxial tension
24 p3102 A73-44507
- The strength of unidirectionally reinforced plastics subjected to tension at an angle to the direction of reinforcement
24 p3102 A73-44511
- The strength of orthogonally reinforced plastics during uniaxial tension
24 p3145 A73-44522
- Hardening and softening of aluminum alloys under load at 135-150 C.
24 p3100 A73-45271
- TENSILE TESTERS**
U TENSILE TESTS
TENSILE TESTS
- Influence of metallurgical factors on the corrosion cracking under tension of TA6V titanium alloy in an aqueous medium at ambient temperature
[ONERA, TP NO. 1100] 01 p0061 A73-10231
- Application of the VEDS-200A electrodynamic vibrator to fatigue tests in symmetric tension and compression
01 p0029 A73-10492
- Time characteristics of rupture and creep in metals during tension under hydrostatic pressure conditions
01 p0064 A73-10605
- An analysis of the breaking elongation in high velocity impact of the power law hardening materials.
01 p0117 A73-11123
- Mechanical properties of glassy carbon fibres derived from phenolic resin.
01 p0068 A73-11498
- Mechanical properties of aluminum matrix composites.
02 p0184 A73-12849

- Tensile, compressive and shear strength and absolute modulus of PRD fibers from reinforced plastic honeycomb and filament wound strand tests
03 p0330 A73-13015
- Characterization of an epoxy system for filament winding.
03 p0330 A73-13016
- Interference grating production for viscoelasticity investigation by moire method, noting tensile tests of viscoelastic plates
03 p0306 A73-13159
- Crack shapes and stress intensity factors for edge-cracked specimens.
04 p0506 A73-14681
- Fatigue crack propagation growth rates under a wide variation of Delta K for an ASTM A517 Grade F /T-1/ steel.
04 p0459 A73-14687
- Sharp-notch tension testing of thick aluminum alloy plate with cylindrical specimens.
04 p0460 A73-14698
- Center cracked tension specimen geometry effects on plane stress fracture toughness of high strength Al, Ti and steel alloy sheets
04 p0460 A73-14699
- Elastic-plastic deformation in edge-notched tension specimens under plane stress conditions.
[ASME PAPER 72-WJ/MAT-3] 04 p0514 A73-15809
- Evaluation of the compact tension specimen for determining plane strain fracture toughness of high strength materials.
05 p0581 A73-16126
- Bending and rolling methods for tensile testing of metals without local necking, considering fracture under reduced axial stress
05 p0581 A73-16130
- Frame photography for temporary creep in cylindrical Al alloy specimen necks under tensile loads, calculating creep diagrams
05 p0634 A73-16748
- Material deformations determined with the aid of X rays in the case of elongations remaining after a uniaxial tensile test involving titanium and TiAl6V4
05 p0588 A73-17243
- Torsional fatigue fixture for high temperature investigation of high strength steels crack growth rate in tensile mode
05 p0563 A73-17254
- Observations on the deformation properties of sandwich materials.
06 p0761 A73-17819
- Tensile tests and heat treatment for creep rupture and fracture strengths of heat resistant steel, noting crack initiation and propagation
06 p0706 A73-17884
- An experimental investigation into the mechanics of deep semielliptical surface cracks in mode I loading.
06 p0763 A73-18478
- Metallographic investigation and notch, tensile and hardness tests for electroslag welding of austenitic stainless steels
07 p0831 A73-19949
- The Kaiser effect in stress wave emission testing of carbon fibre composites.
07 p0843 A73-20185
- Effects of heat treatment on the properties of a molybdenum-carbon-nickel alloy and joints in it.
07 p0840 A73-20371
- Study of the formation process of corrosion cracks under tension in an aluminum alloy
[ONERA, TP NO. 1213] 09 p1098 A73-21925
- Variable-load endurance criteria for steels under conditions of uniaxial and biaxial static tension
09 p1100 A73-22152
- Stress corrosion cracking of commercial Al-Mg alloys and its prevention.
09 p1102 A73-22422
- Deep drawability of titanium sheets.
09 p1104 A73-22522
- Artificial slow crack growth under constant stress - The R-curve concept in plane stress.
09 p1108 A73-23255
- Fatigue and creep testing of unidirectional carbon fibre reinforced plastics.
10 p1238 A73-23965
- The effect of specimen and testing variables on the fracture of some fibre reinforced epoxy resins.
10 p1240 A73-24281
- Application of a digital computer in the processing and presentation of tensile test results.
10 p1192 A73-24569
- Machine for life testing materials under varying tension in working media with high temperatures and pressures.
10 p1204 A73-24946
- Influence of small local deviations in specimen diameter on conventional strain at maximum load in tensile test
11 p1380 A73-25448
- A servo-controlled axial fatigue machine with strain rate feedback for testing polymers and composites.
11 p1344 A73-26311
- Fracture characteristics of thermally strengthened titanium beta-alloys
12 p1510 A73-26914

- Effect of prestraining on the brittleness of molybdenum.
12 p1511 A73-27058
- Yield point phenomenon in Al-Ti alloy.
12 p1511 A73-27060
- A modernized device for testing metal sheet and welded joints under conditions of planar tension
12 p1486 A73-27446
- Facility for conducting fatigue tests with sheet materials in cyclic tension
13 p1597 A73-29050
- Effect of tensile prestrain on fatigue strength of aluminum alloy in high cycle fatigue.
[ASME PAPER 72-MAT-N] 13 p1636 A73-29197
- German monograph - Effect of creep strains at 700 C on the hardening characteristics of the steel X 8 C NiMoNb 16 16 at room temperature.
13 p1637 A73-29281
- Biaxial tensile test facility for three dimensional characterization of nonlinear viscoelastic materials based on variable ratio principal strains in plane stress
13 p1598 A73-29300
- Aluminum foils crack propagation observation with electron microscope during tensile tests, noting crystal dislocation role in ductile fracture process
13 p1639 A73-29461
- Brittle fracture strength and non-crack propagation.
13 p1639 A73-29470
- Plane strain elastic-plastic state and fracture in cracked blunt notched steel plates under tensile loads
13 p1701 A73-29471
- Influence of temperature on the initial yield of notched strength.
13 p1641 A73-29511
- Present situation of Japanese research on the long time creep and creep rupture properties of steels.
13 p1642 A73-29513
- On fatigue damage and debonding of glass fiber reinforced plastics.
13 p1647 A73-29544
- Deformation criteria of failure under simple and composite stresses.
13 p1703 A73-29623
- The use of a type VEDS-200A vibrostand for fatigue tests under conditions of symmetrical tension-compression.
14 p1743 A73-30311
- Strain ratio data for commercial Al alloys in various temper conditions as drawability criterion for sheet press performance, discussing single tensile test method
14 p1762 A73-30644
- Testing assembly for sheet metals and welded joints under static and low-cycle biaxial tension under low temperature conditions
15 p1855 A73-31140
- Testing machine to determine perforated plate biaxial tension creep rupture strength and fatigue life at high temperature
15 p1858 A73-31614
- Effect of temperature on titanium plasticity
15 p1894 A73-32520
- Effect of thermomechanical treatment on the stress corrosion cracking of metastable beta III titanium.
15 p1896 A73-32570
- Some mechanical properties of carbon fibre reinforced aluminum.
16 p2025 A73-32848
- High temperature tensile and stress rupture tests of tungsten /Nichrome laminar composites and tungsten alloy /Inconel sheet and foil specimens
17 p2193 A73-35502
- Fiber orientation effects on fatigue failure of aligned short fibre composite materials.
17 p2198 A73-35546
- On stress concentration factors in orthotropic glass fiber reinforced plastics.
18 p2327 A73-36470
- Low temperature tensile tests for strength and plasticity of pure bcc, hcp and fcc polycrystalline metals, indicating stacking fault energy role
18 p2324 A73-36806
- Crack resistance tests of polymethyl methacrylate specimens under tensile stress
18 p2366 A73-36820
- Apparatus for fatigue tests on sheet materials subject to cyclical extension.
18 p2297 A73-36898
- The characteristics of hydraulic tensile-test machines of the pendulum type and their effect on the tensile test
20 p2545 A73-39626
- An improved test for interfacial shear strength.
21 p2719 A73-40939
- Criteria relating to the fatigue life of steels subjected to alternating loads under conditions of uniaxial and biaxial static strain.
22 p2874 A73-42110
- Testing set-up for cyclic torsion with tension on a small number of loading cycles.
22 p2861 A73-42511
- Response of glass-fiber-reinforced epoxy specimens to high rates of tensile loading.
23 p2996 A73-43331

Free-edge effects in the characterization of composite materials. 23 p3040 A73-43632

Effects of specimen geometry on the strength of composite materials. 23 p2996 A73-43633

Graphite fiber tensile property evaluation, discussing single filament method and improved dry bundle test including electrical resistivity measurement and stress-strain curve analysis. 23 p2996 A73-43644

Investigation of the initial stage of crack development during compression and tension of polymethylmethacrylate samples. 23 p2998 A73-44278

Testing of composite materials with the aid of annular samples. 23 p2998 A73-44295

Strip weakened by array of holes, investigating plastic zone initiation and propagation under uniaxial tension for load bearing capacity estimation. 24 p3147 A73-44685

TENSION

Curve fitting by application of splines under tension, discussing polynomial interpolation drawbacks and linear system solution for unknown second derivatives. 24 p3070 A73-45090

TENSION TESTERS

U TENSILE TESTS

TENSOMETERS

Strain gauge for measuring longitudinal and transverse strains. 07 p0826 A73-20518

Characteristics and properties of WED-05 tensometers. 07 p0827 A73-20537

Tensometric strain gage evaluation of stress analysis methods for hollow cylindrical shells under uniform internal pressure. 13 p1698 A73-29057

Application of refractory oxide coatings in extensometry. 18 p2314 A73-35886

Tensometric strain gage evaluation of stress analysis methods for hollow cylindrical shells under uniform internal pressure. 18 p2366 A73-36889

Strain gauge for measurement of axial and transverse strains. 19 p2430 A73-37794

TENSION ANALYSIS

Collisionless magnetoactive plasma nonlinear responses tensors symmetry properties, stressing Anisotropy relations generalization. 01 p0083 A73-10454

Newtonian force field effect on gyroscopic motion for coordinate axes coincident with inertia tensor axes, solving equations of motion by energy integral. 02 p0192 A73-11769

Curvilinear coordinates for deformation tensor and stress analysis of structures, using finite element method. 02 p0231 A73-11812

Russian book on tensor calculus fundamentals covering tensor algebra and analysis and applications to mechanics of discrete and continuous systems. 02 p0192 A73-11888

Analytical representation of boundary conditions in the technical theory of shells. 03 p0384 A73-13127

Tensor analysis for micropolar elastic body deformation and stresses, solving differential equations of thermoelasticity. 03 p0386 A73-13153

Strength limits correlation to modulus of elasticity for compact bone material from compression tests, noting anisotropy tensor analysis. 03 p0267 A73-13744

Anisotropic material characteristics due to plastic deformation during fabrication processes, presenting tensor analysis. 04 p0511 A73-15169

Invariant criterion generalization for pure gravitational waves in tetrad formulation of general relativity theory, noting electromagnetic field energy tensor. 04 p0476 A73-15638

The variational derivative of degenerate Lagrange densities. 06 p0718 A73-18504

Tensor-linear approach to the stability problem of nonlinearly elastic isotropic plates. 06 p0765 A73-18690

Tensor theory of perturbations in atmospheric dynamics. 09 p1115 A73-23150

Rigorous analogies between elastic and electromagnetic systems. 10 p1250 A73-24873

Combined electromagnetic and gravitational field equations derivation with explicit interaction term and tensors for curved space-times unrestrained in Einstein-Maxwell equations framework. 11 p1401 A73-26658

The general form of constitutive equations in relativistic physics. 13 p1658 A73-28374

First derivative discontinuities of space-time metric tensor in Einstein equations solution for nonisotropic and isotropic hypersurfaces, proving coordinate system existence for continuity. 14 p1774 A73-30328

Quantum and relativity theories compatibility based on hypothesis of matter tensor delta structure and Planck's constant for action singularity. 14 p1775 A73-30425

Metric tensor properties of physical space with deformable continuum in terms of kinetic stress function, approximating Einstein constant. 15 p1945 A73-31041

Geomagnetic variations total field confinement described by Parkinson, discussing primary and secondary fields Maxwell equations linear relationship by induction tensor. 15 p1871 A73-31777

General properties of electromagnetic scattering by inhomogeneous anisotropic composite obstacles of arbitrary shape. 15 p1844 A73-31930

Symmetric vector-type tensor functions of elastic bodies related to strain measure invariants, formulating limited hardness principle in terms of Poisson ratio. 15 p1954 A73-32123

The inertia tensor of the atmosphere, annual variations in its components, and variations in the earth's rotation. 17 p2158 A73-34343

Relativistic rocket motion tensor equations analogous to particle motion in electromagnetic fields, discussing Hamiltonian functions, Lagrangian coordinates and variable mass body mechanics. 18 p2356 A73-37038

The method of virtual powers in mechanics of continuous media. I - Theory of the second gradient. 19 p2495 A73-37424

Rotational line structure in three-photon scattering by symmetric top molecules. 20 p2574 A73-39723

Finite plasticity theory in acoustic tensor calculation for elastic, viscoplastic and plastic wave propagation. 21 p2740 A73-40947

Gravitational waves in a space-time of any dimension. 22 p2885 A73-41773

Centrosymmetric metric generator of field models of particles, discussing Einstein tensor components representation. 22 p2887 A73-42431

Anisotropic composite material swelling coefficients and elastic compliances data averaging and reduction, using tensor transformation and associated scalar invariants. 23 p3041 A73-43636

Mandel viscoplasticity theory constitutive equations satisfying causality principle, considering finite deformations tensor representation by partial differentials. 23 p3044 A73-43970

Tensorial norms properties with respect to Hilbert spaces, constructing perfect ideals in Banach space. 24 p3105 A73-45010

Conductivity tensor of a collisional plasma in a magnetic field. 21 p2749 A73-41628

Bounds on effective dielectric constant of inhomogeneous material. 22 p2896 A73-42263

Matter representation in general theory of relativity in terms of sourceless metric tensor and Einstein matter tensor, examining Mach principle status. 22 p2887 A73-42435

An operational approach to the energy of gravitational waves. 22 p2888 A73-42929

Numerical realization of a possible way of determining the tensor of elastic constants in an anisotropic body. 24 p3144 A73-44506

Automated terminal area ATC operations under FAA ten year plan, investigating analytical model of pilot-aircraft control loop decision making by computer program
17 p2206 A73-34437

The functions of regional airports and the resulting requirements for the ground installations
17 p2146 A73-34476

The financing of essential communication, navigation and terminal aids.
17 p2257 A73-34535

Simulation of a surface traffic control system for John F. Kennedy International Airport.
17 p2147 A73-34818

A simulation study for the design of an air terminal building.
17 p2149 A73-35826

Simulating the introduction of 747 aircraft into airport operations.
18 p2296 A73-36423

Airport simulation program describing passenger flow and scheduling considerations, including automobile parking, baggage handling, rapid transit, arrival and departure peaks and passenger decisions
18 p2296 A73-36841

Floating offshore airport in Osaka Bay, Japan - Digest of preliminary engineering study.
19 p2418 A73-37747

Operational considerations in the design of airports.
19 p2418 A73-37820

Seattle-Tacoma's unconventional concept.
22 p2839 A73-42315

Schiphol as a tourist attraction.
22 p2839 A73-42316

GASP simulation of terminal air traffic system. [ASCE PREPRINT 2059]
22 p2839 A73-42868

TERMINAL GUIDANCE

Discrete control algorithms for spaceborne terminal systems.
01 p0075 A73-11194

Optimal horizontal guidance law for aircraft in the terminal area.
03 p0340 A73-13518

Suboptimal guidance for attitude angle constrained flight trajectories.
06 p0721 A73-18825

Area navigation systems integration with terminal ATC approach procedures, considering computerized data linkage with aircraft navigation system
07 p0849 A73-19351

Stochastically optimal terminal control system synthesis for loss function dependence on finite phase coordinates of dynamic system, considering soft landing of flight vehicle
07 p0805 A73-20037

A discrete separation principle with a stochastic terminal constraint.
07 p0806 A73-20599

All-weather aircraft landing automation, discussing efficient optimal feedback control law selection based on trajectory termination or terminal control requirements
10 p1247 A73-24010

Optimal trajectory solution for minimum transfer time in terminal control problem involving locally controllable final point
16 p2032 A73-33306

Terminal and flight control navigation guidance systems for restricted and short takeoff and landing aircraft air traffic and approach techniques [RAE-TM-AVIONICS-135/BLUE]
17 p2100 A73-34490

Real-time hybrid hardware-in-the-loop simulation of a terminal homing missile.
18 p2291 A73-36834

Results and problems of a theory of final-position control systems with a nonstationary singular feedback
20 p2540 A73-38707

Direct statistical evaluation of nonlinear guidance systems.
[AIAA PAPER 73-836]
20 p2584 A73-38779

System performance prediction by modeling test data in digital simulations.
[AIAA PAPER 73-880]
20 p2543 A73-38816

Optimal guidance for aerodynamically controlled reentry vehicles.
[AIAA PAPER 73-891]
20 p2588 A73-38827

Nonlinear trajectory following in the terminal area - Guidance, control and flight mechanics concepts using the microwave landing system.
[AIAA PAPER 73-903]
20 p2589 A73-38837

Statistically optimal sampled data terminal guidance algorithm for complex probabilistic multipurpose control system, using linearized equations
20 p2590 A73-39344

Nonlinear trajectory-following and control techniques in the terminal area using the Microwave Landing System Navigation Sensor.
21 p2734 A73-40038

Ground based microwave landing system for aircraft navigation, guidance and control in terminal area, discussing system requirements for flight safety
21 p2735 A73-40047

Relationships between operational flexibility and capacity in contemporary terminal air traffic control operations.
21 p2736 A73-40048

Microwave landing system elevation data or altimeter information for flare-out guidance, considering airport, aircraft autopilot and ground equipment and cost factors
21 p2736 A73-40050

Low cost airport surveillance and Localized Cable Radar with runway or taxiway vehicle guidance capability for ground traffic control, using solid state equipment
21 p2736 A73-40051

Approximate solution of Bellman's equation for a class of problems involving optimal terminal control
21 p2668 A73-40179

TERMINAL VELOCITY

Terminal velocity equations for ice crystal growth forms and precipitation rates calculation in clouds, using drag coefficients, aspect ratios and densities
02 p0189 A73-12783

Pontryagin maximum principle for optimal terminal velocity control of automatic space probe descent in Mars atmosphere
03 p0383 A73-14556

TERMINATOR LINES

VLF field diurnal variations and terminator crossing effect on signal path during transmission in earth-ionosphere waveguide
05 p0549 A73-16393

Properties of solar halos in the Martian limb zone and at the terminator
07 p0902 A73-20322

Properties of solar halos in the limb zone and at the terminator of Mars.
12 p1540 A73-27294

Mariner 9 ultraviolet spectrometer experiment - Afternoon terminator observations of Mars.
19 p2479 A73-37220

TERMINOLOGY

Space and terrestrial pollution definitions, discussing control and preventive measures by national and international public and private organizations
04 p0522 A73-15139

Remarks on the ISO international standards relating to 'Terms and Symbols for Flight Dynamics'
10 p1174 A73-23657

Fluidics terminology and vocabulary development and practical use, describing control functions and symbols
11 p1307 A73-25378

TERNARY ALLOYS

Amorphous magnetism in F.C.C. Vicalloy II.
01 p0087 A73-10242

Critical thickness effect of fatigue notched specimens on stress intensity factor and fracture toughness behavior of Ti-Al-V alloys
04 p0462 A73-15244

Growth of ternary composites from the melt. I, II.
04 p0463 A73-15310

Microstructures and transformation kinetics of continuously cooled carbon free Fe-Mo-Ni alloys.
04 p0463 A73-15311

Molybdenum corner in Mo-Ti-B and Mo-Zr-B ternary systems
04 p0464 A73-15494

Structure and composition of certain Laves phases and identification of chi phases in Fe-Mn-Ti alloys
06 p0708 A73-18100

Stability of reactive and refractory metal borides in ternary chromium-base alloys.
07 p0838 A73-19122

On relationship between stress corrosion resistance and grain shape of extruded Al-Zn-Mg alloys with heavy section.
08 p0977 A73-21140

Phase separation analysis of ternary Co-W-Ti alloy during high temperature aging by X ray and electron microscopy method
09 p1099 A73-21963

Metallurgical investigations of phase equilibria in the titanium-niobium-germanium ternary system
10 p1231 A73-23692

Phase equilibria in three-component alloys containing an interstitial element, and the stability of composite materials
10 p1233 A73-24317

Elements distribution in ternary alloy system during simultaneous saturation and burning-out of two components and successive diffusion into third
10 p1236 A73-24953

Determination of alpha plus gamma/gamma phase boundaries in Fe-Cr-Ni, Fe-Cr-Co, and Fe-Cr-Mn systems
11 p1384 A73-26108

Constitution and phase relationships in copper-silver-aluminum ternary system.
11 p1385 A73-26566

Order-disorder alpha and gamma phase transformations as function of temperature in Co-Fe-V alloy by dilatometric, magnetostuctural, neutron diffraction and X ray analyses
12 p1508 A73-26834

Carbide separation and carbide equilibrium in the Co-Cr-C system
12 p1509 A73-26895

Interaction of molybdenum with elements of the iron group and carbon
12 p1510 A73-26903

Mo-W-B alloy phase equilibria, isothermal cross sections, liquidus, solubility and mechanical properties by thermal, X ray and microstructural analyses
12 p1510 A73-26904

Mo-Nb-Ta alloys phase and composition-hardness diagrams for 20-1100 C, establishing mutual solubility of system components
12 p1510 A73-26905

Phase equilibria in the aluminum-chromium-zirconium system
12 p1510 A73-26906

Crack propagation in some aluminum alloys with tensile stresses
12 p1511 A73-26910

X-ray structural investigations of Dy-Fe-Al system alloys in the region of 0 to 33 at. % dysprosium
12 p1512 A73-27243

Hardening by tempering of Fe-Ni-Mo and Fe-Ni-Co-Mo martensites
12 p1514 A73-27987

Quasi-ternary Mo-Ti-C-Zr system
13 p1630 A73-28014

Solubility of nitrogen and hydrogen in cobalt and cobalt alloys - A review.
13 p1637 A73-29245

Stability of metal-based composite materials
15 p1888 A73-31596

Oxygen in titanium alloyed with aluminum and zirconium
15 p1889 A73-31812

Investigation of titanium alloys containing refractory elements
15 p1889 A73-31813

Study of a niobium-aluminum-silicon system. I - Partial isothermal sections at 1500 and 1300 deg C, and the behavior of the Nb/Si, Al/2 phase
15 p1890 A73-31991

Study of a niobium-aluminum-silicon system. II - Analysis of ternary niobium-aluminum-silicon alloys by atom absorption spectrophotometry
15 p1890 A73-31992

Investigation of the phase equilibrium of ternary Ti-Al-Nb system alloys
15 p1893 A73-32514

Characteristics of the distribution of elements in the diffusive layers of titanium-based three-component systems
15 p1893 A73-32521

The role of yttrium in high-temperature oxidation behavior of Ni-Cr-Al alloys.
16 p2025 A73-33077

Phase constitution of the Ni-Cr-S alloy system between 600 and 850 C.
16 p2025 A73-33112

Effects of high omnidirectional pressures and residual stresses on the superconductivity of alloys of the V3Si1-xGex system
16 p2027 A73-34062

Polythermal and isothermal sections of Ti-Al-W phase diagram for Ti corner investigation, determining phase region boundary locations by X ray analysis
17 p1888 A73-34568

Metallurgical investigations of atomic ordering and transformation behavior of close packed ordered nine-layered hexagonal structure /kappa phase/ in V-Co-Ni ternary alloys
17 p2190 A73-34646

The effect of heat treatment on the tensile strength and hardness of a quenched ternary zirconium-base alloy /Zr-0.5 wt. % Nb-1 wt. % Cr/.
21 p2717 A73-40319

Ta-Nb-Re system phase diagram plotted by physicochemical analysis methods, establishing region of existence of ternary solid solutions and temperature dependence
21 p2718 A73-40488

Carbide precipitation and carbide equilibrium in the Co-Cr-C system.
21 p2720 A73-41028

Observations of solid/liquid interfaces in dilute binary and ternary Al-rich alloys.
21 p2721 A73-41120

Russian book - The structure of zirconium alloys.
22 p2873 A73-41973

Ternary systems: Rare earth metal - iron family metal - silicon /Component interaction and crystal structures of compounds/
22 p2873 A73-42084

Investigation of the phase composition of alloys in the Ti-Al-Fe ternary system
22 p2873 A73-42086

Specific structural features of the phase diagrams of the Ti-Cr-V, Ti-Cr-Nb and Ti-Cr-Ta ternary systems
22 p2873 A73-42087

Structure of the phase diagrams of the ternary systems /Mo, W/ - /Ti, Zr, Hf, V, Nb, Ta/ - C
22 p2877 A73-42455

- Isothermal cross sections of the phase diagram of the nickel-molybdenum-tungsten system at 1200 and 1000 C 22 p2877 A73-42459
- Interaction of molybdenum with cobalt and carbon 22 p2877 A73-42460
- Intergranular corrosion of iron-nickel-chromium alloys. 23 p2990 A73-43458
- Ni-based ternary alloy element segregation after addition of third element during crystallization, showing the additional influence on segregation direction of Co, Cr and Mo 23 p2992 A73-43915
- A thermodynamic calculation of the iron-chromium-nickel equilibrium diagram. 23 p2993 A73-43918
- The metallurgy of Remendur - Effects of processing variations. 23 p2993 A73-43987
- On the age-hardening of Fe-Pt-Mn ternary alloys. 23 p2994 A73-44139
- Stability of the gamma-prime Co₃Ti compound in simple and complex cobalt alloys. 24 p3099 A73-45075
- Oxygen in alloys of titanium with aluminum and zirconium. 24 p3100 A73-45275
- Alloys of titanium with refractory elements. 24 p3100 A73-45276
- TERNARY SYSTEMS**
- On the ternary compound G in the Al-Mn-Cr system. 02 p0179 A73-11598
- Disilicides solubility in silver and tin melts, discussing ternary phase formation 02 p0181 A73-12367
- The dynamical evolution of triple star systems - A numerical study. 02 p0221 A73-12702
- Linear and nonlinear optical properties of some ternary selenides. 03 p0350 A73-14458
- Successive diffusion in a ternary system of the iron-tantalum-carbon type 07 p0841 A73-20520
- Ternary nickel-vanadium-oxygen compound and solid solutions formation by vacuum calcination of vanadium and nickel oxides mixtures 13 p1634 A73-28203
- The vanadium-iron-boron, vanadium-cobalt-boron, and vanadium-nickel-boron systems 15 p1887 A73-31202
- Effect of oxygen on the structure and properties of ZrTi₃-based alloys 15 p1923 A73-31209
- Titanium hydride and hydronitride thermal stability analysis from hydrogen vapor pressure and decomposition measurements in vacuum at 400-1100 C 15 p1888 A73-31601
- TERNARY SYSTEMS [DIGITAL]**
- DIGITAL SYSTEMS**
- PENES**
- Volatiles terpenoids from aeciospores of Cronartium sinuatum. 12 p1462 A73-27145
- RACES [LANDFORMS]**
- The use of near-infrared photography in the analysis of surface morphology of an Argentine alluvial floodplain. 22 p2850 A73-42728
- RAIN**
- Radiation pattern of a low-frequency beacon antenna in the presence of a semi-elliptical terrain irregularity. 16 p1979 A73-32913
- The boundary layer above 30 m. III. 19 p2448 A73-38214
- An engineering flight simulation visual display system. 22 p2838 A73-41970
- RAIA PAPER 73-924]**
- RAIN ANALYSIS**
- Computerized airborne multilateration radar with de-beam antenna and narrow pulsewidth for high resolution terrain image mapping 01 p0019 A73-11479
- Side-look radar provides a new tool for topographic and geological surveys. 02 p0140 A73-11850
- Computerized terrain classification system software features for automatic interpretation of aerial photographic imagery by laser scanning system 04 p0445 A73-15772
- Synthetic aperture SLAR systems and their application for regional resources analysis. 05 p0578 A73-17133
- Supervised and unsupervised category identification and classification systems consistency with ERTS ellipses high rate multispectral data requirements 05 p0572 A73-17142
- Radar brightness mapping of Venus surface, noting roughness of terrain from polarization studies and signal processing for extraction of echo power 06 p0744 A73-17440
- Mariner 9 map analysis of Mars geology, covering cratering, circular basins, volcanism, canyons, chaotic terrain, channels and eolian activity 06 p0745 A73-17476
- Geological framework of the south polar region of Mars. 06 p0745 A73-17477
- Radar imagery and aerial photography for geological remote sensing applications in coastal mapping, landform analysis, engineering and reconnaissance 06 p0667 A73-18282
- Clustering phenomena in side-looking radar /SLR/ microtexture. 06 p0667 A73-18285
- Isostasy and relief of the Earth, the Moon and Mars 07 p0878 A73-19661
- Airborne photogrammetric system with mapping and geodetic surveying data acquisition capability, discussing inertial navigation subsystem, terrain profile recorder and electronic distance measuring equipment 09 p1081 A73-22380
- Interpretation of wetlands imagery based on spectral reflectance characteristics of selected plant species. 09 p1077 A73-22388
- Analytical transformation of photographs for plotting topographic and photographic maps in prescribed projections 10 p1219 A73-24483
- First order effects of terrain on the radiation pattern of a non-directional LF beacon. 11 p1332 A73-26204
- Evaluation of remote sensor imagery for military geographic information. 16 p2016 A73-33365
- Remote sensing techniques for support of coastal zone resource management. 18 p2306 A73-36020
- Validation of digital radar landmass simulation utilizing terrain elevation data comparison. 18 p2292 A73-36842
- Martian lowland terrains fretted and chaotic characteristics, hypothesizing evolutionary processes based on escarpment recession, subsurface ground ice and magma collapse 19 p2477 A73-37205
- Variable features on Mars. II - Mariner 9 global results. 19 p2478 A73-37212
- Martian south polar region pitted and etched terrain features, interpreting surface layered blanketing material as due to wind action 19 p2478 A73-37215
- Nature and origin of layered deposits of the Martian polar regions. 19 p2478 A73-37216
- Airborne and spaceborne microwave imaging techniques for earth surface surveys, discussing resolution capabilities and applications for side-looking radar, microwave radiometers and scatterometers [AAS PAPER 73-111] 20 p2533 A73-38577
- Surface microwave emissivities dependence on humidity, vegetation cover and surface structure, considering water influence on sand emissivity 20 p2556 A73-39839
- Utilizing remote sensing data for land use decisions for Indian lands in South Dakota. 20 p2557 A73-39850
- Radiometric terrain mapping at 3 mm wavelength. 20 p2568 A73-39870
- Automatic terrain mapping by texture recognition. 20 p2568 A73-39873
- Ultraviolet, panchromatic, infrared and radar remote sensing of Mesabi Range /Minnesota/, discussing Precambrian rock formations, geological faults, predawn and daytime photography and vegetation patterns 20 p2561 A73-39894
- Small scale Gemini photographs of Indian regions for interpretation of tonal variations, geomorphologic, geologic and structural features and drainage patterns 20 p2561 A73-39898
- Multispectral scanner imagery in aerial photography of plant communities, discussing reflectance effects, digital processing, vegetation types, classification errors and spectrum analysis 20 p2561 A73-39901
- The use of near-infrared photography in the analysis of surface morphology of an Argentine alluvial floodplain. 22 p2850 A73-42728
- The precision of contour lines and contour intervals of large- and medium-scale maps. 23 p2979 A73-44123
- TERRESTRIAL DUST BELT**
- Mesospheric cosmic dust concentration measurements from particle collection rocket flights, discussing interference from uplifted aerosols of terrestrial or cosmic origin 02 p0215 A73-12259
- Optical sounding methods for the upper atmosphere and the earth's dust cloud 07 p0817 A73-19584
- Qualitative detection of space dust particle layers in the lower thermosphere by the twilight method 07 p0817 A73-19586
- TERRESTRIAL MAGNETISM**
- U GEOMAGNETISM**
- TERRESTRIAL RADIATION**
- The effects of aerosols on the outgoing terrestrial radiation. 01 p0072 A73-10357
- The global distribution of outgoing long-wave radiation derived from SIRS radiance measurements. 01 p0038 A73-10391
- Calculation of averaged values for short- and long-wave fluxes and influxes in a real atmosphere 05 p0593 A73-16243
- Measurement of short- and longwave radiant fluxes from the Kosmos-320 satellite. 08 p0961 A73-21586
- Radio Astronomy Explorer /RAE/. I - Observations of terrestrial radio noise. 11 p1356 A73-25920
- Stratospheric aerosol properties and their effects on infrared radiation. 11 p1357 A73-26344
- Radiative properties of terrestrial clouds at visible and infra-red thermal window wavelengths. 13 p1652 A73-28274
- Radiation temperatures of the earth's blankets in the microwave and infrared ranges according to experiment data on the Cosmos-384 artificial earth satellite 13 p1609 A73-29154
- Earth radiation pressure and the determination of density from atmospheric drag. 18 p2308 A73-36051
- Density of the radiation of the earth/atmosphere system into space 18 p2309 A73-36112
- Effect of cloud cover on the variability of outgoing radiation. 18 p2314 A73-37069
- Remote sensing of terrestrial resources 19 p2426 A73-38176
- Equipment for checking of terrestrial resources 19 p2431 A73-38177
- The radiation balance of the earth's surface and inclinations of isodioptric surfaces 19 p2428 A73-38556
- Spatial distribution of outgoing long wave radiation fluxes according to Cosmos-320 satellite data 20 p2555 A73-39188
- Use of space techniques for the determination and monitoring of climate parameters and air contaminants 23 p3003 A73-43780
- Tropospheric vertical energy transfer due to terrestrial and atmospheric water vapor and carbon dioxide radiation calculated for vertical atmospheric temperature and composition distributions 24 p3082 A73-44736
- TESSERAL HARMONICS**
- Synchronous satellite ground track drift analysis for ecological survey application, discussing zonal, tesseral and sectorial harmonics and perturbation compensation 03 p0370 A73-13150
- Venus gravity anomalies and physical properties arising from convection currents and topography deduced from geodetic aspects derived from mass, radius and surface temperature 04 p0496 A73-14812
- Satellite motion near the equatorial plane of a slowly rotating planet 05 p0617 A73-16468
- Effects of resonant tesseral gravity coefficients on Viking-type orbits. 06 p0748 A73-17648
- [AIAA PAPER 73-146]
- Literary theory of the motion of a satellite in the tesseral-harmonic field of the earth's gravitational potential at small eccentricities 09 p1143 A73-22097
- TEST BEDS**
- U TEST EQUIPMENT**
- TEST CHAMBERS**
- NT ANECHOIC CHAMBERS**
- NT HYPERBARIC CHAMBERS**
- NT PRESSURE CHAMBERS**
- NT VACUUM CHAMBERS**
- Test chamber for on board moving parts in ultrahigh vacuum. 01 p0030 A73-11148
- A device for working with extraterrestrial material in an inert-gas medium 02 p0151 A73-12465
- Two chamber adiabatic test compression system design with controlled throttle for high temperature nitrogen- and nitrous oxide-type gases with exothermal reactions 06 p0683 A73-17413
- Testing assembly for sheet metals and welded joints under static and low-cycle biaxial tension under low temperature conditions 15 p1855 A73-31147
- An apparatus for work with extraterrestrial water in an inert gas atmosphere. 15 p1859 A73-32615

TEST EQUIPMENT

- A closed-loop automatic control system for high-intensity acoustic test systems. 16 p1994 A73-33147
- Climate simulation via environmental test chambers examining mechanical, thermal and pressure effects to determine functional component suitability 16 p1997 A73-33382
- Design and construction of a reverberation chamber for high-intensity acoustic testing. 16 p1998 A73-33677
- Parametric test results of a swirl-can combustor. 17 p2222 A73-35471
- Wideband VHF whip antenna impedance simulation using Al cylindrical chamber to simplify impedance-controlling network tuning and power testing 17 p2148 A73-35705
- A monkey metabolism pod for space-flight weightlessness studies. 18 p2270 A73-35963

TEST EQUIPMENT

- Device for measuring the instantaneous value of current and voltage in the operation of a pulsed plasma accelerator 02 p0196 A73-11792
- Apparatus for testing reinforced plastics during nonuniform heating, with due allowance for the gas permeability of the material. 02 p0150 A73-12143
- Electron beam heating test arrangement for high temperature testing of refractory materials in vacuum, describing temperature control systems 02 p0150 A73-12220
- Effects of test capability on system reliability and availability. 03 p0313 A73-13736
- High speed testing of materials mechanical behavior over range of impact loading rates 03 p0394 A73-14023
- Experiments on the stability of various water-lubricated fixed geometry hydrodynamic journal bearings at zero load. 03 p0315 A73-14350
- [ASME PAPER 72-LUB-46] Digitized radar experiments project for data acquisition and processing and weather forecasting techniques development, describing test bed configuration, equipment and operation 03 p0288 A73-14515
- Some results using the ultrasonic goniometer - The corner reflector method. 04 p0447 A73-14930
- A new measurement device for measuring harmonic forces 06 p0695 A73-18434
- Friction in ultrahigh vacuum, discussing test program definition and testing machine design taking into account space environment effects 07 p0829 A73-18907
- Circuit design, manufacture and testing of static memory for D2 satellite computer, considering test equipment, quality control and fabrication 07 p0796 A73-18958
- Transistor tester circuit design with mutually independent collector-emitter voltage, collector current, generator and load resistance adjustment for arbitrary operating point selection 07 p0803 A73-20303
- Fluidics test methods and instrumentation. [SAE ARP 1254] 08 p0928 A73-20695
- Use of open-structure channel electron multipliers in sounding rocket experiments. 09 p1080 A73-22105
- Arava STOL turboprop passenger aircraft flutter flight test program, describing measurement instrumentation and data recording system 09 p1031 A73-22185
- Equipment for highly accurate and repeatable strain gauge factor determination. 10 p1220 A73-24574
- Solid body contact interaction devices at high temperatures in vacuum, gas and air for evaluation of surface coatings, adhesion, diffusion, mechanical properties, etc 10 p1222 A73-24966
- Test rails possibilities for rain erosion phenomena study on aircraft or missile structures 11 p1335 A73-25296
- Development of propellant loading systems and checkout systems for the TD-1A and AEROS satellite projects 11 p1430 A73-25354
- Solar cell battery operational performance test equipment and computerized simulation programs for post-1975 satellite and space station systems integration and design 11 p1309 A73-25986
- Optical fiber breaking stress distributions obtained by a cantilever method. 11 p1344 A73-26312
- An experimental method for determining the characteristics of ablative materials 12 p1557 A73-27068
- A modern mechanical laboratory for the support of aircraft engine design 12 p1486 A73-27385

Machine for measuring hardness and microhardness at high temperatures. 13 p1613 A73-28524

Testing machine with control panel and vacuum chamber for microhardness measurement at high temperatures with precise test point selection and indentation observation capability 13 p1613 A73-28525

Test equipment for thermal stability determination of brittle refractory material, noting data processing procedure and formulas for temperature distribution and thermal stress 13 p1599 A73-29629

High frequency model U-20P fatigue testing unit with program control of the specimen vibration amplitude. 13 p1599 A73-29637

Tape recorder instrumentation for structural dynamic load test data analysis, discussing cable crosstalk, lead length and electrical noise effects in crack propagation measurements 14 p1751 A73-29775

Digital circuits test equipment functional principles, considering time, instantaneous voltage and pulse height measurements 14 p1731 A73-29873

Test assembly for structural component members under different climatic conditions 14 p1743 A73-30689

Testing machine to determine perforated plate biaxial tension creep rupture strength and fatigue life at high temperature 15 p1858 A73-31617

Setting of sensitivity of ultrasonic equipment for weld inspection. 15 p1882 A73-32025

The most important characteristics of magnetizing equipment in the leakage-flux technique - Their measurement and application 15 p1882 A73-32054

Standard Hydraulic Impulse Machine design for testing hose assemblies, tubing, coils and fittings, including circuit diagrams and component identifications [SAE AIR 1228] 16 p1970 A73-33018

MIL-STD-810 uniform test methods for determining military equipment environmental resistance, discussing inadequacies, misapplications and planned revision for improvement 16 p2087 A73-33144

Experimental evaluation of the strength of elements of thin-walled pressure vessels during severe cooling 17 p2177 A73-34331

Solid state Digital Slip Sync Strobe/Camera Control System design for powered wind tunnel helicopter models testing 17 p2101 A73-34622

JFTOT - A new fuel thermal stability test [A summary of a Coordinating Research Council activity]. [SAE PAPER 730385] 17 p2147 A73-34722

An automatic flash photomicrographic system for fatigue crack initiation studies. 18 p2316 A73-36588

Cyclic inelastic deformation and the fatigue notch factor. 18 p2364 A73-36590

Method of measuring the size of defects without using calibrating standards and adjusting the sensitivity of ultrasonic defectoscopes. 19 p2432 A73-38358

Method of holography in nondestructive testing. 19 p2432 A73-38359

Performance test equipment of Transit generator with lightweight Isotec thermoelectric panels 19 p2455 A73-38395

Digital control of a pneumatic isolation system for inertial instrument testing. [AIAA PAPER 73-830] 20 p2543 A73-38775

Apparatus for creep and long-term strength testing of materials in aggressive media under irradiation 20 p2544 A73-39368

The characteristics of hydraulic tensile-test machines of the pendulum type and their effect on the tensile test 20 p2545 A73-39629

Equipment for measuring cross-modulation distortions in high-frequency power transistors 21 p2660 A73-40014

Inexpensive portable vibration-insensitive wave front shearing interferometer developed at NBS for lens testing 21 p2704 A73-41259

Interferometric test of an f/8, 24-inch /60.96 cm/ diameter paraboloidal mirror in the atmosphere. 21 p2704 A73-41260

Procedure and device for the study of the behavior of metals subjected to dynamic torsional stresses 22 p2868 A73-43171

Pulse generator for testing and measurement, describing pulse frequency, duration and sequence capacity, digital design and normal and alarm sequences 23 p2955 A73-44150

TEST FACILITIES

NT ANECHOIC CHAMBERS

NT BALLISTIC RANGES

NT BLOWDOWN WIND TUNNELS

NT CASCADE WIND TUNNELS

NT ENGINE TESTING LABORATORIES

NT ENVIRONMENTAL LABORATORIES

NT HOTSHOT WIND TUNNELS

NT HYPERSONIC WIND TUNNELS

NT HYPERVELOCITY WIND TUNNELS

NT LOW DENSITY WIND TUNNELS

NT LOW SPEED WIND TUNNELS

NT MISSILE RANGES

NT PLASMA JET WIND TUNNELS

NT RECTANGULAR WIND TUNNELS

NT ROCKET TEST FACILITIES

NT SHOCK TUNNELS

NT SLOTTED WIND TUNNELS

NT SUBSONIC WIND TUNNELS

NT SUPERSONIC WIND TUNNELS

NT TEST RANGES

NT TEST STANDS

NT TRANSONIC WIND TUNNELS

NT WIND TUNNELS

Dual sensitivity liquid penetrants for improving NDT inspection of minute defects in military aircraft structures during rework and repair, noting comparative advantages 02 p0173 A73-11984

Test facility for determination of S-3A aircraft landing gear behavior during critical pulse loads while rolling over carrier deck, discussing moving platform components 02 p0150 A73-11999

A fundamental method for evaluating the contaminant tolerance of fluid power control valves. 02 p0132 A73-12000

An altitude test facility for large turbofan engines. [AIAA PAPER 72-1069] 03 p0287 A73-13399

Tubular materials plane stress-strain test facility for combined axial load and internal pressure effects 03 p0288 A73-14023

Resonance type facility using dynamic hysteresis loop method to test metal fatigue and anelasticity in torsion at room and high temperatures 03 p0288 A73-14023

Tutorial lecture notes for experimental modelling in testing. 04 p0452 A73-14710

Cs ion bombardment engines for communications satellites stationkeeping and attitude control, noting mission life and test facilities 04 p0488 A73-15710

Design and development of a high pressure facility for droplet combustion experiments. 05 p0562 A73-16440

Experimental studies of a Ludwig tube high Reynolds number transonic tunnel. [AIAA PAPER 73-212] 06 p0645 A73-17660

Anechoic funnel and rectangular chambers for antenna measurements 06 p0674 A73-17820

Facility for roller bearing parameters testing during high speed rotation in ultrahigh vacuum, discussing circuitry and principal elements 07 p0807 A73-18900

Vibration, radiation and thermal vacuum test procedures and facilities for evaluating spacecraft reliability during launching and in space environment. 07 p0807 A73-18996

Rocket sled facility for impact tests with friable balloon platforms, describing braking and accelerating configurations, vibration damping measures and telemetry system 07 p0808 A73-19000

Facility for studying the strength and rigidity of circular plates prepared from an anisotropic material 07 p0809 A73-20510

Vibration test facilities and control techniques for application to industrial products, discussing shakers, signal generation and amplification, and data recording and reduction 07 p0809 A73-20570

Photo-optic instrumentation of magnetic flyer plate facility for pressure-time response measurement of impact loaded test specimens, using streak and high speed framing cameras 09 p1083 A73-22510

Application of Range Commanders Council Document 118-71 test methods to range management at SAMTEC. 09 p1057 A73-23400

Varying-temperature test installation for the interior design of the Concorde 11 p1342 A73-25100

Russian book on thermal stability of refractory ceramics covering strength and thermophysical characteristics, high temperature thermal fracture and facilities for normal and cyclic load tests 11 p1386 A73-25120

Low temperature vacuum fatigue testing facility for materials testing under space environment conditions 11 p1343 A73-25440

The design of components for an advanced Rankine cycle test facility. 11 p1344 A73-25990

- Long term temperature control and calibration system for creep testing facility temperature drift monitoring and correction 13 p1597 A73-28841
- Biaxial tensile test facility for three dimensional characterization of nonlinear viscoelastic materials based on variable ratio principal strains in plane stress 13 p1598 A73-29309
- Impact body or medium damage prediction and modification technology, discussing test facilities and applications 13 p1699 A73-29310
- An airdrop system for testing large parachutes for recovery of loads in excess of 50,000 lb. [AIAA PAPER 73-471] 15 p1828 A73-31455
- Water towing tank facility for studies of boundary layers, aircraft ground effects, wakes and unsteady and stratified fluid flows 15 p1858 A73-32041
- The shock wind tunnel of the Institute of Aerodynamics and Gasdynamics of Stuttgart University 15 p1858 A73-32042
- Objectives and employment of the integration and system test equipment for Aeros 15 p1943 A73-32180
- Monograph - Development of hotshot wind tunnels for hypersonic aerodynamic studies. 15 p1859 A73-32595
- Subway system vertical tunnel simulation facility including plenum assembly, instrumentation, model uncher, subway car simulation models, tube scaffolding and data acquisition 16 p1994 A73-33148
- Problems and methods of simulating the environment; Annual Meeting, Karlsruhe, West Germany, September 27-29, 1972, Reports 16 p1997 A73-33376
- Missile and explosive environmental tests for mechanical properties, outlining test facilities, climatological effects, salt spray, vibration, shock, dropping, vacuum effects and crack propagation 16 p1997 A73-33387
- Influence of acceleration on the combustion of solid propellants - Measurement and prediction of the effects 16 p2045 A73-33391
- The pressure-shock simulation of the Ernst-Mach-Institute in the test location Wintersweiler 16 p1998 A73-33395
- Wind tunnel acoustic and vibration test facilities, including anechoic chambers, subsonic boundary layer tunnels, acoustic ducts, reverberation rooms, and rotor noise chambers 17 p2148 A73-35334
- Book - Experimental methods of hypersonics. 17 p2097 A73-35338
- Fracture mechanics testing systems, discussing closed loop assembly, programming, readout and failure units and fully automated computer-controlled technique 17 p2175 A73-35672
- Device for studying the strength and rigidity of bond plates of anisotropic material. 19 p2418 A73-37793
- Building a dynamic test complex near an inertial test facility and general test pad considerations. [AIAA PAPER 73-827] 20 p2543 A73-38772
- A real-time six-degree-of-freedom hybrid simulation facility for guidance system testing. [AIAA PAPER 73-876] 20 p2543 A73-38813
- SAM-D guidance system simulator for design verification, preflight checkout and performance demonstration based on real time digital communication between missile computer and simulator hybrid computer [AIAA PAPER 73-877] 20 p2587 A73-38814
- Closed loop preflight qualification testing of a military vehicle roll rate control system. [AIAA PAPER 73-878] 20 p2587 A73-38815
- A high-performance test facility for laboratory simulation of the Large Space Telescope orbiting vehicle in a single-degree-of-freedom mode of rotation. [AIAA PAPER 73-884] 20 p2544 A73-38820
- An aerodynamic test facility with free molecular flow and high stagnation temperature 20 p2545 A73-39615
- FFTF probe-type eddy-current flowmeter - Wet versus dry performance evaluation in sodium. 21 p2738 A73-40768
- NBS radiometric calibration services extended to UV spectrum with dc high power hydrogen wall stabilized arc as primary standard of spectral radiance 21 p2703 A73-41256
- Test facilities for B-1 components prior to construction and flight testing, discussing wind tunnel tests for aerodynamic characteristics, stall performance, drag factor and spin 21 p2675 A73-41431
- Electromagnetic compatibility specifications for aircraft communication and electronic equipment, discussing control and test plans, test facilities, cost effectiveness and British standard 22 p2821 A73-41696
- Electromagnetic radiation hazard test facility, instrumentation, and weapon system susceptibility evaluation for providing environment protection and military standards 22 p2822 A73-41791
- A magnetogasdynamics accelerometer for the simulation of micrometeoroids 23 p2966 A73-43781
- Society of Flight Test Engineers, National Symposium, 3rd, Arlington, Tex., September 11-14, 1972, Proceedings. 23 p3050 A73-44052
- Flight test programs management and control, considering weapon systems performance tests relative to contractual requirements, personnel allocation and supporting facilities 23 p3051 A73-44060
- NAFEC test facilities. 23 p2966 A73-44063
- The capabilities of army test facilities. 23 p2966 A73-44064
- The capabilities of government test facilities at the Air Force Systems Command. 23 p2966 A73-44065
- Naval test and evaluation capabilities for aircraft, emphasizing organizational relationships 23 p3051 A73-44066
- Some results from tests in the NAE high Reynolds number two-dimensional test facility on shockless and other airfoils. 24 p3054 A73-44995
- Analysis of the process of combustion of a single dose of liquid fuel in a constant-volume chamber 24 p3158 A73-45384
- TEST FIRING**
- NT STATIC FIRING
- Filament wound boron/epoxy rocket motor chamber fabrication and hydroproof, burst and firing tests, including failure and deformation evaluation 03 p0331 A73-13024
- Hypergol rocket engines restart difficulties investigation via cold flow and hot firing tests, simulating worst case environmental conditions [AIAA PAPER 72-1160] 03 p0357 A73-13461
- Data quality assurance in a shipboard computer-controlled telemetry system. 09 p1057 A73-23410
- TEST METHODS**
- U TESTS
- TEST PILOTS**
- Psychiatric and psychometric predictability of test pilot school performance. 03 p0269 A73-14165
- 1972 report to the aerospace profession; Proceedings of the Sixteenth Symposium, Beverly Hills, Calif., September 28-30, 1972. 09 p1030 A73-22176
- Test pilots role in aircraft flying qualities evaluation, discussing spin and longitudinal stability testing 09 p1031 A73-22181
- The role of the test pilot in evaluating auto landing systems. I. 09 p1115 A73-22182
- The role of the test pilot in evaluating auto landing systems. II. 09 p1115 A73-22183
- TEST PROGRAMS**
- U TESTS
- TEST RANGES**
- NT BALLISTIC RANGES
- NT MISSILE RANGES
- Survey improvement and calibration analysis for the Air Force Eastern Test Range with Geos C. 04 p0437 A73-14786
- TEST STANDS**
- Application of the VEDS-200A electrodynamic vibrator to fatigue tests in symmetric tension and compression 01 p0029 A73-10492
- Some methodological questions concerning the simulation of turbine blade operation on gasdynamic stands 07 p0809 A73-20509
- The use of a type VEDS-200A vibrostand for fatigue tests under conditions of symmetrical tension-compression. 14 p1743 A73-30317
- On some problems of the method of simulating the working conditions of turbine blades on gas-dynamic benches. 19 p2418 A73-37784
- A gasdynamic test stand and its use in studying sprayer nozzles for spraying metallic solutions. I 24 p3075 A73-44742
- TEST VEHICLES**
- NT FLIGHT TEST VEHICLES
- Possibility of utilizing the ERIDAN rocket probe as an experimental vehicle 16 p2071 A73-32817
- Manned and unmanned aerospace launch vehicle liquid and solid rocket propulsion system effectiveness survey questionnaire response data concerning various tests 21 p2781 A73-41202
- Planetary Atmosphere Experiments Test vehicle reentry into earth atmosphere for flight experience, discussing onboard instrumentation 24 p3088 A73-44440
- TESTERS**
- U TEST EQUIPMENT
- TESTES**
- Regulation of testis function in golden hamsters - A circadian clock measures photoperiodic time. 02 p0134 A73-12422
- Morphological changes in the testicles of dogs exposed to chronic and combined gamma-radiation 08 p0929 A73-20981
- TESTING MACHINES**
- U TEST EQUIPMENT
- TESTING TIME**
- Gas turbine engine hot part equivalent accelerated tests duration determination by analytical method based on Larson-Miller parametric description of long term strength 02 p0236 A73-12216
- Thermoelectric panel array of hybrid thermocouples with p-type Si-Ge encapsulated PbTe/Si-Ge n-legs, presenting performance test results as function of test time 09 p1134 A73-22766
- Truncated sequential life tests for a 3-way decision procedure. 15 p1883 A73-32260
- Strength and plasticity of tantalum in rapid tests 17 p2188 A73-34561
- Antenna radiation pattern recording as functions of two simultaneous parameters, considering measurement time savings 17 p2129 A73-35699
- Thermal conductivity measurement for particulate materials in vacuum, comparing line and differential-line source methods in terms of test and data reduction times 20 p2565 A73-38882
- TESTS**
- NT SALT SPRAY TESTS
- Book - The role of testing in achieving aerospace systems effectiveness. 21 p2675 A73-41201
- NASA program manned and unmanned spacecraft system effectiveness survey questionnaire response data concerning various tests 21 p2781 A73-41203
- TETHERED BALLOONS**
- The measurement of atmospheric turbulence from a captive balloon. 04 p0473 A73-15698
- Instrument suspended from tethered balloon for oceanic measurement of average lower atmosphere vertical electric field profile 05 p0579 A73-17251
- TETHERING**
- Investigation of the dynamics of a rotation scheme of a spacecraft composed of two units 10 p1286 A73-23877
- Theoretical and practical aspects of an automatic hover control system for an unmanned tethered rotor-platform. 10 p1175 A73-24009
- Experimental autostabilized tethered rotor platform for reconnaissance, communications and ECM, discussing control system effectiveness from flight test results 16 p1969 A73-33736
- Dynamics of a twisting mode for a two-section space vehicle. 20 p2614 A73-38896
- A study of planar deployment control and libration damping of a tethered orbiting interferometer satellite. 21 p2781 A73-40900
- TETHERLINES**
- Dynamics of an astronaut's movement on a tether towards a spacecraft and a spacecraft control concept based on the variable-structure systems theory 05 p0628 A73-16411
- TETRAD THEORY**
- Relativistic MHD formulation in terms of non-holonomic tetrad field for rotating plasma coupled to frozen-in magnetic field, noting Alfvén waves propagation velocity 09 p1131 A73-22921
- TETRAFLUOROHYDRAZINE**
- Mass spectrometric studies of tetrafluorohydrazine and the difluoroamino radical. 08 p0936 A73-21173
- TETRAHEDRONS**
- Tetrahedral Mylar plastic balloon drag coefficient measurement as function of Reynolds numbers from experimental free flight test data 23 p3004 A73-44263
- TETRODES**
- Superposition method for potential distribution in plane tetrode field with unipotential and bipotential grids, noting electro-optical effect in cylindrical lenses 13 p1591 A73-28667
- TEXAS**
- Regional land inventory systems development in the Houston area. 20 p2629 A73-39832

TEXTILES

TEXTILES

NT RAYON

Composite materials of today and tomorrow: New materials and conventional industries; International Conference, 1st, Lyons, France, September 22-24, 1971, Proceedings

03 p0334 A73-13579

Stockings, extensible plane structures and three dimensional textile fiber blocks reinforced materials, noting application to structures of revolution under external pressure

03 p0334 A73-13585

Application of simultaneous DTA/TGA and DTA/MS analysis for predicting the flammability of composite textile fabrics and polymers.

09 p1110 A73-22515

Processing aerospace textiles into fabric composite reinforcements 'The weaver's viewpoint.'

16 p2018 A73-33065

Flame resistant and nonflammable textile fibers.

17 p2198 A73-35839

TEXTURES

Textures of deformation and of primary and secondary recrystallization in high-purity nickel

01 p0064 A73-10614

Dependence of the deformability of the Kh17-chromium steel on texture

03 p0326 A73-13827

Secondary maximum grain size and even-grained texture in the region of low and moderate deformations during recrystallization of certain nickel- and iron-based alloys

03 p0326 A73-13967

Mineralogy and texture of Haverd ureilite, noting preterrestrial shock evidence, recrystallized olivine and metal grain, and graphite conversion into diamonds from petrographic observation

09 p1140 A73-21870

Characteristics of elastic anisotropy and the textural development of sheet titanium

09 p1099 A73-21968

Texture and anisotropy of the thermal cmf of sheet titanium

09 p1099 A73-21969

Characteristics of deformation texture development in austenitic steel in a plane stressed state

17 p2188 A73-34564

A comparison of the Ponzo illusion with a textural analogue.

21 p2639 A73-41180

Drop forged Ti alpha-beta alloy textures after heat treatment, quenching, aging and surface machining

22 p2866 A73-42089

TF-30 ENGINE

TF-30-P1 engine mixed flow augmentor test for combustion instability under operation with abnormal fuel zone combination, comparing with predicted pressure oscillations from model

03 p0358 A73-13489

TF-34 ENGINE

TF-34 turbofan engines for S-3A and AX aircraft respectively, discussing technological development, and components and characteristic features

07 p0868 A73-20350

TFX AIRCRAFT

U F-111 AIRCRAFT

THALAMUS

Polysensory responses and sensory interaction in pulvinar and related postero-lateral thalamic nuclei in cat.

09 p1040 A73-22696

Examination of responses evoked in the sensory cortex by thalamic stimulation.

10 p1178 A73-23772

Intranuclear organization of the center median nucleus of the thalamus.

13 p1576 A73-29175

Role of specific and nonspecific thalamic nuclei in the genesis of certain slow rhythms on the human electrocorticogram

19 p2395 A73-37939

Two visual systems in the frog.

21 p2640 A73-41302

Effect of the stimulation of nonspecific thalamic nuclei on spontaneous and evoked spindles in the auditory cortex

22 p2802 A73-41958

Anatomic and functional organization of the ventral anterior and reticular nuclei of the thalamus

24 p3059 A73-44675

THALLIUM

NT THALLIUM COMPOUNDS

NT THALLIUM ISOTOPES

Umbra spectra absorption line feature observation by photoelectric spectroscopy, suggesting TI abundance in solar atmosphere

03 p0378 A73-14423

Polymorphous transformation mechanism in thallium

06 p0735 A73-18045

Experimental investigation of the excitation functions of thallium atoms

09 p1121 A73-21952

THALLIUM COMPOUNDS

Electrophysical parameters of TlSbSe2 thin films

10 p1260 A73-24471

THALLIUM ISOTOPES

Thallium isotope analysis of terrestrial chondrites and achondrite and lunar soil, noting lunar chronology information from lead isotope extinct radioactivity

03 p0375 A73-14109

THAWING

U MELTING

THEMATIC MAPPING

Cartographic applications of high-altitude aircraft photographs.

16 p2016 A73-33362

A study of the statistical patterns of visual perception of a black and white raster image

21 p2644 A73-40861

THEODOLITES

NT CINETHEODOLITES

Design and field tests of astronomical optical theodolite, noting latitude, longitude and azimuth determination and objective aberration

04 p0447 A73-14849

THEOREM PROVING

Reasoning by analogy as an aid to heuristic theorem proving.

01 p0020 A73-11453

THEOREMS

NT BAYES THEOREM

NT BERNULLI THEOREM

NT CASTIGLIANO VARIATIONAL THEOREM

NT EXISTENCE THEOREMS

NT FLOUQUET THEOREM

NT LAGRANGE SIMILARITY HYPOTHESIS

NT LEBESGUE THEOREM

NT LIOUVILLE THEOREM

NT MICHELL THEOREM

NT POYNTING THEOREM

NT RECIPROCAL THEOREMS

NT SIMILARITY THEOREM

NT STOKES THEOREM [VECTOR CALCULUS]

NT UNIQUENESS THEOREM

Theorems on general fluid particle vorticity acquisition by nonanalytic process

03 p0292 A73-13309

Theorems on periodic noncritical approximate solutions of nonlinear oscillations differential equations

04 p0469 A73-14667

Tree-manipulating systems and Church-Rosser theorems.

08 p0941 A73-20962

THEORETICAL PHYSICS

NT NEWTON THEORY

NT QUANTUM THEORY

Gravitational waves astrophysical nature and origin, discussing current theories and possible applications in astronomy

01 p0094 A73-10063

Automation of solutions to mathematical physics problems described by partial differential equations

01 p0019 A73-10100

Book - Astrometry - Theoretical astrophysics instrumentation - Spectroscopy - Galactic structure - Galaxies.

01 p0095 A73-10293

Classical mechanics and field theory derivation based on material points motion in space, discussing space-time metric, electromagnetic and gravitational fields and quantum mechanics

01 p0076 A73-10599

A simple illustration of the principle of correspondence in quantum mechanics

02 p0193 A73-12542

Design of a space probe for the experimental investigation of Einstein's theory of gravitation

03 p0381 A73-13296

Conformally invariant cosmological and physical models in terms of Einstein, Maxwell and Dirac equations

08 p1009 A73-21228

Coleman-Noll concept of rational thermodynamic theory, discussing homogeneous and inhomogeneous fading memory systems and logical structures

10 p1296 A73-24690

Russian papers on mathematical physics boundary value problems covering electrodynamics, electromagnetic fields in conducting channels and ferromagnetic cylinders, heat transfer, shell theory, etc

12 p1525 A73-27803

Cosmological theories historical review, discussing observational background for big bang, steady state and astrophysical theories based on theoretical physics

14 p1797 A73-30059

Relationship of theoretical physics to molecular biology, considering synthesis, ontogenesis, phylogenesis, evolution models, thermodynamic applications and Eugen prebiological evolution theory

15 p1835 A73-31823

Book - Atomic physics and astrophysics, Volume 2.

18 p2356 A73-36969

The Cauchy problem and some basic problems of mathematical physics about parabolic systems with discontinuous coefficients

20 p2582 A73-39252

Relation between the fundamental solutions in cylindrical and spherical coordinates /with identical

03 p0396 A73-13111

coordinate origins/ for certain equations of mathematical physics

21 p2753 A73-41011

THERAPY

NT CHEMOTHERAPY

NT RADIATION THERAPY

Possibilities of barotherapy in ophthalmology

21 p2637 A73-40861

Hemotherapy of coagulation system disturbances: hepatolienal origin

23 p2947 A73-44231

THERMAL ABSORPTION

NT POLAR CAP ABSORPTION

Assessment of temperature rise suppression by eddy losses during irradiation.

09 p1045 A73-22515

Thermal analysis of thin-film micromachining wafers.

15 p1882 A73-31941

Kinetics of gas absorption by refractory metals in dissociated environments - The nitrogen/tantalum system.

22 p2879 A73-42521

THERMAL ACCOMMODATION COEFFICIENTS

U ACCOMMODATION COEFFICIENT

THERMAL AGITATION

U THERMAL ENERGY

THERMAL BLOOMING

Thermal defocusing of high intensity continuous wave laser radiation in absorbing medium with allowance for spherical aberrations

04 p0458 A73-15555

Change in sign of thermal lens of glass laser rods with change in thermo-optical constant of glass.

06 p0703 A73-18621

Numerical solutions to wave and hydrodynamic equations for thermal blooming of pulsed focused Gaussian laser beams in heated gas medium

08 p0974 A73-21041

Influence of thermo-optical distortions on the emission spectrum of a rhodamine 6G laser with incoherent pumping

09 p1096 A73-22991

Theory of thermally-induced interference and lensing in transparent materials.

12 p1523 A73-26801

Absorption saturation effects on high-power CO₂ laser beam transmission.

13 p1628 A73-29391

Thermal blooming of pulsed laser radiation.

17 p2184 A73-34611

IR laser induced change in atmospheric temperature as function of time, using kinetic model with intermolecular energy transfer rates for thermal blooming

17 p2163 A73-35401

Atmospheric turbulence effects on CW carbon dioxide laser propagation, investigating thermal blooming via theoretical diffusion model and experiment

19 p2437 A73-37211

Thermal lensing of laser beams in optically transmitting materials. I.

19 p2438 A73-38011

Intensity limitation and energy spreading in an optical field under transient thermal defocusing conditions.

20 p2574 A73-39011

Coherent oscillation modes of optical waveguide resonators, noting selectivity and thermooptic insensitivity to pumping and active medium deformation

20 p2574 A73-39011

Thermal defocusing avoidance by short pulse duration reduction to permit IR laser window operation before temperature rise, considering changes in index of refraction

21 p2710 A73-40101

Emission of aqueous solutions of rhodamine 6G with detergent additives in the presence of flash lamp excitation

21 p2711 A73-40311

GaAs two-photon absorption coefficient obtained from transmission measurements with Q switched Nd:YAG laser, noting thermal self focusing

21 p2713 A73-40411

Thermal lensing of laser beams in optically transmitting materials. II - Numerical computations.

22 p2870 A73-42521

THERMAL BOUNDARY LAYER

Transient variation of martian ground-atmospheric thermal boundary layer structure.

01 p0097 A73-10411

A boundary value problem for a system of temperature boundary layer equations

01 p0123 A73-11411

Study of the natural convection between two parallel vertical plates parallel and isothermal

02 p0238 A73-12211

Isothermal vertical plate turbulent thermal boundary layer during free convection, noting temperature pulsations dispersion

03 p0396 A73-13111

Calculation of metric coefficients for streamlines coordinates.

03 p0247 A73-14111

Solution of the general heat-transfer problem for flow past cylindrical bodies by the Tolubinskii integral method.

06 p0766 A73-17407

Calculation of the thermal fluxes and the temperatures of the surfaces of a plate with heat transfer between fluids flowing around the plate.

06 p0766 A73-17408

Solutions of thermal boundary layer equations when temperature gradient at the moving flat plate in parabolic flow is prescribed.

06 p0769 A73-18251

Thermal boundary layer thickness for laminar forced convection to flat plates with uniform heating and uniform wall temperature.

06 p0769 A73-18260

Effect of plasma inhomogeneity on the spectral-line profile and the reversal temperature

09 p1129 A73-22662

Approximate calculation of a thermal boundary layer at a flat plate with allowance for a magnetic field

09 p1167 A73-22859

Boundary-value problem for a system of equations with a temperature boundary layer.

11 p1452 A73-26055

Influence function of a nonheated region and the relationship between the method of superposition and the method of expanding solutions in series of form parameters

12 p1558 A73-27312

Investigations regarding the heat exchange integral in turbulent incompressible flows

16 p2085 A73-33256

Recent progress in boundary layer research.

19 p2419 A73-37451

Unsteady thermal boundary-layer on an infinite yawed wedge whose temperature gradient is prescribed.

19 p2377 A73-37575

Global stability of time-dependent flows - Impulsively heated or cooled fluid layers.

21 p2790 A73-40249

Large scale heat transfer in turbulent boundary layer at heated flat plate in incompressible viscous fluid, discussing temperature fluctuation spatial correlation as function of wall law and flow core

21 p2678 A73-41062

Nonisothermal surface cooling for arbitrary temperature distribution and Prandtl number approaching zero, solving thermal boundary layer equations by series expansion

21 p2792 A73-41323

Thermal response of an unsteady laminar boundary layer on a flat plate due to step changes in wall temperature and in wall heat flux.

23 p3049 A73-43802

Dynamic and temperature boundary layers of a submerged jet of viscous fluid spreading over the bottom

24 p3080 A73-45503

HERMAL BUCKLING

Coupled thermoelastic stability effect on critical thermal buckling of strip under compression in temperature field

06 p0765 A73-18686

Reducing the thermal bending of a gravity-gradient stabilizer with the aid of a protective covering

10 p1286 A73-23894

Reduction of thermal deflection of gravitational stabilizer using shielding cover.

20 p2614 A73-38913

Acoustic fatigue resistance of aircraft structures at elevated temperatures.

24 p3056 A73-44829

HERMAL COMFORT

Thermoregulatory behavior of man during rest and exercise.

10 p1178 A73-23572

The effects of core temperature elevation and thermal sensation on performance.

15 p1839 A73-32396

Thermal comfort - New directions and standards.

18 p2283 A73-36785

HERMAL CONDUCTIVITY

Heating of a viscoelastic beam subjected to transverse vibrations

01 p0112 A73-10003

Orthogonal function approximation of uniform thickness plate temperature distribution, using reduced two dimensional unsteady heat conduction equations

01 p0119 A73-10010

Application of the Meler-Fok complex conversion formulas in the solution of certain problems of heat conductivity

01 p0119 A73-10011

Influence of the polarization of phonons on the thermal conductivity of single crystals of indium phosphide between 300 and 800 K

01 p0087 A73-10430

French monograph - Experimental study of the thermal conductivity of rare gases and helium-argon mixtures as functions of temperature and pressure.

01 p0120 A73-10604

Liquid- and wall-temperature calculations for a flow in tubes with allowance for heat losses into the ambient medium and for axial heat conduction

01 p0122 A73-10860

Singularities of the temperature dependences of the heat conduction coefficients of solid solutions of the niobium-zirconium system.

01 p0066 A73-11338

Effect of ion viscosity on the stability of a finite-pressure plasma.

02 p0198 A73-12104

Thermal conductivity of polyethylene - The effects of crystal size, density and orientation on the thermal conductivity.

02 p0185 A73-12431

Thermally conducting alumina and boron nitride filled silicone and polysulfide elastomer sheet materials for electrical insulation and heat sink applications

03 p0331 A73-13028

Cs vapors thermal conductivity at various temperatures and pressures, using low emissivity Ni cylinders.

03 p0396 A73-13181

The thermal and electrical conductivities of tantalum at high temperatures.

03 p0322 A73-13182

High melting point transition metals carbides, nitrides, borides, silicides and oxides thermal conductivity as function of characteristic temperature

03 p0322 A73-13191

Thermal conductivity and hot magnetic poles of pulsars.

03 p0374 A73-13796

Thermal design and tests of transcatal solid state power thyristor, rectifier and transistor devices, using heat pipe-silicon wafer construction

03 p0283 A73-13940

Cauchy problem and mixed boundary value problems for parabolic and hyperbolic wave equations of heat conductivity for boundary operators given on hyperplane

04 p0517 A73-14935

Electric and thermal conductivity, elastic properties, and resistance to bending of porous tungsten throughout the porosity range

04 p0464 A73-15371

Thermal analysis of combustion of fabric in oxygen-enriched atmospheres.

[ASME PAPER 72-WA/HT-22] 04 p0519 A73-15832

Thermal conductivity in vibrationally excited gases.

05 p0600 A73-16048

Frost and ice column models for analysis of heat and mass transfer and effective thermal conductivity relationship to density in frost layer

05 p0638 A73-16225

Earth crust materials high temperature lattice and radiative thermal conductivity from laser IR measurements, discussing single crystal and polycrystal forsterite-rich olivines and enstatite

05 p0569 A73-16378

Heat conductivity of system composed of a silicorganic elastomer and a powdered mineral filler

05 p0589 A73-16771

Thermal conductivity measurements of porous materials in several gaseous environments at subatmospheric pressures.

[AIAA PAPER 73-95] 05 p0640 A73-16858

Thermal conductance of gasket materials for spacecraft joints.

[AIAA PAPER 73-119] 05 p0640 A73-16875

Thermal resistance /conductance shape factor/ prediction for thermal components, considering cylindrical and rotational coordinate systems

[AIAA PAPER 73-121] 05 p0640 A73-16877

Relativistic thermodynamics of simple heat conducting fluids.

05 p0641 A73-17235

Effect of ion viscosity and thermal conductivity on the drift instability in an inhomogeneous high-pressure collisional plasma.

05 p0604 A73-17362

Condensate droplets heat conductivity as function of drop geometry and vapor mass transport interaction with interior heat conduction, using finite difference method

06 p0768 A73-17920

Thermal conductivity and resonant multipole interactions.

06 p0725 A73-18121

Approximate analytical solution of an asymmetrical problem of unsteady heat conduction with nonlinear boundary conditions

06 p0768 A73-18128

Heat conductivity and the Lorentz number of tungsten-rhenium alloys within the solid-solution limits from 0 to 27% Re at temperatures between 1200 and 3000 K

06 p0710 A73-18556

Si and silicon carbide effects on silicided graphite thermal and electrical conductivities

06 p0714 A73-18558

Temperature dependence of diatomic gases thermal conductivity coefficient from shock tube tests, noting molecular gases above dissociation temperature

06 p0687 A73-18561

Influence of the distortion of the temperature field at the point of thermocouple fixation on measurements of the heat conduction coefficient by the steady-state method of radial thermal flux

06 p0770 A73-18566

High temperature compressed gas heat conductivity calculation by least squares and basis isotherm methods

06 p0770 A73-18569

Microwave heating of a plasma and longitudinal electronic thermal conductivity in a magnetic field.

06 p0732 A73-18606

Measurement of high-temperature thermal conductivity of Lucalox (Al₂O₃) using a heat pipe technique.

06 p0715 A73-18778

Experimental study of the effective thermal conductivity of liquid saturated sintered fiber metal wicks.

06 p0770 A73-18836

Determination of thermal conductivity of gases by shock-tube studies.

07 p0918 A73-19187

Apollo 14 returned lunar rock fine thermal conductivity measurement as function of temperature under vacuum conditions, using least squares curve fitting method

07 p0895 A73-19856

Application of a variational technique to wedge flow with variable properties.

07 p0775 A73-19963

Thermal conductivity of nineteen igneous rocks. I - Application of the needle probe method to the measurement of the thermal conductivity of rock. II - Estimation of the thermal conductivity of rock from the mineral and chemical compositions.

07 p0788 A73-20031

The propagation and growth of acceleration waves in heat-conducting elastic materials.

07 p0917 A73-20441

Magnetic field effects on effective thermal conductivity of partially ionized plasmas, indicating neutral component role in solar magnetoplasma heat transport

08 p1001 A73-20755

Dynamic method for measuring thermal conductivity of liquids and gases at high pressures.

08 p1021 A73-20861

Solution of the asymmetric steady-state heat conduction problem for a two-layer hollow cylinder of finite length

08 p1021 A73-20995

Application of the solution to an inverse heat conduction problem to the calculation of the heat transfer coefficient from experimentally measured temperatures at internal point of the body

08 p1021 A73-20996

Temperature distribution in a wedge-shaped prism

08 p1022 A73-21098

Electrical and thermal conductivities of a relativistic degenerate plasma.

08 p0992 A73-21161

Heat conductivity, plasma instabilities, and radio star scintillations in the solar wind.

08 p0998 A73-21165

New formulations of the corresponding states principle for the transport properties of pure dense fluids.

08 p1023 A73-21258

Momentum method extension to thermal conductivity laser heating of nonhomogeneous plasma, obtaining closed form solutions for plane waves

09 p1126 A73-22171

Use of the linear heat flow for poor conductors and its application to the thermal conductivity of nylon.

[AD-758307] 09 p1166 A73-22200

An axisymmetrical nonstationary heat-conduction problem for a system of two cylinders contacting at the end faces

09 p1166 A73-22363

Heat conductivity of cermets with titanium carbide as function of temperature and metal content

09 p1103 A73-22471

Thermal conductivity approximation for gasdynamic equations describing stellar gravitational collapse, calculating neutrino and antineutrino energy and momentum transport processes

09 p1147 A73-22701

Thermal conductivity of mixed-composition plasma-sprayed coatings.

09 p1111 A73-23464

Temperature dependent thermal conductivity coefficient and electron and phonon components for group IV-VI transition metal diborides at 2300 K, using Wiedemann-Frantz law

10 p1236 A73-23518

Temperature dependent heat conductivity, Lorentz number and electrical resistivity of high melting Ti, Zr, Nb, Cr, Mo and W carbides and borides at 300-1200 K.

10 p1230 A73-23519

Temperature distribution in a plasma with turbulent thermal conductivity.

10 p1255 A73-24211

Thermal conductivity of the plasma electron component across the magnetic field

10 p1258 A73-24890

Foamed Al production from Al powder mixture with aluminum hydroxide and orthophosphoric acid,

discussing mechanical, thermal conductivity and electrical insulating properties 10 p1236 A73-24919

Effect of electron-electron collisions on the thermal conductivity of a dense plasma. 11 p1402 A73-25120

Acoustical method for determining thermal diffusivity and relative difference in molar heat capacities of tantalum and vanadium. 11 p1448 A73-25127

Pressure shocks in thermally and electrically conducting viscous gas, discussing growth equation and radiation effects 11 p1403 A73-25164

Experimental study of shock-wave reflection from a thermally accommodating wall. 11 p1449 A73-25252

Method of solving heat conduction problems with nonideal thermal contact 11 p1450 A73-25624

Investigation of the heat conductivity of aluminum oxide deposited by plasma spraying 11 p1373 A73-25731

Thermal diffusivity and thermal conductivity of pyrolytic titanium and niobium carbides and of titanium nitride at high temperatures 11 p1380 A73-25740

Ten-micron eclipse observations of Io, Europa, and Ganymede. 11 p1424 A73-26133

Apollo 12 fines vacuum thermal conductivity as function of temperature for different densities, comparing to terrestrial basalt under vacuum and pressure 11 p1425 A73-26137

A method of measuring thermal conductivity in the presence of extraneous heat currents and the thermal conductivity of brass at low temperatures. 11 p1367 A73-26307

Accuracy and convergence of absolutely stable finite difference procedures for solution of multidimensional heat conductivity equation with discontinuous coefficients 11 p1452 A73-26327

Thermodynamic theory of heat conducting fluids with constitutive quantities dependence on rate of density, gradient, velocity and temperature 11 p1453 A73-26746

Integral emittance of silicon alloyed with iron, cobalt, and nickel in the temperature range from 900 to 1750 C 12 p1513 A73-27309

Photon conductivity analysis for homogeneous isotropic solid body based on convective-radiant transfer equations, determining molten quartz thermal conductivity and diffusivity 12 p1516 A73-27311

Mathematical model of heat conduction medium thermophysical properties based on one dimensional nonlinear thermal conductivity equation solution 12 p1559 A73-27444

Liquid and wall temperature during flow in tubes with heat loss to the surrounding medium and axial heat conduction. 12 p1560 A73-27909

Influence of viscosity, thermal conduction, and ion drag on the propagation of atmospheric gravity waves in the thermosphere. 13 p1606 A73-28154

Entropy supply for classical and relativistic heat conducting fluids, assuming linearity for momentum and energy supplies 13 p1704 A73-28286

Investigation at the Moscow University of the thermal characteristics of material 13 p1704 A73-28426

Nonlinear least squares - An aid to thermal property determination. 13 p1706 A73-28806

Influence of longitudinal thermal conductivity on the ohmic heating of plasma in the Tuman-1 facility 13 p1666 A73-28959

The lattice heat conductivity of aluminium alloys during age-hardening. 13 p1636 A73-29068

Coupled thermoplasticity model of two stress-strain regions characterized by nonevolutionary plastic flow equations and simple wave collapse, with and without thermal conductivity 13 p1698 A73-29087

The thermal conductivity of a number of alloys at elevated temperatures. [ECTP PAPER B1-4] 14 p1760 A73-30435

Red arc data from Richland /WA/ and by Ogo 6 satellite observations, discussing thermal conduction formation theory 14 p1749 A73-30500

Constant line sources of heat in infinite media, whose thermal resistivities are linear functions of the temperature. 14 p1817 A73-30610

Thermal conductivity of carbon fibers 15 p1896 A73-31214

Method for boundary condition selection in the heat transfer problem with phase transition 15 p1958 A73-31872

On the observability and stability of the temperature distribution in a composite heat conductor. 16 p2034 A73-33311

Transport coefficients of ionized argon. 16 p2039 A73-33318

Thermal properties of rhenium single crystals at high temperatures. 16 p2026 A73-33581

Thermal conductivity and Lorenz number of tungsten-rhenium alloys in the solid-solution region /0-27% Re/ at temperatures of 1200-3000 K. 16 p2026 A73-33582

Si and silicon carbide effects on silitized graphite thermal and electrical conductivities 16 p2030 A73-33584

Temperature dependence of diatomic gases thermal conductivity coefficient from shock tube tests, noting molecular gases above dissociation temperature 16 p2086 A73-33586

Effect of temperature field distortions caused by embedded thermocouples on the measurement of the thermal conductivity coefficient by the steady radial heat flux method. 16 p2086 A73-33591

High temperature compressed gas heat conductivity calculation by least squares and isotherm methods 16 p2086 A73-33594

One dimensional shock waves in heat conducting materials with memory. III - Evolutionary behaviour. 16 p2081 A73-33747

Ionospheric electron thermal conductivity obtained for power law dependence of electron-neutral collision frequency dependence on velocity 16 p2010 A73-33923

Investigation of the thermophysical and antifiraction characteristics of polyethylene composites. III - The effect of fillers on the heat conductivity of polyethylene 16 p2030 A73-33930

Thermal conductivity and temperature dependence of energy gaps in niobium samples containing large amounts of impurity atoms 16 p2027 A73-34061

Infinitesimal canonical transformation for obtaining the thermal conductivity coefficient under the theory of linear response 17 p2253 A73-34126

Heat conductivity measurements for a hydrogen plasma in a stabilized electric arc 17 p2214 A73-34129

Certain thermophysical properties of isotropic pyrolytic graphite 17 p2253 A73-34132

Comparison of the solutions obtained by Tikhonov's and Sparrow's methods for the inverse unsteady-heat-conductivity problem 17 p2253 A73-34134

Certain physical properties of a new alloy of the nickel-rhenium-molybdenum system 17 p2186 A73-34137

Experimental determination of thermal conductivity of nitrogen in the temperature range 100-2200 C. 17 p2254 A73-34372

Heat conductivity and electrical properties of vanadium-alloyed titanium at 100 to 350 K 17 p2188 A73-34554

Temperature dependent thermal conductivity coefficient and electron and phonon components for group IV-VI transition metal diborides at 2300 K, using Wiedemann-Frantz law 17 p2196 A73-35198

Temperature dependent heat conductivity, Lorenz number and electrical resistivity of high melting Ti, Zr, Nb, Cr, Mo and W carbides and borides at 300-1200 K 17 p2191 A73-35199

Thermal contact conductance of porous metallic materials in a vacuum environment. [AIAA PAPER 73-747] 18 p2323 A73-36363

Radiative heat transfer through composite materials. 18 p2371 A73-36621

Coordinate function construction in solving the boundary value problems of heat conductivity by direct methods 18 p2372 A73-36818

Application of heat pipes and their thermal transport capability. 19 p2502 A73-37445

Coupled thermoplasticity model of two stress-strain regions characterized by nonevolutionary plastic flow equations and simple wave collapse, with and without thermal conductivity 19 p2498 A73-37637

A theoretical model for lunar surface material thermal conductivity. [ASME PAPER 73-HT-35] 20 p2603 A73-38571

The thermal and electrical conductivities of porous copper and stainless steel to elevated temperatures. [ASME PAPER 73-HT-47] 20 p2575 A73-38572

Thermal conductivity measurement for particulate materials in vacuum, comparing line and differential-line source methods in terms of test and data reduction times 20 p2565 A73-38882

Method for determining the unsteady thermal field of piecewise homogeneous plates of complex shape 20 p2627 A73-39256

Solution of a nonlinear problem of heat conductivity concerning a multilayer cylindrical wall with a nonideal thermal contact 20 p2627 A73-39257

Thermal conductivity of mercury vapors 20 p2595 A73-39607

Model for lunar near surface thermal conductivity in terms of contact conductivity, pressure and packing density 20 p2613 A73-39719

NiO and CoO single crystal thermal conductivities, reporting specific heat and electrical resistivity near magnetic transition 20 p2600 A73-39826

The equations of fast-process hydrodynamics 21 p2676 A73-40205

Thermal contraction of a system of glassfibre and epoxy resin between 300 and 77 K. 21 p2724 A73-41107

Investigation of the effective heat conductivity of plasma-sprayed alumina coatings subject to radiative heating in the temperature range from 100 to 900 C 21 p2792 A73-41220

Thermal conductivities of the elements - Results of a critical evaluation. 21 p2792 A73-41300

Transverse electron thermal conductivity for a plasma in a magnetic field. 21 p2749 A73-41665

Thermal conductivity of superconducting layer in intermediate state with Andreev electron excitation trajectories in magnetic field, using Green function and impurity distribution technique 22 p2896 A73-41728

Coupling between thermal conduction and radiative transfer in a moving atmosphere. 22 p2907 A73-42305

Electrical resistivity and thermal conductivity of alloys of the tungsten-molybdenum system. [ECTP PAPER B1-6] 22 p2876 A73-42402

Thermal characterization of reusable external insulation for the space shuttle. [ECTP PAPER B2-8] 22 p2931 A73-42403

Thermal conductivity of low density carbon. [ECTP PAPER C-5] 22 p2881 A73-42404

New measurements of the thermal conductivity of argon and nitrogen to 200 C and 1600 atmospheres. 22 p2932 A73-42502

Experimental study of the thermal conductivity coefficient of noble gas mixtures at low and moderate densities. 22 p2932 A73-42503

The temperature dependence of viscosity and thermal conductivity of dilute noble gases at moderate and high temperatures. 22 p2932 A73-42504

Determination of thermal contact resistance using a pulse technique. 22 p2878 A73-42511

Theoretical studies and experimental verifications of thermal and electrical conductivity, molecular diffusivity and viscosity of a partially ionized suspension in an electric field. 22 p2894 A73-42512

Direct methods for solving inverse linear problems of thermal conductivity 23 p3048 A73-43444

Extrapolation algorithm for inverse thermal conductivity problem solution of body heat flux and temperature gradients, using successive approximations 23 p3048 A73-43445

Papers on heat pipes covering incompressible laminar vapor flow behavior, startup dynamics, wicking material liquid transport properties, high thermal conductance structures, etc 23 p3049 A73-43459

Effect of longitudinal thermal conductivity on ohmic heating in Tuman-1. 23 p3013 A73-44311

Effect of modified thermal conductivity on the temperature distribution in the protonosphere. 24 p3082 A73-44727

Pulse method for determining heat-transfer coefficients of coatings 24 p3155 A73-44756

Thermal diffusivity and conductivity of titanium and zirconium carbides at high temperatures 24 p3099 A73-44760

Influence of porosity on the effective heat conductivity of graphite 24 p3104 A73-45082

Temperature field boundary value problem with variable heat transfer coefficients and specific heat, using Laplace transformation and variation methods 24 p3156 A73-45083

Numerical solution of a nonlinear inverse heat-conduction problem 24 p3156 A73-45084

Gaseous plasma thermal conductivity in dynamic equilibrium, relating particle binary correlation to shielding distance under temperature gradients 24 p3116 A73-45243

Effects of thermal conductivity in radiative magnetohydrodynamic channel flow. 24 p1317 A73-45370

THERMAL CONDUCTIVITY GAGES
System for measuring the thermal diffusivity of electrically conducting materials at high temperatures 19 p2432 A73-38543

THERMAL CONDUCTORS
Installing the heater cable directly in the redesigned leading edge. 16 p1970 A73-32924
An unsteady heat-conduction problem in a system of diathermally separated bodies 24 p3154 A73-44422

THERMAL CONTROL COATINGS
Electron spin resonance of ultraviolet radiation induced defects in ZnO thermal control coating pigment. 01 p0088 A73-11276
Apparatus for investigations into long-term strength and creep of coated materials at temperatures above 1400 C in air. 02 p0150 A73-12219
Selection and application of the protective coating system for the AWACS radome. 03 p0329 A73-13008
Materials and processes for thermal control surfaces. 03 p0329 A73-13009
Analysis of sublimation-cooled coated mirrors in convective and radiative environments. 05 p0641 A73-17108
Investigation of high-temperature evaporation of heat-resistant ceramic coatings on metals 06 p0714 A73-18656
White and black paints for satellite thermal control coatings, discussing space environment radiation effects on emissivity and solar absorptance 07 p0841 A73-18909
Chemical and electrolytic coatings for satellite surface thermal control, discussing surface anodic oxidation treatment of adhesive Au platings on Al alloys 07 p0829 A73-18910
Solar radiation absorptivity control by metal film coatings, noting thermal control coatings for heat shielding 07 p0778 A73-19300
Thermal conductivity of mixed-composition plasma-sprayed coatings. 09 p1111 A73-23464
Investigation of the heat conductivity of aluminum oxide deposited by plasma spraying 11 p1373 A73-25731
Determination of the required thickness of thermal insulation casings and evaluation of the weight-based effectiveness of materials 12 p1558 A73-27092
High-temperature protective coatings; All-Union Conference on Heat Resistant Coatings, 5th, Kharkov, Ukrainian SSR, May 12-16, 1970, Transactions 18 p2318 A73-35876
High temperature coatings on graphite 18 p2318 A73-35885
Application of refractory oxide coatings in extensometry 18 p2314 A73-35886
Radiative property degradation of water impinging on thermally-controlled surfaces under space conditions. [AIAA PAPER 73-733] 18 p2336 A73-36350
Optical stability of coatings exposed to four years space environment on OSO-III. [AIAA PAPER 73-734] 18 p2336 A73-36351
Thermal control coatings for heat shielding of high-temperature high-speed chemically aggressive gas flows, noting turbine blade shielding application 18 p2371 A73-36812
Spacecraft thermal control coatings development, discussing zinc orthotitanate/silicone properties as solar reflector [ASME PAPER 73-ENAS-7] 19 p2389 A73-37969
Spacecraft environmental optical contamination problems associated with thermal control surface outgassing. [ASME PAPER 73-ENAS-32] 19 p2395 A73-37987
Precession damping of solar probes by radiative forces. 21 p2737 A73-40767
Measurement of the thermo-optical characteristics of satellite thermal control coatings 22 p2929 A73-41872
Book - Thermal radiative properties; Coatings. 22 p2937 A73-42857

THERMAL CONVECTION
U FREE CONVECTION
THERMAL CURRENTS
U CONVECTIVE FLOW
THERMAL CYCLING TESTS
Thermal cycle influence in heat resistant materials plastic strain and time to failure for different stress and temperature conditions 01 p0112 A73-10009
Assembly for studying the characteristics of materials under cyclic loads at elevated temperatures 01 p0029 A73-10024

Nickel structure stabilization by multiply alternated thermocyclic treatment and isothermal annealing 01 p0062 A73-10253
Deformation and failure of heat-resistant materials under conditions of thermal fatigue and creep as functions of the nature of the temperature change cycle and of the boundary conditions 01 p0063 A73-10478
Influence of cyclic heating on the mechanical fatigue of titanium alloys and their weld joints 02 p0180 A73-11933
Application of the basic concepts of structural-energetic theory to the problem of physical fatigue limit. 02 p0235 A73-12131
The influence of preliminary thermocycling on the high-temperature strength of austenitic steel. 02 p0180 A73-12139
A temperature-programmed apparatus for fatigue testing metals. 02 p0150 A73-12218
Thermal cycling and frequency tests for lunar soil dielectric constant, loss tangent and dc conductivity, noting moisture effects 02 p0220 A73-12481
Resonance type facility using dynamic hysteresis loop method to test metal fatigue and anelasticity in torsion at room and high temperatures 03 p0288 A73-14025
B-Al matrix composites environmental properties, costs and development for aerospace systems, considering corrosion, erosion and thermal cycling effects on tensile strength 04 p0467 A73-15934
Thermal-influence region properties in a maraging steel as a function of welding heat cycles 06 p0697 A73-17880
Failure analysis of semiconductor device bonds under on-off operation, noting fatigue testing machine for accelerated life tests 08 p0972 A73-20744
Certain regularities in the deformation and rupture of molybdenum-, niobium-, and tantalum-based high-melting-point alloys under programmed temperature changes 09 p1100 A73-22151
A strain criterion for failure of materials subjected to stress and temperature cycles 09 p1159 A73-22570
Plasticity and failure of heat-resistant materials at a low number of cycles of simultaneous fluctuations of temperature and load. 09 p1105 A73-23154
Refractory materials cyclic elastoplastic tests under shear with holding creep, showing relationship between creep rate and recurrent static deformation 09 p1161 A73-23155
Temperature dependence of conditions for static, quasi-static and fatigue failure of titanium alloys 09 p1107 A73-23193
Failure analysis and heat resistance optimization factors of reinforced metal sheet under thermal cycling 10 p1233 A73-24369
Electron fractography of fatigue failure and macrocrack propagation in dual phase Ti alloy during cyclic loading at minus 140 to plus 150 C 10 p1236 A73-24931
Varying-temperature test installation for the interior design of the Concorde 11 p1342 A73-25103
Stabilization of the austenitic phase of iron-nickel base alloys by cumulative thermal cycling 11 p1379 A73-25323
Structural failures in light weight solar cell arrays under thermal cycling. 11 p1310 A73-25999
Testing machine for thermal fatigue with variable constraint ratio. 13 p1611 A73-28195
Thermal stress analysis of metals with temperature dependent mechanical properties. 13 p1701 A73-29507
Creep test diagrams plotted to estimate heat resistance for turbine blades design, predicting fatigue life with allowance for loading cycle form and duration 13 p1703 A73-29616
Deformation and destruction of heat-resistant materials in conditions of thermal fatigue and creep as a function of the nature of the cyclic change in temperature and boundary conditions. 14 p1759 A73-30303
Thermal cycling effects on void formation in boron-aluminum matrix composites at 70-670 F, considering jet turbine compressor blade applications 16 p2084 A73-33037
The role of temperature in the environmental acceptance testing of electronic equipment. 16 p1989 A73-33606
The metallurgical implications of welding processes. 16 p2021 A73-33863
Method of recording the deformation diagram in thermal-fatigue tests. 17 p2165 A73-34278

Durability of the Kh18N10T steel under the combined influence of creep and thermal cycling 17 p2187 A73-34335
Thermal cyclization of 1,2-polybutadiene and 3,4-polyisoprene. 17 p2119 A73-34925
Creep in VT-14 titanium alloy under low-cycle load conditions 18 p2323 A73-36758
High temperature cyclic oxidation resistance tests on Ni-, Co- and Fe-base alloys for aircraft gas turbine engines 19 p2440 A73-37496
Torque and thermal cycling as methods of testing reliability of reflow-soldered chip-to-substrate joints. 19 p2436 A73-38445
Long term life tests for thermal shock cycles effects on plastic encapsulated semiconductor device reliability, presenting salt atmosphere testing data for silicone package 19 p2471 A73-38454
Method of studying thermal fatigue from the parameters of the hysteresis loop in temperature-force coordinates 20 p2619 A73-39362
Thermal contraction of a system of glassfibre and epoxy resin between 300 and 77 K. 21 p2724 A73-41107
Some patterns of deformation and failure of refractory alloys of molybdenum, niobium and tantalum during a programmed change of temperature. 22 p2874 A73-42101
Grain boundary cavitation and sliding in copper/tungsten composites due to thermal stresses. 22 p2876 A73-42339
Development of a hybrid microelectronics solid state relay for 2500 volts isolation and -120 C to 80 C thermal cycling range. 22 p2835 A73-42914

THERMAL DECOMPOSITION U PYROLYSIS THERMAL DEFOCUSING U THERMAL BLOOMING THERMAL DEGRADATION

The accurate prediction of radiation environment and solar cell degradation. 01 p0006 A73-11164
Thin film CdS solar cell stability improvement by etching, noting cuprous sulfide oxidation effects on degradation from short term tests at high temperature 03 p0255 A73-14221
The thermal decomposition of nitroglycerin and its relation to the stability of CMDB propellants. [WSCI PAPER 72-30] 05 p0605 A73-16685
Deformation and destruction of heat-resistant materials in conditions of thermal fatigue and creep as a function of the nature of the cyclic change in temperature and boundary conditions. 14 p1759 A73-30303
Microorganism heat sterilization process design and control based on logarithmic thermal destruction and Bigelow temperature coefficient models, determining lethality by statistical procedure 16 p1976 A73-33695
Analysis and temperature control of hybrid microcircuits. [ASME PAPER 73-ENAS-6] 19 p2412 A73-37968
Degradation studies of diffused GaAs electroluminescent diodes subjected to mechanical stress. 19 p2439 A73-38458

THERMAL DIFFUSION

Thermal diffusion theory for deformations of thin isotropic shells and plates subjected to nonuniform temperature and stress concentration fields 01 p0113 A73-10019
Thermal intermittency coefficient distribution across turbulent boundary layer as function of free stream turbulence level 01 p0031 A73-10412
The diffusion of point defects to a propagating crack tip. 01 p0116 A73-11000
Diffusive thermal bonding of cermet elements on steel and iron substrates in vacuum 02 p0172 A73-11537
Experimental values of turbulence length scales in Lagrange variables in the vicinity of a flat wall 02 p0154 A73-12541
Diffusion and conduction processes in CdS-Cu/X/S thin film photocells. 03 p0350 A73-14217
Study of the specific characteristics of the diffusion method for measuring turbulence characteristics under conditions of a free homogeneous jet 05 p0576 A73-16617
Use of ion implantation in the fabrication of semiconductor devices 06 p0672 A73-17449
Three component static thermosphere model for oxygen radiative recombination and thermal diffusion dependence on underlying layers and solar UV radiation 06 p0689 A73-17539

Correlation between the diffusion activation energy, the heat of fusion, and the bond energy in metals
06 p0708 A73-18046

Diffusion on a particle in the shear flow of a viscous fluid - Approximation of the diffusion boundary layer.
07 p0809 A73-19021

Influence of thermal-diffusion coatings on the physicochemical properties of heat-resistant metals
07 p0840 A73-20512

Analysis of indicator distribution in the determination of cardiac output by thermal dilution.
08 p0933 A73-21216

Choice of detection site for the determination of cardiac output by thermal dilution - The injection-thermistor-catheter.
08 p0933 A73-21217

Spun on arsenosilica films as sources for shallow arsenic diffusions with high surface concentration.
08 p0995 A73-21478

Estimate of the influence of thermal diffusion on the surface burnout rate in a nonhomogeneous turbulent boundary layer
09 p1167 A73-22618

Development of a procedure for measuring the degree of turbulence at the axis of a free two-phase jet by a thermal-diffusion method
09 p1167 A73-22847

Dissipation of mechanical energy in a deformable body during thermal diffusion processes
10 p1291 A73-24351

Diffusion layer structure and phase composition during quenched and annealed steel saturation by Cr at high heating rates
10 p1236 A73-24962

The stability of a layer of binary gas mixture heated below.
11 p1449 A73-25222

On the turbulent thermal diffusion parallel to a plane wall for y/δ equals 2 to 300
11 p1451 A73-25870

Diffusion of heat from a line source downstream of a turbulence grid.
11 p1451 A73-25870

Austenite stabilization during inverse transformation in Cr-Co-Mo and Cr-Ni-Co-Mo steels
13 p1630 A73-28012

Effects of deformation on diffusion in iron-nickel and iron-chrome systems
14 p1760 A73-30379

Determining unknown coefficients in a nonlinear heat conduction problem.
14 p1817 A73-30406

Diffusion creep by dislocation climb in beryllium and Be-Cu single crystals.
14 p1761 A73-30633

Layered and aggregate product displacement reaction kinetics in solid state/metal-metal oxide/ couples for metal matrix composites at 1000 C from thermodynamic and diffusion data
14 p1783 A73-30634

Subscale inclusions formation in solid Fe alloys with small amounts of Mn and other elements, noting inward oxygen thermal diffusion role and metallurgical implications
15 p1891 A73-32171

Electrical network analogy application to thermal energy steady diffusion within Knudsen gas filled enclosure, discussing free molecule limit and transition regime
15 p1959 A73-32283

Characteristics of the distribution of elements in the diffusive layers of titanium-based three-component systems
15 p1893 A73-32521

Crystal growth by vapor transport of GeSe, GeSe₂, and GeTe and transport mechanism and morphology of GeTe.
15 p1842 A73-32652

Three component static thermosphere model for oxygen radiative recombination and thermal diffusion dependence on underlying layers and solar UV radiation
16 p2001 A73-32763

Charge transfer in overlapping gate charge-coupled devices.
16 p1988 A73-33396

Effect of thermomodification coatings on the physicochemical properties of refractory metals.
19 p2440 A73-37787

Generation of vacancies in tungsten by rapid-rate deformation at elevated temperature.
20 p2578 A73-39492

Vertical plate steady flow thermal diffusion chamber for cloud condensation nucleus counter, featuring long available growth time for operation below 0.2 percent supersaturation
21 p2697 A73-40059

Global stability of time-dependent flows - Impulsively heated or cooled fluid layers.
21 p2790 A73-40249

Interdiffusion in the titanium-zirconium system
22 p2874 A73-42099

On the thermomodification effect in the CW He-Ne laser.
22 p2871 A73-43080

Diffusion in thin film couples of platinum-gold.
23 p3015 A73-43528

Concentration curves and phase diagram plotted for Nb-Zr system diffusion layers during annealing at 700 to 1700 C
23 p2991 A73-43649

Temperature field and motion oscillations in water-methanol and water-isopropanol Benard cells, taking into account thermal diffusion
23 p3049 A73-43936

Experimental investigation of transient supersaturations in a thermal diffusion chamber.
23 p3004 A73-44259

Influence of the type of loading on high-temperature creeping of zirconium carbide
23 p2998 A73-44287

Temperature range for centrifugal thermal diffusion sintering in Cr-Ni powder coatings, relating upper and lower bounds to heating rate
24 p3092 A73-44419

Diffusion treatment of CdS and ZnO crystals and their applications in microwave acoustics.
24 p3120 A73-45433

THERMAL DIFFUSIVITY

Thermal conductivity measurements of porous materials in several gaseous environments at subatmospheric pressures.
05 p0640 A73-16858

Directional dependence of the thermal conductivity of crystal-oriented pyrolytic graphite at high temperatures.
06 p0713 A73-17405

Lunar fines thermal diffusivity measurement, calculating lunar surface temperature distribution [AIAA PAPER 73-40]
06 p0767 A73-17622

Elastic wave velocities and thermal diffusivities of Apollo 14 rocks.
07 p0894 A73-19851

Thermal diffusivity of lunar rocks under atmospheric and vacuum conditions.
09 p1148 A73-22872

Acoustical method for determining thermal diffusivity and relative difference in molar heat capacities of tantalum and vanadium.
11 p1448 A73-25127

Thermal diffusivity and thermal conductivity of pyrolytic titanium and niobium carbides and of titanium nitride at high temperatures
11 p1380 A73-25740

Photon conductivity analysis for homogeneous isotropic solid body based on convective-radiant transfer equations, determining molten quartz thermal conductivity and diffusivity
12 p1516 A73-27311

A comparative study of the thermal diffusivities of stainless steel, hafnium, and Zircaloy.
13 p1630 A73-28051

Investigation at the Moscow University of the thermal characteristics of material
13 p1704 A73-28426

Carrier heating or cooling in semiconductor devices.
13 p1590 A73-28540

Thermal diffusivity measuring technique for hazardous materials.
14 p1752 A73-29914

Development of the method and investigation of the intensity of turbulence at the axis of a two-phase turbulent jet
15 p1862 A73-31298

Certain thermophysical properties of isotropic pyrolytic graphite
17 p2253 A73-34132

Effects of thermal and mass diffusivities on the burning of fuel droplets.
20 p2626 A73-39249

Thermal conductivity of low density carbon.
22 p2881 A73-42404

A two-layer slab method for measuring thermal diffusivity of polymer by irradiated light heat-wave. I. II - Transient response of temperature sensor attached on a polymer substrate. III - Quantitative evaluation of the effect of edge losses in a parallelepiped.
23 p3049 A73-44363

Thermal diffusivity and conductivity of titanium and zirconium carbides at high temperatures
24 p3099 A73-44760

THERMAL DISSOCIATION

Dissociative recombination at elevated temperatures. IV - N₂/+ dominated afterglows.
07 p0853 A73-19149

Dissociation of semiconductor compounds under the action of a laser beam
11 p1378 A73-26675

Thermal dissociation and recombination of hydrogen according to the reversible reactions H₂ + H to H + H + H.
16 p1977 A73-33674

Determination of dissociation energies for some alkaline earth/hydro-/ oxides in CO/N₂O flames.
24 p3156 A73-44985

THERMAL EFFECTS

U TEMPERATURE EFFECTS
THERMAL EFFICIENCY
U THERMODYNAMIC EFFICIENCY
THERMAL EMISSION
NT THERMIONIC EMISSION

Inference of stratospheric temperature structure from limb radiance profiles.
01 p0072 A73-10356

21-micron observations of H II regions.
01 p0104 A73-11045

Michelson interferometer on Mariner 9 space probe for thermal emission spectrum measurement, discussing spectral resolution, external vibration problem and instrument performance
01 p0054 A73-11228

The possibilities of determining the temperature profile in the Venusian atmosphere from the thermal radio emission of the planet
02 p0219 A73-12463

Thermal radio source DR 21 centimeter flux density measurements for antenna aperture calibration, comparing with standard sources
03 p0366 A73-12932

Spatial-temporal coherent processing technique application to thermal radio emission random signal reception, deriving ambiguity function
05 p0547 A73-16057

Lunar polarized 1420 MHz thermal radio emission aperture synthesis maps evaluation
06 p0752 A73-18237

Theoretical possibilities for determining the moisture content of the atmosphere through the thermal radio emission in the submillimeter range.
07 p0848 A73-20347

Carbon stars molecular band strength variations in two-micron spectral region due to thermal emission from circumstellar dust shell
09 p1149 A73-23129

Balloon observations of galactic and extragalactic objects at 100 microns.
09 p1150 A73-23134

The emissivity of a system consisting of a semitransparent isothermal coating and a flat opaque substrate
10 p1294 A73-23514

Electrical resistance and emissivity of certain transition metals and alloys in the high-temperature range
10 p1230 A73-23520

Thermal radio emission from Jupiter and Saturn.
11 p1420 A73-25883

Integral emittance of silicon alloyed with iron, cobalt, and nickel in the temperature range from 900 to 1750 C
12 p1513 A73-27309

Temperature calculation for heat emitting surface in transparent gas flow, using linearizing function method for heat transfer problems with nonlinear boundary conditions
12 p1558 A73-27316

Ground-based measurement of millimetre-wavelength emission by upper stratospheric O₂.
14 p1751 A73-29718

High-resolution survey of thermal sources of radio emission at the 8.2-mm wavelength
15 p1938 A73-31952

The possibilities of determining the temperature profile in Venus' atmosphere from the planet's thermal radio emission.
15 p1942 A73-32613

Radiating power of a system consisting of a semitransparent isothermal coating and a flat non-transparent substrate.
17 p2212 A73-35194

Electrical resistivity and emissivity of some transition metals and alloys in the high-temperature range.
17 p2191 A73-35200

Microwave signatures of first-year and multiyear sea ice.
17 p2163 A73-35466

Soft X-ray flux of the Coma cluster of galaxies.
19 p2475 A73-37626

Thermal positive ions in the dayside polar cusp measured on the ISIS 1 satellite.
21 p2690 A73-41368

Lower atmospheric intensity-calibrated thermal emission spectra with digital recording near IR spectrometer, discussing applications to pollutant detection
21 p2692 A73-41574

Measurement of the thermo-optical characteristics of satellite thermal control coatings
22 p2929 A73-41872

The emittance of blackbody cavities.
22 p2930 A73-41981

The emissivities of liquid metals at their fusion temperatures.
22 p2930 A73-41981

High-resolution survey of thermal radio sources at 8.2 mm.
24 p3131 A73-44477

THERMAL ENERGY

Review of laboratory measurements of aerodynamic ion-neutral reactions.
01 p0014 A73-10335

Experimental investigation of thermal and induced molecular scattering of light in solutions within a wide spectral range
02 p0195 A73-11947

- Thermal energy charge transfer reactions of rare-gas ions to methane, ethane, propane, and silane - The importance of Franck-Condon factors. 02 p0195 A73-12084
- Rate coefficient calculation for near resonant charge transfer reaction between oxygen cations and hydrogen atoms as function of temperature at thermal energies 02 p0217 A73-12391
- Arrhenius rate law for thermally activated processes, deriving master equation based on rates of transition between quantum states 03 p0397 A73-13289
- Geothermal energy extraction from hot rocks via deep dry wells by pressurized water circulation, solving numerically fluid flow, heat transport and rock fracture equations 05 p0569 A73-16382
- Thermal processes in metals exposed to high power laser pulses 06 p0702 A73-18571
- Thermal-activation parameters of plastic deformation in alpha-titanium single crystals 09 p1099 A73-21964
- Thermal wave generation and transformation into shock waves due to energy release in stellar interior, considering nova outburst 09 p1146 A73-22547
- The Solar Collector Thermal Power System - Its potential and development status. 09 p1035 A73-22792
- Electron impact ionization, three body recombination and thermal energy balance effects on gas discharge positive column between plane parallel walls 10 p1255 A73-24265
- Lower thermosphere thermal energy and oxygen transport due to photochemical reactions, noting Schumann-Runge band absorption, atomic recombination and collisional deactivation 11 p1358 A73-26706
- Turbulent flow energy transfer paths and irreversible dissipation as internal thermal energy analyzed by Reynolds convection for turbulent velocity 13 p1605 A73-29267
- Concentric, uniform elastic spherical wave excited by thermal explosion of the envelope. 14 p1816 A73-30251
- Aluminum structure effects on thermal activation parameters of plastic deformation, proposing strain rate control mechanism 14 p1764 A73-30867
- Efficiency of the recovery of high thermal energy densities during porous vaporization of alkali metals 15 p1957 A73-31864
- Thermal processes in metals irradiated by powerful laser pulses. 16 p2086 A73-33596
- Thermal synthesis of amino acids from a simulated primitive atmosphere. 17 p2112 A73-34572
- On the temperature of the Jovian thermosphere. 17 p2232 A73-34860
- Cylindrical Poiseuille flow and thermal creep of a rarefied gas. 18 p2300 A73-36635
- Conditions for thermal explosion occurrence during branched-chain reactions 19 p2502 A73-37501
- Thermodynamic heat concept, discussing kinetic and potential particle energy, internal energy, heat absorption and release and thermal energy 20 p2627 A73-39293
- A numerical, thermo-mechanical model for the welding and subsequent loading of a fabricated structure. 24 p3150 A73-45231
- Excitation mechanisms in He-Cd and He-Zn ion lasers. 24 p3097 A73-45418
- THERMAL ENVIRONMENTS**
- A derivation of thermal mathematical model with measured nodal temperatures. 01 p0123 A73-11142
- Sensitivity analysis method application to spacecraft thermal environment control system design, determining mathematical model input parameters uncertainty effects on temperature determination 01 p0123 A73-11143
- Thermal mathematical model development for spacecraft design as exemplified by small scientific satellite, comparing analytical results with test data 01 p0110 A73-11144
- Scaling of performance and thermal environment in fuel-vortex cooled rocket engines. 03 p0354 A73-13399
- [AIAA PAPER 72-1075]
- Stress analysis and design of silicon solar cell arrays and related material properties. 03 p0255 A73-14224
- An experimental investigation of some heat transfer characteristics on an orbiter/HO-tank/SRM Space Shuttle configurations, freestream Mach number equal to 8.0. 05 p0640 A73-16856
- Lumped parameter network modeling for spacecraft surface thermal environment analysis, discussing computer program and application to Skylab ATM 07 p0919 A73-19496
- Thermal hereditary constitutive law for linear viscoelastic materials time response in transient temperature environment 08 p1018 A73-21409
- On the functional significance of subcuticular single unit activity during sleep. 14 p1714 A73-29993
- Simultaneous control of temperature and humidity in a confined space. I - Mathematical modeling of the dynamic behavior of temperature and humidity in a confined space. 15 p1959 A73-32597
- Eleven ribs and spars made of flat Rene 41 caps based on hot structure concept for thermal environment 16 p2072 A73-33061
- A comparison of hydraulic fluid characterizations in two evaluation systems. [ASLE PREPRINT 73AM-9A-2] 17 p2196 A73-34997
- Human performance at elevated environmental temperatures. 18 p2283 A73-36787
- An insight into the features of the OAO-C thermal design. [ASME PAPER 73-ENAS-4] 19 p2493 A73-37966
- An assembly for electrophysiological and thermometric studies 22 p2815 A73-42663
- Aquatic and diving mammals in fresh water and marine environments, discussing aquatic thermal conditions, body temperature distribution, thermoregulation, metabolic heat production, etc 22 p2809 A73-42861
- Spinal cord heating effects on frog thermoregulatory behavior in aqueous thermal gradient, noting preference for colder ambient temperature 23 p2947 A73-43994
- THERMAL EXPANSION**
- NT THERMAL BUCKLING**
- Subsonic plasma motion in continuous laser light. 01 p0084 A73-10472
- Experimental investigation of the thermal expansion of filamentary composite materials 01 p0068 A73-10859
- Preparation and high-temperature properties of carbon fiber-Ni composites. 03 p0321 A73-12919
- Thermal expansion of Apollo lunar samples and Fairfax diabase. 07 p0895 A73-19855
- Lattice dynamics, third-order elastic constants, and thermal expansion of titanium. 07 p0839 A73-20173
- On optimizing thermal stresses in cylindrical shells. 08 p1015 A73-20674
- Effects of thermal loading on fiber-reinforced composites with constituents of differing thermal expansivities. [ASME PAPER 72-MAT-F] 08 p0979 A73-21573
- Thermal expansion at elevated temperatures. IV - Carbon-fibre composites. 09 p1110 A73-22121
- The thermal expansion coefficients of some glass-reinforced plastics and their components at low and high temperatures. 09 p1111 A73-23063
- Analysis, test, and comparison of composite material laminates configured for isotropic low thermal expansion. 10 p1237 A73-23960
- 'Invar' and 'Elinvar' - Alloys with controllable thermal expansion and elastic properties 11 p1385 A73-26564
- The thermal expansion of composites based on polymers. 12 p1515 A73-27030
- Experimental investigation of thermal expansion in composite fibrous materials. 12 p1516 A73-27908
- Anisotropy of gallium elasticity and thermal expansion 12 p1531 A73-27936
- Thermal expansion of tungsten from 293 to 1800 K. [ECTP PAPER E-1] 13 p1631 A73-28052
- An equation for thermal expansion coefficient at high pressures. 13 p1673 A73-28206
- German monograph on calculation of thermal and transformation stresses in long circular cylinders covering austenite-martensite transformation, thermal expansion and viscous bodies 13 p1699 A73-29284
- Thermal deformation of an injection laser crystal during the passage of pumping current pulses. 13 p1630 A73-29443
- Effects of buoyancy and of acceleration owing to thermal expansion on forced turbulent convection in vertical circular tubes - Criteria of the effects, velocity and temperature profiles, and reverse transition from turbulent to laminar flow. 14 p1818 A73-30614
- Thermal expansion, Young's modulus, and magnetostriction of a stainless iron-chromium-nickel alloy in the temperature range between 80 and 280 K 14 p1764 A73-30868
- Thermal expansion coefficient measurement of diffusely reflecting samples by holographic interferometry. 15 p1877 A73-31980
- Thermal expansion coefficient measurements of specularly reflecting samples. 15 p1877 A73-31981
- Russian book - Precision alloys with specific thermal-expansion and elastic properties 15 p1893 A73-32293
- X-ray diffraction at high temperatures for a study of thermal expansion of MnSe and MnSe₂ 15 p1925 A73-32651
- The relationship between thermal history, X-ray crystallographic structure and thermal properties of Pyco-bond rayon precursor carbon-carbon composites. 16 p2028 A73-33044
- Thermal expansion compatibility of ceramic chip capacitors mounted on alumina substrates. 16 p1989 A73-33472
- High precision photoelastic and ultrasonic techniques for determining absolute and differential thermal expansion of titania-silica glasses. 17 p2171 A73-35410
- A solar engine using the thermal expansion of metals. 19 p2392 A73-38473
- Latitude distribution of the regularity in F2-region irregularities. 20 p2553 A73-39132
- Liquid anorthite viscosity and thermal expansion at 1450-1620 C and 820-950 C, noting agreement with Bottinga-Weill model predictions 20 p2555 A73-39718
- Influence of grain size on effects of thermal expansion anisotropy in MgTi₂O₅. 21 p2752 A73-40893
- Possibility of predicting the residual stress pattern in boronized steels 21 p2721 A73-41229
- Investigation of the thermal expansion of molybdenum and tungsten at high temperatures. [ECTP PAPER E-5] 22 p2876 A73-42406
- Anomalous concentration dependence of thermal expansion coefficients of tungsten-rhenium and tungsten-niobium alloys. 22 p2878 A73-42509
- Thermodynamic expansion processes for argon plasma in a convergent-divergent nozzle. 22 p2894 A73-42632
- Statistical theory of solid heterogeneous materials, discussing constant elastic bounds, fiber reinforced cell model, thermal expansion and stress-strain relations 23 p3038 A73-43303
- THERMAL FATIGUE**
- Deformation and failure of heat-resistant materials under conditions of thermal fatigue and creep as functions of the nature of the temperature change cycle and of the boundary conditions 01 p0063 A73-10478
- A temperature-programmed apparatus for fatigue testing metals. 02 p0150 A73-12218
- Characteristics of the fatigue curve of plastics. 02 p0185 A73-12699
- Strength and microstructure of nickel-base superalloys after long term heating. 05 p0587 A73-16622
- Thermal fatigue resistance of borided alloy KhN70VMYuT. 06 p0709 A73-18215
- The challenge to unify treatment of high-temperature fatigue - A partisan proposal based on strainrange partitioning. 07 p0917 A73-20461
- Service failures and fracture mechanisms under cyclic load at high temperature. 11 p1442 A73-25845
- Testing machine for thermal fatigue with variable constraint ratio. 13 p1611 A73-28195
- Effect of temperature and strain rate on the high temperature, low cycle fatigue behaviour of a 17Cr-10Ni-2Mo stainless steel. 13 p1708 A73-29504
- Metallurgical and strength studies of heat resisting alloys for gas turbines after long term service. 13 p1625 A73-29519
- Investigation of the thermal fatigue of type Kh18Ni9Ti steel under complex stress distributions. 13 p1643 A73-29623
- Deformation and destruction of heat-resistant materials in conditions of thermal fatigue and creep as a function of the nature of the cyclic change in temperature and boundary conditions. 14 p1759 A73-30303

- Method of recording the deformation diagram in thermal-fatigue tests. 17 p2165 A73-34278
- A study of thermal ratchetting using closed-loop, servo-controlled test machines. 18 p2296 A73-36585
- Method of studying thermal fatigue from the parameters of the hysteresis loop in temperature-force coordinates. 20 p2619 A73-39362
- ### THERMAL INSTABILITY
- Some aspects of the instability of superrefractory alloys rich in nickel. 01 p0062 A73-10270
- Thermal instability of nonuniform plasma in steady state D-T fusion reactor operated by charged particle heating with spatially uniform fuel injection. 01 p0084 A73-10465
- Stationary state of the radially symmetrical motion of vapors heated by laser radiation with allowance for thermal and ionizational nonequilibrium. 02 p0175 A73-11601
- On the origin of small-scale type II irregularities in the equatorial electrojet. 02 p0157 A73-11760
- Ni-Cd battery thermal runaways caused by self sustaining temperature increases, discussing operational and maintenance procedures for avoidance or correction. 03 p0251 A73-12906
- Thermal instability of the hydrogen-burning shell in nondegenerate stars. 03 p0366 A73-12937
- Boundary conditions for temperature perturbations in stability problems of compressible gas flows. 03 p0245 A73-13672
- Influence of thermal nonstationarity on convective heat-transfer intensity. 05 p0640 A73-16773
- A study of germanium monoxide at high temperatures. 06 p0739 A73-18659
- Dwarf binary component convective shell behavior under gravitational field periodic tidal action, noting conditions for thermal instability. 08 p0102 A73-21548
- Thermal instability in a viscoelastic fluid layer in hydromagnetics. 09 p1166 A73-22418
- Thermal instability of coronal neutral sheets and the formation of quiescent prominences. 11 p1422 A73-25940
- Stellar evolution lifetime shortening due to thermal instability of nuclear energy generation shell, discussing relaxation oscillations and S-process nucleosynthesis. 13 p1683 A73-28990
- Theory of the thermal explosion in the hydrogen shell of a white dwarf. 13 p1683 A73-29091
- Thermal instability of the helium-burning shell in massive stars. 15 p1936 A73-31557
- Development of convection in horizontal layers of a non-Newtonian fluid. 16 p2084 A73-32679
- Magneto-gravitational and thermal instability in the Galactic disk. 17 p2231 A73-34752
- Free convection and thermal explosion in reactive systems. 17 p2255 A73-35662
- Thermal instabilities and energy relations in convective shells of slowly rotating stars. 19 p2481 A73-37346
- Stability of the sun against spherical thermal perturbations. 20 p2608 A73-39428
- Rotating cylinder model for plasma gradient-temperature instability in gravitational field, showing heat convection due to Coriolis-caused particle drift. 21 p2769 A73-40730
- Propagating thermal waves in force-cooled superconducting devices. 22 p2938 A73-42953
- Rayleigh-Taylor problem of thermal instability of density-stratified layer of incompressible fluid heated from above, considering oscillatory and nonoscillatory modes stability. 23 p3048 A73-43346
- Gradient instabilities in a system of gravitating point masses. 24 p3132 A73-44479
- Density variation and radiative exchange effects on convective instability of plane-parallel polytropic atmosphere heated from below with application to solar granulation. 24 p3135 A73-44628
- Unsteady convective heat exchange for various hot-gas cooling laws in tubes. 24 p3156 A73-45077
- Magnetically induced electrothermal instability in unseeded partially ionized shock heated argon plasma. 24 p3117 A73-45454

THERMAL INSULATION

- Determination of a time-dependent thermal stress on a finite cylinder [DGLR PAPER 72-112]. 02 p0230 A73-11671
- German monograph - Propagation of ion acoustic waves in a weakly ionized plasma. 03 p0398 A73-13814
- Thermophysical properties of thermally insulating materials in the cryogenic temperature region. 04 p0520 A73-15938
- Hypersonic rarefied flow past an insulated flat plate with suction/injection. 04 p0520 A73-15939
- Insulating materials fireproofing effectiveness prediction by finite element method for combined time dependent convective-radiative boundary conditions. 05 p0637 A73-16132
- Free convective heat transfer between vertical parallel plates One plate isothermally heated and the other thermally insulated. 05 p0638 A73-16221
- Temperature distribution at a thermally insulated crack in a plate for various boundary conditions. 05 p0640 A73-16774
- High performance cryogenic multilayer thermal insulation with plastic films coated by vapor deposited metal, discussing heat transfer mechanism for comparison with microsphere insulation. 05 p0642 A73-17285
- Thermal performance evaluation of REI panel gaps for Space Shuttle Orbiter. 07 p0919 A73-19487
- Radiative heat transfer in fiberglass insulation. 08 p1021 A73-20866
- Steady turbulent boundary layer of compressible perfect gas on heat insulated surface with suction and longitudinal pressure gradient. 08 p0954 A73-21177
- Turbulent incompressible boundary layer on porous heat insulated plate with uniform suction, calculating ratio of friction drag coefficients. 08 p0954 A73-21178
- Principles of evacuated cryogenic insulations. 11 p1450 A73-25581
- Determination of the required thickness of thermal insulation casings and evaluation of the weight-based effectiveness of materials. 12 p1558 A73-27092
- Spatial problem of thermoelasticity of a body with an insulated external circular crack. 14 p1814 A73-30725
- Space shuttle lightweight thermal protective insulation materials rain erosion resistance determination at 200-400 MPH and various angles of attack, using rotating arm test apparatus. 16 p2071 A73-33030
- Coating development of Martin Marietta's reusable surface insulation /MAR-SI/ for Space Shuttle applications. 16 p2071 A73-33059
- Cryogenic insulation heat transfer. 17 p2254 A73-34355
- Reinforced plastics under ablative conditions for thermal insulation and structural applications. 17 p2195 A73-34805
- Wind tunnel and flight tests for Saturn S-2 stage polyurethane spray foam insulation erosion under aerodynamic heating, shear stress and static pressure [AIAA PAPER 73-740]. 18 p2326 A73-36357
- IR spectral measurements of reusable surface insulations via radiative four flux model [AIAA PAPER 73-745]. 18 p2370 A73-36361
- Russian book - High-temperature strain gauges based on heat-resistant oxides. 21 p2704 A73-41286
- Nonstandard thermocouple materials, discussing metal and nonmetal thermocouples and ceramic insulating materials. 22 p2857 A73-42036
- Tungsten-rhenium thermocouple, describing alloys behavior, fabrication, insulation sheaths, calibration, stability and applications. 22 p2857 A73-42037
- Fabrication of high-reliability sheathed thermocouples. 22 p2865 A73-42041
- Some designs using sheathed thermocouple wire for jet engine applications. 22 p2858 A73-42042
- Equivalent circuit modeling of insulator shunting errors in high temperature sheathed thermocouples. 22 p2858 A73-42045
- Approximate calculation of the optimal section of a compressible gas on a thermally insulated surface at Prandtl numbers other than unity. 22 p2795 A73-42118
- Thermal characterization of reusable external insulation for the space shuttle. [ECTP PAPER B2-8]. 22 p2931 A73-42403
- ### THERMAL NEUTRONS
- Neutron diffusion from a distributed source in a homogeneous atmosphere. 06 p0742 A73-17549

- Epithelial neutron differential flux spectrum in equilibrium layers of atmosphere at 57 degrees north. 08 p1000 A73-21350
- Theory of fluctuations and particle scattering in ferromagnetic semiconductors and metals. 09 p1134 A73-22678
- Neutron diffusion from a distributed source in an inhomogeneous atmosphere. 16 p2052 A73-32777
- Recoilless nuclear transition based gamma laser using resonant gamma rays or thermal neutron beam irradiation and selective photoionization. 16 p2024 A73-34072
- ### THERMAL NOISE
- The noise of microwave Schottky diodes at 70 MHz. 06 p0673 A73-17570
- Cubic /four-index/ theory of thermal noises in nonlinear resistances. 07 p0792 A73-19910
- Measurement of amplifier noise. 08 p0949 A73-21623
- Thermal noise calculation of single-carrier space-charge-limited current in a non-insulating solid. 12 p1530 A73-27029
- Gunn microwave oscillators electron temperature dependent noise in absence of 1/f type, considering thermal or Johnson noise augmented by carriers hopping. 12 p1478 A73-27111
- Electrical fluctuations in ideal forward-biased non-degenerate diodes. 12 p1480 A73-27272
- Silicon semiconductor resistance strain gage intrinsic thermal noise characteristics at 20 Hz-10 kHz, noting 1/f type as dominant noise component in audio frequency range. 13 p1611 A73-28021
- Thermal noise measurements on space-charge-limited hole current in silicon. 13 p1668 A73-28542
- SNR improvement by negative feedback and deterioration by positive feedback in amplifiers, discussing input circuit thermal noise. 13 p1591 A73-28735
- Extension of the theory of frequency noise of oscillating masers. 13 p1630 A73-29558
- A contribution to the proof of the formula for resistance noise. 16 p1978 A73-32910
- Thermal noise behavior of a FET as a function of the doping profile of the gate-channel junction. 16 p1988 A73-33274
- A study of millimeter-wave GaAs IMPATT oscillator and amplifier noise. 17 p2133 A73-34217
- Natural fluctuations in linear quantum amplifiers. 20 p2574 A73-39699
- Thermally induced FM noise in Gunn oscillators and jitter in Gunn-effect digital devices. 21 p2660 A73-40096
- Quantum mechanics /semiclassical/ theory investigation of shot and thermal noise effects on laser behavior, deriving Fokker-Planck equations for field probability distribution. 21 p2711 A73-40215
- Noise in solid travelling-wave tubes using coupled-mode analysis. 21 p2665 A73-41122
- Short-term frequency stability of the Rb-87 maser. 21 p2716 A73-41148
- Noise of space-charge-limited current in solids is thermal. 21 p2668 A73-41559
- Refraction, convection, and diffusion flame effects in combustion-generated noise. 22 p2934 A73-42780
- Josephson junction I-V characteristics and measurements of phase modulated quasi-particle current in superconducting weak links, taking into account thermal noise. 23 p3018 A73-44174
- ### THERMAL PLASMAS
- Solar coronal plasma cyclotron radiation, taking into account temperature effects. 01 p0096 A73-10309
- Model development of supersonic trough wind with shocks. 03 p0298 A73-12887
- Magnetospheric thermal plasma and hydrogen cation density profile characteristics in different local time regions explained by time-varying convection model. 03 p0303 A73-13879
- Behavior of thermal plasma in the magnetosphere and topside ionosphere. 04 p0442 A73-15336
- Cumulation-laser heating of two-temperature plasma, the recovered energy of nuclear fusion being taken into consideration. 04 p0480 A73-15596
- Recent results of plasma-wall heat transfer studies in highly ionized, dense plasmas. 05 p0603 A73-16762

- Monochromatic plasma wave instability due to induced scattering on thermal plasma electrons and ions with and without magnetic field
05 p0604 A73-17361
- Solar soft X-ray bursts data recorded by satellite telemetry, considering production by thermal plasma and nonrelativistic electrons with power law energy distribution
08 p0996 A73-20765
- Electromagnetic effects on electrostatic modes in a magnetized plasma.
08 p0991 A73-20820
- Impedance of an ion-sheathed spherical probe in a warm, isotropic plasma.
09 p1127 A73-22431
- Wave transformation in warm magnetoplasma slab with parabolic density profile and two lower hybrid layers, discussing long wavelength energy tunneling and conversion efficiency
[TTU-SR-2] 09 p1129 A73-22637
- Numerical simulation of small amplitude whistler waves in thermal plasma, describing particle motion under self consistent and external magnet fields via Lorentz equation
10 p1255 A73-24269
- On what ionospheric workers should know about the plasmopause-plasmasphere.
10 p1215 A73-24781
- Shock wave large particle model of ion density discontinuity decay in nonisothermal plasma, assuming high electron temperature and Boltzmann distribution
13 p1667 A73-29171
- Split Langmuir probe measurements of current density and electric fields in an aurora.
14 p1748 A73-29970
- Ion heating in thermal plasma flows.
16 p2042 A73-33465
- Probability distribution of electric fields in thermal and nonthermal plasmas.
21 p2744 A73-40216
- A study of geosynchronous corpuscles and photoelectrons on the Cosmos 261 satellite. VI - Epithermal electrons in the energy range from 30 to 150 eV in the region of the dayside and nightside polar cusps
21 p2686 A73-40909
- Theory of a corner-driven loop antenna immersed in a warm plasma.
24 p3070 A73-45486
- THERMAL POLLUTION**
Thermal effects of urbanization and industrialization in the boundary layer A numerical study.
06 p0720 A73-18330
- Thermal mapping at electrical power generating sites for outfall from fossil or nuclear fuel plants, considering airborne application
16 p2015 A73-33360
- Multispectral survey of power plant thermal effluents in Lake Michigan.
20 p2558 A73-39862
- THERMAL POWER**
U TURBOGENERATORS
THERMAL PROPERTIES
U THERMODYNAMIC PROPERTIES
THERMAL PROTECTION
The development of the heat control system of the Helios solar probe
[DGLR PAPER 72-102] 02 p0227 A73-11652
- Book - Fundamentals of spacecraft thermal design.
02 p0237 A73-11885
- Fabrication of a lightweight circular orbit passive radiative cooler.
03 p0329 A73-13010
- Titan III convective base heating from solid rocket motor exhaust plumes.
[AIAA PAPER 72-1169] 03 p0382 A73-13467
- Application of an improved transpiration cooling concept to space shuttle type vehicles.
03 p0397 A73-13492
- Push-pull ac modulator design allowing balanced thermal load on plasma electrodes in pulsed high power short arc Xe flash lamps
03 p0282 A73-13933
- RF sputtered integral covers of glass coating for thermal protection of Si solar cells, noting intrinsic stress, adhesion, transparency and radiation damage resistance
03 p0256 A73-14227
- Time-temperature safety thresholds for human epidermal injury related to materials thermal properties
05 p0637 A73-16138
- Aerothermodynamics of the Space Shuttle reaction control system.
[AIAA PAPER 73-93] 05 p0629 A73-16857
- Effectiveness of the thermal protection of a plane wall during injection of air through two rows of rectangular holes arranged in a checkered order
06 p0768 A73-18127
- Thermal protective garment using independent regional control of coolant temperature.
07 p0785 A73-19481
- Thermal behavior of a plasma-heated tungsten probe in the presence of tungsten vapor.
[ECS PAPER 88] 07 p0788 A73-20447
- Post impact behavior of mobile reactor core containment systems.
07 p0850 A73-20468
- Electronic equipment burn-in for repairable equipment.
08 p0945 A73-20949
- Reducing the thermal bending of a gravity-gradient stabilizer with the aid of a protective covering
10 p1286 A73-23894
- Nb refractory alloy sheet mechanical properties for application in space shuttle thermal protection system /TPS/ and space tug aerobraking system
10 p1235 A73-24445
- Hypervelocity tactical missile radome materials with noncharring ablator and fiberglass substructure for thermal protection against aerodynamic heating with negligible effects on radio transmission
11 p1336 A73-25307
- Evaluation of columbium alloy thermal protection systems for space shuttle.
[AIAA PAPER 73-378] 11 p1380 A73-25508
- Heat pipe cooling of electronic components for design requirements of high voltage insulation, small size, low temperature and protection from external heat sources
11 p1451 A73-25990
- Compact gas transpiration cooling system for thermal protection of hypersonic flight leading edges, discussing computer program
11 p1452 A73-26212
- Surface materials ablation cooling for thermal protection during reentry, discussing chemical reactions, plastics pyrolysis and propulsion chemistry
14 p1724 A73-30133
- Influence of stress concentrations on the mechanical properties of cast molybdenum with protective coatings
14 p1763 A73-30688
- Bioassay method for thermal protective clothing fabrica evaluation, measuring skin damage with various fabric combinations under exposure to calibrated flame source
16 p1974 A73-32671
- Space shuttle lightweight thermal protective insulation materials rain erosion resistance determination at 200-400 MPH and various angles of attack, using rotating arm test apparatus
16 p2071 A73-33030
- Low-cost fabrication and installation of ablative heat shields for the space shuttle orbiter.
16 p2072 A73-33060
- Thermal shielding by subliming volume reflectors in convective and intense radiative environments.
17 p2253 A73-34183
- Evolution of the Space Shuttle. II.
17 p2240 A73-35660
- Spacecraft microbial burden reduction due to atmospheric entry heating - Jupiter.
18 p2281 A73-36100
- Heat shielding for Venus entry probes.
[AIAA PAPER 73-712] 18 p2368 A73-36332
- Thermoelectric device application to spacecraft thermal control.
[AIAA PAPER 73-722] 18 p2369 A73-36339
- Evaluation of aerodynamic heating uncertainties for Space Shuttle.
[AIAA PAPER 73-737] 18 p2359 A73-36354
- Four Space Shuttle wing leading edge concepts.
[AIAA PAPER 73-738] 18 p2359 A73-36355
- Initial development of an ablative leading edge for the Space Shuttle orbiter.
[AIAA PAPER 73-739] 18 p2369 A73-36356
- Temperature control of the Mariner class spacecraft - A seven mission summary.
[AIAA PAPER 73-769] 18 p2360 A73-36383
- Space Shuttle Orbiter radiative, ablative and insulative thermal protection system design, performance and reliability
19 p2492 A73-37596
- Reduction of thermal deflection of gravitational stabilizer using shielding cover.
20 p2614 A73-38913
- Method for determining the heat conductivity coefficient of high-temperature materials during unsteady heating
20 p2629 A73-39616
- Thermal design and analysis aspects of advanced communication spacecraft.
20 p2531 A73-39773
- Space shuttle design program with Mark I and II stages, considering thermal protection weight analysis for minimum maintenance and turnaround time
21 p2780 A73-40416
- Catalytic activity in platinum group temperature sensors, discussing elimination by noncatalytic coatings
22 p2857 A73-42034
- High reliability protective coatings for high temperature technology.
22 p2879 A73-42596
- Two stage recoverable space shuttle structural design, discussing configurations, costs and orbiter and booster materials and thermal protection systems
23 p3038 A73-43786
- THERMAL RADIATION**
NT PHONON BEAMS
Spatial-temporal processing of thermal radio signals from emitters moving in the near zone of an interferometer
01 p0017 A73-10213
- The effect of solar radiation reflected from water surfaces on airborne and surface measurements in the thermal infrared.
01 p0038 A73-10385
- Model analysis for heat radiation effect on development and evolution of single buoyant thermal rising in neutrally stratified atmosphere, noting radiative relaxation time
[AD-755499] 01 p0039 A73-10398
- Radiation in the reacting boundary layer.
01 p0121 A73-10642
- Brightness temperature measurement of Callisto satellite thermal radio emission, using ice layer model
01 p0101 A73-10845
- Calculation of the spectral, angular and altitudinal distributions of the thermal radiation field of the atmosphere and the earth's surface
01 p0040 A73-10871
- Direct Monte Carlo simulation of two-dimensional radiative heat transfer in absorbing-emitting medium bounded by the non-isothermal gray walls.
01 p0123 A73-11139
- Interaction of thermal radiation with laminar free convection from a heated vertical plate.
01 p0123 A73-11141
- Thermal effect of optical radiation on water drops of small size
01 p0074 A73-11244
- Nonstationary interaction of thermal radiation with surfaces of pure metals
01 p0124 A73-11434
- Cloud characteristics in problems of radiation energetics in the earth's atmosphere.
02 p0159 A73-12146
- Seasonal and monthly global atmosphere radiative profiles of thermal and solar heating due to ozone and cooling due to carbon dioxide
02 p0165 A73-12780
- The propagation of small disturbances in radiative magnetogasdynamics.
03 p0345 A73-12923
- The radioastronomy of the planets
03 p0372 A73-13273
- Radiation base heating from solid propellant launch vehicle exhaust plumes.
[AIAA PAPER 72-1168] 03 p0397 A73-13466
- IR observations of comets Bennett and Tago-Satoko, noting thermal origin of flux, source structure and material temperature, emissivity and composition
04 p0494 A73-14754
- The influence of fuel preparation and operating conditions on flame radiation in a gas turbine combustor.
[ASME PAPER 72-WA/HT-26] 04 p0519 A73-15828
- Luminous flames thermal radiation total emissivity analysis, considering water vapor, carbon dioxide and soot particles overlapping spectral bands
[WSCI PAPER 72-41] 05 p0638 A73-16677
- A non-similar solution of heat transfer in external non-Newtonian flow with thermal radiation.
[AIAA PAPER 73-116] 05 p0640 A73-16873
- New method for determining the total radiating power of partially transparent materials at high temperatures.
06 p0722 A73-17414
- Brightness temperature of Mars thermal emission in two orthogonal polarizations by microwave radiometry from Mars 2 and 3 orbiters
06 p0747 A73-17490
- Mars microwave spectra computation by improved thermal model with seasonal polar cap effects and accurate aspect geometry, noting lunar-like planetary subsurface nature
06 p0747 A73-17492
- Some averaged properties of wave solutions for a hypersonic thermal wave.
06 p0728 A73-17890
- Pyroelectric tubes for thermal imaging system, discussing materials, electron beam read-out, SNR and performance limit compared with scanned photon detectors
07 p0798 A73-19224
- Electrical components heat dissipation via thermal radiation, determining nonlinear temperature dependence from Stefan-Boltzmann law
08 p1020 A73-20775
- Plane or axisymmetric inviscid optically gray hot gas jet radiating near optically thin limit, considering thermal radiation-gas dynamics coupling effects
08 p1020 A73-20783
- Specular reflection of heat radiation from an arbitrary reflector surface to an arbitrary receiver surface.
08 p1022 A73-21254
- Heat flux contours on a plane for parallel radiation specularly reflected from a cone, a hemisphere and a paraboloid.
08 p1022 A73-21255
- A numerical model of thermal radiation in a dusty atmosphere.
08 p0960 A73-21383
- Assessment of temperature rise suppression by edge losses during irradiation.
09 p1045 A73-22533

THERMAL RADIO EMISSION

Apollo 14 lunar fines thermal radiation properties as function of bulk density, illumination angle and wavelength, calculating solar albedo and total emittance

10 p1277 A73-24080

Construction of the solution to a nonlinear boundary value problem for a heat-radiating body of complex shape

10 p1296 A73-24510

The thermal radiation spectra of supermassive stars and X-ray sources.

10 p1270 A73-24902

Book - Thermal radiative properties: Nonmetallic solids.

11 p1387 A73-25275

Experimental determination of the integral radiative capacity of nickel

11 p1398 A73-25739

Nonstationary interaction of thermal radiation with surfaces of pure metals.

11 p1452 A73-26061

IR spectra of quasars and Seyfert galaxies interpreted as thermal radiation from dust envelopes around cores, considering graphite and silica dust particles

12 p1547 A73-27876

IR thermographic scanners and viewers operational principles, equipment performance specifications and thermal radiation distribution

13 p1611 A73-28020

Results of lunar surface investigations based on its intrinsic radiation

13 p1672 A73-28116

The spectral, angular, and altitudinal distributions of the earth and sky thermal radiation field.

13 p1607 A73-28695

Thermal IR radiation receiver with ferroceramic capacitor for amplification and transformation of signals from RF oscillator

13 p1618 A73-29133

The stability of a thermally radiating stratified shear layer.

14 p1816 A73-30169

Solution of certain nonlinear boundary value problems for regions of complex shape by a structural method

14 p1769 A73-30349

The annual radiation balance of the earth-atmosphere system during 1969-70 from Nimbus 3 measurements.

14 p1750 A73-30762

Calculation of a subsonic radiating gas flow by an adjustment method

15 p1821 A73-30969

Brightness temperature measurement of Callisto thermal radio emission, using ice layer model

15 p1928 A73-30981

Integral transmittance function of the thermal radiation

15 p1904 A73-31782

Estimation of errors arising in calculations of the fluxes and influxes of thermal radiation due to errors in the initial meteorological parameters

15 p1905 A73-31786

Some field characteristics of outgoing thermal radiations in the Venusian and Martian atmospheres

15 p1937 A73-31819

The synergistic inactivation of biological systems by thermoradiation.

16 p1976 A73-33696

Sterilization technology in the United States space program.

16 p1976 A73-33697

Spectral intensity of thermal radiation in a medium for frequencies in the neighbourhood of an absorption line.

16 p2038 A73-34028

Emission of an isothermal, isotropically scattering medium.

18 p2336 A73-36324

Photodetection volume of coherence for thermal optical source with given intensity and spectral density, defining photon phase space cell concept

20 p2570 A73-38610

Dynamics of step heat waves in gases and plasmas.

20 p2592 A73-38863

Integral moisture content determination in rain clouds by simultaneous thermal radiation and radar measurements

20 p2584 A73-39190

Thermal IR image recording, processing and enhancement, discussing prevention of defects or irregularities caused by aircraft motion, weather and electronic noise

20 p2566 A73-39670

Utilization of thermal infra-red ground measurements for determination of adequate surveying periods in remote sensing.

20 p2558 A73-39868

Isothermal mapping of temperature patterns from thermal discharges in Italian coastal waters.

20 p2560 A73-39888

Thermal activity of the Uson Caldera based on infrared and photographic aerial survey.

20 p2561 A73-39895

The decay of perturbations in an electrically conducting and thermally radiating gas.

21 p2789 A73-40246

Precession damping of solar probes by radiative forces.

21 p2737 A73-40767

Theory and measurement of emittance properties for radiation thermometry applications.

22 p2886 A73-41982

Microwave radiometric systems.

22 p2859 A73-42059

Optimal utilization of redundant information in thermal radiation in thermophysical measurements.

22 p2931 A73-42408

Thermal stresses due to an internal source of heat in a solid elastic hemisphere with radiating curved surface and the plane base resting on a smooth rigid insulating plane surface.

22 p2932 A73-42469

Tungusk meteorite event with thermal radiation and severe blast wave attributed to black hole of substellar mass

22 p2909 A73-42488

Viscous laminar Hartmann flow of electrically conducting liquid between parallel walls in transverse magnetic field, assessing thermal radiation effects and temperature distribution

23 p3008 A73-43207

Burner dimension and flame size effects on relative contributions of luminous soot and nonluminous molecular band radiations from combustion fires

23 p3048 A73-43329

THERMAL RADIO EMISSION

U RADIO EMISSION

U THERMAL EMISSION

THERMAL REACTORS

Reactor-thermoelectric power systems for NASA Space Station/Space Base.

11 p1395 A73-26012

Low temperature-reactor Brayton cycle for Space Station/Base application.

11 p1311 A73-26013

Unmanned reactor-thermoelectric systems for applications in the 1970's.

11 p1395 A73-26024

Thermionic reactor systems for electric propulsion.

11 p1395 A73-26025

THERMAL RESISTANCE

Assessment of the heat resistance of graphites over a wide range of temperatures

02 p0184 A73-11619

Structural hardening calculation procedures and thermal strength problems.

02 p0235 A73-12201

Moisture effects on the high-temperature strength of fiber-reinforced resin composites.

03 p0328 A73-13002

Non polar thermosetting resins for high temperature electrical/electronic components.

03 p0332 A73-13035

Increasing the heat resistance of steel Kh14G14N3T with microadditions of boron.

03 p0327 A73-14006

Thermal shock produced edge effect in thermoelastic heated cylinder analyzing brittle material heat resistance and failure

03 p0394 A73-14019

Experience with the application parametric diagrams to the calculation of the heat resistance of construction materials

04 p0466 A73-15665

Thermal resistance /conductance shape factor/ prediction for thermal components, considering cylindrical and rotational coordinate systems

05 p0640 A73-16877

P-n junction size effect on thermal resistance of reverse biased Si mesa-type diode, considering junction area, mesa height and power dissipation

06 p0674 A73-17795

Weldability, corrosion resistance and heat resistance increase in Nb alloyed steels, noting aging temperature effects and microstructure

06 p0706 A73-17886

Heat resistance of alloys of the compound TiAl with niobium at 800 and 1000 C

06 p0708 A73-18049

Choice of thermal parameters for a photoelectric switch operating with a capacitive load

06 p0676 A73-18087

Mechanical properties of heat and corrosion resistant nonmagnetic Ni-Cr-Nr spring alloys with W addition tested in aggressive and nitric acid base media

06 p0709 A73-18211

Russian book - Heat resistance of welded joints.

07 p0831 A73-20230

Experimental investigation of heat transfer using facilities for testing heatproof materials

08 p1022 A73-21094

Method for determining the thermal resistance of channel-wall deposits

08 p1022 A73-21198

Steel and Ni-based alloys structural stability during long term high temperature creep, noting matrix struc-

ture dependence on initial dislocation and interparticle spacing

08 p0980 A73-21780

The effect of creep strain on stacking-fault precipitation in Nb-stabilized 20/25 austenitic stainless steels.

08 p0981 A73-21787

The influence of nickel content on the structure and high temperature properties of a 12% Cr Mo V Nb steel.

08 p0982 A73-21799

W-Ta alloys prepared by electron beam melting, testing Ta content effects on oxidation resistance and hardness at high temperatures

09 p1103 A73-22424

Weibull distribution government of dispersion of destructive temperature gradients characteristic of fireproof ceramic materials heat resistance

09 p1110 A73-23061

Forced air cooling of dual-in-line packages.

10 p1193 A73-23607

Effects of Ni and Fe addition on various properties in heat-resisting aluminum casting alloys.

10 p1231 A73-23675

Preparation and performance characteristics of flammable and inflammable polyimide foams as sand-wich fillers

10 p1239 A73-24098

Influence of temperature on the damping characteristics of heat resistant EP452 and EI696 steels in a uniform stress-strain state produced by tension and compression

10 p1233 A73-24358

Failure analysis and heat resistance optimization factors of reinforced metal sheet under thermal cycling

10 p1233 A73-24369

Effect of chemical composition on the heat resistance of steel Kh25N16G7AR.

10 p1236 A73-24932

Thermal resistance and aging properties of polybenzimidazoles, polyimides and polyamides-imides used for Mach 3 aircraft radomes

11 p1335 A73-25291

Methods and means of studying the characteristics of heat-resistant strain gauges by means of devices heated by electric current

11 p1362 A73-25457

Consideration of creep probability in a low-alloyed heat-resistant CrMoV steel

11 p1384 A73-26111

The relations between superplasticity and high temperature resistance alloys of metallic systems.

13 p1639 A73-29457

Development of austenitic heat-resistant steel containing a high concentration of nitrogen.

13 p1642 A73-29516

Creep test diagrams plotted to estimate heat resistance for turbine blades design, predicting fatigue life with allowance for loading cycle form and duration

13 p1703 A73-29616

Constant line sources of heat in infinite media, whose thermal resistivities are linear functions of the temperature.

14 p1817 A73-30610

Ceramics replacement for Ni-Cr superalloys to improve automotive gas turbine performance by increasing inlet temperature, considering material selection

15 p1897 A73-31250

Investigation of the influence of certain elements on the heat resistance of titanium aluminide Ti3Al

15 p1894 A73-32530

Properties of titanium-niobium based stable beta alloys

15 p1894 A73-32534

Void free high temperature resistant bismaleimide/woven fiberglass composite laminates, discussing synthesis, processing and fabrication

16 p2028 A73-33046

Coating development of Martin Marietta's reusable surface insulation /MAR-SI/ for Space Shuttle applications.

16 p2071 A73-33059

Some physicochemical and technological aspects of obtaining annealed coatings from melts and semimelts

18 p2318 A73-35887

Modeling the effect of air and oil upon the thermal resistance of a sphere-flat contact.

18 p2370 A73-36362

Prediction of the heat-resistance characteristics of high melting materials

18 p2323 A73-36757

Ti rich corner of Ti-Al alloys phase diagrams investigated by differential thermal analysis and radiography for thermal resistance and intermetallic compounds existence

19 p2441 A73-37838

The nature of chemoreception in posterior hypothalamic structures

21 p2636 A73-40279

Effect of supersonic gas flows on the structure and heat resistance of metal alloys

21 p2717 A73-40481

A study of the heat resistance of Nb-Mo alloys containing titanium and zirconium 21 p2718 A73-40489

Heat resistance of chromium-nickel and chromium-nickel-molybdenum steels with additions of boron 21 p2718 A73-40734

Effect of mechanicochemical treatment on the heat-resistant properties of 1Kh14N18V2B steel with boron additives 21 p2718 A73-40735

Hot-pressed eutectics of oxides and metal fibers. 21 p2723 A73-40895

Ti, Al, W and Mo concentrations effect on heat resistance of precipitation hardened Ni-based alloys 21 p2720 A73-41035

Calculation of the heat resistance of metals at variable temperatures 21 p2721 A73-41230

Influence of the method of preparing a Ni + ThO₂ composite and of its strengthening-oxide content on heat resistance 23 p2990 A73-43486

The relation between the internal thermal resistance of transistors and the method of alloying 23 p2960 A73-43677

Research and development of aerospace adhesive bonded systems and concepts. 24 p3093 A73-44763

Development of methods for long-term prediction of heat-resistance characteristics 24 p3099 A73-44768

Effect of aluminum-containing components on phase alloying in periclase ceramic materials 24 p3104 A73-44953

THERMAL SHIELDING
U HEAT SHIELDING
THERMAL SHOCK

Circular cylindrical shell stability for thermal shock on end face, calculating critical thermal flux 02 p0232 A73-11818

Thermal shock produced edge effect in thermoelastic heated cylinder analyzing brittle material heat resistance and failure 03 p0394 A73-14019

Sonic degradation of thermally shocked ceramics. 04 p0448 A73-15124

One-dimensional shock waves in heat conducting materials with memory. II. 04 p0511 A73-15225

Transient heat transfer through a thin-walled circular pipe. 06 p0766 A73-17443

Thermal shock induced transverse vibrations in rectangular plate with combined simple and clamped edge supports, deriving infinite series solutions 06 p0761 A73-17896

The thermal shock on the shell of revolution-coupled and uncoupled theory. 06 p0763 A73-18452

Transversal vibrations of the thin shell of revolution produced by the thermal shock. 06 p0763 A73-18453

Thermal and mechanical history of breccias 14306, 14063, 14270, and 14321. 07 p0883 A73-19729

Propagation of one-dimensional disturbances in a linear viscoelastic half-space under thermal shock 10 p1293 A73-24677

The state of technology of ceramic radomes, their use and possibilities for the future. 11 p1335 A73-25286

Differential equations of thermoelastic state for shells receiving a thermal shock at the surface 12 p1555 A73-27790

Spherical concentric shock wave excitation in elastic medium by hypersonic thermal wave in terms of displacements, particle velocity and stresses 14 p1817 A73-30252

Long term life tests for thermal shock cycles effects on plastic encapsulated semiconductor device reliability, presenting salt atmosphere testing data for silicone package 19 p2471 A73-38454

Integration of a nonlinear partial differential mixed boundary value problem 21 p2792 A73-41065

Improvement of thermal shock resistance by surface prestressing. 22 p2921 A73-42462

A coupled thermo-elastic problem of a half-space under the action of a thermal shock on the bounding surface. 22 p2922 A73-42467

Resistance to crack propagation in ceramics subjected to thermal shock. 23 p2997 A73-44031

THERMAL SIMULATION

Propellants selection to provide an air simulant for hot gas testing or ramjets. 03 p0351 A73-13397

Russian papers on thermal stresses investigation in machine and structural elements covering stress simulation and strain gage methods for model and full scale structures 11 p1435 A73-25451

Methods of simulating the thermal and stressed state at the edges of gas turbine blades 13 p1698 A73-29054

Simulation of a steady-state integrated human thermal system. 15 p1839 A73-32225

Thermal modeling of a plate with coupled heat transfer modes. 18 p2370 A73-36364

[AIAA PAPER 73-748] Mathematical modeling for ATS-F spacecraft louvers and heat pipes thermal control heat rejection capacity, noting correlation with solar environment simulation data 18 p2360 A73-36387

[AIAA PAPER 73-773] Methods of modeling thermal and stressed states in the edges of gas turbine blades. 18 p2366 A73-36886

Functional tests with hypersonic flight vehicles, using an infrared heating system to simulate the temperature loads in flight 19 p2419 A73-38269

Thermal model for streamers in nonequilibrium plasmas. 19 p2470 A73-38317

Book on engineering dynamics similarity and scaling methods covering blast waves and gas dynamics, transient loads, fluid-structure interaction, soil dynamics, thermal modeling, etc 23 p3039 A73-43460

THERMAL STABILITY

Construction materials selection for thermal dimensional stability in critically sensitive precision instruments and mechanical components, considering economic factors 01 p0066 A73-11293

Austenite deformation effect on thermal stability and hardness of Ni steels at various C and Ni concentrations 01 p0067 A73-11349

Thermogravimetry of thermally stable aromatic and heterocyclic polymers. 01 p0015 A73-11447

Investigation of cryogenic stability and reliability of operation of Nb3Sn coils in helium gas environment. 02 p0200 A73-11838

The Viking Orbiter 1975 beryllium INTEREGEN rocket engine assembly. 03 p0382 A73-13438

[AIAA PAPER 72-1131] High efficiency Cu2S-CdS-solar cells with improved thermal stability. 03 p0255 A73-14216

Measurement of small-scale turbulence and thermal stability in the lower atmosphere by radar. 03 p0279 A73-14536

Influence of the nonlinear thermomechanical effect on the thermal stability of rubber-metallic couplings of vibration machines 04 p0509 A73-14981

Thermal pulses in helium shell-burning stars. 04 p0499 A73-15364

Thermal collapse theory of hydrodynamic oil lubrication films failure for slider bearing, noting frictional forces role 05 p0580 A73-16105

Thermal stability improvement of variable inductance electronic circuits for analog magnitudes conversion to frequencies, noting instrument errors compensation 05 p0577 A73-16987

Linear series and of stellar models. I - Thermal stability of stars. 05 p0621 A73-17069

Thermodynamic stability of ordered phase atomic structure state for antiphase domain formation, noting superstructures in face centered and body centered cubic solutions 06 p0736 A73-18118

Coupled thermoelastic stability effect on critical thermal buckling of strip under compression in temperature field 06 p0765 A73-18686

Morphology of gamma prime and gamma double prime precipitates and thermal stability of Inconel 718 type alloys. 06 p0711 A73-18755

Thermally stable heterocyclic ladder polymer films preparation techniques in manufacture of solar cells with CdS or CdTe thin films for space applications 07 p0841 A73-18903

Stability of reactive and refractory metal borides in ternary chromium-base alloys. 07 p0838 A73-19122

Temperature effects on transistor input and output static characteristics, proposing thermal stabilization by collector circuit resistance decrease and heat dissipation increase 07 p0798 A73-19294

New high performance silicone greases and their applications. 07 p0842 A73-19557

Prediction of the low-temperature stability of type 304 stainless steel from a room temperature deformation test. 07 p0840 A73-20414

Contribution to the theory of the resonant thermal self-stabilization in ferroelectric vibrational systems 08 p0948 A73-21519

The effect of niobium content on the steady-state creep of stabilized 20/25 austenitic stainless steels. 08 p0981 A73-21786

Thermal stability of the microstructure in the eutectic composition Al-Al3Ni 09 p1099 A73-21966

Solid polymer electrolyte fuel cell technology application to space shuttle orbiter requirements, noting 2000 hours maintenance free life and thermal stability 09 p1035 A73-22786

Influence of thermally stabilizing alloying additions on the antifiraction properties of lamellar graphites with a organic silicon binders 09 p1110 A73-22978

A new FM system with a novel modulator design yielding high linearity and thermal stability. 09 p1058 A73-23430

Temperature recovery coefficients during turbulent flow of liquid in a circular pipe 10 p1204 A73-23509

Electronic equipment thermal management for energy dissipation rejection, summarizing heat pipe, phase-change heat transfer and high pressure gas convection techniques 10 p1295 A73-23789

Solid composite material thermostats and overall thermoelectric modulus determination, considering arbitrarily anisotropic phases, binary composite and self consistent theory 10 p1295 A73-24099

Thermostable polymers for freezing and cryogenic temperatures, noting theory, methodology and preparation for science and industry 10 p1241 A73-24675

IR-spectroscopic investigation of the thermal stability of albumin at different levels of its ionization 10 p1182 A73-24685

Russian book on thermal stability of refractory ceramics covering strength and thermophysical characteristics, high temperature thermal fracture and facilities for normal and cyclic load tests 11 p1386 A73-25174

Stability of nickel coated sapphire whiskers. 11 p1389 A73-26044

Elevated temperature stability of carbon-fibre, nickel-matrix composites Morphological and mechanical property degradation. 11 p1384 A73-26047

Relaxation stability of iron and nickel alloys at high temperatures 12 p1509 A73-26898

Analysis of the thermal stability of high- and low-power silicon planar transistors in the dynamic regime 12 p1478 A73-26949

Stability of heat transfer during boiling at a nonisothermal surface 12 p1558 A73-27314

Ditantalum carbide thermodynamic stability determination from measurement of carbon monoxide pressure in equilibrium with tantalum carbide-tantalum oxide-tantalum mixture at 1470-1620 C 13 p1632 A73-28128

Directionally solidified eutectic alloy composites for high temperature turbine blade and vane applications, considering morphology, crystallography and thermal stability properties 13 p1635 A73-28778

Mode factor and stress concentration parameter for sudden heating of solid cylinders and disks, noting thermal stability criterion with allowance for statistical strength 13 p1703 A73-29611

Test equipment for thermal stability determination of brittle refractory material, noting data processing procedure and formulas for temperature distribution and thermal stress 13 p1599 A73-29629

Natural and synthetic thermally stable polymers, discussing pyrolysis, structure-property relationships and bond strengths 14 p1724 A73-30132

Emission instability of thermionic converters. 14 p1713 A73-30474

Temperature stability of the disperse phase component of the output emission of an optical quantum amplifier 14 p1758 A73-30576

Stability of the thermomechanical hardening effect in 60N20 nickel steel 14 p1760 A73-30590

Failure under thermal loads of cylindrical bodies consisting of brittle materials 14 p1813 A73-30683

High temperature solid lubricants lubricating and environmental stability characteristics, discussing ball and journal bearings wear test results [ASME PAPER 73-DE-9] 14 p1767 A73-30818

Stellar nuclear hydrogen burning shell thermal stability to radial perturbations, discussing growth rate, energy generation and temperature increases 15 p1929 A73-31058

- Thermal convective instability in uniformly rotating magnetized isothermal stellar atmosphere with constant Alfvén speed, discussing heat loss mechanism dependence on temperature
15 p1929 A73-31060
- Compatibility of silicon carbide fiber with a tungsten base and a titanium matrix
15 p1888 A73-31595
- Stability of metal-based composite materials
15 p1888 A73-31596
- Titanium hydride and hydronitride thermal stability analysis from hydrogen vapor pressure and decomposition measurements in vacuum at 400-1100 C
15 p1888 A73-31601
- Effect of prepregging solvent on high-temperature stability of KERIMID 601 composites.
16 p2029 A73-33049
- Synthetic foam from Pyrrone prepolymer and hollow carbon microsphere mixtures, discussing low curing shrinkage and high thermal stability
16 p2029 A73-33051
- On the observability and stability of the temperature distribution in a composite heat conductor.
16 p2034 A73-33311
- Thermal stability of radiating fluids - The Benard problem.
16 p2085 A73-33313
- Thermal stability of radiating fluids - Asymmetric slot problem.
16 p2085 A73-33314
- Transistor design and thermal stability.
17 p2133 A73-34218
- JFTOT - A new fuel thermal stability test / A summary of a Coordinating Research Council activity. [SAE PAPER 730385]
17 p2147 A73-34722
- Temperature restitution coefficients for turbulent fluid flow in a circular pipe.
17 p2155 A73-35189
- Plastic bonded, thermally stable explosive for an Apollo experiment.
18 p2341 A73-36152
- Stability of the output oscillation amplitude in a linear laser amplifier
18 p2322 A73-36665
- Richardson number profiles through shear instability wave regions observed in the lower planetary boundary layer.
19 p2448 A73-38228
- Multilayer foil insulated Si-Ge thermoelectric converters with multihundred watt power capacity, presenting thermal performance stability under vacuum operating conditions
19 p2392 A73-38423
- Nonspherically symmetric thermal instabilities implied by discrepancy between theory and observation for solar neutrino problem, noting absence in solar numerical model
20 p2608 A73-39429
- Relaxation resistance of alloys based on iron and nickel at high temperatures.
21 p2720 A73-41031
- Stability of 25 ohm platinum thermometer up to 1100 C.
22 p2855 A73-42007
- The high temperature stability of platinum resistance thermometers.
22 p2855 A73-42008
- Reproducibility, stability and linearization of thermistor resistance thermometers.
22 p2855 A73-42012
- Tungsten-rhenium thermocouple, describing alloys behavior, fabrication, insulation sheaths, calibration, stability and applications
22 p2857 A73-42037
- On the stability of metal sheathed noble metal thermocouples.
22 p2858 A73-42044
- The travelling gradient approach to thermocouple research.
22 p2859 A73-42049
- Thin film temperature sensor with polymer coating for medical research providing good sensitivity and stability for rapid temperature changes in biochemical reactions
22 p2813 A73-42055
- Polyquinazolines, thermostable polymers with thermoplastic properties [ONERA, TP NO. 1228]
22 p2881 A73-42218
- A method for thermal stabilization of the parameters of devices with ferrite cores
22 p2833 A73-42371
- The stability of sapphire whiskers in nickel at elevated temperatures. I - General morphological and chemical stability. II - The kinetics of morphological changes over the temperature range 1100 to 1400 C.
23 p2986 A73-44032
- Thin shell theory for thermal stresses in ogival shell used in nose cone design
01 p0113 A73-10016
- Approximate solution of equations describing the thermal stressed state of a shallow spherical shell
01 p0113 A73-10017
- Iterative solution of thermal bending problem for nonuniformly heated thin rectangular plate with discrete boundary conditions
01 p0113 A73-10020
- Unsteady temperature and stress distribution in variable thickness disk under convective heat transfer with ambient medium, using approximation method
01 p0113 A73-10021
- Temperature fields and stresses in bodies of simple geometry when the ambient medium temperature is unsteady
01 p0113 A73-10023
- Temperature stresses in an elastic infinite strip due to sudden heating and heat transfer at the boundary of the strip
01 p0113 A73-10091
- Research performed on the thermomechanics of deformable solids at the Ukrainian Academy of Sciences
01 p0114 A73-10569
- Unsteady thermal stress in an infinite strip with mixed boundary conditions
01 p0115 A73-10916
- Photoelastic stress analysis of solid propellant grains.
01 p0090 A73-11118
- Solar cell generator design for Helios solar probe, considering thermal stresses at sun proximity and sufficient power generating capacity at orbital apogee [DGLR PAPER 72-091]
02 p0131 A73-11663
- Determination of a time-dependent thermal stress on a finite cylinder [DGLR PAPER 72-112]
02 p0230 A73-11671
- Plastic material turbine blades adaptability under nonsteady start-stop thermal and mechanical stress cycle conditions, noting residual stress effects
02 p0235 A73-12129
- Calculation of thermal stresses in spherical storage vessels.
02 p0236 A73-12215
- Mercury thermal stress and strain fields of elastic deformation from solar heating variations due to resonance rotation
02 p0223 A73-12721
- Mathematical models for elastic solid bodies via similarity theory, noting rheoelectrical simulation for thermal stress analysis
03 p0386 A73-13146
- The stability theory of elastic bodies and the theory of thermal stresses of piecewise anisotropic bodies
03 p0386 A73-13156
- Thermal stresses due to a moving heat source in a circular disk.
03 p0389 A73-13328
- Thermal stress analysis of reentry vehicle nose tips at angle of attack.
03 p0392 A73-13688
- Compensation, by the layer winding method, for thermal stresses in articles manufactured from reinforced plastics
03 p0313 A73-13740
- Finite difference theory for bending stress concentration in shells of revolution, noting constitutive equation for thermal stress analysis
03 p0393 A73-13793
- Note on the thermal stresses in an elastic semi-circular disc due to an internal source of heat, the curved boundary being exposed to radiation while the straight insulated boundary is in contact with a smooth rigid surface.
04 p0511 A73-15173
- Heated rolls application in hot rolling of metals, estimating residual thermal stresses and heat transfer [ASME PAPER 72-WA/MAT-2]
04 p0457 A73-15810
- Thermally induced stress waves in an elastic layer. [ASME PAPER 72-WA/APM-22]
04 p0516 A73-15894
- Thermal stresses in circular plates including the influence of transverse shear.
05 p0633 A73-16539
- A numerical solution of an elastoplastic thick-walled tube subjected to thermal loading.
05 p0635 A73-16978
- Weight sensitivity of a space shuttle orbiter to thermal structural combined loads design criteria. [AIAA PAPER 73-257]
05 p0635 A73-16979
- Vibration of thermally stressed plates with various boundary conditions.
05 p0636 A73-17101
- Change in sign of thermal lens of glass laser rods with change in thermo-optical constant of glass.
06 p0703 A73-18635
- Effect of overheating on creep resistance in metastable alloys.
06 p0710 A73-18639
- Monatomic gas flow around uniformly heated sphere for small Reynolds numbers, noting drag decrease due to thermal stresses
06 p0646 A73-18884
- Solar generator technology on the Symphonic satellite.
07 p0778 A73-18976
- Transient stresses induced by heating a plane boundary.
07 p0907 A73-19077
- On the torsional static stability and response of open section tubes subjected to thermal radiation loading.
07 p0908 A73-19086
- Some effects of temperature on material properties and device reliability.
07 p0797 A73-19134
- The measurement of thermal strain using self-temperature compensated strain gauges.
07 p0823 A73-19567
- Analysis of the thermal stress-strain state and cooling effectiveness of some turbine-blade designs
07 p0868 A73-20085
- Thermal stresses in an anisotropic plate with a circular hole.
07 p0914 A73-20199
- Theoretical and experimental prediction for pulsating creep failure.
07 p0917 A73-20489
- Thermal stresses in a spherical vessel filled with liquefied gas
07 p0917 A73-20507
- Influence of thermal-diffusion coatings on the physicochemical properties of heat-resistant metals
07 p0840 A73-20512
- Time optimal heating of thin plates with constraints placed on the thermal stresses
07 p0923 A73-20634
- On optimizing thermal stresses in cylindrical shells.
08 p1015 A73-20674
- Effects of thermal loading on foil and sheet composites with constituents of differing thermal expansivities. [ASME PAPER 72-MAT-E]
08 p0979 A73-21572
- Effects of thermal loading on fiber-reinforced composites with constituents of differing thermal expansivities. [ASME PAPER 72-MAT-F]
08 p0979 A73-21573
- Solution of the three-dimensional thermoelasticity problem for a long cylinder with mixed heating conditions
08 p1019 A73-21758
- Steady temperature fields and stresses in a half-space heated by a linear inductive source
08 p1019 A73-21759
- Some problems in the assessment of high temperature properties for engineering purposes.
08 p0981 A73-21782
- Thermal stresses in cooled gas turbine blade foils and roots with allowance for thermoelastic effects
09 p1136 A73-22568
- Determination of the optimal physical load in the local heating of a cylindrical shell
09 p1159 A73-22589
- Influence of the Reynolds number on nonstationary convective heat transfer in a pipe during a change in the thermal load
10 p1204 A73-23511
- Thermal stresses in an elastic solid weakened by two coplanar circular cracks.
10 p1287 A73-23563
- Optimal conductive heating of hollow cylinder inner surface with temperature dependent thermal stress limits for internal/external surfaces
10 p1289 A73-24063
- The temperature field and thermal stresses in a symmetrical system of three infinite plates
10 p1293 A73-24795
- An experiment to correlate the thermal stress failure level to modulus of rupture in ceramic materials.
11 p1387 A73-25304
- Comparison of the metabolic effects of centrifugation and heat stress in man.
11 p1315 A73-25338
- Approximate calculation of thermoelastic stresses in an arbitrarily heated slab
11 p1434 A73-25393
- Russian papers on thermal stresses investigation in machine and structural elements covering stress simulation and strain gage methods for model and full scale structures
11 p1435 A73-25451
- Strain gages and photoelastic coating methods of thermal stress determination for model and full scale tests
11 p1435 A73-25452
- Mechanical simulation of thermoelastic stresses on the basis of a given temperature field
11 p1435 A73-25453
- Investigation of thermoelastic stresses by means of 'freezing' involving the realization of a prescribed temperature gradient
11 p1435 A73-25454
- Concentration of thermal stresses at joints between heterogeneous materials
11 p1435 A73-25458
- Prediction of inelastic high temperature materials behavior by strain-rate approach. [AIAA PAPER 73-386]
11 p1450 A73-25515

Crippling allowables for elevated temperature and creep environments. 11 p1439 A73-25517
[AIAA PAPER 73-388]
Vibration and local edge buckling of thermally stressed, wedge airfoil cantilever wings. 11 p1441 A73-25557
[AIAA PAPER 73-327]
On the design of air-cooled radial turbine blades. 11 p1410 A73-25843
Automation of thermal design calculations for electrical machines 11 p1313 A73-26115
Thermal stresses arising in high-frequency fatigue tests 12 p1512 A73-27259
Solution of the dynamic problem of thermoelasticity for a circular plate with allowance for the finite velocity of heat propagation 12 p1552 A73-27263
Stability of a nonuniformly heated circular shell 12 p1554 A73-27471
Thermally activated low temperature creep of solids at constant load, considering creep curve stages and plastic deformation mechanism 13 p1635 A73-28263
Methods of simulating the thermal and stressed state at the edges of gas turbine blades 13 p1698 A73-29054
German monograph on calculation of thermal and transformation stresses in long circular cylinders covering austenite-martensite transformation, thermal expansion and viscous bodies 13 p1699 A73-29284
Shock wave produced in a solid by means of supersonic thermal sources. 13 p1700 A73-29390
Thermal stress analysis of metals with temperature dependent mechanical properties. 13 p1701 A73-29507
Test equipment for thermal stability determination of brittle refractory material, noting data processing procedure and formulas for temperature distribution and thermal stress 13 p1599 A73-29629
Nonlinear thermal elastoplastic structural analysis, using principle of virtual work in finite element method 14 p1808 A73-30192
Thermal stress in an anisotropic elastic half-space. 14 p1810 A73-30407
Failure under thermal loads of cylindrical bodies consisting of brittle materials 14 p1813 A73-30683
Mechanical deformation and failure of metals under the action of a 0.01-sec laser light pulse 14 p1758 A73-30714
Thermal stresses and couple-stresses in square cylinder with a circular hole. 14 p1815 A73-30919
Solution of axisymmetrical thermoelasticity problems for an infinite region with several spherical cavities 15 p1945 A73-31039
The effects of couple-stresses on thermal stress distributions in multiply-connected domains. 15 p1947 A73-31362
Russian book - Strength of turbine wheels. 15 p1948 A73-31578
Response-optimal heating of thin plates with constraints on the temperature stresses. 15 p1957 A73-31688
Monatomic gas flow around uniformly heated sphere for small Reynolds numbers, noting drag decrease due to thermal stresses 15 p1824 A73-32409
Aerodynamic and thermal problems related to wall deformations 16 p2076 A73-32801
Thermal stress in and bending of elastic rectangular plates from Kantorovich method combined with iterative techniques 16 p2077 A73-32993
Transient analysis of ceramic vanes for heavy duty gas turbines. 16 p2048 A73-33507
Investigation of thermal deformations by methods of holographic interferometry 17 p2164 A73-34172
Transient thermal stresses in a disc of linearly strain-hardening material. 17 p2243 A73-34547
Effect of Reynolds number on nonstationary convective heat exchange in a tube with variable heat load. 17 p2255 A73-35191
Stresses in molybdenum coatings obtained by thermal decomposition of Mo/CO₂ 18 p2319 A73-35892
A note on uniqueness in the linear theory of heat conduction with finite wave speeds. 18 p2371 A73-36692
Strength of nonuniformly heated rotating disks 18 p2366 A73-36755
Methods of modeling thermal and stressed states in the edges of gas turbine blades. 18 p2366 A73-36886

Thermal stresses in axially connected circular cylinders. 19 p2495 A73-37435
Two dimensional steady and transient thermal stress analysis in rectangular solid with varying surface temperature, noting thermoelastic problems solution by analog method 19 p2498 A73-37668
Thermal stresses in spherical reservoirs while filling with liquefied gas. 19 p2499 A73-37782
Effect of thermomaterial coatings on the physicomaterial properties of refractory metals. 19 p2440 A73-37787
Study of the phenomenon of stress relaxation of flow in the case of titanium 19 p2442 A73-37840
Investigation of a thermomechanical surface during unloading according to the theory of thermoplasticity 20 p2617 A73-39264
Thermoelasticity of coupled bodies in the case of stress-dependent heat transfer 20 p2618 A73-39327
Approximate solutions for heat conduction and thermal stresses in thermoelasticity of solids and beam and ring structures, considering dynamic, coupling, melting and solidification effects 20 p2620 A73-39514
Nonsymmetric buckling of cylinders with axisymmetric thermal discontinuities. 21 p2784 A73-40425
Influence of nonuniform heating on the stability of plates beyond the elastic limit 21 p2786 A73-40983
Thermal stress calculation for elastic half strip in nonuniform temperature field by functions in terms of Castigliano variational principle 21 p2786 A73-40986
Temperature stresses in a partly reinforced orthotropic plate 21 p2787 A73-40991
Temperature and stress fields in a cylindrical shell subjected to induction heat treatment 21 p2787 A73-41233
Grain boundary cavitation and sliding in copper/tungsten composites due to thermal stresses. 22 p2876 A73-42339
Thermal stresses due to an internal source of heat in a solid elastic hemisphere with radiating curved surface and the plane base resting on a smooth rigid insulating plane surface. 22 p2932 A73-42469
Evaluation of error bounds in an optimization problem using the finite-element method. 22 p2924 A73-42882
[ASME PAPER 73-APMW-15]
Multiphase incompressible half-space as simplified earth model for investigating surface displacements due to time- and depth-dependent heat sources 23 p2973 A73-43797
Determination of the temperature fields and thermal stresses in a bimetallic layer subjected to induction heating 23 p3046 A73-44194
Thermal stresses in heated orthotropic plates with variable heat-transfer coefficients 23 p3046 A73-44195
Thermal stresses in rotationally symmetric semi-infinite elastic body with heat input along hole boundary and on plane bounding surface, reducing to solution of Fredholm equation 24 p3147 A73-44745
Radiation pyrometric probe /homogeneous thermally insulated rod/ for measuring body surface thermal loads and heat transfer coefficients 24 p3089 A73-44758
THERMAL VACUUM TESTS
Outgassing and contamination properties of prospective Apollo Telescope Mount materials. 03 p0330 A73-13020
Aeros satellite component tests for design and manufacturing error detection and failure prevention, using structural, thermal and electrical integration models 03 p0288 A73-13918
Mo addition effect on high temperature creep resistance and diffusion activation energy of Nb alloys tested in torsion and tension at 1100-1500 C in vacuum 03 p0328 A73-14018
High vacuum thermal desorption mass spectrometry for electron bombardment activated nitrogen desorption from W surface, discussing lambda state population 04 p0414 A73-14999
Vibration, radiation and thermal vacuum test procedures and facilities for evaluating spacecraft reliability during launching and in space environment 07 p0807 A73-18999
Radiative heat transfer in fiberglass insulation. 08 p1021 A73-20866
Deformation and rupture of molybdenum under conditions of creep 09 p1100 A73-22161
Russian book on space flight radiative heat transfer problems covering spacecraft thermal conditions,

solar and planetary heat flux, radiant cooling and vacuum tests 09 p1166 A73-22348
Solid body contact interaction devices at high temperatures in vacuum, gas and air for evaluation of surface coatings, adhesion, diffusion, mechanical properties, etc 10 p1222 A73-24966
Creep and long-term strength of molybdenum with a boron silicide coating in vacuum at temperatures from 1000 to 1400 C 12 p1512 A73-27257
Nickel-cadmium cells for low earth orbit applications. 13 p1572 A73-29584
A high temperature vacuum assembly for precision creep tests 14 p1743 A73-30694
Influence of heating to high temperatures in vacuum on the electrophysical properties of niobium single crystals 14 p1763 A73-30722
Phenomena associated with bench and thermal-vacuum testing of superconductors - Heat pipes. 16 p2084 A73-33131
Analyses of flight model spacecraft performance during thermal-vacuum tests. 16 p2072 A73-33149
Gas flow analysis during thermal vacuum test of a spacecraft. 16 p1994 A73-33150
Surface diffusion and migration on dispersed silicon and basalt during weak heating in a vacuum 16 p1977 A73-33757
Thermal contact conductance of porous metallic materials in a vacuum environment. 18 p2323 A73-36363
Applications Technology Satellite F aluminum-ammonia heat pipes design, fabrication and life and thermal vacuum testing [ASME PAPER 73-ENAS-46] 19 p2493 A73-37993
Concepts of high-capacity communications satellites. 20 p2613 A73-38714
An arrangement for carrying out metal creep and stress-rupture strength tests under high vacuum conditions 20 p2545 A73-39384
Effect of ultrasound on the dislocation structure and mechanical properties of molybdenum 20 p2579 A73-39745
The deformation and fracture of molybdenum under creep conditions. 22 p2874 A73-42109
Changes in surface structure during high-temperature creep flow. 23 p2994 A73-44159
THERMALIZATION [ENERGY ABSORPTION]
NT NEUTRON THERMALIZATION
Relaxation of ion beam injected into a plasma transversely to a magnetic field. 05 p0602 A73-16550
Energy loss of charged particles in Maxwellian plasmas. 08 p0992 A73-20823
Electrostatic turbulence and ion thermalization in modified Penning discharge, investigating ion heating processes 10 p1251 A73-24259
Kinetic equations describing thermalization of anisotropic solar wind plasma via linear and nonlinear wave-particle interaction 10 p1270 A73-24912
Thermally induced nonlinear propagation of a laser beam in an absorbing fluid medium. 11 p1377 A73-26229
Midlatitudinal standard ionospheric profile to construct F-region noon electron density profiles and thermal response to solar activity changes 12 p1493 A73-27761
Implication of contact thermalization effect in two-valley semiconductors for the high frequency device performance. 14 p1783 A73-29929
Thermalization and transport of photoelectrons - A comparison of theoretical approaches. 24 p3086 A73-45124
THERMIONIC CATHODES
Plasma diagnostics in overcompensation operated Knudsen thermionic converter with Cs-Ba filler, noting W cathode surface properties 10 p1177 A73-24204
Dynamic viscosity and current distribution model of inhomogeneous Cs plasma flow in coaxial plasma gun with thermionic cathode 10 p1258 A73-24886
Cermet cathode materials for electric vacuum equipment 12 p1503 A73-27562
Analysis and investigation of cathode processes in a high-current arc discharge 19 p2466 A73-37360
Thermionic properties of zirconium carbide/rhenium composites 21 p2751 A73-40530

THERMIONIC CONVERSION SYSTEMS

- Dynamic viscosity and current distribution model of inhomogeneous Cs plasma flow in coaxial plasma gun with thermionic cathode
21 p2749 A73-41661
- Apparatus and methods for the precise determination of Boltzmann temperature.
22 p2856 A73-42021
- Low temperature thermionic cathode.
22 p2834 A73-42695
- ## THERMIONIC CONVERSION SYSTEMS
- ### U THERMIONIC POWER GENERATION
- #### THERMIONIC CONVERTERS
- Characteristics of a thermionic converter with a cesium-barium filling at a high anodic temperature
01 p0006 A73-10855
- Plasma diagnostics in overcompensation operated Knudsen thermionic converter with Cs-Ba filler, noting W cathode surface properties
04 p0481 A73-15614
- Russian book - Power systems of spacecraft.
04 p0408 A73-15704
- Performances of the better metallic electrodes in cesium thermionic converters.
09 p1036 A73-22817
- Performance improvement of cesium thermionic converters by addition of oxygen.
09 p1036 A73-22818
- An out-of-core version of a six-cell heat-pipe heated thermionic converter array.
09 p1036 A73-22820
- Development of thermionic radioisotope batteries.
09 p1038 A73-23281
- Development of an actinium fueled thermionic converter.
09 p1038 A73-23282
- Plasma diagnostics in overcompensation operated Knudsen thermionic converter with Cs-Ba filler, noting W cathode surface properties
10 p1177 A73-24204
- Experimental operation of constant temperature heat pipes.
11 p1451 A73-25989
- Characteristics of thermionic converter with cesium-barium filling at high anode temperature.
12 p1461 A73-27905
- Emission instability of thermionic converters.
14 p1713 A73-30474
- Potential distribution in a two-gas thermionic converter at current saturation.
15 p1832 A73-32638
- Development costs for a nuclear electric propulsion stage.
19 p2458 A73-38434
- A possibility of creating a new type of thermionic converter
19 p2392 A73-38560
- Dynamic characteristics of a plasma diode with a low-voltage arc discharge. II - Experimental study of dynamic characteristics
22 p2833 A73-42386
- #### THERMIONIC DIODES
- ##### NT CESIUM DIODES
- Transit mode operation of thermionic injection diodes
02 p0145 A73-11575
- Temperature dependence of thermionic emission current density of Pt additive powdered zirconium carbide deposit on diode cathode working surface
17 p2109 A73-35171
- #### THERMIONIC EMISSION
- Comments on the conduction mechanism in Schottky diodes.
01 p0088 A73-10474
- The effect of stress on metal semiconductor junctions.
08 p0995 A73-21482
- Thermionic constants and electron reflection for Ta/100 by the Shelton retarding field method.
10 p1259 A73-23695
- Work function of the principal faces of single crystals of rhenium solutions in molybdenum
10 p1231 A73-23818
- Thermionic emission properties of refractory metal borides
13 p1634 A73-28201
- Emission instability of thermionic converters.
14 p1713 A73-30474
- Current-voltage characteristic of a metal-dielectric contact with allowance for thermionic and field emission of electrons
16 p1972 A73-34010
- Temperature dependence of thermionic emission current density of Pt additive powdered zirconium carbide deposit on diode cathode working surface
17 p2109 A73-35171
- Exploding wires as a source of flash X-rays.
21 p2738 A73-39975
- On the source of the slowly varying component at centimeter and millimeter wavelengths.
21 p2778 A73-41496
- #### THERMIONIC EMITTERS
- Performances of the better metallic electrodes in cesium thermionic converters.
09 p1036 A73-22817

- Spatially dependent electron relaxation near a thermionic emitting electrode.
14 p1713 A73-30473
- Electron gun with concentric hemispherical anode and space charge limited thermionic emitter for potential field simulation, measuring electron energy distribution for comparison with calculation
17 p2143 A73-35764
- A possibility of creating a new type of thermionic converter
19 p2392 A73-38560

THERMIONIC POWER GENERATION

- Thermionic reactor ion propulsion system /TRIPS/ - Its multi-mission capability.
[AIAA PAPER 72-1060]
03 p0381 A73-13389
- Multiparametric optimization of a thermionic electric power generating element
07 p0778 A73-19286
- Thermionic reactor power systems design for spacecraft auxiliary power supply and electrical propulsion, discussing performance and design guidelines for various applications
09 p1118 A73-22798
- AEC/NASA thermionic reactor program with emphasis on technology utilization, comparing with French, German and Soviet programs
09 p1036 A73-22815
- Thermionic fuel unit cell major component materials selection for life and performance improvements, giving out-of-pile and in-pile results
09 p1036 A73-22816
- Thermionic fuel elements for in-core reactor power plant space applications, summarizing operating and environmental requirements and technology development
09 p1036 A73-22819
- Thermionic reactor systems for electric propulsion.
11 p1395 A73-26025
- In-core 100 kWe thermionic power system design to meet manned spacecraft shielding requirements, discussing waste heat removal and integration with space base
11 p1395 A73-26026
- Nuclear thermionic power plants in the 50-300 kWe range.
11 p1396 A73-26027
- Development of a plutonium-fueled miniature power supply based on thermionic conversion.
11 p1396 A73-26028
- Multiparameter optimization of a thermionic fuel cell.
13 p1571 A73-28686
- Russian book - Physical bases of thermionic energy conversion.
22 p2890 A73-41876

THERMIONIC REACTORS

- ### U ION ENGINES
- ### U NUCLEAR ROCKET ENGINES

THERMISTORS

- Linear response transistorized FM temperature measuring transducer with thermistor, noting low distortion and digital display convenience
01 p0044 A73-10032
- Amplitude stability and distortion in thermistor-controlled oscillators.
20 p2535 A73-39131
- Thermistors as cryogenic thermometers.
22 p2854 A73-41998
- Reproducibility, stability and linearization of thermistor resistance thermometers.
22 p2855 A73-42012
- Precision measurements of temperature differences with thermistors by a simple technique.
22 p2855 A73-42014
- Development of a thermistor type temperature probe for use at low absolute pressures.
22 p2856 A73-42016
- A method for thermal stabilization of the parameters of devices with ferrite cores
22 p2833 A73-42371

THERMO-PHOTOVOLTAIC GENERATORS

- ### U PHOTOELECTRIC GENERATORS
- ### U THERMOELECTRIC GENERATORS

THERMOAEROELASTICITY

- ### U AEROELASTICITY
- ### U THERMOELASTICITY

THERMOCHEMICAL PROPERTIES

- ### NT HEAT OF COMBUSTION
- ### NT HEAT OF FORMATION
- Analysis of volatile combustion products and a study of their toxicological effects.
02 p0138 A73-12429
- Nd laser radiation thermochemical effects on oxide formation on thin Cr films, Fe-Ni-Co and Cr-SiO alloys and MgO-MnO ferrites, noting resistance and etching rates
11 p1376 A73-25636
- Thermochemical calculation for high temperature and pressure formation of interstellar molecules in compact H II regions, considering prestellar and late stellar atmospheres
11 p1423 A73-26105
- Influence of air oxygen concentration on the thermochemical stability of jet fuels
15 p1925 A73-31833

- Variation with temperature of free enthalpy of formation of certain carbides
15 p1898 A73-32644

- High temperature thermal cavity system with vitreous carbon tube and end plugs for material and thermochemical environment investigations, discussing mass spectroscopic measurement
17 p2149 A73-35757

- Thermochemical properties of a silicone elastomeric ablator.
[AIAA PAPER 73-741]
18 p2326 A73-36338
- Nd laser radiation thermochemical effects on oxidation formation on thin Cr films, noting resistance and etching rates
19 p2438 A73-38148

- High-temperature gas-solid reactions.
19 p2403 A73-38558
- Estimation of rate constants of elementary processes - A review of the state of the art.
22 p2933 A73-42739

THERMOCHEMISTRY

- ### NT AEROTHERMOCHEMISTRY
- Analysis of NO formation in single droplet combustion.
01 p0014 A73-10645
- Temperature changes in hydrogen-oxygen explosions.
01 p0121 A73-10646
- Nitrogen thermochemistry during the combustion of zirconium droplets in N₂/O₂ mixtures.
01 p0123 A73-10922
- Boron combustion, covering thermochemistry application to chemical propulsion systems, temperature effects on oxidation, single particle ignition and powder burning
01 p0089 A73-11122
- Oxygen and nonmetallic inclusions in chromium and aluminothermic ferrochrome
04 p0465 A73-15662
- Influence of fretting on the endurance of 40KhNMA steel with various thermochemical processing
11 p1386 A73-26735
- Thermochemical and thermo-oxidative reactions of polyacrylonitrile fibers.
16 p1976 A73-33038
- Applications in aerospace construction and fallout of ONERA thermochemical techniques
[ONERA, TP NO. 1246]
18 p2320 A73-36688
- Numerical integration of the equations of chemical kinetics
24 p3065 A73-44703

THERMOCHROMATIC MATERIALS

- Thermochromic cuprous mercuric iodide for IR recording applications, observing phase transition hysteresis from reflectance-vs-temperature, specific heat and sensitivity measurements
01 p0054 A73-11230

THERMOCOMPRESSION

- ### U COMPRESSING
- ### U HEATING

THERMOCOUPLE PYROMETERS

- Instrument errors of film type thermocouple pyrometers for surface temperature measurement, discussing effects of shunting and junction geometry
02 p0166 A73-11636
- Influence of the distortion of the temperature field at the point of thermocouple fixation on measurements of the heat conduction coefficient by the steady-state method of radial thermal flux
06 p0770 A73-18566
- Determination of the sensitivity of an infrared pyrometer with a thermocouple
06 p0695 A73-18567
- Effect of temperature field distortions caused by embedded thermocouples on the measurement of the thermal conductivity coefficient by the steady radial heat flux method.
16 p2086 A73-33591
- Determination of sensitivity of infrared pyrometer with a thermopile.
16 p2016 A73-33592
- Methods for cryogenic thermocouple thermometry.
22 p2857 A73-42029
- Gold-iron alloys for low temperature thermocouples.
22 p2857 A73-42030
- Reference data for thermocouple materials below the ice point.
22 p2857 A73-42031
- Revision of the standard reference data for thermocouples.
22 p2857 A73-42032
- The effects of catalysis in measuring the temperature of incompletely-burned gases with noble-metal thermocouples.
22 p2857 A73-42035
- Nonstandard thermocouple materials, discussing metal and nonmetal thermoelements and ceramic insulating materials
22 p2857 A73-42036
- Tungsten-rhenium thermocouple, describing alloys behavior, fabrication, insulation sheaths, calibration, stability and applications
22 p2857 A73-42037

Studies of the performance of W-Re type thermocouples. 22 p2858 A73-42039

Fabrication of high-reliability sheathed thermocouples. 22 p2865 A73-42041

Some designs using sheathed thermocouple wire for jet engine applications. 22 p2858 A73-42042

On the stability of metal sheathed noble metal thermocouples. 22 p2858 A73-42044

Measured drift of irradiated and unirradiated W3%Re/W25%Re thermocouples at a nominal 2000 K. 22 p2858 A73-42046

The travelling gradient approach to thermocouple research. 22 p2859 A73-42049

Error accumulation in thermocouple thermometry. 22 p2859 A73-42052

Utilization of semiautomatic thermocouples in gas-turbine engine tests 23 p2982 A73-43743

HERMOCOUPLS

NT THERMOCPILES

Doped CdSb single crystal production and physical properties for IR detectors and thermocouple use. 01 p0087 A73-10040

Thermocouple circuits for measurement of unsteady temperatures in gases by the two-thermoreceiver method and an analysis of thermocouple circuit errors. 02 p0166 A73-11710

Experimental investigation of unsteady-state thermoelectric cooling. III - Combined regime. 05 p0639 A73-16772

Gas flow temperature determination in the presence of radiation heat exchange between the heat sensor and some surrounding structures. 05 p0578 A73-16996

Thermoelectric panel array of hybrid thermocouples with p-type Si-Ge encapsulated PbTe/Si-Ge n-legs, presenting performance test results as a function of test time. 09 p1134 A73-22766

Status of silicon germanium air-vac converter development. 11 p1312 A73-26032

Inert gas injection for W-Re thermocouple wire corrosion protection during temperature measurement in aggressive media. 12 p1497 A73-27319

Fast response coaxial miniature thermoelements for rapid temperature change measurements in droplets, turbulence and bubbles. 12 p1499 A73-27875

Use of inertial heat sensors for measuring the rate of temperature variation. 13 p1617 A73-28865

Temperature determination in a gas flow with the aid of two thermocouples. 15 p1876 A73-31870

Accuracy of type K thermocouple wire below 500 F - A statistical analysis. 17 p2167 A73-34624

Thermoelectric nuclear batteries fabrication in milliwatt power range combining bismuth telluride thermopiles with plutonia fuel capsules. 19 p2455 A73-38410

The multi-hundred watt RTG - Technology background and flight systems program. 19 p2456 A73-38418

Multihundred watt power supply with Si-Ge thermoelectric couples for Pu-238 source heat energy conversion into electric power, discussing computer model for performance projection. 19 p2456 A73-38422

Curium 244 heat source design for multihundred watt radioisotope thermoelectric generator with Si-Ge thermocouples for energy conversion, noting low cost. 19 p2457 A73-38429

Long-term drift of some noble- and refractory-metal thermocouples at 1600 K in air, argon, and vacuum. 22 p2857 A73-42033

Thermal properties of tungsten-rhenium alloys used in high temperature thermocouples. 22 p2858 A73-42038

Material preparation and fabrication techniques for the production of high reliability thermocouple devices. 22 p2858 A73-42040

Equivalent circuit modeling of insulator shunting errors in high temperature sheathed thermocouples. 22 p2858 A73-42045

High temperature core thermocouple development for the Nuclear Rocket Engine Program /Rover/. 22 p2885 A73-42047

Measurement of temperature distribution over metal objects using single-wire thermocouples. 22 p2858 A73-42048

A new conceptual model for components in measurement/control systems - Practical application to thermocouples. 22 p2859 A73-42050

Theory and performance of plated thermocouples. 22 p2859 A73-42051

Electrical and mechanical characteristics of thermocell arms reinforced by metal frames. 24 p3058 A73-45252

THERMODYNAMIC COUPLING

Dynamic coupling of the stratosphere with the troposphere and sudden stratospheric warmings. 19 p2449 A73-38288

Thermoelectric wave propagation in a random medium and some related problems. 21 p2789 A73-41667

THERMODYNAMIC CYCLES

NT BRAYTON CYCLE

NT CARNOT CYCLE

NT RANKINE CYCLE

NT STIRLING CYCLE

Thermodynamic cycle processes in liquid propellant rocket engines, taking into account combustion products chemical dissociation, wall and nozzle heat losses, friction effects, etc. 10 p1263 A73-24700

Gas-turbine processes with interrupted expansion and interrupted compression. 11 p1452 A73-26371

Perfect thermal cycles family definition for heat supply and extraction as function of temperature. 13 p1706 A73-28911

Engine cycle considerations for future transport aircraft. 17 p2222 A73-34693

[SAE PAPER 730345] Subsonic aircraft turbojet engines, discussing thermodynamic cycles, entry temperature increase, propulsion efficiency and economy improvements and ecological requirements. 18 p2343 A73-36994

THERMODYNAMIC EFFICIENCY

Thermodynamic determination of power loss in hydraulic components. 04 p0435 A73-15848

Thermodynamic performance analysis of gas turbine power plants with intercooler. II - Performance of intercooling-regeneration-reheat type and precise calculation method. 11 p1411 A73-26343

Gas-turbine processes with interrupted expansion and interrupted compression. 11 p1452 A73-26371

Nonuniform heat transfer coefficient effect on double-pipe heat exchanger analysis with effectiveness method, discussing exchanger sizing. 12 p1559 A73-27693

Thermosiphon evaporation-condensation-evaporation cycle cooling system operation and effectiveness in thermoelectric cooling and generator devices. 14 p1713 A73-30950

Effectiveness of a gas screen in plasmatrons of axial configuration. 15 p1917 A73-31191

Comparative analysis of turbine loss parameters. 16 p1964 A73-33529

[ASME PAPER 73-GT-91] Turbine engine control system design based on linearized and nonlinear mathematical models accounting for thermodynamic performance. 18 p2343 A73-36995

A solar engine using the thermal expansion of metals. 19 p2392 A73-38473

Porous cooling in a supersonic turbulent boundary layer. 20 p2628 A73-39609

Direct conversion of thermonuclear plasma energy by high magnetic compression and expansion. 21 p2750 A73-41676

Effectiveness of film cooling in a curvilinear channel formed by guide vanes. 23 p3048 A73-43442

Thermodynamics of an air-cooled gas-turbine stage. 23 p3019 A73-43733

THERMODYNAMIC EQUILIBRIUM

Global mean radiative equilibrium model for Venusian mesosphere, determining horizontal variation of thermal heating and cooling. 01 p0097 A73-10361

LTE fine analysis of omicron-tw C Ma line profiles, showing chemical composition near iota Her. 02 p0221 A73-12705

Description of classical homogeneous systems in terms of dressed particles. II - Application to the Debye plasma. 02 p0199 A73-12722

Classical hard-sphere gas in spherical box with coupling between local thermodynamics and gravitation, noting stellar core-halo structure from equilibrium state calculations. 03 p0366 A73-12936

Relative importance of forces of interaction which create, between the grains of a very thin metallic film, the radiation of thermodynamic equilibrium on the one hand, and zero oscillations of the field on the other hand. 03 p0349 A73-13605

THERMODYNAMIC EQUILIBRIUM

EUV emitting plasma structure of solar quiet and active atmospheres, noting extreme departures from LTE. 03 p0363 A73-13952

Thermodynamic equilibrium and relaxation models of ideal and real high temperature gas flows for reversible and irreversible processes [DFVLR-SONDDR-282]. 04 p0517 A73-15678

Rayleigh and Brillouin scattering from fluids in thermal equilibrium and light scattering from macromolecules in solution, discussing light and medium properties interrelationship. 05 p0583 A73-16345

The possibility that nongaseous hydrogen supplies the missing cosmological mass. 05 p0625 A73-17328

Thermodynamic short range order models for dense substance equilibrium properties calculation, assuming molecular interaction independence and self similar radial function. 07 p0851 A73-19397

Departure from thermodynamic equilibrium of an ionized cesium vapor - Experimental study and comparison with a statistical model. 07 p0854 A73-20607

Ar plasma diagnostics from stabilized arc emission spectra, noting thermodynamic equilibrium in central zone of arc channel. 08 p0992 A73-20855

Establishment of thermal equilibrium in a liquid near the critical point. 08 p1021 A73-20857

Validity criteria for local thermodynamic equilibrium and coronal equilibrium. 08 p0992 A73-21007

Spectroscopic measurement of the source function as a test for deviations from local thermodynamic equilibrium /L.T.E./ in arc plasmas. 08 p0992 A73-21018

The influence of dust upon the dynamics and thermal stability of planetary nebulae. 09 p1142 A73-22032

A non-LTE study of silicon line formation in early-type main-sequence atmospheres. 10 p1272 A73-23532

Quantum theory of line formation in a magnetic field. 10 p1249 A73-24134

Thermodynamic equilibrium calculation and demonstration of Mo siliiding by circulation method in hydrogen-free gaseous medium containing silicon chlorides. 10 p1227 A73-24961

Numerical simulation and theory of plasma diffusion across magnetic field at thermal equilibrium, noting collective mode domination at moderate and high fields. 11 p1403 A73-25257

One dimensional temperature equalization process in planar plate, infinitely long cylinder and sphere for range of Biot and Fourier numbers, estimating approximate solution error. 11 p1452 A73-26372

Thermodynamic methods applied to self gravitating n-body systems for different boundary conditions, considering energy transfer. 11 p1427 A73-26604

Global climatic model based on time and space averaged thermodynamic energy equation for idealized land-water distribution, allowing for continents-oceans seasonal interactions. 12 p1519 A73-26801

Taking into account heat-transfer irreversibility in calculating the total change in entropy of individual substances. 12 p1557 A73-26939

Possibility of gasdynamic effects at the critical point of the phase equilibrium. 12 p1487 A73-27418

Some remarks on the thermal equilibrium equation of hot-wire probes. 13 p1613 A73-28528

Kinetic equations for the Green functions describing equilibrium states of a gas. 13 p1662 A73-28551

Solar photosphere turbulent velocity relation to optical depth and deviation from LTE based on Goldberg-Unno method. 13 p1683 A73-29093

Human thermoregulatory system examination under thermodynamic equilibrium based on conductive and convective metastable heat transfer from skin to environment [ASME PAPER 73-AUT-J]. 13 p1577 A73-29414

Cosmological arrow of time theory describing approach to equilibrium in closed systems, noting relation to cosmic expansion. 15 p1933 A73-31310

Thermal and ionization equilibrium in a dense hydrogen cloud. 16 p2059 A73-32841

Transport coefficients of ionized argon. 16 p2039 A73-33318

THERMODYNAMIC PROPERTIES

Decay of a high temperature helium plasma - Validity of local thermodynamic equilibrium and estimation of recombination coefficients for $He^+ + I$, $He + I$, and $He_2^+ + I$.

16 p2043 A73-33867

Calculation of components, electrical conductivity, and total radiative source strength of nitrogen plasma in local thermodynamic equilibrium.

[AIAA PAPER 73-744] 18 p2339 A73-36360

Radiative equilibrium of a gray medium in a rectangular enclosure.

18 p2371 A73-36800

Early type stellar line spectra, discussing LTE, hydrogen and helium lines, stellar element abundance and O and B stars

18 p2356 A73-36875

Book - Physics of stellar interiors.

18 p2356 A73-36965

Equilibrium properties of a one-dimensional kinetic system.

19 p2463 A73-37899

The approach to thermal equilibrium in systems of coupled quantum oscillators initially in a generalized Gaussian state.

20 p2571 A73-38634

Resource exchange and allocation /a generalized thermodynamic approach/. I

20 p2629 A73-39349

Resource exchange and allocation /a generalized thermodynamic approach/. II

20 p2629 A73-39351

Local thermodynamic equilibrium validity limits in short spaced cesium plasmas, discussing electron density and temperature, Maxwell and Boltzmann distributions and total pressure

20 p2599 A73-39673

Relationship between the equilibrium vapor pressure of the solvent and the surface activity in dilute solutions of inactive and surface-active materials

21 p2646 A73-40122

Thermodynamic formation of negative rarefaction/shock waves in single-phase viscous fluids by approximate continuous model

21 p2790 A73-40251

Effect of small perturbations on the behavior of thermodynamic variables near the point of a phase transition of the second kind

21 p2790 A73-40445

The effects of departures from LTE in stellar spectra.

21 p2772 A73-41243

Microturbulence and the effect of departures from LTE on photospheric iron lines.

21 p2777 A73-41481

Energy of an equilibrium fluctuating electromagnetic field in matter

21 p2741 A73-41515

Russian book - The structure of zirconium alloys.

22 p2873 A73-41973

Irreversible heat transfer in the total entropy change for a pure substance.

22 p2930 A73-42273

Effect of the absorbers upon the thermal structure of a LTE atmosphere, hydrogen and helium.

22 p2908 A73-42309

Saha's equation under deviation from thermodynamic equilibrium.

22 p2915 A73-43040

Effects of translational disequilibrium on the structure of a shock wave in an ionized monatomic gas

22 p2895 A73-43045

Study of aluminum-oxygen equilibrium in liquid iron at 1600 deg C with the aid of a solid ThO₂-Y₂O₃ electrolyte cell

23 p2995 A73-44178

Least squares methods for thermal equations of state parameters of substances and solutions, taking into account phase equilibrium lines

24 p3155 A73-44753

Critical two phase He flow rates prediction based on homogeneous thermal equilibrium model, Henry-Fauske data and empirical correction factor curve

24 p3077 A73-44823

Physical particle description of moderately dense gases. II - Equilibrium properties.

24 p3111 A73-45397

Radiating optically thick gas boundary layer based on approximation of gray gas in LTE, noting similarity to Knudsen layer

24 p3158 A73-45535

NT SURFACE ENERGY

NT THERMAL BUCKLING

NT THERMAL CONDUCTIVITY

NT THERMAL DIFFUSION

NT THERMAL DIFFUSIVITY

NT THERMAL EXPANSION

NT THERMAL INSTABILITY

NT THERMAL STABILITY

NT THERMOCHEMICAL PROPERTIES

NT THERMOPHYSICAL PROPERTIES

NT VAPOR PRESSURE

NT VOLATILITY

Difference of thermal properties between threshold type and memory type chalcogenide glass semiconductors.

01 p0087 A73-10432

On a method of determining the interaction coefficient in convective clouds

01 p0074 A73-11273

Microstructure, hardness, electrical resistivity and thermal properties of Ni alloys with Al and Ta, noting composition of heat resistant alloys

01 p0067 A73-11436

North American Thermal Analysis Society, Annual Meeting, 3rd, Waco, Tex., February 7, 8, 1972, Proceedings.

01 p0015 A73-11446

Models of extreme arctic and subarctic winter atmospheres between 20 and 90 km.

02 p0160 A73-12274

The high temperature thermodynamic properties of Ni-Ti alloys.

02 p0182 A73-12753

Shock wave and isentropic compression/expansion in plasma with anomalous thermodynamic properties due to strong particle interactions, discussing phase transitions types

03 p0346 A73-13190

Stress analysis and design of silicon solar cell arrays and related material properties.

03 p0255 A73-14224

Thermodynamics and shocks in nonelastic mediums

04 p0520 A73-15994

Time-temperature safety thresholds for human epidermal injury related to materials thermal properties

05 p0637 A73-16138

Layout of a thermodynamical theory of the life time scattering in materials testing

05 p0635 A73-17066

Thermodynamic characteristics of molybdenum silicides in the temperature interval between 400 and 1200 K

06 p0710 A73-18560

The distribution of chromium between ferrite and austenite and the thermodynamics of the alpha/gamma equilibrium in the Fe-Cr and Fe-Mn systems.

06 p0712 A73-18759

Beryllium for nonstructural and structural applications in aerospace systems, considering high dimensional stability, mechanical and thermodynamic properties, and metal sintering techniques for production

07 p0828 A73-18904

Thermodynamic properties of gases dissolved in electrolyte solutions.

07 p0789 A73-20642

Dislocation glide controlled by linear elastic obstacles - A thermodynamic analysis.

08 p1019 A73-21628

On the solution of the nonlinear heat conduction equations by numerical methods.

08 p1024 A73-21636

Thermodynamic and optical properties of elements vaporized by monochromatic laser light, considering carbon and aluminum vapor stream characteristics

09 p1095 A73-22612

'Flux quantization' type of oscillation effects in a normal metal

09 p1130 A73-22709

Mode of thickening of a low morning convective layer in clear sky

09 p1115 A73-23036

Comparative estimation of thermodynamic characteristics for reduction of tungsten and molybdenum oxides

09 p1107 A73-23226

Orthogonal polynomials for computerized construction of equations of state for substances under thermodynamic restrictions

10 p1293 A73-23505

Thermodynamic properties of the nickel-tungsten system as determined from its hydrogen solubility

10 p1231 A73-23689

Preparation and thermomechanical properties of pyrrone moldings.

10 p1237 A73-23961

Carbon-felt, carbon-matrix composites - Dependence of thermal and mechanical properties on fiber volume percent.

10 p1240 A73-24278

Mechanical, thermal and electrical properties of machinable glass ceramics, discussing application as electromagnetic window materials

11 p1387 A73-25293

Thermodynamic parameters for metallic hydrogen-helium alloy of Saturn and Jupiter interiors, using Monte Carlo chains and dielectric function theory

11 p1420 A73-25888

Lattice model calculation of elastic and thermodynamic properties at high pressure and temperature.

11 p1399 A73-25900

The present thermal state of the terrestrial planets.

11 p1421 A73-25905

Microstructure, hardness, electrical resistivity and thermal properties of Ni alloys with Al and Ta, noting composition of heat resistant alloys

11 p1384 A73-26063

Galilean satellites surface thermal properties from radiometry of 20-micron band during eclipses of Jupiter

11 p1424 A73-26132

Application of the principle of corresponding states to two-phase choked flow.

11 p1349 A73-26744

A quantum model for bending vibrations and thermodynamic properties of C₃.

12 p1526 A73-27019

Study on ionizing shock waves in argon. III - Thermodynamic properties of the plasma.

12 p1527 A73-27173

Carbon dioxide thermodynamic and transport characteristics calculation, treating gas as multicomponent ideal mixture including carbon monoxide and oxygen and carbon atoms and ions

12 p1526 A73-27308

Thermal and mechanical properties of zirconium cloth, felt and braid for heat shielding of reusable space shuttle

12 p1548 A73-27379

Partial and integral molar thermodynamic properties of solid Ta-W alloys at 1050-1300 K, discussing negative deviations from ideality

13 p1632 A73-28126

Ditantulum carbide thermodynamic stability determination from measurement of carbon monoxide pressure in equilibrium with ditantalum carbide-tantalum oxide-tantalum mixture at 1470-1620 C

13 p1632 A73-28128

Experimental and thermodynamic study of the equilibria between ferrite, austenite and intermediate phases in the Fe-Mo, Fe-W, and Fe-Mo-W systems.

13 p1633 A73-28136

A high-temperature thermodynamic investigation of the Nb-Mo system.

13 p1633 A73-28140

On the electrical properties of nonstoichiometric oxides alpha-Nb₂O₅, MnO, and CoO at high temperature

13 p1634 A73-28202

The effect of lattice disorder on the thermodynamic properties of the f.c. tetragonal beta-one NiZn alloys.

13 p1635 A73-28262

The general form of constitutive equations in relativistic physics.

13 p1658 A73-28374

The connection between the thermodynamics of chemisorption on semiconductor surfaces and surface scattering of carriers.

13 p1668 A73-28454

Plastic crystals structural, thermodynamic and mechanical properties, noting high deformability due to molecular rotational freedom

15 p1923 A73-31415

Russian book - Physics of carbographite materials.

15 p1897 A73-31583

Transition metal alloys solid solutions, discussing thermodynamics, interatomic interactions, Debye temperatures, free energy, entropy, magnetic effects and incomplete d shells

15 p1892 A73-32213

Investigation of titanium alloys at high temperatures in vacuum

15 p1894 A73-32541

The relationship between thermal history, X-ray crystallographic structure and thermal properties of Pyco-bond rayon precursor carbon-carbon composites.

16 p2028 A73-33044

The relationship between thermal history, X-ray crystallographic structure and thermal properties of rayon precursor carbon-carbon composites A literature review.

16 p2028 A73-33045

Book - Equilibrium compositions and thermodynamic properties of mixed plasmas. III - Argon-hydrogen plasmas at .01 to 1000 atmospheres between 2,000 and 35,000 K.

16 p2042 A73-33420

Thermodynamic properties of molybdenum silicides in the temperature range 400-1200 K.

16 p2026 A73-33585

Thermodynamic characteristics of the lower atmosphere of Venus on the basis of the results of an experiment conducted with the descent vehicle of the Venus 4 interplanetary probe

16 p2067 A73-33800

Experimental methods regarding the thermodynamics of metals and alloys. I

16 p2026 A73-33953

THERMODYNAMIC PROPERTIES

NT CRITICAL POINT

NT CRITICAL PRESSURE

NT CRITICAL TEMPERATURE

NT EMISSIVITY

NT ENTHALPY

NT ENTROPY

NT FREE ENERGY

NT GIBBS FREE ENERGY

NT HEAT OF COMBUSTION

NT HEAT OF FORMATION

NT MELTING POINTS

NT PYROELECTRICITY

NT SPECIFIC HEAT

NT SUPERCRITICAL PRESSURES

- Book - Foundations of fluid flow theory.
17 p2151 A73-34466
Thermodynamic analysis of liquid metal systems by using a cluster model
17 p2188 A73-34555
Thermodynamic analysis of the distribution of silver in the Cu-Cu₂S system in the presence of Ni₃S₂ and FeS
17 p2188 A73-34556
The operational performance of reentry vehicle heatshield thermodynamic instrumentation.
17 p2238 A73-34605
Orthogonal polynomials for computerized construction of equations of state for substances under thermodynamic restrictions
17 p2255 A73-35185
Moldability, storage stability and thermal, mechanical and electrical properties of epoxy molding compounds for electronic devices
17 p2196 A73-35340
Thermodynamics of b.c.c. solid solutions of hydrogen in niobium, vanadium and tantalum.
17 p2193 A73-35623
Effect of oxides on certain properties of glass-ceramic coatings for titanium
18 p2319 A73-35889
New thermodynamic functions for the C₃ molecule.
18 p2287 A73-36326
Calculations of real gas properties from tables of thermodynamic functions
18 p2372 A73-36817
The F-12 series aircraft aerodynamic and thermodynamic design in retrospect.
19 p2380 A73-37472
Mechanical, thermal and electrical properties of polymers as functions of temperature, radiation and frequency for cryogenic environment material and design selection
19 p2443 A73-37525
Thermal structure and stability study of internal and Kelvin-Helmholtz waves in low Reynolds number flows by sampling and stratified wind tunnel methods
19 p2422 A73-38235
A unified theory of thermoviscoplasticity of crystalline solids.
19 p2501 A73-38256
Unified thermodynamics of dissipative structures and coherence in nonlinear optics.
20 p2571 A73-38633
Experimental characteristics of certain types of semi-open, multi-circuit microwave ferrite filters.
20 p2535 A73-38920
Russian papers on thermophysical properties, analytical method application to thermodynamics, gaseous and liquid equations of state covering metal structures, specific heat measurement, etc
20 p2627 A73-39292
A semiempirical description of the structure of metals
20 p2577 A73-39295
System of experimentally verified equations for calculating the thermodynamic characteristics of some technologically important gases at temperatures ranging from the normal boiling point to 1300 K at pressures up to 1000 bar
20 p2627 A73-39297
Thermodynamic properties of air and thermal equation of state as function of pressure and temperature from piezometer measurement
20 p2627 A73-39298
Determination of the thermodynamic characteristics of a liquid-propellant rocket engine with nonisobaric combustion
21 p2754 A73-40402
Thermodynamic conditions of conservation of irrotational or oligotropic motions across a shock wave
21 p2677 A73-40948
The partial molar thermodynamic magnitudes of oxygen and the nonstoichiometry of oxides - Model with interactions
21 p2791 A73-40950
Oxygen and nitrogen thermodynamic state equation determination by least squares fitting to experimental PVT, isochoric heat capacity and saturation density data
21 p2740 A73-41104
Dense cloud formation and gravitational collapse onset, discussing thermal properties and magnetic field presence
21 p2772 A73-41244
Pure two band superconductor theory, discussing thermodynamic and electromagnetic properties, London group, mixed state, critical field and weak field penetration
21 p2753 A73-41299
Thermodynamic properties and Cr activity measurements in solid Cr-Ni-Fe alloys by solid oxide electrolyte technique
22 p2878 A73-42577
Regularities in the behavior of semiconductors and dielectrics in connection with deviation from stoichiometry
23 p2959 A73-43479
Phase equilibrium technique to measure oxygen solubility in liquid Co at 1510 to 1700 C, determining thermodynamic characteristics and deoxidation curves
23 p2990 A73-43482
Thermodynamic properties and phase composition of the In-Ni system
23 p2991 A73-43706
A thermodynamic calculation of the iron-chromium-vanadium equilibrium diagram.
23 p2993 A73-43918
Mixed finite element models for nonlinear thermomechanical responses of continuous dissipative media based on Oden variational principle and theory of thermoplastically simple materials
23 p3044 A73-44049
Least squares methods for thermal equations of state parameters of substances and solutions, taking into account phase equilibrium lines
24 p3155 A73-44753
Transfer phenomena in nonreactive binary fluid mixtures analyzed by nonlinear continuum thermodynamics of irreversible processes
24 p3156 A73-45081
Thermokinetics and combustion phenomena in non-flowing gaseous systems - An invited review.
24 p3157 A73-45165
Physical particle description of moderately dense gases. II - Equilibrium properties.
24 p3111 A73-45397
Thermodynamics of white dwarf matter in crystalline phase.
24 p3143 A73-45435
- THERMODYNAMICS**
NT AEROTHERMODYNAMICS
NT COMBUSTION PHYSICS
NT NONEQUILIBRIUM THERMODYNAMICS
Differing roles of electron scattering processes in the thermodynamics of metals in the normal and superconducting states
01 p0088 A73-10613
Equations of state and dissociation equilibrium for CsCl plasma, noting thermodynamic model for phase transitions of liquid metal into nonideal ion plasma
01 p0084 A73-10851
Thermodynamic functions and molecular parameters of rhombic dimeric molecules of alkali metal halides
01 p0080 A73-10857
Nonequilibrium thermodynamics description of convective motion, using internal energy and absolute mass flows as generalized convective flow
01 p0123 A73-10867
Liapunov function relation to entropy production in irreversible processes, noting thermodynamic constraints on kinetic equation functions
02 p0191 A73-11613
Semidiscrete-least squares methods for a parabolic boundary value problem.
02 p0188 A73-12615
Existence and uniqueness of heat equation two phase free boundary problem classical solutions
03 p0336 A73-12922
Influence of the nonlinear thermomechanical effect on the thermal stability of rubber-metallic couplings of vibration machines
04 p0509 A73-14981
Relativistic thermodynamics of simple heat conducting fluids.
05 p0641 A73-17235
Use of approximations of thermodynamic functions in gasdynamics calculations
06 p0644 A73-17470
A non-equilibrium thermodynamical analysis of the origin of life.
06 p0651 A73-17931
Thermodynamics of self assembly - An empirical example relating entropy and evolution.
06 p0651 A73-17932
Thermodynamics and morphological orders - A generalized concept of information transfer.
06 p0749 A73-18003
Melchey thermodynamics hypotheses based on average electron energy for examination of equilibrium and steady state conditions in semiconductor p-n junctions
06 p0770 A73-18840
Irreversible thermodynamics and losses in energy conversion, discussing N-port storage representation, flux rate, power flow and electro-caloric and state space relations
07 p0779 A73-20396
Designing electrical analogs for solving a hyperbolic energy equation
08 p1022 A73-20999
Thermodynamic probability and statistical interpretations of entropy, with particular attention to information theory, negentropy and Boltzmann-Gibbs theory
08 p1022 A73-21234
Thermo-acoustic oscillations in forced convection heat transfer to supercritical pressure water.
08 p1022 A73-21253
Stability of certain finite-difference schemes for solving heat conduction equations with a nonself-conjugate elliptic operator
09 p1167 A73-22582
- Method of integral equations in the statistical theory of fluids
09 p1121 A73-22724
Heat conductivity equation solution stabilization for Cauchy problem with oblique derivative and arbitrary number of geometrical variables
10 p1295 A73-24061
Coleman-Noll concept of rational thermodynamic theory, discussing homogeneous and inhomogeneous/fading memory/ systems and logical structures
10 p1296 A73-24690
German handbook of functions and numerical values in physics, chemistry, astronomy, geophysics and engineering covering thermodynamics, combustion physics and heat transfer
11 p1450 A73-25473
Thermodynamic theory of heat conducting fluids with constitutive quantities dependence on rate of density, gradient, velocity and temperature
11 p1453 A73-26746
Improving the properties of the MA5 magnesium alloy by high-temperature thermomechanical treatment
12 p1510 A73-26910
Planck relativistic equations of moving body heat and absolute temperature transformation /1907/ and alternative equations by Ott /1963/, comparing validity
12 p1557 A73-26973
Thermodynamics of relativistic rotating perfect fluids.
12 p1525 A73-27886
Equations of state and dissociation equilibrium for CsCe plasma, noting thermodynamic model for phase transitions of liquid metal into nonideal ion plasma
12 p1529 A73-27901
Nonequilibrium thermodynamics description of convective motion, using internal energy and absolute mass flows as generalized convective flow
12 p1560 A73-27917
Thermodynamics relativistic and quantic structure, considering Lorentz transformation relationship to first principle for entropy and action
13 p1706 A73-28550
A new approach to the problem of predicting the performance of centrifugal compressors.
13 p1565 A73-29012
The numerical solution of parabolic partial differential equations using the method of Lanczos.
13 p1650 A73-29398
Second law of thermodynamics revision to include only spontaneous processes made to yield work, discussing heat flow, solutes diffusion and Gibbs free energy
14 p1816 A73-29735
Quantum irreversible statistical thermodynamics with allowance for occurrence of many temperatures based on principle of isentropic motion, applying to laser action
14 p1756 A73-30150
Book on statistical mechanics, covering thermodynamics, canonical ensembles, quantum statistics, simple gases, ensemble theory, phase transitions, cluster expansions and interacting systems
14 p1775 A73-30360
Nonlinear thermodynamics of irreversible processes for polymer microfracture process under mechanical, thermal, diffusion and chemical actions
14 p1766 A73-30479
Irreversible thermodynamics with internal inertia - Principle of stationary total dissipation.
14 p1817 A73-30484
Some thermodynamic considerations of phenomenological theory of non-isothermal elastic-plastic deformations.
14 p1811 A73-30490
Biological order, structure and instabilities in terms of irreversible thermodynamic processes, entropy, dissipative structures, randomness, abiogenesis, hierarchic organization, chemical reactions and molecular biology
15 p1835 A73-31824
Constraints theory for Cosserat surfaces with applications in thermomechanics and shell theory, investigating equilibrium laws transformation properties and constitutive equations restrictions
16 p2076 A73-32936
On thermodynamics of deformations and variational methods in reversible thermoelectrostatics.
16 p2077 A73-32977
Thermomechanical theory of ferromagnetic and dielectric materials magnetoelectrostatic and electroelastic properties, using variational principles
16 p2037 A73-33228
One dimensional shock waves in heat conducting materials with memory. III - Evolutionary behaviour.
16 p2081 A73-33747
Existence of thermodynamic limits in some models of quantum field theory
17 p2254 A73-34633
Equivalency and macrophysical validity of Thomson and Clausius theorems for second law of thermodynamics, considering Carathéodory theorem relative to entropy and temperature properties
19 p2504 A73-37654

THERMOELASTICITY

- Thermodynamic heat concept, discussing kinetic and potential partial energy, internal energy, heat absorption and release and thermal energy 20 p2627 A73-39293
- Methods for identification of thermodynamically similar substances 20 p2593 A73-39296
- Numerical solution of hydrothermodynamics equations for atmospheric processes on a flat earth 20 p2584 A73-39471
- Thermodynamics of the Al-O and Al-O-C systems 21 p2718 A73-40847
- Continuum thermodynamics-based formulation of mixture theory using Boolean algebra with emphasis on partial stress tensors, considering force, moment and energy balance equations 22 p2885 A73-41771
- Mixed boundary value problem solution for dynamical thermoelasticity, using Laplace transforms in cylindrical coordinates 22 p2918 A73-41952
- Calorimetric measurement of thermodynamic temperatures above 0 C using total blackbody radiation. 22 p2853 A73-41980
- The asynchronous formulation of relativistic statics and thermodynamics. 22 p2931 A73-42436
- Critical slope of the vapor pressure curve of a pure substance. 22 p2932 A73-42506
- Real gas turbocompressor calculations based on equations of state for fundamental thermodynamic processes in ideal gas 22 p2797 A73-42645
- Method of integral equations in statistical theory of liquids. 23 p3007 A73-44324
- Optimal macroscopic control and resource exchange model for open market-like systems in economic and thermodynamic terms 24 p3154 A73-44665
- A simple thermodynamic method of estimating the shock compression temperature of a condensed medium 24 p3155 A73-44709
- Line of symmetry for the classical equation of state. 24 p3110 A73-44987
- Continuous body kinematics and thermodynamics covering frame and motion, differential calculus in Euclidean spaces, deformations, interactions, force equilibrium, entropy and dissipation principle 24 p3112 A73-45472
- Plasticity theory development taking into account thermodynamics of elastoplastic materials, considering existence theorems for plastic flow and variational principle for equilibrium problems solution 24 p3153 A73-45500
- THERMOELASTICITY**
- NT AEROTHERMOELASTICITY**
- Singular integral equations analysis of elasticity theory boundary value problem to determine axisymmetric thermoelastic stress-strain state of half space with cylindrical cavity 01 p0112 A73-10012
- Solution of the thermoelasticity problem for half-spaces with boundary conditions divided by circular lines 01 p0113 A73-10013
- Axisymmetric thermoelasticity problem for an infinite body weakened by two parallel circular cracks 01 p0113 A73-10014
- Stress function for estimating mutual effects of strain and temperature fields in dynamic coupled thermoelasticity problem for thin circular plates 01 p0113 A73-10094
- Research performed on the thermomechanics of deformable solids at the Ukrainian Academy of Sciences 01 p0114 A73-10569
- Unsteady thermal stress in an infinite strip with mixed boundary conditions 01 p0115 A73-10916
- Acceleration waves in anisotropic thermoelastic materials with internal state variables. 01 p0118 A73-11367
- Some variational principles pertaining to non-stationary heat conduction and coupled thermoelasticity. 01 p0118 A73-11369
- Assessment of the heat resistance of graphites over a wide range of temperatures 02 p0184 A73-11619
- Thermoelastic equilibrium of a doubly connected spherical shell 02 p0231 A73-11804
- Russian book on temperature and stress distributions in thin plates covering unsteady heat transfer and thermoelasticity of isotropic and anisotropic plates 02 p0232 A73-11891
- Generalized dynamic problem of thermoelasticity for an infinite plate with a circular hole 02 p0232 A73-11931
- Boundary value problems of thermoelastic wave diffraction in elasticity theory of multiply connected domains bounded by circular cylindrical surfaces 02 p0233 A73-11940

- Three dimensional linear theory of thermoelasticity covering homogeneous and isotropic bodies, work, free energy, boundary value problems and variational principles 02 p0233 A73-11978
- Small disturbance propagation in infinitely extended thermoelastic medium with initial finite homogeneous deformation, determining longitudinal and transverse wave propagation velocities 02 p0234 A73-12018
- Reduction of a three-dimensional quasi-static problem of thermoelasticity for plates to a two-dimensional problem by a symbolic method and by the method of passing to the limit 02 p0235 A73-12194
- Calculation of thermal stresses in spherical storage vessels. 02 p0236 A73-12215
- Uniqueness theorem for linear thermoelasticity theory allowing for second sound, discussing acceleration waves propagation in isotropic material 02 p0237 A73-12796
- Tensor analysis for micropolar elastic body deformation and stresses, solving differential equations of thermoelasticity 03 p0386 A73-13153
- On higher-order theory for thermoelastic analysis of heterogeneous orthotropic cylindrical shells. 03 p0389 A73-13327
- Thermal shock produced edge effect in thermoelastic heated cylinder analyzing brittle material heat resistance and failure 03 p0394 A73-14019
- Radially symmetrical thermoelastic disturbances in generalised dynamical theory of thermoelasticity. 03 p0395 A73-14311
- Thermoelastic wave propagation in a transversally isotropic circular cylinder 04 p0512 A73-15501
- Thermally induced stress waves in an elastic layer. [ASME PAPER 72-WA/APM-22] 04 p0516 A73-15894
- Stress-strain state of a spheroidal inclusion/measuring device/ embedded in a thermoelastic medium 05 p0633 A73-16616
- Coupled thermoelasticity with a finite heat propagation rate 05 p0634 A73-16770
- Temperature distribution at a thermally insulated crack in a plate for various boundary conditions 05 p0640 A73-16774
- The influence of the reference geometry on the response of elastic shells. 05 p0637 A73-17236
- Surface tractions, heat fluxes and body forces required for deformation of flat perforated thermoelastic circular plate into pierced spherical cap 06 p0759 A73-17757
- Thermal shock induced transverse vibrations in rectangular plate with combined simple and clamped edge supports, deriving infinite series solutions 06 p0761 A73-17896
- The linear thermoelastic problem of uniform heat flow disturbed by a two-dimensional crack in a strip. 06 p0762 A73-17985
- Book - On elastic stability under nonconservative loads. 06 p0762 A73-18275
- Coupled thermoelastic stability effect on critical thermal buckling of strip under compression in temperature field 06 p0765 A73-18686
- On the torsional static stability and response of open section tubes subjected to thermal radiation loading. 07 p0908 A73-19086
- Thermoelastic problem for plate with an elliptic insert in the case of nonideal thermal contact 07 p0911 A73-19316
- A review of thermoelastohydrodynamic lubrication in rolling and sliding contacts. 07 p0931 A73-20223
- Thermoelastic bending theory based on structural analysis of multilayer reinforced shells and plates 08 p0107 A73-21373
- Solution of the three-dimensional thermoelasticity problem for a long cylinder with mixed heating conditions 08 p0109 A73-21758
- Thermal stresses in cooled gas turbine blade foils and roots with allowance for thermoelastic effects 09 p1136 A73-22568
- Thermal stresses in an elastic solid weakened by two coplanar circular cracks. 10 p1287 A73-23563
- Solid composite material thermomechanics and overall thermoelastic modulus determination, considering arbitrarily anisotropic phases, binary composite and self consistent theory 10 p1295 A73-24099
- Thermoelastic boundary value problem for heat conduction in elastic bodies with linear and three dimensional inserts 10 p1290 A73-24305
- Boundary conditions model calculations for thermoelastic deformations of continuum body with surface tractions on interface, discussing energy balance laws derivation for loading devices 10 p1292 A73-24696

- Thermoelastic response of a cylinder in the generalised dynamical theory of thermoelasticity. 11 p1433 A73-25160
- Stress-strain state of a thermoelastic spheroidal insert in a thermal viscoelastic medium 11 p1434 A73-25300
- Approximate calculation of thermoelastic stresses in an arbitrarily heated slab 11 p1434 A73-25309
- Mechanical simulation of thermoelastic stresses on the basis of a given temperature field 11 p1435 A73-25401
- Investigation of thermoelastic stresses by means of 'freezing' involving the realization of a prescribed temperature gradient 11 p1435 A73-25454
- Nonlinear thermo-elastic-plastic and creep analysis by the finite element method. [AIAA PAPER 73-358] 11 p1437 A73-25494
- Solution of the dynamic problem of thermoelasticity for a circular plate with allowance for the finite velocity of heat propagation 12 p1552 A73-27262
- Differential equations of thermoelastic state for shells receiving a thermal shock at the surface 12 p1555 A73-27790
- Thermo-acoustical waves in linear thermo-elastic materials. 13 p1691 A73-28088
- Wave propagation in the two temperature theory of thermoelasticity. 13 p1691 A73-28162
- Influence of the diathermancy of an arc-shaped crack on the thermoelastic state of the area about the crack 14 p1814 A73-30720
- Spatial problem of thermoelasticity of a body with an insulated external circular crack 14 p1814 A73-30722
- Solution of axisymmetrical thermoelasticity problems for an infinite region with several spherical cavities 15 p1945 A73-31030
- The effects of couple-stresses on thermal stress distributions in multiply-connected domains. 15 p1947 A73-31362
- On thermodynamics of deformations and variational methods in reversible thermoelasticity. 16 p2077 A73-32977
- Variational principles in nonlinear continuum mechanics. 16 p2036 A73-32979
- Thermal stress in and bending of elastic rectangular plates from Kantorovich method combined with iterative techniques 16 p2077 A73-32992
- Isotropic bonded thermoelastic laminar bodies calculations for thermal flux and temperature fields using linear quasi-static thermal elasticity equations 16 p2080 A73-33242
- Propagation of thermoelastic waves in an unbounded isotropic soil 16 p2081 A73-33363
- Coupled thermally induced vibrations of beams. 17 p2241 A73-34190
- Russian book on elastic equilibrium boundary value problems for isotropic and anisotropic bodies under load or temperature field induced plane deformation 18 p2361 A73-35871
- Protective coating-metal adhesion dependence on chemical bonds, double electric layers at interface and thermoelastic stresses 18 p2319 A73-35895
- Thermoelastic state of an anisotropic plate with an elliptic hole and mixed boundary conditions 18 p2363 A73-36406
- Homogeneous isotropic body thermoelasticity boundary value problems solved by quadrature series using Green function of Laplace equation, determining circular cylinder stress concentration 18 p2366 A73-36753
- Two dimensional steady and transient thermal stress analysis in rectangular solid with varying surface temperature, noting thermoelastic problems solution by analog method 19 p2498 A73-37668
- Minimum principles and some theorems on the elastoplastic equilibrium of bodies subjected to non-stationary physical and thermal effects 19 p2499 A73-37762
- Elastic bodies nonlinear thermomechanical stability under conditions of loaded equilibrium configuration using Liapunov type energy-like functionals 20 p2615 A73-39010
- Thermoelasticity of coupled bodies in the case of stress-dependent heat transfer 20 p2618 A73-39327
- Group properties of the equations of strain theory of thermoelasticity 20 p2618 A73-39329

Approximate solutions for heat conduction and thermal stresses in thermoelasticity of solids and beam and ring structures, considering dynamic, coupling, melting and solidification effects 20 p2620 A73-39514

The incremental theory of three dimensional transient thermoelastoplasticity - Formulation and solution. 20 p2622 A73-39552

Stability of waves and shock structure in generalised thermoelasticity at low temperatures. 20 p2624 A73-39564

Russian book on elastic and thermoelastic waves in continuous deformable bodies covering steady and unsteady deformation dynamics, viscoelasticity and non-linear elasticity using computer methods 21 p2785 A73-40800

Thermal stress calculation for elastic half strip in nonuniform temperature field by functions in terms of Castigliano variational principle 21 p2786 A73-40986

Temperature stresses in a partly reinforced orthotropic plate 21 p2787 A73-40991

Thermoelasticity problems and related particular solutions of a nonhomogeneous Bessel equation 21 p2787 A73-41273

Continuous distributions of dislocations in bonded half spaces. 21 p2742 A73-41666

Thermoelastic wave propagation in a random medium and some related problems. 21 p2789 A73-41667

Thermoelastic dilatational deformation in two perfectly bonded orthotropic half-planes, showing linear relations between elastic and homogeneous field 21 p2789 A73-41674

Mixed boundary value problem solution for dynamic thermoelasticity, using Laplace transforms in cylindrical coordinates 22 p2918 A73-41952

Unsteady state coupled thermoelasticity problem solution based on reducing order of Laplace transform equation, using coupling coefficient as small parameter in series expansion 22 p2921 A73-42279

A coupled thermo-elastic problem of a half-space under the action of a thermal shock on the bounding surface. 22 p2922 A73-42467

Thermal stresses due to an internal source of heat in a solid elastic hemisphere with radiating curved surface and the plane base resting on a smooth rigid insulating plane surface. 22 p2932 A73-42469

Modes of one-dimensional wave propagation in an infinite thermoelastic medium with finite heat propagation rates 22 p2927 A73-42928

Transformation temperatures of martensite in beta-phase nickel aluminide. 23 p2989 A73-43275

A minimum principle in dynamics of elastic-plastic continua at finite deformation. 24 p3146 A73-44678

Transverse coupled thermoelastic vibrations of elastically supported rectangular and circular plates under nonstationary harmonic temperature field 24 p3147 A73-44682

The static axisymmetric problem of the micropolar theory of elasticity and thermoelasticity 24 p3148 A73-44913

Thermoelasticity problem of a spherical shell with multiply connected regions 24 p3149 A73-45175

Variation of amplitudes of thermo-acoustical waves of arbitrary form in isotropic linear thermo-elastic materials. 24 p3157 A73-45372

THERMOELECTRIC CONVERSION SYSTEMS

U THERMOELECTRIC POWER GENERATION

THERMOELECTRIC COOLING

Pipe array design for thermoelectric air conditioners, noting temperature distribution in half-cell and heat conductor junction 01 p0006 A73-10618

Experimental investigation of unsteady-state thermoelectric cooling. III - Combined regime 05 p0639 A73-16772

Low power thermoelectric cascade for cooling substrates to 145 K, discussing materials electrical and thermal properties, design optimization, computerized performance simulation, fabrication and testing 06 p0683 A73-18316

Thermosiphon evaporation-condensation-evaporation cycle cooling system operation and effectiveness in thermoelectric cooling and generator devices 14 p1713 A73-30950

THERMOELECTRIC GENERATORS

NT SNAP 19
NT SNAP 27
NT SNAP 29

Radioactive isotope powered thermoelectric generators operation and performance characteristics and design trends, discussing radiation hazards 01 p0005 A73-10475

Design point characteristics of a 500 - 2500 watt isotope-Brayton power system. [AIAA PAPER 72-1059] 03 p0252 A73-13388

Russian book - Power systems of spacecraft. 04 p0408 A73-15704

Nature of anisotropy in half-cells made of cold-pressed Bi-Te-Se-Sb alloys 06 p0738 A73-18653

Thermoelectric radioisotope generators and nuclear thermoelectronic reactors, noting anaerobic self contained reliable operation and suitability for underwater energy sources 09 p1032 A73-22203

Silicon-germanium technology program of the Jet Propulsion Laboratory. 09 p1117 A73-22759

Thermoelectric generators long term tests, discussing SNAP 11, 19 and 27, TEM-10 and SiGe/PbTe cascaded generator performance characteristics 09 p1136 A73-22760

Vaporization and compatibility of SiGe radioisotope thermoelectric generators. 09 p1117 A73-22761

Radioisotope thermoelectric generator SiGe thermopile power degradation and operating temperature changes, discussing performance prediction model 09 p1117 A73-22763

Co-60 fueled tubular radioisotope thermoelectric generator, correlating long term test data with performance prediction model results 09 p1117 A73-22764

SNAP 19 thermoelectric generator long term performance tests, attributing output degradation to sublimation and hot junction bond loss due to internal gas cover depletion 09 p1118 A73-22765

Thermoelectric panel array of hybrid thermocouples with p-type Si-Ge encapsulated PbTe/Si-Ge n-legs, presenting performance test results as function of test time 09 p1134 A73-22766

Radioisotope thermoelectric converter for Navy TRANSIT navigational satellite 5 year power supply, describing design and performance test data 09 p1034 A73-22767

Computer program for the transient analysis of radioisotope thermoelectric generators. 09 p1060 A73-22768

Isotope Brayton electric power system for the 500 to 2500 watt range. 09 p1118 A73-22793

Radioisotope thermoelectric generators for Nimbus 3 weather satellite, Pioneer 10 Jupiter probe and SNAP 27 powered ALSEP station missions, summarizing operational experience 09 p1154 A73-22795

Navy transit RTG safety and test integration from users viewpoint. 09 p1118 A73-22796

The modeling and design optimization of a space-oriented thermoelectric power supply. 09 p1118 A73-22797

SNAP 19/Pioneer radioisotope thermoelectric generator program status report, stressing Jupiter first mission converters performance prediction 09 p1118 A73-22800

Power from radioisotopes; International Symposium, 2nd, Madrid, Spain, May 29-June 1, 1972, Proceedings 09 p1037 A73-23276

Comparison of strontium-90 and plutonium-238 milliwatt thermoelectric generators. 09 p1037 A73-23277

Five year lifetime space radioisotope thermoelectric generator with lead telluride panels and plutonium 238 dioxide heat source, analyzing reliability, design and performance 09 p1038 A73-23284

Testing of the improved SNAP 19-primary power for advanced space missions. 09 p1038 A73-23285

A review of radioisotope power source development at Atomic Energy of Canada Limited. 09 p1038 A73-23286

Experimental operation of constant temperature heat pipes. 11 p1451 A73-25989

Unmanned interplanetary spacecraft power systems with nickel-cadmium batteries, solar panels or radioisotope thermoelectric generators 11 p1312 A73-26022

Multi-Hundred Watt converter design considerations. 11 p1396 A73-26029

The calculated long-term performance characteristics of a typical silicon-germanium RTG. 11 p1312 A73-26030

THERMOELECTRIC GENERATORS

Analytical model for radioisotope thermoelectric generator performance prediction in air and vacuum, taking into account modified heat transfer rates 11 p1312 A73-26031

Detailed mathematical models of a radioisotope thermoelectric generator. 11 p1396 A73-26033

TRANSIT radioisotope thermoelectric generator technology, discussing structural design, thermal efficiency, performance prediction, panel configurations and life test data 11 p1312 A73-26034

Performance of the thermoelectric converter for the zirconium hydride reactor thermoelectric space power supply. 11 p1396 A73-26036

The SNAP-19 radioisotopic thermoelectric generator experiment - Flight performance on the Nimbus III observatory. 11 p1396 A73-26037

Preliminary testing of a SNAP-19 TAGS RTG in support of the Pioneer F and G missions. 11 p1396 A73-26039

Solar independent power source with radioisotope thermoelectric generator for Grand Tour missions, discussing radiation and thermal interfaces 11 p1313 A73-26042

Thermosiphon evaporation-condensation-evaporation cycle cooling system operation and effectiveness in thermoelectric cooling and generator devices 14 p1713 A73-30950

Thermoelectric device application to spacecraft thermal control. [AIAA PAPER 73-722] 18 p2369 A73-36339

The behavior of xenon when used as a fill-gas in a silicon germanium radioisotope thermoelectric generator. 19 p2455 A73-38388

Cost-effective radioisotope thermoelectric generator designs involving Cm-244 and Pu-238 heat sources. 19 p2455 A73-38389

High temperature material interactions of thermoelectric systems using silicon germanium. 19 p2455 A73-38390

Analytical model for long term performance prediction of multihundred watt radioisotope thermoelectric generator with Si-Ge alloy as thermoelectric material, noting degradation mechanisms 19 p2390 A73-38391

Extending the useful life of radioisotope thermoelectric generators through active power control. 19 p2455 A73-38392

Standardized space shuttle launched multipurpose spacecraft design using nuclear electric power systems with radioisotope thermoelectric generators or Brayton cycle alternators 19 p2455 A73-38393

Transit satellite-borne radioisotope thermoelectric generators launch aboard Scout missile into circular polar orbit, obtaining electrical and thermal data 19 p2494 A73-38394

Performance test equipment of Transit generator with lightweight Isotec thermoelectric panels 19 p2455 A73-38395

Feasibility analysis of satellite solar/thermal power generation and transmission to earth, describing Brayton cycle heat engine for initial energy conversion 19 p2391 A73-38404

Thermoelectric nuclear batteries fabrication in milliwatt power range combining bismuth telluride thermopiles with plutonia fuel capsules 19 p2455 A73-38410

Isotope organic Rankine cycle electric power systems for the 150 to 1500 watt range. 19 p2456 A73-38414

The multi-hundred watt RTG - Technology background and flight systems program. 19 p2456 A73-38418

Multihundred watt radioisotope thermoelectric generator design for on-pad and orbital conditions, discussing configurations, Pu-238 heat source and operating characteristics 19 p2456 A73-38419

The MHW heat source - An advance in radioisotope heat source technology for space applications. 19 p2456 A73-38420

Multihundred watt radioisotope thermoelectric generator full scale thermal performance, vibration, shock, acoustic, acceleration and magnetic field tests 19 p2456 A73-38421

Multihundred watt power supply with Si-Ge thermoelectric couples for Pu-238 source heat energy conversion into electric power, discussing computer model for performance projection 19 p2456 A73-38422

Multilayer foil insulated Si-Ge thermoelectric converters with multihundred watt power capacity, presenting thermal performance stability under vacuum operating conditions 19 p2392 A73-38423

Multilayer foil insulated Si-Ge thermopile design for multihundred watt radioisotope thermoelectric generator to withstand launch environments, evaluating performance under shock and vibration loads 19 p2392 A73-38424

Curium 244 heat source design for multihundred watt radioisotope thermoelectric generator with Si-Ge thermocouples for energy conversion, noting low cost 19 p2457 A73-38429

Design of a nuclear isotope heat source assembly for a spaceborne mini-Brayton power module. 19 p2457 A73-38431

Fuel capsule vent system development for the Viking radioisotope thermoelectric generator. 21 p2737 A73-40766

High-efficiency converter and battery charger for an RTG power source. 22 p2801 A73-42906

THERMOELECTRIC MATERIALS

Room temperature electrical properties and dopant precipitation for SiGe thermoelectric alloys. 09 p1134 A73-22758

SiGe alloys thermoelectric properties long term time and temperature dependent behavior, using diffusion limited dopant precipitation model 09 p1136 A73-22762

The development of SiGe-PbTe segmented thermoelectric couples involving pressure-contacted junctions. 11 p1409 A73-26035

High temperature material interactions of thermoelectric systems using silicon germanium. 19 p2455 A73-38390

Isotope organic Rankine cycle electric power systems for the 150 to 1500 watt range. 19 p2456 A73-38414

Multihundred watt radioisotope thermoelectric generator heat source materials compatibility with thermochemical environment, considering maximum operational and reentry temperatures 19 p2457 A73-38427

Reference data for thermocouple materials below the ice point. 22 p2857 A73-42031

Theory and performance of plated thermocouples. 22 p2859 A73-42051

Comparison of temperature sensors for space instrumentation. 22 p2859 A73-42064

Electrical and mechanical characteristics of thermocell arms reinforced by metal frames 24 p3058 A73-45252

THERMOELECTRIC OUTER PLANET SPACECRAFT

U TOPS [SPACECRAFT]

Zirconium hydride space power reactor design and fabrication technology evaluation, emphasizing requirements for coupling with power conversion and applications for thermoelectric power generation 09 p1118 A73-22801

Autonomous power subsystem design for an Outer Planet Spacecraft. 09 p1154 A73-22805

An integrated radiation physics computer code system. 11 p1334 A73-25997

Reactor-thermoelectric power systems for NASA Space Station/Space Base. 11 p1395 A73-26012

SNAP-27/ALSEP power subsystem used in the Apollo program. 11 p1312 A73-26021

Unmanned reactor-thermoelectric systems for applications in the 1970's. 11 p1395 A73-26024

Status of silicon germanium air-vac converter development. 11 p1312 A73-26032

Five-year lifetime thirty-watt radioisotope thermoelectric generator for NAVY Transit Navigational Satellite, discussing system design, major components, reliability and performance tests 11 p1397 A73-26041

A high resolution dynamic technique of thermoelectric power measurements. 13 p1612 A73-28370

Thermoelectric effects and power calculation of solid electrolyte silver-silver iodide-silver thermocell as function of impurity ion concentration and temperature 21 p2636 A73-40842

THERMOELECTRIC SPACECRAFT

U TOPS [SPACECRAFT]

THERMOELECTRICITY

Gold high temperature thermoelectric properties from electron model based on scattering resulting from d band-Fermi level relative position changes 04 p0463 A73-15313

Effect of irradiation on the absolute thermal emf of metals and alloys 06 p0706 A73-17901

Thermal emf of indium antimonide of a p- and n-type of conductivity at room temperature 06 p0738 A73-18652

Texture and anisotropy of the thermal emf of sheet titanium 09 p1099 A73-21969

Mixing properties of germanium thermoelectric indicators of SHF radiation with 'hot' charge carriers 09 p1063 A73-22456

Thermoelectricity in tungsten at low temperatures. 09 p1135 A73-23335

Influence of heating to high temperatures in vacuum on the electrophysical properties of niobium single crystals 14 p1763 A73-30722

Electrophysical properties of TiC-Nb, TiC-Ta, TiC-Mo, and TiC-W cermet 15 p1892 A73-32242

A method for the determination of the multiplicative constants of thermoelectric pyranometers 15 p1879 A73-32350

A square-law voltmeter based on elements with a thermal coupling 24 p3071 A73-44544

THERMOGRAMS

U RECORDING INSTRUMENTS

U TEMPERATURE MEASURING INSTRUMENTS

THERMOGRAPHS

U RECORDING INSTRUMENTS

U TEMPERATURE MEASURING INSTRUMENTS

THERMOGRAVIMETRY

Thermogravimetric-quadrupole mass-spectrometric analysis of geochemical samples. 01 p0015 A73-11251

Thermogravimetry of thermally stable aromatic and heterocyclic polymers. 01 p0015 A73-11447

Thermogravimetry system designed for use in dispersion strengthening studies. 01 p0015 A73-11449

Vacuum thermogravimetric analysis system for determination of continuous weight change and total condensable materials. 03 p0330 A73-13018

Comparative evaluations of outgassing results between the vacuum thermogravimetric method and the SRI method. 03 p0330 A73-13019

Application of simultaneous DTA/TG and DTA/MS analysis for predicting the flammability of composite textile fabrics and polymers. 09 p1110 A73-22515

THERMOLUMINESCENCE

Refrigeration of lunar samples destined for thermoluminescence studies. 02 p0219 A73-12439

Trapped electrons decay to ground state via nonthermal process in lunar samples during thermoluminescence emission at lunar day temperatures, proposing quantitative model 03 p0369 A73-13101

Phosphor crystals for electromagnetic emission recording based on optical and thermal effects on luminescent screens, considering optimal extinguishing and color alteration conditions 05 p0584 A73-16552

Solar flare and galactic cosmic ray studies of Apollo 14 and 15 samples. 07 p0871 A73-19876

Thermoluminescence of Apollo 14 lunar samples following irradiation at -196 C. 07 p0897 A73-19879

Thermoluminescence of Apollo 12 samples - Implications for lunar temperature and radiation histories. 07 p0897 A73-19880

Thermoluminescence of individual grains and bulk samples of lunar fines. 07 p0897 A73-19883

Spectral emission of natural and artificially induced thermoluminescence in Apollo 14 lunar sample 14163,147. 07 p0897 A73-19884

Saint Severin meteorite irradiation age from thermoluminescence measurements, considering saturation of natural thermoluminescence from calibration curves 09 p1148 A73-22875

Radiophotoluminescence dosimetry for personnel monitoring, discussing thermoluminescence of phosphate and silver activated glasses, energy compensation filters and measurement techniques 11 p1362 A73-25425

Thermoluminescence and activation energies in Al₂O₃, MgO and LiF (TLD-100). 12 p1530 A73-27031

Fossil track and thermoluminescence studies of Luna 20 material. 13 p1675 A73-28312

Fading of thermoluminescence induced in lunar fines. 22 p2915 A73-43027

THERMOMAGNETODYNAMICS

U THERMOMAGNETIC EFFECTS

THERMOMAGNETIC EFFECTS

Influence of the magnetic field on the heat transfer of a ferromagnetic viscoplastic fluid 03 p0347 A73-14323

Investigation of the phonon drag effect in n-GaAs. 04 p0482 A73-14866

Natural remanent magnetization and thermomagnetic properties of the Allende meteorite. 05 p0619 A73-16840

Thermomagnetic shunt for compensation of instrument errors due to temperature effects on magnetoelectric transducers material, calculating magnetic circuit 05 p0577 A73-16988

X ray analysis of high coercivity Ticonal alloy single crystal microstructure after isothermal thermomagnetic treatment 06 p0709 A73-18210

Optimum thickness for thermomagnetic laser writing on Fe doped EuO films on quartz substrate 06 p0702 A73-18372

Thermomagnetic effect in plasma located in an inhomogeneous magnetic field. 07 p0859 A73-20135

Mossbauer and X-ray spectral studies of a nickel cobalt ferrite subjected to thermomagnetic treatment 15 p1886 A73-31034

Studies of galvanomagnetic and thermomagnetic phenomena in selenium and tellurium doped InSb. 15 p1924 A73-32159

On the propagation of relativistic thermo-magneto-viscoelastic waves in a material of Voigt-type. 19 p2459 A73-37648

Theory of quantum oscillations of the Nernst-Ettingshausen thermomagnetic coefficient in semiconductors 20 p2599 A73-39397

Knudsen free molecular flow explanation of thermomagnetic torque on circular cylinder suspended in axial molecular field, noting apparatus tilt effect 22 p2842 A73-42233

Digital microstress gauge for magneto-thermal gas transport studies. 24 p3089 A73-44815

THERMOMAGNETISM

U THERMOMAGNETIC EFFECTS

THERMOMECHANICS

U THERMODYNAMICS

THERMOMETERS

NT RESISTANCE THERMOMETERS

Portable electronic thermometer for temperature measurement during exercise elevation of body temperature in heat acclimatization experiment 10 p1185 A73-24567

CW NMR millidegree thermometer using oscillator to detect resonance, noting Curie law, magnetogyric ratio, spin-lattice relaxation time and low electrical conductivity 13 p1618 A73-29072

Dynamic katathermometer for measuring the cooling effect of an ambient medium 15 p1838 A73-31512

Thermometric applications of ferrite permeability dependence on temperature, describing thermometer for magnetically levitated substrate 21 p2702 A73-41108

Symposium on Temperature, 5th, Washington, D.C., June 21-24, 1971, Proceedings. Part 1 - Basic methods. Scales and fixed points. Radiation. Part 2 - Resistance, electronic and magnetic thermometry. Controls and calibration. Bridges. Part 3 - Thermocouples. Biology and medicine. Geophysics and space. 22 p2852 A73-41976

Theory and measurement of emittance properties for radiation thermometry applications. 22 p2886 A73-41982

Ultrasonic thermometry using resonance techniques. 22 p2854 A73-41993

Ultrasonic pulse techniques based on acoustic velocity for inert gas thermometry, discussing electroacoustic transducer response time, temperature sensitivity and momentary contact coupling technique 22 p2854 A73-41994

Liquid helium temperature range thermometry using superconducting tunnel junction devices with temperature dependent I-V characteristics 22 p2856 A73-42018

Accuracy of gallium arsenide diode thermometers in the range 4-300 K. 22 p2856 A73-42019

A low-temperature, glass-ceramic capacitance thermometer. 22 p2856 A73-42020

Instrumentation errors in nuclear resonance thermometry. 22 p2856 A73-42023

High field NMR thermometry below 1 K using HD. 22 p2856 A73-42024

Methods for cryogenic thermocouple thermometry. 22 p2857 A73-42029

THERMOMETRY

U TEMPERATURE MEASUREMENT

THERMONUCLEAR ENERGY

U THERMONUCLEAR POWER GENERATION

THERMONUCLEAR EXPLOSIONS

Stellar explosive nucleosynthesis foundations in nuclear experiments and numerical schemes for solutions in limits of strong and weak coupling of abundances by nuclear reactions 21 p2771 A73-41238

THERMONUCLEAR POWER GENERATION

Laser-initiated fusion - Key experiments looming. 06 p0727 A73-17570

Review of controlled fusion research using laser heating.
[AIAA PAPER 73-258] 06 p0728 A73-17667
Reaction equilibrium and energy balance in thermonuclear fusion propulsion for interstellar space flight, discussing nuclear fuel and ion temperature effects
10 p1262 A73-24544
Direct conversion of thermonuclear plasma energy by high magnetic compression and expansion.
21 p2750 A73-41676

THERMONUCLEAR PROPULSION
U NUCLEAR PROPULSION
THERMONUCLEAR REACTIONS
NT CONTROLLED FUSION
NT NUCLEAR FUSION
Neutrino archaeology - The simulation of double beta-decay by solar neutrinos.
03 p0344 A73-13293
Gravitational contraction and energy dissipation and compensation in stellar nuclear reactions, noting He thermonuclear reactions and nucleosynthesis
06 p0751 A73-18158
The effect of a metallic reflector upon cyclotron radiation.
08 p0990 A73-20813
Thermonuclear reactor model with core surrounded by dense cold plasma, noting temperature profile effects on fusion and energy release locations
08 p0991 A73-20818
Evolution from the main sequence to the helium flash for population II stars.
08 p1005 A73-20915
Charged particle thermonuclear reactions in nucleosynthesis.
10 p1271 A73-23479
Nuclear reactions in carbon stars.
13 p1672 A73-28038
Thermonuclear reactions and nucleosynthesis in stellar interiors, initial big bang, supermassive objects and supernovae explosions
13 p1663 A73-28989

THERMOPHILES
Spin-labeling studies on the membrane of a facultative thermophilic bacillus.
07 p0782 A73-20027

THERMOPHILIC PLANTS
NT BLUE GREEN ALGAE
Purification of *Synechococcus lividus* by equilibrium centrifugation and its synchronization by differential centrifugation.
18 p2274 A73-36503

THERMOPHYSICAL PROPERTIES
NT CRITICAL POINT
NT CRITICAL PRESSURE
NT CRITICAL TEMPERATURE
NT EMISSIVITY
NT MELTING POINTS
NT PYROELECTRICITY
NT SPECIFIC HEAT
NT SUPERCRITICAL PRESSURES
NT THERMAL CONDUCTIVITY
NT THERMAL DIFFUSION
NT THERMAL DIFFUSIVITY
NT THERMAL STABILITY
NT VAPOR PRESSURE
NT VOLATILITY
Research performed on the thermomechanics of deformable solids at the Ukrainian Academy of Sciences
01 p0114 A73-10569
Thermophysical properties of arc-cast tungsten using the TPRC multi-property apparatus/direct heating method/.
01 p0067 A73-11483
Microstructural, mechanical and thermal properties of Nb-W-Ti-Zr alloys, noting cold rolled sheet products
02 p0182 A73-12580
Thermal properties of tantalum-tungsten alloys at high temperatures.
03 p0322 A73-13192
Thermophysical properties of methane.
04 p0517 A73-15050
Thermophysical properties of thermally insulating materials in the cryogenic temperature region.
04 p0520 A73-15938
Influence of thermal nonstationarity on convective heat-transfer intensity
05 p0640 A73-16773
Cholesteric liquid crystals thermophysical properties application in aerospace sciences and engineering, noting temperature measurement and nondestructive tests
06 p0733 A73-17767
Phase diagram and certain properties of alloys of the neodymium-antimony system
06 p0707 A73-18041
Change in sign of thermal lens of glass laser rods with change in thermooptical constant of glass.
06 p0703 A73-18635
Optical and thermal properties of hydrated yttrium vanadates in aqueous solutions, showing decomposition during thermal dehydration
06 p0739 A73-18655

Ion thruster thermal characteristics and performance.
07 p0867 A73-19488
Lubricants thermophysical properties effects on gas turbine engine design, considering thermal stability, vapor pressure, autoignition, load capacity and bearing life
07 p0843 A73-19563
Weld quality of explosive welded industrial metals, noting role of thermal processes and materials thermophysical properties
07 p0831 A73-19995
Numerical method of transient heat conduction with temperature dependent thermal properties.
07 p0921 A73-20118
SiGe alloys thermoelectric properties long term time and temperature dependent behavior, using diffusion limited dopant precipitation model.
09 p1136 A73-22762
Thermophysical effects of solidification on dendritic structure and mechanical properties of cast stainless and low alloy carbon steels for different crystallization rates
09 p1107 A73-23198
Thermophysical and electrical properties of powdered boron carbonitride as high temperature insulating and refractory material at 1800-2020 C
10 p1241 A73-24687
Book - Thermal radiative properties: Nonmetallic solids.
11 p1387 A73-25275
Measurement of a set of thermal properties of metals at high temperatures by the periodic-heating method
11 p1379 A73-25426
Thermal characteristics of constantan, Ni-Cr-Fe, Ni-Mo, Ce-Al-Fe and Ni-Cr alloy filaments for high temperature strain gages
11 p1362 A73-25456
Mathematical model of heat conducting medium thermophysical properties based on one dimensional nonlinear thermal conductivity equation solution
12 p1559 A73-27444
Application of the method of power series to derive solutions for one-dimensional problems of thermophysically nonhomogeneous media
12 p1560 A73-27808
Thermophysical properties of high temperature electrical insulating materials on the basis of non-metallic compounds with high melting point [ECTP PAPER D2-3]
14 p1766 A73-30436
High speed pyrometer for high temperature measurement of thermophysical properties, presenting experiment computer program outline [ECTP PAPER I2-3]
14 p1753 A73-30438
Influence of the diathermancy of an arc-shaped crack on the thermoelastic state of the area about the crack
14 p1814 A73-30720
Russian book - Thermophysical properties and gasdynamics of high-temperature materials.
15 p1957 A73-31851
A high-speed /subsecond/ system for accurate thermophysical measurements at high temperatures.
18 p2316 A73-36359
Application of thermal analysis to the determination of the thermophysical properties and combustion characteristics of metallic particle conglomerates in an oxidizer flow
18 p2342 A73-37119
Thermal limit of heterogeneous ignition
19 p2503 A73-37512
Russian papers on thermophysical properties, similarity method application to thermodynamics, gaseous and liquid equations of state covering metal structures, specific heat measurement, etc
20 p2627 A73-39292
Russian book on low temperature plasmatron-generated plasmas covering physical and transport properties, optical, thermophysical and gasdynamic analytic methods, etc
21 p2746 A73-40516
Thermal conductivities of the elements - Results of a critical evaluation.
21 p2792 A73-41300
Thermal properties of tungsten-rhenium alloys used in high temperature thermocouples.
22 p2858 A73-42038
European Conference on Thermophysical Properties, 3rd, Turin, Italy, June 20-23, 1972, Proceedings.
22 p2876 A73-42401
Optimal utilization of redundant information in thermal radiation in thermophysical measurements.
22 p2931 A73-42408
Symposium on Thermophysical Properties, 6th, Atlanta, Ga., August 6-8, 1973, Proceedings.
22 p2932 A73-42501
Book - Thermal radiative properties: Coatings.
22 p2937 A73-42857
The relationship of certain mechanical and thermophysical properties of polymer composites with the reduced filler concentration
24 p3102 A73-44512

THERMOPHYSICS
U THERMODYNAMICS

THERMOPILES

Thermal fluxometry - Heat well influence on detector response
08 p0967 A73-21500
Radioisotope thermoelectric generator SiGe thermopile power degradation and operating temperature changes, discussing performance prediction model
09 p1117 A73-22763
Thin film thermopile for Symphonie geostationary satellite attitude determination based on absorbed energy transformation into heat, discussing design and applications
16 p1988 A73-33275
Investigation of the design parameters and experimental parameters of medium-temperature thermopiles based on lead, germanium and tin tellurides
17 p2108 A73-34282
Multilayer foil insulated Si-Ge thermopile design for multihundred watt radioisotope thermoelectric generator to withstand launch environments, evaluating performance under shock and vibration loads
19 p2392 A73-38424

THERMOPLASTIC FILMS

U POLYMERIC FILMS

THERMOPLASTIC RESINS

Characteristics of the fatigue curve of plastics.
02 p0185 A73-12699
Solid phase stretch forming of thermoplastic polypropylene at temperatures below crystalline melting point
03 p0332 A73-13034
On the re-inforcement of thermoplastics by imperfectly aligned discontinuous fibres.
04 p0469 A73-15986
The mechanical properties of thermoplastics strengthened by short discontinuous fibres.
05 p0589 A73-16434
Glass fiber reinforced thermoplastic molding materials mechanical and thermal-dimensional stability properties, considering time dependent behavior under static and dynamic loads
06 p0714 A73-18450
Effect of fiber-matrix adhesion on the properties of short fiber reinforced ABS.
10 p1237 A73-23956
Gear and bearing designs with lubricated and reinforced thermoplastics.
10 p1223 A73-23957
Evaluation of the smoke and flammability characteristics of polymer systems.
12 p1515 A73-27143
Structural analysis via thermoplastic scale model testing with resistance strain gages, considering temperature and humidity effects on measurement accuracy and reliability
14 p1750 A73-29701
The anisotropy of creep behaviour in oriented thermoplastics.
17 p2196 A73-35342
Tensile creep in short fibre reinforced thermoplastics.
17 p2197 A73-35344
Fundamentals of fatigue and creep rupture of a thermoplastic.
17 p2197 A73-35345
Creep, self heating and failure of thermoplastics under pulsating tensile stress.
17 p2197 A73-35346
Thermoplastic temperature range extended up to 260 C by polysulphones.
18 p2326 A73-36068
Mechanical characteristics of thermoplastic materials reinforced with short glass fibers, taking into account various degrees of reinforcement
18 p2327 A73-36479
Interfacial, mechanical and fracture properties of fibre reinforced polycaprolactam.
18 p2328 A73-36480
An improved method of production for high strength fibre-reinforced thermoplastics.
18 p2329 A73-37092
Polyquinazolines, thermostable polymers with thermoplastic properties [ONERA, TP NO. 1228]
22 p2881 A73-42218

THERMOPLASTICITY
Numerical solution to the axisymmetric thermoplasticity problem of a shell of revolution
01 p0112 A73-10007
Nonlinear initial and boundary value problems of thermoviscoplasticity, discussing uses of Vainberg theorem and functional convolution in variational principle formulation [AD-758580]
02 p0236 A73-12516
Temperature, velocity, and stress distribution in thermo-viscoplastic boundary layers
03 p0386 A73-13145
Extremum principles on time independent elastoplastic solids nonisothermal deformation properties based on yield function dependence on temperature
06 p0763 A73-18456
Rheological materials thermodynamics with plastic deformations, discussing thermoplastic boundary value problems, thermal shock and heat generation
07 p0914 A73-20180

THERMORECEPTORS

Nonlinear thermo-elastic-plastic and creep analysis by the finite element method.
[AIAA PAPER 73-358]

Property control in reinforced plastics through interface tailoring.

Coupled thermoplasticity model of two stress-strain regions characterized by nonevolutionary plastic flow equations and simple wave collapse, with and without thermal conductivity

Effect of temperature on titanium plasticity

Joining of plastics to plastics and to metals.

Coupled thermoplasticity model of two stress-strain regions characterized by nonevolutionary plastic flow equations and simple wave collapse, with and without thermal conductivity

Minimum principles and some theorems on the elastoplastic equilibrium of bodies subjected to nonstationary physical and thermal effects

Constitutive equations for isotropic and anisotropic perfectly plastic materials derived from Clausius-Duhem inequality, considering thermal influences, plastic flow, entropy and elastic deformation

Investigation of a thermomechanical surface during unloading according to the theory of thermoplasticity

Group properties of the equations of strain theory of thermoplasticity

Anisotropy of low-temperature plasticity and the tendency of deformed molybdenum toward exfoliation

The incremental theory of three dimensional transient thermoelastoplasticity - Formulation and solution.

Propagation velocities and amplitudes of thermoacoustic waves in thermo-plastic materials.

High-molecular compounds and recording of information on thermoplastic films

Combustion of thermoplastic polymer particles in various oxygen atmospheres - Comparison of theory and experiment.

Mixed finite element models for nonlinear thermomechanical responses of continuous dissipative media based on Oden variational principle and theory of thermoplasticity simple materials

THERMORECEPTORS

Thermosensitive interoreceptors and their interaction with thermosensitive structures of the hypothalamus

Differential thermal sensitivity in the human skin.

THERMOREGULATION

Cardiovascular and temperature regulatory changes during progressive dehydration and euhydration.

Response of single units of the posterior hypothalamus to thermal stimulation.

Heat flow meter and calorimeter measurements of heat transfer between human body and environment under various climatic conditions for temperature regulation studies

Deep hypothermia induced in the golden hamster by altering cerebral calcium levels.

Energy balance and lactic acid production in the exercising rabbit.

Thermoregulatory reactions of animals in a helium-oxygen medium

Thermal protective garment using independent regional control of coolant temperature.

Thermoregulatory reactions of rats in a nitrogen and helium-diluted hypoxic atmosphere

Energy requirements of ouabain-sensitive Na-K positive ion membrane pump during norepinephrine induced thermogenesis of brown adipose tissue in cold-exposed hamsters

Thermoregulatory behavior of man during rest and exercise.

Thermosensitive interoreceptors and their interaction with thermosensitive structures of the hypothalamus

Cerebral temperature oscillations and vascular responses in man

Quantitative influence of CO₂ inhalation on thermal sweating in man.

Hypothalamus, septum and ventrobasal thalamus nuclei single neuron responses to skin thermal stimulation, indicating afferent connections between cerebrum thermoregulation center and peripheral thermoreceptors

Helium-cold induced hypothermia in the white rat.

Step-wise changes in thermoregulatory responses to slowly changing thermal stimuli.

Human thermoregulatory system examination under thermodynamic equilibrium based on conductive and convective metastable heat transfer from skin to environment

Differential thermal sensitivity in the human skin.

Dynamic katathermometer for measuring the cooling effect of an ambient medium

Simulation of a steady-state integrated human thermal system.

Changes in the electrical activity of the brain and in some thermoregulation indices of nonanesthetized male cats during cooling

Control of forearm skin blood flow during periods of steadily increasing skin temperature.

Tolerance to heat following cold stress.

Blood electrolytes and exercise in relation to temperature regulation in man.

The inhibiting action of 5-oxytryptophan on thermal regulation during the awakening from hibernation

Model of evaporation responses to heat load increases

Brain calcium - Role in temperature regulation.

Determinants of hypothalamic neuronal thermosensitivity in ground squirrels and rats.

Changes in thermosensitive characteristics of hypothalamic units over time.

Contraction kinetics of ventricular muscle from hibernating and nonhibernating mammals.

An assembly for electrophysiological and thermometric studies

Book on comparative physiology of thermoregulation covering primitive and aquatic mammals, torpidity aspects, evolution and newborns

Primitive mammals phylogeny relationship to homeothermic abilities, discussing body temperature, thermoregulation, basal metabolism rates, hibernation, nycthemeral rhythms and responses to heat and cold

Aquatic and diving mammals in fresh water and marine environments, discussing aquatic thermal conditions, body temperature distribution, thermoregulation, metabolic heat production, etc

Torpor and hibernation physiology in mammals covering evolution, hypothermia, energy conservation, cell and organ adaptations, nervous and cardiovascular system changes, etc

Thermoregulation evolution in various animals, discussing body size and composition effects, body temperature variations, control mechanisms, heat loss and production, behavior and ontogeny

Spinal cord heating effects on frog thermoregulatory behavior in aqueous thermal gradient, noting preference for colder ambient temperature

Metabolic and myoelectric reactions under chemical thermoregulation in rats after accelerated cold adaptation

Cardiovascular adjustments to progressive dehydration.

THERMOSETTING RESINS

NT EPOXY RESINS

NT NYLON [TRADEMARK]

NT PHENOLIC RESINS

NT POLYAMIDE RESINS

Non polar thermosetting resins for high temperature electrical/electronic components.

The influence of temperature on the wear of carbon fiber reinforced resins.

Flat laminated FRP-FRTP and carbon FRP-FRTP composites, testing lamination effects on bending and impact strengths

Evaluation of the smoke and flammability characteristics of polymer systems.

THERMOSIPHONS

Thermosiphon evaporation-condensation-evaporation cycle cooling system operation and effectiveness in thermoelectric cooling and generator devices

Papers on heat transfer covering thermosiphon technology, flowing gas-solid mixtures, condensation, free convection, flow stability and cryogenic insulation

Thermosiphon technology advances covering open and closed single-phase natural convection and mixed convection systems, two phase systems and turbine blade cooling

THERMOSPHERE

Neutral composition measurements of the mesosphere and lower thermosphere.

Atomic oxygen profiles in the lower thermosphere.

The diurnal variations of hydrogen and oxygen constituents in the mesosphere and lower thermosphere.

Neutral composition measurements in the lower thermosphere by means of a mass spectrometer with helium cooled ion source.

Drag derived density analysis for geomagnetic disturbances effect in thermosphere, noting atmospheric reaction time delay and exospheric temperature increment per unit Kp

Structure of the thermosphere as inferred from incoherent scatter measurements.

Global distributions of thermal energy content and losses in thermosphere, discussing energy sources, continuity equations and transport mechanisms for heat balance

Theoretical model of diurnal variations of the equatorial thermosphere at equinox.

Effects of vertical mass motions on the composition structure in the thermosphere.

Quiet time magnetosphere-thermosphere couplings, describing global wind system model and convection and auroral Joule heating

Inaccuracy sources in winds calculation from thermospheric models, considering neutral air motions due to global pressure variations

Momentum deposition by atmospheric waves, and its effects on thermospheric circulation.

Enhanced N₂ vibrational temperatures in the thermosphere.

Thermospheric parameters seasonal and latitudinal variations calculation based on atmospheric model with components ionization and molecular oxygen dissociation as main heat sources

Changes in thermospheric molecular oxygen abundance inferred from twilight 6300 Å airglow.

Theoretical model for the latitude dependence of the thermospheric annual and semiannual variations.

Numerical solution for the composition of a thermosphere in the presence of a steady subsolar-to-antisolar circulation with application to Venus.

Three component static thermosphere model for oxygen radiative recombination and thermal diffusion dependence on underlying layers and solar UV radiation

Global mean thermosphere temperature profiles as function of solar EUV flux, considering neutral gas heating and ionospheric electron temperature

Comparison of the correlation of incoherent scatter and ionosonde measurements of temperature with calcium plage and 2800-Megahertz intensities.

Parametric description of thermospheric ion composition results.

Thermosphere kinetic temperature diurnal variation from heat conduction equation periodic solution, determining heat sources from solar radiation atmospheric absorption

Qualitative detection of space dust particle layers in the lower thermosphere by the twilight method

Diurnal temperature variations in the thermosphere with solar activity

Neutral thermosphere temperatures from density scale height measurements.

Effect of atomic oxygen on the N₂ vibrational temperature in the lower thermosphere.

Variations of the structural parameters of the thermosphere from satellite braking data

The effects of thermospheric winds on the ionosphere at low and middle latitudes during magnetic disturbances.

A two-component model of the diurnal variations in the thermospheric composition.

Stellar occultation measurements of molecular oxygen in the lower thermosphere.

The variation of temperature with latitude in the lower thermosphere /80-100 km/.

Lower thermosphere thermal energy and oxygen transport due to photochemical reactions, noting Schumann-Runge band absorption, atomic recombination and collisional deactivation

Lower thermosphere density and composition model from satellite drag and accommodation coefficients

Atomic oxygen loss in ion source of sounding rocket-borne mass spectrometer for determining lower thermosphere neutral composition

Magnetic control of near equatorial neutral thermosphere, calculating F region ionization anomaly and molecular nitrogen and atomic oxygen density latitudinal variations

Auroral heating and the composition of the neutral atmosphere.

Diurnal thermospheric heat budget in terms of electron-ion recombination, photodissociation and neutral wind energy transfer and conductive and radiative cooling

Thermospheric neutral gas dynamics, discussing acoustic, gravity, tidal and planetary waves disturbance spectrum, propagation characteristics, latitude structure and energy sources

The heating of the thermosphere by atmospheric gravity waves

Influence of viscosity, thermal conduction, and ion drag on the propagation of atmospheric gravity waves in the thermosphere.

Atmosphere Explorer mission of lower thermosphere and ionosphere physics investigation, discussing orbit selection

Atmosphere Explorer for satellite observation of thermosphere, discussing design goals, spacecraft components and data system

A neutral-atmosphere composition experiment for the Atmosphere Explorer-C, -D, and -E.

Conventional filter photometer onboard Explorer satellite for 3000-7500 Å airglow and auroral thermospheric emission features monitoring

Energy and diffusive mass transport relation to thermospheric circulation, composition, temperature and mass density from three dimensional two constituent magnetic storm model

A thermosphere composition measurement using a quadrupole mass spectrometer with a side energy focusing quasi-open ion source.

Meteor trail drift observations in equatorial region /Somalia/ for lower thermosphere wind velocity and direction calculation via harmonic analysis

Equatorial ionospheric anomaly related neutral thermospheric composition variation observation from

OGO-6 mass spectroscopic data, noting static diffusion model limitations

Three component static thermosphere model for oxygen radiative recombination and thermal diffusion dependence on underlying layers and solar UV radiation

Primary scattering theory for twilight luminance calculation, considering luminance atmospheric scale height growth in thermosphere and seasonal variation

Mesospheric and lower thermospheric ozone concentration measurement at sunset via occultation technique from rocket payloads

Lower thermospheric oxygen photodissociation evaluation for global average and hemispheric imbalance, discussing wind system to compensate for solar thermal input imbalance

On the temperature of the Jovian thermosphere.

A study of the time lag of the 27-day variation in the thermospheric density.

Latitudinal and temporal variability of temperature in the lower thermosphere.

A study of the diurnal variation in the thermosphere as derived by satellite drag.

Results of simultaneous wind velocity profile measurements in the lower thermosphere by the meteor radar and rocket methods.

Rocket investigation of the intensity and composition of the corpuscular radiation at altitudes 180 km up to the polar region.

Atomic hydrogen and water vapour in the lower arctic thermosphere during geomagnetic storm and PCA event.

A model of formation of the mean diurnal state of the upper atmosphere and its diurnal variations.

Thermospheric observations combining chemical seeding and ground-based techniques. II - Ionospheric drifts and the Sq current system.

Thermospheric density variations associated with auroral electrojet activity.

Semiannual effect in thermosphere due to solar heat input associated with subsolar point migration and auroral heating by magnetic storms

Interpretation of the H-alpha atmospheric emissions observed by the D-2A Tourmesol satellite around the magnetic equator

Variations in the temperature of the thermosphere in the course of the day and with solar activity.

Wave-mean flow interactions in the upper atmosphere.

Atomic oxygen and helium concentrations variation at 120 km in thermospheric composition models, discussing association with geomagnetic activity

Interaction of the lower thermosphere with the solid component of the interplanetary medium.

On the diurnal variations of total mass density, number density and temperature in the upper thermosphere.

Atmospheric models for 110-2000 km region, considering composition, temperature profiles, thermosphere and exosphere variations, density and boundary condition computation, etc

Exospheric and thermospheric structure variations with solar activity, diurnal variation, geomagnetic activity, seasonal-latitudinal variations of He, H and density waves

A generalized aeronomic model of the mesosphere and lower thermosphere including ionospheric processes.

Study of neutral composition of lower thermosphere at Fort Churchill.

Lower thermospheric atomic oxygen profile from 18 May 1971 nitric oxide release and mass spectroscopic observation, noting monotonic density increase to 0.8 trillion/cc

Measurements of thermospheric temperatures by incoherent scatter radar.

Equatorial thermospheric composition and its variations.

Thermospheric structural parameter diurnal variations from satellite orbit decay, rocket measurements of vertical temperature distribution and atmospheric component concentrations and incoherent scatter observations

Neutral composition and its variations in the lower thermosphere.

Estimates of thermospheric neutral constituents from ion composition measurements.

Thermospheric density diurnal and seasonal variations from cosmos drag data, discussing amplitude, density distribution, coefficients of expansion, summer solstice spherical functions

Global thermospheric wind distribution computed by solving Navier-Stokes equations with models at upper atmospheric densities and ion distribution

Aeronomical consequences of solar flux variations between 2000 and 1325 angstroms.

Temperature measurements in the thermosphere and ionosphere.

Global distribution of thermospheric heat sources - EUV absorption and Joule dissipation.

Rocket-borne spectrometer measurement of solar UV flux for thermospheric vertical distribution of molecular oxygen

A numerical study of three-dimensional diurnal variations within the thermosphere.

The thermospheric heating function. III - The function describing the heating of the thermosphere by short-wave solar radiation during a period of high solar activity

Helium in the terrestrial atmosphere.

Atomic oxygen densities in the lower thermosphere as derived from in situ 5577-Å night airglow and mass spectrometer measurements.

THERMOSTABILITY

U THERMAL STABILITY

THERMOSTATS

Low weight thermostat for temperature compensation of Sharpe quartz gravimeters

Possibilities of improving the characteristics of operational amplifiers by using thermostated input cascades

THERMOTROPISM

U ANISOTROPY

U TEMPERATURE EFFECTS

THERMOVISCOELASTICITY

Basic behavioral characteristics of viscoelastic orthotropic shell prepared from a generalized thermorheologically simple material

Thermomechanical dissipation analysis of thermoviscoelastic solids by finite elements.

Nonisothermal instability of flows of viscoelastic media

Plane strain dynamics on magneto-thermoviscoelastic materials, noting conductivity, heat sources, potential and rotation

Stress-strain state of a thermoelastic spheroidal insert in a thermal viscoelastic medium

Approximate method for solving dynamic problems in thermoviscoelasticity

Finite element approximations in nonlinear thermoviscoelasticity.

Propagation of steady shock waves in non-linear thermoviscoelastic solids.

Practical implementation of the perturbation method in an inhomogeneous boundary value problem of thermoviscoelasticity

Solution of boundary value problems in thermoviscoelasticity with allowance for mass forces exhibiting a potential

The method of forces for thermoviscoelastic rod systems

Variational principles in dynamic thermoviscoelasticity.

THETA PINCH

THETA PINCH

- Energy and mass analysis of neutral particles emitted from a toroidal theta-pinch plasma. 01 p0084 A73-10466
- Turbulence spectra of collisionless magnetized plasma produced in high voltage theta pinch, considering initial magnetic field orientation and instability theories tests 07 p0857 A73-19527
- Straight plasma column confined by static axial and oscillating transverse magnetic fields, deriving stability criteria via viscous fluid model 10 p1255 A73-24264
- Heating of theta-pinch plasmas by pulsed CO₂ lasers. 10 p1256 A73-24527
- Experimental study of a conical theta-pinch plasma gun. 14 p1779 A73-29928
- The use of fast magnetic compression for the production and heating of plasma in Tokamak-like geometries. 14 p1780 A73-30121
- Damping of Alfvén and magnetoacoustic waves at high beta. 17 p2217 A73-35524
- Interaction between an ion beam and a turbulent low-pressure theta-pinch plasma 18 p2340 A73-36667
- Streaming plasma interaction with variable longitudinal magnetic fields. 19 p2465 A73-37171
- An argon ion laser with a gas-discharge tube of relatively large diameter 21 p2714 A73-40556
- Direct conversion of thermonuclear plasma energy by high magnetic compression and expansion. 21 p2750 A73-41676
- Theta-pinch instability of plasma beam, relating plasma oscillation frequency to microwave emission and electromagnetic wave scattering 23 p3011 A73-43710
- THIAMINE**
- Effect of accelerations on the thiamine-S/35/ distribution in the organism of white mice 08 p0929 A73-20977
- Physiological shifts in the human organism under increased neuropsychic stresses 19 p2393 A73-37392
- THICK FILMS**
- Thin film and thick metal film technology comparison and production cost analysis, emphasizing thin film resistors application in hybrid circuits 01 p0026 A73-11399
- Microelectronic technology development and applications in transistor-transistor logic, medical devices, computers and thick film hybrid assemblies 02 p0148 A73-12593
- Microelectronic technologies for SAM-D system, discussing thick film hybrid circuits and microstrip applications 02 p0148 A73-12594
- Preparation and corrosion properties of a tantalum sputtered thick film. 04 p0456 A73-15759
- The influence of ion bombardment on the microstructure of thick deposits produced by high rate physical vapor deposition processes. 04 p0456 A73-15760
- Failure modes of hybrid microcircuits in thick films 07 p0800 A73-19410
- The load life characteristics of thick-film resistors. 09 p1065 A73-23048
- Adjustment of thick-film resistors by laser and new pastes for the thick-film technology 13 p1627 A73-28574
- Thick film multilayer IC for electro-optical applications, discussing package techniques, sealing materials, ultrathick printing cold cathode panel and liquid crystal displays 13 p1669 A73-29395
- Microwave energy absorbing elements based on Pd/Ag 17 p2141 A73-35549
- Ferrite thick film deposition by arc plasma spraying, discussing apparatus, process and film properties after annealing 19 p2435 A73-38096
- Angular distribution patterns of thick-film holograms. 20 p2567 A73-39701
- Angular distribution patterns of thick-film holograms obtained by rigorous solution of the diffraction problem. 20 p2567 A73-39702
- Study of the properties of thick-film chalcogenide glass holograms 21 p2701 A73-40571
- THICK WALLS**
- Spiral wrap - A technique for fabricating thick-wall carbon composites. 01 p0057 A73-11294
- Stress intensity factors for internally pressurized thick-wall cylinders. 04 p0505 A73-14680

- Thick elastic or inelastic shells finite deformation, presenting multicouple theory for stress-strain distribution 04 p0508 A73-14941
- A numerical solution of an elastoplastic thick-walled tube subjected to thermal loading. 05 p0635 A73-16978
- Viscoelastic strains in a thick-walled cylinder under the long-term effect of a gravitational load 08 p1017 A73-21371
- A method for obtaining stresses and displacements in thick cylindrical shells under arbitrary boundary conditions. 11 p1442 A73-25708
- Vibration analysis of thick-walled hollow spheres and cylinders, determining periodic response and fundamental frequency as function of wave reflection number and dimensions 13 p1695 A73-28489
- Elastoplastic stressed state of a long thick-walled cylinder subjected to the action of a magnetic field 21 p2786 A73-40981
- Experimentally determined shape factors for deep part-through cracks in a thick-walled pressure vessel. 22 p2866 A73-42157
- Vibration analysis of laminated plates and shells by a hybrid stress element. 22 p2923 A73-42566

THICKENED LEADING EDGES

U LEADING EDGES

THICKENERS (MATERIALS)

- Lubricating grease technological development trends, discussing petroleum oils, esters, silicones, ethers and fluorocarbons base types and different thickeners 07 p0842 A73-19556
- Polytetrafluoroethylene and fluorinated ethylene-propylene grease lubricants. [ASLE PREPRINT 73AM-1A-2] 17 p2195 A73-34977

THICKNESS

NT FILM THICKNESS

- Computerized radial turbine blades thickness identification, considering temperature distribution and effects and mathematical model parameters for constraints 03 p0312 A73-13565
- Critical thickness effect of fatigue notched specimens on stress intensity factor and fracture toughness behavior of Ti-Al-V alloys 04 p0462 A73-15244
- Thermal boundary layer thickness for laminar forced convection to flat plates with uniform heating and uniform wall temperature. 06 p0769 A73-18260
- Bending of nonuniform plates with asymmetric thickness variation inclusion of shear deformation. 08 p1015 A73-20716
- Metal barrier maximum puncturable thickness dependence on high velocity meteorite particle impact parameters 12 p1554 A73-27642
- A comparative study of the thermal diffusivities of stainless steel, hafnium, and Zircaloy. [ECTP PAPER C-6] 13 p1630 A73-28051

THICKNESS RATIO

- Effect of the thickness on the stressed state of rotating disks 03 p0384 A73-13128
- Velocity corrected theory of laminated plates applied to free plate strip vibrations. 04 p0513 A73-15588
- Numerical solution of the radiative transfer equation in spherical shells. 21 p2727 A73-41000
- The wave drag of circular nose cones at zero angle of attack at Mach numbers from 1.5 to 4 and thickness ratios from 0.05 to 0.5 23 p2940 A73-43782

THIN AIRFOILS

NT THIN WINGS

- Mathematical prediction for pressure distribution over arbitrary thin airfoil in inviscid potential and real fluid flows, determining velocity increment at leading edge 05 p0527 A73-16593
- Unsteady thin-airfoil theory for subsonic flow. 08 p0925 A73-20718
- Multiphase flow past thin symmetrical airfoil, applying three velocity model with incident two phase and reflected particle flow components 09 p1027 A73-21993
- A note on the lift coefficient of a thin jet-flapped airfoil. 12 p1457 A73-27171
- An inexpensive technique for the fabrication of two-dimensional wind tunnel models. 17 p2149 A73-35762
- Multiplicative rule failure in matched asymptotic expansion solutions for velocity distribution in steady incompressible flow of thin elliptic airfoils 20 p2550 A73-39814
- Closed-form lift and moment for Osborne's unsteady thin-airfoil theory. 21 p2632 A73-40442

- Airfoil theory calculation of bent thin foil lift coefficient and longitudinal moment characteristics at arbitrary flow separation point location 23 p2940 A73-43720

THIN BODIES

- On the uniformly valid approximate solutions of Laplace equation for an inviscid fluid flow past a three-dimensional thin body. 04 p0433 A73-15094
- [ONERA, TP NO. 1145] 04 p0433 A73-15094
- On the shearing flow of a fluid, heavy or not, with constant vortex, around a thin profile placed under a free line, in linear theory 08 p0926 A73-21490
- Asymptotic approximation of an infinitely thin, elastic, nonlinear cylinder by a curvilinear medium 10 p1288 A73-23765
- Dynamic characteristics of space thin beams. 11 p1433 A73-25126
- Thin uniform circular rings axial and radial bending vibrations under perturbing effect of circumferentially attached small cylinder, comparing theoretical with experimental results 11 p1444 A73-26290
- Approximate shock-free transonic solution for a symmetric profile at zero incidence. 13 p1564 A73-28823
- Flows past thin blunt bodies with shock layer separation 15 p1822 A73-31291
- Inspecting thin tubes by ultrasounds - Choice of examination frequency 21 p2707 A73-41068
- Calculation of the two-dimensional turbulent wake behind a thin obstacle [ONERA, TP NO. 1253] 22 p2796 A73-42222
- THIN FILMS**
- NT ENERGY ABSORPTION FILMS**
- NT FERROMAGNETIC FILMS**
- NT MONOMOLECULAR FILMS**
- Semiconductor thin film image amplifiers and converters based on electroluminescent and photoconducting films 01 p0022 A73-10037
- Contribution to the theory of the current-voltage characteristic of a contact between a metal and a thin-film semiconductor 01 p0087 A73-10042
- X-ray investigation of textures in thin films 01 p0050 A73-10800
- Thin film and thick metal film technology comparison and production cost analysis, emphasizing thin film resistors application in hybrid circuits 01 p0026 A73-11399
- Axisymmetric problem of the equilibrium of a cylindrical film under hydrostatic pressure 01 p0035 A73-11412
- Superconducting Mo-Re alloy thin film prepared by sputtering and deposition onto sapphire substrate, measuring transition temperature, critical current and magnetic field characteristics 02 p0200 A73-11841
- Operating characteristics of cylindrical thin film weak link circuits used as the sensing element in ultra-sensitive magnetometer systems. 02 p0200 A73-11845
- Weakly superconducting, thin-film structures as radiation detectors. 02 p0167 A73-11849
- Experimental approaches to well controlled studies of thin-film nucleation and growth. 02 p0201 A73-12633
- Vapor deposition of thin films of DPPH and BDPA. 02 p0201 A73-12639
- Access to uncombined titanium through an inhibiting film in sublimation pumping of deuterium. 02 p0194 A73-12844
- Multilayer thin film microcircuit and printed circuit conductors partial capacitance and potential coefficients, using matrix method for approximate calculation 03 p0284 A73-14070
- Diffusion and conduction processes in CdS-Cu_xS thin film photocells. 03 p0350 A73-14217
- New results on the development of a thin-film p-CdTe-n-CdS heterojunction solar cell. 03 p0255 A73-14220
- Lubricating characteristics of polyimide bonded graphite fluoride and polyimide thin films. [ASLE PREPRINT 72LC-7C-3] 03 p0317 A73-14372
- Thin films durability increase of poly(n-alkyl methacrylate) polymers with alkyl group length, noting friction coefficient behavior [ASLE PREPRINT 72LC-7C-4] 03 p0317 A73-14373
- The design of broad-band resistive radiation probes. 03 p0310 A73-14492
- Amplification of the displacement of Goos-Hanchen by interposition of thin films 03 p0320 A73-14605
- Russian book - Heat transfer in liquid films. 04 p0517 A73-15710
- Electrical conductivity of very thin gold films. 04 p0484 A73-15948

- Critical failure conditions in thin film lubrication - Preliminary results. 05 p0581 A73-16109
- High density coupled flat thin film magnetic memories for large capacity storage, using point density/signal amplitude simulation model 05 p0553 A73-16169
- Electronic transport in insulating films. 05 p0604 A73-16503
- Waveguide properties, modes and optical pumping effects on thin film organic dye lasers, noting temperature effects on refractivity and laser modes 06 p0699 A73-17808
- On the origin of strongly conducting states in thin insulator films. 06 p0734 A73-17812
- Conversion of electromagnetic into acoustic energy via indium films. 06 p0734 A73-17834
- Intermetallics formation and diffusion of contacting Al-Au thin films dependence on temperature, thickness ratio and contact time 06 p0706 A73-17903
- Exciton-phonon interaction in recrystallized CdTe layers 06 p0737 A73-18219
- Determination of the specific surface resistance of thin metallic layers in the microwave range, based on transmission coefficient measurements 06 p0737 A73-18221
- Low-resistance CdTe films exhibiting a constant emf under the action of an ac field 06 p0737 A73-18222
- Proton irradiation at 30 K and isochronal annealing of reactively sputtered Ta thin-film resistors. 06 p0737 A73-18352
- Normal-mode analysis of anisotropic and gyrotropic thin-film waveguides for integrated optics. 06 p0702 A73-18365
- The mechanism of surface mass transfer in the thin-film Ge-Al system 06 p0738 A73-18651
- Electro-optic contrast observations in single-domain epitaxial films of bismuth titanate. 06 p0739 A73-18748
- Preswitching and postswitching phenomena in amorphous semiconducting films. 06 p0739 A73-18800
- An improved thin-film gauge for shock-tube thermal studies. 06 p0696 A73-18845
- Continuous ultrasonic joining of thin plastic films 07 p0828 A73-18902
- Determination of some kinetic recrystallization parameters of thin films by mathematical and graphical analysis of crystallite boundary shapes 07 p0861 A73-19329
- Reliability of thin nickel-chromium resistance layers deposited by sublimation under vacuum on a glass substrate 07 p0862 A73-19424
- Tantalum thin film capacitors fabrication procedure for hybrid ICs, presenting temperature and frequency responses and I-V characteristics of test samples 07 p0801 A73-19535
- Phase matching in second-harmonic generation using artificial periodic structures. 07 p0834 A73-19538
- Reversible high speed high resolution imaging in amorphous semiconductors. 07 p0862 A73-19609
- Transconductance and distortion of a thin-film transistor 07 p0801 A73-20025
- Comparative studies of noise limitations in superconducting thin-film radiation detectors. 07 p0863 A73-20105
- Theory of excitation of microwave elastic waves by multifilm transducers /considering the effect of metallic and insulator layers/. 07 p0801 A73-20139
- Wall contraction in Bloch wall films. 07 p0864 A73-20218
- An X-ray monitor for measurement of a titanium trioxide target thickness. 07 p0809 A73-20466
- A statistical model for electromigration induced failure in thin film conductors. 08 p0944 A73-20745
- Thin film nickel-chromium resistor failures in integrated circuits. 08 p0944 A73-20746
- Tantalum-glass cermet thin-film resistors. 08 p0945 A73-20809
- Laser oscillation modes in corrugated optical waveguides with passive core, calculating wavelengths for hybrid modes 08 p0975 A73-21060
- Fabrication, electrical properties and reliability of thin film capacitors, noting surface irregularity and impurity effects on reliability 08 p0946 A73-21082
- Thin film YAG-Nd laser light sources, discussing material selection, incoherent pumping sources, geometrical configuration, heat dissipation, gain saturation and feedback methods 08 p0975 A73-21143
- Spun on arsenosilica films as sources for shallow arsenic diffusions with high surface concentration. 08 p0995 A73-21478
- Interdigitated power junction transistor technology assessment for power gain, bandwidth and frequency performance, noting packaging effect and thin film module advantage 08 p0949 A73-21648
- Processes determining the composition of a two-dimensional oxide film on a molybdenum surface 09 p1098 A73-21886
- Proposal of periodic layered waveguide structures for distributed lasers. 09 p1090 A73-21935
- Switching and memory effects in amorphous chalcogenide thin films. 09 p1133 A73-21987
- Amorphous chalcogenide Te-As-Si-Ge thin film switch, discussing pressure effect energy accumulation time delay and behavior after voltage removal 09 p1133 A73-21988
- Application circuits for amorphous semiconductor switching devices with thin film active components, discussing electrical characteristics 09 p1061 A73-21990
- Improved responsivity and sensitivity characteristics of the thin-film bismuth bolometer. 09 p1080 A73-22087
- Spectroscopic investigation of the interaction of oxides with a metallic surface. III - Systems Al₂O₃-Me/Al, Cu, Ti, Khl8N9T steel, Ni, Co, Mo, W, Si/ 09 p1103 A73-22470
- Electrical and structural properties of low-temperature bismuth films 09 p1133 A73-22603
- Plane film elements demagnetizing factor measurement from material-element hysteresis loop comparison 09 p1084 A73-22655
- Photographic process based on ultrathin photosensitive molecular dispersion layer of benzenediazophenyl and autocatalytic Ag deposition during development process 09 p1084 A73-22691
- Thin In film sealing techniques at temperatures below 300 C for binding Pyrex to various materials, using Au layer as alloy flux 09 p1085 A73-22950
- The influence of substrate properties on microwave losses in thin films of semiconductors. 09 p1064 A73-23041
- Thickness dependence of effective coupling factors of ZnO thin-film surface-wave transducers. 09 p1086 A73-23097
- Topological design of thin-film resistors with the aid of a digital computer 09 p1066 A73-23119
- Pulse amplitude modulation of a CO₂ laser in an electro-optic thin-film waveguide. 09 p1098 A73-23337
- Some principles of domain device designing for data processing and means of control. 10 p1198 A73-24022
- Electrophysical properties of BiTeI thin films 10 p1259 A73-24154
- Conduction mechanisms in resistive films deposited by the silk-screen process 10 p1259 A73-24412
- Fabrication procedures, structure, and mechanical properties of BiTeI thin films 10 p1260 A73-24470
- Electrophysical parameters of TiSbSe₂ thin films 10 p1260 A73-24471
- Roentgenographic investigations of thin films of lead chalcogenide based alloys 10 p1260 A73-24472
- Accelerated testing of solid film lubricants. 10 p1225 A73-24635
- On the nature of films over corrosion pits in stainless steel. 11 p1378 A73-24975
- CsI thin film photoemission spectra resolution maximization, rejecting localized ionic state transitions model 11 p1407 A73-24986
- Nd laser radiation thermochemical effects on oxide formation on thin Cr films, Fe-Ni-Co and Cr-SiO alloys and MgO-MnO ferrites, noting resistance and etching rates 11 p1376 A73-25636
- The effect of surface films on fatigue crack initiation. 11 p1381 A73-25810
- IR spectroscopic study of polydimethylsiloxane thin film structure and polymerization under glow discharge 11 p1400 A73-26144
- Amorphous thin films of rare earth transition metal alloys for magneto-optic applications, noting SNR in thermomagnetically written film 11 p1409 A73-26325
- Indirect transitions in thin quantized semiconductor films 11 p1410 A73-26450
- Preparation and investigation of EuS thin films 11 p1410 A73-26672
- High field superconductivity in alkali metal intercalates of MoS₂. 11 p1410 A73-26745
- Frequency selective coupler with thin film waveguides in periodic medium, discussing bandwidth and coupling factor from Brillouin diagram 12 p1504 A73-26827
- Copper deposition on ceramic plate, discussing interdigital slow wave structure and thin film meander-line coupling impedance and dispersion characteristics 12 p1480 A73-27581
- V and Cr thin film lattice parameter decrease with thickness, discussing vacuum effects and surface energies estimation 12 p1531 A73-27935
- Determination of the temperature dependence of the Debye-Waller factor for thin gold films by electron diffraction observations 12 p1532 A73-27944
- Exciton absorption band splitting in the PbI₂ spectrum 12 p1532 A73-27945
- Fluctuating shift in the transition temperature of thin superconducting films 12 p1532 A73-27984
- Historical development of solar cells. 13 p1573 A73-29590
- The shear strength of thin lubricant films. 14 p1754 A73-30050
- CdTe thin film fabrication by direct synthesis of vacuum evaporated Cd and Te, noting solar cell efficiency increase after storage in room temperature exsiccator 14 p1713 A73-30475
- Thin dielectric films as protective coatings for metallic mirrors and antireflective coatings for semiconductors and active laser materials 15 p1884 A73-31416
- Thermal analysis of thin-film micro machining with lasers. 15 p1882 A73-31938
- Cadmium mercury telluride thin film coatings preparation by HgTe layers deposition onto previously vapor deposited CdTe layers under isothermal conditions 15 p1924 A73-32158
- Thin film thermopile for Symphonie geostationary satellite attitude determination based on absorbed energy transformation into heat, discussing design and applications 16 p1988 A73-33275
- Epoxy adhesive materials evaluation for microelectronic assemblies of hermetically sealed hybrid circuits with semiconductor chips and thin film substrates 16 p1989 A73-33468
- Scattering of a nonlocalized exciton on phonons in thin quantized semiconductor films 17 p2218 A73-34118
- Electrical properties and photoconductivity of CdS thin films obtained in a hydrogen atmosphere 17 p2219 A73-34281
- Composition of a two-dimensional oxide film on a molybdenum surface. 17 p2186 A73-34309
- Structure of sputtered molybdenum disulfide films at various substrate temperatures. [ASLE PREPRINT 73AM-3C-3] 17 p2196 A73-34988
- Solid film lubricant corrosion study employing salt spray test with sulfur dioxide and synthetic sea water, examining molybdenum disulfide, antimony trioxide and graphite films [ASLE PREPRINT 73AM-3C-4] 17 p2196 A73-34989
- Application of the hydrogen-bubble technique for velocity measurements in thin liquid films. [ASME PAPER 73-APM-8] 17 p2153 A73-35033
- Thin film hybrid microwave integrated circuit. 17 p2141 A73-35323
- Thin turbulent film analysis with approximation for relationship between flow and wall shear stress and effects of surface roughness and inertia at steps [ASME PAPER 73-LUBS-17] 17 p2181 A73-35396
- Low loss light guiding polymer thin film with continuously adjustable refractivity, discussing fabrication and refractivity and scattering loss measurements 17 p2172 A73-35423
- Electrical properties of single-crystal films of p-type PbTe 17 p2219 A73-35556
- Determination of ultramicro-impurities in CdS-type semiconductor materials - Determination of copper 17 p2220 A73-35558
- Papers on integrated optics covering waveguides, mode launching, radiation losses, lasers, parametric devices, light deflectors and thin film deposition 17 p2185 A73-35599

THIN PLATES

A reflectance analog computer for the determination of thin film optical properties. 17 p2132 A73-35773

Solar energy conversion into thermal, chemical or electric energy, discussing high efficiency collector design with thin film for absorber and glass envelope improvement. 18 p2269 A73-36331 [ALAA PAPER 73-710]

Application of the four-probe method to the determination of the resistance of thin films deposited on various substrates. 19 p2470 A73-37953

Nd laser radiation thermochemical effects on oxide formation on thin Cr films, noting resistance and etching rates. 19 p2438 A73-38148

An elusive open-circuit failure mode in thin-film chip resistors. 19 p2410 A73-38444

Improve reliability of electron devices through optimized coverage of surface topography. 19 p2411 A73-38453

Microwave integrated circuit technology. 19 p2411 A73-38535

Influence of electric field strength on effective carrier mobility in polycrystalline CdSe thin films. 20 p2536 A73-39200

Silicon-on-sapphire thin film junction diodes, investigating second breakdown onset delay time and minimum energy dependence on high resistivity side heating. 20 p2536 A73-39415

Acoustic surface wave thin film guides for nonlinear signal processing, discussing relative advantages over nonguided arrangements, and application to transverse wave front imaging. 20 p2531 A73-39596

Measurement of superheating and supercooling fields of superconducting thin films. 20 p2599 A73-39724

Superconductivity of films made from aluminum oxide and niobium mixtures. 20 p2579 A73-39744

A high vacuum, low temperature specimen transfer device for use in measuring optical properties of thin films. 21 p2693 A73-39925

Perturbation analysis of holographic grating couplers in thin film waveguides, discussing coupling efficiency dependence on evanescent tail length, refractive index and gelatin film thickness. 21 p2699 A73-40149

Large mercuric iodide single crystals application to high resolution X ray detectors, discussing fabrication by coating platelet face with thin Aquadag film and mounting upon carbon substrate. 21 p2699 A73-40465

Thin film capacitor with anodic tantalum oxide overlaid with silicon dioxide deposited by RF sputtering, noting reliability under various voltage, temperature and humidity conditions. 21 p2663 A73-40771

A bilevel thin film hybrid circuit containing cross-overs, resistors, capacitors, and integrated circuits. 21 p2669 A73-40773

Thin film temperature sensor with polymer coating for medical research providing good sensitivity and stability for rapid temperature changes in biochemical reactions. 22 p2813 A73-42055

Experimental investigation of a simple squeeze film damper. [ASME PAPER 73-DET-101] 22 p2865 A73-42078

Characteristics of thin-film metal arrays for laser-beam information storage. 22 p2869 A73-42254

Properties of thin-film holograms on chalcogenide glasses. 22 p2860 A73-42409

Low temperature thermionic cathode. 22 p2834 A73-42695

German monograph - Investigation of time-variable currents in Al-Al₂O₃-Al thin-film structures. 22 p2897 A73-42855

Diffusion in thin film couples of platinum-gold. 23 p3015 A73-43528

Theory for the steady-state operation of a thin-film regenerative optron. 23 p2959 A73-43617

The detectability limits of thin coatings measured with the electron microprobe. 23 p2985 A73-43917

Transverse elastic wave propagation in CdS crystal wafer coated on both sides with AgBr, titanium oxide, Si or polystyrene. 23 p3017 A73-44038

Bulk and surface damage mechanisms of laser crystalline and nonlinear optical materials and thin films, noting plasma thresholds and surface polishing. 23 p2989 A73-44210

THIN PLATES

Thermal diffusion theory for deformations of thin isotropic shells and plates subjected to nonuniform temperature and stress concentration fields. 01 p0113 A73-10019

Iterative solution of thermal bending problem for nonuniformly heated thin rectangular plate with discrete boundary conditions. 01 p0113 A73-10020

Effect of heat propagation rates on the temperature field and stresses in thin plates. 01 p0113 A73-10022

Stress function for estimating mutual effects of strain and temperature fields in dynamic coupled thermoelasticity problem for thin circular plates. 01 p0113 A73-10094

Construction of finite-difference schemes in engineering theory of elasticity on the basis integral representations of the resolvent functions. 01 p0114 A73-10483

Asymptotic analysis of nonlinearly elastic and plastic thin rectilinear panels under combined bending and tensile stress. 01 p0119 A73-11442

Russian book on temperature and stress distributions in thin plates covering unsteady heat transfer and thermoelasticity of isotropic and anisotropic plates. 02 p0232 A73-11891

Fracture resistance curve calculation from fracturing diagram, noting crack propagation in thin plate under tensile deformation. 02 p0232 A73-11930

Stability characteristics of thin elastic plate with time varying temperature under transversal magnetic field, calculating buckling probability. 02 p0234 A73-12016

The effects of frequency of loading and of nonreactive external media on growth of fatigue cracks. 02 p0235 A73-12132

General non-linear plate theory applied to a circular plate with large deflections. 02 p0236 A73-12517

A problem of coupling between the vibration of a thin plate and an acoustic field in a fluid. 03 p0383 A73-12982

Perturbation technique for approximation of sound radiation from controlled boundary layer on thin plate, deriving random stationary functions in terms of Fourier integral. 03 p0291 A73-12992

Finite element analysis of thick, thin and sandwich plates, considering quadrilateral elements with allowance for transverse shear effect. 03 p0390 A73-13344

Dimensionless results for plane stress creep behavior of thin disks with central rigid inserts under combined loading. 03 p0396 A73-14644

A method for including the effects of transverse shear and rotatory inertia on flexural motion of elastic plates. 04 p0510 A73-15074

The motion of a plate in a rotating fluid at an arbitrary angle of attack. 04 p0404 A73-15161

Stress intensity factor for axially stressed thin polymethyl methacrylate plate with cracks, noting fracture angle prediction. 04 p0512 A73-15240

Ion distribution function in plasma cylinder flow around thin plate in magnetic field under ionospheric conditions. 04 p0481 A73-15617

Linearized theory of dynamically loaded thin rigid viscoplastic rectangular plates transient response, investigating strain rate effect. 06 p0760 A73-17760

Galerkin methods for vibration problems in two space variables. 06 p0717 A73-18408

On the buckling of thin tensioned sheets with cracks and slots. 06 p0764 A73-18497

Transmission of microwave through perforated flat plates of finite thickness. 06 p0669 A73-18735

A finite element, linear programming method for the limit analysis of thin plates. 07 p0906 A73-19026

Weight minimization of axisymmetric clamped plates subject to constraints. 07 p0908 A73-19092

A creep bending analysis of plates by the finite element method. 07 p0908 A73-19093

Some contact problems for an infinite plate strengthened by elastic cover pieces. 07 p0910 A73-19305

Thin elastic plate stability characteristic values control through elemental boundary forces variation, applying von Karman nonlinear differential equations system eigenvalue problem. 07 p0915 A73-20289

Time optimal heating of thin plates with constraints placed on the thermal stresses. 07 p0923 A73-20634

An examination of the perforation of a mild steel plate by a flat-ended cylindrical projectile. 08 p1016 A73-20828

Vibration of four point-supported plates by a finite element method. 08 p1017 A73-20945

Acoustic radiation from plates excited by flow noise. 08 p0988 A73-21479

Reflection of a microwave signal from a semiconducting plate of finite thickness. 08 p0995 A73-21517

Secondary terms of thin multilayer plate equations, involving edge and stress-strain state fluctuation effects on boundary condition formulation. 08 p1019 A73-21766

On the self-shielding coefficient of plates against neutron fluxes. 09 p1117 A73-22014

Application of the finite element method to the study of the elastic buckling of thin plates of any form. 09 p1157 A73-22214

Thin panels stresses diffusion analysis, comparing Bleich, variational, Conway finite difference and finite element methods. 09 p1159 A73-22717

A triangular plate bending element for contact problems. 09 p1160 A73-22899

Ion distribution function in plasma cylinder flow around thin plate in magnetic field under ionospheric conditions. 10 p1254 A73-24207

A modification of the moire fringes technique for the analysis of moments and deflexions in a laterally loaded plate. 10 p1220 A73-24573

Stress redistribution and rupture due to creep in a uniformly stretched thin plate containing a circular hole. [ASME PAPER 72-APM-KKK] 11 p1442 A73-25709

Asymptotic analysis of nonlinearly elastic and plastic thin rectilinear panels under combined bending and tensile stress. 11 p1443 A73-26060

Thin piezoelectric plate bending deformation and polarization theory in terms of piezoelectricity, electrostatics and elasticity equations for anisotropic body. 12 p1552 A73-23731

Magnetoelastic vibration of electrically conducting thin shells and plates in steady magnetic field from asymptotic integration of electrodynamic equations. 12 p1553 A73-27413

Vibration of simply supported-clamped skew plates at large amplitudes. 13 p1690 A73-28057

Triangular finite elements for plate bending with constant and linearly varying bending moments. 13 p1692 A73-28230

Natural vibrations of thin, prismatic flat-walled structures. 13 p1694 A73-28247

Thin Al alloy sheet fracture toughness from crack growth resistance curves, discussing failure modes and critical stress intensities. 13 p1640 A73-29480

Stress-strain state of thin circular perforated Cu plate under uniform tensile load, showing applicability of small elastoplastic finite deformation theory. 13 p1703 A73-29601

Analytical solution to problems of eddy current distribution in a thin plate and a conducting spherical shell. 14 p1774 A73-30029

Construction of finite difference diagrams of the engineering theory of elasticity, on the basis of integral representations of the resolvent functions. 14 p1810 A73-30308

Nonlinear vibrations of rectangular plates. 15 p1944 A73-31000

Deflection of a thin, nonlinearly heated, rectangular strip. 15 p1946 A73-31142

Response-optimal heating of thin plates with constraints on the temperature stresses. 15 p1957 A73-31688

The transition from thin plate to membrane in the case of a plate under uniform tension. 15 p1953 A73-32094

Thin plates and shells post-buckling behavior analysis by discrete element method, noting computer program capabilities. 16 p2078 A73-32997

Asymptotic integration method solution for three dimensional equations of geometrically nonlinear theory for thin shells and plates. 16 p2080 A73-33243

Natural frequencies and normal modes of a four plate structure. 16 p2083 A73-33948

Radiation emitted by a charge in a stack of plates at frequencies approaching the Bragg frequencies. 17 p2120 A73-34114

A unified approach to the solution of plane problems of magneto-elasticity with special reference to a hole in a thin infinite conducting plate. 17 p2211 A73-34346

The Sorokin damping hypothesis in the case of aperiodic vibrations 17 p2243 A73-34648

Stiffness matrix displacement analysis via curved elements for plane stress and thin plate bending problems 17 p2252 A73-35606

Determination of stiffness and critical loads of a circular plate from a simple bending test. 18 p2362 A73-36327

Approximate method for determining the natural frequencies of flexible rectangular plates 18 p2363 A73-36408

Transverse bending of an annular slab with supporting ribs 18 p2367 A73-36960

Free harmonic vibrations of thin pretwisted rectangular plates analyzed in terms of torsional and bending vibration coupling based on shell theory 19 p2500 A73-38115

Rigid viscoplastic thin circular plate under uniformly distributed transverse pressure, deriving Mises and Tresca yield surface conditions 20 p2624 A73-39567

Investigation of the hypervelocity impact on thin plastics and metal foils 21 p2696 A73-39990

Influence of the shape of the leading edge on the transition process in the boundary layer on a plate in longitudinal flow 21 p2676 A73-40399

Stress distribution in thin circular plate with equiaxed cruciform crack, obtaining stress intensity factor and crack energy by numerical solution of Fredholm equation 21 p2785 A73-40932

Temperature stresses in a partly reinforced orthotropic plate 21 p2787 A73-40991

Flexural wave propagation in a thin plate with circular holes. 21 p2787 A73-41142

Russian book on R-function method for solving boundary value problems of bending and vibration of thin plates with complex configurations 21 p2787 A73-41250

Free flexural vibrations of elliptical thin plate with free edge, calculating mode shapes and frequencies by use of Mathieu function 22 p2918 A73-41822

Convergence of simplified hybrid displacement method for plate bending 22 p2921 A73-42203

Reduction of the degrees of freedom in solving dynamic problems by the finite element method. 22 p2922 A73-42479

Introduction of shear deformations into a thin plate displacement formulation. 22 p2923 A73-42559

Vibration analysis of laminated plates and shells by a hybrid stress element. 22 p2923 A73-42566

Mixed boundary value problem of thin isotropic plate under edge loading, examining bending moment applied to plate with intermittent edge clamping 22 p2928 A73-43065

Fracture of thin sections containing surface cracks. 23 p2992 A73-43807

Bending of a rectangular piezoelectric plate clamped over its edge 23 p3043 A73-43923

Transverse shear extensions to Ilyushin-Shapiro thin shell and plate theory for yield surfaces in rigid-plastic materials 24 p3147 A73-44746

Determination of shape for apertures of equal strength in thin isotropic plates 24 p3152 A73-45356

Laser-induced deformation modes in thin metal targets. 24 p3097 A73-45417

Thin plate in two dimensional supersonic flow, deriving vibration amplitude response to shock pressure load by numerical analysis with Laplace transform 24 p3055 A73-45432

Operator of thin plate reinforced with thin-walled ribs. 24 p3152 A73-45440

THIN WALLED SHELLS

Numerical solution to the axisymmetric thermoplasticity problem of a shell of revolution 01 p0112 A73-10007

Bubnov-Galerkin method for natural vibration frequencies of thin elastic circular conical shell under thermal loading 01 p0113 A73-10015

Thin shell theory for thermal stresses in ogival shell used in nose cone design 01 p0113 A73-10016

Thermal diffusion theory for deformations of thin isotropic shells and plates subjected to nonuniform temperature and stress concentration fields 01 p0113 A73-10019

Finite difference solution to Vekua thin shell equations, using differential and equivalent energetic operators 01 p0116 A73-11076

Stress analysis of cantilever thin walled cylindrical shell with concentrated force on free reinforcement ring, noting members rigidity relationship to internal stress concentration 02 p0230 A73-11718

Thermoelastic equilibrium of a doubly connected spherical shell 02 p0231 A73-11804

Equilibrium equations in theory of anisotropic shells and plates with arbitrary boundary conditions under external loads, noting thin walled reinforced shells 02 p0231 A73-11807

Thin walled shells strength dependence on residual stresses, noting stress analysis of shallow spherical shell with variable residual deformations 02 p0232 A73-11932

Surfaces of constant rate of energy dissipation and deformation velocity for arbitrary thin walled shell under steady creep with given strain hardening 02 p0233 A73-11937

Prediction of the response of a cylindrical shell to arbitrary or boundary-layer-induced random pressure fields. 02 p0237 A73-12601

Curved element for geometrical approximation of thin shell structures, deriving element stiffness equations in terms of nodal displacement degrees of freedom 03 p0389 A73-13325

Vibrational frequency density analysis of thin spherical and cylindrical shells of revolution, using asymptotic integration method 03 p0394 A73-14051

Effect of a circular hole on the buckling of cylindrical shells loaded by axial compression. 03 p0395 A73-14181

Flexibility matrix derived and applied to finite element production for thin walled open tubes under torsion, taking into account warping constraints 03 p0395 A73-14470

Natural frequencies of a hemispherical shell. 03 p0395 A73-14474

On the application of the SHEBA shell element. 04 p0510 A73-15016

Theoretical formulation of finite-element methods in linear-elastic analysis of general shells. 04 p0510 A73-15026

Analytical investigation of a cylindrical shell embedded in a soft medium. 04 p0511 A73-15172

Dynamic response of pressurized thin cylindrical shells subjected to torsional loads. [ASME PAPER 72-WA/PROD-6] 04 p0514 A73-15807

Dynamic stability of monosymmetrical thin-walled structures. [ASME PAPER 72-APM-SS] 05 p0632 A73-16530

Buckling of a long, axially compressed, thin cylindrical shell with random initial imperfections. [ASME PAPER 72-APM-MMM] 05 p0632 A73-16532

Nonlinear shell theory with finite rotation and stress-function vectors. [ASME PAPER 72-APM-CC] 05 p0633 A73-16533

On the determination of the centers of twist and of shear for cylindrical shell beams. [ASME PAPER 72-APM-XX] 05 p0633 A73-16534

On finite symmetrical strain in thin shells of revolution. 05 p0633 A73-16536

A temperature extrapolation method for hollow cylinders. 05 p0641 A73-17119

Transient heat transfer through a thin-walled circular pipe. 06 p0766 A73-17443

Analysis of noncircular cylindrical shells. 06 p0758 A73-17446

Impact of a cylindrical shell against the surface of a compressible fluid 06 p0758 A73-17451

Calculation of general surface-supporting structures with the aid of dynamic relaxation 06 p0758 A73-17516

Dynamic behaviour of thin cylindrical shells subjected to high-speed travelling inner pressures. 06 p0758 A73-17518

Thin shells stability equations based on Bernoulli normal hypothesis, investigating stresses and deformations for equilibrium state under arbitrary load conditions 06 p0759 A73-17743

The thermal shock on the shell of revolution-coupled and uncoupled theory. 06 p0763 A73-18452

Transversal vibrations of the thin shell of revolution produced by the thermal shock. 06 p0763 A73-18453

Derivation of the linear shell theory from the theory of Cosserat medium. 06 p0763 A73-18454

A linear theory of thin elastic shells, based on conservation of a non-normal straight line. 07 p0908 A73-19091

Study of the stability of nonshallow spherical shells with finite displacements by applying various equations of the theory of shells 07 p0911 A73-19318

Deformation of an elastic spherical shell with random initial imperfections 07 p0911 A73-19319

Influence coefficients for end-loaded conical frustums. 07 p0913 A73-19983

The effect of variable temperature on creep collapse of a cylindrical shell under external pressure 07 p0913 A73-20070

Effects of shearing force and rotary inertia to dynamical behaviours of thin cylindrical shells subjected to impulsive inner pressures. 07 p0915 A73-20286

Cyclically symmetrical heat conduction problems for perforated plates and shells in the presence of heat transfer 08 p1021 A73-20997

Dynamic behaviour of thin cylindrical shells collided with dampers. 08 p1019 A73-21527

Thin-walled pipe designs with a curvilinear axis 09 p1158 A73-22362

Strain boundary conditions and complex representations of joining conditions in the theory of shells with finite shear rigidity 09 p1159 A73-22588

A deficiency in current finite elements for thin shell applications. 09 p1160 A73-22893

Stability of the axisymmetric form of motion of flexible shallow shells 09 p1164 A73-23344

Application of a variational difference method to the calculation of forced vibrations of shells of revolution 10 p1292 A73-24487

A note on the arrangement of strain gauges and the sensitivity of strain measurement. 10 p1219 A73-24572

Geometrical theory for flexure waves in shells. 11 p1432 A73-24977

Application of the extended Newton method to the creep analysis of shells of revolution. 11 p1432 A73-24998

Thin walled elastoplastic cylindrical shells deformations investigation by elliptic quasi-linear equation systems 11 p1433 A73-25044

Stability of a shell in the form of a hyperbolic paraboloid subjected to compression along straight generating lines 11 p1435 A73-25397

The free vibrations of a thin circular finite rotating cylinder. 11 p1443 A73-26088

Axisymmetric buckling of rigidly clamped hemispherical shells. 11 p1447 A73-26648

Shear stress and deformation inclusion in elastic plate bending finite element theory, discussing stiffness matrix improvement for thin shells 11 p1447 A73-26651

On the buckling and postbuckling behavior of thin-walled circular cylinders. [DFVLR-SONDDR-261] 12 p1550 A73-26843

Contribution to the theory of the finite element method applied to the overall stress analysis of a fuselage 12 p1551 A73-27084

Creep analysis of a thin-walled wing on the basis of the plate analogy 12 p1551 A73-27086

Determination of the stressed state of a circular cylindrical shell with stepwise variation in wall thickness along the generatrix under the action of a local load 12 p1552 A73-27261

Magnetoelastic vibration of electrically conducting thin shells and plates in steady magnetic field from asymptotic integration of electrodynamics equations 12 p1553 A73-27413

Instability of asymmetric strongly convex thin shallow shells 12 p1553 A73-27414

Asymptotic distribution of the natural frequencies of elastic shells 12 p1524 A73-27452

The Castigliano variational equation and strain continuity relations for a thin shell 12 p1555 A73-27788

One-dimensional zero-moment problem of a thin elastic shell of variable thickness 12 p1556 A73-27800

Large amplitude vibrations of certain deformable bodies. I - Discs, membranes and rings. 12 p1556 A73-27929

THIN WALLS

Influence of deformation history on the yield locus and stress-strain behavior of aluminum and copper. 13 p1632 A73-28130

Finite element method analysis of thin shells, discussing reference surface geometry and membrane and bending theory 13 p1693 A73-28234

The application of a curved, mixed-type shell element. 13 p1693 A73-28237

Stresses in adhesive bonds of thin cylindrical shells 13 p1698 A73-29063

Nonlinear axisymmetric subcritical deformation effect on elastic stability of locally loaded thin circular cylindrical shells under free end compressive load 13 p1698 A73-29089

Three-dimensional photoelastic tests of thin shell pressure vessels. 13 p1699 A73-29307

Apparent symmetry of certain thin elastic shells. 14 p1805 A73-29763

Maximum stress calculation for I beam and thin walled sphere redundant structures under stationary creep by perturbation method 14 p1811 A73-30487

Linearized constitutive equations for thin viscoplastic shell deflection under dynamic loads 14 p1811 A73-30488

Asymptotic solutions for shells with general boundary curves. 14 p1812 A73-30523

Supersonic flutter of truncated multilayered orthotropic conical thin shells. 14 p1814 A73-30702

Construction of refined applied theories for a truncated hollow cone of variable thickness 14 p1815 A73-30786

Traveling wave solutions of differential equations describing thin elastic shell oscillations due to point source 14 p1815 A73-30951

Limit equilibrium of thin-walled containers composed of joined conical sections 15 p1944 A73-30973

General solution of an equation system on plate equilibrium 15 p1945 A73-31033

Optimal forms of the thin-walled closed cross-section of a beam subjected to bending 15 p1947 A73-31365

On dynamic response of prestressed cylindrical shells - Green's tensor technique. 15 p1947 A73-31367

Stringer stiffened cylindrical shells stability characteristics under axial compression, using Donnell thin-shell and Vlasov thin-walled beam theories 15 p1949 A73-31656

Russian book - Plane bending and tension of curvilinear thin-walled beams. 15 p1956 A73-32296

Resolvent equations, in complex form, of the theory of transversely isotropic shells of revolution 16 p2074 A73-32686

The finite element method in shell stability analysis. 16 p2075 A73-32789

Mixed variational principles based on stationary potential energy concept applied to finite element method in thin shell theory 16 p2077 A73-32986

Ring finite elements for axisymmetric and non axisymmetric thin shell analysis. 16 p2077 A73-32989

Application of the finite element method to cases requiring the combination of elements possessing different numbers of degrees of freedom. 16 p2077 A73-32991

Thin plates and shells post-buckling behavior analysis by discrete element method, noting computer program capabilities 16 p2078 A73-32997

Incremental variational method for the large displacement analysis of shells with geometric imperfections. 16 p2078 A73-32999

Variational geometry optimization of thin rotational membrane shells under axisymmetric loading 16 p2079 A73-33011

Asymptotic integration method solution for three dimensional equations of geometrically nonlinear theory for thin shells and plates 16 p2080 A73-33243

The effect of transverse shear stresses on the yield surface for thin shells. 16 p2082 A73-33905

Thin shell elastoplastic deformation theory development for small strains, using Hooke's law to analyze hardening, stress and unloading 16 p2084 A73-34033

Experimental evaluation of the strength of elements of thin-walled pressure vessels during severe cooling 17 p2177 A73-34331

Strongly curved finite element for shell analysis. 17 p2242 A73-34529

Characteristics of deformation texture development in austenitic steel in a plane stressed state 17 p2188 A73-34564

Reaction of a cylindrical shell to periodic shock waves propagating in its interior 17 p2243 A73-34735

First-order frequency effects in supersonic panel flutter of finite cylindrical shells. 17 p2249 A73-35106

[ASME PAPER 73-APM-K] Large amplitude forced vibrations of simply supported thin cylindrical shells. 17 p2249 A73-35107

[ASME PAPER 73-APM-Q] A new finite element method for analyzing symmetrically loaded thin shells of revolution. 17 p2252 A73-35601

Thin clamped hemispherical shell nonlinear dynamic response to suddenly applied pressure, deriving finite difference formulation of fourth order coupled nonlinear equations 18 p2362 A73-36310

Shells of revolution belonging to a spherical class subjected to local loads at the pole 18 p2362 A73-36402

Stresses in bonded joints of thin cylindrical shells. 18 p2366 A73-36895

Influence of the structure of the material of a three-layered cylindrical shell on the natural frequencies 19 p2494 A73-37184

Nonlinear axisymmetric subcritical deformation effect on elastic stability of locally loaded thin circular cylindrical shells under free end compressive load 19 p2498 A73-37639

Operational temperature and frequency effects on radial driving point mechanical impedance of damped thin walled ring with mass segments attached by viscoelastic material 20 p2616 A73-39051

Numerical solution of problems of stability of three-layer cylindrical shells 20 p2620 A73-39503

Free vibration and buckling loads of anisotropic pressurized thin walled shells of revolution, considering cylinders, barrels and spherical sections 20 p2621 A73-39538

The vibrations of non-circular cylindrical shells with initial stresses. 21 p2783 A73-40288

Some results of fuselage calculations on a digital computer by the finite-element method 21 p2783 A73-40387

Calculation of shear-sensitive orthotropic shells with residual stresses 21 p2786 A73-40977

Deformation of shells with a circular axis and variable cross-section parameters 21 p2786 A73-40978

Steady-state creep of a thin-walled tube in the general case of applied forces 21 p2787 A73-41194

Russian book on structural mechanics of tapered thin walled conical bodies and wings in aviation and rocket technology 21 p2788 A73-41281

A note on the finite elastic inflation of a thin spherical shell. 21 p2789 A73-41688

Asymptotic distribution of the eigenfrequencies of elastic shells. 22 p2881 A73-41811

Vibration analysis of laminated plates and shells by a hybrid stress element. 22 p2923 A73-42566

The Morley-Koiter equations for thin-walled circular cylindrical shells. I - General solution for symmetrical shells of uniform thickness. 22 p2924 A73-42884

[ASME PAPER 73-APMW-22] The Morley-Koiter equations for thin-walled circular cylindrical shells. II - Solution for a line loaded cylinder with close-spaced circumferential grooves. 22 p2925 A73-42885

[ASME PAPER 73-APMW-23] Complex structural dynamic response reduction, discussing methods for mathematical models establishment and application to thin cylindrical shell 22 p2926 A73-42921

Thin Ni shell electroforming for applications in structural tests, discussing plating bath composition, Al and wax mandrels preparation 22 p2867 A73-42999

Buckling of short viscoplastic cylindrical shells subjected to radial impulse. 23 p3045 A73-44080

Traveling wave solutions of differential equations describing thin elastic shell oscillations due to point source 23 p3047 A73-44327

Equations of linear elastic theory of thin shells based on model of anisotropic Cosserat surface 24 p3147 A73-44744

Transverse shear extensions to Ilyushin-Shapiro thin shell and plate theory for yield surfaces in rigid-plastic materials 24 p3147 A73-44746

Convergence of finite difference transient response computations for thin shells. 24 p3150 A73-45228

On the problem of flexure of anisotropic cylindrical shells. 24 p3151 A73-45302

The problem of natural oscillations of a thin shell containing an elastoacoustic medium 24 p3152 A73-45359

THIN WALLS

The post-buckled behaviour of a thin-walled box beam in pure bending. 03 p0384 A73-13114

Computer method for analysis of multistory structures. 03 p0391 A73-13683

Production of porous tungsten thin walls intended for cesium ionization by contact 04 p0454 A73-15721

Effectiveness of the thermal protection of a plane wall during injection of air through two rows of rectangular holes arranged in a checked order 06 p0768 A73-18121

A theoretical and experimental investigation of torsional-flexural buckling in thin-walled prismatic members. 07 p0912 A73-19366

Thin walled beam composed indeterminate elastic framed structures minimum weight design, obtaining solutions by nonlinear programming algorithm 07 p0912 A73-19951

Piecewise linear approximation of thin walled ribs and diaphragm reinforced conical beams under thermal field and axial loads, using limit stress-strain diagrams 07 p0913 A73-20096

Stress-strain state of a piecewise homogeneous plane with thin-walled elastic inclusions of finite length 08 p1019 A73-21765

A new method for the study of the phenomenon of dynamic instability of thin-walled bars used in the construction of aeroplanes, ships and bridges. 12 p1551 A73-27063

Elastic deformation of thin walled U-bars lateral stiffeners under torsion, eccentric tension and bending loads, determining vaulting stiffness by finite element method 15 p1950 A73-31906

Lateral instability of thin-walled beams - Considerations regarding methods of experimental investigation 16 p2081 A73-33372

Estimation of corrosion damage levels in thin-walled structural elements by the punching method 18 p2320 A73-36825

Post-buckling behavior of cold-formed thin-walled stainless steel beams. 19 p2496 A73-37481

Steady-state heat transfer between fluids divided by a thin wall 21 p2792 A73-41224

THIN WINGS

Higher-order delta wings with flow separation at subsonic leading edges 02 p0127 A73-11581

Influence of the boundaries of wind-tunnel flow on the flow past a small-aspect-ratio wing 02 p0128 A73-11707

The pressure on flat and anhedral delta wings with attached shock waves. 02 p0128 A73-12501

Wake vorticity of side-slipping slender thin wings at transonic speeds, deriving integral equation for vortex strength based on Prandtl-Glauert rule 03 p0247 A73-14376

[DGLR PAPER 72-127] Vortex lattice discretization for finite Hilbert transform of two dimensional incompressible thin wing flow integral equation with singularities, noting numerical solution accuracy 04 p0403 A73-15004

The aerodynamic characteristics of the thin delta wing fitted with a conical body in supersonic flow. 04 p0404 A73-15167

Stability of a thin-wing model with one and two degrees of freedom 05 p0632 A73-16297

Thin wing induced undulating viscous wake and far field acoustic wave through interaction with turbulent cylindrical jet, using dipole force field model [AIAA PAPER 73-223] 05 p0532 A73-16950

Aerodynamic characteristics of thin asymmetric wing profiles in supersonic flow 07 p0776 A73-20487

Three dimensional steady flow of incompressible viscous fluid near thin wing trailing edge, using Stewartson-Williams triple layer method 08 p0926 A73-21495

Supersonic flow around a delta wing, taking into account flow separation at the leading edges 12 p1457 A73-27098

Experimental study of a high lift re-entry vehicle configuration. 13 p1564 A73-28822

Nonplanar wings in nonplanar ground effect. 15 p1824 A73-31744

Thin rectangular lifting wing investigation at small angle of attack in parallel flow based on Prandtl acceleration potential theory 15 p1955 A73-32126

- Calculation of flows past wings without thickness in the presence of developing vortex sheets
16 p1965 A73-33963
- Improved aircraft capability through variable camber.
19 p2378 A73-37275
- Thin wall rib structured fan shaped wing design for arbitrary air loads, using strain compatibility conditions
21 p2784 A73-40390
- On the application of a new version of lifting surface theory to non slender and kinked wings.
23 p2939 A73-43210
- Determination of the deflections and stresses in a small-aspect-ratio wing by the displacement method
23 p3041 A73-43723
- HINNERS**
U SOLVENTS
- HIOPLASTICS**
Epoxy-thiocol binder viscoelastic deformation under short and long term loads, noting stress-strain linearity limit
13 p1647 A73-29610
- HUBONIUM**
Observations concerning the combined radiation-protective effect of pantothenic acid and aminoethylisothiuronium
02 p0136 A73-11586
- HOMAS-FERMI MODEL**
Nature of chemical bonds in metal-like compounds based on transition metals
07 p0841 A73-20519
- HOMAS-FERMI THEORY**
U THOMAS-FERMI MODEL
- HOMSON EFFECT**
U THERMOELECTRICITY
- HOMSON SCATTERING**
Effect of Thomson scattering on the emission spectrum of an optically semiopaque plasma.
04 p0493 A73-16024
- Differential light scattering cross section derivation for photon interaction with relativistic electrons, comparing with quantum electrodynamic calculation and Thomson scattering experiment
07 p0851 A73-19516
- Solar corona anomalous polarization degree and E vector vibration direction, interpreting discrepancy from Thomson scattering prediction by scattered electron velocity effects
12 p1545 A73-27845
- Influence of saturation effects on stimulating scattering in laser heating of a plasma.
16 p2041 A73-33079
- Measurement of nonisotropic electron velocity distributions by laser scattering.
19 p2465 A73-37166
- Comparison of Langmuir double probe and laser scattering measurements of plasma parameters.
20 p2595 A73-38880
- Problem of increasing the effectiveness of laser usage in experiments on light scattering in a plasma
23 p2987 A73-43670
- Stellar radiation Thomson scattering by free electrons compared to atomic processes as mechanism for H II regions continuous emission
23 p3030 A73-43756
- HORAX**
Volume-pressure characteristics of rib cage-diaphragm interaction in standing subjects during voluntary relaxation
20 p2518 A73-39778
- Effects of hyperinflation of the thorax on the mechanics of breathing.
22 p2806 A73-42415
- Spinal and spino-bulbo-spinal neuron mechanisms of somatic and visceromotor reflex transfer in the thoracic spinal cord
24 p3061 A73-45249
- HORIUM**
NT THORIUM ISOTOPES
- Radiochemical neutron activation analysis for U and Th abundance measurement in achondrites and pallasite olivines
17 p2120 A73-35802
- HORIUM COMPOUNDS**
NT THORIUM OXIDES
- HORIUM ISOTOPES**
U-Th-Pb measurements of Luna 20 soil.
13 p1677 A73-28335
- Determination of coefficients of vertical diffusion between 0 and 100 m with the help of radon and of ThB
13 p1655 A73-29342
- Solar abundance of Th and Pb based on photospheric line spectrum analysis for comparison with chondritic composition data
24 p3135 A73-44627
- THORIUM OXIDES**
Cold rolling of dispersion-strengthened nickel.
01 p0063 A73-10282
- Activated sintering of ThO₂ and ThO₂-Y₂O₃ with NiO.
01 p0066 A73-11014
- High temperature creep properties of recrystallized W-thoria alloy wires, noting dependence on temperature, grain structure and stress
04 p0463 A73-15306
- The effect of a hydrogen preheat-treatment on the oxidation behavior of Ni-Cr-Al-ThO₂ alloys.
04 p0463 A73-15319
- Thoria stability in TD-NiCr at high temperatures in the presence of chromium in solution.
06 p0713 A73-18771
- The influence of a thoria dispersion on preferred orientation in nickel alloys.
08 p0977 A73-21012
- An observation of vacancy sources during substitutional diffusion in thoriated nickel alloys.
10 p1234 A73-24433
- Thoria particle dispersion TD-nickel creep and tensile deformation at elevated temperature dependence on grain size and L/D ratio
14 p1761 A73-30635
- A scanning electron microscope study of the surface morphology of TD-NiCr oxidized at 800 C to 1200 C.
15 p1892 A73-32270
- Mach 1 oxidation of thoriated nickel chromium at 1204 C /2200 F/.
15 p1892 A73-32271
- Na₂SO₄-induced attack of Ni-20Cr-2ThO₂.
15 p1896 A73-32575
- Diffusional creep and creep-degradation in dispersion-strengthened Ni-Cr base alloys.
16 p2025 A73-33111
- Stress relaxation measurements for strain rate sensitivity of dispersion hardened thoriated Ni alloys as function of applied stress concentration
17 p2190 A73-34647
- Influence of the method of preparing a Ni + ThO₂ composite and of its strengthening-oxide content on heat resistance
23 p2990 A73-43486
- Nd-doped Yttralox ceramic lasing performance and interrelationship between ceramic processing, microstructure and optical quality of sintered product
24 p3097 A73-45414
- THORIUM 228**
U THORIUM ISOTOPES
- THORIUM 230**
U THORIUM ISOTOPES
- THORIUM 234**
U THORIUM ISOTOPES
- THREE BODY PROBLEM**
Gravitational constant anisotropy effects on planets with orbits close to ecliptic in solar system two body problem
01 p0099 A73-10689
- On a new form for the differential equations of relative motion of the three-body problem.
01 p0099 A73-10690
- Planar three body problem singularities due to binary collisions, regularizing equations of motion by Levi-Civita coordinate transformation
01 p0099 A73-10692
- Approximate method to determine collision probabilities, hyperbolas, and direct and retrograde ellipses during single close encounters in three body planetary problem
01 p0099 A73-10693
- Periodic perturbation of the libration points of the restricted three-body problem due to presence of a resisting medium and both gravitational and radiative fields of a fourth body.
01 p1013 A73-11018
- Elliptical orbits of mass point under Newtonian gravitational forces of two fixed centers with different mass in Cartesian coordinates as function of time
02 p0211 A73-11776
- The dynamical evolution of triple star systems - A numerical study.
02 p0221 A73-12702
- Computation of Schwarzschild's periodic solutions in the restricted three-body problem.
02 p0226 A73-12838
- On the stability of triangular points of equilibrium in the restricted elliptic problem
03 p0376 A73-14270
- Sufficient conditions for return in the three-body problem.
03 p0377 A73-14274
- Orbital period variations of eclipsing binary TW Draconis caused by third body effect, apsidal motion and matter exchange
03 p0379 A73-14582
- A variation-of-parameters perturbation theory for the restricted three-body problem.
05 p0619 A73-16893
- [ALAA PAPER 73-144] Minimum impulse three-body trajectories.
05 p0619 A73-16894
- [ALAA PAPER 73-145] Four body problem reduction to three body problem via perturbation region, noting Moon-Earth-Sun system
05 p0623 A73-17198
- Sundman power series convergence enhancement in three body problem by Poincare transformation
07 p0852 A73-20042
- Three body problem of stellar system subjected to isoeenergetic variations, evaluating escape and ejection parameters
08 p1005 A73-20920
- Analytical solution of lunar ephemerides, considering sun-earth-moon problem and required corrections and perturbation methods
09 p1147 A73-22710
- Geometrical dynamics method for orbit geometry in configuration space of dynamical system, using polar coordinates as generalized coordinates for circular restricted three body problem
09 p1148 A73-22911
- Motion equation solutions for three flattened spheroids with coincident equatorial symmetry planes in Lagrange form by Duboshin transforms
10 p1274 A73-23722
- Studies in the application of recurrence relations to special perturbation methods. II - Comparison of the Encke and Cowell methods of integration in the restricted three-body problem.
10 p1283 A73-24668
- A study of commensurable motion in the asteroid belt.
11 p1417 A73-25264
- Periodic solutions of the third sort for restricted problem of three bodies and their stability.
11 p1423 A73-26068
- Out-of-plane motion about libration points - Non-linearity and eccentricity effects.
11 p1423 A73-26069
- Three body system successive states classified as triple approach, simple interplay, ejection without escape and escape /final state/ during course of motion
13 p1683 A73-29140
- Cometary and asteroidal orbits discrimination using Jacobi integral in three body system with sun and Jupiter
14 p1795 A73-29849
- A survey of recent results in differential equations.
14 p1769 A73-30411
- On approximate calculation of the principal part of disturbances in an interior bounded three-body problem.
14 p1802 A73-30953
- Elimination of time and differential equation of trajectories in the problem of three restricted, circular, plane bodies
15 p1930 A73-31175
- Periodic solutions of the restricted three-body problem encompassing a large number of revolutions about the smaller body
15 p1931 A73-31240
- Recent advances of celestial mechanics in the Soviet Union.
15 p1932 A73-31303
- Forward precession motion of the moon caused by attraction to the earth and the sun
15 p1939 A73-31966
- Steady motions of three nonpoint bodies moving freely in space with centers of inertia describing uniform circle
16 p2059 A73-32908
- Global stability and the restricted 3-body problem.
18 p2352 A73-36417
- Stromgen doubly asymptotic orbits analyzed by Hamiltonian functions with two degrees of freedom, investigating homoclinic and heteroclinic orbits in restricted three body problem
18 p2352 A73-36419
- Motion equation solutions for three flattened spheroids with coincident equatorial symmetry planes in Lagrange form by Duboshin transforms
18 p2355 A73-36747
- Numerical analysis of families of periodic orbits in restricted three body problem with change in mass ratio mu
21 p2778 A73-41527
- The cause of the residuals in the motion of Halley's comet.
22 p2907 A73-42210
- On the theoretical possibility of the libration cloud.
22 p2911 A73-42936
- Phase plane analysis of the commensurable restricted three-body problem.
22 p2912 A73-42942
- Numerical exploration of commensurable periodic solutions of the restricted problem of three bodies and their stability.
23 p3029 A73-43746
- A note on relative motion in the general three-body problem.
23 p3031 A73-43834
- Evolution of a 'class two' family of periodic orbits in the general planar problem of three bodies.
23 p3031 A73-43835
- Translational-precessional motion of the moon in the gravitational field of the earth and sun.
24 p3132 A73-44491
- Three body problem triple close approaches within escape mechanism, discussing method to control numerical integrations accuracy
24 p3141 A73-45281

THREE DIMENSIONAL BOUNDARY LAYER

- Rectilinear trajectories of the three-body problem when the constant of line forces is zero
24 p3141 A73-45282
- Parameter distribution of small periodic librations about the equilateral points of the elliptic restricted problem.
24 p3141 A73-45283
- Elliptic restricted three body problem equations derived from linear variational equations with periodic coefficients describing motion near libration centers
24 p3141 A73-45284
- Isoceles case of rectilinear restricted three body problem with two equal mass primaries in rectilinear ellipses, deriving escape and collision conditions
24 p3141 A73-45285
- Periodic symmetric solution properties of restricted three body problem for case with lunar mass parameter tending to zero, discussing bifurcation orbit dynamics
24 p3141 A73-45286
- Periodic solutions of a spring-pendulum system.
24 p3111 A73-45294
- Vertical perturbation stability of three dimensional periodic orbits in restricted three body problem
24 p3142 A73-45295
- Three dimensional computer plots of zero velocity contours for restricted three and four body problems, discussing motion stability near equilibrium points
24 p3142 A73-45297
- Stability of Lagrange solutions to the three-dimensional elliptic problem of three bodies
24 p3111 A73-45299
- The restricted problem of three bodies with rigid dumb-bell satellite.
24 p3142 A73-45300
- A tenth order solution in explicit form to the 'restricted' three-body problem.
24 p3143 A73-45304
- Construction of particular solutions of the restricted plane circular three-body problem
24 p3112 A73-45506
- ## THREE DIMENSIONAL BOUNDARY LAYER
- Method of calculation of the three-dimensional turbulent boundary layer up to separation - Application to a simple gas turbine case
[ONERA, TP NO. 1111] 01 p0001 A73-10233
- A solution of the three-dimensional unsteady compressible boundary layer equations.
01 p0004 A73-11356
- Calculation of metric coefficients for streamline coordinates.
03 p0247 A73-14196
- Two numerical methods for three-dimensional boundary layers.
04 p0433 A73-15003
- Numerical predictions of some three-dimensional boundary layers in ducts.
04 p0433 A73-15006
- Velocity profiles and wall shear stress of three-dimensional turbulent boundary layers.
[ONERA, TP NO. 1134] 04 p0403 A73-15092
- Calculation methods of three-dimensional boundary layers with and without rotation of the walls.
[ONERA, TP NO. 1135] 04 p0403 A73-15093
- Wall shear stress inference from two and three-dimensional turbulent boundary layer velocity profiles.
[ASME PAPER 72-WA/FE-4] 04 p0434 A73-15840
- Secondary flow in the entrance region boundary layers of an expanding square duct.
[ASME PAPER 72-WA/FE-34] 04 p0404 A73-15851
- A momentum integral solution of a three-dimensional turbulent boundary layer.
[ASME PAPER 72-FE-1] 05 p0565 A73-16548
- Solutions of thermal boundary layer equations when temperature gradient at the moving flat plate in parabolic flow is prescribed.
06 p0769 A73-18251
- Perturbation about one dimensional parabolic flow field in three dimensional boundary layer separation, obtaining skin friction from linear equation eigensolutions
[AD-755557] 07 p0774 A73-19502
- An extension of the vector potential concept to the case of a three-dimensional unsteady boundary layer.
07 p0776 A73-20287
- A zero-streamwise-pressure-gradient, three-dimensional turbulent boundary layer in a 90 deg curved rectangular duct.
08 p0953 A73-20796
- A two-layer model of high speed two- and three dimensional turbulent boundary layers with pressure gradient, surface mass injection and entropy layer swallowing.
[AIAA PAPER 73-135] 08 p0956 A73-21800
- Parabolic flow over a flat plate with wave disturbance in the main stream.
09 p1071 A73-21950
- Experimental study of the laminar-turbulent transition on a concave wall in a parallel flow
09 p1071 A73-22450
- Laminar boundary layer on a cone near a plane of symmetry.
09 p1029 A73-23442

- Mean velocity profiles in three-dimensional incompressible turbulent boundary layers.
09 p1029 A73-23445
- Three dimensional boundary layer theory, applying Navier-Stokes equations to Newtonian fluids continuous flow over solid bodies or through finite ducts
10 p1171 A73-23863
- Prandtl's boundary-layer theory from the viewpoint of a mathematician.
10 p1172 A73-23866
- Calculation of a three-dimensional boundary layer in revolving channels of centrifugal rotors
10 p1173 A73-24672
- Prandtl boundary layer equations for unsteady three dimensional axisymmetrical and two dimensional symmetrical incompressible flows about solid bodies, considering approximate solution convergence
10 p1208 A73-24808
- Unsteady three dimensional laminar incompressible boundary layer with free and forced convection, determining flow and temperature fields adjacent to heated body
10 p1208 A73-24810
- Kaplan perturbation method for incipient flow separation, considering three dimensional, compressible and unsteady boundary layers
10 p1208 A73-24815
- Universal equations of the three-dimensional laminar boundary layer in the unsteady state and their treatment
10 p1209 A73-24820
- One method of computing the meteorological variables for mesoscale processes.
11 p1394 A73-26192
- Laminar symmetry-plane boundary layer on a sharp spinning body at incidence.
11 p1303 A73-26397
- Enthalpy restoration coefficient in a three-dimensional laminar boundary layer
11 p1303 A73-26434
- Equilibrium three-dimensional turbulent boundary layer on the end wall of a curved channel.
13 p1602 A73-29015
- Three dimensional turbulent boundary layers prediction methods and flow measurements, considering swept and slender wings
14 p1744 A73-30173
- Use of surface fences to measure wall shear stress in three-dimensional boundary layers.
15 p1874 A73-31118
- Three-dimensional turbulent boundary layer - Calculations and experiments
16 p1961 A73-32806
- The three-dimensional turbulent boundary layer - Theoretical and experimental analysis
16 p1961 A73-32810
- Three dimensional turbulent boundary layer of yawed wing suction surface in uniform flow, examining cross flow profile, velocity distribution and weighting functions
16 p1963 A73-33267
- Approximate method of solution for three-dimensional boundary layers.
17 p2150 A73-34188
- A finite difference solution of the two and three-dimensional incompressible turbulent boundary layer equations.
[ASME PAPER 73-FE-20] 17 p2153 A73-35016
- An assessment of three-dimensional turbulent boundary layer prediction methods.
[ASME PAPER 73-FE-25] 17 p2153 A73-35020
- Study of the similarity solution in three dimensional compressible laminar boundary layer.
17 p2157 A73-35862
- Finite-difference solution of the incompressible three-dimensional boundary layer equations for a blunt body.
18 p2259 A73-36156
- Three-dimensional compressible boundary layer flow over a yawed cone.
[AIAA PAPER 73-634] 18 p2260 A73-36193
- Three-dimensional hypersonic transitional/turbulent mean flow profiles.
[AIAA PAPER 73-635] 18 p2260 A73-36194
- Numerical solution existence for three dimensional boundary layer equations governing corner flow in symmetry plane with critical pressure gradients
19 p2419 A73-37492
- Three dimensional boundary layer flow with streamwise vorticity decay, deriving solutions as expansions in terms of eigenfunctions
19 p2420 A73-37851
- Cross flows in bounded three-dimensional turbulent boundary layers.
19 p2422 A73-38298
- A method for calculating three-dimensional turbulent boundary layer by using streamline co-ordinates.
20 p2546 A73-39225
- A three-dimensional MHD boundary layer in an incompressible fluid
21 p2747 A73-40882
- Asymptotic behavior of the solutions to the Navier-Stokes equations near ribs
21 p2678 A73-41275

THREE DIMENSIONAL COMPOSITES

- Relationship between structure and strength for CVD carbon infiltrated substrates. II - Three dimensional woven, tufted and needled substrates.
06 p0715 A73-18718

THREE DIMENSIONAL FLOW

- ### NT SECONDARY FLOW
- An extremum principle for three-dimensional compressible inviscid flows.
01 p0031 A73-10427
- Three dimensional potential flow past arbitrarily shaped aerodynamic configurations, using Hess-Smith numerical method
[DGLR PAPER 72-105] 02 p0127 A73-11657
- Three dimensional jet stream dynamics based on particle population evolution numerical simulation, interpreting solar system evolution
02 p0218 A73-12415
- Rotor unsteady wakes three dimensional flow analysis by wave front averaging technique, using constant temperature hot-wire anemometer
02 p0129 A73-12504
- Finite element technique application for determining velocity field of three dimensional fluid continuum and pressure distribution of lubrication film described by Reynolds equation
03 p0289 A73-12872
- Three-dimensional MHD duct flows with strong transverse magnetic fields. III - Variable-area rectangular ducts with insulating walls.
03 p0346 A73-13534
- Calculation of the supersonic region of three-dimensional nonequilibrium air flow past bodies
03 p0245 A73-13618
- Three dimensional flow pattern from two dimensional supersonic inviscid gas flows around wedged body
03 p0245 A73-13675
- Inverse Laval problem of three dimensional subsonic and supersonic flows in nozzles and ducts of variable cross section in terms of asymptotic series
03 p0246 A73-14046
- Three dimensional ideal incompressible fluid flows under small velocity perturbation, using Euler equations linearized with respect to steady flow
03 p0296 A73-14048
- Small disturbance theory of rotating subsonic and transonic cascades.
03 p0246 A73-14136
- On the uniformly valid approximate solutions of Laplace equation for an inviscid fluid flow past a three-dimensional thin body.
[ONERA, TP NO. 1145] 04 p0433 A73-15094
- An experimental study of flow fields in bistable fluid amplifiers.
[ASME PAPER 72-WA/FLCS-9] 04 p0409 A73-15864
- Quasi-three-dimensional calculation of velocities in turbomachine blade rows.
[ASME PAPER 72-WA/GT-7] 04 p0490 A73-15871
- The Joukowski condition in three-dimensional flow
04 p0405 A73-15988
- Calculation of transonic flow in three-dimensional nozzles
05 p0527 A73-16447
- Multivortex model for bodies of arbitrary cross-sectional shapes.
[AIAA PAPER 73-104] 05 p0529 A73-16864
- Three-dimensional interaction of jets propagating in a supersonic slipstream
06 p0643 A73-17458
- Three-dimensional MHD duct flows with strong transverse magnetic fields. IV - Fully insulated, variable-area rectangular ducts with small divergences.
06 p0728 A73-17704
- Pressure surfaces and flow lines geometry of three dimensional parallel steady flow, noting geodesics formation on surfaces of constant pressure
06 p0686 A73-18174
- Mass-transfer effects on higher-order boundary layer solutions - The leading edge of a swept cylinder.
06 p0688 A73-18833
- Energy conserving finite difference approximation for solution of unaveraged Navier-Stokes equations of three dimensional incompressible turbulent flow in square duct
07 p0810 A73-19263
- Boundary-layer separation on rotating blades in forward flight.
07 p0774 A73-19955
- Aerodynamic characteristics of thin asymmetric wing profiles in supersonic flow
07 p0776 A73-20487
- Unsteady boundary layer flows at general three-dimensional stagnation points.
08 p0954 A73-21008
- Some remarks on the behaviour of surface source distributions near the edge of a body.
08 p0926 A73-21437
- Three dimensional steady flow of incompressible viscous fluid near thin wing trailing edge, using Stewartson-Williams triple layer method
08 p0926 A73-21495

An experimental investigation of three-dimensionalality of wall jet flows. 08 p0956 A73-21831
 Viscous energy transfer from elliptical orifice originated laminar three dimensional jet, using boundary layer assumptions in jet mixing region 09 p1072 A73-22827
 Book - Turbulence transport modeling. 10 p1206 A73-24350
 Unsteady detachment in the three-dimensional laminar regime 10 p1208 A73-24819
 The stability of simply supported rectangular surfaces in uniform subsonic flow. [ASME PAPER 72-APM-ZZ] 11 p1441 A73-25702
 The shape of a supersonic three-dimensional nozzle with a maximum thrust 11 p1302 A73-26334
 Theory on blades of axial, mixed, and radial turbomachines by inverse method. 11 p1303 A73-26340
 Three dimensional gas flow noncollinear total impulse normal and tangential components calculation leading to pressure force determination 12 p1486 A73-27089
 Using a single hot-wire probe in three-dimensional turbulent flow fields. 13 p1600 A73-28526
 Secondary flow in blade cascades of axial turbomachines and the possibility of reducing its unfavourable effects. 13 p1565 A73-29008
 Flow analysis of three-dimensional diffuser for fluid amplifier. 13 p1603 A73-29033
 Flow visualization of two and three dimensional wall jets on circular cylinder, observing flow characteristics sensitivity to curved boundary 13 p1603 A73-29038
 Temperature fields in a hollow cylinder in presence of heat source under the boundary conditions of the second kind. 13 p1708 A73-29666
 Nonlinear effects in steady supersonic dissipative gasdynamics. II - Three-dimensional axisymmetric flow. 14 p1711 A73-30167
 Three-dimensional motion of a reacting gas mixture around a blunt body 15 p1822 A73-31290
 Computerized three dimensional calculations of hypersonic aircraft in viscous potential flow in terms of boundary layers and wakes 16 p1962 A73-32816
 Steady solutions of a nonlinear problem for the Navier-Stokes equations 16 p2031 A73-32933
 Three dimensional flow analysis for helicopter rotor aerodynamic design, considering Mach number, inclination, angle of attack, trajectory, Reynolds number and vortex shedding 16 p1962 A73-32973
 Computerized stream-curve method for calculation velocity distribution and stream surface twist effects for three dimensional flow through gas turbine blade passage 17 p2092 A73-34378
 Two-variable asymptotic solution to unsteady three dimensional turbulent flow equations describing small scale deformation, determining hot spot or macromolecular size statistical behavior 17 p2201 A73-34800
 The analysis of nonequilibrium, chemically reacting, supersonic flow in three dimensions using a bicharacteristics method. 17 p2151 A73-34891
 Three-dimensional flow field in rocket pump inducers. I - Measured flow field inside the rotating blade passage and at the exit. [ASME PAPER 73-FE-33] 17 p2095 A73-35024
 Numerical calculation of the three dimensional transonic flow over a yawed wing. 17 p2096 A73-35129
 A new shock capturing numerical method with applications to some simple supersonic flow fields. 17 p2096 A73-35144
 Computation of three dimensional flows about aircraft configurations. 18 p2259 A73-36158
 Three dimensional jet flap potential flow theory based on vortex lattice method, comparing iterative solution with slatted unswept blown flapped wing experimental results [AIAA PAPER 73-653] 18 p2263 A73-36260
 Geometry of relaxing gas flows. 18 p2299 A73-36330
 Effect of spanwise circulation on compressor noise generation. 19 p2473 A73-37292
 Smoke visualization of three-dimensional flow patterns in a nominally two-dimensional wake. 19 p2375 A73-37423

A note on Beltrami and complex-lamellar flows behind a three-dimensional curved gasdynamic shock wave. 19 p2420 A73-37753
 Viscous flow over a cone at moderate incidence. II - Supersonic boundary layer. 20 p2507 A73-39093
 Velocity wave interaction and helical turbulence equilibrium spectra for two dimensional and three dimensional flow with quadratic energy and enstrophy states 20 p2549 A73-39812
 Unsteady incompressible fluid flow past a doubly periodic grid 21 p2631 A73-40185
 A numerical study of three-dimensional problems of MHD flow 21 p2747 A73-40887
 Asymptotic unsteady three dimensional flow analysis in axial turbine cascade theory, assuming infinite blade number and unity pitch/chord ratio [ONERA, TP NO. 1249] 22 p2796 A73-42220
 A computer model for three-dimensional flow in furnaces. 22 p2934 A73-42787
 Numerical solution of Fredholm integral equation describing incompressible inviscid potential flow past three dimensional bodies 23 p2939 A73-43474
 Precise method for solving certain problems of the theory of three-dimensional supersonic gas flows. 23 p2939 A73-43582
 Computerized simulation of isotropic three dimensional turbulence velocity field growth and energy decay based on Navier-Stokes equation numerical integration 23 p3001 A73-43588
 Classification of methods for solving the direct problem of axisymmetric flow calculation in turboengines 23 p3020 A73-43736
 A divergent difference scheme for calculation of steady supersonic flows with complex structures 24 p3053 A73-44651
 Total pressure loss distribution in viscous gas flow through annular cascades of axial flow compressors, examining three dimensional flow effects on boundary layer development 24 p3054 A73-44916
 Hypersonic flow about a spatial body with an attached shock wave 24 p3054 A73-45172
 Dynamic and temperature boundary layers of a submerged jet of viscous fluid spreading over the bottom 24 p3080 A73-45503
 Determination of the impulses and moments imparted by shock waves to bodies of revolution 24 p3055 A73-45542
 Linearized theory of two and three dimensional incompressible viscous flows based on locally unstable velocity profiles related to boundary layer instability mechanism 24 p3081 A73-45546

THREE DIMENSIONAL MOTION

NT SECONDARY FLOW

NT THREE DIMENSIONAL FLOW

The relation between three-dimensional and two-dimensional problems in the mechanics of continuous media 01 p0119 A73-11430
 Relationship of spatial and planar problems in the mechanics of continuous media. 11 p1443 A73-26059
 Visual perception of motion in depth - Application of a vector model to three-dot motion patterns. 13 p1577 A73-28091
 Constancy and illusion of apparent direction of rotary motion in depth - Tests of a theory. 13 p1577 A73-28094
 Optimal curved pursuit trajectories of point mass in three dimensional space, establishing search technique via Pontryagin principle calculations and equations of state 16 p2061 A73-33269
 The method of plane-axial vector coordinates in the determination of velocities in the general motion of a rigid solid 19 p2459 A73-37643
 Numerical simulation of three dimensional atmospheric turbulence with emphasis on kinetic energy transfer from large to small scales of motion with heat conversion 24 p3108 A73-45092
 Vertical perturbation stability of three dimensional periodic orbits in restricted three body problem 24 p3142 A73-45295

THRESHOLD CURRENTS

Theory of turbulent heating of an isothermal plasma with a transverse current. 01 p0083 A73-10456

Threshold voltage shift for low voltage operation of transistor circuits with boron ion implanted MOS 04 p0427 A73-15322

Heterojunction injection lasers with high efficiency and low threshold currents, discussing amplification, emission, epitaxial layers, and performance superiority over homostructures 05 p0586 A73-17266

Influence of waveguide properties of heterojunction layers on the principal characteristics of injection lasers. 06 p0702 A73-18585

Preservation of threshold on-regime in amorphous semiconductor threshold switch. 06 p0739 A73-18790

Variation of dc domain threshold in a nematic liquid crystal under continual dynamic scattering. 06 p0739 A73-18794

Gain-current relation for GaAs lasers with n-type and undoped active layers. 09 p1091 A73-22239

Gradual degradation of GaAs double-heterostructure lasers. 09 p1092 A73-22241

Transverse mode control in semiconductor lasers. 09 p1092 A73-22242

/GaAl/As lasers with a heterostructure for optical confinement and additional heterojunctions for extreme carrier confinement. 09 p1092 A73-22243

Time delays and Q switching in homostructure and heterostructure injection lasers. 09 p1092 A73-22246

Behavior of threshold current and polarization of stimulated emission of GaAs injection lasers under uniaxial stress. 09 p1092 A73-22247

Mesa-stripe-geometry double-heterostructure injection lasers. 09 p1093 A73-22251

Semiconductor injection lasers, discussing optical transitions threshold effects, radiative recombination, coherent emission, etc 12 p1506 A73-27136

Empirical estimation of the service life of injection lasers from short-term tests. 12 p1507 A73-27523

Detuned single mode laser detailed balance and line width factor in threshold region expressed by Fokker-Planck equation and nonhermitian eigenvalue 20 p2571 A73-38622

Correlation function of a laser beam near threshold. 20 p2571 A73-38631

Threshold, spectral, and output power characteristics of GaAs/Ga_{1-x}Al_x/As single-heterostructure diode lasers. 21 p2713 A73-40462

Red-light-emitting Al_xGa_{1-x}Al_x/As heterojunction laser diodes. 21 p2716 A73-40971

THRESHOLD DETECTORS [DOSIMETERS]

Optimum detection of an optical image on a photoelectric surface. 21 p2650 A73-40338

THRESHOLD GATES

X-band GaAs FET. 03 p0281 A73-13173

Chalcogenide glass threshold switch conceptual model based on electronic origin of firing, discussing applications to contactless switches, bistable relays decoupling and display triggering 12 p1478 A73-27042

THRESHOLD LOGIC

Analysis of a Schmitt trigger employing a field transistor at the input 03 p0284 A73-14324

Low error rate transmission by iterative probabilistic threshold decoding, noting performance improvement over sequential and low density parity check code techniques from simulation 04 p0425 A73-15399

Majority logic detection scheme of differentially phase-modulated waves. 08 p0937 A73-20802

On the solution of linear inequalities with applications to threshold logic. 10 p1191 A73-23746

High speed parallel multiplier design based on threshold logic adder using integrated logic circuits 17 p2139 A73-35238

Electromagnetic core storage and switching elements design for Setun threshold ternary logic computer 19 p2408 A73-38562

Structural complexity and technical realization of formal neurons by means of magnetic current switches 24 p3063 A73-44901

Synthesis of minimized formal neurons by means of magnetic current switches 24 p3063 A73-44902

THRESHOLD SHIFT

U THRESHOLDS

THRESHOLDS

Threshold pump energy value of liquid lasers in quasi-steady-state operation 06 p0699 A73-17915

THRESHOLDS [PERCEPTION]

- Threshold voltage of nonuniformly doped MOS structures. 09 p1064 A73-23046
- Effect of concentration on laser threshold of organic dye laser. 10 p1229 A73-24695
- Influence of elastic deformations on the lasing-threshold characteristics of a ruby laser 11 p1376 A73-26141
- Evaluation of the performance of a signal detection system by counting the overshoots of an internal threshold 15 p1842 A73-31359
- Characteristics change of Gunn diodes with uniaxial stress and temperature. 16 p1991 A73-33996

THRESHOLDS [PERCEPTION]

- Observers detecting a signal in two multiple observation tasks. 01 p0011 A73-10350
- Changes in the vibratory sensation threshold after exposure to powerful vibration. 01 p0013 A73-10772
- Temporary threshold shift caused by combined steady-state and impulse noises. 01 p0077 A73-10785
- The colour vision characteristics of an observer with unilateral defective colour vision - Results and analysis. 02 p0137 A73-12077
- Scotopic vision - An unexpected threshold elevation produced by dark annuli. 02 p0137 A73-12080
- Vernier acuity as affected by target length and separation. 03 p0266 A73-13063
- Human thresholds for perceiving sudden changes in atmospheric pressure. 03 p0260 A73-13554
- Aerodynamic and temporal parameters of olfactory stimulation - Discussion concerning the lowering of the threshold by prenasal injection in man 03 p0262 A73-13787
- Probability estimate for visual target detection in terms of luminance threshold and target size and duration 06 p0658 A73-18242
- Perception of tone differences from film transparencies. 06 p0695 A73-18388
- The effect of accessory auditory stimulation upon detection of visual signals. 06 p0660 A73-18625
- Dynamic properties of vision. III - Twin flashes, single flashes and flickerfusion. 07 p0783 A73-20253
- Stimulus effect on spatial summation of color receptive pathways and discrimination thresholds as function of color, gradient, retinal illumination and field size 07 p0783 A73-20254
- Electrical stimulation effects of human eye on photic threshold for square wave vision as function of wavelength, orientation and spatial frequency 07 p0783 A73-20260
- Threshold variance analysis of monocular vs binocular visual stimulation in apparent movement perception 07 p0783 A73-20262
- Saccadic suppression for structured background as function of visual image pattern and threshold detection elevation in central nervous system 07 p0783 A73-20267
- Psychophysical areal summation and stimulus contour and threshold visibility effects on size selective adaptation in human vision for single- and multichannel models 08 p0931 A73-21563
- The brightness of coloured flashes on backgrounds of various colours and luminances. 08 p0935 A73-21565
- Visual sensitivity in the presence of alternating monochromatic fields of light. 08 p0932 A73-21567
- Visual discrimination of motion - Stimulus relationships at threshold and the question of luminance-time reciprocity. 09 p1044 A73-21897
- Peripheral threshold of perceived contrast of the human eye. 09 p1046 A73-22964
- Visual acuity as a function of exposure duration. 10 p1184 A73-23838
- On neural inhibition, contrast effects and visual sensitivity. 11 p1318 A73-26197
- Foveal contrast sensitivity edge effect dependence on test stimulus size, form and duration 11 p1321 A73-26716
- The effects of edge sharpness and exposure duration on detection threshold. 11 p1321 A73-26718
- Time course of lateral inhibition in the human visual system. 12 p1462 A73-27124

Visual temporal integration for threshold, signal detectability, and reaction time measures. 13 p1578 A73-28097

Probability summation model for heterochromatic luminance additivity failure at absolute visual threshold. 13 p1578 A73-28099

Interaural difference thresholds in binaural perception of signals nonexistent in normal acoustic environment, considering beats, memory, learning, and stereophony 14 p1716 A73-30285

Influence of the dazzling of an eye on the state of adaptation of the congenic eye in a normal subject 14 p1716 A73-30388

Foveal threshold additivity measurements for monochromatic and mixed light, using grating resolution as brightness criterion 14 p1717 A73-30398

Subjective brightness contrast lack of correlation with steady state evoked potential amplitude in suprathreshold stimuli range 15 p1837 A73-31017

Threshold and suprathreshold perceptual color differences. 15 p1837 A73-31019

Damage-risk criteria - The trading relation between intensity and the number of nonreverberant impulses. 16 p1973 A73-33678

Evidence for non-linear response processes in the human visual system from measurements on the thresholds of spatial beat frequencies. 17 p2112 A73-34839

Hearing conservation studies covering impulse noise produced threshold shift, damage risk criteria, ultrasound hazards and hearing protection 17 p2117 A73-35326

Quantitative studies on optokinetic nystagmus in the monkey. 18 p2273 A73-36459

Contrast sensitivity, Westheimer function and Stiles-Crawford effect in a blue cone monochromat. 19 p2394 A73-37414

Spatial frequency channels in human vision and the threshold for adaptation. 19 p2394 A73-37416

Determinants of hypothalamic neuronal thermosensitivity in ground squirrels and rats. 20 p2513 A73-39600

Changes in thermosensitive characteristics of hypothalamic units over time. 20 p2514 A73-39601

Disparity detectors in human depth perception - Evidence for directional selectivity. 21 p2637 A73-40413

Relation between vibratory sensibility and electric signal of living body. 22 p2816 A73-42680

Spatial integration in the crustacean visual system - Peripheral and central sources of non-linear summation. 22 p2810 A73-42956

Eigenvectors of the sensitivity variations across the human central fovea. 22 p2810 A73-42957

Increment thresholds for multiple identical flashes in the peripheral retina. 23 p2946 A73-43343

Visual perception dominance over touch related to threshold changes, analyzing nervous system reliance on sense with lower threshold 23 p2946 A73-43847

THROMBOCYTES
Hemocoagulation and trombocyte state during hypokinesia after highland adaptation 12 p1463 A73-27713

THROMBOSIS
Effect of heparin on blood platelet aggregation and thrombosis under the action of direct electric current 08 p0931 A73-21321

Intravascular platelet aggregation in the heart induced by stress. 08 p0933 A73-21805

The complications of coronary arteriography. 22 p2806 A73-42343

Significance of arterial obstructive lesions in early diagnosis of coronary heart disease. 22 p2808 A73-42829

THROTTLING
Effect of injection velocity ratio and combustion chamber pressure on experimental performance of throttleable LO2/GH2-rocket engines with coaxial injectors. [AIAA PAPER 72-1079] 03 p0354 A73-13402

The vapour core pump vortex inlet valve. 23 p2941 A73-43393

THRUST
NT HIGH THRUST
NT JET THRUST
NT LOW THRUST
NT MICROTHRUST
NT ROCKET THRUST
NT STATIC THRUST
NT VARIABLE THRUST

THRUST AUGMENTATION

- Recent developments in large area ratio thrust augmentors. [AIAA PAPER 72-1174] 03 p0357 A73-13470
- TF-30-P1 engine mixed flow augmentor test for combustion instability under operation with abnormal fuel zone combination, comparing with predicted pressure oscillations from model 03 p0358 A73-13489
- [AIAA PAPER 72-1206] 03 p0358 A73-13489
- A one-dimensional flow model for an air-augmented rocket. 05 p0607 A73-16848
- A comparative study of augmentor wing, ejector nozzle and power jet flap low noise STOL concepts. 11 p1300 A73-25385
- The shape of a supersonic three-dimensional nozzle with a maximum thrust 11 p1302 A73-26334
- A simple estimate of the effect of ejector length on thrust augmentation. 15 p1824 A73-31745
- Aerodynamic rig and wind tunnel developments of compound ejector thrust augmentor for V/STOL aircraft with combined Coanda and center injection flows [ASME PAPER 73-GT-67] 16 p2048 A73-33519
- An evaluation of hypermixing for VSTOL aircraft augmentors. [AIAA PAPER 73-654] 18 p2267 A73-36208
- Experimental investigation of a gas-liquid thruster model with a ballasting-reinforced thrust 22 p2841 A73-42127
- German monograph - A method for the calculation of mixing and combustion processes in a rocket propulsion system with air-augmentation. 22 p2900 A73-42851
- Experimental study on optimization parameters of a supersonic jet ejector thrust augmentor. 22 p2798 A73-43113
- Pulsated over-heated water rocket /POHWARO/ thrust augmentation system for combat aircraft takeoff runs from short runways under severe weather conditions 24 p3057 A73-45391
- THRUST BEARINGS**
Computer-aided design of externally pressurized bearings. 03 p0311 A73-13202
- The steady state performance of an externally pressurized gas lubricated porous thrust bearing with a uniform film. 03 p0311 A73-13203
- A method of analysing the effect of inertia and compressibility in an externally pressurized gas lubricated thrust bearing. 03 p0312 A73-13209
- Spiral groove thrust bearing with load carrying lubricating oil film between stationary and rotating surfaces, discussing design, manufacturing and applications 03 p0313 A73-13925
- The effects of wall conductance on torque of the MHD viscous coupler and hydrostatic thrust bearing. [ASME PAPER 72-LUB-1] 03 p0313 A73-14326
- Dynamic stability of gimbaled spiral-grooved thrust bearing. [ASME PAPER 72-LUB-13] 03 p0313 A73-14329
- Some refinements of the theory of the viscous screw pump. [ASME PAPER 72-LUB-24] 03 p0314 A73-14337
- Static and dynamic behavior of spherical hydrostatic bearings - Theory and experiments. [ASME PAPER 72-LUB-35] 03 p0315 A73-14344
- Theoretical and experimental pressure distribution in supersonic domain for an inherently compensated circular thrust bearing. [ASME PAPER 72-LUB-43] 03 p0315 A73-14349
- Summary of gas bearing applications in the field of space electric power systems. 09 p1089 A73-22771
- Galerkin method application to approximation functions selection in development of thrust gas bearing with blowing 11 p1375 A73-26429
- Hydrodynamic tilting pad thrust bearings performance estimation in turbulent region based on laminar flow operation data 14 p1755 A73-30062
- A pseudo shock theory of pressure depression in externally pressurized circular thrust gas bearings. 15 p1882 A73-31699
- Experimental investigation of air bearings for gas turbine engines. [ASLE PREPRINT 73AM-2B-1] 17 p2178 A73-34981
- Solution for the pressure and temperature in thrust bearings operating in the thermohydrodynamic turbulent regime. [ASME PAPER 73-LUBS-14] 17 p2181 A73-35394
- Inertia effects in MHD lubricated hydrostatic thrust bearing under axial magnetic field investigated by energy integral method, obtaining flow velocity and load carrying capacity 24 p3092 A73-44410

Hirs turbulent lubrication theory, discussing plane inclined slider thrust bearing applications and performance predictions
24 p3094 A73-44891

THRUST CHAMBERS

Filament wound boron/epoxy rocket motor chamber fabrication and hydroproof, burst and firing tests, including failure and deformation evaluation
03 p0331 A73-13024

Verification of a comprehensive thrust chamber compatibility model for liquid rocket engines.
[AIAA PAPER 72-1078] 03 p0354 A73-13401

Hydrogen-oxygen Space Shuttle ACPS thruster technology review.
[AIAA PAPER 72-1158] 03 p0356 A73-13460

Algorithm for calculating unsteady heat transfer in liquid-propellant rocket-engine chambers with regenerative cooling
07 p0868 A73-20087

Russian book - Fundamentals of the theory of operational processes in solid-propellant rocket systems.
10 p1262 A73-23948

Russian book - Solid-propellant rocket engines.
22 p2900 A73-41880

Russian book on rocketry principles covering jet propulsion, jet engine combustion chambers, rocket propellants, design, aerodynamics, flight control and anti-aircraft rockets
23 p0308 A73-43334

THRUST CONTROL

NT THRUST VECTOR CONTROL

Experimental satellite for attitude control. II - Measurement of low thrust gas jet performance.
01 p0111 A73-11189

Thrust modulation of solid propellant rocket motors [ONERA, TP NO. 1155] 02 p0203 A73-11990

Integrated engine-airframe design with fuselage boundary layer ingestion for subsonic-transonic cruise, discussing STOL thrust control via variable pitch fan for landing
03 p0251 A73-14128

Potential operating advantages of a variable area turbine turbojet.
[ASME PAPER 72-WA/AERO-4] 04 p0490 A73-15906

Correction of a spacecraft with a static corrective thrust chamber
11 p1431 A73-26465

Fluidic control modules with temperature sensor and thrust reverser pneumatic actuator for aerospace system applications, investigating reliability test data
16 p1971 A73-33477

The use of a hybrid computer in the optimization of gas turbine control parameters.
[ASME PAPER 73-GT-13] 16 p2047 A73-33491

Civil STOL aircraft engine thrust reverser and fast selection control system designs for high performance, low specific weight and acoustic compatibility requirements
[SAE PAPER 730358] 17 p2222 A73-34706

Influence of the effectiveness of jet vanes on the characteristics of VTOL aircraft
21 p2634 A73-40401

Orbit osculation control algorithm guaranteeing satellite repeated passage over given point of earth surface, deriving functional for satellite thrust control
23 p3027 A73-43271

THRUST FAULTS

U GEOLOGICAL FAULTS

THRUST LOADS

Analysis of an arched outer-race ball bearing considering centrifugal forces.
[ASME PAPER 72-LUB-28] 03 p0314 A73-14339

Constrained optimal design of columns against buckling.
04 p0510 A73-15029

Inelastic column buckling of internally pressurized tubes.
[SESA PAPER 2049] 13 p1699 A73-29305

THRUST MEASUREMENT

Direct measurement of colloid microthruster thrust and propellant mass flow rate, using microbalance
04 p0433 A73-15727

Laminar liquid jets thrust measurement apparatus for dilute polymer solutions rheological characteristics determination, using air bearing suspended rotor with discharge capillary
05 p0562 A73-16441

Rapid continuous evaluation of thruster performance dependence on system parameters using thrust balance for measurement, noting suitability for electric microthruster characterization
05 p0579 A73-17253

A method of measuring the thrust, the polar, and the performance of an aircraft on the basis of flight tests
10 p1175 A73-24494

Thrust measurement bench for afterbody and hot and cold jet nozzle simulated tests in Sigma 4 wind tunnel
16 p1993 A73-32820

Thrust stand performance measurements of a lithium fueled applied field MPD arcjet.
19 p2473 A73-38320

Wind tunnel test for Dolphin airship model static thrust measurements, discussing thrust direction torque moment coefficients and propeller rotation
21 p2635 A73-41648

Swirling flow effect on jet noise suppression based on acoustic field and engine thrust measurements with and without stationary swirl vanes in exhaust nozzle
[AIAA PAPER 73-1003] 24 p3077 A73-44836

THRUST PROGRAMMING

Minimum time of Earth-to-Mars and Earth-to-Venus flights with an uncontrolled limited-power engine
14 p1795 A73-29856

Intermediate-thrust arcs and their optimality in a central, time-invariant force field.
16 p2062 A73-33305

Geostationary injection dispersions and thrusting error elimination by apogee motor firing attitude optimization
21 p2780 A73-40614

Synthesis of programmed extensive control of a spatial turning maneuver
23 p3005 A73-43718

THRUST REVERSAL

Thrust reversal systems for solid propellant rocket motors last stage separation from payloads, examining pressure decay under isothermal and adiabatic assumptions
[AIAA PAPER 72-1110] 03 p0355 A73-13425

An analytical investigation of the impingement of jets on curved deflectors.
03 p0296 A73-14178

Optimization of commercial transport airplane stopping systems.
[SAE PAPER 720872] 05 p0535 A73-16671

Civil STOL aircraft engine thrust reverser and fast selection control system designs for high performance, low specific weight and acoustic compatibility requirements
[SAE PAPER 730358] 17 p2222 A73-34706

Overall sound pressure levels of STOL thrust reverse noise as function of jet velocity at touchdown
20 p2600 A73-38650

THRUST TERMINATION

Influence of the thrust interruption during passage through the shadow cone of a celestial body on the trajectory of a space vehicle using solar electric propulsion - First-approximation calculation
12 p1540 A73-27393

THRUST VECTOR CONTROL

Pegasus vectored thrust turbofan engine for Harrier class VISTOL aircraft, describing design and operational details
01 p0090 A73-10200

Dynamic response of an on-off type secondary injection thrust vector control.
01 p0091 A73-11196

Recent developments in large area ratio thrust augmenters.
[AIAA PAPER 72-1174] 03 p0357 A73-13470

Constrained low thrust guidance algorithms for three axis and spin stabilized constant power solar electric propelled spacecraft on fixed time rendezvous missions
[AIAA PAPER 73-173] 05 p0595 A73-16917

Three dimensional self oscillating motion study of roll and pitch stabilized vehicle with thrust vector control under resonance, using averaging method
05 p0599 A73-17086

Optimal descent maneuver with a limited-thrust engine for entry at a prescribed angle into the atmosphere of a planet
13 p1689 A73-29139

Time optimal propulsion system parameters for thrust vector control during spacecraft maneuver performance
14 p1772 A73-29855

Intermediate-thrust arcs and their optimality in a central, time-invariant force field.
16 p2062 A73-33305

Estimation and correction of electric thruster misalignment effects on a geostationary satellite.
17 p2238 A73-34866

Space shuttle solid rocket boosters mission and systems requirements, considering thrust vector control and staging/separation, electrical and recovery systems
[AIAA PAPER 73-606] 18 p2358 A73-36086

Recent advances in thrust vector control for tactical missiles.
24 p3144 A73-44693

THRUST-WEIGHT RATIO

Volvo RMB turbofan engine for Viggen fighter and ground attack aircraft, emphasizing low fuel consumption for long range cruise and high thrust/weight ratio
05 p0608 A73-17099

Ion thrusters with cesium contact ionization - Study of the main elements.
07 p0867 A73-18933

THRUSTORS

U ROCKET ENGINES

THULIUM COMPOUNDS

Domain-wall related, natural, submillimeter-wave resonance in orthoferrites
06 p0736 A73-18114

THUNDERSTORMS

Infrasound in the ionosphere generated by severe thunderstorms.
01 p0040 A73-10826

Investigation of the electrical parameters and meteorological elements of the atmosphere close to the ground during thunderstorm and thunderstorm-free periods
02 p0189 A73-12589

Doppler radar evidence of severe storm high-reflectivity cores acting as obstacles to airflow.
03 p0337 A73-14507

Kinematic and thermodynamic structure of thunderstorm, considering updraft, upper air environment, surface features and radar echoes
03 p0338 A73-14511

Contribution to the protection of flight vehicles against lightning effects
06 p0648 A73-18436

Single point thunderstorm ranging method based on two radio frequencies field intensity spectral components ratio
07 p0847 A73-19439

Measurement of point-discharge current density in the atmosphere.
11 p1354 A73-25767

Russian thunderstorms mean annual duration chart and calculation nomograms
12 p1522 A73-27746

Auroras induced attenuation fluctuations of VLF atmospherics associated with remote tropical thunderstorms
12 p1522 A73-27786

Thunderstorm activity determination on lightning discharge number recorders
14 p1754 A73-30792

Radiometric observations of atmospheric water vapor injection by thunderstorms.
[AIAA PAPER 73-512] 16 p2006 A73-33550

Localization of sources of two-hop whistlers observed aboard the Interkosmos 3 satellite over Europe.
19 p2404 A73-38021

Doppler spectrum turbulence spreading updraft velocity estimation from observation by pulsed radar, noting average value and standard deviation in small thunderstorm
21 p2728 A73-40058

Thunderstorm electrification by the inductive charging mechanism. I - Particle charges and electric fields. II - Possible effects of updraft on the charge separation process.
23 p3002 A73-43599

Short-term ground ozone fluctuations at Poona.
23 p2974 A73-43865

Thunderstorm excited cavity resonances between earth and ionosphere measured by solenoidal coil antenna, finding diurnal frequency variations related to solar and geomagnetic effects
24 p3088 A73-45211

THYATRONS

Optimum operation conditions of thyatron generator circuit in electroacoustic system for excitation of quartz piezoelectric vibrators in ultrasonic NDT
02 p0168 A73-12147

Electro-optical transient sampling analyzer with neon laser and hydrogen thyatron pulse generator and minimum optical and electrical jitter
11 p1377 A73-26244

THYRISTORS

NT SILICON CONTROLLED RECTIFIERS

Thermal design and tests of transcathode solid state power thyristor, rectifier and transistor devices, using heat pipe-silicon wafer construction
03 p0283 A73-13940

Circuit design of triode thyristors and companion rectifiers for high frequency power conditioning, discussing emitter selection, lifetime control, encapsulation and interdigitation optimization
03 p0283 A73-13943

Procedure for automatic statistical processing of experimental data in determining the rated current-voltage characteristic of TD-320 thyristors
03 p0285 A73-14325

P-n-p-n junction thyristor turnoff process under reverse anode voltage at high injection level, examining current voltage curve and switching time constant
05 p0556 A73-16068

Microwelding equipment with automatic wire breaking and ball melting blocks and electronically controlled wire feeding, noting heating plate with thyristor temperature control
06 p0683 A73-18433

A magnetic thyristor pulse generator with shock-wave generation in the transmission line
08 p0949 A73-21712

The powering and synchronization of a solid-state laser operating at a repetition rate of several Hertz
08 p0976 A73-21716

Circuit diagram and electrical characteristics of semiconductor memory cell consisting of thyristor and n-p-n transistors, noting parameters stability
09 p1063 A73-22460

Integrated neuristor lines based on p-n-p-n structures with diffused resistors
10 p1193 A73-23727

THYROID GLAND

System for automatic regulation of the constant-absolute-slip mode of an asynchronous electrical actuating element with frequency-modulation control by a thyristor converter

12 p1460 A73-26786

A positional, asynchronous, thyristor-based, electrical servo actuating element with directional shaping of the phase trajectories

12 p1460 A73-26787

High energy ignition systems using silicon controlled rectifiers.

12 p1533 A73-27931

Harmonic analysis of voltages and currents at the output of a frequency converter with direct coupling and artificial commutation

13 p1593 A73-28941

An analog computer study of a thyristor inverter with opposite-parallel diodes under load switched-on between input throttles

15 p1851 A73-31697

Variable speed single- and multi-quadrant drives using thyristor electronic regulating unit with static converter motor and frequency changers

16 p1971 A73-33961

Observation of turn-on action in a gate-triggered thyristor using a new microwave technique.

20 p2543 A73-39414

Semiconductor rectifiers and thyristor devices, discussing transistor switching, Zener diode, controlled and light activated p-n-p-n diodes

21 p2668 A73-41619

Impulse analysis of subharmonic oscillations in control systems with thyristor converters.

22 p2835 A73-42299

Semiconductor rectifiers analysis, considering triac and thyristor tetrode circuits, trigger devices and circuit diagrams

22 p2835 A73-43128

Switching transients in conducting channel-broadened p-n-p-n structure thyristors, predicting voltage change during current growth avalanche phase and settling at saturation point

24 p3072 A73-44932

Possible causes of failures in pulse-switched thyristors

24 p3072 A73-44933

THYROID GLAND

Radioisotopic T-3 and T-4 thyroid function tests in the pig-tailed monkey /Macaca nemestrina/.

02 p0135 A73-12548

Thyroid and adrenal cortical rhythmicity during bed rest.

03 p0263 A73-14122

Effect of high-fat diet on thermal acclimation with special reference to thyroid activity.

05 p0541 A73-16800

High altitude chamber effect on thyroid stimulating hormone and thyroxine concentrations, noting shift from extra to intravascular

09 p1041 A73-22926

Determination of iodo amino acids in plasma by gel chromatography

10 p1178 A73-23760

FFA metabolism in thyroidectomized and normal dogs during rest and acute cold exposure.

20 p2515 A73-39787

Reaction of neurocytes of the paraventricular hypothalamic nucleus to unilateral thyroidectomy

21 p2637 A73-40283

THYROXINE

Radioisotopic T-3 and T-4 thyroid function tests in the pig-tailed monkey /Macaca nemestrina/.

02 p0135 A73-12548

High altitude chamber effect on thyroid stimulating hormone and thyroxine concentrations, noting shift from extra to intravascular

09 p1041 A73-22926

Determination of iodo amino acids in plasma by gel chromatography

10 p1178 A73-23760

TID

U TRAVELING DISTURBANCES

IONOSPHERIC

TIDAL OSCILLATION

U TIDES

TIDES

NT ATMOSPHERIC TIDES

NT EARTH TIDES

NT LUNAR TIDES

Wolf number solar activity and planetary tidal force correlation during 1770-1970, noting 11-year cycle relation

01 p0101 A73-10848

Spectral analysis of geomagnetic variations to study the tidal and the storm modulation effects.

02 p0158 A73-11906

Nonstellar origin of Jupiter from tidal instability considerations, discussing binary star formation

02 p0216 A73-12377

Changes in the gravitational energy of galaxies during collisions.

02 p0217 A73-12392

Binary stars tidal evolution theory, deriving energy and momentum equations for arbitrary internal structures

02 p0218 A73-12411

Theoretical model for tidal evolution induced capture of natural satellite pairs into orbit-orbit resonance, discussing Titan and Hyperion relationship with Saturn

02 p0219 A73-12421

Sunspot number relationship to planetary tides on sun, considering earth-Venus conjunctions and opposition

02 p0219 A73-12436

Lunar tidal phenomena and the lunar Rille system.

03 p0370 A73-13113

Tidal generation of narrow intergalactic filaments from computer simulations, discussing alternative models

03 p0372 A73-13353

Tracking stations interdistances and solid-earth tidal perturbations determination by laser ranging to satellites

04 p0439 A73-14801

On the origin of the commensurabilities amongst the satellites of Saturn.

06 p0752 A73-18238

Dynamic analysis of tidal effects arising from hyperbolic close encounters of massive body past galaxy, calculating matter velocity field and galactic structure distortion

08 p1004 A73-20907

A search for neutral hydrogen remnants of strong tidal disruption of the Small Magellanic Cloud.

09 p1141 A73-22012

Satellite-caused energy dissipation via tides in spinning planet leading to orbital decay induced destruction or escape or to stable synchronism

09 p1142 A73-22041

Close binary systems orbital elements perturbations due to stellar material viscosity effects on dynamical tide lag

10 p1271 A73-23478

Mercury, Venus and Pluto satellite system elimination by tidal friction, discussing possible erosion of earth and Mars small satellites

11 p1419 A73-25778

Lunar origin dynamics, discussing earth-moon tidal evolution, capture probability, fragmentary collisions, precession and auxiliary models

14 p1800 A73-30550

Wolf number solar activity and planetary tidal force correlation during 1770-1970, noting 11-year cycle relation

15 p1928 A73-30984

Evolution of satellite resonances by tidal dissipation.

15 p1938 A73-31950

Remote sensing in a circulatory survey of Boston Harbor.

16 p2003 A73-33356

Angular momentum decrease of slowly rotating Kerr black holes due to stationary distribution of outside matter

21 p2766 A73-40314

Tidal generation of magnetic fields in binary celestial systems, calculating growth times

24 p3134 A73-44578

Gravitational radiation emission by star tidally deformed by black hole, computing energy loss rate

24 p3138 A73-45037

TIG WELDING

U GAS TUNGSTEN ARC WELDING

TILT

U ATTITUDE [INCLINATION]

TILT WING AIRCRAFT

NT CL-84 AIRCRAFT

Suction force suppression during takeoff, landing and transition of VTOL turbojet via wing turning wing about axis parallel to earth plane

02 p0129 A73-11631

Suitability of the CL-84 tilting aircraft for the sea control ship system.

05 p0534 A73-16660

TILTING

U ATTITUDE [INCLINATION]

TILTING ROTORS

A summary of wind tunnel research on tilt-rotors from hover to cruise flight.

08 p0928 A73-21683

Progress in the development of a practically applicable VTOL aircraft with low disk loading

17 p2098 A73-34254

An economical method of analyzing transient motion of gas-lubricated rotor-bearing systems.

17 p2178 A73-34982

TIMBER INVENTORY

Land use classification in the southeastern forest region by multispectral scanning and computerized mapping.

20 p2557 A73-39849

Automatic terrain mapping by texture recognition.

20 p2568 A73-39873

Multi-stage acquisition of forest information from space and aircraft imagery and ground sampling.

21 p2687 A73-41334

Use of earth resources satellites for supranational inventories of forests and agricultural areas

23 p2972 A73-43775

TIMBER VIGOR

Solar activity effects on tree growth, farm crop yield, fish availability and human sickness trends, discussing indirect effects via meteorological factors

05 p0622 A73-17111

TIME

NT ACCESS TIME

NT DOWNTIME

NT EPHMERIS TIME

NT FLIGHT TIME

NT MTBF

NT REACTION TIME

NT RELAXATION TIME

NT RESPONSE TIME [COMPUTERS]

NT SIDEREAL TIME

NT TESTING TIME

NT TRANSIT TIME

NT UNIVERSAL TIME

TIME CONSTANT

NT PERCEPTUAL TIME CONSTANT

Type 3 bursts exciter duration and decay time constant from time profiles analysis in decameter range, explaining coronal temperature

03 p0361 A73-132131

Reaction time as a measure of the temporal response properties of individual colour mechanisms.

03 p0267 A73-137575

P-n-p-n junction thyristor turnoff process under reverse anode voltage at high injection level, examining current voltage curve and switching time constant

05 p0556 A73-160686

Critical lag of the driving element in a parametric system

05 p0561 A73-169901

Choice of thermal parameters for a photoelectric switch operating with a capacitive load

06 p0676 A73-180879

Fast solid state IR detection photodiodes design, properties and utilization, investigating high speed response conditions and quantum efficiency

06 p0678 A73-188536

Dynamic operating regime of multistage diode-capacitor storage networks

09 p1063 A73-224599

Short time constant limits of pulse duration on electromagnetic energy emission as function of frequency, applying to extragalactic radio astronomy observations

12 p1547 A73-278844

Kinetic cooling with CW carbon dioxide laser, observing time constant as function of atmospheric water pressure with three-beam interferometer

13 p1659 A73-285460

Analysis of the operation of a diode phase detector with allowance for the diode recovery time

13 p1591 A73-288666

Heat detector signal transients during time constant fluctuations in terms of mathematical expectation of ambient temperature

18 p2317 A73-368570

Signal to noise ratios of inertial detector of mixtures of stationary, normal, random and harmonic voltages, varying RC circuit time constants

20 p2537 A73-394596

Tunnel diode different time constants two delay-line circuit, noting self oscillation range, constant pulse periods and hysteresis phenomenon elimination

21 p2660 A73-400998

Performance decrement, under prolonged testing, across the visual field.

22 p2802 A73-417300

Germanium resistance thermometers - Resistances vs. temperature and thermal time constant characteristics.

22 p2854 A73-420000

Time constants of spark discharges initiated by a gas-laser beam of 0.3371 micron wavelength.

22 p2869 A73-422570

TIME DEPENDENCE

Electron density measurements in time varying plasmas with a microwave reflectometer system.

01 p0044 A73-101208

Time dependence of carbon monoxide TEA laser emission at 77 K, presenting time resolved transitions spectral data

01 p0058 A73-101281

Reynolds equation time dependent numerical integration errors due to phase shifts, indicating correction by extrapolated Crank-Nicolson scheme

01 p0055 A73-102231

Effects of signal duration and masker duration on detectability under diotic and dichotic listening conditions.

01 p0008 A73-104361

Time evolution and functional form of magnetostatic equilibria in axisymmetry.

01 p0082 A73-104521

- Equations of the time-dependent strength of solid bodies 01 p0114 A73-10479
- Crack formation in orthogonally reinforced fiberglass plastics 01 p0067 A73-10482
- Two X-ray bursts /1 August 1967 and 30 January 1968/ and some associated VLF disturbances. 01 p0091 A73-10556
- Time characteristics of rupture and creep in metals during tension under hydrostatic pressure conditions 01 p0064 A73-10605
- Time variable dynamics of plasma beam discharge oscillations frequency spectra 01 p0084 A73-10633
- Blast wave theory extension to time variable energy input, considering application to laser induced blast waves 01 p0121 A73-10760
- Stability criteria for unsteady motion of incompressible Cosserat fluid in arbitrary time dependent domain, using Liapunov function 01 p0033 A73-10776
- Closed form exact solution to quasi-static problem in linear viscoelasticity for homogeneous anisotropic material with time invariant properties 01 p0116 A73-10967
- Double exposure holographic interferometry for comparison of object of two points in time evolution, discussing space division multiplexing of exposures onto photographic plate 01 p0054 A73-11234
- Time dependence of Cygnus X-3 GHz flux density and spectral index during outburst decay, describing source model 02 p0204 A73-11553
- Determination of a time-dependent thermal stress on a finite cylinder [DGLR PAPER 72-112] 02 p0230 A73-11671
- Absorbing boundary propagation model for solar cosmic rays energy spectrum kink time behavior, using Gleeson-Ng theory [AD-756355] 02 p0205 A73-11753
- Time dependence of the basic variables in the symmetric solution to the problem of the motion of a body having a fixed point 02 p0191 A73-11763
- The acoustic emission response of mechanically stressed ceramics. 02 p0173 A73-11989
- Time correlation between current sheet collapse in plasma focus and X ray production, investigating radiation intensity and distribution 02 p0197 A73-12061
- Statistical analysis of the sound-level distribution of aircraft noise as a function of time. II 02 p0131 A73-12449
- Gamma time-dependency in Blaxter's compartmental model. 02 p0187 A73-12550
- He 4, C 12, O 16, Ne 20, Mg 24, Si 28 and Fe 56 abundance computed as function of time for neutron star atmospheres with strong magnetic fields 02 p0223 A73-12728
- Lunar axis inclination to ecliptic axis as function of time, tabulating variations during 1971 03 p0367 A73-13078
- Type 3 bursts exciter duration and decay time constant from time profiles analysis in decimeter range, explaining coronal temperature 03 p0361 A73-13213
- Radial velocity and microturbulence dependence on excitation potential and time in A type supergiants atmosphere, deriving chemical composition 03 p0371 A73-13215
- Time-dependent characteristics of radio waves passing through the irregular ionosphere. 03 p0275 A73-13645
- Aerodynamic and temporal parameters of olfactory stimulation - Discussion concerning the lowering of the threshold by prenasal injection in man 03 p0262 A73-13787
- Survey of some current aerodynamic problems pertaining to supersonic air intakes [ONERA, TP NO. 1102] 03 p0247 A73-14150
- A brief comparison of the accuracy of time-dependent integration schemes for the Reynolds equation. [ASME PAPER 72-LUB-L] 03 p0297 A73-14352
- Current near the insulator wall in plasma accelerators. 03 p0348 A73-14437
- Hold-time effects on the elevated temperature fatigue-crack propagation of type 304 stainless steel. 03 p0328 A73-14448
- Power output of a pulsed Raman laser with saturable excitation. 03 p0319 A73-14453
- Time behavior of a TEA xenon laser. 03 p0320 A73-14466
- The effect of time of electrical stimulation of the carotid sinus on the amount of reduction in arterial pressure. 03 p0265 A73-14648
- Time dependent hydrodynamic models of solar wind, considering coronal electron density and temperature distribution and magnetic field 04 p0491 A73-14835
- A procedure for estimating maximum time-variant distortion levels with limited instrumentation. [ALAA PAPER 72-1099] 04 p0432 A73-14908
- Air density at heights near 200 km from the orbit of 1969-20B. 04 p0440 A73-14965
- Remarks on the steady and time dependent mathematical convection models. 04 p0443 A73-15341
- Thermally induced stress waves in an elastic layer. [ASME PAPER 72-WA/APM-22] 04 p0516 A73-15894
- Time history of laser power pulses from molecular gas lasers. 04 p0459 A73-16041
- Frequency and time description of mode locked laser system, discussing active and passive phase locking of longitudinal standing wave modes in laser cavity 05 p0583 A73-16338
- Viscoelastic liquid flow in wake past two dimensional grid, investigating vorticity increase with time for double array of vortices 05 p0565 A73-16592
- Turbulent space-time correlation measurements in a plane two-stream mixing layer at velocity ratio 0.3. [AIAA PAPER 73-225] 05 p0566 A73-16951
- Load-time dependent relaxation of residual stresses. 05 p0636 A73-17214
- The correlations of the vortex in a homogeneous turbulence associated with a mean shearing flow 05 p0567 A73-17227
- Time-dependent radiation transfer and a possible explanation of the interpulse in CP 0950. 05 p0623 A73-17302
- The infrared variability of a dust model for Seyfert galaxies. 05 p0624 A73-17311
- Interplanetary cosmic ray low energy electron observation, explaining steep spectrum origin and time variations by model with spectral decomposition 05 p0612 A73-17386
- Structure of the pulsations of the earth's electromagnetic field as a random function of time 06 p0689 A73-17541
- Book - Microwave transmission. 06 p0663 A73-17670
- Small vibrations of isotropic elastic medium under finite strain and with time proportional elongations in three mutually perpendicular directions 06 p0759 A73-17759
- The correspondence principle of linear viscoelasticity for problems that involve time-dependent regions. 06 p0762 A73-17992
- Conservation of quasiparticles in weakly turbulent plasmas. 06 p0730 A73-18273
- Time dependence of the gain of an optically pumped solution of rhodamine 6G 06 p0703 A73-18598
- An identification of time varying linear system without a priori information on variation of system parameters. 06 p0681 A73-18812
- Modeling of linear time-varying systems by linear time-invariant systems of lower order. 06 p0682 A73-18867
- Extended X-ray and radio observations of Scorpius X-1. 07 p0874 A73-19069
- A transformation of the radiative transfer equation useful for problems with steep source gradients. 07 p0918 A73-19265
- Eccentric geomagnetic dipole drift field as function of time dependent parameters, calculating potential components in spherical coordinates 07 p0817 A73-19467
- Pulsed CO laser vibrational distribution function time dependent evolution, considering V-V and V-T processes, spontaneous and stimulated emission, electron impact excitation and kinetic heating 07 p0835 A73-19635
- Air-terminal queues under time-dependent conditions. 07 p0850 A73-20375
- Time variation of metal abundance in galaxies - Super-metal-rich stage. 07 p0902 A73-20446
- The effect of a nonlinearity upon signals in the presence of noise. 07 p0795 A73-20499
- Electron plasma oscillation due to beam plasma interaction with standing wave formation between electrodes, observing temporal growth rate during beam modulation removal 08 p0992 A73-21005
- Diffuser box for holography spatial and temporal coherence requirements relaxation, explaining speckling and SNR reduction by time and frequency domain analysis 08 p0963 A73-21035
- Time variable field recording and reconstruction theory and wave equations of holography and holographic interferometry, including double exposure and time averaged techniques 08 p0965 A73-21137
- Nonaxisymmetric kinematics in galaxies with axisymmetric mass distributions. 08 p1008 A73-21154
- Time dependence of cosmic ray intensity during the anisotropic phase of solar flares 08 p0998 A73-21279
- Spatial-temporal distribution of E/s formations associated with visible forms of polar aurorae 08 p0958 A73-21283
- Characterization of p-n junctions under the influence of a time varying mechanical strain. 08 p0951 A73-21481
- Analysis and space-time reconstitution of the circumferential component of instantaneous velocity in immediate proximity to the wall of a cylinder 08 p0926 A73-21496
- The dependence of the notch sensitivity of Waspaloy at 1000-1400 deg F on the gamma prime phase. [ASME PAPER 72-MAT-J] 08 p0979 A73-21571
- Classical theory of spectral distribution of isolated nonlinear oscillations at combined frequencies 09 p1119 A73-21953
- Solution to a time-dependent Schroedinger equation in the case of a specific potential 09 p1122 A73-22021
- Temperature distribution in gas flow about a linear source of heat variable periodically in function of time. 09 p1166 A73-22169
- Time jitter in line regenerators with pattern dependent pulse waveforms. 09 p1062 A73-22301
- A numerical model for predicting mesoscale winds aloft. 09 p1114 A73-22335
- Kinetics of transformation of carbon- and nitrogen-enriched austenite by carbonitriding in the gas phase 09 p1105 A73-23038
- Images and sound rays in the numerical calculation of echograms 09 p1121 A73-23104
- Time evolution of rotating incoherent matter with vanishing internal pressure by Einstein field equations 09 p1151 A73-23342
- Energy spectrum and time variations of hard X-rays from Cyg X-1. 10 p1263 A73-23488
- Computation of time-dependent laminar flow structure. 10 p1294 A73-23552
- Short time aging characteristics of inconel X-750. 10 p1230 A73-23631
- Time dependent radio stars scintillation spectra with allowance for interplanetary plasma discontinuities velocity dispersion at small solar distances 10 p1274 A73-23716
- Problem of the time dependence of the polarization level of Type III solar radio bursts 10 p1264 A73-23719
- A short periodic irregularity in earth's rotation and the motion of the earth's instantaneous pole 10 p1275 A73-23724
- Best approximation in digital filtering 10 p1242 A73-23764
- Visual acuity as a function of exposure duration. 10 p1184 A73-23838
- Earth-atmosphere-ocean energy balance time dependent model equation, using Sellers radiation relationships and turbulent exchange coefficients for numerical solution 10 p1245 A73-23982
- The methods of time-variable systems analysis based on new trends in theory of these systems. 10 p1200 A73-24047
- Temperature distribution in a plasma with turbulent thermal conductivity. 10 p1255 A73-24211
- Electron content measurements - A method for resolving the n-pi ambiguity. 10 p1214 A73-24746
- Visualization experiments on unsteady viscous flows around cylinders and plates. 10 p1174 A73-24836
- Linear system unperturbed motion stability in finite time interval, formulating first approximation vector matrix equation 11 p1397 A73-25045
- Brownian motion of electrons in time-dependent magnetic fields. 11 p1403 A73-25124
- A theoretical study of lunar variations in foF2 at low latitude. 11 p1354 A73-25764
- Time variations in the X-ray emission of solar active regions. 11 p1412 A73-25944
- Observations on the time and frequency structure of solar decameter radio bursts. 11 p1413 A73-25951

TIME DEPENDENCE

Gaussian light beam transmitted intensity derivation for thermal lensing in solids by vector Kirchhoff approach, obtaining time dependent shift in diffraction focus

11 p1377 A73-26228

Time-related behavior of causal, anticausal, memoryless and crosscausal nonlinear control systems modeled as operator on group-valued function space

11 p1391 A73-26366

Spatial-temporal structure of emission from a ruby laser irradiated by gamma rays

11 p1378 A73-26523

The dependence of the negative afterimage on the duration of the stimulus and the stimulus intensity

11 p1321 A73-26550

Cosmic ray electrons from 0.2 to 8 MeV - Pioneer 8 and 9 measurements of their spectrum, time variations, and interplanetary radial gradient.

12 p1533 A73-26976

Carnauba wax electrets manufactured under the simultaneous action of magnetic and electric fields

12 p1523 A73-27103

Time course of lateral inhibition in the human visual system.

12 p1462 A73-27124

Diameter reduction rate and time dependence of corresponding temperature variation of liquid drop unsteady evaporation in rarefied ambient gas

12 p1558 A73-27392

Solar and lunar eclipses, orbits and perturbations prediction from Saros/recurring time periods/

12 p1540 A73-27481

Time characteristics of a ring laser with a bleachable filter.

12 p1507 A73-27509

Closed form exact solution to quasi-static problem in linear viscoelasticity for homogeneous anisotropic material with time invariant properties

12 p1554 A73-27543

Diffraction of electromagnetic waves on reflectors with parameters that vary periodically in time

12 p1470 A73-27583

Time dependent studies of the aurora. I - Ion density and composition.

12 p1492 A73-27601

Mean time of the failure-free operation of a redundant system with allowance for monitoring of operational efficiency

12 p1504 A73-27619

Temporal intensity fluctuation measurements in K line wing near solar disk center, noting power spectrum peaks and brightness relationship to Fe I line displacement

12 p1544 A73-27830

High resolution space-time structure and centre-limb distribution of solar type I sources observed at 169 MHz.

13 p1671 A73-28032

Temporal and spatial features in detecting one- and two-dimensional constraints in complementary visual displays.

13 p1578 A73-28095

Contribution to the study of the behavior of liquid cobaltous oxide in an oxidizing atmosphere

13 p1634 A73-28204

Mass to wind and wind to mass adjustments in dynamic initialization for primitive equation model of atmospheric motion

13 p1652 A73-28270

Determination of the time interval for orientation of conducting nonmagnetic oblong bodies by a homogeneous alternating magnetic field

13 p1571 A73-28467

Mechanical properties of 6061 Al-Mg-Si alloy after very rapid heating.

13 p1636 A73-28795

Relationship of mechanical characteristics and microstructural features to the time-dependent edge-notch sensitivity of Inconel 718 sheet.

13 p1637 A73-29200

Computer simulations of large-signal oscillation behavior of avalanche diodes.

13 p1594 A73-29235

Quadratically coupled oscillators interaction at semiresonant frequencies, considering time dependent Duffing equation and frequency divider application

13 p1661 A73-29375

A molecular theory of elastomer deformation and rupture.

13 p1646 A73-29528

Behavior of random micro-structural systems.

13 p1701 A73-29530

Temperature fields in a hollow cylinder in presence of heat source under the boundary conditions of the second kind.

13 p1708 A73-29666

Temporal development of longitudinal plasma current radial profile, obtaining effective collision frequency estimation for electron heating, hot plasma production conditions and stability restoration force

14 p1777 A73-29685

Time behavior of hydrogen discharge in ST-Tokamak based on measured radial electron tempera-

ture and density profiles and ohmic-heating current and voltage

14 p1778 A73-29691

Creep analysis of transversely isotropic bodies subjected to time-dependent loading.

14 p1805 A73-29769

Isochronous derivatives of certain spacecraft-trajectory parameters

14 p1796 A73-29857

Satellite oscillation in circular orbit plane, determining gravitational stability in minimum time with least fuel consumption

14 p1803 A73-29868

On the propagation of electromagnetic waves through a time-varying dielectric layer.

14 p1726 A73-29932

Solar wind velocity and proton temperature time dependent relations, considering interplanetary medium nonlinear unsteady processes effects

14 p1786 A73-29955

Equations for the time-dependent strength of a solid.

14 p1810 A73-30304

A criterion for the bounded-input, bounded-output stability of time-varying nonlinear systems.

14 p1738 A73-30404

Inverse problem of linear optimal control.

14 p1738 A73-30451

Time varying linear and constant bilinear dynamic systems state space structure, obtaining canonical decomposition by suitable choice of input/output interaction properties

14 p1739 A73-30778

Nonstationarity effects on planetary boundary layer by numerical integration of time dependent boundary layer model

14 p1772 A73-30903

Time-dependent models of the interstellar gas.

14 p1802 A73-30960

On the transport of charged particles in turbulent fields - Comparison of an exact solution with the quasilinear approximation.

15 p1916 A73-31083

A simplified method of calculating thermofluid curves

15 p1837 A73-31168

The general magnetic field on the sun and its changes with time.

15 p1932 A73-31304

Cosmological arrow of time theory describing approach to equilibrium in closed systems, noting relation to cosmic expansion

15 p1933 A73-31310

A technique for the calculation of the opening-shock forces for several types of solid cloth parachutes. [AIAA PAPER 73-477]

15 p1829 A73-31461

Dwell times of thin exploding wires.

15 p1913 A73-31934

Time-resolved gain of a volume-excited TEA CO₂ laser amplifier.

15 p1885 A73-31945

Time required for the destruction of a nonuniformly heated wall

15 p1953 A73-32098

The stability of a time-variable surface wind

15 p1906 A73-32353

Structure of pulsations of the electromagnetic field of the earth as a random function of time.

16 p2001 A73-32765

Time dependent diffusion equation for solar flare cosmic ray propagation through interplanetary space, specifying continuous emission curve shape and period

16 p2053 A73-32966

Adhesive viscoelasticity effects on sandwich structure performance, presenting mathematical model for adhesive behavior and time dependent loading

16 p2029 A73-33053

Time dependent one dimensional Navier-Stokes differential equations solved via difference scheme, determining reflected shock wave structure and end wall pressure

16 p1999 A73-33251

Critical behaviour in chemically reacting systems. I - Difficulties with the Semenov theory. II - An exactly soluble model.

16 p1976 A73-33342

An adaptive estimation algorithm for time-varying bit synchronizers.

16 p1988 A73-33411

Time dependent worldwide distribution of atmospheric neutrons and of their products. I, II, III.

16 p2055 A73-33427

Time dependent stress-strength models for non-electrical and electrical systems. I.

16 p2020 A73-33621

Censored sample size selection for life tests. [AD-758315]

16 p2033 A73-33630

Pi 2 and geomagnetic bay maximum occurrence dependence on geomagnetic time, discussing computation methods for geomagnetic time

16 p2010 A73-33922

On the numerical computation of parabolic problems for preceding times.

17 p2199 A73-34211

The supporting effect of bending specimens under static load in the temperature range from 400 to 500 C

17 p2187 A73-34521E

Time-dependent radiative cooling of a hot low-density cosmic gas.

17 p2231 A73-34752E

Fast differential thermal analysis.

17 p2119 A73-34793E

Unconditional stability in numerical time integration methods.

17 p2201 A73-35027E

Numerical solution of the three-dimensional Navier-Stokes equations in integro-differential form - Flow about a finite body.

17 p2155 A73-35134E

Turbulent flow research, discussing time domain analysis of velocity, displacement and pressure potential flow models of vortices, and shear flow turbulence

17 p2155 A73-35330

IR laser induced change in atmospheric temperature as function of time, using kinetic model with impulsive molecular energy transfer rates for thermal blooming

17 p2163 A73-35414

Kinetic equations for time behavior of solid state photochromic film in photocoloration, photobleaching and thermal bleaching, evaluating absorption cross sections and quantum yields

17 p2172 A73-35422

Time evolution of pulsating air jets from schlieren photography and velocity measurements, using motor driven piston

17 p2157 A73-35514

The field-effect transistor as a resistance varying linearly in time

17 p2141 A73-35547

A new numerical technique for solving the time-dependent radiation transport equation.

17 p2255 A73-35595

Small perturbations in flat galaxies. II - Time-dependent azimuthal perturbations.

17 p2236 A73-35782

Book - Electromagnetic wave propagation.

17 p2130 A73-35857

Time dependent studies of the aurora. II - Spectroscopic morphology.

18 p2311 A73-36185

Time dependent radio sources scintillation spectra with allowance for interplanetary plasma discontinuities velocity dispersion at small solar distances

18 p2355 A73-36741

Time dependence of the polarization of type III solar radio bursts.

18 p2347 A73-36744

A short-period irregularity in the earth's rotation and the motion of the instantaneous pole.

18 p2355 A73-36749

A direct approach to reduce recording time in stroboscopic holographic interferometry.

19 p2429 A73-37541

Time dependent radiative transfer. III - Development of the formalism.

19 p2503 A73-37565

Poincare-Lighthill and linear-time-scales methods for linear perturbation problems.

19 p2445 A73-37752

Time dependence of cosmic-ray intensity at the anisotropic stage of solar flares.

19 p2476 A73-37908

Space-time distribution of Es formations associated with visible auroral forms.

19 p2424 A73-37912

Instability of feedback systems containing several time-varying nonlinear amplifiers.

19 p2414 A73-38078

Non-linear vibration of beams with time-dependent boundary conditions.

19 p2501 A73-38253

Visual responsiveness repeat variability magnitude during prolonged sessions and time of day

20 p2513 A73-39479

Multispectral reflectance scanning of crop image signatures during April-July growing season, examining time dependent image changes, discrimination tests and crop types

20 p2561 A73-39900

Fog dispersal technique evaluation for cost effectiveness by statistical method, taking into account time dependent probability of natural visibility improvement

21 p2729 A73-40066

Tropospheric model for nitrogen-oxygen-carbon-hydrogen atmosphere with time dependent static chemistry, emphasizing methane conversion to CO via OH attack

21 p2646 A73-40081

Linear wave motion analysis of viscous incompressible fluid of infinite depth at small and large times by asymptotic quadrature method

21 p2676 A73-40207

Global stability of time-dependent flows - Impulsively heated or cooled fluid layers.

21 p2790 A73-40249

A class of heat conduction problems with a time-variable heat transfer coefficient

21 p2790 A73-40396

Upper atmospheric models dealing with diurnal variation and latitudinal density dependence to derive time and space dependencies 21 p2683 A73-40631

Kinetic effects in drilling with the CO2 laser. 21 p2707 A73-40974

A method of treating boundary singularities in time-dependent problems. 21 p2726 A73-40997

Directional plasma transport equations derived from Boltzmann equation by averaging of velocity space subset, applying to plasma confinement by external time dependent electromagnetic fields 21 p2748 A73-41127

Influence of hydrogen on the fracture micromechanism of OT4 and OT4-1 titanium alloys 21 p2721 A73-41231

Phase method of investigation of short time scale disturbances and motions in space plasma. 21 p2748 A73-41373

The impulsive increase in the intensity of solar X-rays. 21 p2761 A73-41388

Solar limb flare observations on 11 August 1972, examining temporal relationships of flash, spray, surge and loop phase 21 p2762 A73-41492

Human recognition of dynamic pattern changes in numerical series displayed on spatiotemporal panels, discussing learning times and reactions to pattern disruptions 22 p2812 A73-41887

Latitude and local time dependence of precipitated low-energy electrons at high latitudes. 22 p2901 A73-41914

Critical evaluation of Zhurkov theory of metallic material fracture by successive rupture of atomic bonds due to atom thermal motion 22 p2874 A73-42108

Semiempirical time dependent climate models formulated for stability of asymptotic steady state equilibrium solutions to perturbations 22 p2883 A73-42540

Diurnal thermospheric and ionospheric variations from time dependent continuity equations for O+, H+, O2+, and NO+ ions, motion and heat conduction equations 22 p2849 A73-42572

Root locus analysis of stability of a class of non-linear systems. 22 p2837 A73-42624

German monograph - Investigation of time-variable currents in Al-Al2O3-Al thin-film structures. 22 p2897 A73-42855

Convergent stable three-time level implicit numerical model for phase change problems, evaluating temperature dependent coefficients of parabolic equations at intermediate level 22 p2937 A73-42951

Increase of error in range correction with elapsed time, evaluated by ray tracing through radiosonde-generated atmospheric models. 22 p2828 A73-43176

Unboundedness of solutions and comparison theorems for time-dependent quasilinear differential matrix inequalities. 23 p3000 A73-44202

Space-time limits of stable oscillations of solar surface active zones spanning multiple solar rotations, noting correlation coefficients for north and south hemispheres 24 p3138 A73-45013

Space-time autocorrelation and cross correlation coefficients for transverse turbulent velocity fluctuations in pipe flow 24 p3080 A73-45451

Time-varying network analysis via matrix manipulation and Peano-Baker solution for second and higher order differential equations with periodic coefficients 24 p3075 A73-45477

TIME DISCRIMINATION

Verbal estimates of perceived time of flashing lights interval, relating to lights separation distance 03 p0260 A73-13552

Space-time relations - The effects of variations in stimulus and interstimulus interval duration on perceived visual extent. 05 p0545 A73-17199

Estimation of the passing of four consecutive hours. 06 p0636 A73-17524

Statistical distribution methods for analyzing formation of reflexes conditioned to time intervals between periodic unconditioned stimuli 06 p0633 A73-18166

On the rate of acquisition of visual information about space, time, and intensity. 17 p2118 A73-35496

Effect of carbon monoxide on time perception. 21 p2642 A73-40000

Sufficient conditions for the discrimination of motion. 21 p2639 A73-41181

TIME DIVISION MULTIPLEXING

Synchronous multiplexing of digital signals using a combination of time- and code-division multiplexing /t.d.m. and c.d.m./ 02 p0140 A73-11588

Experimental validation and design refinement program for air-ground-air data link based on automatic time division multiplex transmission of air traffic messages 02 p0190 A73-11852

A time-division multiplexed telemetry system using delta-modulation. 03 p0270 A73-14279

Active terminal devices for wide band time multiplexed laser PCM communication systems. 04 p0417 A73-15069

A compact low-cost electronic time division multiplexer. 04 p0417 A73-15295

TDM link with digitized voice channel and PCM telemetry sequence coding for error correction, comparing tested performance with prediction and computer simulation 04 p0419 A73-15401

Time division multiple access for tactical trunking via satellite. 04 p0420 A73-15424

Pulsed random process energy spectra methods for spectral distribution of signal power in multichannel AM, FM and PM PCM systems with time division multiplexing 04 p0423 A73-15918

Datran TDM switching system with stored program controller and IC components providing reliability, flexibility and high channel capacity in data transmission 05 p0551 A73-16804

An IRIG FM-FM telemetry system for the Petrel sounding rocket. 05 p0551 A73-16850

Electro-optical multiplexers and demultiplexers for time-multiplexed PCM laser communication systems. 06 p0700 A73-18297

8-phase and 16-phase high speed PSK modems for PCM-TDMA satellite communication. 07 p0791 A73-19370

TDMA system and full scale test programs for Symphonic satellite telecommunication with ground 09 p1049 A73-22316

Study of a phase displacement modulation modem for a time division multiple access system 09 p1050 A73-22318

High capacity digital concentrator of telephone circuits for a TDMA station /CELTIC/ 09 p1050 A73-22319

TDMA satellite telephonic communication network with preassigned channeled radio carrier, describing four phase demodulator and channel units regrouping 09 p1050 A73-22320

Intelsat 4 communications system, discussing radio transponders, earth stations, and multiple access, modulation and multiplexing methods 09 p1051 A73-22700

Second-order phase-lock-loop acquisition time in the presence of narrow-band Gaussian noise. 12 p1468 A73-27010

Multiple access system by time division with synchronization in the S2 TDMA satellite 13 p1584 A73-28908

Study of carrier and bit-timing recovery of ultrahigh speed PSK-TDMA systems 13 p1584 A73-28909

A simple error-protection approach in the case of a transmission of anisochronous data signals over time-division multiplex systems 14 p1726 A73-30071

TACAN based SETAC and L band DME based DLS approach and landing systems for military aircraft, discussing time division multiplexing and antenna array [DGLR PAPER 73-019] 17 p2208 A73-34493

Prototype TDMA system design for Intelsat 4 satellite, discussing separate synchronization and data bursts transmission feature for service quality and reliability improvement 17 p2122 A73-34967

Information transfer system of digital avionics system, examining signal reduction by baseband time division multiplexing and video distribution systems 17 p2138 A73-35230

TDM data bus and interface design for digital avionics system, considering standard remote terminal in terms of system parameters, operation and cost effectiveness 17 p2139 A73-35233

Digital time division multiplexing for integrating avionics equipment, discussing electrical power control signal multiplexing 17 p2139 A73-35246

Multiple access techniques for the Canadian domestic satellite communications systems. 17 p2124 A73-35305

Time division multiple access in the INTEL SAT system. 17 p2124 A73-35306

Time Division Multiple Access for the defense satellite communications system. 17 p2124 A73-35307

Wideband multidrop asynchronous TDM/FDM multichannel data distribution system for space station application, discussing analog and digital buses design 17 p2124 A73-35308

The orbital test satellite for the European Communication Satellites Programme - Performance and growth capability. [DGLR PAPER 73-044] 17 p2126 A73-35481

Range and range-rate measuring equipments for communication satellites. 17 p2130 A73-35813

A proposed time division multiple access /TDMA/ satellite system for Anik I. 20 p2523 A73-38719

A satellite-switched SDMA/TDMA system for a wideband multibeam satellite. 20 p2524 A73-38730

Communication satellite history and present developments, discussing Intelsat and ATS programs and TDMA techniques 20 p2526 A73-38747

Applications of error-correcting codes to TDMA satellite communications. 20 p2526 A73-38751

TDMA system design for small satellite terminals. 20 p2528 A73-38767

Data transmission system based on voice channels time division into blocks using cyclic code redundancy without appreciable loss in error correcting capability 21 p2655 A73-41044

Continuous information theory and modulation methods. 22 p2826 A73-42463

TIME FUNCTIONS

Time-periodic solution of the system of boundary layer equations. 07 p0809 A73-19019

Study of the time correlation of multifrequency-laser emission by the photon coincidence method 09 p1096 A73-22877

Signal processing in a randomly time varying system. 10 p1197 A73-23800

Numerical time integration methods in shell transient response finite element analysis, considering conditionally stable explicit and unconditionally or conditionally stable implicit schemes 14 p1807 A73-30187

Solutions of certain difference equations describing transformation of the temporal characteristics of radiation in a laser 16 p2024 A73-32891

Master equations in the theory of incoherent and coherent spontaneous emission. 20 p2570 A73-38608

A study of systems with time-variable coefficients by the definite-integral method 20 p2542 A73-39037

Russian book on mathematical theory of optimal control of discrete time systems covering multidimensional geometry, convex sets, Pontryagin maximum principle and dynamic programming 21 p2726 A73-40802

TIME LAG

Integrated subnanosecond circuits with low power dissipation and few components 01 p0021 A73-11487

Design and fabrication of helix-like strip meander line delay equalizer in printed circuit technology, noting group delay and insertion loss frequency responses 02 p0145 A73-11823

Automated system with CW signal and feedback to measure delay line group delay and transfer function frequency responses, detailing operation and errors 02 p0146 A73-11952

Drag derived density analysis for geomagnetic disturbances effect in thermosphere, noting atmospheric reaction time delay and exospheric temperature increment per unit Kp 02 p0161 A73-12280

Photoelectric measurement of satellite camera shutter opening time delay and photographic plate motion synchronization, calculating root-mean-square error in observation time 03 p0307 A73-13253

A technique for synoptique measurement of ionospheric propagation delays by ranging from geostationary satellites to a network of unmanned transponders. 03 p0308 A73-13629

Application of electron content observations in navigational ranging. 03 p0275 A73-13654

On the almost-sure sample stability of systems with randomly time-varying delays. 03 p0285 A73-13898

Optimal control of nonlinear time-lag systems. 03 p0285 A73-13899

Optimal control approximations for time delay systems. 03 p0286 A73-14195

Delay effects in fatigue crack propagation. 04 p0459 A73-14690

TIME LAPSE PHOTOGRAPHY

The production and analysis of transmission ionograms. 04 p0440 A73-14953

Choice of a rational control law for control systems for delayed objects subjected to random load disturbances. 04 p0429 A73-15202

Algebraic and transfer-function criteria of fixed-time controllability of delay-differential systems. 04 p0430 A73-15212

Necessary and sufficient conditions of pointwise completeness of linear time-invariant delay-differential systems. 04 p0430 A73-15213

Message switching for multiplexing data of computer users with interactive access onto common facilities, evaluating traffic induced time delay performance. 04 p0425 A73-15428

Properties of different groups of type IV solar radio bursts. 04 p0493 A73-16013

Method for calculating the delay in a time-service photoelectric phase apparatus. 04 p0451 A73-16019

Interferometric CW radar for group delay difference measurement of reflected signal components in ionospheric sounding. 05 p0548 A73-16253

Investigation of a signal scattered in the lower ionosphere on the basis of a group delay model. 05 p0548 A73-16254

Operating modes of a phase-loop AFC system with a low control circuit time lag under the action of additive harmonic noise. 05 p0560 A73-16292

Phase space structure of neutral-type quasi-linear differential equations. 05 p0589 A73-16294

Synthesis of an optimal discrete control system in the presence of control delay. 05 p0560 A73-16295

Critical lag of the driving element in a parametric system. 05 p0561 A73-16990

Low cost electronic method of delaying speech signals based on adaptive delta modulators. 05 p0552 A73-17375

Security system signal detector with time delay and prediction filters and optimal noise suppression, noting detection time dependence on cost effectiveness. 06 p0679 A73-17806

On the controllability conditions for systems with distributed delays in state and control. 06 p0716 A73-17852

An optimum settling problem for time lag systems. 06 p0717 A73-18172

Energy dependent time lag in the long-term modulation of cosmic rays. 07 p0869 A73-19252

The effect of higher alkanes on the ignition of methane-oxygen-argon mixtures in shock waves. [AD-756982] 07 p0918 A73-19389

Effect of impurity gradient on the time delays and Q-switching in junction lasers. 07 p0836 A73-20189

Necessary condition for complete controllability with respect to arbitrary function for linear time-invariant differential equation system with time lag. 08 p0950 A73-21092

The dynamic response of a diaphragm-ejector amplifier. 08 p0929 A73-21830

Dwell times of exploding tungsten wires in air. 09 p1119 A73-21929

Delay-lock discriminator to measure spatial delay time of noise-like signal received by two spaced antennas. 09 p1049 A73-22048

Time behavior of the internal Q switching in GaAs lasers under electron-beam excitation. 09 p1092 A73-22245

Time delays and Q switching in homostructure and heterostructure injection lasers. 09 p1092 A73-22246

Double heterojunction [GaAl]As laser pulse modulation at 200 Mbits/sec continuous operation at room temperature, considering lasing delay time and damped oscillations problems. 09 p1093 A73-22257

Numerical position deviation and release delay time estimates for gyroscope motion in gimbal suspension during rotor start-up. 09 p1081 A73-22345

Mathematical model of equilibrium and steady state stability of pulse frequency modulation feedback systems of second kind with time delay filters. 09 p1069 A73-22723

Optimal control of n-order system with transport delay by variational calculation, comparing with proportional integrator (PI) controller. 09 p1069 A73-22974

Group delay equalization in waveguide communications systems for signal regeneration with tapered meander transmission line. 09 p1053 A73-23110

Design and manufacture of delay equalized comb-line filters. 10 p1193 A73-23608

The optimization of delay equalized comb-line filters. 10 p1193 A73-23609

Microwave system with direct, AM, FM and pulse propagation techniques for swept-frequency group delay measurement, discussing error sources and various distortions. 10 p1193 A73-23610

Discrete-time fixed-lag smoothing algorithms. 10 p1243 A73-24547

Unsteady aerodynamics of separating and reattaching flow on bodies of revolution. 10 p1173 A73-24816

Nonlinear delay-differential control systems described by periodic functional differential equations with small real parameter, investigating asymptotic stability in Liapunov sense. 11 p1390 A73-25190

Sagnac effect on clock synchronization of two clocks moving under equal equatorial westward and eastward velocities. 11 p1398 A73-25860

Optimal control for functional differential systems through Krasovskii generalization for time delay systems and resulting Riccati equations numerical solution. 11 p1392 A73-26581

Restart transients of hybrid rocket engines. 11 p1411 A73-26669

A fast method to determine the nose frequency and minimum group delay of a whistler when the causative spheric is unknown. 11 p1358 A73-26705

Temporal characteristics of spark gaps with discharge initiation by a laser flare. 12 p1506 A73-27212

Relative transit time measurements of high-frequency signals using an FM-CW technique. 12 p1474 A73-27763

Stability of coupled systems of nonlinear differential delayed-argument equations. 12 p1525 A73-27947

Linear systems with aftereffects of delayed feedback described by differential equations, obtaining optimal control solution in terms of parameters and boundary value problem. 12 p1486 A73-27950

Vibrations of a system with memory, non-linear elasticity, friction and relaxation. 13 p1690 A73-28055

Accuracy of switching pressure of fluidic OR-NOR device. 13 p1571 A73-29044

Determination of the absolute-stability domain of nonlinear time-lag systems. 13 p1596 A73-29143

Damping time of a ruby laser with flat mirrors. 13 p1630 A73-29556

Oscillations of higher-order retarded differential equations generated by the retarded argument. 14 p1770 A73-30756

On asymptotic solutions of nonlinear differential equations with time lag. 14 p1770 A73-30759

Oscillations of nonlinear functional differential equations generated by retarded actions. 14 p1770 A73-30761

Mathematical model of equilibrium and steady state stability of pulse frequency modulation feedback systems of second kind with time delay filters. 14 p1740 A73-30956

Optimal control theory for systems with inequality restrictions on control and state variables and time delay, using maximum principle and variational techniques. 15 p1855 A73-32580

Ultrafast spark gaps for electro-optical device control, discussing trigger system design and performance in terms of delay, jitter and internal voltage time response. 16 p2013 A73-32874

Space-time adaptation of visual position constancy. 17 p2114 A73-34223

Russian book - Lectures on the theory of stability of the solutions of systems with an aftereffect. 17 p2211 A73-34224

The effect of colour on time delays in the human oculomotor system. 17 p2112 A73-34847

Optimal pursuit-evasive conflicts with guidance systems containing time delays. 17 p2145 A73-35380

A study of the time lag of the 27-day variation in the thermospheric density. 18 p2303 A73-35961

Performance improvement in remote manipulation with time delay by means of a learning system. 19 p2417 A73-37331

A model for the prediction of the time delay characteristics of turbulence amplifiers. 19 p2389 A73-38075

Time delay statistics of photoelectric emissions - An experimental test of classical radiation theory. 20 p2570 A73-38606

Low power laser-triggered switching at voltages greater than 500 kV. 20 p2572 A73-38801

Application of the averaging method to the study of oscillatory systems with distributed parameters and time lag. 20 p2592 A73-38970

On-off control of an unstable plant with time lag. 20 p2542 A73-39349

Adaptive control of forced motions in discrete external systems with independent search. 20 p2542 A73-39348

Observation of turn-on action in a gate-triggered thyristor using a new microwave technique. 20 p2543 A73-39414

Special periodic solutions and asymptotic properties of a class of quasi-linear differential equations with delayed argument. 20 p2583 A73-39506

Time scanned array radar with time delay or phase gradient for electronic beam steering control by signal. 21 p2652 A73-40669

High resolution beam steering phased array radar antenna design by subarray techniques, using time delay circuit for cost effective driver control simplification. 21 p2653 A73-40672

Application of the method of slipping modulating functions for identification of plants with time lag. 21 p2670 A73-40993

Response delays and the timing of discrete motor responses. 21 p2645 A73-41177

An improved method of triggering oscilloscopes for dynamic-strain measurements. 21 p2704 A73-41267

Refraction of plasma waves in the ionosphere in connection with topside sounding of the ionosphere. 21 p2691 A73-41507

Influence of combustion phenomena on the Pogo effect. 21 p2754 A73-41551

Time-optimal control of a linear plant with time lag. 21 p2671 A73-41607

The accuracy and operational stability of a transistorized time-delay relay with an RC network. 21 p2668 A73-41640

Gravitational radiation detection via computerized delay-dependent coincidence comparisons of squared time derivatives of output powers of Argonne and Maryland cylindrical antenna detectors. 22 p2885 A73-41734

Optimum processing for delay-vector estimation in passive signal arrays. 22 p2825 A73-42198

Radar altimeter signal propagation delay estimation, calculating and plotting noise fluctuation characteristics as function of aircraft ground speed, altitude and other parameters. 22 p2828 A73-43067

Pulsed laser saturation spectroscopy - Observation of power broadening by optical nutations. 22 p2871 A73-43082

Approximation of transfer functions for filters with equalized group-delay characteristics. 23 p2960 A73-43676

L2-stability and L2-instability of linear time-invariant distributed feedback systems perturbed by a small delay in the loop. 23 p2964 A73-43822

Interplanetary radar time delays in different theories of gravitation. 23 p3032 A73-43842

Results of delay-time and Doppler-correction measurements obtained in radar observations of Venus during 1962, 1964, 1969, 1970, and 1972. 23 p3037 A73-44252

Frequency methods for simulation, analysis and identification of multiply-connected dynamic systems with delay. 24 p3074 A73-45097

A criterion for a free choice of decisions involving continuous control systems. 24 p3074 A73-45100

Prefrontal lobe functions and the neocortical commissures in monkeys. 24 p3061 A73-45166

The problem of an iteration method for solving a nonlinear system of partial differential equations given in implicit form with time lag. 24 p3106 A73-45507

TIME LAPSE PHOTOGRAPHY U CHRONOPHOTOGRAPHY TIME MEASUREMENT NT CLOCK PARADOX

Eclipse calculations of lunar features. 01 p0095 A73-10294

Nd glass and ruby lasers in mode locking operation for picosecond light pulses emission, noting pulse duration measurement. 01 p0059 A73-10713

Lunar occultation of stars to determine moon diameter and orbital elements, noting time measurement difficulties due to scintillation effects
01 p0102 A73-10994

Time taken for a laser pulse to make a hole in a metal film.
02 p0176 A73-12114

Paleontological evidence on the earth's rotational history since early Precambrian.
02 p0217 A73-12387

Time and latitude observations of star groups with photographic zenith tube, including random, layer distortion and coordinate errors
03 p0307 A73-13249

Accuracy requirements for an objectivized astrolabe
03 p0307 A73-13250

Determination of systematic errors in time determinations with the passage instrument
03 p0307 A73-13251

Photoelectric measurement of satellite camera shutter opening time delay and photographic plate motion synchronization, calculating root-mean-square error in observation time
03 p0307 A73-13253

Method for calculating the delay in a time-service photoelectric phase apparatus.
04 p0451 A73-16019

Harmonic frames of reference in Einstein's theory of gravitation.
05 p0598 A73-16791

Accurate time and frequency comparisons based on TV frame pulses
06 p0692 A73-17587

Hydrogen maser frequency stability dependence on signal output, magnetic polarization field and relaxation effects, describing automated relaxation rate measurement and atomic line spectrum registration
06 p0699 A73-17588

Ionization-relaxation time measurements upon krypton and xenon in a shock-wave heated plasma
06 p0728 A73-17912

Pulsar timing techniques for planet discovery, interstellar electron density measurement, braking mechanism and neutron star structure investigation and gravitational red shift verification
06 p0750 A73-18008

Time difference measuring instrument for asynchronous and synchronized positive pulses in automatic control system, noting pulse generator and switching, trigger and logic circuits
06 p0677 A73-18384

A new uncomplicated method for the simultaneous determination of various parameters in explosive welding
06 p0698 A73-18446

The influence of recording speed on apexcardiographic timing - A multi-observer study of precision and performance utilizing randomized tracings in multiple subjects.
07 p0785 A73-19932

Analysis of voltage steps with a time resolution of 12 picoseconds
08 p0962 A73-20833

Least squares method for eclipsing binary stars minimum epoch, noting application to artificial and observed light curves
08 p1006 A73-20928

Technique for measuring time-base errors of magnetic instrumentation recorders/reproducers.
08 p0965 A73-21084

Investigation of a single spraying site of a colloid thruster.
08 p0996 A73-21599

Gravitational constant constancy from 1663-1972 earth rotation and 1943-1972 stellar occultations by moon, discussing various time scales used
09 p1079 A73-22948

Digitally implemented clock acquisition loops for low SNR data signals.
09 p1056 A73-23405

Range instrumentation system timing error sources classification and uncertainty reduction for comparison of telemetry inertial guidance data with radar and optical data
09 p1057 A73-23413

Relaxation time measurements by an electronic method.
10 p1217 A73-23998

Application of the characteristics of singular points to the determination of the period of quantization in time
11 p1340 A73-25009

A fast method to determine the nose frequency and minimum group delay of a whistle when the causative spheric is unknown.
11 p1358 A73-26705

Calculation of the average usage time of a channel in an adaptive multichannel communications system
12 p1471 A73-27585

Methods for the comparison and the propagation of time scales
12 p1498 A73-27751

An interpretation of the ambiguity between annual trends obtained by time and latitude observations.
13 p1678 A73-28384

On the comparison of diurnal nutation derived from separate series of latitude and time observations.
13 p1679 A73-28402

Probability density characteristics of elapsed time interval to synchronization disruption in phase locked AFC systems
13 p1584 A73-28890

Airborne clock change from synchronized stationary clock after circumnavigation of earth, discussing directional dependence
13 p1660 A73-28922

Pb 205 as chronometer for s-process nucleosynthesis mechanism, discussing cosmochronology implications and abundance at solidification
13 p1657 A73-28923

Digital circuits test equipment functional principles, considering time, instantaneous voltage and pulse height measurements
14 p1731 A73-29873

Navigation system time dissemination and synchronization, considering timing offset estimation for like events at geographically separated locations and clock characteristics for airborne application
14 p1726 A73-29896

Insensitivity of single particle time domain measurements to laser velocimeter 'Doppler ambiguity.'
15 p1875 A73-31671

Automatic measurement of intervals of shock wave transit across a base section
15 p1876 A73-31862

Differential velocity effects on converging target intersection time estimation accuracy, considering plane conditions and air traffic controller experience
16 p1975 A73-32900

Vibrational relaxation measurements in CO₂ employing an incremental TEA laser gain technique.
16 p2024 A73-33083

Measurement of relaxation time during acceleration of rotation of vessels containing helium II, and superfluidity in pulsars
16 p2038 A73-34065

Pulse time of flight measurements using mode locked laser ranging systems consisting of image converter tubes with deflection plates
17 p2185 A73-35411

Flashlamp pumped CW mode-locked dye laser picosecond light pulse duration measurement by electro-optical streak camera
21 p2694 A73-39946

Holographic method of recording temporal characteristics of optical signals.
21 p2695 A73-39958

Direct determination of universal time based on east-west interferometer observations of radio sources using 5 km radio telescope
21 p2739 A73-40373

Atomic time and frequency standards
21 p2700 A73-40513

Application of long-baseline radio interferometers to astrometric tasks
21 p2701 A73-40726

Errors on the dial of cosmic clocks
21 p2701 A73-40728

Possible scientific utilization of long laser bases
21 p2716 A73-41328

Some characteristics of an operational system for measuring UT 1 using very long baseline interferometry.
21 p2705 A73-41330

An analysis of the altitude dependence of the geomagnetic effect by means of 'equivalent durations.'
21 p2689 A73-41353

Precision comparison of time and frequency by means of TV signals.
22 p2859 A73-42191

Transition probability matrix method for calculating residence times of moving particles in region of space, determining stratosphere residence time against exit to tropopause
22 p2849 A73-42543

Vertical arm reaching movements for various gravitational levels, measuring reach time and angular and lower arm velocities
23 p2948 A73-43218

Total shock-tube working time in the investigation of the discharge through holes in the end face
24 p3076 A73-44755

TIME MEASURING INSTRUMENTS

NT ATOMIC CLOCKS
NT CHRONOMETERS
NT CLOCKS
NT TIMING DEVICES

A digital instrument for measuring amplitude-time parameters of nanosecond-duration pulses
08 p0949 A73-21711

Delay-lock discriminator to measure spatial delay time of noiselike signal received by two spaced antennas
09 p1049 A73-22048

Design principles of digital devices for measuring time intervals /Survey/
12 p1496 A73-27201

Laser transit-time measurements between the earth and the moon with a transportable system.
15 p1873 A73-32265

TIME OF FLIGHT SPECTROMETERS

Speed distribution measurements of N₂ and Ar molecular beams produced by a multichannel source.
06 p0726 A73-18261

Theoretical analysis of a time-of-flight mass spectrometer with spherical electrodes and radial ion paths.
06 p0693 A73-18270

Vacuum sublimation of ammonium perchlorate.
12 p1466 A73-27127

New rate measurements on the reaction of O₃/I, O₃, and OH.
[ALAA PAPER 73-501]
16 p1977 A73-34045

Time of flight spectral measurements of metastable lifetimes in molecular beams with different excited states
24 p3089 A73-44814

A dynamic mass spectrometer for the study of laser-produced plasmas.
24 p3090 A73-44817

TIME OPTIMAL CONTROL

Optimal horizontal guidance law for aircraft in the terminal area.
03 p0340 A73-13518

Discontinuous variational problems in time optimal control of systems describable by ordinary differential equations, deriving Weierstrass optimality conditions
03 p0286 A73-14055

Multichannel communication system in adaptive system with automatic channel selection based on random parameter extremum criterion for maximum usage time of extremal channel
03 p0278 A73-14063

The time optimal control of a class of distributed systems.
04 p0517 A73-15230

An all-regime optimal speed control for a single-shaft jet engine
06 p0741 A73-17721

Switching time dependence on input signal amplitude in self adaptive servosystem with open and closed control loops
06 p0680 A73-18382

Time optimal control for vibrationless starting of electromechanical devices with moving parts, noting linear magnetic circuit
06 p0649 A73-18383

A numerical method for solving optimal control problems with unspecified terminal time.
06 p0681 A73-18520

Investigation of the smoothness characteristics of the Bellman function on the basis of the equation of motion of the system in time-optimal problems. I. Linear case
07 p0806 A73-20633

Time optimal heating of thin plates with constraints placed on the thermal stresses
07 p0923 A73-20634

Two concepts for the reduction of payload attitude slewing times.
09 p1155 A73-23209

[ALAA PAPER 73-290]
On the application of the method of decoupling of motions to the analysis and synthesis of nonlinear systems.
10 p1199 A73-24031

Memory included linear stochastic system optimum control over finite time, using Liapunov-Krasovskii functionals
11 p1398 A73-25618

A time-optimal response inverter.
11 p1308 A73-25981

Control improving variation for optimum speed of response, describing differential equations and vector functions
11 p1342 A73-26078

Synthesis of time-optimal control for linear systems and the minimal-time Lyapunov function.
11 p1342 A73-26225

Quasi time-optimal spacecraft reorientation maneuvers using single gimbal control moment gyros /SG CMG's/.
12 p1548 A73-27153

Fourth order linear differential equations solution for time optimal control synthesis with phase limitations
12 p1483 A73-27403

Linear distributed parameter system minimum time control, considering Hilbert space final value and Banach space inequality solutions
13 p1596 A73-28700

Use of the dynamic programming method for optimization of relay systems
13 p1596 A73-28853

Game problem of the rigid collision of two points with impulsive thrust in a linear central field
13 p1660 A73-29080

The sensitivity of nominally time-optimal control systems to parameter variation.
13 p1597 A73-29567

TIME RESPONSE

Spacecraft single-turn reorientation optimization with respect to fuel expenditure depending on maneuver duration and reaction control torque constraints

14 p1803 A73-29852

Time optimal propulsion system parameters for thrust vector control during spacecraft maneuver performance

14 p1772 A73-29855

Minimum time of Earth-to-Mars and Earth-to-Venus flights with an uncontrolled limited-power engine

14 p1795 A73-29856

Near optimal control laws and controller realization for multilevel feedback and time optimal control design and simulation

14 p1739 A73-30780

Minimum time response control problem of moving point in state space, determining piecewise-continuous vector function for optimal system transfer to coordinate reference point

15 p1931 A73-31231

Study of the smoothness properties of the Bellman function in time-optimal problems, based on the equation of motion of the system. I - The linear case.

15 p1854 A73-31687

Response-optimal heating of thin plates with constraints on the temperature stresses.

15 p1957 A73-31688

Synthesis and analysis of tracking systems with optimal acquisition.

15 p1854 A73-31727

Time optimal control of satellite pitching motions by variable mass distribution, solving nonlinear optimization problem via maximum principle

16 p2072 A73-33233

Time and fuel consumption optimal nutation damping and attitude-angular velocity control of spin-stabilized flight vehicles

16 p2072 A73-33234

Optimal trajectory solution for minimum transfer time in terminal control problem involving locally controllable final point

16 p2032 A73-33306

Computer simulation for time optimal or energy optimal attitude control of spin-stabilized spacecraft.

18 p2360 A73-36837

The sensitivity of optimal flight paths to variations in aircraft and atmospheric parameters.

19 p2386 A73-38051

A dual method for optimal control problems with initial and final boundary constraints.

19 p2446 A73-38376

Spectral analysis and a synthesis of linear systems with variable and random parameters in finite time intervals

20 p2540 A73-38704

Some nonlinear problems in optimal control

20 p2541 A73-38995

An adaptive, time-suboptimal position servomechanism

20 p2511 A73-39664

Study of a method of exponential control of a spacecraft rendezvous

21 p2781 A73-40905

Time-optimal control of a linear plant with time lag

21 p2671 A73-41607

Optimal closed automatic control systems synthesis in terms of minimum integral square error of phase coordinates during transient response time

22 p2836 A73-42609

Synthesis of optimal discrete controls for a continuous plant over a fixed time interval

22 p2837 A73-42619

Utilization of tangential trajectories for lowering high-altitude elliptic orbits of artificial satellites of planets

23 p3027 A73-43265

Synthesis of programmed extensive control of a spatial turning maneuver

23 p3005 A73-43718

Nonlinear regulator theory and an inverse optimal control problem.

23 p2963 A73-43820

On the adaptive control of linear systems using the open-loop-feedback-optimal approach.

23 p2964 A73-43824

Optimal stopping time for stochastic games corresponding to diffusion process, obtaining saddle point characterization via elliptical variational inequality solution

23 p2999 A73-44083

Optimal control over a finite time-interval for discrete systems in the problem of minimizing an inhomogeneous quadratic functional /The case of fixed end-points/.

23 p2965 A73-44331

TIME RESPONSE

ERG late photoreceptor potential components time course in macaque monkey cones and rods, noting pure cone foveal response

03 p0261 A73-13761

Acquisition time evaluation at different input SNR values for pseudonoise signal demodulation, noting common bandwidth detection system advantage

04 p0421 A73-15427

Metal-dielectric-semiconductor junction transistor HF response analysis by digital computer, deriving switching time as function of impurity concentration and electrode voltage

05 p0556 A73-16069

On the analysis of scattering and antenna problems using the singularity expansion technique.

06 p0665 A73-18184

Bandpass error free wideband PCM communications system response to pulse signal

06 p0668 A73-18391

The HR 300 ultrafast photomultiplier with a microchannel plate

06 p0678 A73-18852

Thermal hereditary constitutive law for linear viscoelastic materials time response in transient temperature environment

08 p1018 A73-21409

A linearised theory of parachute opening dynamics.

08 p0928 A73-21692

Photo-optic instrumentation of magnetic flyer plate facility for pressure-time response measurement of impact loaded test specimens, using streak and high speed framing cameras

09 p1083 A73-22512

Airborne atmospheric temperature measurements correction for sensor response lag, deriving numerical scheme based on sensing systems wind tunnel calibration

10 p1217 A73-23991

New criteria for bounded-input-bounded-output and asymptotic stability of nonlinear systems.

10 p1199 A73-24041

Combined effects of noise and vibration on human tracking performance and response time.

11 p1323 A73-25334

A time-optimal response inverter.

11 p1308 A73-25981

Control improving variation for optimum speed of response, describing differential equations and vector functions

11 p1342 A73-26078

Forced guidance and distribution of practice in sequential information processing.

11 p1323 A73-26319

Reduction of the switching time of a liquid-crystal optical transparency.

12 p1498 A73-27514

VHF and microwave surface acoustic wave band-pass filter design with impulse model for frequency response and interdigital transducer input admittance calculation

12 p1484 A73-27563

Signal processing device with parametric interaction between opposite acoustic waves passing through delay line considering real time convolution and time inversion capabilities

12 p1470 A73-27569

Skylink satellite communication service for small dish antenna equipped mobile ground stations, emphasizing necessity of rapid central control response to configuration and propagation condition changes

12 p1471 A73-27660

Effect of laser pulse rise time on heating of a magnetically confined plasma.

15 p1919 A73-31929

Inexpensive fast solid state current drive circuit for injection lasers, using parallel conventional transistor switches operated at avalanche breakdown for pulse generation

16 p2024 A73-33400

Opponent-colors responses in the visually evoked potential in man.

17 p2112 A73-34844

Time-domain analysis of intermodulation effects caused by nonlinear amplifiers.

17 p2136 A73-34868

An integro-differential equation technique for the time-domain analysis of thin wire structures. I - The numerical method.

17 p2246 A73-34892

A simple yet theoretically based time domain model for fluid transmission line systems.

17 p2153 A73-35021

Time domain current interaction coefficients for sheet antenna structures.

17 p2142 A73-35647

A comparison of time- and frequency-domain measurement techniques in antenna theory.

17 p2129 A73-35702

Frequency-time domain stability criterion for nonlinear negative feedback system with linear transfer function, using Zame positive operator theory

17 p2203 A73-35731

A comparative study of two basic approaches to extremum control.

19 p2413 A73-38037

A hybrid fluidic directional gyro.

19 p2430 A73-38055

The domain analysis of intersymbol interference effects on phase shift keyed /PSK/ and quadrature phase shift keyed /QPSK/ communication systems.

20 p2524 A73-38734

Injection-modulation devices as elements of integrated circuits

20 p2534 A73-38851

Ultrahigh-speed unsaturated diode-transistor logic elements with a small logic differential

21 p2660 A73-40000

Interactive effects of intense noise and low-level vibration on tracking performance and response time

21 p2644 A73-41121

Response delays and the timing of discrete motor responses.

21 p2645 A73-41120

Interwire coupling noise and cable resonance equations for fast rise time signal switching at resonance frequencies

22 p2823 A73-41800

Antenna radiation pattern measurement using time-to-frequency transformation /TFT/ techniques.

22 p2831 A73-41840

Synthesis of feedback systems with large plant ignorance for prescribed time domain tolerances.

23 p2962 A73-43282

Certain problems of frequency settling in ideal filters

23 p2959 A73-43515

Apparatus for measurement of vision acuity restoration time after brief macula lutea exposures to light

23 p2949 A73-43799

Frequency to time domain sensitivity matrix for equivalent tolerance field and response error evaluation, using Fourier transform

23 p2955 A73-44110

Opening time of brittle shock-tube diaphragms for dense fluids.

24 p3075 A73-44820

Tunnel diode equivalent circuit analysis based on empirical expressions for composite T-V characteristics, predicting series resistance effect on switching time

24 p3073 A73-45481

TIME SERIES ANALYSIS

Operator remnant power spectral density measurement during compensatory tracking task by serial segments method, noting Fourier coefficient processing

01 p0011 A73-10320

Ground based solar astronomy potential for obtaining photographs with factor of two in resolution and time series, discussing optical performance of vacuum solar telescope

02 p0216 A73-12320

Vector summation dial for analysis of time-nonstationary cyclic biological data, applying to peak time change detection and random walks

03 p0263 A73-14120

Status and prospects of EEG spectral analysis.

04 p0411 A73-15270

Visual time compression. II - Detecting moving targets in dense radar ground clutter.

05 p0550 A73-16715

Sunspots moving magnetic features analysis from longitudinal magnetograms time series and H alpha filtergrams

11 p1422 A73-25934

Traffic analysis by statistical tests for batch model-operated digital computer network design, considering user habits, and interarrival, waiting and partitioning times

12 p1475 A73-27150

An attempt to characterize the 'turbulence burst phenomena' using digital time series analysis.

13 p1604 A73-29260

High-frequency stellar oscillations - The Cerro Tololo search for luminosity-variable white dwarfs.

15 p1935 A73-31482

Meteorological time series persistence tendency representation by autocorrelation coefficients, summation, determining independent values effective number by white noise bandpass filtering

15 p1906 A73-32344

High pass filter and power spectral analysis of periodicity in solar activity time series, applying statistical tests to sunspot and flare indices

16 p2060 A73-32955

Automatic analysis and classification of electroencephalograms

17 p2116 A73-34966

Serial correlation of physiological time series and its significance for a stress analysis

19 p2401 A73-38159

Time sensing and analysis of coastal water dynamic features obtained from aircraft and satellite provided sequential photographic data

20 p2560 A73-39885

Subpicosecond time-resolution image converter - The picochron.

21 p2694 A73-39950

Tape recording, off-line digitalization and time series analysis of dynamic field measurement analog data for computerized power spectral density calculation

22 p2859 A73-42197

Climatic means finite time average estimation standard error calculation by stochastic model with application to long range forecasting

23 p3004 A73-44264

TIME SHARING

- Canadian E.R.T.S. data handling system.
04 p0424 A73-15384
- An improved light gun tracking algorithm based on a recursive digital filter.
21 p2654 A73-40834

TIME SIGNALS

- OMEGA time transmissions and receiver design.
04 p0416 A73-15063
- Unified time recording for aerial photographic surveys, using exact time synchronized control signal sequences in recording camera shutter release
09 p1084 A73-22672
- Automatic recording method for the moments of exact-time radio signals
15 p1878 A73-32143

TIMERS

U TIMING DEVICES

TIMING

U TIME MEASUREMENT

TIMING DEVICES

- Electronic programming timer with crystal oscillator, IC counters and memory core matrix for event sequence radio control during spacecraft or rocket launchings
01 p0020 A73-11167
- Geodetic satellite timing accuracies with Loran C, portable atomic clocks and long baseline interferometry
04 p0446 A73-14807
- OMEGA time transmissions and receiver design.
04 p0416 A73-15063
- Single photon detection and timing - Experiments and techniques.
05 p0576 A73-16603
- Unified time recording for aerial photographic surveys, using exact time synchronized control signal sequences in recording camera shutter release
09 p1084 A73-22672
- Digitally implemented clock acquisition loops for low SNR data signals.
09 p1056 A73-23405
- Range instrumentation system timing error sources classification and uncertainty reduction for comparison of telemetry inertial guidance data with radar and optical data
09 p1057 A73-23413
- Precision low frequency adaptive MOSFET IC electronic oscillators with loose tolerance component timers for cost reduction
12 p1478 A73-27167
- Navigation system time dissemination and synchronization, considering timing offset estimation for like events at geographically separated locations and clock characteristics for airborne application
14 p1726 A73-29896
- A sequential programmer for rocket payloads.
16 p1992 A73-33105

TIN

- Mechanism of transformation of a low-carbon 18-10 stainless steel by reaction in liquid tin
02 p0178 A73-11525
- Sn suppression of Al-Cu-Sn alloy aging at low temperatures, relating to Cu solubility decrease in alpha phase
02 p0179 A73-11599
- Disilicides solubility in silver and tin melts, discussing ternary phase formation
02 p0181 A73-12367
- Hot tinning of aluminum bronze.
11 p1375 A73-26353

TIN ALLOYS

- The effect of tin on the strength and plasticity of titanium at low temperatures.
02 p0181 A73-12212
- Sn alloying effect on heat resistant Ni-Cr alloys plastic strain resistance and strength at room and high temperatures
03 p0327 A73-14003
- Effect of oxygen on the scale resistance of titanium-tin alloys.
06 p0709 A73-18208
- Phase diagrams, microstructure and superconducting properties of thermally diffused Nb-Sn system
12 p1508 A73-26835
- Graphite content effect on vibration damping properties of Al-Sn and Al-Zn alloys
13 p1643 A73-29608
- Moessbauer effect in Nb₃Sn as a function of heat treatment
15 p1922 A73-31180

TIN COMPOUNDS

- NT NIOBIUM STANNIDES
- NT ORGANIC TIN COMPOUNDS
- NT STANNATES
- NT TIN TELLURIDES
- Optical and luminescent properties of CdBr₂-Sn and CdCl₂-Sn single crystals
17 p2219 A73-35553

TIN TELLURIDES

- PbTe-SnTe stripe junction diode lasers, discussing fabrication, electrical properties, and mode characteristics from emission spectra, polarization, mirror illumination and far field pattern measurements
[AD-759093] 09 p1092 A73-22250

Oxidation of powdered germanium, tin and lead tellurides under atmospheric conditions
15 p1887 A73-31594

- Investigation of the design parameters and experimental parameters of medium-temperature thermopiles based on lead, germanium and tin tellurides
17 p2108 A73-34282
- Tunable Pb-Sn-Te junction laser characteristics and fabrication by impurity diffusion for IR CW operation at liquid helium temperatures
21 p2716 A73-40967

TIP DRIVEN ROTORS

- The pressure-jet helicopter propulsion system.
02 p0130 A73-11858

TIP SPEED

- Effect of rotor design tip speed on aerodynamic performance of a model VTOL lift fan under static and crossflow conditions.
[ASME PAPER 73-GT-2] 16 p1963 A73-33480
- Progress in source noise suppression of subsonic tip speed fans.
[AIAA PAPER 73-1032] 24 p3122 A73-44861

TIP VORTICES

- U TIP SPEED
- U VORTICES

TIPS

- NT BLADE TIPS
- NT WING TIPS

TIRES

- NT AIRCRAFT TIRES
- Rubber friction effect on vehicle tire force-slip and breaking behavior in terms of peripheral and sideslip components and structural and operational parameters
03 p0251 A73-13242
- A method for the determination of temperatures in rolling tires
08 p0962 A73-20749
- Analysis of the static deformations of flexible extensible gas-filled shells
15 p1947 A73-31279
- Region of existence of frictional noise and experimental verifications
16 p2036 A73-33215

TIROS M

- Current trends in the refinement of scientific equipment for meteorological satellites
15 p1875 A73-31606

TIROS OPERATIONAL SATELLITE SYSTEM

- Weather satellite capabilities - Present and future.
11 p1429 A73-25149
- Improved Tiros Operational Satellite and future near-polar orbiting environmental system, discussing scanning radiometer and vidicon and automatic picture transmission camera remote sensors
16 p2015 A73-33352

TIROS SATELLITES

- NT ITOS I
- NT TIROS M
- Stratospheric temperature measuring instrument development for Tiros N satellites and ESRO geostationary meteorological satellite development for cloud photography
23 p3004 A73-44103

TISSUES (BIOLOGY)

- NT ENDOTHELIUM
- NT EPITHELIUM
- NT NEUROGLIA
- Effect of increased atmospheric pressure on the dynamics of free oxygen content in animal muscle tissues
01 p0007 A73-10156
- Effects of immersion with the head above water on tissue nitrogen elimination in man.
02 p0135 A73-12563
- Intensity of exercise and heart tissue catecholamine content.
03 p0259 A73-13498
- Experimental determination of shear moduli in a compact bone tissue
03 p0267 A73-13742
- A criterion for oxygen supply optimality in tissues and the capillary circulation rate
03 p0268 A73-13821
- DNA catabolism in rat tissues in response to transverse accelerations
06 p0650 A73-17679
- Possible role of antitissular autoantibodies in the protective mechanism of local shielding during total radiation exposure
06 p0657 A73-17685
- Russian book - Tissue, oxygen in the presence of extremal flight factors.
07 p0780 A73-19425
- A model for the elastic properties of the lung and their effect on expiratory flow.
08 p0934 A73-21502
- Effect of training on enzyme activity and fiber composition of human skeletal muscle.
08 p0935 A73-21508
- Gas dynamic theory of gas exchange in organisms based on oxygen and carbon dioxide permanent partial pressure gradients in tissues, blood and lungs
10 p1181 A73-24523

Effect of excessive glucose administration on the lipid level, glycolysis rates, and oxygen uptake in the tissues of the liver, heart, cerebrum and aorta
11 p1314 A73-25042

Brain tissue functional organization based on models for cell pseudorandom behavior, information processing, learning and memory, considering spontaneous wave and unit firing
11 p1314 A73-25143

Biochemical and morphological studies of lunar material effects on plant tissue culture cells, noting nonpathological increased cellular activity and chloroplast and cytoplasm changes
11 p1320 A73-26482

Response of tobacco tissue cultures growing in contact with lunar fines.
11 p1320 A73-26483

Mammalian tissue response to subcutaneous and intraperitoneal injection of aqueous suspensions of lunar fine material, noting insolubility in tissue and irritant action
11 p1320 A73-26484

Water and salt metabolism in hypokinesia-subjected animals
12 p1462 A73-27704

Study of the relations between various mechanical properties and biochemical composition of bone tissues in man
13 p1577 A73-27996

Analysis of various ultrasonic holographic imaging methods for medical diagnosis.
13 p1615 A73-28589

Protein and nucleic acid contents in animal tissues under hypokinesia
15 p1834 A73-31503

Fatty acids of Pinus eliottii tissues.
15 p1841 A73-32199

Temperature conditions and blood supply of the brain in animals
17 p2111 A73-34229

Responses to graded hypoxia at high and low 2,3-diphosphoglycerate concentrations.
17 p2112 A73-35460

Histopathological and histochemical studies of one year isolation and six months immobilization effects on rhesus monkeys internal organs and tissues
18 p2270 A73-35983

Properties of biological fluids and solids: Mechanics of tissues and organs; Proceedings of the Biomechanics Symposium, Georgia Institute of Technology, Atlanta, Ga., June 20-22, 1973.
18 p2281 A73-36428

Changes in respiration effectiveness during muscular activity
18 p2277 A73-36580

The effects of training on some parameters of hemodynamics and of the oxygen transportation function of the blood during static strains
18 p2277 A73-36581

Continual mechanochemical model of muscular tissue
21 p2643 A73-40182

Advantage or disadvantage of a decrease of blood oxygen affinity for tissue oxygen supply at hypoxia - A theoretical study comparing man and rat.
21 p2641 A73-41620

Urea content variations in blood and tissues during muscular activity in relation to the adaptation level of the organism
22 p2807 A73-42660

Polyparametric information of the electrocardiogram in injured tissue.
22 p2809 A73-42834

A model of heat transfer in a biological tissue perfused by blood of arbitrary temperature.
23 p2948 A73-43292

Spectral emissivity of skin and pericardium.
23 p2950 A73-44213

Influence of histotoxic hypoxia on the activity of lactic dehydrogenase isoenzymes in neurons and neuroglia of various sections of the central nervous system
24 p3058 A73-44429

Activity of acid nucleases in eye tissues under the action of corticosteroidal hormones
24 p3058 A73-44430

Gas chromatography-mass spectrometry study of sterols from Pinus eliottii tissues.
24 p3065 A73-44698

TITAN

Titan atmosphere composition of methane hydrate with ammonia impurity, discussing hydrogen and hydrocarbon production, liquid water existence and greenhouse effects
04 p0497 A73-14973

Titan model arising from observations and methane-rich atmosphere thermodynamics, photochemistry and optical properties, considering origins and volatile content of outer planets satellites
12 p1539 A73-27140

Gaseous ring mechanism of Titan atmosphere, considering atmospheric particle outgassing and recapture under Saturn gravitational field to form torus at Titan orbit
14 p1788 A73-29719

- The escape of H₂ from Titan. 17 p2232 A73-34861
- An upper limit on the 4.9-micron flux from Titan. 18 p2357 A73-37112
- Effect of noble gases on an atmospheric greenhouse [Titan]. 19 p2487 A73-38173
- Titan narrow band observations at 8-13 microns, noting temperature inversion and spectroscopically active component 22 p2905 A73-41770
- A first look at atmospheric dynamics and temperature variations on Titan. 24 p3128 A73-44433
- Titan molecular hydrogen greenhouse effect responsibility for IR temperature disagreement with atmosphere equilibrium temperature from analysis of nonray radiative and gray convective equilibrium 24 p3129 A73-44450
- Disk integrated polarization observation for Titan at small phase angles, noting optically thin Rayleigh atmosphere on opaque cloud deck 24 p3130 A73-44451
- Titan satellite optical polarization observation in three spectral regions, noting inconsistency with scattering from planetary surface or pure molecular atmosphere 24 p3130 A73-44452
- Greenhouse effect for Titanian atmospheric models with different methane, hydrogen, helium and ammonia proportions, deriving brightness temperature spectrum and surface pressure 24 p3130 A73-44457
- ### TITAN LAUNCH VEHICLES
- #### NT TITAN 3 LAUNCH VEHICLE
- #### TITAN 3 LAUNCH VEHICLE
- Titan III convective base heating from solid rocket motor exhaust plumes. 03 p0382 A73-13467
- Titan III-C guidance with the Carousel VB inertial guidance system. 06 p0721 A73-18826
- Short guide to Titan III launch vehicles. 08 p1014 A73-20800
- Titan/Centaur launch vehicle for high payload escape missions and large synchronous orbit spacecraft, describing propulsion, control/guidance and telemetry systems [AIAA PAPER 73-617] 18 p2359 A73-36094
- Navigation of the Titan IIIC space launch vehicle using the Carousel VB IMU. [AIAA PAPER 73-905] 20 p2589 A73-38839
- ### TITANATES
- #### NT BARIUM TITANATES
- #### NT ILMENITE
- #### NT LEAD TITANATES
- #### NT MAGNESIUM TITANATES
- #### NT PEROVSKITES
- #### NT ZIRCONIUM TITANATES
- Electro-optical contrast observations in single-domain epitaxial films of bismuth titanate. 06 p0739 A73-18748
- Ion distribution in the crystal structure of complex spinel phases of the Mn-Fe-Ti-O system 11 p1386 A73-26674
- Apollo 17 basalt ortho- and para-armalcolite, noting differences in optical properties, crystal habit and distribution between coarse and fine grained rocks 14 p1789 A73-29739
- Selection and preliminary evaluation of three structures as potential solid conductors of alkali ions - Two hollandites, a titanate, and a tungstate. 17 p2219 A73-35325
- Spacecraft thermal control coatings development, discussing zinc orthotitanate/silicone properties as solar reflector [ASME PAPER 73-ENAS-7] 19 p2389 A73-37969
- ### TITANIUM
- The Bauschinger effect in annealed and irradiated titanium 01 p0064 A73-10495
- Hydrogenation as a means of utilization of industrial titanium scrap. 01 p0065 A73-10821
- The influence of oxygen concentration on the internal stress and dislocation arrangements in alpha titanium. 02 p0184 A73-12768
- Access to uncombined titanium through an inhibiting film in sublimation pumping of deuterium. 02 p0194 A73-12844
- Titanium powder properties, production, alloying, costs and hardware fabrication by pressing, casting, molding, coining and forging 03 p0322 A73-13263
- Mechanical properties of pressed and sintered titanium powder. 03 p0322 A73-13264
- Covalent bond formation role in Ti strengthening by oxygen from evidence of alpha phase stabilization, ordered structures, abnormal resistivity and high activation energy 03 p0323 A73-13371
- Semihydrostatic hot extrusion for Ti plated Cu anode bar, noting metal bonding and current distribution 03 p0312 A73-13583
- Effects of the state of the surface and of titanium films on the dislocation structure of surface layers in molybdenum single crystals 03 p0326 A73-13969
- Metallurgical, chemical and electrochemical production and refining of refractory metals, including titanium, fluorotitanates and artificial rutile 04 p0465 A73-15660
- The reactions of titanium and silicon with Al₂O₃-CaO-CaF₂ slags in the ESR process. 04 p0455 A73-15744
- Nonstoichiometric yttria crucibles for cold wall Ti melting, noting single batches, cost reduction and alloy homogeneity 04 p0455 A73-15749
- Influence of condensation temperature on microstructure and tensile properties of titanium sheet produced by high-rate physical vapor deposition process. 06 p0711 A73-18752
- Crystal-field effects of iron and titanium in selected grains of Apollo 12, 14, and 15 rocks, glasses, and fine fractions. 07 p0881 A73-19710
- Crack corrosion of titanium in a solution of hot concentrated magnesium chloride 07 p0839 A73-20167
- Lattice dynamics, third-order elastic constants, and thermal expansion of titanium. 07 p0839 A73-20173
- Sliding friction welding of nonferrous Cu, wrought Al alloy and Ti, resting rubbing speed and axial pressure effects on equilibrium condition transition 08 p0973 A73-21238
- Characteristics of elastic anisotropy and the textural development of sheet titanium 09 p1099 A73-21968
- Texture and anisotropy of the thermal emf of sheet titanium 09 p1099 A73-21969
- Determination of hydrogen permeation parameters in alpha titanium using the mass spectrometer. 09 p1102 A73-22412
- Investigation of the compatibility of boron fibers with tungsten substrates and titanium matrices 09 p1103 A73-22469
- Experiment on the mechanical anisotropy of titanium, zirconium, and Zircaloy-2 rolled sheets. 09 p1104 A73-22521
- Deep drawability of titanium sheets. 09 p1104 A73-22522
- Brittle fracture tests of Ti-Cr steels with/without nitrogen hardened layer under shock impact loads 09 p1107 A73-23199
- Physical characteristics of sponge titanium of a hardness below 100 HB units, obtained by heat treatment with magnesium 09 p1107 A73-23227
- Creep and creep-rupture-strength of titanium strengthened by molybdenum fibers 10 p1233 A73-24356
- The effect of carbon and titanium on the hot workability of 25Cr-6Ni stainless steels. 10 p1235 A73-24440
- Microscopic, kinetic and microhardness observations of Ti-W metal matrix composite solid state interface reactions, showing enhanced shear resistance 11 p1384 A73-26049
- Investigation of diffused titanium coatings on refractory metals 13 p1630 A73-28015
- An empirical analysis of titanium stress-strain curves. 13 p1632 A73-28133
- Effect of titanium additions on the aging characteristics of an Al-Zn-Mg alloy. 13 p1632 A73-28134
- Access to uncombined titanium through an inhibiting film in sublimation pumping of deuterium. 13 p1581 A73-28929
- Titanium flow curves in octahedral coordinates for various conditions of deformation 13 p1636 A73-29132
- Factors controlling the corrosion behavior of titanium and titanium-nickel alloys in saline solutions. [NACE PAPER 64] 13 p1637 A73-29311
- Monotonic and cyclic prestrain influence on alpha-Ti fatigue life, suggesting twin/grain boundary dislocation interactions 13 p1640 A73-29486
- Mechanical properties of titanium reinforced with unidirectional molybdenum wires. 13 p1643 A73-29604
- Bauschinger effect in annealed and irradiated titanium. 14 p1759 A73-30320
- German monograph - The effect of interstitial elements and recrystallization on the defined yield point of titanium. 14 p1762 A73-30665
- Some plastic deformation laws for titanium under static and alternating loads 14 p1763 A73-30723
- Titanium and zirconium alpha-omega transformation hysteresis at room temperature from dilatometry X ray phase analysis and electrical resistance and shear measurements 14 p1764 A73-30856
- Compatibility of silicon carbide fiber with a tungsten base and a titanium matrix 15 p1888 A73-31595
- Twin-jet thinning techniques for transmission electron microscopy observation of tantalum and niobium. 15 p1891 A73-31995
- Russian book - Titanium - The new structural material. 15 p1893 A73-32512
- Phase and structural changes in titanium under impulsive loads 15 p1894 A73-32530
- Durability of bonded titanium joints increased by new process treatments. 16 p2017 A73-330525
- Titanium casting technology applications to aircraft structures, considering flap tracks, brake torque tubes and arrestor hook mounting brackets 16 p2018 A73-330717
- Workhardening, slip band formation and crack initiation during fatigue of titanium. 17 p1990 A73-348823
- Study of fretting wear in titanium, Monel-400, and cobalt-25 percent molybdenum using scanning electron microscopy. [ASLE PREPRINT 73AM-8A-3] 17 p1990 A73-34993
- CH-53D titanium main rotor blade, describing spar, fiberglass cover and honeycomb core, fabrication methods, ground and flight tests and vibrational characteristics [AHS PREPRINT 783] 17 p2106 A73-35096
- Filament orientation effect on Al and Ti matrix composite tensile properties, using boron, borosic and silicon carbide fibers 17 p2192 A73-35533
- Effect of oxides on certain properties of glass-ceramic coatings for titanium 18 p2319 A73-35889
- Application of a microanalyzer to the investigation of the interaction between titanium and coatings 18 p2323 A73-35894
- Effects of interstitial content and grain size on the strength of titanium at low temperatures. 19 p2440 A73-37542
- Procedure for preparation of metallic titanium by direct reduction of oxides under flux 19 p2441 A73-37829
- Welded titanium tubes and their applications 19 p2433 A73-37834
- Influence of hydrogen and oxygen on the mechanical behavior of unalloyed titanium 19 p2441 A73-37837
- Some details concerning plastic deformation mechanism of commercial titanium between -100 and 400 C 19 p2441 A73-37839
- Study of the phenomenon of stress relaxation of titanium in the case of titanium 19 p2442 A73-37840
- Titanium cathode blanks in electrolytic production of metals, noting titanium oxide nonstick properties, electron transmission and corrosion resistance 19 p2442 A73-37841
- Grain refinement by titanium in the unidirectionally solidified aluminum alloys. 19 p2442 A73-37945
- Oxidation of titanium between 25 C and 400 C. 19 p2442 A73-37950
- Titanium Stressskin panel fabrication and assembly, discussing forming, cutting, thermal processing, welding and applications [SME PAPER MF 73-158] 19 p2437 A73-38502
- Cleavage fracture in alpha phase Ti, considering embrittling species effects on electronic band structure 20 p2578 A73-39490
- Texture and anisotropy of the properties of titanium sheet 21 p2719 A73-40852
- Diffusion parameters of oxygen in alpha and beta titanium modifications 22 p2874 A73-42098
- Some thermophysical properties of titanium in the neighborhood of the melting point. 22 p2878 A73-42508
- Structure and properties of arc-sprayed titanium coatings. 22 p2879 A73-42597
- Orientation dependent slip in polycrystalline titanium. 23 p2993 A73-44028
- Field electron emission microscopic study of titanium 24 p3098 A73-44474
- Hot closed-die forging of powder titanium 24 p3093 A73-44739

TITANIUM ALLOYS

NT NITINOL ALLOYS

The effect of oxide thickness on the hot salt stress corrosion susceptibility of Ti-6Al-4V.

01 p0061 A73-10137

Influence of metallurgical factors on the corrosion cracking under tension of TA6V titanium alloy in an aqueous medium at ambient temperature [ONERA, TP NO. 1100]

01 p0061 A73-10231

Potential titanium airframe applications.

01 p0063 A73-10285

Processing conditions and sample dimensions and shapes effects on Ti alloy creep characteristics at room temperature

01 p0064 A73-10487

A sintered Nb-Ti-Zr alloy.

01 p0065 A73-10822

Ti-V and Ti-Nb alloys mechanical strength and stress concentration resistance at low temperatures

01 p0067 A73-11348

Effect of temperature and polarization rate on the electrochemical behavior of titanium alloys in a sulfuric medium

02 p0178 A73-11523

Random stresses effect on dynamic creep properties of Ti alloy in high temperature air flow

02 p0180 A73-11625

Ti-Al-V alloys as differential measurement method for metallurgical processing and microstructure effects on superconducting critical temperature and magnetic permeability/susceptibility

02 p0200 A73-11843

AC studies of a superconducting Nb-52 at. % Ti alloy.

02 p0200 A73-11844

Influence of cyclic heating on the mechanical fatigue of titanium alloys and their weld joints

02 p0180 A73-11933

Low-temperature mechanical properties of the alloys AT3 and AT6.

02 p0180 A73-12136

The effect of tin on the strength and plasticity of titanium at low temperatures.

02 p0181 A73-12212

Cooling modes effect on heat treated Ti-Nb alloys as function of Nb content, investigating alpha prime and double prime martensites

02 p0181 A73-12500

Microstructure and phase relations for Ti-Mo-Al alloys.

02 p0182 A73-12751

The high temperature thermodynamic properties of Ni-Ti alloys.

02 p0182 A73-12753

Hydrogen reactions and detection by line broadening in beta transformed Ti-Al-V alloy, using X ray diffraction analysis

02 p0183 A73-12759

High-temperature oxidation of a Ti-15Mo-5Zr alloy at low pressure of oxygen /40 microrr to roughly 0.2 millitorr/.

03 p0321 A73-12918

Effects of alloying elements on the solubility of hydrogen in beta titanium.

03 p0321 A73-12920

A study of environmental degradation of adhesive bonded titanium structures in Army helicopters.

03 p0332 A73-13039

Mechanical properties of Fe, Al, Ti and heat resistant alloys consolidated powders, establishing coupling between fundamental concepts and engineering application

03 p0322 A73-13261

Effects of hot-salt stress corrosion on titanium alloys.

03 p0323 A73-13268

Strengthening and stabilization effects of alloying elements in metastable Ti beta-alloys as function of atom concentration and position in periodic system

03 p0324 A73-13511

Influence of microstructure on the corrosion behavior of Ti-2% Ni in hot acidic chloride solutions with particular reference to weld regions.

03 p0325 A73-13730

Martensitic transformation kinetics and martensite morphology in the N25Kt2 alloy after aging

03 p0325 A73-13826

Phase transformations in the VT9 quenched titanium alloy during heating

03 p0327 A73-13974

Stacking faults in alpha titanium alloys

03 p0327 A73-13977

Low-cycle fatigue of titanium alloys.

03 p0327 A73-14007

Flat Ti alloy sheet creep under variable loads at 300-400 C comparing prediction with test data

03 p0328 A73-14016

Influence of the pinning forces for flux lines on the critical current density in magnetic fields of up to 10 Tesla in superconducting titanium-niobium alloys

03 p0328 A73-14654

Fatigue threshold crack propagation in air and dry argon for a Ti6Al-4V alloy.

04 p0459 A73-14685

High speed tool steel, Ti alloys and vanadium carbide products manufacturing by powder metallurgy, using vacuum and high pressure techniques

04 p0460 A73-14745

Surface effects during fretting fatigue of Ti-6Al-4V.

04 p0461 A73-14998

Study by autoradiography at high resolution power of the role of hydrogen in the mechanism of cracking of TA6V titanium alloy in salt water

04 p0461 A73-15097

Nondestructive detection of hydrides and alpha-case in titanium alloys.

04 p0461 A73-15217

Critical thickness effect of fatigue notched specimens on stress intensity factor and fracture toughness behavior of Ti-Al-V alloys

04 p0462 A73-15244

Characteristics of the ingot crystallization process under conditions of melting in vacuum furnaces with a consumable electrode, and the stability of the cast structure in alloys of the Nb-Ti system

04 p0464 A73-15496

Optimal temperature and strain rate for deformation in superplastic state for alpha-beta Ti alloy

04 p0464 A73-15498

Influence of hydrogen on the technological plasticity of the alloy Ti + 9% Al

04 p0464 A73-15499

Precipitation hardening effect on Co-Ni-Ti alloys stress-strain, grain size and strain resistance behavior in micro- and macrodeformation yield point region

04 p0465 A73-15639

Temperature dependence of the elastic micro- and macro-stiffness of dispersion hardenable Co-Ni-Ti and Co-Ni-Ti-Al alloys. II

04 p0465 A73-15640

Study of transformations of TA6V6E2 titanium alloy with 6.4 per cent zirconium, in isothermal conditions after putting in solution in the beta domain

04 p0466 A73-15691

Study of nitriding by ion bombardment of titanium and titanium alloys

04 p0457 A73-15955

Nondestructive eddy current tests of Al braze alloy fillet size and flatwise distribution in Ti honeycomb sandwich panels

05 p0581 A73-16131

X-ray elastic constants of titanium and TiAl6V4

05 p0588 A73-17242

Material deformations determined with the aid of X rays in the case of elongations remaining after a uniaxial tensile test involving titanium and TiAl6V4

05 p0588 A73-17243

Fractographic aspects of the stress corrosion cracking of titanium in a methanol/HCl mixture.

06 p0705 A73-17800

Investigation of precipitation morphology in Cu-Ti alloys

06 p0707 A73-18037

Heat resistance of alloys of the compound TiAl with niobium at 800 and 1000 C

06 p0708 A73-18049

Martensite transformation in an aged Fe-Ni-Ti alloy

06 p0708 A73-18052

Adhesively bonded multilayer Al and Ti alloy sheet metals for complex airframe components, discussing design, fabrication, tests and performance comparison with monolithic structures

06 p0698 A73-18094

Structure and composition of certain Laves phases and identification of chi phases in Fe-Mn-Ti alloys

06 p0708 A73-18100

Field-ion microscopic investigation of the microstructure of deformable superconducting niobium-based alloys

06 p0736 A73-18115

Surface layer grain boundary corrosion damage of Ti alloys during vacuum annealing, reducing rupture strength, vibration resistance and bending fatigue limit

06 p0698 A73-18205

The mechanical properties of titanium alloys with isomorphous beta-stabilizing elements.

06 p0708 A73-18206

The martensitic transformation during deformation of titanium alloys with metastable beta phase.

06 p0708 A73-18207

Effect of oxygen on the scale resistance of titanium alloys.

06 p0709 A73-18208

Susceptibility to brittle fracture of simulated weld seams in Ti-Al-V alloys.

06 p0698 A73-18209

Diffusion in the titanium-aluminum system. I - Interdiffusion between solid Al and Ti or Ti-Al alloys.

06 p0709 A73-18332

Diffusion in the titanium-aluminum system. II - Interdiffusion in the composition range between 25 and 100 at.% Ti.

06 p0709 A73-18333

Diffusion of hydrogen in titanium alloys due to composition, temperature, and stress gradients.

06 p0712 A73-18764

Environmental hydrogen embrittlement of an alpha-beta titanium alloy - Effect of hydrogen pressure.

06 p0713 A73-18769

The casting of titanium and its alloys by the lost-model method

07 p0831 A73-20161

Hole preparation in titanium and high strength steels.

[SME PAPER IQ 72-208]

07 p0832 A73-20450

Fractographic investigation of the resistance to fracture of aluminum and titanium alloys

07 p0840 A73-20505

Creep-rupture strength of OT4 alloy

07 p0840 A73-20511

Welding airframe structures in titanium alloys using tensile loading as a means of overcoming distortion.

08 p0973 A73-21240

The creep strength of 17 Cr-11 Ni-2.5 Mo austenitic steel stabilised by titanium.

08 p0982 A73-21792

Young modulus anomaly in precipitation-hardening subjected Invars

09 p1099 A73-21962

Thermal-activation parameters of plastic deformation in alpha-titanium single crystals

09 p1099 A73-21964

Electron microscopic determination of orientation relationship and habit plane for Ti-Cu martensite.

09 p1101 A73-22406

Recrystallization in Ti-15 Mo base beta titanium alloys.

09 p1103 A73-22423

Microstructural control of Ti-6Al-4V forgings.

09 p1088 A73-22495

Ni-Ti alloy aging effects on yield strength explained by internal strain due to lattice modulation and Ti rich region volume fraction

09 p1103 A73-22520

Influence of environment on the appearance of fatigue striations in various alloys

09 p1104 A73-22716

Titanium alloys corrosion resistance modification relative to nonoxidizing acid media by hydrogen reduction conditions or anodic dissociation curve alteration

09 p1104 A73-22965

Improvement of the friction and wear behavior of T-A6V alloy by a new anodic oxidation treatment

09 p1104 A73-22966

Comparison of the fracture strength K_{1s} of aluminum /AK4-1T1, V95T1, and D16T/ and titanium /VT8 and VT9/ alloys under static and cyclic loads.

09 p1105 A73-23054

Ti based beta alloy strain hardening and failure characteristics, emphasizing initial deformation phase and microdefect onset and development

09 p1105 A73-23064

The effect of the structure of the titanium alloys VT3-1 and VT-18 on their fatigue resistance under asymmetrical cyclic loading.

09 p1106 A73-23164

Mechanisms of stress corrosion cracking of titanium-aluminum alloys in methanol-HCl solutions.

09 p1106 A73-23166

Galvanic interaction between active and passive titanium.

09 p1106 A73-23167

Influence of heat treatment on the mechanical properties of the VT3-1 titanium alloy

09 p1107 A73-23191

Recrystallization of the IVT-1 beta titanium alloy

09 p1107 A73-23192

Temperature dependence of conditions for static, quasi-static and fatigue failure of titanium alloys

09 p1107 A73-23193

Application of the Moessbauer effect to the study of the mechanism of iron diffusion in beta-titanium

09 p1108 A73-23240

Hot die forging /gatorizing/ technique for Ti and heat resistant alloys jet engine parts, emphasizing material and cost savings

09 p1089 A73-23295

Metallurgical investigations of phase equilibria in the titanium-niobium-germanium ternary system

10 p1231 A73-23692

Overview of corrosion cracking of titanium alloys.

10 p1232 A73-23873

Investigation of the morphology and decomposition kinetics of Co-Ni-Ti alloys

10 p1232 A73-24153

Hot deformation of metal ceramic titanium preforms

10 p1225 A73-24321

Damping properties of VT3-1, VT-9, and VT-18 titanium alloys of various microstructure

10 p1233 A73-24359

Influence of notch and thread rolling on the fatigue strength of samples prepared from VT3-1 and VT16 alloys

10 p1233 A73-24370

Study of the effectiveness of various thermomechanical methods of hardening alpha + beta titanium alloys

10 p1234 A73-24425

Subcritical crack growth measurement during static loading of precracked Ti alloys in salt water, discussing arrested crack propagation at different stress intensities

10 p1234 A73-24429

TITANIUM ALLOYS

Calculation of the elastic anisotropy of Ti-6Al-4V alloy sheet from pole figure data.

10 p1234 A73-24431

An electron microscopy study of precipitation in Cu-Ti sideband alloys.

10 p1234 A73-24434

Importance of slip mode for dispersion-hardened beta-titanium alloys.

10 p1235 A73-24441

Influence of pressure on VT14 alloy wear and friction against 30KhGSA steel

10 p1226 A73-24797

Electron fractography of fatigue failure and macrocrack propagation in dual phase Ti alloy during cyclic loading at minus 140 to plus 150 C

10 p1236 A73-24931

Cumulative damage theories for the prediction of life in the case of vibrational stresses. I - A critical overview

11 p1441 A73-25576

Corrosion fatigue and stress corrosion crack growth in high strength aluminum alloys, magnesium alloys, and titanium alloys exposed to aqueous solutions.

11 p1381 A73-25815

The kinetic and dynamic aspects of corrosion fatigue in a gaseous hydrogen environment.

11 p1382 A73-25817

Fretting fatigue in titanium helicopter components.

11 p1383 A73-25837

Ti alloy coating and surface treatment to prolong fatigue life by eliminating fretting damage, discussing design parameters selection, screening and strength tests and performance evaluation

11 p1383 A73-25838

Reactivity and interface characteristics of titanium-alumina composites.

11 p1384 A73-26043

The effect of an addition of molybdenum on the quenched and aged structure of a Ti-1 wt % Si alloy.

11 p1384 A73-26048

Heat treatment effects on the mechanical properties in Ti-6Al-6V-2Sn.

11 p1385 A73-26172

Cracking of Ti-6Al-4V in methanol solutions containing sulfates.

11 p1385 A73-26175

Localized hydrogen in titanium welds.

11 p1375 A73-26358

Relaxation processes in metastable beta titanium alloys.

11 p1385 A73-26498

Investigation with an electron microscope of the structure of wires prepared from the 60T superconducting alloy

12 p1509 A73-26841

Russian papers on nonferrous metals and alloys metallurgy covering phase equilibria, strengthening, deformation and processing of Al, Mg, Cu and Ti alloys

12 p1510 A73-26902

The nature of the nonuniformity of the structure and properties of semiproductions pressed from titanium and its alpha-alloys

12 p1502 A73-26909

Fracture characteristics of thermally strengthened titanium beta-alloys

12 p1510 A73-26914

Precipitation and its hardening effect in Ni-rich NiTi.

12 p1511 A73-27057

Yield point phenomenon in Al-Ti alloy.

12 p1511 A73-27060

Dissolution of Ti-6Al-4V at cathodic potentials in SN HCL

12 p1512 A73-27249

Investigation of adhesion and diffusional interaction of instrumental materials with titanium alloys

12 p1502 A73-27466

Indenter materials for use in high-temperature hardness measurements

12 p1513 A73-27561

Cermet cathode materials for electric vacuum equipment

12 p1503 A73-27562

The strength differential of steel and Ti alloys as influenced by test temperature and microstructure.

12 p1513 A73-27681

Ti-Al-Sn alloy microstructure effects on low temperature creep, discussing creep stresses, activation energy and yield stress

13 p1632 A73-28127

Stress-corrosion cracking of Ti-8Al-1Mo-IV in aqueous environments. I - The kinetics of subcritical crack propagation. II - Plastic zones, crack morphology, and fractography.

13 p1632 A73-28135

Transverse creep and stress-rupture of Borsic-aluminum composites and Borsic-aluminum composites containing stainless steel and titanium.

13 p1633 A73-28143

Ti-Pd phase diagram eutectoid region configuration determination through alloy thin foil arc melting preparation and microstructure examination by electron microscopy

13 p1633 A73-28146

Dynamic strain ageing in some titanium-silicon alloys.

13 p1634 A73-28184

Influence of niobium on the magnetic properties of high-titanium Al-Ni-Co alloys - Second communication.

13 p1637 A73-29244

Factors controlling the corrosion behavior of titanium and titanium-nickel alloys in saline solutions.

[NACE PAPER 64] 13 p1637 A73-29311

Mechanical behavior of high-strength beta-titanium alloys.

13 p1638 A73-29456

The effect of microstructure on fatigue crack propagation in Ti-6Al-6V-2Sn alloy.

13 p1640 A73-29484

Al and Ti alloy corrosion and fretting fatigue in aqueous environment, noting protective oxide surface film effects

13 p1642 A73-29524

Strain curves of titanium alloys VT-6S and VT-14 in the temperature range 20-400 C.

13 p1643 A73-29612

Creep and fracture in OT-4 titanium alloy at temperatures from 400 to 550 C.

13 p1643 A73-29627

Energy dissipation in metals in high-frequency fatigue tests. II.

13 p1643 A73-29631

Mechanical strength of titanium alloys AT-2 and AT-3 and of their welded seams at extreme temperatures.

13 p1643 A73-29633

Properties and structure of Ti-Nb-base superconducting alloys

13 p1643 A73-29644

Processing conditions and sample dimensions and shapes effects on Ti alloy creep characteristics at room temperature

14 p1759 A73-30312

Alpha phase decomposition and precipitation measurement in titanium rich Ti-Al alloys by electrical resistivity and microscopic methods

14 p1761 A73-30638

Solute aluminum strengthening and strain aging in Ti-Al alloys at 78-810 K

14 p1761 A73-30639

German monograph - The effect of germanium additions on the superconductor characteristics and the transition processes in technical titanium-niobium alloys.

14 p1762 A73-30666

German monograph - Effect of the transformation and heat treatment conditions on the mechanical properties and the creep characteristics of the alloy TiAl6V4.

14 p1762 A73-30668

Fatigue failure of a two-phase titanium alloy in vacuum

14 p1763 A73-30713

Superconductivity and electron structures of a solid solution of titanium in niobium

14 p1784 A73-30811

Influence of alpha- and beta-stabilizers on the plastic deformation mechanism of titanium

14 p1765 A73-30888

Influence of hydrogen on the failure of the VT3-1 titanium alloy in programmed cyclic loading

15 p1886 A73-31035

Specific heat of alloys of the niobium-titanium system near the superconducting transition temperature

15 p1886 A73-31184

Temperature dependence of the electrical resistance of superconducting Ti-Nb and Ti-Nb-Zr alloys subjected to working by hydrostatic pressure

15 p1887 A73-31186

Investigation of some physicochemical and X-ray structural changes in a superconducting wire prepared from 60T alloy, as a function of the strain level and duration of annealing in vacuum

15 p1887 A73-31187

Properties of the superconducting alloy 3SBT

15 p1887 A73-31188

Oxygen in titanium alloyed with aluminum and zirconium

15 p1889 A73-31812

Investigation of titanium alloys containing refractory elements

15 p1889 A73-31813

High strength Ti alloy cracking and brittle fracture prevention during aging by high heat rate treatment at 250-500 C

15 p1889 A73-31814

Gas saturated surface layer effect on Ti alloy resistance to static cyclic tensile loads, noting increased fatigue strength after etching

15 p1890 A73-31815

Comparison of R-curves determined from different specimen types.

15 p1951 A73-31988

The reaction of a titanium alloy with hydrogen gas at low temperatures.

15 p1890 A73-31993

High temperature specific heats of iron-rich iron-titanium alloys between 600 and 1150 K.

15 p1891 A73-31994

Scanning electron microscope analysis of Ti-Al-V specimens under simultaneous fatigue and fretting loads

15 p1883 A73-32148

Transage 129 Ti-Al-V-Sn-Zr alloy fabrication cold reduction through good cold formability and weldability with weight saving due to high strength and fatigue resistance

15 p1891 A73-32172

Study of the isothermal transformations of the titanium alloy beta sub III

15 p1892 A73-32257

A physical basis for solid-solution strengthening and phase stability in alloys of titanium.

15 p1892 A73-32274

Al addition effect on strength of Ti via short range order, considering strengthening by alpha stabilizing solutes

15 p1893 A73-32278

Russian book - Titanium - The new structural material.

15 p1893 A73-32512

Critical survey of studies of the equilibrium phase diagram of the Ti-W system

15 p1893 A73-32513

Investigation of the phase equilibrium of ternary Ti-Al-Nb system alloys

15 p1893 A73-32514

Critical survey of studies of phase diagrams in the titanium-oxygen system in connection with the formation of suboxides

15 p1893 A73-32515

Effect of ordering on the properties of oxygen solid solutions in titanium

15 p1893 A73-32516

Phase transformations in alloys of the titanium-molybdenum system

15 p1893 A73-32517

Transformations during heat treatment of Ti-Mo system alloys with additions of aluminum, zirconium, and tin

15 p1893 A73-32518

Structure and decay characteristics of unstable beta-solid solutions of the Ti-V system

15 p1893 A73-32519

Diffusional and nondiffusional metastable-phase transformations in titanium alpha + beta alloys

15 p1893 A73-32520

Characteristics of the distribution of elements in the diffusive layers of titanium-based three-component systems

15 p1893 A73-32521

Structural transformations in two-phase titanium alloys

15 p1893 A73-32522

Phase transformations during heat treatment of the VT18 alloy

15 p1894 A73-32524

Influence of heating rate on the phase composition of the VT3-1 alloy

15 p1894 A73-32525

Influence of plastic deformation and of alloying with small additions of oxygen on the decomposition of the metastable beta phase in the TS6 alloy

15 p1894 A73-32526

Effect of temperature on titanium plasticity

15 p1894 A73-32527

Properties of the 4201 alloy at elevated temperatures

15 p1894 A73-32528

Failure retardation mechanism in plastic titanium alloys

15 p1894 A73-32529

Investigation of the influence of certain elements on the heat resistance of titanium aluminide Ti3Al

15 p1894 A73-32530

Influence of plastic deformation and of phase transformations at negative temperatures on the properties of titanium alloys

15 p1894 A73-32531

Features of the influence of aluminum on the mechanical properties of titanium

15 p1894 A73-32532

Influence of structure and of stress concentration on the mechanical properties of Ti-Ta-Mo system alloys

15 p1894 A73-32533

Properties of titanium-niobium based stable beta alloys

15 p1894 A73-32534

Investigation of friction behavior in titanium alloy with 3.8% Al

15 p1894 A73-32535

Characteristics of failure in alpha-titanium alloys at high temperatures

15 p1894 A73-32536

Oxidizability of the IVT1 beta titanium alloy and its protection from gaseous corrosion

15 p1894 A73-32537

Oxidizability of AN-type beta titanium alloys and their protection from gaseous corrosion

15 p1894 A73-32538

- Oxidation of OT4 and OT4-1 alloys in the process of prolonged heating in air at temperatures from 200 to 400 deg 15 p1894 A73-32539
- Certain systematic errors in determining parameters of oxygen diffusion in alpha titanium 15 p1894 A73-32540
- Investigation of titanium alloys at high temperatures in vacuum 15 p1894 A73-32541
- Investigation of the structure and corrosion behavior of alloys of the Ti-Ta-Cr system 15 p1895 A73-32542
- Investigation of corrosion stability in alloys of the Ti-Ta-Nb system 15 p1895 A73-32543
- The passivation behaviour of the Ti-6Al-4V alloy. 15 p1895 A73-32567
- Passive alpha structure Ti base alloys with Al, Mn, Sn, Nb, Cr or Mo, investigating dissolution characteristics by chronoamperometric measurement using sulfuric acid 15 p1895 A73-32568
- Investigations of the electrochemical processes in titanium alloys as applied to stress-corrosion crack tip state in sea water. 15 p1896 A73-32572
- Stress corrosion cracking of titanium alloys in hydrogen chloride. 15 p1896 A73-32573
- Effect of thermomechanical treatment on the stress corrosion cracking of metastable beta III titanium. 15 p1896 A73-32574
- Low temperature deformation of commercial Ti alloys. 16 p2024 A73-32848
- Hot isostatic pressing of titanium alloys for turbine engine components. 16 p2019 A73-33516
- [ASME PAPER 73-GT-63] Phase composition and properties of metastable alloys of titanium with nickel 16 p2027 A73-34072
- The martensite composition in quenched alloys of the Ti-Mo system 17 p2187 A73-34374
- Anodic oxidation and stress corrosion cracking /SCC/ of titanium alloys. I - Factors affecting SCC and their influence on the anodic behavior of alloy Ti-6Al-6V-2.5Sn. 17 p2187 A73-34524
- Heat conductivity and electrical properties of vanadium-alloyed titanium at 100 to 350 K 17 p2188 A73-34554
- Microstructure and phase composition of oxide scale formation on Ti-Al alloys, noting dependence on Al concentration 17 p2188 A73-34557
- Microstructure and hardness investigations of alpha prime, alpha double prime and omega metastable phases formed during quenching of Ti-Ru alloys 17 p2188 A73-34567
- Polythermal and isothermal sections of Ti-Al-W phase diagram for Ti corner investigation, determining phase region boundary locations by X ray analysis 17 p2188 A73-34568
- Ti-Ta-V-Mo system phase diagram in Ti corner region for 600-900 C, investigating solubility, electrical resistivity and hardness 17 p2189 A73-34570
- Nickel-titanium memory material stress measurement methods, energy absorption capacity and cyclic response, discussing nickel foil surface temperature sensing devices 17 p2166 A73-34616
- An X-ray examination of deformation in beta Ti-V alloys. 17 p2189 A73-34642
- An electrochemical model for hot-salt stress-corrosion of titanium alloys. 17 p2189 A73-34643
- Hydrogen embrittlement and stress corrosion cracking in Ti-Al binary alloys. 17 p2191 A73-35099
- Solid cadmium cracking of titanium alloys. 17 p2191 A73-35123
- Boronic/Ti-Al-V composite properties, fracture modes and fabrication, discussing tensile strength and temperature dependence of longitudinal strength 17 p2192 A73-35532
- Fatigue and creep behavior of aluminum and titanium matrix composites. 17 p2193 A73-35543
- Influence of cold work on the stress corrosion susceptibility of Ti-13V-11Cr-3Al. 17 p2194 A73-35675
- Emerging aerospace materials and fabrication techniques. 17 p2198 A73-35841
- Creep in VT-14 titanium alloy under low-cycle load conditions 18 p2323 A73-36758
- Fractography of stress corrosion in Ti-8Al tested in fatigue. 18 p2326 A73-36972
- Grain growth in commercial alpha and /alpha + beta/ Ti alloys. 18 p2326 A73-37143
- Special features of the fracture of aluminum and titanium alloys at low temperatures 19 p2439 A73-37267
- The hydrogen evolution reaction on Ti-6Al-4V in acidic solutions of NaCl-HCl. 19 p2402 A73-37585
- Fractographic investigation of the ductility of fracture in aluminum and titanium alloys. 19 p2440 A73-37780
- Short-term creep of OT4 alloy. 19 p2440 A73-37786
- Workshop on Titanium and its Alloys, 3rd, Nantes, France, May 17, 18, 1973, Proceedings 19 p2440 A73-37827
- Surface treatments of titanium and its alloys 19 p2441 A73-37828
- The influence of fabrication and structure processes on the result of control by ultrasonics of semifinished products of titanium alloys 19 p2441 A73-37830
- Microstructural characteristics of the TA6V alloy as a function of thermomechanical treatments in alpha plus beta - Effects on the mechanical characteristics in tension 19 p2441 A73-37831
- Transformations of TA6V6E2Zr alloy in isothermal conditions 19 p2441 A73-37832
- Principal aspects of thermal treatments of the alloy Ti-11, 5 Mo-6, Zr-4, 5 Sn /Beta III/ 19 p2441 A73-37833
- Hot fluomachining of Ti alloy tubes and turbine casings, noting dimensional accuracy dependence on temperature 19 p2441 A73-37835
- Working of titanium by high energy due to detonation of an explosive charge 19 p2433 A73-37836
- Ti rich corner of Ti-Al alloys phase diagrams investigated by differential thermal analysis and radiography for thermal resistance and intermetallic compounds existence 19 p2441 A73-37838
- Book - Criteria for current and advanced aircraft hydraulic tubing. [SAE SP-378] 19 p2434 A73-37863
- Quality requirements for Ti-3Al-2.5V annealed and cold worked hydraulic tubing. [SAE SP-378] 19 p2434 A73-37868
- Production of extruded tube hollows for titanium 3Al-2.5V hydraulic tubing. [SAE SP-378] 19 p2434 A73-37869
- The development and control of crystallographic texture in 3Al-2.5V titanium alloy tubing. [SAE SP-378] 19 p2434 A73-37870
- The effects of crystallographic texture on the mechanical and fracture properties of Ti-3Al-2.5V hydraulic tubing. [SAE SP-378] 19 p2434 A73-37871
- Surface conditioning of titanium alloy tubing. [SAE SP-378] 19 p2434 A73-37872
- Application of the hydrostatic extrusion process toward production of 3Al-2.5V titanium alloy hydraulic tubing. [SAE SP-378] 19 p2434 A73-37873
- Mechanical and corrosion resistant properties of titanium castings. 19 p2442 A73-37947
- French monograph - Mechanical behavior of the titanium alloy TA6V6E2 with reference to hydrogen - Influence of heat treatment and oxygen content. 19 p2443 A73-38362
- Laser cutting of aerospace materials. [SME PAPER EM 73-214] 19 p2436 A73-38496
- Twinned plate structure of martensitic transformation dependence on composition in Zr-Ti alloy investigated by transmission electron microscopy 20 p2575 A73-39023
- Long period superlattice in an aged beta titanium alloy. 20 p2577 A73-39222
- Study of low-cycle fatigue of titanium-base alloys at a temperature of -196 C 20 p2577 A73-39375
- Continuous decomposition of gamma solid solution in iron-nickel-titanium alloys 20 p2579 A73-39736
- Effect of iron on the phase composition and mechanism of plastic deformation of titanium 20 p2579 A73-39737
- Ti-V alloys elastic modulus and paramagnetic susceptibility, considering composition vs property curve salient point indications of changes in interatomic bonding energy and electron structure 21 p2718 A73-40487
- Optimal thick layer nitriding of Ti alloys, discussing boundary conditions, film, hydrogen effect and mechanical properties 21 p2707 A73-40739
- Influence of aluminum on the structure and properties of a Ti + 10% V alloy 21 p2719 A73-40850
- Influence of a magnetic field on the weld-seam structure during electroslag welding of titanium alloys 21 p2707 A73-40891
- Mechanical properties of weldments of AK-3 titanium with an elevated oxygen content. 21 p2720 A73-41036
- Properties and structure of superconducting Ti-Nb alloys. 21 p2720 A73-41037
- Influence of hydrogen on the fracture micromechanism of OT4 and OT4-1 titanium alloys 21 p2721 A73-41231
- Determination of the resistance of VT-14 alloy to brittle fracture 21 p2722 A73-41232
- A titanium-base composite material 21 p2724 A73-41276
- Spectrophotometric study of products formed in the course of superficial oxidation of titanium and TA6V alloy 21 p2722 A73-41587
- Omega-phase stability in the Ti-Zr-O system 22 p2873 A73-42085
- Investigation of the phase composition of alloys in the Ti-Al-Fe ternary system 22 p2873 A73-42086
- Specific structural features of the phase diagrams of the Ti-Cr-V, Ti-Cr-Nb and Ti-Cr-Ta ternary systems 22 p2873 A73-42087
- Drop forged Ti alpha-beta alloy textures after heat treatment, quenching, aging and surface machining 22 p2866 A73-42089
- Decay of the solid beta-solution in beta alloys of titanium and zirconium during tempering 22 p2874 A73-42092
- Effect of the superplasticity of titanium and its alloys, and the use of this phenomenon for welding in a solid state 22 p2866 A73-42093
- Elastic properties of alloys of the Ti-Al-Mo system as a function of the composition and heat treatment 22 p2874 A73-42095
- Nature of the strain-hardening of titanium beta solid solutions 22 p2874 A73-42096
- Interdiffusion in the titanium-zirconium system 22 p2874 A73-42099
- The fretting fatigue of titanium and some titanium alloys in a corrosive environment. 22 p2876 A73-42356
- Technique for measuring the diffusivity of hydrogen in titanium alloys. 22 p2878 A73-42505
- Book - Advances in corrosion science and technology. Volume 3. 23 p2990 A73-43455
- Titanium alloys mechanical, electrochemical and metallurgical parameters effects on stress corrosion cracking, discussing crack growth kinetics, failure features and component hazard minimization 23 p2990 A73-43457
- Porous and dense layers in Nb-Ti-O system analyzed by X-ray spectroscopy, finding element content influence 23 p2990 A73-43481
- Investigation of the structure and properties of annealed alloys of the Ti-Mo system 23 p2990 A73-43484
- Influence of diffusion coating and heat treatment on the wear resistance of VT-8 alloy 23 p2990 A73-43485
- Pitting of titanium. I - Titanium-foil experiments. II - One-dimensional pit experiments. 23 p2991 A73-43521
- Fatigue crack growth retardation after single-cycle peak overload in Ti-6Al-4V titanium alloy. 23 p2992 A73-43809
- The stress corrosion of titanium materials - The present status of research 23 p2992 A73-43910
- Fabrication techniques for Ti alloys in aerospace applications, discussing hot forming, electron beam and diffusion welding under vacuum and stress relaxation annealing 23 p2985 A73-43911
- The effect of cold and hot rolling on the microstructure and fracture characteristics of titanium-to-steel explosion welds. 23 p2985 A73-43912
- Recrystallization and X-ray fine structure studies of the age-hardening characteristics of the metastable titanium alloy Ti-13V-11Cr-3Al 23 p2992 A73-43913
- Aluminum brazed titanium honeycomb sandwich structure - A new system. 23 p2985 A73-44000
- Morphology and crystallography of beta prime martensite in TiNi alloys. 23 p2994 A73-44160
- Diagram of continuous cooling transformation of a titanium alloy with 6 per cent Al, 6 per cent V, and 2 per cent Sn /TA 6-V 6-E 2/ homogenized in the beta /sub 0/ phase 23 p2995 A73-44177

TITANIUM BORIDES

Influence of neutron bombardment on the mechanical properties of titanium and the magnitude of the programmed-hardening effect

23 p2995 A73-44284

Influence of titanium on the beta and beta-two phase properties and brittleness of InNDK35T5-type annealed alloys

24 p3098 A73-44472

Deformation characteristics and ductility of two-phase titanium alloys of laminated structure

24 p3099 A73-44573

Structural adhesive bonding of titanium - Superior surface preparation techniques.

24 p3093 A73-44765

Stability of the gamma-prime Co₃Ti compound in simple and complex cobalt alloys.

24 p3099 A73-45075

Oxygen in alloys of titanium with aluminum and zirconium.

24 p3100 A73-45275

Alloys of titanium with refractory elements.

24 p3100 A73-45276

High strength Ti alloy cracking and brittle fracture prevention during aging by high heat rate treatment at 250-500 C

24 p3100 A73-45277

Gas saturated surface layer effect on Ti alloy resistance to static cyclic tensile loads, noting increased fatigue strength after etching

24 p3100 A73-45278

The precipitation of titanium in copper and copper-nickel base alloys.

24 p3100 A73-45473

Dependence of electrical erosion on the interatomic bond strength in binary titanium alloys

24 p3101 A73-45514

Use of the fractional-distillation effect to increase the sensitivity of spectral analysis of metallic titanium

24 p3066 A73-45515

TITANIUM BORIDES

The hardness of titanium-diboride single crystal grown from metal bath.

23 p2994 A73-44154

Creep during the hot compression of titanium diboride powder

24 p3093 A73-44740

TITANIUM CARBIDES

High temperature effects on near order transformations in TiC-WC solid solutions during heat treatment and cooling, using X ray diffusion scattering measurements

01 p0064 A73-10615

The effect of substrate temperature on the structure of titanium carbide deposited by activated reactive evaporation

04 p0456 A73-15757

Flat dendritic carbide effects on crack formation in Ti and Nb stabilized austenitic Cr-Ni corrosion resistant steels after heating to 1250 C

06 p0705 A73-17850

Heat conductivity of cermet with titanium carbide as function of temperature and metal content

09 p1103 A73-22471

Interaction of graphite with titanium and zirconium

09 p1105 A73-22977

Creep associated with hot pressing titanium carbide powders

10 p1224 A73-24315

Thermal diffusivity and thermal conductivity of pyrolytic titanium and niobium carbides and of titanium nitride at high temperatures

11 p1380 A73-25740

Sintering of refractory titanium carbide with varied bound nitrogen content, discussing crystal dislocation effects on initial stage compaction intensification in nonstoichiometric specimens

12 p1503 A73-27556

Effects of small amounts of carbide-forming elements on the elevated temperature strength of austenitic stainless steel.

13 p1642 A73-29517

Concentration dependence of the degree of occupancy of a lattice element in cubic titanium oxycarbide

15 p1896 A73-31210

Electrophysical properties of TiC-Nb, TiC-Ta, TiC-Mo, and TiC-W cermets

15 p1892 A73-32242

Titanium carbide nitride and zirconium niobium carbide solid solutions electromotive forces, examining temperature-concentration dependencies, carbide and carbonitride conductivity mechanisms, resistivity and Hall effect

18 p2325 A73-36964

Preparation and properties of materials containing titanium carbide

21 p2719 A73-40851

An X-ray spectral study of the electronic structure of nonstoichiometric titanium carbide

21 p2721 A73-41226

Investigation of the dross molding process for titanium carbide

23 p2991 A73-43490

Thermal diffusivity and conductivity of titanium and zirconium carbides at high temperatures

24 p3099 A73-44760

TITANIUM COMPOUNDS

NT BARIUM TITANATES

NT ILMENITE

NT LEAD TITANATES

NT MAGNESIUM TITANATES

NT PEROVSKITES

NT RUTILE

NT TITANATES

NT TITANIUM BORIDES

NT TITANIUM CARBIDES

NT TITANIUM NITRIDES

NT TITANIUM OXIDES

NT ZIRCONIUM TITANATES

Russian book on titanium chemistry covering physicochemical and electrochemical properties, hydrolysis and production of metal-organic and complex titanium compounds

02 p0139 A73-11890

Mo disilicide-Ti disilicide system phase diagram based on metallographic, X ray structural and high temperature differential thermal analyses

05 p0587 A73-16846

On some oxygenated compounds of titanium and alkalies /Li, Na/ - Study of the binaries M2O-TiO₂ in the zones rich in alkaline oxide

05 p0547 A73-17219

On supposedly five-co-ordinate titanium /IV/ complexes - The crystal and molecular structure of Cl₃Ti(C₅H₇O₂)

06 p0661 A73-18266

An X-ray monitor for measurement of a titanium tritide target thickness.

07 p0809 A73-20466

Titanium hydride and hydronitride thermal stability analysis from hydrogen vapor pressure and decomposition measurements in vacuum at 400-1100 C

15 p1888 A73-31601

TITANIUM DIOXIDE

U TITANIUM OXIDES

TITANIUM NITRIDES

Titanium nitrides effect on austenite grains formation by high temperature fusion, considering electric arc and vacuum melting of structural steels

06 p0706 A73-17883

Thermal diffusivity and thermal conductivity of pyrolytic titanium and niobium carbides and of titanium nitride at high temperatures

11 p1380 A73-25740

Preparation of porous electrodes from titanium nitrides

15 p1881 A73-31592

Titanium carbide nitride and zirconium niobium carbide solid solutions electromotive forces, examining temperature-concentration dependencies, carbide and carbonitride conductivity mechanisms, resistivity and Hall effect

18 p2325 A73-36964

Nitride inclusions in titanium ingots - A study of possible sources in the production of magnesium-reduced sponge.

20 p2576 A73-39026

A study of the real structure of titanium mononitride in its homogeneity region

21 p2721 A73-41225

TITANIUM OXIDES

NT ILMENITE

NT RUTILE

Electron beam technique for evaporating titanium and silicon oxides antireflection coatings on solar cells, noting humidity and thermal resistances and UV radiation darkening

03 p0256 A73-14228

Electron microprobe investigations of the oxidation states of Fe and Ti in ilmenite in Apollo 11, Apollo 12, and Apollo 14 crystalline rocks.

07 p0880 A73-19696

A new titanium and zirconium oxide from the Apollo 14 samples.

07 p0885 A73-19749

Plasma sprayed boron fiber reinforced titanium oxide and Al matrix composites, discussing temperature control for particle size and SiC coating effects on strength

11 p1388 A73-25413

Experimental investigation of the enthalpy of titanium oxides at temperatures ranging from 500 to 2000 K

12 p1513 A73-27325

Titanium monoxide system cation self-diffusion coefficients, and quenched-in vacancy concentrations as function of stoichiometry, tabulating Arrhenius parameters

13 p1633 A73-28145

Critical survey of studies of phase diagrams in the titanium-oxygen system in connection with the formation of suboxides

15 p1893 A73-32515

Oxidation of OT4 and OT4-1 alloys in the process of prolonged heating in air at temperatures from 200 to 400 deg

15 p1894 A73-32539

High precision photoelastic and ultrasonic techniques for determining absolute and differential thermal expansion of titania-silica glasses.

17 p2171 A73-35410

Procedure for preparation of metallic titanium by direct reduction of oxides under flux

19 p2441 A73-37821

Titanium cathode blanks in electrolytic production of metals, noting titanium oxide nonstick properties, electron transmission and corrosion resistance

19 p2442 A73-37848

Titanium oxide film dissolution indication by tapering colors and weld tensile strength dependence on film thickness and temperature

21 p2717 A73-40449

Phase relations and diagram investigation for zirconium silicate-titanium dioxide system by quenching method, obtaining solid solution formation conditions and lattice constants

23 p2998 A73-44131

TITRATION

Changes in the quantity of overall sulfhydryl groups in the blood of persons coming in contact with microwave radiation sources

15 p1837 A73-31164

TNT (TRINITROTOLUENE)

U TRINITROTOLUENE

TOBACCO

Response of tobacco tissue cultures growing in contact with lunar fines.

11 p1320 A73-26483

Cigarette-smoking and coronary atherosclerosis.

18 p2275 A73-36535

TOKAMAK FUSION REACTORS

Distribution of flux of charge-exchange atoms from a plasma over the cross section of the plasma filaments in the Tokamak-4 apparatus.

13 p1664 A73-28611

Integral relations for an equilibrium toroidal plasma filament with a noncircular cross section

13 p1665 A73-28951

Ignition condition in Tokamak experiments and role of neutral injection heating.

14 p1777 A73-29684

'Drift' instabilities distorting the magnetic surfaces of Tokamak-type toroidal systems.

14 p1778 A73-29690

Time behavior of hydrogen discharge in ST-1 Tokamak based on measured radial electron temperature and density profiles and ohmic-heating current and voltage

14 p1778 A73-29691

Equilibrium of a plasma contained between two parallel plates by a magnetic field

15 p1921 A73-32338

Magnetic feedback stabilization in a Tokamak.

15 p1922 A73-32638

Tokamak axisymmetric toroidal plasma filament equilibrium in conducting circular and elliptic cylinders for pressure and current distributions, using numerical MHD equation integration

17 p2215 A73-34301

Equilibrium of a toroidal plasma with noncircular cross section.

23 p3013 A73-44305

TOLERANCES [MECHANICS]

Hydrostatic journal bearings design review covering pad coefficients, flow control, optimization, dynamic behavior, thermal effects, turbulence and tolerances

03 p0311 A73-13207

The use of tolerance detectors for data protection in the case of FM data transfer

04 p0415 A73-14773

Study of the influence of asymmetries on the flight behaviour of a sounding rocket.

09 p1155 A73-23203

Determination of parameter tolerances for microstrip transmission lines

12 p1470 A73-27580

Magnetic coil type electrical measurement indicating instruments accuracy dependence on manufacturing tolerances, discussing error reducing design methods

12 p1499 A73-27873

TOLERANCES (PHYSIOLOGY)

NT ACCELERATION TOLERANCE

NT ALTITUDE TOLERANCE

NT COLD TOLERANCE

NT HEAT TOLERANCE

NT HUMAN TOLERANCES

NT RADIATION TOLERANCE

Sensitivity of the brain to repeated exposures of hyperbaric oxygen.

11 p1314 A73-25328

Survival of soil bacteria during prolonged desiccation.

14 p1720 A73-30959

Effect of protein quality in the diet of rats on their tolerance to severe hypoxia

15 p1835 A73-31511

Effect of maximal work load on cardiac function.

16 p1973 A73-33991

TOLLMEIN-SCHLICHTING WAVES

Parametric excitation of Tollmein-Schlichting waves in a boundary layer

11 p1347 A73-25430

Reynolds stresses in plane-parallel flows disturbed by Tollmein-Schlichting waves

15 p1861 A73-31193

ONE
U PITCH
ONOMETRY
U INTRAOCULAR PRESSURE
U PRESSURE MEASUREMENTS
ONUS
U MUSCULAR TONUS
OOLS
NT BORING MACHINES
NT GRINDING MACHINES
NT LATHES
NT MACHINE TOOLS
OPOGRAPHY
NT LUNAR TOPOGRAPHY
NT TERRAIN
Side-look radar provides a new tool for topographic and geological surveys.
02 p0140 A73-11850
Topographic earth observations using radar techniques with a single flight.
04 p0419 A73-15403
Surface topography of the inner planets as related to planetary origins.
06 p0749 A73-18005
Radar techniques for planetary mapping with orbiting vehicle.
06 p0664 A73-18011
Random optical density fields pertaining to analyses of aerial photo imaging of aerial topographic objects
06 p0693 A73-18155
Acousto-optical profilometer system with two diffracted laser beams for surface topography holographic measurements
06 p0694 A73-18290
The ground surface of planet Mars
07 p0900 A73-20243
Ground based radar measurement of Martian topography, surface temperature and thermal properties by microwave and IR radiometry and spectral reflectivity observation
09 p1144 A73-22259
Radar measurement of altitude profiles and reflected power for Martian topography and surface properties, noting heavy cratering
09 p1144 A73-22260
High resolution radar observation of Martian surface topography and scattering properties, noting dielectric constant and rms surface slope variations
09 p1144 A73-22261
Analytical transformation of photographs for plotting topographic and photographic maps in prescribed projections
10 p1219 A73-24483
Moire topography for full size living human body contour stereophotographic pictures with high contrast, discussing instrument construction, performance and accuracy
11 p1365 A73-26239
Panoramic and frame cameras for aerial phototopographic survey, noting photo quality and high resolution advantages
12 p1497 A73-27423
Statistical turbulence model of meteorological and topographical aircraft flight conditions for low altitude critical air turbulence (ILO-LOCAT) environment
13 p1569 A73-28831
Use of a computer to design surveys made by the stereotopographic method
13 p1621 A73-29416
Landmark navigational and topographical mapping techniques for planetary surface exploration using unmanned vehicles and earth based computers
17 p2210 A73-35383
A generalized geologic map of Mars.
19 p2477 A73-37201
Martian lowland terrains fretted and chaotic characteristics, hypothesizing evolutionary processes based on escarpment recession, subsurface ground ice and magma collapse
19 p2477 A73-37205
Mars Hellespontus region identification from Mariner 9 photographs as wind produced dunes, considering albedo features
19 p2477 A73-37210
Wind erosion in the Martian polar regions.
19 p2478 A73-37214
Martian south polar region pitted and etched terrain features, interpreting surface layered blanketing material as due to wind action
19 p2478 A73-37215
A study of Martian topography by analytic photogrammetry.
19 p2480 A73-37230
Improve reliability of electron devices through optimized coverage of surface topography.
19 p2411 A73-38453
Planetary surface reflectivity and topography mapping by ground based radar with emphasis on observational methods
23 p2953 A73-43353
Martian surface albedo compared with Mariner-observed topography, noting dark-banded correlation with maximum topographic irregularity regions
24 p3133 A73-44551

TOPOLOGY
NT FIXED POINTS [MATHEMATICS]

NT HOMOTOPY THEORY
NT IMBEDDINGS [MATHEMATICS]
NT INVARIANT IMBEDDINGS
NT METRIC SPACE
Topologic group theory for stress analysis of non-linearly elastic body under complex load, representing loads set by Lie group
01 p0119 A73-11428
Topological analysis of mechanical vibrating linear systems by the method of structural numbers
03 p0396 A73-14598
Stress principle relationship to mechanical power additivity, presenting topological, measure theory and functional analysis theorems
06 p0760 A73-17762
Topological equivalence of linear systems of Pfaff equations in the neighborhoods of their one-dimensional closed characteristics
06 p0718 A73-18677
Topologies for neutral functional differential equations.
07 p0845 A73-20493
Topological design of thin-film resistors with the aid of a digital computer
09 p1066 A73-23119
Sequential systems fault detection methods based on topological description and Boolean analysis of internal variables, obtaining fanout free equivalent network by tree expansion
10 p1201 A73-24055
Vectorial topological continuous function spaces bounded parts, constructing tunneled, quasi-tunneled and nontunneled spaces
11 p1390 A73-25865
Rockafellar duality theorem generalization to integrands over locally convex sublinear topological vector spaces, permitting Banach space transcendence
11 p1390 A73-25866
Topologic group theory for stress analysis of non-linearly elastic body under complex load, representing loads set by Lie group
11 p1443 A73-26057
Some general questions in the theory of probability measures in linear spaces
12 p1517 A73-27187
Formation and solution of the equations of state of electronic circuits
12 p1485 A73-27623
Automatic mesh generation in two and three dimensional inter-connected domains.
13 p1693 A73-28242
Koethe spaces topological properties, considering vector functions integration
15 p1899 A73-31566
Topology of tunneled locally convex spaces, considering Kelley theorem
15 p1900 A73-32206
Topology of induced lunar magnetic fields.
17 p2235 A73-35736
A topology on a group of measurements of probability defined on a Borelian tribe with an enumerable base, and an associated Glivenko-Cantelli theorem
19 p2444 A73-37534
The properties of bond graph junction structure matrices.
19 p2460 A73-38083
Russian book on topological spaces and groups with continuous operations covering rings, Lie group, compact groups, homomorphism, automorphism, isomorphism, etc
21 p2726 A73-40801
Computer analysis of mixed coordinate base transistor circuits determining matrix numbers without main path or generalized node delineation
21 p2670 A73-41308
Means of improving the effectiveness of designing nonlinear electronic circuits on a digital computer by the method of nodular potentials
21 p2666 A73-41310
Dynamic programming application to extremal fields topological singularity in optimal control theory for flight vehicle with state variables satisfying initial conditions and ordinary differential equations
22 p2917 A73-43030
Topological modification and bounded length of decomposition series for convergence space
23 p3000 A73-44301
Splittability of radically semisimple torsion over local and commutative Noetherian rings
24 p3144 A73-44423
The topological association of H alpha structures and magnetic fields.
24 p3136 A73-44639
Topology of linear operators in Banach space generalized to invariant polynomials for minimum Schatten ideals in Hilbert space
24 p3105 A73-45008
Topological analysis of integral operators with Agmon kernel in Sobolev spaces within Hilbert space framework
24 p3105 A73-45009
TOPS [SPACECRAFT]
Autonomous power subsystem design for an Outer Planet Spacecraft.
09 p1154 A73-22805

TORCHES

Part manufacturing with plasma arc torch by extending plasma spray coating technology to mandrel design and machining with consideration for base materials
13 p1624 A73-28907

TORNADOES

Radar and Nimbus 4 infrared measurements of the Oklahoma City tornadoes, 30 April 1970.
03 p0338 A73-14512
Stability of an electrical discharge surrounded by a free vortex.
07 p0848 A73-19514

TOROIDAL DISCHARGE

Plasma-electromagnetic wave interactions in toroidal discharge chamber, noting possibility of collisionless wave absorption due to conversion to longitudinal plasma waves at hybrid resonance
23 p3014 A73-44340

TOROIDAL PLASMAS

Local hydromagnetic toroidal equilibria without symmetry.
01 p0083 A73-10457
Neoclassical theory of Landau damping and ion and electron transit-time magnetic pumping /TTMP/ in toroidal geometry.
01 p0083 A73-10459
One-fluid MHD model for beta and flow effects on stationary axisymmetric self consistent toroidal equilibria, using Bennett relation
01 p0083 A73-10460
Inward diffusion of Tokamak-trapped particles by slow magnetic pumping.
01 p0083 A73-10461
Use of the virtual-casing principle in calculating the containing magnetic field in toroidal plasma systems.
01 p0084 A73-10464
Energy and mass analysis of neutral particles emitted from a toroidal theta-pinch plasma.
01 p0084 A73-10466
The diffusion-driven current in a toroidal resistive plasma.
03 p0348 A73-14433
Current trapping in toroidal high current discharges.
03 p0348 A73-14435
Hydromagnetic stability of closed plasma configurations
04 p0478 A73-15020
Methods of plasma injection into closed magnetic confinement systems
04 p0479 A73-15041
Measurement of the dc plasma electric resistivity perpendicular to the magnetic surface.
04 p0482 A73-15959
Motion of plasmoids in a toroidal magnetic multipole.
06 p0727 A73-17421
Conversion of trapped charged particles into untrapped particles in a high-frequency electric field.
06 p0732 A73-18608
Fast radial displacement of a toroidal plasma by a transverse magnetic field.
06 p0732 A73-18620
Necessary and sufficient condition for hydromagnetic stability of the Bennett pinch.
06 p0733 A73-18848
Method for experimental determination of the magnetic well depth in stellarator-type systems
07 p0855 A73-19285
Performance of a 12-coil superconducting 'bumpy torus' magnet facility.
07 p0809 A73-20460
Steady state hot toroidal Tokamaks plasma, calculating seed current density for bootstrap effect produced by neutral particle injection parameters control
08 p0991 A73-20814
Trapped electrons instability in Tokamak configuration, calculating plasma wave propagation modes via Fokker-Planck equation
08 p0991 A73-20815
Observation of beam-plasma interaction in a toroidal plasma in a large electric field.
08 p0993 A73-21631
Particle and energy fluxes across magnetic field in axisymmetric toroidal magnetic traps and plasmas with weak collisions, calculating radial electric field
08 p0993 A73-21695
Tokamak axisymmetric toroidal plasma filament equilibrium in conducting circular and elliptic cylinder for pressure and current distributions, using numerical MHD equation integration
09 p1123 A73-21877
Application of a system of orthogonalized windings with automatically regulated current for plasma stabilization in Tokamak systems
09 p1125 A73-21908
A device for experiments on high-beta plasmas in a toroidal geometry
13 p1663 A73-28120
Experimental determination of magnetic well depth in stellarators.
13 p1665 A73-28685

TOROIDAL SHELLS

- Integral relations for an equilibrium toroidal plasma filament with a noncircular cross section
13 p1665 A73-28951
- Stability of flute disturbances in a plasma of toroidal geometry
13 p1666 A73-28954
- Particle trapping effect on conductivity of toroidal plasma with like-particle collisions taken into account, obtaining results applicable to all aspect ratios
14 p1778 A73-29687
- Problems associated with the injection of a high-energy neutral beam into a plasma.
14 p1778 A73-29688
- Energy variational principle formulation for stability determination of scalar-pressure toroidal plasma, writing potential energy as one dimensional integral
14 p1778 A73-29689
- Particle diffusion rate due to poloidal magnetic field component in low beta symmetric toroidal plasma, discussing losses induced by electrostatic field fluctuations
14 p1778 A73-29693
- Magnetohydrodynamic simulation of toroidal belt-pinch experiments.
14 p1778 A73-29694
- The use of fast magnetic compression for the production and heating of plasma in Tokamak-like geometries.
14 p1780 A73-30121
- Tokamak axisymmetric toroidal plasma filament equilibrium in conducting circular and elliptic cylinder for pressure and current distributions, using numerical MHD equation integration
17 p2215 A73-34301
- Trapped-particle scattering by electrostatic turbulence in toroidal plasmas.
21 p2749 A73-41675
- Numerical methods for solving some problems of the theory of plasma equilibrium in toroidal configurations.
21 p2750 A73-41680
- Polarizing interaction between colliding plasma flows in a toroidal magnetic field. II
22 p2893 A73-42384
- Experimental observation of the decay of high-frequency waves in a plasma
22 p2826 A73-42389
- Equilibrium of a toroidal plasma with noncircular cross section.
23 p3013 A73-44303
- Flute stability in a toroidal plasma.
23 p3013 A73-44306
- Investigation of neoclassical diffusion in toroidal systems with a three-dimensional magnetic axis
23 p3014 A73-44337
- Nonpotential gravitationally-dissipative instability of a plasma in toroidal systems
23 p3015 A73-44348
- Experiments on the Polytron, a toroidal Hall accelerator employing cusp containment.
24 p3116 A73-45239

TOROIDAL SHELLS

- Variable thickness orthotropic shell of revolution with bending suppressed.
05 p0633 A73-16537
- Thin-walled pipe designs with a curvilinear axis
09 p1158 A73-22362
- Calculation of the stress-strain state of a toroidal shell with holes
12 p1555 A73-27787
- Nonlinear toroidal curved elastic shell inflated by fluid at constant pressure, discussing existence, uniqueness and asymptotic behavior
14 p1812 A73-30520
- Analysis of the static deformations of flexible extensible gas-filled shells
15 p1947 A73-31279
- Geometrically nonlinear axisymmetric deformation of toroidal shells
18 p2362 A73-36403
- Stability of the state of moment stress of a toroidal shell
20 p2624 A73-39650
- Buckling of segments of toroidal shells.
22 p2923 A73-42553
- Buckling of toroidal shells under hydrostatic pressure.
22 p2923 A73-42560
- Chebyshev solution to elliptical equilibrium equations of elastic reticular cylindrical and toroidal shells under distributed loads, applying to extensible fiber structures /tires/
24 p3146 A73-44652

TOROIDS

- Radial and nonradial oscillation modes of gaseous polytrope with toroidal magnetic field, using variational principle
02 p0217 A73-12400
- Computer analysis of latching phase shifters in rectangular waveguide.
06 p0678 A73-18743
- High-Q toroidal cavities for high frequency klystrons.
07 p0803 A73-20550

- The effect of toroidal magnets on the sensitivity of photomultipliers.
21 p2699 A73-40410

TORPEDO ENGINES NT TURBOROCKET ENGINES NT VERNIER ENGINES

- TORQUE**
The effects of wall conductance on torque of the MHD viscous coupler and hydrostatic thrust bearing. [ASME PAPER 72-LUB-1]
03 p0313 A73-14326
Generalized electromagnetic torque on a vacuum pulsar model.
10 p1284 A73-24914
Structural design errors resulting from conventional treatment of distribution law for local radial and torque loads
11 p1433 A73-25028
On the torques due to tidal friction of the oceans and adjacent seas.
13 p1607 A73-28409
Spacecraft single-turn reorientation optimization with respect to fuel expenditure depending on maneuver duration and reaction control torque constraints
14 p1803 A73-29852
Cryptosteady flow energy separation mechanisms, considering bearing friction and rotor torque effects and rotor nozzle proportion equations [ASME PAPER 73-FE-24]
17 p2153 A73-35019
Basic principles of variable speed drives.
17 p2182 A73-35472
Precision gimbal rate control for single gimbal control moment gyro /CMG/ pointing control systems, designing for high frequency response, bandwidth and output torque dynamic range
20 p2587 A73-38808
[ALAA PAPER 73-871]
Core coupling to mantle precession, discussing model with quantitative consideration of inertial and dissipative coupling torque superposition
21 p2764 A73-39929
Magnetized and nonmagnetized rotating neutron star reactions to applied torques for pulsar slowdown, discussing magnetosphere and wind zone
21 p2778 A73-41529
Journal bearings computerized design optimization by geometric programming with volume, dimensions, torque and horsepower absorption, shaft strength, speed, load, pressure and Sommerfeld number as constraints
21 p2708 A73-41668
Knudsen free molecular flow explanation of thermomagnetic torque on circular cylinder suspended in axial molecular field, noting apparatus tilt effect
22 p2842 A73-42233
Effect of the gyromotor torque on the dynamics of a gyroscope
24 p3091 A73-45021
Relativistic torque detection on freely spinning rotor, obtaining phenomenological expression by incremental Hubble law
24 p3142 A73-45342
- TORQUE MEASURING APPARATUS**
U TORQUEMETERS
TORQUE MOTORS
Start/stop motor incremental motion system design for optimal control with minimized energy dissipation and operating temperature under inertial and constant torque load
10 p1198 A73-24023
Synthesis of the optimal characteristics of the engines of multiengine systems
19 p2388 A73-37187
- TORQUEMETERS**
A fluidic transducer of rotor-shaft torque
06 p0692 A73-17836
Analysis of force interaction in magnetolectric torque sensors
22 p2860 A73-42364
- TORQUERS**
Pneumatic torque generator subsystem of French D2 satellite, discussing engineering technical difficulties
07 p0778 A73-18925
- TORSION**
Resonance type facility using dynamic hysteresis loop method to test metal fatigue and anelasticity in torsion at room and high temperatures
03 p0288 A73-14025
Flexibility matrix derived and applied to finite element production for thin walled open tubes under torsion, taking into account warping constraints
03 p0395 A73-14470
Low cycle torsion fatigue, determining empirical relationship between strain amplitude and fatigue life
08 p0977 A73-21020
Application of holographic interferometry to predict long time torsional relaxation.
13 p1620 A73-29301
Elastoplastic torsion of a cylindrical bar of multiconnected section
14 p1805 A73-29762
Pure torsion of prismatic rods composed of different materials
21 p2787 A73-40990

- Splitability of radically semisimple torsion over local and commutative Noetherian rings
24 p3144 A73-44423

- An inverse torsion pendulum with continuous frequency variation for studies of elastic relaxation and fatigue
24 p3076 A73-45554

TORSIONAL STRESS

- Fracture strength of helical-wound composite cylinders.
01 p0117 A73-11121
Investigation of the interrelation between creep parameters in industrial aluminum during the first and second stages of creep
02 p0179 A73-11567
Isotropy postulate verification for strain vectors measurement in annealed steel tubular specimens, showing coincidence of tension-internal pressure and tension-torsion test values
02 p0235 A73-12206
Effect of strain-rate and temperature on the resistance to torsional deformation of several aluminum alloys.
03 p0384 A73-13117
Elastic-plastic analysis of Saint-Venant torsion problem by a hybrid stress model.
03 p0390 A73-13338
Torsion of certain prismatic bars.
03 p0395 A73-14198
Size effect in fatigue testing of metals explained, considering implications for bending, torsion and axial loading
03 p0396 A73-14646
Torsion of prismatic bars made of various materials
04 p0510 A73-15077
Dynamic response of pressurized thin cylindrical shells subjected to torsional loads. [ASME PAPER 72-WA/PROD-6]
04 p0514 A73-15807
Application of the variational-difference method in solving the problems of torsion for rods of complex form
05 p0636 A73-17094
Torsional fatigue fixture for high temperature investigation of high strength steels crack growth rate in tensile mode
05 p0563 A73-17254
On the torsional static stability and response of open section tubes subjected to thermal radiation loading.
07 p0908 A73-19086
Investigation of the stressed state of a rod with a cut under elastoplastic torsion
07 p0911 A73-19308
Torsion of a viscoelastic prismatic rod under the action of a vibrational load
07 p0911 A73-19315
Inequalities for torsion rigidity of a prismatic rod with steady creep
07 p0912 A73-19323
On the torsional strength of composite materials reinforced with glass fabric laminates and the effect of the voids in matrix.
07 p0915 A73-20332
Determination of stresses during pure elastoplastic bending and torsion
09 p1157 A73-22163
Finite element stress field solution of the problem of Saint Venant torsion.
09 p1158 A73-22390
An analysis of plastic instability in pure shear in high strength AISI 4340 steel.
09 p1101 A73-22405
An investigation into the relationships of fatigue fracture and inelastic deformation of metals in torsion.
09 p1161 A73-23052
On the elastoplastic problem of cantilever subject to combined bending and twisting.
09 p1164 A73-23320
Thin reinforcing coatings effect on mechanical behavior of homogeneous isotropic prismatic bars under torsion, obtaining stress-strain expressions
09 p1165 A73-23358
Tensile creep modulus, creep lateral contraction ratio and torsional creep measurements on small non-rigid specimens.
10 p1218 A73-24120
Elasto-plastic stress analysis of prismatic bar under combined bending and torsion.
10 p1289 A73-24160
The dynamic properties of unidirectional fibre reinforced composites in flexure and torsion.
10 p1240 A73-24279
Effects of shear damage on the torsional behaviour of carbon fibre reinforced plastics.
10 p1240 A73-24280
Combined axial and torsional shear of a tube of incompressible isotropic elastic material.
10 p1291 A73-24336
Torsion of a circular-section bar weakened by two longitudinal circular-cylindrical cavities
10 p1293 A73-24702
Torsion of a sectorially composite hollow circular cylindrical beam.
11 p1432 A73-24996

Stability of elastic bending and torsion of uniform cantilevered rotor blades in hover. 11 p1440 A73-25534
[AIAA PAPER 73-405]
Flexural/torsional deformations of material line in continuous body in terms of curvature and bending vectors, using Frenet-Serret equations 11 p1445 A73-26408
Torsional stress on micropolar prismatic nonsymmetrically elastic rotating cylindrical shaft with six degrees of freedom evaluated in terms of Saint Venant function 11 p1445 A73-26409
Transversely isotropic /anisotropic/ elastic beam bending and torsion, determining frequency dependent compliances by approximate analytic solution via variational method 11 p1447 A73-26655
Constant cross section composite circular rod, deriving torsional stress behavior near division line intersection with rod contour from closed solution 12 p1552 A73-27368
Stability of cylindrical shells of variable thickness during torsion 12 p1553 A73-27462
Conditional margin of plastic strength for shaft-type elements subjected to torsion at low temperatures 12 p1554 A73-27478
One-dimensional zero-moment problem of a thin elastic shell of variable thickness 12 p1556 A73-27800
Evaluation of torsional fatigue damage from changes in the fatigue properties and microhardness. 13 p1635 A73-28522
Torsion of an axisymmetrical anisotropic body with mixed boundary conditions on the edge surface 13 p1698 A73-29086
Application of paired integral equations to the problem of the torsion of an elastic space weakened by a conical slot of finite dimensions 13 p1698 A73-29090
Al alloy rupturing analysis in complex stress state, noting sublimation and self diffusion values of activation energy in torsional to tensile state transition 13 p1643 A73-29624
Effect of deep annular grooves on the strength of some metals under static tension and torsion 14 p1763 A73-30693
A method for studying the stressed state during torsion of hollow prismatic beams 14 p1815 A73-30790
Torsion of a reversible flexible fiber shaft 15 p1946 A73-31140
Fredholm integral equation singularity method solution for calculating stresses and elastic displacements in bodies of revolution of arbitrary shape under torsional loads 15 p1947 A73-31327
Combined tension-torsion creep of polyethylene with abrupt changes of stress. 15 p1897 A73-31613
Theory for cylindrical wavy shells via fiberglass-plastic models, noting application to wavy rod torsion problem 15 p1952 A73-32083
Considerations on the centres of shear and of twist in the theory of beams. 15 p1954 A73-32111
Torsion of an inhomogeneous body of revolution with variable shear moduli 16 p2074 A73-32682
Torsion and extension of a cylinder with an outer annular cut 17 p2240 A73-34143
Torsion of a cylindrical shaft having an annular semicircular cutout 17 p2244 A73-34791
Effect of torsion-flap-lag coupling on hingeless rotor stability. [AHS PREPRINT 731] 17 p2105 A73-35067
Evaluation of finite-plasticity theories for torsion-tension members made of Tresca materials. [SESA PAPER 2109] 17 p2251 A73-35447
A biaxial split Hopkinson bar for simultaneous torsion and compression. 17 p2149 A73-35754
Limiting equilibrium of reinforced cylindrical shells 18 p2363 A73-36412
Internal low-frequency friction in niobium in a normal and superconducting state 18 p2323 A73-36676
Torsional rigidities for bars under fully plastic torsion. 18 p2365 A73-36695
A simple method for studying slow crack growth. 19 p2497 A73-37588
Torsion of an axisymmetric anisotropic body with mixed boundary conditions on the side surface. 19 p2498 A73-37636
Application of dual integral equations to the problem of torsion of an elastic space, weakened by a conical crack of finite dimensions. 19 p2498 A73-37640

Inhomogeneous yield limit effect on elastic-plastic boundary of circular cylinder in torsion, considering radial and angular dependencies 19 p2498 A73-37651
Torque and thermal cycling as methods of testing reliability of reflow-soldered chip-to-substrate joints. 19 p2436 A73-38445
Round bars of an anisotropically hardening material in torsion 20 p2619 A73-39356
Torsional and anti-plane strain delamination of an orthotropic layered composite. 20 p2622 A73-39549
Yield criterion in plane stress state for description of second order effect relating to axial strain accumulation in cyclic torsion 20 p2624 A73-39568
Boundary residual methods limitation on elasticity problem solution accuracy, considering torsional stress analysis of square and hexagonal cylinders with circular hollow cores 21 p2784 A73-40431
Torsional elasticity of human skin in vivo. 21 p2642 A73-41625
Determination of the stresses for pure elastic-plastic flexure and torsion. 22 p2919 A73-42111
The cyclic elastoplastic torsion of the circular cylinder in the case of finite deformations 22 p2922 A73-42527
Testing set-up for cyclic torsion with tension on a small number of loading cycles. 22 p2861 A73-42530
The load transfer problem in shafts coupled through a sleeve. [ASME PAPER 73-APMW-3] 22 p2867 A73-42877
Procedure and device for the study of the behavior of metals subjected to dynamic torsional stresses 22 p2868 A73-43171
Post-yielding behavior of torsionally loaded composite tubes. 23 p3041 A73-43640
Torsion of a cylindrical shell with a lateral surface containing an elastic circular inclusion 23 p3042 A73-43727
Stability under torsion of a moderately long cylindrical shell with different walls 23 p3042 A73-43738
Investigation on the optimum tightening force of bolted joint in torque control method. 23 p2986 A73-44140
Complex elastoplastic torsion of cylindrical shafts 23 p3045 A73-44184
Mixed boundary value problem solution for stress-strain state of anisotropic elastic cylinder and layer under joint torsion, using Fourier and Hankel transforms 24 p3146 A73-44676

TORSIONAL VIBRATION

Random gust response statistics for coupled torsion-flapping rotor blade vibrations. 01 p0004 A73-10046
Stress analysis and dynamic investigation of turbine blades from constrained torsion theory, calculating free torsional vibration frequencies 02 p0229 A73-11621
Lateral displacement of discontinuous vibrating wire, noting solution application to longitudinal vibrations of discontinuous shafts and torsional vibrations of circular shafts 02 p0237 A73-12612
Dynamic stability of monosymmetrical thin-walled structures. [ASME PAPER 72-APM-SS] 05 p0632 A73-16530
Drift phenomena in shaken measurement systems prone to torsional vibrations. III 09 p1086 A73-23116
Sensitivity of rotor blade vibration characteristics to torsional oscillations. 11 p1440 A73-25533
Incremental servomechanism design and application as substitute for step motor, discussing servomotor properties, mechanical torsional vibration and loading moment effects 12 p1483 A73-27422
Selection of optimal rigidities for elastic regions of a mechanical system with resonance oscillations 12 p1524 A73-27473
Mathematical observations in structural dynamics. 12 p1555 A73-27739
Unbalance vibration of a rotor-bearing system supported by floating-ring journal bearings. 13 p1623 A73-28647
Linear aerodynamic model incorporating torsional oscillations about two dimensional airfoil midchord for stall flutter description 13 p1697 A73-28814
Note on forced vibration of a non-homogeneous cone with spherical caps. 14 p1814 A73-30708
Simultaneous flexural and torsional vibrations of multidisk rotors 16 p2075 A73-32691

Modal synthesis technique for natural frequencies and mode shapes of bent rectangular beam in flexure-torsion oscillation under six boundary constraint conditions 16 p2075 A73-32792
Torsional vibrations of a bar of variable cross-section. 16 p2079 A73-33075
Nonlinear magnetoelastic effects in Ni tube torsion spring pendulum due to oscillation damping and stiffness characteristics dependence on amplitude 16 p2025 A73-33214
Torsional vibrations of shells of revolution of variable thickness. 16 p2081 A73-33682
Shear waves in infinitely extended double walls with coupling rods of circular cross section. I - Shear waves in the infinitely extended disk 17 p2241 A73-34246
Lateral bending-torsion vibrations of a thin beam under parametric excitation. [ASME PAPER 73-APM-13] 17 p2247 A73-35037
Program of computation of spectral and modal matrices associated with a linear elastic system 18 p2364 A73-36493
On the torsional oscillations of a sphere placed at the axis of a rotating viscous incompressible fluid. 19 p2419 A73-37422
Flexural wave fields in infinite beam-reinforced plates under point excitation. 19 p2498 A73-37725
Free harmonic vibrations of thin pretwisted rectangular plates analyzed in terms of torsional and bending vibration coupling based on shell theory 19 p2500 A73-38115
An electromagnetic torsional vibrator. 20 p2544 A73-39271
Differential equations for the vibrations of twisted rods with allowance for energy dissipation 20 p2619 A73-39372
Longitudinal-torsional vibrations of rotors 20 p2569 A73-39374
Application of simultaneous iteration method to torsional vibration problems. 21 p2783 A73-40289
Application of the method of integrating matrices to the calculation of the natural vibrations of a propeller blade with allowance for deflection in two planes and for torsion 21 p2783 A73-40389
Flexural wave propagation in a thin plate with circular holes. 21 p2787 A73-41142
Critical analysis of the method of M. A. Biot for determining natural torsional frequencies 22 p2867 A73-43047
Natural, flexural and torsional vibration frequencies and modes for helicopter tail rotor blades 24 p3057 A73-45245

TORSO

Redintegrated somatotyping technique for physique measurement and classification based on limb and torso photographic diameter integration with height, using photoelectric cell and electronics 06 p0659 A73-18474

TORUSES

A 12-coil superconducting 'bumpy torus' magnet facility for plasma research. 02 p0150 A73-11839
Performance of a 12-coil superconducting 'bumpy torus' magnet facility. 07 p0809 A73-20460

TOUCH

NT TACTILE DISCRIMINATION

Psychological test for relative contributions of specific and nonspecific components to intersensory transfer between vision and touch 03 p0266 A73-13525
Teleoperator system incorporating touch feedback and sequenced automatic control for experimental investigation of human touch sensing relation to manipulative skills 19 p2397 A73-37328

TOUCHDOWN

Touchdown performance with a computer graphics night visual attachment. [AIAA PAPER 73-927] 21 p2673 A73-40874

TOUGHNESS

NT NOTCH SENSITIVITY

Impurities effect on Mo plastic properties and toughness, suggesting lower vacuum arc welding rates and increased electron beam zone refining runs 01 p0066 A73-11343
Strength and toughness of Fe-10Ni alloys containing C, Cr, Mo, and Co. 06 p0713 A73-18765
Epoxy resins thermal mechanical properties, considering difference between toughness and flexibility in terms of temperature and loading rate insensitivities 10 p1237 A73-23952
Solid fracture theories based on brittle region toughness parameter and absorbed specific fracture work factor above ductile-brittle transition respectively 13 p1640 A73-29479

TOWED BODIES

Cold rolling of polymers. II - Toughness enhancement in amorphous polycarbonates.
17 p2197 A73-35350

TOWED BODIES

Aerial targets for weapon systems performance testing, discussing converted aircraft, pilotless drones and towed targets
09 p1168 A73-23120

Human physiological responses to high speed aerial tow.
18 p2286 A73-36939

TOWED TARGETS

U TARGETS
U TOWED BODIES

TOWERING CUMULI

U CUMULUS CLOUDS

TOWERS

French Guiana space center Diamant and Europa service towers structure, operational security features and protection against corrosion and contamination
07 p0807 A73-18947

TOWNSEND AVALANCHE

Electroradiography technique involving photoproduction of free electrons via Townsend avalanche amplification in diode/triode gap, noting increased quantum efficiency
23 p2950 A73-44214

TOWNSEND DISCHARGE

NT GAS DISCHARGES
NT TOROIDAL DISCHARGE
Effect of an electric field on the ignition of a reacting binary gas mixture
23 p3009 A73-43441
Electron-molecule collision frequencies in a crossed electric and magnetic field.
24 p3118 A73-45476

TOWNSEND SURFACES

U TOWNSEND AVALANCHE

TOXIC DISEASES

NT CARBON MONOXIDE POISONING
Analysis of the mechanism of the therapeutic action of pressurized oxygen in organic phosphorus poisoning
14 p1722 A73-30848

TOXIC HAZARDS

Action of Freon-114B2 on the activity of lactate-dehydrogenase iso-enzymes
06 p0650 A73-17696
Hydrazine derivative poisoning in industry and clinical medicine treatments, noting causes of vitamin B6 deficiency
10 p1183 A73-23819
The acute inhalation toxicology of chlorine pentafluoride.
15 p1839 A73-32173
Evaluation of hazard presented by gas-off products from polymeric materials intended for use in space cabins.
18 p2286 A73-36931
Reactions of singlet oxygen with pine pollen.
19 p2402 A73-38295

TOXICITY

NT CARBON MONOXIDE POISONING
Analysis of volatile combustion products and a study of their toxicological effects.
02 p0138 A73-12429
A study of Halon 1301 (CBrF3) toxicity under simulated flight conditions.
09 p1045 A73-22537
The effects of mercury compounds on the growth and orientation of cucumber seedlings.
12 p1462 A73-27274
Effects of a synchronizer phase-shift on circadian rhythms in response of mice to ethanol or ouabain.
20 p2513 A73-39481
Solubilization and accumulation of copper from elementary surfaces by Penicillium notatum.
21 p2648 A73-41217

TOXICITY AND SAFETY HAZARD

Combustion products of polymeric materials containing nitrogen in their chemical structure.
08 p0983 A73-21821
A study of Halon 1301 (CBrF3) toxicity under simulated flight conditions.
18 p2285 A73-36930

TOXICOLOGY

Effect of lithium on acute oxygen toxicity and associated changes in brain gamma-aminobutyric acid.
13 p1575 A73-28503
Development and reversibility of pulmonary oxygen poisoning in the rat.
14 p1718 A73-30516

TOXINS AND ANTITOXINS

NT ENDOTOXINS

TRACE CONTAMINANTS

Trace phase analysis as an aid in the study of heterogeneous raw material impurities in powder metallurgy
04 p0464 A73-15370
Amino acid search in lunar fines, considering terrestrial source contamination, bound and free amino acids, processing and analysis contamination
06 p0754 A73-18422

Luna 20 soil and rock fragments chemical composition from neutron activation analysis, noting low rare earth content and contamination with W and Mo
13 p1676 A73-28321

Long-path infrared spectra of CO, NO₂, NO, SO₂ and N₂O observed in a simulated atmosphere in trace amounts.
16 p1976 A73-32700

Correlation interferometric measurement of trace species in the atmosphere.
[AIAA PAPER 73-515]
16 p2006 A73-33552

Determination of ultramicro-impurities in CdS-type semiconductor materials - Determination of copper
17 p2220 A73-35558

Skylab medical experiments altitude test (SMEAT)/chamber atmosphere trace contaminants analysis, describing sample acquisition techniques and instrumentation
[ASME PAPER 73-ENAS-45]
19 p2395 A73-37992
Diffusion profile measurements in the base of a microwave transistor.
21 p2668 A73-41560

TRACE ELEMENTS

Chemical fractionation in iron meteorites and its interpretation.
01 p0108 A73-11474

Trace elements profiles, notably Hg, from a preliminary study of the Apollo 15 deep-drill core.
02 p0220 A73-12477

Hornblende from calc-alkaline volcanic rocks of island arcs and continental margins.
02 p0165 A73-12635

Trace-element variation of individual plagioclase and hornblende phenocrysts.
04 p0414 A73-14986

Luna 20 and Apollo 16 core fines - Large-ion lithophile trace-element abundances.
05 p0546 A73-16828

The chemical composition of soil from the Apollo 16 and Luna 20 sites.
05 p0546 A73-16831

Twin spectrograph measurements at 2520-3375 Å of metal trace elements in biological sample solutions
06 p0657 A73-17692

Abundance patterns of thirteen trace elements in primitive carbonaceous and unequilibrated ordinary chondrites.
07 p0877 A73-19651

Neutron activation analysis for geochemical origin and trace element compositions of moldavites and source rocks from Ries impact crater
07 p0877 A73-19652

On lunar metallic particles and their contribution to the trace element content of Apollo 14 and 15 soils.
07 p0884 A73-19746

Chemical characteristics of trace element rich KREEP basaltic rocks from Apollo 12 landing site
07 p0885 A73-19753

Major, minor, and trace element data for some Apollo 11, 12, 14, and 15 samples.
07 p0886 A73-19759

Rare earths and other trace elements in Apollo 14 samples.
07 p0886 A73-19760

Chondrite normalized major and trace element concentrations of Apollo 14 lunar samples, including basalt, breccia and regolith fines
07 p0886 A73-19761

Major impacts on the moon - Characterization from trace elements in Apollo 12 and 14 samples.
07 p0887 A73-19768

Apollo 14 and 15 samples - Rb-Sr ages, trace elements, and lunar evolution.
07 p0887 A73-19777

Trace element relations between Apollo 14 and 15 and other lunar samples, and the implications of a moon-wide Cl-KREEP coherence and Pt-metal non-coherence.
07 p0890 A73-19810

Atmospheric dust trace elements levels sampled in United Kingdom, considering natural origin
07 p0820 A73-20279

Inter-element relationships between trace elements in primitive carbonaceous and unequilibrated ordinary chondrites.
07 p0903 A73-20619

Chemical fractionations in meteorites. VI - Accretion temperatures of H-, LL-, and E-chondrites, from abundance of volatile trace elements.
07 p0789 A73-20622

Depth variation of Apollo 15 deep drill fines trace elements from neutron activation analysis, noting KREEP abundance
10 p1278 A73-24113

Luna 20 and Apollo 16 lunar soil samples rare earth, iron and other trace elements contents from neutron activation analysis, noting Eu anomaly
13 p1675 A73-28317

Allende carbonaceous chondrite Ca-Al rich inclusion refractory trace metals condensation temperature calculation, indicating high temperature primitive solar nebula condensates
13 p1684 A73-29176

Carbonaceous chondrite neutron activation analysis for trace elements, revealing compositional homogeneity
13 p1684 A73-29181

Volatile elements in Apollo 16 samples - Possible evidence for outgassing of the moon.
15 p1933 A73-31370

Minor and trace elements in some meteoritic minerals.
15 p1941 A73-32387

Chemical fractionations in meteorites. VII - Cosmochemistry and cosmochemistry.
15 p1841 A73-32390

Upper atmosphere pollution and near surface climatic and trace gas distribution
[AIAA PAPER 73-492]
16 p2005 A73-33536

Trace gases, aerosols, and solar radiation in the stratosphere - Explored and unexplored problem areas.
[AIAA PAPER 73-509]
16 p2006 A73-33547

Measurement of trace gases in the stratosphere using far infra-red spectroscopy.
[AIAA PAPER 73-516]
16 p2006 A73-33553

Sample preparation, irradiation, and counting and data reduction scheme for trace element analysis of coal using neutron activation
21 p2737 A73-40632

Major and trace elements in igneous rocks from Apollo 15.
23 p2950 A73-43765

Geochemical coherence between trace elements and K, P and rare earth elements in lunar soils evaluated for samples evolutionary history
23 p2951 A73-43767

Radiochemical neutron activation analysis for extralunar trace elements in Apollo 14 lunar soil 14141, comparing with mature samples and Fra Mauro subregolith materials
23 p2951 A73-43846

Background concentrations of photochemically active trace constituents in the stratosphere and upper troposphere.
23 p2976 A73-43889

Some characteristics of the global distribution of the trace element concentration in the lower troposphere.
24 p3085 A73-44967

TRACERS

Utilization of radioactive isotopes as tracers in the investigation of general atmospheric circulation
05 p0593 A73-16234

A three-dimensional stratospheric point-source tracer experiment and its implications for dispersion of effluent from a fleet of supersonic aircraft.
[AIAA PAPER 73-528]
16 p2007 A73-33562

Flash photography using laser excited fluorescent tracers.
21 p2709 A73-39969

Eole experiment on dispersion of Lagrangian tracers in quasi-stationary two dimensional turbulent flow, noting rms distance between paired balloons
21 p2687 A73-41337

Compartmental analysis of biological system with a digital computer.
22 p2829 A73-42228

Design criteria for finite-difference models for eddy diffusion with winds that guarantee stability, mass conservation, and nonnegative masses.
24 p3085 A73-45018

TRACKERS

U TRACKING [POSITION]

TRACKING [POSITION]

NT COMPENSATORY TRACKING
NT INFRARED TRACKING
NT MISSILE TRACKING
NT OPTICAL TRACKING
NT PHOTOGRAPHIC TRACKING
NT PURSUIT TRACKING
NT RADAR TRACKING
NT RADIO TRACKING
NT RANGE AND RANGE RATE TRACKING
NT SATELLITE TRACKING
NT SPACECRAFT TRACKING
NT STAR TRACKERS
NT WILDLIFE RADIOLOCATION

A simple Fourier analysis technique for measuring the dynamic response of manual control systems.
01 p0027 A73-10321

A method for aiding human operator performance in a noncompensatory tracking task.
01 p0011 A73-10323

Phase and frequency tracking accuracy in direct-detection optical-communication systems.
04 p0416 A73-14993

Nonlinear analysis of double feedback loop tracking system with coupling, obtaining steady state phase error probability density functions with application to satellite transponder
04 p0429 A73-14994

Estimating the mean time until follow-up cutoff in a nonlinear sampled-data servosystem for irregular arrival of the signal.
04 p0430 A73-15205

An autonomous navigation technology system.
04 p0474 A73-15274

- Digital phase locked loops for incoming signal phase tracking, predicting performance from nonlinear difference equation model for comparison with digital simulation 04 p0421 A73-15435
- Step input tracking experiment for testing human psychological refractory period, noting directional error correcting reaction time similarities with keyboard tasks 06 p0659 A73-18470
- Time-invariant single input/output controllable and observable tracking servosystem, discussing dynamic trajectory controller and cost functional selection for zero steady state error 06 p0680 A73-18516
- Adaptive trackers based on continuous learning theory. 06 p0682 A73-18821
- Comparison of human operator critical tracking task performance with aural and visual displays. 08 p0936 A73-21667
- Passive solar array orientation devices for terrestrial application. 09 p1033 A73-22440
- Tracking performance of a phase locked loop with a linear phase detector. 09 p1058 A73-23432
- Convergence criteria for reverse error coefficient expansion under transient conditions for tracking servo system with open loop transfer function 15 p1854 A73-31735
- The mechanism of gyroscopic tracking. I. [ASME PAPER 72-MECH-32] 15 p1883 A73-32284
- The mechanism of gyroscopic tracking. II. [ASME PAPER 72-MECH-33] 15 p1883 A73-32285
- TVAC - A television area correlator tracking system. 17 p2171 A73-35381
- Ocean currents observation by ship and satellite tracking of free-drifting Lagrangian platforms [ASAE PAPER 73-144] 20 p2550 A73-38593
- Imaging system pointing precisions, deriving ground target size relationships to spread function and modulation transfer function respectively 20 p2567 A73-39672
- An improved light gun tracking algorithm based on a recursive digital filter. 21 p2654 A73-40834
- TRACKING ANTENNAS**
U DIRECTIONAL ANTENNAS
TRACKING FILTERS
- Signal search networks for enlargement of locking bandwidth of tracking filters in automatic control systems, examining transistorized signal search and acquisition circuits 02 p0145 A73-17193
- Superconducting time variant filter tracking test for RF signal amplitude modulation, using photoelectric perturbation in semiconductor cavity resonant frequency 02 p0146 A73-11847
- A new filter for optimal tracking in dense multitarget environments. 03 p0286 A73-14477
- Optimal nonlinear estimator algorithms for tracking in face of incorrect sensor returns in multitarget environments, using posteriori probability selective measurements 04 p0431 A73-15260
- A higher measurement space filter for passive tracking. 04 p0431 A73-15262
- Application of adaptive tuning of filters to exoatmospheric target tracking. 04 p0498 A73-15275
- Adaptive nonlinear filtering for tracking with measurements of uncertain origin. 07 p0805 A73-20584
- Comparison of theoretical and simulated performance of optimal and suboptimal filters in a dense multitarget environment. 07 p0806 A73-20604
- Transient analysis of phase-locked tracking systems in the presence of noise. 09 p1066 A73-22113
- Linear regression filtering and prediction for tracking maneuvering aircraft targets. 11 p1333 A73-26640
- Self adaptive filter algorithm for automatic tracking of high performance maneuvering targets in real time surveillance systems in changing environments 13 p1596 A73-29207
- Kalman filter adaptive tracker for ATC applications, modeling aircraft maneuvers by linear system with random noise accelerations based on statistical decision theory 13 p1593 A73-29212
- Aided tracking as applied to high accuracy pointing systems. 15 p1854 A73-31726
- Synthesis and analysis of tracking systems with optimal acquisition. 15 p1854 A73-31727
- TRACKING NETWORKS**
NT DEEP SPACE NETWORK
NT GLOBAL TRACKING NETWORK
- NT MANNED SPACE FLIGHT NETWORK
NT STADAN [SATELLITE TRACKING NETWORK]
- Singularity solutions to critical configurations of geodetic range networks with distributed and in plane ground stations and target satellites 04 p0436 A73-14777
- Secor equatorial network evaluation of satellite geodesy program, discussing range data and geocentric coordinate computation and adjustments 04 p0437 A73-14782
- Secor range observations on Geos 1 satellite in Pacific tracking network, determining station coordinates, relative positions and geodetic heights 04 p0437 A73-14783
- Digital photoelectric tracking systems with accumulation of the mismatch signal 16 p1977 A73-32716
- TRACKING RADAR**
- Linear rapid frequency settling time solid state voltage controlled oscillators /VCO/ for electronic countermeasure and B-scan tracking radar applications 01 p0024 A73-10723
- Real time tracking radar for radio guidance system, obtaining algorithm for rocket motor direction and ignition time for satellite orbit optimization 03 p0339 A73-13067
- Optimal correlation of sensor data with tracks in surveillance systems. 06 p0682 A73-18822
- Adaptive real time control for defense systems - A minimum risk algorithm. 06 p0682 A73-18823
- Tracking radar equipment evolution in connection with French space program development, describing reliability technology 07 p0807 A73-18943
- Automated radar terminal systems /ARTS/. 07 p0849 A73-19184
- A theory of tracking for a dynamic radar scatterer ensemble. 10 p1189 A73-24532
- Linear and nonlinear first order closed loop tracking radar systems, predicting noise performance by Gaussian signal amplitude fluctuation modeling 13 p1585 A73-29206
- Automatic checkout and monitoring in the AN TPQ-27 radar system. 13 p1585 A73-29210
- Solid state null tracking Doppler radar ground velocity sensor for supersonic weapon delivery aircraft precision bombing, discussing design and test with computer simulation 17 p2137 A73-35209
- Optimum cross-coupled tracker for pulse-Doppler radar. 21 p2649 A73-40328
- Russian book - Digital methods and systems in radar technology. 21 p2657 A73-41433
- TRACKING STATIONS**
NT GLOBAL TRACKING NETWORK
NT STADAN [SATELLITE TRACKING NETWORK]
- Unified S-band ground system design and management for Apollo program, deep space and manned space flight network tracking and communications requirements 01 p0030 A73-11184
- Center of mass coordinates of Baker-Nunn camera tracking stations from Geos 1 and Geos 2 optical flash data 04 p0437 A73-14785
- Tracking stations interdistances and solid-earth tidal perturbations determination by laser ranging to satellites 04 p0439 A73-14801
- Two channel multimode feed for circular horn tracking antenna applications, discussing channel patterns, coupling, isolation and frequency response 04 p0428 A73-15417
- Mobile ground station for sounding balloons remote control, telemetry and localization, noting antenna pointing control, tracking receiver and trajectory recording 07 p0790 A73-18972
- Clock synchronization experiments performed via the ATS-1 and ATS-3 satellites. 10 p1217 A73-23996
- Ship positioning by sonar group and ultrasonic transponder beacons with tracking station axis direction definition capability 14 p1741 A73-30083
- TRACKING STUDIES**
U TRACKING [POSITION]
- TRACTION**
- The role of compressional viscoelasticity in the lubrication of rolling contacts. [ASME PAPER 72-LUB-O] 01 p0055 A73-10220
- The role of compressional viscoelasticity in the lubrication of rolling contacts. [ASME PAPER 72-LUB-O] 03 p0315 A73-14354
- On the uniqueness of singular solutions to boundary-initial value problems in linear elastodynamics. 04 p0512 A73-15226
- A lunar surface vehicle concept from the viewpoint of assumptions concerning the mechanics of the vehicle-terrain system 06 p0683 A73-17773
- Frictional traction in elastohydrodynamic lubrication. 13 p1623 A73-28198
- Forced extensional vibrations of isotropic elastic plates with time dependent body forces, surface tractions and nonhomogeneous boundary conditions, using Kane-Mindlin theory 16 p2076 A73-32920
- Computer analysis of clamped-clamped and clamped-supported cylindrical shells. 22 p2927 A73-42995
- TRACTORS**
- Automatic machine test equipment and procedures for hydraulic systems, tractor shafts and automobile wheels 13 p1625 A73-29135
- TRACTS**
U SITES
TRADEOFFS
- Cost/weight tradeoff ratios for fiber reinforced plastic aircraft structural components [SAE PAPER 730338] 17 p2257 A73-34689
- Tradeoff studies for feasibility of multiblade ring rotor configuration for helicopter design, discussing ring drag [AHS PREPRINT 714] 17 p2104 A73-35060
- Control of multiplexed communications channels. 17 p2144 A73-35310
- Spacecraft systems design trade-offs for the Earth Resources Technology Satellite. 17 p2239 A73-35631
- Design, capability, and cost of a Versatile Upper Stage /VUS/ family of vehicles. [AIAA PAPER 73-589] 18 p2357 A73-36078
- Antenna coupling induced intersystem electromagnetic interference prediction, discussing tradeoffs between analysis level, input information, measurements, cost results and user requirements 22 p2822 A73-41795
- TRAFFIC**
NT AIR TRAFFIC
TRAFFIC CONTROL
- NT AIR TRAFFIC CONTROL
- NT RADAR APPROACH CONTROL
- Synchronous satellite systems for civilian air, ship and land vehicle traffic control, communication, navigation and surveillance, discussing technology requirements for continental and oceanic systems [AIAA PAPER 73-583] 18 p2288 A73-36075
- Low cost airport surveillance and Localized Cable Radar with runway or taxiway vehicle guidance capability for ground traffic control, using solid state equipment 21 p2736 A73-40051
- Use of simulation in airport planning and design. [ASCE PREPRINT 2038] 22 p2839 A73-42865
- TRAILING EDGES**
- Effect of streamwise vortices on wake properties associated with sound generation. 01 p0001 A73-10045
- Turbulent wake flow behind two dimensional flat plate trailing edge investigated by Nec-Kovaszay turbulent shear flow differential field theory 01 p0004 A73-11137
- The interaction between turbulent wakes and boundary layers. 03 p0244 A73-13561
- Experimental determination of bound vortex lines and flow in the environment of the trailing edge of a slender delta wing [AD-755630] 05 p0528 A73-16600
- Three dimensional steady flow of incompressible viscous fluid near thin wing trailing edge, using Stewartson-Williams triple layer method 08 p0926 A73-21495
- Some characteristics of the flow downstream of a blunt trailing edge in the presence of a neighbouring wall. 10 p1173 A73-24818
- Unsteady boundary layer and wake near the trailing edge of a flat plate. 10 p1173 A73-24826
- On the Kutta-condition at the trailing edge of a nozzle in a weakly nonstationary jet flow. 10 p1209 A73-24827
- Noise reduction for subsonic fluid flow over flat plate via interposition of secondary fluid layer at trailing edge 11 p1300 A73-25386
- Fish like slender body propulsion and flow theory, discussing fin surface-body thickness interaction, vortex sheets, trailing edges and lifting force 11 p1301 A73-25852
- Flow at the trailing edges of a blade cascade at variable M and Re numbers 12 p1457 A73-27096
- Effect of trailing edge thickness on the cascade performance of circular-arc blades. 13 p1565 A73-29006

TRAILING-EDGE FLAPS

- Theoretical investigation on stall flutter of an aerofoil /the case of trailing edge stall/ 13 p1566 A73-29027
- Equivalence rule and transonic flow theory involving lift. 18 p2264 A73-36328
- Trailing vortex pair instability in inviscid incompressible fluid with rotating and nonrotating isolated and axial velocity jet core 18 p2300 A73-36628
- Gas turbine nozzle guide vane trailing edge protection by air films cooling, measuring gas temperatures with chromel-ahumel thermocouples 20 p2600 A73-39425

TRAILING-EDGE FLAPS

- Fighter aircraft maneuverability improvement at high subsonic speeds by slotted and unslopped leading- and trailing-edge flaps on delta wing [DGLR PAPER 72-126] 03 p0248 A73-14386
- Externally blown flap trailing edge noise reduction by slot blowing - A preliminary study. 05 p0532 A73-16969
- [AIAA PAPER 73-245]
- Mechanisms of externally blown flap noise. [AIAA PAPER 73-1029] 24 p3056 A73-44859

TRAINERS

U TRAINING DEVICES

TRAINING

U EDUCATION

TRAINING AIRCRAFT

- NT JAGUAR AIRCRAFT
- NT T-33 AIRCRAFT
- NT T-39 AIRCRAFT
- SOKO Galeb - 3 cantilever low wing trainer-fighter monoplane with Bristol-Siddeley Viper 20 turbojet engine, describing flight control, loading gear, fuel system and avionics 14 p1712 A73-30240

- HS 1182 multipurpose ground attack trainer aircraft, describing weapon system, hydraulic flight control, power plant and avionics 14 p1713 A73-30934

- Wind tunnel simulation of jet exhaust in low speed testing of Franco-German Alpha-Jet trainer and fire support aircraft 16 p1993 A73-32802

- The simulator industry and its contribution to military training requirements. 16 p1996 A73-33208

- Design and application of a part-task trainer to teach formation flying in USAF Undergraduate Pilot Training. [AIAA PAPER 73-935] 21 p2674 A73-40881

TRAINING DEVICES

NT TEACHING MACHINES

- Computer-controlled differential review-time payoff as a training aid. 05 p0544 A73-16725

- Performance measurement system for combat crew flight training in complex aircraft weapon systems, identifying training research goals 05 p0544 A73-16726

- Computer assisted instruction for commercial programmer and systems analyst education and training, discussing government use, pretest importance and future developments 09 p1168 A73-22222

- Turana drone system design and development for Australian naval guns and guided weapons exercises, describing construction and operational details 09 p1032 A73-23122

- Engineering personnel, technical and flight instructors training for introduction to and effective utilization of new civil and military aircraft and weapon systems 13 p1624 A73-28789

- Astronomical educational aids design and application, including photometers for star cluster detection, ocular comparators and projection devices for photograph examination 16 p2014 A73-32950

- The B.O.A.C. navigation procedures trainer. 19 p2418 A73-37874

- The oculometer - A new approach to flight management research. [AIAA PAPER 73-914] 21 p2702 A73-40862

- A visual display system approach for an advanced spaceflight simulator. [AIAA PAPER 73-923] 21 p2673 A73-40871

TRAINING SIMULATORS

NT COCKPIT SIMULATORS

NT FLIGHT SIMULATORS

- ATC simulator, discussing student training routines and exercises, automatic navigation and aircraft pilot-instruction 02 p0190 A73-11853

- A flight control simulator - A computer system for the training of flight control personnel 13 p1598 A73-29100

- Jet procedures trainer for pilot transition from straight wing propeller plane to swept wing jets, discussing pilot instruction and selection 15 p1837 A73-31095

- Training simulator for civil aviation schools 15 p1859 A73-32511

- British Airline Pilots Association and RAF Institute of Aviation Medicine questionnaire results on training simulator effectiveness, analyzing auditory and visual aids 16 p1996 A73-33213

- Visual scene simulation with computer generated images. 17 p2147 A73-34820

- Monte Carlo simulation on CRT display for training and learning system reliability and early decision effects on life cycle cost effectiveness 17 p2140 A73-35261

- The B.O.A.C. navigation procedures trainer. 19 p2418 A73-37874

- A visual detection simulator /VDS/ for pilot warning instrument evaluation. 21 p2672 A73-40864

- An approach to computer image generator for visual simulation. [AIAA PAPER 73-928] 21 p2673 A73-40875

TRAJECTORIES

- NT ABORT TRAJECTORIES
- NT ASCENT TRAJECTORIES
- NT BALLISTIC TRAJECTORIES
- NT DESCENT TRAJECTORIES
- NT EARTH-MARS TRAJECTORIES
- NT EARTH-MOON TRAJECTORIES
- NT EARTH-VENUS TRAJECTORIES
- NT ELECTRON TRAJECTORIES
- NT HYPERBOLIC TRAJECTORIES
- NT INTERPLANETARY TRAJECTORIES
- NT LUNAR TRAJECTORIES
- NT MISSILE TRAJECTORIES
- NT MOON-EARTH TRAJECTORIES
- NT PARTICLE TRAJECTORIES
- NT REENTRY TRAJECTORIES
- NT RENDEZVOUS TRAJECTORIES
- NT ROUND TRIP TRAJECTORIES
- NT SPACECRAFT TRAJECTORIES

TRAJECTORY ANALYSIS

- Gravity thrust Jupiter orbiter trajectories generated by encountering the Galilean satellites. 01 p0095 A73-10103

- Application of ultrastable oscillators to aerospace [ONERA, TP NO. 1114] 01 p0045 A73-10235

- Systematics of earth-to-moon trajectories. I 01 p1012 A73-10995

- Universal dimensionless formulas for physical property and trajectory computation in cosmic spherical media, applying to Kepler orbits, particle motions and radio wave paths 01 p1013 A73-11019

- Sufficient conditions for the optimal control problem 01 p0071 A73-11269

- Roundoff and uncertain data error analysis, discussing hasty judgements, double precision, trajectory problems, ill-posed problems, computer software and hardware flaws, etc 01 p0021 A73-11460

- Rocket flight in rarefied layers of the atmosphere 02 p0227 A73-11579

- Missile range dispersions produced by meteorological factors, drag differences and mass changes during passive ballistic flight 02 p0211 A73-11787

- Variational method in the invariance problem for controlled systems. 02 p0149 A73-12117

- Shadowing of electron azimuthal-drift motions near the noon magnetopause. 02 p0164 A73-12442

- Electron and muon density fluctuations, trajectory distribution and azimuthal symmetry in cosmic ray air showers 02 p0209 A73-12673

- Monte Carlo classical trajectory calculation of the rates of F-atom vibrational relaxation of HF and DF. 03 p0318 A73-13280

- Monte Carlo classical trajectory calculation of the rates of Hand D-atom vibrational relaxation of HF and DF. 03 p0318 A73-13280

- Short term bounds for the effect of oblateness on ballistic trajectories. 03 p0373 A73-13495

- Phase space trajectory analysis of pulsed laser spot pursuit tracking problem for autonomous line-of-sight interceptor missile with flip-flop controls 03 p0287 A73-14483

- Trajectory analysis for swingby technique using Jovian gravitational field for leaving plane of ecliptic along heliocentric orbit and for solar flyby at specified distance 03 p0378 A73-14552

- Analytical study of the evolution of the normal to the wave during the magnetospheric passage of PC 1's 04 p0440 A73-15248

- Solution structure duality between nonlinear filtering with finite dimensional sensor orbit and nonlinear control with involuntary actuator orbit 04 p0431 A73-15264

- Relaxation algorithms for nonlinear system modal trajectory estimation by approximate step with lower

- triangular matrix inversions sequence, comparing convergence with Gauss-Newton method 04 p0472 A73-15262

- Minimum impulse three-body trajectories. [AIAA PAPER 73-145] 05 p0619 A73-16890

- Flight-path characteristics for few re-entry trajectories. 05 p0623 A73-17274

- On a quadratic first integral for the charged particle orbits in the charged Kerr solution. 06 p0725 A73-17869

- Semiclassical theory of inelastic collisions. II - Momentum-space formulation. 06 p0726 A73-18226

- The effects of trajectory characteristics on scientific objectives for major planetary orbiters. 06 p0757 A73-18370

- Numerical model for three dimensional air parcel trajectories computation from operational wind forecasts, deriving atmospheric moisture, dew and temperature distributions predictions 06 p0720 A73-18700

- Distribution of reaction products /theory/. VIII - C₂ + H₂, C₂ + D₂. 07 p0788 A73-19926

- Steady state slow stellar velocity solution for accretion stream beyond neutral point, estimating cutoff range for braking force of gas cloud 07 p0898 A73-19936

- Asymptotic solution to the problem of optimal low-thrust energy increase. 07 p0899 A73-19962

- The anisotropic Kepler problem in two dimensions. 08 p0988 A73-21204

- Russian book on celestial and space flight mechanics covering trajectory and orbit evolution problems, resonance effects, relative motion dynamics and mathematical treatment 09 p1146 A73-22350

- Russian book on earth satellite, lunar, interplanetary and reentry trajectory analysis and optimal control covering motions under low thrust, aerodynamic heating and ablation 10 p1286 A73-23949

- Phase double plane as a method to study the dynamics of a spacecraft with limited constructional rigidity. 10 p1286 A73-24006

- Solid sphere meandering trajectory in viscous liquid filled cylinder, postulating oscillating molecular surface tension layer at interface 10 p1206 A73-24701

- Determination of the turn start point coordinates for modern commercial aircraft 11 p1307 A73-26723

- Satellite ascent transfer trajectories equations of motion numerical integration, replacing time parameter by regularizing independent variable for gravitational singularity elimination [DFVLR-SONDDR-283] 12 p1537 A73-26822

- Influence of the thrust interruption during passage through the shadow cone of a celestial body on the trajectory of a space vehicle using solar electric propulsion - First approximation calculation 12 p1540 A73-27393

- Nonlinear problems in analyzing the observability of the trajectories of spacecraft motion according to measurement data. 12 p1543 A73-27628

- The sensitivity of nominally time-optimal control systems to parameter variation. 13 p1597 A73-29567

- Pons-Brooks comet orbit calculation based on observations in 1812, 1883-1884 and 1953-1954, noting impossibility of single orbit fitting 14 p1791 A73-29806

- Determination of planetary masses from the motions of comets. 14 p1792 A73-29809

- Methods of evaluation of tracking procedures used at the French Guiana Space Center 14 p1727 A73-30093

- French launching base real time trajectory system for rocket space location information, investigating evolution towards maximum reliability 14 p1773 A73-30094

- Elimination of time and differential equation of trajectories in the problem of three restricted, circular, plane bodies 15 p1930 A73-31175

- Choice of a zero approximation of the angular position of a satellite on a trajectory segment of oriented motion in the case of a dipolar approximation of the geomagnetic field 15 p1942 A73-31237

- Rapid estimation and detection of impulse inputs under continuity constraints for space vehicles. 17 p2144 A73-35375

- Quasi-periodic orbits about the translunar libration point. 18 p2352 A73-36420

- The rocket motion in resisting medium on a given trajectory. 18 p2353 A73-36490

Solving M. A. Aizerman's first problem of absolute stability of nonlinear systems on the basis of the general theory of root trajectories

18 p2337 A73-37025

EOLE balloon clusters horizontal trajectories as indicators of southern hemisphere atmospheric circulation, estimating rms divergence as function of scale

19 p2424 A73-37661

The P-star technique and its application to inertial guidance.

[AIAA PAPER 73-837]

20 p2584 A73-38780

Computerized trajectory estimation for maneuvering reentry vehicles, obtaining minimum variance trajectory parameters by Kalman filtering of radar, optical and inertial reference measurements

[AIAA PAPER 73-902]

20 p2589 A73-38836

Root trajectories method for stability analysis of two channel automatic control systems with antisymmetric and symmetric cross couplings

20 p2541 A73-38980

Interference parameters in the problem of estimating the accuracy of prediction of spacecraft motion

21 p2781 A73-40904

Dynamics of a laser with regulated cavity Q

21 p2716 A73-41510

General relativistic gravitation theories based space-time curvature tests near sun from interplanetary probe motion analysis using probe-borne laser light transmission

[ONERA, TP NO. 1210]

22 p2907 A73-42216

Liapunov-like theorems of quantitative stability information on trajectory bounds in state space subset form

22 p2888 A73-43020

Increase of closed-loop nominal trajectory likelihood in uncertain systems.

23 p2962 A73-43280

Typical characteristics of dynamic systems nearly all of whose trajectories remain stable under steadily acting disturbances

24 p3109 A73-44424

Rectilinear trajectories of the three-body problem when the constant of line forces is zero

24 p3141 A73-45282

TRAJECTORY CONTROL

NT TRAJECTORY OPTIMIZATION

Investigation of the dissipativity of a pulse-frequency modulated system of stabilizing an unsteady plant

01 p0027 A73-10596

Electrical power source for spacecraft reentry trajectory control system, thermal protection and radio communication based on reentry vehicle external surfaces utilization as generator electrodes

01 p0111 A73-11174

Guidance of spacecraft controlled by low-thrust rocket engines and evolving in the plane of the initial trajectory

02 p0227 A73-11580

Development and qualification results of the monergonic propulsion system for the aeronomy satellite Aeros

[DGRL PAPER 72-079]

02 p0228 A73-11696

Propulsion system performance for satellite attitude and orbit correction, discussing hydrogen, ammonia and hydrazine resistojets

[DGRL PAPER 72-078]

02 p0203 A73-11697

Multistep three-parameter algorithm for spacecraft stabilization on an atmospheric reentry trajectory

02 p0229 A73-12451

Game problem of impulse controlled soft rendezvous of two material points under attraction and control forces

03 p0344 A73-14044

Prediction in control of re-entry into the atmosphere.

05 p0627 A73-16076

Estimating trajectory correction requirements for multiple outer planet missions.

05 p0623 A73-17205

Space shuttle flight operations ground support systems for trajectory control and systems/mission management, discussing payloads data acquisition and transmission to user

[AIAA PAPER 73-36]

06 p0755 A73-17620

Trajectory deviation conditions in second order linear differential escape game

07 p0850 A73-19014

Real-time analysis and ground command control to achieve accurate vehicle and payload event functions.

[AIAA PAPER 73-298]

09 p1117 A73-23217

Some problems of optimal control of space-vehicle trajectories in the Martian atmosphere

10 p1247 A73-23878

An algorithm for controlling the descent of a spacecraft from an artificial earth satellite orbit.

12 p1543 A73-27631

AEROS research satellite acquisition phase performance, considering injection, attitude determination and control, trajectory measurement and correction, nutation reduction, solar alignment, etc

13 p1689 A73-28782

AEROS aeronomy satellite successfully completes acquisition phase.

13 p1689 A73-28783

The concept of the flight safeguard interferometer for rocket probes of the French Guiana Space Center

14 p1773 A73-30090

Optimal control synthesis in the observation problem. I, II

14 p1802 A73-30788

Guidance of aircraft according to techniques of trajectory plotting with a clock

15 p1911 A73-32489

Three-parameter multistep algorithms for stabilization of a spacecraft on the descent trajectory through the atmosphere.

15 p1944 A73-32601

F/RF-101 ejection seat upgrade kit for performance improvement, discussing propulsion, trajectory control, snubber system and rapid recovery parachute opening

16 p1966 A73-32667

Mission, project profile, and description of the Symphonic satellite

[DGRL PAPER 73-043]

17 p2126 A73-35480

Optimal guidance for aerodynamically controlled reentry vehicles.

[AIAA PAPER 73-891]

20 p2588 A73-38827

Nonlinear trajectory following in the terminal area - Guidance, control and flight mechanics concepts using the microwave landing system.

[AIAA PAPER 73-903]

20 p2589 A73-38837

Some problems in the optimal control of spacecraft trajectories in the Martian atmosphere.

20 p2589 A73-38897

Nonlinear trajectory-following and control techniques in the terminal area using the Microwave Landing System Navigation Sensor.

21 p2734 A73-40038

Space shuttle orbiter abort guidance for premature or abnormal termination of mission due to system or human failure, discussing predictive algorithm

21 p2735 A73-40045

Utilization of tangential trajectories for lowering high-altitude elliptic orbits of artificial satellites of planets

23 p3027 A73-43265

TRAJECTORY MEASUREMENT

Study of accuracy requirements for autonomous trajectory measurements providing conditions for entering planetary atmospheres

05 p0619 A73-17001

High-speed stereoscopic investigation of paths of luminous objects

08 p0969 A73-21719

Automotive approach systems certification and short distance takeoff and landing trajectory by cinehologues, digital optical, airborne and inertial/radiosonde equipment

10 p1246 A73-23656

AEROS research satellite acquisition phase performance, considering injection, attitude determination and control, trajectory measurement and correction, nutation reduction, solar alignment, etc

13 p1689 A73-28782

The quantity of initial-parameter information contained in trajectory measurements

21 p2726 A73-40916

TRAJECTORY OPTIMIZATION

A Chebyshev minimax technique oriented to aerospace trajectory optimization problems.

01 p0100 A73-10729

Trajectory optimization of pursuer vehicle for multitarget rendezvous, noting algorithm for dynamic programming

01 p0105 A73-11124

The optimum reentry trajectory of a lifting vehicle.

01 p0105 A73-11126

Reentry trajectory optimization at superorbital velocities by aerodynamic lift control, using Pontryagin maximum principle

01 p0105 A73-11127

A fast computational algorithm for optimum digital control systems.

01 p0021 A73-11463

Second order trajectory optimization tests in terms of Kelley-Contensou extremals and conjugate points, applying to astrodynamical singular arc

02 p0187 A73-11996

Application of the conditional-gradient method to the solution of an optimum control problem in a Hilbert space

02 p0187 A73-12188

Three parameter boundary value problem for trajectory optimization of maximum weight station injection from earth orbit into interplanetary flight trajectory

02 p0219 A73-12454

Minimization of spacecraft maximum acceleration in atmosphere after reentry, applying results to reentry trajectory optimization and associated optimal control problems

02 p0219 A73-12457

Algorithms for spacecraft trajectory optimization programs for orbit perturbations caused by random measurement errors and minimum mathematical expectancy of energy dissipation

02 p0220 A73-12468

Real time tracking radar for radio guidance system, obtaining algorithm for rocket motor direction and ignition time for satellite orbit optimization

03 p0339 A73-13067

Nearly-optimal single impulsive transfers between coplanar elliptical satellite orbits with identical pericenter altitude

03 p0372 A73-13299

Optimal horizontal guidance law for aircraft in the terminal area.

03 p0340 A73-13518

Spacecraft optimal control after transfer from hyperbolic trajectory to planetary orbit by atmospheric drag, minimizing engine thrust

03 p0340 A73-14570

Optimum elliptic orbit characteristics of planetary artificial satellite based on earth-planet-earth flight

03 p0379 A73-14572

Reorientation of a spacecraft

04 p0504 A73-14885

Optimal trajectory control system synthesis via Pontryagin maximum principle, taking into account system dynamics, control constraints and boundary conditions

04 p0429 A73-15201

Method of solving the interplanetary orbit optimization problem with an invariant nomographic scale.

05 p0613 A73-16093

Russian book - Control of moving objects.

05 p0628 A73-16401

Problems of realization of optimal trajectories for spacecraft entry into the dense layers of the earth's atmosphere

05 p0616 A73-16409

Optimal correction of a planetary-approach trajectory for transfer to an artificial-satellite orbit

05 p0616 A73-16428

Minimum impulse three-body trajectories.

05 p0619 A73-16894

Aircraft performance augmentation by energy management instruments or systems, considering energy/energy rate meter and algorithm for real time onboard flight path optimization

05 p0536 A73-16953

Long-range energy-state maneuvers for minimum time to specified terminal conditions.

05 p0536 A73-16954

Energy management in aerial combat weapon systems maneuvering and delivery tactics, computing optimal feedback control laws for supersonic aircraft minimum time turning trajectories

05 p0536 A73-16956

Soft constraint trajectory optimization formulation as real time optimal feedback guidance method for multiburn orbital maneuvers

05 p0596 A73-16972

Orbital parameters optimization of circular orbit earth satellites network for continuous earth observation, using group theory

05 p0620 A73-17004

Optimization of multiple target electric propulsion trajectories.

06 p0748 A73-17658

Optimum flight paths of rocket powered vehicles for general thrust law.

06 p0756 A73-17742

Time-invariant single input/output controllable and observable tracking servosystem, discussing dynamic trajectory controller and cost functional selection for zero steady state error

06 p0680 A73-18516

Space /rocket/ launch vehicle computer guidance and targeting equations, discussing Q, Delta, explicit, linear tangent, optimal, numerical integration and parameter optimization techniques

06 p0721 A73-18824

Impulsive deboost analysis for maximum and minimum atmospheric entry angles for hyperbolically orbiting rocket vehicles

07 p0875 A73-19207

Asymptotic solution to the problem of optimal low-thrust energy increase.

07 p0899 A73-19962

Computational aspects of multilevel trajectory optimization.

07 p0903 A73-20589

Theory and application of the optimal linear approximation of linear processes

08 p0983 A73-20645

Powered-flight trajectory optimization for an inertial-guidance ballistic vehicle.

08 p0101 A73-21427

Optimal entry algorithm and multiimpulse correction times for spacecraft guidance trajectory of minimum fuel consumption

10 p1247 A73-23881

Russian book on earth satellite, lunar, interplanetary and reentry trajectory analysis and optimal control covering motions under low thrust, aerodynamic heating and ablation

10 p1286 A73-23949

Space shuttle ascent-flyback trajectory optimization with in-flight inequality constraints based on ac-

TRANQUILIZERS

- celerated gradient parameters determination including attitude control angles 10 p1276 A73-24002
- Trajectory optimization for the nonlinear combined estimation and control problem. 10 p1200 A73-24044
- Maximum range flight path during climb with specified fuel supply and variable lift coefficient, solving differential equations system by conjugate gradient procedure 10 p1175 A73-24542
- Guidance methods for heat-optimal three-dimensional descent paths of aerodynamic reentry bodies 11 p1430 A73-25350
- An optimal control approach to terminal area air traffic control. 11 p1394 A73-25786
- Hohmann trajectories efficiency for interplanetary transfers of spacecraft between circular coplanar orbits, considering earth-Mars-earth flight and transition to parabolic trajectory 12 p1538 A73-27065
- Supermemory gradient-restoration algorithm in flight-path optimization problems 12 p1548 A73-27082
- General theory of optimal trajectory for rocket flight in a resisting medium. 12 p1538 A73-27119
- Evaluation of glide paths for landing a VTOL airplane using linear regulator theory. 12 p1458 A73-27154
- The selection of measurable parameters in the determination of the trajectory of a space vehicle. 12 p1543 A73-27626
- Optimal descent maneuver with a limited-thrust engine for entry at a prescribed angle into the atmosphere of a planet 13 p1689 A73-29139
- Minimum time of Earth-to-Mars and Earth-to-Venus flights with an uncontrolled limited-power engine 14 p1795 A73-29856
- Optimal control of discrete systems 14 p1738 A73-30348
- Suboptimal terminal feedback control of nonstationary, nonlinear systems. 14 p1739 A73-30507
- Russian book - Mechanics of controlled motion and problems of cosmic dynamics. 15 p1930 A73-31226
- Optimization of descent maneuvers for a section of a satellite in a planetary orbit 15 p1931 A73-31227
- Optimal orbital transfer in the equatorial plane of an axisymmetric planet with a supplementary accuracy requirement 15 p1931 A73-31228
- Optimal transfer between weakly elliptic orbits with a supplementary accuracy requirement and with allowance for nonsphericity 15 p1931 A73-31229
- Energy optimal four impulse transfer maneuver with return between two moving points in circular coplanar orbits under transit time and stay duration constraints 15 p1931 A73-31230
- Minimum time response control problem of moving point in state space, determining piecewise-continuous vector function for optimal system transfer to coordinate reference point 15 p1931 A73-31231
- Optimal transfer between coplanar elliptic orbits with the aid of tangential impulses applied at the apsidal points 15 p1931 A73-31232
- Three parameter boundary value problem for trajectory optimization of maximum weight station injection from earth orbit into interplanetary flight trajectory 15 p1941 A73-32604
- Minimization of spacecraft maximum acceleration in atmosphere after reentry, applying results to reentry trajectory optimization and associated optimal control problems 15 p1941 A73-32607
- Algorithms for spacecraft trajectory optimization programs for orbit perturbations caused by random measurement errors and minimum mathematical expectancy of energy dissipation 15 p1942 A73-32618
- Optimal curved pursuit trajectories of point mass in three dimensional space, establishing search technique via Pontryagin principle calculations and equations of state 16 p2061 A73-33269
- Intermediate-thrust arcs and their optimality in a central, time-invariant force field. 16 p2062 A73-33305
- Optimal trajectory solution for minimum transfer time in terminal control problem involving locally controllable final point 16 p2032 A73-33306
- Closed loop formulations of optimal control problems for minimum sensitivity. 17 p2144 A73-34363

- Chattering arcs and chattering controls. 18 p2294 A73-36639
- Synthesis of a class of optimal discrete systems for correcting the trajectories of dynamic systems 20 p2592 A73-38697
- A new approach to performance optimization of the 1975 Mars Viking lander. 20 p2614 A73-38825
- [AIAA PAPER 73-889] An indirect trajectory optimization algorithm based on the continuation method for solution of nonlinear equations. 20 p2588 A73-38826
- [AIAA PAPER 73-890] Optimal entry algorithm and multiimpulse correction times for spacecraft guidance trajectory at minimum fuel consumption 20 p2590 A73-38900
- Some nonlinear problems in optimal control 20 p2541 A73-38995
- Synthesis of multidimensional automatic optimization systems with allowance for constraints 20 p2542 A73-39040
- Optimal control of stochastic systems with random shocks and discontinuous trajectories, using functional minimization 20 p2582 A73-39388
- Space shuttle ascent guidance, using quadratic performance index and reference trajectory kinematics to obtain optimal time-varying feedback control gain 21 p2735 A73-40044
- Geostationary injection dispersions and thrusting error elimination by apogee motor firing attitude optimization 21 p2780 A73-40614
- Station acquisition fuel minimization for third stage apogee motor impulse compensation of geostationary transfer orbit dispersions 21 p2781 A73-40618
- Time-optimal control of a linear plant with time lag 21 p2671 A73-41607
- Integrals for optimal flight over a spherical earth. 22 p2884 A73-42561
- Sensitivity of optimal control systems with bang-bang control. 22 p2837 A73-43068
- Optimal landing flare control of aircrafts with sensitivity consideration. 23 p2940 A73-43284

TRANQUILIZERS

- Psychopharmacology in treating psychiatric diseases, negative emotions, and nerve stimulation, discussing tranquilizers synthesis and effects 12 p1465 A73-27497

TRANSCIEVERS

- U TRANSMITTER RECEIVERS
- EXPONENTIAL FUNCTIONS
- LOGARITHMS
- PERIODIC FUNCTIONS
- TRIGONOMETRIC FUNCTIONS
- Transcendental equations solution for satellite Kepler orbit determination from coordinates, velocity and time components, using Lambert-Euler relation 12 p1543 A73-27629

TRANSDUCERS

- DIGITAL TRANSDUCERS
- ELECTROACOUSTIC TRANSDUCERS
- ELECTRONIC TRANSDUCERS
- IMAGE TRANSDUCERS
- LOUDSPEAKERS
- MAGNETIC TRANSDUCERS
- MICROPHONES
- MODE TRANSFORMERS
- PIEZOELECTRIC GAGES
- PIEZOELECTRIC TRANSDUCERS
- PIEZORESISTIVE TRANSDUCERS
- PRESSURE SENSORS
- QUARTZ TRANSDUCERS
- SOUND TRANSDUCERS
- THERMOPILES
- TORQUEUS
- ULTRASONIC WAVE TRANSDUCERS
- An infrared pneumatic transducer with capacitive detection. 08 p0968 A73-21682
- [ONERA, TP NO. 1150] Semiconductor strain transducer 08 p0950 A73-21720
- Stress distortion coefficient of uniaxial tension /compression/ of elastic isotropic medium with flattened ellipsoidal sensor from sensor stress recording 09 p1159 A73-22590
- Electrical measurement of mechanical forces and displacements, discussing transducers design and measurement standards and units 10 p1215 A73-23633
- Problems in constructing aerodynamically active elements - Converters of input and output signals in automatic control systems 12 p1459 A73-26769
- Low noise temperature measurement converter with electrical oscillation frequency output, presenting computer calculations of sensor components 13 p1617 A73-28860
- Experimental force data reduction equations solved by iterative method for multicomponent force transducers used in load tests, discussing wind tunnel balances 17 p2148 A73-35437

balances 17 p2148 A73-35437

Application of information theory to the study of mechanical systems 20 p2592 A73-39268

A new conceptual model for components in measurement/control systems - Practical application to thermocouples. 22 p2859 A73-42056

Further experiments on balancing of a high-speed flexible rotor. [ASME PAPER 73-DET-99] 22 p2865 A73-42077

Measuring characteristics of the displacement cardiograph. 22 p2815 A73-42670

TRANSEQUATORIAL PROPAGATION

- Off-path transequatorial propagation in decametric waves. II - Application to the study by diffusion of ionospheric irregularities 01 p0017 A73-10334
- VLF modal interference effects observed on transequatorial paths. 07 p0793 A73-20059
- Propagational mode deduced from signal strengths in the VHF band on the trans-equatorial path. 09 p1051 A73-22749
- Anomalous diurnal changes of transequatorial VLF radio waves. 11 p1330 A73-25760
- Investigation of the phase variation of a NWC signal /22.3 kHz/ along a transequatorial path 12 p1469 A73-27339
- Result of medium- and long-wave observations at distances of about 7500 km 12 p1474 A73-27768
- Ionospheric tilts and long-range short-wave communications. 15 p1843 A73-31525
- Equatorial spread-F irregularities observed at Nairobi and on the transequatorial path Lindau-Tsumber. 15 p1870 A73-31765
- Signal fading and topside electron density profile observation over VHF transequatorial path between Europe and Southern Africa, noting great circle transmission role 15 p1844 A73-31766
- Study of phase changes of the NWC signal /22.3 kHz/ on a transequatorial path. 23 p2952 A73-43237

TRANSFER FUNCTIONS

- Towards faithful radio transmission of very wide bandwidth signals. 01 p0015 A73-10176
- Variational methods for linear numerical filtering with operator and transfer function spreads compromise, presenting graphical data [ONERA, TP NO. 1127] 01 p0070 A73-10236
- Astronomical seeing and microthermal fluctuations of the atmosphere 01 p0050 A73-10562
- Automated system with CW signal and feedback to measure delay line group delay and transfer function frequency responses, detailing operation and errors 02 p0146 A73-11952
- Planetary observation by earth based photography, discussing resolution limitation and improvement in terms of modulation transfer function 02 p0216 A73-12330
- On combined operations method for transfer problems in homogeneous, cylindrical media. 02 p0193 A73-12383
- Sound propagation in a combustion can with axial temperature and density gradients. 02 p0238 A73-12608
- Satellite transmitted impulse response transfer function evaluation by ray tracing technique for ionospheric model with Chapman ionization vertical profile 03 p0299 A73-13630
- German monograph - Effect of spatial partial coherence on the measurement of optical transfer functions. 03 p0343 A73-13813
- German monograph - Contributions to the calculation of natural frequencies of undamped oscillator chains by the transfer method. 03 p0343 A73-13815
- Magnetic pulse width modulator and power switch subsystem of switching-mode dc regulator, deriving describing function from transfer functions 03 p0282 A73-13928
- Algebraic and transfer-function criteria of fixed-time controllability of delay-differential systems. 04 p0430 A73-15212
- Optical transfer function /OTF/ measurement standards and specification for high quality aerial photographic mapping lens, discussing error sources 05 p0573 A73-16147
- Effect of additive damping on transfer function characteristics of structures. [SAE PAPER 720811] 05 p0634 A73-16641
- Integral Laplace-Fourier transform stability during transient response functions reconstruction from

- transfer function frequency characteristics in linear circuits 05 p0591 A73-16779
- Transfer and moment equations obtained for radiation transfer in spherically moving medium with relativistic corrections, discussing matter-radiation coupling and energy conservation 05 p0612 A73-17382
- Determination of the transfer function of a digital filter from the real part of the frequency response. 06 p0674 A73-17811
- A new method of calculating controller constants according to an optimal modulus criterion 06 p0680 A73-18169
- Display of microwave pulse response via the real-time Fourier transform of the transfer function. 06 p0677 A73-18346
- Dc servomotor transfer function equalization, noting stability conditions for linear system design 06 p0680 A73-18380
- Transfer matrices determination for two terminal pair network derived from four terminal pair network, considering bandpass filter circuit design 06 p0677 A73-18397
- Describing functions, circle criteria and multiple-loop feedback systems. 06 p0680 A73-18444
- Complete identification of some non-linear closed-loop systems. 06 p0681 A73-18525
- Design of active filter sections performing biquadratic transfer functions on the basis of a branched operational-amplifier configuration 07 p0796 A73-18895
- Determination of the transfer function for the spectral albedo of the surface-atmosphere system of the planet 07 p0818 A73-19659
- On the approximation of the optical modulation transfer function (MTF) by analytical functions. 07 p0786 A73-20264
- Engineering systems structure and parameter identification using transfer function, learning model and nonlinear filtering 07 p0796 A73-20427
- Repeated cascade structure and kinetic description for homogeneous turbulence spectrum, considering coupled hierarchies origin from transfer function and eddy viscosity development 07 p0812 A73-20472
- Improvement of frequency characteristics of digital filters. 08 p0945 A73-20801
- Low pass symmetrical filters of composite attenuation with infinite and flat points of attenuation around a given frequency 08 p0945 A73-20967
- Analysis of thermal spread in a pyroelectric imaging system. 08 p0967 A73-21420
- Measurement of admittance of Gunn diodes in passive and active regions of bias voltage. 08 p0947 A73-21432
- Velocity ratio in the analysis of linear dynamical systems. 08 p0988 A73-21467
- On the control of linear systems using two level periodic output feedback. 09 p1067 A73-22231
- Features of the application of the root-locus method to the study of sampled-data automatic systems on the basis of the w-transform 09 p1068 A73-22341
- Realization of two-dimensional state space digital filters. 09 p1068 A73-22398
- Theoretical fundamentals of constructing parametric filters equivalent to linear filters 09 p1063 A73-22451
- Determination of the transfer function of a planet atmosphere by spectrophotometry of the planet surface from space 09 p1077 A73-22488
- An approximate continuous representation of discrete control systems 09 p1068 A73-22564
- Sensitivity of variable-amplifier circuits to variation of the controlled parameters 09 p1069 A73-22651
- Least-squares monotonic lowpass filters with sharp cutoff. 09 p1065 A73-23093
- Synthesis of gyrator RC filters from the cascaded model 10 p1193 A73-23729
- Feedback control system transfer function matrix synthesis, determining design specifications for required compensation filters from compatibility conditions 10 p1200 A73-24049
- A representation of uncorrelated random processes by stochastic integrals 11 p1340 A73-25010
- Modification of the two-flow approximation in radiant-transfer calculations 11 p1450 A73-25623
- Transfer function model for analog simulation of transient unsteady heat conduction through flat and cylindrical walls, optimizing moving polymer film heating 11 p1451 A73-25732
- Analytical fit of the transfer function of a logarithmic electrometer and correction for ambient temperature variations. 11 p1367 A73-26306
- High Q bandpass low sensitivity RC amplifier-filter networks, discussing two-step decomposition of denominator polynomial of second order filter transfer function 11 p1338 A73-26417
- The wave length dependence of the transfer properties of photographic materials for holography. 11 p1370 A73-26536
- On identifying transfer functions and state equations for linear systems. 11 p1342 A73-26641
- Rational methods for controlling multistable elements on the basis of an analysis of the preferential domains of steady states 12 p1482 A73-26774
- Determination of the polarization transfer function in space-based spectrophotometric observations of natural formations on a planetary surface 12 p1488 A73-26965
- IMCON reflection mode dispersive delay line in large time-bandwidth product pulse compression systems, deriving operational characteristics from transfer function 12 p1480 A73-27565
- An algorithmic procedure for determining discrete transfer matrices of controlled plants 12 p1485 A73-27624
- The resolving power and the modulation transfer function of terrestrial and aerial cameras in working conditions. 12 p1501 A73-27963
- Relationship between pointing precision, spread functions and modulation transfer functions. 12 p1501 A73-27969
- A comparison of electrophysiological and psychophysical temporal modulation transfer functions of human vision. 13 p1575 A73-28360
- Response of a jet to a pressure gradient and its relation to edgetones. 13 p1603 A73-29035
- High gain hydromechanical servomechanism with multispurting, mass damping and feedback control, deriving transfer function response, with application to aircraft control surface actuator design 13 p1596 A73-29150
- German monograph - Rapid excitation of quasi-harmonic oscillations in a class of nonlinear oscillators. 13 p1594 A73-29285
- Michelson shearing interferometer with piezoelectric scanner for atmospheric optical mean transfer function measurements from airborne platform, using laser or white light sources 13 p1621 A73-29332
- A proximity focused ultraviolet-sensitive SEC camera tube. 14 p1732 A73-29910
- Point-spread functions, line-spread functions, and edge-response functions associated with MTFs of the form negative exp/n-th power of the ratio of spatial frequency to the MTF frequency constant/. 14 p1768 A73-30158
- Ionospheric model impulse response transfer functions phase and amplitude dependence on profile parameters and TE C, using ray tracing technique 14 p1728 A73-30231
- Dynamic properties of human and animal middle ear in terms of acoustic impedance, transfer function, impulse response, sound diffraction and reflex sensitivity 14 p1715 A73-30279
- Optimal feedback characteristics of transistor amplifiers 14 p1736 A73-30372
- Necessary and sufficient conditions for stability for n-input, n-output convolution feedback systems with a finite number of unstable poles. 14 p1739 A73-30509
- Possibility of independent control of frequency characteristic and coverage band in a PAFPC system. 15 p1842 A73-30987
- Effects of flexibility on a momentum-stabilised communication-satellite attitude-control system. 15 p1942 A73-31099
- Influence of the substrate on the transfer admittance of a saturated MOS transistor 15 p1850 A73-31495
- Modulation-transfer functions of scattering media, derived from observations in direct light. 15 p1914 A73-32189
- Dynamic analysis procedure to locate vibration sources without simulated service tests, mapping structural surfaces at all frequencies via transfer function or mechanical impedance analysis 16 p2019 A73-33098
- Angular quadrature perturbations in radiative transfer theory. 16 p2037 A73-33738
- Acceleration waves in simple elastic materials. 16 p2081 A73-33746
- Rapid interferometric technique for MTF measurements in the visible or infrared region. 17 p2171 A73-35404
- Applications of the speckle pattern techniques to the visualization of modulation transfer functions and quantitative study of vibrations of mechanical structures. 17 p2173 A73-35433
- Comparison of three techniques for solving the radiative transport equation. 18 p2337 A73-36367
- [AIAA PAPER 73-751] Calculation of the eigenfrequencies for a shaft/bearing system with the aid of transfer matrices 19 p2433 A73-37548
- A comparison of errors in linear digital models. 19 p2413 A73-38059
- Equivalent circuit and transfer function of the multimode glass fiber with random mode conversions. 20 p2521 A73-38658
- Controllability and synthesis of optimal dynamic systems 20 p2591 A73-38672
- Synthesis of low-sensitivity automatic control systems 20 p2540 A73-38706
- Amplitude stability and distortion in thermistor-controlled oscillators. 20 p2535 A73-39131
- Approximation of the characteristics of two-port networks with a complex nonlinearity 20 p2537 A73-39464
- Imaging system pointing precisions, deriving ground target size relationships to spread function and modulation transfer function respectively 20 p2567 A73-39672
- Phase contrast transfer damping functions for various beam apertures in high resolution electron microscopy 21 p2702 A73-40949
- Graphical analysis of traveling-wave-tube oscillator with external feedback loop. 21 p2663 A73-41046
- Short-term frequency stability of the Rb-87 maser. 21 p2716 A73-41148
- Method of analyzing electronic circuits on the basis of a hybrid-parameter matrix in a canonical system of coordinates 21 p2670 A73-41306
- Polynomial approximations of the characteristics of low-sensitivity filters 21 p2666 A73-41315
- Influence of combustion phenomena on the Pogo effect 21 p2754 A73-41551
- On the design of wave digital filters with low sensitivity properties. 22 p2835 A73-41950
- Structural methods of multichannel systems synthesis with the aid of the graph theory 22 p2836 A73-42602
- Structural sensitivity transfer matrix for dynamic multiple link control system response minimization with corrections within frequency range 22 p2836 A73-42613
- Transfer function root method for synthesis of multiply connected determinate automatic control systems with asymmetrical channels and limited nonautonomous control elements 22 p2836 A73-42614
- Iteration methods for identification of multiple-link controlled plants for self-adaptation purposes 22 p2836 A73-42617
- Stability circle criteria extended to signal power gain mean-square criteria for nonlinear feedback distributed parameter system defined by transfer function 22 p2837 A73-43066
- Microchannel image intensifiers for detection at low light levels 23 p2979 A73-43222
- The state space and transfer function approaches in practical linear multivariable systems design. 23 p2962 A73-43281
- Synthesis of feedback systems with large plant ignorance for prescribed time domain tolerances. 23 p2962 A73-43282
- A simplified minimal-realization algorithm for a symmetric transfer-function matrix. 23 p2999 A73-43382
- Approximation of transfer functions for filters with equalized group-delay characteristics. 23 p2960 A73-43676
- Three-component sonic anemometer for wind speed measurement, calculating transfer functions for effect of line averaging and path separation on spectral response 23 p2983 A73-44266

- Broadband noise generation by aerofoils and axial flow fans.
[ALAA PAPER 73-1018] 24 p3054 A73-44850
Spectral analysis of frequency noise of oscillators by the Hadamard variance
24 p3073 A73-44974
Nonminimum-phase difficulties in multivariable-control-system design.
24 p3074 A73-45258
Effect of unity-rank feedback on the transfer-function matrix of a multivariable system.
24 p3075 A73-45263

TRANSFER OF TRAINING

- Need for within-trial feedback as a function of task similarity in adaptive training of manual control.
05 p0543 A73-16709
Computer-controlled differential review-time payoff as a training aid.
05 p0544 A73-16725
Performance measurement system for combat crew flight training in complex aircraft weapon systems, identifying training research goals
05 p0544 A73-16726
Airline flight simulation program, examining visual system capacity for replacement of in-flight training with pilot learning transfer estimation and simulation effectiveness appraisal
16 p1995 A73-33204
Studies of pilot performance. III - Validation of objective performance measures for rotary-wing aircraft.
21 p2644 A73-41154
Response surface methodology analysis of training transfer in pursuit rotor tracking task, relating three independent variables through multiple-regression prediction equations
24 p3063 A73-44774
Two components and two stages in search performance - A case study in visual search.
24 p3065 A73-45339

TRANSFER ORBITS

- NT INTERPLANETARY TRANSFER ORBITS
Optimization of the apogee impulse during the positioning of a geostationary satellite.
[ONERA, TP NO. 1218] 02 p0228 A73-11992
Meteor dust motion in the upper atmosphere and in the vicinity of the earth's orbit.
02 p0214 A73-12255
Synthesis of optimal control over the motion of a material point in a thin spherical layer of a central gravitational field with noncollinear vectors of the final gross error in the radius vector and velocity vector
02 p0193 A73-12452
Analytical expressions for postmaneuver velocity and transfer impulse optimizing elliptic-to-hyperbolic orbital transfer
02 p0219 A73-12453
Nearly-optimal single impulsive transfers between coplanar elliptical satellite orbits with identical pericenter altitude
03 p0372 A73-13299
The transition from elliptic to hyperbolic orbits in the two-body problem by slow loss of mass.
03 p0377 A73-14273
Interplanetary spacecraft transfer maneuver for hyperbolic trajectory change into eccentric orbit, using aerodynamic drag to obtain nearly circular orbit
03 p0379 A73-14571
Orbit transfer, -corrections, and attitude control of a lightweight direct broadcasting satellite for Europe.
04 p0505 A73-15738
Transfer from a standby to a stationary orbit using electric propulsion
04 p0505 A73-15740
Considerations on transfer into geostationary orbit using ion propulsion - Application to the Europa III booster
04 p0505 A73-15742
An optimal orbit control system for a stationary artificial earth satellite
05 p0616 A73-16427
Minimum impulse three-body trajectories.
[ALAA PAPER 73-145] 05 p0619 A73-16894
Launch and orbital injection of Intelsat IV satellites.
09 p1152 A73-22699
Russian book on analytical theory of optimization in gravitational fields covering orbital transfer trajectories, variational optimization problems, Lagrange multiplier properties, etc
10 p1284 A73-24800
Optimal orbital transfer in the equatorial plane of an axisymmetric planet with a supplementary accuracy requirement
15 p1931 A73-31228
Optimal transfer between weakly elliptic orbits with a supplementary accuracy requirement and with allowance for nonsphericity
15 p1931 A73-31229
Energy optimal four impulse transfer maneuver with return between two moving points in circular coplanar orbits under transit time and stay duration constraints
15 p1931 A73-31230

- Optimal transfer between coplanar elliptic orbits with the aid of tangential impulses applied at the apsidal points
15 p1931 A73-31232
Contribution to the synthesis of optimum control of motion of a point mass in a spherical lamella of a central gravitational field with finite miss vectors noncollinear with respect to radius vector and velocity vector.
15 p1915 A73-32602
Analytical expressions for postmaneuver velocity and transfer impulse optimizing elliptic-to-hyperbolic orbital transfer
15 p1941 A73-32603
Optimal trajectory solution for minimum transfer time in terminal control problem involving locally controllable final point
16 p2032 A73-33306
Realization of a geostationary orbit by means of an electromagnetic propulsion system /quasi-steady MPD/
17 p2239 A73-34954
Selection of a trajectory for the return to earth from lunar orbit of an artificial satellite
18 p2351 A73-36106
Spacecraft rendezvous in orbit, discussing launching, transfer maneuver, target location, approach phase, docking and mechanical coupling
19 p2487 A73-38302
The fastest transfer from one circular orbit to another under the action of a small thrust
20 p2604 A73-38990
Geostationary injection dispersions and thrusting error elimination by apogee motor firing attitude optimization
21 p2780 A73-40614
Station acquisition fuel minimization for third stage apogee motor impulse compensation of geostationary transfer orbit dispersions
21 p2781 A73-40618
Realisation of rendezvous by the transfer orbit which is tangential to the original and terminal orbits.
21 p2779 A73-41550
Trajectory of a solar-electric propelled vehicle passing through the shadow cone of a celestial body
21 p2779 A73-41556
Utilization of tangential trajectories for lowering high-altitude elliptic orbits of artificial satellites of planets
23 p3027 A73-43265
- TRANSFERRING**
NT DROP TRANSFER
TRANSFORM INTEGRALS
U INTEGRAL TRANSFORMATIONS
TRANSFORMATION TENSORS
U TENSORS
TRANSFORMATIONS [MATHEMATICS]
NT COORDINATE TRANSFORMATIONS
NT FAST FOURIER TRANSFORMATIONS
NT INTEGRAL TRANSFORMATIONS
NT LAPLACE TRANSFORMATION
Relativistic gas dynamics problems reduction to equivalent Newtonian flow via transformation of governing equations
01 p0034 A73-11138
Matrix transformations for spacecraft attitude determination.
02 p0228 A73-11905
Elliptic partial differential equations may be related by a change of independent variables.
02 p0186 A73-11975
Damping perturbation of high order nonlinear autonomous Liapunov system, reducing system equations integration to quadratures via transformation to lower order quasi-linear nonautonomous system
03 p0344 A73-14054
Matrix method for canonical transformations in many body problem of celestial mechanics
03 p0379 A73-14587
Transformation group theory for Poisson equation solutions to boundary value problem of steady heat conduction with generation
03 p0400 A73-14631
New developments in EEG signal processing.
04 p0411 A73-15279
A transformation for the numerical solution of two-dimensional free mixing flow problems.
[ASME PAPER 72-WA/FE-3] 04 p0434 A73-15841
Existence theorem for integral manifolds of point mappings in resonant and nonresonant cases for differential equations systems with fast rotating phases
05 p0560 A73-16290
Affine and nonlinear transformations for aerial photography film deformation effects on photogrammetry accuracy
05 p0575 A73-16315
A solution of the bilinear matrix equation $AY + YB$ equals -Q.
[DFVLR-SONDDER-274] 05 p0591 A73-16607
Transformation of the hypersonic compressible Navier-Stokes equations.
05 p0567 A73-17120
Matrix transformation in hyperplanes method for successive solution of boundary value problems of

- multidimensional differential equations, using space-time functions
06 p0715 A73-17718
Evaluations of matrix functions by real similarity transformation.
06 p0718 A73-18534
Differential operators transformation into integral functions by Green function and distributions theory methods in structural analysis
06 p0719 A73-18727
Nonlinear time-varying control systems transformation, deriving conditions for existence of observable system representation and corresponding scalar differential equation
06 p0719 A73-18807
Invariant imbedding and a transformation procedure for reducing classes of boundary value problems into equivalent initial value systems.
06 p0719 A73-18804
A transformation of the radiative transfer equation useful for problems with steep source gradients.
07 p0918 A73-19263
Wave transformation by a phase corrector
07 p0973 A73-19923
Sundman power series convergence enhancement in a three body problem by Poincare transformation
07 p0852 A73-20042
Hadamard transform spectrometer designed for airborne IR astronomical observations of Mars, using binary orthogonal pseudonoise codes in multiplexing scheme
08 p0972 A73-21753
Features of the application of the root-locus method to the study of sampled-data automatic systems on the basis of the w-transform
09 p1068 A73-22341
Initial circuit equation transformation into equation of variable states, noting linear and nonlinear circuits in static and dynamic regimes
09 p1068 A73-22452
Error analysis of approximate formula for transformation of rarefied gas particle reflection from homogeneous anisotropic random surface
09 p1123 A73-22615
Book - Iterative methods for nonlinear optimization problems.
10 p1242 A73-23947
Analytical transformation of photographs for plotting topographic and photographic maps in prescribed projections
10 p1219 A73-24483
Symmetry properties of the collision integral and nonisotropic steady-state solutions in the theory of weak turbulence
10 p1207 A73-24759
On nonlinear transformation and stabilization of beam-plasma instability.
11 p1404 A73-25274
Application of the invariant of a homographic transformation to measure the series resistance of semiconductor elements
11 p1336 A73-25319
A dynamic transformation method for modal synthesis.
[ALAA PAPER 73-396] 11 p1440 A73-25525
Possibility of correlating the field of a wide wave beam in a smoothly nonhomogeneous medium with the field of a beam in vacuum
11 p1331 A73-26161
Geometric programming with signomial transformation into equivalent posynomials minimized under inequality constraints and generalization by equilibrium solutions to reverse programs in larger class
11 p1391 A73-26576
Second order approximation to autocorrelation matrix of random variable nonlinear transformation, discussing application to Poisson process and monopulse radar receiver AGC effects
11 p1333 A73-26695
Planck relativistic equations of moving body heat and absolute temperature transformation /1907/ and alternative equations by Ott /1963/, comparing validity
12 p1557 A73-26973
Stability of nonlinear systems with a transformed argument
12 p1524 A73-27416
Lorentz contraction and transformation of equilibrium forces and moments in inertial reference systems transition, discussing special relativity theory
12 p1525 A73-27733
On the unity of the constant strain/constant moment finite element methods.
13 p1691 A73-28079
Symmetries of differential equations - The hypergeometric and Euler-Darboux equations.
13 p1648 A73-28538
An algorithm for the computation of the higher order G-transformation.
13 p1649 A73-28601
Classification theorem for analytical transformations of second order differential equations of motion at arbitrary resonance based on group theory
13 p1661 A73-29081

- Haralick-Dinstein iterative clustering procedure limitation and explanation as T transformation linear structure effect in matrix theory 14 p1768 A73-30040
- Linear transformations of variable in system of normal equation in differential correction processes, reducing process to algorithm 15 p1930 A73-31115
- Book on perturbation methods for nonlinear differential equations covering canonical transformation theory, Hamiltonian and integrable systems, area preserve mapping and resonance problem 15 p1899 A73-31472
- Riccati transformation for optimal control linear two-point boundary value problems formulated from first order numerical integration methods 15 p1908 A73-31666
- Dual principles of elastodynamics finite element applications. 17 p2245 A73-34833
- The transformational behaviour of perturbation theories. 18 p2352 A73-36421
- The effect of nonlinear transformations on the computation of weak solutions. 18 p2330 A73-36610
- Classification theorem for analytical transformations of second order differential equations of motion at arbitrary resonance based on group theory 19 p2445 A73-37632
- Hypersonic polytropic transformations of an ideal fluid. II 19 p2420 A73-37645
- Electromagnetic wave propagation in inhomogeneous multilayered structures of arbitrarily varying thickness - Generalized field transforms. 19 p2461 A73-38379
- Symmetry transformations of the classical Kepler problem. 19 p2446 A73-38382
- Nonlinear transformation by a travelling wave tube and power spectral density of a PSK-signal. 20 p2522 A73-38718
- Study of methods of computing transition matrices /Computer-program description/. 20 p2532 A73-39129
- The symmetry method and its application to plane problems of elasticity theory 20 p2618 A73-39325
- Exact solutions of some problems of the Stefan type 20 p2627 A73-39335
- Construction of a transformation matrix and the differentiability of the formal solution of a system of partial differential equations 20 p2582 A73-39475
- Selection of an optimal structure for a tabular model of a control plant 21 p2670 A73-40995
- Laguerre transform of a continuous signal - Application to the study of the asymptotic regime of a Kalman filter 22 p2832 A73-42352
- Prestressing force and tendon configuration optimization for indeterminate structure with prescribed cross sectional dimensions, using linear programming and design variable transformation 22 p2922 A73-42476
- Reference image /brightness distribution functions/ existence and normalization under additive and multiplicative groups of transformations in visual field. 24 p3064 A73-44908
- The formation of resonance lines in multidimensional media. II - Radiation operators and their numerical representation. 24 p3113 A73-45041
- Kustaanheimo-Stiefel transformation in Kepler motion perturbation theory derived from general solution of two body problem, noting application to collision orbits and Lagrange solutions 24 p3142 A73-45298
- TRANSFORMERS**
- NT MODE TRANSFORMERS
- NT VOLTAGE CONVERTERS [AC TO AC]
- High efficiency dc-to-dc converter with second non-saturable transformer for eliminating collector current spike to reduce electromagnetic interference and transistor damage 01 p0005 A73-10247
- Reducing the smoke hazard in small transformer failures. 03 p0252 A73-13572
- Switch transistor control using an intensity transformer 04 p0489 A73-15736
- Characteristics of the OT-series transformer-type transducers of linear displacements 07 p0779 A73-20528
- Conditions derived for reactive two-terminal-pair matching transformer networks operation at maximum power transfer efficiency 09 p1061 A73-22046
- Electrically controlled microwave polarization transformer 09 p1064 A73-22675
- Optoelectronic step-up voltage transformer with optical coupling electrical isolation, using light emitting diode and semiconductor film with high photovoltage levels 12 p1496 A73-26964
- A device for experiments on high-beta plasmas in a toroidal geometry 13 p1663 A73-28120
- Antenna impedance measurement with Weissfloch transformer between terminals and point in input transmission line for achieving high precision 17 p2129 A73-35704
- Microstrip junction circulators with fixed ferrite disks, achieving broadband impedance matching between center conductor and transmission line by transformer on alumina substrate 20 p2538 A73-39668
- TRANSFORMS**
- U TRANSFORMATIONS [MATHEMATICS]
- TRANSFUSION**
- Hemotherapy of coagulation system disturbances of hepatolienal origin 23 p2947 A73-44299
- TRANSHORIZON RADIO PROPAGATION**
- Experimental investigation of the parameters of a statistical Gaussian model of the field below the radio horizon at centimeter wavelengths. 07 p0794 A73-20131
- Trans-horizon propagation techniques for examining disturbances in stratified tropospheric layers. 19 p2405 A73-38221
- Angle and Doppler measurements of the quasi-coherent and incoherent components of microwave transhorizon signals. 22 p2824 A73-41859
- TRANSIENT HEATING**
- NT PULSE HEATING
- NT SHOCK HEATING
- Computer programs for radiative heat transfer and thermal equilibrium equations, noting transient temperature distribution measurement of two stage radiant cooler 01 p0111 A73-11151
- Transient free-convection horizontal laminar flow between two parallel plates. 04 p0517 A73-15681
- Numerical method of transient heat conduction with temperature dependent thermal properties. 07 p0921 A73-20118
- The study of film boiling crises and transient boiling of cryogenic liquids. 07 p0922 A73-20410
- Transfer function model for analog simulation of transient unsteady heat conduction through flat and cylindrical walls, optimizing moving polymer film heating 11 p1451 A73-25732
- Comparison of the solutions found for the inverse transient heat-conduction problem by the method of successive intervals and the method of Sparrow, Haji-Sheikh, and Lundgren. 12 p1560 A73-27911
- A high-speed /subsecond/ system for accurate thermophysical measurements at high temperatures. [AIAA PAPER 73-743] 18 p2316 A73-36359
- Unsteady heat transfer characteristics of a two dimensional laminar wall jet. 20 p2628 A73-39339
- Measuring transient high temperatures by optical pyrometry. 22 p2853 A73-41989
- Transient heat conduction in laminated composites. [ASME PAPER 73-HT-R] 22 p2930 A73-42286
- On some further applications of the variational formulation based on local potential to the solution of diffusion equation. I - Temperature distribution in a transpiration cooled half-space with variable thermal properties. II - Heat conduction in an ablating solid with variable thermal properties. 22 p2931 A73-42468
- TRANSIENT LOADS**
- NT BLAST LOADS
- NT GUST LOADS
- NT IMPACT LOADS
- NT LANDING LOADS
- NT SHOCK LOADS
- Data analysis criteria and instrumentation requirements for the transient measurement of mechanical impedance. 03 p0343 A73-13837
- Extension of an interface flaw under the influence of transient waves. 07 p0908 A73-19080
- Bending stress in an impulsively loaded cylindrical shell of exponentially varying thickness. 07 p0913 A73-19973
- Axially symmetric transient wave propagation in elastic rods with nonuniform section. 11 p1447 A73-26652
- Service life determination in heat-resistant alloys under unsteady working conditions with allowance for brief overloading 14 p1763 A73-30690
- Optimal design of layered structures under dynamic loading. 16 p2075 A73-32790
- Behavior of a wing panel under transient conditions in a gas flow 17 p2091 A73-34139
- Two dimensional steady and transient thermal stress analysis in rectangular solid with varying surface temperature, noting thermoelastic problems solution by analog method 19 p2498 A73-37668
- Transient stress distribution caused by water-jet impact. 19 p2435 A73-38300
- Influence of initial transients on stress relaxation and creep measurements on visco-elastic materials. 22 p2868 A73-43172
- TRANSIENT OSCILLATIONS**
- Shubnikov-de Haas oscillations in graphite selective scattering by charged impurities. 04 p0468 A73-14871
- Nonlinear longitudinal combustion instability in rocket motors. [AIAA PAPER 73-217] 05 p0641 A73-16947
- Relaxation time measurements by an electronic method. 10 p2127 A73-23998
- Nonlinear transient stress-waves in cylindrical and conical shells. 11 p1432 A73-24978
- Spatial oscillations of a vehicle with a nonlinear stabilization system during reentry 14 p1803 A73-29853
- On the nature and origin of the solar five-minute oscillations. 20 p2606 A73-39071
- Analysis of transient oscillations in nonlinear control systems. 22 p2837 A73-43019
- Analysis of microwave circuit for characterization of negative-conductance devices by transients. 23 p2964 A73-44076
- Transient vibration processes during diamond grinding and their statistical evaluation 24 p3094 A73-44971
- TRANSIENT PRESSURES**
- Determination of solid-propellant transient regression rates using a microwave Doppler shift technique. [AIAA PAPER 72-1118] 03 p0351 A73-13433
- Solid propellant ballistic properties from pressure changes due to combustion, considering transient effects 13 p1669 A73-28997
- Role of pressure transients in the detection and identification of lunar surface gas sources. 14 p1752 A73-29963
- Exact steady-state analogy of transient gas compression by coalescing waves. 21 p2790 A73-40439
- TRANSIENT RESPONSE**
- Measurement of transient heat transfer coefficients in the contact between solid materials 01 p0120 A73-10413
- Axisymmetric plastic response of rings to short-duration pressure pulses. 01 p0115 A73-10759
- Rise time and pressure measurements in transient flow during quasi-steady gas injection into vacuum with piston valve, using fast ionization gage 02 p0168 A73-11963
- Jet element output impedance for pneumatic circuits transients determination considering load dynamic properties influence 02 p0133 A73-12120
- Transient curve construction for analysis and synthesis of automatic control systems with asymmetrical nonlinearities, comparing with harmonic linearization 02 p0149 A73-12342
- Evaluation of the method of characteristics applied to a pressure transient analysis of the B.A.C./S.N.I.A.S. Concorde refuelling system. 02 p0133 A73-12645
- Experimental verification of a digital computer simulation method for predicting gas turbine dynamic behaviour. 02 p0204 A73-12647
- Research on combustion instability and application to solid propellant rocket motors. II. [AIAA PAPER 72-1049] 03 p0353 A73-13380
- Transient response of inelastic shells of revolution. 03 p0392 A73-13686
- Current distribution prediction in transient response of rotating disk electrode, noting mass transfer for cathodic reduction of ferricyanide 03 p0273 A73-13728
- Time-averaged power stage models transient and frequency responses characterization and circuit component values derivation for switched dc-dc converters design 03 p0282 A73-13927
- Operation, fabrication, characterization, I-V performance and application of transient voltage suppressor using metal oxide varistor 03 p0283 A73-13941

Reliable uninterrupted controlled transient voltage dc power supplies with active energy storage element, comparing three system configurations, design features and applications

03 p0253 A73-13946

Transient analysis of an electronically tunable dye laser. I - Simulation study.

03 p0320 A73-14457

Propellant grain surface contamination effect on ignition transient characteristics of solid rocket motor [AIAA PAPER 72-1198]

04 p0487 A73-14920

Elastic force minimization during transient process in mechanical multimass system under time dependent external load

04 p0509 A73-14976

Piezoelectric transducers for the study of short-duration mechanical loads

04 p0448 A73-15374

Transient phenomena in a phase-locked loop with a noisy reference.

04 p0421 A73-15437

Transient axisymmetric response of a conical shell frustum.

04 p0513 A73-15585

Dynamic response of pressurized thin cylindrical shells subjected to torsional loads. [ASME PAPER 72-WA/PROD-6]

04 p0514 A73-15807

A finite element based procedure for simulating the transient response and failure of a two-dimensional continuum with nonlinear material characteristics. [ASME PAPER 72-WA/DE-4]

04 p0515 A73-15875

Second order phase lock AFC system transient response duration calculation for rectangular and sawtooth characteristics of phase detector, using averaging method

05 p0547 A73-16059

Transient ionizing radiation effects on IMPATT diode oscillators.

05 p0558 A73-16519

Transient dynamic response of viscoelastic structures. [SAE PAPER 720812]

05 p0634 A73-16649

Integral Laplace-Fourier transform stability during transient response functions reconstruction from transfer function frequency characteristics in linear circuits

05 p0591 A73-16779

Transient heat transfer through a thin-walled circular pipe.

06 p0766 A73-17443

Dynamic behaviour of thin cylindrical shells subjected to high-speed travelling inner pressures.

06 p0758 A73-17518

An optimization technique for the transient response of passively stable satellites.

06 p0755 A73-17566

Linearized theory of dynamically loaded thin rigid viscoplastic rectangular plates transient response, investigating strain rate effect

06 p0760 A73-17760

A time hardening transient creep solution for steadily loaded uniaxial tension panels containing circular and elliptical holes under conditions of plane stress.

06 p0761 A73-17820

A diode model with a current-dependent series resistance

06 p0674 A73-17828

Computer control algorithms for transient response optimization in on/off motor control system synthesis

06 p0741 A73-17963

A program for the analysis and design of general dynamic mechanical systems. [AD-754496]

06 p0671 A73-18063

Emission risetime fluctuations in a gas laser with nonlinear resonant absorption

06 p0700 A73-18104

Response of edge- and face-electroded pyroelectric detectors to infrared laser signals.

06 p0704 A73-18798

Adaptive trackers based on continuous learning theory.

06 p0682 A73-18821

Transient stresses induced by heating a plane boundary.

07 p0907 A73-19077

Cusped wave fronts in anisotropic elastic plates.

07 p0907 A73-19079

Transient response of a plastically anisotropic cylinder in plane strain.

07 p0908 A73-19081

Approximate analysis of containment/deflection ring responses to engine rotor fragment impact.

07 p0910 A73-19188

Transient radiation in homogeneous anisotropic cold plasmas.

07 p0856 A73-19381

Integral method for nonlinear transient heat transfer in a semi-infinite solid.

07 p0919 A73-19493

Analysis of active RC circuits with nonhomogeneously distributed parameters in the time domain

07 p0805 A73-20024

An analysis of an arbitrary n-element adaptive array.

07 p0795 A73-20583

Evolution equations of motion for program manifold of continuous control system with given transient response

07 p0852 A73-20632

Gas turbine engine transient performance presentation for digital computer programs. [SAE ARP 1257]

08 p0996 A73-20696

Internal additive noise generated by a random pulse process

08 p0939 A73-21395

Correlation techniques in the analysis of transient processes.

08 p0988 A73-21466

Integral methods of calculating unsteady processes in nonlinear electric systems

08 p0951 A73-21556

Analysis of transient visual sensations above the flicker fusion frequency.

08 p0932 A73-21566

Mechanisms of transient and steady state creep in a gamma-prime hardened austenitic steel.

08 p0980 A73-21778

Bulk lifetime determination from current and capacitance transient response of MOS capacitors.

09 p1062 A73-22307

Transient functions to estimate thermal inertia of gas temperature sensors with film resistance thermometer mounted on wedge shape insulating base

09 p1081 A73-22346

Construction of quality diagrams for transient processes in nonlinear systems

09 p1068 A73-22558

Computer program for the transient analysis of radioisotope thermoelectric generators.

09 p1060 A73-22768

Method of variation of parameters starting with linear damped vibration solution as its generating solution.

09 p1121 A73-23324

First order phase locked loop statistical transient behavior in presence of noise from differential equation numerical solution, noting correlation with computer simulation

09 p1056 A73-23404

Missile and spacecraft radio telemetry data acquisition site polarization diversity signal combiner transient response requirements, comparing bench test with flight test data

09 p1057 A73-23414

Finite-element method applied to heat conduction in solids with nonlinear boundary conditions.

10 p1295 A73-23778

Some characteristics of transition processes in He-Ne lasers operating at the 0.63-micron wavelength

10 p1227 A73-24073

Local transient phenomena induced in an inert gas plasma by a short pulse.

10 p1257 A73-24626

Transient viscous laminar incompressible flow pattern after sudden vanishing of semiinfinite flat plate based on two dimensional unsteady boundary layer equations with boundary conditions

10 p1208 A73-24811

Nonlinear transient analysis of shells and solids of revolution by convected elements. [AIAA PAPER 73-359]

11 p1437 A73-25495

Transient characteristics of simple systems to modulated random noise. [ASME PAPER 72-APM-FFF]

11 p1398 A73-25703

Shock wave formation in an elastic half-space during one-dimensional nonlinear transient wave processes generated by a continuous force

11 p1445 A73-26456

Space-time cross spectral method to resolve transient disturbances into quasi-standing wave oscillations, giving formulas for node and antinode location

12 p1521 A73-26814

Transient processes in an inductive energy storage element for a plasma injector

12 p1460 A73-26931

A mechanistic model for analysis of pulse-mode engine operation. [AIAA PAPER 72-1184]

12 p1533 A73-27100

Analysis of the distortions of an FM signal in a servo loop with external control

12 p1470 A73-27576

Transient cooling of a solid cylinder by combined convection and radiation at its surface.

13 p1704 A73-28086

Composite materials transient thermal boundary conditions analytical derivation from initial and time dependent internal temperature distribution or gradient

13 p1705 A73-28436

Relaxation rates of lower laser levels in CO₂.

13 p1626 A73-28544

Kinetic cooling with CW carbon dioxide laser, observing time constant as function of atmospheric water pressure with three-beam interferometer

13 p1659 A73-28546

Modified separable kernel method for heat conduction with a nonlinear boundary condition

13 p1706 A73-28819

Dynamic losses in a transistorized switch operating on an active-capacitance load

13 p1593 A73-28944

Computer plotted dynamic stability and transient response of linear continuous systems described by high order differential equations of motion

13 p1661 A73-29144

Transient processes in second harmonic excitation by ultrashort laser light pulse train related to crystal length and phase matching

13 p1629 A73-29433

Theory of the shape of pulses produced by transient parametric generation of light.

13 p1629 A73-29433

Transient self focusing theory of high power laser pulse for homogeneous isotropic transparent solid dielectric with allowance for electrostriction and thermal effects

13 p1629 A73-29444

Transient analysis of multiple-input integrated digital structures.

13 p1595 A73-29580

Book - Theory of vibration with applications.

13 p1703 A73-29675

Detection of transient absorption in YAG laser crystals using combined laser.

14 p1756 A73-29930

Determination of some characteristics of random processes describing the operation of transient action systems with allowance for reliability

14 p1730 A73-30037

Numerical time integration methods in shell transient response finite element analysis, considering conditionally stable explicit and unconditionally one conditionally stable implicit schemes

14 p1807 A73-30187

Method of reducing the order of a differential equation when studying transient processes in mechanical systems

14 p1774 A73-30286

The transient response of non-uniform, non-homogeneous beams.

14 p1813 A73-30644

Influence of transient conditions on the overall service life of turbine blades

14 p1785 A73-30676

Dynamic structural model of transient processes over discrete jet element chain with duct joints

15 p1832 A73-31145

Equivalent circuit HF model of MOS transistor active region based on transient response equation, voltage and structural parameters

15 p1850 A73-31492

Construction of equations of motion for program manifold of continuous control system with given transient response

15 p1913 A73-31680

Convergence criteria for reverse error coefficient expansion under transient conditions for tracking servo system with open loop transfer function

15 p1854 A73-31735

Stability and oscillation characteristics of finite element, finite-difference, and weighted-residuals methods for transient two-dimensional heat conduction in solids.

15 p1958 A73-32270

[ASME PAPER 73-HT-E] Simultaneous control of temperature and humidity in a confined space. I - Mathematical modeling of the dynamic behavior of temperature and humidity in a confined space.

15 p1959 A73-32597

Theory of transient radiation in a waveguide with a piecewise-homogeneous dielectric filler

16 p1978 A73-32890

Arc discharge properties in ionized gases: discussing interruption and reignition in terms of instabilities, decay processes, and circuit breaker problems

16 p2040 A73-32940

Transient oscillator analysis of a high-pressure electrically excited CO laser.

16 p2024 A73-33083

Transient current overshoot to electrostatic processes in continuum, slightly ionized plasmas.

16 p2041 A73-33310

Transient analysis of ceramic vanes for heavy duty gas turbines. [ASME PAPER 73-GT-46]

16 p2048 A73-33507

Transient analysis of complementary MOS IC inverter.

16 p1990 A73-33680

Book - Diffraction of elastic waves and dynamic stress concentrations.

17 p2242 A73-34468

Transient thermal stresses in a disc of linearly strain-hardening material.

17 p2243 A73-34574

Transient response in a receiving system with AGC under the influence of fluctuating signals

17 p2121 A73-34590

Transient temperature response of semiconductor devices under pulsed power operation.

17 p2135 A73-34728

An economical method of analyzing transient motion of gas-lubricated rotor-bearing systems. [ASLE PREPRINT 73-AM-28-2]

17 p2178 A73-34982

Anisotropic laminated fiber composite plates under short duration impact line forces, calculating one

dimensional transient stress and displacement waves by fast Fourier transform
[ASME PAPER 73-APM-L] 17 p2249 A73-35108

Tekite ablation calculation taking into account transient effects, internal radiation, melting and nonequilibrium vaporization of glass and drag effect of flanges
17 p2233 A73-35272

Transient temperatures in a plate from a Gaussian distribution of normal heat flux and current flow with application to the free arc discharge.
17 p2255 A73-35843

Russian book - Nonlinear oscillations and transient processes in machines.
18 p2319 A73-35895

Transient flow and expansion of a pinch discharge plasma in self-induced magnetic fields.
[AIAA PAPER 73-689] 18 p2338 A73-36240

Nonlinear transient responses of structures by the spatial finite-element method.
18 p2362 A73-36309

Cardiorespiratory transients in exercising man. I - Tests of superposition. II - Linear models.
18 p2278 A73-36656

A preliminary study of the transient response of the atmosphere produced by mid-tropospheric heating.
18 p2332 A73-36701

Heat detector signal transients during time constant fluctuations in terms of mathematical expectation of ambient temperature
18 p2317 A73-36857

Synthesis of the optimal characteristics of the engines of multiengine systems
19 p2388 A73-37187

A comparative study of two basic approaches to extremum control.
19 p2413 A73-38037

The transient response of certain third-order nonlinear systems.
19 p2460 A73-38109

A path-independent integral for transient crack problems.
19 p2500 A73-38114

Some transient MHD-flows with finite magnetic Reynolds numbers.
19 p2470 A73-38319

Internal additive interference produced by a pulsed random process.
19 p2407 A73-38353

Mathematical analysis of the operation of regulatory mechanisms of the spinal cord
20 p2517 A73-39005

Investigation of the transient process quality of automatic control systems with variable parameters using the method of the biased characteristic equation
20 p2541 A73-39036

Vibration test techniques used to simulate transients and match shock spectra.
20 p2544 A73-39268

A method of analyzing transient processes in digital fluidic circuits
20 p2510 A73-39352

Transient processes in FM discriminators
20 p2537 A73-39458

Nonlinear response of plates subjected to inplane and lateral pressure pulses.
20 p2622 A73-39547

The incremental theory of three dimensional transient thermoelectroplasticity - Formulation and solution.
20 p2622 A73-39552

Transient ventilatory response to hypoxia with and without controlled alveolar PCO₂.
20 p2515 A73-39777

Practical lasers for photographic and holographic recording.
21 p2709 A73-39973

Laser transient behavior analysis by quantum theory, obtaining density matrix equation solution in terms of exponentially decaying eigenmodes by truncation method
21 p2711 A73-40214

Effects of non-linearity due to large deflections in the derivation of frequency response data from the impulse response of structures.
21 p2783 A73-40287

A mixture theory of the response of a laminated plate to impulsive loads.
21 p2783 A73-40291

Statistical effects in the transient response of a He-Ne laser with a given initial photon distribution
21 p2714 A73-40568

Transient frequency response analysis and far field measurement of linear phased array with tandem series feed network, noting instantaneous bandwidth
21 p2653 A73-40673

Thermal response of microwave transistors under pulsed power operation.
21 p2663 A73-40774

Means of improving the effectiveness of designing nonlinear electronic circuits on a digital computer by the method of nodular potentials
21 p2666 A73-41310

Transient response simulation model for stability analysis of flexible high speed rotor-bearing system dynamics, examining nonlinear effects
[ASME PAPER 73-DET-102] 22 p2865 A73-42079

Transients in inductive energy-storage devices for plasma injectors.
22 p2891 A73-42265

Optimal closed automatic control systems synthesis in terms of minimum integral square error of phase coordinates during transient response time
22 p2836 A73-42609

Experimental determination of the transient uniaxial stress in a bar by dynamic photoplasticity.
[ASME PAPER 73-APMW-37] 22 p2926 A73-42894

Input admittance or impedance and effective height measurement for small metal antennas of prolate and oblate spheroidal and spherical shape, noting transient response
22 p2829 A73-43180

The steady-state and transient performance of some large-scale vortex diodes.
23 p2942 A73-43407

Experimental investigation of transient supersaturations in a thermal diffusion chamber.
23 p3004 A73-44259

A two-layer slab method for measuring thermal diffusivity of polymer by irradiated light heat-wave. I. II - Transient response of temperature sensor attached on a polymer substrate. III - Quantitative evaluation of the effect of edge losses in a parallelepiped.
23 p3049 A73-44363

Sealed carbon dioxide laser output anomalous transient pulsed behavior attributed to gas dissociation and recombination from electron density and temperature measurements
24 p3095 A73-44408

Fluctuations of the radiation rise time in a gas laser with nonlinear resonant absorption.
24 p3095 A73-44494

Transient process due to pressure increase during combustion of condensed material, using fractional-differentiation operator method to determine unsteady burning velocity
24 p3155 A73-44715

Nonlinear transient effects of separated unstable flow on vortex generated acoustic waves in cavities
[AIAA PAPER 73-1014] 24 p3078 A73-44846

Switching transients in conducting channel-broadened p-n-p structure thyristors, predicting voltage change during current growth avalanche phase and settling at saturation point
24 p3072 A73-44932

Switching of semiconductor devices in pulsed voltage regulators
24 p3072 A73-44938

Convergence of finite difference transient response computations for thin shells.
24 p3150 A73-45228

TRANSIENTS [SURGES]
U SURGES

TRANSISTOR AMPLIFIERS
M/W power transistors and MIC amplifiers - State-of-the-art.
01 p0024 A73-10719

A wideband transistor amplifier at the 4 GHz band for communication satellite use.
01 p0026 A73-11176

Russian book on nanosecond multiphase multivibrators covering transistorized single- and dual-stage amplifiers and wave shaping circuits for digital control and computer logic applications
02 p0146 A73-11887

Single circuit amplifier design characterized by cascade connections of transistors to resonance network
03 p0284 A73-14036

Computer-aided design of high-frequency transistor amplifiers.
04 p0427 A73-15053

Neutron irradiation effects on microwave transistor amplifiers.
05 p0558 A73-16520

Large-signal behaviour of R.F. power transistors. I - Analysis of the equivalent circuit.
05 p0559 A73-17125

Circuit parameters and performance of monolithic IC operational amplifiers, noting data sheets with voltage and temperature ranges and frequency response characteristics
06 p0672 A73-17450

Matching of capacitive sensors to low-noise amplifiers based on field effect transistors
07 p0802 A73-20296

Common emitter/common base cascode amplifier overall gain and frequency response dependence on first transistor parameters
07 p0802 A73-20301

X- and Ku-band amplifiers with GaAs Schottky-barriers field-effect transistors.
07 p0803 A73-20555

1-2 GHz high-power linear transistor amplifier.
08 p0947 A73-21146

Two stage microwave monolithic integrated circuit power amplifier design with matched transistors, calculating distributed matching network
08 p0950 A73-21826

Design a 4 to 8 GHz FET amplifier with a 7 dB NF.
08 p0950 A73-21827

Sensitivity of variable-amplifier circuits to variation of the controlled parameters
09 p1069 A73-22651

Temperature measuring devices based on operational amplifier circuits, considering design and applications
09 p1085 A73-22924

Modification and updating of the bioelectric DS2C amplifier for a FET input.
09 p1046 A73-22936

Microstrip solid state power amplifiers with transistors and varactors for spaceborne applications in L and S band ranges
09 p1066 A73-23428

VHF preamplifier with FET for resolving crosstalk and overload problems comparing designed and observed specifications
09 p1066 A73-23429

Spread of transistor parameters as a factor in the design of IF amplifiers with pairs of staggered stages.
10 p1197 A73-24937

Microwave transistor power amplifier.
11 p1338 A73-26149

An electronic relay constructed according to the principle of amplifiers with a controlled amplitude characteristic
12 p1477 A73-26791

Considerations about jump effect in microwave power amplifier.
12 p1478 A73-27073

Output characteristics of high frequency transistor power amplifiers.
12 p1479 A73-27169

Some features of the application of controlled-gain transistors.
12 p1480 A73-27271

Design of sinusoidal and pulsed signal amplification stages with emitter high-frequency compensation.
12 p1480 A73-27273

Errors of the formal theory of amplifiers with a feedback
12 p1481 A73-27594

Pulse amplifier with active gain adjustment for constant bandwidth
13 p1590 A73-28571

A simple method for obtaining a constant input resistance in broadband amplifiers
13 p1590 A73-28572

Optimization of the operating conditions of planar transistors in stages with inductive correction.
13 p1591 A73-28733

Influence of the parasitic capacitance of a field effect transistor and of the input capacitance of the amplifier on the null shift of a modulator
13 p1591 A73-28856

Evaluation of the noise and dynamic range of transistorized selective RC amplifiers with controlled tuning
13 p1591 A73-28868

Null level of a field-effect-transistor modulator of small constant-voltage signals
13 p1592 A73-28873

Effect of the input capacitance of an ac amplifier on the performance of key modulators
13 p1592 A73-28874

A wideband transistor amplifier at the 4-GHz band for communication satellite use.
13 p1594 A73-29228

Gain-bandwidth limitations of microwave transistor amplifiers.
14 p1735 A73-30247

Optimal feedback characteristics of transistor amplifiers
14 p1736 A73-30372

Some operational aspects of an inductively loaded transistorized pulse amplifier at short time intervals
15 p1851 A73-31831

Si transistor amplifier design for power gain stability against temperature variations, considering emitter and collector base voltage as stability parameters
16 p1988 A73-33399

Parameters and energy resolution of the KP303 field effect transistors at low temperatures
17 p2133 A73-34162

Book - Design of modern transistor circuits.
17 p2134 A73-34458

Performance and advantages of FET's as microwave solid state amplifiers.
17 p2141 A73-35322

Book - Solid state electronic circuits: For engineering technology.
18 p2292 A73-35899

A pulse-width modulator operating on dc integral amplifiers
18 p2293 A73-36855

Matching of capacitive pickups to low-noise junction-gate field-effect transistor amplifiers.
18 p2294 A73-37133

Common emitter/common base cascode amplifier overall gain and frequency response dependence on first transistor parameters

18 p2294 A73-37138

A distributed amplifier using bipolar transistors in a common-base circuit

19 p2409 A73-37719

Design and application of low noise GaAs FET amplifiers.

20 p2534 A73-38749

Analysis of a resonant amplifier with stagger-tuned circuits at the input and output

20 p2538 A73-39466

Feedback in microminaturized transistor amplifiers

21 p2659 A73-40010

Circuit variants and applications of series regulated transistor amplifiers, considering trigger circuit, bistable switch, power amplifier, tape recorder monitoring amplifier, etc

21 p2659 A73-40011

Determination of optimal regimes of a common-emitter transistor cascade which ensure minimal distortions

21 p2659 A73-40012

Equipment for measuring cross-modulation distortions in high-frequency power transistors

21 p2660 A73-40014

Design of MOS-transistor integrated-circuit amplifiers

21 p2660 A73-40021

Possibilities of improving the characteristics of operational amplifiers by using thermostated input cascades

21 p2660 A73-40023

The Ebers-Moll effect transistor used as a low-value controlled resistor in ACC and other variable-gain applications.

21 p2661 A73-40229

A 50-W VHF amplifier with transistors

21 p2664 A73-41088

Method of calculating the amplitude and phase-amplitude characteristics of high-frequency amplifiers

21 p2666 A73-41314

Russian book on semiconductor radio transmitter design covering power amplifiers, frequency multipliers, oscillators and Gunn effect devices for sub-microwave frequencies

21 p2666 A73-41424

Russian book on operation and design of bipolar transistor circuits for video amplifiers covering TV, radar, oscilloscope, automatic control and computer applications

22 p2832 A73-41878

Noise characteristics in bipolar transistor differential amplifiers, discussing current sources, circuit configurations, feedback amplifiers and equivalent circuits

22 p2832 A73-41897

Pulse push-pull power amplifier

22 p2833 A73-42361

Two channel transistor amplifier design with negative capacitance correction for microelectrode applications

24 p3062 A73-44723

Investigation of the input impedance of an emitter-input transistor amplifier at near-cutoff frequencies

24 p3072 A73-44935

Aspects of field-effect transistor applications in amplifier stages with feedback

24 p3072 A73-44936

TRANSISTOR CIRCUITS

Transistorized varicap diode frequency modulator circuit with restricted parasitic AM, using phase shift control and frequency multiplication

01 p0022 A73-10031

Influence of strong external factors on the characteristics of semiconductor devices sensitive to the state of the surface /Review/

01 p0022 A73-10036

High efficiency dc-to-dc converter with second non-saturable transformer for eliminating collector current spike to reduce electromagnetic interference and transistor damage

01 p0005 A73-10247

Reliability-performance comparisons between tube and transistor power modules for ground-based and airborne radar applications

01 p0024 A73-10718

New design concepts for microwaves power transistor.

01 p0024 A73-10721

Resonant feedback loops and impedance matching network analysis of pulsed and CW transistor microwave power oscillators

01 p0024 A73-10722

New transistor squaring stage with a 'smooth' parabolic characteristic for realizing a simple high-precision parabolic multiplier

01 p0024 A73-10924

Integrated subnanosecond circuits with low power dissipation and few components

01 p0021 A73-11487

Photodetector array for a holographic optical memory system.

02 p0169 A73-12163

Linear characteristics of transistorized Schmitt trigger pulse width regulators in response to sinusoidal and sawtooth signals for automatic control systems

02 p0149 A73-12343

Measuring hybrid parameters of composite transistors.

02 p0148 A73-12855

Circuit variants of dynamically operated MIS /metal-insulator-semiconductor/ structures

03 p0281 A73-13241

Analysis of limit cycles in a two-transistor saturable-core parallel inverter.

03 p0252 A73-13929

The IHTS - A new building block for power conditioners.

03 p0282 A73-13934

Parasitic oscillations in external excitation oscillators due to internal feedback in transistor, investigating frequency dependence of stability coefficient in common emitter stage

03 p0284 A73-14032

Analysis of a Schmitt trigger employing a field transistor at the input

03 p0284 A73-14324

Threshold voltage shift for low voltage operation of transistor circuits with boron ion implanted MOS

04 p0427 A73-15322

Switch transistor control using an intensity transformer

04 p0489 A73-15736

Self regulated transistorized voltage and frequency converters for multiple motor drives power supply, discussing circuit design, performance characteristics and overload protection

05 p0556 A73-16074

Description and utilization of the TMS 4062 dynamic memory

05 p0553 A73-16171

Three channel transistorized pulse generator for electric stimuli used in electrophysiological studies

05 p0545 A73-16739

Book - Transistor circuit design.

06 p0673 A73-17672

Distributed base resistance effect on stripline geometry transistor input characteristic, using equivalent circuit with pseudo-junction having high saturation current

06 p0677 A73-18396

Effects of ionizing radiations on MOS components

07 p0860 A73-18914

Improving the performance of M.I.S. circuits under radiation.

07 p0797 A73-18918

Analysis of active RC circuits with nonhomogeneously distributed parameters in the time domain

07 p0805 A73-20024

Investigation of the fluctuation characteristics of quartz-crystal harmonic generators

07 p0802 A73-20300

Transistor tester circuit design with mutually independent collector-emitter voltage, collector current, generator and load resistance adjustment for arbitrary operating point selection

07 p0803 A73-20303

A procedure for the evaluation and failure analysis of M.O.S. memory circuits using the scanning electron microscope in potential contrast mode.

08 p0943 A73-20730

Probabilistic analysis of the statistical accuracy of a transistor blocking generator with a common emitter

08 p0949 A73-21590

Circuit diagram and electrical characteristics of semiconductor memory cell consisting of thyristor and n-p-n transistors, noting parameters stability

09 p1063 A73-22460

Amplitude selector for linear transistorized devices

09 p1064 A73-23006

Block diagram of transistorized phase instability meter for statistical analysis of one dimensional density distributions, noting two series connected identical delay lines

09 p1064 A73-23008

Transistor harmonic oscillator design.

10 p1192 A73-23573

Noncrystal controlled oscillator with transistor and tunnel diode, noting high frequency stability due to automatic regulation of dc operating conditions

10 p1194 A73-23735

Narrow band microwave active bandpass filter with inverted-common-collector transistor circuit, discussing design algorithm, insertion loss, stability, sensitivity and frequency selectivity

10 p1201 A73-24169

Study of the behavior of a monostable transistor circuit in the avalanche mode

10 p1195 A73-24413

Transistor sawtooth voltage generator design for accelerated rise time piecewise linear leading edge, using capacitor charge/discharge acceleration

10 p1196 A73-24604

Multistage diffusion model of IC transistor electrical characteristics and impurity distributions as function of surface concentrations and junction depths during fabrication

10 p1196 A73-24606

Avalanche mode I-V characteristics of diffused and alloyed junction transistors at large collector currents

10 p1196 A73-24606

Inductance and Q factor measurements of inductive p-n-p transistor element in IC circuit as function of frequency, temperature and junction capacitance

10 p1196 A73-24610

Multivibrator with p-n-p and n-p-n transistors, noting circuit diagram, operation and power dissipation

10 p1197 A73-24944

Self excited LC and RC oscillator networks based on FETs, discussing frequency tuning and FET methods

10 p1197 A73-24944

Analysis of the thermal stability of high- and low-power silicon planar transistors in the dynamic regime

12 p1478 A73-26944

Characteristics of amplitude discriminators built with transistors operating in the avalanche mode

12 p1479 A73-27292

Certain problems in controlling phase of microwave electromagnetic oscillations using an inductive transistor.

13 p1591 A73-28676

Avalanche transistor circuit with controlled S-shaped I-V characteristics, discussing equivalent circuits and operating points stability

13 p1591 A73-28737

Dynamic losses in a transistorized switch operating on an active-capacitance load

13 p1593 A73-28944

Truncated general equations and a characteristic equation of a self-excited transistor oscillator

14 p1736 A73-30566

Linearization of the relaxation time control of a transistor multivibrator.

15 p1849 A73-30994

Book - The physics and circuit properties of transistors.

15 p1850 A73-31573

Noise properties of a transistor in an integrated circuit

16 p1987 A73-33080

Inexpensive fast solid state current drive circuit for injection lasers, using parallel conventional transistor switches operated at avalanche breakdown for pulsed generation

16 p2024 A73-33400

Wideband varactor-tuned solid-state sources to 20 GHz.

16 p1991 A73-33899

Inductive relaxation oscillator design using common-emitter avalanche transistors with N-shaped I-V characteristics at base input

17 p2133 A73-34150

Book - Design of modern transistor circuits.

17 p2134 A73-34450

Pulse modulation of Gunn-effect oscillator.

17 p2142 A73-35640

Capacitance of a field-effect MOS transistor gate

18 p2293 A73-36720

Investigation of the fluctuation characteristics of quartz harmonic oscillators.

18 p2294 A73-37138

Nonsinusoidal EM waves - State of development

19 p2403 A73-37420

Analysis and design of single-cycle stages in MOS transistors with allowance for nonlinear distortions

20 p2535 A73-38828

A calculation of the equilibrium temperature distributions in multiple-emitter microwave transistors.

20 p2535 A73-38899

Approaches to the design of low-voltage pulsed generators using avalanche semiconductor devices

20 p2538 A73-39466

Ultrafast streaking camera for picosecond laser diagnostics.

21 p2694 A73-39944

Optimization and design of varicap-diode tuned transistor oscillators

21 p2659 A73-40000

Mathematical equipment of a system of automatic designing of components of logic-type semiconductor integrated circuits

21 p2660 A73-40010

Present state and future prospects of the design of large-scale integrated circuits using MIS transistors

21 p2660 A73-40010

Analysis of limit cycles in a two-transistor saturable-core parallel inverter.

21 p2662 A73-40323

Computer analysis of mixed coordinate base transistor circuits determining matrix numbers without main path or generalized node delineation

21 p2670 A73-41300

An effective algorithm for optimizing electronic circuits

21 p2671 A73-41313

Electronic circuit optimization via Powell iterative method, describing search techniques, matrix method and transistor hybrid equivalent circuit application

21 p2671 A73-41313

Semiconductor rectifiers and thyristor devices, discussing transistor switching, Zener diode, controlled and light activated p-n-p-n diodes
21 p2668 A73-41619

The accuracy and operational stability of a transistorized time-delay relay with an RC network
21 p2668 A73-41640

Voltage-to-frequency converters with an avalanche-recombination discharge diode
22 p2832 A73-42357

Dynamic properties of transistor current switches
22 p2833 A73-42369

Analysis of starting circuits for a class of hard oscillators - Two-transistor saturable-core parallel inverters.
22 p2834 A73-42909

Development of a hybrid microelectronics solid state relay for 2500 volts isolation and -120 C to 80 C thermal cycling range.
22 p2835 A73-42914

Logic-controlled solid-state switches for 270 volt dc.
22 p2802 A73-42915

Bilateral power conditioner with common filters and transistor control circuits for battery charge and discharge functions onboard near earth orbit spacecraft
22 p2802 A73-42916

Complementary MOS transistor inverter application to quartz oscillator in terms of frequency, temperature and supply voltage
23 p2960 A73-44112

Cascade n-phase transistorized astable multivibrator circuit design for digital and tool control clock applications
23 p2983 A73-44142

Parameters of low-power transistors in the avalanche mode of operation
24 p3072 A73-44934

Switching of semiconductor devices in pulsed voltage regulators
24 p3072 A73-44938

Darlington composite transistor frequency properties concerning alpha and beta cut-off points and high frequency power gain in common-emitter configuration
24 p3073 A73-45481

TRANSISTOR LOGIC
Microelectronic technology development and applications in transistor-transistor logic, medical devices, computers and thick film hybrid assemblies
02 p0148 A73-12593

Low-dissipation memories by p-channel MOS technology with special processes and by complementary-channel MOS technology
08 p0945 A73-21073

A method for the assessment of the electrical stability of TTL gates
10 p1194 A73-23995

Monolithic IC digital circuits using Si planar technology with Schottky diodes in DTL and TTL gates for high computational speed
11 p1341 A73-25345

Microwave tunnel diode ring counter with displaced nonlinear load line in multistage transistor driver and current switching configuration
13 p1593 A73-29120

Suppressing spurious signals in saturated switching systems.
13 p1595 A73-29394

Book - RCA COS/MOS technology.
20 p2533 A73-38653

Ultrahigh-speed unsaturated diode-transistor logic elements with a small logic differential
21 p2660 A73-40013

TRANSISTORS
NT BIPOLAR TRANSISTORS
NT FIELD EFFECT TRANSISTORS
NT JUNCTION TRANSISTORS
NT PHOTOTRANSISTORS
NT SILICON TRANSISTORS

The performance of recently developed high voltage high current power transistors.
03 p0283 A73-13944

Method of calculating high-frequency parameters of m.o.s. transistors in the nonpinchoff region
05 p0556 A73-16163

Transconductance and distortion of a thin-film transistor
07 p0801 A73-20025

Encapsulated common base microwave transistors mathematical models, determining transfer scattering parameters
10 p1195 A73-24420

Equivalent circuit HF model of MOS transistor active region based on transient response equation, voltage and structural parameters
15 p1850 A73-31492

Influence of the substrate on the transfer admittance of a saturated MOS transistor
15 p1850 A73-31495

Microwave power transistors - The present and the future.
15 p1852 A73-32275

Device for nondestructive measurement of secondary-breakdown parameters in transistors
17 p2133 A73-34161

Avalanche properties of low-power epitaxially-planar transistors
18 p2293 A73-36719

The relation between the internal thermal resistance of transistors and the method of alloying
23 p2960 A73-43677

Some results in predicting the states of semiconductor triodes from noise factors on the basis of the statistical theory of pattern recognition
23 p2961 A73-44297

TRANSIT SATELLITES
A simple apparatus for signal reception of transit system satellites and principal results.
03 p0308 A73-13649

Radioisotope thermoelectric converter for Navy TRANSIT navigational satellite 5 year power supply, describing design and performance test data
09 p1034 A73-22767

Navy transit RTG safety and test integration from users viewpoint.
09 p1118 A73-22796

Circular, hyperbolic, hybrid and angular measurement procedures of satellite navigation, describing Transit system
10 p1246 A73-23660

TRANSIT radioisotope thermoelectric generator technology, discussing structural design, thermal efficiency, performance prediction, panel configurations and life test data
11 p1312 A73-26034

Five-year lifetime thirty-watt radioisotope thermoelectric generator for NAVY Transit Navigational Satellite, discussing system design, major components, reliability and performance tests
11 p1397 A73-26041

Satellites for maritime applications.
19 p2494 A73-38099

Transit satellite-borne radioisotope thermoelectric generators launch aboard Scout missile into circular polar orbit, obtaining electrical and thermal data
19 p2494 A73-38394

Navy Transit Navigation System precision improvements for stationary and nonstationary users, considering uncertainties due to satellite position and instrumentation errors and user motion
21 p2734 A73-40039

Navy Transit navigation satellite system, discussing flight test for feasibility of military application to YP-3C Antisubmarine Warfare Weapons System aircraft
21 p2735 A73-40040

TRANSIT TIME
Large-signal calculations on IMPATT oscillators with voltage waveforms giving close-to-optimum efficiency.
01 p0026 A73-11297

Transit mode operation of thermionic injection diodes
02 p0145 A73-11575

Accuracy requirements for an objectivized astrolabe
03 p0307 A73-13250

Determination of systematic errors in time determinations with the passage instrument
03 p0307 A73-13251

Transit effects in grid plate gap of triode for generating microwave oscillations in regime similar to IMPATT diode
03 p0284 A73-14069

Quantitative radionuclide angiocardiology for determination of chamber to chamber cardiac transit times.
04 p0409 A73-14767

Method for calculating the delay in a time-service photoelectric phase apparatus.
04 p0451 A73-16019

A graph-analytical method for precalculation of the moments of solar transition through the field of view of electrooptical systems
05 p0575 A73-16313

Hypobaric hypoxia - Within-subject transition effects in albino rats.
06 p0649 A73-17525

On the theory of the avalanche transit-time diode reflection amplifier.
06 p0678 A73-18838

Microwave baritt /barrier-injection-transit-time/ diodes large signal performance, noting phase delay between injected and total current densities
08 p0945 A73-21074

Transient photocurrent pulse shapes and transit times in insulators with uniform and exponential trapped space charge in excitation layer or insulator surface
09 p1119 A73-21945

TRAPATT amplifiers for phased-array radar systems.
09 p1051 A73-22497

Neurological fatigue-indices of flight crews of long-range and military transport aviation
11 p1321 A73-25040

Prototype distance measuring instrument for modulated light beam transit time determination
11 p1367 A73-26308

Relative transit time measurements of high-frequency signals using an FM-CW technique
12 p1474 A73-27763

Measuring the positions of satellites with the aid of laser pulses.
13 p1582 A73-28149

Circuits for power density reduction in TRAPATT diodes.
14 p1732 A73-29927

Temperature-dependent design parameters of TRAPATT diodes.
14 p1736 A73-30446

Determination of a probable interval for the mean transit time of geomagnetic-storm /SSC/ solar particles
15 p1926 A73-31647

Laser transit-time measurements between the earth and the moon with a transportable system.
15 p1873 A73-32265

Air-ground transportation interface at airports, examining baggage handling, ticketing, security procedures, rapid transit access, in-airport time and walking distances
16 p1995 A73-33178

Atmospheric refractivity fluctuation caused transit time variation effects on propagation noise and frequency stability in microwave radio link signal reception at 36 GHz
16 p1982 A73-33714

Linear theory of an IMPATT diode distributed microwave amplifier.
16 p1991 A73-33983

Concorde aircraft introduction into airline network, discussing time gain over various routes, operating costs, passenger service, departure and arrival problems, maintenance, etc
[SAE PAPER 730351]
17 p2102 A73-34699

Periodic analysis of arrival times in delayed cosmic-ray coincidences.
19 p2476 A73-38086

Active electronic devices - Microwave diodes
20 p2535 A73-39054

Book - Gallium arsenide microwave bulk and transit-time devices.
20 p2536 A73-39137

TRANSITION
Transition theory application to creep deformation, considering spherical shells
15 p1954 A73-32117

TRANSITION FLOW
An experimental investigation of naturally developing turbulent flow and flow with fixed transition in a parallel pipe.
[ASME PAPER 72-WA/FE-38]
04 p0435 A73-15855

Full scale reentry vehicle laminar to turbulent wake transition characteristics from electrostatic probe inflight measurements of charged particle density fluctuations
[AIAA PAPER 73-109]
05 p0529 A73-16868

Measurements in a transitional/turbulent Mach 10 boundary layer at high-Reynolds numbers.
[AIAA PAPER 73-165]
06 p0645 A73-17649

Numerical prediction of the phenomenon of transition for a flow between two parallel planes
06 p0687 A73-18537

Possible construction of semiempirical turbulent flow theories
07 p0812 A73-20092

Instability, transition, and turbulence in buoyancy-induced flows.
10 p1205 A73-23859

Evaluation of the characteristics of the boundary layer in transitional flow on a flat plate
10 p1296 A73-24497

Study of flow around a rotating circular cylinder.
11 p1302 A73-26337

Calculation of transitional boundary-layer flows.
11 p1348 A73-26394

Influence of the surface-radiation law on the calculation of the aerodynamic coefficients in the near free molecular flow transient regime
12 p1487 A73-27391

Free stream turbulence and transition in a circular duct.
13 p1602 A73-29014

Turbulent source flow between parallel stationary and co-rotating disks.
15 p1862 A73-31337

Photographic studies of the transition between continuum and free molecular flow.
15 p1864 A73-31935

Electrical network analogy application to thermal energy steady diffusion within Knudsen gas filled enclosure, discussing free molecule limit and transition regime
15 p1959 A73-32283

Critical Reynolds number for nondelayed transition in environmental testing for internal and external fluid flows
16 p1999 A73-33146

Natural convection flow equations and stability of laminar and transition flows, external and free boundary flows and boundary layer regimes

17 p2254 A73-34354

The axial flow molecular pump. IV - Performance of a rotor with a single blade row in the transition flow regime.

19 p2433 A73-37673

Some further studies on the transition to turbulent convection.

23 p3003 A73-43935

Air flow in circular convection chamber, investigating transition to turbulence by simultaneous measurements of heat flux and temperature field at low Rayleigh number

24 p3157 A73-45311

TRANSITION LAYERS

Temperature structure and conductive flux in the chromosphere-corona transition region.

01 p0107 A73-11380

Energy balance in the chromosphere-corona transition region.

10 p1279 A73-24138

A model for the polar transition layer and corona for November 1967.

10 p1279 A73-24139

Model solar atmosphere with quiet component involving supergranular velocity field in corona-chromosphere transition layer and vertical magnetic field

10 p1279 A73-24140

Simultaneous determination of the electron temperature and density in the chromospheric-coronal transition region of the sun.

10 p1281 A73-24409

Model of the chromosphere and the transition layer between the chromosphere and solar corona

16 p2057 A73-32703

Application of a microanalyzer to the investigation of the interaction between titanium and coatings

18 p2323 A73-35894

Models of the chromospheric-coronal transition layer and lower corona derived from extreme-ultraviolet observations.

18 p2357 A73-37107

Absorption and transformation of electrostatic surface waves in the transition layer of a magneto-active plasma.

19 p2467 A73-37438

Numerical analysis of magnetic field lines of force reconnection along transition layers or at flow stagnation point of incompressible conducting viscous fluid

22 p2894 A73-42396

Particle number fluctuations and transient effects in electron-photon showers in lead at energies above 20 GeV

23 p3021 A73-43531

Identification of hadrons with 500 GeV energies in cosmic rays by using transitional emission

23 p2981 A73-43566

TRANSITION METALS

NT CADMIUM
NT CHROMIUM
NT COBALT
NT COBALT ISOTOPES
NT COBALT 60
NT GOLD
NT HAFNIUM
NT IRIIDIUM
NT IRON
NT IRON 57
NT MANGANESE
NT MANGANESE ISOTOPES
NT MOLYBDENUM
NT NICKEL
NT NIOBIUM
NT OSMIUM
NT PALLADIUM
NT PLATINUM
NT REFRACTORY METALS
NT RHENIUM
NT RHENIUM ISOTOPES
NT SCANDIUM
NT SILVER
NT TANTALUM
NT TITANIUM
NT TUNGSTEN
NT VANADIUM
NT YTTRIUM
NT ZINC
NT ZIRCONIUM

Certain characteristics of the initial phase of the nitriding process

01 p0055 A73-10255

The valence states of 3d - Transition elements in Apollo 11 and 12 rocks.

03 p0369 A73-13097

High melting point transition metals carbides, nitrides, borides, silicides and oxides thermal conductivity as function of characteristic temperature

03 p0322 A73-13191

Influence of electron concentration on the formation of phases with bcc, fcc, and hexagonal close packed lattices in certain transition-metal alloys

03 p0324 A73-13510

Hardness-controlling additions in transition metal-beryllium alloys

03 p0328 A73-14655

Temperature dependence of impurity resistivity in dilute Al-based Ti, V, Fe, Cu, Zn alloys between 78 and 930 K.

04 p0461 A73-14875

Transition metals nitrides, carbides and silicides applications as electrocatalysts in fuel cells for economic operation, considering hydrogen, formaldehyde and formic acid oxidation

04 p0414 A73-16038

Certain electrophysical properties of zinc oxide base semiconductor ceramics with admixtures of transition-metal oxides

06 p0735 A73-18079

Concentration dependence of the hardness of non-stoichiometric group IV and V transition metal carbides

06 p0710 A73-18658

Nature of chemical bonds in metal-like compounds based on transition metals

07 p0841 A73-20519

Electron and X ray transitions between conduction band and bound level and between two bound levels in transition metals, investigating edge singularity and spectrum shape

07 p0864 A73-20614

The solubility of hydrogen in rhodium, ruthenium, iridium and nickel.

09 p1047 A73-21981

Electron-spectroscopic investigations of two modifications of the alloy steel Kh18N10T

09 p1104 A73-22690

Morphology and spontaneous crystallization conditions of silicides of the transition metals from solutions in metallic melts

09 p1104 A73-22976

Laves phases in hafnium alloys containing period-IV transition metals

09 p1108 A73-23234

Temperature dependent thermal conductivity coefficient and electron and phonon components for group IV-VI transition metal diborides at 2300 K, using Wiedemann-Frantz law

10 p1236 A73-23518

Electrical resistance and emissivity of certain transition metals and alloys in the high-temperature range

10 p1230 A73-23520

Phase equilibria in three-component alloys containing an interstitial element, and the stability of composite materials

10 p1233 A73-24317

Transition metal borides ESCA spectra observation for metal-boron bonding energy based on spectral sensitivity to surface oxidation, discussing relevant features

11 p1325 A73-25202

Thermionic emission properties of refractory metal borides

13 p1634 A73-28201

Body centered cubic lattice transition metals favored cleavage plane prediction for crack propagation

13 p1635 A73-28261

The electrical resistivity of transition metals at high temperatures.

14 p1759 A73-29746

Concentration dependence of the degree of occupancy of a lattice element in cubic titanium oxycarbide

15 p1896 A73-31210

Electronic specific heat of nickel-base alloys containing small amounts of transition metals

15 p1924 A73-32210

Transition metal alloys solid solutions, discussing thermodynamics, interatomic interactions, Debye temperatures, free energy, entropy, magnetic effects and incomplete d shells

15 p1892 A73-32213

Russian book on single crystals of high melting and rare metals and alloys covering structure, interatomic bonds, growth, plastic deformation, heat treatment, etc

15 p1893 A73-32297

Investigation of the influence of certain elements on the heat resistance of titanium aluminide Ti3Al

15 p1894 A73-32530

Influence of plastic deformation and of phase transformations at negative temperatures on the properties of titanium alloys

15 p1894 A73-32531

Heat conductivity and electrical properties of vanadium-alloyed titanium at 100 to 350 K

17 p2188 A73-34554

Effect of group VIII elements on the temperature of plastic-to-brittle transition of states in molybdenum-carbon alloys

17 p2189 A73-34576

Effect of small group-VIII metal additions on the structure and properties of cast molybdenum

17 p2189 A73-34578

Temperature dependent thermal conductivity coefficient and electron and phonon components for group

IV-VI transition metal diborides at 2300 K, using Wiedemann-Frantz law

17 p2196 A73-35198

Electrical resistivity and emissivity of some transition metals and alloys in the high-temperature range.

17 p2191 A73-35206

Superconductivity of beryllides of some transition metals

18 p2340 A73-36678

X ray diffraction analysis of Mo-Ta and Mo-C solid solutions, relating transition and nontransition metal electronic structures and stacking fault energy

18 p2325 A73-36808

The oxidation of binary alloys of chromium with metals of the first long period.

19 p2442 A73-38099

Energy spectrum of transition metals in the superconducting state

20 p2600 A73-39727

Binary and ternary Laves phases in systems composed of zirconium and transition metals of the V through VII groups of the periodic system

21 p2718 A73-40848

Elements of a model of oxygen interactions under low pressure with transition metals at high temperature

21 p2648 A73-41562

The emissivities of liquid metals at their fusion temperatures.

22 p2930 A73-41983

Ternary systems: Rare earth metal - iron family metal - silicon /Component interaction and crystal structures of compounds/

22 p2873 A73-42084

Phase diagrams and composition selections for strengthening of multicomponent deformable Mg alloys with rare earth and transition elements

22 p2874 A73-42094

Patterns of the structure of transition metal/interstitial element diagrams /Me - B, C, N, O, H/

22 p2877 A73-42452

Specific structural features of the binary phase diagrams of some transition metals in a region containing Laves phases

22 p2877 A73-42453

The mechanism of electrical erosion in composite materials during electric arc alloying

24 p3093 A73-44743

TRANSITION POINTS

Investigations into film failure /transition point/ of oil lubricated concentrated contacts.

05 p0580 A73-16100

Efficiency transition point for inductively loaded monopole.

11 p1337 A73-25368

TRANSITION PROBABILITIES

Theoretical treatment of the translational absorption spectrum induced in mixtures of rare gases

01 p0079 A73-10500

Two quantum induced photon-plasma transition probability for hydrogen atom in processes of nebulae and stellar chromospheres

01 p0080 A73-11300

Multiphonon transition theory for electron transitions probability between conduction and forbidden bands, noting semiconductor surface states with longer relaxation time

01 p0089 A73-11438

Blanketed model atmospheres for cool hydrogen-rich white dwarfs.

03 p0371 A73-13222

Solution of the transfer equation for interlocked multiplets by probabilistic method.

05 p0599 A73-17320

Kolmogorov's differential equations for non-stationary, countable state Markov processes with uniformly continuous transition probabilities.

06 p0718 A73-18509

Recombination of H/+ and H/- ions in slow collisions.

07 p0852 A73-19148

Ergodicity criteria of homogeneous Markov chains in a special phase space. I, II

07 p0844 A73-19320

Air-terminal queues under time-dependent conditions.

07 p0850 A73-20370

Calculation of probabilities of energy transfer - Application to the vibrational relaxation of the CS radical in the presence of argon

07 p0854 A73-20604

Dependence of He-Ne laser output power on discharge current, gas pressure and tube radius.

08 p0976 A73-21465

On the theory of tunnelling in electron and proton transfer reactions.

09 p1133 A73-22194

Flux magnitude and single transition probabilities as function of electron density and temperature in relaxation model ionization and recombination channels

10 p1253 A73-23500

Probabilities of infrared and RF transitions in OH and CH molecules

10 p1250 A73-23711

- Probability model of mode interactions, radiation density and output gain of gas laser channels with common lower energy level in active medium
10 p1227 A73-24071
- Light scattering from weakly ionized nonhomogeneous plasmas.
11 p1405 A73-25971
- Transitions between Zeeman atomic sublevels in a medium
11 p1405 A73-26155
- An evaluation of molecular constants and transition probabilities for the NH free radical.
11 p1402 A73-26582
- Atomic L2 and L3 vacancy states absolute width from photoelectron spectroscopy, investigating discontinuities, Auger intensity ratio and Coster-Kronig transition probability
13 p1662 A73-28189
- Exponential bounds for error and equivocation based on Markov chain observations.
13 p1651 A73-29600
- Laser photons multiple absorption by atoms, determining transition probabilities from Schrodinger equation solution via space translation operation
14 p1776 A73-29698
- Transition probabilities of neutral and singly ionized germanium.
14 p1783 A73-30243
- Calculation of the nonlinear polarizability of a gas at a laser transition with allowance for capture of resonance emission
14 p1757 A73-30367
- Probabilistic properties and spectral characteristics of the duobinary code in the baseband
14 p1729 A73-30897
- Certain aspects of the asymptotic behavior of generalized random systems with complete connections
15 p1901 A73-32208
- A proposed correction to the solar abundances of carbon and oxygen utilizing new and accurate theoretical forbidden transition probabilities.
16 p2060 A73-32952
- Flux magnitude and single transition probabilities as function of electron density and temperature in relaxation model ionization and recombination channels
17 p2217 A73-35183
- Transition probability approach to the theory of plasmas.
17 p2218 A73-35819
- Infrared and radio transition probabilities of OH and CH.
18 p2338 A73-36735
- Photoelectric plasma arc measurements of Si I oscillator line intensities in 2500-8000 A range, relating with transition probabilities
20 p2595 A73-39590
- Turbulent diffusion in Schwinger formulation of quantum field theory, deriving transition probabilities from Dyson and Saffman equations
20 p2599 A73-39674
- Probability balance equations for energy level population analysis of ultrashort pulse solid state laser regeneration and amplification
21 p2712 A73-40309
- Detailed balance as check on impact parameter calculations, discussing proton-hydrogen collisions with small transition amplitudes and interpolation errors
21 p2743 A73-40467
- Triply ionized Pm in lithium yttrium fluoride laser, calculating crystal field split energy levels and radiative transition probabilities.
21 p2715 A73-40764
- Evaluation of burst error correcting codes using a simple partitioned Markov chain model.
21 p2656 A73-41168
- Absolute oscillator strengths in neutral chromium and the solar chromium abundance.
22 p2905 A73-41764
- Pitfalls of configuration interaction - Transition probabilities in Fe XIII.
22 p2908 A73-42312
- Transition probability matrix method for calculating residence times of moving particles in region of space, determining stratosphere residence time against exit to tropopause
22 p2849 A73-42543
- Unitary transition probabilities for atom-atom oscillator collisions.
24 p3113 A73-44982
- Multiphotonic absorption spectroscopy without Doppler effect
24 p3096 A73-45327
- TRANSITION TEMPERATURE**
Superconducting-normal phase boundary as function of applied magnetic field and transition temperature in Nb-Ga alloys
02 p0200 A73-11840
- Superconducting Mo-Re alloy thin film prepared by sputtering and deposition onto sapphire substrate, measuring transition temperature, critical current and magnetic field characteristics
02 p0200 A73-11841
- Ti-Al-V alloys as differential measurement method for metallurgical processing and microstructure effects on superconducting critical temperature and magnetic permeability/susceptibility
02 p0200 A73-11843
- Two phase recrystallization temperatures and structural inhomogeneity of dispersion hardened Ni after cold working and annealing at 1300-1400 C
03 p0324 A73-13508
- Relationship between material fracture toughness using fracture mechanics and transition temperature tests.
04 p0506 A73-14703
- Stabilization of superconducting beryllium by addition of aluminum.
05 p0605 A73-16794
- The VDTA-3 apparatus for high-temperature differential thermal analysis
06 p0693 A73-18043
- Dependence of martensite morphology on the isothermal transformation temperature of the Fe-24Ni-3Mn alloy
09 p1100 A73-21974
- Austenite stabilization in Kh17N6M3 transition-type steel
09 p1107 A73-23201
- High temperature superconductivity in three dimensional systems of metals and nonmetals, discussing electron collectivization in metals, dielectrics, organic compounds, semiconductors and molecular crystals
10 p1261 A73-24692
- Change in the superconducting properties of vanadium after the introduction of tantalum impurity atoms
10 p1261 A73-24761
- Characteristics of viscous vortex flows in superconducting alloys near the critical temperature
10 p1261 A73-24765
- Critical transition temperatures and magnetic moment measurements of superconducting state of binary Be alloys
11 p1409 A73-25630
- High field superconductivity in alkali metal intercalates of MoS₂.
11 p1410 A73-26745
- Fluctuating shift in the transition temperature of thin superconducting films
12 p1532 A73-27984
- Superconductivity of cadmium-magnesium alloys.
13 p1668 A73-28223
- Possibility of a superconducting transition in a semiconductor subjected to high-power laser radiation.
13 p1629 A73-29439
- Dependence of the variation of the electronic dislocation drag force in a superconducting transition on the stress, temperature, and velocity.
14 p1783 A73-30341
- Model of degenerate semiconductor transition to superconducting state in terms of electron interactions with phonons of low-lying spectral branch
14 p1783 A73-30343
- German monograph - The effect of germanium additions on the superconductor characteristics and the transition processes in technical titanium-niobium alloys.
14 p1762 A73-30666
- Resistance of superconductors near the critical field H_{c2}
14 p1784 A73-30813
- Some characteristics of the influence of alloying elements on the polymorphous transformation temperature of zirconium
14 p1765 A73-30886
- Russian book - Superconducting alloys and compounds.
15 p1922 A73-31176
- Attempted prediction of the superconducting transition temperature for some metallic compounds with the aid of a computer
15 p1922 A73-31177
- Electron characteristics of sprayed vanadium-gallium alloys
15 p1922 A73-31178
- Structure and properties of alloys of the V3Si-V3Ga-V3Al system
15 p1922 A73-31179
- Moessbauer effect in Nb3Sn as a function of heat treatment
15 p1922 A73-31180
- Structure and superconducting properties of alloys of the vanadium-tantalum system
15 p1923 A73-31183
- Specific heat of alloys of the niobium-titanium system near the superconducting transition temperature
15 p1886 A73-31184
- Changes in the superconducting transition temperature of alloys of variable composition, as exemplified by the niobium-tantalum system
15 p1887 A73-31189
- Structure and properties of alloys of the V3Si-V3Ga-V3Ge system
15 p1923 A73-31190
- An X-ray diffraction and DTA study of the ferroelectric transition in barium sodium niobate.
15 p1924 A73-31839
- Effects of high omnidirectional pressures and residual stresses on the superconductivity of alloys of the V3/Si1-xGex system
16 p2027 A73-34062
- Superfluidity of the Fermi component in a Fermi-Bose gas and in He3-He4 solutions
16 p2038 A73-34067
- Effect of group VIII elements on the temperature of plastic-to-brittle transition of states in molybdenum-carbon alloys
17 p2189 A73-34576
- Relation between the brittle-viscous transition temperature and structural characteristics in certain low-alloyed chromium alloys
17 p2189 A73-34579
- Superconductivity of beryllides of some transition metals
18 p2340 A73-36678
- Superconducting properties of alloys of the vanadium-niobium-chromium system
18 p2325 A73-36898
- Ultrahigh-speed quenching of niobium and vanadium
19 p2439 A73-37250
- Effect of impurities on the temperature of the superconducting transition in W3Si type compounds
20 p2600 A73-39731
- Theory of the phase transition in group IV-VI compound semiconductors
21 p2751 A73-40369
- Effect of high pressure on the superconducting transition temperature of Pd-H.
21 p2753 A73-41126
- Transformation temperatures of martensite in beta-phase nickel aluminide.
23 p2989 A73-43275
- Conductivity of Type II superconductors near the transition temperature
23 p3016 A73-44019
- Superconductivity of copper containing small amounts of niobium.
23 p3017 A73-44033
- Thermal and electrical properties of superconducting vanadium silicide tapes, plotting transition temperature vs heat treatment time and temperature and critical current vs current density
24 p3119 A73-44411
- TRANSITS**
NT CINETHEODOLITES
NT THEODOLITES
The accuracy of measurements of star transits
01 p0098 A73-10553
- Automatic electronic pendulum astrolabe featuring altitude and azimuth tracking mechanisms, azimuth setter and 180 degree turning mechanism
13 p1612 A73-28394
- A punched tape recorder for observation data
15 p1878 A73-32142
- TRANSLATIONAL MOTION**
NT SECONDARY FLOW
NT THREE DIMENSIONAL FLOW
NT THREE DIMENSIONAL MOTION
Theoretical treatment of the translational absorption spectrum induced in mixtures of rare gases
01 p0079 A73-10500
- Relativistic stress tensor in general relativity theory
05 p0597 A73-16469
- Piston motion in semiclosed tube under high initial pressure, using gas-to-piston mass ratio as perturbation parameter in analysis based on Lagrange solution [DFVLR-SONDDR-255]
06 p0685 A73-17739
- First-order perturbations of the two finite body problem.
07 p0877 A73-19594
- Flight-mechanics analysis of various flight conditions of conventional aircraft. VII - Mechanical foundations: Dynamic equations of motion of the translational motion of a rigid body
11 p1307 A73-26725
- Movement of viscous incompressible fluids through annular interstices with walls in relative alternating translational motion
12 p1486 A73-26795
- Translational temperature and atomic velocity distribution functions in rarefied binary gas jets by electron beam excited Doppler line measurement
13 p1618 A73-29163
- Choice of the geometrical parameters, R, r, and r1, of a roller-ring mechanism as a function of maximum load capacity
15 p1832 A73-31277
- Forward precession motion of the moon caused by attraction to the earth and the sun
15 p1939 A73-31966
- Analysis of vestibular effects in experiments on swings
17 p2111 A73-34235
- Canonical elements of the translational-rotational motion of a planet satellite
19 p2476 A73-37199

TRANSLUNAR SPACE

Motion cue method featuring coordinated adaptive washout circuitry in flight simulator using nonlinear filter, discussing heave, yaw and six degrees of freedom application
[AIAA PAPER 73-930] 21 p2674 A73-40877

Translational-precessional motion of the moon in the gravitational field of the earth and sun.
24 p3132 A73-44491

TRANSLUNAR SPACE

U INTERPLANETARY SPACE

TRANSMISSION

NT AERODYNAMIC HEAT TRANSFER
NT AUTOMATIC PICTURE TRANSMISSION
NT CONDUCTIVE HEAT TRANSFER
NT CONVECTIVE HEAT TRANSFER
NT DATA TRANSMISSION
NT DIFFRACTION PROPAGATION
NT DOUBLE SIDEBAND TRANSMISSION
NT ELECTRIC POWER TRANSMISSION
NT ELECTROMAGNETIC WAVE TRANSMISSION
NT GROUND WAVE PROPAGATION
NT HEAT TRANSFER
NT HEAT TRANSMISSION
NT HYPERSONIC HEAT TRANSFER
NT IONOSPHERIC F-SCATTER PROPAGATION
NT IONOSPHERIC PROPAGATION
NT LAMINAR HEAT TRANSFER
NT LIGHT SCATTERING
NT LIGHT TRANSMISSION
NT MICROWAVE ATTENUATION
NT MICROWAVE TRANSMISSION
NT MULTIPATH TRANSMISSION
NT MULTIPLEXING
NT RADAR TRANSMISSION
NT RADIATIVE HEAT TRANSFER
NT RADIO TRANSMISSION
NT SATELLITE TRANSMISSION
NT SCATTER PROPAGATION
NT SHOCK WAVE PROPAGATION
NT SHORT WAVE RADIO TRANSMISSION
NT SIGNAL TRANSMISSION
NT SINGLE SIDEBAND TRANSMISSION
NT SOUND TRANSMISSION
NT STRESS PROPAGATION
NT SUPERSONIC HEAT TRANSFER
NT TELEPHONY
NT TELEVISION TRANSMISSION
NT TIME DIVISION MULTIPLEXING
NT TRANSEQUATORIAL PROPAGATION
NT TURBULENT HEAT TRANSFER
NT WAVE PROPAGATION

TRANSMISSION EFFICIENCY

Experimental investigation of a test-model two-beam TWT /electron-wave TWT/
01 p0025 A73-10986

Plane electromagnetic wave diffraction by periodic grid of dielectric cylindrical filaments, determining reflection and transmission coefficients of radome composite materials
02 p0141 A73-12024

Noise characteristics, channel capacities, power requirements and transmission efficiencies of various semiconductor transmitter designs for FM directional radio systems
03 p0284 A73-14125

Ways for increasing the efficiency of data transmission systems.
04 p0420 A73-15421

Conditions derived for reactive two-terminal-pair matching transformer networks operation at maximum power transfer efficiency
09 p1061 A73-22046

Bandwidth as measure of dimensions added to signal space per unit time in digital transmission power spectral density computation, presenting comparison for telemetry signals
09 p1054 A73-23384

Amplitude-phase-keying with M-ary alphabets - A technique for bandwidth reduction.
09 p1054 A73-23385

Pretransmission normalization procedure to suppress transmission error accumulation in receivers of differential PCM systems
09 p1055 A73-23388

Experimental investigation of undulatory multiplication gear systems
10 p1222 A73-23597

Method of calculation of radioelectric performances of airborne radomes
11 p1327 A73-25282

Influence of the illumination law on the radioelectric performance of radomes - Contribution to the determination of apparent illumination of the antenna
11 p1328 A73-25284

Information transmission reliability enhancement via digital code group symbol transmission by wide-band linear FM radio signals
12 p1471 A73-27593

Approximate procedure for synthesis of interdigital bandpass filters with lumped capacitance loaded bar ends, deriving transmission response from Kirchhoff nodal law
16 p1986 A73-32911

Parasitic mode conversion loss measurement for circular waveguide section quality evaluation, determining transmission coefficient from signal envelope
17 p2121 A73-34588

Single beam spectrophotometer for transmittance measurement constructed from off-axis parabolic mirrors and plane grating monochromator, considering systematic errors
17 p2172 A73-35426

Linear antenna directivity loss for fluctuating signal reception, noting effects of signal to noise ratio and antenna length
17 p2129 A73-35709

Asymptotic methods for the effectiveness computation of a sampling scheme of active sub-channels in an adaptive, multi-channel communication system.
17 p2129 A73-35712

Signal set design for bandwidth constrained multiple phase amplitude shift keyed /MPASK/ communication system, considering minimum error probability for given energy/noise ratio
20 p2522 A73-38717

Transmission strategy and optimal block size in high-speed data communication.
20 p2530 A73-39128

Method for the computation of radio paths up to 4000 km long
20 p2530 A73-39180

Acoustic surface wave thin film guides for nonlinear signal processing, discussing relative advantages over nonguided arrangements, and application to transverse wave front imaging
20 p2531 A73-39596

Digital communication channel with noisy errors, discussing statistical analysis of binary burst sequences for coding design
21 p2655 A73-41090

A new method for calculating correction factors for near-field gain measurements.
22 p2830 A73-41829

ATS-1 borne Random Access Discrete Address System for multiple access satellite communication, discussing repeater performance concerning CW signal transmission efficiency, intermodulation and SNR
22 p2825 A73-42187

Continuous information theory and modulation methods.
22 p2826 A73-42463

TRANSMISSION LINES

NT BEAM WAVEGUIDES
NT COAXIAL CABLES
NT COMMUNICATION CABLES
NT FLUID TRANSMISSION LINES
NT PLASMA GUIDES
NT POWER LINES
NT STRIP TRANSMISSION LINES
NT WAVEGUIDES

Book - Handbook of microwave techniques and equipment.
01 p0021 A73-10025

Rational and irrational matrix functions for analysis and synthesis of distributed microwave networks with multiwire lines and lumped nonreactive elements
01 p0027 A73-10578

Book on electromagnetic field theory covering free space Maxwell equations, Lorentz force law, vector analysis, Laplace equation, lossless transmission lines and dipole antennas
03 p0343 A73-13988

Stationary waves properties dependence on weak skin effect in distributed tunnel diode type of nonlinear active transmission lines
04 p0429 A73-15911

Lambda/4 directional coupler in an inhomogeneous medium with deviations of even and odd mode parameters from the ideal value
05 p0559 A73-17000

Requirements for the production of several, mutually independent beams by a transmission-line fed antenna
05 p0559 A73-17238

Book - Microwave transmission.
06 p0663 A73-17670

Calculation of the asymptotic behaviour of the TDR step response related to the asymptotic behaviour of dielectrics in the frequency domain.
07 p0797 A73-19107

Evaluation of the norm of the wave-impedance distribution function in the synthesis of an inhomogeneous line for wide-band matching
08 p0946 A73-21105

A magnetic thyristor pulse generator with shock-wave generation in the transmission line
08 p0949 A73-21712

Group delay equalization in waveguide communications systems for signal regeneration with tapered meander transmission line
09 p1053 A73-23110

Integrated neuristor lines based on p-n-p-n structures with diffused resistors
10 p1193 A73-23727

Tuning nonlinearity of oscillatory systems made of long-line segments containing a varicap
10 p1193 A73-23728

Equivalent circuit analysis of noise in bulk semiconductor devices.
10 p1197 A73-24869

Low loss fiber optics communication technology with almost infinite bandwidth potential, discussing transmission lines, light sources, detectors, integrated circuits, systems and applications
11 p1399 A73-26118

Calculation of the statistical characteristics of a long waveguide line in a two-wave model
12 p1469 A73-27189

Measurement equipment for the PCM transmission system KPK 30/32
14 p1736 A73-30373

Remote feed, control, and signalization in transmission lines of multichannel systems with pulse code modulation
14 p1728 A73-30374

Thunderstorm activity determination on lightning discharge number recorders
14 p1754 A73-30797

Photoelectron statistics and calculation of the characteristics of optical communications lines
15 p1842 A73-31257

Optical transceiver system requirements for local communications, discussing GaAs light emitting and laser modes, transmission links, installation, maintenance and environmental error factors
16 p1978 A73-32887

Linear cross-polarisation and attenuation measurements at 11 and 36 GHz.
16 p1982 A73-33723

Modular MOS LSI digital data bus system design for integrated avionics and remote sensors interconnection in aerospace vehicles
17 p2139 A73-35232

TDM data bus and interface design for digital avionics system, considering standard remote terminal in terms of system parameters, operation and cost effectiveness
17 p2139 A73-35233

Currents in Florida lightning return strokes.
17 p2163 A73-35465

The generalized multiprobe reflectometer and its application to automated transmission line measurements.
17 p2143 A73-35691

Book - Electromagnetic wave propagation.
17 p2130 A73-35857

Glass fiber transmission characteristics as optical waveguides for communication systems, considering transit time and attenuation
20 p2522 A73-38660

Detachable liquid filled capillary waveguide connector for glass fiber multimode optical transmission lines, discussing propagation efficiency as function of dimensional tolerances
20 p2522 A73-38662

A pulse-regenerating optical transmission line.
20 p2522 A73-38668

Effects of dispersion on steady state electromagnetic shock profiles.
20 p2595 A73-38864

Experimental correlation techniques for the characterization of vibration transmission paths.
20 p2617 A73-39267

Calculation of structurally compressed satellite radio lines
20 p2531 A73-39469

Tunnel diode different time constants two delay-line circuit, noting self oscillation range, constant pulse periods and hysteresis phenomenon elimination
21 p2660 A73-40099

Statistical analysis of microwave transmission line coefficients, discussing line losses, inhomogeneity distribution, input voltage standing wave ratios and rms deviations
21 p2648 A73-40204

Insulated electrically thin dipole antenna with surrounding large wave number isotropic medium, discussing transmission line properties and current and charge distribution
22 p2829 A73-43183

Crosstalk interference and regenerative amplifier noise effects on PCM signal transmission over twin- and four-conductor lines
23 p2954 A73-43784

A quantitative estimate of the electromagnetic compatibility of high-frequency leads in electronic equipment
24 p3071 A73-44596

German book on HF technology, Volume 1, covering coupling filters, transmission lines, antennas, Lecher waves, waveguides, etc
24 p3073 A73-44999

Efficient numerical solution of the transmission-line equivalent-circuit model of a semiconductor.
24 p3119 A73-45261

Self and excited oscillations in a circuit composed of a non-linear element and a delay line.
24 p3075 A73-45487

TRANSMISSION LOSS

Fast spectrograph and image slicers for avoidance of light transmission loss caused by central obscuration

tion in astronomical telescope and image intensifier tubes

01 p0048 A73-10526

Optical power handling capacity of low loss optical fibers as determined by stimulated Raman and Brillouin scattering.

01 p0078 A73-11216

Diffraction losses and corrections for lower order transverse modes and resonance conditions in optical resonators with cylindrical mirrors

03 p0319 A73-14079

Loss compensation in the case of filters with additional resistors

03 p0284 A73-14124

Coupling losses between cylindrical multimode fibers and laser diodes

04 p0458 A73-15321

Higher-order scattering losses in dielectric waveguides.

05 p0549 A73-16366

Higher-order loss processes and the loss penalty of multimode operation.

05 p0549 A73-16367

An aluminum waveguide of oval cross section, which can be wound on a drum, with favorable wave resistance transformations /ALFORM waveguide/

06 p0663 A73-17582

Measurement of dielectric constant of nonmagnetic materials in a waveguide system with an unknown movable reflecting load.

06 p0696 A73-18618

The a.c. losses of non-ideal type II superconductors under parallel configurations of electric currents and magnetic fields.

07 p0864 A73-20403

Circular electric waveguide of minimum loss and elastic flexibility.

08 p0938 A73-20838

Transmission loss at high frequencies on 3260 km temperate-latitude path.

09 p1052 A73-22958

Influence of fabrication inaccuracies on the axis deviation of an airborne radome

11 p1328 A73-25295

Optical beam hybrid lens waveguide with central aperture and surrounding lens, comparing transmission loss and bending effects with iris guides

11 p1365 A73-26230

Lowest-order mode selection in a laser interferometer.

12 p1504 A73-26842

Shimazaki formula corrected for F 2 layer altitude estimation for 2-30 MHz field intensity and transmission losses calculations

12 p1493 A73-27762

Monomode optical fiber waveguide propagation attenuation due to random curvature, analyzing radiation losses for clad cores with uniform and gradient refractive index profiles

14 p1729 A73-30695

Microwave filters physical volume relation to losses, discussing intrinsic and loaded Q factors from frequency attenuation curves and graphical design procedures

15 p1850 A73-31252

Atmospheric lens effect - Another loss for the radar range equation.

16 p1980 A73-33407

Optimal parallel-type varactor frequency multiplier calculation for reverse-biased conditions in terms of nonlinear conductance loss and diffusion capacitance Q factor

16 p1991 A73-33981

Parasitic mode conversion loss measurement for circular waveguide section quality evaluation, determining transmission coefficient from signal envelope

17 p2121 A73-34588

Scattering of waves at a step in a circular multiwave waveguide.

17 p2123 A73-35152

Low loss light guiding polymer thin film with continuously adjustable refractivity, discussing fabrication and refractivity and scattering loss measurements

17 p2172 A73-35423

The effect of stiffeners on the sound radiation and the transmission loss of metal walls

19 p2460 A73-38181

Determining the absorption coefficients of low-loss bulk glass materials.

20 p2563 A73-38663

Statistical analysis of microwave transmission loss coefficients, discussing line losses, inhomogeneity distribution, input voltage standing wave ratios and rms deviations

21 p2648 A73-40204

Lyot birefringent filter contrast element thickness effects on SNR performance and transmission loss

21 p2706 A73-41505

Microwave acoustic surface wave devices design tradeoffs, considering propagation losses, air loading, beam steering and diffraction, and transducer effects in curves and data

22 p2833 A73-42399

Theoretical and experimental investigations of the coupling of two glass-fiber light waveguides

22 p2861 A73-42424

Nonlinear transmission loss in Ge beam splitter in pulsed HF and DF lasers operating at 2.5 to 4 microns

22 p2897 A73-43145

Sealed carbon dioxide laser design for transverse mode output power in terms of beam, transmission loss, Fresnel number and cavity parameters

22 p2872 A73-43155

Losses and impulse response of a parabolic index fiber with random bends.

23 p2987 A73-43989

Electronically tunable microwave bandpass filters

24 p3071 A73-44606

Parameter evaluation method for lossy strip transmission lines, assuming microwave propagation in waveguide system with dielectric between two conducting plates

24 p3074 A73-45007

TRANSMISSIVITY

Two beam optical recording instrument for atmospheric IR transmissivity, discussing spectrophotometers with changeable NaCl, KBr and LiF prisms

04 p0450 A73-15575

TRANSMITTANCE

Line-by-line computations of transmittance for non-homogeneous paths in designing application-oriented representations for water vapor and carbon dioxide channels IR spectral responses

01 p0037 A73-10365

Transmittance functions for satellite temperature sounding.

01 p0037 A73-10367

Reflection and transmission coefficients for stratified media, considering total optical reflection attenuator and metal film reflector

01 p0078 A73-11229

Complex transmission coefficient of waveguide with two arbitrarily spaced infinitely thin plane parallel inhomogeneities, using Galerkin method for single-parameter approximation of electrodynamic problem

03 p0278 A73-14057

Atmospheric windows for HF laser radiation between 2.7 and 3.2 microns.

03 p0319 A73-14431

Atmospheric transmittance calculation from 0.76-micron oxygen band fine structure parameters

04 p0473 A73-15571

Spectral transmittance of cryodeposits on a transmitting substrate.

05 p0598 A73-16897

Determination of the specific surface resistance of thin metallic layers in the microwave range, based on transmission coefficient measurements

06 p0737 A73-18221

Contrast transmittance Monte Carlo computation for atmospheric haze models based on aircraft measurement data from various geographical areas

06 p0694 A73-18302

Measurement of the vertical transparency of the atmosphere in the infrared using an artificial source.

07 p0848 A73-20349

Equipment and procedures for measurement of atmospheric spectral transmittance in the infrared region of the spectrum

11 p1363 A73-25643

Coated laser windows characterized by strong surface absorption, calculating absorptivity, transmittance and reflectivity under assumption of insignificant interference effects within substrate

11 p1377 A73-26243

Photon conductivity analysis for homogeneous isotropic solid body based on convective-radiant transfer equations, determining molten quartz thermal conductivity and diffusivity

12 p1516 A73-27311

Polarization-dependent intensity transmittance of optical systems.

15 p1913 A73-31125

Measuring earth-to-space contrast transmittance from ground stations.

15 p1914 A73-32386

Method to apply homogeneous-path transmittance models to inhomogeneous atmospheres.

17 p2205 A73-34856

Infrared transmittances for indirect soundings of the atmosphere from satellite-based measurements.

18 p2308 A73-36043

Spatial frequencies of clear sky radiance in the range 4.5 to 5.2 microns

18 p2314 A73-36899

Low pass wide and medium band far IR filter obtained by cooling crystalline material to liquid He or nitrogen temperatures, tabulating transmission characteristics

21 p2697 A73-40127

Image contrast and efficiency of nonlinearly recorded holograms of diffusely reflecting objects.

21 p2703 A73-41133

Electromagnetic radiation excited by electric or magnetic line source near inhomogeneous dielectric

layer, evaluating reflected and transmitted fields by saddle point technique

22 p2824 A73-41831

Determination of the transmittance of an optically not dense plasma by an intracavity method

24 p3115 A73-44762

TRANSMITTER RECEIVERS

Design curves for PIN diode transmitter receiver switch based on lumped circuit filter suited to high frequency bands

09 p1063 A73-22496

Solid-state devices and components for mm-wave receiver-transmitter systems.

09 p1064 A73-22498

Optical transceiver system requirements for local communications, discussing GaAs light emitting and lasing modes, transmission links, installation, maintenance and environmental error factors

16 p1978 A73-32887

Experimental test of optical antenna-gain reciprocity.

19 p2439 A73-38487

TRANSIMITTERS

NT IONOSONDES
NT RADAR TRANSMITTERS
NT RADIO BEACONS
NT RADIO TRANSMITTERS
NT RADIOSONDES
NT RADIO/TELEPHONES
NT RAWINSONDES
NT REPEATERS
NT TRANSMITTER RECEIVERS

Circuit technology of a temperature-measurement transmitter for biotelemetric applications

13 p1579 A73-28575

TRANSMUTATION

Preparation of high-level alpha-particle sources for the Surveyor Alpha Scattering Experiment.

16 p2035 A73-32975

Cosmic radiation intensity constancy from observations of cosmic ray induced transmutations in meteorites

17 p2223 A73-34419

Nuclide production rates in stone meteorites and lunar samples by galactic cosmic radiation.

20 p2612 A73-39716

TRANSOCEANIC COMMUNICATION

Transoceanic telephony via communication satellites, discussing satellite reliability and placement in synchronous orbit

06 p0663 A73-17577

AEROSAT - An aeronautical communications satellite for oceanic areas.

06 p0771 A73-17624

[AIAA PAPER 73-46] Omega v.l.f. wave propagation and the 1922-23 Marconi expedition.

06 p0668 A73-18442

The Aeronautical Satellite Programme - ATC aspects.

07 p0848 A73-19141

TRANSOCEANIC SYSTEMS

NT TRANSOCEANIC COMMUNICATION

Multisatellite systems for transoceanic aircraft communications and ATC, discussing day and night operations, cost-benefit optimization and adaptive techniques for capacity augmentation

01 p0018 A73-11201

Operational utilization of an aeronautical satellite system for air traffic control over the North Atlantic.

15 p1911 A73-32487

The transatlantic charter policy of the United States.

24 p3158 A73-44575

TRANSONIC AIRCRAFT

U SUPERSONIC AIRCRAFT

TRANSONIC COMPRESSORS

Some experiences in the scaling of the NASA 8-stage transonic axial flow compressor.

02 p2023 A73-12008

[SAE PAPER 720711] Design and development of a small highly loaded, two-stage, transonic axial compressor.

02 p2023 A73-12009

[SAE PAPER 720712] Study of the waves configuration in an axial-flow supersonic compressor

03 p0246 A73-14135

[ONERA, TP NO. 1104] Experimental method for analyzing the unsteady flow in a transonic aircraft compressor

09 p1028 A73-22715

Calculated leading-edge bluntness effect on transonic compressor noise.

18 p2260 A73-36192

[AIAA PAPER 73-633]

TRANSONIC FLIGHT

Aeromechanical measurements in free flight on piloted aircraft

09 p1032 A73-22447

Buffeting pressures on a swept wing in transonic flight - Comparison of model and full scale measurements.

11 p1305 A73-25542

[AIAA PAPER 73-311]

TRANSONIC FLOW

Secondary jet interaction with emphasis on outflow and jet location.

03 p0243 A73-13496

Magnetogasdynamic characteristics, transonic and compression regions and pressure losses of conduct-

TRANSONIC FLUTTER

ing gas flow in circular tube within axisymmetric magnetic field
03 p0346 A73-13620

Transonic profile theory - Critical comparison of various procedures
03 p0247 A73-14377

Theoretical investigation of transition phenomena in the boundary layer on an infinite swept wing
[DGLR PAPER 72-124] 03 p0248 A73-14379

Buffet boundaries for arrow wings in transonic flow, presenting methods for pressure distribution and three dimensional turbulent boundary layer calculation
[DGLR PAPER 72-123] 03 p0248 A73-14382

The Green's function of the linearized viscous transonic equation
05 p0527 A73-16446

Calculation of transonic flow in three-dimensional nozzles
05 p0527 A73-16447

Characteristics of an argon RF plasma - Active discharge and laminar sonic flow region.
05 p0602 A73-16559

Unsteady transonic flow analysis for low aspect ratio, pointed wings.
[AIAA PAPER 73-122] 05 p0530 A73-16878

Evaluation of numerical viscosity effects in transonic flow calculations.
[AIAA PAPER 73-131] 05 p0530 A73-16884

Shock wave-boundary layer interactions in laminar transonic flow.
[AIAA PAPER 73-239] 05 p0532 A73-16964

Inverse method of designing two-dimensional transonic airfoil sections.
05 p0533 A73-17104

Calculation of subsonic and transonic flow at the stern of bodies of revolution
06 p0643 A73-17468

Equivalence rule and transonic flows involving lift.
[AIAA PAPER 73-88] 06 p0644 A73-17642

Variational mixed boundary value problems of subsonic gas flows for plane parallel symmetric Laval nozzle and transonic wedge, using singular integral equation
06 p0646 A73-18888

Transonic nozzle flow with a parabolic temperature distribution.
07 p0811 A73-19985

Transonic nozzle flow with nonuniform gas properties.
08 p0925 A73-20719

Quasi isothermal, transonic flow of radiating gases
08 p1024 A73-21497

Calculation of the transonic flow around an airfoil, taking account of the exact law of compressibility
09 p1027 A73-22210

Method of experimental study of cascades of transonic blades with strong deflection
09 p1027 A73-22211

Transonic airfoils - Recent developments in theory, experiment, and design.
10 p1171 A73-23856

Experimental determination of the transonic flow on circular cones at angle of attack
10 p1172 A73-24496

Transonic gas flow in rotating turbomachine cascade channels, reducing flow equations to second order differential equation
10 p1172 A73-24507

Study of the fluctuations of wall pressures in transonic flow on a cone-cylinder group presenting a constriction
10 p1173 A73-24825

Compressible magnetorelativistic flow character in subsonic, supersonic and transonic regions, obtaining pressure coefficient, free stream Mach number and Alfvén speed interrelationships
10 p1210 A73-24921

Calculation of unsteady transonic aerodynamics for oscillating wings with thickness.
[AIAA PAPER 73-316] 11 p1301 A73-25547

The theoretical and experimental methods used in France for flutter prediction.
[AIAA PAPER 73-329] 11 p1305 A73-25558

Quasi-linear partial differential equations of non-linear pulse shock wave propagation in two- and three-dimensional steady transonic gas flow near critical point
11 p1302 A73-25854

Large particle method for calculation of transonic supercritical vortex flow fields around flat and axisymmetric bodies
11 p1302 A73-26330

Transonic similarity solution for aligned field MHD nozzle flow.
13 p1599 A73-28089

Approximate shock-free transonic solution for a symmetric profile at zero incidence.
13 p1564 A73-28823

Transonic flow past lifting wings.
13 p1564 A73-28824

Transonic flow about lifting configurations.
13 p1564 A73-28828

Ballistite burning rate in sonic gas flow in super-sonic conical nozzles as function of flow velocity and combustion chamber pressure
13 p1706 A73-28972

Experimental studies on high speed performance of two-dimensional turbine cascades.
13 p1566 A73-29019

The transonic aerofoil problem with embedded shocks.
15 p1821 A73-31122

A numerical solution for the transonic flow around blunt wedges
15 p1823 A73-31330

Spectroscopic observations of subsonic and sonic vapor flow inside an open-ended heat pipe.
15 p1958 A73-31936

Variational mixed boundary value problems of subsonic gas flows for plane parallel symmetric Laval nozzle and transonic wedge, using singular integral equation
15 p1824 A73-32412

Numerical method for mixed elliptical-hyperbolic nonlinear Cauchy problem with boundary conditions, applying to sonic flow around wing sections
16 p1961 A73-32807

Transonic flow through a turbine stator treated as an axisymmetric problem.
[ASME PAPER 73-GT-51] 16 p1964 A73-33510

Relaxation solutions for inviscid axisymmetric transonic flow over blunt or pointed bodies.
17 p2095 A73-35128

Numerical calculation of the three dimensional transonic flow over a yawed wing.
17 p2096 A73-35129

Relaxation factors for supercritical flows.
17 p2154 A73-35131

Transonic flow analysis using a streamline coordinate transformation procedure.
[AIAA PAPER 73-657] 18 p2261 A73-36211

Transonic inviscid flows over lifting airfoils with embedded shock wave using method of integral relations.
[AIAA PAPER 73-658] 18 p2261 A73-36212

Experimental and theoretical investigations in two-dimensional transonic flow.
[AIAA PAPER 73-659] 18 p2261 A73-36213

On viscous and wind tunnel wall effects in transonic flows over airfoils.
[AIAA PAPER 73-660] 18 p2263 A73-36261

Equivalence rule and transonic flow theory involving lift.
18 p2264 A73-36328

Unsteady aerodynamic forces in transonic turbomachines
18 p2266 A73-37084

A synthesis of transonic, 2-D airfoil technology.
[AIAA PAPER 73-792] 19 p2375 A73-37459

Transonic laminar boundary layers with surface curvature.
19 p2423 A73-38480

Shock oscillation associated with Hartmann resonance tubes excited by underexpanded sonic jets, using schlieren streak photography
21 p2677 A73-40616

Analysis of the effects of a probe in the transonic region of a nozzle.
22 p2796 A73-42568

Unsteady transonic flows with shock waves in two-dimensional channels.
23 p2969 A73-43938

Transonic equation for flow in apertures between compressor and turbine blades, examining gas dynamic and geometric parameter influence on near-sonic flow
24 p3054 A73-45024

TRANSONIC FLUTTER
Flutter of pairs of aerodynamically interfering delta wings.
[AIAA PAPER 73-314] 11 p1301 A73-25545

Flutter technology in the United Kingdom - A survey.
[AIAA PAPER 73-330] 11 p1441 A73-25559

TRANSONIC INLETS
U SUPERSONIC INLETS

TRANSONIC NOZZLES
Approximate method based on quasi-one dimensional theory for calculation of transonic wave propagation in slender nozzles
01 p0034 A73-11368

TRANSONIC SPEED
Criteria concerning the adaptation of the rear components of a propulsion system to the subsonic and transonic altitude flight
[DGLR PAPER 72-065] 02 p0128 A73-11690

Wake vorticity of side-slipping slender thin wings at transonic speeds, deriving integral equation for vortex strength based on Prandtl-Glauert rule
[DGLR PAPER 72-127] 03 p0247 A73-14376

Toward simpler prediction of transonic airfoil lift, drag, and moment.
09 p1028 A73-22434

Some noise generation mechanisms in transonic gas jets
14 p1712 A73-30947

Drag and stability characteristics of high-speed parachutes in the transonic range.
15 p1828 A73-31457

Experimental results in the case of the Nonweiler wave-rider in the subsonic, transonic, and supersonic range
16 p1963 A73-33265

Experimental evaluation of the effects of a blunt leading edge on the performance of a transonic rotor.
[ASME PAPER 73-GT-60] 16 p1964 A73-33512

An inexpensive technique for the fabrication of two dimensional wind tunnel models.
17 p2149 A73-35762

Reynolds number effects on the shock wave - Turbulent boundary layer interaction at transonic speeds.
[AIAA PAPER 73-661] 18 p2298 A73-36215

TRANSONIC TURBINES
U SUPERSONIC TURBINES

TRANSONIC WIND TUNNELS
A method of testing full-scale inlet/engine systems at high angles of attack and yaw at transonic velocities.
[AIAA PAPER 72-1097] 03 p0287 A73-13417

Supersonic blowdown wind tunnel modification for transonic airfoil profile aerodynamic characteristics measurement, discussing design criteria and operational range
[DGLR PAPER 72-133] 03 p0288 A73-14380

Comparative measurements involving three geometrically similar calibration models of a transport aircraft type in the transonic wind tunnel of the AVA Goettingen (Proposal: ONERA/
[DGLR PAPER 72-122] 03 p0248 A73-14383

A method for transonic wind-tunnel corrections.
05 p0563 A73-17104

Experimental studies of a Ludwig tube high Reynolds number transonic tunnel.
[AIAA PAPER 73-212] 06 p0645 A73-17665

Correction for change in fluid flow curvature about a lift-generating airfoil in a two-dimensional test section with perforated walls
11 p1302 A73-25864

Calculation of wall corrections in a transonic wind tunnel
16 p1961 A73-32808

Effects of wall boundary layers in wind tunnels on blocking phenomena
16 p1962 A73-32815

Example of utilization of a wind tunnel with perforated variable-geometry walls
16 p1993 A73-32815

TRANSONIC
U TRANSONIC FLOW

TRANSPARENCE
Importance of Fresnel reflections in laser surface damage of transparent dielectrics.
01 p0076 A73-10139

Interaction of opposed beams of electromagnetic waves in a transparent nonlinear medium
01 p0016 A73-10202

Theoretical calculation of light scattering and measurements with grating UV double monochromator for anomalous atmospheric transparency
01 p0039 A73-10408

Transmittance of the atmosphere and the relationship among optical parameters in the ultraviolet spectral region
01 p0040 A73-10873

Role of absorbing inclusions in the fracture mechanism of transparent dielectrics by laser emission
01 p0026 A73-11235

New method for determining the total radiation power of partially transparent materials at high temperatures.
06 p0722 A73-17470

Dioptric powers of transparent plates in a plane state of tension
06 p0765 A73-18699

The emissivity of a system consisting of semitransparent isothermal coating and a flat opaque substrate
10 p1294 A73-23512

Giant polaritons and selfinduced transparency - Frenkel-excitons.
10 p1249 A73-24694

Measurement of the transparency of the atmospheric ground layer at different wavelengths
11 p1363 A73-25656

Theory of thermally-induced interference and lensing in transparent materials.
12 p1523 A73-26833

Reconstruction of the images of transparencies with a semiconductor laser.
12 p1498 A73-27515

Controllable liquid-crystal transparency for recording of holograms.
12 p1498 A73-27515

Reduction of the switching time of a liquid-crystal optical transparency.
12 p1498 A73-27515

Analysis of the information capacity of optically matched filters.
12 p1498 A73-27515

- Spectral and boundary effects on coupled conduction-radiation heat transfer through semitransparent solids. 12 p1559 A73-27695
- Atmospheric transparency and the relationships between optical variables in the ultraviolet. 13 p1607 A73-28697
- Mechanism of damage of the surface of a transparent dielectric during illumination with short light pulses. 13 p1629 A73-29429
- Transient self focusing theory of high power laser pulse for homogeneous isotropic transparent solid dielectric with allowance for electrostriction and thermal effects. 13 p1629 A73-29440
- A nephelometric method for transparency determination in scattering media. 14 p1771 A73-30463
- Concorde cockpit windows design modifications for weight reduction and reliability optimization, discussing transparencies and crew seat movement. 14 p1712 A73-30927
- Radiative heat transfer through semitransparent solid plane layer, measuring temperature profile and heat flux for comparison with rectangular multiband model calculation. 15 p1958 A73-32276
- Mechanism of failure in transparent organic-glass-type dielectrics under the action of laser radiation. 16 p2030 A73-33927
- Radiating power of a system consisting of a semitransparent isothermal coating and a flat non-transparent substrate. 17 p2212 A73-35194
- Studies of fibreglass plastic under tensile load with the aid of transparency measurements. 18 p2327 A73-36476
- Amorphous material conduction, discussing glass transparency relation to electronic properties, semiconducting glasses and switching behavior. 21 p2723 A73-40272
- Use of the backscattering method to measure the atmospheric transparency in oblique directions. 21 p2731 A73-40495
- The role of absorbing impurities in laser-induced damage of transparent dielectrics. 23 p2959 A73-43512
- TRANSPARENT MATERIALS**
- U TRANSPARENCY**
- TRANSPARATION**
- The transpired turbulent boundary layer in an adverse pressure gradient. 04 p0520 A73-15936
- TRANSPARATION COOLING**
- U SWEAT COOLING**
- TRANSPONDERS**
- A technique for synoptic measurement of ionospheric propagation delays by ranging from geostationary satellites to a network of unmanned transponders. 03 p0308 A73-13629
- Communications technology satellite (CTS) with transponder and TWT operating into steerable antenna, discussing experiments on TV broadcast, data transmission, FM and transportable terminals. 04 p0422 A73-15446
- Intelligible crosstalk and AM/PM transfer in commercial communications satellites. 06 p0663 A73-17589
- Ground based and airborne collision avoidance systems comparison, discussing interrogator/transponder concept, pilot warning indicator, and air traffic handling capacity and economics. 07 p0848 A73-18900
- Intelsat 4 communications system, discussing radio transponders, earth stations, and multiple access, modulation and multiplexing methods. 09 p1051 A73-22700
- Symphonic satellite communication equipment payload, discussing mission requirements, receiving and transmitting antennas, transponder and ground testing methods and arrangements. 11 p1417 A73-25356
- A wideband transistor amplifier at the 4-GHz band for communication satellite use. 13 p1594 A73-29228
- Communications systems of television-radio satellites. 17 p2126 A73-35487
- Transponder for European communications satellite systems (ECS and OTS program). 17 p2126 A73-35490
- Aeronautical/maritime satellite borne two-way L-band transponder weight and power limitation effects on channel capacity. 20 p2531 A73-39771
- Three dimensional transponders array for exact solution to positioning problem, discussing large measurements sequential interrogation effects on accuracy. 21 p2734 A73-40034
- High altitude remotely piloted vehicle (RPV) platforms for tactical pseudo-satellite multichannel relay transponder systems. 22 p2826 A73-42423
- TRANSPORT AIRCRAFT**
- NT A-300 AIRCRAFT
- NT AN-2 AIRCRAFT
- NT AN-24 AIRCRAFT
- NT BOEING 727 AIRCRAFT
- NT BOEING 737 AIRCRAFT
- NT BOEING 747 AIRCRAFT
- NT C-5 AIRCRAFT
- NT C-130 AIRCRAFT
- NT C-141 AIRCRAFT
- NT CARGO AIRCRAFT
- NT CH-46 HELICOPTER
- NT CH-47 HELICOPTER
- NT CL-84 AIRCRAFT
- NT CONCORDE AIRCRAFT
- NT DC 9 AIRCRAFT
- NT DC 10 AIRCRAFT
- NT DHC 5 AIRCRAFT
- NT DO-31 AIRCRAFT
- NT H-53 HELICOPTER
- NT H-56 HELICOPTER
- NT HFB-320 AIRCRAFT
- NT L-1011 AIRCRAFT
- NT MERCURE AIRCRAFT
- NT S-61 HELICOPTER
- NT SHORT HAUL AIRCRAFT
- Multivariate analysis applied to aircraft optimisation - Some effects of research advances on the design of future subsonic transport aircraft. 02 p0130 A73-11661
- [DGLR PAPER 72-093]
- Comparison of propulsion system concepts for V/STOL commercial transports. 03 p0250 A73-13472
- [AIAA PAPER 72-1176]
- Subsonic commercial transport aircraft reduced noise and increased cruise Mach number effects on nacelle design in terms of inlet, fan, cowl and nozzle. 03 p0558 A73-13488
- [AIAA PAPER 72-1204]
- Comparative measurements involving three geometrically similar calibration models of a transport aircraft type in the transonic wind tunnel of the AVA Goettingen/Proposal: ONERA/ [DGLR PAPER 72-122] 03 p0248 A73-14381
- Air transportation system planning - Progress in noise reduction. 04 p0406 A73-14895
- Transport aircraft wheels and brakes operational cost minimization, discussing contributory roles of governmental regulations (FAA), aircraft manufacturer, supplier and user. 05 p0534 A73-16650
- [SAE PAPER 720867]
- Optimization of commercial transport airplane stopping systems. 05 p0535 A73-16671
- [SAE PAPER 720872]
- Aerodynamic technology developments including advanced transonic airfoils, low-drag/high-lift systems and stability augmentation for transport aircraft performance, economics and noise improvements. 06 p0644 A73-17604
- [AIAA PAPER 73-9]
- Structural design of future commercial transports. 06 p0759 A73-17613
- [AIAA PAPER 73-20]
- Research on future short-haul aircraft at the NASA Langley Research Center. 06 p0647 A73-17616
- [AIAA PAPER 73-27]
- Flight control techniques for advanced commercial transports. 06 p0647 A73-17618
- [AIAA PAPER 73-30]
- Multiple purpose STOL aircraft for passenger or cargo transport, discussing design features, performance and market prospects. 06 p0648 A73-17999
- Slender delta-wings for future subsonic passenger planes. 09 p1027 A73-21992
- Russian book - Transport aircraft maintainability. 09 p1032 A73-22375
- Air cushion landing gears for transport aircraft, discussing peripheral jet stream performance prediction and system installation on Buffalo STOL. 10 p1174 A73-23659
- Civil transport aircraft future design trends, discussing subsonic, supersonic, hypersonic and V/STOL aircraft, engine design, fuels and noise reduction. 10 p1174 A73-23682
- Neurological fatigue-indices of flight crews of long-range and military transport aviation. 11 p1321 A73-25040
- Transport aircraft maintenance program, discussing safety and reliability correlation with design. 11 p1306 A73-26591
- Russian book - Practical aerodynamics of the An-24 aircraft /2nd revised and enlarged edition/. 15 p1829 A73-31547
- Maintenance of public transportation aircraft - Evolution of methods. 15 p1925 A73-32556
- Maintenance of pitot-static systems of transport aircraft. 16 p2014 A73-33014
- [SAE AIR 975]
- NASA research commercial VTOL transport propulsion system specifications and components development, discussing lift fan propulsion method for aircraft attitude control. 16 p2047 A73-33498
- [ASME PAPER 73-GT-24]
- VTOL jet transport aircraft commercial applications, describing lift engine system, hover flight control, engine failure problems and operating cost analysis. 17 p2099 A73-34257
- Hypersonic transports - Economics and environmental effects. 17 p2099 A73-34435
- Longitudinal motion of a transport aircraft during steep landing approaches. 17 p2100 A73-34482
- Icing conditions of modern transport aircraft according to cruise flight data. 17 p2100 A73-34545
- Engine cycle considerations for future transport aircraft. 17 p2222 A73-34693
- [SAE PAPER 730345]
- Profitable transport engines for the environment of the eighties. 17 p2257 A73-34695
- [SAE PAPER 730347]
- Key factors in developing a future wide-bodied twin-jet transport. 17 p2103 A73-34702
- [SAE PAPER 730354]
- The Air Force/Boeing advanced medium STOL transport prototype. 17 p2103 A73-34710
- [SAE PAPER 730365]
- Technical basis for the STOL characteristics of the McDonnell Douglas/USAF YC-15 prototype airplane. 17 p2103 A73-34711
- [SAE PAPER 730366]
- Applications and concepts for the incorporation of composites in large military transport aircraft. 17 p2104 A73-34816
- The C-401, a STOL transport for many applications. 17 p2107 A73-35666
- DHC-7 four engine turboprop transport aircraft, emphasizing quietness and STOL capability. 18 p2266 A73-36067
- Influences of international operations on aircraft-transport design /Second William Littlewood Memorial Lecture/. 18 p2373 A73-36165
- Commercial transport aircraft structural design and technology advances, discussing materials and fabrication processes with respect to costs, durability and reliability. 18 p2266 A73-36166
- Noise certification of a transport airplane. 19 p2378 A73-37279
- A parameter optimisation technique applied to the design of flight control systems. 19 p2378 A73-37409
- Air cushion landing systems application to tactical airlift aircraft for personnel, and equipment delivery to dispersed sites under diverse climatic, terrain and combat conditions. 19 p2380 A73-37678
- Air cushion landing systems for STOL transport aircraft, investigating structural and power requirements, ground and in-flight handling, mission capability, operational life, weight and cost. 19 p2381 A73-37682
- Air cushion landing system applications and operational considerations. 19 p2381 A73-37684
- Transport aircraft external operational environment factors, discussing navigation, ATC, airspace, flight and pilot workload conditions. 19 p2450 A73-37727
- Transport aircraft noise reduction in airport areas through low noise engine design, traffic control, flight maneuvers and architectural planning. 19 p2384 A73-37818
- Aircrew workload during the approach and landing. 19 p2401 A73-38005
- Rocket vehicle concepts for global transport application, discussing space shuttle technology use, commercial markets, international fleets, single stage feasibility, etc. 20 p2613 A73-38600
- [AAS PAPER 73-163]
- Optimum propulsion system design for advanced technology commercial transport, emphasizing low noise and emission, performance, reliability, maintainability and economics. 20 p2600 A73-38648
- [AIAA PAPER 72-760]
- Application of direct side force control to commercial transport. 20 p2588 A73-38822
- [AIAA PAPER 73-886]
- Future technology and economy of jet-supported VTOL transport aircraft. 21 p2793 A73-40448
- Some method of nonlinear programming suitable for solving the task of optimization of a small transport aircraft. 21 p2634 A73-40478
- Russian book - Economic efficiency and planning of air freight transportation. 21 p2793 A73-41294
- Electromagnetic interference in military transport aircraft, discussing RF terminal voltage and current,

- radiated field, fuselage attenuation and power supply impedance measurements 22 p2821 A73-41693
- TRANSPORT COEFFICIENTS**
- U COEFFICIENTS**
- U TRANSPORT PROPERTIES**
- TRANSPORT EQUATION**
- U BOLTZMANN TRANSPORT EQUATION**
- TRANSPORT PROPERTIES**
- NT ATMOSPHERIC CONDUCTIVITY
- NT CARRIER MOBILITY
- NT DIFFUSION COEFFICIENT
- NT EDDY VISCOSITY
- NT ELECTRICAL RESISTIVITY
- NT ELECTRON MOBILITY
- NT GAS VISCOSITY
- NT GASEOUS DIFFUSION
- NT GASEOUS SELF-DIFFUSION
- NT HOLE MOBILITY
- NT IONIC MOBILITY
- NT IONOSPHERIC CONDUCTIVITY
- NT MAGNETORESISTIVITY
- NT PHOTOCONDUCTIVITY
- NT PLASMA CONDUCTIVITY
- NT SUPERCONDUCTIVITY
- NT THERMAL CONDUCTIVITY
- NT THERMAL DIFFUSIVITY
- NT VISCOSITY
- Transport phenomena in turbulent plasma with electromagnetic waves. 01 p0081 A73-10117
- Book - Lectures in mathematical models of turbulence. 01 p0031 A73-10123
- The early stages of the mechanism of sintering. 01 p0062 A73-10277
- Wave motion of low-tension interfaces with electrical double layers. 02 p0196 A73-12038
- Application of the turbulent eddy diffusivity transport equation to the analysis of turbulent flow in the radial face seal. 03 p0293 A73-13315
- Physical mechanisms of magnetospheric processes, discussing matter and energy exchange between solar wind and magnetosphere, substorms, interaction with ionosphere, etc 03 p0302 A73-13853
- Book - Kinetic theory. Volume 3 - The Chapman-Enskog solution of the transport equation for moderately dense gases. 03 p0345 A73-13991
- Propagation of solar cosmic rays in the solar wind. 04 p0491 A73-14837
- Transport phenomena of reactive fluid flow in heterogeneous combustion processes. [ASME PAPER 72-WA/HT-30] 04 p0519 A73-15825
- The measurement of plasma transport properties in a free-burning electric arc. 05 p0603 A73-16763
- Measurements of turbulence-transport properties with a laser Doppler velocimeter. [AIAA PAPER 73-169] 05 p0566 A73-16914
- On the transport properties of charged particles in one dimension in random electric fields. 05 p0612 A73-17384
- Hydrodynamics equations for multicomponent mixtures with higher-order approximations of transport coefficients 06 p0684 A73-17467
- Flow equations of a multiphase mixture with one coherent liquid or gaseous phase. 06 p0685 A73-17758
- Some evaluations of drag and bulk transfer coefficients over water bodies of different sizes. 06 p0720 A73-18328
- Calculation of the transfer coefficients for planetary atmospheres consisting of CO₂-N₂ mixtures 06 p0754 A73-18568
- Manifestation of the adsorption-induced loss of strength in metals under conditions of selective transfer in boundary friction. 06 p0698 A73-18637
- New formulations of the corresponding states principle for the transport properties of pure dense fluids. 08 p1023 A73-21258
- Book - Turbulence transport modeling. 10 p1206 A73-24350
- Temperature dependence of kinetic properties of photoconductivity produced by carrier redistribution across attachment centers, discussing results with Ag and Al doped ZnS single crystals 10 p1260 A73-24468
- Collisional transverse MHD shock wave structure within magnetic field inducing anisotropic plasma transport properties, using singular perturbation approach 11 p1403 A73-25254
- The transport coefficients and material functions of a plasma with different electron and gas temperatures 11 p1404 A73-25343
- Transport properties of liquid metal hydrogen under high pressures. 11 p1401 A73-25907
- Thermodynamics of heterogeneous gas equilibria. VII - Gas phase composition and chemical transport reactions in the tungsten-oxygen-hydrogen system 11 p1386 A73-26568
- Carbon dioxide thermodynamic and transport characteristics calculation, treating gas as multicomponent ideal mixture including carbon monoxide and oxygen and carbon atoms and ions 12 p1526 A73-27308
- Temperature calculation for heat emitting surface in transparent gas flow, using linearizing function method for heat transfer problems with nonlinear boundary conditions 12 p1558 A73-27316
- Turbulent transport coefficients for compressible heterogeneous mixing. 13 p1705 A73-28435
- International Conference on the Physics of Semiconductors, 11th, Warsaw, Poland, July 25-29, 1972, Proceedings. Volumes 1 & 2. 14 p1783 A73-30572
- Structure-dependent transfer parameters of interdigital transducers for surface waves. I 14 p1754 A73-30895
- Transport coefficients of ionized argon. 16 p2039 A73-33318
- Calculation of the transfer coefficients of planetary atmospheres formed by mixtures of CO₂ and N₂. 16 p2039 A73-33593
- Experimental determination of small scale transport mechanisms in the stratosphere. [AIAA PAPER 73-496] 16 p2010 A73-34044
- Transport coefficients of air at temperatures from 3000 to 25,000 K and at pressures of 0.1, 1, 10, and 100 atm 17 p2253 A73-34264
- Interior of Jupiter and Saturn. 17 p2226 A73-34357
- Development of a high capacity cryogenic heat pipe. [AIAA PAPER 73-729] 18 p2369 A73-36346
- Jupiter and Saturn interior structure models based on state equations and transport properties of hydrogen and helium at high pressures and temperatures 18 p2354 A73-36644
- Weakly ionized continuum plasma turbulent shear flow and transport properties calculation, noting ratio of Debye shielding length to local integral scale 19 p2463 A73-37153
- Transport of charged particles in the earth's magnetosphere 19 p2474 A73-37348
- Increasing the transport capacity in a viscous fluid flow by the injection method 19 p2420 A73-37552
- Oxygen transport augmentation mechanism for human hemoglobin, considering hemoglobin translational mobility absence effects 20 p2515 A73-39795
- Russian book on low temperature plasmatron-generated plasmas covering physical and transport properties, optical, thermophysical and gasdynamic analytic methods, etc 21 p2746 A73-40516
- Anomalous transport due to the dissipative trapped-ion instability. 21 p2750 A73-41682
- State variables and transport coefficients of binary gaseous mixtures. I - A simple method for the accurate determination of the second virial coefficient of binary gaseous mixtures [DFVLR-SONDDR-273] 22 p2931 A73-42373
- State variables and transport coefficients of binary gaseous mixtures. II - The binary interaction between identical and nonidentical molecules [DFVLR-SONDDR-279] 22 p2931 A73-42374
- State variables and transport coefficients of binary gaseous mixtures. III - The calculation of transport coefficients with the aid of consistent potential parameters [DFVLR-SONDDR-280] 22 p2931 A73-42375
- Papers on heat pipes covering incompressible laminar vapor flow behavior, startup dynamics, wicking material liquid transport properties, high thermal conductance structures, etc 23 p3049 A73-43459
- Influence of a random transport-velocity component on the space-time correlations of signal fluctuations 23 p2954 A73-43647
- Measurement of turbulence transport properties in a supersonic boundary-layer flow using laser velocimeter and hot-wire anemometer techniques. [AIAA PAPER 73-1045] 24 p3090 A73-44869
- Transfer phenomena in nonreactive binary fluid mixtures analyzed by nonlinear continuum thermodynamics of irreversible processes 24 p3156 A73-45081
- TRANSPORT THEORY**
- NT CHAPMAN-ENSKOG THEORY
- NT MIXING LENGTH FLOW THEORY
- Book - Radiation transport in spectral lines. 02 p0194 A73-11876
- Near earth electron spectra applied to cosmic ray transport equation numerical solution extension to 1968-1970, providing models for modulation and gradients reproduction 03 p0361 A73-13362
- Numerical studies of the transport of solar protons in interplanetary space. 07 p0870 A73-19664
- Radiative transfer theory application to stellar images in photographic emulsions, deriving theoretical relation between star brightness and photographic effective radius 08 p1006 A73-20924
- New formulations of the corresponding states principle for the transport properties of pure dense fluids. 08 p1023 A73-21258
- Ultrarelativistic cosmic plasma analysis of high density electron beams transport across strong magnetic fields with application to pulsar NP 0532 spectrum 08 p0999 A73-21334
- Nonequilibrium transport process calculation by theoretical microscopic model for interaction between ionized gas and solid particles in suspension, noting free electron concentration change 09 p1130 A73-22826
- A rigorous cosmic-ray transport equation with no restrictions on particle energy. 11 p1414 A73-26609
- Iterative-zonal method for studying and calculating the local characteristics of radiative heat transfer. 12 p1560 A73-27913
- Transport phenomena in a fully ionized ultrarelativistic plasma 15 p1919 A73-31709
- Flux-corrected transport - A minimum-error finite-difference technique designed for vector solution of fluid equations. 17 p2202 A73-35145
- A new numerical technique for solving the time-dependent radiation transport equation. 17 p2255 A73-35595
- Aircraft wake vortex transport model. [AIAA PAPER 73-679] 18 p2267 A73-36230
- New thermodynamic functions for the C₃ molecule. 18 p2287 A73-36326
- Computer-aided two-dimensional analysis of bipolar transistors. 20 p2536 A73-39410
- Propagation of protons injected near 1 AU in a medium with a constant transport length 21 p2756 A73-40583
- Propagation of electromagnetic waves through turbulent plasma using transport theory. 22 p2824 A73-41860
- Quantum transport theory of high-field conduction in semiconductors. 23 p3016 A73-43775
- Singular eigenfunction solution of the monoenergetic neutron transport equation for finite radially reflected critical cylinders. 24 p3109 A73-44700
- TRANSPORT VEHICLES**
- Comparison of modern aircraft engines with other power plants used in transportation 03 p0352 A73-13072
- Utilization of composite materials for the fabrication of fuel cells 03 p0334 A73-13595
- TRANSPORTATION**
- NT AIR TRANSPORTATION
- NT RAIL TRANSPORTATION
- NT RAPID TRANSIT SYSTEMS
- NT SPACE TRANSPORTATION
- NT URBAN TRANSPORTATION
- Airport internal transportation systems for passengers and baggage, considering time scheduled, continuously moving and individually controlled systems 01 p0029 A73-10306
- International Conference on Transportation and the Environment, Washington, D.C., May 31-June 2, 1972, Proceedings. Part 1. 04 p0405 A73-14889
- Prediction models for surface and air transportation dynamic environments, considering broadband and single frequency continuous and recurrent and intermittent discrete excitation modes 09 p1032 A73-22718
- Book - The aerodynamics of high speed ground transportation. 17 p2097 A73-35854
- TRANSURANIUM ELEMENTS**
- NT CURIUM ISOTOPES
- NT CURIUM 244
- NT PLUTONIUM ISOTOPES
- NT PLUTONIUM 238
- TRANSVERSE ACCELERATION**
- DNA catabolism in rat tissues in response to transverse accelerations 06 p0650 A73-17679
- Cardiovascular system reactions to alternating transverse accelerations in man 06 p0650 A73-17687

- Morphological changes in the juxtaglomerular apparatus of rat kidneys exposed to the action of diversely directed accelerations for many hours
08 p0929 A73-20978
- TRANSVERSE FAULTS**
U GEOLOGICAL FAULTS
TRANSVERSE OSCILLATION
NT H WAVES
Transverse resonance solutions for a long slot leaky wave antenna.
01 p0023 A73-10187
Criteria for self loosening of fasteners under vibration.
01 p0058 A73-11512
Transverse vibrations generated in a bracket bar by the reciprocating linear displacements of its seal which are damped in the course of time.
02 p0235 A73-12127
Lateral displacement of discontinuous vibrating wire, noting solution application to longitudinal vibrations of discontinuous shafts and torsional vibrations of circular shafts
02 p0237 A73-12612
The influence of axial load on eigenfrequencies of a vibrating lateral restraint cantilever.
03 p0384 A73-13115
Rotatory inertia and hub radius effects on transverse vibrational characteristics of clamped Rayleigh beam, using Galerkin method
03 p0388 A73-13316
HF transverse resonant vibrations of annular Al plates with polychlorovinyl and polyamide base coatings, noting damping and strain relationship to energy dissipation
03 p0394 A73-14009
Beam transverse vibration with nonlinear-spring supported free end and concentrated mass, determining free vibration frequencies
04 p0508 A73-14940
Transverse oscillations produced by dynamic loads in structural elements of parabolic arc shape
04 p0513 A73-15506
Crystal transverse modulators for laser Q-switching, discussing electro-optical properties of various materials
06 p0699 A73-17753
Thermal shock induced transverse vibrations in rectangular plate with combined simple and clamped edge supports, deriving infinite series solutions
06 p0761 A73-17896
Transversal vibrations of the thin shell of revolution produced by the thermal shock.
06 p0763 A73-18453
He-Se laser low order transverse modes self mode locking at six transition wavelengths, attributing effect to oscillating modes reduction due to hole burning and cross relaxation
10 p1229 A73-24616
Emission field structure during transverse mode synchronization in a laser
13 p1626 A73-28005
Transverse vibration of membranes of arbitrary shape by the method of constant-deflection contours.
13 p1690 A73-28058
Oscillating laser transverse modes locking into off-centered pure Gaussian beam
13 p1626 A73-28347
Nonlinear transverse vibrations of beams with properties that vary along the length.
13 p1695 A73-28488
Heterodyne detection of frequency sweeping in the output of transverse-excitation CO₂ lasers.
13 p1628 A73-29186
Transverse vibrations of variable rectangular cross section rod, reducing fourth order differential equation to second order via Kirchhoff relation
16 p2080 A73-33259
The transverse vibration of spinning acleotrophic disk.
16 p2084 A73-34026
Natural transverse vibrations of sandwich beams of unsymmetrical structure.
18 p2367 A73-37141
Transverse oscillations of a beam lying on an elastic base under the action of a perturbation force which has several harmonics with frequencies close to the first natural frequency
20 p2620 A73-39512
Transverse deflection of guided projectile tail fins during deployment.
22 p2797 A73-42629
Human reactions to whole-body transverse angular vibrations compared to linear vertical vibrations.
23 p2948 A73-43216
Nonlinear transverse vibration analysis of a rectangular plate with lumped M-S-D systems.
23 p3048 A73-44384
Transverse coupled thermoelastic vibrations of elastically supported rectangular and circular plates under nonstationary harmonic temperature field
24 p3147 A73-44682
- TRANSVERSE WAVES**
Heating of a viscoelastic beam subjected to transverse vibrations
01 p0112 A73-10003
Momentum formulae derived for quasi-monochromatic wave packets of transverse and longitudinal waves in plasma without magnetic field
02 p0195 A73-11522
Electromagnetic self induced vibrations in homogeneous unbounded electron beam moving with time dependent velocity, noting longitudinal and transverse wave generation
02 p0198 A73-12102
Radially conducting cone wave spectrum calculation for noncophasal excitation, noting circularly polarized TEM and elliptically polarized TM wave amplitudes
03 p0278 A73-14058
Axial and transverse wave motions of inviscid perfect gas in isothermal solid-body rotation in cylinder
04 p0434 A73-15163
Secondary flow in the entrance region boundary layers of an expanding square duct.
04 p0404 A73-15851
Resonance coupling of a transverse magnetic response to a transverse electric excitation by the axial density gradient of a bounded plasma.
05 p0601 A73-16364
Quasi-hydrodynamic equations for transverse quanta in inhomogeneous plasma, using geometric optics approximation
06 p0728 A73-17969
Scattering of a transverse elastic wave by an elastic sphere in a solid medium.
06 p0737 A73-18351
Galerkin methods for vibration problems in two space variables.
06 p0717 A73-18408
Drift instabilities in nonuniform streaming plasmas.
07 p0855 A73-19337
Transverse hydromagnetic plane waves in the presence of a temperature gradient.
07 p0856 A73-19339
Arbitrary source emitted electromagnetic radiation in anisotropic stratified media, evaluating transverse and scattered fields and plane wave response
07 p0791 A73-19382
Ionosphere heating effects produced by transverse electric field, discussing strong nighttime source
07 p0815 A73-19431
Equilibrium and stability of large-amplitude magnetic Bernstein-Greene-Kruskal waves.
07 p0857 A73-19524
H alpha observations of vertical velocity distribution periodic oscillations in sunspot, noting transverse waves formation and propagation to penumbral boundary
08 p1001 A73-20757
Electromagnetic effects on electrostatic modes in a magnetized plasma.
08 p0991 A73-20820
Effect of transverse shear deformation on vibrations of planar structures composed of beam-type elements.
08 p1017 A73-21192
Propagation of a transverse harmonic wave in a plate with a statistically rough circular hole
08 p1020 A73-21770
Waves in magnetoactive plasma in the presence of a distinct transverse ion velocity
09 p1125 A73-21904
Kinetic equation derived for collective linear fluid oscillations development, applying to longitudinal and transverse wave propagation in fluids
09 p1072 A73-22574
Continuum theory of wave propagation in laminated composites.
10 p1287 A73-23565
Analysis of electromagnetic-wave modes in lens-like media.
10 p1248 A73-23834
Electromagnetic instability for plasma waves propagating perpendicular to uniform magnetic field in counterstreaming electron-ion plasmas based on linearized Vlasov-Maxwell equations
10 p1255 A73-24262
Straight plasma column confined by static axial and oscillating transverse magnetic fields, deriving stability criteria via viscous fluid model
10 p1255 A73-24264
Geometrical theory for flexure waves in shells.
11 p1432 A73-24977
Collisional transverse MHD shock wave structure within magnetic field inducing anisotropic plasma transport properties, using singular perturbation approach
11 p1403 A73-25254
EM induction in a semi-infinite solid, impulsively moving in a uniform magnetic field.
11 p1397 A73-25371
Radiation pattern produced by open ended radial waveguide with TM mode excitation, comparing computed with measured patterns
11 p1329 A73-25677
- Stability of transverse waves in a spinning membrane disk.
[ASME PAPER 72-APM-MM] 11 p1441 A73-25706
Physical interpretation of the diurnal behavior of the TM and TE components of VLF fields in the far zone
11 p1331 A73-26152
Properties of a radial mode CO₂ laser.
12 p1505 A73-27016
Electromagnetic fields due to dipole antennas over stratified anisotropic media.
[AD-756044] 12 p1523 A73-27146
Waves in a magnetoplasma with an isolated transverse ion velocity component.
15 p1922 A73-32629
Edge instability of transverse electromagnetic waves in a weakly ionized plasma
17 p2214 A73-34249
Phase velocity dispersion for transverse normal elastic wave propagation through sandwiched CdS and molten quartz or germanium layers
18 p2340 A73-36672
Excitation of transverse extraordinary mode in an inhomogeneous magnetoplasma.
20 p2598 A73-39300
Experimental study of the stressed state of an elastic beam undergoing transverse impact
20 p2620 A73-39385
Instability of transverse electromagnetic waves in a drifting electron-hole plasma
21 p2751 A73-40368
Mindlin theory extension to transverse shear effects in laminate plates, taking into account continuous stress across thickness and discontinuous shear strain
21 p2784 A73-40432
Saturation effect in RF spectroscopy for transverse optical pumping.
21 p2713 A73-40473
On the reflection of transverse waves from a cold plasma.
21 p2748 A73-40930
Flexural wave propagation in a thin plate with circular holes.
21 p2787 A73-41142
Dynamic stability of transverse axisymmetric waves in circular/cylindrical shells.
[ASME PAPER 73-APMW-26] 22 p2925 A73-42887
Transverse elastic wave propagation in CdS crystal wafer coated on both sides with AgBr, titanium oxide, Si or polystyrene
23 p3017 A73-44038
Energy conversion between longitudinal and transverse waves by mode-mode coupling in a relativistic plasma.
24 p3116 A73-45240
Variation of amplitudes of thermo-acoustical waves of arbitrary form in isotropic linear thermo-elastic materials.
24 p3157 A73-45372
Longitudinal and transverse shock and acceleration waves propagation and decay in anisotropic and isotropic elastic bodies based on theory of singular surfaces
24 p3153 A73-45498
Small transverse vibrations of a flexible rod under the action of a variable axial force
24 p3153 A73-45504
- TRANSVERSELY EXCITED ATMOSPHERIC LASERS**
U TEA LASERS
TRAPATT DIODES
U AVALANCHE DIODES
TRAPEZOIDAL WINGS
Computational program for calculating the Re-number-dependent polar of a glider with arbitrary double trapezoidal wing
16 p1967 A73-33024
Thin wall rib structured fan shaped wing design for arbitrary air loads, using strain compatibility conditions
21 p2784 A73-40390
- TRAPPED MAGNETIC FIELDS**
Suppression of the flute instability of a dense plasma by a magnetic system of feedbacks in an open trap
13 p1666 A73-28953
The effect of interstellar medium parameters on the accretion by neutron stars.
13 p1687 A73-29658
Suppression of the flute instability in a dense plasma in an open system by magnetic feedback.
23 p3013 A73-44305
- TRAPPED PARTICLES**
NT INNER RADIATION BELT
NT MAGNETICALLY TRAPPED PARTICLES
NT OUTER RADIATION BELT
NT PROTON BELTS
NT RADIATION BELTS
Inward diffusion of Tokamak-trapped particles by slow magnetic pumping.
01 p0083 A73-10461
The accurate prediction of radiation environment and solar cell degradation.
01 p0006 A73-11164

Role of trapped particles in plasma waves and instabilities.

02 p0197 A73-12067

Resonance, particle trapping, and Landau damping in finite amplitude obliquely propagating waves.

02 p0197 A73-12068

Trapped electrons decay to ground state via nonthermal process in lunar samples during thermoluminescence emission at lunar day temperatures, proposing quantitative model

03 p0369 A73-13101

Magnetospheric structure studies during 1969-1971, discussing bow shock magnetosheath, magnetopause, polar cusps, electric fields and trapped particle composition

03 p0302 A73-13852

Magnetospheric charged particle populations in magnetosheath, plasma sheet, extraterrestrial ring current, electron trough and trapping regions

03 p0302 A73-13856

New observations of the proton population of the radiation belt between 1.5 and 104 MeV.

03 p0362 A73-13862

ESRO IA/B observations at high latitudes of trapped and precipitating protons with energies above 100 keV.

03 p0362 A73-13863

Some parameters affecting the poleward boundary of trapped electrons.

03 p0363 A73-13869

High energy proton model for the inner radiation belt.

03 p0363 A73-13880

Trapped and precipitated electron energy spectra in relativistic electron precipitation events (REP), discussing bremsstrahlung measurements deductions

03 p0304 A73-14591

Instability of a large-amplitude plasma wave due to inverted trapped particle population.

04 p0480 A73-15194

Magnetospheric trapped particle populations boundaries properties, discussing dynamic boundaries during magnetic disturbances and substorm effect on night magnetosphere configuration

04 p0442 A73-15332

Bottleneck of 29/cm phonons in ruby.

04 p0484 A73-15471

Silicon X band oscillation TRAPATT diodes with high power efficiency, presenting electric field variation with distance

05 p0559 A73-16809

Strong pitch angle diffusion and magnetospheric solar protons.

07 p0869 A73-19229

Theory and simulation of turbulent heating by the modified two-stream instability.

07 p0857 A73-19526

The sideband instability of electrostatic waves in an inhomogeneous medium.

07 p0858 A73-19667

Trapped solar wind noble gases in Apollo 12 lunar fines 12001 and Apollo 11 breccia 10046.

07 p0871 A73-19800

Trapped electrons instability in Tokamak configuration, calculating plasma wave propagation modes via Fokker-Planck equation

08 p0991 A73-20815

Transient photocurrent pulse shapes and transit times in insulators with uniform and exponential trapped space charge in excitation layer or insulator surface

09 p1119 A73-21945

Resonant enhancement of photoexcited nitrogen trap n-type GaAs laser electron-hole recombination probability by crystal composition variation and gamma conduction band degeneration

09 p1093 A73-22255

Effect of the plasma inhomogeneity on the nonlinear damping of monochromatic waves.

09 p1126 A73-22281

Electrostatic turbulence parametric excitation by electric field with frequency near plasma frequency, accounting for saturation electric field in anomalous plasma heating via electron trapping theory

11 p1403 A73-25256

Unstable Langmuir or ion acoustic wave saturation in collisionless plasma due to electron trapping, estimating amplitude via adiabatic and sudden approximation

11 p1404 A73-25258

Influence of electric drift on the cone instability of a plasma in adiabatic traps

12 p1527 A73-26930

Neutron emission after muon capture in Ce, Ba and Sn, analyzing delayed gamma ray energies and branching ratios to excited nuclear states

13 p1662 A73-28650

Particle trapping effect on conductivity of toroidal plasma with like-particle collisions taken into account, obtaining results applicable to all aspect ratios

14 p1778 A73-29687

On electron trapping in ion sound waves in turbulent plasma.

16 p2040 A73-32800

Observation of quasitrapped and precipitating electrons at midlatitude.

18 p2344 A73-35927

An investigation on the spatial distribution of the quasi-trapped energetic electrons observed on board the satellite 'Shinsei.'

18 p2344 A73-35929

Observation of trapped and solar particles since 2 October 1972.

18 p2344 A73-35931

Some characteristics of charged particle flux studies using traps and analyzers. II - Modulation trap utilization for investigating the solar wind

18 p2345 A73-36113

Influence of thermal effects and particle capture by plasma waves on the dispersion characteristics of nonlinear waves

19 p2469 A73-37960

Precipitating protons with E greater than 12.4 keV to 500 keV near the midnight trapping boundary.

21 p2760 A73-40822

Trapped solar wind noble gases and exposure age of Luna 16 lunar fines.

21 p2770 A73-41001

Trapped-particle scattering by electrostatic turbulence in toroidal plasmas.

21 p2749 A73-41675

Enhancement of 0.24- to 0.96-MeV trapped protons during the May 25, 1967, magnetic storm.

22 p2901 A73-41909

Inner zone population of trapped 2.14-9.0 MeV alpha particles, noting strong peak in pitch angle and intensity decrease with L value decrease

22 p2901 A73-41910

Effect of electric drift on the loss-cone plasma instability.

22 p2891 A73-42264

A new type of charge trapping in MOS systems.

22 p2896 A73-42275

Containment stability of charged particles captured by a plane electromagnetic wave propagating at a slowly varying velocity

22 p2826 A73-42377

Computer simulation of the acceleration of charged particles captured by plane electromagnetic waves

22 p2826 A73-42378

TRAPPED RADIATION

U RADIATION BELTS

U TRAPPED PARTICLES

TRAPPING

Current trapping in toroidal high current discharges.

03 p0348 A73-14435

Theory of dynamic charge and capacitance characteristics in MIS systems containing discrete surface traps.

04 p0427 A73-15344

Theory of dynamic charge current and capacitance characteristics in MIS systems containing distributed surface traps.

04 p0427 A73-15345

Radiation produced trapping effects in devices.

05 p0605 A73-16521

A unified approach to the theory of double injection in solids with traps uniformly and non-uniformly distributed in the energy band gap.

09 p1135 A73-23045

TRAPS

NT COLD TRAPS

NT ION TRAPS (INSTRUMENTATION)

Dual spin spacecraft minimum energy and nutational dynamic trap states due to asymmetric or unbalanced rotors, analyzing single degree of freedom dynamic model

[AIAA PAPER 73-908]

20 p2614 A73-38842

TRAVELING CHARGE

Disturbance of a magnetized plasma by a fast traveling charge

10 p1257 A73-24758

Electron-neutral particle collisions effect on potential of test charge moving at velocity lower than plasma electrons, using BGK model and Lorentz collision operator

11 p1404 A73-25260

Emission from a point charge during motion along the plane boundary of a dielectric with periodically varying density

11 p1402 A73-26448

A two-dimensional field induced by travelling sources.

21 p2740 A73-41016

TRAVELING IONOSPHERIC DISTURBANCES

Mesoscale traveling ionospheric disturbances in electron density interpretation in terms of acoustic gravity waves

02 p0162 A73-12295

Statistical properties of traveling ionospheric disturbances in F region from phase height and angle of arrival data

02 p0162 A73-12296

Traveling ionospheric disturbance analysis based on quasi-periodic perturbations in satellite transmitted VHF signal Faraday rotation, obtaining wave-like variations in electron content

03 p0300 A73-13634

On the use of running means in the power spectrum analysis of ionospheric data.

09 p1078 A73-22831

Internal atmospheric gravity wave effect on ionospheric columnar electron content on basis of viscous atmosphere model with isothermal layers

11 p1359 A73-26700

Analytic ray trajectory model of radio wave lateral incidence on traveling large scale ionospheric inhomogeneities as function of location and departure angle

13 p1583 A73-28720

Acoustic-gravity modes and large-scale traveling ionospheric disturbances of a realistic, dissipative atmosphere.

14 p1748 A73-29971

Study of traveling ionospheric perturbations

15 p1872 A73-31900

Ionospheric response to internal gravity waves observed at Delhi.

16 p2010 A73-33919

Measurement of the dispersion of waves in the ionosphere.

21 p2682 A73-40232

Atmospheric gravity wave observations after the solar eclipse of June 30, 1973.

22 p2847 A73-42487

Periodic variations in geostationary satellite polarisation observations.

24 p3082 A73-44735

Current instability of atmospheric gravitational waves

24 p3083 A73-44786

Determination of the difference in group paths by the method of frequency-diversity reception

24 p3068 A73-44810

TRAVELING WAVE AMPLIFIERS

The effect of the surface electric charge on the gain of a solid-state traveling-wave amplifier

01 p0023 A73-10429

Theory of the signal suppression effect in an M-type TWT amplifier with preliminary modulation of the electron beam

01 p0025 A73-10983

Analysis of a dual-signal balanced TWT amplifier

01 p0025 A73-10988

Spontaneous active medium emission effect on amplification characteristics of linear and nonlinear traveling wave IR gas laser amplifier

01 p0060 A73-11084

Optimization of input-signal levels during amplification in a TWT

01 p0026 A73-11266

The GaAs traveling-wave amplifier as a new kind of microwave transistor.

06 p0673 A73-17788

Optimum R.F.-power transport in Nd-limited gallium-arsenide travelling-wave amplifiers.

07 p0798 A73-19159

Characteristics of a gallium-arsenide travelling-wave amplifier with Schottky-barrier contacts.

08 p0946 A73-21118

Influence of external self-focusing on the performance of laser amplifiers

11 p1364 A73-26156

Frequency response of helix and coupled cavity traveling wave tubes and amplifiers power output, discussing electronic countermeasures and space communications

11 p1339 A73-26692

An efficient multiplexing approach for adaptive aircraft communications via a relay satellite.

14 p1726 A73-29899

Harmonic enhancement for airborne low voltage, lightweight TWT amplifier band edge performance improvement to provide bandwidth in excess of two octaves

16 p1988 A73-33298

Optimization of input signal levels in TWT amplifiers.

17 p2134 A73-34319

Design of the 14/11 GHz repeater for the European Orbital Test Satellite.

20 p2525 A73-38745

An investigation of the combined amplification of monochromatic and noise signals in a TWT.

20 p2529 A73-38930

Natural fluctuations in linear quantum amplifiers.

20 p2574 A73-39699

Coupled mode analysis for solid traveling-wave amplifiers.

21 p2665 A73-41120

Microwave cross field and traveling wave tube amplifier characteristics for ECM systems, discussing bandwidth, dual mode, modulation and size and weight tradeoffs

22 p2834 A73-42872

Complete photon conversion in backward-travelling-wave parametric amplification and oscillation.

23 p2955 A73-44108

TRAVELING WAVE MASERS

Superconducting magnet for a Ku-band maser.

02 p0200 A73-11839

- Frequency-locking band of a traveling-wave laser.
22 p2869 A73-42255
- Measurement of the natural linewidth of a traveling wave neon-helium laser in the 0.63-micron range
22 p2870 A73-42411
- Radio astronomical traveling wave maser with ruby or doped rutile single crystals, superconducting magnet, cryogenic equipment and low noise temperature
23 p2953 A73-43375
- Low-noise microwave receiving systems in a world-wide network of large antennas.
23 p2958 A73-43376
- TRAVELING WAVE MODULATION**
Electromagnetic wave propagation velocity modulation in dispersionless linear medium with dielectric constant variation in space and time, evaluating approximation with neglected multiple reflections
10 p1249 A73-24526
- TRAVELING WAVE TUBES**
NT HELITRONS
Nonlinear computation of a resonant O-type oscillator featuring constant wave amplitude in the presence of losses
01 p0025 A73-10984
- Two-beam TWT /electron-wave TWT/ under large input-signal conditions - Effects of parameters
01 p0025 A73-10985
- Experimental investigation of a test-model two-beam TWT /electron-wave TWT/
01 p0025 A73-10986
- Experimental investigation of the coupling impedance in resonator chains with a positive mutual inductance coefficient
01 p0025 A73-10987
- TWT power gain, efficiency and output variations compensation methods during electron beam switching between pulsed and CW modes
02 p0148 A73-12570
- Traveling wave tube for satellite applications.
03 p0281 A73-13174
- High power SHF transmitter experiment using TWT depressed collector beam microwave amplifier for flight testing on communications technology satellite /CTS/
04 p0428 A73-15447
- One dimensional periodic slow wave structure interaction with charged particles beam, considering system operation as TWT and backward wave tube
05 p0556 A73-16063
- 50 GHz helix type travelling wave tube 'W-5028.'
07 p0799 A73-19372
- Reduction of phase non linearities in Traveling Wave Tubes /TWT/.
09 p1062 A73-22305
- Frequency response of helix and coupled cavity traveling wave tubes and amplifiers power output, discussing electronic countermeasures and space communications
11 p1339 A73-26692
- High power linear beam microwave klystrons, coupled cavity TWTs and hybrid tubes design and operation, considering electron gun and focusing system
11 p1339 A73-26693
- Differential equations of motion for analog model of M-type TWT performance, proposing block diagram for electron phase and trajectory and field distribution calculations
12 p1478 A73-26950
- The Canadian/U.S. High-Power Communications Technology Satellite.
12 p1472 A73-27669
- Dual mode microwave tube parameters for ECM power amplifiers based on systems rationale analysis, considering TWT and injected-beam crossed field amplifier
14 p1736 A73-30621
- TWT for air-to-air missile fire control radar transmitter application, considering high average power, RF gain and PPM focusing requirements
14 p1737 A73-30624
- ECM systems with TWT dual moding to provide distinct CW and pulsed microwave power levels, evaluating performance beyond octave in bandwidth
16 p1990 A73-33849
- Broadband TWT microwave amplifier failure modes in airborne systems related to physical mechanism, fabrication processes and field operator handling
17 p2140 A73-35259
- Baseplate heat pipe system for waste heat dispersion and temperature control of TWT microwaves amplifier in space shuttle communication equipment, discussing design and performance
18 p2370 A73-36371
- Generalized representation of electric fields in interaction gaps of klystrons and traveling-wave tubes.
18 p2292 A73-36595
- Designing high efficiency TWT's.
18 p2293 A73-36777
- Nonlinear transformation by a travelling wave tube and power spectral density of a PSK-signal.
20 p2522 A73-38718
- Effect of nonlinear channel characteristics on QPSK system performance.
20 p2526 A73-38752
- High-bit-rate transmissions through a channelized repeater.
20 p2526 A73-38753
- An investigation of the combined amplification of monochromatic and noise signals in a TWT.
20 p2529 A73-38930
- Satellite-borne power amplifier state of art, comparing TWT development to different technological solutions
20 p2538 A73-39772
- Graphical analysis of traveling-wave-tube oscillator with external feedback loop.
21 p2663 A73-41046
- Reduction of noise in high-power crossed-field amplifiers.
21 p2665 A73-41114
- Noise in solid travelling-wave tubes using coupled-mode analysis.
21 p2665 A73-41122
- Helix support, focusing, fabrication and performance tests of miniature traveling wave tubes /TWT/, using rare earth-cobalt /RAECO/ magnets
22 p2834 A73-42696
- Construction techniques for an S-band high-power fluid-cooled TWT helix.
22 p2834 A73-42697
- TRAVELING WAVES**
Antenna synthesis via inverse electrodynamic problem solution for infinite impedance cylinder excited by traveling wave, noting directional antenna with rotating polarization
01 p0017 A73-10217
- On the stability of nonlinear cold plasma waves.
01 p0087 A73-11497
- Wideband microwave device with diode and single component correction circuits Q factors measurement from frequency dependence of input traveling wave coefficients
04 p0429 A73-15927
- O-type synchronous electron beam waves interaction with electrostatically structured traveling wave, noting linear gain dependence on beam current and magnetic field
05 p0556 A73-16066
- Progressive waves analysis, considering nonlinear convective, dissipative and dispersive effects
05 p0528 A73-16756
- Light signal modulation by traveling wave in circular waveguide with coaxial KDP crystal
05 p0558 A73-16781
- Threshold value of the input impedance of a propagating-wave fed, long radiator series
05 p0559 A73-17240
- Polarization properties of a traveling-wave laser.
06 p0703 A73-18611
- Resonator polarization parameters effect on backward wave attenuation in three and four mirror TW ring laser, noting colliding waves intensity dependence on polarization angle
06 p0703 A73-18619
- Radio wave propagation in stratified media with nonuniform boundaries and varying electromagnetic parameters - Full wave analysis.
07 p0791 A73-19261
- Synthesis of a traveling wave antenna
08 p0946 A73-21103
- Influence of combinational coupling on the spectral and statistical properties of multimode fluctuations in a traveling-wave laser
09 p1094 A73-22599
- Amplification of a travelling wave in a non-homogeneous elastic medium.
11 p1400 A73-26407
- Competition between longitudinal modes in a ring laser with an anisotropic resonator.
12 p1507 A73-27508
- Implicit separation of variables /via superposition principle/ and explicit and implicit traveling wave methods of solving nonlinear partial differential equations
13 p1648 A73-28437
- Influence of a traveling acoustic wave on spectral line profiles. II - Asymmetry of weak Fraunhofer lines
13 p1683 A73-29092
- Radiation from travelling wave circular loop antenna in compressible electron plasma.
14 p1731 A73-29709
- Traveling wave solutions of differential equations describing thin elastic shell oscillations due to point source
14 p1815 A73-30951
- Bragg diffraction of light by two orthogonal ultrasonic waves in water.
15 p1914 A73-32256
- Geometric magnification and collimation of traveling wave unidirectional unstable ring lasers, comparing with standing wave resonators
15 p1886 A73-32382
- Monochromatic field frequency misalignment effect on polarization and population ratio instabilities of single frequency traveling wave laser with broadened active medium
16 p2024 A73-32894
- Reliability of diversity reception by antennas with different polarizations.
16 p1991 A73-33984
- Oscillatory flow phenomena in diffusers at low Reynolds numbers.
17 p2152 A73-35011
- Concentrated vortex nonlinear oscillations, discussing vortex ring and helical vortex filament stability, mode shape and frequency changes and standing and traveling wave solutions
18 p2301 A73-37004
- Traveling longitudinal electrostatic waves excitation in warm nonuniform plasma by external HF electric fields, using kinetic theory
19 p2468 A73-37857
- Spectral analysis of traveling planetary scale waves - Vertical structure in middle latitudes of Northern Hemisphere.
23 p2978 A73-43982
- Traveling wave solutions of differential equations describing thin elastic shell oscillations due to point source
23 p3047 A73-44327
- TREADMILLS**
Exercise testing for detecting changes in cardiac rhythm and conduction.
03 p0260 A73-13542
- Thirty-month follow-up of maximal treadmill stress test and double Master's test in normal subjects.
08 p0932 A73-21803
- Laddermil and ergometry - A comparative summary.
11 p1322 A73-25183
- TREADS**
Aircraft tire improvements and possible developments, discussing fibers, rubber compounds, tread, carcass and retreading
05 p0581 A73-16653
- TREES [MATHEMATICS]**
Electronic computer design and programming for solving high order linear equations, using matrix determinants and graph trees in letter symbols
01 p0019 A73-10033
- A partitioning algorithm with application in pattern classification and the optimization of decision trees.
06 p0670 A73-17805
- Generalized m series in tree enumeration.
06 p0717 A73-18000
- A 2-cycle algorithm for source coding with a fidelity criterion.
06 p0671 A73-18142
- Tree-manipulating systems and Church-Rosser theorems.
08 p0941 A73-20962
- Objective trees as technological forecasting technique in structuring program options for selected strategies, considering R and D, marketing and other functional business programs
08 p1026 A73-21699
- Method of analyzing electronic circuits on the basis of a hybrid-parameter matrix in a canonical system of coordinates
21 p2670 A73-41306
- TREES [PLANTS]**
Fatty acids of Pinus elliptioides tissues.
15 p1841 A73-32199
- Point discharge current measurements in trees and metal points during storms, discussing implications for structure of electrified clouds
21 p2684 A73-40779
- Gas chromatography-mass spectrometry study of sterols from Pinus elliptioides tissues.
24 p3065 A73-44698
- TREILLED DRAINAGE**
U DRAINAGE PATTERNS
TRENCHES
U GEOLOGICAL FAULTS
TRESCA FLOW
Large deflection calculation of circular and annular strain hardenable rigid plastic plates under axisymmetric load, using Kirchhoff-Love hypothesis and Tresca flow condition
03 p0394 A73-14022
- Tresca type plastic material shear, considering hypoelastic yield interrelation to Tresca yields
06 p0763 A73-18457
- Tresca-type plastic materials in the theory of hypoelasticity. I Mechanical constitutive equations and simple shear deformation.
07 p0909 A73-19161
- Tresca-type plastic materials in the theory of hypoelasticity. II Optical constitutive equations and birefringence in simple shear.
11 p1447 A73-26649
- Yield conditions for plastic deformation of anisotropic bodies, using stress tensor invariants and Tresca form
14 p1811 A73-30480
- Note on the application of the Tresca criterion to the problem of circular bending of an elastoplastic cylinder
14 p1811 A73-30485
- Evaluation of finite-plasticity theories for torsion-tension members made of Tresca materials.
17 p2251 A73-35447

TRIANGLES

Rigid viscoplastic thin circular plate under uniformly distributed transverse pressure, deriving Mises and Tresca yield surface conditions
20 p2624 A73-39567

Prior to failure extension of flaws in a rate sensitive Tresca solid.
22 p2880 A73-42136

Slow growth of cracks in a rate sensitive Tresca solid.
23 p2992 A73-43810

Dynamical bending resistance of circular piecewise nonhomogeneous rigid-plastic plates in terms of Tresca yield condition for pressure pulse loads
24 p3146 A73-44679

TRIANGLES

On the conforming cubic triangular element for plate bending.
03 p0391 A73-13682

Triangular obstacle caused microwave shadow zone diffraction pattern calculation by ray optics theory, comparing with scale model test results
06 p0666 A73-18201

Corner supported equilateral triangular plates.
08 p1016 A73-20827

Axisymmetric triangular finite elements for the scalar Helmholtz equation.
09 p1120 A73-22392

Images of truncated triangular-wave periodic targets in optical systems in the presence of linear image-motion.
10 p1248 A73-23614

Aerodynamic forces on a triangular cylinder.
21 p2782 A73-40003

TRIANGULAR WINGS

U DELTA WINGS

TRIANGULATION

Adjustment of large observation systems in networks of satellite triangulation.
02 p0159 A73-12169

Absolute topocentric directions and geograv coordinate system for satellite triangulation, using photographs against star background from different camera sites
04 p0436 A73-14779

Status of data reduction and analysis methods for the worldwide geometric satellite triangulation program.
04 p0437 A73-14780

Computation of the minimum bandwidth for aerotriangulation.
08 p0968 A73-21705

Apollo 15 photogrammetric measurements of lunar figure, describing system characteristics and analytical triangulation techniques
12 p1501 A73-27967

Experience in constructing analytical planar phototriangulation grids from 1:40,000 and 1:75,000 scale aerial photographs for the preparation of 1:10,000 scale photographic maps
14 p1753 A73-30416

Martian surface primary and secondary triangulation networks based on multiphotograph stereophotogrammetry and rectified photographs by Mariner 9, discussing control nets and points
19 p2479 A73-37227

Conditional equations of astronomical latitudes, longitudes, and azimuths
19 p2490 A73-38559

Analysis of the results of the geometric satellite world network
22 p2849 A73-42589

TRIATOMIC MOLECULES

Nitrous oxide laser optical pumping at high pressures with TEA hydrogen bromide laser, considering application to other linear triatomic molecules
06 p0704 A73-18796

A quantum model for bending vibrations and thermodynamic properties of C₃.
12 p1526 A73-27019

TRIAXIAL STRESSES

Triaxial plastic compression soil theory generalization to three dimensional complex stress fields, discussing yield surface for granular materials
03 p0390 A73-13332

The effect of the intermediate principal stress on triaxial fatigue of 7075-T6 aluminum alloy.
23 p3047 A73-44351

TRIAXIALITY

U TRIAXIAL STRESSES

TRIBOLIA

Influence of simulated weightlessness on the mutational rate of *Tribolium confusum*.
18 p2270 A73-35984

Interaction between radiation effects, gravity and other environmental factors in *Tribolium confusum*.
21 p2643 A73-40808

TRICHLORIDES

U CHLORIDES

TRIGGER CIRCUITS

Parameter calculation and design of synchronization circuit for firing pumping lamp of laser with modulator employing total internal reflection prism for Q switching
01 p0059 A73-10831

Double discharge TEA carbon dioxide laser trigger circuit, using plastic materials with selected dielectric constant and resistivity for trigger current increase
02 p0175 A73-11958

Linear characteristics of transistorized Schmitt trigger pulse width regulators in response to sinusoidal and sawtooth signals for automatic control systems
02 p0149 A73-12343

Overload tolerance formulas for differential voltage null measuring system with amplifier for trigger circuit drive
02 p0170 A73-12345

Analog simulation for transient and steady state performance of group-triggered cycloconverter supplying controlled slip induction motor, discussing commutation failures
03 p0253 A73-13932

Analysis of a Schmitt trigger employing a field transistor at the input
03 p0284 A73-14324

Time difference measuring instrument for asynchronous and synchronized positive pulses in automatic control system, noting pulse generator and switching, trigger and logic circuits
06 p0677 A73-18384

Electrodynamic exciter power amplifier with pulse width modulation and Schmitt trigger output stage for structural vibration tests
07 p0803 A73-20535

Operating conditions of a triggered pulse generator with a limiter diode
10 p1195 A73-24380

External static and dynamic characteristics of input-output sequences of logic elements
12 p1475 A73-26764

Triggering apparatus for optimal recording of slowly evolving phenomena using electrical impulse or mechanical contact signal
13 p1617 A73-28840

A tunnel diode trigger with an optical output
14 p1737 A73-30797

Triggering characteristics of TEA CO₂ laser.
15 p1885 A73-32019

Ultrafast spark gaps for electro-optical device control, discussing trigger system design and performance in terms of delay, jitter and internal voltage time response
16 p2013 A73-32874

Low power laser-triggered switching at voltages greater than 500 kV.
20 p2572 A73-38883

Observation of turn-on action in a gate-triggered thyristor using a new microwave technique.
20 p2543 A73-39414

Low voltage self triggering vacuum gap characteristics under dc conditions, comparing with thyatron pulse generator technique
21 p2692 A73-39917

Ultrafast streaking camera for picosecond laser diagnostics.
21 p2694 A73-39948

An improved method of triggering oscilloscopes for dynamic-strain measurements.
21 p2704 A73-41267

High voltage waveform generation at low power levels by circuit techniques and system configurations involving parallel series chains of light triggered bilateral switches
22 p2834 A73-42907

Semiconductor rectifiers analysis, considering triac and thyristor tetrode circuits, trigger devices and circuit diagrams
22 p2835 A73-43128

TRIGGERS

U ACTUATORS

TRIGONOMETRIC FUNCTIONS

Conditions for localization of Cesaro's rectangular means and of Abel's method means in the limited summing of a multiple trigonometric Fourier series in the Liouville classes
01 p0071 A73-11439

Functions of a generalized restricted variation and the convergence of their Fourier series and conjugate trigonometric series
02 p0188 A73-12551

Trigonometric series for earth rotation velocity around solar system center of mass
07 p0902 A73-20325

Application of double trigonometric series to the calculation of shell plates of variable thickness
11 p1446 A73-26600

Trigonometric series for earth rotation velocity around solar system center of mass
12 p1540 A73-27297

Method of trigonometric sums in the metric theory of Diophantine approximations of dependent variables
13 p1648 A73-28343

The problem of choosing a zero approximation of the angular position of an oriented satellite in the case of a nondipolar approximation of the geomagnetic field
15 p1942 A73-31238

German monograph - The computation of periodic motions of multipath nonlinear systems.
22 p2888 A73-42854

TRIM [BALANCE]

U AERODYNAMIC BALANCE

TRINITROTOLUENE

Dense air plasma compression and heating by TNT explosive charge, noting shock tube flow patterns
10 p1203 A73-23519

Dense air plasma compression and heating by TNT explosive charge, noting shock tube flow patterns
17 p2147 A73-35159

TRIODES

Investigation of the structure of an electron beam formed by a high-perveance triode gun under controlled-current conditions
01 p0025 A73-10969

Transit effects in grid plate gap of triode for generating microwave oscillations in regime similar to DM PATT diode
03 p0284 A73-14065

Dependence of the current-voltage characteristic of a p-n-p drift triode on the donor concentration in the active base
06 p0675 A73-18081

Long life 100 W triode for ATC and telemetry transponders.
09 p1066 A73-23427

A high-power oscillator triode with zero bias
15 p1850 A73-31259

Some results in predicting the states of semiconductor triodes from noise factors on the basis of theoretical statistical theory of pattern recognition
23 p2961 A73-44297

TRIPHENYLS

Electron absorption spectra of benzochromium-dicarbonyltriphenylphosphine and benzochromium-tricarbonyl and their application to studies of the decomposition kinetics of these compounds
10 p1186 A73-24457

TRIPLET EXCITATION

U ATOMIC ENERGY LEVELS

TRIPLET STATE

U ATOMIC ENERGY LEVELS

TRIPROPELLANTS

U LIQUID ROCKET PROPELLANTS

TRITIUM

Thermal instability of nonuniform plasma in steady state D-T fusion reactor operated by charged particle heating with spatially uniform fuel injection
01 p0084 A73-10465

Argon, radon, and tritium radioactivities in the sample return container and the lunar surface.
07 p0870 A73-19799

Solar flare intensity estimation based on measurements for Ar 37 radioactivities and depth dependences of tritium in Apollo 11 and 12 lunar rock samples
07 p0889 A73-19794

Argon-37, argon-39, and tritium radioactivities in the Haverro meteorite.
09 p1140 A73-21865

Leak testing of tritium fuelled experimental batteries.
09 p1038 A73-23288

Thermal cumulation equations for concentric conductive laser heating of two temperature D-T plasma with nuclear fusion energy recovery
11 p1406 A73-26411

Laser concentric conduction heating of two-temperature D-T plasma.
11 p1406 A73-26412

Concentric laser cumulation of plasma with consideration of the heat of nuclear fusion.
13 p1667 A73-29392

Theory and performance of a tritium battery for the microwatt range.
21 p2737 A73-39922

Simplified averaged equations of concentric laser compression of plasma.
24 p3117 A73-45427

TROCHOIDS

U PIVOTS

TROILITE

The isotopic composition of 'graphitic' carbon from iron meteorites and some remarks on the troilite sub-fur of iron meteorites.
13 p1684 A73-29180

TROJAN ORBITS

Orbital characteristics of comets passing through the 1:1 commensurability with Jupiter.
14 p1790 A73-29785

Horseshoe and Trojan orbits associated with Jupiter and Saturn.
15 p1937 A73-31948

TROPICAL METEOROLOGY

Tropical atmospheric radiative heating estimates for BOMEX/Barbados Oceanographic and Meteorological Experiment/ from direct radiation measurements, satellite images and surface and rawinsonde data
01 p0038 A73-10387

Numerical simulations of the tropical air-sea planetary boundary layer.
01 p0073 A73-10496

On the application of satellite data on cloud brightness to the study of tropical wave disturbances.
02 p0190 A73-12790

Utilization of meteorological data from earth satellites in the analysis of global weather maps and in studies of planetary atmospheric circulation
05 p0593 A73-16246

Note on the extratropical transformation of a typhoon in relation with cold outbreaks.
05 p0594 A73-16349

Equatorial stratosphere quasi-biennial oscillation variations from temperatures and zonal winds measured at Canton Island, Ascension Island and Balboa /Canal Zone/
05 p0594 A73-16573

Baroclinic model of zonal atmospheric circulation in the equatorial region
05 p0594 A73-17351

Theory of inertial atmospheric oscillations in low latitudes
06 p0691 A73-18729

Equatorial Kelvin wave oscillations of zonal wind at 100 mb over Eastern Hemisphere
07 p0847 A73-19043

Meridional circulation zonal averaging effects on summer hemisphere Hadley cell in tropical regions
07 p0847 A73-19046

Measurements of absorbed short-wave energy in a tropical atmosphere.
08 p0958 A73-21267

Low latitude density variations in the earth's neutral atmosphere between 200 and 400 km, from August 1969 to May 1970.
09 p1079 A73-22840

Intratropical convergence zone in the eastern portion of the Pacific Ocean
09 p1115 A73-22990

Characteristics of the development of the quasi-biennial cycle above the Indian Ocean
09 p1115 A73-22991

Application of some numerical techniques in combining satellite and conventional data in the tropics.
09 p1115 A73-23175

A synoptic investigation of anomalous warmth in the mid and upper troposphere during February 1964.
10 p1244 A73-23978

Statistical aspects of lower atmospheric disturbances delineated from conventional and satellite data over the tropical Pacific.
11 p1394 A73-25724

Physics and chemistry of upper atmospheres.
11 p1425 A73-26209

Southeast Asia weather during southwest monsoon in summer, discussing relation to westward moving equatorial waves from wind, pressure and cloudiness synoptic pattern analysis
12 p1520 A73-26805

Role of commercial aircraft in global monitoring systems.
13 p1568 A73-28499

A baroclinic model of the atmospheric zonal circulation in the equatorial region.
15 p1902 A73-31001

Results of the numerical modeling of steady zonal circulation of the atmosphere in the equatorial region
15 p1905 A73-31817

Book - The general circulation of the tropical atmosphere and interactions with extratropical latitudes. Volume 1.
15 p1907 A73-32423

Global circulation numerical modeling problems and numerical weather forecasting status as basis for GARP programs, considering tropical experiment on deep convective cloud systems
17 p2205 A73-34927

Some features of the equatorial D-region as revealed from the Langmuir probe experiments conducted at Thumba.
18 p2303 A73-35954

Proton whistlers in the ionospheric F-region over the South American equatorial area.
18 p2304 A73-35970

The large-scale displacement of subtropical jet stream over Western Europe in winter.
19 p2446 A73-37431

The effect of solar activity on temperatures in the equatorial mesosphere.
19 p2426 A73-38015

Magnetic equatorial ionospheric characteristics, discussing E and F regions, diurnal drift variations, field strength, equatorial electrojet, spread F and sporadic E
20 p2555 A73-39633

Neutral air wind influences deduced from solar cycle changes in the F2 region equatorial anomaly.
21 p2679 A73-39932

Wind modification of structure of thermally driven tropical undercurrent, considering stratified and constant density models, surface winds, monsoons, thermocline jets and meridional circulation
21 p2679 A73-40069

A generalized aeronomical model of the mesosphere and lower thermosphere including ionospheric processes.
21 p2683 A73-40778

Point discharge current measurements in trees and metal points during storms, discussing implications for structure of electrified clouds
21 p2684 A73-40779

Heating of the low-latitude upper atmosphere caused by the decaying magnetic storm ring current.
21 p2684 A73-40786

Post GARP Global Experiment programs, considering tropical vertical wind structure, satellite temperature measurement accuracy increase, data handling for real time and long term prediction
21 p2732 A73-40819

Equatorial thermospheric composition and its variations.
21 p2688 A73-41347

Energetic protons at low L-values of the equatorial magnetosphere.
21 p2761 A73-41379

Effects of interhemisphere transport on plasma temperatures at low latitudes.
22 p2844 A73-41919

Structure of global geopotential fields in view of the quasi-two-year cyclicity in the equatorial stratosphere
23 p3001 A73-43463

Nonlinear theory of the formation and structure of the intertropical convergence zone.
23 p3001 A73-43586

On the interaction between the zonal mean flow and equatorial waves excited by diabatic heat sources at 20 deg latitude.
23 p3001 A73-43587

Mediterranean, south Sahara and northwest India rainfall records analysis, correlating general circulation changes with winter-spring and monsoon rainfall fluctuations
23 p3003 A73-43954

Statistical analysis of satellite-observed trade wind cloud clusters in the western North Pacific.
23 p3003 A73-43980

Upper tropospheric disturbances of the equatorial atmosphere and their influence on rainfall near the equator.
23 p3004 A73-44104

Provisional climatology of most probable wind for application to low latitude operational weather analysis and forecasting, based on ATS-3 observed low level winds
23 p3004 A73-44262

Motion of a tropical hurricane in the field of the North Atlantic trade wind
24 p3107 A73-44428

Northern summer tropical upper tropospheric large scale flow dynamics, energy exchange diagram and limited area numerical weather prediction problems
24 p3108 A73-45094

TROPICAL REGIONS

Positive ion composition measurements in the D and E regions of the equatorial ionosphere.
01 p0041 A73-10889

Electron density profiles in the equatorial lower ionosphere at Thumba.
01 p0043 A73-10908

Energetic protons detection below radiation belt at equatorial latitudes from Azur satellite measurements, hypothesizing exospheric and upper atmospheric charge exchange processes
01 p0043 A73-11514

Magnetic field strength change in equatorial plasma-sphere, considering quiet ring current as equatorial sheet current extension of neutral sheet current in magnetospheric tail
02 p0155 A73-11732

Tropospheric and ionospheric refraction errors in satellite tracking over the Indian sub-continent.
02 p0141 A73-12299

Equatorial scintillation diurnal and seasonal variations and F region electron density irregularities, noting unusual post sunset behavior of Faraday rotation angle
04 p0440 A73-14951

Longitudinal variation of the equatorial anomaly.
04 p0440 A73-14960

Nonuniformities of the ion density at an altitude of 600 km in the ionosphere.
05 p0567 A73-16083

A numerical study of the influence of advective accelerations in an idealized, low-latitude, planetary boundary layer.
05 p0592 A73-16192

A numerical study of coupling between the boundary layer and free atmosphere in an accelerated low-latitude flow.
05 p0592 A73-16193

Investigation of the characteristics of atmospheric motion at low latitudes
05 p0592 A73-16227

6300 A night airglow enhancements in low latitudes.
07 p0818 A73-20051

Calculated distributions of hydrogen and helium ions in the low-latitude ionosphere.
07 p0818 A73-20052

A climatological analysis of oscillations of Kelvin wave period at 50 mb.
08 p0984 A73-21377

Low dispersion whistlers observed simultaneously at two low latitude stations.
08 p0940 A73-21651

Evening/forenoon asymmetry in the 27-day oscillation of the low-latitude magnetic field.
09 p1076 A73-22140

Low latitude equatorial electrojet analysis based on three dimensional electric field equation for ionosphere and magnetosphere
10 p1211 A73-24215

Excitation of oxygen permitted line emissions in the tropical nightglow.
10 p1214 A73-24739

The effects of thermospheric winds on the ionosphere at low and middle latitudes during magnetic disturbances.
11 p1353 A73-25752

Equatorial ionospheric electron drift rate measurement over Thumba, deriving north-south component
13 p1609 A73-28921

International Symposium on Equatorial Aeronomy, 4th, University of Ibadan, Ibadan, Nigeria, September 4-9, 1972, Proceedings.
15 p1868 A73-31750

Solar and lunar effects on neutral atmospheric tidal winds and induced electrostatic and geomagnetic fields effects on low latitude F2 and sporadic E layers
15 p1868 A73-31751

The field levels near midnight at low and equatorial geomagnetic stations.
15 p1869 A73-31758

Semi-annual variation in the true height of the F2-peak in low latitudes /at Puerto Rico/.
15 p1869 A73-31762

Equatorial spread-F irregularities observed at Nairobi and on the transequatorial path Lindau-Tsumeb.
15 p1870 A73-31765

Simultaneous observations of Pcl micropulsation polarization at four low latitude sites.
16 p2008 A73-33877

On the motion of the tropical red arc north boundary.
16 p2008 A73-33882

Particle entry into the equatorial magnetosphere.
18 p2344 A73-35928

Comparison of electron density profiles in the lower ionosphere at Equator and midlatitudes.
18 p2305 A73-36007

Differences in circulation of the upper atmosphere in low latitudes of the southern and northern hemispheres.
18 p2310 A73-36138

Spectrum analysis of tropical cloudiness. II.
19 p2446 A73-37430

On the propagation of ionospheric whistlers at low latitude.
19 p2404 A73-38018

Density measurements in the equatorial atmosphere by means of the San Marco 3 satellite
19 p2426 A73-38151

Photodensity and the impact of shifting agriculture on subtropical vegetation - A case study in the Bahamas.
20 p2562 A73-39905

Low latitude whistler activity during geomagnetic storms related to spread F conditions and magnetospheric and ionospheric electron density
23 p2972 A73-43696

On the large scale vertical movements of the F-layer and its effects on the total electron content over low latitude during the magnetic storm of 25 May 1967.
23 p2972 A73-43699

Studies of variations in the vertical ozone profiles over India.
23 p2975 A73-43871

Studies of the vertical distribution of atmospheric ozone in association with western disturbances over India.
23 p2975 A73-43872

The nighttime distribution of ozone in the low-latitude mesosphere.
23 p2975 A73-43881

Effect of neutral winds on ionospheric F-region at a pair of conjugate stations in low latitude.
24 p3082 A73-44729

TROPICAL STORMS

NT HURRICANES

NT TYPHOONS

A method for incorporating nested finite grids in the solution of systems of geophysical equations.
02 p0165 A73-12776

Tropical cyclone track statistical forecasting comparing methods based on synoptic, empirical and combined data
10 p1245 A73-23984

Rapid intensification and low-latitude weakening of tropical cyclones of the western North Pacific Ocean.
10 p1245 A73-23986

Auroras induced attenuation fluctuations of VLF at-mospherics associated with remote tropical thunderstorms
12 p1522 A73-27786

Relation between the pressure at the center of a tropical cyclone and the dimension of its cloud system
15 p1904 A73-31610

TROPICS

U TROPICAL REGIONS

TROPISM

NT AEOLOTROPISM

NT GEOTROPISM

NT GYROTROPISM

TROPOAUSE

Contrail ice budget measurements with optical array particle size spectrometer onboard Sabreliner, noting water abundance reduction at subtropopause jet traffic levels
02 p0189 A73-12785

Turbulence and tropopause evolution in northeast jet stream over Treviso airport, noting Richardson criterion value as diagnostic and short range prognosis tool
08 p0986 A73-21487

Diurnal tropopause maps divergence from average tropopause altitude profile, commenting on Eole experiment
13 p1605 A73-28073

Mountain range effects on tropopausal turbulence with mountain waves, examining tropopause layer inversions, vertical wind vectors, temperature distribution and buffeting intensity
17 p2204 A73-34542

Gravity-shear waves in jet flow near tropopause with arbitrary temperature-wind stratification
23 p3001 A73-43462

On the vertical ozone and wind profiles near the tropopause.
23 p2977 A73-43907

TROPOSPHERE

Hemispheric synoptic analysis of upper stratospheric warming for energy transformations in troposphere and lower and middle stratosphere
01 p0072 A73-10141

The magnitude and character of the radiation induced vertical circulation of the troposphere.
01 p0039 A73-10394

Troposphere turbulence kinetic energy dependence on height and scales of motions, presenting vertical energy profiles
01 p0074 A73-10869

Mobile FM-CW radar sounder with scanning capability for high resolution remote sensing in lower troposphere, discussing design and performance
02 p0140 A73-11959

Tropospheric and ionospheric refraction errors in satellite tracking over the Indian sub-continent.
02 p0141 A73-12299

Status of remote sensing of the troposphere.
03 p0299 A73-13061

A study of tropospheric radar propagation characteristics during an unusual spell of persistent dust haze followed by thunderstorm over Delhi during May 1966.
03 p0280 A73-14547

Tropospheric refraction effects on satellite range measurements.
04 p0415 A73-14750

Atmospheric correction for the troposphere and stratosphere in radio ranging of satellites.
04 p0439 A73-14808

Interrelation between processes occurring along a vertical, and the forecasting of stratospheric wind
05 p0592 A73-16232

Relationship of atmospheric processes in the troposphere and stratosphere
05 p0593 A73-16233

Diurnal variability of temperature and of isobaric surface heights in the troposphere and lower stratosphere
05 p0593 A73-16241

Computation of upper tropospheric reference heights from winds for use with vertical temperature profile observations.
05 p0569 A73-16575

Engineering models for Jupiter's troposphere and the NH3-H2O cloud systems.
[AIAA PAPER 73-129] 05 p0619 A73-16882

Fine structure of the temperature stratification in the troposphere and stratosphere.
07 p0848 A73-20348

Short-wave spectral radiant heat influx in the atmosphere
08 p0984 A73-21133

Correlation of microthermal turbulence data with meteorological soundings in the troposphere.
08 p0985 A73-21382

Preliminary results of studies of the Martian atmosphere with the aid of the Mars-2 satellite
09 p1146 A73-22486

A synoptic investigation of anomalous warmth in the mid and upper troposphere during February 1964.
10 p1244 A73-23978

The transition from locked to leaky modes in tropospheric radio propagation.
11 p1327 A73-25122

Venus - Microwave opacity of the minor atmospheric constituents.
11 p1417 A73-25267

Southern Hemisphere troposphere atmospheric carbon dioxide monitoring program based on aircraft air sampling, discussing vertical profile data
11 p1358 A73-26472

Experimental determination of two-dimensional spatiotemporal power spectra of stellar light scintillation - Evidence for a multilayer structure of the air turbulence in the upper troposphere.
12 p1521 A73-27120

Photochemistry of minor constituents in the troposphere.
12 p1466 A73-27603

Statistical description of the wind field in the upper troposphere and lower stratosphere with allowance for the scale of motion
12 p1521 A73-27741

Subsynoptic rainbands within precipitation ahead of surface warm front, discussing midtropospheric large-scale dynamic ascent interaction with upper boundary potential instability
13 p1651 A73-28265

Troposphere turbulence kinetic energy dependence on height and scales of motions, presenting vertical energy profiles
13 p1653 A73-28693

Near horizon anomalies in astronomical refraction due to ground air layer effects on tropospheric processes
13 p1610 A73-29322

Preliminary results of Martian-atmosphere research with the Mars-2 satellite.
14 p1798 A73-30321

Analysis of cases of intense turbulence in the troposphere
17 p2205 A73-34544

A preliminary study of the transient response of the atmosphere produced by mid-tropospheric heating.
18 p2332 A73-36701

The remote sensing of wind velocity in the lower troposphere using an acoustic sounder.
19 p2427 A73-38208

On the use of forward scatter techniques in the study of turbulent stratified layers in the troposphere.
19 p2427 A73-38219

Trans-horizon propagation techniques for examining disturbances in stratified tropospheric layers.
19 p2405 A73-38221

Small-scale atmospheric structure deduced from measurements of temperature, humidity and refractive index.
19 p2448 A73-38224

Dynamic coupling of the stratosphere with the troposphere and sudden stratospheric warmings.
19 p2449 A73-38288

New evidence for effects of variable solar corpuscular emission on the weather.
21 p2755 A73-40073

Tropospheric and stratospheric vertical profiles of methane concentration via air sampling and gas chromatography, noting temporal and spatial variations
21 p2680 A73-40077

Tropospheric model for nitrogen-oxygen-carbon-hydrogen atmosphere with time dependent static chemistry, emphasizing methane conversion to CO via OH attack
21 p2646 A73-40081

Photochemical model for homogeneous gas phase radical chain mechanism to remove tropospheric methane, carbon monoxide, molecular hydrogen and formaldehyde
21 p2646 A73-40082

Interpretation of the results of photometric observations of noctilucent clouds
21 p2732 A73-40859

Tropospheric and stratospheric response to solar influence during geomagnetic disturbances.
21 p2690 A73-41364

Lidar measurements for the exploration of the atmosphere
22 p2823 A73-41825

The effect of atmospheric and physiological conditions on the homogeneity of observations of noctilucent clouds
22 p2847 A73-42448

Increased influx of stratospheric air into the lower troposphere after solar H alpha and X ray flares.
22 p2848 A73-42538

Spectral structure of tropospheric vertical temperature profiles over Cape Kennedy, Florida.
22 p2849 A73-42544

Tropospheric aerosol - The relative contribution of marine and continental components.
22 p2849 A73-42547

Study of laser radiation propagation and the diagnostics of a randomly inhomogeneous troposphere.
23 p2954 A73-43572

Meridional distribution of tropospheric ozone from measurements aboard commercial airliners.
23 p2974 A73-43859

A theoretical investigation of tropospheric ozone and stratospheric-tropospheric exchange processes.
23 p2974 A73-43861

The average tropospheric ozone content and its variation with season and latitude as a result of the global ozone circulation.
23 p2974 A73-43862

Remote sensing of the global distribution of total ozone and the inferred upper-tropospheric circulations from Nimbus IRIS experiments.
23 p2975 A73-43876

A discussion of the chemistry of some minor constituents in the stratosphere and troposphere.
23 p2951 A73-43889

Upper tropospheric disturbances of the equatorial atmosphere and their influence on rainfall near the equator.
23 p3004 A73-44100

Tropospheric vertical energy transfer due to terrestrial and atmospheric water vapor and carbon dioxide radiation calculated for vertical atmospheric temperature and composition distributions
24 p3082 A73-44773

Fluctuation characteristics of the electric component of the troposphere.
24 p3084 A73-44940

Some characteristics of the global distribution of trace element concentration in the lower troposphere
24 p3085 A73-44967

Relationship between midtropospheric temperatures and tropospheric synoptic features.
24 p3107 A73-45014

Northern summer tropical upper tropospheric large-scale flow dynamics, energy exchange diagram and limited area numerical weather prediction problems
24 p3108 A73-45094

TROPOSPHERIC RADIATION

Microwave range-difference measurements on 65-km slant overwater path, interpreting tropospheric noise power spectra and rms values as function of baseline length
11 p1330 A73-25685

Rotational spectral lines of water vapor dimers in the upper troposphere
13 p1609 A73-29152

Experimental investigations of solar radiation fluxes in the lower troposphere in the presence of St and Sc clouds
15 p1905 A73-31788

Events in a photoemulsion indicating the formation of superheavy fireballs
23 p3021 A73-43535

TROPOSPHERIC SCATTERING

Russian book on radio wave propagation covering ground, ionospheric and tropospheric propagation, ratio attenuation, scattering and ionospheric and tropospheric reflection
02 p0143 A73-12775

Gaussian channel model for long tropospheric scatter link verification by time varying bandpass impulse response measurements, using Kolmogoroff-Smirnov tests
04 p0418 A73-15392

Frequency dependence of losses by radio-wave scattering at turbulent discontinuities in the troposphere
08 p0939 A73-21398

Imaging properties of monostatic and bistatic troposcatter radars.
09 p1050 A73-22426

Applications of methods of geometric optics in the case of tropospheric propagation
12 p1473 A73-27755

Microwave-propagation studies regarding the isotropy characteristics of the turbulent fine structure of the refractive index in the troposphere
15 p1874 A73-32361

Measurements of wind-induced Doppler shifts at 16 GHz over a long range bistatic scatter link.
16 p1983 A73-33726

Frequency dependence of the loss when radio waves are scattered by turbulent inhomogeneities in the troposphere.
19 p2407 A73-38356

TROPOSPHERIC WAVES

Self focusing of two dimensional cylindrical waves propagating in inhomogeneous natural duct, noting tropospheric communications and ionospheric and sound propagation applications
02 p0142 A73-12527

TROUBLESHOOTING

U MAINTENANCE

TROUGHS

Model development of supersonic trough wind with shocks.
03 p0298 A73-12887

Mars troughs from Mariner 9 pictures, interpreting evolutionary origin in terms of surface and core processes
19 p2477 A73-37204

TRUNCATION [MATHEMATICS]

U APPROXIMATION

TRUNCATION ERRORS

Artificial viscosity truncation error analysis for finite difference analogs of linear advection equations
01 p0035 A73-11466

Finite difference method for boundary layer flow, noting truncation errors due to nonuniform grid
01 p0035 A73-11468

Optimum Runge-Kutta-Fehlberg methods for second-order differential equations.
04 p0471 A73-15231

Practical techniques for estimating the accuracy of finite-difference solutions to parabolic equations. [ASME PAPER 72-WA/APM-12] 04 p0472 A73-15900

Performance of M-ary PSK systems in Gaussian noise and intersymbol interference. 06 p0665 A73-18140

Newton method for calculation of viscous flow around circular cylinder with Fourier series truncation for stream function and vorticity, evaluating numerical error 11 p1345 A73-25115

A dynamic transformation method for modal synthesis. [AIAA PAPER 73-396] 11 p1440 A73-25525

Linear regression filtering and prediction for tracking maneuvering aircraft targets. 11 p1333 A73-26640

A simulative study of correlated error propagation in various finite-precision arithmetics. 15 p1899 A73-31350

A modified Butcher formula for integration of stiff systems of ordinary differential equations. 17 p2199 A73-34212

Word length problems in the on-board computer implementation of digital flight control systems. 17 p2145 A73-35384

Magnitude error bounds for sampled-data frequency response obtained from the truncation of an infinite series. 17 p2145 A73-35640

Forecast of mode variation subsequent to structure modifications 18 p2367 A73-37083

Statistical models for rounding-off error studies in linear algebraic problems 18 p2292 A73-37144

Digital filter tasks and applications, discussing recursive and transversal filters, waveforms, SNR, truncation errors and complex filtering 19 p2414 A73-38301

Image restoration filter with preprocessing to minimize distortion due to truncation errors and edge effects 21 p2697 A73-40131

On the construction of accurate difference schemes for hyperbolic partial differential equations. 23 p3000 A73-43208

Computerized structural analysis by finite element method, discussing round-off and truncation errors with emphasis on inherited error effects minimization 24 p3150 A73-45233

Truncation error in the solution of integral equations. 24 p3106 A73-45344

TRUNKS (LINES)
U TRANSMISSION LINES

TRUNNONS
U SHAFTS (MACHINE ELEMENTS)

TRUSSES
A note on optimality conditions for trusses with a zero minimum cross-section. 01 p0115 A73-10766

Design, development, fabrication and qualification load testing of high modulus graphite-epoxy reflector support truss for ATS F and G 03 p0330 A73-13021

On optimal design of prestressed elastic structures. 03 p0384 A73-13119

Optimality criteria for structural design of statically determinate or indeterminate truss with prescribed compliance and cross sectional area 03 p0391 A73-13679

Minimum weight design of plastic and elastic grillages and fiber reinforced plates of given strength or stiffness, presenting optimal solutions for various boundary conditions 04 p0509 A73-15011

The concept of snap-buckling illustrated by a simple model. 07 p0909 A73-19163

The minimum weight structural configuration of pin-jointed truss cantilevers of given external shape. 08 p1015 A73-20671

The method of internal force parameters in elastokinetics 08 p1016 A73-20782

Application of Krylov's method to the solution of the frequency equation describing the weak vibrations of a truss structure 10 p1288 A73-23624

Small parameter method, with the parameter proportional to the friction forces, in the case of forced vibrations of complex trusses 11 p1435 A73-25395

Russian book on linear truss systems potential strain energy and displacements covering matrix and graph-analytic methods, influence functions, simple and complex strains, etc 11 p1442 A73-25775

Book - Introductory structural analysis with matrix methods. 12 p1554 A73-27548

Blocking procedure for large scale structural analysis in conjunction with plane truss using stiffness matrix method, considering computer subroutines in finite element method 16 p1985 A73-32793

Matrix theory algorithms for static stresses and elastic deformations in truss structures, deriving equilibrium equations in terms of forces, deformations and node displacements 16 p2080 A73-33258

Designing equal-life minimum-weight truss structures 20 p2619 A73-39357

Comparison of some penalty function based optimization procedures for the synthesis of a planar truss. 22 p2922 A73-42478

A new approach to optimal design of elastic structures. 23 p3042 A73-43798

TRYPSIN
Informational biopolymer structure in early living forms. 06 p0652 A73-17946

Trypsinogen activation peptides - An example of molecular epigenesis. 06 p0652 A73-17947

TRYPTAMINES
NT SEROTONIN
Influence of certain brain structures on the sulfhydryl-group, diphosphopyridine-nucleotide, and serotonin contents of the blood 09 p1040 A73-22856

Binding of Melatonin to human and rat plasma proteins. 10 p1182 A73-24657

TRYPTOPHAN
Brain serotonin content - Physiological regulation by plasma neutral amino acids. 01 p0008 A73-10408

Application of the method of polarizational ultraviolet fluorescence microscopy to study giant muscle fibers Balanus rostratus Hock 08 p0930 A73-21135

Serum tryptophan level after carbohydrate ingestion - Selective decline in non-albumin-bound tryptophan coincident with reduction in serum free fatty acids. 12 p1464 A73-27975

The inhibiting action of 5-oxtryptophan on thermal regulation during the awakening from hibernation 19 p2393 A73-37252

Serum tryptophan level after carbohydrate ingestion - Selective decline in non-albumin-bound tryptophan coincident with reduction in serum free fatty acids. 21 p2640 A73-41218

TSUNAMI WAVES
The tsunami model of the origin of ring structures concentric with large lunar craters. 11 p1419 A73-25791

TU-134 AIRCRAFT
Russian book - The Tu-134 aircraft: Its design and operation. 18 p2266 A73-35870

TUBE CATHODES
NT COLD CATHODES
NT HOT CATHODES
NT PHOTOCATHODES
NT PHOTOMULTIPLIER TUBES
NT THERMIONIC CATHODES
Analysis of the static modes of a magnetron with allowance for electron-velocity scatter 11 p1332 A73-26163

TUBE GRIDS
Transit effects in grid plate gap of triode for generating microwave oscillations in regime similar to IMPATT diode 03 p0284 A73-14069

Superposition method for potential distribution in plane tetraode field with unipotential and bipotential grids, noting electro-optical effect in cylindrical lenses 13 p1591 A73-28667

Physicochemical properties of metal filaments under vacuum at high temperatures, assessing suitability as antiemission materials on Mo grids in high power vacuum electron tubes 15 p1898 A73-31842

TUBE HEAT EXCHANGERS
Shell-and-coil condenser for packed air conditioners, testing heat transfer coefficients relationship to Reynolds number, heat flux and condensed refrigerant level 05 p0638 A73-16220

Heat transfer characteristics of air conditioner finned tube heat exchanger surfaces from steady state heat balance, monitoring fluid temperature response at outlet 05 p0638 A73-16223

Transient heat transfer through a thin-walled circular pipe. 06 p0766 A73-17443

Heat exchanging and catalytic dissociation of ammonia flowing through tubes - Application to micropropulsion. 07 p0867 A73-18931

Computerized optimal tube heat exchanger design, discussing programming for heat transfer surface area and operating point determination 11 p1448 A73-25102

Karman vortex street characteristics of single circular cylinders and heat exchanger tube bundles, presenting drag, lift and Strouhal number as function of Reynolds number 11 p1299 A73-25108

Nonuniform heat transfer coefficient effect on double-pipe heat exchanger analysis with effectiveness method, discussing exchanger sizing 12 p1559 A73-27693

Experimental investigation of heat transfer and resistance in crimped tubes 19 p2505 A73-38561

Unsteady convective heat exchange for various hot-gas cooling laws in tubes 24 p3156 A73-45077

TUBERCULOSIS
Thoracic X ray photography technique for tubercular lesion detection in flight personnel, comparing to standard radiography and radioscopy 02 p0137 A73-12155

TUBES
Tubular materials plane stress-strain test facility for combined axial load and internal pressure effects 03 p0288 A73-14024

Flexibility matrix derived and applied to finite element production for thin walled open tubes under torsion, taking into account warping constraints 03 p0395 A73-14470

A quality criterion test for tubes intended for measurement of acoustic absorption and impedance coefficients 09 p1121 A73-23105

Ultrasonic closure welding of small aluminum tubes. 19 p2435 A73-38003

Inspecting thin tubes by ultrasounds - Choice of examination frequency 21 p2707 A73-41068

Combined radial-axial large amplitude oscillations of hyperelastic cylindrical tubes. 22 p2923 A73-42637

TUBING
U PIPES (TUBES)

TUMBLING MOTION
Maneuvering a tumbling dual-spin spacecraft - The recovery of OSO-7. [AIAA PAPER 73-248] 05 p0630 A73-16971

Stable tumbling motions of a dual-spin satellite subject to gravitational torques. 17 p2237 A73-34177

Dynamic passivation of a spinning and tumbling satellite using free-flying teleoperators. 19 p2490 A73-37306

TUNGSTATES
Spectroscopic and lasing studies of a new laser crystal, KY(WO₄)₂-Nd³⁺/+ 09 p1134 A73-22984

A mass spectrometric investigation of reactions involving tungsten and molybdenum with potassium-seeded H₂/O₂ flames. 10 p1186 A73-23554

Selection and preliminary evaluation of three structures as potential solid conductors of alkali ions - Two hollandites, a titanate, and a tungstate. 17 p2219 A73-35325

TUNGSTEN
Fabrication of porous tungsten foils for contact ionization of cesium [ONERA, TP NO. 1113] 01 p0055 A73-10234

Hot extrusion and properties of rods from sintered molybdenum and tungsten blanks. 01 p0065 A73-10817

Effect of high isostatic pressures on the compressibility and sinterability of tungsten powders. 01 p0065 A73-10819

Thermophysical properties of arc-cast tungsten using the TPRC multi-property apparatus /direct heating method/. 01 p0067 A73-11483

Study of polarization during electrodeposition of tungsten simultaneously with nickel 02 p0174 A73-12539

Metal-metal laminar composites for high-temperature applications. 02 p0182 A73-12620

The rate of vaporization of tungsten in argon. 02 p0183 A73-12767

Consolidation of tungsten and molybdenum powders. 03 p0322 A73-13262

Oxidation and nitridation of Cr-W alloy. 03 p0325 A73-13803

Adsorbed barium films on tungsten and molybdenum /011/ face. 04 p0460 A73-14867

High vacuum thermal desorption mass spectrometry for electron bombardment activated nitrogen desorption from W surface, discussing lambda state population 04 p0414 A73-14999

The influence of the electron-phonon scattering on the total energy distribution of field emitted electrons from tungsten.

04 p0477 A73-15000

High temperature tests for chemical vapor deposited W ring and tensile specimens mechanical properties, investigating slip traces and fracture surfaces

04 p0462 A73-15305

Effect of a temperature gradient on bubble growth in tungsten.

04 p0463 A73-15307

Electric and thermal conductivity, elastic properties, and resistance to bending of porous tungsten throughout the porosity range

04 p0464 A73-15371

Plasma diagnostics in overcompensation operated Knudsen thermionic converter with Cs-Ba filler, noting W cathode surface properties

04 p0481 A73-15614

Impurities and cooling rate effects on cast W structure during crystallization from optical metallography

04 p0466 A73-15668

Production of porous tungsten thin walls intended for cesium ionization by contact

04 p0454 A73-15721

On the establishment of a diffusion barrier between a boron fiber and its tungsten substrate

05 p0589 A73-17049

Chemisorption and catalysis of hydrogen on polycrystalline wires of tungsten and nickel.

06 p0661 A73-18253

Superlattice of voids in neutron-irradiated tungsten.

06 p0709 A73-18353

Energy spectra of Cs⁺ ions scattered from the surface of a tungsten single crystal.

06 p0726 A73-18615

Electrical explosion of tungsten wires in a vacuum.

06 p0724 A73-18782

Thermal behavior of a plasma-heated tungsten probe in the presence of tungsten vapor.

07 p0788 A73-20447

Dislocation structure of tungsten single crystals grown by electron-beam zone refining

07 p0841 A73-20523

Dwell times of exploding tungsten wires in air.

09 p1119 A73-21929

Investigation of the compatibility of boron fibers with tungsten substrates and titanium matrices

09 p1103 A73-22469

Recrystallization of electron-beam-melted tungsten with tantalum and zirconium carbide additions

09 p1106 A73-23189

Niobium and tungsten cementation in a glow-discharge plasma

09 p1089 A73-23197

Thermoelectricity in tungsten at low temperatures.

09 p1135 A73-23335

Variation of the work function of W(100) by adsorption of oxygen, cesium, and coadsorption of oxygen and cesium

10 p1186 A73-23696

Certain results of flight tests of a model ion thruster employing contact ionization of cesium on tungsten

10 p1262 A73-23892

Coadsorption of oxygen and carbon monoxide on tungsten - Desorption spectra, electron stimulated desorption and field emission microscopy.

11 p1325 A73-25204

Hydrogen promoted corrosion of tungsten by oxygen in an electric field A field ion microscope study.

11 p1325 A73-25205

Production and properties of tungsten-wire reinforced NiCr 80 20

11 p1379 A73-25407

Microscopic, kinetic and microhardness observations of Ti-W metal matrix composite solid state interface reactions, showing enhanced shear resistance

11 p1384 A73-26049

Thermodynamics of heterogeneous gas equilibria. VII - Gas phase composition and chemical transport reactions in the tungsten-oxygen-hydrogen system

11 p1386 A73-26568

Field-ion microscopic study of the high-speed deformation of tungsten

12 p1509 A73-26838

Solubility of vanadium and tungsten in alpha and gamma phases in the Fe-V and Fe-W binary systems

12 p1513 A73-27683

Thermal expansion of tungsten from 293 to 1800 K. [ECTP PAPER E-1]

13 p1631 A73-28052

Effect of the degree of purity on the dislocation structure of tungsten single crystals

13 p1631 A73-28104

Study of the structure and properties of oriented tungsten single crystals

13 p1631 A73-28105

The interaction between two hydrogen atoms adsorbed on 100/tungsten.

13 p1580 A73-28215

Temperature dependence of the cross section of O⁺ ion desorption by electrons from an oxygen layer adsorbed on a tungsten surface

13 p1663 A73-28969

ESCA study of fractional monolayer quantities of chemisorbed gases on tungsten.

14 p1724 A73-30421

Investigation of the influence of the method of supplying hydrogen to the furnace on the properties of tungsten metal

14 p1765 A73-30885

Compatibility of silicon carbide fiber with a tungsten base and a titanium matrix

15 p1888 A73-31595

The interaction of tungsten and molybdenum melts with gaseous oxygen

15 p1890 A73-31924

Reflection-absorption infrared spectrum of alpha-CO chemisorbed on polycrystalline tungsten.

15 p1841 A73-31971

Effect of specimen thickness on the fracture surface energy of 100 axis tungsten single crystals.

15 p1891 A73-32022

Mechanical treatment of tungsten powder compacts

15 p1892 A73-32246

High temperature tensile and stress rupture tests of tungsten/Nichrome laminar composites and tungsten alloy/Inconel sheet and foil specimens

17 p2193 A73-35545

Phase formation investigation in the Mo-Al and W-Al systems when the Mo and W surfaces are saturated with aluminum by diffusion from a vapor phase in a vacuum

18 p2318 A73-35879

Influence of a solid-phase nickel coating on the sintering kinetics of tungsten wire

18 p2320 A73-36858

Molecular beam study of the desorption of cesium ions from tungsten crystals.

18 p2338 A73-36976

Chemisorption of CO on tungsten /100/- Combined flash desorption and electron stimulated desorption study. II.

18 p2287 A73-37033

Fine structure of rolled annealed tungsten sheet, discussing subsurface layer recrystallization and deformation effects based on radiographic examinations

19 p2440 A73-37443

Brittleness of coated tungsten wire

20 p2577 A73-39361

Generation of vacancies in tungsten by rapid-rate deformation at elevated temperature.

20 p2578 A73-39492

Structural changes during plastic deformation and annealing of tungsten single crystals

20 p2579 A73-39738

Reflection of conductivity electrons from an atomically pure 110/ face of a tungsten crystal

21 p2751 A73-40367

Influence of hydrogen, alcohols, and moisture on the ultimate strength and electrical resistance of tungsten and steel wire samples

21 p2721 A73-41227

Field-ion-microscopic study of interstitial plasticity of tungsten microcrystals.

22 p2872 A73-41726

High temperature thermophysical properties of tungsten.

[ECTP PAPER D1-5]

Investigation of the thermal expansion of molybdenum and tungsten at high temperatures.

[ECTP PAPER E-5]

Chemisorption of H₂ on W(211).

22 p2817 A73-42444

Thermodynamics of transition metal-hydrogen solid solutions.

22 p2880 A73-43076

Investigation of temperature pulsations accompanying the heating of a laminar sample by alternating and pulsating currents

23 p3048 A73-43446

Temperature dependence of the cross section for electron-induced O⁺ desorption from tungsten.

23 p3008 A73-44321

Oxygen-W(100) surface interactions investigated simultaneously by secondary ion mass spectrometry (SIMS) and electron induced desorption (EID)

24 p3066 A73-45330

TUNGSTEN ALLOYS

Structural changes following annealing in a dispersion-strengthened tungsten alloy

01 p0062 A73-10261

Sintered chromium-nickel steel of high tungsten content.

01 p0065 A73-10816

Mechanical properties of molybdenum alloys.

01 p0065 A73-10818

Preparation and sintering of tungsten-rhenium alloy powders.

01 p0065 A73-10820

Creep and durability of tungsten wire.

02 p0180 A73-12137

Thermal properties of tantalum-tungsten alloys at high temperatures.

03 p0322 A73-13192

Ni-Mo-W alloys hardness rating and corrosion resistance to sulfuric and hydrochloric acids, discussing dispersion hardening, quenching and aging treatments

03 p0327 A73-14001

High temperature creep properties of recrystallized W-thoria alloy wires, noting dependence on temperature, grain structure and stress

04 p0463 A73-15306

Phase transformations in Al-rich Al-W alloys rapidly quenched from the melt.

04 p0468 A73-15983

Temperature and concentration effects on heterodiffusion coefficient of diffusion welded Mo-W alloy rods

06 p0707 A73-17907

Heat capacity of the TV-10 tantalum-tungsten alloy at low temperatures

06 p0708 A73-18051

Heat conductivity and the Lorentz number of tungsten-rhenium alloys within the solid-solution limits from 0 to 27% Re at temperatures between 1200 and 3000 K

06 p0710 A73-18556

Phase separation analysis of ternary Co-W-Ti alloy during high temperature aging by X ray and electron microscopy method

09 p1099 A73-21963

W-Ta alloys prepared by electron beam melting, testing Ta content effects on oxidation resistance and hardness at high temperatures

09 p1103 A73-22424

Study of the W-Ta-Re phase diagram by the diffusion layer method

09 p1108 A73-23236

Thermodynamic properties of the nickel-tungsten system as determined from its hydrogen solubility

10 p1231 A73-23689

Mo-W-B alloy phase equilibria, isothermal cross sections, liquidus, solubility and mechanical properties by thermal, X ray and microstructural analyses

12 p1510 A73-26904

Inert gas injection for W-Re thermocouple wire corrosion protection during temperature measurement in aggressive media

12 p1497 A73-27319

Cermet cathode materials for electric vacuum equipment

12 p1503 A73-27562

Partial and integral molar thermodynamic properties of solid Ta-W alloys at 1050-1300 K, discussing negative deviations from ideality

13 p1632 A73-28126

Experimental and thermodynamic study of the equilibria between ferrite, austenite and intermediate phases in the Fe-Mo, Fe-W, and Fe-Mo-W systems.

13 p1633 A73-28136

Grain growth of chemical vapour deposited tungsten-22 wt % rhenium alloy.

13 p1636 A73-28927

Investigation of interdiffusion in the nickel-tungsten and palladium-tungsten systems

14 p1764 A73-30864

Mo-W-C phase equilibria study at 1000 C, obtaining isothermal cross sections for various carbon contents from X ray and microstructural analysis

15 p1888 A73-31598

Electrical resistance of tungsten-rhenium cermet alloys

15 p1892 A73-32243

Critical survey of studies of the equilibrium phase diagram of the Ti-W system

15 p1893 A73-32513

Thermal conductivity and Lorenz number of tungsten-rhenium alloys in the solid-solution region 0-27% Re/ at temperatures of 1200-3000 K.

16 p2026 A73-33582

Polythermal and isothermal sections of Ti-Al-W phase diagram for Ti corner investigation, determining phase region boundary locations by X ray analysis

17 p2188 A73-34568

Certain law controlling the temperature dependence of the microdeformation of Fe-Cu-Ti, W, and W-Re bcc alloys

18 p2324 A73-36803

Some electron structure characteristics of W-Re solid solutions

18 p2325 A73-36809

Mo-W alloys mechanical characteristics dependence on temperature and W content

19 p2439 A73-37265

Structure and mechanical properties of internally oxidized Ta-8 pct W-2 pct Hf /T-111/ alloy.

20 p2576 A73-39025

Possible reinforcement of the tungsten-nickel-iron composite with tungsten fibers.

21 p2722 A73-41586

Deformation and microfracture characteristics of two-phase tungsten-composite materials sintered with the liquid phase

22 p2872 A73-41948

Tungsten-rhenium thermocouple, describing alloys behavior, fabrication, insulation sheaths, calibration, stability and applications

22 p2857 A73-42037

Thermal properties of tungsten-rhenium alloys used in high temperature thermocouples. 22 p2858 A73-42038

Studies of the performance of W-Re type thermocouples. 22 p2858 A73-42039

Electrical resistivity and thermal conductivity of alloys of the tungsten-molybdenum system. [ECTP PAPER B1-6] 22 p2876 A73-42402

Isothermal cross sections of the phase diagram of the nickel-molybdenum-tungsten system at 1200 and 700 C 22 p2877 A73-42459

Anomalous concentration dependence of thermal expansion coefficients of tungsten-rhenium and tungsten-niobium alloys. 22 p2878 A73-42509

Substitution of molybdenum for tungsten in heat resistant cobalt-base alloys 23 p2989 A73-43436

TUNGSTEN CARBIDES

High temperature effects on near order transformations in TiC-WC solid solutions during heat treatment and cooling, using X ray diffraction scattering measurements 01 p0064 A73-10615

The tempering of low carbon steels containing tungsten. 02 p0183 A73-12760

Bipolar noble-metal free electrodes for fuel cells with acid electrolytes. 04 p0407 A73-15113

Bubbles and operating voltage effects in electrochemical machining of tungsten carbide and discharge machining of glass [ASME PAPER 72-WA/PROD-21] 04 p0456 A73-15804

Dependence on the cobalt content of the strength of a WC-Co cutting alloy in tension 09 p1159 A73-22473

Grain growth inhibition by carbide additives in hard metal alloys of the ISO-K 10 type 10 p1231 A73-23688

Mechanical behavior of WC-Co composite alloys. 13 p1643 A73-29545

Hard WC-Co alloys as dispersion strengthened materials 15 p1887 A73-31591

Precipitation and magnetic hardening in sintered WC-Co composite materials. 23 p2997 A73-43776

TUNGSTEN COMPOUNDS

NT TUNGSTATES

NT TUNGSTEN CARBIDES

NT TUNGSTEN OXIDES

Optical band gap energies and stacking sequences of molybdenum tellurides and tungsten selenides derived from dielectric constant measurements 04 p0482 A73-14868

Dinuclear anions of molybdenum VI and tungsten VI with the 'fluoro' and 'oxalato' coordinates 05 p0547 A73-17218

High-temperature oxidation of tungsten boride in oxygen and the effect of scale evaporation. 16 p1976 A73-33076

A study on some metal-base self-lubricating composites containing tungsten disulfide. [ASLE PREPRINT 73AM-3C-1] 17 p2196 A73-34986

Effect of impurities on the temperature of the superconducting transition in W3Si type compounds 20 p2600 A73-39731

TUNGSTEN INERT GAS WELDING

U GAS TUNGSTEN ARC WELDING

TUNGSTEN OXIDES

Cold shortness of W and related refractory metals, noting oxide phases and impurities effects on mechanical properties temperature dependence 01 p0066 A73-11341

Comparative estimation of thermodynamic characteristics for reduction of tungsten and molybdenum oxides 09 p1107 A73-23226

Reduction kinetics and phase transformations of tungsten and molybdenum oxides 13 p1636 A73-28938

Specific surface changes in tungsten and molybdenum oxides during reduction processes 24 p3099 A73-44738

TUNGUSK METEORITE

Optical anomalies due to scattered disperse cosmic matter in upper atmosphere from Tungusk meteorite fall 10 p1213 A73-24681

Tungusk meteorite event with thermal radiation and severe blast wave attributed to black hole of substellar mass 22 p2909 A73-42488

TUNING

The generation of tunable near IR radiation using a nitrogen laser pumped dye laser. 03 p0318 A73-12869

Optical sweep generator using single frequency He-Ne lasers with Michelson interferometer for mode

selection to provide smooth tuning throughout Doppler width 03 p0319 A73-14065

Transient analysis of an electronically tunable dye laser. I - Simulation study. 03 p0320 A73-14457

Internal upconversion and doubling of an optical parametric oscillator to extend the tuning range. 03 p0320 A73-14463

Advances in YIG-tuned Gunn effect oscillators. 04 p0426 A73-14734

Tunable polarized violet light pulse emission from anthracene doped organic molecular fluorene crystal laser pumped with nitrogen laser, noting pulse amplitude and duration 04 p0458 A73-14873

Application of adaptive tuning of filters to exoatmospheric target tracking. 04 p0498 A73-15275

Tunable dye lidar techniques for measurement of atmospheric constituents. 04 p0423 A73-15769

Organic dye lasers use as continuously tunable sources of coherent light, discussing molecular energy level systems and transitions 05 p0583 A73-16337

Electromechanical techniques for rapid frequency tuning of lasers. 05 p0584 A73-16443

GaAs transferred electron /Gunn/ device microwave oscillator with harmonic tuning, noting reactive termination and bias voltage effects on efficiency optimization 05 p0559 A73-16813

Varactor or YIG tuned Gunn effect microwave oscillators for ECM applications, noting low noise octave tuning and high sweep rates 06 p0675 A73-17842

Microwave oscillator subharmonic phase locking, discussing nonlinear capacitance and linear frequency-dependent parameter and broadband tuning characteristics comparison with fundamental injection locking 06 p0677 A73-18739

Angular dispersion of an acousto-optic Bragg cell used in the wavelength tuning of an organic dye laser. 08 p0975 A73-21056

Angular dispersion of diffraction gratings used for tuning organic dye lasers. 08 p0975 A73-21057

A tunable flashlamp-pumped dye ring laser of extremely narrow bandwidth. 09 p1091 A73-22083

A linear voltage-tunable distributed null device. 09 p1066 A73-23246

Tuning nonlinearity of oscillatory systems made of long-line segments containing a varicap 10 p1193 A73-23728

Distribution of equivalent attenuations and generalized detunings in a stagger single-tuned IF amplifier with critical staggering. 10 p1197 A73-24936

Single mode ion laser tuning over entire emission range via intracavity etalon tilting by piezoelectric drive 11 p1376 A73-26104

On combined frequency oscillations of the forced Van der Pol oscillator. 11 p1339 A73-26696

Frequency-agile coaxial magnetrons. 12 p1477 A73-26925

Optical parametric oscillators. 16 p2023 A73-32857

Pb-salt tunable diode lasers. 16 p2023 A73-32859

Wideband varactor-tuned solid-state sources to 20 GHz. 16 p1991 A73-33898

Q band /38 GHz/ varactor-tuned Gunn oscillators. 16 p1991 A73-34018

State-space analysis of a magnetically tuned IMPATT oscillator lumped model. 17 p2136 A73-34973

An X-band Gunn-diode generator with varactor tuning 17 p2126 A73-35550

Pulse modulation of Gunn-effect oscillator. 17 p2142 A73-35652

Wideband VHF whip antenna impedance simulation using AI cylindrical chamber to simplify impedance-controlling network tuning and power testing 17 p2148 A73-35705

Detuned single mode laser detailed balance and line width factor in threshold region expressed by Fokker-Planck equation and nonhermitian eigenvalue 20 p2571 A73-38622

Tuning and bandwidth control of laser pumped continuous dye lasers for obtaining stable single axial mode operation 20 p2571 A73-38624

Analysis of a resonant amplifier with stagger-tuned circuits at the input and output 20 p2538 A73-39466

Optimization and design of varicap-diode tuned transistor oscillators 21 p2659 A73-40009

Dye laser operation at independently tunable wavelengths via utilization of holographic wavelength selectors in succession, discussing limitations on multiple frequency tuning range 21 p2713 A73-40460

Generation of internal modes and its influence on the operation of a tunable ruby laser 21 p2714 A73-40558

Dye laser tuning with pellicles. 22 p2870 A73-42707

Some general observations on the tuning characteristics of 'electromechanically' tuned Gunn oscillators. 23 p2960 A73-44070

Increasing the locking bandwidth of a waveguide-cavity oscillator through the use of a double-tuned circuit. 23 p2965 A73-44109

Dipole antenna with variable capacitance diodes for wideband tuning, calculating and measuring input impedance frequency response 23 p2960 A73-44110

Far IR grating spectrometer using InSb detector with narrow spectral band responsivity and tunability due to cyclotron resonance absorption in magnetic field 23 p2984 A73-44364

Q switched Nd-YAG laser third harmonic for pumping dye laser, extending tunable output range to blue region 23 p2989 A73-44373

Gunn diode negative resistance microwave oscillators with simultaneous lower frequency mode and individual tunings of two frequencies 24 p3073 A73-45483

TUNNEL DIODES

Phase-frequency characteristics of a tunnel-diode regenerative frequency multiplier 01 p0026 A73-11263

Full binary adder circuit with p-n-p junction transistor loaded tunnel diode, noting 200 MHz operation rates capability 01 p0026 A73-11480

Optimal output power of tunnel drift diode oscillator in millimeter band as function of electric field and diode geometry 03 p0284 A73-14086

Superconducting tunnel junctions as phonon sources and detectors. 04 p0428 A73-15466

Stationary waves properties dependence on weak skin effect in distributed tunnel diode type of nonlinear active transmission lines 04 p0429 A73-15911

Stabilization bandwidth reduction in microwave parallel tuned tunnel diode amplifier circuits synthesis 04 p0429 A73-15919

Computerized synthesis of wideband series stabilized tunnel diode amplifier based on distributed constant elements 05 p0555 A73-16061

Influence of fluctuations on the electromagnetic properties of the Josephson tunnel junction. 06 p0733 A73-17425

Semiconductor-insulator-semiconductor /SIS/ tunneling current characteristics, noting negative resistance feature for degenerate p-i-n diode 06 p0677 A73-18359

Effects of electropolishing on the tunneling current in aluminum-aluminum-oxide-aluminum diodes. 06 p0678 A73-18744

Solid state microwave electronics technology review covering parametric amplifier, maser, tunnel and avalanche diodes, transistors, and transmission, filtering and passive signal processing techniques 08 p0942 A73-20701

Noncrystal controlled oscillator with transistor and tunnel diode, noting high frequency stability due to automatic regulation of dc operating conditions 10 p1194 A73-23735

Improved analysis of the steady-state operation of a resistive parametron 10 p1189 A73-24381

Tunnel diodes in receivers to reduce noise level and improve selectivity, discussing distortions, crosstalk and passband dependence on signal amplitude 10 p1195 A73-24385

Tunnel and Gunn diode oscillators coupled to superconducting cavity as S and X band frequency standards 10 p1195 A73-24397

Effect of the nonlinearity of the junction capacitance on the spectral characteristics of the current of a tunnel diode. 10 p1197 A73-24939

Active electromagnetic horn antenna with tunnel diode. 11 p1331 A73-26124

A tunnel diode regenerative frequency multiplier with a high multiplication factor. 13 p1591 A73-28734

Microwave tunnel diode ring counter with displaced nonlinear load line in multistage transistor driver and current switching configuration

13 p1593 A73-29120

High-speed frequency count-down circuit using a tunnel diode and a delay line.

13 p1594 A73-29226

Synthesis of a reflection-type broadband Esaki-diode amplifier using rectangular waveguide.

13 p1594 A73-29229

Tunnel diode oscillator synchronization by external harmonic force with frequency close to generator natural frequency, discussing loading effects

14 p1728 A73-30267

A tunnel diode trigger with an optical output

14 p1737 A73-30797

Phase-frequency responses of a tunnel diode regenerative frequency multiplier.

17 p2134 A73-34316

Physical and chemical analysis of germanium tunnel diodes.

17 p2219 A73-34865

Current-voltage characteristic of a real diode with a Schottky barrier, allowing for tunneling through the spatial charge region

18 p2293 A73-36718

Optimum nonlinear characteristic of the supply element in the astable multivibrator with a tunnel diode.

19 p2410 A73-38309

The optimal nonlinear characteristic of the drive element in an astable multivibrator with a tunnel diode

20 p2536 A73-39201

Synchronization of the frequency of tunnel-diode, IMPATT-diode, and Gunn-device oscillators

20 p2537 A73-39460

Tunnel diode different time constants two delay-line circuit, noting self oscillation range, constant pulse periods and hysteresis phenomenon elimination

21 p2660 A73-40099

Uses of tunnel diodes for zero-transition discrimination in phasometric devices

23 p2959 A73-43477

Zero-transition discrimination in phase-measuring devices with amplifier-limiters and tunnel diodes

23 p2959 A73-43478

Shot noise of a real Schottky-barrier diode during tunneling through the space charge region

23 p2960 A73-43619

Influence of radiation on the current-voltage characteristic of tunnel diodes /Survey/

24 p3072 A73-44926

Experimental investigation of the frequency dependence of the steady-state noise temperature of reverse-biased tunnel diodes between 0.001 and 30 MHz

24 p3072 A73-44931

Analysis of a frequency-modulated tunnel-diode oscillator.

24 p3072 A73-44941

Tunnel diode equivalent circuit analysis based on empirical expressions for composite T-V characteristics, predicting series resistance effect on switching time

24 p3073 A73-45485

Self and excited oscillations in a circuit composed of a non-linear element and a delay line.

24 p3075 A73-45487

TUNNEL RESISTORS

U ELECTRON TUNNELING

U RESISTORS

TUNNELING (EXCAVATION)

Subway system vertical tunnel simulation facility including plenum assembly, instrumentation, model launcher, subway car simulation models, tube scaffolding and data acquisition

16 p1994 A73-33148

TUNNELS

Experimental aerodynamic studies for intra-urban trains traveling in tunnels.

[AIAA PAPER 73-155]

05 p0566 A73-16903

TUPOLEY AIRCRAFT

NT TU-134 AIRCRAFT

TUPOLEY TU-134 AIRCRAFT

U TU-134 AIRCRAFT

TURBIDITY

Return of normal stratospheric turbidity and a new short dust event during October 1971.

01 p0038 A73-10374

Laser radar measurements of atmospheric backscattering turbidity.

01 p0073 A73-10403

Measurements and interpretation of the polarization of radiation emerging from the atmosphere at an altitude of 28 km over south-western New Mexico /USA/.

13 p1652 A73-28269

Reflection and transmission of a narrow beam of light in a thick turbid medium layer with isotropic scattering and absorption

13 p1609 A73-29158

TURBINE BLADES

Stress analysis and dynamic investigation of turbine blades from constrained torsion theory, calculating free torsional vibration frequencies

02 p0229 A73-11621

Model tests regarding the characteristics of the boundary layer at effusion-cooled turbine blades

[DGLR PAPER 72-059]

02 p0127 A73-11655

Optimum heat transfer characteristics of semi-circular surfaces cooled by air impingement from airjet arrays and row of air jet nozzles.

[DGLR PAPER 72-061]

02 p0237 A73-11692

Method of calculating vortex-free flow around hydrodynamic cascades composed of arbitrary profiles

02 p0128 A73-11788

Preparation of information for programming machining operations during grinding of a blade profile by the continuous-shaping method

02 p0172 A73-11799

Behavior of certain turbine-blade materials under asymmetric loading.

02 p0180 A73-12128

Plastic material turbine blades adaptability under nonsteady start-stop thermal and mechanical stress cycle conditions, noting residual stress effects

02 p0235 A73-12129

Surface roughness of turbine blades machined by circular milling

02 p0174 A73-12579

Pyrometer for measurement of surface temperature distribution on a rotating turbine blade.

02 p0171 A73-12617

Material and structural studies of metal and polymer matrix composites.

02 p0182 A73-12621

Computerized radial turbine blades thickness identification, considering temperature distribution and effects and mathematical model parameters for constraints

03 p0312 A73-13565

High pressure stage efficiency of the turbines of modern turbojets

03 p0359 A73-14137

Three dimensional dynamic characteristics of solid particles suspended by polluted air flow in a turbine stage.

[AIAA PAPER 73-140]

05 p0531 A73-16889

Inspection of fir-tree roots of gas-turbine rotor blades

05 p0578 A73-17025

Turbine blade radiation pyrometer system.

06 p0692 A73-17844

Effects of ash deposition on the fatigue strength of the working blade material in gas turbines

06 p0741 A73-18662

Investigation of the corrosion-erosion resistance of niobium alloys

06 p0711 A73-18668

Analysis of the thermal stress-strain state and cooling effectiveness of some turbine-blade designs

07 p0868 A73-20085

Investigation of the heat transfer between the gas and casing in the area of the apertures between the nozzle diaphragm blades and guide vanes of turbines

07 p0868 A73-20086

Calculation of temperature fields in cooled gas-turbine blades on a digital computer

07 p0868 A73-20099

Some methodological questions concerning the simulation of turbine blade operation on gasdynamic stands

07 p0809 A73-20509

Aerodynamic experimental investigation of annular cascade of gas turbine nozzle blade in subsonic and supersonic flow.

08 p0925 A73-20939

Prediction of aeroelastic instabilities in turbines

09 p1135 A73-22204

Method of experimental study of cascades of transonic blades with strong deflection

09 p1027 A73-22211

Thermal stresses in cooled gas turbine blade foils and roots with allowance for thermoelastic effects

09 p1136 A73-22568

A gas turbine stage with additional blades between the rotor waves

10 p1263 A73-24670

Gas turbine engine turbine blades service life increase by Cr and Al vacuum diffusion metallization, presenting full scale endurance test results

10 p1227 A73-24965

Tests concerning the production of gas turbine blades with directionally solidified structure

11 p1372 A73-25104

On the design of air-cooled radial turbine blades.

11 p1410 A73-25843

Theory on blades of axial, mixed, and radial turbomachines by inverse method.

11 p1303 A73-26340

Turbine blades cooling effectiveness for engines gas temperature energy gain compensation

12 p1532 A73-27090

Investigation of the throughput capacity of the longitudinal cooling ducts of gas turbine blades

12 p1532 A73-27093

Use of blowing during tests of blade cascades

13 p1623 A73-28469

Directionally solidified eutectic alloy composites for high temperature turbine blade and vane applications,

considering morphology, crystallography and thermal stability properties

13 p1635 A73-28777

Effect of trailing edge thickness on the cascade performance of circular-arc blades.

13 p1565 A73-29000

Influence of the variation of cascade geometry on the performance in axial flow machinery.

13 p1565 A73-29000

Potential flow about arbitrary thick blades of large camber in cascade.

13 p1565 A73-29000

Effect of solidity on rocket pump inducer performance.

13 p1624 A73-29010

Experimental studies on high speed performance of two-dimensional turbine cascades.

13 p1566 A73-29010

Fundamental study on compressible transient flow and leakage in partially admitted axial and radial flow turbines.

13 p1566 A73-29020

Methods of simulating the thermal and stress state at the edges of gas turbine blades

13 p1698 A73-29050

Metallurgical and strength studies of heat resistant alloys for gas turbines after long term service.

13 p1625 A73-29510

Creep test diagrams plotted to estimate heat resistance for turbine blades design, predicting fatigue life with allowance for loading cycle form and duration

13 p1703 A73-29610

Turbine vane vibration simulation tests with phase shift generation, using tube type phase inverters

13 p1599 A73-29630

Radio telemetry for strain measurements in turbine blades.

14 p1752 A73-30060

Providing a model of flow round a turbine blade when investigating the vibration of flat blading.

14 p1743 A73-30310

Influence of transient conditions on the overall service life of turbine blades

14 p1785 A73-30670

Three-dimensional stress-strain state of turbine blades

14 p1813 A73-30670

Critical rpm of a radial-flow turbine wheel of the closed type

14 p1814 A73-30680

Service life determination in heat-resistant alloys under unsteady working conditions with allowance for brief overloading

14 p1763 A73-30690

A method of analytical error identification in the inspection of the working profiles of blades

16 p2019 A73-33300

Calculation of temperature distribution in multistage axial gas turbine rotor assemblies when blades are uncooled.

[ASME PAPER 73-GT-8]

16 p2047 A73-33480

Prediction of flow outlet angle in blade rows with conical stream surfaces.

[ASME PAPER 73-GT-32]

16 p2048 A73-33500

Welding techniques for high strength superalloy turbine blades and vane repair, discussing controlled preheating and cooling methods for crack prevention

[ASME PAPER 73-GT-44]

16 p2019 A73-33500

The computation and utilization of Busemann's analysis of potential flow in an impeller.

[ASME PAPER 73-GT-45]

16 p1964 A73-33500

Transonic flow through a turbine stator treated as an axisymmetric problem.

[ASME PAPER 73-GT-51]

16 p1964 A73-33510

Calculation of compressible subsonic flow in cascades with varying blade height.

[ASME PAPER 73-GT-59]

16 p1964 A73-33510

Turbulence downstream of stationary and rotating cascades.

[ASME PAPER 73-GT-80]

16 p1964 A73-33520

Nondestructive inspection method for jet engine turbine blades.

[ASME PAPER 73-GT-92]

16 p2019 A73-33530

The unsteady response of a blade row from measurements of the time-mean total pressure.

[ASME PAPER 73-GT-94]

16 p1964 A73-33530

Damping properties of turbine blade materials at operational temperatures

17 p2221 A73-34320

Theoretical and experimental work on losses in 2-D turbine cascades with supersonic outlet flow.

17 p2092 A73-34370

Computerized stream-curvature method for calculation velocity distribution and stream surface twist effects for three dimensional flow through gas turbine blade passage

17 p2092 A73-34370

Secondary loss measurements in a cascade of turbine blades.

17 p2092 A73-34380

A survey and comparison of methods for predicting the profile loss of turbine blades.

17 p2093 A73-34390

Thermal control coatings for heat shielding of high-temperature high-speed chemically aggressive gas flows, noting turbine blade shielding application 18 p2371 A73-36812

Methods of modeling thermal and stressed states in the edges of gas turbine blades. 18 p2366 A73-36886

Aeronautical turbine blade and vane materials selection, considering Ni alloys with powder metallurgy and oriented solidification, composite materials and eutectics 18 p2326 A73-36993

On some problems of the method of simulating the working conditions of turbine blades on gas-dynamic benches. 19 p2418 A73-37784

Gas turbine blade effusion cooling by air blowing, determining heat transfer coefficients for laminar and turbulent boundary layer 19 p2504 A73-38156

Brazing of nickel base alloys. [SME PAPER AD 73-222] 19 p2436 A73-38494

Effect of deflector geometry on the heat transfer in the coolant passages of deflector blades. 21 p2754 A73-41322

An analytical method of designing long turbine blades 22 p2918 A73-41960

Laser Doppler instrument for measurement of vibration of moving turbine blades. 22 p2869 A73-42297

Effect of the circumferential nonuniformity of a temperature field in front of a turbine on the vibrational stresses in the turbine blades 23 p3020 A73-43740

The problem of extrapolating test data on the efficiency of turbine-blade cooling to actual conditions 23 p3020 A73-43741

Improved turbine blade attachment profiles with shoulder locks 23 p2986 A73-44291

Aircraft gas turbine engines with single crystal blades to avoid conventional casting grain boundary weakness and premature damage 24 p3094 A73-45155

Principal failures of turbines during turbine engine operation 24 p3122 A73-45196

TURBINE ENGINES

NT BRISTOL-SIDDELEY BS 53 ENGINE

NT BRISTOL-SIDDELEY VIPER ENGINE

NT GAS TURBINE ENGINES

NT J-33 ENGINE

NT J-85 ENGINE

NT JET ENGINES

NT PULSEJET ENGINES

NT RAMJET ENGINES

NT SUPERSONIC COMBUSTION RAMJET ENGINES

NT TF-30 ENGINE

NT TURBOFAN ENGINES

NT TURBOJET ENGINES

NT TURBOPROP ENGINES

Influence of acceleration on tip clearances in aircraft engine turbines and compressors 02 p0204 A73-12447

System for in-flight recording of the rotational speed of the turbine of a jet engine 07 p0828 A73-20546

Performance of an auxiliary power unit on anhydrous hydrazine. 11 p1308 A73-25980

Investigation of the aerodynamic performance of small axial turbines. [ASME PAPER 73-GT-3] 16 p1963 A73-33481

Hot isostatic pressing of titanium alloys for turbine engine components. [ASME PAPER 73-GT-63] 16 p2019 A73-33516

A current turbine engine maintenance program and the experience and logic upon which it is based. [ASME PAPER 73-GT-81] 16 p2049 A73-33526

Comparative analysis of turbine loss parameters. [ASME PAPER 73-GT-91] 16 p1964 A73-33529

A performance data acquisition and analysis system for turbine engine component testing. 17 p2146 A73-34610

The development of a turbine engine maintenance program from a new reliability model. [SAE PAPER 730374] 17 p2177 A73-34713

Hovercraft propeller and turbine engine fan blades with glass and carbon fiber reinforced plastics respectively, discussing design and constructions 17 p2103 A73-34813

Helicopter turboshaft engine vibration reduction through engine-airframe interface compatibility design and torsional stability of drive trains with automatic fuel control [AHS PREPRINT 774] 17 p2106 A73-35092

Aircraft turbine engine exhaust emissions under simulated high altitude, supersonic free-stream flight conditions. [AIAA PAPER 73-507] 17 p2223 A73-35625

Turbine engine research activity evolution, considering entry temperature increase, pollution sources

nonstationary aerodynamics and aeroelasticity in compressors, and noise problem 18 p2343 A73-36991

Turbine engine control system design based on linearized and nonlinear mathematical models accounting for thermodynamic performance 18 p2343 A73-36995

Corrosiveness of naturally occurring sulfur compounds and organic peroxides in aviation turbine fuels toward Cu and Ag, detailing maximum tolerable ratios 20 p2600 A73-39637

Application of electron beam welding to aircraft turbine engine parts. 22 p2866 A73-42196

Technological change measurement methodology for cost and production estimates with application to aircraft turbine engine development 23 p3020 A73-44219

Ram air turbine with hydraulic pitch change servo regulated speed as emergency power source for aircraft control in event of main engine failure 24 p3058 A73-45475

TURBINE EXHAUST NOZZLES

Theoretical and experimental analysis of the design and off-design performance of supersonic turbine nozzles. 17 p2093 A73-34387

Gas turbine nozzle guide vane trailing edge protection by air films cooling, measuring gas temperatures with chromel-alumel thermocouples 20 p2600 A73-39425

TURBINE PUMPS

Unsteady modes of operation of a centrifugal compressor with a vaneless diffuser 02 p0203 A73-11790

A procedure for optimum rocket engine system/turbopump integration. [AIAA PAPER 72-1183] 03 p0357 A73-13477

Linearized Kalman filtering for turbopump rotating assembly inertial and bearing parameter identification and state estimation, noting state-space model feasibility 03 p0313 A73-13904

Theoretical, quasi-steady analysis of cavitation compliance in turbopumps. 11 p1349 A73-26667

Calculation of the pumping characteristic of a turbomolecular vacuum pump 12 p1461 A73-27475

Effect of solidity on rocket pump inducer performance. 13 p1624 A73-29011

TURBINE WHEELS

Development of IN-100 powder-metallurgy disks for advanced jet engine application. 01 p0063 A73-10283

Application of the theory of linear fracture mechanics to the assessment of turbine rotor strength 02 p0229 A73-11620

Some characteristics of the passage of a circular nonuniformity zone through the working wheel grid of an axial-flow compressor 02 p0203 A73-11709

Flexible rotor balancing of a high-speed gas turbine engine. [SAE PAPER 720741] 02 p0203 A73-12007

Equations of motion for mathematical models of turbine rotors with elastic shaft in unsteady operation, calculating resonant angular velocity 04 p0514 A73-15654

Investigation of the plastic state of disks by the hardness measurement method 07 p0917 A73-20514

Some empirical relationships between creep strain, stress, time and temperature in 1Cr-Mo-V rotor forgings. 08 p0981 A73-21783

Stress concentration and groove design as factors in crack failure of low power single stage gas turbine rotor disk, using optical polarization technique 09 p1157 A73-22166

A gas turbine stage with additional blades between the rotor waves 10 p1263 A73-24670

Stability predictions with the aid of energy expressions in the case of a turborotor with gyroscopic effects 11 p1432 A73-24999

A reappraisal of design methods for inward flow radial gas turbines. 11 p1411 A73-26370

Study on material for investment cast turbine wheel. 13 p1642 A73-29518

Investigation of the structure of turbine disc materials after use. 13 p1643 A73-29632

Rotors and turbine disks fracture resistance optimization at high temperatures from plane strain toughness criteria 14 p1813 A73-30679

Rotating turbine disks ultimate strength relation to stress-strain state, material mechanical properties and plastic deformation 14 p1814 A73-30684

TURBOCOMPRESSORS

Critical rpm of a radial-flow turbine wheel of the closed type 14 p1814 A73-30685

Critical rpm of conical shells incorporated in turbine rotors 14 p1814 A73-30686

Russian book - Strength of turbine wheels. 15 p1948 A73-31578

Flow studies in radial inflow turbines interspace between nozzles and rotors. 17 p2093 A73-34392

A method of measuring three-dimensional rotating wakes behind turbomachinery rotors. 17 p2095 A73-35023

[ASME PAPER 73-FE-31] Strength of nonuniformly heated rotating disks 18 p2366 A73-36755

Plastic state of disks studied from hardness measurements. 19 p2499 A73-37789

Longitudinal-torsional vibrations of rotors 20 p2569 A73-39374

Investigation of different air-cooling methods for the first-stage disk of a two-stage gas turbine 21 p2754 A73-40397

Relationship between the hydraulic losses of a centrifugal wheel and the energy imparted by the wheel to the fluid by circulation in the relative motion 21 p2676 A73-40407

Stress concentration and groove design as factors in crack failure of low power single stage gas turbine rotor disk, using optical polarization technique 22 p2920 A73-42114

Turbine wheel strength, lifetime and safety margin calculations based on classical elasticity and plasticity theories 23 p3020 A73-44225

TURBINES

NT AXIAL FLOW TURBINES

NT GAS TURBINES

NT SHROUDED TURBINES

NT STEAM TURBINES

NT SUPERSONIC TURBINES

Aerodynamic noise and alternating loads in an idealised turbine stage. 03 p0242 A73-12981

TURBOALTERNATORS

U AC GENERATORS

U TURBOGENERATORS

TURBOCHARGERS

U SUPERCHARGERS

U TURBOCOMPRESSORS

TURBOCOMPRESSORS

Unstable operation and rotating stall in axial flow compressors. [ONERA, TP NO. 1090] 01 p0001 A73-10228

Behaviour of boundary layers on plane or annular fixed or mobile supersonic blade cascades [ONERA, TP NO. 1110] 01 p0001 A73-10232

Device signaling unsteady modes of compressor operation 02 p0166 A73-11635

Some characteristics of the passage of a circular nonuniformity zone through the working wheel grid of an axial-flow compressor 02 p0203 A73-11709

Some experiences in the scaling of the NASA 8-stage transonic axial flow compressor. [SAE PAPER 720711] 02 p0203 A73-12008

Design and development of a small highly loaded, two-stage, transonic axial compressor. [SAE PAPER 720712] 02 p0203 A73-12009

Design and test of a small, high-pressure ratio, axial compressor with tandem and swept stators. [SAE PAPER 720713] 02 p0203 A73-12010

Influence of acceleration on tip clearances in aircraft engine turbines and compressors 02 p0204 A73-12447

Radiation properties of propeller and helicopter /free field/ rotors and fans and gas turbine compressors /ducted rotors/ 02 p0131 A73-12611

Peripheral turbocompressors for high pressure rise with small mass flow rate, discussing operational principles, design and performance 02 p0175 A73-12793

Inlet sound power of axial compressors. 03 p0241 A73-12956

Inlet flow distortion induced axial flow compressor stall, converting stagnation pressure and temperature maps into vorticity maps via Crocco theorem [AIAA PAPER 72-1116] 03 p0243 A73-13431

A discussion of the Marsh matrix technique applied to fluid flow problems. 03 p0244 A73-13563

An axial-flow compressor for an air-cushion vehicle 03 p0358 A73-13724

Study of the waves configuration in an axial-flow supersonic compressor [ONERA, TP NO. 1104] 03 p0246 A73-14135

Some recent work on aspect ratio effects in compressor cascades. [SAE PAPER 72-WA/FE-41] 04 p0404 A73-15858

Gas velocity measurements within a compressor rotor passage using the laser Doppler velocimeter. [ASME PAPER 72-WA/GT-2] 04 p0451 A73-15866

TURBOCONVERTERS

- A combined theoretical and empirical method of axial compressor cascade prediction.
[ASME PAPER 72-WA/GT-5] 04 p0404 A73-15869
- A description of two low cost turbo-compressors built for powered lift research.
07 p0867 A73-19942
- Influence of regulated unequal guide-vane spacing on the alternating stress level in the working blades of a compressor
09 p1157 A73-22165
- Graphoanalytic method of calculating plane potential flows
09 p1029 A73-23106
- Piston engine turbocharging system based on split low and high pressure exhaust gas discharge porting, discussing different turbine staging arrangements
10 p1263 A73-24925
- Researches on the two-dimensional retarded cascade. III - Cascade performances at high inlet angles.
11 p1302 A73-26338
- Researches on the two-dimensional retarded cascade. IV - Determination of blade elements at retarded blade row.
11 p1302 A73-26339
- Theory on blades of axial, mixed, and radial turbomachines by inverse method.
11 p1303 A73-26340
- Unstable operation and rotating stall in axial flow compressors.
13 p1566 A73-29024
- Generalized relations for the parameters at the flow separation boundary in compressor cascades
13 p1567 A73-29551
- Axial and radial turbocompressor analysis and design, presenting literature survey on cascade aerodynamics, iterative and hodograph computational methods, etc
14 p1712 A73-30429
- A method for complex design of axial-flow compressor stages at the mean streamline
15 p1925 A73-32203
- Acoustic generation and propagation in annular ducts of axial flow fans, discussing techniques for in-duct fan noise modal distribution measurement
16 p1999 A73-32846
- Small turbomachinery compressor and fan aerodynamics.
[ASME PAPER 73-GT-6] 16 p2047 A73-33484
- Interface effects between a moving supersonic blade cascade and a downstream diffuser cascade.
[ASME PAPER 73-GT-23] 16 p1964 A73-33497
- Upstream attenuation and quasi-steady rotor lift fluctuations in asymmetric flows in axial compressors.
[ASME PAPER 73-GT-30] 16 p2048 A73-33501
- Remanufacture of jet engine compressor components.
[ASME PAPER 73-GT-43] 16 p2048 A73-33504
- Experimental evaluation of the effects of a blunt leading edge on the performance of a transonic rotor.
[ASME PAPER 73-GT-60] 16 p1964 A73-33515
- Pressure measurements on the rotating blades of an axial-flow compressor.
[ASME PAPER 73-GT-79] 16 p2049 A73-33524
- Conditions of rotating stall suppression in axial compressors
16 p2049 A73-33964
- Effect of 'bulk' heat transfers in aircraft gas turbines on compressor surge margins.
17 p2221 A73-34382
- Low-speed performance of a compressor cascade designed for prescribed velocity distribution and tested with variable axial velocity ratio.
17 p2093 A73-34393
- The effect of heat transfer on boundary layer stability in axial flow compressors.
17 p2093 A73-34394
- Turbine engine research activity evolution, considering entry temperature increase, pollution sources nonstationary aerodynamics and aeroelasticity in compressors, and noise problem
18 p2343 A73-36991
- High performance supersonic axial and centrifugal compressors theoretical and experimental research, assessing and forecasting technological developments
18 p2343 A73-36992
- Recent studies of fan noise generation and reduction.
19 p2473 A73-37293
- Blade synchronous rotation about pitch axis in single stage axial compressor at front of gas turbine engine during fan rotation
20 p2601 A73-39663
- Trimming and checking aircraft gas-turbine engines with the aid of the ratio of total pressure behind the turbine to total pressure in front of the compressor
21 p2754 A73-40403
- A method of complex design of the meridional form of the air flow path of a multistage axial-flow compressor
21 p2633 A73-40477
- Effect of an adjustable nonuniform pitch in the distributor on the alternating stresses in compressor rotor blades.
22 p2919 A73-42113

Real gas turbocompressor calculations based on equations of state for fundamental thermodynamic processes in ideal gas
22 p2797 A73-42645

Calculation of the maximum attainable efficiency of a moving compressor blade cascade
22 p2797 A73-42646

Total pressure loss distribution in viscous gas flow through annular cascades of axial flow compressors, examining three dimensional flow effects on boundary layer development
24 p3054 A73-44916

TURBOGENERATORS

TURBOELECTRIC CONVERSION

TURBOGENERATORS

TURBOFAN AIRCRAFT

- NT A-7 AIRCRAFT
NT BOEING 727 AIRCRAFT
NT BOEING 737 AIRCRAFT
NT C-141 AIRCRAFT
NT CONCORDE AIRCRAFT
NT DO-31 AIRCRAFT
NT F-111 AIRCRAFT
NT IL-62 AIRCRAFT
NT TU-134 AIRCRAFT

STOL jet aircraft with variable pitch fan, discussing engine handling, noise reduction and efficiency
16 p2046 A73-33189

Maximum air transportation service with minimum community noise.
[AIAA PAPER 73-796] 19 p2388 A73-38369

TURBOFAN ENGINES

- NT BRISTOL-SIDDELEY BS 53 ENGINE
NT TF-30 ENGINE
NT TF-34 ENGINE

Pegasus vectored thrust turbofan engine for Harrier class VISTOL aircraft, describing design and operational details
01 p0090 A73-10200

A rapid matching procedure for twin-spool turbopumps.
02 p0202 A73-11593

An altitude test facility for large turbofan engines.
[AIAA PAPER 72-1069] 03 p0287 A73-13396

Prediction of inlet duct overpressures resulting from engine surge.
[AIAA PAPER 72-1142] 03 p0243 A73-13448

Gearing fan engine systems - Their advantages and potential reliability.
[AIAA PAPER 72-1173] 03 p0357 A73-13469

The application of adhesive bonded structures and composite materials on advanced turbofan engines.
03 p0359 A73-14134

Noise sources analysis for high and low bypass ratio turbofan engines, considering jet, compressor, fan and turbine sound generation mechanisms
03 p0359 A73-14138

Estimation of engine emissions at altitude through ground testing.
04 p0485 A73-14892

The evolution and development status of the ALF 502 turbofan engine.
[SAE PAPER 720840] 05 p0607 A73-16654

TF34 and F101 turbofan engines for Navy S-3A ASW aircraft and USAF B-1 strategic bomber, respectively, discussing design features, manufacturing techniques and testing procedures
[SAE PAPER 720841] 05 p0607 A73-16655

F100/F401 augmented turbofan engines - High thrust-to-weight propulsion systems.
[SAE PAPER 720842] 05 p0607 A73-16657

Volvo RM8 turbofan engine for Viggen fighter and ground attack aircraft, emphasizing low fuel consumption for long range cruise and high thrust/weight ratio
05 p0608 A73-17099

Engine noise reduction by fan blade tip speed reduction and high lift coefficient operation, presenting full scale test results
06 p0740 A73-17571

Results of an experimental program for the development of sonic inlets for turbofan engines.
[AIAA PAPER 73-222] 06 p0645 A73-17664

TF-34 turbofan engines for S-3A and AX aircraft respectively, discussing technological development, and components and characteristic features
07 p0688 A73-20350

Variable-pitch fans - Progress in Britain.
14 p1785 A73-29770

Variable-pitch fans - Hamilton Standard and the Q-fan.
14 p1785 A73-29771

Multibladed shrouded fan /Q-fan/ with rotary or piston engines as propulsion system for light/medium business aircraft, noting noise and drag reduction
14 p1785 A73-29996

Inlet duct sonic fatigue induced by the multiple pure tones of a high bypass ratio turbofan.
16 p2046 A73-33141

High bypass fan engines for quiet propulsion and optimal aircraft performance in military and commercial applications
16 p2046 A73-33190

Control of turbofan lift engines for VTOL aircraft.
[ASME PAPER 73-GT-20] 16 p2047 A73-33496

Aerodynamic study of a turbine designed for a small low-cost turbofan engine.
[ASME PAPER 73-GT-29] 16 p2048 A73-33505

High bypass ratio quiet turbofan engine for STOL aircraft, emphasizing noise reducing design based on low-speed variable pitch fan concept
16 p2049 A73-34040

Progress in the development of optimally quiet turbofan engines and installations.
[SAE PAPER 730287] 17 p2221 A73-34040

'Quiet' aspects of the Pratt & Whitney Aircraft JT15D turbofan.
[SAE PAPER 730289] 17 p2101 A73-34040

Variable pitch turbofan driven at constant speed through reduction gear to obtain cost-efficiency compromise for future STOL and business aircraft applications
18 p2343 A73-36995

Jet engine noise reduction technology and design: discussing sonic pressure probes, high bypass turbofan engines, noise source fluctuations and far field measurements
19 p2472 A73-37282

Aircraft engine fan noise radiation from inlet and discharge ducts, describing wind tunnel tests and noise spectra at various blade tip speeds
19 p2472 A73-37282

Effect of spanwise circulation on compressor noise generation.
19 p2473 A73-37282

Recent studies of fan noise generation and reduction.
19 p2473 A73-37282

Aircraft installation requirements and considerations for variable pitch fan engines.
[AIAA PAPER 73-807] 19 p2379 A73-37444

Noise from turbomachinery.
[AIAA PAPER 73-815] 19 p2473 A73-37444

Turbofan suction noise level measurements: discussing octave noise analysis, angular velocity distributions, discharge coefficient, takeoff and landing operations
19 p2473 A73-37800

RB-211 turbofan engine development, in-service problems and modifications for performance improvement
20 p2600 A73-39664

Rolls-Royce RB-211 jet engine noise reduction program, considering fan, compressor, turbine and tail pipe noise and acoustic linings and powerplant configurations
22 p2900 A73-41770

The influence of aerodynamic flow noise in turbofan engines.
[AIAA PAPER 73-1016] 24 p3121 A73-44880

Multiple pure tone noise generation and control.
[AIAA PAPER 73-1021] 24 p3122 A73-44880

Inlet geometry and axial Mach number effects on fan noise propagation.
[AIAA PAPER 73-1022] 24 p3122 A73-44880

Turbofan engine core noise prediction and measurement, considering sources from flow passage obstructions, combustion chamber and turbine noise due to interaction with upstream turbulence
[AIAA PAPER 73-1026] 24 p3122 A73-44880

Progress in source noise suppression of subsonic speed fans.
[AIAA PAPER 73-1032] 24 p3122 A73-44880

TURBOFANS
High-pressure axial fan for air-cushion vehicles
02 p0203 A73-11770

Variable pitch fan experimental design for quiet STOL propulsion, testing blade designs for aerodynamic and acoustic performance
03 p0359 A73-14134

Variable-pitch fans - Hamilton Standard and the Q-fan.
14 p1785 A73-29770

Small turbomachinery compressor and fan aerodynamics.
[ASME PAPER 73-GT-6] 16 p2047 A73-33484

New low-pressure-ratio fans for quiet business aircraft propulsion.
[SAE PAPER 730288] 17 p2221 A73-34040

Noise reduction modifications in JT3D and JTF gas turbine engine by single stage fan replacements
[SAE PAPER 730346] 17 p2222 A73-34040

Calculated leading-edge bluntness effect on transonic compressor noise.
[AIAA PAPER 73-633] 18 p2260 A73-36100

Design method of the axial-flow blade row: modified isolated aerofoil theory with interference coefficient. II - The influence of the aerodynamic parameter on the fan performance at low flow rate.
19 p2377 A73-37600

Turbofan suction noise level measurements: discussing octave noise analysis, angular velocity distributions, discharge coefficient, takeoff and landing operations
19 p2473 A73-37800

Design of axial flow fans by cascade method.
21 p2631 A73-40100

Noise comparisons from full-scale fan tests
NASA Lewis Research Center.
[AIAA PAPER 73-1017] 24 p3121 A73-44880

Broadband noise generation by aerofoils and axial flow fans.
[AIAA PAPER 73-1018] 24 p3054 A73-44850

TURBOGENERATORS
Calculation of the deflections of fast-rotating rotors on elastic-damping supports with allowance for unilateral electromagnetic attraction forces
07 p0779 A73-20084
3000 hour endurance test of a 6 kWe organic Rankine cycle power system.
09 p1034 A73-22769
Summary of gas bearing applications in the field of space electric power systems.
09 p1089 A73-22771
Parallel operation of two Brayton-cycle alternators with parasitic speed controllers.
09 p1035 A73-22773
Space shuttle orbiter electrical power system requirements and constraints, considering hydrogen/oxygen fuel cell for compact energy storage and turbine driven generators
09 p1153 A73-22776
Open cycle hydrogen-oxygen turbine driven generator system for space shuttle auxiliary power supply, discussing components, control mode and performance potential
09 p1153 A73-22779
Concepts for application of 500- to 2500-Wa Brayton power systems for shuttle-launched missions.
09 p1154 A73-22794
Ram air turbines for aircraft emergency power supply, discussing design, performance and control
10 p1177 A73-23525
The optimization of nuclear reactor energy supply installations with turbogenerators
11 p1395 A73-25352
Brayton cycle solar dynamic turboalternator space electric power system technology developments during 1962-1972, considering power efficiency, components reliability and future missions
11 p1309 A73-25982
A power and load priority control concept as applied to a Brayton cycle turbo-electric generator.
11 p1309 A73-25984
Space shuttle orbiter power system requirements and design tradeoffs, comparing fuel cells, solar array/battery and radioisotope Brayton cycle and cryogenic fueled turboalternators
11 p1312 A73-26017
Isotope organic Rankine cycle electric power systems for the 150 to 1500 watt range.
19 p2456 A73-38414

TURBOJET AIRCRAFT
UJET AIRCRAFT
TURBOJET ENGINE CONTROL
Suction force suppression during takeoff, landing and transition of VTOL turbojet via wing turning wing about axis parallel to earth plane
02 p0129 A73-11631
Investigation of damping methods for low frequency augmentor combustion instability.
[AIAA PAPER 72-1207] 03 p0358 A73-13490
Potential operating advantages of a variable area turbine turbojet.
[ASME PAPER 72-WA/AERO-4] 04 p0490 A73-15906
An all-regime optimal speed control for a single-shaft jet engine
06 p0741 A73-17721
Control and stability analysis of supersonic aircraft jet engines with afterburner for improved low altitude operation
06 p0741 A73-17722
Influence of the turbine air cooling system on the characteristics of a turbojet engine during regulation of the latter
12 p1532 A73-27091

TURBOJET ENGINES
NT BRISTOL-SIDDELEY BS 53 ENGINE
NT BRISTOL-SIDDELEY VIPER ENGINE
NT J-33 ENGINE
NT J-85 ENGINE
NT TF-30 ENGINE
NT TURBOFAN ENGINES
NT TURBOPROP ENGINES
Experimental verification of a digital computer simulation method for predicting gas turbine dynamic behaviour.
02 p0204 A73-12647
Electric generator inside turbojet or turbofan aircraft engine to reduce need for external gearbox, simplifying nacelle assembly and increasing aircraft design flexibility
[AIAA PAPER 72-1056] 03 p0252 A73-13387
Implementing the design of airplane engine exhaust systems.
[AIAA PAPER 72-1112] 03 p0355 A73-13427
Vibrational and chemical nonequilibrium in a stoichiometric turbojet engine using kerosene-type fuel.
[AIAA PAPER 72-1208] 03 p0273 A73-13491
Development of the Olympus turbojet to meet supersonic civil transport requirements.
03 p0359 A73-14131

High pressure stage efficiency of the turbines of modern turbojets
03 p0359 A73-14137
Modeling of nonlinear systems for the example of a single-shaft jet turbine engine
03 p0360 A73-14615
Turbojet exhaust reactions in stratospheric flight.
[AIAA PAPER 73-99] 05 p0608 A73-16859
Analysis of the operational parameters of a bypass turbojet
12 p1532 A73-27069
Concorde Olympus 593 axial flow turbojet engine design, detailing variable geometry intake and exhaust nozzles, noise abatement, combustion chamber, gearing and fuel system
13 p1669 A73-28156
German monograph on bypass turbojet propulsion systems with jet mixing covering engine parts, thrust characteristics and fuel consumption
14 p1785 A73-30671
Sand erosion tests and protective coatings for aircraft jet and turbojet engines and helicopter compressor airfoils
16 p2046 A73-33029
Remanufacture of jet engine compressor components.
[ASME PAPER 73-GT-43] 16 p2048 A73-33504
Navy development of low-cost supersonic turbojet engines.
[SAE PAPER 730362] 17 p2222 A73-34708
Turbine powerplants for missiles - Cost improvement requirements.
[SAE PAPER 730364] 17 p2222 A73-34709
Russian book - Aerodynamics and flight dynamics of turbojet aircraft /2nd revised and enlarged edition/.
17 p2104 A73-34900
Reliability of aircraft turbojet bearings
18 p2320 A73-36691
Subsonic aircraft turbojet engines, discussing thermodynamic cycles, entry temperature increase, propulsion efficiency and economy improvements and ecological requirements
18 p2343 A73-36994
The effect of afterburning on the emission of pollutants by turbojets
18 p2343 A73-36996
Nitrogen oxide turbojet emissions minimization with hydrogen compared to kerosene /JP/ fuels due to flammability limits, burning velocity and introduction in combustor as gas
19 p2473 A73-37498
Vibrations of turbojet-engine components containing structural dampers of the type of sandwich rods
23 p3020 A73-43735

TURBOMACHINE BLADES
NT COMPRESSOR BLADES
NT ROTOR BLADES [TURBOMACHINERY]
NT STATOR BLADES
NT TURBINE BLADES
Simulation of the flow past turbomachine blades in the study of plane-cascade vibrations
01 p0029 A73-10494
Free three-dimensional vibration processing of gas-turbine engine blades
02 p0172 A73-11723
Problems regarding the use of electronic data processing for the calculation of diagonal cascades in turbomachines
03 p0242 A73-13169
An automated jet-engine-blade inspection system.
03 p0312 A73-13524
Effect of wake-wake interactions on the generation of noise in axial-flow turbomachinery.
03 p0246 A73-14129
Practical application of boundary layer theory to flow and heat transfer problems in turbomachines.
03 p0398 A73-14145
Axial flow turbomachines annulus wall boundary layer growth calculation methods, deriving momentum integral equations from passage averaged equations of motion through cascaded blades
03 p0249 A73-14645
Russian book on aerodynamic design of axial flow turbomachine blades covering direct and inverse problems for axisymmetric flow in axial turbomachines
04 p0404 A73-15709
Quasi-three-dimensional calculation of velocities in turbomachine blade rows.
[ASME PAPER 72-WA/GT-7] 04 p0490 A73-15871
The effect of the degree of turbulence on the aerodynamic characteristics of planar decelerating cascades
[DFVLR-SONDDR-275] 07 p0773 A73-19197
Compressibility effects on unsteady forces generated by jet engine blade rows aerodynamic interference, considering potential flow and viscous wake interactions
09 p1029 A73-23443
Flow through moving cascades of lifting lines with fluctuating lift.
10 p1171 A73-23697

Transonic gas flow in rotating turbomachine cascade channels, reducing flow equations to second order differential equation
10 p1172 A73-24507
Graphic-interactive analysis of the velocity field around blade cascades for turbomachines
12 p1458 A73-27387
Design method of the axial-flow blade row on modified isolated aerofoil theory with interference coefficient, I.
13 p1564 A73-28649
Secondary flow in blade cascades of axial turbomachines and the possibility of reducing its unfavourable effects.
13 p1565 A73-29008
A comparison between potential flow studies through blade cascade by theoretical and rheo-electric analogy methods.
13 p1565 A73-29010
Experimental study by resonance method of unsteady aerodynamic forces acting on cascading blades.
13 p1566 A73-29028
Numerical representation of inlet and exit boundary conditions in transient cascade flow.
[ASME PAPER 73-GT-55] 16 p2048 A73-33511
The correlation between the kinematic structure of the flow and the energy transfer in the rotors of fluid flow machines
18 p2299 A73-36487
Calculation of plane blade cascades in isentropic flow
18 p2266 A73-37085
An aeroelastic whirl phenomenon in turbomachinery rotors.
[ASME PAPER 73-DET-97] 22 p2900 A73-42076

TURBOMACHINERY
NT AXIAL FLOW TURBINES
NT CENTRIFUGAL COMPRESSORS
NT CENTRIFUGAL PUMPS
NT GAS TURBINES
NT J-33 ENGINE
NT SHROUDED TURBINES
NT STEAM TURBINES
NT SUPERSONIC TURBINES
NT TURBINE PUMPS
NT TURBINES
NT TURBOCOMPRESSORS
NT TURBOFANS
NT TURBOGENERATORS
Total-pressure averaging in pulsating flows.
02 p0171 A73-12618
Optimal stabilization conditions of turboreactor combustor initial recirculation zone determined by hydraulic analogy technique, describing vorticity generation and mass flow rates
[ONERA, TP NO. 1105] 03 p0359 A73-14126
Turbomachinery design for Space Shuttle auxiliary power systems.
[SAE PAPER 720835] 05 p0537 A73-16633
Probability theory for vibrational strength of turbomachine parts, calculating statistical maximum stress for given stress distribution conditions
07 p0917 A73-20502
Inlet air flow distortion in high hub/tip ratio mixed flow turbomachines, using modified actuator disc theory
08 p0925 A73-20784
Secondary flows - Theory, experiment, and application in turbomachinery aerodynamics.
10 p1171 A73-23860
Fluid machinery and fluidics; Proceedings of the Second International Symposium, Tokyo, Japan, September 4-9, 1972. Volumes 1 & 2 - Fluid machinery. Volume 3 - Fluidics. Volume 4 - General lectures, discussions, events.
13 p1602 A73-29004
Two dimensional steady subsonic flow through airfoil cascades, predicting turbomachine performance from boundary layer calculation for comparison with experiments
13 p1565 A73-29005
The use of averaged flow equations of motion in turbomachinery aerodynamics.
13 p1603 A73-29047
Effect of radial total pressure gradients on the Mach number distribution in turbomachines
13 p1567 A73-29450
Plane unsteady irrotational flow of ideal incompressible fluid through turbomachine stage due to interaction between stationary and moving grids
16 p2001 A73-34015
Study of incidence loss models in radial and mixed-flow turbomachinery.
17 p2092 A73-34384
General solution to the subsonic through-flow problem in a turbomachine including losses.
17 p2092 A73-34385
Viscous flow in radial turbomachine blade passages.
17 p2093 A73-34389
Total pressure tube measurements in turbomachine-simulating pulsating nozzle flow generator supplemented by pneumatic tube probes for averaging error comparison
17 p2166 A73-34608

- A method of measuring three-dimensional rotating wakes behind turbomachinery rotors.
[ASME PAPER 73-FE-31] 17 p2095 A73-35023
- Unsteady aerodynamic forces in transonic turbomachines 18 p2266 A73-37084
- Problems of minimum-weight turbomachine rotor designs 18 p2367 A73-37140
- Probability theory for vibrational strength of turbomachine parts, calculating statistical maximum stress for given stress distribution conditions 19 p2499 A73-37777
- Russian book on turbomachinery using compressible and incompressible working fluids covering gas and fluid flow equations, energy losses in axial and radial flow stages, etc 21 p2633 A73-40807
- Classification of methods for solving the direct problem of axisymmetric flow calculation in turboengines 23 p3020 A73-43736

TURBOPROP AIRCRAFT

- NT AN-24 AIRCRAFT
NT C-130 AIRCRAFT
NT CL-84 AIRCRAFT
NT DHC 5 AIRCRAFT
- Arava STOL turboprop passenger aircraft flutter flight test program, describing measurement instrumentation and data recording system 09 p1031 A73-22185
- The C-401, a STOL transport for many applications 17 p2107 A73-35666
- DHC-7 four engine turboprop transport aircraft, emphasizing quietness and STOL capability 18 p2266 A73-36067

TURBOPROP ENGINES

- Progress in the development of optimally quiet turboprop engines and installations.
[SAE PAPER 730287] 17 p2221 A73-34652
- Noise generation by turbulent combustion, discussing sound power, spectral content, enclosure effect, and importance in turbopropulsion system core engine noise
[AIAA PAPER 73-1023] 24 p3155 A73-44855

TURBOPUMPS

- U TURBINE PUMPS
TURBOROCKET ENGINES
- Technology applied to the Space Shuttle Main Engine.
[AIAA PAPER 73-60] 06 p0741 A73-17633

TURBOROTORS

- U TURBINE WHEELS
TURBOshafts
- Influence of a change in the throughput of the power turbine on the parameters of a dual-shaft gas turbine engine 10 p1262 A73-23599
- Turboshaft engine for 5-8 passenger single and twin engine commercial helicopter, discussing cost reduction design emphasis, gearbox module and particle separator 17 p2220 A73-34253

TURBOSUPERCHARGERS

- U SUPERCHARGERS
U TURBOCOMPRESSORS

TURBULENCE

- NT ATMOSPHERIC TURBULENCE
NT CLEAR AIR TURBULENCE
NT GUSTS
NT HOMOGENEOUS TURBULENCE
NT ISOTROPIC TURBULENCE
NT LOW LEVEL TURBULENCE
NT LOW TURBULENCE
NT MAGNETOHYDRODYNAMIC TURBULENCE
NT PLASMA TURBULENCE
- Low order models representing realizations of turbulence. 01 p0032 A73-10450
- Boundary layer transition on cones in hypersonic He wind tunnel tests, obtaining turbulent spot geometry and propagation velocity by spark schlieren photography 01 p0003 A73-10762
- Test field model for nonstationary inhomogeneous turbulence with mean shearing velocity 04 p0434 A73-15164
- Primordial turbulence and the formation of galaxies. 04 p0499 A73-15354
- Symmetry properties of the collision integral and nonisotropic steady-state solutions in the theory of weak turbulence 10 p1207 A73-24759
- Determination of damping constants and turbulent speed in the solar photosphere by the Voigt method 15 p1938 A73-31958
- On galaxy formation from primeval universal turbulence. II. 20 p2609 A73-39572
- Damping constants and turbulence velocities in the solar photosphere determined by the Voigt method. 24 p3132 A73-44483

TURBULENCE EFFECTS

- Correlation and structure functions for pulse propagation in a turbulent atmosphere. 01 p0016 A73-10195
- Displacements of spatially bounded light beams in a turbulent medium using the approximation of a random Markov process 01 p0076 A73-10214
- Analytical method of gasdynamic semibounded-space parameter computation allowing for velocity profile inhomogeneity and turbulent combustion of condensed systems 01 p0121 A73-10619
- Turbulent flame velocities in premixed sprays. I - Experimental study. 01 p0121 A73-10635
- On turbulent flows with fast chemical reactions. I - The closure problem. 01 p0032 A73-10637
- Beam spread of laser light propagating through the atmosphere. 01 p0060 A73-11056
- Reynolds stresses and turbulent kinetic energy production in wall jets on flat and concave walls 01 p0034 A73-11357
- The kinematical behaviour of the plasma tail of Comet Tago-Sato-Kosaka 1969 IX. 02 p0221 A73-12704
- Free stream turbulence effect on flat plate boundary layer turbulent behavior, considering Reynolds stress dependence on turbulence intensity 03 p0292 A73-13170
- Unsteady laminar natural and forced convection at transparent medium boundary layer radiating surface, noting turbulence effects on heat exchange 03 p0397 A73-13187
- Application of the turbulent eddy diffusivity transport equation to the analysis of turbulent flow in the radial face seal. 03 p0293 A73-13315
- Turbulent flow velocity pulsations damping in wind tunnel chamber by wire grids, calculating grid turbulence effect 03 p0245 A73-13670
- Acoustic-Doppler-radar scattering equation and general solution. 03 p0276 A73-13830
- Application of the spatial spectral power density to the calculation of resolution limits. 03 p0277 A73-13916
- Turbulence effect on wall pressure fluctuations. 04 p0403 A73-14939
- Galaxy formation from amihilation-generated super-sonic turbulence in the baryon-symmetric big-bang cosmology and the gamma-ray background spectrum. 04 p0499 A73-15353
- Influences of free stream turbulence on mean velocities of turbulent boundary layer without pressure gradient. 04 p0435 A73-15972
- Beam trajectory distortions due to turbulent air refractive index fluctuations in optical waveguides 05 p0551 A73-16785
- Analysis of flight vehicle response to nonstationary atmospheric turbulence including wing bending flexibility. 05 p0535 A73-16921
- He 3 burning burst complication of mixing in solar core for solar luminosity variations resulting from central temperature decrease 05 p0611 A73-17187
- Protoplanet formation models with floccule accumulation, discussing momentum considerations and supersonically turbulent collapsing gas cloud 05 p0625 A73-17318
- Distortion of near-sonic shocks by layers with weak thermal fluctuations. 05 p0537 A73-17374
- A new approach to the problem of wave fluctuations in localized smoothly varying turbulence. 06 p0665 A73-18183
- Limited cavitation and the related scale effects problem. 06 p0686 A73-18435
- Stochastic ion heating by ion-acoustic turbulence. 06 p0733 A73-18850
- The effect of the degree of turbulence on the aerodynamic characteristics of planar decelerating cascades [DFVLR-SONDDR-275] 07 p0773 A73-19197
- Optical beam spread in a turbulent medium - Effect of the outer scale of turbulence. 07 p0851 A73-19274
- Wave propagation in a stratified turbulent magnetized plasma. II. 07 p0858 A73-19534
- Origin of magnetic fields in the early universe. 07 p0877 A73-19607
- Electrostatic turbulence at colliding plasma streams as the source of ion heating in the solar wind. 08 p0997 A73-20886
- The energy spectrum of small-scale solar magnetic fields. 08 p1003 A73-20888

Atmospheric turbulence effects on laser beam transmitted signals, considering filtering and detection based on doubly stochastic Poisson process 09 p1067 A73-22228

A differential method for the prediction of the effects of atmospheric boundary layer turbulence using the turbulence kinetic energy equation. 09 p1071 A73-22288

Remote sensing of the turbulence characteristics of a planetary atmosphere by radio occultation of a space probe. 09 p1146 A73-22428

Measurement of log-irradiance fluctuation of He-Ne laser in the atmosphere. 09 p1096 A73-22737

Number of gust series in turbulent velocity pulsations 09 p1115 A73-22949

Influence of ionizational turbulence on the operation of an MHD generator with nonequilibrium plasma 10 p1253 A73-23533

Fluid film lubrication fluid mechanical theory, considering non-Newtonian fluids, turbulence, inertia and elastohydrodynamic effects in various bearing types. 10 p1223 A73-23859

Depolarization of laser radiation in an optical channel 10 p1229 A73-24616

Turbulent loss mechanism of ring current protons in plasmapause vicinity via electrostatic drift cyclotron loss cone waves 10 p1270 A73-24747

Statistical velocity and temperature characteristics of turbulent electron beams in crossed HF electric and magnetic fields, comparing with Brillouin flow 10 p1258 A73-24888

On the application of Cramer's theorem to axisymmetric, incompressible turbulence. 10 p1284 A73-24909

Electrostatic turbulence parametric excitation by electric field with frequency near plasma frequency, accounting for saturation electric field in anomalous plasma heating via electron trapping theory 11 p1403 A73-25258

Correlation of the shift in the center of gravity of focused light beam in a turbulent atmosphere 11 p1331 A73-26166

Theory of sound scattering by turbulence applied to scattering cross section calculation for turbulent jet flow and wind, discussing jet noise reduction 11 p1349 A73-26449

Lossless Fourier transform holography with mutual coherent reference source close to object, investigating atmospheric turbulence effects on wavefront reconstructed image quality 11 p1370 A73-26536

Investigation of the influence of temperature and velocity fields on the quality of an astronomical image 12 p1546 A73-27869

Solar rotational and vibrational temperature based on turbulent velocity determined from CN molecular line profiles half widths 12 p1547 A73-27874

Diffuser static pressure recovery coefficient for varying turbulence intensity at inlet, considering performance correlation with geometrical and/or velocity profile parameters 12 p1488 A73-27976

Scintillation and vibration of stars and structure of a turbulent atmosphere. 13 p1680 A73-28516

An attempt to characterize the 'turbulence burst phenomena' using digital time series analysis. 13 p1604 A73-29245

Angle-of-arrival difference spectrum of a simple interferometer in turbulent air. 13 p1621 A73-29378

Turbulence dissipation model for galactic origin, accounting for masses and angular momenta of large galaxies 14 p1796 A73-30000

On the influence of inertia forces in hydrostatic turbulent lubrication. 14 p1755 A73-30709

Short-term average optical-beam spread in a turbulent medium. 15 p1913 A73-31010

Calibration of turbulence and visual and photographic scintillation parameters in Pulkovo, Tashkent and Shternberg Institute astroclimate systems for 2 inch reflector 15 p1934 A73-31424

Random/turbulent/ excitation of flutter in wind tunnel dynamic models and flight test aircraft, comparing prediction and damping measurement results [ONERA, TP NO. 1234] 15 p1830 A73-31633

Stochastic heating of a plasma during development of a Langmuir turbulence instability 15 p1918 A73-31707

Earth magnetosphere ion acoustic turbulence generation by longitudinal currents and electric fields relating turbulence induced current dissipation plasma heating 15 p1872 A73-31898

Multiple scattering of sound by turbulence and other inhomogeneities.

15 p1865 A73-32151

On the possibility of turbulent thickening of weak shock waves.

16 p1967 A73-32794

Criteria regarding the predetermination of the laminar-turbulent boundary layer transition in the case of flows about body contours

16 p1965 A73-33750

Generalized random forces in time domain for rectangular panels under subsonic and supersonic boundary layer turbulence, investigating probabilistic nature by Monte Carlo method

17 p2241 A73-34182

Magnetohydrodynamics, hydrodynamics and dynamics of solar system model as contracting rotating cloud, discussing effects of turbulence

17 p2226 A73-34403

Mass transport rate in solar nebula model due to turbulence induced by convection

17 p2229 A73-34432

Holography of large objects in a turbulent atmosphere with a CW laser.

17 p2167 A73-34896

Effect of ionization turbulence on the operation of an MHD generator operating with a nonequilibrium plasma.

17 p2217 A73-35182

Feedback control configured vehicles ride control system design for B-52 aircraft load alleviation and mode stabilization during flight through atmospheric turbulence

17 p2107 A73-35245

Turbulent lubrication - Its genesis and role in modern design.

[ASME PAPER 73-LUBS-19] 17 p2181 A73-35398

Slant-path scintillation in the planetary boundary layer.

17 p2185 A73-35417

Analysis of multiwavelength observations of optical scintillation.

17 p2212 A73-35418

Interaction between high-frequency turbulence and magnetospheric micropulsations.

18 p2352 A73-36277

Response of a rigid aircraft to nonstationary atmospheric turbulence.

18 p2267 A73-36305

Hot gaseous jet noise emission calculation for dependence on turbulent flow characteristics based on Lighthill theory, using computer program

18 p2343 A73-36997

Atmospheric turbulence effects on CW carbon dioxide laser propagation, investigating thermal blooming via theoretical diffusion model and experiment

19 p2437 A73-37260

Optical and millimeter line-of-sight propagation effects in the turbulent atmosphere.

19 p2405 A73-38220

Scintillation measurements for large integrated-path turbulence.

19 p2461 A73-38486

Experimental test of optical antenna-gain reciprocity.

19 p2439 A73-38487

Effects of temperature and velocity fields on the quality of astronomical images.

20 p2608 A73-39238

Solar rotational and vibrational temperature based on turbulent velocity determined from CN molecular line profiles half widths

20 p2608 A73-39244

Analysis of airplane response to nonstationary turbulence including wing bending flexibility. II.

21 p2784 A73-40437

Light scattering from electrohydrodynamic turbulence in liquid crystals.

21 p2744 A73-41020

Turbulent flow velocity pulsations damping in wind tunnel chamber by wire grids, calculating grid turbulence effect

21 p2633 A73-41319

Bole experiment on dispersion of Lagrangian tracers in quasi-stationary two dimensional turbulent flow, noting rms distance between paired balloons

21 p2687 A73-41337

Accuracy of coordinate measurements with the aid of a variable-profile antenna

21 p2667 A73-41472

Model for galactic cluster formation after radiation decoupling from matter in Einstein-De Sitter universe, discussing turbulence in primeval cosmos

21 p2778 A73-41526

Statistical velocity and temperature characteristics of turbulent electron beams in crossed HF electric and magnetic fields, comparing with Brillouin flow

21 p2749 A73-41655

Acoustic turbulence generation of shock waves in compressed gas or plasma excited by random potential forces based on energy transfer along spectrum

22 p2840 A73-41809

On turbulent stress and the structure of young convective stars.

22 p2908 A73-42306

High resolution image formation through the turbulent atmosphere.

22 p2863 A73-43097

Turbulence generation by supersonic nozzle gas flow interaction with plasmas, discussing high current electric arc in axis

22 p2895 A73-43166

Photometric strip blurring and brightness contrast measurements of visual perception in turbulent atmosphere as function of distance, turbulence and exposure

23 p3001 A73-43573

Influence of a random transport-velocity component on the space-time correlations of signal fluctuations

23 p2954 A73-43647

Ultrasonic holography free from phase turbulence - Construction of the device and experimental results.

23 p2983 A73-44087

Response of panels to turbulence-induced, surface-pressure fluctuations and resulting acoustic radiation to the flow field.

24 p3077 A73-44828

[AIAA PAPER 73-993] On aeroacoustic coupling in free-stream turbulence manipulators.

24 p3054 A73-44847

Noise generation by turbulent combustion, discussing sound power, spectral content, enclosure effect, and importance in turbopropulsion system core engine noise

24 p3155 A73-44855

[AIAA PAPER 73-1023] Combustion noise radiation by open turbulent flames.

24 p3156 A73-44856

[AIAA PAPER 73-1025] Turbofan engine core noise prediction and measurement, considering sources from flow passage obstructions, combustion chamber and turbine noise due to interaction with upstream turbulence

24 p3122 A73-44857

[AIAA PAPER 73-1026] TURBULENCE METERS

Laser measurement of turbulence in exhaust jets.

03 p0308 A73-13568

Turbulence measurements in a compressible boundary layer subjected to a shock-wave-induced adverse pressure gradient.

05 p0566 A73-16912

[AIAA PAPER 73-167] Propeller anemometers as sensors of atmospheric turbulence.

06 p0695 A73-18329

Turbulent transport measurements with a laser Doppler velocimeter.

07 p0826 A73-20462

The development of a hot-foil probe for measurements in turbulent flows

08 p0962 A73-20748

Measurements and graphs of turbulence autocorrelations in space and time.

09 p1071 A73-22332

Development of a procedure for measuring the degree of turbulence at the axis of a free two-phase jet by a thermal-diffusion method

09 p1167 A73-22847

The response of a hot-wire anemometer in flows of gas mixtures.

10 p1222 A73-24971

Turbulent interface detector using a multiple array of single hot wires.

13 p1619 A73-29252

The comparison of a new constant temperature anemometer with several laser anemometer configurations.

13 p1620 A73-29268

A comparison of turbulence measurements by different instruments - Tsimlyansk field experiment 1970.

13 p1656 A73-29343

Turbulence measurements with hot-wire anemometry in a non-homogeneous jet.

17 p2174 A73-35512

Frequency-domain analysis of laser Doppler signals for estimation of turbulence parameters.

20 p2572 A73-39130

A universal static calibration procedure for yawed hot wires.

21 p2693 A73-39926

The laser-Doppler velocimeter and its application to the measurement of turbulence.

23 p2982 A73-43937

On the correction of hot wire turbulence measurements for spatial resolution errors.

24 p3089 A73-44691

Measurement of turbulence transport properties in a supersonic boundary-layer flow using laser velocimeter and hot-wire anemometer techniques.

24 p3090 A73-44869

[AIAA PAPER 73-1045] TURBULENT AIR CURRENTS

U AIR CURRENTS

U TURBULENT FLOW

TURBULENT BOUNDARY LAYER

Method of calculation of the three-dimensional turbulent boundary layer up to separation - Application to a simple gas turbine case

[ONERA, TP NO. 1111] 01 p0001 A73-10233

Mathematical and statistical modeling of wall flow turbulence, considering experimental velocity and temperature measuring techniques

01 p0031 A73-10292

TURBULENT BOUNDARY LAYER

Thermal intermittency coefficient distribution across turbulent boundary layer as function of free stream turbulence level

01 p0031 A73-10412

French monograph - A method of calculating the turbulent boundary layer using an equation for the behavior of the Boussinesq coefficient.

01 p0032 A73-10602

A comparison of two prediction methods with experiment for compressible turbulent boundary layers with air injection.

02 p0129 A73-12505

Turbulent pressure fluctuations on smooth and rough walls.

03 p0289 A73-12960

The scattering characteristics of a sonic boom at the passage through a turbulent layer

03 p0290 A73-12967

Incompressible fluid turbulent boundary layer flow stability, considering effect of high polymer additives

03 p0291 A73-13168

Free stream turbulence effect on flat plate boundary layer turbulent behavior, considering Reynolds stress dependence on turbulence intensity

03 p0292 A73-13170

A relation between the energy distribution of the main flow and the corresponding fluctuating quantities in boundary layers

03 p0292 A73-13171

Incompressible flow characteristics and temperature transverse behavior in completely turbulent wall boundary layer

03 p0292 A73-13172

Isothermal vertical plate turbulent thermal boundary layer during free convection, noting temperature pulsations dispersion

03 p0396 A73-13184

Hypersonic turbulent boundary layer flow parameters and heat transfer during blowing of coolant air and He through slot

03 p0242 A73-13186

Conditionally sampled measurements near the outer edge of a turbulent boundary layer.

03 p0293 A73-13526

Heat transfer in the turbulent boundary layer of an incompressible fluid flow past a surface when the pressure gradient and temperature on the surface are variable

03 p0295 A73-13622

Experimental investigation of a turbulent boundary layer on a highly elongated body of revolution in a supersonic flow

03 p0245 A73-13669

Turbulent properties of a compressible boundary layer.

03 p0296 A73-14177

Calculation of compressible turbulent boundary layers with roughness and heat transfer.

03 p0296 A73-14179

Role of the anelastic behavior of the ablation material on cross-hatching.

03 p0398 A73-14189

Plateau pressure in hypersonic turbulent boundary-layer interactions.

03 p0296 A73-14200

Buffet boundaries for arrow wings in transonic flow, presenting methods for pressure distribution and three dimensional turbulent boundary layer calculation

03 p0248 A73-14382

[DGLR PAPER 72-123] Velocity profiles and wall shear stress of three-dimensional turbulent boundary layers.

04 p0403 A73-15092

[ONERA, TP NO. 1134] Calculation methods of three-dimensional boundary layers with and without rotation of the walls.

04 p0403 A73-15093

[ONERA, TP NO. 1135] A free-streamline theory for bluff bodies attached to a plane wall.

04 p0403 A73-15160

Mean velocity and turbulence intensity profiles of asymptotic sink flow turbulent boundary layers, measuring Reynolds and wall shear stresses

04 p0434 A73-15166

Study of the effect of surface roughness on the laminar boundary layer transition in a turbulent boundary layer

04 p0404 A73-15653

Wind profile models for atmospheric turbulent boundary layers over smooth and rough surfaces, using Heisenberg energy transfer theory and von Karman constant

04 p0473 A73-15695

Enthalpy driving forces for gas cooling data correlation in convective heat transfer in reacting turbulent boundary layers with mass injection

04 p0519 A73-15824

[ASME PAPER 72-WA/JHT-31] Wall shear stress inference from two and three-dimensional turbulent boundary layer velocity profiles.

04 p0434 A73-15840

[ASME PAPER 72-WA/FE-4] Eddy-viscosity distribution in thick axisymmetric turbulent boundary layers.

04 p0435 A73-15845

[ASME PAPER 72-WA/FE-18] Calculation of interacting turbulent shear layers - Duct flow.

04 p0435 A73-15849

[ASME PAPER 72-WA/FE-25]

TURBULENT BOUNDARY LAYER

The transpired turbulent boundary layer in an adverse pressure gradient.

04 p0520 A73-15936

Temperature and heat flux distributions in incompressible turbulent equilibrium boundary layers.

04 p0520 A73-15942

Influences of free stream turbulence on mean velocities of turbulent boundary layer without pressure gradient.

04 p0435 A73-15972

A momentum integral solution of a three-dimensional turbulent boundary layer.

[ASME PAPER 72-FE-1] 05 p0565 A73-16548

Numerical analysis of eddy viscosity models in supersonic turbulent boundary layers.

[AIAA PAPER 73-164] 05 p0566 A73-16910

Calculations of turbulent shear stress in supersonic turbulent boundary layer zero and adverse pressure gradient flow.

[AIAA PAPER 73-166] 05 p0566 A73-16911

Unsteady flow generated by shock-turbulent boundary layer interactions.

[AIAA PAPER 73-168] 05 p0566 A73-16913

Shock wave-turbulent boundary layer interactions in rectangular channels. II - The influence of sidewall boundary layers on incipient separation and scale of the interaction.

[AIAA PAPER 73-234] 05 p0566 A73-16959

Shear stress distribution from measured nondimensional mean velocity profile measured in plane turbulent mixing layer formed at cascade wind tunnel exit

05 p0567 A73-17106

Heat transfer downstream of attachment of a turbulent supersonic shear layer.

05 p0533 A73-17112

Measurement of the velocity profile in a turbulent boundary layer on a permeable plate.

06 p0643 A73-17409

Flow visualization of the near-wall region in a drag-reducing channel flow.

06 p0685 A73-17709

Turbulent boundary layers with negligible wall stress - A singular-perturbation theory.

06 p0686 A73-17988

On the determination of the height of the Ekman boundary layer.

06 p0720 A73-18326

Heat transfer from hypersonic turbulent flow at a wedge compression corner.

06 p0646 A73-18531

Transition of the boundary layer on a cone in a supersonic flow

06 p0646 A73-18540

Asymptotic formulas for the thickness of the Ekman boundary layer

06 p0691 A73-18730

Heat transfer in two-dimensional turbulent confined flows.

07 p0920 A73-19570

Plane equilibrium turbulent boundary layer with longitudinal pressure gradient

07 p0811 A73-19619

Turbulent boundary layer separation in supersonic air flow around flat rectangular plate, calculating flow geometry and pressure distribution

07 p0775 A73-20082

Locally similar solutions of equations of a turbulent boundary layer on a circular cone

08 p0925 A73-20646

Mixing length flow theory for turbulent boundary layer calculation, with allowance for mass transfer

08 p0953 A73-20721

Reference temperature method for predicting turbulent compressible skin-friction coefficient.

08 p0925 A73-20722

A generalized correlation of roughness density effects on the turbulent boundary layer.

08 p0953 A73-20724

A zero-streamwise-pressure-gradient, three-dimensional turbulent boundary layer in a 90 deg curved rectangular duct.

08 p0953 A73-20796

Heat transfer and friction in the turbulent boundary layer of a compressible gas on a permeable surface

08 p0926 A73-20992

Steady turbulent boundary layer of compressible perfect gas on heat insulated surface with suction and longitudinal pressure gradient

08 p0954 A73-21177

Turbulent incompressible boundary layer on porous heat insulated plate with uniform suction, calculating ratio of friction drag coefficients

08 p0954 A73-21178

Microsensor measurement of spatial correlation between pressure fluctuations of turbulent boundary layer

08 p0965 A73-21188

The mixing length derived from Karman's similarity hypothesis.

08 p0955 A73-21442

Flow parameters and cylinder elongation effects on turbulent boundary layer characteristics for compressible fluid flow, calculating velocity distribution

08 p0956 A73-21602

Cylinder surface roughness and transverse curvature effects on turbulent boundary layer in incompressible and compressible flows, deriving formula for skin friction coefficient

08 p0956 A73-21603

A two-layer model of high speed two- and three dimensional turbulent boundary layers with pressure gradient, surface mass injection and entropy layer swallowing.

[AIAA PAPER 73-135] 08 p0956 A73-21800

Hydrodynamic wind tunnel investigation of drag reduction and propulsion effect by flexible walls, observing boundary layer transition and turbulence

09 p1071 A73-22207

Buoyancy effects in a turbulent boundary layer.

09 p1071 A73-22330

An investigation of the application of Taylor's hypothesis to atmospheric boundary layer turbulence.

09 p1114 A73-22331

A differential method for the prediction of the effects of atmospheric boundary layer turbulence using the turbulence kinetic energy equation.

09 p1071 A73-22334

Structure of a collisionless boundary layer and the turbulent braking of ions

09 p1127 A73-22607

Estimate of the influence of thermal diffusion on the surface burnout rate in a nonhomogeneous turbulent boundary layer

09 p1167 A73-22618

Study of average and turbulent characteristics of boundary layers stratified in temperature - Comparison with the corresponding characteristics in low layers of the atmosphere

09 p1072 A73-23028

Mean velocity profiles in three-dimensional incompressible turbulent boundary layers.

09 p1029 A73-23445

Experimental study of the heat transfer in the separation zones in front of cylindrical projections

10 p1294 A73-23587

Hot-wire anemometer probe operation in constant current in continuous high-temperature hypersonic turbulent boundary layer, computing velocity and temperature fluctuations

10 p1205 A73-24254

Some heat transfer measurements in compressible turbulent boundary layers.

10 p1296 A73-24648

Unsteady turbulent boundary layer flow past infinite flat plates with free stream acceleration or deceleration, computing characteristics by finite difference method

10 p1209 A73-24834

Some solutions of the unsteady two-dimensional turbulent boundary layer equations.

10 p1209 A73-24835

Noise radiated from a turbulent boundary layer.

11 p1344 A73-24979

A higher order theory for compressible turbulent boundary layers at moderately large Reynolds number.

11 p1346 A73-25218

A simple model of normal shock wave and turbulent boundary-layer interaction.

11 p1347 A73-25710

Investigation of the transition of a turbulent boundary layer into a laminar boundary layer in the presence of deep negative pressure gradients

11 p1347 A73-25737

Calculation of turbulent boundary layers and wall jets over curved surfaces.

11 p1348 A73-26383

Calculation of turbulent skin friction on a rotating disk.

11 p1348 A73-26387

Prediction of heat transfer for turbulent boundary layer with pressure gradient.

11 p1453 A73-26393

Effects of upstream wall temperatures on hypersonic tunnel wall boundary-layer profile measurements.

11 p1344 A73-26395

Shock attenuation in a shock tube due to boundary layer.

12 p1486 A73-27174

Application of small perturbation method in calculations of turbulent boundary layers on a curvilinear surface with suction

13 p1600 A73-28447

Air injection from wall slot into turbulent boundary layer of high temperature gas channel flow, calculating film cooling effectiveness in flat plate

13 p1706 A73-28675

Incipient separation pressure rise for a Mach 3.8 turbulent boundary layer.

13 p1601 A73-28827

Base drag calculations in supersonic turbulent axisymmetric flows.

13 p1564 A73-28835

Effects of free stream velocity profile on turbulent boundary layer, with some reference to the effects of free stream turbulence.

13 p1602 A73-29013

Equilibrium three-dimensional turbulent boundary layer on the end wall of a curved channel.

13 p1602 A73-29013

The thick turbulent boundary layers on rotating cylinders in axial flow.

13 p1602 A73-29013

An approximate method for calculating the interaction between shock wave and turbulent boundary layer.

13 p1602 A73-29013

Experiments in the determination of turbulent layer thickness in monochromatic-type waves

13 p1655 A73-29160

Wavevector/frequency spectrum of turbulent boundary-layer pressure.

13 p1604 A73-29262

Turbulent velocity and pressure fields in boundary layer flows over rough surfaces.

13 p1604 A73-29264

German monograph on compressible turbulent boundary layer equations solution for heat transfer in divergent nozzle flow based on modified Patankar-Spalding difference method

13 p1605 A73-29276

Turbulent surface layer shear convection analysis, using similarity model based on weak interaction between vertical motion and mechanical turbulence

13 p1655 A73-29340

Experimental investigation of the convection inversion process in the viscous sublayer of a turbulent boundary layer during blowing of carbon dioxide through a vertical porous heated surface under conditions of natural convection

13 p1708 A73-29407

Three dimensional turbulent boundary layers prediction methods and flow measurements, considering swept and slender wings

14 p1744 A73-30173

Two dimensional incompressible turbulent boundary layer flow theory, considering Bradshaw turbulence field and Felsch integral methods

14 p1745 A73-30298

Experimental investigations regarding the behavior of turbulent boundary layers in the case of small periodic pressure changes

14 p1745 A73-30299

Heat transfer to a strongly accelerated turbulent boundary layer - Some experimental results, including transpiration.

14 p1818 A73-30615

Velocity profile determination in a turbulent boundary layer

14 p1746 A73-30795

Acoustic radiation intensity of a turbulent boundary layer on a plate

14 p1746 A73-30952

Effective-viscosity model for turbulent wall boundary layers.

15 p1860 A73-31119

Influence of weak viscous interaction on the drag of a wing profile

15 p1822 A73-31195

The turbulent boundary layer on a long thin filament

15 p1822 A73-31197

Application of the energy equation for turbulence in the theory of jet flows

15 p1862 A73-31288

Analysis of turbulent skin friction in thick axisymmetric boundary layers.

15 p1863 A73-31658

Experimental investigation of a turbulent boundary layer on a porous plate with intense injection

15 p1824 A73-31858

Interferometric and thermoacoustic methods of studying binary boundary layers

15 p1876 A73-31859

Film-cooling effectiveness in the near-slot region.

15 p1958 A73-32278

Three-dimensional turbulent boundary layer - Calculations and experiments

16 p1961 A73-32806

The three-dimensional turbulent boundary layer - Theoretical and experimental analysis

16 p1961 A73-32810

The simulation of the atmospheric surface layer with volumetric flow control.

16 p1994 A73-33152

Investigations regarding the heat exchange integral in turbulent incompressible flows

16 p2085 A73-33256

Three dimensional turbulent boundary layer of yawed wing suction surface in uniform flow, examining cross flow profile, velocity distribution and weighting functions

16 p1963 A73-33267

A wake and an eddy in a rotating, radial-flow passage. II - Flow model.

[ASME PAPER 73-GT-58] 16 p1964 A73-33513

Turbulence downstream of stationary and rotating cascades.

[ASME PAPER 73-GT-80] 16 p1964 A73-33525

Axisymmetric turbulent boundary layer along a slender cylinder.

17 p2150 A73-34400

A modified wall wake velocity profile for turbulent compressible boundary layers. 17 p2150 A73-34439

Experimental study of turbulent boundary layer along a flat plate with linear increase of roughness height. 17 p2151 A73-34537

Measurements of temperature fluctuations behind a linear heat source placed in a turbulent boundary layer. 17 p2254 A73-34550

Oscillatory flow phenomena in diffusers at low Reynolds numbers. [ASME PAPER 73-FE-14] 17 p2152 A73-35011

A finite difference solution of the two and three-dimensional incompressible turbulent boundary layer equations. [ASME PAPER 73-FE-20] 17 p2153 A73-35016

An assessment of three-dimensional turbulent boundary layer prediction methods. [ASME PAPER 73-FE-25] 17 p2153 A73-35020

A method for calculating unsteady turbulent boundary layers in two- and three-dimensional flows. 17 p2154 A73-35135

Finite difference solution of Prandtl boundary layer equations for steady incompressible laminar and turbulent boundary layer flows. 17 p2154 A73-35136

Unsteady turbulent boundary layers in two-dimensional, incompressible flow. [AIAA PAPER 73-650] 18 p2260 A73-36205

Finite difference theory predictions for turbulent boundary layer swirling flames, discussing flow simulation, turbulence models and flame size, shape and stability characteristics. [AIAA PAPER 73-651] 18 p2267 A73-36206

Prediction of turbulent separated boundary layers. [AIAA PAPER 73-663] 18 p2261 A73-36214

Turbulent boundary layer flow separation measurements using holographic interferometry. [AIAA PAPER 73-664] 18 p2261 A73-36215

Supersonic, turbulent boundary layer separation measurements at Reynolds number of 10,000,000 to 100,000,000. [AIAA PAPER 73-665] 18 p2261 A73-36216

Separation of a supersonic turbulent boundary layer at moderate to high Reynolds numbers. [AIAA PAPER 73-666] 18 p2261 A73-36217

Supersonic turbulent boundary-layer flows with tangential slot injection. [AIAA PAPER 73-696] 18 p2262 A73-36245

Effect of adverse pressure gradient on film cooling effectiveness. [AIAA PAPER 73-697] 18 p2268 A73-36246

Computation of hypersonic turbulent boundary layers with heat transfer. [AIAA PAPER 73-699] 18 p2263 A73-36248

An integral procedure for estimating boundary layer parameters and heat transfer in arbitrary pressure gradients. [AIAA PAPER 73-700] 18 p2298 A73-36249

Reynolds number effects on the shock wave - Turbulent boundary layer interaction at transonic speeds. [AIAA PAPER 73-661] 18 p2298 A73-36262

Turbulent boundary-layer flow from stationary to moving surfaces. 18 p2298 A73-36313

Probability distributions and correlations in a turbulent boundary layer. 18 p2300 A73-36626

Ratio of Reynolds shear stress to turbulence kinetic energy in a boundary layer. 18 p2300 A73-36633

Calculation of turbulent boundary layers over flat plates with different phenomenological theories of turbulence and variable turbulent Prandtl number. 18 p2301 A73-36699

Turbulent free convection in a boundary layer with variable wall temperature. 18 p2301 A73-36815

Pulsation-energy balance equation in turbulent boundary layer theory. 18 p2301 A73-37002

Investigation of the flow in regions of turbulent boundary layer separation in front of a subsonic jet blown from a circular nozzle. 18 p2265 A73-37003

Plasma channel flow theoretical and experimental review, considering heat transfer studies, turbulent nonequilibrium plasma boundary layers and plasma sheaths. 19 p2464 A73-37161

Recent progress in boundary layer research. [AIAA PAPER 73-780] 19 p2419 A73-37451

The velocity profile in the wall region of a turbulent boundary layer. 19 p2420 A73-37554

Non-reacting and equilibrium chemically reacting turbulent boundary-layer flows. 19 p2421 A73-38187

Waves and turbulence in stable layers and their effects on EM propagation; Proceedings of the Third Symposium, La Jolla, Calif., June 5-15, 1972. Parts 1 & 2. 19 p2447 A73-38202

Acoustic echo-sounding techniques and their application to gravity-wave, turbulence, and stability studies. 19 p2405 A73-38207

Earth surface turbulent boundary layer analysis, considering similarity theory limitation, flux profiles, velocity, temperature and humidity spectra, energy budgets, local isotropy, etc. 19 p2427 A73-38212

On the use of forward scatter techniques in the study of turbulent stratified layers in the troposphere. 19 p2427 A73-38219

Planetary boundary-layer turbulence studies from acoustic echo sounder and in-situ measurements. 19 p2448 A73-38223

The lower atmosphere in hydrostatically stable conditions. 19 p2449 A73-38245

Velocity distributions of rough wall turbulent boundary layers without pressure gradient. 19 p2422 A73-38284

Cross flows in bounded three-dimensional turbulent boundary layers. 19 p2422 A73-38298

Development of a turbulent boundary layer in MHD channel. 19 p2470 A73-38316

Aerodynamic sound and the low-wavenumber wall-pressure spectrum of nearly incompressible boundary-layer turbulence. 20 p2545 A73-39053

The balance of turbulence energy and its components in incompressible turbulent boundary layers. 20 p2546 A73-39096

A method for calculating three-dimensional turbulent boundary layer by using streamline co-ordinates. 20 p2546 A73-39225

Energy spectra of velocity pulsations in a turbulent boundary layer on a permeable plate. 20 p2547 A73-39286

Friction, heat transfer and material removal in a turbulent boundary layer of a compressible high-enthalpy gas under conditions of marked nonisothermicity, injection and negative pressure gradient. 20 p2628 A73-39422

The turbulent boundary layer with stepwise varying boundary conditions at a permeable surface. 20 p2628 A73-39423

Study of shock wave and turbulent boundary layer interaction using the energy integral equation. 20 p2548 A73-39524

Incompressible turbulent boundary layer separation from a curved axisymmetric body. 20 p2548 A73-39525

Porous cooling in a supersonic turbulent boundary layer. 20 p2628 A73-39609

Experiment on convex curvature effects in turbulent boundary layers. 21 p2676 A73-40245

Influence of the shape of the leading edge on the transition process in the boundary layer on a plate in longitudinal flow. 21 p2676 A73-40399

Burnout of a graphite surface during the blowing of an inert gas through it. 21 p2790 A73-40698

Hot-wire anemometer investigation of turbulent boundary layers at a permeable plate with injection. 21 p2678 A73-41055

Large scale heat transfer in turbulent boundary layer at heated flat plate in incompressible viscous fluid, discussing temperature fluctuation spatial correlation as function of wall law and flow core. 21 p2678 A73-41062

Drag due to regular arrays of roughness elements of varying geometry. 21 p2633 A73-41569

Boundary layer induced cockpit noise. 22 p2795 A73-41706

Turbulent boundary layer velocity distribution skewness and flatness factors over smooth wall compared with rough wall, discussing Reynolds shear stress fluctuations. 22 p2842 A73-42231

Aerodynamic interference of pitot tubes in a turbulent boundary layer at supersonic speed. 22 p2796 A73-42552

Experimental investigation of a turbulent boundary layer on a triangular plate with a wedge. 23 p2939 A73-43473

Mean Reynolds stress tensor model for analytical prediction of turbulence structure of density-stratified atmospheric boundary layer. 23 p3002 A73-43592

A method for calculating the burning rates of solid fuels in a turbulent gaseous oxidizer flow at Le unequal to unity. 23 p3049 A73-43729

Approximate method for calculating the turbulent boundary layer in front of a recess. 23 p2968 A73-43732

Heat transfer from a hypersonic turbulent boundary layer on a flat plate. 23 p3049 A73-43933

Turbulent boundary layer noise minimization by acoustic oscillation control, discussing suction and gas injection techniques. 23 p2969 A73-43976

Intensity of sound radiation from a turbulent boundary layer on a plate. 23 p2969 A73-44328

Response of panels to turbulence-induced, surface-pressure fluctuations and resulting acoustic radiation to the flow field. [AIAA PAPER 73-993] 24 p3077 A73-44828

Pressure fluctuations underlying attached and separated supersonic turbulent boundary layers and shock waves. [AIAA PAPER 73-996] 24 p3053 A73-44831

Surface pressure fluctuations in hypersonic turbulent boundary layers. [AIAA PAPER 73-997] 24 p3053 A73-44832

Emission of sound from a rectangular plate vibrating under the action of pressure pulsations in a turbulent boundary layer. 24 p3109 A73-44899

Investigation of the flow pattern in the wall region of a turbulent boundary layer during injection with a positive pressure gradient. 24 p3079 A73-45080

Measurements of the structure of the Reynolds stress in a turbulent boundary layer. 24 p3079 A73-45310

Parametrizing turbulent-friction effects in a planetary boundary layer. 24 p3108 A73-45450

Heat and mass transfer in a turbulent layer above permeable plates. 24 p3081 A73-45528

TURBULENT DIFFUSION

Book on momentum, heat and mass transfer at various interfaces based on Prandtl eddy mixing length concept. 01 p0030 A73-10049

The spectral density technique for the determination of eddy fluxes. 01 p0072 A73-10145

Lower ionosphere variability due to atmospheric dynamics, considering temperature variations, minor constituent transport and eddy diffusion. 01 p0041 A73-10885

Turbopause effect on latitudinal diurnal variation of upper atmosphere neutral species, using turbulent diffusion coefficients and photochemical transport theory. 02 p0161 A73-12278

Statistical theory of light propagation in a turbulent medium /Survey/. 02 p0141 A73-12485

Application of the turbulent eddy diffusivity transport equation to the analysis of turbulent flow in the radial face seal. 03 p0293 A73-13315

Concentration probability of a passive admixture in turbulent shear flows. 03 p0294 A73-13614

Study of the specific characteristics of the diffusion method for measuring turbulence characteristics under conditions of a free homogeneous jet. 05 p0576 A73-16617

The stability of lifted turbulent diffusion and premixed flames. [WSCI PAPER 72-39] 05 p0638 A73-16678

Solutions of the chemical kinetic equations for initially inhomogeneous mixtures. [AIAA PAPER 73-101] 05 p0546 A73-16861

Mass transfer coefficient measurement in turbulent ducted flow, obtaining numerical solution to diffusion equation. 06 p0770 A73-18835

A note on Eulerian-Lagrangian time scale transformation for large-scale atmospheric turbulence. 08 p0985 A73-21424

Turbulent dynamo theory based on functional analysis, noting equation with variational derivatives of characteristic functional. 08 p0989 A73-21697

Determination of the turbulent exchange coefficients in the case of tube bundles in crossflow. 11 p1448 A73-25109

Atmospheric convection and its effect on relaxation time and charge distribution. 11 p1394 A73-25759

On the turbulent thermal diffusion parallel to a plane wall for y/δ equals 2 to 300. 11 p1451 A73-25870

Turbulent diffusion downstream of a linear source in a plane parietal jet. 13 p1599 A73-28070

Nongray radiative transfer and simultaneous turbulent diffusion in layer of molecular gas enclosed by parallel black walls, presenting temperature profiles. 13 p1705 A73-28433

A comparison of time-varying concentrations of air admixtures with those of the corresponding stationary cases. 13 p1653 A73-28742

TURBULENT FLOW

- Dependence of the diffuse expansion characteristics of a crystallization zone on the vertical stability of the atmosphere 13 p1862 A73-28879
- The photochemistry of hydrocarbons in the Jovian atmosphere. 14 p1802 A73-30766
- Influence of a longitudinal pressure gradient on turbulent diffusion in ducts 15 p1862 A73-31297
- Calculation of the flow of a two-phase mixture in a Laval nozzle with allowance for turbulent diffusion of particles 15 p1822 A73-31300
- Role meteorological balloon sounding experiment in Southern Hemisphere, discussing mean circulation, eddy diffusion and data collection and satellite tracking system 15 p1904 A73-31723
- Gravity wave magnitudes and horizontal and vertical scales measured and applied to eddy diffusion coefficients in upper stratosphere [ALAA PAPER 73-495] 16 p2005 A73-33538
- Monthly mean values of eddy diffusion coefficients in the lower stratosphere. 16 p2005 A73-33540
- A simple technique to estimate large-scale eddy coefficients in the stratosphere. 16 p2005 A73-33541
- The effect of large-scale eddies on climatic change. 17 p2160 A73-34851
- Microscopic aspects of turbulent and laminar mixing in terms of molecular, eddy and bulk diffusional operations 17 p2156 A73-35502
- Statistical theory of weakly interacting perturbations and low amplitude turbulence in fluids, considering diffusion, dispersive and acoustic wave characteristics and plasma instabilities 18 p2299 A73-36504
- Droplet transfer in two phase anular mist flow. II - Prediction of droplet transfer rate. 19 p2423 A73-38350
- Turbulent diffusion in Schwinger formulation of quantum field theory, deriving transition probabilities from Dyson and Saffman equations 20 p2599 A73-39674
- The measurement of turbulent spectra and diffusion coefficients in the altitude region 95 to about 110 km. 21 p2688 A73-41341
- Wave-induced eddy diffusion coefficients in the upper atmosphere of Mars. 22 p2906 A73-41903
- Auroral electron and proton flux density, energy spectra, acceleration and precipitation mechanisms and turbulent diffusion from rocket and satellite measurements 22 p2850 A73-42748
- Turbulent diffusion flame velocity, concentration, temperature and momentum flux measurements for hydrogen round jet in co-flowing air stream 22 p2935 A73-42788
- The generation and dissipation of solar and galactic magnetic fields. 22 p2911 A73-42934
- Ammonia density profiles and photochemical destruction above Jovian tropopause as function of eddy diffusion coefficient, considering background atmosphere scale height 23 p3028 A73-43601
- On the behavior of nitrogen oxides in the stratosphere. 23 p2976 A73-43896
- Eddy heat/momentum diffusivity ratio dependence on Richardson number relationship between Deacon numbers of wind and temperature profiles in Antarctic surface layer 23 p3003 A73-43983
- Design criteria for finite-difference models for eddy diffusion with winds that guarantee stability, mass conservation, and nonnegative masses. 24 p3085 A73-45018
- Superposition technique in numerical integration of generalized Ekman equation for wind profile determination, taking into account eddy diffusivity variation 24 p3108 A73-45019
- Atmospheric mixing effects for interpretation of oxygen atom concentration in Mars and Venus upper atmospheres obtained by Mariner and Venera space probes 24 p3139 A73-45134
- Fuel combustion rate and turbulent diffusion induced self ignition in pulsejet engine combustion chamber from schlieren photography and pressure distribution measurements 24 p3123 A73-45377
- TURBULENT FLOW**
NT CAVITATION FLOW
NT SUPERCAVITATING FLOW
 Book - Lectures in mathematical models of turbulence. 01 p0031 A73-10123
- Mixed convection over a heated horizontal plane. 01 p0120 A73-10440
- A study of the kinematic and dynamic characteristics in the wake behind a plate in an unbounded flow 01 p0032 A73-10620
- On turbulent flows with fast chemical reactions. I - The closure problem. 01 p0032 A73-10637
- On turbulent flows with fast chemical reactions. II - The distribution of reactants and products near a reacting surface. 01 p0032 A73-10638
- Experimental study of the turbulent flow of a suspension: Trajectories and velocities of particles - Heat transfers between the two phases 01 p0122 A73-10810
- Drag reduction in non-Newtonian turbulent flow, considering viscosity change with strain in long-chain molecules/polymers/ fluid solutions 01 p0034 A73-11134
- Numerical method for describing turbulent, compressible, subsonic separated jet flows. 01 p0035 A73-11467
- Turbulent non-Newtonian liquid power dissipation steadiness during motion as function of viscous forces balanced variation 02 p0152 A73-11571
- Theory of the electrodiffusion method for measuring the spectral characteristics of turbulent flows 02 p0165 A73-11614
- Computation of the sound energy radiated from turbulent flows [DGLR PAPER 72-074] 02 p0153 A73-11699
- Statistical mechanics of the Burgers model of turbulence. 02 p0153 A73-12039
- Laser Doppler shift velocity correlation meter operation in turbulent flow analyzed by optical mixing theory 02 p0153 A73-12049
- Nondecaying turbulence field production by mean shear in spite of flow viscosity effects 02 p0154 A73-12056
- Turbulence measurements with a laser anemometer measuring individual realizations. 02 p0168 A73-12057
- Experimental values of turbulence length scales in Lagrange variables in the vicinity of a flat wall 02 p0154 A73-12541
- Local transport equations for turbulent shear flow. 02 p0154 A73-12825
- Heat flow and magnetic field diffusion in turbulent fluids. 02 p0199 A73-12841
- Line and continuous excitation sources for measuring wavelength dependence, angular distribution and polarization of scattered light intensity in turbulent and laminar flames 03 p0396 A73-12925
- Aerodynamic noise characteristics, discussing turbulent fluid acoustic propagation equation modification and antinoise legislation 03 p0241 A73-12952
- Measurements of pressure and velocity fluctuations in turbulent pipe flow 03 p0290 A73-12963
- Hot-wire anemometers calibration characteristics for steady channel turbulent air flow measurement, noting linearization error analysis 03 p0306 A73-13166
- Free stream turbulence effect on flat plate boundary layer turbulent behavior, considering Reynolds stress dependence on turbulence intensity 03 p0292 A73-13170
- Carbon dioxide turbulent flow heat transfer in single phase near-critical region under forced and free convection 03 p0396 A73-13185
- Application of the turbulent eddy diffusivity transport equation to the analysis of turbulent flow in the radial face seal. 03 p0293 A73-13315
- Concentration probability of a passive admixture in turbulent shear flows 03 p0294 A73-13614
- Subsonic wind tunnel tests for laminar boundary layer investigation in low level turbulence flow, noting turbulence measurement with hot-wire anemometers 03 p0308 A73-13666
- Turbulent flow velocity pulsations damping in wind tunnel chamber by wire grids, calculating grid turbulence effect 03 p0245 A73-13670
- Influence of distributed grit-type roughness on the spectrum of wall pressure fluctuations of turbulent flow in a tube. 03 p0295 A73-14038
- Singular characteristics of turbulent wall pressure fluctuations associated with flow in a tube. 03 p0295 A73-14041
- Turbulent shear flow structure parameters in conical diffuser, investigating Reynolds number and turbulent kinetic energy effects 03 p0247 A73-14176
- Basic relationships in turbulent lubrication and their extension to include thermal effects. [ASME PAPER 72-LUB-16] 03 p0314 A73-14332
- Amplification of turbulence level by a flame and turbulent flame velocity. 03 p0399 A73-14390
- Test field model for nonstationary inhomogeneous turbulence with mean shearing velocity 04 p0434 A73-15166
- A model for eddy conductivity and turbulent Prandtl number. [ASME PAPER 72-WA/HT-13] 04 p0434 A73-15834
- Secondary flow in the entrance region boundary layers of an expanding square duct. [ASME PAPER 72-WA/FE-34] 04 p0404 A73-15850
- An experimental investigation of naturally developing turbulent flow and flow with fixed transition in a parallel pipe. [ASME PAPER 72-WA/FE-38] 04 p0435 A73-15859
- An analytical and empirical basis for the design of turbulence amplifiers. I - Analysis and experimental confirmation. [ASME PAPER 72-WA/FLCS-1] 04 p0408 A73-15896
- An analytical and empirical basis for the design of turbulence amplifiers. II - Empirical relationships and design procedure. [ASME PAPER 72-WA/FLCS-2] 04 p0408 A73-15860
- Heat and mass transfer laws for fully turbulent wall flows. 04 p0520 A73-15935
- An optical system for measurement of mean and fluctuating concentrations in a turbulent air stream. 05 p0576 A73-16437
- Measurement of longitudinal and normal velocity fluctuations by sensing the temperature downstream of a hot wire. 05 p0576 A73-16438
- Measurements of turbulence-transport properties with a laser Doppler velocimeter. [ALAA PAPER 73-169] 05 p0566 A73-16914
- The correlations of the vortex in a homogeneous turbulence associated with a mean shearing flow 05 p0567 A73-17227
- Experimental investigation of worsened heat-transfer conditions with the turbulent flow of carbon dioxide at supercritical pressure. 06 p0766 A73-17410
- An analytical fluid dynamic model of turbulent inlet flow. [ALAA PAPER 73-138] 06 p0644 A73-17647
- Measurements in a transitional/turbulent Mach 10 boundary layer at high-Reynolds numbers. [ALAA PAPER 73-165] 06 p0645 A73-17649
- Phillips aerodynamic noise theory application to directional patterns of high speed hot jets, discussing convection laws and sound field-turbulence correlation response [ALAA PAPER 73-185] 06 p0684 A73-17654
- Experiment on the geometry of the fine-structure regions in fully turbulent fluid. 06 p0684 A73-17705
- Effects of spanwise rotation on the structure of two-dimensional fully developed turbulent channel flow. 06 p0685 A73-17708
- Computerized mathematical models of two- and three-dimensional turbulent flow combustion, considering temperature and concentration fluctuations, particle size, NO formation and radiative transfer 06 p0767 A73-17727
- Scaling invariance hypothesis for local structure of turbulence, using quantum field theory methods 06 p0686 A73-17977
- Eddy cavitation flow past a wedge 06 p0686 A73-18071
- Possibilities of changing the microstructure of turbulent flow in investigations of convective heat transfer 06 p0686 A73-18133
- Singular perturbation and turbulent shear flow near walls. 06 p0686 A73-18378
- Asymptotic analysis of turbulent channel and boundary-layer flow. 06 p0687 A73-18528
- Approximate calculations of the hydrodynamic characteristics of a turbulent flow of liquid in annular channels 06 p0688 A73-18562
- The use of aerosols for the visualization of flow phenomena. 06 p0683 A73-18837
- Elastic waves induced fluctuating stresses in turbulent parallel mean flow, deriving hyperbolic relations consistent with Taylor frozen field hypothesis 07 p0810 A73-19109
- Energy conserving finite difference approximation for solution of unaveraged Navier-Stokes equations of three dimensional incompressible turbulent flow in square duct 07 p0810 A73-19263
- Intermittent behavior of a plasma discharge in turbulent gas flow. 07 p0856 A73-19517
- Turbulent flow characteristics of an impinging jet. 07 p0810 A73-19569

Two dimensional semibounded jets in laminar and turbulent flows, discussing boundary layers skin and stream regions, step flow velocities, temperatures and self similar problems

07 p0811 A73-19612

Velocity and resistance profiles for unsteady turbulent flow in rough pressure channels, using Prandtl hypothesis

07 p0811 A73-19614

Turbulent energy variations in unsteadily moving flow with structural shift, emphasizing formation of vortices with various inertia scales

07 p0811 A73-19620

Viscous incompressible gas turbulent flow in axisymmetric channel under preliminary test conditions at inlet, using computer numerical solution

07 p0774 A73-19621

Flow velocity fluctuation intensity relationship to turbulent energy dissipation based on Kolmogoroff similarity hypothesis

07 p0811 A73-19624

Effect of low heat-shield ablation rates on flight test turbulent base pressure.

07 p0920 A73-19975

Stroboscopic investigation of the effect of standing acoustic waves on turbulent flames

07 p0920 A73-19992

Possible construction of semiempirical turbulent flow theories

07 p0812 A73-20092

Heat transfer, adiabatic enthalpy /temperature/ of the wall, and hydrodynamic resistance associated with the turbulent and laminar flow of a compressible fluid in a circular tube.

08 p0954 A73-20858

Velocity distribution of the turbulent motion of a fluid between two plane-parallel walls

08 p0954 A73-21175

Turbulent hydrodynamics and heat transfer in rotating flows of incompressible fluid

08 p0954 A73-21184

Effect of Doppler ambiguity on the measurement of turbulence spectra by laser Doppler velocimeter. [AD-756047]

08 p0965 A73-21211

A unified view of the law of the wall using mixing-length theory. [AD-759043]

08 p0926 A73-21441

Acoustic radiation from plates excited by flow noise.

08 p0988 A73-21470

Swirl injector driven air flow in cylindrical tube, measuring flow velocity and turbulent stress tensor components

08 p0956 A73-21601

Heat transfer for turbulent flow with suction in a porous tube.

08 p1024 A73-21637

An evaluation of the heat pulse anemometer for velocity measurement in inhomogeneous turbulent flow. [AD-758460]

09 p1071 A73-22102

Velocity distribution in tubes of circular cross section

09 p1072 A73-22846

Turbulent friction drag of a dusty gas. I - Theoretical study.

09 p1072 A73-23325

Temperature recovery coefficients during turbulent flow of liquid in a circular pipe

10 p1204 A73-23509

Experimental investigation of turbulent flow structure in a circular pipe with delivery through a porous wall

10 p1204 A73-23512

Variable-property turbulent flow in a horizontal smooth tube during uniform heating and constant surface-temperature cooling.

10 p1295 A73-23779

Strong irradiance fluctuations in turbulent air - Plane waves.

10 p1248 A73-23837

Book - Annual review of fluid mechanics. Volume 5.

10 p1205 A73-23851

Statistical properties of intermittency in large scale turbulent flows, considering boundary layer, shear and convective flows

10 p1205 A73-23855

Instability, transition, and turbulence in buoyancy-induced flows.

10 p1205 A73-23859

Experimental determination of the turbulent transfer coefficient in the case of homogeneous isotropic turbulence.

10 p1205 A73-24176

Turbulent interface structure from eddy viscosity models, discussing equations of motion and Nee-Kovaszny and Prandtl models

10 p1205 A73-24253

Book - Turbulence transport modeling.

10 p1206 A73-24350

An experimental study of turbulent flow in pipes with artificial wall roughness

10 p1206 A73-24460

Turbulent Hartmann flow based on differential equations for steady isothermic turbulent motion of incompressible electrically conducting fluid in magnetic field

10 p1256 A73-24591

Semiempirical determination of the anisotropy of turbulent MHD flow in a longitudinal field

10 p1256 A73-24592

Studies of the atmospheric fine structure with the aid of microwave propagation experiments

10 p1213 A73-24682

Incompressible turbulent axisymmetrical impulsive air injection at moderate pressure into stagnant surroundings, measuring flow velocity distribution

10 p1210 A73-24849

Unsteady uniform-length turbulent flow of incompressible fluid in circular pipe studied via Reynolds and turbulence energy balance equations

10 p1210 A73-24851

Heat transfer and friction coefficients for turbulent flow of air in smooth annuli at high temperatures.

10 p1297 A73-24970

Turbulence in a conical diffuser with fully developed flow at entry.

11 p1345 A73-25057

Pressure distributions on circular cylinders at critical Reynolds numbers.

11 p1300 A73-25151

Fluid turbulence equations for large molecular drift velocity gradients in rarefied gas, near surface and stellar system motions, using Predvoditelev hydrodynamic equations

11 p1347 A73-25733

Determination of the convective heat transfer coefficient by 'half-space period' method

11 p1451 A73-25741

Spectra of turbulent pulsations in velocity, temperature, and their correlations for air flow in a circular pipe

11 p1301 A73-25744

Low speed wind tunnel test section anisotropic turbulence decay rates representation by power type laws, comparing with grid and nearly isotropic turbulence

11 p1348 A73-26390

Diffusion of heat from a line source downstream of a turbulence grid.

11 p1453 A73-26399

Mathematical description of the turbulent isobaric flow of a chemically reacting gas in a heated pipe

11 p1453 A73-26428

Turbulence intensity and turbulent transfer characteristics behind grids in tubes

11 p1349 A73-26431

Effect of polymer additions on some energy balance components in a turbulent flow

11 p1349 A73-26433

Considerations concerning the inadequacy of the classical concept of equivalent diameter in calculations of heat transfer in elliptical pipes

12 p1557 A73-26796

The limits and the nature of the onset of influence of thermogravitational forces on turbulent flow and heat transfer in vertical tubes

12 p1487 A73-27313

Asymptotic mechanics of turbulent flows - Energy and entropy

12 p1487 A73-27411

Equations for finitely-dimensional probability distributions of pulsating variables in a turbulent flow

13 p1599 A73-28287

Using a single hot-wire probe in three-dimensional turbulent flow fields.

13 p1600 A73-28526

Influence of wall proximity on hot-wire velocity measurements.

13 p1613 A73-28527

A study of systematic errors in measurements with the constant-temperature anemometer in high-turbulence flows with and without hot-wire signal linearization.

13 p1613 A73-28529

Error estimates for turbulent flow characteristics by visualization and solid particle photography

13 p1601 A73-28738

Study of kinematic and dynamic characteristics in a wake behind a plate in an unbounded flow.

13 p1601 A73-28739

A survey of the mean turbulent field closure models.

13 p1601 A73-28801

Simultaneous comparison of turbulent gas fluctuations by laser Doppler and hot wire.

13 p1616 A73-28821

Representative shear wave passage through plane flame front, determining wave refraction and modification, flame generated turbulence and noise and perturbation of front

13 p1707 A73-28993

Free stream turbulence and transition in a circular duct.

13 p1602 A73-29014

Calculation of the basic characteristics of turbulent flows in a state of structural equilibrium

13 p1604 A73-29168

Problems of theory and practical application of Doppler-laser rate measuring devices in turbulent flow studies

13 p1628 A73-29169

Turbulence in liquids; Proceedings of the Symposium, University of Missouri, Rolla, Mo., October 4-6, 1971.

13 p1604 A73-29251

Turbulent interface detector using a multiple array of single hot wires.

13 p1619 A73-29252

Turbulence measurements with the split-film anemometer probe.

13 p1619 A73-29253

Hot-wire anemometric velocity measurements in nonisothermal turbulent flows, compensating for local temperature effects on downstream wire

13 p1620 A73-29255

Turbulent shear research, considering nondimensional data correlation, governing equations solution for parameters, statistical and experimental methods for structure determination

13 p1604 A73-29259

An attempt to characterize the 'turbulence burst phenomena' using digital time series analysis.

13 p1604 A73-29260

Turbulence in journal bearings, considering Taylor vortices development beyond laminar range and theoretical models based on mixing length flow theory

13 p1625 A73-29261

Energy relations for turbulent flow in rough pipes.

13 p1604 A73-29265

Phase velocities and angle of inclination for frequency components in fully developed turbulent flow through pipes.

13 p1604 A73-29266

Turbulent flow energy transfer paths and irreversible dissipation as internal thermal energy analyzed by Reynolds convention for turbulent velocity

13 p1605 A73-29267

Spectral analysis of the signal from the Laser Doppler Velocimeter - Turbulent flows.

14 p1752 A73-29919

Optimization of turbulence models by means of a logical search algorithm.

14 p1744 A73-29931

Rough estimate of the heat transfer coefficient of a liquid in laminar and turbulent flow through plane ducts

14 p1744 A73-30012

Mass transfer approximation model in unidirectional swirled two phase flow, considering transfer resistance of liquid phase

14 p1816 A73-30016

Derivation of a chain of equations for characteristic functions of a turbulent velocity field from the Hopf equation

14 p1744 A73-30021

Hydrodynamic tilting pad thrust bearings performance estimation in turbulent region based on laminar flow operation data

14 p1755 A73-30062

The origin of secondary flow in turbulent flow along a corner.

14 p1744 A73-30164

Rotating flow evolution in long circular tubes, deriving mathematical formulation for laminar and turbulent flow

14 p1745 A73-30296

The calculation of low-Reynolds-number phenomena with a two-equation model of turbulence.

14 p1746 A73-30606

Effects of buoyancy and of acceleration owing to thermal expansion on forced turbulent convection in vertical circular tubes - Criteria of the effects, velocity and temperature profiles, and reverse transition from turbulent to laminar flow.

14 p1818 A73-30614

Homogeneous turbulent forward and inverted flame front structure during hydrocarbon combustion, investigating gas flow velocity distribution, activation energy levels and burning zone boundaries

14 p1818 A73-30871

Pseudospectral approximation to two-dimensional turbulence.

14 p1746 A73-30909

Intermittency in fully developed turbulence as a consequence of the Navier-Stokes equations

15 p1860 A73-31092

Experimental investigation of the velocity structure and of hydraulic resistances in unsteady forced turbulent flows

15 p1862 A73-31287

Turbulent source flow between parallel stationary and co-rotating disks.

15 p1862 A73-31337

Influence of a magnetic field on turbulent shear flow

15 p1917 A73-31402

Magnetic field induced energy dissipation in conducting fluid isotropic turbulent flow velocity pulsations, noting Joule dissipation effect on damping

15 p1917 A73-31403

Uses of the equation of pulsation energy balance in the theory of MHD flows in channels and tubes

15 p1917 A73-31404

Effect of intense injection on flow stability and turbulence development 15 p1864 A73-31857

Momentum and moment of momentum differential equations of turbulent flow, reviewing and extending Matlioli theory to three dimensional flow 15 p1865 A73-32119

A theoretical analysis of the recovery factor for high-speed turbulent flow. 15 p1865 A73-32280

Subsonic free jet wind tunnel turbulence damping in settling chamber via screen, yielding uniform velocity profile and low turbulence level in nozzle exit 16 p1996 A73-33266

Approximate calculations of the hydrodynamic characteristics of turbulent fluid flow in annular ducts. 16 p2000 A73-33587

Theoretical investigation of the incompressible, turbulent, and axisymmetric internal flow with vanishing wall friction 16 p1964 A73-33749

Criteria regarding the predetermination of the laminar-turbulent boundary layer transition in the case of flows about body contours 16 p1965 A73-33750

Isolation and sampling of random signals transmitted by several hot-wire anemometers 16 p2017 A73-34016

Flow of a dust suspension over an ellipsoid of revolution. 17 p2091 A73-34348

Book on energy equations for small and large scale atmospheric motion covering laminar and turbulent flow and space-time scales for atmospheric energy balance 17 p2158 A73-34463

Two-variable asymptotic solution to unsteady three dimensional turbulent flow equations describing small scale deformation, determining hot spot or macromolecular size statistical behavior 17 p2201 A73-34800

Leakage and frictional characteristics of turbulent helical flow in fine clearance. 17 p2152 A73-35001

An upper bound on the stress in plane Couette flow. [ASME PAPER 73-FE-8] 17 p2152 A73-35007

Performance of low-aspect-ratio diffusers with fully developed turbulent inlet flows. I - Some experimental results. [ASME PAPER 73-FE-12] 17 p2152 A73-35009

Performance of low-aspect-ratio diffusers with fully developed turbulent inlet flows. II - Development and application of a performance prediction method. [ASME PAPER 73-FE-13] 17 p2152 A73-35010

Turbulent viscosities for swirling flow in a stationary annulus. [ASME PAPER 73-FE-16] 17 p2152 A73-35013

Temperature restitution coefficients for turbulent fluid flow in a circular pipe. 17 p2155 A73-35189

Experimental investigation of turbulent flow structure in a circular tube with expansion through a porous wall. 17 p2155 A73-35192

Turbulent flow research, discussing time domain analysis of velocity, displacement and pressure, potential flow models of vortices, and shear flow turbulence 17 p2155 A73-35330

Book - Buoyancy effects in fluids. 17 p2155 A73-35336

An analytical and experimental investigation of turbulent flow in bearing films including convective fluid inertia forces. [ASME PAPER 73-LUBS-1] 17 p2181 A73-35388

On the possibilities of improving the accuracy of the evaluation of inertia forces in laminar and turbulent films. [ASME PAPER 73-LUBS-3] 17 p2181 A73-35389

Turbulent lubrication theory - Application to design. [ASME PAPER 73-LUBS-10] 17 p2181 A73-35392

Experimental study on the interference of inertia and friction forces in turbulent lubrication. [ASME PAPER 73-LUBS-12] 17 p2181 A73-35393

Solution for the pressure and temperature in thrust bearings operating in the thermohydrodynamic turbulent regime. [ASME PAPER 73-LUBS-14] 17 p2181 A73-35394

Thermohydrodynamic lubrication in laminar and turbulent regimes. [ASME PAPER 73-LUBS-15] 17 p2181 A73-35395

Thin turbulent film analysis with approximation for relationship between flow and wall shear stress and effects of surface roughness and inertia at steps [ASME PAPER 73-LUBS-17] 17 p2181 A73-35396

Application of energy model of turbulence to calculation of lubricant flows. [ASME PAPER 73-LUBS-18] 17 p2181 A73-35397

Calculation of pressure, shear, and flow in lubricating films for high speed bearings. [ASME PAPER 73-LUBS-21] 17 p2182 A73-35399

Light beam absorption correlation with axial dispersion of ink injected into turbulent water flow in pipe 17 p2156 A73-35509

Turbulent heat transfer and the periodic viscous sublayer. 17 p2255 A73-35844

Rotor noise due to inflow turbulence. [AIAA PAPER 73-632] 18 p2259 A73-36191

Three-dimensional hypersonic transitional/turbulent mean flow profiles. [AIAA PAPER 73-635] 18 p2260 A73-36194

Turbulent flow fields with two dynamically significant scales. [AIAA PAPER 73-646] 18 p2297 A73-36201

Unsteady turbulent boundary layers in two-dimensional, incompressible flow. [AIAA PAPER 73-650] 18 p2260 A73-36205

Turbulent correlation measurements in a two-stream mixing layer. 18 p2298 A73-36311

Swirling flows in streamtubes of variable cross section. 18 p2298 A73-36314

Statistical theory of weakly interacting perturbations and low amplitude turbulence in fluids, considering diffusion, dispersive and acoustic wave characteristics and plasma instabilities 18 p2299 A73-36504

On Burgers' model equations for turbulence. 18 p2299 A73-36507

Simple universal equilibrium spectrum. 18 p2300 A73-36634

Numerical calculation of heat exchange and frictional resistance for a turbulent flow in a tube in the case of a gas with variable physical characteristics 18 p2301 A73-36816

Rheology of steady turbulent flows of an incompressible fluid 18 p2301 A73-37001

Weakly ionized continuum plasma turbulent shear flow and transport properties calculation, noting ratio of Debye shielding length to local integral scale 19 p2463 A73-37153

Fan acoustic measurements by hot-wire anemometers in anechoic chamber, discussing turbulent flow characteristics, noise spectra, wire velocity spectra and blade tip shape 19 p2472 A73-37289

Kinematic theory of magnetic field reconnection rate for analysis of turbulent flows in solar photosphere, flare phenomena and galaxy 19 p2467 A73-37439

The lift on a wing in a turbulent flow. 19 p2376 A73-37487

Turbulent Couette flow statistical theory, applying stochastic analysis to Navier-Stokes equation 19 p2421 A73-37855

Experimental study of turbulent flow in pipes with artificially roughened walls. 19 p2421 A73-38130

Turbulent flow development characteristics in channel inlets. 19 p2421 A73-38184

Laboratory observations of shear-layer instability in a stratified fluid. 19 p2422 A73-38232

Turbulence in stably stratified fluids - A review of laboratory experiments. 19 p2449 A73-38234

Some properties of horizontally homogeneous, statistically steady turbulence in a stratified fluid. 19 p2449 A73-38236

Interactions between internal gravity waves and their traumatic effect on a continuous stratification. 19 p2422 A73-38237

Measurements of internal waves and turbulence in two-dimensional stratified shear flows. 19 p2422 A73-38238

Practical calculations of transitional boundary layers. 19 p2423 A73-38479

Use of turning ring electrodes for study of the transport of matter in fluid in a laminar or turbulent hydrodynamic regime 19 p2432 A73-38481

Bounding flow existence for turbulent convection in fluid and porous layers analysis between parallel plates based on calculus of variations in Banach spaces 20 p2626 A73-39012

Subsonic and supersonic turbulent shear layer aerodynamic noise emission derivation from differential wave equations via Fourier transformation and WKB method 20 p2507 A73-39087

The structure of internal intermittency in turbulent flows at large Reynolds number - Experiments on scale similarity. 20 p2546 A73-39090

Velocity wave interaction and helical turbulence equilibrium spectra for two dimensional and three dimensional flow with quadratic energy and enstrophy spectra 20 p2549 A73-39812

On the coexistence of laminar and turbulent flow in a narrow triangular duct. 20 p2549 A73-39813

Aerodynamic forces on a triangular cylinder. 21 p2782 A73-40001

Viscoelastic panel vibration damping material for ventilation ducts to reduce LF vibrations induced by turbulent air flow 21 p2723 A73-40221

Asymmetric heat transfer in turbulent flow through a plane slot 21 p2790 A73-40351

Investigation of secondary flows between coaxial rotating cylinders 21 p2676 A73-40574

Convective heat transfer with allowance for three-dimensional heat sources in the fluid for turbulent flow in a plane slit 21 p2792 A73-41191

Subsonic wind tunnel tests for laminar boundary layer investigation in low level turbulence flow, noting turbulence measurement with hot-wire anemometers 21 p2704 A73-41311

Turbulent flow velocity pulsations damping in wind tunnel chamber by wire grids, calculating grid turbulence effect 21 p2633 A73-41311

Hole experiment on dispersion of Lagrangian tracers in quasi-stationary two dimensional turbulent flow, noting rms distance between paired balloons 21 p2687 A73-41333

Autocorrelation and space-time correlations for probe separations aligned with mean flow to test Pielke-Panofsky hypothesis, comparing laboratory tests to atmospheric turbulence 21 p2733 A73-41577

Dispersion of a harmonic signal within a turbulent pipe flow. 21 p2678 A73-41681

Noise from an isolated rotor due to inflow turbulence. 22 p2795 A73-41711

Inertial range differences between Kolmogorov energy spectrum formula for turbulence and modified Navier-Stokes equation, considering mu value deductibility 22 p2840 A73-41731

Equations for the finite-dimensional probability distributions of pulsating variables in a turbulent flow. 22 p2840 A73-41831

Some results of experimental investigations of turbulent flow in flexible tubes 22 p2841 A73-42121

Experimental investigations of the effects of polymer additions on the kinematic characteristics of a plane turbulent flow in a tube with variable wall roughness 22 p2841 A73-42121

Turbulent line vortex decay dependence of Reynolds number, suggesting triple vortex structure with outer and inner regions and viscous core with varying circulation distribution 22 p2842 A73-42271

Combustion in high speed swirling flow in gas turbine combustion chamber, discussing flame stability, pressure measurements and chamber configuration 22 p2935 A73-42791

Turbulent flow reactor for oxidation of moist C₂H₄ and postoxidation phase oxidation of methane, using chemical sampling and gas chromatographic analysis 22 p2820 A73-42841

Experimental determination of the turbulent Prandtl number near a smooth wall 22 p2937 A73-42931

Laser cross-beam intensity-correlation spectrum for a turbulent flow. 22 p2872 A73-43111

Turbulence amplifier with transition process control for multi-input fluid logic OR device operation at very low pressures and flow rates 23 p2942 A73-43331

An experimental investigation of the induced turbulence in laminar channel flow due to a transverse jet current and its applications to fluidic turbulence amplifiers. 23 p2942 A73-43441

Experimental investigation of turbulent flow characteristics in a rotating channel 23 p2968 A73-43441

An approximate model of a separated turbulent flow in an abruptly widening channel 23 p2968 A73-43441

Statistical analysis of two dimensional turbulence, noting probability characteristics ergodicity with respect to class of two dimensional characteristic functions with converging mean squares 23 p2968 A73-43441

Computerized simulation of isotropic three dimensional turbulence velocity field growth and energy decay based on Navier-Stokes equation numerical integration 23 p3001 A73-43511

Effect of pressure on the flame propagation velocity in a turbulent flow 23 p3019 A73-43711

Some further studies on the transition to turbulent convection. 23 p3003 A73-43901

Anisotropic turbulent distributions for waves with a nondecay-type dispersion law 23 p3012 A73-44018

Turbulent mean emf in presence of nonvanishing mean conducting fluid flow, modifying Green tensor of induction equation for constant strain rate velocity fields 23 p2969 A73-44050

Modal analysis of turbulent correlations in compressible flow. 23 p2970 A73-44382

Applicability of difference methods for solving Navier-Stokes equations at large Reynolds numbers 24 p3076 A73-44426

The momentum potential field description of fluctuating fluid motion as a basis for a unified theory of internally generated sound. 24 p3077 A73-44835

Hirs turbulent lubrication theory, discussing plane inclined slider thrust bearing applications and performance predictions 24 p3094 A73-44891

Air flow in circular convection chamber, investigating transition to turbulence by simultaneous measurements of heat flux and temperature field at low Rayleigh number 24 p3157 A73-45311

On the problem of nonlinear interactions in fluid dynamics. 24 p3080 A73-45449

Space-time autocorrelation and cross correlation coefficients for transverse turbulent velocity fluctuations in pipe flow 24 p3080 A73-45451

TURBULENT HEAT TRANSFER

Thermal intermittency coefficient distribution across turbulent boundary layer as function of free stream turbulence level 01 p0031 A73-10412

Influence of geometrical parameters on the energetic separation of superheated water vapor in a conical vortex tube 02 p0153 A73-11789

Hydrodynamics of the convective zone of the sun 03 p0373 A73-13608

Heat transfer in the turbulent boundary layer of an incompressible fluid flow past a surface when the pressure gradient and temperature on the surface are variable 03 p0295 A73-13622

Temperature distribution in a plasma filament in the presence of turbulent heat conduction 04 p0482 A73-15621

Empirical formulae for the universal functions $M_{sub} \mu/mu$ and N_{mu}/m in the resistance law for a barotropic and diabatic planetary boundary layer. 04 p0473 A73-15696

Combustion chamber temperature profiles analytical derivation from simultaneous radiative and turbulent diffusion heat transfer of turbulent flame front [ASME PAPER 72-WA/HT-27] 04 p0519 A73-15827

Heat and mass transfer laws for fully turbulent wall flows. 04 p0520 A73-15935

Statistical transfer theory in non-homogeneous turbulence. 04 p0520 A73-15937

Study of local heat transfer coefficients in a tube in the case of a local flow swirling by swirl vanes 05 p0639 A73-16768

Possible mechanisms of turbulent heating of a plasma by ultrashort pulses of laser radiation. 05 p0603 A73-16792

Evaluation of turbulent heating predictions with flight data. 05 p0532 A73-16943

Current induced drift rate of plasma electrons in electric and magnetic fields, noting electron velocities in turbulent heating of plasma 06 p0732 A73-18621

Dynamics of axial heat transfer in turbulent duct flow 06 p0770 A73-18831

Theory and simulation of turbulent heating by the modified two-stream instability. 07 p0857 A73-19526

Heat transfer in two-dimensional turbulent confined flows. 07 p0920 A73-19570

Nonthermal turbulent heating in the solar envelope. 08 p1003 A73-20887

Turbulent heating of colliding streams in the solar wind. 08 p0998 A73-21164

Turbulent hydrodynamics and heat transfer in rotating flows of incompressible fluid 08 p0954 A73-21184

Heat transfer for turbulent flow with suction in a porous tube. 08 p1024 A73-21637

Variable-property turbulent flow in a horizontal smooth tube during uniform heating and constant surface-temperature cooling. 10 p1295 A73-23779

Temperature distribution in a plasma with turbulent thermal conductivity. 10 p1255 A73-24211

Measurement of the ion energy distribution resulting from the turbulent heating of a plasma. 11 p1404 A73-25269

Prediction of heat transfer for turbulent boundary layer with pressure gradient. 11 p1453 A73-26393

Turbulent heat transfer to a fin leading edge - Flight test results. 11 p1303 A73-26405

Flight test correlation technique for turbulent base heat transfer with low ablation. 11 p1453 A73-26671

Convective heat transfer in the region of interaction between a supersonic overexpanded jet and an oblique obstacle 12 p1458 A73-27324

Theory of turbulent plasma heating by anomalous absorption of magnetosonic waves. 14 p1777 A73-29683

Study of the effect of heat influxes on the formation of lower and higher baric fields in the Northern Hemisphere 15 p1903 A73-31602

Keraug near-ground wind profiles approximation by Monin-Obuchov universal function, obtaining solutions for turbulent heat flux and shear flow velocity 15 p1906 A73-32343

Turbulent heat transfer role in atmospheric thermal budget, deriving smoothed local temperature time derivative 15 p1906 A73-32348

Lagrangian description of phase space flow - Turbulent heating. 16 p2041 A73-33322

Calculation of turbulent heat transfer and skin friction. 17 p2150 A73-34196

Turbulent heat transfer and the periodic viscous sublayer. 17 p2255 A73-35844

The prediction of turbulent heat transfer and pressure on a swept leading edge near its intersection with a vehicle. 18 p2368 A73-36228

Mass transfer effects on turbulent heating in the vicinity of slots. 18 p2371 A73-36381

Heat transfer in the case of turbulent and laminar trickle films 19 p2505 A73-38477

Bounding flow existence for turbulent convection in fluid and porous layers analysis between parallel plates based on calculus of variations in Banach spaces 20 p2626 A73-39012

Study of turbulent transfer with strong injection, longitudinal pressure gradient and nonisothermicity. 20 p2547 A73-39421

Friction, heat transfer and material removal in a turbulent boundary layer of a compressible high-enthalpy gas under conditions of marked nonisothermicity, injection and negative pressure gradient. 20 p2628 A73-39422

Large scale heat transfer in turbulent boundary layer at heated flat plate in incompressible viscous fluid, discussing temperature fluctuation spatial correlation as function of wall law and flow core 21 p2678 A73-41062

Analysis of the heat transfer associated with the evaporation of a fluid film on a rotating disk 24 p3156 A73-45078

TURBULENT JETS

Sound generation at an elastic plate acting as an obstruction in a turbulent free jet [DGLR PAPER 72-085] 02 p0152 A73-11667

The ordered structure of free-jet turbulence and its significance for the free-jet noise [DGLR PAPER 72-075] 02 p0128 A73-11701

Further studies of the aeroacoustics of jets perturbed by screens. 02 p0154 A73-12200

Swirling jet of gases mixture into vacuum. 03 p0289 A73-12908

Structural and aerodynamic characteristics changes in turbulent propane-butane and air jets interacting with sound 03 p0290 A73-12971

Some details of the pressure and velocity fields near the nozzle of a round turbulent jet. 03 p0293 A73-13311

Laser measurement of turbulence in exhaust jets. 03 p0308 A73-13568

German monograph - Axisymmetric free jets and free-jet flames and a numerical procedure for calculating them. 03 p0398 A73-13810

Cross correlations between turbulent jet flow and noise from hot-film and acoustic signal measurement, using Proudman form of Lighthill integral 03 p0246 A73-13842

Flammable fuel-air mixture ignition by transient turbulent hot inert gas jet, calculating minimum required jet size 03 p0399 A73-14390

Turbulent flow characteristics of swirling jets with opposite rotation, discussing lateral spreading into potential ambient fluid [ASME PAPER 72-WA/FE-17] 04 p0435 A73-15844

The swirling turbulent jet. 05 p0564 A73-16544

Pollutant formation in reacting turbulent jet flow field with recirculation, presenting methane-air system pointwise properties determination by numerical analysis [WSCI PAPER 72-21] 05 p0638 A73-16676

Analytical and experimental supersonic jet noise research. 05 p0531 A73-16926

Thin wing induced undulating viscous wake and far field acoustic wave through interaction with turbulent cylindrical jet, using dipole force field model [AIAA PAPER 73-223] 05 p0532 A73-16950

Solid particle transport effect on structure and axial speed characteristics of two phase submerged turbulent jet 06 p0684 A73-17455

Two-dimensional turbulent jets at a porous wall. 07 p0811 A73-19613

Turbulent jet diffusion and vortex models, noting velocity profile in mixing and turbulent boundary layers 07 p0811 A73-19617

Supersonic flow past notch in lateral body surface or in two closely lying coaxial bodies, applying turbulent jet theory to separation zone 07 p0774 A73-19618

Numerical calculations for the turbulent arc constrictor. 07 p0858 A73-19960

Motion of a fluid outside a turbulent jet system 07 p0812 A73-20091

Effect of jet turbulence on the flow in a wall boundary layer 10 p1205 A73-23586

A new criterion for the length of a gaseous turbulent diffusion flame. 11 p1449 A73-25372

Pneumatic sensors without contact 11 p1308 A73-25381

Noise intensity in the field of subsonic turbulent jets 11 p1347 A73-25738

Theory of sound scattering by turbulence applied to scattering cross section calculation for turbulent jet flow and wind, discussing jet noise reduction 11 p1349 A73-26496

Pulsation energy calculations in axisymmetric turbulent jet flows of incompressible fluids with a zero excess impulse 13 p1600 A73-28448

Turbulent jet noise generation theory relationship between flow and acoustic characteristics, obtaining intensity expression with velocity space-time derivatives for moving and stationary coordinates 13 p1603 A73-29138

The application of photon correlation spectroscopy to the measurement of turbulent flows. 13 p1622 A73-29421

Behavior of a weak turbulent jet in a cross flow 15 p1822 A73-31199

Probability distribution of the concentration and intermittency in turbulent jets 15 p1862 A73-31286

Application of the energy equation for turbulence in the theory of jet flows 15 p1862 A73-31288

Development of the method and investigation of the intensity of turbulence at the axis of a two-phase turbulent jet 15 p1862 A73-31298

Interaction position and static pressure measurements of two opposing plane turbulent wall jets in still air in terms of frozen flow 15 p1863 A73-31342

Mean flow data analysis of supersonic combustion ramjet turbulent jet mixing at high free stream Mach number 16 p2000 A73-33268

Turbulent jet deflection and impingement in confined cross flow occurring in gas turbine blade impingement cooling schemes [ASME PAPER 73-FE-15] 17 p2152 A73-35012

Monograph - Two causality correlation techniques applied to jet noise. 17 p2155 A73-35150

Mixing and structural characteristics of turbulent pulsating jets based on hot-wire anemometer velocity measurement data 17 p2157 A73-35513

Experiments on confined turbulent jets in cross flow. 18 p2260 A73-36202

Mathematical approximation of turbulent cylindrical jets: Initial core - Velocity distribution 18 p2301 A73-36690

- Electromagnetic interactions with turbulent plasmas. 19 p2465 A73-37167
- Parametric analysis of turbulent wall jets. 19 p2376 A73-37491
- Experimental investigation of premixed swirling jet flames - Combustion characteristics. 19 p2504 A73-37946
- Turbulent incompressible plane wall jet flow in still air, examining maximum velocity, total thickness and inner length scale with parametric analysis. 21 p2678 A73-41191
- Langmuir probe signal analysis of root-mean-square electron density fluctuations in turbulent Ar plasma jet. 22 p2893 A73-42394
- Refraction, convection, and diffusion flame effects in combustion-generated noise. 22 p2934 A73-42780
- Recirculation and mixing characteristics prediction for enclosed turbulent jet flames in flow regions, using similarity parameters. 22 p2934 A73-42782
- Measurements of the distribution of sound source intensities in turbulent jets. 24 p3053 A73-44826 [AIAA PAPER 73-989]
- Introduction of the viscous force sensing fluctuating probe technique, with measurement in the mixing zone of a circular jet. 24 p3090 A73-44868 [AIAA PAPER 73-1044]
- Development of a mathematical model for vortex configuration in jets and flames. 24 p3157 A73-45376
- ### TURBULENT MIXING
- Turbulent flame velocities in premixed sprays. II - Theoretical analysis. 01 p0121 A73-10636
- Two-stream heterogeneous mixing measurements using laser Doppler velocimeter. 01 p0050 A73-10741
- Supersonic mixing and combustion of confined coaxial hydrogen-air streams. 03 p0397 A73-13473 [AIAA PAPER 72-1178]
- The interaction between turbulent wakes and boundary layers. 03 p0244 A73-13561
- Magnetic field effect on friction shear stress in turbulent slipstreams of conducting fluids, calculating mixing zone width. 03 p0346 A73-13609
- Studies leading to the realization of supersonic combustion in propulsion applications. 03 p0398 A73-14141
- Analysis of free turbulent mixing flows without a net momentum defect. 03 p0296 A73-14187
- Turbulent gas mixing measurements using a laser schlieren technique. 03 p0296 A73-14202
- A nondimensional parameter characterizing mixing processes in a model of thermal gas ignition. 03 p0399 A73-14389
- Buoyancy forces contribution to heat flux during turbulent mixing in upper atmosphere, noting kinetic turbulence balance components. 04 p0473 A73-15573
- A transformation for the numerical solution of two-dimensional free mixing flow problems. [ASME PAPER 72-WA/FE-3] 04 p0434 A73-15841
- Turbulent flow characteristics of swirling jets with opposite rotation, discussing lateral spreading into potential ambient fluid. [ASME PAPER 72-WA/FE-17] 04 p0435 A73-15844
- Free turbulent mixing in axial pressure gradients. [ASME PAPER 72-WA/APM-31] 04 p0435 A73-15888
- Hemispheric single level model of atmospheric action centers formation due to horizontal baroclinicity, including turbulent mixing and circulation index effects. 05 p0592 A73-16229
- Analytical and experimental supersonic jet noise research. [AIAA PAPER 73-188] 05 p0531 A73-16926
- Turbulent space-time correlation measurements in a plane two-stream mixing layer at velocity ratio 0.3. [AIAA PAPER 73-225] 05 p0566 A73-16951
- Shear stress distribution from measured nondimensional mean velocity profile measured in plane turbulent mixing layer formed at cascade wind tunnel exit. 05 p0567 A73-17106
- Some observations on flows described by coupled mixing and kinetics. 06 p0767 A73-17729
- Temperature field structure in strongly heated buoyant thermals. 07 p0919 A73-19504 [AD-754728]
- Turbulent mixing at homogeneous wakes boundary, using heat conduction equivalence. 07 p0810 A73-19610
- Minimum mixing losses of axisymmetric turbulent wakes in profiled wall channels. 07 p0811 A73-19611
- Euler, Lagrange and time turbulence scales for Prandtl mixing length, relating with velocity and pressure pulsations in steady turbulent gas flow. 10 p1204 A73-23474
- Book - Annual review of fluid mechanics. Volume 5. 10 p1205 A73-23851
- Turbulent viscosity distribution in axisymmetric compressible wake and coaxial mixing flows via Navier-Stokes equations, taking into account pressure gradients. 10 p1206 A73-24545
- The response of a hot-wire anemometer in flows of gas mixtures. 10 p1222 A73-24971
- Turbulent transport coefficients for compressible heterogeneous mixing. 13 p1705 A73-28435
- Fuel-air turbulent mixing process in double concentric jet type burner, measuring average velocity, pressure distribution, turbulence intensity and shear stress. 13 p1601 A73-28648
- Probability distribution of the concentration and intermittency in turbulent jets. 15 p1862 A73-31286
- A simple estimate of the effect of ejector length on thrust augmentation. 15 p1824 A73-31745
- Stratospheric mixing estimated from high altitude turbulence measurements. 16 p2005 A73-33539 [AIAA PAPER 73-497]
- Chemical laser power output prediction by laminar analysis modification with conventional gross mixing concept of turbulent flow in population inversion. 17 p2183 A73-34193
- Development of a turbulent mixing region in a liquid. 17 p2150 A73-34265
- Turbulent mixing in the developing region of coaxial jets. [ASME PAPER 73-FE-19] 17 p2153 A73-35015
- Fluid mechanics of mixing; Proceedings of the Joint Meeting, Georgia Institute of Technology, Atlanta, Ga., June 20-22, 1973. 17 p2156 A73-35501
- Microscopic aspects of turbulent and laminar mixing in terms of molecular, eddy and bulk diffusional operations. 17 p2156 A73-35502
- A generalized theory for the turbulent mixing of axially symmetric compressible free jets. 17 p2156 A73-35505
- Mean flow and turbulence measurements in a Mach 5 shear layer. 17 p2097 A73-35506
- Statistical models of turbulent free shear mixing layer structure in incompressible air streams. 17 p2156 A73-35507
- Application of laser Raman spectroscopy to the study of factors that influence turbulent gas mixing rates. 17 p2185 A73-35510
- Turbulence measurements with hot-wire anemometry in a non-homogeneous jet. 17 p2174 A73-35512
- Turbulent mixing of cylindrical jet with parallel stream in terms of mixing length concepts and velocity profiles. 17 p2157 A73-35515
- Calculation of free turbulent mixing by interaction approach. [AIAA PAPER 73-649] 18 p2297 A73-36204
- Multiphase underexpanded plume computational technique including turbulent mixing and nonequilibrium chemistry. [AIAA PAPER 73-695] 18 p2368 A73-36244
- Turbulent correlation measurements in a two-stream mixing layer. 18 p2298 A73-36311
- Turbulent mixing of gas flows in the presence of a pressure gradient. 18 p2266 A73-37016
- A study on opposing jets in air stream and their flame. I - A structure of two dimensional opposing jets in the state without flames. 19 p2377 A73-37945
- On the prediction of turbulence in baroclinic zones. 19 p2449 A73-38246
- The effect of the wedge angle on the similarity parameter of the turbulent mixing region in the case of an incompressible flow. 20 p2547 A73-39408
- Euler, Lagrange and time turbulence scales for Prandtl mixing length, relating with velocity and pressure pulsations in steady turbulent gas flow. 21 p2678 A73-41321
- On turbulent stress and the structure of young convective stars. 22 p2908 A73-42306
- Mathematical modeling of combustors based on turbulent mixing, droplet evaporation and chemical kinetics, considering stirred reactor heat balance and combustor performance prediction. 22 p2935 A73-42789
- Effects of turbulent mixing and chemical kinetics on nitric oxide production in a jet-stirred reactor. 22 p2820 A73-42796
- Nitric oxide generation in turbulent diffusion flames, discussing limits for constant pressure turbulent reacting mixing zone between parallel flowing streams of fuel and oxidizer. 22 p2935 A73-42796
- Laminar and turbulent mixing of compressible jets at low Reynolds numbers. 23 p2967 A73-43403
- ### TURBULENT WAKES
- #### NT PROPELLER SLIPSTREAMS
- #### NT SLIPSTREAMS
- Effect of streamwise vortices on wake properties associated with sound generation. 01 p0001 A73-10040
- Turbulent swirling wake behind spinning axisymmetric body of revolution having axis aligned with free stream direction, obtaining velocity profiles variations. 01 p0004 A73-11121
- Turbulent wake flow behind two dimensional flat plate trailing edge investigated by Nee-Kovaszay turbulent shear flow differential field theory. 01 p0004 A73-11121
- Rotor unsteady wakes three dimensional flow analysis by wave front averaging technique, using constant temperature hot-wire anemometer. 02 p0129 A73-12555
- The interaction between turbulent wakes and boundary layers. 03 p0244 A73-13561
- Observations on the macroscopic structure of a near turbulent wake with a Mach number M sub infinity equal 2.3. [ONERA, TP NO. 1176] 03 p0244 A73-13553
- Fluctuations in geomagnetic wake region at 50 earth radii connected with magnetotail Kelvin-Helmholtz instability, using plasma cylinder model. 04 p0445 A73-15559
- Structure of turbulent wakes of hypersonic spheres as inferred with ion probes. 05 p0527 A73-16569
- Thin wing induced undulating viscous wake and far field acoustic wave through interaction with turbulent cylindrical jet, using dipole force field model. [AIAA PAPER 73-223] 05 p0532 A73-16953
- Numerical analysis of far turbulent wakes in ideal gas, determining hydrodynamic field moments, turbulence levels and mean square enthalpy fluctuations. 06 p0643 A73-17430
- Wind tunnel study of flow structure and turbulent wakes on base surfaces of sharp or blunt edged bodies at various Mach and Reynolds numbers. 06 p0643 A73-17430
- Ion density and current distribution measurements in hypersonic turbulent wakes behind sphere flow in ballistic range, using cylindrical electrostatic probes. 06 p0645 A73-18170
- The aircraft wake turbulence problem. 06 p0648 A73-18140
- Turbulent mixing at homogeneous wakes boundary using heat conduction equivalence. 07 p0810 A73-19610
- Minimum mixing losses of axisymmetric turbulent wakes in profiled wall channels. 07 p0811 A73-19611
- Turbulent intensity induced by wakes near secondary air jet inlet to gas turbine engine flame tube. 07 p0867 A73-19610
- Dynamic model of flow separation of plane flow past body in channel with eddy wake formation. 08 p0954 A73-21101
- Temperature fluctuations in the turbulent wake behind an optically heated sphere. 10 p296 A73-24220
- Turbulent viscosity distribution in axisymmetric compressible wake and coaxial mixing flows via Navier-Stokes equations, taking into account pressure gradients. 10 p1206 A73-24545
- Turbulent wake development in oscillating flow deriving flow equations for sinusoidally time dependent orifice flow. 10 p1208 A73-24840
- Unsteady boundary layer and wake near the trailing edge of a flat plate. 10 p1173 A73-24840
- Conditional sampling and other measurements in plane turbulent wake. 11 p299 A73-25000
- Earliest classic result for the turbulent hydraulic wake behind body of revolution. 11 p1348 A73-25710
- Influence of the shape of a body on the characteristics of a self-similar axisymmetric wake. 12 p1457 A73-26960
- Correlation and statistical characteristics of turbulence fronts in the wakes of hypervelocity bodies. 13 p1567 A73-29220
- A modified wall wake velocity profile for turbulent compressible boundary layers. 17 p2150 A73-34440
- Aircraft wing tip turbulent wakes producing swirling vortices, discussing wake hazards, wind tunnel research and vortex dissipation procedures. [SAE PAPER 730294] 17 p2094 A73-34600

A method of measuring three-dimensional rotating wakes behind turbomachinery rotors.
[ASME PAPER 73-FE-31] 17 p2095 A73-35023
Application of turbulence model equations to axisymmetric wakes.
[AIAA PAPER 73-648] 18 p2260 A73-36203
Turbulence measurements in interacting wakes.
18 p2301 A73-36698
Experimental investigation of the velocities in the turbulent wake behind bodies of revolution
18 p2266 A73-37017
Influences of the shape of a body on the characteristics of a self-similar axisymmetric wake.
19 p2377 A73-38129
Asymptotic behaviour of a scalar in an axisymmetric final period turbulent wake.
20 p2507 A73-39086
Study of turbulent wakes behind cones in hypersonic flight using Schlieren photograph correlation
21 p2696 A73-39985
Calculation of the two-dimensional turbulent wake behind a thin obstacle
[ONERA, TP NO. 1253] 22 p2796 A73-42222
Aeroballistic range facilities development and application to reentry physics, discussing program for turbulent wake properties of hypersonic projectiles
24 p3054 A73-44993

TURING MACHINES

Russian book - Problems in the synthesis of finite automata.
15 p1848 A73-31909
Length minimization in the internal-state code of an asynchronous finite automatic system with a two-step memory
15 p1848 A73-31910
Logic circuit distribution algorithms for asynchronous finite automata synthesis on basis of universal homogeneous medium
15 p1848 A73-31911
State minimization of incompletely defined deterministic automaton by imbedding one-to-one mapping into homomorphism
24 p3074 A73-44664

TURNING FLIGHT

NT MINOR CIRCLE TURNING FLIGHT
Sonic boom avoidance by flight path maneuvers, investigating shock front development in curved flight
02 p0130 A73-11856
Linearized theory for infinite span wing small unsteady motions in curved flight in inviscid incompressible fluid, obtaining time dependent forces, pressure and velocity fields
[AIAA PAPER 73-90] 05 p0529 A73-16854
Energy management in aerial combat weapon systems maneuvering and delivery tactics, computing optimal feedback control laws for supersonic aircraft minimum time turning trajectories
[AIAA PAPER 73-231] 05 p0536 A73-16956
Optimal 3-dimensional minimum time turns for an aircraft.
06 p0648 A73-18377
Minimum fuel rocket maneuvers in horizontal flight.
08 p1014 A73-20714
Determination of the turn start point coordinates for modern commercial aircraft
11 p1307 A73-26723
'Bank-to-turn steering' for highly maneuverable missiles.
[AIAA PAPER 73-860] 20 p2586 A73-38798
Horizontal aircraft maneuver strategy for maximum miss distance and minimum course deviation, examining filtering techniques, collision avoidance system and signal error analysis
21 p2734 A73-40032
Synthesis of programmed extensive control of a spatial turning maneuver
23 p3005 A73-43718

TURNSTILE ANTENNAS

A novel VHF turnstile antenna for the SMS satellite.
04 p0428 A73-15456
Study of two types of turnstile aerial immersed in a warm plasma.
14 p1731 A73-29712

VC (CONTROL)

U THRUST VECTOR CONTROL
WENTY-FOUR HOUR ORBITS
A system of four geosynchronous satellites for global observations
15 p1903 A73-31605
WENTY-SEVEN DAY VARIATION
Winter anomaly in ionospheric absorption of radio waves on 1.725 MHz during sunspot minimum.
01 p0043 A73-10910
Spectral analysis of geomagnetic variations to study the tidal and the storm modulation effects.
02 p0158 A73-11906
Further study of the theta component of the interplanetary magnetic field.
07 p0875 A73-19230
Comparison of the correlation of incoherent scatter and ionosonde measurements of temperature with calcium plage and 2800-Megahertz intensities.
07 p0815 A73-19250

Evening/forenoon asymmetry in the 27-day oscillation of the low-latitude magnetic field.
09 p1076 A73-22140
Relationship between the 27-day cosmic-ray variations and various solar-activity indices during the period from 1957 to 1970
10 p1266 A73-23918
Solar cosmic ray anisotropy 27-day variations during IGY from global network stations neutron component data
10 p1268 A73-24237
A study of the time lag of the 27-day variation in the thermospheric density.
18 p2303 A73-35961
An analysis of the solar-activity effects in the upper atmosphere.
18 p2309 A73-36060
Characteristics of the influence of the solar wind on cosmic-ray intensity during 1969
18 p2345 A73-36108
Periodic variations of the cosmic radiation. III - The 27-day variation.
18 p2345 A73-36180
The 27-day variations of the hard cosmic ray component and the atmospheric ozone X-layer according to IGY data
21 p2755 A73-40109
Differences in the correlations of 27-day and 11-year cosmic ray variations with solar activity parameters
21 p2758 A73-40598
Certain features of the 27-day variations in cosmic-ray anisotropy
21 p2758 A73-40599
Solar cycle control in the 27-day variation of geomagnetic activity.
22 p2846 A73-41945
Polar magnetic storm temporal properties and distribution patterns, discussing solar activity, annual and twenty-seven day variations and sudden commencement
22 p2851 A73-42749

TWILIGHT

U TWILIGHT GLOW
TWILIGHT GLOW
Meteor shower and cosmic dust effects on twilight sky brightness from mountain top and balloon observations
02 p0215 A73-12261
Changes in thermospheric molecular oxygen abundance inferred from twilight 6300 A airglow.
04 p0440 A73-14963
The contrast and the visibility of noctilucent clouds in the twilight sky
04 p0441 A73-15293
Study of the scattering properties of the atmosphere by light polarization measurements in a twilight sky
05 p0572 A73-17355
Optical sounding methods for the upper atmosphere and the earth's dust cloud
07 p0817 A73-19584
Qualitative detection of space dust particle layers in the lower thermosphere by the twilight method
07 p0817 A73-19586
Scattered twilight light variations at 5500 to 6600-A wavelengths according to spectral observations in 1962 through 1968 at Abastumani
07 p0817 A73-19587
Analysis of light polarization variations in a twilight sky in terms of upper atmosphere effects
07 p0817 A73-19588
Determination of the concentration and scattering indicatrix of atmospheric dust from primary twilight brightness
07 p0817 A73-19589
Twilight sounding method for earth upper atmosphere investigation, taking into account earth shadow and effective altitude of solar radiation attenuation/shielding/zone
07 p0818 A73-19591
Photoelectric measurement of twilight sky brightness distribution for separation of primary brightness component, noting possibility of secondary component due to dust
07 p0818 A73-19593
Increase of Na twilight emission after the earth's crossing of the orbital planes of Comets Halley and Encke.
07 p0899 A73-20063
Twilight airglow. I - Photoelectrons and forbidden O I 5577-angstrom radiation.
10 p1214 A73-24737
Twilight circular polarization due to Mie scattering, analyzing polarimeter measurements in IR and UV spectral bands
12 p1490 A73-27150
Derivation of scattering properties of the atmosphere from polarization measurements on the light of the twilight sky.
15 p1865 A73-31005
Spectral investigations of 6300 A forbidden OI twilight emission at Abastumani
15 p1867 A73-31264

Twilight enhancement of forbidden-OI 6300 A airglow.
15 p1868 A73-31382
Sky brightness observation of post-dusk effect in Spanish Sierra Nevada for relationship to predawn enhancement, noting insufficient evidence for quantitative analysis
16 p2008 A73-33880
Primary scattering theory for twilight luminance calculation, considering luminance atmospheric scale height growth in thermosphere and seasonal variation
16 p2009 A73-33889
A comparison of two methods of analysis for the twilight sodium airglow data.
16 p2009 A73-33891
Thermal electron energy distribution measurements in the ionosphere.
21 p2681 A73-40156
Investigation of mid-latitude ionospheric currents by combined rocket techniques.
21 p2689 A73-41359
Mie scattering computation of cosmic dust flux in upper atmosphere from twilight luminance increase during meteor showers
21 p2775 A73-41418
Satellite ultraviolet measurements of nitric oxide fluorescence with a diffusive transport model.
22 p2845 A73-41925
Description of a photometer suitable for measuring twilight ozone content variations from a stratospheric balloon gondola
23 p2982 A73-43875

TWINNING
NT MECHANICAL TWINNING
Microtwinning factors in plastic deformation, volume changes and carbon solution content of Ni martensite
06 p0710 A73-18645
Lunar plagioclase and pyroxene observation for lamella thicknesses by X ray diffraction, noting twinning, exsolution and crystal disorder effects
07 p0788 A73-19711
Twin laws, optic orientation, and composition of plagioclases from rocks 12051, 14053, and 14310.
07 p0881 A73-19713
Observations on the interaction of twins with grain boundaries in Mo-35 at.% Re alloy.
09 p1100 A73-21982
Twinning deformation of mild steel at low temperatures as function of stress-strain state
09 p1100 A73-22154
Plastic strain rates within discrete crack tip zones at running brittle cracks in mild steel plates, identifying twinning as main deformation mode
09 p1163 A73-23258
Gliding, twin formation and fracture of iron-single crystals at 78 K and at 4 K
11 p1386 A73-26571
Deformation and recrystallization of twin crystals in aluminum and magnesium alloys
12 p1510 A73-26913
Nickel niobide tested along crystal growth direction for twinning mode of intermetallic phase in tensile deformation, projecting crystallographic structure upon crystal plane
14 p1762 A73-30640
Twinned plate structure of martensitic transformation dependence on composition in Zr-Ti alloy investigated by transmission electron microscopy
20 p2575 A73-39023

TWISTING
Thermomechanical dissipation analysis of thermoviscoelastic solids by finite elements.
03 p0389 A73-13326
On the determination of the centers of twist and of shear for cylindrical shell beams.
[ASME PAPER 72-APM-XX] 05 p0633 A73-16534
Hamilton variational principle for deriving equations of motion for small elastic displacements of thin circular rings, noting twist equation occurrence
11 p1446 A73-26493
Singular nonaxisymmetric shallow shell equation solutions for concentrated normal and tangential forces and bending and twisting moments
12 p1550 A73-27034
Considerations on the centres of shear and of twist in the theory of beams.
15 p1954 A73-32111
Differential equations for the vibrations of twisted rods with allowance for energy dissipation
20 p2619 A73-39372
Curved twisted space beam elements, expressing displacement function and inertia property by rotation and mass matrices
20 p2621 A73-39533
The plastic deformation of NiAl single crystals between 300 K and 1050 K. I - Experimental evidence on the role of kinking and uniform deformation in crystals compressed along the 001 direction. II - The mechanism of kinking and uniform deformation.
23 p2991 A73-43773

TWO BODY ORBITS

U TWO BODY PROBLEM

TWO BODY PROBLEM

Gravitational constant anisotropy effects on planets with orbits close to ecliptic in solar system two body problem

01 p0099 A73-10689

Dynamics of gravitating systems against the neutrino background of the universe

01 p0100 A73-10712

Distortion of particle trajectories by dynamic effects in the problem of two bodies with corpuscular emission

01 p0102 A73-10947

Circular orbit stability in restricted two body problem with secular variations, giving disturbing function secular terms to eighth order

02 p0222 A73-12710

The transition from elliptic to hyperbolic orbits in the two-body problem by slow loss of mass.

03 p0377 A73-14273

Space-time transformation for equation of relative motion of two bodies on gravitating matter background of Einstein-de Sitter universe

06 p0724 A73-18689

First-order perturbations of the two finite body problem.

07 p0877 A73-19594

Dynamical effects of the curvature of particle trajectories in the two-body problem with corpuscular radiation.

09 p1148 A73-22742

Exact analytical solutions basic to a class of two-body orbits.

11 p1423 A73-26072

Equilibrium configurations and attitude stability criteria for articulated satellite idealized as point-connected rigid two gyrostair problem

14 p1802 A73-29757

A note on the relations between true and eccentric anomalies in the two-body problem.

15 p1930 A73-31116

Two dimensional nonlinear oscillations around center of mass of vehicle moving along circular orbit with magnetic damping under gravitational field and external perturbation

15 p1942 A73-31233

Third Kepler law application to quanta hypothesis of two body systems of physical nature involving centers of attraction

16 p2071 A73-34004

Spatial motion of a two body cluster under the action of gravitational and aerodynamic forces

18 p2351 A73-36119

Elliptical orbit of two coupled material points in Newtonian central gravitation field, discussing flexible weightless filament coupling, equations of motion and sinusoidal oscillations

20 p2608 A73-39319

Gravitational red shift - A simple quantum field-theoretical consideration in a curved space.

23 p3006 A73-43607

Kustaanheimo-Stiefel transformation in Kepler motion perturbation theory derived from general solution of two body problem, noting application to collision orbits and Lagrange solutions

24 p3142 A73-45298

TWO DIMENSIONAL BODIES

Determination of elastic stresses at notches and corners by integral equations.

02 p0234 A73-12075

A free-streamline theory for bluff bodies attached to a plane wall.

04 p0403 A73-15160

Note on the wave propagation problems in isotropic discretized bodies.

06 p0723 A73-17893

Two-dimensional temperature fields in straight rectangular fins

06 p0768 A73-17921

Asymptotic theory of the Boltzmann equation at large Knudsen number.

07 p0853 A73-20473

Unsteady thin-airfoil theory for subsonic flow.

08 p0925 A73-20718

An exploratory investigation of the unsteady aerodynamic response of a two-dimensional airfoil at high reduced frequency.

[AIAA PAPER 73-309]

11 p1301 A73-25540

Finite element elastic-plastic-creep analysis of two-dimensional continuum with temperature dependent material properties.

19 p2496 A73-37483

Analytic solutions for potential flow over a class of semi-infinite two-dimensional bodies having circular arcs.

23 p2940 A73-43931

TWO DIMENSIONAL BOUNDARY LAYER

Separation of turbulent boundary layer - Wall pressure distribution near separation.

02 p0154 A73-12523

The universalization of unsteady boundary layer equations

10 p1207 A73-24805

Transient viscous laminar incompressible flow pattern after sudden vanishing of semi-infinite flat plate

based on two dimensional unsteady boundary layer equations with boundary conditions

10 p1208 A73-24811

Two dimensional laminar boundary layer separation for unsteady flow or flow past moving walls, considering singularity due to bifurcating wake bubble

10 p1208 A73-24813

A higher order theory for compressible turbulent boundary layers at moderately large Reynolds number.

11 p1346 A73-25218

Two dimensional incompressible turbulent boundary layer flow theory, considering Bradshaw turbulence field and Felsch integral methods

14 p1745 A73-30298

A numerical method for integrating the unsteady boundary-layer equations when there are regions of backflow.

16 p1998 A73-32799

The principle of spatial variations - Application to the boundary layer theory.

16 p1999 A73-32978

A finite difference solution of the two and three-dimensional incompressible turbulent boundary layer equations.

[ASME PAPER 73-FE-20]

17 p2153 A73-35016

Practical calculations of transitional boundary layers.

19 p2423 A73-38479

Boundary-layer separation at a free streamline. III - Axisymmetric flow and the flow downstream of separation.

20 p2549 A73-39806

The asymptotic analysis of canonical problems in high-frequency scattering theory. I - Stratified media above a plane boundary. II - The circular and parabolic cylinders.

22 p2886 A73-42347

On the generalization of the Mangler transformation for axisymmetric boundary layers.

23 p2967 A73-43226

Plane boundary layer equations for viscous incompressible fluid with asymmetric stress tensor produced by moment stresses and mass moments

23 p2968 A73-43922

Boundary layer equations of magnetohydrodynamics with moment stresses

23 p3015 A73-44385

TWO DIMENSIONAL FLOW

NT COUETTE FLOW

Plane flow past vortex of inviscid incompressible fluid jets bound by free surface and horizontal wall, considering complex potential function and submerged lifting airfoils

01 p0031 A73-10304

Streaming two dimensional Oseen MHD flow of conducting fluid past semi-infinite needle within aligned field

01 p0031 A73-10305

An investigation of particle trajectories in two-phase flow systems.

01 p0002 A73-10439

Two-dimensional boundary layers in a free stream which oscillates without reversing.

01 p0032 A73-10446

Free and forced convection from fine hot wires.

01 p0120 A73-10447

French monograph - A method of calculating the turbulent boundary layer using an equation for the behavior of the Boussinesq coefficient.

01 p0332 A73-10602

Vibrational instability of plane-parallel convective motion in a vertical duct

01 p0034 A73-10966

Shear waves and perturbations in linearized steady plane flows of a thermally nonconducting compressible ideal fluid

[ONERA, TP NO. 1169]

01 p0034 A73-11359

Experimental investigation of the supersonic two-dimensional flow past a sail at small angles of attack

01 p0004 A73-11371

Hydromagnetic flow about a curved neutral sheet.

01 p0086 A73-11495

Two-dimensional, unsteady, self-similar flows in gas dynamics.

02 p0152 A73-11569

Some exact statistics of two-dimensional viscous flow with random forcing.

02 p0153 A73-12041

On the uniqueness of solutions of the Falkner-Skan equation.

02 p0154 A73-12798

Integral transformations and conformal mapping for velocity distribution of steady two dimensional potential flow along given profile curve

03 p0241 A73-12904

Calculation of the potential created and the velocity induced by a uniform source distribution on a polygon and on a periodic distribution of polygons for the solution of two-dimensional Poisson fields

03 p0241 A73-12910

The boundary layer of particulate gas flow.

03 p0289 A73-12914

Sturm-Liouville solution of unsteady stratified two dimensional Couette flow equations of motion

03 p0292 A73-13363

Applying quasilinearization to the steady laminar flow between two parallel porous plates.

03 p0292 A73-13363

Effects of transverse ribs on pressure recovery of two-dimensional subsonic diffusers.

[AIAA PAPER 72-1141]

03 p0243 A73-13444

Plane Poiseuille flow with small amplitude modulated pressure gradient, noting disturbance shear wave and stability from energy transfer calculation

03 p0293 A73-13510

Boundary-layer development at a two-dimensional rear stagnation point.

03 p0294 A73-13511

The interaction between turbulent wakes and boundary layers.

03 p0244 A73-13512

Three dimensional flow pattern from two dimensional supersonic inviscid gas flows around wedge body

03 p0245 A73-13568

Steady transverse plane magnetogasdynamic flows

03 p0346 A73-13621

Two-dimensional unsteady flow by hydraulic analogy.

03 p0295 A73-13731

Nonlinear instability of two dimensional unbounded incompressible viscous fluid flows under periodic small perturbation

03 p0296 A73-14048

Extension of the Miles-Howard theorem to the circular flows of a compressible fluid.

03 p0297 A73-14448

Vortex lattice discretization for finite Hilbert transform of two dimensional incompressible thin film flow integral equation with singularities, noting a numerical solution accuracy

04 p0403 A73-15010

Finite difference technique for numerical calculation of two dimensional stratified incompressible fluid flows

04 p0433 A73-15112

Study of plane flows of viscous fluid around a boomerang

04 p0404 A73-15113

Study of the laminar free convection wake above an isothermal vertical plate.

[ASME PAPER 72-WA/HT-41]

04 p0518 A73-15180

A transformation for the numerical solution of two dimensional free mixing flow problems.

[ASME PAPER 72-WA/FE-3]

04 p0434 A73-15181

Theoretical low-speed particles collision with symmetrical and cambered aerofiles.

[ASME PAPER 72-WA/FE-35]

04 p0404 A73-15182

Inverse problem approach to the design of slender two-dimensional diffusers.

[ASME PAPER 72-WA/GT-6]

04 p0404 A73-15183

Incompressible plane flow subject to infinitely small vibrations, expressing complex potential as Abel integral

[ONERA, TP NO. 1191]

04 p0472 A73-15184

Hydrodynamic stability of a laminar boundary layer in a flow past a planar plate

05 p0601 A73-16041

Numerical solutions of the Navier-Stokes equations in inlet regions.

[ASME PAPER 72-APM-DD]

05 p0564 A73-16042

On the numerical solution of two-dimensional laminar compressible flows with imbedded shock waves.

[ASME PAPER 72-FE-7]

05 p0564 A73-16043

Two-dimensional viscid MHD flows in cascade channels

05 p0603 A73-16044

Viscoelastic liquid flow in wake past two dimensional grid, investigating vorticity increase with for double array of vortices

05 p0565 A73-16045

Study of the steady motion of a ballistic antenna in plane homogeneous flow

05 p0528 A73-16046

A non-similar solution of heat transfer in external non-Newtonian flow with thermal radiation.

[AIAA PAPER 73-116]

05 p0640 A73-16047

Unsteady flow generated by shock-turbulent boundary layer interactions.

[AIAA PAPER 73-168]

05 p0566 A73-16048

Inverse method of designing two-dimensional transonic airfoil sections.

05 p0533 A73-16049

Shear stress distribution from measured nondimensional mean velocity profile measured in plane turbulent mixing layer formed at cascade wind tunnel exit

05 p0567 A73-16050

Two dimensional jet stream dynamics from simulation particle population evolution in different collision models

05 p0623 A73-16051

Two dimensional cascade acoustic resonance frequencies estimation by variational method, presenting results for three cavity modes

05 p0599 A73-16052

06 p0684 A73-16053

- Small perturbation stability of two dimensional incompressible viscous fluid flow with periodic velocity function, reduced to undulating surface boundary layer problem 06 p0684 A73-17452
- Effects of spanwise rotation on the structure of two-dimensional fully developed turbulent channel flow. 06 p0685 A73-17708
- Discharge of a capillary fluid from under a rectilinear shield 06 p0686 A73-18070
- Heat transfer in a periodic boundary layer near a two-dimensional stagnation point. 06 p0769 A73-18526
- Spatial stability of stagnation water boundary layer with heat transfer. 07 p0919 A73-19503
- Heat transfer in two-dimensional turbulent confined flows. 07 p0920 A73-19570
- German monograph - An iteration procedure for the calculation of planar compressible flows around circular profiles. 07 p0774 A73-19580
- Plane equilibrium turbulent boundary layer with longitudinal pressure gradient 07 p0811 A73-19619
- Two dimensional steady nonrotational flow of perfect compressible fluid around symmetric convex profile, reducing to variational inequality in hodograph plane. 07 p0776 A73-20147
- Quasi two dimensional turbulence model of energy spectra and potential enstrophy transfer in synoptic large scale quasi-horizontal atmospheric motions 07 p0820 A73-20342
- Numerical studies of two-dimensional vortex motion by a system of point vortices. 08 p0954 A73-21010
- Dynamic model of flow separation of plane fluid past body in channel with eddy wake formation 08 p0954 A73-21183
- A special form of Galerkin's method applied to heat transfer in plane Couette-Poiseuille flows. 08 p1023 A73-21412
- Problems of mixing and supersonic combustion of hydrogen in a hypersonic ramjet (ONERA, TP NO. 973) 08 p1025 A73-21684
- Difference schemes for two dimensional gas flows with detonation in frame of Lagrange variables, comparing point explosion with self similar solution 09 p1070 A73-21923
- Unsteady nonlinear flow around an airfoil or a blade cascade with emission of turbulent vortices 09 p1027 A73-22212
- Steady nonviscous nonheat-conducting plane flow of compressible fluid, calculating entropy, speed and pressure under assumption of variable pressure along streamlines 09 p1071 A73-22419
- Intrinsic coordinate method of characteristics application to supersonic steady two dimensional nonisentropic inviscid flow, noting shock wave interaction (ONERA, TP NO. 1186) 09 p1072 A73-22714
- Rayleigh-Ritz solution of boundary value problem for plane compressible subsonic flow past aerofoil noting convergence 09 p1028 A73-22954
- Finite element method for solution of two dimensional flow equations with applications to passive advection and nonlinear gravity wave problems, noting computing time 09 p1113 A73-22955
- Graphoanalytic method of calculating plane potential flows 09 p1029 A73-23106
- Flow through moving cascades of lifting lines with fluctuating lift. 10 p1171 A73-23697
- Transonic airfoils - Recent developments in theory, experiment, and design. 10 p1171 A73-23856
- Prandtl's boundary-layer theory from the viewpoint of a mathematician. 10 p1172 A73-23866
- Some solutions of the unsteady two-dimensional turbulent boundary layer equations. 10 p1209 A73-24835
- Unsteady two dimensional flow within circular cavity with arbitrary velocity distribution on cylinder wall, investigating recirculating flow initiation 10 p1210 A73-24838
- A numerical study of unsteady laminar combined convective flow over vertical plates. 10 p1296 A73-24848
- Conditional sampling and other measurements in a plane turbulent wake. 11 p1299 A73-25056
- Two dimensional inviscid flow model of shear layer motion and vortex shedding in near wake of bluff-based body, using Schwarz-Christoffel transformation 11 p1300 A73-25155
- On Howard's technique for perturbing neutral solutions of the Taylor-Goldstein equation. 11 p1345 A73-25157
- On the stability of plane Couette flow to infinitesimal disturbances. 11 p1346 A73-25158
- Steady plane flow of viscous fluid in symmetrical channels with curved walls, considering approximate series for stream function 11 p1347 A73-25646
- A linearized potential flow theory for airfoils with spoilers. 11 p1301 A73-25853
- Researches on the two-dimensional retarded cascade. III - Cascade performances at high inlet angles. 11 p1302 A73-26338
- Researches on the two-dimensional retarded cascade. IV - Determination of blade elements at retarded blade row. 11 p1302 A73-26339
- Calculation of nozzle flows using Padé fractions. 11 p1303 A73-26386
- Nonlinear plane cavity flow past flexible barrier, deriving uniqueness theorem by variational operator formulation in terms of potentialness conditions 11 p1391 A73-26547
- Two-dimensional steady magneto-fluid-dynamic flows with orthogonal magnetic and velocity field distributions. 12 p1527 A73-27020
- Hydromagnetic stability of plane heterogeneous shear flow. 12 p1527 A73-27129
- On oscillatory instability of plane-parallel convective motion in a vertical channel. 12 p1559 A73-27542
- Flows with wakes about a zero-inclination symmetric profile 13 p1599 A73-28069
- Some comparisons between observed wind profiles at Riso and theoretical predictions for flow over inhomogeneous terrain. 13 p1652 A73-28272
- The wave patterns produced by a moving body in a compressible, density-stratified fluid. 13 p1606 A73-28273
- Two dimensional incompressible steady potential electrohydrodynamic flows past flat dielectric plate, using quasi one dimensional and boundary layer approximation 13 p1664 A73-28442
- Two-dimensional calculation of revolution of the relaxed flow of a gas in a convergent-divergent sonic nozzle 13 p1563 A73-28563
- Plane strain slip line theory for anisotropic rigid/plastic materials. 13 p1697 A73-28793
- Two dimensional steady subsonic flow through airfoil cascades, predicting turbomachine performance from boundary layer calculation for comparison with experiments 13 p1565 A73-29005
- Effect of trailing edge thickness on the cascade performance of circular-arc blades. 13 p1565 A73-29006
- Potential flow about arbitrary thick blades of large camber in cascade. 13 p1565 A73-29009
- Two dimensional flow of viscous incompressible fluid, discussing formulation in analytic functions with applications to flows past elliptic cylinder and flat plates 13 p1603 A73-29048
- Asymptotic solution of initial value problem for weakly nonlinear wave system including dispersive and diffusive effects related to plane Poiseuille flow instability 14 p1744 A73-30171
- On the connection between the elliptic equations of the Navier-Stokes type and the theory of harmonic functionals. 14 p1769 A73-30521
- Pseudospectral approximation to two-dimensional turbulence. 14 p1746 A73-30909
- Multistep computer algorithm for Navier-Stokes equations of two dimensional viscous incompressible flow in channel with complex geometry 15 p1860 A73-30965
- Nonlinear development of disturbances in a plane-parallel Poiseuille flow 15 p1861 A73-31285
- Unsteady shock wave interaction with plane hypersonic flow about a blunt body investigated by second order difference method 15 p1862 A73-31326
- Stability, solvability and adjoint conditions for time periodic perturbation solutions to subcritical bifurcating plane Poiseuille flow 15 p1863 A73-31340
- Noncirculative MHD inviscid conducting fluid flow past circular cylinder and plane profile in magnetic field, using Fredholm equation 15 p1918 A73-31414
- Two dimensional unsteady vortex flow of ideal fluid past inflating decelerating wedge, obtaining pressure distribution on wedge surface [AIAA PAPER 73-449] 15 p1823 A73-31435
- German book - Theoretical gasdynamics. Volume I - Theory of the flows of compressible media. 15 p1863 A73-31474
- Pressure distribution on multicompound airfoils in two dimensional incompressible potential flow, using Martensen-Jacob vorticity distribution method to derive Fredholm type circulation equation 15 p1823 A73-31637
- Local potential variational method for analytic approximation of stagnation in plane flow, discussing generalized entropy method for accuracy improvement 15 p1957 A73-31665
- Calculation of wall corrections in a transonic wind tunnel 16 p1961 A73-32803
- Acoustic radiation from the end of a two-dimensional duct - Effects of uniform flow and duct lining. 16 p1999 A73-32914
- Two dimensional wedge flow singularities for free and fixed boundaries at flow separation points, applying to water entry problem 16 p1999 A73-32928
- The solutions of the boundary layer equations in the case of extremely intensive blowing or suction 16 p1963 A73-33250
- The numerical integration of the Navier-Stokes equations for the two-dimensional incompressible flow along a planar plate 16 p2000 A73-33261
- On the solution of magnetohydrodynamic elastico-viscous flow past a plane porous plate. 16 p2042 A73-33370
- Plane unsteady irrotational flow of ideal incompressible fluid through turbomachine stage due to interaction between stationary and moving grids 16 p2001 A73-34015
- Test techniques for high lift, two-dimensional airfoils with boundary layer and circulation control for application to rotary wing aircraft. 17 p2091 A73-34292
- Book - Lectures on fluid mechanics. 17 p2150 A73-34457
- Two dimensional diffuser flow measurement and model calculation for curvature effects on wall pressure and boundary layer velocity distributions [ASME PAPER 73-FE-2] 17 p2152 A73-35002
- An upper bound on the stress in plane Couette flow. [ASME PAPER 73-FE-8] 17 p2152 A73-35007
- Foppl vortices stability for two dimensional inviscid irrotational steady flow past circular cylinder 17 p2154 A73-35117
- Supersonic and hypersonic two-dimensional laminar flow over a compression corner. 17 p2096 A73-35134
- Near continuum impact of an underexpanded jet plume on a wall. 17 p2096 A73-35137
- Boundary condition calculation procedures for inviscid supersonic flow fields. 17 p2155 A73-35143
- An investigation of velocity flowfields in chemical laser nozzles. 18 p2322 A73-36199
- Calculation of free turbulent mixing by interaction approach. 18 p2297 A73-36204
- Unsteady turbulent boundary layers in two-dimensional, incompressible flow. 18 p2260 A73-36205
- Transonic flow analysis using a streamline coordinate transformation procedure. 18 p2261 A73-36211
- Experimental and theoretical investigations in two-dimensional transonic flow. 18 p2261 A73-36213
- Turbulence measurements in interacting wakes. 18 p2301 A73-36698
- Quantitative study of an aerodynamic flow by holographic interferometry 18 p2317 A73-37082
- Calculation of two-dimensional unsteady plasma flows in channels 19 p2467 A73-37369
- Compressible fluid dynamic theory, using stress tensors to derive constitutive equations for plane homogeneous and shear flows 19 p2420 A73-37644
- Boundary conditions and stability of inviscid plane-parallel flows. 19 p2420 A73-37751
- Measurements of internal waves and turbulence in two-dimensional stratified shear flows. 19 p2422 A73-38238
- Blade tip clearance loss between centrifugal impellers and shrouds during two dimensional viscous laminar flow, discussing energy dissipation and pressure and temperature distribution 19 p2474 A73-38417
- Numerical study of viscous flow in a cavity. 20 p2545 A73-38971

Thin steady two dimensional potential flow with free and/or rigid boundaries in presence of gravity, determining outer and inner expansions characteristics
20 p2546 A73-39085

Steady separated flow over finite flat plate in linearly decelerated free stream, using numerical solution of two dimensional Navier-Stokes equation
20 p2546 A73-39089

Nonlinear model for plane unsteady flow resulting from collapse of homogeneous density region in heavy ideal density-stratified fluid
20 p2547 A73-39287

The two-dimensional slow flow of a conducting fluid.
20 p2598 A73-39340

The local role of the limit line in the well-posing of steady state problems in gas dynamics. II - Two dimensional plane flow.
20 p2549 A73-39562

General two-dimensional problem in the theory of ideal plasticity of anisotropic materials
20 p2624 A73-39643

Velocity wake interaction and helical turbulence equilibrium spectra for two dimensional and three dimensional flow with quadratic energy and enstrophy states
20 p2549 A73-39812

Two dimensional flow theory of Weis-Fogh lift generation in insect motions of insect wings involving viscous effects
21 p2631 A73-40244

Linearized models of two dimensional steady air flow around mountain obstacle for constant temperature gradients and invariant velocity
21 p2731 A73-40741

Turbulent incompressible plane wall jet flow in still air, examining maximum velocity, total thickness and inner length scale with parametric analysis
21 p2678 A73-41191

Eole experiment on dispersion of Lagrangian tracers in quasi-stationary two dimensional turbulent flow, noting rms distance between paired balloons
21 p2687 A73-41337

The method of the false transient for the solution of coupled elliptic equations.
21 p2727 A73-41473

On unsteady flow of an elastico-viscous fluid past an infinite plate with variable suction.
22 p2840 A73-41747

Calculation of the two-dimensional turbulent wake behind a thin obstacle
[ONERA, TP NO. 1253]
22 p2796 A73-42222

Spatial stability of incompressible two-dimensional Gaussian wake in steady viscous flow.
22 p2796 A73-42243

Heat transfer in plane Couette flow of rarefied gas between parallel plates, determining temperature jumps at plates from transfer equations
23 p3048 A73-43206

An approximate model of a separated turbulent flow in an abruptly widening channel
23 p2968 A73-43471

Stability of a plane boundary layer with allowance for nonparallelism
23 p2968 A73-43472

Statistical analysis of two dimensional turbulence, noting probability characteristics ergodicity with respect to class of two dimensional characteristic functions with converging mean squares
23 p2968 A73-43475

Free point method finite difference solution for two dimensional nonstationary hydrodynamic problem of continuous media, demonstrating feasibility by plasma pinch effect calculation
23 p2968 A73-43799

Analytic solutions for potential flow over a class of semi-infinite two-dimensional bodies having circular-arc noses.
23 p2940 A73-43931

Unsteady transonic flows with shock waves in two dimensional channels.
23 p2969 A73-43938

A Riemann-Hilbert problem for a heat conduction in a finned surface.
23 p3049 A73-44051

Some results from tests in the NAE high Reynolds number two-dimensional test facility on shockless and other airfoils.
24 p3054 A73-44995

Thin plate in two dimensional supersonic flow, deriving vibration amplitude response to shock pressure load by numerical analysis with Laplace transform
24 p3055 A73-45432

Flows past exponential bodies in the presence of strong compression in the shock layer
24 p3055 A73-45534

Moment equation solutions for plane nonisothermal Poiseuille gas flow slip rate and temperature and pressure gradients in terms of molecular models
24 p3081 A73-45541

Linearized theory of two and three dimensional incompressible viscous flows based on locally unstable velocity profiles related to boundary layer instability mechanism
24 p3081 A73-45546

TWO DIMENSIONAL JETS

Flow and heat transfer on a flat plate normal to a two-dimensional laminar jet issuing from a nozzle of finite height.
01 p0033 A73-10804

Closed form linearized solutions of plane laminar jets boundary layer equations based on Legendre functions
03 p0297 A73-14628

Planar jet vortex growth control by excitation through transverse periodic disturbances, studying jet flow field by visualization via hydrogen bubble technique
[ASME PAPER 72-WA/APM-21]
04 p0435 A73-15895

Numerical solution of laminar jet mixing with and without free stream.
05 p0564 A73-16174

Similarity solution for the curved two-dimensional jet.
[ASME PAPER 72-APM-JJ]
05 p0564 A73-16527

Turbulent flow characteristics of an impinging jet.
07 p0810 A73-19569

Two dimensional semibounded jets in laminar and turbulent flows, discussing boundary layers skin and stream regions, step flow velocities, temperatures and self similar problems
07 p0811 A73-19612

Two-dimensional turbulent jets at a porous wall.
07 p0811 A73-19613

Experimental investigation of two-dimensional, supersonic flow impingement on a normal surface.
08 p0925 A73-20720

Plane subsonic jet free boundaries flapping measurements from oppositely placed hot-wire probes
11 p1346 A73-25251

Turbulent diffusion downstream of a linear source in a plane parietal jet
13 p1599 A73-28070

Two dimensional opposing incompressible viscous fluid jets impingement, investigating stagnation surface stability characteristics
13 p1603 A73-29036

Flow visualization of two and three dimensional wall jets on circular cylinder, observing flow characteristics sensitivity to curved boundary
13 p1603 A73-29038

Wall effects on the motion of a two-dimensional jet switching between two parallel flat plates.
13 p1571 A73-29043

Interaction position and static pressure measurements of two opposing plane turbulent wall jets in still air in terms of frozen flow
15 p1863 A73-31342

Discrete vortex method of two-dimensional jet flaps.
17 p2091 A73-34179

Experiments on confined turbulent jets in cross flow.
[AIAA PAPER 73-647]
18 p2260 A73-36202

The investigation on the secondary flow induced by jets. I.
19 p2422 A73-38349

Non-parallel flow corrections for the stability of shear flows.
20 p2546 A73-39092

Unsteady heat transfer characteristics of a two dimensional laminar wall jet.
20 p2628 A73-39339

Contribution to the study of the development of a jet issuing from a nozzle of small elongation and confined between two lateral walls
21 p2677 A73-40620

Interaction of sound with jets.
22 p2795 A73-41704

Of fluid mechanics and fluidics and of analysis and physical insight.
23 p2945 A73-43432

TWO FLUID MODELS

Fluid undercutting in the successive channel flow of two gases.
[AIAA PAPER 73-214]
05 p0566 A73-16944

Discontinuity conditions for two fluid model of liquid helium 2 from total energy and superfluid linear momentum balance and entropy production inequality postulations
07 p0850 A73-19106

The structure of a weak shock wave in a gas/liquid medium
08 p0954 A73-21129

Remarks on variational principle for an inviscid, perfect, magnetized plasma.
09 p1126 A73-21222

Effects of collisions and gyroviscosity on gravitational instability in a two-component plasma.
09 p1127 A73-22286

The asymptotic behavior of the supersonic solutions of the two-fluid solar wind equations.
10 p1268 A73-24147

Stellar magnetism origin via fossil, battery and dynamo theories, discussing two fluid plasma model and turbulence
13 p1683 A73-28992

Alfven waves in a two-fluid model of the solar wind.
14 p1787 A73-30005

Structure of a weak shock wave in a gas-liquid medium.
15 p1864 A73-32064

Two fluid models for solar wind heating under boundary conditions, considering enhanced energy transfer between electrons and protons in kinetic theory calculations
17 p2224 A73-34513

Shock waves within the two fluid model in the presence of the magnetic field.
19 p2464 A73-37160

Unsteady shock waves in a rarefied plasma
20 p2597 A73-39277

Shock wave structure in liquid/gas bubble medium from theoretical two-phase model and experimental piezoelectric pressure profile measurements
20 p2547 A73-39283

Self-similar solutions of the plasma equations
21 p2747 A73-40552

Solar-wind properties at the earth as predicted by the two-fluid model.
21 p2763 A73-41502

Experimental study of the thermal conductivity coefficient of noble gas mixtures at low and moderate densities.
22 p2932 A73-42500

Heat current and anisotropy-driven instabilities in connection with the solar wind.
24 p3126 A73-45126

TWO PHASE FLOW

An investigation of particle trajectories in two phase flow systems.
01 p0002 A73-10439

Viscous steady Couette flow between two parallel flat walls with particle injection, obtaining velocity and temperature distribution
01 p0033 A73-10800

Experimental study of the turbulent flow of a suspension: Trajectories and velocities of particles
Heat transfers between the two phases
01 p0122 A73-10816

Pressure drop, gas content, liquid drop size and nozzle length effects on flow velocity and heat transfer in two phase nozzle flow
01 p0033 A73-10861

Flow rate sensor selectivity and additivity transformation functions for two component gas-liquid flowmeter with constrictive device
02 p0167 A73-11860

The boundary layer of particulate gas flow.
03 p0289 A73-12914

Axisymmetric gas-particle flows maximum through nozzle design, investigating particle size, nozzle geometry and heat transfer coefficient effects
[AIAA PAPER 72-1189]
03 p0357 A73-13477

Dynamic radiography - A new imaging technique using penetrating radiation.
05 p0573 A73-16277

Drag coefficient for particles in rarefied, low Mach number flows.
05 p0564 A73-16350

Study of the specific characteristics of the diffusion method for measuring turbulence characteristics under conditions of a free homogeneous jet
05 p0576 A73-16614

Three dimensional dynamic characteristics of solid particles suspended by polluted air flow in a turbulent stage.
[AIAA PAPER 73-140]
05 p0531 A73-16889

Solid particle transport effect on structure and axis speed characteristics of two phase submerged turbulent jet
06 p0684 A73-17420

Mathematical models for critical flow rates of annular two phase mixtures under various discharge conditions
06 p0688 A73-18502

Experimental investigation of the electrical conductivity of a coaxial high-temperature jet with dispersed particles of Ti
07 p0858 A73-20012

Experimental study of water drop evaporation in a heated air flow
07 p0922 A73-20414

Equation of motion and bubble size distribution function for nucleate boiling, noting balance equation for two phase fluid
08 p1022 A73-21090

Pressure changes produced by sudden expansion of a two-phase flow
08 p0955 A73-21151

Supersonic flow of a gas with solid particles about a wedge
08 p0926 A73-21440

Two phase channel flow behavior from three dimensional phase diagram for one dimensional steady flow of ideal gas carrying solid particles
09 p1072 A73-22610

Development of a procedure for measuring the degree of turbulence at the axis of a free two-phase jet by a thermal-diffusion method
09 p1167 A73-22810

A one-dimensional problem concerning the discharge of a two-phase fluid from a nozzle
09 p1073 A73-23310

Nonstationary wave propagation in equilibrium liquid-vapor flow, noting pressure jumps due to expansion
10 p1204 A73-23513

The behavior of vapors of soluble binary systems during expansion in supersonic nozzles - Droplet coalescence in a potential vortex flow
10 p1205 A73-24162

Features of the mechanism of vapor condensation from humid air in narrow channels and the hydrodynamics of two-phase flow during droplet condensation
11 p1451 A73-25735

Anomalous lower dynamic pressure in piezometer of pitot tube in liquid flow containing solid particles, using seeds in aqueous solution of calcium chloride
11 p1367 A73-26476

Application of the principle of corresponding states to two-phase choked flow.
11 p1349 A73-26744

Pressure drop, gas content, liquid drop size and nozzle length effects on flow velocity and heat transfer in two phase nozzle flow
12 p1560 A73-27912

High Reynolds number fluid dynamics and heat and mass transfer in real concentrated particulate two-phase systems.
13 p1704 A73-28427

Emulsion and suspension effective viscosity dependence on dispersed phase volume concentration and particle interactions in two phase flows
13 p1580 A73-28465

Fundamental equations of a mixture of gas and small spherical solid particles from simple kinetic theory.
13 p1600 A73-28616

Structure of the wall zone of a longitudinal disperse flow over a plane plate
14 p1711 A73-30014

Mass transfer approximation model in unidirectional swirled two phase flow, considering transfer resistance of liquid phase
14 p1816 A73-30016

Heat transfer behind a shock wave in a two-phase gasdynamic flow
15 p1862 A73-31294

Development of the method and investigation of the intensity of turbulence at the axis of a two-phase turbulent jet
15 p1862 A73-31298

Calculation of the flow of a two-phase mixture in a Laval nozzle with allowance for turbulent diffusion of particles
15 p1822 A73-31300

Mathematical models for critical flow rates of annular two phase mixtures under various discharge conditions
16 p2000 A73-33588

Study of gas-phase reactions in particle-laden, ducted flows.
17 p2150 A73-34194

Papers on heat transfer covering thermosiphon technology, flowing gas-solid mixtures, condensation, free convection, flow stability and cryogenic insulation
17 p2254 A73-34351

Thermosiphon technology advances covering open and closed single-phase natural convection and mixed convection systems, two phase systems and turbine blade cooling
17 p2254 A73-34352

Heat transfer to flowing gas-solid mixtures.
17 p2254 A73-34353

Nonstationary wave propagation in equilibrium liquid-vapor flow, noting pressure jumps due to expansion
17 p2155 A73-35193

Continuum mechanics analysis of solid particle suspension flow of viscous gas, noting demixed region near wall
17 p2156 A73-35508

The dynamic-bias in radiation interrogation of two-phase flow.
17 p2256 A73-35846

Some characteristics of two-phase nozzle flows
18 p2265 A73-37005

Flow of a mixture consisting of a fluid and gas bubbles past a corner
18 p2301 A73-37007

Forces acting on a small body in an arbitrary incompressible fluid flow and equations of motion of a two-phase medium
18 p2302 A73-37008

Application of a holographic technique to the determination of the dispersity of a two-phase gas/liquid flow
18 p2318 A73-37122

Droplet transfer in two phase annular mist flow. II - Prediction of droplet transfer rate.
19 p2423 A73-38350

Flow film boiling heat transfer correlations - Parametric study with data comparisons.
[ASME PAPER 73-HT-50] 20 p2626 A73-38574

Unsteady combustion of a confined spray.
[AIChE PREPRINT 23] 20 p2626 A73-39250

Exact solutions of some problems of the Stefan type
20 p2627 A73-39335

Spectroscopic studies of supersonic heterogeneous flows with a combustible condensed phase
21 p2754 A73-40702

Motion of a two-component stratified gas-liquid flow in a horizontal pipe
21 p2677 A73-40989

Experimental investigations of the effects of polymer additions on the kinematic characteristics of a plane turbulent flow in a tube with variable wall roughness
22 p2841 A73-42121

Approximate estimation of the possibility of using the viscoelasticity hypothesis for the formulation of an equation of motion for a liquid with polymer additions
22 p2841 A73-42122

Flows with and without suspensions in channels with curvilinear segments
22 p2842 A73-42229

On laminar two-phase flows in magnetohydrodynamics.
23 p3013 A73-44228

A laser Doppler velocimeter for studying fast gasdynamic flows
24 p3089 A73-44714

Critical heat flux for two-phase flow of helium I.
24 p3155 A73-44822

Critical two phase He flow rates prediction based on homogeneous thermal equilibrium model, Henry-Fauske data and empirical correction factor curve
24 p3077 A73-44823

TWO PHASE SYSTEMS
U BINARY SYSTEMS [MATERIALS]
TWO REFLECTOR ANTENNAS
Results of an experimental investigation of a two-mirror antenna with a modified counter reflector
02 p0146 A73-12019

Diffraction by double circular irises and scattering by two elliptical reflectors.
06 p0666 A73-18196

Analysis of generalized dual-mirror antennas
08 p0947 A73-21399

The concentric double spherical reflector as an antenna for simple scanning over a limited angular range
10 p1187 A73-23739

Characteristics of a dual-mirror antenna producing a sum-difference type of radiation pattern
12 p1480 A73-27234

Approximate calculation of the small-reflector surface from the deformations of the large reflector of a Cassegrainian antenna
12 p1480 A73-27235

A simplification in the analysis of four- and five-horn fed Cassegrainian reflectors when the horns have nearly symmetric patterns.
14 p1735 A73-30224

A dual-mirror antenna with beam scanning over a ninety-degree sector
14 p1736 A73-30561

Radiation patterns and structural design of two mirror millimeter wave Cassegrain antennas with horn radiator
16 p1991 A73-33985

A limited steerable dual reflector antenna.
18 p2293 A73-36881

Analysis of two-mirror antennas of a general type.
19 p2410 A73-38357

Implementation of fixed multiple beam spherical antenna systems and measured test results.
20 p2525 A73-38740

Design of coincident dual-frequency mirror antennas
21 p2661 A73-40194

Synthesis and analysis of optimal dual-mirror antennas
23 p2959 A73-43516

A fan-beam dual reflector antenna.
24 p3069 A73-45030

TYPE 2 BURSTS
Propagation through the solar corona of the shock waves responsible for type II radio bursts.
01 p0093 A73-11314

Close connexion between flare-generated coronal and interplanetary shock waves.
17 p2232 A73-35147

A density scale for the interplanetary medium from observations of a type II solar radio burst out to 1 astronomical unit.
18 p2348 A73-37113

TYPE 3 BURSTS
Relative polarization of type III solar radio bursts at 23.5 and 30 MHz.
01 p0093 A73-11315

The role of energetic electrons in the correlation of meter and decimeter type III bursts with 4 keV X-ray emission.
01 p0093 A73-11391

A search of a connection between the polarization of Decam-type III bursts and magnetic fields in different heights of the solar atmosphere.
01 p0093 A73-11392

Particle motions in coronal streamers and type III radio bursts.
01 p0093 A73-11393

Type 3 bursts exciter duration and decay time constant from time profiles analysis in decimeter range, explaining coronal temperature
03 p0361 A73-13213

Type 3 radio bursts correlation with solar flares and electron events from OGO 5, IMP 5 and Explorer 35 observations
05 p0610 A73-17047

Evidence for a common origin of the electrons responsible for the impulsive X-ray and type III radio bursts.
08 p0996 A73-20766

Landau damping of type III solar radiobursts.
08 p0997 A73-20902

Problem of the time dependence of the polarization level of Type III solar radio bursts
10 p1264 A73-23719

Direct observations of low-energy solar electrons associated with a Type III solar radio burst.
10 p1268 A73-24145

Detailed correlation of type III radio bursts with H alpha activity. I - Active region of 22 May 1970.
11 p1413 A73-25950

Non-existence of linear polarization in type III solar bursts at 80 MHz.
16 p2053 A73-32962

On some transient H-alpha features associated with metric type III bursts.
16 p2053 A73-32963

The prevalence of second harmonic radiation in type III bursts observed at kilometric wavelengths.
16 p2053 A73-32964

Solar wind density model from km-wave type III bursts.
16 p2053 A73-32965

19-20 May 1969, an example of type III emission during the impulsive phase of flares.
18 p2344 A73-36013

Time dependence of the polarization of type III solar radio bursts.
18 p2347 A73-36744

Decay time of type III solar bursts observed at kilometric wavelengths.
21 p2762 A73-41497

TYPE 4 BURSTS
Spectral behaviour and proton effects of the type IV broad-band continua.
01 p0093 A73-11394

The self absorption of gyro-synchrotron emission in a magnetic dipole field - Microwave impulsive burst and hard X-ray burst.
03 p0364 A73-14416

Properties of different groups of type IV solar radio bursts.
04 p0493 A73-16013

Solar energetic particles and wide-band continuum storms from metric to hectometric frequencies.
07 p0870 A73-19663

The time-latitude distribution of solar flares accompanied by type IV radio bursts during the period 1956 to 1969.
08 p0997 A73-20770

On the S- and B-components of solar radio and X-emission and their relationships to energetic solar events.
08 p0997 A73-20771

Type IV bursts on August 4 and 7, 1972.
12 p1535 A73-27784

On the generation of high-energy particles in solar flares.
15 p1925 A73-31068

Development of moving type IV solar radio bursts and relation to expanding magnetic bottles from flare regions.
16 p2054 A73-33096

Origination of Type-IV decimetric bursts in the solar corona
23 p3036 A73-44248

Interpretation of distinct type IVm-A- and IVmu-bursts on the basis of micro-instabilities and of resonant nonlinear interaction of waves.
24 p3123 A73-44645

TYPE 5 BURSTS
Harmonic structure of flare related type 5 burst, suggesting plasma wave emission
11 p1412 A73-25856

TYPEWRITERS
NT AUTOMATIC TYPEWRITERS
NT TELETYPEWRITERS
TYPHOONS
Note on the extratropical transformation of a typhoon in relation with cold outbreaks.
05 p0594 A73-16349

Radiosonde soundings for typhoons and hurricanes isobaric surfaces heights, temperatures and humidities, calculating correlation coefficients between sea level pressure and other parameters
10 p1245 A73-23985

U.S.S.R. SPACE PROGRAM

Objectives and first results of the Mars 2, Mars 3 and Mariner 9 planetary probes

01 p0103 A73-10996

Sunspot fine structure from photographs taken on U.S.S.R. Stratospheric Solar Station, noting high Rayleigh resolution of small elements

05 p0621 A73-17031

U.S. and U.S.S.R. Venus probes data on Venus atmosphere, discussing atmospheric heat transfer mechanism and cloud structure

07 p0874 A73-19110

U.S.S.R. sponsored international space communication system, discussing technological, organizational and legal aspects

07 p0923 A73-19202

Apollo-Soyuz docking project for flight testing systems compatibility for safe and reliable crew transfer, discussing program objectives, technical requirements and solutions

09 p1152 A73-22187

Soviet-French cooperation in space exploration

14 p1818 A73-30250

Soviet Mars 1, 2 and 3 lander failure description from western sources, discussing further attempts in July or August 1973 launch windows

17 p2234 A73-35656

Soviet communications satellite systems

18 p2289 A73-36400

Russian book on Soviet news agency space exploration articles for 1971 covering Soyuz, Salyut, Molniya, Luna, Meteor and Lunokhod programs, agricultural satellites and lunar exploration

19 p2486 A73-37771

UBV SPECTRA

Southern open star clusters. I - UBV-H beta photometry of 15 clusters between Galactic longitudes 231 and 256 deg.

01 p0096 A73-10318

An investigation of four southern open clusters.

01 p0096 A73-10320

Three color photometric study of open cluster NGC 1647, obtaining distance, B-V and U-B excesses and ages

01 p0098 A73-10554

Photometry of supernova 1972 in NGC 5253.

01 p0104 A73-11046

Stellar sources UV photography from sounding rocket, obtaining mean interstellar absorption, stars magnitudes and distribution and UBV spectrum

02 p0216 A73-12326

Light variation and extinction of the variable WW Vulpeculae

02 p0226 A73-12836

On the extended van Wijk sequence in the Large Magellanic Cloud.

03 p0371 A73-13217

A search for He-weak stars in very young clusters.

03 p0372 A73-13227

Measured physical and optical properties of the passive geodetic satellite /Pages/ and Echo 1.

04 p0446 A73-14809

Ultraviolet photometry from the orbiting astronomical observatory. V - The helium-weak stars.

04 p0499 A73-15363

UBV photometry of the metal-rich globular cluster NGC 6171.

04 p0500 A73-15487

The pulse shape of the Crab Nebula pulsar NP 0532 as a function of color.

04 p0501 A73-15685

Some relations between the photometric characteristics of the brightness curves and color indexes of Cepheid variables in the system U, B, V. II

05 p0613 A73-16209

The old open cluster NGC 6819.

05 p0618 A73-16744

Ultraviolet photometry from the orbiting astronomical observatory. IV - Photometry of late-type stars.

05 p0626 A73-17381

Light variations of high luminosity O and B stars in the Large Magellanic Cloud.

07 p0877 A73-19597

Optical variability of the nuclei of Seyfert galaxies

07 p0901 A73-20306

The history of star formation and the colors of late-type galaxies.

08 p1008 A73-21155

White dwarf flares UBV energy spectra, assuming mechanism of nonthermal bremsstrahlung due to fast electrons

09 p1146 A73-22296

UBV photometry of the irregular galaxies NGC 5363 and NGC 5360

09 p1146 A73-22548

Cosmic absorption of stellar light in the belt of a local system

09 p1148 A73-22861

Differential UBV photometry of beta Lyrac. III.

11 p1415 A73-25072

Photometric characteristics and structure of nebulae NGC 6914a, IC 5076, and Ced 201

11 p1416 A73-25228

Iapetus UBV light curve minima depths difference explained by two-hemisphere model

11 p1425 A73-26134

Photoelectric observations of the close binary system SZ Camelopardalis.

11 p1425 A73-26266

UBV photometry of 32 Cygni during the 1971 eclipse.

11 p1426 A73-26268

Spectral types and UBV photometry of G-K giants at the North Galactic Pole.

11 p1429 A73-26678

Multicolor photoelectric photometry of Neptune.

11 p1429 A73-26682

Optical variability of the nuclei of Seyfert galaxies.

12 p1539 A73-27278

Iris photometer electronic control system, presenting NGC 1778 cluster stars photoelectric UBV magnitudes

12 p1498 A73-27723

High-speed UBV photometry of Scorpius X-1 flares.

14 p1801 A73-30646

Optical study of BL Lacertae. II - Brightness variation from March 1969 to January 1971

15 p1928 A73-31052

The spectrum variable a Centauri /HD 125 823/.

15 p1935 A73-31485

On the use of UBV photometric diagrams for inferring the existence of an open star cluster.

16 p2058 A73-32833

Application of a photoelectric area scanner to various astronomical problems

19 p2430 A73-37605

Minor planets and related objects. IX - Photometry and polarimetry of /1685/ Toro.

20 p2607 A73-39119

Investigation of the planetary nebula NGC 1360 and its nucleus

21 p2768 A73-40715

Variations in the abundance of chemical elements in the classical Cepheids of the Galaxy

21 p2768 A73-40718

Extra-atmospheric photoelectric study of the brightness of the earth's atmosphere

21 p2686 A73-40912

Photometry of southern globular clusters. I - Bright stars in omega Centauri. II - Bright stars in NGC 6752.

22 p2907 A73-42206

Wolf-Rayet stars effective temperature estimation from UBV photometry of surrounding ring nebulae with optically thick H II region excited by stellar Lyman radiation

23 p3025 A73-43195

Photometric study of new variable stars in NGC 2264

23 p3037 A73-44353

UBV spectral and photographic observations of blue objects around M 92 globular cluster

23 p3037 A73-44355

Interstellar reddening calculation with respect to U-B/V diagram for hot and main sequence stars as function of luminosity based on model stellar atmospheres

24 p3138 A73-45012

Galactic structure in the direction of Cepheus

24 p3140 A73-45191

The 35-day cycle of HZ Herculis.

24 p3143 A73-45491

UDIMET ALLOYS

The mechanisms of growth of gamma prime particles and tensile yield in Udimet 520.

04 p0464 A73-15578

Prediction of inelastic high temperature materials behavior by strain-rate approach.

[AIAA PAPER 73-386]

Udimet 700 creep behavior under cyclic tensile stresses at 925 C from hodograph of monotonic stress-strain relations, taking into account strain rate effects

[AIAA PAPER 73-387]

11 p1439 A73-25516

UH-1 HELICOPTER

A study of environmental degradation of adhesive bonded titanium structures in Army helicopters.

03 p0332 A73-13039

UHTREX (NUCLEAR REACTORS)

U HIGH TEMPERATURE NUCLEAR REACTORS

UHURU SATELLITE

The Uhuru catalog of X-ray sources.

05 p0625 A73-17326

Star sensor of spin stabilized Uhuru satellite for detection and location of stellar X ray sources with accuracies of one arc-minute

06 p0695 A73-18323

Uhuru satellite observations of X ray sources, discussing binary sources and identification in visible stars

07 p0872 A73-20525

Balloon flight observations of Uhuru sources for spectral characteristics, noting hard X ray band sources

09 p1137 A73-22173

Uhuru extragalactic X ray observations including normal galaxies, quasars, giant radio galaxies, Seyferts and galactic clusters

16 p2050 A73-32741

UK SATELLITES

NT ARIEL 4 SATELLITE

ULCERS

Digestive hemorrhages in aircrew - Individual and collective safety

18 p2280 A73-36952

ULM [LIGHT MODULATION]

U ULTRASONIC LIGHT MODULATION

ULNA

Three models of the vibrating ulna.

19 p2398 A73-37543

ULTRA SHORT WAVE RADIO EQUIPMENT

U VERY HIGH FREQUENCY RADIO EQUIPMENT

Parametric amplification of a UHF signal by plasma-beam interaction in the presence of a magnetic field of finite amplitude

04 p0424 A73-15996

Si varactor diode series resistance resonance measurements in UHF band, noting approximate invariance with frequency

06 p0678 A73-18842

GaAs Schottky-barrier diodes for ultrahigh-frequency communication systems.

08 p0945 A73-20808

Preemphasis for an S-band constant bandwidth FM/FM system.

08 p0939 A73-21085

Microstrip solid state power amplifiers with transistors and varactors for spaceborne applications in L and S band ranges

09 p1066 A73-23428

Ionospherically diffracted monochromatic VHF/UHF plane wave statistics characterization, noting Gaussian and log-normal distributions from ATS-3 satellite data recording

10 p1190 A73-24896

Distortions of UHF pulse signals propagating along the earth at distances below the radio horizon

14 p1729 A73-30559

Technologies applicable to the development of an onboard L-band transmitter

15 p1852 A73-32481

Frequency hopping principle for precision L band DME as complementary aid to microwave landings system

15 p1911 A73-32490

Solid-state transmitter for VHF/UHF space telemetry.

16 p1979 A73-33104

S band radio occultation measurements of the atmosphere and topography of Mars with Mariner 9 - Extended mission coverage of polar and intermediate latitudes.

19 p2479 A73-37223

Pulsed RF life of an L-band power transistor.

19 p2411 A73-38466

Diversity combining of UHF signals under rapid fading conditions.

20 p2523 A73-38724

UHF airborne antenna diversity combiner for signal reception using correlation technique for phase variation removal to improve SNR and gain

20 p2523 A73-38725

Analysis of VHF/UHF frequency dependences, space, and polarization properties of ionospheric scintillation in the equatorial region.

20 p2525 A73-38744

Russian book on UHF meteorological radar techniques and applications covering precipitation and cloud monitoring radiolocation stations, lidar, sonar, echo signals and meteorological satellites

20 p2584 A73-39758

Aeronautical/maritime satellite borne two-way L band transponder weight and power limitation effects on channel capacity

20 p2531 A73-39777

Pulsar searches at 408 MHz with Northern Cross radio telescope, comparing discovered objects with previously known pulsars

21 p2778 A73-41530

ULTRAHIGH VACUUM

Test chamber for on board moving parts in ultrahigh vacuum.

01 p0030 A73-11144

Ultrahigh vacuum quartz spring microbalance for determination of evaporation rate and vapor pressure

02 p0168 A73-11966

An ultrahigh-vacuum arrangement for studying extraterrestrial material

02 p0151 A73-12466

Initially uniform gas expansion into ambient atmosphere and subsequent flow into perfect vacuum, noting infinite-strength shock separation from gas-vacuum interface

03 p0294 A73-13538

Friction in ultrahigh vacuum, discussing physicochemical problems, self lubricating materials advantages and drawbacks, and solid lubricant choices for space applications

07 p0828 A73-18900

Friction in ultrahigh vacuum, discussing test program definition and testing machine design taking into account space environment effects

07 p0829 A73-18900

Facility for roller bearing parameters testing during high speed rotation in ultrahigh vacuum, discussing circuitry and principal elements 07 p0807 A73-18908

A cryogenic ultrahigh-vacuum pump with a small liquid-helium flow rate 07 p0830 A73-19288

Cryopumping use in clean ultrahigh vacuum technology, considering cold surface heat load, condensate layer growth rate and heat conductivity, cryosorption and cryotrapping 07 p0852 A73-20402

Ion gun sputter cleaning of thin film metal substrate for in situ corrosion studies by UHV transmission electron microscopy 08 p0990 A73-21616

UHV outgassing measurements on various carbons. 08 p0937 A73-21621

High and ultra-high vacuum by pumping with cryocooled surfaces. 11 p1398 A73-25579

Cryogenic ultrahigh-vacuum pump with low liquid-helium consumption. 13 p1659 A73-28688

Ultrahigh-vacuum apparatus for studying extraterrestrial material. 15 p1859 A73-32616

Oxidation of titanium between 25 C and 400 C. 19 p2442 A73-37950

A harmonic drive used as an ultrahigh vacuum rotary feedthrough. 21 p2671 A73-39919

Vacuum Technology Workshop, Versailles, France, May 30-June 3, 1972, Proceedings 22 p2886 A73-41867

Influence of the wall temperatures of gauges on the measurement of limit pressures 22 p2852 A73-41870

The VAK-2 unit with heated condenser pumps for obtaining a vacuum better than 0.1 pm Hg. 23 p2966 A73-43672

ULTRALOW FREQUENCIES

U EXTREMELY LOW RADIO FREQUENCIES

ULTRAPURE METALS

Textures of deformation and of primary and secondary recrystallization in high-purity nickel 01 p0064 A73-10614

Anomalous slip in high-purity niobium single crystals deformed at 77 K in tension. 04 p0467 A73-15931

Study of pitting corrosion and stress corrosion in stainless steels with the aid of alloys of very high purity 07 p0838 A73-19114

Ultrasonic treatment of alloy MA2-1 during solidification. 10 p1236 A73-24930

Solid solution strengthening of high purity niobium alloys. 14 p1761 A73-30631

Superconductivity and electronic structure of ultrahigh-purity niobium. I - Synthesis of ultrahigh-purity niobium 20 p2600 A73-39732

Electrical resistance variation kinetics in deformed beryllium after annealing 20 p2579 A73-39746

ULTRASONIC AGITATION

Internal friction and heat release in engineering and tool steels in the presence of intense ultrasonic oscillations 01 p0065 A73-10926

Influence of an ultrasonic field on the behavior of a vapor bubble in liquid hydrogen 01 p0077 A73-10929

Fatigue of duralumin under cyclic loads at ultrasonic frequencies 02 p0179 A73-11566

Investigation of the possibility for ultrasonic dispersion of certain corrosion inhibitors introduced in easily removable film coatings 02 p0184 A73-11643

Cleaning and activation of beryllium-copper electron multiplier dynodes. 02 p0146 A73-11966

Skin sensitivity of palms, wrists and forearms to focused ultrasound, noting evoked touch, pulsation, cold, warmth and prick sensations and applications in receptor physiology 05 p0540 A73-16695

Effect of an ultrasonic field on the behavior of a vapor bubble in liquid hydrogen. 10 p1249 A73-24189

Ultrasonic treatment of alloy MA2-1 during solidification. 10 p1236 A73-24930

Effect of ultrasound on the dislocation structure and mechanical properties of molybdenum 20 p2579 A73-39745

ULTRASONIC LIGHT MODULATION

Ultrasonic probes sound fields from thermal effects via IR camera or liquid crystals, sound pressure via Pohlmann image converter and light modulation via schlieren method 15 p1882 A73-32055

Generation of complex phase-shift-keyed signals by the optical correlation method 24 p3067 A73-44595

ULTRASONIC MACHINING

Ultrasonic treatment of nonmetallic materials with a diamond instrument 24 p3094 A73-44969

ULTRASONIC RADIATION

Dislocation damping in ultrasound-irradiated molybdenum single crystals 01 p0061 A73-10251

Ultrasonic waves generation by plasma of activated flame, presenting sound pressure and light emission graphs 01 p0086 A73-11272

Russian papers on nonlinear optics and hyperacoustics covering laser use in ultrasound propagation study and thermal and stimulated molecular light scattering effects 02 p0194 A73-11944

Use of ultrasonic emission in nondestructive inspection. 02 p0169 A73-12148

Russian book on ultrasonic processing in metal crystallization covering design of vibrators and transducers and acoustic power measurement 02 p0175 A73-12800

Acoustical studies of rotational relaxation in gases. 03 p0342 A73-12986

Linear schlieren photography with concave mirror and variable ultrasonic source for high resolution display of acoustic free field pressure gradient on TV screen 03 p0342 A73-12990

Correlation analysis as applied to the observation of fluctuations of laser light diffracted on an ultrasonic wave in an inhomogeneous medium. 03 p0318 A73-12994

Approximate formulas for calculating intensity distributions of intense laser light diffracted on an ultrasonic wave. 03 p0318 A73-12995

Space-modulated side radiation from an ultrasonic beam in a solid. 03 p0344 A73-14042

Acoustic properties of fluid mixtures for ultrasonic delay lines, noting temperature and composition effects on water-glycol mixture parameters 03 p0280 A73-14620

Influence of nonlinear polarization on the ultrasonic gain factor in piezosemiconductors 05 p0605 A73-16821

Structural changes arising in nickel under the action of ultrasound and subsequent thermal annealings 06 p0708 A73-18053

Bragg diffraction by standing ultrasonic waves with application to optical demultiplexing. 06 p0701 A73-18364

Device for studying the effect of ultrasonic oscillations on contact interaction in high vacuum 07 p0822 A73-19295

Ultrasonic P and S waves velocity of Apollo 14 and 15 lunar igneous and breccia rocks for elastic properties determination, noting cracks distribution function 07 p0894 A73-19853

Comparison between a Hall configuration and a Corbino configuration for the amplification of ultrasonic waves 07 p0864 A73-20613

Influence of ultrasound and of a superhigh-frequency electromagnetic field in the three-centimeter band on the oxidative phosphorylation of liver and kidney mitochondria 09 p1044 A73-22368

Ultrasonic holography by one-dimensional moving of the source or the object. 10 p1216 A73-23664

Radar direction measurements by phase comparison of ultrasonic echo pulses reflected from targets in water tank, using piezoelectric sensors for receiving antennas simulation 10 p1194 A73-23736

Characteristics of the electrical activity of the superior olivary bodies of Vespertilionidae and Rhinolophidae bats in response to ultrasonic stimuli of different frequencies 10 p1182 A73-24596

New techniques of acoustic image detection. 11 p1360 A73-25073

Freezing-in phenomenon and acoustical streaming in standing ultrasonic waves 11 p1400 A73-26291

Solid ultrasonic cylindrical lens design for off-axis aberration minimization for focusing properties improvement, using method analogous to chromatic aberration correction in optics 13 p1612 A73-28491

Acoustical hologram recording by electrostatic transducers using rigid backplate electrode insulated with thin dielectric film transparent to ultrasonic radiation 13 p1614 A73-28584

Analysis of various ultrasonic holographic imaging methods for medical diagnosis. 13 p1615 A73-28589

Ultrasonic acoustic holography for wave source and object in relative motion, predicting reconstructed image aberration elimination performance in point-by-point mapping technique 13 p1616 A73-28597

Parametric excitation of ultrasonic waves in piezoelectric semiconductors. 14 p1783 A73-29916

Attenuation of an ultrasonic signal in aluminum deformed according to a harmonic law 14 p1764 A73-30857

Ultrasonic probes sound fields from thermal effects via IR camera or liquid crystals, sound pressure via Pohlmann image converter and light modulation via schlieren method 15 p1882 A73-32055

Bragg diffraction of light by two orthogonal ultrasonic waves in water. 15 p1914 A73-32256

Ultrasound absorption coefficient measurement in semiconductor crystal lattices based on acoustoelectrical effect 17 p2218 A73-34159

Verification of sensitivity enhancement factors for CW ultrasonic resonators. 20 p2565 A73-38887

A periodicity phenomenon occurring instantly when a standing ultrasonic wave is switched off 21 p2738 A73-39982

Acoustic emission measurements during plastic deformation of metals. 22 p2919 A73-41975

Influence of ultrasonic vibrations on the mechanical properties and fine structure of aluminum and an aluminum-magnesium alloy 24 p3098 A73-44570

ULTRASONIC SPEEDS

U SUPERSONIC SPEEDS

ULTRASONIC TESTS

The resolution of flaw depth of angle probes for ultrasonic testing 01 p0056 A73-10589

Generation and detection of helical surface waves at cylindrical bodies by means of contactless electrodynamic transducers 01 p0051 A73-10974

Ultrasonic studies of the nonlinear properties of solids. 01 p0057 A73-11003

Utilization of polarized ultrasound in stress investigations 02 p0166 A73-11645

Computer based data processing system with display for improving ultrasonic pulse echo NDT test equipment resolution and SNR 02 p0173 A73-11983

Ultrasonic measurements of cold-work percentages in Type 316 stainless steel. 02 p0173 A73-11987

Circuitum operation conditions of thyatron generator circuit in electroacoustic system for excitation of quartz piezoelectric vibrators in ultrasonic NDT 02 p0168 A73-12147

Determining the size of defects in standardizing sensitivity using a spherical reflector. 02 p0169 A73-12149

Ultrasonic inspection of nickel-base alloy products. 02 p0174 A73-12150

Echocardiographic analysis of mitral valve motion in atrial septal defect. 02 p0138 A73-12444

Echocardiographic findings in experimental myocardial infarction of the posterior left ventricular wall. 02 p0138 A73-12446

Applications of dynamic photoelasticity in flaw detection analysis. I. 02 p0175 A73-12868

Ultrasonic attenuation measurement of a microplastic memory effect in aluminum single crystals. 03 p0323 A73-13331

Gas phase separation following decompression in asymptomatic rats - Visual and ultrasound monitoring. 03 p0263 A73-14162

Ultrasonic holography application to NDT, discussing small angle approximation to spherical beam, hologram formation, image reproduction and wavelength change effect 04 p0446 A73-14674

Rayleigh waves for continuous monitoring of a propagating crack front. 04 p0452 A73-14691

NDT applications of acoustic or stress wave, ultrasonic spectroscopy, imaging, critical angle reflectivity and holography 04 p0447 A73-14927

- Some results using the ultrasonic goniometer - The corner reflector method. 04 p0447 A73-14930
- Acoustic emission source location using single and multiple transducer arrays. 04 p0448 A73-15121
- Frequency spectra of acoustic emissions generated by deforming metals and ceramics. 04 p0448 A73-15122
- Nondestructive detection of hydrides and alpha-case in titanium alloys. 04 p0461 A73-15217
- Application of graphic display to ultrasonic testing. 05 p0574 A73-16282
- Ultrasonic isometric imaging. 05 p0574 A73-16283
- Determination of the angle of incidence of angle probes for ultrasonic testing. 05 p0582 A73-17068
- Ultrasonic Doppler locators for peripheral vessel blood circulation and myocardium and valvular motor activity measurements. 06 p0656 A73-17682
- Determination of the extent of ultrasonically detected defects - Application to welded butt joint quality control. 07 p0831 A73-19904
- Some new developments in nondestructive testing. 08 p0963 A73-20869
- Radiography and ultrasonic tests for weldment and flaw inspection, discussing choice based on economic, technical and application considerations. 08 p0952 A73-21076
- Non-destructive testing in industry - Non-ferrous metals. 08 p0973 A73-21077
- Visualization of pulsed ultrasound using stroboscopic photoelasticity. 08 p0973 A73-21078
- Unconventional methods of generating, detecting and coupling of ultrasound in non-destructive testing. 09 p1088 A73-22218
- Simple test apparatus for a 100% defect-detection probability in ultrasonic surface scanning of plates and strips. 09 p1070 A73-22219
- Defect size determination by ultrasonic scanning with a relative threshold. 09 p1088 A73-22220
- Ultrasonic structure analyzer for nondestructive inspection of fine grained metallic materials. 09 p1080 A73-22298
- Investigation of the detectability of defects in the ultrasonic testing of joints obtained by friction welding. 09 p1088 A73-22299
- Acoustic emission for monitoring fatigue crack growth. 09 p1083 A73-22511
- Acoustical holography applications in nondestructive testing. 09 p1083 A73-22514
- Intravascular changes associated with hyperbaric decompression - Theoretical considerations using ultrasound. 09 p1045 A73-22534
- Elastic wave analysis in nondestructive testing. 10 p1292 A73-24630
- The effect of environmental relative humidity upon the ultrasonic fatigue endurance of an age hardening aluminum alloy. 11 p1382 A73-25825
- An ultrasonic device for the study of fatigue crack initiation in anodized aluminum alloys. 11 p1363 A73-25830 [AD-760070]
- Ultrasonic measurement of elastic moduli in slender specimens using extensional and torsional wave pulses. 11 p1365 A73-26171
- Ultrasonic investigation of the nematic-isotropic phase transition in MBBA. 11 p1409 A73-26213
- An ultrasonic technique for the inspection of magnetic and explosive welds, using a facsimile recording system. 12 p1502 A73-27037
- Optical interferometry for ultrasonic surface wave detection, using two coherent light beams focusing for recording standing wave ratio, attenuation, transmission and harmonic content. 13 p1613 A73-28497
- Graphic display for ultrasonic nondestructive testing. 13 p1615 A73-28586
- Cylindrical scan acoustical holographic transmitter/sensor system for ultrasonic under ocean surveillance and NDT applications. 13 p1615 A73-28588
- Russian book on ultrasonic methods for weld testing covering flaw detection, emitters/receivers, acoustic channels, echo and mirror shadow methods, automatic testing, etc. 13 p1624 A73-28949
- Ultrasonic attenuation measurements in metals at low temperatures. 13 p1662 A73-29639
- The ultrasonic pulse-echo technique as applied to adhesion testing. 15 p1882 A73-31673
- Setting of sensitivity of ultrasonic equipment for weld inspection. 15 p1882 A73-32025
- The use of the terms nearfield and farfield in ultrasonic non-destructive testing. 15 p1882 A73-32052
- The attenuation of ultrasonic waves in cylindrical work pieces with central bore-hole. 15 p1882 A73-32053
- Residual stress measurement and analysis using ultrasonic techniques. 15 p1879 A73-32249
- Application of frequency analysis to ultrasonic non-destructive testing. 16 p2016 A73-34014
- High precision photoelastic and ultrasonic techniques for determining absolute and differential thermal expansion of titania-silica glasses. 17 p2171 A73-35410
- A nondestructive measurement of the elastic constants of unidirectional boron fiber reinforced aluminum composites. 17 p2182 A73-35439 [SC-72-1644]
- Some applications of spectral analysis in ultrasonic testing. 18 p2316 A73-36485
- The measurement and analysis of fatigue crack growth in cylindrical shapes. 18 p2363 A73-36486
- DONAR - A computer processing system to extend ultrasonic pulse-echo testing. 19 p2407 A73-37448
- The influence of fabrication and structure processes on the result of control by ultrasonics of semifinished products of titanium alloys. 19 p2441 A73-37830
- Schlieren and computer studies of the interaction of ultrasound with defects. 19 p2461 A73-38201
- Method of measuring the size of defects without using calibrating standards and adjusting the sensitivity of ultrasonic defectoscopes. 19 p2432 A73-38358
- Electrodeposited Au on TO-5 headers, discussing discoloration measurement and ultrasonic test for bondability from correlation between optical reflectivity and bond pull strength. 19 p2435 A73-38441
- On the ultrasonic inspection of separation in solid propellant rocket motors. 20 p2568 A73-38646
- Changes in the disorientation of the substructure of a nickel-aluminum alloy under ultrasonic treatment and creep. 20 p2579 A73-39748
- Inspecting thin tubes by ultrasounds - Choice of examination frequency. 21 p2707 A73-41068
- Materials testing via ultrasonic spectroscopy developed from pulse-echo technique, discussing application to metal grain size determination and carbon fiber composite quality control. 21 p2707 A73-41136
- Contactless on-line NDT of metal plates for concealed defects by Lamb wave excitation through wave generation from air. 21 p2708 A73-41138
- Ultrasonic pulse techniques based on acoustic velocity for inert gas thermometry, discussing electroacoustic transducer response time, temperature sensitivity and momentary contact coupling technique. 22 p2854 A73-41994
- Book - Ultrasonic investigation of mechanical properties. 22 p2861 A73-42575
- Experimental verification of dispersion relations for layered composites. 22 p2924 A73-42881 [ASME PAPER 73-APMW-14]
- Fatigue test apparatus for metals at ultrasonic frequencies consisting of transducers, strain amplitude monitor, cooling circuit and static stress mechanism, discussing S-N response. 22 p2867 A73-43169
- Ultrasonic determination of shape and size of hidden defects in solids. 23 p2984 A73-43298
- Ultrasonic spectroscopy for NDT of composite material tube, noting role of frequency signature and pulse spreading in flaw detection. 23 p2984 A73-43641
- High modulus carbon fiber reinforced epoxy composite elastic constant determination by ultrasonic wave propagation velocity measurement in immersion tank, discussing data error sources. 23 p2985 A73-43642
- Expanding the capability of a laboratory ultrasonic testing facility. 23 p2966 A73-44168
- Some results of the application of the nondestructive ultrasonic method to the measurement of residual stresses. 23 p2996 A73-44289
- Fiberglass reinforced plastic laminate creep rate for ultrasonic vibrational and static tensile loads, showing nonlinear viscoelasticity and stress amplitude effects. 24 p3102 A73-44500
- ## ULTRASONIC WAVE TRANSDUCERS
- Generation and detection of helical surface waves on cylindrical bodies by means of contactless electrodynamic transducers. 01 p0051 A73-10975
- Ultrasonic sensing apparatus and eddy current method in NDT, noting radiography, sonic, penetrants and magnetic particles. 01 p0057 A73-11000
- Russian book on ultrasonic processing in metal crystallization covering design of vibrators and transducers and acoustic power measurement. 02 p0175 A73-12800
- Piezoelectric material constants, vibration model, radiation directivity and VHF and UHF operation of ultrasonic transducers. 03 p0306 A73-12950
- Acoustic emission source location using single and multiple transducer arrays. 04 p0448 A73-15121
- Velocity measurements of microwave ultrasonic waves in quartz. 06 p0724 A73-18771
- On the mechanical response of a non-uniform piezoelectric transducer with elastic compliances having damping characteristics. 08 p0994 A73-20870
- HF CW ultrasonics, discussing elimination of electromagnetic leakage or crosstalk between transmitter and receiver by sampling technique. 13 p1612 A73-28480
- A high resolution pulse transmission technique for determining ultrasonic velocities. 20 p2564 A73-38865
- Ultrasonic thermometry using resonance techniques. 22 p2854 A73-41994
- Ultrasonic transducer instrument with broad beam dispersal for blood vessel displacement recording in chronic animal experimentation. 22 p2817 A73-43100
- Oblique radiation of ultrasound by an electromechanical-acoustical method. 24 p3109 A73-44640
- ## ULTRASONIC WAVES
- ### ULTRASONIC RADIATION
- ### ULTRASONIC WELDING
- Russian book on ultrasonic welding of metals and plastics covering equipment, transducers, welded joints stabilization, quality control and efficiency. 04 p0457 A73-15970
- Continuous ultrasonic joining of thin plastic films. 07 p0828 A73-18900
- An experimental model of the microelectronic ultrasonic wire bonding mechanism. 08 p0972 A73-20770
- Solar cell interconnections with different wet types, discussing semiautomatic and automatic ultrasonic processes, solder thickness control and quality inspection methods and criteria. 09 p1035 A73-22280
- Ultrasonic closure welding of small aluminum tubes. 19 p2435 A73-38600
- ## ULTRASONICS
- Non-invasive technique for diagnosing atrial septal defect and assessing shunt volume using direction Doppler ultrasound - Correlations with phasic flow velocity patterns of the shunt. 01 p0014 A73-11500
- The value of the ultrasonic Doppler method as apexcardiography as reference tracings in phonocardiography. 01 p0014 A73-11500
- Ultrasonics Symposium, Boston, Mass., October 7, 1972, Proceedings. 04 p0448 A73-15121
- Relationship between cavitation and decontamination during ultrasonic processing of aluminum and magnesium alloys. 04 p0454 A73-15060
- Left ventricular blood flow velocity in man studied with the Doppler ultrasonic flowmeter. 09 p1042 A73-23160
- State of art of flowmetering, discussing acceptability factors, weirs, laser Doppler velocity method, ultrasonic type, pressure difference technique and ultrasonic and electromagnetic devices. 10 p1221 A73-24200
- Book - Ultrasonics: The low- and high-intensity applications. 11 p1366 A73-26160
- Multi-information recording and reproduction in ultrasono-cardio-tomography. 13 p1579 A73-28497
- Orbit and superior orbital fissure acoustic window for cranium posterior structures imaging by echocardiographic techniques. 22 p2815 A73-42100
- Simple simulated human head for checking echocardiographic equipment. 22 p2815 A73-42100

Ultrasonic holography free from phase turbulence - Construction of the device and experimental results.
23 p2983 A73-44087

ULTRAVIOLET ABSORPTION

Time variations of the ultraviolet absorption in the continuous spectrum of Jupiter and Saturn
01 p0101 A73-10843

Broad band solar EUV absorption in the earth's upper atmosphere.
10 p1214 A73-24747

Measurement of the absorption of solar ultraviolet radiation with the aid of a photoelectron analyzer
11 p1350 A73-25080

Stellar occultation measurements of molecular oxygen in the lower thermosphere.
11 p1356 A73-25911

Temporal variation of ultraviolet absorption in continuous spectra of Jupiter and Saturn.
15 p1928 A73-30979

Atomic oxygen profiles determined by EUV absorption analysis.
18 p2308 A73-36049

Photo-absorption of the upper atmosphere in the middle ultraviolet region.
18 p2308 A73-36050

The absorption cross sections of N₂, O₂, CO, NO, CO₂, N₂O, CH₄, C₂H₄, C₂H₆, and C₄H₁₀ from 180 to 700 Å.
22 p2890 A73-42992

Global distribution of thermospheric heat sources - EUV absorption and Joule dissipation.
23 p2971 A73-43681

Quantum yield of metastable oxygen atoms and molecules via ozone photolysis by UV absorption, noting uncertainties in secondary reaction kinetics
23 p2951 A73-43899

A megarad plastic film dosimeter.
23 p2949 A73-44212

ULTRAVIOLET FILTERS

Report on results of research conducted by the Thin Film Department of SEAVOM, under CNES contract.
07 p0821 A73-18980

Broadband ultraviolet reflectance filters for space applications.
15 p1914 A73-32381

Evaluation of pinholes in unbacked metal film filters to be used in rocket- and satellite-borne XUV spectroheliographs.
19 p2429 A73-37262

ULTRAVIOLET LIGHT**U ULTRAVIOLET RADIATION****ULTRAVIOLET MICROSCOPY**

Application of the method of polarizational ultraviolet fluorescence microscopy to study giant muscle fibers Balanus rostratus Hock
08 p0930 A73-21135

ULTRAVIOLET PHOTOGRAPHY

Stellar sources UV photography from sounding rocket, obtaining mean interstellar absorption, stars magnitudes and distribution and UVB spectrum
02 p0216 A73-12326

Planet wide circulation in Venus upper atmosphere from UV photographs, noting apparent 4.06 day rotation period
06 p0743 A73-17431

Retrograde rotation of the upper atmosphere of Venus.
06 p0744 A73-17433

Magnetically focused electronographic cameras for far UV imagery and spectrography in astronomical and optical geophysical observations from sounding rockets and space vehicles
08 p0971 A73-21744

Stellar survey at 2000-4100 Å via balloon-borne observations, discussing intensity distributions and earth atmospheric ozone layer density
09 p1140 A73-22006

Ultraviolet measurements of the moon in the 1950- to 2750-Å band
16 p2064 A73-33765

Rapid motions of ultraviolet clouds on Venus
16 p2067 A73-33810

UV photography of star field by Eridan rocket-borne wide angle camera, noting inertial guidance system pointing errors data reduction problems
18 p2315 A73-35994

Ultraviolet, panchromatic, infrared and radar remote sensing of Mesabi Range (Minnesota), discussing Precambrian rock formations, geological faults, pre dawn and daytime photography and vegetation patterns
20 p2561 A73-39894

Location in magnetic latitude and local time of the tropical ultraviolet bands seen from Apollo 16.
21 p2684 A73-40788

Apollo 16 far-ultraviolet camera/spectrograph - Instrument and operations.
22 p2864 A73-43165

ULTRAVIOLET PHOTOMETRY
Ultraviolet photometry of the moon with the telescope experiment on the OAO-II.
01 p0096 A73-10317

Importance of high time resolution in flare star observations.
03 p0373 A73-13373

Ultraviolet photometry from the orbiting astronomical observatory. V - The helium-weak stars.
04 p0499 A73-15363

Ultraviolet photometry from the Orbiting Astronomical Observatory. VI - Magnesium II 2800 Å emission in cool stars.
05 p0625 A73-17336

Ultraviolet photometry from the orbiting astronomical observatory. IV - Photometry of late-type stars.
05 p0626 A73-17381

Ultraviolet photometry from the Orbiting Astronomical Observatory. VII alpha squared Canum Venaticorum.
08 p1008 A73-21158

Preliminary results of a spectrophotometric survey of the sky in the ultraviolet with the aid of the TD-1 A satellite
08 p0967 A73-21499

Preliminary results of the determination of altitudes on Mars from CO₂ 2-micron wavelength bands aboard the Mars 3 interplanetary automatic station
13 p1673 A73-28288

An extreme UV photometer for solar observations from Atmosphere Explorer.
13 p1688 A73-28638

OAO-2 observations of Beta Lyrae and a provisional interpretation.
15 p1935 A73-31489

Photometric device for an ISP-28 spectrograph in optical atmospheric studies
15 p1875 A73-31822

Study of the influence of various parameters on the method used for determining the attenuation lengths through photoelectric yield measurements in the far ultraviolet
15 p1878 A73-32211

The Schottky-barrier silicon photodetector in perspective with other detection devices in the 200 nm to 1100 nm range.
16 p2013 A73-32885

Preliminary results of Martian altitude determinations with CO₂ bands /2 micron wavelength/ from the automatic interplanetary space station Mars 3.
22 p2905 A73-41807

Basic method for realization of temperature scale at 10,000 K by photometric comparison between vacuum-UV-blackbody radiation of a plasma and synchrotron radiation.
22 p2852 A73-41978

ULTRAVIOLET RADIATION**NT FAR ULTRAVIOLET RADIATION****NT LYMAN ALPHA RADIATION****NT NEAR ULTRAVIOLET RADIATION**

UV astronomy advances from rocket and satellite observations, discussing early stars, interstellar extinction and gas, galaxies and globular clusters
01 p0094 A73-10059

Pulsed UV-radiation source for producing highly ionized low-density initial plasmas
01 p0082 A73-10325

Electron spin resonance of ultraviolet radiation induced defects in ZnO thermal control coating pigment.
01 p0088 A73-11276

Secondary ionisation and its possible bearing on the performance of a solar cell.
02 p0132 A73-12048

The feasibility of producing laser plasmas via photoionization.
[AD-753308]
02 p0177 A73-12572

UV light intensities calibration in astrophysics and high temperature metrology with thermal arc plasma as radiation sources, discussing intensity standard establishment
02 p0199 A73-12715

Tago-Sato-Kosaka and Bennett comets Lyman alpha radiation explanation via resonant scattering on neutral hydrogen formed by water vaporized from ice core
02 p0224 A73-12742

Outgassing and contamination properties of prospective Apollo Telescope Mount materials.
03 p0330 A73-13020

Uncertainties in determining the effective UV radiation at various altitudes.
[AIAA PAPER 73-102]
05 p0570 A73-16862

The infrared variability of a dust model for Seyfert galaxies.
05 p0624 A73-17311

The formation of diatomic molecules in interstellar clouds.
05 p0625 A73-17333

Mars UV reflectance properties from Mariner 9 spectrometer, giving topographic map based on ultraviolet light scattering from atmosphere
06 p0746 A73-17483

Preliminary results of measurements of UV emissions scattered in the Martian upper atmosphere.
06 p0746 A73-17486

Correlations between X-rays and UV ionizing radiation in the E region from data obtained during the solar eclipse of 25 February 1971
06 p0742 A73-17534

Pulsed nitrogen laser emitting at 3371 Å.
06 p0702 A73-18587

Laser-induced gas breakdown initiated by ultraviolet photoionization.
06 p0703 A73-18749

An efficient electrical CO₂ laser using preionization by ultraviolet radiation.
06 p0704 A73-18797

Photomultipliers for UV radiation detection, discussing high sensitivity and speed features, components, photon detection, tube types and applications
07 p0821 A73-18981

Rocket-borne measurement of UV background radiation at 1115, 1425 and 1446 Å, setting upper limit to flux from Coma galactic cluster.
07 p0868 A73-19057

UV-induced lipid peroxidation in human epidermis, dermis, and hypodermis in vitro
09 p1038 A73-21873

On ultraviolet absorption by molecular hydrogen in stellar atmospheres.
09 p1148 A73-22867

Ultraviolet effects on the chemical composition and optical properties of interstellar grains.
09 p1150 A73-23138

Optical identifications of radioresources from the B2 catalogue - Quasi stellar sources.
10 p1280 A73-24403

Ultraviolet luminescence and nonlinear extinction in ruby
10 p1260 A73-24579

A finding list of faint UV-bright stars in the galactic plane.
11 p1414 A73-25067

Theory of cooperative defect formation in a biopolymer molecule under the action of radiation
11 p1323 A73-25637

A high resolution position sensitive detector for ultraviolet and X-ray photons.
11 p1363 A73-25958

Photoemission diode standards with high sensitivity, time stability and response uniformity for accurate measurement of monochromatic UV light, discussing design and construction
11 p1365 A73-26234

Feasibility of high-pressure noble-gas lasers.
11 p1378 A73-26360

An experimental basis for carcinogenic effects of ultraviolet radiation.
11 p1320 A73-26485

Plant growth response to low temperature and UV treatment, discussing chlorophyll synthesis, carbohydrate levels, ion balance and enzyme characteristics
11 p1320 A73-26486

Some effects of magnetospheric acceleration mechanisms on variations in ultraviolet intensity height profiles, and on consequent rocket spectrograph sensitivities.
11 p1358 A73-26703

The generation of tunable coherent radiation in the wavelength range 2300-3000 Å using lithium formate monohydrate.
12 p1504 A73-26826

Commutation of spark gaps with the aid of a pulsed gas laser emitting in the ultraviolet range
12 p1506 A73-27211

UV radiation effects on gamma irradiated Cr ions spin lattice relaxation rate in ruby and on resonant phonon scattering
13 p1668 A73-28219

Investigation of scattered ultraviolet radiation in the upper Martian atmosphere from the Mars-3 automatic interplanetary station
14 p1796 A73-29866

A proximity focused ultraviolet-sensitive SEC camera tube.
14 p1732 A73-29910

Possibility of using semiconductor photocells as receivers of ultraviolet radiation
14 p1713 A73-30949

Fluorescent cross sections and yields of CO₂ +/- from threshold to 185 Å.
15 p1915 A73-31274

Variable star observations from outside the earth's atmosphere - Review and prospects.
15 p1935 A73-31488

Correlations between X-rays and ionizing ultraviolet radiation in the E-region, according to data from the solar eclipse of February 25, 1971.
16 p2052 A73-32758

Nitrogen pulsed ultraviolet laser.
16 p2023 A73-32861

The characteristics of the solar ultraviolet radiation at Arosa.
[AIAA PAPER 73-523]
16 p2056 A73-33558

Study of ultraviolet radiation from the Venera interplanetary probe
16 p2056 A73-33803

The ultraviolet flux envelopes of main-sequence B stars.
17 p2234 A73-35613

Repetitively pulsed high power nitrogen laser for UV radiation at room temperature, discussing electrical design and construction
17 p2185 A73-35767

ULTRAVIOLET REFLECTION

On the ionization of the intercloud medium by ultraviolet stars. 19 p2484 A73-37611

Mariner 9 ultraviolet spectrometer experiment - Mars atomic oxygen 1304-A emission. 20 p2604 A73-38932

Extraterrestrial ultraviolet radiation and the parameter of the HI medium near the sun 20 p2601 A73-39074

Latitude distribution of the regularity in F2-region irregularities. 20 p2553 A73-39132

The interaction of a laser with matter as an intense source of UV and soft X-ray radiation - Application to X-ray cinematography 21 p2709 A73-39944

Low-inertia ultraviolet hygrometer 21 p2701 A73-40744

Enhancements of the photoelectron-excited dayglow during solar flares. 21 p2761 A73-41389

Spectrum sensitive high amplification solar blind UV sensor for flame surveillance in jet engine environments at 1000 F, using miniature Geiger-Mueller tube 22 p2861 A73-42694

On the backscatter of solar He II, 304 A radiation from interplanetary He+/. 23 p3024 A73-43695

UV radiation measurements of Ar-Hg gas discharge plasma as function of temperature and pressure with emphasis on fluorescent light design 23 p3011 A73-43830

The Nimbus-4 backscatter ultraviolet /BUV/ atmospheric ozone experiment Two years' operation. 23 p2975 A73-43877

Variations in the stratospheric ozone field inferred from Nimbus satellite observations. 23 p2975 A73-43878

Aerosols - A limitation on the determination of ozone from BUV observations. 23 p2975 A73-43879

The mean ozone distribution from several series of rocket soundings to 52 km at latitudes from 58 deg S to 64 deg N. 23 p2975 A73-43880

Rocket-borne spectrometer measurement of solar UV flux for thermospheric vertical distribution of molecular oxygen 24 p3135 A73-44632

Hardening with UV radiation in the manufacture of glass-fiber-reinforced unsaturated polyester resin molding materials 24 p3093 A73-44889

Interstellar trace element ionization predictions by cosmic ray, X-ray and UV star models with hydrogen allowance, showing disagreement with satellite observation 24 p3125 A73-45056

ULTRAVIOLET REFLECTION

Side-viewing detector for a vacuum ultraviolet reflectometer. 03 p0309 A73-14430

Far ultraviolet reflectivity of lunar dust samples - Apollo 11, 12, and 14. 15 p1932 A73-31270

Broadband ultraviolet reflectance filters for space applications. 15 p1914 A73-32381

Ultraviolet observations of Mars made by the Orbiting Astronomical Observatory. 24 p3128 A73-44397

Posteclipse brightening of Io observed at 3500 and 4000 A suggested as transient partial covering of high-albedo material 24 p3134 A73-44564

ULTRAVIOLET SPECTRA

Optical, far UV and radio spectra observations and results for solar spicules, considering morphology, spectroscopic properties and dynamic models 01 p0094 A73-10055

Observational data on galaxies with UV continuum, listing objects with emission lines, s-d classification and quasar spectral energy distribution 01 p0099 A73-10701

Nature of galaxies with an ultraviolet continuum. I - Basic spectral and color characteristics 01 p0099 A73-10702

Nature of the emission of UV Ceti-type stars 01 p0100 A73-10708

Transmittance of the atmosphere and the relationship among optical parameters in the ultraviolet spectral region 01 p0040 A73-10873

Polarimetric investigations of the giant planets. II - Phase variation of the polarization of selected regions on the Saturn disk 01 p0102 A73-10941

UV Ceti-type variable star quiet state and flare spectra, discussing flare mechanism relation to magnetic effects and star evolutionary position 01 p0102 A73-10970

Solar UV spectra with high angular resolution from rocket observations, obtaining center to limb intensity variations 02 p0207 A73-12325

The data-handling problem with television recording of spectra. 02 p0170 A73-12340

Apollo 16 ultraviolet astronomy observations. 02 p0220 A73-12475

New ultraviolet line identifications for early-type stars. 02 p0226 A73-12831

Rocket-ultraviolet spectra of eight stars in Ophiuchus and Scorpius. 03 p0366 A73-12942

Rocket-ultraviolet spectra of six stars in Perseus. 03 p0366 A73-12943

Ultraviolet and X-ray spectroscopy of astrophysical and laboratory plasmas; Proceedings of the Third Symposium, Utrecht, Netherlands, August 24-26, 1971. 03 p0363 A73-13951

Cometary heads observations indicating precursor decay lengths from 100-10,000 km, considering visible and UV molecular and atomic emissions 04 p0495 A73-14764

Investigations of a Kr-Hg mixture regarding laser action 04 p0458 A73-14896

The spectra of highly ionized aluminum /Al VI-X/ in the extreme-ultraviolet and soft X-ray regions. 04 p0492 A73-15369

Secondary component minimum deepening in UV light curve of Beta Lyr eclipsing binary star, suggesting black hole model 04 p0501 A73-15637

Extreme-ultraviolet emission from solar prominences. 05 p0612 A73-17337

Analysis of the extreme-ultraviolet quiet solar spectrum. 05 p0625 A73-17338

Carbon monoxide Cameron bands limb intensity profile in Martian airglow from Mariner 9 UV spectrum observations 06 p0746 A73-17485

Interstellar molecular hydrogen observed in the ultraviolet spectrum of delta Scorpii. 07 p0874 A73-19071

Dawn airglow far UV spectrum observed by scanning Ebert spectrophotometer aboard Aerobee rocket, obtaining altitude profiles at 100-244 km 07 p0814 A73-19247

Distribution of the total ozone content in the atmosphere according to satellite observations. 07 p0820 A73-20346

Photoabsorption cross section of argon in the 180-700-A wavelength region. 08 p0990 A73-21050

On the source of the 3840 A persistent emission by meteors. 08 p1010 A73-21318

Aberrations, astigmatism and coma control for far UV stellar spectrograph design by grating shape and ruling space modification 08 p0972 A73-21752

The interstellar reddening law in the ultraviolet deduced from filter photometry obtained by the OAO-2 satellite. 09 p1141 A73-22029

The extreme-ultraviolet spectrum of Fe XV in a solar flare. 09 p1137 A73-22039

Polarimetric observations of the major planets. II - Phase dependence of the polarization for selected areas on the disk of Saturn. 09 p1147 A73-22736

Further observations of the solar limb spectrum in the region 550-2000 A. 10 p1278 A73-24128

Ultraviolet ion chamber measurements of the solar minimum brightness temperature. 10 p1279 A73-24136

Excitation of oxygen permitted line emissions in the tropical nightglow. 10 p1214 A73-24739

High resolution rocket EUV solar spectrograph. 11 p1360 A73-25059

Ultra-violet argon dayglow lines in the atmosphere of Mercury. 11 p1421 A73-25916

Simplified photoionization analysis of quasar emission spectra. 11 p1427 A73-26616

Absorption spectrum of Cu I in the vacuum ultraviolet. 12 p1526 A73-27122

Ultraviolet spectrum emitted from a laser-produced uranium plasma. 12 p1527 A73-27123

Fraunhofer line data reduction and wavelengths identification in solar UV spectra recorded during flight of Skylark rocket SL 601 12 p1544 A73-27827

Atmospheric transparency and the relationship between optical variables in the ultraviolet. 13 p1607 A73-28699

LTE and hydrogen and ionized He lines approximations for model atmosphere computations of hot early stars, discussing UV line blanketing 13 p1686 A73-29360

Interstellar gas abundances from rocket observations of ultraviolet absorption lines. 14 p1801 A73-30734

An analysis of the solar extreme-ultraviolet spectrum between 50 and 300 A. 14 p1801 A73-30740

Mariner 9 ultraviolet spectrometer experiment - Upper limits on the Lyman-alpha flux from clusters of galaxies. 15 p1936 A73-31584

The extreme-ultraviolet spectrum of a solar active region. 15 p1936 A73-31560

Spectrophotometric results from the Copernicus satellite. VI - Extinction by grains at wavelength between 1200 and 1000 A. 15 p1936 A73-31563

Rocket flight observations of solar UV chromosphere at 1190-1320A, considering spectral and angular resolutions 15 p1936 A73-31564

Quasi-monochromatic measurements of homogeneous arc plasmas. 15 p1841 A73-32395

Observations of the inner F and K coronas below 2220-A wavelength. 16 p2060 A73-32954

The extreme ultraviolet emissions of solar flares - A comparison between OSO-6 spectroheliograph observations and SFDs. 16 p2053 A73-32953

Concentration of OH and NO in YJ93-GE-3 engine exhausts measured in situ by narrow-line UV absorption. [AIAA PAPER 73-506] 16 p2045 A73-33540

Lamp pumping system for lasers based on organic compound solutions 17 p2183 A73-34170

Intrinsic ultraviolet colors from OAO-2 Telescope observations for stars on the main sequence. 17 p2225 A73-34290

Models of the chromospheric-coronal transition layer and lower corona derived from extreme-ultraviolet observations. 18 p2357 A73-37107

The absorption spectrum of Rb I between 350 and 810 A. 19 p2462 A73-37622

TD 1 A astronomical satellite detection of UV dayglow emissions above F 2 peak in equatorial zone considering Mg ions resonance scattering to account for emission features 20 p2551 A73-38940

Observations of ultraviolet stellar spectra by the Utrecht Orbiting Stellar Spectrophotometer S59. 21 p2769 A73-40818

The near ultraviolet spectrum of early type stars obtained with S 59. 21 p2769 A73-40828

Line identifications in the near ultraviolet spectrum of the peculiar A star epsilon Ursae Majoris. 21 p2769 A73-40828

NBS radiometric calibration services extended to far UV spectrum with dc high power hydrogen wall stabilized arc as primary standard of spectral radiance 21 p2703 A73-41256

Solar corona observations in white light by OSO 7 and in XUV by Naval Research Laboratory, discussing contributions from other observatories and satellites 21 p2773 A73-41383

Ultraviolet stellar spectra obtained with the Utrecht orbiting stellar spectrophotometer S 59 aboard the ESO TD-1 A satellite. 21 p2773 A73-41395

Further observations of the structure of the chromosphere-corona transition region from limb and disk intensities. 21 p2779 A73-41537

The far-ultraviolet spectrum of Jupiter. 22 p2905 A73-41768

Excitation of the CO fourth positive system by the dissociative recombination of CO2+/ions. 22 p2843 A73-41904

Analysis of the ultraviolet spectrum of A-type stars observed by the OAO II satellite. 22 p2907 A73-42301

Cerenkov-effect based standard radiation sources designed for the calibration of space experiments - Spectral energy distribution measurement 22 p2860 A73-42307

French monograph - Preparation of a space experiment intended for high resolution study of the far ultraviolet spectrum of the star gamma Gemini. 22 p2910 A73-42714

Energy level transitions in Ca XVII and Ti XIX UV spectra, basing identifications on extrapolation method 22 p2914 A73-43016

Wolf-Rayet stars UV spectra from OAO-2 satellite-borne spectrometer measurements, considering radio spectra of W stars with symmetrical nebulae from ground based observations 23 p3025 A73-43194

Ozone related spectral measurements of total solar radiation. 23 p2975 A73-43882

Looking at the solar system in the far-ultraviolet. 23 p3034 A73-44220

ULTRAVIOLET SPECTROGRAPHS

U ULTRAVIOLET SPECTROMETERS

ULTRAVIOLET SPECTROMETERS

Mariner 9 ultraviolet spectrometer experiment - Mars airglow spectroscopy and variations in Lyman alpha. 06 p0746 A73-17484

Mariner 9 ultraviolet spectrometer experiment - Seasonal variation of ozone on Mars. 08 p1009 A73-21223

Balloon-borne UV stellar spectrometer telescope pointing and stabilization, discussing in-house feasibility studies by small scale test payload experiments 08 p0971 A73-21750

Balloon-borne telescope-UV spectrometer for stellar spectrophotometric measurement with high spectral resolution, discussing system design and operation, image motion compensation and data acquisition 08 p0971 A73-21751

Far UV scanning spectrometer aboard Apollo 17 CSM to measure lunar atmospheric composition, observing spectral albedo, LEM atmosphere, and galactic and solar system atmospheres 12 p1497 A73-27485

Atmosphere Explorer satellite-borne two channel fixed grating Ebert spectrometer for measurement of airglow at 2150 A, yielding altitude profiles of nitric oxide density 13 p1689 A73-28640

Mariner 9 ultraviolet spectrometer experiment - Interstellar absorption at Lyman alpha in OB stars. 15 p1936 A73-31556

The Harvard experiment on OSO-6 - Instrumentation, calibration, operation, and description of observations. 18 p2357 A73-37108

A mechanically scanned interferometer-echelle spectrometer for the middle ultraviolet. 21 p2692 A73-39924

Satellite ultraviolet measurements of nitric oxide fluorescence with a diffusive transport model. 22 p2845 A73-41925

ULTRAVIOLET SPECTROPHOTOMETERS

Solar UV Lyman alpha radiation intensity measurements, using Vertikal-1 rocket-borne photometer and photoelectron analyzer 03 p0379 A73-14565

Lunar Surface Ultraviolet Spectrographic Camera for location and extent determination of gaseous material, describing capability for acquisition of direct imagery and spectroscopy 05 p0576 A73-16746

Atlas S183 spectrophotometer for Skylab orbital laboratory UV observations, discussing electrical, optical and mechanical interface problems 07 p0822 A73-19007

Stellar UV observations with spectrophotometer onboard ESO TD-1A satellite in retrograde near polar orbit 07 p0875 A73-19259

Aberrations, astigmatism and coma control for far UV stellar spectrograph design by grating shape and ruling space modification 08 p0972 A73-21752

The evacuating and outgassing of a vacuum UV spectrophotometer for rockets 10 p1220 A73-24683

EUV spectrophotometer onboard Atmosphere Explorer satellites, discussing design, aeronautical mission objectives, constraints and economic factors 13 p1688 A73-28637

Spectrophotometric results from the Copernicus satellite. I - Instrumentation and performance. 14 p1754 A73-30744

Spectrophotometric results from the Copernicus satellite. III - Ionization and composition of the intercloud medium. 14 p1801 A73-30746

Spectrophotometric results from the Copernicus satellite. IV - Molecular hydrogen in interstellar space. 14 p1802 A73-30747

Spectrophotometric results from the Copernicus satellite. V - Abundances of molecules in interstellar clouds. 14 p1802 A73-30748

Inference of total ozone from photometric measurements of sky radiation. 23 p2973 A73-43856

ULTRAVIOLET SPECTROSCOPY

Recent results of the Goddard rocket program for observing stars. 02 p0215 A73-12324

Twin spectrograph measurements at 2520-3375 A of metal trace elements in biological sample solutions 06 p0657 A73-17692

Mariner 9 Ultraviolet Spectrometer experiment - Observations of ozone on Mars. 09 p1144 A73-22267

Reflectance and optical constants of evaporated osmium in the vacuum ultraviolet from 300 to 2000 A. 13 p1660 A73-28936

Spectrophotometric results from the Copernicus satellite. II - Composition of interstellar clouds. 14 p1801 A73-30745

Optical and UV astronomical telescopes and instrumentation for quasar detection, emphasizing observational requirements and emission line red shift problem 17 p2233 A73-35277

Television sensors for ultraviolet space astronomy. 17 p2170 A73-35292

The detector system of the International Ultraviolet Explorer satellite. 17 p2170 A73-35295

Report on the telescope ultraviolet observations from the OAO-2 satellite and associated research at the Smithsonian Astrophysical Observatory. 18 p2349 A73-35996

Mariner 9 ultraviolet spectrometer experiment - Afternoon terminator observations of Mars. 19 p2479 A73-37220

French monograph - Contribution to the ultraviolet spectrophotometry of the night sky /1900 to 3400 A/. 22 p2850 A73-42742

Mariner 9 ultraviolet spectrometer experiment - 1971 Mars' dust storm. 24 p3127 A73-44396

UMBRA (SHADOWS)

U SHADOWS

UMKEHR EFFECT

Fourteen-year series of vertical ozone distribution over Arosa, Switzerland, from Umkehr measurements. 23 p2974 A73-43869

UNCAMBERED WINGS

NT RING WINGS

Nonplanar wings in nonplanar ground effect. 15 p1824 A73-31744

UNCERTAINTY

U PROBABILITY THEORY

UNCONSCIOUSNESS

NT BLACKOUT [PHYSIOLOGY]

NT NARCOSIS

Military aircraft pilot in-flight consciousness loss etiologies, discussing rapid decompression, hypoxia, dysbarism, seizure, improper maneuver, vasovagal syncope, acceleration sensitivity, etc 17 p2115 A73-34747

Sudden incapacitation in flight - 1 Jan. 1966-30 Nov. 1971. 20 p2512 A73-39112

UNDAMPED OSCILLATIONS

German monograph - Contributions to the calculation of natural frequencies of undamped oscillator chains by the transfer method. 03 p0343 A73-13815

UNDERGROUND NUCLEAR EXPLOSIONS

U NUCLEAR EXPLOSIONS

UNDERGROUND STORAGE

Evaluation of materials for underground exposure in extreme environments. 03 p0329 A73-13006

UNDERWATER ACOUSTICS

Sonic boom induced underwater pressure oscillations, noting strong attenuation with depth 03 p0250 A73-13835

Deformation of a spherical shell under the action of an unsteady spherical hydroacoustic wave 09 p1165 A73-23354

Radar direction measurements by phase comparison of ultrasonic echo pulses reflected from targets in water tank, using piezoelectric sensors for receiving antennas simulation 10 p1194 A73-23736

Real-time reconstruction of images from hydroacoustic holograms. 13 p1614 A73-28578

Cylindrical scan acoustical holographic transmitter/sensor system for ultrasonic under ocean surveillance and NDT applications 13 p1615 A73-28588

Diffraction of acoustic waves on plates interconnected at right angles 17 p2211 A73-34140

UNDERWATER COMMUNICATION

Implementation problems of a multichannel digital filter in the case of beat frequencies in the MHz range 23 p2957 A73-43316

UNDERWATER PROPULSION

Fish like slender body propulsion and flow theory, discussing fin surface-body thickness interaction, vortex sheets, trailing edges and lifting force 11 p1301 A73-25852

UNDERWATER SOUND

U UNDERWATER ACOUSTICS

UNDERWATER TESTS

Cardiorespiratory responses to exercise in air and underwater. 01 p0007 A73-10161

Body thermotopography and some metabolic process characteristics in scuba divers under various underwater exposure conditions 05 p0545 A73-16734

Respiration mechanics during weightlessness simulation in an immersion medium 08 p0929 A73-20986

Investigation of certain indices of higher nervous activity in man during prolonged stay in a water environment 09 p1039 A73-22364

Role of mineralocorticoids in the natriuresis of water immersion in man. 09 p1040 A73-22676

Study of the far wake vortex field generated by a rectangular airfoil in a water tank. 18 p2262 A73-36233

[AIAA PAPER 73-682] Thermographic evaluation of relative heat loss areas of man during cold water immersion. 18 p2283 A73-36781

Tolerance to immersion in cold water 18 p2280 A73-36943

Influence of physical stress on the state of human higher nervous activity under conditions of underwater labor 24 p3059 A73-44672

UNDERWATER VEHICLES

NT SUBMARINES

UNAXIAL STRAIN

U AXIAL STRAIN

UNIFORM FLOW

NT BLASIUS FLOW

The optimisation of sound attenuation in lined ducts containing uniform, axial, subsonic, mean flow. 03 p0291 A73-12987

Highly uniform inlet velocity profile influence on conical diffuser characteristics 07 p0774 A73-19615

Out-of-plane force on a circular cylinder at large angles of inclination to a uniform stream. 09 p1029 A73-23124

Unsteady boundary layer flow of homogeneous viscous fluid in nonrotating environment or bounded by oscillating flat plates, determining velocity field by exact solutions 11 p1346 A73-25165

Acoustic radiation from the end of a two-dimensional duct - Effects of uniform flow and duct lining. 16 p1999 A73-32914

The propagation and attenuation of sound in lined ducts containing uniform or 'plug' flow. 16 p1970 A73-33944

Acoustic energy flow in lined ducts containing uniform or 'plug' flow. 16 p2038 A73-33945

Measurements of surface pressure on an elliptic airfoil oscillating in uniform flow. 19 p2375 A73-37374

Neighboring body effects on bluff body form drag. 20 p2507 A73-39519

Neighboring body effects on bluff body tipping moment. 20 p2507 A73-39520

Hot-wire investigation of the steady laminar wake behind a thin flat plate placed perpendicularly to a uniform flow. 21 p2703 A73-41118

Vortex shedding from and base pressure distribution on bluff body measured in shear or uniform flow, calculating Strouhal number 23 p2940 A73-43939

Study of the field of fluctuating pressures at the surface of a circular cylinder 24 p3079 A73-45220

UNIPOLAR TRANSISTORS

U FIELD EFFECT TRANSISTORS

UNIQUENESS THEOREM

Uniqueness and continuous dependence for the equations of elastodynamics without strain energy function. 01 p0115 A73-10777

A priori estimate of the solution to a Cauchy problem with data prescribed on a time-like surface for a 2-nd order parabolic equation and the uniqueness theorems associated with it 01 p0071 A73-11426

Uniqueness of a solution to an inverse problem in the case of a second order equation with continuous boundary conditions: Regularized sums of a portion of eigenvalues - Factorization of the characteristic determinant 01 p0071 A73-11440

Second-order abstract and Schroedinger linear differential equations in Beurling spaces 02 p0186 A73-11570

Uniqueness and stability of positive periodic solutions of differential equations with a delayed argument 02 p0187 A73-12357

Uniqueness theorem for linear thermoelasticity theory allowing for second sound, discussing acceleration waves propagation in isotropic material
02 p0237 A73-12796

On the uniqueness of solutions of the Falkner-Skan equation.
02 p0154 A73-12798

Existence and uniqueness of heat equation two phase free boundary problem classical solutions
03 p0336 A73-12922

A class of neutral functional differential equations.
04 p0469 A73-14666

Hyperbolic equations and systems with multiple characteristics.
04 p0471 A73-15224

On the uniqueness of singular solutions to boundary-initial value problems in linear elastodynamics.
04 p0512 A73-15226

Necessary conditions for optimal controls of elliptic or parabolic problems.
05 p0590 A73-16487

A note on a general linear initial-boundary value problem.
06 p0716 A73-17980

Uniqueness of non-linear elastic equilibrium for prescribed boundary displacements and sufficiently small strains.
06 p0719 A73-18700

Feedback law choice for autonomy properties of controlled object, noting existence and uniqueness theorems
08 p0951 A73-21127

On the lateral boundary conditions for the primitive equations.
08 p0985 A73-21387

The use of operators with degenerated kernel for nonlinear system investigation.
10 p1242 A73-24043

Equivalent formulations of quasilinear Dirichlet problem driven by positive sources, examining limiting and similarity singular solutions and uniqueness properties
10 p1250 A73-24785

Displacement boundary value problem of linearized elastodynamics with superimposed small and large deformations in homogeneous anisotropic elastic solid, proving solution uniqueness theorem
11 p1444 A73-26282

Algorithm for solution of inverse Stefan problem for flow characteristics determination, stating necessary and sufficient conditions for solution existence and uniqueness
11 p1452 A73-26328

Comparison and oscillation theory for Lienard's equation with positive damping.
11 p1391 A73-26367

Nonlinear plane cavity flow past flexible barrier, deriving uniqueness theorem by variational operator formulation in terms of potentialness conditions
11 p1391 A73-26547

A uniqueness theorem for the solution of the inverse problem of spectral analysis in the case of a differential equation with periodic boundary conditions
12 p1518 A73-27727

Boundary value problem solution uniqueness in dynamic linear theory of hereditary-elastic rheologically composite media
12 p1555 A73-27793

Wave propagation aspects of the generalized theory of heat conduction.
13 p1704 A73-28414

Characteristic initial value problem for class of differential equations, proving solution existence and uniqueness as generic properties
13 p1648 A73-28536

Generalized smoothing spline functions for operators.
13 p1649 A73-28604

Uniqueness of Chebyshev approximation representation by ratios of exponential functions with restricted number of zeros
13 p1651 A73-29400

Uniqueness theorems for the Dirichlet boundary value problem in the case of elliptic-parabolic differential equations and lower bounds for the smallest eigenvalue
14 p1767 A73-29765

Integral equation formulation for electromagnetic scattering by conducting cylinders, investigating coupling between complementary boundary value problem and nonuniqueness consequences on numerical resolution
14 p1727 A73-30215

On the uniqueness of solutions of stress equations of motion of the Beltrami-Michell type.
14 p1809 A73-30254

A uniqueness theorem for a system of stress equations of motion in linear elasticity.
14 p1809 A73-30255

Group data handling theorems on uniqueness of mathematical model for regression curve reconstruction in polynomial domain with small number of points
14 p1738 A73-30288

Third basic boundary value problem of dynamics for a three-dimensional elastic body
14 p1810 A73-30383

Existence and uniqueness theorems for differential equations with deviating arguments of mixed type.
14 p1770 A73-30760

Weak solutions existence and uniqueness for boundary value problem in linearized theory for mixtures of two isotropic incompressible elastic solids, obtaining differentiability conditions
15 p1947 A73-31336

Uniqueness and existence estimates of third order differential equation solutions for nonlinear boundary value problem in fluid mechanics
15 p1863 A73-31363

Russian book on inverse problems for hyperbolic differential equations covering functionals, uniqueness theorems, integral geometry and earth interior structure from seismological data
15 p1899 A73-31581

Solution uniqueness for elasticity problem with modulus diversity based on deformation potential energy as convex function
15 p1950 A73-31826

Feedback law choice for autonomy properties of controlled object, noting existence and uniqueness theorems
15 p1855 A73-32062

Existence and uniqueness of positive eigenfunctions for a class of quasilinear elliptic boundary value problems of sublinear type.
15 p1900 A73-32181

Existence and uniqueness of solutions of boundary value problems for third order differential equations.
15 p1902 A73-32398

New problems pertaining to nonlinear integro-differential equations with several independent variables. I - Search for solutions in the case of initial integral boundary conditions
16 p2032 A73-33172

Regularity theorems for the solution of a second-order abstract linear differential equation
16 p2032 A73-33373

Analyticity of the plane steady state solutions of the Navier-Stokes equation.
17 p2150 A73-34324

Uniqueness theorems for infinite systems of linear equations
17 p2201 A73-34631

Uniqueness requirements for calculated jump conditions across embedded shock waves based on relaxation methods, comparing to time dependent finite difference calculation
17 p2154 A73-35130

A note on uniqueness in the linear theory of heat conduction with finite wave speeds.
18 p2371 A73-36692

Unique solution of boundary value problem of Boltzmann equation for unsteady rarefied gas flow of formless particles past arbitrary surface
19 p2462 A73-37843

Uniqueness of solutions and some approximate methods of solving problems in linear viscoelasticity
21 p2782 A73-40186

On the uniqueness of search directions in variable-metric algorithms.
21 p2726 A73-40837

Proof for the existence of a solution to the fundamental quadrantal problem of dynamics for a three-dimensional elastic body, and approximate computation of the solution
22 p2918 A73-41951

Local and global theorems of existence and uniqueness for solutions to nonlinear singular integral equations on a denumerable set of contours
22 p2882 A73-42472

Optimal feedback control solution existence and uniqueness conditions for asymptotic stability, discussing relationships with Pontryagin equations and linear regulator problem with quadratic cost functionals
22 p2837 A73-43070

Quasi-periodic solutions existence, uniqueness and asymptotic behavior to quasi-linear parabolic equations, demonstrating vanishing conditions at boundary
23 p3049 A73-43611

The Minkowski problem generalized for ovaloids
23 p2999 A73-43613

Uniqueness theorems and variational principles derivation for free viscoplastic flow and constrained plastic deformation, obtaining Castiglione theorem from boundary value problem solution
23 p3044 A73-43974

An existence and uniqueness theorem for the solution of a stochastic integrodifferential equation
23 p2999 A73-44101

Boundary value problem solutions uniqueness and existence for ordinary differential equations under Cauchy condition
23 p3000 A73-44209

Static theory of plane micropolar strain for homogeneous orthotropic elastic solids, deriving existence and uniqueness theorems and reducing boundary value problems to Fredholm equations
24 p3147 A73-44684

An elastoplastic strain-hardening material - Quasi-static evolution of the stress distribution
24 p3147 A73-44749

Classical MHD differential equations solution for uniqueness and existence of shock wave structures based on thermodynamic potential concept
24 p3116 A73-45222

On global existence and uniqueness theorems for gravitational systems.
24 p3141 A73-45280

On the existence, uniqueness, and stability of solutions of a new boundary layer problem concerning certain nonlinear integral-differential polyvibratory systems. I
24 p3106 A73-45390

UNITED NATIONS

International law principles application to space liability codification, noting United Nations role in Draft Convention on space liability
04 p0524 A73-151905

UN accomplishments in space law, discussing ESRO and ELDO application satellites and international agreements
14 p1819 A73-308980

UNITED STATES OF AMERICA

NT ALABAMA

NT COLORADO

NT GEORGIA

NT KANSAS

NT MISSISSIPPI

NT OKLAHOMA

NT OREGON

NT SOUTH DAKOTA

NT TEXAS

Monopoly, concentration, and competition in the air transportation industry of the United States
01 p0124 A73-10568

Detailed gravimetric geoid computation for U.S. area from satellite spherical harmonic and surface gravity data, comparing with astrogeodetic geoid
04 p0439 A73-14798

UNITS OF MEASUREMENT

NT INTERNATIONAL SYSTEM OF UNITS

Solar-planetary system mechanical parameters determination based on astronomical unit, discussing conversion into terrestrial units via radar distance measurements
03 p0376 A73-14174

A note on the quantity /effective/ perceived noise in mass and units of perceived noise level.
04 p0406 A73-15587

Aircraft performance calculations in SI units, considering conversion factors for forces, pressures and specific fuel consumption
06 p0648 A73-18511

Electrical measurement of mechanical forces and displacements, discussing transducers design and measurement standards and units
10 p2125 A73-23633

Metric technical, Imperial /British/ and SI dimensional systems, discussing conversion rules for mass, force, length, area, volume, density, moment of inertia and stress relationships
[SAWE PAPER 963]
19 p2499 A73-37881

UNIVERSAL TIME

VLF navigation development at NAE.

Topside ionospheric winter and summer diurnal electron density variations in Arctic regions as function of universal time, showing Ariel 3 measurements graphically
21 p2682 A73-40171

Direct determination of universal time based on east-west interferometer observations of radio sources using 5 km radio telescope
21 p2739 A73-40373

Errors on the dial of cosmic clocks
21 p2701 A73-40728

Some characteristics of an operational system for measuring UT 1 using very long baseline interferometry.
21 p2705 A73-41330

UNIVERSE

Closed time as an explanation of the black body background radiation.
02 p0193 A73-12440

CP-noninvariance model of baryon asymmetry of universe, postulating kappa particle /neutral massive fermion/
02 p0221 A73-12669

Cosmological vacuum solutions in Brans and Dicke's scalar-tensor theory.
03 p0373 A73-13356

A hypothesis, unifying the structure and the entropy of the universe.
04 p0500 A73-15492

The universe as a black hole.
04 p0501 A73-15624

Cosmological models based on 18th and early 19th century physics for sky darkness resulting from universe expansion, speculating upon Olbers paradox resolution
05 p0614 A73-16308

Universe evolution model, considering quasar number density, radio source counts and big-bang cosmologies 05 p0614 A73-16309

Quantum cosmology for universe beginning and first microseconds, treating quantum gravitation, time and cycles, superspace and quantum foam 05 p0614 A73-16310

Cosmological aspects of order, relevance, and information theory. 06 p0749 A73-18002

Thermodynamics and morphological orders - A generalized concept of information transfer. 06 p0749 A73-18003

A redshift magnitude relation for radiation universe. 08 p1007 A73-21002

Friedman expanding universe model based on Gamow theory of weakly interacting black body radiation-filled space at 3 K temperature 08 p1010 A73-21230

Energy release mechanism during early universe expansion leading to distortion of relic black body spectrum, noting Comptonization effects 08 p1013 A73-21693

Nonzero neutrino rest mass to account for virial mass discrepancy in Coma cluster and missing cosmological mass needed to close universe 09 p1141 A73-22027

Universe isotropic state evolution from initial chaotic conditions, considering attractive and repulsive cosmological constants 10 p1271 A73-23526

Multiple subuniverses concept for wide mean space density variations in closed universe, considering radio and optical observation possibility. 10 p1275 A73-23822

Evolution of universe filled with cold baryons at cosmological singularity from Friedmann solution and equation of state for cold baryons 10 p1284 A73-24753

Model universe generalization to minisuperspace with Einstein equation solution and nondiagonal metric replacing wave equation, considering commutation relations for quantization in curved space 11 p1397 A73-25309

Gravitational instability of regular model-universes in a modified theory of general relativity. 11 p1423 A73-26106

Galaxies as local perturbations in homogeneous universe, considering galactic manufacture within Einstein theory context 12 p1539 A73-27141

Universe evolution explanation via interstellar deuterium investigation, discussing galactic gas chemical composition history 12 p1543 A73-27692

Vortex motions of cosmic matter as cosmological evolution mechanism, considering galactic and solar system kinetics 13 p1681 A73-28780

Absorber theory of radiation and the future of the universe. 19 p2460 A73-38172

Primordial explosion model for universe origin, noting radio astronomy counts of galaxies invalidation of Hoyle steady state cosmology 20 p2604 A73-39008

On galaxy formation from primeval universal turbulence. II. 20 p2609 A73-39572

UNKNOWN

U DEPENDENT VARIABLES

U PROBLEM SOLVING

UNLOADING

Shock unloading phenomena in fiber-reinforced composites. 17 p2247 A73-34916

Investigation of a thermomechanical surface during unloading according to the theory of thermoplasticity 20 p2617 A73-39264

UNLOADING WAVES

Elastic and elastoviscoplastic unloading waves propagation in semiinfinite bar under axial impact stress, considering bilinear stress-strain curve 11 p1447 A73-26646

UNMANNED SPACECRAFT

NT BEACON SATELLITES
NT ECHO 1 SATELLITE
NT ECHO 2 SATELLITE
NT GEODETIC SATELLITES
NT GEOS 1 SATELLITE
NT GEOS 2 SATELLITE
NT GEOS-C SATELLITE
NT JUPITER PROBES
NT LUNAR PROBES
NT LUNIK LUNAR PROBES
NT LUNIK 9 LUNAR PROBE
NT LUNIK 13 LUNAR PROBE
NT LUNIK 16 LUNAR PROBE
NT LUNIK 17 LUNAR PROBE
NT LUNIK 20 LUNAR PROBE
NT MARINER SPACE PROBES
NT MARINER SPACECRAFT
NT MARINER VENUS-MERCURY 1973

NT MARINER 3 SPACE PROBE
NT MARINER 5 SPACE PROBE
NT MARINER 7 SPACE PROBE
NT MARINER 9 SPACE PROBE
NT MARS PROBES
NT MARS 2 SPACECRAFT
NT NAVIGATION SATELLITES
NT OSO
NT OSO-7
NT PAGEOS SATELLITE
NT PIONEER SPACE PROBES
NT PIONEER 6 SPACE PROBE
NT PIONEER 8 SPACE PROBE
NT PIONEER 9 SPACE PROBE
NT PIONEER 10 SPACE PROBE
NT SOLAR OBSERVATORIES
NT SOLAR PROBES
NT SPACE PROBES
NT SURVEYOR LUNAR PROBES
NT SURVEYOR 3 LUNAR PROBE
NT TRANSIT SATELLITES
NT VENERA SATELLITES
NT VENERA 4 SATELLITE
NT VENERA 6 SATELLITE
NT VENERA 7 SATELLITE
NT VENUS PROBES
NT VIKING 75 ENTRY VEHICLE
NT ZOND SPACE PROBES

Unmanned planetary spacecraft chemical rocket propulsion. 01 p0090 A73-10102

Unmanned rendezvous applications for space rescue. 01 p0105 A73-11156

Missions for the systematic unmanned exploration of Mars. 01 p0105 A73-11160

Unmanned spacecraft adhesives and adhesive bonding applications in solar panels, mirrors, circuit boards, antennas, platforms, lunar capsules and reentry heat shields 03 p0333 A73-13049

Unmanned outer planets and round trip mission nuclear rocket engine design for carrying payload into orbit by single earth orbital shuttle [AIAA PAPER 72-1090] 03 p0340 A73-13411

Application of heat pipes to unmanned space power systems. 11 p1452 A73-25994

Unmanned reactor-thermoelectric systems for applications in the 1970's. 11 p1395 A73-26024

Thermionic reactor systems for electric propulsion. 11 p1395 A73-26025

Terrestrial quarantine considerations for unmanned sample return missions. 18 p2349 A73-35977

An analysis of recent advances in autonomous navigation for near earth applications. [AIAA PAPER 73-875] 20 p2587 A73-38812

NASA program manned and unmanned spacecraft system effectiveness survey questionnaire response data concerning various tests 21 p2781 A73-41203

UNSTABLE BURNING

U COMBUSTION STABILITY

UNSTEADY FLOW

NT OSCILLATING FLOW

Unstable operation and rotating stall in axial flow compressors. [ONERA, TP NO. 1090] 01 p0001 A73-10228

Unsteady viscous flow due to the impulsive motion of a flat plate, with special reference to the initial period. 01 p0031 A73-10422

A nonlinear analysis of pulsatile flow in arteries. 01 p0011 A73-10449

Numerical solution of one-dimensional non-steady flow with supersonic and subsonic flows and heat transfer. 01 p0003 A73-10765

Stability criteria for unsteady motion of incompressible Cousserant fluid in arbitrary time dependent domain, using Liapunov function 01 p0033 A73-10776

A note on the flow regimes in the unsteady, rectilinear flow of a perfect gas. 01 p0034 A73-11005

A solution of the three-dimensional unsteady compressible boundary layer equations. 01 p0004 A73-11356

Two-dimensional, unsteady, self-similar flows in gas dynamics. 02 p0152 A73-11569

Gasdynamics calculations for a pulsating flow in pipelines 02 p0152 A73-11610

Boundary layer growth of a micropolar fluid. 02 p0154 A73-12093

Total-pressure averaging in pulsating flows. 02 p0171 A73-12618

Sturm-Liouville solution of unsteady stratified two dimensional Couette flow equations of motion 03 p0292 A73-13304

Incompressible viscous fluid creep flow past deforming sphere for small Reynolds numbers, considering cases of different Strouhal numbers 03 p0244 A73-13529

Initially uniform gas expansion into ambient atmosphere and subsequent flow into perfect vacuum, noting infinite-strength shock separation from gas-vacuum interface 03 p0294 A73-13532

Decoding of the thermoanemometer data for a flow with velocity, pressure, and temperature pulsations 03 p0308 A73-13667

Slowly oscillating lifting surfaces at subsonic and supersonic speeds. 03 p0245 A73-13704

Two-dimensional unsteady flow by hydraulic analogy. 03 p0295 A73-13769

On similarity solution of an unsteady laminar boundary layer along a flat plate. 03 p0297 A73-14314

Unsteady one-dimensional compressible frictional flow with heat transfer. 03 p0298 A73-14639

Transient free-convection horizontal laminar flow between two parallel plates. 04 p0517 A73-15681

Analysis of unsteady laminar boundary layer flow by an integral method. 04 p0434 A73-15839

The measurement of a pulsating air flow using a sharp-edged orifice meter. 04 p0451 A73-15853

Experimental analysis of lift on a fixed cylinder subjected to a flow perpendicular to its axis at high Reynolds numbers 04 p0405 A73-15990

Numerical solution of a boundary value problem for the Navier-Stokes equations 05 p0564 A73-16449

The effects of leading-edge serrations on reducing flow unsteadiness about airfoils. [AIAA PAPER 73-89] 05 p0529 A73-16853

Finite element analysis of unsteady incompressible flow around an oscillating obstacle of arbitrary shape. [AIAA PAPER 73-91] 05 p0529 A73-16855

Unsteady transonic flow analysis for low aspect ratio, pointed wings. [AIAA PAPER 73-122] 05 p0530 A73-16878

Unsteady compressible boundary layers with arbitrary pressure gradients. [AIAA PAPER 73-132] 05 p0565 A73-16885

Unsteady flow generated by shock-turbulent boundary layer interactions. [AIAA PAPER 73-168] 05 p0566 A73-16913

Unsteady compressible potential flow around lifting bodies - General theory. [AIAA PAPER 73-196] 05 p0531 A73-16931

Flow of a gas in a flat channel at a diminishing flow rate 05 p0533 A73-17090

An improved kernel function formulation for unsteady subsonic flow. 05 p0567 A73-17122

A momentum integral solution for pulsatile flow in a rigid tube with and without longitudinal vibration. 05 p0567 A73-17273

On unsteady forced flow against a rotating disk. 06 p0643 A73-17394

Temperature of a duct flow under conditions of unsteady-state heat transfer 06 p0769 A73-18131

Model tests on unsteady rotor wake effects. 07 p0773 A73-19191

A computational method for low Mach number unsteady compressible free convective flows. 07 p0918 A73-19268

Characteristics of the unsteady shock-induced laminar boundary layer on a flat plate. 07 p0810 A73-19505

Velocity and resistance profiles for unsteady turbulent flow in rough pressure channels, using Prandtl hypothesis 07 p0811 A73-19614

Turbulent energy variations in unsteadily moving flow with structural shift, emphasizing formation of vortices with various inertia scales 07 p0811 A73-19620

Copper resistance thermoanemometer for channel unsteady air flow rate measurement, discussing design, operation principles and maximum error 07 p0823 A73-19623

Unsteady motion of a viscous electrically conducting fluid around a flat plate in the case of orthogonal fields 07 p0858 A73-19999

Determination of the hydraulic resistance of throates by short unsteady blowing 07 p0779 A73-20083

An extension of the vector potential concept to the case of a three-dimensional unsteady boundary layer. 07 p0776 A73-20287

On unsteady magnetohydrodynamic boundary layers in a rotating flow. 07 p0859 A73-20290

Decaying unsteady viscous vortex flow under conditions of streamlines and vortex lines coincidence, deriving Navier-Stokes equations solution

07 p0812 A73-20340

Unsteady laminar flow in a pipe with arbitrarily changing flow rate.

08 p0954 A73-20867

Unsteady heat transfer in dispersion media at small values of time

08 p1021 A73-20994

Unsteady boundary layer flows at general three-dimensional stagnation points.

08 p0954 A73-21008

Boundary layer theory approximation for hydrodynamic parameters of unsteady laminar boundary layer on body moving in incompressible fluid

08 p0956 A73-21546

Characteristics of unsteady interaction between a supersonic jet and an infinite obstacle

08 p0927 A73-21609

Heat transfer through the unsteady laminar boundary layer on a semi-infinite flat plate. I - Theoretical considerations. II - Experimental results from an oscillating plate.

08 p1024 A73-21635

A theoretical study of natural convection heat transfer from downward-facing horizontal surfaces with uniform heat flux.

08 p1024 A73-21638

Periodic nozzle flow with heat addition.

[AD-758555] 08 p1025 A73-21669

Parabolic flow over a flat plate with wave disturbance in the main stream.

09 p1071 A73-21950

Unsteady nonlinear flow around an airfoil or a blade cascade with emission of turbulent vortices

09 p1027 A73-22212

Experimental method for analyzing the unsteady flow in a transonic aircraft compressor

09 p1028 A73-22715

Slip parameter for electrogasdynamic generators with unsteady flow.

09 p1037 A73-22825

Filling tests in single and double arm plenum configuration models used in gasdynamic laser systems, noting wave controlled unsteady flow processes

09 p1030 A73-23447

Influence of the Reynolds number on nonstationary convective heat transfer in a pipe during a change in the thermal load

10 p1204 A73-23511

Some peculiarities of flames stabilized in pulsating streams.

10 p1294 A73-23551

Periodic semi-integral solutions of secondary unsteady convective flows in external force field for critical Rayleigh numbers by Liapunov-Schmidt method

10 p1204 A73-23584

Effect of jet turbulence on the flow in a wall boundary layer

10 p1205 A73-23586

Unsteady MHD duct flow by the finite element method.

10 p1256 A73-24289

Unsteady flow of a conducting viscous fluid between parallel porous walls with heat transfer

10 p1256 A73-24587

Unsteady viscoplastic electrically conducting MHD flow in moving-wall channel, assuming time-variable pressure gradient and uniform transverse magnetic field

10 p1256 A73-24588

Electrically conducting unsteady viscoplastic plane channel Hartmann and Couette MHD flows in presence of uniform transverse magnetic field and time variable electric field

10 p1256 A73-24589

Unsteady motion of a viscoplastic medium in a plane MHD channel at a constant flow rate

10 p1256 A73-24590

Recent research on unsteady boundary layers; Symposium, Université du Québec, Québec, Canada, May 24-28, 1971, Proceedings. Volumes 1 & 2

10 p1207 A73-24801

Unsteady boundary layer flow, considering Stokes, Rayleigh and Heisenberg-Tollmien theories application to oscillatory, fluctuating, impulsive and rotational effects

10 p1207 A73-24802

The universalization of unsteady boundary layer equations

10 p1207 A73-24805

Energy method for unsteady flow stability analysis, exemplifying by oscillatory Stokes layer and impulsively heated fluid layer

10 p1208 A73-24806

Similarity solutions of unsteady, compressible plane and axisymmetric laminar boundary layer equations.

10 p1208 A73-24807

Prandtl boundary layer equations for unsteady three dimensional axisymmetrical and two dimensional symmetrical incompressible flows about solid bodies, considering approximate solution convergence

10 p1208 A73-24808

Unsteady three dimensional laminar incompressible boundary layer with free and forced convection, determining flow and temperature fields adjacent to heated body

10 p1208 A73-24810

Transient viscous laminar incompressible flow pattern after sudden vanishing of semiinfinite flat plate based on two dimensional unsteady boundary layer equations with boundary conditions

10 p1208 A73-24811

Two dimensional laminar boundary layer separation for unsteady flow or flow past moving walls, considering singularity due to bifurcating wake bubble

10 p1208 A73-24813

Kaplan perturbation method for incipient flow separation, considering three dimensional, compressible and unsteady boundary layers

10 p1208 A73-24815

Unsteady detachment in the three-dimensional laminar regime

10 p1208 A73-24819

Universal equations of the three-dimensional laminar boundary layer in the unsteady state and their treatment

10 p1209 A73-24820

Unsteady wakes of bluff and streamlined bodies with screens behind them.

10 p1173 A73-24823

Unsteady boundary layer and wake near the trailing edge of a flat plate.

10 p1173 A73-24826

On the Kutta-condition at the trailing edge of a nozzle in a weakly nonstationary jet flow.

10 p1209 A73-24827

Unsteady boundary layer over a flat plate started from rest.

10 p1209 A73-24829

On structure of the laminar boundary layer in the presence of a fluctuating free stream.

10 p1209 A73-24830

Development of unsteady boundary layers under variable suction.

10 p1209 A73-24831

On some aspects of unsteady boundary layers induced by shock waves.

10 p1209 A73-24832

Recent studies in the field of unsteady boundary layers

10 p1173 A73-24833

Unsteady turbulent boundary layer flow past infinite flat plates with free stream acceleration or deceleration, computing characteristics by finite difference method

10 p1209 A73-24834

Some solutions of the unsteady two-dimensional turbulent boundary layer equations.

10 p1209 A73-24835

Visualization experiments on unsteady viscous flows around cylinders and plates.

10 p1174 A73-24836

Unsteady flow between a fixed porous disk and a rotating disk

10 p1209 A73-24837

Unsteady two dimensional flow within circular cavity with arbitrary velocity distribution on cylinder wall, investigating recirculating flow initiation

10 p1210 A73-24838

On unsteady magnetohydrodynamic boundary layers in a rotating flow.

10 p1257 A73-24841

Hydrodynamic visualization technique application to unsteady flow patterns around models and analysis of boundary layers, separation and wakes

10 p1174 A73-24842

A numerical study of unsteady laminar combined convective flow over vertical plates.

10 p1296 A73-24848

Study of the phase of the wall transfer of heat or mass in incompressible pulsed flow

10 p1297 A73-24850

Unsteady uniform-length turbulent flow of incompressible fluid in circular pipe studied via Reynolds and turbulence energy balance equations

10 p1210 A73-24851

Unsteady viscous jet flow into stationary surroundings.

11 p1345 A73-25117

Unsteady boundary layer flow of homogeneous viscous fluid in nonrotating environment or bounded by oscillating flat plates, determining velocity field by exact solutions

11 p1346 A73-25165

Unsteady laminar convection in uniformly heated vertical pipes.

11 p1449 A73-25221

A note on the unsteady motion of a viscous conducting liquid between two porous concentric circular cylinders acted on by a radial magnetic field.

11 p1404 A73-25368

An exploratory investigation of the unsteady aerodynamic response of a two-dimensional airfoil at high reduced frequency.

[AIAA PAPER 73-309]

11 p1301 A73-25540

Unsteady subsonic compressible flow around finite thickness wings.

[AIAA PAPER 73-313] 11 p1301 A73-25544

Calculation of unsteady transonic aerodynamics for oscillating wings with thickness.

[AIAA PAPER 73-316] 11 p1301 A73-25547

Development and applications of supersonic unsteady consistent aerodynamics for interfering parallel wings.

[AIAA PAPER 73-317] 11 p1301 A73-25548

An investigation of unsteady aerodynamics on an oscillating airfoil.

[AIAA PAPER 73-318] 11 p1301 A73-25549

Flow near the stagnation point of a body which undergoes a sudden change in a steady stream.

[ASME PAPER 72-APM-UU] 11 p1347 A73-25701

Investigation of heatproof materials under unsteady operating conditions

11 p1450 A73-25730

Spectra of turbulent pulsations in velocity, temperature, and their correlations for air flow in a circular pipe

11 p1301 A73-25744

Quasi-linear partial differential equations of nonlinear pulse shock wave propagation in two- and three-dimensional steady transonic gas flow near critical point

11 p1302 A73-25854

Nonlinear problem of a shock-tube interaction-region boundary layer.

11 p1348 A73-26391

Variational equations of unsteady near-similar perfect gas flow at strong shock front in terms of mass, energy and momentum in perturbed region

12 p1487 A73-27408

Possibility of gasdynamic effects at the critical point of the phase equilibrium

12 p1487 A73-27418

Classical solutions to the second boundary value problem for the unsteady free convection equations

12 p1559 A73-27421

Equations for finitely-dimensional probability distributions of pulsating variables in a turbulent flow

13 p1599 A73-28287

Pulsation energy calculations in axisymmetric turbulent jet flows of incompressible fluids with a zero excess impulse

13 p1600 A73-28448

Wing-fuselage junctions fairings compromise design, describing rotational eddies formation mechanism for unsteady ducted flow and wing root phenomena

[ONERA, TP NO. 1217] 11 p1564 A73-28836

Calculation of the unsteady subsonic aerodynamic pressures on compressor blades

[ONERA, TP NO. 1221] 13 p1565 A73-28839

Periodic gust and wake induced unsteady air flow, calculating velocity variation with distance from rotor blade for cascade effect

13 p1566 A73-29026

Calculation of the basic characteristics of turbulent flows in a state of structural equilibrium

13 p1604 A73-29168

Visualization of unsteady flow over oscillating airfoils.

13 p1620 A73-29270

Greenstadt binary index criterion for laminar and pulsating bow shock crossings separation in terms of angle, solar wind velocity and Galilean invariance

14 p1748 A73-29979

Radiation from line vortex filaments exhausting from a two-dimensional semi-infinite duct.

14 p1744 A73-30168

Chandrasekhar equations for axisymmetric MHD flows generalized for steady and unsteady flows

14 p1781 A73-30701

Investigation of the stability of a hollow vortex bounded by a rigid wall

15 p1861 A73-31156

Experimental investigation of the velocity structure and of hydraulic resistances in unsteady forced turbulent flows

15 p1862 A73-31287

MHD acceleration in the unsteady expansion of a shock tube driver.

15 p1917 A73-31376

Magnetic field induced energy dissipation in conducting fluid isotropic turbulent flow velocity pulsations, noting Joule dissipation effect on damping

15 p1917 A73-31403

Uses of the equation of pulsation energy balance in the theory of MHD flows in channels and tubes

15 p1917 A73-31404

Two dimensional unsteady vortex flow of ideal fluid past inflating decelerating wedge, obtaining pressure distribution on wedge surface

[AIAA PAPER 73-449] 15 p1823 A73-31435

A numerical method for integrating the unsteady boundary-layer equations when there are regions of backflow.

16 p1998 A73-32799

Longitudinal evolution of the velocity and pressure in a circular duct in pulsating flow

16 p1998 A73-32805

Lift and measurements in an aerofoil in unsteady flow.
[ASME PAPER 73-GT-41] 16 p1964 A73-33503

The unsteady response of a blade row from measurements of the time-mean total pressure.
[ASME PAPER 73-GT-94] 16 p1964 A73-33531

Plane unsteady irrotational flow of ideal incompressible fluid through turbomachine stage due to interaction between stationary and moving grids
16 p2001 A73-34015

Sinusoidal pulse flow through an axial flow gas turbine.
17 p2093 A73-34395

Book - Physical fluid dynamics.
17 p2151 A73-34472

Pulsatile Newtonian frictional losses in a rigid tube.
17 p2151 A73-34532

Total pressure tube measurements in turbomachine-simulating pulsating nozzle flow generator supplemented by pneumatic tube probes for averaging error comparison
17 p2166 A73-34608

A dynamic modeling method of unsteady flows in long fluid lines with turbulent bulk velocities.
[ASME PAPER 73-FE-18] 17 p2153 A73-35014

Numerical solution procedure for calculating the unsteady, one-dimensional flow of compressible fluid with allowance for the effects of heat transfer and friction.
[ASME PAPER 73-FE-30] 17 p2153 A73-35022

Unsteady Couette flow in hydromagnetics.
17 p2154 A73-35121

A method for calculating unsteady turbulent boundary layers in two- and three-dimensional flows.
17 p2154 A73-35135

Computational considerations in application of the finite element method for analysis of unsteady flow around airfoils.
17 p2096 A73-35138

Effect of Reynolds number on nonstationary convective heat exchange in a tube with variable heat load.
17 p2255 A73-35191

Mixing and structural characteristics of turbulent pulsating jets based on hot-wire anemometer velocity measurement data
17 p2157 A73-35513

Time evolution of pulsating air jets from schlieren photography and velocity measurements, using motor driven piston
17 p2157 A73-35514

The dynamic-bias in radiation interrogation of two-phase flow.
17 p2256 A73-35846

On the solution of the unsteady Navier-Stokes equations including multicomponent finite rate chemistry.
18 p2259 A73-36157

Unsteady turbulent boundary layers in two-dimensional, incompressible flow.
[AIAA PAPER 73-650] 18 p2260 A73-36205

Analytical investigation of compressibility and three-dimensionality on the unsteady response of an airfoil in a fluctuating flow field.
[AIAA PAPER 73-683] 18 p2262 A73-36234

The response of unsteady boundary-layer separation to impulsive changes of outer flow.
[AIAA PAPER 73-684] 18 p2298 A73-36235

Solution by characteristics at fixed time interval of the equations of one dimensional unsteady flow.
18 p2300 A73-36608

Pulsation-energy balance equation in turbulent boundary layer theory
18 p2301 A73-37002

Experiments of shock waves in a fully ionized plasma flow.
19 p2464 A73-37159

Calculation of two-dimensional unsteady plasma flows in channels
19 p2467 A73-37369

Analysis of pressure waves as a mean of diagnosing vascular obstructions.
19 p2398 A73-37524

Unsteady thermal boundary-layer on an infinite yawed wedge whose temperature gradient is prescribed.
19 p2377 A73-37575

Unique solution of boundary value problem of Boltzmann equation for unsteady rarefied gas flow of formless particles past arbitrary surface
19 p2462 A73-37843

Numerical investigation of unsteady boundary-layer separation.
19 p2420 A73-37852

Vibration of tubes containing flowing fluid.
[MERL-TN-72-2] 20 p2616 A73-39147

Unsteady combustion of a confined spray.
[AICHE PREPRINT 23] 20 p2626 A73-39250

Energy spectra of velocity pulsations in a turbulent boundary layer on a permeable plate
20 p2547 A73-39286

Nonlinear model for plane unsteady flow resulting from collapse of homogeneous density region in heavy ideal density-stratified fluid
20 p2547 A73-39287

Non-steady, stratified Couette flow between concentric rotating spheres.
20 p2548 A73-39521

A new method of solving one-dimensional unsteady flow equations and its application to shock wave stability in sonic inlets.
20 p2548 A73-39522

Hankel transforms and boundary layer solutions for pulsating laminar flow in curved circular tube under sinusoidal pressure gradients
20 p2549 A73-39809

Unsteady incompressible fluid flow past a doubly periodic grid
21 p2631 A73-40185

Closed-form lift and moment for Osborne's unsteady thin-airfoil theory.
21 p2632 A73-40442

Convective heat transfer with allowance for three-dimensional heat sources in the fluid for turbulent flow in a plane slit
21 p2792 A73-41196

Russian book on nonlinear waves in dispersive media covering unsteady waves, gravity waves in deep water, electromagnetic waves in nonlinear dielectric, etc
21 p2741 A73-41285

Interpretation of hot-wire anemometer readings in a flow with velocity, pressure and temperature fluctuations.
21 p2705 A73-41317

Fluctuating flow and heat transfer from a vertical surface.
21 p2792 A73-41524

Hybrid finite methods for linear and nonlinear unsteady heat conduction problems
21 p2793 A73-41617

On unsteady flow of an elastico-viscous fluid past an infinite plate with variable suction.
22 p2840 A73-41747

Equations for the finite-dimensional probability distributions of pulsating variables in a turbulent flow.
22 p2840 A73-41810

Experimental investigation of the development of a cavern in the case of unsteady gas-induced cavitation
22 p2841 A73-42128

Asymptotic unsteady three dimensional flow analysis in axial turbine cascade theory, assuming infinite blade number and unity pitch/chord ratio
[ONERA, TP NO. 1249] 22 p2796 A73-42220

The unsteady aerodynamics of a finite supersonic cascade with subsonic axial flow.
[ASME PAPER 73-APMW-6] 22 p2797 A73-42879

Use of a fluidic distributor for the calibration of unsteady flow probes.
23 p2945 A73-43430

Technically oriented algorithms for unsteady pipe flow.
23 p2968 A73-43800

Unsteady transonic flows with shock waves in two-dimensional channels.
23 p2969 A73-43938

Nonlinear transient effects of separated unstable flow on vortex generated acoustic waves in cavities
[AIAA PAPER 73-1014] 24 p3078 A73-44846

Broadband noise generation by aerofoils and axial flow fans.
[AIAA PAPER 73-1018] 24 p3054 A73-44850

Unsteady plasma flows behind a moving leading boundary
24 p3119 A73-45539

UNSTEADY STATE

Flutter analysis method for unsteady aerodynamic forces on wings and rotating blades under harmonic vibrations and uniform flow
[ONERA, TP NO. 1099] 01 p0001 A73-10230

Unsteady-state conjugated heat transfer between a semi-infinite surface and incoming flow of a compressible fluid. I - Reduction to the integral relation. II - Determination of a temperature field and analysis of results.
04 p0520 A73-15944

Non-steady-state thermal analysis of a rolling aircraft tire.
[SAE PAPER 720871] 05 p0535 A73-16667

Experimental and theoretical investigations regarding the unsteady aerodynamical derivatives of the longitudinal motion in the case of slender flight bodies at moderate velocity
[DFVLR-SONDDR-206] 05 p0528 A73-16757

Linearized theory for infinite span wing small unsteady motions in curved flight in inviscid incompressible fluid, obtaining time dependent forces, pressure and velocity fields
[AIAA PAPER 73-90] 05 p0529 A73-16854

Couplings effect on Liapunov stability estimation of higher order linear nonstationary systems, using aggregation method
05 p0599 A73-17084

Investigation of nonstationary processes in the ionosphere and space with quantum frequency standards.
10 p2121 A73-24214

Unsteady processes in multimode lasers with a nonuniformly widening line of lasing
15 p1886 A73-32329

A method of obtaining approximate solutions to unsteady-state heat conduction problems
20 p2627 A73-39258

On-off control of an unstable plant with time lag
20 p2542 A73-39345

Unsteady convective heat transfer attending the cooling of gas in tubes.
21 p2791 A73-41053

Unsteady state coupled thermoelasticity problem solution based on reducing order of Laplace transform equation, using coupling coefficient as small parameter in series expansion
22 p2921 A73-42279

UNSWEPT WINGS

NT RECTANGULAR WINGS

NT RING WINGS

Analysis of high aspect ratio jet flap wings of arbitrary geometry.
[AIAA PAPER 73-125] 05 p0530 A73-16880

Three dimensional jet flap potential flow theory based on vortex lattice method, comparing iterative solution with slatted unswept blown flapped wing experimental results
[AIAA PAPER 73-653] 18 p2263 A73-36260

UPCONVERTERS

U PARAMETRIC FREQUENCY CONVERTERS

UPDRAFTS

U VERTICAL AIR CURRENTS

UPPER AIR

U UPPER ATMOSPHERE

UPPER ATMOSPHERE

NT D REGION

NT E REGION

NT EXOSPHERE

NT F REGION

NT F 1 REGION

NT F 2 REGION

NT IONOSPHERE

NT LOWER IONOSPHERE

NT MAGNETOPAUSE

NT MAGNETOSPHERE

NT MESOPAUSE

NT MESOSPHERE

NT SPORADIC E LAYER

NT THERMOSPHERE

NT UPPER IONOSPHERE

Optical manifestations of meteoric aerosols. I - The 1970 Orinoids
01 p0096 A73-10332

Rocket measurements of electron fluxes in the upper atmosphere at midlatitudes.
01 p0041 A73-10887

Observation of upper atmospheric constituents by laser radar systems.
01 p0018 A73-11202

Rocket flight in rarefied layers of the atmosphere
02 p0227 A73-11579

Scientific payload of Aeros German aeronomy satellite for atmospheric upper layers investigation, discussing instruments operation and location and measurement technique
[DGLR PAPER 72-069] 02 p0190 A73-11656

Simultaneous upper atmospheric measurements of electric field at points differing in altitude via balloon-borne instruments
02 p0156 A73-11736

Upper-atmosphere motion, as determined by observations of radio echoes from meteor trails.
02 p0159 A73-12145

Meteor dust motion in the upper atmosphere and in the vicinity of the earth's orbit.
02 p0214 A73-12255

Upper atmospheric dust concentrations in polar regions.
02 p0215 A73-12260

Turbopause effect on latitudinal diurnal variation of upper atmosphere neutral species, using turbulent diffusion coefficients and photochemical transport theory
02 p0161 A73-12278

Corpuscular radiation as an upper atmospheric energy source.
02 p0205 A73-12289

Auroral and magnetospheric phenomena caused by solar wind particles entry and energization via magnetosheath into magnetosphere and upper atmosphere
04 p0492 A73-15331

Buoyancy forces contribution to heat flux during turbulent mixing in upper atmosphere, noting kinetic turbulence balance components
04 p0473 A73-15573

Prediction of the density of the upper atmosphere for the duration of artificial earth satellites.
05 p0567 A73-16091

Electron density increase in the F region after proton bursts
05 p0609 A73-16257

Vertical-ray structure /horizontal inhomogeneity/ of emission from the earth's upper atmosphere on the basis of observations from the Soutz 3 spacecraft
05 p0570 A73-16845

Approximate analytical solutions of the diffusion equation for Jacchia's statistical models of the upper atmosphere
05 p0570 A73-17014

UPPER ATMOSPHERE

Light flash induced by a pulsed X-ray source in the upper atmosphere 05 p0610 A73-17016

Upper atmospheric dust particle temperature and related Na atom abundance seasonal variation based on energy budget and Na sublimation rate considerations 05 p0571 A73-17061

Basic formulas for the determination of the altitude of artificial clouds 05 p0572 A73-17160

Planet wide circulation in Venus upper atmosphere from UV photographs, noting apparent 4.06 day rotation period 06 p0743 A73-17431

Retrograde rotation of the upper atmosphere of Venus. 06 p0744 A73-17433

Jovian atmosphere upper layers high temperature evidenced during star Beta Scorpion occultation by Jupiter 06 p0745 A73-17475

Preliminary results of measurements of UV emissions scattered in the Martian upper atmosphere. 06 p0746 A73-17486

Earth magnetosphere essential processes, discussing outermost atmosphere, solar wind theory and sector structure, models, plasmopause, polar cusps, tail theory and ionospheric currents 06 p0688 A73-17502

Dependence of the length of polar rays on the auroral activity level 06 p0690 A73-17558

Sounding balloon system SITES for upper atmosphere physical parameters measurement, noting PCM telemetry, remote control and vehicle localization 07 p0790 A73-18971

Upper atmosphere structure from rocket and satellite observations, considering COSPAR International Reference Atmosphere /CIRA 1972/ 07 p0813 A73-19221

Upper atmosphere thermodynamic and circulation characteristics for high altitude aircraft flights, including geomagnetic disturbance factors 07 p0847 A73-19298

Compact laser radar probes the upper atmosphere. 07 p0834 A73-19573

Optical sounding methods for the upper atmosphere and the earth's dust cloud 07 p0817 A73-19584

Analysis of light polarization variations in a twilight sky in terms of upper atmosphere effects 07 p0817 A73-19588

Twilight sounding method for earth upper atmosphere investigation, taking into account earth shadow and effective altitude of solar radiation attenuation/shielding/zone 07 p0818 A73-19591

Molecular beam study on BaO and SrO formation for clarifying interaction of metal-vapors with upper atmosphere oxygen. 07 p0818 A73-19668

Energy spectra of cosmic pions and nucleons at the top of the atmosphere. 07 p0872 A73-20015

Heating of the upper atmosphere during aurorae and auroral rays length. 08 p0957 A73-20663

Observations of the variation of temperature with latitude in the upper solar photosphere. II - Magnetic-field comparison, implications for solar-oblateness measurements, and harmonic analysis. 08 p1009 A73-21166

Generation of vibrationally excited O₂ and nonthermal infrared emission in the upper atmosphere 08 p0959 A73-21289

Measurement of the temperature of an optically thick luminous gas layer in the upper atmosphere by the homodyne detection method 08 p0960 A73-21304

High energy electrons and gamma quantum flux in upper atmospheric layers from high altitude balloon measurements 08 p0999 A73-21337

A method for the analysis of artificial clouds in the upper atmosphere. 08 p0961 A73-21391

The Federal Republic's AEROS Satellite Programme. 08 p1026 A73-21659

Observation of mesospheric ozone at low latitudes. 09 p1079 A73-22841

An operational upper air analysis using the variational method. 10 p1244 A73-23645

Upper atmosphere analytical density model for satellite motion prediction, allowing for diurnal and semiannual density variations and solar activity and geomagnetic disturbances effects 10 p1211 A73-23883

Capture of primary cosmic rays in the upper atmosphere as a source of excess radiation 10 p1268 A73-23931

Determination of upper atmosphere parameters from measurements of the ambipolar diffusion coefficient by radar observations of meteor trails. 10 p1212 A73-24223

Investigation of the motion of artificially ionized clouds in the upper atmosphere. 10 p1212 A73-24225

Vibrationally-excited nitrogen in the upper atmosphere. 10 p1212 A73-24226

Optical anomalies due to scattered disperse cosmic matter in upper atmosphere from Tungusk meteorite fall 10 p1213 A73-24681

Broad band solar EUV absorption in the earth's upper atmosphere. 10 p1214 A73-24747

On empirical models of the upper atmosphere in the polar regions. 11 p1356 A73-25915

Physics and chemistry of upper atmospheres. 11 p1425 A73-26209

Temperature variations in the upper atmosphere during a period of minimum solar activity from topside ionospheric sounding data 12 p1491 A73-27346

Upper atmospheric temperatures from Doppler line widths. V - Auroral electron energy spectra and fluxes deduced from the 5577 and 6300 A atomic oxygen emissions. 12 p1492 A73-27605

Turbulence, billows and gravity waves in a high shear region of the upper atmosphere. 12 p1492 A73-27608

Analogies between substorm phenomena of the visual polar aurora and the radio aurora 12 p1493 A73-27757

Detection of a temporary ozone content decrease in the upper atmosphere at the moment of sunrise 13 p1605 A73-28074

Metal ion density measurement in sporadic E layer during beta Taurids shower by rocket-borne mass spectrometry, noting origin in cosmic debris ablation 13 p1673 A73-28277

Results of optical observations of dust in upper atmosphere and interplanetary space. 13 p1680 A73-28520

Solar Lyman alpha radiation scattering analysis to determine neutral hydrogen atom distribution in upper atmosphere 14 p1747 A73-29865

Investigation of scattered ultraviolet radiation in the upper Martian atmosphere from the Mars-3 automatic interplanetary station 14 p1796 A73-29866

Jupiter, Saturn, Uranus and Neptune upper atmospheric ionization equilibrium distribution, emphasizing ionosphere 14 p1799 A73-30353

Structure and time variations of the Jovian ionosphere. 15 p1929 A73-31066

Spatial distribution of H alpha emission in the earth's upper atmosphere, the variations of the emission during a solar cycle, and the dependence of the emission on geomagnetic perturbations 15 p1867 A73-31262

Investigation of the hydrogen in the upper atmosphere and geocorona from observations of the H-alpha emission line in the nightglow spectrum /Survey/ 15 p1867 A73-31267

Observations of aerosol layers in the upper atmosphere by laser radar. 15 p1868 A73-31383

Dependence of the length of auroral rays on auroral activity level. 16 p2002 A73-32782

Study of high energy electrons at upper layers of atmosphere during magnetic perturbations. 16 p2054 A73-33282

Thermospheric wind effects on the distribution of helium and argon in the earth's upper atmosphere. 16 p2004 A73-33441

Magnetic field of a horizontal current above a conducting earth. 16 p2004 A73-33448

Upper atmosphere pollution and near surface climate due to aerospace operations, discussing dynamics and trace gas distribution [ALAA PAPER 73-492] 16 p2005 A73-33536

Gravity wave magnitudes and horizontal and vertical scales measured and applied to eddy diffusion coefficients in upper stratosphere [ALAA PAPER 73-495] 16 p2005 A73-33538

Electrophotometric equipment in the Stara Zagora Observatory 16 p2016 A73-33663

OH emission band, studying effect of adiabatic infrasonic oscillations on upper atmospheric temperature and intensity 16 p2008 A73-33883

A comparison of two methods of analysis for the twilight sodium airglow data. 16 p2009 A73-33891

Enhancement of upper atmospheric sodium from sporadic dust influxes. 16 p2010 A73-33917

Diffusive motion of initially ellipsoidal plasma irregularities or ion clouds in upper atmosphere, considering space charge electric field effects 17 p2160 A73-34787

The Budrio station of the meteoric radar system of the CNR for the systematic study of the upper atmosphere 17 p2147 A73-34959

The theory of charged particle temperatures in the upper atmosphere. 17 p2224 A73-35555

Combined temperature, diffusion coefficient and density measurements of photoluminescent AlCl₃ releases. 18 p2303 A73-35949

The atmospheric mixing in the atmospheres of Mars and Venus. 18 p2349 A73-36034

Photo-absorption of the upper atmosphere in the middle ultraviolet region. 18 p2308 A73-36053

Air density at heights near 200 km from the orbit of 1970-65D. 18 p2309 A73-36052

Rocket sounding of upper atmosphere vertical wind profiles, shear, temperature distribution and diffusion coefficient for model atmosphere calculation 18 p2309 A73-36057

An analysis of the solar-activity effects in the upper atmosphere. 18 p2309 A73-36060

Interpretation of short period density changes shown by the drag of satellites. 18 p2310 A73-36133

Differences in circulation of the upper atmosphere in low latitudes of the southern and northern hemispheres. 18 p2310 A73-36138

Ion composition measurements at altitudes 100-180 km in 1972. 18 p2310 A73-36143

A model of formation of the mean diurnal state of the upper atmosphere and its diurnal variations. 18 p2311 A73-36147

Temperature determination of the upper atmosphere by the low-level detection of artificial luminous cloud radiation. 18 p2311 A73-36149

Thermospheric density variations associated with auroral electrojet activity. 18 p2312 A73-36280

Upper atmospheric turbulence kinetic energy spectrum from radio meteor trails observations, noting relationship to structure function for isotropic turbulence 18 p2312 A73-36288

Energetic neutrons leaking from the top of the atmosphere. 19 p2474 A73-37299

On the Zeeman photometer observing upper atmospheric winds in the daytime. 19 p2429 A73-37377

Sulfuric acid in the Venus clouds. 19 p2483 A73-37579

Diurnal and annual temperature variations in the 30-60 km region as indicated by statistical analysis of rocketsonde temperature data. 19 p2424 A73-37662

Production of vibrationally excited O₂ and nonthermal infrared emission in the upper atmosphere. 19 p2424 A73-37918

Measurement of the temperature of an optically dense layer of luminous gas in the upper atmosphere by the homodyne detection method. 19 p2425 A73-37933

Wave-mean flow interactions in the upper atmosphere. 19 p2427 A73-38217

Upper atmosphere analytical density model for satellite motion prediction, allowing for diurnal and semiannual density variations and solar activity and geomagnetic disturbances effects 20 p2550 A73-38902

Electron flux variation measurements in the upper atmosphere at altitudes of 200 to 500 km 20 p2554 A73-39168

Theoretical model of vertical distributions of CO and CH₄ in the mesosphere and upper stratosphere. 21 p2680 A73-40085

Venus upper atmosphere four-day retrograde rotation derived from statistical analysis of telephotographic observation of Y-shaped feature 21 p2767 A73-40566

Upper atmospheric models dealing with diurnal variation and latitudinal density dependence to derive time and space dependencies 21 p2683 A73-40631

Heating of the low-latitude upper atmosphere caused by the decaying magnetic storm ring current. 21 p2684 A73-40786

Complex studies of corpuscular radiation in the upper atmosphere at midlatitudes during geomagnetic perturbations

21 p2760 A73-40918

The aurora oval in the region of influx of electrons into the earth's atmosphere

21 p2686 A73-40919

The establishment of the winter polar vortex in middle latitudes in 1971.

21 p2687 A73-41338

Internal gravity waves and turbulence in simultaneous upper atmosphere temperature and wind measurements.

21 p2732 A73-41342

Global thermospheric wind distribution computed by solving Navier-Stokes equations with models at upper atmospheric densities and ion distribution

21 p2689 A73-41354

Mie scattering computation of cosmic dust flux in upper atmosphere from twilight luminance increase during meteor showers

21 p2775 A73-41418

Wave-induced eddy diffusion coefficients in the upper atmosphere of Mars.

22 p2906 A73-41903

Spectroscopic measurement of upper atmospheric temperature.

22 p2846 A73-42062

Diurnal thermospheric and ionospheric variations from time dependent continuity equations for O⁺, H⁺, O₂⁺, and NO⁺ ions, motion and heat conduction equations

22 p2849 A73-42572

The 4-day rotation of the upper atmosphere of Venus.

22 p2913 A73-42982

Upper Venusian atmosphere four-day retrograde zonal circulation, discussing moving flame phenomenon, convective instability to mean shear and tidal forcing

22 p2913 A73-42983

Jupiter and terrestrial upper atmospheres compared, discussing solar wind interactions with planetary magnetic fields, Jovian Van Allen belt and cold plasma distribution

22 p2913 A73-42985

Apollo 16 far-ultraviolet camera/spectrograph - Instrument and operations.

22 p2864 A73-43165

Temperature variations in the upper atmosphere during the solar activity minimum based on data of topside sounding of the ionosphere.

23 p2970 A73-43243

Venus upper atmosphere retrograde rotation above main cloud cover, investigating equatorial bulge from pressure surfaces at high elevations

23 p3029 A73-43604

Radiation production and energy deposition by ring current protons precipitated into the mid-latitude upper atmosphere.

23 p3024 A73-43685

Behavior of excited atoms and molecules in the upper atmosphere at heights from 40 to 300 km

24 p3084 A73-44803

Distribution of atomic oxygen in the upper atmosphere deduced from Ogo 6 airglow observations.

24 p3086 A73-45121

Atmospheric mixing effects for interpretation of oxygen atom concentration in Mars and Venus upper atmospheres obtained by Mariner and Venera space probes

24 p3139 A73-45134

UPPER IONOSPHERE

NT F REGION

NT F1 REGION

NT F2 REGION

The global morphology of electron temperature in the topside ionosphere, as measured by an a.c. Langmuir probe.

02 p0158 A73-12027

On investigation of the electron concentration and inhomogeneous structure of the outer ionosphere by means of coherent radiowaves emitted from artificial earth satellites.

03 p0299 A73-13631

Behavior of thermal plasma in the magnetosphere and topside ionosphere.

04 p0442 A73-15336

Shallow-solar-zenith-angle control to topside ionospheric parameters.

04 p0445 A73-15636

Ionospheric double layer theory extended to conditions including gravity and expansion effects in diverging geomagnetic flux tubes

05 p0568 A73-16145

Storms and the seasonal anomaly in the topside ionosphere.

09 p1075 A73-22132

Direct measurements of plasma convection in the upper ionosphere

10 p1211 A73-23885

Autocorrelation and cross correlation coefficients for maximum electron densities and total electron con-

tent in E and F regions and upper and lower ionosphere

11 p1351 A73-25093

Ariel 3 satellite observations of the ionosphere at high southern latitudes.

11 p1353 A73-25754

The topside ionosphere at mid-latitudes during local sunrise.

11 p1353 A73-25757

Satellite-borne electrostatic wave topside ionosphere sounder for electron plasma resonance measurement, discussing data spectra preservation, frequency synthesizer and gain-change mechanism features

11 p1339 A73-26629

Computerized simulation of Ionosphere Sounding Satellite topside sounder system techniques for observation of critical frequencies and apparent distance-frequency characteristic relation

13 p1586 A73-29248

Studies of the equatorial anomaly in the F region and outer ionosphere with the aid of spherical ion traps

14 p1746 A73-29860

Direct measurements of ion drift velocity in the upper ionosphere during a magnetic storm. I - Methodological aspects and some results of measurements in magnetically quiet periods. II - Results of measurements during the magnetic storm of November 3, 1967

14 p1746 A73-29863

The low-latitude and equatorial outer ionosphere during the magnetic storm of January 2-4, 1964

15 p1871 A73-31881

Ion heating in thermal plasma flows.

16 p2042 A73-33465

The behaviour of the topside ionosphere during magnetically disturbed conditions.

16 p2010 A73-33912

The latitudinal variation of the electron concentration in the topside ionosphere in winter.

16 p2010 A73-33913

Direct measurements of plasma convection in the upper ionosphere.

20 p2550 A73-38904

Venus topside ionosphere He content estimated from ionization profiles and discovery of radioactive materials in crust

20 p2604 A73-38942

Topside ionospheric winter and summer diurnal electron density variations in Arctic regions as function of universal time, showing Ariel 3 measurements graphically

21 p2682 A73-40171

The behaviour of the upper ionosphere over North America at sunset.

24 p3087 A73-45203

Enhancement of the equatorial anomaly in the topside ionosphere during magnetic storms.

24 p3088 A73-45216

UPPER STAGE ROCKET ENGINES

Design, capability, and cost of a Versatile Upper Stage (VUS) family of vehicles.

[AIAA PAPER 73-589]

18 p2357 A73-36078

UPSTREAM

Doppler spectrum turbulence spreading updraft velocity estimation from observation by pulsed radar, noting average value and standard deviation in small thunderstorm

21 p2728 A73-40058

UPWASH

A general solution for lift interference in rectangular ventilated wind tunnels.

[AIAA PAPER 73-209]

05 p0563 A73-16940

Unsteady thin-airfoil theory for subsonic flow.

08 p0925 A73-20718

The lift on a wing in a turbulent flow.

19 p2376 A73-37487

UPWELLING

U UPWELLING WATER

UPWELLING WATER

NOAA environmental satellites with IR remote sensors for detection of upwelling off Mexican Pacific Coast and cold water eddies in Sargasso Sea

20 p2560 A73-39890

URANIUM

NT URANIUM ISOTOPES

NT URANIUM PLASMAS

NT URANIUM 238

Uranium and potassium fractionation in pre-Imbrian lunar crustal rocks.

07 p0880 A73-19695

Radiochemical neutron activation analysis for U and Th abundance measurement in achondrites and pallasite olivines

17 p2120 A73-35802

URANIUM ALLOYS

Intercrystalline structures effect on precipitation reactions in supersaturated solid solutions, noting Widmanstatten structure growth in U alloy

04 p0467 A73-15953

Stabilized gamma phase U-Nb-Zr alloy observation by electron microscopy, noting displacement reaction role in transition phase formation

20 p2578 A73-39489

URANIUM ISOTOPES

NT URANIUM 238

Moon geochronology from U-Pb systematics applied to lunar basalt data, discussing two and three stage evolutionary models based on Pb isotope ratios

05 p0618 A73-16834

Uranium and extinct Pu-244 effects in Apollo 14 materials.

07 p0888 A73-19784

Np-237, U-236, and other actinides on the moon.

07 p0888 A73-19785

U-Th-Pb measurements of Luna 20 soil.

13 p1677 A73-28335

A response to a comment on U-Pb systematics in lunar basalts.

18 p2354 A73-36512

URANIUM PLASMAS

Ultraviolet spectrum emitted from a laser-produced uranium plasma.

12 p1527 A73-27123

On the emission coefficient of uranium plasmas.

23 p3005 A73-43388

URANIUM 238

Ultraviolet spectrum emitted from a laser-produced uranium plasma.

12 p1527 A73-27123

URANUS [PLANET]

A near-infrared view of the Uranus system.

01 p0109 A73-11491

The transmission of mass and angular momentum from a satellite or planetary system to its primary.

02 p0225 A73-12810

High-resolution imagery of Uranus obtained by Stratoscope II.

05 p0627 A73-17388

Temperatures of Uranus and Neptune at 24 microns.

07 p0874 A73-19067

Uranus atmosphere - Structure and composition.

07 p0874 A73-19068

Intensity variation across Uranus disk during limb darkening-brightening cycles observations to test cloud absence theory, predicting limb brightening in methane bands

08 p1003 A73-20889

Survey of the outer planets Jupiter, Saturn, Uranus, Neptune, Pluto, and their satellites.

11 p1417 A73-25315

Scientific considerations for a common Saturn/Uranus atmospheric entry probe.

18 p2350 A73-36080

Thermal control subsystem design of a Saturn/Uranus atmospheric entry probe for descent missions to 20 bars.

[AIAA PAPER 73-770]

18 p3604 A73-36384

Atmospheric Uranus and Neptune models with massive atmospheres above solid cores, discussing Uranus solid methane cloud layer

22 p2913 A73-42987

The wavelength dependence of the albedos of Uranus and Neptune from 0.3 to 1.1 micron.

22 p2914 A73-43014

Observation of the Raman effect in the spectrum of Uranus.

22 p2916 A73-43126

H2 pressure-induced lines in the spectra of the major planets.

24 p3138 A73-45050

URBAN DEVELOPMENT

Thermal effects of urbanization and industrialization in the boundary layer A numerical study.

06 p0720 A73-18330

Regional airport systems study for San Francisco bay area, discussing commercial and general aviation future needs, environmental and economic aspects and alternative options

11 p1454 A73-26125

Dallas/Fort Worth regional airport land use planning for airport-community compatibility assurance via airspace distribution

13 p1598 A73-29107

London third airport planning, discussing site selection, large scale urbanization, land use and reclamation, operational aspects and environmental factors

15 p1857 A73-31539

EHF radio wave limitations and potentialities for high speed data communications systems, considering applications in urban short range relays

16 p1981 A73-33705

Passenger response to airline service and resultant competition dynamics among air carriers in metropolitan area, indicating satellite airports importance

21 p2671 A73-40210

Technology transfer in New York City - The NASA/NYC Applications Project. [AIAA PAPER 73-978]

22 p2938 A73-42532

URBAN PLANNING

Urban-change detection systems - Remote-sensing inputs.

03 p0301 A73-13845

Remote sensing applications in urban and regional planning in the Los Angeles metropolis - Problems and accomplishments.

05 p0642 A73-17132

- Air transportation systems problems - The airport operators' view. 06 p0683 A73-17602
[AIAA PAPER 73-6]
- Toronto airport relocation project, summarizing provincial government planning and decision making process, site choice and community resistance to airport. 16 p1995 A73-33181
- Utility of remote-sensing data for urban land use planning. 16 p2003 A73-33363
- Feasibility of downtown heliport facilities in terms of public concerns including fear, noise and economics. 17 p2146 A73-34443
- City center heliport design and location for scheduled intercity helicopter services, discussing terminal facilities, economic factors, elevated sites, etc. 17 p2146 A73-34444
- A proposed littoral airport. 19 p2415 A73-37280
- Inglewood /California/ airport noise abatement monitoring program, discussing landing approach slopes, monitoring equipment and techniques and noise effects on property value. 19 p2505 A73-37283
- Urban and regional planning aspects of offshore airport technology. 19 p2417 A73-37743
- Urban land use from RB-57 photography - Computer graphics of the Boston area. 20 p2556 A73-39845
- Interdisciplinary research on the application of ERTS-1 data to the regional land use planning process. 20 p2563 A73-39910
- URBAN RESEARCH**
- Model study of aircraft noise reverberation in a city street. 02 p0130 A73-12199
- Feasibility experiments for high capacity Hertzian cables to distribute and collect data within urban areas, using cylindrical mirrors. 16 p1982 A73-33715
- Anthropogenic CO sources and urban concentrations, considering meteorological factors, nonanthropogenic sources, temporal variations and background levels in remote areas. 21 p2729 A73-40080
- A technology tool for urban applications - The remotely piloted blimp. 22 p2799 A73-42533
[AIAA PAPER 73-981]
- Helicopter noise experiments in an urban environment. 22 p2800 A73-42944
- URBAN TRANSPORTATION**
- Geology, hydrology, land use and transportation net of Dallas-Fort Worth area from Apollo 6 photographs, comparing with ground based data. 01 p0035 A73-10139
[AIAA PAPER 73-155]
- Experimental aerodynamic studies for intra-urban trains traveling in tunnels. 05 p0566 A73-16903
[AIAA PAPER 73-25]
- Review of New York Airways helicopter operations. 06 p0647 A73-17614
[ASCE PREPRINT 1507]
- Benefit-cost analysis of delay reduction with STOL. 08 p1025 A73-21000
- Helicopter use for urban transportation to meet economic growth needs and alleviate traffic congestion, considering IFR equipment and noise reduction. 14 p1712 A73-30470
- Interaction of an air-cushioned vehicle with an elastic guideway. 17 p2098 A73-34181
- Airtransit - The Canadian demonstration interurban STOL service. 17 p2103 A73-34704
[SAE PAPER 730356]
- ACLS equipped vehicles in inter-city transportation. 19 p2381 A73-37686
- The role ground transportation can play in the airport site selection process. 23 p2966 A73-43497
[ASME PAPER 73-ICT-70]
- UREAS**
- A numerical analysis of some practical aspects of airborne urea seeding for warm fog dispersal at airports. 21 p2728 A73-40056
- Urea content variations in blood and tissues during muscular activity in relation to the adaptation level of the organism. 22 p2807 A73-42660
- URETHANES**
- The chemistry of urethane adhesives incorporating silane coupling agents. 03 p0332 A73-13037
- Liquid rubber formulation for cold and hot urethane casting of photoelastic models, including membranes and thin walled structures. 07 p0843 A73-19566
- URINALYSIS**
- Accelerated chromatographic method for determination of hydroxyproline. 03 p0273 A73-13600

- Proteinuria and civil aviation aircrew. 08 p0931 A73-21538
- Proteinuria and military aircrew. 08 p0931 A73-21539
- Microchemical urinalysis. VIII - Determination of urinary 17-hydroxycorticosteroids. 11 p1324 A73-25138
- Physiological time zone entrainment and stressor effects during prolonged C-141 transmeridian flights, using endocrine-metabolic indices in urine specimens. 13 p1574 A73-28283
- Physiological cost in 36- and 48-hour simulated flights. 20 p2512 A73-39101
- Microchemical urinalysis. IX - Determination of hydroxyproline in urine. 21 p2648 A73-41213
- URINE**
- Serum creatine phosphokinase activity and urinary excretion of creatine and creatinine in man during acclimatization to high altitude and in high altitude natives. 11 p1315 A73-25333
- Circadian rhythm of urinary calcium excretion during immobilization. 14 p1717 A73-30512
- Fibrinolytic activity of urine in healthy persons. 15 p1833 A73-31165
- Effects of the hypodynamics and other factors of a spaceflight on the excretion of 17-oxy corticosteroids and aldosterone. 17 p2111 A73-34233
- USA [UNITED STATES]**
- U UNITED STATES OF AMERICA**
- USNS KINGSFORT**
- U SATELLITE COMMUNICATIONS SHIPS**
- UTILITY AIRCRAFT**
- NT DHC 5 AIRCRAFT
- NT HH-43 HELICOPTER
- NT P-531 HELICOPTER
- NT T-39 AIRCRAFT
- NT UH-1 HELICOPTER
- An-2R aircraft conversion to flying test bed for feasibility studies of jet engine use in agricultural aircraft, describing structural design modifications. 12 p1458 A73-26823
- M-15 agricultural turbojet aircraft design for slow low level flight, tabulating dimensions, weights and performance data. 13 p1568 A73-28026
- Rogallo variable geometry flexible cambered wing structure and aerodynamic performance for low speed agricultural flight applications. 13 p1568 A73-28027
- Helicopters for business executive transport between cities or to isolated locations, police use, ambulance service, etc. 17 p2256 A73-34445
- Trends in avionics simplification for light utility aircraft. 19 p2450 A73-37801
- UTILIZATION**
- NT WASTE UTILIZATION**
- V**
- V BAND**
- U EXTREMELY HIGH FREQUENCIES**
- V GROOVES**
- Diffraction effects encountered in the measurement of bidirectional reflectance from square pyramids. 05 p0598 A73-16898
[AIAA PAPER 73-150]
- V groove MOS transistor fabrication by preferential silicon etching and masking process with noncritical alignment tolerances. 23 p2960 A73-44115
- V/STOL AIRCRAFT**
- NT AUTOGYROS
- NT CH-46 HELICOPTER
- NT CH-47 HELICOPTER
- NT CL-84 AIRCRAFT
- NT COMPOUND HELICOPTERS
- NT DHC 5 AIRCRAFT
- NT DO-31 AIRCRAFT
- NT FLYING PLATFORMS
- NT H-53 HELICOPTER
- NT H-56 HELICOPTER
- NT HELICOPTERS
- NT HH-43 HELICOPTER
- NT MILITARY HELICOPTERS
- NT P-531 HELICOPTER
- NT RIGID ROTOR HELICOPTERS
- NT ROTARY WING AIRCRAFT
- NT S-61 HELICOPTER
- NT SHORT TAKEOFF AIRCRAFT
- NT UH-1 HELICOPTER
- NT VERTICAL TAKEOFF AIRCRAFT
- NT X-22 AIRCRAFT
- Pegasus vectored thrust turbofan engine for Harrier class VISTOL aircraft, describing design and operational details. 01 p0090 A73-10200

- The significance of the aerodynamic jet interference for the development and the testing of the V/STOL transport DO 31. 02 p0127 A73-11651
[DGLR PAPER 72-106]
- Problems of the integration of aircraft and flight control system in the case of new approach procedures. 02 p0190 A73-11696
[DGLR PAPER 72-096]
- Recent developments in large area ratio thrust augmentors. 03 p0357 A73-13470
[AIAA PAPER 72-1174]
- Installation effects on performance of multiple model V/STOL lift fans. 03 p0250 A73-13471
[AIAA PAPER 72-1175]
- Comparison of propulsion system concepts for V/STOL commercial transports. 03 p0250 A73-13472
[AIAA PAPER 72-1176]
- The steady-state flow quality of an open return wind tunnel model. 04 p0433 A73-15512
- NASA lift fan V/STOL transport technology status. 05 p0535 A73-16663
[SAE PAPER 720856]
- Russian book on aviation fundamentals covering aerodynamics and flight theory, designs, components, engines and instrumentation of aircraft, including helicopters, VTOL and STOL. 09 p1032 A73-23224
- Hydraulic powered integrated actuator package /IAP/ for V/STOL aircraft flight control, noting advantages in system weight, mechanical complexity and power loss reduction. 11 p1313 A73-26271
[SAE PAPER 720856]
- Augmentor wing design and performance tests for multimitmission XFV-12 V/STOL prototype aircraft. 12 p1459 A73-27731
- Short haul V/STOL air transportation social and economic aspects in comparison with ground transportation modes, emphasizing convenience and frequency of service. 16 p2088 A73-33193
- Royal Aircraft Establishment Aerodynamics Flight Division flight simulators for V/STOL and helicopters, emphasizing handling, aircraft mathematical models and cockpit simulation. 16 p1996 A73-33211
- Design considerations for supersonic V/STOL aircraft. 16 p1969 A73-33517
[ASME PAPER 73-GT-65]
- Conceptual study of high performance V/STOL fighters. 16 p1969 A73-33518
[ASME PAPER 73-GT-66]
- Aerodynamic rig and wind tunnel developments of compound ejector thrust augmentor for V/STOL aircraft with combined Coanda and center injection flows. 16 p2048 A73-33519
[ASME PAPER 73-GT-67]
- Lift engine bleed flow management for a V/STOL fighter reaction control system. 16 p2048 A73-33521
[ASME PAPER 73-GT-70]
- V/STOL airframe/propulsion integration problem areas. 16 p2048 A73-33522
[ASME PAPER 73-GT-76]
- Performance of jet V/STOL tactical aircraft nozzles. 16 p1969 A73-33523
[ASME PAPER 73-GT-77]
- V/STOL aircraft pilot-in-loop flight control/display system to overcome pilot limitations with performance and decision making flexibility enhancement. 17 p2105 A73-35063
[AHS PREPRINT 722]
- Flight simulator evaluation of control moment usage and requirements for V/STOL aircraft. 17 p2147 A73-35076
[AHS PREPRINT 743]
- Wind tunnel test technique to establish rotor system aeroelastic characteristics. 17 p2095 A73-35083
[AHS PREPRINT 760]
- V/STOL hydraulic controls including internal and external blown jet flap and augmentor wing, describing integrated flight control actuator packages and aircraft configuration. 17 p2108 A73-35851
- Digital V/STOL flight simulation test procedures for aircraft navigation, guidance and control, detailing display device panels, flight path simulation and software configuration. 17 p2210 A73-35853
- An evaluation of hypermixing for VSTOL aircraft augmentors. 18 p2267 A73-36208
[AIAA PAPER 73-654]
- Experimental developments in V/STOL wind tunnel testing at the National Aeronautical Establishment. 18 p2265 A73-36774
- Noise reducing choked /sonic/ inlet design for V/STOL jet aircraft, discussing aerodynamic theoretical and experimental studies. 19 p2375 A73-37295
- V/STOL aircraft testing for the sea control ship environment. 19 p2379 A73-37466
[AIAA PAPER 73-810]
- Integrated hydraulic flight control actuator packages replacing mechanical linkages for aerodynamic surface control during V/STOL operation. 20 p2510 A73-39015

Experience with the NRC 10 ft. x 20 ft. V/STOL propulsion tunnel - Some practical aspects of V/STOL engine model testing.

21 p2672 A73-40855

French automatic beam coupler system for V/STOL and helicopter low speed and low altitude instrument approach

21 p2737 A73-40975

VACANCIES [CRYSTAL DEFECTS]

NT FRENKEL DEFECTS

Activation energy volume relation to heat of fusion and lattice characteristics for vacancy diffusion along crystal grains in melting metals

01 p0087 A73-10256

Electron-vacancy prediction methods for sigma phase precipitation in residual matrix compositions of austenitic Niand Co-base superalloys

02 p0183 A73-12757

The mechanism of stage III recovery of electron irradiated molybdenum.

04 p0461 A73-14870

The diffusion coefficient during plastic deformation in AlMg5

08 p0977 A73-21019

On the influence of grain size and vacancy annihilation on the Portevin-Le Chatelier-effect

08 p0977 A73-21021

An observation of vacancy sources during substitutional diffusion in thoriated nickel alloys.

10 p1234 A73-24433

Titanium monoxide system cation self-diffusion coefficients, and quenched-in vacancy concentrations as function of stoichiometry, tabulating Arrhenius parameters

13 p1633 A73-28145

Crystallographic analysis of hexagonal vacancy type Al-Mg alloy cube plane dislocation loops produced by specimen deformation before quenching

13 p1634 A73-28260

The Portevin-Le Chatelier effect in the case of alloys of copper with aluminum, gallium, germanium, arsenic, and indium

14 p1760 A73-30443

The influence of vacancies on the nucleation of incoherent germanium precipitates in aluminum-germanium alloys. III - The effect of germanium nuclei on precipitation at higher temperatures

16 p2026 A73-33959

Vacancy precipitation in quenched and aged Zr-Al alloys and Zircaloy 2, obtaining evidence by transmission electron microscopy for detailed dislocation structure examination

20 p2578 A73-39488

Generation of vacancies in tungsten by rapid-rate deformation at elevated temperature.

20 p2578 A73-39492

Microdefects in dislocation-free silicon crystals.

22 p2896 A73-42276

VACUUM

NT HIGH VACUUM

NT ULTRAHIGH VACUUM

Cosmological vacuum solutions in Brans and Dicke's scalar-tensor theory.

03 p0373 A73-13356

Type-III Einsteinian void spaces with a G/2 Abelian group of motions and solvable G/3 groups

17 p2212 A73-35565

Y-covariant formulation of the relativistic electrodynamics of material media

17 p2213 A73-35569

VACUUM APPARATUS

NT CONDENSATION PUMPS

NT ION PUMPS

NT IONIZATION GAGES

NT KNUDSEN GAGES

NT MOLECULAR PUMPS

NT PHILIPS IONIZATION GAGES

NT VACUUM CHAMBERS

NT VACUUM FURNACES

NT VACUUM GAGES

NT VACUUM PUMPS

An ultrahigh-vacuum arrangement for studying extraterrestrial material

02 p0151 A73-12466

Development and evaluation of materials for vacuum power interrupters.

04 p0456 A73-15763

An evaluation of pyrolytic techniques with regard to the Apollo 11, 12 and 14 lunar samples analyses.

06 p0753 A73-18411

High vacuum coaxial and coaxial push-pull rotary motion feedthroughs with continuous well shielded low noise cable mounted on vacuum flange

11 p1344 A73-26314

Cermet cathode materials for electric vacuum equipment

12 p1503 A73-27562

Ultrahigh-vacuum apparatus for studying extraterrestrial material.

15 p1859 A73-32616

A high vacuum, low temperature specimen transfer device for use in measuring optical properties of thin films.

21 p2693 A73-39925

VACUUM CHAMBERS

The space environment simulation chamber of Toulouse.

07 p0807 A73-19000

Vacuum system for an infrared calibration facility.

08 p0968 A73-21622

Experimental investigation of the excitation functions of thallium atoms

09 p1121 A73-21952

Assembly for measurement of free surface energy, contact angles, and melt densities by a lying drop technique

09 p1085 A73-23017

A distribution of molecular flow in the interior of a cylindrical space-simulation chamber with spherical gas source

11 p1343 A73-25111

Ionization vacuum chambers for radiation measurement, discussing secondary emission, Greening theory and dosimeters, electron beam monitors, pulse measurement, energy spectrometers and interface dosimetry applications

11 p1362 A73-25422

Low temperature vacuum fatigue testing facility for materials testing under space environment conditions

11 p1343 A73-25445

A compact demountable superleak-tight seal for low temperature experiments.

11 p1375 A73-26317

Gas flow analysis during thermal vacuum test of a spacecraft.

16 p1994 A73-33150

Low voltage self triggering vacuum gap characteristics under dc conditions, comparing with thyratron pulse generator technique

21 p2692 A73-39917

Telecontrol system for particle accelerator target displacement via micromotor electronic control with emphasis on adaptation to ultrahigh vacuum chamber simulating ionospheric plasma

22 p2838 A73-41868

Development of a vacuum chamber for ionospheric plasma simulation - Utilization of liquid helium cryopumping

22 p2838 A73-41869

VACUUM DEPOSITION

Access to uncombined titanium through an inhibiting film in sublimation pumping of deuterium.

02 p0194 A73-12844

Electron beam technique for evaporating titanium and silicon oxides antireflection coatings on solar cells, noting humidity and thermal resistances and UV radiation darkening

03 p0256 A73-14228

Phase structure of vacuum deposited thin Ta films and molecular beam composition obtained by mass spectroscopy

04 p0484 A73-15667

High current low voltage magnetically confined hollow cathode discharge for vacuum evaporation and ionization, noting vacuum deposition of quartz and copper

04 p0455 A73-15755

Vacuum deposition of alloys - Theoretical and practical considerations.

04 p0456 A73-15756

Low-frequency creep in CoNiFe films.

[IEEE PAPER 7.1] 07 p0861 A73-19362

Gas turbine engine turbine blades service life increase by Cr and Al vacuum diffusion metallization, presenting full scale endurance test results

10 p1227 A73-24965

Optical studies of the inhomogeneities of metallic layers deposited in vacuum

13 p1660 A73-28761

CdTe thin film fabrication by direct synthesis of vacuum evaporated Cd and Te, noting solar cell efficiency increase after storage in room temperature exsiccator

14 p1713 A73-30475

Vacuum evaporation method for manufacturing neutral density filters with nonlinear density profiles.

15 p1914 A73-32380

Phase formation investigation in the Mo-Al and W-Al systems when the Mo and W surfaces are saturated with aluminum by diffusion from a vapor phase in a vacuum

18 p2318 A73-35879

Superconductivity of films made from aluminum oxide and niobium mixtures

20 p2579 A73-39744

Role of electron processes in the vaporization mechanism and in the formation of binary semiconductor alloy compositions with ion bonds

23 p3016 A73-43711

Some experiments to crystallize the metal thin films on quartz plates.

23 p3018 A73-44136

VACUUM EFFECTS

The technique and results of ground tests of Lunokhod's friction members.

01 p0030 A73-11154

Water, alkalis and oxygen selective volatilization losses from hot silicate liquids erupted into high vacuum at lunar surface

02 p0219 A73-12438

An ultrahigh-vacuum arrangement for studying extraterrestrial material

02 p0151 A73-12466

Effect of vacuum solidification on the porosity of wound fiberglass-reinforced plastics

02 p0174 A73-12577

Swirling jet of gases mixture into vacuum.

03 p0289 A73-12908

The evaporation of various lubricant fluids in vacuum.

[ASLE PREPRINT 72LC-6C-2]

03 p0335 A73-14366

Electron beam float zone melting and vacuum degassing of niobium single crystals

04 p0456 A73-15762

Investigation of the effect of vacuum environment on the fatigue and fracture behavior of 7075-T6.

04 p0466 A73-15764

Influence of vacuum conditions in fabrication on the structure and electrophysical properties of epitaxial silicon films on sapphire

06 p0736 A73-18089

Surface layer grain boundary corrosion damage of Ti alloys during vacuum annealing, reducing rupture strength, vibration resistance and bending fatigue limit

06 p0698 A73-18205

Electrostatic field effects on the fatigue of steel in vacuum

06 p0711 A73-18661

Electrical explosion of tungsten wires in a vacuum.

06 p0724 A73-18782

Spherical and cylindrical gaseous expansions into a vacuum.

07 p0920 A73-19980

Influence of an external electric field on the initial phase of the explosion of wires in a vacuum

09 p1119 A73-21883

Acceleration of ions during the formation of an electron beam from a stationary vacuum-arc plasma

09 p1125 A73-21909

Thermal diffusivity of lunar rocks under atmospheric and vacuum conditions.

09 p1148 A73-22872

Volatilization studies on a terrestrial basalt and their applicability to volatilization from the lunar surface.

10 p1275 A73-23738

Radiative heat transport models for evacuated powder to specify IR radiation environment on lunar surface

10 p1282 A73-24645

Generalized electromagnetic torque on a vacuum pulsar model.

10 p1284 A73-24914

Leakable gases and water vapor loss rates and service life predictions for sealed alkaline cells in vacuum or aerospace environments, using mass transfer equations

11 p1307 A73-24973

The solid-vacuum interface; Proceedings of the Second International Symposium on Surface Physics, Technische Hogeschool Twente, Enschede, Netherlands, June 21-23, 1972.

11 p1325 A73-25201

Vacuum state of a relativistic system interacting with an external field

11 p1397 A73-25245

The effect of vacuum on the high temperature, low cycle fatigue behavior of structural metals.

11 p1383 A73-25834

The long term performance characteristics of a SNAP-19 generator operating under vacuum conditions.

11 p1396 A73-26038

Apollo 12 fines vacuum thermal conductivity as function of temperature for different densities, comparing to terrestrial basalt under vacuum and pressure

11 p1425 A73-26137

Possibility of correlating the field of a wide wave beam in a smoothly nonhomogeneous medium with the field of a beam in vacuum

11 p1331 A73-26161

Influence of proton irradiation in vacuum on the properties of polymer films

11 p1389 A73-26740

Vacuum sublimation of ammonium perchlorate.

12 p1466 A73-27127

V and Cr thin film lattice parameter decrease with thinness, discussing vacuum effects and surface energies estimation

12 p1531 A73-27935

Fatigue failure of a two-phase titanium alloy in vacuum

14 p1763 A73-30713

Nitrides and oxides formed on a niobium surface at high temperatures in vacuum

15 p1887 A73-31203

High strength steel fracture characteristics in vacuum and gaseous medium, noting hydrogen adsorption effect on crack resistance

15 p1887 A73-31248

VACUUM FURNACES

- Physicochemical properties of metal silicides under vacuum at high temperatures, assessing suitability as antineutron materials on Mo grids in high power vacuum electron tubes 15 p1898 A73-31842
- Scattering of electromagnetic waves by a disk positioned at the boundary between two media 15 p1846 A73-32318
- Investigation of titanium alloys at high temperatures in vacuum 15 p1894 A73-32541
- Ultrahigh-vacuum apparatus for studying extraterrestrial material. 15 p1859 A73-32616
- Ion acceleration in the formation of an electron beam in a vacuum arc. 15 p1922 A73-32634
- Effect of an external electric field on exploding wires in vacuum. 17 p2211 A73-34307
- Microwave amplifier design with discrete variable components, testing power output and efficiency, bandwidth, and temperature, vacuum and vibration effects on performance 17 p2141 A73-35324
- Friction of hard alloys in vacuum at low temperatures 18 p2320 A73-36861
- Multilayer foil insulated Si-Ge thermoelectric converters with multihundred watt power capacity, presenting thermal performance stability under vacuum operating conditions 19 p2392 A73-38423
- Method allowing biological and biochemical studies of vacuum-exposed bacteria. 20 p2513 A73-39483
- Ion acceleration upon expansion of a rarefied plasma. 22 p2890 A73-41724
- Vacuum effects on materials and environment contamination - Screening method and results obtained at CNES 22 p2880 A73-41873
- Experimental investigation of the strength and deformability of vacuum-prepared fiberglass-reinforced plastic shells 22 p2881 A73-43062
- Scattering of electromagnetic waves by a disk at the interface between two media. 24 p3067 A73-44624
- Expansion of a plane rarefied gas layer into a vacuum 24 p3076 A73-44655

VACUUM FURNACES

- A process for delubrication, presintering, and rapid cooling in a vacuum induction furnace. 04 p0455 A73-15751

VACUUM GAGES

- NT IONIZATION GAGES
- NT KNUDSEN GAGES
- NT PHILIPS IONIZATION GAGES
- Hot wire probe applications to radiation, fluid flow, vacuum and temperature measurements, deriving mathematical expressions for physical laws 08 p0962 A73-20750
- UHV outgassing measurements on various carbons. 08 p0937 A73-21621
- The problem of temperature in vacuum metrology. II 11 p1371 A73-26552

VACUUM MELTING

- Mechanical properties anisotropy in heat resistant Ni alloys due to strengthening phase nonmetallic inclusions distribution, suggesting purification by vacuum melting 01 p0066 A73-11346
- Vacuum arc melting for improved heat resistance and mechanical properties of Ni alloy blanks, comparing with electro-beam and plasma arc melting and powder sintering 03 p0323 A73-13502
- Characteristics of the ingot crystallization process under conditions of melting in vacuum furnaces with a consumable electrode, and the stability of the cast structure in alloys of the Nb-Ti system 04 p0464 A73-15496
- Importance of arc gap control in vacuum consumable arc remelting of superalloys. 04 p0454 A73-15743
- Cr heat vacuum decarburization equipment for stainless steel vacuum melting, noting cost analysis, vacuum pumping curve and desulfurization 04 p0455 A73-15745
- Improved M50 aircraft bearing steel through advanced vacuum melting processes. 04 p0455 A73-15746
- Nonstoichiometric yttria crucibles for cold wall Ti melting, noting single batches, cost reduction and alloy homogeneity 04 p0455 A73-15749
- Titanium nitrides effect on austenite grains formation by high temperature fusion, considering electric arc and vacuum melting of structural steels 06 p0706 A73-17883

Recrystallization of electron-beam-melted tungsten with tantalum and zirconium carbide additions 09 p1106 A73-23189

Structure and properties of electron-beam-melted 1Kh12N3M3B steel 09 p1107 A73-23194

A study of the extraction of oxygen from molybdenum by dissolving it in metallic carbon-containing melts in a vacuum 21 p2717 A73-40479

Effect of chemically activated elements on the properties of electron-beam-melted nickel 21 p2718 A73-40482

VACUUM PUMPS

- NT CONDENSATION PUMPS
- NT ION PUMPS
- NT MOLECULAR PUMPS
- Cr heat vacuum decarburization equipment for stainless steel vacuum melting, noting cost analysis, vacuum pumping curve and desulfurization 04 p0455 A73-15745
- The large space simulation chamber of Toulouse and its evacuations pumps 07 p0808 A73-19003
- A cryogenic ultrahigh-vacuum pump with a small liquid-helium flow rate 07 p0830 A73-19288
- Cryopumping use in clean ultrahigh vacuum technology, considering cold surface heat load, condensate layer growth rate and heat conductivity, cryosorption and cryotrapping 07 p0852 A73-20402
- Cryopumping adsorption-desorption theory and cryosorption and condensation pumps, including bare surface, adsorbents and frozen deposit pumps 08 p0989 A73-21619
- High and ultra-high vacuum by pumping with cryocooled surfaces. 11 p1398 A73-25579
- Cryogenic ultrahigh-vacuum pump with low liquid-helium consumption. 13 p1659 A73-28688
- The performance characteristics of modern vacuum pumps. 21 p2707 A73-39915
- Vacuum Technology Workshop, Versailles, France, May 30-June 3, 1972, Proceedings 22 p2886 A73-41867

VACUUM SPECTROSCOPY

- Application possibilities of atomic resonance absorption spectroscopy in vacuum metallurgy. 04 p0455 A73-15754
- Rise time and pressure measurements in transient flow during quasi-steady gas injection into vacuum with piston valve, using fast ionization gage 02 p0168 A73-11963
- Vacuum thermogravimetric analysis system for determination of continuous weight change and total condensable materials. 03 p0330 A73-13018
- Comparative evaluations of outgassing results between the vacuum thermogravimetric method and the SRI method. 03 p0330 A73-13019
- Vacuum technology at low temperatures; Proceedings of the Symposium, Denver, Colo., August 31, 1970. 11 p1398 A73-25578
- Semiconductor lasers pumped by pulsed electric discharge in vacuum. 13 p1626 A73-28545
- Camera design with deep-cooled photographic emulsion for low intensity light photography, discussing gas filling and vacuum techniques for water condensation avoidance 14 p1753 A73-30275
- A harmonic drive used as an ultrahigh vacuum rotary feedthrough. 21 p2671 A73-39919
- Modified poppet valve for quasisteady gas injection into vacuum. 24 p3093 A73-44813

VACUUM SYSTEMS

- Rise time and pressure measurements in transient flow during quasi-steady gas injection into vacuum with piston valve, using fast ionization gage 02 p0168 A73-11963
- Vacuum thermogravimetric analysis system for determination of continuous weight change and total condensable materials. 03 p0330 A73-13018
- Comparative evaluations of outgassing results between the vacuum thermogravimetric method and the SRI method. 03 p0330 A73-13019
- Vacuum technology at low temperatures; Proceedings of the Symposium, Denver, Colo., August 31, 1970. 11 p1398 A73-25578
- Semiconductor lasers pumped by pulsed electric discharge in vacuum. 13 p1626 A73-28545
- Camera design with deep-cooled photographic emulsion for low intensity light photography, discussing gas filling and vacuum techniques for water condensation avoidance 14 p1753 A73-30275
- A harmonic drive used as an ultrahigh vacuum rotary feedthrough. 21 p2671 A73-39919
- Modified poppet valve for quasisteady gas injection into vacuum. 24 p3093 A73-44813

VACUUM TESTS

- NT THERMAL VACUUM TESTS
- VACUUM TUBE OSCILLATORS
- NT BACKWARD WAVE TUBES
- NT CATHODE RAY TUBES
- NT CELESTROSCOPES
- NT GAS DISCHARGE TUBES
- NT HELITRONS
- NT IMAGE ORTHICONS
- NT IMAGE TUBES
- NT KLYSTRONS
- NT MAGNETRONS
- NT MICROWAVE OSCILLATORS
- NT MICROWAVE TUBES
- NT PHOTOMULTIPLIER TUBES
- NT PLANOTRONS
- NT THERMIONIC DIODES
- NT THYRATRONS
- NT TRAVELING WAVE TUBES
- NT VIDICONS

Intersynchronization processes in Thomson oscillators with constraints of different nature placed on their amplitudes 08 p0948 A73-21518

Phase effect in RC transistor oscillator with single transistor or tube as amplifying element, determining vibration frequency, reverse communication amplification and frequency dependence 14 p1737 A73-30790

Distortions of signal frequency in FM oscillators. 17 p2136 A73-35150

VACUUM TUBES

- NT BACKWARD WAVE TUBES
- NT CATHODE RAY TUBES
- NT CELESTROSCOPES
- NT GAS DISCHARGE TUBES
- NT HELITRONS
- NT IMAGE ORTHICONS
- NT IMAGE TUBES
- NT KLYSTRONS
- NT MAGNETRONS
- NT MICROWAVE OSCILLATORS
- NT MICROWAVE TUBES
- NT PHOTOMULTIPLIER TUBES
- NT PICTURE TUBES
- NT PLANOTRONS
- NT THERMIONIC DIODES
- NT THYRATRONS
- NT TRAVELING WAVE TUBES
- NT VACUUM TUBE OSCILLATORS
- NT VIDICONS

VACUUM ULTRAVIOLET RADIATION

- U FAR ULTRAVIOLET RADIATION
- VALENCE
- L-beta /2/ and K-alpha X ray spectra of niobium and carbon in NbC compound, assuming collectivized valence electrons 02 p0180 A73-12174
- Diffusion processes electron mechanism in metal-metal and metal-nonmetal systems, using configurational model for valence electrons localization 10 p1236 A73-24951
- Deformable body with reticular structure, studying microstructural transitions using physical model with isolated-valence bond coupling 13 p1690 A73-27992
- Valency transfers of vanadium ions in ruby 14 p1783 A73-30582
- Europium anomaly in plagioclase feldspar - Experimental results and semiquantitative model. 16 p1976 A73-32902
- Theoretical assignments of the low-lying electronic states of carbon dioxide. 19 p2462 A73-37583
- X-ray spectral data on the valence and conduction band structures in V3X-type vanadium compounds 23 p3017 A73-44041

VALKYRIE AIRCRAFT

- U B-70 AIRCRAFT
- VALLEYS

- Lunar tidal phenomena and the lunar Rille system. 03 p0370 A73-13113
- Experimental studies on the formation of lunar surface features by fluidization - Discussion. 10 p1280 A73-24349
- Lunar sinuous rilles as inverted eskers formed by volatiles /water and carbon dioxide/ moving in channel between basement surface and permafrost layer 17 p2237 A73-35859

VALSALVA EXERCISE

- Hemodynamic effects of physical maneuvers /Valsalva, effort, respiration/ and of pharmacodynamic tests - Their clinical application 02 p0138 A73-12159
- Effect of the Valsalva maneuver on tolerance to +Gz acceleration. 14 p1714 A73-29754

VALSALVA MANEUVER

- U VALSALVA EXERCISE
- VALUE ENGINEERING
- Value engineering methodology for quality control and reliability, noting cost effectiveness 09 p1168 A73-22644
- Aerospace systems evaluation and optimization via systems analysis, discussing capability, dependability and availability and cost 12 p1561 A73-27384
- Testing and evaluation community role in weapon system acquisition, describing R and D philosophy 13 p1569 A73-28902

VALVES

- NT ARTIFICIAL HEART VALVES
- NT AUTOMATIC CONTROL VALVES
- NT CONTROL VALVES
- NT FUEL VALVES
- NT GAS VALVES
- NT HEART VALVES
- The vapour core pump vortex inlet valve. 23 p2941 A73-43393
- VAN ALLEN RADIATION BELTS
- U RADIATION BELTS
- VAN DER WAAL FORCES
- Generalized van der Waals theories for surface tension and interfacial width. 11 p1400 A73-26214

Determination of van der Waals broadening of Fe I emission lines induced by neutral He
13 p1685 A73-29360

Evaluation of the intermolecular energy between two hydrogen molecules near the van der Waals minimum, from a perturbative procedure.
17 p2213 A73-35179

Van der Waals energy calculation from electromagnetic mode quantum energy in spheres and cylinders, considering finite boundary conditions, Green function techniques, and periodic lattices
20 p2538 A73-39706

VANADATES
Optical and thermal properties of hydrated yttrium vanadates in aqueous solutions, showing decomposition during thermal dehydration
06 p0739 A73-18655

The investigation of the middle infrared absorption spectrum of DyVO₄ at low temperatures.
08 p0994 A73-21219

A mass spectrometric investigation of reactions involving vanadium and chromium with potassium-seeded H₂/O₂ flames.
10 p1186 A73-23555

VANADIUM
Spectrophotometric determination of vanadium with 4-/2-pyridylazo/resorcinol by extraction of tetraphenylphosphonium and arsonium salts.
06 p0661 A73-18269

Color centers in gamma-irradiated ruby with vanadium additions
10 p1259 A73-24069

Change in the superconducting properties of vanadium after the introduction of tantalum impurity atoms
10 p1261 A73-24761

Acoustical method for determining thermal diffusivity and relative difference in molar heat capacities of tantalum and vanadium.
11 p1448 A73-25127

Solubility of vanadium and tungsten in alpha and gamma phases in the Fe-V and Fe-W binary systems
12 p1513 A73-27683

V and Cr thin film lattice parameter decrease with thickness, discussing vacuum effects and surface energies estimation
12 p1531 A73-27935

The effect of neutron irradiation damage on the low temperature deformation characteristics of b.c.c. metals and their alloys.
13 p1638 A73-29454

The low-temperature embrittlement of niobium and vanadium by both dissolved and precipitated hydrogen.
14 p1761 A73-30630

Effect of adsorption on the electrical conductivity of thin vanadium films
17 p2220 A73-35557

Thermodynamics of b.c.c. solid solutions of hydrogen in niobium, vanadium and tantalum.
17 p2193 A73-35623

Ultrahigh-speed quenching of niobium and vanadium
19 p2439 A73-37250

VANADIUM ALLOYS
Ti-V and Ti-Nb alloys mechanical strength and stress concentration resistance at low temperatures
01 p0067 A73-11348

Carbide hardening of chromium-molybdenum-vanadium steel.
03 p0327 A73-14005

Susceptibility to brittle fracture of simulated weld seams in Ti-Al-V alloys.
06 p0698 A73-18209

Phase equilibria in V-N-Sc/Y, Ce, Pr alloys
09 p1108 A73-23238

Mechanical properties of recrystallized molybdenum containing vanadium microadditions
10 p1233 A73-24361

Temperature dependence of the Moessbauer spectra of iron-cobalt-vanadium alloys
12 p1509 A73-26839

Increase in the boundary strength of cast electron-beam-melted molybdenum by microadditions of vanadium.
13 p1643 A73-29634

Electron characteristics of sprayed vanadium-gallium alloys
15 p1922 A73-31178

Structure and properties of alloys of the V3Si-V3Ga-'V3Al' system
15 p1922 A73-31179

Structure and superconducting properties of alloys of the vanadium-tantalum system
15 p1923 A73-31183

Structure and properties of alloys of the V3Si-V3Ga-V3Ge system
15 p1923 A73-31190

The vanadium-iron-boron, vanadium-cobalt-boron, and vanadium-nickel-boron systems
15 p1887 A73-31202

Structure and decay characteristics of unstable beta-solid solutions of the Ti-V system
15 p1893 A73-32519

Characteristics of the distribution of elements in the diffusive layers of titanium-based three-component systems
15 p1893 A73-32521

Effects of high omnidirectional pressures and residual stresses on the superconductivity of alloys of the V3Si/xGex/ system
16 p2027 A73-34062

Heat conductivity and electrical properties of vanadium-alloyed titanium at 100 to 350 K
17 p2188 A73-34554

Ti-Ta-V-Mo system phase diagram in Ti corner region for 600-900 C, investigating solubility, electrical resistivity and hardness
17 p2189 A73-34570

An X-ray examination of deformation in beta Ti-V alloys.
17 p2189 A73-34642

Influence of cold work on the stress corrosion susceptibility of Ti-13V-11Cr-3Al.
17 p2194 A73-35675

Superconducting properties of alloys of the vanadium-niobium-chromium system
18 p2325 A73-36898

The effect of vanadium, niobium, and tantalum on the electrical resistance of nickel
20 p2578 A73-39396

Ti-V alloys elastic modulus and paramagnetic susceptibility, considering composition vs property curve salient point indications of changes in interatomic bonding energy and electron structure
21 p2718 A73-40487

Influence of aluminum on the structure and properties of a Ti + 10% V alloy
21 p2719 A73-40850

Electrical conductivity and superconductivity of vanadium, niobium, and chromium solid solutions
22 p2873 A73-41963

Study of the structure and properties of alloys of the V-Al, Cr-Al and V-Cr-Al systems in the region of solid solution bec ordering
22 p2873 A73-42088

A thermodynamic calculation of the iron-chromium-vanadium equilibrium diagram.
23 p2993 A73-43918

The metallurgy of Remendur - Effects of processing variations.
23 p2993 A73-43987

VANADIUM CARBIDES
Activity of carbon and solubility of carbides in the fcc Fe-Mo-C, Fe-Cr-C, and Fe-V-C alloys.
02 p0183 A73-12755

High speed tool steel, Ti alloys and vanadium carbide products manufacturing by powder metallurgy, using vacuum and high pressure techniques
04 p0460 A73-14745

Equilibrium of vanadium carbide with an alpha or gamma solid solution in the iron-rich Fe-Cr-V-C system at temperatures from 700 to 1150 C and at a carbon concentration of 0.30%
12 p1513 A73-27684

Ostwald ripening of transition-metal carbides in liquid nickel and cobalt
14 p1760 A73-30441

VANADIUM COMPOUNDS
NT VANADATES
NT VANADIUM CARBIDES
NT VANADIUM OXIDES
X-ray spectral investigation of some vanadium compounds with a Cr3Si structure
05 p0588 A73-17295

Ternary nickel-vanadium-oxygen compound and solid solutions formation by vacuum calcination of vanadium and nickel oxides mixtures
13 p1634 A73-28203

Vanadium galliumide tape preparation and critical temperature and current as function of heat treatment temperature and applied magnetic field, considering pancake current capacity
13 p1669 A73-29069

Investigation of the oxygen content in superconducting vanadium- and niobium-base compounds
15 p1922 A73-31181

X-ray spectral data on the valence and conduction band structures in V3X-type vanadium compounds
23 p3017 A73-44041

Thermal and electrical properties of superconducting vanadium silicide tapes, plotting transition temperature vs heat treatment time and temperature and critical current vs current density
24 p3119 A73-44411

VANADIUM ISOTOPES
Vanadium isotopic composition and the concentrations of it and ferromagnesian elements in lunar material.
07 p0889 A73-19797

VANADIUM OXIDES
Phase equilibrium in the TeO₂-V₂O₅ system
05 p0589 A73-17173

Experimental studies and applications of vanadium oxides.
16 p2044 A73-33471

Hartree-Fock model for metal to insulator transition in vanadium oxide based on electronic band structure at zero and finite temperatures
23 p2961 A73-44163

VANELESS DIFFUSERS
Unsteady modes of operation of a centrifugal compressor with a vaneless diffuser
02 p0203 A73-11790

Development trends in aircraft-engine compressor design methods. III
07 p0867 A73-19605

Features of flow-parameter measurement by a cylindrical probe in the vaneless diffuser of a small centrifugal compressor
13 p1568 A73-29552

VANES
NT GUIDE VANES
NT JET VANES
Turbine vane vibration simulation tests with phase shift generation, using tube type phase inverters
13 p1599 A73-29638

Aeronautical turbine blade and vane materials selection, considering Ni alloys with powder metallurgy and oriented solidification, composite materials and eutectics
18 p2326 A73-36993

The use of analytic surfaces for the design of centrifugal impellers by computer graphics.
22 p2900 A73-42477

The scale effect and design method of the regenerative pump with non-radial vanes.
23 p2986 A73-44274

VAPOR DEPOSITION
NT VACUUM DEPOSITION
Experimental approaches to well controlled studies of thin-film nucleation and growth.
02 p0201 A73-12633

Vapor deposition of thin films of DPPH and BDPA.
02 p0201 A73-12639

Carbon and pyrolytic graphite isothermal chemical vapor deposited /CVD/ composite coated and free standing products fluid bed manufacturing and applications
03 p0333 A73-13053

High temperature tests for chemical vapor deposited W ring and tensile specimens mechanical properties, investigating slip traces and fracture surfaces
04 p0462 A73-15305

The influence of ion bombardment on the microstructure of thick deposits produced by high rate physical vapor deposition processes.
04 p0456 A73-15760

Preparation of alloy deposits by continuous electron beam evaporation from a single rod-fed source.
04 p0456 A73-15761

Preparation of transmitting coatings for As2S3 glass
05 p0605 A73-17293

Influence of condensation temperature on microstructure and tensile properties of titanium sheet produced by high-rate physical vapor deposition process.
06 p0711 A73-18752

High-energy electron-beam deposition onto a hot graphite surface.
08 p0990 A73-21210

Fabrication procedures, structure, and mechanical properties of BiTeI thin films
10 p1260 A73-24470

Investigation of diffused titanium coatings on refractory metals
13 p1630 A73-28015

Vapor-phase deposition of elementary boron at substrate temperatures in the range from 1100 to 1400 C
13 p1645 A73-28181

Grain growth of chemical vapour deposited tungsten-22 wt % rhenium alloy.
13 p1636 A73-28927

Cadmium mercury telluride thin film coatings preparation by HgTe layers deposition onto previously vapor deposited CdTe layers under isothermal conditions
15 p1924 A73-32158

Boron fiber coating by chemical vapor deposition of boron carbide for improved mechanical properties and incorporation in Al alloy matrices
16 p2030 A73-33070

Improve reliability of electron devices through optimized coverage of surface topography.
19 p2411 A73-38453

Combined LEED, Auger electron and flash desorption spectroscopy of metals on single crystal surfaces.
21 p2706 A73-41596

A new vapor growth method for GaP using a single flat temperature zone.
24 p3119 A73-44412

VAPOR JETS
Thermodynamic and optical properties of elements vaporized by monochromatic laser light, considering carbon and aluminum vapor stream characteristics
09 p1095 A73-22612

VAPOR LIQUID EQUILIBRIUM
U LIQUID-VAPOR EQUILIBRIUM

VAPOR PHASES

VAPOR PHASES

- Accurate relative acidities in the gas phase - Hydrogen sulfide and hydrogen cyanide. 02 p0139 A73-12634
- Gas phase separation following decompression in asymptomatic rats - Visual and ultrasound monitoring. 03 p0263 A73-14162
- Steady two-dimensional heat and mass transfer in the vapor-gas region of a gas-loaded heat pipe. [ASME PAPER 72-WA/HT-34] 04 p0518 A73-15821
- Diffusion freezeout in gas-loaded heat pipes. [ASME PAPER 72-WA/HT-33] 04 p0518 A73-15822
- Condensate droplets heat conductivity as function of drop geometry and vapor mass transport interaction with interior heat conduction, using finite difference method 06 p0768 A73-17920
- The gas-phase reaction of perchloric acid with hydrogen. 07 p0787 A73-19387
- Vapor phase crystallization in Apollo 14 breccia. 07 p0882 A73-19724
- Gas-phase ignition model for some solid fuels in a shock tube 07 p0865 A73-19989
- Prolonged luminescence of complex molecules in the gas phase 09 p1123 A73-23334
- The gas-phase reaction of perchloric acid with ethylene. 10 p1186 A73-23556
- The behavior of vapors of soluble binary systems during expansion in supersonic nozzles - Droplet coalescence in a potential vortex flow 10 p1205 A73-24162
- Thermodynamics of heterogeneous gas equilibria. VII - Gas phase composition and chemical transport reactions in the tungsten-oxygen-hydrogen system. 11 p1386 A73-26568
- Saturation of Kh18N10T steel by molybdenum from the vapor phase 15 p1889 A73-31807
- Phenomena of precipitation observed in carburized tantalum in the vapor phase 15 p1896 A73-32645
- Combustion of fuel vapor-drop-air systems. I - Open burner flames. II - Spherical flames in a vessel. 16 p2085 A73-33343
- Spectroscopy of the vapors of weakly volatile compounds, supercooled in a supersonic flow 16 p2038 A73-34054
- Study of gas-phase reactions in particle-laden, ducted flows. 17 p2150 A73-34194
- The gas carrier problem during the crystallization of metals from a gas phase 18 p2323 A73-35880
- Quasi-steady gas-phase flame theory in unsteady burning of a homogeneous solid propellant. 21 p2790 A73-40430
- Saturation of steel Kh18N10T with molybdenum from the vapor phase. 24 p3100 A73-45270
- ## VAPOR PRESSURE
- Experimental study of the saturated-vapor pressure of rubidium and cesium 01 p0080 A73-10858
- Ultrahigh vacuum quartz spring microbalance for determination of evaporation rate and vapor pressure. 02 p0168 A73-11965
- Vacuum deposition of alloys - Theoretical and practical considerations. 04 p0456 A73-15756
- Vapour density variations in a pulsed mercury discharge. 05 p0601 A73-16432
- Investigation of the vapor pressure of cesium by the boiling-point method. 06 p0722 A73-17404
- Vapor pressure of supersonic aircraft fuels 07 p0865 A73-20014
- Nonstationary wave propagation in equilibrium liquid-vapor flow, noting pressure jumps due to expansion 10 p1204 A73-23513
- Experimental investigation of the pressure of the saturated vapor of rubidium and cesium. 12 p1526 A73-27907
- High-temperature electrical conductivity relaxations induced in CdTe crystals by variations in cadmium vapor pressure 15 p1923 A73-31201
- Evaporation rate and vapor pressure of selected polymeric lubricating oils. [ASLE PREPRINT 73AM-1A-3] 17 p2195 A73-34978
- Nonstationary wave propagation in equilibrium liquid-vapor flow, noting pressure jumps due to expansion 17 p2155 A73-35193
- New vapour pressure measurements for argon and nitrogen and a new method for establishing rational vapour pressure equations. 19 p2461 A73-38200

Methods for identification of thermodynamically similar substances

- 20 p2593 A73-39296
- Relationship between the equilibrium vapor pressure of the solvent and the surface activity in dilute solutions of inactive and surface-active materials 21 p2646 A73-40122
- Vapour pressures of liquid oxygen and nitrogen. 22 p2930 A73-41979
- Critical slope of the vapor pressure curve of a pure substance. 22 p2932 A73-42506
- Revision of high temperature and critical properties of cesium. 22 p2932 A73-42513

VAPOR TRAILS U CONTRAILS

- ### VAPORIZING
- NT BOILING
- NT EVAPORATION
- NT FILM BOILING
- NT LEIDENFROST PHENOMENON
- NT NUCLEATE BOILING
- NT PROPELLANT EVAPORATION
- NT SUBLIMATION
- NT TRANSPIRATION
- Thermal effect of optical radiation on water drops of small size 01 p0074 A73-11244
- Water, alkalis and oxygen selective volatilization losses from hot silicate liquids erupted into high vacuum at lunar surface 02 p0219 A73-12438
- The rate of vaporization of tungsten in argon. 02 p0183 A73-12767
- Fog droplet vaporization and fragmentation by a 10.6-micron laser pulse. [AD-758948] 06 p0698 A73-17494
- Thermal processes in metals exposed to high power laser pulses 06 p0702 A73-18571
- Volatilized lead from Apollo 12 and 14 soils. 07 p0890 A73-19809
- Thermal volatilization studies on lunar samples. 07 p0890 A73-19811
- Correlation of the vaporization onset heat flux for cylinders in saturated liquid helium-II. 07 p0922 A73-20411
- Surface and body vaporization mechanisms during intense energy flux interaction with substance, relating flux density to mean depth of surface-to-bulk vaporization shift 09 p1095 A73-22611
- Thermodynamic and optical properties of elements vaporized by monochromatic laser light, considering carbon and aluminum vapor stream characteristics 09 p1095 A73-22612
- Volatilization studies on a terrestrial basalt and their applicability to volatilization from the lunar surface. 10 p1275 A73-23738
- Effect of heating water droplets by optical radiation. 10 p1246 A73-24181
- Influence of liquid circulation within a droplet on the vaporization rate and drag in a viscous flow 10 p1206 A73-24680
- Liquid droplet drag in vapor flow as function of drop vaporization rate, using Stokes formula 11 p1451 A73-25736
- Dynamics and energetics of the explosive vaporization of fog droplets by a 10.6-micron laser pulse. 11 p1377 A73-26231
- Effects of prevaporized fuel on exhaust emissions of an experimental gas turbine combustor. 11 p1411 A73-26424
- Chemical volatilization as a technique for the detection of extraterrestrial biopolymers and possible metabolic products. 11 p1319 A73-26479
- An approximate estimate of the reaction coefficient during the motion of a vaporizing droplet of fuel in a gas flow 12 p1532 A73-27088
- Laboratory modeling of 'vaporization-condensation and spilling' type processes taking place on the lunar surface 13 p1672 A73-28118
- Efficiency of the recovery of high thermal energy densities during porous vaporization of alkali metals 15 p1957 A73-31864
- Thermal processes in metals irradiated by powerful laser pulses. 16 p2086 A73-33596
- Vaporization theory of cometary nucleus prediction of law of dependence of nongravitational force on heliocentric distance 17 p2228 A73-34427
- Effect of atom self-diffusion on evaporation processes and porosity development in solid bodies during electron-beam treatment 18 p2320 A73-36900
- Existence and uniqueness conditions for solid surface vaporization products dispersion into vacuum formulated for equations of motion of ideal gas under variable energy release 20 p2573 A73-39282

Combustion of a solid fuel in a gaseous oxidized flow

- 21 p2754 A73-40700
- Role of electron processes in the vaporization mechanism and in the formation of binary semiconductor alloy compositions with ion bonds 23 p3016 A73-43711

VAPORS

- NT CESIUM VAPOR
- NT MERCURY VAPOR
- NT METAL VAPORS
- NT SODIUM VAPOR
- NT WATER VAPOR

VARACTOR DIODE CIRCUITS

- Microwave varactor upconverter in radio repeater for domestic wideband communication satellite emphasizing transmission characteristics design 01 p0006 A73-11177
- Optimize Gunn circuits for wideband varactor tuning. 06 p0675 A73-17844
- Varactor or YIG tuned Gunn effect microwaves oscillators for ECM applications, noting low noise octave tuning and high sweep rates 06 p0675 A73-17844
- Analysis of the nonlinearity of the modulation characteristic of a single-circuit phase modulator employing a varactor 10 p1195 A73-24381
- Certain features of the analysis of a crystal-controlled FM oscillator at high modulating voltage levels 12 p1477 A73-26877
- Varactor frequency multipliers of the parallel type - Spectrum analysis of the voltage on a partially open-circuited varactor. 15 p1849 A73-30991
- Optimal parallel-type varactor frequency multiplier calculation for reverse-biased conditions in terms of nonlinear conductance loss and diffusion capacitance Q factor 16 p1991 A73-33981
- An X-band Gunn-diode generator with varactor tuning 17 p2126 A73-35550
- An analytical solution of the problem of a frequency tripler employing a varactor diode with an arbitrary voltage-charge characteristic 24 p3072 A73-44922
- ## VARACTOR DIODES
- Wideband varactor-tuned Gunn effect oscillators. 04 p0426 A73-14733
- Some theoretical and practical considerations in the design of wideband varactor tuned Gunn oscillators. 04 p0426 A73-14733
- Parametric subharmonic oscillators - Statistical behaviour. 04 p0429 A73-15920
- P-n junction size effect on thermal resistance of reverse biased Si mesa-type diode, considering junction area, mesa height and power dissipation 06 p0674 A73-17792
- Si varactor diode series resistance resonance measurements in UHF band, noting approximate invariance with frequency 06 p0678 A73-18843
- Quality control of semiconductor elements manufactured in low-run series production - Ultrahigh frequency components 07 p0801 A73-19422
- Solid-state devices and components for mm-wave receiver-transmitter systems. 09 p1064 A73-22490
- Microstrip solid state power amplifiers with transistors and varactors for spaceborne applications in L and S band ranges 09 p1066 A73-23420
- Tuning nonlinearity of oscillatory systems made of long-line segments containing a varicap 10 p1193 A73-23720
- Wide-band varactor-tuned X-band Gunn oscillators in full-height waveguide cavity. 10 p1197 A73-24863
- Ge-doped p-type epitaxial GaAs for microwave device application. 15 p1923 A73-31399
- Wideband varactor-tuned solid-state sources to 200 GHz. 16 p1991 A73-33890
- Q band /38 GHz/ varactor-tuned Gunn oscillators. 16 p1991 A73-34018
- An electronically tuned Gunn oscillator circuit. 17 p2134 A73-34222
- Method for plotting frequency cutoff measurements for GaAs varactor diodes. 18 p2292 A73-36590
- Preparation and RF properties of MIS mesa varactors. 19 p2409 A73-37720
- Millimeter wave solid state technology for 60 GHz communication systems, discussing silicon Schottky diode and varactor mixer/receiver, parametric amplifiers and upconverters 20 p2534 A73-38740
- Optimization and design of varicap-diode tuned transistor oscillators 21 p2659 A73-40000

- Ion-implanted varicaps with a steep capacitance-voltage characteristic 21 p2664 A73-41096
- Dipole antenna with variable capacitance diodes for wideband tuning, calculating and measuring input impedance frequency response 23 p2960 A73-44110
- Experimental study of the dynamic parameters of varactor diodes 24 p3072 A73-44929

VARIABLES

U VARACTOR DIODES

VARIABLE AREA WINGS

U TRAILING-EDGE FLAPS

VARIABLE GEOMETRY STRUCTURES

- Study of a series of variable-geometry wings derived from delta wings of different aspect ratios. I - Aerodynamic characteristics of delta wings 04 p0404 A73-15651
- Improved flexible supersonic wind-tunnel nozzle operated by a single jack. 07 p0808 A73-19972

- Dynamics of variable sweep wing aircraft in the course of changing geometry. 10 p1175 A73-24012

- Rogallo variable geometry flexible cambered wing structure and aerodynamic performance for low speed agricultural flight applications 13 p1568 A73-28027

- Swing wing - Modifications in variable geometry configuration concepts. 13 p1568 A73-28157

- Kneeling landing gear - The CS variable geometry development. 13 p1568 A73-28158

- Example of utilization of a wind tunnel with perforated variable-geometry walls 16 p1993 A73-32818

- Time optimal control of satellite pitching motions by variable mass distribution, solving nonlinear optimization problem via maximum principle 16 p2072 A73-33233

- Potential payoffs of variable geometry engines in fighter aircraft. 17 p2099 A73-34436

- Feasibility and optimization of variable-geometry wing for jet amphibian business aircraft. [SAE PAPER 730330] 17 p2102 A73-34683

- Experimental investigation of model variable-geometry and ogee tip rotors. [AHS PREPRINT 703] 17 p2104 A73-35054

- Improved aircraft capability through variable camber. 19 p2378 A73-37275

- The RATAN-600 radio telescope 21 p2675 A73-41441

- Adjustment of a variable-profile antenna 21 p2675 A73-41456

- A radio-astronomical method of adjusting variable-profile antennas 21 p2667 A73-41458

- The prediction of the performance of variable geometry free gas turbines. 23 p3019 A73-43297

VARIABLE LIFT

U LIFT

VARIABLE MASS SYSTEMS

- Investigation of conditions corresponding to the existence of an energy integral in the generalized n-body problem with variable masses 01 p0077 A73-10918

- Distortion of particle trajectories by dynamic effects in the problem of two bodies with corpuscular emission 01 p0102 A73-10947

- Variable mass system dynamic maneuver for maximum payload and given initial weight, noting mathematical model for time optimization 04 p0475 A73-15079

- Calculus of variations for maximum payload of partitioned variable mass system, considering optimal weight control effect on motion 04 p0475 A73-15084

- Motion of a body of variable mass in a many-body gravitational field near collision 05 p0615 A73-16326

- Rocket rectilinear motion, comparing Meshcherskii and Gantmacher-Levin equations in light of contact interaction hypothesis 08 p1014 A73-21181

- Mass variation laws in light of Taiolkovskii hypothesis, considering particle separation rates and thermal energy losses for actual jet engines 08 p1014 A73-21182

- Dynamical effects of the curvature of particle trajectories in the two-body problem with corpuscular radiation. 09 p1148 A73-22742

- Investigation of the motion of a body of variable mass within a multibody gravitational field with the aid of a regularizing variable 09 p1121 A73-22852

- Relativistic rocket motion tensor equations analogous to particle motion in electromagnetic fields, discussing Hamiltonian functions, Lagrangian coordinates and variable mass body mechanics 18 p2356 A73-37038

- Application of the Gauss principle in the dynamics of systems having rigid solids of variable mass as constituent elements 19 p2459 A73-37652

- Dynamics of the rotary motions with respect to the center of mass of a system of solids with a variable geometry of the masses 23 p3007 A73-44187

VARIABLE PITCH PROPELLERS

- Investigation of an axial-flow blower during variation of axial clearance and of blade mounting angles in the stator and rotor sections 02 p0131 A73-11791

- Variable pitch fan experimental design for quiet STOL propulsion, testing blade designs for aerodynamic and acoustic performance 03 p0359 A73-14147

- Variable-pitch fans - Progress in Britain. 14 p1785 A73-29770

- Variable-pitch fans - Hamilton Standard and the Q-fan. 14 p1785 A73-29771

- STOL jet aircraft with variable pitch fan, discussing engine handling, noise reduction and efficiency 16 p2046 A73-33189

- Rotorcraft stability augmentation and gust alleviation by collective and cyclical rotor blade pitch angle changes, discussing nonlinear dynamic effects 18 p2267 A73-36397

- Variable pitch turboprop driven at constant speed through reduction gear to obtain cost-efficiency compromise for future STOL and business aircraft applications 18 p2343 A73-36998

- Aircraft installation requirements and considerations for variable pitch fan engines. [AIAA PAPER 73-807] 19 p2379 A73-37465

- Blade synchronous rotation about pitch axis in single stage axial compressor at front of gas turbine engine during fan rotation 20 p2601 A73-39663

VARIABLE STARS

NT CEPHEID VARIABLES

NT HERCULES NOVA

NT NOVAE

NT SUPERNOVAE

NT T TAURI STARS

- Study of variable stars in two stellar fields in the Lacerta and Lyra constellations 01 p0098 A73-10558

- Photometry and spectroscopy of red variables in Omega Centauri. 01 p0098 A73-10584

- Periodic components of the density variations of the radio source VRO 42.22.01 / BL Lacertae / 01 p0101 A73-10933

- UV Cet-type variable star quiet state and flare spectra, discussing flare mechanism relation to magnetic effects and star evolutionary position 01 p0102 A73-10970

- The classification of intrinsic variable stars. II - The red variables of S and related types. 01 p0104 A73-11038

- A study of the spectrum-variable silicon Ap star 56 Ari. 01 p0106 A73-11305

- Polarization of light by circumstellar material. 02 p0226 A73-12828

- Statistical fractions of variable A and F stars, considering main sequence stars, giants, subgiants and open clusters NGC 2548, Praesepe and Coma 02 p0226 A73-12834

- Light variation and extinction of the variable WW Vulpeculae 02 p0226 A73-12836

- Rapid changes in the new shell star HR 6000. 03 p0366 A73-12941

- The location and size of the hot spot in cataclysmic variable stars. 04 p0499 A73-15486

- The angular diameter of X Cancr. 04 p0500 A73-15518

- Hard X-ray observations of Hercules X-1 by OSO-7. 05 p0612 A73-17343

- Multiple and intrinsic variable stars, considering pulsars, binary systems, Cepheids, stellar structure and evolution 06 p0750 A73-18014

- HD 215441 and 53 Camelopardalis - Intrinsic polarization of H-beta and the continuum. 07 p0874 A73-19075

- VV 281-427, variable stars in a Cepheus-Lacerta field of the Milky Way. 07 p0874 A73-19117

- RR Lyrae, V Virginis and RV Tauri population II variables, considering pulsation problem, instability mechanisms and He ionization 07 p0903 A73-20630

- Population II variable stars shock waves detection via Balmer lines emission and metal line doubling, discussing model for numerical calculations of radiating shock structures 07 p0903 A73-20631

- Cyclic variations of the Be star beta-one Monocerotis. 08 p1006 A73-20924

- The spectral classification of the beta Cephei stars and their location in the theoretical Hertzsprung-Russell Diagram. 08 p1006 A73-20927

- Luminous blue variables in M 31 and 33, discussing light curves, color index and luminosity 09 p1141 A73-22014

- Infra-red observations of young stars. I - Stars in young clusters. II - T Tauri stars and the Orion population. III - Nebulous emission-line stars. 09 p1143 A73-22112

- Photoelectric observation of variable star V725 Sagittarii for significant magnitude and period changes since 1935 09 p1147 A73-22728

- Periodic components in the flux-density variation of the radio source VRO 42.22.01 / BL Lacertae / 09 p1146 A73-22449

- Carbon stars molecular band strength variations in two-micron spectral region due to thermal emission from circumstellar dust shell 09 p1149 A73-23129

- Molecular absorption spectra of S-type stars in the one-micron region. 09 p1123 A73-23130

- An abundance analysis of the delta Scuti variable delta Delphini. 10 p1275 A73-23831

- Delta Scuti variables observational and theoretical data, discussing pulsation properties and relationships to other pulsators and nonvariable stars 10 p1281 A73-24405

- Spectrophotometric investigation of the star alpha-2 CVn. II 11 p1416 A73-25232

- Her X-1 optical counterpart observed for B magnitude, relating light curve scatter to 35-day cycle 11 p1428 A73-26627

- The light variation and orbital elements of VW Bootis. 11 p1429 A73-26680

- Photometric characteristics of the star AC Herculis 12 p1537 A73-26851

- Two-color electrophotometric observations of the BD Dra variable 12 p1537 A73-26852

- SMC X-1 binary source observation via USCD OSO-7 X ray telescope, discussing luminosity and optical identification with variable star SK 160 14 p1786 A73-29738

- Book on variable stars, covering high energy astrophysics, low energy outbursts, extensive convection, galaxies, pulsations, white dwarfs, cepheids, flares and gravitational collapse 14 p1796 A73-29950

- Optical study of BL Lacertae. II - Brightness variation from March 1969 to January 1971 15 p1928 A73-31052

- A problem in distance-determination for Mira variables with an appendix on OB-star distances. 15 p1932 A73-31306

- Bands of the light molecules in Mira variables. 15 p1932 A73-31307

- Photoelectric photometric investigation of brightness behavior of Orion nebula variable stars 15 p1934 A73-31422

- New directions and new frontiers in variable star research; Colloquium on Variable Stars, 5th, Bamberg, West Germany, August 31-September 3, 1971, Proceedings. 15 p1934 A73-31476

- Flare star implications for stellar evolution, noting observational data relating to stars in associations and clusters 15 p1934 A73-31478

- Spectral investigations of UV Ceti-type flare stars and search for new variables of this type carried out at Crimea. 15 p1934 A73-31479

- The red dwarf stars of the UV Ceti-type in the neighbourhood of the sun. 15 p1935 A73-31480

- Techniques and results of observations of rapid and ultrarapid variable stars. 15 p1935 A73-31481

- High-frequency stellar oscillations - The Cerro Tololo search for luminosity variable white dwarfs. 15 p1935 A73-31482

- Duplicity and its consequences among variable stars in general. 15 p1935 A73-31484

- The spectrum variable a Centauri / HD 125 823 / 15 p1935 A73-31485

- Variable star observations from outside the earth's atmosphere - Review and prospects. 15 p1935 A73-31488

Period determination method for variable stars using interpolation in light curves, noting applicability to light curves with few branches

15 p1936 A73-31645

Polarization observations of variable stars and extragalactic objects. I - Instruments and methods of observation and data processing. II - Polarization of the EV Lac flare

16 p2057 A73-32708

Spectrographic investigation of the flare star YZ CMi in January 1969

16 p2057 A73-32709

Changes of the Balmer-series lines of hydrogen in the spectrum of the spectrally variable silicon Ap star CU Vir

16 p2057 A73-32711

Nature of the light variation of the peculiar A-star HD 221568.

16 p2058 A73-32836

The radial velocity variations of HD 125823 a Centauri.

16 p2059 A73-32843

HZ Hercules periodically pulsating variable star in binary system detected by Uhuru satellite, detailing X ray emission, rotation pattern and mass exchange mechanism

16 p2059 A73-32948

Poisson frequency distribution of flare stars in Pleiades, including statistical analysis of photographic amplitudes

17 p2226 A73-34364

Stability of periodic oscillations of stars.

20 p2606 A73-39081

Optical studies of Uhuru sources. VI - Photoelectric photometry of HD 153919 = 2U 1700-37.

22 p2905 A73-41766

Observations of the highly variable X-ray source GX 339-4.

22 p2905 A73-41767

On turbulent stress and the structure of young convective stars.

22 p2908 A73-42306

Sanduleak 160 variability confirmed, discussing double peaked optical variation, mass ratios and X ray eclipse

22 p2916 A73-43123

Telescopic observation of Pleiades I flare stars, determining stellar magnitudes and flare brightness

23 p3037 A73-44352

Photometric study of new variable stars in NGC 2264

23 p3037 A73-44353

Photometry of selected flare stars in the Pleiades

23 p3037 A73-44354

W-Ursa-Major stars

24 p3137 A73-44825

Infrared and X-ray variability of Cyg X-3.

24 p3143 A73-45347

The 35-day cycle of HZ Herculis.

24 p3143 A73-45491

Absence of cosmic gamma-ray bursts in association with normal stellar flares.

24 p3127 A73-45492

VARIABLE SWEEP WINGS

SST aircraft wing design for sonic boom avoidance and noise reduction in airport vicinity, describing aerodynamic characteristics from wind tunnel and flying model tests

04 p0405 A73-14673

Dynamics of variable sweep wing aircraft in the course of changing geometry.

10 p1175 A73-24012

Swing wing - Modifications in variable geometry configuration concepts.

13 p1568 A73-28157

VARIABLE THRUST

Potential operating advantages of a variable area turbine turbojet. [ASME PAPER 72-WA/AERO-4]

04 p0490 A73-15906

VARIANCE [STATISTICS]

NT ANALYSIS OF VARIANCE
NT MULTIVARIATE STATISTICAL ANALYSIS

Variance estimate of random process second order moment by nonlinear correlator in presence of additive amplitude and phase modulated and normal noise processes

03 p0278 A73-14075

Uncertainties in coherent measurement of the mean frequency and variance of the Doppler spectrum from meteorological echoes.

03 p0279 A73-14525

Pulse pair estimation of Doppler spectrum parameters.

03 p0279 A73-14527

Limit analysis of structures with stochastic strength variations.

04 p0510 A73-15027

Evaluation of the performance of a variance estimation algorithm using order statistics.

04 p0471 A73-15259

Minimum variance linear filter with partial state elimination by linear transformation for reduction of

computational burden and storage requirements in Kalman filter

04 p0431 A73-15268

Variance reduction in remotely sensed multispectral data caused by random noises and systematic variations in system angular response and in apparent scene radiance

05 p0554 A73-17148

Automatic classification by sequential statistical variance and K-means clustering techniques for remote multispectral earth resource observation data

05 p0555 A73-17154

On the variance spectra and spatial coherences of equatorial winds.

07 p0846 A73-19038

Linear stochastic, multivariable, optimal control, realization and time-varying systems theory developments covering external and internal representations and variance computation problems

10 p1200 A73-24045

Optimal control theory for constant gain radar filter design with weighted variance average minimization comparable with Kalman filter performance

11 p1339 A73-26643

Expected value and variance of failure time in redundant systems.

15 p1901 A73-32264

Scintillation measurements for large integrated-path turbulence.

19 p2461 A73-38486

Unsupervised maximum likelihood classification technique multispectral remote sensing data, using two-part statistical clustering technique of sequential variance analysis

20 p2559 A73-39879

VARIATION METHOD

U CALCULUS OF VARIATIONS

VARIATIONAL PRINCIPLES

An extremum principle for three-dimensional compressible inviscid flows.

01 p0031 A73-10427

Some variational principles pertaining to non-stationary heat conduction and coupled thermoelasticity.

01 p0118 A73-11369

Linearly elastic materials theory covering kinematics, momentum balance, constitutive relation, boundary value problems and field equations

02 p0233 A73-11977

Three dimensional linear theory of thermoelasticity covering homogeneous and isotropic bodies, work, free energy, boundary value problems and variational principles

02 p0233 A73-11978

Optimal energetic characteristics of the parallel guidance method in satellite rendezvous

02 p0219 A73-12456

Nonlinear initial and boundary value problems of thermoviscoplasticity, discussing uses of Vainberg theorem and functional convolution in variational principle formulation

02 p0236 A73-12516

A variational principle for wave propagation in random media.

02 p0194 A73-12732

Convergence of consistently derived Timoshenko beam finite elements.

03 p0390 A73-13342

A variational principle for the nonrotational flow of a perfect compressible liquid in a flexible tank [ONERA, TP NO. 1178]

03 p0294 A73-13601

Theoretical formulation of finite-element methods in linear-elastic analysis of general shells.

04 p0510 A73-15026

Variational principle application to nonself adjoint lifting surface integral equation from finite element viewpoint, considering two dimensional flat plate [AIAA PAPER 73-87]

05 p0529 A73-16852

Application of the variational-difference method in solving the problems of torsion for rods of complex form

05 p0636 A73-17094

A note on a general linear initial-boundary value problem.

06 p0716 A73-17980

Variational methods in solid media linear theory of elasticity, discussing Rayleigh-Ritz method application to linear static, harmonic response and linearized stability problems

06 p0765 A73-18724

Variational mixed boundary value problems of subsonic gas flows for plane parallel symmetric Laval nozzle and transonic wedge, using singular integral equation

06 p0646 A73-18888

Determination of properties of cold stars in general relativity by a variational method.

07 p0874 A73-19065

Variational algorithms for numerical simulation of collisionless plasma with point particles including electromagnetic interactions.

07 p0854 A73-19264

Finite element analysis of buckling and post-buckling behaviors of arches with geometric imperfections.

07 p0914 A73-20211

Dual characterizations of optimal control systems governed by linear and nonlinear differential equations with dynamic constraints, using complementary variational principle in Hilbert space

07 p0846 A73-20598

Variational bounds of unidirectional fiber-reinforced composites.

09 p1157 A73-21931

Remarks on variational principle for an inviscid, perfect, magnetized plasma.

09 p1126 A73-22122

Convergent iterative smoothing algorithm for aircraft stability parameter identification from measurement, using variational optimization procedure

09 p1067 A73-22233

Thin panels stresses diffusion analysis, comparing Bleich, variational, Conway finite difference and finite element methods

09 p1159 A73-22717

Semivariational approximation for solution of parabolic differential equation with inhomogeneous mixed boundary conditions and abstract equation with operators, noting convergence and stability

09 p1113 A73-23025

Inelastic buckling of shallow spherical shells under external pressure. [ASME PAPER 72-PVP-6]

09 p1164 A73-23270

Hybrid stress finite element models for elastic continuum, discussing variational principle and macroscopic equilibrium

09 p1166 A73-23457

An operational upper air analysis using the variational method.

10 p1244 A73-23645

Optimization methods in control systems design, discussing nonlinear and linear programming, variational and maximum principles, dynamic programming and game and graph theories

10 p1242 A73-24032

Application of a variational difference method to the calculation of forced vibrations of shells of revolution

10 p1292 A73-24487

Application of general variational methods with discontinuous fields to bending, buckling, and vibration of beams.

11 p1435 A73-25436

A case of application of the variational method in the theory of the eigenfunctions of nonlinear equations

11 p1391 A73-26076

Entropy minimum principle applied to boundary value problem of non-linear heat conduction.

11 p1452 A73-26342

Nonlinear plane cavity flow past flexible barrier, deriving uniqueness theorem by variational operator formulation in terms of potentialness conditions

11 p1391 A73-26547

Variational aspect of the integration of partial differential equations for the oscillations of elastic bodies

12 p1517 A73-27097

The mathematical foundations of the finite element method with applications to partial differential equations; Proceedings of the Symposium, University of Maryland, Baltimore, Md., June 26-30, 1972.

12 p1519 A73-27921

Finite element method applied to analysis of flow over a spillway crest.

13 p1563 A73-28078

Variational treatment of the elastic constants of disordered materials.

13 p1692 A73-28169

Finite element incremental solutions for geometrically nonlinear problems based on second variations of variational functionals, discussing numerical integration and variational principles

13 p1692 A73-28228

Complementary energy method in elastodynamics.

13 p1694 A73-28249

Alpha-omega dynamo problem of electrically conducting sphere magnetic field, obtaining eigenvalues from variational principle with free decay modes as trial functions

13 p1685 A73-29365

Application of a variational method to dissipative, non-conservative problems of elastic stability.

13 p1700 A73-29376

A variational method for micromechanics of composite materials.

13 p1702 A73-29534

Energy variational principle formulation for stability determination of scalar-pressure toroidal plasma, writing potential energy as one dimensional integral

14 p1778 A73-29689

Variational principles application to finite element method in elastostatic and elastodynamic and elastodynamic small and finite displacement theories

14 p1806 A73-30178

Finite element models for continuum structural analysis, considering variational principles, element base functions and general purpose computer program

14 p1807 A73-30183

Frame structures dynamic analysis, comparing force method derived from stress and velocities varia-

tional principles with displacement method derived from Hamilton principle

14 p1807 A73-30188

Extremum principles in the dynamics of rigid-plastic bodies and mathematical programming.

14 p1813 A73-30547

Local potential variational method for analytic approximation of stagnation in plane flow, discussing generalized entropy method for accuracy improvement

15 p1957 A73-31665

Variational principles of three-dimensional linearized theory of elasticity problems with large initial deformations

15 p1953 A73-32091

Hilbert space of states, considering variational principles, linear elasticity pointwise bounds for homogeneous/inhomogeneous problems and potential theory

15 p1954 A73-32112

A variational principle for finite deformations of quasi-shallow shells.

15 p1955 A73-32162

Variational mixed boundary value problems of subsonic gas flows for plane parallel symmetric Laval nozzle and transonic wedge, using singular integral equation

15 p1824 A73-32412

Book on perturbation methods covering parameter variation, strained coordinates, averaging, multiple scale and matched and composite asymptotic expansions

15 p1902 A73-32578

Optimal control theory for systems with inequality restrictions on control and state variables and time delay, using maximum principle and variational techniques

15 p1855 A73-32580

Optimum energetic characteristics of the parallel-guidance method of bringing satellites into proximity.

15 p1941 A73-32606

The variational principle and the virial theorem for uniformly rotating magnetohydrodynamic systems.

16 p2040 A73-32926

International Conference on Variational Methods in Engineering, University of Southampton, Southampton, England, September 25-29, 1972, Proceedings. Sessions 1-4, 6-12.

16 p2076 A73-32976

On thermodynamics of deformations and variational methods in reversible thermoelasticity.

16 p2077 A73-32977

The principle of spatial variations - Application to the boundary layer theory.

16 p1999 A73-32978

Variational principles in nonlinear continuum mechanics.

16 p2036 A73-32979

Rayleigh-Ritz coefficient application in variational principle calculations of instability and flutter load of nonconservative systems

16 p2031 A73-32980

Convolutional variational principles for stress distribution in anisotropic plates of linear viscoelastic material

16 p2077 A73-32981

Application of extended variational principles to finite element analysis.

16 p2077 A73-32982

Variational principles for plate bending - A unified approach.

16 p2077 A73-32983

Finite element methods by variational principles with relaxed continuity requirement.

16 p2031 A73-32985

Mixed variational principles based on stationary potential energy concept applied to finite element method in thin shell theory

16 p2077 A73-32986

Variational methods applied to nonconservative stability problems of elastic continua.

16 p2078 A73-32995

Nonlinear shell theory, obtaining differential equilibrium equations and boundary conditions from three dimensional variational energy expression by kinematic hypothesis and Ritz method

16 p2078 A73-32996

Incremental variational method for the large displacement analysis of shells with geometric imperfections.

16 p2078 A73-32999

Stability analysis of shell-like structures by complementary energy.

16 p2078 A73-33000

Variational principle with penalty for finite element solution of model Poisson equation with homogeneous Dirichlet boundary conditions, noting convergence

17 p2199 A73-34209

Book on wave propagation in continuous media covering Hamilton principle, energy theorems, elastic waves, electromagnetic and hydromagnetic waves, Green function and nonlinear effects

17 p2211 A73-34280

Dual principles of elastodynamics finite element applications.

17 p2245 A73-34833

Solution of coupled and singular perturbation methods using duality theory.

17 p2202 A73-35358

Field penetration through a flush mounted coaxial aperture - Variational calculation.

17 p2127 A73-35630

On the existence of an optimal solution of the epsilon variational problem.

18 p2330 A73-36641

A variational principle for the laminar boundary layer theory.

19 p2421 A73-38026

Variational analysis of the flow development in the entrance region of circular tubes and parallel-plate channels.

20 p2548 A73-39527

A direct method of stability analysis for elastic circulatory systems.

20 p2621 A73-39535

Column instability under nonconservative forces, with internal and external damping - Finite element using adjoint variational principles.

20 p2621 A73-39540

Finite-element formulations for elastic plates by general variational statements with discontinuous fields.

20 p2623 A73-39558

Complementary variational principle existence condition and duality in linear and quadratic programming in Hilbert space setting, considering relationship to Kuhn-Tucker saddle point theory

21 p2724 A73-40296

The numerical solution of nonlinear parabolic problems by variational methods.

21 p2725 A73-40382

Rarefied gas flows based on variational principle.

22 p2840 A73-41741

Complementary variational principles and error bounds for biharmonic boundary value problems.

22 p2921 A73-42433

The calculation of open circular cylindrical shells with the aid of partial discretization

22 p2922 A73-42528

Papers on computer techniques for electromagnetic radiation and scattering problems via integral equation formulation covering iterative and variational methods and antenna patterns

22 p2827 A73-42839

Variational and iterative methods for waveguides and arrays.

22 p2834 A73-42843

Study of a dynamic problem in viscoelasticity and ideal plasticity with conditions of friction at the boundary

23 p3044 A73-43973

Uniqueness theorems and variational principles derivation for free viscoplastic flow and constrained plastic deformation, obtaining Castiglione theorem from boundary value problem solution

23 p3044 A73-43974

Sandwich shells nonlinear theory with stress-strain relations in tensor notation, using Hamilton principle for equations of motion and boundary conditions

23 p3044 A73-44078

Optimal stopping time for stochastic games corresponding to diffusion process, obtaining saddle point characterization via elliptical variational inequality solution

23 p2999 A73-44083

Computational methods for studying acoustic propagation in nonuniform waveguides. [AIAA PAPER 73-1006]

24 p3078 A73-44839

Differential and integral formulations of variational principles in mechanics, discussing Hoelder-Voss, d'Alembert-Lagrange, Gauss and Jourdain principles

24 p3110 A73-45246

Variational principles in dynamic thermoviscoelasticity.

24 p3151 A73-45306

The governing equations and extremum principles of elasticity and plasticity generated from a single functional. I.

24 p3152 A73-45315

Constitutive equations, creep laws, stress functions, variational principles and differential operators in dynamic and static linear viscoelasticity theory

24 p3153 A73-45496

Plasticity theory development taking into account thermodynamics of elastoplastic materials, considering existence theorems for plastic flow and variational principle for equilibrium problems solution

24 p3153 A73-45500

VARIATIONS

NT ANNUAL VARIATIONS
NT DIURNAL VARIATIONS
NT GEOMAGNETIC MICROPULSATIONS
NT GEOMAGNETIC PULSATIONS
NT MAGNETIC VARIATIONS
NT NOCTURNAL VARIATIONS
NT PERIODIC VARIATIONS
NT TWENTY-SEVEN DAY VARIATION
NT WIND VARIATIONS

VARIOMETERS

Automatic technique for extending magnetograms and for determining variometer sensitivity

05 p0573 A73-16267

Electrical operational and pneumatic /variometer/ differentiation recording of displaced volume derivative from pneumotachograph in spontaneous breathing

09 p1046 A73-22937

Earth crustal conductivity structure from micropulsation activity cycle using magnetic variometer array

12 p1488 A73-26986

Electronic developments for performance gliding.

16 p2014 A73-33023

VARIATORS

Operation, fabrication, characterization, I-V performance and application of transient voltage suppressor using metal oxide varistor

03 p0283 A73-13941

VARNISHES

The testing of varnishing products used in aeronautics

21 p2724 A73-41557

VASCULAR SYSTEM

NT AORTA
NT ARTERIES
NT BLOOD VESSELS
NT CAPILLARIES [ANATOMY]
NT GLOMERULUS
NT VFINS

Microvascular responses to alterations in oxygen tension.

01 p0009 A73-11010

Book - Peripheral vascular diseases: Diagnosis and management.

06 p0651 A73-17871

Cerebral temperature oscillations and vascular responses in man

10 p1179 A73-23805

Analysis of pressure waves as a mean of diagnosing vascular obstructions.

19 p2398 A73-37524

Changes in respiration accompanying a diencephalic vegetative-vascular syndrome under the action of a hypoxic mixture

21 p2636 A73-40280

An analogue-computer simulation of the facultative water-reabsorption process in the human kidney - A vascular role for a.d.h.

22 p2815 A73-42668

VASOCONSTRICTION

Microvascular responses to alterations in oxygen tension.

01 p0009 A73-11010

Studies of blood gas analysis at abnormal environment.

01 p0013 A73-11210

Independent effects of changes in H+ and CO2 concentrations on hypoxic pulmonary vasoconstriction.

10 p1182 A73-24565

Sustained human skin and muscle vasoconstriction with reduced baroreceptor activity.

15 p1833 A73-31344

Measurements of arterial pressure and of pressoreceptor reactions during prolonged pressure shifts in carotid arteries

24 p3062 A73-44720

VASOCONSTRICTOR DRUGS

NT SEROTONIN

VASODILATION

Studies in stress-relaxation and distensibility characteristics of small skin veins in vivo by a combined photoelectric-photographic and plethysmographic technique.

05 p0541 A73-17098

Characteristics of vasomotor alterations during brief arbitrary hyperventilation according to data from rheographic and plethysmographic studies

11 p1314 A73-25041

Changes in microvascular diameter and oxygen tension induced by carbon dioxide.

11 p1317 A73-26116

Xenon 133 measurement of cerebral volumetric circulation rates during papaverin and intensin vasodilation of canine and feline intracranial vessels, showing vessel resistance reduction

13 p1576 A73-29074

A new method of measuring arterial dilation and its application.

22 p2815 A73-42669

The presence in the heart of compounds which participate in the neurohumoral regulation of coronary circulation

24 p3059 A73-44769

VASOMOTOR NERVOUS SYSTEM

U NERVOUS SYSTEM

VECTOR ANALYSIS

NT COLLINEARITY
NT COPLANARITY
NT CURL [VECTORS]
NT VORTICITY

Book on electromagnetic field theory covering free space Maxwell equations, Lorentz force law, vector analysis, Laplace equation, lossless transmission lines and dipole antennas

03 p0343 A73-13988

VECTOR CALCULUS

- Nonlinear shell theory with finite rotation and stress-function vectors.
[ASME PAPER 72-APM-CC] 05 p0633 A73-16533
Vector characteristics use in dimensional analysis, solving Huntley method inconsistencies
07 p0916 A73-20438
- Methods of quadratic Liapunov vector-function construction for linear systems
12 p1525 A73-27895
- Principle of virtual work and equations of shells
14 p1805 A73-29761
- Waveform vector analysis of orthogonal electrocardiograms - Quantification and data reduction.
16 p1975 A73-33115
- Flux-corrected transport - A minimum-error finite-difference technique designed for vector solution of fluid equations.
17 p2202 A73-35145
- Methods of constructing quadratic Lyapunov vector functions for linear systems.
18 p2330 A73-36600
- Computer program for determining system resonance frequencies and damping via numerical analysis of vector modal response loci plots
21 p2783 A73-40290
- Proposal of a new criterion for evaluating the adequacy of models
21 p2669 A73-40499
- Vector theory of the glory and rainbow
21 p2731 A73-40742
- Analysis of force interaction in magnetolectric torque sensors
22 p2860 A73-42364
- The recursive generation, differentiation, and integration of Hermite interpolation polynomials together with an example concerning the application of the method
23 p3044 A73-44048
- Study of the existence of compact laminar for certain complex analytical laminated structures
23 p2999 A73-44097

VECTOR CALCULUS

U VECTOR SPACES

VECTOR CONTROL

U DIRECTIONAL CONTROL

VECTOR SPACES

NT ADJOINTS

NT BANACH SPACE

NT CANONICAL FORMS

NT EIGENVALUES

NT EIGENVECTORS

NT HILBERT SPACE

NT JORDAN FORM

NT MATRICES [MATHEMATICS]

NT STATE VECTORS

NT STOKES THEOREM [VECTOR CALCULUS]

NT VECTORS [MATHEMATICS]

NT VORTICITY

Conformal transformation of semiordered linear space via inclusion statement, considering second order differential operators
01 p0069 A73-10068

Mathematical formulation of linear programming problem, reducing vector valued optimal management plan determination to quadratic programming problem
02 p0144 A73-12126

Method of branches and bounds as a regular method for the solution of irregular mathematical programming problems. I.
06 p0716 A73-17961

Event manifold curvature tensor as six dimensional bivector space via dyadic projections, applying to gravitational waves description
08 p0989 A73-21521

Scalar sequence spaces theory extension to vectorial sequence spaces based on bounded ensemble concept
10 p1241 A73-23763

On the duality of sequence spaces with vectorial values
10 p1243 A73-24123

Vectorial topological continuous function spaces bounded parts, constructing tunneled, quasi-tunneled and nontunneled spaces
11 p1390 A73-25865

Rockafellar duality theorem generalization to integrands over locally convex sublinear topological vector spaces, permitting Banach space transcendence
11 p1390 A73-25866

Errors associated with Rodrigues-Hamilton parameters /vector space basis quaternions/ calculation by numerical integration of kinematic equations of moving body orientation
11 p1400 A73-26454

Phase coordinates estimation optimization, deriving observable vector relations from sampling laws
12 p1524 A73-27417

Estimation of the state vector of a linear plant by the method of distance minimization in metric space on the basis of continuous measurement of plant inputs and outputs
12 p1485 A73-27894

Hilbert boundary value problem solution for piecewise holomorphic vector in singly connected region with Liapunov contour bound
15 p1900 A73-32086

Book - Non-homogeneous boundary value problems and applications. Volume 3.
17 p2200 A73-34464

Type-III Einsteinian void spaces with a G/2 Abelian group of motions and solvable G/3 groups
17 p2212 A73-35565

The method of plane-axial vector coordinates in the determination of velocities in the general motion of a rigid solid
19 p2459 A73-37643

Certain results of the application of the method of sections to typical classes of nonlinear automatic systems
20 p2541 A73-38985

Multicriterial optimization problems solution by method of effective sets defined in criterion or variable vector spaces, noting advantages over global criteria and additive value methods
21 p2670 A73-40992

Geometrical properties of normed spaces, associated with the convexity and smoothness moduli of a unit sphere
24 p3106 A73-45353

VECTOCARDIOGRAPHY

Automated system of storing and processing vectorcardiograms
01 p0012 A73-10660

Usefulness of vectorcardiography combined with His bundle recordings and cardiac pacing in evaluation of the preexcitation /Wolff-Parkinson-White/ syndrome.
02 p0138 A73-12445

Diagnostic value of vectorcardiogram in strictly posterior infarction.
03 p0268 A73-13891

Clinical electrocardiographic and vectorcardiographic diagnosis of left posterior subdivision block, isolated or associated with RBBB.
04 p0409 A73-15200

Mathematical analysis of body surface potentials.
04 p0412 A73-15646

Orthogonal versus planar vector-electrocardiography.
07 p0785 A73-19930

A model to predict respiration from VCG measurements.
07 p0787 A73-20578

Cardiac potential measuring and recording instrument with 240 probes, presenting circuit and block diagrams
10 p1184 A73-24422

Depolarization phase of the spatial velocity electrocardiogram in normal and ventricular overloading.
10 p1185 A73-24900

Computer analysis of the orthogonal electrocardiogram and vectorcardiogram in 939 cases with hypertensive cardiovascular disease.
11 p1324 A73-26361

Waveform vector analysis of orthogonal electrocardiograms - Quantification and data reduction.
16 p1975 A73-33115

Phase progression of the QRS complexes in electrocardiograms versus the inscribing directions of the QRS loops in vectorcardiograms.
16 p1975 A73-33116

A new method for diagnosing myocardial damage in patients with normal electrocardiograms and vectorcardiograms.
16 p1973 A73-33375

Book on vectorcardiography covering equipment, techniques, lead systems and abnormalities associated with atrial and ventricular hypertrophy, bundle branch blocks, myocardial infarction and arrhythmia
17 p2114 A73-34452

Current status of correlations between vectorcardiogram and hemodynamic data.
18 p2274 A73-36526

Russian book - Integral topograms of heart potentials.
22 p2807 A73-42489

VECTORS [MATHEMATICS]

NT EIGENVECTORS

NT STATE VECTORS

NT VORTICITY

Estimate of the probability density and distribution function of a scalar product of vectors with independent, normally distributed components
07 p0845 A73-20050

Optimal control system design with respect to vector quality criterion, noting linear system described by differential equations
09 p1068 A73-22560

Boundary value problems for a nonlinear differential equation with a deviating argument of neutral type
10 p1241 A73-23742

Possibility of determining the secular variation of geomagnetic field components from the distribution of variations of the absolute value of the total vector.
10 p1212 A73-24234

Linear system unperturbed motion stability in finite time interval, formulating first approximation vector matrix equation
11 p1397 A73-25049

Method of Liapunov vector functions in the analysis of complex systems with distributed parameters /Survey/
11 p1398 A73-25617

Geometric interpretation of conditions for resonance wave interactions valid under nondispersive conditions, noting relevance for acoustic waves in crystals and slowness vectors
11 p1400 A73-26278

Coordinate systems standardization in stress analysis, considering vector orientation definitions
11 p1444 A73-26378

Nonlinear vector matrix differential equations for automatic control systems dynamics, discussing stability, dissipativity and convergence
14 p1768 A73-30344

Constitutive equations and directors in plastic anisotropic viscoplastic media
15 p1947 A73-31366

Koethe spaces topological properties, considering vector functions integration
15 p1899 A73-31666

Vector field representation of curved elastic membranes oscillatory motions, particularizing equations of motion for small displacements from equilibrium configurations
16 p2076 A73-32937

Examination of the parameters in solutions to systems of two-dimensional nonlinear Volterra-type integral equations
17 p2203 A73-35590

Vector partition of probability /Brier/ score providing reliability and resolution measures of weather forecasts
18 p2332 A73-36703

Approximate methods for the mathematical description and analysis of processes controlling the spectral characteristics of random vector signals
20 p2542 A73-39047

Asymptotic representation of the fundamental solution of an elliptic equation with a small parameter in the presence of a higher derivative
20 p2582 A73-39474

Rate of convergence of the distribution of the maximum of successive sums of independent variously distributed random vectors toward the limiting law
20 p2583 A73-39476

Concentration functions of finite-dimensional and infinite-dimensional random vectors
22 p2882 A73-42649

VEGETATION

The use of stress situations in vegetation for detecting ground conditions on aerial photographs.
03 p0301 A73-13844

Measurements regarding the color of aerial photographs in studies of the vegetation
06 p0695 A73-18437

Physiological factors and optical parameters as bases of vegetation discrimination and stress analysis.
16 p2003 A73-33355

Satellite imagery in national resource surveys and vegetation growth monitoring on mine dumps from ERTS-1 data
18 p2311 A73-36151

Eutrophication assessment using remote sensing techniques.
20 p2558 A73-39861

Multispectral scanner imagery in aerial photography of plant communities, discussing reflectance effects, digital processing, vegetation types, classification errors and spectrum analysis
20 p2561 A73-39901

Plant canopy models for simulating composite scene spectroradiance in the 0.4 to 1.05 micrometer region.
20 p2562 A73-39906

VEGETATION GROWTH

NT CROP GROWTH

VEHICLE WHEELS

NT NOSE WHEELS

Lunokhod 1 vehicle chassis design and mobility characteristics in Mare Imbrium, discussing wheels, suspension, movement control, traction, cohesion and lunar surface maneuverability
02 p0151 A73-12235

Rubber friction effect on vehicle tire force-slip and braking behavior in terms of peripheral and sideslip components and structural and operational parameters
03 p0251 A73-13242

Automatic machine test equipment and procedures for hydraulic systems, tractor shafts and automobile wheels
13 p1625 A73-29135

Russian book - Aircraft wheel and braking system designs.
19 p2384 A73-37768

VEHICULAR TRACKS
The development of light tracked vehicles for lunar and planetary exploration
08 p0952 A73-20781

VEINS

- Telemetry of venous blood pressure at rest and at muscle activity during running. 03 p0271 A73-14290
- Studies in stress-relaxation and distensibility characteristics of small skin veins in vivo by a combined photoelectric-photographic and plethysmographic technique. 05 p0541 A73-17098
- Mixed-venous oxygen tension by nitrogen rebreathing - A critical, theoretical analysis. 06 p0654 A73-18336
- Vein wall changes as the main cause of acute disturbance of blood circulation in the Vena centralis retinae system 15 p1833 A73-31173

VELA SATELLITES

- Vela 4 Lyman-alpha observations - Evidence for an aspherical hydrogen geocorona at 18 earth radii. 04 p0492 A73-15528

VELOCITY

- NT ACOUSTIC VELOCITY
- NT AIRSPEED
- NT ANGULAR VELOCITY
- NT CRITICAL VELOCITY
- NT ESCAPE VELOCITY
- NT EXHAUST VELOCITY
- NT FLOW VELOCITY
- NT GROUND SPEED
- NT GROUP VELOCITY
- NT HIGH SPEED
- NT HYPERSONIC SPEED
- NT LANDING SPEED
- NT LIGHT SPEED
- NT LOW SPEED
- NT ORBITAL VELOCITY
- NT PHASE VELOCITY
- NT PROPAGATION VELOCITY
- NT RADIAL VELOCITY
- NT RELATIVISTIC VELOCITY
- NT ROTOR SPEED
- NT SOLAR VELOCITY
- NT SUBSONIC SPEED
- NT SUPERSONIC SPEEDS
- NT TERMINAL VELOCITY
- NT TIP SPEED
- NT TRANSONIC SPEED
- NT WIND VELOCITY
- Medium-velocity and electric-current concepts in restricted relativity 19 p2459 A73-37535

VELOCITY DISTRIBUTION

- Velocity structures in hydrogen profiles. 01 p0096 A73-10315
- Curves of spatial isocorrelations and space-time isocorrelations relative to longitudinal velocity fluctuations in a smooth circular duct 01 p0031 A73-10418
- Mixed convection over a heated horizontal plane. 01 p0120 A73-10440
- An investigation of high-wavenumber temperature and velocity spectra in air. 01 p0039 A73-10448
- A nonlinear analysis of pulsatile flow in arteries. 01 p0011 A73-10449
- Stellar proper motion effects on precession and galactic rotation constants determination, considering star velocity fields in solar neighborhood 01 p0098 A73-10583
- The interaction of primordial gravitational waves with groups of galaxies. 01 p0098 A73-10585
- Analytical method of gasdynamic semibounded-space parameter computation allowing for velocity profile inhomogeneity and turbulent combustion of condensed systems 01 p0121 A73-10619
- Velocity variation of a star as a purely discontinuous random process. III Stars with different masses in an open cluster 01 p0100 A73-10711
- Representation of a $1/N$ power law boundary layer in the sheared flow acoustic transmission problem. 01 p0033 A73-10783
- Velocity, temperature and component concentration distributions in laminar boundary layer at blown surface for binary mixture flow 01 p0034 A73-10957
- Turbulent swirling wake behind spinning axisymmetric body of revolution having axis aligned with free stream direction, obtaining velocity profiles variations 01 p0004 A73-11136
- Exact vorticity solutions of the incompressible Navier-Stokes equations. 01 p0034 A73-11358
- The empirical determination of line source functions, beta-L-values, and the microturbulent and convective velocity components as functions of depth in the photosphere-chromosphere transition region. 01 p0107 A73-11378
- Trapped gravity waves velocity oscillations in solar plagues under magnetic field, comparing with Bilderberg continuum atmosphere 01 p0108 A73-11386

Determination of the molecular velocity distribution function in a molecular beam by the method of mechanical selection 02 p0194 A73-11606

Infinite set of velocity fields to describe geomagnetic field lines and interpret discrepancy in plasma sheet motion observations during substorms 02 p0157 A73-11754

Special features of the calculation of electromechanical instrument servosystems with velocity feedbacks 02 p0148 A73-11861

Statistical mechanics of the Burgers model of turbulence. 02 p0153 A73-12039

Turbulence measurements with a laser anemometer measuring individual realizations. 02 p0168 A73-12057

MHD equations for velocity distribution of magnetic field motion in conducting fluid, noting evolution equations of geomagnetic field 02 p0164 A73-12555

Finite element technique application for determining velocity field of three dimensional fluid continuum and pressure distribution of lubrication film described by Reynolds equation 03 p0289 A73-12872

Integral transformations and conformal mapping for velocity distribution of steady two dimensional potential flow along given profile curve 03 p0241 A73-12904

Alfvén wave induced bulk velocity amplitudes in lower solar atmosphere, discussing relationship between energy flux, bulk velocity, wavelengths and scale height 03 p0360 A73-12944

Temperature, velocity, and stress distribution in thermo-viscoplastic boundary layers 03 p0386 A73-13145

Boundary value problem for flow equation of multiphase viscous fluid with given velocity distribution, noting equations of motion for incompressible micropolar fluid flow 03 p0291 A73-13164

Optimum performance of static propellers and rotors. 03 p0242 A73-13308

Some details of the pressure and velocity fields near the nozzle of a round turbulent jet. 03 p0293 A73-13311

Saturn ring dynamics via numerical simulations of jet streams, discussing non-Maxwellian velocity distribution and energy consumption decrease with thickness 03 p0373 A73-13355

Erosive burning rate perturbation in colloidal propellant slab combustor channel as function of lateral velocity gradient and chamber pressure [AIAA PAPER 72-1108] 03 p0351 A73-13423

Hydrodynamics and heat transfer in a fluid with an asymmetrical stress tensor 03 p0398 A73-13722

Two-dimensional unsteady flow by hydraulic analogy. 03 p0295 A73-13769

Study of the asymptotic behavior of axial perturbation velocities in the vicinity of singularities 03 p0245 A73-13770

German monograph - Axisymmetric free jets and free-jet flames and a numerical procedure for calculating them. 03 p0398 A73-13810

Three dimensional ideal incompressible fluid flows under small velocity perturbation, using Euler equations linearized with respect to steady flow 03 p0296 A73-14048

Boltzmann equation model approach for prediction of velocity profiles and gas flow rates through trapezoidal microgaps [ASME PAPER 72-LUB-15] 03 p0297 A73-14331

Use of airborne radar to evaluate hurricane modification experiments. 03 p0338 A73-14513

Doppler radar measurements of the velocity field associated with a turbulent clear air layer. 03 p0338 A73-14532

Inverse problem in the theory of turbulence filtering by the radar pulse volume. 03 p0279 A73-14538

Radar observations of intense undulance in an evaporating cloud layer. 03 p0339 A73-14541

Observation and spectral analysis of instantaneous signals of velocity fluctuation in the laminar boundary layer 03 p0297 A73-14602

Velocity distribution of plasma electrons in the negative H₂- and He-glow with superimposed longitudinal magnetic field. 04 p0477 A73-14897

Ion velocity distributions in the auroral ionosphere. 04 p0440 A73-14966

Hydrodynamic and kinetic instability and oscillations of plasma with non-Maxwellian particle velocity distribution, noting laboratory and cosmic plasmas 04 p0478 A73-15018

Velocity profiles and wall shear stress of three-dimensional turbulent boundary layers. [ONERA, TP NO. 1134] 04 p0403 A73-15092

Mean velocity and turbulence intensity profiles of asymptotic sink flow turbulent boundary layers, measuring Reynolds and wall shear stresses 04 p0434 A73-15166

Droplets size and velocity distribution in air-kerosene atomized spray flame as function of fuel-air ratio from double image high speed photographic measurements [ASME PAPER 72-WA/HT-25] 04 p0519 A73-15829

Wall shear stress inference from two and three-dimensional turbulent boundary layer velocity profiles. [ASME PAPER 72-WA/FE-4] 04 p0434 A73-15840

Eddy-viscosity distribution in thick axisymmetric turbulent boundary layers. [ASME PAPER 72-WA/FE-18] 04 p0435 A73-15845

Calculation of interacting turbulent shear layers - Duct flow. [ASME PAPER 72-WA/FE-25] 04 p0435 A73-15849

Theoretical low-speed particles collision with symmetrical and cambered aerofoils. [ASME PAPER 72-WA/FE-35] 04 p0404 A73-15852

Inverse problem approach to the design of short two-dimensional diffusers. [ASME PAPER 72-WA/GT-6] 04 p0404 A73-15870

Quasi-three-dimensional calculation of velocities in turbomachine blade rows. [ASME PAPER 72-WA/GT-7] 04 p0490 A73-15871

Free turbulent mixing in axial pressure gradients. [ASME PAPER 72-WA/APM-31] 04 p0435 A73-15888

The transpired turbulent boundary layer in an adverse pressure gradient. 04 p0520 A73-15936

Influences of free stream turbulence on mean velocities of turbulent boundary layer without pressure gradient. 04 p0435 A73-15972

Effect of accommodation coefficient on thermal creep flow of rarefied gas. 04 p0436 A73-15973

Electron velocity distribution function in the ionosphere 05 p0568 A73-16252

Similarity solution for the curved two-dimensional jet. [ASME PAPER 72-APM-II] 05 p0564 A73-16527

The swirling turbulent jet. [ASME PAPER 72-FE-18] 05 p0564 A73-16544

Isentropic compressible flow equations for pressure and velocity distributions across vortex in axial core mass flow, noting atmospheric circulation and pressure effects [AIAA PAPER 73-106] 05 p0529 A73-16866

Mean radial velocity of Virgo galactic cluster from red shift data, approximating velocity distribution of elliptical-lenticular and spiral galaxies 05 p0622 A73-17074

Kinematic eddy viscosity at low Reynolds numbers. 05 p0567 A73-17111

Numerical model for calculation of the geopotential field with a new generalized vertical velocity profile incorporating the influence of orography 05 p0572 A73-17352

Measurement of the velocity profile in a turbulent boundary layer on a permeable plate. 06 p0643 A73-17409

Solar wind rotational and tangential velocity discontinuities in anisotropic media, discussing Ivanov, Burlage and Hudson data 06 p0742 A73-17528

Hot wire measurement of velocity gradients in a fluid flow. [AIAA PAPER 73-50] 06 p0692 A73-17626

An investigation of shock strengthening in a conical convergent channel. 06 p0684 A73-17706

Turbulent boundary layers with negligible wall stress - A singular-perturbation theory. 06 p0686 A73-17988

Airfoil profile determination in inverse hydrodynamics problem for given flow velocity distribution, discussing univalent solvability conditions 06 p0686 A73-18067

On the determination of the height of the Ekman boundary layer. 06 p0720 A73-18326

Instability of a two-layer geostrophic flow with an antisymmetric velocity profile in the upper layer 06 p0691 A73-18728

Velocity distribution of quasi-steady and steady flow of ideal incompressible fluids with congruent streamlines, investigating conditions for vortex and irrotational flow 07 p0809 A73-19017

Velocity dispersions in galaxies. II - The ellipticals NGC 1889, 3115, 4473, and 4494. 07 p0873 A73-19054

German monograph - Free convection of air in a horizontal circular gap in the case of temperature- and pressure-dependent density.

07 p0920 A73-19579

Velocity and resistance profiles for unsteady turbulent flow in rough pressure channels, using Prandtl hypothesis

07 p0811 A73-19614

Highly uniform inlet velocity profile influence on conical diffuser characteristics

07 p0774 A73-19615

Circular conical diffuser inlet velocity profile effect on efficiency, presenting experimental results for different cone angles and expansion ratios

07 p0774 A73-19616

Flow of an ideal incompressible ponderable fluid around a thin profile placed under a free line. I, II

07 p0811 A73-19998

On unsteady magnetohydrodynamic boundary layers in a rotating flow.

07 p0859 A73-20290

Supersonic-hypersonic motion around a porous circular cone

07 p0776 A73-20615

Simulation of velocity profiles by shaped gauze screens.

08 p0953 A73-20717

Vertical velocity field oscillations in photospheric sunspot umbra interpretation in terms of gravity or acoustic waves traveling along magnetic field lines

08 p1001 A73-20756

H alpha observations of vertical velocity distribution periodic oscillations in sunspot, noting transverse waves formation and propagation to penumbral boundary

08 p1001 A73-20757

Observations of sunspot umbral velocity oscillations.

08 p1001 A73-20758

The kinematical distribution of dark clouds surveyed in the 4830 MHz H₂CO line.

08 p1004 A73-20904

The distribution of neutral hydrogen and the velocity field of the galaxy NGC 3109.

08 p1004 A73-20905

Unsteady boundary layer flows at general three-dimensional stagnation points.

08 p0954 A73-21008

Numerical calculation of the laminar inlet flow. I.

08 p0954 A73-21011

Velocity distribution of the turbulent motion of a fluid between two plane-parallel walls

08 p0954 A73-21175

Unsteady laminar boundary layers calculation for arbitrary velocity distributions at inner boundary in presence of suction/blowing through porous surface

08 p0954 A73-21176

Boundary layers calculation for nonporous surface extended to porous with suction by replacing velocity distribution with longitudinal pressure gradient

08 p0954 A73-21179

Determination of the elements of an orbit from known values of the velocity vector at three different moments of time

08 p1012 A73-21550

Flow parameters and cylinder elongation effects on turbulent boundary layer characteristics for compressible fluid flow, calculating velocity distribution

08 p0956 A73-21602

Effect of the plasma inhomogeneity on the nonlinear damping of monochromatic waves.

09 p1126 A73-22281

Buoyancy effects in a turbulent boundary layer.

09 p1071 A73-22330

Calculation of forces on stores in the vicinity of aircraft.

09 p1028 A73-22433

Velocity distribution in tubes of circular cross section

09 p1072 A73-22846

Number of gust series in turbulent velocity pulsations

09 p1115 A73-22992

Laminar boundary layer on a cone near a plane of symmetry.

09 p1029 A73-23442

Mean velocity profiles in three-dimensional incompressible turbulent boundary layers.

09 p1029 A73-23445

Prandtl's boundary-layer theory from the viewpoint of a mathematician.

10 p1172 A73-23866

Model solar atmosphere with quiet component involving supergranular velocity field in corona-chromosphere transition layer and vertical magnetic field

10 p1279 A73-24140

Hot-wire anemometer probe operation in constant current in continuous high-temperature hypersonic turbulent boundary layer, computing velocity and temperature fluctuations

10 p1205 A73-24254

Unsteady MHD duct flow by the finite element method.

10 p1256 A73-24289

Statistical laws governing the wind velocity distribution in the atmospheric boundary layer

10 p1246 A73-24373

An upper bound solution for rectangular plate in plane stress compression.

10 p1292 A73-24640

Spatial amplitude distribution of vibrating ribbon two dimensional wake mean, periodic and random velocity components measured in uniform flow by hot-wire anemometry

10 p1173 A73-24828

Unsteady two dimensional flow within circular cavity with arbitrary velocity distribution on cylinder wall, investigating recirculating flow initiation

10 p1210 A73-24838

Velocity field determination for limitless steady boundary layer on circular cylinder and swirling flow produced by generalized vortex

10 p1210 A73-24843

Recent measurements of flow using nuclear magnetic resonance techniques.

10 p1185 A73-24855

Errors in the velocity-area method of measuring asymmetric flows in circular pipes.

10 p1221 A73-24861

On the application of Cramer's theorem to axisymmetric, incompressible turbulence.

10 p1284 A73-24909

Symmetrical airfoils optimized for small flap deflection.

10 p1174 A73-24915

Unsteady boundary layer flow of homogeneous viscous fluid in nonrotating environment or bounded by oscillating flat plates, determining velocity field by exact solutions

11 p1346 A73-25165

Frequencies and virtual masses of a liquid in a cavity formed by eccentric cylinders

11 p1347 A73-25391

Flow and velocity fields simulation by calculating dynamic loads in moving liquid from pressure distribution, viscosity and gravitational acceleration [AIAA PAPER 73-409]

11 p1441 A73-25537

Low velocity wind tunnel design with adjustable pressure gradient, determining contraction section wall contour to avoid boundary layer separation via velocity distribution improvement

11 p1347 A73-25714

Some considerations on the atmospheric internal boundary layer over the ground surface.

11 p1394 A73-25725

On the turbulent thermal diffusion parallel to a plane wall for y^+ equals 2 to 300

11 p1451 A73-25870

The effect of the earth's bow shock and magnetosheath on the interaction of a discontinuity in the solar wind with the magnetosphere.

11 p1357 A73-25924

Analysis of the static modes of a magnetron with allowance for electron-velocity scatter

11 p1332 A73-26163

Calculation of nozzle flows using Padé fractions.

11 p1303 A73-26386

Sonic line for a coaxial axisymmetric nozzle.

11 p1303 A73-26403

On the evolution of turbulent magnetic fields in a collision dominated plasma.

11 p1406 A73-26559

Velocity gradients and microturbulence in Cepheids.

11 p1427 A73-26607

Analysis of the behavior of the electron velocity distribution function of beam interacting with a plasma

12 p1527 A73-26933

Magnetic field line velocity associated with Euler potentials set, considering flux preservation properties of particle motion

12 p1489 A73-27000

Two-dimensional steady magneto-fluid-dynamic flows with orthogonal magnetic and velocity field distributions.

12 p1527 A73-27020

Graphic-interactive analysis of the velocity field around blade cascades for turbomachines

12 p1458 A73-27387

Ray method for solving dynamic problems in viscoelastoplastic media

12 p1553 A73-27415

Compressional wave velocity profile of lunar near-surface and crust derived from seismic refraction data at Apollo 14 and 16 sites

12 p1541 A73-27486

Velocity, temperature and component concentration distributions in laminar boundary layer at blown surface for binary mixture flow

12 p1487 A73-27533

Investigation of the influence of temperature and velocity fields on the quality of an astronomical image

12 p1546 A73-27864

High Galactic latitude intermediate-negative velocity neutral hydrogen properties, noting large complexes and systematic velocity pattern

13 p1671 A73-28029

The pressure and velocity fields of convected vortices.

13 p1599 A73-28067

Boundary layer due to sphere rotation in a medium at rest

13 p1599 A73-28068

MHD free convective flow in a vertical channel.

13 p1663 A73-28164

Some comparisons between observed wind profiles at Riso and theoretical predictions for flow over a homogeneous terrain.

13 p1652 A73-28277

RF field space-time modulation devices to obtain molecular beam velocity distribution and Zeeman pattern components shift

13 p1662 A73-28349

Conjugating a Chaplygin operator with a differential operator in gasdynamics

13 p1563 A73-28443

Influence of wall proximity on hot-wire velocity measurements.

13 p1613 A73-28522

A numerical method for highly accelerated laminar boundary-layer flows.

13 p1600 A73-28608

A note on the effect of Hall currents on hydromagnetic flow near an accelerated plate.

13 p1664 A73-28617

Flow of viscous fluid at small Reynolds numbers past a porous body.

13 p1601 A73-28623

Near-satellite neutral gas temperature determination from measurement of molecular nitrogen velocity distribution

13 p1687 A73-28630

Parameter calculation for laminar incompressible fluid jet expanding in gradient slipstream along moving surface, determining velocity distribution in jet axis

13 p1601 A73-28736

Effects of free stream velocity profile on turbulent boundary layer, with some reference to the effects of free stream turbulence.

13 p1602 A73-29013

Periodic gust and wake induced unsteady air flow, calculating velocity variation with distance from rotor blade for cascade effect

13 p1566 A73-29028

Translational temperature and atomic velocity distribution functions in rarefied binary gas jets by electron beam excited Doppler line measurement

13 p1618 A73-29163

Turbulent velocity and pressure fields in boundary-layer flows over rough surfaces.

13 p1604 A73-29264

Numerical experiments on the stability of spherical stellar systems.

13 p1685 A73-29358

Effect of radial total pressure gradients on the Macromolecular number distribution in turbomachines

13 p1567 A73-29450

Solar wind velocity fluctuations with heliocentric distance beyond one AU via nonlinear fluid dynamic equations numerical solution, considering interplanetary plasma turbulence effects

14 p1786 A73-29556

Derivation of a chain of equations for characteristic functions of a turbulent velocity field from the Hopf equation

14 p1744 A73-30023

Two-dimensional bubbles in slow viscous flows. II.

14 p1744 A73-30178

Initial plastic deformations due to surface defects, deriving corresponding elastic distortions and velocity fields of medium from equilibrium equations

14 p1812 A73-30544

Magnetospheric collisionless drift waves from AT-5 electron and proton velocity distribution measurements, comparing with predicted perturbation distribution function

14 p1750 A73-30659

Velocity profile determination in a turbulent boundary layer

14 p1746 A73-30795

A numerical model of the geopotential field with a new profile of the generalized vertical velocity that takes orography into account.

15 p1865 A73-31002

Experimental investigation of the laminar flow along a straight 135-deg corner.

15 p1861 A73-31124

Probability distribution of the concentration and intermittency in turbulent jets

15 p1862 A73-31286

Experimental investigation of the velocity structure and of hydraulic resistances in unsteady forced turbulent flows

15 p1862 A73-31287

Experimental study of wakes produced by hyper-sonic cones in free flight.

15 p1823 A73-31312

Solar nearby star velocity field variation model from Oort constants derivation with application to faint stars motion analysis and galactic center distance calculation

15 p1933 A73-31397

Motion of a magnetized fluid between parallel plates
15 p1918 A73-31408

Velocity structure of a flow in a magnetic field periodically varying along the flow
15 p1918 A73-31413

Incidence of pulsation wind velocities exceeding a given value
15 p1904 A73-31609

Reynolds equation solutions for transverse velocity and pressure variations in incompressible fluids within journal bearings and between rotating eccentric cylinders
15 p1882 A73-31639

Transient forced convection heat transfer from an isothermal flat plate.
15 p1957 A73-31664

A simple estimate of the effect of ejector length on thrust augmentation.
15 p1824 A73-31745

Experimental investigation of longitudinal flow over a flat plate during strong blowing of a foreign gas under isothermal conditions
15 p1957 A73-31856

Experimental investigation of a turbulent boundary layer on a porous plate with intense injection
15 p1824 A73-31858

Magnetohydrodynamic boundary layer control with suction or injection.
15 p1864 A73-31931

Plasma fine velocity structure and dynamics from diffraction pattern of interplanetary radio sources scintillation
15 p1919 A73-31959

Natural convective heat transfer between vertical parallel plates - One plate with a uniform heat flux and the other thermally insulated.
15 p1958 A73-32057

The large-scale velocity field, the magnetic fields, and the brightness of the solar atmosphere
16 p2057 A73-32701

Velocity field in the active regions of the sun
16 p2057 A73-32702

Three-dimensional turbulent boundary layer - Calculations and experiments
16 p1961 A73-32806

The three-dimensional turbulent boundary layer - Theoretical and experimental analysis
16 p1961 A73-32810

Galactic neutral hydrogen observations along loop III, noting loop effects on gas velocity distribution
16 p2058 A73-32835

Supersonic laminar wakes past wedge, determining pressure distribution, velocity profiles and stream line patterns in recirculation region
16 p1962 A73-32905

Subsonic free jet wind tunnel turbulence damping in settling chamber via screen, yielding uniform velocity profile and low turbulence level in nozzle exit
16 p1996 A73-33266

Three dimensional turbulent boundary layer of yawed wing suction surface in uniform flow, examining cross flow profile, velocity distribution and weighting functions
16 p1963 A73-33267

Observations of two-stream ion wave instability.
16 p2041 A73-33335

Transonic flow through a turbine stator treated as an axisymmetric problem.
[ASME PAPER 73-GT-51] 16 p1964 A73-33510

Turbulence downstream of stationary and rotating cascades.
[ASME PAPER 73-GT-80] 16 p1964 A73-33525

Computerized stream-curve method for calculation velocity distribution and stream surface twist effects for three dimensional flow through gas turbine blade passage
17 p2092 A73-34378

Low-speed performance of a compressor cascade designed for prescribed velocity distribution and tested with variable axial velocity ratio.
17 p2093 A73-34393

The determination of the static pressure and relative velocity distribution in a two-dimensional radially bladed rotor.
17 p2093 A73-34396

Effect of axial velocity variation on the subsonic flow through a compressor cascade.
17 p2094 A73-34397

Axisymmetrical turbulent boundary layer along a slender cylinder.
17 p2150 A73-34400

A modified wall wake velocity profile for turbulent compressible boundary layers.
17 p2150 A73-34439

Speed variation in the earth's rotation and the baric field of the earth's Northern Hemisphere
17 p2159 A73-34637

Two dimensional diffuser flow measurement and model calculation for curvature effects on wall pressure and boundary layer velocity distributions
[ASME PAPER 73-FE-2] 17 p2152 A73-35002

On the free shear layer downstream of a backstep in supersonic flow.
[ASME PAPER 73-FE-3] 17 p2095 A73-35003

Turbulent mixing in the developing region of coaxial jets.
[ASME PAPER 73-FE-19] 17 p2153 A73-35015

An assessment of three-dimensional turbulent boundary layer prediction methods.
[ASME PAPER 73-FE-25] 17 p2153 A73-35020

Three-dimensional flow field in rocket pump inducers. I - Measured flow field inside the rotating blade passage and at the exit.
[ASME PAPER 73-FE-33] 17 p2095 A73-35024

Solution for the pressure and temperature in thrust bearings operating in the thermohydrodynamic turbulent regime.
[ASME PAPER 73-LUBS-14] 17 p2181 A73-35394

Turbulence measurements with hot-wire anemometry in a non-homogeneous jet.
17 p2174 A73-35512

Ionospheric drift measurements. I - A new method for ionospheric drift measurements. II - The effect of random drift velocities upon the determination of ionospheric drift velocities.
18 p2304 A73-35989

Auroral ion velocity distributions using a relaxation model.
18 p2311 A73-36178

An investigation of velocity flowfields in chemical laser nozzles.
[AIAA PAPER 73-641] 18 p2322 A73-36199

Application of turbulence model equations to axisymmetric wakes.
[AIAA PAPER 73-648] 18 p2260 A73-36203

The response of unsteady boundary-layer separation to impulsive changes of outer flow.
[AIAA PAPER 73-684] 18 p2298 A73-36235

Forces acting on conical diffusers and their relation to integral performance parameters.
[AIAA PAPER 73-686] 18 p2262 A73-36237

Velocity distribution in hypersonic helium flow near the leading edge of a flat plate.
[AIAA PAPER 73-691] 18 p2262 A73-36242

Turbulent boundary-layer flow from stationary to moving surfaces.
18 p2298 A73-36313

Transformation, transmission, and reflection of plasma waves in the presence of a tangential velocity discontinuity
18 p2339 A73-36551

Two-point correlation model and the redistribution of Reynolds stresses.
18 p2300 A73-36627

Velocity profiles in steady and unsteady rotating flows for a finite cylindrical geometry. II.
18 p2300 A73-36629

Mathematical approximation of turbulent cylindrical jets: Initial core - Velocity distribution
18 p2301 A73-36690

Numerical calculation of heat exchange and frictional resistance for a turbulent flow in a tube in the case of a gas with variable physical characteristics
18 p2301 A73-36816

Certain vortical flows with variable vorticity past a circular cylinder
18 p2302 A73-37009

Possibility of computing the cloud field on the basis of vertical velocities.
18 p2334 A73-37055

Measurement of nonisotropic electron velocity distributions by laser scattering.
19 p2465 A73-37166

Experimental determination of the velocity characteristics of a pulsed crosion-type accelerator
19 p2467 A73-37366

Interference between a wing and a surface of velocity discontinuity.
19 p2376 A73-37490

The velocity profile in the wall region of a turbulent boundary layer
19 p2420 A73-37554

The method of plane-axial vector coordinates in the determination of velocities in the general motion of a rigid solid
19 p2459 A73-37643

Hypersonic polytropic transformations of an ideal fluid. II
19 p2420 A73-37645

Laminar boundary layers along an infinite flat plate with oblique suction.
19 p2420 A73-37646

Studies on the hydraulic loss in pipe bends - Results for 90-deg screw type elbows.
19 p2420 A73-37672

Third integral of motion and the velocity field for a quasi-Newtonian potential. I
19 p2486 A73-37848

Nonequilibrium velocity distributions and reaction rates in fast highly exothermic reactions.
19 p2402 A73-37897

A study on opposing jets in air stream and their flame. I - A structure of two dimensional opposing jets in the state without flames.
19 p2377 A73-37945

Earth surface turbulent boundary layer analysis, considering similarity theory limitation, flux profiles, velocity, temperature and humidity spectra, energy budgets, local isotropy, etc
19 p2427 A73-38212

Velocity distributions of rough wall turbulent boundary layers without pressure gradient.
19 p2422 A73-38284

Cross flows in bounded three-dimensional turbulent boundary layers.
19 p2422 A73-38298

Calculation and measurement of MHD generator boundary layer velocity profiles.
19 p2470 A73-38315

Effects of temperature and velocity fields on the quality of astronomical images.
20 p2608 A73-39238

Energy spectra of velocity pulsations in a turbulent boundary layer on a permeable plate
20 p2547 A73-39286

Study of shock wave and turbulent boundary layer interaction using the energy integral equation.
20 p2548 A73-39524

Study of the redshift structure of the Coma cluster.
20 p2610 A73-39580

Flow through non-uniform gauze screens.
20 p2508 A73-39811

Multiplicative rule failure in matched asymptotic expansion solutions for velocity distribution in steady incompressible flow of thin elliptic airfoils
20 p2550 A73-39814

Cumulus congestus cloud circulation velocity field measurement by balloon, comparing with radar, cameras, satellite and ground based observed meteorological model computations
21 p2728 A73-40060

Streamline curvature and velocity gradient behind curved shocks.
21 p2632 A73-40441

Demodulated Doppler signal analyzed for uniform steady flow, noting non-Gaussian phase fluctuations statistics
21 p2699 A73-40454

Nuclear spin analogue of a molecular beam maser with cavities in series.
21 p2713 A73-40469

Investigation of the laminar boundary layer at a permeable surface.
21 p2678 A73-41054

Hot-wire anemometer investigation of turbulent boundary layers at a permeable plate with injection.
21 p2678 A73-41055

Hot-wire investigation of the steady laminar wake behind a circular cylinder.
21 p2703 A73-41117

Hot-wire investigation of the steady laminar wake behind a thin flat plate placed perpendicularly to a uniform flow.
21 p2703 A73-41118

Directional plasma transport equations derived from Boltzmann equation by averaging of velocity space subset, applying to plasma confinement by external time dependent electromagnetic fields
21 p2748 A73-41127

Stellar chromospheric velocity fields and the width luminosity relations.
21 p2779 A73-41540

Drag due to regular arrays of roughness elements of varying geometry.
21 p2633 A73-41569

High temperature jet noise dependence on velocity and temperature, discussing Lighthill source term, Reynolds stresses, entropy fluctuations and velocity critical threshold
22 p2795 A73-41703

Calculation of the two-dimensional turbulent wake behind a thin obstacle
[ONERA, TP NO. 1253] 22 p2796 A73-42222

Turbulent boundary layer velocity distribution skewness and flatness factors over smooth wall compared with rough wall, discussing Reynolds shear stress fluctuations
22 p2842 A73-42231

Variation of electron velocity distribution function in the beam-plasma interaction.
22 p2891 A73-42267

Flow of a viscous gas at a slot with strong suction
22 p2796 A73-42283

An attempt to interpret the mean properties of the velocity field of young stars in terms of Lin's theory of spiral waves.
22 p2908 A73-42310

Analysis of the effects of a probe in the transonic region of a nozzle.
22 p2796 A73-42568

Luminosity and velocity distribution of high-luminosity stars near the sun. II - The young disk giants.
22 p2909 A73-42585

Shkhabzian I compact galactic cluster, discussing red shift, angular size, galactic type, velocity dispersion, mass/light ratio and photographic plates
22 p2909 A73-42586

Electric analogy method for subsonic wind tunnel contraction cone design providing uniform velocity distribution in test section, obtaining pressure distribution in cone boundary
22 p2797 A73-43000

Nozzle design for subsonic flow in axisymmetric contractions based on potential flow theory and visual observation, obtaining velocity distribution along wall
22 p2798 A73-43029

Velocity distribution in aortic flow.
22 p2811 A73-43104

Transcutaneous measurement of blood velocity profiles and flow.
22 p2817 A73-43108

Computerized simulation of isotropic three dimensional turbulence velocity field growth and energy decay based on Navier-Stokes equation numerical integration
23 p3001 A73-43588

Single particle approximation analysis of particle velocity changes influence on plasma motion across nonhomogeneous magnetic field, examining energy exchange between particles
23 p3010 A73-43662

Analytic solutions for potential flow over a class of semi-infinite two-dimensional bodies having circular-arc noses.
23 p2940 A73-43931

Turbulent mean emf in presence of nonvanishing mean conducting fluid flow, modifying Green tensor of induction equation for constant strain rate velocity fields
23 p2969 A73-44050

The effects of the exit velocity profile on the flow of a circular jet exhausting normal to the free stream.
23 p2969 A73-44125

Density and velocity fluctuations in young nebulae of Orion type
23 p3035 A73-44232

Velocity field determination in meridional plane of potential field using third isolating integral of motion
23 p3035 A73-44238

Equilibrium configurations of electron beams in a plasma
23 p3014 A73-44338

Plasma fine velocity structure and dynamics from diffraction pattern of interplanetary radio sources scintillation
24 p3132 A73-44484

Solar wind proton thermal anisotropy association with moments of proton velocity distribution and dependence on temperature decrease
24 p3125 A73-45105

Space-time autocorrelation and cross correlation coefficients for transverse turbulent velocity fluctuations in pipe flow
24 p3080 A73-45451

Laser Doppler velocimeter measurement of laminar velocity profiles for developing MHD flow in rectangular duct, noting inlet effects on flow development
24 p3118 A73-45464

Linearized theory of two and three dimensional incompressible viscous flows based on locally unstable velocity profiles related to boundary layer instability mechanism
24 p3081 A73-45546

VELOCITY ERRORS

Errors in measuring the angles of rotation of an object with a triaxial gyro stabilized platform with allowance for its drift
09 p1115 A73-22343

Correction of a spacecraft with a static corrective thruster chamber
11 p1431 A73-26465

Differential velocity effects on converging target intersection time estimation accuracy, considering plane conditions and air traffic controller experience
16 p1975 A73-32900

On the correction of anemometric measurements in air flows of slowly varying temperature
19 p2429 A73-37529

Errors of a single-axis gyrostabilizer as an angular velocity integrator
22 p2860 A73-42366

VELOCITY FIELDS

U VELOCITY DISTRIBUTION

VELOCITY MEASUREMENT

NT WIND VELOCITY MEASUREMENT

Measurement of the macroscopic velocity of the neutral component of weakly ionized gas in the crossed fields.
01 p0081 A73-10116

Mathematical and statistical modeling of wall flow turbulence, considering experimental velocity and temperature measuring techniques
01 p0031 A73-10292

Possibilities of measuring the velocity of circulation of the magnetospheric plasma with the help of a quadrupole probe used in the vicinity of the low hybrid frequency
01 p0035 A73-10326

Photoelectric determination of radial velocities.
01 p0047 A73-10517

The spectrum of the compact galaxy III Zw 43.
01 p0098 A73-10557

Two-stream heterogeneous mixing measurements using laser Doppler velocimeter.
01 p0050 A73-10741

Measurement of particle size, number density, and velocity using a laser interferometer.
01 p0053 A73-11226

Quasi-steady heat transfer equation for frequency response of wedge shaped hot film sensors for flow temperature, velocity and turbulence measurement
02 p0166 A73-11711

Position locus by measurement of the ascension speed of a real or fictitious star
02 p0190 A73-12011

Laser Doppler shift velocity correlation meter operation in turbulent flow analyzed by optical mixing theory
02 p0153 A73-12049

Laser interferometer for measuring high velocities of any reflecting surface.
02 p0171 A73-12818

A polarimetric method of measuring radial velocities.
02 p0171 A73-12830

Interplanetary gas. XVII - An astrometric determination of solar-wind velocities from orientations of ionic comet tails.
03 p0361 A73-12947

Measurement of radial velocities with coude spectrograph of the 152-cm telescope of the Haute Provence Observatory
03 p0371 A73-13223

Laser anemometry developments review covering reference-beam, fringe and single-beam modes optical arrangements, signal processing systems and light scattering particles
03 p0308 A73-13535

Doppler turbulence spectrum and intensity measurement in stalactites region at base of cloud deck cooled by evaporation and destabilized by convection
03 p0339 A73-14539

The effects of a finite radar pulse volume on turbulence measurements.
03 p0279 A73-14540

Gas velocity measurements within a compressor rotor passage using the laser Doppler velocimeter.
04 p0451 A73-15866

Venus atmosphere wind velocity profiles from analysis of Venera 7 descent stage radial velocity measurements
05 p0612 A73-16086

Void fraction measurement based on gas-liquid volume ratio by local void velocity measurement with single probe
05 p0638 A73-16224

Velocity measurements made holographically of diffusely reflecting objects.
05 p0574 A73-16287

Laser Doppler velocity measurements in a supersonic flow without artificial seeding.
05 p0576 A73-16361

How to measure the earth's velocity with respect to absolute space.
05 p0615 A73-16363

Measurement of longitudinal and normal velocity fluctuations by sensing the temperature downstream of a hot wire.
05 p0576 A73-16438

A signal simulator for testing laser-Doppler fluid-flow velocimeter systems.
05 p0562 A73-16442

Optical anemometers applicability to steady atomized fuel sprays, obtaining particle velocity profiles and probability density distributions
05 p0565 A73-16761

A study of vortex rings using a laser Doppler velocimeter.
05 p0565 A73-16865

Measurements of turbulence-transport properties with a laser Doppler velocimeter.
05 p0566 A73-16914

Lateral velocity measurement error analysis in inertial guidance system, noting automatic compensation of mass imbalance effects
05 p0596 A73-16992

Shear stress distribution from measured nondimensional mean velocity profile measured in plane turbulent mixing layer formed at cascade wind tunnel exit
05 p0567 A73-17106

Laser velocity meters - A comparative study.
05 p0580 A73-17265

Application of constant temperature anemometry in measurement of intra-arterial blood flow velocity.
05 p0545 A73-17274

Measurement of the velocity profile in a turbulent boundary layer on a permeable plate.
06 p0643 A73-17409

A method for measuring the sublayer velocity profile of a liquid with polymer additive.
06 p0692 A73-17621

Hot wire measurement of velocity gradients in a fluid flow.
06 p0692 A73-17626

A sampling FM wide-band demodulator useful for laser Doppler velocimeters.
06 p0673 A73-17786

Directional measurements of the solar wind by the ESRO HEOS 1 probe, S 58-73
06 p0749 A73-17863

Speed distribution measurements of N₂ and Ar molecular beams produced by a multichannel source.
06 p0726 A73-18261

Propeller anemometers as sensors of atmospheric turbulence.
06 p0695 A73-18329

Velocity measurements of microwave ultrasonic waves in quartz.
06 p0724 A73-18740

Copper resistance thermoanemometer for channel unsteady air flow rate measurement, discussing design, operation principles and maximum error
07 p0823 A73-19621

A modified sensor of linear accelerations, velocities, and displacements over a path of 0 to 1500 mm
07 p0826 A73-20523

Strain-gauge sensor of flow velocity and fluid discharge
07 p0828 A73-20544

A new probe for measurement of velocity and flow direction in separated flows.
08 p0963 A73-20871

Some problems in the theory of an electrochemical velocity sensor for current-conducting fluids
08 p0965 A73-21108

Effect of Doppler ambiguity on the measurement of turbulence spectra by laser Doppler velocimeter.
08 p0965 A73-21211

Determination of the velocity of a radio meteor with minimum rms error.
08 p1012 A73-21581

Broadening of the measured frequency spectrum by a differential laser anemometer due to interference plane gradients.
08 p0967 A73-21594

An evaluation of the heat pulse anemometer for velocity measurement in inhomogeneous turbulent flow.
09 p1071 A73-22100

Flow velocity measurement method based on laser light frequency Doppler shift in scattering experiments on particle seeded liquid, presenting velocity profiles
09 p1094 A73-22311

An optical Doppler meter of the velocity of a moving surface
09 p1096 A73-22971

Book - Annual review of fluid mechanics. Volume 9
10 p1205 A73-23851

Use of lasers for local measurement of velocity components, species densities, and temperatures.
10 p1217 A73-23851

Statistical analysis and computer simulation of laser Doppler velocimeter systems.
10 p1217 A73-23999

Calibration of a hot-wire anemometer for velocity perturbation measurement.
10 p1218 A73-24120

Induction flowmeter theory in a T-tube of circular section.
10 p1220 A73-24610

Variable area, positive displacement, turbine type electromagnetic and pressure difference flowmeters noting reliability, repeatability and accuracy
10 p1221 A73-24850

Laser Doppler velocimeter configuration and operation, discussing applications and test results
10 p1229 A73-24850

Flow measurement in the presence of strong swirl using a laser Doppler anemometer.
10 p1221 A73-24850

An evaluation of optical anemometers for volumetric flow measurement of liquids and gases.
10 p1221 A73-24850

Long bore thick plate orifices performance in flow velocity measurement at low Reynolds numbers, calculating uncalibrated uncertainty in discharge coefficient
10 p1221 A73-24860

State of art of flowmetering, discussing acceptability factors, weirs, laser Doppler velocity method, ultrasonic type, pressure difference technique and turbine and electromagnetic devices
10 p1221 A73-24860

Remote measurement of wind speed by laser Doppler systems.
11 p1375 A73-25061

Shock wave determination of shear velocity at high pressures for understanding of planetary interior behavior with abrupt change in density from seismic interpretation
11 p1355 A73-25898

Light velocity from Io eclipse times observation by Picard and Roemer, noting rms deviation with present value
11 p1429 A73-26681

Precipitation patterns effective fall velocity determination from three dimensional radar scan data discussing interpolation/extrapolation technique to improve coarse sampling time effects
12 p1520 A73-26801

Application of lasers, radioisotopes, and the correlation method for measuring flow velocity
12 p1495 A73-26840

A low-velocity hot-wire anemometer.
12 p1496 A73-27021

Measurements of free stream velocity and ionization relaxation behind a shock in xenon.
12 p1527 A73-27172

Some remarks on the thermal equilibrium equation of hot-wire probes. 13 p1613 A73-28528

Simultaneous comparison of turbulent gas fluctuations by laser Doppler and hot wire. 13 p1616 A73-28821

Measurement of rarefied gas flow rates from the drift of an ion mark produced by an electron beam. 13 p1619 A73-29167

Problems of theory and practical application of Doppler-laser rate measuring devices in turbulent flow studies 13 p1628 A73-29169

Turbulence measurements with the split-film anemometer probe. 13 p1619 A73-29253

Hot-wire anemometric velocity measurements in nonisothermal turbulent flows, compensating for local temperature effects on downstream wire 13 p1620 A73-29255

An attempt to characterize the 'turbulence burst phenomena' using digital time series analysis. 13 p1604 A73-29260

Phase velocities and angle of inclination for frequency components in fully developed turbulent flow through pipes. 13 p1604 A73-29266

Spectral analysis of the signal from the Laser Doppler Velocimeter - Turbulent flows. 14 p1752 A73-29919

Temperature and velocity profiles measurement in hybrid rocket engine combustion, using optical method based on Na line reversal technique 15 p1957 A73-31636

Insensitivity of single particle time domain measurements to laser velocimeter 'Doppler ambiguity.' 15 p1875 A73-31671

Automatic measurement of intervals of shock wave transit across a base section 15 p1876 A73-31862

A combinational method of calculating the average velocity and the mean-mass temperature of a gas flow from the phase diagram of the substance 15 p1957 A73-31865

Spectroscopic observations of subsonic and sonic vapor flow inside an open-ended heat pipe. 15 p1958 A73-31936

Measurement using the Doppler effect of small velocities in flows occurring in the free convection of fluids. 15 p1864 A73-32069

On the polarographic measurement of the wall gradient of velocity in the upstream stagnation zone or of detachment from the cylinder 15 p1878 A73-32209

Noctilucent clouds seasonal distribution, altitude and displacement velocity from German observations during 1885-1941 15 p1873 A73-32347

Two-component dual-scatter laser Doppler velocimeter with frequency burst signal readout. 15 p1880 A73-32383

Remote measurement of the thickness, distance and velocity of objects by means of a piezoelectric laser beam deflector. 16 p2023 A73-32877

Experimental study of fluctuations of the difference frequency in a ring laser 16 p2024 A73-32895

Nonlinear filter evaluation for estimating vehicle position and velocity using satellites. 16 p1988 A73-33410

Airglow green cells diameter, speed and brightness measurements from isophote patterns in diagrams of UT versus distance 16 p2008 A73-33881

Laser anemometer for the measurement of air flow velocities 17 p2167 A73-34775

Application of the hydrogen-bubble technique for velocity measurements in thin liquid films. [ASME PAPER 73-APM-8] 17 p2153 A73-35033

Solid state null tracking Doppler radar ground velocity sensor for supersonic weapon delivery aircraft precision bombing, discussing design and test with computer simulation 17 p2137 A73-35209

Doppler radar measurements and observations of precipitation velocity fields. 17 p2125 A73-35361

Real-time estimates of mean velocity by averaging quantized phase displacements of Doppler radar echoes. 17 p2125 A73-35362

Mixing and structural characteristics of turbulent pulsating jets based on hot-wire anemometer velocity measurement data 17 p2157 A73-35513

Time evolution of pulsating air jets from schlieren photography and velocity measurements, using motor driven piston 17 p2157 A73-35514

The application of a scanning laser Doppler velocimeter to trailing vortex definition and alleviation. [AIAA PAPER 73-680] 18 p2315 A73-36231

Rapid scanning, three-dimensional, hot-wire anemometer surveys for wing tip vortices in the Ames 40-by 80-foot wind tunnel. [AIAA PAPER 73-681] 18 p2315 A73-36232

Measurements of aerosol size distributions with a laser Doppler velocimeter (LDV). [AIAA PAPER 73-705] 18 p2315 A73-36254

Velocity decay and acoustic characteristics of various nozzle geometries with forward velocity. [AIAA PAPER 73-629] 18 p2263 A73-36256

Probability distributions and correlations in a turbulent boundary layer. 18 p2300 A73-36626

Experimental investigation of the velocities in the turbulent wake behind bodies of revolution 18 p2266 A73-37017

On the correction of anemometric measurements in air flows of slowly varying temperature 19 p2429 A73-37529

Determination of a combustion wave in a conical supersonic flow 19 p2503 A73-37551

Radial velocity measurements of the Cetus Arc nebula around Loop II. 19 p2483 A73-37571

Calculation and measurement of MHD generator boundary layer velocity profiles. 19 p2470 A73-38315

A high resolution pulse transmission technique for determining ultrasonic velocities. 20 p2564 A73-38881

Radial velocity fluctuations of the Ap star HD 224801 20 p2607 A73-39083

Frequency-domain analysis of laser Doppler signals for estimation of turbulence parameters. 20 p2572 A73-39130

Argon laser application in a study of velocity in flames 20 p2573 A73-39620

A universal static calibration procedure for yawed hot wires. 21 p2693 A73-39926

Hypervelocity projectile holography for application to bullets and shells, calculating rotational velocity and flight direction from fringe on wave front reconstruction 21 p2694 A73-39957

Holographic investigations and measurements in a cloud of moving microparticles 21 p2696 A73-39979

Cumulus congestus cloud circulation velocity field measurement by balloon, comparing with radar, cameras, satellite and ground based observed meteorological model computations 21 p2728 A73-40060

FFTF probe-type eddy-current flowmeter - Wet versus dry performance evaluation in sodium. 21 p2738 A73-40768

Laser Doppler velocity measuring system parameters and SNR analysis, comparing photomultiplier, p-i-n and avalanche photodiode detectors for performance 22 p2825 A73-42298

Turbulent diffusion flame velocity, concentration, temperature and momentum flux measurements for hydrogen round jet in co-flowing air stream 22 p2935 A73-42788

Confocal backscatter laser velocimeter with on-axis sensitivity. 22 p2864 A73-43162

Vertical arm reaching movements for various gravitational levels, measuring reach time and angular and lower arm velocities 23 p2948 A73-43218

The laser-Doppler velocimeter and its application to the measurement of turbulence. 23 p2982 A73-43937

Globular cluster mass determination from analysis of field stars proper motions 23 p3035 A73-44237

Temperature compensation in a thermoanemometer 24 p3089 A73-44548

Some comments on the photographic subtraction method of determining chromospheric velocities. 24 p3135 A73-44631

On the correction of hot wire turbulence measurements for spatial resolution errors. 24 p3089 A73-44691

A laser Doppler velocimeter for studying fast gas-dynamic flows 24 p3089 A73-44714

Hypersonic flow velocity measurements using laser velocimeter. [AIAA PAPER 73-1046] 24 p3090 A73-44870

Reducing the level of additive noise in the output signal of a laser velocimeter 24 p3096 A73-44958

VELOCITY MODULATION

Electromagnetic wave propagation velocity modulation in dispersionless linear medium with dielectric constant variation in space and time, evaluating approximation with neglected multiple reflections 10 p1249 A73-24526

A three-dimensional picture of the development of instability during the interaction of a modulated electron beam with a plasma. 17 p2216 A73-35170

Rotor noise due to inflow turbulence. [AIAA PAPER 73-632] 18 p2259 A73-36191

Solar wind alpha particle abundance variations as function of wind velocity from HEOS-1, Vela 3-A and 3-B observations 21 p2763 A73-41500

VELOCITY POTENTIALS

U FLOW DISTRIBUTION

U VELOCITY DISTRIBUTION

VELOCITY PROBES

U PITOT TUBES

U SPEED INDICATORS

VELOCITY PROFILES

U VELOCITY DISTRIBUTION

VENERA SATELLITES

NT VENERA 4 SATELLITE

NT VENERA 6 SATELLITE

NT VENERA 7 SATELLITE

Venera satellite parachute probe method for Doppler measurement of Venus atmosphere wind velocity and turbulence 03 p0379 A73-14566

Data on dynamics of the subcloud Venus atmosphere from Venera spaceprobe measurements. 06 p0744 A73-17436

Optical properties of the lower atmosphere of Venus (for interpreting measurements of the Venera 8 planetary probe) 21 p2686 A73-40913

Results of direct measurements of the illumination in the atmosphere and on the surface of the planet Venus during the flight of the Venera 8 interplanetary probe 21 p2773 A73-41274

VENERA 4 SATELLITE

Investigation of the chemical composition of the atmosphere of Venus by the automatic station Venus 4 16 p2066 A73-33799

Thermodynamic characteristics of the lower atmosphere of Venus on the basis of the results of an experiment conducted with the descent vehicle of the Venus 4 interplanetary probe 16 p2067 A73-33800

Study of ultraviolet radiation from the Venera interplanetary probe 16 p2056 A73-33803

Plasma near Venus - Comparison of results obtained with the aid of Venus 4 and Mariner 5 16 p2067 A73-33804

Certain results of a combined treatment of the Venera 4 interplanetary probe and ground-based radio-astronomical and radar measurements 16 p2068 A73-33819

VENERA 6 SATELLITE

Determination of the velocity of shock waves in the interplanetary medium. 10 p1279 A73-24236

VENERA 7 SATELLITE

Results of the Venus atmosphere measurements made by the landing station Venera 7. 02 p0214 A73-12252

Solar cosmic ray bursts in November-December 1970 according to data from Venus 7 space probe and Lunokhod 1 station. 02 p0206 A73-12321

Venus atmosphere wind velocity profiles from analysis of Venera 7 descent stage radial velocity measurements 05 p0612 A73-16086

The results of measurements of the intensity of cosmic rays by the automatic station 'Venera-7'. 12 p1535 A73-27638

VENTILATION

A general solution for lift interference in rectangular ventilated wind tunnels. [AIAA PAPER 73-209] 05 p0563 A73-16940

Effects of lung volume and disease on the lung nitrogen decay curve. 08 p0934 A73-21501

Ventilation measured by body plethysmography in hibernating mammals and in poikilotherms. 08 p0932 A73-21612

Preventing the shut-off punkah louver from jamming. 16 p1970 A73-32925

VENTILATORS

Viscoelastic panel vibration damping material for ventilation ducts to reduce LF vibrations induced by turbulent air flow 21 p2723 A73-40235

VENTS

Fuel capsule vent system development for the Viking radioisotope thermoelectric generator. 21 p2737 A73-40766

Diaphragm ejector pulse shortener for transforming periodic input signal into sharp pulses by adjusting vent areas of two fluid amplifiers 23 p2942 A73-43408

VENTURI TUBES

Venturi exhausts for air pumping augmentation in ram air operated aircraft heater or combustor, discussing experimental data on suction variation
18 p2343 A73-36396
Herschel-type venturimeter discharge coefficients at low Reynolds number.
20 p2566 A73-39116

VENUS [PLANET]

Soviet Venus probes data on planetary atmosphere composition, temperature and pressure profiles, magnetic field, diameter, mass density and rotation period
01 p0102 A73-10992

Venus gravity anomalies and physical properties arising from convection currents and topography deduced from geodetic aspects derived from mass, radius and surface temperature
04 p0496 A73-14812

Far IR brightness temperature, opacity and emissivity of Jupiter, Venus, Mars and Saturn
05 p0626 A73-17348

Symposium on Planetary Atmospheres and Surfaces, Madrid, Spain, May 10-13, 1972, Proceedings.
06 p0743 A73-17427

High resolution interferometric observations of Venus at three radio wavelengths.
06 p0744 A73-17437

Venus - Measurements of brightness temperatures in the 7-15 cm wavelength range and theoretical radio and radar spectra for a two-layer subsurface model.
06 p0744 A73-17438

Radar brightness mapping of Venus surface, noting roughness of terrain from polarization studies and signal processing for extraction of echo power
06 p0744 A73-17440

Choosing the optimal distribution of radar and optical observations of Venus
09 p1142 A73-22091

Natural radioactive element contents in Venusian rock - Results of a Venus-8 station experiment
11 p1418 A73-25635

Mercury, Venus and Pluto satellite system elimination by tidal friction, discussing possible erosion of earth and Mars small satellites
11 p1419 A73-25778

Bullen solid core model for earth and Venus vindicated by free earth oscillations records and detection of PKIKP seismic phase, discussing compressibility effects
11 p1421 A73-25897

Simultaneous recording of solar cosmic rays near Venus and in the earth magnetosphere
12 p1534 A73-27354

Xenoliths in maars and diatremes with inferences for the moon, Mars, and Venus.
13 p1681 A73-28848

Thermal history of the terrestrial planets
16 p2066 A73-33795

Plasma near Venus - Comparison of results obtained with the aid of Venus 4 and Mariner 5
16 p2067 A73-33804

The magnetic field in the vicinity of Venus
16 p2067 A73-33805

Computer analysis of reflected signals obtained during radar sounding of Venus
16 p2067 A73-33807

Monochromatic and radiometric albedo of Mars and Venus
16 p2067 A73-33811

The current level of volcanic activity on Venus
16 p2068 A73-33813

Spectrophotometry of individual regions of Venus
16 p2068 A73-33814

Radio emission from Venus and Jupiter at 2 and 8 mm wavelengths
16 p2068 A73-33817

High-resolution interferometric observations of Venus at the 3.1-cm wavelength
16 p2068 A73-33818

Measurement of cosmic rays and searches for radiation belts near Venus
16 p2057 A73-33829

Venus and Jupiter telescopic observation aiming errors using Wanschaff vehicle circle, suggesting error sources and correction procedures
17 p2230 A73-34593

Two layer cores in terrestrial planets with emphasis on Mars and Venus, discussing pressure at earth mantle-core boundary, equations of state and composition
17 p2235 A73-35743

Mission planning for remote exploration of the surface of Venus.
[AIAA PAPER 73-580]
18 p2350 A73-36072

Content of natural radioactive elements in Venusian rock Results of experiment with Venera-8 station.
19 p2486 A73-38142

The brightness temperature of Venus at 70 centimeters.
19 p2489 A73-38526

The brightness temperature of Venus and the absolute flux-density scale at 608 MHz.
19 p2489 A73-38527

Simultaneous recording of solar cosmic-rays near Venus and the earth's magnetosphere.
23 p3020 A73-43251

VENUS ATMOSPHERE

NT VENUS CLOUDS

Global mean radiative equilibrium model for Venusian mesosphere, determining horizontal variation of thermal heating and cooling
01 p0097 A73-10361

Radiative and convective heating during Venus entry.
01 p0003 A73-10757

Soviet Venus probes data on planetary atmosphere composition, temperature and pressure profiles, magnetic field, diameter, mass density and rotation period
01 p0102 A73-10992

Results of the Venus atmosphere measurements made by the landing station Venera 7.
02 p0214 A73-12252

Diurnal variation of the exospheric temperatures on Venus and Mars.
02 p0214 A73-12253

The possibilities of determining the temperature profile in the Venusian atmosphere from the thermal radio emission of the planet
02 p0219 A73-12463

Venera satellite parachute probe method for Doppler measurement of Venus atmosphere wind velocity and turbulence
03 p0379 A73-14566

Venus atmospheric parameters below critical refraction and surface refractive index from signal amplitude measurement by radio holographic occultation techniques
03 p0379 A73-14567

Venus atmosphere wind velocity profiles from analysis of Venera 7 descent stage radial velocity measurements
05 p0612 A73-16086

Certain optical properties of the atmosphere of Venus and the possibilities of interpreting photometric and polarization measurements.
05 p0612 A73-16087

Infrared radiative heating and cooling in the Venusian mesosphere. I - Global mean radiative equilibrium.
05 p0613 A73-16197

Numerical solution for the composition of a thermosphere in the presence of a steady subsolar-to-antisolar circulation with application to Venus.
05 p0613 A73-16198

Venus atmosphere engineering models for use in spacecraft design and mission planning from Mariner 5 and Venera spacecraft and earth based measurements
[AIAA PAPER 73-130]
05 p0619 A73-16883

The runaway Greenhouse in the Venus atmosphere.
05 p0622 A73-17124

Review of surface and atmosphere studies of Venus and Mercury.
06 p0743 A73-17428

Planet wide circulation in Venus upper atmosphere from UV photographs, noting apparent 4.06 day rotation period
06 p0743 A73-17431

Retrograde rotation of the upper atmosphere of Venus.
06 p0744 A73-17433

Venus atmosphere water vapor content from IR spectra observed by airborne Fourier interferometric spectrometer, discussing different models for abundance
06 p0744 A73-17434

Venus high resolution spectra for carbon dioxide abundance variations, discussing CO, HF and HCl composition
06 p0744 A73-17435

Data on dynamics of the subcloud Venus atmosphere from Venera spaceprobe measurements.
06 p0744 A73-17436

Some characteristics of the Venus surface.
06 p0744 A73-17439

The thermal structure within the stratospheres of Venus and Mars.
06 p0747 A73-17493

Calculation of the transfer coefficients for planetary atmospheres consisting of CO₂-N₂ mixtures
06 p0754 A73-18568

U.S. and U.S.S.R. Venus probes data on Venus atmosphere, discussing atmospheric heat transfer mechanism and cloud structure
07 p0874 A73-19110

Venus - Radar determination of gravity potential.
07 p0875 A73-19167

Stagnation region radiative heating with steady-state ablation during Venus entry.
08 p1025 A73-21817

Venus - New microwave measurements show no atmospheric water vapor.
09 p1151 A73-23171

Venus - Microwave opacity of the minor atmospheric constituents.
11 p1417 A73-25267

Infrared radiative heating and cooling in the Venusian mesosphere. II - Day-to-night variation.
11 p1418 A73-25719

The planet Venus - A new periodic spectrum variable.
11 p1428 A73-26621

Determination of the characteristics of light-scattering particles in the atmosphere of Venus from photometric measurements.
12 p1543 A73-27640

Venus atmospheric model based on spectroscopic evidence of carbon dioxide spectral lines phase variation due to two scattering layers
13 p1680 A73-28452

Some field characteristics of outgoing thermal radiation in the Venusian and Martian atmospheres
15 p1937 A73-31819

The possibilities of determining the temperature profile in Venus' atmosphere from the planet's thermal radio emission.
15 p1942 A73-32613

The O I 1304- and 1356-A emissions from the atmosphere of Venus.
16 p2062 A73-33431

Calculation of the transfer coefficients of planetary atmospheres formed by mixtures of CO₂ and N₂.
16 p2039 A73-33595

Radio astronomical, radar and interplanetary probe measurements of Venus rotation, dimensions, atmosphere and magnetic field
16 p2066 A73-33798

Investigation of the chemical composition of the atmosphere of Venus by the automatic station Venus 4
16 p2066 A73-33799

Thermodynamic characteristics of the lower atmosphere of Venus on the basis of the results of an experiment conducted with the descent vehicle of the Venus 4 interplanetary probe
16 p2067 A73-33800

Atmosphere and ionosphere of Venus on the basis of data obtained by Mariner 5 in the S band during radio occultation
16 p2067 A73-33801

Radio-occultation measurements of the Venusian atmosphere conducted by Mariner 5 in the 10-centimeter band
16 p2067 A73-33802

Study of ultraviolet radiation from the Venera interplanetary probe
16 p2056 A73-33804

Radar observations of Venus at 3.8 cm
16 p2067 A73-33807

Spectral studies of the atmospheres of Mars and Venus
16 p2067 A73-33811

The current level of volcanic activity on Venus
16 p2068 A73-33813

Distribution of radio brightness across the disk of Venus at the 8-mm wavelength
16 p2068 A73-33817

Certain results of a combined treatment of the Venera 4 interplanetary probe and ground-based radio-astronomical and radar measurements
16 p2068 A73-33818

Absorption of centimeter radio waves in the Venusian atmosphere
16 p2068 A73-33820

Analysis of radio-wave propagation in the Venusian atmosphere
16 p1984 A73-33821

Estimates of water content in the atmosphere of Venus on the basis of radio-astronomical measurements and space probe data
16 p2068 A73-33822

Influence of horizontal inhomogeneity in the Venusian atmosphere on the accuracy of measurements of its parameters by a radio occultation method
16 p2068 A73-33823

The thermal regime and convective motions in the lower layers of the Venusian atmosphere
16 p2068 A73-33824

Venus 4 chemical composition and pressure data for construction of Venus atmospheric model, emphasizing Greenhouse effect
16 p2068 A73-33825

Optical properties of the Venus atmosphere
16 p2069 A73-33828

Estimates of the intensity of turbulence in the atmospheres of Mars and Venus
16 p2069 A73-33829

The atmospheric mixing in the atmospheres of Mars and Venus.
18 p2349 A73-36030

Heat shielding for Venus entry probes.
[AIAA PAPER 73-712]
18 p2368 A73-36330

Pioneer Venus mission plan for atmospheric probe and an orbiter.
[AIAA PAPER 73-579]
18 p2353 A73-36490

Numerical models of the circulation of the atmosphere of Venus.
19 p2485 A73-37650

Linear filtering of ballistic-entry-probe data for atmospheric reconstruction.
[AIAA PAPER 73-904]
20 p2589 A73-38830

Venus topside ionosphere He content estimates from ionization profiles and discovery of radioactive materials in crust
20 p2604 A73-38940

Venus upper atmosphere four-day retrograde rotation derived from statistical analysis of telephotographic observation of Y-shaped feature
21 p2767 A73-40566
Calculations of the limb radiance of Venus in the 600 to 700 per cm region and their application to spacecraft navigation.
21 p2767 A73-40693
Dissipation of the Venusian atmosphere
21 p2769 A73-40733
Optical properties of the lower atmosphere of Venus /for interpreting measurements of the Venera 8 planetary probe/
21 p2686 A73-40913
Results of direct measurements of the illumination in the atmosphere and on the surface of the planet Venus during the flight of the Venera 8 interplanetary probe
21 p2773 A73-41274
Venus atmosphere water vapor phase transformation possibilities, discussing ice crystal and supercooled water drop formation
22 p2911 A73-42736
The 4-day rotation of the upper atmosphere of Venus.
22 p2913 A73-42982
Upper Venusian atmosphere four-day retrograde zonal circulation, discussing moving flame phenomenon, convective instability to mean shear and tidal forcing
22 p2913 A73-42983
Venera 8 - Measurements of temperature, pressure and wind velocity on the illuminated side of Venus.
23 p3028 A73-43602
Venera 8 - Measurements of solar illumination through the atmosphere of Venus.
23 p3029 A73-43603
Venus upper atmosphere retrograde rotation above main cloud cover, investigating equatorial bulge from pressure surfaces at high elevations
23 p3029 A73-43604
The optical properties of Venus and the Jovian planets. I - The atmosphere of Jupiter according to polarimetric observations.
24 p3129 A73-44442
General atmospheric circulation driven by polar and diurnal surface temperature variations.
24 p3131 A73-44463
Venus carbon dioxide production kinetics involving quartz reaction with calcite to form wollastonite and carbon dioxide
24 p3133 A73-44540
Atmospheric mixing effects for interpretation of oxygen atom concentration in Mars and Venus upper atmospheres obtained by Mariner and Venera space probes
24 p3139 A73-45134
VENUS CLOUDS
Ultraviolet clouds on Venus - Observational bias.
06 p0744 A73-17432
Comment on 'The composition of the Venus cloud tops in light of recent spectroscopic data.'
07 p0874 A73-19076
Rapid motions of ultraviolet clouds on Venus
16 p2067 A73-33810
Mars blue haze, earth noctilucent clouds and Venus blue clouds, considering mechanism and condensate chemical composition for formation
16 p2069 A73-33833
Sulfuric acid in the Venus clouds.
19 p2483 A73-37579
Possibilities of calculating the spectral albedo of Venus in the near infrared
21 p2770 A73-40914
The 4-day rotation of the upper atmosphere of Venus.
22 p2913 A73-42982
Venus upper atmosphere retrograde rotation above main cloud cover, investigating equatorial bulge from pressure surfaces at high elevations
23 p3029 A73-43604
Sulfuric acid solution composition to account for Venus cloud temperature, stratosphere dryness and IR spectrum
24 p3129 A73-44441
An expanded theoretical interpretation of the Venus 1.05-micron CO2 line and the Venus 0.8226-micron H2O line.
24 p3139 A73-45052
VENUS PROBES
NT MARINER 5 SPACE PROBE
NT VENERA SATELLITES
Data return maximization for unpredictable channel capacity, considering planetary entry probe to Venus or Jupiter with unknown atmospheric transmission characteristics
04 p0420 A73-15425
U.S. and U.S.S.R. Venus probes data on Venus atmosphere, discussing atmospheric heat transfer mechanism and cloud structure
07 p0874 A73-19110
Optimization of descent maneuvers for a section of a satellite in a planetary orbit
15 p1931 A73-31227

Mission planning for remote exploration of the surface of Venus.
[AIAA PAPER 73-580] 18 p2350 A73-36072
Heat shielding for Venus entry probes.
[AIAA PAPER 73-712] 18 p2368 A73-36332
Pioneer Venus mission plan for atmospheric probes and an orbiter.
[AIAA PAPER 73-579] 18 p2353 A73-36499
VENUS RADAR ECHOES
Moon and Venus relief from backscattering diagrams based on radar echoes, calculating root-mean-square angles of surface inclination
03 p0379 A73-14568
Specific effective scattering area of the surface of the moon, Mars, and Venus in the radio-frequency range.
12 p1543 A73-27639
Radio astronomical, radar and interplanetary probe measurements of Venus rotation, dimensions, atmosphere and magnetic field
16 p2066 A73-33798
Determination of elements of Venusian rotational motion and of coordinates of surface regions with higher reflectivity at radio frequencies
16 p2067 A73-33808
Comparison of determinations of the rotational velocity of Venus by radar, optical Doppler effect, and spot measurement methods
16 p2067 A73-33809
Interpretation of radar measurements of Venus in the microwave range
16 p2068 A73-33820
Results of delay-time and Doppler-correction measurements obtained in radar observations of Venus during 1962, 1964, 1969, 1970, and 1972
23 p3037 A73-44252
VERBAL COMMUNICATION
The employment of a spoken language computer applied to an air traffic control task.
05 p0544 A73-16728
Studies in interactive communication. I - The effects of four communication modes on the behavior of teams during cooperative problem-solving.
06 p0658 A73-18241
Simultaneous motor and verbal processing of visual information in a modified Stroop test.
09 p1044 A73-21896
Russian book on multichannel magnetic tape recorders in civil aviation ATC for speech communication monitoring and preservation covering design and operation principles
09 p1086 A73-23245
Speech data rate reduction. I - Applicability of modern estimation theory. II - Applicability of sensitivity and error analysis.
13 p1585 A73-29201
VOLMET transmission automation with the aid of the 'DECLAM' system using a speech synthesizer
15 p1846 A73-32429
Telephone line echo reduction by adaptive filter compensation, using statistical speech-white noise relations
23 p2952 A73-43318
VERNIER ENGINES
An operational satellite propulsion system providing for vernier velocity, high and low level attitude control and spin trim.
[AIAA PAPER 72-1130] 04 p0486 A73-14916
Scattering of light by the medium generated by a space vehicle. I - Emission of vapor jets by spacecraft microthrusters.
12 p1549 A73-27641
VERTEBRAE
A method of determining spinal alignment and level of vertebral fracture during static evaluation of ejection seats.
16 p1967 A73-32676
Radiological assessment of the vertebral column from the point of view of aviation medicine
22 p2817 A73-43131
VERTEBRAL COLUMN
Surveillance of the vertebral column in pilots who have undergone an ejection
18 p2284 A73-36914
VERTEBRATES
NT AMPHIBIA
NT BATS
NT BIRDS
NT CATS
NT CHIMPANZEES
NT FISHES
NT FROGS
NT HOMEOTHERMS
NT MAMMALS
NT MICE
Comparative anatomy of the vestibular nuclear complex in submammalian vertebrates.
06 p0655 A73-18575
Electrophysiological investigation of suprasegmental motor control systems evolution through Cyclostoma-Primate series, noting preservation of reticulomotor neuron projection characteristics
07 p0781 A73-20001

Vertebrate photoreceptor cell /rods and cones/ development and structure, discussing light pathway, ciliary connective and microtubules, outer and inner segments, etc.
09 p1042 A73-23303
The morphological organization of the vertebrate retina.
09 p1042 A73-23304
Optical properties of vertebrate eyes.
09 p1043 A73-23312
Light-induced potential and resistance changes in vertebrate photoreceptors.
09 p1043 A73-23313
VERTICAL AIR CURRENTS
The magnitude and character of the radiation induced vertical circulation of the troposphere.
01 p0039 A73-10394
Instrument requirements for eddy correlation measurements.
01 p0052 A73-11057
Effects of vertical mass motions on the composition structure in the thermosphere.
02 p0162 A73-12291
Kinematic and thermodynamic structure of thunderstorm, considering updraft, upper air environment, surface features and radar echoes
03 p0338 A73-14511
Asymptotic solution for vertical propagation of equatorial planetary waves in shear, noting gravity-Rossby and Kelvin waves and wind effects on diurnal tides
05 p0591 A73-16190
Convective storm updraft shape calculation based on horizontal momentum changes in rising air, noting effects of mixing and aerodynamic drag
05 p0592 A73-16195
Numerical model for calculation of the geopotential field with a new generalized vertical velocity profile incorporating the influence of orography
05 p0572 A73-17352
Turbulence energy spectra in thick convective cumulonimbus cloud zone, using aircraft measurements
08 p0984 A73-21186
Barotropic model of local forecasts of katabatic winds
08 p0985 A73-21451
Mode of thickening of a low morning convective layer in clear sky
09 p1115 A73-23036
Periodic solutions of the set of equations governing the nonadiabatic convection of dry isolated thermals.
11 p1393 A73-23690
Turbulent surface layer shear convection analysis, using similarity model based on weak interaction between vertical motion and mechanical turbulence
13 p1655 A73-29340
A numerical model of the geopotential field with a new profile of the generalized vertical velocity that takes orography into account.
15 p1865 A73-31002
Electron concentrations increase observed at 60-90 km altitudes during anomalous winter radio wave absorption, noting association with upward aerosol transport decrease
15 p1844 A73-31889
Possibility of computing the cloud field on the basis of vertical velocities.
18 p2334 A73-37055
A comparison between axisymmetric and slab-symmetric cumulus cloud models.
19 p2447 A73-37659
Rate of growth of the upper boundary of cumulus clouds
21 p2730 A73-40117
Experimental investigation of the velocities of vertical motions in convective clouds
21 p2730 A73-40121
Thunderstorm electrification by the inductive charging mechanism. I - Particle charges and electric fields. II - Possible effects of updraft on the charge separation process.
23 p3002 A73-43599
Short-term ground ozone fluctuations at Poona.
23 p2974 A73-43865
Stormy weather vertical air motion velocity calculation for use in synoptic field and atmospheric energy budget evaluations
23 p3003 A73-43996
VERTICAL DISTRIBUTION
NT STAR DISTRIBUTION
Variations of the auroral electron energy spectra during substorms.
01 p0036 A73-10339
Troposphere turbulence kinetic energy dependence on height and scales of motions, presenting vertical energy profiles
01 p0074 A73-10869
Mass spectrometric measurements of minor constituents in the lower thermosphere.
01 p0041 A73-10880
A vertical profile of OH in the mesosphere.
01 p0041 A73-10883

Atmospheric atomic oxygen density vertical distribution measurement by rocket-borne cryocooled mass spectrometer ion source

02 p0157 A73-11756

A technique for recovering the vertical number density profile of atmospheric gases from planetary occultation data.

02 p0158 A73-11913

Changes of lower ionosphere electron concentrations with solar activity.

02 p0159 A73-12029

Earth vertical gravity field probing by observing body free fall from several hundred kilometers altitude

02 p0159 A73-12167

Neutral wind measurement during daytime in the thermosphere.

02 p0159 A73-12224

Results of the Venus atmosphere measurements made by the landing station Venera 7.

02 p0214 A73-12252

Models of extreme arctic and subarctic winter atmospheres between 20 and 90 km.

02 p0160 A73-12274

Ionospheric bottom side electron density profiles from measured monthly median values, using CCIR and ITS computer programs for critical frequencies

02 p0163 A73-12302

Ion concentration measurements in the earth's ionosphere at altitudes from 200 to 6000 km

02 p0164 A73-12462

Trace elements profiles, notably Hg, from a preliminary study of the Apollo 15 deep-drill core.

02 p0220 A73-12477

Lunar rock C 14 production rate as function of depth, discussing solar and galactic cosmic radiation induced nuclear reactions

02 p0220 A73-12479

Extensive air showers vertical distribution at aircraft heights, constructing integral spectrum based on particle number

02 p0209 A73-12674

Extensive air shower characteristics and muon counts at different level observations relative to particle number and primary energy spectra

02 p0209 A73-12678

Energy spectrum of muon formed electromagnetic cascades in vertical cosmic radiation flux

02 p0209 A73-12681

Vertical resolution of temperature profiles obtained from remote radiation measurements.

02 p0165 A73-12778

On investigation of the electron concentration and inhomogeneous structure of the outer ionosphere by means of coherent radiowaves emitted from artificial earth satellites.

03 p0299 A73-13631

On the altitude dependence of the atmospheric X-rays in the energy range 0.1-1 MeV.

03 p0365 A73-14441

E region electron collision frequency vertical distribution from ground and rocket measurements of radio wave absorption and electron density respectively

03 p0304 A73-14562

Electron excitation and auroral emission parameters.

04 p0440 A73-14959

Airglow height profiles of forbidden O I 6300 and 5577 Å line emissions in morning ionosphere from rocket photometric measurement

04 p0444 A73-15542

Adiabatic inviscid quasi-geostrophic planetary scale perturbations forced by stratospheric disturbance, obtaining vertical propagation from layered models representation for zonal wind

05 p0591 A73-16189

Computation of upper tropospheric reference heights from winds for use with vertical temperature profile observations.

05 p0569 A73-16575

Vertical distribution of minor atmospheric constituents as derived from air-borne measurements of atmospheric emission and absorption infrared spectra. [AIAA PAPER 73-103]

05 p0570 A73-16863

Fluctuations of the ion concentration level in the terrestrial ionosphere at altitudes from 200 to 1300 km

05 p0570 A73-17012

IR radiation source shape and size effects on aerial IR surveys at various flight altitudes, noting spectral composition change with height

05 p0578 A73-17140

The thermal structure within the stratospheres of Venus and Mars.

06 p0747 A73-17493

Quantitative temperature data from Direct-Readout Infrared (DRIR) pictures. [AD-759891]

06 p0696 A73-18711

Dawn airglow far UV spectrum observed by scanning Ebert spectrophotometer aboard Aerobee rocket, obtaining altitude profiles at 100-244 km

07 p0814 A73-19247

Variation with altitude of the scatter coefficient in the stratosphere, based on measurements from the Soiuz-3 spacecraft

07 p0817 A73-19585

Sharply defined upper limit existence for lunar ash flow with heat transfer, presenting altitude dependence of pressure, gas density, temperature and velocity distributions

07 p0895 A73-19864

Theoretical vertical profiles of minor ions at the Equator.

07 p0819 A73-20053

Vertical velocity field oscillations in photospheric sunspot umbras interpretation in terms of gravity or acoustic waves traveling along magnetic field lines

08 p1001 A73-20756

H alpha observations of vertical velocity distribution periodic oscillations in sunspot, noting transverse waves formation and propagation to penumbral boundary

08 p1001 A73-20757

Vertical profiles of liquid water content and other cloud parameters for cumulus and cumulus congest clouds from aircraft measurements over Ukraine

08 p0985 A73-21454

Nitric oxide densities during sunrise derived from overhead emission measurement as function of altitude

09 p1074 A73-22065

Es-q layer at Huancayo during the March 1970 geomagnetic storm.

09 p1078 A73-22836

A probabilistic evaluation of helicopter lift capability.

10 p1175 A73-23775

Altitude and latitude dependences of the partial coefficients and integral multiplicity of the cosmic-ray neutron component

10 p1268 A73-23933

Depth variation of Apollo 15 deep drill fines trace elements from neutron activation analysis, noting KREEP abundance

10 p1278 A73-24113

Correct statement of the problem of computing the N/h profiles of the lower ionosphere.

10 p1212 A73-24241

Statistical laws governing the wind velocity distribution in the atmospheric boundary layer

10 p1246 A73-24373

Observations of the Helium II 304-Å and Helium I 584-Å atmospheric dayglow radiation.

10 p1213 A73-24735

Vertical electron density and temperature data from geophysical rocket borne Langmuir probes and electrode traps

11 p1350 A73-25078

Ionospheric vertical electron density profiles from geophysical rocket-borne microwave dispersing interferometer

11 p1350 A73-25079

Formation of the density profile of charged particles at heights from 10 to 90 km

11 p1411 A73-25082

Forecast maps for seasonal variations in the geometrical parameters of the F2 layer

11 p1351 A73-25094

Calculation of the N/h profiles in the ionosphere from two magnetoionic components

11 p1351 A73-25096

Influence of vertical wind shear on the development of convective cloudiness

11 p1393 A73-25640

An observational study of the vertical profile of the high frequency fluctuations of the wind in the atmospheric boundary layer.

11 p1393 A73-25691

A study of convective elements in the atmospheric surface layer.

11 p1393 A73-25692

The topside ionosphere at mid-latitudes during local sunrise.

11 p1353 A73-25757

Atmospheric convection and its effect on relaxation time and charge distribution.

11 p1394 A73-25759

Vertical distribution of viscosity and convection conditions in earth mantle, discussing shallow convection model and geophysical evidence for validity

11 p1356 A73-25906

Convection near critical Rayleigh numbers in the case of an almost vertical temperature gradient

11 p1453 A73-26435

Southern Hemisphere troposphere atmospheric carbon dioxide monitoring program based on aircraft air sampling, discussing vertical profile data

11 p1358 A73-26472

Some effects of magnetospheric acceleration mechanisms on variations in ultraviolet intensity height profiles, and on consequent rocket spectrograph sensitivities.

11 p1358 A73-26703

A two-satellite microwave occultation system for determining pressure altitude references.

12 p1521 A73-26813

Dropsonde for continuous temperature measurement during descent through lower atmospheric level, discussing receiving unit and data conversion unit

12 p1495 A73-26815

Three-dimensional analytical model of the electron density distribution in a quiet ionosphere

12 p1490 A73-27338

Averaged nighttime altitude profile of atmospheric emission at 6300 Å

12 p1491 A73-27340

Spherical harmonic analysis of the geomagnetic field during the epoch 1965.0 up to $n = 23$ from group data. II - Results

12 p1491 A73-27342

Atmosphere Explorer satellite-borne two channel fixed grating Ebert spectrometer for measurement of airglow at 2150 Å, yielding altitude profiles of nitric oxide density

13 p1689 A73-28640

Troposphere turbulence kinetic energy dependence on height and scales of motions, presenting vertical energy profiles

13 p1653 A73-28644

Calculation of the growth and melting of ice particles and the radar signal reflection profiles in cumulonimbus clouds

13 p1653 A73-28844

Dependence of the diffuse expansion characteristics of a crystallization zone on the vertical stability of the atmosphere

13 p1654 A73-28847

A mode theory of radio wave propagation in an inhomogeneous atmosphere with jointed-segment profile.

13 p1586 A73-29217

Similarity theory of diffusion and the observed vertical spread in the diabatic surface layer.

13 p1655 A73-29319

Determination of coefficients of vertical diffusion between 0 and 100 m with the help of radon and ^{222}Rn

13 p1655 A73-29323

Distribution of water vapor in the stratosphere determined from balloon measurements of atmospheric emission spectra in the 24- to 29-micron region.

14 p1749 A73-30119

A technique for the calculation of the opening-shock forces for several types of solid cloth parachutes. [AIAA PAPER 73-477]

15 p1829 A73-31404

Semi-annual variation in the true height of the H peak in low latitudes [at Puerto Rico].

15 p1869 A73-31708

Features of the long-wave radiant influx in the presence of stratified cloudiness [A numerical experiment]

15 p1904 A73-31710

A critical study on the reliability of electron temperature measurements with a Langmuir probe.

15 p1871 A73-31808

Calculation of ionospheric N/z profiles with the use of radio-wave absorption data

15 p1871 A73-31810

D region partial reflection mechanism model based on multiple reflector concept, presenting electron density vertical distribution

15 p1845 A73-32020

Upper stratosphere and lower mesosphere vertical mixing implications of methane observations at 50 km assuming modelability by eddy transport

15 p1873 A73-32210

Measurement of the ion density in the earth's ionosphere at altitudes from 200 to 6000 km.

15 p1874 A73-32212

Vertical profiles of molecular H₂ and CH₄ in the stratosphere.

[AIAA PAPER 73-518]

16 p2006 A73-33040

Global balloon monitoring program of stratospheric dust, ozone, water vapor, temperature and aerosol determination in northern and southern hemisphere. [AIAA PAPER 73-521]

16 p2007 A73-33042

Analysis of radio-wave propagation in the Venus atmosphere

16 p1984 A73-33044

Vertical distribution and temperature profile of the night time atmospheric sodium layer obtained by laser backscatter.

16 p2009 A73-33120

The lateral distribution of muons in near vertical EAS.

17 p2223 A73-34010

Critical analysis of the results obtained by SIR3 in remote sensing of the temperature field over the Mediterranean

17 p2205 A73-34012

A synoptic model for evaluation of vertical temperature and geopotential profiles from satellite pictures

17 p2206 A73-34014

Influence of the vertical structure of the wind field on the development of cumulus and cumulonimbus clouds

18 p2332 A73-31712

ALADDIN II ionospheric composition measurements, obtaining ion and neutral vertical density profiles and dynamic parameters for E region nighttime ion layering prediction model

18 p2303 A73-31714

Vertical ozone profiles from observations of eclipsing satellites.

18 p2304 A73-31716

- Meteor radar study of tides in the 80 to 100 km altitude range. 18 p2305 A73-35999
- Vertical temperature profiles from satellites - Results from second generation instruments aboard Nimbus-5. 18 p2307 A73-36029
- Ion composition measurements at altitudes 100-180 km in 1972. 18 p2310 A73-36143
- Theoretical analysis of improvements in remote sensing of atmospheric and pollutant gases through high resolution detection of individual infrared emission lines. [AIAA PAPER 73-703] 18 p2315 A73-36252
- Cosmic ray total ionization - 1970-1972. 18 p2347 A73-36293
- Review of current sonic boom studies. 18 p2267 A73-36393
- Variability of eigenvectors and eigenvalues of correlation matrices for vertical temperature profiles. 18 p2334 A73-37062
- Assessment of characteristics of the atmospheric moisture distribution with the aid of satellite measurements. 18 p2334 A73-37064
- Interrelationship between developments of synoptic processes and evolution of the integral moisture field according to satellite measurements. 18 p2334 A73-37065
- Some characteristics of the vertical structure of the humidity field over the North Atlantic. 18 p2334 A73-37076
- Comparison of vertical profile turbulence structure with stellar observations. 19 p2446 A73-37259
- Accuracy and coverage of temperature data derived from the IR radiometer on the NOAA 2 satellite. 19 p2424 A73-37665
- Vertical profiles of small-scale temperature structure in the atmosphere. 19 p2448 A73-38209
- The boundary layer above 30 m. III. 19 p2448 A73-38214
- Height distribution of O⁺ and H⁺ ions in the ionosphere F2 region. I 19 p2427 A73-38333
- Atmospheric temperature and humidity vertical profiles from satellite-borne IR spectral radiance measurements, using linear extrapolation and statistical regression techniques. [AAS PAPER 73-124] 20 p2521 A73-38584
- Altitude distribution of the drift velocity and direction of ionosphere inhomogeneities over Ashkhabad in years of maximum and minimum solar activity. 20 p2554 A73-39162
- Altitude dependence of F 2 layer electron density annual anomaly, discussing summer-winter density discrepancies and nighttime critical frequencies. 20 p2555 A73-39177
- Moon production in large air showers, determining mean origin height via magnetic spectrography, distance from shower core, geomagnetic deflection and trajectory angles. 20 p2603 A73-39707
- A survey on the recent measurements of the absolute vertical cosmic-ray muon flux at sea level. 20 p2603 A73-39825
- Design and performance characteristics of the Vertical Temperature Profile Radiometer (VTPR) for atmospheric temperature soundings. 20 p2567 A73-39852
- Anomalies in geomagnetic variations across the central Gulf of California. 21 p2679 A73-39928
- Low value atmospheric density extremes evaluation covering ground elevations up to 15,000 feet for engine power calculation in aircraft design. 21 p2729 A73-40063
- Tropospheric and stratospheric vertical profiles of methane concentration via air sampling and gas chromatography, noting temporal and spatial variations. 21 p2680 A73-40077
- CO atmospheric vertical distribution from balloon-borne IR grating spectrometer observations, noting concentration decrease with altitude. 21 p2680 A73-40078
- Theoretical model of vertical distributions of CO and CH₄ in the mesosphere and upper stratosphere. 21 p2680 A73-40085
- Ground based and rocket techniques for vertical ionospheric electron density distribution measurement, considering incoherent scatter, partial reflection, wave interaction, and Faraday rotation. 21 p2685 A73-40809
- An analysis of the altitude dependence of the geomagnetic effect by means of 'equivalent durations.' 21 p2689 A73-41353
- Steady state coefficients in the D region during solar particle events. 21 p2760 A73-41372
- A numerical diffusion model for continuous releases. 21 p2732 A73-41568
- Airborne IR spectrometer with solar sensor for stratospheric minor molecular constituents vertical distribution, indicating spectral resolution for vibrational-rotational absorption bands. [ONERA, TP NO. 1216] 22 p2847 A73-42221
- Characteristics of the redistribution of charged particles in the nighttime E region at mid-latitudes. 22 p2847 A73-42331
- Measurements of absolute intensities of cosmic-ray muons in the vertical and greatly inclined directions at geomagnetic latitudes 16 N. 22 p2903 A73-42437
- Measurement of the absolute vertical integral and differential cosmic-ray single-muon flux at 3.6 GeV and a measurement of the showerless penetrating particle-pair flux above 3.6 GeV. 22 p2903 A73-42440
- Spectral structure of tropospheric vertical temperature profiles over Cape Kennedy, Florida. 22 p2849 A73-42544
- Tropospheric aerosol - The relative contribution of marine and continental components. 22 p2849 A73-42547
- Three-dimensional analytical model of electron density distribution of the quiet ionosphere. 23 p2970 A73-43232
- Average nighttime vertical profile of the 6300 A atmospheric emission. 23 p2970 A73-43242
- Spherical harmonic analysis of the geomagnetic field for the 1965 epoch up to n = 23 according to ground-based data. II - Results. 23 p2971 A73-43250
- Venera 8 - Measurements of solar illumination through the atmosphere of Venus. 23 p3029 A73-43603
- Metastable oxygen atoms radiative lifetime quenching rate as function of altitude in lower ionosphere based on auroral observations and atmospheric model. 23 p2972 A73-43692
- Fourteen-year series of vertical ozone distribution over Arosa, Switzerland, from Umkehr measurements. 23 p2974 A73-43869
- Six years of regular ozone soundings over Switzerland. 23 p2974 A73-43870
- Studies of variations in the vertical ozone profiles over India. 23 p2975 A73-43871
- Studies of the vertical distribution of atmospheric ozone in association with western disturbances over India. 23 p2975 A73-43872
- Statistical characteristics of the vertical ozone distribution in mid-latitudes. 23 p2975 A73-43874
- Aerosols - A limitation on the determination of ozone from UV observations. 23 p2975 A73-43879
- The concentration of molecular H₂ and CH₄ in the stratosphere. 23 p2976 A73-43891
- Recent developments in photochemistry of atmospheric ozone. 23 p2951 A73-43892
- On the vertical distribution of carbon monoxide and methane in the stratosphere. 23 p2976 A73-43894
- On the behavior of nitrogen oxides in the stratosphere. 23 p2976 A73-43896
- On the theoretical model for vertical ozone density distributions in the mesosphere and upper stratosphere. 23 p2977 A73-43898
- On the vertical ozone and wind profiles near the tropopause. 23 p2977 A73-43907
- IR absorption spectrometry to determine vertical distribution of nitric oxide abundance in stratosphere. 23 p2978 A73-43959
- Zonally symmetric global general circulation models with and without the hydrologic cycle. 23 p2978 A73-43981
- A numerical method for determining the temperature structure of planetary atmospheres. 24 p3130 A73-44456
- Rocket-borne spectrometer measurement of solar UV flux for thermospheric vertical distribution of molecular oxygen. 24 p3135 A73-44632
- Layering of the neutral metals of meteoric origin in the lower ionosphere. 24 p3066 A73-44733
- Tropospheric vertical energy transfer due to terrestrial and atmospheric water vapor and carbon dioxide radiation calculated for vertical atmospheric temperature and composition distributions. 24 p3082 A73-44736
- Vertical and latitudinal development of a seasonal anomaly in the daytime F2 region. I 24 p3083 A73-44791
- Formation of the sporadic E layer and the nighttime E region of the ionosphere at midlatitudes. 24 p3083 A73-44794
- Comparative analysis of rocket measurements of n sub e/h/ and of ground-based vertical sounding data. 24 p3083 A73-44795
- Positive nitrogen ions in midlatitude atmosphere, discussing concentration dependence on height, solar zenith angle and activity level. 24 p3084 A73-44801
- Height distribution and directionality of 2-12 A X-ray flare emission in the solar atmosphere. 24 p3124 A73-45046
- ISIS 2 scanning photometric analysis of E and F region airglow at O 15577 A, noting height difference of airglow components at midlatitudes and near equator. 24 p3088 A73-45214
- VERTICAL FINS
U FINIS
VERTICAL FLIGHT
Vertical aircraft flight control and navigation instrumentation avionics developments, emphasizing inertial-lead Vertical Speed Indicator design and command and advisory information displays. 13 p1621 A73-29345
- A flight evaluation of pilotage error in area navigation with vertical guidance. 21 p2733 A73-40029
- VERTICAL LANDING
Performance characteristics of a model VTOL lift fan in crossflow. 11 p1301 A73-25782
- VERTICAL MOTION
On the effect of the vertical drift in the equatorial F region. 04 p0443 A73-15476
- Vertical motion of the lower ionosphere during a solar eclipse. 05 p0569 A73-16262
- Vertical scintillation propagation from ground characterized by log normal probability distribution, universal spectral function and variance behavior dependent on near ground meteorological conditions. 05 p0569 A73-16625
- The vertical thermal structure of the Martian atmosphere - Modification by motions. 09 p1145 A73-22271
- Upper sporadic E layer downward velocity, considering corkscrew mechanism, ionization following gravity wave particular phase and velocity decrease. 10 p1215 A73-24750
- Precipitation patterns effective fall velocity determination from three dimensional radar scan data, discussing interpolation/extrapolation technique to improve coarse sampling time effects. 12 p1520 A73-26808
- Vertical free vibrations of rectangular vessel partially filled with perfect incompressible liquid analyzed by power series. 15 p1860 A73-31045
- Stochastic wind field effects on baroclinic wave disturbances vertical propagation through turbulent atmosphere, obtaining stream function and dispersion equation. 15 p1907 A73-32356
- Solar convective motions and associated magnetic fields, discussing photospheric cellular and chromospheric vertical motions, fibril structures, sunspot magnetic properties and faculae. 16 p2061 A73-33283
- Downward transport of nighttime Es layers into the lower E-region at Arecibo. 18 p2302 A73-35941
- Dynamic processes as derived from the mean circulation in the upper mesosphere and lower thermosphere. 18 p2307 A73-36036
- Distortions of the nighttime ionosphere during magnetospheric substorms. 18 p2312 A73-36279
- A three-level model for calculating vertical motions generated by planetary orography. 18 p2314 A73-37073
- The upward propagation of LF waves /electron whistlers/ into the ionosphere and the turning of the Poynting vector towards the earth's magnetic field. 21 p2654 A73-40782
- Wind component exchange and the rapid vertical movement of a sporadic E layer. 22 p2845 A73-41922
- Internal gravity wave-mean wind interaction. 23 p3000 A73-43339
- Cumulus-scale vertical transport of mass, heat and momentum calculated from radar and rain gage precipitation measurement. 23 p3002 A73-43596
- On the large scale vertical movements of the F-layer and its effects on the total electron content over low latitude during the magnetic storm of 25 May 1967. 23 p2972 A73-43699
- Influence of the vertical motion field on ozone concentration in the stratosphere. 23 p2977 A73-43904

VERTICAL PERCEPTION

The effect of dissipation on the vertical propagation of planetary waves in the vicinity of critical levels.
23 p3032 A73-43906

VERTICAL PERCEPTION

Muscular activity control mechanism interactions in vertical posture maintenance from stabilogram, mechanogram and electromyogram data
02 p0137 A73-12119

Effect of forward head inclination on visual orientation during lateral body tilt.
03 p0266 A73-13000

Moving visual scenes influence the apparent direction of gravity.
04 p0411 A73-15250

Effect of lateral body tilts and visual frames on perception of the apparent vertical.
22 p2811 A73-41736

Optimal input rates for tilt adaptation.
22 p2814 A73-42500

VERTICAL STABILIZERS

U STABILIZERS [FLUID DYNAMICS]

VERTICAL TAILS

U STABILIZERS [FLUID DYNAMICS]

U TAIL ASSEMBLIES

VERTICAL TAKEOFF

Performance characteristics of a model VTOL lift fan in crossflow.
11 p1301 A73-25782

VERTICAL TAKEOFF AIRCRAFT

NT FLYING PLATFORMS

NT X-22 AIRCRAFT

Suction force suppression during takeoff, landing and transition of VTOL turbojet via wing turning wing about axis parallel to earth plane
02 p0129 A73-11631

A procedure for the barometric altitude control in the case of hovering devices and helicopters
03 p0249 A73-12916

Light combat aircraft with hover capability.
03 p0251 A73-13923

Russian book - VTOL aircraft power plants.
04 p0487 A73-15706

Choices for the future - An industry viewpoint on prototyping.
05 p0534 A73-16659

SAE PAPER 720848] VTOL aircraft and short-haul transportation.
06 p0648 A73-18150

A proposed design for the construction of a VTOL simulator
08 p0952 A73-21249

Evaluation of glide paths for landing a VTOL airplane using linear regulator theory.
12 p1458 A73-27154

Prediction of height-velocity boundaries for rotorcraft by application of optimization techniques.
12 p1459 A73-27175

Anthropotechnical investigation of an above-ground indication and of an artificial horizon with preindication in connection with the manual control of VTOL aircraft
15 p1839 A73-32044

VTOL and STOL projects flight simulation trials for autostabilization, head-up displays and flight controls effectiveness in handling qualities improvement and pilot workload reduction
16 p1996 A73-33209

A flight research program to define VTOL visual simulator requirements.
16 p1996 A73-33210

Effect of rotor design tip speed on aerodynamic performance of a model VTOL lift fan under static and crossflow conditions.
16 p1963 A73-33480

Control of turbofan lift engines for VTOL aircraft.
16 p2047 A73-33496

NASA research commercial VTOL transport propulsion system specifications and components development, discussing lift fan propulsion method for aircraft attitude control
16 p2047 A73-33498

SAE PAPER 73-GT-24] Future technology and economy of the VTOL aircraft; International Helicopter Forum, 10th, Bueckeburg, West Germany, June 5-7, 1973, Proceedings
17 p2098 A73-34251

Progress in the development of a practically applicable VTOL aircraft with low disk loading
17 p2098 A73-34254

Military VTOL combat and commercial efficiency considerations, including convertiplane substitution, Mach number effects and reverse flow on blades, rotor design and speed limitations
17 p2098 A73-34256

VTOL jet transport aircraft commercial applications, describing lift engine system, hover flight control, engine failure problems and operating cost analysis
17 p2099 A73-34257

VTOL and helicopter design considerations, including nonsymmetrical rotor flow characteristics, rotor types, airspeed capacities, compound helicopters, tilt wing and tilt rotor aircraft
17 p2099 A73-34259

A manual-control approach to development of VTOL automatic landing technology.
17 p2209 A73-35075

AHS PREPRINT 742] VTOL applications in civil aviation, discussing safety, noise reduction, fatigue life, industrial applications, economic factors, short haul utilization and wind tunnel tests
19 p2384 A73-37813

Possibilities and problems of achieving community noise acceptance of VTOL.
19 p2386 A73-38010

VFW-FOKKER VAK-191B VTOL fighter aircraft structural and aerodynamic design, describing airframe construction, power plant arrangement, flight controls, hydraulic and electrical systems
19 p2387 A73-38167

Influence of the effectiveness of jet vanes on the characteristics of VTOL aircraft
21 p2634 A73-40401

Future technology and economy of jet-supported VTOL transport aircraft
21 p2793 A73-40448

Flight simulation requirement in artificial stabilizer design for VTOL aircraft flight control system, noting agreement with flight tests
22 p2838 A73-41751

VERTICAL TAKEOFF AND LANDING

U VERTICAL LANDING

U VERTICAL TAKEOFF

VERTOL MILITARY HELICOPTERS

U BOEING AIRCRAFT

VERY HIGH FREQUENCIES

Frequency independent characteristic time scales in meter wave intensity structure of pulsars CP 0950 and 1133, using predetection dispersion removal technique
03 p0374 A73-13715

Meter-wavelength observations of the solar radio burst storm of August 17-22, 1968.
08 p0997 A73-20768

Propagation mode deduced from signal strengths in the VHF band on the trans-equatorial path.
09 p1051 A73-22749

VHF preamplifier with FET for resolving crosstalk and overload problems comparing designed and observed specifications
09 p1066 A73-23429

A new VHF interferometer with three steerable high-gain-antennas for satellite-tracking.
09 p1070 A73-23434

Ionospherically diffracted monochromatic VHF/UHF plane wave statistics characterization, noting Gaussian and log-normal distributions from ATS-3 satellite data recording
10 p1190 A73-24896

On some transient H-alpha features associated with metric type III bursts.
16 p2053 A73-32963

Solid-state transmitter for VHF/UHF space telemetry.
16 p1979 A73-33104

Wideband VHF whip antenna impedance simulation using Al cylindrical chamber to simplify impedance-controlling network tuning and power testing
17 p2148 A73-35705

Radio interferometer for the range from 136 to 138 MHz in the central German ground station
19 p2432 A73-38273

Analysis of VHF/UHF frequency dependence, space, and polarization properties of ionospheric scintillation in the equatorial region.
20 p2525 A73-38741

Digitally switched phase shifter operating at metric wavelengths
21 p2662 A73-40544

A 50-W VHF amplifier with transistors
21 p2664 A73-41088

VLF input impedance of a loop antenna embedded in the magnetosphere.
23 p2954 A73-43700

VERY HIGH FREQUENCY RADIO EQUIPMENT

Design and performance of VHF telemetry transmitter and remote controlled radio receiver for Eole satellite, noting production technology and block diagram
07 p0790 A73-18961

Low noise VHF preamplifier design for backscatter radar, presenting circuit diagram
07 p0801 A73-19536

VERY LOW FREQUENCIES

Two X-ray bursts /1 August 1967 and 30 January 1968/ and some associated VLF disturbances.
01 p0091 A73-10556

Studies of the lower ionosphere by means of VLF propagation over long distances
01 p0044 A73-11515

Preliminary findings of a petrel rocket experiment to investigate the VLF emission 'chorus' in the ionosphere.
02 p0141 A73-12319

A theory on the latitude and local time distribution of precipitating electrons during a sudden commencement.
03 p0304 A73-13885

VLF wave propagation properties in waveguide formed by ground and ionospheric shell, noting diurnal phase and amplitude anomalies due to ionospheric disturbances
04 p0416 A73-15060

A model of VLF band radio wave propagation in the earth-ionosphere waveguide channel
05 p0549 A73-16391

Effect of the earth's electrical properties on the characteristics of VLF wave propagation in the earth-ionosphere waveguide
05 p0550 A73-16398

A theoretical and experimental study of non-ducted VLF waves after propagation through the magnetosphere.
05 p0551 A73-17054

A satellite study of the mid-latitude trough in electron density and VLF radio emissions during the magnetic storm of 25-27 May 1967.
05 p0571 A73-17060

Omega v.l.f. wave propagation and the 1922-23 Marconi expedition.
06 p0668 A73-18442

Incoherent Cerenkov radiation in the magnetosphere and the ground observations of VLF hiss.
07 p0814 A73-19240

Measurement of the dielectric constant of polyvinyl chloride at very low frequencies, and influence of the superposition of a continuous voltage
08 p0942 A73-20648

Use of electron and proton beams for production of very low frequency and hydromagnetic emissions.
09 p1074 A73-22061

A magnetically controlled tube generator of very-low-frequency sinusoidal oscillations
09 p1063 A73-22337

Anomalous diurnal changes of transequatorial VLF radio waves.
11 p1330 A73-25760

VLF radio signals propagational effects relationship to ionospheric polar substorm different phases
11 p1330 A73-25765

Physical interpretation of the diurnal behavior of the TM and TE components of VLF fields in the far zone
11 p1331 A73-26152

Tunneling transmission through the equatorial lower ionosphere of ELF and VLF electromagnetic waves.
11 p1358 A73-26707

Employment of mode theory and ray theory for their interpretation of very-long-wave measurements at medium distances
12 p1474 A73-27766

VLF atmospheric measurement and geophysical analysis, discussing meteorological, geoelectric and propagation aspects
13 p1582 A73-28152

Intercomos 5 investigation of VLF electromagnetic signals and emissions, discussing onboard instruments to measure particle fluxes
13 p1622 A73-29663

Spiral top-loaded antenna (STLA) characteristics and design procedure derivation via self consistent field method, noting VLF applications
14 p1734 A73-30204

The values of ionospheric absorption of VLF electromagnetic waves in middle geomagnetic latitudes.
15 p1868 A73-31522

Digital correlator-computer-pattern recognition system for VLF phenomena investigation, discussing electromagnetic waves structure and spectrum analysis
15 p1845 A73-32233

Penetration and reflection of VLF waves through the ionosphere - Full wave calculations with ground effect.
16 p1984 A73-33921

A device for qualifying very low frequency vibration exciters
16 p2083 A73-33977

VLF and Omega signal air navigation at 3 to 30 kHz supplementing VOR-DME and Loran-A navigation frequencies, considering transmission techniques
17 p2209 A73-34616

Aircraft VLF radio navigation, discussing propagation characteristics, Omega and Global Navigation systems and historical development
17 p2209 A73-34657

SAE PAPER 730313] Space probe observed VLF hiss powers disappear with theoretical prediction for incoherent Cerenkov radiation, considering Landau instability generated wave amplification
17 p2160 A73-34777

VLF navigation development at NAE.
17 p2209 A73-34844

Propagation of VLF waves in the earth-ionosphere waveguide under nighttime ionospheres.
17 p2126 A73-35626

Ducted propagation of VLF waves through the magnetosphere.
18 p2288 A73-35994

VLF pulse ionosonde measurements of the reflection properties of the lower ionosphere.
18 p2305 A73-36004

- Measurements of ionospheric reflectivity from 6 to 35 kHz. 18 p2289 A73-36286
- Localization of sources of two-hop whistlers observed aboard the Interkosmos 3 satellite over Europe. 19 p2404 A73-38021
- Whistlers association with sudden changes in amplitude of long distance nighttime subionospheric VLF transmission 20 p2530 A73-38944
- Ariel 3 evidence of zones of VLF emission at medium invariant latitudes which co-rotate with the earth. 21 p2691 A73-41382
- Non-linear propagation of VLF waves in a magnetoplasma including the effect of ions. 23 p3012 A73-44143
- Generation of VLF waves in the ionosphere near the low-frequency plasma resonance. I 24 p3115 A73-44788
- Short-time fluctuations of the VLF field along polar paths 24 p3067 A73-44809
- ## VESSELS
- Rational winding of vessels with nonlinear winding programs 18 p2319 A73-36470
- ## VESTA ASTEROID
- The light-curve for the minor planet 4/ Vesta. 03 p0379 A73-14578
- ## VESTIBULAR TESTS
- Semicircular canals as a primary etiological factor in motion sickness. 02 p0135 A73-12560
- Auditory rail task for acoustic stimuli effects on human equilibrium under axisymmetric intermittent tone exposure, discussing acoustic energy effect on vestibular receptors 03 p0260 A73-13551
- Vestibular adaptation in man - Effects of increased acceleration during different phases of adaptation. 04 p0411 A73-15218
- Vestibular reactions to Coriolis accelerations under hypoxia conditions 06 p0650 A73-17691
- Caloric vestibular stimulation via UHF-microwave irradiation. 10 p1178 A73-23650
- The role of vestibulometry in medical evaluation of flight personnel 10 p1183 A73-23821
- Clinical applications of averaging techniques in studies of vestibulo-oculomotor function. I - Basic techniques and illustrative cases. 11 p1315 A73-25339 [AD-758545]
- Posture responses of upper limb muscles during electric stimulation of the vestibular apparatus 11 p1317 A73-26087
- Vestibular stresses effects on systemic and cerebral hemodynamics, considering human acceleration adaptation and compensation mechanisms 12 p1463 A73-27714
- Changes in visual functions after the action of weak vestibular stimuli 12 p1464 A73-27719
- Harmonic spectral analysis of nystagmus waveform frequency content for clinical vestibular examination via digital computer 13 p1579 A73-28502
- Nystagmic response persistence to Fitzgerald-Hallpike caloric tests as function of directional cupular deflections due to head movement 13 p1576 A73-28510
- Asymmetry of otolith responses in fish 15 p1834 A73-31507
- Effect of antiradiation drugs on the functional condition of the vestibular analyzer 15 p1838 A73-31509
- Influence of stimulation of the vestibular analyzer under conditions of hypoxia on certain functions of the visual analyzer 15 p1835 A73-31516
- Calculation of a Coriolis acceleration acting on semicircular canal receptors of man in rotating systems 15 p1835 A73-31518
- Experimental-mathematical analysis of the effects of rotational accelerations on the vestibular apparatus 17 p2110 A73-34120
- Effectiveness of some hemodynamic indices in the detection of vestibulo-vegetative disorders under ordinary conditions and those of hypoxia 17 p2110 A73-34121
- Analysis of vestibular effects in experiments on swings 17 p2111 A73-34235
- Certain features of hemodynamics during orthostatic tests with persons of different vestibulo-vegetative tolerance levels 17 p2111 A73-34236
- Skylab astronaut vestibular function experiment in orbital flight, discussing motion sickness susceptibility, stimulation thresholds and space perception measurements 17 p2115 A73-34741
- Cross coupling between effects of linear and angular acceleration on vestibular nystagmus. 18 p2272 A73-36441
- Visual-vestibular interaction and motion perception. 18 p2273 A73-36460
- Effect of sonic boom on hearing and vestibular equilibrium 18 p2284 A73-36910
- Aircraft pilot spatial disorientation and illusory perceptual break-off sensations during flight associated with minor vestibular asymmetry 20 p2512 A73-39111
- Effects of round window stimulation on unit discharges in the visual cortex and superior colliculus. 20 p2513 A73-39146
- A descriptive model of multi-sensor human spatial orientation with applications to visually induced sensations of motion. 21 p2644 A73-40863 [AIAA PAPER 73-915]
- On the electronic simulation of acceleratory nystagmus. 22 p2816 A73-42683
- ## VESTIBULES
- Vestibular influences on orientation in zero gravity, produced by parabolic flight. 06 p0653 A73-18032
- Comparative anatomy of the vestibular nuclear complex in submammalian vertebrates. 06 p0655 A73-18575
- Electrophysiological study of the topographic organization of Deiters' lateral vestibular nucleus 10 p1181 A73-24515
- Adequate vestibular stimulants on earth and in space 17 p2110 A73-34122
- Histological studies on the vestibular organ of frog embryos and larvae after the influence of simulated weightlessness. 18 p2270 A73-35979
- Vestibular and cerebellar control of oculomotor functions. 18 p2271 A73-36438
- ## VER (RULES)
- ### U VISUAL FLIGHT RULES
- ### VHF OMNIRANGE NAVIGATION
- A system for the precise calibration of air navigational receivers. 03 p0310 A73-14501
- PRS-system for determination of position of flight inspection aircraft for control of ILS-and VOR facilities. 15 p1909 A73-32449
- Doppler VOR equipment, economics, blending function and antenna system, discussing ground measurement and monitoring, sideband generation and reference modulation 15 p1859 A73-32452
- French VOR system with single type equipment for operation on site at performance levels to meet ICAO standards, emphasizing antenna design 15 p1909 A73-32453
- A VOR sensor of advanced design - The Bendix RVA-33A. 15 p1909 A73-32454
- Doppler VOR area navigation operational principles, emphasizing bearing accuracy improvement compared to conventional VOR systems 15 p1909 A73-32456
- The application of digital techniques to a VOR signal generator. 16 p1979 A73-33405
- Ground and flight test results for standard VOR and double parasitic loop counterpoise antennas. 17 p2129 A73-35700
- Plane coordinate transformations for area navigation based on existing VOR/DME network 18 p2336 A73-37043
- Data compression in recursive estimation with applications to navigation systems. 20 p2589 A73-38835 [AIAA PAPER 73-901]
- ## VIABILITY
- Survival of Arthrobaacter crystallopoietes during prolonged periods of extreme desiccation. 07 p0782 A73-20026
- ## VIBRATION
- NT BENDING VIBRATION
- NT BREATHING VIBRATION
- NT COMBUSTION VIBRATION
- NT FLUTTER
- NT FORCED VIBRATION
- NT FREE VIBRATION
- NT LATTICE VIBRATIONS
- NT LINEAR VIBRATION
- NT PANEL FLUTTER
- NT POGO EFFECTS
- NT RANDOM VIBRATION
- NT RESONANT VIBRATION
- NT SELF INDUCED VIBRATION
- NT STRUCTURAL VIBRATION
- NT SUBSONIC FLUTTER
- NT SUPERSONIC FLUTTER
- NT TORSIONAL VIBRATION
- NT TRANSONIC FLUTTER
- Statistics of laser beam fade induced by pointing jitter. 08 p0975 A73-21058
- Development of data analysis in sound and vibration. 17 p2131 A73-35335
- Laser absorption study of carbon monoxide vibrational relaxation behind incident shock waves, discussing vibration-rotation levels, shock tubes, oscilloscope traces and Boltzmann distributions 19 p2437 A73-37900
- Non-linear vibration of beams with time-dependent boundary conditions. 19 p2501 A73-38253
- Russian papers on vibration theory of lumped and distributed systems covering pendulums, virial theorem, electric filters, solids, Fourier series, degrees of freedom and sinusoidal waves 21 p2741 A73-41434
- ## VIBRATION DAMPERS
- ### U VIBRATION ISOLATORS
- ### VIBRATION DAMPING
- Damping in copper-aluminum-nickel alloys and its causes 01 p0064 A73-10611
- Synthesis of active controllers for vibratory systems. 01 p0057 A73-10697
- A linearized analysis for frictionally damped systems. 01 p0090 A73-10782
- Recent developments in testing unstable burning characteristics of solid propellants. 01 p0089 A73-11115
- Reaction of a damped system to the simultaneous action of an isolated semisinusoidal impact pulse and of vibrational oscillations 01 p0054 A73-11418
- Determination of attenuation factors from experimental vibrograms of multifrequency attenuating oscillations 02 p0233 A73-11942
- A selfadjoint formulation of overdamped systems. 02 p0193 A73-12090
- Low-frequency oscillations in a bounded low-density plasma. 02 p0198 A73-12105
- Transverse vibrations generated in a bracket bar by the reciprocating linear displacements of its seal which are damped in the course of time. 02 p0235 A73-12127
- Oscillation damping by pulsed dynamic dampers. 02 p0235 A73-12209
- Neutron star vibration damping from semirealistic neutron star models with magnetic field, superfluid component, outer crust, normal neutron composition and quantum crystals 02 p0222 A73-12714
- Liapunov function for Hamilton-Jacobi equation for motion stability of linear and nonlinear mechanical systems, calculating vibration damping factor 03 p0342 A73-13157
- Frequency dependence of the damping of mechanical vibrations in some commercially pure metals 03 p0327 A73-13976
- HF transverse resonant vibrations of annular Al plates with polychlorovinyl and polyamide base coatings, noting damping and strain relationship to energy dissipation 03 p0394 A73-14009
- Governing equations for vibrating constrained-layer damping sandwich plates and beams. [ASME PAPER 72-WA/APM-24]
- Non-linear damping of longitudinal ion oscillations in a collisionless non-isothermal plasma. 04 p0515 A73-15892
- Study of the dynamics of the preliminary-damping system of a gravitationally stable satellite with allowance for constraints on its sensors and on the flexural vibrations of the stabilizer 04 p0482 A73-16042
- Porcelain enamels for heat resistant alloys low temperature fatigue strength and high temperature vibration damping increase [SAE PAPER 720809] 05 p0633 A73-16629
- Modal damping predictions using substructure testing. [SAE PAPER 720810] 05 p0634 A73-16643
- Study of modeling of substructure damping matrices. [SAE PAPER 720813] 05 p0634 A73-16645
- The calculation of the natural vibration parameters of a damped system on the basis of the results of a vibration test in an exciter configuration 05 p0634 A73-16758
- Measurement of vibration characteristics by impact testing. 05 p0637 A73-17233
- Nonlinearity of Helmholtz resonators 05 p0599 A73-17269
- Anisotropic flexible bearings mounted rotors backward and forward precessional motion excitation,

noting internal viscous damping forces effect on vibration amplitude

06 p0758 A73-17515

Magnetic articulation damping for gravity gradient satellite stabilization, using digital simulation

07 p0904 A73-18937

Rocket sled facility for impact tests with friable balloon platforms, describing braking and accelerating jet configurations, vibration damping measures and telemetry system

07 p0808 A73-19004

Kron algorithm for complex eigenvalue problems of damped vibrating mechanical systems, using Newton method

07 p0909 A73-19098

The status of engineering knowledge concerning the damping of built-up structures.

07 p0909 A73-19099

German monograph - Harmonically excited forced oscillations of a spring/mass system with controlled Coulomb damping.

07 p0851 A73-19581

Connecting measured objects with sensors measuring the parameters of vibrational motion

07 p0826 A73-20531

Prediction of aeroelastic instabilities in turbines

09 p1135 A73-22204

Double heterojunction [GaAl]As laser pulse modulation at 200 Mbits/sec continuous operation at room temperature, considering lasing delay time and damped oscillations problems

09 p1093 A73-22257

Damping of plasma waves in the lower hybrid frequency range.

09 p1131 A73-22908

Experimental study of the damping of bending vibrations in supported square plates with coatings.

09 p1161 A73-23153

Method of variation of parameters starting with linear damped vibration solution as its generating solution.

09 p1121 A73-23324

Three layered sandwich rings damped vibrations under time-harmonic radial concentrated load, comparing experimental and theoretical mechanical impedance data

09 p1165 A73-23440

High-damping measurements and a preliminary evaluation of an equation for constrained-layer damping.

09 p1166 A73-23458

Criteria for oscillations in closed isothermal reacting systems.

10 p1294 A73-23561

Improving reliability and eliminating maintenance with elastomeric dampers for rotor systems.

10 p1175 A73-23950

Damping properties of VT-1, VT-9, and VT-18 titanium alloys of various microstructure

10 p1233 A73-24359

An analytical estimate of the effect of mobility of a small internal mass on oscillations of a body during deceleration in the atmosphere

10 p1286 A73-24451

Damping of an aerial photo camera with the aid of polymeric materials

10 p1219 A73-24478

Calculation of forced vibrations in damped centrifugal pumps with a given level of rotor imbalance

10 p1263 A73-24673

Effect of atomic oxygen on the N2 vibrational temperature in the lower thermosphere.

10 p1214 A73-24748

Beam and plate flexural vibration damping by free or uncompressed rigid viscoelastic coatings applied on sides

10 p1293 A73-24794

Distribution of equivalent attenuations and generalized detunings in a stagger single-tuned IF amplifier with critical staggering.

10 p1197 A73-24936

Formulation of Pontryagin's maximality principle in a problem of structural mechanics.

11 p1434 A73-25185

Experimental investigation of oscillation damping in shells with holes

11 p1435 A73-25398

Synthesis of shuttle vehicle damping using substructure test results.

11 p1430 A73-25529

[AIAA PAPER 73-400]

Analysis of stall flutter of a helicopter rotor blade.

11 p1305 A73-25532

[AIAA PAPER 73-403]

European contribution to structural response to noise.

11 p1305 A73-25561

[AIAA PAPER 73-332]

Comparison and oscillation theory for Liénard's equation with positive damping.

11 p1391 A73-26367

In-flight flutter testing methods for determining aircraft structure natural frequencies and vibration damping ratios with air flow

11 p1306 A73-26593

[ONERA, TP NO. 1224]

Small oscillations of gravity gradient satellite in circular near-equatorial orbit, discussing operational efficiency of magnetic damping systems

12 p1549 A73-27648

Frequency method of synthesis for an active dynamic vibration damper

12 p1525 A73-27948

Improvement of damping characteristics of structural members with high damping elastic inserts.

13 p1690 A73-28056

Effect of shroud eccentricity on suppression of flow induced vibrations.

13 p1690 A73-28059

Piezoelectric sound pressure sensor for damping measurement of structural element coatings under intense acoustic loads

13 p1618 A73-29060

Bending vibration test of glass-textolites, noting temperature effect on vibration damping properties

13 p1647 A73-29607

Graphite content effect on vibration damping properties of Al-Sn and Al-Zn alloys

13 p1643 A73-29608

Vibration analysis of sandwich beam with constrained viscoelastic layers on both sides.

14 p1806 A73-30046

Russian book on elastic structures vibration in aircraft covering integral equations for beams, damping principles and transcendental equations for flexural and torsional vibrations natural frequencies

14 p1810 A73-30354

Book - Optimal control theory for the damping of vibrations of simple elastic systems.

14 p1813 A73-30674

Gravity oriented satellite librational damping by solar radiation pressure, comparing WKB method with numerical integration results

15 p1943 A73-31640

Whirling shafts motion stability necessary and sufficient conditions analysis based on Liapunov method, taking into account internal and external damping effects

15 p1955 A73-32166

Nonlinear magnetoelastic effects in Ni tube torsion spring pendulum due to oscillation damping and stiffness characteristics dependence on amplitude

16 p2025 A73-33214

Self induced vibration of friction bearing mounted rigid rotor, considering oscillation damping or enhancing effect of oil film

16 p1968 A73-33236

Effects of attenuation on the stability characteristics in the case of combination resonances

16 p2080 A73-33260

Damped lateral vibration in an axially creeping beam with random material parameters.

16 p2082 A73-33902

Damping properties of turbine blade materials at operational temperatures

17 p2221 A73-34327

Assembly for studying oscillation damping in rod elements in the field of centrifugal forces

17 p2145 A73-34340

The Sorokin damping hypothesis in the case of aperiodic vibrations

17 p2243 A73-34648

Estimation of the response of a mechanical structure to arbitrary excitation

17 p2243 A73-34649

Helicopter turboshaft engine vibration reduction through engine-airframe interface compatibility design and torsional stability of drive trains with automatic fuel control

[AHS PREPRINT 774]

17 p2106 A73-35092

High frequency vibration of aircraft structures.

17 p2250 A73-35329

Oscillation theorems for a second order damped nonlinear differential equation.

18 p2330 A73-36694

Piezoelectric sound pressure sensor for damping measurement of structural element coatings under intense acoustic loads

18 p2317 A73-36892

Vibration isolation and the use of controlled flexibility for noise reduction.

19 p2495 A73-37298

Comparison of optimized active and passive vibration absorbers.

19 p2435 A73-38084

Analytical estimate of the effect of the motion of a small internal mass on the oscillation of a body decelerating in the atmosphere.

19 p2494 A73-38131

Flexural vibrations of rods with viscoelastic coating subjected to axial force.

19 p2502 A73-38347

Building a dynamic test complex near an inertial test facility and general test pad considerations.

20 p2543 A73-38772

Operational temperature and frequency effects on radial driving point mechanical impedance of damped thin walled ring with mass segments attached by viscoelastic material

20 p2616 A73-39051

Virtual motion principle implication for structural damping differential equations for cases of homogeneous, inhomogeneous and aerodynamic flutter for various degrees of freedom

20 p2616 A73-39098

Shock spectrum analysis and structural design.

20 p2617 A73-39270

Damping of glass-like materials at high temperatures.

20 p2580 A73-39272

Hydrodynamic bearing damping in infinitely broad gap between oppositely oscillating parallel boundary surfaces, discussing inertia, Reynolds number and coefficient of friction

20 p2547 A73-39409

Zeroth-order approximation by multiple scaling method to analyze nonlinear oscillations with small speed-dependent damping, applying to pendulum problem

20 p2593 A73-39536

Flutter-divergence transition criteria in certain viscoelastic polymeric systems.

20 p2623 A73-39556

Optimal active damping of vibrations

20 p2594 A73-39638

Resiliently mounted objects holographic system sensitivity threshold control by proper selection of support stiffness and vibration damping

21 p2698 A73-40132

Viscoelastic panel vibration damping material for ventilation ducts to reduce LF vibrations induced by turbulent air flow

21 p2723 A73-40235

Vibration and noise damping of steel structures by prebonded laminates or viscoelastic layer additions, discussing steel sheets

21 p2717 A73-40236

Computer program for determining system resonance frequencies and damping via numerical analysis of vector modal response loci plots

21 p2783 A73-40290

Control law synthesis and sensor design for active flutter suppression.

[AIAA PAPER 73-832]

21 p2784 A73-40502

Parametric study of multiple-layer damping treatments on beams.

21 p2785 A73-40750

A study of planar deployment control and librational damping of a tethered orbiting interferometer satellite.

21 p2781 A73-40900

Tuned dampers for randomly excited dynamical systems.

[ASME PAPER 73-DET-70]

22 p2919 A73-42070

A numerical study of damping in viscoelastic sandwich beams.

[ASME PAPER 73-DET-73]

22 p2919 A73-42070

Improvement of damping capacity of structural members by introduced stress concentration.

[ASME PAPER 73-DET-76]

22 p2919 A73-42070

Sinusoidal response of composite-material plate with material damping.

[ASME PAPER 73-DET-120]

22 p2919 A73-42080

Book - Dynamics in engineering structures.

22 p2922 A73-42490

German monograph - Passive and active satellite attitude control with the aid of rod-like torsion pendula.

22 p2917 A73-42590

Analysis of a damped, non-linear, non-autonomous system.

22 p2887 A73-42620

Studies of the relaxation of internal energy of molecular hydrogen.

22 p2898 A73-42760

German monograph - Characteristics of motion of an elastically supported rotor with interior damping.

22 p2867 A73-42840

Complex structural dynamic response reduction discussing methods for mathematical models establishment and application to thin cylindrical shells

22 p2926 A73-42920

Isolation of machinery vibration from nonrigid substructures using multiple antivibration mountings.

22 p2927 A73-42920

A study of a fluidic open loop damping flight stability augmentation system.

23 p2941 A73-43390

Study and calculation of the vibrations of a rotating rotor with allowance for clearances in the bearings

23 p3041 A73-43720

Damping of mechanical systems with the aid of viscoelastic liquids

24 p3109 A73-44900

Small transverse vibrations of a flexible rod under the action of a variable axial force

24 p3153 A73-45560

The motion of a body containing a liquid-filled cavity with elastic radial ribs and exhibiting perturbation relative to the longitudinal axis

24 p3112 A73-45510

VIBRATION EFFECTS
NT POGO EFFECTS

Polysynaptic pathways role in tonic vibration at monosynaptic reflexes due to muscle vibratory

nerve electric stimulation, respectively, discussing tetanization effects
01 p0008 A73-10409

Peripheral electromyography spike and ventral root unit discharge intervals during tonic vibration reflex of cat soleus motoneuron
01 p0008 A73-10410

Mathematical description of certain properties of human sensitivity to vibration
01 p0012 A73-10659

Michelson interferometer on Mariner 9 space probe for thermal emission spectrum measurement, discussing spectral resolution, external vibration problem and instrument performance
01 p0054 A73-11228

Criteria for self loosening of fasteners under vibration.
01 p0058 A73-11512

Non-linear vibration of rotating cantilever blades treated by the Ritz averaging process.
02 p0232 A73-11859

Convection heat transfer in a contained fluid subjected to vibration.
03 p0398 A73-13547

Oscillation effects upon film boiling from a sphere.
03 p0398 A73-13548

German monograph - Investigations concerning perception levels and transferred vibrational forces in the case of a vertical action of periodic vibrational mixtures on man.
03 p0268 A73-13818

Absence of appreciable cardiovascular and respiratory responses to muscle vibration.
03 p0263 A73-14119

Laser frequency fluctuations due to mechanical vibrations.
03 p0319 A73-14451

Changes in whole body force transmission of dogs exposed repeatedly to vibration.
[ASME PAPER 72-WA/BHF-11]

Analysis of the resistance of reed contacts to shock and vibration impacts
04 p0410 A73-15878

A momentum integral solution for pulsatile flow in a rigid tube with and without longitudinal vibration.
05 p0559 A73-17237

Some finite element solutions for plate bending problems by simplified hybrid displacement method.
05 p0567 A73-17273

Biophysical properties of vibration energy transfer to human body structure, noting harmful effects dependence on frequency range
06 p0758 A73-17444

Criteria for self loosening of fasteners under vibration. II.
06 p0657 A73-17748

Stability of a gyroscope on a vibrating base under resonance conditions
08 p0972 A73-20948

Some delinearization problems in the dynamics of complex vibrational systems
08 p0972 A73-21763

Criteria for self loosening of fasteners under vibration. III.
08 p0989 A73-21768

Combined effects of noise and vibration on human tracking performance and response time.
10 p1222 A73-23524

Effect of whole-body vibration on peripheral nerve conduction time in the Rhesus monkey.
11 p1315 A73-25335

Dynamic error of solid body-elastic rod pendulum system hinged on vibrating suspension point in terms of tensile rigidity finiteness
11 p1399 A73-26096

Incremental servomechanism design and application as substitute for step motor, discussing servomotor properties, mechanical torsional vibration and loading moment effects
12 p1483 A73-27422

Shallow spherical shell dynamic stability under axisymmetric loads, noting small HF vibrations effect on static stability
12 p1556 A73-27814

Determination of the time interval for orientation of conducting nonmagnetic oblong bodies by a homogeneous alternating magnetic field
13 p1571 A73-28467

Vibrating string total field /absolute gravity meter/ accelerometer, discussing calibration at single reference point
13 p1617 A73-28849

Simultaneous recording of acceleration and brain waves.
14 p1721 A73-29995

Vibrational relaxation effects in weak shock waves in air and the structure of sonic bangs.
14 p1711 A73-30174

Gradient instabilities in a system of gravitating point masses
15 p1938 A73-31954

Gas turbine vibration limits - A fundamental view.
[ASME PAPER 73-GT-48]

16 p2048 A73-33509

A statistical analysis of product reliability due to random vibration.
16 p2020 A73-33637

Experimental investigation of the effect of vibrations on the creep of glassfiber-reinforced plastics in the presence of complex stress conditions
16 p2030 A73-33939

Roentgenographic study of relative heart motion during vibration in water-immersed cats.
16 p1973 A73-34039

The problem of electron-pair tunneling in a sound field in superconductors
16 p2045 A73-34069

Cosmic ray pulses conduction to interstellar gas by magnetic field, describing effects on sound vibration
17 p2223 A73-34369

U.S. Army helicopter vibration data for OH-6A, OH-58A, UH-1H and CH-54B models obtained from triaxial accelerometer locations, presenting spectral and statistical analyses
[AHS PREPRINT 763]

Microwave amplifier design with discrete variable components, testing power output and efficiency, bandwidth, and temperature, vacuum and vibration effects on performance
17 p2106 A73-35086

Human response to transportation noise and vibration.
17 p2141 A73-35324

Effect of dynamic factors of space flights on green alga *Chlorella vulgaris*.
17 p2117 A73-35328

Microwave equipment reliability design for aerospace environment applications, considering vibration, shock, humidity and temperature effects and frequency stability
18 p2270 A73-36098

Influence of clearances on the behavior of a gyroscope on a vibrating base
18 p2293 A73-36778

Three models of the vibrating ulna.
19 p2428 A73-37188

Electro-mechano-hydraulic servovalve system, calculating dynamic frequency response in vibrating accelerated field under external disturbance
19 p2398 A73-37543

Theory of a two-mass model of a vibrational impactor
19 p2388 A73-37670

Vibration of tubes containing flowing fluid.
[MERL-TN-72-2]

Vibrations in environmental engineering; Proceedings of the Symposium, Imperial College of Science and Technology, London, England, July 4, 5, 1973.
20 p2592 A73-39891

Investigation of the motion of a gyroscopic pendulum on a randomly vibrating base
20 p2616 A73-39147

Interactive effects of intense noise and low-level vibration on tracking performance and response time.
21 p2644 A73-41153

Specifications of a cryostat for a vibrating sample magnetometer between 1.7 and 300 K
21 p2706 A73-41592

Scattering of electromagnetic waves from rough oscillating surfaces using spectral Fourier method.
22 p2824 A73-41855

Relation between vibratory sensibility and electric signal of living body.
22 p2816 A73-42680

Synthesis of optimal control of the longitudinal motion of an elastic tank containing liquid
22 p2843 A73-43059

Time-average holography of objects vibrating sinusoidally and moving with constant acceleration.
22 p2863 A73-43092

Radiological assessment of the vertebral column from the point of view of aviation medicine
22 p2817 A73-43131

Human reactions to whole-body transverse angular vibrations compared to linear vertical vibrations.
23 p2948 A73-43216

Optimal work-rest schedules under prolonged vibration.
23 p2948 A73-43217

Finite element analysis on L-L type vibration energy concentrator/divider considering its design.
23 p2961 A73-44138

The drifts of a gyroscope mounted on the oscillating housing.
23 p2983 A73-44271

Influence of ultrasonic vibrations on the mechanical properties and fine structure of aluminum and an aluminum-magnesium alloy
24 p3098 A73-44570

Use of the conditioned reflex method to study the motor analyzer during hygienic evaluation of working conditions in the presence of vibrations
24 p3062 A73-44673

Decrements in tracking and visual performance during vibration.
24 p3063 A73-44777

Influence of a discrete component of acoustic vibration on flow in a supersonic jet with a nondesign ratio of active to passive pressure
24 p3055 A73-45538

VIBRATION ISOLATORS

Vibration resistant holographic table consisting of polished iron plate resting on four elastic dampers mounted on two concrete supports
09 p1085 A73-23016

Shock absorbing-vibration insulating viscoelastic systems design under singular influence function assumption, determining ranges of parameters change
12 p1516 A73-27177

Hydraulic system noise measurements and control, discussing source, vibrating parts isolation, transmission path and acoustic barriers and enclosures
16 p1971 A73-33993

Vibration isolation and the use of controlled flexibility for noise reduction.
19 p2495 A73-37298

Comparison of optimized active and passive vibration absorbers.
19 p2435 A73-38084

Vibrations in environmental engineering; Proceedings of the Symposium, Imperial College of Science and Technology, London, England, July 4, 5, 1973.
20 p2544 A73-39265

High performance vibration isolated tables.
20 p2544 A73-39266

Resiliently mounted objects holographic system sensitivity threshold control by proper selection of support stiffness and vibration damping
21 p2698 A73-40132

Isolation of mechanical vibration, impact, and noise; Proceedings of the Colloquium, Cincinnati, Ohio, September 9-12, 1973.
22 p2926 A73-42920

Automatic control theory application to random vibration passive and active isolators synthesis, considering vehicle suspension systems and electrohydraulic damper
22 p2927 A73-42922

Isolation of machinery vibration from nonrigid substructures using multiple antivibration mountings.
22 p2927 A73-42923

Biodynamic applications regarding isolation of humans from shock and vibration.
22 p2816 A73-42926

Vibrations of turbojet-engine components containing structural dampers of the type of sandwich rods
23 p3020 A73-43735

VIBRATION MEASUREMENT

Interferometric measurements of the vibrostaticity of a holographic stand
01 p0050 A73-10798

A versatile Moessbauer spectrometer and its applications in structural mechanics.
03 p0305 A73-12875

Vibrational analysis with the aid of holographic interferometry vibrational analysis of acoustic radiators with the aid of holographic interferometry
03 p0306 A73-12985

Some applications of interferometry in coherent light
05 p0586 A73-17321

Application of holographic subtraction to time-average hologram interferometry of vibrating objects.
06 p0691 A73-17499

Acquisition and processing system of vibration measurements
07 p0807 A73-19001

Load amplifiers for vibration and shock measurements
07 p0808 A73-19009

Measurement of dynamic mechanical quantities; Scientific-Engineering Conference, 3rd, Warsaw, Poland, October 26-28, 1972, Summaries
07 p0826 A73-20526

Properties of electrocapillary transducers and possibilities of their application in vibration measurements
07 p0826 A73-20530

Connecting measured objects with sensors measuring the parameters of vibrational motion
07 p0826 A73-20531

Electromagnetic measurement of frequency and amplitude of mechanical vibration, based on echo signal phase modulation, explaining heterodyne detection system
07 p0827 A73-20532

Six-channel strain-gauge system for dynamic measurements
07 p0827 A73-20539

Vibration measurement by vibrating-plate holograms.
09 p1079 A73-21997

Fringe control in real time and double exposure holography for nondestructive testing of multilaminated and thin laminated structures and vibration analysis
11 p1370 A73-26541

Nondestructive flaw detection by holographic interferometry, discussing methods, equipment and applications for materials testing and vibrational analysis
11 p1371 A73-26551

Piston engine or turboprop aircraft photography, measuring camera vibration components in roll, pitch and yaw by flashing light technique for image quality improvement

12 p1500 A73-27954

A modified interferometer for vibration amplitude measurement.

16 p2013 A73-32878

Measurement of small movements and vibrations by laser photography.

16 p2013 A73-32879

A hologram interferometer with a retro-reflected speckle reference beam for the real time visualization of vibration patterns.

16 p2013 A73-32880

Region of existence of frictional noise and experimental verifications

16 p2036 A73-33215

ABC helicopter stability, control, and vibration evaluation on the Princeton Dynamic Model Track.

[AHS PREPRINT 744]

Vibration analysis of circular cylinders by holographic interferometry.

21 p2701 A73-40756

Diffractionographic techniques for vibration measurement.

[ASME PAPER 73-DET-116]

Laser Doppler instrument for measurement of vibration of moving turbine blades.

22 p2869 A73-42297

Reflex arch liability in rabbits at synchronous maximum frequency of electromyographic and muscle stretching vibration measurement

22 p2807 A73-42659

Application of holographic subtraction to time-average hologram interferometry of vibrating objects.

22 p2863 A73-43141

Speckle effect use in laser photography for vibration and displacement measurement of mechanical systems, discussing diffraction patterns and measurement methods

23 p2982 A73-43675

VIBRATION METERS

NT LUNAR SEISMOGRAPHS

NT SEISMOGRAPHS

Instrument Society of America, Annual Conference, 27th, New York, N.Y., October 9-12, 1972, Proceedings, Part 2.

09 p1082 A73-22501

VIBRATION MODE

A method of construction and the structure of asymptotic approximations of the solutions of nonlinear mixed boundary value problems in studies of multifrequency oscillation modes

01 p0076 A73-10097

A study of basilar membrane vibrations. I - Fuzziness-detection: A new method for the analysis of microvibrations with laser light.

01 p0013 A73-10973

The five-minute oscillations as nonradial pulsations of the entire sun.

01 p0104 A73-11049

Vibrational resonance modes of balanced gyroscope on fixed base, determining gimbal vibration amplitude and gyro drift rate as function of perturbation frequency

01 p0054 A73-11401

Dynamics of flexible satellites with active attitude control.

02 p0228 A73-11994

Radial and nonradial oscillation modes of gaseous polytrope with toroidal magnetic field, using variational principle

02 p0217 A73-12400

Similar normal mode vibrations in certain conservative systems with two degrees-of-freedom.

02 p0193 A73-12515

Morphic effects. III - Effects of an external magnetic field on the long wavelength optical phonons.

02 p0201 A73-12638

Piezoelectric material constants, vibration mode, radiation directivity and VHF and UHF operation of ultrasonic transducers

03 p0306 A73-12954

Numerical simulation of initial value problem of axisymmetric equatorially trapped oscillation modes of constant density viscous fluid in rotating spherical shell

03 p0384 A73-13064

An accurate approximate formula for assessing the vibration frequency of structures axially loaded.

03 p0384 A73-13116

Beam vibration frequencies tables handbook preparation technique

03 p0388 A73-13317

Oscillation modes and cathode potential drop in plasma generated by continuous electric discharge at low pressure between anode and cold cathode.

03 p0346 A73-13603

Small steady free oscillations of liquid in rigid tanks, considering HF modes

03 p0296 A73-14047

N degrees of freedom system resonant vibration mode and frequencies determination from forced vibration of complementary body

04 p0509 A73-14979

Considerations concerning the orthogonality of the natural oscillation modes in elastic systems with many degrees of freedom

04 p0476 A73-15658

Low order spatial modes principal resonance region of in-plane loaded skew stiffened plate, obtaining equation of motion by Hamilton principle

[ASME PAPER 72-WA/AFM-32]

04 p0515 A73-15887

The vibration of cantilever beams of fiber reinforced material.

05 p0631 A73-16115

Modal damping predictions using substructure testing.

[SAE PAPER 720810]

05 p0634 A73-16643

Free vibrations in nonlinear systems with two degrees of freedom

05 p0599 A73-17087

Influence of a moving load on the vibrational characteristics of plates

05 p0636 A73-17093

Comparison of eigenvalues and characteristic vibration modes of circular ring bars, circular ring disks, and circular ring fibers

06 p0758 A73-17584

Comparison of the characteristic values and characteristic vibration forms of a circular ring beam, a circular ring disk, and a circular ring fiber. II

06 p0759 A73-17586

Small vibrations of isotropic elastic medium under finite strain and with time proportional elongations in three mutually perpendicular directions

06 p0759 A73-17759

Galerkin methods for vibration problems in two space variables.

06 p0717 A73-18408

Natural frequencies and vibration modes determination for skew plates with different edge conditions involving support and clamping based on Ritz variational method

07 p0909 A73-19094

Non-linear resonant attitude motions in gravity-stabilized gyrostatt satellites.

07 p0905 A73-19162

Free vibration of multi-degree-of-freedom nonlinear systems.

07 p0909 A73-19164

Lateral vibration and stability relationship of elastically restrained circular plates.

07 p0913 A73-19967

Designing turbomachine blades for forced vibrations under various excitation conditions

07 p0917 A73-20503

IMPATT diode anomalous microwave oscillation mode performance analysis, calculating I-V variation, power and efficiency from equivalent circuit

08 p0943 A73-20708

The oscillation probability of self-excited multimode oscillators.

08 p0945 A73-20803

Laser oscillation modes in corrugated optical waveguides with passive core, calculating wavelengths for hybrid modes

08 p0975 A73-21060

Optimized design - Characteristic vibration shapes and resonators.

08 p1017 A73-21191

Dynamic analysis of helicopter structures

09 p1031 A73-22206

Transverse mode control in semiconductor lasers.

09 p1092 A73-22242

Recursive solution for steady forced vibration modes of tensed string under concentrated harmonic forces

09 p1120 A73-22583

Optimal beam frequencies by the finite element displacement method.

09 p1160 A73-22898

Explicit addition of rigid-body motions in curved finite elements.

09 p1165 A73-23441

Kinetic equations for vibrational energy relaxation in a polyatomic gas mixture

10 p1250 A73-23579

Resonance phenomena associated with nonlinear vibrations of solid bodies

10 p1249 A73-24303

Axisymmetric vibrations of circular plates with stepped thickness.

10 p1291 A73-24394

Vibrations of segmented shells.

10 p1293 A73-24720

Overlength modes of transferred-electron oscillators.

11 p1337 A73-25359

Structure statistical identification method based on experimental measurements of natural frequencies and mode shapes to modify finite element model structural parameters

[AIAA PAPER 73-339]

11 p1436 A73-25479

Computer generated displays of structures in vibration.

[AIAA PAPER 73-362]

11 p1334 A73-25498

Gradient optimization of structural weight for specified flutter speed.

[AIAA PAPER 73-390]

11 p1439 A73-25519

A dynamic transformation method for modal synthesis.

[AIAA PAPER 73-396]

Multiple shaker resonance testing for structural dynamic characteristics, considering natural frequencies, mode shapes, damping and generalized masses

[AIAA PAPER 73-402]

11 p1440 A73-25548

Stabilizing the elastic modes of the Space Shuttle vehicle during launch.

[AIAA PAPER 73-319]

Vibration and local edge buckling of thermally stressed, wedge airfoil cantilever wings.

[AIAA PAPER 73-327]

Rayleigh-Ritz method for natural frequencies of transversely vibrating polar orthotropic annular perforated plates, proposing coordinate transformation for asymmetric mode solutions

11 p1446 A73-26494

Live fringes time averaging, fringe spooling, stroboscopic and speckle pattern real time recording techniques in holographic interferometry for surface vibration modes analysis

11 p1369 A73-26535

Deformation equations of a propeller blade and the orthogonality characteristics of its normal mode shapes of vibration

12 p1458 A73-27080

Static, vibration and buckling analysis of axisymmetric circular plates using finite elements.

12 p1555 A73-27772

Vibration of simply supported-clamped skew plate at large amplitudes.

13 p1690 A73-28001

Transverse vibration of membranes of arbitrary shape by the method of constant-deflection contours

13 p1690 A73-28002

Axisymmetric vibrations of circular plates with linearly varying thickness.

13 p1695 A73-28444

Ultraharmonic motion of a viscously damped nonlinear beam.

13 p1697 A73-28808

Periodic rectilinear solutions close to normal mode shapes of vibration of nonlinear conservative systems described by differential equations generated in homogeneous potential systems

13 p1661 A73-29008

Blocking oscillator multipulse mode operation with digital control by supply voltage regulation

13 p1593 A73-29101

Parametric vibrations of elastically connected two mass system with two degrees of freedom, considering dynamic response to excitation by external compression loads

13 p1700 A73-29360

Book - Theory of vibration with applications.

13 p1703 A73-29604

Free vibrations of shells of revolution with variable thickness.

14 p1805 A73-29708

Russian book on elastic structures vibration in aircraft covering integral equations for beams, damping principles and transcendental equations for flexural and torsional vibrations natural frequencies

14 p1810 A73-30000

Calculation of natural frequencies and modes of steadily rotating systems - A teaching note.

15 p1946 A73-31000

Apparent added masses of a plate array in an incompressible liquid

15 p1861 A73-31000

Multiplicity of dielectric local modes - Bound states of phonons with impurity centers

15 p1885 A73-31000

Gradient instabilities in a system of gravitating point masses

15 p1938 A73-31000

The geometrical stability of non-linear normal modes in two degree of freedom systems.

15 p1955 A73-32000

Implementation of simultaneous iteration for vibration analysis.

16 p2075 A73-32000

Modal synthesis technique for natural frequencies and mode shapes of bent rectangular beam in flexural torsion oscillation under six boundary constraint conditions

16 p2075 A73-32000

Speckle reference beam /by retro reflection/ holography for the real time visualisation of vibration terms.

16 p2012 A73-32000

Finite element analysis of coupled vibrations tapered twisted blades.

16 p2078 A73-32000

Transverse vibrations of variable rectangular cross section rod, reducing fourth order differential equation to second order via Kirchhoff relation

16 p2080 A73-32000

Newkirk effect - Thermally induced dynamic instability of high-speed rotors.

[ASME PAPER 73-GT-26]

16 p2047 A73-32000

Flexural vibrations of clamped orthotropic plates

16 p2081 A73-32000

Natural frequencies and normal modes of a four plate structure. 16 p2083 A73-33948

Determination of the eigenmodes of a structure by vibration tests with nonadjusted excitation 16 p2074 A73-33967

The transverse vibration of spinning aeolotropic disk. 16 p2084 A73-34026

Combined Rayleigh-Ritz and Lagrange multiplier technique for investigation of free vibrations of constrained cylindrical shell, considering axisymmetric mode 17 p2241 A73-34198

Asymptotic characteristics of the problem involving intrinsic asymmetrical vibrations of circular conical shells 17 p2241 A73-34267

The influence of pitch and twist on blade vibrations. 17 p2099 A73-34440

Statistics calculation method for natural frequencies and mode shapes of vibration for structures under external static loads 17 p2242 A73-34527

Variational methods for vibratory bending equations of asymmetrical sandwich plates with mode families in terms of displacement ratios, taking into account inertia effects 17 p2243 A73-34548

Finite element method application to solution of structural dynamics problems, considering equations of motion and vibration mode shapes 17 p2245 A73-34836

High speed oscillating tests of lubricating composites. [ASLE PREPRINT 73AM-3C-2] 17 p2179 A73-34987

Vibration of plates subject to arbitrary in-plane loads - A perturbation approach. [ASME PAPER 73-APM-26] 17 p2248 A73-35042

Modes and frequencies of transversely isotropic slightly curved Timoshenko beams. [ASME PAPER 73-APM-27] 17 p2248 A73-35043

On the question of adequate hingeless rotor modeling in flight dynamics. [AHS PREPRINT 732] 17 p2105 A73-35068

First-order frequency effects in supersonic panel flutter of finite cylindrical shells. [ASME PAPER 73-APM-K] 17 p2249 A73-35106

Applications of the speckle pattern techniques to the visualization of modulation transfer functions and quantitative study of vibrations of mechanical structures. 17 p2173 A73-35433

Mass condensation and simultaneous iteration for vibration problems. 17 p2252 A73-35605

Forecast of mode variation subsequent to structure modifications 18 p2367 A73-37083

Calculation of the natural frequencies and the principal modes of helicopter blades. 18 p2367 A73-37090

Extraneous modes in sound absorbent ducts. 19 p2459 A73-37294

Computer based analyses of the response of box type structures to random pressures. 19 p2497 A73-37485

Periodic solutions close to rectilinear normal mode shapes of vibration of nonlinear conservative system described by differential equations generated by homogeneous potential systems 19 p2459 A73-37634

Calculating the fundamental oscillations in turboengine blades with different types of excitation. 19 p2499 A73-37778

On the modal equations of large amplitude flexural vibration of beams, plates, rings and shells. 19 p2501 A73-38254

Asymptotic expansion of random processes depending on a small parameter 20 p2582 A73-39387

A direct method of stability analysis for elastic circulatory systems. 20 p2621 A73-39535

Coherent oscillation modes of optical waveguide resonators, noting selectivity and thermooptic insensitivity to pumping and active medium deformation 20 p2574 A73-39692

Large amplitude flexural vibration of simply supported skew plates. 21 p2784 A73-40423

Evaluation of various analytical models for buckling and vibration of stiffened shells. 21 p2784 A73-40424

Coupled bending-twisting vibrations of a single boom flexible solar array and spacecraft. 21 p2781 A73-40619

Eigenmodes in vibrations of circular cylindrical shells with free boundaries, calculating frequencies from theory of inextensional vibrations 21 p2788 A73-41614

Dynamic behaviour of orthotropic plates using finite difference technique. 22 p2917 A73-41716

In-plane free vibrations of tapered oval rings, determining normal modes and resonant frequencies from differential force and moment equilibrium equations 22 p2918 A73-41818

Free flexural vibrations of elliptical thin plate with free edge, calculating mode shapes and frequencies by use of Mathieu function 22 p2918 A73-41822

Vibration of beams with overhangs. 22 p2923 A73-42563

Exact hydroelastic solution for an ideal fluid in a hemispherical container. 22 p2843 A73-42631

German monograph - Lifetime detection in the case of acoustically loaded structures on the basis of the appropriate form of vibration. 22 p2924 A73-42741

Newton method relationship to Floquet theory for nonlinear vibration problems, considering Van der Pol equation periodic solutions for breathing and bending modes [ASME PAPER 73-APMW-20] 22 p2924 A73-42883

Stress amplification in a ring caused by dynamic instability. [ASME PAPER 73-APMW-35] 22 p2925 A73-42893

Asymptotic method for approximate elastodynamic plate theories derivation from elasticity equations with application to plate free extensional and forced flexural vibration frequency spectrum 22 p2926 A73-42900

Equilibrium structure of polytropes with toroidal magnetic fields. 22 p2912 A73-42941

Critical analysis of the method of M. A. Biot for determining natural torsional frequencies 22 p2867 A73-43047

Reconciliation of calculated and measured natural frequencies and normal modes. 22 p2929 A73-43136

Normal modes of elastically connected circular plates. 22 p2929 A73-43140

A general conclusion regarding the large amplitude flexural vibration of beams and plates. 23 p3039 A73-43305

On the computation of natural modes of an unsupported vibrating structure by simultaneous iteration. 23 p3042 A73-43801

Finite element analysis on L-L type vibration energy concentrator/divider considering its design. 23 p2961 A73-44138

A method for the study of the gain and the oscillating modes of a CO2 laser. 23 p2989 A73-44176

Nonlinear transverse vibration analysis of a rectangular plate with lumped M-S-D systems. 23 p3048 A73-44384

A new weighting function for solving nonlinear oscillation problems. 24 p3148 A73-44893

Calculation of the energetic characteristics of Gunn diode oscillators in retarded- and quenched-domain modes 24 p3072 A73-44928

Vibration characteristics of aluminum plates reinforced with boron-epoxy composite material. 24 p3149 A73-45148

Natural, flexural and torsional vibration frequencies and modes for helicopter tail rotor blades 24 p3057 A73-45245

Vibration of rectangular plates with mixed boundary conditions. 24 p3151 A73-45268

On the gyroscopic coupling of a Van der Pol oscillator in the forced regime and of a free linear oscillator 24 p3111 A73-45396

VIBRATION PERCEPTION

Changes in the vibratory sensation threshold after exposure to powerful vibration. 01 p0013 A73-10772

German monograph - Investigations concerning perception levels and transferred vibrational forces in the case of a vertical action of periodic vibrational mixtures on man. 03 p0268 A73-13818

Interindividual differences in homomodal and heteromodal scaling of auditory and vibrotactile stimulation intensity and duration, using magnitude estimation method 12 p1464 A73-26750

VIBRATION PICKUPS

U TRANSDUCERS

VIBRATION METERS

VIBRATION PROTECTION

U VIBRATION ISOLATORS

VIBRATION SIMULATORS

Simulation of the flow past turbomachine blades in the study of plane-cascade vibrations

01 p0029 A73-10494

Electrodynamic exciter power amplifier with pulse width modulation and Schmitt trigger output stage for structural vibration tests 07 p0803 A73-20535

Device for endurance testing of materials at low temperatures 09 p1070 A73-22168

Turbine vane vibration simulation tests with phase shift generation, using tube type phase inverters 13 p1599 A73-29638

Providing a model of flow round a turbine blade when investigating the vibration of flat blading. 14 p1743 A73-30319

Optimization of a vibration generator in the presence of external perturbations 16 p2083 A73-33969

A device for qualifying very low frequency vibration exciters 16 p2083 A73-33970

Theory of a two-mass model of a vibrational impactor 20 p2592 A73-38981

Simulation of complex excitation of structures in random vibration by one-point excitation. 20 p2617 A73-39269

An electromagnetic torsional vibrator. 20 p2544 A73-39271

A unit for fatigue testing of materials at low temperatures. 22 p2838 A73-42116

VIBRATION TESTING MACHINES

U VIBRATION SIMULATORS

VIBRATION TESTS

NT DAMPING TESTS

Application of the VEDS-200A electrodynamic vibrator to fatigue tests in symmetric tension and compression 01 p0029 A73-10492

Simulation of the flow past turbomachine blades in the study of plane-cascade vibrations 01 p0029 A73-10494

A digital system for shaping, analysis and control of a random vibration spectrum 01 p0027 A73-10598

Criteria for self loosening of fasteners under vibration. 01 p0058 A73-11512

Investigation of the fitness for space travel of the electric propulsion plant ESKA 18 [DGLR PAPER 72-087] 02 p0131 A73-11694

Inherent limitations in digital incremental oscillator-analyser systems for mechanical vibration testing. 02 p0171 A73-12610

Diagnostic instrumentation on J-85 engines for gas path and vibration analysis, noting flight test program and installation of remote pressure transducers and signal conditioners 03 p0308 A73-13404

German monograph - Investigations concerning perception levels and transferred vibrational forces in the case of a vertical action of periodic vibrational mixtures on man. 03 p0268 A73-13818

Sonic degradation of thermally shocked ceramics. 04 p0448 A73-15124

Determination of Young's modulus and of the Poisson coefficient by a method of resonant bars 04 p0462 A73-15247

Digital vibration control systems for structural design dynamic testing and evaluation, discussing state of art and trends toward multichannel and multi-axis control [SAE PAPER 720820] 05 p0553 A73-16628

Field experience with digital control systems for vibration and acoustic testing. 05 p0554 A73-16637

[SAE PAPER 720821] Vibration, radiation and thermal vacuum test procedures and facilities for evaluating spacecraft reliability during launching and in space environment 07 p0807 A73-18999

Vibration test facilities and control techniques for application to industrial products, discussing shakers, signal generation and amplification, and data recording and reduction 07 p0809 A73-20575

Prediction of IC and LSI performance by specialized vibration/detection test for presence of conductive particles. 08 p0943 A73-20732

Dynamic analysis of freely supported axisymmetric shells. 08 p1018 A73-21473

Automated vibration shaker calibration data acquisition and analysis system with minicomputer for working transfer standard voltage monitoring and acceleration level determination 09 p1070 A73-22508

Generator of rectilinear vibrations for the study of structures at low frequency [ONERA, TP NO. 1185] 09 p1084 A73-22713

An 'orthogonalization' method for determining the dynamic characteristics of an elastic body from static vibration tests 09 p1161 A73-23090

Multiple shaker resonance testing for structural dynamic characteristics, considering natural frequencies, mode shapes, damping and generalized masses [AIAA PAPER 73-402] 11 p1440 A73-25531

The dependence of piezo-electric accelerometer response on method of attachments. 12 p1496 A73-26974

- Turbine vane vibration simulation tests with phase shift generation, using tube type phase inverters
13 p1599 A73-29638
- The use of a type VEDS-200A vibrostand for fatigue tests under conditions of symmetrical tension-compression.
14 p1743 A73-30317
- Providing a model of flow round a turbine blade when investigating the vibration of flat blading.
14 p1743 A73-30319
- Performance and methodology of a digital random vibration control system.
16 p1993 A73-33134
- Vibration and shock qualification testing of an airborne early warning radar.
16 p1987 A73-33137
- The relation of tests with electrodynamic vibrators to the Woelher testing technique
16 p2037 A73-33379
- Evaluation of machinery characteristics through on-line vibration spectrum monitoring.
[ASME PAPER 73-GT-68] 16 p2048 A73-33520
- Intensity of mechanical influences and mechanical degradation of hard polymers
16 p2030 A73-33940
- Determination of the eigenmodes of a structure by vibration tests with nonadjusted excitation
16 p2074 A73-33967
- A device for qualifying very low frequency vibration exciters
16 p2083 A73-33970
- Lateral bending-torsion vibrations of a thin beam under parametric excitation.
[ASME PAPER 73-APM-13] 17 p2247 A73-35037
- Wind tunnel acoustic and vibration test facilities, including anechoic chambers, subsonic boundary layer tunnels, acoustic ducts, reverberation rooms, and rotor noise chambers
17 p2148 A73-35334
- An optimization technique utilizing the deflected gradient algorithm for dynamic testing of electromechanical equipment.
17 p2202 A73-35386
- A closed-loop automatic control system for high-intensity acoustic test systems.
18 p2296 A73-36712
- Multihundred watt radioisotope thermoelectric generator full scale thermal performance, vibration, shock, acoustic, acceleration and magnetic field tests
19 p2456 A73-38421
- Experimental correlation techniques for the characterization of vibration transmission paths.
20 p2617 A73-39267
- Vibration test techniques used to simulate transients and match shock spectra.
20 p2544 A73-39268
- Vibration tests with rotors as a rotor identification problem
21 p2707 A73-40395
- Analysis of the accuracy of a system for controlling vibration tests with sinusoidal excitation
21 p2674 A73-40996
- Technical progress on new vibration and acoustic tests for proposed MIL-STD-810C, 'environmental test methods.'
21 p2674 A73-41200
- Increasing the critical rotational speed of the tail rotor drive shaft in SM-1 and SM-2 helicopters
24 p3057 A73-45195
- VIBRATIONAL FREEZING**
Freezing-in phenomenon and acoustical streaming in standing ultrasonic waves
11 p1400 A73-26291
- VIBRATIONAL FREQUENCIES**
U VIBRATIONAL SPECTRA
VIBRATIONAL RELAXATION
U MOLECULAR RELAXATION
VIBRATIONAL SPECTRA
Semiclassical theory for low-energy molecular collisions - H₂/+H₂ vibrational excitation.
01 p0080 A73-10564
- Accuracy of the determination of the spectral density of a vibrational process with the aid of a spectrum analyzer
01 p0077 A73-10677
- Thermodynamic functions and molecular parameters of rhombic dimeric molecules of alkali metal halides
01 p0080 A73-10857
- Ionic reaction mechanism for F region nitrogen vibrational temperature, using positive ion composition
01 p0042 A73-10894
- Vibration-rotation bands of NH in the spectrum of alpha Orionis.
01 p0104 A73-11041
- Laser power density calculation with complete rotational analysis for molecular hydrogen Lyman and Werner bands vibrational-rotational transitions
01 p0061 A73-11224
- Energy transfer between impurity molecules in the presence of relaxation
01 p0080 A73-11243

- Stress analysis and dynamic investigation of turbine blades from constrained torsion theory, calculating free torsional vibration frequencies
02 p0229 A73-11621
- Frequency distribution function for free rotation and uniform angular distribution of molecules, detecting conformations from vibrational spectrum characteristics
02 p0195 A73-12099
- Algorithms for equations of oscillatory motion about moving center, noting disturbing force effect on vibrational frequency
02 p0193 A73-12196
- Cation determinative curves for Mg-Fe-Mn olivines from vibrational spectra.
02 p0139 A73-12636
- Numerical model of energy transfer in carbon monoxide-nitrogen laser, considering electron-molecule excitation and vibration-vibration exchange
02 p0178 A73-12816
- Vibrational frequency density analysis of thin spherical and cylindrical shells of revolution, using asymptotic integration method
03 p0394 A73-14051
- Natural vibration frequency spectra of circular cylindrical and spherical shells of revolution, using Bessel function
03 p0395 A73-14052
- Vibrational excitation in CO by electron impact in the energy range 10-90 eV.
04 p0477 A73-14770
- Existence theorem for nonlinear oscillatory equations of motion transformation into normal form, noting quasi-periodic functions with arbitrary frequencies
04 p0475 A73-14888
- Vibrational and energy spectra of welding electron beam interacting with beam produced plasma, noting interaction length effect on instability
04 p0454 A73-15609
- Vibrational spectra and structure of tetrakis(trifluoromethyl)hydrazine in the crystalline and fluid states.
04 p0414 A73-16036
- Group theory application to in-plane vibrations natural frequencies of nth order polygonal particle elastic system, obtaining analytical solution through eigenvalue problem simplification
05 p0599 A73-17373
- Reaction mechanisms of the CS₂-O₂ chemical laser.
06 p0702 A73-18370
- Studies in molecular dynamics by collision-induced infrared absorption in H₂-rare gas mixtures. I - Profile analysis and the intercollisional interference effect.
08 p0990 A73-21630
- Change of vibrational temperature due to laser action in CO₂ lasers.
09 p1089 A73-21933
- Classical theory of spectral distribution of isolated nonlinear oscillations at combined frequencies
09 p1119 A73-21953
- Vibrational relaxation theory of diatomic and multiatomic single component and gas mixture systems for molecular laser mechanisms, using oscillator simulation
09 p1097 A73-23331
- Free particle gravitating cylindrical model for gravitational kinetic instabilities, calculating natural vibration spectrum and parameters for beam instability development
10 p1253 A73-23714
- Energy transfer between impurity molecules during relaxation.
10 p1251 A73-24180
- Vibrational and energy spectra of welding electron beam interacting with beam produced plasma, noting interaction length effect on instability
10 p1224 A73-24199
- Vibrationally-excited nitrogen in the upper atmosphere.
10 p1212 A73-24226
- Measurement of vibrational temperature of CO and N₂ using the He/2 3S/ Penning ionization technique.
10 p1218 A73-24246
- Influence of an intermediate stiffener on the vibration frequency spectrum of a cantilever plate
10 p1291 A73-24357
- Spectroscopic study of the vibrational-energy dissipation of the I₂ molecule excited by a He-Ne laser
10 p1228 A73-24577
- Temperature-induced changes of the electron-vibration spectrum of LaAlO₃-Cr³⁺/ crystals
10 p1260 A73-24578
- IR spectrum line reversal for measurement of CO and gas mixture laser plasma vibrational temperatures as function of discharge current and gas pressure
10 p1230 A73-24884
- Characteristics of the vibrational spectrum of laminar As₂S₃ semiconductors
11 p1408 A73-25244
- Low frequency vibrations and molecular structure of /CH₃/2NPF₂.
11 p1326 A73-25567
- Rotational and vibrational hydroxyl excitation in the laboratory and in the night airglow.
11 p1354 A73-25761

- Vibrational relaxation in hydrogen-rare-gases mixtures.
11 p1402 A73-25969
- An evaluation of molecular constants and transition probabilities for the NH free radical.
11 p1402 A73-26582
- Determination of the temperature of a methane-fluorine diffusion flame by means of the vibration-rotation spectrum of the HF molecule
11 p1453 A73-26586
- Vibrational level populations in diatomic molecules during steady pumping
12 p1504 A73-26888
- A quantum model for bending vibrations and thermodynamic properties of C₃.
12 p1526 A73-27019
- Approximate dependences for the vibration frequencies of smooth cylindrical shells and for ones with concentrated inclusions
12 p1555 A73-27789
- Influence of rotational inertia on the frequency spectrum of the natural vibrations of a cylindrical shell
12 p1556 A73-27801
- Stability of gravitating systems with a quadratic potential. I - Methods of investigating the stability of systems with a limited phase volume: Vibration spectrum of the Maclaurin stellar disk
12 p1546 A73-27856
- Luminescence quenching and zero-phonon line broadening associated with defect interactions in diamond.
13 p1667 A73-28212
- The vibrational frequency of Fe-57 atoms in Pt-Fe solid solution from measurements of the second-order Moessbauer Doppler shift.
13 p1634 A73-28258
- Contribution to the theory of the natural vibration spectra of a nonequilibrium resonant cavity
13 p1589 A73-28290
- Line and rectangular plane finite element models for accurate and efficient dynamic vibration frequency analysis of frames and shear walls respectively
13 p1700 A73-29377
- Interaction between a plasma and an electron beam modulated by low-frequency oscillations.
14 p1780 A73-30335
- Boundary value problem solutions for parallelogram and elliptical thin plates vibration frequencies and mode shapes based on eigenvalues domain dependence and parameter differentiation technique
14 p1810 A73-30408
- Investigation of the excitation of vibrational levels of the /N-14/H₃ molecule by carbon dioxide laser radiation
14 p1758 A73-30801
- Errors in the absolute method of measuring the frequency of difference oscillations
15 p1853 A73-31256
- Computation of upper and lower bounds to the frequencies of elastic systems by the method of Lehmann and Maehly.
15 p1951 A73-32027
- Vibrational spectra of substituted hydrazines. IV - Raman and far-infrared spectra and structure of tetramethylhydrazine.
15 p1841 A73-32220
- Vibrational spectrum of bis(trifluoromethyl) trioxide.
15 p1841 A73-32221
- Classical calculation of intensity distribution in the oscillatory-rotational spectra of diatomic molecules
15 p1916 A73-32338
- Evaluation of machinery characteristics through on-line vibration spectrum monitoring.
[ASME PAPER 73-GT-68] 16 p2048 A73-33520
- Modes and frequencies of transversely isotropic slightly curved Timoshenko beams.
[ASME PAPER 73-APM-27] 17 p2248 A73-35043
- Temperature effects on modulation sensitivity and vibrational spectra in Gunn diode oscillators, suggesting frequency stability improvement method
17 p2136 A73-35162
- Flexural vibration frequencies of right circular cylindrical tensor gravitational wave detectors in regime with sound wavelength comparable to diameter
17 p1276 A73-35763
- Free particle gravitating cylindrical model for gravitational kinetic instabilities, calculating natural vibration spectrum and parameters for beam instability development
18 p2340 A73-36739
- Oscillator strength calculations for vibrational transitions of X-A electronic system of interstellar CH positive ion, noting agreement with astrophysical observations of line spectra
19 p2488 A73-38512
- Stability of gravitating systems with a quadratic potential. I - Systems bounded in phase space - Oscillation spectrum for a Maclaurin stellar disk.
20 p2608 A73-39230
- Low-frequency vibrations of a high-frequency E-discharge plasma in a magnetic field
20 p2598 A73-39398
- The carbon monoxide laser - Mechanism of formation of population inversion
21 p2712 A73-40444

Far infrared and Raman spectra of gaseous carbon suboxide and the potential function for the low frequency bending mode.

21 p2740 A73-40935

IR spectrum line reversal for measurement of CO and gas mixture laser plasma vibrational temperatures as function of discharge current and gas pressure

21 p2717 A73-41659

Theory of eigenmode spectra of a nonequilibrium resonator.

22 p2830 A73-41814

The inference of temperature from the infrared spectra of planets.

22 p2906 A73-42065

Cylindrical circular shell vibrational frequencies, examining free surface or solid plane influence on shell natural vibrations in incompressible fluids

22 p2920 A73-42130

Vibrational relaxation of oxygen in an unsteady expansion wave.

22 p2889 A73-42441

Transient vibration processes during diamond grinding and their statistical evaluation

24 p3094 A73-44971

Bending potential of an H₂O molecule.

24 p3113 A73-44977

The problem of natural oscillations of a thin shell containing an elastoacoustic medium

24 p3152 A73-45359

Boundaries of natural frequency variations during the longitudinal oscillations of rods

24 p3152 A73-45360

VIBRATIONAL STRESS

Alternating-pressure measurements involving mushroom-nozzle flows with regard to dynamic stresses in the case of the skin structures of reusable carrier rockets

[DGLR PAPER 72-076] 02 p0128 A73-11686

Experimental investigation of stresses in plates acted on by acoustic loads.

02 p0235 A73-12135

Vibrational strength of structural members from Woehler lines, calculating service life from S-N diagrams

03 p0385 A73-13138

Changes in whole body force transmission of dogs exposed repeatedly to vibration. [ASME PAPER 72-WA/BHF-11]

04 p0410 A73-15878

Crew performance in extended operation under vibrational stress.

05 p0543 A73-16717

Biophysical properties of vibration energy transfer to human body structure, noting harmful effects dependence on frequency range

06 p0657 A73-17748

Probability theory for vibrational strength of turbomachine parts, calculating statistical maximum stress for given stress distribution conditions

07 p0917 A73-20502

Influence of regulated unequal guide-vane spacing on the alternating stress level in the working blades of a compressor

09 p1157 A73-22165

Cumulative damage theories for the prediction of life in the case of vibrational stresses. I - A critical overview

11 p1441 A73-25576

Failure criterion for metallic materials in the case of multiaxial vibrational stress

15 p1952 A73-32045

German monograph on frictional fatigue failure covering microcrack initiation due to shear induced vibrational stresses

15 p1956 A73-32587

Interpretation of the results of simulation tests, taking into account scatter effects

16 p2019 A73-33378

Vibration and shock stresses in the case of ballistic rockets. II - Measurement, evaluation, simulation

16 p2072 A73-33388

Vibration and shock stresses in the case of ballistic rockets. III - Evaluation of the results and comparison with the specifications available

16 p2073 A73-33389

Accelerated testing of air-to-air guided missiles.

16 p2073 A73-33612

Probability theory for vibrational strength of turbomachine parts, calculating statistical maximum stress for given stress distribution conditions

19 p2499 A73-37777

Changes in whole body force transmission of dogs exposed repeatedly to vibration.

20 p2512 A73-39106

Oscillations of a spinning satellite due to small deflections of its dipole antennae.

21 p2780 A73-40089

A model to predict the mechanical impedance of the sitting primate during sinusoidal vibration. [ASME PAPER 73-DET-78]

22 p2813 A73-42073

Effect of an adjustable nonuniform pitch in the distributor on the alternating stresses in compressor rotor blades.

22 p2919 A73-42113

Forced vibrations of a cylindrical shell in the presence of gas pressure fluctuations

22 p2928 A73-43057

High frequency vibrations and waves in laminated orthotropic plates.

22 p2928 A73-43135

Effect of the circumferential nonuniformity of a temperature field in front of a turbine on the vibrational stresses in the turbine blades

23 p3020 A73-43740

Fiberglass reinforced plastic laminate creep rate for ultrasonic vibrational and static tensile loads, showing nonlinear viscoelasticity and stress amplitude effects

24 p3102 A73-44504

VIBRATORS

U ELECTRIC CHOPPERS

VIBRATORY LOADS

Vibratory loads effect on metal microstructure under sliding friction, noting rheological criteria for fretting corrosion wear resistance

02 p0180 A73-11934

Torsion of a viscoelastic prismatic rod under the action of a vibrational load

07 p0911 A73-19315

Damage accumulation hypotheses concerning lifetime prediction during vibrational loading. II - A critical review

11 p1384 A73-25849

Effect of loading frequency and directional anisotropy on the fatigue strength of grade AMg6BM aluminum alloy sheet.

13 p1643 A73-29606

Resonant frequency, fatigue and energy dissipation relations for endurance limit determination in Al alloy specimens under vibrational loads

13 p1643 A73-29618

Vibration of plates subject to arbitrary in-plane loads - A perturbation approach. [ASME PAPER 73-APM-26]

17 p2248 A73-35042

Behavior of materials under multiaxial vibrating loads. II - Experimental investigations

24 p3153 A73-45447

VIBRATORY POLISHING

Free three-dimensional vibration processing of gas-turbine engine blades

02 p0172 A73-11723

VIBROCARDIOGRAPHY

U PHONOCARDIOGRAPHY

VIBROMETERS

U VIBRATION METERS

VIDEO COMMUNICATION

Video signals differential pulse code modulation, improving SNR by quantizing characteristics modification via nonlinear coder

09 p1054 A73-23375

Communication system for digital image processing services over Advanced Research Project Agency computer network, describing hardware facilities and software capacity

09 p1061 A73-23390

Block quantizers for encoding pictures at low bit rates, noting maximum nonstationary error signal incurred at block edges

10 p1186 A73-23497

An optimal electrooptical method of signal processing in coherent pulse reception

12 p1468 A73-26947

Video-signal improvement using comb filtering techniques.

12 p1468 A73-27012

Communications aspects of broadcast TV satellites.

14 p1725 A73-29716

Two-way wideband microwave communication system oriented toward PCM-TDM digital technique for covering telephone, videophone and radio broadcasting services

17 p1213 A73-34968

The problem of applying information theory to efficient image transmission.

17 p2124 A73-35302

An error correction method for DPCM picture transmission

19 p2432 A73-38268

Multiple-beam satellite repeater tradeoffs applied to a multifunctional system.

20 p2524 A73-38732

Digital codings of multi-dimensional information sources and applications to image coding.

21 p2655 A73-41043

VIDEO DATA

Digital storage of graphs and curves and their representation on visual displays

01 p0021 A73-11484

Computerized multichannel alphanumeric TV system for ATC operational information display, describing data acquisition, processor and software peripherals and video display subsystem

02 p0165 A73-11594

System design, breadboard construction and tests of slope reversal video processor based on tapped delay line estimation with timing discriminator

02 p0167 A73-11957

Universal data system for image processing of earth resources observations, discussing input/output film,

tape and multispectral data, interactive control and video color displays

05 p0555 A73-17155

Storage and transmission of sequences of moving images

08 p0941 A73-21559

Delta modulation and differential PCM systems performance comparison at high sampling rates for color video signal coding

09 p1055 A73-23389

A probabilistic model of an optical-field and the statistical properties of a videosignal from a vidicon target

11 p1360 A73-25025

Instruments and techniques for cartographic processing of space photographs.

12 p1500 A73-27959

Video-to-film color-image recorder.

13 p1619 A73-29240

A real-time simulator for image data systems.

17 p2147 A73-34903

Digital processing of Mariner 9 television data.

17 p2168 A73-34907

Real time digital videomagnetograph at the Aerospace San Fernando Solar Observatory.

17 p2168 A73-34909

Operational principles and testing of a digital radar target extractor

19 p2404 A73-37584

Biplane roentgen videometric system for dynamic, 60/sec, studies of the shape and size of circulatory structures, particularly the left ventricle.

19 p2399 A73-37798

Secondary surveillance radar - Current usage and improvements.

19 p2451 A73-37808

Conference on Video and Data Recording, University of Birmingham, Birmingham, England, July 10-12, 1973, Proceedings.

19 p2431 A73-38195

An optimized video output from a wide angle optical probe. [AIAA PAPER 73-918]

21 p2673 A73-40866

Parametric amplification and generation of pulses in nonlinear distributed systems

22 p2826 A73-42333

Multidimensional Fourier transforms and image processing with finite scanning apertures.

22 p2864 A73-43150

Use of a response surface to optimize digital telecommunication systems.

23 p2948 A73-43214

Long baseline interferometry with high angular resolution widely separated radio telescopes and video signal magnetic recording tapes, discussing coherence and timing requirements and calibration

23 p2980 A73-43349

Orbit improvement from satellite imaging data obtainable from outer planet missions.

23 p3032 A73-43840

VIDEO EQUIPMENT

Type and time of integration in precision digital video integrator for meteorological radar, describing equipment and operation

03 p0281 A73-14521

High-data-rate, spacecraft tape recorders. [AD-751726]

04 p0449 A73-15383

Viking lander vehicles ground reconstruction equipment for Martian surface digital magnetic tape video data conversion into high quality hard copy

06 p0683 A73-18321

Sensitivity of Josephson junctions in video detection of microwave and millimeter-wave radiation.

06 p0677 A73-18371

Two dimensional photon counting - A design based on the Aerospace-NASA videomagnetograph.

08 p0972 A73-21756

Application of an electronic image analyzer to dimensional measurements from neutron radiographs.

11 p1371 A73-26743

A light amplifier display device.

16 p2013 A73-32882

Video instrumentation for radionuclide angiocardiology.

19 p2399 A73-37796

Use of a video system in the study of ventricular function in man.

19 p2399 A73-37797

Modular airborne video tape recording systems using wideband frequencies, describing wideband channels, power supply, transport unit, servo module and bit storage rates

19 p2431 A73-38199

Russian book on operation and design of bipolar transistor circuits for video amplifiers covering TV, radar, oscilloscope, automatic control and computer applications

22 p2832 A73-41878

VIDICONS

NT RETURN BEAM VIDICONS

Secondary electron conduction /SEC/ vidicon television system for space astronomy, discussing data reduction requirements, costs and quasar spectrum observation

01 p0048 A73-10530

Radiation sensitivity of silicon imaging sensors on missions to the outer planets.

05 p0557 A73-16512

Satellite-borne TV vidicon design requirements and operational specifications, considering storage, relaxation, resolution, sensitivity, electrostatic focusing and deflection, image magnification and enhancement

07 p0821 A73-18982

Satellite-borne vidicon camera and associated control and telemetry electronics for imagery and dimensional parameters of sparks generated by gamma radiation

07 p0822 A73-18987

Electronic imaging systems with TV vidicon competition with film photography for spaceborne solar astronomy, comparing resolution, sensitivity and SNR

08 p0971 A73-21749

Theoretical performance figures for low light level TV cameras.

08 p0972 A73-21757

TV vidicon image converter with arbitrary scanning format and computer-compatible output signals, using power spectrum redistribution functions

09 p1060 A73-22945

A probabilistic model of an optical-field and the statistical properties of a video signal from a vidicon target

11 p1360 A73-25025

Sunspot observations by means of a vidicon camera.

I.

12 p1545 A73-27833

The impact of silicon technology on near-infrared and low-light-level imaging.

16 p2012 A73-32867

Preliminary progress with digital image-tubes at Cerro Tololo.

17 p2169 A73-35281

Application of the SIT vidicon to astronomical measurements.

17 p2169 A73-35285

Astronomical observations with an SEC vidicon system.

17 p2233 A73-35289

A multi-channel coronal spectrophotometer.

17 p2170 A73-35291

Space application of SEC vidicons - The OSO 7 coronagraph.

17 p2170 A73-35293

Ultraviolet proximity focussed converters for use in a satellite SEC-TV system.

17 p2170 A73-35296

VIEW EFFECTS

Spaced annular ring shell-to-shell and shell-to-tube view factors for finite difference radiative heat transfer solutions

22 p2923 A73-42564

VIEWING

Rear projection holographic and interferometric viewing screens using deflected and scattered light, discussing microfilm reading applications, dichromated gelatin film and laser exposures

21 p2699 A73-40151

VIKING LANDER SPACECRAFT

Viking Mars program for surface mapping and exploration, atmospheric composition investigation and life evidence search, discussing orbiter and lander phases

01 p0105 A73-11155

Viking lander-borne gas chromatograph mass spectrometer for Martian atmosphere sampling and soil analyses

02 p0168 A73-12000

Effects of nonequilibrium ablation chemistry on Viking radio blackout.

05 p0551 A73-16981

Viking lander vehicles ground reconstruction equipment for Martian surface digital magnetic tape video data conversion into high quality hard copy

06 p0683 A73-18321

Implementation of the 1975 Mars Viking Lander cameras.

08 p0970 A73-21741

The facsimile camera - Its potential as a planetary lander imaging system.

12 p1495 A73-26875

Aerodynamic decelerator dynamics modeling for Viking lander parachute deployment, analyzing unfurling process with attention to longitudinal and rotational dynamics

12 p1549 A73-27440

Viking lander capsule decelerator system candidate materials evaluation, discussing in-situ testing for high density packing and heat sterilization effects on strength

[ALAA PAPER 73-447] 15 p1881 A73-31433

Development of the Viking parachute configuration by wind tunnel investigation.

[ALAA PAPER 73-454] 15 p1826 A73-31440

Viking 75 Mars lander parachute high altitude qualification flight tests for camera, telemetry and radar performance, using ground based computer-radar monitoring system

[ALAA PAPER 73-456] 15 p1826 A73-31442

Viking 75 Mars lander spacecraft mortar system design and environmental requirements, stressing

manufacturing and qualification tests and parachute ejection

[ALAA PAPER 73-458] 15 p1827 A73-31444

Viking type spacecraft rendezvous with the Martian moons.

19 p2482 A73-37401

Mars almanac /ephemerides, rotation data, coordinate data, etc/ for Viking lander position definition and stellar and planetary observations from Mars surface

21 p2733 A73-40031

VIKING MARS PROGRAM

Viking Mars program for surface mapping and exploration, atmospheric composition investigation and life evidence search, discussing orbiter and lander phases

01 p0105 A73-11155

Viking aerodynamic decelerator for Mars lander mission in 1976, discussing mortared disk-gap-band parachute, qualification flight tests and atmospheric environment effects

[ALAA PAPER 73-442] 15 p1825 A73-31428

Low altitude flight test phase of Viking decelerator system development, considering low density environment loading condition simulation method

[ALAA PAPER 73-455] 15 p1826 A73-31441

Viking 75 lander deceleration system qualification flight tests at expected Mars conditions, discussing design requirements and full scale vehicle simulation in earth atmosphere

[ALAA PAPER 73-457] 15 p1827 A73-31443

Viking Mars 1975 soft landing and search for extraterrestrial life, considering lander transmission of atmospheric and surface data

21 p2766 A73-40414

Fuel capsule vent system development for the Viking radioisotope thermoelectric generator.

21 p2737 A73-40766

VIKING ORBITER SPACECRAFT

NT VIKING ORBITER 1975

Viking Mars program for surface mapping and exploration, atmospheric composition investigation and life evidence search, discussing orbiter and lander phases

01 p0105 A73-11155

Effects of resonant tesseral gravity coefficients on Viking-type orbits.

[ALAA PAPER 73-146] 06 p0748 A73-17648

Viking Orbiter power subsystem performance prediction computer program simulating solar array, battery charge controls, zener diodes and power conditioning equipment characteristics and interactions

09 p1060 A73-22802

VIKING ORBITER 1975

Selection of a surface tension propellant management system for the Viking 75 Orbiter.

[ALAA PAPER 72-1042] 03 p0381 A73-13377

The Viking Orbiter 1975 beryllium INTERGEN rocket engine assembly.

[ALAA PAPER 72-1131] 03 p0382 A73-13438

Second order digital phase locked loop for Viking Orbiter 1975 command system, using filtered sequence of phase error polarity to correct system clocks

09 p1053 A73-23372

VIKING ROCKET VEHICLE

The Viking Orbiter 1975 beryllium INTERGEN rocket engine assembly.

[ALAA PAPER 72-1131] 03 p0382 A73-13438

VIKING 75 ENTRY VEHICLE

Dynamic stress analysis during inflation of disk-gap-band Viking 75 parachute for Mars soft landing

[ALAA PAPER 73-444] 15 p1825 A73-31430

Viking 75 Mars lander parachute high altitude qualification flight tests for camera, telemetry and radar performance, using ground based computer-radar monitoring system

[ALAA PAPER 73-456] 15 p1826 A73-31442

Viking 75 lander deceleration system qualification flight tests at expected Mars conditions, discussing design requirements and full scale vehicle simulation in earth atmosphere

[ALAA PAPER 73-457] 15 p1827 A73-31443

Viking 75 Mars lander spacecraft mortar system design and environmental requirements, stressing manufacturing and qualification tests and parachute ejection

[ALAA PAPER 73-458] 15 p1827 A73-31444

Wake flow model of Viking 75 entry vehicle for different angles of attack at free stream Mach numbers 0.2-3.95

[ALAA PAPER 73-475] 15 p1823 A73-31459

A new approach to performance optimization of the 1975 Mars Viking lander.

[ALAA PAPER 73-889] 20 p2614 A73-38825

VINYL CYANIDE

U ACRYLONITRILES

VINYL POLYMERS

Effects of hardening conditions on the physicochemical and frictional properties of polyvinyl furfural

08 p0982 A73-21591

Vinyl plastisols with high adhesion to metals

10 p1239 A73-24093

Axial alignment of basal planes in polyacrylonitrile base carbon fibers, increasing axial and radial microstructural textures via heat treatment temperature

17 p2198 A73-35837

Investigation of the spectral properties of sensitized polyvinylcinnamate

21 p2646 A73-40256

Investigation of the antistatic properties of lacquer coatings based on quaternary polyvinylpyridine salts

21 p2647 A73-40261

VIRGO STAR CLUSTER

Low frequency, high resolution observations of Virgo A.

01 p0100 A73-10791

VIRIAL THEOREM

Relation of the equation of state of compressed gases with the optical complex and the specific refraction - Virial coefficients of carbon dioxide

01 p0080 A73-10856

Second virial coefficients for polar molecules in steam based on PVT data, using Stockmayer potential for curve fitting at 100-1000 C

02 p0238 A73-12643

Statistical mechanics and virial functions for equation of state of dense gas with spherical nonpolar molecules, calculating compressibility factor for methane and Ar

06 p0726 A73-18555

Connection between the equation of state of compressed gases with an optical complex and the specific refraction - The virial coefficients of carbon dioxide.

12 p1526 A73-27906

Magnetic stars formation from interstellar matter in presence of interstellar magnetic field, considering critical mass based on Chandrasekhar-Fermi virial theorem

14 p1799 A73-30426

The variational principle and the virial theorem for uniformly rotating magnetohydrodynamic systems.

16 p2040 A73-32926

Statistical mechanics and virial functions for equation of state of dense gas with spherical nonpolar molecules, calculating compressibility factor for methane and Ar

16 p2039 A73-33580

A semiempirical description of the structure of metals

20 p2577 A73-39295

State variables and transport coefficients of binary gaseous mixtures. I - A simple method for the accurate determination of the second virial coefficient of binary gaseous mixtures [DFVLR-SONDDR-273]

22 p2931 A73-42373

A new determination of the second virial coefficient of carbon dioxide at temperatures between 0 and 150 C, and an evaluation of its reliability.

22 p2932 A73-42507

VIRTUAL PROPERTIES

Frequencies and virtual masses of a liquid in a cavity formed by eccentric cylinders

11 p1347 A73-25391

The method of virtual powers in mechanics of continuous media. I - Theory of the second gradient

19 p2495 A73-37424

Virtual motion principle implication for structural damping differential equations for cases of homogeneous, inhomogeneous and aerodynamic flutter for various degrees of freedom

20 p2616 A73-39098

Phase integral corrections to radio wave absorption and virtual height for model ionospheric layers.

21 p2654 A73-40777

Synthetic radio direction defining methods with virtual antenna patterns.

21 p2658 A73-41649

VIRTUAL WORK

U EQUILIBRIUM

VISCERA

NT ADRENAL GLAND

NT ESOPHAGUS

NT GONADS

NT INTESTINES

NT KIDNEYS

NT LIVER

NT LUNGS

NT ORGANS

NT PANCREAS

NT PINEAL GLAND

NT PITUITARY GLAND

NT TESTES

NT THYROID GLAND

Spinal and spino-bulbo-spinal neuron mechanisms of somatic and visceromotor reflex transfer in the thoracic spinal cord

24 p3061 A73-45249

VISCOELASTIC CYLINDERS

Stressed state of multilayer spherical vessels, cylindrical tubes and circular disks consisting of a linear viscoelastic material

13 p1690 A73-27994

Solution of the problem of plane deformation for a tube consisting of a physically nonlinear quadratic viscoelastic material

13 p1690 A73-27995

- Analysis of centrifugal stresses in anisotropic viscoelastic cylinder. 13 p1697 A73-28810
- Nonlinear dynamic problem concerning a cylinder with a slowly changing internal boundary 16 p2082 A73-33932
- Flexural vibrations of rods with viscoelastic coating subjected to axial force. 19 p2502 A73-38347
- An approximation for the determination of the dynamic characteristics of long viscoelastic hollow cylinders 21 p2788 A73-41615
- Nonlinear vibrations of viscoelastic cylinder with elastic shell under harmonic forces, showing steady state equilibrium stability conditions 24 p3145 A73-44530
- VISCOELASTIC DAMPING**
U ELASTIC DAMPING
U VISCOUS DAMPING
VISCOELASTIC FLOW
U VISCOELASTICITY
VISCOELASTICITY
NT PHOTOVISCOELASTICITY
NT THERMOVISCOELASTICITY
- Heating of a viscoelastic beam subjected to transverse vibrations 01 p0112 A73-10003
- The role of compressional viscoelasticity in the lubrication of rolling contacts. [ASME PAPER 72-LUB-O] 01 p0055 A73-10220
- Closed form exact solution to quasi-static problem in linear viscoelasticity for homogeneous anisotropic material with time invariant properties 01 p0116 A73-10967
- Ordinary integrodifferential equations for dynamic and quasi-static problems of nonlinear viscoelasticity theory 01 p0119 A73-11431
- Numerical Laplace transform inversion of a function arising in viscoelasticity. 01 p0119 A73-11469
- Determination of the strains and displacements for a rectangular shaped viscoelastic body 02 p0229 A73-11578
- Bending of a physically nonlinear viscoelastic rectangular plate under the action of a transversely distributed load 02 p0237 A73-12587
- Biaxial stress relaxation in glassy polymers - Polymethylmethacrylate. 02 p0186 A73-12811
- Compression and elastic moduli of heterogeneous viscoelastic materials consisting of mechanical mixture of homogeneous phases, using elastic-viscoelastic analogy 03 p0385 A73-13139
- Displacement and stress determination in the case of the profile-planar viscoelastic disk 03 p0385 A73-13141
- Interference grating production for viscoelasticity investigation by moire method, noting tensile tests of viscoelastic plates 03 p0306 A73-13159
- On bending and vibration of reinforced and bircorrelated elastic and viscoelastic shells. 03 p0387 A73-13160
- Numerical integration of nonlinear integrodifferential equations of thin viscoelastic beams deflection, considering cantilever beam under uniformly distributed loads 03 p0390 A73-13343
- Viscoelastic properties of amorphous polymers employed in stress investigations by the optical polarization method 03 p0335 A73-13737
- Stress analysis of thick walled hollow viscoelastic circular cylinder enclosed in elastic shell and subjected to nonlinear creep conditions, noting temperature effects 03 p0394 A73-14021
- Reversible instantaneous deformations and internal energy in viscoelastic incompressible fluids, using Oldroyd and De Witt hydrodynamic models 03 p0296 A73-14053
- The role of compressional viscoelasticity in the lubrication of rolling contacts. [ASME PAPER 72-LUB-O] 03 p0315 A73-14354
- Fracture criteria in quasi-viscoelastic analysis of crack initiation and propagation in polymethyl methacrylate, noting thermal effects on stress intensity factor 04 p0512 A73-15237
- Russian book - Strength of viscoelastic materials relative to solid-propellant rocket-motor charges. 04 p0517 A73-15967
- Viscoelastic liquid flow in wake past two dimensional grid, investigating vorticity increase with time for double array of vortices 05 p0565 A73-16592
- Effect of additive damping on transfer function characteristics of structures. [SAE PAPER 720811] 05 p0634 A73-16641
- Transient dynamic response of viscoelastic structures. [SAE PAPER 720812] 05 p0634 A73-16649
- Three dimensional static and dynamic stability equations of viscoelastoplastic deformation under axial compression 05 p0635 A73-17078
- Approximate method for solving wave propagation problems in viscoelastic materials 05 p0636 A73-17088
- Computing pressure cure viscoelastic effects in solid propellants. 05 p0606 A73-17208
- The influence of viscosity on the stability of a relative motion of two media. 06 p0685 A73-17761
- The correspondence principle of linear viscoelasticity for problems that involve time-dependent regions. 06 p0762 A73-17992
- French monograph - Determination and utilization of the laws of viscoelastic fluid behavior. 06 p0686 A73-18098
- Closed form analytical solution for secondary flow in viscoelastic liquids axisymmetric flow past oblate and prolate ellipsoids 06 p0687 A73-18507
- A note on the Cherepanov calculation of viscoelastic fracture. 07 p0908 A73-19090
- Construction of exact solutions to certain systems of linear and nonlinear Volterra integral equations by using a power series 07 p0844 A73-19129
- Methods of reducing continual nonlinear mechanics problems for deformable solids to discrete problems 07 p0910 A73-19303
- Torsion of a viscoelastic prismatic rod under the action of a vibrational load 07 p0911 A73-19315
- A visco-plasto-elastic expression for stress-strain diagram of fiber reinforced plastics subjected to repeated low frequency loads. 07 p0915 A73-20329
- Effect of diffusion on the growth and decay of acceleration waves in gases. 08 p0955 A73-21189
- Viscoelastic strains in a thick-walled cylinder under the long-term effect of a gravitational load 08 p1017 A73-21371
- Thermal hereditary constitutive law for linear viscoelastic materials time response in transient temperature environment 08 p1018 A73-21409
- Stability of a shallow three-layer shell with a linearly viscoelastic filler 09 p1157 A73-21994
- Inversion of Prony series characterization for viscoelastic stress analysis. 09 p1158 A73-22393
- Thermal instability in a viscoelastic fluid layer in hydromagnetics. 09 p1166 A73-22418
- Propagation of one-dimensional disturbances in a linear viscoelastic half-space under thermal shock 10 p1293 A73-24677
- Ordinary integrodifferential equations for dynamic and quasi-static problems of nonlinear viscoelasticity theory 11 p1443 A73-26066
- Damping properties of soft viscoelastic materials for certain plane stress combinations 12 p1515 A73-27176
- Shock absorbing-vibration insulating viscoelastic systems design under singular influence function assumption, determining ranges of parameters change 12 p1516 A73-27177
- Deformation of zero-moment shells subjected to internal pressure under creep conditions 12 p1551 A73-27179
- Flattening and creep stability loss of nonlinear viscoelastic ring under external pressure 12 p1551 A73-27180
- Elastic and viscoelastic zero moment reinforced and weakened shells of composite materials, calculating deformation mode characteristics 12 p1553 A73-27375
- Ray method for solving dynamic problems in viscoelastoplastic media 12 p1553 A73-27415
- Closed form exact solution to quasi-static problem in linear viscoelasticity for homogeneous anisotropic material with time invariant properties 12 p1554 A73-27543
- Boltzmann-Volterra constitutive law for viscoelastic linear materials, investigating criteria for relaxation properties 13 p1639 A73-28562
- Linear viscoelastic fluid parallel flow in straight duct of uniform cross section under axial pressure gradient 13 p1602 A73-28918
- Biaxial tensile test facility for three dimensional characterization of nonlinear viscoelastic materials based on variable ratio principal strains in plane stress 13 p1598 A73-29309
- Limit of linear viscoelastic behavior - An energy criterion. 13 p1700 A73-29465
- Epoxy-thiocol binder viscoelastic deformation under short and long term loads, noting stress-strain linearity limit 13 p1647 A73-29610
- Heat transfer by fluctuating flow of an elastico-viscous liquid past an infinite plate with time varying suction. 14 p1816 A73-29999
- Vibration analysis of sandwich beam with constrained viscoelastic layers on both sides. 14 p1806 A73-30046
- Quasi-monochromatic viscoelastic waves energy velocity equivalence to phase velocity for medium represented by standard linear solid or Maxwell model 15 p1955 A73-32176
- Finite amplitude dynamic motion of viscoelastic materials. 15 p1956 A73-32223
- Poisson's Ratio and the deflection of a viscoelastic plate. 15 p1956 A73-32342
- Development of convection in horizontal layers of a non-Newtonian fluid 16 p2084 A73-32679
- Convolutional variational principles for stress distribution in anisotropic plates of linear viscoelastic material 16 p2077 A73-32981
- Adhesive viscoelasticity effects on sandwich structure performance, presenting mathematical model for adhesive behavior and time dependent loading 16 p2029 A73-33053
- Viscoelastic body stress-strain state under quasi-static loads, obtaining boundary value problem solution via finite element method 16 p2080 A73-33244
- On the generation of rational function approximations for Laplace transform inversion with an application to viscoelasticity. 16 p2032 A73-33307
- On the solution of magnetohydrodynamic elastico-viscous flow past a plane porous plate. 16 p2042 A73-33370
- Modeling, identification and prediction of a class of nonlinear viscoelastic materials. I. 16 p2082 A73-33904
- Equilibrium conditions for multilayer anisotropic viscoelastic plates in a complex stressed state 16 p2083 A73-33933
- Theory for the flexural vibrations of a rotating viscoelastic cantilever 16 p2083 A73-33936
- Prediction of the deformation properties of polymer materials 17 p2194 A73-34268
- Orthotropic viscoelastic shells and plates dynamic behavior reduced to eigenvalue and quasi-static solutions for nonstabilized oscillation 17 p2241 A73-34326
- Book - Nonlinear viscoelastic solids. 17 p2243 A73-34574
- The Sorokin damping hypothesis in the case of aperiodic vibrations 17 p2243 A73-34648
- Plane finite amplitude viscoelastic wave propagation, deriving expressions for nonlinear, dispersion and dissipation effects 17 p2244 A73-34792
- Acceleration wave propagation in a nonlinear viscoelastic solid. [ASME PAPER 73-APM-2] 17 p2247 A73-35028
- Viscoelastic fracture of solid propellant pressurization condition. [SESA PAPER 2114A] 17 p2220 A73-35449
- The use of a high modulus inclusion gauge in nonlinear viscoelastic materials. [SESA PAPER 2187A] 17 p2173 A73-35457
- A numerical method for creep deformation of solids. 18 p2365 A73-36612
- A note on uniqueness in the linear theory of heat conduction with finite wave speeds. 18 p2371 A73-36692
- On the propagation of relativistic thermo-magneto-viscoelastic waves in a material of Voigt-type. 19 p2459 A73-37648
- A path-independent integral for transient crack problems. 19 p2500 A73-38114
- Random loading on a spherical pressure vessel of Hooke-Norton material. 19 p2501 A73-38252
- A study on the dynamical behaviors of composite materials by dynamical model. 20 p2580 A73-38643
- Successive approximation technique for dynamic-load problems of nonlinear viscoelastic systems 20 p2593 A73-39322
- Mathematical theory of nonlinear viscoelasticity 20 p2618 A73-39330
- Numerical solution of quasi-static problems in viscoelasticity theory 20 p2619 A73-39332

Rotary inertia and energy dissipation effects on dynamic response of three layered symmetrical laminate beam with viscoelastic core vibrating in flexural mode, using variational calculus

20 p2623 A73-39555

Flutter-divergence transition criteria in certain viscoelastic polygenic systems.

20 p2623 A73-39556

Impact generated elastic strain low amplitude pulses propagating in filamentary composite rods, using Fourier transform technique and viscoelastic relation

20 p2623 A73-39557

Uniqueness of solutions and some approximate methods of solving problems in linear viscoelasticity

21 p2782 A73-40186

Viscoelastic panel vibration damping material for ventilation ducts to reduce LF vibrations induced by turbulent air flow

21 p2723 A73-40235

Parametric study of multiple-layer damping treatments on beams.

21 p2785 A73-40752

Russian book on elastic and thermoelastic waves in continuous deformable bodies covering steady and unsteady deformation dynamics, viscoelasticity and nonlinear elasticity using computer methods

21 p2785 A73-40800

Torsional elasticity of human skin in vivo.

21 p2642 A73-41625

The response of viscoelastic materials to slow cyclic stresses.

21 p2789 A73-41689

On unsteady flow of an elastico-viscous fluid past an infinite plate with variable suction.

22 p2840 A73-41747

Approximate estimation of the possibility of using the viscoelasticity hypothesis for the formulation of an equation of motion for a liquid with polymer additions

22 p2841 A73-42122

Large deflection theory for viscoelastic anisotropic thin plates, deriving constitutive, plane stress, plate and nonlinear integrodifferential equations

22 p2923 A73-42638

A new method of measuring arterial dilation and its application.

22 p2815 A73-42669

Thermal response of a viscoelastic rod under cyclic loading.

[ASME PAPER 73-APMW-39] 22 p2926 A73-42896

Linear viscoelasticity theory application to high polymers mechanical properties determination via relaxation spectrum with emphasis on polymethyl methacrylate

22 p2881 A73-43170

Influence of initial transients on stress relaxation and creep measurements on visco-elastic materials.

22 p2868 A73-43172

Finite amplitude dynamic motion of viscoelastic materials.

23 p3038 A73-43273

Prediction of stability of viscoelastic Couette flow based on network rupture hypothesis.

23 p2967 A73-43300

Capillary breakup length and stability of Newtonian and viscoelastic cylindrical liquid jets in terms of dimensionless viscosity and relaxation time

23 p2967 A73-43307

Fatigue failure analysis of low carbon steel endurance under cyclic loading with time dependent viscoelastic effects, using Hooke's-Trouton laws

23 p3040 A73-43469

Slow growth of cracks in a rate sensitive Tresca solid.

23 p2992 A73-43810

Weak longitudinal waves in a nonlinear viscoelastic medium

23 p3045 A73-44182

Numerical approximation of quasi-static and dynamic problems in viscoelasticity by net-point and finite difference methods

24 p3144 A73-44505

Power series solution to Volterra equations in nonlinear viscoelastic dynamic plate and shell theory with application to flexible cylindrical shell vibrations under periodic loads

24 p3145 A73-44518

Solution of physically nonlinear quasi-static problems of viscoelasticity

24 p3145 A73-44519

Dynamic stability of a viscoelastic orthotropic cylindrical shell

24 p3146 A73-44532

Damping of mechanical systems with the aid of viscoelastic liquids

24 p3109 A73-44915

Recent results in nonlinear viscoelastic wave propagation.

24 p3151 A73-45305

Book - Solid-state mechanics 3.

24 p3153 A73-45495

Constitutive equations, creep laws, stress functions, variational principles and differential operators in dynamic and static linear viscoelasticity theory

24 p3153 A73-45496

VISCOMETERS

Navier-Stokes equation solution for steady state, tandem and Rankine capillary viscometer precision measurements, including compressibility correction

11 p1361 A73-25367

VISCOMETRY

An improved acoustic viscosimeter for studies of the viscosity of simple fluids in the critical region.

04 p0448 A73-15123

Absolute viscosity of air down to cryogenic temperatures and up to high pressures.

19 p2422 A73-38296

VISCOPLASTIC FLOW
U VISCOPLASTICITY
VISCOPLASTICITY

Nonlinear initial and boundary value problems of thermoviscoplasticity, discussing uses of Vainberg theorem and functional convolution in variational principle formulation

[AD-758580] 02 p0236 A73-12516

Temperature, velocity, and stress distribution in thermo-viscoplastic boundary layers

03 p0386 A73-13145

Spherical wave propagation in a viscoplastic medium.

03 p0393 A73-13788

Influence of the magnetic field on the heat transfer of a ferromagnetic viscoplastic fluid

03 p0347 A73-14323

Thermodynamics and shocks in nonelastic mediums

04 p0520 A73-15994

Three dimensional static and dynamic stability equations of viscoelastoplastic deformation under axial compression

05 p0635 A73-17078

Time variable stress-strain state of viscoelastoplastic hollow sphere under internal pressure, using piecewise linear differential law

05 p0635 A73-17080

Minimum principles in the dynamics of isotropic rigid-plastic and rigid-viscoplastic continuous media.

06 p0757 A73-17396

Linearized theory of dynamically loaded thin rigid viscoplastic rectangular plates transient response, investigating strain rate effect

06 p0760 A73-17760

Viscoplasticity theory based on strain rate vector perpendicularity to quasi-static yield surface, comparing results to Perzyna theory

07 p0907 A73-19078

A visco-plasto-elastic expression for stress-strain diagram of fiber reinforced plastics subjected to repeated low frequency loads.

07 p0915 A73-20329

Mixed viscous-brittle fracture model of plastic crack distribution and propagation pattern in bcc polycrystal by electron raster microscope analysis

09 p1157 A73-21961

Unsteady viscoplastic electrically conducting MHD flow in moving-wall channel, assuming time-variable pressure gradient and uniform transverse magnetic field

10 p1256 A73-24588

Electrically conducting unsteady viscoplastic plane channel Hartmann and Couette MHD flows in presence of uniform transverse magnetic field and time variable electric field

10 p1256 A73-24589

Unsteady motion of a viscoplastic medium in a plane MHD channel at a constant flow rate

10 p1256 A73-24590

Elastic and elastoviscoplastic unloading waves propagation in semiinfinite bar under axial impact stress, considering bilinear stress-strain curve

11 p1447 A73-26646

Dynamic tensile deformation of viscoplastic filament without bending rigidity, displacement constraints and cross sectional area variations

12 p1552 A73-27300

Dynamically possible finite deformations of isotropic, incompressible, elastic-inelastic solids with temperature independent response.

13 p1695 A73-28416

Evaluation of dissipation and damage in metals submitted to dynamic loading.

13 p1701 A73-29505

Buckling of viscoplastic cylindrical shells loaded by radial pressure impulse.

14 p1811 A73-30481

Linearized constitutive equations for thin viscoplastic shell deflection under dynamic loads

14 p1811 A73-30488

Constitutive equations and directors in plastic and viscoplastic media

15 p1947 A73-31368

Dynamic analysis of viscoelastoplastic anisotropic shells.

16 p2075 A73-32787

A unified theory of thermoviscoplasticity of crystalline solids.

19 p2501 A73-38256

Exact solutions of some problems of the Stefan type

20 p2627 A73-39335

Equations of motion for ideal isotropic viscoplastic medium in axisymmetric space, determining conditions for flow core existence

20 p2619 A73-39336

Rigid viscoplastic thin circular plate under uniformly distributed transverse pressure, deriving Mises and Tresca yield surface conditions

20 p2624 A73-39567

Finite plasticity theory in acoustic tensor calculation for elastic, viscoplastic and plastic wave propagation

21 p2740 A73-40947

Experimental bases and models for the study of the overall behavior of metals

23 p2993 A73-43964

Elementary mechanisms and physical models in plasticity and viscoplasticity

23 p3043 A73-43965

Constitutive equations of elastoplastic and elastoviscoplastic bodies based on thermodynamic state, considering deformation velocity and stress relaxation

23 p3043 A73-43967

Classical viscoplasticity and Mandel plasticity theories comparison with emphasis on strain hardening, acceleration wave propagation and plastic and elastic deformations

23 p3043 A73-43968

Thermodynamic treatment of plastic media with application to viscoplastic materials, elastoplastic deformation and entropy jump across weak shock waves

23 p3043 A73-43969

Mandel viscoplasticity theory constitutive equations satisfying causality principle, considering finite deformations tensor representation by partial differentials

23 p3044 A73-43970

Order of magnitude of the differences between theory and experiment in viscoplasticity under varying stress and temperature

23 p3044 A73-43971

Study of a dynamic problem in viscoelastoplasticity and ideal plasticity with conditions of friction at the boundary

23 p3044 A73-43973

Uniqueness theorems and variational principles derivation for free viscoplastic flow and constrained plastic deformation, obtaining Castigliano theorem from boundary value problem solution

23 p3044 A73-43974

Buckling of short viscoplastic cylindrical shells subjected to radial impulse.

23 p3045 A73-44080

Potential theory-based relationships between plastic deformation and strain hardening properties of elastoviscoplastic and elastoplastic media, considering specific entropy and free energy contributions

23 p3045 A73-44099

Dislocation plasticity theory for slip system in terms of constitutive equations for dislocation speeds and densities, extending to rigid viscoplastic body

23 p3046 A73-44226

A lower bound theorem for dynamically loaded rigid-viscoplastic structures.

24 p3146 A73-44680

VISCOITY

NT EDDY VISCOSITY

NT GAS VISCOSITY

Transport phenomena in turbulent plasma with electromagnetic waves.

01 p0081 A73-10117

The role of compressional viscoelasticity in the lubrication of rolling contacts.

[ASME PAPER 72-LUB-O] 01 p0055 A73-10220

Drag reduction in non-Newtonian turbulent flow, considering viscosity change with strain in long-chain molecules /polymers/ fluid solutions

01 p0034 A73-11134

Artificial viscosity truncation error analysis for finite difference analogs of linear advection equations

01 p0035 A73-11466

Effect of ion viscosity on the stability of a finite-pressure plasma.

02 p0198 A73-12104

The effects of viscous friction on axial rotation of celestial bodies.

02 p0216 A73-12376

The effects of viscous friction on the precession and nutation of celestial bodies.

02 p0217 A73-12396

The statistical evaluation of the measurement of viscosity of a non-Newtonian liquid.

03 p0306 A73-12899

Nonadiabatic temperature change in rapidly expanded or compressed gas, discussing shearing and volume viscosity effects

05 p0597 A73-16350

The Navier-Stokes equations and the bulk viscosity of simple gases.

05 p0597 A73-16591

Hydrodynamic instability of the boundary of a viscous plasma in a magnetic field.

05 p0603 A73-16793

Evaluation of numerical viscosity effects in transonic flow calculations.

[AIAA PAPER 73-131] 05 p0530 A73-16884

Effect of ion viscosity and thermal conductivity on the drift instability in an inhomogeneous high-pressure collisional plasma.

05 p0604 A73-17362

Viscosity investigation of sintered fiberglass in the region of softening and annealing temperatures

06 p0715 A73-18657

Application of a variational technique to wedge flow with variable properties.

07 p0775 A73-19963

Influence of liquid lubricant properties on their performance.

07 p0844 A73-20464

Experimental determination of the temperature and pressure dependence of the absolute viscosity of mineral oils

10 p1237 A73-23661

Viscosity of the moon. I - After mare formation. II - During mare formation.

10 p1277 A73-24081

Vertical distribution of viscosity and convection conditions in earth mantle, discussing shallow convection model and geophysical evidence for validity

11 p1356 A73-25906

Influence of viscosity, thermal conduction, and ion drag on the propagation of atmospheric gravity waves in the thermosphere.

13 p1606 A73-28154

Emulsion and suspension effective viscosity dependence on dispersed phase volume concentration and particle interactions in two phase flows

13 p1580 A73-28465

Artificial viscosity related to shocks for studying anomalous wall heating and solution behavior at interface by substituting Rankine-Hugoniot equation

14 p1775 A73-30908

Effective-viscosity model for turbulent wall boundary layers.

15 p1860 A73-31119

Influence of viscosity on the flow of an under-expanded jet propagating in a supersonic slipstream

15 p1822 A73-31299

Bulk viscosity effects in imperfect fluid Friedmann cosmology, considering implications for singularity problem

15 p1939 A73-32011

Chemo-rheology of two high temperature epoxy resins.

17 p2197 A73-35347

Thermohydrodynamic lubrication in laminar and turbulent regimes.

[ASME PAPER 73-LUBS-15] 17 p2181 A73-35395

Turbulent lubrication - Its genesis and role in modern design.

[ASME PAPER 73-LUBS-19] 17 p2181 A73-35398

Liquid anorthite viscosity and thermal expansion at 1450-1620 C and 820-950 C, noting agreement with Bottlinga-Weill model predictions

20 p2555 A73-39718

Influence of certain hydroxyl- and nitrogen-containing low-molecular-weight substances on the structural viscosity of cellulose acetate solutions

21 p2647 A73-40263

Theoretical studies and experimental verifications of thermal and electrical conductivity, molecular diffusivity and viscosity of a partially ionized suspension in an electric field.

22 p2894 A73-42512

Model experiments on apparent blood viscosity and hematocrit in pulmonary alveoli.

24 p3064 A73-45064

Experimental investigation of the viscosity of lubricating oil containing air

24 p3094 A73-45548

VISCOSITY DAMPING

Floating potential and diffusion coefficients of viscosity damping of convective cells in stellarator for confined He, Ar and Xe plasmas

01 p0083 A73-10462

Harmonic oscillations of elastic system with viscous damping, calculating maximum amplitude of third subharmonic

04 p0509 A73-14978

Transient dynamic response of viscoelastic structures.

[SAE PAPER 720812] 05 p0634 A73-16649

Stability analysis of gyroscopic systems for parametric resonance case, allowing for viscous friction at gimbal axes

05 p0578 A73-17085

Anisotropic flexible bearings mounted rotors backward and forward precessional motion excitation, noting internal viscous damping forces effect on vibration amplitude

06 p0758 A73-17515

Effect of suspension-line viscous damping on parachute opening load amplification.

07 p0777 A73-19495

Frequency response of a dynamic system with statistical damping.

08 p0950 A73-20715

Improving reliability and eliminating maintenance with elastomeric dampers for rotor systems.

10 p1175 A73-23950

Subharmonic resonance of order 1/2 with an asymmetrical restoring force.

10 p1292 A73-24649

Beam and plate flexural vibration damping by free or uncompressed rigid viscoelastic coatings applied on sides

10 p1293 A73-24794

Damping properties of soft viscoelastic materials for certain plane stress combinations

12 p1515 A73-27176

Ultraharmonic motion of a viscously damped nonlinear beam.

13 p1697 A73-28809

Elastic viscously damped ten degree of freedom system with two torsion-elastically mutually pivotally joined rotors, determining eigenfrequencies by equations of motion numerical evaluation

16 p1968 A73-33235

Superharmonic resonance in piecewise-linear system - Effect of damping and stability problem.

19 p2459 A73-37669

A numerical study of damping in viscoelastic sandwich beams.

[ASME PAPER 73-DET-73] 22 p2919 A73-42071

Identification of damping coefficients in multidimensional linear systems.

[ASME PAPER 73-APMW-43] 22 p2926 A73-42899

Resonance conditions for nonlinear interaction of acoustic gravity waves with viscous damping taken into account

22 p2828 A73-43178

Monofrequent oscillations in mechanical systems governed by second order hyperbolic differential equations with small non-linearities.

23 p3044 A73-44077

Damping of mechanical systems with the aid of viscoelastic liquids

24 p3109 A73-44915

VISCOS DRAG

The effect of radiative and viscous dissipation of the propagation of forced planetary waves in the vicinity of critical levels.

01 p0039 A73-10395

Shear layer extent caused by slip surface in inviscid flow with shock interactions, noting viscous effect in hypersonic flow

01 p0033 A73-10747

Ideal fluid flow past a body with an upstream jet

01 p0035 A73-11427

Influence of liquid circulation within a droplet on the vaporization rate and drag in a viscous flow

10 p1206 A73-24680

Liquid droplet drag in vapor flow as function of drop vaporization rate, using Stokes formula

11 p1451 A73-25736

Flow of an ideal fluid past a body with a reverse-stream.

11 p1348 A73-26056

Influence of weak viscous interaction on the drag of a wing profile

15 p1822 A73-31195

The slow unsteady settling of two fluid spheres along their line of centres.

22 p2840 A73-41742

VISCOS FLOW

NT BOUNDARY LAYER FLOW

NT BOUNDARY LAYER SEPARATION

NT COUETTE FLOW

NT REATTACHED FLOW

NT SECONDARY FLOW

NT SEPARATED FLOW

NT STOKES FLOW

Calculation of the flow of a viscous compressible fluid past a parabolic obstacle

[ONERA, TP NO. 1129] 01 p0002 A73-10238

Unsteady viscous flow due to the impulsive motion of a flat plate, with special reference to the initial period.

01 p0031 A73-10422

Effect of viscosity on the motion of the inhomogeneities of a nonequilibrium plasma in a magnetic field

01 p0085 A73-10865

Numerical calculations of the flow field of low Reynolds number viscous flow with or without real-gas-effects in slender-channel-nozzles.

[DGLR PAPER 72-110] 02 p0152 A73-11674

Axisymmetric slow viscous flow past an arbitrary convex body of revolution.

02 p0153 A73-12040

Some exact statistics of two-dimensional viscous flow with random forcing.

02 p0153 A73-12041

Nondecaying turbulence field production by mean shear in spite of flow viscosity effects

02 p0154 A73-12056

Incompressible viscous fluid creep flow past deforming sphere for small Reynolds numbers, considering cases of different Strouhal numbers

03 p0244 A73-13529

The prediction of airfoil pressure distributions for subcritical viscous flow and for supercritical inviscid flow.

03 p0247 A73-14378

Navier-Stokes equation solutions for steady laminar viscous flow of incompressible fluid with mixed no-slip and no-shear conditions

05 p0563 A73-16097

The Green's function of the linearized viscous transonic equation

05 p0527 A73-16446

Calculation of supersonic viscous gas flow past blunt bodies at large Reynolds numbers

05 p0527 A73-16448

Two-dimensional viscid MHD flows in coaxial channels

05 p0603 A73-16588

Viscous shock layer flow in the windward plane of cones at angle of attack.

[ALAA PAPER 73-134] 05 p0530 A73-16886

Nose pressure distribution and separation on an inclined axisymmetric body.

05 p0533 A73-17123

Magnetohydrodynamic viscous flow induced by an oscillating disk.

06 p0728 A73-17792

Low Reynolds number flow past a porous spherical shell.

06 p0687 A73-18506

Small amplitude viscous similarity solution for vertical two dimensional internal wave production by circular cylinder resonant oscillation in incompressible stratified fluid

06 p0646 A73-18527

Viscous compressible flow near right angle corner of two flat plates, presenting streamwise and secondary flow velocities and skin friction coefficient distribution

06 p0687 A73-18532

An extension of the modified Oseen solution for laminar viscous flow past a semi-infinite flat plate.

06 p0688 A73-18849

Development of flow in the entrance region of a converging channel.

07 p0810 A73-19103

The influence of the accommodation coefficients on the flow variables in the viscous interaction region of a hypersonic slip-flow boundary layer.

[DFVLR-SONDDR-267] 07 p0773 A73-19206

Viscous incompressible gas turbulent flow in axisymmetric channel under preliminary twist conditions at inlet, using computer numerical solution

07 p0774 A73-19621

Viscous flow behavior of lunar compositions 14259 and 14310.

07 p0895 A73-19857

Analysis of flow of viscous fluids by the finite-element method.

07 p0811 A73-19953

Experimental and theoretical study of supersonic viscous flow over a yawed circular cone.

07 p0775 A73-19957

Flow of an ideal incompressible ponderable fluid around a thin profile placed under a free line. I, II

07 p0811 A73-19998

Unsteady motion of a viscous electrically conducting fluid around a flat plate in the case of orthogonal fields

07 p0858 A73-19999

Flow of a viscous incompressible fluid between a fixed porous disk and a rotating nonporous disk, with radial discharge

07 p0811 A73-20069

Decaying unsteady viscous vortex flow under conditions of streamlines and vortex lines coincidence, deriving Navier-Stokes equations solution

07 p0812 A73-20340

The Stokes problems for a suspension of particles.

08 p0955 A73-21426

Numerical analysis of the viscous, hypersonic, MHD blunt-body problem.

09 p1132 A73-23455

Numerical study of the flow of a viscous incompressible fluid around a circular cylinder

10 p1171 A73-23766

Breakup length maximum and decrease achievement in laminar viscous jet with velocity increase, discussing effects of ambient gas

10 p1206 A73-24255

The initial flow past an impulsively started circular cylinder.

10 p1172 A73-24338

Flow near an accelerated plate in the presence of a magnetic field.

10 p1206 A73-24528

Influence of liquid circulation within a droplet on the vaporization rate and drag in a viscous flow

10 p1206 A73-24680

Characteristics of viscous vortex flows in superconducting alloys near the critical temperature

10 p1261 A73-24765

Visualization experiments on unsteady viscous flows around cylinders and plates.

10 p1174 A73-24836

Unsteady flow between a fixed porous disk and a rotating disk

10 p1209 A73-24837

An evaluation of cell type finite difference methods for solving viscous flow problems. 11 p1345 A73-25112 [AD-757443]
Viscous flow over a cone at moderate incidence. I - Hypersonic tip region. 11 p1300 A73-25114
Newton method for calculation of viscous flow around circular cylinder with Fourier series truncation for stream function and vorticity, evaluating numerical error 11 p1345 A73-25115
Unsteady viscous jet flow into stationary surroundings. 11 p1345 A73-25117
Unsteady boundary layer flow of homogeneous viscous fluid in nonrotating environment or bounded by oscillating flat plates, determining velocity field by exact solutions 11 p1346 A73-25165
Numerical study of a viscous flow through a pipe orifice. 11 p1346 A73-25213
A note on the unsteady motion of a viscous conducting liquid between two porous concentric circular cylinders acted on by a radial magnetic field. 11 p1404 A73-25368
Newtonian and non-Newtonian liquids rotating adjacent to a stationary surface. 11 p1346 A73-25369
Asymptotic Nusselt numbers for dissipative non-Newtonian flow through ducts. 11 p1346 A73-25370
Solar wind-lunar limb interaction from viscous MHD approach including continuum fluids, kinetic plasma and magnetic boundary layer 12 p1534 A73-27003
Experimental investigation of heat and mass transfer in the condensation of vapor from gas-vapor mixtures under viscous and viscous-gravitational flow conditions 12 p1558 A73-27315
Influence of viscosity on the motion of nonuniformities of a nonequilibrium plasma in a magnetic field. 12 p1529 A73-27914
Steady universal motions of a Navier-Stokes fluid - The case when the velocity magnitude is constant on a Lamb surface. 13 p1599 A73-28285
Integral properties of viscous channel or pipe flow satisfying mixed no-slip and no-shear conditions from total momentum flux considerations 13 p1599 A73-28417
Flow of viscous fluid at small Reynolds numbers past a porous body. 13 p1601 A73-28625
Two dimensional flow of viscous incompressible fluid, discussing formulation in analytic functions with applications to flows past elliptic cylinder and flat plates 13 p1603 A73-29048
Study of a new family of solutions of Navier-Stokes equations 14 p1744 A73-29758
Free convection effects on the oscillatory flow past an infinite, vertical, porous plate with constant suction. I, II. 14 p1816 A73-30049
Two-dimensional bubbles in slow viscous flows. II. 14 p1744 A73-30170
Numerical solution of the viscous flow in the entrance region of parallel plates. 14 p1746 A73-30907
The conservative method of flows and the calculation of a viscous heat conducting gas flow past a body of finite size 15 p1821 A73-30962
The nature of viscous flow around the forward stagnation point in the presence of strong injection of a gas through the surface of a slender pointed body 15 p1821 A73-31043
Steady solutions of a nonlinear problem for the Navier-Stokes equations 16 p2031 A73-32933
The computation of the flow in the gap between two concentrically rotating spherical surfaces 16 p2000 A73-33255
Stability of a viscous fluid between rotating cylinders with axial flow and pressure gradient round the cylinders. 16 p2000 A73-33312
Jet-induced external flows of an incompressible viscous liquid 17 p2149 A73-34138
Mathematical formulation of viscous-inviscid interaction problems in supersonic flow. 17 p2091 A73-34178
Viscous flow in radial turbomachine blade passages. 17 p2093 A73-34389
Book - Lectures on fluid mechanics. 17 p2150 A73-34457
Book - Foundations of fluid flow theory. 17 p2151 A73-34466
Book - Physical fluid dynamics. 17 p2151 A73-34472

Turbulent viscosities for swirling flow in a stationary annulus. 17 p2152 A73-35013 [ASME PAPER 73-FE-16]
Linearized implicit schemes for the computation of viscous incompressible flow - with applications. 17 p2155 A73-35141
Viscous fluid dynamic problem solution method implementation in Eulerian code AZTEC within continuum mechanics-kinetic theory union, preserving conservation properties throughout time integration 17 p2155 A73-35142
Numerical studies of viscous, incompressible flow through an orifice for arbitrary Reynolds number. 17 p2157 A73-35602
Impulsively started viscous flow past a finite flat plate with and without an applied magnetic field. 17 p2217 A73-35604
Turbulent heat transfer and the periodic viscous sublayer. 17 p2255 A73-35844
On the solution of the unsteady Navier-Stokes equations including multicomponent finite rate chemistry. 18 p2259 A73-36157
Numerical solutions of time-dependent incompressible Navier-Stokes equations using an integro-differential formulation. 18 p2297 A73-36159
Theory of supersonic laminar non-adiabatic boundary layer flow past small rearward-facing steps including viscous-inviscid interaction. 18 p2261 A73-36219
On viscous and wind tunnel wall effects in transonic flows over airfoils. 18 p2263 A73-36261
Viscous effects in massively-ablating planetary entry body flow fields. 18 p2264 A73-36335
Effect of downstream massive blowing on Jovian entry heating. 18 p2264 A73-36336
Calculation of viscous gas flows in flat channels 18 p2265 A73-36990
Steady-state solutions to the problem of viscous incompressible fluid flow past a body 19 p2419 A73-37244
Increasing the transport capacity in a viscous fluid flow by the injection method 19 p2420 A73-37552
The velocity profile in the wall region of a turbulent boundary layer 19 p2420 A73-37554
Linear viscous stability theory for stably stratified shear flow - A review. 19 p2421 A73-38227
Numerical study of viscous flow in a cavity. 20 p2545 A73-38971
Nonlinear streaming effects associated with viscous incompressible fluid near oscillating cylinder, considering theory based on outer-inner expansion technique with Stokes drift correction 20 p2546 A73-39088
Viscous flow over a cone at moderate incidence. II - Supersonic boundary layer. 20 p2507 A73-39093
Unsteady heat transfer characteristics of a two dimensional laminar wall jet. 20 p2628 A73-39339
No-slip boundary condition origin for viscous incompressible Newtonian fluid flow over family of models for rough wall 20 p2549 A73-39810
On the coexistence of laminar and turbulent flow in a narrow triangular duct. 20 p2549 A73-39813
Two dimensional flow theory of Weis-Fogh lift generation in inviscid motions of insect wings involving viscous effects 21 p2631 A73-40244
Study of MHD effects in a viscous conducting fluid flow in a traveling magnetic field 21 p2747 A73-40884
Spatial stability of incompressible two-dimensional Gaussian wake in steady viscous flow. 22 p2796 A73-42243
The hydrodynamic analogy and its application to a two-dimensional problem in elasticity theory 22 p2921 A73-42282
Heat transfer in liquids due to second order boundary layer flows with dissipation. 22 p2938 A73-42996
Laminar flow of a viscous barotropic gas through a circular pipe 23 p2968 A73-43721
The flow of a viscous liquid down a variable incline. 24 p3080 A73-45368
A method for solving problems involving viscous flows past bodies at large Reynolds numbers 24 p3081 A73-45530

VISCOUS FLUIDS

Existence and stability of the secondary periodic solution figuring in Navier-Stokes type evolution problems [ONERA, TP NO. 1172] 01 p0033 A73-10780

Viscous steady Couette flow between two parallel flat walls with particle injection, obtaining velocity and temperature distribution 01 p0033 A73-10808
Magnetohydrodynamic flow around a hollow sphere 01 p0085 A73-11259
Turbulent non-Newtonian liquid power dissipation steadiness during motion as function of viscous forces balanced variation 02 p0152 A73-11571
Theory of the electrodiffusion method for measuring the spectral characteristics of turbulent flows 02 p0165 A73-11614
Nonlinear baroclinic instability of a continuous zonal flow of viscous fluid. 02 p0153 A73-12035
Liapunov-Schmidt analysis of convection bifurcation scheme in internally heated viscous fluid layers of infinite horizontal extent 02 p0238 A73-12053
Nonlinear instability of two dimensional unbounded incompressible viscous fluid flows under periodic small perturbation 03 p0296 A73-14049
Some refinements of the theory of the viscous screw pump. 03 p0314 A73-14337
A theoretical analysis of non-isentropic flow of a compressible, viscous gas in narrow passages. [ASLE PREPRINT 72LC-3A-1] 03 p0297 A73-14355
An improved acoustic viscosimeter for studies of the viscosity of simple fluids in the critical region. 04 p0448 A73-15123
The motion of a plate in a rotating fluid at an arbitrary angle of attack. 04 p0404 A73-15161
Study of plane flows of viscous fluid around a body 04 p0404 A73-15652
Numerical solution of a boundary value problem for the Navier-Stokes equations 05 p0564 A73-16449
Effect of the asymmetry of an external magnetic field on a viscous fluid flow in an annular MHD channel 05 p0603 A73-16589
Steady rectilinear universal motions of a Navier-Stokes fluid. 06 p0685 A73-17861
French monograph - Determination and utilization of the laws of viscoelastic fluid behavior. 06 p0686 A73-18098
Boundary value problems of viscous fluid dynamic system generated by Navier-Stokes equations, using Hopf theory 06 p0724 A73-18634
On generalized hydrodynamic equations used in heat transfer theory. 06 p0688 A73-18834
Diffusion on a particle in the shear flow of a viscous fluid - Approximation of the diffusion boundary layer. 07 p0809 A73-19021
Flow of a conductive fluid through a cylindrical duct with periodic deformations in the presence of an azimuthal magnetic field 07 p0858 A73-20073
Cylindrical pores in viscous incompressible liquid film, considering existence duration and pore wall motion under surface tension forces 07 p0923 A73-20420
New formulations of the corresponding states principle for the transport properties of pure dense fluids. 08 p0223 A73-21258
Blood vessels simulation by muscle pump represented by elastically deformable pipe with valves, solving Navier-Stokes equation for viscous fluid flow 08 p0934 A73-21375
Interaction of pulsating bubbles in a viscous fluid 08 p0955 A73-21446
Three dimensional steady flow of incompressible viscous fluid near thin wing trailing edge, using Stewartson-Williams triple layer method 08 p0926 A73-21495
Two approximate methods for describing the steady motions of an incompressible viscous fluid with a free boundary 09 p1072 A73-22619
Supersonic flow of a viscous gas about a spherically blunt cooled object 09 p1028 A73-22620
Putting an electrically conducting fluid in rotation by a rotating magnetic field 10 p1254 A73-24125
Finite element solution algorithm for viscous incompressible fluid dynamics. 10 p1243 A73-24296
Unsteady flow of a conducting viscous fluid between parallel porous walls with heat transfer 10 p1256 A73-24587
An extended boundary-layer analysis of the impulsive motion of a flat plate in a viscous fluid. 10 p1208 A73-24809

On unsteady magnetohydrodynamic boundary layers in a rotating flow.

10 p1257 A73-24841

The motion of a viscous, stratified fluid subjected to forced oscillations.

10 p1210 A73-24844

Parallel magnetic field effect upon plane interface stability between two conducting viscous fluids in uniform relative motion, obtaining neutral shear flow stability curves

11 p1402 A73-25054

Pressure shocks in thermally and electrically conducting viscous gas, discussing growth equation and radiation effects

11 p1403 A73-25164

Viscous incompressible Jeffery-Hamel fluid flow in divergent channel, discussing secondary supercritical flow, winding and vortex formation

11 p1346 A73-25223

Steady plane flow of viscous fluid in symmetrical channels with curved walls, considering approximate series for stream function

11 p1347 A73-25646

Oscillations arising when parallel flows of a viscous liquid lose stability relative to periodic long-wave disturbances

11 p1349 A73-26430

Internal atmospheric gravity wave effect on ionospheric columnar electron content on basis of viscous atmosphere model with isothermal layers

11 p1359 A73-26709

Movement of viscous incompressible fluids through annular interstices with walls in relative alternating translational motion

12 p1486 A73-26795

Motion of a conducting gas with variable properties between rotating cylinders

12 p1487 A73-27798

Memory effects associated with bulk viscosity on the spectrum of stimulated Brillouin scattering.

13 p1626 A73-28372

Viscous fluid sloshing in rectangular vessel, studying forced oscillations, ejected flow and frequency equation based on Navier-Stokes equations and boundary conditions

13 p1600 A73-28444

On the concepts of viscous fluids, of elastic solids, and of heat conduction in relativity

13 p1661 A73-29555

Low Hartmann number MHD flow of weakly conducting viscous fluid past nonconducting sphere within aligned uniform magnetic field

14 p1781 A73-30655

Computerized three dimensional calculations of hypersustained aircraft in viscous potential flow in terms of boundary layers and wakes

16 p1962 A73-32816

Leading edge effects on displacement thickness and skin friction variations of unsteady boundary layer on flat plate under impulsive motion in viscous fluid

16 p1962 A73-32927

Approximate method based on the application of hydrodynamic analogy

17 p2244 A73-34794

Continuum mechanics analysis of solid particle suspension flow of viscous gas, noting demixed region near wall

17 p2156 A73-35508

Analysis of nonequilibrium particulate flow.

[AIAA PAPER 73-687] 18 p2298 A73-36238

Mises variables in problems with a free boundary for the Navier-Stokes equations

19 p2419 A73-37245

On the torsional oscillations of a sphere placed at the axis of a rotating viscous incompressible fluid.

19 p2419 A73-37422

Heat transfer from a vibrating circular cylinder.

19 p2505 A73-38478

Vortex interaction with plane in viscous fluid, discussing free parameter related to insufficient boundary conditions for solving Navier-Stokes equations

20 p2547 A73-39289

Convection in a liquid heated from below in a closed cavity with temperature-dependent viscosity

20 p2628 A73-39612

The equations of fast-process hydrodynamics

21 p2676 A73-40205

Linear wave motion analysis of viscous incompressible fluid of infinite depth at small and large times by asymptotic quadrature method

21 p2676 A73-40207

Thermodynamic formation of negative/rarefaction shock waves in single-phase viscous fluids by approximate continuum model

21 p2790 A73-40251

Vibrations of a rotating solid body with a cavity partly filled with an arbitrary viscous fluid

21 p2677 A73-40988

Steady-state heat transfer between fluids divided by a thin wall

21 p2792 A73-41224

Eddies development downstream a pipe orifice.

22 p2840 A73-41738

Flow of a viscous gas at a slot with strong suction

22 p2796 A73-42283

Flow stability of viscous homogeneous incompressible electrically conducting fluid between nonconducting walls at large magnetic Reynolds numbers

22 p2894 A73-42639

Electron paramagnetic resonance studies of a viscous nematic liquid crystal. II - Evidence counter to a second-order phase change.

22 p2897 A73-42711

Vibrations of a rotating solid body containing a cavity partially filled with a viscous fluid

22 p2843 A73-43058

Nonstationary mass transfer during the longitudinal flow of a nonlinearly viscous fluid past a flat plate and the forward stagnation point

23 p2967 A73-43440

Plane boundary layer equations for viscous incompressible fluid with asymmetric stress tensor produced by moment stresses and mass moments

23 p2968 A73-43922

Calculation of supersonic flow around blunt bodies using complete and simplified Navier-Stokes equations

24 p3053 A73-44657

Dynamic and temperature boundary layers of a submerged jet of viscous fluid spreading over the bottom

24 p3080 A73-45503

VISIBILITY

NT LOW VISIBILITY

The contrast and the visibility of noctilucent clouds in the twilight sky

04 p0441 A73-15293

Visibility of lunar surface features - Apollo 14 orbital observations and lunar landing.

05 p0617 A73-16713

Haven View project for atmospheric visibility and radiation measurements, describing airborne and ground based instrumentation and measurement results

11 p1352 A73-25444

Scotopic visibility curve in man obtained by the VER.

13 p1575 A73-28356

Weather condition caused aircraft accident avoidance, considering meteorological factors of air temperature, humidity, cloud formation, fog, haze, precipitation and visibility deterioration

13 p1568 A73-28554

The effect of the size distribution of the rain drops on the standard visibility

15 p1902 A73-31139

Runway visual range equation derivation, taking into account background luminance, atmospheric absorption and illumination

15 p1906 A73-32351

Fully automatic assessment of RVR, and comparison with observers.

15 p1910 A73-32466

Aircraft in-flight visibility /consciousness/ during daytime, discussing exterior paints, tapes and high intensity lighting effectiveness for midair collision avoidance

16 p1965 A73-32661

Instrument landing monitor /ILM/ evaluation program for potential and actual capability to restore poor and/or missing visibility

20 p2590 A73-39211

VISIBLE RADIATION

U LIGHT [VISIBLE RADIATION]

VISIBLE SPECTRUM

U LIGHT [VISIBLE RADIATION]

VISION

NT BINOCULAR VISION

NT COLOR VISION

NT MONOCULAR VISION

NT NIGHT VISION

NT PERIPHERAL VISION

NT STEREOSCOPIC VISION

Psychological test for relative contributions of specific and nonspecific components to intersensory transfer between vision and touch

03 p0266 A73-13525

Papers on visual function assessment covering visual acuity, fields and adaptation, night, color and rod vision, depth perception and electrophysiological measurements

05 p0539 A73-16476

Rod vision chemistry in terms of rhodopsin, visual cycle and pigment-vision relations, considering dark and light adaptation

05 p0540 A73-16479

Electroretinography /ERG/, electro-oculography /EOG/, visual evoked response /VER/ and electric evoked response /EER/ procedures for electrophysiological investigation of visual system

05 p0542 A73-16484

Human visual system model based on neurological connectivity data from anatomical dissection, in vivo physiological measurements and psychological experimentation

17 p2116 A73-35239

Interaction of vision with optical aids.

21 p2645 A73-41608

VISIOPLASTICITY

U FLOW VISUALIZATION

U PLASTIC FLOW

VISUAL ACCOMMODATION

Correlations between motor learning and visual and arm adaptation under conditions of computer-simulated visual distortion.

03 p0267 A73-13556

Reduced illumination effects on visual acuity, color vision, dark adaptation, accommodation, visual fields and glare

05 p0540 A73-16480

Polarity cue for visual accommodation response of trained subjects to target motion direction change, considering retinal image blur and feedback relation

08 p0932 A73-21569

Laser speckle for determining ametropia and accommodation response of the eye.

11 p1377 A73-26232

Absolute motion parallax and the specific distance tendency.

13 p1578 A73-28096

Scalar perceptions with binocular cues of distance.

13 p1578 A73-28176

Accommodation of the eye during sleep and anesthesia.

14 p1716 A73-30391

Pupil movements to light and accommodative stimulation - A comparative study.

14 p1717 A73-30395

The problem of early presbyopia in aircrew.

18 p2285 A73-36923

Visual problems among senior flight personnel.

18 p2285 A73-36924

Problems related to high-performance flight in the Arctic regions

18 p2287 A73-36953

Invariance of visual receptive-field size and visual acuity with viewing distance.

19 p2396 A73-38484

Performance decrement, under prolonged testing, across the visual field.

22 p2802 A73-41730

VISUAL ACUITY

A minor perturbing effect of retinal locus on dot pattern recognition - Rejection of a possible artifact.

02 p0135 A73-12524

Vernier acuity as affected by target length and separation.

03 p0266 A73-13063

Visibility, resolution and spatial acuities in terms of target-background contrast, diffraction, luminance, stimuli wavelength and anatomical variations effects on retinal images

05 p0542 A73-16477

Visual function as sum of visual acuity and visual field, considering role of resolution and detection tasks in retinal function examinations

05 p0539 A73-16478

Reduced illumination effects on visual acuity, color vision, dark adaptation, accommodation, visual fields and glare

05 p0540 A73-16480

Ophthalmological assessment of visual functional impairment due to glare, stimulus motion and aging changes

05 p0540 A73-16485

The control of sensitivity in the retina.

06 p0655 A73-18673

Vernier alignment acuity task accuracy related to retinal image line position location, noting effect of high contrast grating background

07 p0782 A73-20159

Meridional amblyopia - Evidence for modification of the human visual system by early visual experience.

08 p0931 A73-21562

Human retina-patterned ideal perceiving machine to calculate visual acuities for spatial arrangement in line figures

08 p0932 A73-21564

Eye dominance measurement relationship to image sharpness or visual acuity from binocular and monocular tests, obtaining dominance normal distribution

09 p1039 A73-21893

Visual acuity as a function of exposure duration.

10 p1184 A73-23838

Deficits in visual function associated with laser irradiation.

10 p1182 A73-24563

Influence of stimulation of the vestibular analyzer under conditions of hypoxia on certain functions of the visual analyzer

15 p1835 A73-31516

Visual acuity dependence on background brightness, object contrast, pupil diameter and visual time lag

17 p2114 A73-34639

Evidence for non-linear response processes in the human visual system from measurements on the thresholds of spatial beat frequencies.

17 p2112 A73-34839

Localized electroretinography capable of maintaining constant light scattering with small angular dimensions by employing Ulbricht principle of uniformly illuminated sphere

17 p2116 A73-34963

- The problem of early presbyopia in aircrew.
18 p2285 A73-36923
- Visual problems among senior flight personnel.
18 p2285 A73-36924
- The significance of retinal pathology in ageing aircrew.
18 p2285 A73-36925
- Remote viewing system with TV cameras to duplicate human visual field and acuity functions, featuring operator command and data link bandwidth minimization
19 p2416 A73-37319
- Contrast sensitivity, Westheimer function and Stiles-Crawford effect in a blue cone monochromat.
19 p2394 A73-37414
- Invariance of visual receptive-field size and visual acuity with viewing distance.
19 p2396 A73-38484
- Visual cues and six degree of freedom motion flight simulation for F-4 aircraft energy maneuvering performance, discussing pilot evaluations
[AIAA PAPER 73-934] 21 p2674 A73-40880
- Developments as regards maximum visual acuity with age among cockpit crew members.
21 p2645 A73-41164
- Apparatus for measurement of vision acuity restoration time after brief macula lutea exposures to light
23 p2949 A73-43791
- Decrements in tracking and visual performance during vibration.
24 p3063 A73-44777
- VISUAL AIDS**
- Image transformation in visual condition simulators of aircraft training equipment
01 p0029 A73-10666
- Visual systems for indicating approach slope during aircraft landing
09 p1116 A73-22975
- Flight Simulation Symposium, 2nd, London, England, May 16, 17, 1973, Proceedings.
16 p1995 A73-33201
- Airline flight simulation program, examining visual system capacity for replacement of in-flight training with pilot learning transfer estimation and simulation effectiveness appraisal
16 p1995 A73-33204
- The simulator industry and its contribution to military training requirements.
16 p1996 A73-33208
- Ground visual aids for civil STOL aircraft steep gradient approach and blind landing, discussing flight trials and simulator experiments
[RAE-TM-AVIONICS-136/BLUEU/] 17 p2208 A73-34489
- Interaction of vision with optical aids.
21 p2645 A73-41608
- VISUAL CONTROL**
- Role of visual and articular afferentation in the implementation of motor reactions involving complex coordination and precision
06 p0653 A73-18164
- Airport lighting systems as visual landing aids, discussing runway disposition, brightness levels, beam orientation, visibility factors and flashing lights
16 p1993 A73-32974
- A Lie algebra of visual piloting
20 p2590 A73-39038
- VISUAL CUES**
- U CUES**
- U VISUAL PERCEPTION**
- VISUAL DISCRIMINATION**
- Observers detecting a signal in two multiple observation tasks.
01 p0011 A73-10350
- Investigation of the edge vision contrast phenomenon using the null method
01 p0009 A73-10654
- Target detection during picture transmission through a TV system
[DGLR PAPER 72-099] 02 p0166 A73-11682
- Color effects in visual discrimination, measuring response times in letter matching task
02 p0135 A73-12525
- The effect of illumination level, stroke width and figure ground on legibility of NAMEL numbers.
05 p0544 A73-16729
- Sensory, learned, and cognitive mechanisms of size perception.
06 p0657 A73-18031
- Perception of tone differences from film transparencies.
06 p0695 A73-18388
- Color naming and hue discrimination in congenital tritanopia and tritanomaly.
07 p0782 A73-20251
- Stimulus effect on spatial summation of color receptive pathways and discrimination thresholds as function of color, gradient, retinal illumination and field size
07 p0783 A73-20254
- Analysis of transient visual sensations above the flicker fusion frequency.
08 p0932 A73-21566

- Visual sensitivity in the presence of alternating monochromatic fields of light.
08 p0932 A73-21567
- Single cell analysis of saturation discrimination in the macaque.
08 p0932 A73-21568
- Visual discrimination of motion - Stimulus relationships at threshold and the question of luminance-time reciprocity.
09 p1044 A73-21897
- Single unit and evoked potential responses in cat optic tract to paired light flashes.
11 p1317 A73-25647
- Colour selectivity in orientation masking and aftereffect.
11 p1323 A73-26196
- Apparent contraction and disappearance of moving objects in the peripheral visual field.
11 p1318 A73-26198
- Binocular rivalry and binocular fusion of afterimages.
11 p1318 A73-26200
- Tachistoscopically measured independent image size and visual field recognition capacities of human eye
12 p1462 A73-27109
- Temporal and spatial features in detecting one- and two-dimensional constraints in complementary visual displays.
13 p1578 A73-28095
- Probability summation model for heterochromatic luminance additivity failure at absolute visual threshold.
13 p1578 A73-28099
- Monocular contribution to binocular vision in normals and amblyopes.
13 p1575 A73-28359
- Detection of informational constraints related to multi-variate visual displays.
13 p1580 A73-29185
- Behavioral and electrophysiological correlates during flash-frequency discrimination learning in monkeys.
14 p1714 A73-29989
- Binocular color resolution capability of the eyes as a function of the characteristics of vision during anisometropia
15 p1832 A73-30999
- Acquisition of signal concepts under conditions of aversion activation. I - Theoretical part and form interpretation test
16 p1972 A73-33091
- Information processing in the visual periphery.
17 p2113 A73-34150
- On the rate of acquisition of visual information about space, time, and intensity.
17 p2118 A73-35496
- The superiority of the pair-comparisons method for scaling visual illusions.
17 p2118 A73-35497
- Successive differentiation of visual stimuli in monkeys under various conditions of presentation
20 p2516 A73-39805
- Compensating for distortion in viewing pictures obliquely.
21 p2639 A73-41178
- Sufficient conditions for the discrimination of motion.
21 p2639 A73-41181
- Two visual systems in the frog.
21 p2640 A73-41302
- Interaction of vision with optical aids.
21 p2645 A73-41608
- Increment thresholds for multiple identical flashes in the peripheral retina.
23 p2946 A73-43343
- Noise blurred image recognition probability characteristics from experimental investigation, showing difference from statistical decision theory data
24 p3062 A73-44667
- Prefrontal lobe functions and the neocortical commissures in monkeys.
24 p3061 A73-45166
- VISUAL DISPLAYS**
- U DISPLAY DEVICES**
- VISUAL FIELDS**
- Extraretinal feedback and visual localization.
01 p0008 A73-10437
- Investigation of the edge vision contrast phenomenon using the null method
01 p0009 A73-10654
- Induced retinal image blurring effects on rabbit mid-brain single cell trigger features and response efficiencies, noting receptive field responsive area
01 p0010 A73-11503
- Scotopic vision - An unexpected threshold elevation produced by dark annuli.
02 p0137 A73-12080
- Analysis of the response characteristics of optic tract and geniculate units and their mutual relationship.
02 p0134 A73-12162
- Orientation illusion and masking in central and peripheral vision.
03 p0266 A73-12999

- Test field surround effects on onset and offset reaction time to foveal stimulation
03 p0261 A73-13558
- A relationship between the detection of size, rate, orientation and direction in the human visual system.
03 p0261 A73-13578
- Psychophysical effects of night vision perceptual contrast in terms of central visual receptive field organization
03 p0261 A73-13759
- Stereoscopic depth magnitude in viewing background-contrasted superimposed half-fields, noting relation to binocular disparity detection
03 p0261 A73-13762
- Source locations of pattern-specific components of human visual evoked potentials. I - Component of striate cortical origin. II - Component of extrastriate cortical origin.
04 p0409 A73-15024
- Visual receptive fields sensitive to absolute and relative motion during tracking.
04 p0409 A73-15072
- Visual field image analysis via investigation of receptor-furnished signal analysis by network of neuron-like structures
04 p0413 A73-15789
- An optical model of a detector of oriented segments of the visual analyzer in animals
04 p0413 A73-15795
- Angular velocity magnitude conversion into visually perceived apparent velocity, using psychophysical mathematical model based on axisymmetric annular visual field perception
04 p0413 A73-15796
- Visual function as sum of visual acuity and visual field, considering role of resolution and detection tasks in retinal function examinations
05 p0539 A73-16478
- Reduced illumination effects on visual acuity, color vision, dark adaptation, accommodation, visual fields and glare
05 p0540 A73-16480
- Observer target acquisition performance dependence on target position within restricted visual field
05 p0543 A73-16711
- Role of the visual cortex in the organization of nystagmic reactions evoked by optokinetic stimulation
06 p0653 A73-18165
- Physiological mechanisms of evoked-potential habituation in the visual analyzer
07 p0782 A73-20006
- Attention field and perception probability distribution mechanisms of Muller-Lyer illusion due to angle contour
07 p0783 A73-20255
- Random dot pattern luminance and contrast effects on limiting inter-stimulus interval for visual apparent motion masking by bright field
07 p0783 A73-20256
- Visual sensitivity in the presence of alternating monochromatic fields of light.
08 p0932 A73-21567
- Visibility of an afterimage alone and in the presence of one or two additional afterimages.
09 p1039 A73-21894
- Receptive fields of retinal ganglion cells.
09 p1043 A73-23315
- Independence of the recognition of an object's orientation and position in the field of vision
10 p1180 A73-24331
- A probabilistic model of an optical-field and the statistical properties of a videosegment from a vidicon target
11 p1360 A73-25025
- Field of view and target uncertainty in visual search and inspection.
11 p1322 A73-25181
- Apparent contraction and disappearance of moving objects in the peripheral visual field.
11 p1318 A73-26198
- Differential effects of central versus peripheral vision on egocentric and exocentric motion perception.
11 p1318 A73-26221
- Single unit reactions in the visual cortex of the unanesthetized rabbit to the light flashes of different intensities.
11 p1321 A73-26719
- Tachistoscopically measured independent image size and visual field recognition capacities of human eye
12 p1462 A73-27109
- Temporal and spatial features in detecting one- and two-dimensional constraints in complementary visual displays.
13 p1578 A73-28095
- Brightness functions for a complex field with changing illumination and background.
13 p1578 A73-28100
- Influence of stimulation of the vestibular analyzer under conditions of hypoxia on certain functions of the visual analyzer
15 p1835 A73-31516
- Residual visual function after brain wounds involving the central visual pathways in man.
16 p1975 A73-33218

Information processing in the visual periphery.
17 p2113 A73-34150

Choice of optimal light characteristics for marks in optical sighting devices
17 p2114 A73-34241

The visual cortex as a spatial frequency analyzer.
17 p2112 A73-34840

Extended border enhancement during intermittent illumination - Binocular effects.
17 p2112 A73-34842

Distance perception and the ambiguity of visual stimulation - A theoretical note.
17 p2117 A73-35492

Some functional characteristics of the superior colliculus of the Rhesus monkey.
18 p2272 A73-36442

Optomotor integration in the colliculus superior of the cat.
18 p2272 A73-36443

The role of the superior colliculus in visually-evoked eye movements.
18 p2272 A73-36445

Frontal eye-field lesions in monkeys.
18 p2272 A73-36446

Visual-vestibular interaction and motion perception.
18 p2273 A73-36460

Visual perception of direction and voluntary saccadic eye movements.
18 p2274 A73-36463

Interaction between contours in visual masking
19 p2393 A73-37395

Spatial characteristics of chromatic induction - The segregation of lateral effects from straightly artefacts.
19 p2394 A73-37419

Orientation specificity and response variability of cells in the striate cortex.
19 p2394 A73-37421

Invariance of visual receptive-field size and visual acuity with viewing distance.
19 p2396 A73-38484

Effects of round window stimulation on unit discharges in the visual cortex and superior colliculus.
20 p2513 A73-39146

Visually evoked cortical potentials to patterned stimuli in monkey and man.
20 p2514 A73-39760

Use of gyro technology to measure small random angular motion.
21 p2700 A73-40504

[AIAA PAPER 73-839]
A visual display system approach for an advanced spaceflight simulator.
21 p2673 A73-40871

[AIAA PAPER 73-923]
Optical mosaics for large field visual simulation display systems.
21 p2673 A73-40873

[AIAA PAPER 73-926]
Comparison of tilt and displacement adaptation in visual perception, establishing qualitative differences by interocular transformation magnitude and exposure time methods
21 p2640 A73-41188

Visual field defects after missile injuries to the geniculate-striate pathway in man.
21 p2641 A73-41600

Performance decrement, under prolonged testing, across the visual field.
22 p2802 A73-41730

Effect of lateral body tilts and visual frames on perception of the apparent vertical.
22 p2811 A73-41736

Visual perception of relative object dimension during monocular and binocular rod equalization experiment in various visual field restriction conditions, recording eye movements and focusing characteristics
22 p2812 A73-41890

Spatial integration in the crustacean visual system - Peripheral and central sources of non-linear summation.
22 p2810 A73-42956

Investigation of complex and hypercomplex receptive fields of visual cortex of the cat as spatial frequency filters.
22 p2810 A73-42958

Fringe localization and visibility in hologram and classical broad source interferometry.
22 p2863 A73-43094

Image formation by light intensification and thermographic imagery compared from energy viewpoint, considering effect of parasitic light sources in visual field
23 p2979 A73-43223

Gamma-aminobutyric acid antagonism in visual cortex - Different effects on simple, complex, and hypercomplex neurons.
23 p2946 A73-43338

Mathematical model for physical space transformation into subjective field metric for monocular vision
24 p3064 A73-44906

Reference image /brightness distribution functions/ existence and normalization under additive and multiplicative groups of transformations in visual field
24 p3064 A73-44908

Optical electronic model of local detectors of the visual analyzer
24 p3064 A73-44912

Comparison of visual evoked potentials to stationary and to moving patterns.
24 p3061 A73-45168

VISUAL FLIGHT

Airport runway lights system location and use for aircraft takeoff operations and visual indication of landing approach angle
14 p1743 A73-30242

A flight research program to define VTOL visual simulator requirements.
16 p1996 A73-33210

An optimized video output from a wide angle optical probe.
[AIAA PAPER 73-918]
21 p2673 A73-40866

Touchdown performance with a computer graphics night visual attachment.
[AIAA PAPER 73-927]
21 p2673 A73-40874

Frequency of anti-collision observing responses by solo pilots as a function of traffic density, ATC traffic warnings, and competing behavior.
21 p2645 A73-41158

VISUAL FLIGHT RULES

Curved landing approaches under visual and instrument flight conditions, investigating steep glide slope display configurations and flight control modes
13 p1569 A73-28901

Air traffic control and the prevention of collisions
19 p2450 A73-37386

VISUAL OBSERVATION

Synoptic Jupiter visual observation during 1966-1968, noting band activity and Red Spot longitude change
01 p0101 A73-10849

Meteorological and atmospheric physics observations by Soyuz manned spacecraft, analyzing spectrophotometry, photography and visual observation data of twilight, night and day horizons
02 p0160 A73-12265

High resolution limitations and improvement for earth based visual and photographic planetary observation, considering atmospheric boundary layer and use of elevated stations
02 p0169 A73-12331

Adaptation of the electronic camera to the coronagraph
02 p0170 A73-12544

Mathematical models for distance perception of earth surface features observed from ascending vehicle, considering convergence, accommodation and monocular parallax mechanisms
04 p0413 A73-15785

Vertical-ray structure /horizontal inhomogeneity/ of emission from the earth's upper atmosphere on the basis of observations from the Soiuz 3 spacecraft
05 p0570 A73-16845

Color structure in Jupiter observations, discussing use of binoculars and graphical representation methods
05 p0578 A73-17097

3C 120, BL Lacertae, and OJ 287 - Coordinated optical, infrared, and radio observations of intraday variability.
05 p0625 A73-17342

Mars diameter optical measurements by earth based refractor telescopes with birefringent double image micrometer
06 p0747 A73-17489

Astronaut observations from lunar orbit and their geologic significance.
07 p0879 A73-19682

The epsilon-Lyrid, alpha-Coronid, and phi-Draconid meteor streams in 1969
08 p1007 A73-21069

A method for the analysis of artificial clouds in the upper atmosphere.
08 p0961 A73-21391

Periodic comet disintegration considerations, discussing comet Tempel 2 absolute magnitude from visual brightness estimates and Meisel statements on secular decrease
09 p1146 A73-22544

VHF Doppler spectra of radar echoes associated with a visual auroral form - Observations and implications.
12 p1468 A73-26996

Determination of the circular orbit of an artificial earth satellite from optical observations at undetermined moments of time
12 p1547 A73-27867

Synoptic Jupiter visual observation during 1966-1968, noting band activity and Red Spot longitude change
15 p1928 A73-30985

Calibration of turbulence and visual and photographic scintillation parameters in Pulkovo, Tashkent and Shternberg Institute astrolimate systems for 50 inch reflector
15 p1934 A73-31425

Cloud cover probability computation models, showing averaged values for direction of sighting and cumulus cloud cover estimations
15 p1905 A73-31797

Differential velocity effects on converging target intersection time estimation accuracy, considering plane conditions and air traffic controller experience
16 p1975 A73-32900

Visualization of the amplitude-phase structure of electromagnetic fields in the millimeter and submillimeter ranges
17 p2121 A73-34158

Visual observation of the picture of a CO₂-laser radiation field
17 p2182 A73-34166

Choice of optimal light characteristics for marks in optical sighting devices
17 p2114 A73-34241

Analysis of visibility conditions during aircraft landing in radiation fog
17 p2204 A73-34540

Frequency analysis of spatio-temporal visually evoked cortical potentials during binocular rivalry.
17 p2118 A73-35645

Russian book - Optical phenomena in the atmosphere as observed from piloted spacecraft.
18 p2348 A73-35898

The meteor showers epsilon-Lyrids, alpha-Coronids, and phi-Draconids in 1969.
18 p2355 A73-36870

Determination of a circular orbit for an earth satellite from optical observations at unknown times.
20 p2608 A73-39241

Solar eclipse of 10 July 1972 observed by visual and photographic method from aircraft, taking into account coronal structure
21 p2767 A73-40565

Comparison of Apollo and earth-based observations - Definition of surface units in Mare Serenitatis.
21 p2769 A73-40821

MK spectral classification system validity, discussing standards for O4-G2 spectral range and limits in visual spectral classification
21 p2771 A73-41236

Occultation of beta Scorpio by Jupiter on May 13, 1971.
21 p2779 A73-41544

Airborne photographic and visual observation of material from Comet Giacobini-Zinner produced meteor showers due to orbit perturbation and perihelion changes by Jupiter
22 p2909 A73-42588

Sky region mobile barrier concept to predict satellite appearance for telescopic visual observation
22 p2910 A73-42642

Nozzle design for subsonic flow in axisymmetric contractions based on potential flow theory and visual observation, obtaining velocity distribution along wall
22 p2798 A73-43029

Eye movements of trained inspectors recorded during visual inspection of colored slides of IC chips, determining performance with emphasis on speed
23 p2947 A73-43212

Visual observations of the earth and of the circumterrestrial space environment from manned orbital stations
23 p2971 A73-43331

Photoelectric and visual observation of the total eclipse of the moon of August 6, 1971.
24 p3134 A73-44568

VISUAL PERCEPTION

NT AUTOKINESIS
NT CRITICAL FLICKER FUSION
NT SPACE PERCEPTION
NT VISUAL DISCRIMINATION

Axiomatic formulation of a mathematical model for visual adaptation
01 p0012 A73-10655

Two stage mathematical model of brightness perception operation for stimuli having luminance field with asymmetric discontinuity
02 p0137 A73-12078

Cat optic tract and geniculate unit responses corresponding to human visual masking effects.
02 p0134 A73-12161

Effect of forward head inclination on visual orientation during lateral body tilt.
03 p0266 A73-13000

On the apparent visual forms of relativistically moving objects.
03 p0343 A73-13294

Study of variations of retinal disparities around the fixation point by the binocular vernier method in the foveal region
03 p0261 A73-13763

Moving visual scenes influence the apparent direction of gravity.
04 p0411 A73-15250

Information theory mathematical models applied to different visual function activity phases, covering Shannon and Fisher probability models, Shreider semantic theory and Kolmogorov algorithm
04 p0412 A73-15784

Mathematical description of some visual inertia effects
04 p0413 A73-15786

Axiomatic mathematical model for human visual edge contrast based on additivity, one-dimensionality and contrast continuity parameters

04 p0413 A73-15788

Psychophysical studies of visual image normalization mechanisms in man

04 p0413 A73-15791

Mathematical and physical models of human long and short term memory, considering information processing and memorization at lower visual perception levels

04 p0413 A73-15793

An optical model of a detector of oriented segments of the visual analyzer in animals

04 p0413 A73-15795

Characteristic of collicular responses to stimulation of various sections of the visual afferent pathway in cats

05 p0539 A73-16332

Papers on visual function assessment covering visual acuity, fields and adaptation, night, color and rod vision, depth perception and electrophysiological measurements

05 p0539 A73-16476

Color vision in terms of spectral sensitivity, color appearance and discrimination, chromatic stimuli production, pigments spectral response, etc

05 p0540 A73-16481

The interaction of auditory noise and subjective noise annoyance sensitivity with peripheral visual sensitivity.

05 p0543 A73-16703

A computer-generated display to isolate essential visual cues in landing.

05 p0595 A73-16704

Mislocation of visual stimuli during voluntary saccades.

05 p0541 A73-17174

Visual after-images in athletes and coaches as a prestart condition index

06 p0658 A73-18161

Visual performance with high-contrast cathode-ray tubes at high levels of ambient illumination.

06 p0658 A73-18243

The effect of accessory auditory stimulation upon detection of visual signals.

06 p0660 A73-18625

Inter-hemispheric transfer of meaningful visual information in normal human subjects.

07 p0782 A73-20123

Human receptive visual field adaptation characteristics for stabilized retinal images by psychophysical probe detection technique

07 p0782 A73-20252

Attention field and perception probability distribution mechanisms of Muller-Lyer illusion due to angle contour

07 p0783 A73-20255

Intrinsic light brightness and intensity estimation tests for foveal and peripheral retina under photopic and scotopic stimuli

07 p0783 A73-20257

Neural channel mechanism for real light and equivalent background coding, using test flashes under bleaching and field adaptation

07 p0783 A73-20258

Electrical stimulation effects of human eye on photic threshold for square wave vision as function of wavelength, orientation and spatial frequency

07 p0783 A73-20260

Threshold variance analysis of monocular vs binocular visual stimulation in apparent movement perception

07 p0783 A73-20262

The role of colour perception and 'pattern' recognition in stereopsis.

07 p0783 A73-20266

Information processing in the visual system.

07 p0786 A73-20374

Contrast and assimilation effects analysis based on receptive field models of vertebrate retinal function

08 p0929 A73-20812

The brightness of coloured flashes on backgrounds of various colours and luminances.

08 p0935 A73-21565

Visibility of an afterimage alone and in the presence of one or two additional afterimages.

09 p1039 A73-21894

Peripheral threshold of perceived contrast of the human eye.

09 p1046 A73-22964

Retinal S-potential receptive field relationship to light energy and wavelength, considering cone and rod potentials, ganglion cells and vision

09 p1043 A73-23314

Retinal mechanisms of colour vision.

09 p1043 A73-23316

Duplex vision theory of photoreceptor (rods and cones) light and dark adaptation, discussing rhodopsin regeneration, bleaching and desensitization mechanisms

09 p1043 A73-23317

Effect of passive 70-deg head-up tilt on peripheral visual response time.

10 p1185 A73-24566

Short-term latent reactions of the lateral geniculate body neurons in the rat to electrical stimulation of the optical tract

10 p1182 A73-24595

Pattern recognition based on visual perception relation to transformations and identification by coded sentences

11 p1334 A73-25621

Retention of information in the iconic visual memory during recognition of images of varying complexity

11 p1323 A73-26084

On neural inhibition, contrast effects and visual sensitivity.

11 p1318 A73-26197

Possible stimulus hypothesis and visual space perception.

11 p1324 A73-26321

Human visual evoked response signal decomposition by complex demodulation in terms of after-discharge time, envelope and frequency parameters

11 p1324 A73-26497

The effects of edge sharpness and exposure duration on detection threshold.

11 p1321 A73-26718

After-effects of movement contingent on direction of gaze.

11 p1324 A73-26721

Time course of lateral inhibition in the human visual system.

12 p1462 A73-27124

Changes in visual functions after the action of weak vestibular stimuli

12 p1464 A73-27719

Brightness functions for a complex field with changing illumination and background.

13 p1578 A73-28100

The visual system: Neurophysiology, biophysics, and their clinical applications; Proceedings of the Ninth Symposium, Brighton, England, July 1971.

13 p1574 A73-28351

A comparison of electrophysiological and psychophysical temporal modulation transfer functions of human vision.

13 p1575 A73-28360

Flashblindness recovery following exposure to constant energy adaptive flashes.

13 p1579 A73-28505

Longitudinal and lateral magnification distortion correction in three dimensional long wavelength holography from standpoint of observer visual perception

13 p1616 A73-28596

Anatomical and neurophysiological investigations of centrifugal control of retinal activity via efferent optic nerve fibers

14 p1714 A73-29875

Foveal threshold additivity measurements for monochromatic and mixed light, using grating resolution as brightness criterion

14 p1717 A73-30398

A visual stimulator employing a T.V. raster display.

14 p1722 A73-30400

Normal fixation of eccentric targets.

15 p1837 A73-31018

Threshold and suprathreshold perceptual color differences.

15 p1837 A73-31019

Spatial information coding in the human visual system - Psychophysical data.

17 p2116 A73-35240

Pattern recognition techniques suggested from psychological correlates of a model of the human visual system.

17 p2116 A73-35241

Book - The psychology of visual perception.

17 p2117 A73-35474

Neuronal elements of the orienting response - Microrecordings and stimulation experiments in rabbits.

18 p2272 A73-36444

Neurophysiological correlates of eye movements in the visual cortex.

18 p2272 A73-36450

Eye movements necessary for continuous perception during stabilization of retinal images.

18 p2273 A73-36461

Real-time, three-dimensional, visual scene generation with computer generated images.

18 p2291 A73-36831

Evaluation of human operator visual performance capability for teleoperator missions.

19 p2397 A73-37327

Linear summation of spatial harmonics in human vision.

19 p2393 A73-37411

Spatial frequency channels in human vision and the threshold for adaptation.

19 p2394 A73-37416

An electrical model of the inertial and adaptive properties of vision as a self-regulating system with delayed feedback

20 p2517 A73-39004

Inverted posture illusion phenomenon in astronauts during weightless space flight, discussing vestibular

organ function, acceleration effects and body gravitation sensing system

20 p2513 A73-39149

Visual responsiveness repeat variability magnitude during prolonged sessions and time of day

20 p2513 A73-39479

Human miniature eye movement relationship to visibility and saccades position-correcting reflex function and suppression

21 p2637 A73-40411

A study of the statistical patterns of visual perception of a black and white raster image

21 p2644 A73-40861

A descriptive model of multi-sensor human spatial orientation with applications to visually induced sensations of motion.

[AIAA PAPER 73-915]

21 p2644 A73-40863

Carrier landing simulation for pilot visual perception, describing Fresnel lens optical landing system, periscopes, cockpit equipment and glide paths

[AIAA PAPER 73-917]

21 p2634 A73-40865

Illuminance and albedo variations (whiteness constancy) category judgments for stimuli with unpatterned and patterned surfaces

21 p2639 A73-41183

Spatial frequency selectivity of a visual tilt illusion.

21 p2642 A73-41642

Performance decrement, under prolonged testing, across the visual field.

22 p2802 A73-41730

Soviet book on visual image formation on retina covering perception, stabilization, manipulative ability, etc

22 p2810 A73-42869

Performances and physical limitations of image intensifiers

23 p2979 A73-43221

Bezold-Bruecke effect and visual nonlinearity.

23 p2946 A73-43342

Bee image detection by ommatidium based on physical model using electromagnetic analysis of light absorption in photoreceptor

23 p2946 A73-43344

Photometric strip blurring and brightness contrast measurements of visual perception in turbulent atmosphere as function of distance, turbulence and exposure

23 p3001 A73-43573

Visual perception dominance over touch related to threshold changes, analyzing nervous system reliance on sense with lower threshold

23 p2946 A73-43847

Asymmetry in perception - Attention versus other determinants.

24 p3065 A73-45338

VISUAL PHOTOMETRY

Irregular auroral pulsation commencement and termination times from photometric recordings compared with geomagnetic micropulsations

06 p0690 A73-17557

Two-color electrophotometry of RW in the Northern Crown

11 p1416 A73-25233

Satellite rotation period determination from visual photometric observations reduction, noting solar and geomagnetic activity effects

15 p1843 A73-31649

Fully automatic assessment of RVR, and comparison with observers.

15 p1910 A73-32466

Irregular auroral pulsation commencement and termination times from photometric recordings compared with geomagnetic micropulsations

16 p2002 A73-32781

ISIS-II scanning auroral photometer.

19 p2428 A73-37256

ISIS-2 red line photometer for global distribution mapping of atomic oxygen 6300 A emission in airglow and auroras, discussing atomic excitation processes in upper atmosphere

19 p2428 A73-37257

Design and test of a photometer with nine wavelength bands for the measurement of astronomical objects

22 p2852 A73-41784

Determination of radii of satellites and asteroids from radiometry and photometry.

24 p3130 A73-44453

Area-scanning photometric observations of Galilean satellite surface color variations due to orbital phase and Jupiter environment

24 p3130 A73-44455

VISUAL PIGMENTS

Modified rhodopsin in the pigment epithelium.

07 p0783 A73-20263

The structure and reactions of visual pigments.

09 p1042 A73-23306

Duplex vision theory of photoreceptor (rods and cones) light and dark adaptation, discussing rhodopsin regeneration, bleaching and desensitization mechanisms

09 p1043 A73-23317

Spectral sensitivities of colour mechanisms isolated by the human visual evoked response.

12 p1461 A73-26919

Human cone optical density estimation implications of conflicting results for luminosity at bleaching intensities in dichromats related to use of psychophysical data
14 p1717 A73-30402

Contrast sensitivity, Westheimer function and Stiles-Crawford effect in a blue cone monochromat.
19 p2394 A73-37414

Recovery of cone receptor activity in the frog's isolated retina.
22 p2810 A73-42962

Frog red rod dark adaptation from recorded receptor potentials of isolated retina, examining permanent sensitivity loss due to pigment bleaching
22 p2810 A73-42963

Inhibition by selenium of the free-radical states of the retina of the eye
24 p3059 A73-44724

VISUAL SIGNALS

Cortical potentials evoked by confirming and disconfirming feedback following an auditory discrimination.
09 p1039 A73-21895

Group performance in a visual signal-detection task.
11 p1322 A73-25182

Manipulating the response criterion in visual monitoring.
14 p1722 A73-30499

Non-linearity of visual signals in relation to shape-sensitive adaptation responses.
19 p2394 A73-37418

Ability of a human operator to estimate the probability characteristics of alternative stimuli
22 p2813 A73-41893

Adaptive measurement of vigilance decrement.
23 p2947 A73-43211

VISUAL STIMULI

Some differences among figural aftereffects, apparent motion, and paracontrast.
01 p0011 A73-10435

Extraretinal feedback and visual localization.
01 p0008 A73-10437

Influence of observing strategies and stimulus variables on watchkeeping performances.
01 p0012 A73-10771

Photopic luminous efficiency measured by critical flicker frequency method, noting dependence on intermittence frequency of light stimulus or overall radiance level
[AD-754344] 02 p0137 A73-12076

Two stage mathematical model of brightness perception operation for stimuli having luminance field with asymmetric discontinuity
02 p0137 A73-12078

Influence of border and background on perception of straightness.
02 p0137 A73-12081

Cat optic tract and geniculate unit responses corresponding to human visual masking effects.
02 p0134 A73-12161

Analysis of the response characteristics of optic tract and geniculate units and their mutual relationship.
02 p0134 A73-12162

Orientation illusion and masking in central and peripheral vision.
03 p0266 A73-12999

Vernier acuity as affected by target length and separation.
03 p0266 A73-13063

Verbal estimates of perceived time of flashing lights interval, relating to lights separation distance
03 p0260 A73-13552

Tests for binocular rivalry of light contours for detection of randomness in disappearance patterns
03 p0261 A73-13557

Test field surround effects on onset and offset reaction time to foveal stimulation
03 p0261 A73-13558

Reaction time as a measure of the temporal response properties of individual colour mechanisms.
03 p0267 A73-13757

A relationship between the detection of size, rate, orientation and direction in the human visual system.
03 p0261 A73-13758

Stereoscopic depth magnitude in viewing background-contrasted superimposed half-fields, noting relation to binocular disparity detection
03 p0261 A73-13762

Cortical area of neural loci involved in monoptic and dichoptic metacontrast occurring for target and masking stimuli imaged on different retinal regions
03 p0261 A73-13764

Recording and discrimination of pulsed neuron activity responses to stimulus application and removal
03 p0268 A73-13823

Source locations of pattern-specific components of human visual evoked potentials. I - Component of striate cortical origin. II - Component of extrastriate cortical origin.
04 p0409 A73-15024

Influence of a visual frame and vertical-horizontal illusion of shape and size perception.
04 p0411 A73-15219

The stereoscopic frame of reference in asymmetric convergence of the eyes - Response to 'point' stimulation of the retina.
05 p0573 A73-16149

Characteristic of collicular responses to stimulation of various sections of the visual afferent pathway in cats
05 p0539 A73-16332

Visibility, resolution and spatial acuities in terms of target-background contrast, diffraction, luminance, stimuli wavelength and anatomical variations effects on retinal images
05 p0542 A73-16477

Color vision in terms of spectral sensitivity, color appearance and discrimination, chromatic stimuli production, pigments spectral response, etc
05 p0540 A73-16481

Mislocation of visual stimuli during voluntary saccades.
05 p0541 A73-17174

Space-time relations - The effects of variations in stimulus and interstimulus interval duration on perceived visual extent.
05 p0545 A73-17199

Functional alterations in the auditory and visual analyzer systems of monkeys during experimental neurosis
06 p0653 A73-18163

Role of the visual cortex in the organization of nystagmic reactions evoked by optokinetic stimulation
06 p0653 A73-18165

Visual evoked responses elicited by rapid stimulation.
06 p0654 A73-18350

Central tracking task performance simultaneously with response to peripheral stimulus under high heat stress environments
06 p0659 A73-18473

Tilt discrimination and motion aftereffect independence of flicker rate of stroboscopically illuminated contours visual stimuli
06 p0660 A73-18624

Dynamic properties of vision. III - Twin flashes, single flashes and flickerfusion.
07 p0783 A73-20253

Stimulus effect on spatial summation of color receptive pathways and discrimination thresholds as function of color, gradient, retinal illumination and field size
07 p0783 A73-20254

Random dot pattern luminance and contrast effects on limiting inter-stimulus interval for visual apparent motion masking by bright field
07 p0783 A73-20256

Cyclofusional stimulation effects on retinal image disparity in terms of central component and Panum fusional areas
07 p0783 A73-20265

Saccadic suppression for structured background as function of visual image pattern and threshold detection elevation in central nervous system
07 p0783 A73-20267

Evoked potential correlates of expected stimulus intensity.
08 p0930 A73-21225

Psychophysical areal summation and stimulus contour and threshold visibility effects on size selective adaptation in human vision for single- and multichannel models
08 p0931 A73-21563

Simultaneous motor and verbal processing of visual information in a modified Stroop test.
09 p1044 A73-21896

Visual discrimination of motion - Stimulus relationships at threshold and the question of luminance-time reciprocity.
09 p1044 A73-21897

Polysensory responses and sensory interaction in pulvinar and related postero-lateral thalamic nuclei in cat.
09 p1040 A73-22696

Limulus photoreceptor response to single photon stimulation, discussing flash intensity, dim lights, discrete waves and subliminal responses
09 p1042 A73-23308

Effect of light deprivation on the metabolic reaction development in retinal ganglion cells
10 p1178 A73-23681

Corpus callosum role in monocular system transmissural interactions from binocular interaction studies of stimulus-evoked potentials in rat visual cortex
10 p1180 A73-24332

Electroretinogram recovery cycle during light adaptation and after dark adaptation
10 p1181 A73-24518

Backward masking and enhancement of multisegmented visual targets.
11 p1321 A73-25133

The influence of wavelength on visual adaptation to spatially periodic stimuli.
11 p1318 A73-26199

Adjustment of saccade characteristics during head movements.
11 p1319 A73-26222

Influence of synchronized sleep upon spontaneous and induced discharges of single units in visual system.
11 p1319 A73-26223

Possible stimulus hypothesis and visual space perception.
11 p1324 A73-26321

The dependence of the negative afterimage on the duration of the stimulus and the stimulus intensity
11 p1321 A73-26550

Foveal contrast sensitivity edge effect dependence on test stimulus size, form and duration
11 p1321 A73-26716

The effects of edge sharpness and exposure duration on detection threshold.
11 p1321 A73-26718

Single unit reactions in the visual cortex of the unanesthetized rabbit to the light flashes of different intensities.
11 p1321 A73-26719

Estimation of the variability of the latency of responses to brief flashes.
11 p1321 A73-26720

Spectral sensitivities of colour mechanisms isolated by the human visual evoked response.
12 p1461 A73-26919

The role of analyzers of conditional and unconditional stimuli in the functional system of the behavioral conditioned-reflex action
12 p1461 A73-27105

Time course of lateral inhibition in the human visual system.
12 p1462 A73-27124

Dynamics of certain characteristics of the evoked potential of the optic cortex in rabbits under conditions of increasing hypoxia
12 p1463 A73-27709

Photostimulation significance in electroencephalographic examinations of pilots and aviation school applicants
12 p1465 A73-27717

Apparent motion of stimuli presented stroboscopically during pursuit movement of the eye.
13 p1577 A73-28093

Constancy and illusion of apparent direction of rotary motion in depth - Tests of a theory.
13 p1577 A73-28094

Theoretical models of the generation of steady-state evoked potentials, their relation to neuroanatomy and their relevance to certain clinical problems.
13 p1574 A73-28354

Evoked potentials to changes in the chromatic contrast and luminance contrast of checkerboard stimulus patterns.
13 p1575 A73-28355

Scotopic visibility curve in man obtained by the VER.
13 p1575 A73-28356

A clinical method for obtaining pattern visual evoked responses.
13 p1575 A73-28357

Scotopic electroretinography and visual evoked responses under adaptive illumination, comparing blind spot stray light with parafoveal stimulation
13 p1575 A73-28361

New method of stimulation for the study of photoreceptors.
13 p1578 A73-28362

Stimulus luminance-duration relationship of adapting light effect in human electroretinography, referring to Bunsen-Roscoe and Bloch constant law
13 p1575 A73-28363

The macular and paramacular local electroretinograms of the human retina and their clinical application.
13 p1575 A73-28364

Late visual cortical region reactions during the convergence of light stimulation and electrocutaneous stimulation
13 p1576 A73-29073

Visual pattern matching - An investigation of some effects of decision task, auditory codability, and spatial correspondence.
13 p1579 A73-29123

Properties of human visual orientation detectors - A new approach using patterned afterimages.
13 p1579 A73-29124

Influence of the dazzling of an eye on the state of adaptation of the congenic eye in a normal subject
14 p1716 A73-30388

Saccadic eye movement control system, investigating response characteristics to variously timed pulse stimuli
14 p1716 A73-30389

The Mach-Dvorak phenomenon and binocular fusion of moving stimuli.
14 p1717 A73-30392

Oscillatory waves in intraretinally recorded electroretinograms in primates, considering electrode depth, stimulus duration and intensity and background illumination, anesthesia and tetrodotoxin effects
14 p1717 A73-30393

Voluntary small saccadic eye movements in presence of stationary visible target, considering scanning function of fixation saccades
14 p1717 A73-30394

Pupil movements to light and accommodative stimulation - A comparative study. 14 p1717 A73-30395

A visual stimulator employing a T.V. raster display. 14 p1722 A73-30400

Servo-controlled moving stimulus generator for single unit studies in vision. 14 p1722 A73-30401

Subjective brightness contrast lack of correlation with steady state evoked potential amplitude in suprathreshold stimuli range. 15 p1837 A73-31017

Electrophysiological evidence that abnormal early visual experience can modify the human brain. 15 p1838 A73-31371

Histochemical correlates of changes in the primate brain associated with varying environmental light conditions. 15 p1837 A73-32600

Space-time adaptation of visual position constancy. 17 p2114 A73-34223

The visual cortex as a spatial frequency analyzer. 17 p2112 A73-34840

Stereoscopic depth aftereffects with random-dot patterns. 17 p2115 A73-34841

Temporal factors of movements in visual aftereffects. 17 p2115 A73-34843

Opponent-colors responses in the visually evoked potential in man. 17 p2112 A73-34844

Movement perception during voluntary saccadic eye movements. 17 p2112 A73-34845

Stabilized target visibility as a function of contrast and flicker frequency. 17 p2112 A73-34846

The effect of colour on time delays in the human oculomotor system. 17 p2112 A73-34847

Amplitude of visual suppression during the control of binocular rivalry. 17 p2117 A73-35491

Distance perception and the ambiguity of visual stimulation - A theoretical note. 17 p2117 A73-35492

Factors affecting processing mode in visual search. 17 p2117 A73-35493

Influence of stimulus symmetry on visual scanning patterns. 17 p2118 A73-35494

On the perception of a class of bilaterally symmetric forms. 17 p2118 A73-35495

On the rate of acquisition of visual information about space, time, and intensity. 17 p2118 A73-35496

The superiority of the pair-comparisons method for scaling visual illusions. 17 p2118 A73-35497

Frequency analysis of spatio-temporal visually evoked cortical potentials during binocular rivalry. 17 p2118 A73-35645

Stereoscopic vision - Cortical limitations and a disparity scaling effect. 18 p2269 A73-35922

Supranuclear connections to oculomotor nuclei in terms of stimulus relation to eye movements. 18 p2271 A73-36435

The role of the superior colliculus in visually-evoked eye movements. 18 p2272 A73-36445

Saccade correlated events in the lateral geniculate body. 18 p2272 A73-36449

Central programming and peripheral feedback during eye-head coordination in monkeys. 18 p2273 A73-36452

The control of eye movements in the saccadic system. 18 p2273 A73-36453

Comparative physiology of movement-detecting neuronal systems in lower vertebrates (anura and urodela). 18 p2273 A73-36454

Rabbit optokinetic reactions and retinal direction-selective cells (A preliminary model). 18 p2273 A73-36455

Optokinetic stimulation of an immobilized eye in the monkey. 18 p2273 A73-36457

Ambivalent optokinetic stimulation and motion detection. 18 p2273 A73-36458

Quantitative studies on optokinetic nystagmus in the monkey. 18 p2273 A73-36459

Eye movements necessary for continuous perception during stabilization of retinal images. 18 p2273 A73-36461

Scanning movements in space perception in terms of convergence role during cue conflict and cue isolation experiments. 18 p2274 A73-36462

Involuntary eye movements in the presence and absence of points. 18 p2276 A73-36568

The value of data processing in the analysis of visual evoked potentials. 18 p2279 A73-36911

Interaction between contours in visual masking. 19 p2393 A73-37395

Linear summation of spatial harmonics in human vision. 19 p2393 A73-37411

Monkey rod receptor potential suppression at photopic stimulus intensities by neurophysiological inhibitory mechanism for clearing cone initiated visual pathway. 19 p2393 A73-37412

Slowed decay of the monkey's cone receptor potential by intense stimuli, and protection from this effect by light adaptation. 19 p2394 A73-37413

Spatial determinants of the aftereffect of seen motion. 19 p2394 A73-37415

Spatial frequency channels in human vision and the threshold for adaptation. 19 p2394 A73-37416

The interaction between horizontal and vertical eye rotations in tracking tasks. 19 p2394 A73-37417

Orientation specificity and response variability of cells in the striate cortex. 19 p2394 A73-37421

Effects of prestimulus cuing and target load variability on maintenance of response strategies in a visual search task. 19 p2402 A73-38378

Inversion of lighting regimen alters acrophase relations of circadian rhythms in body temperature, heart rate and movement of pocket mice. 20 p2513 A73-39480

Visually evoked cortical potentials to patterned stimuli in monkey and man. 20 p2514 A73-39760

Role of associations in the formation of evoked potentials from the human cerebral cortex. 20 p2515 A73-39798

Successive differentiation of visual stimuli in monkeys under various conditions of presentation. 20 p2516 A73-39805

A visual detection simulator (VDS) for pilot warning instrument evaluation. 21 p2672 A73-40864

[ALAA PAPER 73-916] Symmetry of the visual evoked potential in normal subjects. 21 p2638 A73-41012

Compensating for distortion in viewing pictures obliquely. 21 p2639 A73-41178

A comparison of the Ponzo illusion with a textural analogue. 21 p2639 A73-41180

Reaction times for focal and nonfocal/peripheral/processing of simultaneously presented color and form stimuli. 21 p2639 A73-41182

Illuminance and albedo variations /whiteness constancy/ category judgments for stimuli with unpatterned and patterned surfaces. 21 p2639 A73-41183

Effect of eye movements on backward masking and perceived location. 21 p2639 A73-41184

Visual search, complex backgrounds, mental counters, and eye movements. 21 p2639 A73-41185

Visually perceived motion in depth resulting from proximal changes. I, II. 21 p2640 A73-41186

Individual physiological differences in evoked potential reactions to light sources, discussing latent periods, potential amplitude distribution and EEG measurement techniques. 22 p2812 A73-41888

Optimal input rates for tilt adaptation. 22 p2814 A73-42500

Spatial integration in the crustacean visual system - Peripheral and central sources of non-linear summation. 22 p2810 A73-42956

Investigation of complex and hypercomplex receptive fields of visual cortex of the cat as spatial frequency filters. 22 p2810 A73-42958

Stimulus specificity in the human visual system. 22 p2810 A73-42960

Rectifier-like color dependent phase shifts in electrophysiological responses to different colored stimuli at evoked potential and single neuron levels. 22 p2810 A73-42961

Neuronal activity of the sensorimotor and visual cortex in rabbits during development of a summation focus in the reticular formation. 24 p3058 A73-44550

Cortical and intracortical study of the frontal visual evoked potential in photosensitive Papio papio. 24 p3061 A73-45159

Visual evoked potentials to changes in the motion of a patterned field. 24 p3061 A73-45167

Comparison of visual evoked potentials to stationary and to moving patterns. 24 p3061 A73-45168

VISUAL TASKS

Observers detecting a signal in two multiple observation tasks. 01 p0011 A73-10356

Influence of observing strategies and stimulus variables on watchkeeping performances. 01 p0012 A73-10771

Color effects in visual discrimination, measuring response times in letter matching task. 02 p0135 A73-12523

Vernier acuity as affected by target length and separation. 03 p0266 A73-13063

Effects of intermittent and continuous noise on serial search performance. 03 p0267 A73-13560

Asymmetries related to cerebral dominance in returning the eyes to specified target positions in the dark. 03 p0261 A73-13760

Identification and adjustment of psychological factors to improve solar patrol observing. 04 p0411 A73-14841

Psychophysical studies of visual image normalization mechanisms in man. 04 p0413 A73-15791

Visual function as sum of visual acuity and visual field, considering role of resolution and detection tasks in retinal function examinations. 05 p0539 A73-16478

Visual work duration and intensity effects on optic papillae expansions and shape alterations, noting differences between trained and untrained subjects. 05 p0540 A73-16694

Visibility of lunar surface features - Apollo 14 orbital observations and lunar landing. 05 p0617 A73-16713

A human factors approach to lighting recommendations and standards. 05 p0545 A73-16730

Effects of noise and response complexity upon vigilance performance. 06 p0656 A73-17523

Visual-motor coordination characteristics of parachute jumpers. 06 p0657 A73-17750

Probability estimate for visual target detection in terms of luminance threshold and target size and duration. 06 p0658 A73-18242

Visual performance with high-contrast cathode-ray tubes at high levels of ambient illumination. 06 p0658 A73-18243

Human performance measures relationship determination across sense modes under visual, auditory and combined stimulus conditions by controlling for task difficulty on individual basis. 06 p0658 A73-18244

Functional state alteration of the visual analyzer in pilots. 06 p0659 A73-18257

The superior colliculus of the brain. 06 p0654 A73-18347

Physical work induced hyperthermia effects on detection rate in visual vigilance task performance in hot and humid environment. 06 p0659 A73-18469

Autokinetic movement as a function of the implied movement of target shape. 07 p0785 A73-19549

Vernier alignment acuity task accuracy related to retinal image line position location, noting effect of high contrast grating background. 07 p0782 A73-20159

Polarity cue for visual accommodation response of trained subjects to target motion direction change, considering retinal image blur and feedback relation. 08 p0932 A73-21569

Influence of high ambient temperatures on the performance and some physiological parameters in a tracking problem and an optical vigilance problem. 08 p0935 A73-21575

Comparison of human operator critical tracking task performance with aural and visual displays. 08 p0936 A73-21667

Neuroendocrine, cardiorespiratory, and performance reactions of hypoxic men during a monitoring task. 09 p1044 A73-25257

Fatigue levels of cerebral hemispheres in response to visual task and test stimuli, noting left handed reduced performance capacity. 09 p1040 A73-22925

Backward masking and enhancement of multisegmented visual targets. 11 p1321 A73-25133

Field of view and target uncertainty in visual search and inspection. 11 p1322 A73-25181

Group performance in a visual signal-detection task. 11 p1322 A73-25182

Combined effects of noise and vibration on human tracking performance and response time. 11 p1323 A73-25334 [AD-759329]

Ergonomic endurance limits, physiological strains and fatigue assessment in video coding information task performance as function of work shift time length 11 p1323 A73-25649

Target-detection performance as a function of noise intensity and task difficulty. 11 p1323 A73-26320

Visual perception of motion in depth - Application of a vector model to three-dot motion patterns. 13 p1577 A73-28091

Implications of measurement of eye fixations for a psychophysics of form perception. 13 p1577 A73-28092

Visual temporal integration for threshold, signal detectability, and reaction time measures. 13 p1578 A73-28097

Visual pattern matching - An investigation of some effects of decision task, auditory codability, and spatial correspondence. 13 p1579 A73-29123

Optimal lighting for visual tasks, discussing color, type, transillumination, crossed polarization, brightness patterns, diffuse reflection and surface shadowgraphing 14 p1722 A73-30498

Manipulating the response criterion in visual monitoring. 14 p1722 A73-30499

Normal fixation of eccentric targets. 15 p1837 A73-31018

Self-estimates of distractibility as related to performance decrement on a task requiring sustained attention. 15 p1839 A73-32394

A comparison of visual, auditory, and cutaneous tracking displays when divided attention is required to a cross-adaptive loading task. 15 p1839 A73-32395

Motivation in vigilance - A test of the goal-setting hypothesis of the effectiveness of knowledge of results. 17 p2113 A73-34149

Informative parameters of the psychophysiological state of flight personnel when working with indicators 17 p2114 A73-34237

Factors affecting processing mode in visual search. 17 p2117 A73-35493

On the perception of a class of bilaterally symmetric forms. 17 p2118 A73-35495

Searching for many targets - An analysis of speed and accuracy. 17 p2118 A73-35498

Investigations of the eye tracking system through stabilized retinal images. 18 p2273 A73-36456

Study of performances in a warm environment in case of air conditioning breakdown on a supersonic transport 18 p2286 A73-36947

Gaze-positioning eye movement perturbations during somnolence states 18 p2280 A73-36950

Illumination and television considerations in teleoperator systems. 19 p2416 A73-37318

The interaction between horizontal and vertical eye-rotations in tracking tasks. 19 p2394 A73-37417

Interference of 'attend to and learn' tasks with tracking. 19 p2401 A73-38377

Effects of prestimulus cuing and target load variability on maintenance of response strategies in a visual search task. 19 p2402 A73-38378

The oculometer - A new approach to flight management research. [AIAA PAPER 73-914] 21 p2702 A73-40862

The psychophysical inquiry into binocular summation. 21 p2640 A73-41187

Individual and simultaneous tracking of a step input by the horizontal saccadic eye movement and manual control systems. 22 p2811 A73-41735

Dynamic operative image formation and function features during extrapolation tracking of visibly moving target, noting image reaction to operator performance 22 p2812 A73-41886

Visual perception of relative object dimension during monocular and binocular rod equalization experiment in various visual field restriction conditions, recording eye movements and focusing characteristics 22 p2812 A73-41890

Cognitions and 'placebos' in behavioral research on ambient noise. 22 p2816 A73-42950

Recognition of component differences in two-dimensional oculomotor tracking tasks. 22 p2810 A73-42959

Signal and noise in the human oculomotor system. 22 p2810 A73-42964

Adaptive measurement of vigilance decrement. 23 p2947 A73-43211

Use of a digital computer for studying velocity judgements of radar targets. 23 p2948 A73-43213

Use of a response surface to optimize digital telecommunication systems. 23 p2948 A73-43214

Keeping track of sequential events - Implications for the design of displays. 23 p2948 A73-43215

Two components and two stages in search performance - A case study in visual search. 24 p3065 A73-45339

VISUAL TRACKING

U OPTICAL TRACKING

VISUALIZATION OF FLOW

U FLOW VISUALIZATION

VITAMIN B

U THIAMINE

VITAMIN B COMPLEX

U BIOTIN

VITAMIN B 06

U PYRIDOXINE

VITAMINS

NT BIOTIN

NT PYRIDOXINE

NT THIAMINE

Vitamin metabolism alteration under increased atmospheric pressure 11 p1321 A73-25036

VITON RUBBER [TRADEMARK]

The effect of environmental factors on seal performance of VITON E-60C fluoroc elastomer. 03 p0331 A73-13027

VITREOUS MATERIALS

High temperature thermal cavity system with vitreous carbon tube and end plugs for material and thermochemical environment investigations, discussing mass spectroscopic measurement 17 p2149 A73-35752

Photoelectric phenomena in amorphous chalcogenide semiconductors. 20 p2599 A73-39133

Damping of glass-like materials at high temperatures. 20 p2580 A73-39272

VLASOV EQUATIONS

Theoretical and numerical results in the case of the nonlinear Vlasov equation 01 p0069 A73-10073

Theoretical and experimental study of the H.F. current associated with a plasma wave. 01 p0081 A73-10118

Third order collisionless electron plasma echo signal wavelength and rise and fall rate about central position, comparing experiment with Vlasov equation theory 02 p0197 A73-12064

A method of solution of Vlasov's equation - Application to a nonlinear overall theory of the galactic rotation and of the galactic spiral structure 03 p0380 A73-14608

Equilibrium and stability of large-amplitude magnetic Bernstein-Greene-Kruskal waves. 07 p0857 A73-19524

Small perturbations solution for spatially homogeneous expanding gravitating medium, using Vlasov kinetic equation with self consistent Newtonian field 07 p0901 A73-20315

Feedback stabilization of a multimode two-stream instability. 11 p1406 A73-26556

Long wavelength instability in a perpendicular shock. 11 p1406 A73-26557

Small perturbations solution for spatially homogeneous expanding gravitating medium, using Vlasov kinetic equation with self consistent Newtonian field 12 p1539 A73-27287

Nonlinear plasma oscillations in terms of Van Kampen modes. 14 p1780 A73-30350

On an initial value problem for a nonlinear system of Vlasov-Maxwell equations. 17 p2200 A73-34320

Resolvent boundary solutions for Vlasov shallow shell equations in terms of force and deflection functions over entire contour 22 p2928 A73-43055

Stability of two-dimensional collision-free plasmas. 24 p3116 A73-45237

VLF EMISSION RECORDERS

Ground based geomagnetic observations of medium and high latitude VLF emissions due to transverse resonance instability and auroral oval Cerenkov radiation from magnetosheath 03 p0276 A73-13884

Low dispersion whistlers observed simultaneously at two low latitude stations. 08 p0940 A73-21651

VOCODERS

Speech data rate reduction. I - Applicability of modern estimation theory. II - Applicability of sensitivity and error analysis. 13 p1585 A73-29201

VOICE

Utilization of human voice for estimation of man's emotional stress and state of attention. 11 p1322 A73-25329

VOICE COMMUNICATION

NT TELEPHONY

NT VOICE DATA PROCESSING

Current and near future data transmission via satellites of the Intelsat network. 03 p0280 A73-14659

A digital echo suppressor for satellite circuits. 04 p0416 A73-14995

Channel filters with longitudinally coupled flexural mode resonators. 04 p0427 A73-15320

TDM link with digitized voice channel and PCM telemetry sequence coding for error correction, comparing tested performance with prediction and computer simulation 04 p0419 A73-15401

Low cost electronic method of delaying speech signals based on adaptive delta modulators 05 p0552 A73-17375

Canadian Anik I synchronous domestic communication satellite for color TV broadcasting or telephony, considering northerners reaction and community beneficiaries 06 p0668 A73-18432

Canadian telecommunications satellite system for TV, voice and analog or digital data transmission, describing space segment, satellite control and ground station network 11 p1431 A73-26259

Direct conversion s.s.b. receivers - A comparison of possible circuit configurations for speech communication. 12 p1467 A73-26800

Use of semiconductor lasers in compact communication systems. 12 p1470 A73-27521

Modulation and speech processing techniques for a maritime-satellite service. 12 p1472 A73-27662

The use of satellites for aircraft communications and air traffic control. 12 p1472 A73-27666

Balloon-aircraft ranging, data, and voice experiment. 12 p1473 A73-27680

Intelligibility improvement of analog communication systems using an amplitude control technique. 14 p1726 A73-29901

FAA air traffic control systems projected improvements, including microwave landing system, aeronautical satellites, electronic voice switching and discrete address radar beacon 16 p2087 A73-33179

Two-way wideband microwave communication system oriented toward PCM-TDM digital technique for covering telephone, videophone and radio broadcasting services 17 p2123 A73-34968

System aspects of the initial Telesat Thin Route satellite communication system. 20 p2523 A73-38720

Error rate of a 4-phase coherent PSK satellite channel with non-Gaussian interference. 20 p2523 A73-38721

A digital communications system for manned spaceflight applications. 20 p2527 A73-38763

Communications and position fixing experiments using the ATS satellites. 21 p2733 A73-40024

Maritime communications via satellites employing phased arrays. 21 p2649 A73-40330

Data transmission system based on voice channels time division into blocks using cyclic code redundancy without appreciable loss in error correcting capability 21 p2655 A73-41044

Speech scrambling by the matrixing of amplitude samples. 21 p2657 A73-41206

VOICE DATA PROCESSING

Speech data rate reduction. I - Applicability of modern estimation theory. II - Applicability of sensitivity and error analysis. 13 p1585 A73-29201

VOID RATIO

VOID RATIO

The dynamic growth of a void in a plastic material and an application to fracture.

03 p0394 A73-13984

Upper bound tensile strength analysis of reinforced composite materials in terms of matrix/particle bond strength, void formation and geometrical factors [ASME PAPER 72-WA/PROD-7]

04 p0469 A73-15805

Void fraction measurement based on gas-liquid volume ratio by local void velocity measurement with single probe

05 p0638 A73-16224

Superlattice of voids in neutron-irradiated tungsten.

06 p0709 A73-18353

Thermal cycling effects on void formation in boron-aluminum matrix composites at 70-670 F, considering jet turbine compressor blade applications

16 p2084 A73-33037

Low void polyimide/glass and graphite reinforced composite properties and fabrication, showing improved interlaminar shear and wet strength

16 p2029 A73-33048

The yielding of a two-dimensional void assembly in an organic glass.

19 p2444 A73-38090

Small angle X ray scattering study of submicroscopic voids in glassy carbon, using two density theory

19 p2444 A73-38091

Surveyor 3 lunar soil shear strength measurements for range of bulk densities obtained by different packing procedures, calculating void ratios

23 p3031 A73-43761

VOIDS

Alloying elements effects on voids nucleation in irradiated Al alloys, tabulating defect concentration

09 p1101 A73-22175

Ductile fracture strain criteria from known stress-strain relationships, predicting microscopic crack and void nucleation strain

09 p1164 A73-23322

Localized hydrogen in titanium welds.

11 p1375 A73-26358

VOIGT EFFECT

Determination of damping constants and turbulent speed in the solar photosphere by the Voigt method

15 p1938 A73-31958

On the propagation of relativistic thermo-magneto-viscoelastic waves in a material of Voigt-type.

19 p2459 A73-37648

Damping constants and turbulence velocities in the solar photosphere determined by the Voigt method.

24 p3132 A73-44483

VOLATILITY

Volatile-rich lunar soil - Evidence of possible cometary impact.

05 p0615 A73-16321

Compounds of carbon and other volatile elements in Apollo 14 and 15 samples.

07 p0891 A73-19822

Volatile terpenoids from aciosporites of *Cronartium fusiforme*.

12 p1462 A73-27145

Pulsed gas laser employing substances of low volatility

12 p1506 A73-27218

Luna 16 and 20 sample carbon chemistry analysis for volatilizable species by vacuum pyrolysis and mass spectrometry

13 p1580 A73-28333

Volatile elements in Apollo 16 samples - Possible evidence for outgassing of the moon.

15 p1933 A73-31370

JP8 and JP4 aircraft fuel fire and explosion susceptibility from gunfire hits, discussing combat survivability relative to fuel volatility

16 p2045 A73-32670

Cosmogonic prerequisites for the accumulation of volatile substances in the upper mantle of the earth

22 p2912 A73-42972

VOLATILIZATION

U VAPORIZING

VOLCANICS

U VOLCANOLOGY

VOLCANOLOGY

Hornblendes from calc-alkaline volcanic rocks of island arcs and continental margins.

02 p0165 A73-12635

Response of lunar atmosphere to volcanic gas releases.

03 p0365 A73-12880

Lunar mare ridge formation with broad gentle arch overlaid by sharper contorted ridge, discussing ring structures and volcanic ring complexes

03 p0368 A73-13091

Lunar and planetary topography formation by exogenous and endogenous mechanisms, considering fluidization by volcanism

03 p0369 A73-13109

Distributions of lunar and Martian craters in relation to their origin

05 p0613 A73-16202

Some observations on the cenozoic volcano-tectonic evolution of the Great Basin, western United States.

05 p0570 A73-16841

Mars surface volcano and canyon features from Mariner 9 photographs and geological map, suggesting internal heating, water erosion, atmospheric evolution and life problem solution

06 p0754 A73-18672

Mariner spacecraft photographed Mars surface volcanic mountains and water in polar caps, suggesting recurring rainfall and rivers during successive interglacial periods

07 p0875 A73-19166

New geological findings in Apollo 15 lunar orbital photography.

07 p0878 A73-19680

Role of water in the evolution of the lunar crust: An experimental study of sample 14310 - An indication of lunar calc-alkaline volcanism.

07 p0880 A73-19691

The nature and effect of the volatile cloud produced by volcanic and impact events on the moon as derived from a terrestrial volcanic model.

07 p0890 A73-19812

Icelandic geothermal activity and the mercury of the Greenland icecap.

09 p1079 A73-22949

Identification, distribution and significance of lunar volcanic domes.

10 p1276 A73-24076

Lunar cinder cone deposits in Taurus-Littrow region of Apollo 17 landing site as counterparts of terrestrial pyroclastic eruptions

11 p1426 A73-26375

Laboratory modeling of 'vaporization-condensation and spilling' type processes taking place on the lunar surface

13 p1672 A73-28118

Magnetic anomalies in New Guinea-New Zealand region from proton magnetometer measurements, noting effects of andesite-basalt volcanic processes and nuclear precession signal variations

13 p1608 A73-28727

Xenoliths in maars and diatremes with inferences for the moon, Mars, and Venus.

13 p1681 A73-28848

Orange colored lunar soil from Shorty crater associated with volcanic fumarolic activity of water vapors reacting with lava

14 p1789 A73-29721

Aerological investigation of the volcanic beds of Kamchatka by polarizational and spectral methods

16 p1977 A73-33760

General features of lunar volcanism

16 p2065 A73-33785

The current level of volcanic activity on Venus

16 p2068 A73-33813

Lunar volcanism - Age of the glass in the Apollo 17 orange soil.

17 p2230 A73-34522

Evidence of active and ancient volcanism on Mars - A review.

17 p2233 A73-35482

Martian volcanic and tectonic features from Mariner 9 photography, comparing evolutionary phases with lunar and terrestrial morphology

19 p2477 A73-37203

Circularity of Martian craters.

19 p2486 A73-37800

Geological analysis of aerial thermography of the Canary Islands, Spain.

20 p2561 A73-39896

Engineering applications of geophysical phenomena covering earthquakes, volcanology, hydrology, glaciology and wind stress effects during severe storms

23 p2979 A73-44007

VOLT-AMPERE CHARACTERISTICS

Influence of strong external factors on the characteristics of semiconductor devices sensitive to the state of the surface [Review]

01 p0022 A73-10036

Contribution to the theory of the current-voltage characteristic of a contact between a metal and a thin-film semiconductor

01 p0087 A73-10042

Electrode phenomena with plasma-MIG welding.

01 p0055 A73-10114

Controlled low-resistance shunt method for determining the volt-ampere characteristics of composite superconductors

01 p0088 A73-10617

Semiconductor device with current regulated switching from high voltage/low current to low voltage/high current state, noting I-R characteristics

01 p0026 A73-11096

Three point check method of solar panel characteristics for satellite.

01 p0006 A73-11162

Indium phosphide as a new material for microwave/transferred electron effect/oscillators.

02 p0199 A73-11536

Change in critical current of superconducting NbTi by neutron irradiation.

02 p0200 A73-11842

Josephson tunnel junction fabrication technology evaluation in terms of electrode materials, native oxide and artificial barriers, noting factors affecting stability and I-V characteristics

02 p0200 A73-11846

Weakly superconducting, thin-film structures as radiation detectors.

02 p0167 A73-11849

A simple method for determining static parameters of large signal semiconductor diode and transistor models.

02 p0147 A73-12044

A two-dimensional analysis of gallium arsenide junction field effect transistors with long and short channels.

02 p0147 A73-12047

Possibility of the occurrence of self-oscillations in a circuit containing a constant source of current and a homogeneous semiconductor specimen with small response times

03 p0349 A73-12907

Calculation of the complex conductivity of a monopolar semiconductor with a finite-injection contact

03 p0349 A73-13662

Frequency conversion using the real current-voltage characteristic of a metal-semiconductor contact

03 p0349 A73-13663

Effect of illumination on the form of current-voltage characteristics of SbSI in the paraelectric region

03 p0350 A73-13756

Operation, fabrication, characterization, I-V performance and application of transient voltage suppressor using metal oxide varistor

03 p0283 A73-13941

The performance of recently developed high voltage high current power transistors.

03 p0283 A73-13944

Amplifier stability in optimal frequency regime, relating cut-off voltage and plate current as function of magnetic field, input power and geometrical parameters

03 p0284 A73-14068

Pulse discharge plasma in Ar with gas ionization level near unity, noting plasma cylinder parameters, electron temperature and I-V characteristics

03 p0347 A73-14091

Effect of alternating current on the steady-state characteristics of a Josephson junction.

03 p0344 A73-14097

An experimental investigation into the feasibility of higher efficiency silicon solar cells.

03 p0254 A73-14206

Solar cell graded band gap materials, determining I-V characteristics, junction capacitance and photovoltaic spectral response

03 p0254 A73-14207

Vertical multijunction solar cells light generated current spectral response and I-V characteristics derivation from minority carrier diffusion equations

03 p0254 A73-14208

Diffusion, recombination and combined models demonstrating shunting and second current conduction effects on forward I-V characteristics for dark and illuminated Si solar cells

03 p0254 A73-14211

High efficiency Cu₂S-CdS-solar cells with improved thermal stability.

03 p0255 A73-14216

Diffusion and conduction processes in CdS-Cu_x/S thin film photocells.

03 p0350 A73-14217

New results on the development of a thin-film p-CdTe-n-CdS heterojunction solar cell.

03 p0255 A73-14220

Photovoltaic and I-V characteristics of integral diode solar cells as function of temperature and radiation exposure

03 p0256 A73-14231

Breakdown phenomena in reverse biased silicon solar cells.

03 p0256 A73-14234

Solar Array System for the Skylab Orbital Workshop.

03 p0257 A73-14238

Voltage and power relationships in lithium-containing solar cells.

03 p0257 A73-14241

Fabrication criteria, mission design factors and I-V characteristics of Li solar cells

03 p0257 A73-14242

Electron irradiated float-zone Si solar cell I-V performance degradation due to photon irradiation, noting base region minority carrier lifetime role

03 p0257 A73-14246

Procedure for automatic statistical processing of experimental data in determining the rated current-voltage characteristic of TD-320 thyristors

03 p0285 A73-14325

Oscillations of injected carriers in p-type indium antimonide.

04 p0482 A73-14869

Impurity centers effect on I-V characteristics of double injection level semiconductors, noting negative resistance region

04 p0482 A73-14877

Effects of 10-150 keV proton bombardment on silicon solar cells.

04 p0406 A73-14984

Pre-threshold conductance and polarization effects in amorphous semiconductor switches.

04 p0427 A73-15343

Proton beam effect on carbon dioxide laser discharge I-V characteristics and emission power

04 p0458 A73-15559

I-V characteristics and luminescence changes in Cs vapor arc discharge at various spark gap widths, noting pressure effect on gas stratification

04 p0481 A73-15613

Ion engines with ion emission from liquid metal drops under electric field, noting emitter I-V characteristics and engine design

04 p0488 A73-15726

Russian book on plasma cutting covering electrophysical and thermophysical principles of arc discharges application for metal cutting, arc I-V characteristics, plasmatrons and operation

04 p0457 A73-15962

P-n-p-n junction thyristor turnoff process under reverse anode voltage at high injection level, examining current voltage curve and switching time constant

05 p0556 A73-16068

Book - Superconductive tunnelling and applications.

05 p0556 A73-16357

Purity evaluation of n type GaAs LSA diodes from low-field temperature-dependent mobility.

05 p0556 A73-16435

Current saturation mechanisms in junction field-effect transistors.

05 p0558 A73-16605

Transverse magnetic field effects on n-type GaAs Gunn diodes microwave power, coherence and dynamic I-V characteristics

05 p0558 A73-16784

Electrical properties of nickel-low-doped n-type gallium arsenide Schottky-barrier diodes.

05 p0559 A73-17072

Reliable starting technique for an ion laser tube with internal gas return bores.

05 p0586 A73-17263

Third side of the Lampert triangle - Evidence of traps-filled-limit single-carrier injection.

05 p0605 A73-17349

The current-voltage characteristics of boron implanted silicon diodes.

06 p0674 A73-17797

On the origin of strongly conducting states in thin insulator films.

06 p0734 A73-17812

Influence of recombinations in the base contact and on the base surface upon static and dynamic characteristics of the p-n junction.

06 p0674 A73-17816

Energy absorption inelastic surface mechanisms effect on I-V characteristics profile for bounded semiconductor with negative differential conductivity

06 p0735 A73-17974

Investigation of regularities characterizing impact ionization within a high-field domain in Gunn diodes.

06 p0675 A73-18076

Dependence of the current-voltage characteristic of a p-n-p drift triode on the donor concentration in the n-type base

06 p0675 A73-18081

Energy structure, I-V characteristics and optical and photoelectrical properties of heterojunctions between different semiconductor materials, noting interface state effects

06 p0736 A73-18091

Investigation of static and transient current-voltage characteristics of diodes made of nickel-modified silicon

06 p0676 A73-18248

Effects of electropolishing on the tunneling current in aluminum-aluminum-oxide-aluminum diodes.

06 p0678 A73-18744

Electrical contacts to ion cleaned n-type gallium arsenide.

07 p0797 A73-19136

A two-dimensional numerical FET model for dc, ac, and large-signal analysis.

07 p0799 A73-19342

On the form and stability of electric-field profiles within a negative differential mobility semiconductor.

07 p0799 A73-19344

Tunneling observation of bound states in a normal metal-superconductor sandwich.

07 p0862 A73-19606

Influence of the Schottky effect and the peculiarities in the distribution of the applied voltage on the thickness of the depletion layer and the volt-ampere characteristics of a semiconductor with blocking contact.

07 p0802 A73-20191

IMPATT diode microwave oscillator performance analysis for I-V characteristics, output power, efficiency and starting current from equivalent circuit

08 p0943 A73-20707

IMPATT diode anomalous microwave oscillation mode performance analysis, calculating I-V variation, power and efficiency from equivalent circuit

08 p0943 A73-20708

Gunn diode effect in n-type GaAs, discussing electron drift velocity relationship to electric field, I-V characteristics and fabrication

08 p0943 A73-20709

On the mechanism for microwave amplification in 'supercritically' doped n-GaAs.

08 p0947 A73-21212

Surface oxide transistor with MIS and base contacts, investigating I-V characteristics as function of oxide thickness and contact separation distance

08 p0948 A73-21480

Diffusion effects in the double injection negative-resistance problem.

08 p0948 A73-21483

Thermal free electron constant approximation in space charge current theory, considering I-V characteristics and ionized donor concentrations at injection levels

08 p0951 A73-21484

Probabilistic analysis of the statistical accuracy of a transistor blocking generator with a common emitter

08 p0949 A73-21590

Ion saturation currents to planar Langmuir probes in a collision-dominated flowing plasma.

08 p0993 A73-21597

Possibilities of determining the permissible reverse-bias current and voltage in semiconductor devices by a nondestructive method

09 p1061 A73-21979

Electronic conduction and switching in chalcogenide glasses.

09 p1133 A73-21985

A system for the evaluation of solar cell samples.

09 p1033 A73-22438

Calculation of series and shunt resistances on the basis of the current-voltage characteristics of a solar cell

09 p1033 A73-22720

Sealed cylindrical high energy density Ni-Cd batteries, discussing electrode design and performance characteristics

09 p1034 A73-22754

Large area wraparound contact silicon solar cell, application and development.

09 p1036 A73-22812

A unified approach to the theory of double injection in solids with traps uniformly and non-uniformly distributed in the energy band gap.

09 p1135 A73-23045

MOSFET devices with trapezoidal gates - I-V characteristics and magnetic sensitivity.

10 p1194 A73-24157

I-V characteristics and luminescence changes in Cs vapor arc discharge at various spark gap widths, noting pressure effect on gas stratification

10 p1254 A73-24203

Study of the behavior of a monostable transistor circuit in the avalanche mode

10 p1195 A73-24413

Calculation of the characteristics of nonlinear elements in first-order circuits for given signal conversion conditions

10 p1196 A73-24603

Avalanche mode I-V characteristics of diffused and alloyed junction transistors at large collector currents

10 p1196 A73-24609

Stabilization of relaxation oscillators based on devices with an S-type current-voltage characteristic.

10 p1197 A73-24933

Switching in amorphous selenium.

11 p1407 A73-25147

Performance studies on a rechargeable hydrogen-oxygen fuel cell.

11 p1309 A73-25988

Solar cell dark I-V characteristics and their applications.

11 p1310 A73-26003

Design and performance of the TACSAT power subsystem.

11 p1312 A73-26020

Analytical fit of the transfer function of a logarithmic electrometer and correction for ambient temperature variations.

11 p1367 A73-26306

A nanovolt-level MOSFET reversing switch for low temperature applications.

11 p1367 A73-26310

Characteristics of amplitude discriminators built with transistors operating in the avalanche mode

12 p1479 A73-27209

Analog voltage squaring circuits with series-connected resistors shunted by semiconductor diodes or ladder network, discussing design, construction and operation principles

12 p1481 A73-27591

Biased wall heat transfer in electric arc chamber, noting I-V characteristics and electron current saturation in superimposed axial flow

12 p1560 A73-27700

Thermal noise measurements on space-charge-limited hole current in silicon.

13 p1668 A73-28542

Cylindrical electrostatic probes onboard Explorer C, D and E, presenting I-V characteristics of collector

13 p1688 A73-28636

Avalanche transistor circuit with controlled S shaped I-V characteristics, discussing equivalent circuits and operating points stability

13 p1591 A73-28731

Nonlinear elements piecewise and continuous approximations for constructing current-voltage characteristic functions

13 p1596 A73-28871

Analysis of primary currents in a three-phase/single-phase frequency converter with direct coupling and artificial commutation

13 p1592 A73-28940

Harmonic analysis of voltages and currents at the output of a frequency converter with direct coupling and artificial commutation

13 p1593 A73-28941

Analysis of primary currents and voltages in single-modulation frequency converters

13 p1593 A73-28942

Hypersonic wind tunnel MHD accelerator design and operating principles, discussing flux density, I-V characteristics, cooling losses, plasma temperature, gas pressure and velocity, etc

14 p1743 A73-30295

Phenomenon of negative differential resistance in silicon carbide crystals

14 p1783 A73-30384

Switching effect in amorphous semiconductors at discontinuous changes in the heat transfer from the sample.

14 p1783 A73-30434

Investigation of high-voltage photoelectric converters at low radiation intensities

14 p1713 A73-30948

The influence of Auger recombination on the forward characteristic of semiconductor power rectifiers at high current densities.

15 p1850 A73-31130

Russian book - Radiation receivers of automatic electron optics devices.

15 p1875 A73-31588

Ion current at the forward stagnation region of an electrically conducting body.

15 p1918 A73-31669

S-type current-voltage characteristic in Gunn diodes.

15 p1923 A73-31674

The most important characteristics of magnetizing equipment in the leakage-flux technique - Their measurement and application

15 p1882 A73-32054

Current-voltage characteristics of multispike diodes operating under conditions of explosive emission of electrons

15 p1852 A73-32315

Electric properties of dense plasmas in high current pulsed discharge.

16 p2040 A73-32943

Continuum analysis of the photoionization chamber in the transition from low to high rates of ionization.

16 p2015 A73-33321

Experimental studies and applications of vanadium oxides.

16 p2044 A73-33471

Transient analysis of complementary MOS IC inverter.

16 p1990 A73-33688

Current-voltage characteristic of a metal-dielectric contact with allowance for thermionic and field emission of electrons

16 p1972 A73-34010

Theory for the inelastic tunneling effect in normal metals

16 p2027 A73-34063

Inductive relaxation oscillator design using common emitter avalanche transistors with N-shaped I-V characteristics at base input

17 p2133 A73-34154

Light sensitive MNOS /metal-nitride-oxide-silicon/ memory transistor space charge layers current-field relationships and steady state I-V measurements

17 p2134 A73-34221

Design of nonlinear resistive networks with prescribed input-output behavior.

17 p2145 A73-35378

Electronically-regulated power supplies for microwave backward-wave oscillators.

17 p2142 A73-35643

Determination of the dispersion relation in tunnel structures - Influence of the barrier shape and validity of the WKB approximation.

17 p2220 A73-35655

Detection of optical and infrared radiation with dc-biased electron-tunneling metal-barrier-metal diodes.

17 p2143 A73-35792

Influence of the reflection forces and the tunnel effect on the current-voltage characteristic of a metal-semiconductor contact with a Schottky barrier

18 p2340 A73-36668

Current-voltage characteristic of a real diode with a Schottky barrier, allowing for tunneling through the spatial charge region

18 p2293 A73-36718

- A study of the static S-shaped current-voltage characteristics of chalcogenide glass switching devices 18 p2293 A73-36722
- Injection and field processes in thin semiconductor films in the current jump region 18 p2341 A73-36723
- Formulation of the basic approximations of the field theory of static current-voltage characteristics of quasi-monopolar semiconductors 18 p2341 A73-36724
- Double-probe measurements of electron temperatures on low pressure diffusion flames - Criticism of the methods for determining the electron temperature from the double-probe current voltage characteristic. 18 p2317 A73-37097
- Continuum thick sheath probe studies in hypersonic ionized boundary layers. 19 p2375 A73-37164
- Coaxial Ar plasma accelerator for spacecraft propulsion, discussing quasi-steady state I-V characteristics and exhaust velocity 19 p2466 A73-37180
- Two cascade plasma accelerator with conical and ring electrodes, investigating plasma jet-cascade current interaction dynamics via magnetic probes and I-V characteristics 19 p2467 A73-37362
- Electrical properties and simplified theory of a particular junction field-effect transistor operating with a forward gate-source bias. 19 p2409 A73-37428
- Low-frequency $1/f$ noise in MOSFET's. 19 p2409 A73-37581
- Application of cylindrical Langmuir probes to streaming plasma diagnostics. 19 p2469 A73-37862
- Optimum nonlinear characteristic of the supply element in the astable multivibrator with a tunnel diode. 19 p2410 A73-38309
- A computer study of the design and operating performance of a photovoltaic cell for thermophotovoltaic energy conversion applications. 19 p2391 A73-38405
- Dynamic thermal properties of IMPATT diodes. 19 p2411 A73-38459
- MIS structures with reversible charge capture capability, discussing I-V characteristics and applications similar to FET, image storage and charge coupled devices 20 p2534 A73-38853
- Analysis and design of single-cycle stages in MOS transistors with allowance for nonlinear distortions 20 p2535 A73-38857
- Some photoelectrical characteristics of photoelectric converters with a p-n structure 20 p2510 A73-39448
- Determination of the parameters A and j/sub 0/ in the loaded portion of the current-voltage characteristic of a photoelectric converter 20 p2510 A73-39450
- Substrate effect estimation for space charge limited current in intrinsic materials and planar structures, discussing I-V curves 20 p2543 A73-39593
- Design of Gunn-diode oscillators on the basis of normalized characteristics 21 p2659 A73-40007
- Possibilities of improving the characteristics of operational amplifiers by using thermostated input cascades 21 p2660 A73-40023
- Superconductor-semiconductor Schottky barrier diode video detector with proper doping and electron tunneling to obtain high degree nonlinearity in I-V characteristics 21 p2662 A73-40463
- The theory of the current-voltage characteristic of diodes fabricated out of compensated semiconductors 21 p2663 A73-40795
- Planar conductance transistor based on charge carrier accumulation due to n-n junction, featuring steep negative resistance characteristics and low sustaining voltage 21 p2655 A73-41048
- Ion-implanted varicaps with a steep capacitance-voltage characteristic 21 p2664 A73-41096
- Liquid helium temperature range thermometry using superconducting tunnel junction devices with temperature dependent I-V characteristics 22 p2856 A73-42018
- Voltage-to-frequency converters with an avalanche-recombination discharge diode 22 p2832 A73-42357
- Dynamic characteristics of a plasma diode with a low-voltage arc discharge. II - Experimental study of dynamic characteristics 22 p2833 A73-42386
- Interpretation of measurement results with ion traps in a bicomponent medium. 22 p2911 A73-42735
- Analysis of starting circuits for a class of hard oscillators - Two-transistor saturable-core parallel inverters. 22 p2834 A73-42909

Optimum design of electron beam-semiconductor linear low-pass amplifiers. II - Output capabilities. 23 p2958 A73-43454

Influence of the surface level on the differential slope of the semilogarithmic current-voltage characteristic of Schottky diodes 23 p2960 A73-43620

Diffusionless theory of the current-voltage characteristics of a metal/monopolar semiconductor contact in the case of current limiting by an arbitrary space charge 23 p3015 A73-43621

Diamagnetism of Penning discharge plasma as function of gas pressure, magnetic field strength and applied voltage, discussing plasma energetic lifetime and current characteristics 23 p3009 A73-43653

Investigation of a turbulent plasma in a reflex discharge with the aid of a double electric probe 23 p3011 A73-43668

Uniaxial pressure effects on diode structures volt-ampere characteristics, examining potential barrier height and photo emf changes 23 p2960 A73-43787

Oscillation amplitude curve determination of negative resistance oscillator connected to LC circuit, obtaining device I-V characteristics 23 p2961 A73-44147

Josephson junction I-V characteristics and measurements of phase modulated quasi-particle current in superconducting weak links, taking into account thermal noise 23 p3018 A73-44174

Volt-ampere characteristics of double electrical plasma probe measuring ionization level in low temperature dense plasma under interelectrode gap near-breakdown conditions 23 p2983 A73-44344

Off state I-V characteristics and thermal switching phenomena for tellurium selenium germanide chalcogenide glass semiconductors, assuming internal heat generation 24 p3119 A73-44607

Evolution of the shape of the current-voltage characteristics of n-p-n and p-n-p three-layer degenerate semiconductor structures 24 p3072 A73-44926

Influence of radiation on the current-voltage characteristic of tunnel diodes /Survey/ 24 p3072 A73-44926

Calculation of the energetic characteristics of Gunn diode oscillators in retarded- and quenched-domain modes 24 p3072 A73-44928

Switching transients in conducting channel-broadened p-n-p-n structure thyristors, predicting voltage change during current growth avalanche phase and settling at saturation point 24 p3072 A73-44932

Stationary charge transport in metal-semiconductor-metal /MSM/ structures. 24 p3120 A73-45421

Tunnel diode equivalent circuit analysis based on empirical expressions for composite T-V characteristics, predicting series resistance effect on switching time 24 p3073 A73-45485

Self and excited oscillations in a circuit composed of a non-linear element and a delay line. 24 p3075 A73-45487

VOLTAGE U ELECTRIC POTENTIAL VOLTAGE AMPLIFIERS

On the calibration system of the amplifying tract of spherical ion trappers. 02 p0169 A73-12186

The use of selective RC amplifiers in the RF amplifier of a superheterodyne receiver. 16 p1991 A73-33982

High loop gain operational amplifiers voltage changes as slewing rates using nonlinear circuit model, discussing equivalent circuits, frequency characteristics and bandwidth 22 p2832 A73-41896

VOLTAGE BREAKDOWN

U ELECTRICAL FAULTS

VOLTAGE CONVERTERS [AC TO AC]

High-frequency converter for power supply applications. [IEEE PAPER 17.3] 07 p0779 A73-19363

VOLTAGE CONVERTERS [DC TO DC]

A computer-aided design procedure for flyback step-up dc-to-dc converters. [IEEE PAPER 4.4] 07 p0779 A73-19361

Instrument providing dc voltage corresponding to amplitude of uniform pulse train, using differential comparator as sensing element and closed loop control scheme 11 p1313 A73-26316

Repetitively switched circuit analysis via matrix formalism and eigenvalue techniques with application to dc-dc converter 16 p1992 A73-33409

Computer-aided design and graphics applied to the study of inductor-energy-storage dc-to-dc electronic power converters. 21 p2635 A73-40340

High-efficiency converter and battery charger for an RTG power source. 22 p2801 A73-42906

Requirements of switching devices in dc-to-dc converters. 22 p2801 A73-42908

Linearized stability analysis and design of a flyback dc-dc boost regulator. 22 p2801 A73-42910

System oscillations from negative input resistance at power input port of switching-mode regulator, amplifier, dc/dc converter, or dc/ac inverter. 22 p2802 A73-42911

Dynamic behaviour and z-transform stability analysis of dc/dc regulators with a non linear P.W.M. control loop. 22 p2837 A73-42912

The application of standardized control and interface circuits to three dc to dc power converters. 22 p2802 A73-42918

A symmetry correcting pulse-width modulator for power conditioning applications. 22 p2802 A73-42919

VOLTAGE GENERATORS

NT PHOTOVOLTAIC CELLS

Logic network design for digital waveform shaping of polyphase voltage generator, noting application for airborne and marine gyroscope power supply 03 p0258 A73-14618

Transistor sawtooth voltage generator design for accelerated rise time piecewise linear leading edge, using capacitor charge/discharge acceleration 10 p1196 A73-24604

Error analysis of a generator with a uniform probability distribution of instantaneous values 11 p1331 A73-26100

VOLTAGE MEASUREMENT

U ELECTRICAL MEASUREMENT

VOLTAGE REGULATORS

Linear rapid frequency settling time solid state voltage controlled oscillators /VCO/ for electronic countermeasure and B-scan tracking radar applications 01 p0024 A73-10723

A sequenced PWM controlled power conditioning unit for a regulated bus satellite power system. 03 p0252 A73-13930

Processing power for a low voltage source-pulse load system. 03 p0253 A73-13939

Reliable uninterrupted controlled transient voltage dc power supplies with active energy storage element, comparing three system configurations, design features and applications 03 p0253 A73-13946

Self regulated transistorized voltage and frequency converters for multiple motor drives power supply, discussing circuit design, performance characteristics and overload protection 05 p0556 A73-16074

Battery charge regulator for Eole meteorological balloons power supply, describing printed circuit design and construction 07 p0778 A73-18970

Power system for a 4.1 kilowatt synchronous satellite. 11 p1312 A73-26023

Optoelectronic step-up voltage transformer with optical coupling electrical isolation, using light emitting diode and semiconductor film with high photovoltage levels 12 p1496 A73-26964

Blocking oscillator multipulse mode operation digital control by supply voltage regulation 13 p1593 A73-29119

The cause and effects of dc offset voltage in solid state ac power controllers. 17 p2109 A73-35255

Electronically-regulated power supplies for microwave backward-wave oscillators. 17 p2142 A73-35643

Electrical design requirements for electrolytic capacitors used in regulated low voltage DC power supplies. 21 p2663 A73-40772

System oscillations from negative input resistance at power input port of switching-mode regulator, amplifier, dc/dc converter, or dc/ac inverter. 22 p2802 A73-42911

Dynamic behaviour and z-transform stability analysis of dc/dc regulators with a non linear P.W.M. control loop. 22 p2837 A73-42912

Analysis of processes occurring during no-load operation of a ferroresonant voltage regulator with an improved shape of the output voltage curve 24 p3057 A73-44608

Switching of semiconductor devices in pulsed voltage regulators 24 p3072 A73-44938

VOLTAGE VARIATION INDICATORS U VOLTMETERS

VOLTERRA EQUATIONS

A method for phenomenological analysis of ecological data. 02 p0188 A73-12629

Close coupled calculations of electron-hydrogen atom scattering using a noniterative integral equation technique. 04 p0477 A73-14818

Iterative methods for best approximate solutions of linear integral equations of the first and second kinds. 06 p0717 A73-18170

Construction of exact solutions to certain systems of linear and nonlinear Volterra integral equations by using a power series 07 p0844 A73-19129

Application of the regularization principle to the construction of approximate solutions to inverse heat-conduction problems 08 p1022 A73-21097

Integral methods of calculating unsteady processes in nonlinear electric systems 08 p0951 A73-21556

Numerical solution of Volterra integral equations. 09 p1113 A73-23020

Spline approximation to the solution of the Volterra integral equation of the second kind. 10 p1241 A73-23642

Method of solving heat conduction problems with nonideal thermal contact 11 p1450 A73-25624

Application of the Chaplygin method to the solution of Volterra-type nonlinear integro-differential equations 11 p1391 A73-26521

Existence and stability of the solution of the Volterra nonlinear integral equation 12 p1517 A73-27101

Singular perturbation analysis of a certain Volterra integral equation. 13 p1648 A73-28412

Modified separable kernel method for heat conduction with a nonlinear boundary condition. 13 p1706 A73-28819

Stability considerations for a Volterra integral equation with discontinuous nonlinearity. 14 p1769 A73-30403

Asymptotic stability and perturbations for linear Volterra integrodifferential systems. 14 p1770 A73-30757

Modeling, identification and prediction of a class of nonlinear viscoelastic materials. I. 16 p2082 A73-33904

Asymptotic expansions for product integration. 17 p2200 A73-34213

Examination of the parameters in solutions to systems of two-dimensional nonlinear Volterra-type integral equations 17 p2203 A73-35590

Diffraction of an acoustic wave at a moving plate 18 p2265 A73-37012

On the noniterative solution of integral equations for scattering of electromagnetic waves. 19 p2407 A73-38381

Nonlinear control systems analysis, discussing phase space method, Taylor-Cauchy transform, Volterra functions, Liapunov stability, Popov-Kalman-Yakubovich theorems and limit cycle oscillations 20 p2592 A73-38691

Solution of a multipoint problem about the eigenvalues and eigenfunctions of an ordinary linear differential operator using a decomposition technique. 20 p2582 A73-39251

Successive approximation technique for dynamic-load problems of nonlinear viscoelastic systems 20 p2593 A73-39322

Direct methods for solving inverse linear problems of thermal conductivity 23 p3048 A73-43444

Power series solution to Volterra equations in nonlinear viscoelastic dynamic plate and shell theory with application to flexible cylindrical shell vibrations under periodic loads 24 p3145 A73-44518

Solution of physically nonlinear quasi-static problems of viscoelasticity 24 p3145 A73-44519

Solutions of boundary value problems with integral conditions for linear ordinary differential equations by the method of decomposition 24 p3106 A73-45351

VOLTMETERS

Determination of the optimal structure of a unit measuring the effective value of a nonsinusoidal periodic voltage 05 p0560 A73-16330

A square-law voltmeter based on elements with a thermal coupling 24 p3071 A73-44544

VOLUME

A criterion for establishing the principal dimensions of metallic standard measures of volume 03 p0306 A73-12897

VOLUMETRIC ANALYSIS

Void fraction measurement based on gas-liquid volume ratio by local void velocity measurement with single probe 05 p0638 A73-16224

'Closing volumes' and decreased maximum flow at low lung volumes in young subjects. 09 p0141 A73-22929

Theory of mass flow measurement - Its advantages and instrumentation related to same. 17 p2166 A73-34619

Burnett cell design and fabrication for error reduction in high precision P-V-T data generation without volume or mass measurements 17 p2182 A73-35772

The effect of immobilization on body fluid volume in the rat. 20 p2513 A73-39487

VON KARMAN EQUATION

The mixing length derived from Karman's similarity hypothesis. 08 p0955 A73-21442

The observed relation between the Kolmogorov and von Karman constants in the surface boundary layer. 11 p1393 A73-25694

Logarithmic wind profile in neutral barotropic planetary boundary layers, discussing von Karman constant 11 p1394 A73-25717

Simple universal equilibrium spectrum. 18 p2300 A73-36634

VON MISES THEORY

U STRESS FUNCTIONS

VON ZEIPPEL METHOD

Temperature difference between pole and equator of the sun. 21 p2776 A73-41479

VOR SYSTEMS

U VHF OMNIRANGE NAVIGATION

VORTEX BREAKDOWN

Wing-tip vortex breakdown and dissipation, deriving closed form transcendental solutions for viscous core flow quasi-cylindrical momentum integral equations 02 p0128 A73-12036

Aircraft wake dissipation by sinusoidal instability and vortex breakdown. 05 p0529 A73-16867

Observations of atmospheric effects on the transport and decay of trailing vortex wakes. 05 p0529 A73-16869

The influence of acoustic disturbances on the mechanics in shear layer behind a circular cylinder in air flow. 13 p1563 A73-28530

Trapped wave vortex breakdown model for long weakly nonlinear wave propagation on critical flows in tubes of variable cross sections 16 p1998 A73-32796

Trailing vortex pair instability in inviscid incompressible fluid with rotating and nonrotating isolated and axial velocity jet core 18 p2300 A73-36628

Formation and decay of vortex filaments in a plasma current sheath. 19 p2465 A73-37173

Turbulent line vortex decay dependence on Reynolds number, suggesting triple vortex structure with outer and inner regions and viscous core with varying circulation distribution 22 p2842 A73-42230

VORTEX COLUMNS

U VORTICES

VORTEX DISTURBANCES

U VORTICES

VORTEX FLOW

U VORTICES

VORTEX GENERATION

U VORTEX GENERATORS

VORTEX GENERATORS

Planar jet vortex growth control by excitation through transverse periodic disturbances, studying jet flow field by visualization via hydrogen bubble technique [ASME PAPER 72-WA/APM-21] 04 p0435 A73-15895

Vortex core precession in water or air high swirl flows above critical Reynolds number 13 p1602 A73-29017

Study of the far wake vortex field generated by a rectangular airfoil in a water tank. 18 p2262 A73-36233

The vapour core pump vortex inlet valve. 23 p2941 A73-43393

Vortex shedding from and base pressure distribution on bluff body measured in shear or uniform flow, calculating Strouhal number 23 p2940 A73-43939

VORTEX INJECTORS

A note on compressible flow through a vortex swirl cup. 17 p2154 A73-35120

VORTEX RINGS

Flame propagation in premixed propane /air or propane/ oxygen vortex rings, describing normal and schlieren photographic techniques 03 p0399 A73-14399

A study of vortex rings using a laser Doppler velocimeter. 05 p0565 A73-16865

One parameter family of axisymmetric vortex rings propagating steadily through unbounded ideal fluid at rest at infinity 11 p1345 A73-25051

Finite core model of self induced motions and stability of filament vortex rings in inviscid fluid under small sinusoidal perturbation 11 p1348 A73-26202

A Hamiltonian theory for weakly interacting vortices. 13 p1609 A73-28917

Flow deceleration as mechanism of vortex ring formation, showing liquid mass variability and vortex clusters of spheroid and hemisphere shapes 15 p1861 A73-31282

Concentrated vortex nonlinear oscillations, discussing vortex ring and helical vortex filament stability, mode shape and frequency changes and standing and traveling wave solutions 18 p2301 A73-37004

VORTEX SHEETS

Vortex sheath formalism based on coupled integral equations for rectangular wing-slipstream aerodynamic interference 03 p0244 A73-13562

The Joukowski condition in three-dimensional flow 04 p0405 A73-15988

Multivortex model for bodies of arbitrary cross-sectional shapes. 05 p0529 A73-16864

Numerical studies of two-dimensional vortex motion by a system of point vortices. 08 p0954 A73-21010

Discrete vortex scheme of a wing of finite span 08 p0927 A73-21611

Trailing vortex sheet roll-up behind finite aspect ratio wings for different loading conditions, discussing drag penalties for tip vortices strength improvements 09 p1029 A73-23125

Fish like slender body propulsion and flow theory, discussing fin surface-body thickness interaction, vortex sheets, trailing edges and lifting force 11 p1301 A73-25852

Calculation of flows past wings without thickness in the presence of developing vortex sheets 16 p1965 A73-33963

The instability due to acoustic radiation striking a vortex sheet on a supersonic stream. 17 p2151 A73-34824

Harmonic and impulsive acoustic source-produced sound propagation across vortex sheet separating two subsonic fluids; investigating instability waves 17 p2151 A73-34825

Vortex sheet model of directional acoustic wave radiation near nozzle exit from supersonic helium jet shear layer instability 21 p2677 A73-40617

Interaction of sound with jets. 22 p2795 A73-41704

The reflexion of an acoustic pulse by a plane vortex sheet. 22 p2842 A73-42348

VORTEX STREETS

NT KARMAN VORTEX STREET

Synthesis of helicopter rotor tips for less noise. 11 p1299 A73-24981

Dimensional inviscid flow model of shear layer and vortex shedding in near wake of bluff-based body, using Schwarz-Christoffel transformation 11 p1300 A73-25155

VORTEX TUBES

U HILSCH TUBES

U VORTICES

VORTICES

Effect of streamwise vortices on wake properties associated with sound generation. 01 p0001 A73-10045

The spectral density technique for the determination of eddy fluxes. 01 p0072 A73-10145

Plane flow past vortex of inviscid incompressible fluid jets bound by free surface and horizontal wall, considering complex potential function and submerged lifting airfoils 01 p0031 A73-10304

Taylor vortices nonoscillation theory for outward decrease of circulation square, investigating system eigenvalues [AD-754480] 01 p0033 A73-10779

Instrument requirements for eddy correlation measurements. 01 p0052 A73-11057

Pregalactic vortex motion decay calculation from kinetic equation of hot expanding universe model 01 p0106 A73-11307

Exact vorticity solutions of the incompressible Navier-Stokes equations.

01 p0034 A73-11358

Three linear invariant relations in the problem of motion of a heavy solid body with a liquid filler

02 p0153 A73-11773

Method of calculating vortex-free flow around hydrodynamic cascades composed of arbitrary profiles

02 p0128 A73-11788

Influence of geometrical parameters on the energetic separation of superheated water vapor in a conical vortex tube

02 p0153 A73-11789

Wing-tip vortex breakdown and dissipation, deriving closed form transcendental solutions for viscous core flow quasi-cylindrical momentum integral equations

02 p0128 A73-12036

Finite amplitude waves on aircraft trailing vortices.

02 p0129 A73-12506

An investigation of the near wake properties which lead to the generation of vortex shedding sound from airfoils.

03 p0242 A73-12976

Aerodynamic noise and alternating loads in an idealized turbine stage.

03 p0242 A73-12981

The Rankine-Hilsh vortex tube and its application to spacecraft environmental control systems.

03 p0287 A73-13313

Steady flow of neutrally buoyant flat-faced rigid cylindrical capsules along pipeline under hydraulic pressure gradient effect, noting toroidal vortices

03 p0293 A73-13528

Lee-side vortices on delta wings at hypersonic speeds.

03 p0247 A73-14180

Thrust coefficient of artificially excited vortex trail behind a jet flap aerofoil.

03 p0247 A73-14186

Vortex lattice discretization for finite Hilbert transform of two dimensional incompressible thin wing flow integral equation with singularities, noting numerical solution accuracy

04 p0403 A73-15004

Magnetospheric convection, discussing ionospheric twin vortex pattern, reconnection model for solar wind induced generation, plasmasphere response and magnetotail dynamics

04 p0442 A73-15337

Turbulent flow characteristics of swirling jets with opposite rotation, discussing lateral spreading into potential ambient fluid

[ASME PAPER 72-WA/FE-17] 04 p0435 A73-15844

Vortex induced vibration of circular cylindrical structures.

[ASME PAPER 72-WA/FE-39] 04 p0404 A73-15856

Significant vortex structures occurrences from ESSA 3 and 5 global cloud observations, discussing source and formation patterns over Northern and Southern Hemisphere regions

05 p0593 A73-16346

Experimental determination of bound vortex lines and flow in the environment of the trailing edge of a slender delta wing

[AD-755630] 05 p0528 A73-16600

Study of local heat transfer coefficients in a tube in the case of a local flow swirling by swirl vanes

05 p0639 A73-16768

Isentropic compressible flow equations for pressure and velocity distributions across vortex in axial core mass flow, noting atmospheric circulation and pressure effects

[AIAA PAPER 73-106] 05 p0529 A73-16866

The correlations of the vortex in a homogeneous turbulence associated with a mean shearing flow

05 p0567 A73-17227

The aircraft wake turbulence problem.

06 p0648 A73-18149

Velocity distribution of quasi-steady and steady flow of ideal incompressible fluids with congruent streamlines, investigating conditions for vortex and irrotational flow

07 p0809 A73-19017

A synoptic climatology of satellite observed cloud vortices over the Southern Hemisphere.

07 p0846 A73-19039

Wing tip vortex modification by tip-mounted upstream and downstream directed air jets, discussing wind tunnel test results

07 p0773 A73-19193

Stability of an electrical discharge surrounded by a free vortex.

07 p0848 A73-19514

Turbulent jet diffusion and vortex models, noting velocity profile in mixing and turbulent boundary layers

07 p0811 A73-19617

Turbulent energy variations in unsteadily moving flow with structural shift, emphasizing formation of vortices with various inertia scales

07 p0811 A73-19620

Stationary vortices behind a flat plate normal to the freestream in incompressible flow.

07 p0775 A73-19974

Decaying unsteady viscous vortex flow under conditions of streamlines and vortex lines coincidence, deriving Navier-Stokes equations solution

07 p0812 A73-20340

The secondary flow about circular cylinders mounted normal to a flat plate.

08 p0926 A73-21440

On the shearing flow of a fluid, heavy or not, with constant vortex, around a thin profile placed under a free line, in linear theory

08 p0926 A73-21490

Unsteady nonlinear flow around an airfoil or a blade cascade with emission of turbulent vortices

09 p0127 A73-22212

Atmospheric turbulent fluctuations explained via eddy-wind shear and convective rolls-gravity wave interactions, using wind-temperature data from White Sands

09 p1114 A73-22329

Causes of the rotation of galaxies in terms of the nonlinear theory of gravitational instability

10 p1274 A73-23712

Closed form solution for heat transfer through Rankine vortex, noting square root dependence of Nusselt number on Peclet number

10 p1295 A73-23780

Secondary flows - Theory, experiment, and application in turbomachinery aerodynamics.

10 p1171 A73-23860

Aircraft wake vortex avoidance systems with current locus detection and/or prediction capability, discussing design based on hazard assessment and computer simulation for performance

10 p1172 A73-24557

Characteristics of viscous vortex flows in superconducting alloys near the critical temperature

10 p1261 A73-24765

Unsteady wakes of bluff and streamlined bodies with screens behind them.

10 p1173 A73-24823

Electrodynamics analysis of superconducting vortices interaction with cylindrical cavities (pinning), calculating critical currents in type II superconductors in external magnetic field

11 p1409 A73-26191

Large particle method for calculation of transonic supercritical vortex flow fields around flat and axisymmetric bodies

11 p1302 A73-26330

Aerodynamics of wake vortices.

11 p1303 A73-26385

The pressure and velocity fields of convected vortices.

13 p1599 A73-28067

Vortex motions of cosmic matter as cosmological evolution mechanism, considering galactic and solar system kinetics

13 p1681 A73-28780

A Hamiltonian theory for weakly interacting vortices.

13 p1609 A73-28917

Turbulence in journal bearings, considering Taylor vortices development beyond laminar range and theoretical models based on mixing length flow theory

13 p1625 A73-29261

Barotropic and baroclinic contribution to eddy kinetic energy increase in disturbance amplification using quasi-geostrophic equations of motion and omega equation

13 p1610 A73-29335

Helicopter rotor blade passing close to tip vortex, calculating fluctuating lift induced harmonic blade loads and generated cyclic banging noise

13 p1570 A73-29382

Existence of a corner-type steady flow for an ideal fluid with a free surface

13 p1605 A73-29554

Radiation from line vortex filaments exhausting from a two-dimensional semi-infinite duct

14 p1744 A73-30168

Equilibrium equations for vortex lines with allowance for interaction with boundary of ideal superconductor, calculating extremum values of magnetic field

14 p1774 A73-30342

NMR measurements of the speed of vortices in flux flow in a type II superconductor.

14 p1783 A73-30433

Book - A course in continuum mechanics. Volume 3 - Fluids, gases and the generation of thrust.

14 p1745 A73-30594

Further investigations on the nonlinear behavior of a system of parallel line vortices.

14 p1746 A73-30652

Investigation of the stability of a hollow vortex bounded by a rigid wall

15 p1861 A73-31156

Two dimensional unsteady vortex flow of ideal fluid past inflating decelerating wedge, obtaining pressure distribution on wedge surface

15 p1823 A73-31435

Vortex conservation mechanism of earth atmosphere jet stream formation in terms of Hadley cell in meridional divergence/convergence velocity region

15 p1903 A73-31603

Finite chord effects on vortex induced large aspect ratio wing loads, noting rolling moment magnitude overestimate from lifting line solution

15 p1823 A73-31670

Optimal grid arrangement in vortex lattice method of lifting surface aerodynamic analysis, comparing numerical with kernel function results for simple wing planforms

15 p1824 A73-31746

Theory of turbulence with a vortex-type anisotropy

15 p1864 A73-32084

Instabilities in charge sheets and current sheets and their possible occurrence in the aurora.

15 p1873 A73-32235

Book on Cartesian vortex theory of planetary motions covering celestial mechanics theories of Galileo, Kepler, Descartes, Leibniz and Newton

15 p1960 A73-32422

Wavelength and cell size determination of steady supercritical Taylor vortex flow for long rotating cylinders with radius, viscosity and end boundary variations

16 p1998 A73-32798

Calculation of the characteristics of tail fins in the vertical field of a wing

16 p1962 A73-32819

A wake and an eddy in a rotating, radial-flow passage. I - Experimental observations.

[ASME PAPER 73-GT-57] 16 p1964 A73-33512

A wake and an eddy in a rotating, radial-flow passage. II - Flow model.

[ASME PAPER 73-GT-58] 16 p1964 A73-33513

Discrete vortex method of two-dimensional jet flaps.

17 p2091 A73-34179

Vortex-lift prediction for complex wing planforms.

17 p2094 A73-34438

Aircraft wake vortex avoidance system for safety management and capacity optimization in airport operations related to ATC, considering various sensors and display subsystem requirements

17 p2166 A73-34613

Aircraft wing tip turbulent wakes producing swirling vortices, discussing wake hazards, wind tunnel research and vortex dissipation procedures

[SAE PAPER 730294] 17 p2094 A73-34658

Flight test studies of the formation and dissipation of trailing vortices.

[SAE PAPER 730295] 17 p2094 A73-34659

Discontinuity of the vortex on a shock in thermodynamic variables

17 p2154 A73-35047

Experimental investigation of model variable-geometry and ogee tip rotors.

[AHS PREPRINT 703] 17 p2104 A73-35054

An investigation of the vibratory and acoustic benefits obtainable by the elimination of the blade tip vortex.

[AHS PREPRINT 735] 17 p2105 A73-35071

Foppl vortices stability for two dimensional inviscid irrotational steady flow past circular cylinder

17 p2154 A73-35117

Turbulent flow research, discussing time domain analysis of velocity, displacement and pressure, potential flow models of vortices, and shear flow turbulence

17 p2155 A73-35330

Development and effects of super-critical Taylor-vortex flow in a lightly-loaded journal bearing.

[ASME PAPER 73-LUBS-4] 17 p2181 A73-35390

The Taylor vortex regime in the flow between eccentric rotating cylinders.

[ASME PAPER 73-LUBS-8] 17 p2181 A73-35391

A jet-wing lifting-surface theory using elementary vortex distributions.

[AIAA PAPER 73-652] 18 p2260 A73-36207

A conceptual study of leading-edge-vortex enhancement by blowing.

[AIAA PAPER 73-656] 18 p2261 A73-36210

Aircraft wake vortex transport model.

[AIAA PAPER 73-679] 18 p2267 A73-36230

The application of a scanning laser Doppler velocimeter to trailing vortex definition and alleviation.

[AIAA PAPER 73-680] 18 p2315 A73-36231

Rapid scanning, three-dimensional, hot-wire anemometer surveys for wing tip vortices in the Ames 40-by-80-foot wind tunnel.

[AIAA PAPER 73-681] 18 p2315 A73-36232

Three dimensional jet flap potential flow theory based on vortex lattice method, comparing iterative solution with slatted unswept blown flapped wing experimental results

[AIAA PAPER 73-653] 18 p2263 A73-36260

Swirling flows in streamtubes of variable cross section.

18 p2298 A73-36314

On Burgers' model equations for turbulence.

18 p2299 A73-36507

Gulf Stream eddies - Recent observations in the western Sargasso Sea. 18 p2313 A73-36642

Development of rotation in galaxies in the nonlinear theory of gravitational instability. 18 p2354 A73-36737

Concentrated vortex nonlinear oscillations, discussing vortex ring and helical vortex filament stability, mode shape and frequency changes and standing and traveling wave solutions 18 p2301 A73-37004

Certain vortical flows with variable vorticity past a circular cylinder 18 p2302 A73-37009

Some parameters of cyclonic cloud vortices. 18 p2333 A73-37053

Cloud eddy formation in wakes of single mountain islands similar to Karman vortex streets, noting application to wind field forecasting 18 p2334 A73-37075

Formation and decay of vortex filaments in a plasma current sheath. 19 p2465 A73-37173

Investigations of the 500mb level in relation to the general circulation. I - Transport of relative angular momentum at the 500mb level, by considering daily and monthly eddies that were obtained by applying Fisher's partitioning. 19 p2446 A73-37499

Aircraft wake vortex detection and avoidance systems, examining acoustic sensors, bistatic Doppler sensors, pulsed radar, aircraft spacing techniques and ground wind measurement 19 p2452 A73-37823

Study of control system effectiveness in alleviating vortex wake upsets. [AIAA PAPER 73-833] 20 p2507 A73-38776

Structure of vortical motion systems in the ionosphere that generate Sq variations of the geomagnetic field 20 p2553 A73-39153

Taylor vortex occurrences between rotating eccentric cylinders 20 p2547 A73-39284

Vortex interaction with plane in viscous fluid, discussing free parameter related to insufficient boundary conditions for solving Navier-Stokes equations 20 p2547 A73-39289

The description of vortex-excited oscillations of prismatic bodies by means of a sequence of pulses having random time differences 20 p2594 A73-39770

The initial development of a submerged laminar round jet. 20 p2550 A73-39815

Design of axial flow fans by cascade method. 21 p2631 A73-40124

Strouhal number and flat plate oscillation in an air stream. 21 p2782 A73-40125

Investigation of secondary flows between coaxial rotating cylinders 21 p2676 A73-40574

Thermodynamic conditions of conservation of irrotational or oligotropic motions across a shock wave 21 p2677 A73-40948

The establishment of the winter polar vortex in middle latitudes in 1971. 21 p2687 A73-41338

Sound propagation in rotating vortex flow downstream from delta wing in wind tunnel, discussing acoustic ray refraction by flow 22 p2839 A73-41715

Eddies development downstream a pipe orifice. 22 p2840 A73-41738

Effect of combustion upon precessing vortex cores generated by swirl combustors. 22 p2934 A73-42781

Navier-Stokes equation formulation in parabolic coordinates for flow in trailing vortex, obtaining asymptotic expansions for stream function and angular momentum 23 p2939 A73-43205

Axial vortex and Coanda vortex flow controllers. 23 p2941 A73-43392

Oil hydraulic button vortex valve optimization experiment for power consumption reduction, noting Reynolds number effects on turn down and pressure ratios 23 p2942 A73-43404

Dynamic range and frequency response of the vortex rate sensor. 23 p2942 A73-43406

The steady-state and transient performance of some large-scale vortex diodes. 23 p2942 A73-43407

Fluidic vortex-type proximity sensor with analog to digital converter, optimizing output nozzle diameter and pressure by steepest ascent method 23 p2981 A73-43431

The structure and dynamics of horizontal roll vortices in the planetary boundary layer. 23 p3002 A73-43594

Relation between the intensity of the stratospheric circumpolar vortex and the accumulation of ozone in the winter hemisphere. 23 p2977 A73-43905

Stellar vortex formation in solar apex region in terms of retrograde motion and solar orbit characteristics 23 p3036 A73-44240

Aircraft aerodynamics problems covering slender body theory, atmospheric turbulence and boundary layers, wind tunnel contractions, radiator blocks, vortex induced oscillations, etc 24 p3053 A73-44690

Nonlinear transient effects of separated unstable flow on vortex generated acoustic waves in cavities [AIAA PAPER 73-1014] 24 p3078 A73-44846

Stability of a potential vortex with a non-rotating and rigid-body rotating top-hat jet core. 24 p3055 A73-45309

Vortex model for flames and free jets characteristic velocities based on three dimensional turbulent combustible flow 24 p3158 A73-45387

Nonlinear stability of cylindrical vortex enclosing a central jet of light or dense fluid. 24 p3080 A73-45452

VORTICITY

An asymmetrically rotating fluid disc with applications. [AD-751727] 02 p0217 A73-12393

Theorems on general fluid particle vorticity acquisition by nonanalytic process 03 p0292 A73-13309

Inlet flow distortion induced axial flow compressor stall, converting stagnation pressure and temperature maps into vorticity maps via Crocco theorem [AIAA PAPER 72-1116] 03 p0243 A73-13431

Wake vorticity of side-slipping slender thin wings at transonic speeds, deriving integral equation for vortex strength based on Prandtl-Glauert rule [DGLR PAPER 72-127] 03 p0247 A73-14376

The influence of planetary vorticity gradient and vertical entropy gradient on the stability of an atmospheric shear layer. 04 p0441 A73-15288

Viscoelastic liquid flow in wake past two dimensional grid, investigating vorticity increase with time for double array of vortices 05 p0565 A73-16592

Geomagnetic storms and wintertime 300-mb trough development in the North Pacific-North America area. 08 p0961 A73-21384

Wind tunnel study of flows generated by slender cones in subcritical Reynolds number regime, examining vortex shedding and drag 10 p1174 A73-24845

A numerical solution of the Navier-Stokes equations using the finite element technique. 11 p1345 A73-25116

Comment on the effect of a vorticity centre on a frontal boundary. 13 p1656 A73-29663

The process of galaxy formation according to the universal turbulence hypothesis. 14 p1798 A73-30142

Some computation-steeples in fluid mechanics. 14 p1745 A73-30412

Free stream vorticity effect on incompressible boundary layer stability via Orr-Sommerfeld equation, considering self-similar flows with pressure gradients 14 p1712 A73-30651

A generalized flux-vorticity theorem. I. 15 p1916 A73-31088

Vorticity advection and geopotential change due to dynamic causes as two-layer problem 15 p1907 A73-32355

The analytical aspects of the reduction of boundary errors in the case of numerical weather predictions 16 p2034 A73-33074

Upstream attenuation and quasi-steady rotor lift fluctuations in asymmetric flows in axial compressors. [ASME PAPER 73-GT-30] 16 p2048 A73-33501

Atmospheric vorticity effects on hexagonal convection cells formation, considering temperature profiles nonlinearity, turbulent viscosity and perturbation scale 18 p2333 A73-37052

Three dimensional boundary layer flow with streamwise vorticity decay, deriving solutions as expansions in terms of eigenfunctions 19 p2420 A73-37851

Quasi-stationary atmospheric waves and mean monthly vorticity production from development term of two level model 19 p2447 A73-38153

The investigation on the secondary flow induced by jets. I. 19 p2422 A73-38349

Asymptotic behaviour of a scalar in an axisymmetric final period turbulent wake. 20 p2507 A73-39086

Material indifference - A principle or a convenience. 20 p2619 A73-39337

Numerical forecasting experiments based on the conservation of potential vorticity on isentropic surfaces. 21 p2728 A73-40053

VORTICITY EQUATIONS

An efficient, one-level, primitive-equation spectral model. 01 p0072 A73-10248

An extremum principle for three-dimensional compressible inviscid flows. 01 p0031 A73-10427

Vorticity equation advection, divergence and curl terms effects on vorticity changes over isobaric surfaces and on weather and cyclonic development in synoptic meteorology 13 p1653 A73-28745

Generalized expressions for secondary vorticity using intrinsic co-ordinates. 18 p2299 A73-36506

The vorticity equation as an angular momentum equation. 22 p2842 A73-42349

Dynamics of quasigeostrophic flows and instability theory. 22 p2842 A73-42450

VORTICITY TRANSPORT HYPOTHESIS

Flow in the entrance region at low Reynolds numbers. [ASME PAPER 72-WA/FE-21] 04 p0435 A73-15847

VOYAGEUR HELICOPTER

U CH-46 HELICOPTER

U TO FIGHTER AIRCRAFT

U FIGHTER AIRCRAFT

U VERTICAL TAKEOFF AIRCRAFT

VTOL

U VERTICAL LANDING

U VERTICAL TAKEOFF

VTOL AIRCRAFT

U VERTICAL TAKEOFF AIRCRAFT

VULCANIZATES

U VULCANIZED ELASTOMERS

VULCANIZED ELASTOMERS

Layer strength and vulcanization effects on rubber/metal bonding with MEGUM agent 10 p1239 A73-24095

VULNERABILITY

Laser guided weapon system optical countermeasures /OCM/ vulnerability evaluation, discussing use of LED laser in computerized simulation at low cost 17 p1247 A73-35208

W

W WINGS

U VARIABLE SWEEP WINGS

WAFERS

Method of calculating yield for LSI arrays considering radial distribution of defects on wafers. 10 p1193 A73-23668

Use of Sirtl etch for silicon-slice evaluation. 12 p1530 A73-27044

WAKEFULNESS

Developmental changes in neurochemistry during the maturation of sleep behavior. 03 p0264 A73-14261

Development of wakefulness-sleep cycles and associated EEG patterns in mammals. 03 p0264 A73-14263

Patterns of reflex excitability during the ontogenesis of sleep and wakefulness. 03 p0264 A73-14264

Wakefulness and sleep states in developing organism, discussing REM sleep deprivation effects on behavior, brain excitability, pharmacology and biochemistry 03 p0265 A73-14265

Diurnal psychic working capacity dynamics under conditions of continuous 72-hr wakefulness 08 p0930 A73-20989

The effects of Dalmane /flurazepam hydrochloride/ on human EEG characteristics. 08 p0931 A73-21464

Investigation of the sleep and wakefulness rhythms in the crewmembers of Soyuz-3 through Soyuz-9 spacecraft prior to, during, and after space flight 10 p1182 A73-24697

Influence of synchronized sleep upon spontaneous and induced discharges of single units in visual system. 11 p1319 A73-26223

Spiral aftereffect durations following awakening from REM sleep and non-REM sleep. 21 p2639 A73-41179

WAKES

NT AIRCRAFT WAKES

NT HELICOPTER WAKES

NT HYPERSONIC WAKES

NT LAMINAR WAKES

NT NEAR WAKES

NT PROPELLER SLIPSTREAMS

NT SLIPSTREAMS

NT SUPERSONIC WAKES

NT TURBULENT WAKES

WALKING

- A study of the kinematic and dynamic characteristics in the wake behind a plate in an unbounded flow 01 p0032 A73-10620
- Electric fields and conductivities derived from wake measurements on a rocket. 02 p0164 A73-12311
- On the importance of the wake for the noise of an obstacle placed in a flow 03 p0291 A73-12974
- Effect of wake-wake interactions on the generation of noise in axial-flow turbomachinery. 03 p0246 A73-14129
- Wake vorticity of side-slipping slender thin wings at transonic speeds, deriving integral equation for vortex strength based on Prandtl-Glauert rule [DGLR PAPER 72-127] 03 p0247 A73-14376
- Scaling relations to predict size of submarine generated wake in stratified water flow, measuring velocity and temperature profiles [AIAA PAPER 73-108] 06 p0644 A73-17644
- Model tests on unsteady rotor wake effects. 07 p0773 A73-19191
- Flow in the wake of a cascade of oscillating airfoils. 07 p0774 A73-19954
- Atmospheric dispersion of air pollutants, analyzing buoyant plumes and wakes 10 p1205 A73-23857
- Unsteady wakes of bluff and streamlined bodies with screens behind them. 10 p1173 A73-24823
- Spatial amplitude distribution of vibrating ribbon two dimensional wake mean, periodic and random velocity components measured in uniform flow by hot-wire anemometry 10 p1173 A73-24828
- Study of flow around a rotating circular cylinder. 11 p1302 A73-26337
- Study of kinematic and dynamic characteristics in a wake behind a plate in an unbounded flow. 13 p1601 A73-28739
- Unstable operation and rotating stall in axial flow compressors. 13 p1566 A73-29024
- Wake past an obstacle in a magnetized plasma flow. 15 p1916 A73-31089
- Wake flow model of Viking 75 entry vehicle for different angles of attack at free stream Mach numbers 0.2-3.95 [AIAA PAPER 73-475] 15 p1823 A73-31459
- A wake and an eddy in a rotating, radial-flow passage. I - Experimental observations. [ASME PAPER 73-GT-57] 16 p1964 A73-33512
- A wake and an eddy in a rotating, radial-flow passage. II - Flow model. [ASME PAPER 73-GT-58] 16 p1964 A73-33513
- Experimental investigation of model variable-geometry and ogee tip rotors. [AHS PREPRINT 703] 17 p2104 A73-35054
- Study of the far wake vortex field generated by a rectangular airfoil in a water tank. 18 p2262 A73-36233
- Smoke visualization of three-dimensional flow patterns in a nominally two-dimensional wake. 19 p2375 A73-37423
- Numerical integration method for Navier-Stokes equation of time dependent flow past impulsively started circular cylinder, calculating length of separated wake and pressure distribution 21 p2631 A73-40248
- Large space vehicles - Platforms for second generation in-situ wake observations. 21 p2781 A73-40901
- F region disturbances in wake of burnt-out Black Brant rocket body, discussing electron depletion from ground based Digisonde 21 p2690 A73-41363
- Spatial stability of incompressible two-dimensional Gaussian wake in steady viscous flow. 22 p2796 A73-42243
- Experimental studies on the flame structure in the wake of a burning droplet. 22 p2937 A73-42816
- Liquid fuel spray burning characteristics in stabilizer disk wake of luminous hollow cone pressure jet flame, using spark photographic technique 22 p2937 A73-42818

WALKING

- Striding devices for astronautical application areas. 04 p0433 A73-15630
- Features of supraspinal control of the reflex paths of the spinal cord during walking 10 p1178 A73-23677
- Relationship of physiological strain to change in heart rate during work in the heat. 15 p1836 A73-32548

WALKING MACHINES

- Some aspects of the inverted pendulum problem for modeling of locomotion systems. 19 p2460 A73-38035
- Physical model selection for the balance preservation system in man 24 p3063 A73-44903

WALL FLOW

- Mathematical and statistical modeling of wall flow turbulence, considering experimental velocity and temperature measuring techniques 01 p0031 A73-10292
- Plane flow past vortex of inviscid incompressible fluid jets bound by free surface and horizontal wall, considering complex potential function and submerged lifting airfoils 01 p0031 A73-10304
- French monograph - A method of calculating the turbulent boundary layer using an equation for the behavior of the Boussinesq coefficient. 01 p0032 A73-10602
- Nonlinear boundary-value problem for a conducting source flow in an inhomogeneous magnetic field. 01 p0085 A73-11064
- Influence of the boundaries of wind-tunnel flow on the flow past a small-aspect-ratio wing 02 p0128 A73-11707
- Integral method of calculating a semibounded laminar jet 02 p0153 A73-11784
- Experimental values of turbulence length scales in Lagrange variables in the vicinity of a flat wall 02 p0154 A73-12541
- Turbulent pressure fluctuations on smooth and rough walls. 03 p0289 A73-12960
- Incompressible flow characteristics and temperature transverse behavior in completely turbulent wall boundary layer 03 p0292 A73-13172
- Existence in the laminar boundary layer of a natural instability not predicted by theory and connected to a wall deformation 03 p0294 A73-13576
- Study of the boundary layers of a completely ionized two-temperature plasma on the nonconducting wall of an MHD channel 03 p0346 A73-13610
- Current near the insulator wall in plasma accelerators. 03 p0348 A73-14437
- Velocity profiles and wall shear stress of three-dimensional turbulent boundary layers. [ONERA, TP NO. 1134] 04 p0403 A73-15092
- Calculation methods of three-dimensional boundary layers with and without rotation of the walls. [ONERA, TP NO. 1135] 04 p0403 A73-15093
- A free-streamline theory for bluff bodies attached to a plane wall. 04 p0403 A73-15160
- Wall shear stress inference from two and three-dimensional turbulent boundary layer velocity profiles. [ASME PAPER 72-WA/FE-4] 04 p0434 A73-15840
- Heat and mass transfer laws for fully turbulent wall flows. 04 p0520 A73-15935
- Heat transfer in fully developed laminar flow between flat parallel boundary walls, deriving approximations to higher eigenvalues 05 p0563 A73-16101
- Surrounding wall electrical resistivity effects on plasma pinch stabilized by outer region force-free current flow, deriving instability growth rate 05 p0604 A73-17363
- Flow visualization of the near-wall region in a drag-reducing channel flow. 06 p0685 A73-17709
- Turbulent boundary layers with negligible wall stress - A singular-perturbation theory. 06 p0686 A73-17988
- Effectiveness of the thermal protection of a plane wall during injection of air through two rows of rectangular holes arranged in a checkered order 06 p0768 A73-18127
- Singular perturbation and turbulent shear flow near walls. 06 p0686 A73-18378
- Determination of the shape of jets flowing off the walls of an asymmetrically positioned bucket 07 p0776 A73-20098
- A generalized correlation of roughness density effects on the turbulent boundary layer. 08 p0953 A73-20724
- Impurity transport in a cylinder in the case of a time-dependent flow rate and gas exchange with the wall 08 p1022 A73-20998
- A unified view of the law of the wall using mixing-length theory. [AD-759043] 08 p0926 A73-21441
- Experimental study of the laminar-turbulent transition on a concave wall in a parallel flow 09 p1071 A73-22450
- Effect of jet turbulence on the flow in a wall boundary layer 10 p1205 A73-23586
- An experimental study of turbulent flow in pipes with artificial wall roughness 10 p1206 A73-24460

Two dimensional laminar boundary layer separation for unsteady flow or flow past moving walls, considering singularity due to bifurcating wake bubble 10 p1208 A73-24813

Some characteristics of the flow downstream of a blunt trailing edge in the presence of a neighbouring wall. 10 p1173 A73-24818

Study of the phase of the wall transfer of heat or mass in incompressible pulsed flow 10 p1297 A73-24850

A higher order theory for compressible turbulent boundary layers at moderately large Reynolds number. 11 p1346 A73-25218

On the turbulent thermal diffusion parallel to a plane wall for y/δ equals 2 to 300 11 p1451 A73-25870

On MHD flow along an infinite flat wall with constant suction. 11 p1405 A73-25975

Linear stability theory applied to stability characteristics of laminar condensate film flow along inclined wall, noting critical Reynolds number for disturbance amplification 12 p1559 A73-27697

Perforated water tunnel to decrease wall effect on deflected cavitation flow, studying suction coefficient, pressure losses and blowing parameters 13 p1597 A73-28450

Influence of wall proximity on hot-wire velocity measurements. 13 p1613 A73-28527

Equilibrium three-dimensional turbulent boundary layer on the end wall of a curved channel. 13 p1602 A73-29015

An approximate method for calculating the interaction between shock wave and turbulent boundary layer. 13 p1602 A73-29018

The switching of wall-reattachment fluidic devices. 13 p1571 A73-29041

Wall effects on the motion of a two-dimensional jet switching between two parallel flat plates. 13 p1571 A73-29043

Structure of the wall zone of a longitudinal dispersion flow over a plane plate 14 p1711 A73-30014

Experimental investigations regarding the behavior of turbulent boundary layers in the case of small periodic pressure changes 14 p1745 A73-30299

The calculation of low-Reynolds-number phenomena with a two-equation model of turbulence. 14 p1746 A73-30606

The theory of fluctuating flow fields near walls. 14 p1746 A73-30704

Use of surface fences to measure wall shear stress in three-dimensional boundary layers. 15 p1874 A73-31118

Effective-viscosity model for turbulent wall boundary layers. 15 p1860 A73-31119

Investigation of the stability of a hollow vortex bounded by a rigid wall 15 p1861 A73-31156

Supersonic flow along a wavy wall in a channel 15 p1823 A73-31332

Experimental investigation of the pressure distribution in constrained MHD flows past cylinders 15 p1917 A73-31401

Determination, by a wall probe, of the changing regime of the flow between two off-center cylinders with very close radii 15 p1863 A73-31568

Determination of the thickness of a wall layer by an approximate method in the presence of intense injection 15 p1876 A73-31861

On the polarographic measurement of the wall gradient of velocity in the upstream stagnation zone of detachment from the cylinder 15 p1878 A73-32209

Aerodynamic and thermal problems related to wall deformations 16 p2076 A73-32801

Calculation of wall corrections in a transonic wind tunnel 16 p1961 A73-32803

Qualitative study of flow deviation by a wall cavity 16 p1962 A73-32811

Experimental investigation of secondary instabilities in the unstable laminar boundary layer of a concave wall in parallel flow 16 p1999 A73-33247

Planar free convection flow over horizontal cylinders with a small Grashof number under the influence of a planar wall 16 p2085 A73-33254

A modified wall wake velocity profile for turbulent incompressible boundary layers. 17 p2150 A73-34439

Pressure distributions in porous ducts of arbitrary cross section. [ASME PAPER 73-FE-9] 17 p2152 A73-35008

- Application of the hydrogen-bubble technique for velocity measurements in thin liquid films.
[ASME PAPER 73-APM-8] 17 p2153 A73-35033
- Thin turbulent film analysis with approximation for relationship between flow and wall shear stress and effects of surface roughness and inertia at steps
[ASME PAPER 73-LUBS-17] 17 p2181 A73-35396
- Continuum mechanics analysis of solid particle suspension flow of viscous gas, noting demixed region near wall
17 p2156 A73-35508
- Experiments on confined turbulent jets in cross flow.
[AIAA PAPER 73-647] 18 p2260 A73-36202
- The singularity at boundary layer separation due to mass injection.
18 p2301 A73-36696
- Laminar boundary layers in low pressure argon plasma.
19 p2464 A73-37163
- On the flow of a nonequilibrium ionized gas past a wall in the presence of a magnetic field.
19 p2465 A73-37178
- The velocity profile in the wall region of a turbulent boundary layer
19 p2420 A73-37554
- Experimental study of turbulent flow in pipes with artificially roughened walls.
19 p2421 A73-38130
- Velocity distributions of rough wall turbulent boundary layers without pressure gradient.
19 p2422 A73-38284
- Stationary water flow stability through 90-deg bend with rectangular cross section, noting preserved laminar structure of flow along convex wall
20 p2549 A73-39565
- No-slip boundary condition origin for viscous incompressible Newtonian fluid flow over family of models for rough wall
20 p2549 A73-39810
- Contribution to the study of the development of a jet issuing from a nozzle of small elongation and confined between two lateral walls
21 p2677 A73-40620
- Creeping flow of Newtonian fluids in curved rectangular channels.
22 p2840 A73-41745
- High Reynolds number flow in a moving corner.
22 p2840 A73-41746
- Equations of the boundary perturbations of a cavity moving near a solid wall
22 p2841 A73-42124
- Turbulent boundary layer velocity distribution skewness and flatness factors over smooth wall compared with rough wall, discussing Reynolds shear stress fluctuations
22 p2842 A73-42231
- Experimental determination of the turbulent Prandtl number near a smooth wall
22 p2937 A73-42952
- Shear layer effect on acoustic duct wall impedance for sound propagation in uniform flow in terms of parabolic cylinder functions
22 p2900 A73-43138
- The effect of walls on the lifting force of a solid-foil wing
23 p2940 A73-43722
- Effect of wall conduction on convective heat transfer with laminar boundary layer.
23 p3049 A73-43833
- Stability of a flow bounded by elastic walls
24 p3079 A73-44898
- Investigation of the flow pattern in the wall region of a turbulent boundary layer during injection with a positive pressure gradient
24 p3079 A73-45080
- WALL JETS**
- Boundary-layer separation - Effect of low-speed wall jets.
01 p0030 A73-10047
- Plane flow past vortex of inviscid incompressible fluid jets bound by free surface and horizontal wall, considering complex potential function and submerged lifting airfoils
01 p0031 A73-10304
- Reynolds stresses and turbulent kinetic energy production in wall jets on flat and concave walls
01 p0034 A73-11357
- An experimental study of flow fields in bistable fluid amplifiers.
[ASME PAPER 72-WA/FLCS-9] 04 p0409 A73-15864
- Two dimensional semibounded jets in laminar and turbulent flows, discussing boundary layers skin and stream regions, step flow velocities, temperatures and self similar problems
07 p0811 A73-19612
- Central shock position in supersonic jet impinging on wall, noting flow velocity dependence on pressure
08 p0927 A73-21605
- An experimental investigation of three-dimensionality of wall jet flows.
08 p0956 A73-21831
- Calculation of turbulent boundary layers and wall jets over curved surfaces.
11 p1348 A73-26383
- Turbulent diffusion downstream of a linear source in a plane parietal jet
13 p1599 A73-28070
- Flow visualization of two and three dimensional wall jets on circular cylinder, observing flow characteristics sensitivity to curved boundary
13 p1603 A73-29038
- Interaction position and static pressure measurements of two opposing plane turbulent wall jets in still air in terms of frozen flow
15 p1863 A73-31342
- Film-cooling effectiveness in the near-slot region.
15 p1958 A73-32278
- An analytical model for the response of fluevic wall attachment amplifiers.
16 p1970 A73-33474
- Parametric analysis of turbulent wall jets.
19 p2376 A73-37491
- Unsteady heat transfer characteristics of a two dimensional laminar wall jet.
20 p2628 A73-39339
- Turbulent incompressible plane wall jet flow in still air, examining maximum velocity, total thickness and inner length scale with parametric analysis
21 p2678 A73-41191
- Output pressure-displacement and flow pattern characteristics of digital limit Schrenk, wall attachment and nozzle receiver fluidic switches
23 p2945 A73-43426
- Of fluid mechanics and fluidics and of analysis and physical insight.
23 p2945 A73-43432
- WALL PRESSURE**
- Separation of turbulent boundary layer - Wall pressure distribution near separation.
02 p0154 A73-12523
- Separated flow noise.
03 p0291 A73-12975
- Consideration of wall friction in the streamline procedure with the aid of a modified boundary layer calculation for laminar flows according to the momentum method
03 p0291 A73-13126
- Oblique shock wave interaction with approach boundary layer at combustor entrance in supersonic scramjet engines, observing wall pressure distribution [AIAA PAPER 72-1181] 03 p0357 A73-13476
- Influence of distributed grit-type roughness on the spectrum of wall pressure fluctuations of turbulent flow in a tube.
03 p0295 A73-14038
- Singular characteristics of turbulent wall pressure fluctuations associated with flow in a tube.
03 p0295 A73-14041
- Turbulence effect on wall pressure fluctuations.
04 p0403 A73-14939
- Motion of a fluid outside a turbulent jet system
07 p0812 A73-20091
- Study of the fluctuations of wall pressures in transonic flow on a cone-cylinder group presenting a constriction
10 p1173 A73-24825
- Wavevector/frequency spectrum of turbulent-boundary-layer pressure.
13 p1604 A73-29262
- Time dependent one dimensional Navier-Stokes differential equations solved via difference scheme, determining reflected shock wave structure and end wall pressure
16 p1999 A73-33251
- Procedure for the simulation of sonic fields, particularly for fatigue tests
16 p1997 A73-33384
- Two dimensional diffuser flow measurement and model calculation for curvature effects on wall pressure and boundary layer velocity distributions [ASME PAPER 73-FE-2] 17 p2152 A73-35002
- Aerodynamic sound and the low-wavenumber wall-pressure spectrum of nearly incompressible boundary-layer turbulence.
20 p2545 A73-39053
- The balance of turbulence energy and its components in incompressible turbulent boundary layers
20 p2546 A73-39096
- Correlation of hypersonic zero-lift drag data.
22 p2797 A73-42635
- WALL TEMPERATURE**
- Liquid- and wall-temperature calculations for a flow in tubes with allowance for heat losses into the ambient medium and for axial heat conductivity
01 p0122 A73-10860
- Temperature characteristics in the wall of an annular channel heated internally at supercritical pressures
01 p0123 A73-10861
- Scaling of performance and thermal environment in fuel-vortex cooled rocket engines.
[AIAA PAPER 72-1075] 03 p0354 A73-13399
- Heat transfer in the turbulent boundary layer of an incompressible fluid flow past a surface when the pressure gradient and temperature on the surface are variable
03 p0295 A73-13622
- German monograph - Propagation of ion acoustic waves in a weakly ionized plasma.
03 p0398 A73-13814
- Nonstoichiometric yttria crucibles for cold wall Ti melting, noting single batches, cost reduction and alloy homogeneity
04 p0455 A73-15749
- A proposed method for calculating film-cooled wall temperatures in gas turbine combustion chambers.
[ASME PAPER 72-WA/HT-24] 04 p0519 A73-15830
- Experimental investigation of worsened heat-transfer conditions with the turbulent flow of carbon dioxide at supercritical pressure.
06 p0766 A73-17410
- Heat transfer in the thermal entrance region of rectangular channels with a circumferential only partially heated
06 p0768 A73-17918
- Investigation of friction drag during gas flow in a tube with wall temperatures up to 2800 K
06 p0686 A73-18126
- Thermal boundary layer thickness for laminar forced convection to flat plates with uniform heating and uniform wall temperature.
06 p0769 A73-18260
- Thermal stresses in a spherical vessel filled with liquefied gas
07 p0917 A73-20507
- Reference temperature method for predicting turbulent compressible skin-friction coefficient.
08 p0925 A73-20722
- Heat transfer, adiabatic enthalpy /temperature/ of the wall, and hydrodynamic resistance associated with the turbulent and laminar flow of a compressible fluid in a circular tube.
08 p0954 A73-20858
- Variable properties laminar gas flow heat transfer in the entry region of parallel porous plates.
[AD-759455] 08 p1024 A73-21640
- Application of the method of Bhatnagar-Gross-Krook-Morse to the Knudsen layer of a polyatomic gas which is solidified or in equilibrium - Expression of discontinuities of wall temperatures
09 p1072 A73-23033
- Entrance region heat transfer between parallel plates with uniform wall temperature.
09 p1167 A73-23460
- Certain results of an experimental study of local heat transfer under supercritical pressure in a unilaterally heated rectangular channel
10 p1293 A73-23510
- Isothermal wall conical cavity radiant energy streaming, determining annular baffle effects by Monte Carlo method
10 p1295 A73-23835
- Experimental study of shock-wave reflection from a thermally accommodating wall.
11 p1449 A73-25252
- Transfer function model for analog simulation of transient unsteady heat conduction through flat and cylindrical walls, optimizing moving polymer film heating
11 p1451 A73-25732
- Forced convection heat transfer in laminar boundary layer at low Prandtl numbers.
11 p1452 A73-26123
- Initial conditions for the hypersonic-shock/boundary-layer interaction problem.
11 p1303 A73-26384
- Effects of upstream wall temperatures on hypersonic tunnel wall boundary-layer profile measurements.
11 p1344 A73-26395
- Liquid and wall temperature during flow in tubes with heat loss to the surrounding medium and axial heat conduction.
12 p1560 A73-27909
- Temperature conditions at the wall of an annular channel with internal heating at supercritical pressures.
12 p1560 A73-27910
- Increase of boundary-layer heat transfer by mass injection.
13 p1706 A73-28816
- Construction of solutions for the equations of a compressible laminar boundary layer on a plate with abruptly changing boundary conditions
13 p1567 A73-29408
- Artificial viscosity related to shocks for studying anomalous wall heating and solution behavior at interface by substituting Rankine-Hugoniot equation
14 p1775 A73-30908
- Calculation of a subsonic radiating gas flow by an adjustment method
15 p1821 A73-30969
- Time required for the destruction of a nonuniformly heated wall
15 p1953 A73-32098
- A theoretical analysis of the recovery factor for high-speed turbulent flow.
15 p1865 A73-32280
- Results of an experimental investigation of local heat transfer at supercritical pressure in a rectangular channel heated from one side.
17 p2255 A73-35190
- Turbulent free convection in a boundary layer with variable wall temperature
18 p2301 A73-36815

WALL TEMPERATURE DISTRIBUTION

- Laminar boundary layers along an infinite flat plate with oblique suction. 19 p2420 A73-37646
- Thermal stresses in spherical reservoirs while filling with liquefied gas. 19 p2499 A73-37782
- Heat transfer in the case of turbulent and laminar trickle films 19 p2505 A73-38477
- Study of turbulent transfer with strong injection, longitudinal pressure gradient and nonisothermicity. 20 p2547 A73-39421
- The turbulent boundary layer with stepwise varying boundary conditions at a permeable surface. 20 p2628 A73-39423
- Effectiveness of film cooling of an adiabatic wall downstream of the perforated section. 20 p2628 A73-39424
- Heat release by free convection from horizontal cylinders to CO₂ under near-critical conditions 20 p2628 A73-39613
- Asymmetric heat transfer in turbulent flow through a plane slot 21 p2790 A73-40398
- Improvement to Klineberg's method for the calculation of viscous-inviscid interactions in supersonic flow. 21 p2632 A73-40429
- Large scale heat transfer in turbulent boundary layer at heated flat plate in incompressible viscous fluid, discussing temperature fluctuation spatial correlation as function of wall law and flow core 21 p2678 A73-41062
- Influence of the wall temperatures of gauges on the measurement of limit pressures 22 p2852 A73-41870
- Reflection of a shock wave from a thermally accommodating wall - Molecular simulation. 22 p2842 A73-42234
- Thermal response of an unsteady laminar boundary layer on a flat plate due to step changes in wall temperature and in wall heat flux. 23 p3049 A73-43802
- Hot plasma in contact with cold wall, calculating dynamic behavior in magnetic field from numerical solution of one-fluid two-temperature equations 24 p3117 A73-45456
- The incompressible boundary layer of higher order at the axisymmetrical stagnation point in the case of strong suction or blowing 24 p3056 A73-45545

WALL TEMPERATURE DISTRIBUTION

U TEMPERATURE DISTRIBUTION

U WALL TEMPERATURE

WALLOPS ISLAND

- Organization and operations at National Aeronautics and Space Administration Wallops Station. 14 p1741 A73-30078

WALLS

- NT POROUS WALLS
- NT THICK WALLS
- NT THIN WALLS
- NT WIND TUNNEL WALLS
- Line and rectangular plane finite element models for accurate and efficient dynamic vibration frequency analysis of frames and shear walls respectively 13 p1700 A73-29377

WALSH FUNCTION

- Comparison of digital-signal multiplexing methods by means of sequencing 01 p0021 A73-11485

- Digital multiplicity filters analysis via Walsh functions, considering time discrete dyadic invariant systems 09 p1065 A73-23111

- Nonsinusoidal EM waves - State of development 19 p2403 A73-37432

- Signal theory problems of discrete signal representation decomposition and characterization by Walsh and orthogonal functions, noting voiced speech analysis 23 p2952 A73-43309

WANKEL ENGINES

- One dimensional model for spark ignition Wankel engine combustion, presenting unsteady turbulent flame propagation equations 09 p1136 A73-22824

WARFARE

NT ANTISUBMARINE WARFARE

NT COMBAT

- Electronic warfare tactics against remotely piloted unmanned aircraft used for reconnaissance or weapons delivery, considering onboard countermeasures 04 p0418 A73-15379

WARHEADS

- Russian book - Physical principles of rocket weaponry. 15 p1944 A73-32419

WARMING

U HEATING

WARNING DEVICES

U WARNING SYSTEMS

WARNING SIGNALS

U WARNING SYSTEMS

WARNING SYSTEMS

- Manoeuvre in response to collision warning from airborne devices. 01 p0074 A73-10349

- Laser system for fire detection based on induced air refractive index changes and smoke induced light transmission loss, using photocell detectors 06 p0699 A73-17751

- Ground based and airborne collision avoidance systems comparison, discussing interrogator/transponder concept, pilot warning indicator, and air traffic handling capacity and economics 07 p0848 A73-18900

- The ABC method of providing warning of an impending solar flare. 07 p0899 A73-19941

- Aircraft wake vortex avoidance systems with current locus detection and/or prediction capability, discussing design based on hazard assessment and computer simulation for performance 10 p1172 A73-24557

- Electronic safety test replaces radioactive test source. 14 p1712 A73-30928

- Survival and Flight Equipment Association, Annual Symposium, 10th, Phoenix, Ariz., October 2-5, 1972, Proceedings. 16 p1965 A73-32653

- Behavioral stress response related to passenger briefings and emergency warning systems on commercial airlines. 16 p1965 A73-32660

- USAF Airborne Warning and Control System with overland downlook Doppler radar for low-fly aircraft detection in severe clutter environment, discussing design and performance 17 p2121 A73-34371

- A new approach to aircraft exterior lighting. 17 p2108 A73-35808

- Behavioral stress response RE - Passenger briefings and emergency warning systems on commercial airlines. 18 p2285 A73-36922

- Aircraft wake vortex detection and avoidance systems, examining acoustic sensors, bistatic Doppler sensors, pulsed radar, aircraft spacing techniques and ground wind measurement 19 p2452 A73-37823

- Air based collision avoidance system feasibility appraisal, discussing YG1054 proximity warning indicator, cost analysis and implementation prognosis 19 p2454 A73-38468

- A visual detection simulator /VDS/ for pilot warning instrument evaluation. 21 p2672 A73-40864

WASHING

- Evaluation of 165 deg F reverse osmosis modules for wastewater purification. 19 p2399 A73-37964

- Reverse osmosis for wash water recovery in space vehicles. 19 p2399 A73-37971

WASHOUT [RADIOACTIVITY]

U FALLOUT

WASPALOV

- The dependence of the notch sensitivity of Waspalov at 1000-1400 deg F on the gamma prime phase. 08 p0979 A73-21571

WASTE DISPOSAL

- Ni-base alloy powder metallurgy from production waste cuttings by oxidation and subsequent oxide reduction with hydrogen and calcium hydride 12 p1503 A73-27553

- Trash management during Skylab and long duration missions with compactors, autoclaves, biocides and isotope powered water recovery/waste management systems 19 p2401 A73-37986

- Zero-gravity and ground testing of a waste collection subsystem for the Space Shuttle. 19 p2401 A73-37989

- The transportation of highly active nuclear waste products to the sun 20 p2590 A73-39148

WASTE UTILIZATION

- Advanced methods of recovery for space life support systems. 19 p2398 A73-37711

- Waste Management System overview for future spacecraft. 19 p2400 A73-37974

- Reverse osmosis for recovering and recycling water in Space Station Prototype Environmental Thermal Control/Life Support System Integrated Water and Waste Management 19 p2400 A73-37978

- The availability and cost of curium-244 from power reactor fuel reprocessing wastes. 19 p2457 A73-38430

- Recovery of nonferrous metals from scrap automobiles by magnetic fluid levitation. 22 p2878 A73-42531

WASTES

NT HUMAN WASTES

NT METABOLIC WASTES

NT RADIOACTIVE WASTES

NT URINE

WATCHES

U CLOCKS

WATER

NT COASTAL WATER

NT COLD WATER

NT GROUND WATER

NT HEAVY WATER

NT POTABLE WATER

NT SEA WATER

NT SHALLOW WATER

- The effect of solar radiation reflected from water surfaces on airborne and surface measurements in the thermal infrared. 01 p0038 A73-10385

- Heat transfer as function of temperature on small horizontal wires in water and organic liquids noting application for heater low gravity behavior prediction 01 p0122 A73-10801

- Experimental investigation of the evaporation rate of water droplets in atmospheres of air and carbon dioxide under conditions of a thermostatic droplet surface 04 p0517 A73-14881

- Longitudinal rolls and Benard cells in water layer natural convection, predicting wavelength-depth relations and Rayleigh numbers for comparison with experiments 06 p0684 A73-17623

- [AIAA PAPER 73-42] A dual polarization laser backscatter system for water quality studies. 06 p0700 A73-18306

- Laboratory determinations of water surface emissivity. 06 p0691 A73-18713

- Mariner spacecraft photographed Mars surface volcanic mountains and water in polar caps, suggesting recurring rainfall and rivers during successive interglacial periods 07 p0875 A73-19166

- Role of water in the evolution of the lunar crust: An experimental study of sample 14310 - An indication of lunar calc-alkaline volcanism. 07 p0880 A73-19691

- Restrictions on the intensity of cosmic masers and the possibility of detecting new OH and H₂O sources in a rapid sky survey 10 p1275 A73-23725

- Optical constants of water in the 200-nm to 200-micron wavelength region. 11 p1350 A73-25060

- Electron impact excitation of H₂O. 12 p1526 A73-27687

- Isotope separation factor of carbon dioxide-water system and isotopic composition of atmospheric oxygen. 15 p1873 A73-32252

- Criteria for the existence of H₂O crystals on Mars 16 p2069 A73-33836

- Silicates and water identification in interstellar grains, considering possibility of iron and carbon components 17 p2227 A73-34410

- Constraints on cosmic maser intensity, and the possibility of detecting new OH and H₂O radio sources by a rapid sky survey. 18 p2355 A73-36750

- The steady-state thickness of a liquid water film on the surface of hailstones of various shapes 21 p2730 A73-40118

- Indices of backscattering and attenuation of light by a water aerosol 21 p2731 A73-40747

- Water damage in polyester/glass laminates. II - Microscopic evidence. 21 p2723 A73-40921

- Calibration of capsule platinum resistance thermometers at the triple point of water. 22 p2857 A73-42027

- Water condensation coefficient for 3-micron radius droplets, noting expected error confirmation with standard deviation in experiment 22 p2883 A73-42548

- High altitude infrared spectroscopic evidence for bound water on Mars. 24 p3127 A73-44395

- Influence of the microstructure of water aerosol on the phase function, its asymmetry, and polarization of scattered light 24 p3084 A73-44963

- Bending potential of an H₂O molecule. 24 p3113 A73-44977

- Dipole moment of water from Stark measurements of H₂O, DHO, and D₂O. 24 p3113 A73-44978

- Charge transfer from a highly electrically stressed water surface during drop impact. 24 p3108 A73-45206

WATER BALANCE

- Water-salt homeostasis mathematical model, solving equations with analog and digital computers 10 p1184 A73-23941

Responses of men and women to two-hour walks in desert heat. 20 p2518 A73-39784

Multispectral remote sensing of elements of water and radiation balances. 20 p2558 A73-39864

Russian book - Mutual relationship of water and salt secretion functions in digestive and excretory organs under conditions of high temperature. 21 p2641 A73-41438

Effect of altitude on renin-aldosterone system and metabolism of water and electrolytes. 22 p2806 A73-42420

An analogue-computer simulation of the facultative water-reabsorption process in the human kidney - A vascular role for a.d.h. 22 p2815 A73-42668

Energy balance and change in body weight and body water in man during a 2-day cold exposure. 24 p3060 A73-45059

WATER CIRCULATION
NT OCEAN CURRENTS
NT WATER CURRENTS
WATER COLOR

Remote sensing of ocean color as an index of biological and sedimentary activity. 18 p2307 A73-36030

WATER CONSUMPTION

The effect of prolonged immobilization on diuresis and water intake in rats. 11 p1320 A73-26489

The role of the amygdaloid nuclei in the regulation of water intake. 21 p2636 A73-40278

WATER CONTENT
U MOISTURE CONTENT
WATER CURRENTS
NT OCEAN CURRENTS

Shallow lake or sea with large class of bottom topographies, obtaining wind-driven current analytic solution with conformal mapping technique. 21 p2686 A73-41015

WATER DEPRIVATION

Survival of soil bacteria during prolonged desiccation. 14 p1720 A73-30959

WATER EROSION

Resistance to hydroerosion of hard-faced maraging steels. 06 p0706 A73-17881

The erosion of carbon fibre reinforced plastic by repeated liquid impact. 07 p0843 A73-20224

Test rails possibilities for rain erosion phenomena study on aircraft or missile structures. 11 p1335 A73-25296

Airliner radomes erosion by atmospheric precipitation, water penetration, icing, bird and stone impact and lightning. 11 p1335 A73-25297

Rain-erosion resistance and other properties of Schott infrared-transmitting glasses. 11 p1387 A73-25299

Aircraft and missile radomes technology in France, discussing materials, antenna radiation pattern calculation, computer programming for transmission and angular aberrations, and raindrop erosion tests. 11 p1336 A73-25301

Space shuttle lightweight thermal protective insulation materials rain erosion resistance determination at 200-400 MPH and various angles of attack, using rotating arm test apparatus. 16 p2071 A73-33030

Rain erosion of reinforced plastics for aerospace applications in terms of drop size, impact angle and velocity effects and protective coatings. 17 p2195 A73-34806

Lubricant testing as an aid to bearing damage analysis. [ASLE PREPRINT 73AM-3B-1] 17 p2178 A73-34983

Lunar sinuous rilles as inverted eskers formed by volatiles /water and carbon dioxide/ moving in channel between basement surface and permafrost layer. 17 p2237 A73-35859

Radiative property degradation of water impinging on thermally-controlled surfaces under space conditions. [AIAA PAPER 73-733] 18 p2336 A73-36350

Water and processes of degradation in the Martian landscape. 19 p2477 A73-37202

Scaling relations to predict size of submarine generated wake in stratified water flow, measuring velocity and temperature profiles [AIAA PAPER 73-108] 06 p0644 A73-17644

Spatial stability of stagnation water boundary layer with heat transfer. 07 p0919 A73-19503

Liquid and gas flow visualization methods, discussing water tests and hydraulic analogies [ONERA, TP NO. 1222] 10 p1172 A73-23864

State of art of water flow measurement by weirs and flumes in artificial channels. 10 p1221 A73-24854

Experimental investigation of hydrodynamic stability at rigid and elastic-damping surfaces. 11 p1349 A73-26440

Finite element method applied to analysis of flow over a spillway crest. 13 p1563 A73-28078

Rain fall deceleration effect on flow velocity of infinitely deep water mass, solving Navier-Stokes equations via Laplace transforms. 13 p1600 A73-28419

Vortex core precession in water or air high swirl flows above critical Reynolds number. 13 p1602 A73-29017

Interpretation of hot-film anemometer response in a non-isothermal field. 13 p1620 A73-29256

Light beam absorption correlation with axial dispersion of ink injected into turbulent water flow in pipe. 17 p2156 A73-35509

Techniques for studying the aerodynamic characteristics of the bronchial tree of man. 18 p2282 A73-36576

Water resources systems modelling today and its research opportunities. 19 p2426 A73-38074

Stationary water flow stability through 90-deg bend with rectangular cross section, noting preserved laminary structure of flow along convex wall. 20 p2549 A73-39565

Experimental determination of the turbulent Prandtl number near a smooth wall. 22 p2937 A73-42952

Gaseous fuel combustion in water flow by introducing fuel-oxygen mixture in stagnation region behind body for flame stabilization. 24 p3158 A73-45386

WATER INJECTION

Air/water mist spray coolant for high gas temperature and pressure environment at gas turbine inlet. 17 p2221 A73-34388

WATER JETS
U HYDRAULIC JETS
WATER LANDING
NT DITCHING [LANDING]

Two dimensional wedge flow singularities for free and fixed boundaries at flow separation points, applying to water entry problem. 16 p1999 A73-32928

Preliminary results from dynamic model tests of an air cushion landing system. 19 p2382 A73-37694

WATER MANAGEMENT

Multipurpose properties and conflict situations in automatic control systems. 16 p1992 A73-33666

Reverse osmosis for recovering and recycling water in Space Station Prototype Environmental Thermal Control/Life Support System Integrated Water and Waste Management [ASME PAPER 73-ENAS-22] 19 p2400 A73-37978

Water resources systems modelling today and its research opportunities. 19 p2426 A73-38074

ERTS-1 multispectral scanner analysis of Kansas reservoirs color and water content, discussing turbidity, gray coloration levels, water management possibilities and water sample data. 20 p2563 A73-39912

Assessment of applications of space-borne remote sensing to hydrology and water resources - An overview. 21 p2686 A73-40832

WATER POLLUTION

Legal aspects of water pollution detection through remote sensing. 05 p0642 A73-17138

Airborne remote sensing for forestry and agricultural land imagery and water pollution detection, discussing use of color films and picture processing. 17 p2161 A73-34933

The use of satellites for remote sensing of the sea surface. 17 p2162 A73-34956

Oil spills - Measurements of their distributions and volumes by multifrequency microwave radiometry. 17 p2164 A73-35806

Environmental considerations for offshore airports. 19 p2417 A73-37742

Microbial contamination of water - Traditional and space-age problems and approaches. [ASME PAPER 73-ENAS-33] 19 p2395 A73-37988

Contributions of the DFVLR to environmental research and environment protection. II - Noise control, water environment protection, nature and landscape, environmental protection techniques. 19 p2506 A73-38266

Remote sensing applications in the Metropolitan Washington Council of Governments. 20 p2556 A73-39833

Multispectral survey of power plant thermal effluents in Lake Michigan. 20 p2558 A73-39862

Water quality determinations in the Virgin Islands from ERTS-A data. 20 p2558 A73-39867

Polarization - A key to an airborne optical system for the detection of oil on water. 23 p2979 A73-43225

WATER PRESSURE

Thermo-acoustic oscillations in forced convection heat transfer to supercritical pressure water. 08 p1022 A73-21253

WATER PURIFICATION
U WATER TREATMENT
WATER QUALITY

Development of a practical remote sensing water quality monitoring system. 20 p2567 A73-39830

Water quality determinations in the Virgin Islands from ERTS-A data. 20 p2558 A73-39867

WATER RECLAMATION

Progress in the development of the reverse osmosis process for spacecraft wash water recovery. 02 p0137 A73-11993

Effectiveness of the application of tightly bonded sulfo-cation exchange resins in water recycling by the sorption method. 06 p0656 A73-17677

Advanced methods of recovery for space life support systems. 19 p2398 A73-37711

Design considerations for space mission wash water processing by reverse osmosis. 19 p2493 A73-37965

[ASME PAPER 73-ENAS-3] 19 p2493 A73-37965

Development of sulfonated polyphenylene oxide membranes for the reverse osmosis purification of wash water at sterilization temperatures /165 F/. [ASME PAPER 73-ENAS-16] 19 p2399 A73-37973

NS-1 membranes - Potentially effective new membranes for treatment of wastewater in space cabins. [ASME PAPER 73-ENAS-19] 19 p2400 A73-37975

Hyperfiltration technique applied to wash water reclamation at elevated temperatures. [ASME PAPER 73-ENAS-27] 19 p2400 A73-37982

Trash management during Skylab and long duration missions with compactors, autoclaves, biocides and isotope powered water recovery/waste management systems. [ASME PAPER 73-ENAS-31] 19 p2401 A73-37986

WATER RECOVERY
U WATER RECLAMATION
WATER RESOURCES

Remote sensing applications in agriculture and forestry including land inventories, soil classification and water resources detection. 17 p2162 A73-34948

Applications of the ERTS-1 satellite in remote sensing of water resource data in Canada. 18 p2307 A73-36026

WATER TEMPERATURE

Optical method for studying the heat transfer mechanism in bubble boiling. 13 p1708 A73-29173

Isothermal mapping of temperature patterns from thermal discharges in Italian coastal waters. 20 p2560 A73-39888

Remote measurement of subsurface sea water temperature by airborne Raman scattering with cross polarizer in front of light source and detector, noting precision. 20 p2568 A73-39889

Improvements brought to the measurement of the ocean surface temperature by utilization of a polarizing infrared radiometer. 21 p2698 A73-40142

A direct comparison of satellite and aircraft infrared /10 to 12 microns/ remote measurements of surface temperature. 22 p2850 A73-42729

Aquatic and diving mammals in fresh water and marine environments, discussing aquatic thermal conditions, body temperature distribution, thermoregulation, metabolic heat production, etc. 22 p2809 A73-42861

WATER TREATMENT

Chlorination studies. I - The reaction of aqueous hypochlorous acid with cytosine. 02 p0139 A73-12631

Radiation-induced oxidation of impurities in the water obtained from human moisture-containing bioactivity products. 08 p0933 A73-20984

WATER TUNNELS

Investigation of the disinfecting properties of sorbents which are used in a spacecraft life support system

17 p2114 A73-34240

Advanced methods of recovery for space life support systems.

19 p2398 A73-37711

Evaluation of 165 deg F reverse osmosis modules for wastewater purification.

[ASME PAPER 73-ENAS-2] 19 p2399 A73-37964

Design considerations for space mission wash water processing by reverse osmosis.

[ASME PAPER 73-ENAS-3] 19 p2493 A73-37965

Reverse osmosis for wash water recovery in space vehicles.

[ASME PAPER 73-ENAS-12] 19 p2399 A73-37971

Development of sulfonated polyphenylene oxide membranes for the reverse osmosis purification of wash water at sterilization temperatures /165 F/.

[ASME PAPER 73-ENAS-16] 19 p2399 A73-37973

NS-1 membranes - Potentially effective new membranes for treatment of wastewater in space cabins.

[ASME PAPER 73-ENAS-19] 19 p2400 A73-37975

Microbial contamination of water - Traditional and space-age problems and approaches.

[ASME PAPER 73-ENAS-33] 19 p2395 A73-37988

Eutrophication assessment using remote sensing techniques.

20 p2558 A73-39861

WATER TUNNELS

U HYDRAULIC TEST TUNNELS

WATER VAPOR

Line-by-line computations of transmittance for non-homogeneous paths in designing application-oriented representations for water vapor and carbon dioxide channels IR spectral responses

01 p0037 A73-10365

Precipitable water vapor temperature-geopotential height profiles from satellite IR spectrometer /SIRS/ measurements, using stepwise regression technique

01 p0073 A73-10380

Rates of clustering of oxygen negative ions with water vapor.

01 p0014 A73-10902

Mars polar caps formation at aerographic latitudes, assuming water vapor condensation on ground and water presence in carbon dioxide snow

01 p0106 A73-11322

Influence of geometrical parameters on the energetic separation of superheated water vapor in a conical vortex tube

02 p0153 A73-11789

Microwave radiometric measurements of atmospheric temperature and water from an aircraft.

02 p0164 A73-12361

Investigation of the radio wave absorption spectrum of atmospheric water vapor in the 1.15 to 1.5-mm range

02 p0142 A73-12487

Search for OH-IR stars with emission concentrated in main lines, considering water vapor line emission or absorption band in near IR

02 p0222 A73-12717

Gain and frequency characteristics of a 20 mW C.W. water vapour laser oscillating at 118.6 microns.

02 p0177 A73-12724

Gas-temperature measurement in pulsed H₂O laser discharges.

[AD-755012] 02 p0178 A73-12814

Solar spectra line intensities in band 201 of visible and near IR regions, noting water vapor bands presence in sunspot spectra

03 p0377 A73-14412

Venus atmosphere water vapor content from IR spectra observed by airborne Fourier interferometric spectrometer, discussing different models for abundance

06 p0744 A73-17434

Dynamics of moisture diffusion through a partially liquid filled porous matrix.

06 p0649 A73-18259

Lunar water vapor spectra during Apollo 14 ALSEP suprathermal ion detector experiment /SIDE/ and total ion detector /TID/ observations

07 p0891 A73-19829

On calculating the radiation from two plane isothermal layers of carbon dioxide and/or water vapor.

08 p1021 A73-20859

Radiation absorption calculation for nonisothermal gas containing combustion products, noting approximation for water vapor radiation

08 p1021 A73-20860

Absorption measurements of carbon monoxide laser radiation by water vapor.

08 p0974 A73-21033

Determination of the statistical characteristics of temperature fluctuation in pool boiling.

08 p1022 A73-21252

Direct measurement of water vapor absorption of solar radiation in the free atmosphere.

08 p0985 A73-21389

Destabilization of vapor film boiling around spheres.

08 p1024 A73-21641

Pulsed and CW water vapor lasers, investigating He addition effects on time-varying gas temperature and power output

[AD-760377] 09 p1091 A73-22082

Exchange of water vapor between the atmosphere and surface of Mars.

09 p1145 A73-22270

Leakable gases and water vapor loss rates and service life predictions for sealed alkaline cells in vacuum or aerospace environments, using mass transfer equations

[ECS PAPER 32] 11 p1307 A73-24973

Seasonal variations in the telluric lines of oxygen and water vapor

11 p1392 A73-25614

Water vapor lines controlled atmospheric absorption spectrum in 220 GHz window region, discussing approximate calculation for submillimeter lines residual effect

11 p1330 A73-25688

Analysis of external mass transfer and choice of its parameters for convective removal of reaction-product vapors in a hydrogen-oxygen fuel cell with a capillary membrane

11 p1308 A73-25727

Features of the mechanism of vapor condensation from humid air in narrow channels and the hydrodynamics of two-phase flow during droplet condensation

11 p1451 A73-25735

Effect of water vapor on fatigue behavior of an aluminum-boron composite.

11 p1383 A73-25828

The absorption spectrum of atmospheric water vapor in the vicinity of the He 10830 A triplet.

11 p1421 A73-25933

Optical absorption cell with water vapor cross flow instrument designed for wall decontamination and open air meteorological simulation, examining thermodynamic parameters effects

11 p1367 A73-26318

Preliminary measurement data on the H₂O content of the Martian atmosphere from the Mars-3 automatic interplanetary station

12 p1540 A73-27451

Gasdynamic laser with a high water vapor content.

12 p1507 A73-27510

The determination of the evaporation from a class-A pan by means of empirical evaporation formulas

13 p1653 A73-28746

Rotational spectral lines of water vapor dimers in the upper troposphere

13 p1609 A73-29152

Orange colored lunar soil from Shorty crater associated with volcanic fumarolic activity of water vapors reacting with lava

14 p1789 A73-29721

Rocket-based mass spectrometric measurements of midlatitude and north polar region ionospheric ion composition, discussing ionization of water and heavy water vapors

14 p1747 A73-29864

Distribution of water vapor in the stratosphere as determined from balloon measurements of atmospheric emission spectra in the 24- to 29-micron region.

14 p1749 A73-30160

Effect of H₂O, SF₆ and CCl₃F additions on the electron concentration in highly heated air

15 p1840 A73-31852

Determination of atmospheric water-vapor densities from measurements of the 6943.8-A absorption line strength.

15 p1845 A73-32227

Water vapor from a lunar breccia - Implications for evolving planetary atmospheres.

16 p2060 A73-33124

High altitude aircraft water vapor measurements using aluminum oxide hygrometer, noting comparison with remote sounders

[AIAA PAPER 73-511] 16 p2006 A73-33549

Radiometric observations of atmospheric water vapor injection by thunderstorms.

[AIAA PAPER 73-512] 16 p2006 A73-33550

Correction of electrical path length by passive microwave radiometry.

16 p1983 A73-33729

Role of water vapor in the meteorology of Mars

16 p2069 A73-33831

Balloon-borne phosphoric anhydride electrolytic gage measurement of water vapor mixing ratio to 35 km, noting decrease to minimum near tropopause

16 p2008 A73-33884

The effects of water vapor and oxides of nitrogen on the ozone and temperature structure of the stratosphere.

17 p2160 A73-34857

Study of the conditions defining the passivating action of surface-active substances on hygroscopic condensation nuclei

18 p2332 A73-35918

Atomic hydrogen and water vapour in the lower arctic thermosphere during geomagnetic storm and PCA event.

18 p2310 A73-36141

Causes of changes in the properties of resite in aqueous and alkaline media

18 p2328 A73-36822

Interrelationship between developments of synoptic processes and evolution of the integral moisture field according to satellite measurements.

18 p2334 A73-37065

Ignition limit of metallic particles in a mixture of two oxidizers

19 p2503 A73-37511

Water masers in a protostellar gas cloud.

19 p2483 A73-37573

A study of the CW 28-micron water-vapor laser.

19 p2438 A73-38270

Combined forced convection and radiation heat transfer in the thermal entrance region of a non-isothermal parallel plate channel - Optical thin gases.

[ASME PAPER 73-HT-14] 20 p2625 A73-38566

Effect of water vapor on output power of CO₂ gas-dynamic laser.

20 p2573 A73-39300

Correlation between output power and composition of discharge products in a water vapor laser.

20 p2574 A73-39699

Growth mechanism of charged ice crystals in water vapor

21 p2742 A73-40123

Evaporation of a water drop

21 p2791 A73-40745

Observations of far infrared atmospheric windows at 44/cm and 50/cm from Pikes Peak.

21 p2780 A73-41647

Preliminary results of measurements of the H₂O content of the Martian atmosphere by the unmanned spacecraft Mars 3.

22 p2905 A73-41806

Observations of water vapor ions at the lunar surface.

23 p0301 A73-43764

Atmospheric water vapor concentration in upper stratosphere above tropopause from balloon observations of solar IR absorption spectra

23 p2976 A73-43890

The effects of water vapour and oxides of nitrogen on ozone and temperature structure of the stratosphere.

23 p2977 A73-43900

Development of an H₂O atmosphere around Comet Kohoutek /1973f/ and its possible detection.

23 p0303 A73-43950

Experimental investigation of transient supersaturations in a thermal diffusion chamber.

23 p3004 A73-44250

Martian W cloud diurnal brightening observation by Mariners 6 and 7 flyby missions, considering probable water ice formation

24 p3128 A73-44390

An expanded theoretical interpretation of the Venus 1.05-micron CO₂ line and the Venus 0.8226-micron H₂O line.

24 p3139 A73-45000

Strengths and air-broadened widths of H₂O lines in the 2950 to 3400 per cm region.

24 p3066 A73-45320

WATER VEHICLES

NT AIRCRAFT CARRIERS

NT CARGO SHIPS

NT NUCLEAR POWERED SHIPS

NT SATELLITE COMMUNICATIONS SHIPS

NT SHIPS

NT SUBMARINES

NT TANKER SHIPS

WATER WAVES

Heaving and pitching response of a hovercraft moving over regular waves.

01 p0004 A73-10700

Doppler spectral width of radar signal reflected from sea surface as function of illuminated region dimensions, waviness scale and emission factors

04 p0423 A73-15900

Frequency spectra of the inner and outer structures of wind waves at different stages of wave development

05 p0594 A73-17320

Study of the surface layer of drift currents in the laboratory

08 p0985 A73-21400

Intermittence effects in the equilibrium range of developing wind waves

08 p0986 A73-21400

Group velocity and nonlinear dispersive wave propagation.

10 p1249 A73-24770

Experiments in the determination of turbulent layer thickness in monochromatic-type waves

13 p1655 A73-29100

Bragg diffraction of light by two orthogonal ultrasonic waves in water.

15 p1914 A73-32210

Korteweg-de Vries equation solution for long nonlinear wave amplification and decay in rotating stratified fluids with application to shallow water waves

16 p1998 A73-32770

Optical wave measurement technique and experimental comparison with conventional wave height probes.

19 p2458 A73-37263

Reconstruction of surface-wave fields in liquids with the aid of holographic methods

19 p2431 A73-38158

Relationship between sea wave parameters and the spectra of aerial photography and radar imagery of sea surface.

20 p2531 A73-39891

Two frequency radar interferometry applied to the measurement of ocean wave height.

22 p2843 A73-41832

WATERPROOFING

An advanced printed circuit board system having outstanding resistance to humid environments.

03 p0281 A73-13047

Performance of a water-repellent radome coating in an airport surveillance radar.

21 p2648 A73-40101

WATTMETERS

Problem of using the magnetoresistance effect to measure transferred SHF power

01 p0023 A73-10215

WAVE AMPLIFICATION

Amplification of signal by Cerenkov resonance interaction.

04 p0415 A73-14958

Comparison between a Hall configuration and a Corbino configuration for the amplification of ultrasonic waves

07 p0864 A73-20613

Nonlinear theory of plasma heating by parametric instabilities.

[TTU-SR-2]

09 p1128 A73-22633

Stimulated emission of acoustic power as analog to lasers and masers, noting nonpreservation of phase between incident and stimulated pressure

10 p1249 A73-24388

Wave amplification during the reflection from a rotating 'black hole'

10 p1283 A73-24752

Absorption and amplification of electromagnetic waves in a nonstationary magnetoactive plasma with allowance for spatial dispersion

11 p1405 A73-26151

Amplification of a travelling wave in a non-homogeneous elastic medium.

11 p1400 A73-26407

The theoretical situation with the investigations of parametric instabilities in gaseous plasmas.

[IPPCZ-167]

12 p1528 A73-27432

Amplification of cylindrical electromagnetic waves reflected from a rotating body.

14 p1728 A73-30333

Korteweg-de Vries equation solution for long nonlinear wave amplification and decay in rotating and stratified fluids with application to shallow water waves

16 p1998 A73-32795

Space probe observed VLF hiss powers disparity with theoretical prediction for incoherent Cerenkov radiation, considering Landau instability generated wave amplification

17 p2160 A73-34788

The theoretical situation with the investigations of parametric instabilities in gaseous plasmas.

20 p2597 A73-39195

Amplification of backscattering by bodies placed in a medium with random inhomogeneities

21 p2657 A73-41513

Amplification of electromagnetic and gravitational waves during scattering on a rotating black hole

23 p0304 A73-44008

WAVE ATTENUATION

NT ACOUSTIC ATTENUATION

NT MANDELSTAM REPRESENTATION

NT RADAR ATTENUATION

NT RADIO ATTENUATION

NT SHOCK WAVE ATTENUATION

Role of trapped particles in plasma waves and instabilities.

02 p0197 A73-12067

Alfven waves nonlinear damping mechanism due to magnetosonic wave dissipation, presenting nonlinear coupling rates

02 p0217 A73-12401

Field distribution formulas for fast wave attenuation in thin walled tubular dielectric waveguide within external absorbing diaphragms

02 p0142 A73-12495

Equations of motion in electrohydrodynamics of multiphase one dimensional flow, noting shock wave propagation and attenuation

03 p0346 A73-13611

Far field solution for stress wave attenuation and dispersion in composite materials, noting pulse shape

05 p0633 A73-16540

Effect of bulk-reacting liners on wave propagation in ducts.

[AIAA PAPER 73-227]

05 p0566 A73-16952

Radiation field in a scattering medium after a long time interval following exposure to a light pulse

05 p0599 A73-17354

Nonlinear damping of potential monochromatic waves in inhomogeneous plasma, obtaining resonance particle distribution function

06 p0728 A73-17967

Damping of an ion acoustic wave in a weakly ionized plasma

06 p0730 A73-18460

Resonator polarization parameters effect on backward wave attenuation in three and four mirror TW ring laser, noting colliding waves intensity dependence on polarization angle

06 p0703 A73-18619

Wave attenuation in superconducting elliptical waveguides

07 p0793 A73-19924

The theory of a coaxial gas-discharge oscillator loaded by a helical line.

07 p0801 A73-20138

Collision absorption of a rapid hydromagnetic wave in a plasma of two kinds of ions - Experiment

07 p0859 A73-20149

Measurement of the attenuation of an electromagnetic wave in a bounded hot electron plasma.

07 p0860 A73-20478

Comparison between a Hall configuration and a Corbino configuration for the amplification of ultrasonic waves

07 p0864 A73-20613

Fast wave propagation and damping at the second harmonic of the ion cyclotron frequency.

[TTU-SR-2]

09 p1128 A73-22631

Operating features of an ion-cyclotron-wave plasma apparatus running in the RF-sustained mode.

09 p1128 A73-22632

Plasma low density regions caused by Langmuir turbulence, discussing energy dissipation of long wave oscillations and wave collapse

11 p1406 A73-26185

Dissipation of hydromagnetic waves with application to the outer solar corona. III - Transition from collisional to collisionless protons.

11 p1428 A73-26619

Excitation and damping-mechanism of waves and resonances in bounded magnetoactive media.

[IPPCZ-167]

12 p1528 A73-27431

Microwave signal source amplitude stabilization, analyzing circuit with doubly balanced electronically regulated attenuator with p-i-n diodes

14 p1733 A73-30055

Monomode optical fiber waveguide propagation attenuation due to random curvature, analyzing radiation losses for cladded cores with uniform and gradient refractive index profiles

14 p1729 A73-30695

The light field existing in a scattering medium long after its illumination by a light pulse.

15 p1912 A73-31004

Structure of the current front of an electron-acoustic wave in a plasma

15 p1920 A73-32301

Effect of a sheath on the fields of a probe in a hot magnetized plasma.

16 p2041 A73-33330

Damping of Alfven and magnetoacoustic waves at high beta.

17 p2217 A73-35524

Field penetration through a flush mounted coaxial aperture - Variational calculation.

17 p2127 A73-35630

Arbitrary propagation of HM waves along the F region.

18 p2312 A73-36285

Absorption and transformation of electrostatic surface waves in the transition layer of a magneto-active plasma.

19 p2467 A73-37438

Magnetohydrodynamic waves in the solar wind plasma

21 p2763 A73-41506

Langmuir wave attenuation in collisionless plasma of variable density due to field generated by resonant particle currents moving toward lower density region

23 p3015 A73-44349

Structure of the current front of an electron-acoustic wave in a plasma.

24 p3114 A73-44609

Radiative damping of trapped gravity waves in the solar atmosphere.

24 p3135 A73-44629

Damping of a plane shock wave during high-velocity impact

24 p3076 A73-44712

Enhanced scattering and decay of electromagnetic waves in the ionosphere.

24 p3086 A73-45130

Book - Solid-state mechanics 3.

24 p3153 A73-45495

Longitudinal and transverse shock and acceleration waves propagation and decay in anisotropic and isotropic elastic bodies based on theory of singular surfaces

24 p3153 A73-45498

WAVE DIFFRACTION

A comparison of geometrical theory of diffraction and integral equation formulation for analysis of reflector antennas.

01 p0022 A73-10179

Geometrical theory to approximate HF electromagnetic wave diffraction from moving conducting strip under incident field

01 p0016 A73-10192

Reflexion and diffraction of shocks interacted by yawed wedges.

01 p0002 A73-10272

Diffraction and nonlinearity characteristics of amplitude holograms for reconstructed nonlinear images on photosensitive layer

01 p0052 A73-11085

Interferometric testing of large optical components with circular computer holograms.

01 p0053 A73-11225

Conical solutions for diffraction of plane pulse wave by three dimensional trihedron corner via boundary conditions reduction to eigenvalue problem, presenting sonic boom example

01 p0019 A73-11424

Book - Light transmission optics.

02 p0192 A73-11881

Linear equations for steady wave diffraction and propagation in deformable bodies in multiply connected regions, considering circular cylinders, spherical cavities and fibrous media

02 p0232 A73-11889

Boundary value problems of thermoelastic wave diffraction in elasticity theory of multiply connected domains bounded by circular cylindrical surfaces

02 p0233 A73-11940

Plane electromagnetic wave diffraction by periodic grid of dielectric cylindrical filaments, determining reflection and transmission coefficients of radome composite materials

02 p0141 A73-12024

Diffraction of elastic waves by two coplanar and parallel rigid strips.

02 p0234 A73-12088

Dual integral equations and diffraction of electromagnetic waves by a thin conducting strip.

02 p0141 A73-12101

Approximate formulas for calculating intensity distributions of intense laser light diffracted on an ultrasonic wave.

03 p0318 A73-12995

Determination of the flow past a cylinder and a sphere in the presence of an incident shock wave

03 p0294 A73-13615

Diffraction losses and corrections for lower order transverse modes and resonance conditions in optical resonators with cylindrical mirrors

03 p0319 A73-14079

The effect of polarity on the diffraction of plane elastic waves by a cylindrical cavity.

03 p0396 A73-14627

Geometrical optics calculation of radar cross sections.

04 p0416 A73-15058

Diffraction of a two-dimensional electromagnetic field by an ideally conducting plane with a boundless rectilinear slit

04 p0423 A73-15608

Orthogonalization method application to problems of wave diffraction from several bodies through reduction to integral equations

05 p0547 A73-16053

Electromagnetic wave diffraction by ideally conducting homogeneous bodies of revolution with arbitrary complex permittivity and permeability, using separation of variables method

05 p0547 A73-16054

Bragg-diffraction imaging and it's application for non destructive testing.

05 p0574 A73-16281

Diffraction of waves generated by a magnetic-dipole current system on a variable-radius sphere

05 p0550 A73-16397

Boundary value problems of elastic wave diffraction by spherical cavities, using vector equation of motion solutions

05 p0636 A73-17091

An investigation of shock strengthening in a conical convergent channel.

06 p0684 A73-17706

Diffraction of the emission field of a horizontal dipole on a circular hole in a plane screen in the presence of a circular disk coaxial with the hole

06 p0664 A73-17716

Reflector antenna radiation pattern analysis by equivalent edge currents.

06 p0665 A73-18179

Errors in the predicted gain of pyramidal horns.

06 p0676 A73-18180

Applications of conformal mappings to the diffraction of electromagnetic waves by a grating.

06 p0665 A73-18182

Theory of double parasitic loop counterpoise antenna radiation patterns.

06 p0666 A73-18190

A comparison of mode match, geometrical theory of diffraction, and Kirchhoff radiation.

06 p0666 A73-18192

Diffraction by double circular irises and scattering by two elliptical reflectors.

06 p0666 A73-18196

Triangular obstacle caused microwave shadow zone diffraction pattern calculation by ray optics theory, comparing with scale model test results

06 p0666 A73-18201

Diffraction of an arbitrary plane electromagnetic wave by a half-plane.

06 p0667 A73-18203

Diffraction of electromagnetic plane wave by an infinite slit embedded in an anisotropic plasma.

06 p0668 A73-18356

Iterative formula for wave functions related to sources situated on prism symmetry plane with application to electromagnetically polarized wave diffraction by dielectric wedge

06 p0669 A73-18841

Electrooptic liquid crystal devices - Principles and applications.

07 p0861 A73-19135

E-polarized plane wave diffraction by conducting wedge loaded with thin dielectric slab, obtaining Fresnel integral solution with application to cylindrical wave excitation

07 p0792 A73-19383

Diffraction of a plane electromagnetic wave at an array of circular cylinders with a spiral slot

07 p0793 A73-19917

Application of the Lorentz lemma to the calculation of diffraction mode excitation coefficients

07 p0793 A73-19918

Inverse problem of diffraction for a reactance plane

07 p0793 A73-19919

Diffraction of a plane wave by a random phase screen.

07 p0793 A73-20056

Diffraction of plane electromagnetic wave at anisotropic halfspace in free space and in planar waveguide.

07 p0793 A73-20126

Averaged boundary conditions for a grid consisting of nonparallel and nonrectilinear conductors placed on a nonplane surface.

07 p0801 A73-20127

Application of impedance treatment to diffraction problems for rectangular waveguide.

07 p0802 A73-20143

A mathematical analysis concerning the edge effect of sound absorbing materials.

08 p0987 A73-21124

The diffraction of fast magneto-acoustic waves by a plasma layer of a periodically varying density.

08 p0993 A73-21459

Diffraction on an infinite grating made of cylindrical elements of random cross section

09 p1051 A73-22851

A local point method for problems of diffraction on an array

09 p1051 A73-22860

Diffraction of a two-dimensional electromagnetic field on an ideally conducting plane with an infinite straight slit.

10 p1188 A73-24198

Propagating radio wave field strength from double knife edge diffraction signals

10 p1189 A73-24335

Allowance for diffraction occurring in the interaction between a weak shock wave and a plate

10 p1206 A73-24488

Ionospherically diffracted monochromatic VHF/UHF plane wave statistics characterization, noting Gaussian and log-normal distributions from ATS-3 satellite data recording

10 p1190 A73-24896

Quasi-optical diffraction-type radiation generator

11 p1331 A73-26159

Thermally induced nonlinear propagation of a laser beam in an absorbing fluid medium.

11 p1377 A73-26229

A numerical method for solving the stationary diffraction problem of electromagnetic waves on bodies of revolution

11 p1332 A73-26332

Circular carrier-frequency photography for observing phase objects.

12 p1495 A73-26832

Diffraction of electromagnetic waves on reflectors with parameters that vary periodically in time

12 p1470 A73-27583

Book - Mathematical problems in wave propagation theory.

12 p1524 A73-27625

Diffraction theory treatment of long wave holography to demonstrate spiral scan and other circular sampling formats in microwave or acoustic hologram recording

13 p1615 A73-28585

Spatial filtering considerations in Bragg diffraction imaging.

13 p1615 A73-28593

Acoustic imaging by Bragg diffraction using point sources and spherical optics

13 p1616 A73-28594

Paraxial electromagnetic wave packets diffraction on thin conducting periodic structures and dielectric plate, noting packet width and phase front curvature changes

13 p1582 A73-28653

Plane and cylindrical electromagnetic waves diffraction on infinitely long cylindrical bodies, calculating induced currents, diffraction patterns and near fields

13 p1582 A73-28654

Diffraction of a plane wave at an array of planar waveguides with projecting dielectric plates.

13 p1582 A73-28655

Plane TE polarized electromagnetic wave diffraction on infinite conducting cylinder in nonhomogeneous medium, calculating far field diffraction patterns

13 p1582 A73-28656

Plane electromagnetic wave diffraction by ideally conducting circular cylinder in far and bright spot zones, using Green theorem for field calculation

13 p1583 A73-28851

Asymptotic pressure calculation of plane acoustic wave diffraction by infinitely long isotropic solid elastic circular cylinder in viscous liquid medium

13 p1583 A73-28863

Solution of a boundary value problem for the oblique incidence of a plane E-polarized wave on a metallic strip array with an optically active medium

13 p1623 A73-29682

Dynamic properties of human and animal middle ear in terms of acoustic impedance, transfer function, impulse response, sound diffraction and reflex sensitivity

14 p1715 A73-30279

Theory of diffraction efficiency maximization for thin-layer amplitude holograms

14 p1753 A73-30364

Investigation of the dependence of the quality of a reconstructed holographic image on the parameters of the photoemulsion layer. I - Diffractive efficiency of the hologram

14 p1753 A73-30370

Russian book - Asymptotic theory of diffraction of electromagnetic waves by finite structures.

15 p1845 A73-32294

German monograph on data transmission by laser covering analysis of electromagnetic wave diffraction by narrow slits via Mathieu function solution of boundary value problem

15 p1847 A73-32585

Diffraction of an electromagnetic wave on a plane hologram

16 p2011 A73-32823

Steady state diffraction of stress waves by semi-infinite running crack in elastic solid under dynamic loading, obtaining solution based on Wiener Hopf technique

16 p2082 A73-33910

Diffraction of acoustic waves on plates interconnected at right angles

17 p2211 A73-34140

Book - Diffraction of elastic waves and dynamic stress concentrations.

17 p2242 A73-34468

Diffraction of a plane electromagnetic wave on arrays of periodically spaced cylinders

17 p2121 A73-34583

Effect of orthotropy on singular stresses for a finite crack.

[ASME PAPER 72-APM-VVV] 17 p2249 A73-35109

Short-wave asymptotics of the Green's function in the problem of diffraction at a plane layer

18 p2290 A73-36987

Diffraction of an acoustic wave at a moving plate

18 p2265 A73-37012

Diffraction of waves at finite bodies of revolution

19 p2458 A73-37182

A comparison of the efficiency and focused stray light characteristics of a conventionally ruled- and a holographically produced-concave diffraction grating in the vacuum ultraviolet.

19 p2431 A73-38164

Bounded spherical body wave diffraction field represented by diverging wave series expansion, examining Rayleigh hypothesis, Butrov algebraic solution and converging waves

19 p2406 A73-38339

General remarks concerning theories dealing with scattering and diffraction in random media.

20 p2528 A73-38845

Electromagnetic scattering by discontinuities in weakly inhomogeneous parallel plane waveguides or ducts, noting edge diffraction singularities role from ray optical calculation

20 p2528 A73-38847

Application of method of fringe waves to problems of diffraction from bodies placed in a smoothly inhomogeneous medium.

20 p2529 A73-38919

Diffraction of optical radiation by a reflecting disk in a turbulent atmosphere.

20 p2531 A73-39680

Angular distribution patterns of thick-film holograms obtained by rigorous solution of the diffraction problem.

20 p2567 A73-39702

A method of locating defective elements in large phased arrays.

21 p2653 A73-40682

Diffraction of a plane electromagnetic wave by a slit in a thick screen placed between two different media.

22 p2821 A73-41744

Diffraction of a plane electromagnetic wave by a perfectly conducting elliptic cylinder.

22 p2822 A73-41749

Equivalent filamentary current derivation for bi-static field diffracted by ring singularity based on geometrical theory

22 p2824 A73-41838

Electromagnetic wave diffraction by a metallic cylinder surrounded by a plasma layer

22 p2892 A73-42336

Energy propagation lines in the diffraction of a plane electromagnetic wave by a slot in a conductive plane

22 p2826 A73-42353

Diffraction and reflection of shocks from corners.

22 p2843 A73-42567

Monograph - Generation of acoustic waves in piezoelectric devices.

22 p2861 A73-42700

Self diffraction of coherent wave radiation by absorption from excited levels of Nd laser light induced phase diffraction gratings in thin layer rhodamine

22 p2870 A73-42723

Hybrid numerical solution to electromagnetic wave scattering and diffraction with application to microstrip transmission lines, echelette gratings and dielectric step discontinuities in waveguides

22 p2828 A73-42844

Derivation of diffraction coefficients for a thin wire of finite length.

23 p2955 A73-44106

Wave propagation and diffraction in bodies with noncircular cylindrical boundaries

23 p3045 A73-44181

Investigation of the diffraction of strong shock waves on convex corners

24 p3081 A73-45536

WAVE DISPERSION

Numerical solution for propagation of longitudinal waves along the geomagnetic field using a three-fluid ionosphere model.

01 p0016 A73-10197

Relativistic dispersion equation for a circular waveguide with a rotating tubular electron beam, allowing for the effect of the space charge

01 p0017 A73-10982

Quasi-linear theory of plasma waves resonant diffusion, proceeding from Vlasov equation to derive frequency, wavenumber and velocity by quantum methods

01 p0086 A73-11492

Fiber-dispersion measurements using a mode-locked krypton laser.

02 p0177 A73-12574

Numerical and analytic solutions for dispersion equation for flute-like ion cyclotron instabilities in high beta plasma, noting magnetic field inhomogeneity effect

03 p0348 A73-14436

Turbulent wave field growth rate and saturation amplitude for nonresonant instability in weak cold beam plasma system, using Dupree plasma turbulence theory

04 p0479 A73-15193

A technique for making dispersion relation measurements of electrostatic waves.

04 p0450 A73-15554

Plane time-harmonic wave propagation through periodically arranged composite material, determining displacement mode shapes and dispersion relations by variational method [ASME PAPER 72-WA/APM-10]

04 p0516 A73-15902

Periodic axisymmetric waveguide with complex structure, obtaining slow wave dispersion equation solutions

04 p0429 A73-15910

The dispersion diagram of the plasma waves on the plasma branch in a beam-created plasma.

04 p0482 A73-15949

Geometric dispersion of acoustic waves by a fibrous composite.

05 p0597 A73-16114

Dispersion relations for electromagnetic radiation in random media.

05 p0597 A73-16494

Far field solution for stress wave attenuation and dispersion in composite materials, noting pulse shape

05 p0633 A73-16540

Progressive waves analysis, considering nonlinear convective, dissipative and dispersive effects

05 p0528 A73-16756

Lower F region ionospheric wave dispersion observation for horizontal phase and group velocities rela-

tionship to period, considering interpretation by internal gravity wave hypothesis

Electrodynamics of anisotropic media with space and time dispersion.

Dispersion equations for E and H waves in multilayer plasma, defining amplitudes correlation for incident, transmitted and reflected waves

Spectra of potential ion-cyclotron plasma oscillations

Analysis of dispersion equation of a two-layer elliptical waveguide in critical regime.

Gauge invariant and covariant description of plasma response to electromagnetic disturbances, deriving waves dispersion properties in arbitrary reference frame

Study of the dynamic theory of BaTiO₃ in the cubic phase

Angular dispersion of diffraction gratings used for tuning organic dye lasers.

Dispersion of axially symmetric waves in empty and fluid-filled cylindrical shells.

Low dispersion whistlers observed simultaneously at two low latitude stations.

High-resolution study of anomalous dispersion in the ruby R lines.

Dissipation of hydromagnetic waves with application to the outer solar corona. I - Collisionless protons and collisional electrons. II - Transition from collisional to collisionless electrons.

Equation of motion derived for laser resonator with frequency dispersion effect on emission kinetics and spectral features, analyzing unsteady /transient/ processes

Influence of dispersion on the nonlinear evolution of quasi-monochromatic spiral waves in a magnetoactive plasma

Damping of plasma waves in the lower hybrid frequency range.

Conductivity tensor and dispersion equation for collisional magnetoactive plasma.

Conversion of the wave spectrum in a medium with smooth spatial-temporal fluctuations

Laminated composites displacement equations of motion, obtaining stored kinetic and strain energy and free harmonic waves dispersion normal and along layers

Characteristics of waveguides filled with homogeneous lossy anisotropic drifting plasma.

Bending waves dispersion properties in rod applied to acoustic LF dispersion delay line design, analyzing signal distortion and attenuation during propagation

Dispersion equation and spectrum conversions for slow wave excitation and propagation in plane waveguide with homogeneous isotropic impedance

Symmetry properties of the collision integral and nonisotropic steady-state solutions in the theory of weak turbulence

Group velocity and nonlinear dispersive wave propagation.

Small amplitude surface and plate waves propagation in incompressible biaxially stressed elastic media, obtaining dispersion equation for various phase velocities

Nose extension method based on approximate dispersion function for calculating ducted whistler frequency and associated travel time, discussing ionosphere-magnetosphere interactions

Laddertron oscillator /klystron/ cavity dispersion characteristics via electrodynamic analysis of dispersion equation for surface wave operation and coupled modes

An association of magnetospheric whistler dispersion characteristics with changes in local plasma density.

Dispersion characteristics of multiloop cylindrical spiral antennas with opposite winding

An inversion method for the determination of the electron density profile of the ionosphere on the basis of satellite tracking data

The wave patterns produced by a moving body in a compressible, density-stratified fluid.

Dispersion equations for E and H waves in multilayer plasma, defining amplitudes correlation for incident, transmitted and reflected waves

Electrostatic ion-cyclotron plasma oscillations.

Theory of surface wave dispersion in an inhomogeneous plasma situated in a strong HF field

The design and applications of highly dispersive acoustic surface-wave filters.

Calculation of dispersion in delay systems composed of resonator sequences with mixed excitation

Asymptotic solution of initial value problem for weakly nonlinear wave system including dispersive and diffusive effects related to plane Poiseuille flow instability

Modeling of pulsed propagation problems of radio waves excited by an infinite electric current filament in homogeneous dispersing media

Dispersion equation for nonpotential oscillations and hydrodynamic instabilities in hot ion plasma with transverse current in magnetic field

Stochastic wind field effects on baroclinic wave disturbances vertical propagation through turbulent atmosphere, obtaining stream function and dispersion equation

Fiber laser amplifier properties and light dispersion due to fiber structure and materials in optical communication

Dispersion of gravitational waves by a collisionless gas.

Waves in a plasma amid magnetic and gravitational fields

Results of numerical solution of the complex dispersion equation for the HE₁₁/ wave in a two-layer circular waveguide.

Interaction between a tubular electron beam and a plasma

High-frequency plasma turbulence in outer-space

Influence of thermal effects and particle capture by plasma waves on the dispersion characteristics of nonlinear waves

Linear dispersive shear waves in two-layer elastic medium.

Dispersion characteristic of a three-mode gas laser during modulation of relative excitation

Bounded spherical body wave diffraction field represented by diverging wave series expansion, examining Rayleigh hypothesis, Butrov algebraic solution and converging waves

Rectangular waveguide loaded by a semiinfinite chain of ferrite spheres

General remarks concerning theories dealing with scattering and diffraction in random media.

Effects of dispersion on steady state electromagnetic shock profiles.

An integral-equation approach to dispersion relations for guided elastic surface waves.

Dispersion curve computation for elastic acoustic waves propagation in /001/-cut cubic free anisotropic plate, noting relationship with slowness curves for bulk waves

Multiwave interactions in nonlinear distributed systems

The role of Korteweg-de Vries equation in plasma physics.

Wave dispersion equation for large eccentric elliptic jet stability calculations for noise suppression, using approximate Mathieu functions

Measurement of the dispersion of waves in the ionosphere.

Instability of transverse electromagnetic waves in a drifting electron-hole plasma

A two-dimensional field induced by travelling sources.

Energy of an equilibrium fluctuating electromagnetic field in matter

Dispersion of a harmonic signal within a turbulent pipe flow.

Dispersion relations for parallel-plane waveguide containing transversely magnetized uniaxial and warm plasma in relative motion.

New dispersion relation for a strongly magnetized degenerate electron plasma with anisotropic pressure.

Investigation of the waveguide properties of a plasma cylinder for axially asymmetric waves

Experimental verification of dispersion relations for layered composites.

A theoretical and experimental study of the insulated loop antenna in a dissipative medium.

Anisotropic turbulent distributions for waves with a nondecay-type dispersion law

TEM-TE coupled transmission line model for microstrip, calculating frequency-dependent wave dispersion curves for comparison with experiment

Dispersion equation for nonpotential oscillations and hydrodynamic instabilities in hot ion plasma with transverse current in magnetic field

Dispersion characteristics of whistler atmospherics during higher geomagnetic activity.

Dielectric coaxial waveguide modal cut-off, dispersion and attenuation characteristics, discussing guide geometry and dielectric properties effects

WAVE DRAG

The influence of the Mach number on fuselages and profiles with optimized wave resistance in the case of supersonic flow

Thermodynamic considerations for the design of a sonic-boom reducing powerplant.

Critique of paper on supersonic aircraft configuration with zero wave drag, discussing tubular outer structure and convergent-divergent inner duct

The wave drag of circular nose cones at zero angle of attack at Mach numbers from 1.5 to 4 and thickness ratios from 0.05 to 0.5

WAVE EQUATIONS

Book - Sound, structures, and their interaction.

Coupled wave equations for propagation in generally inhomogeneous compressible magnetoplasma.

The convergence of separation /Galerkin/ formulations in the case of time-dependent equations

Cauchy problem and mixed boundary value problems for parabolic and hyperbolic wave equations of heat conductivity for boundary operators given on hyperplane

Asymptotic waves and Cauchy problem with singular data for a system of linear equations with a double characteristic

Semiclassical theory of inelastic collisions. I - Classical picture and semiclassical formulation.

High-frequency sound waves to eliminate a horizon in the mixmaster universe.

Classical solvability of a problem of conjugation of two equations with the third boundary condition

Estimate of the time of occurrence of discontinuities in the solution of a boundary value problem for a second order quasilinear hyperbolic system.

Application of the theory of multiple wave scattering to the derivation of the radiative transfer equation for a statistically inhomogeneous medium

Acoustic radiation from two concentric cylindrical shells.

07 p0851 A73-19958

Time variable field recording and reconstruction theory and wave equations of holography and holographic interferometry, including double exposure and time averaged techniques

08 p0965 A73-21137

Book on boundary value problems in physics and engineering covering Fourier series and integrals, heat, wave and potential equations, Laplace transforms and numerical methods

09 p1113 A73-23300

S matrix method featuring eigenenergy and eigenfunction trials number reduction for rapid numerical determination of bound states of partial-wave-projected Schroedinger equation

10 p1248 A73-23669

A four-component hypermass equation possibly applying to unstable neutrinos.

10 p1251 A73-23754

Analysis of electromagnetic-wave modes in lens-like media.

10 p1248 A73-23834

Finite element method for solution of Laplace or wave equation in cylindrical coordinates through base matrices, applying to electromagnetic wave propagation in waveguides

13 p1581 A73-28077

Dyadic formalism in two dimensional distributions in general relativity theory, discussing gravitational, diffusive, wave, Einstein and preservation equations

14 p1776 A73-30942

Integral equations for piecewise-homogeneous media in the solution of boundary value problems of electrodynamics

15 p1913 A73-31693

A note on the use of the finite difference method for predicting steady state sound fields.

16 p2036 A73-33217

Explicit formulas for the representation of the Green's functions of covariant wave equations in the case of a weak gravitational field. I, II

16 p2038 A73-34021

On the interaction of shocks and simple waves of the same family. II.

20 p2545 A73-39011

The role of Korteweg-de Vries equation in plasma physics.

20 p2599 A73-39625

Numerical solution of nonlinear resonant wave equation of radiating gas between parallel walls by parametric differentiation

21 p2790 A73-40250

Scalar waves in the mixmaster universe. I - The Helmholtz equation in a fixed background.

21 p2766 A73-40317

The effect of magnetic mass on Alfvén waves.

21 p2701 A73-40624

Wave equation solutions for free plane standing wave fields formation in unbounded elastic media

21 p2740 A73-40794

Molecular collisions. XIX - The distorted wave approximation to atom-rigid symmetric top rotational excitation.

22 p2889 A73-42445

Finite difference scheme for wave equation solution for wave propagation in layered composite materials, obtaining matrix eigenvalues with Floquet condition for various methods

[ASME PAPER 73-APMW-40] 22 p2926 A73-42897

Self-focusing and self-trapping of light beams in a non-linear medium.

22 p2888 A73-43050

WAVE EXCITATION

NT ACOUSTIC EXCITATION

NT HARMONIC EXCITATION

Excitation of electromagnetic waves in a plasma by a flux of phased oscillators

01 p0082 A73-10207

Excitation of space charge waves in a one-carrier semiconductor with variable doping.

01 p0088 A73-10680

Analog computer study of the effect of initial conditions on the excitation and sustaining of lower harmonic oscillations in a single-phase electroferromagnetic oscillatory circuit

02 p0147 A73-12352

Radially conducting cone wave spectrum calculation for noncircular excitation, noting circularly polarized TEM and elliptically polarized TM wave amplitudes

03 p0278 A73-14058

Investigation of fluctuation and wave phenomena in argon low-current low-pressure discharges, taking place under the influence of a 'brief' axial magnetic field

03 p0348 A73-14623

Multiple soliton excitation by ion acoustic square pulse wave in double plasma device in frame of Korteweg-de Vries equation

04 p0477 A73-14771

Excitation of electromagnetic waves in a plasma with the aid of longitudinal electric fields

04 p0481 A73-15606

Electromagnetic-emission energy flux during the development of beam instability in a magnetically confined plasma

04 p0481 A73-15607

Shadowgraph photography for electromagnetic excitation of shock waves in normal pressure gas, noting plasma and shock compressed regions in shock tube

04 p0434 A73-15618

The excitation mechanism for the filaments in the Crab Nebula.

05 p0617 A73-16471

Excitation of a magnetohydrodynamic waveguide by a moving source

05 p0603 A73-16820

Hydromagnetic waves excited by transverse magnetic dipole in finite-conductivity plasma

07 p0816 A73-19462

Application of the Lorentz lemma to the calculation of diffraction mode excitation coefficients

07 p0793 A73-19918

Theory of excitation of microwave elastic waves by multifilm transducers /considering the effect of metallic and insulator layers/.

07 p0801 A73-20139

Collision absorption of a rapid hydromagnetic wave in a plasma of two kinds of ions - Experiment

07 p0859 A73-20149

Parametric excitation of circularly polarized and Langmuir waves in a magnetized plasma.

07 p0859 A73-20197

Waves in a hot uniaxial plasma excited by a current source.

07 p0860 A73-20477

Electron plasma oscillation due to beam plasma interaction with standing wave formation between electrodes, observing temporal growth rate during beam modulation removal

08 p0992 A73-21005

Parametric excitation of surface waves in a non-homogeneous magnetized plasma

09 p1124 A73-21892

Collisional effect on the saturation amplitude of nonlinearly excited plasma waves.

09 p1125 A73-22023

Electron-beam excitation of finite-sized plasma near the lower-hybrid frequency.

09 p1129 A73-22638

Excitation of long-wave oscillations by a secondary electron stream in a plasma generated by an ion beam

09 p1129 A73-22684

Parametric excitation of circularly polarized and ion waves in a magnetized plasma.

09 p1131 A73-22905

Excitation of magnetosonic waves in a plasma with nonequilibrium ions

09 p1131 A73-23076

Internal equation numerical solution for excitation of multilayer arbitrary shape dielectric body of revolution, considering radome curvature effects on antenna radiation pattern

09 p1052 A73-23084

Excitation of electromagnetic waves in a plasma by longitudinal electric fields.

10 p1254 A73-24196

Electromagnetic energy in the two-stream instability in a magnetized plasma.

10 p1254 A73-24197

Shadowgraph photography for electromagnetic excitation of shock waves in normal pressure gas, noting plasma and shock compressed regions in shock tube

10 p1205 A73-24208

Dispersion equation and spectrum conversions for slow wave excitation and propagation in plane waveguide with homogeneous isotropic impedance

10 p1190 A73-24601

Effect of concentration on laser threshold of organic dye laser.

10 p1229 A73-24695

On hydromagnetic Rossby waves excited by travelling forcing effects.

11 p1403 A73-25154

Parametric excitation of Tollmein-Schlichting waves in a boundary layer

11 p1347 A73-25430

Harmonic generation and parametric excitation of waves in a laser-created plasma.

11 p1405 A73-25972

Contribution to the nonlinear theory of kinetic instability of an electron beam in plasma.

11 p1405 A73-26183

Czechoslovak Seminar on Plasma Physics, 6th, Liblice, Czechoslovakia, May 10-12, 1972, Research Report.

[IPPCZ-167] 12 p1528 A73-27430

Excitation and damping-mechanism of waves and resonances in bounded magnetoactive media.

[IPPCZ-167] 12 p1528 A73-27431

The theoretical situation with the investigations of parametric instabilities in gaseous plasmas.

[IPPCZ-167] 12 p1528 A73-27432

Dynamics of strongly nonlinear beam-plasma interaction.

[IPPCZ-167] 12 p1529 A73-27434

Parametric excitation of ultrasonic waves in piezoelectric semiconductors.

14 p1783 A73-29916

O I 4368 airglow tropical emission excitation due to conjugate photoelectron escape flux, discussing radiative recombination contribution to intensity

14 p1749 A73-29981

Calculation of dispersion in delay systems composed of resonator sequences with mixed excitation

14 p1733 A73-30028

Offset parabolic reflector antennas linearly and circularly polarized excitations, discussing dependence on angle between dual mode feed and axis

14 p1734 A73-30212

Concentric, uniform elastic spherical wave excited by thermal explosion of the envelope.

14 p1816 A73-30251

Spherical concentric shock wave excitation in elastic medium by hypersonic thermal wave in terms of displacements, particle velocity and stresses

14 p1817 A73-30252

Excitation of an electron semicyclotron wave and its harmonics during the interaction of high-current opposed electron beams

15 p1920 A73-32312

Parametric excitation of surface waves in an inhomogeneous magnetized plasma.

17 p2215 A73-34315

An integro-differential equation technique for the time-domain analysis of thin wire structures. I - The numerical method.

17 p2246 A73-34892

Excitation of electromagnetic waves in a plasma with a relativistic electron beam.

17 p2216 A73-35159

Quadratic antenna systems and noise excited antennas.

17 p2128 A73-35682

Wave transformation due to oblique incidence on the boundary of a magnetoactive plasma

18 p2289 A73-36553

Nonlinear excitation of an ion-acoustic wave in a bounded plasma

18 p2340 A73-36675

Load currents in missile circuits excited by a plane polarized field.

19 p2409 A73-37272

Traveling longitudinal electrostatic waves excitation in warm nonuniform plasma by external HF electric fields, using kinetic theory

19 p2468 A73-37857

Excitation of electromagnetic waves propagating along a magnetic field in a cold plasma by a beam of phased oscillators

19 p2406 A73-38330

Excitation of the earth-ionosphere waveguide by point dipoles at satellite heights.

20 p2528 A73-38846

The theory of parametric excitation of electrostatic surface waves in a plasma layer

20 p2597 A73-39194

The theoretical situation with the investigations of parametric instabilities in gaseous plasmas.

20 p2597 A73-39195

Excitation of transverse extraordinary mode in an inhomogeneous magnetoplasma.

20 p2598 A73-39300

Contactless on-line NDT of metal plates for concealed defects by Lamb wave excitation through wave generation from air

21 p2708 A73-41138

Nonlinear conversion of electromagnetic waves at the boundary of a magnetoactive plasma

21 p2658 A73-41517

Electromagnetic radiation excited by electric or magnetic line source near inhomogeneous dielectric layer, evaluating reflected and transmitted fields by saddle point technique

22 p2824 A73-41831

Electron wave excitation and propagation in low density large volume plasmas near electron Langmuir frequency

22 p2891 A73-42241

On the interaction between the zonal mean flow and equatorial waves excited by diabatic heat sources at 20 deg latitude.

23 p3001 A73-43587

Excitation of electron-cyclotron waves by high-current counter-streaming electron beams.

24 p3115 A73-44620

Enhanced scattering and decay of electromagnetic waves in the ionosphere.

24 p3086 A73-45130

Wave-wave contribution to the high-frequency resistivity of nonequilibrium plasma.

24 p3117 A73-45457

WAVE FRONT DEFORMATION

Comparison of observed and predicted phase-front distortion in line-of-sight microwave signals.

11 p1330 A73-25687

Improvement on moire technique for in-plane deformation measurements.

11 p1365 A73-26241

Passage of pulses through an inhomogeneous plasma medium

19 p2406 A73-38329

Far field effects of weak spatially periodic inhomogeneities.

[AIAA PAPER 73-1036] 24 p3109 A73-44864

WAVE FRONT RECONSTRUCTION

NT KINOFORM
Hologram reconstruction by incoherent light. II - Experimental results. 01 p0045 A73-10431

Diffraction and nonlinearity characteristics of amplitude holograms for reconstructed nonlinear images on photosensitive layer 01 p0052 A73-11085

Limiting resolution of reconstructed image of focused hologram in electron microscopes as function of aberration and spatial coherence 03 p0309 A73-14088

Ultrasonic holography application to NDT, discussing small angle approximation to spherical beam, hologram formation, image reproduction and wavelength change effect 04 p0446 A73-14674

Holographic correlation offers new possibilities for acoustical NDT. 04 p0446 A73-14675

Velocity measurements made holographically of diffusely reflecting objects. 05 p0574 A73-16287

Wavefront sampling in holographic interferometry. 05 p0579 A73-17223

Application of holographic subtraction to time-average hologram interferometry of vibrating objects. 06 p0691 A73-17499

On the numerical reconstruction of images from a microwave hologram. 06 p0669 A73-18737

Evaluation of the wavefront aberration in holography. 08 p0963 A73-21013

Holographic optical element for visual display applications. 08 p0963 A73-21034

Speckle reduction by simulation of partially coherent object illumination in holography. 08 p0964 A73-21037

Recording and reconstruction method for image plane hologram multiplexed tenfold in small area, using He-Cd laser 08 p0964 A73-21052

Time variable field recording and reconstruction theory and wave equations of holography and holographic interferometry, including double exposure and time averaged techniques 08 p0965 A73-21137

Holographic system parameter relations from wave phase analysis of undistorted reconstructed image 09 p1079 A73-21915

Two direct methods for reconstructing pictures from their projections - A comparative study. 09 p1080 A73-22224

Holographic recording and reproduction of wave polarization information by correlation matrix and Stokes parameter method 09 p1087 A73-23333

Reconstruction of analog signals and choice of sampling rates in telemetry. 09 p1058 A73-23421

Ultrasonic holography by one-dimensional moving of the source or the object. 10 p1216 A73-23664

Nonlinear /binary/ transformation effects on acoustic hologram spatial signal amplitude noting multiple images and reconstructed image distortion 10 p1218 A73-24209

Image holography through convective fog. 11 p1361 A73-25365

Phase characteristic function of holographic images of objects in parabolic motion. 11 p1366 A73-26248

Optical and acoustical holography; Proceedings of the Advanced Study Institute, Milan, Italy, May 24-June 4, 1971. 11 p1369 A73-26526

Wave front reconstruction principle application to side-looking radar, diffused holograms, holographic interferometry and computer storage 11 p1369 A73-26527

Volume holograms reconstruction differences due to interferences, noting color and directional selectivity effects 11 p1369 A73-26528

Lesser Fourier transform holography with mutual coherent reference source close to object, investigating atmospheric turbulence effects on wavefront reconstructed image quality 11 p1370 A73-26539

The application of holography to sonic boom investigations. 11 p1371 A73-26633

Reversible recording of holograms on chalcogenide glass films 12 p1495 A73-26940

Book - An introduction to acoustical holography. 12 p1496 A73-27052

Holographic focused image recording and reconstruction in white light, considering source size, shape and spectral composition effects and interferometry 12 p1497 A73-27424

Reconstruction of the images of transparencies with a semiconductor laser. 12 p1498 A73-27512

Investigation of coherence with the aid of the diffraction shearing interferometer. 12 p1507 A73-27515

Real-time reconstruction of images from hydroacoustic holograms. 13 p1614 A73-28578

Acoustic hologram irradiation with sound waves to yield image as acoustic intensity pattern, noting parallels in optical holography 13 p1615 A73-28587

The effects of scanning position and motion errors on hologram resolution. 13 p1615 A73-28590

Ray optics model analysis for spherical aberration effects on acoustic hologram resolution in image reconstruction, discussing computer generated correction for quality improvement 13 p1615 A73-28591

Phase and amplitude only scanned acoustical holograms, noting Fraunhofer diffraction region reconstructed images 13 p1615 A73-28592

Ultrasonic acoustic holography for wave source and object in relative motion, predicting reconstructed image aberration elimination performance in point-by-point mapping technique 13 p1616 A73-28597

A Fabry-Perot acoustic surface vibration detector-application to acoustic holography. 13 p1622 A73-29422

Solution of linear equations in remote sensing and picture reconstruction. 14 p1767 A73-29767

Geometrical projection for holographic image reconstruction, assuming configuration and wavelength differences from reference wave 14 p1752 A73-30024

Effect of laser pulse shape on the form of holographic velocity fringes. 14 p1752 A73-30153

Investigation of the dependence of the quality of a reconstructed holographic image on the parameters of the photoemulsion layer. I - Diffractive efficiency of the hologram 14 p1753 A73-30370

A technique to retain the hologram reconstruction efficiency in elimination of the intense reference beam by the method of pre- or postexposure. 15 p1874 A73-31137

Limiting information capacity of a holographic system 15 p1879 A73-32317

Optical model of a holographic television system 15 p1879 A73-32331

Holographic system parameter relations from wave phase analysis of undistorted reconstructed image 15 p1880 A73-32641

Diffraction of an electromagnetic wave on a plane hologram 16 p2011 A73-32823

Role of cooperative effects in hologram generation and in the formation of reconstructed images 17 p2168 A73-34921

Image quality of binary and multigradation microwave holograms, noting HF components and background noise 17 p2168 A73-35164

Reference radiation frequency shift for holographic interferometry of vibrating objects 17 p2172 A73-35428

Distortionless recording in double-exposure holographic interferometry. 17 p2173 A73-35430

Holographic coding plate - A new application of holographic memory. 17 p2173 A73-35431

Visualization of surface elastic waves on structural materials. 19 p2432 A73-37449

Reconstruction of surface-wave fields in liquids with the aid of holographic methods 19 p2431 A73-38158

Image reconstruction from the modulus of the correlation function - A practical approach to the phase problem of coherence theory. 20 p2570 A73-38616

Hypervelocity projectile holography for application to bullets and shells, calculating rotational velocity and flight direction from fringe on wave front reconstruction 21 p2694 A73-39957

Holographic method of recording temporal characteristics of optical signals. 21 p2695 A73-39958

Color holographic technique through wave front coding of colored object, discussing He-Ne, He-Cd and argon laser irradiation, coding masks and image reconstruction 21 p2697 A73-40128

Elimination of a fundamental defect of two-dimensional holograms 21 p2700 A73-40570

On numerical reconstruction of the image from a microwave hologram. 21 p2655 A73-41045

Application of transverse reference beams in holographic investigations of small particles. 22 p2860 A73-42253

Holographic image nonlinear distortion analysis based on photographic film material characteristic curve representation by Taylor series 22 p2861 A73-42410

Ultrahigh resolution holographic spectroscopy by double exposure of light scattering medium interferogram recording and reconstruction, noting equivalence to use of narrower laser line width 22 p2861 A73-42413

German monograph on holographic interferometry for displacement and deformation determination of diffusely reflecting bodies covering wave front reconstruction methods and diffraction pattern characteristics 22 p2862 A73-42719

Electromagnetic theory of Fresnel holograms in the first perturbation theory approximation 22 p2862 A73-42927

Holographic thin-beam reconstruction technique for the study of 3-D refractive-index field. 22 p2862 A73-43087

Interference patterns from spatially separate holograms and holograms superimposed on same region of recording medium, comparing to double exposure holography performance 22 p2862 A73-43091

Speckle noise reduction by the composition of diffused Fraunhofer holograms. 22 p2863 A73-43093

Fringe localization and visibility in hologram and classical broad source interferometry. 22 p2863 A73-43094

Application of holographic subtraction to time-average hologram interferometry of vibrating objects. 22 p2863 A73-43141

Numerical method for computer generated kinoform image reconstruction error minimization, comparing with random phase method 22 p2863 A73-43148

The imaging properties and aberrations of thick transmission holograms. 23 p2982 A73-43705

The nature of quasi-axial reconstructed pictures generated by 'nonreferenced' focused-image holograms 23 p2987 A73-43717

Study of the parameters of three-dimensional holographic gratings in LiNbO₃ crystals 24 p3089 A73-44623

Maximum information capacity of a holograph system. 24 p3091 A73-44944

Radon transform application in holographic interferometry for reconstructing two and three dimensional spatial distribution of refractivity in object

WAVE FRONTS

NT SHOCK FRONTS

Wave front propagation velocity definition valid for classical and relativistic fluid dynamics 02 p0152 A73-11572

The thickness of perpendicular collisionless shocks in a hot plasma. 04 p0479 A73-15191

Cusped wave fronts in anisotropic elastic plates. 07 p0907 A73-19079

Two zone model of multizone condensed system combustion, showing front velocity dependence on leading heat zone and dispersion depth 10 p1294 A73-23589

Automatic sensor with parabola null test and ray intercept error measurement for optical system wave front error determination, noting interferometric sensitivity 11 p1365 A73-26242

Calculation of the constants of an infinitely narrow beam in spectral devices 13 p1660 A73-28769

IR seeing disks /blurred interference patterns of corrugated wave fronts/ speckles and intensity profiles from atmospheric turbulence models 15 p1929 A73-31061

Small perturbation method study of nonlinear weak D-type unsteady ionization front geometry with radiation source in interstellar incompressible gas medium 15 p1932 A73-31295

Structure of the current front of an electron-acoustic wave in a plasma 15 p1920 A73-32301

The dynamic field of a growing plane elliptical shear crack. 16 p2082 A73-33907

Wavefront investigation of a Fourier transform lens with the fan trace interferometer. 17 p2172 A73-35427

Compactness criterion for the formation of averaged trapped surfaces in gravitational collapse. 17 p2234 A73-35734

WAVE FUNCTIONS

Intracellular-extracellular action potentials - Considerations for the formation of wavefronts and their detection on the body surface. 18 p2282 A73-36518

Incident-light double-refracting interference microscope with variable wavefront shear. 21 p2703 A73-41134

Inexpensive portable vibration-insensitive wave front shearing interferometer developed at NBS for lens testing. 21 p2704 A73-41259

Acoustic wave fronts in ideal membrane traversed by steady pressure distribution, noting abrupt displacement gradient changes across pressure front. 22 p2918 A73-41823

Structure of the current front of an electron-acoustic wave in a plasma. 24 p3114 A73-44609

WAVE FUNCTIONS

NT MOLECULAR ORBITALS

Multiquantum ionization of a molecule represented by a nonorthogonal wave function system. 01 p0080 A73-10622

Inelastic scattering calculations with projected Hartree-Fock wave functions. II - Coupled-channel treatment. 03 p0345 A73-13806

Linear integral equation, wave function and parameter optimization for numerical analysis of remote sensing problem. 03 p0337 A73-14488

Holography without fringes in the electron microscope. 04 p0447 A73-15049

P II Zeeman effect spectral line observation for J-value assignments with check on wave functions obtained from energy level least squares fitting. 05 p0600 A73-16497

Eigenvalues of a class of spherical wave functions. 06 p0665 A73-18177

Semiclassical theory of inelastic collisions. II - Momentum-space formulation. 06 p0726 A73-18262

Iterative formula for wave functions related to sources situated on prism symmetry plane with application to electromagnetically polarized wave diffraction by dielectric wedge. 06 p0669 A73-18841

Oxygen anions excited electronic states, analyzing energy curves and wave functions via configuration-interaction results obtained by multiconfiguration self consistent field techniques. 07 p0853 A73-19333

Line broadening of Lyman alpha wings due to protons calculated via positive molecular hydrogen ion wave functions. 08 p0997 A73-20892

Wave functions and energies of the autoionization states of the cesium atom. 09 p1122 A73-21976

Ionization of 6s- and 5p-electrons of the cesium atom by electron impact. 09 p1122 A73-21977

Calculation of the magnetic properties of a hydrogen molecule with the aid of the method of varying the vector potential and the method of varying the induced current. 09 p1122 A73-22017

Quantum mechanical operator for photon flux density passing through spatial point over infinite time, interpreting photon wave functions. 09 p1094 A73-22598

Quantum mechanical formalism for unitary transformations of wave functions, gauge transformations and current conservation, discussing use of gauge invariant atomic orbitals. 10 p1251 A73-24245

Electronic charge densities in semiconductors. 11 p1408 A73-25374

Normalization properties of resonance wave functions of quantum systems associated with poles of Green function in terms of Siegert and Kapur-Peierls energy definitions. 14 p1776 A73-30244

Eigenstate localization parameter calculation for wave functions in one dimensional disordered potential chain, considering extension to coupled oscillators and electromagnetic waves in stratified media. 21 p2750 A73-40227

Spin contamination in unrestricted Hartree-Fock calculations. 22 p2889 A73-42442

Hartree-Fock equation with allowance for the correlation. 22 p2889 A73-42647

Energy spectra of localized elementary excitations for dilute solutions of He 3 atoms in superfluid He 4 using Feynman type wave function, considering Raman scattering. 23 p3007 A73-44173

Electrostatic Hellmann-Feynman theorem applied to long-range interatomic forces - The hydrogen molecule. 24 p3113 A73-44981

WAVE GENERATION

Linear MHD equations for inviscid medium under external forces, discussing magnetoacoustic wave generation by radially pulsating cylinder and sphere. 02 p0196 A73-11605

Electromagnetic self induced vibrations in homogeneous unbounded electron beam moving with time dependent velocity, noting longitudinal and transverse wave generation. 02 p0198 A73-12102

Atmospheric gravity waves to be expected from the solar eclipse of June 30, 1973. 02 p0159 A73-12223

A possible mechanism of the generating of the unusually long lunar seismic oscillations. 03 p0368 A73-13092

Compression shock formation in arbitrary medium described by first order quasi-linear partial differential equations, considering strongly radiating and emission dominated gases. 03 p0400 A73-14629

Fermions spin polarization reversal for HF high intensity gravitational waves generation and detection, suggesting superconducting metals for waves receiver. 04 p0476 A73-15633

Diffraction of waves generated by a magnetic-dipole current system on a variable-radius sphere. 05 p0550 A73-16397

Frequency spectra of the inner and outer structures of wind waves at different stages of wave development. 05 p0594 A73-17359

Evolutionary aspects of shock waves in the Chew, Goldberg, and Low approximation. 06 p0727 A73-17471

Hall current effects on waves in an electrically conducting rotating fluid. 07 p0854 A73-19104

Ion cyclotron wave generation in a two-ion plasma. 08 p0991 A73-20817

Compression wave interaction induced shock wave formation in shock tube, studying unsteady gas flow near opening diaphragm. 08 p0955 A73-21520

Thermal wave generation and transformation into shock waves due to energy release in stellar interior, considering nova outburst. 09 p1146 A73-22547

Supersonic generation of atmospheric gravity waves, via atmospheric cooling by moon shadows during lunar eclipses, noting analogy to terminator action. 10 p1211 A73-23825

Particle scattering in interplanetary space and the properties of solar corpuscular streams. 10 p1265 A73-23902

An investigation of internal gravity waves generated by a buoyantly rising fluid in a stratified medium. 11 p1351 A73-25152

Holographic interferograms for demonstration of acoustic field near supersonic air, nitrogen and helium jets, noting generated Mach wave convection velocity. 11 p1346 A73-25382

Waves produced by a source of harmonic oscillations located in a cylindrical layer of liquid. 11 p1349 A73-26468

Application of acoustic surface-wave technology to spread spectrum communications. 12 p1470 A73-27570

Generation of opposed waves polarized in different planes in a ring laser. 14 p1757 A73-30368

Shock-wave generation in a randomly inhomogeneous gas. 15 p1860 A73-31014

Permeable elastic piston models of shock wave formation before flame front during inflammable gas mixture combustion in channels. 15 p1957 A73-31868

Evaluation of the directivity of gravitational wave radiators. 15 p1914 A73-31944

Electrostatic waves with frequencies above the gyrofrequency in a plasma with a loss-cone. 17 p2218 A73-35831

PPM pulse waveform synthesis with SNR performance improvement while retaining bandwidth-mean-square error properties inherent in wideband modulation system. 20 p2524 A73-38736

Acoustic turbulence generation of shock waves in compressed gas or plasma excited by random potential forces based on energy transfer along spectrum. 22 p2840 A73-41809

Atmospheric gravity wave observations after the solar eclipse of June 30, 1973. 22 p2847 A73-42487

Monograph - Generation of acoustic waves in piezoelectric devices. 22 p2861 A73-42700

Diurnal harmonic oscillation instability of atmospheric boundary layer as mesoscale internal gravity waves generation mechanism in lower atmosphere, considering unsteady flow equations. 23 p3001 A73-43589

Large amplitude baroclinic waves generation via instabilities of two layer fluid in rapidly rotating cylinder compared with mathematical model based on quasi-geostrophic equations. 23 p3001 A73-43590

Weak longitudinal waves in a nonlinear viscoelastic medium. 23 p3045 A73-44182

Generation of VLF waves in the ionosphere near the low-frequency plasma resonance. I. 24 p3115 A73-44788

Hydromagnetic gradient waves in the ionosphere. 24 p3083 A73-44789

WAVE INTERACTION

NT SHOCK WAVE INTERACTION

A method for nonlinear plasma wave kinetics. 01 p0082 A73-10419

The interaction of primordial gravitational waves with groups of galaxies. 01 p0098 A73-10581

Light waves interaction in nonlinear medium, noting operational principles and optical properties of parametric optical generators with semiconductors. 01 p0059 A73-10717

Reflection coefficients for acoustic waves interacting with stratified media. 01 p0078 A73-110979

Collision between an electromagnetic wave and a gravitational wave packet. 01 p0019 A73-112808

Gas and solid state lasers amplitude and phase fluctuations calculated from Langevin equations, noting spectral line width and ring laser wave coupling. 01 p0061 A73-113555

Energy transfer between interacting electromagnetic waves propagating in half space media, applying to acoustic surface wave excitation by electromagnetic converter. 02 p0140 A73-115686

Book - Sound, structures, and their interaction. 02 p0192 A73-118808

Interaction between gravity waves and ionization in the ionospheric F region. 02 p0162 A73-122964

Wave coupling at a collisionless plasma discontinuity. 02 p0198 A73-124080

Spectral characteristics of nonlinear plasma oscillations near collapse limit, discussing wave interaction energy exchange and velocity corrections. 02 p0198 A73-124849

Acoustic and shock waves interaction in axisymmetric gas flow through variable section channel, calculating flow characteristics variations via isentropic theory of steady flow. 03 p0295 A73-13677

Magnetospheric observations inOGO-5 plasma wave experiment, emphasizing electrostatic wave particle interaction with plasma. 03 p0303 A73-13881

Rayleigh wave propagation at the boundary between a piezoelectric insulator and a semiconductor. 03 p0350 A73-14030

Amplification of signal by Cerenkov resonance interaction. 04 p0415 A73-14951

LF spectrum of plasma oscillations from amplitude modulation of plasma SHF radiation, noting Langmuir and magnetoacoustic waves interaction. 04 p0478 A73-15034

Spatial echo and nonlinear interaction of waves in a plasma. 04 p0478 A73-15034

One dimensional analysis of saturation spectral lines for energy transfer in plasma waves interaction, noting Landau damping effect on parametric instability. 04 p0482 A73-15656

O-type synchronous electron beam waves interaction with electrostatically structured travelling wave, noting linear gain dependence on beam current and magnetic field. 05 p0556 A73-16060

Interaction between long waves and zonal circulation in a baroclinic atmosphere. 05 p0592 A73-16230

Electro-optical media for initial light radiation frequency shift maximum, analyzing circular light/modulating wave interactions. 05 p0551 A73-16780

Possibility of radar observation of nonlinear wave interaction in ionospheric plasma. 05 p0570 A73-17020

Geomagnetic micropulsations within magnetosphere, investigating MHD waves and particle-wave interactions. 05 p0570 A73-17020

The theory of the reflection of low frequency radio waves in the ionosphere near critical coupling conditions. 05 p0551 A73-17020

Possibility of observing the decay interaction of plasma waves in top-side sounding experiments. 06 p0689 A73-1751

D region electron density profiles analytical determination from pulsed wave interaction measurements 07 p0791 A73-19242

Dynamics of the non-linear interaction of magnetohydrodynamic waves. 07 p0859 A73-20236

Compression wave interaction induced shock wave formation in shock tube, studying unsteady gas flow near opening diaphragm 08 p0955 A73-21520

Mathematical model for nonlinear interactions between HF waves and LF acoustic waves applied to electromagnetic wave stability in plasmas and dielectrics 09 p1128 A73-22614

Coupled waves and particle scattering processes in ferromagnetic semiconductors and metals 09 p1133 A73-22677

Theory of fluctuations and particle scattering in ferromagnetic semiconductors and metals 09 p1134 A73-22678

High-frequency instability of an electromagnetic wave in a nonequilibrium magnetized plasma 09 p1130 A73-22705

Wave-wave interactions in turbulent plasma and ion sound turbulence enhancement of three wave interaction processes, considering plasma heating experiments 09 p1131 A73-22901

Nonlinear interactions between Langmuir waves in a weakly inhomogeneous plasma 10 p1253 A73-23576

Probability model of mode interactions, radiation density and output gain of gas laser channels with common lower energy level in active medium 10 p1227 A73-24071

Computer simulation of two dimensional plasma diffusion via wave interactions descriptions by nonlinear differential equations, considering electric field and particle velocity correlations 10 p1255 A73-24266

Negative energy mode loss to positive energy mode in positive-negative energy wave interactions within magnetized plasma, considering ion acoustic waves 11 p1402 A73-25123

Coupling coefficients for resonant interaction between three waves with well-defined phases in cold magnetized plasma, applying to solar corona 11 p1405 A73-25917

The interaction of weak gravitational waves with a gas. 11 p1400 A73-26177

Geometric interpretation of conditions for resonant wave interactions valid under nondispersive conditions, noting relevance for acoustic waves in crystals and slowness vectors 11 p1400 A73-26278

Ring laser output calculation in the region of capture 12 p1504 A73-26885

Signal processing device with parametric interaction between opposite acoustic waves passing through delay line considering real time convolution and time inversion capabilities 12 p1470 A73-27569

Nonlinear theory of parametric wave instability in a plasma 12 p1530 A73-27981

Extension of the hodograph method for the one-dimensional elastic-plastic wave propagation. 13 p1696 A73-28646

Amplitude characteristics of a helium-neon laser at the 0.63-micron wavelength in the region of strong interaction between two modes. 13 p1630 A73-29446

Parametric instabilities and anomalous absorption and heating of plasmas. 14 p1779 A73-30118

Direct nonlinear coupling of electromagnetic waves and electrostatic waves in a plasma - Theory. 14 p1781 A73-30656

Possibility of observing the decay interaction of plasma waves in topside sounding experiments. 16 p2002 A73-32775

Influence of a reflected signal on the operation of a laser 16 p1978 A73-32892

Detection and measurement of low-level backscattering of laser radiation 16 p1978 A73-32893

Klein-Gordon equation for a charged particle interacting with an electromagnetic wave. 16 p1979 A73-33164

Satellite waves effects on dynamic behavior of resonant wave-triplet coupling from comparison with isolated triplet in explosive and decay instabilities 16 p2041 A73-33334

Nonlinear theory of wave interaction in a plasma 16 p2042 A73-33735

Nonlinear wave interaction and fluctuations in plasma. 17 p2217 A73-35818

On the explosive instabilities of waves in plasmas with special regard to dissipation and phase effects. 17 p2218 A73-35820

Five wave interaction - A possibility for enhancement of optical or microwave radiation by nonlinear coupling to explosively unstable plasma waves. 17 p2218 A73-35821

On the stabilization of explosive instabilities by nonlinear frequency shifts. 17 p2218 A73-35822

Direct nonlinear coupling of electromagnetic waves and electrostatic waves in a plasma - Experiment. 19 p2469 A73-37860

Interactions between internal gravity waves and their traumatic effect on a continuous stratification. 19 p2422 A73-38237

Dynamic coupling of the stratosphere with the troposphere and sudden stratospheric warmings. 19 p2449 A73-38288

Interaction of parametrically coupled waves in nonequilibrium media /Survey/ 19 p2406 A73-38326

A generalized extinction theorem and its role in scattering theory. 20 p2591 A73-38613

Second harmonic amplitude modulation of an electromagnetic wave by an acoustic wave in a dispersive plasma. 20 p2597 A73-39199

Multwave interactions in nonlinear distributed systems 20 p2593 A73-39511

Study of shock wave and turbulent boundary layer interaction using the energy integral equation. 20 p2548 A73-39524

Absolute instability of the interaction between optical and acoustic waves. 20 p2594 A73-39679

Velocity wave interaction and helical turbulence equilibrium spectra for two dimensional and three dimensional flow with quadratic energy and entropy states 20 p2549 A73-39812

Second-harmonic resonance in the interaction of an air stream with capillary-gravity waves. 20 p2550 A73-39816

Rocket experiments on nonlinear wave-wave interaction in the ionospheric plasma. 21 p2685 A73-40823

Russian book on nonlinear waves in dispersive media covering unsteady waves, gravity waves in deep water, electromagnetic waves in nonlinear dielectric, etc 21 p2741 A73-41285

Gravity wave nonlinear interactions producing secondary waves of opposite polarization, discussing tide polarization 21 p2688 A73-41343

Interaction of sound with jets. 22 p2795 A73-41704

Propagation mode with fine structure interpreted as quasi-cylindrical electrostatic wave interference with cold plasma field from potential measurements near point source antenna 22 p2895 A73-43021

Resonance conditions for nonlinear interaction of acoustic gravity waves with viscous damping taken into account 22 p2828 A73-43178

Internal gravity wave-mean wind interaction. 23 p3000 A73-43339

Collision between an electromagnetic wave and a gravitational wave packet. 23 p3006 A73-43501

Nonlinear interaction of high-amplitude Langmuir waves in a collisionless plasma 23 p3012 A73-44015

Hydrodynamic equations for nonlinear stability of plasma ionization wave interactions in absence of magnetic field 23 p3012 A73-44040

Plasma-electromagnetic wave interactions in toroidal discharge chamber, noting possibility of collisionless wave absorption due to conversion to longitudinal plasma waves at hybrid resonance 23 p3014 A73-44340

Interpretation of distinct type IVmA- and IVmubursts on the basis of micro-instabilities and of resonant nonlinear interaction of waves. 24 p3123 A73-44645

Amplification of magnetostatic surface waves in the YIG-Ge hybrid system. 24 p3120 A73-45431

WAVE MOTION

U WAVES

WAVE OSCILLATORS

U OSCILLATORS

WAVE PACKETS

Momentum formulae derived for quasi-monochromatic wave packets of transverse and longitudinal waves in plasma without magnetic field 02 p0195 A73-11522

Wave spectrum transformation in an active nonlinear medium 07 p0792 A73-19907

The energy-momentum tensor for an electromagnetic wave in plasma. 10 p1254 A73-24115

Paraxial electromagnetic wave packets diffraction on thin conducting periodic structures and dielectric plate, noting packet width and phase front curvature changes 13 p1582 A73-28653

Valve effect of inhomogeneities on anisotropic wave propagation. 14 p1780 A73-30165

Phenomena of scattering of electromagnetic and gravitational wave packets in the gravitational field of a black hole 15 p1932 A73-31245

On the existence of critical levels, with applications to hydromagnetic waves. 16 p2043 A73-33869

Propagation of frequency-modulated pulses in a randomly stratified plasma. 17 p2214 A73-34095

Application of the ray method to a study of the propagation of large-scale perturbations in a barotropic atmosphere with a mean wind 17 p2204 A73-34345

Wave-trains in the solar wind. I - General theory and its application to an ideal, isotropic, one-fluid plasma. 17 p2224 A73-34505

Interaction of parametrically coupled waves in nonequilibrium media /Survey/ 19 p2406 A73-38326

Nonlinear theory of a quasi-monochromatic electrostatic wave packet in an inhomogeneous plasma 21 p2745 A73-40363

Polarizable particle entrainment in electromagnetic field consisting of wave packets propagating in opposite directions 22 p2889 A73-43099

Collision between an electromagnetic wave and a gravitational wave packet. 23 p3006 A73-43501

WAVE PROPAGATION

NT DIFFRACTION PROPAGATION

NT GROUND WAVE PROPAGATION

NT IONOSPHERIC F-SCATTER PROPAGATION

NT IONOSPHERIC PROPAGATION

NT LIGHT SCATTERING

NT MANDELSTAM REPRESENTATION

NT MICROWAVE TRANSMISSION

NT MULTIPATH TRANSMISSION

NT SCATTER PROPAGATION

NT SHOCK WAVE PROPAGATION

NT TRANSEQUATORIAL PROPAGATION

Application of the averaging method to the problem of plane wave propagation in a dissipative heat conducting medium 01 p0075 A73-10086

Wave motion in an elastic solid due to a nonuniformly moving line load. 01 p0114 A73-10301

The effect of radiative and viscous dissipation of the propagation of forced planetary waves in the vicinity of critical levels. 01 p0039 A73-10395

Nongray theory for temperature wave propagation without turbulent or convective motions, discussing diurnal waves simulation for planetary atmospheres 01 p0039 A73-10396

Ultrasonic studies of the nonlinear properties of solids. 01 p0057 A73-11003

Elastic waves originating at the surface of a spherical opening in nonhomogeneous isotropic media. 01 p0116 A73-11065

Wave propagation in elastic laminates using a multi-continuum theory. 01 p0117 A73-11364

Acceleration waves in anisotropic thermoelastic materials with internal state variables. 01 p0118 A73-11367

Approximate method based on quasi-one dimensional theory for calculation of transonic wave propagation in slender nozzles 01 p0034 A73-11368

Numerical Laplace transform inversion of a function arising in viscoelasticity. 01 p0119 A73-11469

Wave front propagation velocity definition valid for classical and relativistic fluid dynamics 02 p0152 A73-11572

Linear equations for steady wave diffraction and propagation in deformable bodies in multiply connected regions, considering circular cylinders, spherical cavities and fibrous media 02 p0232 A73-11889

Scheme for calculating the process of elastic wave propagation in a composite beam 02 p0233 A73-11943

Small disturbance propagation in infinitely extended thermoelastic medium with initial finite homogeneous deformation, determining longitudinal and transverse wave propagation velocities 02 p0234 A73-12018

Ionizing potential wave analysis for gas breakdown, noting photoionization role in avalanche propagation and velocity, electron densities and temperature as function of electric field 02 p0197 A73-12063

Resonance, particle trapping, and Landau damping in finite amplitude obliquely propagating waves.

02 p0197 A73-12068

Nonlinear waves in a multicomponent plasma with weak dissipation.

02 p0198 A73-12103

Propagation of surface waves along a plane boundary between two magnetoactive plasmas.

02 p0198 A73-12107

Statistical theory of light propagation in a turbulent medium /Survey/

02 p0141 A73-12485

Finite amplitude waves on aircraft trailing vortices.

02 p0129 A73-12506

A variational principle for wave propagation in random media.

02 p0194 A73-12732

Uniqueness theorem for linear thermoelasticity theory allowing for second sound, discussing acceleration waves propagation in isotropic material

02 p0237 A73-12796

The ducted propagation of PP micropulsations in the magnetosphere and PP dotting.

03 p0298 A73-12877

Converging lens effect of air jet for upstream moving waves, describing experimental procedure

03 p0290 A73-12968

Long wave disturbance propagation analysis via equations of motion from mathematical model of liquid-gas mixture, determining velocity, pressure and density perturbation propagation

03 p0294 A73-13612

Spherical wave propagation in a viscoplastic medium.

03 p0393 A73-13788

Propagation of elastic waves in a cylindrical bar subject to a moving load on its lateral surface.

03 p0343 A73-13833

An analysis of thermally-induced plane waves in elastic-plastic single crystals.

03 p0394 A73-13980

Rayleigh wave propagation at the boundary between a piezoelectric insulator and a semiconductor.

03 p0350 A73-14037

Parametric instability of a spatially modulated plasma.

03 p0347 A73-14089

Finite elements for axisymmetric solids under arbitrary loadings with nodes on origin.

03 p0395 A73-14192

Propagation of ion acoustic waves in a weakly ionized plasma

03 p0348 A73-14625

A mechanism of steady-turbulence development in a plasma

04 p0477 A73-14876

Microfracture effects on seismic wave propagation velocity and Q factor in lunar rocks by Rayleigh ultrasonic surface wave technique

04 p0497 A73-15125

Comparison of wave propagation in the stationary and moving plasma - Motion and wave propagation along the magnetic field.

04 p0479 A73-15190

Analytical study of the evolution of the normal to the wave during the magnetospheric passage of PC 1's

04 p0440 A73-15248

Thermoelastic wave propagation in a transversally isotropic circular cylinder

04 p0512 A73-15501

Elastic waves in an infinite cylinder with micropolar structure

04 p0513 A73-15502

Elastic wave propagation in a circular cylinder subjected to finite deformation Compressible material

04 p0513 A73-15503

Radiation energy distribution in laser pulse heating of moving plasma without reflection, noting thermal wave propagation

04 p0481 A73-15605

Propagation of harmonic waves in orthotropic circular cylindrical shells.

[ASME PAPER 72-WA/APM-23]

04 p0515 A73-15893

A continuum theory for wave propagation in laminated composites. I - Propagation normal to the laminates.

[ASME PAPER 72-WA/APM-20]

04 p0516 A73-15896

Plane time-harmonic wave propagation through periodically arranged composite material, determining displacement mode shapes and dispersion relations by variational method

[ASME PAPER 72-WA/APM-10]

04 p0516 A73-15902

Elastic wave propagation in filamentary composite materials.

05 p0631 A73-16122

Sinusoidal thermal wave propagation in horizontal fluid layer with small Prandtl number, deriving induced mean flow from nonlinear equation solution by perturbation approach

05 p0591 A73-16188

Book - Calculation of wave propagation by nomograms - Frequencies above 30 MHz.

05 p0548 A73-16325

Open spiral density wave propagation and distortion due to differential rotation in Lindblad resonance region

05 p0616 A73-16455

Effect of bulk-reacting liners on wave propagation in ducts.

[AIAA PAPER 73-227]

05 p0566 A73-16952

Approximate method for solving wave propagation problems in viscoelastic materials

05 p0636 A73-17088

Running waves in quiet sunspots with well developed penumbras, noting intensity fluctuation in H alpha centerline or wing

05 p0626 A73-17347

Stream instabilities in a cold plasma in the presence of a magnetic field.

06 p0728 A73-17793

Large amplitude waves in bounded media. I - Reflexion and transmission of large amplitude shockless pulses at an interface.

06 p0761 A73-17874

Wave normal and ray propagation in lossless positive bianisotropic media.

06 p0723 A73-17875

Note on the wave propagation problems in isotropic discretized bodies.

06 p0723 A73-17893

Further exact and approximate considerations of the barrier problem.

06 p0716 A73-17981

Wave propagation in a micro-isotropic, micro-elastic solid.

06 p0762 A73-17990

Nonlinear mode-mode coupling of Alfvén waves in the interstellar medium.

06 p0730 A73-18465

Small amplitude viscous similarity solution for vertical two dimensional internal wave production by circular cylinder resonant oscillation in incompressible stratified fluid

06 p0646 A73-18527

Propagation of one-dimensional, plane waves in a physically nonlinearly-elastic medium

06 p0765 A73-18691

Equatorial Kelvin wave oscillations of zonal wind at 100 mb over Eastern Hemisphere

07 p0847 A73-19043

Stress-induced rotation of polarization directions of elastic waves in slightly anisotropic materials.

07 p0908 A73-19083

Stress wave propagation in a laminated plate under impulsive loads.

07 p0908 A73-19089

Diffraction effects from cylindrical transducers in a piezo-elastic medium of hexagonal symmetry /class C6v/6mm/.

07 p0822 A73-19108

Conservation of energy in random media, with application to the theory of sound absorption by an inhomogeneous flexible plate.

07 p0851 A73-19153

Propagation of a nonlinear wave in a weakly turbulent plasma

07 p0854 A73-19276

Wave propagation in a stratified turbulent magnetized plasma. II.

07 p0858 A73-19534

Elastic velocity and Q factor measurements on Apollo 12, 14, and 15 rocks.

07 p0894 A73-19852

Wave spectrum transformation in an active nonlinear medium

07 p0792 A73-19907

Lateral expansion of a laser-supported detonation wave in a gas.

07 p0920 A73-19979

On the detection of gravitational radiation by its interaction with electromagnetic fields.

07 p0852 A73-20227

An exact helical wave solution to the equations of magnetohydrodynamics.

07 p0859 A73-20233

The propagation and growth of acceleration waves in heat-conducting elastic materials.

07 p0917 A73-20441

Trapped electrons instability in Tokamak configuration, calculating plasma wave propagation modes via Fokker-Planck equation

08 p0991 A73-20815

Lower-hybrid-resonance heating of a plasma in a parallel-plate waveguide.

08 p0991 A73-20816

Electromagnetic effects on electrostatic modes in a magnetized plasma.

08 p0991 A73-20820

Wave propagation along radially inhomogeneous glass fibres.

08 p0937 A73-20832

Landau damping of type III solar radiobursts.

08 p0997 A73-20902

Generalization of J. K. Lunde's method for determining the flow around models in a rectangular-section test tank

08 p0955 A73-21195

Characteristics of hydromagnetic wave propagation in a slowly varying magnetic field /Geometrical optics approximation/

08 p0959 A73-21294

A climatological analysis of oscillations of Kelvin wave period at 50 mb.

08 p0984 A73-21377

Quasi-static ion acoustic surface wave propagation along warm plasma layer-dielectric boundary

08 p0993 A73-21460

Propagation of a transverse harmonic wave in a plate with a statistically rough circular hole

08 p0120 A73-21770

On dynamic plasticity. I

08 p0120 A73-21823

Propagation of backward surface wave along an annular plasma guide with azimuthal electron density variation.

09 p1125 A73-21930

Proposal of periodic layered waveguide structures for distributed lasers.

09 p1090 A73-21935

Effects of collisions and gyroviscosity on gravitational instability in a two-component plasma.

09 p1127 A73-22286

Green operator evaluation by Fourier transform method for wave propagation in bianisotropic media, obtaining constitutive equations

09 p1049 A73-22311

Elastic wave propagation in a cylindrical shell containing a filler

09 p1158 A73-22357

Wave number space analysis of propagation in nonuniform media.

09 p1120 A73-22474

Asymptotic scheme for a class of partial differential equations

09 p1112 A73-22477

Kinetic equation derived for collective linear fluid oscillations development, applying to longitudinal and transverse wave propagation in fluids

09 p1072 A73-22574

Fast wave propagation and damping at the second harmonic of the ion cyclotron frequency.

09 p1128 A73-22631

Operating features of an ion-cyclotron-wave plasma apparatus running in the RF-sustained mode.

09 p1128 A73-22632

Lower-hybrid-resonance heating of a plasma in a parallel-plate waveguide.

09 p1129 A73-22639

One-dimensional finite amplitude wave propagation in a compressible elastic half-space.

09 p1160 A73-22895

A continuum mixture theory of wave propagation in laminated and fiber reinforced composites.

09 p1160 A73-22897

Propagation of surface waves and instability wave growth in an ion beam-plasma system.

09 p1131 A73-22906

Propagation of monochromatic waves in an initially stressed infinite micropolar elastic plate.

09 p1160 A73-23024

Propagation of discharges and confinement of a dense plasma by electromagnetic fields

09 p1132 A73-23327

Use of modal solutions in elastic wave propagation problems.

09 p1166 A73-23456

Nonstationary wave propagation in equilibrium liquid-vapor flow, noting pressure jumps due to expansion

10 p1204 A73-23513

Continuum theory of wave propagation in laminated composites.

10 p1287 A73-23565

Strong irradiance fluctuations in turbulent air - Plane waves.

10 p1248 A73-23837

Radiation energy distribution in laser pulse heating of moving plasma without reflection, noting thermal wave propagation

10 p1254 A73-24195

A numerical method for the analysis of longitudinal elastic-plastic stress wave propagation.

10 p1290 A73-24297

Transient compressional wave propagation in a two-layered circular rod with imperfect bonding.

10 p1291 A73-24390

Elastic wave analysis in nondestructive testing.

10 p1292 A73-24630

Half-harmonic modes for different frequency ranges and wave vectors from infinite homogeneous plasma model for high frequency electrostatic wave propagation in magnetosphere

10 p1213 A73-24733

Group velocity and nonlinear dispersive wave propagation.

10 p1249 A73-24775

Range of earth structure nonuniqueness implied by body wave observations.

10 p1215 A73-24779

Geometrical theory for flexure waves in shells.

11 p1432 A73-24977

Small amplitude surface and plate waves propagation in incompressible biaxially stressed elastic media, obtaining dispersion equation for various phase velocities

11 p1434 A73-25166

The ion cyclotron drift loss-cone instability with a coexisting cold plasma.

11 p1404 A73-25271

European contribution to structural response to noise.

[AIAA PAPER 73-332]

11 p1305 A73-25561

A photon rest mass and the propagation of longitudinal electric waves in interstellar and intergalactic space.

11 p1417 A73-25562

Stress waves in finite longitudinally layered shells.

11 p1442 A73-25712

Shear correction factors for orthotropic laminates under static load.

11 p1442 A73-25713

Possibility of correlating the field of a wide wave beam in a smoothly nonhomogeneous medium with the field of a beam in vacuum

11 p1331 A73-26161

Temperature-waves in connection with drift type instabilities in a Q-plasma.

11 p1406 A73-26558

Elastic and elastoviscoplastic unloading waves propagation in semiinfinite bar under axial impact stress, considering bilinear stress-strain curve

11 p1447 A73-26646

An existence proof for permanent capillary gravity waves with general vortex distributions

11 p1349 A73-26747

Calculation of the statistical characteristics of a long waveguide line in a two-wave model

12 p1469 A73-27189

Power series solution of quasi-linear parabolic heat conduction equation for temperature wave propagation in soil

12 p1560 A73-27807

A general theory of harmonic wave propagation in linear periodic systems with multiple coupling.

13 p1658 A73-28066

Influence of viscosity, thermal conduction, and ion drag on the propagation of atmospheric gravity waves in the thermosphere.

13 p1606 A73-28154

Wave propagation in the two temperature theory of thermoelasticity.

13 p1691 A73-28162

Nonlinear wave propagation processes in elastic tubes

13 p1692 A73-28165

Wave propagation aspects of the generalized theory of heat conduction.

13 p1704 A73-28414

Propagation of a nonlinear wave in a weakly turbulent plasma.

13 p1665 A73-28676

Planar shear wave motions polarized in plane of bonded elastic orthotropic layered plates with each layer having distinct mechanical and inertial properties and thickness

13 p1697 A73-28820

Representative shear wave passage through plane flame front, determining wave refraction and modification, flame generated turbulence and noise and perturbation of front

13 p1707 A73-28993

Extension of Mandel inequalities to plastic acceleration wave velocities in a finitely deformed medium

13 p1703 A73-29553

Wave propagation in the ion sheath of an antenna immersed in a plasma

14 p1731 A73-29730

Interplanetary plasma inhomogeneities effect on Alfvén wave propagation direction from Pioneer 6 magnetic measurements

14 p1796 A73-29957

Influence of flow and pressure on wave propagation in the canine aorta.

14 p1715 A73-30066

Implicit predictor-corrector difference scheme for boundary value problem solution in propagation of spherical and cylindrical N waves /asymptotic pulse forms/

14 p1745 A73-30175

Patterns of waves in galactic disks.

14 p1801 A73-30728

Boundary conditions in primitive equation weather prediction models with special emphasis on the control of gravity wave propagation.

14 p1772 A73-30902

Propagation constant and wave resistance in the case of coaxial and hollow conductors with lossy dielectric and magnetic materials

14 p1730 A73-30920

Propagation of elastic Lamb waves in an initially stressed body

15 p1945 A73-31030

Hydraulic impact in coaxial cylindrical tubes

15 p1860 A73-31046

The effect of temperature perturbations on ion-acoustic and drift waves in a weakly collisional plasma.

15 p1916 A73-31087

Hadamard theorem on wave propagation existence in elastic body with infinitesimal stability condition proved by linear elliptical partial differential equations systems theory techniques

15 p1914 A73-32120

Quasi-monochromatic viscoelastic waves energy velocity equivalence to phase velocity for medium represented by standard linear solid or Maxwell model

15 p1955 A73-32176

Current distribution on an infinite tubular antenna immersed in a cold collisional magnetoplasma

15 p1920 A73-32236

Russian book - Asymptotic theory of diffraction of electromagnetic waves by finite structures.

15 p1845 A73-32294

Nonlinear ion-acoustic and electron-acoustic waves of a plasma in a magnetic field

15 p1921 A73-32324

Hydrodynamic theory of high-amplitude ionization waves

15 p1921 A73-32326

Trapped wave vortex breakdown model for long weakly nonlinear wave propagation on critical flows in tubes of variable cross sections

16 p1998 A73-32796

Planar pressure waves propagation across wall with elastically supported and damped edges, considering induced gas flow characteristics behind wall

16 p2000 A73-33257

Weak disturbances upstream propagation in supersonic boundary layer, deriving homogeneous boundary value problem for complex amplitude function

16 p2000 A73-33263

Propagation of thermoelastic waves in an undefined isotropic soil

16 p2081 A73-33369

Acceleration waves in simple elastic materials.

16 p2081 A73-33746

Spatially growing wave trails of an inviscid fluid discontinuity.

16 p2001 A73-33868

On the existence of critical levels, with applications to hydromagnetic waves.

16 p2043 A73-33869

Flexural wave mechanics - An analytical approach to the vibration of periodic structures forced by convected pressure fields.

16 p2083 A73-33947

The effect of plasma resonance on the propagation of surface waves along plasma-vacuum channel.

16 p2043 A73-34023

Book on wave propagation in continuous media covering Hamilton principle, energy theorems, elastic waves, electromagnetic and hydromagnetic waves, Green function and nonlinear effects

17 p2211 A73-34280

Book - Diffraction of elastic waves and dynamic stress concentrations.

17 p2242 A73-34468

The propagation of Alfvén waves and their directional anisotropy in the solar wind.

17 p2223 A73-34501

Wave propagation in the magnetosphere of Jupiter.

17 p2229 A73-34506

Wave propagation in uniform laminar cylindrical shells, discussing group and phase velocities on wave numbers in sandwich walls

17 p2243 A73-34734

Plane finite amplitude viscoelastic wave propagation, deriving expressions for nonlinear, dispersion and dissipation effects

17 p2244 A73-34792

Nonstationary wave propagation in equilibrium liquid-vapor flow, noting pressure jumps due to expansion

17 p2155 A73-35193

Book - Applied nonlinear optics.

17 p2212 A73-35274

Electrostatic waves with frequencies above the gyrofrequency in a plasma with a loss-cone.

17 p2218 A73-35831

Book - Electromagnetic wave propagation.

17 p2130 A73-35857

Meteor radar observations of long period waves in the 80-100 km altitudes range.

18 p2304 A73-35968

Ducted propagation of VLF waves through the magnetosphere.

18 p2288 A73-35995

Alfvén waves in the solar wind - Wave pressure, Poynting flux, and angular momentum.

18 p2346 A73-36264

Nonlinear radial wave propagation in low density expanding flows with application to the free jet.

18 p2300 A73-36630

Phase velocity dispersion for transverse normal elastic wave propagation through sandwiched CdS and molten quartz or germanium layers

18 p2340 A73-36672

A note on uniqueness in the linear theory of heat conduction with finite wave speeds.

18 p2371 A73-36692

Weak perturbation propagation in magnetic gasdynamics

19 p2468 A73-37550

Calculation of reflection and transmission coefficients for a class of one-dimensional wave propagation problems in inhomogeneous media.

19 p2459 A73-37587

On the propagation of relativistic thermo-magneto-viscoelastic waves in a material of Voigt-type.

19 p2459 A73-37648

Characteristics of hydromagnetic wave propagation in a slowly varying magnetic field /in the approximation of geometric optics/.

19 p2425 A73-37923

On the kinetic theory of wave propagation in random media.

19 p2460 A73-38103

Two dimensional wave problems in rotating elastic media.

19 p2460 A73-38183

Occurrence and features of ducted modes of internal gravity waves over Western Europe and their influence on microwave propagation.

19 p2405 A73-38225

Thermal structure and stability study of internal and Kelvin-Helmholtz waves in low Reynolds number flows by sampling and stratified wind tunnel methods

19 p2422 A73-38235

Measurements of internal waves and turbulence in two-dimensional stratified shear flows.

19 p2422 A73-38238

Book - Stress wave propagation in solids: An introduction.

19 p2502 A73-38363

Dynamics of step heat waves in gases and plasmas.

20 p2592 A73-38863

Verification of sensitivity enhancement factors for CW ultrasonic resonators.

20 p2565 A73-38887

Propagation of stress wave with plastic deformation in metal obeying the constitutive equation of the Johnson-Gilman type.

20 p2615 A73-38888

Convective amplification of type I irregularities in the equatorial electrojet.

20 p2551 A73-38938

Application of the method of normal waves to the study of the oscillations of a cylindrical shell in contact with an elastic medium

20 p2615 A73-38984

Potential oscillations with frequencies higher than the gyrofrequency in a plasma containing a cone of losses

20 p2597 A73-39207

Propagation velocities and amplitudes of thermo-acoustical waves in thermo-plastic materials.

21 p2789 A73-40088

Effects of propagation parallel to the magnetic field on the Type I electrojet irregularity instability.

21 p2682 A73-40160

Deviation of the solution of a quasi-linear wave equation from the solution of the linear equation in the region of continuous first derivatives

21 p2724 A73-40181

Linear wave motion analysis of viscous incompressible fluid of infinite depth at small and large times by asymptotic quadrature method

21 p2676 A73-40207

Carrier-frequency distance dependence of a pulse propagating in a two-level system.

21 p2649 A73-40224

Surface wave propagation parallel to applied magnetic field in electron hole plasma, explaining observed resonances in InSb by LF mode

21 p2751 A73-40325

A wave propagation method for conversion of grey pictures into line figures.

21 p2654 A73-40688

Flexural wave propagation in a thin plate with circular holes.

21 p2787 A73-41142

Statistical model for phase relations derived from observations of photospheric oscillations, criticizing horizontal propagation theory for phase propagation

21 p2777 A73-41482

Umbral flashes and running penumbral waves relation to overstable hydromagnetic oscillation in sunspots, noting depth dependence and electrical conductivity variation effects

21 p2777 A73-41487

Magnetohydrodynamic waves in the solar wind plasma

21 p2763 A73-41506

Thermoelastic wave propagation in a random medium and some related problems.

21 p2789 A73-41667

Acceleration waves in ideal fluid mixtures with several temperatures.

22 p2929 A73-41772

Gravitational waves in a space-time of any dimension.

22 p2885 A73-41773

WAVE RADIATION

Wave amplitude calculation for propagation in inhomogeneous isotropic media by optical ray tracing consisting of integration of first and second order differential equations 22 p2885 A73-41817

Electron wave excitation and propagation in low density large volume plasmas near electron Langmuir frequency 22 p2891 A73-42241

Contribution to the theory of wave propagation in a one-dimensional randomly inhomogeneous medium 22 p2826 A73-42334

Short-wave propagation in a randomly inhomogeneous medium with an arbitrary law of permittivity fluctuations 22 p2826 A73-42335

An exact solution on the propagation of small disturbances in a radiating grey gas with isotropic scattering. 22 p2932 A73-42570

On detonation waves supported by diffusion flames. 22 p2936 A73-42810

Dynamic stability of transverse axisymmetric waves in circular/cylindrical shells. [ASME PAPER 73-APMW-26] 22 p2925 A73-42887

Finite difference scheme for wave equation solution for wave propagation in layered composite materials, obtaining matrix eigenvalues with Floquet condition for various methods [ASME PAPER 73-APMW-40] 22 p2926 A73-42897

Modes of one-dimensional wave propagation in an infinite thermoelastic medium with finite heat propagation rates 22 p2927 A73-42928

Propagating thermal waves in force-cooled superconducting devices. 22 p2938 A73-42953

Vertically nonpropagating magnetatmospheric waves investigation based on local dispersion relations governing magnetoacoustic and magnetogravitational wave propagation with emphasis on solar atmosphere conditions 22 p2914 A73-43010

Observation of extraordinary wave propagation near the lower hybrid resonance frequency. 22 p2895 A73-43023

High frequency vibrations and waves in laminated orthotropic plates. 22 p2928 A73-43135

Small amplitude Alfvén waves propagation in solar wind under interplanetary magnetic field, relating wave and wind velocity 23 p3029 A73-43612

The effect of dissipation on the vertical propagation of planetary waves in the vicinity of critical levels. 23 p3032 A73-43906

Classical viscoplasticity and Mandel plasticity theories comparison with emphasis on strain hardening, acceleration wave propagation and plastic and elastic deformations 23 p3043 A73-43968

Transverse elastic wave propagation in CdS crystal wafer coated on both sides with AgBr, titanium oxide, Si or polystyrene 23 p3017 A73-44038

Non-linear propagation of VLF waves in a magnetoplasma including the effect of ions. 23 p3012 A73-44143

Wave propagation and diffraction in bodies with noncircular cylindrical boundaries 23 p3045 A73-44181

On the generation of umbral flashes and running penumbral waves. 24 p3136 A73-44638

Current instability of atmospheric gravitational waves 24 p3083 A73-44786

Use of a relaxation technique in nozzle wave propagation problems. [AIAA PAPER 73-1011] 24 p3078 A73-44843

Successively forward-scattered wave propagating through a random medium. 24 p3110 A73-45028

Solid fuels combustion stability and shock wave induced detonations propagation stability in aerosols investigation based on one dimensional turbulence, using multistage mathematical models 24 p3157 A73-45383

WAVE RADIATION

U ELECTROMAGNETIC RADIATION

WAVE REFLECTION

Ground reflection effects upon radiated and received signals as viewed via image theory. 01 p0015 A73-10181

Discussion of radiative-transfer methods applied to electromagnetic reflection from turbulent plasma. 01 p0081 A73-10196

Shock wave reflections along the axis in a steady axisymmetric flow [ONERA, TP NO. 1128] 01 p0001 A73-10237

Reflection and diffraction of shocks interacted by yawed wedges. 01 p0002 A73-10272

Reflection of plane stress waves in an elastoplastic medium with a variable yield limit 01 p0114 A73-10570

Reflection coefficients for acoustic waves interacting with stratified media. 01 p0078 A73-11097

Determining the size of defects in standardizing sensitivity using a spherical reflector. 02 p0169 A73-12149

Russian book on radio wave propagation covering ground, ionospheric and tropospheric propagation, ratio attenuation, scattering and ionospheric and tropospheric reflection 02 p0143 A73-12775

Applications of dynamic photoelasticity in flaw detection analysis. I. 02 p0175 A73-12868

Polar streamline directions at the triple point of Mach interaction of shock waves. 03 p0244 A73-13566

Total reflection of a plane wave by a semi-infinite random medium. 04 p0480 A73-15198

FM Gaussian electromagnetic pulse distortion during reflection from ionospheric model with linear electron density profile and constant collision frequency 04 p0422 A73-15479

Mirror corner for use with overmoded circular waveguide. 05 p0548 A73-16165

Error analysis of Wentzel-Kramers-Brillouin approximation for electromagnetic wave reflection from nonuniform absorbing half space 05 p0549 A73-16392

Dielectric layers in the radiation field of microwave antennas 05 p0550 A73-16475

A universal method of calculation of the state of a real gas behind primary and reflected shock waves. 06 p0684 A73-17700

Anechoic funnel and rectangular chambers for antenna measurements 06 p0674 A73-17822

Large amplitude waves in bounded media. I - Reflexion and transmission of large amplitude shockless pulses at an interface. 06 p0761 A73-17874

Reflection and transmission of electromagnetic waves obliquely incident on a relativistically moving uniaxial plasma slab. 06 p0665 A73-18185

Distortion of electromagnetic pulses undergoing total internal reflection from a moving dielectric half-space. 06 p0666 A73-18200

Measurement of dielectric constant of nonmagnetic materials in a waveguide system with an unknown movable reflecting load. 06 p0696 A73-18618

Electromagnetic wave reflection by two level medium analog of moving molecular beam, considering fields penetration and surface impedance effects 06 p0668 A73-18647

Antenna design for Eole satellite radio communications with balloons, noting wave polarization and sea reflection effects 07 p0797 A73-18963

On the reflection of harmonic waves in fiber-reinforced materials. 07 p0909 A73-19096

Ionospheric attenuation of 3-100 MHz radio waves, interpreting scatter mode propagation mechanism as total reflection from lower ionizational irregularities 07 p0792 A73-19458

The laws of reflection and refraction of incompressible magnetohydrodynamic waves at a fluid-solid interface. 07 p0858 A73-20028

On the transmission of the energy in an incompressible magnetohydrodynamic wave into a conducting solid. 07 p0858 A73-20029

Transmission of electromagnetic waves through a conducting slab. IV - A simple multiple-reflection method. 07 p0852 A73-20172

Reflection from the earth's surface of shock waves generated by falling meteorites 08 p0958 A73-21065

Hemispherical reflectivity and transmissivity of an absorbing, isotropically scattering slab with a reflecting boundary. 08 p1025 A73-21643

Ionospheric electron density profile observation by partial reflection experiment, discussing radio signal amplitude and phase data recording sensitivity requirement 09 p1075 A73-22071

Experimental observations of the amplitudes of Es and F-region reflections and their comparison with the thin-layer model for Es. 09 p1076 A73-22138

Quasi-monochromatic radiation pulse reflection from rough surfaces, analyzing echoes statistical properties 09 p1120 A73-22575

Kinetic theory for the reflection of waves obliquely incident on the boundary of a magnetoactive plasma 09 p1052 A73-23078

Coefficients of hydromagnetic wave reflection from conjugate ionospheres 10 p1211 A73-23895

Electromagnetic wave reflection at interface between anisotropic Vlasov plasma and vacuum with external magnetic field, deriving electric and magnetic field characteristics 10 p1255 A73-24260

Wave amplification during the reflection from a rotating 'black hole' 10 p1283 A73-24752

Experimental study of shock-wave reflection from a thermally accommodating wall. 11 p1449 A73-25252

Calculation of the radiation diagram of an antenna in the presence of a radome 11 p1328 A73-25285

Effect of edge reflections on the performance of antenna ground screens. 11 p1329 A73-25673

Reflection plate interferometer with thin glass shearing plate replacing knife edge in Schlieren system, noting optimum operating range and fringe spacing 11 p1365 A73-26238

Single reflection Fresnel rhomb for quarter-wave retardation in the infrared. 11 p1400 A73-26251

Use of reflection-coefficient amplitude-phase diagrams for choosing and analyzing the operating modes of a radio defectoscope. 11 p1375 A73-26363

Kramers-Kronig analysis of relative reflectance spectra measured at an oblique angle. 11 p1400 A73-26421

Precise measurement of reflection coefficients by means of tuned microwave reflectometers. 12 p1478 A73-27047

Reflection of electromagnetic waves from non-homogeneous anisotropic plasma layers /normal incidence/ 12 p1470 A73-27356

The use of surface-elastic-wave reflection gratings in large time-bandwidth pulse-compression filters. 12 p1480 A73-27566

Vibration analysis of thick-walled hollow spheres and cylinders, determining periodic response and fundamental frequency as function of wave reflection number and dimensions 13 p1695 A73-28489

Electromagnetic wave reflection and transmission by slant air/dielectric interface in rectangular waveguide investigated by Green function technique 14 p1724 A73-29706

Electromagnetic wave radiation and reflection at guiding structure discontinuity, calculating TE mode surface wave by boundary perturbation technique 14 p1727 A73-30214

A null-reading method of measuring the complex reflection coefficient in the short-wave end of the millimeter band 14 p1728 A73-30271

Investigation of rough surfaces by a method based on the scattering of coherent light by the sound reflected from such surfaces 14 p1753 A73-30583

Frequency dependence of radio-wave absorption in a reflecting layer 15 p1844 A73-31884

Reflection and transmission of electromagnetic waves obliquely incident on a relativistically moving isotropic plasma slab. 15 p1919 A73-31947

Reflection of electromagnetic waves from a moving plasma 15 p1846 A73-32303

Asymptotic development method for the determination of the field reflected by a random surface 16 p1984 A73-33966

Determination of changes in the reflection coefficient of absorbing coatings in the millimeter wavelength band 17 p2120 A73-34156

Radiometric measurements of temperature of the ocean surface - Improvement brought by use of a polarizing radiometer 17 p2161 A73-34946

Physics and chemistry of the ionosphere 17 p2162 A73-35050

Non-coherent scattering in transfer problems in spherical shell media. I - Frequency-independent source function. 17 p2236 A73-35780

One-dimensional model for nonlinear reflection of laser radiation by an inhomogeneous plasma layer. 17 p2218 A73-35824

Evidence of frontal structures in nonblanketing sporadic-E layers. 18 p2304 A73-35990

Transformation, transmission, and reflection of plasma waves in the presence of a tangential velocity discontinuity 18 p2339 A73-36551

Reflection of meteorite generated shock waves from the earth's surface. 18 p2313 A73-36866

- Oblique reflection of a plane acoustic wave from a burning surface 19 p2503 A73-37513
- Calculation of reflection and transmission coefficients for a class of one-dimensional wave propagation problems in inhomogeneous media. 19 p2459 A73-37587
- The interaction between atmospheric microstructure and acoustic and electromagnetic waves. 19 p2406 A73-38242
- Reflection of powerful radio waves from the lower ionosphere 19 p2406 A73-38334
- Reflection coefficients of hydromagnetic waves from conjugate ionospheres. 20 p2551 A73-38914
- Regular reflection of an oblique shock in a plane flow of ideally dissociating gas in the presence of a transverse magnetic field 21 p2744 A73-40189
- Digitally scanned planar phased arrays, deriving optimum phase perturbation function for quantization and reflection lobe dispersion in terms of aperture distribution amplitude 21 p2652 A73-40667
- On the reflection of transverse waves from a cold plasma. 21 p2748 A73-40930
- Reflection and transmission of plane waves at a boundary between two conducting media. 21 p2655 A73-41047
- Image contrast and efficiency of nonlinearly recorded holograms of diffusely reflecting objects. 21 p2703 A73-41133
- Russian book on statistical properties of ionosphere reflected signals covering statistical modeling, random processes, perturbation method and wave reflection problems 21 p2657 A73-41284
- Reflection of a shock wave from a thermally accommodating wall - Molecular simulation. 22 p2842 A73-42234
- Yagi type antenna array of vertical monopoles with optimized slot reradiation to modify foreground reflection for performance improvement 22 p2832 A73-42295
- Incident electromagnetic wave reflection in inhomogeneous plasma with local nonlinearity, discussing reflection point shift and dielectric permittivity effect 22 p2892 A73-42328
- The reflexion of an acoustic pulse by a plane vortex sheet. 22 p2842 A73-42348
- Diffraction and reflection of shocks from corners. 22 p2843 A73-42567
- Elastic-plastic wave reflection and refraction obtained by method of singular surfaces, discussing interface and plastic deformation effects [ASME PAPER 73-APMW-38] 22 p2926 A73-42895
- On an integral equation governing the reflection of electromagnetic waves by a random surface 22 p2888 A73-42948
- Reflection and transmission of electromagnetic waves at a moving magnetoplasma half-space. 22 p2896 A73-43179
- Reflection of electromagnetic waves from inhomogeneous anisotropic plasma sheets /normal incidence/. 23 p2952 A73-43255
- Scattering and transmission functions of radiation by finite atmospheres with reflecting surfaces. 23 p3030 A73-43755
- Reflection of electromagnetic waves from a moving plasma. 24 p3067 A73-44611
- Similarity of flows arising during reflection of weak shock waves from a rigid wall and from a free surface 24 p3076 A73-44713
- Winds and wave motions /70-100 km/ as measured by a partial reflection radiowave system. 24 p3088 A73-45212
- Lagrangian analysis of multiple scatter in acoustic and electromagnetic reflexion. 24 p3111 A73-45394
- WAVE RESISTANCE**
- Propagation constant and wave resistance in the case of coaxial and hollow conductors with lossy dielectric and magnetic materials 14 p1730 A73-30920
- Construction of a minimum-wave-drag profile in inhomogeneous supersonic flow 21 p2631 A73-40184
- WAVE SCATTERING**
- NT ACOUSTIC SCATTERING
- NT ATMOSPHERIC SCATTERING
- NT ELECTROMAGNETIC SCATTERING
- NT HALOS
- NT IONOSPHERIC F-SCATTER PROPAGATION
- NT LIGHT SCATTERING
- NT MICROWAVE SCATTERING
- NT MIE SCATTERING
- NT RAMAN SPECTRA
- NT RAYLEIGH SCATTERING
- NT REVERBERATION

NT TROPOSPHERIC SCATTERING

NT X RAY SCATTERING

- Incident plane wave fluctuations effect on diffraction pattern formed by scattering on reflecting sphere, calculating amplitude distribution in Fresnel and Fraunhofer regions 01 p0016 A73-10211
- Book - Radiation and scattering of waves. 02 p0192 A73-11882
- Wave scattering in collisionless magnetoactive plasma, taking into account magnetic field effects, spiral motion of scattering particle and shielding fields 03 p0346 A73-13357
- Time-periodic fluid surface wave radiation and scattering by partially immersed objects in short wave asymptotic limit of nondimensional wavelength approaching zero 03 p0397 A73-13533
- Monochromatic plasma wave instability due to induced scattering on thermal plasma electrons and ions with and without magnetic field 05 p0604 A73-17361
- Nonequilibrium plasma wave scattering cross section dependence on energy bands shape and field orientation in semiconductors 06 p0735 A73-17975
- Application of the theory of multiple wave scattering to the derivation of the radiative transfer equation for a statistically inhomogeneous medium 07 p0792 A73-19913
- The compressional modulus of a material permeated by a random distribution of circular cracks. 07 p0915 A73-20335
- Backscattering of a scalar wave field by an ideally reflecting object situated near the caustic surface 09 p1052 A73-23081
- Inverse scattering method application to plane wave incident on perfectly conducting sphere, comparing results to simulation experiments 11 p1329 A73-25680
- Scattering of a cylindrical wave in an elastic plate in the presence of an absolutely rigid cylindrical inclusion 12 p1551 A73-27240
- Scattering from a periodic corrugated surface - Semi-infinite alternately filled plates. 13 p1659 A73-28484
- Ion acoustic wave scattering effects on stochastic ion heating in turbulent plasma 14 p1780 A73-30340
- Phenomena of scattering of electromagnetic and gravitational wave packets in the gravitational field of a black hole 15 p1932 A73-31245
- Obliquely incident plane wave scattering from moving perfectly conducting cylinder, discussing mode coupling, Doppler shift and far field scattered power 15 p1845 A73-32238
- Diffraction of a plane electromagnetic wave on arrays of periodically spaced cylinders 17 p2121 A73-34583
- Scattering of waves at a step in a circular multiwave waveguide. 17 p2123 A73-35152
- Scattering of a spherical wave by spherical inhomogeneity with arbitrary refractive index distribution along the radius. 17 p2123 A73-35163
- On the kinetic theory of wave propagation in random media. 19 p2460 A73-38103
- Limits of applicability of the Delano model for describing the process of wave scattering by a complex-shaped body 19 p2407 A73-38343
- Laser beam incidence in active nonlinear medium, considering Kerr effect, beam generation, Green function and intensity calculations for wave scattering 21 p2710 A73-40153
- On the surface-to-bulk mode conversion of Rayleigh waves. 21 p2705 A73-41429
- Raman scattering of SHF radiation in a bounded plasma of a solid 21 p2657 A73-41509
- WAVE SUPERHEATERS**
- U HYPERVELOCITY WIND TUNNELS
- U SHOCK TUBES
- WAVEFORMS**
- NT PULSE AMPLITUDE
- NT PULSE DURATION
- NT SAWTOOTH WAVEFORMS
- NT SQUARE WAVES
- Ultrasonic studies of the nonlinear properties of solids. 01 p0057 A73-11003
- Limited space charge accumulation oscillations in gallium arsenide 02 p0199 A73-11530
- Ionospheric resonance signal envelope and waveform observation by rocket-borne RF sounder, noting electron gyrofrequency third harmonic due to beating waves 02 p0140 A73-11750

- Russian book on nanosecond multiphase multivibrators covering transistorized single- and dual-stage amplifiers and wave shaping circuits for digital control and computer logic applications 02 p0146 A73-11887
- Average return pulse form and bias for the S193 radar altimeter on Skylab as a function of wave conditions. 04 p0446 A73-14804
- Complex detection - A waveform preserving technique for single-sideband demodulation. 04 p0415 A73-14989
- Detection of multichannel FSK signals using chirp dispersion method. 04 p0419 A73-15407
- The pulse shape of the Crab Nebula pulsar NP 0532 as a function of color. 04 p0501 A73-15685
- Nonlinear analysis for local microwave oscillator voltage waveform across nonlinear junction of Schottky barrier mixer diode, comparing results with analog simulation 06 p0677 A73-18740
- Common-bandwidth transmission of data signals and wide-band pseudonoise synchronization waveforms. 07 p0790 A73-19200
- A study on accumulation of waveform distortions in PCM hybrid transmission. 07 p0791 A73-19369
- Photocurrent pulse shape in thin organic semiconductor films 07 p0862 A73-20008
- Transient photocurrent pulse shapes and transit times in insulators with uniform and exponential trapped space charge in excitation layer or insulator surface 09 p1119 A73-21945
- A new approach to picosecond laser pulse analysis shaping and coding. 09 p1090 A73-22077
- Investigation of the dielectric waveguide modes in homostructure GaAs laser. 09 p1091 A73-22238
- Time jitter in line regenerators with pattern dependent pulse waveforms. 09 p1062 A73-22301
- Images of truncated triangular-wave periodic targets in optical systems in the presence of linear image-motion. 10 p1248 A73-23614
- Signal synthesis based on desired autocorrelation function for pulse shaping applications in radar and communications, discussing nonlinear equations solution by decomposition into source polynomials 10 p1187 A73-23730
- Experimental verification of new Gunn-effect reflection-insensitive pulse regenerator. 11 p1337 A73-25361
- Sampling circuit for HF repetitive waveforms reproduction on standard x-y recorder, noting SNR improvement by signal averaging 11 p1366 A73-26304
- A programmable surface acoustic wave matched filter for phase-coded spread spectrum waveforms. 12 p1484 A73-27574
- The effect of wave form and cyclic frequency on the fatigue life of aluminium alloys. 13 p1640 A73-29491
- Wide integrated pulse profiles of pulsars. 16 p2071 A73-34036
- Parasitic mode conversion loss measurement for circular waveguide section quality evaluation, determining transmission coefficient from signal envelope 17 p2121 A73-34588
- Performance measurements of aircraft electrical systems having highly distorted voltage and current waveforms. 17 p2135 A73-34604
- Automatic recognition of electrocardiographic patterns 17 p2116 A73-34964
- Currents in Florida lightning return strokes. 17 p2163 A73-35465
- Effect of rotational level coupling on pulse sharpening in CO2 amplifiers. 17 p2143 A73-35791
- Central nervous system influence upon electrocardiographic waveforms. 18 p2275 A73-36530
- Digital filter tasks and applications, discussing recursive and transversal filters, waveforms, SNR, truncation errors and complex filtering 19 p2414 A73-38301
- PPM pulse waveform synthesis with SNR performance improvement while retaining bandwidth-mean-square error properties inherent in wideband modulation system 20 p2524 A73-38736
- Contingent negative variation expectancy waveform relation to human psychic state in response to visual and imperative acoustic stimuli 20 p2516 A73-39804

WAVEGUIDE ANTENNAS

Harmonic frequency content analysis from fluxgate magnetometer recorded Pi 2 pulsation spectral waveform, noting agreement with earth current spectrum

21 p2681 A73-40154

Q switched carbon dioxide laser pulse forms and spectrum, covering mirror and prism configurations, sodium chloride plate irradiation, laser wavelengths and pressure effects

21 p2714 A73-40572

Shaping device for frequency analysis of electrical processes in peripheral neural stems and ganglia

22 p2815 A73-42664

High voltage waveform generation at low power levels by circuit techniques and system configurations involving parallel series chains of light triggered bilateral switches

22 p2834 A73-42907

WAVEGUIDE ANTENNAS

NT HORN ANTENNAS

Performance of a protruding-dielectric waveguide element in a phased array.

01 p0022 A73-10180

Dual frequency antenna design using hollow fin as TE mode waveguide with sidewall radiating elements, calculating attenuation for comparison with experiment

01 p0023 A73-10189

Propagation and radiation characteristics of corrugated horns.

07 p0798 A73-19156

Influence of horn length on radiation pattern of oblique-flare-angle corrugated horn.

07 p0798 A73-19160

Rectangular horn with dielectric-slab insert.

08 p0946 A73-21117

Radiation characteristics of waveguide-excited dielectric spheres with matched sphere-air boundary.

08 p0947 A73-21121

Near-field technique for inferring aperture antenna radiation patterns.

09 p1052 A73-22960

Computational estimate of applicability of infinite-array theory.

09 p1065 A73-23099

Horn antennas dephasing based on quadrupole with circular guides, cones of revolution and air space

11 p1327 A73-25279

Two mode rectangular waveguide longitudinal and transverse narrow half wave slots properties, discussing measurement apparatus and techniques and radiation patterns

11 p1328 A73-25661

Diffraction of a plane wave at an array of planar waveguides with projecting dielectric plates.

13 p1582 A73-28655

Radiating waveguide antenna elliptical beam off-axis gain maximization, applying to geostationary satellite

13 p1587 A73-29671

Corrugated circular waveguide horn as monopulse antenna feed for optimal tracking performance, using difference-sum patterns with hybrid modes

14 p1731 A73-29705

Broad-band impedance matching of rectangular waveguide phased arrays.

14 p1734 A73-30205

Radial mode analysis of electromagnetic wave propagation on slotted cylindrical structures.

14 p1727 A73-30208

Radiation characteristics of a waveguide excited dielectric sphere backed by a metallic hemisphere.

14 p1728 A73-30225

A wide-band square-waveguide array polarizer.

14 p1735 A73-30228

Radiating slot antenna immittance reactive term due to energy storage in feeding waveguide, discussing resonance characteristics

15 p1849 A73-31097

Radiation efficiency of an X-band waveguide antenna.

17 p2127 A73-35637

Equivalent conductivity of a longitudinal slot on the broad wall of a uniformly curved rectangular waveguide

21 p2648 A73-40199

Tilted, off-center, matched slots on the broad wall of a uniformly curved rectangular waveguide

21 p2648 A73-40200

Phased array element types comparison, discussing dipole and open-ended waveguide radiator designs with emphasis on driving point impedance accuracy and active element pattern

21 p2663 A73-40649

Analysis of infinite planar array of rectangular waveguides by generalized scattering matrix approach.

21 p2651 A73-40652

A new procedure for the design of a waveguide element for a phased-array antenna.

21 p2652 A73-40658

Wide-angle impedance matching of phased-array antennas - A survey of theory and practice.

21 p2652 A73-40659

The design of a wide band wide scan-angle waveguide radiating element.

21 p2652 A73-40660

Multimode phased array element for wide scan angle impedance matching.

21 p2652 A73-40661

Realized gain function for a cylindrical array of open-ended waveguides.

21 p2653 A73-40677

Dual beam antenna - A unique waveguide phased array with independently steered beams.

21 p2653 A73-40683

Narrow-beam antennas using cylindrical columns of isotropic plasma.

21 p2665 A73-41124

Circularly polarized linear waveguide array.

22 p2831 A73-41843

WAVEGUIDE FILTERS

Microwave-power attenuation in Gunn diodes

01 p0025 A73-10979

Modulation type microwave receiver with selective filter and ferrite resonator in waveguide coupling

08 p0949 A73-21561

General cavity analysis for corrugation in rectangular waveguide microwave filters, using admittance method with consideration for propagation modes

10 p1192 A73-23606

Tapered corrugated waveguide low-pass filters.

21 p2666 A73-41427

Coupling coefficient/frequency characteristics of rectangular dielectric waveguide channel dropping coupled line filter for millimeter wave

23 p2961 A73-44118

WAVEGUIDE WINDOWS

Regenerative amplifier based on multiple IMPATT diodes

07 p0802 A73-20295

Analysis of thick rectangular waveguide windows with finite conductivity.

18 p2292 A73-36605

Regenerative multidiode IMPATT amplifier.

18 p2294 A73-37132

WAVEGUIDES

NT BEAM WAVEGUIDES

NT OPTICAL WAVEGUIDES

NT PLASMA GUIDES

Book - Handbook of microwave techniques and equipment.

01 p0021 A73-10025

Ray optical procedure to obtain scalar Green function for polygonal waveguides by image diagram identification from rectangular guide equivalent combinations

01 p0024 A73-10684

Unit for wideband measurements of dielectric parameters at millimeter wavelengths

01 p0050 A73-10794

Experimental investigation of millimeter-band electromagnetic wave propagation in a waveguide filled with n-type InSb under a magnetic field

01 p0017 A73-10977

Relativistic dispersion equation for a circular waveguide with a rotating tubular electron beam, allowing for the effect of the space charge

01 p0017 A73-10982

Field distribution formulas for fast wave attenuation in thin walled tubular dielectric waveguide within external absorbing diaphragms

02 p0142 A73-12495

The ducted propagation of PP micropulsations in the magnetosphere and PP dotting.

03 p0298 A73-12877

Complex transmission coefficient of waveguide with two arbitrarily spaced infinitely thin plane parallel inhomogeneities, using Galerkin method for single-parameter approximation of electrodynamic problem

03 p0278 A73-14057

Study of bends in long distance waveguides - The case of metallic guides

04 p0427 A73-14900

Eigenvalues and eigenfunctions of electric and magnetic waves of shielded strip transmission line, calculating electromagnetic field in cylindrical waveguide

04 p0417 A73-15089

Periodic axisymmetric waveguide with complex structure, obtaining slow wave dispersion equation solutions

04 p0429 A73-15910

Higher-order evanescent modes on slow-wave structures.

05 p0547 A73-16160

Mirror corner for use with overmoded circular waveguide.

05 p0548 A73-16165

Pulse propagation in a two-mode waveguide.

05 p0548 A73-16365

Higher-order scattering losses in dielectric waveguides.

05 p0549 A73-16366

Higher-order loss processes and the loss penalty of multimode operation.

05 p0549 A73-16367

Eigenvalues of normal waves in a plane waveguide channel

05 p0549 A73-16385

Vertical electric dipole excited electromagnetic fields in triple layer medium with plane boundaries, noting waveguide thickness effect on electromagnetic wave propagation

05 p0549 A73-16386

Variational method of moments and some iteration procedures for determining the characteristics of VLF wave propagation in the earth-anisotropic ionosphere waveguide channel. I

05 p0549 A73-16387

Vertical electric dipole excited electromagnetic field in earth-ionosphere waveguide, using Galerkin method for VLF electromagnetic wave propagation equation

05 p0549 A73-16389

The field of a vertical electric dipole over a spherical earth having an atmosphere that is nonhomogeneous with height

05 p0549 A73-16390

A model of VLF band radio wave propagation in the earth-ionosphere waveguide channel

05 p0549 A73-16391

VLF field diurnal variations and terminator crossing effect on signal path during transmission in earth-ionosphere waveguide

05 p0549 A73-16393

Effect of the earth's electrical properties on the characteristics of VLF wave propagation in the earth-ionosphere waveguide

05 p0550 A73-16398

Light signal modulation by traveling wave in circular waveguide with coaxial KDP crystal

05 p0558 A73-16781

Excitation of a magnetohydrodynamic waveguide by a moving source

05 p0603 A73-16820

An aluminum waveguide of oval cross section, which can be wound on a drum, with favorable wave resistance transformations /ALFORM waveguide/

06 p0663 A73-17582

Dimensional and material effects on microwave waveguide damping and bandwidth characteristics in long distance communications

06 p0663 A73-17583

The solution of Maxwell's equation for inhomogeneous dielectric slabs.

06 p0699 A73-17809

Eigenvalues of a class of spherical wave functions.

06 p0665 A73-18177

Aperture fields and gain of open-ended parallel-plate waveguides.

06 p0676 A73-18178

A comparison of mode match, geometrical theory of diffraction, and Kirchhoff radiation.

06 p0666 A73-18192

Waveguide resonator structure of an electron-beam-pumped semiconductor laser.

06 p0702 A73-18584

Influence of waveguide properties of heterojunction layers on the principal characteristics of injection lasers.

06 p0702 A73-18585

Measurement of dielectric constant of nonmagnetic materials in a waveguide system with an unknown movable reflecting load.

06 p0696 A73-18618

Cut-off frequency calculation for TE and TM modes in doubly ridged circular and elliptical microwave waveguides, using Mathieu function and eigenfunctions

06 p0669 A73-18736

Satellite S-band telemetry evanescent mode waveguide diplexer design with foreshortened band-pass filters to eliminate I junction and connecting flanges

06 p0678 A73-18741

Computer analysis of latching phase shifters in rectangular waveguide.

06 p0678 A73-18743

Satellite dimensional resonances in microwave helicon transmission through semiconductors.

06 p0739 A73-18788

Fluctuations in the level and phase of a field in a waveguide with a random boundary

07 p0793 A73-19916

Electromagnetic wave propagation in a circular waveguide with spirally conducting inserts

07 p0793 A73-19920

Complex wave existence in some two-layer isotropic structures

07 p0793 A73-19921

Wave transformation by a phase corrector

07 p0793 A73-19923

Wave attenuation in superconducting elliptical waveguides

07 p0793 A73-19924

Diffraction of plane electromagnetic wave at anisotropic halfspace in free space and in planar waveguide.

07 p0793 A73-20126

The computation of critical frequencies of waves of higher types in a hollow elliptical waveguide.

07 p0802 A73-20141

Analysis of dispersion equation of a two-layer elliptical waveguide in critical regime.

07 p0802 A73-20142

Parametric radiation of relativistic electron bundles in a waveguide with a stratified dielectric filling.

07 p0802 A73-20145

Waveguide cavity multistage Gunn reflection amplifiers for FM-CW systems, discussing stabilization techniques, bandwidth, noise, power variation with temperature and group delay distortion

07 p0803 A73-20552

Waveguide millimeter wave diode, ECL-2173.

07 p0804 A73-20568

Horizontal-polarization biconical horn antenna excited by TE/sub-11/ mode in circular waveguide.

08 p0945 A73-20805

Semicircular waveguide-type, band-splitting filter for millimeter waves.

08 p0945 A73-20807

Optical modulator based on coupled waveguides for integrated optical circuits, presenting design and dynamic characteristics

08 p0974 A73-20810

Lower-hybrid-resonance heating of a plasma in a parallel-plate waveguide.

08 p0991 A73-20816

Circular electric waveguide of minimum loss and elastic flexibility.

08 p0938 A73-20838

On the procedures of measuring microwave Faraday rotation in semiconductors.

08 p0994 A73-21016

Frequency-dependent transmission properties of coupled strip lines in a laminar dielectric

08 p0945 A73-21072

Band-splitting filters in oversized rectangular waveguide.

08 p0946 A73-21119

Calculation of the field amplitude and phase velocity of low-frequency waves in the earth's spherical waveguide

08 p0939 A73-21285

Reflection of a microwave signal from a semiconductor plate of finite thickness

08 p0995 A73-21517

Resonant excitation of a circular cylinder with a longitudinal slit by a plane wave

09 p1048 A73-21905

On the interaction of the electromagnetic field with electron beams in resistive wall waveguides

09 p1062 A73-22324

Propagation in periodically loaded waveguides with higher symmetries.

09 p1063 A73-22490

Lower-hybrid-resonance heating of a plasma in a parallel-plate waveguide.

[TTU-SR-2] Electrically controlled microwave polarization transformer

09 p1129 A73-22639

640 Mbit/sec waveguide transmitter at 38 GHz.

09 p1065 A73-23095

Group delay equalization in waveguide communication systems for signal regeneration with tapered meander transmission line

09 p1053 A73-23110

Dielectric gradient waveguides inhomogeneous core layer, solving differential equation by perturbation method

09 p1065 A73-23113

Wideband squintless linear arrays.

10 p1192 A73-23605

Determination of eigenvalues in a class of waveguides of doubly connected cross section.

10 p1249 A73-24392

A measurement stand for reciprocal circuits in a waveguide

10 p1189 A73-24417

Dispersion equation and spectrum conversions for slow wave excitation and propagation in plane waveguide with homogeneous isotropic impedance

10 p1190 A73-24601

Wide-band varactor-tuned X-band Gunn oscillators in full-height waveguide cavity.

10 p1197 A73-24865

Perturbation theory for the surface-wave multistrip coupler.

11 p1337 A73-25363

Radiation pattern produced by open ended radial waveguide with TM mode excitation, comparing computed with measured patterns

11 p1329 A73-25677

Design and performance of electrically regulated phase shifter comprising rectangular waveguide section containing two ferrite resonators magnetized at ferromagnetic-resonance frequency

12 p1477 A73-26945

Calculation of the statistical characteristics of a long waveguide line in a two-wave model

12 p1469 A73-27189

Propagation of low-frequency electromagnetic waves in the spherical waveguide formed by the earth and the ionosphere

12 p1469 A73-27340

A magnetosonic resonator of Pc2,3 pulsations in the earth's magnetosphere

12 p1491 A73-27351

Book - Microwave power measurement.

12 p1480 A73-27425

Anisotropic piezoelectric heterogeneous acoustic surface waveguides of arbitrary cross section computing mode spectrum by efficient and accurate numerical techniques

12 p1480 A73-27568

Certain methods of numerical calculation in problems of microwave scattering from cylindrical obstacles

13 p1581 A73-28125

High power latching ferrite phase shifters for AEGIS.

13 p1591 A73-28620

High power microwave nanosecond pulse generator with waveguide standing wave resonator, noting power gain and pulse shape

13 p1583 A73-28672

Critical frequencies of electromagnetic wave propagation in H waveguides with a dielectric cross-piece

13 p1595 A73-29411

Calculation of dispersion in delay systems composed of resonator sequences with mixed excitation

14 p1733 A73-30028

Narrowband time domain reflectometer uses pulse modulated Gunn-oscillator to measure small reflections in 6 and 7.5 GHz band waveguides.

14 p1733 A73-30057

The scattering matrix of a double truncated corner in a waveguide

14 p1726 A73-30073

Electromagnetic wave radiation and reflection at guiding structure discontinuity, calculating TE mode surface wave by boundary perturbation technique

14 p1727 A73-30214

Analysis of EH inhomogeneities and singular H inhomogeneities in a rectangular-section waveguide

14 p1729 A73-30560

Relativistic electron beam focusing by neutral gas filled conical guide tube, comparing efficiency, fluence gain, energy loss and pressure variation predictions with experiments

14 p1777 A73-30658

Propagation constant and wave resistance in the case of coaxial and hollow conductors with lossy dielectric and magnetic materials

14 p1730 A73-30920

Ferrite component for waveguide commutator used as microwave switching element and modulator, noting application in navigation instruments and avionics

15 p1849 A73-30995

Study in curvature of long distance wave guides - The case of helicoidal guides. I

15 p1842 A73-31360

Resonant excitation of a circular cylinder with a longitudinal slot by a plane wave.

15 p1847 A73-32630

Theory of transient radiation in a waveguide with a piecewise-homogeneous dielectric filler

16 p1978 A73-32898

Several parallel-plate guides with screen as phased array - Effect of the coupling on the directive gain

16 p1979 A73-33374

Ceramic waveguide microwave integrated circuits.

16 p1989 A73-33470

Eddy power flow of electromagnetic waves.

16 p1980 A73-33690

Broad X band multichannel waveguide matrix for high speed switching from one input to one of four outputs at high power levels

16 p1990 A73-33897

Reflection coefficient of an electromagnetic wave by a plasma column of variable electron density in a waveguide.

16 p1984 A73-33994

Transient radiation in a shortened waveguide

17 p1210 A73-34116

Parasitic mode conversion loss measurement for circular waveguide section quality evaluation, determining transmission coefficient from signal envelope

17 p1211 A73-34588

Quenched-domain mode oscillation in waveguide circuits.

17 p1216 A73-34969

On the optimum design of tapered waveguide transitions.

17 p1216 A73-34970

Scattering of waves at a step in a circular multiwave waveguide.

17 p1213 A73-35152

An experimental investigation of the propagation of electromagnetic waves in a rectangular waveguide, partially filled with n-InSb in a transverse magnetic field.

17 p1213 A73-35166

The effects of the microwave structure parameters on the behavior of X-band Gunn oscillator.

17 p1214 A73-35650

Results of numerical solution of the complex dispersion equation for the HE₁₁/ wave in a two-layer circular waveguide.

17 p1213 A73-35718

A circular waveguide 'hybrid-T' and its applications.

18 p2292 A73-36606

Spatial coherence characteristics of noise emission in active waveguide channel, considering Raman scattering of focused beam

19 p2437 A73-37247

Wave propagation between two plane, parallel reactive walls.

19 p2404 A73-37721

Waveguide transitions especially for excitation of the H sub 11 mode in a circular waveguide

19 p2404 A73-37722

An approximation method for calculating the attenuation characteristic of dielectric-lined circular waveguides.

19 p2404 A73-37723

Computations of the field amplitude and phase velocity of low-frequency waves in a spherical surface waveguide.

19 p2404 A73-37914

Waveguide channel point source electric field level and phase derived by Rytov smooth perturbation technique, obtaining correlation functions, energy spectra and phase fluctuations

19 p2406 A73-38338

Using the new fundamental system of modified cylindrical functions for designing optical core fiber waveguides with cladding of finite thickness.

20 p2522 A73-38661

Electromagnetic scattering by discontinuities in weakly inhomogeneous parallel plane waveguides or ducts, noting edge diffraction singularities role from ray optical calculation

20 p2528 A73-38847

Surface strip coplanar waveguide characteristic impedance measurement as function of aspect ratio and substrate thickness

20 p2538 A73-39595

Acoustic surface wave thin film guides for nonlinear signal processing, discussing relative advantages over nonguided arrangements, and application to transverse wave front imaging

20 p2531 A73-39596

Corrugated circular waveguide boundary value problem solution to predict lower attenuation for HE sub 11 mode

20 p2538 A73-39598

A survey of the simulator technique for designing a radiating element in a phased-array antenna.

21 p2652 A73-40657

Elaborated attenuation computation for elliptic waveguide with corrected expressions for axial and transverse surface impedances and TE and TM modes

21 p2656 A73-41112

Russian book on wave propagation in stratified media covering elastic and electromagnetic fields, waveguides, whispering galleries, diffraction rays, caustic surfaces, etc

21 p2741 A73-41279

On inhomogeneously filled rectangular waveguides.

21 p2657 A73-41430

A projection method in the problem of the excitation of a dielectric antenna

21 p2667 A73-41512

Contribution to the theory of wave propagation in a one-dimensional randomly inhomogeneous medium

22 p2826 A73-42334

Variational and iterative methods for waveguides and arrays.

22 p2834 A73-42843

Hybrid numerical solution to electromagnetic wave scattering and diffraction with application to microstrip transmission lines, echelette gratings and dielectric step discontinuities in waveguides

22 p2828 A73-42844

Propagation of low-frequency electromagnetic waves in a spherical earth-ionosphere waveguide.

23 p2952 A73-43238

Magnetosonic resonator of Pc2,3 pulsations in the earth's magnetosphere.

23 p2970 A73-43248

Damping in a strip waveguide with a central conductor composed of two equipotential strips

23 p2959 A73-43517

Oversize waveguide polarization diplexers based on metal grating or dielectric plate at Brewster angle, measuring performances in microwave circuit and with HCN IR laser

23 p2960 A73-44071

Modified H guide for millimeter and submillimeter wavelengths.

23 p2960 A73-44072

Finite-boundary corrections to the coplanar waveguide analysis.

23 p2954 A73-44075

Increasing the locking bandwidth of a waveguide-cavity oscillator through the use of a double-tuned circuit.

23 p2965 A73-44109

The eigenvalue solution of asymmetric-ridge waveguides using the mode-matching method.

23 p2955 A73-44146

WAVELENGTHS

- The damping of electromagnetic waves in smooth, superconductive waveguides. 24 p3068 A73-44945
- Parameter evaluation method for lossy strip transmission lines, assuming microwave propagation in waveguide system with dielectric between two conducting plates 24 p3074 A73-45007
- Dielectric coaxial waveguide modal cut-off, dispersion and attenuation characteristics, discussing guide geometry and dielectric properties effects 24 p3069 A73-45407
- Coherence of an electromagnetic field propagating in a weakly guiding fiber. 24 p3097 A73-45416

WAVELENGTHS

- Morphic effects. III - Effects of an external magnetic field on the long wavelength optical phonons. 02 p0201 A73-12638
- The deflection of light at the sun and the change of its velocity and wavelength 02 p0225 A73-12809
- A dual wavelength ground-based auroral scanner. 03 p0299 A73-12888
- Time-periodic fluid surface wave radiation and scattering by partially immersed objects in short wave asymptotic limit of nondimensional wavelength approaching zero 03 p0397 A73-13533
- Wavelength dependence of moire patterns 05 p0577 A73-16822
- The influence of wavelength on visual adaptation to spatially periodic stimuli. 11 p1318 A73-26199
- Programmed radiation spectrum control in a ruby laser 12 p1504 A73-26883
- Linear Z pinch magnetohydrodynamic instability mode and characteristic wavelength determined by discharge tube radius and current buildup rate 15 p1918 A73-31703
- Forward scattering method for determination of atmospheric aerosols particle size distribution, considering angle-dependent scattering at fixed wave number 17 p2161 A73-34938
- Accurate wavelengths of stellar and telluric absorption lines near lambda 7000 A. 22 p2907 A73-42208

WAVES

- Quasi-stationary atmospheric waves and mean monthly vorticity production from development term of two level model 19 p2447 A73-38153

WAXES

- Carnauba wax electrets manufactured under the simultaneous action of magnetic and electric fields 12 p1523 A73-27103

WEAPON SYSTEM MANAGEMENT

- Naval air weaponry logistics support, discussing criteria for management effectiveness evaluation 13 p1709 A73-29573
- Safety management of air to surface nuclear short range attack missile /SRAM/ at fabrication, testing and operation levels 16 p2073 A73-33640
- A rational basis for determining the EMC capability of a system. 20 p2528 A73-38770
- Management of Air Force test and evaluation activities. 23 p3050 A73-44055
- Management and control of flight test programs of the Naval Air Systems Command. 23 p3050 A73-44056
- Management and control of military flight test programs at McDonnell Douglas St. Louis, Missouri. 23 p3050 A73-44059
- Flight test programs management and control, considering weapon systems performance tests relative to contractual requirements, personnel allocation and supporting facilities 23 p3051 A73-44060

WEAPON SYSTEMS

- NT GROUND OPERATIONAL SUPPORT SYSTEM
- NT MISSILE SYSTEMS
- Air Force weapon system procurement needs, considering industry technological capabilities, nonlinear estimation in cruise navigation and nonlinear systems design, test and implementation 04 p0430 A73-15252

- Electronic warfare tactics against remotely piloted unmanned aircraft used for reconnaissance or weapons delivery, considering onboard countermeasures 04 p0418 A73-15379

- Performance measurement system for combat crew flight training in complex aircraft weapon systems, identifying training research goals 05 p0544 A73-16726

- Energy management in aerial combat weapon systems maneuvering and delivery tactics, computing optimal feedback control laws for supersonic aircraft minimum time turning trajectories [AIAA PAPER 73-231] 05 p0536 A73-16956

- Air combat roles identification by reachable sets technique, evaluating aircraft/weapon systems potential performance vs given threat [AIAA PAPER 73-232] 05 p0536 A73-16957
- Digital Avionics Information System /DAIS/ development for military supersonic all-weather precision weapon delivery system, emphasizing modular design for different aircraft types 06 p0672 A73-17572

- Data quality assurance in a shipboard computer-controlled telemetry system. 09 p1057 A73-23410

- Book - The Polaris system development: Bureaucratic and programmatic success in government. 12 p1561 A73-27400

- Testing and evaluation community role in weapon system acquisition, describing R and D philosophy 13 p1569 A73-28902

- Development and testing of ballute stabilizer/decelerators for aircraft delivery of a 500-lb munition. [AIAA PAPER 73-485] 15 p1829 A73-31467
- Russian book - Physical principles of rocket weaponry. 15 p1944 A73-32419

- Vibration and shock stresses in the case of ballistic rockets. II - Measurement, evaluation, simulation 16 p0272 A73-33388

- AEGIS AN/SPY-1 radar system - Design for availability. 16 p1980 A73-33607

- AEGIS Demineralizer/Water Cooler - Design for availability. 16 p1989 A73-33608

- AEGIS Operational Readiness Test System - Design for system effectiveness. 16 p2073 A73-33609

- Tactical weapon system final test for random failures, discussing electronic component defects effects and semiconductor device screening for system reliability improvement 16 p1990 A73-33624

- Safety aspects in documentation system for orientation, training and maintenance of equipment for Poseidon Missile System 16 p2073 A73-33639

- Laser guided weapon system optical countermeasures /OCM/ vulnerability evaluation, discussing use of LED laser in computerized simulation at low cost 17 p2147 A73-35208

- Solid state null tracking Doppler radar ground velocity sensor for supersonic weapon delivery aircraft precision bombing, discussing design and test with computer simulation 17 p2137 A73-35209

- An in-flight investigation of the influence of flying qualities on precision weapons delivery. [AIAA PAPER 73-783] 19 p2378 A73-37453

- Aircraft-store separation design for angular momentum increase of external weapon with internally mounted spinning flywheel 20 p2508 A73-38652

- GDC/EOSS - Real-time visual and motion simulators for evaluation of fire control and electro-optical guidance systems. [AIAA PAPER 73-919] 21 p2673 A73-40867

- International cooperation in weapons systems development, discussing military R and D technology interdependence within NATO, duplication and security 21 p2793 A73-41173

- Overview of Department of Defense Electromagnetic Radiation Hazards Standardization Program. 22 p2822 A73-41790

- Electromagnetic radiation hazard test facility, instrumentation, and weapon system susceptibility evaluation for providing environment protection and military standards 22 p2822 A73-41791

- Russian book on rocket weapon systems safety handling covering HF electromagnetic, noise and vibration effects, ionizing radiation, fire, etc 22 p2812 A73-41874

- Remotely piloted vehicle /RPV/ for reconnaissance, electronic warfare systems, target acquisition, weapon delivery, air-air combat and different combinations 24 p3057 A73-45399

WEAPONS

- NT NUCLEAR WEAPONS
- NT WARHEADS

WEAPONS DEVELOPMENT

- U.S. double-base solid propellant tactical rockets of the 1940-1955 era. [AIAA PAPER 73-274] 09 p1135 A73-23248

- Book - The Polaris system development: Bureaucratic and programmatic success in government. 12 p1561 A73-27400

- Approach to reliability for the SM-2 missile. 16 p2073 A73-33610

- International cooperation in weapons systems development, discussing military R and D technology interdependence within NATO, duplication and security 21 p2793 A73-41173

WEAR

- Investigations into film failure /transition point/ of lubricated concentrated contacts. 05 p0580 A73-16103

- Boundary lubrication and wear of slow moving sliding concentrated hardened steel contacts as function of geometry, load, speed, lubricant and oxygen content 05 p0580 A73-16104

- Factors affecting coefficient of friction and wear of friction materials for brakes, discussing fillers use as reinforcements and friction modifiers 05 p0580 A73-16106

- Metal components wear mechanisms of friction and adhesion, tribooxidation, abrasion and surface fatigue, discussing prevention by lubrication, suitable mating of materials and surface treatments 11 p1373 A73-25577

- 'Glazes' produced on nickel-base alloys during high temperature wear. 12 p1513 A73-27598

- Errors due to electrode-instrument wear during the electric-erosion treatment of cavities 15 p1881 A73-31146

- Failure data evaluation, determining wear out, degradations, environments causing system failures, repairs, maintenance and sub par performers 16 p2021 A73-33649

- Influence of hydrodynamics on the performance of radial lip seals. [ASLE PREPRINT 73AM-9B-2] 17 p2179 A73-34998

- Corrosion wear mechanism with emphasis on chemical and mechano-chemical reaction products formation and removal from friction surface /tribo-mechanical processes/ 18 p2320 A73-36494

WEAR INHIBITORS

- Molybdenum disulfide in oils and greases under boundary conditions. [ASME PAPER 72-LUB-37] 03 p0335 A73-14345

- Antifriction bearing with lubricated rubber and metal laminations for wear elimination in limited rotation applications, discussing design guidelines and advantages 03 p0317 A73-14424

- Some aspects of the metallurgy and wear resistance of surface coatings. 05 p0580 A73-16102

- Study of the wear resistance of nitrided electrolytic chromium coatings on certain alloy steels 10 p1223 A73-24065

- Possibility of reducing the wear of the VD-17 aluminum alloy in a jet of free abrasive particles with the aid of metallic coatings 10 p1226 A73-24797

- Influence of pressure on VT14 alloy wear and friction against 30KhGSA steel 11 p1371 A73-24992

- Wear-resistant surfaces through electrical spark hardening 17 p2178 A73-34980

- Grease lubrication of helicopter transmissions. [ASLE PREPRINT 73AM-2A-1] 17 p2196 A73-34996

- Amine phosphates as antiwear additives in neopentyl polyol esters. [ASLE PREPRINT 73AM-9A-1] 17 p2196 A73-34996

- The role of physicochemical processes in surface wear under rolling friction in low-molecular hydrocarbon media 18 p2343 A73-36821

WEAR TESTS

- An autoradiographic investigation of material transfer and wear during high speed/low load sliding. 01 p0056 A73-10438

- Elemental analysis of a friction and wear surface during sliding using Auger spectroscopy. 01 p0057 A73-11277

- Laboratory experience with long-term bearing lubrication. 01 p0057 A73-11278

- Cr and V additions effects on Mn steels mechanical properties and wear resistance, noting strength limit increase 01 p0067 A73-11351

- Vibratory loads effect on metal microstructure under sliding friction, noting rheological criteria for fretting corrosion wear resistance 02 p0180 A73-11934

- Effect of laser working on the wear of machine parts in an abrasive-lubricant medium 02 p0173 A73-11935

- Performance tests for steel-steel lubrication capability of dimethyl silicone oils and greases modified by soluble, heat-stable extreme pressure and antiwear additives 03 p0329 A73-13011

- Wear and energy dissipation of contacts vibrated at high frequencies, analyzing mechanism of fretting wear [ASME PAPER 72-LUB-20] 03 p0314 A73-14335

Investigation of anti wear additives under various loads and at different sliding speeds.
[ASLE PREPRINT 72LC-3C-4]

03 p0316 A73-14359
The influence of temperature on the wear of carbon fiber reinforced resins.
[ASLE PREPRINT 72LC-5B-3]

03 p0335 A73-14363
Transitions in the friction coefficients, the wear rates, and the compositions of the wear debris produced in the unlubricated sliding of chromium steels.
[ASLE PREPRINT 72LC-7B-2]

03 p0316 A73-14369
Solid-state sliding friction and wear in the case of iron, cobalt, copper, silver, magnesium, and aluminum, kept in an oxygen-nitrogen mixture at pressures from 760 torr to 0.2 microtorr

05 p0581 A73-16107
A technical note on the correspondence between Amontons' law and wear-scar data in a 4-ball machine.

05 p0581 A73-16108
Investigation of the friction and wear behavior of polytetrafluoro-ethylene composite materials as compared to synthetic carbon and sintered metal. I

06 p0714 A73-18449
Evaluation of the lubricating properties of chemically upgraded MoS₂.

07 p0842 A73-19553
The erosion of carbon fibre reinforced plastic by repeated liquid impact.

07 p0843 A73-20224
Photographic and metallographic evidence of two stage ductile materials erosion mechanism under particle impact, describing impact velocity, particle size and angle effects

07 p0839 A73-20225
Friction and wear of graphite fiber composites.

07 p0833 A73-20500
Characteristics of the microstructural wear pattern of carburized chromium coatings

09 p1088 A73-22592
Improvement of the friction and wear behavior of T-A6V alloy by a new anodic oxidation treatment

09 p1104 A73-22966
Emission spectrographic analysis of used aero engine oil - A tool of maintenance.

09 p1136 A73-23242
Effects of metal grain size on friction and wear characteristics

10 p1223 A73-24067
Polytetrafluoroethylene friction and wear properties as function of heat treatment, speed and temperature, attributing high wear rate to slippage in banded fine structure

10 p1224 A73-24164
Accelerated testing of ball bearings.

10 p1225 A73-24636
Effect of solid lubricants on the physicochemical and friction properties of materials

10 p1225 A73-24686
Ag- or Cu-based fiber reinforced composite materials for springs in electrical contact devices, investigating mechanical strength and contact and wear resistances

11 p1387 A73-25410
Friction, wear, and noise of slip ring and brush contacts for synchronous satellite use.

11 p1374 A73-26211
Friction and wear of self-lubricating composite materials.

13 p1624 A73-28776
The tolerance of fluid machinery to contaminant wear.

13 p1571 A73-29031
Book on fretting corrosion covering contacting surface theory, damage characteristics, wear variables effect, fatigue, adhesion and electrochemical properties, etc

13 p1643 A73-29575
Investigation of the friction and wear behavior of polytetrafluoroethylene composite materials as compared with that of artificial coal and sintered metal. II

13 p1647 A73-29652
Behavior of the electrode potential of a metal under conditions of fretting corrosion

14 p1763 A73-30711
Russian book - Accelerated wear-resistance tests for machine components and machinery.

15 p1881 A73-31582
Investigation of friction and wear mechanisms in a friction coupling with a small overlapping coefficient

15 p1882 A73-31599
Effect of treatment factors on the properties of friction materials. II - Effect of sintering conditions on the structure and friction and wear properties of friction materials

15 p1892 A73-32244
Investigation of friction behavior in titanium alloy with 3.8% Al

15 p1894 A73-32535
German monograph - Model wear investigations concerning the effect of the intermediate medium on

the sliding characteristics in the case of a contact between different materials.

15 p1883 A73-32593
High speed oscillating tests of lubricating composites.
[ASLE PREPRINT 73AM-3C-2]

17 p2179 A73-34987
Study of fretting wear in titanium, Monel-400, and cobalt-25 percent molybdenum using scanning electron microscopy.
[ASLE PREPRINT 73AM-8A-3]

17 p2190 A73-34993
Comparative evaluation of the wear resistance of electrolytic and plasma chromium coatings

18 p2318 A73-35883
Friction of hard alloys in vacuum at low temperatures

18 p2320 A73-36861
Mechanical, chemical and physical characteristics of glass and ceramics with respect to adhesion, friction and wear behavior

21 p2707 A73-40633
An application of topographical analysis to the wear of polymers.

22 p2881 A73-42355
Influence of diffusion coating and heat treatment on the wear resistance of VT-8 alloy

23 p2990 A73-43485
Influence of cooling on surface dispersion during the friction process

24 p3092 A73-44417

WEATHER

NT COLD WEATHER

WEATHER CHARTS

U METEOROLOGICAL CHARTS

WEATHER CONTROL

U WEATHER MODIFICATION

WEATHER DATA RECORDERS

Investigation of the electrical parameters and meteorological elements of the atmosphere close to the ground during thunderstorm and thunderstorm-free periods

02 p0189 A73-12589
Technological weather forecasting advances, including use of satellites, global meteorological network, computer techniques and mechanical recorders

15 p1902 A73-31149

WEATHER FORECASTING

NT LONG RANGE WEATHER FORECASTING

NT NUMERICAL WEATHER FORECASTING

NT STATISTICAL WEATHER FORECASTING

Digitized radar experiments project for data acquisition and processing and weather forecasting techniques development, describing test bed configuration, equipment and operation

03 p0288 A73-14515
Experiments on objectively predicting some atmospheric and oceanic variables for the winter of 1971-72.

[AD-758469] 06 p0720 A73-18702
Weather forecasting with the aid of satellite data.
[AIAA PAPER 73-21] 07 p0848 A73-19582

Turbulence and tropopause evolution in northeast jet stream over Treviso airport, noting Richardson criterion value as diagnostic and short range prognosis tool

08 p0986 A73-21487
Mandelstam-Brillouin laser light scattering theory and application to atmospheric parameters remote sensing

09 p1094 A73-22327
Ordinal relationships between measures of the 'accuracy' and 'value' of probability forecasts - Preliminary results.

10 p1244 A73-23646
Hedging, proper and improper skill scoring rules for meteorological probability forecasts

10 p1246 A73-23992
Weather satellite capabilities - Present and future.

11 p1429 A73-25149
Bounds upon the growth rate of errors in quasi-non-divergent prediction models.

13 p1652 A73-28271
Momentum and mass transfer in atmospheric boundary layer from surface drag and evaporation data for weather prediction models

13 p1652 A73-28275
Weather forecasting in the recent past, at the present time, and in the near future

13 p1655 A73-29189
Mesoscale cloud systems analysis from meteorological observations and weather satellite data nephanalysis, applying to weather forecasting

13 p1655 A73-29191
Technological weather forecasting advances, including use of satellites, global meteorological network, computer techniques and mechanical recorders

15 p1902 A73-31149
Cloud-free line-of-sight calculations.

15 p1903 A73-31317
Operations research methods application to meteorological forecasting, discussing optimization algorithm and feedback systems

15 p1907 A73-32354

Experiments in objectivization of a forecasting method for lower cloud boundary altitudes

17 p2204 A73-34541
All-Union Meteorological Conference, 5th, Leningrad, USSR, June 21-25, 1971, Transactions. Volume 1 - General information, resolutions and plenary reports.

Volume 2 - Weather prediction section. Volume 3 Climate section. Volume 4 - Section on seeding effects on atmospheric processes

18 p2331 A73-35905
Evolution of the hydrodynamic methods for weather forecasting

18 p2331 A73-35906
Current status and immediate problems of hydrodynamic short-term weather forecasting

18 p2331 A73-35908
Medium-range forecasting of large-scale atmospheric circulation components on the basis of a nonlinear spectral model

18 p2331 A73-35910
Development of methods of forecasting meteorological conditions for aviation

18 p2331 A73-35912
Providing satellite systems for the national weather satellite services.

[AIAA PAPER 73-586] 18 p2373 A73-36077
International cooperation in the field of spatial meteorology

18 p2373 A73-36391
Comparison and synthesis of the characteristics of long- and short-duration blocking systems over the Euroatlantic region

19 p2447 A73-38124
On the prediction of turbulence in baroclinic zones.

19 p2449 A73-38246
Hurricane prediction - Progress and problem areas.

21 p2731 A73-40641
Post GARP Global Experiment programs, considering tropical vertical wind structure, satellite temperature measurement accuracy increase, data handling for real time and long term prediction

21 p2732 A73-40819
Micrometeorite and cosmic dust studied for solar system and universe origin and evolution and for medium range weather forecasting, discussing cosmic matter infall to earth

22 p2913 A73-42988
On the variation with height of the top brightness of precipitating convective clouds.

23 p3005 A73-44270

WEATHER FRONTS

U FRONTS [METEOROLOGY]

WEATHER MAPS

U METEOROLOGICAL CHARTS

WEATHER MODIFICATION

NT CLOUD SEEDING

Use of airborne radar to evaluate hurricane modification experiments.

03 p0338 A73-14513
Possibility of affecting the coagulation of droplets in warm clouds and fog by electrical methods

06 p0719 A73-17840
Russian book - Physics of clouds and seeding effects.

13 p1653 A73-28876
Artificial inducement of drizzling rain in an uncloudy atmosphere at relatively high humidity

16 p2034 A73-33109
Simulated weather records experiment for polluted atmosphere effects on climatic change, using numerical circulation model

[AIAA PAPER 73-537] 16 p2007 A73-33568
Scheme for evaluating the influence of convective-cloud modifications aimed at controlling precipitations artificially, and the results of cumulus cloud structure investigations from aircraft

18 p2332 A73-35917
Experimental and theoretical investigation of the process of artificial crystallization and dissipation of supercooled clouds

18 p2332 A73-35919
Light beam dispersal of fog with various drop sizes based on energy equation, considering cloud water content, cross wind effects and front velocity

18 p2337 A73-36561
Fog dispersal technique evaluation for cost effectiveness by statistical method, taking into account time dependent probability of natural visibility improvement

21 p2729 A73-40066
Weather modification activities, discussing state and local funding, research, federal programs, precipitation, hail and warm fog

21 p2729 A73-40092

WEATHER RADAR

U METEOROLOGICAL RADAR

WEATHER STATIONS

Meteorological radar site selection factors, discussing antenna towers installation

03 p0288 A73-14514
Principal trends of investigations in the field of theoretical meteorology performed in Hungary

04 p0473 A73-15284

WEATHERING

- Weather radar surveillance data short term distribution to airline users through weather message switching center, describing data coding, teletype network and data plotting operations 10 p1189 A73-24550
- Rational distribution of meteorological stations as a problem of operation studies 15 p1903 A73-31604
- Participation of the Air Force Weather Service in the Eole experiment 17 p2206 A73-34940
- Hydrometeorological data processing and dissemination techniques and equipment, with emphasis on computerized regional centers and space-based systems 18 p2295 A73-35907
- Russian book on UHF meteorological radar techniques and applications covering precipitation and cloud monitoring radiolocation stations, lidar, sonar, echo signals and meteorological satellites 20 p2584 A73-39758

WEATHERING

- Hammond Downs, a new chondrite from the Tenham area, Queensland, Australia. 13 p1680 A73-28618
- Studies on testing methods and weatherability of plastics. 13 p1646 A73-29532
- Mechanism of breakdown in the interface region of glass reinforced polyester by artificial weathering. 15 p1898 A73-31838
- Mechanism of surface microcracking of matrix in glass-reinforced polyester by artificial weathering. 23 p2997 A73-44034

WEBBING

- Parachute webbing designs for opening shock energy absorption and force limitation, discussing drop tower and ballistic piston test results for various designs 16 p2018 A73-33066

WEBS [MEMBRANES]

- U MEMBRANES

WEBS [SUPPORTS]

- Flange-to-web connection requirements on beams with corrugated webs. 10 p1223 A73-23632

WEDGE FLOW

- Reflexion and diffraction of shocks interacted by yawed wedges. 01 p0002 A73-10272
- On the multi-parameter characteristic perturbation method - Application to nonlinear supersonic nonequilibrium flow over a wedge. 01 p0004 A73-11425
- Solution of the wedge entry problem by numerical conformal mapping. 03 p0244 A73-13537
- Rates of change of flutter Mach number and flutter frequency. 03 p0395 A73-14188
- A non-similar solution of heat transfer in external non-Newtonian flow with thermal radiation. [AIAA PAPER 73-116] 05 p0640 A73-16873
- Shockwave-boundary layer interference heating analysis. [AIAA PAPER 73-237] 05 p0532 A73-16962
- Closed form solutions for dust density and temperature distributions in shock layer of hypersonic wedge flow 05 p0533 A73-17115
- High Reynolds number steady separated flow past a wedge of negative angle. 06 p0685 A73-17710
- Measurements of base pressure upon a plate and a wedge in the 2.8 to 6.8 Mach number range. [DFVLR-SONDDR-256] 06 p0645 A73-17740
- Eddy cavitation flow past a wedge 06 p0686 A73-18071
- Heat transfer from hypersonic turbulent flow at a wedge compression corner. 06 p0646 A73-18531
- Variational mixed boundary value problems of subsonic gas flows for plane parallel symmetric Laval nozzle and transonic wedge, using singular integral equation 06 p0646 A73-18888
- Corner pressures and fillet shock locations for symmetrical corners by an approximate method. 07 p0774 A73-19494
- Application of a variational technique to wedge flow with variable properties. 07 p0775 A73-19963
- Laminar flow heat transfer from wedge-shaped bodies with limited heat conductivity. 08 p1023 A73-21257
- Supersonic flow of a gas with solid particles about a wedge 08 p0926 A73-21404
- A numerical solution for the transonic flow around blunt wedges 15 p1823 A73-31330

Linearized theory of finite conductivity steady ideal MGD flow past thin wedge in aligned magnetic field, using Fourier integral transform 15 p1917 A73-31338

Two dimensional unsteady vortex flow of ideal fluid past inflating decelerating wedge, obtaining pressure distribution on wedge surface [AIAA PAPER 73-449] 15 p1823 A73-31435

Variational mixed boundary value problems of subsonic gas flows for plane parallel symmetric Laval nozzle and transonic wedge, using singular integral equation 15 p1824 A73-32412

Supersonic laminar wakes past wedge, determining pressure distribution, velocity profiles and stream line patterns in recirculation region 16 p1962 A73-32905

Two dimensional wedge flow singularities for free and fixed boundaries at flow separation points, applying to water entry problem 16 p1999 A73-32928

Inviscid supersonic far wake flow past pointed bodies using the method of integral relations. [AIAA PAPER 73-671] 18 p2262 A73-36222

Unsteady thermal boundary-layer on an infinite yawed wedge whose temperature gradient is prescribed. 19 p2377 A73-37575

The effect of the wedge angle on the similarity parameter of the turbulent mixing region in the case of an incompressible flow 20 p2547 A73-39408

Experimental investigation of a turbulent boundary layer on a triangular plate with a wedge 23 p2939 A73-43473

Supersonic laminar flow over wedge or backward-facing step for large Reynolds number and small base or step height, predicting pressure distribution at reattachment 24 p3055 A73-45314

Flow field over pointed wedges in isoelectric flow of thermally and calorically perfect gases with nonuniform incident supersonic flow, noting attached shock formation 24 p3056 A73-45547

WEDGES

Three dimensional flow pattern from two dimensional supersonic inviscid gas flows around wedged body 03 p0245 A73-13675

Source excited dielectric wedge surface magnetic field local mode solution compared with plane wave method, noting inaccuracy near surface wave cutoff 06 p0666 A73-18197

Singular integrodifferential and linear integral equations for load transfer from stringer to wedge under concentrated force and for stringer-coupled wedge shaped regions 07 p0910 A73-19306

Infinite triangular wedge, with a notch at its bisectrix, under the action of concentrated forces applied to the edges of the notch 07 p0911 A73-19312

Elastic wedge whose apex section is reinforced with a rod of variable cross section 07 p0911 A73-19313

E-polarized plane wave diffraction by conducting wedge loaded with thin dielectric slab, obtaining Fresnel integral solution with application to cylindrical wave excitation 07 p0792 A73-19383

Temperature distribution in a wedge-shaped prism 08 p1022 A73-21098

Transient functions to estimate thermal inertia of gas temperature sensors with film resistance thermometer mounted on wedge shape insulating base 09 p1081 A73-22346

Edge condition of a perfectly conducting wedge with its exterior region divided by a resistive sheet. 11 p1329 A73-25676

Plane wave expansion approximation for wave field on dielectric wedge representing tapered antenna, considering lateral wave contribution 11 p1329 A73-25681

Infinite elastically isotropic solid under external tensile stress, deriving condition for complete fracture from wedge crack 15 p1951 A73-32023

Diffraction and reflection of shocks from corners. 22 p2843 A73-42567

WEIBULL DENSITY FUNCTIONS

Generalized gamma distribution with a negative shape parameter as a model of the lifetime distribution of electrical elements with a single-maximum failure rate 02 p0145 A73-11585

Weibull flaw distribution models for fracture strength and failure analysis of brittle materials and fiber reinforced composites 04 p0468 A73-14726

Stress and strength theory application to mechanical failure of electronic equipment, showing Weibull law use in reliability analysis 07 p0800 A73-19420

Weibull distribution government of dispersion of destructive temperature gradients characteristic of fireproof ceramic materials heat resistance 09 p1110 A73-23061

Random yield limit of stochastically non-homogeneous elements in tension. 14 p1811 A73-30489

Solution of the three-parameter Weibull equations by constrained modified quasilinearization /progressively censored samples/. 15 p1901 A73-32263

A consistent shape parameter estimator for the Weibull distribution. 16 p2032 A73-33602

New relationships between stress testing, failure and reliability. 17 p2178 A73-34730

Bayesian estimation of life parameters in the Weibull distribution. 17 p2204 A73-35810

Statistical representation of the strength of fiberglass-reinforced plastic samples 22 p2880 A73-41956

The robustness of reliability predictions for series systems of identical components. 22 p2867 A73-42967

Sequential determination of inspection epochs for reliability systems with general lifetime distributions. 24 p3093 A73-44576

An empirical Bayes estimator for the scale parameter of the two-parameter Weibull distribution. 24 p3105 A73-44577

WEIERSTRASS FUNCTIONS

Discontinuous variational problems in time optimal control of systems describable by ordinary differential equations, deriving Weierstrass optimality conditions 03 p0286 A73-14055

WEIGHT [MASS]

NT BODY WEIGHT

NT ORGAN WEIGHT

NT STRUCTURAL WEIGHT

Rotary and fixed wing aircraft growth factors from implicit differentiation of gross weight relative to fixed weight [SAWE PAPER 952] 19 p2385 A73-37880

Aircraft fuselage structure weight estimation method assuming bending, shear, torque and internal pressurization loading for skin-stringer-shallow frame types [SAWE PAPER 981] 19 p2385 A73-37887

Early operational experience with the L-1011 On-Board Weight and Balance System. [SAWE PAPER 986] 19 p2386 A73-37890

WEIGHT ANALYSIS

Structural weight analysis of single stage and multistage spacecraft for given payload and initial vehicle weight, considering optimization problem 02 p0229 A73-12469

Structural weight optimization of single stage and multistage spacecraft for given payload and initial vehicle weight 15 p1944 A73-32619

Avionics systems simplification for cost, weight and space reduction, considering ease of maintenance, failure points reduction and flight director/autopilot computers and couplers elimination 16 p1968 A73-33187

High strength organic fiber PRD-49 reinforced plastics compared to materials reinforced with glass, graphite and boron, discussing weight required to achieve Al faced sandwich performance 17 p2194 A73-34802

Helicopter power transfer systems analysis in terms of weight reduction and reliability improvement [AHS PREPRINT 773] 17 p2106 A73-35091

Problems of minimum-weight turbomachine rotor designs 18 p2367 A73-37140

A parametric weights study of a composite material prop/rotor blade. [SAWE PAPER 950] 19 p2385 A73-37878

The weight/performance interface - An argument for weight control. [SAWE PAPER 967] 19 p2385 A73-37884

THE STAN /R/ 'S' Integral Weight and Balance System for the C-130 aircraft. [SAWE PAPER 985] 19 p2385 A73-37889

Space shuttle design program with Mark I and II stages, considering thermal protection weight analysis for minimum maintenance and turnaround time 21 p2780 A73-40416

Weight reduction in stiffened panels with specified initial buckling load in uniform longitudinal compression by stiffeners utilization 21 p2787 A73-41190

Russian book on aircraft onboard instruments and equipment arrangement and housing for weight reduction covering electric, radar, navigation, control, display and auxiliary devices 21 p2635 A73-41425

Light weight shaft design using minimum principle for nonlinear multipoint boundary value problem [ASME PAPER 73-DET-10] 22 p2919 A73-42068

Fracture mechanics technology for optimum pressure vessel design. 22 p2920 A73-42155

Analytic treatment of minimum weight design of cantilevers. [ASME PAPER 73-APMW-29] 22 p2925 A73-42889

WEIGHT FACTORS

U WEIGHT [MASS]

WEIGHT INDICATORS

NT MICROBALANCES

NT STRAIN GAGE BALANCES

Digital readout top-loading balance adaptation as micromanometer, discussing accuracy, sensitivity and repeatability characteristics 03 p0309 A73-14471

Fabrication of high precision strain gage dynamometers and balances at the O.N.E.R.A. Modane Centre. [ONERA, TP NO. 1196] 22 p2839 A73-42217

WEIGHT MEASUREMENT

Vacuum thermogravimetric analysis system for determination of continuous weight change and total condensable materials. 03 p0330 A73-13018

Determination of the mass of Saturn from the motion of Trojans. 17 p2234 A73-35615

Vacuum effects on materials and environment contamination - Screening method and results obtained at CNES 22 p2880 A73-41873

WEIGHTING FUNCTIONS

Homogeneous linear partial differential equation for optimal control with boundary condition formed by terminal component, noting weighting functions for linear plant 02 p0149 A73-12116

Weighted estimates of the error in the grid method of solving the Laplace and Poisson equations 02 p0187 A73-12177

An identification of time varying linear system without a priori information on variation of system parameters. 06 p0681 A73-18812

The algorithms of accuracy research of nonstationary linear systems with continuous and discrete elements. 10 p1200 A73-24048

Method of designing digital devices for bandpass filtration of signals 11 p1333 A73-25023

Multiinput multioutput linear time invariant discrete system optimal approximation, noting algorithms and weighting matrices computational difficulties 11 p1390 A73-25192

Determining the trend of a random sequence 12 p1518 A73-27224

Comparison of different methods of reconstitution of a signal furnished under a sampled form 13 p1582 A73-28475

The influence of properties of a set of observations on the weights of determination of the orbital elements of a one-apparition comet. 14 p1790 A73-29794

Boundary value properties of weighting space functions and applications of the functions in boundary value problems 15 p1900 A73-32101

Weighted residual processes in finite element with particular reference to some transient and coupled problems. 17 p2245 A73-34835

Use of weighting functions in conjugate gradient methods 18 p2295 A73-37079

A note on the period of oscillation of non-linear systems. 19 p2460 A73-38108

Optical and millimeter line-of-sight propagation effects in the turbulent atmosphere. 19 p2405 A73-38220

Determination of an optimal dynamic system according to complex statistical criteria in the presence of constraints 20 p2539 A73-38680

Analysis of methods for selecting significant attributes in the classification of patterns 20 p2532 A73-38999

The effect of weighting upon signal-to-noise ratio in pulse bursts. 21 p2649 A73-40327

Electromagnetic absorption in magnetized cold plasma, discussing definition and use of velocity dependent collision frequencies with Legendre polynomials as weighting functions 21 p2654 A73-40818

On the construction of accurate difference schemes for hyperbolic partial differential equations. 23 p3000 A73-43208

A new weighting function for solving nonlinear oscillation problems. 24 p3148 A73-44893

WEIGHTLESSNESS

Gravity selection by animals in fields of centrifugal acceleration superimposed on weightlessness during sounding rocket flights. 01 p0009 A73-11209

Zero-g propellant gauging 06 p0755 A73-17573

Vestibular influences on orientation in zero gravity, produced by parabolic flight. 06 p0653 A73-18032

Findings on American astronauts bearing on the issue of artificial gravity for future manned space vehicles. 09 p1045 A73-22531

Development of neurosurgical instrumentation and procedures for emergency use in null and low-gravity environments - A speculative approach. 11 p1323 A73-25342

Sortie module/pallet scientific European space program based on system performing orbital zero-g or earth/celestial bodies observation platforms functions 12 p1549 A73-27381

Inversion illusion in the so-called zero-gravity conditions of parabolic flight. 14 p1722 A73-30511

International literature survey of microbiological space research for 1930-1970, discussing high altitude balloon, rocket and satellite experiments, weightlessness effects, mutagenesis, etc 15 p1838 A73-31501

Space flight exercise regimen proposals, exploring moving picture/electric muscle stimuli program as earth gravity simulator in weightlessness 15 p1838 A73-31515

Annual Scientific Meeting, Las Vegas, Nev., May 7-10, 1973, Preprints. 16 p1973 A73-33421

Physiological effects of acceleration and weightlessness during space flight, discussing cardiovascular system, renal function, respiration, blood volume, metabolism, work capacity, etc [AFOSR-72-2451TR] 17 p2113 A73-35856

Russian book - Fundamentals of the dynamics and heat and mass transfer of fluids under conditions of weightlessness. 18 p2297 A73-35868

Gravity, weightlessness and organismic genetic structures. 18 p2269 A73-35923

A monkey metabolism pod for space-flight weightlessness studies. 18 p2270 A73-35963

Prolonged space flight and hypokinesia. 18 p2278 A73-36789

Inverted posture illusion phenomenon in astronauts during weightless space flight, discussing vestibular organ function, acceleration effects and body gravitation sensing system 20 p2513 A73-39149

Apollo 16 flight program for investigating physiological effects of prolonged weightlessness on central nervous system, vestibular, neuromuscular and cardiovascular functions, metabolism, radiation sensitivity and body weight 22 p2814 A73-42176

WEIGHTLESSNESS SIMULATION

A comparison of neutral buoyancy and free fall for liquid propellant system zero-G simulations. [AIAA PAPER 72-1041] 03 p0287 A73-13376

Respiration mechanics during weightlessness simulation in an immersion medium 08 p0929 A73-20986

Zero Gravity Facility for space vehicle fluid systems research. 16 p1994 A73-33151

Histological studies on the vestibular organ of frog embryos and larvae after the influence of simulated weightlessness. 18 p2270 A73-35979

Influence of simulated weightlessness on the mutational rate of *Tribolium confusum*. 18 p2270 A73-35984

WEIGHTS [COEFFICIENTS]

U COEFFICIENTS

WELD STRENGTH

Structural changes in Kh18N9T steel during explosion welding 01 p0055 A73-10262

Influence of cyclic heating on the mechanical fatigue of titanium alloys and their weld joints 02 p0180 A73-11933

Structure and properties of the weld metal in maraging N18K9M5T steel 06 p0697 A73-17879

Composition affects tensile strength of welded aluminium-magnesium alloy. 06 p0709 A73-18385

Small-scale explosion seam welding. 10 p1223 A73-23626

Effect of welding variables on aluminum alloy weldments. 10 p1230 A73-23627

Influence of welding parameters on the strength properties of spot welds of MST1X steel with protective coatings 11 p1374 A73-26293

Mechanical properties of weld, base metal and coated columbium alloy Cb 752. 11 p1375 A73-26356

Measuring projection weld strength by acoustic emission. 12 p1502 A73-27038

The strength of welded joints in high strength stainless steels at cryogenic temperatures. 13 p1625 A73-29615

Conditions of brittle strength of weld joints at different temperatures and applied loading rates. 13 p1626 A73-29628

Estimation of fatigue-crack propagation life in butt welds. 14 p1755 A73-30147

A comparison of the capabilities of continuous drive friction and inertia welding. [SME PAPER AD 73-221] 19 p2436 A73-38493

Titanium oxide film dissolution inhibition by tempering colors and weld tensile strength dependence on film thickness and temperature 21 p2717 A73-40480

How composition affects properties of a ferritic stainless steel. 21 p2721 A73-41084

The creep characteristics of the heat-resistant ferritic steels X 20 CrMoV 12 1 and X 18 CrMoNi V Nb 12 1 and their welded connections 22 p2872 A73-41780

Gas metal arc welding of 9% Ni steel using ferritic filler metal. 22 p2866 A73-42226

WELD TESTS

Fatigue crack propagation in stainless steel weldments at high temperature. 01 p0067 A73-11372

Electron microanalysis of backfilled hot cracks in Inconel 600. 01 p0067 A73-11373

Fracture characteristics of aluminum alloy welds in Charpy impact test at super-low temperatures. 02 p0172 A73-11596

Influence of microstructure on the corrosion behavior of Ti-2% Ni in hot acidic chloride solutions with particular reference to weld regions. 03 p0325 A73-13730

Local stress-strain response of notched members to predict fatigue life of stress relieved and as-received weldments with internal cavities 04 p0453 A73-14864

Weld quality of explosive welded industrial metals, noting role of thermal processes and materials thermophysical properties 07 p0831 A73-19995

Russian book - Heat resistance of welded joints. 07 p0831 A73-20230

Investigation of the low-cycle fatigue of light-alloy welds 07 p0833 A73-20506

Influence of low temperatures on the fatigue life of welds 07 p0833 A73-20508

An experimental model of the microelectronic ultrasonic wire bonding mechanism. 08 p0972 A73-20734

Sliding friction welding of nonferrous Cu, wrought Al alloy and Ti, resting rubbing speed and axial pressure effects on equilibrium condition transition 08 p0973 A73-21238

Problems in electron-beam welding of non-ferrous metals. 08 p0973 A73-21243

Effect of process variables on partial penetration electron beam welding. 10 p1223 A73-23629

Flange-to-web connection requirements on beams with corrugated webs. 10 p1223 A73-23632

Embrittlement of 2-1/4Cr-1Mo steel weld metal by postweld heat treatment. 11 p1375 A73-26354

An ultrasonic technique for the inspection of magnetic and explosive welds, using a facsimile recording system. 12 p1502 A73-27037

Measuring projection weld strength by acoustic emission. 12 p1502 A73-27038

A modernized device for testing metal sheet and welded joints under conditions of planar tension 12 p1486 A73-27464

Russian book on ultrasonic methods for weld testing covering flaw detection, emitters/receivers, acoustic channels, echo and mirror shadow methods, automatic testing, etc 13 p1624 A73-28949

Mechanical strength of titanium alloys AT-2 and AT-3 and of their welded seams at extreme temperatures. 13 p1643 A73-29633

WELDABILITY

- Solidification structure and tensile properties of 2014 aluminum alloy welds. 14 p1755 A73-30149
- Testing assembly for sheet metals and welded joints under static and low-cycle biaxial tension under low temperature conditions 15 p1855 A73-31147
- Setting of sensitivity of ultrasonic equipment for weld inspection. 15 p1882 A73-32025
- Forecasting failures with acoustic emission. 16 p2022 A73-33992
- Investigation of low-cycle fatigue of welded joints in light alloys. 19 p2433 A73-37781
- Effect of low temperature on the fatigue limit of welded joints. 19 p2433 A73-37783
- Scribe line technique detects incomplete fusion in EB welds. 21 p2708 A73-41251
- Prediction of weld metal hydrogen levels obtained under test conditions. 21 p2708 A73-41252
- An investigation of pulsed GTA welding variables. 21 p2708 A73-41254
- Weldability and weld metal capabilities of a new precipitation-hardenable alloy. 21 p2708 A73-41255
- A technique for placing known defects in weldments. 23 p2986 A73-44170

WELDABILITY

- Weldability, corrosion resistance and heat resistance increase in Nb alloyed steels, noting aging temperature effects and microstructure 06 p0706 A73-17886
- Effects of the initial structures of pressed semi-finished products made of AK-8 alloy on their weldability. 07 p0832 A73-20370
- Filler wire welded joints of Al-Zn-Mg and Al-Mg alloys, testing weldability and mechanical properties susceptibility to hot cracking 07 p0840 A73-20372
- Possibility of argon-nitrogen gas metal-arc welding of some non-ferrous metals. 08 p0973 A73-21237
- Transage 129 Ti-Al-V-Sn-Zr alloy fabrication cost reduction through good cold formability and weldability with weight saving due to high strength and fatigue resistance 15 p1891 A73-32172
- Weldability and weld metal capabilities of a new precipitation-hardenable alloy. 21 p2708 A73-41255

WELDED JOINTS

- NT SPOT WELDS
- Structured changes and phase transformations of welded joints of Al alloy with Cu addition during welding thermal cycles 01 p0067 A73-11352
- Temperature fields and stresses during local tempering of helical welds of a cylindrical shell 01 p0118 A73-11413
- Influence of cyclic heating on the mechanical fatigue of titanium alloys and their weld joints 02 p0180 A73-11933
- State-of-technology for joining TD-NiCr sheet. 02 p0174 A73-12619
- Comparison and analysis of residual stress measuring techniques and the effect of post-weld heat treatment on residual stresses in Inconel 600, Inconel X-750 and Rene 41 weldments. 03 p0313 A73-13596
- Russian book on ultrasonic welding of metals and plastics covering equipment, transducers, welded joints stabilization, quality control and efficiency 04 p0457 A73-15970
- Evaluation of fracture toughness in aluminum alloys and welds by the Charpy impact test. 05 p0587 A73-16578
- HF dc straight polarity current pulsations effects on quality and mechanical properties of gas tungsten arc welds in Al alloy [SAE PAPER 720874] 05 p0582 A73-16669
- Diffusion welding of beryllium. II - The role of the microalloying elements. 06 p0704 A73-17597
- Structure and properties of the weld metal in maraging N18K9M5T steel 06 p0697 A73-17879
- Susceptibility to brittle fracture of simulated weld seams in Ti-Al-V alloys. 06 p0698 A73-18209
- Reflections on the nature of the bond in welding of metals - The particular case of fusion welding 06 p0698 A73-18693
- Mechanical behavior of assemblies welded by fusion on steel 06 p0698 A73-18694
- Surface preparation and heating and control processes in diffusion brazing and welding, illustrating with turboreactor construction 06 p0698 A73-18695

Determination of the extent of ultrasonically detected defects - Application to welded butt joint quality control 07 p0831 A73-19904

Russian book - Heat resistance of welded joints. 07 p0831 A73-20230

Fine grained weld structures. 07 p0832 A73-20273

Effects of heat treatment on the properties of a molybdenum-carbon-nickel alloy and joints in it. 07 p0840 A73-20371

Filler wire welded joints of Al-Zn-Mg and Al-Mg alloys, testing weldability and mechanical properties susceptibility to hot cracking 07 p0840 A73-20372

On optimizing thermal stresses in cylindrical shells. 08 p1015 A73-20674

Some fatigue properties of welded high temperature alloys. 08 p0978 A73-21241

Investigation of the detectability of defects in the ultrasonic testing of joints obtained by friction welding. 09 p1088 A73-22299

Solar cell interconnections with different weld types, discussing semiautomatic and automatic ultrasonic processes, solder thickness control and quality inspection methods and criteria 09 p1035 A73-22807

Small-scale explosion seam welding. 10 p1223 A73-23626

Flange-to-web connection requirements on beams with corrugated webs. 10 p1223 A73-23632

Welded joints fatigue properties, considering porosity, nonmetallic occlusions and cracks effects 11 p1372 A73-25105

Fatigue-crack growth in Type 304 stainless steel weldments at elevated temperatures. 11 p1379 A73-25131

Crack propagation behavior in type 304 stainless steel weldments at elevated temperature. 11 p1375 A73-26357

Localized hydrogen in titanium welds. 11 p1375 A73-26358

A modernized device for testing metal sheet and welded joints under conditions of planar tension. 12 p1486 A73-27464

The strength of welded joints in high strength stainless steels at cryogenic temperatures. 13 p1625 A73-29615

Conditions of brittle strength of weld joints at different temperatures and applied loading rates. 13 p1626 A73-29628

Estimation of fatigue-crack propagation life in butt welds. 14 p1755 A73-30147

Fatigue crack propagation in butt welds containing joint penetration defects. 14 p1755 A73-30148

Determination of fatigue strength of welded joints with artificial flaws by radiographic examination 15 p1882 A73-32051

Competitive processes in joining; Proceedings of the Twenty-sixth Autumn Review Course, Eastbourne, England, October 27-29, 1972. 16 p2021 A73-33859

The metallurgical implications of welding processes. 16 p2021 A73-33863

Structure and phase composition of welded joints of zirconium alloy with 2.5% Nb 19 p2439 A73-37266

Weldbonding/rivetbonding - Application testing of thin gauge aircraft components. [AIAA PAPER 73-805] 19 p2433 A73-37464

Effect of low temperature on the fatigue limit of welded joints. 19 p2433 A73-37783

Effect of heat input on properties of Inconel filler metal 82 weld deposits. 19 p2435 A73-38002

Development of a lightweight body-mounted solar cell array with a high power to weight ratio. 19 p2391 A73-38408

Influence of a magnetic field on the weld-seam structure during electroslag welding of titanium alloys 21 p2707 A73-40891

Scribe line technique detects incomplete fusion in EB welds. 21 p2708 A73-41251

Effect of technological and metallurgical treatment on the properties of electroslag-welded joints in heat resistant steels 22 p2865 A73-41778

Effect of the superplasticity of titanium and its alloys, and the use of this phenomenon for welding in a solid state 22 p2866 A73-42093

WELDED STRUCTURES

NT STEEL STRUCTURES

Application of the theory of linear fracture mechanics to the assessment of turbine rotor strength 02 p0229 A73-11620

Welded structural components fatigue behavior representation by characteristic curves derived from S-N diagrams, describing data reduction procedure 07 p0910 A73-19216

Static and dynamic behavior of welded aluminum beams. 07 p0839 A73-20270

Acoustic emission weld monitoring of nuclear components. 07 p0832 A73-20274

Effects of the initial structures of pressed semi-finished products made of AK-8 alloy on their weldability. 07 p0832 A73-20370

Radiography and ultrasonic tests for weldment and flaw inspection, discussing choice based on economic, technical and application considerations 08 p0952 A73-21076

Implosive and explosive welding of mono- and bimetallic duplex cylinders. 08 p0973 A73-21239

Welding airframe structures in titanium alloys using tensile loading as a means of overcoming distortion. 08 p0973 A73-21240

Failure of high-strength welded structures with initial cracks 10 p1225 A73-24368

Improvement of damping characteristics of structural members with high damping elastic inserts. 13 p1690 A73-28056

Thermal stress analysis of metals with temperature dependent mechanical properties. 13 p1701 A73-29507

Welded steel beam fatigue behavior evaluation via stable crack growth concepts, developing fracture mechanics model for cracks originating from pores 17 p2246 A73-34887

Welded titanium tubes and their applications 19 p2433 A73-37834

Ultrasonic closure welding of small aluminum tubes. 19 p2435 A73-38003

Mechanical properties of weldments of AK-3 titanium with an elevated oxygen content. 21 p2720 A73-41036

WELDING

- NT ARC WELDING
- NT BRAZING
- NT DIFFUSION WELDING
- NT ELECTRIC WELDING
- NT ELECTRON BEAM WELDING
- NT ELECTROSLAG WELDING
- NT EXPLOSIVE WELDING
- NT FLASH WELDING
- NT FUSION WELDING
- NT GAS TUNGSTEN ARC WELDING
- NT GAS WELDING
- NT PLASMA ARC WELDING
- NT PRESSURE WELDING
- NT ULTRASONIC WELDING
- State-of-technology for joining TD-NiCr sheet. 02 p0174 A73-12619
- Assembling by welding and bonding - Introductory report on assemblies 06 p0698 A73-18692
- Calibration procedure for instruments to measure the delta ferrite content of austenitic stainless steel weld metal. 07 p0832 A73-20272
- Lamellar tearing and the slice bend test. 07 p0832 A73-20275
- Welding and fabrication of non-ferrous metals; Proceedings of the International Conference, Eastbourne, Sussex, England, May 2, 3, 1972, Volume 1. 08 p0973 A73-21235
- Mechanism by which hot cracks form during welding aluminium and its alloys. 08 p0977 A73-21236
- The phenomenon of superplasticity of polymorphous metals and alloys and its use for welding and hardening in the solid state. 08 p0978 A73-21242
- Welding techniques for high strength superalloy turbine blades and vanes repair, discussing controlled preheating and cooling methods for crack prevention [ASME PAPER 73-GT-44] 16 p2019 A73-33505
- Competitive processes in joining; Proceedings of the Twenty-sixth Autumn Review Course, Eastbourne, England, October 27-29, 1972. 16 p2021 A73-33859
- Joining and assembly by welding. 16 p2021 A73-33860
- Joining of plastics to plastics and to metals. 16 p2021 A73-33861
- A numerical, thermo-mechanical model for the welding and subsequent loading of a fabricated structure. 24 p3150 A73-45231
- WELDING MACHINES
- Cutting and welding using a CO₂ laser. 05 p0582 A73-17264
- Microwelding equipment with automatic wire breaking and ball melting blocks and electronically controlled wire feeding, noting heating plate with thyristor temperature control 06 p0683 A73-18433
- Problems in electron-beam welding of non-ferrous metals. 08 p0973 A73-21243

Plasma-MIG arc welding with deposition from automatic reel fed wire via rotating arc, noting suitability for stainless steel sheet

09 p1089 A73-22693

High speed welding of sheet steel with a CO₂ laser.

11 p1375 A73-26351

Cape Kennedy Space Center ground support equipment welding machines and techniques, emphasizing propellant storage tanks and mobile launcher transporters

16 p1995 A73-33195

Development of a data-processing installation for the automatic quality control of spot-welding joints

16 p2019 A73-33222

Book - Welding and welding technology.

17 p2177 A73-34454

An accurate method for determining electron beam welding voltages.

19 p2435 A73-38001

Research carried out by the Aviation Institute on electric welding in protective atmospheres

21 p2708 A73-41578

Application of electron beam welding to aircraft turbine engine parts.

22 p2866 A73-42196

WENTZEL-KRAMER-BRILLOUIN METHOD

Propagation of electromagnetic waves in media which vary slowly with position and time.

[AD-753304] 04 p0423 A73-15483

Error analysis of Wentzel-Kramers-Brillouin approximation for electromagnetic wave reflection from nonuniform absorbing half space

05 p0549 A73-16392

Internal gravity waves in an atmosphere with wind shear - Validity of the WKB approximation at critical layers in the presence of buoyancy forces.

11 p1394 A73-25721

Gravity oriented satellite librational damping by solar radiation pressure, comparing WKB method with numerical integration results

15 p1943 A73-31640

Determination of the dispersion relation in tunnel structures - Influence of the barrier shape and validity of the WKB approximation.

17 p2220 A73-35655

WEST GERMANY

U GERMANY

WESTLAND AIRCRAFT

NT P-531 HELICOPTER

Westland Sea Lynx naval variant aircraft design and development for multiservice multirole application, emphasizing high reliability and maintenance ease requirements

[AHS PREPRINT 711] 17 p2104 A73-35057

WESTLAND P-531 HELICOPTER

U P-531 HELICOPTER

WETLANDS

Interpretation of wetlands imagery based on spectral reflectance characteristics of selected plant species.

09 p1077 A73-22388

Wetlands mapping in New Jersey.

13 p1619 A73-29237

Applications of high-altitude remote sensing to coastal zone ecological studies.

16 p2003 A73-33364

WETNESS

U MOISTURE CONTENT

WETTABILITY

Wettability and interfacial tension of magnesia single crystals by molten magnesium oxide-aluminum trioxide-silicon dioxide glasses, discussing contact angle relationship to temperature

23 p2998 A73-44132

WETTING

The wetting of carbon and carbides by copper alloys.

15 p1897 A73-31837

Effect of skin wetting on finger cooling and freezing.

20 p2518 A73-39779

Physicochemistry of the deposition of gelatinous photographic emulsion layers on a substrate

21 p2647 A73-40268

Influence of certain wetting agents on the optical sensitization and retention of the photographic properties of a finished layer

21 p2647 A73-40271

The effect of impregnation and wetting characteristics on the mechanical parameters of glass-fiber-reinforced plastics

24 p3103 A73-44877

WHEATSTONE BRIDGES

A dc amplifier operating with a measuring bridge circuit

07 p0803 A73-20540

Photoelectric servo simulator for pupil, using Wheatstone bridge with CdS light dependent resistor

14 p1722 A73-30399

Electron beam current fluctuation reduction by placing hot filament into Wheatstone bridge arm for temperature regulation in power supply for electron gun

17 p2176 A73-35776

Detuning of Wheatstone-bridge circuit during the measurement with wire strain gages - Influence and elimination of undesired effects on detuning

20 p2566 A73-39630

WHEEL BRAKES

Rubber friction effect on vehicle tire force-slip and breaking behavior in terms of peripheral and sideslip components and structural and operational parameters

03 p0251 A73-13242

Hydraulic system on de Havilland Twin Otter STOL aircraft for flaps, wheel brakes and nose wheel steering, noting power supply mounting

03 p0252 A73-13350

Transport aircraft wheels and brakes operational cost minimization, discussing contributory roles of governmental regulations (FAA), aircraft manufacturer, supplier and user

[SAE PAPER 720867] 05 p0534 A73-16650

Cantilever aircraft tires - More than a break for brakes.

[SAE PAPER 720870] 05 p0534 A73-16652

Hydraulic drive and control systems used for landing gear retraction and extension on Piper Cherokee Arrow and for main wheel braking on F-111

07 p0779 A73-19604

Investigation of friction and wear mechanisms in a friction coupling with a small overlapping coefficient

15 p1882 A73-31599

Design and development of lightweight wheel braking equipment.

[SAE PAPER 995] 19 p2434 A73-37894

WHEELS

NT FLYWHEELS

NT NOSE WHEELS

NT REACTION WHEELS

NT TURBINE WHEELS

NT VEHICLE WHEELS

WHIP ANTENNAS

Amplifier design for continuous recording of plasma frequency, using dipolar resonance signal obtained from parallel whip antennas surrounded by plasma sheath

10 p1216 A73-23747

Wideband VHF whip antenna impedance simulation using AI cylindrical chamber to simplify impedance-controlling network tuning and power testing

17 p2148 A73-35705

The effect of snow on antenna radiation patterns - A presentation of results.

22 p2831 A73-41850

WHIRL INSTABILITY

U ROTARY STABILITY

WHIRLING

U ROTATION

WHIRLING TESTS

U SPIN TESTS

WHISKER COMPOSITES

Directionally solidified NiAl-Cr and NiAl-Mo eutectic composites microstructural stability as function of time and temperature

06 p0711 A73-18753

Morphological factors influencing the initial stages of coarsening in the Al-Al₃Ni eutectic composite.

06 p0712 A73-18761

Networks of polycrystalline metal whiskers for composite materials

11 p1379 A73-25408

Silicon carbide whisker reinforced Al composite production by powder metallurgy, discussing mechanical strength and extrusion process for fiber orientation

11 p1373 A73-25414

Reactivity and interface characteristics of titanium-alumina composites.

11 p1384 A73-26043

Stability of nickel coated sapphire whiskers.

11 p1389 A73-26044

Monograph - Fibre reinforcement.

17 p2240 A73-34125

The stability of sapphire whiskers in nickel at elevated temperatures. I - General morphological and chemical stability. II - The kinetics of morphological changes over the temperature range 1100 to 1400 C.

23 p2986 A73-44032

Shear strength of whiskered-fiber reinforced composites

24 p3102 A73-44513

Whiskers as reinforcing component of composite materials, process-technical alignment methods

24 p3104 A73-44888

WHISKERS [SINGLE CRYSTALS]

Strength and elastic characteristics of ammonium perchlorate whiskers grown with potassium permanganate additions, discussing crystal dislocations and physico-chemical properties

14 p1767 A73-30829

Ultrahigh speed cinematography with rotating Ti drums bound by monocrystalline boron fibers, noting prototype performance

21 p2693 A73-39937

Special features of the structure and growth of pyrocarbon whiskers

23 p2996 A73-43624

Whisker junctions between growth structures on CdS layers.

23 p2997 A73-44027

The creep of sapphire filament with orientations close to the c-axis.

23 p2997 A73-44029

The effect of halide impurities on the mass production of metal whiskers by reduction.

24 p3098 A73-44401

Whiskers as reinforcing component of composite materials, process-technical alignment methods

24 p3104 A73-44888

WHISTLERS

Refraction of whistler-mode waves by large-scale gradients in the middle-latitude ionosphere.

01 p0017 A73-10328

Comparative study of monthly and diurnal occurrences of whistlers and gyroelectric echoes in conjugate regions of Europe and South Africa

01 p0043 A73-11274

Diurnal effects in pc 1 hydromagnetic whistlers - An early afternoon source model.

02 p0158 A73-11909

Quasimonochromatic whistler mode packets of slowly varying amplitude.

02 p0140 A73-11920

Quasi-linear interaction of whistler-mode waves and nonthermal electrons.

02 p0141 A73-12390

The effects of ions of VLF and ELF propagation in an abnormally ionized atmosphere.

02 p0143 A73-12851

Transmission and reflection of magnetospheric whistlers in the ionosphere and lower exosphere at high latitudes.

03 p0298 A73-12884

Parametric instability and anomalous heating due to electromagnetic waves in plasma.

03 p0345 A73-13060

Helicon /whistler/ turbulence spectra in collisionless plasma, noting ion scattering relation to self trapping and concentration along magnetic field with Landau absorption decay

04 p0480 A73-15564

Investigations of high-energy charged particles and VLF radiation with the Interkosmos 3 satellite.

05 p0608 A73-16085

Nonducted whistlers observed in the plasmasphere.

05 p0572 A73-17165

Self trapping modulational instability of electron cyclotron wave whistler in cold and hot dense plasmas, discussing relevance to phenomena in magnetosphere

07 p0814 A73-19239

Computerized simulation for nonlinear evolution of whistler instabilities in anisotropic collisionless plasmas with various Maxwellian electron distributions

07 p0857 A73-19523

R and L modes of ion cyclotron whistler propagation in ionosphere, noting refractive indexes and wave polarization for multicomponent plasma

07 p0819 A73-20060

Annual and semi-annual variations in the electron density of the inner magnetosphere deduced from whistler dispersion.

07 p0819 A73-20061

Propagation modes of radio whistlers and gyroelectric echoes received in middle latitudes

08 p0937 A73-20651

VLF ion cyclotron whistler propagation in upper ionosphere, noting polarization reversal and mode coupling from satellite observation

08 p0937 A73-20653

Low dispersion whistlers observed simultaneously at two low latitude stations.

08 p0940 A73-21651

Whistler observations of the depletion of the plasmasphere during a magnetospheric substorm.

09 p1074 A73-22060

Effect of geomagnetic activity on occurrence of whistler atmospherics.

09 p1077 A73-22373

Nonducted whistlers observed in the plasmasphere.

09 p1078 A73-22748

Enhanced energetic electron intensities at 100 km altitude and a whistler propagating through the plasmasphere.

09 p1079 A73-22839

Numerical simulation of small amplitude whistler waves in thermal plasma, describing particle motion under self consistent and external magnet fields via Lorentz equation

10 p1255 A73-24269

Nonlinear hydrodynamic VLF wave scattering in the earth's magnetosphere.

11 p1331 A73-25913

Nose extension method based on approximate dispersion function for calculating ducted whistler frequency and associated travel time, discussing ionosphere-magnetosphere interactions

11 p1358 A73-26704

WHITE BLOOD CELLS

A fast method to determine the noise frequency and minimum group delay of a whistler when the causative spheric is unknown. 11 p1358 A73-26705

Steady ELF plasmaspheric hiss, studying whistler mode turbulence, band limitation, power spectra and peak intensities 12 p1488 A73-26984

An association of magnetospheric whistler dispersion characteristics with changes in local plasma density. 12 p1488 A73-26985

Measurements of wave normal direction of whistler mode signals in the ionosphere by means of the rocket-Doppler technique. 12 p1492 A73-27610

The values of ionospheric absorption of VLF electromagnetic waves in middle geomagnetic latitudes. 15 p1868 A73-31523

Magnetospheric electric field under quiet conditions on the basis of ground-based observations of whistlers 15 p1872 A73-31903

Theory and computer simulation of whistler turbulence and velocity space diffusion in the magnetospheric plasma. 16 p2003 A73-33439

The plasmasphere during a magnetic recovery period - A combined study of the OGO 4 and OGO 5 satellite data and of whistlers received at the ground 16 p2008 A73-33876

Simultaneous observations of Pc1 micropulsation polarization at four low latitude sites. 16 p2008 A73-33877

Penetration and reflection of VLF waves through the ionosphere - Full wave calculations with ground effect. 16 p1984 A73-33921

VLF goniometer observations at Halley Bay, Antarctica. I - The equipment and the measurement of signal bearing. II - Magnetospheric structure deduced from whistler observations. 17 p2159 A73-34777

Proton whistlers in the ionospheric F-region over the South American equatorial area. 18 p2304 A73-35970

Interaction between high-frequency turbulence and magnetospheric micropulsations. 18 p2352 A73-36277

Simulation of gyroresonant electron-whistler interactions in the outer radiation belts. 18 p2347 A73-36296

A unified picture of the parallel whistler mode instability. 19 p2403 A73-37440

On the propagation of ionospheric whistlers at low latitude. 19 p2404 A73-38018

Ducted propagation of low-latitude whistlers deduced from simultaneous observations at multi-stations. 19 p2404 A73-38019

The effect of geomagnetic disturbance on the duct propagation of low-latitude whistlers. 19 p2426 A73-38020

Localization of sources of two-hop whistlers observed aboard the Interkosmos 3 satellite over Europe. 19 p2404 A73-38021

Whistler-mode hiss at low and medium frequencies in the dayside-cusp ionosphere. 20 p2529 A73-38935

Whistlers association with sudden changes in amplitude of long distance nighttime subionospheric VLF transmission 20 p2530 A73-38944

Magnetospheric implications of the nonlinear whistler instability obtained in a computer experiment. 20 p2553 A73-38961

Effects of collisions on whistler-mode ray tracing. 20 p2531 A73-39404

The upward propagation of LF waves /electron whistlers/ into the ionosphere and the turning of the Poynting vector towards the earth's magnetic field. 21 p2654 A73-40782

Modulation of spectrum and amplitude of VLF signal in the magnetosphere. 21 p2657 A73-41381

Balloon and VLF whistler measurements of electric fields, equatorial electron density, and precipitating particles during a barium cloud release in the magnetosphere. 22 p2845 A73-41934

Nonlinear development and Fourier analysis of the whistler mode instability. 22 p2893 A73-42391

Absorption of vlf and elf waves in whistler mode - Sunrise and sunset effects. 22 p2849 A73-42622

Absorption of whistler waves during night. 22 p2850 A73-42623

Low latitude whistler activity during geomagnetic storms related to spread F conditions and magnetospheric and ionospheric electron density 23 p2972 A73-43696

VLF input impedance of a loop antenna embedded in the magnetosphere. 23 p2954 A73-43700

The determination of whistler noise-frequency and minimum group delay and its implication for the measurement of the east-west electric field and tube content in the magnetosphere. 24 p3087 A73-45210

Dispersion characteristics of whistler atmospheric during higher geomagnetic activity. 24 p3088 A73-45365

WHITE BLOOD CELLS

Differentiations and maturations in red and white blood cells construction in red bone marrow, noting hematopoietic system formation from single source cell 06 p0649 A73-17473

WHITE DWARF STARS

Evolutionary models for helium white dwarves with uniformly accreting hydrogen shell, noting thermally unstable laminar energy source formation in shell lower layers 01 p0100 A73-10709

White dwarfs gravitational red shifts, radial velocities and mass-radius relationships, considering colors and luminosities 01 p0104 A73-11036

Nuclear energy sources in superdense celestial bodies. 01 p0106 A73-11311

Blanketed model atmospheres for cool hydrogen-rich white dwarfs. 03 p0371 A73-13225

Discovery of circular polarization in the red degenerate star G99-47. 04 p0502 A73-15687

Subnuclear density state equation for minimum mass and binding energy of neutron star converting into white dwarf 04 p0502 A73-15978

Scorpius X-1 representation via old-nova model consisting of standing shock and X ray source formed by mass accretion at white dwarf surface 07 p0874 A73-19063

Supernova explosions in close binary systems 09 p1145 A73-22289

Radial pulsations of a white dwarf in the case of nonuniform rotation 09 p1145 A73-22290

Evolution of a white dwarf during accretion of hydrogen-rich matter. II 09 p1145 A73-22291

White dwarf flares UVB energy spectra, assuming mechanism of nonthermal bremsstrahlung due to fast electrons 09 p1146 A73-22296

Quasi-radial pulsations of rotating white dwarfs and neutron stars in the relativistic theory of gravitation 10 p1274 A73-23711

Her X-1 optical counterpart observed for B magnitude, relating light curve scatter to 35-day cycle 11 p1428 A73-26627

Criticism of Galactic cosmic ray production model with rotating magnetic white dwarfs, noting contrary evidence in magnetic field observations and decay theories 12 p1539 A73-27149

Blue OB stars detection by flicker comparison, astronomical photography and two color diagrams, discussing classification as quasars and white dwarfs 13 p1673 A73-28148

White dwarfs model based on zero temperature Fermi gas theory, determining mass-radius relation and limit mass 13 p1682 A73-28982

Theory of the thermal explosion in the hydrogen shell of a white dwarf 13 p1683 A73-29091

Book on variable stars, covering high energy astrophysics, low energy outbursts, extensive convection, galaxies, pulsations, white dwarfs, cepheids, flares and gravitational collapse 14 p1796 A73-29950

White dwarfs, neutron stars and black hole identification by satellite X ray astronomy, discussing gas temperature and mass relation to cluster parameters 14 p1797 A73-30075

High-frequency stellar oscillations - The Cerro Tololo search for luminosity-variable white dwarfs. 15 p1935 A73-31482

Variable X ray sources Cyg X-1, Cen X-3 and Sco X-1 behavioral analysis from Uhuru satellite data, considering pulsating white dwarf model for Cen X-3 15 p1935 A73-31483

The magnetohydrodynamic stability of white dwarfs and neutron stars. 16 p2062 A73-33573

Quasiradial pulsation of rotating white dwarfs and neutron stars in general relativity. 18 p2354 A73-36736

Viscous effects in rapidly rotating stars with application to white-dwarf models. I, II. 18 p2357 A73-37106

The effect of hot white dwarfs on the interstellar medium. II - The changes in its structure with height above the galactic plane and some consequences of the finite lifetimes and velocities of the white dwarfs. 19 p2483 A73-37561

Light curves of the gravitational lens-like action for binaries with degenerate stars. 19 p2483 A73-37563

Temperature aspects of Landau orbital ferromagnetism in white dwarfs and neutron stars. 20 p2610 A73-39573

Quantized magnetic bremsstrahlung from white dwarfs surface layer as possible source of Galactic center infrared radiation 20 p2611 A73-39709

Configurations of hot white dwarfs with nuclear energy sources 23 p3025 A73-44360

Thermodynamics of white dwarf matter in crystalline phase. 24 p3143 A73-45435

WHITE NOISE

NT THERMAL NOISE

White noise signal correction for nonlinear nonstationary systems, using orthonormalized functionals 01 p0027 A73-10593

State and integral equations formulations for signal design problem of channels with known time dispersion and additive white Gaussian noise 04 p0419 A73-15405

Kalman-Bucy method solution to time-space dependent random fields optimal filtration under additive white noise 07 p0804 A73-20635

Kalman filtering theory application to optimal causal demodulator for pulse amplitude modulated signals in white Gaussian noise 09 p1067 A73-22116

Functional state of the cerebral cortex and of the mesencephalic reticular formation during prolonged action of impulsive and stable noise 10 p1181 A73-24334

Combinational noise and interference effects during frequency conversion, noting mathematical methods 10 p1189 A73-24376

A representation of uncorrelated random processes by stochastic integrals 11 p1340 A73-25010

Optimal passband of a double-tuned selective amplifier during the simultaneous passage of rectangular radio pulses and white noise 12 p1477 A73-26874

Temperature field in front of or behind gas turbine with additive white noise, deriving optimal filter for dynamic programming technique in random fields analysis 12 p1483 A73-27080

Other stability criteria for distributed and Gaussian stochastic systems with diagonal nonlinearity 13 p1596 A73-28564

Kalman-Bucy method for optimal filtering of time and space dependent random fields in Hilbert space in presence of additive white noise 15 p1854 A73-31689

Meteorological time series persistence tendency representation by autocorrelation coefficients, summation, determining independent values effective number by white noise bandpass filtering 15 p1906 A73-32344

An algebraic method for linear dynamical systems with stationary excitations. 16 p2076 A73-32919

Dynamic systems stability under influence of white noise-Gaussian random processes, discussing optical control, Markov processes, linear equations and vector fields 20 p2583 A73-39768

Noise of space-charge-limited current in solids is thermal. 21 p2668 A73-41559

IMPATT diode frequency-independent small-signal equivalent circuit incorporated with negative resistance element and white noise source for terminal behavior prediction 23 p2964 A73-44074

Studies on a band limited white noise with a uniform bispectrum. 23 p2965 A73-44135

Eigenfunction expansions for randomly excited non-linear systems. 24 p3151 A73-45265

WHITHAM RULE

On the higher approximations of the supersonic projectile theory. [AIAA PAPER 73-669] 18 p2262 A73-36220

WHITTAKER FUNCTIONS

A study of systems with time-variable coefficients by the definite-integral method 20 p2542 A73-39037

WICKS

Predicting performance of heat pipes with partially saturated wicks. [ASME PAPER 72-WA/HT-38] 04 p0518 A73-15817

Arterial wick heat pipes self filling capability theoretical and experimental investigation, deriving expressions for mesh size, artery radius and stem height relationships
[ASME PAPER 72-WA/HT-36] 04 p0518 A73-15819

Experimental study of the effective thermal conductivity of liquid saturated sintered fiber metal wicks.
06 p0770 A73-18836

Development of a high capacity variable conductance heat pipe.
[AIAA PAPER 73-728] 18 p2369 A73-36345

Development of a high capacity cryogenic heat pipe.
[AIAA PAPER 73-729] 18 p2369 A73-36346

WIDE ANGLE LENSES

An optimized video output from a wide angle optical probe.
[AIAA PAPER 73-918] 21 p2673 A73-40866

A compound wide angle color visual display system and a high resolution, high sensitivity close circuit color television camera developed for wide angle color visual systems.
[AIAA PAPER 73-925] 21 p2702 A73-40872

WIDEBAND

U BROADBAND

WIDEBAND COMMUNICATION

Towards faithful radio transmission of very wide bandwidth signals.
01 p0015 A73-10176

Microwave varactor upconverter in radio repeater for domestic wideband communication satellite, emphasizing transmission characteristics design
01 p0006 A73-11177

Constant-envelope spread spectrum random access satellite communication system, discussing message and multiple access modems, signal acquisition, tracking, ranging, etc
01 p0018 A73-11178

Multifrequency radio beacon on polar orbiting satellite for wideband transmission through ionosphere without significant signal distortion
03 p0275 A73-13627

Active terminal devices for wide band time multiplexed laser PCM communication systems.
04 p0417 A73-15069

The ERTS wideband image communication system.
04 p0418 A73-15382

Bandpass error free wideband PCM communications system response to pulse signal
06 p0668 A73-18391

On near-field distributions along the leaky coaxial cable.
08 p0937 A73-20804

Application of equiangular conical antennas with thick leads
08 p0938 A73-20963

Investigation of the mutual ambiguity function of a wideband signal with complex angle modulation
10 p1187 A73-23731

Multichannel wideband FM communication systems, discussing method for channel density increase with reduced linearity requirement and enhanced noise immunity
10 p1187 A73-23732

High volume wideband PSK system design for minimal sidelobe, calculating signal number relationship to maximum sidelobe level of cross correlation and autocorrelation
10 p1187 A73-23733

Study of ionospheric phase distortion at Ahmedabad.
10 p1188 A73-24170

Commercial communications satellite technology trends, stressing wideband capabilities, flexibility, multiple access and channel capacity increase
10 p1189 A73-24561

Low loss fiber optics communication technology with almost infinite bandwidth potential, discussing transmission lines, light sources, detectors, integrated circuits, systems and applications
11 p1399 A73-26118

Discrete wideband FM signals optimal filter synthesis by coupling two nonlinear servosystems
12 p1467 A73-26869

The impact of satellites on military communications.
14 p1729 A73-30874

Broad X band multichannel waveguide matrix for high speed switching from one input to one of four outputs at high power levels
16 p1990 A73-33897

Two-way wideband microwave communication system oriented toward PCM-TDM digital technique for covering telephone, videophone and radio broadcasting services
17 p2123 A73-34968

A 180-deg phase-shift keying modulator for microwave broadband application
18 p2292 A73-36398

Modular airborne video tape recording systems using wideband frequencies, describing wideband channels, power supply, transport unit, servo module and bit storage rates
19 p2431 A73-38199

A satellite-switched SDMA/TDMA system for a wideband multibeam satellite.
20 p2524 A73-38730

The design of a wide band wide scan-angle waveguide radiating element.
21 p2652 A73-40660

New developments regarding wide-band communication with waveguide, glass fiber, and superconductivity
21 p2655 A73-41072

WIDMANSTATTEN STRUCTURE

Inter-crystalline structures effect on precipitation reactions in supersaturated solid solutions, noting Widmanstatten structure growth in U alloy
04 p0467 A73-15953

Laminar precipitation hardening in Al alloy during aging by microscopic, X ray and Widmanstatten structure analyses
12 p1510 A73-26912

The precipitation behavior of a commercial aluminum-copper-lithium alloy. I - The microstructure after isothermal heat treatment
16 p2026 A73-33954

The structure of a meteorite, its formation and transformation during heating
17 p2230 A73-34565

X ray and electron diffraction studies of Ni-containing etched brown rims in meteoritic taenite /Ni-Fe alloy/ associated with kamacite, noting Widmanstatten pattern
23 p2951 A73-43844

WIENER FILTERING

Analysis of certain nonstationary processes by using Wiener functionals
01 p0026 A73-10026

Wiener-Kolmogoroff optimal filtration theory for synthesis of linear stabilization systems under steady random external perturbations, noting control optimality conditions
01 p0028 A73-10670

Equivalence of the likelihood ratio processor, the maximum signal-to-noise ratio filter, and the Wiener filter.
03 p0282 A73-13917

Optimal matched Wiener discrete filters investigated with operator-matrix concepts, considering signal decorrelation
03 p0278 A73-14030

Wiener and Kalman-Bucy filters design with error covariance bound for performance divergence prevention under stochastic processes with unknown signal and noise densities
07 p0806 A73-20603

Wiener and Kalman filters theory for stochastic processes in communication, demonstrating optimum demodulator derivation by Kalman-Bucy theory application to double sideband amplitude modulation
09 p1065 A73-23112

Analysis of a method for obtaining near-diffraction-limited information in the presence of atmospheric turbulence.
19 p2461 A73-38485

Nonnegative additive functionals of Markov processes and certain limit theorems
20 p2582 A73-39389

Reproduction of a useful signal by linear feedback systems
20 p2543 A73-39506

Phase-tracking performance of direct-detection optical receivers.
21 p2656 A73-41169

A new approach to gust alleviation of a flexible aircraft using an open loop device
[ONERA, TP NO. 1236] 22 p2799 A73-42219

Representation of functions of Markov processes as solutions of stochastic equations.
23 p3000 A73-44207

WIENER HOPF EQUATIONS

Fourier transformations and Wiener-Hopf equations for stress intensity factor of crack propagation in linearly elastic homogeneous isotropic strip
04 p0512 A73-15238

Thin walled open ended cylindrical antenna in cold magnetoplasma, calculating current distribution by approximations based on Wiener-Hopf procedure
06 p0729 A73-18193

Discrete Wiener-Hopf equations composed of the Fourier coefficients of piecewise Wiener functions
10 p1243 A73-24459

WIGHTMAN THEORY

U FIELD THEORY (PHYSICS)

U QUANTUM THEORY

U RELATIVISTIC THEORY

WIGNER COEFFICIENT

Gasdynamics equations for low temperature monatomic gas, showing Wigner distribution function independence of density gradient in agreement with nonequilibrium statistical thermodynamics concepts
23 p2939 A73-43704

WILDLIFE

NT BATS

NT BIRDS

NT CHIMPANZEES

WILDLIFE RADIOLOCATION

The potential application of space technology to the radio tracking and biotelemetry of unrestrained animals.
05 p0545 A73-17134

WIND [METEOROLOGY]

NT CIRCUMPOLAR WESTERLIES

NT CYCLOGENESIS

NT GEOSTROPHIC WIND

NT GROUND WIND

NT GUSTS

NT JET STREAMS [METEOROLOGY]

NT MONSOONS

NT WINDS ALOFT

A method for incorporating nested finite grids in the solution of systems of geophysical equations.
02 p0165 A73-12776

Barotropic model of local forecasts of katabatic winds
08 p0985 A73-21451

Monograph - The quasi-biennial oscillation in the stratosphere.
08 p0986 A73-21841

An operational upper air analysis using the variational method.
10 p1244 A73-23645

A comparative study of the wind structure in the stratosphere at Sonmiani vis-a-vis CIRA 1965.
10 p1244 A73-23647

Equatorial spread F formation convective electric fields generation by neutral winds and conductivity caused by metallic ion concentrations
14 p1749 A73-29988

Kinetic models of the solar and polar winds.
15 p1926 A73-31847

A prediction of the phenomena that take place during so called 'sudden warmings.'
18 p2308 A73-36038

Atmospheric density, temperature and winds measured during Aladdin II.
18 p2309 A73-36055

WIND CIRCULATION

U ATMOSPHERIC CIRCULATION

WIND DIRECTION

Interrelation between processes occurring along a vertical, and the forecasting of stratospheric wind
05 p0592 A73-16232

Meridional circulation zonal averaging effects on summer hemisphere Hadley cell in tropical regions
07 p0847 A73-19046

Meteor trail drift observations in equatorial region /Somalia/ for lower thermosphere wind velocity and direction calculation via harmonic analysis
15 p1902 A73-31223

A comparison of geostrophic and rocket winds at stratospheric levels, measured from a small network of rocket sounding stations.
19 p2424 A73-37604

Reversing barchan dunes in lower Victoria Valley, Antarctica.
21 p2687 A73-41214

Mapping of North Atlantic winds by HF radar sea backscatter interpretation.
22 p2882 A73-41836

Upper tropospheric disturbances of the equatorial atmosphere and their influence on rainfall near the equator.
23 p3004 A73-44104

Motion of a tropical hurricane in the field of the North Atlantic trade wind
24 p3107 A73-44428

WIND EFFECTS

On the dependence of quietness and sharpness of solar image on local and large scale atmospheric circulation.
01 p0098 A73-10561

An evaluation of the scale of mesospheric wind disturbances.
02 p0160 A73-12272

Observation and interpretation of ionization drift measurements in the F region at St-Santin-Nancay.
02 p0161 A73-12284

Model for meteorite impact generated gas flow on moon as function of mass, velocity and composition, noting wind effects on lunar erosion
02 p0223 A73-12719

Atmospheric wind and temperature inhomogeneity induced sound wave refraction effects on acoustic sounder measurements, noting scattering volume displacement and Doppler shift
03 p0276 A73-13831

Energy conversion in the atmospheric boundary layer
04 p0441 A73-15286

The steady-state flow quality of an open return wind tunnel model.
04 p0433 A73-15512

Asymptotic solution for vertical propagation of equatorial planetary waves in shear, noting gravity-Rossby and Kelvin waves and wind effects on diurnal tides
05 p0591 A73-16190

Study of the steady motion of a ballistic antenna in a plane homogeneous flow
05 p0528 A73-16750

Computing meteorological effects on aircraft noise.
05 p0536 A73-17121

Frequency spectra of the inner and outer structures of wind waves at different stages of wave development

05 p0594 A73-17359

Some evaluations of drag and bulk transfer coefficients over water bodies of different sizes.

06 p0720 A73-18328

Dynamic response of a vertical cantilever structure in the natural wind.

07 p0823 A73-19565

Ionospheric winds in the F-region and their effects on the limiting periods of gravity waves.

07 p0818 A73-19673

Ionospheric plasma interaction with neutral meridional wind, noting effects of east-west gradients in electron concentration

07 p0819 A73-20057

Earth surface and background wind effects on mesoscale and large scale meteorological processes in free stably stratified atmosphere

07 p0848 A73-20343

Study of the surface layer of drift currents in the laboratory

08 p0985 A73-21455

Intermittence effects in the equilibrium range of developing wind waves

08 p0986 A73-21458

Spectra of short-term fluctuations of line-of-sight signals - Electromagnetic and acoustic.

10 p1190 A73-24893

Missile ablation shields erosion by high velocity dust, considering wind tunnel test data on phenolic cork for various dust materials, particle sizes and velocities

[AIAA PAPER 73-379]

11 p1388 A73-25509

Launch vehicle response to inflight winds during ascent, modeling wind velocity as nonstationary random process

[AIAA PAPER 73-398]

11 p1392 A73-25527

The effects of thermospheric winds on the ionosphere at low and middle latitudes during magnetic disturbances.

11 p1353 A73-25752

Theory of sound scattering by turbulence applied to scattering cross section calculation for turbulent jet flow and wind, discussing jet noise reduction

11 p1349 A73-26496

Periodic gust and wake induced unsteady air flow, calculating velocity variation with distance from rotor blade for cascade effect

13 p1566 A73-29026

Barotropic and baroclinic contribution to eddy kinetic energy increase in disturbance amplification using quasi-geostrophic equations of motion and omega equation

13 p1610 A73-29335

Analysis of various automatic homing techniques for gliding airdrop systems with comparative performance in adverse winds.

[AIAA PAPER 73-462]

15 p1827 A73-31448

Solar and lunar effects on neutral atmospheric tidal winds and induced electrostatic and geomagnetic fields effects on low latitude F2 and sporadic E layers

15 p1868 A73-31751

Equatorial electrojet. I - Development of a model including winds and instabilities. II - Use of the model to study the equatorial ionosphere.

15 p1904 A73-31756

Stochastic wind field effects on baroclinic wave disturbances vertical propagation through turbulent atmosphere, obtaining stream function and dispersion equation

15 p1907 A73-32356

Critical study of the effects of gusts on an aircraft

16 p1961 A73-32808

Three bladed model rotor gust induced impulsive discrete noise characteristics prediction by point dipole and rotational noise theories for comparison with measurement

16 p1967 A73-32917

Thermospheric wind effects on the distribution of helium and argon in the earth's upper atmosphere.

16 p2004 A73-33441

Measurements of wind-induced Doppler shifts at 16 GHz over a long range bistatic scatter link.

16 p1983 A73-33726

Atmospheric refractivity variation, precipitation and wind effects on two orthogonal linearly polarized microwave signals transmission over radio link at 22 and 37 GHz

16 p1983 A73-33733

Application of the ray method to a study of the propagation of large-scale perturbations in a barotropic atmosphere with a mean wind

17 p2204 A73-34345

The permissible scale of spatial averaging of geopotential values in the stratosphere when the impact of wind on the flight of a supersonic aircraft is taken into account

17 p2100 A73-34546

Lower thermospheric oxygen photodissociation evaluation for global average and hemispheric imbalance, discussing wind system to compensate for solar thermal input imbalance

17 p2159 A73-34784

Kinesonde studies of cesium ion clouds in the E-region.

18 p2304 A73-35988

Light beam dispersal of fog with various drop sizes based on energy equation, considering cloud water content, cross wind effects and front velocity

18 p2337 A73-36561

Some problems associated with wind drag and infrared images of the sea surface.

18 p2313 A73-36643

Mariner 9 evidence for wind erosion in the equatorial and mid-latitude regions of Mars.

19 p2477 A73-37210

Mars Hellespontus region identification from Mariner 9 photographs as wind produced dunes, considering albedo features

19 p2478 A73-37211

Martian sandstorms and wind erosion, discussing theoretical calculation methods and wind tunnel experiments

19 p2478 A73-37212

Variable features on Mars. II - Mariner 9 global results.

19 p2478 A73-37212

Wind erosion in the Martian polar regions.

19 p2478 A73-37214

Martian south polar region pitted and etched terrain features, interpreting surface layered blanketing material as due to wind action

19 p2478 A73-37215

Direct side force control for STOL crosswind landings.

[AIAA PAPER 73-811]

19 p2379 A73-37467

Effect of wind shear on atmospheric wave instabilities revealed by FM/CW radar observations.

19 p2447 A73-38206

A note on the FM-CW radar as a remote probe of the Pacific Trade-Wind Inversion.

19 p2448 A73-38211

Structure of vortical motion systems in the ionosphere that generate Sq variations of the geomagnetic field

20 p2553 A73-39153

Wind modification of structure of thermally driven tropical undercurrent, considering stratified and constant density models, surface winds, monsoons, thermocline jets and meridional circulation

21 p2679 A73-40069

Analysis of airplane response to nonstationary turbulence including wing bending flexibility. II.

21 p2784 A73-40437

Shallow lake or sea with large class of bottom topographies, obtaining wind-driven current analytic solution with conformal mapping technique

21 p2686 A73-41015

Surface wind stress and threshold friction velocity required to raise dust on Mars, discussing mechanisms for production of strong winds in Ekman layer

22 p2912 A73-42981

Critical velocities of the steady motion of a pliable thread in plane homogeneous flow.

22 p2928 A73-43061

Engineering applications of geophysical phenomena covering earthquakes, volcanology, hydrology, glaciology and wind stress effects during severe storms

23 p2979 A73-44007

Effect of neutral winds on ionospheric F-region at a pair of conjugate stations in low latitude.

24 p3082 A73-44729

The behaviour of the upper ionosphere over North America at sunset.

24 p3087 A73-45203

Critical frequency evolution during F2 region storms at middle and low latitudes, showing random global patterns and relation to neutral wind flow

24 p3087 A73-45205

WIND EROSION

Ventifact evolution in Wright Valley, Antarctica.

21 p2687 A73-41211

WIND MEASUREMENT

NT WIND VELOCITY MEASUREMENT

The spectral density technique for the determination of eddy fluxes.

01 p0072 A73-10145

Instrument requirements for eddy correlation measurements.

01 p0052 A73-11057

Upper-atmosphere motion, as determined by observations of radio echoes from meteor trails.

02 p0159 A73-12145

Neutral wind measurement during daytime in the thermosphere.

02 p0159 A73-12224

An evaluation of the scale of mesospheric wind disturbances.

02 p0160 A73-12272

Measurement of wind gradients in convective storms by Doppler radar.

[AD-751716]

03 p0278 A73-14508

E region wind and density measurements by VHF radar and atmosphere temperature measurement by radio acoustic sounding technique, describing instrumentation and computerized data reduction

03 p0339 A73-14546

The measurement of atmospheric turbulence from a captive balloon.

04 p0473 A73-15698

Computation of upper tropospheric reference heights from winds for use with vertical temperature profile observations.

05 p0569 A73-16575

Measurements and graphs of turbulence autocorrelations in space and time.

09 p1071 A73-22332

Low level wind measurement error as it affects sounding rocket dispersion.

[AIAA PAPER 73-296]

09 p1116 A73-23215

The measurement of winds in the D-region of the ionosphere by the use of partially reflected radio waves.

11 p1358 A73-26707

Method for calculating turbulent flows from network data

12 p1521 A73-27744

Wind profile measurements in proximity of a moderate storm.

13 p1651 A73-28205

Terrestrial atmospheric general circulation theoretical and observational research, considering Reynolds or eddy stress distribution across horizontal and vertical surfaces

13 p1610 A73-29333

Digital readout wind measurement and indicator system for data acquisition, processing and display in airports for aircraft wind information service

15 p1874 A73-31318

Coordinated measurements of atmospheric parameters at stratospheric levels.

[AIAA PAPER 73-526]

16 p2007 A73-33560

Experimental determination of small scale transport mechanisms in the stratosphere.

[AIAA PAPER 73-496]

16 p2010 A73-34044

Buffalo aircraft fiberglass laminated polyester nose boom for mounting horizontal and vertical wind sensing probes, describing instruments and measurement procedures

17 p2174 A73-35576

Climatological studies based on satellite data, including cloud, snow and ice cover, wind measurement, convection currents, temperature fields and earth thermal balance

18 p2331 A73-35914

Wind measurement by magnetometers, optical and static pressure sensors.

18 p2310 A73-36136

Pulsed-Doppler velocity isotach displays of storm winds in real time.

18 p2333 A73-36707

On the Zeeman photometer observing upper atmospheric winds in the daytime.

19 p2429 A73-37377

Techniques for deriving winds from cloud movement.

[AAS PAPER 73-126]

20 p2583 A73-38586

Radio techniques applied to oceanography and earth science - Oceanic wind measurement and overland imaging as examples.

21 p2654 A73-40817

Results of simultaneous wind measurements in the stratosphere, mesosphere and low thermosphere.

21 p2732 A73-41340

Internal gravity waves and turbulence in simultaneous upper atmosphere temperature and wind measurements.

21 p2732 A73-41342

Provisional climatology of most probable wind for application to low latitude operational weather analysis and forecasting, based on ATS-3 observed low level winds

23 p3004 A73-44262

Polar wind measurements by electrically neutral luminous by-product clouds from Ba ion releases, discussing ion drag

24 p3085 A73-45120

WIND PRESSURE

Turbulence effect on wall pressure fluctuations.

04 p0403 A73-14939

Development and employment of a measurement transformer for a difference in pressure. I

16 p2014 A73-33224

WIND PROFILES

Atmospheric moisture and wind field synoptic analysis based on Nimbus 4 temperature-humidity IR radiometer /THIR/ measurements

01 p0073 A73-10379

Commencement of routine meteorological rocket observation at Ryori, Japan.

02 p0188 A73-12271

Atmospheric stratification stability at heights of 30-90 km from grenade test determined wind and temperature data, presenting Richardson number latitudinal and seasonal distribution

02 p0160 A73-12273

Incoherent scatter observations of meridional winds in the 150-225 km region.

02 p0161 A73-12283

Simultaneous measurements of height wind profiles and electron concentration for verifying theory of

sporadic E layer formation in midlatitudes under wind shear action

02 p0163 A73-12306

Electron density and wind structure observations in lower ionosphere by rocket, noting sporadic E layer due to wind shear

02 p0163 A73-12307

The effect of the baroclinicity of the atmosphere on the structure of the wind field in the steady planetary boundary layer

04 p0441 A73-15289

Wind profile models for atmospheric turbulent boundary layers over smooth and rough surfaces, using Heisenberg energy transfer theory and von Karman constant

04 p0473 A73-15695

Relative importance of terms in the turbulent-energy and momentum equations as applied to the problem of a surface roughness change.

05 p0591 A73-16191

Midlatitude sporadic E layer vertical electron and ion distributions from rocket experimental wind velocity profile, assuming molecular and metallic ions in ionosphere

06 p0742 A73-17535

Time spectra and cross-spectra of kinetic energy in the planetary boundary layer.

07 p0847 A73-19044

The Leipzig wind profile and the boundary layer wind-stress relationship.

07 p0847 A73-19045

An analytical and numerical study of the Martian planetary boundary layer over slopes.

08 p1011 A73-21381

Correlation of microthermal turbulence data with meteorological soundings in the troposphere.

08 p0985 A73-21382

Boundary layer wind profile model in a steady state, diabatic, baroclinic atmosphere.

09 p1114 A73-22328

A numerical model for predicting mesoscale winds aloft.

09 p1114 A73-22335

Intratropical convergence zone in the eastern portion of the Pacific Ocean

09 p1115 A73-22990

Characteristics of the development of the quasi-biennial cycle above the Indian Ocean

09 p1115 A73-22991

Logarithmic wind profile in neutral barotropic planetary boundary layers, discussing von Karman constant

11 p1394 A73-25717

Application of Nimbus 4 THIR 6.7-micron observations to regional and global moisture and wind field analyses.

12 p1520 A73-26812

Statistical description of the wind field in the upper troposphere and lower stratosphere with allowance for the scale of motion

12 p1521 A73-27741

Wind profile measurements in proximity of a moderate storm.

13 p1651 A73-28205

Some comparisons between wind observed wind profiles at Riso and theoretical predictions for flow over inhomogeneous terrain.

13 p1652 A73-28272

The wind profile very close to the ground.

14 p1772 A73-30904

General circulation of the tropical lower stratosphere.

15 p1906 A73-31845

Sporadic E random electron concentration due to wind shift spectral composition, determining empirical autocorrelation functions for frequency parameters

15 p1871 A73-31885

Keraug near-ground wind profiles approximation by Monin-Obuchov universal function, obtaining solutions for turbulent heat flux and shear flow velocity

15 p1906 A73-32343

Vorticity advection and geopotential change due to dynamic causes as two-layer problem

15 p1907 A73-32355

Book - The general circulation of the tropical atmosphere and interactions with extratropical latitudes. Volume 1.

15 p1907 A73-32423

Midlatitude sporadic E layer vertical electron and ion distributions from rocket experimental wind velocity profile, assuming molecular and metallic ions in ionosphere

16 p2052 A73-32759

F region neutral wind profiles and electron densities measured at midlatitude station during equinox months for medium sunspot year

16 p2009 A73-33888

Influence of the vertical structure of the wind field on the development of cumulus and cumulonimbus clouds

18 p2332 A73-35920

Results of simultaneous in-situ-observations in Spain of electron concentration, neutral wind and air pressure in the D-region in different seasons and dur-

ing an SID-event and their relevance to the winter-anomalous state of the atmosphere.

18 p2305 A73-36001

Rocket sounding of upper atmosphere vertical wind profiles, shear, temperature distribution and diffusion coefficient for model atmosphere calculation

18 p2309 A73-36057

Results of simultaneous wind velocity profile measurements in the lower thermosphere by the meteor radar and rocket methods.

18 p2310 A73-36130

Influence of longitudinal variations on the structure of temperature, pressure and wind fields in the stratosphere and mesosphere of the Northern Hemisphere.

18 p2310 A73-36139

Objective analysis method tested via comparison to known function at radiosonde observation stations, considering description of spectral analyses of wind field kinetic energy

18 p2332 A73-36702

Effectiveness of utilizing cloudiness data obtained from satellites in objective analysis of the wind field.

18 p2334 A73-37071

Cloud eddy formation in wakes of single mountain islands similar to Karman vortex streets, noting application to wind field forecasting

18 p2334 A73-37075

The boundary layer above 30 m. III.

19 p2448 A73-38214

Matching the geopotential and wind fields with the aim of improving the accuracy of objective analysis

19 p2449 A73-38544

Determination of the wind field from the pressure field and the latitudinal effect of the geomagnetic field in the ionosphere

21 p2681 A73-40105

Wind profiles over Heiss Island.

21 p2685 A73-40812

Post GARP Global Experiment programs, considering tropical vertical wind structure, satellite temperature measurement accuracy increase, data handling for real time and long term prediction

21 p2732 A73-40819

Global thermospheric wind distribution computed by solving Navier-Stokes equations with models at upper atmospheric densities and ion distribution

21 p2689 A73-41354

Horizontal wind fluctuations coherence at different meteorological sites compared to wind tunnel experiment

21 p2732 A73-41573

An exact solution to the system of prognostic equations of a barotropically divergent model of the atmosphere

23 p3001 A73-43461

The structure and dynamics of horizontal roll vortices in the planetary boundary layer.

23 p3002 A73-43594

The effect of dissipation on the vertical propagation of planetary waves in the vicinity of critical levels.

23 p3032 A73-43906

On the vertical ozone and wind profiles near the tropopause.

23 p2977 A73-43907

Application of general circulation models to the study of stratospheric ozone.

23 p2978 A73-43909

Ionosphere dynamic process investigations, describing wind models, E region drift velocity curves and energy distribution chart

23 p2978 A73-43978

Eddy heat/momentum diffusivity ratio dependence on Richardson number relationship between Deacon numbers of wind and temperature profiles in Antarctic surface layer

23 p3003 A73-43983

Analysis of hurricane data using the variational optimization approach with a dynamic constraint.

23 p3004 A73-44258

Superposition technique in numerical integration of generalized Ekman equation for wind profile determination, taking into account eddy diffusivity variation

24 p3108 A73-45019

Winds and wave motions 70-100 km/ as measured by a partial reflection radiowave system.

24 p3088 A73-45212

WIND SHEAR
Simultaneous measurements of height wind profiles and electron concentration for verifying theory of sporadic E layer formation in midlatitudes under wind shear action

02 p0163 A73-12306

Electron density and wind structure observations in lower ionosphere by rocket, noting sporadic E layer due to wind shear

02 p0163 A73-12307

Wind shear near the ground and aircraft operations.

03 p0337 A73-13702

Internal gravity wave-atmospheric wind interaction - A cause of clear air turbulence.

04 p0473 A73-15071

The influence of planetary vorticity gradient and vertical entropy gradient on the stability of an atmospheric shear layer.

04 p0441 A73-15288

The Leipzig wind profile and the boundary layer wind-stress relationship.

07 p0847 A73-19045

Atmospheric turbulent fluctuations explained via eddy-wind shear and convective rolls-gravity wave interactions, using wind-temperature data from White Sands

09 p1114 A73-22329

Influence of vertical wind shear on the development of convective cloudiness

11 p1393 A73-25640

Some observations of the influence of geostrophic shear on the cross-isobar angle of the surface wind.

11 p1393 A73-25695

Internal gravity waves in an atmosphere with wind shear - Validity of the WKB approximation at critical layers in the presence of buoyancy forces.

11 p1394 A73-25721

Parawing-drag chute system operation on wind shear energy to maintain payload flight altitude

11 p1305 A73-25787

Turbulence, billows and gravity waves in a high shear region of the upper atmosphere.

12 p1492 A73-27608

Theory of cyclogenesis, taking into account condensation

13 p1653 A73-28744

Turbulent surface layer shear convection analysis, using similarity model based on weak interaction between vertical motion and mechanical turbulence

13 p1655 A73-29340

A three-dimensional model of cumulus cloud development.

14 p1771 A73-30764

Formation of blanketing sporadic E-layers at the magnetic equator due to horizontal wind shears.

15 p1866 A73-31070

Low level wind shear and clear air turbulence effects on flight safety and aircraft accidents

17 p2098 A73-34084

Influence of the vertical structure of the wind field on the development of cumulus and cumulonimbus clouds

18 p2332 A73-35920

Rocket sounding of upper atmosphere vertical wind profiles, shear, temperature distribution and diffusion coefficient for model atmosphere calculation

18 p2309 A73-36057

Skylark rocket magnetometer measurement of sporadic E layer magnetic fields, testing wind shear theory of ionization redistribution at midlatitudes

19 p2426 A73-38022

Effect of wind shear on atmospheric wave instabilities revealed by FM/CW radar observations.

19 p2447 A73-38206

Richardson number profiles through shear instability wave regions observed in the lower planetary boundary layer.

19 p2448 A73-38228

Interpretation of the results of photometric observations of noctilucent clouds

21 p2732 A73-40859

Wind component exchange and the rapid vertical movement of a sporadic E layer.

22 p2845 A73-41922

Resonant oscillations of intermediate frequency in a stratified atmosphere.

22 p2848 A73-42539

Internal gravity wave-mean wind interaction.

23 p3000 A73-43339

Rocket-borne magnetometer measurement of magnetic field changes associated with electron density fluctuations and wind structure, testing wind shear theory of sporadic E formation

23 p3024 A73-43701

Experimental test of the wind-shear theory: A reply - Rocket-borne magnetometers do measure B.

23 p3024 A73-43702

Statistical analysis of satellite-observed trade wind cloud clusters in the western North Pacific.

23 p3003 A73-43980

WIND TUNNEL APPARATUS
NT WIND TUNNEL DRIVES
NT WIND TUNNEL NOZZLES

Some development of hypersonic flow experiment by the gun tunnel.

01 p0003 A73-11129

Holographic interferometry applied to aerodynamics [ONERA, TP NO. 1161F]

08 p0968 A73-21677

A precise position and attitude measurement system for free-flying wind-tunnel models

11 p1362 A73-25443

Laser activated, model surface recession compensator system for testing ablative materials.

11 p1343 A73-25510

[AIAA PAPER 73-380]
Hypersonic wind tunnel MHD accelerator design and operating principles, discussing flux density, I-V characteristics, cooling losses, plasma temperature, gas pressure and velocity, etc

14 p1743 A73-30295

Experimental force data reduction equations solved by iterative method for multicomponent force transducers used in load tests, discussing wind tunnel balances 17 p2148 A73-35437

Fabrication of high precision strain gauge dynamometers and balances at the O.N.E.R.A. Modane Centre. [ONERA, TP NO. 1196] 22 p2839 A73-42217

Electric analogy method for subsonic wind tunnel contraction cone design providing uniform velocity distribution in test section, obtaining pressure distribution in cone boundary 22 p2797 A73-43000

WIND TUNNEL BALANCES

U WEIGHT INDICATORS

U WIND TUNNEL APPARATUS

WIND TUNNEL CALIBRATION

Some development of hypersonic flow experiment by the gun tunnel. 01 p0003 A73-11129

Comparative measurements involving three geometrically similar calibration models of a transport aircraft type in the transonic wind tunnel of the AVA Goettingen (Proposal: ONERA/ [DGLR PAPER 72-122] 03 p0248 A73-14381
A method for transonic wind-tunnel corrections. 05 p0563 A73-17105

Experimental studies of a Ludwig tube high Reynolds number transonic tunnel. [AIAA PAPER 73-212] 06 p0645 A73-17661

WIND TUNNEL DRIVES

Fluid undercutting in the successive channel flow of two gases. [AIAA PAPER 73-214] 05 p0566 A73-16944

The RAE 5m low-speed wind tunnel. 11 p1344 A73-26499

WIND TUNNEL MODELS

Some development of hypersonic flow experiment by the gun tunnel. 01 p0003 A73-11129

Experimental investigation of the supersonic two-dimensional flow past a sail at small angles of attack 01 p0004 A73-11371

Experimental investigation of the frequency response of a planar rigid airfoil 03 p0241 A73-12915

Method for increasing wind tunnel Mach number for large-scale inlet testing. [AIAA PAPER 72-1096] 03 p0287 A73-13416

Powered model wind tunnel investigation to determine performance trends with nacelle location. [AIAA PAPER 72-1114] 03 p0243 A73-13429

Experimental investigation of the base pressure on slender circular cylinders 03 p0245 A73-13674

Investigations on incipient boundary layer separation on axisymmetric compression surfaces. 03 p0246 A73-14127

Comparative measurements involving three geometrically similar calibration models of a transport aircraft type in the transonic wind tunnel of the AVA Goettingen (Proposal: ONERA/ [DGLR PAPER 72-122] 03 p0248 A73-14381

The steady-state flow quality of an open return wind tunnel model. 04 p0433 A73-15512

Flight and wind tunnel investigation of the effects of Reynolds number on installed boattail drag at subsonic speeds. [AIAA PAPER 73-139] 05 p0530 A73-16888

Nose pressure distribution and separation on an inclined axisymmetric body. 05 p0533 A73-17123

Wind tunnel study of flow structure and turbulent wakes on base surfaces of sharp or blunt edged flat bodies at various Mach and Reynolds numbers 06 p0643 A73-17456

Icing testing in the large Modane wind-tunnel on full-scale and reduced scale models 07 p0808 A73-20244

A summary of wind tunnel research on tilt-rotors from hover to cruise flight. [ONERA, TP NO. 1133] 08 p0928 A73-21683

High Reynolds number experimental data for forebody axial force. 09 p1030 A73-23453

Wind tunnel study of flows generated by slender cones in subcritical Reynolds number regime, examining vortex shedding and drag 10 p1174 A73-24845

A precise position and attitude measurement system for free-flying wind-tunnel models 11 p1362 A73-25443

Design and evaluation of miniature control surface actuation systems for aeroelastic models. [AIAA PAPER 73-323] 11 p1305 A73-25553

Flutter technology in the United Kingdom - A survey. [AIAA PAPER 73-330] 11 p1441 A73-25559

Wake flow model of Viking 75 entry vehicle for different angles of attack at free stream Mach numbers 0.2-3.95 [AIAA PAPER 73-475] 15 p1823 A73-31459

Theoretical and experimental study of a swept-back wing at low velocity over a wide range of angles of attack 16 p1962 A73-32814

Development of experimental turbine facilities for testing scaled models in air or freon. 17 p2145 A73-34381

An inexpensive technique for the fabrication of two-dimensional wind tunnel models. 17 p2149 A73-35762

Automated structural design and analysis of advanced composite wing models. 19 p2497 A73-37486

Basic acoustic considerations for model noise experiments in wind-tunnels. 22 p2838 A73-41705

Experimental investigation of a turbulent boundary layer on a triangular plate with a wedge 23 p2939 A73-43473

Surface pressure fluctuations in hypersonic turbulent boundary layers. [AIAA PAPER 73-997] 24 p3053 A73-44832

WIND TUNNEL NOZZLES

Investigation of flow characteristics behind diffusers with large cone angles 03 p0245 A73-13671

Improved flexible supersonic wind-tunnel nozzle operated by a single jack. 07 p0808 A73-19972

Automated machining and surface finishing of heat resistant stainless steel nozzles for wind tunnel applications 15 p1855 A73-31200

Subsonic free jet wind tunnel turbulence damping in settling chamber via screen, yielding uniform velocity profile and low turbulence level in nozzle exit 16 p1996 A73-33266

WIND TUNNEL STABILITY TESTS

Three-degree-of-freedom motions of a slender asymmetric cone in a hypersonic wind tunnel. 03 p0287 A73-13494

B-1 airplane model support and jet plume effects on aerodynamic characteristics. [AIAA PAPER 73-153] 05 p0563 A73-16901

Experimental investigation of flow stability during intense injection 06 p0643 A73-17462

Wing tip vortex modification by tip-mounted upstream and downstream directed air jets, discussing wind tunnel test results 07 p0773 A73-19193

Aerodynamic studies of spacecraft in the freestream Mach number range of 3 to 10 at high Reynolds numbers [DFVLR-SONDDR-286] 13 p1567 A73-29447

Forced vibration solution and wind tunnel investigation of shallow cylindrical shells under moving pulsating pressure discontinuities, noting compression shock effects 13 p1703 A73-29602

Separate surfaces for automatic flight controls. [SAE PAPER 730304] 17 p2101 A73-34665

Surface effect take-off and landing system for high performance aircraft. 19 p2382 A73-37695

WIND TUNNEL TESTS

The application of dual hologram interferometry to wind tunnel testing. [AIAA PAPER 73-210] 05 p0577 A73-16941

Experimental study of a high lift re-entry vehicle configuration. 13 p1564 A73-28822

Experimental studies on high speed performance of two-dimensional turbine cascades. 13 p1566 A73-29019

Wind tunnel tests as part of rotary wing aircraft development, discussing technical and economic aspects 14 p1743 A73-30469

Development of the Viking parachute configuration by wind tunnel investigation. [AIAA PAPER 73-454] 15 p1826 A73-31440

A parachute snatch force theory incorporating line disengagement impulses. [AIAA PAPER 73-464] 15 p1827 A73-31450

A 14.2-ft Do variable-porosity conical ribbon chute for supersonic application. 15 p1828 A73-31456

Drag and stability characteristics of high-speed parachutes in the transonic range. [AIAA PAPER 73-473] 15 p1828 A73-31457

Parachute gore shape and flow visualization during transient and steady-state conditions. [AIAA PAPER 73-474] 15 p1828 A73-31458

Random /turbulent/ excitation of flutter in wind tunnel dynamic models and flight test aircraft, comparing prediction and damping measurement results [ONERA, TP NO. 1234] 15 p1830 A73-31638

Wind tunnel simulation of jet exhaust in low speed testing of Franco-German Alpha-Jet trainer and fire support aircraft 16 p1993 A73-32802

Wind tunnel gust simulation for STOL aircraft behavior during low velocity flight in turbulent atmosphere near ground 16 p1962 A73-32813

Theoretical and experimental study of a swept-back wing at low velocity over a wide range of angles of attack 16 p1962 A73-32814

Thrust measurement bench for afterbody and hot and cold jet nozzle simulated tests in Sigma 4 wind tunnel 16 p1993 A73-32820

Aspects of investigating STOL noise using large-scale wind-tunnel models. 16 p1994 A73-33170

Lift and measurements in an aerofoil in unsteady flow. [ASME PAPER 73-GT-41] 16 p1964 A73-33503

Test techniques for high lift, two-dimensional airfoils with boundary layer and circulation control for application to rotary wing aircraft. 17 p2091 A73-34292

Experimental study of turbulent boundary layer along a flat plate with linear increase of roughness height. 17 p2151 A73-34537

Pressure measurements for establishing inlet/engine compatibility. 17 p2221 A73-34609

Solid state Digital Slip Sync Strobe/Camera Control System design for powered wind tunnel helicopter models testing 17 p2101 A73-34622

Aircraft wing tip turbulent wakes producing swirling vortices, discussing wake hazards, wind tunnel research and vortex dissipation procedures [SAE PAPER 730294] 17 p2094 A73-34658

Some effects of camber on swept-back wings. [SAE PAPER 730298] 17 p2094 A73-34661

A detailed experimental analysis of dynamic stall on an unsteady two-dimensional airfoil. [AHS PREPRINT 702] 17 p2095 A73-35053

Wind tunnel test technique to establish rotor system aeroelastic characteristics. [AHS PREPRINT 760] 17 p2095 A73-35083

Tail rotor performance in presence of main rotor, ground, and winds. [AHS PREPRINT 764] 17 p2106 A73-35087

Wind tunnel acoustic and vibration test facilities, including anechoic chambers, subsonic boundary layer tunnels, acoustic ducts, reverberation rooms, and rotor noise chambers 17 p2148 A73-35334

Support wire disturbances in near viscous wakes of slender supersonic bodies. 18 p2295 A73-36155

A conceptual study of leading-edge-vortex enhancement by blowing. [AIAA PAPER 73-656] 18 p2261 A73-36210

Experimental and theoretical investigations in two-dimensional transonic flow. [AIAA PAPER 73-659] 18 p2261 A73-36213

Turbulent boundary layer flow separation measurements using holographic interferometry. [AIAA PAPER 73-664] 18 p2261 A73-36215

Rapid scanning, three-dimensional, hot-wire anemometer surveys for wing tip vortices in the Ames 40- by 80-foot wind tunnel. [AIAA PAPER 73-681] 18 p2315 A73-36232

Slightly ionized low density hypersonic flow about a sharp plate and its diagnostics. [AIAA PAPER 73-690] 18 p2262 A73-36241

Investigation of the expansion side of a delta wing at supersonic speed. 18 p2263 A73-36312

Mass transfer effects on turbulent heating in the vicinity of slots. [AIAA PAPER 73-766] 18 p2371 A73-36381

A finite-element method for calculating aerodynamic coefficients of a subsonic airplane. 18 p2265 A73-36394

Experimental developments in V/STOL wind tunnel testing at the National Aeronautical Establishment. 18 p2265 A73-36774

Aircraft engine fan noise radiation from inlet and discharge ducts, describing wind tunnel tests and noise spectra at various blade tip speeds 19 p2472 A73-37288

Development of an Air Cushion Landing System. [AIAA PAPER 73-812] 19 p2379 A73-37468

Thermal structure and stability study of internal and Kelvin-Helmholtz waves in low Reynolds number flows by sampling and stratified wind tunnel methods 19 p2422 A73-38235

Airfoil profiles aerodynamic characteristics from laminar flow wind tunnel measurements 19 p2377 A73-38361

S-3A aircraft systems, performance and design, discussing flight simulation, wind tunnel tests, weapons systems, flutter tests, avionics, TF-34 engine, stalls and computer programming [AIAA PAPER 73-778] 19 p2387 A73-38367

Multihundred watt radioactive isotope heat source wind tunnel tests to obtain aerodynamic coefficients, 19 p2387 A73-38367

heating rate, stability and ablation for reentry protection design

19 p2456 A73-38425

Visualization of gas flows by means of high-speed holography

21 p2696 A73-39978

Influence of the shape of the leading edge on the transition process in the boundary layer on a plate in longitudinal flow

21 p2676 A73-40399

Freon-22 circular and flat jet propagation in air cross flow in wind tunnel, examining air-gas dynamic pressure ratio effects

21 p2676 A73-40405

Experience with the NRC 10 ft. x 20 ft. V/STOL propulsion tunnel - Some practical aspects of V/STOL engine model testing.

21 p2672 A73-40855

Investigation of multi-element airfoils with external flow jet flap.

21 p2633 A73-41087

Hot-wire investigation of the steady laminar wake behind a circular cylinder.

21 p2703 A73-41117

Hot-wire investigation of the steady laminar wake behind a thin flat plate placed perpendicularly to a uniform flow.

21 p2703 A73-41118

Turbulent flow velocity pulsations damping in wind tunnel chamber by wire grids, calculating grid turbulence effect

21 p2633 A73-41319

Test facilities for B-1 components prior to construction and flight testing, discussing wind tunnel tests for aerodynamic characteristics, stall performance, drag factor and spin

21 p2675 A73-41431

Horizontal wind fluctuations coherence at different meteorological sites compared to wind tunnel experiment

21 p2732 A73-41573

Study of flow around an airfoil with a spoiler at Mach numbers ranging from 0.5 to 2.3

21 p2634 A73-41584

Wind tunnel test for Dolphin airship model static thrust measurements, discussing thrust direction torque moment coefficients and propeller rotation

21 p2635 A73-41648

Reattachment of a separated boundary layer to a convex surface.

22 p2843 A73-42554

The panel method for the calculation of the pressure distribution on missiles in the subsonic range

22 p2797 A73-43028

An experimental investigation of a jet issuing from a wing in crossflow.

22 p2798 A73-43111

Aircraft aerodynamics problems covering slender body theory, atmospheric turbulence and boundary layers, wind tunnel contractions, radiator blocks, vortex induced oscillations, etc

24 p3053 A73-44690

On problems of flight over an extended angle-of-attack range.

24 p3056 A73-44692

Comparison of aircraft noise measured in flight test and in the NASA Ames 40- by 80-foot wind tunnel.

[AIAA PAPER 73-1047]

24 p3056 A73-44871

The behavior of hot-film anemometers in gas mixtures.

24 p3091 A73-45325

WIND TUNNEL WALLS

Influence of the boundaries of wind-tunnel flow on the flow past a small-aspect-ratio wing

02 p0128 A73-11707

A method for transonic wind-tunnel corrections.

05 p0563 A73-17105

Hydrodynamic wind tunnel investigation of drag reduction and propulsion effect by flexible walls, observing boundary layer transition and turbulence

09 p1071 A73-22207

Low velocity wind tunnel design with adjustable pressure gradient, determining contraction section wall contour to avoid boundary layer separation via velocity distribution improvement

11 p1347 A73-25714

Correction for change in fluid flow curvature about a lift-generating airfoil in a two-dimensional test section with perforated walls

11 p1302 A73-25864

Effects of upstream wall temperatures on hypersonic tunnel wall boundary-layer profile measurements.

11 p1344 A73-26395

Wind tunnel interference on oscillating airfoils in low supersonic flow.

13 p1563 A73-28166

Calculation of wall corrections in a transonic wind tunnel

16 p1961 A73-32803

Effects of wall boundary layers in wind tunnels on blocking phenomena

16 p1962 A73-32815

Example of utilization of a wind tunnel with perforated variable-geometry walls

16 p1993 A73-32818

On viscous and wind tunnel wall effects in transonic flows over airfoils.

[AIAA PAPER 73-660]

18 p2263 A73-36261

WIND TUNNELS

NT BLOWDOWN WIND TUNNELS

NT CASCADE WIND TUNNELS

NT HOTSHOT WIND TUNNELS

NT HYPERSONIC WIND TUNNELS

NT HYPERVELOCITY WIND TUNNELS

NT LOW DENSITY WIND TUNNELS

NT LOW SPEED WIND TUNNELS

NT PLASMA JET WIND TUNNELS

NT RECTANGULAR WIND TUNNELS

NT SHOCK TUNNELS

NT SLOTTED WIND TUNNELS

NT SUBSONIC WIND TUNNELS

NT SUPERSONIC WIND TUNNELS

NT TRANSONIC WIND TUNNELS

Turbulent flow velocity pulsations damping in wind tunnel chamber by wire grids, calculating grid turbulence effect

03 p0245 A73-13670

Wind tunnel experimental verification of flight vehicles aerodynamic characteristics during preliminary design stage, discussing correction procedures for model data extrapolation to full scale parameters [SAE PAPER 720861]

05 p0528 A73-16665

Wind tunnel facilities in India for subsonic, transonic and supersonic aerodynamic R and D, describing design layouts, power requirements, operational functions and instrumentation

07 p0808 A73-20249

French project of anechoic chamber with wind tunnel for studying jets, turbojets blowers, helicopter rotors and V/STOL aircraft

08 p0953 A73-21529

On the response of laminar boundary layers to periodic changes in free-stream speed.

10 p1207 A73-24803

Hailstones icicle lobe formation growth in wind tunnel, using supercooled or frozen hydrometeors

12 p1521 A73-26817

Inlet system design procedures and wind tunnel facility modifications allowing for verification on large scale models at Mach 4.5

15 p1824 A73-31743

The simulation of the atmospheric surface layer with volumetric flow control.

16 p1994 A73-33152

Book - Experimental methods of hypersonics.

17 p2097 A73-35338

Plasma accelerators in gas dynamics, discussing ion propulsion systems, high velocity wind tunnels with electric arc heating and electromagnetic shock tubes

19 p2466 A73-37354

Experiment on convex curvature effects in turbulent boundary layers.

21 p2676 A73-40245

WIND VARIATIONS

Tethered balloon measurements of turbulent wind, temperature and humidity fluctuations up to 200 meters over open sea, allowing for wave induced ship motion

01 p0072 A73-10142

Solar-activity effects and zonal wind in the stratosphere and lower mesosphere

01 p0043 A73-10945

Equatorial stratosphere quasi-biennial oscillation variations from temperatures and zonal winds measured at Canton Island, Ascension Island and Balboa /Canal Zone/

05 p0594 A73-16573

On the variance spectra and spatial coherences of equatorial winds.

07 p0846 A73-19038

Meteorological rocket observations of amplitudes and phases of zonal wind quasi-biennial oscillations at 25-60 km during 1962-1969

07 p0846 A73-19040

Equatorial Kelvin wave oscillations of zonal wind at 100 mb over Eastern Hemisphere

07 p0847 A73-19043

Charge separation induced vertical electric field calculated for wind motion periodic with height, latitude and longitude at magnetic equator, noting relationship to electrojet

09 p1074 A73-22067

Effects of solar activity on zonal winds in the stratosphere and lower mesosphere.

09 p1078 A73-22740

Rapid intensification and low-latitude weakening of tropical cyclones of the western North Pacific Ocean.

10 p1245 A73-23986

The diurnal wind variation in the lowest 1500 ft in central Oklahoma - June 1966-May 1967.

10 p1245 A73-23987

The stability of a time-variable surface wind

15 p1906 A73-32353

Diurnal and seasonal variations of neutral winds and electric fields above 90 km in the vicinity of the auroral electrojet.

21 p2690 A73-41365

Horizontal wind fluctuations coherence at different meteorological sites compared to wind tunnel experiment

21 p2732 A73-41573

WIND VELOCITY

Estimation of the global circulation characteristics of planetary atmospheres with various hypotheses concerning the nature of dissipation

01 p0040 A73-10868

Inaccuracy sources in winds calculation from thermospheric models, considering neutral air motions due to global pressure variations

02 p0189 A73-12293

Venera satellite parachute probe method for Doppler measurement of Venus atmosphere wind velocity and turbulence

03 p0379 A73-14566

Annual and semi-annual zonal wind components and corresponding temperature and density variations, 60-130 km.

04 p0440 A73-14961

Venus atmosphere wind velocity profiles from analysis of Venera 7 descent stage radial velocity measurements

05 p0612 A73-16086

Interrelation between processes occurring along a vertical, and the forecasting of stratospheric wind

05 p0592 A73-16232

Lunisolar tidal effects and motions in the F region

05 p0568 A73-16255

The specific ozone destruction at the ocean surface and its dependence on horizontal wind velocity from profile measurements.

05 p0594 A73-16348

Planetary-scale fluctuations of pressure in the E-layer, f-min, and pressure in the stratosphere.

05 p0571 A73-17057

A method for the analysis of artificial clouds in the upper atmosphere.

08 p0961 A73-21391

Some diagnostic applications of wind speed and component spectra for mesoscale through synoptic scale frequencies.

09 p1114 A73-22336

Number of gust series in turbulent velocity pulsations

09 p1115 A73-22992

Explicit and implicit weather forecast expressions based on differential hydrodynamics equation relating horizontal and vertical wind velocity, geopotential and temperature gradients

10 p1244 A73-23813

Statistical laws governing the wind velocity distribution in the atmospheric boundary layer

10 p1246 A73-24373

Remote measurement of wind speed by laser Doppler systems.

11 p1375 A73-25062

An observational study of the vertical profile of the high frequency fluctuations of the wind in the atmospheric boundary layer.

11 p1393 A73-25691

Estimates of global circulation characteristics of planetary atmospheres.

13 p1607 A73-28692

The determination of the evaporation from a class-A pan by means of empirical evaporation formulas

13 p1653 A73-28746

Spatial correlation functions of velocity and temperature components in the atmospheric boundary layer

13 p1654 A73-29153

Ground wind component calculations from synoptic parameters

13 p1655 A73-29190

Meteor trail drift observations in equatorial region /Somalia/ for lower thermosphere wind velocity and direction calculation via harmonic analysis

15 p1902 A73-31223

Incidence of pulsation wind velocities exceeding a given value

15 p1904 A73-31609

A numerical integration method for the determination of flutter speeds.

15 p1955 A73-32163

Neutral winds in the F-region obtained from new models of density and temperature.

18 p2309 A73-36056

Neutral wind velocities calculated from temperature measurements during a magnetic storm and the observed ionospheric effects.

18 p2311 A73-36150

An explanation of anomalously large Reynolds stresses within the convective planetary boundary layer.

23 p3002 A73-43593

Influence of a random transport-velocity component on the space-time correlations of signal fluctuations

23 p2954 A73-43647

The specific ozone destruction rate of the ocean surface and its dependence on horizontal wind velocity.

23 p2974 A73-43867

WIND VELOCITY MEASUREMENT

Stormy weather vertical air motion velocity calculation for use in synoptic field and atmospheric energy budget evaluations

23 p3003 A73-43996

WIND VELOCITY MEASUREMENT

Measurements of microturbulent pulsations of the wind velocity derivative in the ground layer of the atmosphere

01 p0074 A73-10870

Doppler radar evidence of severe storm high-reflectivity cores acting as obstacles to airflow.

03 p0337 A73-14507

Atmospheric microthermal turbulence vertical distribution from balloon flights compared with stellar scintillation data, predicting irradiance spectra from turbulence and wind velocity measurement

03 p0305 A73-14656

Surface winds from sun-glitter measurements from a spacecraft.

04 p0474 A73-15777

Analysis of the meteor wind data.

05 p0622 A73-17167

Data on dynamics of the subcloud Venus atmosphere from Venera spaceprobe measurements.

06 p0744 A73-17436

LF boundary of inertial range in lowest atmospheric layer, comparing turbulence scale and wind velocity components

08 p0954 A73-21185

Lidar anemometry and atmospheric sounding [ONERA, TP NO. 1151]

08 p0986 A73-21680

Thermoanemometer errors in turbulent wind velocity pulsations measurement

11 p1367 A73-26436

Statistical description of the wind field in the upper troposphere and lower stratosphere with allowance for the scale of motion

12 p1521 A73-27741

Measurements of turbulent microfluctuations of the wind-velocity derivative in the surface layer.

13 p1653 A73-28694

Statistical model of gust factor relation to lake and terrain surface roughness and height from wind velocity measurement data

13 p1655 A73-29341

A comparison of turbulence measurements by different instruments - Tsimsyansk field experiment 1970.

13 p1656 A73-29343

Stratospheric mixing estimated from high altitude turbulence measurements.

16 p2005 A73-33539

Measurements of wind-induced Doppler shifts at 16 GHz over a long range bistatic scatter link.

16 p1983 A73-33726

Meteor radar observations of long period waves in the 80-100 km altitudes range.

18 p2304 A73-35968

Results of simultaneous wind velocity profile measurements in the lower thermosphere by the meteor radar and rocket methods.

18 p2310 A73-36130

Temperature and wind velocity variations in winter mesosphere of polar regions.

18 p2310 A73-36140

Corrections for response errors in a three-component propeller anemometer.

18 p2316 A73-36710

The remote sensing of wind velocity in the lower troposphere using an acoustic sounder.

19 p2427 A73-38208

Doppler spectrum turbulence spreading updraft velocity estimation from observation by pulsed radar, noting average value and standard deviation in small thunderstorm

21 p2728 A73-40058

Rate of growth of the upper boundary of cumulus clouds

21 p2730 A73-40117

Experimental investigation of the velocities of vertical motions in convective clouds

21 p2730 A73-40121

Wind profiles over Heiss Island.

21 p2685 A73-40812

A numerical diffusion model for continuous releases.

21 p2732 A73-41568

Zonal wind semiannual variations at 20-65 km, noting wave maximum amplitude and maximum location

22 p2883 A73-42550

Fluidic jet deflection anemometer design and tests of directional wind velocity measurement in rain/sand environments

23 p2981 A73-43429

Venera 8 - Measurements of temperature, pressure and wind velocity on the illuminated side of Venus.

23 p3028 A73-43602

Analysis of hurricane data using the variational optimization approach with a dynamic constraint.

23 p3004 A73-44258

Forward scatter CW radar effectiveness for cross path wind velocity profile measurements compared with radiosonde and pilot balloon observations

23 p3004 A73-44261

Three-component sonic anemometer for wind speed measurement, calculating transfer functions for effect of line averaging and path separation on spectral response

23 p2983 A73-44266

Wind speed variability /standard deviation difference/ over 16.25 km distance between observation sites compared to generalized models for varying conditions of cyclonic activity

23 p3004 A73-44267

Meteorological Doppler radar for measurements of particle velocity and horizontal winds inside convective storms, discussing signal processing and multiple radar method

24 p3107 A73-44687

Signal conditioning electronics for a laser vector velocimeter.

24 p3090 A73-44819

Nighttime meridional neutral winds near 350 km at low to mid-latitudes.

24 p3087 A73-45209

WINDING

NT FILAMENT WINDING

NT HELICAL WINDINGS

NT WIRE WINDING

Compensation, by the layer winding method, for thermal stresses in articles manufactured from reinforced plastics

03 p0313 A73-13740

WINDMILLING

U AUTOROTATION

WINDOWS

Atmospheric windows in different spectral bands due to various gases, comparing continuum and line absorption spectra properties

01 p0037 A73-10364

Thin polypropylene window proportional counters for the observation of cosmic soft X-rays.

01 p0046 A73-10433

Absorption in the 220 GHz atmospheric window.

04 p0418 A73-15394

The acoustic response of rooms with open windows to airborne sounds.

05 p0537 A73-17369

The transmission of sonic boom signals into rooms through open windows.

05 p0537 A73-17370

International Conference on Electromagnetic Windows, 2nd, Ecole Nationale Supérieure de Techniques Avancées, Paris, France, September 8-10, 1971, Proceedings. Volume 1, 2 & 3

11 p1334 A73-25276

Electromagnetic window for a trajectory radar

11 p1327 A73-25280

Concorde cockpit windows design modifications for weight reduction and reliability optimization, discussing transparencies and crew seat movement

14 p1712 A73-30927

WINDOWS [APERTURES]

Electromagnetic wave transmission through 8-12 micron atmospheric window, investigating particulate matter effects on radiation energy extinction

01 p0037 A73-10372

Radiation effects on multiplier phototubes.

11 p1363 A73-25960

Coated laser windows characterized by strong surface absorption, calculating absorptivity, transmittance and reflectivity under assumption of insignificant interference effects within substrate

11 p1377 A73-26243

Cryostats with and without radiation passage through window into vacuum space in balloon-borne far IR instruments requiring cooling to liquid He temperature

11 p1453 A73-26516

A high performance large aperture window for photography from a space platform.

13 p1621 A73-29326

Spectracon camera for astronomical telescope prime focus operation, discussing image tube extended area photocathode and mica window

14 p1751 A73-29906

Thermal defocusing avoidance by short pulse duration reduction to permit IR laser window operation before temperature rise, considering changes in index of refraction

21 p2710 A73-40134

Ocular hazard from viewing the sun unprotected and through various windows and filters.

21 p2698 A73-40143

Indoor azimuth reference systems specifications, characteristics and results, discussing optical windows, theodolites, reflectors, bulk monument structure measurements and rocket applications

21 p2671 A73-40505

[AIAA PAPER 73-842]

Stress and temperature analysis for surface cooling or heating of laser window materials.

21 p2716 A73-40966

WINDOWS [INTERVALS]

NT LAUNCH WINDOWS

WINDS ALOFT

NT GEOSTROPHIC WIND

NT JET STREAMS [METEOROLOGY]

The establishment of the winter polar vortex in mid-latitude latitudes in 1971.

21 p2687 A73-41338

Results of simultaneous wind measurements in the stratosphere, mesosphere and low thermosphere.

21 p2732 A73-41340

Internal gravity waves and turbulence in simultaneous upper atmosphere temperature and wind measurements.

21 p2732 A73-41342

Zonal wind semiannual variations at 20-65 km, noting wave maximum amplitude and maximum location

22 p2883 A73-42550

Polar wind measurements by electrically neutral luminous by-product clouds from Ba ion releases, discussing ion drag

24 p3085 A73-45120

WINDSCREENS

U WINDSHIELDS

WINDSHIELDS

Theory of light deviation by sheets of circular cone geometry

11 p1397 A73-25565

Mathematical method for calculating the optical characteristics of cone-shaped cockpit windscreens.

18 p2266 A73-36069

Aircraft windshield stretched acrylic plastic, chemically strengthened glass, and clad polycarbonate curved composite materials

22 p2799 A73-41863

WINDWARD

U UPSTREAM

U WIND [METEOROLOGY]

WING CAMBER

Conically cambered triangular wings with reflex spanwise curvature.

08 p0925 A73-20938

Some effects of camber on swept-back wings. [SAE PAPER 730298]

17 p2094 A73-34661

WING FLAPS

NT LEADING EDGE SLATS

NT TRAILING-EDGE FLAPS

STOL aircraft with mechanical high-lift systems in comparison to STOL aircraft with wings having blown flaps [DGLR PAPER 72-057]

02 p0130 A73-11665

Variations in the sound field of a STOL aircraft as a function of wing-flap deflection

11 p1306 A73-26592

Analysis of the aerodynamic characteristics of wing lift augmentation devices

12 p1457 A73-26824

WING LOADING

Nonstationary load distribution on an arbitrary-planform wing in supersonic motion

08 p0927 A73-21725

Trailing vortex sheet roll-up behind finite aspect ratio wings for different loading conditions, discussing drag penalties for tip vortices strength improvements

09 p1029 A73-23125

Aerodynamics of wake vortices.

11 p1303 A73-26385

Finite chord effects on vortex induced large aspect ratio wing loads, noting rolling moment magnitude overestimate from lifting line solution

15 p1823 A73-31670

Beyond the buffet boundary.

17 p2100 A73-34538

Interference between a wing and a surface of velocity discontinuity.

19 p2376 A73-37490

A fatigue test program for the wing of the Jantar SZD-37 sailplane

20 p2509 A73-39245

Pressure fields over hypersonic wing-bodies at moderate incidence.

20 p2508 A73-39808

Thin wall rib structured fan shaped wing design for arbitrary air loads, using strain compatibility conditions

21 p2784 A73-40390

Influence of wing flexibility on sailplane loading by individual gusts

21 p2635 A73-41577

Determination of the deflections and stresses in a small-aspect-ratio wing by the displacement method

23 p3041 A73-43723

WING OSCILLATIONS

Experimental investigation of the frequency response of a planar rigid airfoil

03 p0241 A73-12915

Slowly oscillating lifting surfaces at subsonic and supersonic speeds.

03 p0245 A73-13704

High-frequency vibrations of a circular wing in the flow of an ideal fluid

05 p0636 A73-17089

An automated method for determining the flutter velocity and the matched point.

06 p0645 A73-17656

Parametric studies of the wing flutter behavior of a STOL transport.

11 p1304 A73-25523

Calculation of unsteady transonic aerodynamics for oscillating wings with thickness. 11 p1301 A73-25547
[AIAA PAPER 73-316]
Response-optimum control of the angular and torsional oscillations of an elastic flying wing. 12 p1459 A73-27459
Lifting-surface theory for a wing oscillating in yaw and sideslip with an angle of attack. 13 p1564 A73-28802
Downwash-velocity potential method for oscillating surfaces. 13 p1564 A73-28803
Semiempirical method for flutter prediction of unsteady lift and aerodynamic forces acting on oscillating airfoil in stall regime, using separation function. 13 p1566 A73-29029
Unsteady separated free jet flow of an ideal fluid past a wing. 15 p1861 A73-31155
An approximate method for the calculation of the velocities induced by a wing oscillating in subsonic flow. 15 p1824 A73-31905
Automatic electronic feedback control systems for active wing/external store flutter suppression. 17 p2107 A73-35244
Simplified aerodynamic theory of oscillating thin surfaces in subsonic flow. 21 p2632 A73-40427
Analysis of airplane response to nonstationary turbulence including wing bending flexibility. II. 21 p2784 A73-40437

WING PANELS
Investigation of fatigue life and residual strength of wing panel for reliability purposes. 03 p0387 A73-13233
Behavior of a wing panel under transient conditions in a gas flow. 17 p2091 A73-34139
Contribution to the theory of biplane wing sections. 17 p2091 A73-34325

WING PLANFORMS
NT ARROW WINGS
NT DELTA WINGS
NT SWEPTBACK WINGS
NT TRAPEZOIDAL WINGS
NT VARIABLE SWEEP WINGS
The influence of a strake on the flow field of a delta wing $\lambda = 0.2$ at near-sonic velocities [DGLR PAPER 72-125] 03 p0248 A73-14385
Leading-edge force features of the aerodynamic finite element method. 05 p0533 A73-17213
Nonstationary load distribution on an arbitrary-planform wing in supersonic motion. 08 p0927 A73-21725
Unsteady subsonic compressible flow around finite thickness wings. 11 p1301 A73-25544
Development and applications of supersonic unsteady consistent aerodynamics for interfering parallel wings. 11 p1301 A73-25548
Optimal grid arrangement in vortex lattice method of lifting surface aerodynamic analysis, comparing numerical with kernel function results for simple wing planforms. 15 p1824 A73-31746
German monograph - The flow around wings of arbitrary planform in the case of supersonic flow - A computational method. 15 p1824 A73-32581
Three dimensional turbulent boundary layer of yawed wing suction surface in uniform flow, examining cross flow profile, velocity distribution and weighting functions. 16 p1963 A73-33267
Vortex-lift prediction for complex wing planforms. 17 p2094 A73-34438
Numerical calculation of the three dimensional transonic flow over a yawed wing. 17 p2096 A73-35129
A jet-wing lifting-surface theory using elementary vortex distributions. 18 p2260 A73-36207
[AIAA PAPER 73-652]
The lift on a wing in a turbulent flow. 19 p2376 A73-37487
A theoretical note on the lift distribution of a non-planar ground effect wing. 19 p2376 A73-37493
Russian book on structural mechanics of tapered thin walled conical bodies and wings in aviation and rocket technology. 21 p2788 A73-41281
Methods for calculating nonlinear flows with attached shock waves over conical wings. 22 p2796 A73-42562
Monograph - Quasi homogeneous approximations for the calculation of wings with curved subsonic leading edges flying at supersonic speeds. 22 p2797 A73-42675

WING PROFILES
NT WING SPAN

Stability characteristics of re-entry wing shapes and their measurement. 03 p0244 A73-13567
Asymptotic solution for inviscid conducting fluid flow past arbitrary wing profile in magnetic field. 03 p0347 A73-14045
Supercritical shock free transonic profiles for transport aircraft wings of large and medium aspect ratio, discussing straight and yawed wing tests [DGLR PAPER 72-130] 03 p0248 A73-14383
Aerodynamic characteristics of thin asymmetric wing profiles in supersonic flow. 07 p0776 A73-20487
Discrete vortex scheme of a wing of finite span. 08 p0927 A73-21611
Analysis of the aerodynamic characteristics of wing-lift augmentation devices. II. 11 p1301 A73-25796
Solid profile wing motion in ideal incompressible fluid at variable distance from screen in terms of small perturbation theory. 12 p1488 A73-27815
Rogallo variable geometry flexible cambered wing structure and aerodynamic performance for low speed agricultural flight applications. 13 p1568 A73-28027
Transonic flow past lifting wings. 13 p1564 A73-28824
Influence of weak viscous interaction on the drag of a wing profile. 15 p1822 A73-31195
Numerical method for mixed elliptical-hyperbolic nonlinear Cauchy problem with boundary conditions, applying to sonic flow around wing sections. 16 p1961 A73-32807
STOL light aircraft wing with circulation control through blowing around trailing edge, boundary layer control through suction, leading edge modification and increase in chord length. 17 p2094 A73-34682
[SAE PAPER 730328]
Feasibility and optimization of variable-geometry wing for jet amphibian business aircraft. 17 p2102 A73-34683
[SAE PAPER 730330]
Analysis of the aerodynamic characteristics of devices for increasing wing lift. III - Influence of ground proximity on the aerodynamic characteristics of the flaps. 18 p2266 A73-37022
The optimisation of wing design. 19 p2495 A73-37408
The aerodynamic development of the wing of the A 300B. 21 p2633 A73-41192
Approximate calculation of the optimal suction of a compressible gas on a thermally insulated surface at Prandtl numbers other than unity. 22 p2795 A73-42118
The effect of walls on the lifting force of a solid-foil wing. 23 p2940 A73-43722

WING ROOTS
Wing-fuselage junctions fairings compromise design, describing rotational eddies formation mechanism for unsteady ducted flow and wing root phenomena. 13 p1564 A73-28836
[ONERA, TP NO. 1217]
Wing spar static and fatigue tests and S-N curve for lifetime measurement of root sections of small trainer and passenger aircraft. 15 p1955 A73-32190
Some findings from a preliminary fatigue experiment with model light-alloy specimens. 15 p1955 A73-32191

WING SLATS
U LEADING EDGE SLATS
WING SPAN
An improved nonlinear lifting-line theory. 13 p1564 A73-28817
Equivalence rule and transonic flow theory involving lift. 18 p2264 A73-36328

WING STALL
U BOUNDARY LAYER SEPARATION
WING TANKS
Convective fluid motion and heat transfer in aircraft wing fuel tanks due to aerodynamic heating, comparing analytical with experimental results. 15 p1957 A73-31643
Technical and safety aspects of maintenance work on commercial aircraft wing fuel tanks, considering wing deformation effects and sealant materials and reapplications. 18 p2286 A73-36932

WING TIPS
Wing-tip vortex breakdown and dissipation, deriving closed form transcendental solutions for viscous core flow quasi-cylindrical momentum integral equations. 02 p0128 A73-12036
Wing tip vortex modification by tip-mounted upstream and downstream directed air jets, discussing wind tunnel test results. 07 p0773 A73-19193

Calculation of the aerodynamic characteristics of a rectangular wing with tip plates moving at a low subsonic speed in the proximity of a screen. 07 p0775 A73-20094
A theory for rectangular wings with small tip clearance in a channel. 15 p1821 A73-31120
Aircraft wing tip turbulent wakes producing swirling vortices, discussing wake hazards, wind tunnel research and vortex dissipation procedures [SAE PAPER 730294] 17 p2094 A73-34658
Rapid scanning, three-dimensional, hot-wire anemometer surveys for wing tip vortices in the Ames 40-by-80-foot wind tunnel. [AIAA PAPER 73-681] 18 p2315 A73-36232

WINGED ROCKET BOOSTERS
U LAUNCH VEHICLES
WINGS
NT ARROW WINGS
NT CAMBERED WINGS
NT CARET WINGS
NT DELTA WINGS
NT FIXED WINGS
NT FLEXIBLE WINGS
NT LIFTING ROTORS
NT LOW ASPECT RATIO WINGS
NT PARAWINGS
NT RECTANGULAR WINGS
NT RIGID ROTORS
NT RING WINGS
NT ROTARY WINGS
NT SLENDER WINGS
NT SUPERCRITICAL WINGS
NT SWEPT WINGS
NT SWEPTBACK WINGS
NT THIN WINGS
NT TILTING ROTORS
NT TIP DRIVEN ROTORS
NT TRAPEZOIDAL WINGS
NT UNCAMBERED WINGS
NT UNSWEPT WINGS
NT VARIABLE SWEEP WINGS
Aerodynamic interference between jet propulsion system and airframe for supersonic transport with wing-mounted nacelles, noting wing performance role in lift effectiveness. 03 p0243 A73-13428
Powered model wind tunnel investigation to determine performance trends with nacelle location. [AIAA PAPER 72-1114] 03 p0243 A73-13429
Selective reinforcement of wing structure for flutter prevention. 03 p0392 A73-13705
Optimum design for air superiority fighter, noting conventional, delta and coupled canard wing configurations and SAAB Viggen aircraft. 03 p0250 A73-13922
Induced drag of finite wing with antisymmetric incidence distribution due to rolling, deriving relations between wing lift distribution and induced downwash. 03 p0248 A73-14472
Linearized theory for infinite span wing small unsteady motions in curved flight in inviscid incompressible fluid, obtaining time dependent forces, pressure and velocity fields. 05 p0529 A73-16854
[AIAA PAPER 73-90]
Trailing vortex sheet roll-up behind finite aspect ratio wings for different loading conditions, discussing drag penalties for tip vortices strength improvements. 09 p1029 A73-23125
Creep analysis of a thin-walled wing on the basis of the plate analogy. 12 p1551 A73-27086
The evolution and application of lofting techniques at Hawker Siddeley Aviation. 13 p1623 A73-28054
Fiberglass-reinforced plastics for glider laminate wing spars, describing elastic properties and strength characteristics. 14 p1809 A73-30241
Aircraft recovery by inflatable wing canopy with steel cable or fiber suspension lines, discussing aerodynamic characteristics, suspension system and centrifugal compressor performance. 15 p1828 A73-31454
[AIAA PAPER 73-470]
Applications and concepts for the incorporation of composites in large military transport aircraft. 17 p2104 A73-34816
A three-dimensional wing/jet interaction analysis including jet distortion influences. 18 p2261 A73-36209
[AIAA PAPER 73-655]
Four Space Shuttle wing leading edge concepts. 18 p2359 A73-36355
[AIAA PAPER 73-738]
Automated structural design and analysis of advanced composite wing models. 19 p2497 A73-37486
New contributions to the iterative method for aerodynamic calculations of wings in subsonic flows. 19 p2376 A73-37545
An experimental investigation of a jet issuing from a wing in crossflow. 22 p2798 A73-43111

WINTER

WINTER

- Models of extreme arctic and subarctic winter atmospheres between 20 and 90 km.
02 p0160 A73-12274
- Rocket sounding and grenade experiments for stratosphere-mesosphere interaction, showing simultaneous winter temperature changes of opposite sign.
02 p0165 A73-12789
- Auroral sporadic E layer diurnal distribution correlation to charged particle integral flux diurnal variations observed by satellite in winter, noting Kp index effect.
07 p0816 A73-19455
- Geomagnetic storms and wintertime 300-mb trough development in the North Pacific-North America area.
08 p0961 A73-21384
- Models of the extremal arctic winter atmosphere at heights between 20 and 80 km.
09 p1115 A73-22993
- Results of ship-borne ionospheric absorption measurements on the North Atlantic during winter.
11 p1359 A73-26713
- Blocking anticyclones over Siberia in the cold half-year period and the possibility of forecasting them.
12 p1521 A73-27745
- Electron concentrations increase observed at 60-90 km altitudes during anomalous winter radio wave absorption, noting association with upward aerosol transport decrease.
15 p1844 A73-31889
- Anomalous winter time absorption of radio waves in the middle latitude ionosphere.
15 p1844 A73-31900
- The latitudinal variation of the electron concentration in the topside ionosphere in winter.
16 p2010 A73-33913
- The use of the LF A3 absorption measurements in studying the winter anomaly.
18 p2303 A73-35947
- The southern boundary region of the winter anomaly in ionospheric absorption in winter 1971/72 observed on board the cargo vessel 'Hanau' of Hapag-Lloyd moving between 10 deg and 55 deg N.
18 p2305 A73-36002
- Spatial extent of the winter anomaly in absorption.
18 p2305 A73-36003
- Some results obtained from the European Cooperation concerning studies of the winter anomaly in ionospheric absorption.
18 p2305 A73-36004
- Midwinter mesospheric cooling during stratospheric warming, discussing circulation, stratosphere-mesosphere interactions and summertime temperature values at midwinter mesopause.
18 p2308 A73-36037
- A prediction of the phenomena that take place during so called 'sudden warmings'.
18 p2308 A73-36038
- Temperature and wind velocity variations in winter mesosphere of polar regions.
18 p2310 A73-36140
- Structure variations in the winter polar atmosphere.
21 p2685 A73-40827
- The establishment of the winter polar vortex in middle latitudes in 1971.
21 p2687 A73-41338
- Variations of the total amount of ozone and the behaviour of some ionospheric parameters in the winter time upper atmosphere.
23 p2976 A73-43885
- Ozone and temperature change in the winter stratosphere.
23 p2977 A73-43901
- Relation between the intensity of the stratospheric circumpolar vortex and the accumulation of ozone in the winter hemisphere.
23 p2977 A73-43905
- WIRE**
- NT ELECTRIC WIRE**
- NT EXPLODING WIRES**
- Resonances of an antenna associated with the excitation of ion Bernstein modes.
02 p0198 A73-12071
- Creep and durability of tungsten wire.
02 p0180 A73-12137
- Lateral displacement of discontinuous vibrating wire, noting solution application to longitudinal vibrations of discontinuous shafts and torsional vibrations of circular shafts.
02 p0237 A73-12612
- High temperature creep properties of recrystallized W-thoria alloy wires, noting dependence on temperature, grain structure and stress.
04 p0463 A73-15306
- Determination of the modulus of elasticity of metallic and nonmetallic fibers based on bending oscillations.
10 p1231 A73-23691
- Torsion of a reversible flexible wire shaft.
15 p1946 A73-31140
- Reflection coefficients for wires, cables, ropes and chains from scanning laser radar, discussing wire avoidance system for airplanes and helicopters.
17 p2210 A73-35421

Influence of cold work on the stress corrosion susceptibility of Ti-13V-11Cr-3Al.
17 p2194 A73-35675

Influence of a solid-phase nickel coating on the sintering kinetics of tungsten wire.
18 p2320 A73-36858

A bonding-wire failure mode in plastic encapsulated integrated circuits.
19 p2410 A73-38442

Brittleness of coated tungsten wire.
20 p2577 A73-39361

Influence of hydrogen, alcohols, and moisture on the ultimate strength and electrical resistance of tungsten and steel wire samples.
21 p2721 A73-41227

Structure of lanthanum-hexaboride-coated rhenium filaments.
24 p3105 A73-45401

WIRE BRIDGE CIRCUITS

NT WHEATSTONE BRIDGES

Self balancing ac resistance bridge design with digital readout for low temperature carbon resistance thermometers.
21 p2659 A73-39921

WIRE CLOTH

Simulation of velocity profiles by shaped gauze screens.
08 p0953 A73-20717

Flow deflection characteristics of short pyramid wire gauze conical diffuser with high expansion ratio, showing satisfactory uniformity, pressure loss and flow steadiness.
16 p2001 A73-34032

WIRE MESH

U WIRE CLOTH

WIRE WINDING

Feasibility model of airborne ac synchronous generator with rotating superconducting field winding, comparing predicted performance, size and weight with conventional technology.
02 p0131 A73-11827

Rotating electrical machine superconducting field winding design requirements in terms of size, magnetic energy storage, power level, rotation speed and pole number.
02 p0132 A73-11828

Flooded rotor, direct current acyclic motor, with superconducting field winding.
02 p0132 A73-11829

Synchronous electric generators with superconducting field windings, discussing fundamental characteristics, operating modes, refrigeration and cryogenic equipment and applications.
02 p0132 A73-11834

Change in critical current of superconducting NbTi by neutron irradiation.
02 p0200 A73-11842

Technology assessment of superconductivity application to windings of electric machinery.
07 p0863 A73-20108

Influence of wave currents on the windings of electrical equipment during short circuiting.
09 p1037 A73-22942

Mechanical properties of titanium reinforced with unidirectional molybdenum wires.
13 p1643 A73-29604

Optimum windings for linear induction machines.
19 p2389 A73-38312

WIRING

A design approach for LSI using chip selection and circuit modification techniques.
21 p2670 A73-41049

WIRING SYSTEMS

U WIRING

WKB APPROXIMATION

U WENZEL-KRAMER-BRILLOUIN METHOD

WOOD

NT CORK (MATERIALS)

NT PLYWOOD

WOOD AIRCRAFT CONSTRUCTION

U AIRCRAFT STRUCTURES

WORDS (LANGUAGE)

NT MESSAGES

German monograph - The design of digital filters with minimal storage word length for coefficients and state parameters.
14 p1737 A73-30667

WORK

NT PHYSICAL WORK

Second law of thermodynamics revision to include only spontaneous processes made to yield work, discussing heat flow, solutes diffusion and Gibbs free energy.
14 p1816 A73-29735

WORK CAPACITY

Russian papers on human adaptability covering altitude and temperature acclimatization, work capacity and anthropogenetic and medicogenetic factors.
02 p0133 A73-11921

Comparative evaluation of the general and specific efficiencies of athletes under normal barometric pressure and in the process of training and acclimatization under highland conditions of Pamir.
02 p0136 A73-11925

Exercise testing for evaluation of cardiac performance.
03 p0259 A73-13538

Multiple hormonal responses to prolonged exercise in relation to physical training.
03 p0263 A73-14117

Telemetric transmission of ergonomic and time study data to describe work load of radar controllers.
03 p0272 A73-14308

An evaluation of sinus arrhythmia as a measure of mental load.
05 p0543 A73-16718

Work requirements test program for operator proficiency in tasks analogous to aircraft piloting under difficulty variation, deriving workload capability limits.
05 p0544 A73-16722

Transinformation and real time identification applied to the study of pilot workload.
05 p0545 A73-17195

Statistical correlations of maximum oxygen consumption, body weight and endurance /work/ performance in exercise-oxygen studies.
06 p0659 A73-18472

German monograph - Work-physiological investigations for the objectivization of the tracking behavior, the mental load, and its psychopharmacological modularity.
07 p0786 A73-20388

Diurnal psychic working capacity dynamics under conditions of continuous 72-hr wakefulness.
08 p0930 A73-20989

Influence of developmental adaptation on aerobic capacity at high altitude.
09 p1041 A73-22928

Kinetics of oxygen uptake and recovery for supramaximal work of short duration.
11 p1323 A73-25648

German monograph - Investigation concerning a consideration of the human circadian rhythm by means of a variable working time.
13 p1580 A73-29283

Oxygen consumption alteration effects on human endurance capacity as function of relative work, muscle blood flow and anaerobic metabolism.
14 p1714 A73-29753

Towards an objective assessment of cockpit workload. I - Physiological variables during different flight phases.
14 p1718 A73-30515

Commercial aircraft flight control instrumentation for safe and efficient flight path management, emphasizing aircrew work load relief under stressful air traffic conditions.
15 p1830 A73-32473

Relationship of physiological strain to change in heart rate during work in the heat.
15 p1836 A73-32548

Effect of maximal work load on cardiac function.
16 p1973 A73-33991

Physical energy expenditure in long-haul cabin crew.
18 p2283 A73-36793

The capacity for muscular work in acute hypoxia.
18 p2286 A73-36946

Pilot workload and performance measures in terms of physiological activity in flight deck environment for reduced aircraft accidents due to human error.
19 p2398 A73-37732

Pilot workload immediate, duty day and long term period evaluation from heart rate, subjective, psychological, biochemical stress and sleep pattern measurements.
19 p2398 A73-37734

Cockpit mock-ups and simulator design for pilot workload assessment for Concorde program and V/STOL research.
19 p2384 A73-37735

The air traffic controller and control capacity.
19 p2451 A73-37811

Comparison of the job attitudes of personnel in three air traffic control specialties.
20 p2517 A73-39108

Human intrapair twin differences, examining age, height, weight, heart volume, metabolism, respiratory rate and monozygous/dizygous differences.
20 p2519 A73-39792

Oxygen uptake during maximal work at lowered and raised ambient air pressures.
21 p2638 A73-41132

SkyLab 1 medical experiments concerning astronaut physiological responses and work capability as affected by exposure to space flight environment.
21 p2778 A73-41519

Work-heat tolerance derived from interval training.
22 p2806 A73-42416

Climbing and cycling with additional weights on the extremities.
22 p2806 A73-42418

The effect of anxiety control on the level of information processing.
23 p2946 A73-43848

Oxygen kinetics for constant work loads at various altitudes.
24 p3060 A73-45062

**WORK DECREMENT
U WORK CAPACITY
WORK FUNCTIONS**

Determination of the complete set of physical parameters of Schottky-barrier diodes
01 p0022 A73-10041

Comments on the conduction mechanism in Schottky diodes.
01 p0088 A73-10474

Influence of light on the electron work function of GaAs single crystals at low temperatures
01 p0088 A73-10631

X-band GaAs FET.
03 p0281 A73-13173

Buried channel MOS, double junction and Schottky barrier charge coupled devices, noting higher speeds, charge transfer efficiencies and radiation resistance
05 p0559 A73-16810

MIS and Schottky barrier microstrip devices consisting of microstrip transmission line fabricated on semiconductor substrate, causing capacitance dependence on electric field
05 p0559 A73-16818

The noise of microwave Schottky diodes at 70 MHz
06 p0673 A73-17579

Shot noise in a Schottky barrier diode in the presence of surface electronic states at the contact
06 p0675 A73-18077

Shot noise in diodes with a Schottky barrier in the case of a disturbed carrier distribution function
06 p0676 A73-18090

Influence of the Schottky effect and the peculiarities in the distribution of the applied voltage on the thickness of the depletion layer and the volt-ampere characteristics of a semiconductor with blocking contact.
07 p0802 A73-20191

X- and Ku-band amplifiers with GaAs Schottky-barriers field-effect transistors.
07 p0803 A73-20555

Point contact and Schottky barrier microwave mixer diodes reliability under X band RF pulse operating conditions, considering burnout alleviating fabrication techniques
08 p0943 A73-20735

GaAs Schottky-barrier diodes for ultrahigh-frequency communication systems.
08 p0945 A73-20808

Characteristics of a gallium-arsenide travelling-wave amplifier with Schottky-barrier contacts.
08 p0946 A73-21118

Electric charges on stainless steel surfaces - The effects of hydrogen, charged particles, illumination, and electric fields on the work function.
09 p1133 A73-22195

Work function measurements by the field emission retarding potential method.
09 p1133 A73-22196

The effect of an interfacial layer on minority carrier injection in forward-biased silicon Schottky diodes.
09 p1135 A73-23044

Variation of the work function of W(100) by adsorption of oxygen, cesium, and coadsorption of oxygen and cesium
10 p1186 A73-23696

Work function of the principal faces of single crystals of rhenium solutions in molybdenum
10 p1231 A73-23818

Equivalent noise temperature equation relating HF noise in mm wave Schottky barrier diodes to barrier transport mechanism
11 p1339 A73-26697

On the existence in Schottky diodes of correlation laws between the parameters of the direct characteristic and the amplitude of low frequency background noise
13 p1590 A73-28565

Sources of spurious background in the Spectracon.
14 p1732 A73-29907

Work function and surface ionization currents in steatite ceramics from nickel electrode and thermocouple measurements, plotting temperature dependent Paschen curves
16 p2031 A73-34011

Effect of adsorption on the electrical conductivity of thin vanadium films
17 p2220 A73-35557

Influence of the reflection forces and the tunnel effect on the current-voltage characteristic of a metal-semiconductor contact with a Schottky barrier
18 p2340 A73-36668

The role of surface states in the formation of a Schottky barrier at a metal/gallium arsenide contact
18 p2341 A73-36717

Thermionic properties of zirconium carbide/rhenium composites
21 p2751 A73-40530

Determination of work functions near melting points of refractory metals by using a direct-current arc.
21 p2722 A73-41563

Gunn effect digital functional device.
22 p2829 A73-42204

Chemisorption of H₂ on W(211).
22 p2817 A73-42444

**WORK HARDENING
NT STRAIN HARDENING**

Effect of diamond smoothing on the surface finish and fatigue strength of EI961 steel.
02 p0174 A73-12141

Deep drawability of titanium sheets.
09 p1104 A73-22522

Temperature dependent combined hardening theory within plasticity formulations for finite element analysis of aerospace vehicle engines under plastic strain and cyclic fatigue
09 p1166 A73-23463

Plasticity theory, strength-differential /SD/ phenomenon, and volume expansion in metals and plastics.
10 p1234 A73-24428

On the identification of the unknown functions in Drucker's work-hardening relation for plastic deformation of crystalline materials.
10 p1292 A73-24652

The role of annealing twins in the primary recrystallization of nickel 270 work hardened in tension
12 p1514 A73-27988

Stability of the thermomechanical hardening effect in 60N20 nickel steel
14 p1760 A73-30590

Some effects of prestraining nickel at various rates on its subsequent tensile properties.
14 p1761 A73-30637

Note on volume integrals of the elastic field around an ellipsoidal inclusion.
15 p1946 A73-31104

Work hardened plastic material mechanical properties changes manifested by Bauschinger effect defined as acquired anisotropy, examining plastic deformation conditions
15 p1952 A73-32079

Rectangular cross section isotropic elastoplastic material behavior under combined compressive and bending stresses with allowance for work hardening
16 p2076 A73-32931

Unconventional processes for faster extrusion of aluminum hard alloys
16 p2021 A73-33951

Workhardening, slip band formation and crack initiation during fatigue of titanium.
17 p190 A73-34882

A procedure for solving problems of elasto-plastic flow.
19 p2496 A73-37484

Plastic deformation anisotropy and work-hardening of composite materials.
19 p2444 A73-38261

Fine structure of an explosion-hardened chromium-nickel-manganese austenitic steel
21 p2718 A73-40484

Work hardening of copper, nickel, and alloy H31 by compression and explosion
21 p2707 A73-40705

Fatigue hardening in niobium single crystals.
24 p3101 A73-45474

WORK-REST CYCLE

Role of the sympathico-adrenal system during a period of rest and in adaptation to muscular activity
01 p0007 A73-10157

Crew performance in extended operation under vibrational stress.
05 p0543 A73-16717

Daily rhythm of biogenic amine /histamine and serotonin/ contents in human blood during usual and shifted work schedules
06 p0650 A73-17688

Adenonucleotides, NAD⁺, and NADIN in skeletal muscles during intensive work and at rest
07 p0780 A73-19475

Determination of the optimal time of continuous work for operators in man-machine systems
09 p1046 A73-22849

Intermittent exercise - Metabolites, oxygen pressure, and acid-base equilibrium in the blood.
09 p1041 A73-22933

Investigation of the sleep and wakefulness rhythms in the crewmembers of Soiuz-3 through Soiuz-9 spacecraft prior to, during, and after space flight
10 p1182 A73-24697

Astronauts diurnal life cycle inversion during space flight missions, considering social factors and work-rest cycle effects
12 p1463 A73-27715

Bactericide activity of the integument of man at different times of the day
12 p1463 A73-27716

German monograph - Investigation concerning a consideration of the human circadian rhythm by means of a variable working time.
13 p1580 A73-29283

Work-rest cycle effects on airline pilots performance, considering central nervous system changes measurement techniques
15 p1839 A73-32059

Circadian rhythms in human mental performance from waking day, round of clock and simulated shift-work studies
16 p1972 A73-33156

Industrial work rhythm and between-day fluctuation studies 1920-1969, emphasizing industrial record and between-day fluctuations
16 p1975 A73-33160

Investigation of the possibility of human adaptation to a 16-hour day
17 p2114 A73-34238

Ultradian rhythms in human telemetered gross motor activity.
20 p2512 A73-39102

Sleep loss in air cabin crew.
20 p2517 A73-39109

Effect of a subjective ambiguity estimate concerning the duration of work on activity regulation
22 p2812 A73-41892

Optimal work-rest schedules under prolonged vibration.
23 p2948 A73-43217

Ventilation at transition from rest to exercise.
24 p3061 A73-45375

WORKING FLUIDS

Microcorrosion studies with functional fluids.
[ASLE PREPRINT 72LC-4C-1]
03 p0335 A73-14360

3000 hour endurance test of a 6 kW organic Rankine cycle power system.
09 p1034 A73-22769

Low peak temperatures and hydrodynamic bearings - Key to long life organic Rankine cycle systems.
09 p1034 A73-22770

Hall current effects in the Lewis magnetohydrodynamic generator.
09 p1130 A73-22823

Boundary layer efficiency as working fluid in ram-jets for high aircraft speeds, obtaining external efficiency as function of boundary layer parameters and flow rate
09 p1073 A73-23360

Review of liquid-metal magnetohydrodynamic spacecraft energy conversion cycles.
11 p1308 A73-25977

Heat pipe substituting polarization electrohydrodynamic force effects for capillarity to collect, guide and pump working fluid condensate liquid phases
13 p1705 A73-28434

Heat pipe operational principle and liquid metal working fluids, discussing design, construction and experiments
13 p1706 A73-28674

Heat pipe operation and characteristics, considering working fluid properties, choice and figure of merit
16 p2086 A73-34043

Differential temperature measurements in engine fluids.
18 p2315 A73-36071

Development of a high capacity cryogenic heat pipe.
[AIAA PAPER 73-729]
18 p2369 A73-36346

Russian book on turbomachinery using compressible and incompressible working fluids covering gas and fluid flow equations, energy losses in axial and radial flow stages, etc
21 p2633 A73-40807

**WORLD
U EARTH [PLANET]
WOUND HEALING**

Low calcium diet produced chronic decalcification effect on osseous repair of experimentally induced cortical bone defect in chickens
18 p2270 A73-35981

WRINKLING

Unsymmetric wrinkling of circular plates.
14 p1812 A73-30522

WROUGHT ALLOYS

Characterization of age-hardenable and stress-rupture properties of some cobalt-base alloys.
04 p0465 A73-15579

The influence of some structural factors on the creep strength of wrought precipitation-hardened Ni-Cr alloys.
08 p0982 A73-21793

The resistance of wrought high strength aluminum alloys to stress corrosion cracking.
10 p1232 A73-23872

Zr additions effect on quenched and aged Al-Mg-Li alloy having phases in equilibrium with solid solution
10 p1236 A73-24928

Investigation of the hardening process of alloy D16 in liquid nitrogen.
10 p1226 A73-24929

WURTZITE

Anisotropy of piezoelectrical scattering in semiconductors with a wurtzite structure
06 p0738 A73-18648

Generalized theory of nonlinear susceptibilities and linear electrooptic coefficients based on a three-dimensional anharmonic oscillator model.
14 p1756 A73-29926

X

**X BAND
U SUPERHIGH FREQUENCIES**

X RAY ABSORPTION

X RAY ABSORPTION

- Theoretical consideration of soft X-ray absorption by the metallic films of lanthanum and cerium
06 p0737 A73-18220
- The process of reinforcement of lead shields in electroradiography
07 p0822 A73-19330
- Electron-spectroscopic investigations of two modifications of the alloy steel Kh18NiOT
09 p1104 A73-22690
- Conjugate asymmetries in sudden commencement absorption and the sudden commencement absorption event of February 28, 1969.
12 p1534 A73-26982
- X-ray spectral study of the K state in a nickel-chromium alloy
12 p1514 A73-27943
- Optical appearance of binary X-ray sources.
17 p2232 A73-35146
- X-ray absorption K-spectra of zirconium and its compounds with elements of the second period in the periodic table
18 p2325 A73-36811
- X-ray absorption and optical extinction in interstellar space.
19 p2475 A73-37567
- On the detection of X-rays from celestial sources through their ionization of the terrestrial atmosphere.
21 p2762 A73-41394
- ### X RAY ANALYSIS
- X-ray fine structure of dense plasma in a co-axial accelerator.
01 p0086 A73-11493
- X-ray study and MOessbauer spectroscopy on lunar ilmenites [Apollo 11].
02 p0220 A73-12480
- The growth process of oxide layers during the initial oxidation of a 80Ni-20Cr alloy.
03 p0321 A73-12917
- Dispersion-free X-ray-fluorescent analysis in studies of space and terrestrial objects
05 p0546 A73-17019
- X ray analysis of high coercivity Ticonal alloy single crystal microstructure after isothermal thermomagnetic treatment
06 p0709 A73-18210
- X-ray spectral studies of manganese-aluminum binary alloy systems
06 p0710 A73-18644
- A new method of local X-ray structural analysis - The method of an X-ray beam converging in a solid angle
08 p0965 A73-21131
- X-ray electronic studies of metallic iron in the lunar regolith
08 p1008 A73-21134
- Preliminary results of studies of the Martian atmosphere with the aid of the Mars-2 satellite
09 p1146 A73-22486
- Cast, annealed and hardened zirconium binary alloys cubic to hexagonal phase transitions from X ray and differential thermal analysis
10 p1233 A73-24318
- Roentgenographic investigations of thin films of lead chalcogenide based alloys
10 p1260 A73-24472
- X-ray structural investigations of Dy-Fe-Al system alloys in the region of 0 to 33 at. % dysprosium
12 p1512 A73-27243
- X-ray investigation of the fine crystalline structure of aluminum with creep
17 p2186 A73-34117
- An X-ray examination of deformation in beta Ti-V alloys.
17 p2189 A73-34642
- X ray data refinement on proteins, discussing backbone and side chain dihedral angles adjustment by least squares fitting to relieve atomic overlaps
17 p2112 A73-34893
- Application of a microanalyzer to the investigation of the interaction between titanium and coatings
18 p2323 A73-35894
- X-ray investigation of the mechanism of effects of alloying on defect formation in refractory metal alloys
22 p2877 A73-42454
- Improvement of the electron optics of X-ray image-intensifiers.
23 p2982 A73-43678
- ### X RAY APPARATUS
- Design and operation of high power pulsed X ray tube with photocathode and nitrogen laser illumination for electron beam generation
02 p0175 A73-11960
- Multilayer X ray film chamber for gamma quanta energy spectrum determination by primary photon impact and absorber calorimetric methods
02 p0208 A73-12660
- An X-ray tube emitting soft and hard radiation with controlled focusing
08 p0969 A73-21721
- A position sensitive proportional counter with high spatial resolution.
13 p1622 A73-29643
- Intercosmos satellite-borne X ray polarimeter measurements of solar flares
18 p2345 A73-36144

- Portable pulse X-ray micro and nanosecond range apparatus for studying fast-going processes in opaque media.
21 p2696 A73-39977
- Electrofluoroplanigraphy for human body layer single-plane sections synchronization, using X ray tomography and TV imaging followed by roentgenogram electronic summation
21 p2645 A73-41216
- Semiautomatic recorder for photometry of black spots produced by electron-photon cascades on RT-6 type X-ray films
23 p2982 A73-43568

X RAY ASTRONOMY

- ### NT X RAY SOURCES
- Thin polypropylene window proportional counters for the observation of cosmic soft X-rays.
01 p0046 A73-10433
- Binary stars as X-ray sources.
01 p0102 A73-10969
- Galactic and extragalactic X and gamma ray sources identification from satellite, rocket and high altitude balloon observations, discussing radiation generation theories
01 p0092 A73-10990
- Galactic-latitude dependence of low-energy diffuse X-rays.
01 p0092 A73-11030
- [AD-760196]
Observations of soft X-rays - Two supernova remnants in the constellation Lupus and the diffuse background.
01 p0103 A73-11031
- The nature of the first Cygnus X-3 radio outburst.
02 p0204 A73-11551
- X ray intensity observations of Cygnus X-3 by Uhuru satellite before/during September 1972 radio flare
02 p0210 A73-11554
- Cygnus X-3 intensity drop and principal period observation by X ray instrument onboard OAO Copernicus
02 p0204 A73-11563
- Observational evidence relating to a recent theory on the origin of the universal X-ray background [Research note].
02 p0207 A73-12395
- Cosmic soft X rays observations by rocket-borne polypropylene window proportional counters, analyzing X ray sources spectra and intensity distributions
02 p0207 A73-12404
- Spectrum of the cosmic X- and gamma ray background in the energy range 1 keV-1 MeV.
02 p0210 A73-12730
- Possibility of continuous monitoring of celestial X-ray sources through their ionization effects in the nocturnal D-region ionosphere.
03 p0361 A73-13361
- Matrix method for direct reduction of astronomical X ray spectral data, taking into account detector resolution and fluorescent escape phenomena effects
03 p0361 A73-13366
- A balloon-borne observation of the X-ray source Cygnus XR-1.
03 p0361 A73-13367
- Asymmetry of soft X-ray emission near M87.
03 p0361 A73-13713
- Observation of a correlated X-ray-radio transition in Cygnus X-1.
03 p0361 A73-13714
- GX 17 + 2 X ray source optical counterpart identification, noting interstellar absorption role in magnitude estimation
03 p0374 A73-13795
- Spectroscopic techniques in X-ray astronomy.
03 p0375 A73-13961
- Advances in solar and cosmic X-ray astronomy - A survey of experimental techniques and observational results.
03 p0364 A73-14167
- Distances and absolute luminosities of galactic X-ray sources.
04 p0492 A73-15358
- Physical significance of interstellar matter accretion on rotating magnetized star with emphasis on implications for X ray sources
04 p0493 A73-15979
- Measuring rocket attitude by starlight.
05 p0594 A73-16300
- High energy /X ray, gamma ray and cosmic ray/ astronomy research impact on astrophysical and cosmological models
05 p0610 A73-16932
- The Uhuru catalog of X-ray sources.
05 p0625 A73-17326
- Observations of the extended X-ray sources in the Perseus and Coma clusters from Uhuru.
05 p0625 A73-17327
- Soft X-ray spectra of the Cygnus Loop and Cygnus X-2 in the energy range of 0.16-6.7 keV.
05 p0612 A73-17332
- Hard X-ray observations of Hercules X-1 by OSO-7.
05 p0612 A73-17343
- Spectroscopic observations of HZ Herculis and a model for Hercules X-1.
05 p0625 A73-17344

- Small Magellanic Cloud X-1 X ray source binary nature, occultation, energy spectrum and intensity from Uhuru satellite observation
05 p0626 A73-17345
- Positional evidence of Virgo X ray source correspondence with spiral galaxy IC 3576, noting optical and radio data incompatibility
05 p0626 A73-17346
- Search for coronal line emission from the Cygnus Loop.
05 p0626 A73-17380
- A soft X-ray survey of the galactic plane from Cygnus to Norma.
05 p0612 A73-17389
- Observations of Vela XR-1 by the UCSD X-ray telescope on OSO-7.
05 p0627 A73-17390
- High energy astronomy research in space, discussing HEAO A and B, UV astronomy, X ray astronomy, gamma rays, cosmic rays, hot stars, stellar energy sources and elementary particles
06 p0743 A73-18016
- Star sensor of spin stabilized Uhuru satellite for detection and location of stellar X ray sources with accuracies of one arc-minute
06 p0695 A73-18323
- Consequences of a universal cosmic-ray theory for gamma-ray astronomy.
07 p0872 A73-20154
- Analysis procedure of gamma ray astronomy spark chamber data.
07 p0828 A73-20644
- Observations of spatial structure in the soft X-ray diffuse flux.
08 p0997 A73-20881
- Models for extragalactic objects with very high IR and X-ray luminosity.
09 p1141 A73-22007
- UK5 X ray astronomy satellite, discussing structural design, attitude sensing for pointing control, data handling, attitude control and power supply systems
09 p1155 A73-22920
- Cosmic gamma ray observations for choice between galactic and metagalactic models of cosmic ray origin, discussing proton nuclear component
09 p1138 A73-22952
- The observation of relic radiation as a test of the nature of X-ray radiation from the clusters of galaxies.
09 p1138 A73-22953
- Gamma-ray emission from the region of the Galactic center.
10 p1264 A73-23530
- A high resolution position sensitive detector for ultraviolet and X-ray photons.
11 p1363 A73-25958
- Collimator corrections to the measured diffuse X-ray background.
12 p1537 A73-27885
- Coaxial anode for background suppression in X-ray proportional counters.
13 p1612 A73-28367
- On Compton models of the isotropic X-ray background.
14 p1796 A73-30001
- White dwarfs, neutron stars and black hole identification by satellite X ray astronomy, discussing gas temperature and mass relation to cluster parameters
14 p1797 A73-30075
- Wolter-Schwarzschild telescopes for X-ray astronomy.
14 p1752 A73-30159
- Gamma and cosmic ray astronomy review, covering balloon and rocket measurements, galactic and metagalactic source locations and radio source information
15 p1926 A73-31148
- Low energy X-ray map of Puppis A supernova remnant.
15 p1933 A73-31353
- Gamma-ray observations of the galactic centre.
15 p1933 A73-31354
- X- and gamma-ray astronomy; Proceedings of the Symposium, Madrid, Spain, May 11-13, 1972.
16 p2049 A73-32727
- Galactic and extragalactic X ray observations at 20-500 keV, considering supernova remnants, Sco-1 and Cyg 1 type sources, M31, Magellanic Clouds and Crab Nebula
16 p2049 A73-32731
- Sco X 1, Cygnus and galactic center X ray sources radio observations, discussing identification, properties and variabilities
16 p2050 A73-32733
- Pulsar X ray emission relation to general X ray sources, considering NP 0532, Sco X-1 and Cen X-3
16 p2050 A73-32740
- Uhuru extragalactic X ray observations including normal galaxies, quasars, giant radio galaxies, Seyferts and galactic clusters
16 p2050 A73-32741
- Extragalactic X-ray sources and their contribution to the diffuse background [Invited paper].
16 p2051 A73-32744

Soft X ray background observations at 0.1-10 keV, considering interstellar absorption effects, galactic radiation and extragalactic components
16 p2051 A73-32745

X ray background and emission mechanism nature, considering evolutionary effects and unresolved sources
16 p2051 A73-32747

Diffuse background X ray origin theories with emphasis on soft flux in galactic plane and at poles
16 p2051 A73-32748

Extragalactic diffuse X ray background above 30 keV, discussing spectral breaks and bumps at various energies
16 p2051 A73-32749

X-ray and radio emission from stellar coronae.
16 p2052 A73-32827

Hard X-ray solar bursts observed from the OSO-6 satellite.
16 p2052 A73-32828

Gamma ray astronomical state-of-art, discussing cosmic gamma ray sources observation and diffuse radiation measurement
16 p2055 A73-33290

Imaging techniques in spaceborne X ray astronomy, discussing ray focusing, data processing and observational requirements of single photon detection and high time resolution
17 p2170 A73-35294

Grazing incidence X ray telescope lens design for radio and optical identifications of radiation sources by satellites
17 p2171 A73-35409

Book - Atomic physics and astrophysics, Volume 2.
18 p2356 A73-36969

Cosmic X-ray sources - A progress report.
19 p2474 A73-37149

Copernicus satellite observation of eclipsing binary Her X-1 to search for steady soft X ray flux strong enough to heat companion star
19 p2482 A73-37391

Astronomische Gesellschaft, Scientific Meeting, Vienna, Austria, September 18-23, 1972, Reports
20 p2605 A73-39056

Cosmic sources of X rays and gamma rays
20 p2601 A73-39061

Monte-Carlo-method based calculation of the linearity and resolving power of a Cerenkov spectrometer for purposes of gamma astronomy
21 p2701 A73-40613

Clusters of galaxies - A possible source of background emission in the X-ray band
21 p2759 A73-40709

Diffuse X and gamma radiation at 0.1-100 MeV, discussing nonthermal mechanisms, thermal emission from uniform intergalactic medium, isotropic background, galactic clusters, etc
21 p2760 A73-41246

Pulsed high-energy gamma rays from the Crab Nebula.
22 p2901 A73-41760

Galactic and extragalactic gamma ray bursts contribution to diffuse cosmic X ray flux, noting superposition of supernovae outbursts
23 p3025 A73-43957

Are the recently observed soft gamma-ray bursts from stellar superflares.
24 p3124 A73-44989

The effect of the Gum Nebula on soft X-rays from galactic sources.
24 p3138 A73-45044

Long-term X-ray observations of Scorpius X-1 by OSO-III.
24 p3138 A73-45045

Infrared and X-ray variability of Cyg X-3.
24 p3143 A73-45347

X RAY DENSITY MEASUREMENT
Pulsed X-ray photography of a shock wave in cesium vapor using two X-ray tubes
06 p0731 A73-18554

Preliminary interpretation of the polarization measurements performed on "Intercosmos-4" during three X-ray solar flares.
10 p1268 A73-24142

Pulse X-ray photography of a shock wave in cesium vapor using two X-ray tubes.
16 p2042 A73-33579

Bremsstrahlung X ray measurements over subauroral latitudes during substorms, noting e folding energy correlated with local electrojet and anticorrelated with conjugate electrojet
21 p2760 A73-41366

Some diagnostic methods for dense plasmas from high-pressure pulse discharges
23 p3011 A73-43667

X RAY DIFFRACTION
X-ray investigation of textures in thin films
01 p0050 A73-10800

Polychromatic X-ray diffraction - A rapid and versatile technique for the study of solids under high pressure and high temperature.
01 p0054 A73-11482

Hydrogen reactions and detection by line broadening in beta transformed Ti-Al-V alloy, using X ray diffraction analysis
02 p0183 A73-12759

X ray diffraction measurement of ordering kinetics in Ni-Pt alloy at annealing temperatures, showing disorder-order transitions relation to nucleation and growth
04 p0467 A73-15982

Wavelength dependence of moire patterns
05 p0577 A73-16822

A method for performing high precision lattice parameter change measurements on quenched aluminum.
05 p0580 A73-17257

Study of fatigue crack propagation by X-ray diffraction approach.
06 p0698 A73-18496

Crystallography and chemical trends of orthopyroxene-pigeonite from rock 14310 and coarse fine 12033.
07 p0881 A73-19703

Lunar plagioclase and pyroxene observation for lamella thicknesses by X ray diffraction, noting twinning, exsolution and crystal disorder effects
07 p0788 A73-19711

Forms of carbon in the new Haverø ureilite of Finland.
09 p1140 A73-21863

Investigation of stress state at fatigue crack tip by means of X-ray microbeam.
10 p1293 A73-24918

Stony-iron meteorite shock histories, determining crystallographic character of kamacite in samples via back reflection X ray diffraction technique
11 p1419 A73-25780

Iron silicate disproportionation by ruby laser and static heating in resistance furnace, discussing X ray diffraction patterns
11 p1409 A73-25901

Rare earth-rhodium systems intermediate phase equilibria and crystal structures, using powder X ray diffraction technique
11 p1410 A73-26569

Compositional and X-ray data for Luna 20 feldspar.
13 p1677 A73-28334

X-ray investigation of fatigue-crack growth - On critical strain for fracture at the crack tip.
13 p1625 A73-29482

Further consideration of crack propagation by oscillating crystal X-ray microbeam diffraction technique.
13 p1625 A73-29483

Residual surface stress changes dependence on fatigue life and steel specimen size during rotating bending fatigue tests from X ray diffraction study
13 p1625 A73-29485

An X-ray study of hydrogen induced phenomena affecting mechanical behaviours of austenitic stainless steels.
13 p1625 A73-29522

An X-ray diffraction and DTA study of the ferroelectric transition in barium sodium niobate.
15 p1924 A73-31839

X-ray diffraction at high temperatures for a study of thermal expansion of MnSe and MnSe2
15 p1925 A73-32651

The relationship between thermal history, X-ray crystallographic structure and thermal properties of Pyco-bond rayon precursor carbon-carbon composites.
16 p2028 A73-33044

The relationship between thermal history, X-ray crystallographic structure and thermal properties of rayon precursor carbon-carbon composites A literature review.
16 p2028 A73-33045

A survey of nondestructive testing techniques.
18 p2320 A73-36484

Recording of diffraction patterns by X-ray pulses of materials subjected to a shock wave compression
21 p2695 A73-39967

New tubes and techniques for flash X-ray diffraction and high contrast radiography.
21 p2696 A73-39974

Study of precipitates in an aged Mg-3.6 wt%Zn alloy by an X-ray method.
23 p2993 A73-44124

X RAY FLUORESCENCE
Light flash induced by a pulsed X-ray source in the upper atmosphere
05 p0610 A73-17016

Dispersion-free X-ray-fluorescent analysis in studies of space and terrestrial objects
05 p0546 A73-17019

Lunar surface chemical composition mapping with onboard Apollo 15 X ray fluorescence spectrometer, showing Al, Mg and Si ratios
07 p0871 A73-19825

Soviet Lunokhod 2 lunar rover design, guidance systems, mineralogical analyses by X ray fluoroscopic spectroscopy, magnetic field measurements and operations site
16 p1996 A73-33225

Ultraminiature X-ray fluorescence spectrometer for in-situ geochemical analysis on Mars.
21 p2765 A73-40241

X RAY FLUORESCENCE ANALYSIS
U X RAY ANALYSIS
U X RAY FLUORESCENCE
X RAY INSPECTION
The influence of X-ray parameters on crack detection capability.
[NA-72-779]
02 p0173 A73-11985

An X-ray monitor for measurement of a titanium tritide target thickness.
07 p0809 A73-20466

Comparative investigation of sensitivities of the xeroradiographic and the roentgenographic methods of flaw detection.
11 p1375 A73-26364

A wave propagation method for conversion of grey pictures into line figures.
21 p2654 A73-40688

Real-time X-ray inspection system for fast flux test facility fuel.
23 p2966 A73-44169

A technique for placing known defects in weldments.
23 p2986 A73-44170

X RAY IRRADIATION
Radiation protective effect of a mixture of ATP, AET, and serotonin on yields of 600-R X-ray-induced chromosome aberrations in the rat.
02 p0134 A73-12187

Electron-microscopic investigations regarding the protective effect of hypothermia on cell organelles in the case of whole-body X-irradiation
03 p0262 A73-13824

Russian book on auto-antibodies of X ray irradiated animal and human blood and organisms covering cell formation, isolation, preparations, sickness treatment and auto-immune reactions
04 p0410 A73-15711

Absolute yields of X-ray induced photoemission from metals.
05 p0604 A73-16515

Permanent and transient radiation effects in BARITT microwave oscillators.
05 p0558 A73-16518

Effect of impurities and X-ray irradiation on the motion of pores in ionic crystals under the action of an external electric field
11 p1401 A73-25242

Study of lymphocyte chromosome aberrations in human peripheral blood under in vitro exposures to 645-MeV protons and X-rays
15 p1835 A73-31517

Thermal structure and evolution of interstellar gas exposed to a soft X-ray burst.
17 p2231 A73-34757

The effect of low X-ray doses on the central nervous system
23 p2947 A73-44179

X RAY PHOTOGRAPHY
U PHOTOGRAPHY
RADIOGRAPHY
X RAY SCATTERING
Charge density distribution in Be single crystals from X ray structure amplitudes for lowest angle Bragg reflections, comparing with Hartree-Fock and free electron plane wave models
04 p0467 A73-15932

Dynamic radiography - A new imaging technique using penetrating radiation.
05 p0573 A73-16278

Intensity calculation of X-ray scattering by the atom and ion of aluminum
06 p0725 A73-18216

Investigation of X-ray atomic scattering functions taking into consideration the tetrahedral covalent bonds in some semiconductors
06 p0736 A73-18217

Liquid Ni-Si alloy short range order structure analyzed by X ray scattering, revealing Ni atoms position relation to Si atoms
14 p1764 A73-30870

Small angle X ray scattering study of submicroscopic voids in glassy carbon, using two density theory
19 p2444 A73-38091

X RAY SOURCES
Radio outbursts observation in X ray source Cyg X-3, showing relativistic electrons sporadic injection dominance of synchrotron radio emission characteristics
02 p0210 A73-11564

Sharp focused short pulse X ray source with laser flash synchronization for radiographic plasma diagnostics
06 p0732 A73-18609

Scorpius X-1 representation via old-nova model consisting of standing shock and X ray source formed by mass accretion at white dwarf surface
07 p0874 A73-19063

Observations of Taurus X-1 by the I-60 keV X-ray detector on the OSO-7.
07 p0868 A73-19064

Extended X-ray and radio observations of Scorpius X-1.
07 p0874 A73-19069

Observations of the neutral-hydrogen absorption spectrum of Cygnus X-3.
07 p0874 A73-19073

- Physics of the X-radiation from clusters of galaxies.
07 p0874 A73-19074
The interpretation of the X-ray emission detected from some nearby radio galaxies.
07 p0872 A73-19940
Soft X-ray pulsations from PSR 0833-45.
07 p0872 A73-20153
Lambda-Sco, a possible source of soft X-rays.
07 p0900 A73-20183
Observations of periodic variations in the X-ray intensity of Cygnus X-3.
07 p0872 A73-20240
Isotropic X ray and optical emissions from supernovae and pulsars, deriving pulsar synchrotron emission evolution formulas
07 p0900 A73-20304
The disc model of gaseous accretion on a relativistic star in a close binary system
07 p0901 A73-20305
Uhuru satellite observations of X ray sources, discussing binary sources and identification in visible stars
07 p0872 A73-20525
Spectroscopic observations of the Cygnus X-1 optical candidate.
08 p1003 A73-20895
Spectroscopic observations of the optical candidate for Cygnus X-1.
08 p1004 A73-20896
A search for hard X-rays from extragalactic objects.
08 p0997 A73-21153
Neutron-star accretion in a stellar wind - Model for a pulsed X-ray source.
08 p0997 A73-21160
A soft X-ray survey from the galactic center to Cassiopeia.
08 p1008 A73-21163
X-ray emission of coronal condensations during the eclipse on 20 May 1966 and its connection with optical and radio observations.
08 p0998 A73-21310
Mass differentiation of X ray sources based on Roche model, identifying pulsating sources with neutron stars and black holes as nonpulsating sources
08 p1013 A73-21810
The X-ray surface brightness of the Cygnus Loop.
08 p1013 A73-21811
Cen X-3 and Her X-1 X ray sources emission pulsation explained by model with neutron star accretion of matter from companion via magnetic funnel
09 p1141 A73-22010
Balloon flight observations of Uhuru sources for spectral characteristics, noting hard X ray band sources
09 p1137 A73-22173
The problem of laser sources of radiation in the far-ultraviolet and X-ray regions of the spectrum
09 p1094 A73-22600
Isotropic cosmological models of X ray background radiation, presenting observational constraints on source distribution and radiation mechanisms
09 p1138 A73-22869
IR galaxy model consisting of low energy cosmic or X rays at center of dust shell, discussing physical dimensions of radiating region
09 p1151 A73-23146
Rotating neutron star gas cocoon heating by LF radiation absorption, noting X ray emission
10 p1263 A73-23481
Energy spectrum and time variations of hard X-rays from Cyg X-1.
10 p1263 A73-23488
Sco X-1 hard X rays and optical emission time variations from simultaneous observations, using balloon-borne counter telescopes
10 p1263 A73-23493
X ray background emission and behavior of infalling intergalactic gas into Galaxy resulting from shock wave generation and heating in accretion process
10 p1264 A73-23495
The dependence of Compton X-ray emission from clusters of galaxies on the velocity dispersion of the cluster.
10 p1264 A73-23544
Short-term temporal studies of the X-ray emission from Cassiopeia A, Tycho, and Scorpius X-1.
10 p1264 A73-23547
Quasi-periodic variations in X ray emission from black holes for accretion-formed disk with surface bright spots
10 p1273 A73-23703
Spectroscopic changes in the suspected X-ray source X Persei.
10 p1275 A73-23846
Black holes existence and tentative configuration, discussing galaxies great group missing mass mystery and X ray source investigation
10 p1282 A73-24653
Nuclear laser realizability for gamma quanta production from population inversion during radiative capture of neutrons, considering constraints imposed on heating of active medium
10 p1229 A73-24754
The thermal radiation spectra of supermassive stars and X-ray sources.
10 p1270 A73-24902
Remarks on the soft X-ray emission from the galactic radio spurs.
10 p1270 A73-24904
Production of metagalactic X-rays by relativistic dust grains.
10 p1270 A73-24907
The distribution of X-ray sources in our galaxy.
11 p1415 A73-25178
Supernova remnant Cas A identification as extended source of soft X rays from grazing incidence X ray telescopes aboard OAO Copernicus
11 p1412 A73-25776
X ray source identified with galaxy NGC 5128 located at center of radio source Cen A, noting 3.4 keV low energy cutoff in X ray spectrum
11 p1427 A73-26603
Evidence for the binary nature of 2U 1700-37.
11 p1428 A73-26628
Isotropic X ray and optical emissions from supernovae and pulsars, deriving pulsar synchrotron emission evolution formulas
12 p1539 A73-27276
Disk model of gas accretion on a relativistic star in a close binary system.
12 p1539 A73-27277
X ray sources in Centaurus X-3 and Hercules X-1 eclipsing binaries, determining upper and lower limits on physical parameters from assumption involving mass function
12 p1536 A73-27878
Gamma-ray emission above 20 MeV from the Crab Nebula and NP 0532.
14 p1785 A73-29737
SMC X-1 binary source observation via UCS2 OSO-7 X ray telescope, discussing luminosity and optical identification with variable star SK 160
14 p1786 A73-29738
Extragalactic X ray source data increase from Uhuru catalog publication, discussing relevance to X ray background
14 p1787 A73-30598
Transition radiation production by relativistic electrons traversing cosmic grains as source of celestial X rays, discussing formation zone effect
14 p1787 A73-30730
Galactic origin, distance and flux estimates of transient X ray sources, rejecting extragalactic and supernova event hypotheses
14 p1788 A73-30732
The number-intensity distribution of X-ray sources observed by Uhuru.
14 p1788 A73-30733
Black holes in binary systems, discussing radiation spectrum, disk formation, optical luminosity, X rays, UV regions and temperature distribution
15 p1928 A73-31051
Variable X ray sources Cyg X-1, Cen X-3 and Sco X-1 behavioral analysis from Uhuru satellite data, considering pulsating white dwarf model for Cen X-3
15 p1935 A73-31483
Production of astrophysical X-rays by transition radiation.
15 p1926 A73-31553
X-ray pulse profile and celestial position of Hercules X-1.
15 p1936 A73-31563
Model for X-ray sources based on magnetic field twisting.
15 p1927 A73-32047
Uhuru observed galactic X ray sources, discussing whole-galaxy X ray emission, Sco X-1 type binary sources and emissions in GX263+2 and Small Magellanic Cloud
16 p2049 A73-32728
Observations of cosmic X-ray sources by the MIT instrument on the OSO-7.
16 p2049 A73-32729
X ray power derivation from gravitational energy release during matter accretion onto surface of component of mass transfer binary star
16 p2049 A73-32730
Galactic and extragalactic X ray observations at 20-500 keV, considering supernova remnants, Sco-1 and Cyg 1 type sources, M31, Magellanic Clouds and Crab Nebula
16 p2049 A73-32731
Sco X-1 noncorrelation of radio with optical or X ray intensities, noting paucity of simultaneous observations of other X ray sources
16 p2050 A73-32732
Radio counterparts of X-ray sources and X-ray counterparts of radio stars.
16 p2050 A73-32734
Supernovae remnant X radiation observations, discussing Crab Nebula, Cas A, SN 1572, Cygnus Loop, Vela X and Puppis A and possibilities from Uhuru catalog
16 p2050 A73-32735
Compact X ray source models from statistical analysis of Uhuru catalog sources with respect to luminosities, lifetimes and stellar populations
16 p2050 A73-32737
Models for compact pulsing X-ray sources.
16 p2050 A73-32738
Pulsar X ray emission relation to general X ray sources, considering NP 0532, Sco X-1 and Cen X-3
16 p2050 A73-32740
The properties of extragalactic X-ray sources from visible light observations.
16 p2050 A73-32742
Extragalactic X ray source physical properties, discussing thermal bremsstrahlung X ray generation by synchrotron mechanism or by Compton scattering
16 p2051 A73-32743
Extragalactic X-ray sources and their contribution to the diffuse background [Invited paper].
16 p2051 A73-32744
Absorption and production of soft X-rays in the Galaxy.
16 p2051 A73-32746
Observation of excess gamma-radiation fluxes from the region of the northern galactic pole.
16 p2054 A73-33078
International Conference on Cosmic Rays, 12th University of Tasmania, Hobart, Tasmania, Australia, August 16-25, 1971, Papers. Volume 7 & Invited and Rapporteur Papers.
16 p2054 A73-33276
Luminosity of thermal X-ray sources with a strong magnetic field.
16 p2062 A73-33574
On limits to Jupiter's magnetospheric diffusion rates.
17 p2224 A73-34511
Observations of soft X-rays - Upper limits on the flux from SN 1972E and measurements of the diffuse background in Centaurus.
17 p2224 A73-34754
Optical appearance of binary X-ray sources.
17 p2232 A73-35146
Cylindrical X ray source with Al K-alpha radiation production for spherical photoelectron spectrometer, discussing radiation intensity with minimum bremsstrahlung
17 p2176 A73-35765
Properties of cosmic X-ray sources.
18 p2343 A73-35924
Extragalactic radio sources modeled as bubbles of relativistic plasma rising through hot gas, producing galactic clusters X ray emission
18 p2353 A73-36508
Quasi-periodic variations in X ray emission from black holes for accretion-formed disk with surface bright spots
18 p2354 A73-36728
Evidence for the softening of the cosmic-ray electron spectrum at a few hundred GeV and the origin of the galactic-ridge X-radiation.
18 p2348 A73-37102
Cosmic X-ray sources - A progress report.
19 p2474 A73-37149
X-ray absorption and optical extinction in interstellar space.
19 p2475 A73-37567
Soft X-ray flux of the Coma cluster of galaxies.
19 p2475 A73-37626
Upper limits to the X-ray emission from Beta Persei during radio flares.
19 p2475 A73-37630
The X-ray structure of the Vela X region observed from Uhuru.
19 p2488 A73-38514
GX-5-1 X ray source position determination from lunar occultation observations by Copernicus satellite, noting error bounds
20 p2605 A73-39014
X ray source Hercules X-1 observation from Uhuru satellite, relating regular dips in intensity to orbital phase
20 p2602 A73-39440
Balloon X ray observations of GX 301-2, GX 304-1, GX 1+4, GX 5-1 and GX 3+1 X ray spectra, noting coincidence with Uhuru low energy sources
20 p2602 A73-39441
A model for compact X-ray sources - Accretion by rotating magnetic stars.
20 p2602 A73-39443
X-ray spectrum of Cassiopeia A - Evidence for iron line emission.
20 p2603 A73-39446
The interaction of a laser with matter as an intense source of UV and soft X-ray radiation - Application to X-ray cinematography
21 p2709 A73-39944
Exploding wires as a source of flash X-rays.
21 p2738 A73-39957
X-ray studies of the Crab nebula occultations, 1974-75.
21 p2765 A73-40300
X ray background radiation intensity fluctuations from random discrete point sources, indicating extragalactic origin
21 p2759 A73-40710
Radio binaries observation, noting black hole, large magnetic field or thermal bremsstrahlung as possible origin of strong X-ray radiation
21 p2770 A73-40940

- Balloon measurement of angular extent of Coma and Virgo clusters hard X-ray emission
21 p2762 A73-41393
- Effect of Gaunt factors on analysis of X-ray spectra - Viability of a thermal intergalactic medium in the Coma cluster.
22 p2900 A73-41753
- Further observations of Cygnus X-3 at 8 GHz during the September 1972 outbursts.
22 p2915 A73-43026
- Isothermal gas-sphere model with thermal bremsstrahlung for X-ray emission from Coma, Perseus and Virgo galactic clusters, noting gas distribution
22 p2904 A73-43120
- Cepheus X-4 X-ray source observation by X-ray telescope on OSO-7, confirming position by second telescope aboard
22 p2904 A73-43122
- Interaction of the X-ray source radiation with the atmosphere of the normal star in close binary systems.
23 p3030 A73-43750
- Clusters of galaxies with a wide range of X-ray luminosities.
24 p3139 A73-45055
- Observations of Cyg X-1 and Cyg X-3 above 7 keV from OSO-7.
24 p3144 A73-45494
- X RAY SPECTRA**
Positive detection of an excess of low-energy diffuse X-rays at high galactic latitude.
[AD-760197] 01 p0092 A73-11029
- L-beta 2/ and K-alpha X-ray spectra of niobium and carbon in NbC compound, assuming collectivized valence electrons
02 p0180 A73-12174
- Fe ions optical transition lines in solar flares soft X-ray spectra, noting continuum emission near 8 Å
03 p0367 A73-12945
- Matrix method for direct reduction of astronomical X-ray spectral data, taking into account detector resolution and fluorescent escape phenomena effects
03 p0361 A73-13366
- Ultraviolet and X-ray spectroscopy of astrophysical and laboratory plasmas; Proceedings of the Third Symposium, Utrecht, Netherlands, August 24-26, 1971.
03 p0363 A73-13951
- The coronal X-spectrum - Problems and prospects.
03 p0363 A73-13954
- Mapping the solar corona in X-ray lines of O VII and Ne IX.
03 p0375 A73-13956
- X-ray spectra of solar flares at 0.4-250 keV, emphasizing soft X-ray spectra and emission line and continuum features interpolation
03 p0364 A73-13958
- Scorpio X-1, Crab Nebula, extragalactic, thermal and diffuse background source X-ray spectra
03 p0364 A73-13962
- X-ray line emission associated with solar flares.
04 p0490 A73-14832
- The spectra of highly ionized aluminum /Al VI-X/ in the extreme-ultraviolet and soft X-ray regions.
04 p0492 A73-15369
- Dielectronic satellite spectra for highly-charged helium-like ion lines.
04 p0500 A73-15490
- Soft X-ray spectra of the Cygnus Loop and Cygnus X-2 in the energy range of 0.16-6.7 keV.
05 p0612 A73-17332
- X-ray K absorption spectra shifts /Bergard additivity rule deviations/ in Fe-Cr, Fe-V, Fe-Ni and Fe-Co systems due to lattice characteristics and electron structure changes
06 p0707 A73-18039
- Structure of lunar glasses by Raman and soft X-ray spectroscopy.
07 p0788 A73-19737
- Electron and X-ray transitions between conduction band and bound level and between two bound levels in transition metals, investigating edge singularity and spectrum shape
07 p0864 A73-20614
- Measurements of the solar spectrum between 30 and 128 Å.
[AD-757958] 08 p1002 A73-20760
- Gamma-ray lines from an expanding supernova shell.
08 p1008 A73-21162
- X-ray temperature measurements of laser produced plasmas in large radiation fields.
09 p1125 A73-22024
- Chemical composition of the interstellar gas - X-ray determinations.
10 p1263 A73-23480
- Observation of structure in the X-ray spectrum of Puppis A.
10 p1264 A73-23548
- Interpretation of K X-ray emission spectra and chemical bonding in oxides of Mg, Al and Si using quantitative molecular orbital theory.
10 p1211 A73-24107
- Fine structure of X-ray spectra of nickel and some of its alloys with a nickel arsenide lattice and lattices resembling it
10 p1259 A73-24152
- X-ray and electron spectra from the double inverse pinch device.
10 p1251 A73-24258
- On the morphology of auroral-zone X-ray events. II - Events during the early morning hours.
11 p1354 A73-25762
- D-region recombination coefficients and the short wavelength X-ray flux during a solar flare.
11 p1356 A73-25914
- X-ray source identified with galaxy NGC 5128 located at center of radio source Cen A, noting 3.4 keV low energy cutoff in X-ray spectrum
11 p1427 A73-26603
- Radioactive spallation induced scintillator errors in satellite measurements of diffuse cosmic X-ray spectrum, considering astrophysical implications
12 p1537 A73-27882
- X-ray spectral study of the K state in a nickel-chromium alloy
12 p1514 A73-27943
- New observations of Fe XVII in the solar X-ray spectrum.
13 p1685 A73-29357
- Galactic X-ray polarimetry and high-resolution X-ray spectroscopy.
16 p2058 A73-32736
- Extragalactic diffuse X-ray background above 30 keV, discussing spectral breaks and bumps at various energies
16 p2051 A73-32749
- Spectra of solar flares from 8.5 Å to 16 Å.
16 p2053 A73-32960
- The solar albedo of hard X-ray flares.
16 p2053 A73-32961
- Balloon observations of Sco X-1 in the energy interval 17-106 keV.
17 p2225 A73-35783
- Analysis of solar flare X-ray radiation with Bragg spectrometers.
18 p2344 A73-36014
- Limits to the spectra of the Perseus and Coma clusters above 7 keV from the OSO-7.
18 p2357 A73-37101
- X-ray spectrum of the entire Cygnus Loop.
18 p2357 A73-37103
- Hard X-ray spectrum of Hercules X-1.
19 p2475 A73-37388
- Bragg spectroscopy of Scorpius X-1 in search of the Fe XXV emission lines.
19 p2485 A73-37627
- Balloon X-ray observations of GX 301-2, GX 304-1, GX 1+4, GX 5-1 and GX 3+1 X-ray spectra, noting coincidence with Uhuru low energy sources
20 p2602 A73-39441
- Low energy gamma ray spectrum following muon capture by oxygen 16 leading to bound states of nitrogen 16
21 p2743 A73-40475
- Analysis of the solar X-ray spectrum of 20 August 1971.
21 p2760 A73-40826
- Galactic positronium annihilation gamma ray spectrum with 476 keV photon peak, indicating possible origin in supernova explosive nucleosynthesis of positrons
21 p2770 A73-40941
- Observations of the X-ray emission of solar active regions on 28 November 1970 and 20 August 1971.
21 p2761 A73-41387
- The impulsive increase in the intensity of solar X-rays.
21 p2761 A73-41388
- Lunar orbital gamma ray measurements from Apollo 15 and Apollo 16.
21 p2762 A73-41397
- Exponential projectile charge dependence of Ar K and Ne K X-ray production by fast, highly ionized argon beams in thin neon targets.
22 p2890 A73-42710
- Asymptotic forms of solutions to nonrelativistic Compton Fokker-Planck equation for bremsstrahlung X-ray spectra changes due to Compton scattering in emitting gas
22 p2904 A73-43018
- X-ray spectral data on the valence and conduction band structures in V3X-type vanadium compounds
23 p3017 A73-44041
- X RAY SPECTROGRAPHY**
U X RAY SPECTROSCOPY
X RAY SPECTROMETRY
U X RAY SPECTROSCOPY
X RAY SPECTROSCOPY
- Investigation of the chemical composition of lunar surface along the route of Lunokhod 1.
02 p0212 A73-12228
- Spectroscopic remote sensing of lunar surface composition.
[AD-756154] 04 p0448 A73-15181
- X-ray spectral investigation of some vanadium compounds with a Cr3Si structure
05 p0588 A73-17295
- ESCA-investigation of lunar regolith from the Seas of Fertility and Tranquility.
07 p0887 A73-19770
- A soft X-ray survey from the galactic center to Cassiopeia.
08 p1008 A73-21163
- Spectroscopic measurement method for the electron temperature and density of a focusing discharge of the 'plasma focusing' type
11 p1404 A73-25270
- Use of soft X-ray spectroscopy to study corrosion and oxidation products on metals and alloys.
[NACE PAPER 124] 13 p1638 A73-29319
- ESCA study of fractional monolayer quantities of chemisorbed gases on tungsten.
14 p1724 A73-30421
- Mossbauer and X-ray spectral studies of a nickel-cobalt ferrite subjected to thermomagnetic treatment
15 p1886 A73-31034
- An electronically gated gamma and X-ray calibration scheme.
15 p1879 A73-32222
- Characteristics of the distribution of elements in the diffusive layers of titanium-based three-component systems
15 p1893 A73-32521
- Apollo 15 and 16 lunar orbital X and gamma ray spectrometer for lunar surface composition and radioisotopes surveys, detailing experimental results
16 p2015 A73-33353
- Detection of a gamma-ray spectral line from the galactic-center region.
20 p2602 A73-39438
- Study of the electronic structure of iron, cobalt, and nickel monosilicides by X-ray photoelectron spectroscopy and X-ray spectroscopy
20 p2578 A73-39734
- Large mercuric iodide single crystals application to high resolution X-ray detectors, discussing fabrication by coating platelet face with thin Aquadag film and mounting upon carbon substrate
21 p2699 A73-40465
- An X-ray spectral study of the electronic structure of nonstoichiometric titanium carbide
21 p2721 A73-41226
- First results of the solar hard X-ray spectrometer on board the ESRO TD-1 A satellite.
21 p2761 A73-41386
- Crystal spectrometry of active regions on the sun.
21 p2706 A73-41602
- The detectability limits of thin coatings measured with the electron microprobe.
23 p2985 A73-43917
- X RAY STRESS ANALYSIS**
X-ray elastic constants of titanium and TiAl6V4
05 p0588 A73-17242
- Calculation of X-ray elastic constants on the basis of single crystal coefficients of metals with a hexagonal structure
05 p0588 A73-17244
- X RAY STRESS MEASUREMENT**
Material deformations determined with the aid of X-rays in the case of elongations remaining after a uniaxial tensile test involving titanium and TiAl6V4
05 p0588 A73-17243
- X RAY TELESCOPES**
Supernova remnant Cas A identification as extended source of soft X-rays from grazing incidence X-ray telescopes aboard OAO Copernicus
11 p1412 A73-25776
- A light and compact X-ray image read-out system for space applications.
11 p1364 A73-26050
- A telescope for soft gamma ray astronomy.
12 p1499 A73-27892
- Wolter-Schwarzschild telescopes for X-ray astronomy.
14 p1752 A73-30159
- Grazing incidence X-ray telescope lens design for radio and optical identifications of radiation sources by satellites
17 p2171 A73-35409
- Acoustical spark chamber in a telescope designed for investigations of primary cosmic gamma radiation
21 p2701 A73-40612
- X RAY TESTING**
U X RAY INSPECTION
X RAYS
- NT SOLAR X-RAYS
Properties of H I regions heated by X-rays and cosmic rays
01 p0092 A73-10935
- Auroral X-ray and conjugate ionospheric absorption observations of an electron precipitation event accompanying a sudden impulse in the geomagnetic field.
02 p0157 A73-11759
- Time correlation between current sheet collapse in plasma focus and X-ray production, investigating radiation intensity and distribution
02 p0197 A73-12061
- Cosmic diffuse soft X-rays intensity distribution, taking interstellar absorption into account
02 p0207 A73-12402
- The spectrum of diffuse cosmic X-rays in the 20-125 keV range.
02 p0210 A73-12738

X-Y PLOTTERS

- Local time variations of X ray substorm activity observed at auroral zone station, including atmospheric passage and energy spectrum measurements
03 p0363 A73-13889
- Laboratory-produced radiation related to the solar flare emission.
03 p0364 A73-13957
[AD-758606]
- On the altitude dependence of the atmospheric X-rays in the energy range 0.1-1 MeV.
03 p0365 A73-14441
- Projectile structure effects on neon K X-ray production by fast, highly ionized argon beams.
04 p0476 A73-14769
- Auroral-zone X-ray measurements at Kiruna in 1970.
04 p0492 A73-15100
- X ray background radiation measurement in outer space for proof of Gamow hypothesis on universe chemical composition, indicating improved cosmological models
05 p0613 A73-16210
- Mechanisms of optical, X-ray and gamma-radiation from Crab pulsar.
05 p0611 A73-17314
- Some questions on the evidence of laser X-ray emission from CuSO₄ doped gelatin.
08 p0975 A73-21061
- Balloon observations of auroral-zone X-rays in conjugate regions.
09 p1137 A73-22135
- Properties of H I regions heated by X rays and cosmic rays.
09 p1147 A73-22730
- Bremsstrahlung X-rays in the stratosphere and auroral activity on January 21 and February 3, 1969.
10 p1268 A73-24224
- X ray ionization and heating of H I regions refuted from energy input rate computations of observed flux in Galactic plane
11 p1415 A73-25118
- On the morphology of auroral-zone X-ray events. III - Large-scale observations in the midnight-to-morning sector.
11 p1354 A73-25763
- A position-sensitive X-ray detector for the HEAO-A satellite.
11 p1364 A73-25963
- Correlation between pulsations in auroral luminosity variations and X-rays.
11 p1359 A73-26710
- Midlatitude bremsstrahlung X rays, VLF propagation disturbances and electron precipitation during magnetospheric substorm
12 p1468 A73-26983
- Observations of narrow microburst trains in the geomagnetic storm of August 4-6, 1972.
12 p1490 A73-27007
- Collimator corrections to the measured diffuse X-ray background.
12 p1537 A73-27885
- Effect of a magnetic field on the soft X-ray radiation of a laser plasma
12 p1530 A73-27977
- On the longitudinal extension of electron precipitation during magnetospheric substorms.
13 p1606 A73-28152
- Magnetopause plasma oscillations excitation and transformation into electromagnetic waves, estimating magnetic bremsstrahlung and X ray emission intensities
15 p1926 A73-31892
- Large area focusing collector for the observation of cosmic X rays.
15 p1876 A73-31976
- Radiation emitted by a charge in a stack of plates at frequencies approaching the Bragg frequencies
17 p2120 A73-34114
- Absorption of ultrahigh energy photons in the universe
17 p2223 A73-34368
- Description of small-scale fluctuations in the diffuse X-ray background.
17 p2224 A73-34753
- Transition radiation from interstellar dust grains.
17 p2231 A73-34755
- Large-scale auroral-zone electron precipitation event, briefly interrupted during a negative magnetic impulse.
18 p2344 A73-35951
- X-ray bremsstrahlung at subauroral latitudes
18 p2345 A73-36111
- Advanced radiographic imaging techniques.
18 p2316 A73-36680
- X radiation arising during collisions between metal bodies
19 p2458 A73-37249
- X-ray emission in laser-produced plasmas.
20 p2595 A73-38890
- Coherent X ray emission from plasma generated by laser irradiation of copper sulfate doped thin gelatin layer
21 p2710 A73-40126
- A gas density control system for X-ray proportional counters in space.
22 p2851 A73-41699

- Electron precipitation caused auroral zone bremsstrahlung X rays classification with respect to magnetic storm phases
22 p2851 A73-42750
- Interstellar trace element ionization predictions by cosmic ray, X-ray and UV star models with hydrogen allowance, showing disagreement with satellite observation
24 p3125 A73-45056

X-Y PLOTTERS

- FORTAN subroutine for X-Y plotting and display of two dimensional alphanumeric finite element mesh on line printer
03 p0280 A73-13340
- Numerically controlled plotters THD 605.
07 p0795 A73-18944
- Sampling circuit for HF repetitive waveforms reproduction on standard x-y recorder, noting SNR improvement by signal averaging
11 p1366 A73-26304
- X-22 AIRCRAFT
Total In-Flight Simulator for X-22A aircraft based on variable stability-and-control system concept for reliability design
24 p3057 A73-45153

XB-70 AIRCRAFT

U B-70 AIRCRAFT

XENON

NT XENON ISOTOPES

NT XENON 129

- Time behavior of a TEA xenon laser.
03 p0320 A73-14466
- An estimate of radiative emission from an isothermal xenon plasma at temperatures up to 50,000 K.
05 p0602 A73-16561
- Feasibility of high-pressure noble-gas lasers.
11 p1378 A73-26360
- Measurements of free stream velocity and ionization relaxation behind a shock in xenon.
12 p1527 A73-27172
- Electric properties of dense plasmas in high current pulsed discharge.
16 p2040 A73-32943
- Vacuum UV radiation of electron beam excited high pressure Xe laser, measuring optical gain due to diatomic state-repulsive ground state transitions
17 p2186 A73-35794
- The behavior of xenon when used as a fill-gas in a silicon germanium radioisotope thermoelectric generator.
19 p2455 A73-38388

XENON ISOTOPES

NT XENON 129

- Xenon in carbonaceous chondrites.
04 p0501 A73-15631
- Isotopic composition of solar wind xenon in carbonaceous chondrites, discussing evolution of meteoritic matter
17 p2233 A73-35266
- Non-Gaussian statistics of superradiant radiation from saturated xenon 3.5-micron laser amplifier.
20 p2570 A73-38620
- On Pu-244 in lunar rocks from Fra Mauro and implications regarding their origin.
23 p2951 A73-43771

XENON LAMPS

- Design and performance of solar simulator with water cooled Xe lamp, calculating irradiance distribution by ray tracing method
01 p0030 A73-11149
- Push-pull ac modulator design allowing balanced thermal load on plasma electrodes in pulsed high power short arc Xe flash lamps
03 p0282 A73-13933
- Lens projection system for a solar simulator providing irradiance of 100 solar constants.
08 p0952 A73-21042
- Maximum loads on pulse-discharge light sources producing short flashes.
13 p1629 A73-29437

XENON 129

- Extinct lunar radio activities - Xenon from Pu-244 and I-129 in Apollo 14 breccias.
08 p0936 A73-20843
- Orgueil chondrite magnetite age via I 129/Xe 129 method compared to Karoonda magnetite age
13 p1684 A73-29250

XEROGRAPHY

- Comparative investigation of sensitivities of the xeroradiographic and the roentgenographic methods of flaw detection.
11 p1375 A73-26364

Y

Y AXIS

U COORDINATES

YAG [GARNET]

U YTTRIUM-ALUMINUM GARNET

YAG LASERS

- Pulse pumped Q switched Nd-YAG and ruby lasers single longitudinal mode selection by providing intracavity resonator with active medium
03 p0320 A73-14464
- High-power Y3Al5O12:Nd³⁺/laser with an explosion-type lamp.
06 p0703 A73-18597
- Optimization of the parameters of a quasi-CW YAG:Nd³⁺/laser with a nonlinear element in the resonator.
06 p0703 A73-18599
- Efficient pumping of a CW garnet laser by water-cooled metal-halide lamps.
06 p0703 A73-18600
- Direct overtone excitation of hydrogen fluoride second vibrational level, measuring global deactivation rate by temperature tuned Nd-YAG laser excited fluorescence technique
06 p0703 A73-18750
- Light emitting diode pumped Nd-YAG laser analysis for pumping rate and output dependence on temperature, using circular and transverse intensity distribution
06 p0704 A73-18787
- A stabilized mode-locked Nd:YAG laser using electronic feedback.
07 p0834 A73-19537
- Thin film YAG-Nd laser light sources, discussing material selection, incoherent pumping sources, geometrical configuration, heat dissipation, gain saturation and feedback methods
08 p0975 A73-21143
- Megawatt power IR output of Nd-YAG 50 micron pulse laser, using antireflection coated lithium niobate crystal for Q switch with high polarization contrast ratio
09 p1091 A73-22088
- Internally modulating and multiplexing mode locked Nd-YAG laser techniques for one gigabit optical communication, noting system efficiency improvement over conventional approaches
10 p1227 A73-23783
- High data rate YAG laser communication experimental systems with partial cavity dumping, orthogonal setup or harmonic mode locking, investigating internal modulation feasibility
11 p1378 A73-26246
- Stabilized two-pulse operation of the phase-modulated, frequency-doubled laser.
12 p1504 A73-26831
- Continuous-wave laser with a vortex-stabilized lamp.
12 p1506 A73-27503
- The laser - A unique tool for the time being/unique applications
15 p1884 A73-31325
- Burst-mode frequency-doubled YAG:Nd³⁺/laser for time-sequenced high-speed photography and holography.
15 p1886 A73-32384
- Current status of Nd:YAG lasers.
16 p2022 A73-32855
- A neodymium-doped yttrium-aluminum-garnet laser amplifier with an integrated design
20 p2572 A73-38669
- Low power laser-triggered switching at voltages greater than 500 kV.
20 p2572 A73-38883
- Nd doped YAG laser crystal relaxation time, describing population inversion, beam gain time dependence and phonon spectra
20 p2574 A73-39695
- Miniaturized Nd-YAG laser end pumped by single incoherent gallium-arsenide-phosphide light emitting diode to achieve threshold at room temperature
21 p2713 A73-40457
- GaAs two-photon absorption coefficient obtained from transmission measurements with Q switched Nd-YAG laser, noting thermal self focusing
21 p2713 A73-40459
- Surface and bulk laser-damage statistics and the identification of intrinsic breakdown processes.
21 p2714 A73-40758
- Generation of reproducible giant pulses with an optically regenerative Q switch.
21 p2715 A73-40959
- Ideal laser amplifier as a phase measuring system of a microscopic radiation field.
22 p2870 A73-42516
- Q switched Nd-YAG laser third harmonic for pumping dye laser, extending tunable output range to blue region
23 p2989 A73-44373
- Pulsed Nd-YAG laser output spiking for control of materials machining parameters
24 p3098 A73-45552
- YAGI ANTENNAS
Directivity and bandwidth of single-band and double-band Yagi arrays.
01 p0023 A73-10188
- Nonlinear optimization reduces the sidelobes of Yagi antenna.
22 p2831 A73-41847

Yagi type antenna array of vertical monopoles with optimized slot reradiation to modify foreground reflection for performance improvement
22 p2832 A73-42295

Numerical solution of wire antenna boundary value problems based on integral equations formulation, considering Yagi-Uda array, antenna design and radiation patterns
22 p2827 A73-42840

YARNS

High strength and low density graphite fiber yarn for reinforcement in structural composite components on heavily loaded flight vehicles
06 p0715 A73-18716

High modulus graphite fiber preparation from polyacrylonitrile yarn, discussing graphitization, properties and stabilization oxidation treatment
16 p2028 A73-33042

YAW

A method of testing full-scale inlet/engine systems at high angles of attack and yaw at transonic velocities.
[AIAA PAPER 72-1097] 03 p0287 A73-13417

Experiments on flow about a yawed circular cylinder.
[ASME PAPER 72-FE-2] 05 p0527 A73-16546

A laser optical lever system for measuring the pitch and yaw of a ground-launched rocket.
08 p0974 A73-20669

Lifting-surface theory for a wing oscillating in yaw and sideslip with an angle of attack.
13 p1564 A73-28802

Three dimensional turbulent boundary layer of yawed wing suction surface in uniform flow, examining cross flow profile, velocity distribution and weighting functions
16 p1963 A73-33267

Numerical calculation of the three dimensional transonic flow over a yawed wing.
17 p2096 A73-35129

Three-dimensional compressible boundary layer flow over a yawed cone.
[AIAA PAPER 73-634] 18 p2260 A73-36193

Effect of yaw on supersonic and hypersonic flow over delta wings.
19 p2377 A73-38008

Automatic control of adverse yaw in the landing environment using optimal control theory.
[AIAA PAPER 73-861] 20 p2586 A73-38799

Diffraction and reflection of shocks from corners.
22 p2843 A73-42567

YAWING MOMENTS

Flight simulator evaluation of control moment usage and requirements for V/STOL aircraft.
[AHS PREPRINT 743] 17 p2147 A73-35076

YAWMETERS

U ATTITUDE INDICATORS

U YAW

YEAST

On the mechanism of adaptation of micro-organisms to conditions of extreme low humidity.
22 p2803 A73-42164

YHU-1 HELICOPTER

U UH-1 HELICOPTER

YIELD POINT

Reflection of plane stress waves in an elastoplastic medium with a variable yield limit
01 p0114 A73-10570

Characteristics of the process of plastic deformation of bcc metals in the microyield zone
02 p0179 A73-11622

Determination of yield locus curves for copper and aluminum crystals with the aid of Knoop hardness measurements
02 p0181 A73-12364

The influence of texture on the yield loci of copper and aluminium.
02 p0181 A73-12365

On the influence of acceleration stresses on the yielding of disks of uniform thickness.
03 p0384 A73-13118

Finite plastic deformation of pressurized membranes of revolution.
03 p0384 A73-13120

Yield and plastic flow theory for porous metal powder compacts and preforms, discussing stress-strain and deformation-densification relations
03 p0388 A73-13260

Triaxial plastic compression soil theory generalization to three dimensional complex stress fields, discussing yield surface for granular materials
03 p0390 A73-13332

Plane strain limit analysis of plastic material described by piecewise analytic nonlinear yield condition and associated flow rule
03 p0393 A73-13778

The mechanisms of growth of gamma prime particles and tensile yield in Udimet 520.
04 p0464 A73-15578

Upper yield point removal in pure Ta by reversed cyclic stressing at room temperature, indicating cumulative mobile dislocation multiplication
05 p0586 A73-16136

Mathematical models for yield point dependence on statistical arrangements of ordered precipitated phases, noting crystal dislocations interaction effect
06 p0735 A73-18044

Deformation by Pibbert-Lueders bands observed on composites of oriented solidification
[ONERA, TP NO. 1192] 06 p0708 A73-18099

Yield surface equation derivation for plastically prestrained anisotropic material from simple tension and compression tests
06 p0763 A73-18455

Grain size effects on iron substitutional alloys yield stress, investigating Hall-Petch relation
06 p0713 A73-18770

A new relationship between pre-strain and yield stress drop due to Bauschinger effect.
06 p0713 A73-18772

Temperature and loading rate effects on yield stress and specific fracture work in tempered carbon steel from notch tests, correlating with linear fracture mechanics
07 p0838 A73-19215

The yield point phenomenon in a Be-Al composite.
07 p0839 A73-20115

Influence of annealing under load on the structure and properties of a self-ordering Ni3Mn alloy
09 p1099 A73-21957

Rigidly plastic shells yield point, deriving yield surface in generalized stress space
09 p1158 A73-22360

Tensorial expansions for the plastic flow of partially compressible media.
10 p1290 A73-24325

Cylindrical metal projectile impact induced elastoplastic deformation, determining dynamic yield point by computer simulation of Taylor stress wave propagation model
10 p1292 A73-24529

The soft surface effect in plastic deformation and fatigue of metals and alloys.
11 p1381 A73-25808

Plane strain plastic yielding due to bending of end-loaded cantilevers containing circular, triangular or diamond-shaped holes.
11 p1443 A73-26091

Yield point phenomenon in Al-Ti alloy.
12 p1511 A73-27060

Ideal plasticity theory for solid bodies of isotropic materials with different yield points in extension and compression
12 p1553 A73-27374

Influence of deformation history on the yield locus and stress-strain behavior of aluminum and copper.
13 p1632 A73-28130

Plane strain slip line theory for anisotropic rigid/plastic materials.
13 p1697 A73-28793

Thin ferrosilicon intermediate cylindrical layer tensile strength, microhardness and yield point determination at 20-1000 C
13 p1624 A73-29064

Stability criteria for rigid plastic cylindrical shells at yield point load as function of deformation rate and geometry changes
14 p1809 A73-30257

Yield conditions for plastic deformation of anisotropic bodies, using stress tensor invariants and Tresca form
14 p1811 A73-30480

Limit state solution to equilibrium equation of elliptical plate with Johansen yield condition under uniform load, using Abel differential equation
14 p1811 A73-30486

Random yield limit of stochastically non-homogeneous elements in tension.
14 p1811 A73-30489

Solid solution strengthening of high purity niobium alloys.
14 p1761 A73-30631

German monograph - The effect of interstitial elements and recrystallization on the defined yield point of titanium.
14 p1762 A73-30665

German monograph - Elevation of the yield point and pronounced yield range of multicrystalline aluminum-magnesium alloys.
14 p1762 A73-30673

Hard WC-Co alloys as dispersion strengthened materials
15 p1887 A73-31591

Yielding in unidirectional composites under external loads and temperature changes.
15 p1949 A73-31679

Polycarbonate as a model material for three-dimensional photoplasticity.
17 p2247 A73-35029

[ASME PAPER 73-APM-4] Yielding and failure of metals in a complex state of stress
18 p2366 A73-36756

Temperature dependence of the yield point in grain-oriented beryllium
18 p2324 A73-36773

Thin ferrosilicon intermediate cylindrical layer tensile strength, microhardness and yield point determination at 20-1000 C
18 p2320 A73-36896

Inhomogeneous yield limit effect on elastic-plastic boundary of circular cylinder in torsion, considering radial and angular dependencies
19 p2498 A73-37651

The yielding of a two-dimensional void assembly in an organic glass.
19 p2444 A73-38090

Yield surfaces of metals at elevated temperatures.
20 p2615 A73-38640

On the relationship of stress crazing and yielding of polymethyl methacrylate.
20 p2579 A73-38641

Effects of misalignment on the pre-macroyield region of the uniaxial stress-strain curve.
20 p2576 A73-39030

Sandwich plates minimum volume design for elliptical, triangular and annular structures, discussing Mises criterion and bending coordinates
20 p2623 A73-39559

Rigid viscoplastic thin circular plate under uniformly distributed transverse pressure, deriving Mises and Tresca yield surface conditions
20 p2624 A73-39567

Yield criterion in plane stress state for description of second order effect relating to axial strain accumulation in cyclic torsion
20 p2624 A73-39568

Stability of the bending equilibrium of shells beyond the elastic limit
20 p2625 A73-39657

Effect of the yield point of the material on the stability of cylindrical shells under axial compression
20 p2625 A73-39658

Determination of the limiting equilibrium of a brittle body weakened by a system of cracks whose form on a plane approaches a circular form
22 p2921 A73-42284

Unified plastic yield criterion for ductile solids.
22 p2923 A73-42555

Generalized initial yield surfaces for unidirectional composites.
[ASME PAPER 73-APMW-24] 22 p2925 A73-42886

The yield stress of Ni3Al, W.
22 p2880 A73-43075

Certain methods in the physically nonlinear theory of three-layer plates
23 p3043 A73-43921

Experimental bases and models for the study of the overall behavior of metals
23 p2993 A73-43964

Critical equilibrium of cylindrical shells made from an ideal rigid-plastic material with different yield points in tension and compression
23 p3047 A73-44280

Influence of dislocation density and aging on the yield point of Al-Cu-Mg-Mn alloys
23 p2995 A73-44285

Limit loads of circular plates under combined loading.
[ASME PAPER 73-APM-G] 23 p3047 A73-44379

Dislocation locking by interstitial oxygen atoms and the temperature dependence of the yield point in niobium
24 p3099 A73-44574

Transverse shear extensions to Ilyushin-Shapiro thin shell and plate theory for yield surfaces in rigid-plastic materials
24 p3147 A73-44746

Plastic plate bending under concentrated forces, defining stress and strain principles at yield limit
24 p3148 A73-44919

Continuity equation and equations of motion for ideal plastic body based on von Mises yield condition, considering stress discontinuity and boundary value problems
24 p3153 A73-45499

YIELD STRENGTH

Mechanical properties and stress analysis of elastoplastic body, noting yield conditions and Bauschinger effect
03 p0386 A73-13155

The dependence of the lower yield strength in iron and steel on grain size and temperature.
04 p0463 A73-15308

A plastic-strip specimen for fatigue crack propagation studies in low yield strength alloys.
05 p0581 A73-16127

Partial yielding of cylindrical pressure vessel with elastic modulus and yield function as arbitrary functions of radial coordinate, assuming elastoplastic strain hardening material
06 p0761 A73-17895

Tresca type plastic material shear, considering hypoelastic yield interrelation to Tresca yields
06 p0763 A73-18457

Influence of local variations of yield strength on plastic zones at crack tips.
06 p0709 A73-18480

Strength and toughness of Fe-10Ni alloys containing C, Cr, Mo, and Co.
06 p0713 A73-18765

YIG [GARNET]

Dynamic yield, compressional, and elastic parameters for several lightweight intermetallic compounds. 09 p1099 A73-21926

Influence of the type of the stress-strain state on strain-hardening of materials 09 p1157 A73-22155

Ni-Ti alloy aging effects on yield strength explained by internal strain due to lattice modulation and Ti rich region volume fraction 09 p1103 A73-22520

Yield and fracture of D16T alloy at low temperatures in the presence of a complex stress pattern. 09 p1105 A73-23055

Linear elastic and general yielding fracture mechanics compatibility, investigating crack opening displacement relationship to stress intensity factor 09 p1109 A73-23263

Stress-strain relations for materials with different tension, compression yield strengths. 09 p1166 A73-23452

Yield criteria derivation for laminated media with isotropic and anisotropic layers based on strength constants characterization as tensors 10 p1289 A73-24277

Plasticity theory, strength-differential /SD/ phenomenon, and volume expansion in metals and plastics. 10 p1234 A73-24428

The effect of strain rate on the characteristic value of the linear-elastic fracture mechanics determined on large and small specimens 11 p1380 A73-25446

Effect of cyclic stress form on corrosion fatigue crack propagation below K_{Isc} in a high yield strength steel. 11 p1382 A73-25822

Mechanical properties of 6061 Al-Mg-Si alloy after very rapid heating. 13 p1636 A73-28795

Strength and ductility of two-phase iron alloy composed of austenite and martensite. 13 p1638 A73-29453

Influence of temperature on the initial yield of notch strength. 13 p1641 A73-29511

Two dimensional analysis of yielding to fracture process in angle-ply filament wound laminates under biaxial tension and compression 13 p1702 A73-29543

Automatic evaluation of strain gauge data reliability by comparison with a preset parameter and determination of a statistical yield strength. 13 p1622 A73-29549

Influence of vanadium, niobium, carbon, and silicon on the properties of low-pearlite steel 15 p1889 A73-31810

The effect of transverse shear stresses on the yield surface for thin shells. 16 p2082 A73-33905

On the transverse strength of fiber-reinforced materials. [ASME PAPER 72-APM-EEE] 17 p2249 A73-35111

A necessary condition for the nonoccurrence of von Mises yielding in impulsively loaded plates. 17 p2250 A73-35118

Dynamic yield strength determination at elevated temperatures after nanosecond pulse heating. [SESA PAPER 2141A] 17 p2148 A73-35450

Book - Elevated temperature properties as influenced by nitrogen additions to types 304 and 316 austenitic stainless steels. 18 p2325 A73-36971

The effect of very short time-at-temperature on the yield stress of 6061-T651 aluminum. 19 p2440 A73-37590

Effect of heat input on properties of Inconel filler metal 82 weld deposits. 19 p2435 A73-38002

The compression yield behaviour of polymethyl methacrylate over a wide range of temperatures and strain-rates. 19 p2444 A73-38097

Influence of non-singular stress terms and specimen geometry on small-scale yielding at crack tips in elastic-plastic materials. 19 p2501 A73-38264

General theory of constrained continuous media and plastic materials, deriving Huber-Mises yield condition by finite element method 19 p2501 A73-38304

Isotropic elastic material fracture and yield criteria in terms of frame-indifferent relation between stress and strain increments 20 p2623 A73-39563

Maraging steels with strengths from 110 to 130 kgf/sq-mm 21 p2718 A73-40736

Influence of hydrogen, alcohols, and moisture on the ultimate strength and electrical resistance of tungsten and steel wire samples 21 p2721 A73-41227

The Bauschinger effect and its role in mechanical anisotropy. 21 p2722 A73-41547

Effect of stressed state on strain hardening. 22 p2919 A73-42104

Fatigue and corrosion-fatigue crack growth of 4340 steel at various yield strengths. 22 p2875 A73-42142

Influence of the offset on the experimental yield surfaces of metals - A theoretical evaluation. 24 p3147 A73-44747

Effect of the characteristics of diamond grinding on the stressed state and strength of hard alloy VK6 24 p3094 A73-44968

Effect of vanadium, niobium, and silicon on the properties of low-pearlite steel. 24 p3100 A73-45273

YIG [GARNET]

U YTTRIUM-IRON GARNET

YJ-85 ENGINE

U J-85 ENGINE

YO-YO DEVICES

Experimental satellite for attitude control. II - Numerical analysis and a test of a yo-yo de-spinner. 01 p0111 A73-11190

Yo-yo system despin mechanism for the Aeros aeronomy satellite. 03 p0382 A73-13919

British X4 spacecraft mechanical design configuration with honeycomb sandwich panels, on yo-yo principle based despin system and flexible solar array 20 p2615 A73-39774

YOUNG MODULUS

U MODULUS OF ELASTICITY

YTTERBIUM

Cooperative luminescence in trivalent ytterbium and erbium ions in cadmium fluoride crystals 06 p0738 A73-18543

Transfer of Yb/3+/- excitation energy to TR/3+/- in CaF2 and BaF2 crystals 07 p0837 A73-20206

Crystallochemical analogy between europium, ytterbium, calcium, and barium in their alloys with manganese 09 p1135 A73-23235

YTTERBIUM COMPOUNDS

Chromium-ytterbium energy transfer in silicate glass. 21 p2752 A73-40963

YTTRIUM

The role of yttrium in high-temperature oxidation behavior of Ni-Cr-Al alloys. 16 p2025 A73-33077

YTTRIUM ALLOYS

Phase diagram of the neodymium-yttrium system 01 p0088 A73-10919

Influence of deformations on the mechanical properties of magnesium alloys containing yttrium 03 p0324 A73-13509

A study of precipitation at elevated temperatures in a Mg-8.7 pct Y alloy. 04 p0463 A73-15318

High temperature and metallographic investigation of Nd-Y alloys, measuring heat and electrical conductivity, thermal expansion and emf, magnetic susceptibility and Hall coefficient 06 p0735 A73-18050

Cast and annealed chromium-yttrium and chromium-lanthanum alloys peak solubility from metallographic, durometric and differential thermal analyses 12 p1512 A73-27245

YTTRIUM COMPOUNDS

NT YTTRIUM OXIDES

NT YTTRIUM-ALUMINUM GARNET

NT YTTRIUM-IRON GARNET

Enthalpy and specific heat of the orthophosphates of lanthanum, neodymium, and yttrium at high temperatures 06 p0738 A73-18654

Optical and thermal properties of hydrated yttrium vanadates in aqueous solutions, showing decomposition during thermal dehydration 06 p0739 A73-18655

Conductivity and solubility measurements and potentiometry for composition of yttrium nitrate-potassium metaniobate/potassium niobate/-water system 09 p1134 A73-22979

Spectroscopic and lasing studies of a new laser crystal, KY/WO4/2-Nd/3+/- 09 p1134 A73-22984

YTTRIUM OXIDES

Activated sintering of ThO2 and ThO2-Y2O3 with NiO. 01 p0066 A73-11014

The high-temperature oxidation of cobalt-21 wt % chromium-3 vol. % Y2O3 alloys. 04 p0461 A73-14925

Nonstoichiometric yttria crucibles for cold wall Ti melting, noting single batches, cost reduction and alloy homogeneity 04 p0455 A73-15749

Investigation in the sintering of Y2O3 powders in the temperature range 1000 to 1400 C. 04 p0457 A73-15987

Determination of the boundaries of fluorite-type Y2O3 solid solutions in HfO2 13 p1645 A73-28292

Nd-doped Yttralox ceramic lasing performance and interrelationship between ceramic processing, microstructure and optical quality of sintered product 24 p3097 A73-45414

YTTRIUM-ALUMINUM GARNET

Optical absorption spectrum of excited Cr/3+/- ions in yttrium aluminum garnet. 13 p1629 A73-29432

Observation of dislocations and inclusions in neodymium-doped yttrium aluminum garnet by transmission electron microscopy. 14 p1782 A73-29744

Detection of transient absorption in YAG laser crystals using combined laser. 14 p1756 A73-29930

Chromium-rare-earth energy transfer in YAlO3. 21 p2752 A73-40957

YTTRIUM-IRON GARNET

Advances in YIG-tuned Gunn effect oscillators. 04 p0426 A73-14734

Varactor or YIG tuned Gunn effect microwave oscillators for ECM applications, noting low noise octave tuning and high sweep rates 06 p0675 A73-17842

Compact YIG bandpass filter with finite-pole frequencies for applications in microwave integrated circuits. 06 p0678 A73-18742

Microwave filters with single crystal YIG sample as ferrimagnetic resonators, determining magnetic field and temperature effects on resonator cut-off frequency 08 p0942 A73-20705

Parallel spin-wave pumping in yttrium garnet single crystals. 11 p1409 A73-26188

Use of an yttrium-iron garnet sphere as the tuning element in Gunn oscillators 12 p1481 A73-27592

Application of the superregeneration principle to a ferromagnetic amplifier 13 p1592 A73-28910

Optical and polarization study of magnetization processes around individual dislocations in yttrium-iron garnet single crystals 23 p3017 A73-44024

Amplification of magnetostatic surface waves in the YIG-Ge hybrid system. 24 p3120 A73-45431

YUH-1 HELICOPTER

U UH-1 HELICOPTER

YUKAWA POTENTIAL

Time-dependent Yukawa-potentials of a class of weak gravitational fields. 02 p0193 A73-12182

Z

Z AXIS

U COORDINATES

Z TRANSFORM

U LAPLACE TRANSFORMATION

ZEEMAN EFFECT

Nitric oxide detection by use of Zeeman-effect and CO laser. 03 p0318 A73-12871

P II Zeeman effect spectral line observation for J-value assignments with check on wave functions obtained from energy level least squares fitting 05 p0600 A73-16497

Magnetic field effect on laser radiation intensity and polarization, noting Zeeman component change 09 p1095 A73-22666

Solar Fraunhofer spectral lines having simple Zeeman triplet splitting with large Lande g-factors tabulated, noting missing lines in identification 11 p1421 A73-25932

Asymmetric intensities of Zeeman components of electronic transitions of diatomic molecular spectra in sunspots, considering CN red lines 11 p1422 A73-25936

Transitions between Zeeman atomic sublevels in a medium 11 p1405 A73-26155

Field spinning Zeeman modulation in microwave spectroscopy with cosine distribution magnets. 11 p1366 A73-26302

RF field space-time modulation devices to obtain molecular beam velocity distribution and Zeeman pattern components shift 13 p1662 A73-28345

High temperature-microwave spectrometer for Zeeman-effect measurements involving diamagnetic molecules 14 p1753 A73-30235

On the Zeeman photometer observing upper atmospheric winds in the daytime. 19 p2429 A73-37377

Zeeman effect in the X-ray star candidates HD 77581 and theta super 2 Orionis. 19 p2482 A73-37399

Solar magnetic field spatial structure in relation to solar activity phenomena, discussing measurements based on Zeeman effect in absorption line spectra formation 20 p2605 A73-39059

ZENER DIODES
U AVALANCHE DIODES
ZENER EFFECT
 Zener diodes for overvoltage spark protection circuits in automatic control and measuring equipment operating in explosive environment 02 p0147 A73-12175
 Laws governing the behavior of the electrical resistance during process of inelastic-strain relaxation 23 p3040 A73-43574

ZENITH
 The accuracy of measurements of star transits 01 p0098 A73-10553
 Possible dependence of the differential shifts of Fraunhofer telluric lines on the solar zenith distance 01 p0106 A73-11241
 On automatic angle measurements and a proposition of their application into zenith distance measurements on the surface of the moon. 03 p0307 A73-13258
 Possible dependence of differential shifts of telluric Fraunhofer lines on zenith distance of the sun. 10 p1279 A73-24177
 Functional relation between the F2-layer ionization state in daylight time and the zenith angle of the sun 20 p2555 A73-39178
 Operational features of variable-profile antennas during near-zenith observations 21 p2666 A73-41445
 Short wave radio signal fadeout due to ionospheric disturbances, obtaining experimental equation on magnitude relationship with solar zenith angle and operating frequency 22 p2825 A73-42194

ZERO ANGLE OF ATTACK
 An investigation into the flow around a family of elliptically nosed cylinders at zero incidence at free-stream Mach numbers of 2.5 and 4. 02 p0129 A73-12507
 A mechanism for ablation-induced spin-up. 11 p1431 A73-26402
 Supersonic-hypersonic motion past a permeable cone at zero angle of attack 19 p2376 A73-37544
 The wave drag of circular nose cones at zero angle of attack at Mach numbers from 1.5 to 4 and thickness ratios from 0.05 to 0.5 23 p2940 A73-43782

ZERO CROSSINGS
U ROOTS OF EQUATIONS
ZERO FORCE CURVES
 Realization of a zero-force magnetic field configuration in the case of axisymmetric magnetohydrodynamic flows 09 p1146 A73-22541
 Synchrotron emission, adiabatic invariant, and gradient drift of particles in a linearly inhomogeneous magnetic field 09 p1132 A73-23079
 Some characteristics of the motion and acceleration of particles in a linearly inhomogeneous magnetic field with a neutral plane 09 p1132 A73-23080

ZERO GRAVITY
U WEIGHTLESSNESS
ZERO-ZERO WEATHER
U. CEILINGS [METEOROLOGY]
ZINC
 The inhibition of the dendritic electrocrystallization of zinc from doped alkaline zincate solutions. 03 p0273 A73-13727
 Influence of the intercrystalline structure on the diffusion of zinc in the symmetrical joints of bending of aluminum 11 p1379 A73-25324

ZINC ALLOYS
 Loading-rate dependence of the deformation mechanism in a Zn-22% Al superplastic alloy 03 p0326 A73-13970
 Influence of the composition and structure on the mechanical properties of ultraplasic alloys of the Al-Zn system 04 p0464 A73-15497
 Double aging time effects on hardness of solution treated, quenched and heat treated two phase Al-Zn-Mg alloy specimens, obtaining transmission electron micrographs 05 p0587 A73-16577
 Effect of titanium additions on the aging characteristics of an Al-Zn-Mg alloy. 13 p1632 A73-28134
 Tensile properties of high strength Al-Zn-Mg and Al-Zn-Mg-Cu alloy products processed by T-AHA type final thermomechanical treatments 13 p1633 A73-28141
 The effect of lattice disorder on the thermodynamic properties of the f.c. tetragonal beta-one NiZn alloys. 13 p1635 A73-28262

Fracture toughness-strength relationships in aluminum-zinc-magnesium-copper alloys. 13 p1639 A73-29473
 Graphite content effect on vibration damping properties of Al-Sn and Al-Zn alloys 13 p1643 A73-29608
 Tensile deformation and fracture in high-strength Al-Zn-Mg alloys. 20 p2575 A73-39019
 The influence of heat treatment on the stress-corrosion susceptibility of a ternary Al-5.3 pct Zn-2.5 pct Mg alloy. 20 p2576 A73-39031
 Superplasticity and residual tensile properties of a microduplex copper-nickel-zinc alloy. 22 p2879 A73-42582
 Study of precipitates in an aged Mg-3.6 wt%Zn alloy by an X-ray method. 23 p2993 A73-44124

ZINC COMPOUNDS
NT WURTZITE
NT ZINC OXIDES
NT ZINC SELENIDES
NT ZINC SULFIDES
NT ZINC TELLURIDES
NT ZINCBLENDE
 Preferential adsorption in the lubrication process of zinc dialkylidithiophosphate. [ASLE PREPRINT 72LC-3C-3] 03 p0274 A73-14358
 Spacecraft thermal control coatings development, discussing zinc orthotitanate/silicone properties as solar reflector 19 p2389 A73-37969
 High temperature creep of lithium zinc silicate glass-ceramics. I - General behaviour and creep mechanisms. II - Compression creep and recovery. 23 p2997 A73-44030

ZINC NICKEL BATTERIES
U NICKEL ZINC BATTERIES
ZINC OXIDES
 Electron spin resonance of ultraviolet radiation induced defects in ZnO thermal control coating pigment. 01 p0088 A73-11276
 Certain electrophysical properties of zinc oxide base semiconductor ceramics with admixtures of transition-metal oxides 06 p0735 A73-18079
 Concentration and mobility of electrons in indium-doped zinc oxide crystals 07 p0862 A73-20016
 Thickness dependence of effective coupling factors of ZnO thin-film surface-wave transducers. 09 p1086 A73-23097
 Measurement of zincate permeation in a polyethylene battery separator with controlled external hydrodynamic conditions. 11 p1307 A73-24974
 Oxidation of organic molecules by photoproducts of ZnO. 15 p1841 A73-31969
 RF sputtering of ZnO shear-wave transducers. 21 p2702 A73-40952
 Diffusion treatment of CdS and ZnO crystals and their applications in microwave acoustics. 24 p3120 A73-45433

ZINC SELENIDES
 The growth and electrical characteristics of epitaxial layers of zinc sulphide and of zinc selenide on p-type gallium phosphide. 01 p0088 A73-10683

ZINC SILVER BATTERIES
U SILVER ZINC BATTERIES
ZINC SILVER OXIDE BATTERIES
U SILVER ZINC BATTERIES
ZINC SULFIDES
NT WURTZITE
NT ZINCBLENDE
 The growth and electrical characteristics of epitaxial layers of zinc sulphide and of zinc selenide on p-type gallium phosphide. 01 p0088 A73-10683
 IR and thermal extinction spectra of luminescence and photoconductivity of zinc cadmium sulfide solid solution films doped with Cu and Cl 06 p0738 A73-18643
 Nonlinear optical susceptibility measurements for zinc silver indium sulfide quaternary compounds, noting agreement with bond charge theory 09 p1120 A73-22090
 Emission spectra of ZnS.Cu single crystals 21 p2751 A73-40311

ZINC TELLURIDES
 Spontaneous luminescence of ZnTe single crystals and mixed zinc cadmium telluride crystals at low temperatures, describing spectral lines 01 p0088 A73-10628
 Photoluminescence of ZnTe during laser stimulation 11 p1376 A73-26145
 Effect of an electric field on the negative photoconductivity of high-resistance ZnTe-CdTe crystals 17 p2219 A73-35552

ZINCBLENDE
 The exciton energy spectrum in diamond and sphalerite type crystals 09 p1134 A73-22683

ZIRCALOY 2 [TRADEMARK]
 A comparative study of the thermal diffusivities of stainless steel, hafnium, and Zircaloy. [ECTP PAPER C-6] 13 p1630 A73-28051
 The effect of plastic anisotropy in the low-cycle fatigue behavior of Zircaloy. 13 p1640 A73-29487

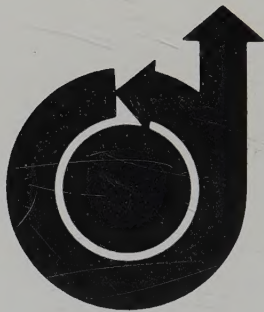
ZIRCALOYS [TRADEMARK]
NT ZIRCALOY 2 [TRADEMARK]
 Cracking of Zircaloy as a result of unusual localized texturing. 02 p0183 A73-12756
 Experiment on the mechanical anisotropy of titanium, zirconium, and Zircaloy-2 rolled sheets. 09 p1104 A73-22521

ZIRCONATES
 Raman spectrum of PbZrO₃. 21 p2752 A73-40894

ZIRCONIUM
 Nitrogen thermochemistry during the combustion of zirconium droplets in N₂/O₂ mixtures. 01 p0123 A73-10922
 Influence of the degree of decomposition of a solid solution of zirconium in aluminum on the recrystallization temperature of an aluminum-zinc-magnesium-zirconium system alloy 03 p0327 A73-13972
 An experimental investigation of the significance of zirconium partitioning in lunar ilmenite and ulvöspinel. 05 p0619 A73-16838
 Features of the structure and of plastic deformation in zirconium saturated with nitrogen and oxygen 09 p1099 A73-21967
 Experiment on the mechanical anisotropy of titanium, zirconium, and Zircaloy-2 rolled sheets. 09 p1104 A73-22521
 Anomalous creep behavior of crystal bar alpha-Zr during dynamic strain aging at 723-823 K as function of temperature, stress and oxygen content 14 p1760 A73-30626
 Titanium and zirconium alpha-omega transformation hysteresis at room temperature from dilatometry, X ray phase analysis and electrical resistance and shear measurements 14 p1764 A73-30863
 Zirconium sorption by and release from carboxyl cationites in nitric and sulfuric acids, discussing pH dependence 14 p1765 A73-30884

ZIRCONIUM ALLOYS
NT ZIRCALOY 2 [TRADEMARK]
NT ZIRCALOYS [TRADEMARK]
 Grain growth in alloyed molybdenum under conditions of creep 01 p0063 A73-10486
 Mechanical properties of molybdenum alloys. 01 p0065 A73-10818
 A sintered Nb-Ti-Zr alloy. 01 p0065 A73-10822
 Singularities of the temperature dependences of the heat conduction coefficients of solid solutions of the niobium-zirconium system. 01 p0066 A73-11338
 Hydrogen self-diffusion in the niobium-zirconium-hydrogen system 03 p0327 A73-13973
 Solubility of zirconium and niobium in solid-state copper 04 p0464 A73-15495
 Phase composition of Nb-1% Zr-C and Nb-2% Hf-C alloys 09 p1108 A73-23237
 Cast, annealed and hardened zirconium binary alloys cubic to hexagonal phase transitions from X ray and differential thermal analysis 10 p1233 A73-24318
 Zr additions effect on quenched and aged Al-Mg-Li alloy having phases in equilibrium with solid solution 10 p1236 A73-24928
 Phase equilibria in the aluminum-chromium-zirconium system 12 p1510 A73-26906
 Grain growth during creep of alloyed molybdenum. 14 p1759 A73-30311
 Some characteristics of the influence of alloying elements on the polymorphous transformation temperature of zirconium 14 p1765 A73-30886
 Properties of the superconducting alloy 35BT 15 p1887 A73-31188
 Simultaneous measurement of specific heat, electrical resistivity, and hemispherical total emittance of niobium-1 /wt. % zirconium alloy in the range 1500 to 2700 K by a transient /subsecond/ technique. 17 p2187 A73-34499
 A study of the process of oxidation of zirconium-oxygen alloys 17 p2188 A73-34558
 Structure and phase composition of welded joints of zirconium alloy with 2.5% Nb 19 p2439 A73-37266

- Electron diffraction study of a noncrystalline Zr-Ni phase. 20 p2575 A73-39021
- Twinned plate structure of martensitic transformation dependence on composition in Zr-Ti alloy investigated by transmission electron microscopy. 20 p2575 A73-39023
- Vacancy precipitation in quenched and aged Zr-Al alloys and Zircaloy 2, obtaining evidence by transmission electron microscopy for detailed dislocation structure examination. 20 p2578 A73-39488
- Effect of zirconium concentration on creep of niobium-zirconium alloys. 20 p2579 A73-39739
- The effect of heat treatment on the tensile strength and hardness of a quenched ternary zirconium-base alloy /Zr-0.5 wt. % Nb-1 wt. % Cr/. 21 p2717 A73-40319
- Preparation of zirconium-niobium alloy by carbide-oxide reaction. 21 p2717 A73-40321
- Influence of hydrogen on the mechanical properties of zirconium and some of its alloys. 21 p2718 A73-40483
- Phase diagram thermal sections and concentration corner of Mo-Zr-B system by microstructure, X ray and electron microscope analysis. 21 p2718 A73-40490
- Binary and ternary Laves phases in systems composed of zirconium and transition metals of the V through VII groups of the periodic system. 21 p2718 A73-40848
- Russian book - The structure of zirconium alloys. 22 p2873 A73-41973
- Omega-phase stability in the Ti-Zr-O system. 22 p2873 A73-42085
- Decay of the solid beta-solution in beta alloys of titanium and zirconium during tempering. 22 p2874 A73-42092
- Interdiffusion in the titanium-zirconium system. 22 p2874 A73-42099
- Concentration curves and phase diagram plotted for Nb-Zr system diffusion layers during annealing at 700 to 1700 C. 23 p2991 A73-43649
- ZIRCONIUM CARBIDES**
- Influence of high-temperature annealing on the rupture characteristics of zirconium carbide. 02 p0178 A73-11541
- Zirconium carbide creep characteristics and limit at 2450-2810 K, examining test conditions effects on parameters. 03 p0328 A73-14017
- Solubility of oxygen in ZrC. 07 p0838 A73-19199
- Interaction of graphite with titanium and zirconium. 09 p1105 A73-22977
- Recrystallization of electron-beam-melted tungsten with tantalum and zirconium carbide additions. 09 p1106 A73-23189
- Effect of neutron irradiation on the structure and properties of zirconium carbide. 12 p1512 A73-27200
- Diffusion-controlled processes in the homogeneity region of zirconium carbide. 15 p1881 A73-31593
- Temperature dependence of thermionic emission current density of Pt additive powdered zirconium carbide deposit on diode cathode working surface. 17 p2109 A73-35171
- Titanium carbide nitride and zirconium niobium carbide solid solutions electromotive forces, examining temperature-concentration dependencies, carbide and carbonitride conductivity mechanisms, resistivity and Hall effect. 18 p2325 A73-36964
- Thermionic properties of zirconium carbide/rhenium composites. 21 p2751 A73-40530
- Influence of the type of loading on high-temperature creeping of zirconium carbide. 23 p2998 A73-44287
- Thermal diffusivity and conductivity of titanium and zirconium carbides at high temperatures. 24 p3099 A73-44760
- ZIRCONIUM COMPOUNDS**
- NT ZIRCONATES**
- NT ZIRCONIUM CARBIDES**
- NT ZIRCONIUM HYDRIDES**
- NT ZIRCONIUM NITRIDES**
- NT ZIRCONIUM OXIDES**
- NT ZIRCONIUM TITANATES**
- Interaction between the ZrCr₂ intermetallic compound and some zirconium compounds with iron, cobalt, and nickel. 06 p0708 A73-18056
- Interaction between zirconium diboride and molybdenum. 09 p1105 A73-22981
- Confirmation of electronic paramagnetic resonance of the existence of an ordered phase in the zirconium-calcium system. 09 p1135 A73-23031
- X-ray absorption K-spectra of zirconium and its compounds with elements of the second period in the periodic table. 18 p2325 A73-36811
- Phase relations and diagram investigation for zirconium silicate-titanium dioxide system by quenching method, obtaining solid solution formation conditions and lattice constants. 23 p2998 A73-44131
- ZIRCONIUM HYDRIDES**
- Zirconium hydride space power reactor design and fabrication technology evaluation, emphasizing requirements for coupling with power conversion and applications for thermoelectric power generation. 09 p1118 A73-22801
- ZrH space power reactors design, discussing long life fuel elements, high temperature hard vacuum irradiation environment control drive components and shield fabrication. 11 p1395 A73-26011
- Performance of the thermoelectric converter for the zirconium hydride reactor thermoelectric space power supply. 11 p1396 A73-26036
- ZIRCONIUM NITRIDES**
- Investigation of the electrical resistivity of zirconium and hafnium nitrides. 06 p0714 A73-18559
- ZIRCONIUM OXIDES**
- Electrical evaluation of doped and undoped cobalt chromite as the interconnection material for high-temperature, zirconia-electrolyte, fuel-cell batteries. [ECS PAPER 16] 01 p0006 A73-10724
- Calcium stabilized zirconia electrolyte with appreciable oxygen ionic diffusivity used as permeation membrane for oxygen leak source. 02 p0167 A73-11955
- A new titanium and zirconium oxide from the Apollo 14 samples. 07 p0885 A73-19749
- Thermal and mechanical properties of zirconia cloth, felt and braid for heat shielding of reusable space shuttle. 12 p1548 A73-27379
- Resistance to crack propagation in ceramics subjected to thermal shock. 23 p2997 A73-44031
- ZIRCONIUM TITANATES**
- Dielectric breakdown of shock-loaded PZT 65/35. 09 p1132 A73-21927
- ZODIACAL DUST**
- Influence of nongravitational effects on the evolution of dust particles moving along elliptic orbits around the sun. 23 p3036 A73-44251
- ZODIACAL LIGHT**
- Interplanetary dust particle flux curves, number densities and size distributions from zodiacal light investigations. 02 p0215 A73-12262
- The zodiacal light as seen from the Pioneer F/G and Helios probes. 02 p0215 A73-12263
- A photometric model of the zodiacal light. 07 p0876 A73-19359
- Photography of the zodiacal light outside the ecliptic in quadrature and in opposition with the sun. 09 p1073 A73-22001
- Optical properties of single-component zodiacal light models. 11 p1357 A73-25926
- Observations of the inner F and K coronas below 2220-A wavelength. 16 p2060 A73-32954
- Observations of zodiacal light from the Pioneer 10 Asteroid-Jupiter probe - Preliminary results. 21 p2776 A73-41423
- French monograph - Preliminary photometric study in the far ultraviolet of the zodiacal and galactic emission. 22 p2910 A73-42716
- Photometric study of a diffuse reinforcement observed in the zodiacal light at a distance of 100 solar radii from the sun. 24 p3134 A73-44566
- ZONAL HARMONICS**
- Energy balance and field equations of dissipative atmosphere oscillations for zonal semidiurnal Pedersen region, using K-Hermicity. 02 p0158 A73-11907
- Synchronous satellite ground track drift analysis for ecological survey application, discussing zonal, tesseral and sectorial harmonics and perturbation compensation. 03 p0370 A73-13150
- Short term bounds for the effect of oblateness on ballistic trajectories. 03 p0373 A73-13495
- Improvement of zonal harmonics by the use of observations of low-inclination satellites Dial, SAS, and Peole. 04 p0438 A73-14795
- Relationship between the coefficients of spherical and ellipsoidal expansion of the gravity force in the case of the biaxial earth ellipsoid. 11 p1352 A73-25431
- Geoid equatorial section approximation by zonal spherical harmonics using axially-symmetric features. 15 p1940 A73-32050
- Zonal gravity harmonics from long satellite arcs by a seminumeric method. 17 p2233 A73-35269
- Density scale height and geopotential coefficients evaluations from analysis of Cosmos 54 rocket orbit perturbations due to drag and odd-zonal harmonics. 18 p2351 A73-36176
- Secular perturbations of third order with respect to oblateness from all zonal harmonics of the gravitational potential of a planet. 23 p3037 A73-44253
- Satellite intermediate orbit and secular perturbations due to second zonal harmonics of planetary potential and outer body attraction. 23 p3037 A73-44254
- ZOND SPACE PROBES**
- Measurements of the isotopic composition of particle fluxes carried out on spacecrafts Soyuz, Zond 8 and Luna 16. 02 p0206 A73-12317
- Photometric analysis of earth photographs from Zond space station, determining earth sidereal magnitude. 10 p1281 A73-24477
- ZONE MELTING**
- Impurities effect on Mo plastic properties and toughness, suggesting lower vacuum arc welding rates and increased electron beam zone refining runs. 01 p0066 A73-11343
- Electron beam float zone melting and vacuum degassing of niobium single crystals. 04 p0456 A73-15762
- Zone refining of chromium alloys with rare-earth metals. 06 p0707 A73-18042
- Dislocation structure of tungsten single crystals grown by electron-beam zone refining. 07 p0841 A73-20523
- Determination of the composition of Ni-NiMo eutectic by the zone recrystallization method. 09 p1108 A73-23239
- Investigation of structure and imperfections in molybdenum single crystals grown by electron-beam zone refining techniques. 13 p1631 A73-28106
- ZONE REFINING**
- U ZONE MELTING**



AIAA TECHNICAL INFORMATION SERVICE

750 THIRD AVENUE

NEW YORK, N. Y. 10017